Canadian Journal of Chemistry

Issued by THE NATIONAL RESEARCH COUNCIL OF CANADA

VOLUME 40 JANUARY 1962 NUMBER 1

CORRELATIONS OF ETHYLENIC PROTON COUPLING CONSTANTS WITH ELECTRONEGATIVITY

T. SCHAEFER

The Department of Chemistry, University of Manitoba, Winnipeg, Manitoba

Received September 11, 1961

ABSTRACT

A strong correlation is found between the electronegativity, E_X, and the three proton coupling constant of the vinyl group in over a hundred compounds of the type $CH_2 = CHX$. This correlation extends over the range $E_X = 4$ to 1 and over the range $J_{gem}+J_{cis}+J_{trans} = 14$ to 50 c.p.s. Simple implications and some useful applications of this correlation are discussed.

A recent publication notes that for a number of vinyl compounds the sums of the three proton coupling constants in the vinyl radical fall into two groups, one of about 20 c.p.s. and one of about 30 c.p.s. (1). Vinyl fluoride is an exception, with a sum of 14.3 c.p.s. At present there are data available for about 140 vinyl compounds (2–10). The sums of the coupling constants, $J_{gem}+J_{cis}+J_{trans}$, are found to lie in the range 14.3 to 50.2 c.p.s. (see Table I). It appears that there is a regular progression from low to high values.

Banwell *et al.* (3) have recently plotted values of coupling constants for seven vinyl compounds against the electronegativities derived by Dailey and Shoolery from chemical-shift differences in ethyl halides (11). They find an inverse proportionality, E_X, for the compounds $CH_2 = CHX$ over the range $E_X = 2.5$ to 4.0. It is of interest to see whether this inverse proportionality extends to lower values of E_X.

In Table I the known coupling constants for a large number of vinyl compounds are collected. Opposite each group X is given the value of E_X used in Figs. 1 and 2. The apparent electronegativity of a group will be dominated by the atom at which the vinyl group is attached. With this in mind, the values of E_X are given for the atom to which the vinyl group is bonded. Thus we use the same values of E_X for aryl and alkyl ethers and so on. Two exceptions are to be noted. The value $E_X = 3.35$ has been taken for the nitro group and $E_X = 3.0$ for the vinyl sulphones. These values appear approximately correct from the work of Clifford (13).

In Fig. 1, the values of the coupling constants are plotted against E_X. There certainly is a strong correlation between the two parameters. Whether it is a linear relationship is perhaps questionable, but illustrative straight lines are drawn through the points. The values for bromine fall consistently far from the "straight line".

Inspection of the methods used for the analysis of the proton resonance spectra, which are all of the *ABC* type (15), shows that the sum of the coupling constants is a much more accurate experimental parameter than the individual values. This is so because this

TABLE I

Average values of coupling constants in compounds $CH_2 = CHX$ in c.p.s.

X	E_X	No. of values	J_{gem}	J_{cis}	J_{trans}	Reference
1. —F	3.95*	3	−3.2	4.65	12.75	2, 3, 5
2. —Cl	3.2*	2	−1.4	7.3	14.6	2, 3
3. —Br	3.0*	4	−1.8	7.1	15.2	2, 3, 4, 5
4. —OR (alkyl)	3.5*	17	−1.9	6.7	14.2	2, 3
5. —OR (aryl)	3.5*	13	−1.5	6.5	13.7	2
6. —OOCR	3.5†	12	−1.4	6.3	13.9	2
7. —Phosphates	3.5†	5	−2.3	5.8	13.2	2
8. —NO_2	3.35‡	1	−2.0	7.6	15.0	2
9. —NR	3.0*	5	0	9.4	16.1	2, 5
10. —COOR	2.5†	14	1.7	10.2	17.2	2
11. —CN	2.5†	1	1.3	11.3	18.2	7
12. —COR	2.5†	2	1.8	11.0	18.0	2, 5
13. —R (alkyl)	2.5†	18	1.6	10.3	17.3	2, 8
14. —R (aryl)	2.5†	9	1.3	11.0	18.0	2
15. —Pyridyl	2.5†	3	1.1	10.8	17.5	2
16. —Sulphones	3.0‡	9	−0.6	9.9	16.6	2
17. —Sn	1.9*	4	2.8	14.1	20.3	2, 10
18. —As	2.1*	4	1.7	11.6	19.1	2
19. —Sb	2.0*	1	2.0	12.6	19.5	2
20. —Pb	1.9†	1	2.0	12.1	19.6	2
21. —Hg	1.9†	1	3.5	13.1	21.0	10
22. —Al etherate	1.5†	1	6.3	15.3	21.4	10
23. —Li	1.0†	1	7.1	19.3	23.9	9

*Reference 12.
†Reference 14.
‡Reference 13.

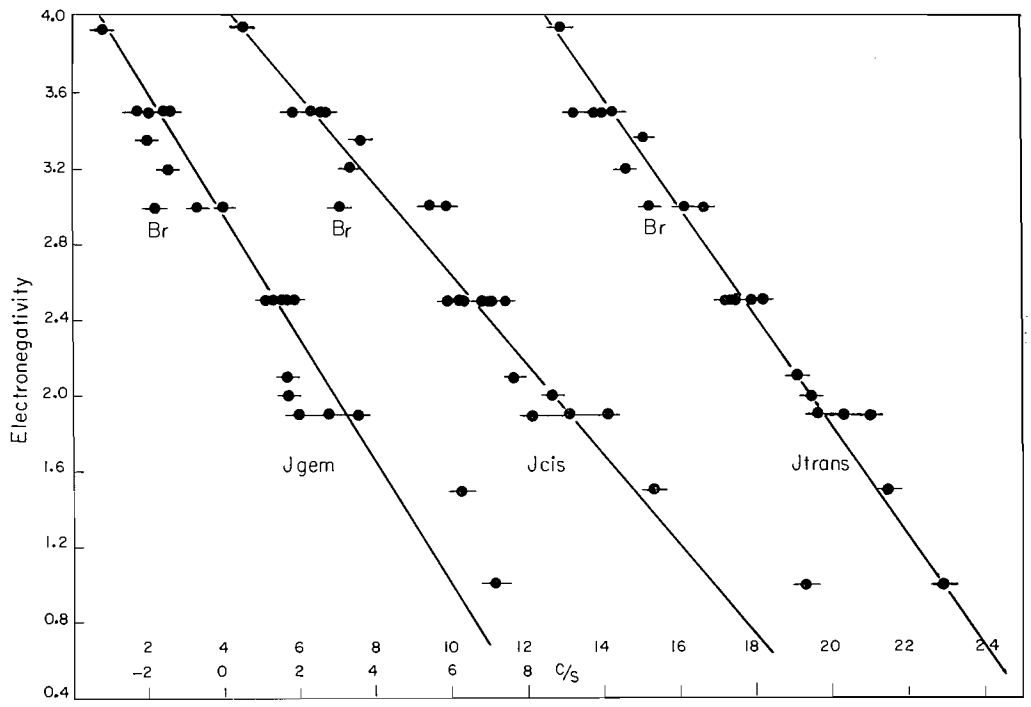

FIG. 1. The values of J_{gem}, J_{cis}, and J_{trans} in c.p.s. are plotted against the electronegativity E_X. Data are from Table I. Note that J_{cis} and J_{trans} are referred to the scale running from 0 to 24 c.p.s.

parameter can be gotten directly from the repeated line spacings in the spectrum (7), whereas the individual values must be extracted by a complete analysis involving the three chemical-shift parameters as well. The percentage error in J_{gem} is bound to be particularly large, since its magnitude is so small. Therefore it is gratifying that the best correlation between J and E_X is found for J_{trans}.

In Fig. 2, the sum of the coupling constants is plotted against E_X. Since in almost all

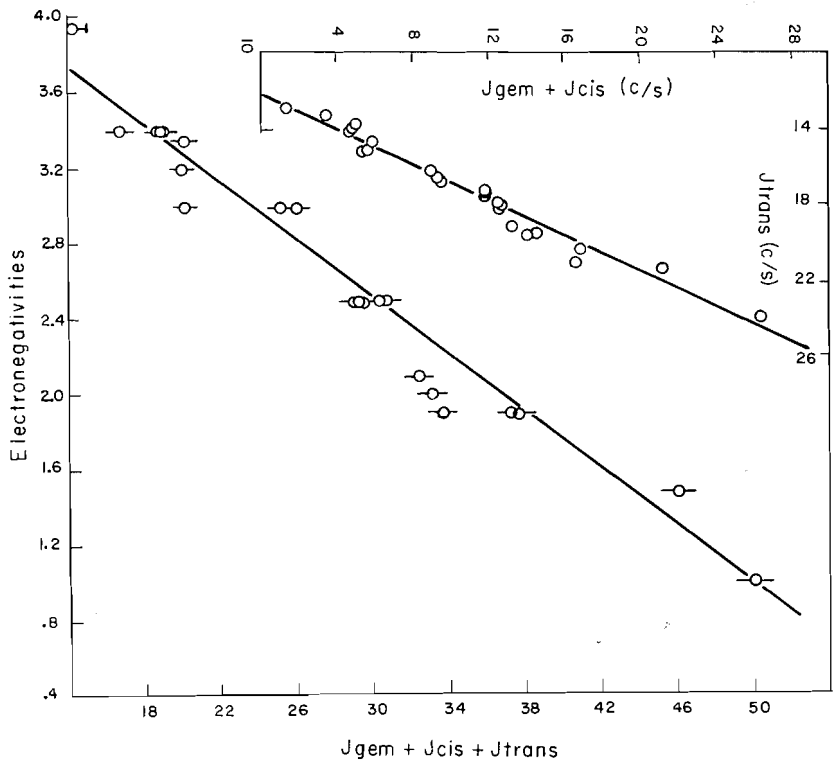

FIG. 2. The sum $J_{gem}+J_{cis}+J_{trans}$ in c.p.s. plotted against the electronegativity E_X; also sum $J_{gem}+J_{cis}$ plotted against J_{trans}, all in c.p.s. Data are from Table I.

the compounds this sum was accurately derived with a maximum error of about 0.5 c.p.s. (2), we can conclude from Fig. 2 that the scatter in most cases is due to factors other than that of large errors in the coupling constants. It would be surprising, I think, if there were a precise relationship between the two parameters. Extensive calculations suggest strongly that the value of J_{gem} should depend only on the angle between the two C—H bonds (5). In that case, Fig. 1 suggests that an approximate relationship exists between the bond angle and the electronegativity of the substituent on the β-carbon atom. In particular, the value of the CH_2 bond angle for metal vinyls should then lie between 110° and 120° (5).

It follows from Figs. 1 and 2 that there will be linear relationships between the coupling constants themselves. This has been found over a restricted range by Banwell and Shepherd (16). In order to minimize the relatively large errors in J_{gem}, Fig. 2 also shows a plot of $J_{gem}+J_{cis}$ against J_{trans}. The plot is linear, as expected.

An obvious practical application of the above correlations is in the analysis of the proton resonance spectra of other vinyl compounds. If the values found lie too far off

the lines in Fig. 1 they are probably incorrect. There are a number of examples in the literature. A striking one is tetravinylsilane (2). The coincidence of a large number of the 15 possible lines in the spectrum is probably the reason for the wrong assignment.

Another useful application is as a discriminant between two reasonable sets of parameters derived from a single spectrum. The iterative method for solving the ABC system does not always converge on the correct ones (7). The exact analysis of three spin spectra is now possible (7). In the exact analysis one always finds *all* the possible solutions, but the final choice is not always completely unambiguous; a consequence of the errors in peak-intensity measurements. An example is the ABC proton spectrum of acrylonitrile, the most reliable analysis of which is, no doubt, that of Castellano and Waugh (7). They find two sets of coupling constants, both of which would be accepted as reasonable if reached by the usual iterative method. They suggest that a final decision be made by running the spectrum in a magnetic field strength considerably different from the one they use. This has been done in these laboratories and, at the cost of considerable work, their preferred assignment has been substantiated. It is interesting to note that the reference to the plot of Fig. 1 would have resulted in the same conclusion.

ACKNOWLEDGMENTS

I would like to thank the National Research Council at Ottawa and the Research Corporation for financial aid.

REFERENCES

1. G. S. Reddy and J. H. Goldstein. J. Chem. Phys. **35**, 389 (1961).
2. W. Bruegel, Th. Ankel, and F. Krueckeberg. Z. Elektrochem. **64**, 1121 (1960).
3. C. N. Banwell, N. Sheppard, and J. J. Turner. Spectrochim. Acta, **16**, 794 (1960).
4. T. Schaefer and W. G. Schneider. Can. J. Chem. **37**, 2066 (1960).
5. H. S. Gutowsky, M. Karplus, and D. M. Grant. J. Chem. Phys. **31**, 1278 (1959).
6. E. O. Bishop and R. E. Richards. Mol. Phys. **3**, 114 (1960).
7. S. Castellano and J. S. Waugh. J. Chem. Phys. **34**, 295 (1961).
8. A. A. Bothner-By and C. Naar-Colin. J. Am. Chem. Soc. **83**, 231 (1961).
9. C. S. Johnson, Jr., M. A. Weiner, J. S. Waugh, and D. Seyferth. J. Am. Chem. Soc. **83**, 1306 (1961).
10. D. W. Moore and J. A. Haape. J. Phys. Chem. **65**, 224 (1961).
11. B. P. Dailey and J. N. Shoolery. J. Am. Chem. Soc. **77**, 3977 (1955).
12. M. L. Huggins. J. Am. Chem. Soc. **75**, 4123 (1953).
13. A. F. Clifford. J. Phys. Chem. **63**, 1227 (1959).
14. W. Gordy and J. O. Thomas. J. Chem. Phys. **24**, 439 (1956).
15. H. J. Bernstein, J. A. Pople, and W. G. Schneider. Can. J. Chem. **35**, 65 (1957).
16. C. N. Banwell and N. Sheppard. Mol. Phys. **3**, 350 (1960).

THE RATE OF REACTION OF ACTIVE NITROGEN WITH AMMONIA AND ETHYLENE[1]

A. N. WRIGHT AND C. A. WINKLER
The Physical Chemistry Laboratory, McGill University, Montreal, Que.

Received August 14, 1961

ABSTRACT

The rate constants for the reactions of C_2H_4 and NH_3 are determined by termination of the reactions in the gas phase after different times of reaction. The average value for the rate constant of the N atom – C_2H_4 reaction at 150° C is 1.8×10^{10} cc mole^{-1} sec^{-1}, when the initial N-atom concentration is determined from the maximum production of HCN. The average value for the rate constant for the over-all reaction of NH_3 with excited nitrogen molecules, at 104° C in the "poisoned" system, and 83° C in the "unpoisoned" system, for low initial flow rates of NH_3, or short reaction time, is 2.2×10^{10} cc mole^{-1} sec^{-1}. The decrease in value of this rate constant at higher initial flow rates of NH_3 and longer reaction times in the "poisoned" system indicates that the species responsible for NH_3 decomposition is generated during the decay of N atoms in the presence of NH_3. The value for the NH_3 reaction is discussed in terms of energy transfer.

INTRODUCTION

Previous investigations (1) have indicated that the reaction of active nitrogen with C_2H_4 involves a direct attack of nitrogen atoms on the hydrocarbon, with production of HCN to the extent of about 96% of the nitrogen atoms destroyed. On the other hand, the corresponding reaction of NH_3 (2) appears to involve its destruction by excited nitrogen molecules. The maximum extent of NH_3 destruction, by active nitrogen, produced in a condensed discharge, is about one sixth the maximum production of HCN from C_2H_4 and other hydrocarbons. The reaction with NH_3 appears to be unaffected in extent by increase in reaction temperature, and to proceed at a quite rapid rate (2). With active nitrogen produced by a microwave discharge, Kistiakowsky and Volpi observed (3) that addition of NH_3 partially quenched the yellow nitrogen afterglow, without measurable destruction of NH_3, or decrease in N-atom concentration, as measured by a mass spectrometer. These authors estimated that the rate constant for a reaction between N atoms and NH_3 must be less than 10^8 cc mole^{-1} sec^{-1}. Since the reaction $N + NH_3 = NH + NH_2$ is endothermic to the extent of approximately 19 kcal, while the process $N + NH_3 = N_2 + H_2 + H$ conflicts with spin-conservation rules, they concluded that the efficient quenching of the afterglow was due to reaction between NH_3 and electronically excited nitrogen molecules. The concentration of the latter was estimated to be very low in the active nitrogen produced by the microwave discharge.

Further evidence that the destruction of NH_3 does not involve N atoms, in the rate-controlling step, is provided by the observation that addition of excess NH_3 to active nitrogen of microwave origin does not affect the ability of the active nitrogen to destroy nitric oxide (4). Moreover, it has recently been established (5) that its addition to active nitrogen produced by a condensed discharge, wherein appreciable destruction of NH_3 is observed, does not decrease either the ability of the active nitrogen to destroy NO, nor its capacity to produce HCN from C_2H_4. Hence, if the concentration of nitrogen atoms indicated by reaction of active nitrogen with NO is greater than that inferred from the

[1]*This work supported by the Geophysics Research Directorate, Air Force Cambridge Research Division, and by the Defence Research Board of Canada.*

maximum production of HCN from C_2H_4, as observed by Verbeke and Winkler (6), and this discrepancy is due to reactions of NO with excited nitrogen molecules, as these authors suggest, the excited molecules responsible for NH_3 decomposition might not be the same species as those responsible for reaction with NO.

Since NH_3 quenches the afterglow which originates in a transition between the B and A states of the nitrogen molecule, it seemed reasonable to assume (3) that $N_2(B^3\Pi_g)$ was probably responsible for the destruction of NH_3. However, recent work (7) has indicated that other precursors of the afterglow, such as the $^5\Sigma_g^+$ state, might also be involved. The destruction of NH_3 has also been attributed (8) to the $A^3\Sigma_u^+$ state of the nitrogen molecule, with a lifetime of at least 10^{-2} second (9, 10). This suggestion seems more plausible if it is assumed that the $A^3\Sigma_u^+$ molecules responsible for NH_3 decomposition have sufficient vibrational energy to permit crossover (7, 11) into the B state at vibrational levels high enough to give rise to at least part of the Lewis–Rayleigh nitrogen afterglow. Although vibrationally excited *ground-state* nitrogen molecules have a long lifetime (12, 13), and certain levels of this state could cause the decomposition of NH_3 (14), it is difficult to see how their removal by NH_3 would affect the afterglow (15).

The results of Kelly and Winkler (8) indicated that the excited nitrogen molecule responsible for NH_3 destruction is probably formed during homogeneous decay of nitrogen atoms. However, measurable amounts of NH_3 destruction have been observed only in active nitrogen produced by a condensed discharge, and it has been suggested (4) that the production of excited molecules might depend upon the mode of excitation of the nitrogen. In fact, recent studies of Beale and Broida (16), and Young and Clark (15), have indicated a large number of energetic species that *may* survive, at low concentrations, into the afterglow region. On the other hand, if the excited molecule is *formed* during homogeneous decay of ^4S nitrogen atoms, its concentration should be proportional to the square of the N-atom concentration, and, consequently, should be quite small in active nitrogen produced at low concentrations in a microwave system. It might be difficult, therefore, to detect destruction of NH_3 in such a system, even if the rate constant for the over-all reaction is relatively high.

The rate of reaction of active nitrogen with unsaturated hydrocarbons is quite fast (1). At the time this study was begun, no accurate determination of the rate constant for these reactions had been reported, although Greenblatt and Winkler (17) had obtained a rough estimate for the rate constant of the active nitrogen – ethylene reaction by a diffusion-flame technique. The average value, at a reaction temperature of about 52° C, was 4.0×10^{10} cc mole^{-1} sec^{-1}.

The purpose of the present work was to compare the rate constants, by a method involving variation in time of reaction, for the reactions of active nitrogen with C_2H_4 and NH_3. Active nitrogen was generated at relatively high concentrations in a condensed discharge (1), so that the ammonia reaction proceeded to an easily measurable extent. The reactions were terminated in the gas phase, after different times of reaction, by "flooding" the reaction mixture with another reactant. The reactions were studied only in an unheated reaction vessel, with temperatures in the reaction zones up to about 105° C with ammonia and 151° C with ethylene.

The rate constant for the NH_3 reaction presumably corresponds to the over-all reaction

$$N_2^* + NH_3 \rightarrow NH_3^* + N_2 \rightarrow \text{decomposition products} + N_2, \qquad [1]$$

where N_2^* and NH_3^* represent excited molecules. The previous studies of Freeman and Winkler (2) and Willey and Rideal (18) both indicated that the products of this reaction

are only N_2 and H_2. As in the photodecomposition of NH_3 (see, for example, reference 19), the excited NH_3 molecule probably breaks down to an hydrogen atom and the NH_2 radical, which is then followed by the reaction

$$2NH_2 \rightarrow N_2 + 2H_2. \qquad [2]$$

EXPERIMENTAL

The condensed discharge was operated for a "warm-up" period of at least 20 minutes prior to each experiment of 100-seconds duration. The reaction vessel was a straight, pyrex-glass tube of 25-mm i.d., with a fixed reactant jet 14.5 cm below the discharge and a *mobile reactant jet* (20) that could range from 0.1 to 45 cm below the fixed jet. Both jets contained six small holes placed symmetrically around their bulbous ends to produce an even flow of reactant into the active-nitrogen stream.

Because of the complicating reactions of hydrogen atoms with NH_3 at higher temperatures (2), the present experiments were made in an unheated reaction vessel. The pressure in the system was 3 mm of Hg, with a flow rate of molecular nitrogen of 378×10^{-6} mole sec^{-1}, corresponding to a linear flow rate of 478 cm sec^{-1}. The apparatus was "poisoned" against nitrogen-atom recombination by the introduction of less than 0.03×10^{-6} mole sec^{-1} of water vapor to the molecular nitrogen before the discharge. Such a small quantity of water vapor does not appear to affect the reactions of active nitrogen (21), but is an effective "poison" for wall recombination of atoms (22).

Nitrogen (Linde "bone-dry") was used without further purification, except during experiments in the "unpoisoned" system, when a liquid-air trap was used to ensure that no traces of moisture remained in the gas. Commercial NO (Matheson Co.) was freed from nitrogen by evacuation, while the NO was kept at liquid-nitrogen temperature; N_2O_3 was removed by three distillations of the NO from a bath held at $-78°$ C. Anhydrous ammonia (Canadian Industries Ltd.) and C. P. ethylene (Ohio Chemical Co.) were used after three bulb-to-bulb distillations during which only the middle fractions were retained. The reaction products were trapped at liquid-air temperature, and the production of HCN, or destruction of NH_3, was followed by the usual titration method.

The concentration of nitrogen atoms available for reaction at the fixed upper jet was estimated by the two methods in current use, i.e., by a gas-phase titration with NO (23, 24), and from the maximum production of HCN from C_2H_4 (1, 8).

RESULTS

After the 20-minute warm-up period, the temperature of the active-nitrogen stream, as measured with a glass-encased thermocouple 3 cm below the fixed jet, was found to be constant, for about 5 minutes, at 106° C in the "poisoned" system, and at 85° C in the "unpoisoned" system. The temperature measured during the C_2H_4 reaction, at flow rates of ethylene in the plateau region (see ref. 1), was 151° C in the "poisoned" system. The addition of excess NH_3 to the active nitrogen caused a *decrease* of 1° to 2° C in both the "poisoned" and "unpoisoned" systems. Possibly the reaction of NH_3 with N_2* removed a species from active nitrogen, which otherwise readily loses energy to the wall.

In the "poisoned" system, the maximum, or "plateau value", production of HCN from C_2H_4, when the reaction products were trapped 120 cm downstream from the fixed jet, was found to be independent of the reaction temperature in a cylindrical reaction vessel (5, 25) and indicated a flow rate of N atoms equal to 24.7×10^{-6} mole sec^{-1} at the fixed upper jet. The NO "titration" indicated a flow rate of N atoms equal to 45.0×10^{-6} mole sec^{-1} at the same point. The ratio NO/HCN of 1.8 is similar to that found by Verbeke and Winkler (6) at a pressure of 3 mm. This discrepancy between the two methods for estimating the N-atom concentration will be discussed elsewhere (5). Both values are used for calculating rate constants in the present study, to enable comparison with published values that are based on N-atom concentrations inferred from either method.

The experimentally observed quantities were measured as flow rates. These may be expressed as concentrations for calculations of rate constants by a multiplying factor equal to the ratio of molecular nitrogen concentration in the system, determined from the ideal gas law to be $1.43_3\times10^{-7}$ mole cc^{-1} at 3 mm and 25° C, to the molecular nitrogen flow

rate. The numerical value of this factor at 25° C was 3.79×10^{-4} sec cc^{-1}. The same value was used for other temperature conditions encountered in the study, since neither the pressure within the system, nor the linear flow rate of gas, showed appreciable variation with temperature between 25° C and 106° C, with the discharge off and on respectively. The flow rates mentioned above for the "poisoned" system corresponded to concentrations of N atoms at the fixed jet of $1.7_0\times10^{-8}$ and $0.93_6\times10^{-8}$ mole cc^{-1} for the NO and HCN methods respectively. In the "unpoisoned" system, the two methods indicated N-atom flow rates of 18.0×10^{-6} and 10.6×10^{-6} mole sec^{-1}, corresponding to N-atom concentrations of $0.68_1\times10^{-8}$ and $0.40_1\times10^{-8}$ mole cc^{-1} respectively.

The Reaction with Ethylene

The addition of an excess of NO (46.0×10^{-6} mole sec^{-1}) through the mobile jet, at different levels downstream from C_2H_4 introduced through the fixed upper jet, was found to decrease the HCN production from C_2H_4. The HCN production was reduced by only about 5% when NO was added at the 45- and 30-cm levels downstream, compared with the amount normally produced when the reaction was allowed to proceed to completion, i.e., for 120 cm, before the products were trapped. However, addition of NO at distances of 15, 10, 5, and 1.2 cm below the C_2H_4 inlet, corresponding to reaction times with C_2H_4 of 31.4, 20.9, 10.5, and 2.5 milliseconds respectively, decreased HCN production to a larger extent, as indicated by the results in Table I. The very rapid reaction of NO with nitrogen atoms (26) appeared to terminate the C_2H_4 reaction, by the rapid removal of any N atoms remaining in the gas stream.

TABLE I

Second-order rate constants for N+C_2H_4 at 150° C

Reaction time, milliseconds	Flow rate of C_2H_4, mole sec^{-1} ($\times10^6$)	HCN recovered, mole sec^{-1} ($\times10^6$)	k_{NO},* cc mole^{-1} sec^{-1} ($\times10^{-9}$)	k_{HCN},† cc mole^{-1} sec^{-1} ($\times10^{-9}$)
31.4	46.0	22.6	1.59	5.91
20.9	46.0	22.0	2.29	7.88
10.5	46.0	18.9 (23.0)	3.6 (4.9)	9.7 (19.5)
10.5	16.0	10.5 (13.3)	5.6 (8.2)	12.6 (18.9)
2.5	46.0	15.9 (18.1)	10.5 (13.9)	24.3 (36.2)

*k_{NO} is calculated for $[N]_0 = 1.7_0\times10^{-8}$ mole cc^{-1} (based on NO titration).
†k_{HCN} is calculated for $[N]_0 = 0.93_6\times10^{-8}$ mole cc^{-1} (based on maximum HCN production).

Rate constants were calculated from the integrated second-order rate equation, assuming that the initial N-atom attack on C_2H_4 is rate determining for HCN production, and that 1 molecule of C_2H_4 yields 1.5 molecules of HCN (1, 5) under the prevailing conditions. The equation then takes the form

$$k = \frac{1.5}{t}\frac{2.303}{a-1.5b}\log\frac{b(a-x)}{a\left(b-\frac{x}{1.5}\right)},$$

where x represents the concentration of HCN produced, and the other symbols have their usual significance.

When NO was added at distances of 5 cm or less from the C_2H_4 jet, considerable reaction of N atoms with NO occurred (the green NO_2 glow was observed), and condensation of ozone became a hazard. This was avoided by placing silver wire in the gas stream just before the trap, to remove oxygen atoms. However, the presence of silver oxide

decreased the amount of HCN recoverable by distillation from the product trap, and this decrease persisted even when the C_2H_4 reaction was allowed to go to completion, i.e., when no NO was added. The previously established HCN production for complete reaction at the particular initial flow rate of C_2H_4 used could be reproduced only after the product trap was cleaned with acid. This decrease in recoverable HCN was slightly variable, and a normalization factor for HCN loss was derived by making an experiment at the same C_2H_4 flow rate, but without added NO, immediately following each reaction that involved addition of NO at distances of 5 cm or less. The figures in parentheses in Table I are normalized in this way, to take into account the loss in HCN when silver oxide was present in the system. The normalization factor for a reaction time of 10.5 milliseconds, at a flow rate of 46.0×10^{-6} mole sec^{-1} of C_2H_4, was apparently a little too high, but the rate constant, based on an initial N-atom concentration inferred from the NO titration, lies somewhere between 3.6×10^{9} and 4.9×10^{9} cc $mole^{-1}$ sec^{-1}.

The values for the rate constant must be considered as minima, since the method assumes that neither NO, nor oxygen atoms, interferes with the *production* of HCN from the reaction of nitrogen atoms with ethylene. The averages (27) of the normalized values for the rate constant, based on the two methods for estimating the initial N-atom concentration, are $k_{NO} = 6.2\times10^{9}$ cc $mole^{-1}$ sec^{-1} and $k_{HCN} = 1.8\times10^{10}$ cc $mole^{-1}$ sec^{-1}. These are in fair agreement with the value previously obtained by observations on the length of the reaction flame (17).

The Reaction with Ammonia

Flooding the NH_3 – active nitrogen mixture with NO, to terminate the NH_3 reaction, would not be satisfactory because of the reaction of oxygen atoms with NH_3, and the reaction of NO with its decomposition products (19). However, it was found that the extent of NH_3 destruction was decreased by the addition of excess C_2H_4 (in the range 52×10^{-6} to 60×10^{-6} mole sec^{-1} in the "poisoned" system, and 46×10^{-6} mole sec^{-1} in the "unpoisoned" system) at the 45-, 30-, 15-, and 1.2-cm levels below the NH_3 inlet, corresponding to times for the NH_3 reaction of 94.3, 62.7, 31.4, and 2.5_1 milliseconds respectively. For a given flow rate of NH_3, the decrease became larger as the C_2H_4 was added closer to the NH_3 jet, and, at each level, became smaller as the flow rate of NH_3 was increased. The results are summarized in Table II.

It appeared that the excess of C_2H_4 quickly removed not only the N atoms remaining in the gas stream, but probably also removed (14) most of the excited nitrogen molecules remaining in the system. Experiments in which C_2H_4 was added at 15 and 30 cm above the point of introduction of NH_3 showed that the ability of active nitrogen to decompose NH_3 was completely destroyed. It should be noted that, even though C_2H_4 could deactivate many possible forms of N_2*, and became itself excited by a collision of the second kind, direct formation of HCN from this reaction is highly unlikely. Moreover, subsequent production of HCN from a possible breakdown product of the excited C_2H_4, such as C_2H_3 or CH_3, would still require consumption (14) of N atoms.

Experiments in the "poisoned" system, with a flow rate of NH_3 of $2.5_0\times10^{-6}$ mole sec^{-1}, represent those where the amount of NH_3 introduced is less than the maximum amount of NH_3 destroyed ($4.5_0\times10^{-6}$ mole sec^{-1}) at high flow rates of NH_3, when the reaction goes to completion. Under conditions of complete reaction, no NH_3 is recovered at an initial flow rate of $2.5_0\times10^{-6}$ mole sec^{-1}, and it appears, from the reaction for 94.3 milliseconds, that about 90% of the NH_3 introduced at that flow rate is destroyed at the 45-cm level. In all other experiments in the "poisoned" system, the initial flow rate of

TABLE II

Second-order rate constants for reaction of NH_3 with active nitrogen

Time of reaction, milliseconds	Initial flow rate of NH_3, mole sec^{-1} ($\times 10^6$)	NH_3 destroyed, mole sec^{-1} ($\times 10^6$)	k_{obs}* cc $mole^{-1}$ sec^{-1} ($\times 10^{-10}$)
"Poisoned" system: reaction temperature ~104° C			
94.3	2.5_0	2.2_3	2.2
	8.0_0	3.2_6	0.60
	12.5	3.9_3	0.60
62.7	2.5_0	1.8_8	1.9
	8.0_6	2.5_0	0.47
	12.5	3.1_0	0.46
31.4	2.5_0	1.2_0	1.5
	2.5_0	1.2_1	1.5
	8.0_0	1.9_0	0.55
	12.5	2.0_6	0.44
2.5_1	2.5_0	0.3_6	3.8
	8.0_0	0.8_0	1.7
	11.7	1.0_7	2.6
	12.5	1.4_3	3.5
"Unpoisoned" system: reaction temperature ~83° C			
94.3	2.2_0	0.9_0	1.6
62.7	2.2_0	0.8_7	2.3
31.4	2.8_0	0.6_7	1.8

*k_{obs} based on initial [active nitrogen] given by maximum amount of NH_3 destruction = $1.7_6\times10^{-9}$ mole cc^{-1}, "poisoned" system; = $0.55_6\times10^{-9}$ mole cc^{-1}, "unpoisoned" system.

NH_3 is greater than the maximum destruction of NH_3 when the reaction goes to completion. At an initial flow rate of NH_3 of 12.5×10^{-6} mole sec^{-1}, its destruction at the 45-cm level appears to be only 88% of the maximum destruction obtained at this flow rate when the reaction is not interrupted by the addition of C_2H_4. In the "unpoisoned" system, the initial NH_3 flow rates are slightly larger than the maximum destruction of NH_3 for complete reaction, $1.4_7\times10^{-6}$ mole sec^{-1}.

The selection of a value for the initial concentration of active nitrogen at the fixed jet, capable of reaction with NH_3, poses a problem. If one assumes that the reaction is due to excited molecules produced directly in the discharge, or formed by homogeneous recombination of N atoms between flashes within the discharge (8), the most obvious value to use for $[N_2^*]_{initial}$ would be the maximum destruction of NH_3 when the reaction goes to completion. When the reaction was allowed to proceed to the trap (120 cm from the fixed jet), the extent of NH_3 destruction in the "poisoned" system increased only by 0.2×10^{-6} mole sec^{-1} for an increase in NH_3 flow rates from $8.0_0\times10^{-6}$ to 13.0×10^{-6} mole sec^{-1}. In the "unpoisoned" system, the extent of NH_3 destruction after complete reaction ($1.4_7\times10^{-6}$ mole sec^{-1}) was quite independent of the initial flow rate of NH_3 between the same limits. These "plateau" values for NH_3 destruction indicated concentrations of active nitrogen capable of NH_3 destruction, at the fixed jet, of $1.7_0\times10^{-9}$ and $0.55_6\times10^{-9}$ mole cc^{-1}, in the "poisoned" and "unpoisoned" systems repectively.

Using these values for $[N_2^*]_{initial}$, second-order rate constants were calculated for the destruction of NH_3 by active nitrogen, on the assumption that excitation of NH_3, by a collision of the second kind, leads to its dissociation with an efficiency of 100% at the pressure of 3 mm used in the experiments. Precedent for the latter assumption is obtained from the observation that the photolytic decomposition of NH_3 proceeds with a primary quantum yield of unity (see ref. 19). The absence of collisional transfer of energy from

excited NH_3 to NO, added as a radical scavenger, at a pressure of 4 mm or less, has been explained (28) by a very short lifetime of the excited NH_3 molecule.

The calculated values of k_{obs} agreed well for initial flow rates of NH_3 of about $2.5_0 \times 10^{-6}$ mole sec^{-1}, at different reaction times, in both the "poisoned" and "unpoisoned" systems. However, consistently lower values were obtained for higher initial flow rates of NH_3, except for the shortest reaction time. The average value of k_{obs}, for all reaction times at the lowest flow rate of NH_3, and for the shortest reaction time for all flow rates, was found to be 2.2×10^{10} cc $mole^{-1}$ sec^{-1} (27). For the "poisoned" system, the experiments with higher initial flow rates of NH_3, and reaction times greater than 2.5_1 milliseconds, gave an average value of 0.52×10^{10} cc $mole^{-1}$ sec^{-1}.

DISCUSSION

The Reaction with Ethylene

The few experiments on this system indicated a minimum value for the second-order rate constant that compares well with two recently published values.

Herron (29) obtained an average value of 5.8×10^{10} cc $mole^{-1}$ sec^{-1} over the temperature range 200 to 330° C. The N-atom concentration was measured with a mass spectrometer after a fixed reaction time, with negligible decomposition of C_2H_4. The "absolute" value of the N-atom concentration was estimated by the NO titration.

Milton and Dunford (25) obtained a value for k of 9.63×10^{10} cc $mole^{-1}$ sec^{-1}, at 40° C, by a flame-diffusion technique. The initial N-atom concentration was inferred from the maximum production of HCN from ethylene. The method differed from that of Greenblatt and Winkler (17) in that the active nitrogen diffused into the hydrocarbon reactant. However, the flame technique must assume that the flame, emitted mostly by excited CN radicals (30), parallels the reaction of which the rate is presumably measured:

$$N + C_2H_4 \xrightarrow{k} HCN + CH_3\cdot \,. \qquad [3]$$

In fact, Bayes has recently presented evidence (31) that, for certain organic reactants at least, light emission in active-nitrogen reactions may be initiated by a second reactive species, possibly $A^3\Sigma_u^+$ metastable nitrogen molecules.

Although the minimum values, obtained by the present method, had to be normalized as outlined earlier, the method does involve variation of the fundamental reaction parameter, time, and an analysis for the products of the reaction of which the rate is presumably measured. With decrease of reaction time, the rate constant shows a trend toward higher values, and improved agreement with those obtained by the other methods (25, 29). Complicating factors probably became more significant at larger reaction times in this system, e.g., loss of N atoms by recombination at the wall, and disappearance of $CH_3\cdot$ radicals, produced in reaction [3], by reactions other than their rapid attack by N atoms to produce HCN (1).

The Reaction with Ammonia

The addition of excess C_2H_4 appeared to terminate the NH_3 reaction satisfactorily, since calculation of rate constants, at least for low flow rates of NH_3, in the "poisoned" system, gave reasonably constant values for k_{obs} after different reaction times. Moreover, the few experiments in the "unpoisoned" system, with its lower active-nitrogen concentration, gave values of k_{obs} similar to those obtained at low NH_3 flow rates, or at the shortest reaction time, in the "poisoned" system. Since addition of C_2H_4 always caused a decrease in the amount of NH_3 destroyed, reactions of NH_3 with C_2H_4, or its decomposition products, appeared to be insignificant at the temperature of reaction.

The variation in k_{obs} for the over-all reaction leading to NH_3 decomposition, based on an active-nitrogen concentration given by the maximum destruction of NH_3, would seem to give some information about the source of the reactive species in active nitrogen responsible for NH_3 destruction. The values for k_{obs} decrease only in the "poisoned" system, for reaction times greater than 2.5_1 milliseconds, and initial flow rates of NH_3 greater than $2.5_0\times10^{-6}$ mole sec^{-1}. This decrease indicates strongly that *part* of the N_2^* responsible for NH_3 destruction is formed, in the presence of NH_3, during the decay of N atoms down the reaction tube. The work of Kelly and Winkler (8) suggested that the N_2^* involved in destruction of NH_3 was formed during homogeneous recombination of N atoms prior to introduction of NH_3. Also, observations with a photomultiplier tube (32) have shown that a decrease in the intense active-nitrogen afterglow, produced in the present system, persists, upon addition of excess NH_3, for at least 45 cm in a "poisoned" reaction tube.

It is possible to estimate a concentration of N_2^* available for reaction with NH_3, in the "poisoned" system, at the fixed jet. Studies on the decrease of "plateau" values for HCN production from C_2H_4 have indicated (5) that a concentration of N_2^* equivalent to 1.5×10^{-6} mole sec^{-1} *may* be formed during homogeneous decay of N atoms between the fixed jet and the 45-cm level. The maximum destruction of NH_3 observed after a reaction time of 94.3 milliseconds shows that the maximum concentration of N_2^* formed between the 45-cm level and the trap is equivalent to a flow rate of $0.5_7\times10^{-6}$ mole sec^{-1}. The maximum concentration of N_2^* formed after the fixed jet is then equivalent to $\sim2.1\times10^{-6}$ mole sec^{-1}. An approximation to the concentration of N_2^* available at the fixed jet, deduced by subtracting this value from the maximum destruction of NH_3 for complete reaction, is equivalent to a flow rate of $\sim2.4\times10^{-6}$ mole sec^{-1}. The NH_3 destruction at a reaction time of 2.5_1 milliseconds, and a flow rate of 12.5×10^{-6} mole sec^{-1} of NH_3, gives direct evidence that a concentration of N_2^* equivalent to at least $1.4_5\times10^{-6}$ mole sec^{-1} is available at the fixed jet, since the formation of N_2^* from termolecular recombination of N atoms is negligible in this reaction time.

The k_{obs} values suggest that most of the reaction of NH_3, in the "poisoned" system, at least at low initial flow rates, occurs with a slowly decaying N_2^* formed prior to the fixed jet, at a concentration at least equivalent to $1.4_5\times10^{-6}$ mole sec^{-1}. Further reaction appears to occur at a slower over-all rate, which is governed by the rate of formation of excited nitrogen molecules during homogeneous decay of N atoms. At a flow rate of $2.5_0\times10^{-6}$ mole sec^{-1}, the maximum decomposition of NH_3 given in Table II is $2.2_3\times10^{-6}$ mole sec^{-1}, after a 94.3-milliseconds reaction time. Since the concentration of N_2^* required for this destruction of NH_3 is probably available at the fixed jet, the calculated values for k_{obs} at this flow rate do not vary appreciably with reaction time. At the shortest reaction time of 2.5_1 milliseconds, the concentration of N_2^* available at the fixed jet is sufficient to maintain the relation between extent of NH_3 destruction and reaction time, even at the higher flow rates of NH_3, and consequently the calculated values of k_{obs} do not show a decrease. (The experiment at a reaction time of 31.4 milliseconds, and an initial flow rate of NH_3 of $8.0_0\times10^{-6}$ mole sec^{-1}, indicates that the amount of N_2^* available at the fixed jet may be less than a flow rate of 1.9×10^{-6} mole sec^{-1}, since the calculated value for k_{obs} for this experiment falls into the low range of values.)

In the "unpoisoned" system, k_{obs} values are not "low" for initial flow rates of NH_3 somewhat greater than the concentration of active nitrogen indicated by maximum NH_3 destruction for complete reaction. However, in this system of low N-atom concentration,

formation of N_2^* beyond the fixed jet is probably insignificant, since recombination of N atoms occurs predominantly on the wall. Experiments on the present system have indicated (5) that homogeneous recombination in the "unpoisoned" system accounts for only one eighth of the total decay of N atoms between the fixed jet and the 45-cm level, whereas it accounts for about one half in the "poisoned" system.

From the previous discussion, the higher average value for $k_{obs} = 2.2\times10^{10}$ cc mole^{-1} sec^{-1} may be considered a more accurate measure of the over-all rate of reaction of active nitrogen with NH_3. This average value is probably a little low, since a rather large value is used for the initial concentration of active nitrogen, capable of NH_3 destruction, in the "poisoned" system. Nevertheless, this average value for k_{obs} is as high as that obtained for the fast reaction between N atoms and ethylene. It may be concluded, therefore, that failure to observe NH_3 destruction in active nitrogen, produced by a microwave discharge, is due to the low N-atom concentration, hence low N_2^* concentration, and is not due to a slow rate for over-all NH_3 destruction, nor to some unique characteristic of active nitrogen produced by a condensed discharge.

Since energy is not transferred from excited NH_3 during the photodecomposition of NH_3 (28), it may be assumed that its lifetime is probably very short at the pressure of 3 mm in the present system. Consequently, if the over-all reaction leading to NH_3 decomposition is represented by

$$N_2^* + NH_3 \underset{k_{-1}}{\overset{k_1}{\rightleftarrows}} NH_3^* + N_2 \qquad [4]$$

$$NH_3^* \xrightarrow{k_2} NH_2 + H, \qquad [5]$$

a steady-state approximation for the rate of change of $[NH_3^*]$ leads to the following expression for the over-all rate of the reaction:

$$-d[NH_3]/dt = k_2[NH_3^*] = k_1[N_2^*][NH_3]. \qquad [6]$$

This corresponds to the "low pressure" form of the rate expression for unimolecular decomposition. The values of k_{obs} may then be identified with k_1, the rate constant for a process involving a collision of the second kind.

If the exchange of energy occurred on every "kinetic" collision, the value of the rate constant would be approximated by the rate of binary collisions for molecules of moderate dimensions at room temperature, i.e., $10^{14.7}$ cc mole^{-1} sec^{-1} (33).

Terenin and Ermolaev (34) have shown that simultaneous transition, in which the *total spin* is conserved, can have a high probability of occurrence. Kistiakowsky and Volpi (3) suggested that decomposition of NH_3 by N_2^* in, say the $B^3\Pi_g$ state, could well occur as the result of an inelastic collision in which total spin is conserved, and in the course of which the nitrogen molecule undergoes a triplet–singlet transition to the $X^1\Sigma_g^+$ ground state, while the NH_3 molecule undergoes a singlet–triplet transition to an excited state capable of decomposition. However, these authors (3) were doubtful of the high efficiency of the transfer of energy to NH_3 molecules required in this mechanism. The present study indicates that the transfer of energy need not be particularly efficient, especially since it appears to occur with an excited state of the nitrogen molecule of rather long life.

Electronic energy transfer is probably greater for *molecules* when there is a large overlap of the emission spectrum of the donor and absorption spectrum of the acceptor, and when both radiative transitions have a high probability of occurrence (35). In the present

system, although the over-all reaction conserves spin, the transition in the N_2 molecule, for example, is not optically allowed, whether the N_2^* molecule be in the $B^3\Pi_g$ or $A^3\Sigma_u^+$ (the Vegard–Kaplan bands) states. Consequently, the mutual coupling would not be as strong as it would be (36) if the corresponding optical transitions in both molecules were allowed for electric-dipole radiation. The impact between electronically excited nitrogen molecules and NH_3 probably corresponds more closely to that involving triplet–singlet transition, with a value for the rate constant for energy transfer of 4.8×10^5 cc mole^{-1} sec^{-1} (34), than to the sensitization of the fluorescence of perylene by 1-chloroanthracene, which involves a singlet–singlet transition and gives a value of k_1 (corresponding to k_t of ref. 35) of the order of 10^{15} cc mole^{-1} sec^{-1} (37). If the N_2^* molecule capable of donating the energy to NH_3 is in the A state, the lower cross section, or probability of energy transfer, in the present system, may be compensated, as in the system studied by Terenin and Ermolaev (34), by the long lifetime of the donor molecule, the excited N_2 molecule in this case.

REFERENCES

1. H. G. V. Evans, G. R. Freeman, and C. A. Winkler. Can. J. Chem. **34**, 1271 (1956).
2. G. R. Freeman and C. A. Winkler. J. Phys. Chem. **59**, 371 (1955).
3. G. B. Kistiakowsky and G. G. Volpi. J. Chem. Phys. **28**, 665 (1958).
4. J. T. Herron, J. L. Franklin, P. Bradt, and V. H. Dibeler. J. Chem. Phys. **30**, 879 (1959).
5. A. N. Wright, R. L. Nelson, and C. A. Winkler. To be published.
6. G. J. Verbeke and C. A. Winkler. J. Phys. Chem. **64**, 319 (1960).
7. K. D. Bayes and G. B. Kistiakowsky. J. Chem. Phys. **32**, 992 (1960).
8. R. Kelly and C. A. Winkler. Can. J. Chem. **38**, 2514 (1960).
9. W. Lichten. J. Chem. Phys. **26**, 306 (1957).
10. P. G. Wilkinson and R. S. Mulliken. J. Chem. Phys. **31**, 674 (1959).
11. P. Harteck, R. R. Reeves, and G. Mannella. Can. J. Chem. **38**, 1648 (1960).
12. S. J. Lukasik and J. E. Young. J. Chem. Phys. **27**, 1149 (1957).
13. F. Kaufman and J. R. Kelso. J. Chem. Phys. **28**, 510 (1958).
14. H. G. V. Evans and C. A. Winkler. Can. J. Chem. **34**, 1217 (1956).
15. R. A. Young and K. C. Clark. J. Chem. Phys. **32**, 604 (1960).
16. G. E. Beale, Jr. and H. P. Broida. J. Chem. Phys. **31**, 1030 (1959).
17. J. H. Greenblatt and C. A. Winkler. Can. J. Research, B, **27**, 732 (1949).
18. E. J. B. Willey and E. K. Rideal. J. Chem. Soc. 669 (1927).
19. A. Serewicz and W. A. Noyes, Jr. J. Chem. Phys. **63**, 843 (1959).
20. A. Ung. Thesis, McGill University, Montreal, Que. 1961.
21. R. A. Back and C. A. Winkler. Unpublished results.
22. C. B. Kretschner and H. C. Peterson. J. Chem. Phys. **33**, 948 (1960).
23. G. B. Kistiakowsky and G. G. Volpi. J. Chem. Phys. **27**, 1141 (1957).
24. F. Kaufman and J. R. Kelso. J. Chem. Phys. **27**, 1209 (1957).
25. E. R. V. Milton and H. B. Dunford. J. Chem. Phys. **34**, 51 (1961).
26. M. A. A. Clyne and B. A. Thrush. Nature, **189**, 56 (1961).
27. R. L. Nelson, A. N. Wright, and C. A. Winkler. Symposium on Some Fundamental Aspects of Atomic Reactions, McGill University, Montreal, Que. September 1960.
28. R. Srinivason. J. Phys. Chem. **64**, 679 (1960).
29. J. T. Herron. J. Chem. Phys. **33**, 1273 (1960).
30. K. R. Jennings and J. W. Linnet. Trans. Faraday Soc. **56**, 1737 (1960).
31. K. D. Bayes. Can. J. Chem. **39**, 1074 (1961).
32. A. N. Wright and C. A. Winkler. Unpublished results.
33. A. F. Trotman-Dickenson. Gas kinetics. Butterworths Scientific Publ., London. 1955. p. 23.
34. A. N. Terenin and V. L. Ermolaev. Trans. Faraday Soc. **52**, 1042 (1956).
35. R. Livingston. J. Phys. Chem. **61**, 860 (1957).
36. T. Förster. Discussions Faraday Soc. **27**, 7 (1957).
37. E. J. Bowen and R. Livingston. J. Am. Chem. Soc. **76**, 6300 (1954).

METAL OXIDE ALKOXIDE POLYMERS

PART III. THE HYDROLYSIS OF SECONDARY AND TERTIARY ALKOXIDES OF ZIRCONIUM[1]

D. C. BRADLEY[2] AND D. G. CARTER[3]
The Department of Chemistry, Birkbeck College, London, W.C.1, England

Received June 21, 1961

ABSTRACT

The hydrolysis of zirconium alkoxides with secondary or tertiary alkoxide groups $Zr(OR)_4$, where R = Pr^i, Bu^s, Bu^t, and Am^t, has been studied. The relatively low polymers formed by the metal oxide alkoxides have been interpreted on the basis of structural models involving octahedrally 6-co-ordinated zirconium.

INTRODUCTION

Previous work (1) on the hydrolysis of some primary alkoxides of zirconium showed that polymeric oxide alkoxides $[ZrO_x(OR)_{4-2x}]_n$ were formed. A satisfactory interpretation of the number-average degree of polymerization as a function of degree of hydrolysis was developed on the basis of three structural models involving 6-co-ordinated zirconium and identical with those originally proposed for titanium (2, 3). Model I was based on the unsolvated trimeric alkoxide $Zr_3(OR)_{12}$ and gave rise to a series of co-ordination – condensation polymers having the general formula $Zr_{3(x+1)}O_{4x}(OR)_{4(x+3)}$. The requirement of relatively low polymers by this structural model was a consequence of the highly compact structures which are made possible by the sharing of common faces of octahedra. Even lower polymers are predicted by the solvated species $Zr_2(OR)_8,(ROH)_2$ (model II) and $Zr(OR)_4,(ROH)_2$ (model III), where the zirconium achieves some or all (respectively) of its increase in co-ordination by bonding with alcohol molecules instead of by intermolecular bonding with alkoxide groups. The degrees of polymerization of zirconium secondary alkoxides (4) in benzene are lower than for the normal alkoxides, whilst the tertiary alkoxides (5) are monomeric. This behavior was ascribed to the powerful steric effects of secondary and, especially, tertiary alkoxide groups which prevent intermolecular co-ordination. The steric effect thus provides an entirely different process for the formation of low polymers and it was therefore important to study the polymeric nature of zirconium oxide alkoxides involving secondary and tertiary alkoxide groups. In this communication we report results on the hydrolysis of zirconium isopropoxide, *sec*-butoxide, *tert*-butoxide, and *tert*-amyloxide under carefully controlled conditions.

EXPERIMENTAL AND RESULTS

Zirconium Alkoxides

These were prepared and analyzed using previously described methods (4, 5). The *sec*- and *tert*-butoxides and the *tert*-amyloxide were redistilled *in vacuo* prior to each experiment. The tetraisopropoxide was distilled *in vacuo* and then crystallized from isopropanol as the solvate $Zr(OPr^i)_4,Pr^iOH$.

Ebulliometric Studies

The variation of number-average degree of polymerization with degree of hydrolysis for the zirconium oxide alkoxides in their respective boiling alcohols was determined by

[1]*For Part II, see ref. 6.*
[2]*Present address: The University of Western Ontario, London, Ontario.*
[3]*Present address: Norwood Technical College, London, England.*

the ebulliometric method which was described in detail in a previous paper (1). In the following tables we present the value for n (the number-average degree of polymerization) at each value of the degree of hydrolysis h (the ratio of water molecules added per metal atom).

(a) Zirconium Isopropoxide

TABLE I

(Initial concentration of zirconium isopropoxide = 0.382 g-mol./kg isopropanol)

h	0.000	0.115	0.269	0.462	0.761	1.043	1.329	1.612	1.905	2.19
n	1.91	2.17	2.52	2.99	3.84	5.48	9.49	12.8	16.0	20.3
n_{calc}	2.00	2.17	2.44	2.89	4.06	6.57	17.55	—	—	—

The solution remained clear up to $h = 2.19$ but the next addition of water (to $h = 2.47$) caused precipitation. Values of n_{calc} are derived from the theoretical equation $n = 6/(3-2h)$, which applies to the polymer series $Zr_{2(x+1)}O_{3x}(OR)_{2(x+4)},(ROH)_{2(x+1)}$ model II based on the solvated dimer $Zr_2(OPr^i)_8,(Pr^iOH)_2$.

(b) Zirconium sec-Butoxide

TABLE II

(Initial concentration of zirconium *sec*-butoxide = 0.101 g-mol./kg *sec*-butanol)

h	0.000	0.130	0.474	0.831	1.178	1.527	1.879
n	1.94	2.16	3.12	5.15	11.3	20.8	19.9
n_{calc}	2.00	2.19	2.92	4.48	9.31	—	—

The solution remained clear up to $h = 1.879$ but the next addition of water (to $h = 2.235$) resulted in unsteady readings on the differential water thermometer. The latter phenomenon was ascribed to the presence of "unreacted" water. Values of n_{calc} are derived from the theoretical equation $n = 6/(3-2h)$.

(c) Zirconium tert-Butoxide

When zirconium *tert*-butoxide was added to boiling *tert*-butanol in the ebulliometer the thermometer readings were unsteady and gave rise to an abnormally high value for the molecular weight of $Zr(OBu^t)_4$, which is known to be monomeric in benzene (3). However, it was shown that $Zr(OBu^t)_4$ was appreciably volatile in boiling *tert*-butanol and that the ebulliometric method was inapplicable.

(d) Zirconium tert-Amyloxide

Successive additions of $Zr(OAm^t)_4$ to boiling *tert*-amyl alcohol gave a linear increase of the elevation of boiling point (ΔT) with increase in concentration, and from the slope of this, the correct (monomeric) value for the molecular weight of $Zr(OAm^t)_4$ was calculated. Unfortunately the line did not pass through the origin but gave a negative intercept on the ΔT axis. It appeared that the first addition of $Zr(OAm^t)_4$ must be interacting with some impurity in the *tert*-amyl alcohol (possibly water), so that the elevation of the boiling point was less than it should be. This effect persisted in spite of various attempts to purify the alcohol and at present it defies explanation. In the determination of the molecular weight of $Zr(OAm^t)_4$ this effect could be ignored because several additions of alkoxide were made and the slope of the ΔT versus Δm line was used for the calculations. However, in the ebulliometric hydrolysis technique the molecular weight of each zirconium oxide *tert*-amyloxide is determined from the ΔT value for a single point and would be sensitive to errors in the absolute value of ΔT.

An empirical method was devised (7) for correcting the value of h to allow for this deviation but the results are probably less accurate than for the other alkoxides. Accordingly we show the results graphically in Fig. 1 but have not tabulated the data. The initial concentration of $Zr(OAm^t)_4$ was 0.0584 g-mol./kg *tert*-amyl alcohol.

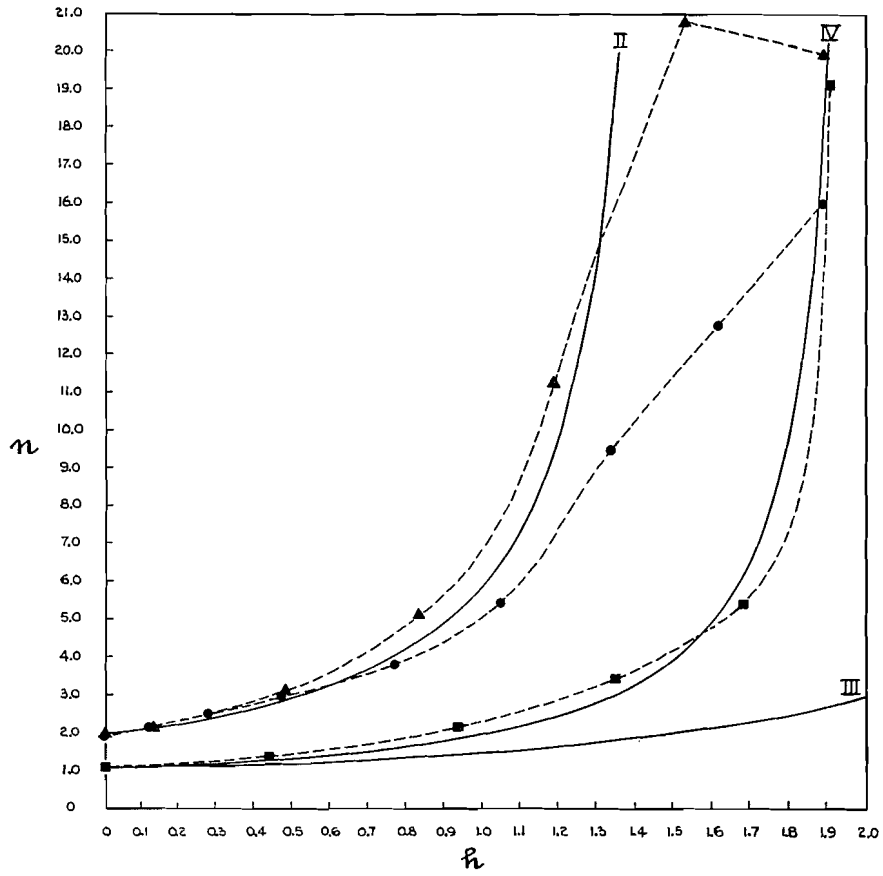

FIG. 1. The hydrolysis of $Zr(OPr^i)_4$, $Zr(OBu^s)_4$, and $Zr(OAm^t)_4$ in their alcohols: ●, $Zr(OPr^i)_4$; ▲, $Zr(OBu^s)_4$; ■, $Zr(OAm^t)_4$; II, $n = 6/(3-2h)$; III, $n = 3/(3-h)$; IV, $n = 2/(2-h)$.

Soluble Zirconium Oxide tert-Amyloxides

To establish the composition of zirconium oxide *tert*-amyloxides, samples (ca. 5 g) of $Zr(OAm^t)_4$ were hydrolyzed in boiling *tert*-amyl alcohol (ca. 25 cc) by the addition of measured amounts of aqueous *tert*-amyl alcohol (10% H_2O, w/w). The solution of the alkoxide was boiled under reflux and the lower, uncooled zone of the condenser was plugged with Fenske glass helices. The latter ensured that the added aqueous alcohol was rapidly mixed with the refluxing alcohol and thus diluted before entering the solution. Refluxing was continued for $\frac{1}{2}$ hour following the addition of water, and the solution was allowed to cool and then evaporated at room temperature under a pressure of 0.1 mm. When the product appeared to be free from alcohol the pumping was continued for another hour. The product was then analyzed for zirconium. The results are given in Table III. The calculated zirconium values are based on the formula $ZrO_h(OAm^t)_{4-2h}$

TABLE III

Ratio (h) of H_2O:$Zr(OAm^t)_4$	Nature of product	% Zr	
		Found	Calc.
0.211	Viscous liquid	22.3	22.4
0.360	Viscous liquid	23.6	23.8
0.597	Viscous liquid	26.8	26.4
0.780	Gum	28.2	28.8
0.982	Gum	30.2	32.1
1.007	Glass	31.3	32.5
1.340	Glass	38.2	40.1
1.691	Glass	42.4	53.0

and assume that hydroxyl groups are absent. Agreement between observed and calculated percentage of Zr is satisfactory up to $h = 0.780$ but for higher values the observed values are significantly lower than the calculated. However, these products were glassy and it is possible that some solvent was tenaciously bound in the product.

Insoluble Products

(a) An Insoluble Zirconium Oxide Isopropoxide

In the ebulliometric hydrolysis (Table I) of the isopropoxide no precipitation occurred up to $h = 2.19$ but the next addition of water ($h = 2.47$) caused the formation of a precipitate, which was dried and analyzed. Model II would give an infinite linear polymer $Zr_2O_3(OR)_2,2ROH$, which should be insoluble. The insoluble zirconium oxide isopropoxide was close in analysis to $Zr_2O_3(OPr^i)_2$ (found: Zr, 53.6; calc.: Zr, 52.4%).

(b) Insoluble Zirconium Oxide tert-Butoxides

A solution of $Zr(OBu^t)_4$ in *tert*-butanol was inadvertently exposed to the atmosphere for <1 minute and during the following 2 days it deposited some needle-shaped crystals (found: Zr, 27.0; $Zr(OBu^t)_4$ requires: Zr, 23.8; $Zr_2O(OBu^t)_6$ requires: Zr, 28.4; $Zr_2O_3(OBu^t)_2,(Bu^tOH)_4$ requires: Zr, 27.1%). A hydrolysis product ($h = 1.01$; found: Zr, 32.2; $ZrO_{1.01}(OBu^t)_{1.98}$ requires: Zr, 36.2%) was heated at 200° at 0.1 mm until the formation of volatile products appeared complete. The volatile products consisted of a small quantity of *tert*-butanol (sufficient to explain the low percentage of Zr of the original material) and $Zr(OBu^t)_4$. The insoluble, non-volatile residue was reasonably similar in composition to that of the infinite trilinear polymer of model I (found: Zr, 40.9; $Zr_3O_4(OBu^t)_4$ requires: Zr, 43.5%). A material balance was in reasonable agreement with the following disproportionation equation:

$$4/x[ZrO(OBu^t)_2]_x \rightarrow Zr_3O_4(OBu^t)_4 + Zr(OBu^t)_4.$$

DISCUSSION

Zirconium Oxide Isopropoxides

The variation of number-average degree of polymerization for zirconium oxide isopropoxides (Fig. 1) as a function of h is clearly in accordance with the predictions of the theory (1) for model II species between $h = 0$ and 0.76. This behavior is particularly significant because zirconium isopropoxide gives a relatively stable solvate which is dimeric $Zr_2(OPr^i)_8,(Pr^iOH)_2$ and lends strong support to the postulate of Bradley, Gaze, and Wardlaw (2) that such solvated species might exist in solution. The coefficient of variation for n (n_{calc} listed in Table I) for the region $h = 0$–0.76 is ±4%, which is of the order of probable experimental error. For $h > 0.76$ the experimental values of n deviate significantly from the $n = 6/(3-2h)$ equation with n less than n_{calc}. This suggests that as the

molar concentration of oxide isopropoxide decreases, solvation based on the monomer species $Zr(OPr^i)_4,(Pr^iOH)_2$ model III comes into play. It is interesting to note that although the polymer series based on model II should form infinite polymers at $h = 1.5$ and these would be expected to be insoluble, nevertheless, no precipitation occurred before $h > 2$. According to the calculations of Bradley and Holloway (6) based on the analogous structures for tantalum oxide ethoxides the failure to form insoluble products at $h > 1.5$ may be attributed to a disproportionation of h between the model II and model III series. However, this will not satisfactorily explain the present results because it would be necessary in making $h_{II} < 1.5$ to have $h_{III} > 2$ in view of the high proportion (83% at $h = 1.612$) of the model II polymers in the system. This suggests that at $h > 1.5$ the hydrolysis is incomplete, although there was no indication of "unreacted" water in the ebulliometer. On the other hand the absence of precipitation at $h = 2.19$ adds support to the suggestion that hydrolysis is incomplete as $h \rightarrow 2$. The situation is further complicated by the interesting fact that the solid $Zr_2O_3(OPr^i)_2$ which eventually precipitated at $h = 2.47$ had a degree of hydrolysis near that required by the infinite polymer of the model II series $Zr_2O_3(OPr^i)_2,(Pr^iOH)_2$, although it lacked the co-ordinated alcohol. Hence it appears that at $h > 1.5$, hydrolysis is incomplete, probably because of the presence of Zr—OH groups, and that the value of h_{II} for model II is less than h_{III} for model III. The material which precipitates is the model II infinite polymer, which loses its alcohol in the drying process.

Zirconium Oxide sec-Butoxides

The data in Fig. 1 show that the number-average degree of polymerization of a zirconium oxide *sec*-butoxide conforms reasonably well to the prediction of the theoretical equation $n = 6/(3-2h)$ based on the model II series over the range of hydrolysis $h = 0$–1.2. Thus the coefficient of variation for n (n_{calc} listed in Table II) for the first three points is ±4.5% and for the first five points it is ±12.5%. We have already pointed out (6) that n becomes rather sensitive to errors in h for $h > 1$ and the larger errors in the fourth and fifth points is understandable. For $h > 1.3$ it is clear that further solvation is setting in and that polymers from the model III series are present. The similarity of the n versus h curves for the zirconium oxide isopropoxides and the zirconium oxide *sec*-butoxides over the range $h = 0$–1.0 is quite striking. In fact zirconium *sec*-butoxide forms a crystalline solvate, $Zr_2(OBu^s)_8,(Bu^sOH)_2$, but it is less stable than the solvated isopropoxide and readily loses its alcohol of addition when dried *in vacuo*. Actually the similarity in hydrolytic behavior of these compounds is rather closer than might be expected. For example, in boiling benzene $Zr(OBu^s)_4$ is less polymeric than $Zr(OPr^i)_4$ (4) and this is believed to be due to a slightly greater steric effect of the *sec*-butoxide groups. Moreover, as *sec*-butanol has a higher boiling point than isopropanol and it is believed that an increase in temperature favors depolymerization and solvation of the alkoxide (3), we would have predicted that the degree of polymerization of $Zr(OBu^s)_4$ in boiling Bu^sOH should be significantly less than that of $Zr(OPr^i)_4$ in boiling Pr^iOH. Furthermore, we would have expected the zirconium oxide *sec*-butoxides to exhibit lower values of n than the corresponding oxide isopropoxides, whereas over a fair range in h (0.5–1.5) the opposite is true.

Zirconium Oxide tert-Butoxides

The high volatility of $Zr(OBu^t)_4$ in *tert*-butanol precluded the use of the ebulliometric method of studying its hydrolysis. However, some ebulliometric experiments were carried out with the view to determining at what value of h precipitation occurred. Values of $h > 2$ were required, in one case $h > 3.28$, and this behavior suggested that hydrolysis

was incomplete at the higher values of h, possibly due to the presence of ZrOH groups which were stable in the boiling solution. Two interesting insoluble products were isolated. A crystalline compound deposited when a solution of $Zr(OBu^t)_4$ in *tert*-butanol was inadvertently allowed to hydrolyze. The zirconium analysis corresponded to $Zr_2O_3(OBu)_2$, $(BuOH)_4$, which is the species for $h = 1.5$ in the solvated monomer model III series. Unfortunately there is ambiguity concerning this type of compound because of the alternative formulation involving say Zr(OH)(OR) in place of ZrO,ROH. Thus the above formula could be rearranged to $Zr_2(OH)_3(OBu)_5$,BuOH, which is also not very different from $Zr(OH)(OBu)_3$. The other insoluble product, obtained by the more extreme process of thermal disproportionation at 200°, had a zirconium content a little less than that for $Zr_3O_4(OBu^t)_4$, the infinite linear polymer for the unsolvated trimer model I series. Under the conditions of this experiment we should not expect Zr—OH groups to survive nor alcohol molecules to remain co-ordinated so it is not surprising that the product conforms to the model I series. The tendency towards model I would also be expected on the grounds that steric hindrance is alleviated by the small number of *tert*-butoxide groups per metal atom.

Zirconium Oxide tert-Amyloxides

The data presented in Table III show that for h values up to about 0.78 the hydrolysis of $Zr(OAm^t)_4$ produces unsolvated zirconium oxide *tert*-amyloxides. The intractable nature of the more highly hydrolyzed materials raises the doubt of whether or not they were completely dried free from alcohol. Alternatively, the low zirconium analyses may indicate the presence of solvated products or products containing ZrOH groups. Nevertheless it is clear that hydrolysis with the formation of zirconium oxide *tert*-amyloxides is substantially complete for h up to about 1.0. The ebulliometric data shown in Fig. 1 suggest that the polymeric species in solutions are initially close to the requirements of the solvated monomer model III (1) but tend towards the less solvated dimer model II as the hydrolysis is increased. This is the type of behavior to be expected if powerful steric effects are operating in the less-hydrolyzed species and thus preventing condensation polymerization. As the number of *tert*-amyloxide groups per zirconium atom decreases the molecules become capable of adopting the more compact structure of model II. An alternative possibility is that another structural model IV is adhered to by the zirconium oxide *tert*-amyloxides. This is based on the solvated monomer $Zr(OR)_4,(ROH)_2$ too but the oxide *tert*-amyloxide species involve condensation through ZrOZr groups sharing edges of the octahedra, as shown in Figs. 2 and 3. Structures in this model should conform

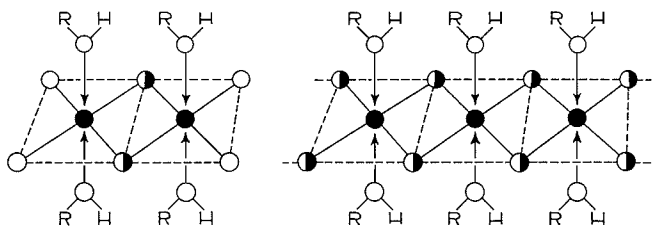

2 3

FIG. 2. The dimer $Zr_2O_2(OR)_4,(ROH)_4$: ●, Zr; ◑, oxygen in Zr·O·Zr; ○, oxygen in OR (R groups omitted).
FIG. 3. Section of the infinite polymer $[ZrO_2,(ROH)_2]_\infty$: ●, Zr; ◑, oxygen in Zr·O·Zr.

to the equation $n = 2/(2-h)$ and it is evident in Fig. 1 that the first five points in the hydrolysis of $Zr(OAm^t)_4$ are in reasonable agreement with the predicted curve IV.

CONCLUSIONS

1. The hydrolysis of zirconium alkoxides $Zr(OR)_4$, where R = Pr^i, Bu^s, Bu^t, and Am^t_2 leads to the formation of polymeric zirconium oxide alkoxides having low number-average degrees of polymerization.

2. No evidence of the formation of zirconyl compounds was obtained.

3. The variation of number-average degree of polymerization as a function of the degree of hydrolysis for zirconium isopropoxide and zirconium *sec*-butoxide conformed to the requirements of a structural model for the polymers based on octahedrally 6-co-ordinated zirconium.

4. At high degrees of hydrolysis it appears that highly solvated species are present and that hydrolysis may be incomplete in solution.

REFERENCES

1. D. C. Bradley and D. G. Carter. Can. J. Chem. **39**, 1434 (1961).
2. D. C. Bradley, R. Gaze, and W. Wardlaw. J. Chem. Soc. 3977 (1955).
3. D. C. Bradley, R. Gaze, and W. Wardlaw. J. Chem. Soc. 469 (1957).
4. D. C. Bradley, R. C. Mehrotra, and W. Wardlaw. J. Chem. Soc. 5020 (1952).
5. D. C. Bradley, R. C. Mehrotra, and W. Wardlaw. J. Chem. Soc. 4204 (1952).
6. D. C. Bradley and H. Holloway. Can. J. Chem. **39**, 1818 (1961).
7. D. G. Carter. Ph.D. Thesis, London University, London, England. 1959.

CONSTITUTION OF AN ALDOTETRAOURONIC ACID FORMED ON ENZYMIC HYDROLYSIS OF A 4-*O*-METHYLGLUCURONOXYLAN FROM THE WOOD OF WHITE BIRCH (BETULA PAPYRIFERA MARSH.)

T. E. TIMELL

The Pulp and Paper Research Institute of Canada and the Department of Chemistry, McGill University, Montreal, Que.

Received September 12, 1961

ABSTRACT

An aldotetraouronic acid has been isolated by enzymic hydrolysis of a 4-*O*-methylglucuronoxylan from the wood of white birch. It has been shown to be *O*-4-*O*-methyl-α-D-glucosyluronic acid-(1 → 2)-*O*-β-D-xylopyranosyl-(1 → 4)-*O*-β-D-xylosyl-(1 → 4)-D-xylose.

In a previous communication (1) an account was given of preliminary results obtained on treatment of a 4-*O*-methylglucuronoxylan from the wood of white birch with a commercial pectinase preparation. The enzymic hydrolysis was carried out inside a semipermeable membrane (2) and the oligosaccharides formed were allowed to diffuse rapidly through the latter, thus escaping further hydrolysis. Two series of oligosaccharides, one neutral and the other acidic, were obtained in high yields. The shortest acid oligomer formed was an aldotetraouronic acid. This paper is concerned with the structure of this new compound.

RESULTS AND DISCUSSION

The mixture of sugars obtained after the enzymic hydrolysis was resolved into an acidic and a neutral portion with an anion exchange resin. The sugar acids were separated either by gradient elution from a charcoal–Celite column or by preparative paper chromatography. The lowest acid was obtained as an amorphous powder, $[\alpha]_D^{20}$ +23°, in a yield of 11% of the original sugar mixture. Its rate of movement on the paper chromatogram was identical with that of an aldotetraouronic acid previously (3) isolated from a similar polysaccharide. The values for methoxyl, carboxyl, and reducing groups indicated the presence of an *O*-methylglucuronosyl xylotriose. Mild partial hydrolysis gave an aldotriouronic acid (4) and xylose, while an aldobiouronic acid was formed under more vigorous conditions. On oxidation with periodate, the compound consumed 5 moles of oxidant with concomitant formation of 2 moles of formic acid. From the structure of the parent polysaccharide (5), it appeared probable that the acid groups were attached to the 2-position of β-D-xylopyranose residues and that the latter were linked through their 1- and 4-positions. Consideration of the three possible structures of the aldotetraouronic acid showed that under these conditions only that alternative where the acid group was located at the non-reducing end was compatible with the above results.

A specimen of the aldotetraouronic acid which had been obtained from the charcoal–Celite column was methylated, first with dimethyl sulphate and alkali and subsequently according to Kuhn and co-workers (6). The fully methylated sugar acid was subjected to methanolysis, saponified, acidified, and resolved into an acidic and a neutral portion with an anion exchange resin. The acid fraction, a fully methylated aldobiouronic acid, was esterified and reduced with lithium aluminum hydride to give a partially methylated disaccharide, which could not be induced to crystallize. Hydrolysis yielded equimolar quantities of a di-*O*-methylxylose and a tri-*O*-methylglucose which were separated by gradient elution from charcoal–Celite. The first sugar was identified as 3,4-di-*O*-methyl-

D-xylose and the second as 2,3,4-tri-*O*-methyl-D-glucose. This shows that the methylated aldobiouronic acid was methyl 2-*O*-[methyl(2,3,4-tri-*O*-methyl-α-D-glucosyl)uronate]-3,4-di-*O*-methyl-D-xyloside. The neutral fraction contained only one compound, characterized as 2,3-di-*O*-methyl-D-xylose, 2 moles being obtained per mole of tri-*O*-methylglucose. A similar methylation of a specimen obtained by preparative paper chromatography gave the same results.

Of the three structures possible for the aldotetraouronic acid, only the alternative suggested by the periodate oxidation data would give 2 moles of 2,3-di-*O*-methyl-D-xylose in the neutral and 1 mole of 3,4-di-*O*-methyl-D-xylose in the acid fraction after methanolysis. The results obtained by the methylation technique are therefore unequivocal. The combined evidence shows that the acid isolated was *O*-4-*O*-methyl-α-D-glucosyluronic acid-(1 → 2)-*O*-β-D-xylopyranosyl-(1 → 4)-*O*-β-D-xylosyl-(1 → 4)-D-xylose. The aldotriouronic acid formed on mild partial hydrolysis was presumably *O*-4-*O*-methyl-α-D-glucosyluronic acid-(1 → 2)-β-D-xylopyranosyl-(1 → 4)-D-xylose, a compound which has previously been isolated from several xylans. The corresponding isomer with the acid group attached to the reducing xylose moiety of the triouronic acid does not seem to have been obtained so far, probably because of the much greater stability of the first isomer (3, 7, 8). This stability is also indicated by the fact that hardly any aldobiouronic acid was obtained on mild acid hydrolysis of the present aldotetraouronic acid.

The constitution of the other uronic acids, the physical characteristics of the neutral oligosaccharides, and the possible mechanism of the enzymic hydrolysis will be discussed elsewhere (9).

EXPERIMENTAL

All specific rotations were equilibrium values and were determined at 20° C. Melting points are corrected. Evaporations were carried out at 40–50° C *in vacuo*.

Paper Chromatography

Sugars were separated by the descending technique on Whatman No. 1 or, for preparative purposes, No. 3MM filter papers. Solvents (v/v) used were ethyl acetate – acetic acid – water in the proportions (A) (9:2:2), (B) (3:1:3), or (C) (18:7:8); butanone–water (D) (89:11); and ethanol–benzene–water (E) (47:200:15). Paper electrophoresis was carried out in 0.05 *M* borate solution with Whatman No. 3MM paper at 700 volts for 5 hours. *o*-Aminodiphenyl was used as a spray reagent (10).

Isolation and Preliminary Characterization of the Aldotetraouronic Acid

The enzymic hydrolysis and the isolation of the various oligosaccharides will be described in detail elsewhere (9). Two methods were used for obtaining a chromatographically pure aldotetraouronic acid, one involving gradient elution with aqueous ethanol from a charcoal–Celite column, the other separation on strips of filter paper with solvent C.

The aqueous solution of the aldotetraouronic acid was neutralized with sodium bicarbonate to pH 2.5 and concentrated to 250 ml. The solution was treated with Amberlite IR-120 (acid form) exchange resin, filtered, and evaporated to near dryness *in vacuo* at 25° C. Repeated evaporations from acetone gave a white, fluffy material (5–6 g by each method), $[\alpha]_D$ +23° (*c*, 3.0 in water). Anal. Calc. for $C_{22}H_{36}O_{19}$: OCH_3, 5.13%; equiv. wt. (acid), 604; equiv. wt. (reducing group), 604. Found: OCH_3, 5.18%; equiv. wt. (acid), 604; equiv. wt. (reducing group), 580 (11).

Partial hydrolysis at 100° C with 0.02 *N* hydrochloric acid for 2 hours gave an aldotriouronic acid and xylose, tentatively characterized from their rate of movement on the paper chromatogram with solvents A, B, and C. Hydrolysis at 100° C with *N* hydrochloric acid yielded an aldobiouronic acid and xylose.

Periodate Oxidation of the Aldotetraouronic Acid

Samples of aldotetraouronic acid (30–40 mg) were dissolved in 0.05 *M* aqueous sodium metaperiodate and the reaction was allowed to proceed in the dark at 30° C for various lengths of time. Remaining oxidant was determined by the excess arsenite method. The results, given as moles per mole tetraouronic acid, were as follows:

Time, hr	5	15	20	24	45	67
Periodate consumption	4.3	4.5	4.7	5.0	5.3	5.2

Samples of tetraouronic acid (30–40 mg) were dissolved in water (5–10 ml) and carefully neutralized with 0.01 *N* sodium hydroxide. Periodate solution (50 ml) was added and the oxidation was allowed to proceed in the dark. After the desired time, the reaction was interrupted by addition of excess ethylene glycol. After 30 minutes, formic acid was determined either by titration with 0.01 *N* sodium hydroxide or by the iodide–iodate method, the final titration being carried out with 0.01 *N* sodium thiosulphate in this case. The two procedures gave identical results throughout. The following moles of formic acid per mole of aldotetraouronic acid were produced:

Time, hr	24	48	72	96	240
Formic acid	1.8	1.9	2.0	2.1	2.5

Overoxidation with periodate was apparently very slow with the aldotetraouronic acid. In contrast, a sample of 2-*O*-(4-*O*-methyl-α-D-glucosyluronic acid)-D-xylopyranose, under the same conditions and within the first 15 hours, consumed 6.0 moles of periodate with concomitant formation of 4.3 moles of formic acid, the expected consumption of periodate being 2 moles with no formic acid produced.

The previously reported formation of 3 moles of formic acid on oxidation of the aldotetraouronic acid (1) was due to an experimental error.

Methylation of the Aldotetraouronic Acid

Aldotetraouronic acid (4.0 g) was dissolved in water (100 ml) containing sodium bicarbonate (5.0 g). Dimethyl sulphate (50 ml) and 40% (w/w) aqueous sodium hydroxide (50 ml) were added dropwise with stirring over a period of 4 hours at 10° C in a nitrogen atmosphere. Solid sodium hydroxide (30 g) was added, followed by dropwise addition of dimethyl sulphate (50 ml) over 1 day. The same amounts of reagents were then added once more. The reaction mixture was acidified to pH 2.0 with sulphuric acid and extracted three times with chloroform. The chloroform solution was dried over anhydrous sodium sulphate, filtered, evaporated to dryness, and dissolved in ethyl acetate. After filtration, the clear solution was evaporated to dryness and further dried *in vacuo* over calcium chloride to yield a crisp, white solid (4.4 g).

The partly methylated material was dissolved in dry dimethyl formamide (75 ml) (6), and silver oxide (30 g) and methyl iodide (30 ml) were added. After the mixture had been shaken in the dark at 30° C for 1 day, silver oxide (60 g), methyl iodide (75 ml), and some Drierite were added. The mixture was shaken for 3 days, after which the solid residue was washed with chloroform by filtration. The solution (1.5 liter) was concentrated to 250 ml and washed once with 10% aqueous potassium cyanide and then twice with water. The chloroform solution was dried with anhydrous sodium sulphate, filtered, and evaporated to dryness to give a sirup (3.1 g). Anal. Calc. for $C_{32}H_{56}O_{19}$: OCH_3, 45.8%. Found: OCH_3, 44.2%. The infrared diagram indicated the absence of hydroxyl groups.

Methanolysis of the Aldobiouronic Acid and Separation of Acidic and Neutral Sugars

A portion of the methylated aldotetraouronic acid (2.0 g) was boiled under reflux with 0.7 *N* methanolic hydrogen chloride in the presence of Drierite for 8 hours. After neutralization with silver carbonate and filtration through Celite, the sirup obtained (2.1 g) was heated at 60° C in 5% aqueous barium hydroxide (50 ml) for 2 hours. Barium hydroxide was removed by addition of solid carbon dioxide and filtration through Celite, and the solution was treated with Amberlite IR-120 exchange resin (acid form). After filtration and concentration to 100 ml, the solution was added to the top of a column (3.5×15 cm) containing Dowex 1-X4 anion exchange resin (acetate form). Neutral glycosides (765 mg) were removed by washing with water (2 liters), followed by elution with 30% aqueous acetic acid (2 liters) for recovery of acid glycosides (800 mg).

Characterization of Acid Fraction

The acid fraction was boiled under reflux with 0.7 *N* methanolic hydrogen chloride in the presence of Drierite, after which the methyl ester – methyl glycoside was dissolved in dry tetrahydrofuran (50 ml) and reduced in the usual way with lithium aluminum hydride (1.5 g). The partly methylated disaccharide obtained, which could not be induced to crystallize, was boiled under reflux with *N* sulphuric acid (100 ml) for 7 hours. After neutralization with barium carbonate, filtration through Celite, treatment with Amberlite IR-120 exchange resin (acid form), filtration, and evaporation, a sirup was obtained (780 mg). Paper chromatography (solvents D and E) suggested the presence of a di-*O*-methylxylose and a tri-*O*-methylglucose.

The sugar mixture was dissolved in water (25 ml) and added to the top of a column (3.5×55 cm) containing a 1:1 mixture of Darco G-60 charcoal and Celite. The sugars were separated by gradient elution with 3 liters each of 10% and 30% aqueous ethanol. Fractions, 25 ml each, were collected at an average rate of two per hour. Aliquots of 1 or 2 ml were withdrawn from every third test tube and examined by paper chromatography (solvent E). Di-*O*-methylxylose was collected from fractions 48–70, tri-*O*-methylglucose from fractions 140–210.

Identification of 3,4-Di-O-methyl-D-xylose

The colorless, clear sirup (275 mg) had $[\alpha]_D$ +21° (*c*, 2.0 in water). Anal. Calc. for $C_7H_{14}O_5$: OCH_3,

34.8%. Found: OCH_3, 34.0%. On paper electrophoresis and paper chromatography (solvent D), the compound had a rate of movement identical with that of an authentic sample of 3,4-di-*O*-methyl-D-xylose. A portion of the sirup (100 mg) was oxidized with bromine in the usual way (12). After removal of bromine and hydrobromic acid, the aqueous solution was treated with Amberlite IR-120 exchange resin (acid form) and evaporated to dryness. The remaining sirup was distilled at 150–200° C (bath temperature) and 0.05 mm Hg to give a clear sirup (50 mg) which crystallized spontaneously. After three recrystallizations from a 1:1 mixture of ethyl ether – petroleum ether (b.p. 30–60° C), the 3,4-di-*O*-methyl-D-xylono-δ-lactone had m.p. 66–67° C, $[\alpha]_D$ −22° (*c*, 1.0 in water). The 3,4-di-*O*-methyl-*N*-phenyl-D-xylosylamine, after one recrystallization from ethyl ether – petroleum ether, had m.p. 119–120° C (13).

Identification of 2,3,4-Tri-O-methyl-D-glucose

The colorless, clear sirup had $[\alpha]_D$ +71° (*c*, 3.5 in water). Anal. Calc. for $C_9H_{18}O_6$: OCH_3, 41.8%. Found: OCH_3, 40.0%. The 2,3,4-tri-*O*-methyl-*N*-phenyl-D-glucosylamine had m.p. and mixed m.p. 143–144° C (14).

Identification of the Neutral Fraction 2,3-Di-O-methyl-D-xylose

The neutral glycoside fraction was hydrolyzed in the usual way with *N* sulphuric acid to give a colorless, clear sirup (650 mg). Paper electrophoresis and paper chromatography (solvent D) indicated the presence of only 2,3-di-*O*-methylxylose. The sirup crystallized on standing, m.p. and mixed m.p. 93–94° C (15), $[\alpha]_D$ +22.4° (*c*, 1.0 in water). Anal. Calc. for $C_7H_{14}O_5$: OCH_3, 34.8%. Found: OCH_3, 34.5%. The dimorphic (16) 2,3-di-*O*-methyl-*N*-phenyl-D-xylopyranosylamine had m.p. 136.5–137.5° C, unchanged on further recrystallization from ethyl acetate, and $[\alpha]_D$ +148° (*c*, 1.7 in ethanol). Anal. Calc. for $C_{13}H_{19}O_4N$: OCH_3, 24.5%. Found: OCH_3, 24.5%.

Second Methylation of the Aldotetraouronic Acid

A sample of aldotetraouronic acid (3.0 g), obtained by preparative paper chromatography, was methylated as described above. The molar ratio between the 3,4-di-*O*-methylxylose, 2,3,4-tri-*O*-methylglucose, and 2,3-di-*O*-methylxylose obtained was 1:1:2.

Identification of Component Sugars

3,4-Di-O-methyl-D-xylose.—This sugar had $[\alpha]_D$ +20° (*c*, 1.0 in water). The corresponding δ-lactone had m.p. and mixed m.p. 65–66° C.

2,3,4-Tri-O-methyl-D-glucose.—This compound had $[\alpha]_D$ +70° (*c*, 1.0 in water). The aniline derivative had m.p. and mixed m.p. 143–144° C. Calc. for $C_{15}H_{23}O_5N$: OCH_3, 31.3%. Found: OCH_3, 30.0%.

2,3-Di-O-methyl-D-xylose.—The crystalline compound had m.p. and mixed m.p. 91–92° C and $[\alpha]_D$ +22° (*c*, 2.0 in water). Methoxyl content: 34.5%. The aniline derivative (16) had m.p. 142–143° C after three recrystallizations from ethyl acetate – petroleum ether and OCH_3, 24.3%.

ACKNOWLEDGMENTS

The author wishes to express his gratitude to Professor F. Smith, the University of Minnesota, for a specimen of an aldotriouronic acid. This investigation was supported in part by a United States Public Health Service Research Grant A-4258 from the National Institute of Arthritis and Metabolic Diseases, Public Health Service.

REFERENCES

1. T. E. TIMELL. Chem. & Ind. 999 (1959).
2. T. J. PAINTER. Can. J. Chem. **37**, 497 (1959).
3. J. K. HAMILTON and N. S. THOMPSON. J. Am. Chem. Soc. **79**, 6464 (1957).
4. D. V. MYHRE and F. SMITH. J. Agr. Food Chem. **8**, 359 (1960).
5. C. P. J. GLAUDEMANS and T. E. TIMELL. J. Am. Chem. Soc. **80**, 941, 1209 (1958).
6. R. KUHN, H. TRISCHMANN, and I. LÖW. Angew. Chem. **67**, 32 (1955).
7. R. H. MARCHESSAULT and B. G. RÅNBY. J. Polymer Sci. **36**, 561 (1959).
8. R. H. MARCHESSAULT and B. G. RÅNBY. Svensk Papperstidn. **62**, 230 (1959).
9. T. E. TIMELL. To be published.
10. T. E. TIMELL, C. P. J. GLAUDEMANS, and A. L. CURRIE. Anal. Chem. **28**, 1916 (1956).
11. E. L. HIRST, L. HOUGH, and J. K. N. JONES. J. Chem. Soc. 928 (1949).
12. S. P. JAMES and F. SMITH. J. Chem. Soc. 739 (1945).
13. J. K. N. JONES and L. E. WISE. J. Chem. Soc. 3389 (1952).
14. S. PEAT, E. SCHLÜCHTERER, and M. STACEY. J. Chem. Soc. 581 (1939).
15. J. K. HAMILTON, E. V. PARTLOW, and N. S. THOMPSON. Tappi, **41**, 811 (1958).
16. I. EHRENTHAL, M. C. RAFIQUE, and F. SMITH. J. Am. Chem. Soc. **74**, 1341 (1952).

THERMOCHEMICAL STUDIES OF SOME ALCOHOL–ISOCYANATE REACTIONS

EDWARD G. LOVERING AND KEITH J. LAIDLER
The Department of Chemistry, University of Ottawa, Ottawa, Canada
Received September 13, 1961

ABSTRACT

The heats of reaction of normal-, iso-, and secondary-butyl alcohols reacting with phenyl isocyanate, the three tolyl isocyanates, and 2,4-tolylene diisocyanate were measured at 25° C, using a differential calorimeter of the Tian–Calvet type. The results are interpreted in terms of substituent effects.

From bond energy considerations the heats of formation of phenyl isocyanate and tolyl isocyanate have been estimated.

INTRODUCTION

Polyurethanes, formed by the reaction of a diisocyanate with a dihydroxy alcohol or polyol, are playing an increasingly important role in plastics technology. There is a lack of heat of reaction data for reactions of this type, and heats of formation for aryl isocyanates and urethanes do not appear to be available. In view of this situation it was decided to measure the heats of reaction of some simple alcohol–isocyanate reactions, since these are relevant to the more complicated reactions giving rise to polyurethanes. The reactions studied were those of normal-, iso-, and secondary-butyl alcohols with phenyl isocyanate, the three tolyl isocyanates, and 2,4-tolylene diisocyanate.

The only heats of formation available concerning isocyanates are those of Lemoult (1), who measured the heat of combustion of methyl and ethyl isocyanates. He reported the heat of combustion of liquid ethyl isocyanate to be 424.4 kcal mole^{-1}, but reported no analysis of the combustion products. Heats of formation do not appear to be available for any urethane of the type R—NH—COO—R′, although Kharasch (2) gives the heat of formation of urethane itself. The heat of formation of a few di-*N*-substituted urethanes are given by Schmidt (3). Recently Skinner and Snelson (4) have determined the heats of combustion of the four butyl alcohols at 25° C. The heats of formation of normal-, iso-, and secondary-butyl alcohols in the liquid state were given as -78.49 ± 0.20, -80.00 ± 0.20, and -81.88 ± 0.22 kcal mole^{-1} respectively.

EXPERIMENTAL

Purification and Preparation of Materials

The normal- and iso-butyl alcohols used were Fisher Certified Reagents. Secondary-butyl alcohol was a Fisher "Highest Purity" grade material. The alcohols were dried by refluxing over freshly ignited calcium oxide for 4 hours followed by fractionation through a 40-cm column packed with short lengths of 4-mm glass tubing. Only the middle fractions (collected at 117.7°, 108.4°, and 99.5° C for normal-, iso-, and secondary-butyl alcohols respectively) were retained. The alcohols were tested for dryness using the method suggested by Dyer, Taylor, Mason, and Samson (5). One or two drops of phenyl isocyanate were added to a sample of the alcohol; if no crystals of insoluble *sym*-diphenyl urea formed the alcohol was considered to be suitable for the experiments.

The phenyl and tolyl isocyanates used were manufactured by Eastman Organic Chemicals. They were purified by double vacuum distillation, the last distillation taking place immediately prior to use. Analysis of the distilled isocyanate using the Stagg technique (6) indicated that the isocyanates were between 99.5% and 100.5% pure. The boiling points and approximate boiling pressures for the isocyanates were phenyl: 46° C, 5 mm; *o*-tolyl: 57° C, 10 mm; *m*-tolyl: 62° C, 5 mm; *p*-tolyl: 66° C, 10 mm. The 2,4-tolylene diisocyanate was obtained from the Canadian Armaments Research and Development Establishment at Valcartier, Que. It was treated as were the other isocyanates; the boiling point was 165° C at approximately 50 mm.

Urethanes were prepared by causing isocyanate to react with a small excess of alcohol; in certain cases the reaction was catalyzed with ferric acetylacetonate. The urethanes were purified by recrystallization from petroleum ether. The urethanes of *m*-tolyl isocyanate are liquids at room temperature; they were purified by a double vacuum distillation, only the middle portion being retained in each case. In cases where the urethanes have been previously reported the melting point of the prepared material was compared with that given in the literature. In the cases of previously unreported urethanes a carbon and hydrogen analysis was carried out. For each urethane prepared, the melting or boiling point and, where appropriate, the literature melting point and the results of the elemental analysis are given in Table I.

TABLE I

Urethanes: melting points and analytical results

Urethane	M.p. (°C)	Literature m.p. (°C)	% carbon		% hydrogen	
			Exptl.	Theory	Exptl.	Theory
N-Phenyl-*n*-butyl	57.5	57 (7)				
N-Phenyl-*i*-butyl	85.5–86.0	86 (7)				
N-Phenyl-*s*-butyl	64–65	65 (7)				
N-*o*-Tolyl-*n*-butyl	45.5–46.0	45.5 (8)				
N-*o*-Tolyl-*i*-butyl	41–42		70.05	69.52	8.27	8.27
N-*o*-Tolyl-*s*-butyl	42.5–43.0		69.58	69.52	8.18	8.27
N-*m*-Tolyl-*n*-butyl	185 (b.p. at 5 mm)		69.75	69.52	8.61	8.27
N-*m*-Tolyl-*i*-butyl	183 (b.p. at 15 mm)		69.47	69.52	8.27	8.27
N-*m*-Tolyl-*s*-butyl	179 (b.p. at 20 mm)		69.53	69.52	8.67	8.27
N-*p*-Tolyl-*n*-butyl	63	63 (8)				
N-*p*-Tolyl-*i*-butyl	52.5–53.0		70.01	69.52	8.25	8.27
N-*p*-Tolyl-*s*-butyl	32–33		69.86	69.52	7.95	8.27
N,*N*′-2,4-Tolylene-di-*n*-butyl	79		63.56	63.40	7.94	8.14
N,*N*′-2,4-Tolylene-di-*i*-butyl	122–123		63.07	63.40	7.90	8.14
N,*N*′-2,4-Tolylene-di-*s*-butyl	90–91		63.57	63.40	7.95	8.14

Calorimetry

The heats of reaction were measured using a differential microcalorimeter of the Tian–Calvet (9) type. The instrument was fitted with electronic amplifier and integrator circuits as described by Attree, Cushing, Ladd, and Pieroni (10). It can be shown (9) that the area under the curve of amplified thermopile voltage vs. time is directly proportional to the amount of heat which produces the thermopile voltage. It was found experimentally that equal amounts of heat, liberated simultaneously in each cell of the calorimeter, gave rise to a net area of zero, indicating that the two opposing thermopiles are properly balanced.

The calorimeter was calibrated electrically; a curve of total area against heat was constructed by liberating various amounts of heat in the reaction cell of the calorimeter, and recording the resulting area. Because of a tendency for the electronic components of the system to drift, the calibration was checked after every measurement. This was done by duplicating, by electrical heating, the area due to the chemical reaction. The electrical calibration procedure was checked by measuring the heat of solution of anhydrous lithium sulphate crystals in water. The heat of solution for the process

$$Li_2SO_4\,(c.) + 220H_2O\,(l.) = Li_2SO_4.220\,(aq.)$$

was found to be -6.54 ± 0.10 kcal mole^{-1}. This is in good agreement with the value of -6.61 kcal mole^{-1} obtained from the N.B.S. tables (11).

In order to compensate for the heat evolved on mixing the alcohol and isocyanate reactants, an amount of urethane equivalent to the amount of isocyanate was dissolved in one cell of the calorimeter, while the reaction took place in the other cell. Since the calorimeter is a differential one, the net heat measured was that due to the heat of reaction.

The reaction cell assembly consists of a stainless steel capsule, with ends of aluminum foil, containing either the isocyanate or the urethane. It is suspended in a glass cylindrical cell which contains the alcohol. The reaction is initiated by piercing the ends of the cylinder with a length of wire held in place directly above the capsule. There is a calibrating resistor in the cell containing the isocyanate. The cells are stirred gently during the initial period of the reaction by a mechanical suction device; stirring was necessary to obtain reproducible results.

There is a tendency towards the formation of disubstituted ureas instead of urethanes during alcohol–isocyanate reactions. The tendency increases on going from normal to secondary to tertiary alcohols, and also as the temperature increases (5). Dyer *et al.* (5) report urea formation during the reaction between phenyl isocyanate and secondary-butyl alcohol at 25° C. None was observed under our reaction conditions. Because of the possibility of side reactions, however, the product of each reaction was examined

in the following way. The solution of the product in alcohol (the final state after reaction) was examined for the presence of crystals of the disubstituted urea (these ureas are insoluble in the butyl alcohols). The excess alcohol was removed under vacuum and an infrared spectrum of the solid product was taken. This was compared with the spectrum of the expected urethane, obtained from the previously prepared material. Only in the case of the reaction between *p*-tolyl isocyanate and secondary-butyl alcohol was there evidence of appreciable side reaction. Since only a few insoluble crystals were seen in the reaction vessel, the side reaction was estimated to involve less than 5% of the isocyanate. No correction to the observed heat was made; such a correction will be small since the reaction involving tertiary-butyl alcohol, which yields considerable urea, gives approximately the same heat of reaction as do the reactions which yield only urethane as product.

The calories used in this paper are defined calories, equal to 4.1840 joules.

EXPERIMENTAL RESULTS

The heats evolved per mole when normal-, iso-, and secondary-butyl alcohols react with phenyl isocyanates, the three tolyl isocyanates, and 2,4-tolylene diisocyanate, are given in Table II. In the table the weight of isocyanate used is given, as well as the heat measured experimentally. The measured heat is the heat evolved when the given weight of isocyanate is introduced into 10 ml of the given alcohol, less the heat evolved when a weight of urethane equivalent to the isocyanate is dissolved in 10 ml of the alcohol. The heat of reaction in kcal mole^{-1} calculated from the measured heat is also given in the table. The molecular weights of the isocyanates were taken to be for phenyl, 119.12; for tolyl, 133.14; and for 2,4-tolylene diisocyanate, 174.06.

In the case of certain reactions, a catalyst was used to shorten the reaction time and decrease the experimental error due to drift in the electronic components of the calorimeter over long periods of time. The heats of reaction measured in the presence of a catalyst are clearly marked in the table. In order to be certain that the added catalyst did not affect the heat of reaction, certain reactions were measured with and without a catalyst. As expected, the presence of catalyst does not affect the heat of reaction. The catalysts used were either ferric acetylacetonate or dimethylcetylamine.

Although the experimental deviation is usually less than $\frac{1}{2}$% for each reaction, we have attached a somewhat larger experimental error to our work because of our inability to detect side reactions, unless they are appreciable. The estimated error for each reaction is given in the table.

DISCUSSION

The heats of alcohol–isocyanate reactions do not appear to have been previously measured, and there are insufficient heat of formation data to permit their calculation. Consequently no comparison with previous measurements is possible. The heats of formation of the isocyanates can, however, be estimated using an empirical bond energy scheme. The scheme used is that devised by Laidler (12) together with certain modifications to it which are applicable to aromatic ring compounds.

Lemoult's value for the heat of combustion of ethyl isocyanate (424.4 kcal mole^{-1}) has been used without correction to calculate the heat of atomization of ethyl isocyanate as 976.3 kcal mole^{-1}. The bonds contributing to this value are

$$c_1+3p+2s+n = 976.3,$$

where, following Laidler, the carbon–carbon bond energy is c_1, primary carbon – hydrogen bonds are represented by p, and secondary carbon – hydrogen bonds by s. The contribution to the heat of atomization by the isocyanate group is denoted by n. Laidler gives values of 85.40, 98.96, and 98.23 kcal for the contributions to the heat of atomization of a compound in the liquid state for c_1, p, and s respectively. From these values

TABLE II

The heats of isocyanate reactions at 25° C

n-Butyl alcohol			*i*-Butyl alcohol			*s*-Butyl alcohol		
Weight of isocyanate (g)	Observed heat of reaction (cal)	Heat of reaction (kcal mole^{-1})	Weight of isocyanate (g)	Observed heat of reaction (cal)	Heat of reaction (kcal mole^{-1})	Weight of isocyanate (g)	Observed heat of reaction (cal)	Heat of reaction (kcal mole^{-1})
Phenyl isocyanate								
0.1305	27.36	24.97*	0.1292	26.17	24.13	0.1204	23.72	23.47
0.1259	26.50	25.07*	0.1264	25.52	24.05	0.1174	23.02	23.36
0.1449	30.45	25.03*	0.1282	26.00	24.16	0.1166	22.92	23.42
0.1474	31.10	25.12						
0.1155	24.32	25.08						
		Mean 25.1±0.3			Mean 24.1±0.3			Mean 23.4±0.3
o-Tolyl isocyanate†								
0.1257	22.10	23.41	0.1199	19.90	22.10	0.1267	20.65	21.70
0.1198	21.04	23.38	0.1280	21.15	22.00	0.1263	20.53	21.64
0.1168	20.60	23.48	0.1281	21.25	22.09	0.1257	20.55	21.76
0.01605	2.840	23.55	0.1168	19.84	22.16			
		Mean 23.5±0.3			Mean 22.1±0.3			Mean 21.7±0.3
m-Tolyl isocyanate‡								
0.1784	26.11	19.49	0.1750	25.10	19.10	0.1918	26.65	18.50
0.1692	24.84	19.55	0.1779	25.52	19.10	0.1848	26.05	18.55
0.1710	25.00	19.46	0.1809	25.89	19.05	0.1811	25.21	18.53
		Mean 19.5±0.3			Mean 19.1±0.3			Mean 18.5±0.3
p-Tolyl isocyanate§								
0.1370	25.44	24.74	0.1405	25.35	24.02	0.1534	27.12	23.54
0.1236	22.98	24.75	0.1291	23.23	23.96	0.1537	27.10	23.47
0.1222	22.65	24.68	0.1315	23.60	23.90‖	0.1482	26.45	23.76
0.1198	22.30	24.78	0.1311	23.50	23.86‖	0.1548	27.50	23.65
0.1191	22.10	24.71				0.1485	26.35	23.62
		Mean 24.7±0.3			Mean 23.9±0.3			Mean 23.6±0.6
2,4-Tolylene diisocyanate¶ **								
0.1114	28.18	44.03	0.0944	23.11	42.61	0.0879	20.86	41.31
0.1008	25.46	43.96	0.1005	24.67	42.73	0.943	22.40	41.35
0.1012	25.58	44.00	0.0939	22.90	42.45	0.1077	25.60	41.37
0.0951	24.04	44.00	0.1011	24.85	42.78	0.1034	24.58	41.38
		Mean 44.0±0.6			Mean 42.6±0.8			Mean 41.3±0.6

*Reaction catalyzed by dimethylcetylamine (0.05 g/100 ml alcohol).
†Reaction with *i*-butyl alcohol catalyzed with ferric acetylacetonate (0.15 g/100 ml alcohol).
‡The urethanes of *m*-tolyl isocyanate are in the liquid state at 25° C.
§A small amount of *N,N'*-di-*p*-tolyl urea was formed in reactions with *s*-butyl alcohol. The amount is estimated to be less than 5%.
‖Reaction catalyzed with ferric acetylacetonate (0.15 g/100 ml alcohol).
¶*N,N'*-2,4-tolylene di-*i*-butyl urethane is slow to dissolve in *i*-butyl alcohol. It was necessary to stir the second cell violently to achieve solution, with a considerable decrease in experimental reproducibility.
**Reactions with *i*- and *s*-butyl alcohol catalyzed by ferric acetylacetonate (0.15 g/100 ml alcohol).

and the heat of atomization of ethyl isocyanate, the value of n, the bond energy of the isocyanate group, is calculated to be 397.6 kcal. Preliminary work on a bond energy scheme for aromatic compounds indicates that carbon–carbon bonds in an aromatic ring should have a special value, denoted by c_b, as should carbon–hydrogen bonds, denoted by t_b, when the carbon atom is part of the ring. Values of 124.29 and 97.55 kcal for c_b and t_b respectively have been used. The heat of atomization of phenyl isocyanate is given by $6c_b+5t_b+n$, yielding a value of 1631.01 kcal mole^{-1} for the heat of atomization of liquid phenyl isocyanate; from this, ΔH_f^0 (l., 25° C) = 3.5 kcal mole^{-1} is obtained. Similarly, for the tolyl isocyanates, ΔH_f^0 (l., 25°) is found to be -5.3 kcal mole^{-1}. There are insufficient data available to attempt to make allowance in ΔH_f^0 for the ring positions of the three tolyl isocyanate isomers. It is expected that two isocyanate groups on an aromatic ring would lead to considerable interaction; this would affect the heat of formation which, therefore, has not been calculated for 2,4-tolylene diisocyanate.

The heats of formation of the urethanes are readily approximated using the heats of formation of the alcohols, the estimated heats of formation of the isocyanates, and the appropriate heat of reaction.

The results of the heat of reaction measurements can be interpreted in terms of substituent effects. As far as the effect of changing the alcohol from normal- to iso- to secondary-butyl is concerned, a decrease in stability of the resulting urethane (the heat of reaction being a measure of the stability of the resulting urethane) would be expected on the grounds of steric hindrance. The inductive effect will act in the same direction, tending to put a partial negative charge on to the urethane group. This will decrease the resonance stabilization of the urethane group with the aromatic ring to which it is attached. It is observed in the case of every isocyanate that the heat of reaction decreases in the order normal > iso > secondary. Turning to the effects of a methyl group substituted into the aromatic ring of the urethane, it is expected that partial negative charges would appear ortho and para to the methyl group, due to the resonance effect. There will be, in addition, a small charge on the ring due to the inductive effect, which decreases in the order ortho > meta > para. Steric effects will also be of importance in cases of ortho substitution. From these considerations phenyl isocyanate should show the largest heat of reaction, *m*-tolyl isocyanate would be expected to yield a smaller value, followed by *p*-tolyl isocyanate. Because of the steric effect, the heat of formation of ortho urethanes should be considerably less than for the others. These predictions are substantiated by the experimental results; because of the difference in state the predicted behavior of *m*-tolyl isocyanate reactions cannot be verified.

This work was supported by Grant No. 1028-28 Defence Research Board.

REFERENCES

1. P. LEMOULT. Ann. de chim. et phys. Ser. VII, **16**, 338 (1899).
2. M. S. KHARASCH. J. Research Natl. Bur. Standards, **2**, 359 (1929).
3. A. SCHMIDT. Z. ges. Schiess- u. Sprengstoffw. **29**, 259 (1934).
4. H. A. SKINNER and A. SNELSON. Trans. Faraday Soc. **56**, 1776 (1960).
5. E. DYER, H. A. TAYLOR, S. J. MASON, and J. SAMSON. J. Am. Chem. Soc. **71**, 4106 (1949).
6. H. E. STAGG. Analyst, **71**, 557 (1946).
7. R. L. SHRINER and R. C. FUSON. The systematic identification of organic compounds. John Wiley and Sons, Inc., New York. 1948.
8. BEILSTEIN'S HANDBUCH DER ORGANISCHEN CHEMIE. Vol. 12. Vierte Auflage. Zweites Erganzungswerk. Springer-Verlag, Berlin. 1950. pp. 444, 511.
9. E. CALVET and H. PRAT. Microcalorimetrie. Masson et Cie, Paris. 1956.
10. R. W. ATTREE, R. L. CUSHING, J. A. LADD, and J. J. PIERONI. Rev. Sci. Instr. **29**, 491 (1958).
11. U.S. NATIONAL BUREAU OF STANDARDS. Selected values of chemical thermodynamic properties. Ser. I. Washington. 1952.
12. K. J. LAIDLER. Can. J. Chem. **34**, 626 (1956).

KINETIC STUDIES OF SOME ALCOHOL–ISOCYANATE REACTIONS

EDWARD G. LOVERING AND KEITH J. LAIDLER
The Department of Chemistry, University of Ottawa, Ottawa, Canada
Received September 13, 1961

ABSTRACT

The kinetics of 12 alcohol–isocyanate reactions have been studied at a series of temperatures. The reactions were studied by a calorimetric technique, as well as the usual analytical method. The results are shown to be in agreement with a mechanism previously proposed by Baker. Certain objections to Baker's mechanism are discussed.

INTRODUCTION

The preceding paper described the measurement of the heats of reaction of normal-, iso-, and secondary-butyl alcohols with phenyl isocyanate, the three tolyl isocyanates, and 2,4-tolylene diisocyanate. During the course of these measurements it became apparent that kinetic rate constants could be deduced from the data obtained calorimetrically. In order to verify the rate constants so obtained the reactions were studied by the usual analytical technique of following the disappearance of one of the reactants with time. In addition, two mechanisms for the alcohol–isocyanate reactions have been suggested, and it was felt that the additional data would help to decide between them.

Kinetic rate constants were deduced from the calorimetric data using a method suggested by Baumgartner and Duhaut (1). In essence the method consists of obtaining the ratio of product concentration to initial reactant concentration at a given time, from the ratio of the heat evolved at that time, to the heat evolved at infinite time. The pseudo first-order rate constant can be readily calculated from this ratio.

The first kinetic study of an alcohol–isocyanate reaction appears to be that of Davies and Farnum (2), who measured relative rates by causing two alcohols to compete for a limited amount of isocyanate. Baker and Holdsworth (3), Baker and Gaunt (4), and Baker, Davies, and Gaunt (5) have carried out an extensive series of investigations of alcohol–isocyanate reactions. On the basis of their findings, they propose the following mechanism:

$$\phi\text{—N=C=O} + \text{ROH} \underset{k_2}{\overset{k_1}{\rightleftharpoons}} \phi\text{—N=C(—O}^-\text{)—ROH}^+ \qquad [1a]$$

$$\phi\text{—N=C(—O}^-\text{)—ROH}^+ + \text{ROH} \xrightarrow{k_3} \phi\text{—NH—C(=O)—OR} + \text{ROH}. \qquad [1b]$$

The alcohol is believed to function as a catalyst through its basic oxygen atom, as well as a reactant. Application of the steady-state treatment to this mechanism yields the following relationship:

$$\frac{[\text{ROH}]}{k_0} = \frac{k_2}{k_1 k_3} + \frac{[\text{ROH}]}{k_1}, \qquad [2]$$

where k_0 is the experimental second-order rate constant. Consideration was given to the possibility that a complex not containing isocyanate reacts with isocyanate; this,

however, was rejected, because such a mechanism would not fit equation [2], and because of evidence obtained in studies of the reaction in the presence of basic catalyst. This evidence clearly indicates that the isocyanate forms part of the initial complex. Baker and co-workers also report that the reaction is autocatalyzed by the urethane produced. The proposed mechanism has been tested by plotting $[ROH]/k_0$ vs. [ROH]. Such a plot should yield a straight line of slope $1/k_1$ and intercept k_2/k_1k_3. Baker and co-workers have studied reactions between phenyl isocyanate and methyl, ethyl, and isopropyl alcohols at 20° C and 30° C. In each case straight lines were obtained, except at very low alcohol concentrations.

The second-order rate constant was found to be dependent upon the ratio of alcohol to isocyanate. This effect is thought to be due to stabilization of the activated complex by polar alcohol molecules. The reported increase of rate in benzene solution, as compared with dibutyl ether solution, is thought to be due to the presence of monomeric alcohol molecules. The reactions were also studied in the presence of basic catalysts.

Dyer, Taylor, Mason, and Samson (6) have measured the reaction rates, at a series of temperatures, of phenyl isocyanate with *n*-butyl and *s*-butyl alcohols. They have interpreted their results in terms of Baker's mechanism.

The reaction between phenyl isocyanate and methyl alcohol has been studied at 20° C in a series of solvents by Ephraim, Woodward, and Mesrobian (7). They claim that the logarithm of the rate constant decreases as the dielectric constant of the solvent increases; a plot of their experimental data, however, shows that there is no significant correlation of this kind. These authors also find that deviations from second-order kinetics increase as the hydrogen bonding capability of the solvent increases. They propose the mechanism:

$$2ROH \overset{K_{1a}}{\rightleftharpoons} \text{complex 1}$$

$$ROH + \text{solvent} \overset{K_{1b}}{\rightleftharpoons} \text{complex 2}$$

$$ROH + \text{urethane} \overset{K_{1c}}{\rightleftharpoons} \text{complex 3}$$

$$\text{Complex 1} + RNCO \xrightarrow{k_{2a}} \text{urethane} + ROH$$

$$\text{Complex 2} + RNCO \xrightarrow{k_{2b}} \text{urethane} + \text{solvent}$$

$$\text{Complex 3} + RNCO \xrightarrow{k_{2c}} 2\text{urethane}.$$

No mention is made of Baker's argument that this type of mechanism is improbable.

Studies of amine-catalyzed alcohol–isocyanate reactions have been reported by Kogon (8), Burkus and Eckert (9), and Sato (10).

EXPERIMENTAL

The method used to purify the chemicals used in the experiments was completely described in the preceding paper.

Isocyanates were analyzed using a modification of Stagg's technique (11). The method consists of allowing the unknown isocyanate to react with an excess of a standard solution of dibutylamine in toluene, followed by back titration of the excess amine with standard hydrochloric acid to a bromphenol blue end point. Isopropyl alcohol is added to prevent the formation of a second phase during the titration.

The reaction was carried out in a round-bottomed flask with a ground-glass stopper. A weighed amount of alcohol was placed in the flask, which was put into the thermostat. When equilibrium was reached isocyanate was added by means of a hypodermic syringe. The weight of isocyanate was found by weighing the isocyanate container before and after addition of isocyanate to the reaction vessel. Five-milliliter samples of the reacting mixture were withdrawn by pipette at regular intervals; the reaction was stopped

by draining the pipette into a standard solution of dibutylamine. The time at which the pipette was half empty was recorded; the excess amine was back titrated with standard hydrochloric acid. The rate constant, k, was obtained from the integrated expression for a pseudo first-order reaction:

$$k = (1/tb) \ln (a/a-x),$$

where t is the time, b the concentration of alcohol, a the initial concentration of isocyanate, and x the concentration of product at time t. The experimental data were also treated by the differential method by plotting log rate vs. log concentration. The slope of the curve gives the order, and the intercept the rate constant.

The results of a typical calorimetric run are shown in Fig. 1. Figure 1(a) is a curve of electromotive

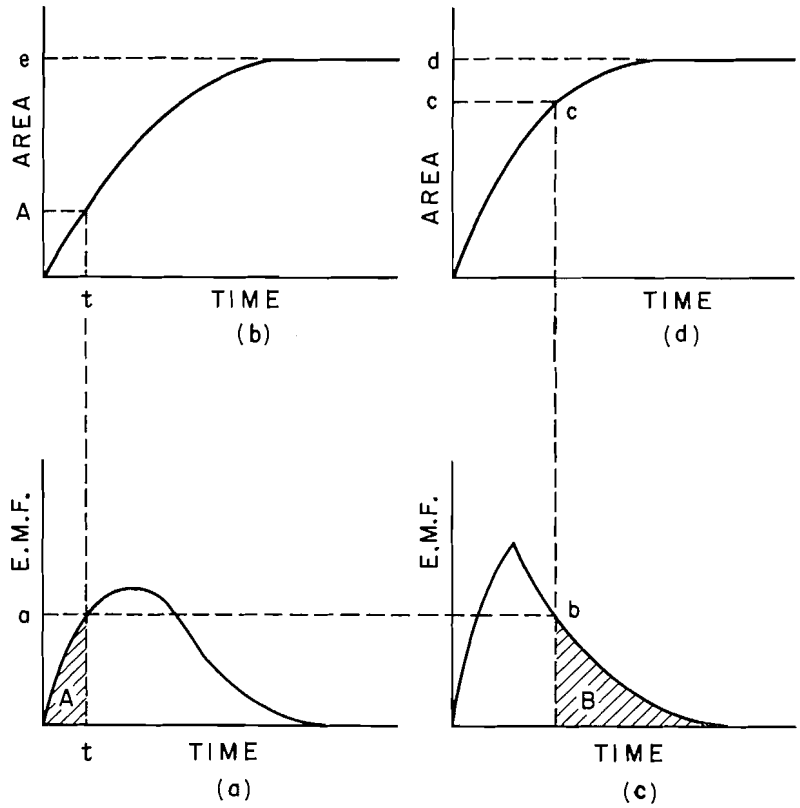

FIG. 1. Typical time–voltage curves: (a) chemical reaction, (b) integral of the chemical reaction, (c) electrical heating, (d) integral of the electrical heating.

force vs. time for a chemical reaction, and Fig. 1(b) shows the integral of this curve with time. The E.M.F.-vs.-time results for electrical heating are shown in Fig. 1(c); the integral of this curve appears in 1(d). It is desired to obtain values for the ratio a/x at a series of times. The heat evolved from the reaction cell from $t = 0$ to $t = t$ is the shaded area A in Fig. 1(a). The value of this area A is read directly from the plot of area vs. time in Fig. 1(b). The heat remaining in the reaction cell at time t is evolved in the same way that heat is evolved from the system after an electrical heating. Hence the area B under the electrical cooling curve from E.M.F. = b to E.M.F. = 0 is a measure of the unevolved heat in the reaction cell at time t. The sum of A+B gives the total heat produced by the reaction up to time t. Area B is obtained from Fig. 1(d) by subtracting c from d. The ratio of the heat produced at infinity to the heat produced at time t is a measure of a/x. This ratio is evaluated at a series of times, and the rate constant is calculated using the integrated pseudo first-order expression. The results for each run are averaged.

EXPERIMENTAL RESULTS

The rates of the reactions between normal-, iso-, and secondary-butyl alcohol and phenyl isocyanate and the three tolyl isocyanates have been measured at a series of

temperatures. The data were treated by the integral and differential method to obtain the second-order rate constant. The rate constant at a series of temperatures and the activation energy for each reaction is given in Table I. The rate constants at 25° C, deduced from the calorimetric measurements described in the preceding paper, are given in Table II, where they are compared to the rate constants determined analytically. The percentage difference between the two is also given.

DISCUSSION

It is seen from Table II that all the rate constants deduced calorimetrically are within 10% of those determined by chemical analysis. These results are satisfactory, as there are important sources of error present for which allowance could not be made. These are the increase in temperature as the reaction proceeds and the time lag between an event occurring in the reaction cell and its appearance as a signal on the recorder. Attempts to apply an empirical correction to the rate constant obtained in this way were unsuccessful. However, if steps were taken to ensure identical conditions of contact between the reaction cell and the calorimeter from one run to the next, we believe that an empirical time lag correction could be applied, with a considerable improvement in the accuracy of the rate constants so obtained.

The experimental results are in accord with the previously determined data for alcohol–isocyanate reactions and fit the mechanism suggested by Baker and his co-workers (3, 4, 5). Most of the reactions exhibit small deviations from pseudo first-order kinetics toward the end of the reaction. These deviations are probably due to autocatalysis.

The only previous work which is directly comparable to the results obtained here is that due to Dyer *et al.* (6), who measured rates and activation energies for reactions of phenyl isocyanate with normal- and secondary-butyl alcohols. They report activation energies of 8.1 and 9.9 kcal mole^{-1} for normal- and secondary-butyl alcohol reactions respectively; the values reported here are 11.5 and 12.5 kcal mole^{-1} respectively. This change in activation energy confirms the observations of Baker and his co-workers that the activation energy increases as the ratio of alcohol to isocyanate increases. The reactions reported here were carried out in a large excess of alcohol, while the work of Dyer *et al.* was in xylene solution.

For the reactions reported here it was found that the activation entropies are all in the region of −38 e.u. A large negative entropy of activation is an indication of an activated complex in which oppositely charged centers are separated from each other. The activated complex of Baker's mechanism is just such a species; it is doubtful if the formation of an alcohol–alcohol, an alcohol–solvent, or a urethane–alcohol complex, as suggested by Ephraim *et al.* (7), could account for this large negative entropy of activation.

It is of interest to note, at least for the reaction between *n*-butyl alcohol and phenyl isocyanate, that the free energy of reaction appears to be approximately independent of the reaction conditions, whereas the energy and entropy of activation are not. From the activation energy of 7.5 kcal mole^{-1} in xylene solution reported by Dyer, an activation entropy and free energy of −48 e.u. and 22.0 kcal mole^{-1} are calculated. For the same reaction in toluene catalyzed by triethylamine, Burkus and Eckert (9) report an activation entropy of −61 e.u. and a free energy of activation of 21.2 kcal mole^{-1}; the values reported here are −37 e.u. and 21.9 kcal mole^{-1}. The increase in activation energy as the alcohol concentration increases is probably an indication that more and more hydrogen bonds must be ruptured before the activated complex is formed. The increase in the entropy of activation probably indicates a decreasing amount of solvent

TABLE I

Isocyanate reactions: rate constants and activation energies

Alcohol	Rate constant (l. mole^{-1} sec^{-1}) 35° C	25° C	15° C	7° C	5° C	0° C	Activation energy (kcal mole^{-1})	Entropy of activation (cal mole^{-1} deg^{-1})
Phenyl isocyanate								
n-Butyl		4.57×10^{-4}	2.35×10^{-4}		1.15×10^{-4}		11.5	−36.9
i-Butyl		2.99×10^{-4}	1.54×10^{-4}		7.35×10^{-5}		11.8	−36.9
s-Butyl		1.44×10^{-4}	6.97×10^{-5}		3.14×10^{-5}		12.5	−35.9
o-Tolyl isocyanate								
n-Butyl	9.01×10^{-5}	4.49×10^{-5}	2.08×10^{-5}				12.9	−37.0
i-Butyl	6.22×10^{-5}	3.07×10^{-5}	1.43×10^{-5}				12.9	−37.5
s-Butyl	3.05×10^{-5}	1.51×10^{-5}	6.82×10^{-6}				13.1	−38.4
m-Tolyl isocyanate								
n-Butyl		2.50×10^{-4}	1.29×10^{-4}	7.72×10^{-5}		4.04×10^{-5}	11.7	−37.4
i-Butyl		1.73×10^{-4}	8.62×10^{-5}	5.48×10^{-5}		2.82×10^{-5}	11.7	−38.1
s-Butyl		7.94×10^{-5}	4.06×10^{-5}	2.18×10^{-5}		1.25×10^{-5}	12.5	−37.2
p-Tolyl isocyanate								
n-Butyl		2.46×10^{-4}	1.21×10^{-4}			3.86×10^{-5}	11.9	−36.8
i-Butyl		1.65×10^{-4}	8.21×10^{-5}			2.57×10^{-5}	12.0	−37.4
s-Butyl		7.64×10^{-5}	3.66×10^{-5}			1.13×10^{-5}	12.3	−37.9

TABLE II

Calorimetric rate constants at 25° C

Alcohol	Isocyanate	Rate constants (l. mole^{-1} sec^{-1})		Percentage difference
		Calorimetric	Analytical	
i-Butyl	Phenyl	2.98×10^{-4}	2.99×10^{-4}	0.3
s-Butyl	Phenyl	1.60×10^{-4}	1.44×10^{-4}	−10.0
n-Butyl	*m*-Tolyl	2.28×10^{-4}	2.50×10^{-4}	10.0
i-Butyl	*m*-Tolyl	1.57×10^{-4}	1.73×10^{-4}	10.0
s-Butyl	*m*-Tolyl	8.02×10^{-5}	7.94×10^{-5}	−0.7
i-Butyl	*p*-Tolyl	1.84×10^{-4}	1.65×10^{-4}	−10.4
s-Butyl	*p*-Tolyl	8.40×10^{-5}	7.64×10^{-5}	−9.0

rearrangement as the activated complex is formed. That is, the reactants are probably already well solvated with alcohol, and the formation requires mainly rearrangement of the solvent, and not addition of new solvent molecules. The lower entropy of activation for the amine-catalyzed reaction is probably an indication that the activated complex contains the amine molecule.

It would thus appear that all the experimental facts currently available support the mechanism proposed by Baker and his co-workers.

This work was supported by a grant from the Defence Research Board.

REFERENCES

1. P. Baumgartner and P. Duhaut. Bull. soc. chim. France, 1187 (1960).
2. T. L. Davies and M. C. Farnum. J. Am. Chem. Soc. **56**, 883 (1934).
3. J. W. Baker and J. B. Holdsworth. J. Chem. Soc. 713 (1947).
4. J. W. Baker and J. Gaunt. J. Chem. Soc. 9, 19, 27 (1949).
5. J. W. Baker, M. M. Davies, and J. Gaunt. J. Chem. Soc. 24 (1949).
6. E. Dyer, H. A. Taylor, S. J. Mason, and J. Samsom. J. Am. Chem. Soc. **71**, 4106 (1949).
7. S. Ephraim, A. E. Woodward, and R. B. Mesrobian. J. Am. Chem. Soc. **80**, 1326 (1958).
8. I. C. Kogon. J. Org. Chem. **24**, 438 (1959).
9. J. Burkus and C. F. Eckert. J. Am. Chem. Soc. **80**, 5948 (1958).
10. M. Sato. J. Am. Chem. Soc. **82**, 3893 (1960).
11. H. E. Stagg. Analyst, **71**, 557 (1946).

THE SYSTEM SILVER–INDIUM–GALLIUM

A. N. CAMPBELL AND W. F. REYNOLDS[1]
The Chemistry Department, University of Manitoba, Winnipeg, Manitoba
Received April 17, 1961

ABSTRACT

The system silver–indium–gallium has been investigated by the standard techniques of thermal analysis, photomicrography, X-ray photography, and hardness testing. The smallness of the heat effects made the determination of the liquid surface indefinite, at least in the low-temperature region where the pronounced tendency for metastable liquid phase to persist rendered all measurements indefinite, but the room-temperature isotherm was determined with more certainty. Owing to the complexity of the diagram there is still some uncertainty about some areas.

A one-phase area (α phase) exists in the silver-rich region of the ternary isotherm, representing the solid solubility of indium and gallium in silver. The silver-rich intermediate phase in the system silver–indium, δ, is shown to have a close-packed hexagonal structure and its lattice constants have been determined. The structure of γ, the corresponding phase in the system silver–gallium is more complex and was not determined. δ and γ phases do not form a continuous one-phase region.

Ternary peritectics exist at 623° C and 600° C (approximately). It is possible that two peritectics exist at the latter temperature, in close proximity.

The ternary eutectic lies at 14.5° C and has an approximate composition of 2% silver, 24% indium, and 74% gallium.

The system silver–indium–gallium has not been investigated previously; it is of interest because certain of the alloys can be used in transistors. In the present investigation, the liquidus surface and the location of the ternary peritectics and eutectics were investigated, as well as the room-temperature isotherm. Thermal analysis, X-ray and photomicrographic methods, as well as hardness testing, were used. A complete investigation of the system would involve the determination of the regions of stable existence of all phases at all temperatures and this would require quenching techniques. As two of the component binary systems are quite complicated the amount of work involved would be considerable. We did not undertake this, because the room-temperature condition is the most important.

The literature deals only with the component binary systems, as follows.

1. Gallium–indium: The first investigation was by de Boisbaudron (1), the discoverer of gallium. Other workers are French, Sidney, Saunders, and Ingle (2); Denny, Hamilton, and Lewis (3). The latest investigation is that of Svirbely and Selis (4), who investigated the system in its entirety from a study of the electrical resistivity of alloys over a range of temperature. All investigators agree that the system is of the eutectic type.

2. Silver–gallium: This system was studied in detail by Weibke, Meisel, and Weigels (5). Their results are shown in Fig. 1.

Investigations by Hume-Rothery and Andrews (6) indicated that β phase decomposes peritectically at 611° C and that β phase has a hexagonal close-packed structure. It transforms eutectoidally into α and γ phases at 378° C.

3. Silver–indium: Weibke and Eggers (7) carried out a systematic investigation of this system, using all the conventional techniques. Their results are shown in Fig. 2.

Frevel and Ott (8) report the following phases: a cubic phase rich in silver, a hexagonal phase, a pseudohexagonal phase, a face-centered cubic phase, and a tetragonal phase (in order of decreasing silver content). Presumably these correspond to α, δ, ϵ, and γ phases and solid solution of silver in indium.

[1]*Holder of N.R.C. Bursary, 1959–60.*

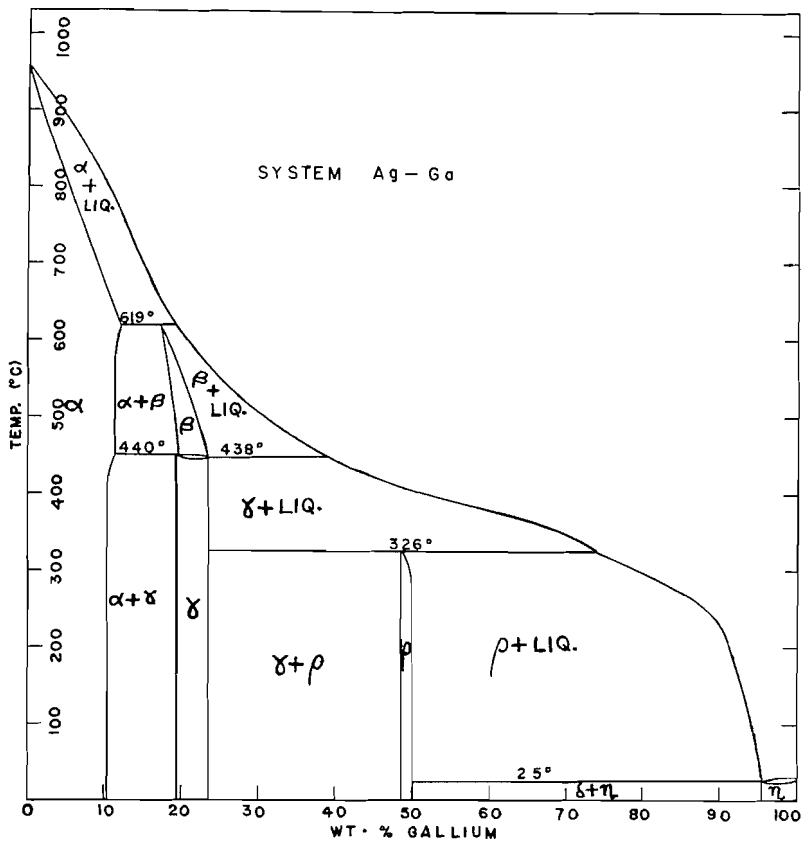

FIG. 1. Silver–gallium.

Hallner and Laues (9) report the following indium–silver phases (by X-ray methods): Ag_2In, cubic; $AgIn_2$, tetragonal; Ag_3In (hexagonal). Goldschmidt (10) reports that Ag_3In (δ) has a hexagonal close-packed structure, with cell dimensions $c = 4.76$ Å, $a = 2.95$ Å, $c/a = 1.626$. Hume-Rothery (11) and associates agree with Weibke and Eggers (7) about the solid solution of indium in silver.

EXPERIMENTAL

The individual metals were of the highest purity, as follows: (1) silver (Johnson, Matthey, Ltd.) 99.995%; (2) indium (Consolidated Mining and Smelting Company of Canada) 99.995%; (3) gallium (United Mineral and Chemical Corporation) 99.99%.

The alloys were prepared by fusion in an induction furnace at a temperature of approximately 1100° C. To prevent oxidation, the metals were sealed in evacuated pyrex tubes. This method was originated by Campbell, Wood, and Skinner (12), when studying the iron–tin system. The glass retains a complete vacuum, despite the fact that it softens at 600° C, if it is supported in the crucible so that it cannot run. The sealed tubes were heated in alundum crucibles packed with powdered alundum to provide the necessary support for the glass. In this way, the alloys could be melted and resolidified with formation of only a thin scum of oxide on the surface.

The alloys were allowed to cool in the furnace from 800° C to 100° C, over a period of about 30 hours. They were then further annealed in an oven at 100° C for 1 week, then left for a week at room temperature, before thermal analysis and preparation of polished sections were carried out.

Liquid was always present (to some extent, at least, metastably) in the lower-melting alloys, even after the above annealing treatment. Attempts were made to bring these alloys into true equilibrium by further

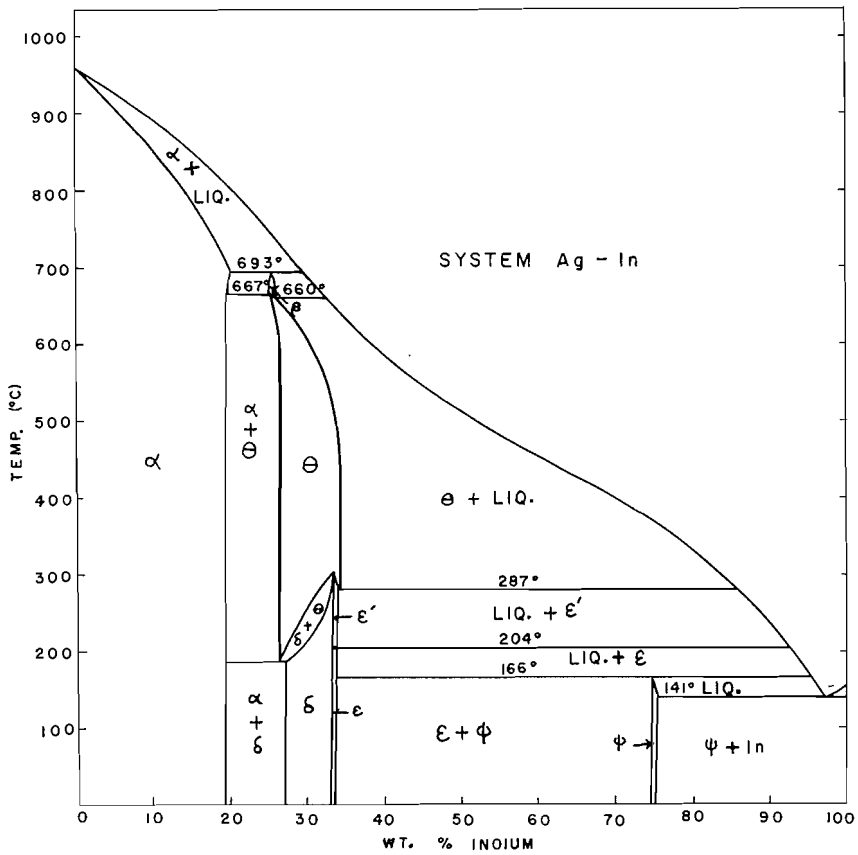

FIG. 2. Silver–indium.

annealing them at temperatures ranging between 50° C and 300° C, for periods of 3 weeks, but no decrease in the amount of liquid was ever noted.

The techniques used were those of thermal analysis, photomicrography, X-ray photography, and Rockwell hardness testing.

Those alloys which were completely solid at temperatures above 600° C were submitted to thermal analysis by the ordinary method of cooling, but the fact that gallium and gallium-rich alloys have a pronounced tendency to supercool makes this form of thermal analysis useless below 600° C. We therefore resorted to a controlled heating process, i.e., the temperature of the furnace was caused to rise as a straight-line function of the time. The furnace, consisting of a pyrex tube wrapped with asbestos paper and nichrome wire, was placed in a copper container packed with asbestos powder. This container was immersed in an ice–salt mixture to provide the necessary cold environment. The temperature was controlled by a "Variac", which was continuously adjusted by a geared-down electric motor. This gave a constant rate of voltage increase and a nearly constant rate of temperature increase (about 1° per minute).

The extreme hardness of gallium, despite its low melting point, renders polishing and etching of the metal difficult. The procedure adopted was as follows: The mounted specimen was polished on a series of successively finer sheets of emery paper, grades 2, 1, 0, and 00. Further polishing was done on a special polishing paper with a surface of alternate rows of fine abrasive and hollow spaces. The washed and dried specimen was then polished on a felt-covered wheel, using a paste of magnesium oxide as abrasive. When no scratches were visible to the naked eye, the polishing cloth was replaced by a velveteen cloth. Using levigated alumina as a fine polishing agent, the metal was polished until it had a mirror-like finish. The washed and dried specimen was examined under the microscope for scratches. If no scratches were visible, the alloy was etched with the following etchant: 98% H_2SO_4, 5 ml; $K_2Cr_2O_7$ (saturated solution), 100 ml; NaCl (saturated solution), 2 ml. This solution was diluted in the proportion of 1 part of etchant to 9 parts of water.

For the X-ray work a 57.3 mm Debye X-ray powder photography camera was used. Powder specimens were obtained in the following manner. The ingot was first cut and then a cleaned file was rubbed against one of the freshly cut surfaces. The second cut surface was then filed. Surface filings were discarded and only subsurface filings were kept as samples. An X-ray tube with copper anticathode and nickel filter was used. Measurements of "*d*" values gave a consistency of about 1% or better. Intensities were estimated visually.

Specimens for hardness testing were about 5 mm thick and had two parallel flat surfaces. A Rockwell hardness tester was used.

EXPERIMENTAL RESULTS

Table I reproduces all the experimental data, as obtained. A selection of the photomicrographs is given (Figs. 3–5). Figure 6 represents the room-temperature equilibrium diagram of the silver-rich region. The X-ray photographs are not reproduced, since most of them were used primarily for identification. In Table II, however, the interplanar distances and line intensities of alloys 5, 11, 14, and 15 are given, since these refer to pure, or almost pure phases, of, however, different compositions.

δ phase is shown to have close-packed hexagonal structure. For alloy 15, the lattice dimensions are $c = 4.725$ Å, $a = 2.942$ Å, and $c/a = 1.606$. This agrees with the theoretical $c/a = 1.633$ for hexagonal close-packed and with the results of Goldschmidt (10) for Ag_3In. Table III gives a summary of the results of photomicrography and (or) X-ray photography, together with hardness, of those alloys which were used for the definition of phase boundaries.

Hardness was used to delineate the regions of existence of δ and γ phases. Both phases showed nearly constant hardness throughout their regions of existence; there was no gradual transition in hardness from one phase to the other. The γ phase is quite hard, B-78 as compared with B-86 for mild steel. The hardness of the two phases is the more remarkable when one considers the relative softness of α phase.

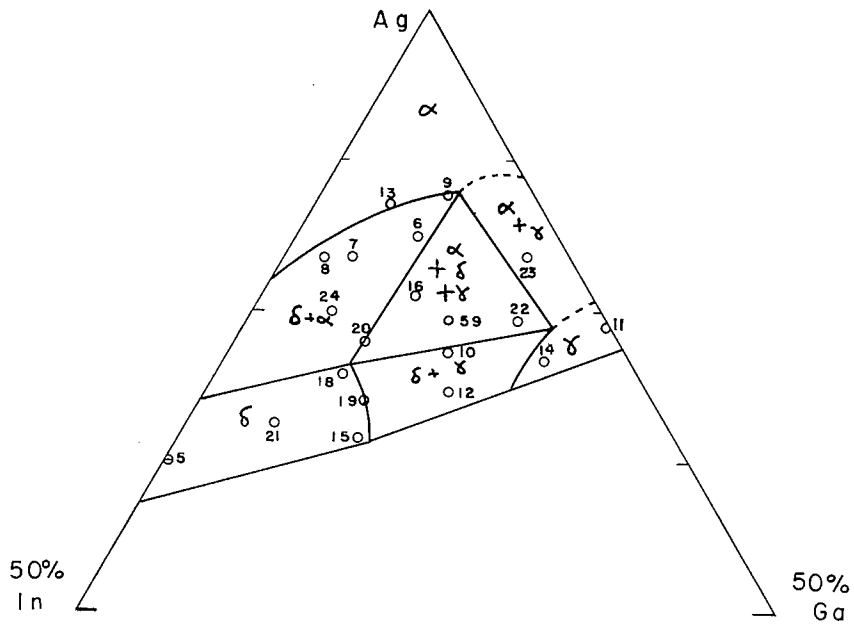

FIG. 6. Room temperature equilibrium diagram of the Ag-rich region.

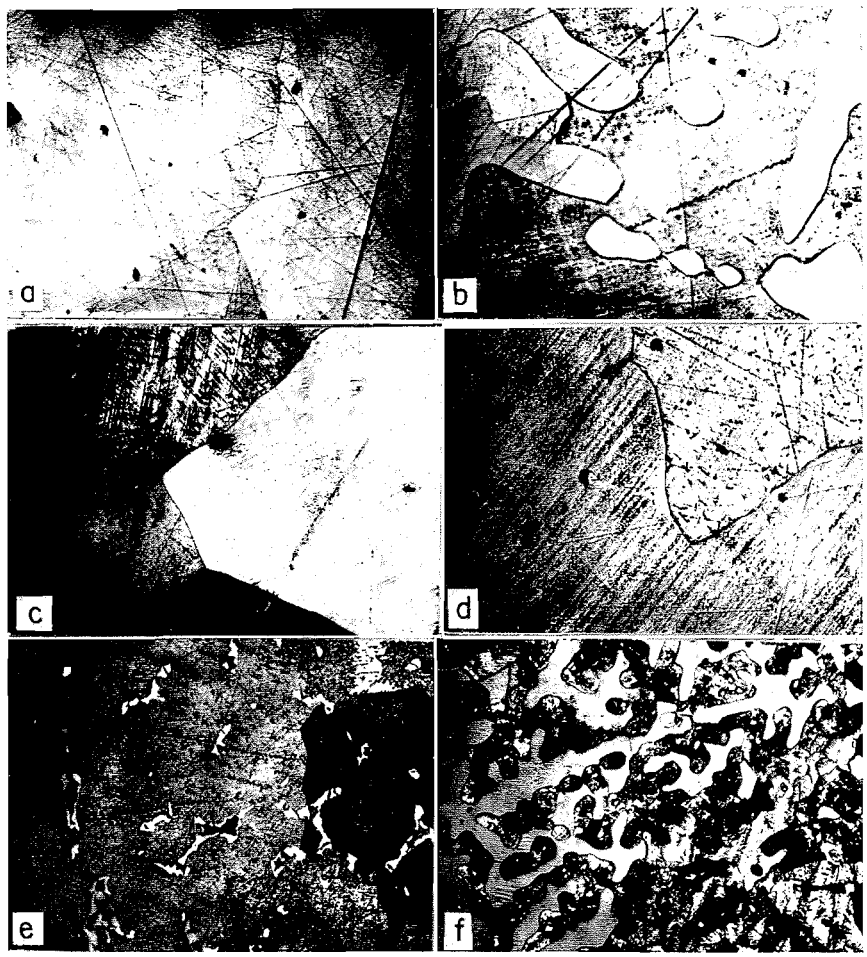

FIG. 3. (*a*) Alloy 1. This alloy is pure α phase. Note the existence of large grains of slightly different coloring due to oriented grain lustre.
(*b*) Alloy 3. This alloy contains α (dark) and δ (light) in approximately the same quantities.
(*c*) Alloy 4. This alloy is Ga-rich α phase. Again the grains show a variety of coloring.
(*d*) Alloy 5. This alloy is pure δ phase, in the Ag–In binary.
(*e*) Alloy 17. This alloy is ϵ phase with slight amounts of ψ phase. The ψ phase has a pitted appearance because it is much softer than ϵ phase and is worn away by polishing.
(*f*) Alloy 25. This alloy contains δ (light) and ϵ (mottled) phase.
NOTE: The magnification of Figs. 3, 4, and 5 is 120×.

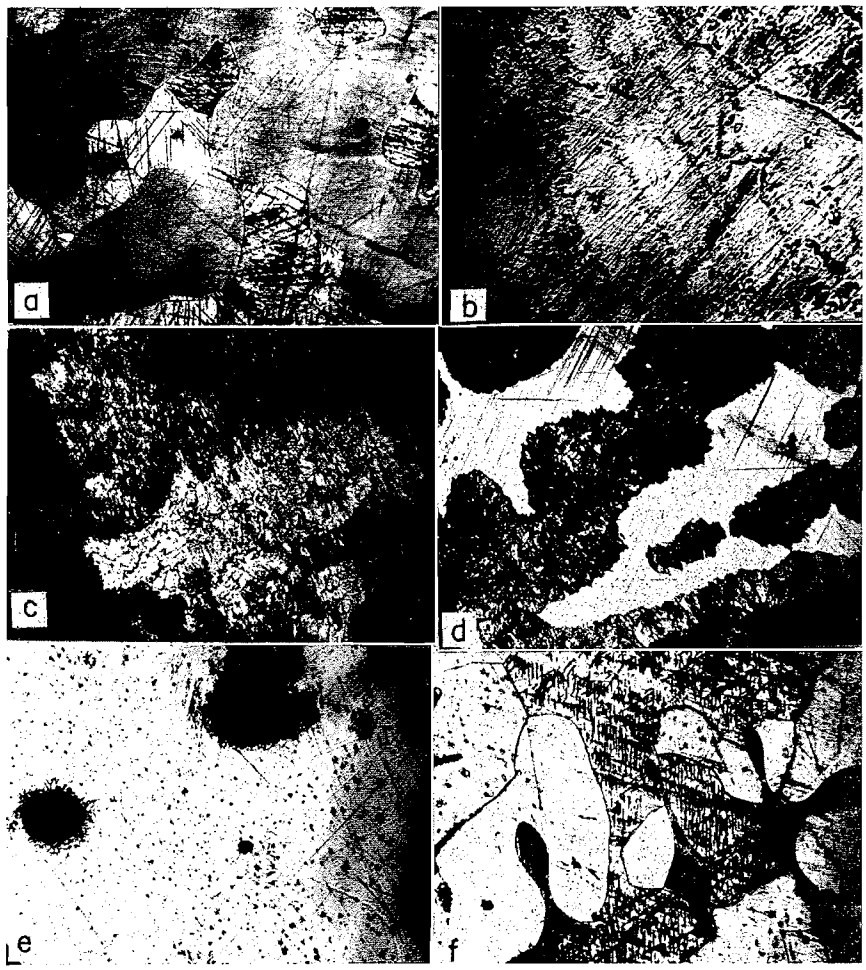

FIG. 4. (*a*) Alloy 6. This alloy contains α (dark) phase with a considerable amount of δ (light) phase.
(*b*) Alloy 21. This alloy contains only δ phase.
(*c*) Alloy 14. This alloy is pure γ phase. Its dark and mottled appearance indicates that is definitely not the same as δ phase.
(*d*) Alloy 12. This alloy contains approximately equal amounts of and δ and γ phases. This alloy definitely appears heterogeneous, indicating δ and γ are not the same phase.
(*e*) Alloy 19. This alloy contains δ phase with medium-sized inclusions of γ phase.
(*f*) Alloy 18. This alloy contains δ and α phases and possibly slight inclusions of γ phase (dark specks).

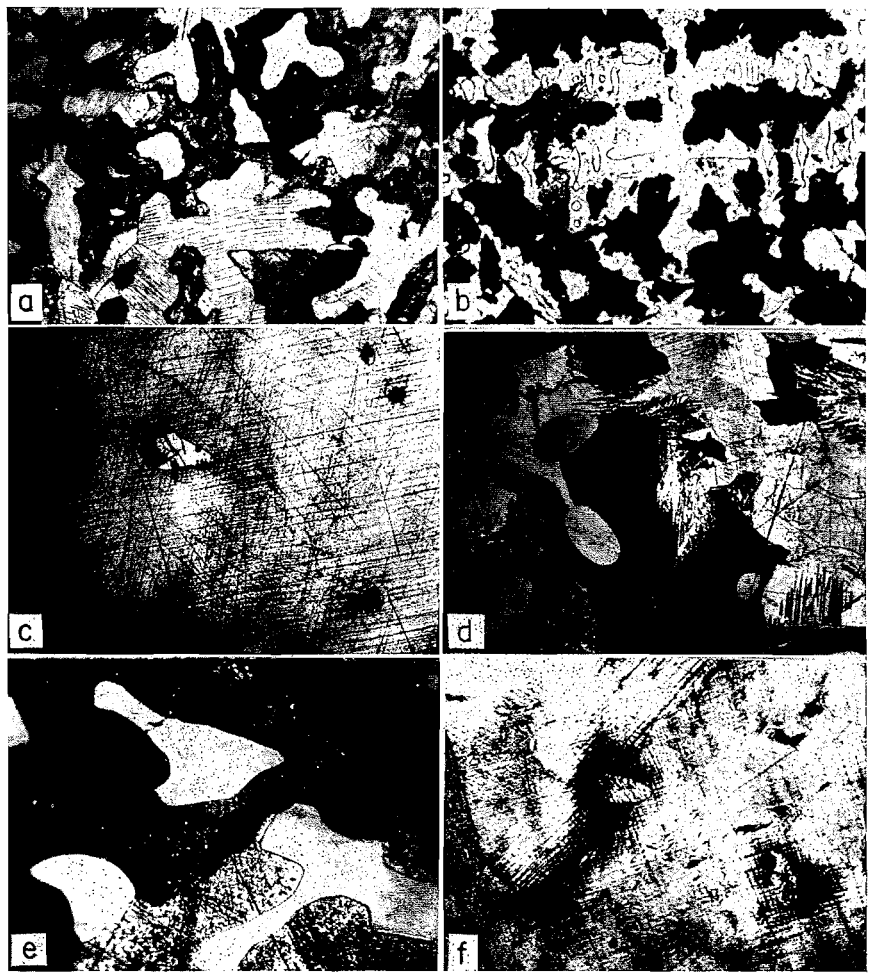

FIG. 5. (*a*) Alloy 22. This alloy contains γ and α phases with possible inclusions of δ phase. The similarity in appearance between α and δ phase makes it difficult to be certain.
(*b*) Alloy 59. This alloy definitely contains 3 phases: γ (mottled, dark), δ (light), and α (medium). This definitely establishes the existence of a ternary three-phase triangle.
(*c*) Alloy 8. This alloy contains α phase with slight inclusions of δ phase.
(*d*) Alloy 23. This alloy contains approximately equal amounts of α and γ phases.
(*e*) Alloy 28. This alloy apparently contains ϵ (mottled) and δ phases.
(*f*) Alloy 8. This shows a polished section from alloy 8 after lengthy annealing as described in the text. Notice the similarity to (*c*).

TABLE I

Results of thermal analysis

Alloy No.	Composition as weighed (%)			Analysis (% Ag)	Thermal analysis	
	Ag	In	Ga		Inflec. points (°C)	Halt points (°C)
1	94.90	5.10	—	94.98	937	—
2	82.00	18.00	—	81.91	830	—
3	77.47	22.53	—	77.52	785	693
4	92.79	—	7.21	92.60	869	—
5	70.17	29.83	—	70.28	693	693, 658
6	84.82	8.16	7.02	84.85	793	—
7	83.53	12.52	3.95	83.44	842	—
8	83.56	14.02	2.50	83.68	851	—
9	87.52	5.00	7.48	87.39	827	—
10	77.51	9.98	12.51	77.54	674	625, 602
11	79.02	—	20.98	79.16	613	—
12	74.98	11.24	13.78	74.87	623	623, 596
13	87.98	7.46	4.56	88.01	871	—
14	76.48	5.04	18.48	76.60	603	—
15	71.97	18.03	10.00	72.01	620	—
16	81.00	8.99	10.01	81.14	726	623, 602
17	63.40	36.60	—	63.46	632	—
18	75.79	16.95	7.26	75.84 75.88	685	643, 619
19	74.09	16.53	9.38	74.22	685	643, 619
20	78.06	14.53	7.41	78.17	731	635, 613
21	72.55	22.51	4.94	72.51	663	660, 613
22	79.06	5.00	15.94	79.16	657	613
23	83.30	2.50	14.20	83.46		
24	80.01	15.50	4.49	79.96	783	648, 618
25	66.67	33.33	—	66.70	654	166
26	50.10	—	49.90	—	—	324, 26
27	59.33	40.67	—	59.38	592	167
28	66.50	31.00	2.50	66.62	637	—
29	55.13	25.12	19.75	—	551	—
30	17.51	55.02	27.47	—	520	14.5
31	17.49	42.60	39.91	—	—	106–100, 14.5
32	17.48	30.02	52.50	—	—	14.5
33	17.49	17.60	64.91	—	—	14.5
34	42.57	17.48	39.95	—	—	30–23, 14.5
35	30.00	30.00	40.00	—	381	23, 14.5
36	42.55	5.25	52.20	—	—	33–23, 14.5
37	30.00	42.50	27.50	—	—	109–102, 14.5
38	30.03	17.48	52.49	—	—	23, 14.5
39	30.01	5.02	64.97	—	—	33–23, 14.5
40	67.40	17.59	15.01	67.52	565	190, 32–23
41	67.51	4.93	27.56	67.60	510	231, 32–23
42	55.04	17.51	27.45	—	462	187, 30–23
43	54.98	5.01	40.01	—	430	170, 30–23
44	54.96	30.03	15.01	—	500	204, 30–23
45	55.08	39.93	4.99	—	—	115–100, 14.5
46	42.01	52.95	5.04	—	463	102, 14.5
47	42.73	42.86	14.41	—	—	105, 14.5
48	42.42	30.60	26.98	—	414	25–23, 14.5
49	29.81	64.67	5.52	—	—	107–100, 14.5
50	30.68	54.41	14.91	—	—	118–105, 14.5
51	17.04	77.76	15.20	—	—	215, 128, 100, 14.5
52	5.72	77.03	17.25	—	—	118, 111–109, 104, 14.5
53	5.00	54.48	40.12	—	—	115, 111–109, 104, 14.5
54	4.98	30.18	64.48	—	—	14.5
55	5.01	17.47	77.52	—	—	32–23, 14.5
56	17.08	5.09	77.83	—	—	34–23, 14.5
57	4.99	5.01	90.00	—	—	31–23, 14.5
58	2.00	24.00	74.00	—	—	14.5
59	80.77	7.87	11.36	80.90	697	623, 601

TABLE II

X-Ray crystallographic data

Alloy No.	Interplanar distance	Line intensity	Alloy No.	Interplanar distance	Line intensity
5	2.60	4	15	2.55	4
	2.41	5		2.37	4
	2.29	10		2.24	10
	1.764	2		1.731	2
	1.495	2		1.469	2
	1.361	2		1.338	2
	1.269	2		1.248	2
	1.248	2		1.228	2
	1.200	1		1.186	1
	1.007	1		0.976	1
	0.957	1		0.943	1
	0.935	1		0.921	1
	0.899	1		2.31 (γ phase)	1
11	4.12	1	14	3.94	1
	2.54	4		2.58	2
	2.39	10		2.34	10
	2.25	8		2.31	10
	2.09	2		2.21	1
	1.734	1		1.922	1
	1.465	4		1.623	3
	1.348	1		1.447	1
	1.250	4		1.370	1
	1.192	2		1.316	2
	0.924	1		1.301	1
				1.263	3
				1.127	1
				0.966	1

DISCUSSION OF RESULTS

Figure 7 indicates the positions of the peritectic troughs in the high-temperature region.

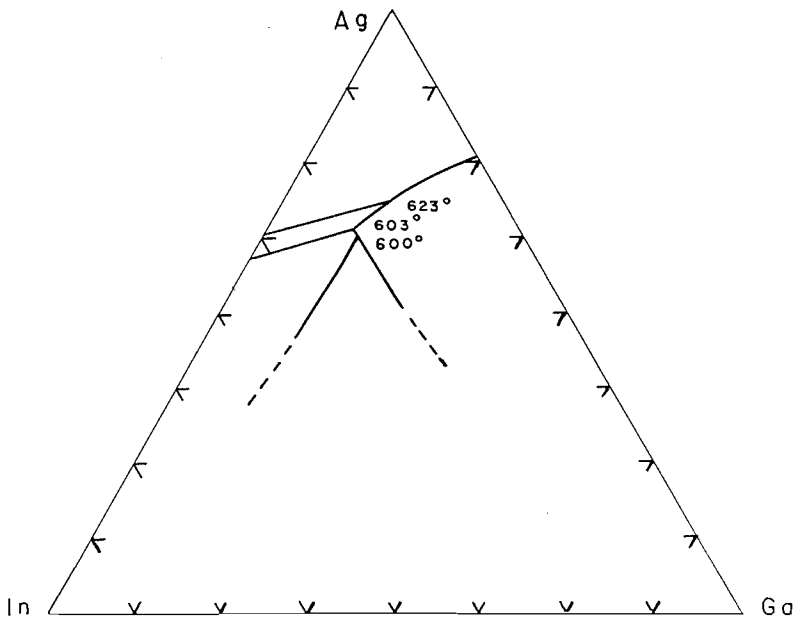

FIG. 7. Positions of peritectic troughs.

TABLE III

Results of microscopic, X-ray, and hardness studies at 25° C

Alloy No.	Phases present		Rockwell hardness
	Microscopy	X-Ray	
1	α	α	—
2	α	α	—
3	$\alpha+\delta$	—	—
4	α	α	—
5	γ	δ	B-42
6	$\alpha+\delta$	—	F-52
7	$\alpha+\delta$	$\alpha+\delta$	—
8	$\alpha+\delta$	α	F-58
9	$\alpha+\delta$	—	—
10	$\gamma+\delta$	$\gamma+\delta$	—
11	—	γ	—
12	$\gamma+\delta$	$\gamma+\delta$	B-52
13	α	—	—
14	γ	γ	B-78
15	$\gamma+\delta$	δ	B-41
16	$\alpha+\gamma+\delta$	—	—
17	$\epsilon+\varphi$	—	—
18	δ	—	—
19	$\gamma+\delta$	—	—
20	$\alpha+\gamma+\delta$	—	—
21	δ	—	B-40
22	$\alpha+\gamma+\delta$	—	—
23	$\alpha+\delta$	—	—
24	$\alpha+\delta$	$\alpha+\delta$	—
25	$\delta+\epsilon$	$\delta+\epsilon$	—
27	$\epsilon+\varphi$	—	—
28	$\delta+\epsilon$	—	—
59	$\alpha+\gamma+\delta$	—	—

There are apparently three peritectic troughs and two ternary peritectics at 623±2° C and 600±4° C. The exact temperature of the second peritectic was indefinite, since decomposition appears to occur over a temperature range. Perhaps, there are two ternary peritectics in close proximity. Alloys on the indium-rich side of the composition triangle tend towards a peritectic or series of peritectics in the temperature region 100 to 118° C. Usually, during thermal analysis a long semihalt was observed over this temperature range, with an irregular series of breaks, alternating with halts. Alloys 52 and 53 gave halts at 118°, 110°, and 104° C. Alloys in the center and on the gallium-rich side gave the same results as for peritectics. This indicates the existence of a "hump" in the liquidus surface on the indium-rich side of the diagram. When heated, alloys in this region usually showed a halt corresponding to eutectic melting at 14.5° C, a change of slope in the region 22° to 30° C, and a halt at 30° to 32° C. The lack of success in thermal analysis is no doubt due to the smallness of the heat effects associated with the various ternary reactions.

The temperature data of Table I are plotted on Fig. 8 for the liquidus points as a function of silver concentration. Essentially this represents a projection of the liquidus surface upon the isopleth for equal gallium and indium concentration.

The cross-hatched line represents the outline of the liquidus in the system Ga–Ag, while the plain line gives the outline for the system Ag–In. Figure 9 shows isothermal lines on the liquidus surface. These two diagrams outline the shape of the liquid surface down to about 400° C (without giving the peritectic troughs in the surface).

Liquidus points below 400° C were not obtained with any degree of certainty and the

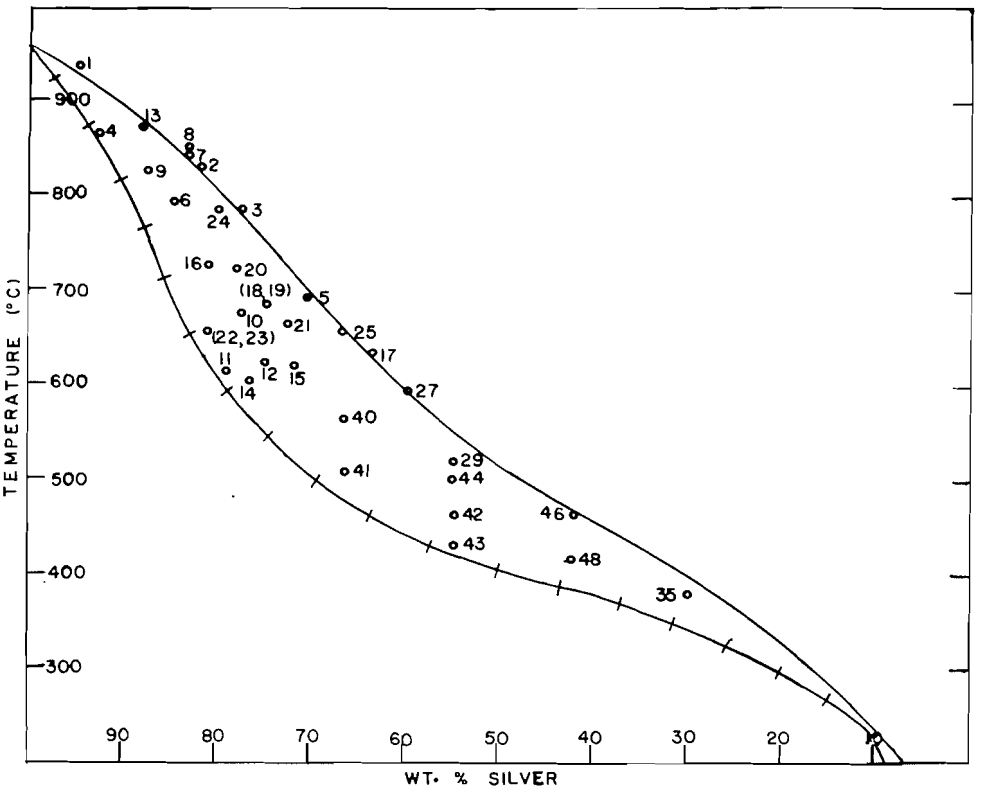

FIG. 8. Liquidus points as a function of silver concentration.

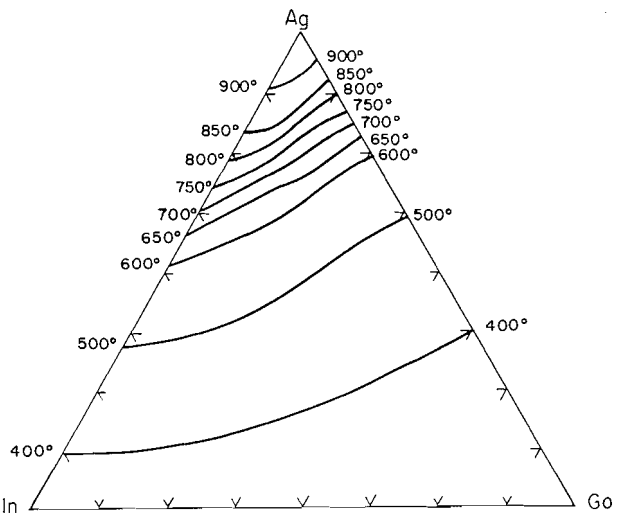

FIG. 9. Isothermal lines on liquidus surface.

peritectic troughs did not show up during thermal analysis. The temperatures of the ternary peritectic halts were obtained, but without a knowledge of the trough leading to the peritectic, it is not possible to specify the composition.

The ternary eutectic temperature is 14.5° C and the ternary eutectic alloy results when 2% silver is added to the binary eutectic indium–gallium.

More success was obtained with the low temperature (25°) isotherm. Our data show that the δ phase of the Ag–In system is different from the γ phase of the Ag–Ga system. Figure 6 represents the 25° isotherm of alloys containing more than 50% silver: each point on the figure is given a number which refers to Table III. There is no ambiguity about this part of the diagram. The diagram is drawn with a break in the line outlining the region of existence of α phase where the line touches the three-phase triangle. This break was not found experimentally, but theoretically it must occur. It is thermodynamically necessary that the extension of boundaries of solid solution must lie either both within the triangle or both within the adjoining two-phase regions (13). This means that of four possible combinations of phases within the three-phase triangle, two are thermodynamically impossible.

The δ phase has been shown to be hexagonal close-packed. The γ phase structure could not be characterized by X-ray powder techniques but it must be nearly hexagonal since well-formed crystals in the shape of a six-sided star were visible to the naked eye in alloys of pure γ phase.

REFERENCES

1. L. DE BOISBAUDRON. Compt. rend. **100**, 701 (1885).
2. J. FRENCH, J. SIDNEY, J. SANDERS, and G. W. INGLE. J. Phys. Chem. **42**, 265 (1938).
3. J. DENNY, J. HAMILTON, and J. LEWIS. Trans. A.I.M.E. **194**, 39 (1952).
4. W. SVIRBELY and S. SELIS. J. Phys. Chem. **58**, 33 (1954).
5. F. WEIBKE, K. MEISEL, and L. WEIGELS. Z. anorg. u. allgem. Chem. **226**, 201 (1938).
6. W. HUME-ROTHERY and K. ANDREWS. J. Inst. Metals, **68**, 133 (1942).
7. F. WEIBKE and H. EGGERS. Z. anorg. u. allgem. Chem. **222**, 145 (1935).
8. L. K. FREVEL and E. J. OTT. J. Am. Chem. Soc. **57**, 228 (1935).
9. E. HALLNER and F. LAUES. Z. Naturforsch. **2a**, 177 (1947).
10. V. M. GOLDSCHMIDT. Ber. **60**, 1294 (1927).
11. W. HUME-ROTHERY, H. MABBOT, and E. CHANNEL-EVANS. Phil. Trans. Roy. Soc. London, Ser. A, **233**, 1 (1934).
12. A. N. CAMPBELL, J. H. WOOD, and G. B. SKINNER. J. Am. Chem. Soc. **71**, 1729 (1949).
13. J. S. MARSH. Principles of phase diagrams. 1st ed. McGraw-Hill Book Co., Inc., New York. 1935. pp. 128–129.

REACTION OF IODOMETHANE WITH TERTIARY ARSINE MERCURIC IODIDE COMPLEXES

M. M. Baig, W. R. Cullen, and D. S. Dawson
The Chemistry Department, University of British Columbia, Vancouver, British Columbia
Received September 27, 1961

ABSTRACT

The reaction of 1:1 tertiary arsine mercuric iodide complexes with iodomethane gives arsonium derivatives of triiodomercury (II).

DISCUSSION AND RESULTS

The reaction of iodoarsines with alkyl iodides in the presence of mercury has been found to yield arsonium derivatives of triiodomercury (II) (1); for example:

$$R_2AsI + Hg + 2CH_3I \rightarrow R_2As(CH_3)_2HgI_3.$$

It has been suggested (1) that such reactions proceed through the formation of 1:1 tertiary arsine mercuric iodide complexes as intermediates which then react further with the alkyl iodide to give the arsonium derivative; for example:

$$R_2AsI + Hg + CH_3I \rightarrow R_2AsCH_3.HgI_2 \xrightarrow{CH_3I} R_2As(CH_3)_2HgI_3.$$

In the present investigation the plausibility of the second part of this reaction sequence has been investigated.

It has been found that the 1:1 mercuric iodide complexes of dimethylphenylarsine, methyldiphenylarsine, dimethyl-α-naphthylarsine react with excess iodomethane to give the corresponding arsonium triiodomercury (II) derivatives; for example:

$$(C_6H_5)_2AsCH_3.HgI_2 + CH_3I \rightarrow (C_6H_5)_2As(CH_3)_2HgI_3.$$

The reaction of the 1:1 complex of triethylarsine and mercuric iodide with iodomethane gives two products, triethylmethylarsonium triiodomercury (II) and bis(triethylmethylarsonium) tetraiodomercury (II). The 1:1 triethylarsine complex is unstable in solution with respect to the 2:3 complex $[(C_2H_5)_3As]_2[HgI_2]_3$ (2) and the tetraiodomercury (II) derivative is most probably formed from reaction of the 2:3 complex with iodomethane rather than from reaction of the 1:1 complex. Iodoethane and trifluoroiodomethane do not react with the 1:1 triethylarsine complex at 20°; however, at 100° some reaction with trifluoroiodomethane takes place producing diethyltrifluoromethylarsine in low yield. This compound is also produced by the reaction of triethylarsine with trifluoroiodomethane at 100° (3) and reaction in the case of the 1:1 complex may be due to dissociation or disproportionation of the complex to produce triethylarsine.

Coates and co-workers (4) have found that in acetone solution iodomethane reacts with some 2:1 tertiary arsine mercuric iodide complexes to give bisarsonium tetraiodomercury (II) derivatives, and in the present work it has been found that the 2:1 complex of triphenylarsine reacts similarly giving bis(methyltriphenylarsonium) tetraiodomercury (II). The triphenylarsine complex does not react with trifluoroiodomethane at 20° but does react slowly with iodoethane. Presumably the product from the latter reaction is the tetraiodomercury (II) derivative, though this was not established.

Similar reactions are known for tertiary phosphine mercuric iodide complexes (4, 5) and also for disubstituted sulphide mercuric iodide complexes (6). The mercuric iodide

complexes are labile and reactions of this sort most likely proceed through addition of the alkyl iodide to the complexing ligand produced by the dissociation of the complex; for example:

$$R_3As.HgI_2 \rightleftharpoons R_3As + HgI_2,$$
$$R_3As + CH_3I \rightarrow R_3AsCH_3I,$$
$$R_3AsCH_3I + HgI_2 \rightarrow R_3AsCH_3HgI_3.$$

Direct formation of the arsonium iodide from the tertiary arsine and iodomethane is known to occur at 20° for all the arsines involved in the above reactions, except triphenylarsine (7). However, the presence of mercuric iodide as an iodide ion acceptor could be expected to facilitate the formation of onium derivatives even when the onium iodides are not easily formed by direct reaction. An alternative mechanism involving "addition" of the alkyl iodide across the, say, As–Hg bond seems much less likely.

Two new 1:1 mercuric halide complexes of dimethyl-α-naphthylarsine were also prepared during this investigation. These are the compounds $C_{10}H_7As(CH_3)_2.HgX_2$ (X = Cl, m.p., 233–235°, X = I, m.p., 192–195°). Attempts to prepare the corresponding 2:1 adducts from hot alcoholic solutions of the components resulted only in the isolation of the 1:1 complexes. Anderson and Burrows (8) found similar difficulties in isolating the 2:1 mercuric halide complexes of dimethylphenylarsine. The 1:1 complex of dimethyl-α-naphthylarsine and mercuric iodide has a significantly low molecular weight when it is determined by the Rast method. This is probably due to dissociation. The corresponding mercuric chloride complex is insoluble in camphor so no measurement of its molecular weight was made.

EXPERIMENTAL

Except where otherwise indicated reactions were carried out at 20° and in sealed tubes in the absence of air and moisture. Volatile reactants and products were manipulated in a vacuum system.

Reaction of the 1:1 Complex of Methyldiphenylarsine and Mercuric Iodide with Iodomethane

Methyldiphenylarsine was prepared by the reaction of phenylmagnesium bromide on diiodomethylarsine (9). On mixing hot alcohol solutions of the arsine (1 mole) and mercuric iodide (1 mole) the 1:1 complex was obtained, m.p. 117° (lit. value 116° (8)). Acetone solutions of the complex (0.7 g) and iodomethane (0.8 g), on mixture in air, gave a yellow precipitate (0.8 g), m.p. 122°. The arsine complex (0.8 g) was soluble in iodomethane (14.5 g) but after 7 days a yellow precipitate had appeared. The unreacted iodomethane was removed under vacuum and the remaining yellow solid melted at 122°. The products from both these reactions when recrystallized from alcohol melted at 131° and were identified as dimethyldiphenylarsonium triiodomercury (II) (m.p. 131° (1)) on the basis of their melting points and mixed melting points with an authentic sample (undepressed), and their X-ray powder photographs.

Reaction of the 1:1 Complex of Dimethylphenylarsine and Mercuric Iodide with Iodomethane

The arsine was prepared from phenylmagnesium bromide and iododimethylarsine (9). The 1:1 arsine mercuric iodide complex was prepared by mixing hot alcohol solutions containing molar proportions of the arsine and mercuric iodide. The yellow precipitate which was obtained gave two fractions on fractional crystallization from alcohol: one, the major product, consisted of orange-yellow needles of the 1:1 complex, m.p. 144° (lit. value, 144° (8)), the other, small pale yellow needles, m.p. 89°. The 1:1 complex (5.4 g) was soluble in excess iodomethane but after 13 days a yellow precipitate had appeared. The excess iodomethane was removed under vacuum, leaving a yellow solid. This solid on recrystallization from acetone–alcohol was identified as trimethylphenylarsonium triiodomercury (II) on the basis of its melting point 128–129° (lit. value, 128° (1)) and the identity of its infrared spectrum and X-ray powder photograph with those of an authentic sample.

Reaction of the 1:1 Complex of Triethylarsine and Mercuric Iodide with Iodomethane

Triethylarsine was prepared from ethylmagnesium bromide and arsenic trichloride (10). The 1:1 arsine mercuric iodide complex was prepared using the procedure of Mann *et al.* (2). The complex so obtained melted at 89° (lit. value, 88–89°). The complex (3.19) was soluble in 22.3 g of iodomethane. The solution

slowly deposited a yellow oil and after 30 days the volatile contents of the tube were removed under vacuum. The residual oil (3.98) slowly solidified and the solid melted at 68°. On crystallization from acetone–alcohol two fractions were obtained. The less soluble pale yellow fraction (1.5 g) melted at 253°. The more soluble yellow fraction melted at 61° after further recrystallization (0.9 g). For the identification of these products reference compounds were prepared from triethylmethylarsonium iodide and mercuric iodide. Triethylmethylarsonium iodide was prepared by direct reaction between triethylarsine and iodomethane. The arsonium iodide was recrystallized from alcohol and melted at 273° (lit. value, 270°). *Triethylmethylarsonium triiodomercury (II)*, m.p. 64°, and *bis(triethylmethylarsonium) tetraiodomercury (II)*, m.p. 253°, were prepared by mixing hot alcohol solutions of the arsonium iodide and mercuric iodide in the calculated proportions (1:1 and 2:1 respectively); the products were recrystallized from alcohol. Anal. Found: C, 11.3; H, 2.39; Hg, 26.0%; mol. wt., 793. Calc. for $C_7H_{18}AsHgI_3$: C, 11.1; H, 2.37; Hg, 26.5%; mol. wt., 759. Found: C, 15.9; H, 3.34; Hg, 18.6%. Calc. for $C_{14}H_{36}As_2HgI_4$: C, 15.8; H, 3.38; Hg, 18.9%.

Comparison of the melting points and X-ray powder photographs of the products from the original reaction with those of the reference compounds showed that the least soluble fraction, m.p. 253°, was the arsonium tetraiodomercury (II) compound and the other fraction, m.p. 61°, was the arsonium triiodomercury (II) derivative.

Reaction of the 2:1 Complex of Triphenylarsine and Mercuric Iodide with Iodomethane

The 2:1 adduct was prepared by reacting together alcoholic solutions of triphenylarsine (2 moles) and mercuric iodide (1 mole). The product was purified by crystallization from alcohol. It melted at 198° (lit. value, 197° (2)). The complex (2.0 g) and iodomethane (9.7 g) were left for 7 days. The volatile contents of the tube were removed under vacuum and a yellow residue (2.1 g, m.p. 174°) was left in the tube. The product was expected to be *bis(triphenylmethylarsonium) tetraiodomercury (II)* so this compound, m.p. 175°, was prepared by reacting alcoholic solutions of commercial triphenylmethylarsonium iodide and mercuric iodide in correct proportion. The complex was recrystallized from alcohol. Anal. Found: C, 34.1; H, 2.64; Hg, 14.4%. Calc. for $C_{38}H_{36}As_2HgI_4$: C, 33.9; H, 2.67; Hg, 14.9%. Comparison of the infrared spectra and melting points of the reference compound and the product of the reaction suggested that they were identical. Confirmation was obtained from an undepressed mixed melting point.

Reactions of Tertiary Arsine Mercuric Iodide Complexes with Other Alkyl Halides and Trifluoroiodomethane

(a) The 1:1 complex of triethylarsine and mercuric iodide with iodoethane.—The complex (3.5 g) and iodoethane (6.4 g) were left for 28 days. The volatile contents of the tube were removed under vacuum, leaving a yellow solid, m.p. 50°. The X-ray powder photograph of this sample showed it to be mainly the starting material and showed the absence of detectable amounts of tetraethylarsonium triiodomercury (II) and bis(tetraethylarsonium) tetraiodomercury (II).

(b) The 1:1 complex of triethylarsine and mercuric iodide with trifluoroiodomethane.—The complex (3.6 g) was soluble in trifluoroiodomethane (16.595 g). After 40 days the volatile contents of the tube were taken into the vacuum system where trap-to-trap distillation showed that only trifluoroiodomethane (16.525 g) was present. The complex (7.3 g) and trifluoroiodomethane (16.3 g) after 48 hours at 100° gave diethyltrifluoromethylarsine (0.202 g) identified by its infrared spectrum (11), and unreacted trifluoroiodomethane (15.9 g).

(c) The 2:1 complex of triphenylarsine and mercuric iodide with iodoethane.—When the complex (2.7 g) and iodoethane (9.097 g) were left for 25 days 0.223 g of iodoethane was consumed. The solid product (2.8 g) melted in the range 89–97°. By recrystallization from alcohol, two products were obtained. The first consisted of 0.914 g of a colorless substance identified as the starting material by comparison of its infrared spectrum, X-ray powder photograph, and melting point (found, m.p., 202° (from acetone); lit. value, 197° (2)). The second product, after further recrystallization, melted at 88° and analysis indicated that it was still impure as the results do not correspond to any likely reaction product. Found: C, 29.5; H, 2.87; Hg, 20.3%; mol. wt., 751.

Reaction of the 1:1 Complex of Dimethyl-α-naphthylarsine and Mercuric Iodide with Iodomethane

Dimethyl-α-naphthylarsine was prepared from iododimethylarsine and α-naphthylmagnesium bromide (9). The product was purified by distillation in a nitrogen atmosphere; the colorless liquid boiled at 178–180° (24 mm). The arsine reacted directly with iodomethane at 20° to give trimethyl-α-naphthylarsonium iodide, m.p. 238° (lit. value, 230°). Anal. Found: C, 42.0; H, 4.35%. $C_{13}H_{16}AsI$ requires: C, 41.8; H, 4.31%. Mixing hot ethanolic solutions of the arsine (1 mole) and mercuric chloride (1 mole) gave the colorless 1:1 adduct, m.p. 233–235°. Anal. Found: C, 29.2; H, 2.89; As, 15.3; Cl, 14.5; Hg, 37.3%. Calc. for $C_{12}H_{13}AsCl_2Hg$: C, 28.7; H, 2.60; As, 14.9; Cl, 14.1; Hg, 39.9%. The same product was obtained on mixture of hot alcoholic solutions of the arsine (2 moles) and mercuric chloride (1 mole). The 1:1 arsine mercuric iodide complex was similarly obtained as a yellow solid, soluble in hot methanol, m.p. 192–195°. Anal. Found: C, 21.2; H, 1.88; Hg, 28.9%; mol. wt., 438. Calc. for $C_{12}H_{13}AsHgI_2$: C, 21.0; H, 1.91; Hg, 29.2%; mol. wt., 687. Attempts to prepare the 2:1 arsine mercuric iodide complex from hot alcoholic solutions gave only the 1:1 adduct. On mixing hot alcoholic solutions of trimethyl-α-naphthylarsonium iodide (1 mole) and mercuric iodide (1 mole) yellow crystals of trimethyl-α-naphthylarsonium triiodomercury (II) were obtained, m.p.

183–185°. Anal. Found: C, 19.0; H, 1.95; Hg, 24.4%; mol. wt., 829. Calc. for $C_{13}H_{16}AsHgI_3$: C, 18.8; H, 1.93; Hg, 24.2%; mol. wt., 850. The same compound was obtained when the 1:1 complex of dimethyl-α-naphthylarsonium iodide and mercuric iodide was left in contact with excess iodomethane in a stoppered flask (12 days). The product was identified by its melting point of 184–186° and its infrared spectrum.

ACKNOWLEDGMENTS

The authors wish to acknowledge financial assistance from the National Research Council of Canada. One of us (M. M. B.) expresses thanks for a scholarship received under the auspices of the Colombo Plan. Microanalyses were carried out by Dr. Alfred Bernhardt.

REFERENCES

1. M. M. Baig and W. R. Cullen. Can. J. Chem. **39**, 420 (1961).
2. R. C. Evans, F. G. Mann, H. S. Peiser, and P. Purdie. J. Chem. Soc. 1209 (1940).
3. W. R. Cullen. To be published.
4. R. C. Cass, G. E. Coates, and R. G. Hayter. J. Chem. Soc. 4007 (1955).
5. G. Deacon and B. O. West. Private communication; J. Inorg. & Nuclear Chem. In press.
6. S. Smiles. J. Chem. Soc. 163 (1900).
7. E. Krause and A. von Grosse. Die chemie der metal-organischen verbindungen. Borntraeger, Berlin. 1937.
8. J. J. Anderson and G. J. Burrows. J. Proc. Roy. Soc. N. S. Wales, **70**, 63 (1936).
9. G. J. Burrows and E. E. Turner. J. Chem. Soc. 1373 (1920).
10. W. J. C. Dyke and W. J. Jones. J. Chem. Soc. 2426 (1930).
11. W. R. Cullen. Can. J. Chem. In press.

THE STRUCTURE OF LICHENIN: SELECTIVE ENZYMOLYSIS STUDIES[1]

A. S. PERLIN AND S. SUZUKI[2]

Prairie Regional Laboratory, National Research Council of Canada, Saskatoon, Saskatchewan

Received September 13, 1961

ABSTRACT

Lichenin, the poly-β-D-glucan of *Cetraria islandica* (Iceland moss), is found by enzymic degradation to differ in fine structure from the poly-β-D-glucans of cereal grains. Enzymolysis has been carried out with a cellulase and a laminarinase preparation, the former yielding mainly *O*-β-D-glucopyranosyl-(1 → 3)-*O*-β-D-glucopyranosyl-(1 → 4)-α-D-glucose, and the latter mainly *O*-β-D-glucopyranosyl-(1 → 4)-*O*-β-D-glucopyranosyl-(1 → 3)-α-D-glucose. Di- and tetra-saccharides are produced in small proportions. Steric aspects of these enzymic degradations are discussed. The basis constitution of lichenin is represented by a tetrameric unit in which two adjacent (1 → 4) linkages alternate with an isolated (1 → 3) linkage; occasionally four consecutive monomers are linked by (1 → 4) bonds. The glucans of cereal origin differ mainly in possessing a higher proportion of the latter structural sequence. Despite their close chemical similarity to cellulose, all of these glucans are soluble, a property that appears to be related to the even distribution of β-(1 → 3) bonds along the chains, with a resulting disruption of linear orientation effects.

Lichenin, a major polysaccharide component of *Cetraria islandica* (Iceland moss) is composed of β-D-glucopyranose units linked in a linear manner by (1 → 4) and (1 → 3) glycosidic bonds (1, 2, 3). The only other known source of polysaccharides of this type is the Gramineae family (notably oats and barley). Careful chemical examination (3) has shown no distinct structural difference between these polymers isolated from such widely divergent botanical origins. In recent studies on the β-glucans of oats and barley (4) it was found that each of two enzymes—a cellulase and a laminarinase—degrades the β-glucans extensively in a highly selective fashion. Hence, it appeared that a study of the comparative behavior of the same enzymes on lichenin might indicate to what degree this polymer resembles the cereal β-glucans.*

The lichenin was isolated by the procedure of Peat, Whelan, and Roberts (3), and purified via the derived acetate. Based on periodate uptake the ratio of (1 → 4) to (1 → 3) linkages present in lichenin, as well as in the cereal glucans (2, 3, 4), is reported to be about 7 to 3. In the present study, overoxidation of the lichenin prevented an accurate measure of this ratio and, in parallel experiments, the oat and barley glucans were found to be overoxidized similarly. However, a comparison of the data (experimental section) indicated that lichenin consumes about 10% less of periodate, and that the incidence of (1 → 3) linkages in this polymer is perhaps 35%, whereas in the cereal polysaccharides it is closer to 25%.

When the lichenin was treated with a cellulase from *Streptomyces* sp. QM B814 (5) the products were found by paper chromatography to consist of a mixture of cellobiose together with tri- and tetra-saccharides. This mixture was readily fractionated by preparative paper chromatography. By far the major product was the trisaccharide *O*-β-D-glucopyranosyl-(1 → 3)-*O*-β-D-glucopyranosyl-(1 → 4)-D-glucopyranose (I), which accounted for about 60% of the polymer (Table I). Previously this trisaccharide had been characterized as the derived undecaacetate (3, 4) but the crystalline α-anomer of

[1]*Issued as N.R.C. No. 6587.*

Presented at the 44th Conference of the Chemical Institute of Canada, Montreal, Que., August 2–5, 1961.

[2]*National Research Council of Canada Postdoctorate Fellow, 1960–1961.*

**This study was made possible through the kind co-operation of Dr. E. T. Reese, who provided the enzyme preparations.*

TABLE I

Products from the enzymolysis of polyglucans

	Initial polymer (mg)	Dimer (mg)	Trimer (mg)	Tetramer (mg)	Trimer / Tetramer
A. By cellulase					
Lichenin	24.4	2.2	14.2	3.6	4.0
Oat glucan	20.4	1.2	10.4	4.8	2.2
Barley glucan	23.0	1.5	11.7	4.8	2.4
B. By laminarinase					
Lichenin	24.4	3.4	13.4	3.7	3.6*
Oat glucan	21.5	2.6	10.2	6.8	1.5*
Barley glucan	21.1	3.4	10.2	5.5	1.8*

*These ratios are minimal values since the tetramer fractions, particularly that from lichenin, contained a substantial proportion of material travelling on the chromatograms at a slightly slower rate.

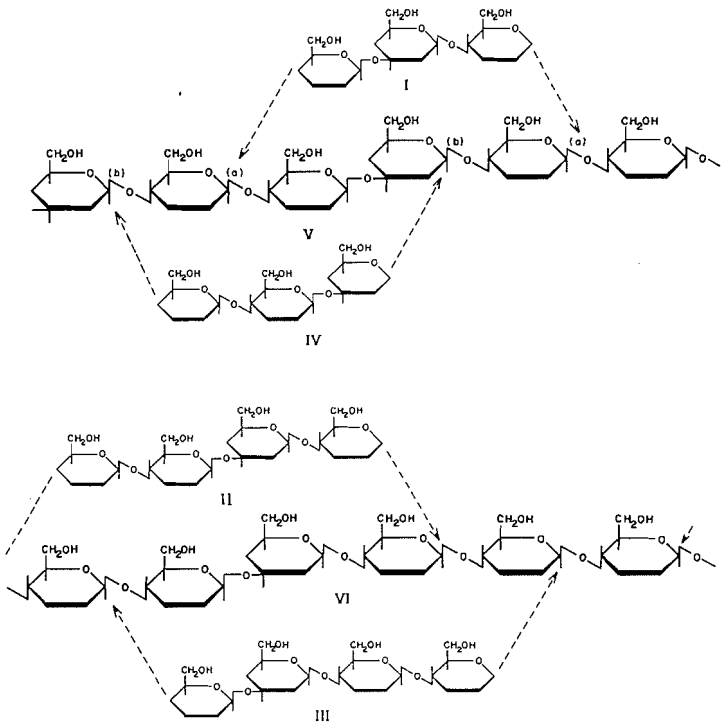

the free sugar has now been obtained. As found earlier with the cereal glucans, the tetrasaccharide fraction contained at least two components. These were not separable chromatographically but their presence was detected by selective degradation (4) to a mixture of two different triitols. One of the tetrasaccharides, which subsequently crystallized from the mixture, was found to be *O*-β-D-glucopyranosyl-(1 → 4)-*O*-β-D-glucopyranosyl-(1 → 3)-*O*-β-D-glucopyranosyl-(1 → 4)-D-glucopyranose (II), the structure of which had been determined previously with an amorphous sample derived from barley glucan (4). By seeding, the latter sample now has been crystallized also. A minor component of the mixture was *O*-β-D-glucopyranosyl-(1 → 3)-*O*-β-D-glucopyranosyl-(1 → 4)-*O*-β-D-glucopyranosyl-(1 → 4)-D-glucose (III) (4).

The main product formed from lichenin by the laminarinase of *Rhizopus arrhizus* QM 1032 (6) was also a trisaccharide, *O*-β-D-glucopyranosyl-(1 → 4)-*O*-β-D-glucopyranosyl-(1 → 3)-D-glucose (IV), accounting for about 55% of the polysaccharide (Table I). This trisaccharide has now been obtained as the crystalline α-anomer, being characterized previously as an undecaacetate.* Other products of the enzymic degradation, detected chromatographically, corresponded to laminaribiose, tetrasaccharide, and higher oligosaccharides, but all of these were minor products and pure fractions of them were not isolated. Cunningham and Manners have also found recently (private communication) that the degradation of lichenin by preparations of laminarinase yields mainly trisaccharide IV.

Peat, Whelan, and Roberts (3) concluded on the basis of data from partial acid hydrolysis that an important type of structural unit in lichenin is one in which four β-D-glucopyranosyl units are linked by a (1 → 3) bond and two consecutive (1 → 4) bonds, as in V. The present data clearly support their conclusion and show, in fact, that sequence V likely represents the major proportion of the lichenin molecule, just as found earlier with the cereal glucans (4). Such a structure is consistent with the formation in high yield of trisaccharide I (by cleavage at (*a*)) and of trisaccharide IV (by cleavage at (*b*)), taking into consideration the ratio of (1 → 4) to (1 → 3) linkages in the polymer, and the evidence available as to the specificity of the two enzymes (4, 9). Since I and IV each contains a (1 → 3) bond and hence accounts for a high percentage of such bonds present, liberation of these trisaccharides must involve mainly the scission of (1 → 4) linkages. Thus, attack at (*a*) by the cellulase appears to be related to a "(→ 4) (1 → 4)" bonding arrangement of the β-D-glucopyranosyl unit (to the left of (*a*) in V). The second unit engaged in forming linkage (*b*) is itself not 4-substituted, which presumably accounts for its lack of susceptibility to cellulase. However, this unit is 3-substituted, an arrangement consistent with the idea that the laminarinase action involves cleavage at (*b*) (4, 9).

Formation of tetrasaccharides II and III by cellulase is indicative of the occurrence of structural units such as VI, in which a single (1 → 3) bond alternates with three consecutive (1 → 4) bonds, as noted with the cereal glucans (4). However, sequence V has relatively much greater prominence in the lichenin structure than in the cereal glucans, since the ratio of trisaccharide (representative of V) to tetrasaccharide (representative of VI) is much higher with lichenin (Table I), i.e., a value of 4 as against 2.3 (average) for the cereal glucans. This difference was detected also with laminarinase, which produced trimer and tetramer from lichenin in a ratio of 3.6 to 1, and from the oat and barley glucan in a ratio of 1.7 (average) to 1 (Table I). Consistent with these findings is the indication from periodate oxidation data that lichenin contains the higher proportion of (1 → 3) linkages. Other differences between these polysaccharides are reflected in the fact that cellulase produces more of tetrasaccharide II than of III from lichenin, whereas the reverse is true for the cereal glucans; also, 3′-*O*-cellotriosyl-D-glucose (4) is a major product of laminarinase action on the cereal glucans, whereas with lichenin much less tetramer (not identified) is produced and higher oligosaccharides are relatively more prominent.

Therefore, although lichenin closely resembles the cereal glucans it can readily be differentiated from them in terms of fine structure. The oat and barley polysaccharides, however, must be regarded, on the basis of the data available, as indistinguishable from each other.

**Two different sets of physical constants have been reported for the acetate of this trisaccharide (3, 4, 7). This complication has now been resolved by Moscatelli, Ham, and Rickes (8), who find that the different acetates represent two modifications, probably anomers, of the same parent trisaccharide.*

Apparently, the cereal glucans contain minor structural features which were not detected in the earlier enzymic study (4) nor by partial hydrolysis (3). With both these methods of examination the presence of only isolated (1 → 3) bonds was indicated, but other methods have shown the occurrence also of two and three consecutive (1 → 3) linkages (10, 11), although quantitative data are not yet available. The possibility that such sequences are present also in lichenin must await further examination.

In formulating structures such as V and VI no account has been taken of the fact that a small quantity of disaccharide (5–15%) is produced by each enzyme from lichenin as well as from the cereal glucans. For the present purposes of comparing the three polysaccharides these dimers are of little significance. From the standpoint of enzymic stereospecificity, however, it may be noted that the cellulase produces cellobiose whereas the laminarinase yields laminaribiose. This pattern of attack on the glucans is characteristic of enzymes of these classes isolated from a variety of sources (E. T. Reese, private communication), and is in agreement with recent suggestions about the specificity of polyglycosidases (9). According to this view, cellobiose is a product consistent with cellulase action since it is liberated by attack on alternate 4-substituted β-D-glucosyl units (which become reducing-end units), but the non-reducing end unit in the dimer is itself not substituted at position 4. In similar fashion, laminaribiose should be formed by attack on alternate β-D-glucose units linked through positions 1 and 3 to adjacent units, but should itself be stable because the non-reducing end unit is not 3-substituted. It is not inconceivable, therefore, that the polyglucans contain a small proportion of sequences such as

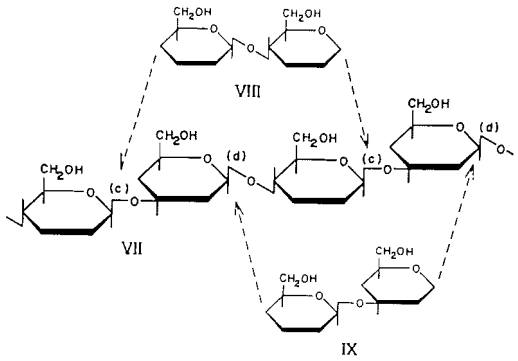

VII, and that cellobiose (VIII) is derived by attack at (*c*) (with actual cleavage of a (1 → 3) bond) whereas laminaribiose (IX) arises from attack at (*d*) (with actual cleavage of a (1 → 4) bond).

Lichenin and the cereal glucans are closely related in structure to cellulose in that they are composed primarily of (1 → 4)-linked β-D-glucopyranosyl units. As pointed out by Hirst (12), these polysaccharides provide a good illustration of how small variations in structure can markedly influence the physical characteristics of such polysaccharides. The insolubility of cellulose is attributed mainly to the high degree of linear orientation and strong intermolecular bonding possible with a molecule of this type (Fig. 1(*a*)). Replacement of a small percentage of the (1 → 4) bonds by (1 → 3) bonds "converts" this alkali-insoluble polymer into one readily soluble in water. This marked variation in solubility is perhaps understandable when the (1 → 3) bonds are seen to be distributed uniformly along the chains at intervals of three or four units, an arrangement (Fig. 1(*b*)) which should greatly minimize orientation effects such as are obtained in cellulose.

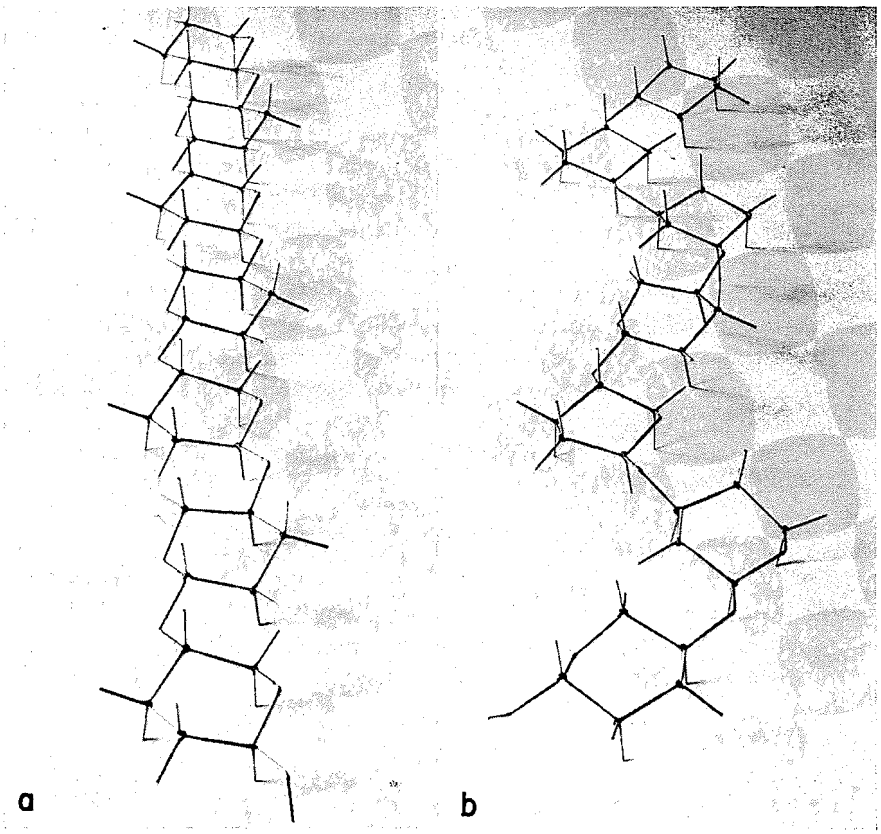

FIG. 1. Representation (Drieding models) of a molecule of (*a*) cellulose, (*b*) lichenin or the poly-β-D-glucans of oats and barley.

EXPERIMENTAL

The cellulase (obtained from *Streptomyces* QM B814) and laminarinase (obtained from *R. arrhizus* QM 1032) preparations were lyophylized powders, prepared by Dr. E. T. Reese.

Analytical and preparative paper chromatography was carried out using as solvents: (A) ethyl acetate – pyridine – water (10:4:3) and (B) ethyl acetate – acetic acid – water (9:2:2).

Evaporations were carried out at 40–45°. Optical rotations were measured at 25±2°. Melting points are corrected.

Isolation and Purification of Lichenin

The isolation procedure was essentially that described by Peat, Whelan, and Roberts (3). A commercial sample of powdered Iceland moss was extracted exhaustively with 2% potassium carbonate to remove tannins, and then twice with hot water. The water extract was frozen, then thawed, and the suspended gel collected by centrifugation. A vigorously stirred solution of the gel at 50° (pH 6.5) was treated with salivary amylase to degrade the isolichenin, and the polysaccharide remaining was precipitated out with ethanol and recovered. Yield, 101 g from 1 kg of moss.

Crude lichenin (20 g) was suspended in formamide (200 ml) with vigorous stirring, pyridine (200 ml) and acetic anhydride (100 ml) were added portionwise, and after 4 hours the reaction mixture was poured into ice water. The precipitated material was washed and dried, and reacetylated. Final yield, 24 g. The acetate (20 g) was extracted into acetone (600 ml) and fractional precipitation was carried out by gradual addition of light petroleum (b.p. 60–110°). Four fractions were obtained: (1) 6.0 g, $[\alpha]_D$ −36°; (2) 2.3 g, $[\alpha]_D$ −32°; (3) 1.4 g, $[\alpha]_D$ −31°; (4) 4.7 g, $[\alpha]_D$ −29° (specific rotations measured at 2% concentration in chloroform).

The acetates were deacetylated by dissolving them in acetone and adding excess 0.2 *N* potassium hydroxide, the free polysaccharide being recovered, after acidification with acetic acid, by precipitation with alcohol. Deacetylated fractions 2, 3, and 4 were white, fibrous materials, readily soluble in water at 40–45°. Compared on the basis of glucose content (each 92–95%), periodate uptake, degree of enzymolysis

by cellulase and laminarinase, and chromatographic examination of the enzymolysis products, these fractions appeared to be sufficiently similar to warrant their recombination for use in the experiments described below. Fraction 1 contained a higher percentage of impurities and was less soluble, and was not examined further.

Comparison of Some Properties of Lichenin with Those of Oat and Barley Glucans

(a) Periodate Oxidation

Lichenin was treated with two molar equivalents of sodium periodate at 19° in the dark. The periodate consumption (moles/mole (hours)) was 0.49 (16), 0.57 (40), 0.61 (88), 0.65 (160), 0.67 (208). At 208 hours the yield of formic acid was 0.019 moles/mole.

Oxidized under the same conditions, oat and barley glucans gave periodate uptake data (moles/mole (hours)) similar to those reported earlier (4): for oat glucan, 0.58 (40), 0.61 (88), 0.74 (160), 0.76 (208); for barley glucan, 0.59 (40), 0.66 (88), 0.77 (160), 0.79 (208).

(b) Enzymolysis

Each polysaccharide (20–25 mg) in water (2 ml) was treated at 45° with the enzyme preparation (cellulase or laminarinase, 5 mg). The copper-reducing power of the digest was essentially constant in each experiment within 5 hours' reaction time, the values (calculated as percentage of glucose) then being:

	Cellulase	Laminarinase
Lichenin	35.6	27.0
Oat glucan	37.6	26.9
Barley glucan	34.8	29.2

Each digest was heated on the steam bath for 10 minutes, concentrated, and chromatographed on Whatman No. 1 paper, using solvent A. The various components detected were eluted with water and estimated (Table I) with Nelson's reagent (13), using as standards cellobiose and trisaccharide I for the cellulase experiments, and laminaribiose and trisaccharide IV for the laminarinase experiments.

Degradation of Lichenin with Cellulase

Lichenin (1.0 g) in water (100 ml) was incubated at 44° with cellulase (0.12 g) for 5 hours. The digest was heated on the steam bath for 10 minutes, filtered, and the filtrate was concentrated and chromatographed on Whatman No. 3 MM paper sheets. The chromatogram was developed, first with solvent B and then with solvent A. The major products detected were eluted with water, and the eluates were purified by treatment with mixed-bed ion-exchange resins.

*O-β-*D*-Glucopyranosyl-(1 → 3)-O-β-*D*-glucopyranosyl-(1 → 4)-α-*D*-glucopyranose (I)*

The trisaccharide fraction (0.5 g) crystallized and was recrystallized from water–ethanol; m.p. 229–231°, $[\alpha]_D$ 18.7° → 13.0° (*c*, 1.4, H_2O). Calculated for $C_{18}H_{32}O_{16}$: C, 42.86%; H, 6.39%; molecular weight, 502. Found: C, 42.80%; H, 6.45%; molecular weight (vapor pressure osmometry (14), in water), 481.

On acetylation with acetic anhydride – sodium acetate at 95°, the compound afforded a derivative, m.p. 121–123°, undepressed by admixture with the β-undecaacetate of trisaccharide I.

An amorphous sample of I, obtained earlier from oat glucan (4), was induced to crystallize by seeding with the current crystalline material, and the identity of the two trisaccharide preparations was shown by a comparison of X-ray powder diagrams.

*O-β-*D*-Glucopyranosyl-(1 → 4)-O-β-*D*-glucopyranosyl-(1 → 3)-O-β-*D*-glucopyranosyl-(1 → 4)-*D*-glucopyranose (II)*

The tetrasaccharide fraction (0.15 g) was chromatographically homogeneous. However, degradation of a portion of this material by the procedure described previously (4)—involving lead tetraacetate oxidation, reduction, and partial hydrolysis—afforded two products, one corresponding chromatographically to 2-*O*-β-D-laminaribiosyl-D-erythritol (major component) and the other to 2-*O*-β-D-cellobiosyl-D-erythritol (minor component). This finding showed that at least two tetrasaccharides were present.

After prolonged storage in water–methanol the tetrasaccharide fraction afforded crystalline material (65 mg) which was recrystallized from the same solvent, m.p. 223–226°. This product served as seed for crystallization of an amorphous preparation of tetrasaccharide II ($[\alpha]_D$+19.8°), characterized earlier (4), the identity of the two products being shown by a comparison of X-ray powder diagrams. Calculated for $C_{24}H_{42}O_{21}.H_2O$: C, 42.10%; H, 6.48%. Found: C, 41.80%; H, 6.65%.

*O-β-*D*-Glucopyranosyl-(1 → 3)-O-β-*D*-glucopyranosyl-(1 →4) -O-β-*D*-glucopyranosyl-(1 → 4)-β-*D*-glucopyranose (III)*

The supernatant solution remaining after the isolation of II afforded a second product which, after three recrystallizations from water–methanol, had m.p. 187–188°; this product was found to be the dihydrate of III (4) by mixed melting point and from its X-ray powder diagram.

Degradation of Lichenin with Laminarinase

Lichenin (0.14 g) in water (15 ml) was incubated at 44° with laminarinase (25 mg) for 6 hours. The digest was heated at 95° for 10 minutes, concentrated, and chromatographed on Whatman No. 3 MM paper sheets using solvent A.

O-β-D-Glucopyranosyl-(1 → 4)-O-β-D-glucopyranosyl-(1 → 3)-α-D-glucose (IV)

The eluted trisaccharide fraction, after purification with mixed ion-exchange resins, crystallized and was recrystallized from water–ethanol; m.p. 236–239°, $[\alpha]_D$ 16.5° → 11.7° (*c*, 1.5, H_2O). Calculated for $C_{18}H_{32}O_{16}$: C, 42.86%; H, 6.39%; molecular weight, 502. Found: C, 42.81%; H, 6.47%; molecular weight (vapor pressure osmometry, in water), 480. The X-ray powder diagram was indistinguishable from that of trisaccharide IV, obtained previously as amorphous material from oat glucan (4) but which also has now been crystallized (m.p. 234–237°).

ACKNOWLEDGMENTS

The authors express their deep appreciation to Dr. E. T. Reese for his kindness in providing the enzyme preparations used. They also thank Mrs. J. Nuttall for able technical assistance. Microanalyses were performed by Mr. M. Mazurek. X-Ray powder diagrams were prepared by Miss I. Gaffney and Mr. W. Haid.

REFERENCES

1. K. H. Meyer and P. Gürtler. Helv. Chim. Acta, **30**, 751 (1947).
2. N. B. Chanda, E. L. Hirst, and D. J. Manners. J. Chem. Soc. 1951 (1957).
3. S. Peat, W. J. Whelan, and J. G. Roberts. J. Chem. Soc. 3916 (1957).
4. F. W. Parrish, A. S. Perlin, and E. T. Reese. Can. J. Chem. **38**, 2094 (1960).
5. E. T. Reese, E. Smakula, and A. S. Perlin. Arch. Biochem. Biophys. **85**, 171 (1959).
6. E. T. Reese and M. Mandels. Can. J. Microbiol. **5**, 173 (1959).
7. H. Ono and M. Dazai. Nature, **183**, 1055 (1959).
8. E. A. Moscatelli, E. A. Ham, and E. L. Rickes. J. Biol. Chem. In press.
9. F. W. Parrish and A. S. Perlin. Nature, **187**, 1110 (1960).
10. I. J. Goldstein, G. W. Hay, B. A. Lewis, and F. Smith. American Chemical Society, 135th Meeting Abstracts, 3D (1959).
11. I. A. Preece, N. K. Garg, and J. Hoggan. J. Inst. Brewing, **66**, 33 (1960).
12. E. L. Hirst. Proceedings of the 4th International Congress of Biochemistry. Vol. 1. 1958. p. 31.
13. N. Nelson. J. Biol. Chem. **158**, 375 (1944).
14. A. P. Brady, H. Huff, and J. W. McBain. J. Phys. & Colloid Chem. **55**, 304 (1951).

PHOTOCHEMICAL SYNTHESES

2. THE IRRADIATION OF ACENAPHTHENE WITH BENZIL

P. DE MAYO AND A. STOESSL[1]

The Department of Chemistry, University of Western Ontario, London, Ontario

Received September 15, 1961

ABSTRACT

The irradiation product of acenaphthene and benzil described by Oliveri-Mandalà, Giacalone, and Deleo has been shown to have the structure (III) and not that of the cyclobutane derivative (II, R = H) originally proposed. The main product obtained by the action of acetic anhydride and sulphuric acid on (III) is not the result of an acetylation process, but is the sultone (IV).

The irradiation of hydrocarbons, which are capable of giving stable radicals by hydrogen abstraction, in the presence of carbonyl compounds has been shown to give carbinols (2, 3). Cyclohexene and acetone, for instance, give cyclohexenyldimethylcarbinol (I). The reported irradiation (1), in sunlight, of such a hydrocarbon, acenaphthene, in the presence of a diketone was, therefore, of some interest. The product isolated had an analysis corresponding to 1:1 addition, and structure (II, R = H) was proposed on the basis of diacetate (II, R = Ac) formation on acetylation with acetic anhydride and sulphuric acid. Acetic anhydride and pyridine had no action. If correct, this scheme could well provide a new route to syntheses in the cyclobutane series.

The formation of (II, R = H) was a priori not unreasonable since the expected initial product (III) might well cyclize, such an intramolecular reaction being unexceptional (4). However, the formation of a simple diacetate seemed surprising under conditions of such acidity. Such a strained molecule should provide ample opportunity for acid-catalyzed rearrangement and a number of mechanistically credible routes can be envisaged. Furthermore, the main product of the acetylation process was a substance for which no empirical formula was proposed and which was orange-red in color. Since no simple transformation product of (II, R = H) should be so colored the preparation of the irradiation product was repeated.

Irradiation of benzil and acenaphthene in benzene solution using, however, an ultraviolet lamp, gave the desired product with properties as previously described (1). The structure (II, R = H) was shown to be untenable since the infrared spectrum revealed bands in the carbonyl and hydroxyl region at 1669 and 3460 cm^{-1} compatible with those expected for a benzoin. The alternative structure (III) seemed, therefore, very probable and its correctness was established by the following experiments.

Reduction of (III) with sodium borohydride gave the corresponding diol showing no carbonyl absorption in the infrared. This was further characterized as a monoacetate. Cleavage of the diol with periodic acid then gave benzaldehyde (characterized as the 2,4-dinitrophenylhydrazone) and benzoylacenaphthene. The latter substance had the expected absorption in the infrared and ultraviolet. In addition the n.m.r. spectrum showed a typical ABX pattern for the three non-aromatic hydrogen atoms. (J_{AB} 17.2, J_{AX} 4.7, J_{BX} 7.9 c.p.s.; τ, 6.46, 6.12, and 4.62). However, since the literature (5) records a substance purporting to be 1-benzoylacenaphthene with a melting point differing from

[1]*Present address: Pesticide Research Institute, Canada Department of Agriculture, University Sub Post Office, London, Ontario.*

that of the degradation product by 60°, the ketone was converted to 1-benzylidine-acenaphthene identical with a specimen prepared by a Grignard synthesis from acenaphthenone. The structure of the hydrocarbon was confirmed by ozonolysis to benzaldehyde (isolated as the 2,4-dinitrophenylhydrazone) and by quantitative hydrogenation to the oily 1-benzylacenaphthene, which had the expected spectroscopic properties and yielded a crystalline picrate. In addition, heating the benzoylacenaphthene with sodium ethoxide at 180° in the presence of hydrazine resulted in bond cleavage and the formation, by dealdolization, of acenaphthene, together with benzoic acid presumably derived by a Canizzaro reaction from the first-formed benzaldehyde. The nature of the earlier substance, prepared by the irradiation of benzaldehyde and acenaphthene, remains in doubt. No analysis or properties other than the melting point were recorded.

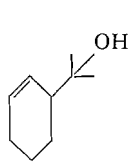

(I)

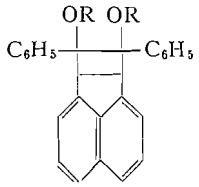

(II)

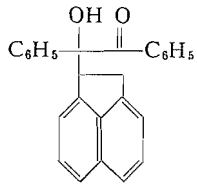

(III)

Treatment of (III) with acetic anhydride and sulphuric acid gave the orange-red main product as described by the Italian workers (1). We were unable, however, to isolate any substance corresponding to the supposed "diacetate" even by chromatography. The original isolation involved hand picking of crystals and the recorded analysis for this substance (only carbon and hydrogen reported) lies midway between the starting material and the main product, as does, indeed, the melting point. It is therefore possible that it was a mixture.

The original carbon and hydrogen analysis for the orange-red substance was confirmed. No band attributable to a carbonyl group was visible in the infrared spectrum. The low value for hydrogen immediately suggested that some element other than carbon, hydrogen, or oxygen might be present. In fact, analysis for sulphur established the empirical formula $C_{26}H_{16}O_3S$. The condition of genesis of the substance suggested unsaturated sultone formation (6) and on mechanistic grounds the structure (IV) seemed probable. Its correctness was established in the following way.

Hydrolysis of (IV) with aqueous alcoholic sodium hydroxide gave 1 molecule equivalent of benzoic acid together with the sodium salt of a yellow sulphonic acid formulated as (V). Its formation may be rationalized as a δ-addition of water to the unsaturated sultone followed by either cleavage of the δ-keto, α-β unsaturated acid, or dealdolization to the mixed anhydride followed by hydrolysis. Ozonolysis of (V) followed by treatment with base gave, by condensation of the intermediate 1,5-diketone (VI), the known hydroxyperinaphthenone (VII), which was identified by comparison with an authentic specimen (7) and by ozonolysis to naphthalic anhydride (VIII).

EXPERIMENTAL

Melting points were taken on the Kofler hot stage. Ultraviolet spectra were determined in 95% ethanol and infrared spectra as Nujol mulls.

Irradiation of Benzil and Acenaphthene

Benzil (15 g) and acenaphthene (11 g) in benzene (50 ml) were irradiated in a pyrex flask under nitrogen with an 85 w HC3 (Hanovia) lamp. After 2 days the precipitate was collected (1.28 g) and crystallized from ethyl acetate to give the adduct, m.p. 237–239° (lit. 234°). Calc. for $C_{26}H_{20}O_2$: C, 85.69; H, 5.53%. Found: C, 85.33; H, 5.35%. The substance showed λ_{max} 228 mμ (ϵ, 64,000) in the ultraviolet.

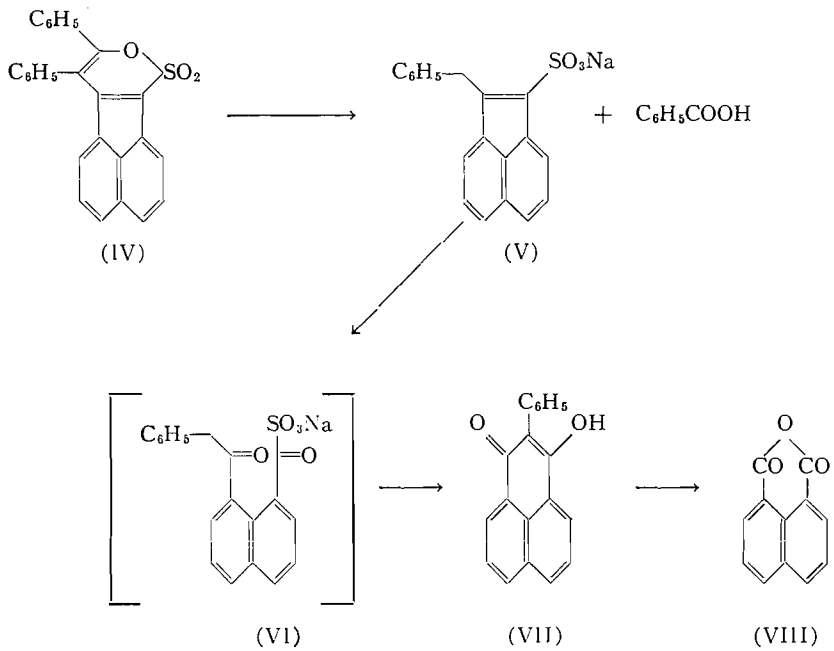

Reduction of the Adduct to the Diol

The adduct (102 mg) in dioxan (5 ml) was treated with a solution of sodium borohydride (21 mg) in methanol (5 ml) at 10°. After 1 hour, the mixture was poured onto ice water and the product isolated with chloroform containing methanol. The combined extracts were washed with water and dried (Na_2SO_4) and the solvent removed to give, after crystallization from methanol, the diol, m.p. 222–224°. Calc. for $C_{26}H_{22}O_2$: C, 85.21; H, 6.05%. Found: C, 85.12; H, 6.32%. The substance showed λ_{max} 230 mμ (ϵ, 64,000).

Acetylation (acetic anhydride – pyridine at 55° for 20 hours) of the diol (29 mg) gave the monoacetate, m.p. (from ethyl acetate) 264–266°. Calc. for $C_{28}H_{24}O_3$: C, 82.33; H, 5.92%. Found: C, 81.96; H, 6.13%.

Periodate Oxidation of the Diol

To the diol (25.4 mg) in ethyl acetate (3 ml) and methanol (6 ml) was added aqueous periodic acid (0.4 *N*; 2 ml) and the mixture allowed to stand overnight. The mixture was then steam distilled (after reduction of excess periodic acid with arsenite) and the distillate treated with 2,4-dinitrophenylhydrazine in hydrochloric acid. The precipitate (81% yield) was identified as benzaldehyde 2,4-dinitrophenylhydrazone (m.p. and mixed m.p. 236–240°) by comparison with an authentic specimen.

In a similar experiment on a larger scale (120 mg) the oxidizing mixture was allowed to stand 64 hours. After dilution with water the mixture was extracted with benzene and the isolated benzoyl acenaphthene crystallized from methanol and from ethyl acetate (charcoal), with m.p. 137–138.5°. Calc. for $C_{19}H_{14}O$: C, 88.34; H, 5.46%. Found: C, 88.56; H, 6.00%. The ketone (36 mg) when heated in a sealed tube at 180° in ethanol (1.25 ml) containing sodium (85 mg) and hydrazine (1 ml) (Wolff–Kishner conditions) gave, by isolation with benzene and sublimation, acenaphthene (12 mg), identified by melting point and mixed melting point, with an authentic specimen. Acidification of the aqueous phase and steam distillation gave, after extraction and crystallization from water, benzoic acid (7 mg), identified by m.p. and mixed m.p.

1-Benzylidine-acenaphthene

(a) From 1-Benzoylacenaphthene

The ketone (49 mg) was reduced with sodium borohydride as described above. The syrupy product was transferred to a Dean and Stark apparatus and refluxed overnight in toluene (100 ml) containing *p*-toluenesulphonic acid (200 mg). After it was washed with sodium hydroxide solution and water, the solution was evaporated under reduced pressure and the residue chromatographed on alumina (Brockmann Grade 1, 5 g). Light petroleum eluted a gummy fraction (15 mg) which, on hydrogenation, afforded 1-benzylacenaphthene (see below) identified by infrared spectrum and by m.p., mixed m.p., and infrared spectrum of picrate. Further elution of the column with benzene in light petroleum (1:9) furnished a crystalline compound (25 mg) which, after repeated recrystallization from acetone, was identical in all respects with a synthetic specimen of 1-benzylidineacenaphthene.

(b) From Acenaphthenone

Benzyl Grignard reagent was prepared from Mg (360 mg) essentially as described by Adkins and Zartmann (8). To the cooled ethereal solution was added acenaphthenone (9) (2.1 g) in cold dry benzene (18 ml) and the mixture was stirred at ice-temperature (10) for 2 hours, and for a further 1.5 hours while it was allowed to reach room temperature. The complex was decomposed with ice-cold hydrochloric acid (6 *N*; 100 ml) and the product isolated in the usual way as a syrup. A portion (950 mg) was intimately mixed with boric acid (925 mg) and heated at 160° for 30 minutes (11). The mixture was extracted with light petroleum and the extracts chromatographed on alumina (50 g).

Elution with light petroleum gave a yellow oil (473 mg) which was retained (fraction I). Elution with benzene – light petroleum (1:4) then gave an orange oil (fraction II) (92 mg) which crystallized slowly from ethyl acetate. Repeated crystallization from acetone gave a product having a melting point of 98.0–98.5°. In a similar experiment fraction II was sublimed *in vacuo* at 110° to give material which, on crystallization from acetone, was identical with that obtained by chromatography. Found: C, 93.66; H, 5.77%. Calc. for: $C_{19}H_{14}$: C, 94.18; H, 5.82%. The substance showed λ_{max} 246 mμ (ϵ, 27,000) in the ultraviolet.

1-Benzylacenaphthene

(*a*) 1-Benzylideneacenaphthene (m.p. 98–98.5°) (15.5 mg) in ethyl acetate (5 ml) was hydrogenated in the presence of palladized charcoal (5%; 15 mg) with the uptake of 0.94 molecule equivalent of hydrogen. The resultant oil was identical in every respect with that described under (*b*) below, and gave an identical picrate.

(*b*) Fraction I (473 mg) obtained from the boric acid treatment described above was hydrogenated in the presence of palladized charcoal with the uptake of 1 molecule equivalent of hydrogen. The oily product was converted, in ethanolic solution, to the picrate (618 mg) m.p. 81–82° unchanged by further crystallization from alcohol. Found: C, 63.42; H, 4.31; N, 8.90%. Calc. for $C_{25}H_{19}O_7N_3$: C, 63.42; H, 4.04; N, 8.88%. The picrate (320 mg) was filtered through a column of alumina (8 g) and the column washed with benzene. Isolation of the eluted hydrocarbon and sublimation gave benzylacenaphthene as an oil, λ_{max} 228 mμ (ϵ, 78,500), n_D^{25} 1.6409. Found: C, 93.20; H, 6.45%. Calc. for $C_{19}H_{16}$: C, 93.42; H, 6.60%.

Ozonolysis of 1-benzylideneacenaphthene

The crystalline hydrocarbon (20 mg) in ethyl acetate (2 ml) was treated with a stream of ozone at −10° for 10 minutes and the residue distilled from water containing a few drops of dilute sulphuric acid and a little Zn dust. The distillate was treated with 2,4-dinitrophenylhydrazine in dilute sulphuric acid and the precipitate (10 mg), purified by chromatography on bentonite–celite (1:1 by volume) and crystallization from benzene, was identified as the benzaldehyde derivative by melting point and mixed melting point.

Treatment of the Adduct (III) with Acetic Anhydride

The adduct (0.49 g) was suspended in acetic anhydride (3 ml) and sulphuric acid added dropwise with shaking until the solid had dissolved (about 10 drops). After 24 hours the precipitate (240 mg; m.p. 184–190°) was collected and crystallized from ethyl acetate to give the sultone, m.p. 190–191.5°. (Oliveri-Mandalà *et al.* (1) give 187–188°.) Calc. for $C_{26}H_{16}O_3S$: C, 76.45; H, 3.95; O, 11.75; S, 7.85%. Found: C, 75.87, 76.26; H, 3.72; 4.16; O, 12.30; S, 7.97%. The substance showed λ_{max} 450, 384, 366, 346, 289, 238 (inf) (ϵ, 6,200, 14,600, 15,100, 12,900, 11,700, and 14,000 respectively) in the ultraviolet.

Careful examination of the mother liquor in the manner previously described (1), and by chromatography failed to reveal any trace of the substance, m.p. 195–196°, reported by Oliveri-Mandalà *et al.* (1).

Hydrolysis of the Sultone (IV)

The sultone (999 mg) was refluxed in aqueous ethanol (80%; 800 ml) containing sodium hydroxide (32 g) until solution was complete (1 hour) and 1 hour further. After acidification the product was isolated by extraction with ethyl acetate. This was washed with saturated sodium sulphate solution and concentrated to 70 ml. The lower aqueous layer which separated was then further extracted with ethyl acetate and the organic phases dried over sodium sulphate,[2] evaporated to dryness, and added to a silica column (50 g) in benzene. Elution with chloroform gave benzoic acid (317 mg, 1.06 molecule equivalent) identified by melting point and mixed melting point and infrared spectrum with an authentic specimen.

Elution of the column with ethanol–chloroform (1:4) gave a crystalline mixture. This was extracted with boiling ethyl acetate and the residue crystallized from ethanol to give the sulphonic acid sodium salt (V), m.p. 280° (decomp.). Calc. for $C_{19}H_{13}O_3SNa.\frac{1}{2}H_2O$, C, 64.56; H, 3.99; S, 9.07; Na_2SO_4, 20.11%. Found: C, 64.16; H, 3.93; S, 8.92; ash (sulphated), 20.12%. The substance showed λ_{max} 350, 343, 328, 314, 264, 251, 233 mμ (ϵ 6,700, 6,700, 13,900, 9,200, 3,600, 2,800, 39,600 respectively) in the ultraviolet.

Ozonolysis of the Sulphonic Acid, Sodium Salt (V)

The sodium salt (49.5 mg) in ethanol (5 ml) was treated with a stream of ozone at −20° until the yellow color was discharged (about 10 minutes). Hydrogen peroxide (30%; 0.25 ml) was added, followed by sodium hydroxide solution (10%; 1 ml) and the mixture refluxed 30 minutes. After acidification the orange-yellow precipitate (18.4 mg, m.p. 218–221°) was recrystallized from ethyl acetate to give 3-hydroxy-2-phenylperinaphthenone, m.p. 219–221°, undepressed on admixture with an authentic specimen. The infrared spectra were superposable.

[2]*The sulphonic acid, being a strong acid, exchanged with the sodium sulphate, probably on drying.*

Ozonolysis of 3-Hydroxy-2-phenylperinaphthenone

The perinaphthenone, 18.4 mg, in alcohol (10 ml) was treated with ozonized oxygen at ca. −25° until just colorless. Water (100 ml) containing sodium hydroxide (80 mg) and hydrogen peroxide (30%; 0.2 ml) was added and the solution was concentrated on the steam bath to ca. 5 ml, cooled, and acidified. The precipitate was collected and crystallized from acetic acid containing a drop of acetic anhydride to furnish naphthalic anhydride (9.0 mg), m.p. and mixed m.p. 270–271°, further identified by the infrared spectrum.

The aqueous filtrate from which the naphthalic anhydride had separated was extracted with ether (3×10 ml). Evaporation of the extracts and sublimation of the residue followed by recrystallization from water gave benzoic acid (3.5 mg), m.p. and mixed m.p. 120–122°.

ACKNOWLEDGMENTS

We wish to thank Imperial Oil of Canada, Ltd., and the National Research Council of Canada for financial support. We are grateful to Dr. J. B. Stothers for the determination of the n.m.r. spectra.

REFERENCES

1. E. OLIVERI-MANDALÀ, A. GIACALONE, and E. DELEO. Gaz. chim. ital. **69**, 104 (1939).
2. P. DE MAYO, J. B. STOTHERS, and W. TEMPLETON. Can. J. Chem. **39**, 488 (1961).
3. E. PATERNO and G. CHIEFFI. Gaz. chim. ital. **39**, 415 (1904); see G. S. HAMMOND, W. P. BAKER, and W. M. MOORE. J. Am. Chem. Soc. **83**, 2795 (1961).
4. N. C. YANG and D-D. H. YANG. J. Am. Chem. Soc. **80**, 2913 (1958).
5. R. DE FAZI. Atti accad. naz. Lincei, **9**, 1004 (1929).
6. T. MOREL and P. E. VERKADE. Rec. trav. chim. **68**, 619 (1949).
7. F. KOELSCH and R. H. ROSENWALD. J. Am. Chem. Soc. **59**, 2166 (1937).
8. H. ADKINS and W. ZARTMANN. Org. Syntheses. Coll. Vol. II. p. 606.
9. L. F. FIESER and T. CASON. J. Am. Chem. Soc. **62**, 432 (1940).
10. B. R. BROWN and D. L. L. HAMMICK. J. Chem. Soc. 1395 (1948).
11. G. L. BUCHANAN and D. R. LOCKHARDT. J. Chem. Soc. 3586 (1959).

METAL OXIDE ALKOXIDE POLYMERS

PART IV. THE HYDROLYSIS OF SOME TANTALUM ALKOXIDES[1]

D. C. BRADLEY[2] AND H. HOLLOWAY[3]
The Department of Chemistry, Birkbeck College, London, W.C.1, England
Received June 21, 1961

ABSTRACT

Ebulliometric studies on the hydrolysis of tantalum pentaalkoxides $Ta(OR)_5$, where R = Me, Pr^n, Bu^n, and Bu^s, have furnished important data on the polymeric nature of tantalum oxide alkoxides. It is shown from the variation of number-average degrees of polymerization as a function of degree of hydrolysis that the polymers conform to certain structural models. The structural models involve 6-co-ordinated tantalum.

INTRODUCTION

Recent work on the controlled hydrolysis of the tetraalkoxides of titanium (1, 2) and zirconium (3, 4) has revealed that the polymeric metal oxide alkoxides thus formed conform to certain structural models based on octahedral 6-co-ordination of the metal. These structural models give rise to unique equations describing the dependence of the number-average degree of polymerization on the degree of hydrolysis. A remarkable feature of these series of co-ordination – condensation polymers is that for a given degree of hydrolysis the number-average degree of polymerization is independent of the distribution of polymer sizes. The fundamental nature of these structural models was foreshadowed by our results on the products of hydrolysis of tantalum pentaethoxide in which the quinquevalent metal also appears to assume a co-ordination number of six. The introduction of a single parameter, namely the proportion of tantalum atoms conforming to one of the two appropriate structural models, was sufficient to define the number-average degree of polymerization as a function of degree of hydrolysis over a considerable range of hydrolysis. In order to test further the validity of the theory we have extended the work to include the hydrolysis of other tantalum pentaalkoxides which were amenable to study by the ebulliometric technique. We now report the results of the hydrolysis of the following alkoxides: $Ta(OR)_5$, where R = Me, Pr^n, Bu^n, and Bu^s.

EXPERIMENTAL AND RESULTS

Preparation of Tantalum Alkoxides

The pentaalkoxides were prepared using previously described procedures (6, 7) based on two methods: (i) the reaction involving $TaCl_5$ and the appropriate alcohol in the presence of excess of ammonia, (ii) alcoholysis of a lower alkoxide. We found that tantalum penta-*sec*-butoxide could be synthesized by the alcoholysis involving tantalum pentamethoxide and excess *sec*-butanol in benzene. Removal of the liberated methanol was achieved by fractional distillation of the minimum boiling binary azeotrope $MeOH/C_6H_6$. This result was of interest since Bradley *et al.* (8) have reported that tantalum pentaisopropoxide cannot be obtained by alcoholysis of the pentamethoxide because the reaction ceases with the formation of the stable mixed alkoxide $Ta(OMe)(OPr^i)_4$.

[1]*For Part III, see ref. 4.*
[2]*Present address: The University of Western Ontario, London, Ontario.*
[3]*Present address: Post Office Research Station, Dollis Hill, London, N.W.2, England.*

Drying of the Alcohols

Methanol

Absolute methanol was refluxed over magnesium methoxide for 4 hours and distilled. The distillate was kept in contact with "molecular sieve" granules in an all-glass apparatus and samples were withdrawn under an atmosphere of dry nitrogen.

Propanol

Commercially available *n*-propanol was dried and purified by "azeotropic drying" after the addition of benzene. The water was removed as the ternary minimum boiling azeotrope $Pr^nOH/C_6H_6/H_2O$, b.p. 69° C, and then the benzene as the binary azeotrope Pr^nOH/C_6H_6, b.p. 89° C. Fractionation was carried out at a very high reflux ratio in a Podbielniak column (150 cm long) with an efficiency of approximately 80 theoretical plates. The pure *n*-propanol was stored in contact with molecular sieve (Linde type 4A, previously dried at 210° C at 0.01 mm for 16 hours). The molecular-sieve drying apparatus consisted of a glass column (120 cm×2.5 cm diameter) surmounted by a reservoir (approx. 1 liter) and fitted with a grease-free ground-glass tap at the base of the column.

n-Butanol and sec-Butanol

Since these alcohols do not form ternary azeotropes with benzene and water the "azeotropic drying" was effected by the addition of ethanol, followed by fractional distillation to remove, in turn, the ternary azeotrope $EtOH/C_6H_6/H_2O$, b.p. 65° C; the binary azeotrope $EtOH/C_6H_6$, b.p. 68° C; and the remaining benzene, b.p. 80° C. Finally the butanol was distilled into a molecular-sieve column and dispensed under dry nitrogen.

The water content was shown in all cases to be less than 0.005% by the Karl Fischer method.

Ebulliometric Technique and Results

An all-glass ebulliometer using a differential water thermometer was used as described in Part II (5). The alkoxides were freshly distilled *in vacuo* immediately prior to the ebulliometric hydrolysis.

Tantalum Methoxide

Three separate experiments, each involving several additions of solute, were carried out on the determination of the molecular weight of tantalum pentamethoxide in boiling methanol. The elevation of the boiling point was a linear function of solute concentration within the probable experimental error over a wide concentration range (0.0195–0.330 g-mol./kg methanol). The three values for the number-average degree of polymerization, 1.78, 1.75, 1.74, gave an average of 1.76 ± 0.02. This value is significantly higher than that reported earlier (6).

The results of the ebulliometric hydrolysis of tantalum methoxide in two seperate experiments are reported in Table I, where n is the observed number-average degree of polymerization of the tantalum oxide methoxide of degree of hydrolysis h (number of g-mol. H_2O per g-atom Ta). No precipitation was observed in these experiments, which were terminated when the elevation of the boiling point became too low to be measured with reasonable accuracy.

Tantalum n-Propoxide

Two separate determinations of the molecular weight of tantalum penta-*n*-propoxide in *n*-propanol, each involving several additions of solute over a range of concentration (0.02–0.12 g-mol./kg), gave values of 1.62 and 1.57 for the number-average degree of polymerization for the alkoxide. The average value 1.59 ± 0.03 was taken. There was no evidence of concentration dependence of the molecular weight over the wide range of

TABLE I

Initial concentration of $Ta_2(OMe)_{10}$ = 0.157 g-mol./kg									
h	0.067	0.203	0.353	0.491	0.635	0.805	0.978	1.15	
n	1.79	2.01	2.27	2.65	3.06	3.89	5.24	7.63	
n_{calc}	1.83	2.03	2.31	2.64	3.10	3.91	5.32	8.29	
h	1.34	1.43	1.51	1.65	1.74				
n	12.0	14.3	19.9	20.5	20.9				
Initial concentration of $Ta_2(OMe)_{10}$ = 0.165 g-mol./kg									
h	0.082	0.169	0.299	0.424	0.530	0.625	0.747	0.875	
n	1.83	1.98	2.23	2.53	2.83	3.09	3.67	4.47	
n_{calc}	1.85	1.98	2.20	2.47	2.75	3.06	3.59	4.38	
h	1.00	1.13	1.27	1.37	1.48	1.59	1.70	1.81	1.94
n	5.81	7.60	11.4	14.1	17.5	20.3	22.9	24.0	23.3
n_{calc}	5.59	7.81							

concentrations studied, although the non-integral value of n shows that more than one species must be present. The results of two ebulliometric hydrolyses are recorded in Table II. No precipitation was observed but the experiments were terminated at $h > 1.6$

TABLE II

Initial concentration of $Ta_2(OPr^n)_{10}$ = 0.075 g-mol./kg							
h	0.161	0.423	0.677	0.847	1.061	1.29_5	1.55
n	1.73	2.10	2.67	3.27	4.49	7.01	7.20
n_{calc}	1.73	2.10	2.64	3.27	4.49		
Initial concentration of $Ta_2(OPr^n)_{10}$ = 0.0745 g-mol./kg							
h	0.162	0.345	0.589	0.806	1.037	1.26	1.50_5
n	1.71	1.94	2.38	2.99	4.11	6.25	6.90
n_{calc}	1.74	1.98	2.43	3.04	4.16		

when characteristic fluctuations in the thermometer reading indicated the presence of traces of water.

Tantalum sec-Butoxide

Two separate determinations of the molecular weight of $Ta(OBu^s)_5$ in boiling *sec*-butanol gave number-average degrees of polymerization of 1.08 and 1.06. The mean value of 1.07 ± 0.01 was taken for subsequent calculations. The measurements were made over a concentration range of approximately 0.0073–0.052 g-mol./kg and no evidence for a concentration dependence of molecular weight was detected. The results of two ebulliometric hydrolyses are recorded in Table III. No precipitation was observed but fluctuations of the thermometer reading at $h > 1.6$ indicated the presence of traces of water.

TABLE III

Initial concentration of $Ta(OBu^s)_5$ = 0.0982 g-mol/kg							
h	0.080	0.234	0.357	0.477	0.604	0.740	0.870
n	1.18	1.33	1.47	1.60	1.78	2.02	2.33
h	1.01	1.17	1.30	1.43	1.57		
n	2.80	3.58	4.71	6.76	9.8		
Initial concentration of $Ta(OBu^s)_5$ = 0.0861 g-mol./kg							
h	0.120	0.269	0.412	0.540	0.660	0.833	
n	1.22	1.39	1.54	1.70	1.90	2.26	
h	1.005	1.175	1.37	1.48	1.61		
n	2.79	3.59	5.37	7.22	10.1		

Tantalum n-Butoxide

Separate determinations of the molecular weight of $Ta(OBu^n)_5$ over the concentration range 0.00398–0.0308 g-mol./kg gave values of 1.34 and 1.37 for the number-average degree of polymerization, with no indication of concentration effects. The average value of 1.36 ± 0.02 was taken. In the ebulliometric hydrolysis of $Ta(OBu^n)_5$ it was found that the addition of aqueous *n*-butanol to the boiling solution of the tantalum compound caused an immediate *increase* in the elevation of the boiling point (ΔT). This was followed by a slow decrease in ΔT until a steady value was reached which was lower than the original value. This behavior was probably due to the partition of water between solution and vapor phases, coupled with a slow hydrolysis of $Ta(OBu^n)_5$. In the early stages of hydrolysis the time required to reach a steady value of ΔT after an increment $\Delta h \sim 0.2$ was about 45 minutes but in the later stages hydrolysis was slower and over 90 minutes was required to reach a steady ΔT. The ebulliometric measurements in boiling *n*-butanol were less accurate than in the other alcohols due to technical problems caused by the high boiling point of *n*-butanol. Elaborate precautions against heat loss by the thermometer were required. Also, the water thermometer was so sensitive at this temperature that random fluctuations in the temperatures of the two bulbs made accurate reading difficult. The results for two ebulliometric hydrolyses are recorded in Table IV. No

TABLE IV

Initial concentration of $Ta(OBu^n)_5$ = 0.0617 g-mol./kg								
h	0.300	0.659	0.838	1.26	1.46	1.71	1.95	
n	1.45	1.75	2.02	2.84	3.36	3.59	3.74	
n_{calc}	1.46	1.74	1.93	2.58				
Initial concentration of $Ta(OBu^n)_5$ = 0.0798 g-mol./kg								
h	0.142	0.264	0.409	0.633	0.907	1.15	1.54	1.74
n	1.37	1.41	1.50	1.59	1.90	2.36	3.33	3.51
n_{calc}	1.36	1.44	1.53	1.72	2.01	2.37		

precipitation was observed but at $h > 2$ addition of water produced an increase in ΔT which persisted for over 2 hours and indicated the presence of water.

DISCUSSION

Tantalum Oxide Methoxides

It is clear from the plot of n versus h in Fig. 1 that for h = 0–1.15, the tantalum oxide methoxides conform substantially to the bilinear polymer series based in structural model II, as was found for the tantalum oxide ethoxides (5). However, it is also evident from the lower number-average degree of polymerization for tantalum pentamethoxide compared with the pentaethoxide that a higher proportion of monomer species must be present in the tantalum oxide methoxide system. Following the procedure developed in Part II (5) we have taken all of the data from h = 0 to 1.15 inclusive and determined by the method of least squares the best fit for n^{-1} versus h. The equation $n^{-1} = 0.5721 - 0.3929h$ was thus derived and the coefficient of variation for the percentage error in n, $\sigma_n = \sqrt{[\Sigma\ (100\delta n/n)^2/(m-1)]}$ (where $\delta n = n_{calc} - n$, and m is the number of points), for the 19 points was $\pm 2.8\%$. There were 13 changes in sign in δn, showing that the linear equation was statistically valid. Values of n_{calc} from the least-squares equation are given in Table I. Examination of the errors ($\delta n = n_{calc} - n$) showed that the major contribution was caused by the last 3 points (h = 1.00, 1.13, and 1.15) and that the coefficient of variation for the first 16 points was $\pm 1.65\%$, which is close to the error ($\pm 1.2\%$) in determining the molecular weight of tantalum methoxide. Moreover, extrapolation of

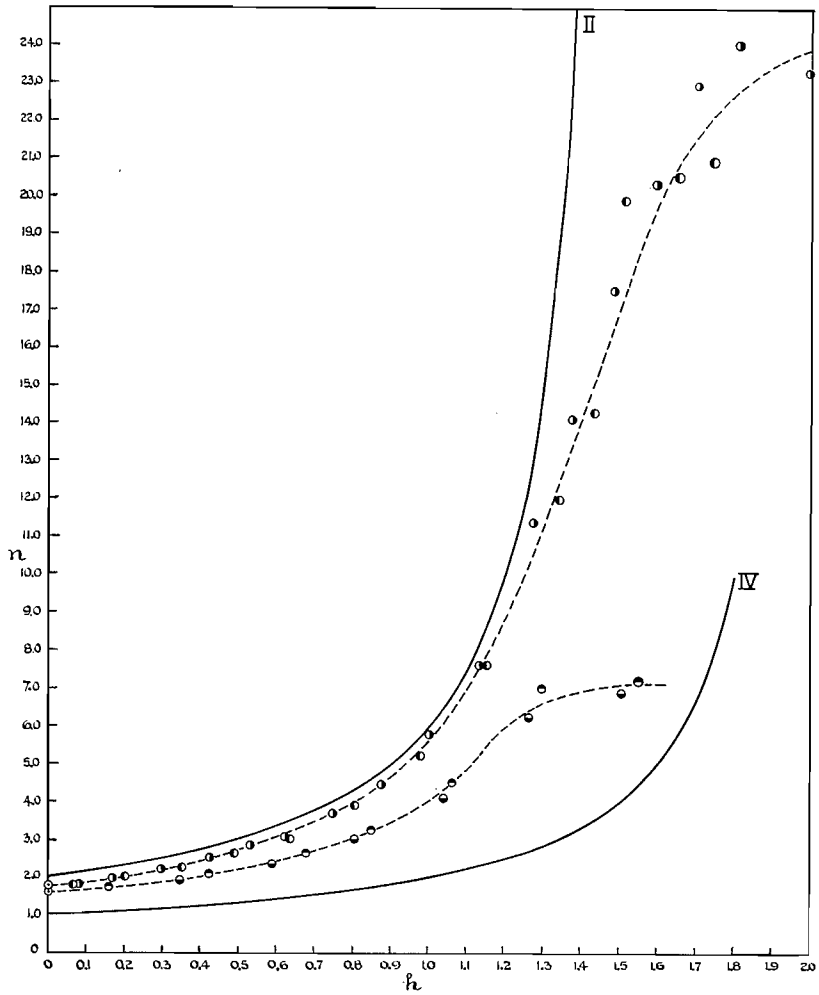

FIG. 1. The variation of n with h for tantalum oxide methoxides and oxide n-propoxides: ◐, tantalum oxide methoxides (Table I); ◑, tantalum oxide methoxides (Table II); ◓, tantalum oxide n-propoxides (Table III); ◒, tantalum oxide n-propoxides (Table IV); curve II, $n = 6/(3-2h)$; curve IV, $n = 2/(2-h)$.

the least-squares equation for the tantalum oxide methoxides to $h = 0$ leads to a value for n_0, the number-average degree of polymerization of tantalum methoxide, of 1.75, compared with the experimental value of 1.76 ± 0.02. Let us now consider the problem of which polymer series based on the solvated monomer $Ta(OMe)_5$,MeOH is present with model II. The intercept $n^{-1} = 0.5721$ ($h = 0$) shows that α_{II} (5), the proportion of metal atoms in the dimer series, is equal to 0.856 (cf. 0.908 for the tantalum oxide ethoxides) but this does not determine which monomer series is present. However, the slope $d(n^{-1})/dh$ is determined by which monomer species is present. Thus we showed for the tantalum oxide ethoxides (5) that for a system involving a mixture of the dimer series model II with the monomer series model III the predicted slope was -0.333_4, but for the mixture of model II and the monomer model IV the slope was $-(0.5000-0.166_7\alpha_{II})$. Substituting the value of α_{II} in the last expression gives a calculated slope of -0.357 to be compared with the slope -0.393 obtained for the least-squares equation. Clearly the

experimental slope favors the model II – model IV system for the tantalum oxide methoxides. For values of $h > 1.3$ it is evident from Fig. 1 that α_{II} is decreasing as solvation becomes more extensive and model IV is favored. This type of behavior has also been noted in the oxide alkoxides of titanium (1, 2) and zirconium (3, 4) and is believed to be due to the decrease in molar concentration which results from the formation of higher polymers. An interesting feature of the ebulliometric experiments on the hydrolysis of tantalum methoxide was the absence of precipitation even up to $h = 1.94$. Thus the model II polymer series predicts infinite polymers at $h = 1.5$ and these would presumably be insoluble. As in the case of the tantalum oxide ethoxides at $h > 1.5$ we suggest that disproportionation may be taking place, so that h for the species in model (h_{II}) is <1.5 (i.e. gives soluble species) while $h_{IV} > 1.5$. The limitation will be that h_{IV} must not reach 2.0 since this model gives an infinite polymer at $h_{IV} = 2$. It is noteworthy that the deviations of the experimental points from curve II become very marked at around $h = 1.6$ and it seems likely that for $h > 1.6$ the hydrolysis is incomplete due to the formation of Ta—OH bonds which are stable in solution. The presence of traces of water in this system would not cause the characteristic fluctuations of the thermometer readings noted in experiments involving the higher alcohols and would thus not be detectable.

Tantalum Oxide n-Propoxides

In Fig. 1 it can be seen that the number-average degrees of polymerization for tantalum oxide *n*-propoxides are between the values calculated for the dimer and monomer models from $h = 0$ to 1.06. However, the lower value of n_0 (1.59, cf. 1.76 for the methoxide) suggests that there should be a smaller proportion of model II species than was found in the oxide methoxides. This low value of n_0 is probably due to the higher boiling point of *n*-propanol compared with methanol since it has been suggested (1, 2, 3, 9) that a higher temperature causes depolymerization of the metal alkoxide co-ordination polymers and the metal is forced to maintain its higher co-ordination by the solvation mechanism. The experimental data for $n = 0$–1.06 were treated by the method of least squares to determine the best straight line for the variation of n^{-1} with h. The equation $n^{-1} = 0.6382 - 0.3838h$ was obtained and there were six changes of sign of δn when the 11 points were arranged in ascending order of h, showing that the straight line was statistically valid. The values of n_{calc} are given in Table II. The coefficient of variation for the percentage errors in n was $\pm 1.83\%$, which is near the probable experimental error. From the intercept at $h = 0$ a value for $n_0 = 1.57$ was obtained which is in good agreement with the value 1.59 ± 0.03 obtained from the measurements on tantalum penta-*n*-propoxide. The intercept also corresponds to $\alpha_{II} = 0.724$ for the proportion of model II species in the system. This value of α_{II} leads to a calculated value of -0.379 for the slope $d(n^{-1})/dh$, assuming that the structural model IV is present with model II, whereas for model III and model II the slope must be -0.333_4. The least-squares value of the slope is -0.384, in good agreement with that calculated for the participation of model IV. It appears from the data in Fig. 1 that for $h > 1.06$ increasing solvation (decrease in α_{II}) becomes quite marked and is greater than that found in the tantalum oxide methoxides. The behavior of the thermometer at $h = 1.6$ indicated the presence of traces of water and there seems little doubt that hydrolysis is incomplete at $h > 1.6$.

Tantalum Oxide sec-Butoxides

Tantalum *sec*-butoxide was of special interest because it is practically monomeric in both benzene ($n_0 = 1.06$) (7) and *sec*-butanol ($n_0 = 1.07$). Since benzene could hardly be regarded as a good donor solvent it is assumed that polymerization of the alkoxide

is prevented by the steric effect of the bulky alkoxide groups. Thus the tantalum penta-*sec*-butoxide has its tantalum predominantly in the 5-co-ordinated form in boiling benzene and this might still be true in boiling *sec*-butanol. However, in the latter solvent it is possible that the monomeric species is solvated as $Ta(OBu^s)_5,Bu^sOH$ and the tantalum is 6-co-ordinated because steric effects are smaller in the solvated monomer than in the dimer. This is evident from the drawings in Fig 2. For example, in the dimer the steric

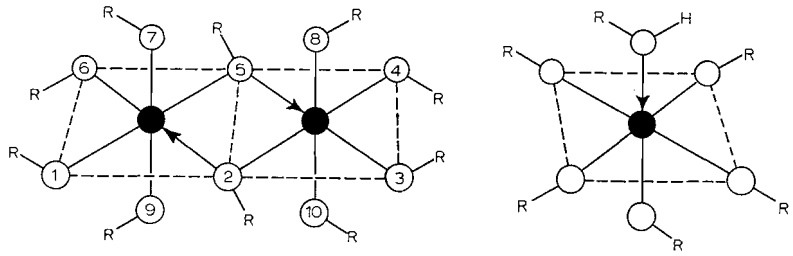

FIG. 2. $Ta_2(OR)_{10}$ and $Ta(OR)_5,ROH$: ●, Ta.

effects are strongest in the bridging alkoxide groups 2 and 5 since they are equidistant from six neighboring alkoxide groups. Next in steric effect are the four apical groups 7, 8, 9, and 10, which are each equidistant from five neighbors, while the least steric interaction is experienced by the four terminal groups 1, 3, 4, and 6, which have only four nearest neighbors. In the solvated monomer the steric interaction must be considerably less because each alkoxide group has only four nearest neighbors. However, as a result of hydrolysis and the formation of Ta.O.Ta groups (condensation polymerization) the alkoxide groups are progressively removed and the steric effects in the tantalum oxide *sec*-butoxides will be smaller than in the penta-*sec*-butoxide. In Fig. 3 we depict polymers

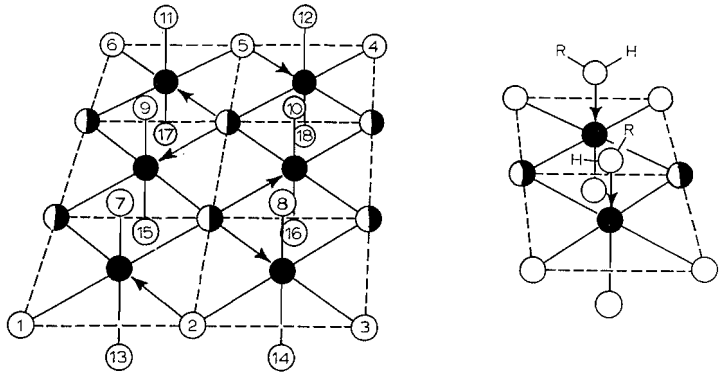

FIG. 3. $Ta_6O_6(OR)_{18}$ and $Ta_2O_2(OR)_6,(ROH)_2$: ●, Ta; ◑, oxygen attached to Ta only. R groups omitted from OR groups.

from the dimer series model II $Ta_6O_6(OR)_{18}$, and the monomer series model IV $Ta_2O_2(OR)_6,(ROH)_2$, both having the same value of h. Comparing first the model II polymer (Fig. 3) with the dimer (Fig. 2) we note that the proportion of highly hindered bridging alkoxide groups (2 and 5) is reduced from 1/5 in $Ta_2(OR)_{10}$ to 1/9 in $Ta_6O_6(OR)_{18}$. Moreover, the apical groups 7, 8, 11, 12, 13, 14, 17, and 18 have only four nearest-neighbor alkoxide groups and groups 9, 10, 15, and 16 have only three nearest neighbors compared with the apical groups in the dimer $Ta_2(OR)_{10}$, which have five. Also,

the terminal alkoxide groups 1, 3, 4, and 6 in $Ta_6O_6(OR)_{18}$ have only three nearest-neighbor akoxides whereas in $Ta_2(OR)_{10}$ the terminal groups have four nearest neighbors. Evidently the steric hindrance per alkoxide group to the formation of $Ta_6O_6(OR)_{18}$ will be considerably smaller than in $Ta_2(OR)_{10}$ and this release of steric strain is cumulative as the degree of hydrolysis increases. There is also a decrease in steric interaction on passing from $Ta(OR)_5$,ROH (all OR groups have four nearest neighbors) to the model IV polymer $Ta_2O_2(OR)_6$,$(ROH)_2$ (all OR groups have three nearest neighbors). It was clear from this analysis of steric factors that the polymeric nature of the tantalum oxide *sec*-butoxides might show some novel features.

The variation of n with h for these compounds is shown in Fig. 4 where it is clear

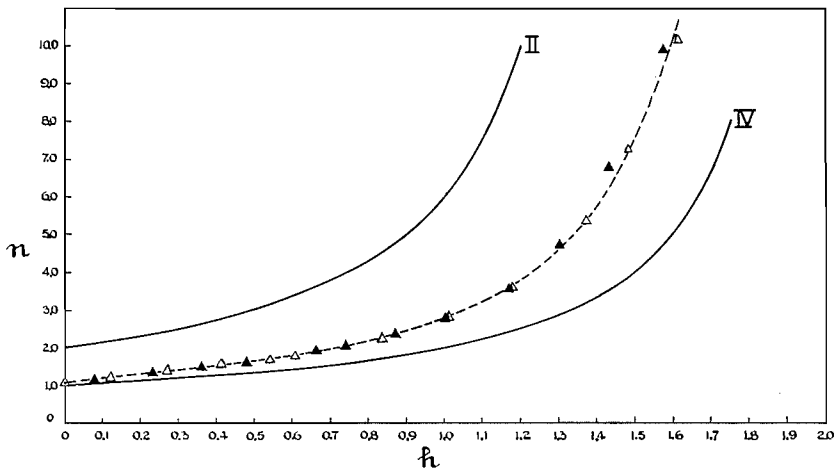

FIG. 4. The variation of n with h for tantalum oxide *sec*-butoxides: ▲, from Table V; △, from Table VI; curve II, $n = 6/(3-2h)$; curve IV, $n = 2/(2-h)$.

that experimental points deviate away from curve IV as h increases. A plot of n^{-1} against h showed curvature at the lowest and also at the highest values of h, with an intermediate region ($h = 0.3$ to 1.3) which was approximately linear.

Applying the method of least squares to the data between $h = 0.357$ and $h = 1.30$ inclusive gave the equation $n^{-1} = 0.857-0.494h$. Extrapolation to $h = 0$ for n_0 resulted in the value of $\alpha_{II} = 0.286$. Hence for a system consisting of models II and IV the calculated value of $d(n^{-1})/dh$ is -0.45 compared with the least-squares slope of -0.49 and the calculated slope of -0.33 for a system consisting of models II and III. Accordingly we conclude that over the range $h = 0.36$–1.3 the polymers conform to the structural models II and IV. Values for α_{II} were then calculated for each value of n from $h = 0$ to 1.61 and the results are shown graphically in Fig. 5. The rapid initial increase in α_{II} is quite striking and suggests strongly that the increase in the proportion of the model II polymers is due to the relief of steric hindrance as the branched alkoxides are removed in the hydrolysis. The continued steady rise in α_{II} over the rest of the range is not surprising, since our analysis of the steric interactions in the model II series of polymers showed that the steric hindrance becomes steadily less with increase in the degree of hydrolysis. However, it would be expected that as the bilinear polymer became large the steric factor would gradually become constant. Unfortunately our ebulliometric investigations were limited by the detection of water in the system at $h > 1.6$ presumably due to incomplete hydrolysis.

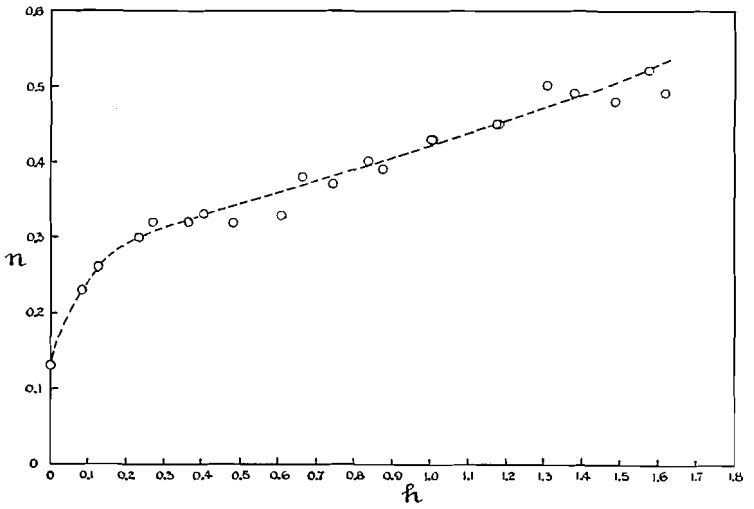

FIG. 5. The variation of α_{II} with h for tantalum oxide *sec*-butoxides.

Tantalum Oxide n-Butoxides

Tantalum penta-*n*-butoxide is dimeric in boiling benzene whereas in boiling *n*-butanol $n_0 = 1.36 \pm 0.02$. It seems reasonable to assume that the lower value in the alcohol is a result of solvation and that a considerable proportion of the monomer species is present. The results shown graphically in Fig. 6 indicate that the tantalum oxide

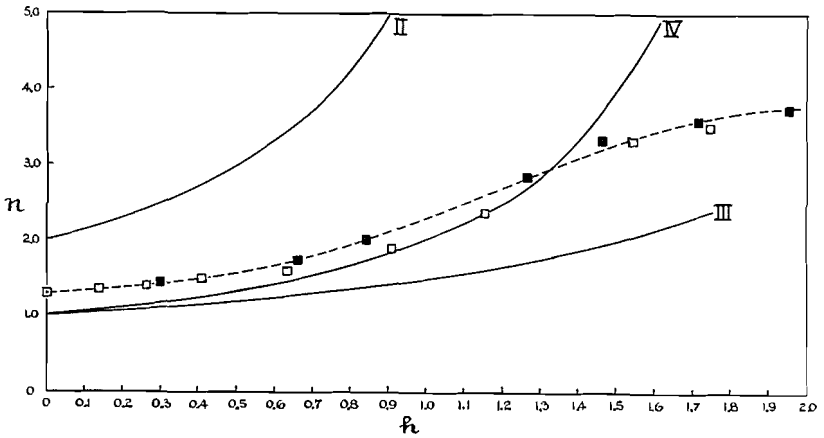

FIG. 6. The variation of n with h for tantalum oxide *n*-butoxides: ■, from Table VII; □, from Table VIII; curve II, $n = 6/(3-2h)$; curve III, $n = 3/(3-h)$; curve IV, $n = 2/(2-h)$.

n-butoxides contain a considerable proportion of polymers based on the model III or model IV series together with the model II polymers. However, a plot of n^{-1} versus h showed some unusual features. For example, there was pronounced curvature at both ends of the graph whilst in the middle section the scatter in the points was rather marked, with the values from one experiment following a slightly different path from that followed by the data from the second experiment. The curvature at high values of h is typical and is probably caused by incomplete hydrolysis but the curvature at low values of h

is perplexing since it is in the opposite sense to that observed in the hydrolysis of $Ta(OBu^s)_5$. Thus it appears that the degrees of polymerization of the tantalum oxide *n*-butoxides are abnormally low in the region $h = 0-0.2$ and two alternative possible explanations seem worthy of consideration. Firstly, there might be some specially preferred species with an abnormally low degree of polymerization which is formed in the early stages of hydrolysis. For example a stable metal–oxygen double bond might give rise to a 6-co-ordinated tantalum species such as $O{=}Ta(OR)_3,(ROH)_2$. Unfortunately this would require the presence of monomeric species at $h = 1.0$ and this is not found to be the case. The second possibility is that, for technical reasons, the hydrolysis may be incomplete in the very early stages of the experiment. This might well be the case due to the high boiling point of *n*-butanol (see the experimental section), which causes a considerable fraction of the added water to assume the vapor state and thus slows down the rate of hydrolysis. If the rate of hydrolysis is some function of the concentration of water in solution then the approach to the true degree of hydrolysis will obviously increase with increasing h. Since the hydrolysis is cumulative the error due to incomplete hydrolysis will become less as h becomes greater. This might also explain the scatter between the results of the two separate experiments. Nevertheless a least-squares fit of n^{-1} versus h for all the points from $h = 0$ to 1.26 gave the line $n^{-1} = 0.778-0.310h$, with a coefficient of variation $\sigma_n = \pm 5\%$. The calculated values of n are listed in Table IV. From the intercept n_0^{-1} ($h = 0$) a value of $\alpha_{II} = 0.44$ for the proportion of dimer species was obtained. Using this value of α_{II} leads to a calculated value of the slope $d(n^{-1})/dh$ of -0.426 for a mixture of model II and model IV polymers. However, the least-squares slope of -0.31 is clearly in much closer agreement with the predicted value of -0.33 required for a mixture of model II and model III polymer species.

CONCLUSIONS

1. The polymeric nature of the products of hydrolysis of tantalum pentaalkoxides can be rationalized in terms of structural models based on 6-co-ordinated tantalum.

2. The number-average degrees of polymerization of tantalum oxide *n*-alkoxides $TaO_x(OR)_{(5-2x)}$, where R = Me, Et, Pr^n, and Bu^n, are accurately described over a considerable range of degrees of hydrolysis by simple linear equations of the form $n^{-1} = a-bh$. From the numerical values of the constants a and b, deductions have been made concerning the participation of different structural models. When R = Me, Et, or Pr^n, the polymers are predominantly based on an unsolvated model II which is related to the dimeric alkoxide $Ta_2(OR)_{10}$ with smaller proportions of either models III or IV, which are related to the solvated monomer $Ta(OR)_5$,ROH. When R = Bu^n the polymers favor model III.

3. The tantalum oxide *sec*-butoxides show an interesting behavior which can be interpreted in terms of the changes in steric hindrance to polymerization as the degree of hydrolysis is increased.

4. The structural models which explain the polymeric nature of tantalum oxide alkoxides are directly related to the ones which were used to explain the behavior of the oxide alkoxides of titanium and zirconium. It appears, therefore, that these structures are of fundamental significance to metal oxide alkoxides in general.

ACKNOWLEDGMENTS

We are pleased to acknowledge the support of the Department of Scientific and Industrial Research through a Maintenance Grant (to H. H.).

REFERENCES

1. D. C. BRADLEY, R. GAZE, and W. WARDLAW. J. Chem. Soc. 3977 (1955).
2. D. C. BRADLEY, R. GAZE, and W. WARDLAW. J. Chem. Soc. 469 (1957).
3. D. C. BRADLEY and D. G. CARTER. Can. J. Chem. **39**, 1434 (1961).
4. D. C. BRADLEY and D. G. CARTER. Can. J. Chem. This issue.
5. D. C. BRADLEY and H. HOLLOWAY. Can. J. Chem. **39**, 1818 (1961).
6. D. C. BRADLEY, W. WARDLAW, and A. WHITLEY. J. Chem. Soc. 726 (1955).
7. D. C. BRADLEY, W. WARDLAW, and A. WHITLEY. J. Chem. Soc. 1139 (1956).
8. D. C. BRADLEY, B. N. CHAKRAVARTI, A. K. CHATTERJEE, W. WARDLAW, and A. WHITLEY. J. Chem. Soc. 99 (1958).
9. D. C. BRADLEY, W. WARDLAW, and A. WHITLEY. J. Chem. Soc. 5 (1956).

THE SOLUBILITY OF BERYLLIUM OXIDE IN AQUEOUS BERYLLIUM SULPHATE SOLUTIONS

S. L. Bennett and W. J. Biermann
The Parker Chemistry Laboratory, University of Manitoba, Winnipeg, Manitoba
Received July 21, 1961

ABSTRACT

It is observed that ignited beryllium oxide was soluble in concentrated aqueous solutions of beryllium sulphate to the extent of 1 mole of oxide per 2 moles sulphate, saturation being virtually complete within 6 hours at 180° C. Since the molar solubility of aluminum oxide is much lower under similar conditions, it is suggested that partial resolution of oxide mixtures might be made on this basis.

INTRODUCTION

The majority of processes for the preparation of beryllium compounds from beryllium minerals employ a fusion of the mineral, with or without a flux, giving a mixture of oxides which can be taken into solution, usually with sulphuric acid (1, 2). Because beryllium oxide is more slowly dissolved by acids than are the oxides of aluminum, iron, and other accompanying metallic elements, standard procedures involve complete solution of all the metallic constituents, followed by addition of a succession of reagents to remove these until only beryllium compounds remain in solution, at which point beryllium is precipitated as an hydroxide. A solvent having a selective action on beryllium oxide would seem to have potential application by simplifying the chemical metallurgy of beryllium, provided, however, that its net cost were not so great as to wipe out any economies which might be brought about through its use.

Aqueous solutions of beryllium salts are known to dissolve considerable quantities of the carbonate and hydroxide. Some time ago, Sidgwick and Lewis (3) found that upon addition of beryllium carbonate to a concentrated solution of beryllium sulphate, followed by boiling of the mixture to remove carbon dioxide, there is an increase in the solubility of beryllium sulphate. A polynuclear species was postulated in accordance with the data that 1 molecule of salt dissolved for every 4 molecules of oxide added. This suggested to us the possibility that some equivalent compound could be formed between beryllium oxide and soluble beryllium salts. Such a reaction, should it be possible to be brought about, promised to be relatively specific with respect to attack of beryllium oxide in a mixture of metallic oxides, provided no highly basic oxide were present.

EXPERIMENTAL

Both the "nuclear grade" beryllium oxide, supplied by A. D. MacKay, Inc., and the beryllium sulphate tetrahydrate, supplied by Fisher Scientific Co., were analyzed by standard procedures (4, 5) to confirm the absence of any significant amount of foreign material. A solution of beryllium sulphate tetrahydrate, saturated at 22.5° C (0.002704 mole $BeSO_4$/g of saturated solution or 28.41 g $BeSO_4$/100 g saturated solution), was prepared and it was verified that the ratio of equivalents of beryllium and sulphate was unity. The beryllium oxide was ignited to 900° C to insure that no hydroxide would be present.

About 0.5 ml of beryllium sulphate solution and an amount of ignited beryllium oxide slightly in excess of the amount that, from preliminary work, was anticipated to dissolve, were weighed into a piece of heavy-walled Pyrex glass tubing about 1 × 10 cm O.D. and sealed on one end. The excess of solid phase in all runs was taken as an indication that supersaturation effects were unlikely. After a tube was filled the second end was sealed with a flame and the tube placed inside a short length of iron pipe, which was then closed by screwing on perforated caps. The pipe was, of course, intended for the protection of personnel. A

number of these assemblies were then placed in an air thermostat, whose regulation was about ±1° C and then withdrawn after an appropriate time interval.

After cooling, the tubes were broken and the contents washed onto a filter with the aid of distilled water. The undissolved beryllium oxide was collected on the filter, ignited to 900° C, and weighed. This mass, when used in conjunction with the masses of the liquid and solid reactants and the known analysis of the beryllium sulphate solution, permitted a calculation of the mole ratio of beryllium oxide dissolved per mole of beryllium sulphate in the original charge.

Studies were made to show (*a*) the effect of temperature on the amount of beryllium oxide dissolved, as summarized by the upper curve in Fig. 1, (*b*) the effect of time on the amount of beryllium oxide dissolved, as summarized by the upper curve in Fig. 2, and (*c*) the effect of the concentration of beryllium sulphate on the amount of beryllium oxide dissolved, as summarized in Fig. 3. The essential data on which these curves are based are tabulated in Tables I, II, and III.

TABLE I

The effect of temperature on the number of moles of beryllium oxide and on the number of moles of aluminum oxide dissolved per mole of beryllium sulphate (The beryllium sulphate solution was saturated at 22.5° C and the time in all cases is 6 hours)

Temperature (° C)	Moles beryllium oxide dissolved per mole beryllium sulphate	Moles aluminum oxide dissolved per mole beryllium sulphate
90	0.182	
105	0.245	
120	0.299	
	0.314	
135	0.359	
	0.352	
150	0.378	
165	0.432	
180	0.454	0.0353
200	0.457	0.0345
215	0.454	0.0377
230	0.454	0.0396

TABLE II

The effect of time on the number of moles of beryllium oxide and on the number of moles of aluminum oxide dissolved per mole of beryllium sulphate (The beryllium sulphate was saturated at 22.5° C and the temperature in all cases is 180° C)

Time (hours)	Moles beryllium oxide dissolved per mole beryllium sulphate	Moles aluminum oxide dissolved per mole beryllium sulphate
3	0.310	0.0216
5	0.417	0.0261
6	0.454	0.0353
	0.452	
8	0.458	0.0311
19	0.480	0.0399
	0.489	
24	0.497	0.0382
96	0.492	—
134	0.501	—
144	—	0.0496

FIG. 1. The effect of temperature on the number of moles of beryllium oxide and on the number of moles of aluminum oxide dissolved per mole of beryllium sulphate. The beryllium sulphate solution was saturated at 22.5° C and the time in all cases is 6 hours.

FIG. 2. The effect of time on the number of moles of beryllium oxide and on the number of moles of aluminum oxide dissolved per mole of beryllium sulphate. The beryllium sulphate was saturated at 22.5° C and the temperature in all cases is 180° C.

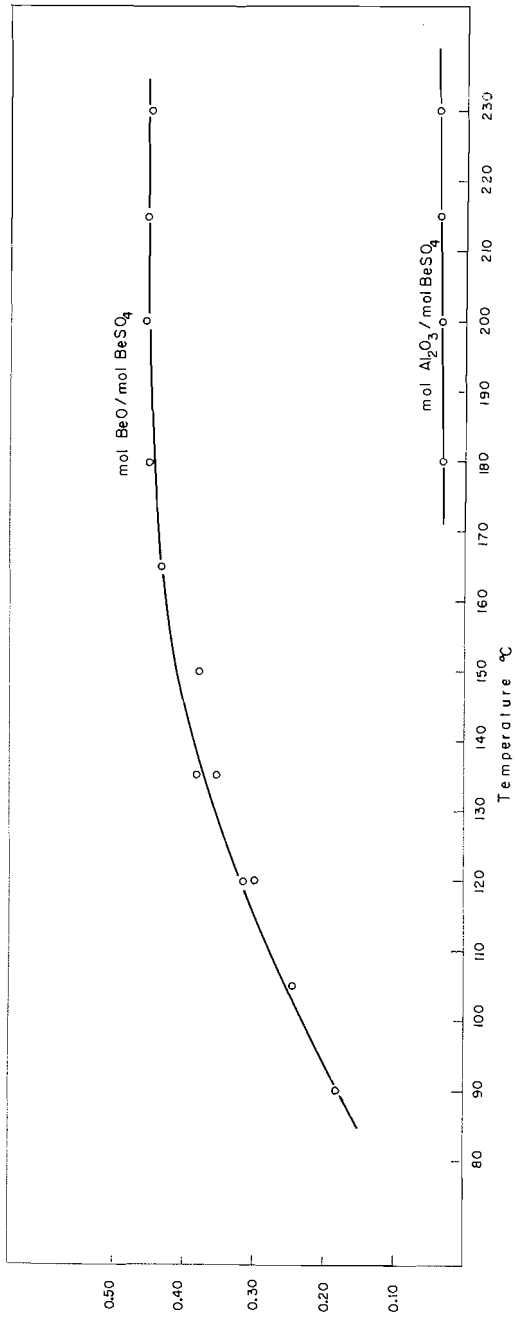

FIG. 1.

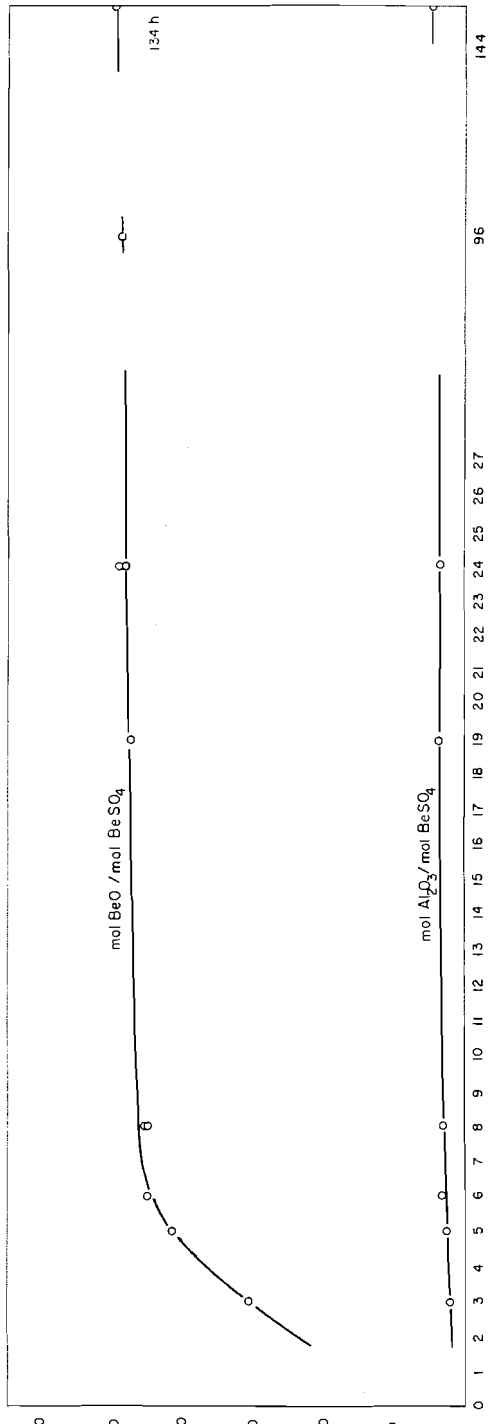

FIG. 2.

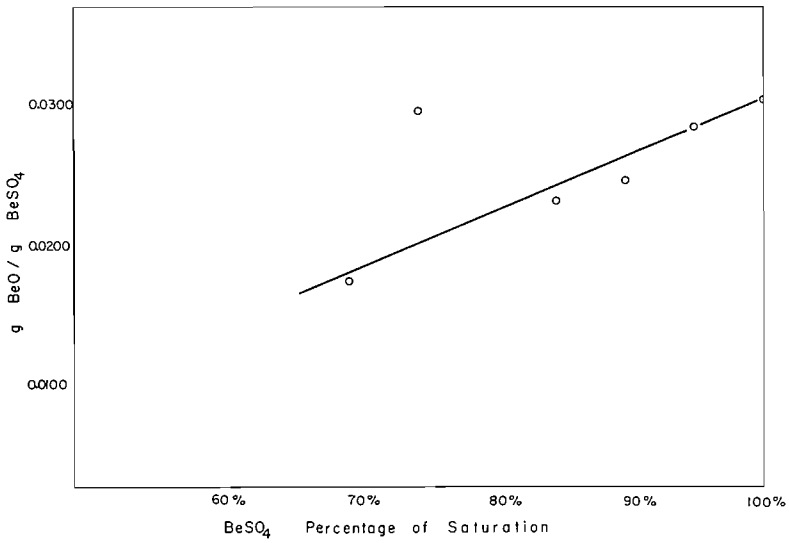

FIG. 3. The effect of the concentration of beryllium sulphate solution on the number of moles of beryllium oxide which will dissolve per mole of beryllium sulphate at 180° C in 6 hours.

TABLE III

The effect of the concentration of beryllium sulphate solution on the number of moles of beryllium oxide which will dissolve per mole of beryllium sulphate at 180° C in 6 hours

Concentration, relative saturation at 22.5° C = 100.0	Moles BeO dissolved per mole $BeSO_4$
70.9	0.355
75.1	0.589
84.4	0.410
92.3	0.396
95.5	0.444
100.0	0.454

Because aluminum and beryllium generally occur together in nature, and because of the general chemical similarity of this pair, ignited aluminum oxide was used as the solid reactant in a second series of determinations designed to give some indication of the amount of separation that could be expected. The lower curves of Figs. 1 and 2 summarize the effect of time and of temperature on the solubility of aluminum oxide in beryllium sulphate solutions. The numerical data on which these curves are based are contained in Tables I and II.

DISCUSSION

The data collected indicate that the optimum conditions for dissolving beryllium oxide in beryllium sulphate solutions are 180° C and a time of 6 hours; a high concentration of beryllium sulphate increased the rate of reaction considerably. Figures 1 and 2, and also some isolated runs not included here, indicate that some species with an empirical formula $2BeSO_4.BeO.xH_2O$, very stable in solution, is formed, the rate of formation being favored by high temperatures. The region of stability of this compound must be fairly extensive since highly diluted solutions obtained in washing the undissolved beryllium oxide onto a filter show no tendency to reprecipitate the dissolved beryllium oxide, even when allowed to stand for several months at room temperature. It seems unlikely that this apparent stability can be explained in terms of the inertness sometimes observed

with polynuclear species. Further studies of the chemical nature of this compound will be undertaken on the basis of inherent interest from a chemical, if not metallurgical, viewpoint.

The limited solubility of aluminum oxide is most likely due to its having a basicity similar to that of beryllium oxide and simply displacing some of the aquoberyllium ions from solution, the displaced beryllium then entering into polynuclear formation.

With the existence of a preferential solvent for beryllium oxide and suitable experimental conditions for its use established, this study will be continued by examining specific metallurgical situations in which it appears useful. One of the most obvious situations, of course, would be the partial resolution of the oxide mixture obtained when beryllium is fused and quenched.

ACKNOWLEDGMENT

The authors are much indebted to Sudbay Beryllium Mines, Ltd., for their generous support of our studies of the chemical metallurgy of beryllium.

REFERENCES

1. P. SILBER. *In* Nouveau traite de chimie minerale. Vol. IV. *Edited by* P. Pascal. Masson et Cie, Paris. 1958.
2. D. W. WHITE and J. E. BURKE (*Editors*). The metal beryllium. American Society for Metals, Cleveland, Ohio. 1955.
3. N. W. SIDGWICK and N. B. LEWIS. J. Chem. Soc. 1287 (1926).
4. L. G. BOSSETT and F. S. TOMKINS. *In* Analytical chemistry of the Manhattan project. *Edited by* C. J. Rodden. McGraw-Hill Book Co., Inc., New York. 1950.
5. J. A. VINCI. Anal. Chem. **25**, 1580 (1953).

THE ESTABLISHMENT OF CONFIGURATION IN DIELS–ALDER ADDUCTS BY N.M.R. SPECTROSCOPY[1]

ROBERT R. FRASER
The Department of Chemistry, University of Ottawa, Ottawa, Ontario
Received August 11, 1961

ABSTRACT

It has been shown that the magnetically anisotropic double bond in bicyclic Diels–Alder adducts exerts a paramagnetic effect on protons in an *exo* configuration and a diamagnetic effect on protons in an *endo* configuration. Thus the configuration of a proton or proton-bearing substituent can be ascertained by observing the change in its chemical shift when the double bond is removed by hydrogenation. However, caution must be used in applying the method to compounds in which the double bond bears a magnetically anisotropic substituent.

The Diels–Alder reaction between cyclic dienes and derivatives of ethylene may produce either of two diastereomeric adducts, the *endo* or the *exo* isomer. In most instances the *endo* isomer predominates in accordance with Alder's rule (1). However, exceptions to this rule have been observed (2, 3) so that each new adduct synthesized requires proof of its stereochemistry. Several chemical methods have been employed to establish the configuration of Diels–Alder adducts (4). Lactonization (5), iodolactonization (6), and titrimetric analysis (4) have been used for this purpose with carboxylic acid derivatives of bicyclo[2.2.1]hept-2-ene. The first two suffer the disadvantage that rearrangements do occur under the reaction conditions. Classical degradative procedures (7) are often unambiguous but exceedingly arduous.

The use of physical methods obviates both of these difficulties. Alder and co-workers (3) have employed infrared spectroscopy to assign configurations to the two 5-cyano-bicyclo[2.2.2]oct-2-enes formed from cyclohexadiene and acrylonitrile. Nuclear magnetic resonance has already proved itself capable of differentiating between diastereoisomers in cyclohexanes (8) and cyclopentanes (9) and between geometrical isomers in many olefin derivatives (10, 11). It therefore seemed worth while to investigate the ability of n.m.r. to be used in assigning structures to diastereomeric Diels–Alder adducts.

It has already been found that in the camphane-2,3-diols (12), in α and α' chloro-camphor (13), and in 3,8-cyclocamphor (14) the magnitude of the coupling of an *exo* proton with the adjacent bridgehead proton is larger (4–5 cycles/sec) than when the proton is *endo* (0–1 cycles/sec). Thus when such a proton is well separated from the rest of the absorption pattern, the size of its spin–spin interaction with the bridgehead proton will establish the configuration of the compound. A more general method would be possible if the chemical shift of a proton could be correlated with its *endo* or *exo* position. To explore this possibility we have examined the spectra of five derivatives of bicyclo[2.2.1]hept-2-ene whose configurations had been previously established (22). These are the two diastereomeric adducts of α-methacrylic acid and cyclopentadiene, the two adducts of *trans*-crotonic acid and cyclopentadiene, and the *exo* adduct of methyl methacrylate and cyclopentadiene. After removal of the double bond by hydrogenation, the spectra of the five dihydrocompounds were also measured.

[1]*This paper was presented at the 44th Annual Conference of the Chemical Institute of Canada, Montreal, Que., Aug. 3–5, 1961.*

The spectra of 5-*endo*-methylbicyclo[2.2.1]hept-2-ene-5-*exo*-carboxylic acid (I) and its dihydro derivative (II) are illustrated in Fig. 1. The assignments in A are as follows. The

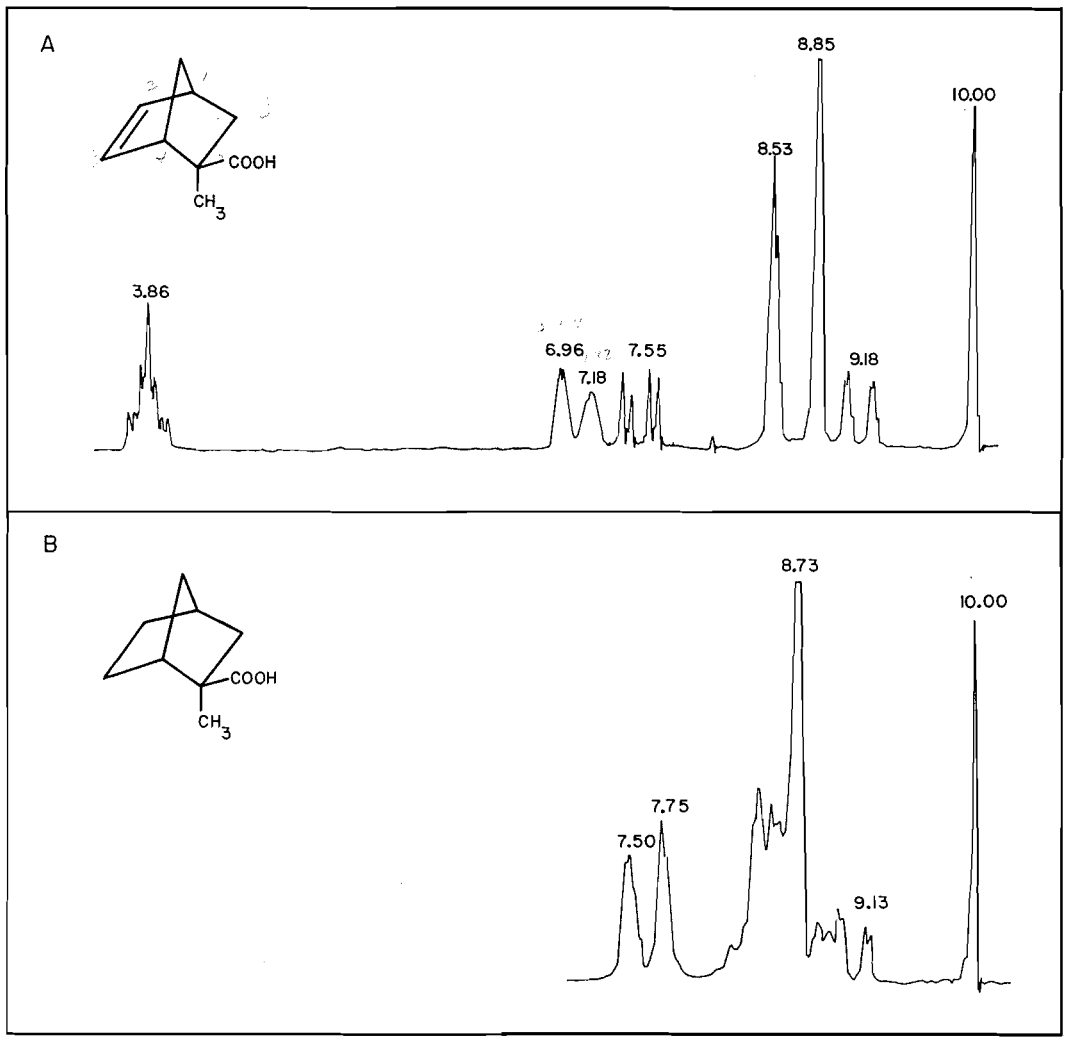

FIG. 1. (A) Spectrum of 5-*endo*-methylbicyclo[2.2.1]hept-2-ene-5-*exo*-carboxylic acid (I). (B) Spectrum of 5-*endo*-methylbicyclo[2.2.1]heptane-5-*exo*-carboxylic acid (II). The chemical shifts are given as τ values.

multiplet at low field has a τ value of 3.86, characteristic of protons attached to a carbon–carbon double bond (15). The two broad peaks at 6.96 and 7.18 τ are assigned to the two bridgehead protons at C_4 and C_1 (15), although the reverse assignment is not excluded. The quartet centered at 7.55 τ represents a proton coupled by 12.0 and 3.8 cycles/sec with two other protons. One of these must be the proton at 9.18 τ, which also possesses a 12.0 cycles/sec splitting. The second must be one of the bridgehead protons, as is indicated by the pronounced skewness of the two doublets at 7.55 τ. The peak at 7.55 τ is assigned to the proton in the *exo* C_6 position and the peak at 9.18 τ to the proton in the *endo* C_6 position. This accounts for the large 12.0 cycles/sec geminal coupling constant (16) and the *exo* bridgehead coupling constant of 3.8 cycles/sec. Under

very slow sweep each portion of the doublet at 9.18 τ appeared to be further split into a triplet of spacing 1.0 cycle/sec. This suggests that the *endo* C_6 proton is weakly coupled with a proton two carbons removed, in addition to being coupled slightly with the bridgehead proton. Similar long range coupling has been observed in this ring system previously (12). The remaining peaks at 8.53 and 8.85 τ are assigned, on the basis of their relative intensities, to the hydrogens at C_7 and the methyl group at C_5 respectively. The proton on the carboxyl group occurs at -2.45 and is not shown in the figure.

The spectrum of the hydrogenated adduct (II) shows fewer well-resolved peaks. The two peaks at 7.50 and 7.75 τ are assigned to the protons at the bridgehead positions. The *exo* proton absorption is likely obscured by one of these, presumably the more intense band at 7.75 τ. This assumption is supported by the spectrum of II in benzene, in which solvent a part of the *exo* multiplet is visible between the two bridgehead peaks. The only other identifiable bands are the methyl absorption at 8.73 τ and the band due to the *endo* C_6 proton at 9.13 τ. This is a pair of doublets of spacings 12.0 and 1.0 cycles/sec. The spectra of the other four adducts and their dihydroderivatives were examined and the assignments for individual protons were made in the same way. The chemical shifts of the protons in each of the compounds is given in Fig. 2. Blank spaces are present wherever the proton was not sufficiently separated to allow an unambiguous assignment.

Compound	Olefinic	Bridgehead	Hx	Hn	C_7-H_2	CH_3
I	3.86	6.96, 7.18	7.55	9.18	8.53	8.85
II		7.50, 7.75		9.13		8.73
III	3.88	7.22	8.72	8.08		8.53
IV		7.79				8.71
V	3.87	6.89, 7.55	7.65	8.24	8.51	8.81
VI		7.46, 8.10	7.79			9.03
VII	3.85	6.99, 7.31	7.61		8.34	9.06
VIII		7.54, 7.92				8.94
IX	3.92	6.37 ($COOCH_3$) 7.04, 7.23	7.59	9.22	8.62	8.94
X		6.42 ($COOCH_3$) 7.58, 7.77		9.19		8.81

FIG. 2. The chemical shifts of all identifiable protons in compounds I–X.

From the beginning it was recognized that the absolute τ value of a proton could not be used to assign its configuration. However, much is now known about the neighboring anisotropy effect from a study of aromatic rings (10, p. 176) and Jackman (17) has cited evidence indicating that a double bond also possesses an appreciable anisotropy. By this effect the absorption frequency of protons which lie above the plane of a double bond* are shifted upfield whereas a downfield frequency shift is experienced by protons which lie in the plane of the double bond (17). Figure 3 illustrates this diagrammatically. Therefore, because it is anisotropic, the double bond in any Diels–Alder adduct will provide

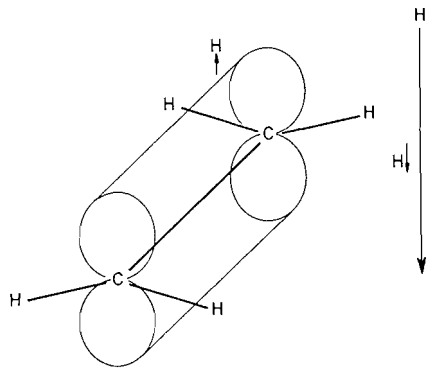

FIG. 3. A diagrammatic illustration of the magnetic anisotropy of the olefinic bond in ethylene. In the presence of a strong field *H*, the proton situated above the plane of the sp^2 bonds experiences a diamagnetic shielding. The proton at the right in the sp^2-bond plane is deshielded by the double bond.

a contribution to the total shielding of all neighboring protons, which will depend in magnitude and in sign upon the spatial position of the proton with respect to the double bond. In the bicyclo[2.2.1]hept-2-enes an *exo* proton is in a position approximately in the plane of the double bond and should therefore be shifted downfield by it. When the double bond is removed by hydrogenation the chemical shift of this *exo* proton should now be at higher field. In other words, if the τ value for the proton in the adduct is τ_1, and in the dihydro adduct is τ_2, then $\Delta\tau = \tau_2 - \tau_1$ represents the change in chemical shift upon hydrogenation and should be positive for an *exo* proton. Since the *endo* proton lies well above the plane of the double bond it should experience a negative $\Delta\tau$ upon hydrogenation. From the data in Fig. 2, all the $\Delta\tau$ values observable for protons in the *exo* and *endo* positions are compiled in Table I. It can be seen that when the proton or

TABLE I

Change in chemical shift ($\Delta\tau$) on hydrogenation

Compounds	H_{endo}	H_{exo}	$CH_{3\ endo}$	$CH_{3\ exo}$
I → II	−.05		−.12	
III → IV				+.18
V → VI		+.14		+.22
VII → VIII			−.12	
IX → X	−.03		−.13	+.05 (ester methyl)

proton-bearing methyl group is *exo* then $\Delta\tau$ is positive, when the proton or methyl group is *endo* then $\Delta\tau$ is negative.

**The "plane of the double bond" refers to the plane passing through the two carbon atoms of the double bond and the four atoms bonded to them.*

The theoretical relation of $\Delta\sigma$, the contribution of anisotropy to the total screening of the proton, with the distance R of the proton from the center of the double bond and the angle θ which the line joining the proton to the center of the double bond makes with the plane of the double bond can be written $\Delta\sigma = k(1/R^3)(1-3\cos^2\theta)$, where k is a constant proportional to the difference in the magnetic susceptibilities in the plane of and perpendicular to the double bond (10, p. 178). From Barton models θ_{exo} was estimated to be 25°, θ_{endo} 60°. The ratio R_{exo}/R_{endo} was measured and found to be 1.26. From these estimates $\Delta\sigma_{exo}/\Delta\sigma_{endo}$ is calculated from the above relationship to be -3.0. This is in reasonable agreement with the observed ratio of $\Delta\tau_{exo}/\Delta\tau_{endo}$, which was $0.14/-0.04 = -3.5$. This provides further justification for the reliability of our results.

We have used the method to establish the configuration of the nitro group in 5-nitronorbornene. This compound was prepared by the addition of nitroethylene to cyclopentadiene following the procedure of Roberts and co-workers (18). The spectra of 5-nitronorbornene and 5-nitronorbornane are reproduced in Fig. 4. In the 5-nitronorbornene spectrum the peaks at 3.87, 5.07, 6.47, and 7.01 τ are assigned to the olefinic protons, the proton on C_5, and the two bridgehead protons, in that order. The multiplet at higher field represents the remaining four protons. The proton at C_5 appears as a quintet of spacing 3.9 cycles/sec. Its structure is attributed to strong coupling (7.8 cycles/sec) with the *exo* proton at C_6 and weak coupling (3.9 cycles/sec) with both the *endo* proton at C_6 and the bridgehead proton at C_4. The magnitude of the C_4–C_5 proton–proton coupling constant indicates that the proton on C_5 is *exo* and that the nitro group is therefore *endo*. The fact that this quintet is shifted upfield upon hydrogenation by 12 cycles/sec ($\Delta\tau = +0.2$) corroborates this conclusion. Thus Robert's tentative assignment of the nitro group to the *endo* position (18) is confirmed.

It is interesting to note that the *endo* and *exo* adducts of benzyne to bicycloheptadiene show the same behavior in their n.m.r. spectra. Simmons (19) has recently published the spectra of both adducts and their hydrogenation products. His data shows that when the aromatic ring is *exo*, $\Delta\tau = +0.05$ for the aromatic protons, and when the ring is *endo* $\Delta\tau = -0.20$. The application of this method need not be confined to the bicyclo[2.2.1]heptane system. In fact we have observed the same behavior in the bicyclo-[2.2.2]octane system (20). The main limitation to its use will be the ability to observe and identify the desired protons in the spectra of both the adduct and its hydrogenation product. It should be noted that, if the double bond bears a substituent other than hydrogen, the method will not necessarily be applicable, especially if the substituent possesses an appreciable magnetic anisotropy. In this case the change in position of this substituent on hydrogenation could produce a greater effect than the removal of the double bond.

EXPERIMENTAL

All spectra were recorded on a Varian V-4302 high-resolution n.m.r. spectrometer operating at a radio frequency of 60 Mc/sec. All spectra were measured on 10% (w/v) solutions in carbon tetrachloride containing 1% of tetramethylsilane as an internal standard. Calibrations were performed by the side-band technique (10, p. 74). All τ values which were employed in calculating $\Delta\tau$'s are the average of six determinations and are accurate to ± 0.6 cycles/sec. The remaining τ values are the average of two determinations and are probably accurate to within 1 cycle/sec.

With the exception of the methyl esters described below, all the compounds were prepared by Alder's procedure (22). The nitroethylene used in the preparation of 5-nitronorbornene was prepared as previously described (21).

5-endo-Methyl-5-exo-carbomethoxybicyclo[2.2.1]hept-2-ene (IX)

To a solution of 1.3 g of 5-*endo*-methylbicyclo[2.2.1]hept-2-ene-5-*exo*-carboxylic acid in 5 ml of ether was added an ethereal solution of diazomethane until the yellow color of diazomethane persisted. The

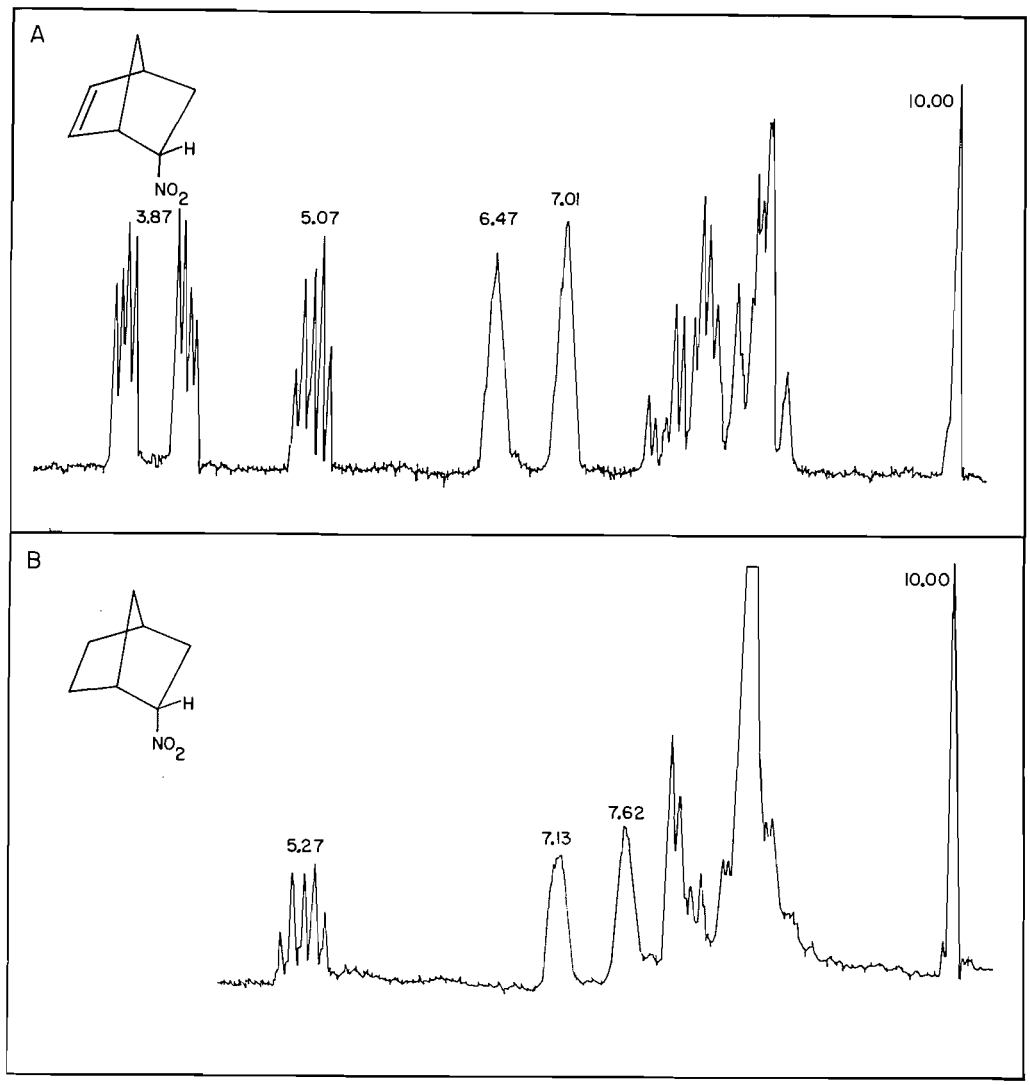

FIG. 4. (A) Spectrum of 5-nitronorbornene. (B) Spectrum of 5-nitronorbornane.

excess of diazomethane and ether was removed by distillation and the residue, 1.3 g, was distilled under reduced pressure to give 1.05 g of liquid, b.p. 62°, 5 mm. Both the infrared and n.m.r. spectra of this liquid showed no trace of an impurity and were completely consistent with the structure IX. Calc. for $C_{10}H_{14}O_2$: C, 73.2; H, 8.5. Found: C, 71.0, 70.8; H, 8.3, 8.1. Repeated analysis gave consistently low C and H values, which is attributed to the very high volatility of this compound.

5-endo-Methyl-5-exo-carbomethoxybicyclo[2.2.1]heptane (X)

A solution of 293 mg of IX in 7 ml of ethyl acetate was added to 7 ml of ethyl acetate containing 29.5 mg of prehydrogenated platinum dioxide in a hydrogenation apparatus. The mixture was stirred at room temperature until the uptake of hydrogen had ceased. The catalyst was removed by filtration through celite and the ethyl acetate was distilled off. The residue, 290 mg, was distilled in a capillary under a reduced pressure of 7 mm. The infrared spectrum of the distillate did not absorb above 3000 cm^{-1}. Calc. for $C_{10}H_{16}O_2$: C, 71.4; H, 9.6. Found: C, 71.8; H, 9.5.

ACKNOWLEDGMENTS

The author wishes to express his thanks to the Imperial Oil Company of Canada for a grant in aid of this research. The financial assistance of the National Research

Council of Canada is also acknowledged. The technical assistance of Mrs. L. Westland and Mrs. N. Stojanac was of great aid to this work. Microanalyses were determined by Miss E. Busk.

REFERENCES

1. K. ALDER and G. STEIN. Angew. Chem. **50**, 510 (1937).
2. M. SCHWARZ and M. MAIENTHAL. J. Org. Chem. **25**, 449 (1960).
3. K. ALDER, K. HEIMBACH, and R. REUBKE. Ber. **91**, 1516 (1958).
4. H. STOCKMANN. J. Org. Chem. **26**, 2025 (1961).
5. S. BECKMANN and H. GEIGER. Ber. **94**, 48 (1961).
6. C. S. RONDESTVEDT, JR. and C. D. VER NOOY. J. Am. Chem. Soc. **77**, 4878 (1955).
7. K. ALDER and S. SCHNEIDER. Ann. **524**, 189 (1936).
8. R. U. LEMIEUX, R. K. KULLNIG, H. J. BERNSTEIN, and W. G. SCHNEIDER. J. Am. Chem. Soc. **80**, 6098 (1958).
9. D. Y. CURTIN, H. GRUEN, and B. A. SHOULDERS. Chem. & Ind. 1205 (1958).
10. J. A. POPLE, W. G. SCHNEIDER, and H. J. BERNSTEIN. High resolution nuclear magnetic resonance. McGraw-Hill Book Co., Inc., New York. 1959. p. 238.
11. L. M. JACKMAN and R. H. WILEY. J. Chem. Soc. 2881 (1960).
12. F. A. L. ANET. Can. J. Chem. **39**, 789 (1961).
13. W. D. KUMLER, J. N. SHOOLERY, and F. V. BRUTCHER, JR. J. Am. Chem. Soc. **80**, 2533 (1958).
14. E. J. COREY, M. OHNO, S. W. CHOW, and R. A. SCHERRER. J. Am. Chem. Soc. **81**, 6305(1959).
15. G. V. D. TIERS. N.M.R. summary. Minnesota Mining and Manufacturing Co., St. Paul, Minn. 1958.
16. H. S. GUTOWSKY, M. KARPLUS, and D. M. GRANT. J. Chem. Phys. **31**, 1278 (1959).
17. L. M. JACKMAN. Applications of nuclear magnetic resonance spectroscopy in organic chemistry. Pergamon Press, New York. 1959. p. 129.
18. J. D. ROBERTS, C. C. LEE, and W. H. SAUNDERS, JR. J. Am. Chem. Soc. **76**, 4501 (1954).
19. H. E. SIMMONS. J. Am. Chem. Soc. **83**, 1657 (1961).
20. R. R. FRASER and S. O'FARRELL. Unpublished results.
21. R. R. FRASER. Can. J. Chem. **38**, 2226 (1960).
22. K. ALDER and W. GUNZL. Chem. Ber. **93**, 809 (1960).

INFRARED ABSORPTION OF FORMALDEHYDE AT LOW TEMPERATURES

EVIDENCE FOR MULTIPLE TRAPPING SITES IN AN ARGON MATRIX

K. B. HARVEY AND J. F. OGILVIE[1]

The Department of Chemistry, University of British Columbia, Vancouver, British Columbia

Received September 22, 1961

ABSTRACT

The infrared absorption of formaldehyde in both the polycrystalline and the monomeric form has been measured at 4° K. In the latter case the molecules were suspended in an inert matrix of Ar or N_2. The fine structure of the matrix spectra is discussed from the point of view of rotation of the monomers but this interpretation is ruled out in favor of one based on multiple trapping sites in the matrix.

INTRODUCTION

In the past few years, the matrix isolation technique has become established as one of the principal aids in the investigation of free radicals and other chemically reactive species (1, 2, 3). More recently, however, interest has arisen in the physical aspects of the matrix environment particularly as related to the spectra of the trapped molecules. Milligan and his co-workers have published infrared evidence for the rotation of H_2O, D_2O, HDO (4), and NH_3 (5) in inert-gas matrices and were able in the latter case to assign the rotational transitions. Glasel (6) placed the same interpretation on fine structure observed in the O—H stretching region of H_2O in matrices of Xe and Ar. In the field of electronic spectroscopy, Robinson and McCarty have explained the spectrum of trapped NH_2 radicals in terms of rotation (7), and have achieved also considerable success in the theoretical interpretation of spectral shifts using a Lennard-Jones (6–12) potential function to represent the interaction between the trapped atoms or simple molecules and the matrix (8). The present high-resolution infrared study was undertaken with a view to providing further information on the interactions which take place between the matrix and trapped molecules. In particular, it provides optical spectroscopic evidence for multiple trapping sites, a feature which has also been investigated by electron spin resonance (9, 10).

EXPERIMENTAL

The low-temperature cell constructed for this work is basically of the Duerig–Mador type (11) equipped with optical windows of cesium iodide. The only major modification is a rotatable liquid helium chamber which makes it possible to spray the gaseous sample onto the trapping surface from the side rather than from below. A Au–Cu:Ag–Au thermocouple mounted directly below the cesium iodide trapping surface enables us to measure the approximate temperature of the sample during warmup.

Gaseous mixtures to be investigated were prepared in 5-liter bulbs in ratios determined by the partial pressures of the components. It is interesting that, even though the dilute component was introduced first, proper mixing of the components was not a trivial consideration. It was found necessary to heat parts of the bulb to produce convection currents to ensure effective mixing, and even then care had to be exercised to make certain that no pockets of pure formaldehyde were trapped in side arms etc. No attempt was made to measure absolute flow rates during the deposition of the sample, but reproducible conditions could be obtained through pressure measurements on the low-pressure side of the controlling needle valve.

The formaldehyde vapor was produced by heating paraformaldehyde (polyoxymethylene) until the required pressure of vapor was obtained in the bulb. Considerable care was taken to make certain that the paraformaldehyde contained a minimum of water, as indicated by its infrared spectrum. The purest material was that precipitated from a basic formalin solution (12) and then well dried under vacuum. Absorption in the O—H stretching region was very weak and since the O—H units terminate the chains, we were led to

[1]*Present address: Department of Physical Chemistry, University of Cambridge, Cambridge, England.*

the conclusion that the polymer units were quite large. This was further substantiated by the very weak intensity of the band attributable to the C—O stretching mode of the methoxyl group, also at the end of the chain. The matrix materials, Ar and N_2, were analyzed mass spectrometrically and contained less than 40 p.p.m. impurities. They were admitted directly from the gas cylinders, through an evacuated capillary, to the sample bulb to avoid the introduction of impurities through the use of a gas regulator.

Spectroscopic measurements were carried out on a Perkin–Elmer 112G spectrometer with a modified source unit. Calibration was effected through established grating spectra and the reported frequencies are estimated to be precise to ± 2 cm^{-1}. Spectral slit widths are indicated on the individual spectra.

RESULTS

In addition to the matrix isolation spectra, we examined the spectrum of polycrystalline formaldehyde at 4° K and 77° K. Figure 1 shows the more interesting spectra, and the

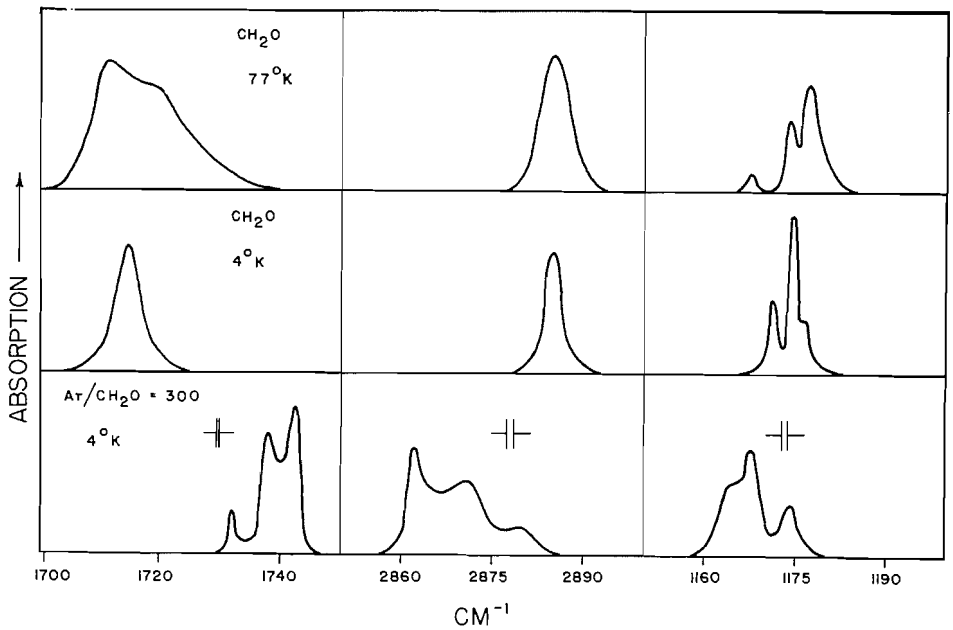

FIG. 1. The fundamentals ν_2, ν_4, and ν_6. Upper spectra are of normal associated CH_2O at 77° K and 4° K, lower spectrum is that of monomer dispersed in argon matrix at 4° K.

observed bands are summarized completely in Table I along with the gas phase measurements of Blau and Nielson (13) and previous low-temperature spectra of Schneider and Bernstein (14). Our results differ significantly from those of the latter authors in the fine structure observed in some of the bands, probably because of the higher resolution and lower temperatures used in our work. None of these lines coincide with those of the higher-temperature modification reported by Schneider and Bernstein, nor did we observe any effects to indicate the presence of two crystalline forms. On the other hand, our films were probably deposited much more slowly and we did not extensively investigate the effect of temperature on the spectrum. Our primary interest was in obtaining spectra of associated molecules at low temperatures for comparison with the matrix spectra.

With regard to the matrix spectra, our chief concern must be to estimate the degree of isolation attained. This can be done in a number of ways, all of which lead us to the conclusion that the matrix spectra are those of isolated monomers. That little or none of the normal associated species is present is confirmed by an inspection of the fundamentals ν_1 and ν_2. In these cases, the shifts from polycrystalline solid to matrix are quite

TABLE I

Infrared absorption of formaldehyde (frequencies in cm^{-1})*

Mode	Blau and Neilson	Schneider and Bernstein	This work			
					Matrix	
	gas	77° K	77° K	4° K	Ar	N_2
					2809.5m	2808w
					2800.5m	
$\nu_1(\nu CH)a_1$	2766.4	2834s	2829vs	2829vs	2796vs	2799s
			1720sh			
$\nu_2(\nu CO)a_1$	1746.0	1712s	1711vs	1715vs	1742vs	
					1738s	1739m
					1732m	1736.5m
			1506sh			
$\nu_3(\delta CH_2)a_1$	1500.6	1491s	1495vs	1494vs	1498m	1495
			1490sh			
					2880m	
					2871w	
$\nu_4(\nu CH)b_1$	2843.4	2890s	2885s	2885s	2862s	2865m
$\nu_5(\rho CH_2)b_1$	1247.4	1247m	1250vs	1250vs	1245w	
			1246s	1246s	1247vw	
			1239.5w	1244sh		
				1241w		
				1176sh	1174vw	
$\nu_6(\omega CH_2)b_2$	1163.5	1177w	1177s	1174.5m	1167.5m	
			1174m	1172w	1164w	
			1167.5vw			
$2\nu_2a_1$		3414w	3402w	3404w		
$2\nu_3a_1$		2960m				
$(\nu_2+\nu_5)b_1$	3003.3	2997s	2991vs	2993m	2996m	
$(\nu_3+\nu_5)b_1$		2729w	2727m	2727w	2718w	2720w
					2721sh	
$(\nu_1+\nu_2)a_1$			4535vw	4545vw		
			4539sh			
$(\nu_2+\nu_4)b_1$			4562w	4562vw		

*The approximate relative intensities are quoted after the frequencies of absorption according to the following abbreviations: vs = very strong, s = strong, m = medium, w = weak, vw = very weak; sh = shoulder.

large and any associated species in the matrix would be readily detected. The presence of smaller polymer units (dimers, trimers, etc.) was investigated by varying the matrix ratio or rate of deposition, and by observing the spectrum of the deposit as it warmed. The mixture used in most cases was $Ar/CH_2O = 300$ but if this were reduced below 100 or so, then spectra of the type shown in Fig. 2 were observed. In the warmup spectra, it will be seen that the lines assigned to monomers disappear as the broadened bands due to absorption by polymers grow in intensity. We may, therefore, assume with reasonable certainty that the absorption of interest is due to monomers.

DISCUSSION

Polycrystalline Solid

There are several possible explanations for the fine structure observed in the spectrum of the crystalline solid. The fundamentals ν_2 and ν_3 both become considerably narrower as the temperature is lowered from 77° K to 4° K, suggesting a rotational envelope decreased in width by the depopulation of upper rotational levels. This interpretation is ruled out, however, by the n.m.r. spectrum at 77° K.* Alternatively, some of the weaker

**These spectra were very kindly run for us by Mr. D. Gilson on samples of formaldehyde specially prepared by double distillation. The observed doublet splitting was of the order of 7 gauss, much larger than the 3 gauss expected if the proton pair in CH_2O were rotating.*

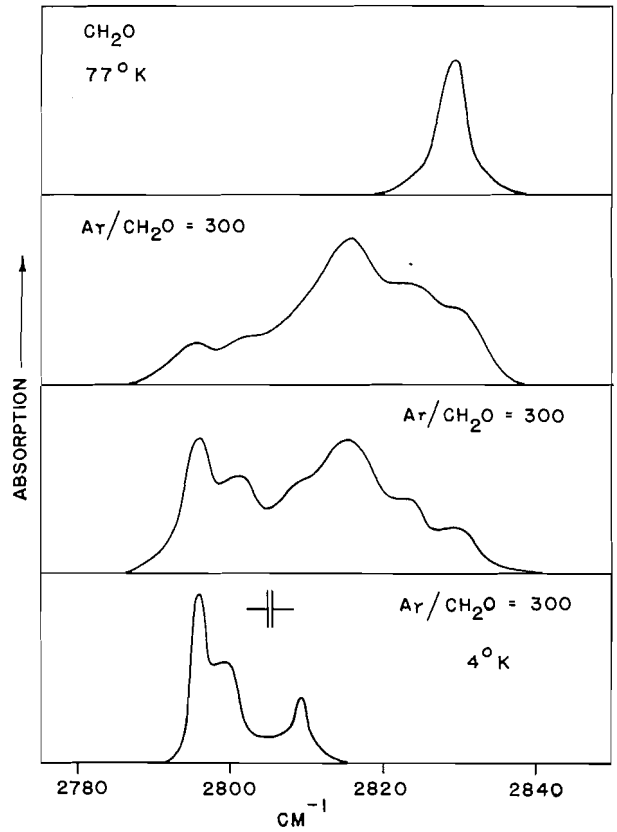

FIG. 2. Behavior of ν_1 fundamental during warmup of the deposit. Lowest spectrum is that of monomer at 4° K dispersed in argon and uppermost is that of normal associated CH_2O at 77° K. The middle two are matrix spectra at intermediate temperatures (about 35 and 50° K).

lines may be due to the presence of the isotopic species $C^{13}H_2O$, which has a natural abundance of about 1%. The expected shifts may be readily estimated for the two vibrations of species b_1 using the FG matrix method and introducing the appropriate symmetry co-ordinates. The calculated shifts were found to be -12 cm^{-1} and -9 cm^{-1} for ν_4 and ν_5 respectively. For the out-of-plane bending mode ν_6, the calculated shift was -12 cm^{-1}. It is possible then, that the weak lines at 1167.5 cm^{-1} and 1241 cm^{-1} are due to the presence of $C^{13}H_2O$. The lack of a corresponding line for ν_4 might be due to the low relative intensity of this mode. On the other hand, even if this assignment to isotopic species is correct, a number of lines remain unassigned. These are likely due to intermolecular effects, but since the crystal structure of formaldehyde is unknown, little can be done in the way of interpretation. They might arise, for example, from the existence of crystallographically non-equivalent molecules in the unit cell.

Matrix Spectra

Dealing with the argon matrix spectra first, it is noted that for four of the six fundamentals a triplet structure is observed. Only ν_3 and ν_5 lack this structure and in these two cases, the shift ν_{solid} to ν_{gas} is very small. Furthermore, the shapes of these bands are such as to suggest a closely spaced, unresolved fine structure. These observations alone tend to rule out rotation as the cause of the fine structure but this can be shown even more convincingly by considering the spectrum to be expected in the case of rotation.

Using the rotational constants of Lawrence and Strandberg (15), and treating the formaldehyde molecule as a prolate symmetric top (16), one may calculate the first few rotational energy levels. These are listed in Table II along with the appropriate Boltzmann

TABLE II
Rotational energy levels of formaldehyde

		Boltzmann factors	
$F(J,K)$	E (cm^{-1})	4° K (eq.)	4° K ($A \leftrightarrow B$)
(0,0)	0	1	1
(1,0)	2.44	0.42	0.42
(2,0)	7.32	0.07	0.07
(1,1)	10.63	0.01	1
(2,1)	15.51	0.01	0.17

factors. If thermal equilibrium obtains, then only the two lowest levels are significantly populated at 4° K so that the number of observable transitions is severely limited. For parallel bands (ν_1, ν_2, ν_3) the selection rules are: $\Delta K = 0$, $\Delta J = 0, \pm 1$ if $K \neq 0$ and $\Delta K = 0$, $\Delta J = \pm 1$ if $K = 0$; and three transitions $R(0,0)$, $R(1,0)$, and $P(1,0)$ are permitted. In the case of perpendicular bands (ν_4 and ν_5), $\Delta K = \pm 1$, $\Delta J = 0, \pm 1$ so that a Q branch is allowed and the transitions would be $Q(1,0)$, $R(0,0)$, and $R(1,0)$. The remaining vibration, ν_6, while of a different symmetry, may also be considered a perpendicular band in this approximation. Thus, if the trapped formaldehyde molecules were rotating, we might expect to see fine structure, as illustrated in Fig. 3.

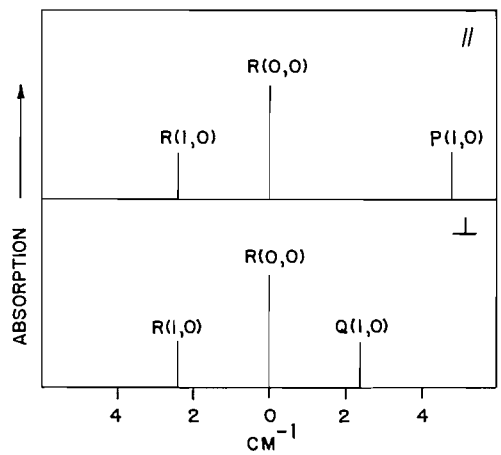

FIG. 3. Calculated rotational structure of parallel and perpendicular bands of CH_2O in thermal equilibrium at 4° K.

Comparison of the calculated fine structure with that observed reveals no agreement other than the fact that they are both triplets. Not only are the observed spacings far too large, but ν_1 and ν_2, which are of the same symmetry, do not exhibit the same band structure. A number of refinements might be considered in the theoretical treatment but these only serve to worsen the agreement. If, for example, the selection rule ortho $\leftrightarrow$ para were not violated during the freezing process, then a state of thermal non-equilibrium would be expected in which the (1,1) and (2,1) levels would also have a significant population. (These levels correlate with levels of species B in the more accurate asymmetric

rotor treatment while the (0,0) and (1,0) levels are of species A.) The main effect of this on the calculated spectra would be to introduce a Q branch into the parallel band and a P branch into the perpendicular band, giving more lines than observed. A similar situation would obtain if some of the selection rules were violated or if the rotational temperature were higher than 4° K. Alternatively, if the motion of the molecule were hindered in such a way that rotation about only one axis were allowed, the band structure would be like that of a linear or diatomic molecule. This would be a series of lines with a regular spacing of about 2.5 cm^{-1} or 18 cm^{-1} depending on the axis of rotation. Such an interpretation, like the others discussed, fails to account for the observed spectra so we must rule out rotation as the cause of the fine structure.

On the other hand, a strong argument can be presented for multiple trapping sites. In the three best-resolved bands, ν_1, ν_2, and ν_4, it is seen that the strongest lines are nearest to the gas phase absorption frequency while the weaker lines are shifted in the direction of the frequency of absorption in the polycrystalline solid. This suggests that the molecules are trapped in three types of holes of different sizes. The majority of the molecules occupy the largest type of hole and, being least perturbed, absorb at a frequency closest to that observed for the gas. A lesser number of molecules are present in somewhat smaller holes where the packing is more like that existing in the polycrystalline solid. From the small size of the gas-to-solid shifts for ν_3 and ν_5 it can be deduced that these vibrations are least perturbed by the close-packed environment of a solid. Hence the triplet splitting in the matrix spectrum should be small in these cases, in agreement with observation.

In speculating on the nature of the trapping sites, it is interesting to compare the present work with that of Foner *et al.*, who reported the trapping of hydrogen atoms on both substitutional and interstitial sites in inert-gas matrices. Specifically, they proposed that in these cubic close-packed structures, hydrogen atoms occupy substitutional sites and octahedral holes in both argon and xenon and possibly also tetrahedral holes in xenon. The sizes of these holes in argon are

$$r_{sub} = 1.88 \text{ Å}, r_{oct} = 0.77 \text{ Å}, r_{tet} = 0.43 \text{ Å},$$

so that a hydrogen atom may apparently squeeze into a hole considerably smaller than its own van der Waals radius (1.2 Å). The fact that the size of the tetrahedral hole in xenon is about the same as that of the octahedral hole in argon suggests that this is about the minimum size of hole which can accommodate a hydrogen atom. Taking into account the much larger size of the formaldehyde molecule it seems extremely unlikely that it could be accommodated in anything smaller than the environment of a substitutional site in argon. The distortion required to accommodate a formaldehyde molecule in an octahedral hole would likely be so large that the site would simply lose its identity as an octahedral hole and become a substitutional site. It is proposed, therefore, that the lines at 2809.5 cm^{-1}, 1732 cm^{-1}, and 2880 cm^{-1} in ν_1, ν_2, ν_4, respectively, be assigned to absorption by formaldehyde molecules replacing a single argon atom in the cubic close-packed structure. The remaining lines must be assigned to absorption by formaldehyde molecules occupying larger holes, presumably those in which two and three argon atoms are displaced. The environment of these sites would be such as to prevent rotation while still allowing greater freedom of vibration.

The spectrum exhibited by formaldehyde in a nitrogen matrix is less complex than that in argon. This was not unexpected since others have reported similar phenomena (4) and we have observed it ourselves for H_2O and D_2O. On the basis of the observed spectra,

it would appear that two types of sites are occupied but it is difficult to specify what these might be. In solid α nitrogen, which is the stable form below 35° K, the arrangement of the molecule centers is face-centered cubic with the axes of the molecules inclined at the tetrahedral angle to one another (17). The cylindrical substitutional site with a radius of about 1.5 Å and a length of approximately 4 Å, could probably accommodate a formaldehyde molecule with a small amount of distortion of the N_2 lattice. The other hole would have to be larger and likely corresponds to the case in which a formaldehyde molecule replaces two N_2 molecules.

ACKNOWLEDGMENTS

The authors are indebted to Mr. Rudolf Muelchen for his very capable assistance in the construction and maintenace of the apparatus. We wish also to thank Dr. R. Snider for many helpful discussions and Professor C. A. McDowell for criticizing the manuscript. The financial assistance of the National Research Council of Canada is gratefully acknowledged.

RÉSUMÉ

On a mesuré l'absorption infrarouge de formaldéhyde à 4° K dans l'état polycristallin et de forme monomérique. Dans le dernier cas, les molécules ont été suspendues dans une matrice inerte d'argon ou d'azote. Les fondamentales des monomères ont une structure qui suggère une rotation des molécules, mais cette interprétation est à écarter en faveur d'une explication basée sur l'existence de plusieurs emplacements différents dans la matrice.

REFERENCES

1. A. M. Bass and H. P. Broida. Formation and trapping of free radicals. Academic Press, New York. 1960.
2. E. D. Becker and G. C. Pimentel. J. Chem. Phys. **25**, 224 (1956).
3. G. C. Pimentel. Spectrochim. Acta, **12**, 94 (1958).
4. C. Catalano and D. E. Milligan. J. Chem. Phys. **30**, 45 (1959).
5. D. E. Milligan, R. M. Hexter, and K. Dressler. J. Chem. Phys. **34**, 1009 (1961).
6. J. A. Glasel. J. Chem. Phys. **33**, 252 (1960).
7. G. W. Robinson and M. McCarty. J. Chem. Phys. **30**, 999 (1959).
8. M. McCarty and G. W. Robinson. Mol. Phys. **2**, 415 (1959).
9. S. N. Foner, E. L. Cochrane, V. A. Bowers, and C. K. Jen. J. Chem. Phys. **32**, 963 (1960).
10. F. J. Adrian. J. Chem. Phys. **32**, 972 (1960).
11. W. H. Duerig and I. L. Mador. Rev. Sci. Instr. **23**, 421 (1952).
12. J. F. Walker. Formaldehyde. Reinhold, New York. 1953.
13. H. H. Blau and H. H. Nielson. J. Mol. Spectroscopy, **1**, 124 (1957).
14. W. G. Schneider and H. J. Bernstein. Trans. Faraday Soc. **52**, 13 (1956).
15. R. B. Lawrence and M. P. W. Strandberg. Phys. Rev. **83**, 363 (1951).
16. G. Herzberg. Infrared and Raman spectra. Van Nostrand, New York. 1945.
17. L. H. Bolz, M. E. Boyd, F. A. Mauer, and H. S. Peiser. Acta Cryst. **12**, 247 (1959).

THE DIELECTRIC BEHAVIOR AT LOW TEMPERATURES OF SEVERAL GASES ADSORBED UPON POROUS VYCOR GLASS

I. D. CHAPMAN AND R. MCINTOSH
The Department of Chemistry, University of Toronto, Toronto, Ontario
Received June 28, 1961

ABSTRACT

The complex dielectric constants of several systems comprising a gas adsorbed on Vycor glass have been measured at temperatures between 0° C and −180° C and frequencies between 3 kc/sec and 4 Mc/sec. The real and imaginary parts of the dielectric constant of the adsorbed phase have been computed. Loss maxima occurring at low temperatures are observed for some of the matter in the monolayer and are assumed to be due to complexes formed between the gas first admitted and hydroxyl groups which are covalently attached to the surface of the glass. The complexes may be considered either as dipoles having two equilibrium positions, or as highly damped oscillators. Ethyl chloride adsorbed in the first molecular layer and not bonded to OH behaves as an oscillatory system for which no loss is observed in the frequency and temperature ranges studied. Ethyl chloride adsorbed in the multilayers behaves similarly but shows a slightly greater temperature coefficient of ϵ'. Both these types of adsorbed ethyl chloride interact with the complexes and reduce the threshold temperature at which loss is observed in the complex. Methyl chloride interacts with OH groups in a similar fashion, but *n*-butane does not.

INTRODUCTION

The investigation of the dielectric properties of gases adsorbed upon solids can provide a useful means of investigating the modes of motion of molecules held upon the surface and in subsequent layers. In particular, the variation of the dielectric constant of the adsorbed phase with temperature and with frequency (especially in the dispersion region) can give useful information in the case of polar adsorbates. For such adsorbates the temperature coefficient of the dielectric constant will be negative if the molecule is free to rotate in three dimensions in an applied field (1) or, as McIntosh, Rideal, and Snelgrove (2) have shown, is free to rotate in a plane having random orientation in the field. Further, dipolar molecules in the liquid state and free to align themselves with the field, or dipoles in solids which may exhibit several orientations relative to the field, will reveal a characteristic dielectric dispersion, as Debye (1) and Fröhlich (3) have shown. The temperatures and frequencies at which dispersion occurs are dependent upon the nature of the molecules. The variation of dispersion with frequency or temperature will be different from that dispersion known as resonance absorption. Fröhlich (4) points out that resonance absorption is expected for rotational oscillators undergoing dispersion. Adsorbed oscillators should reveal a small temperature coefficient of the dielectric constant as Kurbatov (5) and Snelgrove and McIntosh (6) have demonstrated.

In this investigation the real and imaginary parts of the dielectric constant of systems consisting of gases adsorbed on porous Vycor glass have been measured over a wide range of temperature, from 0° C to −180° C, and of frequency, from 3 kc/sec to 4 Mc/sec. The real and imaginary parts of the dielectric constant of the adsorbate were calculated using the extended Böttcher treatment discussed by earlier workers (2, 7, 8). Allowance had to be made for the losses, both in the adsorbate and adsorbent, and, due to the complicated nature of the equations so obtained (see McCowan and McIntosh (9)), the results were computed on the IBM 650 computer. The value of the dielectric constant of the adsorbed ethyl chloride was approximately 7 for amounts less than monolayer coverage in the range of temperature where there were no losses. This value agrees

quite well with results of other workers (2, 7, 9) when one considers the very different temperatures and frequencies employed in the various assemblies. The major part of this work was undertaken using ethyl chloride. Methyl chloride and *n*-butane were also employed to test various hypotheses but were not investigated extensively.

The findings may be summarized as follows:

(1) A negative temperature coefficient of the dielectric constant was found for ethyl chloride in the monolayer. Its value was approximately one-sixth that of the bulk liquid. For matter adsorbed in the multilayers the coefficient was one-third that of the bulk liquid. These values were established for adsorbate at temperatures above $-130°$ C where the losses in the adsorbate were negligible.

(2) Broad loss maxima were obtained at temperatures below $-130°$ C for ethyl and methyl chlorides adsorbed in quantities less than the monolayer. A corresponding decrease in the real part of the dielectric constant was also observed. Over the narrow range of temperature within which loss maxima could be observed, it was found that the maxima of the loss curves did not change with change in temperature. The losses persisted in the region corresponding to capillary condensation but were not due to the quantities of gas adsorbed after the monolayer. It was possible to show further that the losses were due only to a part of the total gas adsorbed in the monolayer. Interaction between the material first adsorbed and that adsorbed at higher relative pressures was revealed by the fact that the temperature at which losses became observable was reduced with increasing amounts of adsorbate.

(3) No losses other than those already present for the glass alone were detected when a small quantity of *n*-butane was adsorbed. The computed values of ϵ' for *n*-butane were approximately constant over the entire range of temperature and agreed well with the values for liquid butane.

During the preparation of this paper an excellent study of the dielectric properties of small amounts of ammonia adsorbed upon a similar Vycor glass has been described by Fiat, Folman, and Garbatski (10). As the procedure employed by them to calculate molar polarization of the adsorbed matter differs from that employed here, some discussion of their paper will be given.

EXPERIMENTAL

The adsorbent used in this investigation was a tube of porous Vycor glass, Code No. 7930, obtained from the Corning Glass Works, Corning, New York. It weighed 8.751 g *in vacuo* and measured 10.00 cm in length, 1.50 cm O.D., and 1.19 cm I.D. The glass was cleaned by being boiled in a 30% nitric acid solution and heated in distilled water with repeated changes of water. The glass was then heated in the cell to 300° C and pumped to a pressure of 10^{-6} mm Hg. The adsorbates were obtained from the Ohio Chemical Co., and were purified by repeated trap-to-trap distillation under vacuum. Their purity was checked by vapor pressure measurements.

The test cell was made of Invar steel, of the same coefficient of expansion as the glass, and consisted of two coaxial cylinders which fitted around the glass tube and acted as the plates of a condenser. The inner or high-frequency voltage plate was insulated from the outer or ground plate by a glass spacer. The cell fitted into a thin-walled Monel tube which acted as a cell housing and was attached to the system as shown in Fig. 1. The cell could be heated to 350° C without leaks developing in the indium gasket at the top of the housing. The high-potential lead was brought into the housing through a metal–glass seal. The cell housing was further surrounded by a Monel jacket which could be evacuated to reduce heat transfer from the cell. This jacket was cooled with liquid air which enabled temperatures as low as $-180°$ C to be reached in the cell. Higher temperatures were obtained by means of a heating coil wound on the cell and regulated using a Variac. The temperature of the cell was measured with a calibrated copper–constantin thermocouple, and was controlled by a vapor pressure thermometer which operated a switch in the heating circuit.

The frequency range 3 kc/sec to 100 kc/sec was covered using a modified Schering bridge of standard design. Frequencies above 100 kc/sec to 4 Mc/sec were covered by a resonance system described in detail in other papers (7).

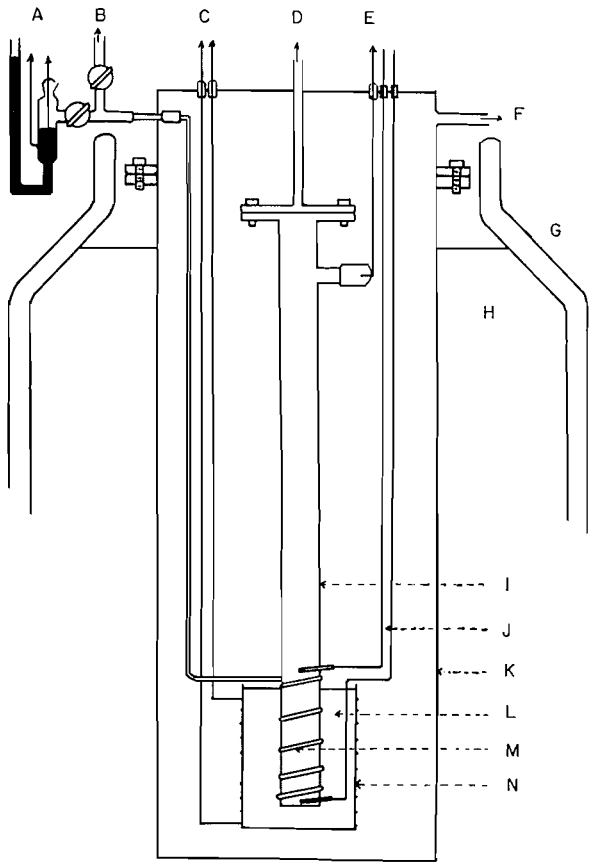

FIG. 1. Cell assembly and system for temperature control.

A = to relay	H = liquid air
B = to storage	I = cell housing
C = to variac	J = thermocouples
D = to system	K = 0.020-in. Monel
E = HF lead	L = copper turnings
F = to vacuum system	M = 2-mm copper tubing
G = Dewar	N = heating wire

A correction of the capacitance readings due to the gap (estimated as 0.002 in.) between the glass tubes and the electrodes of the cell had to be made. This involved a consideration of the potentials across the two air gaps and the glass in the cell. The capacitance reading could then be directly related to the dielectric constant if the radii of the sections in the cell were known:

$$[1] \qquad 1/c = 2 \ln (b/a) + [2\epsilon']/[(\epsilon')^2 + (\epsilon'')^2] \ln (c'/b) + 2 \ln (d/c'),$$

where c is the capacitance per unit length, a, b, c', and d refer to the distances of glass, etc., from the center of the coaxial system. The magnitude of this correction was about 5%. Although the dimensional changes of the adsorbent due to a phase change of the adsorbate are not known, Hodgson and McIntosh (11) have observed expansion when adsorbed water freezes. From the magnitude of this expansion it may be estimated that the gap would not change by more than 4×10^{-5} in., that is, about 2%. Such a variation would be undetectable through the dielectric measurements. After each addition of gas, the system was investigated throughout the entire frequency and temperature range possible. Twenty-four hours elapsed between frequency measurements after a temperature change and no evidence of temperature hysteresis was ever found.

RESULTS

The dielectric constant of a system such as ethyl chloride and Vycor glass is a function of three variables—the volume adsorbed, temperature, and frequency. The variation of ϵ or cell capacitance with each one of these variables, the other two being kept constant, is used to summarize the data.

(i) If one plots the change in cell capacitance with volume of material adsorbed (Fig. 2)

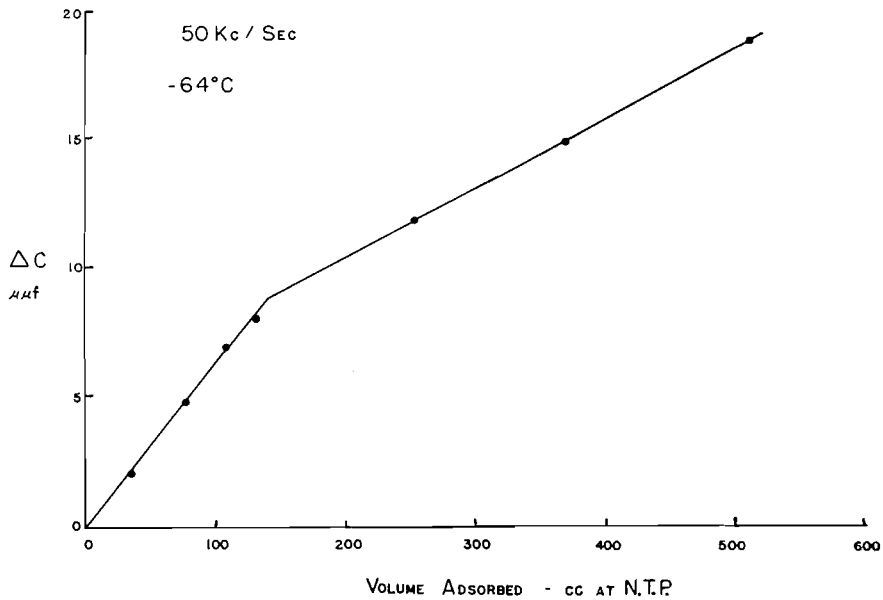

FIG. 2. Plot of change in cell capacitance against volume of gas adsorbed (cc at N.T.P.).

two linear sections result. The second has a lesser slope than the first, which confirms the observations of previous workers (2, 7, 9). To calculate the dielectric constant of the adsorbed phase the extended Böttcher formulae were used (2). The appropriate terms of equation [2] and the analogue of equation [4] were made complex in the program used in computing the results on the IBM 650 computer, and typical results are given in Table I both for the primary data for the composite material and the computed values for the adsorbed phase.

Values of the dielectric constant corresponding to points along the second section of Fig. 2 were, as expected, when computed in this way, lower than for points along the first section, and grew progressively smaller as more gas was adsorbed. This latter result was due to the method of using equation [2], where δ_3 is the volume fraction of free space, to

$$[2] \qquad \frac{\epsilon+2}{3}-\frac{3\epsilon\delta_3}{2\epsilon+1}=\frac{\epsilon_0-1}{4\pi C_1}+\frac{\epsilon-\epsilon_0}{4\pi C_2},$$

compute the results. The reason may be understood by considering an example using data which are not complex. In that event the term $(\epsilon_0-1)/(4\pi C_1)$ would be the intercept of the plot of the left-hand side of equation [2] against $\epsilon-\epsilon_0$. The plot would consist of two linear sections, and the slopes of these sections would yield the respective values of C_2 for the two regions of adsorption. If, however, the equation is solved analytically for

TABLE I

Amount adsorbed (cc at N.T.P.)	Temperature (°C)	ϵ' of composite dielectric	$\epsilon'' \times 10^2$ of composite dielectric	ϵ' of glass	ϵ'' of glass
0.0	−43.0	2.26	2.54	3.30	0.05
	−95.1	2.29	2.97	3.38	0.06
	−131.6	2.31	2.82	3.39	0.05
				ϵ_2'	ϵ_2''
33.1	−34.2	2.33	2.12	6.16	0.03
	−75.7	2.37	2.40	6.78	0.02
	−110.4	2.39	3.17	7.68	0.03
76.6	−32.5	2.45	2.26	6.10	0.02
	−61.0	2.49	2.40	6.89	0.07
	−116.5	2.52	2.83	7.46	0.06
109.2	−68.0	2.59	2.65	6.94	0.03
	−95.2	2.61	2.83	7.20	0.07
	−121.1	2.62	2.69	7.33	0.03
132.1	−79.5	2.65	2.55	7.23	0.04
	−126.5	2.68	2.98	7.76	0.004
251.4	−64.4	2.81	2.41	5.04	0.02
	−95.5	2.87	2.70	5.52	0.04
	−137.6	2.92	3.12	6.11	0.02
361.9	−38.6	2.90	3.27	4.18	0.004
367.9	−83.1	3.01	2.84	4.71	0.005
	−124.0	3.08	2.85	5.23	0.004
510.4	−85.3	3.20	3.13	4.34	0.02
	−129.6	3.27	2.99	4.72	0.002

NOTE: true cell capacitance = 22.2 $\mu\mu$f; end capacitance = 2.0 $\mu\mu$f; frequency = 50 kc/sec.

each point along the second linear region, while retaining the value of the intercept $(\epsilon_0-1)/(4\pi C_1)$ as one point, and the value of the point on the second section as the other quantity defining the line, varying and progressively lesser values of C_2 would be obtained. This is essentially what is done in the procedure employed in using the computer. Previous workers had avoided this difficulty by using the values of the slopes of the two sections, and had thus obtained unique values of the dielectric constant for material corresponding to the first section (assumed to be monolayer) and the second section (assumed to be multilayer). In order to calculate the dielectric constant of the material in the region adsorbed in the multilayer (ϵ_{22}), the polarization/cc (C_2) calculated for the total adsorbed material was assumed to be made up of contributions from the monolayer (C_{21}) and the multilayer (C_{22}), which were further assumed to add on a volume fraction basis:

$$[3] \qquad C_2 = C_{21}\frac{V_1}{V_2+V_1} + C_{22}\frac{V_2}{V_2+V_1},$$

where V_1 represents the volume of material required to complete the monolayer and V_2 is the volume of material in the multilayer. Hence C_{22} can be evaluated and ϵ_{22} calculated from the equation

$$[4] \qquad \frac{\epsilon_{22}-1}{\epsilon_{22}+2} = \frac{4}{3}\pi C_{22}.$$

Some results for different temperatures, and amounts of gas adsorbed, are given in Table II and compared with results obtained graphically by plotting the left-hand side of equation [2] against $(\epsilon-\epsilon_0)$ and obtaining two straight lines of which the second slope gives C_{22} and hence ϵ_{22}. Results were not a function of frequency for temperatures above −130° C.

TABLE II

Dielectric constant of adsorbate from equation [3] and graphically

Volume adsorbed (cc at N.T.P.)	Temp. (°C)	Equation [3]	Temp. (°C)	Graphical method*
251.4	−64.4	3.55	−85.0	3.50
	−137.6	4.67	−95.0	3.51
			−130.0	3.57
367.9	−83.1	3.81		
	−124.0	4.12		
510.4	−85.3	3.74		
	−129.5	4.04		

NOTE: frequency = 10 kc/sec.
*Since the graphical method is based upon the slope of the second linear section of plots such as Fig. 2, the value of ϵ_2' is independent of amount adsorbed.

(ii) Figure 3 shows the variation of cell capacitance with temperature for glass and for various quantities of adsorbed ethyl chloride. It can be seen that there is a negative

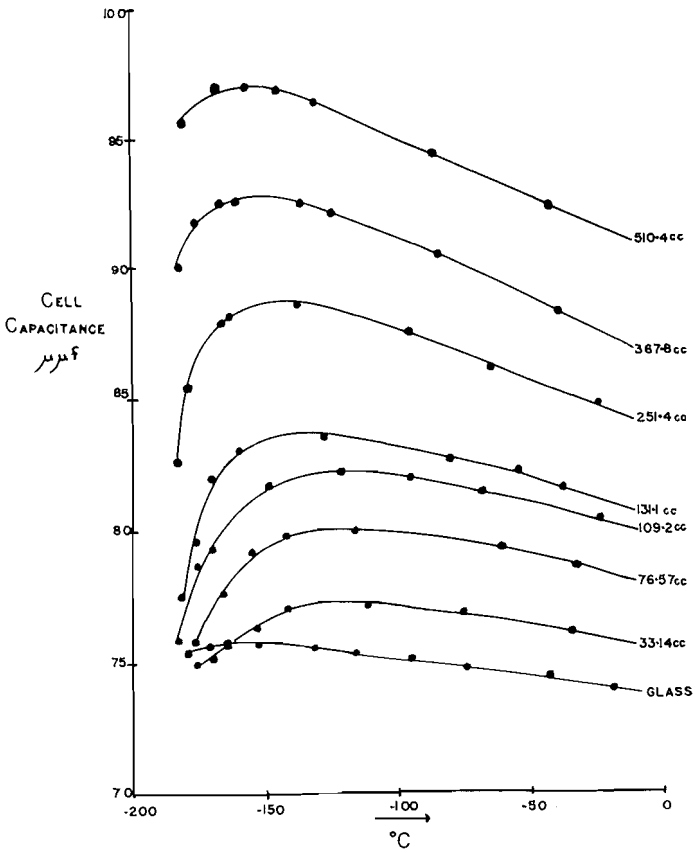

FIG. 3. Plot of cell capacitance against temperature with, and without, adsorbed ethyl chloride.

temperature coefficient for the glass alone, which was attributed to the presence of OH groups on the surface of the glass. Infrared studies by Folman and Yates (12) and Sidorov (13) have indicated the presence of these OH groups.

Treatment of the glass with a 3% aqueous solution of NH_4F, which reduced the concentration of the surface OH groups by replacing them with F (14), showed that the temperature coefficient was reduced. The effect of the OH groups on the dielectric constant can be estimated by extrapolating ϵ to high temperatures. When ethyl chloride is added, in quantities less than those that correspond to the monolayer, the curve virtually parallels that for glass alone down to $-130°$ C. Quantitative treatment of the data shows the temperature coefficient to have about one-sixth the magnitude expected for liquid ethyl chloride. However, as the low-temperature measurements and infrared studies (15) show, hydrogen bonding occurs between the surface OH groups and the ethyl chloride. We might, therefore, consider the OH—ClC_2H_5 complex as an entity and evaluate its variation of ϵ_2 with temperature using the baseline value of ϵ for the glass without OH groups. The temperature coefficient now increases to about one-half that of liquid ethyl chloride but more significantly the value of μ, the dipole moment, calculated using ϵ_2 of the complex and the Onsager (16) equation is still much lower than expected, namely, 1.66 D as compared with 2.0 D, which is the value of the dipole moment of ethyl chloride in the gaseous state. In the multilayer region, the temperature coefficient (from values of ϵ_{22} which were calculated by equations [3] and [4]) is about twice that in the monolayer.

Below $-130°$ C Fig. 3 indicates dispersion both for the glass and the complexed ethyl chloride. A plot for glass plus *n*-butane (not shown), however, parallels the curve for glass alone and therefore shows no dispersion and evidence of adsorbate–adsorbent interaction.

(iii) In the low-temperature region below $-130°$ C the real part of the dielectric constant ϵ' decreases and ϵ'' increases with increasing frequency for the glass and glass–chloride systems. Broad peaks are discernible for these latter systems and do not change in height as the temperature changes (see Fig. 4 and Table III). The behavior with either

TABLE III

Frequency	ϵ_2'*	ϵ_2''*	ϵ_2'†	ϵ_2''†
3 kc/sec	6.10	0.50	5.01	1.20
5	5.97	0.67	4.82	1.31
8	5.51	0.75	4.09	1.28
10	5.56	0.83	4.08	1.81
30	4.61	1.15	2.89	1.25
50	4.32	1.25	2.64	1.16
80	4.89	1.29	2.16	1.06
100	3.69	1.22	2.07	1.01
1 mc/sec	3.34	0.78	2.58	0.66
2.5	3.03	0.72	3.03	0.46
4.0	2.05	0.54	2.41	0.46

NOTE: amount adsorbed in cc at N.T.P. = 109.2.
*Temperature = $-170.4°$ C.
†Temperature = $-183.9°$ C.

of the chlorides clearly shows the interaction of the adsorbate with the adsorbent, since in Fig. 3 the second curve crosses the first in the low-temperature region. This is due to the presence of the complex, which has a different dielectric dispersion behavior than do the OH groups alone on the glass. Methyl chloride, which is a lighter molecule than ethyl chloride, also showed the same effect, but because of its molecular weight, the inception of loss occurred at a lower temperature than for ethyl chloride. Beyond about one-quarter of the monolayer coverage (on the assumption that monolayer completion is revealed by the sudden change of dielectric constant with amount adsorbed), further addition of ethyl chloride does not increase the loss.

DISCUSSION

The loss peaks shown in Fig. 4 resemble Debye-type curves in that the amplitude and width appear constant over the narrow temperature range in which peaks could be defined.

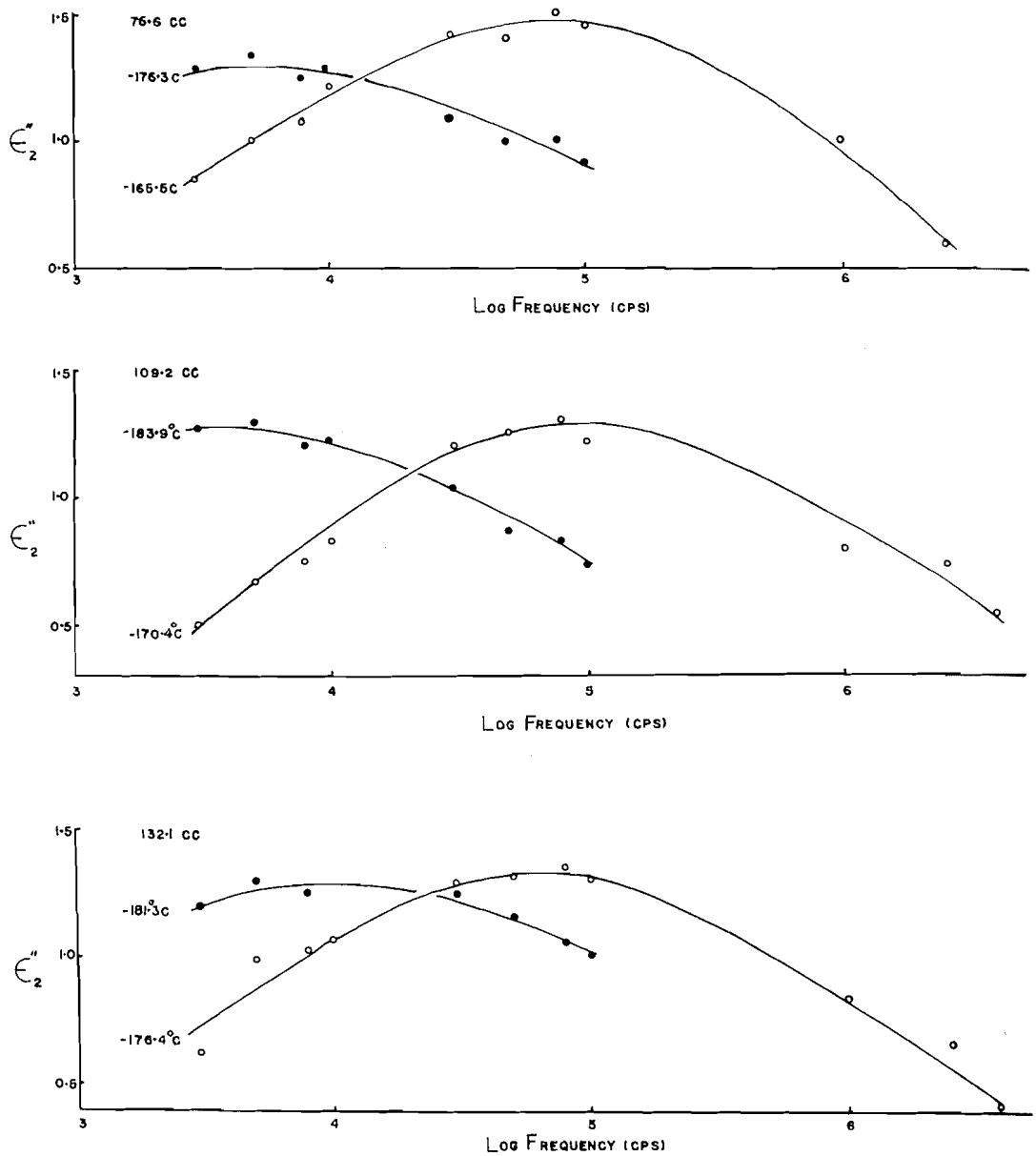

FIG. 4. Plot of ϵ_2'' for ethyl chloride against log frequency (c.p.s.).

However, it was not possible to obtain a typical Cole–Cole plot (17), which is usually taken as a criterion of Debye-type behavior. This failure could be due to the uncertain absolute values of ϵ_2'. As already stated, the temperature coefficient calculated for the

complexed ethyl chloride was smaller than expected. However, if one takes the form of the loss curves as a sufficient criterion of Debye-type behavior in the dielectric, a mechanism can be advanced based on a model having two positions between which the complex makes rotational transitions (1). As Fröhlich (3) points out, this leads, in the presence of a field, to an exponential approach to equilibrium and hence to the Debye equation. In particular, the well-known equation

$$\tau = \frac{1}{\omega_{max}} = \tau_0 e^{-H/RT}$$

may be applied if values of ω_{max} and τ are known. Table IV below gives values of τ_0 and H

TABLE IV

Volume adsorbed (cc at N.T.P.)	τ_0	H (kcal/mole)
76.6	6×10^{13}	4.47
109.2	1×10^{14}	4.30
132.1	5×10^{18}	6.72

calculated from Fig. 4. As can be seen the consistency between different doses of gas is moderately good, although the value of τ_0 is somewhat higher than expected; the small temperature range and the broad maxima of the peaks make the accuracy doubtful.

The two-position theory is the best available to explain Debye-type losses. A treatment based on an order–disorder theory as discussed by Fröhlich (18) cannot be valid in this case. One of the deductions of this latter theory is the decreasing value of the low-frequency value of ϵ_2' with decreasing temperature and no evidence of this was observed for adsorbed ethyl chloride. The fact that such a differentiation between theories is possible is due to a knowledge of ϵ_2', which can also provide a value of the temperature coefficient and dipole moment. This emphasizes the deficiencies in some of the work done on adsorbent–adsorbate systems, in which not only is no attempt made to calculate values of ϵ_2' and ϵ_2'' for the adsorbate itself, but values of ϵ' for the composite dielectric are sometimes not reported.

If the low value of temperature coefficient of the complexed ethyl chloride is considered too low for the Debye behavior discussed immediately above, the entity could be considered as an oscillator. This would require an explanation of the low frequency at which losses appear when the natural frequency (ω_0) would be close to 10^{12} oscillations/sec. The shape of the dispersion curves would also be anomalous if resonance absorption were advanced to explain the dielectric behavior. Von Hippel (19) gives the equation

$$[5] \qquad \hat{\epsilon} = A + \frac{B}{\omega_0^2 - \omega^2 + 2j\omega\alpha},$$

which results from the differential equation of motion

$$[6] \qquad \frac{d^2z}{dt^2} + 2\alpha\frac{dz}{dt} + \omega_0^2 z = \frac{e}{M}E',$$

where M is the mass of the oscillator, e the electronic charge, etc. In equation [5] A is the contribution of oscillators with natural frequencies very different from that of the species of natural frequency ω_0. The measuring frequency is ω and α is the damping coefficient. Since $\omega \ll \omega_0$, rationalization shows that ϵ' decreases continuously with ω, and ϵ'' goes through a maximum as a function of ω provided α is sufficiently large. Experimental finding may therefore be interpreted on the basis of the assumption of large α.

Although the following procedure does not provide an independent check of this interpretation, it was considered instructive to attempt to evaluate α from the known energy dissipation in the dielectric. The energy dissipation is given in ergs cm^{-3} sec^{-1} by $\omega E_0^2 \epsilon''/8\pi$, where E_0 is the applied field. The number of complexed ethyl chloride molecules has been estimated as 6×10^{21} per cc and ϵ'' may be taken as 0.5 at 10^5 cycles/sec. Thus, the ergs dissipated per molecule per second is 1×10^{-20}. One may relate α to this by means of the expression $[m\alpha(dz)/(dt)]\times[d/t]$, where m is the weight of one molecule and $(dz)/(dt)$ and d/t are the same quantity, namely, the distance moved by a molecule in 1 second. From the estimated size of the complex, namely 9×10^{-8} cm, one complete revolution would be about 5×10^{-7} cm. The distance turned by each molecule was evaluated on the assumption of a dielectric constant of about 12 in a field of about 10 volts cm^{-1}, giving a moment per cc of 0.03 e.s.u. Assuming a moment of 2.6 D for the complex, each molecule turns about 2×10^{-6} of a revolution each half cycle. Thus, in 1 second a distance of 10^{-7} cm is traversed by each molecule, so that $\alpha = 10^{-20}/(10^{-22}\times10^{-14}) = 10^{16}$ and $\omega\alpha = 10^{16}\times6\times10^5 \approx 10^{22}$. This is about the correct order of magnitude.

Thus it can be seen that a sufficiently large value of the damping coefficient will rationalize the shape of the absorption peak and also will predict a gradual decrease in the real part of the dielectric constant with frequency.

As already indicated, ethyl chloride, in greater quantity than about one quarter of the unimolecular layer capacity, does not enhance the losses. It is not only loss free but alters, towards lower temperatures, the condition for which loss is detected in the complexes which have formed. This situation is also recognized in the multilayer region. If the volume polarizability method of calculating the dielectric constant is extended to the region of loss, the added material in the multilayer appears to have a negative loss, which indicates that the condition for which loss was originally found in the monolayer has altered. There is, therefore, clear evidence of interaction between matter in the first and subsequent adsorbed layers.

The observation that an adsorbate may interact with the substrate yielding an unexpectedly low ϵ_2' could provide a second explanation for the phenomenon shown by Fig. 2. The lower dielectric constants in the multilayer region have previously been thought to be due to the location of the adsorbate in a region where the internal field is wrongly assessed by the Böttcher treatment. However, it could also be explained on the basis of interaction of the adsorbate and adsorbent through which the polarization of the substrate is reduced. However, in contrast with the matter adsorbed at the lowest relative pressures, the matter adsorbed in this range of pressure shows no dielectric loss, and there is, therefore, no positive evidence of interaction between adsorbate and adsorbent.

Since about three quarters of the ethyl chloride which enters the first molecular layer shows no loss and a low temperature coefficient, it would seem reasonable to consider the motion of this matter as oscillatory. Losses would presumably not be shown for such oscillators until much higher frequencies (20). Loss is also absent in matter going into the multilayer so that the behavior of these molecules does not resemble that of bulk liquid, on the presumption that bulk liquid would show losses at low temperatures and a frequency of 4 Mc/sec.

The recent paper by Fiat, Folman, and Garbatski (10), which deals with the adsorption of small amounts of ammonia on porous Vycor glass, should be discussed in relation to the present work. Fiat, Folman, and Garbatski calculate the molar polarization of the adsorbed ammonia by assuming that the heterogeneous dielectric may be considered as a solution, and the specific polarization of each constituent was added in proportion

to its volume fraction to yield the specific polarization of the composite dielectric. This polarization is related to the dielectric constant of the composite dielectric by the Onsager (15) equation. A somewhat similar solution treatment was given by Channen and McIntosh (8), but was not considered preferable by them. For example, ammonia adsorbed upon rutile showed a moment of 0.55 D, sulphur dioxide 0.0 D, ethyl chloride 0.55 D, in contrast with the gaseous moments of 1.47 D, 1.61 D, and 2.02 D, respectively. Miss Shimizu (21) employed the Onsager equation and the weight additivity of polarization in another attempt to treat these systems as solutions. Values obtained by Miss Shimizu were critized by Benson, Channen, and McIntosh (20). Nevertheless, in the present situation, when the evaluation of the property of the adsorbate must still be considered as somewhat empirical, the suitability of a given procedure must be judged, at least partly, by the apparent reasonableness of the values. On this basis Fiat, Folman, and Garbatski can report an excellent value for the dielectric constant of the glass alone. Differential molar polarizations of the adsorbed ammonia are considered satisfactory by them in view of the bonding with hydroxyl groups. Whether temperature variations of polarization are consistent with the calculated value of the moment is not demonstrated, however.

In general, the question remains as to whether an adsorbed molecule should show an increased or diminished value of the orientational polarization in comparison with bulk matter. This problem has been touched upon by Benson, Channen, and McIntosh (19). It was pointed out by them that a dipolar molecule which had created in it, by induction due to the surface field, an additional moment equivalent to one-half that of its moment in the gaseous state, would contribute no more than an additional 3% to the normal orientational polarization. Admittedly, the model discussed was one in which the dipole diminished with displacement from the position of minimum energy when no applied field was operating, but at the same time, the molecule was considered as free to rotate and the restoring force to the original position was ignored. Thus, an unrealistically large orientational polarization was calculated. In the present instance, Fiat, Folman, and Garbatski apparently calculated the moment on the basis of the molar polarization and the relation $P = 4/3\pi N[\alpha' + (\mu')^2/(3kT)]$, which implies a form of the orientational polarization which may well not be valid. As in the case of ethyl chloride bonded to hydroxyl, reported above, until a realistic model of the adsorbed entity can be analyzed, the deduction of values of dipole moments is open to serious doubt. In the experiments with ethyl chloride it has been shown that the increase of dielectric constant with quantity adsorbed is linear. Thus, the polarization of bonded ethyl chloride must be that of physically adsorbed ethyl chloride in the first layer. This latter material does not have a large contribution to the polarization from orientation if the value of the dielectric constant of 7 is accepted and the Onsager equation is used to calculate the dipole moment. The dipole moment (1.66 D) is less than that of the gaseous molecule. Such an assignment of a dipole moment is clearly unwarranted in view of the fact that no account has been taken of the mode of motion of the adsorbed molecule.

One further comment is indicated. A positive temperature coefficient of the polarization is observed at low coverages of ammonia by Fiat, Folman, and Garbatski. A similar result was found by McCowan and McIntosh (9) for very much higher measuring frequencies, and evidence of dispersion or loss was found associated with the positive temperature coefficient. One would expect losses for conditions in which the rotation of molecules is hindered, but the measurement of loss was not feasible with the device

and procedure employed by Fiat, Folman, and Garbatski. Interesting results should be obtained in the frequency and temperature ranges employed by them.

In summary, it appears that complexes form between the first quantities of adsorbed ethyl chloride and hydroxyl groups. To explain the losses of this species at low temperature the complexes may be considered either as dipoles having two equilibrium positions relative to the field, or as highly damped oscillators. Ethyl chloride adsorbed in the first molecular layer and not bonded to OH behaves as an oscillatory system for which no loss is observed in the frequency and temperature ranges studied. Multilayer ethyl chloride behaves similarly, but shows a slightly greater temperature coefficient of ϵ_2'. Both these types of adsorbed ethyl chloride interact with the complexes $OHClC_2H_5$ and reduce the temperature at which loss is observed.

ACKNOWLEDGMENTS

It is a pleasant duty to acknowledge the financial support of this investigation by the National Research Council, Ottawa, and the Advisory Committee on Research of the University of Toronto.

REFERENCES

1. P. DEBYE. Polar molecules. Chemical Catalogue Company, New York. 1929.
2. R. McINTOSH, E. K. RIDEAL, and J. A. SNELGROVE. Proc. Roy. Soc. (London), A, **208**, 292 (1951).
3. H. FRÖHLICH. Theory of dielectrics. Oxford Univ. Press. 1949. p. 70.
4. H. FRÖHLICH. Theory of dielectrics. Oxford Univ. Press. 1949. p. 102.
5. L. N. KURBATOV. J. Phys. Chem. (U.S.S.R.), **24**, 899 (1950).
6. J. A. SNELGROVE and R. McINTOSH. Can. J. Chem. **31**, 84 (1953).
7. S. E. PETRIE and R. McINTOSH. Can. J. Chem. **35**, 183 (1957).
8. E. CHANNEN and R. McINTOSH. Can. J. Chem. **33**, 172 (1955).
9. J. D. McCOWAN and R. McINTOSH. Can. J. Chem. **39**, 425 (1961).
10. D. FIAT, M. FOLMAN, and U. GARBATSKI. Proc. Roy. Soc. (London), A, **260**, 409 (1961).
11. C. HODGSON and R. McINTOSH. Can. J. Chem. **38**, 958 (1960).
12. M. FOLMAN and D. J. C. YATES. Trans. Faraday Soc. **54**, 1684 (1958).
13. A. N. SIDOROV. J. Phys. Chem. (U.S.S.R.), **30**, 183 (1956).
14. T. H. ELMER. U.S. Patent No. 2,982,053.
15. D. J. C. YATES, N. SHEPPARD, and C. L. ANGELL. J. Phys. Chem. **23**, 1980 (1955).
16. L. ONSAGER. J. Am. Chem. Soc. **58**, 1486 (1936).
17. K. S. COLE and R. H. COLE. J. Chem. Phys. **9**, 341 (1941).
18. H. FRÖHLICH. Theory of dielectrics. Oxford Univ. Press. 1949. p. 60.
19. A. R. VON HIPPEL. Dielectric materials and applications. John Wiley & Sons, Inc., New York. 1954.
20. G. C. BENSON, E. CHANNEN, and R. McINTOSH. J. Colloid. Sci. **11**, 593 (1956).
21. M. SHIMIZU. J. Chem. Soc. Japan, Pure Chem. Sect. **74**, 587 (1953).

STUDIES ON THE STRUCTURE OF CATALPOSIDE

W. H. LUNN,[1] DEIRDRE WALDRON EDWARD, AND J. T. EDWARD
The Department of Chemistry, McGill University, Montreal, Que.

Received September 25, 1961

ABSTRACT

Catalposide extracted from the unripe fruit of *Catalpa ovata* affords bisdesoxyaucubin on reduction with lithium in liquid ammonia. The reduction is accompanied by the shift of a double bond. From this and other evidence, two possible structures are proposed for the compound.

Claassen (1) in 1888 extracted a colorless crystalline compound from unripe fruit of *Catalpa bignonoides* Wal., and named it catalpin. The compound was renamed catalposide by Colin, Tanret, and Chollet (2) because it was hydrolyzed by emulsin and hence was probably a β-glucoside. This was recently confirmed by Bobbitt, Schmid, and Africa (3), who obtained glucose on acid hydrolysis and *p*-hydroxybenzoic acid on alkaline hydrolysis of catalposide. From the analytical data for the compound and for 12 crystalline derivatives, they calculated for it the formula $C_{22}H_{26}O_{12}$.

Our own investigations, started some time ago, have been carried out with catalposide isolated from the fruit of *Catalpa ovata*. This material after prolonged drying at 110° analyzed as $C_{22}H_{26}O_{12}$, but when dried at 64° analyzed as a monohydrate, $C_{22}H_{28}O_{13}$. Acid hydrolysis afforded glucose, identified by paper chromatography, and an insoluble black solid, while alkaline hydrolysis afforded *p*-hydroxybenzoic acid. The latter compound was also obtained in small yields by the pyrolysis of catalposide. It has previously been obtained by treatment of the fruit of *Catalpa bignonoides* with dilute acid (4).

The close similarity in the ultraviolet absorption spectra of catalposide and of ethyl *p*-hydroxybenzoate in neutral and alkaline solution (Fig.1) shows the phenolic hydroxyl

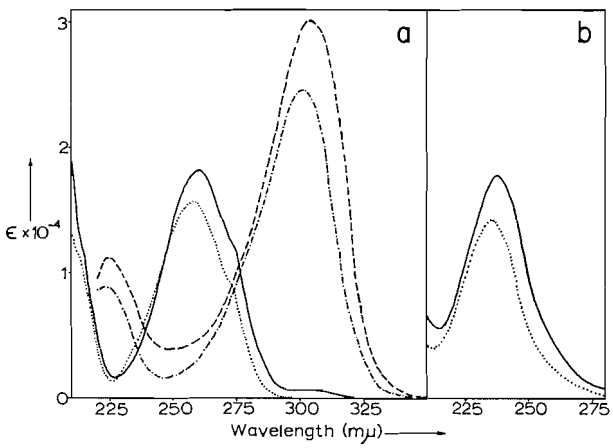

FIG. 1. Ultraviolet absorption of catalposide, ethyl *p*-hydroxybenzoate, heptaacetylcatalposide, and ethyl *p*-acetoxybenzoate.
(*a*) Catalposide: —— in 95% ethanol; — — in 0.01 *N* NaOH in 95% ethanol. Ethyl *p*-hydroxybenzoate: . . . in 95% ethanol; — · in 0.01 *N* NaOH in 95% ethanol.
(*b*) Heptaacetylcatalposide: —— in 95% ethanol. Ethyl *p*-acetoxybenzoate: . . . in 95% ethanol.

[1]*Holder of N.R.C. Studentships 1959–61.*

of the *p*-hydroxybenzoyl group to be free. Titration of the phenolic group in catalposide monohydrate with sodium hydroxide in 10% aqueous ethanol indicated a pK of 8.35, as compared with a pK of 8.45 for ethyl *p*-hydroxybenzoate, and an equivalent weight in good agreement with the formula $C_{22}H_{28}O_{13}$.

Acetylation of catalposide afforded a dimorphous compound which analyzed as a heptaacetate. Bobbitt *et al.* (3) reported obtaining a hexaacetate. The ultraviolet absorption of this compound was, as expected, very similar to that of ethyl *p*-acetoxybenzoate (Fig. 1).

Alkaline hydrolysis of catalposide yielded, besides *p*-hydroxybenzoic acid, a crystalline compound, *catalpol*, $C_{15}H_{22}O_{10}$. This compound also gave a heptaacetate. The analytical results suggested that catalpol might be a hydroxy derivative of aucubin, $C_{15}H_{22}O_9$ (I, R = β-glucosyl = $C_6H_7O(OH)_4$; X = H) (5, 6, 7, 8), a possibility supported by a close similarity in the infrared spectra of the compounds. A close relationship was shown by reducing catalposide with lithium in liquid ammonia, using various alcohols as proton donors, to give bisdesoxyaucubin (II, R = $C_6H_7O(OH)_4$), isolated in low yields as the tetraacetate. This compound had previously been obtained by Grimshaw and Juneja (6) by a similar reduction of aucubin.

In a preliminary communication (9) the structure I (R = $C_6H_7O(OH)_4$; X = $OCOC_6H_4OH$) was proposed for catalposide, on the basis of this evidence, on the assumption that the double bonds of catalposide have the same position as in bisdesoxyaucubin. However, this structure is excluded by a comparison of the nuclear magnetic resonance spectra of catalposide and several derivatives with those of aucubin and the corresponding derivatives. All compounds showed a highly characteristic quartet at low field (τ = 3.45 for aucubin, 3.39 for catalpol, both in D_2O; 3.83 for hexaacetylaucubin (8), 3.65 for heptaacetylcatalposide, 3.62 for heptaacetylcatalpol, all in $CDCl_3$) which must be due to the C-3 proton (8, 10), coupled strongly with the C-4 proton ($J_{34} \approx 5.9$ c.p.s.) and weakly with the C-5 proton ($J_{35} \approx 1.5$ c.p.s.). However, aucubin and hexaacetylaucubin showed complex peaks (τ = 3.93 and 4.20 respectively) due to the olefinic proton at the 7-position (8) which were absent from the spectra of catalposide and its derivatives. This indicates that the second double bond of the latter compounds must be at the Δ^8 position, as shown in formula IV, and that formation of bisdesoxyaucubin (II) in the Birch reduction of catalposide involves a $\Delta^8 \rightarrow \Delta^7$ double-bond shift via the mesomeric anion III (11). Further evidence for this position of the double bond comes from the peaks at highest field. Whereas hexaacetylaucubin has three complex peaks at 6.24, 6.81, and 7.16, which have been ascribed to the protons at C-5 and C-9 of the aglycone and C-5′ of glucose (8), heptaacetylcatalposide (τ = 6.18 and 7.27) and heptaacetylcatalpol (τ = 6.18 and 7.32) have only two peaks in this region, and hence must lack a proton at C-9.

The oxygen functions eliminated in the Birch reduction must be allylic to a Δ^7 or Δ^8 double bond (11), and can only be at the 6, 7, and 10 positions in view of the n.m.r. evidence for a proton at the 5-position; confirmation for the location of an oxygen at the 10-position comes from the failure to detect a C-methyl group in Kuhn–Roth oxidations. Catalpol is accordingly IV (R = $C_6H_7O(OH)_4$; R′ = R″ = H). The large shift in molecular rotation in going from catalpol ($[M]_D$ −443°) to catalposide ($[M]_D$ −841°) indicates that the *p*-hydroxybenzoyloxy group of the latter is probably attached to the 6- or 7-, rather than to the non-asymmetric 10-position, and that catalposide is either IV (R = $C_6H_7O(OH)_4$; R′ = COC_6H_4OH; R″ = H) or IV (R = $C_6H_7O(OH)_4$; R′ = H; R″ = COC_6H_4OH).

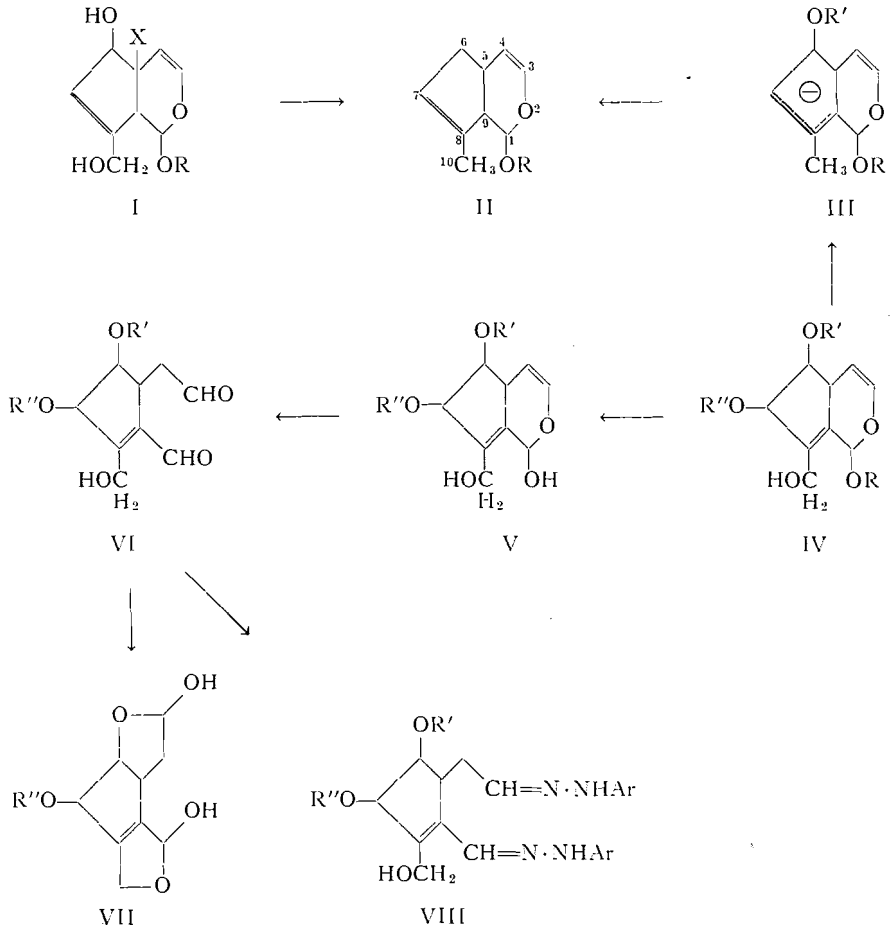

Confirmation of the Δ^8 position of a double bond comes from the properties of catalpogenin, the amorphous but chromatographically homogeneous aglycone given by hydrolysis with emulsion. This formed a crystalline bis-2,4-dinitrophenylhydrazone, $C_{27}H_{26}O_{14}N_8$, which had a broad, flat absorption peak centered at about 367 mμ (ϵ 43,300). A peak at this position and of this shape must be due to the merging of two sharper peaks due to 2,4-dinitrophenylhydrazone chromophores derived from a saturated aldehyde (λ_{max} 348–360 mμ (12)) and an α,β-unsaturated aldehyde (λ_{max} 366–387 mμ (12)). This is in accord with the expected structure VIII. However, the structure of catalpogenin itself is not given by the dialdehyde formula VI, because of the absence of aldehyde C—H stretching peaks in the 2700–2800 cm^{-1} region (13), nor by the formula V, because of the absence of a vinyl ether peak at about 1650 cm^{-1} (13). The formula VII (R″ = COC_6H_4OH) is one of several possible formulae, derived by cyclization from the dialdehyde VI, permitted by the infrared data. Catalpogenin formed an amorphous triacetate.

The treatment of catalposide in liquid ammonia with lithium and various alcohols gave, besides bisdesoxyaucubin, either catalpol or an isomer (isocatalpol), isolated as their heptaacetates. The formation of catalpol by attack of alkoxide ion on catalposide requires no comment; the formation of isocatalpol may possibly be explained by base-catalyzed epimerization at the 1-position. A similar base-catalyzed epimerization was

observed by Wolfrom and Husted (14), who found that the β-forms of the pentaacetates of gluco-, manno-, and galacto-pyranose could be converted to the α-forms by sodium hydroxide in anhydrous dioxane or ether. This formulation for isocatalpol is in accord with the infrared and n.m.r. spectra of its heptaacetate, which are very similar to those of heptaacetylcatalpol and indicate the same functional groups to be present in both compounds.

EXPERIMENTAL

Ultraviolet absorption spectra, except where otherwise noted, are for solutions in 95% ethanol. Nuclear magnetic resonance measurements were made at 60 Mc/sec and peak positions were measured relative to an internal tetramethylsilane reference. Microanalyses were carried out by A. Bernhardt (Mulheim, Germany) and C. Daesslé (Montreal).

Isolation of Catalposide

The procedure was modified slightly from that of Claassen (1). The green beans of *C. ovata* growing on the McGill campus were stripped of their outer coverings, covered with 95% ethanol, and simmered for 1 hour in the presence of a trace of calcium carbonate. The ethanol was poured off, the extraction repeated, and the combined extracts concentrated at reduced pressure to a small volume. The green solution was then washed with ether and left in the refrigerator for 1 week. The solid which separated was taken up in a small volume of ethanol and precipitated with chloroform. It was redissolved in ethanol and filtered through charcoal. The residue from evaporation of the solvent was recrystallized several times from water, giving fine white needles (0.26–0.30% yield). These when dried at 64° at 0.1 mm melted at about 160°, resolidified, and melted again at 209–211° (decomp.); λ_{max} 260 mμ, ϵ_{max} 18,200; in 0.01 *N* sodium hydroxide in ethanol, $\lambda\lambda_{max}$ 225, 305 mμ, $\epsilon\epsilon_{max}$ 11,000, 30,100; ν_{max}^{KBr}: 3540 s,sh, 3400 s, 2910 w, 1708 s, 1654 w, 1613 s, 1597 m, 1519 m, 1393 m, 1355 m, 1315 m, 1290 s, 1257 m, 1232 m, 1177 m, 1105 s, 1090 s, 1074 s, 1055 s, 1015 s, 994 s, 965 s, 921 w, 906 w, 886 w, 874 w, 855 m, 840 m, 813 w, 772 s, 735 w, 704 m, 689 w, and 665 w cm^{-1}. This material analyzed as a *monohydrate*: calc. for $C_{22}H_{28}O_{13}$: C 52.80, H 5.64%; found: C 52.93, H 5.65%. When dried at 110° at 0.1 mm catalposide melted at 209–211° (decomp.), $[\alpha]_D^{22}$ −174° (*c*, 2.11 in ethanol). Calc. for $C_{22}H_{26}O_{12}$: C 54.77, H 5.43, O 39.80%; found: C 54.74, H 5.38, O 39.10%.

Except where otherwise noted, the catalposide used in the experiments described below was dried at room temperature at 15 mm. Such material contained 4–5 molecules of water of crystallization per $C_{22}H_{26}O_{12}$, as shown by combustion analysis and titration, and melted unsharply at about 80°, resolidified, and melted again at about 211° (decomp.). The purity of the compound was checked by ascending chromatography on Whatman No. 1 filter paper with the butanol – acetic acid – water solvent system of Partridge (15). It gave rise to a well-defined black zone (R_f 0.80) when the dried chromatogram was sprayed with 50% aqueous sulphuric acid and warmed gently. It was shown to be essentially free from aucubin (R_f 0.27–0.30), which gave rise to a blue zone when the chromatogram was sprayed with a solution of *p*-dimethylaminobenzaldehyde in acidic ethanol (16); the sensitivity of this chromatographic method was such that less than 0.2% aucubin in catalposide could be detected.

Titration of Catalposide

Aliquots (1.00 ml) of a solution of catalposide monohydrate (132.0 mg) in ethanol (10.0 ml) were diluted to 10.0 ml with distilled water, and the solutions titrated with 0.196 *N* sodium hydroxide in a Radiometer (Copenhagen) continuous automatic titrator. A sigmoid titration curve was obtained; the p*K* of the compound was obtained from the pH value for the midpoint of the curve. Calc. for $C_{22}H_{28}O_{13}$: equivalent 500.5; found: 496, 496, 504.

Acid Hydrolysis of Catalposide

When heated to 100° for 2 hours, a solution of catalposide (220 mg) in 2 *N* sulphuric acid (3 ml) darkened and deposited as infusible black solid. The solution was neutralized with barium hydroxide, centrifuged, and the clear brown supernatant was concentrated to 2 ml. Analysis by paper chromatography, using the solvent systems butanol – acetic acid – water (15) and pyridine – amyl alcohol – water (17) and a developing spray of aniline acid phthalate (15), showed the presence of a substance developing the same brown color and having the same R_f values as glucose.

Alkaline Hydrolysis of Catalposide

Hydrolysis of air-dried catalposide (3 g) in 0.1 *N* barium hydroxide (50 ml) was followed by observing the change in absorption of aliquots diluted with 0.01 *N* sodium hydroxide. After 23 hours λ_{max} had changed from 305 mμ to 280 mμ, characteristic of *p*-hydroxybenzoic acid (18). The solution was slowly acidified with 5 *N* sulphuric acid with cooling and then extracted with ether. Removal of the ether from the dried (magnesium sulphate) extract left a residue (690 mg) which crystallized from acetone–hexane–benzene in needles, m.p. 213–214°, identified as *p*-hydroxybenzoic acid by mixed melting point.

The slightly acidic aqueous solution was neutralized with barium carbonate and filtered, and the water evaporated at reduced pressure at room temperature. A solution of the residue in a few drops of water was diluted gradually with acetone over a period of several days, yielding several gummy crops and finally a colorless crystalline solid. This was recrystallized several times from small volumes of water by addition of acetone, giving stout white needles of *catalpol* (321 mg); m.p. 207.5°–209° (decomp.); $[\alpha]_D^{25}$ −122° (*c*, 0.82 in 90% (v/v) aqueous ethanol); ν_{max}^{KBr}: 3360 s, 2925 m,sh, 2880 m, 1659 m, 1465 w,sh, 1435 w, 1386 m, 1340 w, 1313 m, 1281 w, 1260 w, 1238 m, 1150 m,sh, 1130 m,sh, 1104 s, 1084 s, 1055 s,sh, 1040 s, 1014 s, 989 s, 961 w,sh, 914 m, 900 m,sh, 887 w,sh, 861 w, 836 m, 762 m,sh, 754 m, and 736 m cm^{-1}. Calc. for $C_{15}H_{22}O_{10}$: C 49.71, H 6.12%; found: C 49.64, 49.92, H 6.27, 6.29%.

By ascending chromatography on Whatman No. 1 filter paper and spraying with 50% aqueous sulphuric acid, catalpol gave single, well-defined black zones with the following solvent systems: butanol – acetic acid – water (15), R_f 0.31; phenol saturated with water, R_f 0.77; pyridine – ethyl acetate – water (1:2:2 (vol.)), R_f 0.83. The R_f values of catalposide with these solvent systems were 0.80, 0.78, and 0.93 respectively.

Pyrolysis of Catalposide

A flask containing catalposide (1.5 g) under a pressure of 0.1 mm was heated by immersion in an oil bath, the temperature of which was raised from 170° to 260° C. At the higher temperature a green oil distilled over into a cold trap, and white crystals (70 mg) formed in the neck of the flask. The latter on crystallization from acetone–hexane–benzene had m.p. 213–214° C, undepressed by admixture with authentic *p*-hydroxybenzoic acid, and having an identical infrared spectrum.

Heptaacetylcatalposide

A solution of catalposide (2 g) in pyridine (6 ml) and acetic anhydride (5 ml), after standing overnight at room temperature, was diluted with a large volume of hexane. An oil precipitated which solidified on washing with hexane. The solid crystallized from aqueous isopropanol in white silky needles (2.08 g); m.p. 112.5°–113.5° C; λ_{max} 238 mμ, ϵ_{max} 17,700; ν_{max}^{KBr}: 2946 w, 2900 w,sh, 1750 s, 1720 s,sh, 1654 m, 1606 m, 1508 m, 1435 m, 1373 s, 1275 s,sh, 1247 s,sh, 1220 s, 1195 s,sh, 1164 s, 1100 s, 1065 s, 1040 s, 1015 s, 972 m, 932 s, 910 m, 870 w, 845 w, 762 w, and 700 w cm^{-1}. Calc. for $C_{36}H_{40}O_{19}$: C 55.66, H 5.19%. Found: C 55.77, H 5.29%.

Later preparations of this compound afforded needles, m.p. 142.5°–143.5° C, identical otherwise (ultraviolet and infrared spectra) with lower melting form; $[\alpha]_D$ −108° (*c*, 1.28 in chloroform).

Heptaacetylcatalpol

(a) From Catalpol

A solution of catalpol (127 mg) in pyridine (4 ml) and acetic anhydride (1 ml) was left overnight at room temperature, and then diluted with a large volume of hexane and left a further 24 hours. The precipitated solid was washed with hexane and crystallized from aqueous isopropanol to give large white needles (108 mg); m.p. 140.5°–141.5°; $[\alpha]_D^{23}$ −87° (*c*, 1.83 in chloroform); ν_{max}^{KBr}: 2950 m, 2900 w,sh, 1748 s, 1657 m, 1439 m, 1381 s, 1316 w,sh, 1248 s,sh, 1234 s, 1172 w, 1149 w, 1128 w, 1100 w,sh, 1072 s,sh, 1050 s,sh, 1042 s, 1019 s,sh, 984 m, 971 w,sh, 956 w,sh, 934 m, 921 m, 910 m, 882 w, 868 w, 840 w,sh, 768 m, 745 m, 699 w, 686 w,sh, and 670 w cm^{-1}. Calc. for $C_{29}H_{36}O_{17}$: C 53.04, H 5.53, CH_3CO 45.88%; found: C 53.27, 53.15, H 5.74, 5.71, CH_3CO 45.52, 45.37%.

(b) From Catalposide

Catalposide (2 g) in absolute ethanol (40 ml) was rapidly added dropwise with stirring to a mixture of lithium (2.5 g), liquid ammonia (600 ml), and ethanol (8 ml) cooled in an acetone – dry ice bath. After 20 minutes the cooling bath was removed and the solution left overnight to allow the ammonia to evaporate. Removal of volatile liquids was completed at reduced pressure, and then the residual brown solid was suspended in pyridine (250 ml) and treated with acetic anhydride (100 ml) with stirring and cooling. After standing overnight, the mixture was filtered to remove lithium acetate. The filtrate was concentrated at reduced pressure to 200 ml, diluted with water, and further concentrated to 25 ml. Dilution with water precipitated a viscous oil which was triturated with water, dried at room temperature at 0.1 mm, triturated with hexane, and then left under hexane overnight. The brown solid thus formed was dissolved in methanol, filtered through charcoal, recovered by evaporation at reduced pressure, and recrystallized from aqueous isopropanol. White needles of heptaacetylcatalpol were obtained, m.p. and mixed m.p. 139°–140.5° C, $[\alpha]_D^{20}$ −84° (*c*, 1.64 in chloroform), infrared spectrum identical with that of the compound described above.

Catalpogenin

Optical rotations of an aliquot of a solution of catalposide (3 g) and emulsin (300 mg) in water (1 l.), clarified by filtration through celite, decreased for 2 days and then became constant. The solution was concentrated to about 60 ml at reduced pressure and diluted with acetone to precipitate emulsin and some glucose. The mixture was filtered through celite, and the filtrate taken to dryness at reduced pressure. The yellow residue was dissolved in butanol saturated with water (30 ml) and passed through a column of Whatman cellulose powder (60 g) packed with the same solvent. Elution with water-saturated butanol (250 ml) removed the yellow color from the column. The eluate, taken to dryness at reduced pressure and

dried at 0.1 mm, gave a solid yellow foam (1.98 g). Paper chromatography of this solid, using butanol – acetic acid – water as irrigating solvent and an aniline hydrogen phthalate spray (15), revealed a single yellow spot of R_f 0.90 and no glucose. The solid could not be crystallized and so a portion of it (774 mg) in acetone solution was filtered through charcoal, recovered by evaporation, taken up in isopropanol, and deposited by rotary evaporation on celite (2.5 g). After drying at 0.1 mm, this solid was extracted with anhydrous ether in a Soxhlet apparatus for 3 days. *Catalpogenin* (365 mg) was obtained as a pale yellow amorphous solid on evaporation of the ether; λ_{max} 260 mμ, ϵ_{max} 14,400 (based on formula $C_{16}H_{10}O_7$); ν_{max}^{KBr}: 3440 s, 2950 s, 2886 m,sh, 1712 s, 1692 s, 1614 s, 1604 s, 1599 s,sh, 1519 m, 1468 m,sh, 1451 m, 1350 m, 1311 m, 1282 s, 1217 s,sh, 1170 s, 1112 s, 1068 s, 1030 s, 975 s,sh, 925 m,sh, 895 w, 852 m, 815 w, 773 m, 700 m cm^{-1}. All attempts to crystallize this solid failed, but on paper chromatography it gave rise to a single, well-defined spot.

Triacetylcatalpogenin

A solution of catalpogenin (180 mg) in pyridine (4 ml) and acetic anhydride (1 ml), after standing overnight, was diluted with a large volume of hexane. The brown gum which separated became solid after repeated trituration with hexane, and was taken up in methanol and filtered through charcoal. The colorless residue (60 mg) from the filtrate could not be crystallized, and so was dissolved in carbon tetrachloride, filtered through celite, and recovered by evaporation as an amorphous solid; ν_{max}^{KBr}: 3060 w, 2940 m, 1752 s, 1719 s, 1604 m, 1506 m, 1436 m, 1416 m, 1372 s, 1240 s,sh, 1217 s,sh, 1200 s, 1164 s, 1115 s, 1100 s,sh, 1041 s, 1016 s, 975 m,sh, 914 s, 862 m, 806 w, 764 m, 705 m, and 674 w cm^{-1}; $\nu_{max}^{CCl_4}$: 1757 s, and 1723 s cm^{-1}. Calc. for $C_{22}H_{22}O_{10}$: C 59.20, H 4.97%; found: C 58.64, H 5.45 %.

Catalpogenin bis-2,4-Dinitrophenylhydrazone

A warm solution of 2,4-dinitrophenylhydrazine (260 mg) in ethanol (5.3 ml) – sulphuric acid (1 ml) – water (1.7 ml) was added to a warm solution of catalpogenin (135 mg) in ethanol (3 ml). After 2 hours at room temperature, the mixture was diluted with water (20 ml) and kept for 4 hours in the refrigerator. The yellow-brown solid removed by filtration was washed with water until acid free and then taken up in a small volume of ethyl acetate. Dilution of this solution with boiling ethanol precipitated several crops of brown gum, which were removed by filtration through celite, and finally yellow needles of *catalpogenin bis-2,4-dinitrophenylhydrazone* (40 mg); m.p. 166.5°–167.5° C (decomp.); $[\alpha]_D^{23}$ −378° (*c*, 0.460 in ethyl acetate); $\lambda\lambda_{max}$ 258, 367 mμ, $\epsilon\epsilon_{max}$ 37,100, 43,300 (in ethyl acetate); ν_{max}^{KBr}: 3430 s,w, 3290 s, 3100 w, 1700 m, 1666 s, 1593 s,sh, 1516 s, 1426 m, 1334 s, 1310 s,sh, 1275 s, 1225 m, 1165 m, 1140 s, 1100 s, 1058 w,sh, 925 w, 852 w, 834 m, 772 w, 744 m, and 724 w cm^{-1}. Calc. for $C_{28}H_{24}O_{13}N_8$: C 49.42, H 3.56%; found: C 49.59, 49.40, H 3.90, 3.89%.

Reduction of Catalposide with Lithium in Liquid Ammonia

(a) With Ethanol as Proton Source

Catalposide (2.5 g) in warm absolute ethanol (45 ml) was added to liquid ammonia (320 ml), followed by lithium (10 g) in small pieces over a period of 15 minutes, giving a blue solution with a bronze phase. After 40 minutes, ethanol (25 ml) was added dropwise over a period of 20 minutes, during which the bronze phase disappeared; after another 40 minutes, the addition of more ethanol (20 ml) led to the disappearance of the blue color. The solution was worked up as described above for the preparation of heptaacetylcatalpol from catalposide, yielding a yellow gum (1.39 g) which was chromatographed on Woelm neutral alumina (42 g, activity II). Elution with hexane–benzene, 1:3, removed a solid (60 mg), which after crystallization from aqueous methanol melted at 132°–134.5° C, and was identified as tetraacetylbisdesoxyaucubin by melting point, mixed melting point, and infrared spectrum; $\nu_{max}^{CCl_4}$: 2920 w, 2865 w,sh, 1709 s, 1659 w, 1440 w, 1370 m, 1224 s, 1158 w, 1070 s,sh, 1056 s,sh, 1037 s, 996 w,sh, 965 m, 952 w,sh, 920 w,sh, 910 w, and 881 w cm^{-1}. (Authentic bisdesoxyaucubin was prepared by a similar reduction of aucubin, isolated by Mr. I. Puskas from *Aucuba japonica* leaves (16).)

Elution with benzene containing increasing amounts of ether removed a gum which crystallized from ether–hexane in white needles (53 mg) of *heptaacetylisocatalpol*; m.p. 127°–128° C; $[\alpha]_D^{25}$ −121°, −120° (*c*, 2.21, 2.09 in chloroform); $\nu_{max}^{CCl_4}$: 2950 w, 2883 w,sh, 1751 s, 1655 w, 1433 w, 1369 m, 1221 s, 1160 w, 1125 w, 1062 m, 1038 m, 1010 w,sh, 955 w, and 905 w cm^{-1}. Calc. for $C_{29}H_{36}O_{17}$: C 53.04, H 5.53, CH_3CO 45.88%; found: C 53.06, 53.06, H 5.79, 5.71, CH_3CO 44.51, 44.93%. Larger amounts of organic material were obtained as intractable gums on elution with ether containing 0–3% acetic acid.

(b) With Methanol as Proton Source

Catalposide (2.5 g) in anhydrous methanol (28 ml) was added to liquid ammonia (600 ml), followed by lithium (2 g) over a period of 2 hours. The blue color persisted while the mixture was agitated for a further 2 hours, but disappeared after the addition of methanol (22 ml) over another hour. Ammonium sulphate (70 g) was added, and the mixture left overnight. The solid residue was dissolved in water (150 ml) and the solution evaporated at reduced pressure to yield a near-white residue which was powdered and extracted several times with boiling anhydrous ether, followed by warm methanol. The methanol extract was filtered through charcoal, concentrated, and the residual gum dried and treated with pyridine (10 ml) and acetic anhydride (8 ml) overnight. Dilution of this solution with water precipitated a gum (1.86 g), which was

chromatographed on Woelm neutral alumina, activity grade II (60 g). Elution with hexane–benzene, 1:3 (v/v), removed tetraacetylbisdesoxyaucubin, which, after crystallization from aqueous methanol, melted at 134.7–137.0° (15 mg), $[\alpha]_D - 139°$ (*c*, 0.491 in chloroform), infrared spectrum identical with that of authentic material. Elution with benzene–ether, 9:1 (v/v), removed heptaacetylisocatalpol, which after crystallization from ether–hexane had m.p. and mixed m.p. 127–128° (225 mg).

(c) With Isopropanol as Proton Source

Lithium (3.6 g) and isopropanol (27 ml) were added to catalposide (0.8 g) in isopropanol (16 ml) – ammonia (200 ml) over 90 minutes. Ten minutes later the blue color disappeared and ammonium sulphate (35 g) was added. The reaction was worked up as in (*b*) above to give tetraacetylbisdesoxyaucubin (3 mg), m.p. 132–134°, followed by heptaacetylcatalpol (30 mg), m.p. 140–141°, and then heptaacetylisocatalpol (about 30 mg).

ACKNOWLEDGMENTS

We are grateful to Professor F. A. L. Anet for n.m.r. spectra and for help in their interpretation, to Professor A. J. Birch, for discussions and for suggesting reduction in liquid ammonia, to Mr. H. R. Juneja for details of the reduction of aucubin and for a sample of tetraacetylbisdesoxyaucubin, to Mr. I. Puskas for generous samples of aucubin, to Professor R. D. Gibbs for help and advice, and to the National Research Council for financial support.

REFERENCES

1. E. Claassen. Am. Chem. J. **10**, 228 (1888).
2. H. Colin, G. Tanret, and M.-M. Chollet. Compt. rend. **216**, 677 (1943).
3. J. M. Bobbitt, H. Schmid, and T. B. Africa. J. Org. Chem. **26**, 3090 (1961).
4. A. Piutti and E. Comanducci. Bull. soc. chim. France, (3), **27**, 615 (1902).
5. J. Fujise, H. Obara, and H. Uda. Chem. & Ind. (London), 289 (1960).
6. J. Grimshaw and H. R. Juneja. Chem. & Ind. (London), 656 (1960).
7. M. W. Wendt, W. Haegle, E. Simonitsch, and H. Schmid. Helv. Chim. Acta, **43**, 1440 (1960).
8. W. Haegle, F. Kaplan, and H. Schmid. Tetrahedron Letters. No. 3, 110 (1960).
9. W. H. Lunn, D. W. Edward, and J. T. Edward. Chem. & Ind. (London), 1488 (1961).
10. L. M. Jackman. Applications of nuclear magnetic resonance spectroscopy in organic chemistry. Pergamon Press, London. 1959. p. 62.
11. A. J. Birch. Quart. Revs. (London), **4**, 69 (1950).
12. E. A. Braude and E. R. H. Jones. J. Chem. Soc. 498 (1945).
13. L. J. Bellamy. The infra-red spectra of complex molecules. Methuen, London. 1958. p. 184.
14. M. L. Wolfrom and D. R. Husted. J. Am. Chem. Soc. **59**, 364 (1937).
15. S. M. Partridge. Biochem. J. **42**, 238 (1948); Nature, **164**, 443 (1949).
16. A. R. Trim and R. Hill. Biochem. J. **50**, 310 (1951).
17. I. Werner and L. Odin. Upsala Läkareförens. Forh. **54**, 69 (1949).
18. L. Doub and J. M. Vandenbelt. J. Am. Chem. Soc. **69**, 2715 (1947).

THE INFRARED FREQUENCIES AND INTENSITIES OF THE HYDROXYL BAND OF ORTHO-ALKYL PHENOLS IN THE VAPOR PHASE[1]

K. U. INGOLD

The Division of Applied Chemistry, National Research Council, Ottawa, Canada

Received September 27, 1961

ABSTRACT

The infrared frequencies and intensities of the fundamental stretching vibration of the hydroxyl group have been measured for a number of ortho-alkyl phenols in the vapor phase over a range of temperatures. Both quantities have been shown to depend on internal steric and environmental factors. The differences in enthalpy between the cis and trans isomers of several 2-tert-alkyl phenols have been measured, and it is concluded that the latter are not significantly stabilized relative to the former by solvation in non-polar solvents.

INTRODUCTION

The presence of two fundamental hydroxyl stretching bands in the infrared spectra of *o-t*-alkyl phenols has been reported recently by several workers (1, 2, 3, 4). The two bands are almost certainly due to geometrical isomerism of these phenols, i.e. to cis and trans structures in which the hydroxyl group—coplanar with the ring—points respectively towards and away from the alkyl substituent. In contrast to the related isomerism in which intramolecular hydrogen bonding occurs between the *o*-substituents and the hydroxyl group, the trans isomer predominates in *o-t*-alkyl phenols. We have recently measured the differences in free energy and enthalpy between the two isomers in carbon tetrachloride and hexachlorobutadiene for several different *t*-alkyl groups (1, 2). We suggested that these values might be appreciably higher than the values which would be obtained by measurements in the vapor phase, owing to the increased stabilization of the trans isomer as a result of its interaction with the solvent (5). The present work, in which the differences in enthalpy were measured in the vapor state, was therefore undertaken to estimate the stabilizing effect of the solvents used in the previous measurements. Moreover, enthalpy differences in the vapor are of greater theoretical importance from the point of view of non-bonding interactions in sterically hindered molecules. It was also hoped that the resolution of the two bands would be improved in the vapor, but this was found not to be the case, the resolution being about the same as in carbon tetrachloride at room temperature.

EXPERIMENTAL

The spectrometer and slit conditions have been described previously (1). A simple heated cell was constructed of quartz with a path length of 10.1 cm and a total volume of 207 cc. The temperature of the cell could be read and controlled to about ±2° C. To eliminate traces of air and moisture from the samples the following procedure was used. The cell was heated to 300° C and evacuated overnight, following which it was cooled to room temperature and filled with purified helium. It was then momentarily removed from the gas handling system and a previously weighed quantity of the phenol was dropped in. The cell was re-evacuated for 2 minutes and then sealed off under vacuum. The quantity of the phenol added was sufficient to give a concentration in the vapor of about 10^{-3} mole/liter.

At room temperature none of the phenols showed any absorption in the O—H region. As the temperature was raised the O—H band appeared and increased rapidly in intensity until the phenol was all in the vapor state, after which the maximum band height decreased rather slowly with increasing temperature. Measurements were made in this region at 20° C intervals. In three cases, only one measurement was made since the temperature had to be raised to about 300° C to get these phenols entirely into the vapor state. No measurements were recorded above 300° C since all the phenols examined above this temperature were apparently decomposing quite rapidly.

[1]*Issued as N.R.C. No. 6611.*

RESULTS

Although the main interest in this work was centered on relative band intensities it was found that, if these were obtained from the product of the apparent half-band width and the molecular extinction coefficient, they could differ by as much as 10% from the relative intensities obtained by graphical integration. For this reason, the intensities relative to phenol (A) recorded in Tables I and II were obtained by integration over the entire absorption band. They are probably correct to within ±5%. The integrated intensities are independent of temperature within the accuracy of the measurements, a decrease of about 1–2% every 10° C in the maximum band height, ($\log_{10} I_o/I_m$), being compensated by an increase in the apparent band width. This supports the view that the decrease in intensity with increasing temperature observed previously in solution (2) was due to expansion of the solvent. The primary effect of solvent expansion is to decrease the quantity of material in the cell. A secondary effect is that, as the solvent density decreases, phenol–solvent interaction is also decreased. The intensity therefore decreases, tending towards its smaller value in the vapor phase as the temperature is raised. Thus, the absolute intensity of the OH band of phenol obtained by integration, as far as the flat wings of the band using $\log_{10}(I_o/I)$ and not applying a wing correction, was found to be 0.18×10^4 mole^{-1} liter cm^{-2} in the vapor compared with $0.43_5\times10^4$ in carbon tetrachloride at room temperature (1).* The increase in frequency of the band maximum (ν_m) with increasing temperature in solution was also attributed to this secondary effect, which is confirmed by the fact that ν_m is independent of temperature in the vapor state. Values of A and ν_m, the latter accurate to about ±1 cm^{-1}, are recorded in Table I for those phenols which do not contain just one *o*-*t*-alkyl substituent. ν_m for phenol, which has a very pronounced flat top to the band, is actually the frequency of the band center (ν_c). In most cases ν_m does not differ from ν_c by more than 1 cm^{-1}, but in benzyl alcohol and 4-CHO phenol it is 2 cm^{-1} lower than ν_c and in 4-Me phenol and 2,6-$(Et_3C)_2$-4-Me phenol it is 2 cm^{-1} higher than ν_c. Benzyl alcohol, a fairly typical alcohol (6), is included in Table I and Fig. 1 for comparative purposes.

The band shapes of those phenols which are included in Table I show very marked differences in the vapor phase which are not apparent in solution. For example, $\log_{10}(I_o/I_m)$ increases and the band width decreases with increasing mass of the 4-substituent. Some typical band shapes are shown in Fig. 1. The bands have all been corrected to a concentration of 10^{-3} mole/liter and to a temperature of 250° C. The band shapes have also been indicated in Table I by including the apparent half-band widths ($\Delta\nu_{\frac{1}{2}}$), the ratio of the apparent one-quarter- to three-quarter-band widths ($\Delta\nu_{\frac{1}{4}}/\Delta\nu_{\frac{3}{4}}$), and $\log_{10}(I_o/I_m)$ under these conditions. These values were obtained by extrapolation when necessary, e.g. with 2-*sec*-dodecyl-4-Me phenol, 2,4,6-Am_3^n phenol and 2,6-Oct_2^{tt}-4-CHO phenol,† for all of which only a single high temperature measurement was made.

The bands of some of the substituted phenols show small irregularities which are perhaps due to the presence of overlapping hot bands. The contribution these irregularities make to the values of A obtained by integration over the whole band are probably not significant compared to the accuracy with which A can be measured. Therefore, no correction was applied for these irregularities. With 2,6-Bu_2^t-4-Cl phenol and 2,6-Bu_2^t-4-CHO phenol irregularities appeared on the low frequency side of the band at temperatures above 270° C. They were attributed to the partial decomposition of these phenols involving the loss of one of the *t*-butyl groups. 2,6-$(Et_3C)_2$-4-Me phenol showed a similar

**This value is incorrectly recorded as 4.35×10^4 in reference 1.*

†*The Oct^{tt} or t-t-octyl group is* $(CH_3)_3CCH_2(CH_3)_2C$—.

TABLE I

Frequencies and intensities of phenols in the vapor state

Phenol substituents or compound	$\Sigma\sigma$	A	ν_m, cm^{-1}	$\Delta\nu_{\frac{1}{2}}$,* cm^{-1}	$\Delta\nu_{\frac{1}{4}}/\Delta\nu_{\frac{3}{4}}$*	$\log (I_o/I_m)$* (10^{-3} mole/liter, 10.1 cm path)
Benzyl alcohol		0.36	3659.5	49	2.45	0.123
Phenol	0.00	1.00	3655	37	1.58	0.457
4-Me	−0.17	0.98	3659	30.5	1.82	0.549
4-Oct^{tt}	−0.19	0.97	3655	14.5	3.07	0.980
4-Cl	0.23	1.17	3655.5	26.5	2.43	0.752
4-CHO	1.13	1.28	3644	25	1.82	0.791
2,4,6-Me_3	−0.51	0.87	3655	28	2.54	0.495
2,3,5,6-Me_4	−0.48	0.90	3657.5	24.5	2.38	0.596
2,3,4,5,6-Me_5	−0.65	0.82	3660.5	23.5	2.25	0.517
2-*sec*-dodecyl-4-Me	−0.29	⩾0.93	3649.5	21	2.29	⩾0.614
2,4,6-Bu^s_3	−0.37	1.12	3646	21.5	2.86	0.745
2,4,6-Am^n_3	−0.48	⩾1.06	3646.5	15	2.80	⩾0.874
2,6-Bu^t_2-4-Me	−0.56	2.08	3670.5	27	2.50	1.085
2,6-Bu^t_2-4-Cl	−0.33	2.30	3666.5	23.5	2.66	1.418
2,6-Bu^t_2-4-CHO	0.73	2.77	3656	18.5	3.17	2.174
2,6-Am^t_2-4-Me	−0.55	2.02	3661.5	27	2.53	1.077
2,6-$(Et_3C)_2$-4-Me	−0.52	2.02	3653.5	30	3.59	0.907
2,6-Oct^{tt}_2-4-Me	−0.55	2.08	3653	29	3.40	1.037
2,6-Oct^{tt}_2-4-CHO	0.75	⩾2.70	3636.5	~20	3.46	⩾1.712
2-Bu^t-4-Me-6-Oct^{tt}	−0.56	2.04	3662	31.5	2.42	0.935

*At 250° C.

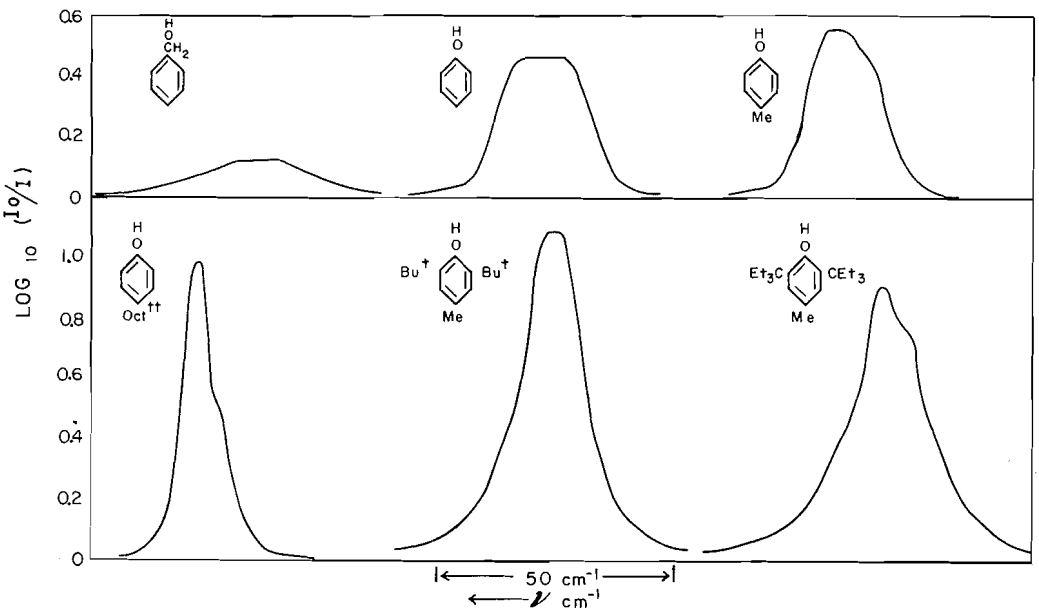

FIG. 1. The O—H vibration bands of benzyl alcohol and some phenols at 250° C and 10^{-3} mole/liter; path length = 10.1 cm.

irregularity even at the lowest experimental temperature (265° C) (Fig. 1). If this irregularity is also due to the partial loss of one of the ortho-alkyl groups the intensity recorded in Table I for this phenol is probably too low.

Phenols containing a single *o-t*-alkyl substituent show the expected double band, but the smaller of the two bands is relatively twice as large as it is in solution in CCl_4. The bands are shown in Fig. 2 at 10^{-3} mole/liter at the lowest temperatures at which they were measured so as to show the maximum resolution achieved. Values of total intensity, ν_m, $\Delta\nu_{\frac{1}{2}}$, etc. are given in Table II. With the exception of the total intensity, these values are not as accurate as those in Table I, owing to the problem of separating the two bands.

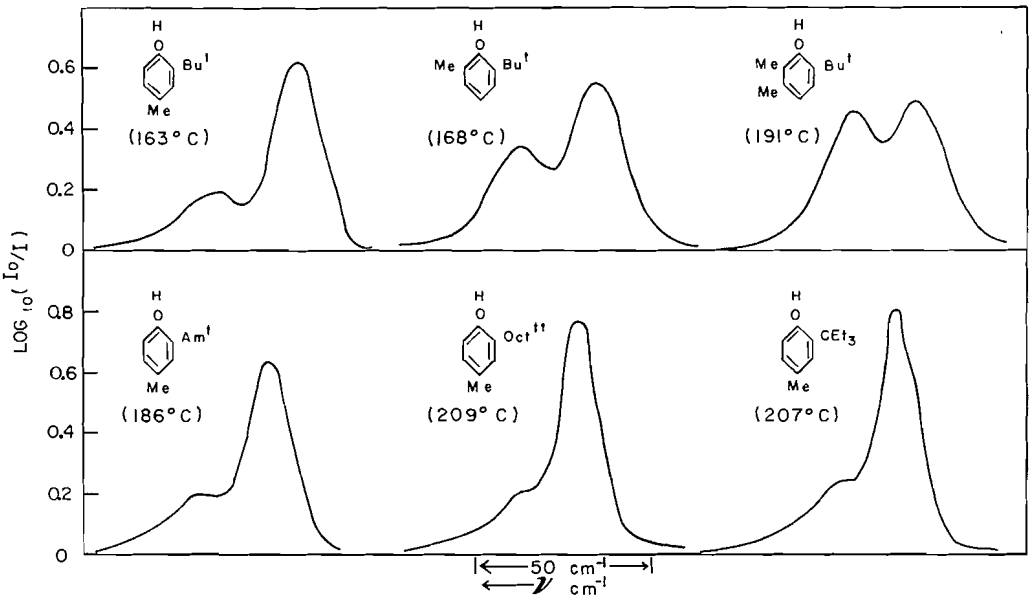

FIG. 2. The O—H vibration bands of ortho-*tert*-alkyl phenols at 10^{-3} mole/liter; path length = 10.1 cm.

TABLE II

Frequencies and intensities of *o-t*-alkyl phenols in the vapor state

Phenol substituents		$\Sigma\sigma$	Total A Meas.	Total A Calc.	ν_m, cm^{-1} Meas.	ν_m, cm^{-1} Calc.	ν_m (meas.) $-\nu_m$ (calc.)	$\Delta\nu_{\frac{1}{2}}$,* cm^{-1}	$\Delta\nu_{\frac{1}{4}}/\Delta\nu_{\frac{3}{4}}$*	log (I_o/I_m)* (10^{-3} mole/liter, 10.1 cm path length)
2-Bu^t-4-Me	t	−0.37	1.07	1.14	3646	3661	−15	22.5	1.97	0.538
	c				3677	3668	9	29.5	2.16	0.175
2-Am^t-4-Me	t	−0.36	1.06	1.13	3645.5	3661	−15.5	20.5	2.14	0.573
	c				3671.5	3659	12.5	27.5	2.37	0.185
2-Et$_3$C-4-Me	t	−0.35	1.09	1.10	3645.5	3661	−15.5	19	2.17	0.684
	c				3666	3651	15	24.5	2.33	0.173
2-Oct^{tt}-4-Me	t	−0.36	1.07	1.09	3644.5	3661	−16.5	18	2.26	0.705
	c				3665	3650.5	14.5	26	2.67	0.157
2-Bu^t-6-Me	t	−0.37	1.27	1.18	3648.5	3653.5	−5	27.5	2.16	0.421
	c				3677.5	3668	9.5	26	2.30	0.291
2-Bu^t-5,6-Me$_2$	t	−0.44	1.34	1.26	3653	3657	−4	~28	~2.5	~0.40
	c				3678	3669	9	~26	~2.4	~0.38

*At 250° C.

DISCUSSION

(i) Phenols Not Containing a Single Ortho-t-alkyl Group

It has been shown previously (7) that ν_m, A, and $\Delta\nu_{\frac{1}{2}}$ for the fundamental O—H stretching mode of 4-substituted phenols and 4-substituted-2,6-di-*t*-butyl phenols can be correlated

in solution with the Hammett σ constants of the 4-substituents. Figure 3 shows the correlations which are obtained for ν_m and A in the vapor state, the σ constant of an ortho substituent being assumed equal to that of the same para substituent.* The error in this assumption (8) is negligible in view of the small σ-para constants of alkyl substituents. Because of their double hydroxyl band, phenols with a single *o*-*t*-alkyl substituent have not been included. For the phenols which do not have two ortho-*t*-alkyl groups, the points have been plotted against the total σ for all the substituents, i.e. $\sum\sigma$. The points for 2,6-di-*t*-butyl and 2,6-di-*t*-*t*-octyl phenols have been plotted against the σ constant of the 4-substituent only so as to make comparisons with the simple 4-substituted phenols easier.

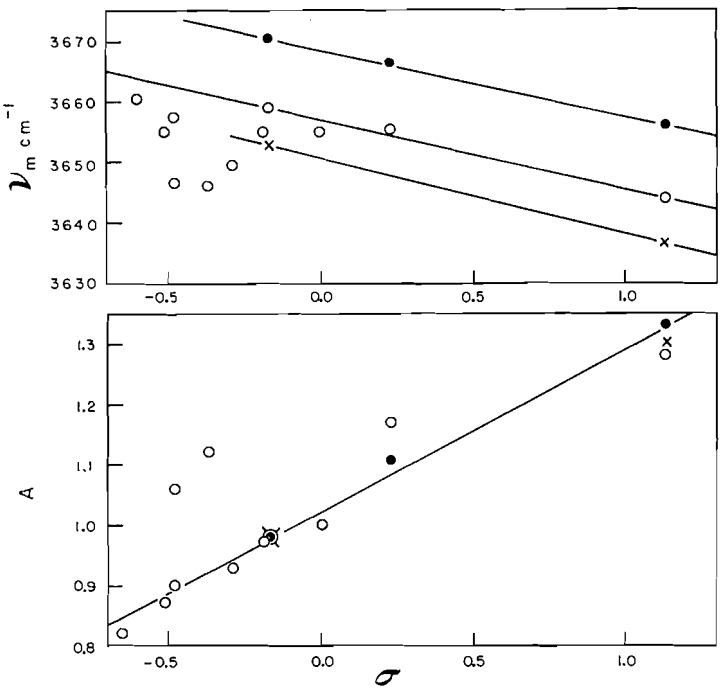

FIG. 3. Variation of A and ν_m with σ: phenols ○; 2,6-Bu_2^t phenols ●; 2,6-Oct_2^{tt} phenols ×.

In carbon tetrachloride and 1,2 dichlorethane a straight line was obtained by plotting A against σ for phenols and 2,6-di-*t*-butyl phenols with a slope $\rho = 0.37$ (7).† In a similar plot in Fig. 3 the intensities of 2,6-di-*t*-butyl and 2,6-di-*t*-*t*-octyl phenols have all been multiplied by 0.98/2.08 so that the A values of their 4-methyl derivatives coincide with

A figure showing the relation between $\Delta\nu_{\frac{1}{2}}$ and σ has not been included because, in the vapor state, the influence of a substituent on $\Delta\nu_{\frac{1}{2}}$ is primarily due to changes in the relative moments of inertia of the phenol and only secondarily due to the electronic effect of the substituent. With 4-substituted 2,6-Bu_2^t and 2,6-Oct_2^{tt} phenols, where changes in the moments of inertia can be neglected, $\Delta\nu_{\frac{1}{2}}$ decreases with an increase in σ, as was found in solution (7). $\Delta\nu_{\frac{1}{2}}$ for simple 4-substituted phenols also shows a decrease with increasing σ when allowance is made for the effect of changes in the moments of inertia. This trend is in the opposite direction to that observed in solution (7). A decrease in $\Delta\nu_{\frac{1}{2}}$ with an increase in σ is probably connected with an increase in the depth of the coplanar potential energy wells resulting from increased resonance of the hydroxyl group with electron-attracting 4-substituents. With non-hindered phenols in solution this effect is more than offset by increasing solvent interaction with the hydroxyl group.

†*It has recently been suggested (9) that $A^{\frac{1}{2}}$, rather than A, should be plotted against σ. The present results do not show any significant improvement when plotted against $A^{\frac{1}{2}}$ and have therefore been plotted against A to facilitate comparison with our previous work.*

4-Me phenol. The points for most 4-substituted phenols, methyl-substituted phenols, 2-*sec*-dodecyl-4-Me phenol, and 2,6-di-*t*-alkyl-4-substituted phenols fall close to a single straight line with a slope of 0.27.* This indicates that the orientation of the hydroxyl group is the same for all these phenols (7), i.e. if the hydroxyl is coplanar with the ring in phenol it is also coplanar in 2,6-di-*t*-alkyl phenols. This conclusion receives further confirmation from the parallel lines obtained with phenols and di-*t*-alkyl phenols in the ν_m versus σ plots. Moreover, the high intensities of all the di-*t*-alkyl phenols compared with a typical alcohol (benzyl alcohol) also suggest a coplanar hydroxyl, since the intensity would be expected to decrease to a value similar to that of an alcohol if the hydroxyl were twisted out of the plane by the alkyl groups.

In the plot of ν_m against σ three straight lines have been drawn to pass through the ν_m values obtained for the 4-Me and 4-CHO derivatives of phenol, 2,6-Bu_2^t phenol and 2,6-Oct_2^{tt} phenol. The lines are nearly parallel with slopes of -11.5, -11.5, and -12.5 cm^{-1} respectively, which are slightly lower than the slope of -13.7 cm^{-1} obtained with the first two phenols in CCl_4 (7). The lower slopes in the vapor are to be expected as a result of the elimination of solvent interaction with the hydroxyl group (7). The divergence of multi-alkyl substituted phenols from this line may be partly due to a saturation of electronic effects owing to the large number of electron-releasing groups attached to the ring. However, since Am_3^n, Bu_3^s, and 2-*sec*-dodecyl-4-Me phenols are further from the line than Me_5 phenol the divergence is probably mainly due to interaction of the hydroxyl with the alkyl groups. The results suggest that ν_m is more sensitive than A to such interactions.

In a previous publication (1) the differences between measured values of ν_m and A in CCl_4 for 2,6-dialkyl phenols and the values calculated from the Hammett equations were plotted against the difference in free energy between the cis and trans isomers of the corresponding *o*-alkyl phenols, i.e. $\Delta\nu_m$ and ΔA were plotted against ΔG. It was pointed out that although this procedure cannot be justified directly, the values of $\Delta\nu_m$ and ΔA for di-*o*-alkyl phenols must be related in some way to the steric interaction of the alkyl groups with the hydroxyl group and the magnitude of this interaction is some function of ΔG. The original plots are reproduced in Fig. 4 with the addition of the $\Delta\nu_m$ and ΔA values for the vapor state plotted against the slightly different values of ΔG found in the vapor (see below). The general shapes of the curves are similar in the vapor and in solution. The discontinuities between the methyl phenols and the *t*-alkyl phenols indicate that *o*-alkyl groups have two different effects on the hydroxyl; the relative magnitudes of the two effects varying with the size of the substituents. The solution curves were tentatively explained on the basis that mild steric interactions narrowed the potential energy well of the O—H stretching vibration, while stronger steric effects tended to polarize the hydroxyl bond (1). However, the present results suggest that changes in the environment around the OH group produced by alkyl substitution play an equally important role in determining $\Delta\nu_m$ and ΔA. The frequency of a "free" phenolic hydroxyl group (e.g. phenol) increases as the surrounding medium is changed from CCl_4 to a hydrocarbon to the vapor, and its intensity decreases (see Table I in reference 2). Alkyl substitution in both ortho positions changes the environment of the hydroxyl to one similar to that encountered by the OH group of phenol in a hydrocarbon. Provided the steric interaction between the OH and alkyl groups is small the environmental change produced

**The divergence of 4-chlorophenol from this plot may be due to the presence of some 2-chlorophenol since this was an unpurified commercial product. The divergence of Bu_3^s and Am_3^n phenols is probably due to the interaction of the ortho-alkyl groups with the hydroxyl. This interaction raises A towards its apparently limiting value of slightly more than 2.0, which is reached in di-o-t-alkyl phenols (Fig. 4).*

by alkyl substitution suggests that $\Delta\nu_m$ will be positive in CCl_4 and negative in the vapor while the reverse should be true of ΔA. The $\Delta\nu_m$ and ΔA values of 2,6-Me_2 and 2,3,5,6-Me_4 phenols show the expected changes in the vapor and in CCl_4, although the intensities do not seem to be as sensitive as the frequencies to environmental changes. The sudden increase in A to a virtually constant value on the substitution of two *o-t*-alkyl groups may be due to the complete enclosure of the hydrogen atom of the hydroxyl group by the alkyl substituents; that is, the OH is no longer "free" whatever the orientation of the alkyl substituents, and its environment should therefore be very similar to that encountered by the OH group of phenol in hexane. This environmental similarity is emphasized by comparing the absolute intensities of phenol in hexane with the absolute intensities of di-*t*-alkyl phenols in the vapor (Table III; the hexane values have been calculated from Table I, reference 2).* The positive values of ΔA observed with di-*t*-alkyl phenols in CCl_4 and hexane, and the small increase in ΔA on going from di-*t*-butyl to di-*t-t*-octyl phenol, are probably both connected mainly with steric effects. Specific solvent interactions may also play a part in these changes in ΔA, since the intensities of these phenols are virtually constant in carbon disulphide solution (2).

TABLE III

Comparison of ν_m and A in hexane and vapor

Substituents	ν_m (vapor) $-\nu_m$ (hexane), cm^{-1}	Absolute intensity, 10^4 $mole^{-1}$ liter cm^{-2}	
		Vapor	Hexane
None (phenol)	$32._5$	0.18	0.39
Me_5	23	0.15	0.24
2,6-Bu_2^t-4-Me	$14._5$	0.37	0.40
2,6-Am_2^t-4-Me	$14._5$	0.36	0.40
2,6-$(Et_3C)_2$-4-Me	15	0.36	0.51
2,6-Oct_2^{tt}-4-Me	14	0.37	0.47
2-Bu^t-4-Me	—	0.19_3	0.27_6
Trans	$26._5$	0.13 (250° C)	0.25 (25° C)
Cis	$18._5$	0.06_3 (250° C)	0.02_6 (25° C)

The increase in $\Delta\nu_m$ from 2,6-Me_2 phenol to 2,6-Bu_2^t phenol is probably connected with a narrowing of the O—H potential energy well because of the increased steric repulsion between the hydroxyl and alkyl groups. The decrease in $\Delta\nu_m$ above 2,6-Bu_2^t phenol is interesting in that it exactly parallels the decrease in the frequencies of these phenols in hexane (see Table III). The cause of the decrease must therefore be intramolecular in origin. A possible explanation would be that the C–$\widehat{O}$–H angle starts to increase as the *t*-alkyl group becomes larger than *t*-butyl, this would tend to decrease the O—H bond strength and hence ν_m.

Bu_3^s and Am_3^n phenols appear to provide a hydrocarbon type environment around the hydroxyl without the simultaneous introduction of large steric effects; that is, their steric effects are probably not much greater than those produced by two ortho-methyl groups, but their $\Delta\nu_m$ values are -15.5 cm^{-1} and -16 cm^{-1} respectively, and their ΔA values are 0.16 and greater than or equal to 0.20 respectively. There is no value of ΔG which will allow either of these phenols to be placed on both the $\Delta\nu_m$ and ΔA curves in Fig. 4. These phenols therefore provide additional evidence that both the frequencies and intensities of

**The calculated absolute intensity of all the 2,6-di-t-alkyl-4-methyl phenols in hexane (based on phenol and an assumed ρ value of 0.30 in hexane) is 0.33.*

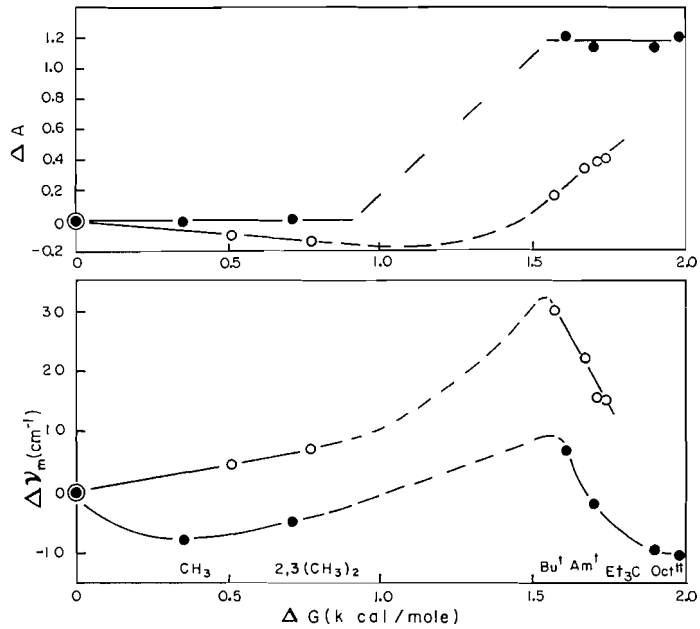

FIG. 4. Differences between measured and calculated frequencies, and intensities, of 2,6-dialkyl phenols plotted against ΔG: in CCl_4 solution ○; in vapor ●.

2,6-dialkyl phenols are determined by environmental as well as by steric factors. It is impossible on the basis of the present work to estimate how the relative importance of these two factors changes with changes in the structure of the alkyl substituents.

(ii) Phenols Containing a Single Ortho-t-alkyl Group

The double hydroxyl bands of *o-t*-alkyl phenols (Fig. 2) are similar to those found in solution (2), that is, the smaller band always occurs at the higher frequency. In solution the larger band was attributed to the trans (to *t*-alkyl) isomer and the smaller to the cis isomer because the frequencies of the two bands were quite close to the frequencies of phenol and the corresponding 2,6-di-*t*-alkyl phenol, respectively. It can be seen from the results in Table II for the measured values of ν_m and for the values calculated from the symmetrically substituted phenols by the Hammett equation that this is far from being the case in the vapor. In particular, the calculated ν_m's for the cis configuration of 2-Am^t-4-Me, 2-Et_2C-4-Me, and 2-Oct^{tt}-4-Me phenols are lower than the ν_m values calculated for the trans isomer (based on 4-Me phenol). This suggests that the identification of the smaller, high frequency, band with the cis isomer might be incorrect. However, the measured and calculated values of ν_m are in the expected order for 2-Bu^t-4-Me, 2-Bu^t-6-Me, and 2-Bu^t-5,6-Me_2 phenols, the calculated ν_m of the trans isomer being based on 4-Me, 2,4,6-Me_3, and 2,3,5,6-Me_4 phenols. Moreover, the measured total intensities of the double bands are in good agreement with the values calculated on the assumption that the smaller band corresponds to the cis isomer (Table II). The calculated intensities were obtained by adding the products of the theoretical intensities of the trans and cis isomers —calculated by the Hammett equation from the A values of the respective symmetrically substituted phenols—and the fraction of each isomer present in the mixture at a given temperature (see below). The agreement between measured and calculated A's would not be achieved if the opposite assignments were made, and therefore the smaller, high frequency, band will henceforth be attributed to the cis isomer.

The relative intensities of the two bands of *o*-*t*-alkyl phenols were estimated at each temperature by a graphical method for 2-*t*-alkyl-4-Me phenols and 2-Bu^t-6-Me phenol. The true ratio of the concentrations of the two isomers, i.e. [trans]/[cis], were obtained by multiplying these relative intensities by a factor which takes account of the intrinsic differences in the intensities of the two isomers. The derivation of this factor from the intensities of the corresponding symmetrically substituted phenols has been described previously (1). Since the A values of 2,6-di-*t*-alkyl-4-Me phenols are nearly constant, and since the A values of 2,4,6-Me_3 and 2,3,5,6-Me_4 phenols are very close to their calculated values (see Figs. 3 and 4), the factor is virtually the same for each phenol. An average correction factor of 2.32 was therefore used in each case. The graphical procedure could not be used to separate the two bands of 2-Bu^t-5,6-Me_2 phenol because they are of nearly equal height. This [trans]/[cis] ratio was therefore obtained by multiplying the ratio of the measured band heights by the correction factor.

The differences in enthalpy (ΔH) and entropy (ΔS) between the two isomers can, in principle, be obtained by plotting $\log_{10}$ [trans]/[cis] against $1/T$ (°K). These plots are shown in Fig. 5. In view of the difficulties involved in separating the two bands and the comparatively small temperature range that was covered the points are not sufficiently accurate to determine ΔS. The straight lines through the points have therefore been drawn to pass through the origin; that is, it was assumed that $\Delta S = 0$ and $\Delta H = \Delta G$, which means that the concentrations of the two isomers become equal as $T \rightarrow \infty$. The points measured at high temperatures for some phenols deviate appreciably from these lines, probably because some decomposition has occurred. The values obtained for ΔH in the vapor are given in Table IV together with the values of ΔG obtained previously at room temperature in CCl_4. ΔH for 2-Me and 2,3-Me_2 phenols was obtained by difference. The agreement between the two sets of data is surprisingly good in view of the expected stabilization of the trans isomer relative to the cis in CCl_4. If this stabilization was appreciable, ΔH in the vapor would be smaller than ΔG in solution. That such stabilization cannot be very large is indicated by the fact that the increases in ν_m for the cis and for the trans isomers on going from CCl_4 to the vapor never differ by more than 10 cm^{-1}. For example, the frequency increase with 2-Bu^t-4-Me phenol is 36 cm^{-1} for the trans and 27.5 cm^{-1} for the cis isomer, a difference of only 8.5 cm^{-1}. These differences are recorded for all the *o*-*t*-alkyl phenols under $\delta\nu_m$ in Table IV.

TABLE IV

Cis–trans isomers in *o*-*t*-alkyl phenols

Phenol substituent	$\delta\nu_m$, cm^{-1}	ΔH (vapor), kcal/mole	ΔG (CCl_4), kcal/mole
2-Bu^t-4-Me	8.5	1.61	1.57
2-Am^t-4-Me	9	1.70	1.67
2-Et_3C-4-Me	10	1.90	1.74
2-Oct^{tt}-4-Me	10.5	1.98	1.71
2-Bu^t-6-Me	3.5	1.26	1.06
2-Bu^t-5,6-Me_2	6	0.90	0.80
2-Me		0.35	0.51
2,3-Me_2		0.71	0.77

It is quite possible that the values of ΔH have been overestimated owing to an overestimation of the intrinsic intensity correction factor; that is, the data in Table II show that ν_m's for the trans isomers of 2-*t*-alkyl-4-Me phenols are about 15 cm^{-1} below the values calculated from 4-Me phenol. A similar, though smaller, effect was observed

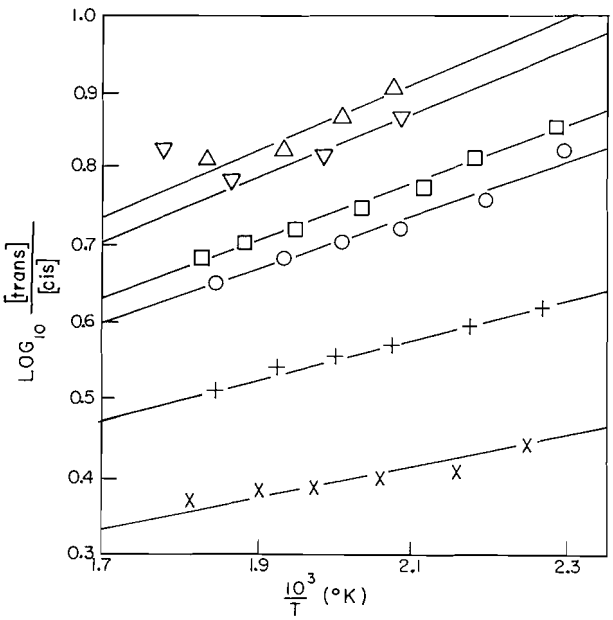

FIG. 5. Effect of temperature on $\log_{10}$ [trans]/[cis] for ortho-*tert*-alkyl phenols in vapor: 2-Bu^t-5,6-Me$_2$ ×; 2-Bu^t-6-Me +; 2-Bu^t-4-Me ○; 2-Am^t-4-Me □; 2-Et$_3$C-4-Me ▽; 2-Oct^{tt}-4-Me △.

previously in solution (1, 7). It was attributed either to van der Waals attraction of the lone pairs of electrons on the oxygen by the trans-*t*-alkyl group (1), or to a steric enhancement of resonance owing to the O—H group being held more rigidly in the plane by the trans-*t*-alkyl group (7). Since a similar effect will probably also be operative in decreasing the ν_m values of 2,6-di-*t*-alkyl phenols it may explain why the measured values of ν_m for the cis isomers of 2-*t*-alkyl phenols are larger than the values calculated from the di-*t*-alkyl phenols by a roughly equal amount (9–15 cm^{-1}). The directions in which the frequencies of the cis and trans isomers differ from their calculated values imply that the intrinsic intensity of the trans isomer will be larger than calculated and that of the cis isomer smaller than calculated. This means that the intrinsic intensity correction factor has probably been overestimated.* The values of ΔH recorded in Table IV are therefore maximum values. Since this source of error is larger in the vapor than in CCl_4, to judge by the differences in the measured and calculated values of ν_m in these two systems, the present results would not be inconsistent with a stabilization energy due to solvation by CCl_4 of a few tenths of a kilocalorie per mole for the trans isomer.

Carbon tetrachloride has been reported to stabilize the trans isomer of *o*-iodophenol ($\delta\nu_m$ = 23 cm^{-1}) by 1.4 kcal/mole with respect to the vapor (5). The present results suggest that this stabilization energy has been overestimated and that much of the observed decrease in the relative intensity of the trans isomer in the vapor is due to a decrease in its intrinsic intensity. If it is assumed that this decrease is of the same magnitude as the decrease observed with phenol in this work (i.e. 0.435/0.18 = 2.4) and that the

**If the measured ν_m values of the cis and trans isomers are used to derive σ constants for the two isomers from the ν_m versus σ plot, and if these σ values are then used to derive intrinsic intensities, the correction factors and ΔH's are reduced but the calculated total intensities are no longer in good agreement with the measured values (e.g. for 2-Bu^t-4-Me phenol the correction factor = 1.29, ΔH = 1.0 kcal/mole, but the total calculated A = 1.39). This again suggests that frequencies are influenced more than intensities by ortho substituents.*

intrinsic intensity of the cis isomer is unaffected by the medium, the stabilization energy only amounts to about 0.5 kcal/mole, which is in better agreement with the present results and with the small value $\delta\nu_m$.

On the basis of the measured steric repulsion of the hydroxyl group by an *o*-*t*-butyl group (~1.6 kcal/mole) and a dielectric measurement of the internal rotational barrier of the OH group in 2,4,6-Bu_3^t phenol (2.8 kcal/mole (10)) we have previously estimated the rotational barrier in phenol to be $\geqslant$4.4 kcal/mole (1). Evans (11) has recently calculated a barrier height of 3.37 from the complete infrared spectrum of phenol vapor. If all these values are assumed to be reasonably accurate, it implies that two *o*-*t*-butyl groups not only raise the coplanar potential minimum of the hydroxyl by 1.6 kcal/mole but also raise the barrier height by about 1.0 kcal, i.e., 4.4 kcal represents the barrier to rotation from the trans to the cis position of the hydroxyl group in 2-*t*-butyl phenol.

CONCLUSION

The frequency and intensity of the fundamental hydroxyl stretching band of a 2-alkyl or 2,6-dialkyl phenol are determined by internal steric and environmental factors in addition to the normal inductive and resonance effects described by the Hammett equation. 2-Alkyl phenols exist as cis and trans isomers both in the vapor and in solution. The trans isomers are not significantly stabilized relative to the cis by solvation in non-polar solvents such as carbon tetrachloride. A 2-*tert*-alkyl group (but probably not a 2-methyl group) can affect the hydroxyl even when the latter points away from it. This interaction may be due either to an attraction of the lone pairs of electrons on the oxygen by the alkyl substituent or to a steric enhancement of resonance between the hydroxyl group and the benzene ring.

ACKNOWLEDGMENTS

The author is indebted to Dr. J. E. Bertie and Dr. I. E. Puddington for several helpful discussions.

REFERENCES

1. K. U. INGOLD and D. R. TAYLOR. Can. J. Chem. **39**, 471 (1961).
2. K. U. INGOLD and D. R. TAYLOR. Can. J. Chem. **39**, 481 (1961).
3. R. F. GODDU. J. Am. Chem. Soc. **82**, 4533 (1960).
4. N. A. PUTTNAM. J. Chem. Soc. 5100 (1960).
5. G. ROSSMY, W. LÜTTKE, and R. MECKE. J. Chem. Phys. **21**, 1606 (1953).
6. T. D. FLYNN, R. L. WERNER, and B. M. GRAHAM. Australian J. Chem. **12**, 575 (1959).
7. K. U. INGOLD. Can. J. Chem. **38**, 1092 (1960).
8. M. CHARTON. Can. J. Chem. **38**, 2493 (1960).
9. T. L. BROWN. J. Phys. Chem. **64**, 1798 (1960).
10. M. DAVIES and R. J. MEAKINS. J. Chem. Phys. **26**, 1584 (1957).
11. J. C. EVANS. Spectrochim. Acta, **16**, 1382 (1960).

ACID-CATALYZED REACTIONS OF VINYL COMPOUNDS

PART I. PRELIMINARY STUDIES ON VINYL ESTERS AND BENZENE[1]

J. M. PEPPER, B. P. ROBINSON, AND G. W. SCHWANBECK
The Department of Chemistry, University of Saskatchewan, Saskatoon, Saskatchewan

Received July 26, 1961

ABSTRACT

A detailed study of the nature, and the mechanism of formation, of the products of the aluminum chloride catalyzed reaction of vinyl esters and benzene has been initiated. Using vinyl acetate the formation of the previously reported acetophenone, 1,1-diphenylethane, and 9,10-dimethylanthracene has been confirmed. By means of both column chromatography and thermal distillation, a similar carbonyl-containing fraction was obtained which, as a result of a gas chromatographic study, has been shown to be a mixture of six compounds. Of these, the two major components have been identified as acetophenone and *p*-ethylacetophenone, the latter previously unreported as a product of this reaction.

The reaction of vinyl formate and benzene has been studied for the first time. High yields of 9,10-dimethylanthracene were obtained but no carbonyl-containing compounds. A study of the effect of a variation in molar ratio of benzene to vinyl acetate indicated that a maximum yield of 9,10-dimethylanthracene was obtained using a 6:1 molar ratio.

The significance of these results is discussed.

A method has been devised for an improved synthesis of 9,10-dimethylanthracene. The generality of this procedure for the synthesis of other substituted polynuclear compounds is indicated.

Some years ago, Hopff, in a patent disclosure (1), indicated that the acid-catalyzed interaction of vinyl acetate and benzene gave rise to 2-phenylethyl acetate. The possibility thereby arose whereby this condensation followed by hydrolysis of the ester could provide a convenient method of synthesis of 2-phenylethanol, a perfume ingredient. Attempts to repeat the initial condensation were not successful, but the products that were obtained were of sufficient interest to warrant further study regarding their nature and mechanism of formation. In 1946, Korshak, Samplavskaya, and Gershanovich (2) reported the identification of acetophenone (I), 1,1-diphenylethane (II), and a compound believed to be 9,10-dimethyl-9,10-dihydroanthracene (III) in the reaction product of vinyl acetate and benzene in the presence of aluminum chloride. They proposed a mechanism involving the initial formation of I and acetaldehyde. Acetaldehyde then reacted further with benzene to produce II, two molecules of which subsequently gave rise to one molecule of III and two molecules of benzene. Some support for this theory was obtained by showing that acetaldehyde and benzene did react to yield these same compounds and also that II gave rise to III in the presence of aluminum chloride. It was also noted that the yield of III increased with increasing time of reaction. Evidence had been given much earlier for this mechanism. In 1895, Radziewanowski (3) showed that in the absence of benzene, aluminum chloride catalyzed the conversion of II to III, and in 1931, Bodendorf (4) reported that acetaldehyde, benzene, aluminum chloride, and hydrogen chloride at 0° gave rise to ethylbenzene, II, and III.

A review of the literature indicated that the acid-catalyzed interaction of vinyl compounds and benzene has been the subject of several reports since as early as 1884. The interaction with vinyl bromide was reported to yield 1-bromo-2-phenylethane and 1,4-di-(β-bromoethyl)benzene by Hanriot and Guilbert (5) in 1884; ethylbenzene, II, and III by Angeblis and Anschütz (6) in 1884. These latter workers suggested the addition of

[1]*Presented at the 44th Annual Conference, Chemical Institute of Canada, at Montreal, August 3–5, 1961.*

hydrogen bromide to vinyl bromide to give 1,1-dibromoethane, which reacted with benzene to give II and III. Later in 1886, Anschütz (7) reported the formation of some styrene, ethylbenzene, II, and III from a similar reaction.

Vinyl chloride and benzene in the presence of a catalyst made from mercuric chloride and aluminum gave rise to II and III according to Böeseken and Bastet (8) in 1913 and similar products plus ethylbenzene were reported by Davidson and Lowy (9) in 1929. The former workers first postulated the formation of styrene to which benzene added to give II. However, styrene as a reactant did not give the same products, so other mechanisms were suggested including that proposed earlier by Angeblis and Anschütz (6) and one involving the intial production of 1-chloro-1-phenylethane, which reacted with benzene to give II. However, no such intermediate was isolated. Schramm (10) had in 1893 reported that 1-chloro-1-phenylethane reacted with benzene to give ethylbenzene, II, and III. The latter investigators showed that styrene could not be an intermediate and also that the major product at 0–5° was II with only traces of III, whereas at 60–70° the yield of II decreased and that of III increased appreciably. In 1946, Korshak, Samplavskaya, and Gervanovich (2) also reported compounds II and III and showed that the yield of II decreases while that of III increases as the time of reaction is increased. These same two products along with some ethylbenzene and styrene were claimed by Malinovskii (11) in 1949 to be formed by the reaction of vinyl chloride and benzene. He claimed that III arises from 1-chloro-1-phenylethane in the presence of the aluminum chloride catalyst. The reaction of benzene with three other vinyl ethers has also been reported. Using vinyl-*n*-butyl ether, Korshak *et al.* (2) in 1946 reported small yields of *n*-butylbenzene and a polymer of the vinyl ether, whilst, in 1938, Hopff (1) claimed that vinyl ethyl ether and acrylic acid reacted with benzene in the presence of an acid catalyst to give β-phenylethyl ether and β-phenylpropionic acid respectively. The interaction of three substituted vinyl compounds with benzene in the presence of aluminum chloride has also been studied. In 1930, Gibson and Johnson (12) reacted $(CHCl{=}CH)_2AsCl$ to yield a compound $C_{16}H_{14}$ (yellow plates, m.p. 179–180°); in 1950 Kirk (13), in a patent, claimed that $C(CH_3)_2{=}CHY$ gave $C_6H_4(C(CH_3)_2CH_2Y)_2$ (Y = Ac or COOH); and in 1952, Hurd and Gershbein (14) reported that isopropenyl acetate gave rise to acetophenone (I).

The structure of the polynuclear product reported in these investigations as 9,10-dimethyl-9,10-dihydroanthracene (III) had been questioned and finally proved incorrect. As early as 1885, Friedel and Crafts (15) believed this product to be 9,10-dimethylanthracene (IV). Later in 1926, Barnett and Matthews (16) suggested that the product obtained by Anschutz (7) was really IV because it had a relatively high melting point, formed a picrate, and was identical with the product obtained by the reaction of methyl magnesium iodide and 9-methylanthrone. The relationship was finally proved when in 1941, Badger, Goulden, and Warren (17) effected a sulphur dehydrogenation of authentic 9,10-dimethyl-9,10-dihydroanthracene to produce a yellow, fully aromatic compound, m.p. 180–182°, identical with the compound III obtained as described above, and when, in 1950, Badger, Jones, and Pearce (18) performed a similar dehydrogenation with aluminum chloride. This last observation suggests the route by which 9,10-dimethylanthracene was formed in all the reactions described earlier.

It was decided, therefore, to reinvestigate the aluminum chloride catalyzed reaction of vinyl derivatives and benzenoid hydrocarbons in an attempt to establish more completely the nature of the products of the reaction and, if possible, to suggest a plausible

mechanism for their formation. In a series of exploratory experiments* I, II, and III were confirmed as the major components of the product of reaction of vinyl acetate, benzene, and aluminum chloride. Compound III was identified by comparison with an authentic sample.† Other acids, including zinc chloride, zirconium tetrachloride, sulphuric acid, boron trifluoride, hydrogen fluoride, and aluminum chloride sulphate, were investigated but only zirconium tetrachloride was found to be equivalent to aluminum chloride for this reaction. Both nitromethane and carbon disulphide were studied as diluents. In the former case, product yields were decreased but with the latter solvent higher yields and less resinous material were obtained than if it had been omitted. The presence of acetophenone (I) suggested a mechanism involving attack by the acetylium ion (CH_3CO^+). It was of interest therefore to investigate the products of reaction in which vinyl formate replaced vinyl acetate. In this case no acetophenone, no benzaldehyde, nor, indeed, any carbonyl-containing fragment was detected. However, good yields of 9,10-dimethylanthracene (III) were again obtained, indicating that the formation of this compound involved the vinyl part of the ester molecule. It was further shown that in reactions involving vinyl formate, carbon monoxide was eliminated as determined by the color tests described by Fiegl (19) using phosphomolybdic acid and palladium chloride.

Conflicting reports have been noted regarding the possible intermediary role of styrene in this reaction. It may be conceived that styrene could arise as a result of the attack by the vinylium ion, $CH_2{=}CH^+$, on benzene, the product of which then may dimerize to 9,10-dimethyl-9,10-dihydroanthracene, which, as has been shown experimentally, may be dehydrogenated by aluminum chloride to give the final product 9,10-dimethylanthracene. Under the conditions used, styrene, in the presence of benzene and aluminum chloride, gave rise only to a polymeric substance, indicating the inadequacy of this mechanism. Similarly β-phenylethyl acetate was tested as a possible intermediate but in this case no anthracene derivative was detected but, instead, appreciable yields of 1,2-diphenylethane were obtained.

These preliminary observations only emphasized the need for a more thorough study of the interaction of vinyl derivatives and aromatic hydrocarbons to clarify the relationship of reaction conditions to the nature of the products and to establish a mechanism for their formation. Furthermore the ease of synthesis of 9,10-dimethylanthracene suggested that the method may be capable of development as a general one for the preparation of 9,10-dialkyl-substituted polynuclear hydrocarbons and their derivatives, depending on the choice of the unsaturated and benzenoid substances. In particular, this method of synthesis of 9,10-dimethylanthracene is an improvement over that involving the aryllithium intermediate as reported by Mikhailov and Kozminskaya (20), either of those involving a Grignard reaction as described by Sandin and Kitchen (21) and Barnett and Matthews (16), and over that in which metallic sodium is used as described by Bachmann and Chemerda (22).

Initially the emphasis has been on the yield and nature of the products of reaction of vinylacetate and benzene in the presence of aluminum chloride. The reaction procedure was essentially that described by Korshak *et al.* (2) and gave a crude reaction product in the form of a brownish yellow paste. Chromatographic separation of this crude product on alumina effected a partial separation, as shown in Table I.

Carried out as an undergraduate thesis requirement by A. Francis (1955), H. Ford (1957), and A. Notation (1958) for the B.E. degree, and in part by A. Currie (1954) for the M.A. degree.

†*Authentic sample of 9,10-dimethylanthracene kindly supplied by Dr. R. Sandin, University of Alberta.*

TABLE I

Chromatographic separation of reaction product of vinyl acetate and benzene*

Eluent	Vol. of eluent (ml)	Nature of product	Remarks
Light petroleum	200	Colorless oil	
	100	Oil and solid	
	200	Pale yellow solid	
	100	Pale yellow solid	
	100	Yellow oil	Carbonyl-containing fraction (1.94 g) (36%)
Light petroleum: benzene (1:1)	1100	Yellow oil	
	600	Yellow solid	"Hydrocarbon fraction" (0.49 g) (9.1%)
Benzene	400	Yellow solid	
Benzene: Et_2O (1:1)	800	Viscous oil	
Methanol	2500	Dark residue	

*Crude reaction product (5.83 g); alumina (200 g).

The pale yellow crystals obtained in the light petroleum eluate were identified as 9,10-dimethylanthracene and a study of the yield of this product is reported later. The product designated as "hydrocarbon fraction" was crystallized from carbon tetrachloride, then methanol, to give white crystals, m.p. 190–210°, which have not been further investigated.

The carbonyl-containing fraction gave a negative aldehyde test but a strong haloform reaction. Attempts were made to separate further the components of this fraction by thermal distillation and rechromatography. In neither case were pure compounds obtained since subsequent gas chromatographic separation using a Beckman, 6-ft silicone column showed that all such fractions were mixtures. It was later found that an initial distillation under reduced pressure (90–140° at 12 mm) of the crude reaction product permitted of a separation of a fraction containing the same components and in the same relative abundance as the carbonyl-containing fraction obtained by column chromatography. Using gas chromatography, and by repeated injections and collections of the compound represented by its peak of the chromatogram, a sample of three of the compounds was obtained. Rechromatography, followed by distillation, gave analytically pure samples, the analytical data of which are given in Table II.

TABLE II

Gas chromatographic separation of carbonyl-containing products*

Compound	Retention time (min)	% of injected sample†	B.p. at 12 mm (°C)	Analyses	
				C (%)	H (%)
1	6	20	88	79.44‡	7.12‡
2	9.3	2.0	85	—	—
3	13	33	120	80.86§	7.77§
4	17.6	2.5	114	82.08‖	9.29‖
5	27	2.2	—	—	—
6	29.6	5.1	—	—	—

*Six-foot silicone column, Beckman No. 17,449; temperature 220°; helium gas 0.91 cc/min; each injection 100 μl.
†Total recovery 64.8%.
‡Calc. for acetophenone: C, 79.97; H, 6.71%.
§Calc. for *p*-ethylacetophenone: C, 81.04; H, 8.16%.
‖Calc. for $C_{12}H_{16}O$: C, 81.77; H, 9.15%.

Compound 3 was readily shown to be *p*-ethylacetophenone by its oxidation to terephthalic acid, and by formation of the oxime, semicarbazone, and 2,4-dinitrophenylhydrazone derivatives. The retention time of an authentic sample of *p*-ethylacetophenone

was also 13 minutes. This is the first report that this compound constitutes a major part (18.5%) of the products of the aluminum chloride catalyzed reaction of vinyl acetate and benzene. Compound 4 has an analysis corresponding to a diethyl acetophenone and its identification is under study.

At this stage it became evident that the reaction, as performed, led to a complex mixture of products. To facilitate a mechanistic study it would be desirable to modify the reaction conditions to minimize the initial number of products and later to determine the nature of any secondary reactions. To this end a study was made of the effect of variation in molar ratio of benzene to vinyl acetate under conditions of excess threefold molar ratio aluminum chloride to vinyl acetate. For comparison the following yields were determined: total product; 9,10-dimethylanthracene; a distillate, b.p. → 150° at 12 mm; a distillate, b.p. 150–175° at 0.17 mm; and the residue. It had been found that a simple washing of the crude reaction product with methanol permitted an effective separation of the slightly soluble anthracene derivative (0.1% soluble) from all other reaction products. The methanol was evaporated from the resulting solution and the residue distilled. The results of this series of experiments are given in Table III.

TABLE III

Effect of ratio of benzene:vinyl acetate in aluminum chloride catalyzed reaction*

Molar ratio benzene:vinyl acetate	Reaction product		9,10-Dimethyl-anthracene (%)‡	Distillate		Residue (%)‡
	(g)	(%)†		→ 150° at 12 mm (%)‡	150–175° at 0.17 mm (%)‡	
100	15.4	63.5	6	38	37	18
50	14.9	61.5	14	42	17	28
50	16.2	67.0	12	42	27	19
50	15.6	64.5	11	46	22	21
10	14.2	58.8	19	36	28	17
7.5	15.6	64.5	24	50	12	14
6	18.2	75.0	29	46	14	11
5	20.0	82.7	24	51	11	16
4.5	17.8	73.5	18	50	15	17
4	18.2	75.0	15	52	20	13
2	18.2	75.0	0	55	19	26

*Each run: vinyl acetate (8.6 g, 0.1 mole); aluminum chloride (40 g, 0.3 mole).
†Based on a calculated yield of addition of 2 moles benzene to 1 mole vinyl acetate.
‡Percentage of total product.

Some observations regarding the mechanism of this reaction may be made from these data. There is a parallel relationship to be found between the variation in yield of 9,10-dimethylanthracene and that of the higher-boiling distillate fraction, the former going through a maximum and the latter a minimum at a molar ratio of benzene to vinyl acetate of about 6:1. The relative constancy of the yield of the lower-boiling distillate, which has already been shown to be the carbonyl-containing fraction, suggests that the components of this fraction arise by a reaction involving the acetoxy part of the ester, whereas the higher-boiling fraction and the anthracene derivative are related by a reaction involving the vinyl part. The observation, too, that the yield of 9,10-dimethylanthracene decreases with dilution greater than a molar ratio of 6:1 supports the belief that this product results by a dimerization of two primary products, and not by a mechanism in which the final step involves reaction with benzene. On the other hand the increasing yield as the ratio varies from 2:1 to 6:1 is difficult to interpret at this time but may involve the availability of the aluminum chloride – vinyl acetate complex. Further identification of the reaction products will aid in the understanding of this reaction.

EXPERIMENTAL

Aluminum Chloride Catalyzed Reaction of Vinyl Formate and Benzene

Vinyl formate (7.2 g, 0.1 mole) (obtained from Monomer–Polymer Inc., Leominster, Mass.) was added slowly over a period of 1 hour to a well-stirred mixture of benzene (78 g, 1 mole) and sublimed anhydrous aluminum chloride (40 g, 0.3 mole) in a 200-ml 3-necked flask equipped with reflux condenser, dropping funnel, and mechanical stirrer. Both the condenser and dropping funnel were fitted with calcium chloride drying tubes. Throughout the addition, the flask was cooled in an ice bath and the color changed from colorless through yellow to orange. The reaction mixture was allowed to warm to room temperature, during which time the color deepened to a brown, and then refluxed for 3 hours, after which the mixture was red colored. Pouring this mixture into a mixture of concentrated hydrochloric acid (75 ml) and crushed ice (75 g) resulted in the formation of a pale yellow precipitate (4.9 g), m.p. 182–185°. A mixed melting point with an authentic sample of 9,10-dimethylanthracene showed no depression.

Aluminum Chloride Catalyzed Reaction of β-Phenylethyl Acetate and Benzene

In a manner similar to that described above, β-phenylethyl acetate (27 g, 0.16 mole) was added dropwise to a mixture of benzene (100 ml) and aluminum chloride (22 g, 0.16 mole) over a period of 0.5 hour. After hydrolysis, the benzene layer was separated and the aqueous layer extracted twice with benzene. The combined benzene extracts were evaporated to yield a pale yellow oil. When the oil was cooled, crystals separated which were removed by filtration and washed with ethanol; yield, 6 g, m.p. 45–46°. Recrystallization from ethanol gave white crystals, m.p. 50–51°. A mixed melting point with an authentic sample of dibenzyl, m.p. 50–51° (prepared by the Clemmensen reduction of benzoin (23)), showed no depression.

Aluminum Chloride Catalyzed Reaction of Vinyl Acetate and Benzene

A typical procedure involved the addition of vinyl acetate (8.6 g, 0.1 mole) to benzene (78 g, 1.0 mole) and sublimed, anhydrous aluminum chloride (40 g, 0.3 mole) followed by treatment as described above. A modification involved washing the benzene extract first with sodium hydroxide (10%), then with water, before drying it over anhydrous sodium sulphate. After removal of the solvent, a semisolid product remained (16.4 g). A portion (5.38 g) of this crude product was chromatographed through alumina (200 g) using successively, light petroleum, light petroleum – benzene (1:1), benzene, benzene – diethyl ether (1:1), and methanol, collecting 100-ml fractions.

In the series of runs involving varying ratios of benzene to vinyl acetate a similar procedure was used. In all cases except those involving the 100:1 and the 2:1 ratios the crude product solidified to a yellow-colored paste. The product was washed from the reaction flask using methanol (15 ml) and filtered. The resulting yellow solid, 9,10-dimethylanthracene, was washed again with methanol (5 ml). Two such samples of crude product melted at 176–181° and 180–184°; reported, 180–181° (21).

ACKNOWLEDGMENTS

Grateful acknowledgment is made to the National Research Council and to Imperial Oil Limited for financial assistance.

REFERENCES

1. H. Hopff. German Patent No. 666,466 (1938).
2. V. V. Korshak, K. K. Samplavskaya, and A. I. Gershanovich. Zhur. Obscheĭ Khim. **16**, 1065 (1946).
3. C. Radziewanowski. Ber. **27**, 3235 (1894).
4. K. Bodendorf. J. prakt. Chem. **129**, 337 (1931).
5. M. Hanriot and J. Guilbert. Compt. rend. **98**, 525 (1884).
6. A. Angeblis and R. Anschütz. Ber. **17**, 167 (1884).
7. R. Anschütz. Ann. **235**, 299 (1886).
8. J. Böeseken and M. C. Bastet. Rec. trav. chim. **32**, 184 (1913).
9. J. M. Davidson and A. Lowy. J. Am. Chem. Soc. **51**, 2978 (1929).
10. J. Schramm. Ber. **26**, 1709 (1893).
11. M. S. Malinovskii. Zhur. Obscheĭ Khim. **17**, 2235 (1947).
12. C. S. Gibson and J. D. A. Johnson. J. Chem. Soc. 2785 (1930).
13. W. Kirk, Jr. U.S. Patent No. 2,497,673 (1950).
14. C. D. Hurd and L. L. Gershbein. J. Am. Chem. Soc. **74**, 3185 (1952).
15. C. Friedel and J. M. Crafts. Ann. chim. et phys. Ser. 6, **1**, 485 (1884).
16. E. de B. Barnett and M. A. Matthews. Ber. B, **59**, 1429 (1926).
17. G. M. Badger, F. Goulden, and F. L. Warren. J. Chem. Soc. 18 (1941).
18. G. M. Badger, M. L. Jones, and R. S. Pearce. J. Chem. Soc. 1700 (1950).
19. F. Fiegl. Spot tests. Vol. II. Elsevier Publishing Co. 1954.
20. B. M. Mikhailov and T. K. Kozminskaya. Doklady Akad. Nauk (U.S.S.R.), **58**, 811 (1947).
21. R. B. Sandin and R. Kitchen. J. Am. Chem. Soc. **67**, 1305 (1945).
22. W. E. Bachmann and J. W. Chemerda. J. Org. Chem. **4**, 583 (1939).
23. L. Gattermann. Laboratory methods of organic chemistry. Macmillan and Co. Ltd., London. 1937. p. 383.

SYNTHESIS OF POTENTIALLY PHYSIOLOGICALLY ACTIVE β-PHENYLETHYLAMINES

PART I. 3,4,5-TRIMETHOXY-α-AMINOMETHYLBENZYL ALCOHOL AND 4-ACETOXY-3,5-DIMETHOXY-α-AMINOMETHYLBENZYL ALCOHOL DERIVATIVES[1]

R. A. HEACOCK AND O. HUTZINGER
The Psychiatric Research Unit, University Hospital, Saskatoon, Saskatchewan

Received July 24, 1961

ABSTRACT

The preparation of several 3,4,5-trisubstituted-β-hydroxy-β-phenylethylamines related to mescaline, by the reduction or reductive alkylation of the corresponding nitroalcohols, is described.

Mescaline (I) has been known for many years to produce marked psychological changes in human subjects (see ref. 1 for some of the more important references), and many chemically similar substances have been prepared and examined for psychopharmacological activity (cf. ref. 2). However, little attention, so far, seems to have been given to the preparation or physiological activity of mescaline-like compounds with a hydroxyl group in the side chain on the carbon atom adjacent to the aromatic ring (i.e. as in adrenaline). As yet, only two compounds of this type have been described, but as far as the authors are aware, there are no reports in the literature of studies on the psychological activity of either of these two substances.

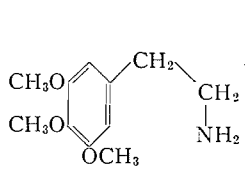

I

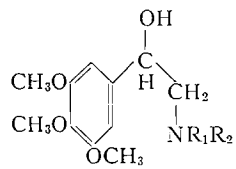

II

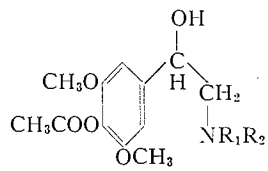

III

3,4,5-Trimethoxy-α-aminomethylbenzyl alcohol (II: $R_1 = R_2 = H$) was first prepared in 1931 by the catalytic reduction of 3,4,5-trimethoxybenzoyl cyanide (3). Twenty years later, it was shown that (II: $R_1 = R_2 = H$) could also be obtained by reduction of the corresponding aryl cyanohydrin (or aroyl cyanide) with lithium aluminum hydride (4, 5). The *N*-methyl analogue (II: $R_1 = CH_3$; $R_2 = H$) has been prepared by the catalytic hydrogenation of ω-(*N*-benzyl-*N*-methyl)-amino-3,4,5-trimethoxybenzophenone (6).

This communication describes a simple method for the synthesis of compounds of this nature by the reduction or reductive alkylation (cf. ref. 7) of suitable α-phenyl-β-nitroethanol derivatives. (These nitroalcohols are readily available by the method of Heacock, Hutzinger, and Nerenberg (8).)

The reduction of α-phenyl-β-nitroethanol derivatives with sodium amalgam and dilute acetic acid to the corresponding α-phenyl-β-aminoethanol was first described by Rosenmund (9). Later, Kanao obtained 3,4-diacetoxy-α-aminomethylbenzyl alcohol from the reduction of 3,4-diacetoxy-α-nitromethylbenzyl alcohol with zinc and dilute acetic acid

[1]*This investigation was supported by grants from the Government of Saskatchewan (Department of Public Health) and the Department of National Health and Welfare, Ottawa.*

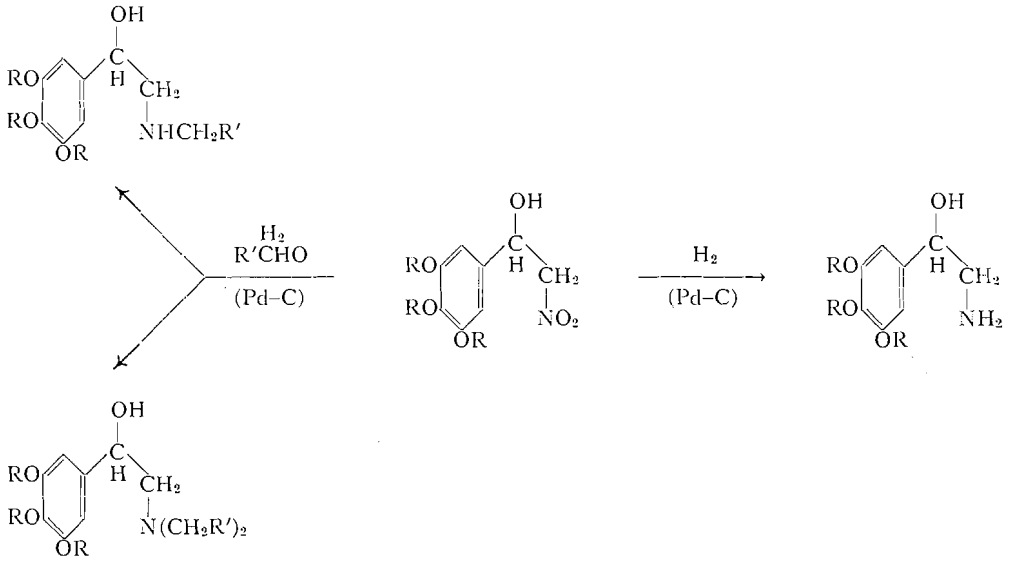

(10). This author also reported several reductive alkylations of 3,4-diacetoxy-α-nitromethylbenzyl alcohol with zinc and dilute acetic acid in the presence of about one mole of a suitable aldehyde (10). Recently, Axelrod *et al.* prepared O^4-benzylnormetanephrine by the catalytic hydrogenation of 4-benzyloxy-3-methoxy-α-nitromethylbenzyl alcohol (11). O^4-Acetylnormetanephrine and O^4-acetylmetanephrine have recently been obtained from 4-acetoxy-3-methoxy-α-nitromethylbenzyl alcohol by catalytic reduction and reductive alkylation respectively (12).

3,4,5-Trimethoxy-α-aminomethylbenzyl alcohol (II: $R_1 = R_2 = H$) has been obtained in high yield (as the hydrochloride or oxalate salt) by catalytic hydrogenation of 3,4,5-trimethoxy-α-nitromethylbenzyl alcohol in aqueous suspension. If the hydrogenation was carried out in the presence of 1 equivalent of formaldehyde, reductive alkylation occurred with the formation of the monomethylamino derivative (i.e. 3,4,5-trimethoxy-α-methylaminomethylbenzyl alcohol; II: $R_1 = CH_3$; $R_2 = H$); reduction in the presence of 3 to 4 equivalents of formaldehyde lead to the formation of the dimethylamino derivative (i.e. 3,4,5-trimethoxy-α-dimethylaminomethylbenzyl alcohol; II: $R_1 = R_2 = CH_3$). 4-Acetoxy-3,5-dimethoxy-α-aminomethylbenzyl alcohol (III: $R_1 = R_2 = H$) and the corresponding *N*-methyl (III: $R_1 = CH_3$; $R_2 = H$) and *N*,*N*-dimethyl (III: $R_1 = R_2 = CH_3$) derivative could be obtained (as the oxalates) in an analogous manner from 4-acetoxy-3,5-dimethoxy-α-nitromethylbenzyl alcohol.

In view of the possibility of an intermolecular cyclization reaction of the Pictet–Spengler type (cf. ref. 13) occurring during the reductive alkylations which would have presumably led to the formation of tetrahydroisoquinoline derivatives, a sample of the product assumed to be 3,4,5-trimethoxy-α-dimethylaminomethylbenzyl alcohol (II: $R_1 = R_2 = CH_3$) was oxidized with aqueous alkaline potassium permanganate. 3,4,5-Trimethoxybenzoic acid was obtained, indicating that cyclization had not occurred, since a phthalic acid derivative would have been expected from the permanganate oxidation products of the tetrahydroisoquinoline ring system.

Further synthetic work in this field is underway and the physiological activity of this group of substances is under investigation. The results will be reported elsewhere in due course.

TABLE I

3,4,5-Trimethoxy-α-aminomethylbenzyl alcohol derivatives[a]

Substance prepared			Reagent employed[b]		Properties		
					Yield[c]		
R_1	R_2	Salt	Acid component	Formaldehyde solution in water (36%)	g	%	M.p. (°C)
H	H	Oxalate[d]	—	—	—	—	190–191 (decomp.)
H	H	Hydrogen oxalate[d]	—	—	—	—	188–189 (decomp.)
H	H	Hydrochloride[e]	3.8 ml *N* HCl	—	0.75	73	202–203
H	CH_3	Hydrogen oxalate	0.5 g oxalic acid[f]	0.33 ml (≡ 1 mole)	0.5	39	202 (decomp.)
H	CH_3	Hydrochloride	3.8 ml *N* HCl	0.33 ml (≡ 1 mole)	0.5	46	172
CH_3	CH_3	Hydrogen oxalate	0.5 g oxalic acid[f]	1 ml (≡ 3 moles)	0.4	30	154–155 (decomp.)
CH_3	CH_3	Hydrochloride	3.8 ml *N* HCl	1 ml (≡ 3 moles)	0.8	70	201

[a]In all cases, the preparation and properties of the DL-mixture of optical isomers are described.
[b]The hydrogenations were carried out in water (150 ml). The quantities of reagents given are for the reduction or reductive alkylation of 1 g of the nitroalcohol.
[c]The yields given are based on the reduction or reductive alkylation of 1 g of the nitroalcohol.
[d]Prepared from base and calculated amounts of oxalic acid. (Hydrogenation in the presence of 1 or 2 moles of oxalic acid invariably led to the formation of mixtures of the neutral and acid oxalates, which proved to be difficult to separate by recrystal-

TABLE II

4-Acetoxy-3,5-dimethoxy-α-aminomethylbenzyl alcohol derivatives[a]

Substance prepared			Reagent employed[b]		Properties	
					Yield[c]	
R_1	R_2	Salt	Acid component	Formaldehyde solution in water (36%)	g	%
H	H	Oxalate	0.22 g oxalic acid[d]	—	0.4	38
H	H	Hydrochloride	3.4 ml *N* HCl	—	0.8	78
H	CH_3[e]	Oxalate	0.22 g oxalic acid[d]	0.3 ml (≡ 1 mole)	0.8	73
CH_3	CH_3	Hydrogen oxalate	0.44 g oxalic acid[d]	0.9 ml (≡ 3 moles)	0.4	76
CH_3	CH_3	Hydrochloride	3.4 ml *N* HCl	0.9 ml (≡ 3 moles)	0.6	53

[a]In all cases, the preparation and properties of the DL-mixture of optical isomers are described.
[b]The hydrogenations were usually carried out in an ethanol/water (1:2) mixture (150 ml). The quantities of reagents given are for the reduction or reductive alkylation of 1 g of the nitroalcohol.
[c]The yields given are based on the reduction or reductive alkylation of 1 g of the nitroalcohol.
[d]Oxalic acid dihydrate was used in all these preparations.

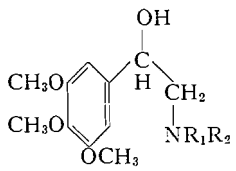

of purified product		Analysis							
		Found				Calculated			
Crystalline form	M.p. reported in literature (°C)	C	H	N	Cl	C	H	N	Cl
Colorless needles from 95% ethanol	—	52.85	6.76	5.17	—	52.93	6.66	5.14	—
Colorless needles from ethanol	—	49.35	6.00	4.43	—	49.21	6.04	4.41	—
Colorless plates from ethanol	189–192 (4) 203 (3)	50.10	6.98	5.41	—	50.09	6.88	5.32	—
Small colorless plates from 95% ethanol	—	50.69	6.39	4.29	—	50.57	6.39	4.23	—
Colorless prisms from isopropanol	168–169 (6)[g]	51.89	7.12	4.91	12.72	51.89	7.25	5.05	12.77
Colorless prisms from 5% light petroleum (b.p. 60–80°) in ethanol	—	52.14	6.71	4.05	—	52.17	6.71	4.06	—
Colorless prisms from isopropanol	—	53.36	7.39	4.66	11.95	53.51	7.60	4.81	12.15

lization.)
[e]The corresponding free base (i.e. 3,4,5-trimethoxy-α-aminomethylbenzyl alcohol) was prepared by treating a solution of the hydrochloride with strong alkali, extracting with benzene, and recrystallizing the product from toluene, m.p. 141°. (Previously reported m.p.'s: 138° (4), 141–142° (5), 144° (3). Analysis: Found: C, 58.20; H, 7.66. Calc. for $C_{11}H_{17}O_4N$: C, 58.13; H, 7.54%.)
[f]Oxalic acid dihydrate was used in all these preparations.
[g]Incorrectly named as 3,4,5-trimethoxy-α-aminomethylbenzyl alcohol hydrochloride in Chem. Abstr. 47, 8036 (1953).

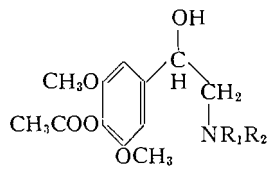

of purified product		Analysis							
		Found				Calculated			
M.p. (°C)	Crystalline form	C	H	N	Cl	C	H	N	Cl
182 (decomp.)	Small colorless plates from 95% ethanol	52.18	6.11	4.60	—	52.00	6.05	4.67	—
197	Small colorless prisms from ethanol	49.18	6.22	4.55	12.18	49.40	6.22	4.81	12.15
211–212 (decomp.)	Small colorless prisms from ethanol	53.36	6.36	4.18	—	53.50	6.41	4.45	—
172 (decomp.)	Colorless needles from ethanol	51.36	6.28	3.71	—	51.47	6.21	3.75	—
177–178	Colorless prisms from MEK[f]	52.49	6.91	4.14	10.83	52.58	6.94	4.38	11.08

[e]It was not possible to prepare a pure sample of the hydrochloride salt of 4-acetoxy-3,5-dimethoxy-α-methylaminomethylbenzyl alcohol, either from attempts to prepare the salt directly by hydrogenation in the presence of hydrochloric acid or by treatment of the corresponding oxalate with calcium chloride. Two different substances, m.p.'s 207–209° and 150–151° respectively, were obtained, but in neither case could a completely satisfactory analysis for the desired product be obtained.
[f]MEK = methyl ethyl ketone.

EXPERIMENTAL

*General Procedure for Reduction and Reductive Alkylation**

A suspension of the nitroalcohol (prepared by the method of Heacock, Hutzinger, and Nerenberg (8)) containing one third of its weight of a palladium catalyst (5% on charcoal), an acid component, and formaldehyde (where applicable, see tables), was shaken in the presence of hydrogen at atmospheric pressure until the calculated amount was taken up. After filtration of the reaction mixture, the product was concentrated to dryness *in vacuo* (below 40°) and the residue was recrystallized from a suitable solvent.

Oxidation of 3,4,5-Trimethoxy-α-dimethylaminomethylbenzyl Alcohol Hydrochloride

A solution of 3,4,5-trimethoxy-α-dimethylaminomethylbenzyl alcohol hydrochloride† (0.2 g) in 1% aqueous sodium hydroxide (10 ml) was oxidized with potassium permanganate (0.6 g), the solution being maintained at 90° C for 2 hours. The reaction mixture was acidified with dilute sulphuric acid, after filtration, and the white solid which separated was recrystallized from aqueous ethanol. Colorless needles, m.p. 171–172°, were obtained, which were identical in all respects (no depression of melting point and identical infrared spectra) with an authentic sample of 3,4,5-trimethoxybenzoic acid.

REFERENCES

1. F. Benington, R. D. Morin, and L. C. Clark. J. Org. Chem. **19**, 11 (1954).
2. F. Benington, R. D. Morin, L. C. Clark, and R. P. Fox. J. Org. Chem. **23**, 1979 (1958).
3. K. Kindler and W. Peschke. Arch. Pharm. **269**, 581 (1931).
4. A. Dornow and G. Petsch. Arch. Pharm. **284**, 160 (1951).
5. A. Dornow and G. Petsch. Arch. Pharm. **285**, 323 (1952).
6. M. Semonský and V. Zikán. Chem. listy, **46**, 667 (1952); Chem. Abstr. **47**, 8036 (1953).
7. W. S. Emerson. *In* Organic reactions. Vol. IV. *Edited by* R. Adams. J. Wiley and Sons. Inc., New York. 1948. p. 174.
8. R. A. Heacock, O. Hutzinger, and C. Nerenberg. Can. J. Chem. **39**, 1143 (1961).
9. K. W. Rosenmund. Ber. **46**, 1034 (1913).
10. S. Kanao. J. Pharm. Soc. Japan, **49**, 239 (1929); Chem. Abstr. **23**, 5162 (1929).
11. J. Axelrod, S. Senoh, and B. Witkop. J. Biol. Chem. **233**, 697 (1958).
12. R. A. Heacock and O. Hutzinger. Chem. & Ind. (London), 595 (1961).
13. W. M. Whaley and T. R. Govindachari. *In* Organic reactions. Vol. VI. *Edited by* R. Adams. J. Wiley and Sons, Inc., New York. 1951. p. 151.

**The specific quantities of reagents used in each case are given in Tables I and II.*

†One example of a substance prepared by reductive alkylation of the nitroalcohol was chosen arbitrarily for oxidation. It was assumed that the other compounds prepared in this fashion would behave similarly on oxidation.

SYNTHESIS OF POTENTIALLY PHYSIOLOGICALLY ACTIVE β-PHENYLETHYLAMINES

PART II. 3,4-METHYLENEDIOXY-α-AMINOMETHYLBENZYL ALCOHOL DERIVATIVES[1, 2]

R. A. HEACOCK, O. HUTZINGER, AND C. NERENBERG[3]
The Psychiatric Research Unit, University Hospital, Saskatoon, Saskatchewan
Received July 24, 1961

ABSTRACT

The preparation of 3,4-methylenedioxy-α-aminomethylbenzyl alcohol and a number of its *N*-alkyl and *N,N*-dialkyl derivatives by the reduction or reductive alkylation of 3,4-methylenedioxy-α-nitromethylbenzyl alcohol is described.

As a prerequisite for an examination of the physiological activity of several groups of compounds related to adrenaline, the preparation of a number of substituted α-aminomethylbenzyl alcohols has been undertaken. The methylenedioxyphenyl group is present in many naturally occurring physiologically important substances and a series of *N*-substituted derivatives of 3,4-methylenedioxy-α-aminomethylbenzyl alcohol has been prepared in order to study the effects of variation of the *N*-substituent on the physiological activity of this particular series of compounds.

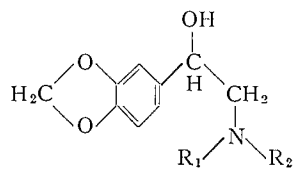

I

3,4-Methylenedioxy-α-methylaminomethylbenzyl alcohol (I: $R_1 = CH_3$; $R_2 = H$) was the first member of this series to be described (1) and was obtained by the action of methylamine on 3,4-methylenedioxy-α-bromomethylbenzyl alcohol. The dimethylamino analogue (I: $R_1 = R_2 = CH_3$) was obtained a few years later by a similar route (2). The analogous primary amino compound, 3,4-methylenedioxy-α-aminomethylbenzyl alcohol (I: $R_1 = R_2 = H$), was prepared, several years later, by the reduction of piperonal cyanohydrin with sodium amalgam in dilute acetic acid (3). Subsequently several authors have repeated and improved the afore-mentioned procedures (4, 5, 6, 7, 8). 3,4-Methylenedioxy-α-aminomethylbenzyl alcohol (I: $R_1 = R_2 = H$) has also been obtained by the catalytic reduction of (*a*) 3,4-methylenedioxybenzoyl cyanide (9) (reported to give better yields than reduction of the corresponding cyanohydrin), and of (*b*) ω-nitro-3,4-methylenedioxyacetophenone (10). Two further methods have been described for the preparation

[1]*This investigation was supported by grants from the Government of Saskatchewan (Department of Public Health) and the Department of National Health and Welfare, Ottawa.*
[2]*Part I. Can. J. Chem. This issue.*
[3]*Present address: Research Division, Columbus Psychiatric Institute and Hospital, Ohio State University Health Center, Columbus 10, Ohio, U.S.A.*

of compounds in this series. Firstly, by the decarboxylation of suitable 3,4-methylenedioxyphenylserine derivatives (11), which are readily available by the condensation of piperonal with an alkylglycine derivative (12), and secondly, 3,4-methylenedioxy-α-methylaminobenzyl alcohol (I: $R_1 = CH_3$; $R_2 = H$) has been obtained by the acid hydrolysis of 3-methyl-5-(3,4-methylenedioxyphenyl)-2-oxazolidone (13).

The preparation of α-aminomethylbenzyl alcohol derivatives by the reduction or reductive alkylation of the corresponding α-phenyl-β-nitroalcohol derivative has been discussed in Part I of this series (14) and these general procedures have been extended to the synthesis of 3,4-methylenedioxy-α-aminomethylbenzyl alcohol and a number of its *N*-alkyl and *N*,*N*-dialkyl derivatives.

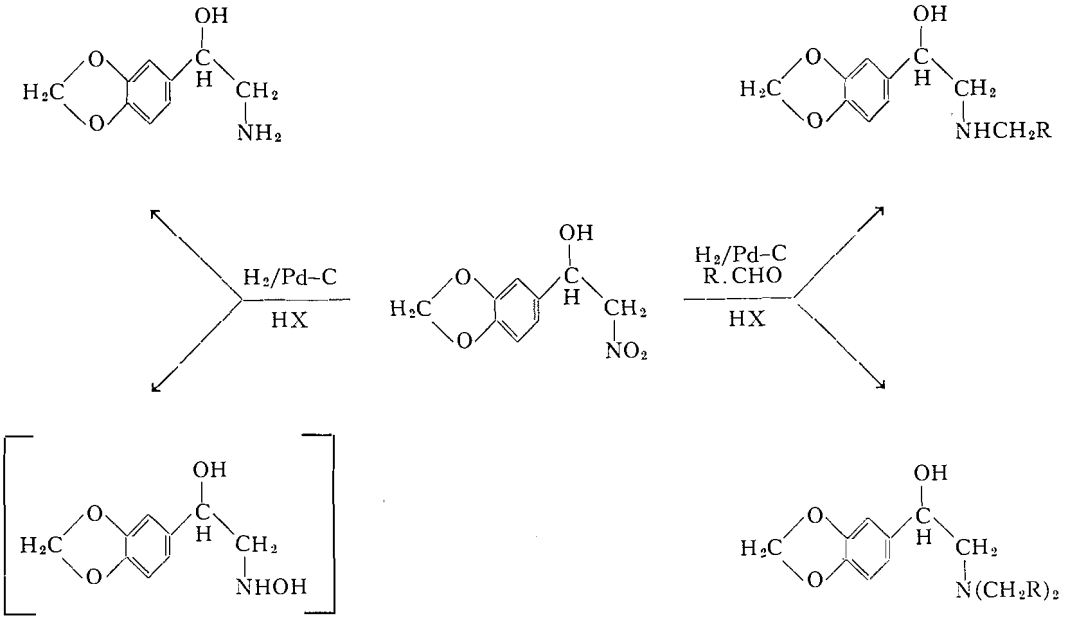

3,4-Methylenedioxy-α-nitromethylbenzyl alcohol was reduced catalytically with hydrogen in aqueous suspension, at atmospheric pressure in the presence of 1 mole of oxalic acid; 3,4-methylenedioxy-α-aminomethylbenzyl alcohol was isolated as the "neutral" oxalate salt after the calculated quantity of hydrogen had been taken up. The presence of oxalic acid enabled the product to be isolated easily, as the oxalate salt crystallizes well. It should be noted that the neutral oxalate was invariably obtained irrespective of the amount of oxalic acid present. The hydrogen oxalate of 3,4-methylenedioxy-α-aminomethylbenzyl alcohol had previously been reported (7, 10) and it was claimed that it could be recrystallized from water (10). During the present investigation, however, it was only found possible to obtain the acid salt by treatment of the neutral oxalate with an excess of oxalic acid in absolute ethanol, followed by recrystallization of the product from a cold, saturated solution of oxalic acid in absolute ethanol. Attempted recrystallization of the acid oxalate from water always led, in our hands, to the formation of the neutral salt.

The catalytic hydrogenation of a number of similar α-phenyl-β-nitroalcohols using a

5% palladium-on-charcoal catalyst in the presence of oxalic acid had previously been reported to give the corresponding α-hydroxylaminomethylbenzyl alcohol derivatives (16). The formation of the hydroxylamino derivatives requires the uptake of 2 molecules of hydrogen as opposed to the 3 molecules required for the total reduction of the nitro group. We have found that with the 3,4-methylenedioxy-α-nitromethylbenzyl alcohol the reaction proceeded to completion easily. However, if the uptake of hydrogen was arrested after approximately 2 molecules of hydrogen had been absorbed, 3,4-methylenedioxy-α-hydroxylaminomethylbenzyl alcohol could be obtained (as the oxalate salt). All attempts to isolate 3,4-methylenedioxy-α-hydroxylaminomethylbenzyl alcohol as the free base from the oxalate salt were unsuccessful. This type of hydroxylamine derivative is known to be unstable in alkali and to rapidly form the corresponding *N*-(β-hydroxy-β-phenylethyl)-isobenzaldoxime (cf. ref. 16). It would thus appear that in the present case attempts to prepare the hydroxylamine derivative as the free base led to the formation of *N*-(β-hydroxy-β-(3,4-methylenedioxyphenyl)-ethyl)-3′,4′-methylenedioxyisobenzaldoxime (II).

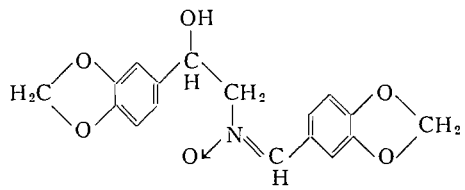

II

Our earlier experiments were carried out with oxalic acid rather than a mineral acid to avoid the possibility of ω-nitrostyrene formation by dehydration of the nitroalcohol (cf. ref. 15) prior to its reduction. However, it was subsequently found that this did not occur readily and the hydrochloride salts could be prepared directly.

The reductive alkylations were carried out with 1 mole or 3–4 moles respectively of the desired carbonyl component, the products usually being the mono- or di-alkylamino derivatives respectively. In cases where steric hindrance could be a factor (e.g. when the carbonyl compound was a branched-chain aldehyde or a ketone, i.e. in the cases studied: acetone and isobutyraldehyde) even in the presence of a large excess of the carbonyl component, only the monoalkyl derivative was obtained.

When the reductive alkylation was carried out in the presence of 1 mole of oxalic acid, usually the mono- and di-alkyl derivatives were obtained as the hydrogen oxalate. In the only case studied (i.e. the *N*-monomethyl derivative) the neutral oxalate was obtained in the presence of a ½ mole of oxalic acid. The *N*-monoethyl derivative behaved anomalously, giving the neutral oxalate under all conditions investigated. The free bases could be obtained by treating the crude reduction mixtures with strong aqueous alkali followed by benzene extraction. In general, the monoalkyl derivatives were solids and the dialkyl derivatives oils at room temperature.

In most cases, the hydrochloride salts can be obtained directly (i.e. hydrogenation in the presence of hydrochloric acid) or by treatment of the free base with 1 equivalent of aqueous hydrochloric acid and removing the solvent *in vacuo* below 40°. Attempts to obtain the hydrochlorides by treating the base in dry ether (or dry benzene) with gaseous hydrogen chloride (or a saturated solution of hydrogen chloride in absolute

ethanol) sometimes led to anomalous results. (Microanalysis often suggested that the product contained two chlorine atoms.) The lability of the side-chain hydroxyl group in compounds of this nature is well known (cf. ref. 17), particularly when under the influence of the 3,4-dialkoxy substitution in the benzene ring. However, the exact nature of this phenomenon is still not fully understood and will be subject to further investigation. Unsuccessful attempts were made to effect reductive alkylation using 1,3-dihydroxyacetone, furfuraldehyde, and benzaldehyde as the carbonyl component. In all cases the unalkylated primary amino derivative was obtained. (Kanao (18) prepared the *N*-benzyl and *N*-furfuryl derivatives of 3,4-diacetoxy-α-aminomethylbenzyl alcohol by the reduction of 3,4-diacetoxy-α-nitromethylbenzyl alcohol with zinc and acetic acid in the presence of benzaldehyde and furfuraldehyde respectively.)

In view of the possibility of an intermolecular cyclization reaction of the Pictet–Spengler type (cf. ref. 19) occurring during the reductive alkylation, which would have presumably led to the formation of tetrahydroisoquinoline derivatives, a sample of the product assumed to be 3,4-methylenedioxy-α-*n*-propylaminomethylbenzyl alcohol* was oxidized with aqueous alkaline potassium permanganate; piperonylic acid was obtained, indicating that cyclization had not occurred, since a phthalic acid derivative would have been expected from the permanganate oxidation products of the tetrahydroisoquinoline ring system.

The physiological activity of these compounds will be the subject of a further study and the results will be reported elsewhere in due course.

EXPERIMENTAL

3,4-Methylenedioxy-α-nitromethylbenzyl Alcohol

3,4-Methylenedioxy-α-nitromethylbenzyl alcohol was prepared by the method of Heacock *et al.* (20).

Reduction and Reductive Alkylation of 3,4-Methylenedioxy-α-nitromethylbenzyl Alcohol

An aqueous suspension† of the above nitroalcohol, together with one third of its weight of a 5% palladium-on-charcoal catalyst, oxalic acid (or hydrochloric acid) (1 mole), and where applicable, 1 or 3–4 moles of the desired carbonyl compound, was shaken in hydrogen (atmospheric pressure; room temperature). After the hydrogen uptake was complete (4–6 hours), the reaction mixture was filtered and the filtrate was concentrated *in vacuo*, below 40°, and the residue recrystallized from a suitable solvent.

For the preparation of the free base, 40% aqueous sodium hydroxide was added to an aqueous solution of the oxalate or hydrochloride salt (or the filtrate from the crude reduction mixture), and the free base extracted with benzene. After concentration of the dried (Na_2SO_4) extract to dryness the crude product was purified either by distillation in high vacuum or by recrystallization from a suitable solvent. In some cases where difficulties were encountered in crystallizing the oxalates or hydrochlorides, the picrates were prepared for the accurate characterization of the bases. In the case of the *N*,*N*-divaleryl base, no crystalline salts could be obtained, but the free base had a satisfactory analysis.

Full details of the compounds prepared are given in Tables I, II, and III.

Oxidation of 3,4-Methylenedioxy-α-n-propylaminomethylbenzyl Alcohol Hydrochloride

A solution of 3,4-methylenedioxy-α-*n*-propylaminomethylbenzyl alcohol hydrochloride (0.2 g) in water (10 ml) and aqueous sodium hydroxide (2 *N*: 0.6 ml) was oxidized with potassium permanganate (0.6 g) at 90° for 2 hours. After filtration, the reaction mixture was acidified with dilute sulphuric acid and the white solid that was obtained recrystallized from aqueous ethanol. Small colorless needles of piperonylic acid, m.p. 230°, were obtained which were identical in all respects (i.e. no depression of melting point and identical infrared spectra) with a sample of authentic piperonylic acid.

**One compound, during the preparation of which a cyclization of this type could have occurred, was chosen arbitrarily for oxidation. It was considered justifiable to assume that other substances prepared in a similar manner would behave similarly on oxidation.*

†Water proved to be the most satisfactory solvent for the reductions and reductive alkylations. Several preliminary runs were made in methanol but the reaction was much slower, possibly due to the relatively low solubility of some of the oxalate salts in methanol. With methanol as a solvent a considerable amount of the product was adsorbed onto the catalyst and unless the catalyst was repeatedly extracted with hot water the yields obtained were very low.

TABLE I

3,4-Methylenedioxy-α-aminomethylbenzyl alcohol derivatives (salts)[a]

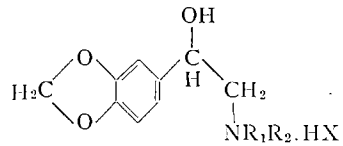

Compound	Substance prepared			Reagents employed[b]		Properties of pure compound				
						Yield[b]				
	R_1	R_2	Salt	Acid component	Carbonyl component	(g)	(%)	M.p. (°C)	Crystalline form	M.p. reported in literature (°C)
1	H	H	Oxalate	0.3 g oxalic acid[c]	—	0.7	54.5	248–249 (decomp.)	Thin colorless plates from water	—
2	H	H	Hydrogen oxalate	*d*	—	—	—	202 (decomp.)	Colorless prisms from a saturated solution of oxalic acid in ethanol	180 (10) 197 (7)
3	H	H	Hydrochloride	4.7 ml *N* HCl	—	0.5	48.5	192	Colorless prisms from ethanol	176 (3); 181–182 (8); 182–183 (7); 192 (9)
4	H	H	Hydrogen tartrate	0.7 g tartaric acid	—	0.8	51	163–165	Small colorless prisms from ethanol	—
5	H	CH_3	Oxalate	0.3 g oxalic acid	0.4 ml HCHO (36% in H_2O)	0.4	35	178–179 (decomp.)	Small colorless prisms from ethanol	—
6	H	CH_3	Hydrogen oxalate	0.6 g oxalic acid	0.4 ml HCHO (36% in H_2O)	0.3	22	168 (decomp.)	Small colorless prisms from ethanol	—
7	H	CH_3	Hydrochloride	—	—	*e*	—	136[f]	Colorless needles from ethanol/MEK[g]	163–165 (8)[f]
8	CH_3	CH_3	Hydrogen oxalate	0.6 g oxalic acid	1.2 ml HCHO (36% in H_2O)	1.0	71	130–132	Colorless prisms from ethanol/benzene	—
9	CH_3	CH_3	Hydrochloride	4.7 ml *N* HCl	1.2 ml HCHO (36% in H_2O)	0.6	52	175–176[h]	Small colorless prisms from ethanol/benzene	151–153 (2)[h]
10	H	C_2H_5	Oxalate	0.3 g oxalic acid	0.27 ml CH_3CHO	0.45	37.5	214–215 (decomp.)	Small colorless prisms from 95% ethanol	—
11	H	C_2H_5	Hydrochloride	4.7 ml *N* HCl	0.27 ml CH_3CHO	0.4	34.5	164–165[i]	Colorless prisms from isopropanol	—
12	C_2H_5	C_2H_5[j]	Hydrochloride	4.7 ml *N* HCl	0.8 ml CH_3CHO	0.6	46	138–139	Small colorless plates from isopropanol/ether	—

TABLE I (*Continued*)

Compound	Substance prepared			Reagents employed[b]		Yield[b]		Properties of pure compound		
	R_1	R_2	Salt	Acid component	Carbonyl component	(g)	(%)	M.p. (°C)	Crystalline form	M.p. reported in literature (°C)
13	H	n-C_3H_7	Hydrogen oxalate	0.6 g oxalic acid	0.35 ml CH_3CH_2CHO	0.6	40.5	180–181 (decomp.)	Colorless prisms from ethanol	—
14	H	n-C_3H_7	Hydrochloride	4.7 ml N HCl	0.35 ml CH_3CH_2CHO	0.8	47	156–157[k]	Colorless plates from isopropanol	—
15	n-C_3H_7	n-C_3H_7[m]	Hydrogen oxalate	0.6 g oxalic acid	1.05 ml CH_3CH_2CHO	0.6	36	98	Colorless prisms from ethanol/LP[l]	—
16	H	n-C_4H_9	Hydrogen oxalate	0.6 g oxalic acid	0.42 ml $CH_3(CH_2)_2CHO$	1.05	67	178 (decomp.)	Colorless prisms from 95% ethanol	—
17	H	n-C_4H_9	Hydrochloride	—	—	*e*	—	162	Colorless prisms from MEK[g]	—
18	n-C_4H_9	n-C_4H_9[n]	Hydrogen oxalate	0.6 g oxalic acid	1.3 ml $CH_3(CH_2)_2CHO$	1.2	66	133–134	Colorless prisms from ethanol/LP[l]	—
19	H	n-C_5H_{11}	Hydrogen oxalate	0.6 g oxalic acid	0.5 ml $CH_3(CH_2)_3CHO$	1.1	67	186	Colorless prisms from MEK[g]	—
20	H	n-C_5H_{11}	Hydrochloride	—	—	*e*	—	196	Colorless plates from MEK[g]	—
21	n-C_5H_{11}	n-C_5H_{11}	—	0.6 g oxalic acid	1.5 ml $CH_3(CH_2)_3CHO$	*o*	—	—	—	—
22	H	i-C_3H_7[p]	Hydrochloride	4.7 ml N HCl	0.35 ml CH_3COCH_3	0.8	47	179	Colorless needles from isopropanol	—
23	H	i-C_4H_9	Hydrogen oxalate	0.6 oxalic acid	0.42 ml CH_3>CH—CHO CH_3	0.5	32	198 (decomp.)	Colorless prisms from ethanol	—
24	H	i-C_4H_9	Hydrochloride	—	—	*e*	—	162–163	Colorless plates from MEK[g]	—

NOTE: Footnotes to table on facing page.

[a]The properties of the compounds described here will be those of DL-mixtures of the two possible optical isomers.
[b]The quantities of reagents used and the yields obtained are for the reduction or reductive alkylation of 1 g of 3,4-methylenedioxy-α-nitromethylbenzyl alcohol.
[c]Oxalic acid dihydrate was used in all these preparations.
[d]The hydrogen oxalate was prepared from the neutral oxalate by treatment with an excess of oxalic acid in ethanolic solution.
[e]The hydrochloride was prepared from the free base and the calculated amount of aqueous hydrochloric acid, followed by concentration of the reaction mixture *in vacuo* below 40°.
[f]All attempts to prepare this hydrochloride directly by carrying out the reductive alkylation in the presence of hydrochloric acid were unsuccessful. Dialkylation invariably occurred and 3,4-methylenedioxy-α-dimethylaminomethylbenzyl alcohol hydrochloride was always obtained. 3,4-Methylenedioxy-α-methylaminomethylbenzyl alcohol hydrochloride (m.p. 136°) was prepared by treatment of the free base with 1 equivalent of hydrochloric acid in aqueous solution. A white crystalline solid (m.p. 156–157° with decomposition) was obtained from an attempt to prepare this hydrochloride by passage of dry hydrogen chloride gas into a solution of the free base in dry benzene. Analysis of this compound indicated that it probably contained two chlorine atoms per molecule (found: C, 49.03; H, 5.13; Cl, 27.60%). Adityachaudhury and Chatterjee report a melting point of 163–165° (with decomposition) for 3,4-methylenedioxy-α-methylaminomethylbenzyl alcohol hydrochloride, prepared by the action of hydrogen chloride gas on a solution of the free base in ether. In view of the proximity of this melting point to that obtained by the authors for the "chlorohydrochloride", it is possible that Adityachaudhury and Chatterjee did not, in fact, have the true hydrochloride, although they do report a satisfactory analysis for this salt (8).
[g]MEK = Methyl ethyl ketone.
[h]As in the case of the monomethylamino derivative, 3,4-methylenedioxy-α-dimethylaminomethylbenzyl alcohol hydrochloride (m.p. 175–176°) was prepared in aqueous solution. Attempts to prepare this salt by passage of dry hydrogen chloride gas into a solution of the free base in dry benzene (or dry ether) gave a white crystalline solid, m.p. 151–152° (with decomposition). Analysis of this compound indicated that it probably contained two chlorine atoms per molecule; probably the β-hydroxy group in the ethylamine side chain had been replaced by chlorine to give 3,4-methylenedioxy-α-dimethylaminomethylbenzyl chloride hydrochloride. Found: C, 49.88; H, 5.78; N, 5.37; Cl, 26.74. Calc. for $C_{11}H_{15}O_2NCl_2$: C, 50.02; H, 5.73; N, 5.31; Cl, 26.85%. The same substance was obtained by treating the free base with thionyl chloride in dry benzene (a reaction known to lead to the replacement of the side-chain hydroxyl group by chlorine (cf. 21)). It is interesting to note that Pyman reported the melting point of 3,4-methylenedioxy-α-dimethylaminomethylbenzyl alcohol hydrochloride as 151–153°, i.e., a melting point very close to that obtained in the current investigation for the anomalous hydrochloride; however, Pyman reported a satisfactory analysis for the true hydrochloride (2).
[i]An attempt to prepare this hydrochloride by treating a solution of the free base in benzene with saturated alcoholic hydrogen chloride gave a crystalline product, m.p. 156–157° (with decomposition), which probably contained two chlorine atoms per molecule (found: C, 50.46; H, 5.78; N, 5.34; Cl, 24.17%).
[j]It was not possible under any circumstances to obtain a crystalline oxalate of 3,4-methylenedioxy-α-diethylaminomethylbenzyl alcohol. However, the picrate of 3,4-methylenedioxy-α-diethylaminomethylbenzyl alcohol was prepared by addition of picric acid to the free base, both in benzene solution; yellow flat prisms from 95% ethanol, m.p. 148–150° (with decomposition). Found: C, 49.03; H, 4.81; N, 11.80. Calc. for $C_{19}H_{22}O_{10}N_4$: C, 48.93; H, 4.75; N, 12.01%.
[k]An attempt to prepare the hydrochloride by treating a solution of the free base in benzene with dry hydrogen chloride gas gave a substance, m.p. 139.5° (with decomposition), which probably contained two chlorine atoms per molecule (found: C, 58.19; H, 7.20; Cl, 24.89%).
[l]LP = light petroleum (boiling range 60–80°) (B.D.H. AnalaR grade).
[m]The picrate of 3,4-methylenedioxy-α-di-*n*-propylaminomethylbenzyl alcohol was prepared by addition of picric acid to the free base, both in benzene solution; yellow needles from ethanol, m.p. 144° (with decomposition). Found: C, 50.88; H, 5.45; N, 11.40. Calc. for $C_{21}H_{26}O_{10}N_4$: C, 51.01; H, 5.30; N, 11.33%.
[n]The picrate of 3,4-methylenedioxy-α-di-*n*-butylaminomethylbenzyl alcohol was prepared by addition of picric acid to the free base, both in benzene solution; yellow prisms from ethanol/benzene, m.p. 101° (with decomposition). Found: C, 53.04; H, 5.89; N, 10.52. Calc. for $C_{23}H_{30}O_{10}N_4$: C, 52.87; H, 5.78; N, 10.72%.
[o]No crystalline salts could be isolated but a satisfactory analysis was obtained for the free base prepared from this reaction mixture (see Table III).
[p]The picrate of 3,4-methylenedioxy-α-isopropylaminomethylbenzyl alcohol was prepared by addition of picric acid to the free base, both in benzene solution; yellow prisms from ethanol/benzene, m.p. 142–144° (with decomposition). Found: C, 47.88; H, 4.47; N, 12.41. Calc. for $C_{18}H_{20}O_{10}N_4$: C, 47.79; H, 4.46; N, 12.39%.

TABLE II

Analysis of 3,4-methylenedioxy-α-aminomethylbenzyl alcohol derivatives (salts)

	Found				Calculated			
Compound	C	H	N	Cl	C	H	N	Cl
1	52.87	5.42	6.06	—	53.09	5.35	6.19	—
2	48.55	4.93	5.08	—	48.71	4.83	5.16	—
3	49.86	5.60	6.43	16.33	49.65	5.51	6.43	16.29
4	47.05	5.20	4.32	—	47.13	5.17	4.23	—
5	54.89	5.86	5.79	—	54.99	5.87	5.83	—
6	50.48	5.39	4.95	—	50.52	5.30	4.91	—
7	51.87	6.02	6.26	15.09	51.83	6.09	6.04	15.30
8	52.31	5.73	4.85	—	52.17	5.73	4.68	—
9	53.50	6.56	5.67	14.78	53.77	6.58	5.71	14.43
10	56.33	6.55	5.60	—	56.68	6.34	5.51	—
11	53.99	6.85	5.85	14.35	53.77	6.58	5.71	14.43
12	57.00	7.31	4.96	13.20	57.03	7.36	5.13	12.95
13	53.95	5.96	4.31	—	53.67	6.11	4.47	—
14	55.51	7.05	5.53	13.55	55.49	6.98	5.39	13.65
15	57.47	7.41	4.00	—	57.45	7.09	3.94	—
16	55.01	6.48	4.25	—	55.04	6.47	4.28	—
17	57.04	7.30	4.87	12.79	57.03	7.36	5.13	12.95
18	59.47	7.58	3.60	—	59.51	7.62	3.65	—
19	56.36	6.83	4.25	—	56.29	6.79	4.10	—
20	58.47	7.76	4.89	12.50	58.42	7.72	4.88	12.32
21	—	—	—	—	—	—	—	—
22	55.71	7.09	5.32	13.41	55.49	6.98	5.39	13.65
23	55.08	6.42	4.32	—	55.04	6.47	4.28	—
24	56.93	7.29	5.16	13.09	57.03	7.36	5.13	12.95

3,4-Methylenedioxy-α-hydroxylaminomethylbenzyl Alcohol Oxalate

Employing the procedure described by Allais for the preparation of similar compounds (16), an aqueous suspension of 3,4-methylenedioxy-α-nitromethylbenzyl alcohol (1 g), a palladium catalyst (0.3 g; 5% on charcoal), and oxalic acid dihydrate (0.3 g) was shaken in the presence of hydrogen at atmospheric pressure until the calculated quantity (i.e. 2 moles) had been taken up. The reaction mixture, after filtration, was concentrated to dryness *in vacuo*, below 40°, and the resulting white solid recrystallized extensively from water and aqueous ethanol, affording 3,4-methylenedioxy-α-hydroxylaminomethylbenzyl alcohol oxalate in colorless prisms, m.p. 173–174°. (Found: C, 51.06; H, 5.33; N, 6.00. Calc. for $C_{20}H_{24}N_2O_{11}$: C, 51.28; H, 5.15; N, 5.98%.)*

Attempted Preparation of 3,4-Methylenedioxy-α-hydroxylaminomethylbenzyl Alcohol as the Free Base

(*a*) An aqueous solution of the oxalate was made alkaline with 40% aqueous sodium hydroxide and the reaction mixture continuously extracted with benzene for 10 hours. After being dried (Na_2SO_4), the benzene extract was concentrated to small bulk; small colorless prisms (m.p. 175°) were obtained when the concentrated extract was cooled.

(*b*) The alkaline reaction mixture, prepared as described above, was repeatedly extracted with ethyl acetate; concentration of the dried (Na_2SO_4) extract gave a white solid, yielding small colorless prisms (m.p. 181–182°) on recrystallization from benzene.

(*c*) An aqueous solution of the oxalate was stirred, under nitrogen, for 3 hours with an excess of calcium carbonate, in the presence of ethyl acetate. The ethyl acetate layer was removed and the remaining aqueous suspension, after filtration, was further extracted with ethyl acetate. On concentration, the combined, dried (Na_2SO_4) extracts gave a white solid, affording small colorless prisms on recrystallization from benzene (m.p. 179°).

**Considerable difficulty was encountered in obtaining a satisfactory analysis for this compound. Several estimations on different samples for carbon, hydrogen, and nitrogen all reported a small amount of an incombustible residue, even when it was impossible to comprehend how the contamination with inorganic material could occur. The above figures are calculated after making allowance for the incombustible residue, it being assumed that complete combustion of this product is difficult to accomplish.*

TABLE III

3,4-Methylenedioxy-α-aminomethylbenzyl alcohol derivatives (bases)

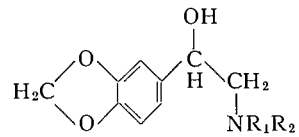

Base prepared[a]		Properties of pure compound				Analysis					
						Found			Calculated		
R_1	R_2	M.p. (°C)	B.p. (°C)	Physical state	M.p. reported in literature (°C)	C	H	N	C	H	N
H	H	72	—	Small colorless prisms from benzene	Oil (3, 8) 75 (9)	59.38	6.03	7.42	59.66	6.12	7.73
H	CH_3	99–100	—	Small colorless prisms from water or benzene	Oil (1, 4, 7) 95–96 (6)	61.33	6.80	7.14	61.52	6.71	7.18
CH_3	CH_3	37	125–130 at 1 mm	Colorless prisms solidified after distillation	Oil (2)	63.01	7.27	6.53	63.14	7.23	6.69
H	C_2H_5	100	—	Small colorless prisms from water or benzene/LP[b]	—	63.31	7.32	6.52	63.14	7.23	6.69
C_2H_5	C_2H_5	—	150 at 0.5–1mm	Pale yellow oil	—	65.43	8.19	5.90	65.80	8.07	5.90
H	n-C_3H_7	94–95	—	Small colorless prisms from ethanol/water or benzene/LP[b]	—	64.84	7.65	6.44	64.55	7.68	6.27
n-C_3H_7	n-C_3H_7	—	160 at 3 mm	Pale yellow oil	—	68.14	8.65	5.37	67.89	8.74	5.28
H	n-C_4H_9	91–92	—	Colorless plates from ethanol/water	—	65.53	7.98	5.71	65.80	8.07	5.90
n-C_4H_9	n-C_4H_9	—	170 at 2.5 mm	Pale yellow oil	—	69.47	9.26	4.86	69.59	9.28	4.77
H	n-C_5H_{11}	93	—	Fine colorless plates from ethanol/water	—	66.84	8.46	5.63	66.90	8.42	5.57
n-C_5H_{11}	n-C_5H_{11}	—	160 at 0.5–1 mm	Pale yellow oil	—	70.87	9.89	4.31	70.99	9.72	4.36
H	i-C_3H_7	88–89	—	Colorless plates from benzene/LP[b] or ethanol/water	—	64.53	7.58	6.46	64.55	7.68	6.27
H	i-C_4H_9	88	—	Colorless plates from ethanol/water	—	65.81	8.07	5.93	65.80	8.07	5.90

[a]The free bases were prepared from the corresponding oxalate or hydrochloride salts or the crude reaction mixtures by treatment with strong alkali; extraction with benzene; and purification either by distillation in high vacuum or crystallization from a suitable solvent.
[b]LP = light petroleum (boiling range 60–80°) (B.D.H. AnalaR grade).

(*d*) 3,4-Methylenedioxy-α-nitromethylbenzyl alcohol (1 g) was dissolved in 95% ethanol (150 ml) and shaken with hydrogen in the presence of a palladium catalyst (0.3 g; 5% on charcoal) until 2 molecules of hydrogen had been absorbed. Concentration of the filtered reaction mixture gave a white solid, giving small colorless needles (m.p. 183–185°) on repeated recrystallization from ethanol.

Comparisons of infrared spectra and mixed melting point determinations showed the identical nature of the substances prepared by the four methods described above. This substance which appeared to crystallize from benzene in small colorless prisms and from ethanol in small colorless needles (m.p. 183–185°) is probably *N*-β-hydroxy-β-(3,4-methylenedioxyphenyl)-ethyl-3′,4′-methylenedioxyisobenzaldoxime (cf. Allais (16)). (Found: C, 62.10; H, 4.60; N, 4.25%; mol. wt., 329. Calc. for $C_{17}H_{15}O_6N$: C, 61.99; H, 4.59; N, 4.25%; mol. wt., 329.3.)

REFERENCES

1. G. Barger and H. A. D. Jowett. J. Chem. Soc. **87**, 967 (1905).
2. F. L. Pyman. J. Chem. Soc. **93**, 1793 (1908).
3. F. A. Mason. J. Chem. Soc. **119**, 1077 (1921).
4. H. Pauly and K. Neukam. Ber. **41**, 4151 (1908).
5. C. Mannich. Apotheker Ztg. **24**, 60 (1909).
6. C. Mannich. Arch. Pharm. **248**, 127 (1910).
7. H. C. Bhatnagar, N. N. Chopra, K. S. Narang, and J. N. Ray. J. Indian Chem. Soc. **14**, 344 (1937).
8. N. Adityachaudhury and A. Chatterjee. J. Indian Chem. Soc. **36**, 585 (1959).
9. K. Kindler and W. Peschke. Arch. Pharm. **269**, 581 (1931).
10. B. Reichert and W. Koch. Ber. **68**, 445 (1935).
11. S. Kanao and K. Shinozuka. J. Pharm. Soc. Japan, **67**, 218 (1947); Chem. Abstr. **45**, 9508 (1951).
12. S. Akabori and K. Momotani. J. Chem. Soc. Japan, **64**, 608 (1943); Chem. Abstr. **41**, 3774 (1947).
13. G. Schroeter. D.R.P. 220852, Sept. 16, 1908; J. Chem. Soc. Abstr. I. **98**, 431 (1910).
14. R. A. Heacock and O. Hutzinger. Can. J. Chem. This issue.
15. K. W. Rosenmund. Ber. **46**, 1034 (1913).
16. M. A. Allais. Bull. soc. chim. France, 536 (1949).
17. B. F. Tullar. J. Am. Chem. Soc. **70**, 2067 (1948).
18. S. Kanao. J. Pharm. Soc. Japan, **49**, 239 (1929); Chem. Abstr. **23**, 5162 (1929).
19. W. M. Whaley and T. R. Govindachari. *In* Organic reactions. Vol. VI. *Edited by* R. Adams. J. Wiley and Sons, Inc., New York. 1951. p. 151.
20. R. A. Heacock, O. Hutzinger, and C. Nerenberg. Can. J. Chem. **39**, 1143 (1961).
21. J. Hukki and N. Seppäläinen. Acta Chem. Scand. **12**, 1231 (1958).

AMINO NITRILES

III. REACTION OF AMINO NITRILES WITH ISOTHIURONIUM SALTS[1]

M.-E. KRELING AND A. F. MCKAY
The L. G. Ryan Research Laboratories of Monsanto Canada Limited, LaSalle, Que.

Received September 25, 1961

ABSTRACT

N-Substituted-N′,N″-di-(2-cyanoethyl)-guanidines have been cyclized with the elimination of acrylonitrile to 2-imino-3-substituted-4-keto-hexahydropyrimidines. These pyrimidine derivatives also were prepared by treating 1-substituted-3-(2-cyanoethyl)-S-methyl isothiuronium iodide salts with ammonia. 1-(3,4-Dichlorobenzyl)-3-(2-cyanoethyl)-urea was cyclized in the presence of absolute ethanolic hydrogen chloride to 2,4-diketo-3-(3,4-dichlorobenzyl)-hexahydropyrimidine.

A series of N-substituted-N′,N″-di-(2-cyanoethyl)-guanidines (I) (Table IA) was prepared from the corresponding thioureas (Table IB) in order to study their propensity for cyclization. The desired bicyclic derivatives (II) were not obtained. Under the reaction

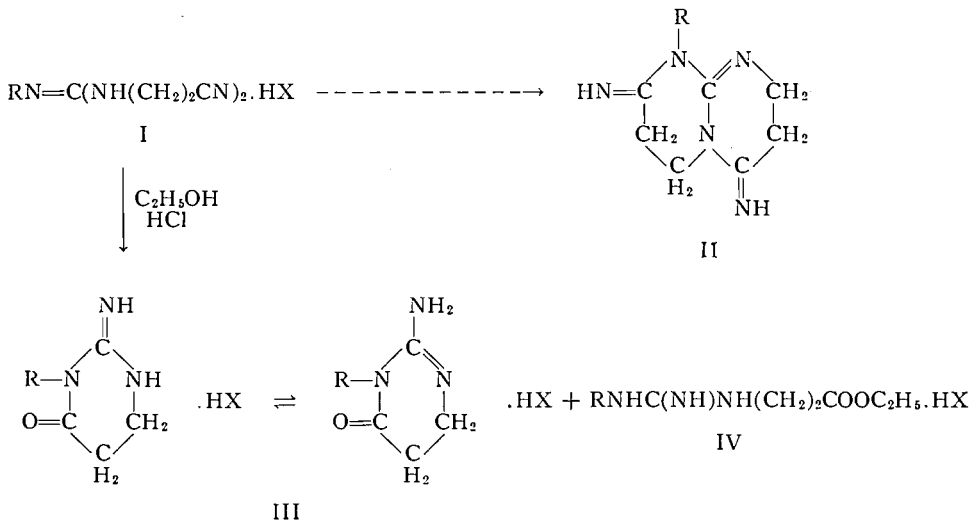

conditions employed, the guanidine derivatives (I) lost 1 mole equivalent of acrylonitrile and the monocyclic 2-imino-3-substituted-4-keto-hexahydropyrimidines (III) were formed together with N-substituted-N′-(2-carbethoxyethyl)-guanidine (IV). When N-(3,4-dichlorobenzyl)-N′,N″-di-(2-cyanoethyl)-guanidine (I, R = 3,4-$Cl_2C_6H_3CH_2$) or its hydrochloride or hydroiodide salts were refluxed in absolute ethanol for 8 hours, the original compounds were recovered unchanged.

1-Phenyl-3-(2-cyanoethyl)-S-methyl-isothiuronium iodide (V, R = C_6H_5) on treatment with anhydrous ammonia in ethanol or anhydrous α-aminoisobutyronitrile gave 2,4-diimino-3-phenyl-hexahydropyrimidinium iodide (VI, R = C_6H_5). When aqueous

[1]*Contribution No. 33.*

TABLE I

R	M.p. (°C)	Yield (%)	Formula	C		H		N		X or S	
				Calc.	Found	Calc.	Found	Calc.	Found	Calc.	Found
A. Guanidine derivatives, $RN{=}C(NH(CH_2)_2CN)_2.HX$											
C_6H_5	208.5–209	59.6	$C_{13}H_{16}IN_5$*	42.30	42.38	4.37	4.38	18.97	18.72	34.38	34.50
	200.5–202	63.8	$C_{19}H_{18}N_8O_7$†	48.51	48.92	3.86	3.97	23.81	23.83		
3,4-$Cl_2C_6H_3$	187–188	90.2	$C_{13}H_{14}Cl_2IN_5$*	35.64	35.67	3.22	3.27	15.99	15.49	45.15	45.12
	218.5–219	79.8	$C_{19}H_{16}Cl_2N_8O_7$†	42.33	42.55	2.99	3.06	20.77	20.41	13.15	13.01
	228–229	80.0	$C_{13}H_{14}Cl_3N_5$‡	45.03	45.32	4.07	4.32	20.20	19.99	30.68	30.61
	180–181	79.3	$C_{13}H_{13}Cl_2N_5$§	50.34	50.35	4.22	4.37	22.58	22.36	22.86	22.68
3,4-$Cl_2C_6H_3CH_2$	156–157	67.1	$C_{20}H_{18}Cl_2N_8O_7$†	43.42	43.70	3.28	3.42	20.25	20.21	12.82	12.82
B. Thiourea derivatives, $RNHC(S)NH(CH_2)_2CN$											
CH_3	115.5–116	93‖	$C_5H_9N_3S$	41.94	41.98	6.33	6.36	29.35	29.60	22.39	22.22
C_6H_5	123.5–125	95¶									
3,4-$Cl_2C_6H_3$	174.5–175.5	91.2	$C_{10}H_9Cl_2N_3S$**	43.79	43.76	3.31	3.24	15.33	15.07	11.69	11.78
3,4-$Cl_2C_6H_3CH_2$	122–122.5	89.7	$C_{11}H_{11}Cl_2N_3S$††	45.83	45.95	3.85	3.91	14.58	14.36	11.13	10.87

*Hydroiodides.
†Picrates.
‡Hydrochloride.
§Free base.
‖Reported m.p. 112–113°, D. J. Brown, J. Appl. Chem. (London), **7**, 109 (1957).
¶Reported m.p. 123–124°, A. F. McKay *et al.*, J. Am. Chem. Soc. **81**, 4328 (1959).
**Cl: calc. 25.86, found 26.18.
††Cl: calc. 24.60, found 24.43.

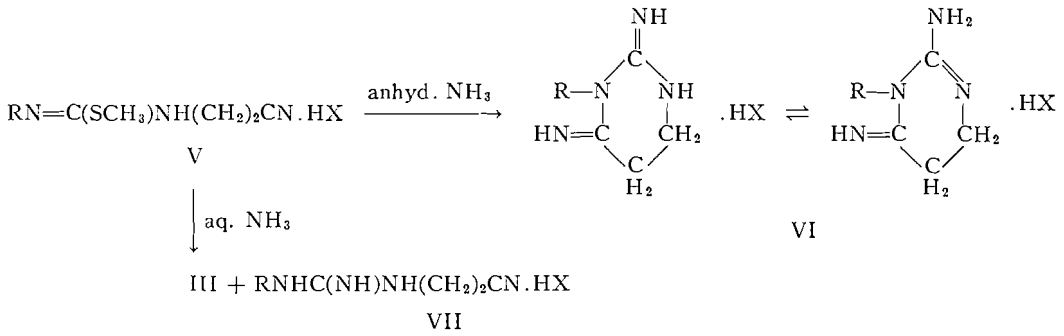

ammonia was employed in the same reaction, then the corresponding 2-imino-3-substituted-4-keto-hexahydropyrimidinium salts (III) were isolated. Treatment of 1-(3,4-dichlorobenzyl)-3-(2-cyanoethyl)-S-methyl-isothiuronium iodide (V, R = 3,4-$Cl_2C_6H_3CH_2$) with aqueous ammonia gave a mixture of 2-imino-3-(3,4-dichlorobenzyl)-4-keto-hexahydropyrimidinium iodide (III, R = 3,4-$Cl_2C_6H_3CH_2$) and N-(3,4-dichlorobenzyl)-N′-(2-cyanoethyl)-guanidinium iodide (VII, R = 3,4-$Cl_2C_6H_3CH_2$). When 1-methyl-3-(2-cyanoethyl)-S-methyl-isothiuronium iodide was heated under reflux in anhydrous ethanolic ammonia solution, it gave N-methyl-N′-(2-cyanoethyl)-guanidinium iodide instead of the expected 2,4-diimino-3-methyl-hexahydropyrimidinium iodide (VI, R = CH_3).

In order to obtain the 2,4-diimino-3-substituted hexahydropyrimidine salts (VI) strictly anhydrous conditions must be employed. The presence of moisture during reaction or during crystallization will convert these salts (VI) into the corresponding 2-imino-3-substituted-4-keto-hexahydropyrimidine salts (III). Also, crystallization of 1-(3,4-dichlorophenyl)-3-(2-cyanoethyl)-S-methyl-isothiuronium iodide (V, R = 3,4-$Cl_2C_6H_3$) from ethanol–ether solution gave some 2-keto-3-(3,4-dichlorophenyl)-4-imino-hexahydropyrimidinium iodide.

Attempts (1) to cyclize 1,3-di-(2-cyanoethyl)-urea and 1-(2-cyanoethyl)-3-(cyanomethyl)-urea by refluxing in ethanol solution were unsuccessful. Now 1-(2-cyanoethyl)-3-(3,4-dichlorobenzyl)-urea has been cyclized by heating with anhydrous ethanolic hydrogen chloride. In the presence of 9.5 mole equivalents of hydrogen chloride an 83% yield of 1-(3,4-dichlorobenzyl)-3-(2-carbethoxyethyl)-urea and an 11.9% yield of 2,4-diketo-3-(3,4-dichlorobenzyl)-hexahydropyrimidine were obtained. The latter compound was obtained in 65% yield when the hydrogen chloride was reduced to 1.2 mole equivalents.

Infrared Spectra

The pyrimidines which are reported here have been described as hexahydropyrimidine derivatives. Spectral evidence (2, 3) at present favors the ketonic structures for 2-hydroxy-, 4-hydroxy-, and 2,4-dihydroxy-pyrimidines. Moreover, the spectra given in Table II indicate that the 4-amino group in this series of 2,4-diamino- and 2-keto-4-amino-dihydropyrimidines exists in the imino form. The amino group in position 2 of the dihydropyrimidines probably exists in the amino form but no conclusion can be drawn from the present spectral data. In this investigation the infrared spectra were used mainly to confirm the formation of cyclic reaction products. A number of the band assignments in the 1500–1750 cm^{-1} region for pyrimidines are still regarded as tentative.

The C ≡ N stretching band between 2250 and 2265 cm^{-1} is a weak band and it disappears completely with some of the salts where the general absorption is high in this region.

TABLE II

Infrared absorption band (cm^{-1}) assignments*

Compounds	Stretching modes				Bending modes
	N—H	C≡N	C=O	C=N	N—H
2,4-Diimino-3-phenyl-hexahydropyrimidinium chloride	3100 (br)			1674, 1638	1615, 1555, 1540
2,4-Diimino-3-(3,4-dichlorobenzyl)-hexahydropyrimidinium chloride	3120			1672, 1627	1568, 1557
2-Keto-3-(3,4-dichlorophenyl)-4-imino-hexahydropyrimidinium iodide	3340, 3180		1683	1745	1608
2-Imino-3-phenyl-4-keto-hexahydropyrimidinium chloride	3180		1730	1680	1613
2-Imino-3-(3,4-dichlorobenzyl)-4-keto-hexahydropyrimidinium chloride	3290, 3180, 3080		1730	1677	1607
2,4-Diketo-3-(3,4-dichlorobenzyl)-hexahydropyrimidine	3245, 3100		1725	1690	1570
1-(3,4-Dichlorobenzyl)-3-(2-carbethoxyethyl)-urea	3350		1726, 1613		1583
1-Methyl-3-(2-cyanoethyl)-thiourea	3345, 3300	2260			1560, 1508
1-(3,4-Dichlorophenyl)-3-(2-cyanoethyl)-thiourea	3400, 3310	2260			1555, 1515
N-Phenyl-N′,N″-di-(2-cyanoethyl)-guanidinium chloride	3245			1642	1604, 1567
N-(3,4-Dichlorophenyl)-N′,N″-di-(2-cyanoethyl)-guanidinium chloride	3220, 3150, 3050	2255		1660	1578, 1553
N-Methyl-N′-(2-cyanoethyl)-guanidinium iodide	3380, 3240, 3175			1638	1620, 1567, 1545
N-(3,4-Dichlorobenzyl)-N′-(2-cyanoethyl)-guanidinium iodide	3320, 3240, 3170			1647	1615, 1542
1-Methyl-3-(2-cyanoethyl)-S-methyl-isothiuronium iodide	3450, 3260, 3160	2265		1613	1560, 1528
1-Phenyl-3-(2-cyanoethyl)-S-methyl-isothiuronium iodide	3170	2250		1608	1589, 1517

*Nujol mulls of the crystalline compounds were used for spectral analyses.

EXPERIMENTAL[2]

1-Substituted-3-(2-cyanoethyl)-thioureas

All of the 1-substituted-3-(2-cyanoethyl)-thioureas which are listed in Table 1B were prepared by the following procedure for the preparation of 1-methyl-3-(2-cyanoethyl)-thiourea.

A solution of methyl isothiocyanate (5.4 g, 0.075 mole) in benzene (20 ml) was added slowly to a stirred solution of 3-aminopropionitrile (5.2 g, 0.075 mole) in benzene (15 ml) while the temperature was maintained at 20–30°. After addition was complete, the stirring was continued at room temperature for 1 hour. The thiourea was recovered by filtration and the product was purified by crystallizing from ethanol.

1-Phenyl-3-(2-cyanoethyl)-S-methyl-isothiuronium Iodide

Methyl iodide (7.4 g, 0.052 mole) was added over a period of 5 minutes to a refluxing solution of 1-phenyl-3-(2-cyanoethyl)-thiourea (9.73 g, 0.047 mole) in absolute methanol (75 ml). After the heating under reflux had been continued for 3 hours, the solution was evaporated to dryness *in vacuo*. The oily product crystallized on trituration with acetone (50 ml), yield 15.1 g (92.6%). Three crystallizations from absolute ethanol – ether (3:1) solution raised the melting point from 152–159° to 165–167°. Anal. calc. for $C_{11}H_{14}IN_3S$: C 38.04, H 4.06, I 36.55, N 12.10, S 9.23%; found: C 38.07, H 4.12, I 36.40, N 12.07, S 9.05%.

A picrate (m.p. 139–141°) was formed in 72% yield in the usual manner in aqueous solution. Anal. calc. for $C_{17}H_{16}N_6O_7S$: C 45.53, H 3.60, N 18.74%; found: C 45.83, H 3.87, N 18.51%.

1-Methyl-3-(2-cyanoethyl)-S-methyl-isothiuronium Iodide

1-Methyl-3-(2-cyanoethyl)-thiourea (9.3 g, 0.065 mole) was methylated by the procedure described above for the methylation of 1-phenyl-3-(2-cyanoethyl)-thiourea with the exception that the reflux period was 1 hour. After evaporation of the solvent *in vacuo*, the residual colorless oil was triturated with absolute ethanol. The crystals (m.p. 109–113°) were recovered by filtration, yield 4.3 g (30.2%). Three crystallizations from absolute ethanol raised the melting point to 116–117°. Anal. calc. for $C_6H_{12}IN_3S$: C 25.27, H 4.24, I 44.50, N 14.73, S 11.25%; found: C 25.16, H 4.39, I 44.34, N 14.61, S 11.25%.

1-(3,4-Dichlorophenyl)-3-(2-cyanoethyl)-S-methyl-isothiuronium Iodide

1-(3,4-Dichlorophenyl)-3-(2-cyanoethyl)-thiourea (10.95 g, 0.04 mole) and methyl iodide (6.25 g, 0.044 mole) in methanol (75 ml) were heated under reflux for 3 hours. Evaporation of the solvent *in vacuo* gave 16.5 g (99.5%) of a semicrystalline product. Since this product lost methyl mercaptan readily it was used without further purification for the next reaction.

An attempt to purify a sample (8.25 g) of the semicrystalline product by crystallizing from ethanol–ether (5:1) solution gave 2.1 g of a white crystalline product melting at 176–288°. This product did not contain sulphur and several crystallizations from ethanol raised the melting point to 301–301.5° decomp. (evac. cap.). Anal. calc. for $C_{10}H_{10}Cl_2IN_3O$: C 31.11, H 2.61, N 10.88, total halogen 51.25%; found: C 31.43, H 2.67, N 11.04, total halogen 50.74%. This product was identified by analyses and infrared spectrum as 2-keto-3-(3,4-dichlorophenyl)-4-imino-hexahydropyrimidine.

1-(3,4-Dichlorobenzyl)-3-(2-cyanoethyl)-S-methyl-isothiuronium Iodide

1-(3,4-Dichlorobenzyl)-3-(2-cyanoethyl)-thiourea (7.35 g, 0.025 mole) and methyl iodide (3.62 g, 0.025 mole) in absolute methanol were stirred at room temperature for 1 hour. The temperature was increased to 45° and the stirring was continued for 15 minutes. On the addition of ether to the cooled solution, crystals (m.p. 127–128°) separated, yield 6.3 g (57.5%). The melting point was not changed by recrystallization. Anal. calc. for $C_{12}H_{14}Cl_2IN_3S$: C 33.51, H 3.28, total halogen 46.00, N 9.77, S 7.45%; found: C 33.50, H 3.40, total halogen 45.56, N 10.06, S 7.38%.

A sample of the hydroiodide salt in methanol solution was converted into its picrate (m.p. 122.5–123.5°) in the usual manner. Anal. calc. for $C_{18}H_{16}Cl_2N_6O_7S$: C 40.69, H 3.04, Cl 13.35, N 15.82, S 6.03%; found: C 40.74, H 3.25, Cl 13.38, N 15.58, S 6.14%.

N-Substituted-N′,N″-di-(2-cyanoethyl)-guanidines

The N-substituted-N′,N″-di-(2-cyanoethyl)-guanidines listed in Table IA were all prepared by the following general procedure.

1-(3,4-Dichlorophenyl)-3-(2-cyanoethyl)-S-methyl-isothiuronium iodide (8.32 g, 0.02 mole) and 3-aminopropionitrile (1.4 g, 0.02 mole) were heated under reflux in absolute ethanol (50 ml) for 3 hours after which the evolution of methyl mercaptan had ceased. Evaporation of the solvent gave a crystalline residue which was purified by crystallizing from absolute ethanol.

A picrate (m.p. 218.5–219°) was prepared in 79.8% yield from aqueous solution in the usual manner. It was purified by crystallization from water.

Conversion of the guanidinium iodides into their corresponding hydrochlorides or free bases was accomplished by one of the following methods.

[2]*All melting points are uncorrected. Microanalyses were performed by Micro-Tech Laboratories, Skokie, Illinois.*

Method A. A solution of N-(3,4-dichlorophenyl)-N′,N″-di-(2-cyanoethyl)-guanidinium iodide (2 g, 0.0046 mole) in absolute ethanol (30 ml) was passed through a column of IRA 400 resin (25 ml in the chloride form). The resin was washed with methanol (50 ml) and the combined washings and eluate were taken to dryness *in vacuo*. The crystalline hydrochloride was obtained in 80% (1.26 g) yield. It was crystallized from ethanol–ether (3:2) solution.

Method B. A solution of N-(3,4-dichlorophenyl)-N′,N″-di-(2-cyanoethyl)-guanidinium iodide (0.32 g, 0.0007 mole) in absolute ethanol was treated with 1.5 mole equivalents of 4% aqueous sodium hydroxide solution at 0°. It was then held at room temperature for 15 minutes after which the solution was diluted with water. The aqueous solution was extracted with chloroform. After the combined chloroform extracts had been washed with water, the chloroform layer was treated with excess 1 *N* hydrochloric acid. An oil separated which crystallized immediately, yield 0.19 g (76.9%).

The free base was obtained by passage of a solution of the iodide salt (0.62 g) in absolute ethanol (45 ml) through a column of IRA 400 resin (in the hydroxyl form). The resin column was washed with ethanol (80 ml) and the washings and eluate were evaporated to dryness *in vacuo* under nitrogen. N-(3,4-Dichlorophenyl)-N′,N″-di-(2-cyanoethyl)-guanidine was obtained in 79.3% (0.44 g) yield. The free base was crystallized from absolute ethanol for analyses.

2,4-Diimino-3-phenyl-hexahydropyrimidinium Iodide

1-Phenyl-3-(2-cyanoethyl)-S-methyl-isothiuronium iodide (3.47 g, 0.01 mole) in absolute ethanol (25 ml) which had been saturated with anhydrous ammonia was heated under reflux for 12.5 hours. After evaporation of the solvent *in vacuo*, the semicrystalline product was crystallized from ethanol–ether solution. The crystals possessed a double melting point of 162–163° and 192°, yield 2.33 g (73.8%).

A sample of the hydroiodide salt in ethanol was converted into its picrate (m.p. 229–231°) in the usual manner. Anal. calc. for $C_{16}H_{15}N_7O_7$: C 46.05, H 3.62, N 23.50%; found: C 46.12, H 3.64, N 23.15%.

Reaction of 1-Phenyl-3-(2-cyanoethyl)-S-methyl-isothiuronium Iodide with 2-Aminoisobutyronitrile

A solution of 1-phenyl-3-(2-cyanoethyl)-S-methyl-isothiuronium iodide (1.87 g, 0.005 mole) and 2-aminoisobutyronitrile (0.45 g, 0.005 mole) in absolute ethanol (25 ml) was heated under reflux for 7 hours. Since a crystalline hydroiodide could not be isolated from the reaction, the crude hydroiodide in ethanol was passed through a column of IRA 400 resin (in the chloride form). The resin was washed with ethanol and the combined washings and eluate were taken to dryness *in vacuo*. The residual semicrystalline solid crystallized on trituration with absolute ethanol, yield 0.6 g (51.7%). Crystallization from ethanol–ether (1:2) solution raised the melting point from 85–216° to 217–218°. This compound gave the correct analyses for 2,4-diimino-3-phenyl-hexahydropyrimidinium chloride. Anal. calc. for $C_{10}H_{13}ClN_4$: C 53.45, H 5.83, Cl 15.78, N 24.93%; found: C 53.55, H 5.93, Cl 16.03, N 24.87%.

The picrate (m.p. 225–230°) was formed in the usual manner from the hydrochloride salt in aqueous medium. Two crystallizations from water raised the melting point to 229°. This picrate did not depress the melting point of 2,4-diimino-3-phenyl-hexahydropyrimidinium picrate (229–231°) formed from the reaction of anhydrous ammonia with 1-phenyl-3-(2-cyanoethyl)-S-methyl-isothiuronium iodide.

Reaction of 1-(3,4-Dichlorobenzyl)-3-(2-cyanoethyl)-S-methyl-isothiuronium Iodide with Ammonia

Concentrated aqueous ammonia solution (5 ml) was added to 1-(3,4-dichlorobenzyl)-3-(2-cyanoethyl)-S-methyl-isothiuronium iodide (1.83 g, 0.004 mole) in ethanol (4 ml). After the solution had been heated under reflux for 10 hours, the solvent was removed *in vacuo*. The residual oil partially crystallized on addition of a small amount of absolute ethanol. The crystals (m.p. 262–264°, decomp.) were removed by filtration, yield 0.12 g (8.6%). Two crystallizations from aqueous ethanol raised the melting point to 267.8–268.6°. The analytical results indicate that two molecules of 2-imino-3-(3,4-dichlorobenzyl)-4-keto-hexahydropyrimidine are associated with one molecule of hydrogen iodide. Anal. calc. for $C_{22}H_{23}Cl_4IN_6O_2$: C 39.31, H 3.45, total halogen 39.98, N 12.50%; found: C 39.40, H 3.84, total halogen 39.92, N 12.39%.

A sample of the crude product in aqueous solution gave a crystalline picrate (m.p. 205–207°) in 94.5% yield on treatment with aqueous picric acid. One crystallization from aqueous ethanol raised the melting point to 206–207°. Anal. calc. for $C_{17}H_{14}Cl_2N_6O_8$: C 40.74, H 2.82, Cl 14.15, N 16.77%; found: C 41.04, H 3.08, Cl 14.00, N 16.74%.

The mother liquor from the above crude hydroiodide gave a second crystalline iodide (m.p. 157–159°) on addition of ether, yield 0.18 g (10.6%). Crystallization from ethanol–ether raised the melting point to 163.2–163.8°. This product was identified as N-(3,4-dichlorobenzyl)-N′-(2-cyanoethyl)-guanidinium iodide by elemental and infrared analyses. Anal. calc. for $C_{11}H_{13}Cl_2IN_4$: C 33.10, H 3.28, total halogen 49.57, N 14.04%; found: C 32.90, H 3.32, total halogen 49.50, N 13.86%.

A picrate (m.p. 198–198.5°) was formed in 80% yield in the usual manner from aqueous solution. Anal. calc. for $C_{17}H_{15}Cl_2N_7O_7$: C 40.80, H 3.02, N 19.60%; found: C 40.95, H 2.97, N 19.74%.

Reaction of 1-(3,4-Dichlorobenzyl)-3-(2-cyanoethyl)-S-methyl-isothiuronium Iodide with 3-Aminopropionitrile

1-(3,4-Dichlorobenzyl)-3-(2-cyanoethyl)-S-methyl-isothiuronium iodide (6.89 g, 0.016 mole) and 3-aminopropionitrile (1.12 g, 0.016 mole) in absolute ethanol (40 ml) were heated under reflux for 4.5 hours. Evaporation of the solvent *in vacuo* gave 7 g of semicrystalline residue.

A portion (0.5 g) of the crude product was converted into a picrate (m.p. 60–65°) in the usual manner in water, yield 0.41 g (67%). Crystallization from aqueous acetone raised the melting point to 156–157°. The analyses are in agreement with those calculated for N-(3,4-dichlorobenzyl)-N′,N″-di-(2-cyanoethyl)-guanidine picrate. Anal. calc. for $C_{20}H_{18}Cl_2N_8O_7$: C 43.42, H 3.28, Cl 12.82, N 20.25%; found: C 43.70, H 3.42, Cl 12.82, N 20.21%.

The remainder of the original semicrystalline residue was dissolved in ethanol and passed through a column of IRA 400 resin (in the OH form). After the column was washed with ethanol, the washings and eluate were evaporated to dryness *in vacuo*. The oily product on solution in ethanol and acidification with concentrated hydrochloric acid gave a crystalline precipitate (m.p. 280–285°), yield 0.6 g (12%). One crystallization from ethanol raised the melting point to 288–290°. The analytical values for this compound agree with those calculated for 2-imino-3-(3,4-dichlorobenzyl)-4-keto-hexahydropyrimidinium chloride. Anal. calc. for $C_{11}H_{12}Cl_3N_3O$: C 42.80, H 3.92, Cl 34.46, N 13.62%; found: C 43.06, H 4.16, Cl 34.62, N 13.70%.

The picrate (m.p. 206–207°) was obtained in the usual manner from aqueous solution in 98% yield. A sample of this picrate on admixture with 2-imino-3-(3,4-dichlorobenzyl)-4-keto-hexahydropyrimidine picrate (m.p. 206–207°) from the reaction of ammonia with 1-(3,4-dichlorobenzyl)-3-(2-cyanoethyl)-S-methyl-isothiuronium iodide did not depress its melting point.

2-Imino-3-(3,4-dichlorophenyl)-4-keto-hexahydropyrimidine

Crude 1-(3,4-dichlorophenyl)-3-(2-cyanoethyl)-S-methyl-isothiuronium iodide (0.83 g, 0.002 mole) was dissolved in ethanol (4 ml) and treated with an excess of concentrated ammonia (5 ml). The solution was heated under reflux for 6.25 hours. Crystals (m.p. 247°) separated from the cooled solution in 60.6% yield. Crystallization from aqueous ethanol raised the melting point to 262–262.5°. Anal. calc. for $C_{10}H_9Cl_2N_3O$: C 46.52, H 3.52, Cl 27.47, N 16.28%; found: C 46.90, H 3.53, Cl 27.16, N 16.36%.

N-Methyl-N′-(2-cyanoethyl)-guanidinium Iodide

1-Methyl-3-(2-cyanoethyl)-S-methyl-isothiuronium iodide (2.3 g, 0.008 mole) in saturated absolute ethanolic ammonia solution (25 ml) was heated under reflux for 21 hours. Evaporation of the solution to dryness *in vacuo* gave 1.92 g (93.7%) of crystals (double melting point at 159–160° and 169–170°). Crystallization from ethanol–ether (2:1) solution gave a product with a double melting point. It melted at 160°, resolidified, and remelted at 173–173.8°. Anal. calc. for $C_5H_{11}IN_4$: C 23.63, H 4.36, I 49.95, N 22.05%; found: C 23.87, H 4.35, I 50.08, N 22.00%.

1-(3,4-Dichlorobenzyl)-3-(2-cyanoethyl)-urea

A solution of 3,4-dichlorobenzyl isocyanate (5.02 g, 0.025 mole) in ether (50 ml) was added to a cooled ethereal solution of 2-aminopropionitrile (1.75 g, 0.025 mole). The reaction mixture was held at room temperature for 2 hours after which the crystals (m.p. 125–127°) were recovered by filtration, yield 6.4 g (94.5%). The melting point was raised to 133.6–134.2° by crystallizing from aqueous ethanol. Anal. calc. for $C_{11}H_{11}Cl_2N_3O$: C 48.55, H 4.07, Cl 26.06, N 15.44%; found: C 48.58, H 4.21, Cl 26.06, N 15.47%.

1-(3,4-Dichlorobenzyl)-3-(2-carbethoxyethyl)-urea

A solution of 1-(3,4-dichlorobenzyl)-3-(2-cyanoethyl)-urea (2.16 g, 0.008 mole) in ethanolic hydrogen chloride (2.8 g, 0.077 mole of hydrogen chloride in absolute ethanol (20 ml)) was heated under reflux for 3.5 hours. When the solution was cooled, a small amount of ammonium chloride separated, yield 0.35 g. The filtrate was evaporated to dryness and the semicrystalline residue was triturated with ethanol (10 ml). The crystals (m.p. 183–185°) were removed by filtration, yield 0.26 g (11.9%). These crystals were identified as 2,4-diketo-3-(3,4-dichlorobenzyl)-hexahydropyrimidine by a mixed melting point determination.

The filtrate on evaporation yielded a solid which melted at 89–93°. Recrystallization from ethanol–ether solution raised the melting point to 110.5–111°. The yield of 1-(3,4-dichlorobenzyl)-3-(2-carbethoxyethyl)-urea was 2.1 g (83%). Anal. calc. for $C_{13}H_{16}Cl_2N_2O_3$: C 48.91, H 5.05, Cl 22.21, N 8.78%; found: C 48.96, H 5.17, Cl 22.20, N 8.90%.

2,4-Diketo-3-(3,4-dichlorobenzyl)-hexahydropyrimidine

1-(3,4-Dichlorobenzyl)-3-(2-cyanoethyl)-urea (0.68 g, 0.0025 mole) in ethanolic hydrogen chloride (0.1 g, 0.003 mole) in absolute ethanol (5 ml) was heated under reflux for 2.3 hours. The reaction mixture on cooling gave crystals (m.p. 180–183°) of 2,4-diketo-3-(3,4-dichlorobenzyl)-hexahydropyrimidine, yield 0.46 g (65%). One crystallization from absolute ethanol raised the melting point to 183.5–185°. Anal. calc. for $C_{11}H_{10}Cl_2N_2O_2$: C 48.37, H 3.69, Cl 25.96, N 10.26%; found: C 48.07, H 3.88, Cl 26.01, N 10.22%.

Attempted Cyclization of N-Substituted-N′,N″-di-(2-cyanoethyl)-guanidines

Method A. N-(3,4-Dichlorobenzyl)-N′,N″-di-(2-cyanoethyl)-guanidinium chloride (1 g) in absolute ethanol was refluxed for 8 hours. After concentration and cooling of the solution, the starting material was recovered unchanged in 81.5% yield. The recovered material was identified by a mixed melting point determination.

Under similar conditions both N-(3,4-dichlorobenzyl)-N′,N″-di-(2-cyanoethyl)-guanidine and its hydroiodide salt were recovered unchanged.

Method B. N-Phenyl-N′,N″-di-(2-cyanoethyl)-guanidinium chloride (0.97 g, 0.0035 mole) was heated under reflux for 2 hours in absolute ethanol (7.5 ml) containing hydrogen chloride (1 g, 0.028 mole). The reaction mixture was cooled and the crystals (m.p. 280–282°) were recovered by filtration, yield 0.43 g (54.8%). Two crystallizations from absolute ethanol raised the melting point to 292.4–292.8°. This product was identified as 2-imino-3-phenyl-4-keto-hexahydropyrimidinium chloride by elemental analyses and infrared spectrum. Anal. calc. for $C_{10}H_{12}ClN_3O$: C 53.21, H 5.36, Cl 15.71, N 18.62%; found: C 53.47, H 5.44, Cl 15.58, N 18.89%.

The picrate (m.p. 242–244°) was formed in 41% yield in the usual manner from aqueous ethanol. Anal. calc. for $C_{16}H_{14}N_6O_8$: C 45.94, H 3.37, N 20.09%; found: C 45.83, H 3.39, N 19.73%.

The mother liquor from the crystals was evaporated to dryness *in vacuo*. A mixture of oil and crystals was obtained, yield 1.14 g. A portion (0.23 g) of this mixture in absolute ethanol on treatment with aqueous picric acid gave a crystalline picrate (m.p. 133.2–133.8°), yield 0.15 g (38.7%). The melting point was raised to 134.4–134.8° by two crystallizations from aqueous ethanol. The analyses agree with those calculated for the picrate of 1-phenyl-3-(2-carbethoxyethyl)-guanidine. Anal. calc. for $C_{18}H_{20}N_6O_9$: C 46.54, H 4.34, N 18.10%; found: C 46.65, H 4.36, N 18.29%.

When N-phenyl-N′,N″-di-(2-cyanoethyl)-guanidinium chloride was treated under the same conditions as above using approximately 1 mole equivalent of hydrogen chloride instead of 8, the starting material was recovered in 44.3% yield and a 42% yield of 2-imino-3-phenyl-4-keto-hexahydropyrimidinium chloride was obtained.

ACKNOWLEDGMENT

The infrared spectra were determined by Dr. C. Sandorfy of the University of Montreal, Montreal, Quebec.

REFERENCES

1. A. F. McKay, G. Y. Paris, and D. L. Garmaise. J. Am. Chem. Soc. **80**, 6276 (1958).
2. H. W. Thompson, D. L. Nicholson, and L. N. Short. Discussions Faraday Soc. No. 9, 222 (1950).
3. L. N. Short and H. W. Thompson. J. Chem. Soc. 168 (1952).

NOTES

THE ENZYMIC SYNTHESIS OF 3-*O*- AND 6-*O*-β-D-GALACTOPYRANOSYL-D-GALACTOSE*

A. M. STEPHEN, S. KIRKWOOD, AND F. SMITH

Chemical synthesis constitutes one approach to the proof of structure of disaccharides but, in general, only limited success has attended these procedures. The usual method, involving the combination of an acetohalogeno derivative (1) of the non-reducing moiety of the required disaccharide with a suitable blocked derivative of the aglycone residue leads, as a rule, to β-linked disaccharides (2). Those disaccharides having a biose linkage which engages C_6 of a hexose or C_5 of a pentose unit can be synthesized without too much difficulty because the necessary acceptor molecules are easily prepared and the reaction proceeds smoothly, giving reasonably good yields (3, 5). On the other hand, however, the synthesis of disaccharides whose biose linkage engages C_2, C_3, or C_4 of either a hexose (2, 3) or a pentose unit (4) is much more difficult because the required acceptor molecules are generally inaccessible and the yields of disaccharide are usually poor.

Certain disaccharides have been obtained as reversion products (6) by the action of acid on concentrated aqueous solutions of monosaccharides, and with the advent of chromatographic techniques for separating closely related isomeric substances, this approach has become useful and relatively simple for the preparation of some disaccharides (7).

Formerly the reversible effect of enzymes upon glycosidic bonds was put to good synthetic use, especially by Bourquelot, for the formation of the (at that time) inaccessible β-D-glucosides (8) and more recently Peat and his co-workers (9) have shown that almond emulsin can be used to transform D-glucose into the disaccharides gentiobiose, cellobiose, laminaribiose, sophorose, and β,β-trehalose. Bourquelot reported that such enzymes could be used to generate oligosaccharides. In particular it was found (10) that emulsin preparations would act on concentrated galactose solutions giving higher molecular weight oligosaccharides, and it has since been suggested (11), from a comparison of physical properties, that two of Bourquelot's crystalline products were probably identical with 3-*O*-β- and 6-*O*-β-D-galactopyranosyl-D-galactose. The widespread occurrence of β 1 → 3 and β 1 → 6 linked galactose units is of special interest in connection with our investigation of gums and mucilages, and it was therefore decided to re-examine the work of Bourquelot to ascertain the feasibility of using enzymes for synthesizing disaccharides and oligosaccharides that are relatively inaccessible by the usual chemical procedures.

In preliminary experiments the effect of a number of readily available enzymes on D-galactose was explored. Accordingly, certain enzyme preparations were incubated at pH 3.6, 4.6, and 6.9 with a 33% aqueous solution of D-galactose, the reaction products being examined chromatographically. As a result of these exploratory tests (12), it was decided to use a commercial β-D-glucosidase (emulsin) preparation at pH 7 (approx.) since this gave evidence of producing at least three oligosaccharides from D-galactose, two of which resembled 3-*O*- and 6-*O*-β-D-galactopyranosyl-D-galactose according to partition chromatographic and electrophoretic tests.

Paper No. 4543, Scientific Journal Series, Minnesota Agricultural Experiment Station.

Production of oligosaccharides from D-galactose with emulsin, the so-called β-D-glucosidase, appeared to reach a maximum after about 5 days at room temperature. The reaction was terminated by heating the digest to 100°, and separation of most of the unchanged D-galactose from the oligosaccharides was effected by passing the solution through charcoal. The oligosaccharides adsorbed by the charcoal were selectively displaced with gradually increasing concentrations of aqueous alcohol. The fraction eluted by 7.5 to 30% aqueous ethanol, which was richest in oligosaccharides, was further fractionated by chromatography on a cellulose column. The mixture of oligosaccharides proved to be quite complex; at least seven components moving faster than 6-*O*-β-D-galactopyranosyl-D-galactose were detected. The two components present in the greatest proportion readily crystallized and proved to be 3-*O*-β-D-galactopyranosyl-D-galactose and 6-*O*-β-D-galactopyranosyl-D-galactose, as suggested by Weinland (11). It is of interest to note that both galactose disaccharides have been previously synthesized chemically (13, 18) and the latter has been found among the products formed by the action of an enzyme from *Saccharomyces fragilis* on lactose (14).

It appears that the enzymatic method shows considerable promise since more suitable sources of β-D-galactosidase would most likely produce purer galactose di- and higher saccharides in better yields. The minor components from the emulsin reaction on D-galactose reported herein may represent disaccharides some of which, from their relatively high positive specific rotation, may be of the α-type. Clearly the use of an α-D-galactosidase would be invaluable for the synthesis of galactose oligosaccharides having α-linkages and it seems reasonable to believe that the enzymic method could be applied quite generally for the synthesis of oligosaccharides, many of which cannot readily be synthesized by chemical means.

EXPERIMENTAL

The Effect of Various Enzymes on Galactose

Solutions of D-galactose were prepared at a concentration of 33% in buffers of varying pH. The solutions were brought to the boiling point and cooled. To each of these solutions of galactose (5 ml) was added one of the enzyme preparations (20 mg), followed by a few drops of toluene to prevent mold growth. The containers were stoppered and the solutions kept at 37°. At intervals a paper chromatographic examination was made to ascertain the progress of oligosaccharide synthesis. The synthesis of oligosaccharides appeared to reach a maximum after about 5 days.

The results showed that the best pH was 6.9; at lower pH's less synthesis was noted. The enzymes, in order of decreasing efficiency, were as follows: "β-glucosidase" (Worthington Chemical Co.), emulsin (Nutritional Biochemicals Corp.), enzyme prepared from germinating alfalfa seeds by the procedure of Hill (12, 15, 16) (enzyme fractions were precipitated with 20% ammonium sulphate, 40% ammonium sulphate, and with saturated ammonium sulphate; the enzyme precipitates were dialyzed to remove ammonium sulphate and freeze-dried), and Cellulase 35 (Rohm and Haas Chem. Co.). Two other enzyme preparations, Lactase C and Cellulase 36, kindly supplied along with Cellulase 35 by the Rohm and Haas Chem. Co., Philadelphia, Pa., had little or no synthetic activity.

Enzymic Synthesis of D-Galactose Oligosaccharides

A solution of D-galactose (10 g) in hot water (30 ml) was cooled to room temperature and treated with a "β-glucosidase" preparation (70 mg, Worthington Biochemical Corp., Freehold, N.J.). The solution was covered with a layer of toluene to prevent growth of microorganisms. After 3 days, paper chromatography revealed the presence of two oligosaccharides whose R_F values corresponded to those of 3-*O*-β-D-galactopyranosyl-D-galactose and 6-*O*-β-D-galactopyranosyl-D-galactose isolated by the graded hydrolysis of *Virgilia oroboides* gum (17). Charcoal (3 g) was added in an attempt to adsorb the oligosaccharides and thus promote synthesis. After storage for 10 weeks (a shorter time, e.g. 1 week, would suffice) the reaction mixture was boiled, filtered through charcoal (60 g) contained in a Büchner funnel, and washed with water (the combined filtrate and washings amounted to 350 ml). The charcoal was then eluted successively with 3% ethanol (500 ml), 7.5% ethanol (500 ml), 10% ethanol (500 ml), 15% ethanol (500 ml), and 30% ethanol (500 ml). Chromatography, using ethyl acetate:pyridine:water (10:4:3), of the 7.5% eluate showed the presence of galactose and oligosaccharides. Galactose was also detected in the 15% eluate. The

fractions recovered were as follows: I (from aqueous filtrate and washings), 5.45 g; II (from 3% ethanol eluate), 2.19 g; and III (from 7.5 to 30% ethanol eluate), 0.65 g.

Separation of Oligosaccharides from Fraction III

Fraction III (0.65 g) obtained above, which was found to contain the two oligosaccharides having R_F values corresponding to 3-*O*-β-D-galactopyranosyl-D-galactose and 6-*O*-β-D-galactopyranosyl-D-galactose, was put on a cellulose column (4.5×60 cm packed dry) and eluted with ethyl acetate:pyridine:water (10:4:3), the eluate being collected automatically in 15-ml fractions every 30 minutes. The results are recorded in Table I.

TABLE I

Column chromatographic separation of oligosaccharides synthesized by emulsin from D-galactose

Fraction	Tube No.	Wt. (mg)	R_{Gal} Solvent A*	R_{Gal} Solvent B†	No. components by electrophoresis‡	Identity of components
1	35–75	—	1.00	1.00	1	D-Galactose
2	90–129	23	0.59	0.50	1	Unknown
3	130–150	17	0.59	0.42–0.50	2	Unknown
4	151–170	74	0.59, 0.50	0.43, 0.36	2	Unknown
5	171–200	23	0.50	0.36	1	β-D-Gal$_p$(1 → 3)D-Gal$_p$ (A)
6	201–205		0.50–0.44	0.36, 0.26	2	A + unknown
7	206–230	6	0.44	0.31	2	Unknown
8	240–261§	84	0.35	0.24	1	β-D-Gal$_p$(1 → 6)D-Gal$_p$ (B)
9	262–271	34	0.35–0.28	0.24–0.15	2	B + unknown

*Solvent A = ethyl acetate:pyridine:water (10:4:3).
†Solvent B = ethyl acetate:acetic acid:formic acid:water (18:3:1:4).
‡Electrolyte: 0.1 *M* borate.
§Composition of eluting solvent changed to ethyl acetate:pyridine:water (10:4:5).

Isolation of 3-O-β-D-Galactopyranosyl-D-galactose

The material from tubes 171 to 205 crystallized spontaneously and had m.p. 165° after washing with methanol and with diethyl ether, $[\alpha]_D^{24}$ +84° in water (*c*, 0.8) (15 minutes), +75° (35 minutes), +69° (1 hour), +64° (4 hours, const.). Lit. m.p. 163–170°, $[\alpha]_D$ +75° (5 minutes) → +60° (2 hours) in water (18). Paper chromatography (1-butanol:acetic acid:water) and paper electrophoresis (0.1 *M* borate buffer) showed that the disaccharide was quite different from 6-*O*-β-D-galactopyranosyl-D-galactose prepared from *V. oroboides* gum. The crystals were dissolved in the minimum volume of methanol containing a drop of water and were seeded with 3-*O*-β-D-galactopyranosyl-D-galactose (m.p. 200°) from *V. oroboides* gum (17). The crystalline material, which separated slowly, had m.p. 203° and showed no depression when mixed with the 3-*O*-β-D-galactopyranosyl-D-galactose used for nucleation. There was, however, a depression of the melting point when it was mixed with 4-*O*-β-D-galactosyl-D-galactose.

Isolation of 6-O-β-D-Galactopyranosyl-D-galactose

The crystalline material from tubes 240–261 was recrystallized from methanol, m.p. 136° with previous sintering at 106° (yield 40 mg). This disaccharide which appeared to crystallize with water and methanol of constitution gave no depression of the melting point when mixed with the 6-*O*-β-D-galactopyranosyl-D-galactose prepared from *V. oroboides* gum and crystallized from methanol (17). This enzymically synthesized disaccharide, which has the same chromatographic mobility (tested with two different solvent systems) as 6-*O*-β-D-galactopyranosyl-D-galactose, showed $[\alpha]_D^{18}$ +24° in water (*c*, 1) (5 minutes) changing in 5 hours to +32° (const. value). Lit. m.p. 114° (11), $[\alpha]_D$ +34° (water) (10, 11). Acid hydrolysis of this disaccharide gave only galactose and, when treated with crystalline β-D-galactosidase, only galactose was generated. When the crystalline disaccharide (20 mg) was treated with phenylhydrazine in the usual way, a phenylosazone was obtained, m.p. 206° (after two recrystallizations from aqueous ethanol). An identical phenylosazone (m.p. and mixed m.p.) was produced by the same procedure from the 6-*O*-β-D-galactopyranosyl-D-galactose obtained from *V. oroboides* gum. Lit. (13, 17) m.p. 207°.

ACKNOWLEDGMENTS

The authors thank Dr. Frank Reithel of the University of Oregon for a specimen of crystalline β-D-galactosidase, and one of us (A. M. S.) wishes to acknowledge the support of the International Cooperation Administration under the Visiting Research Scientists Program administered by the National Academy of Sciences of the United States of America.

1. M. KOENIGS and E. KNORR. Ber. **34**, 957 (1901).
2. B. HELFERICH and W. KLEIN. Ann. **450**, 219 (1926). L. J. HAYNES and F. W. NEWTH. Advances in Carbohydrate Chem. **10**, 207 (1955).
3. B. HELFERICH. Advances in Carbohydrate Chem. **3**, 79 (1948).
4. D. V. MYHRE and F. SMITH. J. Org. Chem. In press.
5. H. BREDERICK, A. WAGNER, H. KUHN, and H. OTT. Ber. **93**, 1201 (1960).
6. E. FISCHER. Ber. **23**, 3687 (1890).
7. J. C. SOWDEN and A. S. SPRIGGS. J. Am. Chem. Soc. **78**, 2503 (1956).
8. E. BOURQUELOT, H. HERISSEY, and J. COIRRE. Compt. rend. **157**, 732 (1913). E. BOURQUELOT and M. BRIDEL. Ann. chim. et phys. Ser. 8, **29**, 145 (1913).
9. S. PEAT, W. J. WHELAN, and K. A. HINSON. Nature, **170**, 1056 (1952).
10. E. BOURQUELOT. Compt. rend. **163**, 60 (1916); **164**, 443, 521 (1917).
11. H. WEINLAND. Z. physik. chem. **305**, 87 (1956).
12. K. HILL. Ber. Verhandl. sächs. Akad. Wiss. Leipzig, Math.-phys. Kl. **86**, 115 (1934).
13. K. FREUDENBERG, A. WOLF, E. KNOPF, and S. H. ZAHEER. Ber. **61**, 1743 (1928).
14. J. H. PAZUR, C. L. TIPTON, T. BUDOVICH, and J. M. MARSH. J. Am. Chem. Soc. **80**, 119 (1958).
15. J. B. SUMNER and K. MYRBÄCK (*Editors*). The enzymes. Vol. I. Academic Press, New York. 1950. p. 624.
16. R. L. WHISTLER, W. H. EOFF, and D. M. DOTY. J. Am. Chem. Soc. **72**, 4938 (1950).
17. F. SMITH and A. M. STEPHEN. J. Chem. Soc. In press.
18. D. H. BALL and J. K. N. JONES. J. Chem. Soc. 905 (1958).

RECEIVED AUGUST 2, 1961.
DEPARTMENT OF AGRICULTURAL BIOCHEMISTRY,
THE UNIVERSITY OF MINNESOTA,
ST. PAUL 1, MINNESOTA.

CIS–TRANS ISOMERS OF ASARONE, THEIR LIQUID–GAS CHROMATOGRAPHIC BEHAVIOR AND THAT OF CERTAIN OTHER PROPENYLPHENOLETHERS*

R. M. BAXTER, M. C. FAN, AND S. I. KANDEL

Previously the isolation of three compounds with hypnotic potentiating activity from the volatile oil of *Acorus calamus* L., Indian, had been reported (1). Two of these proved to be the cis–trans isomers of 1,2,4-trimethoxy-propenyl benzene, namely asarone (α-asarone) and β-asarone (II and I).

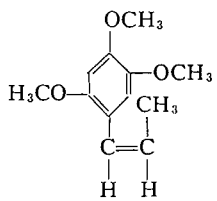

I

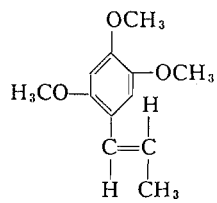

II

The cis–trans relationship of the asarones as well as other propenylbenzenephenolethers, many of which are constituents of volatile oils, has been well established (1, 2, 3). Although the Auwers–Skita rule is not strictly applicable in this series of compounds it has been utilized (3) in an attempt to elucidate the actual stereochemical configuration in this series (4). More recently Naves *et al.*, utilizing infrared spectroscopy, have shown that one of the isomer pair of each of isosafrole (5), anethol (6), isoeugenol, and isoeugenol-methylether (7) possesses a characteristic absorption band in a region at 963–967 cm^{-1}, which is in close proximity to the absorption band of *trans*-ethylenic compounds. The other isomer does not absorb in the same region. The present report is concerned with the

**This paper was presented at the 7th Canadian Conference on Pharmaceutical Research, August 1960.*

1. M. KOENIGS and E. KNORR. Ber. **34**, 957 (1901).
2. B. HELFERICH and W. KLEIN. Ann. **450**, 219 (1926). L. J. HAYNES and F. W. NEWTH. Advances in Carbohydrate Chem. **10**, 207 (1955).
3. B. HELFERICH. Advances in Carbohydrate Chem. **3**, 79 (1948).
4. D. V. MYHRE and F. SMITH. J. Org. Chem. In press.
5. H. BREDERICK, A. WAGNER, H. KUHN, and H. OTT. Ber. **93**, 1201 (1960).
6. E. FISCHER. Ber. **23**, 3687 (1890).
7. J. C. SOWDEN and A. S. SPRIGGS. J. Am. Chem. Soc. **78**, 2503 (1956).
8. E. BOURQUELOT, H. HERISSEY, and J. COIRRE. Compt. rend. **157**, 732 (1913). E. BOURQUELOT and M. BRIDEL. Ann. chim. et phys. Ser. 8, **29**, 145 (1913).
9. S. PEAT, W. J. WHELAN, and K. A. HINSON. Nature, **170**, 1056 (1952).
10. E. BOURQUELOT. Compt. rend. **163**, 60 (1916); **164**, 443, 521 (1917).
11. H. WEINLAND. Z. physik. chem. **305**, 87 (1956).
12. K. HILL. Ber. Verhandl. sächs. Akad. Wiss. Leipzig, Math.-phys. Kl. **86**, 115 (1934).
13. K. FREUDENBERG, A. WOLF, E. KNOPF, and S. H. ZAHEER. Ber. **61**, 1743 (1928).
14. J. H. PAZUR, C. L. TIPTON, T. BUDOVICH, and J. M. MARSH. J. Am. Chem. Soc. **80**, 119 (1958).
15. J. B. SUMNER and K. MYRBÄCK (*Editors*). The enzymes. Vol. I. Academic Press, New York. 1950. p. 624.
16. R. L. WHISTLER, W. H. EOFF, and D. M. DOTY. J. Am. Chem. Soc. **72**, 4938 (1950).
17. F. SMITH and A. M. STEPHEN. J. Chem. Soc. In press.
18. D. H. BALL and J. K. N. JONES. J. Chem. Soc. 905 (1958).

RECEIVED AUGUST 2, 1961.
DEPARTMENT OF AGRICULTURAL BIOCHEMISTRY,
THE UNIVERSITY OF MINNESOTA,
ST. PAUL 1, MINNESOTA.

CIS–TRANS ISOMERS OF ASARONE, THEIR LIQUID–GAS CHROMATOGRAPHIC BEHAVIOR AND THAT OF CERTAIN OTHER PROPENYLPHENOLETHERS*

R. M. BAXTER, M. C. FAN, AND S. I. KANDEL

Previously the isolation of three compounds with hypnotic potentiating activity from the volatile oil of *Acorus calamus* L., Indian, had been reported (1). Two of these proved to be the cis–trans isomers of 1,2,4-trimethoxy-propenyl benzene, namely asarone (α-asarone) and β-asarone (II and I).

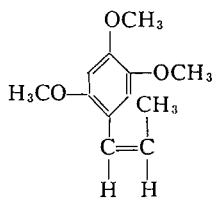

I

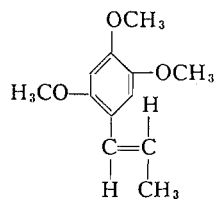

II

The cis–trans relationship of the asarones as well as other propenylbenzenephenolethers, many of which are constituents of volatile oils, has been well established (1, 2, 3). Although the Auwers–Skita rule is not strictly applicable in this series of compounds it has been utilized (3) in an attempt to elucidate the actual stereochemical configuration in this series (4). More recently Naves *et al.*, utilizing infrared spectroscopy, have shown that one of the isomer pair of each of isosafrole (5), anethol (6), isoeugenol, and isoeugenol-methylether (7) possesses a characteristic absorption band in a region at 963–967 cm^{-1}, which is in close proximity to the absorption band of *trans*-ethylenic compounds. The other isomer does not absorb in the same region. The present report is concerned with the

**This paper was presented at the 7th Canadian Conference on Pharmaceutical Research, August 1960.*

stereochemical configuration of asarone and β-asarone as determined by infrared spectroscopy and the chromatographic behavior of the asarones and other propenylphenolethers.

From Fig. 1 it may be seen that asarone absorbs at 964 cm^{-1} in a manner which is characteristic of *trans*-propenyl benzenes and that β-asarone exhibits no absorption in

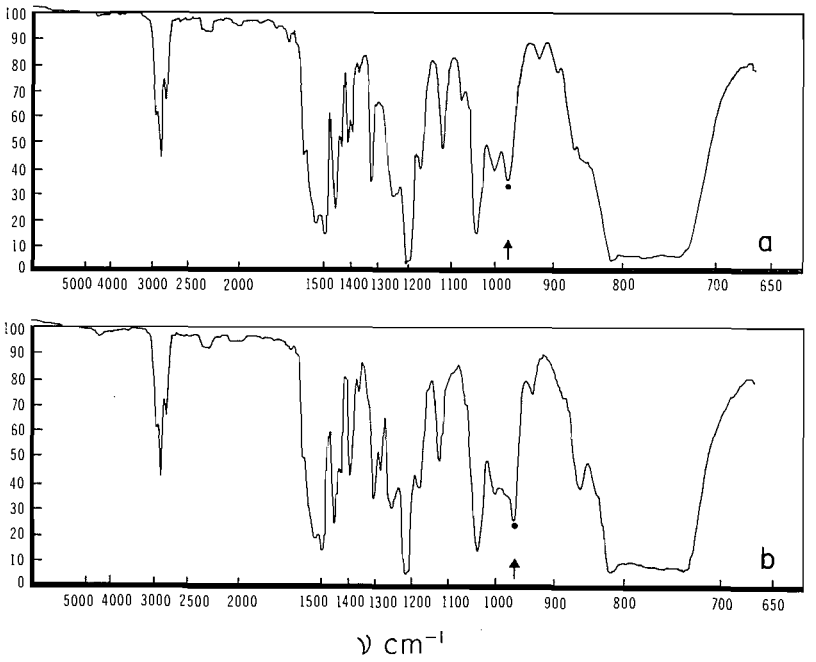

FIG. 1. The infrared spectra of (*a*) asarone and (*b*) β-asarone.

this region. It may therefore be concluded (5) that β-asarone (I) possesses a *cis*- and asarone (II) a *trans*-ethylenic side chain.

It was also found that the isomeric pairs of propenylphenolethers could be separated on each of the liquid–gas chromatographic columns used. The best separation can be achieved with a Ucon polar column where the mixture of *cis–trans*-isosafrole, *cis–trans*-isoeugenolmethylether, *cis–trans*-isoeugenol, and *cis–trans*-asarone (β-asarone and asarone) can be separated (Fig. 2). It will be observed that in each instance the cis

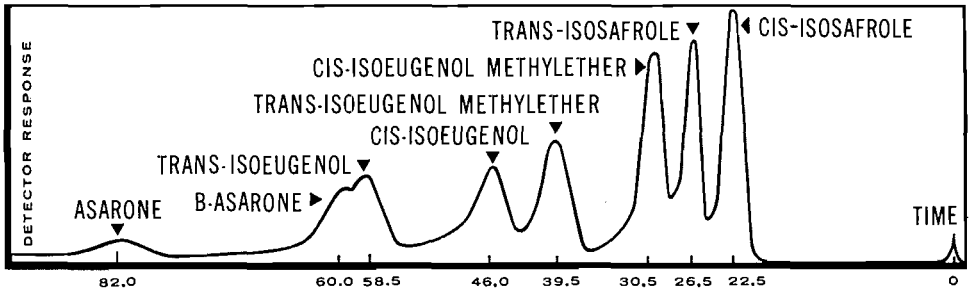

FIG. 2. Separation of certain propenylphenolethers by liquid-gas chromatography on Ucon polar column. Conditions as in Table I.

isomer had a lower retention time than the trans (Table I). There is at present no evidence to indicate that the higher retention times of the trans isomers were due directly to their

TABLE I

The retention time of certain propenylphenolethers as indicated by liquid–gas chromatography

Compounds	Retention times (min)		
	Ucon polar	Reoplex 400	Asphalt
cis-Isosafrole	22.5	13.0	15.0
trans-Isosafrole	26.5	17.0	19.0
cis-Isoeugenolmethylether	30.5	20.5	20.0
trans-Isoeugenolmethylether	39.5	24.5	25.5
cis-Isoeugenol	46.0	27.5	20.5
trans-Isoeugenol	58.5	34.5	26.0
β-Asarone	60.0	38.5	34.5
Asarone	82.0	57.0	50.5

NOTE: Column 10 ft × ¼ in. Liquid phases on chromosorb P (35–80 mesh) in a ratio 25/75 by weight. Temperature: 200° C ±2° C. Outlet flow: 70 ml of helium per minute.

configuration and not to their higher boiling points. It would appear, however, that in the propenylphenolethers studied, the trans isomers should exhibit longer retention times than the cis isomers. It is suggestive that this relationship would be applicable independent of the relative polarity of the chromatographic column. This method may allow for the simultaneous separation and the determination of the quantity and geometrical configuration of each individual cis, trans isomer in this series.

Subsequent to the presentation of this data, Stahl and Trennheuser (8) reported on the liquid–gas chromatographic separation of the same propenylphenolethers.

EXPERIMENTAL

Asarone and β-asarone were isolated from the volatile oil of Indian *Acorus calamus* L. (Fritzsche Bros. Inc.) by liquid–gas chromatography, using a "Ucon" polar column. The samples emerging from the column were collected in acetone and cooled in an acetone – dry ice bath. After the evaporation of the acetone, asarone and β-asarone were purified and identified as described earlier (1). *Cis*- and *trans*-isosafrole, *cis*- and *trans*-isoeugenol, *cis*- and *trans*-isoeugenolmethylether were generously provided by Dr. Y. R. Naves.

Infrared Spectra

The spectra of asarone and β-asarone (1.5% w/v in carbon tetrachloride) were obtained using a Beckman IR-4 recording spectrophotometer.

Liquid–Gas Chromatography

An Aerograph A 100-C liquid–gas chromatography unit was utilized. The column temperature was maintained at 200° C ±2° C. Dried helium was used as carrier gas with a flow rate of 70 ml per minute measured at the outlet of the apparatus. The sample (3–5 μl) was injected into a column with a 10-μl Hamilton fixed needle syringe. In the case of asarone the sample was dissolved in acetone.

The solid support used in the column was chromosorb P, 35–80 mesh. The liquid phase (6 g) was applied to the solid support in the ratio of 3 to 1 by weight dissolved in a solvent. In the case of Ucon polar (monoether of a random copolymer of ethylene oxide and propylene oxide, Wilkins Instrument & Research Inc.) and Reoplex 400 the solvent was acetone (100 ml) and in the case of asphalt the solvent was petroleum ether (100 ml, b.p. 60–80° C). The solution was added to the solid support (18 g) and shaken for 3 hours. The solvent was removed *in vacuo* at 30° C. After it was dried in a vacuum desiccator the material was packed into a 10 ft × ¼ in. (O.D.) copper column with constant tapping.

1. R. M. BAXTER, P. C. DANDIYA, S. I. KANDEL, A. OKANY, and G. C. WALKER. Nature, **185**, 466 (1960).
2. B. S. RAO and K. SUBRAMANIAM. J. Chem. Soc. 1338 (1937).
3. E. GUENTHER and D. ALTHAUSEN. The essential oils. Vol. II. D. Van Nostrand Co., Inc., New York. 1949. pp. 499–546.
4. K. V. AUWERS. Ber. **68**, 1348 (1935).

5. Y. R. NAVES and P. ARDISIO. Bull. soc. chim. France, 1053 (1957).
6. Y. R. NAVES, P. ARDISIO, and C. FAVRE. Bull. soc. chim. France, 566 (1958).
7. Y. R. NAVES and A. V. GRAMPOLOFF. Bull. soc. chim. France, 1233 (1959).
8. E. STAHL and L. TRENNHEUSER. Arch. Pharm. **293/65**, 826 (1960).

RECEIVED AUGUST 24, 1961.
FACULTY OF PHARMACY,
UNIVERSITY OF TORONTO,
TORONTO, ONTARIO.

FLUORINE PERCHLORATE, INFRARED AND NUCLEAR MAGNETIC RESONANCE SPECTRA

H. AGAHIGIAN, A. P. GRAY, AND G. D. VICKERS

The preparation of $FClO_4$ has been reported (1, 2), but spectral data are not available. The infrared and fluorine nuclear magnetic resonance spectra of fluorine perchlorate are reported below.

Since the fluorine resonance appears to shift to low field with increasing electronegativity of an attached atom or group (3, 4*a* and *b*), the fluorine chemical shift of fluorine perchlorate was measured in order to determine the extent of the displacement of the fluorine resonance to low field.

The fluorine n.m.r. spectrum of neat perchloryl fluoride has been reported (3). A low-field fluorine chemical shift as well as fluorine–chlorine spin–spin coupling was observed in perchloryl fluoride (3).

Since the method (3) of measuring the chemical shift and the standard used were different from those used in this laboratory, a comparison among fluorine perchlorate, fluorine oxide, and perchloryl fluoride was made using $CFCl_3$ (5) as a standard and solvent.

The fluorine n.m.r. spectrum of fluorine perchlorate consisted of a single line, and a chemical shift of -225.9 p.p.m. relative to $CFCl_3$ was obtained. The chemical shift of fluorine perchlorate was not measured neat but as a 50% solution in Freon-11. Although the perchlorate will detonate in the pure form, in solution fluorine perchlorate appears to be stable and the data was obtained without incident.

A 50% solution of perchloryl fluoride in Freon-11 was studied in an effort to resolve the spectrum of the proposed quartets (3). However, the use of a solvent did little to help resolve the spectrum. The center of what appeared to be a broad doublet was -287.0 p.p.m. relative to $CFCl_3$. The splitting between the peaks was 460 cycles.

The fluorine chemical shift of fluorine oxide was measured as a gas under 5-atm pressure and relative to $CFCl_3$ in a sealed capillary. The chemical shift was -250.0 p.p.m.

The fluorine chemical shifts relative to $CFCl_3$ are shown below.

$FOClO_3$	-225.9 p.p.m.
FOF	-250.0 p.p.m.
$FClO_3$	-287.0 p.p.m.

The side-band technique (6) was used to measure the chemical shifts. Since different techniques were used, comparison of presented and published (3) data would be difficult, but the chemical shifts of the three compounds $FClO_4$, $FClO_3$, and OF_2, appear to be of the right order of magnitude, and are in the order predicted by theory (4).

The infrared spectrum of fluorine perchlorate was obtained in the sodium chloride region only. As the spectrum of fluorine perchlorate has not previously been reported,

5. Y. R. NAVES and P. ARDISIO. Bull. soc. chim. France, 1053 (1957).
6. Y. R. NAVES, P. ARDISIO, and C. FAVRE. Bull. soc. chim. France, 566 (1958).
7. Y. R. NAVES and A. V. GRAMPOLOFF. Bull. soc. chim. France, 1233 (1959).
8. E. STAHL and L. TRENNHEUSER. Arch. Pharm. **293/65**, 826 (1960).

RECEIVED AUGUST 24, 1961.
FACULTY OF PHARMACY,
UNIVERSITY OF TORONTO,
TORONTO, ONTARIO.

FLUORINE PERCHLORATE, INFRARED AND NUCLEAR MAGNETIC RESONANCE SPECTRA

H. AGAHIGIAN, A. P. GRAY, AND G. D. VICKERS

The preparation of $FClO_4$ has been reported (1, 2), but spectral data are not available. The infrared and fluorine nuclear magnetic resonance spectra of fluorine perchlorate are reported below.

Since the fluorine resonance appears to shift to low field with increasing electronegativity of an attached atom or group (3, 4*a* and *b*), the fluorine chemical shift of fluorine perchlorate was measured in order to determine the extent of the displacement of the fluorine resonance to low field.

The fluorine n.m.r. spectrum of neat perchloryl fluoride has been reported (3). A low-field fluorine chemical shift as well as fluorine–chlorine spin–spin coupling was observed in perchloryl fluoride (3).

Since the method (3) of measuring the chemical shift and the standard used were different from those used in this laboratory, a comparison among fluorine perchlorate, fluorine oxide, and perchloryl fluoride was made using $CFCl_3$ (5) as a standard and solvent.

The fluorine n.m.r. spectrum of fluorine perchlorate consisted of a single line, and a chemical shift of -225.9 p.p.m. relative to $CFCl_3$ was obtained. The chemical shift of fluorine perchlorate was not measured neat but as a 50% solution in Freon-11. Although the perchlorate will detonate in the pure form, in solution fluorine perchlorate appears to be stable and the data was obtained without incident.

A 50% solution of perchloryl fluoride in Freon-11 was studied in an effort to resolve the spectrum of the proposed quartets (3). However, the use of a solvent did little to help resolve the spectrum. The center of what appeared to be a broad doublet was -287.0 p.p.m. relative to $CFCl_3$. The splitting between the peaks was 460 cycles.

The fluorine chemical shift of fluorine oxide was measured as a gas under 5-atm pressure and relative to $CFCl_3$ in a sealed capillary. The chemical shift was -250.0 p.p.m.

The fluorine chemical shifts relative to $CFCl_3$ are shown below.

$FOClO_3$	-225.9 p.p.m.
FOF	-250.0 p.p.m.
$FClO_3$	-287.0 p.p.m.

The side-band technique (6) was used to measure the chemical shifts. Since different techniques were used, comparison of presented and published (3) data would be difficult, but the chemical shifts of the three compounds $FClO_4$, $FClO_3$, and OF_2, appear to be of the right order of magnitude, and are in the order predicted by theory (4).

The infrared spectrum of fluorine perchlorate was obtained in the sodium chloride region only. As the spectrum of fluorine perchlorate has not previously been reported,

the four observed absorptions at 1298, 1049, 885, and 666 cm^{-1} will be briefly discussed. The two high-frequency bands are nearly coincident with those found in both anhydrous $HClO_4$ (7) and Cl_2O_7 (8) and are evidently associated with the covalent perchlorate group. In this case, the 1298 cm^{-1} band is assigned as the approximately degenerate antisymmetric ClO_3 stretches and 1049 cm^{-1} as the corresponding symmetric vibration. With NaCl prism resolution, the 1298 cm^{-1} band has no discernible structure, while a *P*,*R* contour is observed at 1049 cm^{-1}. The 666 cm^{-1} absorption has a similar contour and is consistent in position with the singly bonded Cl—O stretch. The symmetric Cl—O stretch in chlorine monoxide occurs at 688 cm^{-1} (9). The absorption at 885 cm^{-1} has a *PQR* structure and is assigned as the O—F stretch, corresponding to the symmetric vibration in fluorine monoxide at 928 cm^{-1} (10).

Inertially, ClO_3OF is expected to be similar to methanol, with singly bonded Cl—O being the axis of an approximate symmetric top. The 1049 and 666 cm^{-1} bands are therefore expected to have a *PQR* structure, whereas a *Q* branch is not observed. However, this is not considered sufficient reason for rejection of the above assignment, since even for truly symmetric tops, the *Q* branch in parallel bands is frequently unobserved, due to significant differences between upper- and lower-state inertial constants, resulting in non-superposition of the *Q*-branch subbands (11). The *PQR* structure of the O—F stretching at 885 cm^{-1} is that expected for a hybrid band of an approximate symmetric top.

EXPERIMENTAL

The n.m.r. spectrometer was a 56.4 Mc instrument, and the side-band technique (6) was used to measure the chemical shifts.

The fluorine oxide could not be measured in solution but was measured as a gas under pressure. A capillary was filled with $CFCl_3$ and sealed. This was inserted into the 5-mm pyrex tube and fluorine oxide was condensed into the n.m.r. tube and the tube was sealed. The chemical shift for fluorine oxide was uncorrected for bulk susceptibility.

The infrared spectra were obtained in the vapor phase using a 5-cm Monel cell with NaCl windows sealed vacuum tight with Fluorolube wax.

ACKNOWLEDGMENTS

The authors wish to thank Mr. Thomas Hurley for preparing and purifying fluorine perchlorate, as well as preparing the samples of perchloryl fluoride and fluorine oxide; and Dr. Sydney Brownstein of the National Research Council, Ottawa, Canada, for his comments and interesting observations.

1. G. H. Rohrback and G. H. Cady. J. Am. Chem. Soc. **69**, 677 (1947).
2. Fr. Fichter and E. Brunner. Helv. Chim. Acta, **12**, 305 (1929).
3. S. Brownstein. Can. J. Chem. **38**, 1597 (1960).
4. (*a*) H. S. Gutowsky and C. J. Hoffman. J. Chem. Phys. **19**, 1259 (1951).
   (*b*) A. Saika and C. P. Slichter. J. Chem. Phys. **22**, 26 (1954).
5. G. Filipovich and G. V. D. Tiers. J. Phys. Chem. **19**, 1608 (1951).
6. J. T. Arnold and M. E. Packard. J. Chem. Phys. **19**, 1608 (1951).
7. A. Simon and M. Weist. Z. anorg. u. allgem. Chem. **268**, 301 (1952).
8. Unpublished results.
9. K. Hedberg. J. Chem. Phys. **19**, 509 (1951).
10. H. J. Bernstein and J. Powling. J. Chem. Phys. **18**, 685 (1950).
11. G. Herzberg. Infrared & raman spectra of polyatomic molecules. D. Van Nostrand Co., Inc., New York. p. 419.

Received July 3, 1961.
Research Center,
Olin Mathieson Chemical Corp.,
275 Winchester Avenue,
New Haven 4, Connecticut.

PREPARATION OF SYNTHETIC GELS FOR CHROMATOGRAPHY OF MACROMOLECULES*

D. J. Lea† and A. H. Sehon

The introduction of the technique of column chromatography on cross-linked gels (1, 2) has provided a powerful new tool for the fractionation of complex mixtures of biological origin. These gels exhibit both adsorption and molecular sieve properties. Various polymers, such as dextran, starch, and polyvinyl alcohol, cross-linked in an undisclosed manner, have been used for the chromatographic separation of aqueous solutions of proteins, dextrans, and similar materials. So far gels which will permit the entry of materials with molecular weights up to 40,000 into the gel matrix have been prepared (1, 2). However, it has been found in this laboratory that certain compounds, such as pollen pigments, could not be readily desorbed from the dextran gel and that the gel had to be discarded after a single fractionation.

Two modifications of the method using dextran gel have recently been described (3): (i) Diethylaminoethyl-dextran gels, functioning by ion-exclusion, have been prepared, and (ii) the adsorption properties of dextran gels have been changed by using mixed solvent systems, such as acetic acid – pyridine – water, in place of the usual aqueous buffer solutions. A technique using agar gel, which is not cross-linked, has also been published recently (4).

Alternative methods for the preparation of different gels with a wide range of "pore" size and adsorption properties were explored in the present study. Polymerization of readily available charged and neutral monomers,‡ in the presence of cross-linking agents, in water or in mixed solvent systems, permitted the synthesis of gels suitable for the fractionation of mixtures of biological materials. The preparation of three different polymers, using N,N′-methylenebisacrylamide as the cross-linking agent, and the preliminary results of fractionation experiments are described below.

(1) Acrylamide, a water-soluble monomer, can be easily polymerized in aqueous solution to give hydrophilic gels (5). A suitable content of cross-linking agent gives gels which have sufficient mechanical stability to serve as packing materials for columns. Acrylamide§ (4.6 g) and N,N′-methylenebisacrylamide§ (0.4 g) were dissolved in boiled distilled water (98 ml). The initiators, dimethylaminopropionitrile (40 μl), followed by ammonium persulphate (40 mg) were added. The solution was stirred gently and covered by a layer of heavy paraffin oil to exclude oxygen. The appearance of milkiness indicated the beginning of polymerization. Several hours later, a firm white gel had formed, which was cut up into small pieces and washed exhaustively with running tap water to remove unreacted monomer. The pieces of gel were forced through a sieve (1-mm mesh) and the particles were again washed with water, alcohol, and acetone and finally with distilled water, until the ultraviolet-absorbing material ceased to elute from the solid. The finest particles were then removed by decantation or filtration through a sieve (U.S. 50 mesh).

*This study was supported by grants from the National Institute of Allergy and Infectious Diseases, National Institutes of Health, Bethesda, Md., and the National Research Council of Canada, Ottawa, Ont.

†Postdoctoral fellow of the Arthritis and Rheumatism Foundation. Present address: Central Public Health Laboratory, Colindale Avenue, London, England.

‡It should be noted that samples of monomer may require fractional distillation before polymerization is possible.

§These materials were generously supplied by Cyanamid Co. of Canada, Ltd.

(2) A polymer of vinyl ethyl carbitol* (CH_2=$CH \cdot O \cdot CH_2 \cdot CH_2 \cdot O \cdot CH_2 \cdot CH_2 \cdot O \cdot C_2H_5$) was prepared using the same cross-linking agent and initiators.

Vinyl ethyl carbitol (12.75 g) was mixed with boiled distilled water (42.5 ml) and ethyl alcohol (42.5 ml). The solution was treated with Amberlite IR-120 (H^+ form) to remove the inhibitor, then sodium bicarbonate (1 g) and N,N′-methylenebisacrylamide (2.25 g) were added, giving a turbid solution. Dimethylaminopropionitrile (4 μl) and ammonium persulphate (4 mg) were added in turn, with gentle stirring, and the solution was covered with paraffin oil. In a few hours a firm, rather friable, white gel had formed, which was washed and broken up as before.

(3) Vinyl pyrrolidone† was also polymerized to a gel. Vinyl pyrrolidone (12.75 g) was dissolved in boiled distilled water (85 ml) and treated with ion exchange resin, as before, and N,N′-methylenebisacrylamide (2.25 g) was added. The catalyst system was concentrated ammonia solution (0.2 ml) and hydrogen peroxide (0.4 ml, 30%).

To evaluate the possible usefulness of these gels for column chromatography, some preliminary experiments were done with mixtures of materials readily available in this laboratory, such as human serum proteins, lysozyme, and the water-soluble components of ragweed pollen, which include proteins, polysaccharides, lipids, and pigments.

Serum (0.5 ml) containing haemoglobin was applied to a column (60 cm×2.5 cm I.D.) containing acrylamide gel. For elution, a solution of 0.9% saline and sodium phosphate buffer (17.25 g $Na_2HPO_4.7H_2O$ plus 1.417 g $NaH_2PO_4.H_2O$ per liter) was used, 5-ml fractions being collected. From optical density measurements and from immunochemical examination‡ of the eluates it was clear that a partial fractionation had been attained. The lipid present in the serum did not appear to be retained by the gel and appeared first in the eluate after the passage of about 60 ml, representing the dead volume of the column. Methaemoglobin and several serum proteins eluted immediately afterwards. These fractions were virtually free of albumin, which reached maximum concentration after collection of 90–100 ml of eluate. Lysozyme, when examined in the same way, reached maximum concentration at about 140–150 ml. Aqueous ragweed pollen extract on elution with water gave initial fractions containing lipid, followed by protein, and then by various pigments.

Polyvinyl ethyl carbitol under the same conditions gave results similar to those reported above with ragweed pollen preparations. However, polyvinyl pyrrolidone retained some of the pigments, which are derivatives of quercetin, so strongly that elution of these materials was quite difficult. These findings are in accordance with the known properties of polyvinyl pyrrolidone to complex with different compounds (6).

From these preliminary results, it appears that such polymer gels offer a new approach to adsorption chromatography. Obviously, this principle may be extended to the preparation of gels with ion exchange properties conferred by the incorporation of ionic groups, such as diethylaminoethyl, pyridine, and carboxyl groups.

1. J. Porath. Clin. Chim. Acta, **4**, 776 (1959).
2. W. Bjork and J. Porath. Acta Chem. Scand. **13**, 1256 (1959).
3. J. Porath and E. B. Lindner. Nature, **191**, 69 (1961).
4. A. Polson. Biochim. et Biophys. Acta, **50**, 565 (1961).
5. M. L. White. J. Phys. Chem. **64**, 1563 (1960).
6. R. Schubert. Arzneimittel-Forschg. **4**, 42 (1950).

Received October 11, 1961.
Department of Chemistry,
McGill University,
Montreal, Que.

*Kindly supplied by Union Carbide Company of Canada.
†Generously supplied by Antara Chemical Division, General Aniline and Film Corporation, U.S.A.
‡The micro-Ouchterlony gel method with a horse antihuman serum was used for the detection of the different serum proteins eluted.

REACTION OF GROUP V IODIDES WITH IODOMETHANE AND TRIFLUOROIODOMETHANE IN THE PRESENCE OF MERCURY

M. M. Baig and W. R. Cullen

The reaction of alkyl- or aryl-iodoarsines with alkyl iodides in the presence of mercury produces arsonium triiodomercury (II) derivatives (1). Under similar conditions using perfluoroalkyl iodides the products are trifluoromethylarsines (2, 3). It has now been found that arsenic triiodide does not react with trifluoroiodomethane in the presence of mercury to give trifluoromethylarsines and that similar results are obtained for phosphorus, antimony, and bismuth triiodides (see Table I). The reaction of iodomethane with these iodides in the presence of mercury produces tetramethylarsonium triiodomercurate (II) (1); tetramethylstibonium triiodomercurate (II), m.p. 167°; the 1:1 complex of trimethylphosphine and mercuric iodide, $(CH_3)_3P.HgI_2$, m.p. 197–200°; together with another unidentified minor product. In the case of bismuth triiodide a low yield of an unstable yellow solid is also produced.

The phosphine mercuric iodide adduct is a pale yellow solid. Its molecular weight in camphor indicates that it is present in solution largely as the monomer. Similar results have been obtained for other 1:1 tertiary phosphine mercuric iodide complexes (4). The reaction of iododimethylarsine with iodoethane in the presence of mercury similarly produces the 1:1 adduct of ethyldimethylarsine and mercuric iodide though all other reactions of this kind so far investigated produce onium derivatives of triiodomercury (II) if the reactant is an alkyl iodide (1).

Diiodophenylstibine in the presence of mercury does not react with trifluoroiodomethane, and with iodomethane the main product is methylmercury iodide. This compound is also formed as a by-product in similar reactions of iodophenylarsines (1). The reaction of diiodophenylstibine with iodomethane also produces a small amount of a yellow substance, possibly an onium complex, but the yield is not sufficient for easy isolation and identification. The absence of any significant reaction of the phenyliodostibine with both iodomethane and trifluoroiodomethane is surprising in view of the similar behavior of arsenic and antimony triiodides when reacted with iodomethane: both yield onium derivatives in moderately good yield.

It has been found that when the compounds R_nAsI_{3-n} (R = alkyl or aryl, n = 1 or 2) are reacted with trifluoroiodomethane in the presence of mercury the yield of trifluoromethylarsine decreases as the number of iodine atoms to be substituted increases (2, 3). Failure of arsenic triiodide to react with trifluoroiodomethane can thus be regarded as the limiting case.

EXPERIMENTAL

For these experiments commercial phosphorus and bismuth triiodides were used. Arsenic and antimony triiodides were prepared by the procedures given in *Inorganic syntheses* (5). Diiodophenylstibine, m.p. 69° (lit. value, 69°) (6), was prepared by reducing phenylstibonic acid with stannous chloride in the presence of sodium iodide. Phenylstibonic acid was prepared by the action of diazotized aniline on antimony trioxide (6). The reactions reported below were carried out in sealed tubes in the absence of air and light. The reaction temperature was 20° unless otherwise stated. Volatile reactants were manipulated in a vacuum system.

Reaction of Group V Iodides with Trifluoroiodomethane in the Presence of Mercury

Table I shows the results of these experiments. Mercury (ca. 200 g) was also present in the tubes in addition to the reactants listed. After shaking the tubes for the time shown the volatile contents were taken into the vacuum system. Trap-to-trap distillation and infrared examination of the fractions isolated failed in all cases to show that any volatile substance other than trifluoroiodomethane was present.

TABLE I

Reactants*	Time (days)	CF_3I recovered (g)
PI_3 (18.0), CF_3I (82.5)	50	83.0
AsI_3 (9.0), CF_3I (73.2)	7	73.1†
SbI_3 (14.9), CF_3I (54.1)	30	54.0
$C_6H_6SbI_2$ (14.0), CF_3I (43.8)	40	42.3
BiI_3 (19.7), CF_3I (79.0)	14	77.3

*Weight, in grams, of reactants given in parentheses.
†No unreacted arsenic triiodide could be extracted from the solid residue with alcohol.

Reactions of Group V Iodides with Iodomethane in the Presence of Mercury

Phosphorus triiodide.—Phosphorus triiodide (18.5 g), mercury (215 g), and iodomethane (65 g) were shaken for 50 days. The contents of the tube were extracted with acetone and a slightly soluble, pale yellow solid was isolated. Fractional crystallization of this solid gave fractions melting in the range 148–162°. These were combined and recrystallization from a large volume of ethanol gave two fractions, one a pale yellow crystalline solid, m.p. 165–170° (6 g), and the other a small amount of a yellow waxy solid, m.p. 85–106°. Analysis of the first fraction (found: C 5.86, H 1.57, P 5.16, Hg 36.8, I 49.6%) (empirical formula $C_{2.9}H_{9.4}P_1Hg_{1.1}I_{2.4}$) suggested that the substance was mainly the 1:1 adduct of trimethylphosphine and mercuric iodide. A sample of the adduct was prepared by reacting trimethylphosphine (1.278 g, 1 mole) with mercuric iodide (1 mole) at 90° for 6 days. No volatile material was present in the tube after this time. The yellow solid which remained in the tube was only slightly soluble in hot ethanol or acetone but was eventually recrystallized using a large volume of a mixture of ethanol and acetone (2:1 by volume). The product melted at 197–200° and its infrared spectrum was identical with that of the product, m.p. 165–170°, from the reaction of phosphorus triiodide with mercury and iodomethane. The identity of the 1:1 adduct was confirmed by analysis. Found: C 6.90, H 1.65, P 5.75, Hg 37.5, I 47.7%, mol. wt. 565; calc. for $C_3H_9HgI_2P$: C 6.78, H 1.69, P 5.83, Hg 37.8, I 47.8%, mol. wt. 531. The reaction product melting at 85–106° was also analyzed but the results do not approximate to any reasonable compound.

Antimony triiodide.—The triiodide (13.9 g), mercury (219 g), and iodomethane (50.3 g) were shaken for 30 days. Extraction of the contents of the tube with acetone gave, after recrystallization, *tetramethylstibonium triiodomercurate* (II), m.p. 167° (41% yield). Anal.: found: C 6.81, H 1.59, Hg 25.6, I 48.8%; calc. for $C_4H_{12}HgI_3Sb$: C 6.3, H 1.57, Hg 26.3, I 50.0%.

Diiodophenylstibine.—The stibine (8.0 g), mercury (189 g), and iodomethane (31.4 g) were shaken for 40 days. Extraction of the contents of the tube with acetone gave a slightly colored (yellow) solid (15.6 g). This, on recrystallization from acetone, was colorless and was identified as methylmercury iodide. Anal.: found: C 2.98, H 0.74, Hg 57.6, I 37.4%, mol. wt. 316, m.p. 147–148°; CH_3HgI requires: C 3.50, H 0.87, Hg 58.7, I 37.0%, mol. wt. 343, m.p. 152° (7). The yellow impurity was not present in sufficient quantity to enable easy isolation and identification.

Bismuth triiodide.—The triiodide (22.2 g), mercury (300 g), and iodomethane (63.2 g) were shaken for 14 days. The acetone extract was yellow but on crystallization the product appeared to decompose with the liberation of mercuric iodide.

ACKNOWLEDGMENTS

The authors wish to acknowledge financial assistance from the National Research Council. One of us (M. M. B.) expresses thanks for a scholarship received under the auspices of the Colombo Plan. Thanks are also due to Dr. M. A. Beg for a gift of trimethylphosphine. Microanalyses were carried out by Dr. Alfred Bernhardt.

1. M. M. Baig and W. R. Cullen. Can. J. Chem. **39**, 420 (1961).
2. W. R. Cullen. Can. J. Chem. **38**, 439 (1960).
3. W. R. Cullen. Can. J. Chem. **38**, 445 (1960).
4. R. C. Cass, G. E. Coates, and R. G. Hayter. J. Chem. Soc. 4007 (1955).
5. W. C. Fernelius. Inorganic syntheses. Vol. I. McGraw-Hill Book Co., Inc., New York. 1946.
6. H. Schmidt. Ann. **429**, 123 (1922).
7. E. Krause and A. von Grosse. Die Chemie der Metal-organischen Verbindungen. Borntraeger, Berlin. 1937.

Received August 21, 1961.
Chemistry Department,
University of British Columbia,
Vancouver 8, B.C.

IMPROVED SYNTHESIS OF N-ALKYL-ASPARTIC ACIDS

R. Laliberté and L. Berlinguet

N-Alkyl-aspartic acids can now be prepared readily by nucleophilic addition of primary amines to the double bond of monomethyl maleate according to a technique first described by Zilkha and Bachi (1).

During the preparation of some N-alkyl-aspartic acids, we found that triethylamine could advantageously replace pyridine as solvent and catalyst. The yields are about 20% higher and the isolation of a much purer product is possible owing to the absence of colored secondary products.

We have extended this reaction to two more primary amines and we have obtained good yields of the following derivatives: N-ethyl-aspartic acid β-methyl ester (95%) and N-isopropyl-aspartic acid β-methyl ester (75%).

We also found that this method is quite general and that other types of amines can be used to give new N-alkyl-aspartic-acid β-methyl esters. Piperidine, ethanolamine, 2-propanolamine, and glycine methyl ester were condensed with monomethyl maleate to give the expected N-alkyl-aspartic acids β-methyl ester with yields of 76%, 75%, 82%, and 75% respectively.

When 2 equivalents of the amine were used, we obtained the corresponding N,N′-disubstituted asparagine: thus N,N′-dibutyl-asparagine and N,N′-dipiperidyl-asparagine were obtained.

Good yields of the N-alkyl-aspartic acids were obtained by hydrolysis of the corresponding methyl esters with cold barium hydroxide (1). All these amino acids were characterized as such except for N-(2-propanol)-aspartic acid, which is hygroscopic and was isolated as the copper salt.

EXPERIMENTAL

Preparation of N-Alkyl-aspartic Acids β-Methyl Esters

Maleic anhydride (56 g, 0.57 mole) was dissolved in 200 ml of methanol. After the mixture was refluxed on a water bath for 30 minutes, excess methanol was distilled off. One hundred milliliters of triethylamine was added to the residue, cooled in ice, very slowly and with stirring in order to avoid side reactions which could contaminate the product with colored by-products. One-half mole of the desired amine was then added in one portion. This mixture was stirred over a water bath for an hour. Usually the product started to crystallize in 20 minutes. The mixture was filtrated and washed twice with hot acetone or ethyl acetate. After these washings, the product is usually white and can be used without further purification (see Table I).

If necessary, the ester can be crystallized from a minimum volume of hot water by adding a large amount of acetone.

The addition of piperidine goes smoothly at room temperature and it is not necessary to heat the solution. However, in this reaction no solid crystallizes out, and the excess of triethylamine has to be evaporated, because the addition product remains in solution. The residue is taken in hot isopropanol and crystallized in the cold. A further crop of crystals is obtained after the addition of petroleum ether.

In the case of glycine methyl ester, 5 g (0.036 mole) of the hydrochloride were mixed with monomethyl maleate prepared from 5 g of maleic anhydride. To this mixture were added 30 ml of triethylamine and 5 ml of methanol. After heating on a water bath for an hour, the hydrochloride of triethylamine crystallized in the cold and was eliminated by filtration. The methanol and the excess of triethylamine were distilled off. The condensation product was dissolved in water and crystallized by the addition of isopropanol.

Preparation of N-Alkyl-aspartic Acids

The N-alkyl-aspartic acid methyl ester to be hydrolyzed (0.10 mole) was dissolved in 0.125 mole barium hydroxide solution and left for 2 hours at room temperature. The solution was heated for 10 minutes and

TABLE I

N-Alkyl-aspartic acids β-methyl esters

$CH_3—OOC—CH_2—\underset{\displaystyle NH\\ \displaystyle R}{CH}—COOH$

R	Yield (%)	M.p. (°C)	Formula	% nitrogen Calc.	% nitrogen Found
Ethyl	92	217	$C_7H_{13}NO_4$	7.99	7.93
Isopropyl	75	214	$C_8H_{15}NO_4$	7.39	7.35
Butyl*	80	231	$C_9H_{17}NO_4$	6.89	6.82
Cyclohexyl†	90	216	$C_{11}H_{19}NO_4$	6.11	6.16
Allyl‡	84	213	$C_8H_{13}NO_4$	7.48	7.43
Ethanol-2	75	198	$C_7H_{13}NO_5$	7.32	7.35
Propanol-2	82	200	$C_8H_{15}NO_5$	6.82	6.77
Piperidyl	76	164	$C_{10}H_{17}NO_4$	6.50	6.41
Methyl acetate	75	164	$C_8H_{13}NO_6$	6.39	6.57

*Reported (1) m.p. 220° C.
†Reported (1) m.p. 210° C.
‡Reported (1) m.p. 213° C.

then an equivalent of hot sulphuric acid (1.0 *M*) was added. The filtrated solution was evaporated to 30 ml. The amino acid was usually obtained by the slow addition of 200 to 500 ml of an organic solvent (see Table II).

TABLE II

Preparation of N-alkyl-aspartic acids

$HOOC—CH_2—\underset{\displaystyle NH\\ \displaystyle R}{CH}—COOH$

R	Yield (%)	M.p. (°C)	Formula	Solvent used for crystallization	% nitrogen Calc.	% nitrogen Found
Ethyl	95	190	$C_6H_{11}NO_4$	Ethanol	8.68	8.66
Isopropyl	98	185	$C_7H_{13}NO_4$	Ethanol	7.99	7.92
Ethanol-2	90	182	$C_6H_{11}NO_5$	Isopropanol	7.90	7.85
Propanol-2*	95	—	—	—	5.53	5.37
Piperidyl	75	185	$C_9H_{15}NO_4$	Acetone and ether	6.95	6.81
Carboxymethyl†	95	191	$C_6H_9NO_6$	Isopropanol	7.32	7.22

*Hygroscopic, characterized as copper salt.
†Reported (2) m.p. 198–199°.

N,N'-Dipiperidyl-asparagine

Fifty-one grams (0.60 mole) of piperidine (without triethylamine) were added to 38.2 g (0.29 mole) of monomethyl maleate prepared as described previously from 29 g of maleic anhydride. The mixture was heated over a water bath for 6 hours, then dissolved into 150 ml of isopropanol. N,N'-Dipiperidyl-asparagine crystallized slowly in the cold giving 30 g of white solid, which can be crystallized from ethanol by adding petroleum ether. Yield 56%; m.p. 192°. Calc. for $C_{14}H_{24}N_2O_3$: N, 10.43%. Found: N, 10.52%.

N,N'-Dibutyl-asparagine

To the methyl maleate obtained from maleic anhydride (21 g, 0.21 mole) and methanol were added 40 g (0.55 mole) of anhydrous butylamine and 50 ml of triethylamine. The mixture was heated on a water bath with stirring for 3 hours. The solid formed was filtered and washed twice with acetone. The melting point after recrystallization from water was 242°. Yield 70%. Calc. for $C_{12}H_{24}N_2O_3$: N, 11.46%. Found: N, 11.52%.

ACKNOWLEDGMENTS

The authors are indebted to the National Research Council of Canada for a fellowship to one of them (R. L.) and to the Medical Research Council of Canada for financial assistance.

1. A. ZILKHA and M. D. BACHI. J. Org. Chem. **24**, 1096 (1959).
2. S. KORMAN and H. T. CLARKE. J. Biol. Chem. **221**, 113 (1956).

RECEIVED OCTOBER 10, 1961.
DEPARTMENT OF BIOCHEMISTRY,
FACULTY OF MEDICINE,
LAVAL UNIVERSITY,
QUEBEC, QUE.

THE SYNTHESIS OF SOME BASIC DIPHENYL ETHERS

GERASSIMOS FRANGATOS, J. M. DODSWORTH, GEZA KOHAN, AND FRANCIS L. CHUBB

Recently several publications and patents (1–4) have appeared which described the synthesis and physiological activity (4) of 10-dialkylaminoalkylphenoxazines. In this communication we wish to describe the synthesis of some basic aromatic ethers, including two series of compounds, 2-(3-dialkylaminopropionamido)diphenyl ethers (I) (see Table I) and 2-(3-dialkylaminopropyl)diphenyl ethers (II) (see Table II), which may be regarded as open-chain analogues of the corresponding phenoxazine derivatives.

The basic ethers I and II were prepared from 2-aminodiphenyl ether according to the reaction scheme shown below.

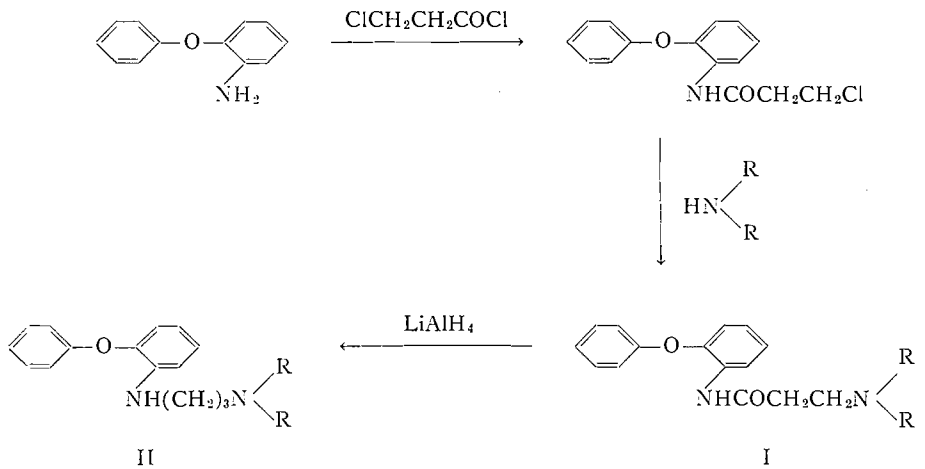

In order to study further the relationship of structure to physiological activity in this series, some 4-(3-dialkylaminopropionamido)-2-nitrodiphenyl ethers (III) (see Table III) were synthesized in the same way as I, starting from 4-amino-2-nitrodiphenyl ether.

ACKNOWLEDGMENTS

The authors are indebted to the National Research Council of Canada for a fellowship to one of them (R. L.) and to the Medical Research Council of Canada for financial assistance.

1. A. ZILKHA and M. D. BACHI. J. Org. Chem. **24**, 1096 (1959).
2. S. KORMAN and H. T. CLARKE. J. Biol. Chem. **221**, 113 (1956).

RECEIVED OCTOBER 10, 1961.
DEPARTMENT OF BIOCHEMISTRY,
FACULTY OF MEDICINE,
LAVAL UNIVERSITY,
QUEBEC, QUE.

THE SYNTHESIS OF SOME BASIC DIPHENYL ETHERS

GERASSIMOS FRANGATOS, J. M. DODSWORTH, GEZA KOHAN, AND FRANCIS L. CHUBB

Recently several publications and patents (1–4) have appeared which described the synthesis and physiological activity (4) of 10-dialkylaminoalkylphenoxazines. In this communication we wish to describe the synthesis of some basic aromatic ethers, including two series of compounds, 2-(3-dialkylaminopropionamido)diphenyl ethers (I) (see Table I) and 2-(3-dialkylaminopropyl)diphenyl ethers (II) (see Table II), which may be regarded as open-chain analogues of the corresponding phenoxazine derivatives.

The basic ethers I and II were prepared from 2-aminodiphenyl ether according to the reaction scheme shown below.

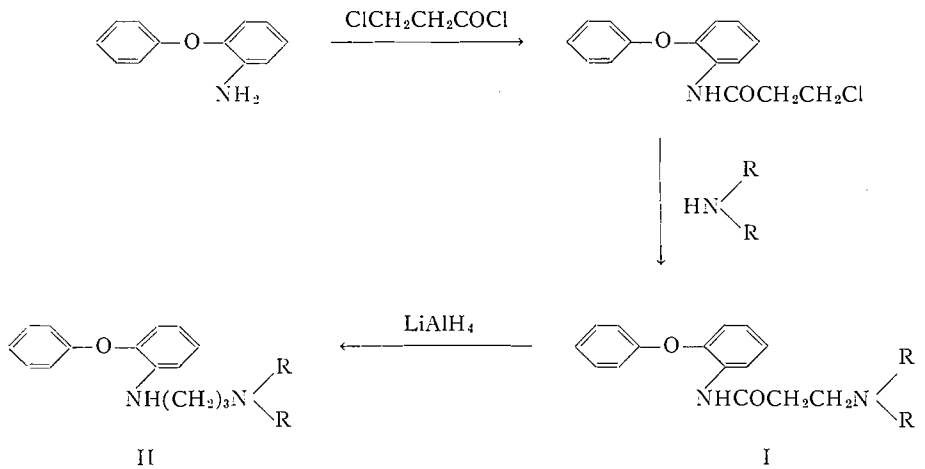

In order to study further the relationship of structure to physiological activity in this series, some 4-(3-dialkylaminopropionamido)-2-nitrodiphenyl ethers (III) (see Table III) were synthesized in the same way as I, starting from 4-amino-2-nitrodiphenyl ether.

TABLE I

2-(3-Dialkylaminopropionamido)diphenyl ethers

—N(R)(R)	Yield (%)	Derivative	M.p.	Molecular formula	Analyses					
					Calculated			Found		
					C	H	N	C	H	N
—N(C_2H_5)(C_2H_5)	51	Hydrochloride	151°	$C_{19}H_{25}ClN_2O_2$	65.41	7.27	8.03	65.38	7.39	7.78
—N(pyrrolidine)	84	Free base	116°	$C_{19}H_{22}N_2O_2$	73.52	7.15	9.03	73.21	7.28	8.98
—N(pyrrolidine)	—	Hydrochloride	179°	$C_{19}H_{23}ClN_2O_2$	65.79	6.68	8.08	65.32	6.88	8.30
—N(piperidine)	75	Hydrochloride	176°	$C_{20}H_{25}ClN_2O_2$	66.56	6.98	7.76	66.06	7.06	7.76
—N(morpholine)	78	Free base	136°	$C_{19}H_{22}N_2O_3$	69.91	6.80	8.58	69.96	6.97	8.88
—N(morpholine)	—	Hydrochloride	172°	$C_{19}H_{23}ClN_2O_3$	62.89	6.39	7.72	62.63	6.42	7.84
—N(N—CH_3-piperazine)	85.6	Free base	131°	$C_{20}H_{25}N_3O_2$	70.77	7.42	12.38	70.38	7.54	11.93

TABLE II

2-(3-Dialkylaminopropyl)diphenyl ethers

—N(R)(R)	Yield (%)	Derivative	M.p.	Molecular formula	Analyses					
					Calculated			Found		
					C	H	N	C	H	N
—N(C_2H_5)(C_2H_5)	71.8	Dihydrochloride	172°	$C_{19}H_{26}Cl_2N_2O$	61.45	7.60	7.55	61.00	7.91	7.42
—N(pyrrolidine)	80	Dihydrochloride	202°	$C_{19}H_{26}Cl_2N_2O$	61.78	7.10	7.59	61.92	7.17	7.62
—N(piperidine)	70.6	Dihydrochloride	205°	$C_{20}H_{28}Cl_2N_2O$	62.66	7.36	7.31	62.40	7.52	7.07
—N(morpholine)	87	Dihydrochloride	184°	$C_{19}H_{26}Cl_2N_2O_2$	59.22	6.80	7.27	58.59	6.93	7.52
—N(4-CH_3-piperazine)	78	Free base	47°	$C_{20}H_{27}N_3O$	73.81	8.36	12.91	73.64	8.63	12.81
—N(4-CH_3-piperazine)		Dipicrate	222°	$C_{32}H_{33}N_9O_{15}$	49.04	4.24	16.09	49.31	4.53	15.74

TABLE III

4-(3-Dialkylaminopropionamido)-2-nitrodiphenyl ethers

—NRR	Yield (%)	Derivative	M.p.	Molecular formula	Analyses					
					Calculated			Found		
					C	H	N	C	H	N
—N(C_2H_5)(C_2H_5)	88.7	Free base	124°	$C_{19}H_{23}N_3O_4$	63.85	6.49	11.76	63.32	6.81	11.66
—N(C_2H_5)(C_2H_5)		Hydrochloride	226°	$C_{19}H_{24}ClN_3O_4$	57.94	6.14	10.67	57.83	6.33	10.55
—N(CH$_2$CH$_2$CH$_2$CH$_2$)	90.3	Free base	151°	$C_{19}H_{21}N_3O_4$	64.21	5.96	11.82	63.68	6.32	11.73
—N(CH$_2$CH$_2$CH$_2$CH$_2$)		Hydrochloride	230°	$C_{19}H_{22}ClN_3O_4$	58.23	5.66	10.72	57.63	5.91	10.20
—N(CH$_2$CH$_2$CH$_2$CH$_2$CH$_2$)	92	Free base	147°	$C_{20}H_{23}N_3O_4$	65.02	6.28	11.38	64.88	6.60	11.29
—N(CH$_2$CH$_2$CH$_2$CH$_2$CH$_2$)		Methiodide	190°	$C_{21}H_{26}N_3O_4I$	49.33	5.13	8.22	48.79	5.34	8.08
—N(CH$_2$CH$_2$OCH$_2$CH$_2$)	79.9	Free base	159°	$C_{19}H_{21}N_3O_5$	61.44	5.70	11.31	61.20	6.05	11.33
—N(CH$_2$CH$_2$OCH$_2$CH$_2$)		Picrate	173°	$C_{25}H_{24}N_6O_{12}$	50.00	4.03	13.99	50.11	4.24	14.23
—N(CH$_2$CH$_2$N—CH$_3$CH$_2$CH$_2$)	98.2	Free base	153°	$C_{20}H_{24}N_4O_4$	62.48	6.29	14.58	62.43	6.35	13.98

The pharmacology of these compounds will be reported elsewhere.

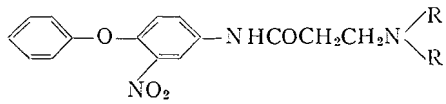

III

EXPERIMENTAL

Melting points are uncorrected. Microanalyses were performed by E. Thommen, Thannerstrasse 45, Basel, Switzerland.

2-(3-Chloropropionamido)diphenyl Ether

The procedure of Roberts and Turner (5) was adopted for the reduction of 2-nitrodiphenyl ether (6) to 2-aminodiphenyl ether.

A solution of 12.7 g (0.1 mole) of 3-chloropropionyl chloride in 50 ml of benzene was added dropwise to a cooled (ice bath) solution of 18.5 g (0.1 mole) of 2-aminodiphenyl ether and 10.1 g (0.1 mole) of triethylamine in 150 ml of benzene. After the addition was complete, the reaction mixture was allowed to stand overnight at room temperature, during which time crystals of triethylamine hydrochloride gradually separated. Water (300 ml) was added and the layers were separated. The aqueous layer was extracted with two 100-ml portions of benzene. After the combined benzene layers over sodium sulphate were dried, the benzene was distilled under reduced pressure. The residual oil which distilled at 207° under 1 mm pressure was recrystallized from benzene–hexane to yield 18.5 g (67.3%) of 2-(3-chloropropionamido)-diphenyl ether, m.p. 62°. Anal. calc. for $C_{15}H_{14}ClNO_2$: C 65.34, H 5.12, N 5.08; found: C 65.11, H 5.36, N 4.99.

2-(3-Morpholinopropionamido)diphenyl Ether

A mixture of 27.6 g (0.1 mole) of 2-(3-chloropropionamido)diphenyl ether, 300 ml of toluene, 8.71 g of morpholine, and 2.5 g of anhydrous potassium carbonate was stirred and refluxed for 5 hours. After the hot reaction mixture was filtered, the solid residue was washed with 150 ml of hot toluene. The combined toluene filtrates were dried over anhydrous sodium sulphate and the toluene was evaporated under reduced pressure. The oily residue crystallized on trituration with a minimum amount of ether. Recrystallization from ether yielded 25.6 g (78.5%) of 2-(3-morpholinopropionamido)diphenyl ether, m.p. 136°. Anal. calc. for $C_{19}H_{22}N_2O_3$: C 69.91, H 6.80, N 8.58; found: C 69.96, H 6.97, N 8.88.

The remainder of the ethers I and III, listed in Tables I and III respectively, were prepared as above.

2-(3-Morpholinopropylamino)diphenyl Ether

A solution of 16.3 g (0.05 mole) of 2-(3-morpholinopropionamido)diphenyl ether in 150 ml of absolute ether was added dropwise to a stirred solution of 8 g of lithium aluminum hydride in 200 ml of ether, at such a rate as to maintain gentle refluxing without external heating. After the addition was complete, the stirring and refluxing was continued for an additional 3 hours. The excess of lithium aluminum hydride was destroyed by the cautious addition of 10 ml of water. An additional 100 ml of water was added and the reaction mixture was filtered. After the solid residue was washed with 100 ml of ether, the combined ether layers were washed with water and dried over anhydrous sodium sulphate. Dry hydrogen chloride was passed into the solution and the dihydrochloride of 2-(3-morpholinopropylamino)diphenyl ether precipitated. Recrystallization from isoamyl alcohol – ethyl acetate yielded 16.8 g (87.2%), m.p. 184°. Anal. calc. for $C_{19}H_{20}Cl_2N_2O_4$: C 59.22, H 6.80, N 7.27; found: C 58.59, H 6.93, N 7.52.

The remaining members of the series (II) were prepared in a similar way and are listed in Table II.

4-(3-Chloropropionamido)-2-nitrodiphenyl Ether

The above compound was obtained from the reaction of 3-chloropropionyl chloride with 4-amino-2-nitrodiphenyl ether (7), using the procedure employed for the preparation of 2-(3-chloropropionamido)-diphenyl ether. The crude product was recrystallized from alcohol and 71.2% of material melting at 144° was obtained. Anal. calc. for $C_{15}H_{13}Cl_2N_2O_4$: C 56.17, H 4.08, N 8.74; found: C 56.71, H 4.27, N 8.65.

1. G. Frangatos, G. Kohan, and F. L. Chubb. Can. J. Chem. **38**, 1021 (1960).
2. Belg. Patent No. 569,697.
3. J. W. Cusic. U.S. Patent No. 2,687,414.
4. Brit. Patent No. 825,312.
5. E. Roberts and E. E. Turner. J. Chem. Soc. **127**, 2008 (1925).
6. Organic synthesis. Coll. Vol. 2. John Wiley & Sons Inc., New York. 1943. p. 445.
7. M. T. Bogert and R. L. Evans. Ind. Eng. Chem. **18**, 299 (1926).

Received June 28, 1961.
Frank W. Horner, Ltd.,
Montreal, Que.

Canadian Journal of Chemistry

Issued by THE NATIONAL RESEARCH COUNCIL OF CANADA

VOLUME 40 FEBRUARY 1962 NUMBER 2

STUDIES OF CHLOROBIUM CHLOROPHYLLS

IV. PREPARATIVE LIQUID–LIQUID PARTITION CHROMATOGRAPHY OF PORPHYRINS AND CHLOROPHYLL DERIVATIVES AND ITS USE TO RESOLVE CHLOROBIUM PHEOPHORBIDE (650) INTO SIX COMPONENTS[1]

D. W. HUGHES[2] AND A. S. HOLT

With the technical assistance of G. BESSERER

The Division of Applied Biology, National Research Council, Ottawa, Canada

Received October 24, 1961

ABSTRACT

Various porphyrins and chlorophyll derivatives have been purified on a preparative scale by distribution between hydrochloric acid and ether on Celite columns. By this technique crude *Chlorobium* pheophorbide (650) was resolved into six components, which possessed almost identical visible absorption spectra, but slightly different acid distribution numbers. Chromic acid oxidation and subsequent gas–liquid partition chromatography of the neutral fractions indicate the presence of more than one *Chlorobium* chlorophyll (650) in the original pigment preparation.

The method most frequently used for resolving mixtures of porphyrins or chlorophyll derivatives is partition between aqueous hydrochloric acid and ether. The resolution obtained by this method depends on how much the compounds differ in basicity and solubility. An approximate quantitative expression of these properties is the "acid number", i.e. the percentage (w/w) of aqueous hydrochloric acid which extracts two thirds of a compound from an equal volume of ether (1). When the "acid numbers" of two pigments differ by several percentage units complete separation may be readily accomplished. However, when components possess almost equal "acid numbers" countercurrent distribution is usually necessary. This method has the disadvantages of requiring special, expensive apparatus and is not usually applicable to large quantities of material.

Liquid–liquid partition chromatography has been applied in a few instances to the resolution of mixtures of porphyrins (2, 3, 4). In particular, Falk (5) has quoted the use by Scott of Celite columns containing hydrochloric acid as the stationary phase and ether as the eluent. No experimental details have, to our knowledge, been published. We have developed such a procedure and have found that by choosing the appropriate strength of hydrochloric acid or by using solvents other than ether, many mixtures of porphyrins and chlorophyll derivatives of similar acid number can be resolved. Our experience fully confirms that of Lemieux *et al.* (6) concerning the ease of construction and extrusion of Celite columns, and of uniform and rapid flow through such columns.

[1]*Issued as N.R.C. No. 6616.*

[2]*National Research Council Postdoctorate Research Fellow, 1959–61. Present address: New Chemicals Group, National Chemical Lab., Teddington, Middlesex, England.*

The method did not resolve the isomers coproporphyrins 3 and 4 and was not applicable to acid-labile substances such as magnesium complexes and esters with high acid numbers. Esters with low acid numbers, e.g. methyl vinylphylloporphyrin (acid number: 1.4 (7)) and methyl phylloporphyrin (acid number: 0.9 (8)) were separated without hydrolysis when the column was developed rapidly (Fig. 1). A mixture of pyropheophorbide *a* and mesopyropheophorbide *a* (acid numbers: 12–13 and 12, respectively (9)) (Fig. 2) and

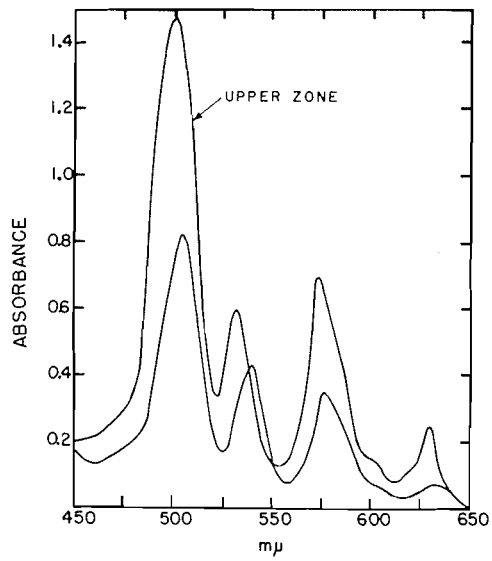

FIG. 1. Spectra of ether solutions of pigments separated on Celite column. Upper zone: methyl phylloporphyrin; lower zone: methyl vinylphylloporphyrin. Stationary phase: 1.5% (w/w) aqueous HCl saturated with ether; mobile phase: ether.

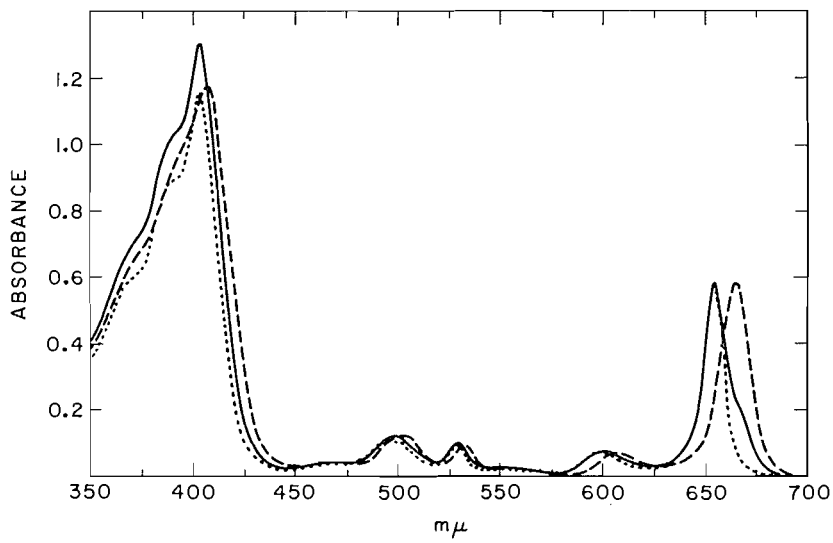

FIG. 2. Spectra of ether solutions of pyro- and mesopyro-pheophorbide *a* separated on Celite column: —— before partition; . . . upper zone (mesopyropheophorbide *a*); – – – lower zone (pyropheophorbide *a*). Stationary phase: 14% (w/w) aqueous HCl saturated with ether; mobile phase: ether.

a mixture of deuteroporphyrin 9 and mesoporphyrin 9 (acid numbers: 0.4 and 0.5, respectively (10)) were also resolved successfully. Neither partition using separatory funnels nor adsorption chromatography on sucrose followed by crystallization had previously given mesopyropheophorbide *a* completely free of pyropheophorbide *a*. Separation of deutero- and meso-porphyrin 9 was accomplished earlier by means of countercurrent distribution between hydrochloric acid and ether (11).

The column technique was applied to the further resolution of crude *Chlorobium* pheophorbide (650), which we have recently reported to be separable into two components by chromatography on sucrose (12). Eight zones were obtained and were designated as fractions 1 to 8 in the relative order of their position on the column, fraction 8 being uppermost. Fractions 7 and 8 were minor constituents and were discarded when they proved to have the same visible absorption spectra as *Chlorobium* pheophorbide (660) (13). The visible absorption spectra of the pigments in fractions 1 to 6 were, for practical purposes, almost identical, and the ratios of absorption at the indicated wavelengths are given in Table I. The percentage of each fraction extracted by two concentrations of

TABLE I

Ratios of absorbance (A) at wavelengths ($m\mu$) indicated for fractions of *Chlorobium* pheophorbide (650)

Fraction	$\frac{A_{531}}{A_{502}}$	$\frac{A_{403}}{A_{657}}$	Fraction	$\frac{A_{531}}{A_{502}}$	$\frac{A_{403}}{A_{657}}$
1	1.05	1.96	4	1.10	1.85
2	1.05	1.92	5	1.05	1.88
3	1.06	1.87	6	1.03	1.88

aqueous hydrochloric acid from ether solution is given in Table II. The latter results were to be expected from the order in which the fractions moved down the Celite column, i.e. fraction 1 was extracted the least and fraction 6 the most.

TABLE II

Percentage of fractions of *Chlorobium* pheophorbide (650) extracted from ether by two concentrations of aqueous hydrochloric acid

Fraction	12.3% HCl	14.0% HCl	Fraction	12.3% HCl	14.0% HCl
1	20	70	4	75	95
2	45	85	5	80	96
3	56	89	6	91	98

Countercurrent distribution of a sample of the same crude pheophorbide (650) between hydrochloric acid (14%) and ether gave partial resolution into four components after 620 transfers (see Fig. 3).

A sample from each of fractions 1 to 6 was oxidized by chromium trioxide in sulphuric acid. The products were resolved into neutral and acidic fractions and after the latter had been methylated each fraction was analyzed by gas–liquid partition chromatography (14). The retention times relative to that of quinoline of the components observed in the respective neutral fractions are given in Table III. Each pigment yielded chiefly one of three products, two of which had the same retention times as methylethylmaleimide and methyl-*n*-propylmaleimide. Fractions 3 and 6 gave evidence of contamination, which

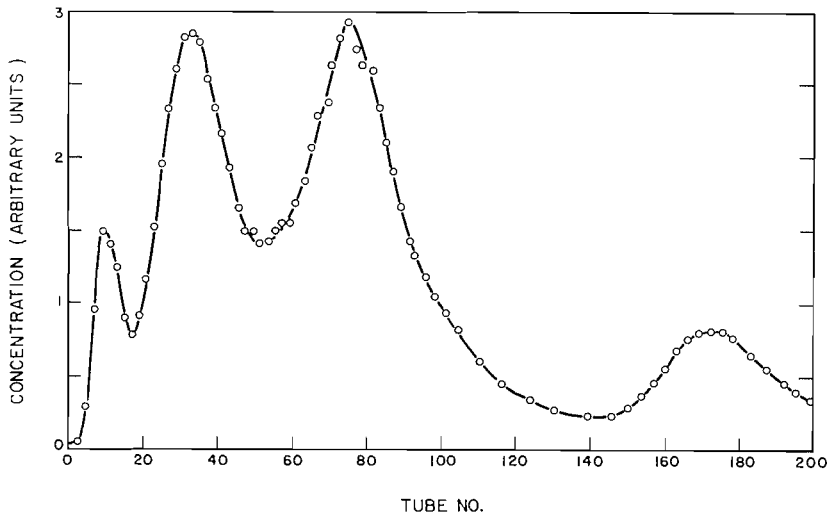

FIG. 3. Separation of components in crude *Chlorobium* pheophorbide (650) (40 mg) by countercurrent distribution between aqueous hydrochloric acid (14%, w/w) and ether.

TABLE III

Gas–liquid partition chromatography of the neutral products formed by oxidation of the fractions of *Chlorobium* pheophorbide (650)

Fraction	Retention time of neutral product relative to quinoline	Fraction	Retention time of neutral product relative to quinoline
1	1.58	5	1.33
2	1.33	6	0.93†
3	1.33*	Methylethylmaleimide	0.93
4	0.93	Methyl-*n*-propylmaleimide	1.33

*Contaminated by a small amount of material with a retention time of 1.58.
†Contaminated by a small amount of material with a retention time of 1.33.

presumably resulted from incomplete fractionation on the Celite column. The unknown product from fractions 1 and 3 has not been isolated in sufficient quantity to permit its identification. Each of the methylated acidic fractions contained one main component which had the same retention time as dihydrohematinic acid imide methyl ester. In addition, a complex mixture of products whose retention times were considerably lower was observed, but the nature of these has not been studied.

The above results show that the original *Chlorobium* chlorophyll (650) extracted from the cells contained more than one chlorophyll. It remains to be shown whether these arise from a mixed culture of different strains of *Chlorobium*, or whether the individual cells synthesize more than one chlorophyll.

EXPERIMENTAL[3]

I. Preparation and Use of Celite Columns

A glass column, plugged at its tapered end with glass wool, was tightly packed with dry, commercial Celite (Johns Manville 535 or 545) under suction and tamped. To protect the surface of the Celite the top was then covered with glass wool onto which the solutions were subsequently poured. Aqueous hydrochloric acid of chosen strength, saturated with ether, was first added to the column under slight suction. Iron

[3]*All visible absorption spectra were measured on a Cary Recording Spectrophotometer, Model 11M.*

impurity in the Celite was removed completely as ferric chloride, which travelled with the acid front. When low acid concentrations had to be used, the Celite was washed previously with concentrated acid. After the ferric chloride had been completely eluted, the "acid-saturated" ether solution was added to the column and allowed to percolate under gravity until separate aqueous and ether layers were observed in the receiver flask. The glass wool was removed, the column was allowed to run dry, retamped, and its upper surface was covered with a filter paper.

The pigment solutions to be partitioned were usually prepared by dissolving the pigment in pyridine and ether and then removing the pyridine with dilute hydrochloric acid. The pigment solution was absorbed at the top of the column and the chromatogram was developed with a continuous flow of ether under gravity or slight suction. The pigments were recovered from the individual bands either by elution or by first extruding the column, and then cutting out the individual bands and washing with acetone containing dilute aqueous hydrochloric acid.

For the resolution of porphyrins whose solubilities in ether were very low, e.g. meso- and deuteroporphyrins 9, alternative procedures of introducing the pigments onto the column were used (see below).

II. Resolution of Mixtures of Known Compounds

(a) Separation of Methyl Vinylphylloporphyrin and Methyl Phylloporphyrin

A mixture of the two porphyrins (ca. 2 mg) was chromatographed on a column (2×15 cm) using 2.5% (w/w) aqueous hydrochloric acid. Two zones, separated by 5 cm, were evident when the leading zone containing methyl vinylphylloporphyrin reached the bottom of the column.

(b) Separation of Deuteroporphyrin 9 and Mesoporphyrin 9

Deuteroporphyrin 9 (6 mg) and mesoporphyrin 9 (3 mg) were dissolved in a mixture of hydrochloric acid (12.5 ml, 0.75%) and tetrahydrofuran (5 ml) and mixed with Celite (25 g). The wet powder was packed on top of a column (5×30 cm) which had been prepared earlier using 0.75% hydrochloric acid. The column was developed for 4 hours, at the end of which time two discrete bands were observed. A more rapid and more satisfactory separation was obtained by using 2.5% hydrochloric acid and a mixture of chloroform and ether (2:1, v/v).

(c) Purification of Mesopyropheophorbide a

Impure mesopyropheophorbide *a* (15 mg), prepared from pyropheophorbide *a* (15, 16), was chromatographed on a column (4.5×30 cm) using 14% (w/w) hydrochloric acid and ether. Two bands were obtained. The products were recovered after the leading zone had moved 20 cm. The separation between the bands was then 6 cm.

(d) Attempted Resolution of Coproporphyrins 3 and 4

A mixture of the porphyrins (ca. 2 mg) was chromatographed on a column (2×48 cm) using hydrochloric acid (0.2%, w/w) and ether. No resolution was observed during 20 hours' development.

III. Growth of Chlorobium thiosulfatophilum (strain L) and Isolation of Chlorobium chlorophyll (650)

Chlorobium thiosulfatophilum (strain L) was cultured in mass in 1-gal bottles at 85–88° F for 7 to 9 days under Sylvania, 30W, Warm White fluoroscent lamps (light intensity: ca. 200 ft-c). Preliminary tests showed that strict asepsis was unnecessary and that maintenance of anaerobic conditions was sufficient to ensure good growth. Otherwise the procedures used were essentially those recommended by Larsen (17). The medium used is given below:

NH_4Cl	0.1%
KH_2PO_4	0.1%
$MgCl_2.6H_2O$	0.054%
NaCl	0.3%
$NaHCO_3$	0.2%
$Na_2S_2O_3.5H_2O$	0.158%
$Na_2S.9H_2O$	0.01%
$CaCl_2$	0.004%
Fe from $FeCl_3.6H_2O$	150 μg%
B from H_3BO_3	100 μg%
Zn from $ZnSO_4.7H_2O$	10 μg%
Co from $Co(NO_3)_2.6H_2O$	20 μg%
Cu from $Cu(SO_4).5H_2O$	10 μg%
Mn from $MnSO_4.H_2O$	1 μg%

The cells were harvested by filtration under suction through a 1-in. pad of Celite (545 and 505, 3 parts to 1) covered with filter paper (Whatman No. 1). The pigment was isolated as follows: the Celite pad and filter papers were blended in cold methanol containing tetrahydrofuran (10%, v/v) and the mixture filtered. The filtrate was poured into ether in a separatory funnel, water added, and the lower layer removed. Successive filtrates were added to the same ethereal solution until the discarded aqueous phase contained

significant amounts of pigment. Calcium chloride was used to break up any emulsion and to dry the solution, which was then filtered and evaporated. The mixture was dissolved in a minimum volume of tetrahydrofuran, and petroleum ether was added to precipitate the chlorophyll. The pigment was collected on Celite, redissolved, reprecipitated, dissolved once again, transferred into ethyl ether, and collected on water as described earlier (18). Material isolated by this procedure had no methoxyl content. It was stored at −25° C.

Crude *Chlorobium* pheophorbide (650) was prepared by adding chlorophyll (1 g in 25 ml of pyridine) to boiling methanolic potassium hydroxide (150 ml, 4%, w/v) under anaerobic conditions. After 20 minutes the mixture was poured into ether (3 l.), acidified with hydrochloric acid (2–3%), and shaken. The ether layer was washed twice with water and evaporated.

IV. Resolution of Chlorobium Pheophorbides (650)

An ether solution (500 ml) of crude pheophorbide, obtained from the chlorophyll (0.25 g), was shaken with 2–3% (w/w) aqueous hydrochloric acid and poured onto a column (9.5×44 cm) of Celite which had been previously prepared using hydrochloric acid (14%) and ether. The column was developed for 5 hours, and the pigments were recovered after extrusion of the Celite. Each fraction was rechromatographed once or twice more. The yields per gram of chlorophyll of fractions 1 to 6 were 39, 128, 55, 88, 42, and 29 mg, respectively.

V. Oxidative Degradation of Fractions 1 to 6 and Identification of the Products

Pigment (10 mg) in a test tube was dissolved in sulphuric acid (2.0 ml, 25%) and cooled to −10° C. Aqueous chromium trioxide (0.5 ml, 6.7%, w/v) was added, and the reaction mixture was stirred for 20 minutes. The pH was raised to 10 to 11 with aqueous sodium carbonate and the volume was adjusted to 10 ml. The solution was transferred to a separatory funnel and neutral products were extracted by 10 separate 25-ml volumes of ethyl acetate (19). Acidic products were removed similarly after the solution had been acidified. The solutions were dried ($MgSO_4$) and reduced to a small volume (ca. 0.1 ml). A Pye Argon Chromatograph was used to establish the identities of the oxidation products by comparing their chromatographic behavior with those of authentic samples of methylethylmaleimide, methyl-*n*-propylmaleimide, and dihydrohematinic acid imide methyl ester. The column (4 mm (I.D.)×117 cm) was packed with 15% (w/w) polyphenyl ether (*m*-bis(*m*-phenoxy-phenoxy)-benzene) on Celite. The flow rate was 100 ml per minute, and the temperatures 175 and 230° C for the neutral and acidic fractions, respectively.

ACKNOWLEDGMENTS

Samples of porphyrins were provided by Dr. S. F. MacDonald of the Division of Pure Chemistry, National Research Council. Gas–liquid partition chromatographic separations were done by Mr. F. Cooper. Cultures of *Chlorobium thiosulfatophilum* were kindly supplied by Drs. J. Lascalles and H. Larsen.

REFERENCES

1. R. Willstätter and W. Mieg. Ann. **350**, 1 (1906).
2. R. E. H. Nicholas and C. Rimington. Scand. J. Clin. & Lab. Invest. **1**, 12 (1949).
3. J. Lucas and J. Orten. J. Biol. Chem. **191**, 287 (1951).
4. M. Morrison and E. Stotz. J. Biol. Chem. **213**, 373 (1955).
5. J. E. Falk. Brit. Med. Bull. **10**, 211 (1954).
6. R. U. Lemieux, C. T. Bishop, and G. E. Pelletier. Can. J. Chem. **34**, 1365 (1956).
7. H. Fischer and S. F. MacDonald. Ann. **540**, 211 (1939).
8. A. Treibs and E. Wiedemann. Ann. **466**, 264 (1928).
9. H. Fischer and A. Stern. Chemie des pyrrols. Vol. II. Pt. 2. Leipzig. 1940. pp. 73, 75.
10. H. Fischer and H. Orth. Chemie des pyrrols. Vol. II. Pt. 1. Leipzig. 1937. pp. 413, 442.
11. S. Granick and L. Bogorad. J. Biol. Chem. **202**, 781 (1953).
12. A. S. Holt and D. W. Hughes. J. Am. Chem. Soc. **83**, 499 (1961).
13. A. S. Holt and H. V. Morley. *In* Comparative biochemistry of photoreactive systems. *Edited by* M. B. Allen. Academic Press, New York. 1960.
14. H. V. Morley and A. S. Holt. Can. J. Chem. **39**, 755 (1961).
15. H. Fischer and E. Lakatos. Ann. **506**, 123 (1933).
16. H. Fischer, J. Riedmair, and J. Hasenkamp. Ann. **508**, 224 (1934).
17. H. Larsen. Kgl. Norske Videnskab. Selskabs, Forh. Skrifter, 1 (1953).
18. E. E. Jacobs, A. E. Vatter, and A. S. Holt. Arch. Biochem. Biophys. **53**, 228 (1954).
19. G. E. Ficken, R. B. Johns, and R. P. Linstead. J. Chem. Soc. 2272 (1956).

STUDIES IN THE PYRROLINE SERIES

I. THE PROTON MAGNETIC RESONANCE SPECTRA OF SOME PYRROLINES

R. Bonnett and D. E. McGreer
The Chemistry Department, University of British Columbia, Vancouver 8, British Columbia
Received August 24, 1961

ABSTRACT

The proton magnetic resonance spectra of some pyrrolines and pyrroline oxides have been determined. The spectra accord with the Δ^1 formulation of the bases.

Interest in the 1-pyrrolines has been stimulated recently by the formulation (1) of the chromophore of vitamin B_{12} as a considerably reduced, ring-contracted porphyrin which can be regarded as being constituted of pyrroline rather than pyrrole nuclei. Up to this time the pyrrolines had attracted little sustained attention, and, except for the 3-pyrrolines, the position of unsaturation was in doubt, although the 2-pyrroline structure

1-Pyrroline

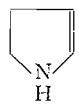

2-Pyrroline

was usually drawn. This question has been debated recently (2, 3, 4, 5, 6), and, in general, the conclusion has been drawn that these substances exist predominantly in the Δ^1 form.

Both chemical and physical evidence have been adduced to support this formulation. The Zerewitinoff determinations (6, 8) have probably been the most significant chemical evidence since they have shown that in the examples studied little or no active hydrogen was immediately available. Physical evidence has been based on some study of ultraviolet spectra (9), but the most significant results have come from infrared studies (2, 3, 4, 6). In general the pyrrolines have shown little or no absorption in the N—H stretching region, but a strong band, attributed to C=N absorption, is present in the 1620–1650 cm^{-1} region. The position of the C=N band, and the hypsochromic shift it undergoes on protonation of the base, are not definitive, however, as is indicated by the values given below.

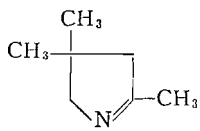

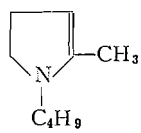

Base	1644 cm^{-1} (5)	1639 cm^{-1} (10)
Salt	1684 cm^{-1} (5)	1685 cm^{-1} (10)

The strength of the C=N absorption band, and, especially, the absence of N—H absorption are, on the other hand, of considerable importance. In the latter area difficulties have arisen in certain instances. Thus Evans (3) reported that 2-methylpyrroline showed

a weak band at 3.02 μ, and Burckhalter and Short (4) considered a similar band at 3.05–3.10 μ in the spectrum of 2-benzylpyrroline to be anomalous since the compound did not contain active hydrogen. Other workers have considered that "the N—H region of the infrared absorption spectra of pyrrolidines and pyrrolines is difficult to interpret" (6, cf. ref. 7), and it is, of course, true that absorption in this region could be caused by species, notably traces of moisture or of dimer, other than the 2-pyrroline, which is presumed to be tautomeric with the Δ^1 form.

Proton magnetic resonance is particularly useful for studying the structures of compounds containing olefinic protons, and would be expected to distinguish clearly between the Δ^1 and Δ^2 forms of the pyrrolines, and also between the corresponding forms of the pyrroline-1-oxides:

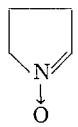

1-Pyrroline-1-oxide

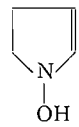

1-Hydroxy-2-pyrroline

The proton magnetic spectra of five pyrrolines, I, II, III, IV, and V, and three pyrroline-1-oxides, VI, VII, and VIII, have therefore been determined for the pure liquids, and are reported in Table I.

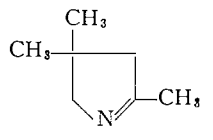

I

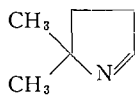

II

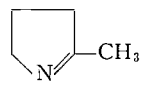

III

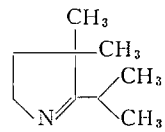

IV

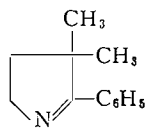

V

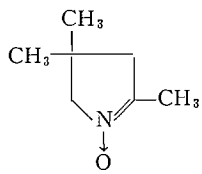

VI

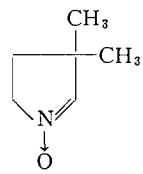

VII

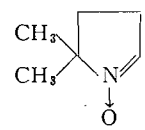

VIII

The spectra of 2-methylpyrroline (III), 2,4,4-trimethylpyrroline (I) and its N-oxide (VI) most clearly show the position of the double bond. The lack of signal in the olefinic proton region (2.0–5.5 τ) (11) is consistent with only that structure containing the double bond in the Δ^1 position (as shown) since all possible tautomers would have olefinic protons. As little as 5% of such tautomeric species would have been detected readily. The spectra of the other compounds studied are also consistent with the Δ^1 formulation. Thus the Δ^2 forms of II and VIII would be expected to show two olefinic proton signals, but area measurement clearly shows that only one proton is absorbing at low field. Again, the exo-Δ^2 form of IV would not be expected to show a septet, which is found here in the 7.8 τ region and which is characteristic of a tertiary proton coupled with six identical protons. Compounds V and VII cannot tautomerize to the Δ^2 form.

TABLE I

Proton magnetic resonance spectra of some pyrrolines and pyrroline-1-oxides

Compound	Proton position*					
	C_2	C_3	C_4	C_5	$(CH_3)_2$	Other
I	—	7.9	—	6.7	9.2	8.3 (CH_3 on C_2)
II†	3.1	7.8	8.8	—	9.1	—
III	—	8.0	8.5	6.7	—	8.4 (CH_3 on C_2)
IV	—	—	8.6	6.6	9.1	7.8 (3°H-septet)
						9.1 (CH_3 of *i*-Pr)
V	—	—	8.7	6.6	9.2	2.4 and 3.1 (Ph)
VI	—	7.4	—	6.5	8.9	8.2 (CH_3 on C_2)
VII‡	3.4	—	8.2	6.2	8.9	—
VIII§	3.4	7.6	8.0	—	8.8	—

*The protons on the saturated ring carbons of II, IV, V, and VII gave triplet signals with splittings of 7–7.5 c.p.s. In these cases and for other multiplets the center of the signal is recorded in units of τ.
†The area ratio of the signals for the H's on C_2 and C_3 was 1.0 to 2.0.
‡The area ratio of the signals for the H's on C_3, C_4, C_5, and the dimethyl group was 1.1:2.0:1.8:6.4 respectively.
§The area ratio of the signals for the H's on C_2 to those on C_3 plus C_4 was 0.9 to 4.0.

The assignment of signals to all other protons is straightforward since in at least one compound in each series the protons on each ring position are replaced by methyl groups. Thus examination of the spectra of the nitrones shows that the protons on ring positions 3, 4, and 5 give signals in the regions 7.5, 8.1, and 6.4 τ respectively. Similar signals for the pyrrolines are found in the regions 7.9, 8.7, and 6.7 τ respectively. These signals appear at higher field than those of the nitrones, presumably because the strong electron-withdrawing effect of the semipolar bond has been removed.

While it is possible that under certain conditions of substitution and environment the Δ^2 form may become detectable, or even isolable (cf. ref. 12), in the present simple but varied examples no evidence for the presence of a Δ^2 isomer has been forthcoming. The proton magnetic resonance spectra have strongly reinforced previous conclusions regarding the Δ^1 structures of these compounds.

EXPERIMENTAL

Pyrrolines

These were prepared by known methods: I and II (5); III (3); IV and V (13). The aliphatic pyrrolines were purified by distillation followed by preparative vapor phase chromatography on a 5-ft Uconpolar column at 85–120° (Aerograph A-100-C instrument) using helium as the carrier gas (cf. ref. 5). The aromatic compound V was purified by distillation.

Pyrroline-1-oxides

Compounds VI and VIII were prepared by known methods (14) and the preparation of VII will soon be reported. The nitrones were purified by distillation *in vacuo*.

Spectra

The proton magnetic resonance spectra were measured on a 40 Mc/s Varian spectrophotometer with field stabiliser VK 3506. Neat samples were used and calibrated to an external standard of hexamethyldisiloxane which had a chemical shift value of 10.3 τ as determined by reference to a solution of tetramethylsilane in carbon tetrachloride. A calibrated audio-frequency unit was used to determine chemical shifts by the side-band technique.

ACKNOWLEDGMENTS

The support of the National Research Council of Canada and the President's Committee on Research in the University of British Columbia is gratefully acknowledged.

REFERENCES

1. D. C. HODGKIN, J. KAMPER, M. MACKAY, J. PICKWORTH, K. N. TRUEBLOOD, and J. G. WHITE. Nature, **178**, 64 (1956). R. BONNETT, J. R. CANNON, V. M. CLARK, A. W. JOHNSON, L. F. J. PARKER, E. LESTER SMITH, and SIR ALEXANDER TODD. J. Chem. Soc. 1158 (1957).
2. B. WITKOP. J. Am. Chem. Soc. **76**, 5597 (1954).
3. G. E. EVANS. J. Am. Chem. Soc. **73**, 5230 (1951).
4. J. H. BURCKHALTER and J. H. SHORT. J. Org. Chem. **23**, 1278 (1958).
5. R. BONNETT, V. M. CLARK, A. GIDDEY, and SIR ALEXANDER TODD. J. Chem. Soc. 2087 (1959).
6. M. C. KLOETZEL, J. L. PINKUS, and R. M. WASHBURN. J. Am. Chem. Soc. **79**, 4222 (1957).
7. W. DAVEY and D. J. TIVEY. J. Chem. Soc. 2276 (1958).
8. P. M. MAGINNITY and J. B. CLOKE. J. Am. Chem. Soc. **73**, 49 (1951). P. M. MAGINNITY and T. J. GAIR. J. Am. Chem. Soc. **74**, 4958 (1952).
9. P. J. A. DEMOEN and P. A. J. JANSSEN. J. Am. Chem. Soc. **81**, 6281 (1959).
10. N. J. LEONARD and V. W. GASH. J. Am. Chem. Soc. **76**, 2781 (1954).
11. L. M. JACKMAN. Applications of nuclear magnetic resonance spectroscopy. Pergamon Press, New York. 1959. p. 60.
12. F. C. UHLE and F. SALLMANN. J. Am. Chem. Soc. **82**, 1190 (1960).
13. A. P. TERENTEV, A. N. KOST, and A. M. BERLIN. Zhur. Obshchei. Khim. **25**, 1613 (1955).
14. R. BONNETT, R. F. C. BROWN, V. M. CLARK, I. O. SUTHERLAND, and SIR ALEXANDER TODD. J. Chem. Soc. 2094 (1959).

STUDIES IN THE PYRROLINE SERIES

II. OXYGEN TRANSFER FROM CYCLIC NITRONES TO TRIPHENYLPHOSPHINE

FRANCO AGOLINI AND R. BONNETT

The Chemistry Department, University of British Columbia, Vancouver 8, British Columbia

Received August 24, 1961

ABSTRACT

Triphenylphosphine, triphenylarsine, triphenylstibine, and triphenylbismuthine have been evaluated as acceptors in oxygen transfer reactions involving 1-pyrroline-1-oxides. The first reagent especially offers a useful route from the nitrones to the corresponding pyrrolines.

The direct reduction of 1-pyrroline-1-oxides to the corresponding pyrrolines has previously been carried out in two ways (1). 2,4,4-Trimethyl-1-pyrroline-1-oxide, I, for example, on treatment with zinc and acetic acid, gave a 66% yield of the corresponding pyrroline picrate, while a smaller yield was obtained when sulphur dioxide in chloroform was the reducing agent. A more convenient method has been sought which would avoid aqueous or acidic conditions and which, moreover, would give the product directly. Such a process is required in cases under examination (2) where the product of a preparative sequence is the 1-pyrroline-1-oxide from which it is then necessary to make the pyrroline; but it also offers a method of removing oxygen from certain of the products of syntheses involving the reactive nitrones.

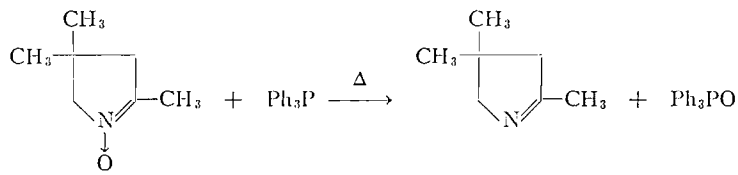

I II

Oxygen transfer to compounds of other elements of group V suggested itself as a potential method, especially since triphenylphosphine has been used successfully to remove oxygen from pyridine oxides and other amine oxides (3, 4) and from oxazirans (5). The reduction of an aldonitrone has been noted (4), but no information appears to be available concerning the applicability of the reaction to purely aliphatic nitrones, including the 1-pyrroline-1-oxides. It was decided to examine as oxygen acceptors the complete range of compounds from triphenylphosphine to triphenylbismuthine, although it was expected that as this series was ascended the increasing instability of both the carbon–metal bond and the pentavalent state of the metal would intervene and at some stage make the reaction inconvenient or useless as a preparative method.

Trial experiments were carried out with 2,4,4-trimethyl-1-pyrroline-1-oxide, I, and triphenylphosphine. It was found that the reaction did not proceed to a useful degree in refluxing benzene or toluene. Reaction occurred speedily, however, when the substances were heated together with a free flame, and the product, 2,4,4-trimethyl-1-pyrroline, II, distilled directly out of the reaction mixture. A broadly similar result was obtained with triphenylarsine. With triphenylstibine and triphenylbismuthine, however,

extensive decomposition was evident, and in the latter case the main product in the distillate was benzene. These results are summarized, and some comparisons drawn, in Table I.

TABLE I

Oxygen transfer from 2,4,4-trimethyl-1-pyrroline-1-oxide

Reagent	Reaction with CH_3I (6)	Dipole moment (7) (Debye)	Effect of heating alone*	Weight of distillate† (g)	% yield	% yield of picrate‡
Ph_3P	Rapid	1.45	Refluxes	0.66	75	57
Ph_3As	Slow	1.07	Refluxes, slight decomp.	0.61	70	42
Ph_3Sb	Nil	0.57	Decomp.	0.74	§	34
Ph_3Bi	Nil	0	Decomp.	1.6	§	Trace

*Under the reaction conditions.
†One-gram portions of nitrone heated with an equimolar amount of the reagent (see Experimental).
‡Prepared in moist ether.
§Distillate extensively contaminated by decomposition products of the organometallic compound.

The triphenylphosphine reaction was examined further, and it was shown that triphenylphosphine oxide was isolable from the residue, thus confirming that the reaction involves oxygen transfer to phosphorus, rather than pyrolytic deoxygenation, a process which has been observed with certain amine oxides (8). The reaction was also applied to 5,5-dimethyl-1-pyrroline-1-oxide, a cyclic aldonitrone. In contrast to the cyclic ketonitrone, I, which is fairly stable to heat, 5,5-dimethyl-1-pyrroline-1-oxide is thermolabile. This decomposition is attended by the development in the infrared spectrum of a broad absorption band in the 1660 cm^{-1} region: this has led to the supposition that isomerization to the corresponding lactam may be one of the reactions involved. However, the oxygen transfer reaction evidently proceeds more rapidly than the decomposition, for the reaction gave a 65% yield of the crude 5,5-dimethyl-1-pyrroline (39% yield as the picrate), and triphenylphosphine oxide (57%) was isolated from the residue.

EXPERIMENTAL

The following equipment was used. Melting points: Fisher–Johns heated block. Infrared spectra: Perkin–Elmer Infracord or Model 21. Vapor phase chromatography: Aerograph model A-100-C with 5′ Uconpolar column.

2,4,4-Trimethyl-1-pyrroline from 2,4,4-Trimethyl-1-pyrroline-1-oxide

(*a*) The nitrone (1) (1 g) and triphenylphosphine (2.5 g) were heated (free flame) under a short Vigreux column. The volatile liquid which formed after a short time was refluxed gently for about 15 minutes and then distilled over at 110–130° (0.66 g, 75%). The infrared spectrum (film) of the basic liquid showed the presence of moisture (present in the hygroscopic starting material), together with a strong sharp band at 1650 cm^{-1} (lit. (9) 1644 cm^{-1}). No nitrone band was present. The picrate (1.52 g, 57%) was prepared in ether, and after recrystallization from ethanol had m.p. and mixed m.p. 195–196° (lit. (9) 195°). The infrared spectrum of the picrate (Nujol mull) was identical with that of an authentic sample.

The residue from the distillation was extracted with cyclohexane, and the solution treated with charcoal to give colorless needles (0.6 g, 23%) of triphenylphosphine oxide, m.p. 156–158°.

(*b*) In three trial experiments the reaction was repeated as above, except that the phosphine was replaced by equimolar amounts of triphenylarsine, triphenylstibine, and triphenylbismuthine. In the last two runs decomposition products (largely benzene) from the organometallic compound were present in the distillates. The results of these experiments are indicated in Table I.

Pyrolysis of 5,5-Dimethyl-1-pyrroline-1-oxide

A sample of 5,5-dimethyl-1-pyrroline-1-oxide was heated in a stoppered flask in an oil bath at 100° and the infrared spectrum of the liquid (film) was taken at intervals. During the course of 3 hours a peak at about 1660 cm^{-1}, very weak initially, increased slightly in intensity. After a further hour at 180° the sample became very dark. The new peak was now as strong as the nitrone peak at 1575 cm^{-1}, and the latter became weaker and less sharp as the experiment continued.

5,5-Dimethyl-1-pyrroline from the Corresponding Nitrone

5,5-Dimethyl-1-pyrroline-1-oxide (1) (1 g) was treated with triphenylphosphine (2.62 g) as before, and the volatile liquid boiling up to 104° was collected as crude 5,5-dimethyl-1-pyrroline (0.55 g, 65%), the infrared spectrum (film) of which showed a sharp peak at 1618 cm^{-1} (lit. (9) 1621 cm^{-1}). The yield was not improved by using a Wood's metal bath at 300° instead of a free flame. After purification by vapor phase chromatography the product had the same infrared spectrum as a similarly purified sample of the authentic base. The picrate, prepared in ether (1.13 g, 39%), was identical with an authentic sample.

Triphenylphosphine oxide (57%) was isolated from the dark residue after chromatography (3).

ACKNOWLEDGMENTS

Dr. W. R. Cullen is thanked for cordial discussions and for certain of the reagents used. The financial support of the National Research Council of Canada is gratefully acknowledged.

REFERENCES

1. R. Bonnett, R. F. C. Brown, V. M. Clark, I. O. Sutherland, and Sir Alexander Todd. J. Chem. Soc. 2094 (1959).
2. R. Bonnett and S. C. Ho. Unpublished results.
3. E. Howard and W. F. Olszewski. J. Am. Chem. Soc. **81**, 1483 (1959).
4. L. Horner and H. Hoffmann. Angew. Chem. **68**, 473 (1956).
5. L. Horner and E. Jurgens. Chem. Ber. **90**, 2184 (1957).
6. W. C. Davies and W. P. G. Lewis. J. Chem. Soc. 1599 (1934).
7. E. Bergmann and W. Schütz. Z. physik. Chem. **19B**, 401 (1932).
8. W. Wernick and R. Wolffenstein. Ber. **31**, 1553 (1898).
9. R. Bonnett, V. M. Clark, A. Giddey, and Sir Alexander Todd. J. Chem. Soc. 2087 (1959).

APPARENT DENSITIES AND INTERNAL SURFACE AREAS OF SELECTED CARBON BLACKS

P. L. WALKER, JR. AND W. V. KOTLENSKY*

The Fuel Technology Department, The Pennsylvania State University, University Park, Pennsylvania, U.S.A.

Received August 28, 1961

ABSTRACT

It is shown that the open pore volume within carbon blacks can be calculated from nitrogen adsorption isotherms (77° K) on the blacks. From this volume and a helium density, the apparent density of a black can be calculated. Other properties of the blacks which then can be calculated are free surface area, internal surface area, surface roughness factor, and the average pore diameter of the internal surface. These data are presented for five selected carbon blacks.

INTRODUCTION

Carbon blacks are more or less porous depending upon the perfection of their crystallite alignment and the extent of their oxidation during preparation (1). The amount of porosity can be of importance in affecting the behavior of carbon blacks in rubber, paints, and plastics; and yet little quantitative information is available on the nature of the porosity within blacks—such information as given by apparent densities and internal surface areas.

Kotlensky and Walker (2) used a mercury porosimeter to measure the apparent densities of some carbon blacks of large particle size. The volume of mercury forced between the particles was followed by the potential drop across a platinum–iridium wire looped and held taut inside a precision bore section of a dilatometer tube. Complete filling of the void volume between particles was taken as the point where a negligible change in potential drop first occurred with increase in pressure. From a knowledge of the weights of sample and mercury and the combined volume of the sample and mercury (with mercury filling the voids between particles), a particle density could be calculated. This technique appears to be satisfactory and convenient for carbon blacks of large particle size. However, for blacks of small particle size the pressure required to completely fill the voids between particles is high. For example, for Carbolac 1, a black having an arithmetic mean diameter of 106 Å (3), a pressure in excess of 20,000 p.s.i. would be required. At such pressures, crushing and distortion of the particles are of concern (4, 5). Therefore, it is of interest to explore another approach to determine apparent densities of carbon black particles. This approach and the information which can be derived therefrom are described in this paper.

EXPERIMENTAL

The carbon blacks studied were supplied by the Cabot Corp. with some of their properties listed by them (3). Some additional properties of interest are summarized by Kotlensky and Walker (2). Carbolac 1, Carbolac 2, Monarch 71, and Mogul A are channel blacks. Vulcan 3 is an oil furnace black.

Adsorption isotherms on the blacks were measured at 77° K using a standard gas adsorption apparatus (6) with nitrogen as the adsorbate. A description of the procedure used to measure helium densities (at 30±0.1° C) has been given previously (2).

RESULTS AND DISCUSSION

Adsorption isotherms for the blacks studied are given in Fig. 1. Typical calculations involved in using isotherm data to calculate apparent densities and other physical properties of the blacks can be demonstrated for Carbolac 1. As suggested by Pierce (7),

**Present address: Jet Propulsion Laboratory, California Institute of Technology, Pasadena, California, U.S.A.*

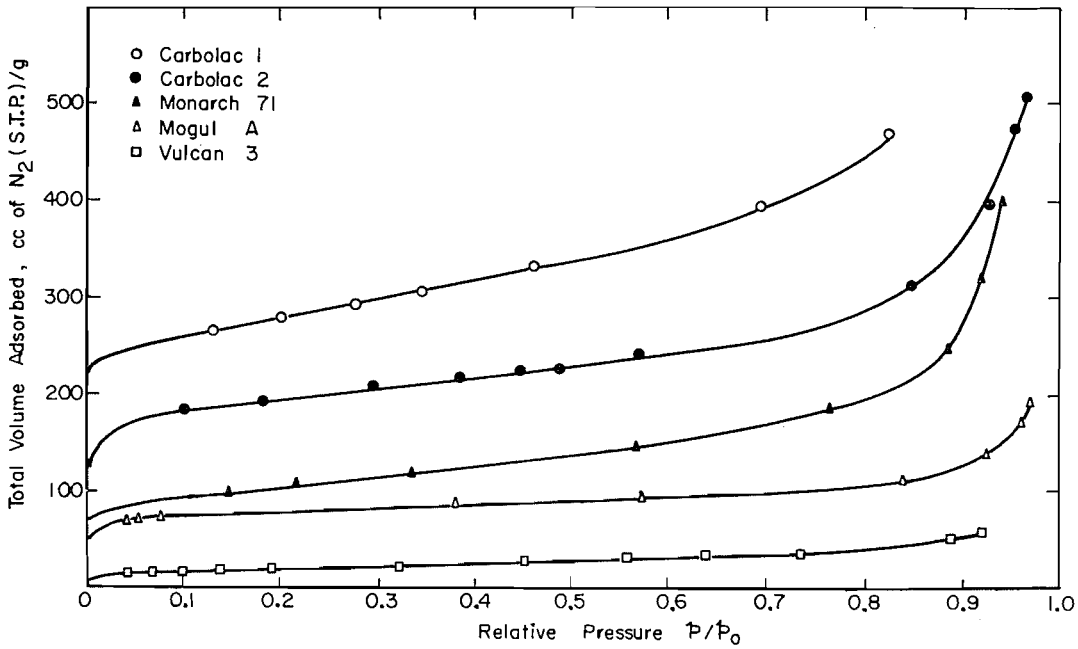

FIG. 1. Adsorption isotherms for nitrogen at 77° K on selected carbon blacks: ○ Carbolac 1, ● Carbolac 2, ▲ Monarch 71, △ Mogul A, □ Vulcan 3.

an isotherm for a porous solid can essentially be divided into three regions. In the middle region of the isotherm (region II), no capillary condensation occurs, but only multilayer adsorption on the free surface. In the lower region of the isotherm, monolayer and then multilayer adsorption is accompanied by the filling of the micropores within particles by capillary condensation. In the upper region of the isotherm, multilayer adsorption is accompanied by capillary condensation within the voids between particles.

In region II of the isotherm, it is possible to solve for the volume of adsorbate which completely fills the micropores (V_c) and the volume of adsorbate which covers the free surface with a monolayer (V_m'). That is, V_t, the total volume adsorbed at any relative pressure in region II, is given by

$$V_t = V_c + nV_m', \quad [1]$$

where n is the statistical number of layers of adsorbate at a particular relative pressure.

Or since V_c is constant in region II,

$$\Delta V_t = V_m' \Delta n. \quad [2]$$

Since n is known as a function of relative pressure for the adsorption of nitrogen on carbon at 77° K (8), ΔV_t can be plotted against Δn. From the slope of this plot, V_m' can be calculated. Figure 2 shows such a plot for Carbolac 1 over the relative pressure range 0.20 to 0.46, giving a value of V_m' of 135 cc N_2/g at S.T.P. From equation [1], then, V_c is calculated to equal 110 cc N_2/g at S.T.P.

As discussed by Pierce (8), if only multilayer adsorption is occurring, the ideal nitrogen isotherm is given by the Frenkel–Halsey–Hill equation

$$(V/V_m)^b = \frac{k}{\log (p_0/p)}, \quad [3]$$

where b equals about 2.75. Or for a porous solid, in region II, the Frenkel–Halsey–Hill isotherm can be re-expressed as

$$[4] \qquad (V_t - V_c)^b = \frac{k'}{\log (p_0/p)}.$$

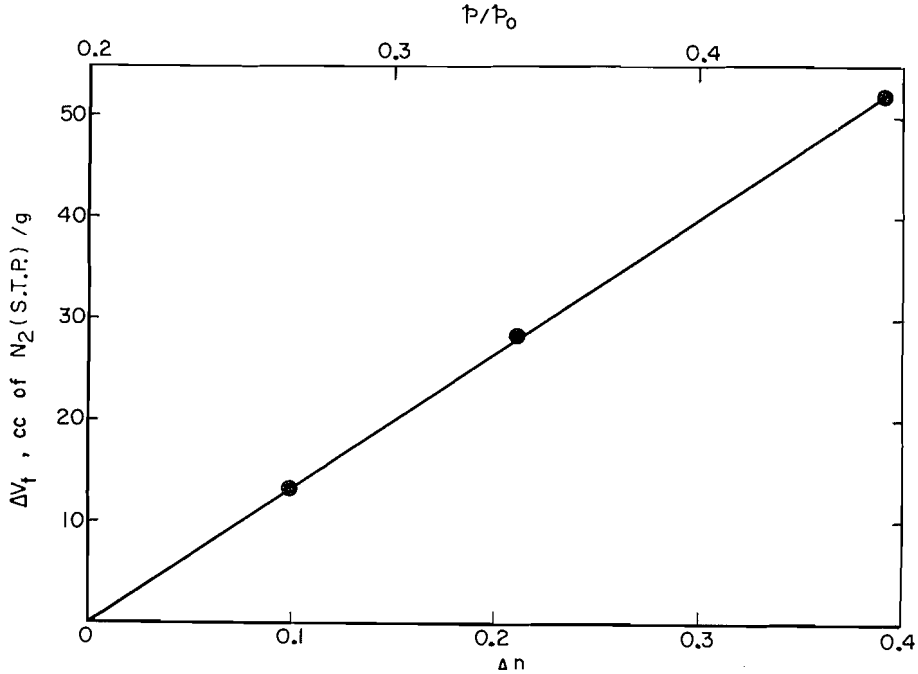

FIG. 2. Plot of ΔV_t versus Δn for Carbolac 1 over the relative pressure range 0.20 to 0.46.

For Carbolac 1, the Frenkel–Halsey–Hill isotherm is plotted between $p/p_0 = 0.20$ and 0.46, as shown in Fig. 3. A good straight line is obtained which has a slope of 2.77.

Taking the density of liquid nitrogen at 77° K as 0.81 g/cc (6), V_c for Carbolac 1 can be re-expressed as 0.170 cc of liquid N_2/g. The total volume of a Carbolac 1 particle equals the volume of solid, plus the volume of pores closed to helium at room temperature, plus the volume of pores open to N_2 at 77° K, plus the volume between the size of pore which helium can enter at room temperature (30 minutes equilibration) and the size of pore which nitrogen can enter at 77° K (30 minutes equilibration). Assuming the latter volume to be negligible,* the specific volume of Carbolac 1 is given by the reciprocal of its helium density plus V_c. For Carbolac 1 the helium density is 2.02 g/cc. Therefore, the specific volume of Carbolac 1 is 0.665 cc/g, or its apparent density is 1.50 g/cc.

From the total surface area, calculated from the simplified BET equation for the isotherm data in Fig. 1, and the free surface area, calculated from V_m', the internal surface area (A) of the blacks can be calculated. Then, assuming cylindrical pores, an approximation of their average diameter can be calculated from the relationship $\bar{d} = 4V_c/A$. Further, a surface roughness factor can be calculated as the ratio of the free surface area of the blacks to the geometric surface area. The geometric surface areas are reported by Cabot (3), from electron micrograph counts.

**From studies on zeolite molecular sieves (9), it appears that this volume is in pores between ca. 2.8 and 4.2 Å in diameter. As will be seen later, the average pore size in the internal pores of the carbon blacks studied is considerably greater than 4.2 Å. Therefore, this assumption appears reasonable.*

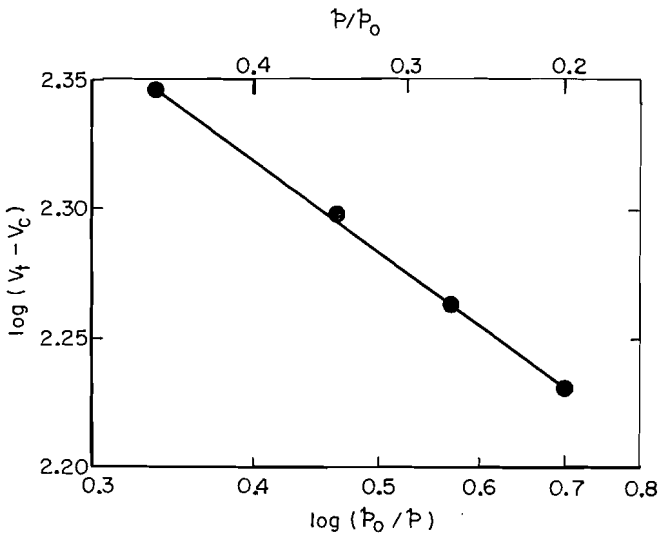

FIG. 3. Frenkel–Halsey–Hill isotherm for nitrogen on Carbolac 1 at 77° K.

Results for the five carbon blacks studied are summarized in Table I. For each black, a middle region of its isotherm was found over which the Frenkel–Halsey–Hill isotherm

TABLE I

Physical data for carbon blacks

Property	Carbolac 1	Carbolac 2	Monarch 71	Mogul A	Vulcan 3
Helium density, g/cc	2.02	2.00	2.04	2.06	2.06
Open pore volume, cc/g	0.170	0.145	0.029	0.062	0.002
Apparent density, g/cc	1.50	1.55	1.93	1.83	2.05
Total surface area, m^2/g	1000	670	372	300	69
Free surface area, m^2/g	587	348	304	130	65
Internal surface area, m^2/g	413	322	68	170	4
Electron microscope surface area, m^2/g (3)	264	178	145	82	74
Surface roughness factor	2.2	2.0	2.1	1.6	(0.9)
Average pore diameter $\bar{d}$, Å	17	18	17	14	20

for adsorption on the free surface was obeyed. The slope of the isotherms varied from 2.64 for Monarch 71 to 2.76 for Carbolac 2.

The results show that considerable variation exists in the extent of internal porosity within carbon blacks. The majority of the variation is thought to be due to differences in the extent of air after-treatment at elevated temperatures, which is a standard manufacturing step used to increase the volatile matter content of blacks (1). Carbolacs 1 and 2, with volatile matter contents of 17 and 12% respectively (3), have undergone considerable oxidation during after-treatment. Smith and Polley (10) have shown that such

oxidation can effectively open up porosity within carbon blacks. In addition, the presence of oxygen during carbon formation is known to inhibit crystallite growth and good crystallite alignment, probably because of crosslinking (11); this can result in higher porosity.

Voet (12) obtained nitrogen adsorption isotherms at 77° K on a series of carbon blacks. From these isotherms and the assumption that the amount of nitrogen filling the internal pores of the carbon blacks by capillary condensation is negligible, he calculated pore size distributions. For Carbolac 1, he reports a distribution in pore diameter between 16 and 48 Å, with the peak in the distribution occurring at ca. 20 Å. He further reports that the internal surface area of Carbolac 1 constitutes 55% of the total surface area. This can be compared with the data presented in this paper for Carbolac 1, where the average diameter of the internal pore system is 17 Å and the internal surface area constitutes 41% of the total surface area. The differences noted could possibly be due to the fact that different black samples were used in these two studies and/or to Voet's assumption of negligible capillary condensation within the internal pore system.

It is noted that the BET surface area for Vulcan 3 is less than the electron microscope surface area. This is relatively common for carbon blacks of low porosity (3, 13), and is probably due, in part, to uncertainty as to what value to use for the apparent density of the black. It does result in a surface roughness factor of less than 1 being calculated for Vulcan 3.

ACKNOWLEDGMENT

This work was supported, in part, by the Atomic Energy Commission on Contract No. AT(30-1)-1710.

REFERENCES

1. W. R. Smith. Encyclopedia of chemical technology. Vol. 3. The Interscience Encyclopedia Inc. 1949. pp. 34–65.
2. W. V. Kotlensky and P. L. Walker, Jr. Proceedings of the Fourth Carbon Conference. Pergamon Press, London. 1960. pp. 423–442.
3. Cabot Carbon Blacks under the Electron Microscope. Cabot Corp. 1950.
4. S. Mrozowski. Proceedings of the Third Carbon Conference. Pergamon Press, London. 1959. pp. 495–508.
5. S. Mrozowski. Industrial carbon and graphite. Society of Chemical Industry (London). 1958. pp. 7–18.
6. P. H. Emmett. A.S.T.M. Tech. Publ. **51**, 95 (1941).
7. C. Pierce. J. Phys. Chem. **63**, 1076 (1959).
8. C. Pierce. J. Phys. Chem. **64**, 1184 (1960).
9. D. W. Breck, W. G. Eversole, R. M. Milton, T. B. Reed, and T. L. Thomas. J. Am. Chem. Soc. **78**, 5963 (1956).
10. W. R. Smith and M. H. Polley. J. Phys. Chem. **60**, 689 (1956).
11. A. E. Austin and W. A. Hedden. Ind. Eng. Chem. **46**, 1520 (1954).
12. A. Voet. Rubber World, **139**, 63 (1958).
13. G. Kraus and J. Dugone. Ind. Eng. Chem. **47**, 1809 (1955).

CHAIN TERMINATION IN THE PHOTOCHLORINATION OF METHYL CHLORIDE

K. G. Mathai and D. J. Le Roy
The Department of Chemistry, University of Toronto, Toronto, Ontario

Received July 28, 1961

ABSTRACT

The photochlorination of methyl chloride has been studied at 2.4°, 25.0°, and 50.1° C using absorbed light intensities of the order of 10^{-10} einstein cm^{-3} sec^{-1} and a wave length of 4358 Å. Chain termination was by chlorine atom removal but two mechanisms were operative. For the first, termolecular collisions, the evidence indicated somewhat different third-body efficiencies for methyl chloride, methylene chloride, and chlorine; the efficiency of SF_6 was lower than for these by a factor of 6 to 9; the efficiency of HCl was, relatively, too small to measure. The second mechanism involved "sticky" collisions. Methylene chloride was particularly efficient in this process, indicating an unusually stable CH_2Cl_2-Cl complex.

In most photohalogenation reactions in which a substance RH is converted to RX + HX the initial production of halogen atoms is followed by a Nernst chain:

$$X + RH \xrightarrow{k_a} R + HX,$$
$$R + X_2 \xrightarrow{k_b} RX + X.$$

In the steady state (X)/(R) will be approximately equal to $[k_b(X_2)]/[k_a(RH)]$, since the rates of the two reactions will be approximately equal. In the presence of roughly equal concentrations of the two reagents X_2 and RH the ratio (X)/(R) will be determined by the value of k_b/k_a. If X ≡ Br the latter ratio will be quite large and hence homogeneous chain termination will occur by the combination of two bromine atoms. If k_a should be comparable in magnitude to k_b, as, for example, in the *addition* of Cl to an olefin (1), homogeneous chain termination may also take place through the combination of a halogen atom with an R radical or through the combination of two R radicals. Because of the current interest attached to the rates of combination of atoms and the paucity of information on the rate of combination of atomic chlorine (2) we have undertaken the present investigation of the mechanism of the photochlorination of methyl chloride.

The choice of methyl chloride was particularly fortunate. Chain termination was found to occur exclusively by chlorine atom removal and evidence was obtained for both of the commonly assumed mechanisms of atom combination,

$$X + X + P = X_2 + P; \quad [I]$$
$$X + M = MX,$$
$$MX + X = X_2 + M. \quad [II]$$

We were also able to obtain some information about the relative efficiencies of various substances, both as third bodies, P, and as participants, M, in "sticky" collisions.

EXPERIMENTAL

The main features of the apparatus have already been described (3), but a few of the improvements are worthy of mention. The stability of the photoelectric photometer used in following chlorine consumption was greatly improved by replacing the Leeds and Northrup type 7673 electrometer with a Curtis Wright Dynamic Capacitor Electrometer (Model NA 100). This same instrument was used to activate a Honeywell recorder which plotted a function proportional to the decrease in chlorine concentration. For a fixed setting of the bridge the rate of change of chlorine concentration is inversely proportional to the apparent extinction

coefficient K_a (3) and directly proportional to the slope on the recorder chart. Since both the chart speed and the sensitivity of the electrometer could be controlled precisely, we were able to obtain values of $-d(Cl_2)/dt$ at any time by drawing tangents. For very slow reactions the off-balance voltage was simply read off the electrometer at regular intervals and plotted.

As in our previous work, the change in K_a during the course of a single experiment was insignificant. As a number of minor changes had been made in the optical system it was of interest to check the validity of our procedure for correcting for reflection, absorption, and scattering (4). As before, K_a was found to be a linear function of the square root of the apparent fraction of light transmitted. Although the slope differed from that found by Dignam and Le Roy for their apparatus, as might be expected, the value of the "true" extinction coefficient, K, for 4358 Å and 25° C was the same, namely 1.51×10^3 cm^2 mole^{-1}. The value of $K_{50.1°}/K_{25.0°}$ was 1.020, that of $K_{25.0°}/K_{2.4°}$ was 1.019, also in good agreement with our previous work.

Absolute light intensities were determined by the ferrioxalate actinometer using the recommended procedures (5) and correcting for reflections. To allow for gradual changes in the intensity of the light source, the intensity of 4358-Å light transmitted through the front window of the cell was related to the potential drop across the fixed resistance in series with the photocell which was exposed to the reference beam. For the "high" light intensity experiments the value of I_o was 1.118×10^{-8} einstein cm^{-2} min^{-1} volt^{-1}; for the "low" light intensity experiments this number was multiplied by 1/18.30, the transmission of the filter used to reduce the light intensity by a known amount. The voltage drop across the fixed resistor was measured accurately for each experiment; its average value was about 1.6 volts. The internal cross section of the cell was 13.07 cm^2, its length was 25.8 cm.

The main products of the reaction were, of course, hydrogen chloride and methylene chloride. A mass spectrographic analysis of the products of typical experiments showed that the amount of methylene chloride produced agreed with the amount of chlorine consumed within 6%. No evidence could be found for more highly chlorinated derivatives. The stoichiometry was, therefore, assumed to be $Cl_2 + CH_3Cl = CH_2Cl_2 + HCl$.

Experiments were performed at 2.4°, 25.0°, and 50.1° C using various concentrations of chlorine and methyl chloride. Hydrogen chloride, methylene chloride, and sulphur hexafluoride were added initially in certain instances. Each experiment consisted of two parts: the first was carried out at high light intensity, the second at low light intensity. The two values of $-d(Cl_2)/dt$ at the point of interruption, R' and R'', and their ratio, $r = R'/R''$, were determined. If λ is the ratio of the high to the low light intensity, 18.30 in the present case, then r would be equal to λ if the rate were proportional to the first power of the light intensity and to $\lambda^{1/2}$ if it were proportional to the square root of the light intensity.

RESULTS AND DISCUSSION

The experimental conditions and some of the results are shown in Table I. The significant features are as follows: (*a*) all values of r lay between λ and $\lambda^{1/2}$; (*b*) the addition of large amounts of hydrogen chloride (expts. 176–178) had no effect on the rate at high light intensity; (*c*) addition of methylene chloride caused a marked decrease in rate (expts. 215–217, 184–187); (*d*) the rate during a given experiment was found to decrease too rapidly to be accounted for by the loss of chlorine and methyl chloride; (*e*) the addition of sulphur hexafluoride caused a modest decrease in the rate (e.g. expts. 179–183); that this was not due to impurities was shown by subjecting the sulphur hexafluoride to an extensive "prephotochlorination" before addition of the methyl chloride; (*f*) addition of large amounts of hydrogen chloride and sulphur hexafluoride had very little effect on r.

Effect (*a*) is usually taken to indicate simultaneous first- and second-order chain termination. As pointed out previously (3), the rates of reactions for which $\lambda^{1/2} < r < \lambda$ can be expressed by the general equation

$$-d(Cl_2)/dt = A[(1+B\bar{I}_a)^{1/2}-1], \qquad [i]$$

in which A and B are combinations of rate constants and (or) concentrations. Substitution of the average rate of light absorption, $\bar{I}_a$, for the *local* rate of light absorption, I_a, was valid (3). Numerical values of B, and hence of A, were obtained for each experiment from a knowledge of r and λ; thus, if $\bar{I}_a''$ is the average rate of light absorption at the low light intensity,

$$B\bar{I}_a'' = 4r(r-1)(\lambda-r)(r^2-\lambda)^{-2}. \qquad [ii]$$

TABLE I

Expt. No.	Concentration (moles cm^{-3}×10^{7}) (Cl_2)	(CH_3Cl)	(HCl)	(CH_2Cl_2)	(SF_6)	R_{obs}' ×10^{9}	r_{obs}	A_{cor} ×10^{10}	B_{cor} ×10^{-12}
2.4° C									
209	13.75	7.36	3.79	3.79	—	1.07	11.25	7.01	3.64
210	13.77	10.47	3.76	3.76	—	1.48	10.87	8.68	4.22
212	2.50	8.47	2.51	2.51	—	0.50	13.95	7.05	6.83
213	12.21	9.73	5.35	5.35	—	1.15	12.70	10.96	2.47
214	12.45	3.72	5.09	5.09	—	0.47	12.72	4.61	2.33
215	13.79	5.49	3.82	9.22	—	0.45	15.32	10.38	0.74
216	13.74	5.41	3.84	6.90	—	0.55	13.95	7.68	1.30
217	13.64	5.48	3.84	12.20	—	0.34	15.94	10.41	0.54
219	13.76	8.11	3.84	3.84	142.1	1.00	9.55	4.30	7.04
25.0° C									
174	14.11	8.56	3.64	3.64	—	1.71	8.60	5.46	10.25
175	14.18	8.78	3.65	3.65	—	1.77	8.58	5.57	10.55
176	14.06	8.66	28.67	3.65	—	1.73	8.62	5.58	10.13
177	14.30	8.44	52.07	3.66	—	1.68	8.58	5.37	10.22
178	14.02	8.34	102.11	3.67	—	1.70	8.55	5.40	10.33
179	14.10	8.30	3.65	3.65	25.0	1.62	8.63	5.26	9.97
180	14.32	8.12	3.68	3.68	50.6	1.40	8.55	4.49	10.20
181	14.16	7.79	3.63	3.63	99.0	1.28	8.50	4.07	10.49
182	13.95	7.85	3.63	3.63	147.4	1.19	7.95	3.18	13.85
183	13.81	7.85	3.67	3.67	195.6	1.12	7.75	2.76	16.10
184	14.01	7.64	3.68	9.10	—	1.05	13.0	11.01	1.84
185	14.22	7.68	3.69	10.87	—	1.00	13.72	12.87	1.39
186	13.65	7.89	3.68	13.71	—	0.84	14.70	14.93	0.96
187	13.97	7.73	3.67	15.82	—	0.77	14.90	14.81	0.85
190	27.86	5.30	2.51	2.51	—	1.42	6.84	2.48	15.55
192	14.23	10.53	3.66	3.66	—	1.95	9.40	7.74	7.22
193	12.89	14.34	4.86	4.86	—	2.23	10.30	11.11	5.58
195	2.79	9.95	2.41	2.41	—	0.75	13.10	8.28	8.21
50.1° C									
197	14.23	12.03	3.58	3.58	—	3.16	7.60	7.06	17.20
198	13.95	9.09	3.60	3.60	—	2.32	7.60	5.53	17.42
199	12.90	14.24	4.75	4.75	—	3.28	9.15	11.92	8.76
203	14.20	8.77	3.59	9.40	—	1.72	12.50	15.69	2.14
204	14.02	7.69	2.60	10.74	—	1.33	13.00	13.93	1.80
205	14.12	7.01	3.57	14.45	—	0.61	14.10	15.08	1.15
207	14.06	8.46	3.56	3.56	74.8	1.98	8.25	5.83	11.63
208	14.17	7.98	3.55	3.55	199.6	1.72	8.50	5.46	10.15

NOTE: All values apply to the time when the light intensity was reduced by the factor 18.30. Units used are moles, cm^3, and seconds.

The numerical evaluation of the two parameters made it possible to study the functional form of A and B and of combinations of the two.

If the values of r were greater than $\lambda^{1/2}$ because of a diffusion-controlled first-order chain termination process, then r would approach $\lambda^{1/2}$ as $\bar{I}_a$ is increased and also when the total pressure is increased by the addition of inert gas. It follows from [i] that the limiting rate expression at low light intensities would be

$$-d(Cl_2)/dt = \tfrac{1}{2}AB.\bar{I}_a. \qquad [iii]$$

For a diffusion-controlled first-order chain termination process the quantity AB would be inversely proportional to the diffusion coefficient of the species involved, and hence directly proportional to the total pressure under otherwise constant conditions. The results of expts. 179–183 show that this is not the case. We feel, therefore, that diffusion of chain carriers to the wall is not an important process.

The inhibiting effect of methylene chloride is difficult to explain on a chemical basis. Its reaction with Cl to form CH_2Cl and Cl_2 would be highly endothermic; its reaction with CH_2Cl would have no effect on the rate if a Cl atom were removed, and would result in the formation of appreciable amounts of higher chlorinated products if an H atom were removed, contrary to our mass spectrometric analysis.

Effect (*d*) could be accounted for if there were inhibition by either HCl or CH_2Cl_2, but effect (*b*) rules out inhibition by HCl. Effect (*e*) is easily accounted for if SF_6 acts as a third body for chain termination; this was shown to be the case.

Of the various attempts to formulate a mechanism in the light of the above considerations only the following was successful:

$$Cl_2 + h\nu = 2Cl \quad [1]$$

$$Cl + CH_3Cl = CH_2Cl + HCl \quad [2]$$

$$CH_2Cl + Cl_2 = CH_2Cl_2 + Cl \quad [3]$$

$$Cl + M = MCl \quad [4]$$

$$MCl = M + Cl \quad [5]$$

$$Cl + MCl = M + Cl_2 \quad [6]$$

$$2Cl + P = Cl_2 + P. \quad [7]$$

The substance or substances M and P are distinguished because of their different roles, but need not be specified further as yet. The group [4], [5], [6], on the one hand, and reaction [7], on the other, comprise the two general types that have been suggested for atom combination. In most cases it is not possible to distinguish between them, and the rates of atom combination reactions are simply expressed as third-order processes. In the present instance it appears to be possible to distinguish between them as a result of $k_5(MCl)$ being considerably smaller than $k_6(Cl)(MCl)$, i.e. M is very "sticky".

Before the results could be treated quantitatively it was necessary to consider the possibility of errors in A and B arising from deviations from isothermal conditions in the reaction vessel. Benson (6) has discussed the problem at some length and given correction terms applicable to spherical reaction vessels. Wilson (7) has derived relations for calculating the maximum temperature rise in cells of various shapes. More recently, Goldfinger *et al.* (8) have applied corrections to photochlorination reactions. In all treatments it was assumed that temperature gradients were controlled by thermal conductivity only, and no account was taken of convection or radiation; we have made the same assumption.

Treating the cell as an infinite cylinder, it is easy to show that if the rate, R, were independent of temperature the difference between the temperature at the central axis and at the wall would be given by the expression

$$\Delta T^0 = \frac{qRD^2}{16K}, \quad [iv]$$

in which q is the heat liberated per unit concentration change at constant volume, R is the corresponding rate, D is the diameter of the cell, and K is the coefficient of thermal conductivity.

Wilson (7) has shown that if the reaction has an activation energy E then the temperature rise at the center will be given, to a good approximation, by

$$\Delta T = \Delta T^0\left(1+\frac{3E\Delta T^0}{4\times 1.987T^2}\right), \quad [v]$$

provided the second term in the brackets is less than unity. In the present case this term is sufficiently small that we have felt justified in neglecting it, particularly since the value of ΔT calculated from [v] would be too large if convection were of any importance. The volume-average temperature rise calculated from [iv] is

$$\Delta\bar{T} = \frac{qRD^2}{32K}. \qquad [vi]$$

If R' is the rate at high light intensity that would obtain at the temperature T (of the cell wall), and $R'+dR'$ the observed rate, then,

$$dR'/R' = \frac{E\Delta\bar{T}}{1.987T^2} = \frac{EqR'D^2}{32\times 1.987T^2K}. \qquad [vii]$$

A similar expression will hold for R'', the rate at low light intensity. The fractional error in r will be given by the expression

$$dr/r = dR'/R' - dR''/R'' = (dR'/R')(1-1/r). \qquad [viii]$$

The fractional error in B is then,

$$d\ln B \equiv d\ln(B\bar{I}_a'') = (dR'/R')(1-1/r)\left(1+\frac{r}{r-1}-\frac{r}{\lambda-r}-\frac{r^2}{r^2-\lambda}\right). \qquad [ix]$$

The corrected values of A and B are given in Table I. The former were obtained from relation [i] using corrected values of R' and $B\bar{I}_a'$. The maximum value of $\Delta\bar{T}$ for any experiment was 1.5° C; the maximum correction to R' was 3.2%, to B, 7.8%. In making the corrections q was taken to be 23.5 kcal and E was assumed to be 3 kcal mole^{-1}. Values of K were calculated from the expression

$$K = \sum_i \frac{K_iN_i}{\sum_j a_{ij}N_j}, \qquad [x]$$

in which K_i is the thermal conductivity of a pure component and N_i and N_j are mole fractions; the coefficients a_{ij} were evaluated from the expression given by Reid and Sherwood (9).

It follows from [i] that the limiting rate equation at high light intensities is given by the expression

$$-d(Cl_2)/dt = AB^{1/2}\bar{I}_a^{1/2} = \frac{k_2}{k_7^{1/2}}\cdot\frac{(CH_3Cl)}{(P)^{1/2}}\cdot\bar{I}_a^{1/2}. \qquad [xi]$$

It is convenient to apply this relation in the form

$$\frac{(CH_3Cl)^2}{A^2B} = \frac{k_7}{k_2^2}(P). \qquad [xii]$$

It was evident from an examination of the values of $(CH_3Cl)^2/A^2B$ that the efficiencies of the various gases as third bodies were not the same; the efficiency of HCl appeared to be negligible in comparison with the other gases, and that of SF_6 considerably less than that of CH_3Cl, CH_2Cl_2, or Cl_2. Taking the efficiency of the latter three as unity, α, and β, and the efficiency of SF_6 as γ, [xii] may be written

$$\frac{(CH_3Cl)}{A^2B} = \frac{k_7}{k_2^2}\left(1+\alpha\frac{(CH_2Cl_2)}{(CH_3Cl)}+\beta\frac{(Cl_2)}{(CH_3Cl)}+\gamma\frac{(SF_6)}{(CH_3Cl)}\right). \qquad [xiii]$$

In Figs. 1 and 3 the left side of [xiii] is plotted for the experiments in which SF_6 was not used on the assumption that $\alpha = \beta = 1$; for these experiments the accuracy of the data did not justify doing otherwise. In Fig. 2(*a*) the corresponding data for 25° C are plotted using the same assumption. While the three curves provide ample justification for the mechanism and the values of $k_2/k_7^{1/2}$ derived from the slopes fit a satisfactory Arrhenius plot, as shown in Fig. 4, the activation energy difference $(E_2 - 1/2E_7) = 1.8$ kcal mole^{-1} must be accepted with reserve.

The sensitivity of the calculated values of $k_2/k_7^{1/2}$ to the assumed values of α and β is illustrated in Fig. 2(*b*). In this case a least-squares treatment gave $\alpha = 0.50$ and $\beta = 0.59$, and these values were used in plotting curve (*b*). While the fit is undoubtedly better than in Fig. 2(*a*), the value of $k_2/k_7^{1/2}$ has been increased by about 50%, from 0.087 to 0.127 sec$^{-1/2}$.

Assuming that $\alpha = \beta = 1$, the value of γ was determined by plotting the function $F = [(RH)^2/A^2B].[k_2^2/k_7].[\{1/[(RH)+(RCl)+(Cl_2)]\}-1]$ against $(SF_6)/[(RH)+(RCl)+(Cl_2)]$ as shown in Fig. 5, using the value of k_2^2/k_7 obtained from Fig. 2(*a*). The value obtained was 0.16. The alternative method, using $\alpha = 0.50$, $\beta = 0.59$, and the value of k_2^2/k_7 from Fig. 2(*b*) gave $\gamma = 0.11$. Average values of γ for 2.4° and 50.1° were 0.08 and 0.09, respectively.

The results obtained on the termolecular combination of chlorine atoms are not as satisfactory as one would wish. Among the reasons for this are (1) the occurrence of a second chain termination process (reactions [4], [5], and [6]) and the consequent necessity of determining two separate constants, A and B, in order to evaluate the quantity $(k_7/k_2^2)(P)$; (2) the impossibility of determining the absolute rate of reaction [7] from the equilibrium constant for the dissociation of chlorine and kinetic data for the thermal reaction in the same temperature range, as was done by Steiner for the case of bromine atoms (10). In spite of these difficulties it would appear, however, that the termolecular combination of chlorine atoms, like that of bromine and iodine (2), has rate constants characteristic of the particular third body involved. The relatively low efficiency of SF_6 is of particular interest.

According to the present mechanism the limiting rate expression at low light intensities given by [iii] takes the form

$$-d(Cl_2)/dt = \frac{AB}{2}\cdot \bar{I}_a = \frac{k_2}{k_4}\cdot\frac{(CH_3Cl)}{(M)}\cdot \bar{I}_a. \qquad [xiv]$$

Using the measured values of A and B, this relation was tested in the form

$$\frac{1}{AB} = \frac{k_4}{2k_2}\left(\frac{(CH_2Cl_2)}{(CH_3Cl)} + a\right), \qquad [xv]$$

in which a is the efficiency of CH_3Cl relative to that of CH_2Cl_2 as an "M". The quantity a was considerably less than unity, and the efficiencies of the other gases were negligibly small. The data are plotted in Figs. 6, 7, and 8. At 2.4° C a appeared to be zero within experimental error, the least-squares value of k_2/k_4 calculated on this basis was 6.5×10^2; at 25° C a was found to be 0.11, k_2/k_4 13.4×10^2; at 50.1° C a was found to be 0.06, k_2/k_4 18.4×10^2. The accuracy of the method is such that an efficiency of less than 10%, relative to that of methylene chloride, could not be readily detected in the case of methyl chloride or chlorine. It is clear, however, that the efficiencies of hydrogen chloride and sulphur hexafluoride as M's must be lower than this by at least another order of magnitude. Points derived from expts. 176, 177, and 178, in which an excess of HCl was used,

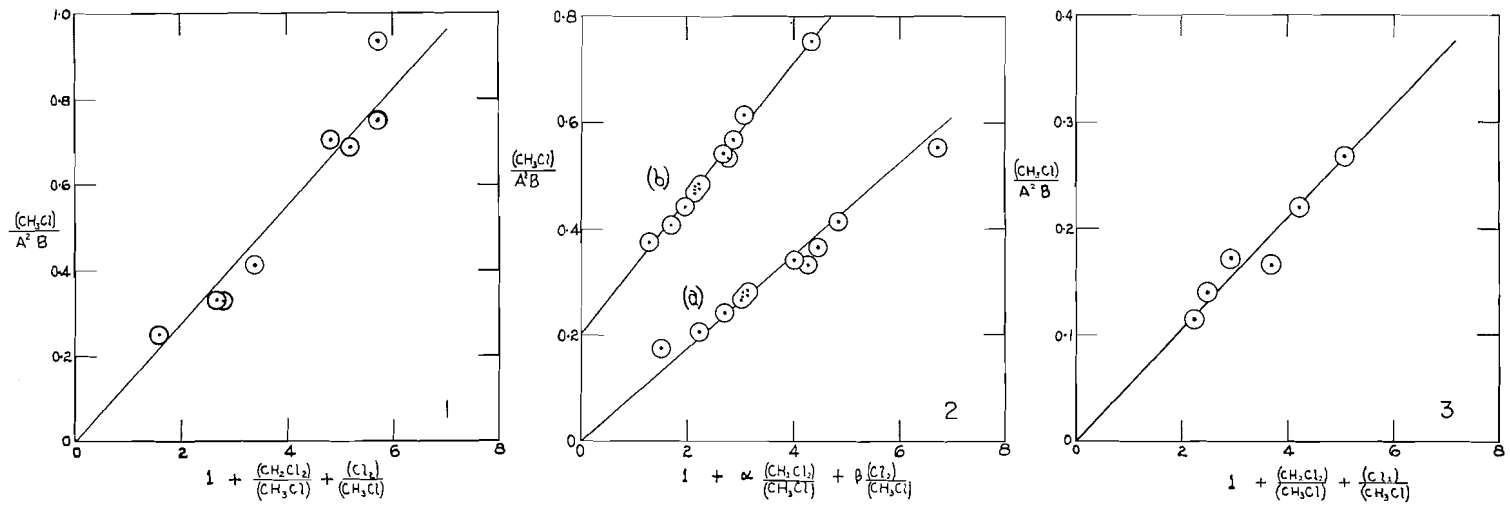

FIG. 1. Test of termolecular mechanism for chlorine atom combination at 2.4° C assuming $\alpha = \beta = 1$.
FIG. 2. Test of termolecular mechanism for chlorine atom combination at 25.0° C assuming (*a*) $\alpha = \beta = 1$; (*b*) $\alpha = 0.50$, $\beta = 0.59$.
FIG. 3. Test of termolecular mechanism for chlorine atom combination at 50.1° C assuming $\alpha = \beta = 1$.

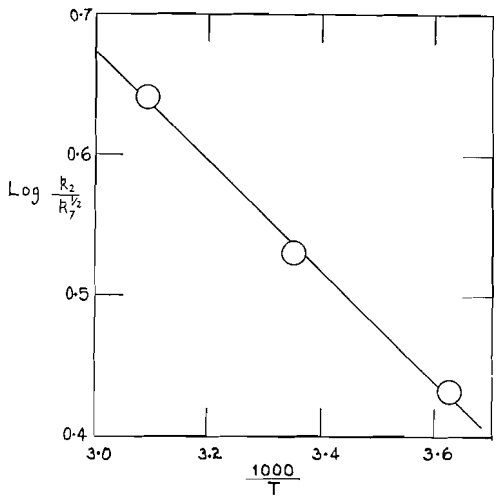

FIG. 4. Arrhenius plot of $k_2/k_7^{1/2}$ using values derived from Figs. 1, 2(*a*), and 3.

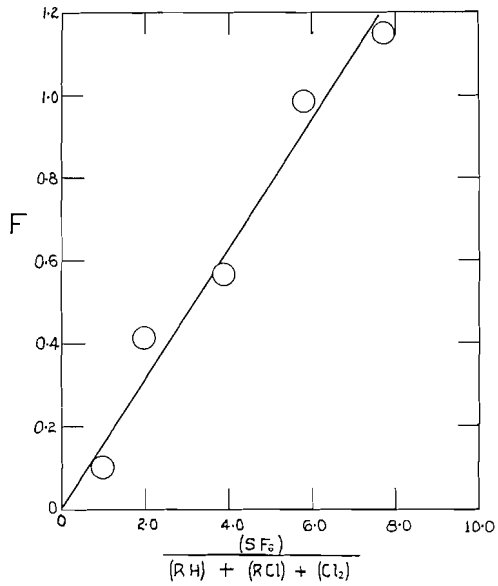

FIG. 5. Determination of γ, the third-body efficiency of SF_6 relative to that of CH_3Cl, CH_2Cl_2, and Cl_2, at 25.0° C.

show no deviation from the curve of Fig. 7. The points derived from the experiments in which SF_6 was added are shaded in Figs. 6, 7, and 8; these show that SF_6 has no measurable efficiency as an M.

A theoretical interpretation of the combination process given by reactions [4], [5], [6] has been offered by Bunker and Davidson (11). These authors are inclined to the view that the "sticky" collision mechanism is quite general, and their theory accounts quite well for the negative activation energy found for the combination of iodine atoms. If k_5(MCl) were comparable in magnitude to k_6(Cl)(MCl) the "sticky" collision mechanism could not be distinguished kinetically from reaction [7]. On the other hand, the present measurements indicate that the bound state (11) of MCl is unusually stable when

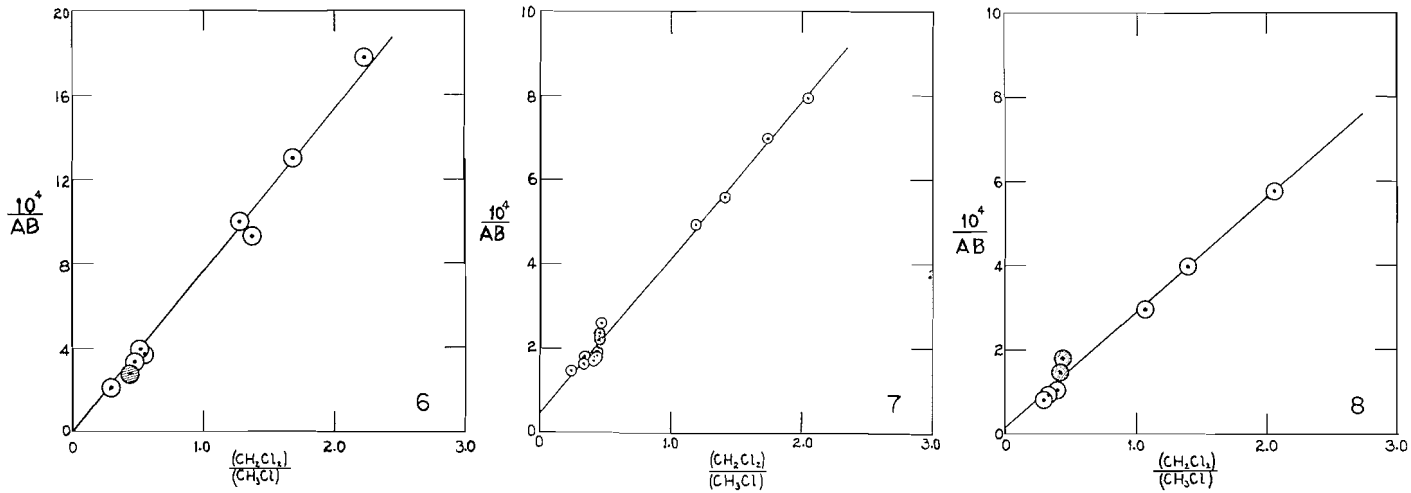

FIG. 6. Test of "sticky" collision mechanism for chlorine atom combination at 2.4° C. Expt. 219, with added SF_6, indicated by shading.
FIG. 7. Test of "sticky" collision mechanism for chlorine atom combination at 25.0° C. Expts. 179–183, with added SF_6, indicated by shading; data from expts. 176–178, with added HCl, included among open circles.
FIG. 8. Test of "sticky" collision mechanism for chlorine atom combination at 50.1° C. Expts. 207 and 208, with added SF_6, indicated by shading.

$M = CH_2Cl_2$; rough calculations indicate a lifetime of the order of 1 second and a heat of formation of the order of 18 kcal mole^{-1}. This is to be compared to the heat of formation of 5.3 kcal mole^{-1} which Bunker and Davidson calculated for the bound state of the $I-I_2$ complex.

In deriving the value for the $Cl-CH_2Cl_2$ complex it was necessary to utilize the data obtained by Pritchard, Pyke, and Trotman-Dickenson (12), who measured k_2 relative to the corresponding value for the abstraction of an H atom from methane. The value for methane was, in turn, relative to that for the reaction $Cl + H_2 = HCl + H$, which had been determined by Ashmore and Chanmugam (13). The significant contribution of the latter authors is that they were able to measure the rate of hydrogen abstraction relative to the known equilibrium constant for the reaction $NO + Cl_2 = NOCl + Cl$ and did not have to rely on assumptions regarding the rate constant and activation energy for the combination of chlorine atoms. While such assumptions have been made in the past the present results indicate quite clearly that even at high light intensities, at which reaction [7] might predominate, errors will arise unless account can be taken of the efficiencies of all third bodies at the temperatures involved.

It should be pointed out that our results, and hence our mechanism, differ in various respects from those of Goldfinger *et al.* (14). They assume that the rate is proportional to $\bar{I}_a^{1/2}$. If this were so then all the values of r in Table I would be equal to $\lambda^{1/2}$, or 4.3, and hence independent of the concentration of methylene chloride. By using the rather large value of λ (18.30) we have been able to show, beyond any experimental error, that the rate is not directly proportional to $I_a^{1/2}$ in the range of light intensities used by us.

They give no evidence for a third-body effect on chain termination, shown clearly in our experiments with added SF_6, and according to their mechanism chain termination occurs by the combination of CH_2Cl with Cl and with CH_2Cl, but not by reaction [7]. If these were the chain termination reactions at high light intensities, at which the rate would be proportional to $I_a^{1/2}$, then the quantity $(Cl_2)^2/A^2B$ should be a linear function of $(Cl_2)/(CH_3Cl)$, with a positive intercept. When this function was plotted for each temperature, using our data, the points were quite scattered, but not about straight lines; furthermore, least-squares curves through the points gave negative intercepts. It does not seem possible, at present, to account for the discrepancies between the results obtained in the two laboratories.

ACKNOWLEDGMENTS

The authors are grateful to the National Research Council of Canada for a grant in aid of the research and to Professor A. G. Harrison for carrying out the mass spectrographic analyses.

REFERENCES

1. J. Adam, P. Goldfinger, and P. A. Gosselain. Bull. soc. chim. Belges, **65**, 549 (1956).
2. S. W. Benson. The foundations of chemical kinetics. McGraw-Hill Inc. 1960.
3. M. J. Dignam, W. G. Forbes, and D. J. Le Roy. Can. J. Chem. **35**, 1341 (1957).
4. M. J. Dignam and D. J. Le Roy. J. Chem. Phys. **26**, 964 (1957).
5. C. G. Hatchard and C. A. Parker. Proc. Roy. Soc. (London), A, **235**, 518 (1956).
6. S. W. Benson. J. Chem. Phys. **22**, 46 (1954).
7. D. J. Wilson. J. Phys. Chem. **62**, 653 (1958).
8. P. Goldfinger, G. Huybrechts, A. M. Mahiew-Van der Auwera, and D. Van der Auwera. J. Phys. Chem. **64**, 468 (1960).
9. R. C. Reid and T. K. Sherwood. The properties of gases and liquids. McGraw-Hill Inc. 1958.
10. W. Steiner. Z. physik. Chem. (Leipzig), B, **30**, 399 (1935).
11. D. L. Bunker and N. Davidson. J. Am. Chem. Soc. **80**, 5090 (1958).
12. H. O. Pritchard, J. B. Pyke, and A. F. Trotman-Dickenson. J. Am. Chem. Soc. **77**, 2629 (1955).
13. P. G. Ashmore and J. Chanmugam. Trans. Faraday Soc. **49**, 254 (1953).
14. R. Eckling, P. Goldfinger, G. Huybrechts, G. Martens, L. Meyers, and S. Smoes. Chem. Ber. **93**, 3014 (1960). G. Chiltz, A. M. Mahieu, and G. Martens. Bull. soc. chim. Belges, **67**, 33 (1958).

A SYSTEM OF MOLECULAR THERMOCHEMISTRY FOR ORGANIC GASES AND LIQUIDS

PART III. EXTENSION TO AROMATIC AND CYCLIC COMPOUNDS

EDWARD G. LOVERING[1] AND OTHMAN BIN M. NOR
The Department of Chemistry, University of Ottawa, Ottawa, Ontario

Received September 21, 1961

ABSTRACT

The empirical bond energy scheme described in Part I has been modified and applied to saturated and aromatic ring compounds. The classes of compounds treated are the alkyl benzenes, alkyl cyclopentanes, and alkyl cyclohexanes. The scheme given permits values for the heats of atomization, formation, combustion, and vaporization to be calculated. Reasons for the failure of the scheme, when applied to aromatic nuclei containing a functional group, are discussed.

INTRODUCTION

In Part I (1) of this series a system of bond energy contributions to heats of formation, combustion, atomization, and vaporization for homologous series of organic compounds was described. Part II (2) described an extension of the scheme given in Part I to certain sulphur- and oxygen-containing compounds.

The scheme described in Part I, as applied to paraffins, contains four parameters; satisfactory agreement between calculated and experimental quantities is obtained, except in the case of compounds which exhibit considerable chain branching. This scheme is equivalent to one which considers only bond energies and interactions between adjacent bonds. Allen (3) has presented a scheme which, in addition, takes account of next-nearest-neighbor interactions, as well as steric effects which are present in certain compounds. A similar treatment has also been given by Skinner (4). This scheme, applied to paraffins, yields excellent agreement between calculated and observed heats of atomization. Recently, improved values of the constants have been calculated for Tatevskii's scheme by Skuratov and Shtekher (5).

A method for calculating thermodynamic properties of alkyl benzenes was also given in Part I. This was done by treating the aromatic nucleus as substituted cyclohexatriene; a resonance correction of 42.2 kcal was added to the calculated heats of atomization to obtain agreement between the calculated and experimental quantities. A somewhat different treatment of aromatic hydrocarbons is described in this paper;* all aromatic carbon–carbon bonds are considered to be identical and a new bond energy term is found for this type of bond. A related method has been applied to cyclohexanes and cyclopentanes.

Alkyl Benzenes

All carbon–carbon bonds, denoted by c_b, within an aromatic ring are considered to make the same bond energy contribution to the heat of atomization. Carbon–hydrogen bond strengths, where the carbon atom is part of an aromatic ring, are denoted by t_b. The strength of the carbon–carbon bond joining an alkyl side chain to the ring is denoted by c_s. As in Part I, the carbon–carbon bond strength of all other non-aromatic carbons is represented by c_1, primary carbon–hydrogen bond strengths by p, secondary carbon–hydrogen bond strengths by s, and tertiary carbon–hydrogen bond strengths by t. The

[1]*Present address: Inorganic Chemistry Laboratory, Oxford, England.*

**Another scheme for aromatic systems has just been published by Mackle and O'Hare, Trans. Faraday Soc., 57, 1521 (1961).*

values of p, s, t, and c_1 have been taken from Laidler (1). The values of c_s, c_b, and t_b were calculated from the heat of atomization data for several alkyl benzenes, which were selected to give the best agreement between experimental and calculated heats of atomization. The scheme also contains an ortho correction term, o_b, which is applied when two alkyl groups occupy adjacent positions on the aromatic nucleus. The value of this term was determined directly from the data for ortho-dialkyl benzenes. The bond energy values are given in Table I.

TABLE I

Bond contributions for heats of atomization, formation, and combustion of gases and liquids and heat of vaporization (at 25° C)

Bond	Symbol	Heat of atomization		Heat of formation		Heat of combustion		Heat of vaporization
		Gas	Liquid	Gas	Liquid	Gas	Liquid	
C—C	c_1	85.4	85.4	−0.45	−0.45	47.48	47.48	0
C—C	c_b	123.44	124.41	8.97	9.94	53.73	52.76	0.968
C—C	c_s	85.4	85.4	−14.76	−14.76	69.62	69.62	0
C—H	p	98.47	98.96	3.45	3.95	54.22	53.73	0.494
C—H	s	97.65	98.23	2.64	3.21	55.04	54.46	0.579
C—H	t	96.80	97.32	1.78	2.30	55.89	55.37	0.518
C—H	t_b	97.05	97.40	−12.27	−11.92	43.62	43.27	0.350
	o_b	−0.70	−0.52	−0.70	−0.52	0.70	0.52	0.18
C—H	s_6	97.71	98.36	2.70	3.35	54.98	54.33	0.654
C—H	t_6	98.21	99.08	3.20	4.07	54.48	53.61	0.867
C—H	p_{r6}	98.33	98.70	3.32	3.69	54.36	53.99	0.374
C—H	s_{r6}	97.21	97.59	2.20	2.58	55.48	55.10	0.378
	s_6	−1.1	−1.0	−1.1	−1.0	1.1	1.0	0.10
	a_6	−2.0	−1.87	−2.0	−1.87	2.0	1.87	0.13
C—H	s_5	97.08	97.76	2.07	2.75	55.61	54.92	0.685
C—H	t_5	96.83	97.59	1.82	2.58	55.86	55.10	0.764
C—H	p_{r5}	98.30	98.73	3.29	3.72	54.39	53.95	0.435
C—H	s_{r5}	97.48	97.96	2.47	2.95	55.21	54.73	0.482
	cis_{12}	−1.6	−1.3	−1.6	−1.3	1.6	1.3	0.3
	cis_{13}	−0.7	−0.7	−0.7	−0.7	0.7	0.7	0

Comparisons between experimental and calculated heats of atomization are made in Table II. The heats of atomization were calculated using heats of atomization of graphite, hydrogen, and oxygen of 171.7, 52.09, and 59.16 kcal/mole respectively. Heat of formation data for the alkyl benzenes were taken from the A.P.I. tables (6).

TABLE II

Alkyl benzenes: heats of atomization (25° C)

Compound	Bonds	Q_f (obs.), kcal/mole	Q_a (obs.), kcal/mole	Q_a (calc.), kcal/mole	Q_a (calc.) − Q_a (obs.)
Benzene	$6c_b+6t_b$	−19.8	1322.92	1322.94	+0.02
Toluene	$6c_b+5t_b+c_s+3p$	−11.9	1606.67	1606.70	+0.03
Ethylbenzene	$6c_b+5t_b+c_s+c_1+3p+2s$	−7.1	1887.37	1887.40	+0.03
n-Propylbenzene	$6c_b+5t_b+c_s+2c_1+3p+4s$	−1.9	2168.51	2168.10	−0.41
i-Propylbenzene	$6c_b+5t_b+c_s+2c_1+3p+4s$	−0.9	2169.44	2169.71	+0.27
n-Butylbenzene	$6c_b+5t_b+c_s+3c_1+3p+6s$	3.3	2449.56	2448.80	−0.76
1,2-Dimethylbenzene	$6c_b+4t_b+2c_s+6p+o_b$	−4.5	1889.96	1889.76	−0.20
1,3-Dimethylbenzene	$6c_b+4t_b+2c_s+6p$	−4.1	1890.38	1890.46	+0.08
1,4-Dimethylbenzene	$6c_b+4t_b+2c_s+6p$	−4.3	1890.21	1890.46	+0.25
1-Methyl-2-ethylbenzene	$6c_b+4t_b+2c_s+c_1+6p+2s+o_b$	−0.3	2170.09	2170.46	+0.37
1-Methyl-3-ethylbenzene	$6c_b+4t_b+2c_s+c_1+6p+2s$	0.5	2170.83	2171.16	+0.33
1-Methyl-4-ethylbenzene	$6c_b+4t_b+2c_s+c_1+6p+2s$	0.8	2171.16	2171.16	0
1,2,3-Trimethylbenzene	$6c_b+3t_b+3c_s+9p+2o_b$	2.3	2172.67	2172.82	+0.15
1,2,4-Trimethylbenzene	$6c_b+3t_b+3c_s+9p+o_b$	3.3	2173.71	2173.52	−0.19
1,3,5-Trimethylbenzene	$6c_b+3t_b+3c_s+9p$	3.8	2174.22	2174.22	0

Bond energy contributions to the heats of vaporization of alkyl benzenes have also been calculated. Bond contributions to the heats of vaporization are given in Table I. Again the experimental data were taken from the A.P.I. tables (6). Comparison between the calculated and experimental heats of vaporization is made in Table III.

TABLE III

Alkyl benzenes: heats of vaporization (25° C)

Compound	ΔH_v (obs.), kcal/mole	ΔH_v (calc.), kcal/mole	Difference (calc. − obs.)
Benzene	8.090	7.908	−0.182
Methylbenzene	9.080	9.040	−0.040
Ethylbenzene	10.097	10.198	+0.101
n-Propylbenzene	11.049	11.356	+0.307
i-Propylbenzene	10.789	11.040	+0.251
1,2-Dimethylbenzene	10.381	10.352	−0.029
1,3-Dimethylbenzene	10.195	10.172	−0.023
1,4-Dimethylbenzene	10.128	10.172	+0.044
1-Methyl-2-ethylbenzene	11.40	11.51	+0.11
1-Methyl-3-ethylbenzene	11.21	11.33	+0.12
1-Methyl-4-ethylbenzene	11.14	11.33	+0.19
1,2,3-Trimethylbenzene	11.725	11.664	−0.061
1,2,4-Trimethylbenzene	11.457	11.480	+0.023
1,3,5-Trimethylbenzene	11.346	11.304	−0.042

Cyclohexanes

It was necessary to calculate six new parameters in order to obtain good agreement between experimental and calculated heats of atomization for alkyl-substituted cyclohexanes. Carbon–carbon bonds within the ring were considered to have the same strength as those in paraffins. New values were obtained for carbon–hydrogen bond strengths, where the carbon is part of the ring. These bonds can be secondary, denoted by s_6, or tertiary, denoted by t_6. In addition, carbon–hydrogen bonds, where the carbon is adjacent to the ring, can be primary, secondary, or tertiary; the strengths of these bonds are denoted by p_{r6}, s_{r6}, and t_{r6} respectively. Unfortunately, there are insufficient data for the calculation of t_{r6}.

The stable form of cyclohexane is the chair form. Side chains on a cyclohexane ring are either equatorial to the ring or axial to it; the equatorial position is the more stable. Thus there are six dimethyl-substituted cyclohexane isomers, of which three are cis and three are trans. The equatorial isomers are *trans*-1,2-, *cis*-1,3-, and *trans*-1,4-dimethylcyclohexane; the other three isomers are axial. In order to take into account the difference in stability of the axial and equatorial isomers an axial correction term, a_e, was introduced. There is, in addition, a steric correction, s_c, which is applied in the case of $n,n+1$ substituted cyclohexanes.

Values for the bond energy contributions to the heat of atomization, found in the usual way, are given in Table I. Calculated heats of atomization are compared to the experimental quantities in Table IV. Heats of atomization were calculated from data given in the A.P.I. tables (6).

Bond energy contributions to the heat of vaporization are given in Table I; experimental results are compared to calculated results in Table V.

Cyclopentanes

The treatment of the cyclopentanes is similar to that applied to the cyclohexanes. Carbon–hydrogen bonds, where the carbon is part of the ring, can be either secondary

TABLE IV

Alkyl cyclohexanes: heats of atomization (25° C)

Compound	Bonds	Q_f (obs.), kcal/mole	Q_a (obs.), kcal/mole	Q_a (calc.), kcal/mole	Q_a (calc.) − Q_a (obs.)
Cyclohexane	$6c_1+12s_6$	29.43	1684.71	1684.92	+0.21
Methylcyclohexane	$7c_1+10s_6+t_6+3p_{r6}$	36.99	1968.15	1968.10	−0.05
Ethylcyclohexane	$8c_1+10s_6+t_6+2s_{r6}+3p$	41.05	2248.09	2248.34	+0.25
n-Propylcyclohexane	$9c_1+10s_6+t_6+2s_{r6}+2s+3p$	46.20	2529.12	2529.04	−0.08
n-Butylcyclohexane	$10c_1+10s_6+t_6+2s_{r6}+4s+3p$	50.95	2809.75	2809.74	−0.01
n-Pentylcyclohexane	$11c_1+10s_6+t_6+2s_{r6}+6s+3p$	55.88	3090.56	3090.44	−0.12
n-Hexylcyclohexane	$12c_1+10s_6+t_6+2s_{r6}+8s+3p$	60.80	3371.36	3371.14	−0.22
1,1-Dimethylcyclohexane	$8c_1+10s_6+6p_{r6}$	43.26	2250.30	2250.28	−0.02
trans-1,2-Dimethylcyclohexane	$8c_1+8s_6+2t_6+6p_{r6}+s_c$	43.02	2250.06	2250.18	+0.12
cis-1,2-Dimethylcyclohexane	$8c_1+8s_6+2t_6+6p_{r6}+s_c+a_e$	41.15	2248.19	2248.18	−0.01
cis-1,3-Dimethylcyclohexane	$8c_1+8s_6+2t_6+6p_{r6}$	44.16	2251.20	2251.28	+0.08
trans-1,3-Dimethylcyclohexane	$8c_1+8s_6+2t_6+6p_{r6}+a_c$	42.20	2249.24	2249.28	+0.04
trans-1,4-Dimethylcyclohexane	$8c_1+8s_6+2t_6+6p_{r6}$	44.12	2251.16	2251.28	+0.12
cis-1,4-Dimethylcyclohexane	$8c_1+8s_6+2t_6+6p_{r6}+a_e$	42.22	2249.26	2249.28	+0.02

TABLE V

Alkyl cyclohexanes: heats of vaporization (25° C)

Compound	ΔH_v (obs.), kcal/mole	ΔH_v (calc.), kcal/mole	Difference (calc. − obs.)
Cyclohexane	7.895	7.848	−0.047
Methylcyclohexane	8.451	8.529	+0.078
Ethylcyclohexane	9.673	9.645	−0.028
n-Propylcyclohexane	10.78	10.803	+0.023
n-Butylcyclohexane	11.96	12.403	+0.443
1,1-Dimethylcyclohexane	9.043	8.784	−0.259
trans-1,2-Dimethylcyclohexane	9.167	9.310	+0.143
cis-1,2-Dimethylcyclohexane	9.492	9.440	−0.052
cis-1,3-Dimethylcyclohexane	9.136	9.210	+0.074
trans-1,3-Dimethylcyclohexane	9.368	9.340	−0.028
trans-1,4-Dimethylcyclohexane	9.052	9.210	+0.158
cis-1,4-Dimethylcyclohexane	9.328	9.340	−0.012

or tertiary; the bond strengths are denoted by s_5 or t_5 respectively. Carbon–hydrogen bonds, when the carbon is adjacent to the ring, can be primary, secondary, or tertiary; these bond strengths are denoted by p_{r5}, s_{r5}, and t_{r5} respectively. There are again insufficient data available for the calculation of t_{r5}. There are five isomers of dimethylcyclopentane of which two are the less stable cis isomers. The correction terms for the cis isomers are different because of the large steric effect in the case of *cis*-1,2-dimethylcyclopentane. These correction terms are denoted by cis_{12} and cis_{13}.

Bond contributions to the heat of atomization are given in Table I. The calculated and experimental heats of atomization are compared in Table VI. Bond contributions to the heat of vaporization, and comparison of the experimental and calculated results are given in Table I and Table VII respectively. The experimental data were taken from the A.P.I. tables (6).

DISCUSSION

The agreement between the experimental and calculated heats of atomization for the benzenes and cycloalkanes is satisfactory. The method used to obtain the bond energy values for these classes of compounds does away with the necessity of adding an arbitrary term to the calculated heats of atomization to account for resonance stabilization or

TABLE VI

Alkyl cyclopentanes: heats of atomization (25° C)

Compound	Bonds	Q_f (obs.), kcal/mole	Q_a (obs.), kcal/mole	Q_a (calc.), kcal/mole	Q_a (calc.) − Q_a (obs.)
Cyclopentane	$5c_1+10s_5$	18.46	1397.86	1397.80	−0.06
Methylcyclopentane	$6c_1+8s_5+t_5+3p_{r5}$	25.50	1680.78	1680.77	−0.01
Ethylcyclopentane	$7c_1+8s_5+t_5+2s_{r5}+3p$	30.37	1961.54	1961.64	+0.10
n-Propylcyclopentane	$8c_1+8s_5+t_5+2s_{r5}+2s+3p$	35.39	2242.44	2242.34	−0.10
n-Butylcyclopentane	$9c_1+8s_5+t_5+2s_{r5}+4s+3p$	40.22	2523.15	2523.04	−0.11
n-Pentylcyclopentane	$10c_1+8s_5+t_5+2s_{r5}+6s+3p$	45.15	2803.96	2803.74	−0.22
n-Hexylcyclopentane	$11c_1+8s_5+t_5+2s_{r5}+8s+3p$	50.07	3084.76	3084.44	−0.32
1,1-Dimethylcyclopentane	$7c_1+8s_5+6p_{r5}$	33.05	1964.22	1964.24	+0.02
trans-1,2-Dimethylcyclopentane	$7c_1+6s_5+2t_5+6p_{r5}$	32.67	1963.84	1963.74	−0.10
cis-1,2-Dimethylcyclopentane	$7c_1+6s_5+2t_5+6p_{r5}+\mathrm{cis}_{12}$	30.96	1962.13	1962.14	+0.01
trans-1,3-Dimethylcyclopentane	$7c_1+6s_5+2t_5+6p_{r5}$	32.47	1963.64	1963.74	+0.10
cis-1,3-Dimethylcyclopentane	$7c_1+6s_5+2t_5+6p_{r5}+\mathrm{cis}_{13}$	31.93	1963.11	1963.04	−0.07

TABLE VII

Alkyl cyclopentanes: heats of vaporization (25° C)

Compound	ΔH_v (obs.), kcal/mole	ΔH_v (calc.), kcal/mole	Difference (calc. − obs.)
Cyclopentane	6.818	6.850	+0.032
Methylcyclopentane	7.560	7.549	−0.011
Ethylcyclopentane	8.720	8.690	−0.030
n-Propylcyclopentane	9.820	9.848	+0.028
n-Butylcyclopentane	11.000	11.006	+0.006
1,1-Dimethylcyclopentane	8.079	8.090	+0.019
trans-1,2-Dimethylcyclopentane	8.259	8.248	−0.011
cis-1,2-Dimethylcyclopentane	8.56	8.548	−0.012
trans-1,3-Dimethylcyclopentane	8.200	8.248	+0.048
cis-1,3-Dimethylcyclopentane	8.26	8.248	−0.012

ring strain, as the case may be. It has the disadvantage, however, that in the case of aromatic compounds it treats σ and π bonds together, instead of individually.

Recent data are also available for methyl-substituted phenols (7) and methyl-substituted pyridines (8). We attempted to treat the phenols in a manner similar to that applied to the methylbenzenes. We used the aromatic carbon–carbon bond strength, c_b, and the carbon–hydrogen bond strength, t_b, as calculated from the data for methylbenzenes. A value for the hydroxide group contribution to the heat of atomization was calculated from phenol. Values for the methyl group contributing in the three aromatic ring positions were obtained from the cresols. We then attempted to calculate the heat of atomization of the xylenols using these terms plus a correction term for ortho-methyl groups. The calculated heats of atomization so obtained were only a first approximation to the experimental values.

The additivity of the data available for methyl pyridines has been discussed by Cox (8), who gives an equation permitting heats of formation to be calculated for α- and γ-picoline, and for all the lutidines. The equation, which is equivalent to the scheme we attempted to apply to the phenols, cannot be applied to β-picoline, demonstrating that the data for methyl pyridines, like those for methyl phenols, are not additive in the sense described here.

From these results it seems reasonable to suppose that heat of formation data for aromatic compounds having a functional group within or attached to the aromatic

nucleus are not, in general, additive in the simple manner described here. The non-additivity of methyl pyridines is attributed (8) to hyperconjugation effects which stabilize α- and γ-picoline but not β-picoline. In the case of phenols we attribute the lack of additivity mainly to resonance and inductive effects which change considerably in going from cresols to xylenols.

The quantum mechanical approximation known as the linear combination of bond orbitals (LCBO) has been applied by Brown (9) to account for the additivity of heats of formation of paraffins. It would be useful if a similar treatment could be applied to aromatic compounds.

This work was supported by grant 1028–28 from the Defence Research Board.

REFERENCES

1. K. J. LAIDLER. Can. J. Chem. **34**, 626 (1956).
2. E. G. LOVERING and K. J. LAIDLER. Can. J. Chem. **38**, 2367 (1960).
3. T. L. ALLEN. J. Chem. Phys. **31**, 1039 (1959).
4. H. A. SKINNER. Anales. real soc. españ. fís. y quím. **56B**, 931 (1960).
5. S. M. SKURATOV and S. M. SHTEKHER. Doklady Akad. Nauk S.S.S.R. **137**, 109 (1961).
6. Selected values of physical and thermodynamic properties of hydrocarbons and related compounds. Carnegie Press, Pittsburgh. 1953.
7. R. J. L. ANDON, D. P. BIDDISCOMBE, J. D. COX, R. HANDLEY, D. HARROP, E. F. G. HERINGTON, and J. F. MARTIN. J. Chem. Soc. 5246 (1960).
8. J. D. COX. Trans. Faraday Soc. **56**, 959 (1960).
9. R. D. BROWN. J. Chem. Soc. 2615 (1953).

AMINO ACIDS

X. PREPARATION AND CHEMISTRY OF 2-(ω-CARBOXYALKYLAMINO)-DIHYDROTHIAZINES, -TETRAHYDROPYRIMIDINES, AND -IMIDAZOLINES[1, 2]

A. F. McKay and M.-E. Kreling
The L. G. Ryan Research Laboratories of Monsanto Canada Limited, Lasalle, Quebec

Received September 22, 1961

ABSTRACT

The preparation and properties of 3-keto-1,2,5,6-tetrahydro-3(H)-imidazo(1,2-*a*)imidazole, 3-keto-1,2,6,7-tetrahydro-3(H),5(H)-imidazo(1,2-*a*)pyrimidine, and 4-keto-2,3,6,7,8,9-hexahydro-4(H)-pyrimido(1,2-*a*)pyrimidine are described. The first two bicyclic systems possess active methylene groups in position 2 and they are oxidized to indigo-type dyes.

INTRODUCTION

The bicyclic compounds 3-keto-1,2,5,6-tetrahydro-3(H)-imidazo(1,2-*a*)imidazole* and 3-keto-1,2,6,7-tetrahydro-3(H),5(H)-imidazo(1,2-*a*)pyrimidine* were previously described (1). It has now been found that the original melting points given for these bicyclic compounds and their picrates are in error. Both of these compounds are readily oxidized and the presence of oxidation products in the original preparations is undoubtedly responsible for the high melting points previously reported. Both 3-keto-1,2,5,6-tetrahydro-3(H)-imidazo(1,2-*a*)imidazole and 3-keto-1,2,6,7-tetrahydro-3(H),5(H)-imidazo (1,2-*a*)pyrimidine may exist in the tautomeric forms I–IV. The presence of the pentad

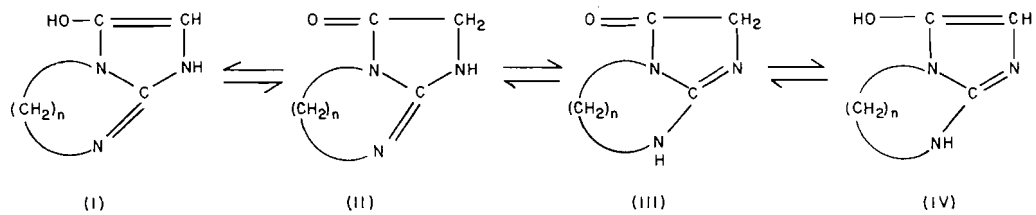

(I) (II) (III) (IV)

n = 2 or 3

system —C=N—CH_2—C=O is responsible for the mobility of the hydrogens at C_2. Further proof of the presence of an active methylene group was obtained by condensing these bicyclic compounds (I, n = 2 and 3) with benzaldehydes to form the corresponding 2-benzylidene derivatives (V).

A comparison of the tautomeric structures I–IV with indoxyl tautomeric structures VI–VIII indicates that the bicyclic compounds (I–IV, n = 2 and 3) would be expected to oxidize to indigo-type dyes, and the residues from the sublimation of the crude preparations of these bicyclic compounds did have typical dye properties. The dark blue residue from 3-keto-1,2,5,6-tetrahydro-3(H)-imidazo(1,2-*a*)imidazole gave a deep blue solution

[1]*Contribution No. 34.*
[2]*Amino Acids. IX, J. Org. Chem.* **23**, *1973 (1958).*
**Named in accordance with the rules on nomenclature of fused ring compounds, The Ring Index, Am. Chem. Soc. 2nd ed. 1960. These compounds were referred to as 3-keto-2,3,5,6-tetrahydro-1-imidaz(1,2-a)imidazole and 3-keto-Δ⁵-hexahydro-1,4,8-pyrimidazole respectively in reference 1.*

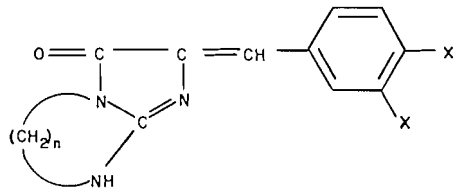

(V)

n = 2 or 3
X = H or Cl

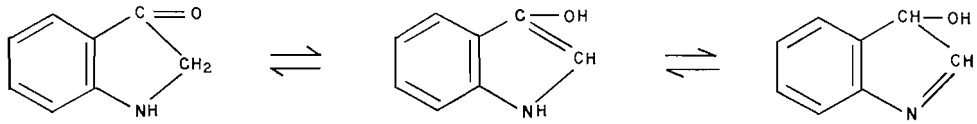

(VI) (VII) (VIII)

on dissolving in concentrated hydrochloric acid while the residue from 3-keto-1,2,6,7-tetrahydro-3(H),5(H)-imidazo(1,2-*a*)pyrimidine gave a wine-red acid solution. These highly colored materials possess high melting points and are very insoluble in the common organic solvents.

Lüttke's (2) molecular orbital calculations and studies on indigo, selenoindigo, thioindigo, etc., have demonstrated that the benzene nucleus is not necessary for the development of indigoid characteristics such as light absorption. The ring-free chromophore IX

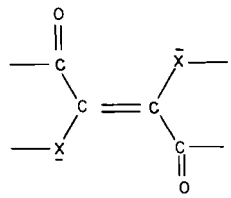

(IX)

X = NH or S

with the double, crossed auxochrome–antiauxochrome groups on a common —C=C— group is considered to be the simplest system which will exhibit the characteristic properties of indigo-type dyes. Thus the formation of dyes from the above bicyclic systems II is understandable.

When 2-carboxymethylamino-Δ^2-dihydro-1,3-thiazine was prepared by refluxing glycine and 2-methylmercapto-Δ^2-dihydro-1,3-thiazine in aqueous methanol, a deep blue-black metallic dye was formed as a by-product. It might be expected that this dye as well as those from compounds II, $n = 2$, and II, $n = 3$, would possess a structure X similar to indigo. However, the analytical values agree with structure XI. This problem of structure is still under investigation.

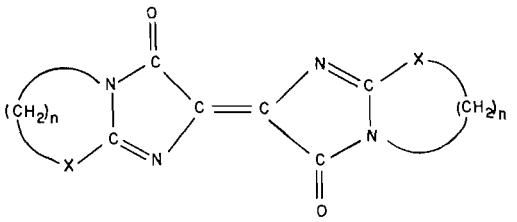

(X)

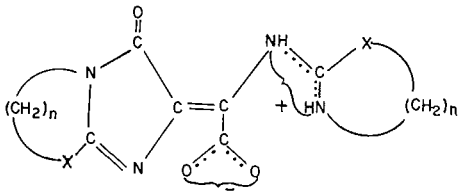

(XI)

DISCUSSION

The three bicyclic derivatives, 3-keto-1,2,5,6-tetrahydro-3(H)-imidazo(1,2-*a*)imidazole (II, $n = 2$), 3-keto-1,2,6,7-tetrahydro-3(H),5(H)-imidazo(1,2-*a*)pyrimidine (II, $n = 3$), and 4-keto-2,3,6,7,8,9-hexahydro-4(H)-pyrimido(1,2-*a*)pyrimidine (XII), have been prepared by an improved procedure. These compounds were finally purified by sublimation *in vacuo* under nitrogen. Special care was required in the isolation of compound XII,

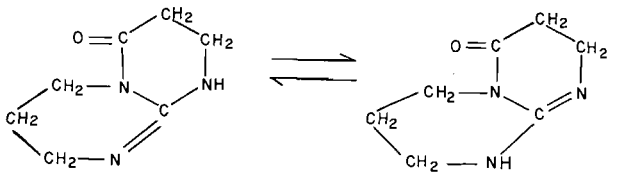

(XII)

which hydrolyzed extremely rapidly to the parent acid, 2-(2-carboxyethylamino)-Δ^2-tetrahydropyrimidine.

An attempt to prepare an analogous bicyclic compound from 2-methylmercapto-5,6-dihydro-4(H)-1,3-oxazine (XIII) and glycine was unsuccessful. This oxazine derivative was not very reactive in comparison with 2-methylmercapto-2-imidazolines (3) and 2-methylmercapto-2-thiazolines (4). After prolonged heating of compound XIII with benzylamine and α-naphthylmethylamine only small yields (10–13%) of the respective 2-benzylamino- (X, R = C_7H_7) and 2-α-naphthylmethylamino-5,6-dihydro-4(H)-1,3-oxazine (X, R = $C_{11}H_9$) were obtained.

Several methods were investigated for the preparation of 3,4,5,6-tetrahydro-2(H)-1,3-oxazine-2-thione. Two of these gave the desired compound in approximately 34% yield.

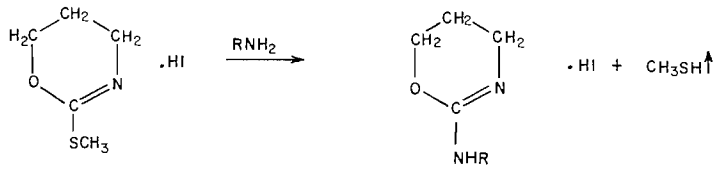

(XIII) (XIV)

On the other hand the procedure used by Fisher (5) for the preparation of 4,4,6-trimethyl-2-thio-tetrahydro-1,3-oxazine gave a 77% yield of 1,3-di-(3-hydroxypropyl)-thiourea and a 20.5% yield of potassium 3-hydroxypropyldithiocarbamate. 1,3-Di-(3-hydroxypropyl)-thiourea was also obtained when 3-amino-1-propanol was heated with carbon disulphide in ethanol for several hours.

3-Keto-1,2,5,6-tetrahydro-3(H)-imidazo(1,2-*a*)imidazole (II, $n = 2$), on being heated under reflux with absolute ethanolic hydrogen chloride for 17 hours, gave a 66% yield of 2-carbethoxymethylamino-2-imidazoline. The other bicyclic compounds II, $n = 3$, and XII were much more stable towards ethanolic hydrogen chloride solution. After 3-keto-1,2,6,7-tetrahydro-3(H),5(H)-imidazo(1,2-*a*)pyrimidine was heated in this reagent for 6 days, 72.3% was recovered unchanged. Compound XII, on being heated with ethanolic hydrogen chloride for 7.5 days, gave 30% of 2-(2-carbethoxyethylamino)-Δ^2-tetrahydropyrimidine and 18% unchanged starting material.

2-(N-3,4-Dichlorobenzylcarbamyl)-methylamino-2-imidazoline was prepared by heating bicyclic compound II, $n = 2$, with ethanolic benzylamine solution.

EXPERIMENTAL*

2-Carboxymethylamino-2-imidazoline

2-Carboxymethylamino-2-imidazoline (m.p. 283° decomp.) was prepared in 86% yield as previously described (1) from 2-methylmercapto-2-imidazolinium iodide, aqueous sodium hydroxide solution, and glycine. The reported (1) melting point is 293° with decomposition.

3-Keto-1,2,5,6-tetrahydro-3(H)-imidazo(1,2-a)imidazole

2-Carboxymethylamino-2-imidazoline (15 g, 0.105 mole) was heated under reflux with hydrogen chloride (11.5 g, 0.315 mole) in absolute ethanol (250 ml) for 3 hours. Benzene (50 ml) was added and the solution was heated for an additional hour. The benzene–water–ethanol azeotrope was distilled and the remaining ethanol solution was again treated with benzene. The removal of benzene–water–ethanol was repeated three times, after which the ethanolic solution was taken to dryness *in vacuo*.

The crude, oily ester hydrochloride in absolute methanol (400 ml) was passed through a column of IRA 400 resin (300 ml in hydroxyl form) which had been previously washed thoroughly with absolute methanol. The column was washed with methanol (300 ml) until the methanol washings were neutral and the combined eluate and washings were evaporated *in vacuo* to dryness. The yellowish crystalline solid melted at 165–170°, yield 9.5 g (72.6%). Crystallization from a minimum amount of ethanol in the presence of Norite gave colorless crystals melting at 168–170°, yield 5.56 g (42.4%). A sample was sublimed at 145–155° *in vacuo* (0.2 mm). The white crystalline sublimate melted at 169–170°. Anal. calc. for $C_5H_7N_3O$: C 48.00, H 5.64, N 33.59%; found: C 47.80, H 5.68, N 33.59%.

The picrate (m.p. 180–181°) was prepared in 86.2% yield in the usual manner with ethanolic picric acid solution. One crystallization from absolute ethanol raised the melting point to 180.5–181.5°. Anal. calc. for $C_{11}H_{10}N_6O_8$: C 37.30, H 2.85, N 23.73%; found: C 37.29, H 2.94, N 23.60%.

Opening One Ring of 3-Keto-1,2,5,6-tetrahydro-3(H)-imidazo(1,2-a)imidazole

A. With Ethanolic Hydrogen Chloride

A solution of 3-keto-1,2,5,6-tetrahydro-3(H)-imidazo(1,2-*a*)imidazole (0.2 g, 0.0016 mole) in ethanolic hydrogen chloride (0.063 g, 0.0017 mole) was refluxed for 17 hours. This solution on treatment with ethanolic picric acid solution gave a 66% yield of 2-carbethoxymethylamino-2-imidazoline picrate (m.p. 190.5–191.5°). The reported (1) melting point is 193–195°.

**All melting points are uncorrected. Microanalyses were determined by Micro-Tech Laboratories, Skokie, Ill.*

B. With 3,4-Dichlorobenzylamine

3,4-Dichlorobenzylamine (0.35 g, 0.002 mole) and 3-keto-1,2,5,6-tetrahydro-3(H)-imidazo(1,2-*a*)-imidazole (0.25 g, 0.002 mole) in absolute ethanol (6 ml) was refluxed for 2 hours. The reaction mixture was evaporated to dryness and the solid product was crystallized from water in the presence of Norite, yield 0.26 g (43.3%). Two crystallizations from water raised the melting point of the 2-(N-(N'-3,4-dichlorobenzylcarbamylmethyl)amino)-2-imidazoline from 155° to 156–157°. Anal. calc. for $C_{12}H_{14}Cl_2N_4O$: C 47.84, H 4.69, Cl 23.54, N 18.60%; found: C 47.80, H 4.89, Cl 23.10, N 18.41%.

A sample in ethanol, on treatment with ethanolic picric acid, gave a 98% yield of a crystalline picrate (m.p. 195–196°). The melting point remained unchanged after crystallization from absolute ethanol. Anal. calc. for $C_{18}H_{17}Cl_2N_7O_8$: C 40.77, H 3.23, Cl 13.37, N 18.49%; found: C 40.60, H 3.48, Cl 13.47, N 18.11%.

2-Methylmercapto-Δ^2-tetrahydropyrimidine

2-Methylmercapto-Δ^2-tetrahydropyrimidinium iodide (6.45 g, 0.025 mole) in water (10 ml) at 0° was treated with an aqueous solution of potassium hydroxide (1.4 g, 0.025 mole in 5 ml water). This solution was extracted with ether (10×100 ml) and the combined ether extracts were dried over anhydrous sodium sulphate. Evaporation of the ether gave a 82.4% yield of the free base (m.p. 89–90°). The melting point of 2-methylmercapto-Δ^2-tetrahydropyrimidine was not changed by crystallization from acetone–hexane solution. Anal. calc. for $C_5H_{10}N_2S$: C 46.13, H 7.74, N 21.53, S 24.63%; found: C 46.35, H 7.74, N 21.94, S 24.78%.

The picrate (m.p. 179.5–180.5°) was formed in the usual manner from water, yield 94%. Anal. calc. for $C_{11}H_{13}N_5O_7S$: C 36.76, H 3.65%; found: C 36.88, H 3.81%.

2-Carboxymethylamino-Δ^2-tetrahydropyrimidine

The original procedure (1) for the preparation of 2-carboxymethylamino-Δ^2-tetrahydropyrimidine was modified because the product was difficult to isolate and purify.

An intimate mixture of 2-methylmercapto-Δ^2-tetrahydropyrimidine (19.53 g, 0.15 mole) and glycine (11.26 g, 0.15 mole) was heated in an oil bath at 90° for 50 minutes. After the mixture melted, white crystals began to form. The heating was continued for 35 minutes at 130°. After the crystalline product had cooled, *n*-amyl alcohol (20 ml) was added and the mixture was refluxed for 60 minutes. The crystalline solid (m.p. 212–214°) was removed by filtration, yield 71.6%. Two crystallizations from aqueous ethanol raised the melting point to 219–220° (reported (1) m.p. 211.5–212°).

2-Carbethoxymethylamino-Δ^2-tetrahydropyrimidine Hydrochloride

This compound was prepared in quantitative yield by the procedure given (1) for the esterification of 2-carboxymethylamino-2-imidazoline. The crude 2-carbethoxymethylamino-Δ^2-tetrahydropyrimidine hydrochloride (m.p. 162–168°) was used to prepare 3-keto-1,2,6,7-tetrahydro-3(H),5(H)-imidazo(1,2-*a*)-pyrimidine.

3-Keto-1,2,6,7-tetrahydro-3(H),5(H)-imidazo(1,2-a)pyrimidine

A solution of 2-carbethoxymethylamino-Δ^2-tetrahydropyrimidine hydrochloride (18.6 g, 0.084 mole) in absolute methanol (370 ml) was passed through a column of IRA 400 resin (300 ml in hydroxyl form) which had been previously washed with methanol. The column was washed with absolute methanol (450 ml) and the eluate and washings were combined. The elution and washing procedures were carried out under nitrogen. The crude product from the evaporation of eluate and washings was dissolved in absolute ethanol (60 ml). A mixture of yellow, red, and white crystals separated from the solution on cooling to −10°, yield 5.85 g (50.2%). This crude mixture melted at 157–168°. Concentration of the mother liquors to a small volume gave an orange-colored microcrystalline powder (m.p. >350°), yield 0.15 g.

The first crop of mixed crystals (3.28 g) was sublimed *in vacuo* (0.2 mm) at a bath temperature of 150–160°. The white crystalline sublimate melted at 179.5–180° in an evacuated capillary tube, yield 2.92 g (89%). Resublimation did not change the melting point. Anal. calc. for $C_6H_9N_3O$: C 51.78, H 6.52, N 30.20%; found: C 51.73, H 6.51, N 30.18%.

The picrate (m.p. 193.8–194.8°) was prepared in 97.2% yield from ethanol solution. Anal. calc. for $C_{12}H_{12}N_6O_8$: C 39.14, H 3.29, N 22.82%; found: C 39.36, H 3.55, N 22.39%.

Treatment of 3-Keto-1,2,6,7-tetrahydro-3(H),5(H)-imidazo(1,2-a)pyrimidine with Ethanolic Hydrogen Chloride

3-Keto-1,2,6,7-tetrahydro-3(H),5(H)-imidazo(1,2-*a*)pyrimidine (0.35 g, 0.0025 mole) was heated under reflux in absolute ethanol containing hydrogen chloride (0.006 mole) for 6 days. Evaporation of the solvent left a semicrystalline hygroscopic mass (0.43 g). A portion (0.15 g) of the crude product in absolute ethanol was converted to its picrate (m.p. 189°) in the usual manner, yield 0.23 g (72.3%). This picrate did not depress the melting point of a known sample of 3-keto-1,2,6,7-tetrahydro-3(H),5(H)-imidazo(1,2-*a*)-pyrimidine picrate (m.p. 193°).

The original crude product was crystallized twice from ethanol–ether solution to give crystals (m.p. 209–210° (block), 214–215° (evac. cap.)) of the hydrochloride of the original bicyclic compound. Anal. calc. for $C_6H_{10}ClN_3O$: C 41.04, H 5.74, Cl 20.19, N 23.93%; found: C 40.87, H 5.68, Cl 20.28, N 23.80%.

2-(2-Carboxyethylamino)-Δ²-tetrahydropyrimidine

2-Methylmercapto-Δ²-tetrahydropyrimidine (28 g, 0.215 mole) and β-alanine (19.15 g, 0.215 mole) were mixed thoroughly and heated at 90° for 20 minutes. After the reaction mixture had melted, crystals began to sublime onto the cooler sides of the reaction flask. The temperature was raised to 105° and held at this temperature for 1 hour after which it was heated at 130° for 30 minutes. Ethanol (35 ml) was added to the solidified mass after it had cooled and the reaction mixture was refluxed for 4.6 hours. The white solid (m.p. 209.5–210°) was removed by filtration, yield 21.6 g (58.9%). This acid was very difficult to free from solvent and the melting point varied considerably on recrystallization from aqueous or anhydrous solvents. Thus the picrate (m.p. 164–165°) was formed in 60.6% yield in the usual manner from absolute ethanol. Crystallization from ethanol did not change the melting point. Anal. calc. for $C_{13}H_{16}N_6O_9$: C 39.00, H 4.03, N 21.00%; found: C 39.02, H 4.10, N 20.82%.

An attempt to purify a sample of 2-β-carboxyethylamino-Δ²-tetrahydropyrimidine by sublimation *in vacuo* at 170° gave a sublimate which melted at 120–123°. This sublimate in ethanol yielded a picrate in 39.1% yield melting at 212–213°. Two crystallizations from absolute ethanol raised the melting point to 214–215°. This picrate did not depress the melting point (214–215°) of 4-keto-2,3,6,7,8,9-hexahydro-4(H)-pyrimido(1,2-*a*)pyrimidine picrate (*vide infra*).

4-Keto-2,3,6,7,8,9-hexahydro-4(H)-pyrimido(1,2-a)pyrimidine

2-(2-Carboxyethylamino)-Δ²-tetrahydropyrimidine (10.01 g, 0.058 mole) was converted in quantitative yield into the hydrochloride salt of its ethyl ester by the procedure previously (1) described. A portion of the colorless oil in alcohol was converted into its picrate (m.p. 117°, resolidified and remelted at 128°) in 76.7% yield. Two crystallizations from absolute ethanol raised the melting point to 121° with resolidification and remelting at 136°. Anal. calc. for $C_{15}H_{20}N_6O_9$: C 42.06, H 4.71, N 19.62%; found: C 42.39, H 4.69, N 19.71%.

2-(2-Carbethoxyethylamino)-Δ²-tetrahydropyrimidine hydrochloride (13.8 g, 0.58 mole) in absolute methanol (250 ml) was passed through IRA 400 resin and the product was recovered. The procedure was the same as described above for the cyclization of 2-carbethoxymethylamino-Δ²-tetrahydropyrimidine hydrochloride to 3-keto-1,2,6,7-tetrahydro-3(H),5(H)-imidazo(1,2-*a*)pyrimidine. The crude product sintered at 110° and melted at 176–188°, yield 8.7 g.

The crude product was sublimed *in vacuo* (0.2 mm) at 120–130°, yield 3.34 g (38.4%). The sublimate of 4-keto-2,3,6,7,8,9-hexahydro-4(H)-pyrimido(1,2-*a*)pyrimidine melted at 127°. Two further sublimations did not change the melting point. This bicyclic compound hydrolyzed extremely rapidly and it was not possible to obtain an analytical sample free from traces of the parent acid, 2-(β-carboxyethylamino)-Δ²-tetrahydropyrimidine. Anal. calc. for $C_9H_{11}N_3O$: N 27.43%; found: N 26.60%. The sublimate in absolute ethanol gave a crystalline picrate (m.p. 214–215°) of 4-keto-2,3,6,7,8,9-hexahydro-4(H)-pyrimido(1,2-*a*)pyrimidine in 91.4% yield. Anal. calc. for $C_{13}H_{14}N_6O_8$: C 40.84, H 3.69, N 21.98%; found: C 40.73, H 3.70, N 22.08%.

Treatment of 4-Keto-2,3,6,7,8,9-hexahydro-4(H)-pyrimido(1,2-a)pyrimidine with Ethanolic Hydrogen Chloride

The bicyclic compound (0.17 g, 0.001 mole) in absolute ethanol containing hydrogen chloride (0.003 mole) was heated under reflux for 7.5 days. Evaporation of the solvent gave a viscous colorless oil which partially crystallized on standing in an evacuated desiccator for several days. A portion (0.09 g) of the product on treatment with ethanolic picric acid solution gave a crystalline picrate (m.p. 208–213°), yield 18.2%. One crystallization from ethanol raised the melting point to 214–215°. It did not depress the melting point of a known sample of 4-keto-2,3,6,7,8,9-hexahydro-4(H)-pyrimido(1,2-*a*)pyrimidine picrate (m.p. 214–215°) on admixture.

The mother liquor from the bicyclic picrate on concentration and cooling gave a second picrate (m.p. 121°, resolidification with remelting at 136–137°), yield 0.05 g (30.6%). This picrate was identified as the picrate of 2-(2-carbethoxyethylamino)-Δ²-tetrahydropyrimidine (m.p. 121° and 136–137°).

Benzylidene Derivative of 3-Keto-1,2,5,6-tetrahydro-3(H)-imidazo(1,2-a)imidazole

3-Keto-1,2,5,6-tetrahydro-3(H)-imidazo(1,2-*a*)imidazole (0.5 g, 0.004 mole), fused sodium acetate (0.58 g), and benzaldehyde (0.6 ml, 0.006 mole) in glacial acetic acid were heated in an oil bath at 140° for 75 minutes. The solution became dark orange in color and after 15 minutes yellow crystals separated. The mixture was allowed to cool to room temperature and the crystals (m.p. 266–274°) were collected by filtration, yield 0.45 g. A second crop (75 mg) of crystals was obtained from the mother liquors on further cooling, total yield 61.2%. Two crystallizations from absolute ethanol raised the melting point to 283.5–284.2°. Anal. calc. for $C_{12}H_{11}N_3O$: C 67.60, H 5.20, N 19.71%; found: C 67.33, H 5.37, N 20.17%. Ultraviolet absorption spectrum (in ethanol): λ_{max} 237 mμ, ε 11,350; λ_{max} 242 mμ (sh), ε 10,650; λ_{max} 347 mμ, ε 27,250.

The picrate (215–217° decomp.) was formed in the usual manner in ethanol solution, yield 38%. Two crystallizations from absolute ethanol raised the melting point to 217.4–218.2° decomp. Anal. calc. for $C_{18}H_{14}N_6O_8$: C 48.88, H 3.19, N 19.00%; found: C 48.94, H 3.33, N 18.51%.

Benzylidene Derivative of 3-Keto-1,2,6,7-tetrahydro-3(H),5(H)-imidazo(1,2-a)pyrimidine

Freshly sublimed 3-keto-1,2,6,7-tetrahydro-3(H),5(H)-imidazo(1,2-*a*)pyrimidine (0.51 g, 0.0037 mole), fused sodium acetate (0.61 g), and benzaldehyde (0.6 ml, 0.006 mole) in glacial acetic acid (4.5 ml) were refluxed for 75 minutes. After the solution was cooled in freezing mixture, crystals of sodium acetate separated, yield 0.27 g. The filtrate was taken to dryness *in vacuo* and the residue was extracted with water

to remove the remaining sodium acetate. The residue melted at 227–232°, yield 0.54 g (63.6%). Two crystallizations from absolute ethanol raised the melting point to 239.2–239.8°. Anal. calc. for $C_{13}H_{13}N_3O$: C 68.70, H 5.77, N 18.49%; found: C 68.21, H 5.83, N 18.50%. Ultraviolet absorption spectrum (in ethanol): λ_{max} 241 mμ, ε 13,600; λ_{max} 247 mμ (sh), ε 12,680; λ_{max} 365 mμ, ε 25,340.

The picrate (m.p. 217–219°) was prepared from ethanol solution in 90.6% yield. Two crystallizations from absolute ethanol raised the melting point to 223.4–224.2°. Anal. calc. for $C_{19}H_{16}N_6O_8$: C 49.99, H 3.53, N 18.42%; found: C 50.01, H 3.55, N 18.34%.

3,4-Dichlorobenzylidene Derivative of 3-Keto-1,2,6,7-tetrahydro-3(H),5(H)-imidazo(1,2-a)pyrimidine

This compound (m.p. 248–256° decomp.) was prepared in 91% yield by the procedure given above for the preparation of 2-benzylidene-3-keto-1,2,5,6-tetrahydro-3(H)-imidazo(1,2-*a*)imidazole. Two crystallizations from absolute ethanol raised the melting point to 265–266° decomp. Anal. calc. for $C_{13}H_{11}Cl_2N_3O$: C 52.73, H 3.74, Cl 23.94, N 14.19%; found: C 52.58, H 3.87, Cl 24.15, N 14.10%.

A crystalline picrate (m.p. 237–240° decomp.) was obtained in quantitative yield from ethanol solution. Two crystallizations from absolute ethanol raised the melting point to 246.2–246.6° decomp. Anal. calc. for $C_{19}H_{14}Cl_2N_6O_8$: C 43.44, H 2.69, Cl 13.50, N 16.00%; found: C 43.45, H 2.89, Cl 12.96, N 16.25%.

2-Carboxymethylamino-Δ^2-dihydro-1,3-thiazine

2-Methylmercapto-Δ^2-dihydro-1,3-thiazine (4) (17.68 g, 0.12 mole) and glycine (9.01 g, 0.12 mole) in methanol–water (1:1) solution (200 ml) were refluxed for 19 hours. The reaction mixture turned a deep blue color after the first few hours of heating. A dark blue crystalline solid (m.p. >360°) separated from the cooled solution, yield 3.53 g. This dye was virtually insoluble in all the common organic solvents. A dilute solution in hydrochloric acid was deep blue in color. Anal. calc. for $C_{12}H_{14}N_4O_3S_2$: C 44.25, H 4.33, N 16.67, S 19.65%; found: C 44.73, H 4.52, N 16.61, S 19.47%.

The filtrate, from which the dye had been removed, was evaporated to dryness. The residue was dissolved in hot methanol with the exception of a small amount (0.37 g) of blue dye. The filtrate from the blue dye, on cooling, gave a mixture of blue and white crystals (m.p. 170–173°), yield 6.49 g. The mother liquors yielded a second crop of crystals (m.p. 169–173°). The total yield of crude 2-carboxymethylamino-Δ^2-dihydro-1,3-thiazine was 9.87 g (46.8%). Two crystallizations from ethanol in the presence of Norite gave grey crystals melting at 174–175° (blue melt). Anal. calc. for $C_6H_{10}N_2O_2S.H_2O$: C 37.48, H 6.30, N 14.58, S 16.68%; found: C 37.29, H 6.41, N 14.82, S 16.42%.

The picrate (m.p. 159–160°, dark blue melt) was prepared in 82% yield in the usual manner from water. Anal. calc. for $C_{12}H_{13}N_5O_9S$: C 35.73, H 3.25, N 17.37, S 9.95%; found: C 36.01, H 3.33, N 17.28, S 7.72%.

3,4,5,6-Tetrahydro-2(H)-1,3-oxazine-2-thione

Method A

3,4,5,6-Tetrahydro-2(H)-1,3-oxazine-2-thione (m.p. 124–125°) was prepared in 34% yield by the method of Menard *et al.* (6).

Method B

A solution of carbon disulphide (31.2 g, 0.4 mole) in chloroform (80 ml) was added dropwise over a period of 40 minutes to a stirred solution of 3-amino-1-propanol (30 g, 0.4 mole) and triethylamine (40.4 g, 0.4 mole) in chloroform (80 ml) at 0°. This reaction mixture was stirred for 5 minutes at 25° and then cooled again to 0°. After ethyl chloroformate (43.2 g, 0.4 mole) was added over a period of 50 minutes, stirring was continued for 20 minutes. A solution of triethylamine (44.4 g, 0.44 mole) in chloroform (150 ml) was added during the next 50 minutes after which stirring was continued for 15 minutes. Then the chloroform solution was washed with 5% aqueous sodium hydroxide (2×150 ml), 5% hydrochloric acid (2×150 ml), and water (5×200 ml). After the chloroform solution was dried over anhydrous sodium sulphate and allowed to stand in the refrigerator for 15 minutes, it was evaporated to dryness. The crude yield of 3,4,5,6-tetrahydro-2(H)-1,3-oxazine-2-thione (m.p. 124–125°) was 15.6 g (33.3%). The structure of this compound was confirmed by its infrared spectrum, analyses, and molecular weight determination. The infrared spectrum of the compound dispersed in Nujol mull gave the following absorption bands: 3195 cm^{-1} (N—H stretching mode), 1573 cm^{-1} (N—H bending mode), and 1376 cm^{-1} (—N—C=S stretching mode (provisional assignment)). One crystallization from acetone raised the melting point to 126.5–127.5°. Anal. calc. for C_4H_7NOS: C 41.00, H 6.01, N 11.95, S 27.36%, mol. wt. 117.05; found: C 41.11, H 6.18, N 11.67, S 27.26%, mol. wt. (Rast) 119.

2-Methylmercapto-5,6-dihydro-4(H)-1,3-oxazine Hydroiodide

Methyl iodide (24.8 g, 0.17 mole) was added portionwise to a suspension of 3,4,5,6-tetrahydro-2(H)-1,3-oxazine-2-thione (15.8 g, 0.13 mole) in absolute ethanol (35 ml). The reaction mixture was heated under reflux for 45 minutes and then the clear solution was evaporated to dryness *in vacuo*. The crystalline residue was treated with cold absolute methanol (50 ml) and the insoluble residue was removed by filtration. Addition of water (20–25 ml) to the methanolic filtrate gave the crystalline product (m.p. 64.5–65.5°), yield 31.84 g (91.4%). Infrared spectrum of the compound in Nujol mull gave the following absorption bands: 3290 cm^{-1} (=N—H^+ stretching mode), 1638 cm^{-1} (C=NH^+ stretching mode), and 1536 cm^{-1} (=NH^+ bending mode). Anal. calc. for $C_5H_{10}INOS$: C 23.18, H 3.89, N 5.41, S 12.38%; found: C 23.15, H 3.78, N 5.08, S 11.94%.

2-Benzylamino-5,6-dihydro-4(H)-1,3-oxazine Picrate

2-Methylmercapto-5,6-dihydro-4(H)-1,3-oxazine hydroiodide (3.9 g, 0.015 mole) and benzylamine (1.6 g, 0.015 mole) in ethanol were refluxed for 17 hours. The solvent was removed *in vacuo* and the residual oil was dissolved in ethanol and treated with aqueous picric acid solution. The solvent was decanted from the oily picrate (yield 10.2%), which crystallized (m.p. 168–170°) on heating with fresh ethanol. Three crystallizations from ethanol raised the melting point to 172.5–173.5. Anal. calc. for $C_{17}H_{17}N_5O_8$: C 48.69, H 4.09, N 16.70%; found: C 48.33, H 4.13, N 16.73%.

A paper chromatogram of the residual oil from this reaction showed that very little reaction had taken place after the prolonged heating period.

2-(α-Naphthylmethylamino)-5,6-dihydro-4(H)-1,3-oxazine Picrate

A solution of α-naphthylmethylamine (2.3 g, 0.015 mole) and 2-methylmercapto-5,6-dihydro-4(H)-1,3-oxazine hydroiodide (3.9 g, 0.015 mole) in ethanol (12 ml) was heated under reflux for 26 hours. Evaporation of the solvent gave 5.53 g of a glasslike, solid mass. A sample (1.1 g) of this product in methanol was treated with aqueous picric acid solution. A mixture of oily and crystalline picrates formed. The crystals were collected by filtration and identified by a mixed melting point determination as α-naphthylmethylamine picrate (m.p. 226–228° decomp.). Treatment of the remaining oily picrate with boiling water (100 ml) and boiling methanol caused partial crystallization to occur. The crystals (m.p. 215–217°) were removed by filtration, yield 0.18 g (12.8%). Several crystallizations from methanol raised the melting point to 219–219.5°. Anal. calc. for $C_{21}H_{19}N_5O_8$: C 53.73, H 4.08, N 14.92%; found: C 53.80, H 4.34, N 14.85%.

1,3-Di-(2-hydroxypropyl)-thiourea

Method A

Carbon disulphide (22.84 g, 0.3 mole) in absolute ethanol (15 ml) was added to a cooled (5–10°) solution of 3-amino-1-propanol (22.53 g, 0.3 mole) in absolute ethanol (35 ml) over a period of 1 hour. The reaction mixture was heated at reflux for 7 hours and then the solvent was removed *in vacuo*. After the oily product had been heated at 110° for 8 hours, it was dissolved in absolute ethanol (50 ml) and heated under reflux for an additional 8 hours. The alcohol was removed *in vacuo* and the waxy solid (30 g, 85.5% yield) was crystallized from ethanol–ether solution. This crystalline product melted at 90.4–91°, yield 20.3 g. Anal. calc. for $C_7H_{16}N_2O_2S$: C 43.71, H 8.39, N 14.57, S 16.67%; found: C 43.58, H 8.33, N 14.19, S 16.68%.

Method B

3-Amino-1-propanol (62.7 g, 0.836 mole) was added to a solution of potassium hydroxide (16 g, 0.28 mole) in absolute ethanol (200 ml). Carbon disulphide (69.9 g, 0.92 mole) was added dropwise to this solution at 30° over a period of 1 hour. After standing at room temperature for 1.5 hours, the reaction mixture was heated under reflux (48°) for 3 hours. A small amount of unreacted carbon disulphide (6 ml) was removed by distillation and the residue was heated under reflux (72–76°) for 6 hours. The solution on standing at room temperature overnight deposited large prisms. The crystals (m.p. 148–152° decomp.) were recovered by filtration, yield 20.23 g. Evaporation of the ethanol filtrate *in vacuo* gave a yellow, mobile oil (95.5 g). Addition of acetone to this oil gave a second crop of the high-melting (150° decomp.) product. Careful fractional crystallization of the remainder with acetone and then hexane gave a total yield of 32.43 g (20.5% based on 3-amino-1-propanol) of the potassium salt of 3-hydroxypropyldithiocarbamic acid and 63.8 g (76.9%) of 1,3-di-(3-hydroxypropyl)-thiourea (m.p. 88–90°). The thiourea gave no depression in melting point on admixture with a sample of the 1,3-di-(3-hydroxypropyl)-thiourea (m.p. 90.4–91°) described above under Method A.

A portion of the crude potassium salt of 3-hydroxypropyldithiocarbamic acid was crystallized twice from warm ethanol–ether solution. The final melting point was 149.5–150.5° with decomposition. Anal. calc. for $C_4H_8KNOS_2$: C 25.37, H 4.26, N 7.40, S 33.87%; found: C 25.76, H 4.35, N 7.13, S 33.71%.

ACKNOWLEDGMENTS

The authors wish to thank Miss G. Schlauch for skillful technical assistance. The preparation of 2-carboxymethylamino-Δ^2-dihydro-1,3-thiazine was performed by Dr. D. J. Whittingham.

REFERENCES

1. A. F. McKay and W. G. Hatton. J. Am. Chem. Soc. **78**, 1618 (1956).
2. W. Lüttke. Angew. Chem. **72**, 421 (1961).
3. A. F. McKay and D. L. Garmaise. Can. J. Chem. **35**, 8 (1957).
4. A. F. McKay, D. J. Whittingham, and M.-E. Kreling. J. Am. Chem. Soc. **80**, 3339 (1958).
5. H. L. Fisher. U.S. Patent No. 2,326,732 (August 10, 1943).
6. M. Menard, A. M. Wrigley, and F. L. Chubb. Can. J. Chem. **39**, 273 (1961).

AROMATIC SUBSTITUTION

PART I. THE REACTION OF PHENYLLITHIUM WITH 3-ALKYLPYRIDINES. STERIC EFFECT AND QUANTITATIVE ANALYSIS OF ISOMER RATIOS[1]

R. A. Abramovitch and Choo-Seng Giam
The Department of Chemistry, University of Saskatchewan, Saskatoon, Saskatchewan

Received September 26, 1961

ABSTRACT

No 4-phenylpyridine is formed in the reaction of phenyllithium with pyridine. When phenyllithium reacts with a 3-alkylpyridine the main product is the 3-alkyl-2-phenylpyridine if the alkyl group is methyl, ethyl, or isopropyl, but it is the 5-alkyl-2-phenylpyridine when the substituent is *t*-butyl. Methods are described for the separation and quantitative analysis of mixtures of 3-alkyl- and 5-alkyl-2-phenylpyridines using vapor phase chromatography. The results are discussed briefly and possible explanations of the observed orientations are mentioned.

The well-known (1, 2) reaction of lithium alkyls and aryls with dry pyridine involves the formation of a dihydroderivative (I) which, on heating, eliminates lithium hydride to give the 2-substituted pyridine (3):

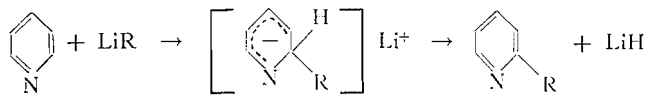

I

The formation of a 4-substituted pyridine has not been reported in such reactions except in those cases where the 2- and 6-positions of the pyridine ring are blocked, e.g. the case of acridine (4). It has now been verified that in the reaction of phenyllithium with pyridine no 4-phenylpyridine can be detected, even by vapor phase chromatography. Thus, the addition of an organo-lithium compound to a 3-substituted pyridine may lead to one isomer, or a mixture of two isomers:

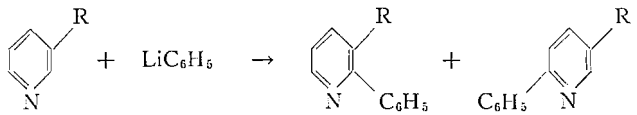

II III IV

In two earlier papers (5, 6) the reaction of phenyllithium with a number of 3-substituted pyridines was examined. When 3-picoline (II; R = CH_3) was treated with phenyllithium the ratio of 2,3:2,5 isomers was found to be 19:1. With nicotine (II; R = 2-*N*-methylpyrrolidyl) the isomer ratio was approximately 1:1. Two further examples were studied: R = NH_2 and R = OCH_3. In both cases the only isomer detected was the 2,3-disubstituted pyridine. It was suggested (6) that in these last two cases the exclusive substitution at the 2-position might be explained by assuming some co-ordination of the lithium atom with a pair of electrons on the 3-substituent such that the phenyl group would be suitably oriented for attack at the 2-position.

[1]*This paper was presented as part of a lecture given at the Stereochemistry Symposium of the C.I.C. at Edmonton in September 1960.*

The preferential attack of the 2-position by the nucleophilic reagent in these and other reactions (for a brief summary of previous work on related reactions see ref. 5) was contrary to what would have been predicted a priori on the basis of a consideration of straightforward electronic and steric effects of the substituents studied. One would expect the 2-position to be somewhat more electron rich than the 6-position and also that attack at that site would be subject to the steric effect of the 3-substituent. That the 3-substituent does exert a steric effect is shown by a comparison of the isomer ratios for the reactions of 3-picoline and of nicotine. Appreciable steric hindrance by an ortho-methyl group in nucleophilic aromatic substitutions has also been observed in the reaction of 1-chloro-2,4-dinitro-6-methylbenzene with piperidine (7), though the geometry of the transition state is probably different from that in our reactions, which involve a more powerful nucleophilic reagent in a less polar solvent. It seems likely that with the more powerful nucleophilic reagent the transition state would resemble the reactants and that its formation would not lead to too much perturbation of the π-electron densities in the ground state (8, 9) (in which case hyperconjugation by the 3-alkyl group would probably be small).

It was clearly of interest to examine the effect of increasing the size of the 3-alkyl group systematically from methyl to *t*-butyl upon the ratio of III:IV obtained and this has now been done.

EXPERIMENTAL

Melting points are uncorrected. Infrared spectra were measured with a Perkin–Elmer Model 21 instrument using sodium chloride optics; only the main peaks are reported. Vapor phase chromatography was carried out with a Beckman GC-2 unit fitted with a fraction collector and modified such that the heated sample inlet block permitted injection as close to the column as possible.

Preparation of 3-Alkylpyridines

3-Picoline was commercially available synthetic material (Reilly Tar and Chemical Corp.); this was dried (KOH) and distilled through a Podbielniak Mini-Cal Spinning Band Column, the fraction b.p. 138–140° at 720 mm being used.

3-Ethylpyridine was prepared by the alkylation of 3-picoline as described by Brown and Murphey (10). An average yield of 50.4% was obtained. However, even after several fractional distillations through a Podbielniak column, the 3-ethylpyridine could not be isolated in a completely pure state; it was always contaminated with small amounts of 3-picoline and 3-isopropylpyridine, as indicated by vapor phase chromatography. Since the 3-ethylpyridine required had to be essentially free of these contaminants it was prepared from 3-acetylpyridine using hydrazine hydrate and potassium hydroxide (11). A yield of 83.5% of pure product was thus obtained.

3-Isopropylpyridine was obtained initially as a by-product of the alkylation of 3-picoline (average yield 10%). When 3-ethylpyridine was the starting material the average yield was raised to 55%; the product, however, could not be freed from 3-ethylpyridine completely by fractional distillation. Pure 3-isopropylpyridine was, therefore, prepared from methyl nicotinate by treating the latter with methyl magnesium iodide (12), dehydrating the alcohol obtained with a mixture of concentrated sulphuric acid and acetic acid (10), and hydrogenating the resulting 3-isopropenylpyridine (in solution in a mixture of glacial acetic acid (1 part) and 95% ethanol (4 parts)) at 25 p.s.i. and room temperature in the presence of Adams' catalyst.

3-*t*-Butylpyridine was prepared by a modification (13) of the method for the alkylation of 3-isopropylpyridine. The time of addition of the methyl chloride was extended to 13 hours. In no case could a conversion of more than 10% be achieved, though Professor Brown informs us that he has obtained yields as high as 37%. Essery and Schofield (14) have recently also been unable to obtain such a high yield using potassium amide instead of sodamide in liquid ammonia. In spite of repeated and careful fractional distillations the product obtained was only 95% pure and had to be used as such in subsequent reactions with phenyllithium.

2-Phenylpyridine (2)

A solution of pyridine (0.93 g) in dry ether (2 ml) was added to a well-stirred, standardized ethereal solution of phenyllithium (6 ml, 0.007 mole) under nitrogen and worked up by the general procedure described below. The crude reaction product was subjected to vapor phase chromatography on a column 3 ft$\times\frac{1}{4}$ in. of "Apiezon N" on "Embacel" (May and Baker), the column temperature being 190° and the helium inlet pressure 50 p.s.i. The product had the same retention time as authentic 2-phenylpyridine (8 minutes, 10 seconds). No peak corresponding to 4-phenylpyridine (9 minutes, 30 seconds) was observed. It was verified that small amounts of 4-phenylpyridine would have been detected by this method by analyzing made-up mixture of authentic samples of 2- and 4-phenylpyridine. Purification of the crude reaction product gave 2-phenylpyridine (0.76 g; 69%).

Reaction of Phenyllithium with 3-Alkylpyridines

The procedure described below was adopted for all the reactions of phenyllithium with 3-picoline, 3-ethyl-, 3-isopropyl-, and 3-*t*-butyl-pyridine. The amounts of the reactants employed and the yields of products obtained are summarized in Table I.

TABLE I

Reaction of phenyllithium with 3-alkylpyridines

Expt. No.	3-Alkyl substituent	Wt. of lithium (g)	Wt. of bromobenzene (g)	Wt. of 3-alkylpyridine (g)	Total % yield of both isomers
1	CH_3	30.0	313.8	204	(*b*)
2	CH_3	0.15	1.05	1.02	41.6
3	CH_3	0.15	1.05	1.02	25.0
4	CH_3	(*a*)	(*a*)	(*a*)	41.6
5	C_2H_5	6.9	52.5	58.9	20.5
6	C_2H_5	0.15	1.05	1.10	22.9
7	C_2H_5	0.15	1.05	1.10	18.0
8	C_2H_5	(*a*)	(*a*)	(*a*)	39.4
9	iso-C_3H_7	0.28	2.1	2.66	(*b*)
10	iso-C_3H_7	3.8	28.8	33.2	15.0
11	iso-C_3H_7	(*a*)	(*a*)	(*a*)	25.2
12	*t*-C_4H_9	0.30	2.1	2.96	22.5
13	*t*-C_4H_9	1.89	13.1	18.7	25.0
14	*t*-C_4H_9	(*a*)	(*a*)	(*a*)	24.2

NOTE: (*a*) In these experiments, 0.007 mole of phenyllithium and 0.010 mole of 3-alkylpyridine were used. (*b*) Yields in these experiments were not determined.

Very finely cut lithium was suspended in anhydrous ether (approximately 300 ml for each mole of lithium) under dry nitrogen and to this was added dropwise a solution of bromobenzene in an equal volume of dry ether. Gentle reflux was continued for 3 hours after which a solution of the 3-alkylpyridine in dry ether was added dropwise so that boiling under gentle reflux was maintained. When the addition was completed the ether was distilled off and simultaneously replaced by an equal volume of dry toluene. The temperature of the reaction mixture was then raised to ca. 110° and kept there for 7½ hours. The mixture was cooled, treated cautiously with an excess of water, and exhaustively extracted with ether. The ether extract was dried (KOH) and the solvent removed by distillation. The residue was divided into two portions, the larger one being used for the isolation and identification of the reaction products and the smaller being used for the quantitative analyses of the isomeric alkylphenylpyridines.

Isolation of the 3-Alkylpyridines

The isomeric alkylphenylpyridines were separated and isolated by preparative vapor phase chromatography. In experiments (1) and (2) a copper tubing column 5½ ft × ¼ in. (I.D.) packed with "Apiezon N" on "Embacel" Kieselguhr (1:4 by weight) was used. In all the other experiments, four 10-in. columns (½ in. I.D.) connected in series and packed with "Apiezon N" on Celite 545 (1:4 by weight) were used.

Differentiation between 3-Alkyl- and 5-Alkyl-2-phenylpyridines by Infrared Spectroscopy

The isomeric alkylphenylpyridines could be characterized by using their infrared spectra as described by Abramovitch, Giam, and Notation (15). The 3-alkyl-2-phenylpyridines exhibited a characteristic absorption band in the range 1577–1589 cm^{-1}, and the 5-alkyl-2-phenylpyridines gave a band in the range 1592–1605 cm^{-1}. Assignment of orientation could also be made from a study of the range 900–750 cm^{-1} as discussed by Podall (16).

Some of the assignments were confirmed by oxidation of the isomers to known compounds and by the behavior on vapor phase chromatography (see below). In the case of the methylphenylpyridines n.m.r. spectroscopy has also been used (5).

3-Ethyl-2-phenylpyridine

B.p. 156–158° at 18 mm. Infrared spectrum (liquid film): 1583 (m), 1568 (m), 1435 (s), 1060 (m), 793 (s), 750 (s), 698 cm^{-1} (s). Calc. for $C_{13}H_{13}N$: C, 85.20; H, 7.15. Found: C, 85.26; H, 7.22. The product was identical with that obtained from authentic 3-methyl-2-phenylpyridine as described below. The picrate was recrystallized from benzene and had m.p. 104°. Calc. for $C_{13}H_{13}N,C_6H_3O_7N_3$: C, 55.34; H, 3.91. Found: C, 55.46; H, 3.96.

5-Ethyl-2-phenylpyridine

B.p. 179–180° at 22 mm. Infrared spectrum (liquid film): 1603 (m), 1567 (m), 1483 (s), 1440 (s), 842 (m), 793 (m), 742 (s), 695 cm^{-1} (s). Found: C, 84.81; H, 7.36. The picrate (from benzene) had m.p. 155–156°; found: C, 55.74; H, 4.04.

3-Isopropyl-2-phenylpyridine

B.p. 152–154° at 22 mm. Infrared spectrum (liquid film): 1580 (m), 1563 (m), 1436 (s), 1385 (m), 1367 (m), 793 (s), 750 (s), 698 cm^{-1} (s). Calc. for $C_{14}H_{15}N$: C, 85.23; H, 7.66. Found: C, 85.28; H, 7.61.

5-Isopropyl-2-phenylpyridine

White crystals, m.p. 53–53.5° (purified by sublimation after vapor phase chromatography). Infrared spectrum (Nujol mull): 1595 (m), 1561 (m), 842 (s), 787 (m), 737 (m), 693 cm^{-1} (s). Found: C, 85.17; H, 7.78.

3-t-Butyl-2-phenylpyridine

B.p. 140° at 18 mm. Infrared spectrum (liquid film): 1578 (w), 1561 (m), 1427 (s), 1395 (w), 1365 (m), 785 (s), 762 (s), 702 cm^{-1} (s). Calc. for $C_{15}H_{17}N$: C, 85.26; H, 8.11. Found: C, 84.90; H, 8.30.

5-t-Butyl-2-phenylpyridine

B.p. 130° at 0.72 mm. Infrared spectrum (liquid film): 1592 (m), 1535 (m), 1480 (s), 1377 (s), 1395 (w), 1365 (w), 845 (s), 750 (s), 730 (s), 690 cm^{-1} (s). Found: C, 85.32; H, 8.18.

A plot of the logarithm of the retention times against the number of carbon atoms in the side-chain alkyl groups in 3-alkyl-2-phenylpyridines gave a straight line as did the corresponding plot of the values for 5-alkyl-2-phenylpyridines. The slope of the latter line was greater than that of the former. This observed linearity in each case serves as confirmatory evidence for the orientation assigned to the various pairs of isomers.

Oxidation of 5-Ethyl-2-phenylpyridine

5-Ethyl-2-phenylpyridine was boiled under reflux with an aqueous solution of potassium permanganate for 8 hours and worked up as described for the oxidation of 3-methyl-2-phenylpyridine (5). 2-Phenylpyridine-5-carboxylic acid, m.p. 232°, was obtained. The melting point was undepressed on admixture with an authentic specimen of this acid (5).

Synthesis of 3-Ethyl-2-phenylpyridine

3-Methyl-2-phenylpyridine (6.9 g) was added to a suspension of sodamide in liquid ammonia (2.3 g of sodium in 80 ml of anhydrous ammonia and 0.03 g of ferric nitrate nonahydrate), followed by methyl chloride (5 g), the addition of the latter taking approximately 15 minutes. The mixture was allowed to stand overnight when the ammonia evaporated and the residue was cautiously treated with water and exhaustively extracted with ether. The ether extract was dried (KOH), the solvent evaporated, and the residue fractionally distilled under vacuum. The fraction b.p. 110–143° at 11 mm was subjected to vapor phase chromatography using a copper column, $5\frac{1}{2}$ ft$\times\frac{1}{4}$ in. (I.D.), packed with "Apiezon N" on "Embacel" (1:4 by weight), the column temperature being 220°. A compound having the same "emergence time" (the time taken for the compound to begin entering the detector cell) as the sample of 3-ethyl-2-phenylpyridine obtained from the reaction of phenyllithium with 3-ethylpyridine was isolated. This compound had an infrared spectrum identical with that of the compound which had been assigned the structure 3-ethyl-2-phenylpyridine on the basis of its infrared spectrum. Both samples formed picrates whose melting points (102–103°) were undepressed on admixture. In the alkylation reaction a 33% conversion of 3-methyl-2-phenylpyridine to 3-ethyl-2-phenylpyridine (2.2 g) was achieved.

Quantitative Analyses

Once the various isomeric alkylphenylpyridines had been isolated and characterized calibration curves were prepared for each individual isomer so that its concentration in a mixture could be estimated from the area under the curve of its vapor phase chromatogram. A linear plot of the areas of their chromatograms versus concentration was obtained for the individual isomers as well as for a number of made-up mixtures of known concentrations of isomeric pairs. The concentrations of the isomers formed during the phenylation reactions could then be read off from the calibration curves, provided the conditions established for the chromatographic analysis of each pair of isomers were kept constant. These conditions are summarized below:

Methylphenylpyridines: $5\frac{1}{2}$ ft$\times\frac{1}{4}$ in. (I.D.) copper tube packed with "Apiezon N" on "Embacel" (1:4 by weight); column temperature 220°; helium inlet pressure 30 p.s.i.

Ethylphenylpyridines: same conditions as for methylphenylpyridines.

Isopropylphenylpyridines: 2 ft$\times\frac{1}{4}$ in. (I.D.) copper tube packed with "Apiezon N" on Celite 545 (1:4 by weight); column temperature 220°; helium inlet pressure 40 p.s.i.

t-Butylphenylpyridines: 3 ft$\times\frac{1}{4}$ in. (I.D.) copper tube packed with "Apiezon N" on "Embacel" (1:4 by weight); column temperature 220°; helium inlet pressure 30 p.s.i.

The results of the quantitative analyses are summarized in Table II, which also contains the data for the reaction of nicotine with phenyllithium (5).

DISCUSSION OF RESULTS

The results given in Table II indicate that the 3-substituent exerts a slight steric effect which becomes quite large when the alkyl group is *t*-butyl. The sudden great increase in steric hindrance to attack at the 2-position on passing from 3-iso-C_3H_7 to 3-*t*-Bu is unexceptional

TABLE II
Ratio of III:IV in the reaction of C_6H_5Li with 3-RC_5H_4N

R	III:IV	No. of runs
CH_3	94.6:5.4 (±0.6)	4
C_2H_5	84.0:16.0 (±0.5)	4
iso-C_3H_7	70.0:30.0 (±4.0)	3
t-C_4H_9	4.5:95.5 (±0.5)	3
2-*N*-Methylpyrrolidyl (5)	49.6:50.4 (±0.2)	2

(17). The fact that the steric effect of the lower alkyl group is only relatively small seems to confirm the suggestion made above that in the transition state leading to the formation of the dihydroderivative the attacking phenyl group is almost perpendicular to the pyridine ring, whose ground-state configuration is only slightly distorted. The results also indicate quite strikingly that in spite of the greater deactivating influence of the +I effect of the alkyl group on the 2- than on the 6-position and some steric hindrance to attack at the 2-position, addition of the nucleophilic reagent takes place preferentially at that carbon atom. In fact, in the case of 3-picoline the ortho/para ratio (with respect to methyl) is as high as 19. This "ortho" effect is reminiscent of those encountered in electrophilic substitutions on compounds bearing substituents such as —NO_2, —CO_2H, —CN, and so on. Similar results to those reported above have been obtained by Brown and his group but using methyllithium instead of phenyllithium (13).

No decision can be made as to the correct explanation of the observed substitution pattern since too little is known about the detailed mechanism of this addition–elimination reaction and the effect of various substituents upon the rates and orientation in such nucleophilic substitutions. Both of these aspects are presently under investigation in these laboratories and the results of such studies should permit a clearer formulation to be made of the mechanisms involved. It is of interest though, to speculate a little about possible explanations of the orientation observed.

There is only one published molecular orbital calculation of the π-electron densities at the various nuclear carbon atoms in the ground state of 3-picoline, that due to Ploquin (18). Dr. K. L. McEwen has kindly repeated for us Ploquin's calculation for several different values of the nitrogen and methyl group inductive parameters. The results indicate that the 2-position would be slightly more favorable than position 6 for nucleophilic attack only if a negative inductive effect (−I) is attributed to the methyl group. With a positive inductive effect attack at the 6-position would be favored over attack at the 2-position. The introduction of methyl hyperconjugation into the ground-state calculations made little difference to the results. The nucleophilic localization energies at C_2 and C_6 were not calculated but if the postulate that the geometry of the transition state is more related to that of the ground state than to that of the intermediate is correct then these would not enter into the picture. A −I effect for methyl has been suggested by Murrell and McEwen to explain the observed shifts in the ultraviolet absorption spectra of some substituted benzenes (19). There is, however, a large body of chemical and physicochemical evidence which indicates that alkyl groups have a +I effect. Indeed, the n.m.r. spectrum of 3-picoline itself is consistent with the effect of the higher electron density in the ring due to the presence of the methyl substituent (20). Another possible explanation involves the contributions made by each of the two Kékulé structures V ↔ VI to the actual state of the 3-picoline molecule. If one assumes that the electrical effect of the 3-methyl substituent is such as to stabilize structure V with respect to VI, then V would have a larger coefficient than VI in the aromatic wave function, and

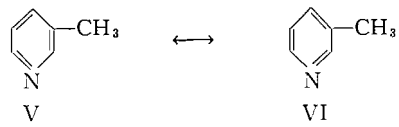

V VI

direction of a polar effect would be that which V would favor. If one then assumes that the phenyl anion (if such is the attacking species) will add at that end of the conjugated system whose other end is the N atom, then addition should take place preferentially at the 2-position.* It is not clear at the moment how an alkyl group would favor the stabilization of V with respect to VI. Yet another explanation possible would involve the hyperconjugation by the methyl group. Structure VIII, being *p*-quinonoïd in nature, might be more stable than VII so that the electron density at the 2-position would consequently

VII VIII

be less than at the 6-position. Similar arguments have been used to explain the high ortho/para ratios observed in the nitration of nitrobenzene and benzonitrile, for example ref. 21. Two further possibilities have to be taken seriously into account: one is that there may be some form of *steric acceleration* favoring substitution at the 2-position and not at the 6-position (the nitrogen atom in the picoline is obviously complexed in some way either with phenyllithium itself or with the lithium bromide present in solution and this would have the same steric effect as a substituent on the N atom). The other is some form of attractive interaction, perhaps of the nature of London dispersion forces, between the polarizable approaching nucleophile and the methyl substituent which would accelerate attack ortho to the methyl group rather than para to it. Dipolar field effects have been similarly suggested to explain the high ortho/para ratios in electrophilic substitutions mentioned above (22). This seems to be a very attractive possibility in the present case and is being investigated.

It should be pointed out that if the second stage in this reaction, the elimination of hydride ion, should be rate-determining, and if it is assumed that the addition step is rapidly reversible, a simple explanation is possible for the observed orientation. The transition state for such an elimination probably involves the abstraction by the lithium cation of the hydrogen atom with its bonding pair of electrons and the electron-repelling ortho-alkyl group should lower the energy of this transition state more than would a para-alkyl substituent.† At present, work is in progress to try to establish which step is the rate-determining one in this reaction, as well as to clarify the effect of alkyl substituents (activating or deactivating), the effect of the lithium bromide present in solution in this particular case, and the effect of quaternizing the ring nitrogen atom. There are some data in the literature on the last point. For example, in the reaction of 3,4-lutidine methiodide with benzyl magnesium chloride the only isomer formed was apparently the 1,2-dihydroderivative (23). Other examples of such reactions are known (24).

The authors would like to express their gratitude to Professor C. K. Ingold for a discussion of this point.

†*A referee has pointed out, however, that hydride expulsion from the ortho-substituted addition product should be less favorable on steric grounds than from the para-substituted addition product since in the former, formation of the transition state brings the alkyl and phenyl substituents closer together. We wish to thank the referee for bringing this to our attention.*

ACKNOWLEDGMENTS

The authors would like to thank Dr. K. L. McEwen for carrying out the molecular orbital calculations reported here and for many discussions, and Professor H. C. Brown for communicating some of the results of his investigations before their publication. Thanks are also offered to the University of Saskatchewan for the award of a Demonstratorship (to C.-S. G.) and to the National Research Council for financial support of this work.

REFERENCES

1. K. ZIEGLER and H. ZEISER. Ber. **63**, 1847 (1930).
2. J. C. W. EVANS and C. F. H. ALLEN. Org. Syntheses Collective, **2**, 517 (1943).
3. E. S. LEWIS and M. C. R. SYMONS. Quart. Revs. (London), **12**, 230 (1958).
4. E. BERGMANN, O. BLUM-BERGMANN, and A. F. VON CHRISTIANI. Ann. **483**, 80 (1930).
5. R. A. ABRAMOVITCH, C.-S. GIAM, and A. D. NOTATION. Can. J. Chem. **38**, 761 (1960).
6. R. A. ABRAMOVITCH and A. D. NOTATION. Can. J. Chem. **38**, 1445 (1960).
7. B. CAPON and N. B. CHAPMAN. J. Chem. Soc. 600 (1957).
8. G. S. HAMMOND. J. Am. Chem. Soc. **77**, 334 (1955).
9. R. D. BROWN and R. D. HARCOURT. J. Chem. Soc. 3451 (1959).
10. H. C. BROWN and W. A. MURPHEY. J. Am. Chem. Soc. **73**, 3308 (1951).
11. T. I. FAND and C. F. LUTOMSKI. J. Am. Chem. Soc. **71**, 2931 (1949).
12. R. GRAF and W. LANGER. J. prakt. Chem. **146**, 103 (1936).
13. H. C. BROWN. Private communication.
14. J. M. ESSERY and K. SCHOFIELD. J. Chem. Soc. 4953 (1960).
15. R. A. ABRAMOVITCH, C.-S. GIAM, and A. D. NOTATION. Can. J. Chem. **38**, 624 (1960).
16. H. E. PODALL. Anal. Chem. **29**, 1423 (1957).
17. J. F. BUNNETT. Quart. Revs. (London), **12**, 1 (1958).
18. J. PLOQUIN. Bull. soc. chim. France, **15**, 640 (1948).
19. J. N. MURRELL and K. L. MCEWEN. J. Chem. Phys. **25**, 1143 (1956).
20. H. J. BERNSTEIN and W. G. SCHNEIDER. J. Chem. Phys. **24**, 469 (1956).
21. E. S. GOULD. Mechanisms and structure in organic chemistry. H. Holt and Co., New York. 1959. p. 439.
22. G. S. HAMMOND. *In* Newman's Steric effects in organic chemistry. John Wiley and Sons, New York. 1956. pp. 176–182.
23. E. L. MAY and E. M. FRY. J. Org. Chem. **22**, 1366 (1957).
24. N. B. EDDY, J. G. MURPHY, and E. L. MAY. J. Org. Chem. **22**, 1370 (1957). M. FREUND and G. BODE. Ber. **42**, 1746 (1909).

ALIPHATIC CHEMISTRY OF FLUORENE

PART VIII. BENZYL 9-FLUORENYL SULPHOXIDE AND SOME 9-FLUORENYL SULPHIDES

P. M. G. BAVIN[1]

The Chemistry Department, the University, Hull, East Yorkshire, England

Received July 31, 1961

ABSTRACT

Allyl 9-fluorenyl sulphide, benzyl 9-fluorenyl sulphide, and di-9-fluorenyl sulphide are stable to boiling ethereal phenyl lithium, in marked contrast to the corresponding ethers. Benzyl 9-fluorenyl sulphoxide has been prepared and shown to be more weakly acidic than 9-fluorenyl sulphones.

Wittig and co-workers have reported (1) that the anions (I) derived from certain 9-fluorenyl ethers rearrange to the corresponding 9-substituted-9-fluorenyl alkoxides (II). Of particular interest to the present study were the anions of the allyl and benzyl ethers (I, R = $CH_2CH{=}CH_2$ and $C_6H_5CH_2$, respectively) which rearranged very rapidly at $-10°$. The anion of di-9-fluorenyl ether rearranged at room temperature but those of other alkyl and aryl ethers required elevated temperatures and longer reaction times.

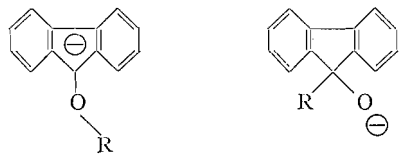

I II

These reactions belong to a wider group known as the Stevens rearrangement (2, pp. 527–528; 3, pp. 282–283; 4). Most of the published work has been concerned with ethers (1, 5, 6, 7, 8) but Hauser and co-workers have examined some sulphides (4). Both benzyl methyl sulphide and dibenzyl sulphide underwent the Stevens rearrangement, more typical of the reactions of quaternary ammonium compounds. Similar rearrangements have been reported for some sulphonium compounds (4, 9). Although allylamine-N-oxides show allylic rearrangement from nitrogen to oxygen (10, 11), related allyl (12) and benzyl (4) sulphoxides and sulphones do not rearrange. Allyl phenyl sulphide and allyl *p*-tolyl sulphide possibly undergo the ortho Claisen rearrangement (13; cf. ref. 14) but more slowly than the corresponding ethers. Unlike the ether, *t*-butyl phenyl sulphide does not rearrange when distilled (15, 16).

We have now prepared by a general method (17) allyl 9-fluorenyl sulphide, benzyl 9-fluorenyl sulphide, and di-9-fluorenyl sulphide. All three sulphides dissolved in ethereal solutions of phenyl lithium with formation of the deep red color associated with fluorene anions of this type (1, 18) but the color was apparently unchanged after boiling under reflux for up to 24 hours. Hydrolysis with water regenerated the original sulphides. Thus the anions of the sulphides are more stable than those of the ethers, resembling the 9-fluorenyl-trialkylammonium compounds in not undergoing the ortho rearrangement (19).

[1]*I.C.I. Fellow, 1958–60. Present address: Smith Kline and French Laboratories Ltd., Mundells, Welwyn Garden City, Herts, England.*

The color of the anion derived from benzyl 9-fluorenyl sulphide was almost immediately discharged by the addition of methyl iodide. Oxidation of the tertiary sulphide gave benzyl 9-methyl-9-fluorenyl sulphone, isomeric with the product of benzylation of methyl 9-fluorenyl sulphone. The non-identity of the two sulphones confirmed that rearrangement of benzyl 9-fluorenyl sulphide anion had not occurred.

Allyl 9-fluorenyl sulphide was not obtained crystalline and decomposed on attempted distillation.* Like other allyl sulphides (22, 23) oxidation gave the sulphone without epoxidation of the double bond. Since allyl fluorene-9-carboxylate rearranges to 9-allylfluorene-9-carboxylic acid when heated with lithamide in toluene (24), the reaction of allyl 9-fluorenyl sulphone with sodamide has been examined. Extensive decomposition occurred, these results paralleling those reported by Cope (12) for other sulphones. The infrequency with which allyl and benzyl groups migrate from sulphur to carbon may be due to *d*-orbital resonance diminishing the charge on the potential migration terminus (cf. the effect of sulphur on the stability of anions (20, 21, 24)). Similar reasons have been put forward to account for the failure of thiophenol acetate to undergo the Fries rearrangement (26). A recent paper (27) has described the pyrolysis of some sulphones which resulted in the formation of rearranged hydrocarbons, but probably by a free radical mechanism.

The reaction between fluorene, thionyl chloride, and aluminum chloride has been reported (28) to yield di-9-fluorenyl sulphoxide, characterized by oxidation to di-9-fluorenyl sulphone (m.p. 199° with decomposition). Although one example of intramolecular acylation at the 9-fluorenyl position has been described (29), Friedel–Crafts and related reactions generally give 2-fluorenyl derivatives (30, p. 277). We have now prepared di-9-fluorenyl sulphone by oxidation of the sulphide and find it to have m.p. 242–244° with decomposition. Paucity of experimental details has prevented repetition of Courtot's preparation (28).

Allyl and benzyl 9-fluorenyl sulphides decomposed rapidly at 258–260° with formation of evil-smelling mixtures. The only product identified was di-9-fluorenyl (8–10%). Di-9-fluorenyl sulphide behaved similarly, giving difluorenyl (11%) accompanied by di-9-fluorenylidene (9%). These observations parallel those reported for the corresponding ethers (1).

In an earlier paper (17) the acidity of 9-fluorenyl sulphones was described. We have now prepared benzyl 9-fluorenyl sulphoxide and examined its reactions. (For a recent discussion of the formation of sulphoxides, see ref. 31.) It dissolves in methanol containing sodium methoxide without formation of the yellow color associated with 9-fluorenyl anions of this type (17, 32, 33). Further, the presence of the alkoxide does not significantly affect the ultraviolet spectrum. Addition to the solution of either methyl or allyl halides led to mixtures from which traces of hydrocarbons were isolated. The infrared spectra showed the presence of sulphones, and fluorenone could be isolated as the 2,4-dinitrophenylhydrazone. Failure to isolate alkylation products is probably due to the low acidity of the sulphoxide since, after 1 hour, dilution precipitated unchanged sulphoxide. Alkylation of the related sulphones is known to be rapid (17). Although disappointing, these results were not unexpected. Unlike the corresponding sulphones, sulphoxides are insoluble in aqueous sodium hydroxide solution (34), and dibutyl sulphoxide undergoes hydrogen exchange very slowly in alkaline media (35). It has been concluded from

**Allylic sulphides are readily isomerized to propenyl sulphides by strong bases (for examples, see refs. 20, 21). In view of the failure of benzyl 9-fluorenyl sulphide anion to undergo rearrangement, the structure of the allyl sulphide was confirmed only by its infrared spectrum (see Experimental).*

spectral and other studies (36) that the electron-accepting properties of the sulphoxide group are only slightly greater than those of the uncharged sulphides. Our results agree with this conclusion.

The infrared spectra of the sulphones reported in this and the earlier paper (17) have been discussed elsewhere (37).

EXPERIMENTAL

Benzyl 9-Fluorenyl Sulphide

Prepared from 9-bromofluorene and benzyl mercaptan in the usual way (17), it crystallized from acetone–methanol as colorless prisms and laths (87%), m.p. 66–67°. Found: C, 83.38; H, 5.80%. Calculated for $C_{20}H_{16}S$: C, 83.26; H, 5.59%.

Benzyl 9-Fluorenyl Sulphoxide

Following a series of trial experiments, the following was found to be reproducible:

The sulphide (2 g) in acetic acid (100 ml) and 50% hydrogen peroxide (15 ml) was heated on the steam bath for 15 minutes. The yellow solution was poured into water, precipitating the *sulphoxide* as a white solid. Crystallization from ethanol gave felted needles (1.45 g), m.p. 147–148° with decomposition to a red liquid. Found: C, 78.55; H, 5.40%. Calculated for $C_{20}H_{16}OS$: C, 78.91; H, 5.30%.

Benzyl 9-Fluorenyl Sulphone

The oxidation described above was continued for 2 hours, additional 50% hydrogen peroxide (10 ml) being added after 1 hour. The *sulphone* formed thick colorless needles from ethanol (82%), m.p. 169–170°. Found: C, 74.64; H, 4.85%. Calculated for $C_{20}H_{16}O_2S$: C, 74.97; H, 5.03%.

Benzyl 9-Methyl-9-fluorenyl Sulphide

Benzyl 9-fluorenyl sulphide (1 g) dissolved in ethereal phenyl lithium (from 2 g bromobenzene) with formation of a deep red color, which was not visibly altered after boiling of the solution under reflux for 24 hours. At the end of this period, methyl iodide (2 g) was added, the solution being almost immediately decolorized. After it was washed with ice water, the ether solution was dried (K_2CO_3), divided into two approximately equal parts, and each part evaporated to dryness.

The oil from one part was left under methanol for 4 weeks, crystallization slowly taking place. Recrystallization from methanol gave small colorless prisms (0.26 g), m.p. 59.5–61.0°. Found: C, 83.61; H, 6.29%. Calculated for $C_{21}H_{18}S$: C, 83.40; H, 6.00%.

The oil from the second part was oxidized in the usual way (17) with hydrogen peroxide. *Benzyl 9-methyl-9-fluorenyl sulphone* crystallized from methanol as colorless needles (0.4 g), m.p. 155–156°. Found: C, 75.66; H, 5.32%. Calculated for $C_{21}H_{18}O_2S$: C, 75.42; H, 5.42%. The same compound (m.p., mixed m.p., and identity of infrared spectra) was obtained by methylating benzyl 9-fluorenyl sulphone in the usual way (17).

Benzylation of 9-fluorenyl methyl sulphone (17) gave *9-benzyl-9-fluorenyl methyl sulphone*, crystallizing from acetone as lustrous plates (69%), m.p. 172–173°, depressed to 141–153° by addition of benzyl 9-methyl-9-fluorenyl sulphone. Found: C, 75.03; H, 5.32%. Calculated for $C_{21}H_{18}O_2S$: C, 75.42; H, 5.42%.

Di-9-fluorenyl Sulphone

9-Fluorenyl mercaptan (10 g) (38) and 9-bromofluorene (13 g) were dissolved in hot ethanol (500 ml). The addition of a solution of sodium methoxide (from 1.2 g sodium) in methanol (50 ml) brought about a vigorous reaction. The *sulphide* started to separate almost at once. Recrystallization from xylene gave colorless lustrous plates (16.5 g, 82%), m.p. 257–259° with decomposition to a red liquid.

Oxidation of the sulphide (1 g) in hot acetic acid (1500 ml) with 50% hydrogen peroxide (15 ml) gave the *sulphone*, which crystallized from xylene as almost colorless prisms (0.7 g), m.p. 242–244° with partial decomposition. Found: C, 78.85; H, 4.43%. Calculated for $C_{26}H_{18}O_2S$: C, 79.16; H, 4.60%.

Allyl 9-Fluorenyl Sulphone

The reaction between 9-bromofluorene (24.5 g), allyl mercaptan (10 g), and sodium methoxide (from 2.5 g sodium) in methanol (250 ml) gave the sulphide as an oil (18 g). It was not obtained crystalline but oxidation in the usual way (17) gave the sulphone (15.2 g) as prisms or plates from acetone–methanol, m.p. 120–121°. Found: C, 70.75; H, 5.23%. Calculated for $C_{16}H_{14}O_2S$: C, 71.08; H, 5.22%.

The sulphide was also obtained as an oil from the reaction between 9-fluorenyl mercaptan and allyl chloride.

9-Allyl-9-fluorenyl Methyl Sulphone

Prepared from 9-fluorenyl methyl sulphone in the usual way (17), it crystallized as elongated prisms from acetone, m.p. 168–169°. Found: C, 71.49; H, 5.33%. Calculated for $C_{17}H_{16}O_2S$: C, 71.80; H, 5.67%.

Pyrolysis of the Sulphides

Di-9-fluorenyl sulphide (2 g) was placed in a 100-ml Erlenmeyer flask, closed with a cotton plug, and maintained at 258–260° (oil bath) for 2 minutes. Crystallization from heptane gave colorless needles (0.2 g, 11%), m.p. 245–246° after two crystallizations. Comparison with an authentic specimen (39) showed the product to be di-9-fluorenyl. The mother liquors slowly formed a crust of red crystals, which were removed and crystallized from carbon tetrachloride – ethanol. The resulting red needles (0.16 g, 9%) had m.p. 185–186° and were identified as di-9-fluorenylidene by comparison with an authentic specimen (39).

The characteristic sulphone bands in the infrared spectra have been discussed elsewhere (37). The structure of allyl 9-fluorenyl sulphide was supported by strong bands at 989 and 912 cm^{-1}, indicative (40) of the vinyl group.

ACKNOWLEDGMENT

The author is indebted to Dr. Brian Saville for kindly reading the manuscript.

REFERENCES

1. G. Wittig, H. Doser, and I. Lorenz. Ann. **562**, 192 (1949).
2. C. K. Ingold. Structure and mechanism in organic chemistry. Cornell University Press, Ithaca, New York. 1953.
3. M. S. Newman (*Editor*). Steric effects in organic chemistry. John Wiley and Sons, New York. 1956.
4. C. R. Hauser, S. W. Kantor, and W. R. Brasen. J. Am. Chem. Soc. **75**, 2660 (1953).
5. G. Wittig and L. Lohman. Ann. **550**, 260 (1942).
6. G. Wittig and W. Happe. Ann. **557**, 205 (1947).
7. C. R. Hauser and S. W. Kantor. J. Am. Chem. Soc. **73**, 1439 (1951).
8. R. L. Letsinger and D. F. Pollart. J. Am. Chem. Soc. **78**, 6079 (1956).
9. L. A. Pinck and G. E. Hilbert. J. Am. Chem. Soc. **68**, 751 (1946).
10. R. F. Kleinschmidt and A. C. Cope. J. Am. Chem. Soc. **66**, 1929 (1944).
11. A. C. Cope and P. H. Towle. J. Am. Chem. Soc. **71**, 3423 (1949).
12. A. C. Cope, D. E. Morrison, and L. Field. J. Am. Chem. Soc. **72**, 59 (1950).
13. C. D. Hurd and H. Greengard. J. Am. Chem. Soc. **52**, 3356 (1930).
14. E. N. Karavlova, D. Sh. Meilanova, and G. D. Galpern. Doklady Akad. Nauk S.S.S.R. **113**, 1280 (1957); Chem. Abstr. **52**, 301*d* (1958).
15. E. A. Bartkus, E. B. Hotelling, and M. B. Neuworth. J. Org. Chem. **25**, 232 (1960).
16. D. S. Tarbell and D. P. Harnish. J. Am. Chem. Soc. **74**, 1862 (1952).
17. P. M. G. Bavin. Can. J. Chem. **38**, 917 (1960).
18. P. M. G. Bavin. Can. J. Chem. **38**, 882 (1960).
19. C. R. Hauser, R. M. Manyik, W. R. Brasen, and P. L. Bayless. J. Org. Chem. **20**, 1119 (1955).
20. D. S. Tarbell and M. A. McCall. J. Am. Chem. Soc. **74**, 48 (1952).
21. D. S. Tarbell and W. E. Lovett. J. Am. Chem. Soc. **78**, 2259 (1956).
22. D. Barnard. J. Chem. Soc. 489 (1956).
23. W. E. Truce and R. J. McManimie. J. Am. Chem. Soc. **75**, 1672 (1953).
24. R. T. Arnold, W. E. Parham, and R. M. Dodson. J. Am. Chem. Soc. **71**, 2439 (1949).
25. D. J. Cram, D. A. Scott, and W. D. Nielsen. J. Am. Chem. Soc. **83**, 3696 (1961).
26. D. S. Tarbell and A. H. Herz. J. Am. Chem. Soc. **75**, 1668 (1953).
27. E. M. La Combe and B. Stewart. J. Am. Chem. Soc. **83**, 3457 (1961).
28. C. Courtot and N. Kozentchouk. Compt. rend. **218**, 973 (1944).
29. P. M. G. Bavin. Can. J. Chem. **38**, 1099 (1960).
30. E. Clar. Aromatische kohlenwasserstoffe. Verlag von Julius Springer, Berlin. 1952.
31. A. Cerniani, G. Modena, and P. E. Todesco. Gazz. chim. ital. **90**, 3, 12 (1960).
32. W. Wislicenus and W. Mocker. Ber. **46**, 2772 (1913).
33. F. A. L. Anet and P. M. G. Bavin. Can. J. Chem. **34**, 991 (1956).
34. R. C. Shriner, H. C. Stuck, and W. J. Jorison. J. Am. Chem. Soc. **52**, 2060 (1930).
35. W. E. Von Doering and A. K. Hoffmann. J. Am. Chem. Soc. **77**, 521 (1955).
36. F. G. Bordwell and P. J. Boutan. J. Am. Chem. Soc. **78**, 854 (1956).
37. P. M. G. Bavin, G. W. Gray, and A. Stephenson. Spectrochim. Acta, **16**, 1312 (1960).
38. M. M. Klenk, C. M. Suter, and S. Archer. J. Am. Chem. Soc. **70**, 3846 (1948).
39. P. M. G. Bavin. Can. J. Chem. **38**, 882 (1960).
40. L. J. Bellamy. The infra-red spectra of complex molecules. Methuen and Co. Ltd., London. 1956.

GLYCOSIDATION OF SUGARS

I. FORMATION OF METHYL-D-XYLOSIDES[1]

C. T. BISHOP AND F. P. COOPER
The Division of Applied Biology, National Research Council, Ottawa, Canada

Received October 2, 1961

ABSTRACT

The reactions of D-xylose, methyl α-D-xylofuranoside, and methyl β-D-xylopyranoside with methanolic hydrogen chloride under controlled conditions have been followed by gas–liquid partition chromatographic analysis of the products. Rate curves were established for each of the four methyl-D-xylosides and the results showed that the following sequence of reactions occurs in the formation of methyl xylosides: (1) xylose → furanosides, (2) anomerization of furanosides, (3) furanosides → pyranosides, (4) anomerization of pyranosides. The relative rates of these four reactions in order of decreasing velocity are 2, 1, 3, 4. Reaction 3 appears to proceed with retention of configuration at the anomeric center. Possible intermediates in these reactions are discussed. Substitution of positions 2 and 3 in the D-xylose molecule by *O*-methyl groups resulted in an increase in the furanoside content of the methanolysis products at equilibrium.

Reaction of sugars with methanolic hydrogen chloride to form methyl glycosides has been known since 1893 (1) and remains of considerable interest and importance in carbohydrate chemistry. The literature on this subject has been reviewed by Shafizadeh (2), who also presented postulated intermediates in the hydrolysis and formation of glycosides via a cyclic or an acyclic mechanism. It is noteworthy that much of the information contributing to those mechanisms was obtained by studies on the *hydrolysis* of glycosides; work on the *formation* of glycosides has been much less extensive and less definitive, probably because of difficulties in analyzing the products. Levene, Raymond, and Dillon (3) studied the methanolysis of nine monosaccharides (glucose, mannose, galactose, fructose, rhamnose, arabinose, lyxose, ribose, and xylose) and presented rate curves showing the changes in proportions of free sugar, furanoside, and pyranoside. Differences in rates of hydrolysis were used to distinguish between furanosides and pyranosides and the results showed that furanosides were formed early in the methanolysis and then decreased gradually with a concurrent increase in pyranosides. The validity of this conclusion has been recognized and substantiated by its general application to the preparation of glycoside mixtures enriched with respect to furanosides or pyranosides (4). However, more recent work has shown differences in rates of hydrolysis for individual furanosides and pyranosides (2) and it is apparent that neither the extent of initial furanoside formation nor the furanoside–pyranoside composition at equilibrium could be determined accurately by the procedure of Levene *et al.* (3). This was recognized by Mowery and Ferrante (5), who re-examined the methanolysis of galactose using modern chromatographic procedures for analyzing the products. These authors separated α- from β-anomers and then estimated the amounts of furanoside and pyranoside in the two fractions from optical rotations. The results showed that β-anomers were formed first and then change to α-anomers, this latter reaction being more "important" than the change of furanoside to pyranoside. Similar results were obtained when a cation exchange resin, rather than hydrogen chloride, was used as catalyst in the methanolysis (6).

[1]*Issued as N.R.C. No. 6628.*
Presented at the 140th Meeting of the American Chemical Society, Chicago, September 3–7, 1961.

Methanolysis of mannose was also investigated and it was found (7) that α-anomers predominate at all times and that furanosides gradually change to pyranosides.

The chromatographic procedures used by Mowery and Ferrante (5) and by Mowery (6, 7) provided more definitive information than the techniques available to Levene *et al.* (3). However, they are time consuming, require large samples, and therefore restrict the convenient analysis of products to relatively few intervals during the reaction. The use of gas–liquid partition chromatography for separating carbohydrate derivatives (8, 9, 10) provides a fast, accurate method for analyzing mixtures of glycosides and requires only small samples. By this means it is possible, with most monosaccharides, to obtain separate rate curves for each of the four methyl glycosides and to establish reliable quantitative data for the equilibrium compositions. The present paper reports the results obtained in the methanolysis of xylose, and the glycoside compositions at equilibrium of its 2-*O*-, 3-*O*-, and 2,3-di-*O*-methyl derivatives.

Reactions were carried out under carefully controlled conditions and products were analyzed by the following procedure. At various times samples were removed, neutralized by sodium methoxide to stop the reaction, and evaporated to dryness. The residue was then methylated by the Kuhn (11) procedure and the fully methylated methyl glycosides were analyzed by gas–liquid partition chromatography (8, 9, 10). Figure 1 shows a

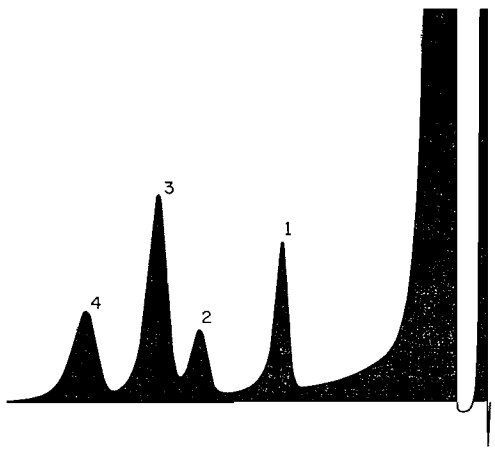

FIG. 1. Separation of fully methylated methyl-D-xylosides. Conditions: column (4 ft×4 mm)—Carbowax 6000 on acid-washed celite 545, 80–100 mesh, 1:9 w/w; temp.—125° C; flow rate—250 ml argon/minute. 1, methyl 2,3,4-tri-*O*-methyl-β-D-xyloside; 2, methyl 2,3,4-tri-*O*-methyl-α-D-xyloside; 3, methyl 2,3,5-tri-*O*-methyl-β-D-xyloside; 4, methyl 2,3,5-tri-*O*-methyl-α-D-xyloside.

typical separation of the four fully methylated methyl-D-xylosides. The components were identified by comparison with authentic samples of each of the four glycosides, and quantitative estimations were made by triangulation of the peaks. Disappearance of reducing sugar was followed by the hypoiodite method (12). Methylation of individual authentic methyl xylosides and gas–liquid partition chromatography of the products showed that no anomerizations or changes in the ring form occurred during these steps and also that complete methylation of each xyloside was achieved under the conditions used.

Figures 2 and 3 show the rate curves for the products from methanolysis of D-xylose at 25° C and 44° C respectively and reveal the general sequence of reactions. Thus, at 25° C (Fig. 2), the concentration of free sugar dropped very quickly to about 9% with concurrent production of furanosides, which then decreased as pyranosides were formed.

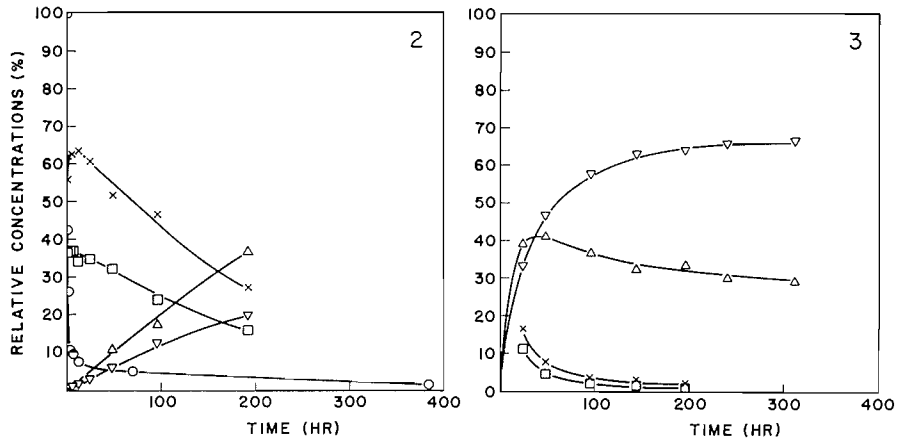

FIG. 2. Products from methanolysis of D-xylose (2% in 0.50% MeOH–HCl) at 25°±0.01° C. ○ D-Xylose, × methyl β-D-xylofuranoside, □ methyl α-D-xylofuranoside, ▽ methyl α-D-xylopyranoside, △ methyl β-D-xylopyranoside.

FIG. 3. Products from methanolysis of D-xylose (2% in 0.50% MeOH–HCl) at 44°±0.01° C. □ Methyl α-D-xylofuranoside, × methyl β-D-xylofuranoside, ▽ methyl α-D-xylopyranoside, △ methyl β-D-xylopyranoside.

The reaction was too slow at 25° C to be followed to equilibrium so it was repeated at 44° C when the rate curves (Fig. 3) showed that the sequence just described was followed by an anomerization of the pyranosides. It was not possible to obtain rate constants of sufficient accuracy to calculate activation energies for any of these reactions because the data did not fit first- or second-order rate kinetics ideally. This was probably caused by the simultaneous occurrence of competing reactions to a small but significant extent and, since the rates were shown to be dependent upon acid concentration, by reaction between methanol and hydrogen chloride. However, approximate *relative* rates could be determined by a comparison of first-order rate constants calculated from data over the same portion of each reaction. At 25° C the ratio of methyl-α-D-xylofuranoside to methyl-β-D-xylofuranoside was the same (1:1.72) throughout the reaction and must therefore be the equilibrium ratio for these two anomers. Any anomerization of furanosides must have occurred too rapidly to have been detected at that temperature. Accordingly, the rate for anomerization of furanosides was determined at 10° C using methyl α-D-xylofuranoside as the starting product and the same concentrations of reactants as used at the higher temperatures. The rate constants, relative to that of the slowest reaction, are given in Table I. The rate constants from which these values were calculated were obtained from the early portions of the reactions when the data fitted first-order

TABLE I

Relative rates of reactions in the methanolysis of D-xylose*

Reaction	Figure†	Relative rate constants	Temp. (°C)
(1) D-Xylose → furanosides	2	324.0	25
(2) Methyl α-furanoside → methyl β-furanoside	—	382.5	10
(3) Furanoside (α+β) → pyranoside (α+β)	2	5.4	25
(4) Methyl β-pyranoside → methyl α-pyranoside	6	1.0	25

*Initial concentration of starting product was 2% in 0.50% methanolic hydrogen chloride at the temperature shown.

†Figure showing rate curves from which rate constants were obtained.

kinetics and when the occurrence of competing reactions would be expected to be at a minimum. It is apparent that reaction 2 was the fastest of the four, at both reaction temperatures, and was followed in order of decreasing velocity by reactions 1, 3, and 4. The results showed that it would be impossible to see if one of the anomeric furanosides is formed predominantly from a solution of D-xylose, in which the equilibrium composition of α and β forms is known, because the furanosides would be anomerized to their equilibrium mixture as soon as they were formed. However, the difference in the rates of reactions 3 and 4 permitted some information to be gained about these two reactions. During the conversion of furanosides to pyranosides the ratio of α- to β-anomers was the same in both ring forms and was constant until the concentrations of furanosides were relatively low. At that stage the anomerization of the pyranosides became the predominant reaction and the ratio of α- to β-anomers changed. These ratios, taken at various times, are shown in Table II. The results indicated that the conversion of

TABLE II

Ratios of α to β anomers in furanoside and pyranoside ring forms during methanolysis of D-xylose*

Time (hr)	α:β furanosides	α:β pyranosides
48	1:1.72	1:1.67
96	1:1.74	1:1.70
120	1:1.75	1:1.71
150	1:1.72	1:1.79
192	1:1.69	1:1.82
Equilibrium	—	1:0.49

*Reaction of a 2% solution of D-xylose in 0.50% methanolic hydrogen chloride at 25° C.

D-xylofuranosides to D-xylopyranosides proceeds with retention of configuration at the anomeric center. This conclusion was supported by the rate curves, shown in Fig. 4, which were obtained by analysis of the products from the reaction of methyl α-D-xylofuranoside with hydrogen chloride in *p*-dioxane. It is readily apparent that the methyl

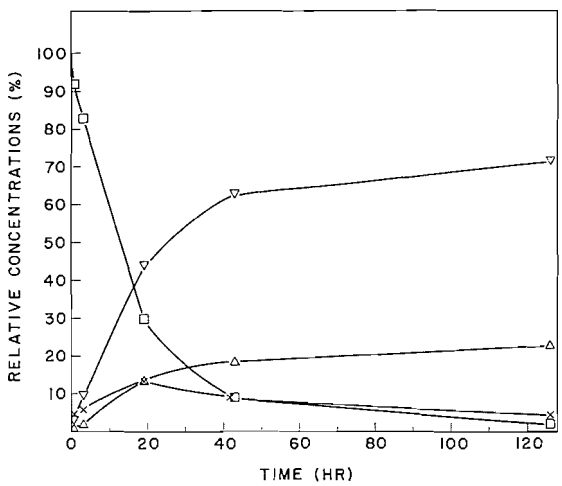

FIG. 4. Products from reaction of methyl α-D-xylofuranoside (2.0%) with hydrogen chloride (0.50%) in *p*-dioxane at 25°±0.01° C. □ Methyl α-D-xylofuranoside, × methyl β-D-xylofuranoside, ▽ methyl α-D-xylopyranoside, △ methyl β-D-xylopyranoside.

α-D-xylofuranoside yielded the methyl α-D-xylopyranoside predominantly. The smaller amounts of β-D-xylopyranoside could have arisen from minor competing reactions, e.g. (*a*) methyl α-furanoside → methyl β-furanoside → methyl β-pyranoside, (*b*) methyl α-pyranoside → methyl β-pyranoside. Very little anomerization of furanoside occurred in this system with *p*-dioxane being used as a solvent. This is in direct contrast to the results obtained with methanolic hydrogen chloride and showed that methanol was necessary for the rapid anomerization of furanosides described earlier.

Glycosidation with methanolic hydrogen chloride results in the formation of 1 mole of water from each mole of sugar. The water so formed could promote reverse reactions in the system. However, the results obtained on reaction of methyl α-D-xylofuranoside (Fig. 5) with methanolic hydrogen chloride were in complete agreement with those

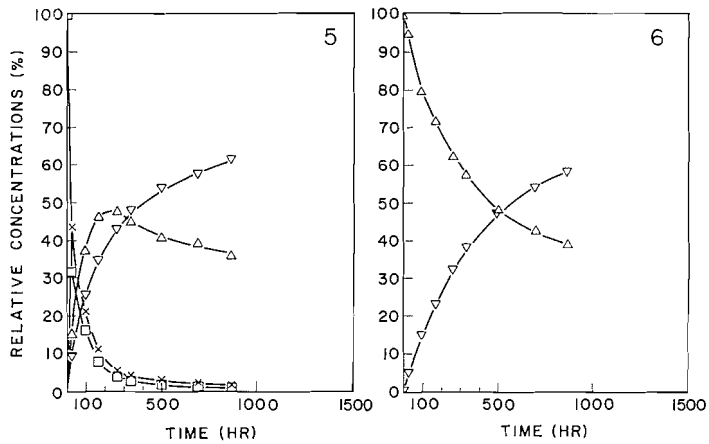

FIG. 5. Products from methanolysis of methyl α-D-xylofuranoside (2% in 0.50% MeOH–HCl) at 25°±0.01° C. □ Methyl α-D-xylofuranoside, × methyl β-D-xylofuranoside, ▽ methyl α-D-xylopyranoside, △ methyl β-D-xylopyranoside.

FIG. 6. Products from methanolysis of methyl β-D-xylopyranoside (2% in 0.50% MeOH–HCl) at 25°±0.01° C. △ Methyl β-D-xylopyranoside, ▽ methyl α-D-xylopyranoside.

given by D-xylose under the same conditions. This showed that, under the conditions used, the 1 mole of water produced from each mole of sugar had no demonstrable effect on the reaction.

The anomerization of methyl-β-D-xylopyranoside in methanolic hydrogen chloride is shown in Fig. 6. These results indicated that no furanoside ring forms were involved in the anomerization of methyl-D-xylopyranosides. Of course, as the reaction progressed, small amounts of furanosides (not shown) appeared due to the reverse reactions. However, the amounts of furanosides were those found at equilibrium (cf. Table III) and were consistent with the view that they arose entirely from the reverse reactions. The rates of all reactions were approximately 4 times faster when the acid concentration was quadrupled.

On the basis of the foregoing results some comments can be made about possible mechanisms for the methanolysis reactions of D-xylose. The sequence of reactions can be established definitely as (1) D-xylose → furanosides, (2) anomerization of furanosides, (3) furanosides → pyranosides, (4) anomerization of pyranosides. As mentioned before, little comment can be made about the first reaction because it was slower than reaction 2. However, from Table I it may be seen that the anomerization of furanosides is about

400 times faster than anomerization of pyranosides. If, by analogy, it may be assumed that the furanose and pyranose forms of D-xylose differ in reactivity in the same way and by the same order of magnitude, then the initial acetal formation would proceed primarily through the furanose form. Very little of the latter would need to be present in the equilibrium mixture given by D-xylose in methanol solution. Figure 7 shows a

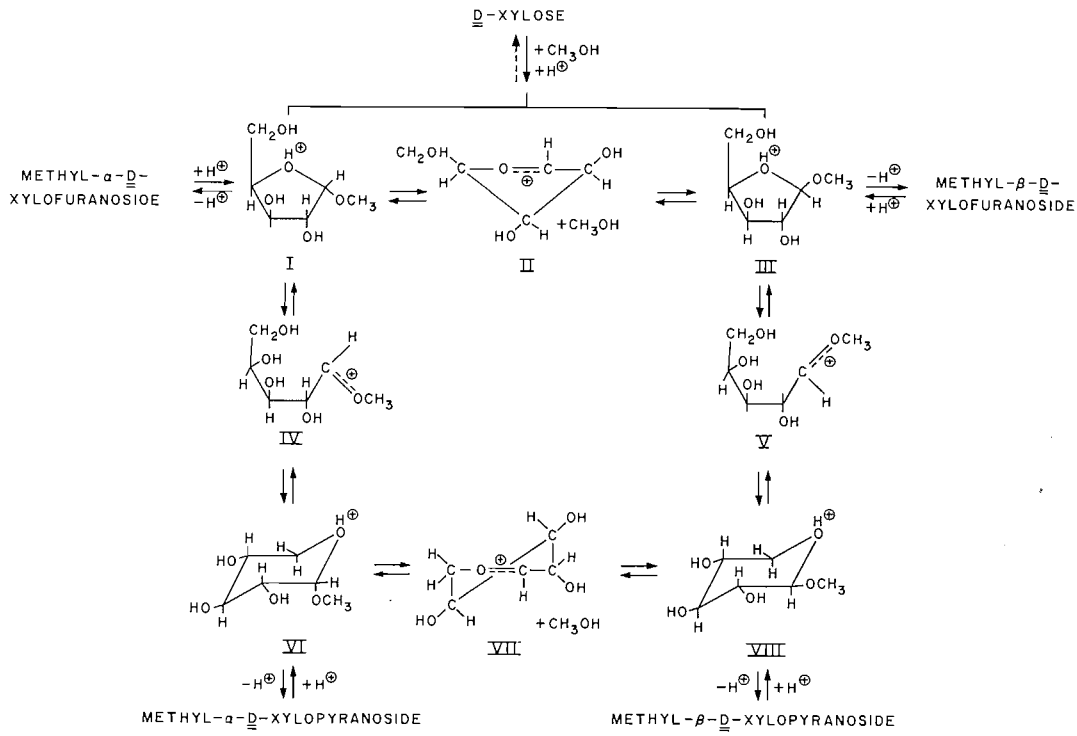

FIG. 7. Postulated mechanism in formation of methyl-D-xylosides.

postulated scheme for reactions 2, 3, and 4. In accordance with the accepted mechanisms for formation and hydrolysis of acetals (13) the proposed scheme is one of specific rather than general acid catalysis. Although probably correct, this requires confirmation by further kinetic studies. The differences in the observed rates of reactions are probably best explained by the postulation of cyclic carbonium ion intermediates (II and VII) for the anomerizations (reactions 2 and 4). Thus, the higher rate of reaction 2, relative to the other three reactions, may be explained by the ease of formation of the ion II from I and III. In the C_s conformation (14) the C_4, ring O, C_1, and C_2 atoms of the methyl-D-xylofuranosides (I and III) would be coplanar and practically no conformational change would be involved in the formation of II. Conversely, the production of ion VII in the half-chair conformation from the stable chair forms VI and VIII requires considerable change in conformation, and the energy demands make the reaction the slowest of the four. The reason for suppression of furanoside anomerization in the reaction of methyl α-D-xylofuranoside (I) with hydrogen chloride in *p*-dioxane is not clear but must be due to a solvent effect. It may be that carbonium ion II is stabilized by solvation with methanol but not with dioxane. This would lead to a shift in the equilibrium in favor of IV in the latter solvent to yield the pyranoside VI.

Retention of anomeric configuration during the furanoside → pyranoside reaction may be explained by considering the geometry of the acyclic ions IV and V. In these two ions, as they are formed from the protonated furanosides I and III, ring closure at C_5 to yield pyranosides requires a rotation about the C_3—C_4 bond of only some 10°. A simultaneous anomerization at C_1 would require a rotation about the C_1—C_2 bond of 180°. It might be expected, therefore, that the compound requiring the smaller change would predominate in the reaction products. For this to be true the ring closure in carbonium ions IV and V must be sufficiently rapid that the H, OCH_3, and C_2 are retained in their original tetrahedral configuration on C_1. Absence of the dimethyl acetal of D-xylose in any of these reactions provided negative evidence for such a rapid ring closure. Had the acyclic ions IV or V existed for any appreciable time it would be expected that a solvent attack at C_1 would yield the dimethyl acetal. Possible alternatives to the acyclic intermediates IV and V could be cyclic, "bridged" compounds involving partial bond formation from C_1 to both the C_4 and C_5 oxygens.

Glycoside compositions at equilibrium in the methanolysis reaction were determined for D-xylose and its 2-*O*-, 3-*O*-, and 2,3-di-*O*-methyl derivatives. Table III shows these

TABLE III

Methyl glycoside compositions at equilibrium in the methanolysis of D-xylose and its 2-*O*-, 3-*O*-, and 2,3-di-*O*-methyl derivatives*

Sugar	Methyl glycoside (%)			
	β-Pyranoside	α-Pyranoside	β-Furanoside	α-Furanoside
D-Xylose	32.0	60.0	6.5	1.4
3-*O*-Methyl-D-xylose	26.7	64.2	5.9	3.1
2-*O*-Methyl-D-xylose	29.2	58.0	9.5	3.3
2,3-di-*O*-Methyl-D-xylose	29.8	53.8	12.7	3.7

*Reaction of the sugar (0.06%) in 2% methanolic hydrogen chloride under reflux for 20 hours.

compositions and it is apparent that the methoxy groups on C_2 and C_3 result in an increase in the amounts of furanoside ring forms in the mixtures at equilibrium. This effect was probably caused by increased non-bonded interactions between the *trans* C_2 and C_3 substituents when hydroxyl groups were replaced by methanol. Since trans C_2 and C_3 substituents are closer together in the pyranoside than in the furanoside ring form, substitution at these positions should decrease the stability of pyranoside more than furanoside, leading to an increase in furanoside content at equilibrium.

EXPERIMENTAL

Reagents

D-Xylose was a purified product supplied by Fisher Scientific Co. Methanol was reagent grade and was distilled from magnesium–iodine immediately before use. Hydrogen chloride was obtained from a cylinder and was dried by passage through a calcium chloride tube. *p*-Dioxane was refluxed with *N* hydrochloric acid, treated with solid potassium hydroxide, and fractionally distilled from sodium; the fraction boiling at 101–102° C was used (15). *N*,*N*-Dimethyl formamide was distilled and stored over barium oxide.

Apparatus

Gas–liquid partition chromatography was carried out on an F and M Model 500 Chromatograph employing a thermal conductivity detector or on a Pye Argon Chromatograph using an ionization detector. On the former, separations of the fully methylated methyl-D-xylosides were made on an 8-ft column of coiled ¼-in. copper tubing packed with 20% w/w Carbowax 20M on Gas-Chrom A (120–140 mesh). Separations were carried out at 150° C with a flow rate of 60 ml of helium per minute. On the latter instrument separations were obtained on straight glass columns (4 ft×4 mm) packed with Carbowax 6000 on acid-washed Celite 545, 80–100 mesh, 1:9 w/w; temperature was 125° C and a flow rate of 250 ml Argon/minute was used.

Preparation of Methyl-D-Xylosides

These compounds were prepared by the method of Augestad and Berner (16). Each xyloside gave a single spot on paper chromatograms run in butanone–water azeotrope. Gas–liquid chromatography of each fully methylated (11) xyloside showed only one component clearly distinguishable (Fig. 1) from the other three xylosides. The methyl xylosides had the following physical constants:

	Our values		Reported values	
	M.p. (°C)	$[\alpha]_D$*	M.p. (°C)	$[\alpha]_D$
Methyl α-D-xylofuranoside	83–84	+181°	84	+182° (16)
Methyl β-D-xylofuranoside	Sirup	− 80°	45	− 89.5° (16)
Methyl α-D-xylopyranoside	89–91	+151°	91–92	+153.9° (17)
Methyl β-D-xylopyranoside	155.5–156.5	− 65°	156–157	− 65.5° (18)

*c, 1–2% in water, T = 25° C.

Glycosidations and Anomerizations

The reactions were carried out in screw-capped bottles fitted with silicone rubber septums and kept in a water bath at 10°, 25°, or 44° C (±0.01°). D-Xylose, methyl α-D-xylofuranoside, or methyl β-D-xylopyranoside (0.300 g) was dissolved in absolute methanol (10 ml) at the required temperature, and the solution was then made up to 15 ml by the addition of 1.50% methanolic hydrogen chloride. In one experiment, to determine the effect of acid concentration on the rate of reaction, 6.0% methanolic hydrogen chloride was added in the same proportions, giving a final acid concentration of 2%. In another experiment purified *p*-dioxane was used instead of methanol.

Analysis of Methyl-D-Xyloside Mixtures

Aliquots (0.5 ml) were withdrawn from the reaction bottles by a hypodermic syringe, neutralized immediately with sodium methoxide in 3-ml test tubes, and evaporated to dryness *in vacuo*. The dried samples were methylated (11) by addition of *N,N*-dimethyl formamide (0.1 ml), methyl iodide (0.1 ml), and silver oxide (0.1 g). The stoppered tubes, covered with foil paper, were shaken for at least 4 hours and sometimes up to 20 hours. The supernatant liquid was then analyzed directly by gas–liquid partition chromatography, the components being identified by comparison with authentic methyl-D-xylosides methylated in the same way. Amounts of individual xylosides were determined from the areas under the peaks.

Effect of Methylation Procedure on D-Xylose

A mixture of D-xylose (15.0 mg) and methyl β-L-arabinopyranoside (16.2 mg) was methylated as described above. Analysis of the products by gas–liquid partition chromatography gave the following results:

Compound	Units of area under peak	Percentage
Methyl 2,3,4-tri-*O*-methyl-β-D-xylopyranoside	1142	74.8
Methyl 2,3,4-tri-*O*-methyl-α-D-xylopyranoside	263	17.2
Methyl 2,3,5-tri-*O*-methyl-β-D-xylofuranoside	79	5.2
Methyl 2,3,5-tri-*O*-methyl-α-D-xylofuranoside	41	2.7
Total methyl tri-*O*-methyl-D-xylosides	1525	
Methyl tri-*O*-methyl-β-L-arabinopyranoside	1528	

This showed that D-xylose was quantitatively converted to fully methylated methyl xylosides by this procedure. Therefore, when D-xylose remained in samples taken for analysis a correction for products arising from the free sugar was made utilizing the percentages shown above.

Analysis for D-Xylose

This was carried out by the alkaline hypoiodite method (12). Reactions in which a methyl-D-xyloside was the starting product were also checked for the presence of free sugar but none was found at any time.

Glycosidation of Partially Methylated D-Xyloses

2-*O*-Methyl-D-xylose, m.p. 103–104° C; 3-*O*-methyl-D-xylose, m.p. 132–133° C; and 2,3-di-*O*-methyl-D-xylose, m.p. 78–79° C, had been characterized previously during work in this laboratory on the structural

investigation of polysaccharides. Samples (15 mg) of each were dissolved in 2% methanolic hydrogen chloride (25 ml) and refluxed for 20 hours. The products, recovered after neutralization with silver carbonate, filtration, and evaporation, were methylated and analyzed as described above.

REFERENCES

1. E. FISCHER. Ber. **26**, 2400 (1893).
2. F. SHAFIZADEH. Advances in Carbohydrate Chem. **13**, 9 (1958).
3. P. A. LEVENE, A. L. RAYMOND, and R. T. DILLON. J. Biol. Chem. **95**, 699 (1932).
4. J. CONCHIE, G. A. LEVVY, and C. A. MARSH. Advances in Carbohydrate Chem. **12**, 157 (1957).
5. D. F. MOWERY and G. R. FERRANTE. J. Am. Chem. Soc. **76**, 4103 (1954).
6. D. F. MOWERY. J. Am. Chem. Soc. **77**, 1667 (1955).
7. D. F. MOWERY. Abstracts of Papers, 130th Meeting, American Chemical Society, 1956. p. 9D.
8. A. G. MCINNES, D. H. BALL, F. P. COOPER, and C. T. BISHOP. J. Chromatog. **1**, 556 (1958).
9. C. T. BISHOP and F. P. COOPER. Can. J. Chem. **38**, 388 (1960).
10. H. W. KIRCHER. Anal. Chem. **32**, 1103 (1960).
11. R. KUHN, H. TRISCHMANN, and I. LÖW. Angew. Chem. **67**, 32 (1955).
12. R. WILLSTÄTTER and G. SCHUDEL. Ber. **51**, 780 (1918).
13. J. HINE. Physical organic chemistry. McGraw-Hill Book Company, Inc., New York. 1956.
14. J. E. KILPATRICK, K. S. PITZER, and R. SPITZER. J. Am. Chem. Soc. **69**, 2483 (1947).
15. A. WEISSBERGER, E. S. PROSKAUER, J. A. RIDDICK, and E. E. TOOPS. Technique of organic chemistry. Vol. VII. Interscience, New York. 1955. p. 372.
16. I. AUGESTAD and E. BERNER. Acta Chem. Scand. **8**, 251 (1954).
17. E. FISCHER. Ber. **28**, 1145 (1895).
18. E. FISCHER. Ber. **28**, 1157 (1895).

SYNTHESIS OF 4-*O*-METHYL-L-ARABINOSE[1]

I. R. SIDDIQUI[2] AND C. T. BISHOP
The Division of Applied Biology, National Research Council, Ottawa, Canada

Received October 18, 1961

ABSTRACT

4-*O*-Methyl-L-arabinose has been synthesized from ethyl 2,3-di-*O*-benzyl-α-L-arabinofuranoside by successive methanolysis, methylation, debenzylation, and hydrolysis; a proof of structure is presented. Ethyl 2,3-di-*O*-benzyl-α-L-arabinofuranoside yielded 57% furanoside and 43% pyranoside at equilibrium in methanolic hydrogen chloride.

Among the mono-*O*-methyl derivatives of L-arabinose the 2-*O*- and 3-*O*-methyl isomers have been known for some time (1) and syntheses of the 5-*O*-methyl derivative have been reported more recently (2, 3). The present paper reports the synthesis and proof of structure of 4-*O*-methyl-L-arabinose, the only monomethyl ether of that sugar which has not been described.

The sequence of reactions in the synthesis was as follows:

Ethyl 2,3-di-*O*-benzyl-α-L-arabinofuranoside, prepared during the synthesis of 5-*O*-methyl-L-arabinose (3), was refluxed with methanolic hydrogen chloride to yield a mixture of the corresponding furanosides and pyranosides. This mixture was methylated, debenzylated, and hydrolyzed to yield 4-*O*- and 5-*O*-methyl-L-arabinose, which were separated by preparative paper chromatography.

The prolonged methanolysis (24 hours in 2% methanolic hydrogen chloride) of ethyl 2,3-di-*O*-benzyl-α-L-arabinofuranoside had been expected to convert the compound to a mixture in which the pyranoside-ring forms predominated (4, 5). However, subsequent analysis of the methyl mono-*O*-methyl-L-arabinosides by gas–liquid partition chromatography (6, 7) of their fully methylated derivatives gave a furanoside:pyranoside ratio of 1:0.75 (57% furanoside, 43% pyranoside). It has been reported (8) that *O*-methyl groups on C_2 and C_3 in the D-xylose molecule increase the ratio of furanoside forms at equilibrium in methanolic hydrogen chloride. The present results indicated that *O*-benzyl groups have a similar effect. In this connection it may be noted that 2,3-di-*O*-methyl-L-arabinose yields 75.4% furanosides at equilibrium in methanolic hydrogen chloride (9).

The 4-*O*-methyl-L-arabinose was a sirup having $[\alpha]_D +132° \pm 2°$ and giving only one spot on paper chromatograms. Complete methylation yielded methyl 2,3,4-tri-*O*-methyl-α,β-L-arabinoside and oxidation by bromine water yielded a δ-lactone. The *O*-methyl group therefore could not be on C_5. The mono-*O*-methyl-L-arabinose yielded a crystalline osazone without loss of methoxyl, showing that the C_2 hydroxyl was not substituted. On methanolysis the mono-*O*-methyl-L-arabinose yielded crystalline α- and β-methyl glycosides, which were separated by fractional crystallization. The configurations of the glycosides were assigned on the basis of Hudson's rules of isorotation (10). Periodate oxidation of a mixture of these two glycosides resulted in the consumption of 0.93 mole of oxidant per mole of glycoside and showed that the C_3 hydroxyl was not substituted. Direct proof that the *O*-methyl group was on C_4 was obtained by reduction and hydrolysis of the periodate-oxidized methyl glycosides (11) to yield 2-*O*-methyl glycerol, identified as its crystalline 1,3-di-*O*-trityl derivative.

[1]*Issued as N.R.C. No. 6632.*
[2]*N.R.C. Postdoctorate Fellow 1958–1960.*

EXPERIMENTAL

Methyl 2,3-Di-O-benzyl-α,β-L-arabinosides (Furanoside/Pyranoside)

Ethyl 2,3-di-*O*-benzyl-α-L-arabinofuranoside (3), 9.0 g, was refluxed for 24 hours in 2% methanolic hydrogen chloride (200 ml). The solution was neutralized with silver carbonate, filtered, and evaporated to a sirup (8.9 g); $[\alpha]_D^{25}$ +11.7°±2° (*c*, 2% in methanol); OCH_3, 7.09%, calc. OCH_3, 9.0%.

Methyl 2,3-Di-O-benzyl-4/5-O-methyl-L-arabinoside (Furanoside/Pyranoside)

The mixture (8.9 g) of methyl 2,3-di-*O*-benzyl-L-arabinosides obtained above was methylated twice by methyl iodide (75 ml) and silver oxide (10 g) (12). The product (7.2 g, 78.2%) showed no hydroxyl absorption in its infrared spectrum; $[\alpha]_D^{25}$ ±0° (*c*, 3.45% in methanol); OCH_3, 17.60%, calc. OCH_3, 17.30%.

Methyl 4/5-O-Methyl-L-arabinosides

The fully methylated di-*O*-benzyl derivative was debenzylated by reduction with sodium in alcohol (13) to yield a sirupy, water-soluble product (2.3 g, 88.4%); $[\alpha]_D^{26}$ −12.0°±1.5° (*c*, 1.3% in methanol).

A sample (5 mg) of this material was methylated by the Kuhn (14) procedure and the fully methylated derivatives were analyzed by gas–liquid partition chromatography (6, 7). Separations were carried out at 180° C on a 4-ft column of polyphenyl ether, 10% (w/w) on Celite 545 (80–100 mesh), with a flow rate of 75 ml argon per minute. Under these conditions the anomeric methyl glycosides of 2,3,5-tri-*O*-methyl-L-arabinose were resolved, those of 2,3,4-tri-*O*-methyl-L-arabinose ran as one component. Measurement of areas under the three peaks showed that the mixture contained 57% of the 2,3,5-tri-*O*-methyl and 43% of the 2,3,4-tri-*O*-methyl isomers.

4-O-Methyl-L-arabinose

The mixture of methyl 4/5-*O*-methyl-L-arabinosides (2.3 g) was hydrolyzed by 1.5 *N* sulphuric acid (50 ml) at 100° C for 8 hours. The solution was neutralized with barium carbonate, filtered, and evaporated to a sirup, $[\alpha]_D^{28}$ +35°±2° (*c*, 1.5% in water). Paper chromatography of the hydrolyzate in butanone saturated with 2% aqueous ammonium hydroxide revealed components, detected by *p*-anisidine hydrochloride spray reagent (15), with R_F values of 0.32 and 0.11. Authentic samples of 2-*O*-, 3-*O*-, and 5-*O*-methyl-L-arabinose had R_F values of 0.19, 0.14, and 0.32 respectively in the same solvent system. Very weak spots with R_F values of 0.56, 0.21, and 0.55 were also detected; these latter components were probably incompletely debenzylated products.

The component of R_F 0.11 was isolated by preparative paper chromatography using the same solvent system. Elution of the appropriate areas of the chromatograms and filtration and evaporation of the eluate yielded 4-*O*-methyl-L-arabinose as a straw-colored sirup (380 mg); $[\alpha]_D^{27}$ +132°±2° (*c*, 1.0% in water).

A sample (1 mg) of this product was methylated (14), and gas–liquid partition chromatography of the reaction mixture, using the conditions described previously, showed only one component which ran the same as methyl 2,3,4-tri-*O*-methyl-α,β-L-arabinoside.

4-O-Methyl-L-arabinolactone

4-*O*-methyl-L-arabinose (100 mg) in water (3 ml) was oxidized by bromine (0.5 ml) in the presence of barium carbonate (75 mg) for 60 hours. Bromine was removed by aeration and the mixture was adjusted to pH 1.0 by addition of *N* hydrochloric acid. The resulting solution was extracted continuously with ethyl acetate for 24 hours. The extract was dried (sodium sulphate) and evaporated to yield a sirup (95.3 mg) which was distilled, b.p. (bath temperature) 130–135° C at 0.02 mm. The distillate showed carbonyl absorption in its infrared spectrum at 1725 cm^{-1} indicative of a six-membered lactone ring (16).

The change in specific rotation of this lactone in aqueous solution, $[\alpha]_D^{27}$ +19.4° (7 minutes) → 0° (100 minutes and constant), was indicative of the rapid hydrolysis characteristic of six-membered sugar–acid lactones.

4-O-Methyl-L-arabinosazone

4-*O*-Methyl-L-arabinose (60 mg) in 20% aqueous acetic acid (3 ml) was heated on a boiling-water bath for 2 hours with sodium bisulphite (50 mg) and phenylhydrazine (0.5 ml). The solution was allowed to stand overnight at room temperature and the osazone that crystallized was removed by centrifugation. The product was recrystallized from ethanol–water to a constant melting point of 176–177.5° C, $[\alpha]_D^{29}$ ±0° (*c*, 0.7% in ethanol). Anal. Calc. for $C_{18}H_{23}O_3N_4$: C, 62.96%; H, 6.75%; N, 16.32%. Found: C, 62.94%; H, 6.55%; N, 16.35%.

Methyl Glycosides of 4-O-Methyl-L-arabinose

4-*O*-Methyl-L-arabinose (100 mg) was refluxed in 4% methanolic hydrogen chloride (15 ml) for 15 hours. Acid was neutralized by Amberlite IR-45 exchange resin and the neutral solution was evaporated to a brown sirup which crystallized spontaneously.

(a) Methyl 4-O-methyl-β-L-arabinoside.—Crystallization of the mixture from ethyl acetate containing a few drops of light petroleum (b.p. 30–60° C) yielded a crop of cubic crystals (36.7 mg) which were recrystallized to a constant melting point of 112–114° C, $[\alpha]_D^{28}$ +213°±2° C (*c*, 0.93% in methanol). Anal. Calc. for $C_7H_{14}O_5$: C, 47.18%; H, 7.92%. Found: C, 47.20%; H, 7.87%.

(b) Methyl 4-O-methyl-α-L-arabinoside.—All of the mother liquors from crystallization of the β-anomer were combined and evaporated to yield a mass of sticky crystals. Recrystallization from ethyl acetate containing a higher proportion (ca. 2:1) of light petroleum (b.p. 30–60° C) yielded crystals in the form of needles, which were recrystallized to a constant melting point of 83–84° C, $[\alpha]_D^{28}$ +58°±2° (*c*, 0.93% in methanol). Anal. Calc. for $C_7H_{14}O_5$: C, 47.18%; H, 7.92%. Found: C, 47.05%; H, 7.75%.

Periodate Oxidation of Methyl 4-O-methyl-α,β-L-arabinoside

Another sample of 4-*O*-methyl-L-arabinose was methanolysed as described above. The mixture of anomeric glycosides was dried to constant weight (178 mg, 1 mmole) and dissolved in 0.0143 *M* sodium metaperiodate (100 ml). The solution was kept at 35° C and the consumption of oxidant was followed spectrophotometrically (17). Consumption of periodate reached a constant value of 0.93 mole per mole of glycoside after 24 hours. The solution was neutralized with sodium bicarbonate, saturated with sodium sulphate, and extracted continuously with ether for 42 hours. The extract was dried (sodium sulphate) and evaporated to a sirup, which was hydrolyzed by 0.5 *N* sulphuric acid (5 ml) at 97° C for 2 hours. The hydrolyzate was neutralized with barium carbonate, filtered, and potassium borohydride (200 mg) was added to the filtrate. The solution was left at room temperature overnight and Amberlite-IR-120 exchange resin was then added until gas evolution ceased. The resin was filtered off, washed thoroughly with water and methanol, and the combined filtrate and washings were evaporated to dryness under reduced pressure at 35° C. Methanol was added to the residue and the solution was again evaporated. This procedure was repeated five times to assure complete removal of boric acid. The residue was then distilled *in vacuo* (b.p. up to 120° C at 0.02 mm). A solution of the distillate and triphenylchloromethane (61.8 mg) in pyridine (5 ml) was kept at room temperature overnight and then poured into water (50 ml). The insoluble, oily product was separated by centrifugation, dried *in vacuo*, and washed through an alumina column with benzene. The eluate was evaporated to a sirupy residue which crystallized from ethanol, m.p. 161–162° C unchanged on admixture with authentic 1,3-di-*O*-trityl-2-*O*-methyl glycerol; mixed melting point with triphenylcarbinol (m.p. 162–164° C) was 133–136° C. Anal. Calc. for $C_{42}H_{38}O_3$: C, 85.39%; H, 6.48%. Found: C, 84.95%; H, 6.24%.

Preparation of 1,3-Di-O-trityl-2-O-methyl Glycerol

1,3-Di-*O*-trityl glycerol (18), m.p. 174–176° C, was methylated by methyl iodide and silver oxide to yield the corresponding 2-*O*-methyl derivative, m.p. 162–163° C, reported (19) m.p. 158.5° C. The product showed no hydroxyl absorption in the infrared and a mixed melting point with triphenylcarbinol (m.p. 162–164° C) was 133–136° C.

ACKNOWLEDGMENTS

The authors gratefully acknowledge the assistance of F. P. Cooper with the gas–liquid chromatography. Analyses were performed by A. E. Castagne, Microanalyst, Division of Applied Biology.

REFERENCES

1. R. A. LAIDLAW and E. G. V. PERCIVAL. Advances in Carbohydrate Chem. **7**, 1 (1952).
2. G. G. S. DUTTON, Y. TANAKA, and K. YATES. Can. J. Chem. **37**, 1955 (1959).
3. I. R. SIDDIQUI, C. T. BISHOP, and G. A. ADAMS. Can. J. Chem. **39**, 1595 (1961).
4. P. A. LEVENE, A. L. RAYMOND, and R. T. DILLON. J. Biol. Chem. **95**, 699 (1932).
5. J. CONCHIE, G. A. LEVVY, and C. A. MARSH. Advances in Carbohydrate Chem. **12**, 157 (1957).
6. A. G. MCINNES, D. H. BALL, F. P. COOPER, and C. T. BISHOP. J. Chromatog. **1**, 556 (1958).
7. C. T. BISHOP and F. P. COOPER. Can. J. Chem. **38**, 388 (1960).
8. C. T. BISHOP and F. P. COOPER. This issue.
9. C. T. BISHOP and F. P. COOPER. Unpublished results.
10. C. S. HUDSON. J. Am. Chem. Soc. **31**, 66 (1909).
11. J. K. HAMILTON, G. W. HUFFMAN, and F. SMITH. J. Am. Chem. Soc. **81**, 2173 (1959).
12. T. PURDIE and J. C. IRVINE. J. Chem. Soc. **83**, 1021 (1903).
13. K. FREUDENBERG and E. PLANKENHORN. Ann. **536**, 257 (1938).
14. R. KUHN, H. TRISCHMANN, and I. LÖW. Angew. Chem. **67**, 32 (1955).
15. L. HOUGH, J. K. N. JONES, and W. H. WADMAN. J. Chem. Soc. 1702 (1950).
16. S. A. BARKER, E. J. BOURNE, R. M. PINHARD, and D. H. WHIFFEN. Chem. & Ind. (London), 658 (1958).
17. G. O. ASPINALL and R. J. FERRIER. Chem. & Ind. (London), 1216 (1957).
18. B. HELFERICH and H. SIEBER. Z. physiol. Chem. **175**, 311 (1928).
19. H. HIBBERT and N. M. CARTER. J. Am. Chem. Soc. **51**, 1601 (1929).

THE ALKALOIDS OF LYCOPODIUM ANNOTINUM

PART V. THE STRUCTURE AND STEREOCHEMISTRY OF LYCOFOLINE[1]

F. A. L. ANET, M. AHMAD, AND N. H. KHAN
The Department of Chemistry, University of Ottawa, Ottawa, Canada

Received October 26, 1961

ABSTRACT

Lycofoline forms a monoacetyl or a diacetyl derivative, depending on the reaction conditions. Hydrogenation of lycofoline yields dihydrolycofoline. Sodium borohydride reduction of acrifoline under non-epimerizing conditions gives the known acrifolinol, but reduction in the presence of sodium hydroxide gives both acrifolinol and lycofoline. From these reactions as well as the evidence of n.m.r. spectra, lycofoline is shown to have structure IV.

The alkaloid lycofoline, $C_{16}H_{25}O_2N$, m.p. 144–145°, $[\alpha]_D$ −75°, was isolated recently by Anet and Khan (1) from *Lycopodium annotinum* L. The infrared spectrum of lycofoline indicated the presence of a double bond and at least one hydroxyl group. A C-methyl group was found by Kuhn–Roth determination and the tertiary nature of the nitrogen atom was shown by the formation of a quaternary methiodide. The present paper deals with the elucidation of the structure and stereochemistry of lycofoline.[3]

The nature of the oxygen atoms in the alkaloid was first investigated. Acetylation with acetic anhydride in pyridine solution at room temperature gave a monoacetyl derivative, $C_{18}H_{27}O_3N$, m.p. 159–160°. This compound still had a hydroxyl group, as shown by a band at 3600 cm^{-1} in the infrared spectrum. Acetylation of the second hydroxyl group was much more difficult, being incomplete even after 7 hours at 80 to 90° with the acetic anhydride – pyridine reagent. The diacetyl derivative, $C_{20}H_{29}O_4N$, m.p. 113–118°, was, however, easily separated from the monoacetyl derivative by chromatography. Thus, there are two hydroxyl groups in lycofoline, and one hydroxyl group is quite strongly hindered.

Hydrogenation of lycofoline proceeded readily in the presence of Adams' catalyst to give dihydrolycofoline, $C_{16}H_{27}O_2N$, m.p. 146–147°. This compound was isomeric but not identical with dihydroacrifolinol (2), α-dihydroannofoline (3), or deacetylfawcettiine (4).

The proton nuclear magnetic resonance (n.m.r.) spectra (5) of lycofoline and its acetyl derivatives provided key information in the structure determination of the alkaloid.

The n.m.r. spectrum of lycofoline is shown in Fig. 1. The doublet (splitting, 6 c.p.s.) at 9.02 τ of intensity corresponding to three protons confirms the presence of a C-methyl group. The position of this band shows that the C-methyl group is attached to a saturated carbon atom, and the splitting of 6 c.p.s., that this carbon bears just one hydrogen atom. The triplet (splitting, 4 c.p.s.) of relative intensity 1:2:1 at 4.71 τ corresponds to one ethylenic proton. The magnitude of the splitting shows that the grouping involved

[1]*Taken in part from the Ph.D. thesis of N. H. Khan, University of Ottawa, 1959.*
[2]*Part III, F. A. L. Anet, Tetrahedron Letters, No. 20, 13 (1960); Part IV, F. A. L. Anet and M. V. Rao, Tetrahedron Letters, No. 20, 9 (1960).*
[3]*After the preparation of this paper was complete, a preliminary communication (R. H. Burnell and D. R. Taylor, Chem. & Ind. (London), 1399 (1961)) appeared in which the same conclusions were reached, but based on different evidence.*

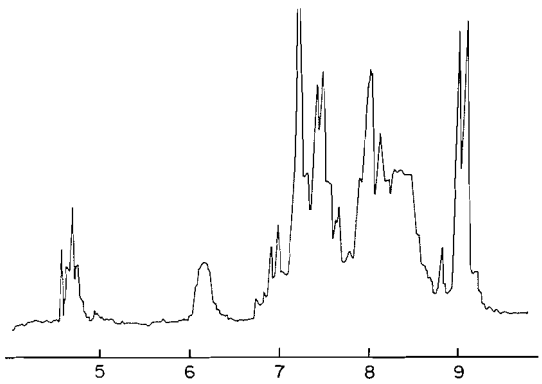

FIG. 1. Nuclear magnetic resonance spectrum of lycofoline in chloroform solution. The sharp band at lowest field is due to $C^{13}HCl_3$.

is $\begin{matrix} C \\ \diagdown \\ \quad C{=}CH{-}CH_2{-} \\ \diagup \\ C \end{matrix}$. Bands at 6.14 τ and 6.82 τ, each corresponding to one proton, can be assigned to $\diagdown CH{-}O{-}$ groups from their chemical shifts and from the effect of acetylation on the position of these bands. The protons of the hydroxyl groups corresponding to these bands probably give rise to the sharp band at 7.2 τ. No coupling is observed owing to fast exchange of the protons of hydroxyl groups caused by the basic nitrogen atom present in the alkaloid. The band at 6.82 τ is a quartet with spacings of 10.8 and 5.4 c.p.s., showing that there is coupling to two protons. The values of the coupling constants are consistent with the following arrangement about the hydroxyl group:

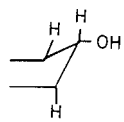

The band at 6.14 τ is quite broad, with a half-band width of 10 c.p.s., indicating coupling to three or four protons. The coupling constants cannot be very large and a structure of the following type is consistent with the evidence:

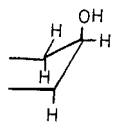

The n.m.r. spectrum of acetyllycofoline shows the same features as that of the parent alkaloid except that the quartet at 6.8 τ is shifted to 5.66 τ. This is consistent with the assignment already made that the proton responsible for this band is attached to a carbon atom bearing an equatorial, and therefore unhindered, hydroxyl group. In diacetyllycofoline, the n.m.r. spectrum is further modified by a shift on the band at 6.14 τ to 4.94 τ. In both acetylated derivatives the protons of the acetyl groups give rise to a sharp band at about 8.00 τ.

On the basis of the above evidence and of a probable structural relationship to other *Lycopodium* alkaloids the most likely structure for lycofoline was thought to be IV. In IV the axial secondary hydroxyl group is highly hindered, as required by the experimental evidence.

That lycofoline indeed has structure IV was proved in the following way. Reduction of acrifoline (I) with sodium borohydride in the presence of sodium hydroxide was

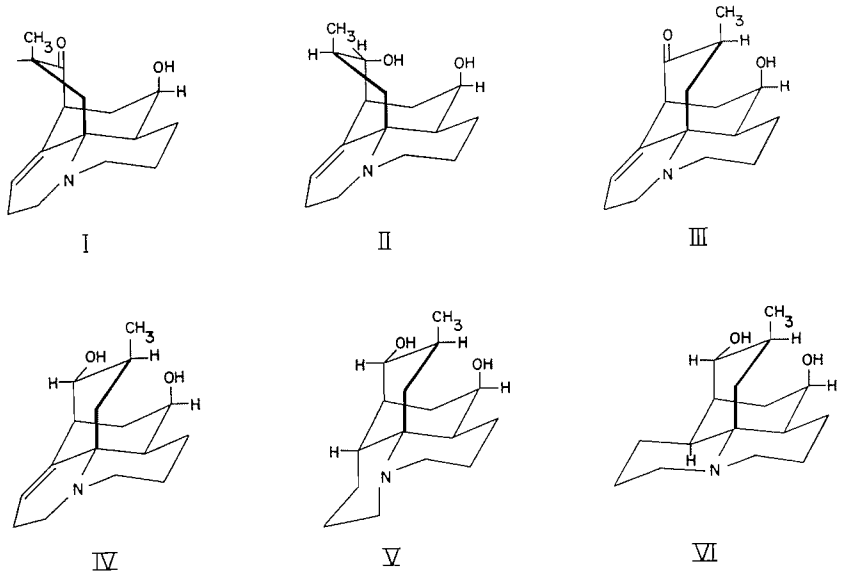

found to give a mixture of acrifolinol (2) and lycofoline. These reduction conditions have already been used to obtain deacetylfawcettiine from annofoline (4). The reaction of acrifoline with lithium aluminum hydride is known (2) to give acrifolinol. Although acrifoline is certainly unchanged by base (2, 6), it must isomerize to some slight extent to give an equilibrium amount of III. The ketone group in acrifoline, like that of annofoline, is highly hindered and therefore undergoes reduction with metal hydrides to give an axial alcohol, acrifolinol (II). This is also consistent with the fact that reduction of acrifoline with lithium and alcohol in liquid ammonia gives a different alcohol (6), in which the new hydroxyl group is presumably equatorial.

In III the carbonyl group is unhindered, and therefore hydride reduction should give the equatorial alcohol IV. In fact, this reduction product is identical with lycofoline.

Since dihydrolycofoline is not identical with deacetylfawcettiine (V), it must have structure VI. Acetyl derivatives of lycofoline occur in *L. fawcettii* (7), but have not been found as yet in *L. annotinum*.

EXPERIMENTAL

Infrared spectra were taken on a Perkin–Elmer Infracord instrument with carbon tetrachloride as the solvent and 1-mm-path-length cells. Paper chromatography was carried out on buffered paper with wet butanol as the developing agent. The n.m.r. spectra were measured on a Varian V-4302 high-resolution spectrometer at a frequency of 60 Mc/sec. Tetramethylsilane was used as an internal standard and chemical shifts are given on the τ scale of Tiers (5) (i.e. in p.p.m. with tetramethylsilane at 10.00). The chemical shifts obtained were not particularly accurate and may be in error by as much as 0.1 τ. The coupling constants should be accurate to 1 c.p.s.

Acetyllycofoline

A mixture of lycofoline (50 mg), pyridine (0.3 ml), and acetic anhydride (0.3 ml) was allowed to stand at room temperature for 5 hours. Methanol was added and the solution evaporated to dryness in a stream of nitrogen. Sublimation of the residue at 110–120° at 0.03 mm gave 45 mg of a compound giving a single spot on paper chromatography (pH 6.0) (R_f 0.66; R_f of lycofoline 0.25). The sublimate was crystallized from acetone–pentane to give 27 mg of acetyllycofoline, m.p. 159–160°, pK_a (50% aqueous ethanol) 8.7. (Found: C, 71.03; H, 8.86. Calc. for $C_{18}H_{27}O_3N$: C, 70.79; H, 8.91%.) In the infrared the compound had bands at 1740 and 3600 cm^{-1}.

Diacetyllycofoline

A mixture of lycofoline (103 mg), pyridine (1 ml), and acetic anhydride (1 ml) was heated at 80–90° for 7 hours. The reaction was worked up as described above to give an oily distillate (117 mg) which gave two spots on paper chromatography (pH 6.0) (R_f 0.61, 0.83; R_f acetyllycofoline 0.61). About two thirds of the product was the required diacetyl derivative. Chromatography of the product on alumina (25 g, deactivated with 5% water) resulted in the separation of diacetyllycofoline, which was eluted first with benzene, from acetyllycofoline, which was eluted with 4:1 benzene–chloroform. The diacetyllycofoline was sublimed at 110–120° at 0.03 mm and then recrystallized from ether and finally resublimed to give 12 mg of crystals, m.p. 113–118°. (Found: C, 68.85; H, 8.13. Calc. for $C_{20}H_{29}O_4N$: C, 69.13; H, 8.41%.) The infrared spectrum had a band at 1740 cm^{-1}, but no hydroxyl band.

Dihydrolycofoline

A mixture of lycofoline (35 mg), ethanol (6 ml), and Adams' catalyst (18 mg) was shaken in an atmosphere of hydrogen for 8 hours. The catalyst was removed and the solvent evaporated. Sublimation of the residue (130–140° at 0.03 mm) gave 30 mg of product which gave one main spot (R_f 0.37; R_f of lycofoline 0.60) on paper chromatography (pH 7.0). Traces of other compounds were also present (R_f 0.21, 0.77). The product was chromatographed on alumina (5 g, deactivated with 5% water). Elution with 2:3 benzene–chloroform gave a product which, after three sublimations, amounted to 12 mg, m.p. 146–147°. (Found: C, 72.12; H, 9.99. Calc. for $C_{16}H_{27}O_2N$: C, 72.41; H, 10.26%.)

Reduction of Acrifoline Hydrobromide with $NaBH_4$ in the Presence of Sodium Hydroxide

Acrifoline hydrobromide (205 mg), ethanolic sodium hydroxide solution (6.1 g in 150 ml), and sodium borohydride (0.712 g) were refluxed for 2 hours. Excess of sodium borohydride was decomposed with acetic acid and most of the ethanol was evaporated. The residue was dissolved in water, made basic with dilute sodium hydroxide solution, and extracted with chloroform. The chloroform extract was evaporated to give the crude reaction product. A paper chromatogram (pH 7.0) of this product gave two spots, R_f 0.50 (lycofoline, minor component) and 0.73 (acrifolinol, major component).

Since the two compounds present in the crude reaction product were well separated on the chromatogram, isolation of them was made by preparative paper chromatography on Whatman No. 3MM paper buffered to pH 7 and developed with butanol saturated with water.

The strip corresponding to the compound with the lower R_f value was cut from the rest of the paper and was eluted with 1% hydrochloric acid. The acid solution was well shaken with chloroform and the chloroform layer was rejected. The acid solution was then made basic with dilute sodium hydroxide solution and the alkaloidal contents were extracted with chloroform. The product obtained on removal of chloroform from the extract was sublimed at 105–115° under vacuum.

The sublimed product (25 mg, m.p. 140–144°) was crystallized from ether, m.p. 143–145°. A mixed melting point with an authentic sample of lycofoline did not show any depression. The infrared spectrum of the product in Nujol mull was identical with that of lycofoline. The product had $[\alpha]_D$ −74.5° (c, 2.0 in ethanol).

ACKNOWLEDGMENTS

This work was supported by the National Research Council of Canada. We wish to thank the Colombo Plan authorities for the award of a scholarship (to N. H. K.) and to the Canadian Commonwealth Scholarship Committee for the award of a scholarship (to M. A.).

REFERENCES

1. F. A. L. ANET and N. H. KHAN. Can. J. Chem. **37**, 1589 (1959).
2. W. N. FRENCH and D. B. MACLEAN. Can. J. Chem. **39**, 2100 (1961).
3. F. A. L. ANET and N. H. KHAN. Chem. & Ind. (London), 1238 (1960).
4. R. H. BURNELL. J. Chem. Soc. 3091 (1959).
5. L. M. JACKMAN. Applications of nuclear magnetic resonance spectroscopy in organic chemistry. Pergamon Press, New York. 1959.
6. F. A. L. ANET and M. AHMAD. Unpublished observation.
7. R. H. BURNELL, B. S. MOOTOO, and D. R. TAYLOR. Can. J. Chem. **38**, 1927 (1960).

THE REACTION OF NITROGEN ATOMS WITH HYDROGEN ATOMS[1]

C. MAVROYANNIS[2] AND C. A. WINKLER
The Upper Atmosphere Chemistry Research Group, McGill University, Montreal, Que.

Received August 18, 1961

ABSTRACT

The reaction has been studied in a fast-flow system by the addition of atomic hydrogen to active nitrogen. Hydrogen atom concentrations were estimated from the maximum destruction of hydrogen bromide in the atomic hydrogen stream. The nitrogen atom consumption, in the reaction mixture, was determined by addition of nitric oxide at different positions along the reaction tube. A lower limit of $4.87 \pm 0.8 \times 10^{14}$ cc^{2}mole^{-2}sec^{-1} was derived for the rate constant of the reaction of nitrogen atoms with hydrogen atoms, over the pressure range 2.5 to 4.5 mm, in an unheated reaction tube, poisoned with phosphoric acid. No reaction between nitrogen atoms and molecular hydrogen was observed, even at 350° C.

INTRODUCTION

A good deal of recent work has provided evidence for the existence, in the gas phase, of radicals consisting of nitrogen and hydrogen, e.g., NH, NH_2, N_2H_2, N_2H_3. Most of these have been identified spectroscopically from studies on such substances as hydrazoic acid, hydrazine, and ammonia (1, 2, 3). The failure of many investigators (4, 5) to find NH radicals, by mass spectrometry, in the dissociation of hydrazoic acid, has been attributed to the ability of the NH radical to abstract hydrogen atoms from chemically stable molecules, without the need for any activation energy. On the other hand, the presence of atomic nitrogen and hydrogen in the reaction products has suggested that nitrogen atoms are more or less passive toward bound hydrogen (4). From chemical studies, Winkler and his co-workers (6, 7) have similarly concluded that nitrogen atoms do not abstract hydrogen atoms in their attack on hydrocarbons or ammonia.

An attempt has been made in the present investigation to establish the kinetics and mechanism of the reaction that occurs in a mixture of nitrogen and hydrogen atoms.

EXPERIMENTAL

The apparatus was a fast-flow system, similar to that used in other studies in this laboratory. Microwave generators (Raytheon 125-watt diathermy unit, operating at a frequency of 2400 Mc/sec) were used to produce atomic nitrogen in one, and atomic hydrogen in a second, quartz discharge tube, each of which was of 12-mm i.d., and 10 cm long. The reaction vessel was a pyrex tube of 20-mm i.d., and 30 cm long, poisoned with 20% phosphoric acid. Five small inlets were placed along the reaction tube at different distances.

Nitrogen and hydrogen, after passage through liquid air traps, were passed into their respective discharge tubes and the emerging gas streams, containing nitrogen and hydrogen atoms, were blended in the reaction vessel. The nitrogen atom consumption, in the reaction mixture, was determined by addition of pure nitric oxide at subsequent jet positions along the reaction tube.

Nitric oxide reacts with hydrogen atoms by the termolecular mechanism (8, 9)

$$NO + H + M \rightarrow HNO + M$$

followed by

$$HNO + H \rightarrow H_2 + NO.$$

Hence, destruction of nitric oxide should occur only as a result of attack by active nitrogen, which permits the nitric oxide titration (10, 11) to be used for estimation of the nitrogen atom flow rate in the presence of hydrogen atoms.

[1]*This work received financial assistance from the Geophysics Research Directorate of the Air Force Cambridge Research Laboratories, Air Force Research Division, the Defence Research Board of Canada, and the National Research Council of Canada.*

[2]*Holder of a "Cominco" Fellowship, 1959–60, and a National Research Council Studentship, 1960–61.*

Hydrogen atom concentrations at the point of mixing were determined, for the same pressure and flow conditions that prevailed during the reaction, but without the nitrogen discharge in operation, by introducing excess hydrogen bromide, and estimating the maximum amount of hydrogen bromide consumed by hydrogen atoms (12). Hydrogen bromide flow rates, and unreacted hydrogen bromide, were estimated by condensing it in a removable trap containing standard NaOH solution, and back titrating the excess alkali with standard acid.

All the experiments were made in an unheated reaction tube, with the one exception that the reaction of nitrogen atoms with molecular hydrogen was studied at temperatures up to 350° C.

RESULTS AND DISCUSSION

A series of experiments was first made in which molecular hydrogen was added to active nitrogen. No product was found from this reaction, and the afterglow intensity was unaffected (except for a possible dilution effect), even at high flow rates of molecular hydrogen, and at temperatures up to 350° C. This observation agrees with that from earlier studies by Kistiakowsky and Volpi (13) and Steiner (14), but is contrary to the results of Varney (15), who found small amounts of ammonia.

The reaction of nitrogen atoms with hydrogen atoms appeared to produce only small amounts of a basic substance, estimated by titration with standard acid. This product was assumed to be ammonia, since hydrazine, if formed, should react rapidly with either nitrogen or hydrogen atoms, which were present in excess in the gas stream (16). Moreover, earlier studies indicate that hydrazine is not a significant product of the reaction (1, 17). The data for ammonia production, in Table I, are in substantial agreement with earlier observations (1, 17).

TABLE I

Ammonia produced in the reaction of nitrogen atoms with hydrogen atoms
(Unheated reaction tube poisoned with phosphoric acid)

Nitrogen pressure, mm	Hydrogen pressure, mm	Total pressure, mm	Nitrogen atom flow rate, mole/sec×10⁶	Hydrogen atom flow rate, mole/sec×10⁶	Ammonia produced, mole/sec×10⁶
2.0	0.50	2.50	2.84	5.2	—
2.5	0.50	3.00	3.25	5.2	—
2.0	0.75	2.75	2.84	7.1	0.054
1.5	1.00	2.50	1.60	8.6	0.013
1.0	1.00	2.00	0.73	8.6	0.027
2.0	1.00	3.00	2.84	8.6	0.027
3.0	1.00	4.00	4.34	8.6	0.027
3.5	1.00	4.50	5.29	8.6	0.027

The following energetically favorable elementary reactions may be involved in a mixture of nitrogen atoms and hydrogen atoms:

	ΔH (kcal/mole)*	
$N + H + M \rightarrow NH + M$	− 85.0	[1]
$NH + N \rightarrow N_2 + H$	−140.0	[2]
$NH + NH \rightarrow N_2 + H_2$	−158.0	[3]
$NH + NH + M \rightarrow N_2H_2 + M$	−104.0±6.0	[4]
$NH + H \rightarrow H_2 + N$	− 18.0	[5]
$NH + H + M \rightarrow NH_2 + M$	− 88.0	[6]
$NH + H_2 + M \rightarrow NH_3 + M$	− 89.0	[7]
$NH_2 + H + M \rightarrow NH_3 + M$	−104.0	[8]
$NH_2 + H \rightarrow NH + H_2$	− 15.0	[9]

**The heats of reaction are approximate, based on the data D_{N-N} = 225 kcal, D_{H-H} = 103 kcal, D_{N-H} = 85 kcal (18), D_{H-NH} = 88 kcal (19), D_{H-NH_2} = 104 kcal (20), D_{HN-NH} = 104±6 kcal (4); but they do indicate the energetics of the reactions considered.*

$NH_2 + NH_2 \rightarrow N_2 + 2H_2$	-85.0	[10]
$NH_2 + N \rightarrow N_2 + H_2$	-155.0	[11]
$NH_2 + H_2 \rightarrow NH_3 + H$	-1.0	[12]
$NH_2 + NH_2 + M \rightarrow N_2H_4 + M$	-68.0	[13]
$N + N + M \rightarrow N_2 + M$	-225.0	[14]
$N + \text{wall} \rightarrow \frac{1}{2}N_2 + \text{wall}$		[15]
$H + H + M \rightarrow H_2 + M$	-103.0	[16]
$H + \text{wall} \rightarrow \frac{1}{2}H_2 + \text{wall}$		[17]

The NH_2 can be formed only by reaction [6] which, followed by reactions [8] and [12], would lead to the formation of ammonia. The very small amount of ammonia produced (Table I) indicates that NH_2 exists in the gaseous mixture only in small amounts, in accordance with its formation from ternary collisions (reaction [6]), and its destruction by the probable reactions [9], [10], [11], and [13]. For a kinetic treatment, reaction [6], and the other termolecular reactions [4], [7], and [8], may be neglected in comparison with the bimolecular reactions [2], [3], and [5]. Reactions [9] to [13], inclusive, may then also be neglected, since they depend upon reaction [6].

From reactions [1], [2], [5], [13], and [15],

$$-d(\mathrm{N})/dt = k_1(\mathrm{M})(\mathrm{H})(\mathrm{N}) + k_2(\mathrm{NH})(\mathrm{N}) - k_5(\mathrm{NH})(\mathrm{H}) + k_{14}(\mathrm{M})(\mathrm{N})^2 + k_{15}(\mathrm{N}). \quad [18]$$

Reaction [2], the attack of NH by N, is probably very fast, since it appears to be quite analogous to the reaction of NO with N, for which a rate constant between 10^{-10} and 10^{-11} cc molecule^{-1}sec^{-1} (21, 22) has been found in recent investigations. No similar basis seems to be available for estimating the rate of reaction [5]. It is quite conceivable that it, too, might be a fast reaction, but there is no reason to suppose that its rate would exceed that of reaction [2], under the conditions of the present experiments.

If it is assumed that the rates of reactions [2] and [5] are equal,

$$-d(\mathrm{N})/dt = k_1(\mathrm{M})(\mathrm{H})(\mathrm{N}) + k_{14}(\mathrm{M})(\mathrm{N})^2 + k_{15}(\mathrm{N}). \quad [19]$$

On the other hand, if it is assumed that reaction [5] may be neglected relative to reaction [2], application of the steady-state approximation to NH yields

$$d(\mathrm{NH})/dt = k_1(\mathrm{M})(\mathrm{H})(\mathrm{N}) - k_2(\mathrm{NH})(\mathrm{N}) - k_3(\mathrm{NH})^2 = 0.$$

Since the NH concentration is expected to be small (the half-life of NH is about 9×10^{-4} second (1), compared with a value of approximately 10^{-2} second for CH and CH_2), the term $k_3(\mathrm{NH})^2$ may be neglected. Then

$$k_1(\mathrm{M})(\mathrm{H})(\mathrm{N}) = k_2(\mathrm{NH})(\mathrm{N})$$

and

$$-d(\mathrm{N})/dt = 2k_1(\mathrm{M})(\mathrm{H})(\mathrm{N}) + k_{14}(\mathrm{M})(\mathrm{N})^2 + k_{15}(\mathrm{N}). \quad [20]$$

Calculation from equation [20] should therefore give a lower limit for the value of k_1, which, however, is not likely to be in error by more than a factor of two.

If the wall recombination of nitrogen atoms is neglected, since the reaction of nitrogen atoms with hydrogen atoms has been studied at pressures higher than 2.5 mm (23, 24, 25), the rate expression is given by

$$-d(\mathrm{N})/dt = 2k_1(\mathrm{M})(\mathrm{H})(\mathrm{N}) + k_{14}(\mathrm{M})(\mathrm{N})^2.$$

Upon integrating,

$$\ln \frac{(\mathrm{N})_0}{(\mathrm{N})_t} = 2k_1(\mathrm{M}) \int_0^t (\mathrm{H})dt + k_{14}(\mathrm{M}) \int_0^t (\mathrm{N})dt. \quad [21]$$

The rate expression for the decay of hydrogen atoms in reactions [16] and [17] is

$$-d(\mathrm{H})/dt = k_{16}(\mathrm{M})(\mathrm{H})^2+k_{17}(\mathrm{H}).$$

This integrates to

$$\ln \frac{(\mathrm{H})_0}{(\mathrm{H})_t}-\ln \frac{[k_{17}+k_{16}(\mathrm{M})(\mathrm{H})_0]}{[k_{17}+k_{16}(\mathrm{M})(\mathrm{H})_t]} = k_{17}t$$

or

$$(\mathrm{H})_t = \frac{k_{17}}{k_{16}(\mathrm{M})} \frac{1}{\left[1+\frac{k_{17}}{k_{16}(\mathrm{M})(\mathrm{H})_0}\right]e^{k_{17}t}-1}.$$

Hence,

$$\int_0^t (\mathrm{H})_t dt = \frac{1}{k_{16}(\mathrm{M})} \ln \left[1+\frac{k_{16}(\mathrm{M})(\mathrm{H})_0}{k_{17}}(1-e^{-k_{17}t})\right]. \qquad [22]$$

Similarly, the nitrogen atom concentration at time t (reaction [14]) is given by

$$(\mathrm{N})_t = \frac{(\mathrm{N})_0}{k_{14}(\mathrm{M})(\mathrm{N})_0 t+1}$$

or

$$(\mathrm{N})_t dt = \frac{(\mathrm{N})_0 dt}{k_{14}(\mathrm{M})(\mathrm{N})_0 t+1}.$$

Upon integrating,

$$\int_0^t (\mathrm{N})_t dt = \frac{1}{k_{14}(\mathrm{M})} \int_0^t \frac{d[k_{14}(\mathrm{M})(\mathrm{N})_0 t+1]}{k_{14}(\mathrm{M})(\mathrm{N})_0 t+1} = \frac{1}{k_{14}(\mathrm{M})} \ln [k_{14}(\mathrm{M})(\mathrm{N})_0 t+1]. \qquad [23]$$

Substitution of [22] and [23] in equation [21] yields the expression

$$k_1 = \frac{k_{16}}{2} \frac{\log \frac{(\mathrm{N})_0}{(\mathrm{N})_t}-\log [1+k_{14}(\mathrm{M})(\mathrm{N})_0 t]}{\log \left[1+\frac{k_{16}(\mathrm{M})(\mathrm{H})_0}{k_{17}}(1-e^{-k_{17}t})\right]}, \qquad [24]$$

where $(\mathrm{N})_0$ = initial nitrogen atom concentration, $(\mathrm{H})_0$ = initial hydrogen atom concentration, $(\mathrm{N})_t$ = nitrogen atom concentration at time t, t = reaction time. The rate constant of reaction [16] was taken as $k_{16} = 10^{16}$ cc^{2}mole^{-2}sec^{-1} (26, 27) with $\gamma = 2\times10^{-5}$ (28), which, for the conditions used, corresponds to $k_{17} = 2.5$ sec^{-1}. For the rate constant of reaction [14], the value of $k_{14} = 1.04\times10^{16}$ cc^{2}mole^{-2}sec^{-1} (25) was used.

Rate constants for the reaction of nitrogen atoms with hydrogen atoms under various conditions, derived from equation [24], on the assumption that atoms and molecules are equally effective as third bodies, are recorded in Table II. The average value of k_1 may be taken as

$$k_1 = 4.87\pm0.8\times10^{14} \text{ cc}^2\text{mole}^{-2}\text{sec}^{-1}$$

over the range of pressures from 2.5 to 4.5 mm, in an unheated reaction tube poisoned with phosphoric acid.

TABLE II

Rate constants for the reaction of nitrogen atoms with hydrogen atoms as a function of reaction time, pressure, and initial reactant concentrations
(Unheated reaction tube poisoned with phosphoric acid)

Nitrogen pressure, mm	Hydrogen pressure, mm	Total pressure, mm	Nitrogen flow rate, mole/sec $\times 10^6$	Hydrogen flow rate, mole/sec $\times 10^6$	Total flow rate, mole/sec $\times 10^6$	M, mole/sec $\times 10^7$	$(N)_0$, mole/cc $\times 10^9$	$(H)_0$, mole/cc $\times 10^9$	$\log \frac{(N)_0}{(N)_t}$	t, sec $\times 10^2$	k_1, $cc^2 mole^{-2} sec^{-1}$ $\times 10^{-14}$
2.0	0.50	2.50	133	44.5	177.5	1.38	2.21	3.91	0.0400	2.69	4.40
"	"	"	"	"	"	"	"	"	0.0659	4.48	5.65
"	"	"	"	"	"	"	"	"	0.0897	6.04	6.30
"	"	"	"	"	"	"	"	"	0.1209	7.50	5.50
											Average $k_1 = 5.46$
2.0	0.75	2.75	133	74.0	207.0	1.47	2.01	5.04	0.0417	2.54	5.75
"	"	"	"	"	"	"	"	"	0.0641	4.23	4.80
"	"	"	"	"	"	"	"	"	0.0841	5.70	5.00
"	"	"	"	"	"	"	"	"	0.1011	7.09	4.55
											Average $k_1 = 5.02$
2.0	1.00	3.00	133	95.0	228.0	1.60	2.00	6.03	0.0417	2.52	4.00
"	"	"	"	"	"	"	"	"	0.0659	4.20	3.34
"	"	"	"	"	"	"	"	"	0.0859	5.66	3.90
"	"	"	"	"	"	"	"	"	0.1109	7.03	5.05
											Average $k_1 = 4.08$
2.5	1.00	3.50	172	95.0	267.0	1.87	2.27	6.03	0.0540	2.51	4.19
"	"	"	"	"	"	"	"	"	0.0854	4.18	4.18
"	"	"	"	"	"	"	"	"	0.1140	5.63	4.62
"	"	"	"	"	"	"	"	"	0.1353	6.99	3.87
											Average $k_1 = 4.22$
3.0	0.50	3.50	219	44.5	263.5	1.87	3.22	3.69	0.0728	2.54	6.25
"	"	"	"	"	"	"	"	"	0.1143	4.24	5.75
"	"	"	"	"	"	"	"	"	0.1452	5.71	5.15
"	"	"	"	"	"	"	"	"	0.1771	7.09	5.60
											Average $k_1 = 5.67$
3.0	0.75	3.75	219	74.0	293.0	2.00	3.10	4.84	0.0728	2.45	4.57
"	"	"	"	"	"	"	"	"	0.1143	4.08	4.50
"	"	"	"	"	"	"	"	"	0.1452	5.48	4.10
"	"	"	"	"	"	"	"	"	0.1771	6.81	4.46
											Average $k_1 = 4.41$
3.0	1.00	4.00	219	95.0	314.0	2.14	2.95	5 85	0.0776	2.44	5.75
"	"	"	"	"	"	"	"	"	0.1256	4.06	6.50
"	"	"	"	"	"	"	"	"	0.1575	5.47	5.65
"	"	"	"	"	"	"	"	"	0.1842	6.79	4.82
											Average $k_1 = 5.68$
3.5	1.00	4.50	235	95.0	330.0	2.40	3.80	6.25	0.1075	2.61	4.50
"	"	"	"	"	"	"	"	"	0.1577	4.35	4.34
"	"	"	"	"	"	"	"	"	0.2116	5.86	5.35
"	"	"	"	"	"	"	"	"	0.2435	7.28	3.60
											Average $k_1 = 4.45$
											Average $k_1 = 4.87 \pm 0.8 \times 10^{14}$ $cc^2 mole^{-2} sec^{-1}$

The number of termolecular collisions may be calculated, using the collision model, and assuming the mechanism of the reaction to be

$$\begin{aligned} N + H &\rightleftarrows NH^* \\ NH^* + M &\rightarrow NH + M, \end{aligned}$$

as given by

$$Z_{ter} = Z_{NH} Z_{NH^*.M} \tau_{NH^*},$$

where Z_{NH} and $Z_{NH^*.M}$ are the binary collision frequencies between N and H and NH* and M respectively, and τ_{NH^*} is the mean life time of the complex NH*. For $T = 300°$ K; M = N_2; collision diameters $\sigma_N = 2.95$ Å, $\sigma_H = 2.4$ Å, $\sigma_{NH} = 2.68$ Å; and $\tau_{NH^*} = 10^{-13}$ second,

$$Z_{ter} = 1.2 \times 10^{16} \text{ cc}^2\text{mole}^{-2}\text{sec}^{-1},$$

and for M = H_2, and $\sigma_{H_2} = 2.7$ Å,

$$Z_{ter} = 9.2 \times 10^{15} \text{ cc}^2\text{mole}^{-2}\text{sec}^{-1}.$$

Thus, the reaction of nitrogen atoms with hydrogen atoms has a probability factor of 4×10^{-2} or 5×10^{-2} depending on whether nitrogen or hydrogen is considered as a third body.

The value of k_1 reported here for the three-body interaction of nitrogen and hydrogen atoms is lower than that found for many atom-combination reactions, but, within experimental error, it probably should be regarded as comparable with the value of 1.83×10^{15} cc^{2}mole^{-2}sec^{-1} found recently for the rate constant of the analogous reaction of nitrogen and oxygen atoms (25), and with the most recent value, 1.0×10^{15} cc^{2}mole^{-2} sec^{-1}, for the rate constant of the O + O + M reaction (29).

REFERENCES

1. F. O. Rice and M. Freamo. J. Am. Chem. Soc. **73**, 5529 (1951); **75**, 548 (1953).
2. I. L. Mador and M. C. Williams. J. Chem. Phys. **22**, 1267 (1954).
3. E. D. Becker, G. C. Pimentel, and M. Van Thiel. J. Chem. Soc. **26**, 145 (1957).
4. S. N. Foner and R. L. Hudson. J. Chem. Phys. **28**, 719 (1958); **29**, 442 (1958).
5. B. A. Thrush. Proc. Roy. Soc. (London), A, **235**, 143 (1956).
6. G. R. Freeman and C. A. Winkler. J. Phys. Chem. **59**, 371 (1955).
7. H. G. V. Evans, G. R. Freeman, and C. A. Winkler. Can. J. Chem. **34**, 1271 (1956).
8. D. E. Hoare and A. D. Walsh. Trans. Faraday Soc. **53**, 1102 (1957).
9. J. K. Cashion and J. C. Polanyi. J. Chem. Phys. **30**, 317 (1959).
10. G. B. Kistiakowsky and G. G. Volpi. J. Chem. Phys. **27**, 1141 (1957).
11. F. Kaufman and J. R. Kelso. J. Chem. Phys. **27**, 1209 (1957).
12. D. Wiles. Ph.D. Thesis, McGill University, Montreal, Que. 1957.
13. G. B. Kistiakowsky and G. G. Volpi. J. Chem. Phys. **28**, 665 (1958).
14. W. Steiner. Z. Elektrochem. **36**, 807 (1930).
15. R. N. Varney. J. Chem. Phys. **23**, 866 (1955).
16. G. R. Freeman and C. A. Winkler. Can. J. Chem. **33**, 692 (1955).
17. R. A. Ruehwein, J. S. Hashman, and J. W. Edwards. Formation and trapping of free radicals. *Edited by* A. M. Bass and H. P. Broida. Academic Press, New York. 1960. p. 279.
18. T. L. Cottrell. The strengths of chemical bonds. 2nd ed. Butterworth Scientific Publications, London. 1958.
19. A. P. Altshuller. J. Chem. Phys. **22**, 1947 (1954).
20. M. Szwarc. Chem. Revs. **47**, 75 (1950).
21. M. A. A. Clyne and B. A. Thrush. Proc. Roy. Soc. (London), A, **261**, 259 (1961).
22. J. T. Herron. J. Chem. Phys. **35**, 1139 (1961).
23. R. Kelly and C. A. Winkler. Can. J. Chem. **37**, 62 (1959).
24. J. Herron, D. Franklin, and P. Bradt. J. Chem. Phys. **30**, 879 (1959).
25. C. Mavroyannis and C. A. Winkler. Can. J. Chem. **39**, 1601 (1961).
26. W. Steiner and F. W. Wicke. Z. physik. Chem. Bodenstein Band, 817 (1931); Trans. Faraday Soc. **31**, 623 (1935).
27. I. Amdur. Phys. Rev. **43**, 208 (1933); J. Am. Chem. Soc. **60**, 2347 (1938).
28. W. V. Smith. J. Chem. Phys. **11**, 110 (1943).
29. J. Morgan and H. I. Schiff. Private communication.

THE KINETICS OF THE DECOMPOSITION AND SYNTHESIS OF SOME DITHIOCARBAMATES[1]

D. M. MILLER AND R. A. LATIMER[2]
The Pesticide Research Institute, Canada Department of Agriculture, London, Ontario
Received July 31, 1961

ABSTRACT

Rate constants, activation energies, and dissociation constants were determined in a kinetic study of the synthesis and decomposition of a number of *N*-substituted dithiocarbamates. These data combined with certain spectral evidence are evaluated and reaction mechanisms suggested.

INTRODUCTION

Studies on the acid-induced decomposition of a number of dithiocarbamates having the general structure I have been reported by Bode (1) and Zahradnik and Zuman (2). Bode made kinetic studies based on the assumption that decomposition occurs as the single reaction

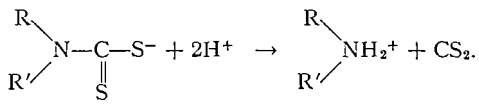

I

Zahradnik and Zuman, on the other hand, showed that the dithiocarbamate ion (A) first combines with a hydrogen ion, giving the protonated form HA, which then decomposes to CS_2 (C) and the corresponding amine (B) thus:

$$H^+ + A \rightleftharpoons HA \rightarrow C + B \overset{+H^+}{\rightleftharpoons} BH^+,$$

so that 2 moles of acid are consumed per mole of dithiocarbamate decomposing. They further suggest two possible structures (II and III) for the protonated form of which, they argue, III is the more likely. These conclusions are re-examined in the present work in the light of new information obtained through a study of a number of compounds, some of which have not been investigated previously.

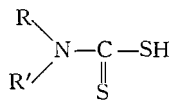

II

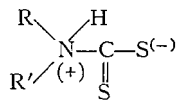

III

EXPERIMENTAL

Materials

The *N*-[β-aminoethyl]-dithiocarbamate inner salt was synthesized by the method of McKay and Hatton (3), while standard methods were used in the synthesis of all other dithiocarbamates.* All these compounds were subjected to frequent recrystallizations while under study. The remaining chemicals used were reagent grade or of equivalent purity.

[1]*This paper constitutes part of a thesis submitted by R. A. Latimer in partial fulfillment of the Ph.D. degree (1959) from the University of Western Ontario, London, Ontario.*
[2]*Present address: John Labatt Ltd., Simcoe St., London, Ontario.*
**The authors wish to thank Dr. G. D. Thorn of this institute, who provided these compounds.*

Methods

(a) Decomposition Reaction

The dithiocarbamate in crystalline form was dropped into a well-stirred, deaerated 500-ml volume of distilled water, previously adjusted to the proper pH, in which it dissolved rapidly, initiating the reaction. The reaction vessel was sealed against the entry of air and a slow stream of nitrogen bubbled through the solution removed the CS_2 produced. A Radiometer titrator (available from Canadian Laboratory Supplies Ltd., Toronto, Ont.) was used to maintain the pH which otherwise would have risen due to the consumption of hydrogen ions. The titrator added standard HCl from a recording burette (4), which provided a record of the course of the reaction.

(b) Synthesis

The same apparatus was used in the study of the synthesis reactions with the following changes in procedure. Nitrogen saturated with CS_2 vapor was bubbled through distilled water at the proper pH and temperature until a saturated solution was attained. The reaction was started with the addition of a solution of the appropriate amine hydrochloride and the pH maintained by the titrator with the addition of standard NaOH solution. Samples of the solution were removed for CS_2 analysis (5) both at the beginning and end of the reaction to establish the concentration of CS_2.

All reactions were studied at a constant temperature (±0.05° C) and most measurements were made within the concentration range of 0.5–1.0 mM. In some cases, however, 10 times this value was used without noticeably altering the kinetics.

(c) Ultraviolet Spectra

Three ultraviolet spectra were obtained as follows using a Beckman D.K.1 recording spectrophotometer:

(1) The spectrum of the *N-methyldithiocarbamate* ion was obtained on a 6×10^{-5} M solution of the sodium salt in distilled water.

(2) The spectrum of the *protonated form* of the same ion was obtained by dissolving the salt in water to a concentration of 6×10^{-3} M and diluting with 100 volumes of 0.1 N HCl, being careful to exclude oxygen from all solutions. Other measurements were made in 1 and 6 N HCl, with no change in the shape of the spectrum.

(3) The *methyl ester* of N-methyldithiocarbamate was dissolved in alcohol to a concentration of 6×10^{-2} M and diluted with 1000 volumes of either water, 0.1 N HCl, or N HCl, giving similar spectra in all three solvents.

Following dilution by the appropriate solvent the solution in each case was introduced into the spectrometer as quickly as possible and the spectrum recorded. This was followed by further recordings at different time intervals to ascertain the rate of dissociation, if any. Only the acid solution of the salt decomposed, causing a drop in the height of the peaks with no change in the shape of the spectrum, provided oxygen was rigorously excluded. Plotting the optical density of the highest peak against time and extrapolating to zero time provided an estimate of the drop in absorption due to decomposition.

RESULTS AND CALCULATIONS

Decomposition of the Alkyldithiocarbamates

Figure 1 is a reproduction of an actual record of acid consumption against time resulting from the decomposition of sodium N-methyldithiocarbamate. Here Q_0 is the initial uptake required to satisfy the equilibrium

$$A + H^+ \rightleftharpoons HA, \qquad K_a = \frac{[H^+][A]}{[HA]}. \qquad [1]$$

For a first-order reaction,

$$dT/dt = k[HA]V, \qquad [2]$$

where V is the volume of solution, T is the total number of moles of dithiocarbamate present at any time t, and k is the first-order rate constant. Since $T/V = [A]+[HA]$ then [1] can be rearranged to give

$$[HA] = \frac{[H^+]}{K_a+[H^+]}\cdot\frac{T}{V} = \alpha\frac{T}{V}. \qquad [3]$$

Substitution of [3] into [2] followed by integration gives for the first-order rate constant,

$$k = \frac{2.303}{\alpha t}\cdot\log\frac{T_0}{T}, \qquad [4]$$

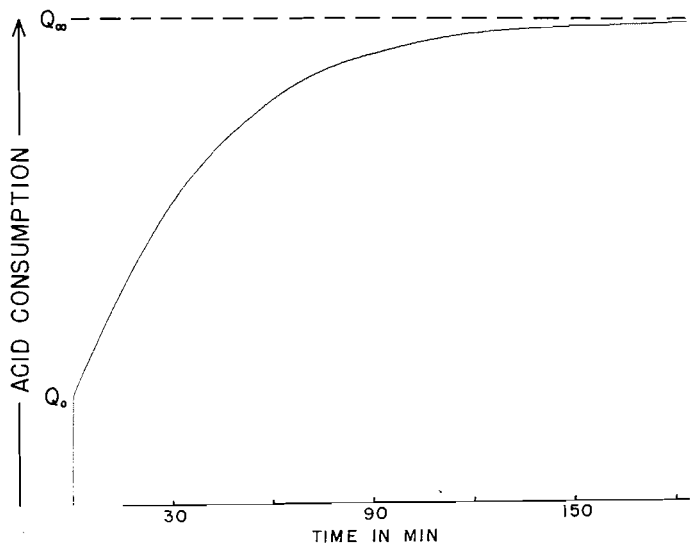

FIG. 1. Titration of sodium methyldithiocarbamate at pH 3.0 and 25° C.

where T_0 is the initial number of moles of dithiocarbamate. The amount of dithiocarbamate which has decomposed at time t will be T_0-T and the amount of acid consumed by this decomposition will be $2(T_0-T)$. Furthermore, some acid will have been consumed in the formation of the protonated form and since this equals $[HA]V$, the total acid consumption to time t will be

$$Q = 2(T_0-T)+[HA]V. \qquad [5]$$

During any given run, since the pH is a constant, α will be a constant. Thus the ratio $[HA]V/T$ at any time will be equal to α, and therefore to its original value $[HA]_0V/T_0$. The initial uptake of acid Q_0 results from the production of sufficient protonated form to satisfy [1] so that $Q_0 = [HA]_0V$. Furthermore, when the reaction is complete all the dithiocarbamate is decomposed, consuming 2 moles of acid per mole of dithiocarbamate initially present or $Q_\infty = 2T_0$. Thus we have $[HA]V = 2Q_0T/Q_\infty$ and $T_0 = Q_\infty/2$. These two expressions may be substituted into [5] to solve for T, which is then introduced into [4] to give [6], an equation for the rate constant in terms of the measurable values Q_0, Q, and Q_∞:

$$k = \frac{2.303}{\alpha t}\log\frac{Q_\infty-Q_0}{Q_\infty-Q}. \qquad [6]$$

To obtain the value of α it is necessary to determine K_a for each compound. This may be obtained directly from the graphs since

$$K_a = \frac{[H^+][A]_0}{[HA]_0} = \frac{Q_\infty-2Q_0}{2Q_0}\cdot[H^+]. \qquad [7]$$

These measurements were made at a number of pH's for each compound and the K_a values averaged. With this information, equation [6] could be applied to recordings of acid consumption at different pH's, allowing the rate constant to be determined at a

number of different time values. All these values were averaged for each compound and standard deviations calculated to provide the information listed in Table I. The activation energies were obtained in the usual way from measurements made at various temperatures.

TABLE I

Constants involved in the decomposition of some *N*-substituted derivatives of dithiocarbamic acid

Derivative	Dissociation constant K_a at 25° C (mole l^{-1})	Rate constant k at 25° C (min^{-1})	Activation energy (kcal)
Methyl	$(1.3\pm0.1)\times10^{-3}$	$(2.5\pm0.4)\times10^{-2}$	15±2
Ethyl	$(9.1\pm0.9)\times10^{-4}$	$(2.4\pm0.2)\times10^{-2}$	19±1
n-Propyl	$(7.9\pm0.8)\times10^{-4}$	$(2.0\pm0.2)\times10^{-2}$	16±3
Dimethyl	$(4.4\pm1.3)\times10^{-4}$	3.1±0.3	18±2
Diethyl	$(2.1\pm0.7)\times10^{-4}$	4.8±0.4	20±1
Di-*n*-propyl	$(1.9\pm0.3)\times10^{-4}$	3.1±0.3	19±3
β-Aminoethyl	$\sim10^{-1}$	$(k/K_a = 16\pm4)$	

Synthesis of the Alkyldithiocarbamates

The synthesis reactions which occur at high pH may be expressed as

$$BH^+ \rightleftharpoons B + H^+ \qquad [8a]$$

$$B + C \rightarrow HA \qquad [8b]$$

$$HA \rightleftharpoons A + H^+. \qquad [8c]$$

Equation [8*a*] is an equilibrium determined by the dissociation constant K_b of the amine and occurs virtually instantaneously as does [8*c*]. Thus we may shorten the over-all reaction to

$$B + C \rightarrow A + H^+. \qquad [9]$$

K_b for the various amines is available in the literature (6, 7). From them may be calculated the concentration of the free amine in each case as

$$[B] = \frac{[OH^-]}{K_b+[OH^-]}\cdot\frac{T_b}{V} = \alpha_b\frac{T_b}{V},$$

where T_b is the total amount of amine present. Reaction [9] is actually second order but since [C] is held constant it is reduced to first order and as in the previous section we may derive the expression

$$k_b = \frac{2.303}{\alpha_b[C]t}\log\frac{Q_\infty - Q_0}{Q_\infty - Q}, \qquad [10]$$

where Q_∞, Q_0, and Q now refer to quantities of base added.

As before, the rate constants were determined at a number of different time values from graphs recorded at a number of pH's and the values averaged to give those recorded in Table II.

Decomposition of β-Aminoethyldithiocarbamate and Disodium Ethylene Bisdithiocarbamate (Nabam)

The decomposition of Nabam ($NaS(S)CNHCH_2CH_2NHC(S)SNa$) is complicated by the fact that the two dithiocarbamate groups are present, resulting in the possible existence of two protonated forms (HA and H_2A) and in the formation of a monodithiocarbamate intermediate (the β-aminoethyl derivative) which itself has two forms (referred

TABLE II

Constants involved in the synthesis of some *N*-substituted derivatives of dithiocarbamic acid

Derivative	Rate constant k (l. mole^{-1}min^{-1})	Activation energy (kcal)
Methyl	14±3	19±6
Dimethyl	22±3	17±6
Diethyl	16±3	
Di-*n*-propyl	14±4	

to below as M and HM). Thus, before a reaction scheme for the decomposition of Nabam can be written the dissociation constants K_1 and K_2 for Nabam and K_3 for the β-aminoethyl compound must be determined, so that we may calculate the concentrations of the various forms from equations [11], [12], and [13].

$$[H_2A] = \alpha\frac{T}{V}, \text{ where } \alpha = \frac{[H^+]^2}{[H^+]^2+K_1[H^+]+K_1K_2}, \quad [11]$$

$$[HA] = \beta\frac{T}{V}, \text{ where } \beta = \frac{K_1[H^+]}{[H^+]^2+K_1[H^+]+K_1K_2}, \quad [12]$$

$$[HM] = \gamma\frac{T_M}{V}, \quad \text{where } \gamma = \frac{[H^+]}{[H^+]+K_3}, \quad [13]$$

where T (and later T_0) refer to the total amount of the various Nabam forms and T_M is the amount of intermediate (monodithiocarbamate) present.

From titration curves of Nabam at various pH's, Q_0 and Q_∞ were measured, and since

$$Q_0 = 2[H_2A]V+[HA]V = 2\alpha T+\beta T$$

and

$$T_0 = Q_\infty/4,$$

then by substitution we obtain

$$\frac{Q_0}{T_0} = \frac{4Q_0}{Q_\infty} = \frac{[H^+](2[H^+]+K_1)}{[H^+]^2+K_1[H^+]+K_1K_2}. \quad [14]$$

Using the values of $4Q_0/Q_\infty$ obtained as a function of $[H^+]$, K_1 and K_2 were obtained from [14] employing a modification of Hartley's statistical method as outlined by Williams (8).* These values are listed in Table III.

TABLE III

Constants involved in the decomposition of ethylenebisdithiocarbamic acid determined at 25° C

Dissociation constants (mole l^{-1})	Rate constants (min^{-1})
$K_1 = (5.0\pm1)\times10^{-3}$	$k_1 = (2.3\pm0.5)\times10^{-3}$
$K_2 = (2.5\pm0.5)\times10^{-4}$	$k_2 = (3.7\pm0.7)\times10^{-2}$

The authors are indebted to Mrs. P. M. Morse, Statistical Research Service, Canada Department of Agriculture, Ottawa, for assistance in these calculations.

The determination of K_3 was attempted using the methods previously described for the alkyl derivatives but it was found that even at pH 2, Q_0 was small, indicating a relatively large value for K_3, which could only be estimated as approximately 10^{-1} mole l^{-1}. This high value is probably due to stabilization of the ionized form as a cyclic inner salt (IV).

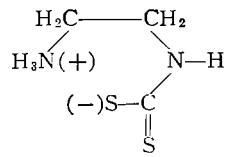

IV

Since K_3 is large relative to the range of $[H^+]$ used in this study (pH 2.5 to 4.0) we may let $\gamma = [H^+]/K_3$. Furthermore, since K_3 is not known accurately only the ratio $R = k_3/K_3$ (where k_3 is the decomposition rate constant) can be obtained employing instead of [6] expression [15] in which R is a constant independent of $[H^+]$. A value for R averaged from measurements made over a range of $[H^+]$ is given in Table I.

$$R = \frac{2.303}{[H^+]t} \log \frac{Q_\infty - Q_0}{Q_\infty - Q} \qquad [15]$$

Turning again to Nabam we may write for the over-all decomposition the following:

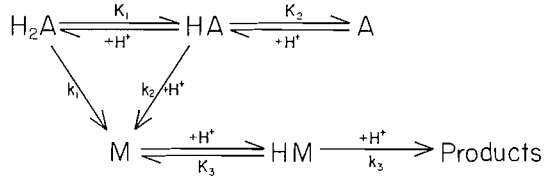

This may be simplified to

$$A \xrightarrow[+2H^+]{k} M \xrightarrow[+2H^+]{k'} \text{products}, \qquad [16]$$

where $k = \alpha k_1 + \beta k_2$ and $k' = \gamma k_3 = [H^+].R$.

The total acid consumption is given by $Q = Q_A + Q_M$, where Q_A is the acid consumed during the first decomposition step in [16] and Q_M acid consumption during the second. These in turn can be seen to be

$$Q_A = 2(T_0 - T) + [HA]V + 2[H_2A]V$$

and

$$Q_M = 2(T_0 - T) - 2T_M,$$

where T_M is the amount of unreacted intermediate, virtually all of which is in the dissociated form. Again, since $[HA]V + [H_2A]V$ is a constant fraction of T and $T_0 = Q_\infty/4$,

$$[HA]V + 2[H_2A] \cdot V = \frac{4Q_0}{Q_\infty} T$$

so that substitution in equation [4] provides the expression

$$k = \frac{2.303}{t} \log \frac{Q_\infty - Q_0}{Q_\infty - Q - 2T_M}. \qquad [17]$$

The amount of the intermediate may be found from the standard expression [18]. Obviously the substitution of [18] into [17] produces an equation much too complex for an easy solution of k, so that an approximation must be made. The first step is to obtain an estimate of k with $T_M = 0$. This value substituted into [18] gives a first approximation

$$T_M = \frac{k}{k'-k} T_0(e^{-kt} - e^{-k't}) \qquad [18]$$

for T_M which when introduced into [17] provides the second approximation for k. Further approximations of k and T_M are made until stabilized values are obtained. Since $k = \alpha k_1 + \beta k_2$ and, from [11] and [12], $\alpha = ([H^+]/K_1)\beta$, then

$$\frac{k}{\beta} = \frac{[H^+]}{K_1} k_1 + k_2$$

so that by plotting $[H^+]/K_1$ against k/β a straight line is obtained whose slope is k_1 and k/β intercept is k_2. Figure 2 represents such a plot from which the values listed in Table III were obtained.

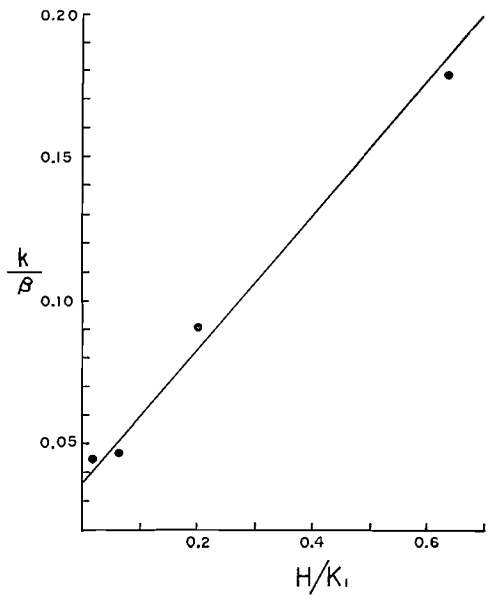

FIG. 2.

The Ultraviolet Spectra

The three spectra are reproduced in Fig. 3, the acid curve appearing twice to allow comparison between it and the others. The ester and salt concentration were 6.0×10^{-5} M while the acid form was estimated to be 5.4×10^{-5} M.

In the presence of oxygen the spectrum of the acid form slowly changed to one having a peak of 240 mμ and a shoulder at about 275 mμ. This later spectrum appeared to be stable with time and reverted to the ion form on neutralization.

DISCUSSION

The experimental results may be discussed most conveniently in three sections as follows:

(a) Spectral Evidence

Janssen (9) has made an extensive study of the ultraviolet spectra of some 70 thion compounds from which he concluded that the longer wavelength peak (shown in Fig. 3)

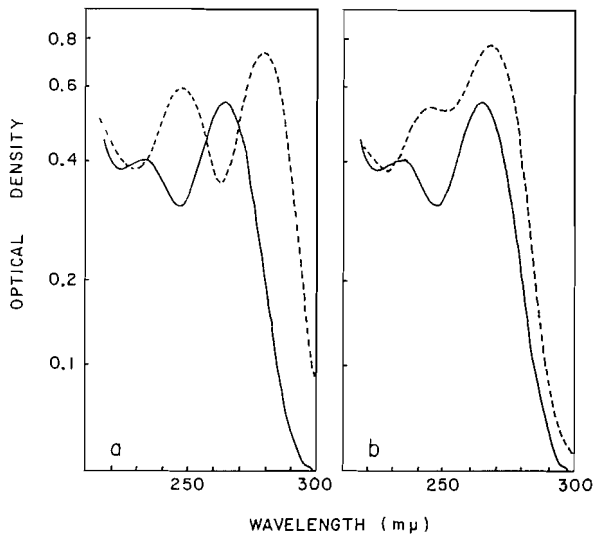

FIG. 3. (*a*) —— acid, – – – salt; (*b*) —— acid, – – – ester.

may be assigned to the structure —N—C(=S)— and the shorter wavelength peak to the structure —C(=S)—S—. This leads to the initial expectation that the addition of a proton to the ion would bring about a change in the shorter wavelength peak if structure II resulted and in the longer wavelength peak if structure III resulted. Actually *both* peaks are seen to shift to shorter wavelengths in Fig. 3. This is not surprising since the change in the ion either to a neutral molecule or a zwitter ion is bound to have profound effects on the entire structure. The *direction* of shift *is* significant, however, since a move to shorter wavelengths generally indicates a reduction in resonance. Structure II, having no free charges, has less resonance than the ion, and seems to be indicated here.

A comparison can also be made in Fig. 3 between the ester, which under the present conditions is not protonated and whose structure resembles that of II, and the acid form of the dithiocarbamate. The similarity between the longer wavelength peaks of these two compounds shows that the electronic configuration around the nitrogen is unchanged on esterification, thus ruling out structure III. The shift in the shorter wavelength peak probably occurs as a result of replacing a hydrogen by a methyl group on the CSS structure.

As there is no change in the spectrum of the acid form in solutions containing between 0.1 and 6 *N* HCl, it seems unlikely that the diprotonated form suggested by Zahradnik and Zuman (2) exists.

(b) The Acid Dissociation Constants

The ability of a compound to release protons depends on its electronegativity. Thus for any given acidic group, the acid dissociation constant K_a will decrease with increasing electron-donating power of the groups to which it is attached. This is the case with the dissociation constants of the alkyl-substituted compounds listed in Table I where the increasing size and number of the electron-donating alkyl groups causes a drop in K_a.

It is the case also for a change in substituent from an uncharged alkyl group to a group such as $^{-}S(S)C—NH—CH_2—CH_2—$ (K_2, Table III) whose negative charge provides it with a greater electron-donating power. Any increase in electron density about the nitrogen atom will be communicated to the sulphur, resulting in a similar dependence of the acidity of both structures II and III on substitution, so that neither is preferred as a result of these observations.

The β-aminoethyl derivative on the other hand, being anomalous, is more useful in regard to a selection of structure. That K_a for this compound should be higher than all the other compounds listed is not unexpected in view of the electrophilic nature of the positive charge on its substituent. However, an increase of at least 1000-fold is excessive and must result from other factors. In its ionized state, this compound is an inner salt in the form of a six-membered ring (IV), which is a very stable structure. The addition of a proton to the sulphur can only occur with the disruption of the salt bond. Thus if protonization is of this type its probability of occurrence is lower and its K_a higher than would be expected as a result of electronic effects alone. Such an argument would not apply if protonization is at the nitrogen since the ring structure would remain, so that once again structure II is preferred.

(c) Rate Constants

The results of the kinetic studies listed in Tables I, II, and III may be summarized as follows:

(1) With the exception of the β-aminoethyl derivative and diprotonated Nabam, the monosubstituted compounds all have decomposition rate constants of the same order. There is some indication that increased electron-donating power of the substituent groups results in a larger decomposition rate, since both increase in the substitution series $HSSCNHCH_2CH_2— <$ alkyl— $< {}^{-}SSCNHCH_2CH_2—$.

(2) The dialkyl decomposition rate constants also follow this rule, having values in excess of those of the monoalkyls. The almost 100-fold increase, however, appears to be too great to be due to electronic effects alone so that steric factors must make an added contribution.

(3) The β-aminoethyl derivative is again anomalous since it should certainly exhibit no greater steric hindrance than exists in Nabam, and furthermore it would be expected to show a reduced rate constant by virtue of the electron-withdrawing powers of the positive charge. In spite of this it was found to have a high rate constant ($\sim$2 min^{-1}) compared to other monosubstituted compounds.

(4) The rate of synthesis of the alkyl compounds is also revealing in that the dialkyls are synthesized at the same or greater rate than the monoalkyls, two of which (ethyl and *n*-propyl) were so slow in the pH range available to the method that they could not be measured. This fact appears to be in conflict with the conclusion reached in (2) since if steric factors aid in the decomposition by placing a strain on the C—N bond, it seems likely that they should hinder synthesis.

To reconcile these apparent contradictions the following reaction mechanism is offered:

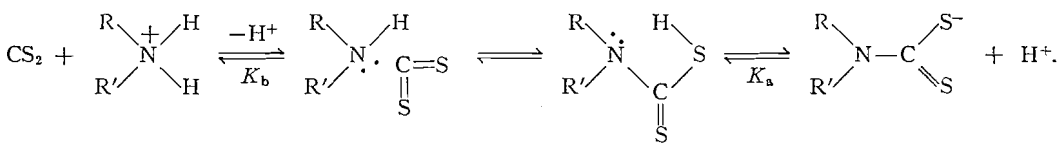

V II

This scheme follows Zahradnik and Zuman's suggestion (2) that CS_2 acting as a Lewis

acid adds to the amine to form V. It also satisfies the overall observation that pH's near or less than the pK_a of the acid bring about decomposition while those near or in excess of the pK_b of the amine result in synthesis.

The crucial step in both synthesis and decomposition is the transfer of the hydrogen between the nitrogen and the sulphur, which occurs in the step between V and II. Groups adding to the electronegativity of the nitrogen should aid in transfer toward the nitrogen, increasing the rate of decomposition and decreasing the rate of synthesis.

The effect of steric factors on transfer is clearly indicated by models of V and II. In both compounds rotation about the N—C bond is virtually unrestricted if only one large group is attached to the nitrogen whereas disubstitution prevents free rotation and brings about important orientation effects. In V the S=C=S structure is forced into a plane at a right angle to that of the substituents so that the S—H distance is near optimal for the transfer. In II the HS group is forced into a position proximal to the free electron pair on the nitrogen, where transfer again should be facilitated. The net result of the addition of a second alkyl to the nitrogen then is that the electronic and steric effects are additive during decomposition, resulting in a large increase in rate, and opposed during synthesis, resulting in little change in rate, as is observed in Tables I and II.

With the β-aminoethyl compound, the hydrogen transfer is aided in another way. The protonated amino group exerts a strong inductive electron shift directly on the S=C bond, as in VI, reducing the electronegativity of the sulphide sulphur and weakening the C—N bond.

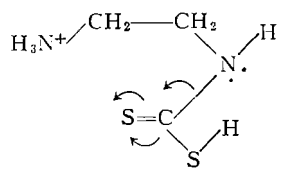

VI

This would promote the transfer step and lead to the unusually high decomposition rate observed.

Since hydrogen bond formation between the nitrogen and the sulphur is possible with structure II it is tempting to suggest that this does in fact occur, the hydrogen assuming a position intermediate to its position in II and III. Accepting this structure, however, leaves us without an explanation for the steric effects, and since such a compound would have some of the free charge characteristics of III, without an explanation of the downward shift in the spectrum of the protonated form. We are therefore forced to acceptance of structure II pending further evidence to the contrary.

ACKNOWLEDGMENTS

The authors wish to thank Mr. A. W. Tatham and Mr. H. J. Murphy for technical assistance in this work and Dr. G. D. Thorn and Dr. A. Stoessl for many helpful discussions.

REFERENCES

1. H. Bode. Z. anal. Chem. **142**, 414 (1954).
2. R. Zahradnik and P. Zuman. Czechoslov. Commun. **24**, 1132 (1959).
3. A. F. McKay and W. B. Hatton. J. Am. Chem. Soc. **78**, 1618 (1956).
4. D. M. Miller. Anal. Chem. **30**, 2067 (1958).
5. D. G. Clarke, H. Baum, E. L. Stanley, and W. F. Hester. Anal. Chem. **23**, 1842 (1951).
6. I. M. Kolthoff and V. A. Stanger. Volumetric analysis. Interscience Publishers, New York. 1947.
7. J. F. J. Dippy. Chem. Revs. **25**, 203 (1939).
8. E. J. Williams. Regression analysis. John Wiley and Sons Inc., New York. 1959. Chap. 4.
9. M. J. Janssen. The electronic structure of organic thion compounds. Ph.D. Thesis. Utrecht, 1959.

FABIANINE[1,2]

O. E. EDWARDS AND N. F. ELMORE[3]
The Division of Pure Chemistry, National Research Council, Ottawa, Canada
Received September 29, 1961

ABSTRACT

The structures of two volatile alkaloids from the plant *Fabiana imbricata* have been elucidated. The occurrence in this plant of *p*-hydroxyacetophenone, large quantities of oleanolic acid, and a yellow pigment is reported.

An extract of the terminal branchlets of the South American plant *Fabiana imbricata* Ruiz and Pav. (common name pichi-pichi) has been used to treat kidney and bladder infections, liver flukes of goats and sheep, etc. (1). In early examinations of the plant Kunz-Krause (1) and Edwards and Rogerson (2) reported the presence of neutral and phenolic compounds and the latter indicated the presence of an alkaloid which gave an amorphous picrate, m.p. 125° (decomp.). In view of the reported physiological activity of the plant and its commercial availability we are undertaking a further examination of its constituents. This report will be mainly concerned with the alkaloids of the plant.

An alcohol extract of the ground plant material when concentrated yielded a large semicrystalline mass with a strong and pleasant odor. The crystals were collected and proved to be oleanolic acid.[4] The filtrate was concentrated and diluted with water and then dilute sulphuric acid was added. A mixture of oleanolic acid and a pale yellow phenolic pigment separated and was collected by filtration. The final filtrate was separated into neutral acidic and basic components. None of the fabiatrin, previously reported as occurring in the plant (2), has been isolated. The basic fraction contained fairly volatile liquid components, which were subjected to short-path distillation *in vacuo*. The most volatile base was relatively free from contamination. It was purified by conversion to its crystalline picrate (m.p. 114–116°) and regeneration. It was a fairly mobile, colorless liquid with negligible optical rotation. We have given this the name fabianine.

Fabianine analyzed for $C_{14}H_{21}NO$. Its infrared spectrum (liquid film) showed the presence of a hydroxyl group (ν_{max} 3280 cm^{-1}), and the bands at 1577 cm^{-1} and 1596 cm^{-1} resembled those of a pyridine ring (3). The presence of a pyridine ring was confirmed by its ultraviolet absorption maxima (Table I) and its low pK_a (5.25 in 50% ethanol). The position of the long-wave-length absorption maximum did not shift in acid solution, but the band increased in intensity, again characteristic of a pyridine, as distinct from an aniline or indoline type. The base failed to give a methiodide even when heated with methyl iodide in dimethyl formamide, behavior suggestive of a 2,6-disubstituted pyridine.

TABLE I

Base	$\lambda\lambda_{max}$	log ϵ	Reference
Fabianine	213, 273	3.9, 3.8	
5,6,7,8-Tetrahydroquinoline	215, 270	3.55, 3.65	4
6,7-Dihydro-5H-pyrindine	215, 275	3.7, 3.7	4

[1]*Issued as N.R.C. No. 6610.*
[2]*Presented at the meeting of the Chemical Institute of Canada in Montreal, August 1961.*
[3]*National Research Council of Canada Postdoctorate Fellow.*
[4]*We are grateful to Dr. G. Just, who identified this component.*

The alkaloid proved inert to chromic acid in acetic acid, hence the hydroxyl was tertiary. It was dehydrated readily by a refluxing mixture of acetic acid and acetic anhydride containing *p*-toluene sulphonic acid or by thionyl chloride – pyridine combination. The double bond of this olefin (A) was terminal (ν_{max} 882, 1645 cm^{-1}). Olefin A was recovered unchanged after refluxing with formic acid for 4 hours, but in refluxing 6 *N* sulphuric acid, it was converted to the isomeric olefin (B) having its double bond in conjugation with the pyridine ring. Olefin B was obtained in a purer state by heating A with potassium hydroxide in ethylene glycol, thus making it very unlikely that B had a rearranged skeleton. Fabianine did not form a derivative with benzaldehyde when sodium hydroxide or acetic anhydride was used as catalyst, a fact which misled us to conclude that no α or γ methyl group was present on the pyridine ring.

The very informative nuclear magnetic resonance spectra[5] of fabianine and of olefins A and B (in CCl_4) are reproduced in Fig. 1. In the spectrum of the alkaloid the aromatic hydrogens appeared as pairs of doublets at 2.5 and 3.0 (J = 8.5), and hence were the γ and β hydrogens of the pyridine ring (6, 7). The hydroxyl group appeared at 2.74 and two 'benzylic' hydrogens were in an ill-defined peak at 7.2. The sharp signal at 7.5 was a methyl group directly attached to the aromatic ring, while three aliphatic methyl groups appeared at 9.1 (3 H) and 8.7 (6 H). The two groups responsible for the signal at 8.7 clearly had the oxygen on the adjacent carbon; hence most probably formed part of a dimethyl carbinol system (I).

The spectrum of olefin A contained bands at 5.25 and 5.8 (terminal methylene) and one methyl now resonated at 8.2. This is compatible with the presence of group II (in olefin A) derived from the dimethyl carbinol. The n.m.r. spectrum of conjugated olefin B (produced by acid-catalyzed rearrangement) showed it to be a mixture containing mainly a tetrasubstituted double bond but also some trisubstituted double bond, while that produced by the base-catalyzed rearrangement of A was almost pure tetrasubstituted

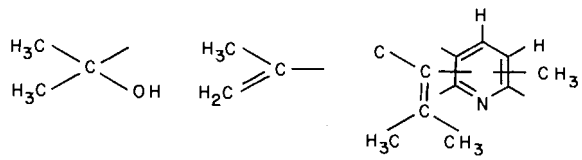

I II III

olefin. In addition to the aromatic methyl signal there were now two other methyls resonating at low field (7.5 and 8.15) which were hence attached to the double bond. It followed that olefin B had partial structure III.

The absence of conjugation other than that to be expected from one double bond and the pyridine ring in olefins A and B meant that to satisfy its empirical formula fabianine had to have two rings. In view of the limited number of carbons left to form it, the only structures compatible with the above evidence had this ring fused to the α and β positions of the pyridine ring.

The carbon in fabianine linking the side chain containing the dimethyl carbinol group to the pyridine ring must carry a tertiary 'benzylic' hydrogen. This left one 'benzylic' hydrogen to account for, from which it followed that the methyl group giving a doublet at 9.1 in the alkaloid had to be on the remaining carbon attached to the pyridine ring. Consideration of the above facts and a possible origin of the aliphatic portion in two

[5]*The n.m.r. data are reported in* τ *values throughout this paper (5).*

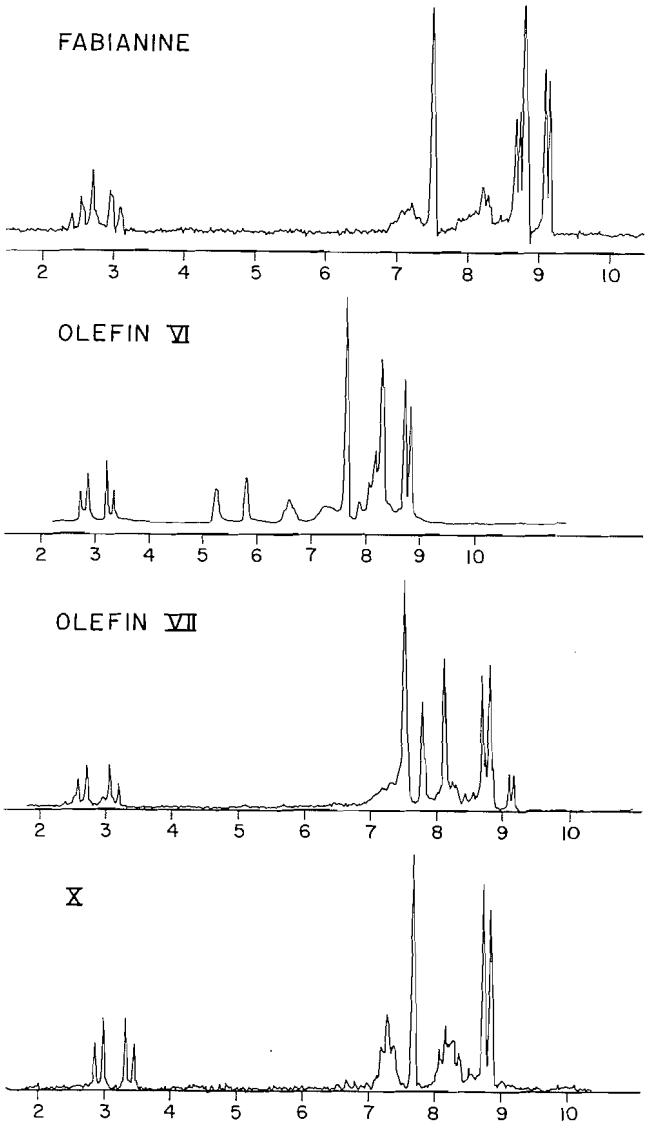

FIG. 1. The n.m.r. spectra (60 Mc, instrument) determined on 10% solutions in CCl_4 with $Si(CH_3)_4$ as internal standard.

isoprene units (see below) led us to consider four expressions for fabianine, IV and (in the unlikely event that rearrangement had taken place in forming olefin B) V and the analogues with the substituents on ring A reversed. The latter possibilities were readily eliminated when it was found that dehydrogenation of both fabianine and olefin B with palladium–charcoal gave 2,5-dimethylquinoline.

Structure IV accounted very neatly for the alkali-catalyzed isomerization of olefin A (VI) to olefin B (VII) via the α-picolyl anion VIII produced by base abstraction of the acidic 8-hydrogen. However, the conditions for the isomerization (180°) were severe enough that this fell short of proving IV to be correct. Similarly, the dehydrogenations

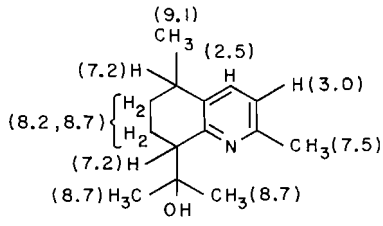

IV

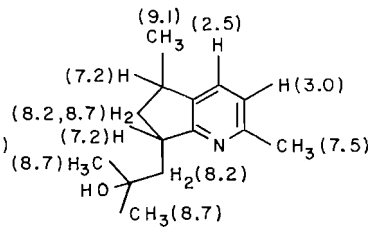

V

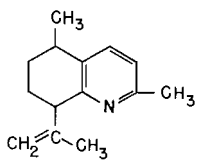

(VI)

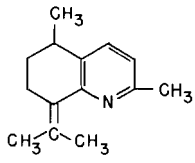

(VII)

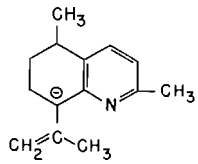

(VIII)

could have involved expansion of a five-membered ring to give the quinoline. The n.m.r. spectrum of fabianine didn't enable us to distinguish between IV and V, although it seemed that it actually fitted V better[6] (see assignments on the formula). However, the n.m.r. spectrum of A fitted structure VI considerably better than that for the terminal olefin derived from V. As indicated earlier, it also appeared very unlikely that both acid- and alkali-catalyzed transformations of A into B would give the same product if a skeletal rearrangement were involved. The n.m.r. spectrum of B fitted formula VII as far as the methyl signals and the absence of olefinic hydrogen were concerned (see Fig. 1) and the spectrum was incompatible with the alternative IX derived from V, thus strongly

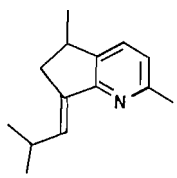

IX

favoring structure IV for the alkaloid. A decisive chemical distinction was sought to strengthen this conclusion.

Inspection of the two structures IV and V suggested that only the former would undergo base-catalyzed fission into acetone and 2,5-dimethyl-5,6,7,8-tetrahydroquinoline (X). When fabianine was heated with potassium hydroxide in ethylene glycol in a slow stream of nitrogen, acetone was formed and was trapped as its 2,4-dinitrophenylhydrazone. After prolonged heating to complete the fission the main fragment was isolated from the reaction mixture; its analysis and n.m.r. (Fig. 1) and infrared spectra were in

[6]*For structure IV the tertiary hydrogen on* C-*8 would be expected to resonate at considerably lower field than the tertiary hydrogen on* C-*5, while for V these should have very similar chemical shifts. Actually these protons were not very well resolved (Fig. 1). In addition the four hydrogens on* C-*6 and* C-*7 might be expected to have chemical shifts near 8.2. Actually, three hydrogens resonate near 8.2 but the fourth appears near 8.7.*

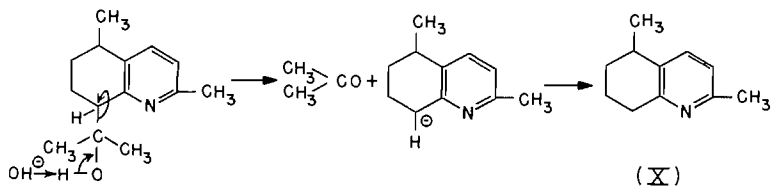

(X)

complete agreement with structure X. We thus consider structure IV for fabianine decisively proved.

It was hoped to deduce the relative stereochemistry of the alkaloid by observing whether or not hydrogenation of A and B produced the same product. Unfortunately similar but not identical mixtures were obtained from both,[7] indicating that double-bond migration had taken place before hydrogenation in the case of A at least.

However, two observations lead us to suggest a cis relation of the substituent at C-5 and C-8 in olefin A. Examination of models (Courtauld) leads us to conclude that the conformation illustrated in XI is the most favorable one for this configuration. This is consistent with the downfield shift of the methyl signal since the double bond and the methyl group are reasonably close, with the methyl in the plane of the double bond. This relative stereochemistry and conformation also account neatly for the large chemical shift difference (33 c.p.s.) between the two vinyl hydrogens since one of them is close to and above the pyridine ring, giving rise to its shielded character (τ = 5.8) (8). The cis relationship of these groups can also be deduced from the argument that only in fabianine is the 5-methyl quasi axial (and resonating at higher field) because the dimethyl carbinol group adopts the quasi-equatorial conformation (stabilized by hydrogen bonding to the nitrogen). When the 5-methyl is quasi equatorial in the two olefins and X, it is deshielded by being in the plane of the pyridine ring.

It is noteworthy that the dehydration of fabianine under two widely different conditions gives rise to the non-conjugated olefin VI instead of the conjugated olefin VII. There is considerable steric hindrance to attack at the 8-hydrogen in fabianine, as opposed to the ready accessibility of the methyl hydrogens and a sixfold multiplicity factor favoring removal of one of these. In addition, if the transition state for the dehydration to the conjugated olefin resembles the product then the serious interaction of the nitrogen and one of the methyl groups (Courtauld model) may impede its development and hence favor formation of the terminal olefin. The nitrogen atom undoubtedly influences the course of the dehydration and we suggest that in the *p*-toluene sulphonic acid catalyzed reaction the positive charge on the nitrogen in the pyridinium salt retards the formation of a proton in its vicinity so the proton is eliminated as far away from this center as

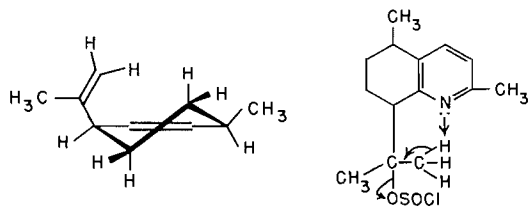

(XI) (XII)

[7]*We are indebted to Dr. H. J. Bernstein for help in analyzing the n.m.r. spectra of these mixtures.*

possible, yielding the terminal olefin. Again, with dehydration by thionyl chloride in pyridine one would expect abstraction of the acidic 8-hydrogen, but the fact that exclusively terminal olefin is produced indicates that an important factor is probably the internal base abstraction of the primary hydrogen in the cyclic process illustrated in XII.

The mother liquors from which fabianine picrate had crystallized yielded another liquid base which was very readily eluted from alumina. Its infrared and n.m.r. spectra were identical with those of 2,5-dimethyl-5,6,7,8-tetrahydroquinoline obtained by degradation of fabianine. Since it could have been formed by the action of the alumina used in regenerating the base from the picrate, a sample of fabianine was adsorbed on alkaline alumina and left for 5 hours. On elution only fabianine was recovered; hence this second tetrahydroquinoline must occur in the plant.

Fabianine is almost certainly constructed in nature from two isoprene units, linked head to tail, and a C_4N unit, probably derived from acetoacetate, as illustrated. The second base (X) could then be produced from it by an enzyme-catalyzed analogue of the retroaldol reaction described earlier.

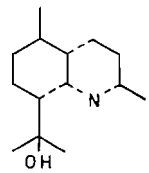

It is interesting to note the recent assignment of structure to skytanthine (9, 10) and actinidine (11), where a monoterpene unit has been used to construct a piperidine and pyridine ring respectively.

EXPERIMENTAL

Ultraviolet spectra were determined in 95% ethanol (ϵ_{max} in parentheses). Unless otherwise stated, Woelm brand neutral alumina was used for chromatography, the cited activity being on the Brockmann scale (12). Distillations were over a short path in a chain of bulbs, the cited temperatures being that of the air bath.

The Extractives of Fabiana imbricata

A 22-kg quantity of twigs and terminal branchlets of *Fabiana imbricata* Ruiz and Pav. were obtained from the S. B. Penick Co. This was finely ground, then percolated exhaustively with ethanol. The resulting extract was concentrated to a thin syrup *in vacuo*. This deposited 180 g of fine crystalline solid which was collected by filtration. The filtrate was taken to a thick syrup on a rotating evaporator, then dilute sulphuric acid added. A further 335 g of solid which separated was removed by filtration, then the neutral and acidic material were extracted from the filtrate into methylene chloride. The organic layer was back extracted with dilute acid. The combined aqueous layers were adjusted to pH 8 using sodium carbonate, then the weak bases (51 g, crude) were extracted into methylene chloride. The aqueous solution was then adjusted to pH 11 using sodium hydroxide and the 'strong bases' (11 g) were extracted into methylene chloride.

The neutral and acidic fractions were separated by distribution between dilute sodium hydroxide solution and methylene chloride. A microcrystalline sodium salt, which separated, was filtered off (wt. 50 g). The neutral extract, with strong aroma, weighed 1900 g, while the acid fraction weighed 1200 g.

The Weak Bases

The crude weak-base fraction was repeatedly extracted with pure ether, leaving a large dark residue of neutral material. The ether extract was concentrated and the residue distilled under 10 mm pressure. The bulk of the base (16 g) distilled as a mobile liquid between 90 and 100°. This still contained considerable neutral material. A further 2.7 g of more viscous distillate was collected at bath temperatures up to 126°.

After a further passage through acid to remove neutral components, the volatile base was redistilled at 70°, 5×10^{-2} mm, giving 11 g of colorless oil. The 'strong-base' fraction proved to be mainly neutral, but a further 2 g of fabianine was recovered from it.

Fabianine

The 13 g of oil was converted to its picrate, which crystallized from concentrated ethanol solution. The salt was recrystallized from ethyl acetate, giving needles, m.p. 114–116°. Calc. for $C_{20}H_{24}N_4O_8$: C, 53.57;

H, 5.39. Found: C, 53.80, 53.76; H, 5.31, 5.50. The pure base was regenerated from the picrate by dissolving the salt in chloroform and passing this solution through a column of alkaline alumina. The eluted base distilled at 74°, 5×10^{-2} mm as a colorless oil with $[\alpha]_D$ less than 1°. Calc. for $C_{14}H_{21}NO$: C, 76.66; H, 9.65; N, 6.39. Found: C, 76.49; H, 9.51; N, 6.17. It had λ_{max} 213 (7440) and 273 (6765) mμ and ν_{max} (liq. film) at 3270 (OH), 1595, and 1575 cm^{-1} (pyridine ring).

Acetylation of Fabianine

Fabianine (120 mg) was dissolved in dry pyridine (5 cc) and acetic anhydride (5 cc) was added. After it was left to stand overnight at room temperature, the mixture was heated for 1 hour on the water bath and the base (117 mg) was isolated. Distillation at 70–75°, 10^{-2} mm gave an oil (62 mg) which was chromatographed on alumina (activity IV). The material eluted with hexane showed strong ester bands ($\nu_{max}^{CHCl_3}$ 1720 and 1280 cm^{-1}) but the substance repeatedly failed to analyze correctly.

Attempted Preparation of Benzylidene Derivative

(*a*) A solution of fabianine (80 mg) and benzaldehyde (80 mg) in 80% ethanol (2 cc) was treated with sodium hydroxide solution (0.2 cc) and left at room temperature for 60 hours. The organic base was isolated in the usual manner. Its infrared spectrum was identical with that of fabianine.

(*b*) Fabianine (100 mg) was dissolved in acetic anhydride (5 cc), and benzaldehyde (2 cc) was added. After 48 hours at room temperature the unchanged base was again recovered.

Attempted Preparation of the Methiodide

(*a*) Fabianine and excess methyl iodide in isopropyl ether were kept at room temperature for 24 hours. After removal of solvent the base was unchanged (infrared spectrum).

(*b*) The base was heated in a sealed tube with methyl iodide and dimethyl formamide for 10 hours at 125°. After tetramethyl ammonium iodide was removed by filtration the residue failed to crystallize.

Attempted Oxidation of Fabianine

(*a*) Fabianine (109 mg, 0.5 mmole) was dissolved in acetic acid (5 cc) and a solution of chromic oxide (50 mg, 0.5 mmole) in water (0.25 cc) was added. After 19 hours at room temperature the solution was still deep red. The base was recovered and its infrared spectrum showed retention of the strong OH band.

Dehydration of Fabianine to VI

(*a*) Fabianine (154 mg) and *p*-toluene sulphonic acid monohydrate (205 mg) were dissolved in acetic acid (10 cc) containing acetic anhydride (1 cc) and the solution was refluxed for 3 hours. After cooling, the solution was diluted to 50 cc with water, neutralized (Na_2CO_3), extracted with ether and the ether extract was dried over magnesium sulphate. Distillation gave a colorless oil (117 mg), b.p. 62–65°, 5×10^{-3} mm. λ_{max} 272 (3925) and 281 (3250) mμ; ν_{max} (liq. film) 882, 1645 cm^{-1} (—CH=CH_2), 1575, 1597 cm^{-1} (pyridine ring). Calc. for $C_{14}H_{19}N$: C, 83.53; H, 9.51; N, 6.96. Found: C, 83.71; H, 9.28; N, 7.05.

(*b*) Fabianine (165 mg) was dissolved in pyridine (2 cc), the flask was cooled in ice water, then thionyl chloride (0.25 cc) was added. The resulting red solution was left to reach room temperature during 2 hours. After hydrolysis with ice, sodium carbonate was added and the solution was extracted with ether. The ether extract was dried ($MgSO_4$), filtered, and evaporated on a rotating evaporator at 40°. The product distilled at 54–59°, 3×10^{-3} mm as a colorless oil (146 mg) whose infrared spectrum was identical with that of the product from the *p*-toluene sulphonic acid dehydration above.

Catalytic Reduction of the Olefin VI

The olefin VI (24 mg) in ethanol (4 cc) was hydrogenated over Pd(C) (20 mg, 10%). Uptake of hydrogen ceased after 90 minutes. The product was isolated in the usual manner and distilled at 52–55°, 10^{-3} mm, giving a colorless, mobile oil. Calc. for $C_{14}H_{21}N$: C, 82.70; H, 10.41. Found: C, 82.34; H, 10.37.

Treatment of Olefin VI with Formic Acid

The olefin (20 mg) in formic acid (10 cc, 98%) was refluxed for 4 hours. After cooling and neutralization (Na_2CO_3) the product was isolated. Its infrared spectrum was identical with that of the starting material.

Dehydrogenation of Fabianine

A bulb containing 190 mg of fabianine and 230 mg of 30% palladium–charcoal was immersed in a bath at 225°. While a slow stream of dry nitrogen was introduced into the bulb the bath temperature was raised during 80 minutes to 250°. This temperature was maintained for 5 hours. After cooling, the mixture was extracted several times with chloroform (total volume 20 cc) and the greenish-brown solution was filtered through a plug of cotton wool. The chloroform was evaporated and the residue on distillation gave 77 mg of a colorless liquid, b.p. 55–60°, 5×10^{-2}. The ultraviolet spectrum of the product had maxima at 234, 236, 282, 293, 306, and 319 mμ and minima at 222 and 249 mμ, corresponding in position and intensity to that of an alkylquinoline (13). The oil was treated with picric acid (100 mg), and ethanol (20 cc) was added. The solution was warmed but all of the solid would not dissolve; when it was cooled a mass of yellow crystals was obtained. The picrate (103 mg) was recrystallized once from ethanol to give yellow needles (71 mg), m.p. 212–216° raised to 217–220° after two crystallizations from methanol. A chloroform solution of the

picrate was filtered through a column of alumina (Fisher) and the base was distilled, giving a colorless oil, b.p. 47–50°, 10^{-3} mm. The n.m.r. spectrum of the base showed 5 aromatic protons and 2 aromatic methyl groups. Calc. for $C_{11}H_{11}N$: C, 84.04; H, 7.05. Found: C, 83.66; H, 6.95. λ_{max} 234 (50,730), 236 (50,360), 293 (4,520), 305 (4,035), and 319 (3,520) mμ.

The infrared spectrum of the base was identical with that of an authentic specimen of 2,5-dimethylquinoline (14).[8] The melting point of authentic 2,5-dimethylquinoline picrate was not depressed on admixture with a sample derived from the dehydrogenation product.

Rearrangement of Olefin VI to Olefin VII

(a) By Sulphuric Acid

The olefin VI (375 mg) was refluxed with sulphuric acid (6 *N*, 20 cc) during 4 hours. After cooling and neutralization (Na_2CO_3) the ether extract was dried ($MgSO_4$) and the product was distilled. Redistillation gave a colorless oil, b.p. 65–75°, 3×10^{-2} mm. λ_{max} 250 (9400) and 296 (7670) mμ; λ_{min} 271 (3455) mμ; ν_{max} (liq. film) 1630 cm^{-1} (tetrasubstituted double bond), 1575 cm^{-1} (pyridine ring). Calc. for $C_{14}H_{19}N$: C, 83.53; H, 9.51. Found: C, 83.28; H, 9.46.

(b) By Potassium Hydroxide

The olefin VI (650 mg) was refluxed for 24 hours with a solution of potassium hydroxide (2 g) in ethylene glycol (30 cc). After dilution with water the olefin was isolated and was dissolved in hexane and chromatographed on a short column of alumina (activity IV). The hexane eluate (60 cc) was evaporated to yield an oil (170 mg), which was distilled, and the fraction boiling at 60–65°, 6×10^{-3} mm was collected. It had λ_{max} 250 (8470) and 296 (6985) mμ; λ_{min} 271 (3760) mμ; ν_{max} (liq. film) 1630 cm^{-1} (double bond), 1570 cm^{-1} (pyridine ring). Calc. for $C_{14}H_{19}N$: C, 83.53; H, 9.51. Found: C, 83.66; H, 9.28.

Reduction of Olefin VII

(*a*) The olefin VII (143 mg) produced by alkaline rearrangement of olefin VI was hydrogenated over Pd(C) (10%) in ethanol at atmospheric temperature and pressure. The product was isolated in the normal manner and distilled at 58–63°, 8×10^{-3} mm as a colorless oil (95 mg).

The infrared spectrum of this reduction product was identical with that of the hydrogenated olefin VI but the n.m.r. spectra showed significant differences.

(*b*) A sample of olefin VII obtained by sulphuric acid rearrangement of olefin VI was reduced in the manner described in (*a*). The product had b.p. 50–54°, 7×10^{-3} mm and its infrared spectrum was almost superimposable upon that of the hydrogenated olefin VI.

Dehydrogenation of Olefin VII

Olefin VII (160 mg), obtained by acid-catalyzed rearrangement of olefin VI, was dehydrogenated by Pd(C) (160 mg, 30%) during 5 hours at 220° in a stream of dry nitrogen. The product (103 mg) was isolated as before and the ether-soluble material was filtered through a short column of alumina (activity IV). The eluted material was distilled up to 125°, 8×10^{-2} mm. The distillate was a pale yellow oil (66 mg) which exhibited a weak alkylquinoline-type ultraviolet spectrum. Picric acid (75 mg) was added to the oil in ethanol and the yellow needles obtained (45 mg) had m.p. 217–218° after recrystallization from methanol. The melting point was undepressed on admixture with a sample of 2,5-dimethylquinoline picrate. The base was regenerated in the usual manner and its infrared spectrum was identical with that of authentic 2,5-dimethylquinoline (14).

Retroaldol Reaction

Fabianine (250 mg) was placed in a two-necked flask connected to two tubes containing 2,4-dinitrophenylhydrazine sulphate in aqueous ethanol. A stream of dry nitrogen was passed through the apparatus. A solution of potassium hydroxide (1.85 g) in ethylene glycol (15 cc) and water (5 cc) was added to the base and the flask was heated slowly in an oil bath. After 4 hours the bath was at 130° and the contents began to boil. An orange solid appeared in the first trap and heating was discontinued after 100 minutes. The hydrazone (38 mg) was filtered and dried and had m.p. 113–119°. It was dissolved in benzene and chromatographed on alumina (Spence 'H'). The derivative was rapidly eluted and the solid obtained on evaporation of the benzene was crystallized three times from methanol and had m.p. 125.5–127°. When mixed with authentic acetone 2,4-dinitrophenyl hydrazone, the m.p. was 126.5–128.5°.

The reaction mixture was refluxed for a further 17 hours and the basic material was isolated in the usual manner. The infrared spectrum still showed some hydroxyl absorption so the oil was dissolved in hexane and filtered through alumina (activity IV). The product (125 mg) distilled as a colorless oil, b.p. 50–55°, 8×10^{-3} mm and was redistilled for analysis. λ_{max} 273 (4810) mμ; λ_{min} 245 (2150) mμ. Calc. for $C_{11}H_{15}N$: C, 81.93; H, 9.38. Found: C, 81.88; H, 9.47.

Isolation of 2,5-Dimethyl-5,6,7,8-tetrahydroquinoline

The mother liquors from the preparation of fabianine picrate were evaporated and the residual gum was dissolved in chloroform. The bases were regenerated from this solution by filtration through alkaline alumina.

[8]*We wish to thank Dr. Léo Marion for a sample of this base.*

Evaporation of the chloroform yielded a red oil which distilled at 85–95°, 5×10^{-2} mm to give a pale yellow oil (920 mg). The oil was dissolved in hexane (3 cc) and was chromatographed on neutral alumina (15 g, activity IV). The first 30 cc of eluate contained 478 mg of base which distilled at 68–73°, 4×10^{-2} mm as a colorless, mobile oil. The n.m.r. and infrared spectra of this oil were identical with those of compound X.

Isolation of p-Hydroxyacetophenone

A neutral component carried with the weak bases in one extraction proved readily separable from fabianine by chromatography on alumina. The more strongly adsorbed fractions yielded the crystalline substance. It crystallized from benzene as colorless needles, m.p. 109–110.5°. It was sublimed at 80°, 5×10^{-1} mm for analysis. Calc. for $C_8H_8O_2$: C, 70.57; H, 5.92. Found: C, 70.90; H, 5.94. A mixed melting point with *p*-hydroxyacetophenone was undepressed.

Isolation of Oleanolic Acid

The insoluble sodium salt described under the general isolation corresponded to the acid which was the main component of the crystalline material obtained directly from the concentrated alcohol extract. After recrystallization from methanol it melted at 299–305° and had $[\alpha]_D$ +76° (*c*, 0.67 in ethanol). It had ν_{max} (nujol mull) at 3400 cm^{-1} (OH) and 1688 cm^{-1} (carboxyl). Its methyl ester (CH_2N_2) melted at 199–201° and had $[\alpha]_D$ +69° (*c*, 0.95 in $CHCl_3$). The acetate was formed from the methyl ester using acetic anhydride–pyridine mixture. It melted at 218–220° and had $[\alpha]_D$ +66° (*c*, 1.65 in $CHCl_3$). Calc. for $C_{33}H_{52}O_4$: C, 77.30; H, 10.22. Found: C, 77.29; H, 10.22. The empirical formulae and physical properties correspond closely to those of oleanolic acid and its derivatives (15).

The Yellow Pigment

The 235 g of solid which precipitated from the concentrated alcohol extract on addition of dilute sulphuric acid was boiled with methanol. The bulk dissolved, leaving a small residue of oleanolic acid. When the solution was concentrated and diluted with water, several small crops of oleanolic acid crystallized, then finally the solution set to a solid mass of fine needles. After repeated recrystallization the compound separated from aqueous methanol as pale yellow needles, m.p. 188–189°. It was insoluble in acetone, chloroform, butanol, and cold water, but dissolved in alkali to give a deep yellow solution. It could be recrystallized from boiling water. It was dried at 100°, 0.1 mm for 4 hours for analysis. Found: C, 49.57; H, 5.93; N, absent. Its infrared spectrum had ν_{max} (nujol) 3405 cm^{-1} (OH), 1658, 1604 cm^{-1} and its ultraviolet spectrum had λ_{max} 258 mμ (E_1^1 = 42.6) and 360 mμ (E_1^1 = 32.1). It had no optical rotation. Further study is needed before an empirical formula can be assigned with confidence.

ACKNOWLEDGMENTS

We are indebted to Mr. A. Knoll for extraction and isolation of the plant constituents, Mr. M. Lesage for the characterization of fabianine, Mr. H. Seguin for the analyses, Mr. R. Lauzon for the infrared spectra, and Mr. J. Nicholson for the n.m.r. spectra.

REFERENCES

1. H. Kunz-Krause. Arch. Pharm. **237**, 1 (1899).
2. G. R. Edwards and H. Rogerson. Biochem. J. **21**, 1010 (1927).
3. L. J. Bellamy. The infrared spectra of complex molecules. Methuen and Co. Ltd., London. 1954. p. 234.
4. E. Godar and R. P. Mariella. J. Am. Chem. Soc. **79**, 1402 (1957).
5. G. V. D. Tiers. J. Phys. Chem. **62**, 1151 (1958).
6. H. J. Bernstein, J. A. Pople, and W. G. Schneider. Can. J. Chem. **35**, 65 (1957).
7. W. G. Schneider, H. J. Bernstein, and J. A. Pople. Can. J. Chem. **35**, 1487 (1957).
8. J. S. Waugh and R. W. Fessenden. J. Am. Chem. Soc. **79**, 846 (1957).
9. C. Djerassi, J. P. Kutney, M. Shamma, J. N. Shoolery, and L. F. Johnson. Chem. & Ind. (London), 210 (1961).
10. G. C. Casinovi, J. A. Garbarino, and G. B. Marini-Bettolo. Chem. & Ind. (London), 253 (1961).
11. T. Sakan, A. Futina, F. Murai, Y. Butsugan, and A. Suzui. Bull. Chem. Soc. Japan, **32**, 315 (1959).
12. H. Brockmann and H. Schodder. Ber. **74**, 73 (1941).
13. R. A. Friedel and M. Orchin. Ultraviolet spectra of aromatic molecules. John Wiley and Sons, Inc., New York. 1951.
14. R. H. F. Manske, L. Marion, and F. Leger. Can. J. Research, B, **20**, 133 (1942).
15. J. L. Simonsen and W. C. J. Ross. The terpenes. Vol. V. Cambridge University Press. 1957. p. 221.

ADSORPTION OF LIGNOSULPHONATES ON SOLIDS

J. BEECKMANS[1]
The Department of Chemistry, Ontario Research Foundation, Toronto, Ontario
Received July 25, 1961

ABSTRACT

The adsorption of various fractionated lignosulphonates on kaolin and on titanium dioxide was studied as a function of acidity and ionic strength. The quantity adsorbed at surface saturation was found to be remarkably dependent on the pH, and to some extent on ionic strength. The adsorption was irreversible with respect to dilution for all but the lowest molecular weight fractions, but desorption could be induced by changes in the pH. This fact was employed to fractionate some lignosulphonates and may be of general utility as a method for fractionating polyelectrolytes. The data are interpreted in terms of the contributions of the electrostatic and hydrogen-bonding forces to the adsorption energy.

INTRODUCTION

The adsorption of the lignosulphonate ion on solids is of interest because of the increasingly widespread use of waste sulphite liquor solids as dispersing agents, but the problem is also of more general interest because of the scantiness of our knowledge of the adsorption of polyelectrolytes. Only a few very limited studies on this subject have appeared in the literature to date, although the subject is potentially very rewarding because of the profound influence of even a very small amount of adsorbed polyion on the electrostatic potential of the surface. Thus polyelectrolytes have been found to act as dispersants in some cases (1) or as flocculating agents (2), or both, depending on the molecular weight. Previous studies with lignosulphonates have indicated that they act as dispersants in neutral solution only in a certain molecular weight range (3). A study on the adsorption of some synthetic polyelectrolytes on kaolin indicated that the pH plays a remarkable role in these systems (4).

Two adsorbents were chosen for this investigation, kaolin because the adsorption of lignosulphonate on clay is of commercial interest, and titanium dioxide, because its zeta potential can be either positive or negative, depending on the pH of the solution (5).

EXPERIMENTAL

Fractionation of Lignosulphonates by Selective Dissolution with Ethanol–Water

The starting material was a commercial paper grade waste sulphite liquor (70% balsam fir, 30% spruce, cooking time 6 hours, maximum cooking temperature 145° C, kindly supplied by Fraser Companies Ltd., Edmundston, New Brunswick). Sugars and other non-lignins were removed by a method described in reference 6. Four liters of waste sulphite liquor were de-ashed on Dowex 50 resin, extracted with 3 volumes of ether, and neutralized to pH 8.1 with calcium hydroxide to precipitate sulphuric and free sulphurous ions. The solution was filtered, de-ashed once more, and shaken with 3.5 liters of 1:4 benzene–butanol containing 10% by volume of tri-*n*-hexylamine. The lignosulphonates combined with the amine and went into the organic phase, and were later back-extracted with sodium bicarbonate solution. The original aqueous phase containing most of the non-lignins was washed with amine solution and discarded. Residual lignosulphonates in the extracted organic phase were stripped out by washing with dilute sodium hydroxide solution. These washings and the main lignosulphonate fraction previously extracted with bicarbonate were de-ashed, neutralized to pH 7, and freeze-dried. The analytical data are given in Table I.

The main-fraction lignosulphonates were separated into three fractions by elution on two grades of Sephadex controlled pore-size gels (Pharmacia, Uppsala, Sweden). Lignosulphonates sufficiently small to enter the grains of Sephadex G25 were labelled fraction 3, and those too large to enter were separated further on a column of Sephadex G50 to give fraction 2 (species sufficiently small to enter the grains) and

[1]*Present address: Department of Physiological Hygiene, School of Hygiene, University of Toronto, Toronto, Ontario.*

TABLE I

Separation of lignosulphonates from waste sulphite liquor

	Weight of solids (g)	Reducing value eq. glucose (g)	Glucose eq. as % of solids	ϵ_{281}* (l. cm^{-1} g^{-1})	Total neutr. eq. (meq.)
Starting material	396	103.2	26.1	10.30	1116
After treatment with $Ca(OH)_2$	435	102.4	23.6	8.38	1018
Main fraction	235.6	7.5	3.18	11.43	657
Washings	20.85	0.5	2.40	12.75	47.7
Sugar fraction	69.5	83.5	120.0	—	28.1

NOTE: some solids were lost in spillage.
*Extinction coefficient at 280 millimicrons.

fraction 1 (species too large to enter the grains). The columns were approximately 80 cm in height and 6 cm in diameter. Samples of the order of 1 g could be processed in one pass. Analytical data on this fractionation are presented in Table II.

TABLE II

Fractionation of purified lignosulphonates on Sephadex gels

Fraction	Weight %	ϵ_{281}	ϵ_{260}	$\epsilon_{231}/\epsilon_{260}$
1	30.1	13.94	10.51	1.327
2	45.3	11.13	7.93	1.405
3	24.6	7.27	4.70	1.547

Each fraction was split into subfractions by selective dissolution with enthanol–water mixtures from a column of Celite 535 (68 cm in height, 3 cm in diameter). The aqueous solution of each fraction was first mixed with a small portion of Celite and freeze-dried. The powdery mixture was then slurried in absolute ethanol and placed on top of the column, which was saturated with ethanol. Successive fractions were obtained by elution with 1-liter portions of ethanol–water followed by 1 liter of absolute ethanol. Results are presented in Table III. Optical absorbencies were measured on a Cary Recording Spectrophotometer Model 14 (Applied Physics Corporation). Equivalent weights were determined by titration with $N/10$ sodium hydroxide using a recording titrimeter. Diffusion coefficients were determined in double-ended cells in $N/20$ KCl, as described in reference 6. Molecular weights were calculated from diffusion coefficients by the equations of McCarthy *et al* (7).

Fractionation by Desorption from Titanium Dioxide

This method of fractionation is based on the observation, to be described below, that a mixture of lignosulphonates may be fractionated by adsorption at low pH followed by desorption induced by stepwise increases in the pH.

Two hundred and fifty milliliters of waste sulphite liquor (ammonia base, paper grade, 10.13% solids) was diluted to 7 liters with N HCl. Five pounds of titanium dioxide (Fisher reagent grade) was dispersed in the solution with vigorous stirring. The slurry was filtered and washed with 4 liters of N HCl, excess fluid being removed by suction. The filtrate and washings were discarded, and the solids were redispersed in 4 liters of 0.1 N sodium acetate – acetic acid buffer, to give a suspension of pH 3.2. The filtrate from this suspension, together with washings (using the same solvent), contained desorbed lignosulphonates which after removal of small anions by elution on Sephadex G25 and neutralization were labelled fraction T1. The procedure was repeated with buffer mixtures of higher pH to yield two more fractions, T2 at pH 4.7 and T3 at pH 6.0. Analytical data on these fractions are given in Table IV. They were not tested for reducing value because of lack of material, but in view of the method of preparation and of the relatively high absorbencies at 281 mμ it seems unlikely that they contained much sugar.

Adsorption Measurements

Adsorption measurements were made in cylindrical Pyrex cells 15 cm long and 2.8 cm in diameter consisting of a body with a 24/40 female ground-glass joint at one end with cap to fit. The insides of these cells and all ground surfaces were made water repellent by treatment with a 10% solution of Dow Corning 200 silicone fluid in toluene, followed by a 1-hour baking period at 265° C to polymerize the silicone into an insoluble film. This treatment practically eliminated any contact between the grease used to lubricate the joint and the contents of the cell. The cells were tumbled at 60 r.p.m. in a water thermostat during

TABLE III

Fractionation of lignosulphonates by elution with ethanol–water

Original fraction	Eluted fractions	% water in eluting solution	Weight % of fraction	ϵ_{231} (l. cm^{-1} g^{-1})	$\epsilon_{231}/\epsilon_{260}$	Equivalent weight	Diffusion coefficient $\times 10^7$ (cm^2/sec)	Molecular weight
1	1A	85	22.6	13.25	1.360	482	17.9	9,300
	1B	83	33.1	13.84	1.317	454	13.2	15,800
	1C	81	27.4	14.27	1.274	595	8.8	32,000
	1D	79	3.9	13.22	1.234			
	1E	75	4.9	13.41	1.250			
	1F	0	8.1	13.12	1.213	542	8.3	34,700
2	2A	86	54.4	11.55	1.571	210	23.4	4,310
	2B	83	31.2	11.96	1.389	363	21.1	5,700
	2C	81	9.6	10.53	1.301			
	2D	77	3.6	10.60	1.230			
	2E	0	1.2	9.65	1.064			
3	3A	0	Negligible	—	—			
	3B	95	20.6	6.48	1.768	255	45.6	580
	3C	92	42.8	9.47	1.584	306	33.9	1,400
	3D	90	24.7	11.40	1.264			
	3E	88	5.6	6.80	1.117			
	3F	85	3.4	3.69	1.090			
	3G	82	2.9	4.46	1.092			
	3H	0	Lost	—	—			

TABLE IV

Lignosulphonate fractions obtained by desorption from titanium dioxide

Fraction	Weight (g)	Equivalent weight	Diffusion coefficient $\times 10^7$ (cm^2/sec)	Molecular weight	ϵ_{281}	$\epsilon_{281}/\epsilon_{260}$
T1	2.59	513	14.4	13,600	13.91	1.389
T2	1.06	584	10.8	21,700	13.50	1.343
T3	0.21	569	9.8	26,400	12.47	1.307

equilibration. Isotherm points were determined in the usual manner by observing the decrease in concentration of a solution of adsorbate in contact with a known quantity of adsorbent. Twenty-five milliliters of solution consisting of lignosulphonate dissolved in buffer was added to a cell containing the adsorbent (usually 1±0.001 g). After a period of agitation (generally 8 hours) the suspension was allowed to settle for a few hours and then 10 ml of supernatant solution was withdrawn with a pipette. The solution was shaken with 1 ml of chloroform to reduce the size of the blank, and in addition, in some cases 0.1 ml of concentrated sulphuric acid was added to assist in clarification. These operations each resulted in a decrease of approximately 1% in the concentration of adsorbate and were allowed for in the calculations. They resulted in very considerable decreases in the blank readings. Finally the solutions were centrifuged at 2000 r.p.m. for 30 minutes and their optical absorbencies at 281 mμ were determined.

The titanium dioxide was obtained from Fisher Scientific Company, and was stated to be in the anastase form. Its specific surface as determined by argon adsorption was 4.65 m^2/g, and by adsorption of the dye crystal violet, 4.96 m^2/g (8).

The kaolin was supplied by the Merck Chemical Company, and its specific surface was 10.2 m^2/g by argon adsorption. Dispersion in water followed by drying at 110° C produced no change in the specific surface of either adsorbent.

RESULTS

Adsorption Isotherms

Adsorption was found to be rapid, irreversible, and independent of temperature in the range 25° to 35° C for most fractions, although some of the lowest molecular weight fractions showed partial reversibility. These findings are in agreement with those of Rezanowich *et al.* (3).

Three types of isotherms were obtained, which could be plotted as straight lines either according to the Langmuir equation or by a modification in which only extensive variables were used. Examples of these isotherms are given in Fig. 1. The modified Langmuir equation may be written as follows:

$$[1] \qquad \frac{Q-\Gamma}{\Gamma} = \frac{Q-\Gamma}{\Gamma_m} + k,$$

where Q is the total quantity of adsorbate added to the system, Γ the quantity adsorbed, Γ_m the quantity adsorbed at surface saturation, and k the intercept. This equation is independent of the volume of solution in the system, as required by the irreversibility of the adsorption process. Incomplete adsorption at less than maximum coverage in a system which adsorbs irreversibly implies fractionation of the adsorbate, and the isotherm provides some information on the heterogeneity of the sample. With a perfect fraction the adsorption is complete up to surface saturation and ceases at this point. Hence $(Q-\Gamma)$ must equal zero in equation [1] for Q less than Γ_m, with Γ equalling Γ_m for Q greater than Γ_m. This implies that the fixed term k equals zero, and the Langmuir plot becomes a straight line of slope Γ_m^{-1} passing through the origin, as the type A isotherm, Fig. 1.

Isotherms obtained with fractions which fractionate even at the limit of zero adsorption will have a positive intercept on the Langmuir plot. In the limit of zero Q and zero Γ,

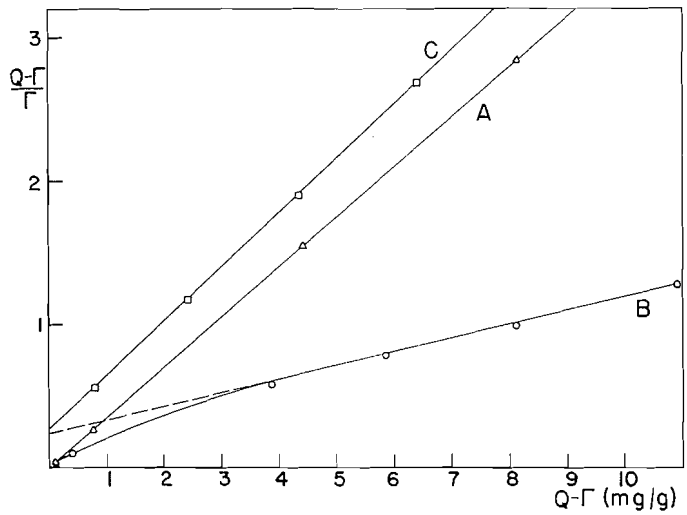

FIG. 1. Typical adsorption isotherms, illustrating three types obtained: A, adsorption of fraction Tl–2 on kaolin at pH 4.7; B, adsorption of fraction 2B on titanium dioxide at pH 1.1; C, adsorption of fraction 2B on kaolin at pH 4.7.

the ratio Γ/Q assumes a value α which equals the proportion of the adsorbate which adsorbs at the limit of zero adsorption. At this point equation [1] condenses to

$$\alpha = 1/(k+1). \qquad [2]$$

The parameter α, together with Γ_m, is used to characterize the results (Tables V and VI).

The partial fit of the data to the Langmuir equation must of course be purely fortuitous, since the considerations used in deriving that equation do not apply in this case. The type C isotherm is a limiting case applicable to an heterogeneous and poorly adsorbing adsorbate which only partially adsorbs at zero coverage. The type B isotherm was more common and represents an intermediate case in which initially the adsorption is total, with fractionation becoming very appreciable, well before completion of the monolayer.

Desorption Experiments

As may be seen in Table V the adsorbed lignosulphonates are much more densely packed on the surface at low pH values. It was found that adsorbed polyions which were attached irreversibly with respect to dilution of the 'equilibrium' solution at constant pH and supporting electrolyte concentration could nevertheless be desorbed by raising the pH, although, as was to be expected with such a system, there was some hysteresis. The saturation adsorption curves for a number of desorbing fractions were determined as follows. One gram of adsorbent was placed in a cell and dispersed with sufficient lignosulphonate dissolved in 0.1 *N* HCl to saturate the surface at that pH. After achievement of equilibrium and settling of the solids, 10 ml of the supernatant solution was withdrawn for analysis and replaced with 10 ml of 0.1 *N* buffer of a higher pH than the solution. The process was then repeated till the pH had reached a value of 11.7. The results are plotted in Figs. 2 and 3.

In the experiments described above, the surfaces of the adsorbents were saturated with adsorbent throughout the course of the run. Another experiment was made with one

TABLE V

Adsorption of fraction T1 lignosulphonates on titanium dioxide at various ionic strengths

	HCl–NaCl pH 1.1		Acetic acid – NaCl pH 2.7		Acetic–acetate buffer – NaCl pH 4.7	
Ionic strength	Γ_m	α	Γ_m	α	Γ_m	α
0.10	10.90	0.947	5.07	0.962	2.25	0.481
0.60	9.57	0.967	6.42	0.769	3.67	0.820
2.60	11.65	0.730	10.72	0.730	5.06	0.629

TABLE VI

Adsorption of lignosulphonates from 0.1 *N* solutions of supporting electrolyte

Fraction	Molecular weight	Hydrochloric acid pH 1.1		Acetic acid pH 2.7		Acetic–acetate buffer pH 4.7		Sodium acetate pH 7.3	
		Γ_m	α	Γ_m	α	Γ_m	α	Γ_m	α
Titanium dioxide									
3B	580	—	Low	—	—	—	—	—	—
3C	1,400	4.63	0.472	2.04	0.333	Low	Low	—	—
2B	5,700	10.52	0.813	4.25	0.784	2.61	0.317	Low	Low
1A	9,300	11.51	0.945	5.88	0.902	3.17	0.394	Low	Low
1C	32,000	13.45	1.00	5.90	1.00	3.43	1.00	2.86	0.50
1F	34,700	14.35	1.00	6.06	1.00	3.14	0.945	1.40	0.769
T1	14,000	10.90	0.947	5.07	0.962	2.25	0.481		
T2	22,000	11.02	0.999	5.45	0.996	1.96	0.972		
Kaolin									
3B	580	—	Low						
3C	1,400	3.69	0.440	3.58	0.424	1.96	0.417		
2B	5,700	6.45	0.730	3.53	0.858	3.26	0.646	2.18	0.757
1A	9,300	7.66	0.894	5.08	0.960	3.29	0.757	2.22	0.885
1C	32,000	8.14	1.00	5.83	1.00	3.82	1.00	2.94	1.00
1F	34,700	9.45	1.00	5.09	1.00	3.60	1.00	3.41	1.00
T1	14,000	6.55	0.834	3.61	0.999	2.54	1.00		
T2	22,000	6.97	0.985	4.19	1.00	2.81	0.980		

NOTE: Γ_m expressed in milligrams adsorbed per gram of adsorbent.

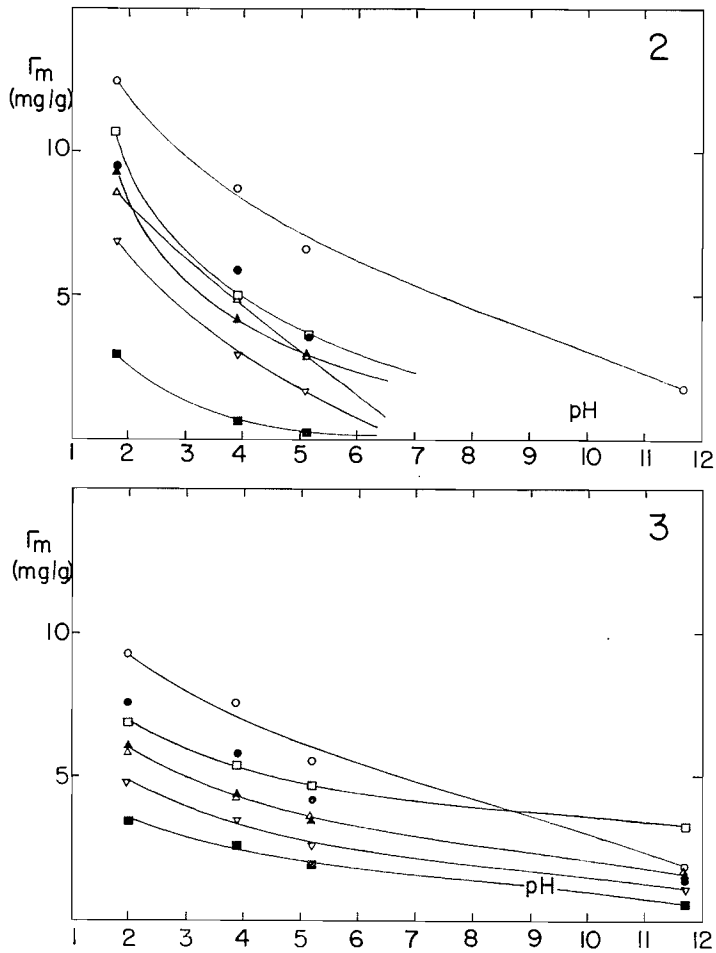

FIG. 2. Desorption of lignosulphonates from titanium dioxide as a function of pH: ○ 1F, ● 1C, □ T2, △ T1, ▲ 1A, ▽ 2B, ■ 3C.

FIG. 3. Desorption lignosulphonates from kaolin as a function of pH: ○ 1F, ● 1C, □ T2, △T1, ▲ 1A, ▽2B, ■ 3C.

system only, fraction 1A on titanium dioxide, at a number of unsaturated surface concentrations. The pH was raised from 1.1 to 4.7 in one step. The Langmuir constants of this run (at pH 4.7) were 3.98 for Γ_m and 0.612 for α. These figures may be compared with 3.17 and 0.394 for adsorption at pH 4.7.

DISCUSSION

The mechanism of the adsorption of a polyelectrolyte may be considered to be basically similar to that of the adsorption of a non-ionic polymer, but modified by the presence of electrostatic forces between the polyion and the solid surface, and by the intra- and inter-molecular forces between the charges on the polyions. The theoretical aspects of the adsorption of flexible non-ionic polymers have been treated in detail by Frish, Eirich, and Simha (9, 10, 11, 12). Their statistical mechanical analysis indicates that only a small number of randomly located segments of the flexible polymer chain are actually adsorbed

on the surface, the intervening segments forming bridges extending away from the surface into the solution. At low surface coverage the number of adsorbed segments per molecule and the heat of adsorption are approximately proportional to $t^{\frac{1}{2}}$, t being the number of segments per molecule. At higher coverage a second term proportional to t must be added. If the interaction potential between polymer and solid extends for a finite distance away from the surface and is large in relation to kT, the heat of adsorption and Γ_m become proportional to t, and the isotherm becomes very steep in the region of zero concentration. These conclusions have on the whole been substantiated by experimental results.

Jenckel and Rumbach (13) found that the quantity of polymer adsorbed was very large compared with that required for monolayer coverage for a number of polymers adsorbed on quartz, aluminum, glass wool, and carbon. Kolthoff, Gutmacher, and Kahn (14) and Kolthoff and Gutmacher (15), working with various rubber fractions adsorbed on carbon blacks, showed that the saturation adsorption on a given adsorbent depended on the solvent and on the pretreatment of the adsorbent. Kraus and Dugone (16), using similar systems, found good agreement of their results with the Frish–Eirich–Simha equation, but this must be to some extent fortuitous since the adsorption was partially irreversible. The high molecular weight species tended to displace lower molecular weight species from the surface in most of these investigations. It should, however, be mentioned that in at least one case the results seemed to indicate that the adsorbate lay flat on the surface (17).

More direct evidence in support of the Frish–Eirich–Simha theory is furnished by the work of Miller and Grahame (18) on the differential capacity of the interface between mercury and a solution containing polymethacrylic acid at low pH. A sharp peak in the differential capacity curve was interpreted as being due to rapid adsorption and desorption of polymer segments in phase with the 1000 cycle superimposed a-c. signal. Since entire polymer molecules would diffuse far too slowly to follow such rapid fluctuations the conclusion was reached that the bulk of the 'adsorbed' molecules lies in a surface phase parallel to but not touching the mercury, being held there by rather loose bonds between the mercury and a small number of segments in contact with it.

Finally, the paper by Heller and Pugh (19) on the protective action of polyethylene glycols of various molecular weights on gold sols may be cited in support of the view that large molecules are adsorbed in such a manner as to hinder the approach of sol particles to within a distance greater than the range of the attractive forces.

There appears to be even less data in the literature on the adsorption of polyelectrolytes than on the adsorption of non-ionic polymers. A systematic study of the effects of variables such as the molecular weight, the pH, and the ionic strength of the supporting electrolyte is still awaited, although some work has been done on the action of polyelectrolytes as flocculating or sensitizing agents. In general, polyions of opposite charge to that of the sol cause flocculation at low values of the surface coverage, and peptize at higher concentrations (20, 21). These facts are easily explicable in terms of an increase or a decrease in the effective surface charge due to adsorption of the polyion.

The adsorption of sodium polyacrylate and hydrolyzed sodium polyacrylamide on kaolin was studied by Michaels and Morelos (4), who found that the adsorption decreased sharply as the pH was raised, and became zero in the region of pH 8. These authors postulated hydrogen bonding between the unionized carboxyl groups and the oxygen atoms of the clay surface, which would favor increased adsorption at low pH.

The quantity of polymer adsorbed at surface saturation should be fairly independent of molecular weight, as the following reasoning will show. Let the polymer molecules of molecular weight M be represented by impenetrable spheres of radius R. If these spheres become attached at random to the surface a saturation value will ultimately be attained. Let θ be defined as the total projected area of the spheres per unit area of surface. The maximum value of θ is clearly $\Pi/4$, corresponding to close packing on a square lattice, but for random deposition θ will be less than this value. At saturation we have

$$[3] \qquad \frac{\Gamma_m}{A} = \frac{M\theta}{4R^2N_0},$$

N_0 being Avogadro's number, and A the specific surface of the adsorbent.

Strictly speaking R should be taken as the radius of the equivalent excluded volume sphere (22), but this is a refinement probably not justified when applied to a polyelectrolyte. As a useful approximation R will be taken as the root mean square distance of the polymer segments from the center of gravity of the molecule, $\overline{S^2}$. The ratio of M to $\overline{S^2}$ is constant for a non-ionic polymer homologous series, and was found to be constant (21.9×10^{16} g cm^{-2}mole^{-1}) for lignosulphonates in the molecular weight range 4,000–19,000 when checked by means of the intrinsic viscosity – number-average molecular weight data of Gardon and Mason (22) (for method of calculation of $\overline{S^2}$, see pp. 612 and 408 of reference 23). Substitution of $\overline{S^2}$ for R^2, 21.9×10^{16} for $M/\overline{S^2}$, and $\Pi/4$ for θ in equation [3] leads to the constant value 7.15×10^{-8} for Γ_m/A. Independence of the saturation adsorption from the molecular weight of the adsorbate has been found in most investigations (1, 15, 16) with non-ionic polymers.

Substitution of appropriate values for A yields the following values for Γ_m:

on titanium dioxide (A = 4.65 m^2/g)	3.33 mg/g,
on kaolin (A = 10.2 m^2/g)	7.30 mg/g.

These values are quite close to the observed saturation adsorptions in the vicinity of the isoelectric point of the adsorbents, approximately at pH 4 for titanium dioxide (5), and presumably at a low pH for kaolin.

The thermodynamic irreversibility of the adsorption process indicates a rather large molar heat of adsorption. On the other hand the ability to desorb on a rise in the pH of the medium points to the presence of strongly repulsive forces between solid and adsorbate or between adsorbate molecules. The forces favoring adsorption must be sufficiently large to overcome the opposing forces of desorption, and by a margin sufficiently great to render the adsorption irreversible. In other words, the net heat of adsorption must be large in relation to product of the absolute temperature and the entropy difference between adsorbed and unadsorbed polymer molecules. It appears unlikely that van der Waals forces alone could account for such an adsorption energy, even in the case of the higher molecular weight species, where the heat of adsorption would increase with molecular weight, since the opposing forces would also be rising functions of the molecular weight. Some kind of bonding, probably hydrogen bonding as suggested by Michaels and Morelos (4) or possibly an interaction with cations attached to ion-exchange site on the solid, appears to be required.

Repulsive forces may arise from electrostatic interactions between the ionized segments of the adsorbed molecules, which would tend to push the adsorbed molecules apart, and between the adsorbent and the charged ionized polymer segments, which would tend to

push the adsorbed molecules away from the surface. Qualitative electrophoretic measurements showed that the positively charged titanium dioxide sol in acid medium changes sign on adsorption of only a fraction of a monolayer of lignosulphonate. Hence even in an acid medium it would appear that the electrostatic surface forces are predominantly repulsive.

The effect of a decrease in the pH should, therefore, favor the adsorption process in three ways: firstly, by increasing the number of available unionized sulphonic acid groups in the polyelectrolyte capable of hydrogen bonding with oxygen atoms in the surface of the solid; secondly, by reducing the mutual repulsion between polyelectrolyte segments; and thirdly, by making the zeta potential of the adsorbent more positive. Similarly, an increase in the ionic strength should favor adsorption, because of reduced ionization and this was observed (Table VI). A more detailed analysis of these phenomena must be deferred until publication of a study of the adsorption of a synthetic polyelectrolyte of constant equivalent weight and constant composition.

The fractionation which occurs on desorption must be due to differences in the balance between attractive and repulsive forces with molecular weight, the larger species presumably having a greater net heat of adsorption at a given pH. This effect would be enhanced by the tendency to an increasing equivalent weight with increasing molecular weight. It may be remarked that a fractionation based on a pH-controlled adsorption–desorption method has theoretical advantages over conventional methods based on a partition between solvents. In the latter all species must be represented in both phases at equilibrium, and it may be shown (22) that a perfect fractionation can only be approached by means of an infinite phase volume ratio, a condition clearly impossible of attainment in practice. The pH-controlled desorption method on the other hand is a non-equilibrium system, and it should be possible to achieve excellent fractionation by very small changes in the pH. The method will shortly be tried with a synthetic polyelectrolyte, in which the complicating factor of variations in the equivalent weight will be absent.

ACKNOWLEDGMENT

This research was made possible by a grant received by the Ontario Research Foundation from the Province of Ontario through the Department of Commerce and Development.

REFERENCES

1. F. M. Ernsberger and W. G. France. Ind. Eng. Chem. **37**, 598 (1945).
2. A. S. Michaels. Ind. Eng. Chem. **46**, 1485 (1954).
3. A. Rezanowich, J. Jaworzyn, and D. A. I. Goring. Pulp and Paper Mag. Can. 62C, T-172 (1961).
4. A. S. Michaels and O. Morelos. Ind. Eng. Chem. **47**, 1801 (1955).
5. P. G. Johansen and A. S. Buchanan. Austr. J. Chem. **10**, 392 and 398 (1957).
6. E. Eisenbraun. To be published.
7. J. Moacanin, V. F. Felicetta, W. Haller, and J. L. McCarthy. J. Am. Chem. Soc. **77**, 3470 (1955).
8. W. W. Ewing and F. W. J. Liu. J. Colloid Sci. **8**, 204 (1953).
9. H. L. Frish, R. Simha, and F. R. Eirich. J. Chem. Phys. **21**, 365 (1953).
10. R. Simha, H. L. Frish, and F. R. Eirich. J. Phys. Chem. **57**, 584 (1955).
11. H. L. Frish and R. Simha. J. Phys. Chem. **58**, 507 (1954).
12. H. J. Frish. J. Phys. Chem. **59**, 633 (1955).
13. E. Jenckel and R. Rumbach. Z. Elektrochem. **55**, 612 (1951).
14. I. Kolthoff, G. S. Gutmacher, and A. Kahn. J. Phys. Chem. **55**, 1240 (1951).
15. I. Kolthoff and G. S. Gutmacher. J. Phys. Chem. **56**, 740 (1952).
16. G. Kraus and J. Dugone. Ind. Eng. Chem. **47**, 1809 (1955).
17. J. S. Binford and A. Gessler. J. Phys. Chem. **63**, 1376 (1959).
18. J. R. Miller and D. C. Grahame. J. Am. Chem. Soc. **78**, 3577 (1956).
19. W. Heller and T. Pugh. J. Chem. Phys. **22**, 1778 (1954).
20. R. A. Ruehrwein and D. W. Ward. Soil Sci. **73**, 485 (1952).
21. W. Heller and T. Pugh. J. Chem. Phys. **24**, 1107 (1956).
22. J. L. Gardon and S. G. Mason. Can. J. Chem. **33**, 1491 (19[illegible]
23. P. J. Flory. Principles of polymer chemistry. Cornell. 195[illegible]

THE CONFIGURATION OF GLYCOSIDIC LINKAGES IN OLIGOSACCHARIDES

X. KÖNIGS–KNORR REACTIONS OF 3,5-DI-*O*-BENZOYL-ARABINO- AND -RIBO-FURANOSYL BROMIDES AND THEIR 2-SUBSTITUTED DERIVATIVES[1]

P. A. J. GORIN

The National Research Council of Canada, Prairie Regional Laboratory, Saskatoon, Saskatchewan

Received August 31, 1961

ABSTRACT

The reactions of 3,5-di-*O*-benzoyl-L-arabinofuranosyl and -D-ribofuranosyl bromides and their 2-substituted 1,2-trans-derivatives (2-acetates, 2-benzoates, 2-*p*-nitrobenzoates, and 2-nitrates) with methanol and 1,2,3,4-tetra-*O*-acetyl-β-D-glucose have been studied. The products of these reactions, the occurrence of retention or inversion of configuration or ortho-ester formation, and the suitability of bromo derivatives for stereospecific synthesis of glycosidic linkages were considered. In general, the syntheses of oligosaccharides are more stereospecific than the corresponding formation of methyl glycosides. As in the α-D-mannopyranosyl bromide series, the reactions with tetra-*O*-acetyl-glucose give products with retention of configuration about C-1, presumably via an intermediate cyclic carbonium ion when there is an ester at C-2, but retention can take place also even when there is no convenient ester group at C-2 of the bromide. The participation of the C-2 substituent is particularly noteworthy in the condensations of the 2-acetate and 2-benzoate derivatives of 3,5-di-*O*-benzoyl-β-D-ribofuranosyl bromide with 1,2,3,4-tetra-*O*-acetyl-β-D-glucose, which yield exclusively disaccharides of the orthoester type.

INTRODUCTION

In a previous paper (1) various derivatives of α-D-mannopyranosyl bromide were used in condensation reactions with hydroxyl compounds under Königs–Knorr conditions. In some cases the configuration of the product was different from that expected on the basis of earlier work (summarized in refs. 2 and 3). For instance, 3,4,6-tri-*O*-acetyl-α-D-mannopyranosyl bromide and its 2-*O*-benzyl derivative both gave disaccharides with an α-configuration on condensation with 1,2,3,4-tetra-*O*-acetyl-D-glucose. Previously, reactions examined in which a substituent in the 2-position could not participate by forming an intermediate cyclic carbonium ion (e.g. 2,3,4,6-tetra-*O*-acetyl-α-D-gluco- and -D-galactopyranosyl bromides) have given products with the configuration opposite to that of the starting material. A qualitative and semi-quantitative study has now been made using 1-bromo derivatives of L-arabino- and D-ribo-furanose benzoates in which the bromo groups are also mainly trans to the C-2 substituent. The nature of the grouping at C-2 was varied and the configuration and structure of the products studied in two series of experiments. These reactions were carried out in the presence of silver oxide (*a*) with pure methanol and (*b*) with an excess of tetra-*O*-acetyl-D-glucose in chloroform in the presence of Drierite.

The current interest in nucleosides and nucleotides has focussed attention on stereospecific Königs–Knorr syntheses of pentofuranosyl glycosidic linkages. β-D-Ribofuranosyl derivatives have been prepared from 2,3,5-tri-*O*-acetyl-α-D-ribofuranosyl chloride (4) and bromide (configuration unknown) (5) and 2,3,5-tri-*O*-benzoyl-β-D-ribofuranosyl bromide (6, 7) whereas α-D-ribofuranosides can be derived from 5-*O*-benzoyl-2,3,-*O*-carbonyl-D-ribofuranosyl bromide (8). In the arabinofuranosyl series the α-configuration is readily attainable and has been synthesized by Wright and Khorana, who used 2,3,5-tri-*O*-benzoyl-α-D- and -L-arabinofuranosyl bromides (9) and a 2,3,5-tri-*O*-acetyl-L-arabinofuranosyl bromide (9) of uncertain configuration. β-D-Arabinofuranosides are of interest

[1]*Issued as N.R.C. No. 6657.*

because of their natural occurrence in the nucleosides of sponges (10, 11). The Königs-Knorr synthesis of this type of linkage does not appear to have been carried out, although it has been formed by the inversion of the C-2 hydroxyl group of a D-ribofuranosyl uracil (12) and thymine (13, 14) derivatives. Although the conditions used above are different from those for disaccharide synthesis, it appeared that some of these bromides could be adapted for the preparation of α-L-arabinofuranosyl and β-D-ribofuranosyl disaccharides. Thus, the condensation of 2,3,5-tri-*O*-benzoyl-α-L-arabinofuranosyl bromide with 2,3,4-tri-*O*-acetyl-L-arabinose diethyl dithioacetal has now led to the synthesis of 5-*O*-α-L-arabinofuranosyl-L-arabinose, a structural component in sugar beet pentosan (15).

The use of substitutents on C-2 of a sugar bromide in order to control the configuration of the product has been demonstrated in the D-ribofuranose (8), the D-glucopyranose (16, 17, 18*a*), and the D-mannopyranose series (1), and use of this technique has now been utilized in the L-arabinofuranosyl and D-ribofuranosyl series. Convenient compounds for such starting materials in the preparation of 1-bromo derivatives of L-arabino- and D-ribo-furanose have been described by Fletcher and Ness (19, 20). These are 1,3,5-tri-*O*-benzoyl-β-L-arabinose and 1,3,5-tri-*O*-benzoyl-α-D-ribose, and from these compounds the 2-acetates (19, 21), 2-nitrates, and 2-*p*-nitrobenzoates can be prepared using conventional reactions. Treatment of these products with chloroform containing hydrogen bromide until constant rotation had been reached furnished the 1-bromo derivatives (Table I),

TABLE I

3,5-Di-*O*-benzoyl-L-arabino- and -D-ribo-furanosyl bromide derivatives and their reaction products with methanol and 1,2,3,4-tetra-*O*-acetyl-β-D-glucose

2-Substituted bromo derivatives	Specific rotations	Product from methanol	Product from 1,2,3,4-tetra-*O*-acetyl-β-D-glucose
3,5-Di-*O*-benzoyl-L-arabinofuranose			
α-2-Acetate	−112°	Mainly orthoacetate*	α-Disaccharide*
		α- and β-Glycoside	Trace of β
α-2-Benzoate		Orthobenzoate	α-Disaccharide
		α- and β-Glycoside (β > α)	Trace of β
α-2-*p*-Nitrobenzoate	−63°	Ortho-*p*-nitrobenzoate	α-Disaccharide
		α- and β-Glycoside (β > α)	Trace of β
α-2-Nitrate	−65°	β-Glycoside	β-Disaccharide
			Trace of α
α-2-Hydroxyl	−103°	β-Glycoside	α and β-Disaccharide (39:61)
3,5-Di-*O*-benzoyl-D-ribofuranose			
β-2-Acetate	−52°	Orthoacetate	Orthoester
		α- and β-Glycoside	
β-2-Benzoate	−11°	Orthobenzoate	Orthoester
		β-Glycoside	
β-2-*p*-Nitrobenzoate	+8°	Ortho-*p*-nitrobenzoate	β-Disaccharide
		α- and β-Glycoside	Orthoester
β-2-Nitrate	−39°	α-Glycoside	α- and β-Disaccharide (32:68)
		Trace of β	
α-2-Hydroxyl	+109°	α- and β-Glycoside	α- and β-Disaccharide (46:54)

*In all these reactions some free arabinose (or ribose) was obtained on de-esterification. However, the purpose of the paper is to compare orthoester and α- and β-glycoside formation.

which were used immediately because of possible instability. From the specific rotations of the bromides it was concluded that all the L-arabinofuranose derivatives were predominantly α and the D-ribofuranose compounds β, with the notable exception of 3,5-di-*O*-benzoyl-D-ribofuranosyl bromide (20), which appeared to be α because of its marked difference in specific rotation from the rest of the series (Table I).

When the 2-benzoates, 2-*p*-nitrobenzoates, and 2-acetates of 3,5-di-*O*-benzoyl-L-arabinofuranosyl bromide and 3,5-di-*O*-benzoyl-D-ribofuranosyl bromide were treated in one series of experiments with methanol and in the other with 1,2,3,4-tetra-*O*-acetyl-β-D-glucose (silver oxide being used in both cases as acid acceptor, with iodine present also in the arabinofuranosyl disaccharide syntheses) the course of reaction could be anticipated to some extent by taking into account participation, prior to glycoside formation, of the 2-substituted group via intermediate cyclic carbonium ions. In the L-arabinose series, methanol treatment of these bromides resulted in the formation of orthoester derivatives and methyl arabinofuranosides of which the β-anomer predominated. These results are essentially analogous to those obtained by Isbell and Frush when 2,3,4,6-tetra-*O*-acetyl-α-D-mannopyranosyl bromide was treated with methanol in the presence of silver carbonate (22) except that in this instance some methyl α-L-arabinofuranoside was formed in addition to the β-anomer. Also analogous were the results from the use of excess 1,2,3,4-tetra-*O*-acetyl-D-glucose as the nucleophilic reagent (1). The disaccharide formed after deacetylation was 6-*O*-α-L-arabinofuranosyl-D-glucose (characterized as the free sugar and its heptaacetate) with little of the β-anomer. However, mixtures of α- and β-disaccharides (39:61) were formed from 3,5-di-*O*-benzoyl-α-L-arabinofuranosyl bromide, in contrast to the product formed from 3,4,6-tri-*O*-acetyl-α-D-mannopyranosyl bromide, which was mainly α in configuration (1). The possibility that the C-5 benzoyl group could participate in this reaction via a cyclic carbonium ion seems unlikely since on treatment with methanol the bromide yielded methyl β-L-arabinofuranoside and no 1,5-orthobenzoate.*

No orthoesters were obtained from the reaction of the arabinofuranosyl bromides with tetra-*O*-acetyl glucose, but their absence may have been due to the excess of acid which was found to be produced in early stages of the condensations. The Königs–Knorr condensations described in this paper were not carried out under optimum conditions in which the halide would be added slowly to an excess of the alcohol (23). Since some of the pentofuranosyl bromides were somewhat unstable, the mixture of alcohol and other components were added in one batch to a flask containing the bromide, immediately after its preparation. Such conditions were probably also responsible in all the condensations for a product in which gentiobiose and higher oligosaccharides could be detected after deacylation. In the case of the reaction using 3,5-di-*O*-benzoyl-α-L-arabinofuranosyl bromide, the disaccharide by-product was isolated and converted by de-esterification to gentiobiose. When 1,2,3,4-tetra-*O*-acetyl-β-D-glucose alone was treated with hydrogen bromide in chloroform, slow-moving spots corresponding to gentiobiose and higher oligosaccharides were noted on paper chromatograms after deacetylation. These results are similar to those described by Haq and Whelan (24), who produced 1,6-*O*-β-D-glucopyranose oligosaccharides by the self-condensation of 2,3,4-tri-*O*-acetyl-α-D-glucopyranosyl bromide. The yields of gentiobiose in the Königs–Knorr reactions in the L-arabinofuranose series appear to correspond to the reactivity of the starting halide towards alcohols. The 2-*p*-nitrobenzoyl and 2-*O*-nitro bromides gave little of the disaccharide by-product whereas the 2-benzoyl, 2-hydroxyl, and 2-acetyl bromides gave appreciable amounts.

Condensations using a 2-*O*-nitro halide have been reported by Wolfrom, Pittet, and Gillam (18), who prepared an α-disaccharide (contaminated with β) by the reaction of 3,4,6-tri-*O*-acetyl-2-*O*-nitro-β-D-glucopyranosyl chloride with 1,2,3,4-tetra-*O*-acetyl-β-D-glucose. From a preparative point of view, 3,5-di-*O*-benzoyl-2-*O*-nitro-α-L-arabino-

**Similarly, no 1,5-orthobenzoate was formed from 3,5-di-O-benzoyl-α-D-ribofuranosyl bromide.*

furanosyl bromide is similarly useful for synthesis of β-arabinofuranosides. Reaction of the 2-*O*-nitro bromide with methanol and 1,2,3,4-tetra-*O*-acetyl-β-D-glucose resulted in the formation of the methyl β-L-arabinofuranoside derivative and a β-disaccharide, respectively, and only traces of the α-anomers were formed. The latter result thus shows that the 2-nitrate group does not participate in the formation of an intermediate nitronium ion.

In the D-ribofuranosyl series the reactions with methanol and 1,2,3,4-tetra-*O*-acetyl-D-glucose gave mixtures of products (Table I), as would be expected on the basis of S_N1 mechanisms. Treatment of the bromides with tetra-*O*-acetyl-glucose gave mainly β-disaccharides, which were adulterated either with orthoester or α-disaccharide. In specific instances, such as the reaction of 3,5-di-*O*-benzoyl-2-*O*-nitro-β-D-ribofuranosyl bromide with methanol and 1,2,3,4-tetra-*O*-acetyl-β-D-glucose, some unexpected reactions took place. The methanol reaction gave complete inversion at C-1 whereas with tetra-*O*-acetyl-glucose there was much retention of configuration. This picture is similar to the condensation of 2-*O*-benzyl-3,4,6-tetra-*O*-acetyl-α-D-mannopyranosyl bromide with methanol and tetra-*O*-acetyl-β-D-glucose, which has been considered in a previous paper (1).

Under certain conditions trans-1-bromides of sugars can be converted to products of the same configuration without the chemical participation of an ester group at C-2. 3,4,6-Tri-*O*-acetyl-2-*O*-trichloroacetyl-β-D-glucosyl chloride yields mainly the α-glycoside and does not, in contrast to trans-2-acetate derivatives, give a 1,2-orthotrichloroacetate on reaction with methanol (25). This has been explained by the reduction of nucleophilic activity of the carbonyl oxygen by the three chloro groups so that a cyclic carbonium ion intermediate is not possible (3). A more limited reduction of carbonyl participation could explain the differing reactions of the 2-acetyl, 2-benzoyl, and 2-*p*-nitrobenzoyl derivatives of 3,5-di-*O*-benzoyl-β-D-ribofuranosyl bromides with 1,2,3,4-tetra-*O*-acetyl-β-D-glucose. The two former derivatives give orthoester products only whereas the 2-*p*-nitrobenzoate derivative gives rise to β-disaccharide also.

The reactions summarized in Table I can give rise to some overall generalizations. It appears that, in the five-membered ring, the ester group at C-2 can participate in the Königs–Knorr reaction by formation of cyclic carbonium ion intermediates to a greater extent than in the 6-membered series. The participation of C-2 is emphasized in the ribofuranosyl series since orthoester yield is very high in attempted ribofuranosyl disaccharide syntheses. This should not be surprising when the favorable stereochemistry of cis-carbon to oxygen bonds at C-1 and C-2 of the five-membered ring is considered. It can also be concluded that the reaction in disaccharide formation is more stereospecific than the corresponding methyl furanoside synthesis. This presumably is due to the size of the nucleophilic reagent, which could be a factor limiting the direction of approach of the tetra-*O*-acetyl glucose, in contrast to that of the smaller methanol molecule.

EXPERIMENTAL

Evaporations were carried out under reduced pressure at 50° C (bath temperature and optical rotations were measured at 23° C).

Preparation of 2-Substituted 1,3,5-Tri-O-benzoyl-β-L-arabinoses

(a) 2-p-Nitrobenzoate

1,3,5-Tri-*O*-benzoyl-β-L-arabinose (1.40 g) was heated at 80° C for 1 hour in pyridine (20 ml) containing *p*-nitrobenzoyl chloride (1.40 g). The mixture was then added to aqueous sodium bicarbonate, shaken for an hour, and the precipitate which formed was filtered off. Two recrystallizations from ethyl acetate – hexane gave the 2-*p*-nitrobenzoate with m.p. 170–171° C and $[\alpha]_D$ +114° (*c*, 1.0, $CHCl_3$). Calculated for $C_{33}H_{25}O_{11}N$: C, 64.8%; H, 4.1%. Found: C, 64.6%; H, 4.2%.

(b) 2-Nitrate

1,3,5-Tri-*O*-benzoyl-β-L-arabinose (1.38 g) dissolved in acetic anhydride (10 ml) was added slowly to a mixture of acetic anhydride (8 ml) and fuming nitric acid (2 ml), cooled in an ice bath. After 30 minutes at 0° C and 15 minutes at room temperature, ice-cold aqueous sodium bicarbonate solution was added to destroy the reagent. Extraction with chloroform and evaporation of the extract yielded a solid which, on two recrystallizations from ethanol, yielded the 2-nitrate (1.06 g) with m.p. 99–100° C and $[\alpha]_D$ +58° (*c*, 0.5, $CHCl_3$). Calculated for $C_{26}H_{21}O_{10}N$: C, 61.5%; H, 4.2%; N, 2.8%. Found: C, 61.3%; H, 4.2%; N, 2.1%.

Preparation of 2-Substituted 1,3,5-Tri-O-benzoyl-α-D-riboses

(a) 2-p-Nitrobenzoate

1,3,5-Tri-*O*-benzoyl-α-D-ribose was *p*-nitrobenzoylated by the above method. Two recrystallizations from ethyl acetate – hexane yielded the 2-*p*-nitrobenzoate with m.p. 112–115° C and $[\alpha]_D$ +100° (*c*, 1.0, $CHCl_3$). Calculated for $C_{33}H_{25}O_{11}N$: C, 64.8%; H, 4.1%; N, 2.3%. Found: C, 64.8%; H, 4.2%; N, 2.2%.

(b) 2-Nitrate

1,3,5-Tri-*O*-benzoyl-α-D-ribose was converted to its sirupy 2-nitrate derivative using the nitration procedure described above. It had $[\alpha]_D$ +69° (*c*, 0.7, H_2O). Calculated for $C_{26}H_{21}O_{10}N$: N, 2.8%. Found: N, 2.2%.

Bromination of 2-Substituted 1,3,5-Tri-O-benzoyl-β-L-arabinoses

To purify the chloroform, it was washed with water, dried with calcium chloride, and distilled, and hydrogen bromide was bubbled through it for 2 minutes to yield an approximately 0.3 *N* solution. A 1% solution of each benzoate derivative in this solvent was prepared and its specific rotation followed. The solution was then evaporated (bath temperature 0° C), and residual hydrogen bromide removed by evaporation three times of chloroform solutions. The specific rotations recorded are as follows, the initial reading being measured in chloroform separately, and the final reading being the constant value reached:

(*a*)	2-acetate	+60° → −112° (immediate),
(*b*)	2-*p*-nitrobenzoate	+114° → −63° (7 minutes),
(*c*)	2-nitrate	+58° → −65° (12 minutes),
(*d*)	2-hydroxyl	+4° → −103° (immediate).

Bromination of 2-Substituted 1,3,5-Tri-O-benzoyl-α-D-riboses

A similar bromination procedure was used, and the following specific rotations were measured:

(*a*)	2-acetate	+74° → −52° (6 minutes),
(*b*)	2-benzoate	+88° → −11° (9 minutes),
(*c*)	2-*p*-nitrobenzoate	+100° → +8° (16 minutes),
(*d*)	2-nitrate	+83° → −39° (2 hours),
(*e*)	2-hydroxyl	+87° → +109° (immediate).

Reactions of Pentofuranosyl Bromides with Methanol

The bromides prepared from the appropriate 1-benzoate derivative (0.50 g) were shaken for 1 hour in methanol (20 ml) containing an excess of silver oxide (2.5 g). The solutions were then filtered and evaporated. De-esterification, when necessary, was carried out in 30 hours using 0.1 *N* sodium methoxide in methanol (0.2 equivalents). Characterization of products was then carried out using paper chromatograms (sprays: *p*-anisidine hydrochloride (26) and ammoniacal silver nitrate (27); solvent: *n*-butanol–ethanol–water (40:11:19 v/v)). Orthoesters had R_F's ~0.8 and methyl α-L-arabinofuranoside was characterized since it moved faster than its β-anomer, both glycosides having R_F's ~0.4.

(a) L-Arabinofuranosyl Series

(i) 2-Acetate derivative.—The material appeared to be mainly the methyl orthoester. The reaction product had $[\alpha]_D$ +15° (*c*, 1.0, $CHCl_3$) and, after crystallization and two recrystallizations from hexane, had m.p. 120–121° C and $[\alpha]_D$ 0° (*c*, 2.3, $CHCl_3$). Calculated for $C_{22}H_{22}O_8$: C, 63.8%; H, 5.35%. Found: C, 63.9%; H, 5.4%. De-esterification did not give methyl arabinosides.

(ii) 2-Benzoate derivative.—The product had $[\alpha]_D$ −20° (*c*, 1.0, $CHCl_3$) and the de-esterified sample showed mainly orthoacetate, some methyl β-arabinoside, and only a small proportion of the α-anomer. Methyl 1,2-orthobenzoyl-L-arabinose was isolated by ethyl acetate extraction of an aqueous solution of the mixture which had been previously extracted with hexane to remove methyl benzoate. The product had no carbonyl absorption in the infrared and had $[\alpha]_D$ −5° (*c*, 2.1, H_2O). Treatment with 0.01 *N* sulphuric acid immediately changed this to +80° (*c*, 1.0) and the material (probably 2-*O*-benzoyl-L-arabinose) obtained after neutralization and evaporation had strong carbonyl absorption at 1710 cm^{-1}.

(iii) 2-p-Nitrobenzoate derivative.—The product had $[\alpha]_D$ +36° (*c*, 1.2, $CHCl_3$) and, on de-esterification, gave a similar picture on a paper chromatogram as the above 2-benzoate. 3,5-Di-*O*-benzoyl-1,2-methyl-ortho-*p*-nitrobenzoyl-L-arabinose crystallized, and two recrystallizations from ethyl acetate – hexane gave

material with m.p. 155–159° C and $[\alpha]_D$ +36° (*c*, 0.8, $CHCl_3$). Calculated for $C_{27}H_{23}O_{10}N$: C, 62.2%; H, 4.95%. Found: C, 61.8%; H, 4.8%. De-esterification gave material corresponding to a methyl ortho-*p* nitrobenzoate derivative on a paper chromatogram.

(iv) 2-Nitrate derivative.—The product, $[\alpha]_D$ +85° (*c*, 1.5, $CHCl_3$), crystallized, and two recrystallizations from hexane yielded methyl 3,5-di-*O*-benzoyl-2-*O*-nitro-β-L-arabinofuranoside with m.p. 98–99° C and $[\alpha]_D$ +85° (*c*, 0.8, $CHCl_3$). Calculated for $C_{20}H_{19}O_9N$: C, 57.55%; H, 4.6%; N, 3.4%. Found: C, 57.8%; H, 4.7%; N, 2.8%. The methyl glycoside (37 mg) was shaken in ethanol (10 cc) containing 5% palladium on charcoal (30 mg) under 2 atmospheres of hydrogen for 24 hours (28). After filtration and evaporation the product was de-esterified to yield methyl β-L-arabinofuranoside (identified on a paper chromatogram).

(v) Hydroxyl derivative.—The methyl glycoside derivative obtained appeared to be methyl 3,5-di-*O*-benzoyl-β-L-arabinofuranoside since only the β-L-glycoside was obtained on de-esterification.

(b) D-Ribofuranosyl Series

The products obtained in this series were sirupy and are summarized in Table I. The specific rotations of the products after treatment with methanol are as follows: 2-acetate +72° (*c*, 0.6, $CHCl_3$); 2-benzoate +90° (*c*, 0.9, $CHCl_3$); 2-*p*-nitrobenzoate +112° (*c*, 1.1, $CHCl_3$); 2-nitrate +69° (*c*, 0.7, $CHCl_3$); and 2-hydroxyl +39° (*c*, 0.8, $CHCl_3$). Methyl ribofuranosides were identified by their relative R_F values (29).

Reactions of L-Arabinofuranosyl Bromides with 1,2,3,4-Tetra-O-acetyl-β-D-glucose

In these experiments 1.0 g of the appropriate bromide was mixed with silver oxide (1.0 g), iodine (0.25 g), and Drierite (5.0 g). Then a solution of 1,2,3,4-tetra-*O*-acetyl-β-D-glucose (4.0 g) in dry chloroform (16 ml) was added, and the mixture was shaken overnight. After filtration and evaporation the sirup was de-esterified with 0.2 equivalents of 0.1 *N* sodium methoxide in methanol over 3 hours. The product was then examined on paper chromatograms in the ethyl acetate – pyridine – water (10:4:3 v/v) solvent using aniline oxalate (30) as spray. 6-*O*-α-L-Arabinofuranosyl-D-glucose had $R_{Galactose}$ 1.2 whereas the β-anomer had $R_{Galactose}$ 1.0. In each addition some gentiobiose and higher homologues were detected and the disaccharide was isolated in the case of the condensation with 2-hydroxyl derivative. The products were fractionated on a cellulose column. *n*-Butanol saturated with water gave a partial separation of the arabinosyl glucosides and *n*-butanol–ethanol–water (4:1:1 v/v) eluted gentiobiose.

(i) 2-O-Benzoyl derivative.—The product was mainly 6-*O*-α-L-arabinofuranosyl-α-D-glucose (0.30 g) with spots corresponding to 1,6-*O*-β-glucopyranosyl oligosaccharides. The former was recrystallized twice from ethanol and had m.p. 163–165° C and $[\alpha]_D$ −15° → −40° (*c*, 1.0, H_2O; constant value, 18 hours). Calculated for $C_{11}H_{20}O_{10}$: C, 42.3%; H, 6.5%. Found: C, 42.3%; H, 6.4%. The sugar was α rather than β since on oxidation in aqueous sodium periodate the specific rotation of the solution changed to −77° (*c*, 0.6, H_2O) (31). The crude disaccharide (0.24 g) was heated in acetic anhydride (2 ml) containing sodium acetate (0.20 g) at 100° C overnight. The anhydride was destroyed with ice water and the mixture extracted with benzene. The solution was evaporated and the residue crystallized from ethanol–hexane. Recrystallization from the same solvent gave hepta-*O*-acetyl-6-*O*-α-L-arabinofuranosyl-β-D-glucose (0.17 g) with m.p. 108–109° C and $[\alpha]_D$ −20° (*c*, 2.0, $CHCl_3$). Calculated for $C_{25}H_{34}O_{17}$: C, 49.5%; H, 5.7%. Found: C, 49.45%; H, 5.7%. The acetate appeared to be β since its mother liquor had a specific rotation of −10° (*c*, 2.0, $CHCl_3$).

(ii) 2-O-Acetyl derivative.—In addition to 6-*O*-α-L-arabinofuranosyl-D-glucose (310 mg) spots corresponding to 1,6-*O*-β-D-glucopyranosyl oligosaccharides were obtained. The arabinosyl glucose was converted to its hepta-*O*-acetate, m.p. and mixed m.p. 106.5–108° C.

(iii) 2-p-Nitrobenzoate derivative.—The product in this case contained only a trace of glucose containing oligosaccharides and in the arabinofuranosyl glucose fraction the α-anomer predominated. The isolated 6-*O*-α-L-arabinofuranosyl-D-glucose (252 mg) was converted to the hepta-*O*-acetate, m.p. and mixed m.p. 107.5–109.5° C.

(iv) 2-Nitrate derivative.—Here the reaction mixture was filtered and evaporated and half of the residue taken up in benzene, which was then washed three times to remove tetra-*O*-acetyl-glucose. On evaporation, the sirup crystallized and after two recrystallizations from ethanol yielded 0.22 g of 6-*O*-β-(3,5-di-*O*-benzoyl-2-*O*-nitryl-L-arabinofuranosyl)-(1,2,3,4-tetra-*O*-acetyl-β-D-glucose) with m.p. 152–153° C and $[\alpha]_D$ +83° (*c*, 1.1, $CHCl_3$). Calculated for $C_{33}H_{35}O_{18}N$: C, 54.0%; H, 4.8%. Found: C, 54.0%; H, 4.8%.

Of this material 0.11 g was denitrated by shaking in ethanol (25 ml) containing 5% palladium charcoal (0.20 g) under 2 atmospheres of hydrogen overnight. After filtration of the catalyst this process was repeated. Refiltration and evaporation gave a product (45 mg) which did not crystallize on seeding with the starting material. The product had $[\alpha]_D$ +49° (*c*, 1.1, $CHCl_3$), and de-esterification gave 6-*O*-β-L-arabinofuranosyl-D-glucose (20 mg) with $[\alpha]_D$ +73° (*c*, 0.6, H_2O).

Repetition of this process on the crude Königs–Knorr product showed that only a trace of the 6-*O*-α-L-arabinofuranosyl-D-glucose derivative was present.

(v) 2-Hydroxyl derivative.—The product consisted of 6-*O*-α- and 6-*O*-β-L-arabinofuranosyl-D-glucose. An attempt was made to fractionate these on a cellulose column and two fractions were obtained, one (373 mg) with $[\alpha]_D$ +34° (*c*, 1.5, H_2O) and the other (79 mg) with $[\alpha]_D$ +8° (*c*, 1.3, H_2O). Based on the known specific rotations of the α- and β-disaccharide, the mixture consisted of 39% of the α- and 61% of the β-anomer.

Gentiobiose (310 mg) was also separated from its higher oligomer and was converted to its β-octaacetate derivative (32). Two recrystallizations from ethanol gave crystals with m.p. 200–202° C and $[\alpha]_D$ −5° (*c*, 1.2, $CHCl_3$). Calculated for $C_{28}H_{38}O_{19}$: C, 49.6%; H, 5.6%. Found: C, 49.6%; H, 5.65%. X-Ray diffraction patterns of this and a specimen of authentic gentiobiose, β-octaacetate, were identical.

Action of Hydrogen Bromide in Chloroform on 1,2,3,4-Tetra-O-acetyl-β-D-glucose

1,2,3,4-Tetra-*O*-acetyl-β-D-glucose (0.48 mmole) was treated with hydrogen bromide (0.96 mmole) in chloroform (5.4 ml) and the specific rotation followed.

Time (minutes)	0	2	4	5	6	10
Specific rotation (in pure $CHCl_3$)	+11°	−26°	−32°	−39°	−43°	−46°

The solution after 10 minutes was washed with aqueous sodium bicarbonate, then water, and evaporated. Deacetylation gave mainly glucose with a small proportion of material corresponding to gentiobiose.

Reactions of D-*Ribofuranosyl Bromides with 1,2,3,4-Tetra-O-acetyl-β-D-glucose*

The conditions used in this series of experiments were identical with those used in the L-arabinofuranosyl series, except that the relative proportion of silver oxide was increased fivefold and no iodine was used.

(i) 2-O-Acetyl derivative.—The product, after deacetylation, gave a yellow spot with $R_{Galactose}$ 0.8 on paper chromatograms (solvent: *n*-butanol–ethanol–water (40:11:19 v/v); spray: *p*-anisidine hydrochloride) and this disappeared on acidification with acetic acid. No normal disaccharide was present.

(ii) 2-O-Benzoyl derivative.—When a similar procedure as for the above 2-acetyl derivative was used a spot with $R_{Galactose}$ 0.9 was obtained, also corresponding to orthoester. No ribofuranosyl-glucose was present.

(iii) 2-p-Nitrobenzoyl derivative.—The product on de-esterification appeared to be a mixture of orthoester and a normal disaccharide. The disaccharide fraction had $R_{Galactose}$ 0.95 (and a trace at 0.90) in the ethyl acetate – pyridine – water (10:4:3 v/v) solvent, and on isolation from a cellulose column it (35 mg) had $[\alpha]_D$ 0° (*c*, 1.0, H_2O). Oxidation with aqueous sodium periodate changed its specific rotation to −94° (*c*, 0.6, H_2O; constant value 5 minutes), indicating a β-linkage. Acetylation of the 6-*O*-β-D-ribofuranosyl-D-glucose by the hot acetic anhydride – sodium acetate method (see earlier in experimental reaction for method) yielded a substance which crystallized, and after two recrystallizations from ethanol–hexane the waxy hepta-*O*-acetate had m.p. 108–110° C and $[\alpha]_D$ +3° (*c*, 1.5, $CHCl_3$). Calculated for $C_{25}H_{34}O_{17}$: C, 49.5%; H, 5.65%. Found: C, 49.6%; H, 5.7%.

(iv) 2-Nitrate derivative.—After denitration (as for denitration of the 2-nitrate of the corresponding L-arabinofuranose derivative) followed by de-esterification the mixture was fractionated on a cellulose column. The product (41 mg) had $[\alpha]_D$ +34° (*c*, 0.9, H_2O), and on oxidation with sodium periodate a value of −48° (*c*, 0.5, H_2O; constant value 1 hour) was obtained. This corresponds to 68% of 6-*O*-β-D-ribofuranosyl-D-glucose and 32% of the α-anomer (31).

(v) 2-Hydroxyl derivative.—After de-esterification paper chromatography showed an almost equal mixture of the β- and α-anomers ($R_{Galactose}$ 0.95 and 0.90 respectively). Column chromatography yielded two fractions, one (16 mg) with $[\alpha]_D$ +77° (*c*, 1.0, H_2O) (after periodate oxidation +54° (*c*, 0.6, H_2O)) consisting mainly of 6-*O*-α-D-ribofuranosyl-D-glucose, and the other (14 mg) had $[\alpha]_D$ +12° (*c*, 0.6, H_2O) (after periodate oxidation −88° (*c*, 0.3, H_2O)) and was mainly β-anomer. The combined fractions thus appear to consist of 54% of β- and 46% of α-disaccharide.

Preparation of 5-O-α-L-Arabinofuranosyl-L-arabinose

5-O-α-L-Arabinofuranosyl-L-arabinose Diethyl Thioacetal

Using the same Königs–Knorr conditions as for the preparation of the other L-arabinofuranosyl disaccharides 2,3,4-tri-*O*-benzoyl-α-L-arabinofuranosyl bromide (1.0 g) was treated with 2,3,4-tri-*O*-acetyl-L-arabinose diethyl thioacetal. The product, after de-esterification, was fractionated on a cellulose column. Benzene–ethanol–water (1000:50:1 v/v) eluted unchanged thioacetal and the (500:50:1 v/v) mixture gave the disaccharide thioacetal (0.41 g). The mercaptal was crystallized twice from ethyl acetate – hexane and had m.p. 56° C and $[\alpha]_D$ −62° (*c*, 1.3, H_2O). Calculated for $C_{19}H_{28}O_8S_2$: C, 43.3%; H, 7.3%. Found: C, 42.9%; H, 7.3%. Oxidation with sodium periodate gave a product with $[\alpha]_D$ −91° (*c*, 0.6, H_2O), thus indicating an α-L-configuration for the disaccharide linkage.

5-O-α-L-Arabinofuranosyl-L-arabinose

The disaccharide thioacetal (100 mg) was acetylated by the hot acetic anhydride – sodium acetate method (see earlier in experimental section for method) to yield the hexa-*O*-acetate (158 mg). This was dissolved in acetone (3 ml) and water (1.5 ml). Mercuric oxide (2.0 g) was added, followed by mercuric chloride (0.40 g) in acetone (4 ml), to the stirred mixture. After 30 minutes the solution was refluxed for 10 minutes, and then filtered and evaporated. The sirup was dissolved in chloroform, which was washed twice with water, dried ($MgSO_4$), filtered, and evaporated. The product was deacetylated and the disaccharide obtained was fractionated on a cellulose column (*n*-butanol 3/4 saturated with water as solvent) to yield the purified material (55 mg) with $[\alpha]_D$ −94° (*c*, 1.4, H_2O). A sample of disaccharide prepared from

sugar beet araban had $[\alpha]_D$ −72° (15). On sodium periodate oxidation the $[\alpha]_D$ changed to −76° (210 minutes; *c*, 0.9, H_2O) (expected value: −79° to −88° (31)), thus indicating that the 5-*O*-α-L-arabinofuranosyl-L-arabinose was not entirely pure.

ACKNOWLEDGMENTS

The author wishes to thank Mrs. S. F. Hector for technical assistance, Mr. M. Mazurek for microanalytical determinations, and Miss I. Gaffney for measuring infrared spectra.

REFERENCES

1. P. A. J. Gorin and A. S. Perlin. Can. J. Chem. **39**, 2474 (1961).
2. R. U. Lemieux. Advances in Carbohydrate Chem. **9**, 1 (1954).
3. L. J. Haynes and F. H. Newth. Advances in Carbohydrate Chem. **10**, 207 (1955).
4. J. Davoll and B. A. Lowry. J. Am. Chem. Soc. **73**, 1650 (1951).
5. G. A. Howard, B. Lythgoe, and A. R. Todd. J. Chem. Soc. 1052 (1947).
6. R. S. Wright and H. G. Khorana. J. Am. Chem. Soc. **77**, 3423 (1955).
7. R. S. Wright and H. G. Khorana. J. Am. Chem. Soc. **78**, 811 (1956).
8. G. M. Tener, R. S. Wright, and H. G. Khorana. J. Am. Chem. Soc. **79**, 441 (1957).
9. R. S. Wright and H. G. Khorana. J. Am. Chem. Soc. **80**, 1994 (1958).
10. W. Bergmann and R. J. Feeney. J. Org. Chem. **16**, 981 (1951).
11. W. Bergmann and D. C. Burke. J. Org. Chem. **20**, 1501 (1955).
12. D. M. Brown, A. R. Todd, and S. Varadarajan. J. Chem. Soc. 2388 (1956).
13. J. J. Fox and N. Yung. Federation Proc. **15**, 254 (1956).
14. J. J. Fox, N. Yung, and A. Bendich. J. Am. Chem. Soc. **79**, 2775 (1957).
15. P. Andrews, L. Hough, and D. B. Powell. Chem. & Ind. (London), 658 (1956).
16. S. Haq and W. J. Whelan. J. Chem. Soc. 1342 (1958).
17. K. Matsuda. Nature, **180**, 985 (1957).
18*a*. M. L. Wolfrom and I. C. Gillam. Science, **130**, 1424 (1959).
18*b*. M. L. Wolfrom, A. O. Pittet, and I. C. Gillam. Proc. Natl. Acad. Sci. U.S. **47**, 700 (1961).
19. R. K. Ness and H. G. Fletcher, Jr. J. Am. Chem. Soc. **80**, 2007 (1958).
20. R. K. Ness and H. G. Fletcher, Jr. J. Am. Chem. Soc. **76**, 1663 (1954).
21. R. K. Ness and H. G. Fletcher, Jr. J. Am. Chem. Soc. **78**, 4710 (1956).
22. H. S. Isbell and H. L. Frush. J. Research Natl. Bur. Standards, **43**, 161 (1949).
23. D. D. Reynolds and W. L. Evans. J. Am. Chem. Soc. **60**, 2559 (1938).
24. S. Haq and W. J. Whelan. J. Chem. Soc. 4543 (1956).
25. W. J. Hickinbottom. J. Chem. Soc. 1676 (1929).
26. L. Hough, J. K. N. Jones, and W. H. Wadman. J. Chem. Soc. 1702 (1950).
27. S. M. Partridge. Nature, **158**, 270 (1946).
28. L. P. Kuhn. J. Am. Chem. Soc. **68**, 1761 (1946).
29. G. R. Barker and D. C. C. Smith. J. Chem. Soc. 2151 (1954).
30. R. H. Horrocks. Nature, **164**, 444 (1949).
31. A. J. Charlson and A. S. Perlin. Can. J. Chem. **34**, 1804 (1956).
32. G. Zemplén. Z. Physiol. Chem. **85**, 399 (1913).

CHEMISTRY OF THE TRIFLUOROMETHYL GROUP

PART IV. DIPHENYLTRIFLUOROMETHYLPHOSPHINE AND COMPLEX FORMATION BY PHENYLTRIFLUOROMETHYLPHOSPHINES[1]

M. A. A. Beg and H. C. Clark

The Department of Chemistry, University of British Columbia, Vancouver, British Columbia

Received October 10, 1961

ABSTRACT

Three methods of preparing diphenyltrifluoromethylphosphine are described. The hydrolysis of the phosphine to diphenylphosphinic acid and fluoroform, and the formation of dibromo- and diiodo-phosphoranes from the phosphine are reported. The adducts $(C_6H_5)_3P.BF_3$ and $(C_6H_5)_2CF_3P.BF_3$ are described and the latter is found to be the less stable. With platinum (II) chloride, the complexes *trans*-$[(C_6H_5)_2PCF_3]_2PtCl_2$ and *trans*-$[C_6H_5P(CF_3)_2]_2PtCl_2$ are formed. The properties of the BF_3 adducts and $PtCl_2$ complexes are interpreted in terms of the electronegativity and size of the trifluoromethyl group.

INTRODUCTION

In the previous paper (1) of this series, the preparation and physical and chemical properties of phenylbistrifluoromethylphosphine were described. We now report the preparation of diphenyltrifluoromethylphosphine, and also the results of experiments designed to determine the abilities of both these phosphines to participate in complex formation.

DISCUSSION AND RESULTS

Three methods have been found successful in preparing diphenyltrifluoromethylphosphine. Since phenylbistrifluoromethylphosphine can be obtained by the addition of trifluoroiodomethane to the P—P bonds of tetraphenylcyclotetraphosphine, one obvious route to diphenyltrifluoromethylphosphine lay in the reaction of tetraphenyldiphosphine with trifluoroiodomethane:

$$(C_6H_5)_2P—P(C_6H_5)_2 + CF_3I \rightarrow (C_6H_5)_2PCF_3 + (C_6H_5)_2PI.$$

This and other reported additions (2, 3) to compounds of the type $R_2P—PR_2$ involve cleavage of the weak P—P bond. Its bond energy is only 50 kcal mole^{-1} (4), much less than that of the P—C bond (62 kcal mole^{-1}), so that the P—P bond will be the potential point of attack by a reactive species.

Tetraphenyldiphosphine is prepared by the reaction of diphenylphosphine and diphenylchlorophosphine (5, 6), preferably in a high-boiling solvent such as xylene. When tetraphenyldiphosphine is heated with excess trifluoroiodomethane at 185°, or when the two reactants are exposed to ultraviolet radiation, a mixture of diphenyltrifluoromethylphosphine and diphenyliodophosphine is produced, from which the former can be extracted with petroleum ether. Since the reaction will occur either thermally or on ultraviolet irradiation, a free-radical mechanism involving the attack of CF_3 radicals on the P—P bond seems probable.

The alternative methods of preparation require the reaction of either diphenylchlorophosphine or triphenylphosphine with trifluoroiodomethane at 185–200°. Although in both cases the yields are not high (approx. 20%), these methods are advantageous in

[1]*From part of the thesis submitted by M. A. A. Beg in partial fulfillment of the requirements for the Ph.D. degree.*

that the reactants are readily available and the preparation of the diphosphine is not required. A number of secondary products are obtained in each case so that the overall reactions can be represented as

$$(C_6H_5)_3P + CF_3I \rightarrow (C_6H_5)_2PCF_3 + (C_6H_5)_2PI + C_6H_5CF_3$$
$$(C_6H_5)_2PCl + CF_3I \rightarrow (C_6H_5)_2PCF_3 + (C_6H_5)_2PI + (C_6H_5)CF_3PCl + C_6H_5CF_3 + CF_3Cl.$$

The nature of the products strongly suggests that these reactions involve a radical mechanism, presumably the attack of CF_3 radicals on the P—C_6H_5 or P—Cl bonds.

Diphenyltrifluoromethylphosphine is a colorless, viscous liquid which boils at 255–257°. This is 28° lower than the boiling point of the methyl analogue, $(CH_3)_2PCF_3$, and 24° lower than that of the secondary phosphine, $(C_6H_5)_2PH$. Such low boiling points are common for the perfluoroalkyl derivatives of the group V elements and reflect the reduced molecular polarity and hence the weaker intermolecular interactions.

Diphenyltrifluoromethylphosphine is stable in air and is not decomposed easily on heating. After being heated to 300° for 24 hours, 85% of the phosphine is recovered. The phosphine is unaffected by water or by hydrochloric acid up to 150°. Only slight hydrolysis occurs with aqueous sodium hydroxide at 100°, in marked contrast to phenylbistrifluoromethylphosphine which is quantitatively hydrolyzed under these conditions. Diphenyltrifluoromethylphosphine can be hydrolyzed with alcoholic potassium hydroxide, although the reaction is only 78% complete after 96 hours at 80°. The hydrolysis products are fluoroform and diphenylphosphinic acid, $(C_6H_5)_2P(O)OH$.

It is of considerable interest that trifluoromethyl-metallic and -metalloidal derivatives are much more susceptible to hydrolytic attack than the analogous alkyl and aryl compounds. Exceptions among the phosphorus–trifluoromethyl compounds are trifluoromethylphosphonic acid (7) and compounds which also contain a phenyl group, e.g. diphenyltrifluoromethylphosphine. These show much greater resistance to hydrolysis, as do the comparable arsenic derivatives (8), this presumably being a consequence of electron delocalization involving the aromatic systems.

In general, however, the ready removal of the trifluoromethyl group on hydrolysis, usually to give fluoroform, can be understood in terms of its high electronegativity, and high electron-withdrawing effect, as shown by the value of the Taft polar substituent constant σ^*.

Group	σ^*	Electronegativity
CH_3	0.00 (9)	2.34 (11)
H	0.49 (9)	2.10 (11)
C_6H_5	0.60 (9)	2.70 (12)
OCH_3	1.46 (9)	2.92 (12)
Br	2.80 (9)	2.94 (12)
CCl_3	2.65 (10)	2.76 (11)
Cl	2.94 (9)	3.19 (12)
CF_3	2.81 (10)	3.3 (13)
F	3.08 (9)	3.93 (12)

These values indicate the high polarity of the M—CF_3 bond compared with M—CH_3 or M—C_6H_5, and suggest that the M—CF_3 bond will therefore be a very likely point of hydrolytic attack.

Bromine and iodine react readily with diphenyltrifluoromethylphosphine to form diphenyltrifluoromethyl-dibromophosphorane and -diiodophosphorane respectively. These

are stable oils which are unaffected by air or water and are stable to 200°. However, they are hydrolyzed quantitatively by aqueous sodium hydroxide to fluoroform, diphenylphosphinic acid, and sodium halide:

$$(C_6H_5)_2CF_3PX_2 + 2NaOH \rightarrow (C_6H_5)_2P(O)OH + CF_3H + 2NaX.$$

The fact that diphenyltrifluoromethyldiiodophosphorane can be prepared, whereas phenylbistrifluoromethyldiiodophosphorane could not be isolated (1), is interesting and must be due, at least in part, to the large steric effect of the CF_3 group. Thus, replacement of one CF_3 group in phenylbistrifluoromethylphosphine by a less bulky phenyl group gives a phosphine which is sterically capable of forming a diiodophosphorane. Similarly, triphenylphosphine in which steric effects are further reduced, also forms a stable diiodophosphorane (14). In its physical and chemical properties, therefore, diphenyltrifluoromethylphosphine is closely related to triphenylphosphine.

In an earlier paper (15), the ability of methyltrifluoromethylphosphines to take part in complex formation was examined, and one purpose of the present investigation has been the study of the corresponding properties of the phenyltrifluoromethylphosphines. Three types of reactions have been examined, namely the tendency of each phosphine to form (*a*) a phosphonium iodide with an alkyl iodide, (*b*) an addition compound with boron trifluoride, and (*c*) a planar complex with platinum (II) chloride.

As might be expected neither phenylbistrifluoromethylphosphine nor diphenyltrifluoromethylphosphine forms a phosphonium iodide with trifluoroiodomethane, nor is phenylbistrifluoromethylphosphine sufficiently basic to react with iodomethane. However, the more basic character of diphenyltrifluoromethylphosphine is shown by its reaction with iodomethane to form diphenylmethyltrifluoromethyl phosphonium iodide, $[(C_6H_5)_2CF_3CH_3P]I$. This yellow crystalline solid melts at 123–125° and is stable in dry air but it is very readily hydrolyzed by cold water to produce fluoroform, hydriodic acid, and methyldiphenylphosphine oxide:

$$(C_6H_5)_2CF_3CH_3PI + H_2O \rightarrow (C_6H_5)_2CH_3PO + CF_3H + HI.$$

Such ease of hydrolysis is consistent with other studies (16) of the decomposition of phosphonium hydroxides, which show that the most electron-withdrawing organic radical is always the one eliminated, the three less electron-withdrawing groups forming the phosphine oxide.

By examining the stability of phosphine – boron trifluoride adducts, information is obtained concerning the strength of the dative σ-bond between phosphorus and boron. Such studies for the phenyltrifluoromethylphosphines give results which parallel those obtained for the methyltrifluoromethylphosphines (15). Triphenylphosphine-boron trifluoride is a stable white solid of low volatility with a melting point of 128–130°. The boron trifluoride adduct of diphenyltrifluoromethylphosphine is an oil whose saturation pressure is greater than that of its triphenylphosphine analogue. Boron trifluoride adducts of phenylbistrifluoromethylphosphine and tristrifluoromethylphosphine could not be formed. In confirmation of our previous results (8), it is therefore clear that the introduction of one CF_3 group causes a very substantial reduction in the basicity of a phosphine, and the introduction of two such groups makes the phosphine such a weak base that a BF_3 adduct is not formed.

In complexes of phosphines with transition metal halides, such as platinum (II) chloride, the metal–phosphorus bonds contain both σ and π components. The way in which each of these components is influenced by the type of group attached to phosphorus

is reasonably well understood and was briefly outlined earlier (15). Bis(triphenylphosphine) dichloroplatinum (II) has been prepared by Jensen (17) as the cis isomer, but preparations of the corresponding complexes of diphenyltrifluoromethylphosphine and phenylbistrifluoromethylphosphine give only the trans isomers. This is shown by their zero dipole moments. Some caution must be used in interpreting these results in terms of the relative stabilities of cis and trans isomers, since the proportions of the two isomers obtained in such cases often varies somewhat according to the preparative method used. Although detailed studies of the cis–trans equilibria would be necessary to reach a conclusion regarding the stabilities of the two isomers, it is of interest that both the phenyltrifluoromethylphosphines seem to give chiefly the trans isomer. As in the methyltrifluoromethylphosphines, therefore, stepwise replacement of methyl by trifluoromethyl imposes steric restrictions on the phosphine which have the effect of stabilizing the trans isomer with respect to the cis. However, in the phenyl series, the introduction of only one CF_3 group seems to have a much greater effect, since methylbistrifluoromethylphosphine gives a very stable cis complex (15). The situation is parallel to that for tri-*n*-butylarsine and phenyldi-*n*-butylarsine, of which the former gives only the trans complex, but for the latter the cis–trans equilibrium is shifted in favor of the cis isomer (18).

Both bis(phenylbistrifluoromethylphosphine) dichloroplatinum (II) and bis(diphenyltrifluoromethylphosphine) dichloroplatinum (II) react with bromine and iodine to form the compounds $[C_6H_5P(CF_3)_2]_2PtCl_2X_2$ and $[(C_6H_5)_2PCF_3]_2PtCl_2X_2$, where X = Br or I. These are stable solids which are presumably Pt (IV) complexes of the type $[R_2R'P]_2PtX_2Cl_2$, although further investigation is required to establish such a formulation.

The above studies on complex formation emphasize the effect of the highly electronegative trifluoromethyl group in reducing the donor properties of phosphines, and they also reveal the importance of steric factors in the chemistry of the trifluoromethyl group.

EXPERIMENTAL

The general techniques used in the preparation, manipulation, and determination of physical and chemical properties of these compounds have been described previously (1).

Diphenylchlorophosphine was prepared by the method of Steube, LeSuer, and Norman (19). After aluminum chloride (222 g) had been added to a mixture of phosphorus pentasulphide (208 g) and benzene (224 g), the mixture was refluxed for 5 hours and after being cooled was poured onto crushed ice. The resultant dark green solution of diphenylphosphinodithiioc acid was diluted with an equal volume of benzene and chlorinated at 0° by a stream of chlorine. Diphenyltrichlorophosphorane crystallized out and, after separation, was heated with red phosphorus (15.5 g) to 180°. After the more volatile products had been removed, the residual mixture was vacuum distilled to give diphenylchlorophosphine (64 g, 63% yield), which boiled at 178° at 20 mm.

Diphenylphosphine was obtained by the reaction of diphenylchlorophosphine with lithium metal in ether solution, followed by hydrolysis (6).

Tetraphenyldiphosphine was prepared by refluxing an ethereal solution of diphenylchlorophosphine (11 g) and diphenylphosphine (9 g). The precipitated white solid was washed with ether and dried.

Preparation of Diphenyltrifluoromethylphosphine

(*a*) Tetraphenyldiphosphine (1.2 g) and excess trifluoroiodomethane (12.2 g) were heated in a sealed Pyrex tube at 185° for 12 hours. Removal of the volatile products, which were excess trifluoroiodomethane and a trace of fluoroform, left an involatile liquid (0.4 g). Analysis of a sample purified by vapor phase chromatography showed it to be diphenyltrifluoromethylphosphine. (Found: C, 60.86%; H, 4.25%; F, 22.69%; P, 11.79%. Calc. for $C_{13}H_{10}F_3P$: C, 61.41%; H, 3.94%; F, 22.45%; P, 12.21%.)

The same product was obtained when tetraphenyldiphosphine (10 g) and trifluoroiodomethane (10 g) were exposed to ultraviolet radiation for 7 days.

(*b*) Triphenylphosphine (2.5 g) was heated with excess trifluoroiodomethane (14.0 g) at 185° for 4 hours. Fractionation of the volatile products gave trifluoroiodomethane (10.6 g), fluoroform (0.46 g), and trifluoromethylbenzene (0.04 g). Vacuum distillation of the involatile residue gave diphenyltrifluoromethylphosphine (0.2 g), which was identified by its infrared spectrum. There remained a residue of diphenyliodophosphine. No reaction occurred between triphenylphosphine and trifluoroiodomethane at 110°, while heating at 214° gave only a resinous material which could not be identified.

(*c*) Diphenylchlorophosphine (5.6 g) and trifluoroiodomethane (17.0 g) were heated at 205° for 12 hours. The reactants were miscible and after being heated gave a reddish brown solution. The volatile products consisted of trace amounts of hexafluoroethane and fluoroform, unreacted trifluoroiodomethane (8.8 g), trifluorochloromethane (1.24 g), and trifluoromethylbenzene (0.04 g). The ethereal extract of the involatile materials was found to contain more trifluoromethylbenzene, phenyltrifluoromethylchlorophosphine, and diphenyltrifluoromethylphosphine. These were separated by distillation.

Diphenyltrifluoromethylphosphine is a colorless, oily liquid which boils at 255–257°. Its vapor pressure equation is $\log P_{mm} = 7.781 - (2598/T)$, whence the latent heat of vaporization is 11,850 kcal mole^{-1}, and Trouton's constant is 22.9. Diphenyltrifluoromethylphosphine is stable in air, and prolonged heating at 300° causes only 15% decomposition.

Hydrolysis Reactions

(*a*) Water: The phosphine (0.22 g) was sealed in a Pyrex tube with water (1.2 g) and heated at 120° for 48 hours. The compounds were immiscible and the phosphine was recovered quantitatively.

(*b*) Hydrochloric acid: Diphenyltrifluoromethylphosphine (0.34 g) was recovered unchanged after being heated with concentrated hydrochloric acid (2.4 g) at 150°.

(*c*) Aqueous sodium hydroxide: Diphenyltrifluoromethylphosphine (0.24 g) was unaffected by heating to 100° for 24 hours with 5 ml of 20% sodium hydroxide solution.

(*d*) Alcoholic potassium hydroxide: The phosphine (0.21 g) was heated to 70° with 5 ml of 20% alcoholic potassium hydroxide solution for 96 hours. The volatile product was fluoroform (0.046 g), corresponding to 78% hydrolysis of the phosphine. From the residual solution, diphenylphosphinic acid was recovered. This was identified by its infrared spectrum and its melting point of 193° (20).

Reactions with Halogens

(*a*) Iodine (0.18 g) reacted with diphenyltrifluoromethylphosphine (0.18 g) in carbon tetrachloride at 25°. After the mixture had stood for an hour, a brown oil separated, which was identified as diphenyltrifluoromethyldiiodophosphorane. (Found: I, 49.32%. Calc. for $C_{13}H_{10}F_3I_2F$: I, 50.0%.) When the phosphorane (0.123 g) was heated to 80° with aqueous sodium hydroxide solution, fluoroform (0.016 g) was evolved, representing 91.7% hydrolysis. The phosphorane was unaffected by water and only slight decomposition occurred after heating of the solution to 200° for 24 hours.

(*b*) Bromine (0.105 g) and diphenyltrifluoromethylphosphine (0.166 g) were reacted in carbon tetrachloride solution. The resulting orange oil was identified as diphenyltrifluoromethyldibromophosphorane. (Found: Br, 38.07%. Calc. for $C_{13}H_{10}F_3Br_2P$: Br, 38.64%.) Diphenyltrifluoromethyldibromophosphorane (0.272 g) was treated with aqueous sodium hydroxide solution at 80° to give fluoroform (0.044 g), representing 96.1% hydrolysis. Acidification of the remaining solution gave diphenylphosphinic acid, m.p. 194°.

Reaction with Trifluoroiodomethane

Diphenyltrifluoromethylphosphine (0.22 g) was quantitatively recovered after being heated with trifluoroiodomethane (0.86 g) at 100° for 24 hours.

Reaction with Iodomethane

Diphenyltrifluoromethylphosphine (0.234 g) was heated with iodomethane (0.269 g) to 100° for 12 hours. An orange oil separated from which the excess iodomethane was removed to give a yellow powder, identified as methyldiphenyltrifluoromethyl phosphonium iodide, m.p. 123–126°. (Found: C, 42.4%; H, 3.3%; F, 14.2%; P, 7.6%. Calc. for $C_{14}H_{13}F_3PI$: C, 42.6%; H, 3.3%; F, 14.3%; P, 7.9%.) Reaction of the phosphonium iodide (0.127 g) with water (3.5 g) gave fluoroform (0.022 g, 99.1%) and left an acidic solution. Evaporation of this solution and extraction of the residue with benzene gave a white solid identified as methyldiphenylphosphine oxide, m.p. 111–112°.

Reactions with Boron Trifluoride

(*a*) The passage of boron trifluoride through a petroleum ether solution of triphenylphosphine (0.368 g) precipitated a white solid which analyzed for triphenylphosphine-boron trifluoride. (Found: C, 65.5%; H, 5.02%. Calc. for $C_{18}H_{15}PBF_3$: C, 64.6%; H, 4.7%.) The adduct melted at 128–130°; it was stable in dry air but was decomposed rapidly by moisture and was insoluble in non-polar solvents. The saturation pressure is given by the equation $\log P_{mm} = 3.840 - (972/T)$ in the range 80–170°, whence the heat of sublimation is 4.43 kcal mole^{-1}.

(*b*) Diphenyltrifluoromethylphosphine (0.254 g) was mixed with boron trifluoride (0.136 g). No reaction occurred at room temperature but when the mixture was cooled to −78°, an oil formed from which excess boron trifluoride (0.063 g) was removed by pumping. This loss of BF_3 corresponds to the formation of a 1:1 compound. The adduct, which is an oil, has the same properties towards air, moisture, and non-polar solvents as the triphenylphosphine adduct. The saturation pressure in the range 40–110° C is given by the expression $\log P_{mm} = 6.609 - (1753/T)$, whence the heat of vaporization is 8.04 kcal mole^{-1}.

No reaction occurred between boron trifluoride and phenylbis(trifluoromethyl)phosphine either at 25° or at −78°.

Reactions with Platinum (II) Chloride

(*a*) Diphenyltrifluoromethylphosphine (0.254 g) in acetone was added to an aqueous solution of potassium chloroplatinite (0.21 g), and the mixture was heated for 30 minutes. Removal of the acetone gave a resinous mass which, after purification with animal charcoal and water, gave a pale yellow solid, bis(diphenyltrifluoromethylphosphine) dichloroplatinum (II). (Found: CF_3, 16.9%. Calc. for $C_{26}H_{20}F_6P_2PtCl_2$: CF_3, 17.8%.) Treatment with ether gave a small portion melting at 230°, while the bulk of the product was soluble in ether, and melted at 63–65°.

Reaction of the complex with a carbon tetrachloride solution of bromine or iodine gave a yellow and brown precipitate respectively. With bromine the product was bis(diphenyltrifluoromethylphosphine) dichlorodibromoplatinum (II). (Found: CF_3, 14.5%. Calc. for $C_{26}H_{20}F_6P_2PtCl_2Br_2$: CF_3, 14.7%.)

(*b*) Phenylbis(trifluoromethyl)phosphine (0.793 g) was heated with platinum (II) chloride (0.308 g) to 100° for 7 days. The product was recrystallized from acetone and was bis(phenylbistrifluoromethylphosphine) dichloroplatinum (II), m.p. 134–136°. (Found: C, 25.6%; H, 1.36%; F, 29.44%. Calc. for $C_{16}H_{10}F_{12}P_2PtCl_2$: C, 25.4%; H, 1.37%; F, 30.16%.) The same product was obtained by adding the phosphine to an aqueous solution of potassium chloroplatinite, although in this case, the product also contained a small amount of material which melted above 300°.

Treatment of the complex with a carbon tetrachloride solution of either bromine or iodine, as in (*a*) above, gave the dibromo or diiodo derivative. These were characterized by weight gain and by alkaline hydrolysis.

Dipole moments were measured as described previously (8); the platinum (II) complexes of both phenylbis(trifluoromethyl)phosphine and diphenyltrifluoromethylphosphine were found to have zero dipole moments.

ACKNOWLEDGMENTS

We gratefully acknowledge the support of the National Research Council, and one of us (M. A. A. B.) expresses thanks for a scholarship received from C.S.I.R. (Pakistan) under the auspices of the Colombo Plan.

REFERENCES

1. M. A. A. Beg and H. C. Clark. Can. J. Chem. **39**, 564 (1961).
2. W. R. Cullen. Can. J. Chem. **38**, 439 (1960).
3. A. B. Burg. J. Am. Chem. Soc. **83**, 2226 (1961).
4. M. L. Huggins. J. Am. Chem. Soc. **75**, 4123 (1953).
5. W. Dorken. Chem. Ber. **21**, 1505 (1888).
6. W. Kuchen and H. Buchwald. Chem. Ber. **91**, 2871 (1958).
7. F. W. Bennett, H. J. Emeleus, and R. N. Haszeldine. J. Chem. Soc. 3886 (1954).
8. W. R. Cullen. Can. J. Chem. **38**, 445 (1960).
9. R. W. Taft. *In* Steric effects in organic chemistry. *Edited by* M. S. Newman. John Wiley & Sons, Inc., New York. 1956.
10. C. E. Griffin. Spectrochim. Acta, **16**, 1464 (1960).
11. R. E. Kagarise. J. Am. Chem. Soc. **77**, 1377 (1955).
12. B. P. Dailey and J. N. Shoolery. J. Am. Chem. Soc. **77**, 3977 (1955).
13. J. J. Lagowski. Quart. Revs. (London), **13**, 233 (1959).
14. M. Issleib and W. Seidel. Z. anorg. u. allgem. Chem. **288**, 201 (1956).
15. M. A. A. Beg and H. C. Clark. Can. J. Chem. **38**, 119 (1960).
16. G. W. Fenton and C. K. Ingold. J. Chem. Soc. 2342 (1929).
17. K. A. Jensen. Z. anorg. u. allgem. Chem. **229**, 237 (1936).
18. J. Chatt and R. G. Wilkins. J. Chem. Soc. 525 (1956).
19. G. Steube, W. M. LeSuer, and G. R. Norman. J. Am. Chem. Soc. **77**, 1864 (1955).
20. G. M. Kosolapoff. Organophosphorus compounds. John Wiley & Sons, Inc., New York. 1950. p. 170.

MODIFICATION OF THE ILKOVIC EQUATION

R. S. SUBRAHMANYA
The Department of Inorganic and Physical Chemistry, Indian Institute of Science, Bangalore-12, South India

Received May 18, 1961

ABSTRACT

Taking into consideration the total amount of the depolarizer that reaches the surface of a flat stationary electrode, the following integral equation was obtained by Stackelberg:

$$\frac{2}{\pi D}.A.{}^{l}\delta_1 = \int_0^t \frac{A}{{}^{l}\delta_1}\,dt.$$

An equation of a similar form was also assumed to hold even in the case of the dropping mercury electrode. By this procedure he obtained the same expression for the flux $D[{}^*C/\sqrt{((3/7)\pi Dt)}]$ as obtained by Ilkovic. In the present work it has been shown that the same expression for the flux is obtained by introducing 'A' as a function of 't' in the basic integral and considering the effect which the moving surface will have on the thickness of the diffusion layer. The application of this new approach to the case of spherical diffusion to the dropping mercury electrode has lead to the following new polarographic equation:

$$i_d = 607\ nD^{1/2}{}^*Cm^{2/3}t^{1/6}(45.1\ D^{1/2}m^{-1/3}t^{1/6}+1).$$

INTRODUCTION

The Ilkovic equation in polarography derived by Ilkovic (1), MacGillavry and Rideal (2), and Stackelberg (3) represents the polarographic diffusion current. The current intensity at any time 't' is given by $i = nFAD(\partial C/\partial x)_{x=0}$. Each of the above authors determined the flux of the depolarizer at the electrode surface by different methods but they all obtained the same final result for the flux $D[{}^*C/\sqrt{((3/7)\pi Dt)}]$. Stackelberg (3, 4) derived the following integral equation taking into consideration the total amount of the depolarizer that reaches the surface of a flat stationary electrode:

$$\frac{2}{\pi D}\cdot A\cdot {}^{l}\delta_1 = \int_0^t \frac{A}{{}^{l}\delta_1}\,dt.$$

Since the area of the dropping electrode is $\propto t^{2/3}$, the following integral equation was assumed to be valid in the case of the dropping mercury electrode:

$$\frac{2}{\pi D}\cdot t^{2/3}\cdot {}^{d}\delta_1 = \int_0^t \frac{t^{2/3}}{{}^{d}\delta_1}\,dt.$$

In the present work it has been shown that the same final expression for ${}^{d}\delta_1$ is obtained when 'A' is introduced as a function of 't' in the basic integral and the effect which the moving surface will have on the thickness of the diffusion layer is considered. The method has also been used in the case of spherical diffusion to the dropping mercury electrode. This approach has led to a new polarographic equation.

NOTATIONS

n: number of electrons involved in the reduction process
A: area of the electrode
F: Faraday
${}^*C$: concentration of the depolarizer in the bulk in millimoles per liter

^0C: concentration of the depolarizer at the surface of the electrode; it becomes zero in the limiting diffusion current region

D: diffusion coefficient of the depolarizer in $cm^2\ sec^{-1}$

t: duration of electrolysis in seconds

$\left(\frac{\partial C}{\partial x}\right)_{x=0} = \frac{^*C - {}^0C}{\sqrt{(\pi Dt)}}$: gradient of the depolarizer at a stationary flat electrode surface

$D(\partial C/\partial x)_{x=0}$: flux of the depolarizer at the stationary flat electrode surface

$^l\delta_1 = \sqrt{(\pi Dt)}$: differential thickness of the diffusion layer at a stationary flat electrode surface

$^d\delta_1$, $^d\delta_s$: differential thickness of the diffusion layer at the dropping mercury electrode surface, for linear and spherical diffusion respectively

δ_s: differential thickness of the diffusion layer at the surface of stationary spherical electrode

$\left(\frac{\partial C}{\partial r}\right)_{r=r_2} = \left(\frac{1}{r_1} + \frac{1}{\sqrt{(\pi Dt)}}\right)\left(^*C - {}^0C\right)$: gradient of the depolarizer at a stationary spherical electrode

i: diffusion-controlled current in microamperes at any time 't'

$r_1 = \left(\frac{3m}{4\pi d}\right)^{1/3} t^{1/3} = a \cdot t^{1/3}$: radius of the mercury drop considered as a sphere at any time 't'. In the case of a stationary spherical electrode 'r_1' is the radius

m: rate of flow of mercury in mg per sec

d: specific gravity of mercury

$4\pi r_1^2 = 4\pi\left(\frac{3m}{4\pi d}\right)^{2/3} t^{2/3} = b \cdot t^{2/3}$: area of the mercury drop at any time 't'

THEORETICAL

Two cases are discussed: (i) linear diffusion to a growing spherical surface and (ii) spherical diffusion to a growing spherical surface.

Case (i). Linear Diffusion to a Growing Spherical Surface

When the surface is stationary the thickness of the diffusion layer is $^l\delta_1$. Let us suppose that when the surface is growing the thickness of the diffusion layer is changed by some factor 'x' so that the new thickness due to drop growing is $x\,^l\delta_1 = {}^d\delta_1$. The amount of the depolarizer reaching the electrode surface in time 'dt' as given by Fick's first law is

$$A \cdot D \frac{^*C - {}^0C}{x\,^l\delta_1}\, dt.$$

The total amount transferred to the electrode surface during the time interval $t = 0$ to $t = t$ is

$$\int_0^t D \cdot A \frac{^*C - {}^0C}{x\,^l\delta_1}\, dt = \int_0^t D \cdot b \cdot t^{2/3} \frac{^*C - {}^0C}{x\,^l\delta_1}\, dt$$

$$= \int_0^t D \cdot b \cdot t^{2/3} \frac{^*C - {}^0C}{x\sqrt{(\pi Dt)}}\, dt = \int_0^t D \cdot b \frac{^*C - {}^0C}{x\sqrt{(\pi D)}}\, t^{1/6} dt$$

$$= 2D \cdot b \cdot t^{2/3} \frac{{}^{*}C - {}^{0}C}{x\pi D} \cdot \frac{3}{7} \sqrt{(\pi Dt)} = 2D \cdot A \frac{{}^{*}C - {}^{0}C}{x^2 \pi D} \cdot \frac{3}{7} x \sqrt{(\pi Dt)}.$$

Hence for the dropping mercury electrode the following integral equation can be written

$$x^2 \int_0^t D \cdot A \frac{{}^{*}C - {}^{0}C}{{}^{d}\delta_1} dt = \frac{3}{7} 2D \cdot A \frac{{}^{*}C - {}^{0}C}{\pi D} {}^{d}\delta_1.$$

When the surface is stationary the following integral equation can be obtained (4):

$$\int_0^t D \cdot A \frac{{}^{*}C - {}^{0}C}{{}^{l}\delta_1} dt = \frac{2D \cdot A ({}^{*}C - {}^{0}C) {}^{l}\delta_1}{\pi D}.$$

Comparison of the integral equation obtained with the moving electrode with the integral equation obtained for the stationary electrode of the same area 'A' with diffusion layer thickness ${}^{l}\delta_1$ indicates that the value of 'x' is $\sqrt{(3/7)}$.

It can therefore be said that the effect of the growing of the mercury drop is to reduce the thickness of the diffusion layer from $\sqrt{(\pi Dt)}$ to $\sqrt{((3/7)\pi Dt)}$. This result is the same as that obtained by Stackelberg.

Case (ii). Spherical Diffusion to a Growing Spherical Electrode

The flux of the depolarizer at the surface of a stationary spherical electrode of radius 'r_1' is given by

$$D\left(\frac{\partial C}{\partial r}\right)_{r=r_1} = D\left(\frac{1}{r_1} + \frac{1}{\sqrt{(\pi Dt)}}\right)({}^{*}C - {}^{0}C).$$

The total amount of the depolarizer reaching the electrode surface during the time interval $t = 0$ to $t = t$ is

$$\int_0^t D \cdot A \left(\frac{1}{r_1} + \frac{1}{\sqrt{(\pi Dt)}}\right)({}^{*}C - {}^{0}C) dt$$

$$= \int_0^t D \cdot A ({}^{*}C - {}^{0}C) \frac{1}{r_1} dt + \int_0^t D \cdot A ({}^{*}C - {}^{0}C) \frac{1}{\sqrt{(\pi Dt)}} dt$$

I term II term

$$= D \cdot A ({}^{*}C - {}^{0}C) \frac{t}{r_1} + \frac{2D \cdot A ({}^{*}C - {}^{0}C)\sqrt{t}}{\sqrt{(\pi D)}}$$

$$= D \cdot 4\pi ({}^{*}C - {}^{0}C) r_1 t + \frac{2}{\pi D} D \cdot A ({}^{*}C - {}^{0}C) \sqrt{(\pi Dt)}.$$

It is clear that for spherical and linear diffusion to electrodes of equal area the reciprocal of the gradient differs by '$1/r_1$', where 'r_1' is the radius of the sphere. Consequently, the integral representing the total amount of the depolarizer can be split up into two portions. The II term is identical with the case of linear diffusion to a plane electrode of the same area. The difference between spherical diffusion and linear diffusion lies in the first term.

Since the thickness of the diffusion layer δ_s at a stationary spherical surface is given by the relation $1/\delta_s = 1/r_1 + 1/\sqrt{(\pi Dt)}$, one might consider the effect of growing surface on $1/\delta_s$ due to the effects on $1/r_1$ and $1/\sqrt{(\pi Dt)}$. Hence one can write $1/{}^{d}\delta_s = 1/yr_1 + 1/x\sqrt{(\pi Dt)}$, where '$y$' and '$x$' must be determined.

The total amount of the depolarizer that reaches the electrode surface in the case of the dropping mercury electrode would be

$$\int_0^t D \cdot A \left(\frac{1}{yr_1} + \frac{1}{x\sqrt{(\pi Dt)}} \right) (*C - {}^0C) dt.$$

This integral can be split up into the following two integrals:

$$\int_0^t D \cdot A \frac{*C - {}^0C}{yr_1} dt + \int_0^t D \cdot A \frac{*C - {}^0C}{x\sqrt{(\pi Dt)}} dt.$$

The two integrals can now be treated separately. Following the procedure that was followed in case (i) it can be shown that $x = \sqrt{(3/7)}$.

The value of 'y' can now be evaluated thus:

When the drop is growing 'A' and 'r_1' become functions of time. Hence

$$\int_0^t D \cdot A \frac{*C - {}^0C}{yr_1} dt = \int_0^t D \cdot 4\pi r_1 \frac{*C - {}^0C}{y} dt$$

$$= \int_0^t 4\pi D \frac{*C - {}^0C}{y} a \cdot t^{1/3} dt = 4\pi D \frac{*C - {}^0C}{y} a \cdot t^{4/3} \frac{3}{4}$$

$$= 4\pi D \frac{*C - {}^0C}{y} a \cdot t^{1/3} \cdot \frac{3}{4} t$$

$$= 4\pi D r_1 \frac{*C - {}^0C}{y} \cdot \frac{3}{4} t$$

$$= 4\pi D \frac{*C - {}^0C}{y^2} (yr_1) \frac{3}{4} t.$$

The following integral equation can be written:

$$y^2 \int_0^t D \cdot A \frac{*C - {}^0C}{(yr_1)} dt = 4\pi D (*C - {}^0C)(yr_1) \frac{3}{4} t.$$

We can now compare this equation with the following that has been obtained in the case of a stationary spherical electrode of area 'A' and radius 'r_1':

$$\int_0^t D \cdot A \frac{*C - {}^0C}{r_1} dt = 4\pi D (*C - {}^0C) r_1 t.$$

These equations are of the same form except that instead of 'r_1', 'yr_1' appears in the case of the dropping mercury electrode. Hence $y^2 = 3/4$ or $y = \sqrt{3}/2$.

The modified expression for the flux at the electrode surface can be written thus:

$$D\left(\frac{\partial C}{\partial r}\right)_{r=r_1} = D(*C - {}^0C)\left(\frac{1}{(\sqrt{3}/2)r_1} + \frac{1}{\sqrt{((3/7)\pi Dt)}}\right).$$

The current at any time 't' is

$$i_t = n.F.A.D.\left(\frac{\partial C}{\partial r}\right)_{r=r_1} = n.F.A.D.(*C - {}^0C)\left(\frac{1}{(\sqrt{3}/2)r_1} + \frac{1}{\sqrt{((3/7)\pi Dt)}}\right)$$

On expressing current in microamperes, 'A' and 'r_1' in terms of the amount of mercury flowing out per second, one gets

$$i_t = 706(*C - {}^0C) D^{1/2} n (51.6 D^{1/2} m^{1/3} t^{1/3} + m^{2/3} t^{1/6})$$

$$= 706(*C - {}^0C) D^{1/2} n m^{2/3} t^{1/6} (51.6 D^{1/2} m^{-1/3} t^{1/6} + 1).$$

The mean current is

$$\bar{i} = \frac{1}{t_{max}} \int_0^{t_{max}} i_t dt = 607\ nD^{1/2}(^*C - {}^0C)m^{2/3}t^{1/6}(45.1\ D^{1/2}m^{-1/3}t^{1/6}+1).$$

The following expression can be written for i_d, the limiting diffusion current:

$$i_d = 607\ nD^{1/2*}Cm^{2/3}t^{1/6}(45.1\ D^{1/2}m^{-1/3}t^{1/6}+1).$$

DETERMINATION OF 'K'

Several authors have treated the problem of the modification of the Ilkovic's equation. They have obtained an equation of the following form:

$$i_d = 607\ nD^{1/2*}Cm^{2/3}t^{1/6}(KD^{1/2}m^{-1/3}t^{1/6}+1),$$

the value of 'K' being 17 (5), 39 (4, 6), or 45.1 as in the present work. The equation derived by Koutecky (12) has the form

$$i_d = 607\ nD^{1/2*}Cm^{2/3}t^{1/6}(1+KD^{1/2}m^{-1/3}t^{1/6}+LDm^{-2/3}t^{1/3}+ \ldots),$$

the value of 'K' being 34. The equation derived in the present paper has only two terms inside the brackets corresponding in form to those derived by Stackelberg (5), Kambara, Suzuki, and Tachi (4), and Lingane and Loveridge (6) but differs from all other equations in that the value of 'K' is 45.1. It has to be pointed out that Kambara, Suzuki, and Tachi have employed the integral equation technique of Stackelberg for the case of diffusion to a growing spherical electrode. They have formulated the integral equation but in the subsequent mathematical operations the integration of $1/r_1$ is masked and hence they get a value of 39 for 'K'. In the present approach to the problem the effect of the growing drop is separately evaluated on each of the terms appearing in the expression for the thickness of the diffusion layer of the stationary spherical electrode leading to a value of 45.1 for 'K'. Lingane and Loveridge (6) obtained a value of 39.1 for 'K' for data for lead ions in 1 N potassium chloride. For the same data Strehlow and Stackelberg drew a least-square straight line and obtained a value of 17.4 for 'K' (7). The experimental determination of 'K' and the consequent verification of the theoretical equations derived by Strehlow and Stackelberg (5), Kambara, Suzuki, and Tachi (4), Lingane and Loveridge (6), and by the present author, are very difficult. Airey and Smales (8) have suggested that when a drop falls from the capillary it leaves a part of the depleted diffusion layer at the end of the capillary. Consequently the succeeding drop grows in a depleted region of the depolarizer solution. Hence the average current that is measured is smaller than the current one would expect from the 'first drop'. Ilkovic (9) has pointed out that the exhaustion effect may cause the diffusion current to decrease by as high as 15%. In order to verify the theoretical equations all experiments have to be conducted on the 'first drop'. In the alternative one has to use Smoler's horizontal capillary (10), where the drop dislodges at right angles to the tip of the capillary. With Smoler's technique there is mixing up of the solution and the impoverishment of the depolarizer does not exist at the tip of the capillary. Polarographers should also give careful thought to the suggestion of McKenzie (11) that one should measure the instantaneous current at the end of the drop life when the effect due to the impoverishment of the depolarizer is largely avoided. A detailed program of work employing Smoler's electrode has been planned in order to find out the exact value of 'K'.

ACKNOWLEDGMENTS

The author wishes to express his thanks to Professor M. R. A. Rao for helpful discussions. He is also thankful to Dr. S. K. Lakshmana Rao, Assistant Professor of Mathematics, Regional Engineering College, Warrangal, for his scrutiny of the mathematical aspects in this paper.

REFERENCES

1. D. Ilkovic. Collection Czechoslov. Chem. Comms. **6**, 498 (1934); J. chim. phys. **35**, 129 (1938).
2. D. MacGillavry and E. K. Rideal. Rec. trav. chim. **56**, 1013 (1937).
3. M. v. Stackelberg. Z. Elektrochem. **45**, 466 (1939).
4. T. Kambara, M. Suzuki, and I. Tachi. Bull. Chem. Soc. Japan, **23**, 219 (1950). T. Kambara and I. Tachi. Bull. Chem. Soc. Japan, **23**, 225 (1950). T. Kambara and I. Tachi. Proceedings of the First International Polarographic Congress, Prague. Vol. 1. 1951. p. 126.
5. H. Strehlow and M. v. Stackelberg. Z. Elektrochem. **54**, 51 (1950).
6. J. J. Lingane and B. A. Loveridge. J. Am. Chem. Soc. **72**, 438 (1950).
7. O. H. Muller. Electrochemical constants. National Bureau of Standards Circular 524. 1953. p. 289.
8. L. Airey and A. A. Smales. Analyst, **75**, 287 (1950).
9. D. Ilkovic. Advances in polarography. Proceedings of the Second International Congress held at Cambridge. 1959, Vol. 1. Pergamon Press. 1960. p. 380.
10. I. Smoler. Collection Czechoslov. Chem. Comms. **19**, 238 (1954).
11. H. A. McKenzie. Australian J. Chem. **11**, 271 (1958).
12. J. Koutecky. Czechoslov. J. Phys. **2**, 50 (1953).

APPENDIX

(i) Constancy of 'x'

In the derivation presented in this paper 'x' has been introduced for the sake of convenience. In fact, it is not necessary to introduce 'x' nor assume anything regarding its dependence on 't'. In the case of linear diffusion to a growing mercury drop surface we have

$$\int_0^t D\cdot A\,\frac{{}^*C-{}^0C}{{}^l\delta_1}\,dt = \int_0^t D\cdot b\cdot t^{2/3}\,\frac{{}^*C-{}^0C}{\sqrt{(\pi Dt)}}\,dt = 2D\cdot A\,\frac{{}^*C-{}^0C}{\pi D}\cdot\frac{3}{7}\sqrt{(\pi Dt)}.$$

Adjustment of 3/7 with ${}^l\delta_1$ or $\sqrt{(\pi Dt)}$ puts the integral equation into the same form as that obtained in the case of stationary electrode. Hence in the case of the dropping mercury electrode it can be written

$$\int_0^t D\cdot A\,\frac{{}^*C-{}^0C}{\sqrt{(3/7)}\,{}^l\delta_1}\,dt = 2D\cdot A\,\frac{{}^*C-{}^0C}{\pi D}\sqrt{(3/7)}\,{}^l\delta_1,$$

where $\sqrt{(3/7)}\,{}^l\delta_1 = {}^d\delta_1$.

The basic technique employed in the present work is to evaluate the integrals of the time-dependent functions and then compare the final integral equation with that obtained in the case of a stationary electrode to obtain the thickness of the diffusion layer in the case of the growing surface. Since this means that the form of integral equations governing diffusion to the stationary and growing surface are the same, it can formally be shown that under these conditions 'x' must be a constant. In the general case let 'x' be equal to $f(t)$. The following integral equation can be written for the case of the growing surface since the relation in the case of a growing surface is identical in structure with that in the case of a stationary surface:

$$H\int_0^t \frac{t^{1/6}}{f(t)}\,dt = Jf(t)t^{7/6},$$

where

$$H = \frac{Db({}^*C-{}^0C)}{\sqrt{(\pi D)}} \quad \text{and} \quad J = 2Db\,\frac{{}^*C-{}^0C}{\sqrt{(\pi D)}}.$$

Differentiating with respect to 't', multiplying both sides of the equation by $t^{7/6}$, and rearranging, one gets

$$\frac{H}{J}\cdot t^{4/3} = f(t)\cdot t^{7/6}\frac{d}{dt}\left(f(t)\cdot t^{7/6}\right).$$

On integration it is found

$$\frac{H}{J}\cdot\frac{3}{7}t^{7/3} = \frac{1}{2}\left(f(t)\cdot t^{7/6}\right)^2 + \text{constant}.$$

The constant must be zero since when $t = 0$ both sides must be zero, which leads to

$$f(t) = \sqrt{(3/7)} = \text{constant}.$$

(ii) Constancy of 'y'

In a similar way it can be proved that 'y' also should be a constant.

A SIMPLE METHOD OF SOLVING ILKOVIC'S DIFFERENTIAL EQUATION FOR THE TRANSFER OF DEPOLARIZER TO THE DROPPING MERCURY ELECTRODE

R. S. SUBRAHMANYA

The Department of Inorganic and Physical Chemistry, Indian Institute of Science, Bangalore-12, South India

Received May 18, 1961

ABSTRACT

The method developed by Ilkovic for solving the differential equation

$$\frac{\partial C}{\partial t} = D\frac{\partial^2 C}{\partial x^2} + \frac{2}{3}\cdot\frac{x}{t}\cdot\frac{\partial C}{\partial x}$$

which governs the diffusion of the depolarizer to the surface of the dropping mercury electrode is very difficult. In the present work a simple method is presented. The above equation is transformed into $\partial C/\partial T = \partial^2 C/\partial s^2$ by introducing the two new variables $s = xt^{2/3}/2.\sqrt{((3/7)D)}$ and $T = (1/4)t^{7/3}$. The boundary conditions for the transformed differential equation are formulated and the equation is solved by the Laplace transform method.

NOTATIONS

$C(x,t)$: concentration of the depolarizer at a distance 'x' from the electrode surface at time 't'.

$C(0,t)$: concentration of the depolarizer at the electrode surface at time 't' (^0C)

$^*C$: bulk concentration of the depolarizer

D: diffusion coefficient of the depolarizer in $cm^2\ sec^{-1}$

A: area of the electrode

p: variable in Laplace transformation

$L(C)$: Laplace transform of C

$L^{-1}u$: inverse transform of 'u'

$s = xt^{2/3}/2\sqrt{((3/7)D)}$: new variable

$T = (1/4)t^{7/3}$: new variable

INTRODUCTION

Several authors have treated the problem of diffusion of depolarizer to the dropping mercury electrode. A critical review of the various methods has been given by Markowitz and Elving (1). The methods employed fall into two classes. To the first class belong the differential methods wherein a differential equation is formulated and the equation solved using the appropriate boundary conditions. To the second class belong the integral methods where the problem is formulated as an integral equation. Ilkovic (2) treated the problem by assuming that the depolarizer reaches the surface of the dropping mercury electrode by linear diffusion. Since the thickness of the diffusion layer is much smaller than the radius of the mercury drop the curvature of the diffusion layer does not significantly differ from that of the mercury drop. In the formulation of the differential equation he also added an additional term to include the effect of the growing drop on the thickness of the diffusion layer. The following differential equation was formulated by him:

[1] $$\frac{\partial C}{\partial t} = D\frac{\partial^2 C}{\partial x^2} + \frac{2}{3}\cdot\frac{x}{t}\cdot\frac{\partial C}{\partial x}.$$

This differential equation was solved by him by employing the Fourier integral method after introducing a new variable $u = xt^{2/3}$. MacGillavary and Rideal (3) treated the problem as three dimensional spherical diffusion, and formulated the following differential equation:

$$\frac{\partial C}{\partial t} = D\left(\frac{\partial^2 C}{\partial r^2}+\frac{2}{r}\cdot\frac{\partial C}{\partial r}\right)-\frac{a^3}{3r^2}\cdot\frac{\partial C}{\partial r},$$

where 'r' is the distance from the center of the mercury drop. Due to the simplifications introduced in the subsequent mathematical operations they obtained the same final equation as Ilkovic for the current. The following equation for the average diffusion current was obtained:

$$i_d = 607nD^{1/2}{}^*Cm^{2/3}t^{1/6}.$$

Ilkovic had noticed that the differential thickness of the diffusion layer in the case of linear diffusion to a stationary electrode was $\sqrt{(\pi Dt)}$ and in the case of linear diffusion to a growing drop $\sqrt{\{(3/7)\pi Dt\}}$. Lingane and Loveridge (4) argued that even in the case of spherical diffusion an equation for the diffusion current can be obtained provided a correction is applied to the gradient obtained in the problem of diffusion to a stationary spherical electrode. The gradient is written

$$^*C(1/r+1/\sqrt{((3/7)\pi Dt)}).$$

The following expression was obtained for the diffusion current:

$$i_d = 607nD^{1/2}{}^*Cm^{2/3}t^{1/6}(1+KD^{1/2}m^{-1/3}t^{1/6}).$$

The value of 'K' was 39.

Strehlow and Stackelberg (5) re-examined the derivation of MacGillavary and Rideal and modified the intermediate mathematical steps and obtained the same equation as above but in which 'K' has the value 17. Kambara and Tachi (6) applied Ilkovic's technique of the formulation of the differential equation to the case of spherical diffusion to a growing drop. They obtained the same differential equation as MacGillavary and Rideal. After introducing a new dependent variable φ $(= rC)$ and transferring the co-ordinates from the center to the surface of the drop they obtained the following differential equation:

$$\frac{\partial \varphi}{\partial t} = D\frac{\partial^2 \varphi}{\partial x^2}+\frac{2x}{3t}\cdot\frac{\partial \varphi}{\partial x}.$$

The above differential equation is of the same form as that obtained by Ilkovic in the case of linear diffusion (eq. [1]). The procedure employed for solving this differential equation is not clear. However, they get the same equation for the diffusion current as Lingane and Loveridge.

The above is only a short account of the differential methods used in solving the problem of diffusion of the depolarizer to the dropping mercury electrode. It is clear that in these problems one meets differential equations of the form of equation [1]. The published procedures for the solution of such equations are either very difficult or not clearly given. Hence work was undertaken in this laboratory to examine the possibilities of solving such equations by suitable mathematical techniques, i.e. conversion of these partial differential equations into standard forms by the technique of change of variables and then solution by the Laplace transform method. In the present paper the method of solving the Ilkovic differential equation is given.

THEORETICAL

(i) Transformation of Ilkovic's Differential Equation

In the differential equation

$$\frac{\partial C}{\partial t} = D\cdot\frac{\partial^2 C}{\partial x^2}+\frac{2}{3}\cdot\frac{x}{t}\cdot\frac{\partial C}{\partial x}$$

'x' and 't' are the independent variables. Let us now express the above differential equation in terms of the new independent variables 's' and 'T'. Employing the chain rule the following transformations can be written:

(*a*)
$$\frac{\partial C}{\partial t} = \frac{\partial C}{\partial T}\cdot\frac{\partial T}{\partial t}+\frac{\partial C}{\partial s}\cdot\frac{\partial s}{\partial t} = \frac{\partial C}{\partial T}\cdot\frac{1}{4}\cdot\frac{7}{3}t^{4/3}+\frac{\partial C}{\partial s}\cdot\frac{x}{2\sqrt{((3/7)D)}}\cdot\frac{2}{3}t^{-1/3}$$

$$= \frac{\partial C}{\partial T}\cdot\frac{1}{4}\cdot\frac{7}{3}t^{4/3}+\frac{\partial C}{\partial s}\cdot\frac{2}{3}\cdot\frac{xt^{2/3}}{2\sqrt{((3/7)D)}}\cdot\frac{1}{t}$$

$$= \frac{\partial C}{\partial T}\cdot\frac{1}{4}\cdot\frac{7}{3}t^{4/3}+\frac{\partial C}{\partial s}\cdot\frac{2}{3}\cdot\frac{s}{t}.$$

(*b*)
$$\frac{\partial C}{\partial x} = \frac{\partial C}{\partial T}\cdot\frac{\partial}{\partial x}\left(\frac{1}{4}t^{7/3}\right)+\frac{\partial C}{\partial s}\cdot\frac{\partial s}{\partial x} = \frac{\partial C}{\partial s}\cdot\frac{t^{2/3}}{2\sqrt{((3/7)D)}}.$$

$$\therefore\ \frac{2}{3}\cdot\frac{x}{t}\cdot\frac{\partial C}{\partial x} = \frac{2}{3}\cdot\frac{x}{t}\cdot\frac{t^{2/3}}{2\sqrt{((3/7)D)}}\cdot\frac{\partial C}{\partial s} = \frac{2}{3}\cdot\frac{s}{t}\cdot\frac{\partial C}{\partial s}.$$

(*c*)
$$\frac{\partial^2 C}{\partial x^2} = \frac{\partial}{\partial x}\cdot\frac{\partial C}{\partial x} = \frac{\partial}{\partial x}\left(\frac{\partial s}{\partial x}\cdot\frac{\partial C}{\partial s}\right).$$

Since

$$\frac{\partial C}{\partial x} = \frac{\partial s}{\partial x}\cdot\frac{\partial C}{\partial s},\quad \frac{\partial}{\partial x} = \frac{\partial s}{\partial x}\cdot\frac{\partial}{\partial s},$$

$$\frac{\partial}{\partial x}\left(\frac{\partial s}{\partial x}\cdot\frac{\partial C}{\partial s}\right) = \frac{\partial s}{\partial x}\cdot\frac{\partial}{\partial s}\left(\frac{\partial s}{\partial x}\cdot\frac{\partial C}{\partial s}\right)$$

$$= \frac{t^{2/3}}{2\sqrt{((3/7)D)}}\cdot\frac{\partial}{\partial s}\left\{\frac{t^{2/3}}{2\sqrt{((3/7)D)}}\cdot\frac{\partial C}{\partial s}\right\} = \frac{t^{4/3}}{\{2\sqrt{((3/7)D)}\}^2}\cdot\frac{\partial^2 C}{\partial s^2}.$$

$$\therefore\ D\frac{\partial^2 C}{\partial x^2} = D\frac{t^{4/3}}{\{2\sqrt{((3/7)D)}\}^2}\cdot\frac{\partial^2 C}{\partial s^2}.$$

On substituting for $\partial C/\partial t$, $D\partial^2 C/\partial x^2$, and $2/3(x/t)(\partial C/\partial x)$ in terms of the new variables 's' and 'T', in equation [1] one gets

[2]
$$\frac{\partial C}{\partial T} = \frac{\partial^2 C}{\partial s^2}$$

(ii) Boundary Conditions for the Equation $\partial C/\partial T = \partial^2 C/\partial s^2$

The boundary conditions for equation [1] can be written as follows:

$$C(x,0) = {}^*C;\ C(0,t) = {}^0C;\ C(x,t) = {}^*C \text{ as } 'x' \rightarrow \infty.$$

Ilkovic transformed equation [1] into $\partial C/\partial t = D(\partial^2 C/\partial u^2)t^{4/3}$ by introducing the new variable $u = xt^{2/3}$ and has given the following boundary conditions:

$$C(u,0) = {}^*C \text{ and } C(0,t) = {}^0C.$$

For equation [2] obtained in the present work the following boundary conditions can be given:

$$C(s,0) = {}^*C,\ C(0,T) = {}^0C, \text{ and } C(s,T) = {}^*C \text{ as } 's' \rightarrow \infty.$$

It is interesting to examine the significance of the boundary conditions that have been given above for equation [2]. The variable 'x' represents the distance of any point from the surface of the electrode and Ilkovic has restricted the range of 'x' such that 'Ax' is always a constant. The significance of this becomes clear if we consider the difference in volume between concentric spheres of radius r_1+x and r_1:

$$\Delta V = 4/3\pi\{(r_1+x)^3-r_1^3\} = 4/3\pi x(3r_1^2+3r_1x+x^2) \simeq 4\pi r_1^2 x$$

$$= 4\pi(3m/4\pi d)^{2/3}t^{2/3}x = Ax \text{ (when '}x\text{' is small as compared to '}r_1\text{')}.$$

It is interesting to find out the error that is introduced in neglecting $3r_1x$ and x^2 in comparison with $3r_1^2$. Let us take the case of a depolarizer with diffusion coefficient 10^{-5} cm^{2}sec^{-1} diffusing to the surface of a dropping mercury electrode with the following capillary characteristics: $m = 1.5$ mg per sec; $t = 5$ sec. At the maximum size of the drop the error introduced when the value of 'x' is equal to $\sqrt{\{(3/7)\pi Dt\}}$ (thickness of the diffusion layer in the case of the dropping mercury electrode) is about 16%. When the value of 'x' is about one eighth the thickness of the diffusion layer, 'Ax' is constant within about 2%. For smaller values of 'x' the error introduced becomes much smaller. It is therefore obvious that the condition put by Ilkovic that 'Ax' be a constant highly restricts the range of 'x'. Similar results are also obtained in calculations made at different times during the life time of a mercury drop.

Introduction of the variable 's', $xt^{2/3}/2\sqrt{((3/7)D)}$, suggests that we are considering the value of C at different concentric spheres from the surface of the electrode. Regarding 'T' it can be said that changes in 't' are similar to changes in 'T'.

(iii) Solution of the Equation $\partial C/\partial T = \partial^2 C/\partial s^2$

The boundary conditions are given by $C(s,0) = {}^*C$, $C(0,T) = {}^0C$, and $C(s,T) = {}^*C$ as 's' $\rightarrow \infty$. $\partial C/\partial T = \partial^2 C/\partial s^2$ is a partial differential equation with constant coefficients. Hence the Laplace transform method can be used for solving this equation.

We define the Laplace transform of $C(s,T)$ (abbreviated as $L\ C(s,T)$) as

$$u(s,p) = p\int_0^\infty e^{-pT}C(s,T)dT.$$

The equation $\partial C/\partial T = \partial^2 C/\partial s^2$ is transformed into

$$pu - p{}^*C = \frac{d^2u}{ds^2} \qquad [3]$$

since ${}^*C$ is the value of the function $C(s,T)$ when $T = 0$.
The solution of [3] is

$$u = u_c+u_p = A_1e^{+\sqrt{(p)}\cdot s}+A_2e^{-\sqrt{(p)}\cdot s}+\frac{-p{}^*C}{-p} = A_1e^{+\sqrt{(p)}\cdot s}+A_2e^{-\sqrt{(p)}\cdot s}+{}^*C.$$

Since the concentration of the depolarizer does not increase indefinitely with an increase in 's', $A_1 = 0$. $C(0,T) = {}^0C$ = constant. A Laplace transformation of a constant is the constant itself.

Therefore

$$L\,C(0,T) = u(0,p) = \text{constant} = {}^{0}C$$

$$A_2 = -(*C - {}^{0}C)$$

$$u = *C - (*C - {}^{0}C)e^{-\sqrt{(p)}.s}$$

$$C(s,T) = L^{-1}u(s,p) = L^{-1}*C - L^{-1}\,(*C - {}^{0}C)e^{-\sqrt{(p)}.s}$$

$$= *C - (*C - {}^{0}C)\left\{1 - \text{erf}\,\frac{s}{2\sqrt{T}}\right\}$$

[4] $$= {}^{0}C + (*C - {}^{0}C)\ \text{erf}\,\frac{s}{2\sqrt{T}}.$$

I n terms of the old co-ordinate system we have

[5] $$C(x,t) = {}^{0}C + (*C - {}^{0}C)\ \text{erf}\,\frac{x}{2\sqrt{((3/7)Dt)}}.$$

The value of $(\partial C/\partial x)_{x=0}$ can be obtained by differentiating with respect to 'x' under the integral sign either from [4] or [5]:

$$\left(\frac{\partial C}{\partial x}\right)_{x=0} = \frac{*C - {}^{0}C}{\sqrt{((3/7)\ \pi Dt)}}.$$

The current at any time 't' is given by

$$n.F.A.D\left(\frac{\partial C}{\partial x}\right)_{x=0} = n.F.A.D\,\frac{*C - {}^{0}C}{\sqrt{((3/7)\ \pi Dt)}}.$$

ACKNOWLEDGMENTS

The author wishes to express his thanks to Professor M. R. A. Rao for helpful discussions. His thanks are also due to Dr. S. K. Lakshmana Rao, Assistant Professor of Mathematics, Regional Engineering College, Warrangal, for his scrutiny of the mathematical aspects of this paper.

REFERENCES

1. J. M. Markowitz and P. J. Elving. Chem. Rev. **58**, 1047 (1958).
2. D. Ilkovic. J. chim. phys. **35**, 129 (1938).
3. D. MacGillavary and E. K. Rideal. Rec. trav. chim. **56**, 1013 (1937).
4. J. J. Lingane and B. A. Loveridge. J. Am. Chem. Soc. **72**, 438 (1950).
5. H. Strehlow and M. von Stackelberg. Z. Elektrochem. **54**, 51 (1950).
6. T. Kambara and I. Tachi. Proceedings of the First International Polarographic Congress, Prague. Vol. 1. 1951. p. 126.

THE INFRARED ABSORPTION SPECTRA OF DEUTERATED ESTERS

III. METHYL LAURATE[1]

R. NORMAN JONES

The Division of Pure Chemistry, National Research Council of Canada, Ottawa, Canada

Received October 17, 1961

ABSTRACT

The infrared absorption spectrum of methyl laurate in carbon tetrachloride and carbon disulphide solutions has been compared with the spectra of seven derivatives deuterated in the ω-methyl group, the α-methylene groups, the carbomethoxy group, and in binary and ternary combinations of these positions. The spectra of *n*-dodecanes deuterated in the terminal methyl groups and of methyl laurates chlorinated in the ω-methyl and α-methylene groups have also been measured.

From an analysis of these spectra, all the bands and inflections between 3100 and 700 cm^{-1} in the spectrum of methyl laurate can be assigned to localized group vibrations. The spectra of some related acid chlorides, alcohols, and bromides are also briefly noted.

INTRODUCTION

The molecular vibrations of open-chain polymethylene compounds have been investigated extensively. The earlier work was reviewed by Sheppard and Simpson (1) in 1953, and the more controversial aspects of recent work have been discussed by Sheppard (2), J. R. Nielsen, and Holland (3), and Krimm (4) among others. Most of these studies have dealt with the solid state in which the chain is extended in the all-trans form. In the liquid state, compounds containing short methylene chains exhibit more complex spectra because a limited number of non-linear conformational isomers are present in equilibrium with the all-trans form. As the chain lengthens the number of conformational isomers increases, but the spectral band envelope simplifies because only the predominating all-trans and a few of the cissoid infrared-active vibrations give rise to discrete resolved bands.

Earlier work from this laboratory (5, 6) has dealt with the effect of chain length on the infrared spectra of straight-chain fatty acids and their methyl esters. It was observed that the spectra of the acids and esters in the C_{14}–C_{21} range were very similar when measured in solution. Only small variations occurred in the relative band intensities and these could not be evaluated quantitatively by the experimental techniques then available. More recently we have studied quantitatively the effect of the chain length on the spectra of *n*-alkanes in solution, using an improved spectrophotometric technique (7). The absorption characteristic of the carbomethoxy group has also been examined by comparing the spectra of methyl and ethyl acetates with the spectra of derivatives in which the methyl and methylene groups have been selectively deuterated (8, 9).

These investigations showed that the carbomethoxy group vibrations of fatty acid methyl esters are "insulated" from the chain vibrations, and it is of interest to determine how precisely such spectra can be treated in terms of sets of independent absorption bands specific respectively to the chain and to the terminal groups. In the long-chain esters the vibrational modes of the α-methylene group are perturbed by the proximity of the carbonyl. Absorption specific to the ω-methyl group is also distinguished

[1]*Issued as N.R.C. No. 6650.*

Presented, in part, at the International Conference of the European Molecular Spectroscopy Group, Bologna, Italy, September 1959.

and the spectra of the long-chain esters can be most conveniently discussed in terms of the four vibrational "zones" (*a*)–(*d*) of structure I.

$$\underset{(a)}{CH_3}—\underset{(b)}{(CH_2)_n}—\underset{(c)}{CH_2}—\underset{(d)}{COOCH_3}$$

I

In order to investigate possible interaction effects among the vibrations assigned to these units of structure, a series of compounds has been prepared in which the ω-methyl group, the α-methylene group, and the carbomethoxy methyl group of a representative long-chain methyl ester have been selectively deuterated. Methyl laurate (II), with $n = 9$, was chosen for this purpose as this length of chain provides an optimum balance between the cumulative intensity of the weak chain methylene bands and the stronger absorption of the carbomethoxy group.

Seven selectively deuterated derivatives of methyl laurate were prepared (III–IX). These include III–V, deuterated respectively in the ω-methyl group, the α-methylene group, and the carbomethoxy group, VI–VIII deuterated at two of these positions, and IX deuterated at all three. The spectrum of *n*-dodecane (X) and its derivatives deuterated in one or both methyl groups (XI, XII) were also examined, as were two chlorinated analogues (XIII, XIV) and two acid chlorides (XV, XVI). Attempts to prepare a third chlorinated analogue (XVII) were not successful. The acetylenic ester XVIII and the alcohols and bromides XIX–XXIV were obtained as intermediates in the syntheses, and certain aspects of the spectra of XIX, XX, XXII, and XXIV will also be discussed.

II	$CH_3—(CH_2)_9—CH_2—COOCH_3$	XIV	$CH_3—(CH_2)_9—CCl_2—COOCH_3$
III	$CD_3—(CH_2)_9—CH_2—COOCH_3$	XV	$CH_3—(CH_2)_9—CH_2—COCl$
IV	$CH_3—(CH_2)_9—CD_2—COOCH_3$	XVI	$CH_3—(CH_2)_9—CCl_2—COCl$
V	$CH_3—(CH_2)_9—CH_2—COOCD_3$	XVII	$[CH_3—(CH_2)_9—CH_2—COOCCl_3]$
VI	$CD_3—(CH_2)_9—CD_2—COOCH_3$	XVIII	$HC\equiv C—(CH_2)_7—CH_2—COOCH_3$
VII	$CD_3—(CH_2)_9—CH_2—COOCD_3$	XIX	$CH_3—(CH_2)_9—CH_2—CH_2OH$
VIII	$CH_3—(CH_2)_9—CD_2—COOCD_3$	XX	$CD_3—(CH_2)_9—CH_2—CD_2OH$
IX	$CD_3—(CH_2)_9—CD_2—COOCD_3$	XXI	$CH_3—(CH_2)_9—CH_2—CD_2OH$
X	$CH_3—(CH_2)_{10}—CH_3$	XXII	$CH_3—(CH_2)_9—CH_2—CH_2Br$
XI	$CD_3—(CH_2)_{10}—CH_3$	XXIII	$CH_3—(CH_2)_9—CH_2—CD_2Br$
XII	$CD_3—(CH_2)_{10}—CD_3$	XXIV	$CD_3—(CH_2)_9—CH_2—CD_2Br$
XIII	$CCl_3—(CH_2)_9—CH_2—COOCH_3$		

EXPERIMENTAL

The deuterated and chlorinated esters were synthesized by Dr. L. C. Leitch and Miss M. E. Isabelle, and their preparation has already been described (10). The hydrocarbons XI and XII, also prepared by Leitch and Isabelle, were obtained from the esters II and III. These esters were reduced with $LiAlD_4$ to the alcohols XXI and XX, which were converted with bromine and phosphorus to XXIII and XXIV respectively. Dehalogenation of these bromides with zinc dust in deuterium oxide gave the hydrocarbons XI and XII. The deuterium content of several of these compounds was assayed by infrared analysis of the water formed on combustion (11) to give the following results, expressed as atoms of deuterium per molecule:

III (2.86, 2.93); VI (4.80); VIII (5.12, 5.09);
IX (8.09, 8.06); XI (2.89, 2.92); XII (5.81);
XX (5.10, 4.90); XXIV (4.91, 4.78).

The infrared spectra were measured on a Perkin–Elmer Model 112 single-beam double-pass spectrometer using LiF, CaF_2, and NaCl prisms. Carbon tetrachloride was used as solvent for the range 3200–1320 cm^{-1} and carbon disulphide below 1320 cm^{-1}.

Measurements were made at 1-mm path length. The spectrometer was calibrated with a ternary mixture of indene, camphor, and cyclohexanone (12) and the estimated precision of the band positions is ± 1 cm^{-1}

below 2000 cm^{-1}, diminishing to ± 3 cm^{-1} at the higher frequencies. A nominal spectral slit width of 2 cm^{-1} was used between 2000 and 650 cm^{-1}, increasing to 4 cm^{-1} at 3200 cm^{-1}. A separate solvent background spectrum was recorded on each chart, and the spectra were plotted as apparent molecular extinction coefficients (ϵ'_{ν}) against wavenumber. The reported intensities are the mean of at least two sets of measurements on separately prepared solutions; all peak intensities were measured at absorbances in the range 0.1–0.8. Between 890 cm^{-1} and 820 cm^{-1}, where carbon disulphide absorbs, the spectra of several of the compounds were also measured qualitatively on capillary films of the undiluted liquids, using a Perkin–Elmer Model 21 spectrophotometer with NaCl prism.

RESULTS

C—H Stretching Vibrations

The spectra of representative compounds in the C—H stretching region are shown in Fig. 1 and the complete data are summarized in Table I. Bands D and F are the

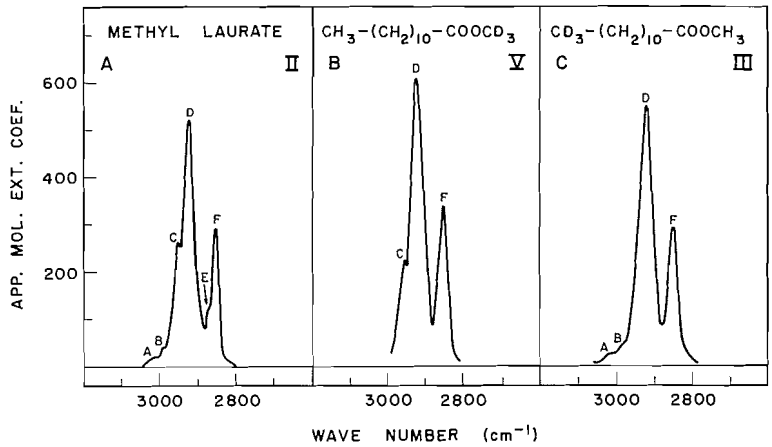

FIG. 1.

TABLE I

C—H stretching bands of methyl laurate and related compounds

Compound	Band[a] A	B	C	D	E	F
II	[3020] (16)	2995 (40)	2950 (260)	2922 (520)	[2870] (120)	2852 (290)
III	3015 (24)	[2990] (42)	—	2923 (550)	—	2851 (300)
IV[b]	3020 (25)	[2995] (40)	[2950] (250)	2923 (490)	[2870] (120)	2856 (270)
V	—	—	2952 (230)	2924 (610)	—	2852 (340)
VI[b]	[3020] (20)	2993 (33)	—	2928 (540)	—	2857 (295)
VII	—	—	—	2921 (575)	—	2849 (300)
VIII[b]	—	—	[2955] (210)	2926 (525)	—	2857 (290)
IX[b]	—	—	—	2926 (510)	—	2857 (285)
X[b, c]	—	—	2955 (310)	2923 (665)	2871 (175)	2854 (360)
XI[b]	—	—	2956 (190)	2926 (600)	—	2857 (335)
XII[b]	—	—	—	2926 (660)	—	2857 (350)
XVIII[d]	3020 (20)	2995 (35)	—	2926 (320)	—	2855 (165)
XX[b]	—	—	—	2926 (555)	—	2857 (305)

[a]The band maxima are in cm^{-1} followed by ϵ^{a}_{max} in parenthesis. The positions of points of inflection are indicated in square brackets.

[b]For spectra measured with a CaF_2 prism at a nominal spectral slit width of 10 cm^{-1}. The other spectra were obtained with a LiF prism at a nominal spectral slit width of 2 cm^{-1}. All measurements are for solutions in carbon tetrachloride at a concentration of approximately 0.01 *M*.

[c]Data obtained at higher resolution are reported in reference 7.

[d]The acetylenic ≡C—H stretching band is at 3310 cm^{-1} (ϵ^{a}_{max} 150) with shoulder at 3295 cm^{-1} (ϵ^{a}_{max} 20). The C≡C stretching band is at 2116 cm^{-1} (ϵ^{a}_{max} 15).

asymmetrical and symmetrical C—H stretching bands of the polymethylene chain. Band C and the inflection E at 2950 cm^{-1} and 2870 cm^{-1} are absent from the spectra of III, VI, VII, IX, XII, XVIII, and XX. These compounds lack the ω-CH_3 group and the bands are assigned to the asymmetrical and symmetrical stretching modes of this group. The spectra of XXII and XXIV were not measured in this region.

Absorption specific to the C—H stretching modes of the carbomethoxy group is less obvious. In the spectrum of $CH_3.COOCH_3$ there are weak bands at 3026, 2999, and 2957 cm^{-1}; these are absent from the spectrum of $CH_3.COOCD_3$ and have been assigned to the carbomethoxy methyl group (8). Similar bands near 3025 cm^{-1} and 3000 cm^{-1} are observed for III, VI, and XVIII but not for V, VII–XII, and XX, consistent with their assignment to the carbomethoxy group. The inflection at 3020 cm^{-1} (band A) and the maximum at 2995 cm^{-1} (band B) in the spectrum of methyl laurate can be assigned similarly. The third band near 2957 cm^{-1} is not observed for methyl laurate, but is presumed to be submerged beneath the stronger absorption of the other C—H bands (band α). Greek letters will be used in general to designate bands that are presumably present but are obscured by overlap in the methyl laurate spectrum.

Wilmshurst (13) has assigned both the 3026 cm^{-1} and the 2999 cm^{-1} bands of methyl acetate to asymmetrical C—H stretching modes of the methoxyl group, assuming that the molecule has the planar *s*-cis conformation XXV. The normally doubly degenerate mode is here split because of the presence of a plane of symmetry. The 3026 cm^{-1} band is attributed to the a' species, symmetrical with respect to the plane, and the 2999 cm^{-1} to the a'' antisymmetrical species. The presence of a similar doublet in the spectrum of methyl laurate indicates that the carbomethoxy group has the same *s*-cis configuration (XXVI). Wilmshurst's evidence for the *s*-cis configuration in methyl acetate is not conclusive, but it is based on analogy with methyl formate and fits the experimental data satisfactorily. Wilmshurst assigns the α band to the symmetrical mode.

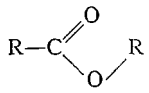

XXV (R = —CH_3)
XXVI (R = —$C_{11}H_{23}$)

Absorption specific to the α-methylene group of methyl laurate should be most readily detected by comparisons among the spectra of VII, IX, and XII, but no significant differences are observed in the contours of these band envelopes.

C—D Stretching Vibrations

On deuteration of the ω-methyl group three bands appear at 2210, 2120, and 2075 cm^{-1} (Table II). These are observed in the spectra of III, XI, and XII, with the intensity for XII approximately twice that for XI. The more intense band is tentatively identified with the asymmetrical C—D stretching mode. The weaker doublet may involve a Fermi resonance of the symmetrical C—D stretching mode with an overtone or combination band.

Deuteration of the carbomethoxy group produces a more complex set of five bands at 2272, 2247, 2192, 2125, and 2080 cm^{-1}. On the basis of Wilmshurst's assignments for methyl acetate, three bands would be expected for the —$COOCD_3$ group.

Exchange of deuterium in the α-methylene group produces a very weak set of bands at 2312, 2220, and 2150 cm^{-1}. Here again the number of bands observed exceeds that anticipated for a pair of antisymmetrical and symmetrical C—D stretching vibrations.

TABLE II

C—D stretching bands of deuterated methyl laurates and related compounds

	Band[a]										
Compound	α-CD_2—	—OCD_3	—OCD_3	α-CD_2—	CD_3—	—OCD_3	α-CD_2—	—OCD_3	CD_3—	—OCD_3	CD_3—
III	—	—	—	—	2210 (17)	—	—	—	2120 (7)	—	2075 (8)
IV	2312 (2)	—	—	2220 (3)	—	—	2150 (3)	—	—	—	—
V	—	2272 (17)	2247 (35)	—	—	2192 (18)	—	2125 (16)	—	2080 (22)	—
VI	—	—	—	....2212 (32)[b]....		—	—	—	2121 (12)	—	2077 (16)
VII	—	[2270] (14)	2248 (23)	—	2212 (32)	[2195] (20)	—	....2125 (22)....		....2078 (37).. ..	
VIII	—	2275 (15)	2252 (24)	—	—	2195 (20)	—	2125 (14)	—	2080 (26)	—
IX	—	2272 (16)	2250 (24)	....2212 (38)[b]....		2195 (26)	—	....2125 (22)		....2078 (36)....	
XI	—	—	—	—	2212 (34)	—	—	—	2120 (10)	—	2077 (15)
XII	—	—	—	—	2212 (67)	—	—	—	2122 (18)	—	2077 (26)

[a]The band maxima are in cm^{-1} followed by ϵ_{max} in parenthesis. The positions of points of inflection are indicated by square brackets. The spectra were measured at a nominal spectral slit width of 2 cm^{-1} in carbon tetrachloride solution at a concentration of approximately 0.1 *M*, except for IV, for which a concentration of 1.3 *M* was used.
[b]Broad band.

Apart from the obvious, but unproved, explanation in terms of Fermi resonance, the additional band could result from restricted rotation about the C—CO bond, leading to an equilibrium between XXVII and XXVIII or related non-eclipsed structures. Some anomalous C—D absorption could result from incomplete exchange of hydrogen, but the deuterium analyses indicate that the concentration of any —CHD— species must be small, and would be unlikely to give a C—D stretching band of significant intensity.

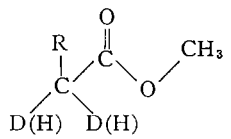

XXVII

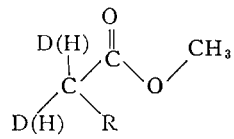

XXVIII

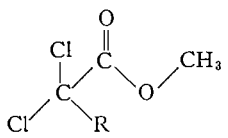

XXIX

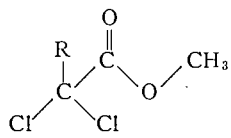

XXX

The spectra of esters deuterated at more than one center exhibit C—D bands that are consistent with the superposition of the spectra discussed above (Table II).

C=O Stretching Vibrations

The positions of the C=O stretching bands are listed in Table III. Deuteration of the carbomethoxy methyl shifts the band to lower frequency, as in methyl acetate. Deuteration in the ω-methyl or α-methylene has no effect. The insensitivity to α-methylene deuteration is notable, since deuteration of $CH_3.COOCH_3$ to $CD_3.COOCH_3$, which similarly involves deuterium replacement on the α-carbon, lowers the carbonyl frequency by 5 cm^{-1} (8, 9).

The spectrum of the α-chloro ester (XIV) has two maxima at 1768 and 1751 cm^{-1}, which probably result from restricted rotation about the C—CO bond (XXIX, XXX). By analogy with the doublet carbonyl maxima of chloroacetone (14, 15) and the ω-halogenated acetophenones (16), the 1768 cm^{-1} peak is attributed to the *s*-cis isomer (XXIX) and the 1751 cm^{-1} peak to the gauche form (XXX). Our sample of XIV had an additional

TABLE III

C=O stretching bands of methyl laurate and related compounds

Compound	Band G[a]	Compound	Band G[a]
II	1742 (550)	XIII	1744 (580)
III	1741 (540)	XIV	1768 (135)
IV	1741 (495)		1751 (250)
			1723 (62)
V	1739 (550)	XV	1803 (365)
VI	1743 (530)		1760 (50)
			1711 (65)
VII	1739 (515)	XVI	1810 (165)
VIII	1738 (540)		1784 (235)
IX	1739 (590)	XVIII	1742 (520)

[a]The band maxima are in cm^{-1} followed by ϵ_{max} in parenthesis. The spectra were measured at a nominal spectral slit width of 2 cm^{-1} in carbon tetrachloride solution at a concentration of 0.01 *M*.

weak maximum at 1723 cm^{-1} which is difficult to explain in terms of conformational isomerism, nor is there any likely impurity that would absorb at this position. The acid chloride XV absorbs at 1803 cm^{-1} with secondary maxima at 1760 and 1711 cm^{-1} and the acid chloride XVI at 1810 and 1784 cm^{-1}. The satellite bands of XV may be due to impurity, but similar secondary absorption below the main C=O maximum is also observed in the spectrum of benzoyl chloride (17) and remains unexplained.

C—H Deformation Vibrations between 1500 and 1300 cm^{-1}

In this region of the spectrum the effects of selective deuteration are most specific. Methyl laurate exhibits eight peaks (bands H–N of Fig. 2A and band O of Fig. 7A). There is also indirect evidence that three bands (β–δ) contribute to the H/I system; an additional weak band (ϵ) is submerged beneath band J and two more weak bands (ζ, η) lie beneath bands L and M. Representative spectra are shown in Figs. 2–6 and the numerical data are summarized in Table IV.

Bands H and I (1467 and 1458 cm^{-1})

This doublet results from the overlapping of several bands. The principal components are the scissoring modes of the chain methylene groups, with secondary contributions from both methyl groups. The dominant methylene contribution (band β) is apparent from the spectra of IX and XII in Figs. 3D and 4C. The contribution from the asymmetrical C—H bending mode of the ω-methyl group (band γ) is indicated by the progressive diminution in the intensity of the H/I band envelope for X, XI, and XII in Fig. 4.

The short-chain *n*-alkanes exhibit a maximum at 1467 cm^{-1} with a satellite peak at 1457 cm^{-1}. With increasing chain length, an intermediate band appears at 1460 cm^{-1} which can be detected by graphical analysis for *n*-tridecane and is visually apparent for *n*-octacosane (7). The 1467 cm^{-1} and the 1460 cm^{-1} bands have been assigned to methylene scissoring vibrations and the 1457 cm^{-1} band to the asymmetrical C—H bend of the methyl groups. The contours and intensities of the H/I band group in Fig. 4 show that although the absorption at 1457 cm^{-1} weakens with deuteration of the methyl some absorption remains at 1457 cm^{-1}, and the 1467 cm^{-1} band of XII is highly asymmetrical on the low-frequency side. This suggests that methylene scissoring modes (probably from coiled or bent chains) are contributing to absorption in the 1460–1455 cm^{-1} region as well as the terminal methyl group vibration. The temperature dependence of these bands is currently under investigation.

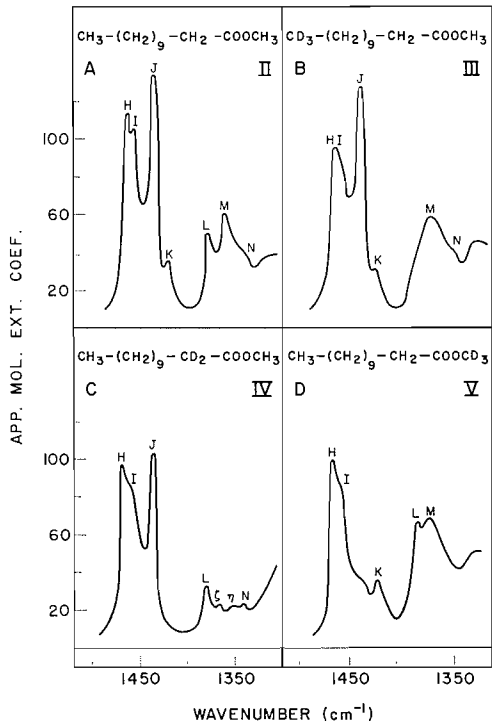

FIG. 2.

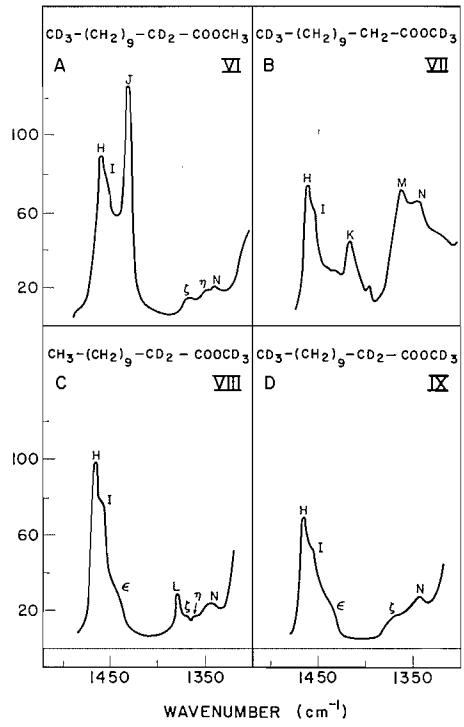

FIG. 3.

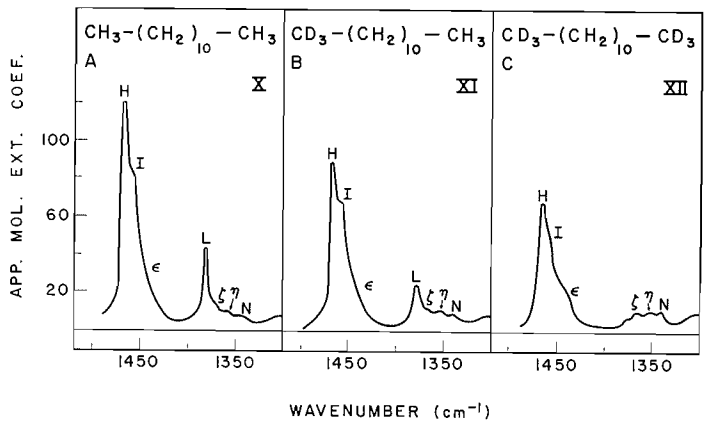

FIG. 4.

The carbomethoxy methyl group of methyl laurate also contributes to the absorption beneath the H/I envelope (band δ). The spectrum of $CD_3.COOCH_3$ has a band at 1456 cm^{-1} which has been attributed to the asymmetrical C—H bending mode (8). This is not distinguishable in the spectrum of methyl laurate, but its presence is suggested by the fall in the intensity of band I when the carbomethoxy group is deuterated (cf. Figs. 2A and 2D; 3A and 3D). If the carbomethoxy group is planar (XXVI) there should be two bands, and Wilmshurst has reported the second (weaker) band at 1469 cm^{-1} in methyl acetate (13).

TABLE IV

C—H deformation bands between 1500 and 1300 cm^{-1} of methyl laurate and related compounds

Compound	Band [a] H	I	ϵ	J	K
II	1467 (113)	1458 (107)	—	1436 (136)	1419 (36)
III	1463	(96).....	—	1436 (130)	1419 (32)
IV	1466 (98)	[1458] (86)	—	1436 (105)	—
V	1465 (102)	[1458] (90)	—	—	1418 (37)
VI	1464 (88)	[1458] (78)	—	1435 (126)	—
VII	1466 (75)	[1458] (63)	—	—	1419 (42)
VIII	1466 (100)	[1458] (75)	[1440] (25)	—	—
IX	1466 (72)	1458 (54)	[1440] (25)	—	—
X	1467 (120)	1457 (86)	[1444] (30)	—	—
XI	1467 (90)	1457 (68)	[1440] (25)	—	—
XII	1465 (68)	[1457] (48)	[1440] (20)	—	—
XIII	1467 (103)	1457 (93)	—	1435 (138)	[1419] (32)
XIV	1468 (105)	1458 (98)	—	1436 (130)	—
XV	1467 (95)	1457 (75)	[1440] (30)	—	1406 (48)
XVI	1466 (95)	1457 (75)	[1434] (30)	—	—
XVIII	1460	(80).....	—	1436 (140)	1420 (37)
XIX	1468 (83)	1458 (65)	[1440] (25)	—	—
XX	1467 (73)	1457 (53)	[1440] (23)	—	—
XXII[c]	1468 (95)	[1457] (75)	—	—	1430 (30)
XXIV	1466 (73)	[1457] (55)	—	—	1430 (20)

Compound	Band [a] L	ζ	M	η	N	O
II	1378 (51)	—	1362 (62)	—	[1340] (40)	[1305] (50)[b]
III	—	—	1362 (60)	—	[1340] (40)	[1305] (46)[b]
IV	1379 (35)	1366 (24)	—	1352 (24)	1340 (24)	[1300] (40)[b]
V	1377 (68)	—	1364 (72)	—	—	[1300] (60)[b]
VI	—	1370 (14)	—	[1353] (18)	1343 (21)	[1300] (60)[b]
VII	—	—	1366 (72)	—	1346 (63)	[1308] (50)[b]
VIII	1378 (30)	1368 (18)	—	[1358] (17)	1344 (25)	[1305] (75)[b]
IX	—	[1368] (18)	—	—	1344 (30)	[1302] (90)[b]
X	1379 (43)	[1368] (15)	—	[1355] (10)	1344 (8)	1304 (12)
XI	1379 (25)	1367 (13)	—	1353 (11)	1342 (10)	1300 (15)
XII	—	1368 (11)	—	1353 (12)	1342 (11)	1292 (16)
XIII	—	—	1364 (65)	—	—	[1300] (50)[b]
XIV	1378 (34)	—	—	1356 (20)	1342 (22)	1310 (40)[b]
XV	1378 (30)	1365 (18)	—	1354 (18)	1342 (19)	1304 (17)
XVI	1379 (30)	[1365] (15)	—	1354 (14)	[1340] (12)	1300 (20)
XVIII	—	—	1362 (62)	—	[1346] (50)	[1298] (45)[b]
XIX	1380 (37)	1368 (22)	—	1353 (16)	1340 (17)	1303 (20)
XX	—	1368 (17)	—	1352 (18)	1342 (18)	—
XXII[c]	1379 (26)	1373 (16)	—	1353 (12)	1341 (11)	[1298] (22)
XXIV	—	1368 (12)	—	1352 (13)	1343 (12)	1296 (20)

[a]The band maxima are in cm^{-1} followed by ϵ^{a}_{max} in parenthesis. The positions of points of inflection are indicated by square brackets. The spectra were measured at a nominal spectral slit width of 2 cm^{-1} in carbon tetrachloride solution at a concentration of approximately 0.05–0.10 *M* except for band O which was measured in carbon disulphide.
[b]Intensified by superposition on other absorption.
[c]Also a band at 1438 cm^{-1} (ϵ^{a}_{max} 42) assigned to C—H scissoring mode of $—CH_2Br$ group.

Band J (1436 cm^{-1}) (Band ϵ (1440 cm^{-1}))

The strong band J is absent from the spectra of esters containing the $—COOCD_3$ group (Figs. 2D, 3B, 3C, 3D). Its identification with a carbomethoxy methyl vibration is substantiated by its prominence in the spectrum of VI (Fig. 3A), and in the spectrum of $CD_3.COOCH_3$ (8). It is assigned to the symmetrical C—H bending mode. The position and intensity of this band make it particularly useful for distinguishing between methyl and other types of alkyl esters.

A considerably weaker broad band near 1440 cm^{-1} is observed as an inflection in the spectrum of *n*-dodecane and other compounds lacking the carbomethoxy group (VIII,

IX–XII, XX, XXI) (Figs. 3C, 3D, 4). This absorption (band ϵ) coincides with the strongly Raman-active methylene vibration of alkanes and probably derives from scissoring modes in which vicinal methylenes move in phase.

Dodecyl bromide (XXII) has a stronger band at 1438 cm^{-1} which is absent from the spectrum of XXIV (cf. Figs. 6C, 6D) and presumably involves a C—H scissoring

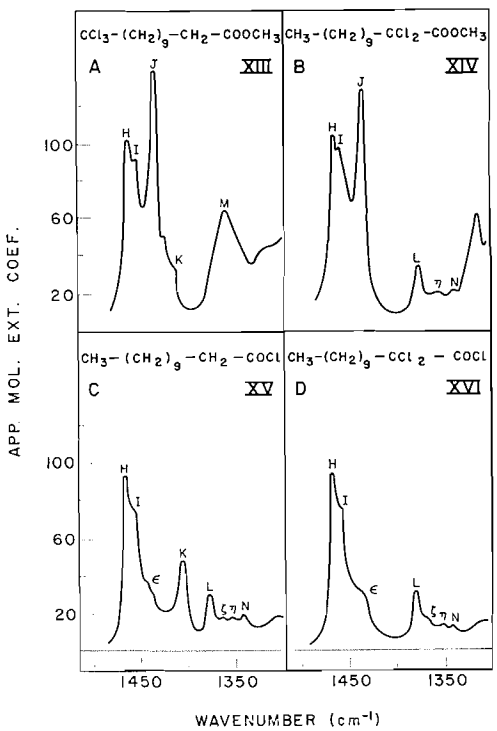

FIG. 5.

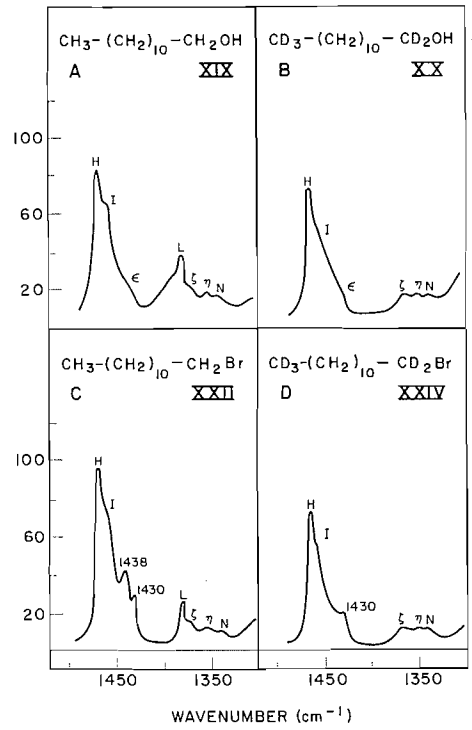

FIG. 6.

mode in the terminal —CH_2Br group. Brown and Sheppard assign a band at 1435 cm^{-1} in the spectrum of 1,2-dibromoethane to a similar vibration (18). Both XXII and XXIV also absorb weakly at 1430 cm^{-1}; possibly this is a scissoring mode of the methlyene α to the —CH_2Br or —CD_2Br group.

Band K (1419 cm^{-1})

The weak band *K* of methyl laurate is absent if the α-methylene is deuterated (Figs. 2C, 3A, 3C, 3D) or chlorinated (Fig. 5B); it is prominent in the spectrum of V (Fig. 2D), and is identified with the scissoring mode of the α-methylene group. In the acid chloride XV it is intensified and displaced to 1406 cm^{-1} (Fig. 5C) and it is absent from the spectrum of XVI (Fig. 5D).*

Band L (1378 cm^{-1})

This is the well-recognized symmetrical C—H bending band of the ω-methyl group. It is absent from the spectra of III, VI, VII, IX, XII, XIII, XVIII, XX, and XXIV and is prominent in the spectra of VIII and X (Figs. 3C and 4A).

**Isabelle and Leitch (10) noted that lauric acid also absorbs near 1419 cm^{-1} but the band does not disappear on α-methylene deuteration. Hadzi and Sheppard (19) have shown this is a skeletal vibration of the carboxylic acid dimer.*

Band M (1362 cm^{-1})

The presence or absence of this band runs parallel with that of band K and it is therefore due to α-methylene. A similar band is observed for diethyl ketone (20) and has been assigned to the wagging mode. Absorption between 1360 and 1320 cm^{-1} in the spectra of propionates and butyrates has been similarly assigned by Katritzky, Lagowski, and Beard (21).

Band N (1340 cm^{-1}) (Bands ζ (1368 cm^{-1}) and η (1353 cm^{-1}))

The weak band N inflection is part of a triplet of which the other two components at 1368 cm^{-1} and 1353 cm^{-1} (bands ζ and η) are overlapped in the methyl laurate spectrum by bands L and M. All three bands are seen in the spectra of IV, VI, X–XII, XIX, XX, XXII, and XXIV. They are most prominent for XII, XX, and XXIV (Figs. 4C, 6B, 6D) where they are free of overlap. Similar bands have been reported in the spectra of *n*-alkanes in the liquid state and are assigned by Sheppard and Simpson (1) to hydrogen deformation modes in non-linear configurations of the chain. Nielsen and Holland (3) assign the 1368 cm^{-1} component to the twisting mode in the all-trans configuration and the 1353 cm^{-1} band to the trans–gauche structure. Sheppard would place all twisting vibrations below 1300 cm^{-1} (2), in which case the 1368, 1353, and 1340 cm^{-1} bands would all be associated with wagging modes. Similar bands in amorphous polymethylene are also assigned to wagging modes by Krimm (4). This is a controversial problem to which the new data presented here makes no direct contribution, apart from emphasizing the association of all these bands with chain methylene groups.

Band O (1305 cm^{-1})

For technical reasons this band was measured in carbon disulphide solution and is illustrated in Figs. 7–10. It is broad and weak in the methyl laurate spectrum and partly obscured by stronger bands at lower frequency. It is seen more clearly in the *n*-alkane spectra (Fig. 10). Nielsen and Holland (3) assign it to a methylene twisting fundamental by analogy with the strongly Raman-active band at 1295 cm^{-1} as also does Krimm (4). The possibility of it being a wagging vibration has also to be considered.

"C—O Stretching" Vibrations between 1300 and 1150 cm^{-1}

Bands P, Q, and R (1248, 1196, and 1169 cm^{-1})

The spectrum of methyl laurate between 1300 and 1150 cm^{-1} is dominated by three bands, P, Q, and R (Fig. 7A). Strong absorption in this region is characteristic of carboxylic esters; the C—O linkages are clearly involved since analogous structure is missing from the spectra of the acid chlorides XV and XVI (Figs. 9B, 9C). Although these bands have been extensively discussed (22–24) no specific vibrational assignments have been made; it has been noted, however, that the spectra of methyl esters show unusual features, particularly near 1190 cm^{-1} (24).

The P, Q, and R bands are all perturbed by deuteration, but the effects are strikingly different for exchange in the α-methylene or carbomethoxy groups. On deuteration of the carbomethoxy group, band Q remains essentially unchanged, P is displaced slightly from 1245 cm^{-1} to 1256 cm^{-1}, but band R is replaced by a prominent narrow band at 1087 cm^{-1} (Fig. 7B). Deuteration in the α-methylene produces a more profound change. None of the P, Q, R band group is any longer recognizable and a new intense band appears at 1252 cm^{-1} (Fig. 8A). Chlorination of the α-methylene has a rather similar effect (Fig. 9A), two new peaks appearing at 1265 cm^{-1} and 1258 cm^{-1}; this doublet may be associated with an equilibrium between *s*-cis and *s*-trans conformations for which other evidence has been noted (band G). If the hydrogen in both the α-methylene and

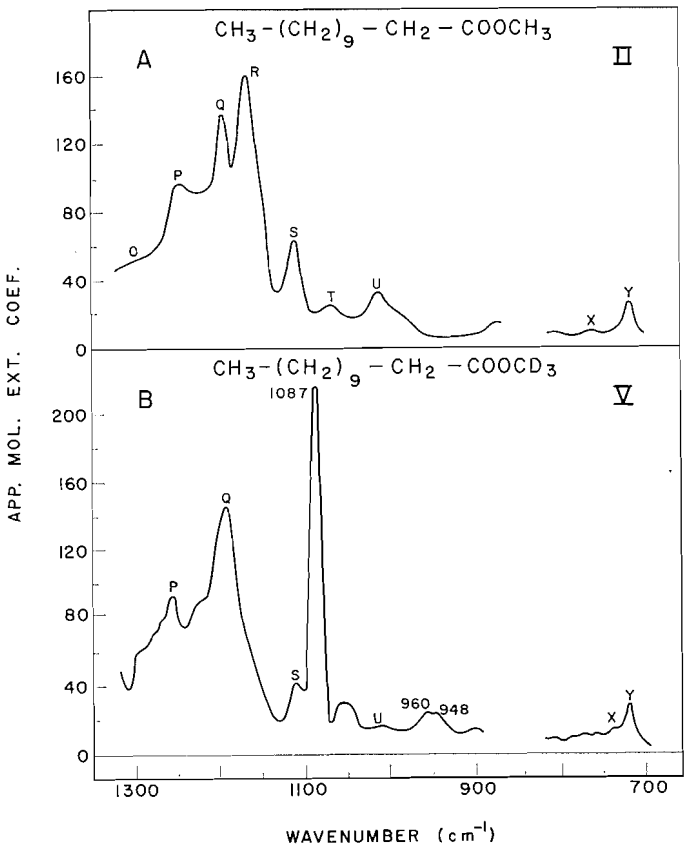

FIG. 7.

the carbomethoxy groups is exchanged (Fig. 8B) the effect on the methyl laurate spectrum approximates to a combination of the two separate exchange effects; the high-frequency band appears at 1275 cm^{-1} and the low-frequency band at 1088 cm^{-1}. As would be expected, deuteration of the ω-methyl group has no significant effect on this absorption (Table V).

In attempting to interpret these changes it is convenient to consider first the fully exchanged structure $R—CD_2—COOCD_3$, which has the simplest spectrum. The pair of strong bands near 1275 and 1088 cm^{-1} resemble structure seen in the spectra of many acetate esters, viz. $CH_3.COOCH_3$, $CH_3.COOCD_3$, $CD_3.COOCH_3$, $CD_3.COOCD_3$ (8); $CH_3.COOC_2H_5$, $CD_3.COOC_2H_5$ (9); $CH_3.COO.CH_2.CH_2.OOC.CH_3$, $CH_3.COO.CD_2.CD_2.OOC.CH_3$, $CH_3.COO.CH(CH_3)_2$, $CH_3.COO.CH_2.CH(CH_3)_2$ (25). The spectra of all the foregoing esters have a pair of strong bands in the ranges 1276–1217 cm^{-1} (ϵ^a_{max} 675–275) and 1106–1034 cm^{-1} (ϵ^a_{max} 395–130). For methyl acetate Wilmshurst assigns the upper band to the CO—O stretching mode and the lower band to the $O—CH_3$ stretching mode (13). It would seem probable that this pair of bands is the "normal" spectrum associated with the $R_1.CO.O.R_2$ structure, though in view of its manifest sensitivity to changes in the R_1 and R_2 groups Wilmshurst's assignments are oversimplified and it would be more realistic to regard both bands as involving skeletal stretching modes extending through the —CO.OC— group.

TABLE VA

Bands between 1300 and 650 cm^{-1} of methyl laurate and related compounds

	Band[a]									
Compound	P	Q	R	S	T	U	V	W	X	Y
II	1245 (97)	1196 (137)	1169 (162)	1112 (64)	1074 (25)	1016 (30)	875[c]	845[c]	755 (8)	721 (27)
III	1246 (86)	1192 (126)	1167 (173)	1108 (54)	—	1015 (32)	870[c]	[840][c]	746 (11)	720 (22)
IV	*1252* (192)	—	—	1120 (63)	1075 (32)	1008 (34)	858[c]	815[c]	742 (15)	720 (25)
V	1256 (92)	1193 (145)	—	1112 (40)	[b]	1012 (16)	—	—	[740] (12)	720 (28)
VI	*1256* (247)	—	—	1123 (100)	1074 (35)	1008 (38)	[b]	[b]	748 (12)	720 (20)
VII	1262 (83)	1195 (132)	—	1115 (34)	[b]	—	[b]	[b]	748 (10)	721 (18)
VIII	*1275* (277)	—	—	1128 (60)	[b]	—	[b]	[b]	752 (12)	721 (23)
IX	*1276* (295)	—	—	1128 (70)	[b]	—	[b]	[b]	750 (14)	721 (22)
X	—	—	—	—	1077 (6)	—	[b]	[b]	[760] (4)	721 (25)
XI	—	—	—	—	[1080] (8)	—	[b]	[b]	748 (7)	721 (20)
XII	—	—	—	—	[1082] (9)	—	[b]	[b]	748 (8)	720 (16)
XIII	1245 (106)	1196 (147)	1170 (180)	1104 (68)	1070 (42)	1014 (36)	880[c]	840[c]	[l]	722 (48)
XIV	*1258* (128)	*1266* (124)	—	1107 (39)	1070 (27)	—	[b]	[b]	755 (20)	722 (31)
XV	—	—	—	1126 (26)	1077 (18)	—	[b]	[b]	[m]	722 (75)[g]
XVI	—	—	—	1126 (23)	[1080] (28)	—	[b]	[b]	[l]	[722] (69)[g]
XVIII	1242 (122)	1196 (140)	1169 (167)	1100 (42)	[1080] (26)	1020 (30)	[b]	[b]	[740] (10)	722 (22)
XIX	—	—	—	1120 (14)	[1070] (50)	—	[b]	[b]	—	721 (24)
XX	—	—	—	[1116] (30)	—	—	[b]	[b]	[748] (10)	721 (22)
XXII	—	—	—	1116 (6)	1075 (6)	—	[b]	[b]	750 (8)	720 (28)
XXIV	—	—	—	1115 (32)	[1080] (15)	—	[b]	[b]	[745] (8)	721 (22)

NOTE: for footnotes to table see table VB.

TABLE VB

Bands between 1300 and 650 cm^{-1} of methyl laurate and related compounds

Compound	Other bands[a]								
II	—								
III	1052 (26)[d]	[985] (22)	908 (12)	687[d, o]					
IV	1205 (85)	1175 (58)	[1162] (52)	[1142] (50)	[1135] (55)	1060 (26)	968 (22)	932 (12)	697 (18)[n]
V	1087 (216)[i]	1055 (30)	960 (23)[j]	948 (22)[j]	895				
VI	1193 (67)	1150 (70)	1055 (47)[d]	988 (23)	[975] (16)	928 (9)	815 (13)		
VII	[1215] (100)	1090 (240)[i]	1054 (38)[d]	[965] (16)[j]	952 (18)[j]	778 (5)			
VIII	1250 (103)	1168 (40)	1088 (230)[i]	1055 (32)	998 (16)[k]	975 (24)[k]	950 (18)[k]		
IX	[1250] (120)	1208 (45)	1160 (50)	1090 (260)[i]	1055 (50)[d]	996 (20)[k]	976 (27)[k]	950 (18)[k]	
X	[1260] (7)	1180 (3)	1136 (4)	1097 (5)	990 (3)	960 (4)	892 (5)		
XI	1160 (4)	[1138] (5)	1114 (8)[d]	1055 (14)[d]	965 (3)	684 (3)[d]	656 (8)[d]		
XII	[1146] (5)	1115 (13)[d]	1054 (36)[d]	965 (3)	925 (3)	[805] (2)	[780] (3)	682 (4)[d]	656 (13)[d]
XIII	1137 (75)	777 (183)[e]	694 (182)[e]						
XIV	[1214] (48)	1204 (47)	1187 (32)	1172 (33)	1131 (33)	1097 (41)	1026 (32)	[1008] (28)	998 (30)
			975 (20)	925 (8)	828 (28)	709 (68)[e]			
XV	996 (48)	952 (72)[f]	[935] (56)	908 (34)	828 (16)	810 (12)	[770] (18)	680 (58)[f]	
XVI	1260 (23)	[990] (45)	966 (57)[f]	910 (34)	802 (36)	744 (78)[f]	692 (88)	[683] (62)[f]	
XVIII	1137 (57)	1131 (56)	992 (23)						
XIX	1050 (66)[h]	[1030] (55)	[960] (13)						
XX	1274 (40)	1160 (33)	1130 (32)	1088 (38)	1054 (38)[d]	959 (90)[h]	890 (17)		
XXII	1252 (35)	1238 (30)	1150 (2)						
XXIV	1055 (27)[d]	994 (30)	957 (23)						

[a]The band maxima are in cm^{-1} followed by ϵ^{n}_{max} in parenthesis. The positions of points of inflection are indicated in square brackets. Bands listed in italics differ significantly in intensity from others in the same vertical column of Table VA; the associated vibrational modes are perturbed by vicinal structure and they are discussed in the text. The spectra were measured at a nominal spectral slit width of 2 cm^{-1} in carbon disulphide solution, except for the bands noted under the footnote *c*.

[b]Region not measured.
[c]Measured qualitatively on a capillary layer of the undiluted liquid.
[d]Attributed to CD_3— (see text).
[e]Attributed to C—Cl (see text).
[f]Attributed to —CO.Cl (see text).
[g]Intensity enhanced by overlap or interaction with —COCl absorption.
[h]Attributed to —OH group.
[i]Characteristic of the —$COOCD_3$ group (see text under *Bands P, Q, R*).
[j]Characteristic of the —CH_2.$COOCD_3$ group (see text under *Band U*).
[k]Characteristic of the —CD_2.$COOCD_3$ group (see text under *Band U*).
[l]Obscured by overlap with strong C—Cl band.
[m]Obscured by overlap with strong —COCl band.
[n]Attributed to α-CD_2—.
[o]See Fig. 10C.

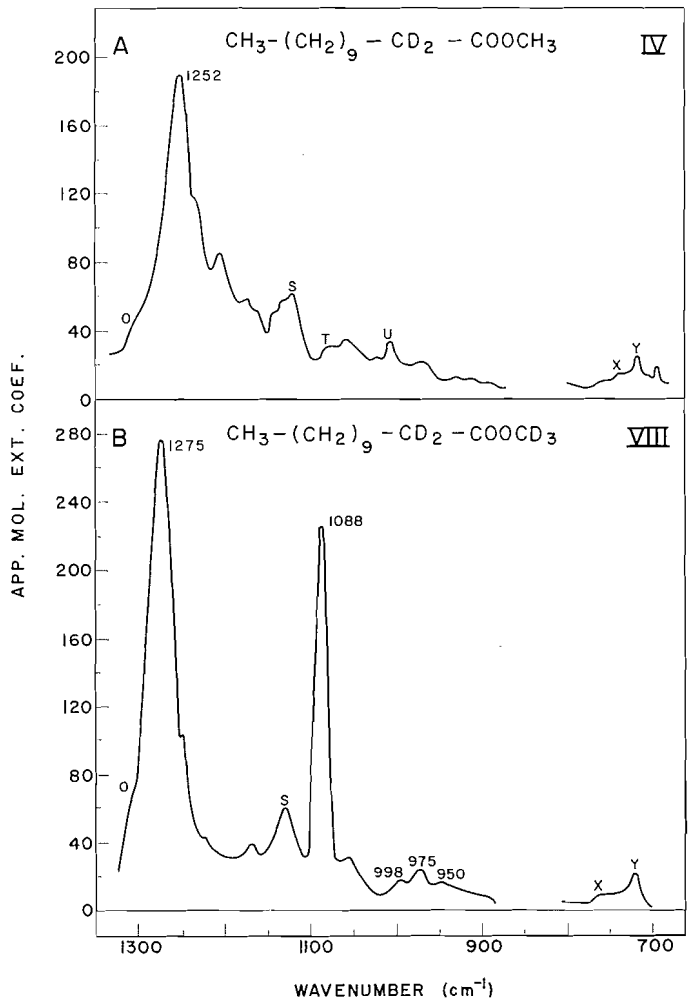

FIG. 8.

Since replacement of the α-methylene deuterium in $R.CD_2.COOCD_3$ by hydrogen strongly perturbs the 1275 cm^{-1} band and gives rise to the P and Q bands of the methyl laurate spectrum, it would appear that the P and Q bands involve strong coupling with a vibration of the α-CH_2 group. If band M is correctly assigned to the α-methylene wagging mode, the twisting mode may be concerned here.

The relation between the 1088 cm^{-1} band of $R.CD_2.COOCD_3$ and band R of the methyl laurate spectrum is more obscure. The 1088 cm^{-1} band is present in all the methyl laurate esters that contain —OCD_3 and is absent from those that do not. It could therefore be associated with an internal vibration of the —OCD_3 group, possibly the asymmetrical C—D bending mode (cf. band J). However, the 1088 cm^{-1} band is considerably more intense than band J, though this intensity might be gained by coupling with a skeletal mode. The band, however, does bear a close similarity to the band in the acetate spectra, noted above, where deuterium is not necessarily involved. A further difficulty is the seeming absence of both band R and the 1088 cm^{-1} band from the spectra

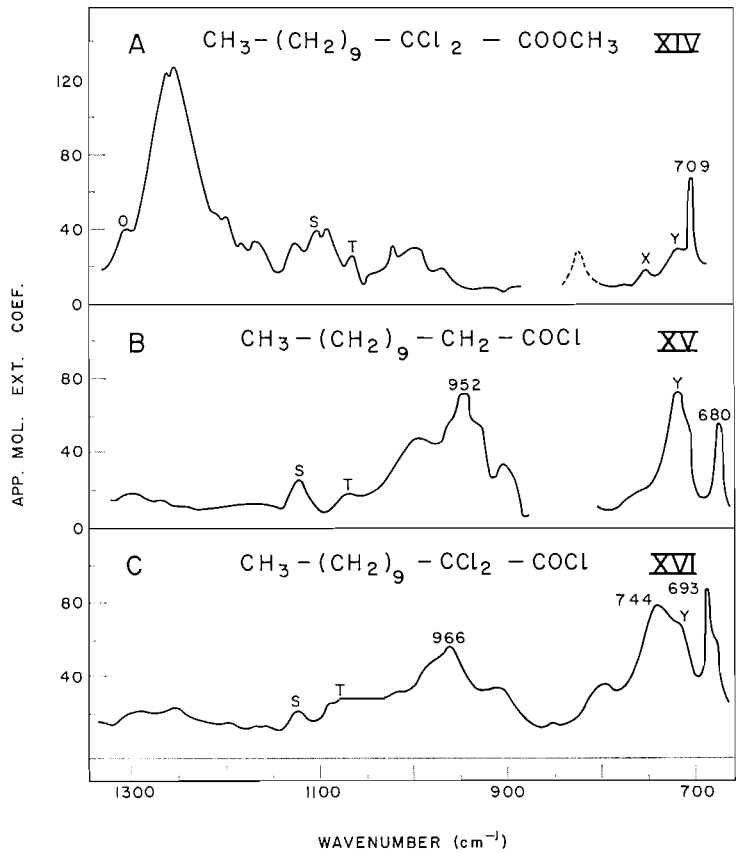

FIG. 9.

of $R.CD_2.COOCH_3$ and $R.CCl_2.COOCH_3$ (Fig. 8A, 9A), neither of which shows any intense absorption below 1200 cm^{-1} that can readily be attributed to the lower of the two postulated C—O stretching modes.

The complexity of these spectra recalls the confusion over attempts to interpret the "amide II" bands of secondary amides in terms of localized bond vibrations. The present studies indicate that the P, Q, and R bands of the methyl laurate spectrum involve vibrational modes that extend through the whole of the $—CH_2.CO.O.CH_3$ unit.

Vibrations below 1150 cm^{-1}

The spectrum of methyl laurate between 1150 and 650 cm^{-1} is weak and the bands are broad. There are well-resolved peaks at 1112, 1074, 1015, 875, 845, 755, and 720 cm^{-1} (bands S–Y). These bands are no doubt superimposed on much unresolved absorption associated with skeletal modes of various chain conformations. Considerable uncertainty still remains concerning the assignment of these bands even in the simplest case of the all-trans polymethylene chain (2, 4).

Band S (1112 cm^{-1})

This band is prominent in the spectra of II, III, V, VII, and XIII, which contain the structure $R.(CH_2)_9.CH_2.COOR$. For the esters IV, VI, VIII, and IX, containing

the group —CD_2.COOR, there is a band near 1130 cm^{-1}; the acid chlorides XV and XVI absorb near 1126 cm^{-1}, the alcohols and bromides XIX, XX, XXII, and XXIV absorb between 1120 and 1115 cm^{-1}, and the acetylenic ester XVIII at 1100 cm^{-1}. The intensities of these bands are variable over the range ϵ^a_{max} 14 to ϵ^a_{max} 100 and there is doubtful justification for assuming that they are necessarily associated with a common vibrational mode. If, however, this assumption is granted, a skeletal vibration of the —$(CH_2)_9$— chain perturbed slightly by the nature of the end groups would appear to be involved. For the homologous series of fatty acid methyl esters, the band shifts progressively from 1095 cm^{-1} to 1115 cm^{-1} with lengthening chain, and for a given chain length the position is the same for the methyl esters as for the free dimeric carboxylic acid (26). For *n*-alkanes Sheppard observes a band that shifts progressively from 965 cm^{-1} in *n*-butane to 1121 cm^{-1} in nonadecane (2, 27). This "1120 cm^{-1} series" has been tentatively assigned to a terminal methyl rocking mode and to a C—C skeletal mode (R_2 and Ψ in Sheppard's nomenclature). On chlorination of the ω-methyl group of methyl laurate this band is displaced by only 6 cm^{-1} from 1112 cm^{-1} (ϵ^a_{max} 62) for II to 1106 cm^{-1} (ϵ^a_{max} 68) for XIII. This would suggest that any coupling with the methyl rocking mode is small and that the vibration is predominantly C—C skeletal.

Band T (1074 cm^{-1})

A weak band between 1080 and 1070 cm^{-1} is observed in the spectra of II, IV, VI, X–XV. The assignment of this to a C—C skeletal mode is supported by the fact that a similar band is observed at 1080 cm^{-1} in the spectrum of XII, sandwiched between bands characteristic of the —CD_3 groups at 1115 cm^{-1} and 1055 cm^{-1}. Brown, Sheppard, and Simpson identify this band with the C—C skeletal mode α (the "1060 cm^{-1} series") as also does Krimm (4). In V and IX this band may be obscured or overlapped by the strong 1088 cm^{-1} band, but failure to observe it in the spectrum of III should be noted.

Band U (1016 cm^{-1})

This band appears prominently in the spectrum of II, III, XIII, and XVIII, all of which contain —CH_2.$COOCH_3$. A narrower band at 1008 cm^{-1} is associated with the —CD_2.$COOCH_3$ structure of IV and VI while a weaker doublet near 960 and 948 cm^{-1} characterizes the —CH_2.$COOCD_3$ group (Fig. 7B) and a triplet at 998, 975, and 950 cm^{-1} the —CD_2.$COOCD_3$ group (Fig. 8B).

Katritzky, Lagowski, and Beard (21) note the 1015 cm^{-1} band, which they locate in the range 1020–995 cm^{-1} in various saturated methyl esters, and assign tentatively to a skeletal mode or to an in-plane O—CH_3 rock of the carbomethoxy group. Wilmshurst (13), however, associates this mode with bands at 1230 cm^{-1} in methyl formate and 1248 cm^{-1} in methyl acetate. Comparison among the deuterated methyl laurates indicates that band U, like the P, Q, R triplet, involves the whole —CH_2.COOR structural unit.

Bands V and W (875, 845 cm^{-1})

The spectra of capillary films of II, III, IV, and V are shown in Fig. 10. Bands near 875 and 845 cm^{-1} are observed for II, III, and XIII, which contain —CH_2.$COOCH_3$. The —CD_2.$COOCH_3$ group of IV absorbs similarly at 855 and 815 cm^{-1} but the spectrum of V, containing the —CH_2.$COOCD_3$ group, shows no resolved absorption between 890 and 755 cm^{-1}. Bands V and W of methyl laurate therefore appear to be associated with the carbomethoxy methyl group and similar absorption is noted for various methyl esters by Katritzky and collaborators (21), who assign it to the methyl out-of-plane rocking mode. Wilmshurst (13) assigns a band at 844 cm^{-1} in the spectrum of methyl acetate to the CH_3.C— rocking mode, and if this is correct there can be no analogy with the methyl laurate spectrum in this respect.

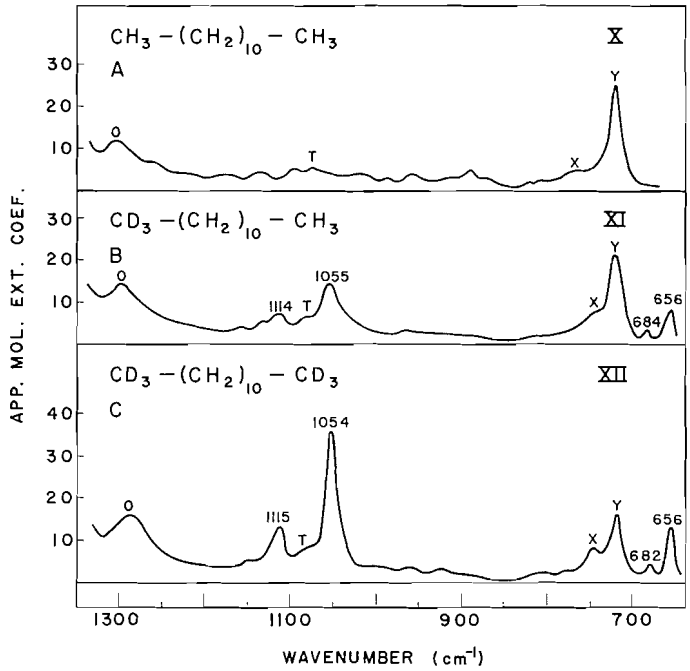

FIG. 10.

Bands X and Y (755, 721 cm^{-1})

Band Y is the well-recognized CH_2 rocking vibration of the polymethylene chain and its behavior is normal in all the compounds. The position of band X varies between 755 and 740 cm^{-1} and it is probably the second member of a progression of CH_2 rocking bands, the higher members of which are too weak for observation.

Other Absorption in the Substituted Compounds

Comparison of the spectra of the hydrocarbons X–XII (Fig. 11) indicates that on introduction of —CD_3 bands appear at 1115, 1054, 684, and 656 cm^{-1}. The two at

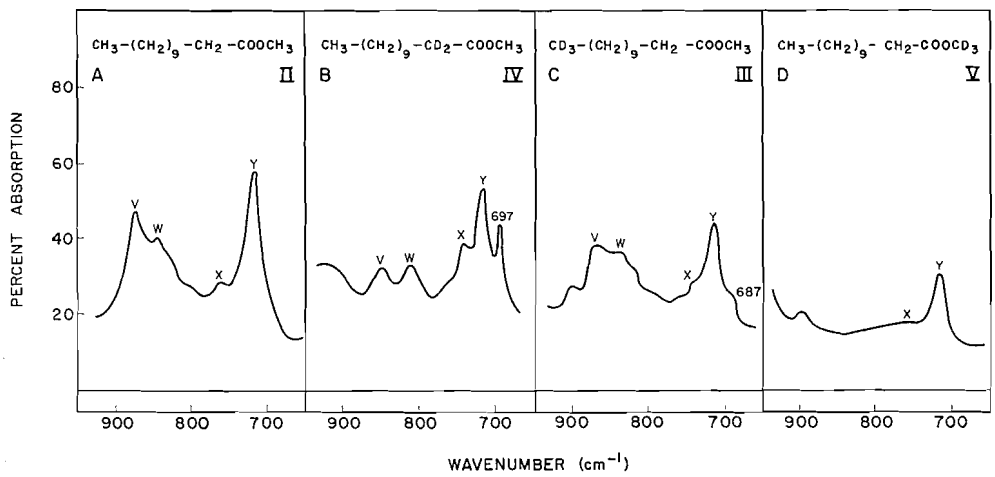

FIG. 11.

higher frequency are probably C—D bending modes and the others may be CD_3—C rocking modes. The 1054 cm^{-1} band is observed for the methyl trideuterolaurates (III, VI, VII, IX) and for the alcohol XX and the bromide XXIV (Table V), but the weaker band at 1115 cm^{-1} is obscured by band S in the ester spectra.

The methyl trichlorolaurate XIII exhibits prominent maxima at 777 and 694 cm^{-1} and the methyl α-dichlorolaurate XIV at 709 cm^{-1}. Presumably these bands involve C—Cl stretching modes. The acid chlorides XV and XVI show strong characteristic bands at 952, 722, 680 cm^{-1} and 966, 744, and 693 cm^{-1} respectively (Figs. 9B, 9C).

CONCLUSIONS

The complete spectrum of methyl laurate is shown in Fig. 12 plotted on a uniform ordinate scale, and the band assignments are summarized in Table VI. All peaks and

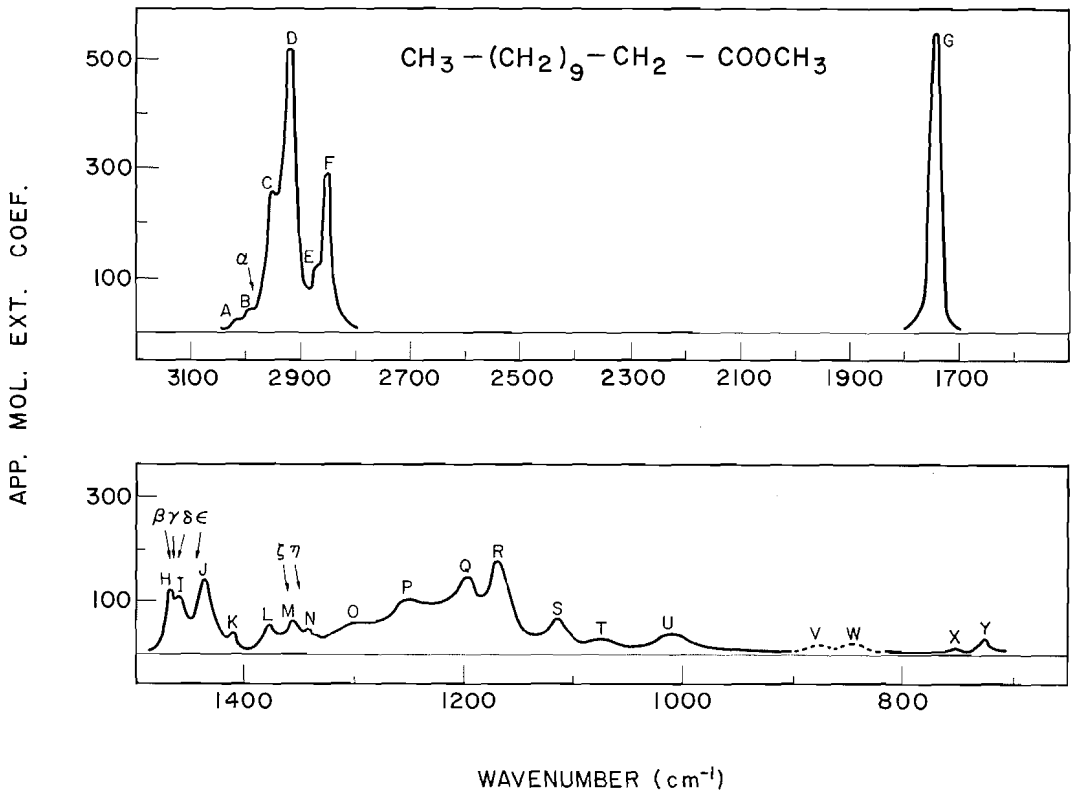

FIG. 12.

inflections in the spectrum can be assigned to the specific units of molecular structure (*a*)–(*d*) of I, except for bands P, Q, R, and U, which involve both the (*c*) and (*d*) units. The remaining uncertainty in the complete interpretation of the spectrum is due more to lack of knowledge concerning the nature of the vibrational modes within these structural units than to their mutual perturbation effects.

The use of the characteristic group frequency concept in analyzing the infrared spectra of complex molecules has been subject to some abuse, and has been used in different connotations by various spectroscopists. Theoretical spectroscopists, in particular, have

TABLE VI

Summary of band assignments for methyl laurate

Band[a]	ν_{max} (cm^{-1})	ϵ^{a}_{max}	Assignment	
			Group	Mode
A	[3020]	16	$-COOCH_3$	asym. C—H stretch (a')
B	2995	40	$-COOCH_3$	asym. C—H stretch (a'')
α	2955	—	$-COOCH_3$	sym. C—H stretch
C	2950	260	CH_3-	asym. C—H stretch
D	2922	520	$-(CH_2)_9-$	asym. C—H stretch
E	[2870]	120	CH_3-	sym. C—H stretch
F	2852	290	$-(CH_2)_9-$	sym. C—H stretch
G	1742	550	$-COOCH_3$	C=O stretch
H	1467	113 band β	$-(CH_2)_9-$	C—H scissor
		band γ	CH_3-	asym. C—H bend
I	1458	107 band δ	$-COOCH_3$	asym. C—H bend (a'')
ϵ	1440	—	$-(CH_2)_9-$	C—H scissor or wag
J	1436	135	$-COOCH_3$	sym. C—H bend
K	1419	36	α-CH_2-	C—H scissor
L	1378	51	CH_3-	sym. C—H bend
ζ	1368	—	$-(CH_2)_9-$	C—H wag or twist
M	1362	62	α-CH_2-	C—H wag
η	1352	—	$-(CH_2)_9-$	C—H wag or twist
N	[1340]	40	$-(CH_2)_9-$	C—H wag or twist
O	[1305]	50	$-(CH_2)_9-$	C—H twist (or wag?)
P	1245	97	$-CH_2-COOCH_3$	C—O skeletal coupled with α-CH_2— deformation
Q	1196	137	$-CH_2-COOCH_3$	C—O skeletal coupled with α-CH_2— deformation
R	1169	162	$-CH_2-COOCH_3$	C—O skeletal coupled with α-CH_2— deformation
S	1112	64	$-(CH_2)_9-$	C—C skeletal coupled with end groups
T	1074	25	$-(CH_2)_9-$	C—C skeletal
U	1016	30	$-CH_2-COOCH_3$	C—O skeletal coupled with α-CH_2— deformation
V	875	—	$-COOCH_3$	Methyl rock ?
W	845	—	$-COOCH_3$	Methyl rock ?
X	755	8	$-(CH_2)_9-$	C—H rock
Y	721	27	$-(CH_2)_9-$	C—H rock

[a]Points of inflection are designated by square brackets. Greek letters identify bands that are not observed in the methyl laurate spectrum but are presumed to be present from the analysis of the spectra of the deuterated derivatives.

been critical of its use for purely descriptive purposes, where there is often insufficient evidence from normal co-ordinate analysis to justify the localization of the vibration to the postulated restricted bond systems. It would be preferable to reserve this term for those situations where the vibration is in fact localized, in reasonable approximation, to motions of small groups of atoms, such as O—H stretching bands of non-hydrogen-bonded hydroxyl groups, and C=O stretching bands of ketones. In other cases, typified by the P, Q, R band system of methyl laurate, the group of three bands, taken as a whole, characterizes the $R.CH_2.COOCH_3$ structure, though the normal vibrations which are responsible for these bands within the group are not yet understood. In these circumstances we would prefer to use the expression "characteristic zone absorption" instead of "characteristic group frequency". The emphasis is here displaced from an individual band to a pattern of absorption that may extend over a wide wavenumber range, and that may characterize a unit of molecular structure consisting of a considerable number of atoms. The word "zone" identifies the region of molecular structure involved, and is consistent with the definition of a zone as "an area or region set off or characterized as distinct from adjoining parts" (28). The P, Q, R bands of methyl laurate provide a rather simple example of this zone concept, which is also being applied to the descriptive analysis of steroid spectra in the 1350–650 cm^{-1} range (29).

In a subsequent paper, the effects of varying the chain length on the fatty acid methyl ester spectra will be considered, and further discussion of the methyl laurate spectrum will be deferred in order that this additional data can also be discussed.

ACKNOWLEDGMENTS

We wish to thank Dr. L. C. Leitch and Miss M. E. Isabelle for synthesizing the deuterated and chlorinated compounds. Thanks are also due to Mr. R. Lauzon, Mr. A. Nadeau, and Mrs. M. A. MacKenzie for technical assistance with the measurement of the spectra. Mrs. MacKenzie was also responsible for the deuterium analyses.

REFERENCES

1. N. SHEPPARD and D. M. SIMPSON. Quart. Revs. (London), **7**, 19 (1953).
2. N. SHEPPARD. Advances in spectroscopy. Vol. 1. *Edited by* H. W. Thompson. Interscience Publishers, Inc., New York, London. 1959. pp. 288–353.
3. J. R. NIELSEN and R. F. HOLLAND. J. Mol. Spectroscopy, **4**, 488 (1960).
4. S. KRIMM. Fortschr. Hochpolymer Forsch. **2**, 51 (1960).
5. R. G. SINCLAIR, A. F. MCKAY, and R. N. JONES. J. Am. Chem. Soc. **74**, 2570 (1952).
6. R. N. JONES, A. F. MCKAY, and R. G. SINCLAIR. J. Am. Chem. Soc. **74**, 2575 (1952).
7. R. N. JONES. Spectrochim. Acta, **9**, 235 (1957).
8. B. NOLIN and R. N. JONES. Can. J. Chem. **34**, 1382 (1956).
9. B. NOLIN and R. N. JONES. Can. J. Chem. **34**, 1392 (1956).
10. M. E. ISABELLE and L. C. LEITCH. Can. J. Chem. **36**, 440 (1958).
11. R. N. JONES and M. A. MACKENZIE. Talanta, **3**, 356 (1960).
12. R. N. JONES, N. B. W. JONATHAN, M. A. MACKENZIE, and A. NADEAU. Spectrochim. Acta, **17**, 77 (1961).
13. J. K. WILMSHURST. J. Mol. Spectroscopy, **1**, 201 (1957).
14. S. MIZUSHIMA, T. SHIMANOUCHI, T. MIYAZAWA, I. ICHISHIMA, K. KURATANI, I. NAKAGAWA, and N. SHIDO. J. Chem. Phys. **21**, 815 (1953).
15. L. J. BELLAMY and R. L. WILLIAMS. J. Chem. Soc. 4294 (1957).
16. R. N. JONES and E. SPINNER. Can. J. Chem. **36**, 1020 (1958).
17. R. N. JONES, C. L. ANGELL, T. ITO, and R. J. D. SMITH. Can. J. Chem. **37**, 2007 (1959).
18. J. K. BROWN and N. SHEPPARD. Discussions Faraday Soc. **9**, 144 (1950).
19. D. HADŽI and N. SHEPPARD. Proc. Roy. Soc. (London), A, **216**, 247 (1953).
20. B. NOLIN and R. N. JONES. J. Am. Chem. Soc. **75**, 5626 (1953).
21. A. R. KATRITZKY, J. M. LAGOWSKI, and J. A. T. BEARD. Spectrochim. Acta, **16**, 954 (1960).
22. R. A. RUSSELL and H. W. THOMPSON. J. Chem. Soc. 479 (1955).
23. R. N. JONES and C. SANDORFY. *In* Technique of organic chemistry. Vol. IX. *Edited by* A. Weissberger. Interscience Publishers, Inc., New York, London. 1956. p. 502.
24. A. R. KATRITZKY, J. M. LAGOWSKI, and J. A. T. BEARD. Spectrochim. Acta, **16**, 964 (1960).
25. Unpublished observation from this laboratory.
26. R. N. JONES. Can. J. Chem. This issue.
27. J. K. BROWN, N. SHEPPARD, and D. M. SIMPSON. Phil. Trans. Roy. Soc. London, Ser. A, **247**, 35 (1954).
28. WEBSTER'S NEW COLLEGIATE DICTIONARY. 1949 edition. G. and C. Merriam Co., Springfield, U.S.A., and T. Allen Ltd., Toronto, Canada. p. 996.
29. R. N. JONES. Trans. Roy. Soc. Can. III, **52**, 9 (1958).

THE EFFECTS OF CHAIN LENGTH ON THE INFRARED SPECTRA OF FATTY ACIDS AND METHYL ESTERS[1]

R. NORMAN JONES
The Division of Pure Chemistry, National Research Council, Ottawa, Canada

Received October 17, 1961

ABSTRACT

The infrared spectra of straight-chain fatty acids and their methyl esters have been measured over the range 1500–650 cm^{-1} in carbon tetrachloride and carbon disulphide solution. The effects of the chain length on the peak intensities of the bands have been analyzed in relation to the group frequency assignments derived from comparative studies of deuterium-substituted methyl laurates.

INTRODUCTION

Comparison of the infrared spectrum of methyl laurate with the spectra of derivatives deuterated at specific sites (1) has shown that all of the 25 maxima and inflections between 3020 and 700 cm^{-1} in the methyl laurate spectrum can be attributed to localized group vibrations. Twenty-one of these bands can be assigned, in good approximation, to one of four "characteristic zones", (*a*)–(*d*) of structure I, while the remaining four bands involve coupled modes extending over zones (*c*) and (*d*).

$$\underset{(a)}{CH_3}\text{—}\underset{(b)}{(CH_2)_n}\text{—}\underset{(c)}{CH_2}\text{—}\underset{(d)}{COOCH_3}$$

I

If the group vibrations are strictly localized within the respective zones, it is easy to predict the effects of increasing the chain length. Bands associated with zones (*a*), (*c*), and (*d*) should be unaffected in position and intensity. For zone (*b*) the bands involving purely internal vibrations of each methylene group should intensify without wavenumber displacement, while for the modes that involve coupling between successive methylene groups, progressive wavenumber shifts may occur.

In order to examine these relationships, the spectra of the straight-chain methyl esters have been measured over the range $n = 0$ to $n = 15$ and the corresponding carboxylic acids (II) have been investigated between $n = 0$ and $n = 18$. The *n*-alkanes (CH_3—$(CH_2)_n$—CH_3) have been studied previously from $n = 4$ to $n = 34$ under the same experimental conditions (2).

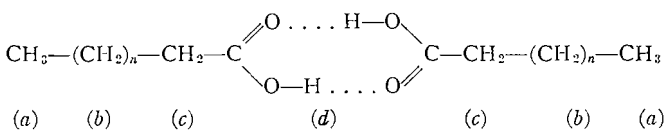

II

EXPERIMENTAL

The acids and esters were obtained from commercial sources. The lower-boiling esters were distilled at atmospheric pressure through a Todd column. Five percent of the third quarter of the distillate was collected, and the homogeneity was checked by vapor-phase chromatography. Propionic and butyric

[1]*Issued as N.R.C. No. 6651.*

acids were dried with anhydrous sodium sulphate and distilled at atmospheric pressure in the presence of potassium permanganate.

The spectra were measured from 1500 to 1300 cm^{-1} in carbon tetrachloride solution and from 1300 to 700 cm^{-1} in carbon disulphide solution on a Perkin–Elmer Model 112 spectrometer under conditions described previously (1, 2).

RESULTS

In the preceding paper, the bands and inflections in the spectrum of methyl laurate were designated alphabetically in order of decreasing wavenumber, and the same identification system will be used here. Since these measurements do not extend above 1500 cm^{-1} only bands H–Y are considered. Bands H–M, P–U, and Y are clearly recognizable in the spectra of all the esters. Bands N, O, V, W, and X, though observed in most of the ester spectra, are unsuitable for quantitative consideration, because of weakness, or for other reasons. They are noted in the last column of Table I but will not otherwise be discussed. The carboxylic acids are predominantly in the dimeric form (II); in their spectra, bands H, I, L, S, T, and Y can be unequivocally identified with their counterparts in the ester spectra. Other bands, common to the acids but not present in the ester spectra, are distinguished by lower case letters (bands *a–f*).

The positions and peak heights of the methyl ester and acid bands are listed in Tables I and II respectively. The ester bands can be identified by reference to Fig. 12 of the preceding paper. The acid bands are shown in the representative spectrum of lauric acid in Fig. 1.

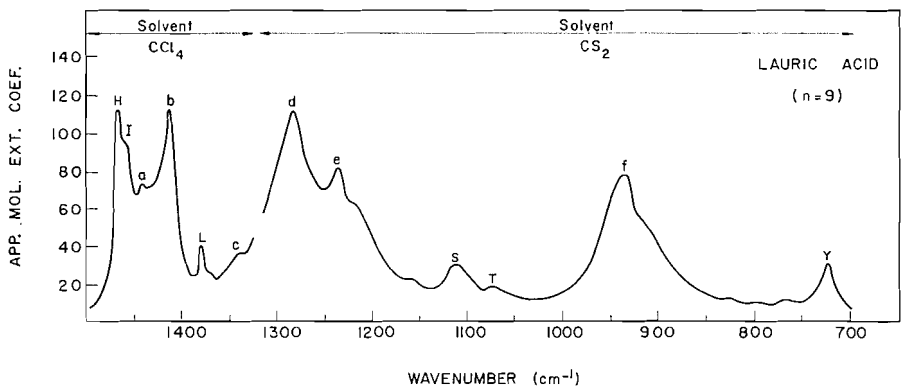

FIG. 1.

DISCUSSION

In an initial analysis of the ϵ^{a}_{max} versus chain length relationships, the band intensities were plotted against n, as was done previously for the n-alkane spectra (2). For most of the bands approximately linear relationships were observed, except in a few cases for low values of n. Representative plots for bands S and Y of both the esters and acids are shown in Figs. 2 and 3. The diagrams for the other bands are not reproduced, but the slopes (α) and the zero abscissal intercepts (β) for a linear least-square fit through the points are reported in Table III together with the standard deviation (S). For the majority of the bands the distribution about the least-square fit appears random, except in a few cases where abnormal departures from linearity are noted for the shorter-chain compounds. In these instances the short-chain homologues were omitted in fitting the data. This is indicated under the column headed n' in Table III. The more significant

TABLE I

Band positions and intensities for methyl esters[a] (CH_3—$(CH_2)_n$—CH_2—$COOCH_3$)

Chain length (n)	Band H (1467 cm^{-1})	Band I (1458 cm^{-1})	Band J (1436 cm^{-1})	Band K (1419 cm^{-1})	Band L		Band M (1362 cm^{-1})	Band P	
					ν_{max}	ϵ^n_{max}		ν_{max}	ϵ^n_{max}
0	—	92[b, c]	117	35[e, i]	1382	26	118	—	—
3	71[d]	72	127	33	1380	43	54	1244	140
4	73[d]	75	131	33	1380	44	56	1234	102
5	77[d]	81	126	34	1379	47	57	1250	98
6	90	87	130	34	1378	48	59	1248	103
7	97	93	133	35	1378	48	60	1244	105
9	113	107	136	36	1378	51	62	1245	97
13	145	125	144	36[i]	1378	54	67	1244	98
15	164	143	149	36[i]	1377	58	69	1244	95

Chain length (n)	Band Q		Band R		Band S		Band U		Band Y		Other bands[g]
	ν_{max}	ϵ^n_{max}	ν_{max}	ϵ^n_{max}	ν_{max}	ϵ_{max}	ν_{max}	ϵ^n_{max}	ν_{max}	ϵ^n_{max}	
0	1198	245	1175	195	1086	72	1023	63	—	—	1328[i] (32); 1272 (50); 968 (16); 955[i] (8); *850* (37); 807 (20).
3	1192	120	1169	232	1100	64	1015	36	733	15	1350[i] (40); 1318 (48); 1287 (48); 1268 (52); 1217 (90); 1110 (60); 970[i] (14); 934 (5); 918 (7); 902 (7); *864*[f] (15); 770 (6); 745[i, j] (6).
4	1198	112	1167	204	1102	66	1022	33	726	16	1318 (44); 1276[i] (60); 1256 (77); 1118[i] (48); 992 (20); 763 (7).
5	1198	132	1166	192	1105	67	1020	26	724	19	1318[i] (42); 1299[k] (48); 1225[i] (92); *860*[f] (13).
6	1196	134	1165	176	1107	66	1020	27	721	21	1303[k] (44); 1050[l] (19); 995[i] (20); *875*[f] (9); *832*[h] (8); 762 (8); 748[j] (6).
7	1198	138	1167	168	1110	63	1016	28	721	23	1064[l] (23); 898 (7); *864*[f] (11); *832*[h] (13).
9	1196	137	1169	162	1112	64	1016	30	721	27	See reference 1.
13	1196	138	1169	170	1115	58	1016	29	721	35	1300[i, k] (55); 1090[i, l] (25); 990[i] (20); *874*[f] (12); *836*[h] (11); 762[i] (10).
15	1196	136	1168	171	1115	57	1015	31	721	41	1300[k] (55); 1090[i, l] (35); 1070[i] (25); 990[i] (25); *865*[f] (11); *835*[h] (10); 765[i] (9).

[a]Bands H–M were measured in carbon tetrachloride solution and bands N–V in carbon disulphide. Unless otherwise indicated the band positions are listed in the column heading, and ϵ^n_{max} in the column.
[b]1456 cm^{-1}.
[c]Band H not observed.
[d]Note that band H is weaker than band I.
[e]1425 cm^{-1}.
[f]Tentatively identified with band V of methyl laurate.
[g]The band positions are given first followed by ϵ^n_{max} in parenthesis. Bands indicated in italics are superimposed on strong solvent absorption bands and their positions and intensities are less certain.
[h]Tentatively identified with band W of methyl laurate.
[i]Inflection.
[j]Tentatively identified with band X of methyl laurate.
[k]Tentatively identified with band O of methyl laurate.
[l]Tentatively identified with band T of methyl laurate.

TABLE II

Band positions and intensities for carboxylic acids[a] (CH_3—$(CH_2)_n$—CH_2—COOH)

Chain length (n)	Band H (1466 cm^{-1})	Band I (1458 cm^{-1})	Band a (1440 cm^{-1})	Band b		Band L		Band c (1336 cm^{-1})	Band d	
				ν_{max}	ϵ^a_{max}	ν_{max}	ϵ^a_{max}		ν_{max}	ϵ^a_{max}
0	115[b]	—	—	1416	112	1385	45	38[i]	1284	83
1	54[c, d]	61[e]	60[i]	1415	109	1383	32	34[f]	1278	113
3	76[c]	63	65[i]	1415	112	1381	37	36	1288	103
4	77[c]	74	65[i]	1414	113	1381	38	36	1281	113
5	83	82	65[i]	1414	114	1380	39	36	1278	105
6	91	84	68[i]	1413	115	1380	39	36[i]	1284	116
7	97	88	68[i]	1413	112	1379	39	36[i]	1278	107
9	112	93	73	1413	113	1379	40	36[i]	1281	110
11	134	113	80	1412	114	1379	42	39	1282	113
13	146	116	83	1413	113	1379	42	39	1280	111
14	159	125	90	1412	114	1379	44	41[i]	1282	115
15	162	131	90	1413	114	1378	44	41	1280	117
16	169	140	92	1412	116	1379	44	41	1280	117
17	180	148	90	1412	117	1378	45	40[i]	1280	120
18	187	156	85	1412	116	1378	46	42	1280	116

TABLE II (*Concluded*)

Chain Length (n)	Band e		Band S		Band f (934 ± 2 cm^{-1})	Band Y		Other bands[g]
	ν_{max}	ϵ^n_{max}	ν_{max}	ϵ^n_{max}		ν_{max}	ϵ^n_{max}	
0	1235	192	1079	48	74[j]	—	—	1425 (82); 1324 (42); 1134 (17); 994 (18); *849*[k] (33); 808[k] (22).
1	1218	108	1091	31	77[j]	749	13	1305[i,n] (76); 1230[i] (76); 1141 (18); 1078 (24); 1045[i] (12); 890[i] (30); *855*[i] (15); 778 (25).
3	[h]	—	1098	31	77	732	19	1308[i,n] (65); 1262[l] (83); 1243[l] (86); 1212 (63); 1138 (16); 1075[i] (22); *860*[i] (20).
4	1235	89	1102	35	77	724	20	1295[i,n] (90); 1205 (55); 1180[i] (30); 1116 (27); *880*[i] (30); *822* (17); 765 (10).
5	1230	86	1105	32	80	723	24	1296[i,n] (90); 1202 (50); 1175[i] (28); 790 (12).
6	1234	82	1108	36	80	721	26	1265[i] (88); 1220[i] (75); 1200[i] (45); 1165[i] (28); 1132 (20); 1050[i,o] (15); *860*[i] (15); *774* (12).
7	[h]	—	1108	30	75	721	27	1245[l] (76); 1227[l] (69); 1212[i] (62); 1198[i] (37); 1163[i] (24); 1060[o] (16); *860* (13); 762 (11); 738[i,o] (14).
9	1235	81	1111	31	78	721	32	1300[i,n] (85); 1260[i] (80); 1220[i] (62); 1160[i] (22); 1070[o] (18); 765 (11); 740[i,m] (12).
11	1234	80	1113[i]	33	78	721	38	1080[i,o] (20); *860* (16); *830* (14); 770 (12); 740[i,m] (15).
13	1238	82	1115	32	79	721	42	1092[o] (26); *860*[i] (24); 762 (14); 740[i,m] (17).
14	1234	83	1115	33	81	721	43	1092[o] (26); *860*[i] (18); 770 (13); 740[i,m] (15).
15	1234	83	1115	32	81	721	45	1092[i,o] (23); *870*[i] (20); 740[i,m] (15).
16	1234	83	1115	33	82	721	48	1092[i,o] (27); *870*[i] (20); 770[i] (14); 740[i,m] (18).
17	1235	84	1115	32	82	721	51	1095[i,o] (27); *875*[i] (25); 765[i] (14); 735 [i,m] (18).
18	1233	83	1116	35	79	721	54	1095[i,o] (32); 1060[i] (20); 1022[i] (18); *850*[i] (17); 778 (12); 740[i,m] (22).

[a]Bands H–c were measured in carbon tetrachloride solutions and bands d–Y in carbon disulphide. Unless otherwise indicated, the band positions are listed in the column headings and ϵ^n_{max} in the column.
[b]1463 cm^{-1}.
[c]1468 cm^{-1}.
[d]Note that band H is weaker than band I.
[e]1460 cm^{-1}.
[f]1340 cm^{-1}.
[g]The band positions are given first followed by ϵ^n_{max} in parenthesis. Bands indicated in italics are superimposed on strong solvent absorption bands and their positions and intensities are less certain.
[h]Anomalous; see section *Bands d and e*.
[i]Inflection.
[j]931 cm^{-1}.
[k]One of these bands may be a methylene rock.
[l]One of these bands may be the analogue of band e.
[m]Tentatively identified with band X of methyl laurate.
[n]Tentatively identified with band O of methyl laurate.
[o]Tentatively identified with band T of methyl laurate (see section *Band T*).

TABLE III

Summary of linear relationships between band intensity and chain length
($\epsilon^{a}_{max} = \beta + n\alpha$ where $n' \leqslant n \leqslant n''$)

	α	β	Number of compounds m	Interpolation range n'	n''	Standard deviation S	Figure of merit $\alpha/2s$
Band H (1468–1466 cm^{-1})							
Alkanes[a]	7.74	40.3	15	6	34	2.21	1.75
Acids	7.88	44.4	12	4	18	2.10	1.87
Esters	8.17	40.1	5	6	15	0.94	4.35
Band J (1436 cm^{-1})							
Esters	1.80	120.5	8	3	15	1.9	0.47
Band K (1419 cm^{-1})							
Esters	0.28	32.5	8	3	15	0.56	0.25
Band *b* (1416–1412 cm^{-1})							
Acids	0.20	111.9	15	3	18	1.06	0.095
Band L (1385–1378 cm^{-1})							
Alkanes[a]	0.437	40.4	13	8	34	0.77	0.28
Acids	0.534	35.8	13	3	18	0.47	0.57
Esters	1.238	39.5	8	3	15	0.84	0.74
Band M (1362 cm^{-1})							
Esters	1.220	51.05	8	3	15	0.40	1.53
Band *d* (1288–1278 cm^{-1})							
Acids	0.72	104.9	13	3	18	3.35	0.11
Band P (1250–1244 cm^{-1})							
Esters	−0.60	104.8	6	5	15	2.7	(−)0.11
Band *e* (1238–1230 cm^{-1})							
Acids	−0.20	85.6	11	4	18	1.74	(−)0.058
Band Q (1198–1196 cm^{-1})							
Esters	0.33	132.8	6	15	15	1.82	0.09
Band R (1169–1165 cm^{-1})							
Esters	−0.083	170.2	5	6	15	4.5	(−)0.009
Band S (1116–1098 cm^{-1})							
Acids	0.022	32.4	13	3	18	1.73	0.006
Esters	−0.78	69.2	8	3	15	1.52	(−)0.26
Band U (1020–1015 cm^{-1})							
Esters	0.40	24.9	6	5	15	0.86	0.23
Band *f* (936–932 cm^{-1})							
Acids	0.25	76.5	14	3	18	1.51	0.084
Band Y (732–721 cm^{-1})							
Alkanes[a]	2.418	0.82	17	4	34	0.60	2.02
Acids	2.308	11.58	17	3	18	0.76	1.52
Esters	2.155	7.90	8	3	15	0.66	1.63

[a]Values for α and β for the *n*-alkanes differ slightly from the values reported in Table 5 of reference 2. They are based on more accurate analysis of the same data.

features of the ϵ^{a}_{max} versus n relationships for some of the individual bands will next be discussed, in relation to the zones with which they are associated.

Zone (a). The Terminal Methyl Group

Band L

Only band L near 1378 cm^{-1} is uniquely identified with the terminal methyl group, and its assignment to the symmetrical C—H deformation is well established. The intensity increases slightly with the lengthening chain; the increment per methylene (α) is about 0.5 for *n*-alkanes and acids and about twice as large for the esters.

This increase in intensity is probably due to weak underlying absorption from zone (*b*), principally band ζ, which is observed at 1368 cm^{-1} in the spectra of methyl laurates and *n*-dodecanes deuterated in the ω-methyl group. The effect of chain length on this

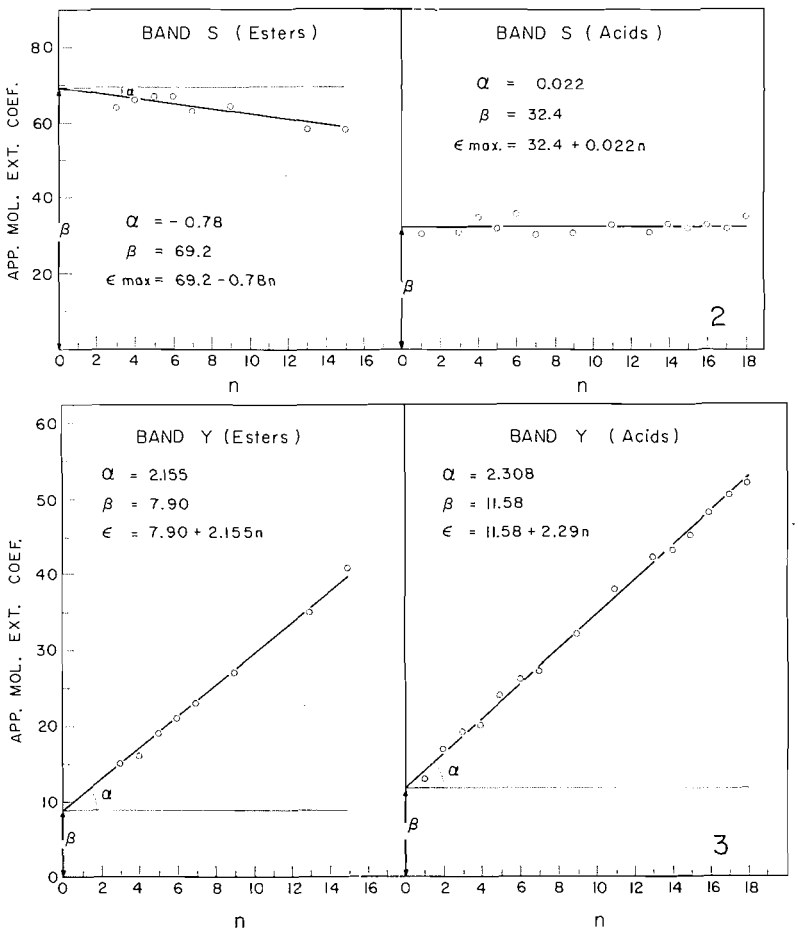

FIGS. 2 AND 3.

underlying absorption is difficult to evaluate quantitatively, but it is apparent from Figs. 4 and 5 of reference 2 that it intensifies considerably in passing from *n*-tridecane ($n = 11$) to *n*-octacosane ($n = 26$). The intercept β must be interpreted cautiously; values of 40.4, 35.8, and 39.5 were obtained for the *n*-alkanes, acids, and esters respectively. Since there are two ω-methyl groups in the *n*-alkanes, the intrinsic intensity per methyl is about 20. The higher value for the acids and esters is probably due to overlap from the shoulders of neighboring bands. In the ester spectra there is obvious enhancement from the shoulder of band M at 1362 cm^{-1}. In the acid spectra there may be contributions from the wings of the strong bands at 1413 and 1281 cm^{-1}. The similarity of the β values of the three classes of homologues therefore appears to be fortuitous and suggests that the transfer of peak-intensity measurements from one class of homologue to another must be treated circumspectly, though significance can probably be attached to the α values.

For the acids, the peak frequency of band L is displaced progressively from 1385 cm^{-1} to 1378 cm^{-1} as the chain lengthens (Table II). This could be a true displacement resulting

from weak coupling with a skeletal mode,* though it could result from a superpositional displacement effect of the underlying zone (*b*) band at 1368 cm^{-1}. Similar displacements are noted for band L in the short-chain methyl esters. They were not observed in the *n*-alkane spectra, where chain lengths below $n = 4$ were not investigated.

Zone (b). The Polymethylene Chain

Bands S, T, X, and Y have been assigned to the polymethylene chain of methyl laurate, also the β component of band H. Band X is too weak and uncertainly located for quantitative consideration and is noted only in Tables I and II. The complex H/I band system is discussed in a later section, and we shall be concerned here only with bands S, T, and Y.

Band Y

It is well established that band Y is associated with the CH_2 out-of-plane rocking mode. The intensity behavior is very similar for the esters, acids, and *n*-alkanes, the α values being 2.418, 2.308, and 2.155 respectively. For the *n*-alkanes β is small (0.8); it is much larger for the esters and acids, indicating that there is underlying unresolved absorption in the spectra of these compounds. In butyric acid ($n = 1$) the band Y maximum is at 748 cm^{-1} and it shifts progressively to 721 cm^{-1} in pelargonic acid ($n = 6$) and the higher homologues. The ester band behaves similarly. It is commonly stated that this band reaches its constant position for a chain of four methylenes. The additional displacements for the $—(CH_2)_5—$ and $—(CH_2)_6—$ systems only amount to 2–3 cm^{-1}, but they are believed to be significant.

Band S

The position of this peak in the ester spectra shifts progressively from 1086 cm^{-1} for $n = 0$ to 1115 cm^{-1} for $n \geqslant 13$. Band S is also observed in the spectra of the acids. For a given chain length it occurs at the same position in both the ester and acid spectra, but the intensity for the acids is only about one half of that for the esters. In neither series of homologues is the intensity much affected by chain length (Fig. 2). In the *n*-alkanes the intensity is lower by a factor of 10 and the band is not clearly recognizable in the solution-phase spectra. For the acids of shorter chain length there is some suggestion of an alteration in the intensity of band S for odd and even values of *n* (Fig. 2). This has not been observed on any other band and may be spurious. The wavenumber shifts with chain length are consistent with the assignment to a predominantly C—C skeletal mode. In several of the lower members of both the acid and ester series band S exhibits pronounced asymmetry on the high-frequency side and in some compounds a second band is resolved (e.g. methyl caproate (Fig. 4)).

Band T

This weaker band was identified in the methyl laurate spectrum with a skeletal mode that Sheppard designated "the 1060 series" (4). In the ester spectra it is only resolved over the narrow range of chain length from $n = 6$ to $n = 9$, and is most prominent for $n = 7$. It shifts progressively from 1050 cm^{-1} for $n = 6$ to merge into the low-frequency shoulder of band S for $n \geqslant 13$. In the spectra of the acids it can be distinguished

**Although the symmetrical* C—H *deformation mode of the methyl group is commonly regarded as an internal vibration, very simple calculations show that appreciable axial motion of the carbon atom is involved, and this must produce some perturbation at the next carbon atom. For the* XY_3 *molecule of* C_{3v} *symmetry Herzberg observes (3) that the motion of the* X *atom amounts to* $3m_Y/m_X.S_2.\sin\beta$, *where* m_X *and* m_Y *are the masses of the* X *and* Y *atoms,* β *is the angle between the* XY *bond and the symmetry axis, and* S_2 *the symmetry co-ordinate. From this it follows that the linear displacement of the carbon atom of the methyl group, in the absence of any coupling with the rest of the chain, would amount to about 8% of the displacement of each hydrogen atom.*

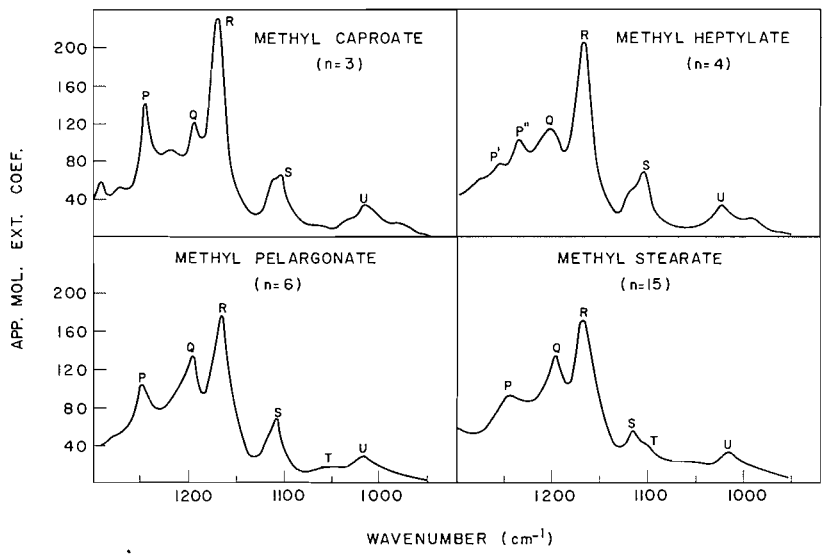

FIG. 4.

as an inflection for $n = 6$, 11, 15–18 and is resolved for $n = 7$, 9, 13, 14. Its position is similar for the esters and acids of the same chain length.

In both the acid and ester spectra there are other weaker inflections in the regions of bands S and T. Presumably these are derived from complex underlying absorption associated with skeletal modes of various subunits of the chain in trans–trans, trans–gauche, and gauche–gauche conformations. These show significant variation from compound to compound.

Zone (c). The α-Methylene Group

On the basis of the selective deuteration of methyl laurate, band K at 1419 cm^{-1} and band M at 1362 cm^{-1} have been assigned respectively to the scissoring and wagging modes of the α-methylene group.

Band K

In the ester spectra band K has an almost constant intensity ($\alpha = 0.2$); it lies on the shoulder of the strong band J, which is also insensitive to chain length. Band K has no obvious counterpart in the spectra of the acids.

Band M

For band M $\alpha = 1.17$ and it is therefore more affected by chain length than is band K. This is almost certainly due to its superposition on the methylene chain absorption (bands ζ, η) and indeed the intensification effect is very similar to that of the neighboring band L, for which $\alpha = 1.24$. The corresponding band in the spectra of the acids has not been positively identified. The acids do possess a band at 1336 cm^{-1} (band *c*) which might be associated with this mode.

Zone (d). The Carbomethoxy Group

Band J

This band, which has been assigned to the carbomethoxy group, shows a small intensity increment with chain length ($\alpha = 1.80$); this can be reasonably attributed to the overlap

effect of the wings of bands H, I, and ϵ. The general appearance of the band is similar in all the ester spectra and there is no significant wavenumber displacement.

Bands Involving Multiple Zones

There are two types of bands involving more than one zone. One is typified by the H/I band system for which three components are recognized (bands β, γ, and δ), associated respectively with zones (*b*), (*a*), and (*d*). The deuterium-substitution studies on methyl laurate lead to the conclusion that the overlap is a simple additive one. The second type of multiple zone absorption is illustrated by the P, Q, R, and U bands of methyl laurate, where there can be no doubt that strongly coupled vibrations involving the participation of the atoms of both zones (*c*) and (*d*) are involved.

Bands H and I

In the H/I band system band H is dominant in the spectra of the long-chain homologues of the acids, esters, and *n*-alkanes. For all three classes of compound the ϵ^{a}_{max}/n plot for band H is linear with $\alpha = 8$ for esters and alkanes in which $n \geqslant 6$ and for acids in which $n \geqslant 4$. For all three homologous series the intercept β is $\sim$40.

For the short-chain compounds, the components of the H/I doublet are separately resolved. Band I becomes more prominent as the chain length diminishes, and the contour changes are qualitatively in accord with the postulated contributions from three component bands associated respectively with the scissoring mode of the chain methylene group (band β), the asymmetrical C—H bending mode of the ω-methyl group (band γ), and the asymmetrical C—H bending mode of the carbomethoxy group (band δ). Band β contributes predominantly to band H and bands γ and δ to band I, though the distinction is not a sharp one. If the carbomethoxy group has the planar conformation III there should be an additional band due to the a', a'' degeneracy

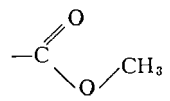

III

splitting of the asymmetrical C—H deformation mode. Wilmshurst (5) has assigned the a' vibration of methyl acetate to a weak band at 1469 cm^{-1} and the a'' vibration to a stronger band at 1450 cm^{-1}. There is no indication of this second band in the spectra considered here, but the a' band could be making an undetected contribution to band H. There is evidence from the C—H stretching region of the methyl laurate spectrum that the carbomethoxy group exists wholly or predominantly in conformation III and it is difficult to see why this should not hold also for the other homologues.

Bands P, Q, R, and U

These bands involve coupled vibrations extending through the (*c*) and (*d*) zones. They are observed with little change in position or intensity in the esters for which $n \geqslant 5$. For methyl heptylate ($n = 4$) band P is replaced by a doublet at 1255 and 1234 cm^{-1}, whereas for methyl caproate ($n = 3$) band P occurs at the normal position but with enhanced intensity. Band Q is "normal" at all chain lengths. The position of band R is unchanged at all chain lengths but it is significantly more intense for $n = 3$ and $n = 4$. The weaker band U is little affected. These bands are shown in Fig. 4. The spectrum of methyl propionate ($n = 0$) has bands at 1223, 1198, and 1175 cm^{-1} which may correspond with the P, Q, and R bands.

From the perturbations in the contours of the P, Q, and R bands of the lower homologues, it can be reasoned that zone (*b*) as well as zones (*c*) and (*d*) exercises some influence on these bands, particularly on band P. If this is so the perturbation effect of the polymethylene chain becomes constant when the number of methylene groups exceeds five. The effect could result from coupling with a skeletal mode of the chain, or it could be due to a steric effect influencing the conformation of the (*c*) and (*d*) zone structure. It would obviously be of interest to investigate the effect of temperature on these band contours for the short-chain esters. For methyl laurate temperature variation from 30° C to −70° C has no pronounced effect on the P, Q, R band contour.*

Other Bands Specific to the Carboxylic Acid Group

Bands *a–f* of the acids (Fig. 1) have no counterparts in the ester spectra.

Band a

This weak band appears as an inflection in the spectra of the short-chain acids and is resolved for $n \geqslant 9$. It might be identified with the scissoring vibration of the α-methylene group, since it is absent from the spectrum of $CH_3.(CH_2)_9.CD_2.COOD$.

Band b

This band, which occurs near 1416 cm^{-1}, exhibits an almost constant intensity. Sinclair, McKay, Myers, and Jones (6) assigned it erroneously to the α-methylene scissoring mode, but later Hadži and Sheppard (7) showed it to be associated with the carboxylic acid dimer group and assigned it to a mode in which C—O stretching vibrations are coupled with an O—H in plane deformation. In the acids substituted in the α-methylene group (e.g. isobutyric acid, α-bromostearic acid) it is displaced to 1430–1420 cm^{-1}.

Band c

This band appears as a weakly resolved peak or inflection near 1336 cm^{-1} and has been tentatively identified with the α-methylene wag (see section *Band M*).

Bands d and e

The prominent P, Q, R triplet of the ester spectra is replaced by the *d* and *e* doublet in the spectra of the acids. These are probably "C—O stretching" bands of the dimer ring system coupled with O—H in-plane deformations (cf. band *b*) (7). The intensity of band *d* is reasonably constant for all chain lengths except $n = 0$, but the position of the peak wanders between 1278 and 1288 cm^{-1} in an unsystematic fashion for the short-chain compounds; for $n \geqslant 9$ it remains steady at 1281 ± 1 cm^{-1}. The weaker band *e* is more variable in position, though it also becomes stabilized for $n \geqslant 9$. A distinct anomaly is observed for caproic acid ($n = 3$), where band *e* is replaced by a doublet at 1262 and 1242 cm^{-1}. Capric acid ($n = 7$) also shows a splitting of the absorption in the neighborhood of band *e*.

The shorter-chain acids show numerous other weakly resolved peaks and inflections in the region of the *d* and *e* bands. These are noted in the last column of Table II. They modulate the contour of the band envelope in a manner that is characteristic for each acid. This region of the acid spectra calls for more detailed examination under high resolution. In the solid phase these compounds exhibit well-defined progressions of equally spaced bands which are commonly attributed to coupled wagging or twisting vibrations of the methylene chain units. These vibrations may also be the cause of the fine structure in the liquid-phase spectra, though the uniform spacing is not apparent.

We wish to thank Dr. R. A. Ripley for making these measurements.

Band f

This characteristically broad band is well known in the spectra of carboxylic acids and has been assigned by Davies and Sutherland (8) to an out-of-plane deformation mode of the carboxylic acid dimer ring. The intensity is remarkably constant ($\alpha = 0.27$), consistent with its localization in zone (*d*). It exhibits a pronounced asymmetry on the low-frequency side.

CONCLUDING REMARKS

Over the range n' to n'', where linear correlations between ϵ^{a}_{max} and n appear to hold, the α values effectively distinguish the bands associated with the internal modes of the zone (*b*) bands, for which $\alpha = 2$–8, from the other types of bands which give much lower values of α. The zone (*b*) bands associated with skeletal modes also show low α values, but are distinguished by progressive frequency displacements. An exception must be made for the small frequency displacement of band L associated with zone (*a*). Most of the bands associated with zones (*a*), (*c*), and (*d*) do exhibit some intensification with increasing chain length, but this can be reasonably attributed to overlap effects from the shoulders of zone (*b*) bands. In the course of this intensity analysis no serious anomalies were observed that are inconsistent with the commonly accepted group frequency assignments for these bands, as reported in the earlier literature and substantiated by the measurements on the deuterium-substituted methyl laurates.

In column 7 of Table III the standard deviation (S) is reported, where

$$[1] \qquad S = \sqrt{\frac{\sum(\epsilon_{obs} - \epsilon_{calc})^2}{m}},$$

in which ϵ_{obs} is the experimentally observed absorption maximum, ϵ_{calc} the value obtained from the least-square fit, and m the number of compounds measured. Statistical considerations suggest that random errors in excess of $2S$ are improbable. The quantity $\alpha/2S$, shown in the final column of Table III, is therefore a convenient measure of the significance of the peak intensity as a criterion of chain length.

In the experimental section the absolute precision of the peak-intensity measurements was not discussed. In the present state of infrared spectrophotometry, it is not possible to evaluate quantitatively the experimental errors affecting absolute peak-intensity measurements. Since the measurements discussed here were made prior to the availability of commercial grating spectrometers, they do not represent the highest standards of photometric accuracy now obtainable with these new instruments. The spectral slit width employed was in the range 1–2 cm^{-1}, and although the majority of the bands are broad, we have preferred to express the intensities in "apparent" and not "absolute" units. Several laboratories are currently concerned with the determination of absolute standards for infrared band intensity measurements. When these data are available it will be of considerable interest to reinvestigate some of these acid and ester bands on a high-resolution grating spectrometer, accurately calibrated with respect to the absolute intensity. We would anticipate that the systematic errors associated with the finite slit function will principally affect the β values and that the increments per methylene will be less sensitive to this variable.

In this and the preceding paper we have dealt in considerable detail with the quantitative analysis of the infrared spectra of a family of compounds of a degree of complexity intermediate between the simple molecules susceptible to a rigid treatment by the methods of vibrational theory, on the one hand, and the large molecules of predominant

biological interest on the other. There are obvious difficulties in attempting to extend to such molecules the techniques of vibrational analysis applicable to small ones. While those concerned with the theory of molecular vibrations are well aware of this difficulty, organic chemists are naturally reluctant to accept the thesis that much of the absorption that they observed in the spectra of complex molecules must be dismissed as of empirical significance only. This creates a strong temptation to overextend the group frequency concept. The breakdown of the spectrum into sets of bands associated with more or less clearly differentiated subunits of molecular structure makes possible an analysis of complex spectra on a zonal basis without the necessity of invoking precise vibrational mechanisms.

In these solution-phase studies of homologous series we have been dealing with systems in which complex conformational equilibria are present, due to the flexibility of the polymethylene chain. The molecular spectroscopist can eliminate this by going to the crystalline state, and most of the literature dealing with the vibrational analysis of the polymethylene chain is restricted to solid-phase studies. The organic chemist seeking information about the contribution of polymethylene chain structure to the spectra of more complex molecules will not always be in a position to lay out the chain in a crystal of known *s*-trans chain configuration. Furthermore, if bulky cyclic groups are also present there can be no assurance that information derived from the analysis of the crystalline polymethylene chain system of simple hydrocarbons will be transferable to the very different packing system in more complex structures. Although the spectra of the liquid–phase polymethylene systems are less informative, the information they do convey is more widely applicable. This problem is currently being investigated with a series of long-chain steroid esters.

ACKNOWLEDGMENTS

We wish to thank Mrs. M. A. MacKenzie and Mr. A. Nadeau for technical assistance with the measurement of the spectra. We are also grateful to Dr. A. S. Hay, who purified the compounds and ran preliminary spectra.

REFERENCES

1. R. N. JONES. Can. J. Chem. This issue.
2. R. N. JONES. Spectrochim. Acta, **9**, 235 (1957).
3. G. HERZBERG. Infrared and Raman spectra of polyatomic molecules. Van Nostrand Co. Inc., New York. 1945. p. 155.
4. J. K. BROWN, N. SHEPPARD, and D. M. SIMPSON. Phil. Trans. Roy. Soc. London, Ser. A, **247**, 35 (1954).
5. J. K. WILMSHURST. J. Mol. Spectroscopy, **1**, 201 (1957).
6. R. G. SINCLAIR, A. F. MCKAY, G. S. MYERS, and R. N. JONES. J. Am. Chem. Soc. **74**, 2578 (1952).
7. D. HADŽI and N. SHEPPARD. Proc. Roy. Soc. (London), A, **216**, 247 (1953).
8. M. DAVIES and G. B. B. M. SUTHERLAND. J. Chem. Phys. **6**, 755 (1938).

THE OBJECTIVE EVALUATION OF THE POSITIONS OF INFRARED ABSORPTION MAXIMA[1]

R. NORMAN JONES, K. S. SESHADRI[2]
The Division of Pure Chemistry, National Research Council of Canada, Ottawa, Canada

AND

J. W. HOPKINS
The Division of Applied Biology, National Research Council of Canada, Ottawa, Canada

Received October 19, 1961

ABSTRACT

The fit of polynomial series of varying degree to infrared absorption bands in the neighborhood of the maxima has been investigated, and, in the instances considered, an acceptable graduation was usually possible with a quartic equation. By differentiation of the polynomial an objective, and independently reproducible, numerical value can be obtained for the band maximum. The abscissal positions computed for the maximum converged as the degree of the polynomial was raised, provided the experimental points did not exhibit gross departures from a smooth distribution. The convergence of the roots of the quadratic, cubic, and quartic functions was employed to check the applicability of the technique in individual cases. A Lorentz curve can be fitted exactly by a parabola if the reciprocal of the absorbance is plotted as ordinate, but in practice no improvement in the fit of power series to real absorption bands was achieved by using the reciprocal ordinates.

Frequency shifts in the infrared spectra of benzene, acetone, and nitromethane on solution in carbon tetrachloride have been measured by this method. The finite displacements observed contradict a recent statement in the literature that the peak frequencies of the bands in the spectra of these and other substances are uninfluenced by solution in non-polar solvents.

INTRODUCTION

In a recent publication, de Maine, Daly, and de Maine (1) have claimed that, contrary to the observations of numerous other workers, the infrared absorption bands of a variety of organic compounds exhibit no frequency shifts between the spectrum of the pure compound in the liquid state and the spectrum in carbon tetrachloride solution over wide concentration ranges.

As part of a study of the factors determining infrared profiles, a technique has been developed in our laboratory by means of which objective and independently reproducible values can be obtained for the maxima of infrared absorption bands with a precision approaching that of the ordinate and abscissal data. The routine application of this technique is facilitated by the availability of a suitable program for the IBM 650 computer.

Several of the absorption bands of benzene, acetone, and nitromethane, which were investigated by de Maine and collaborators, have been remeasured on a high-dispersion grating spectrometer, and the peak positions evaluated by the new technique. This work was undertaken to test the general applicability of the computer program, and to check de Maine's measurements under more rigorous experimental conditions.

LOCATION OF INFRARED BAND MAXIMA

Experience with the evaluation of wavenumber data for the calibration of infrared spectrometers (2) has established that, over limited scanning ranges, an absolute accuracy within ± 0.1 cm^{-1} can be achieved. Our measurements were made with a

[1]*Issued as N.R.C. No. 6656.*
[2]*National Research Council Postdoctorate Fellow.*

Perkin–Elmer Model 112G grating spectrometer, with corrections applied for time-dependent calibration drift. Other investigators have also shown that accuracy of the same order can be achieved with other types of commercially available grating spectrometers (3). These instruments were calibrated from measurements of the rotational fine structure lines of vapor phase spectra, where precise location of the band maximum presents no serious problem.

For the broader bands of spectra measured in condensed phases, both the absolute accuracy and the reproducibility of the measured peak positions are limited by experimental uncertainty in locating the position of zero slope on the band envelope. In favorable cases this might be done with an accuracy approaching the absolute accuracy of the calibration data. Normally, however, the uncertainty in the measured peak position will be considerably greater, particularly if subjective visual methods are used.

In connection with the analysis of infrared band profiles from the truncated band moments (4) the need arose to determine the positions of the band maxima as precisely as possible and to eliminate any personal bias associated with subjective methods. The fit of polynomial power functions of various orders to limited regions of the band envelopes in the neighborhood of the maxima was therefore investigated.

If the equation of the absorption band envelope near the maximum can be approximated with sufficient accuracy by a power series of the form

$$[1] \qquad a_0+a_1x+a_2x^2 \ldots +a_nx^n = y$$

the position of the maximum will be adequately approximated by one of the roots of the first-derivative equation

$$[2] \qquad a_1+2a_2x+3a_3x^2 \ldots +na_nx^{n-1} = 0.$$

The graduation of the experimental points by such an nth degree polynomial equation, using the method of least squares, involves the solution of a series of $n+1$ equations of the form

$$[3] \qquad \begin{aligned} &a_0 \sum x_i^0+a_1 \sum x_i+a_2 \sum x_i^2+ \ldots a_n \sum x_i^n = \sum y_i \\ &a_0 \sum x_i+a_1 \sum x_i^2+a_2 \sum x_i^3+ \ldots a_n \sum x_i^{n+1} = \sum x_iy_i \\ &a_0 \sum x_i^n+a_1 \sum x_i^{n+1}+a_2 \sum x_i^{n+2}+ \ldots a_n \sum x_i^{2n} = \sum x_i^ny_i, \end{aligned}$$

where x_i, y_i are the measured co-ordinates.

On inverting the [X] matrix, these equations can be solved for the coefficients $a_0 \ldots a_n$, and the position of the maximum of the graduation can be obtained from equation [2].

Under idealized conditions, the infrared band profiles probably conform closely to the Lorentz contour

$$[4] \qquad f(x) = a/(b^2+x^2),$$

where $2b$ is the band width at half maximal intensity, a/b^2 is the peak height, and x the wavenumber displacement from the band center. In initial investigations, the fitting of power series of increasing order to the symmetrically disposed ordinates of the Lorentz curve was examined. The results of these computations are summarized in Table I; they show that a fit acceptable within the limits of the observational precision is obtained for a quadratic function over the range $-0.5j$ to $+0.5j$, where $j = x/b$. The Lorentz function has inflection points at $\pm 0.535j$, and the fit is likely to deteriorate if the interpolation is extended beyond $0.5j$ (i.e. beyond one half of the half-band width from the center).

TABLE I

Graduation of symmetrical Lorentz ordinates by polynomials of increasing degree
(ν_0 800 cm^{-1}; a/b^2 1; b 1.2 cm^{-1})

	$-0.25j$ to $+0.25j$		$-0.5j$ to $+0.5j$	
Degree of polynomial*	Discrepance† (cm^{-1})	R.M.S.E.‡ (cm^{-1})	Discrepance† (cm^{-1})	R.M.S.E.‡ (cm^{-1})
2	0.000001471	0.0012	0.0003408	0.0185
4	0.0000000156	0.0001	0.0000020	0.0014

*Because the curve is symmetrical, the values of the discrepance and the R.M.S.E. for 3rd and 5th power functions are the same as for the 2nd and 4th, respectively.
†The discrepance is given by $(y_{\text{Lorentz}}-y_{\text{polynominal}})^2/(\text{number of ordinates})$.
‡The root mean square error is the square root of the discrepance.

The envelopes of absorption bands will not generally conform to the Lorentz contour, and allowance must be made for perturbations that may include appreciable skewness. It was therefore anticipated that at least a quartic function would be needed to obtain an adequate fit for real absorption bands over the same abscissal range, and that an objective value for the maximum might be obtained by successively fitting power series of increasing order. For the technique to have practical value it would be required that above a certain degree the differences in successively computed maxima should fall below the limits of accuracy of the experimental observations (± 0.1 cm^{-1}).

In our experiments the spectra were determined on a single-beam spectrometer with which random errors may be encountered in both the background transmission curve and the experimental absorption curve. These errors involve both electronic noise of a comparatively high frequency, and longer-period perturbations due to variation in amplifier gain, electrical surges, and other uncontrolled factors disturbing the recorder. To avoid subjective influences on the data evaluation, no attempt was made to smooth these irregularities when transposing the chart measurements to absorbance, prior to processing for the calculation of the peak frequency. The magnitude of these random errors depends on the instrumental conditions, and the curves can be classified into three broad categories, as illustrated in Fig. 1. In case A, the band envelope appears smooth to the eye; in case B one or two clearly recognizable irregularities are present, which may reasonably be excluded as "catastrophic" errors affecting the particular ordinates. In case C, large and seemingly random departures from a smooth contour occur extensively through the spectrum. Excluding the exceptional situation where the true band shape is in fact modulated by fine structure, case C is indicative of gross random errors in the measurements, and under these conditions attempts to apply precision techniques for evaluating the center of the band envelope are inapplicable and meaningless.

Some examples of the fit obtained with polynomials of varying degree to real absorption bands are illustrated in Table II. In the majority of instances, as the degree of the polynomial was raised the experimental points were approximated more closely and the abscissal positions computed for the maxima either converged to a constant value or oscillated within the experimentally significant limits of ± 0.1 cm^{-1}. Exceptions were noted and these were usually for data conforming to type C bands (e.g. band IV of Table II).

With the increasing order of the polynomial, the number of roots of the differential equation increases proportionately, and the selection of the correct root may require computation of the ordinates in doubtful cases. This is rarely so for cubic or quartic

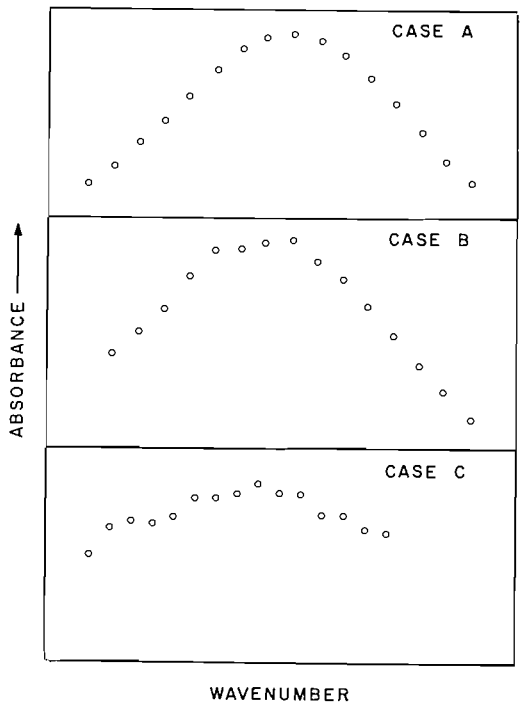

FIG. 1.

TABLE II

Approximation of real absorption bands by power series of increasing order

Degree of polynomial	Abscissal displacement of computed from visually estimated maximum* (cm^{-1})							
	Band I		Band II		Band III		Band IV	
	y	$1/y$	y	$1/y$	y	$1/y$	y	$1/y$
2	−0.10	−0.10	−0.38	−0.41	−0.20	−0.20	+0.66	+0.67
3	−0.14	−0.13	−0.23	−0.18	+0.03	+0.04	+0.73	+0.73
4	−0.08	−0.08	−0.18	−0.25	+0.02	+0.02	−0.70	−0.72
5	−0.08	−0.07						

*Band I: perylene, 5.2×10^{-3} M in CS_2, visually estimated max. 812.7 cm^{-1}; band II, benzene, liquid, visually estimated max. 1036.1 cm^{-1}; band III: benzene, 3.33 M in CCl_4, visually estimated max. 1815.6 cm^{-1}; band IV: benzene, 3.33 M in CCl_4, visually estimated max. 1176.9 cm^{-1}.

The values in the y columns were computed for the absorbance ordinates and in the $1/y$ columns for the reciprocal absorbance ordinates.

Bands I and II were of type A, band III was of type B, and band IV of type C (see Fig. 1).

polynomials, for which the alternative roots are usually displaced by two or more cm^{-1} from the significant root, and the correct choice is seldom in doubt. On the basis of this survey it was concluded that no advantage will normally be gained by fitting polynomials above the fourth degree and that, provided the convergence or oscillation of the computed maxima for the quadratic, cubic, and quartic graduations meet the conditions noted in the preceding paragraph, the quartic value can routinely be accepted.

If the Lorentz function is inverted, the parabolic equation

$$f(x)^{-1} = (b^2+x^2)/a \qquad [5]$$

is obtained. It is therefore possible to fit a Lorentzian absorption band exactly by a quadratic equation if the reciprocal of the absorbance is plotted as ordinate. An extension of this argument would suggest that the perturbed Lorentzian envelopes of real absorption bands might also be graduated more precisely by power series if plotted in terms of the reciprocal absorbance.

The values for the maxima obtained by using the reciprocal absorbances are given in the "$1/y$" columns of Table II, and they show no significant differences from those computed directly. From this it is to be inferred that the perturbations from the Lorentz band profiles in the neighborhood of the maxima are sufficiently large to require significant third- and fourth-order terms in the graduating function of the reciprocal curve.

THE COMPUTER PROGRAM

In handling a problem of this kind with a desk calculator, it is convenient to choose the abscissal origin as close as possible to the band center, and to take equal numbers of points at equal abscissal intervals on either side of the origin. In this way the arithmetic is simplified as the odd powers of x vanish. For the computer program this simplification is not necessary, though it is still advantageous to choose the abscissal origin at the estimated band center. Since it is desirable to restrict the range of the graduation within one half of the half-band width on either side of the maximum, the half-band width with respect to the position of the estimated maximum must be estimated. The difference between this estimated width and the evaluated half-band width, is unlikely to significantly affect the interpolation range. Commonly the polynomials of the second, third, and fourth degree were evaluated, using, as data points, the estimated band center and two points on either side.

Our current program for the IBM 650 computer is based on one published by Spector (5) and consists of two parts. The first part inverts the [X] matrix and gives the coefficients of the graduating polynomial; control cards specify the degree of the polynomial and the number of data points. The second part, using these coefficients, evaluates (*a*) the calculated ordinates, (*b*) the differences between the experimental and calculated ordinates, (*c*) the squares of these differences, (*d*) the sums of the differences and of their squares. The last quantity provides a check on the fit of the graduation. At present the roots of the first-derivative equations are evaluated by a separate program on a Bendix computer, but it is our intention to combine these operations into a single program for the IBM 1620 computer. The technical details of this combined program will be published at a later date.

SOLVENT SHIFTS IN CARBON TETRACHLORIDE SOLUTION

In their investigations of frequency displacements in carbon tetrachloride solution, de Maine, Daly, and de Maine (1) examined several bands in the spectra of benzene, acetone, and nitromethane, as well as other compounds. The solute concentration ranges extended up to 11.25, 13.64, and 18.51 moles per liter respectively for these three substances, corresponding to the concentrations in the pure liquids at 20° C. The authors concluded from their measurements that no measurable frequency shifts were observed for any band in any solute – carbon tetrachloride pair studied, even for large changes in the electrical properties of the solutions. Since the reproducibility of their wavenumber measurements is given as "within 1 cm^{-1}" it is to be assumed that any solvent displacement in excess of 1 cm^{-1} should have been detected, and would have been regarded as significant.

TABLE III

Infrared band shifts in carbon tetrachloride solution (cm^{-1})

Previously reported values				These experiments: Visually estimated values*	Computed values	Accepted value	Solvent	Concn. (mole per liter)	Displacement on solution
Benzene	1967,†	1957,‡	1961§	1959.4	1959.90	1959.9	Liquid	11.24	—
				1960.4	1959.96				
"	—	—	—	1956.6	1956.94	1957.2	CCl_4	3.33	−2.7
				1957.5	1957.51				
"	—	—	—	1956.6	1957.00	1957.1	CCl_4	2.22	−2.8
				1957.5	1957.22				
Benzene	1810,†	1814,‡	1815§	1815.6	1815.68	1815.8	Liquid	11.24	—
				1815.6	1815.90				
"	—	—	—	1814.0	1814.01	1813.6	CCl_4	3.33	−2.2
				1813.2_5	1813.24				
"	—	—	—	1814.0	1813.71	1813.8	CCl_4	2.22	−2.0
				1814.0	1813.87				
Benzene	1480,†	1482,‡	1479§	1479.2	1478.76	1478.8	Liquid	11.24	—
				1479.2	1478.81				
"	—	—	—	1480.2	1479.93	1479.9	CCl_4	3.33	+1.1
				1480.2	1479.92				
"	—	—	—	1480.2	1479.95	1479.8_5	CCl_4	2.22	$+1.0_5$
				1480.2	1479.78				
Benzene	1390,†	1395,‡	1393§	1393.7	1393.68	1393.6_5	Liquid	11.24	—
				1393.7	1393.64				
"	—	—	—	1391.9	1391.70	1391.9	CCl_5	6.98	-1.7_5
				1391.9	1392.07				
"	—	—	—	1391.9	1391.92	1391.9_5	CCl_4	3.33	−1.7
				1391.9	1392.00				
"	—	—	—	1391.9	1391.83	1391.5	CCl_4	2×22	-2.1_5
				1391.9	1391.20				
Benzene	1034,†	1036,‡	1036§	1036.1	1035.95	1036.0	Liquid	11.24	—
				1036.1	1036.05				
"	—	—	—	1036.1	1036.04	1036.1	CCl_4	6.98	(+0.1)
				1036.1	1036.16				
"	—	—	—	1036.1	1036.22	1036.3_5	CCl_4	3.33	$(+0.3_5)$
				1036.1	1036.51				
Acetone	1710,†	1721‖		1715.3	1715.94	1715.9_5	Liquid	13.62	—
				1715.3	1715.94				
"	—	1717¶		1718.0	1718.02	1718.0	CCl_4	0.67	$+2.0_5$
				1718.0	1717.94				
"	—	1717¶		1718.0	1717.58	1717.7	CCl_4	0.47	$+1.7_5$
				1718.0	1717.85				
Acetone	1215†	—		1221.6	1221.81	1221.7	Liquid	13.62	—
				1221.6	1221.61				
"	—	1218¶		1218.5	1218.48	1218.5	CCl_4	0.67	−3.2
				1218.5	1218.56				
"	—	1218¶		1218.5	1218.37	1218.6	CCl_4	0.47	−3.1
				1219.1	1218.88				
Acetone	1085†			1092.2	1092.49	1092.4_5	Liquid	13.62	—
				1092.2	1092.41				
"	—	—		1091.0	1090.78	1090.9	CCl_4	2.71	−1.55
				1091.0	1091.04				
Nitromethane	1378,†	1379**		1377.6	1377.68	1378.0	Liquid	18.50	—
				1378.4	1378.31				
"	—	—		1375.1	1375.17	1375.0_5	CCl_4	0.74	-2.9_5
				1375.1	1374.98				
"	917,†	920**		917.4	917.35	917.3_5	Liquid	18.50	—
				917.4	917.36				
"	—	—		916.6	916.44	916.4_5	CCl_4	3.93	−0.9
				916.6	916.45				
Nitromethane	—	—		656.8	656.65	656.5_5	Liquid	18.50	—
				656.5	656.48				
"	—	—		655.3	655.96	655.9	CCl_4	0.74	-0.6_5
				655.7	655.80				

*Each pair constitutes two independent measurements on different spectra.
†de Maine, Daly, and de Maine (see reference 1).
‡A.P.I. Catalog, infrared spectrum No. 307.
§A.P.I. Catalog, infrared spectrum No. 498.
‖R. N. Hazeldine, J. Chem. Soc. 4145 (1954).
¶S. A. Francis. J. Chem. Phys. **19**, 942 (1951).
**A.P.I. Catalog, infrared spectrum No. 1751.

Our measurements of the positions of five bands in the benzene spectrum, three in the acetone spectrum, and three in the nitromethane spectrum are reported together with other relevant information in Table III. These spectra were measured on a Perkin–Elmer 112G spectrometer, calibrated from the data in Tables 1–34 of the IUPAC calibration tables (2). Scanning speeds in the range 2–3 cm^{-1} per minute were used at chart speeds of 1 cm per minute corresponding to a chart spread of 3.3–5 mm per cm^{-1}. The calibration drift was checked by measurement of the rotational band at 3048.25 cm^{-1} in the spectrum of methane vapor, before and after each run, and did not exceed 0.005 cm^{-1} per minute. The solutes and the solvent were obtained from commercial sources and were distilled through a Todd column immediately before use; the middle 10% fraction was collected.

For the benzene band at 1036.0 cm^{-1} the measured displacement on solution in carbon tetrachloride is insignificantly small. The solvent effects on the benzene band at 1478.8 cm^{-1} and on the nitromethane band at 917.3_5 cm^{-1}, which only amount to about 1 cm^{-1}, could hardly have been detected using de Maine's technique. The nitromethane band at 656.5_5 cm^{-1} is also rather solvent insensitive, but was not accessible for measurement with the sodium chloride optics used in de Maine's experiments. The remaining bands, however, all show significantly large solvent shifts in the range 1.5–3.2 cm^{-1}.

Analysis of the 30 sets of duplicate values in Table III give a standard error of 0.31 cm^{-1} between pairs of measurements on identical bands. From this it may be concluded that the band positions can be reasonably reported to ± 0.3 cm^{-1} and that experimentally observed displacements in excess of 0.6 cm^{-1} are statistically suggestive of physical significance. The half widths of these bands vary considerably and a more precise analysis of the significance of the frequency differences between pairs of measurements should take this into consideration. It would be preferable to express the discrepancies in units of the fractional band width (j-units) instead of cm^{-1}. These considerations will be dealt with in more detail in connection with the discussion of band profiles in a later publication.

CONCLUDING REMARKS

We have to conclude that the general statement that solution in non-polar solvents has no effect on the position of the infrared band maximum is erroneous. In some cases, however, the displacement may be appreciably less than 1 cm^{-1} and will only be detected by refined methods of measurement. In other cases it can be quite large and well within the limits of measurements of simple instrumental techniques.

We do agree with de Maine and collaborators that the Kirkwood–Bauer–Magat equation, and the subsequent modifications that attempt to describe solvent shifts in terms of non-specific perturbing effects of the solvent cavity, are inadequate; the solvent–solute interaction is much more localized. Once this is conceded it is no longer possible to regard a molecule such as carbon tetrachloride as "non-polar", since it is the internal bond polarization and not the over-all dipole of the solvent molecule that is specifically involved. It is interesting in this connection to contrast the very small solvent effect of the nitromethane bands at 656.5_5 and 917.3_5 cm^{-1} with the large effect on the 1380.0 cm^{-1} band. These bands have been assigned (6) respectively to the symmetrical N—O deformation vibration, the C—N stretching vibration, and the symmetrical N—O stretching vibration. For the latter mode the motions of the oxygen atoms project more into the solvent cavity than for the two other modes where the C—N and N—O motions have more internal character. The greater solvent effect on the 1378.0 cm^{-1} band can be visualized in these terms, particularly if there exists some form of weak association between the oxygen atom of the nitromethane molecule and the chlorine atom of the solvent acting along the N—O . . . . . Cl—C bond direction.

ACKNOWLEDGMENT

We wish to thank Dr. S. D. Baxter and Mr. A. Croteau of the Mathematical Analysis Laboratory of the National Research Council for providing the computation facilities and for advice and assistance with the application of the computer program.

REFERENCES

1. P. A. D. DE MAINE, L. H. DALY, and M. M. DE MAINE. Can. J. Chem. **38**, 1921 (1960).
2. Tables of wavenumbers for the calibration of infrared spectrometers. *Prepared by* the Commission on Molecular Structure and Spectroscopy of the International Union of Pure and Applied Chemistry. *Reprinted from* Pure and Appl. Chem. **1**, No. 4 (1961). Butterworths, London. 1961.
3. P. KRUEGER. In press.
4. Unpublished work from this laboratory.
5. J. SPECTOR. IBM 650 Program Library, File No. 6–0–027.
6. D. C. SMITH, CHI-YUAN PAN, and J. R. NIELSEN. J. Chem. Phys. **18**, 706 (1950).

THE CHEMISTRY OF ALUMINUM–NITROGEN COMPOUNDS

II. REACTIONS OF TETRAMETHYLTETRAZENE WITH ALUMINUM HYDRIDE AND TRIALKYLALUMINUM COMPLEXES

NEIL R. FETTER AND BODO BARTOCHA*

The Chemistry Division, U.S. Naval Ordnance Laboratory, Corona, Calif., U.S.A.

Received October 12, 1961

ABSTRACT

The reaction of tetramethyltetrazene with $Me_3Al{:}NMe_3$, Et_3Al, and $H_3Al{:}NMe_3$ has led to a new method for the preparation of $(Me_2Al{-}NMe_2)_2$, $(Et_2Al{-}NMe_2)_2$, and $H_2Al{-}NMe_2$, respectively. The reaction of tetramethyltetrazene with Me_3Al has produced $Al(NMe_2)_3$, $MeAl(NMe_2)_2$, and $Me_2Al{-}NMe_2$, and with $Et_3Al{:}NMe_3$ has produced $Et_3Al{:}Me_2NN{=}NNMe_2$, $Et_2Al{-}NMe_2$, and the polymer $(-AlEtNEt-)_n$. In all but one case, the complexes are formed by the interaction of a dimethylamine radical, which results from the cleavage of $Me_2NN{=}NNMe_2$, with the aluminum moiety and the subsequent elimination of an alkane or hydrogen.

INTRODUCTION

Recently (1) we reported the reactions of several methylhydrazines with trimethylaluminum. As a continuation of this preparative survey on compounds with covalent aluminum–nitrogen bonds, we have found an interesting cleavage of tetramethyltetrazene (hereafter abbreviated as TMT) during its reaction with aluminum hydride trimethylamine, aluminum alkyls, and trialkylaluminum trimethylamine complexes.

The tetra-substituted tetrazenes exhibit thermal instability when heated in inert solvents, and they decompose to form tetra-substituted hydrazines and nitrogen (2):

$$R_2NN{=}NNR_2 \xrightarrow{\Delta} R_2N{-}NR_2 + N_2.$$

However, when TMT is treated with aluminum hydride trimethylamine, the dimethylamino groups do not combine, but react, with the aluminum–hydrogen bond to form $H_2Al{-}NMe_2$ plus hydrogen, nitrogen, and trimethylamine:

$$Me_2NN{=}NNMe_2 + 2H_3Al{:}NMe_3 \rightarrow 2H_2Al{-}NMe_2 + 2NMe_3 + N_2 + H_2.$$

The reactions of TMT with trimethylaluminum and triethylaluminum proceed in a similar manner. However, in several cases more than one alkyl group on aluminum was replaced by a dimethylamino group; thus, in the reaction of Me_3Al with TMT, we obtained $(Me_2Al{-}NMe_2)_2$, $MeAl(NMe_2)_2$, and $Al(NMe_2)_3$.

EXPERIMENTAL

Apparatus and Starting Materials

All the work described here was carried out with the aid of a conventional high-vacuum system. Infrared spectra were taken employing a Model IR-5 Beckman infrared spectrophotometer with sodium chloride optics. The spectra of gases were taken in a 10-cm cell equipped with NaCl windows, and the spectra of liquids were taken in a NaCl cell with a 0.001-inch lead spacer. Molecular weights were determined cryoscopically in an all-glass apparatus† which could be filled in an inert atmosphere chamber.‡ The solvent used was Fisher certified reagent grade cyclohexane.

Tetramethyltetrazene was supplied by the Chemistry Division, U.S. Naval Ordnance Test Station, China Lake, Calif. It was vacuum distilled from CaH_2 before use.

**Present address: U.S. Naval Propellant Plant, Indian Head, Maryland, U.S.A.*
†Bender & Hobein, G.m.b.H., Munich, Germany.
‡Model HE43/HE73, D. L. Herring Co., Inc., Sherman Oaks, Calif., U.S.A.

The trimethylaluminum was purchased from the Ethyl Corp., Baton Rouge, La., and the triethylaluminum, from Texas Alkyls, Inc., Houston, Texas. Both materials were used without further purification. The trimethylaluminum trimethylamine was prepared by a procedure described by Brown and Davidson (3). The compound was purified by vacuum sublimation at 60° C. Triethylaluminum trimethylamine was synthesized in this laboratory (4) and was used without further purification. The aluminum hydride trimethylamine was prepared by a procedure described first by Wiberg (5) and later improved and simplified in this laboratory (4).

The solvents used were reagent grade, and no further purification was required.

Analysis

The compounds obtained were analyzed by hydrolysis, and evolved gases were measured in the vacuum system by fractionating the mixtures through a series of traps into a calibrated volume and removing the non-condensable material with a Toepler pump. Elemental analyses were performed by the Schwarzkopf Microanalytical Laboratory, Woodside, New York.

Reaction of Tetramethyltetrazene with Aluminum Hydride Trimethylamine

By vacuum distillation, 2.40 g (0.0207 mole) of TMT was added to 1.95 g (0.0219 mole) of $H_3Al{:}NMe_3$. The mixture was allowed to warm from −196° C to room temperature and was then maintained at 65° C for 6 hours. During the reaction, 404.5 ml (STP) of a mixture of hydrogen and nitrogen (average molecular weight = 19.1) and 370.0 ml (0.0165 mole) of trimethylamine were evolved. The evolution of trimethylamine did not occur until heating at 65° C began.

The crude product was pumped at room temperature for 1 hour to remove any unreacted TMT. During this period the material changed from a liquid to a crystalline solid, which was then vacuum sublimed at 60° C (0.005 mm Hg) onto a −15° C cold finger. The yield of sublimate (m.p. 89–91° C) was approximately 90 mole%, based on the initial quantity of $H_3Al{:}NMe_3$. Anal. Calc. for C_2H_8NAl: C, 32.87; H, 11.03; N, 19.17; Al, 36.92. Found: C, 32.08; H, 10.72; N, 19.32; Al, 37.37. The melting point and the analytical data agree very well with those reported by Ruff and Hawthorne (6) for $H_2Al{-}NMe_2$ (89–90° C). As a confirmation, $H_2Al{:}NMe_2$ was prepared by the reaction

$$LiAlH_4 + Me_2HN{:}HCl \rightarrow H_2Al{-}NMe_2 + LiCl + 2H_2,$$

and a mixed melting point (90.0–93.0° C) was taken. The infrared spectra were also identical. The equation for the reaction of TMT with $H_3Al{:}NMe_3$ may then be written:

$$2H_3Al{:}NMe_3 + Me_2NN{=}NNMe_2 \rightarrow 2H_2Al{-}NMe_2 + N_2 + H_2 + 2NMe_3.$$

Reaction of Tetramethyltetrazene with Trimethylaluminum Trimethylamine

The TMT (1.54 g, 0.0133 mole) was distilled onto 1.78 g (0.0136 mole) of $Me_3Al{:}NMe_3$ at −196° C. The mixture was allowed to warm to room temperature and was then heated at 90° C for 10 hours. During the heating, the water-clear solution turned a deep red and 301.0 ml (0.0135 mole) of nitrogen, 57.1 ml (0.00255 mole) of methane, and 227.0 ml (0.0101 mole) of trimethylamine were evolved. The red solution was sublimed at 75° C (0.005 mm Hg) onto a −78° C cold finger. The deposit was a light yellow slush. This material was resublimed at room temperature onto a −15° C cold finger, and a white crystalline solid (m.p. 147–149° C) deposited. Resublimed again, the compound had a melting point of 151–153° C, which agrees quite well with that reported for $(Me_2Al{-}NMe_2)_2$ by Brown and Davidson (3) (m.p. 154–156° C). This conclusion was confirmed by elemental analysis and molecular weight determinations: Anal. Calc. for $C_4H_{12}NAl$: C, 47.50; H, 11.97; Al, 26.68. Found: C, 46.72; H, 11.59; Al, 25.79. Calc. for $(Me_2Al{-}NMe_2)_2$: molecular weight, 202.2. Found: molecular weight, 203.0 and 208.0. The reaction therefore proceeded as follows:

$$2Me_3Al{:}NMe_3 + Me_2NN{=}NNMe_2 \rightarrow (Me_2Al{-}NMe_2)_2 + N_2 + 2NMe_3 + 2CH_4.$$

The source of the hydrogen atoms, necessary for the formation of methane, is not known.

The yield of sublimed $(Me_2Al{-}NMe_2)_2$ was approximately 50 mole%, based on the quantity of $Me_3Al{:}NMe_3$.

Reaction of Tetramethyltetrazene with Trimethylaluminum

The TMT (2.82 g, 0.00243 mole) was vacuum distilled onto 1.60 g (0.0222 mole) of Me_3Al dissolved in 25 ml of pentane. The mixture was allowed to warm from −196° C to room temperature and then to remain at ambient temperature for 18 hours. At the end of this period the solution had a faint red color. The pentane and any excess TMT were removed by pumping, and the resulting colored liquid was sublimed at 55° C (0.005 mm Hg) onto a −15° C cold finger. A slushy deposit of white crystals formed on the cold finger, and the liquid in the bottom of the sublimation vessel turned a deep red color.

The solid material was heated in vacuum at 85° C for 1 hour. The mixture turned deep red, but no further gas evolution was observed. This mixture was sublimed at 50° C (0.005 mm Hg) onto a −15° C cold finger, and white crystals (m.p. 150.0–153.0° C) deposited on the cold finger. The melting point indicated that the sublimate was $(Me_2Al{-}NMe_2)_2$ and an elemental analysis confirmed this: Anal. Calc. for $C_4H_{12}NAl$: C, 47.50; H, 11.97; N, 13.85; Al, 26.68. Found: C, 46.94; H, 12.03; N, 13.55; Al, 26.73.

The red liquid from the sublimation vessel was vacuum distilled at 40° C (0.005 mm Hg), and approximately 1 ml of clear liquid was obtained. About 1 ml of deep red gum was left behind in the flask.

The clear distillate (m.p. −30° C) will slowly turn red in about 8 hours if heated to 50° C and will convert almost completely into the dark red gum in about 1 hour at 90° C. In fact, there is evidence that the clear liquid will change color very slowly at room temperature; hence, isolation has been difficult. However, elemental analysis gave results that agree with the empirical formula $C_6H_{18}N_3Al$: Anal. Calc.: C, 45.26; H, 11.39; N, 26.39; Al, 16.95. Found: C, 45.35; H, 11.50; N, 26.40; Al, 16.98. From these data, we propose the formula $Al(NMe_2)_3$ for this complex. Two molecular weight determinations showed the compound to be associated in cyclohexane: Calc. for $Al(NMe_2)_3$: 159.1. Found: 199 and 193.

Characterization of the red tar has been difficult because of purification problems. However, an elemental analysis of this material agrees with the empirical formula $C_5H_{15}N_2Al$. Anal. Calc. for $C_5H_{15}N_2Al$: C, 46.13; H, 11.62; N, 21.52; Al, 20.72. Found: C, 47.90; H, 10.88; N, 20.40; Al, 21.01.

A methanol hydrolysis of 0.1478 g (0.00114 mole) of the red fluid yielded 35.9 ml (0.00160 mole) of methane; hence we assigned the formula $MeAl(NMe_2)_2$ to this material.

The yields of $Me_2Al—NMe_2$ and $Al(NMe_2)_3$ were approximately 30 mole%, based on Me_3Al, and the remainder was the red residue.

The equation for the reaction is somewhat complex, but it appears that at least two routes are possible:

$$2Me_2Al + Me_2NN{=}NNMe_2 \rightarrow (Me_2Al{-}NMe_2)_2 + N_2 + 2CH_4 \quad [1]$$

$$2Me_3Al + 3Me_2NN{=}NNMe_2 \rightarrow 2Al(NMe_2)_3 + 3N_2 + 6CH_4 \quad [2]$$

$$\downarrow \Delta$$

red tar $(MeAl(NMe_2)_2)$

In another reaction, using 1.50 g of Me_3Al (0.0209 mole) and 1.20 g (0.0103 mole) of TMT, at room temperature, 325 ml (0.0145 mole) of nitrogen, but only 85.6 ml (0.00383 mole) of methane, were recovered.

Reaction of Tetramethyltetrazene with Triethylaluminum Trimethylamine

In the reactions discussed so far, the cleavage of TMT into nitrogen and $\cdot NMe_2$ radicals has occurred before products could be isolated. In this reaction, a complex has been isolated which appears to contain an uncleaved TMT molecule.

The TMT (0.982 g, 0.00845 mole) was distilled into 1.054 g (0.00646 mole) of $Et_3Al{:}NMe_3$ at −196° C. The mixture was allowed to warm to room temperature, and it was then heated and maintained at 60° C for 20 hours. During the heating period, 68.5 ml (0.00306 mole) of NMe_3 was evolved, but examination by infrared and mass spectrometry indicated that no ethane was present. The mixture was pumped at room temperature for 1 hour to remove any excess TMT and was then purified by vacuum transfer at 60–65° C (0.005 mm Hg). Approximately 0.5 ml of a clear liquid was obtained. Elemental analysis gave values which agreed with the empirical formula $C_{10}H_{27}N_4Al$: Anal. Calc. for $C_{10}H_{27}N_4Al$: C, 52.14; H, 11.82; N, 24.33; Al, 11.71. Found: C, 50.87; H, 12.01; N, 25.44; Al, 10.52. From these data we propose the formula $Et_3Al{:}Me_2NN{=}NNMe_2$ for the distillate.

Hydrolysis of 0.4416 g (0.00192 mole) of the above product with methanol produced 125.2 ml (0.00560 mole) of ethane. The molar ratio of ethane to $Et_3Al{:}Me_2NN{=}NNMe_2$ is 2.91, close to the calculated value of 3:1. The reaction may thus be written:

$$Et_3Al{:}NMe_3 + Me_2NN{=}NNMe_2 \xrightarrow{60^\circ\ C} Et_3Al{:}Me_2NN{=}NNMe_2 + NMe_3.$$

In another experiment, 0.586 g (0.00505 mole) of TMT was distilled onto 1.509 g (0.00919 mole) of $Et_3Al{:}NMe_3$ and was then heated at 85° C for 6 hours. A crack in the vacuum system prevented measurement of the evolved gases, but the crude product was recovered. It was purified by vacuum transfer at 65° C (0.005 mm Hg), and approximately 1 ml of clear liquid and a viscous orange residue were obtained. Elemental analysis of the liquid gave results which agree with the calculated empirical formula $C_6H_{16}NAl$: Anal. Calc. for $C_6H_{16}NAl$: C, 55.79; H, 12.49; N, 10.84; Al, 20.88. Found: C, 55.08; H, 12.53; N, 14.02; Al, 18.57.

Hydrolysis of 0.4050 g (0.00281 mole) of the distilled product with methanol gave 95.0 ml (0.00423 mole) of ethane. This corresponds to a ratio of 1:1.51 of compound to ethane. The infrared spectrum agreed closely with that obtained from $Et_2Al—NMe_2$ prepared from the reaction of Et_3Al and $HNMe_2$ (7). Based on these data, the formula $Et_2Al—NMe_2$ has been assigned to the complex.

Although the orange residue obtained above could not be distilled or otherwise purified, an elemental analysis gave results which agree with the empirical formula $C_4H_{10}NAl$: Anal. Calc. for $C_4H_{10}NAl$: C, 48.47; H, 10.17; N, 14.13; Al, 27.22. Found: C, 48.20; H, 10.99; N, 14.00; Al, 26.26.

This material is very viscous and appears to be polymeric; hence, we have assigned it the formula

$$\left[\begin{array}{c} Et \quad Et \\ | \quad | \\ -Al-N- \end{array}\right]_n.$$

In order that the evolved gases could be characterized and measured, the experiment was repeated, and 1.283 g (0.00743 mole) of $Et_3Al{:}NMe_3$ was reacted with 2.024 g (0.0174 mole) of TMT under the second set of conditions described above. From the mixture, 74.0 ml (0.00330 mole) of nitrogen, 201.0 ml (0.00895 mole) of trimethylamine, and a trace of TMT were recovered. No ethane or ethylene were detected in the infrared spectra of these gases.

Two molecular weight determinations of $Et_2Al{-}NMe_2$ in cyclohexane gave the values 241 and 235 (calc.: 288.3 for $(Et_2Al{-}NMe_2)_2$).

The reaction of TMT with $Et_3Al{:}NMe_3$ at 60° C appears to involve the formation of a complex in which TMT is exchanged with NMe_3; however, when the reaction is run at 80–85° C, the TMT cleaves:

$$2Et_3Al{:}NMe_3 + Me_2NN{=}NNMe_2 \xrightarrow{80^\circ\ C} Et_2Al{-}NMe_2 + 2NMe_3 + N_2 + C_2H_6(?).$$

Under these reaction conditions $Et_2Al{-}NMe_2$ also appears to lose two methyl groups to form the polymeric material:

$$n Et_2Al{-}NMe_2 \xrightarrow{80^\circ\ C} [{-}AlEtNEt{-}]_n + nC_2H_6.$$

The yields of the two complexes discussed above were approximately 50 mole% (based on $Et_3Al{:}NMe_3$), and the remainder in the second experiment was polymeric material.

Reaction of Tetramethyltetrazene with Triethylaluminum

With 25 ml of pentane as a solvent, 1.952 g (0.0168 mole) of TMT was vacuum distilled onto 1.945 g (0.0170 mole) of Et_3Al at −196° C. The mixture was warmed to room temperature and then heated at 55° C for 18 hours. The pentane was removed in vacuum, and the remaining brown fluid was purified by vacuum transfer at 90° C (0.005 mm Hg) (b.p. from reference 7 66° C at 0.15 mm Hg). A yield of approximately 75%, based on Et_3Al, was obtained. The experiment was repeated in nonane so that the condensable gases could be recovered more easily. Under the conditions described above, 1.422 g (0.0123 mole) of TMT was reacted with 2.330 g (0.0204 mole) of Et_3Al. From the reaction were recovered 252 ml (0.0112 mole) of nitrogen and 82.5 ml of a condensable (−196° C) gas which was estimated, by infrared analysis, to be a mixture consisting of 90% ethane and 10% ethylene. No trimethylamine or dimethylamine was observed.

Elemental analysis of the distillate gave values which agree with those calculated for $Et_2Al{-}NMe_2$: Anal. Calc. for $C_6H_{16}NAl$: C, 55.79; H, 12.49; N, 10.84; Al, 20.88. Found: C, 56.64; H, 12.73; N, 11.64; Al, 20.76. Methanol hydrolysis of 0.2872 g of the distillate (0.00222 mole $Et_2Al{-}NMe_2$) produced 83.4 ml (0.00372 mole) of ethane.

Although $Et_2Al{-}NMe_2$ is a liquid at room temperature, molecular weight data indicate that the complex is a dimer. Two determinations gave the values 285 and 283 (calc. for $(Et_2Al{-}NMe_2)_2$: 288.4).

The infrared spectrum of the complex was compared with that of a sample of $Et_2Al{-}NMe_2$ prepared (7) from the reaction of Et_3Al with $NHMe_2$ and found to be identical.

From these data, the equation for the reaction of Et_3Al and TMT is

$$2Et_3Al + Me_2NN{=}NNMe_2 \rightarrow (Et_2Al{-}NMe_2)_2 + N_2 + 2C_2H_6 + (C_2H_4).$$

No other products were isolated, and there appear to be no side reactions as is the case with $Et_3Al{:}NMe_3$ and TMT.

DISCUSSION

The reaction between $H_3Al{:}NMe_3$ and TMT appears to be straightforward, with the formation of $H_2Al{-}NMe_2$, H_2, N_2, and NMe_3.

However, the reaction between Me_3Al and TMT is more complex. If the latter reaction proceeded in the manner of the former, ethane and not methane should have been observed. The source of the hydrogen atom required to form methane must await further study of the mechanism of this reaction.

The referee of this paper proposed a reaction scheme which would eliminate the problem of the hydrogen atom in methane formation. The reaction would proceed as follows:

$$R_3Al + Me_2N{-}N{=}N{-}NMe_2 \rightarrow R_3Al{:}Me_2N{-}N{=}N{-}NMe_2 \quad [1]$$

$$R_3Al{:}Me_2N{-}N{=}N{-}NMe_2 \rightarrow R_2Al{-}NMe_2 + R{-}N{=}N{-}NMe_2 \quad [2]$$

$$R{-}N{=}N{-}NMe_2 + R_3Al \rightarrow R_2Al{-}NMe_2 + R{-}N{=}N{-}R, \quad [3]$$

where R = Me or Et.

An examination of the infrared spectra of the condensable gas from the reactions of this type showed, for the reaction of $Me_3Al{:}NMe_3$ with TMT, a strong absorption at 2100 cm^{-1} plus a weaker one at 2400 cm^{-1}. These peaks have been shown by Pierson, Fletcher, and Gantz (11) to be characteristic of diazomethane, but not azomethane; hence, a fourth reaction,

$$MeN{=}NMe \rightarrow CH_4 + CH_2N_2, \qquad [4]$$

must be added to the three written above. This mode of decomposition of azomethane does not follow the classical route at high temperature to ethane and nitrogen (12), but is necessary to account for the diazomethane and methane observed in the reaction gases.

An absorption at 2100 cm^{-1} is also present in the condensables from the reaction of Me_3Al with TMT, but it is much weaker than that observed for $Me_3Al{:}NMe_3$.

The infrared spectra of condensables from the reactions Et_3Al and $Et_3Al{:}NMe_3$ with TMT also have weak absorptions in the 2100 cm^{-1} region; hence, this mechanism appears to apply to all of the reactions involving the aluminum alkyls.

Another striking feature of the reaction of Me_3Al with TMT is the formation of a compound to which we have given the formula $Al(NMe_2)_3$. A complex of this composition was first reported by Wiberg and May (8), who prepared it by the reaction of aluminum hydride etherate and dimethylamine:

$$H_3Al.n\mathrm{Et_2O} + 3HNMe_2 \rightarrow Al(NMe_2)_3 + 3H_2 + n\mathrm{Et_2O}.$$

This compound has also been reported recently by Ruff (9) and by Longi, Mazzanti, and Bernardini (10). The former author employed two methods of preparation, namely:

$$H_3Al{:}NMe_3 + 3HNMe_2 \rightarrow Al(NMe_2)_3 + NMe_3 + 3H_2 \qquad [1]$$

$$LiAlH_4 + 4HNMe_2 \rightarrow LiAl(NMe_2)_4 + 4H_2 \qquad [2]$$

$$3LiAl(NMe_2)_4 + AlCl_3 \rightarrow 4Al(NMe_2)_3 + 3LiCl.$$

The latter authors employed the reaction of triisobutyl aluminum with dimethylamine at high temperature:

$$(i\text{-Bu})_3Al + 3HNMe_2 \xrightarrow[\text{heptane}]{195^\circ\,C} Al(NMe_2)_3 + 3i\text{-}C_4H_9.$$

They indicate that the product is a solid but do not report a melting point. The physical constants of the complex (Table I) we have prepared differ markedly from those described previously.

TABLE I

Physical constants of $Al(NMe_2)_3$

	M.p. (° C)	Mol. wt. (calc.: 159.1)
Authors	−30	199, 193* cryoscopically
Wiberg (8)	87–88	162† ebullioscopically
Ruff (9)	87–89	353‡ cryoscopically
Longi *et al.* (10)	Not reported	320‡ cryoscopically

*In cyclohexane.
†In ether.
‡In benzene.

We have repeated the preparation of this complex, and the elemental analysis and other physical properties have been confirmed. It is hoped that instrumental studies being carried out in this laboratory will reveal the structure of this complex.

Finally, it should be noted that the data presented above indicate that it is possible to obtain from this reaction a complete series of dimethylamino substitutions on trimethylaluminum, namely $Me_2Al{-}NMe_2$, $MeAl(NMe_2)_2$, and $Al(NMe_2)_3$. However, there

appears to be a discrepancy in the reaction sequence. Although one would assume that $Al(NMe_2)_3$ would be the most stable complex, heating the liquid $Al(NMe_2)_3$ produces the red fluid which analysis has established as $MeAl(NMe_2)_2$. Hence, this complex and $Me_2Al—NMe_2$ seem to be the most stable materials of this series.

Whether the complex $Et_3Al{:}NMe_2NN{=}NNMe_2$ is the precursor to $(Et_2Al—NMe_2)_2$ is not known, but it does appear that $(Et_2Al—NMe_2)_2$ undergoes an unusual rearrangement in which an ethyl group migrates to the nitrogen atom and two methyl groups are eliminated, presumably to form ethane. It should also be noted that the formula $(—AlEtNMe_2)$ also fits the elemental analysis to which the formula $(—AlEtNEt—)_n$ was assigned. The first formula above would require a structure of the type

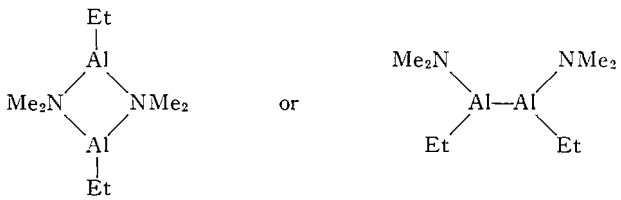

to satisfy the valency of aluminum. In our experience, compounds of this type are rare, if non-existent; hence, for this reason and because of the polymeric character, we have chosen the latter formula.

The structure of $Et_3Al{:}Me_2NN{=}NNMe_2$ may be one of unusual character involving a cyclic ring with a pentavalent aluminum atom:

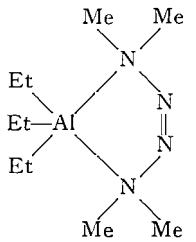

ACKNOWLEDGMENTS

The authors wish to thank Dr. Charles P. Haber and Dr. Frederick E. Brinckman, Jr. of the U.S. Naval Ordnance Laboratory, Corona, California, and Dr. William R. McBride of the U.S. Naval Test Station, China Lake, California, for their assistance and interest during the course of this work. This investigation was supported by funds from the Advanced Research Projects Agency through the U.S. Navy Department, Bureau of Naval Weapons.

REFERENCES

1. N. R. FETTER and B. BARTOCHA. Can. J. Chem. **39**, 2001 (1961).
2. L. F. AUDRIETH and B. A. OGG. The chemistry of hydrazine. John Wiley & Sons, Inc., New York. 1951.
3. H. C. BROWN and N. DAVIDSON. J. Am. Chem. Soc. **64**, 316 (1942).
4. F. M. PETERS, A. J. BILBO, and B. BARTOCHA. To be published.
5. E. WIBERG, H. GRAF, and R. USON LACAL. Z. anorg. u. allgem. Chem. **272**, 221 (1953).
6. J. K. RUFF and M. F. HAWTHORNE. J. Am. Chem. Soc. **82**, 2141 (1960).
7. K. ZIEGLER. Brit. Patent No. 799,823. (August 13, 1958); Chem. Abstr. **53**, 2690h (1959).
8. E. WIBERG and A. MAY. Z. Naturforsch. Part b, **10b**, 234 (1955).
9. J. K. RUFF. J. Am. Chem. Soc. **83**, 2835 (1961).
10. P. LONGI, G. MAZZANTI, and F. BERNARDINI. Gazz. chim. ital. **90**, 180 (1960).
11. R. H. PIERSON, A. N. FLETCHER, and E. C. GANTZ. Anal. Chem. **28**, 1218 (1956).
12. O. K. RICE and D. V. SICKMAN. J. Chem. Phys. **4**, 242 (1936).

THE STRUCTURAL ANALYSIS OF SOME ACIDIC XYLANS BY PERIODATE OXIDATION

G. G. S. DUTTON AND A. M. UNRAU
The Department of Chemistry, University of British Columbia, Vancouver, British Columbia

Received September 18, 1961

ABSTRACT

By determining the amount of formaldehyde produced on periodate oxidation of borohydride-reduced apple- and cherry-wood xylans the degree of polymerization was shown to be 155 and 100 respectively. Acid hydrolysis of the polyols obtained by periodate oxidation and borohydride reduction gave ethylene glycol in amounts indicating that these xylans have a small degree of branching. Mild acid hydrolysis of the polyols demonstrated that in these xylans D-glucuronic acid as well as 4-*O*-methyl-D-glucuronic acid was present and that some of the former occupied non-terminal positions.

The constitution of numerous hemicelluloses has been investigated by graded hydrolysis and characterization of the products and also by methylation followed by identification of the methylated monosaccharides produced on hydrolysis. These methods and the results obtained have been extensively reviewed (e.g. refs. 1, 2).

Recently a modified periodate degradative procedure has been described based on the mild acid hydrolysis of the polyalcohol obtained after borohydride reduction (2, 3). The conditions of hydrolysis are such that true acetal systems are cleaved whereas glycosidic bonds are stable. This method holds great promise as a convenient means of examining the fine structure of polysaccharides. It has so far been applied to oat glucan (3), brome grass hemicellulose (4), and oat hull hemicellulose (5). The present paper reports the application of this method to the 4-*O*-methyl-D-glucurono-xylans obtained from apple and cherry wood.

These two hemicelluloses have previously been examined by the methylation technique and were assumed to have essentially linear structures of D-xylose units joined by $\beta(1 \rightarrow 4)$ linkages. Each polysaccharide carried branches of 4-*O*-methyl-D-glucuronic acid with a xylose:acid ratio of about 6:1. From the quantity of 2,3,4-tri-*O*-methyl-D-xylose found, the chain length was estimated to be 120 for the applewood xylan (6) and 110 for the cherrywood xylan (7).

When the degree of polymerization (D.P.) of these polysaccharides was determined by measuring the formaldehyde produced upon periodate oxidation of the borohydride-reduced xylans (8) a value of 155 was obtained for the applewood xylan and 100 for the cherrywood xylan. These values are based on the assumption that the reducing end-group was not substituted at position 2. Complete acid hydrolysis of the polyalcohol obtained after reduction ($NaBH_4$) of the polyaldehyde from the applewood xylan gave ethylene glycol (1 mole, from terminal, non-reducing xylopyranose units), glycerol (40 moles, from internal $1 \rightarrow 4$-linked xylopyranose units), and xylose (7 moles, from xylose residues substituted at $C_{2\ (3)}$ and C_4, hence immune to periodate attack). The quantity of ethylene glycol found indicated that the xylan possessed a repeating unit consisting of about 50 sugar residues, which suggested that the xylan possessed two branch points other than those caused by the direct attachment of a single uronic acid residue to the main chain.

When the cherrywood xylan was subjected to the same sequence of reactions the ratio of ethylene glycol:glycerol:xylose was 1:42:10. These results suggested that this xylan had one such branch point.

Mild acid hydrolysis (3) of the polyalcohols derived from each xylan followed by adsorption of the acidic fragments of an anion exchange resin left a neutral residue which was composed of ethylene glycol, glycerol, and a non-reducing xyloside identified as 2′-*O*-glyceryl-β-D-xylopyranoside. The three compounds were converted to their crystalline *p*-nitrobenzoates. The xyloside was further characterized by periodate oxidation, reduction ($NaBH_4$), and hydrolysis, which gave a 1:1 ratio of ethylene glycol:glycerol, each characterized as their *p*-nitrobenzoates. The glycoside, 2′-*O*-glyceryl-β-D-xylopyranoside, mainly originated, as anticipated, from the xylose units substituted at $C_{2\ (3)}$ by uronic acid. This glycoside has been prepared previously by Perlin and his associates (9).

The acidic material adsorbed on an anion exchange resin was eluted with alkali, and the free acids were regenerated by passage through a cation resin. Evaporation of the eluate gave an acidic residue, chromatographically free of glycerol, which was subjected to heat under vacuum to effect lactonization. Reduction ($NaBH_4$) of the product (10) and chromatographic examination of the final residue in each case revealed three compounds, two in minor quantities corresponding to glycerol and erythritol and the major component corresponding to a synthetic sample of 2-*O*-methyl-D-erythritol. The molar ratio of erythritol:glycerol:2-*O*-methyl-D-erythritol was about 1:2.2:12 for the apple xylan and 1:1.6:9 for the cherry xylan. The three polyols were converted to their crystalline *p*-nitrobenzoates. The 2-*O*-methyl-D-erythritol arose, as expected, from periodate cleavage of the 4-*O*-methyl-D-glucuronic acid residues. Glycerol possibly arose from D-glucuronic acid residues while erythritol could only arise in this analysis sequence from a D-glucuronic acid residue substituted at C_4 with a residue other than methoxyl, presumably a xylopyranose unit. This structural feature would thus explain the formation of greater amounts of ethylene glycol than anticipated on the basis of the D.P. determinations, had the structures been strictly linear. Approximately equimolar quantities of acids and 2′-*O*-glyceryl-β-D-xyloside were obtained from both xylans. From the ratio of xylose to glycerol it may be deduced that in the apple xylan there is 1 uronic acid per 7 xylose units and that with the cherry xylan the ratio is 1:5.

These results show that both xylans possess similar structures and they largely confirm the earlier findings from the methylation studies (6, 7). The present periodate investigation has, however, revealed several points which were not observed in the earlier work (6, 7). When only small amounts of monomethyl pentoses are obtained in methylation studies it is difficult to ascertain whether these are of constitutional significance or are formed by demethylation. The isolation of ethylene glycol by periodate oxidation, reduction, and hydrolysis appears to be less subject to such uncertainties and indicates that these two xylans have a slightly branched structure.

From the analysis of the acidic fraction after periodate oxidation, reduction, and hydrolysis it is apparent that about 20% of the acid portion of the apple xylan is D-glucuronic acid, rather than its 4-*O*-methyl ether, and that of this about 30% (or 6% of the total acid) occupies non-terminal positions. In the case of the cherry xylan about 22% of the acid is D-glucuronic acid and of this 40% (or 8% of the total acid) occupies non-terminal positions.

In the earlier studies on these xylans chromatographic examination of the aldobiouronic acid fraction, produced on hydrolysis of the polysaccharides, showed in each case a component having an R_{xylose} 0.7. This component only showed faintly on the chromatograms and was assumed to be present in trivial amounts. The present work shows that this assumption was in error and that an unmethylated aldobiouronic acid is a significant

percentage of the acid component. This error in interpretation may well account for our inability to crystallize the methyl 2-*O*-(2,3,4-tri-*O*-methyl-D-glucosyl)-3-*O*-methyl-D-xylopyranoside obtained by reduction of the partly methylated acid fraction (6, 7).

It is thus apparent that the technique introduced by Smith (3) is a powerful tool in the elucidation of the structure of polysaccharides.

EXPERIMENTAL

Chromatographic studies were conducted by the descending technique using Whatman No. 1 filter paper. The solvent systems used were (*a*) 1-butanol:pyridine:water (6:4:3); (*b*) 1-butanol:ethanol:water (4:1:5) (upper phase); and (*c*) butanone–water azeotrope. Non-reducing sugar alcohols were detected with ammoniacal silver nitrate while reducing sugars were detected with *p*-anisidine trichloracetate spray. Whatman No. 3 MM paper was used for preparative separation of compounds.

The melting points reported are uncorrected and the specific rotations quoted are equilibrium values. Unless otherwise stated, all evaporations were carried out under reduced pressure at a bath temperature of 40° C.

Determination of D.P.

The D.P. of applewood xylan, using 62 mg of material, was estimated by a chemical procedure described elsewhere (8). After 72 hours of contact with periodate, the formaldehyde production from the reduced xylitol end-residues became constant. On the basis that 1 mole of formaldehyde was produced from each xylan molecule, the 0.084 mg CH_2O released corresponded to a D.P. of about 155. Similarly, 34.8 mg of cherrywood xylan yielded 0.074 mg CH_2O corresponding to a D.P. of about 100.

A. Applewood Xylan

Periodate Oxidation

Xylan (2.964 g) was dissolved in dilute alkali after which the solution was made slightly acidic and the volume adjusted to 200 ml, and after cooling to 5° C, 0.5 *M* periodic acid was added (50 ml). After 72 hours, 0.878 mole of periodate had been consumed per sugar residue and no change was observed thereafter. To the solution was added $BaCO_3$ to precipitate periodate and iodate, and to the clear filtrate was added $NaBH_4$ (945 mg) and the solution left overnight. The solution was neutralized, evaporated, and borate removed from the polyol by several treatments with methanolic hydrogen chloride.

Partial Hydrolysis of Polyol

The polyol was dissolved in 0.2 *M* hydrochloric acid and left at room temperature for 10 hours. The solution was passed through cation and anion exchange resins in that order and the neutral effluent evaporated to a syrup (1.795 g). Chromatographic examination of the syrup revealed the presence of glycerol, a slow-moving, non-reducing component believed to be a xylosyl glycerol, and a small amount of ethylene glycol. Part of the mixture was resolved using sheets of Whatman No. 3 MM paper and solvent C.

Component No. 1, ethylene glycol, 24 mg by weight, 20.2 mg (0.326 mmole) by chromotropic acid determination. The di-*p*-nitrobenzoate prepared in the usual manner had m.p. and mixed m.p. 139–141° C.

Component No. 2, glycerol, 995 mg by weight, 988 mg (10.7 mmoles) by chromotropic acid determination. An aliquot was treated with *p*-nitrobenzoyl chloride to give the tri-*p*-nitrobenzoate, m.p. and mixed m.p. 188–190° C.

Component No. 3, 2′-*O*-glyceryl-β-D-xylopyranoside, 530 mg by weight, 532 mg (2.38 mmoles) by the phenol – sulphuric acid (11) analysis. The compound in water had $[\alpha]_D^{22}$ −33° (*c*, 4.0), R_{xylose} in solvent *c* of 0.80, R_g was 1.45. Hydrolysis in 1 *N* H_2SO_4 of an aliquot (120 mg) of the compound gave glycerol and xylose in equimolar proportions. *Glycerol*, 43.2 mg (0.47 mmole), was converted to the tri-*p*-nitrobenzoate, m.p. and mixed m.p. 188–190° C. D-*Xylose*, 74.1 mg (0.49 mmole), $[\alpha]_D^{22}$ +18.1° in water (*c*, 1.5). The sugar crystallized from a mixture of acetonitrile, methanol, and petroleum ether, m.p. and mixed m.p. 143–145° C.

The glycoside was further characterized as follows:

(*a*) Preparation of *p*-nitrobenzoate: To the compound (40 mg) dissolved in pyridine (2 ml) was added a 10% molar excess of *p*-nitrobenzoyl chloride, and the solution was heated at 70° C for 40 minutes. After isolation and recrystallization from a petroleum ether – ethyl acetate mixture the penta-*p*-nitrobenzoate had m.p. 101–102° C, $[\alpha]_D^{22}$ −37.1° in ethyl acetate (*c*, 0.47). Calc. for $C_{43}H_{31}O_{22}N_5$: N, 7.23%. Found: N, 7.15%.

(*b*) Periodate oxidation: An aliquot (140 mg, 0.62 mmole) was treated with a 15% molar excess sodium periodate at 5° C. After 14, 24, and 48 hours, between 2.16 to 2.18 moles of periodate had been consumed per mole of compound, the theoretical value being 2.00 moles. The amount of formic acid produced was 0.66 milliequivalent, expected was 0.62 milliequivalent. No formaldehyde was formed. The dialdehyde (120 mg), $[\alpha]_D^{22}$ +11.3°, was reduced ($NaBH_4$); the product, freed from borate, had $[\alpha]_D^{22}$ −16.8° in methanol. The compound was cleaved with 1 *N* sulphuric acid on a steam bath for 10 hours to yield ethylene glycol and glycerol in equimolar quantities as expected. Ethylene glycol gave the corresponding di-*p*-nitrobenzoate, m.p. and mixed m.p. 138–140° C, while the tri-*p*-nitrobenzoate of glycerol had m.p. and mixed m.p. 188–190° C.

Quantitative analysis.—A portion of the syrup obtained by partial hydrolysis of the polyol was separated chromatographically using solvent *c* for 10 hours and the ratio of components 1, 2, and 3 was determined colorimetrically using a periodate – chromotropic acid procedure (8) for the alcohols and the phenol – sulphuric acid method (11) for the xyloside. To the figure for glycerol obtained by the former method was added 1 mole of glycerol for each mole of xylose found. The ratio thus obtained for ethylene glycol: glycerol (total): xylose was 1:40:7. The same ratio was obtained when the polyol (10 mg) was heated at 100° C with sulphuric acid (1 *N*, 15 ml) for 8 hours, thus hydrolyzing the glycoside. When this ratio was determined gravimetrically from the weights of the three components isolated the ratio was 1:38:6.5.

Isolation and characterization of acidic components.—The acidic material previously adsorbed onto the anion exchange resin was eluted with alkali followed by regeneration of the pure acid by passage through cation exchange resin. The acidic solution was evaporated and the residue treated several times with methanol to affect removal of HCl. The residue was transferred to a tube fitted with a cold finger packed with solid CO_2, and the material was heated at 80–90° C *in vacuo* for about 2 hours to affect lactonization. The residue was dissolved in water, $NaBH_4$ added (400 mg), and the solution left overnight. After evaporation, borate was removed as described previously and an aqueous solution of the residue deionized. The final product (285 mg) was examined chromatographically. A major component corresponding to a synthetic sample (12) of 2-*O*-methyl-D-erythritol was observed. Also present in minor quantities were compounds corresponding to glycerol and erythritol. The residue (220 mg) was resolved using Whatman No. 3 MM paper and solvent *c*. *Glycerol*, 20.2 mg (0.22 mmole), was converted to the tri-*p*-nitrobenzoate, m.p. and mixed m.p. 187–190° C. *Erythritol*, 12.0 mg (0.098 mmole) was treated with *p*-nitrobenzoyl chloride to give the tetra-*p*-nitrobenzoate, m.p. and mixed m.p. 248–250° C. *2-O-Methyl-D-erythritol*, 161.5 mg (1.19 mmoles), $[\alpha]_D^{22}$ +28° in methanol (*c*, 3.2), was converted to the tri-*p*-nitrobenzoate, m.p. and mixed m.p. 218–220° C, $[\alpha]_D^{22}$ −17.2° in pyridine (*c*, 1.5). The molar ratio of erythritol:glycerol:2-*O*-methyl-D-erythritol was 1:2.2:12. Using this ratio, the 285 mg of mixed alcohols obtained by reduction of the acidic components correspond to 2.31 mmoles and assuming that this reduction is essentially quantitative there must have been 2.31 mmoles of acidic components. This figure taken in conjunction with those previously determined gives the ratio for ethylene glycol:glycerol:xylose:acids as 1:40:7:7.

B. Cherrywood Xylan

Periodate Oxidation

A quantity (946 mg) of xylan was dissolved in alkali (about 0.2 *N* NaOH), the solution acidified with acetic acid, and the volume adjusted to 100 ml. To the cooled (5° C) solution was added 0.5 *M* periodic acid (20 ml) and the oxidation was allowed to proceed at 5° C in the dark. Periodate consumption was determined periodically, and after 4 days, 0.845 mole of periodate had been consumed per mole of sugar with no further change upon longer standing. The periodate and iodate ions were removed from the solution by precipitation ($BaCO_3$) and the solution was treated with $NaBH_4$ (1.5 g) overnight. The solution was neutralized, evaporated, and the residue treated several times with methanol containing about 1% HCl to remove borate. The residue was dissolved in 0.2 *N* hydrochloric acid, left overnight, and then passed through cation and anion exchange resin columns in that order, and the effluent evaporated.

Characterization of neutral components.—The neutral residue was chromatographed and found to contain ethylene glycol (minor amount), glycerol, and a slower-migrating, non-reducing compound believed to be a xylosyl glycerol. The components were resolved using sheets of Whatman No. 3 MM paper and solvent *c*.

Component No. 1, ethylene glycol, 4.3 mg by weight, 4.0 mg (0.064 mmole) by chromotropic acid determination, was converted to the di-*p*-nitrobenzoate, m.p. and mixed m.p. 138–140° C.

Component No. 2, glycerol, 183 mg by weight, 180 mg (1.96 mmoles) by chromotropic acid determination, was transformed to the tri-*p*-nitrobenzoate, m.p. and mixed m.p. 188–190° C.

Component No. 3, 2′-*O*-glyceryl-β-D-xylopyranoside, 140 mg (0.625 mmole), $[\alpha]_D^{22}$ −30° in water (*c*, 2.8). The compound had an R_g of 1.34 in solvent *a*, 1.45 in solvent *b*, and showed an R_{xylose} of 0.76 in solvent *c*. A portion of the glycoside was characterized as described previously and gave identical results. The compound was boiled in *N* H_2SO_4 for about 10 hours after which the observed rotation had changed to positive. Chromatography of the hydrolyzate showed the presence of xylose and glycerol in equal molar proportions. *Xylose*, 34 mg (0.23 mmole), $[\alpha]_D^{22}$ +18.2 in water (*c*, 1.3), was crystallized from hot acetonitrile after addition of a few drops of ether, m.p. and mixed m.p. 143–145° C. *Glycerol*, 21 mg (0.23 mmole), was converted to the tri-*p*-nitrobenzoate, m.p. and mixed m.p. 188–190° C.

Isolation and characterization of acidic components.—The material derived from the uronic acids and believed to be mainly 3-*O*-methyl-D-erythronic acid was eluted with alkali from the anion exchange column and the effluent passed through a column of cation exchange resin. The residue left after evaporation was transferred to a tube fitted with a cold finger packed with solid CO_2 and the contents heated for about 3 hours at 85–90° C *in vacuo* to effect lactonization. The residue was dissolved in water, $NaBH_4$ (0.3 g) was added, and the reduction mixture was left overnight. After evaporation of the solvent and removal of borate by several treatments with methanolic hydrogen chloride, chromatography of the residue (90 mg) revealed the presence of components presumed to be glycerol and erythritol in addition to the major component co-chromatographing with a sample of 2-*O*-methyl-D-erythritol prepared previously (12). The mixture was resolved using Whatman No. 3 MM paper and solvent *c* as irrigant. *Glycerol*, 9.0 mg by weight, 8.8 mg (0.096 mmole) by chromotropic acid, was converted to the corresponding tri-*p*-nitrobenzoate,

m.p. and mixed m.p. 188–190° C. *Erythritol*, 7.3 mg by weight, 7.1 mg (0.058 mmole) by chromotropic acid, was converted to the tetra-*p*-nitrobenzoate, m.p. and mixed m.p. 248–250° C. *2-O-Methyl-*D*-erythritol*, 73.5 mg by weight, 72.8 mg (0.535 mmole) by chromotropic acid, $[\alpha]_D^{22}$ +29° in methanol (*c*, 1.46), gave upon reaction with *p*-nitrobenzoyl chloride the corresponding tri-*p*-nitrobenzoate, m.p. and mixed m.p. 219–220° C, $[\alpha]_D^{22}$ −17.5° in pyridine (*c*, 1.2).

The molar ratio of alcohols derived from the acidic fraction to 2′-*O*-glyceryl-*β*-D-xylopyranoside was approximately 1:1. The molar ratio of erythritol:glycerol:2-*O*-methyl-D-erythritol was 1:1.6:9, and hence the molar ratio of ethylene glycol:glycerol (including the glycerol in the xylosyl glycerol component):xylose:acids was approximately 1:42:10:10.

ACKNOWLEDGMENTS

The continued financial support of the National Research Council is gratefully acknowledged, and we are indebted to Mrs. A. Aldridge for the nitrogen analyses.

REFERENCES

1. G. O. Aspinall. *In* Advances in carbohydrate chemistry. Vol. 14. Academic Press, New York. 1959.
2. H. O. Bouveng and B. Lindberg. *In* Advances in carbohydrate chemistry. Vol. 15. Academic Press, New York. 1960.
3. I. J. Goldstein, G. W. Hay, B. A. Lewis, and F. Smith. Abstracts, 135th American Chemical Society Meeting, Boston. April 1959. p. 3D.
4. D. V. Myhre and F. Smith. Abstracts, 139th American Chemical Society Meeting, St. Louis. March 1961. p. 6D.
5. G. W. Hay and F. Smith. Abstracts, 139th American Chemical Society Meeting, St. Louis. March 1961. p. 6D.
6. G. G. S. Dutton and T. G. Murata. Can. J. Chem. **39**, 1995 (1961).
7. G. G. S. Dutton and S-A. McKelvey. Can. J. Chem. **39**, 2582 (1961).
8. A. M. Unrau and F. Smith. Chem. & Ind. (London), 330 (1957).
9. A. J. Charlson, P. A. J. Gorin, and A. S. Perlin. Can. J. Chem. **35**, 365 (1957).
10. M. L. Wolfrom and H. B. Wood. J. Am. Chem. Soc. **73**, 2933 (1951).
11. M. Dubois, J. K. Hamilton, K. A. Gilles, P. A. Rebers, and F. Smith. Anal. Chem. **28**, 350 (1956).
12. G. G. S. Dutton and A. M. Unrau. Unpublished results.

SYNTHÈSES D'ACIDES AMINÉS CYCLIQUES À PARTIR DE DÉRIVÉS DE L'ACIDE ADIPIQUE[1]

LISE NICOLE ET LOUIS BERLINGUET
Département de Biochimie, Faculté de Médecine, Université Laval, Québec, Qué.

Reçu le 10 juillet 1961

ABSTRACT

The Dieckmann reaction has been reinvestigated in view of obtaining alkyl-substituted cyclopentanones. Control of the reaction during alkylation now permits either the opening of the cyclopentane ring to give, without the isolation of intermediates, substituted adipic esters in excellent yields or normal substitution on the ring.

Methyl- and allyl-substituted cyclopentanones were obtained from the corresponding Dieckmann esters or from the substituted adipic acids. These ketones were transformed by the Strecker method into their corresponding spirohydantoins. In both cases, two diastereoisomers were isolated and studied.

1-Amino-2-methyl-cyclopentanecarboxylic acid and 1-amino-2-allyl-cyclopentanecarboxylic acid were prepared in good yields from the spirohydantoins and characterized.

INTRODUCTION

L'acide amino-1 cyclopentane-carboxylique possède des propriétés chimiothérapeutiques contre certains types de cancer. Récemment, on a démontré que cet acide aminé non-naturel peut réduire le développement de l'hépatome de Novikoff (1) et du carcinosarcome Walker 256 chez le rat (2*a*, 2*b*) ainsi que le sarcome 180, le carcinome 755 et la leucémie L-1210 chez la souris (3).

Dans le but d'atténuer la toxicité de cette substance, tout en conservant son activité, nous avons pensé en modifier la structure moléculaire en introduisant sur le noyau, en position 2, une chaîne aliphatique.

Pour obtenir ces acides aminés cycliques, nous avons employé la méthode de synthèse de Strecker et Bucherer en partant de la cyclopentanone substituée en position 2. Ces cétones cycliques alkylées peuvent être obtenues par substitution directe au moyen d'halogènes ou d'halogénures d'alkyles en présence de sodium dans l'ammoniac liquide (4). Dans ce cas, il y a presque toujours formation de dérivés bi-substitués lesquels sont souvent difficiles à éliminer. Nos essais biologiques demandant des produits d'une très grande pureté, nous avons préféré utiliser une méthode où il ne peut y avoir de bi-substitution.

L'éther de Dieckmann (II) est un ester β-cétonique qui permet une alkylation simple. Par décarboxylation subséquente, on obtient une cétone cyclique mono-substituée (VII). Cette synthèse de cétones cycliques substituées par l'intermédiaire de l'éther de Dieckmann a été utilisée par plusieurs auteurs, lesquels mentionnent inévitablement que les rendements sont très variables (5–11). Sans raison apparente, on obtient, lors de l'alkylation, soit l'éther de Dieckmann substitué (V), soit le di-ester de l'acide adipique substitué (III).

Cornubert et Borrel en ont étudié les conditions expérimentales (12) et plusieurs auteurs (10, 11, 13) ont avancé des mécanismes de réaction. On admet aujourd'hui (14) que la température, la grosseur de la chaîne alkylée substituée et surtout la concentration en éthoxyde de sodium sont responsables de l'ouverture des éthers de Dieckmann substitués en esters adipiques correspondants.

[1]*Présenté au congrès annuel de l'Institut de Chimie du Canada, tenu à Ottawa en juin 1960.*

Nous avons repris ces travaux dans le but de préparer les cétones cycliques substituées avec le moins possible d'intermédiaires et de contrôler lorsqu'il y a lieu l'ouverture des éthers de Dieckmann.

Lorsqu'on effectue la cyclisation de l'adipate di-éthylique par un équivalent de sodium dans le toluène, il y a élimination d'une molécule d'éthanol, qui peut se combiner avec le sodium résiduel pour donner l'ion éthoxyde $C_2H_5O^-$, responsable de l'ouverture du cycle. En éliminant par distillation partielle l'alcool ainsi formé avant de faire l'alkylation, on parvient à éviter cette ouverture du cycle. Ainsi on obtient avec 88% de rendement la carboxyéthyl-2 méthyl-2 cyclopentanone-1, (V, R = $-CH_3$) par méthylation directe de l'éther de Dieckmann.

Si, au contraire, on veut obtenir le di-ester de l'acide adipique substitué en α, on ajoute, après alkylation, un excès d'éthanol. On obtient sans isoler d'intermédiaires et avec des rendements respectifs de 89% et de 80% les di-esters méthyl-2 adipate de diéthyle (III, R = $-CH_3$) et allyl-2 adipate de diéthyle (III, R = $-CH_2-CH=CH_2$). L'absence ou la présence d'éthanol lors de l'alkylation est donc en grande partie responsable de la stabilité ou de l'ouverture du cycle.

L'obtention des cétones substituées en α présente une autre difficulté. La décarboxylation de l'éther de Dieckmann alkylé en position 2 par ébullition en milieu acide ou en présence de baryte ne se fait bien qui si la chaîne alkylée est inférieure à trois atomes de carbone. Le traitement de l'allyl-2 carboxyéthyl-2 cyclopentanone-1 (V, R = $-CH_2-CH=CH_2$) par l'acide sulfurique à chaud pendant 6 heures, ne permet d'obtenir que 30% de l'allyl-2 cyclopentanone-1. On récupère, inchangé, le produit de départ. Ceci est dû de toute évidence à un empêchement stérique, puisque dans les mêmes conditions la décarboxylation de l'allyl-5 carboxyéthyl-2 cyclopentanone-1 (IV, R = $-CH_2-CH=CH_2$) donne un rendement presque quantitatif. Cope *et al.* (15) rapportent des difficultés analogues lors de la décarboxylation de l'allyl-2 carboxyéthyl-2 cyclopentanone-1, de même que Cornubert et Borrel (12) pour la méthyl-5 propyl-2 carboxyéthyl-2 cyclopentanone-1. Lorsque cet empêchement stérique existe, il y a évidemment avantage à effectuer la décarboxylation sur la carboxyéthyl-2 cyclopentanone-1 substituée en position 5, laquelle s'obtient par cyclisation de l'ester di-éthylique de l'acide adipique substitué. Dans ces conditions l'allyl-2 adipate di-éthylique (III, R = $-CH_2-CH=CH_2$) donne avec un rendement de 66% l'éther de Dieckmann substitué en position 5 (IV, R = $-CH_2-CH=CH_2$) lequel se décarboxyle avec facilité pour donner quantitativement l'allyl-2 cyclopentanone-1 (VII, R = $-CH_2-CH=CH_2$).

On peut aussi cycliser directement, par chauffage, en présence de baryte, suivant la méthode habituelle, un acide adipique substitué. Le rendement est excellent dans le cas de la méthyl-2 cyclopentanone-1.

Dans les mêmes conditions, la cyclisation de l'acide allyl-2 adipique (VIII) donne de faibles rendements (18–50%) en allyl-2 cyclopentanone-1. Il se forme plutôt de la méthyl-4 (3-carboxypropyl)-2 butyrolactone (IX) qu'on obtient aussi avec un excellent rendement par chauffage de l'acide allyl-2 adipique en milieu chlorhydrique. Une lactonisation de même type a déjà été rapportée pour un produit analogue (16).

Par la méthode de Strecker, nous avons transformé les cyclopentanones substituées en spirohydantoïnes correspondantes. L'introduction d'un substituant sur le cycle cyclopentane crée deux centres asymétriques, donc deux paires de diastéréoisomères que nous avons réussi à séparer.

Il est curieux de constater que Granger et Techer (17) n'ont obtenu qu'un seul acétyl amino-1 cyano-1 méthyl-2 cyclopentane à partir de la méthyl-2 cyclopentanone-1.

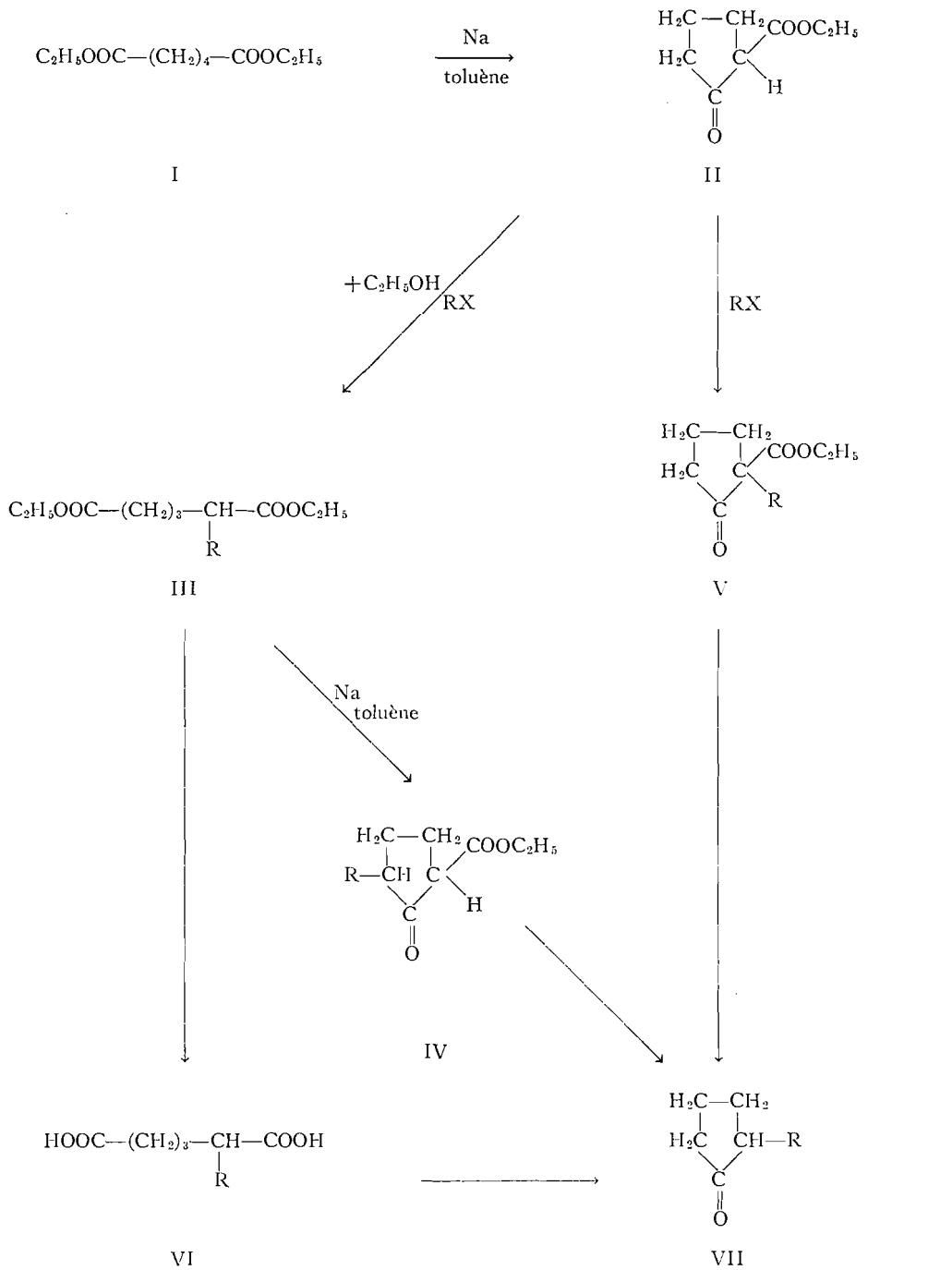

Par cristallisation fractionnée, nous avons pu isoler les deux diastéréoisomères de la méthyl-6 diazaspiro-1,3(4-4) nonane dione-2,4 ayant des points de fusion de 197–199° et 136–138° et les deux diastéréoisomères de l'allyl-6 diazaspiro-1,3(4-4) nonane dione-2,4 dont les points de fusion sont de 170° et 140°.

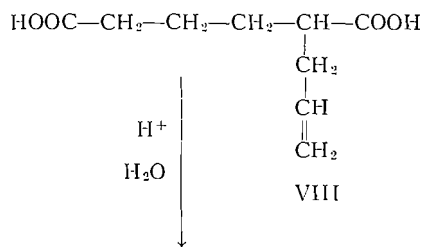

VIII

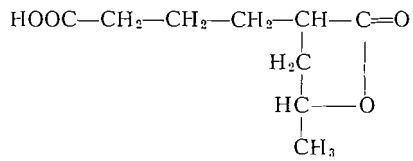

IX

Quantitativement, il y a toujours un rapport de 2 à 1 entre les deux formes isomériques, celle qui a le point de fusion le plus élevé et qui est la moins soluble étant la forme prédominante. L'autre isomère plus soluble est moins stable. C'est ainsi que nous avons traité l'isomère de la (méthyl-2′) cyclopentyl hydantoïne-5 ayant un point de fusion de 136°–138° par une solution de soude à 10% pendant quelques heures. Le produit obtenu fond à 185°, soit le point de fusion du mélange. Dans ces conditions, l'isomère ayant un point de fusion de 197° est stable.

Peu de cas d'isomérie semblable ont été rapportés (18) et à notre connaissance aucun diastéréoisomère de spirohydantoïne n'a été isolé.

Nous avons donc étudié ces produits plus en détail. Les spectres à infrarouge ne permettent pas de mettre en évidence la structure différente des deux diastéréoisomères. Par ailleurs, les spectres obtenus par résonance nucléaire magnétique* suggèrent que les deux produits ayant des points de fusion de 138–140° et 197–199° et dont l'analyse correspond à la formule de la (méthyl-2′) cyclopentyl hydantoïne-5, sont en fait deux diastéréoisomères.

La chromatographie sur papier des deux spirohydantoïnes méthylées suivie de révélation au chlore et à l'iode suivant la technique de Rydon et Smith (19) n'a cependant pas permis de séparer les deux isomères puisque les valeurs R_f ont toujours été identiques dans plusieurs solvants.

L'hydrolyse par la baryte à 160° de ces spirohydantoïnes substituées donne les acides aminés correspondants avec d'excellents rendements. Il est probable que ce traitement alcalin à chaud a pour effet de changer la configuration des deux carbones asymétriques, de telle sorte que même en partant d'un diastéréoisomère de l'hydantoïne on doit s'attendre à obtenir un mélange des deux diastéréoisomères de l'acide aminé correspondant.

Nous n'avons pu isoler d'isomères stériques après hydrolyse alcaline de l'une ou l'autre des (méthyl-2′) cyclopentyl hydantoïne-5. Les produits obtenus ont toujours eu des R_f identiques tant en chromatographie sur colonne de Dowex-50 que par chromatographie sur papier en utilisant différents solvants et même par chromatographie sur papier imbibé de résines échangeuses d'ions.

Varian Associates, 611 Hansen Way, Palo Alto, California, U.S.A.

Par hydrolyse des deux isomères de la (méthyl-2′) cyclopentyl hydantoïne-5 au moyen de l'acide iodhydrique en présence de phosphore rouge, on obtient parallèlement deux produits ayant une solubilité quelque peu différente dans l'eau.

Les picrates de ces deux acides aminés ainsi que les dérivés phényl-uréidos des deux acides correspondants ont dans chacun des cas des points de fusion identiques. Les sels de cuivre ont par ailleurs une solubilité différente dans l'eau et peuvent servir à séparer les diastéréoisomères.

Les deux spirohydantoïnes ayant des points de fusion de 137° et 198° donnent par hydrolyse acide deux acides amino-1 méthyl-2 cyclopentane-carboxyliques. Par traitement avec KOCN, ces deux isomères donnent des acides hydantoïques dont les points de fusion sont différents.

Ces acides hydantoïques redonnent les deux spirohydantoïnes de départ par chauffage en milieu acide. Les acides aminés isolés sont donc bien des isomères qui conservent leur configuration lors de la transformation en hydantoïnes.

L'hydrolyse alcaline de l'(allyl-2′) cyclopentyl hydantoïne-5 donne un acide aminé dont l'analyse correspond à l'acide amino-1 allyl-2 cyclopentane-carboxylique mais qui en réalité doit être un mélange des formes allo et thréo.

Cette hydantoïne est par ailleurs peu stable en milieu acide et on obtient par chromatographie des solutions d'hydrolyse, deux taches d'acides aminés dont une correspond à l'acide amino-1 allyl-2 cyclopentane-carboxylique, l'autre étant probablement un produit d'addition sur la double liaison lequel produit d'addition peut se cycliser ou non.

Ces acides amino-1 cycloalkyl-carboxyliques substitués sont solubles dans l'eau et partiellement dans l'éthanol. Ils sont tout à fait insolubles dans l'acétone d'où ils précipitent sous forme de gels volumineux. Ils se volatilisent sur une plaque chaude pour donner une vapeur se solidifiant rapidement.

Des travaux biologiques avec ces acides aminés sont en cours et seront publiés sous peu.

PARTIE EXPÉRIMENTALE

Adipate de diéthyle (I)

On prépare l'adipate de diéthyle à partir de 400 g (2.74 mole) d'acide adipique, en présence d'acide sulfurique (120 ml), d'éthanol à 95% (600 ml) et de benzène (2000 ml) suivant la méthode de Van Ryssel-berghe (8). Rendement 477 g (86%). P.é. 130° à 15 mm, n_D^{20} 1.427 (lit. p.é. 138° à 20 mm, n_D^{20} 1.427) (8).

Carboxyéthyl-2 cyclopentanone-1 (éther de Dieckmann) (II)

On fait la cyclisation de l'adipate de diéthyle par le sodium dans le toluène suivant la méthode décrite par Cornubert et Borrel (12). À partir de 200 g (0.988 mole) d'adipate de diéthyle, on obtient 110 g d'éther de Dieckmann. Rendement 71%. P.é. 110–115° à 19 mm, n_D^{20} 1.454 (lit. p.é. 114° à 20 mm, n_D^{20} 1.452) (8).

Carboxyéthyl-2 méthyl-2 cyclopentanone-1 (V) (R = —CH_3)

(a) À partir de l'éther de Dieckmann

On fait la méthylation de l'éther de Dieckmann selon la méthode de Cornubert et Borrel (12) par condensation de l'iodure de méthyle avec le dérivé sodé de la carboxyéthyl-2 cyclopentanone-1. Tel que mentionné par Cornubert et Borrel, cette réaction doit être effectuée à très basse température et en présence d'une quantité rigoureusement exacte de sodium. Autrement, on s'expose à obtenir l'ester méthyl-2 adipate de diéthyle qui se forme par ouverture du cycle cyclopentanique.

Même en prenant toutes ces précautions, il arrive, comme l'ont mentionné plusieurs auteurs, que ce soit le di-ester substitué ouvert qu'on obtienne.

À partir de 60 g (0.384 mole) d'éther de Dieckmann, on obtient 57.5 g de carboxyéthyl-2 méthyl-2 cyclopentanone-1. Rendement 88%. P.é. 104° à 12 mm, n_D^{20} 1.440 (lit. p.é. 105° à 13 mm, n_D^{20} 1.4464) (5).

(b) Directement à partir de l'adipate de diéthyle

On chauffe dans un ballon muni d'un réfrigérant et d'un agitateur 14.0 g (0.61 mole) de sodium dans 725 ml de toluène dé-thiophéné. Lorsque le sodium est fondu, on agite vigoureusement pour fractionner le sodium en fines particules. On ajoute alors l'adipate de diéthyle (101 g, 0.50 mole) et on chauffe à reflux

pendant 2 heures. Le sel de sodium de la carboxyéthyl-2 cyclopentanone-1 se présente sous forme de masse spongieuse. On distille alors pour recueillir 125 ml de toluène et d'éthanol formé lors de la cyclisation. On ajoute 75 ml de toluène dé-thiophéné au mélange et on continue la distillation jusqu'à ce que le volume total du distillat atteigne 200 ml.

On refroidit alors dans la glace et on ajoute en une seule fraction 160 g (1.13 mole) d'iodure de méthyle. On chauffe à reflux pendant 16 heures. On ajoute alors de l'eau pour dissoudre l'iodure de sodium. On sépare le toluène, on le sèche et on recueille par distillation sous vide la carboxyéthyl-2 méthyl-2 cyclopentanone-1. Rendement total à partir de l'adipate de diéthyle 69.9 g (82.2%) passant à 100–105° sous 14 mm, n_D^{20} 1.444.

Carboxyéthyl-5 méthyl-2 cyclopentanone-1 (IV) (R = —CH_3)

On cyclise par la méthode de Cornubert et Borrel (12) le méthyl-2 adipate de diéthyle (137.0 g, 0.63 mole) par le sodium dans le toluène. Rendement en carboxyéthyl-5 méthyl-2 cyclopentanone-1 52.0 g (48.3%). P.é. 120–125° sous 25 mm, n_D^{20} 1.450 (lit. p.é. 123–124° sous 31 mm) (7).

Méthyl-2 adipate de diéthyle (III) (R = —CH_3)

En s'inspirant de la méthode de synthèse de l'éther de Dieckmann, décrite par Cornubert et Borrel (12), on place dans un ballon muni d'un réfrigérant et d'un agitateur 15.7 g de sodium dans 600 ml de toluène. Quand le toluène bout, on agite vigoureusement le ballon afin de diviser finement le sodium fondu. On ramène la température du toluène à 60° et on ajoute 112.2 g (0.55 mole) d'adipate de diéthyle. Aux environs de 80°, la réaction devient vive. Lorsqu'elle est entièrement terminée, on prolonge le chauffage encore 1 heure. On ajoute alors l'iodure de méthyle en excès (118.1 g, 0.82 mole). On laisse agiter à reflux, pendant 16 heures, après avoir ajouté 50 ml d'éthanol pour favoriser l'ouverture du cycle. On refroidit et on dissout l'iodure de sodium dans l'eau. On décante et on lave la partie aqueuse avec du toluène que l'on ajoute à la partie toluénique. On distille le toluène à la pression atmosphérique et on distille le résidu dans le vide. Rendement 105.8 g (89%). P.é. 140–145° à 33 mm, n_D^{20} 1.431 (lit. p.é. 141° à 26 mm) (7).

Acide méthyl-2 adipique (VI) (R = —CH_3)

(a) Par hydrolyse alcaline

On fait bouillir à reflux, pendant 16 heures, un mélange de méthyl-2 adipate de diéthyle (140.9 g, 0.65 mole) et d'hydroxyde de potassium (98.0 g, 1.47 mole) dans 1 litre d'éthanol à 95%. On dissout alors les sels par addition d'eau, et on évapore à sec. On reprend par de l'eau, on acidifie avec HCl concentré. On extrait la solution aqueuse plusieurs fois à l'éther qu'on sèche et qu'on évapore. Il reste 82.5 g (79.5%) d'une huile qui cristallise lentement.

(b) Par hydrolyse acide

On fait bouillir à reflux, pendant 16 heures, le méthyl-2 adipate de diéthyle (60 g, 0.278 mole) avec 100 ml d'acide chlorhydrique et 100 ml d'acide acétique glacial. On évapore alors à sec et on reprend le résidu par du benzène chaud. On cristallise l'acide par addition d'éther de pétrole et on porte au froid. Rendement 37.5 g (84.3%). P.f. 57°* (lit. 61°) (20).

Méthyle-2 cyclopentanone-1 (VII) (R = —CH_3)

(a) À partir de la carboxyéthyl-2 méthyl-2 cyclopentanone-1

On effectue la décarboxylation de la carboxyéthyl-2 méthyl-2 cyclopentanone-1 au moyen de l'acide chlorhydrique dilué dans les proportions 1:3, en chauffant à reflux durant 16 heures avec une bonne agitation. On extrait le produit à l'éther et on le distille. À partir de 56.7 g (0.333 mole) de carboxyéthyl-2 méthyl-2 cyclopentanone-1, on obtient 20.7 g de méthyl-2 cyclopentanone-1. Rendement 63%. P.é. 138–140° à 760 mm, n_D^{20} 1.433 (lit. p.é. 139° à 760 mm, n_D^{20} 1.4348) (21). La cétone donne des cristaux orangés avec la dinitro-2,4 phénylhydrazine, qui fondent après recristallisation du méthanol à 160°.

(b) À partir de la carboxyéthyl-5 méthyl-2 cyclopentanone-1

On chauffe avec une bonne agitation la carboxyéthyl-5 méthyl-2 cyclopentanone-1 (52.0 g, 0.30 mole) en présence de 100 ml d'acide sulfurique à 10%. Après 4 heures, on refroidit et on extrait plusieurs fois à l'éther. On fait une distillation de la solution éthérée. La méthyl-2 cyclopentanone-1 passe à 135–138° à 760 mm. Rendement 18.0 g (61.5%).

(c) À partir de l'acide méthyl-2 adipique

En utilisant la méthode décrite pour la cyclopentanone (22), on cyclise à 290° l'acide méthyl-2 adipique (33.5 g, 0.22 mole) en présence d'hydroxyde de baryum (2.0 g). On recueille 19.1 g de méthyl-2 cyclopentanone-1, n_D^{20} 1.435. Rendement 93%.

Méthyl-6 diazaspiro-1,3 (4-4) nonane dione-2,4 (X) (R = —CH_3) (méthyl-2') cyclopentyl hydantoïne-5

À la température de la chambre, on fait réagir la méthyl-2 cyclopentanone-1 (53.5 g, 0.546 mole) avec du cyanure de potassium (65.1 g, 1.0 mole) dissous dans un mélange contenant 150 ml de méthanol, 150 ml d'eau, du chlorure d'ammonium (53.4 g, 1.0 mole) et un peu de résine IR 4-B (23). On agite mécaniquement

**Les points de fusion ne sont pas corrigés.*

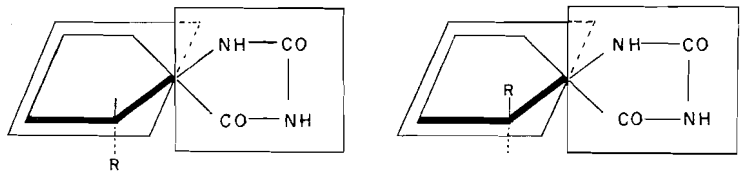

X

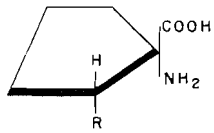

XI R = $-CH_3$

XII R = $-CH_2-CH=CH_2$

durant 3 heures. On ajoute alors au mélange un excès de carbonate d'ammonium et l'on chauffe durant 16 heures à 60° sur un bain-marie. On évapore la solution de moitié pour chasser l'alcool. On filtre la résine, on ajuste le pH à 5–6 et on refroidit. Une première précipitation donne 71.0 g de cristaux, p.f. 168°. En évaporant de nouveau, on obtient une seconde précipitation de cristaux, 11.0 g, p.f. 145°. Rendement brut total 82.0 g (89%).

Le premier précipité (71.0 g) est formé du mélange des deux diastéréoisomères. On peut les séparer par recristallisation fractionnée dans l'eau. Le plus insoluble cristallise facilement. Après filtration, on obtient 41.5 g d'un produit qui commence à sublimer à 130° et qui fond complètement à 197–199°. Anal. Calc. pour $C_8H_{12}N_2O_2$: N, 16.65%. Trouvé: N, 16.82%.

On recristallise de l'eau les 11.0 g de cristaux obtenus lors de la seconde précipitation. Si, à cette solution, on ajoute les eaux-mères du début, on obtient, par concentrations et filtrations successives, un total de 29.5 g du second diastéréoisomère fondant à 136–138°. Anal. Calc. pour $C_8H_{12}N_2O_2$: N, 16.65%. Trouvé: N, 16.82%.

Le rendement total des deux diastéréoisomères est 71.0 g (77%) dont 41.5 g ont un point de fusion de 197–199° et 29.5 g ont un point de fusion de 136–138°.

Les rendements habituels en hydantoïnes varient entre 70 et 85%, mais on a toujours la prédominance de l'isomère fondant à 197° sur l'isomère fondant à 138° dans les proportions de 2 à 1.

Propriétés des diastéréoisomères de la méthyl-6 diazaspiro-1,3 (4-4) nonane dione-2,4

Les deux diastéréoisomères des spirohydantoïnes sont insolubles dans l'éther, l'acétate d'éthyle et le benzène. Ils sont totalement solubles dans l'acétone et partiellement solubles à chaud dans l'eau et dans l'éthanol.

On peut les séparer soit par cristallisation fractionnée de l'eau soit en les dissolvant à chaud dans l'acétone et en ajoutant de l'éther de pétrole jusqu'à turbidité. Le diastéréoisomère le plus insoluble précipite le premier. Son point de fusion est 197–198°. Cet isomère est beaucoup plus stable que l'autre isomère fondant à 138°. Un chauffage de 2 ou 3 heures en présence de soude à 10% ou en tube scellé avec HBr 48% ne parvient pas à le transformer. Tout au plus peut-on déceler une trace de l'acide aminé correspondant par chromatographie sur papier, lequel provient de l'ouverture de l'anneau de l'hydantoïne. Par recristallisation de l'eau, on recueille l'hydantoïne inchangée ayant un point de fusion de 198°.

L'isomère fondant à 138° est par contre moins stable. On peut le transformer en l'autre diastéréoisomère par chauffage prolongé en milieu alcalin ou même en milieu très fortement acide. C'est ainsi que l'on dissout 2.92 g de l'hydantoïne fondant à 138° dans 6 ml de NaOH à 10% et 18 ml d'eau distillée. On laisse sur un bain-marie bouillant toute la nuit. Le lendemain, on acidifie avec HCl concentré et en portant au froid, l'hydantoïne cristallise en gros bâtonnets (1.42 g) qui commencent à sublimer vers 140° mais ne fondent complètement qu'à 182–188°.

Si on traite l'hydantoïne ayant un point de fusion de 138° en tube scellé pendant 2 ou 3 heures avec HBr 48%, on parvient à ouvrir partiellement l'anneau de l'hydantoïne et on peut déceler l'acide aminé correspondant par chromatographie sur papier. On recupère cependant une certaine quantité d'hydantoïne qui maintenant a un point de fusion de 185–190°.

Par ailleurs après une ébullition de 17 heures en présence d'acide chlorhydrique concentré, ou de quelques minutes en présence de soude à 10%, on récupère dans chaque cas les deux hydantoïnes inchangées.

Acide amino-1 méthyl-2 cyclopentane-carboxylique (XI) (R = —CH_3)

(a) Hydrolyse alcaline

Dans un autoclave, on hydrolyse 14.3 g (0.085 mole) de l'hydantoïne ayant un point de fusion de 197° avec 40 g (0.127 mole) d'hydroxyde de baryum dissous dans 120 ml d'eau bouillante. On porte la température à 165° durant une $\frac{1}{2}$ heure. On laisse le mélange refroidir, puis on ajoute 80 g (1.42 mole) de carbonate d'ammonium.

On concentre la solution par ébullition et on filtre le carbonate de baryum. Après avoir évaporé le filtrat sous pression réduite, on reprend le résidu par l'eau bouillante. Par cristallisations successives de l'eau, on obtient l'acide aminé, lequel cristallise avec une molécule d'eau. Anal. Calc. pour $C_7H_{13}NO_2.H_2O$: N, 8.70%. Trouvé: N, 8.79%. Rendement 10.9 g (90%). On sèche le produit à l'étuve à 110° pendant quelques heures. Le produit se décompose en brunissant vers 290°. Anal. Calc. pour $C_7H_{13}NO_2$: N, 9.78%. Trouvé: N, 9.94%.

On procède de la façon décrite plus haut pour hydrolyser l'autre isomère de l'hydantoïne ayant un point de fusion de 138°. En partant de 9.6 g (0.057 mole) d'hydantoïne, on obtient après séchage à l'étuve 5 g d'acide aminé. Rendement 61%. L'acide aminé n'a pas de point de fusion et commence à se décomposer à 290°. Anal. Calc. pour $C_7H_{13}NO_2$: N, 9.78%. Trouvé: N, 9.87%. Il cristallise aussi avec une molécule d'eau. Anal. Calc. pour $C_7H_{13}NO_2$: N, 8.70%. Trouvé: N, 8.62%.

(b) Hydrolyse acide

Dans un ballon muni d'un réfrigérant, on place 11.0 g (0.065 mole) de l'isomère fondant à 198° de la méthyl-6 diazaspiro-1,3(4-4) nonane dione-2,4, 125 ml d'acide iodhydrique 57% et 1 g de phosphore rouge amorphe. On chauffe à reflux pendant au moins 48 heures. En diminuant le temps d'hydrolyse on s'expose à retrouver des quantités importantes d'hydantoïne de départ. Après avoir refroidi la solution, on filtre le phosphore et on évapore à sec sous vide.

On dissout le résidu dans l'eau bouillante et on verse cette solution sur un excès de AgOH fraîchement préparé. Après avoir agité pendant $\frac{3}{4}$ heure, on chauffe à ébullition et on filtre les sels d'argent. On sature le filtrat de sulfure d'hydrogène. On filtre le sulfure d'argent et on rinse à l'eau chaude. Après avoir vérifié que le filtrat ne contient plus d'ions d'argent ou d'iode, on le décolore avec du noir animal et on évapore à sec sous vide. On reprend le résidu dans un minimum d'eau et on porte au froid. On évapore à sec et on reprend par un minimum d'eau bouillante. L'acide aminé précipite au froid. On concentre les eaux-mères pour obtenir d'autres cristaux. Par addition subséquente d'éthanol et d'acétone, on récupère les dernières traces de l'acide aminé. Rendement total en acide aminé 8.41 g (90%). L'acide aminé sublime à partir de 160° et se décompose en brunissant vers 290°. Anal. Calc. pour $C_7H_{13}NO_2$: N, 9.78%. Trouvé: N, 9.73%.

On procède de la façon décrite plus haut pour hydrolyser l'autre isomère de l'hydantoïne ayant un point de fusion de 138°. En partant de 18.2 g (0.109 mole) d'hydantoïne, on obtient 14.5 g d'acide aminé. Rendement 96%. L'acide aminé sublime vers 220° et se décompose à 297–299°. Anal. Calc. pour $C_7H_{13}NO_2$: N, 9.78%. Trouvé: N, 9.94%.

Propriétés de l'acide amino-1 méthyl-2 cyclopentane-carboxylique

L'acide aminé n'est presque pas soluble dans l'éthanol bouillant. Il est insoluble dans la plupart des solvants organiques. Il est plus soluble dans l'eau, à froid, et on peut le recristalliser assez facilement. Il est toutefois partiellement soluble dans un mélange eau–éthanol.

On peut le précipiter très facilement des solutions aqueuses ou alcooliques par addition d'acétone. Il se forme alors un volumineux gel qui se filtre très aisément.

Lorsque l'acide aminé solide est projeté sur une plaque chauffante, maintenue à 300°, il se volatilise en une sorte de sublimé qui se solidifie immédiatement au contact de l'air.

Picrates de l'acide amino-1 méthyl-2 cyclopentane-carboxylique

Les divers échantillons de l'acide aminé obtenus tant par hydrolyse acide que par hydrolyse alcaline des deux diastéréoisomères ont toujours donné des picrates dont le point de fusion est 215–216°. Ces picrates recristallisent de l'eau et ils sont assez solubles dans l'éther. Calculé pour $C_{13}H_{16}N_4O_9$: N, 15.07%. Trouvé: N, 14.84%.

Sels de cuivre de l'acide amino-1 méthyl-2 cyclopentane-carboxylique

On fait bouillir pendant 2 heures une solution aqueuse de l'acide amino-1 méthyl-2 cyclopentane-carboxylique avec un excès de carbonate de cuivre. On filtre à chaud et on recueille après avoir refroidi le sel de cuivre de l'acide aminé.

Les deux diastéréoisomères donnent des cristaux d'un bleu violet en forme d'aiguilles. Les deux sels de cuivre ont des solubilités différentes dans l'eau et par recristallisation fractionnée on peut séparer les deux diastéréoisomères. Ils sont aussi partiellement solubles dans l'éthanol et le méthanol à chaud.

Les sels de cuivre cristallisent avec une molécule d'eau. Calculé pour $C_{14}H_{24}O_4N_2Cu.H_2O$: N, 7.66%. Trouvé: N, 7.64%. Après séchage à l'étuve on obtient le sel anhydre. Calculé pour $C_{14}H_{24}O_4N_2Cu$: N, 8.06%. Trouvé: N, 7.98%.

Chlorhydrate de l'ester éthylique de l'acide amino-1 méthyl-2 cyclopentane-carboxylique

On suspend 2.80 g (0.019 mole) d'acide amino-1 méthyl-2 cyclopentane-carboxylique dans 100 ml d'éthanol bouillant dans lequel barbote HCl gazeux. Après 2 heures d'ébullition, on évapore à sec et on recristallise de l'éthanol par addition d'éther. Rendement 2.7 g (66%). P.f. 200°. Anal. Calc. pour $C_9H_{18}NO_2Cl$: N, 6.76%. Trouvé: N, 6.86%.

Acide uréido-1 méthyl-2 cyclopentane-carboxylique

On chauffe au bain-marie pendant 2 heures, une solution contenant 2.86 g (0.02 mole) d'acide amino-1 cyclopentane-carboxylique et 1.62 g (0.02 mole) de cyanate de potassium dans 40 ml d'eau. On refroidit dans la glace et on acidifie avec HCl concentré. On filtre les cristaux blancs et on les sèche. Rendement 2.86 g (77%). P.f. 205°. Anal. Calc. pour $C_8H_{14}N_2O_3$: N, 15.08%. Trouvé: N, 14.70%. Le poids moléculaire trouvé par neutralisation avec NaOH 0.1 *N* est 194. Calculé: 186. Les analyses ont été faites sur les cristaux séchés à l'étuve, le produit ayant tendance à cristalliser avec des molécules d'eau.

Les deux diastéréoisomères de l'acide amino-1 cyclopentane-carboxylique se comportent de la même façon et donnent avec le même rendement le produit décrit plus haut.

Cyclisation en spirohydantoïnes

On chauffe à reflux pendant 2 heures un mélange de 10 ml d'acide chlorhydrique concentré et 40 ml d'eau dans lequel est dissous 1.0 g d'acide uréido-1 méthyl-2 cyclopentane-carboxylique obtenu à partir de l'isomère le moins soluble de l'acide amino-1 méthyl-2 cyclopentane-carboxylique. On évapore à sec et on reprend le résidu dans l'acétone chaud. Par addition d'éther de pétrole, la méthyl-6 diazaspiro-1,3(4-4) nonane dione-2,4 cristallise. Rendement 0.70 g (79%). P.f. 195°.

Dans les mêmes conditions, l'acide uréido-1 méthyl-2 cyclopentane-carboxylique, obtenu à partir de l'isomère le plus soluble de l'acide amino-1 méthyl-2 cyclopentane-carboxylique, donne l'autre isomère de la spirohydantoïne dont le point de fusion est 140°.

Ces transformations indiquent bien que les deux diastéréoisomères de la spirohydantoïne donnent par hydrolyse acide les diastéréoisomères des acides aminés correspondants. Les acides aminés peuvent être transformés de nouveau par l'intermédiaire des acides uréido correspondants en diastéréoisomères de la spirohydantoïne de départ. Toutes ces transformations se font donc sans perte de configuration pour le deuxième carbone asymétrique.

Acide N-phényluréido-1 méthyl-2 cyclopentane-carboxylique

Dans une fiole conique, on dissout 2.86 g (0.02 mole) d'acide amino-1 méthyl-2 cyclopentane-carboxylique le plus insoluble dans un minimum d'eau. On ajoute ensuite de la soude (0.80 g, 0.02 mole) et on agite la solution. En une seule portion, on ajoute alors l'isocyanate de phényle (0.38 g, 0.02 mole). On agite vigoureusement pendant 15 minutes. Puis on filtre la diphényl urée qui a pu se former et on verse le filtrat sur la glace. L'addition d'acide chlorhydrique concentré précipite l'acide phényluréido-1 méthyl-2 cyclopentane-carboxylique. On filtre le précipité et on recristallise dans un mélange eau-éthanol. Rendement 3.45 g (66%). P.f. 145°. Anal. Calc. pour $C_{14}H_{18}N_2O_3$: N, 10.68%. Trouvé: N, 10.40%.

Méthyl-6 phényl-3 diazaspiro-1,3 (4-4) nonane dione-2,4

On cyclise par chauffage dans 50 ml d'acide chlorhydrique dilué pendant quelques heures, 1.0 g d'acide N-phényluréido-1 méthyl-2 cyclopentane-carboxylique obtenu plus haut (0.0038 mole). En refroidissant, les cristaux de la spirohydantoïne substituée apparaissent. On filtre et on sèche. Rendement 0.8 g (86%). On recristallise de l'eau et de l'éthanol. P.f. 148°. Anal. Calc. pour $C_{14}H_{16}N_2O_2$: N, 11.49%. Trouvé: N, 11.52%.

Essais de séparation des diastéréoisomères

Les acides amino-1 méthyl-2 cyclopentane-carboxyliques, obtenus à partir de l'une ou l'autre des deux formes isomériques des hydantoïnes soit par hydrolyse alcaline soit par hydrolyse acide, ont des propriétés chimiques très voisines. Par recristallisation fractionnée de l'eau, on parvient toutefois à isoler deux fractions dont les solubilités dans l'eau sont assez différentes.

Dans le but de mieux séparer ces diastéréoisomères, nous avons utilisé la chromatographie sur papier dans plusieurs systèmes de solvants. Tel que l'indique le Tableau I, les divers échantillons de l'acide amino-1 méthyl-2 cyclopentane-carboxylique migrent tous avec des valeurs R_f identiques.

N'ayant pu séparer les deux diastéréoisomères par chromatographie sur papier, nous avons utilisé des feuilles de cellulose imbibées de résines échangeuses d'ions.* Plusieurs auteurs ont utilisé avec profit ces feuilles de cellulose pour séparer des acides aminés dont les solubilités sont très voisines dans les solvants utilisés pour la chromatographie classique (24–27). Nous avons surtout utilisé le type WA-2, faiblement acide. Les autres types SA et SB, acide fort et base forte, donnent des mauvaises migrations. Comme l'indique le Tableau II, les diverses valeurs R_f des échantillons d'acide aminé sont très voisines, pour tous les solvants employés. Même dans ces conditions, il a été impossible de séparer les diastéréoisomères attendus.

Nous avons finalement essayé de faire la séparation par adsorption sur une colonne de résine Dowex-50 et élution subséquente avec diverses solutions. Les acides amino-1 méthyl-2 cyclopentane-carboxyliques

**Echantillons gracieusement fournis par Reeve Angel, 9 Bridewell Place, Clifton, N.J.*

TABLEAU I

Acide amino-1 méthyl-2 cyclopentane-carboxylique

Systèmes de solvants	Valeurs R_f (a)	(b)	(c)	(d)
Pyridine–eau (80:20)	0.72	0.72	0.72	0.72
Phénol–eau (92:8)	0.91	0.91	0.91	0.91
Pyridine–CH_3COOH–eau (50:35:15)	0.92	0.92	0.92	0.92
Butanol–éthylméthylcétone–eau–diéthylamine (40:40:20:4)	0.80	0.80	0.80	0.80

(*a*) Obtenu par hydrolyse alcaline de l'hydantoïne fondant à 197°.
(*b*) Obtenu par hydrolyse alcaline de l'hydantoïne fondant à 138°.
(*c*) Obtenu par hydrolyse acide de l'hydantoïne fondant à 197°.
(*d*) Obtenu par hydrolyse acide de l'hydantoïne fondant à 138°.

TABLEAU II

Chromatographie de l'acide amino-1 méthyl-2 cyclopentane carboxylique sur papier de type faiblement acide WA-2

Systèmes de solvants	Valeurs R_f (a)	(b)	(c)	(d)
Acide acétique – eau (90:10)	0.72	0.71	0.73	0.72
Eau	0.69	0.68	0.72	0.72
Tampon véronal (0.05 *M*, pH 8.6)	0.70	0.68	0.70	0.70
Acide acétique – pyridine (pH 6.4)	0.75	0.75	—	—
Phénol–eau (92:8)	0.58	0.60	—	—
Pyridine–eau (80:20)	0.81	0.81	—	—

(*a*) Obtenu par hydrolyse alcaline de l'hydantoïne fondant à 197°.
(*b*) Obtenu par hydrolyse alcaline de l'hydantoïne fondant à 138°.
(*c*) Obtenu par hydrolyse acide de l'hydantoïne fondant à 197°.
(*d*) Obtenu par hydrolyse acide de l'hydantoïne fondant à 138°.

sont fortement adsorbés sur la résine. Ils ne sont élués qu'à l'aide d'une solution d'ammoniaque à 10%. Nous n'avons pu, ici encore, mettre en évidence la présence des deux diastéréoisomères.

La migration de cet acide aminé cyclique lorsqu'on la compare à celle de d'autres acides aminés comme la lysine, la glycine et l'acide glutamique indique que l'acide amino-1 méthyl-2 cyclopentane-carboxylique est relativement basique. Le comportement de cet acide aminé sur la colonne de Dowex-50 confirme le même fait. Tel que démontré par Tillson et Noll (28) pour l'acide amino-1 cyclopentane-carboxylique, l'acide amino-1 méthyl-2 cyclopentane-carboxylique ne peut être titré par un alcali en présence de formol, suivant la méthode classique de Sörensen.

Spectres d'absorption dans l'infrarouge

Les spectres d'absorption dans l'infrarouge ont été pris avec le spectrophotomètre Beckman, modèle IR-4. La comparaison entre les spectres des deux isomères, soit de la (méthyl-2′) cyclopentyl hydantoïne-5, soit de l'(allyl-2′) cyclopentyl hydantoïne-5, ne permet pas de conclure à la présence de deux diastéréoisomères. Les bandes d'absorption sont à toute fin pratique presque identiques.

Spectres magnétiques de résonance nucléaire

Les spectres des deux échantillons de la (méthyl-2′) cyclopentyl hydantoïne-5 ont été pris dans une solution de chloroforme deutéré avec une trace de tétraméthylsilane comme référence interne. La position des bandes est mesurée en cycles par seconde. On voit dans la Figure 1 que les deux bandes situées de chaque côté du spectre du chloroforme à 436 c.p.s. sont dues aux groupes NH. Le doublet que l'on observe à 54 c.p.s. est dû au radical méthyle. Cette bande est séparée en deux par suite de la vibration du proton voisin. Les autres bandes qui forment un complexe proviennent des sept protons du cycle à cinq carbones. Le spectre correspond donc à la structure proposée.

Le spectre de l'autre isomère montre lui aussi deux bandes dues aux groupes NH. Le triplet observé à 61 c.p.s. est en réalité un doublet dont la ligne gauche est superposée sur la ligne droite de l'autre. On retrouve ici aussi le complexe provenant des sept protons du cycle cyclopentanique.

FIG. 1. Spectre magnétique de résonance nucléaire des deux isomères de la méthyl-6 diazaspiro-1,3 (4-4) nonane dione-2,4. Échantillon I (p.f. 197°); échantillon II (p.f. 138°). Les spectres ont été pris dans une solution de chloroforme deutéré avec une trace de tétraméthylsilane comme référence interne. Le taux de balayage est X10-36/300 et la vitesse est de 3 pouces/minute. Le noyau est H′ et la fréquence 60 Mc.

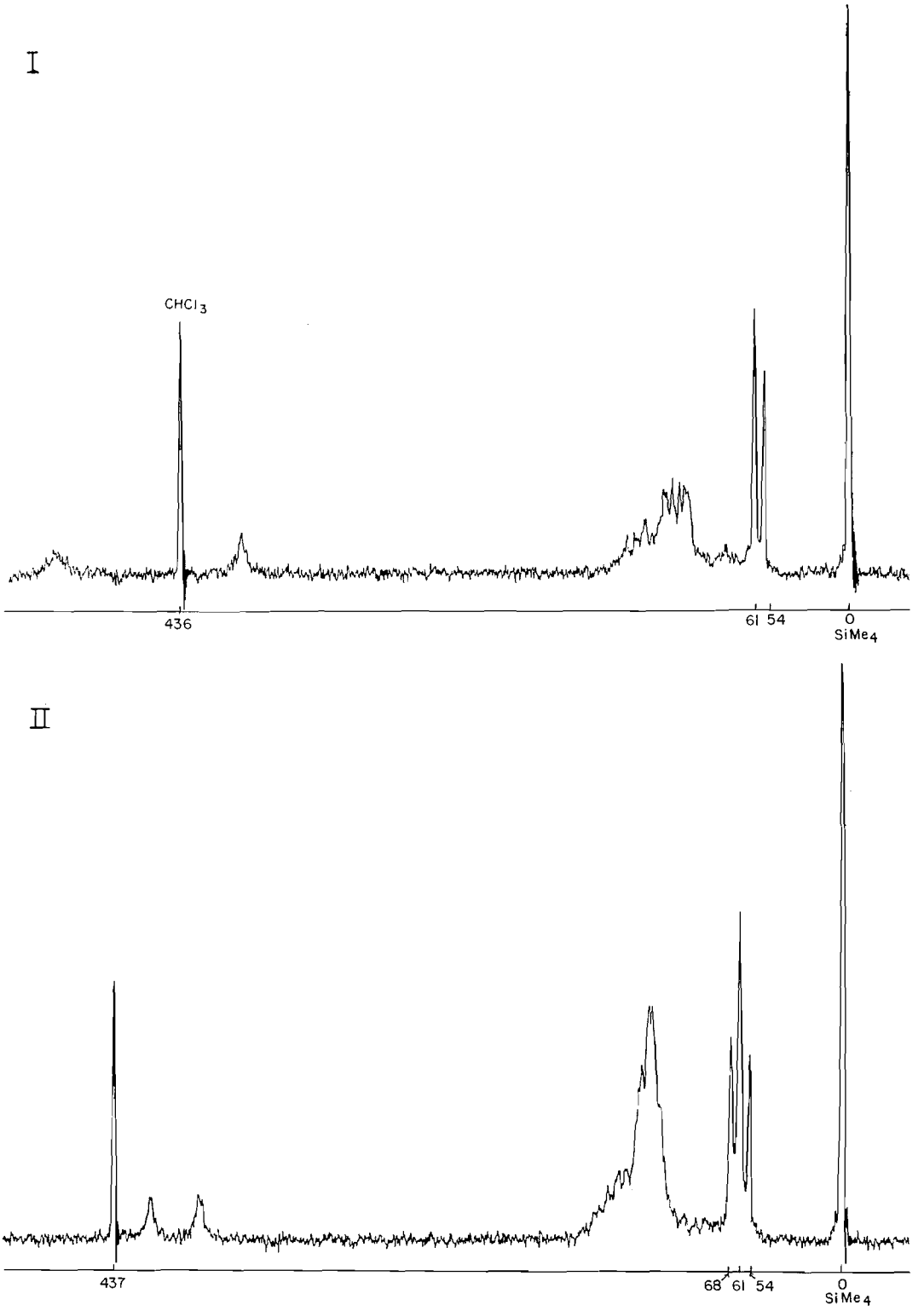

Il semble aussi d'après les spectres que l'isomère dont le point de fusion est 138° ne soit pas pur et qu'il contienne un peu de l'autre isomère.

Toutefois la comparaison des deux spectres indique bien qu'il s'agit là de deux diastéréoisomères, ne différant que par l'orientation du radical méthyle par rapport au noyau hétérocyclique.

Allyl-2 adipate de diéthyle (III) (R = —CH_2—CH=CH_2)

On passe directement de l'adipate de diéthyle non substitué au di-ester substitué en alpha, sans isoler d'intermédiaires.

On chauffe à reflux avec une bonne agitation, l'adipate de diéthyle (303 g, 1.5 mole) dans 1500 ml de toluène sec, en présence de 42.0 g (1.83 mole) de sodium. Après 3 heures d'ébullition, le sel de sodium de l'éther de Dieckmann présente l'aspect d'une masse volumineuse et spongieuse. On ajoute alors 242 g (2.0 moles) de bromure d'allyle en une seule portion et on chauffe à reflux pendant 5 heures.

On ajoute un peu d'eau pour extraire les sels inorganiques et on ramène le pH à 7.0 avec quelques gouttes d'acide acétique. Après avoir séché la couche de toluène, on distille sous vide le toluène et l'ester adipique substitué. Rendement 290 g (80%). P.é. 150° à 14 mm, n_D^{20} 1.443.

Allyl-2 carboxyéthyl-2 cyclopentanone-1 (V) (R = —CH_2—CH=CH_2)

On utilise la méthode décrite par Vavon et Horeau (9) dans laquelle on ajoute lentement à une solution de carboxyéthyl-2 cyclopentanone-1 (40 g, 0.256 mole) et de bromure d'allyle (34 g, 0.281 mole) dans 100 ml d'éthanol, une solution d'hydroxyde de sodium (12 g, 0.300 mole) dans 50 ml d'eau. Rendement 30 g (60%). P.é. 125–127° à 13–15 mm, n_D^{20} 1.459 (lit. 129° à 16 mm) (9).

Allyl-5 carboxyéthyl-2 cyclopentanone-1 (IV) (R = —CH_2—CH=CH_2)

On effectue la cyclisation en ajoutant goutte à goutte l'allyl-2 adipate de diéthyle (121.6 g, 0.5 mole) à une suspension de fines particules de sodium (14.0 g, 0.61 mole) dans 800 ml de toluène sec et dé-thiophéné maintenu à 35–40°. On chauffe ensuite pendant 4 heures à 70°. On acidifie alors à 0° par H_2SO_4 dilué. On extrait au toluène qu'on lave au bicarbonate dilué et qu'on sèche et distille. Rendement 65.0 g (66%). P.é. 127–130° à 10 mm, n_D^{20} 1.462.

Allyl-2 cyclopentanone-1 (VII) (R = —CH_2—CH=CH_2)

(a) Par décarboxylation de l'allyl-2 carboxyéthyl-2 cyclopentanone-1

On place dans un ballon de 500 ml à trois cols, surmonté d'un réfrigérant, l'allyl-2 carboxyéthyl-2 cyclopentanone-1 (21.0 g, 0.107 mole) et 150 ml d'acide sulfurique 6 *N*. On agite fortement de façon à bien mettre en contact les deux couches et on chauffe au bain-marie pendant 6 heures. Après avoir refroidi, on extrait plusieurs fois à l'éther qu'on sèche et qu'on distille dans le vide. On obtient un résidu liquide qui donne après distillation fractionnée dans le vide, deux fractions. La première, l'allyl-2 cyclopentanone-1, pèse 4.0 g (30.7%) passant à 55–57° à 18 mm, n_D^{20} 1.458. La cétone donne avec la dinitro-2,4 phénylhydrazine des cristaux jaunes, recristallisés du méthanol et ayant un point de fusion de 130–132°.

L'autre fraction est surtout formée de l'allyl-2 carboxyéthyl-2 cyclopentanone-1 inchangé. On recueille ainsi 5.0 g (23.8% du produit initial) passant entre 75–125° à 18 mm, n_D^{20} 1.465.

En prolongeant le temps de chauffage, le rendement reste sensiblement le même.

Si l'on effectue la décarboxylation de l'allyl-2 carboxyéthyl-2 cyclopentanone-1 par chauffage en présence d'une solution d'hydroxyde de baryum (12) le rendement diminue sensiblement.

(b) Par décarboxylation de l'allyl-5 carboxyéthyl-2 cyclopentanone-1

Tel que décrit plus haut, on décarboxyle l'allyl-5 carboxyéthyl-2 cyclopentanone-1 (86.0 g, 0.439 mole) par chauffage pendant 4 heures sur un bain-marie bouillant en présence de 300 ml de H_2SO_4 4 *N*. Après extraction à l'éther, on obtient environ 50 g (92%) d'allyl-2 cyclopentanone-1 brute: n_D^{20} 1.458. Par distillation, on obtient 37.5 g (69%) de cétone pure, passant à 77–80° sous 23 mm, ou à 175–180° sous 758 mm, n_D^{20} 1.459.

On peut aussi effectuer la décarboxylation en chauffant à reflux l'allyl-5 carboxyéthyl-2 cyclopentanone-1 (20.0 g, 0.102 mole) pendant 4 heures en présence d'hydroxyde de baryum (20.0 g, 0.063 mole) dissous dans 100 ml d'eau (12). On filtre le carbonate de baryum formé et on extrait plusieurs fois à l'éther qu'on sèche et qu'on distille. On obtient: 11.0 g (88.7%) d'allyl-2 cyclopentanone-1 brute, n_D^{20} 1.459.

(c) Par chauffage de l'acide allyl-2 adipique

On place dans un ballon à trois cols, l'acide allyl-2 adipique (25.0 g, 0.135 mole) intimement mélangé avec de l'hydroxyde de baryum (2.0 g, 0.006 mole). On chauffe pour que la température du mélange se maintienne entre 290–300°, et on recueille le mélange d'eau et d'allyl-2 cyclopentanone-1 qui passe lentement par distillation. Après 6 heures de chauffage, on extrait à l'éther le distillat obtenu. Après avoir séché et évaporé l'éther, on obtient 9.0 g (54%) d'allyl-2 cyclopentanone-1 impure.

La formation de la cétone est fort lente. Si après quelques minutes de chauffage, on distille sous vide le mélange, on obtient plutôt la méthyl-4 (3-carboxypropyl)-2 butyrolactone.

Méthyl-4 (3-carboxypropyl)-2 butyrolactone (IX)

(a) Par traitement de l'acide allyl-2 adipique par l'hydroxyde de baryum

Ainsi par chauffage de l'acide allyl-2 adipique (37.2 g, 0.20 mole) avec de l'hydroxyde de baryum (3.0 g, 0.009 mole) à 290–300°, on obtient après 1 heure de chauffage, environ 7–8 ml d'un mélange azéotropique

d'eau et d'allyl-2 cyclopentanone-1. On fait alors le vide dans l'appareil et on recueille 21.5 g, d'un liquide passant à 210–215° à 17 mm. On reprend les deux distillats dans 50 ml d'eau et on ajoute suffisamment de soude pour avoir un pH alcalin. On extrait à l'éther plusieurs fois et après avoir séché et distillé l'éther, on recueille 4.5 g (18.3%) d'allyl-2 cyclopentanone-1 passant à 180° sous 760 mm.

On acidifie alors la fraction aqueuse avec H_2SO_4 dilué et on extrait au benzène l'huile qui se sépare. On sèche et on distille sous vide le benzène, ce qui laisse un résidu huileux pesant 18.5 g (50%) et qui ne tarde pas à cristalliser. Un échantillon de la méthyl-4 (3-carboxypropyl)-2 butyrolactone est recristallisé du benzène et de l'éther de pétrole. Les cristaux obtenus ont un point de fusion de 90–92°.

Le poids moléculaire trouvé par neutralisation avec NaOH en présence de phénolphtaléine est 187. Calculé pour $C_9H_{14}O_4$: 186.

La distillation sous vide d'un échantillon pesant 7.2 g, donne 5.0 g d'une huile ayant un point d'ébullition de 230° à 20 mm et qui cristallise rapidement en donnant des cristaux fondant à 90°.

(b) À partir de l'acide allyl-2 adipique par l'acide chlorhydrique

On chauffe à reflux pendant 7 heures 48.5 g (0.261 mole) d'acide allyl-2 adipique avec 150 ml d'acide chlorhydrique dilué 1:1. On évapore alors à sec dans le vide sur bain-marie et on obtient un résidu qu'on recristallise du benzène chaud auquel on ajoute de l'éther de pétrole. Rendement en méthyl-4 (3-carboxypropyl)-2 butyrolactone 42.0 g (86.6%). Poids moléculaire trouvé par neutralisation avec NaOH en présence de phénolphtaléine et en calculant une seule fonction acide: 184. Calculé pour $C_9H_{14}O_4$: 186.

(c) À partir de l'allyl-2 adipate de diéthyle

On chauffe à reflux pendant 7 heures l'allyl-2 adipate de diéthyle (81.7 g, 0.337 mole) avec 800 ml d'acide chlorhydrique dilué 1:1. On évapore à sec et on obtient un résidu qu'on distille dans le vide. On recueille 48.0 g (76.5%) de la lactone, passant à 210° sous 5 mm.

Acide allyl-2 adipique (VIII)

On fait bouillir à reflux pendant 17 heures un mélange d'allyl-2 adipate de diéthyle (62.0 g, 0.256 mole) et d'hydroxyde de potassium (35.0 g, 0.625 mole) dans 750 ml d'éthanol. On évapore ensuite l'éthanol dans le vide sur un bain-marie et on reprend le résidu dans l'eau. On extrait à l'éther l'allyl-2 adipate d'éthyle qui aurait pu résister à la saponification. En acidifiant la portion aqueuse avec H_2SO_4 dilué, une épaisse huile incolore vient flotter en surface. Après l'avoir extraite à l'éther, on sèche et on évapore l'éther. L'huile incolore résiduelle pèse 45.1 g (95%). Cette huile cristallise très lentement à température de la chambre pour donner un solide ayant un point de fusion de 55°. On peut recristalliser l'acide d'un mélange benzène – éther de pétrole ou éther – éther de pétrole. P.f. 57°. Poids moléculaire trouvé par neutralisation avec NaOH et en calculant deux fonctions acides: 189. Calculé pour $C_9H_{14}O_4$: 186.

L'acide allyl-2 adipique est relativement stable en milieu aqueux. Si l'on fait bouillir 2.0 g en présence de 150 ml d'eau pendant 5 heures et qu'on extrait le tout à l'éther, on retrouve une huile qui, recristallisée du benzène – éther de pétrole, redonne 1.5 g du produit initial, soit l'acide allyl-2 adipique. P.f. 56°. Poids moléculaire trouvé par neutralisation avec NaOH et en calculant deux fonctions acides: 185. Calculé pour $C_9H_{14}O_4$: 186.

Allyl-6 diazaspiro-1,3 (4-4) nonane dione-2,4 (XII), (allyl-2′) cyclopentyl hydantoïne-5

On ajoute l'allyl-2 cyclopentanone-1 (37.5 g, 0.30 mole) à un mélange de cyanure de potassium (65.1 g, 1.0 mole), de chlorure d'ammonium (53.4 g, 1.0 mole) et environ 5 g de résine IR A-400 (23) en suspension dans 100 ml de méthanol et 100 ml d'eau. On agite à la température de la chambre pendant 2 heures. On ajoute alors un excès de carbonate d'ammonium (2.0 moles) et on chauffe le tout à 60° pendant 15 heures. On filtre la résine insoluble, on évapore alors les trois-quarts du volume total pour chasser le méthanol et en portant au froid, l'hydantoïne cristallise de la solution saline. Rendement brut 49.0 g (83.3%). P.f. 148–155°.

L'(allyl-2′) cyclopentyl spirohydantoïne-5 est soluble à chaud dans l'éther, l'acétate d'éthyle, et partiellement dans l'eau. Elle est aussi soluble à froid dans l'acétone et l'éthanol et insoluble dans l'éther de pétrole.

On peut recristalliser l'hydantoïne brute soit de l'eau, soit de l'éther – éther de pétrole, soit de l'acétate d'éthyle – éther de pétrole.

On obtient ainsi une première précipitation de cristaux dont le point de fusion est 175–176°. Anal. Calc. pour $C_{10}H_{14}N_2O_2$: N, 14.44%. Trouvé: N, 14.41%.

Par cristallisation fractionnée, on obtient le deuxième isomère dont le point de fusion est 142–143°. Celui-ci beaucoup plus soluble que l'autre. Anal. Calc. pour $C_{10}H_{14}N_2O_2$: N, 14.44%. Trouvé: N, 14.43%.

Le point de fusion mixte des deux diastéréoisomères est 150–155°.

Acide amino-1 allyl-2 cyclopentane-carboxylique (XI) (R = —CH_2—CH=CH_2)

(a) Par hydrolyse alcaline

Dans un autoclave, on hydrolyse 37.0 g (0.19 mole) de l'allyl-6 diazaspiro-1,3 (4-4) nonane dione-2,4 avec 120 g (0.38 mole) d'hydroxyde de baryum dissous dans 500 ml d'eau bouillante. On porte la température à 165° durant ½ heure et on isole l'acide aminé tel que décrit pour l'acide amino-1 méthyl-2 cyclopentane-carboxylique. Par évaporations successives des eaux-mères, on isole 23.1 g (71.5%) de l'acide aminé. Dans le système de solvant pyridine–eau (80:20), l'acide aminé donne une tache violette avec la ninhydrine, dont le R_f est de 0.81. Anal. Calc. pour $C_9H_{15}NO_2$: N, 8.29%. Trouvé: N, 8.12%.

L'acide aminé est assez soluble dans l'eau, partiellement dans l'éthanol et il forme un gel volumineux par addition d'acétone à une solution aqueuse. Le picrate donne une huile qui ne cristallise pas de l'eau. Les sels de cuivre, préparés de façon habituelle, sont peu solubles dans l'eau et ils cristallisent en aiguilles soyeuses bleues. Anal. Calc. pour $C_{18}H_{28}N_2O_4Cu$: N, 7.03%. Trouvé: N, 6.60%.

Comme on doit s'y attendre, l'acide aminé n'est pas tellement stable à chaud en milieu chlorhydrique, puisqu'on retrouve après quelques heures d'ébullition deux taches par chromatographie sur papier. Une des taches correspond à l'acide allyl-2 amino-1 cyclopentane-carboxylique de départ. L'autre provient probablement d'un acide aminé bicyclique formé par addition d'eau sur la double liaison et cyclisation subséquente.

Acide N-phényluréido-1 allyl-2 cyclopentane-carboxylique

On agite violemment pendant 10 minutes un mélange formé de 0.845 g (0.005 mole) d'acide amino-1 allyl-2 cyclopentane-carboxylique, 0.20 g (0.005 mole) d'hydroxyde de sodium et 0.6 ml d'isocyanate de phényle (0.005 mole) dans 30 ml d'eau. On acidifie avec HCl concentré et on filtre le précipité obtenu, qu'on recristallise de l'eau et de l'éthanol. Rendement 1.0 g (69.5%). P.f. 138°. Anal. Calc. pour $C_{16}H_{20}N_2O_3$: N, 9.74%. Trouvé: N, 9.75%. Poids moléculaire trouvé par neutralisation avec NaOH: 294. Calculé pour $C_{16}H_{20}N_2O_3$: 288.

REMERCIEMENTS

Les auteurs remercient M. Bertin Girard pour sa précieuse aide technique.

Ils remercient l'Office des recherches scientifiques de la Province de Québec pour une bourse accordée à l'un d'eux (L. N.), ainsi que l'Institut National du Cancer du Canada pour son aide financière.

Ils remercient de plus le Dr. R. Deghenghi pour l'étude des spectres à l'infra-rouge et le Dr. J. N. Shoolery pour l'interprétation des spectres magnétiques de résonance nucléaire.

BIBLIOGRAPHIE

1. F. Martel et L. Berlinguet. Can. J. Biochem. and Physiol. **37**, 433 (1959).
2*a*. T. A. Connors, L. A. Elson et W. C. J. Ross. Biochem. Pharmacol. **1**, 239 (1958).
2*b*. T. A. Connors, L. A. Elson, A. Haddow et W. C. J. Ross. Biochem. Pharmacol. **5**, 108 (1960).
3. R. B. Ross, C. I. Noll, W. C. J. Ross, M. V. Nadkarni, B. H. Morrison, Jr. et M. H. W. Bond. J. Med. Phar. Chem. **3**, 1 (1961).
4. C. A. Vanderwerf et L. V. Lemmerman. Org. Syntheses, **28**, 8 (1948).
5. L. Bouveault. Bull. soc. chim. France, **21** (3), 1021 (1899).
6. F. H. Case et E. E. Reid. J. Am. Chem. Soc. **50**, 3062 (1928).
7. A. Haller et R. Cornubert. Bull. soc. chim. France, **39** (4), 1726 (1926).
8. V. Rysselberghe. Bull. soc. chim. Belges, **35**, 310 (1926).
9. G. Vavon et J. Horeau. Bull. soc. chim. France, **1** (5), 1709 (1934).
10. R. I. Reed et M. B. Thornley. J. Chem. Soc. 2148 (1954).
11. C. N. Habecker et C. I. Noll. Thèse de maîtrise, The Pennsylvania State University. 1958.
12. R. Cornubert et C. Borrel. Bull. soc. chim. France, 47 (4), 301 (1930).
13. C. K. Ingold. Structure and mechanism in organic chemistry. Bell and Sons, Ltd., London. 1953. p. 787.
14. C. R. Hauser et W. B. Renfrow. J. Am. Chem. Soc. **59**, 1823 (1937).
15. A. C. Cope, K. E. Hoyle et D. Heyl. J. Am. Chem. Soc. **63**, 1848 (1941).
16. R. Gaudry, L. Berlinguet, A. Langis et G. Paris. Can. J. Chem. **34**, 502 (1956).
17. R. Granger et H. Techer. Bull. soc. chim. France, 787 (1960).
18. H. Gilman. Organic chemistry. Vol. I. J. Wiley & Sons, Ltd., New York. 1942. p. 340.
19. H. N. Rydon et P. W. G. Smith. Nature, **169**, 922 (1952).
20. L. Bouvreault et R. Locquin. Bull. soc. chim. France, **3** (4), 450 (1908).
21. O. Wallach et F. Collmann. Ann. **331**, 323 (1903).
22. J. F. Thorpe et G. A. R. Kon. Org. Syntheses, Coll. Vol. I, 192 (1941).
23. C. J. Schmidle et R. C. Mansfield. Ind. Eng. Chem. 44, 1389 (1952).
24. D. V. Myhre et F. Smith. J. Org. Chem. **23**, 1229 (1958).
25. M. M. Tuckerman. Anal. Chem. **30**, 231 (1959).
26. H. R. Roberts et M. G. Kolar. Anal. Chem. **31**, 565 (1959).
27. E. Lederer. Chromatographie en chimie organique et biologique. Masson et Cie, Paris. 1959. p. 605.
28. H. C. Tillson et C. I. Noll. Thèse de maîtrise, The Pennsylvania State University. 1948.

THERMODYNAMIC PROPERTIES AND GEOCHEMISTRY OF ISOTOPIC COMPOUNDS OF SELENIUM

H. R. KROUSE* AND H. G. THODE

The Departments of Chemistry and Physics, McMaster University, Hamilton, Ontario

Received August 10, 1961

ABSTRACT

Using "normal vibration equations" and statistical mechanics, the isotopic vibrational frequencies and the partition function ratios for various Se^{76}- and Se^{82}-containing compounds have been calculated. The equilibrium constants for selenium isotope exchange reactions derived from these partition function ratios indicate that noticeable fractionation of selenium isotopes can be expected in the laboratory and in naturally occurring processes.

The Se^{82}/Se^{76} ratios for 16 natural samples have been compared mass spectrometrically. Variations of up to 1.5% found in this ratio are discussed.

A kinetic isotope effect of 1.5% found in a chemical reduction of selenite ion to elemental selenium is also discussed.

INTRODUCTION

It is well known that isotopes of the lighter elements differ in their chemical properties to the extent that significant fractionation of these isotopes occurs in laboratory and natural processes. This is explained theoretically by the dependence of many thermodynamic properties of molecules upon their vibrational frequencies which, in turn, depend upon the masses of the atoms in the molecule. Earlier theoretical studies of possible chemical exchange processes involving the isotopes of many of the lighter elements were made by Urey and Rittenberg (1), Urey and Greiff (2), and Urey (3). Equilibrium constants for isotope exchange reactions were predicted to differ from unity and many of these have been confirmed experimentally.

Because of the large number of isotopes for many of the heavier elements, the percentage mass difference between the lightest and heaviest isotope is often considerable and, therefore, chemical differences are to be expected in these isotopes. With this in mind, investigations of the selenium isotopes were carried out. Selenium, element 34, has six stable isotopes, 74, 76, 77, 78, 80, and 82, with abundances of approximately 1.0, 9.0, 7.5, 23.5, 50.0, and 9.0%. Although the percentage mass difference between Se^{74} and Se^{82} is about 10%, Se^{76} and Se^{82}, in which case the percentage mass difference is greater than 7%, were examined because of the more favorable abundance of Se^{76} over that of Se^{74}.

The examination of the isotopes of selenium was also prompted by the results which had been obtained from studies on sulphur isotope abundances. The variations of up to 5% initially found in the natural S^{34}/S^{32} ratio by Thode *et al.* (4) in 1949 have been widened to 8% by subsequent investigations. Here the percentage mass difference is about 6% and a theoretical study by Tudge and Thode (5) in 1950 predicted equilibrium constants significantly different from unity for exchange of S^{32} and S^{34} between sulphur-containing compounds. The studies on sulphur isotope abundances have proved most interesting because of the wide distribution and the many chemical forms and valence states in which sulphur exists in nature.

Since selenium is, to some extent, chemically similar to sulphur, one might expect to find some analogous fractionations of the selenium isotopes in nature. On the other

**Present address: Department of Physics, University of Alberta, Edmonton, Alberta.*

hand, a study of the selenium isotopes might yield new and interesting information because of the physical differences between selenium and sulphur and their compounds. Therefore, the Se^{82}/Se^{76} ratio has been investigated both theoretically and experimentally to determine the extent to which it might be altered in natural and laboratory processes.

THEORY

Isotopic Equilibrium Exchange Reactions

Since the first application of statistical mechanics to the calculation of isotopic equilibrium exchange constants, Urey (3) and Bigeleisen and Mayer (6) have carried out further simplifications which make it possible to calculate these equilibrium constants, with the exception of the hydrogen isotopes, from a knowledge of the isotopic vibrational frequencies of the participating molecules.

A typical isotope exchange reaction can be written as

$$aA_1 + bB_2 \rightleftharpoons aA_2 + bB_1, \qquad [1]$$

where A and B are molecules containing the element being exchanged and the subscripts 1 and 2 refer to the light and heavy isotopes respectively of this element.

The equilibrium constant for this exchange is given by

$$K = \frac{[Q_{A_2}/Q_{A_1}]^a}{[Q_{B_2}/Q_{B_1}]^b}, \qquad [2]$$

where the Q's are the total partition functions of the molecules. Urey (3) and Bigeleisen and Mayer (6) showed that the equilibrium constant for isotopic exchange reactions could be expressed in terms of isotopic partition function ratios Q_2/Q_1 which depend only on the vibrational frequencies of the isotopic molecules. In the present work, the simplification of Bigeleisen and Mayer (6) was used in which the isotopic partition function ratio is given by

$$\frac{Q_2'}{Q_1'} = \frac{\sigma_1}{\sigma_2}\left[1 + \sum_i \left(\left(\frac{1}{2} - \frac{1}{u_{2_i}}\right) + \frac{1}{e^{u_{2_i}} - 1}\right)\Delta_{u_i}\right], \qquad [3]$$

where $u = hcw/kT$; "w" is the vibrational frequency in cm^{-1} units. The summation is over "i" fundamental vibrational frequencies of the molecule and an n-degenerate frequency is summed "n" times.

$\Delta_{ui} = u_{i1} - u_{2i}$ and is always positive. The σ's are the symmetry numbers of the molecule and σ_1/σ_2 is unity if the molecule contains only one atom of the element being exchanged or more than one atom occupying indistinguishable positions. The function $(1/2 - 1/u_2 + 1/(e^{u_2} - 1))$ has been termed the free energy function $G(u)$ by Bigeleisen and Mayer (6) and has been tabulated for values of u from 0 to 25.

Using this theory, the partition function ratios were calculated for Se^{82}- and Se^{76}-containing compounds. In the absence of specific spectroscopic data for these isotopic molecules, the experimental frequencies available were assumed to apply to the molecule containing the most abundant species Se^{80}, and the frequencies of the Se^{76} and Se^{82} molecular species were calculated by means of "known vibration equations". These equations relate the fundamental vibrational frequencies of molecules to "force constants" and atomic weights on the assumption of a particular model of the molecule in question.

Kinetic Isotope Effects

Since the discovery by Urey and Washburn (7) that partially electrolyzed water is enriched in deuterium because protium is evolved faster at the cathode, it has been shown

that isotopic molecules of other light elements have different rates of reaction and that, in general, the molecule containing the lighter isotope reacts faster.

The ratio of rate constants for competing isotopic reactions, in principle, can be calculated from formulae given by Eyring (8) and Bigeleisen (9). Making only the assumptions inherent in the "theory of absolute reaction rates" of Eyring (8) and Evans and Polanyi (10), Bigeleisen obtains the following expression for the ratio of the reaction rates:

$$\frac{k_1}{k_2} = \frac{K_1}{K_2} S \frac{\nu_{1L}}{\nu_{2L}} \left[1 + \sum_i^{3n-6} G(u_i)\Delta u_i - \sum_i^{3n-7} G(u_i)^{\ddagger}\Delta u_i^{\ddagger} \right], \qquad [4]$$

where, as before, $G(u)$ is the Bigeleisen and Mayer (6) free energy function, $\ddagger$ refers to the transition state of the absolute reaction rate theory, 1 and 2 refer to the light and heavy molecules respectively, S is a statistical factor and depends on the symmetry numbers of the molecules and, finally, ν_L is the imaginary frequency along the reaction co-ordinates in the transition state. The factor ν_{1L}/ν_{2L} gives the ratio of the number of light and heavy molecules in transition state which decompose in unit time. K_1/K_2, the ratio of the transmission coefficients for the isotopic reaction, has been shown by Hirschfelder and Wigner (11) to be nearly unity above room temperature.

According to the theorem of Slater (12), developed for unimolecular reactions, the frequency factor ν_{1L}/ν_{2L} of equation [4] may be replaced by $(\mu_2^{\ddagger}/\mu_1^{\ddagger})^{1/2}$, where μ is the reduced mass across the bond being ruptured. This is based on the premise that only the motions of the two atoms across the ruptured bond are involved.

Bigeleisen and Wolfsberg (13) have suggested a reaction co-ordinate which tears the two decomposition fragments apart. Such a co-ordinate would lead to

$$\nu_{1L}/\nu_{2L} = \left(\frac{\mu_2^{\ddagger}}{\mu_1^{\ddagger}}\right)^{\frac{1}{2}},$$

where μ, the reduced mass across the ruptured bond, is evaluated by using the masses of the two fragments rather than the masses of the two atoms. The choice of the co-ordinate to use, the Slater co-ordinate or the co-ordinate that tears the two fragments apart, will probably depend on the reactions under consideration and the relative bond strengths of the molecules. The usefulness of equation [4] is also limited because of the lack of knowledge concerning the "transition state" and the inability to calculate the last term of the equation $\sum_i G(u_i)^{\ddagger}\Delta u_i^{\ddagger}$. Because of these difficulties, simplifying assumptions must be made in the calculation of kinetic isotope effects.

Results of Theoretical Calculations

Table I summarizes the vibrational frequencies calculated for some Se^{76}- and Se^{82}-containing species. The spectroscopic data and the method of calculation used are found in Herzberg (14). Corrections for anharmonicity were taken into account.

Table II summarizes the fundamental vibrational frequencies that were calculated for Se^{82}- and Se^{76}-containing polyatomic molecules. References are given for the spectroscopic data and the normal vibrational force equations used in the calculations.

Table III summarizes the partition function ratios and the equilibrium constants for Se^{76}–Se^{82} exchange reactions. The method of tabulation is that used by Urey (15). The partition function ratios are listed in the first row under their respective compound at 0° C, 25° C, 100° C, and 250° C, while the equilibrium constants are contained in the main body of the table at the intersection of the pertaining row and column. An equilibrium constant greater than unity indicates that the heavier isotope will concentrate in the compound listed in the left column.

TABLE I

Diatomic molecular frequencies (cm^{-1})

	Molecule							
	PbSe	$Ge^{74}Se$	SnSe	$C^{12}Se$	$Si^{28}Se$	$SeSe^{80}$	Se_2	SeO^{16}
Frequency observed for Se^{80}-containing species (Herzberg)	276.6	404.4	329.8	1026.4	576.5	389.7	389.7	897.9
Frequency calculated for Se^{82}-containing species	274.2	403.0	327.3	1024.7	574.7	387.3	384.9	896.1
Frequency calculated for Se^{76}-containing species	281.8	410.5	334.9	1029.8	580.3	394.7	399.8	901.8

TABLE II

Polyatomic molecular frequencies (cm^{-1})
(The number in parentheses indicates the degeneracy of a frequency)

Molecule	w_1	w_2	w_3	w_4	w_5	w_6	Reference
H_2Se^{80}	2260	1074	2350				Observed (28)
H_2Se^{76}	2260.7	1074.4	2349.7				Calculated (29, 30)
H_2Se^{82}	2259.8	1073.8	2350.7				
$Se^{80}O_4^{=}$	834	875 (3)	416 (3)	339			Observed (31)
$Se^{76}O_4^{=}$	834	880.0 (3)	418.6 (3)	339			Calculated (32)
$Se^{82}O_4^{=}$	834	872.6 (3)	415.1 (3)	339			
$Se^{80}F_6$	708	662 (2)	787 (3)	461 (3)	405 (3)	245 (3)	Observed (33)
$Se^{76}F_6$	708	662 (2)	794.7 (3)	463.8 (3)	405 (3)	245 (3)	Calculated (34)
$Se^{82}F_6$	708	662 (2)	783.9 (3)	459.7 (3)	405 (3)	245 (3)	

EXPERIMENTAL

The Se^{82}/Se^{76} ratios of various samples were compared using selenium hexafluoride gas in a mass spectrometer.

Preparation of Samples

Selenium was extracted in its elemental form from natural samples by the hydrobromic acid – bromine technique as outlined by Noyes and Bray (16). The adaptations of this method to natural samples by Robinson *et al.* (17) and Williams and Lakin (18) were generally followed. The extracted selenium was then fluorinated to SeF_6 in a monel fluorine line. The prepared SeF_6 was handled in monel sample tubes to avoid contaminations.

Reduction of Selenite Ion to Elemental Selenium (Kinetic Isotope Effect Study)

Hydroxylamine hydrochloride was used to reduce sodium selenite to elemental selenium in dilute solution according to the reaction

$$2H^+ + 2NH_2OH + SeO_3^{=} \rightarrow Se\downarrow + N_2O\uparrow + 4H_2O.$$

Five grams of sodium selenite were dissolved in 50 ml of water, and enough hydroxylamine hydrochloride (~0.04 g) in solution was added to slowly precipitate about 1% of the total selenium present. After 2 days, this precipitate was separated from the solution with a centrifuge. The remaining 99% of the selenium was then precipitated with excess hydroxylamine hydrochloride and separated. The Se^{82}/Se^{76} ratios for these two samples were then compared after fluorination to SeF_6.

Mass Spectrometry

In the normal electron bombardment of SeF_6, the most abundant ion species is SeF_5^+. Therefore, a 6-in. radius, 90° mass spectrometer was equipped with two collector slits for the simultaneous collection of $Se^{76}F_5^+$ and $Se^{82}F_5^+$ ions. The well-known null method of recording was used where a measured portion of the voltage produced by the one ion current is fed back inversely to cancel the voltage produced by the other ion current.

The sample handling system was of monel construction and entirely free of grease and mercury, which were found to produce contaminations. This system allowed two samples to be alternately introduced

TABLE III

Equilibrium constants for Se^{82}/Se^{76} exchange reactions

	$\frac{Se^{82}F_6}{Se^{76}F_6}$	$\frac{Se^{82}O_4^{=}}{Se^{76}O_4^{=}}$	$\frac{Se^{82}Se^{82}}{Se^{76}Se^{76}}$	$\frac{Se^{82}O}{Se^{76}O}$	$\frac{H_2Se^{82}}{H_2Se^{76}}$	$\frac{Se^{82}Se^{80}}{Se^{76}Se^{80}}$	$\frac{PbSe^{82}}{PbSe^{76}}$	$\frac{Se^{82-}}{Se^{76-}}$	T (°C)
$\frac{Q_2'}{Q_1'}$	1.059	1.044	1.012	1.009	1.005	1.006	1.005	1.000	0
	1.051	1.038	1.011	1.008	1.005	1.005	1.004	1.000	25
	1.034	1.023	1.007	1.005	1.003	1.003	1.003	1.000	100
	1.019	1.014	1.004	1.003	1.002	1.002	1.001	1.000	250
$\frac{Se^{82}F_6}{Se^{76}F_6}$	1.000	1.014	1.046	1.050	1.054	1.053	1.054	1.059	0
		1.013	1.040	1.043	1.046	1.046	1.043	1.051	25
		1.011	1.027	1.029	1.031	1.031	1.031	1.034	100
		1.005	1.015	1.016	1.017	1.017	1.018	1.019	250
$\frac{Se^{82}O_4^{=}}{Se^{76}O_4^{=}}$		1.000	1.032	1.035	1.039	1.038	1.039	1.044	0
			1.027	1.030	1.033	1.033	1.034	1.038	25
			1.016	1.018	1.020	1.020	1.020	1.023	100
			1.010	1.011	1.012	1.012	1.013	1.014	250
$\frac{Se^{82}Se^{82}}{Se^{76}Se^{76}}$			1.000	1.003	1.007	1.006	1.007	1.012	0
				1.003	1.006	1.006	1.007	1.011	25
				1.002	1.004	1.004	1.002	1.007	100
				1.001	1.002	1.002	1.001	1.004	250
$\frac{Se^{82}O}{Se^{76}O}$				1.000	1.004	1.003	1.004	1.009	0
					1.003	1.003	1.004	1.008	25
					1.002	1.002	1.002	1.005	100
					1.001	1.001	1.002	1.003	250
$\frac{H_2Se^{82}}{H_2Se^{76}}$					1.000	0.999	1.000	1.005	0
						1.000	1.001	1.005	25
						1.000	1.000	1.003	100
						1.000	1.001	1.002	250
$\frac{Se^{82}Se^{80}}{Se^{76}Se^{80}}$						1.000	1.001	1.006	0
							1.001	1.005	25
							1.000	1.003	100
							1.001	1.002	250
$\frac{PbSe^{82}}{PbSe^{76}}$							1.000	1.005	0
								1.004	25
								1.003	100
								1.001	250
$\frac{Se^{82-}}{Se^{76-}}$								1.000	0
									25
									100
									250

into the mass spectrometer under identical conditions. Usually, 5 minutes were required to switch these samples and in this operation, parts of the line used in common by both samples were evacuated and flamed. No difficulties with memory effects were experienced. Up to three continuous recordings of each sample were made in an hour. With this method of comparison, measurements of the ratio in two samples, within a single run, could be obtained with a standard deviation of ± 0.0005. The same reproducibility could be obtained also for comparisons of the same samples on different days and for different chemical extractions from the same natural sample.

Experimental Results

Table IV and Fig. 1 summarize the selenium isotope abundance data obtained for a variety of natural samples.

In view of the remarkable uniformity in the S^{32}/S^{34} ratio in meteorites of all types (15, 19, 20) and the considerable evidence that this ratio represents the primordial ratio of sulphur isotopes in terrestrial sulphur, it seemed reasonable in the first instance to assume that the selenium extracted from troilite in the Canyon Diablo meteorite represents the primordial ratio of the selenium isotopes. The Canyon Diablo meteorite sample was therefore used as a primary standard and a sample of selenium from Noranda was used as a secondary standard because of the small amount of meteoritic selenium available.

In Table IV and Fig. 1, δ_{82} is the enrichment of Se^{82} in ‰ defined by

$$\delta_{82} = \frac{Se^{82}/Se^{76}\text{ sample} - Se^{82}/Se^{76}\text{ meteoritic}}{Se^{82}/Se^{76}\text{ meteoritic}} \times 1000.$$

TABLE IV

Variations of the Se^{82}/Se^{76} ratio in natural samples

Sample No.	Location	Alleged type of deposit	δ_{82} (‰)
1	Canyon Diablo meteorite	Selenium in troilite	0.000
2	Noranda, Quebec	Hypothermal or magmatic hydrothermal massive sulphide	+0.5±0.5
3	Murdochville, Quebec	Hypothermal or magmatic hydrothermal massive sulphide	+1.0±0.5
4	Flin Flon, Manitoba	Hypothermal or magmatic hydrothermal massive sulphide	+0.5±0.5
5	Sudbury, Ontario	Molten magma or igneous origin	+0.5±0.5
6	Mt. Lyell, Australia	Mesothermal	−1.0±1.0
7	Mt. Wingen, N.S.W.	Selenium precipitated below a pyrite bed	−1.0±1.0
8	Beaverlodge Lake, Saskatchewan	Umangite ($Cu_3SeCuSe$) in hydrothermal pitchblende bearing sulphide vein	0.0±0.5
9	Beaverlodge Lake, Saskatchewan	Chalcomenite ($CuSeO_3.2H_2O$) in association with No. 8	+0.5±0.5
10	Unknown	Refined selenium, Phelps Dodge Refining Corp., New York	+0.5±0.5
11	Unknown	Refined selenium, American Smelting and Refining Co.	+0.5±0.1
12	Unknown	Commercial SeF_6, Allied Chemical and Dye Corp., Baton Rouge, Louisiana; selenium was purchased from Company in No. 11.	+0.5±0.5
13	Southwestern U.S.A., exact location unknown	*Astragalus bisulcatus* plant containing selenite and complex organic selenium compounds	+2.0±0.5
14	Southwestern U.S.A., exact location unknown	*Astragalus pattersoni* plant containing selenite and complex organic selenium compounds	−11.0±1.0
15	County Meath, Ireland	Soil sample containing selenite and complex organic selenium compounds	+4.0±0.5
16	Mt. Shirane, Japan	Elemental selenium in volcanic sulphur	−2.0±1.0

Table V summarizes the results obtained on three reductions of Na_2SeO_3 to elemental selenium at 3° C.

TABLE V

Fractionation in reduction of sodium selenite to elemental selenium

Run	R
1	1.014
2	1.016
3	1.016
Average	1.015±0.001

The isotope effect which occurred in the 1% reaction is expressed by

$$R = \frac{Se^{76}/Se^{82} \text{ reduced Se (1\%)}}{Se^{76}/Se^{82} \text{ remainder of solution (99\%)}}.$$

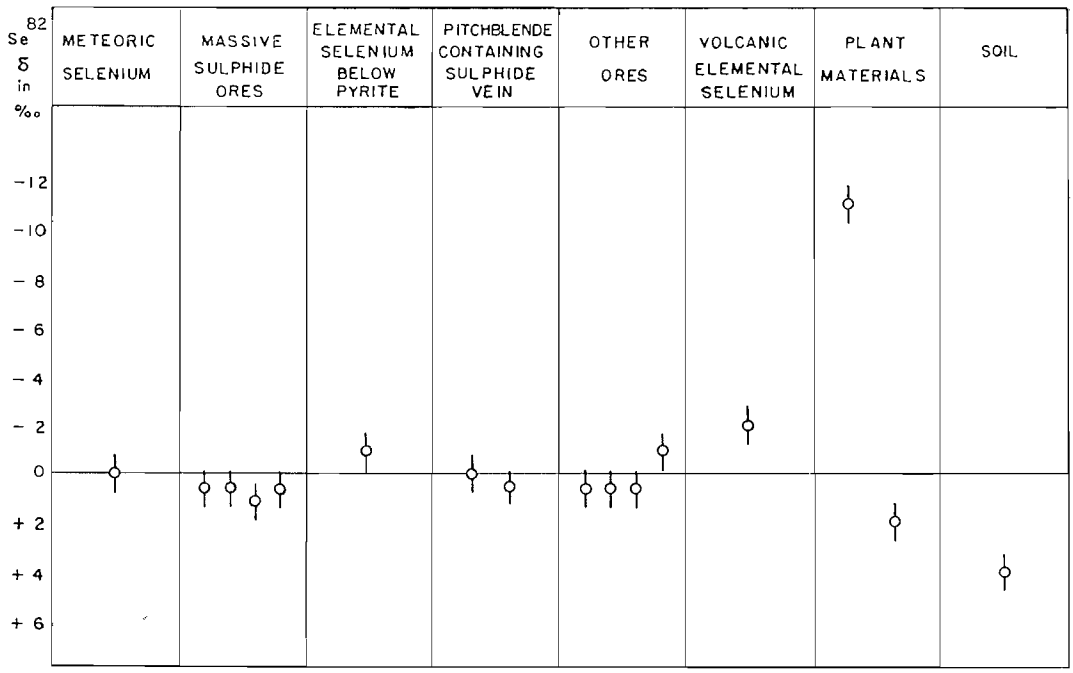

FIG. 1. Variations in the Se^{82}/Se^{76} ratio found for natural samples.

DISCUSSION AND CONCLUSIONS

Isotope Distribution in Nature

It is obvious from the theoretical study (Table III) that Se^{76} and Se^{82} differ in their chemical properties to the extent that isotope fractionations of up to 6% are predicted for Se^{76}–Se^{82} equilibrium exchange processes, provided that mechanisms are available for such exchanges.

Table IV and Fig. 1 show that the Se^{82}/Se^{76} ratio in the natural samples examined varied by 1.5%. The selenium samples from plant materials and soil show the largest variations to both sides of the meteoritic value, whereas selenium in massive sulphide ores shows little or no deviation from the meteoritic selenium value.

It is interesting to compare these selenium isotope results with similar results obtained in sulphur isotope studies.

There is an indication that the selenium extracted from massive sulphide ores is slightly enriched in the heavy isotope Se^{82} ($\delta_{82} = +0.5‰$). The effect in the case of sulphur is more pronounced. For example, samples of Sudbury igneous ore have been found enriched by 0.5 and 2.5‰ in Se^{82} and S^{34} respectively, the meteoritic values being taken as standard in each case (21).

The Se^{82}/Se^{76} ratio for volcanic elemental selenium from Mt. Shirane, Japan, is, of course, not indicative of the average value of the selenium in this volcano, since selenium is also present in other compounds. Since the theoretical study indicates that fractionation of selenium isotopes is possible between such compounds in volcanic gases, the depletion of Se^{82} ($\delta_{82} = -2‰$) found would indicate that such a fractionation occurred in this volcanic sample. Elemental sulphur from the same location is also depleted in the heavy isotope S^{34} ($\delta_{34} = -5‰$) (Sakai *et al.* 22).

The sample from Beaverlodge Lake, Saskatchewan, which contains umangite (Cu_2Se-CuSe) and chalcomenite ($CuSeO_3.2H_2O$) (samples 8 and 9, Table IV), is considered to

have been derived from primary sulphide ore as the selenide and subsequently partially oxidized (Robinson (23)). The results found show that little or no fractionation of the selenium isotopes occurred in this natural oxidation process.

The variations found in the Se^{82}/Se^{76} ratio for selenium extracted from plant material and soils indicate large isotope effects which have occurred probably in oxidation and reduction processes in biological systems. It is now fairly well established that the major portion of sulphur isotope fractionation in biological systems occurs in the bacterial reduction of sulphate (Thode *et al.* (24, 25)). In addition to reducing sulphates, anaerobic bacteria are known to reduce selenates and selenites as well, and these might provide a mechanism for fractionation of the selenium isotopes.

Equilibrium Isotope Effects

The fractionations in the Se^{82}/Se^{76} ratio is not expected to be as high as that found in the S^{34}/S^{32} ratio for two reasons:

(1) From statistical mechanics, the partition function ratios are lower, e.g., for $S^{34}O_4^{=}/S^{32}O_4^{=}$, $Q_2'/Q_1' = 1.088$ at 25° C; while for $Se^{82}O_4^{=}/Se^{76}O_4^{=}$, $Q_2'/Q_1' = 1.038$ at 25° C.

(2) The potential for oxidizing elemental selenium to the +6 valence state is quite high ($Se \rightarrow H_2SeO_4$ −1.89 volts) in comparison to that of sulphur ($S \rightarrow H_2SO_4$ −0.58 volts). For this reason, sulphates are abundant in nature, while selenates are rarely found. Since isotope effects are higher in equilibrium exchanges if a greater valence change is involved (See Table III), the above fact further lowers the natural isotope fractionation expected with selenium in comparison to sulphur.

Kinetic Isotope Effects

It has been found in studies of kinetic isotope effects in the bacterial reduction of sulphate that, while the fractionation varies with the metabolic rate, the maximum value obtained at low metabolic rates approaches that obtained in a direct chemical reduction (Harrison and Thode (25, 26)). For this reason, the isotope effect found in the reduction of selenite is of importance. The results (Table V) indicate a kinetic isotope effect of $(R-1)\times 100 = 1.5\%$ in the chemical reduction of selenite to elemental selenium.

The question may arise about whether this is a true kinetic effect in which case $R = k_1/k_2$ for

$$Se^{76}O_3^{=} \xrightarrow{k_1} Se^{76}$$

$$Se^{82}O_3^{=} \xrightarrow{k_2} Se^{82}$$

or whether some isotopic exchange of selenium has also occurred between the reactant and the product in the course of the experiment. Such an exchange would result in a gradual increase of $(R-1)$ since the equilibrium isotope constant for the exchange

$$Se^{76}O_3^{=} + Se^{82} \rightleftharpoons Se^{82}O_3^{=} + Se^{76}$$

would be considerably larger than 1.015. In this connection, Haissinsky and Pappas (27) observed with tracer experiments that amorphous selenium exchanges with its ions in a 5.5 *N* HCl solution 0.1 *M* with respect to SeO_2. The rate was found to increase with acid concentration approaching 40% in 1 hour at 10 *N* HCl. Since this exchange was found to take place only at high acid concentrations, it would seem that a true kinetic isotope effect was observed in the almost neutral dilute solutions of the present work.

The kinetic isotope effect for the reduction of selenite to elemental selenium could be calculated using the equation of Bigeleisen (9) if the isotopic vibrational frequencies were known for the selenite ion and the activated complex. The former is currently being

calculated, while the latter is unknown. The analogous reduction of sulphates indicated that the rate-controlling step is the initial S—O bond breakage. If the rate-controlling step in the reduction of selenites is assumed to be the initial Se—O bond breakage, a simple calculation can be made by considering a Se—O diatomic model whose bond is completely broken in the activated complex. With this model, k_1/k_2 from the Bigeleisen equation is found to be 1.015 and 1.014 at 0° C and 25° C respectively. In view of the simple model assumed, the close agreement with the experimental value indicates only that the result is of the order expected.

ACKNOWLEDGMENTS

We wish to thank the following people, who have supplied samples for this investigation: E. P. Henderson, Smithsonian Institution; O. A. Beath, University of Wyoming; G. A. Fleming, The Agricultural Institute, Ireland; S. C. Robinson, Geological Survey of Canada; M. Shima, McMaster University; W. C. Cooper, Canadian Copper Refineries, Montreal; Austin Smith, International Nickel Co.; H. Barkell, Phelps Dodge Refining Corp., N.Y.; H. M. Murray, Mount Lyell Mining and R. R. Co. Ltd., Australia; A. F. Evans, Electrolytic Refining and Smelting Co. of Australia.

Thanks are also due to Dr. R. H. Farquhar, who, several years ago, investigated sample preparation methods and made some preliminary calculations of selenium isotope exchange constants. Finally, we wish to acknowledge financial support from the National Research Council of Canada, without which this investigation would not have been possible.

REFERENCES

1. H. C. Urey and D. Rittenberg. J. Chem. Phys. **1**, 137 (1933); J. Am. Chem. Soc. **56**, 1885 (1934).
2. H. C. Urey and L. Greiff. J. Am. Chem. Soc. **57**, 321 (1935).
3. H. C. Urey. J. Chem. Soc. 562 (1947).
4. H. G. Thode, J. Macnamara, and C. B. Collins. Can. J. Research, B, **27**, 361 (1949).
5. A. P. Tudge and H. G. Thode. Can. J. Research, B, **28**, 567 (1950).
6. J. Bigeleisen and M. G. Mayer. J. Chem. Phys. **15**, 261 (1947).
7. H. C. Urey and E. W. Washburn. Proc. Nat. Acad. Sci. **18**, 496 (1932).
8. H. Eyring. J. Chem. Phys. **3**, 107 (1935).
9. J. Bigeleisen. J. Chem. Phys. **17**, 675 (1949).
10. M. G. Evans and M. Polanyi. Trans. Faraday Soc. **31**, 875 (1935).
11. J. O. Hirschfelder and J. Wigner. J. Chem. Phys. **1**, 616 (1939).
12. N. B. Slater. Trans. Roy. Soc. (London), A, **246**, 57 (1953).
13. J. Bigeleisen and M. Wolfsberg. Advances in chemical physics, Vol. 1. Interscience Publishers Inc., New York. 1958, p. 15.
14. G. Herzberg. Molecular spectra and molecular structure. Van Nostrand. 1957.
15. A. V. Trofimov. Doklady Akad. Nauk. S.S.S.R. **66**, 181 (1949).
16. A. A. Noyes and W. C. Bray. A system of qualitative analysis of the rare elements. Macmillan Co., New York. 1927.
17. W. O. Robinson, H. C. Dudley, K. T. Williams, and H. G. Byers. Ind. Eng. Chem. Anal. Ed. **6**, 274 (1934).
18. K. T. Williams and H. W. Lakin. Ind. Eng. Chem. **7**, 409 (1935).
19. J. Macnamara and H. G. Thode. Phys. Rev. **78**, 307 (1950).
20. A. P. Vinogradov. Isotopic composition of S in meteorites and in the earth. Radioisotopes in scientific research. Vol. II. Pergamon Press. 1958.
21. J. Macnamara, W. Fleming, A. Szabo, and H. G. Thode. Can. J. Chem. **30**, 73 (1952).
22. H. Sakai and H. Nagasawa. Geochim. et Cosmochim. Acta, **15**, 32 (1958).
23. S. C. Robinson. Geological Survey of Canada, Bull. 31. 1955.
24. H. G. Thode, R. K. Wanless, and R. Wallouch. Geochim. et Cosmochim. Acta, **5**, 286 (1954).
25. A. Harrison and H. G. Thode. Trans. Faraday Soc. **54**, 84 (1958).
26. A. Harrison and H. G. Thode. Trans. Faraday Soc. **53**, 1 (1957).
27. M. Haissinsky and A. Pappas. J. chim. phys. **47**, 506 (1950).
28. W. C. Sears, D. M. Cameron, and H. H. Nielsen. J. Chem. Phys. **1**, 994 (1939).
29. G. Glocker and J.-Y. Tung. J. Chem. Phys. **13**, 338 (1945).
30. S. Smith and J. W. Linnett. Trans. Faraday Soc. **52**, 891 (1956).
31. A. S. Ganesan. Proc. Indian Acad. Sci. **1**, 156 (1934).
32. D. F. Heath and J. W. Linnett. Trans. Faraday Soc. **44**, 884 (1948).
33. E. Bartholomé and H. Sachsee. Z. Physik. Chem. B, **28**, 251 (1935).
34. D. F. Heath and J. W. Linnett. Trans. Faraday Soc. **45**, 264 (1949).

NOTES

DI-(4-OXA-5α-CHOLESTAN-3α-YL) ETHER

J. T. Edward and I. Puskas

Solutions in water-saturated ether of 4-oxa-5α-cholest-2-ene (I) (1), recovered from experiments carried out at different times, were stored in an unstoppered flask at room temperature. The gradual evaporation of the solvent caused the deposition of a solid which, after purification, melted at 205–208° and analyzed as $C_{52}H_{90}O_3$ (i.e. two molecules of I and H_2O). This compound must be di-(4-oxa-5α-cholestan-3α-yl) ether (III), formed

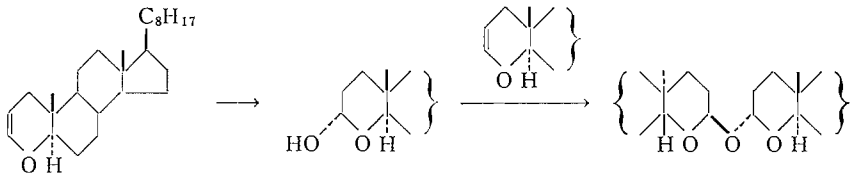

I II III

by hydration of the unsaturated ether (I) to give 4-oxa-5α-cholestan-3α-ol (II) (1), followed by reaction of the latter with a second molecule of I. This second reaction was employed (with a trace of acid as a catalyst) in a more deliberate synthesis of the compound.

Similar results have been obtained in the acid-catalyzed hydration of dihydropyran (2), analogues of II or III being obtained according to conditions.

On hydrolysis with aqueous acid in tetrahydrofuran solution the ether (III), m.p. 205–208°, yielded 4-oxa-5α-cholestan-3α-ol.

Arguments based on optical rotations indicate for the ether the 3α,3′α configuration shown in III. It seems likely (3, 4) that conversion of 4-oxa-5α-cholestan-3α-ol into a 3α- or 3β-alkoxy derivative is accompanied by shifts in molecular rotation of the same sign and of about the same magnitude as those accompanying the conversion of α-D-glucose into the corresponding alkyl α- or β-D-glucoside (1). The conversion of two molecules of α-D-glucose into a molecule of α,α′-trehalose is accompanied by a shift of +271° (both rotations measured in water (5)), fairly close to the difference (+386°, both measurements for chloroform solutions) between the molecular rotation of the ether (III) and of two molecules of 4-oxa-5α-cholestan-3α-ol. The formation of α,β′- and of β,β′-trehalose from two molecules of α-D-glucose involves shifts of −62° and −537° respectively (5).

EXPERIMENTAL

Di-(4-oxa-5α-cholestan-3α-yl) Ether

(a) From 4-Oxa-5α-cholest-2-ene

Ether solutions of 4-oxa-5α-cholest-2-ene were stored in an uncovered flask. The residue, after evaporation of the ether, was recrystallized several times from petroleum ether (b.p. 65–75°), giving *shining plates* melting at 205–208° (apparatus preheated to 190°; m.p. affected by rate of heating); $[\alpha]_D^{23}$ +116° (*c*, 1.30 in chloroform); $\nu_{max}^{CCl_4}$ in cm^{-1} (molar extinction coefficients in parentheses): 2930 (1120), 2860 (620), 1470 (300), 1449 (250), 1385 (235), 1370 (187), 1357 (156), 1339 (127), 1325 (108), 1161 (172), 1143 (313), 1123 (230), 1102 (245), 1092 (240), 1064 (425), 1052 (356), 1032 (520), 947 (236), 935 (233), 914 (104), 899 (142). Calc. for $C_{52}H_{90}O_3$: C, 81.82; H, 11.89%; mol. wt., 763. Found: C, 81.65; H, 11.67; mol. wt., 754 (Rast).

(b) From Reaction of 4-Oxa-5α-cholestan-3α-ol with 4-Oxa-5α-cholest-2-ene

A solution of 4-oxa-5α-cholestan-3α-ol (30 mg) and 4-oxa-5α-cholest-2-ene (30 mg) in anhydrous ether (5 ml) containing a trace of hydrogen chloride was allowed to evaporate at room temperature. The residue was recrystallized from ligroin, and the crystals were washed with ethyl acetate; the remaining solid (7 mg) was shown by melting point and infrared spectrum to be identical with the compound obtained above.

Hydrolysis of Di-(4-oxa-5α-cholestan-3α-yl) Ether

A solution of di-(4-oxa-5α-cholestan-3α-yl) ether (43 mg), water (20 drops), and concentrated aqueous hydrochloric acid (2 drops) in tetrahydrofuran (5 ml) was refluxed for 1 hour. The solvent was removed at reduced pressure, and the residue taken up in ether, washed with water, and dried over sodium sulphate. Evaporation of the ether left a crystalline solid (42 mg), m.p. 120–135°, shown to contain 4-oxa-5α-cholestan-3α-ol by its infrared spectrum. Recrystallization from methanol raised the melting point to 179–182° (28 mg), undepressed by admixture with authentic material.

ACKNOWLEDGMENTS

We are grateful to the National Research Council for a Studentship (to I. P.) and for financial support of the research, and to Miss D. J. Holder for a supply of 4-oxa-5α-cholest-2-ene.

1. J. T. Edward, P. F. Morand, and I. Puskas. Can. J. Chem. **39**, 2069 (1961).
2. L. E. Schniepp and H. H. Geller. J. Am. Chem. Soc. **68**, 1646 (1946). R. Paul. Bull. soc. chim. France, **1**, 971 (1934).
3. D. H. Whiffen. Chem. & Ind. (London), 964 (1956).
4. J. H. Brewster. J. Am. Chem. Soc. **81**, 5475, 5483 (1959).
5. W. N. Haworth and W. J. Hickinbottom. J. Chem. Soc. 2847 (1931).

Received October 10, 1961.
Department of Chemistry,
McGill University,
Montreal, Que.

STEROIDS

III. 12-METHYLENEPROGESTERONE

George Just and R. Nagarajan

We wish to report the synthesis of 12-methyleneprogesterone and an alternative route for the preparation of 12-hydroxy-12-methylpregnane derivatives (1, 2).

Partial succinylation of 3α,12α-dihydroxypregnane-20-one (I) at the 3-position (3, 4), and methylation of the hemisuccinate with diazomethane afforded the methyl succinate I*b*. Ketalization of the methyl succinate I*b* at the 20-position, followed by oxidation of the ketal II with chromium trioxide in pyridine (5) afforded 3α-hydroxypregnane-3,20-dione 20-ethylene ketal methyl succinate (III). This was a suitable intermediate for the introduction of a methyl group at C_{12}, and accordingly the 12-ketone III was reacted with an eightfold excess of methyl magnesium iodide. The Grignard reaction product was treated with *p*-toluene sulphonic acid and acetone, and then with methanolic potassium hydroxide to hydrolyze the ketal and methyl succinate groups respectively. The hydrolyzed product was oxidized with chromium trioxide and chromatographic separation of the oxidation product on alumina afforded the epimeric 12-methyl-12-hydroxypregnan-3,20-diones IV and V (1, 2). The yields of the 12α-alcohol IV and 12β-alcohol V were 25% and 12% respectively, for the reaction sequence III → IV + V. In accordance with our previously published results (1, 2), the 12α-alcohol IV was the major product.

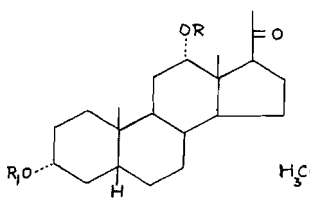

I $R = R_1 = H$

Ia $R = R_1 = COCH_3$

Ib $R = H, R_1 = CO(CH_2)_2CO_2CH_3$

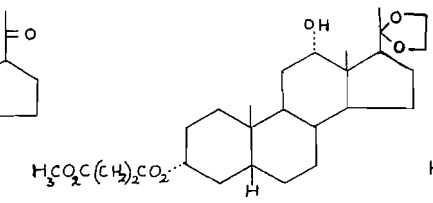

II

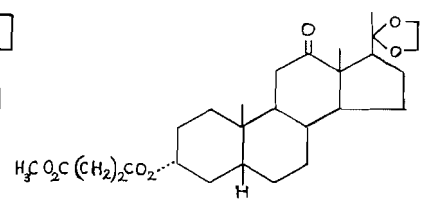

III

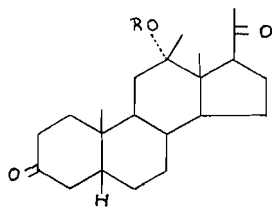

IV $R = H$

IVa $R = COCH_3$

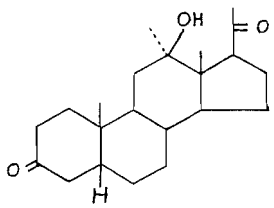

V

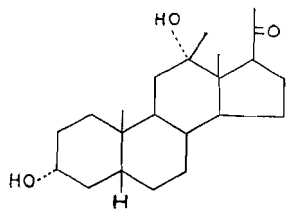

VI

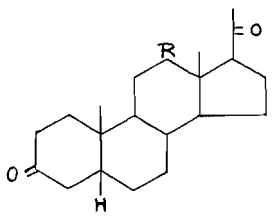

VII $R = =CH_2$

VIIa $R = =O$

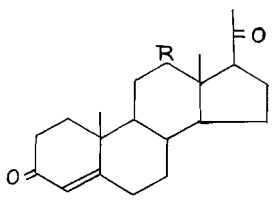

VIII $R = \begin{matrix} OH \\ CH_3 \end{matrix}$

VIIIa $R = =CH_2$

VIIIb $R = \begin{matrix} OCOCH_3 \\ CH_3 \end{matrix}$

Dehydration of the epimeric hydroxy ketones IV and V with phosphorus oxychloride and thionyl chloride in pyridine (6, 7) was unsuccessful. However, treatment of the hydroxy ketone V with acetic acid, acetic anhydride, and *p*-toluene sulphonic acid gave a 53% yield of the 12-methylene compound VII. It had been observed that the epimeric hydroxy ketone IV under similar reaction conditions also affords a 53% yield of the exo olefin VII (2).

Since Δ''-dehydroprogesterone exhibits high progestational activity (8), the effect of the incorporation of a 12,12*a*-double bond by introduction of a methylene group at C_{12} to the parent hormone seemed a worth-while investigation. Consequently, the progesterone

analogue VIII (1) was dehydrated with acetic acid, acetic anhydride, and *p*-toluene sulphonic acid to 12-methyleneprogesterone, VIII*a*. A minor product was obtained as an oil and it was assigned the 12α-acetoxy-12β-methylprogesterone configuration VIII*b* since its infrared spectrum showed absorption bands characteristic of an acetate group, and also because the analogous reaction of 12α-hydroxy-12β-methylpregnane-3,20-dione (IV) with acetic acid, acetic anhydride, and *p*-toluene sulphonic acid gave the exo olefin VII and the 12α-acetate IV*a* (2).

Preliminary biological tests of the two progesterone analogues VIII*a* and VIII*b* did not exhibit any notable progestational, androgenic, diuretic, hypotensive, or anabolic properties.[1]

EXPERIMENTAL[2, 3, 4, 5]

3α,12α-Dihydroxypregnan-20-one 3-Methyl Succinate (Ib) (4)

To a solution of the diol I (12.2 g, m.p. 164–167°; crude product obtained by alkaline hydrolysis of 15.0 g of the diacetate I*a*) in pyridine (125 ml) was added succinic anhydride (32.5 g); the resulting solution was heated at 90° for 2 hours and left at room temperature for 12 hours. The reaction mixture was extracted with ether. The organic layer was washed with 2 *N* hydrochloric acid, water, and then dried over magnesium sulphate. The ethereal solution was methylated with diazomethane. Crystallization from acetone–hexane afforded 13.427 g of the methyl succinate I*b* (4), m.p. 125–127° (yield 84%).

3α,12α-Dihydroxy-20-pregnanone Ethylene Ketal 3-Methyl Succinate (II)

To a solution of 8.99 g of the methyl succinate I*b* in absolute benzene (200 ml) was added ethylene glycol (20 ml) and *p*-toluene sulphonic acid (100 mg), and the reaction mixture was heated at reflux temperature for 12 hours. The water that formed during the reaction was continuously removed. The reaction mixture was extracted with ether, the ethereal layer washed with sodium bicarbonate solution and then with water, until the washings were neutral, and dried over magnesium sulphate. Repeated crystallizations from ether–hexane afforded 3.92 g of broad needles of the ketal II, m.p. 181–184° (yield 40%).

Two crystallizations from ether–hexane raised the melting point of II to 182–184°, $[\alpha]_D^{27}$ 57° (*c* 1.01 in $CHCl_3$). Calc. for $C_{28}H_{44}O_7$: C 68.26, H 9.00; found: C 68.40, H 9.07.

3α-Hydroxy-12,20-pregnandione 20-Ethylene Ketal 3-Methyl Succinate (III)

A solution of 3.2 g of the ketal II in pyridine (36 ml) was added to a slurry of chromium trioxide (3.2 g) in pyridine (32 ml) with stirring and left at room temperature for 16 hours (5). The reaction mixture was poured into 500 ml of water and extracted with chloroform. The organic layer was washed with iced 2 *N* hydrochloric acid, 5% sodium bicarbonate solution, and water, until the washings were neutral. The chloroform solution was dried over magnesium sulphate and evaporated to about 40 ml. On addition of 20 ml of hexane, the ketone III crystallized as needles, 2.404 g, m.p. 239–240°. The mother liquors on crystallization from methylene chloride – hexane afforded 0.364 g, m.p. 237–239° (yield 98%).

Recrystallization of the ketone III for analysis did not raise the melting point, $[\alpha]_D^{27}$ 96° (*c* 0.78 in $CHCl_3$). Calc. for $C_{28}H_{42}O_7$: C 68.55, H 8.63; found: C 68.64, H 8.65.

Reaction of Methyl Magnesium Iodide with 3α-Hydroxy-12,20-pregnandione 20-Ethylene Ketal 3-Methyl Succinate (III)

To 300 ml of an ethereal solution of methyl magnesium iodide (from 700 mg of magnesium and 2.0 ml of methyl iodide) was added with stirring a solution of 1.0 g of the ketone III in benzene, and the resulting mixture was heated at reflux temperature for 18 hours. A solution of ammonium chloride (20 g) in water (500 ml) was added to the reaction mixture. The usual extraction procedure afforded 930 mg of an oil.

To a solution of the Grignard adduct (930 mg of oil) in 50 ml of acetone was added with stirring 75 mg of *p*-toluene sulphonic acid and the reaction mixture left at room temperature for 22 hours. Ether extraction afforded 884 mg of an oil. An infrared spectrum analysis of the oil showed a strong absorption band at 1707 cm^{-1} (C_{20}-ketone), and a weak absorption band at 1725 cm^{-1} (C_3-methyl succinate).

A solution of this oil in 25 ml of 5% methanolic potassium hydroxide was heated at reflux temperature for 45 minutes. The usual extraction procedure afforded 735 mg of foam. It was dissolved in 10 ml of acetic

[1]*Biological tests were carried out by Drs. C. I. Chappel and C. Revesz of Messrs. Ayerst, McKenna and Harrison Ltd., Montreal, Que.*

[2]*All melting points are corrected.*

[3]*Only the best yields obtained were reported.*

[4]*The commercially available aluminum oxide (Woelm) was used for chromatography.*

[5]*The microanalyses were carried out by Dr. A. Bernhardt, Mülheim, Germany, and Dr. C. Daessle, 5757 Decelles St., Montreal, Que.*

acid, and to it was added with stirring a solution of 250 mg of chromium trioxide in 3 ml of 90% acetic acid. The reaction mixture was left at room temperature for 12 hours. Ether extraction afforded 740 mg of oil, and it was chromatographed on 23 g of alumina (4.5% water).

The hexane–benzene (1:1) eluates on crystallization from acetone–hexane afforded 106 mg of the trione VII*a* (1, 9), m.p. 197–199°, identified by mixed melting point and comparison of infrared spectra with an authentic sample. Crystallization of mother liquors from acetone–hexane gave 21 mg, m.p. 192–197°.

The first half of the benzene fractions on crystallization from ether–hexane afforded 67 mg of the hydroxy ketone V, m.p. 123–124°.

The rest of the benzene eluates and the benzene–ether (9:1, 4:1) fractions on crystallization from acetone–hexane afforded 80 mg of the hydroxy ketone IV, m.p. 187–188°. Crystallization of mother liquors gave 29 mg, m.p. 184–187°.

The ether–methanol (9:1) eluates on crystallization from acetone–hexane afforded 34 mg of needles of 3α,12α-dihydroxy-12β-methylpregnan-20-one (VI), m.p. 225–259°. Recrystallization from acetone–hexane raised the melting point to 228–230°, $[\alpha]_D^{27}$ 106° (*c* 0.74 in $CHCl_3$). Calc. for $C_{22}H_{36}O_3$: C 75.80, H 10.41; found: C 75.96, H 10.07.

Chromium trioxide oxidation of the hydroxy ketone VI (10 mg) afforded 3 mg of the hydroxy ketone IV, m.p. 186–188°, identified by mixed melting point and comparison of infrared spectra with an authentic sample (1).

Taking into consideration the unreacted ketone III (isolated as the trione VII*a*), the yields of 12α-alcohol IV and 12β-alcohol V were 25% and 12% respectively.

12-Methylenepregnan-3,20-dione (VII) from 12α-Methyl-12β-hydroxypregnan-3,20-dione (V)

To a solution of 330 mg of the hydroxy ketone V in 25 ml of acetic acid were added 5 ml of acetic anhydride and 330 mg of *p*-toluene sulphonic acid monohydrate (10), and the suspension was stirred until the solid dissolved. The reaction mixture was left at room temperature for 4 hours, then poured into 500 ml of iced water. After 30 minutes, the usual extraction procedure afforded 390 mg of an oil which showed absorption bands in the infrared at 3080 cm^{-1}, 1645 cm^{-1}, 890 cm^{-1} ($>C=CH_2$) (11); 1755 cm^{-1}, 1218 cm^{-1} ($\Delta^{17(20)}$-enol acetate) (12); 1713 cm^{-1} (3-ketone). Under the above reaction conditions the $\Delta^{17(20)}$-enol acetate is known to be formed (2, 13). The enol acetate (390 mg of oil) was converted to the C_{20}-ketone by heating a solution of it in 30 ml of methanol and 700 mg of potassium carbonate in 10 ml of water at reflux temperature for 2 hours. Ether extraction afforded 360 mg of product showing no bands at 1750 cm^{-1} and 1218 cm^{-1} characteristic of enol acetates, and it was chromatographed on 10 g of alumina (4.5% water). The hexane–benzene (4:1, 1:1) eluates containing the olefin VII[6] crystallized from ether–hexane as needles, 134 mg, m.p. 89–90°. Crystallization of mother liquors afforded 33 mg, m.p. 89–90° (yield 53.4%).

A portion of the olefin VII was recrystallized from ether–hexane for analysis, m.p. 89–90°, $[\alpha]_D^{27}$ 133° (*c* 1.02 in $CHCl_3$), $\nu_{max}^{CS_2}$ 3075 cm^{-1}, 1645 cm^{-1}, 888 cm^{-1} ($>C=CH_2$); 1713 cm^{-1} (3,20-ketone). Calc. for $C_{22}H_{32}O_2$: C 80.41, H 9.82; found: C 80.18, H 9.84.

The benzene and benzene–ether eluates on crystallization from acetone–hexane afforded 56 mg of leaflets of IV*a* (1), m.p. 175–176° (yield 15.1%).

12-Methyleneprogesterone (VIIIa) and 12β-Methyl-12α-acetoxyprogesterone (VIIIb)

According to the procedure previously described by us (1), 900 mg of the hydroxy ketone IV was transformed to the progesterone analogue VIII. Crystallization from ether–hexane afforded 330 mg of VIII, m.p. 152–153°. The mother liquors (590 mg) were chromatographed on 17 g of alumina (4.5% water). The benzene and benzene–ether eluates on crystallization from ether–hexane afforded 160 mg of the progesterone analogue VIII, m.p. 152–153°. Crystallization of mother liquors afforded 51 mg, m.p. 135–142° (yield 61%).

In a solution of the progesterone analogue VIII (475 mg, m.p. 152–153°) in 25 ml of acetic acid and 5 ml of acetic anhydride was dissolved 475 mg of *p*-toluene sulphonic acid with stirring. The reaction mixture was left at room temperature for 2 hours. Ether extraction afforded 540 mg of an oil, and it was dissolved in 25 ml of methanol. To the methanol solution was added 750 mg of potassium carbonate dissolved in 10 ml of water and the reaction mixture was heated at reflux temperature for 2 hours. The usual extraction procedure afforded 520 mg of an oil, which was chromatographed on 15 g of alumina (4.5% water). The

[6]*In our previous publication it was concluded that the compound with m.p. 100–101° was the olefin VII and the compound with m.p. 73–74° contained mainly the exo olefin with probably traces of the endo olefin (2). It now seems that all the three forms melting at 73–74°, 89–90°, and 100–101° are different polymorphic forms of the olefin VII on the basis of the following evidence: A mixed melting point of the two forms of olefin VII melting at 73–74° and 89–90° on a Kofler block showed the form melting at 73–74° melted at the latter temperature, but crystallized on further raising the temperature, and the whole mass melted at 89–90°. The two forms of olefin melting at 89–90° and 100–101° were melted side by side, and the molten mass was seeded with a crystal of the form melting at 89–90°, and cooled. The whole mass melted at 89–90°. Furthermore, the infrared spectra and the rotations of the three forms were identical within experimental error.*

hexane–benzene (4:1, 1:1) and benzene eluates on crystallization from ether–hexane afforded 121 mg of cubic crystals of 12-methyleneprogesterone, VIII*a*,[7] m.p. 104–105° (yield 27%). Two recrystallizations from ether–hexane raised the melting point to 105–106°, $[\alpha]_D^{27}$ 189° (*c* 0.92 in $CHCl_3$), λ_{max}^{EtOH} 240 mμ (ε 18,500). $\nu_{max}^{CCl_4}$ 3070 cm^{-1}, 1643 cm^{-1}, 890 cm^{-1} (>CH=CH$_2$); 1707 cm^{-1} (20-ketone); 1675 cm^{-1}, 1617 cm^{-1} (Δ^4-3-ketone). Calc. for $C_{22}H_{30}O_2$: C 80.91, H 9.25; found: C 80.70, H 9.05.

The benzene–ether eluates afforded 210 mg of an oil which resisted crystallization. Its infrared spectrum showed absorption bands at 1727 cm^{-1} (12-acetate); 1705 cm^{-1} (20-ketone); 1675 cm^{-1}, 1617 cm^{-1} (Δ^4-3-ketone). It was tentatively assigned the 12β-methyl-12α-acetoxyprogesterone configuration VIII*b* on the basis of its infrared spectrum, and from the analogous reaction that 12β-methyl-12α-hydroxypregnan-3,20-dione with acetic acid, acetic anhydride, and *p*-toluene sulphonic acid gives 12β-methyl-12α-acetoxypregnan-3,20-dione as the minor product of the reaction (2).

ACKNOWLEDGMENTS

We wish to express our thanks to the National Research Council, and Messrs. Ayerst, McKenna and Harrison Ltd. for generous financial assistance.

1. G. Just and R. Nagarajan. Can. J. Chem. **39**, 548 (1961).
2. R. Nagarajan and G. Just. Can. J. Chem. **39**, 1274 (1961).
3. E. Schwenk, B. Riegel, R. B. Moffett, and E. Stahl. J. Am. Chem. Soc. **65**, 549 (1943). M. Sorkin and T. Reichstein. Helv. Chim. Acta, **29**, 1218 (1946).
4. Ch. R. Engel and W. W. Huculak. Can. J. Chem. **37**, 2031 (1959).
5. G. I. Poos, G. E. Arth, R. E. Beyler, and L. H. Sarett. J. Am. Chem. Soc. **75**, 422 (1953).
6. P. Bladon and W. McMeekin. J. Chem. Soc. 2191 (1960).
7. S. G. Levine and M. E. Wall. J. Am. Chem. Soc. **82**, 3391 (1960).
8. P. Hegner and T. Reichstein. Helv. Chim. Acta, **26**, 715 (1943). J. von Euw and T. Reichstein. Helv. Chim. Acta, **29**, 654 (1946).
9. T. Reichstein and E. v. Arx. Helv. Chim. Acta, **23**, 747 (1940).
10. R. B. Turner. J. Am. Chem. Soc. **75**, 3489 (1953).
11. L. J. Bellamy. The infrared spectra of complex molecules. John Wiley and Sons, Inc., New York. 1958. p. 34.
12. H. Vanderhaeghe, E. R. Katzenellenbogen, K. Dobriner, and T. F. Gallagher. J. Am. Chem. Soc. 74, 2810 (1952).
13. P. Z. Bedoukian. J. Am. Chem. Soc. **67**, 1430 (1945). C. W. Marshall, T. H. Kritchevsky, S. Lieberman, and T. F. Gallagher. J. Am. Chem. Soc. **70**, 1837 (1948).

Received October 20, 1961.
Department of Chemistry,
McGill University,
Montreal, Quebec.

PREPARATION OF ALUMINUM *tert*-ALKOXIDES

M. S. Bains*

The alcohol interchange method for the preparation of aluminum alkoxides has been mentioned by various workers (1, 2) and was used elegantly by Mehrotra (3, 4) in preparing pure primary and secondary aluminum alkoxides for studying their physical properties. It was claimed that repeated attempts to obtain aluminum *tert*-butoxide and aluminum *tert*-amyloxide from aluminum isopropoxide by the interchange method failed since the third isopropoxide group did not interchange. Steric hindrance was considered the main cause for this failure of complete interchange and consequently for steric reasons the dimeric nature of these mixed alkoxides was proposed through isopropoxide bridges as

[7]*The progesterone derivative VIIIa was obtained in another polymorphic modification as needles, m.p. 135–136°.*

**National Research Council of Canada Postdoctoral Fellow. Present address: Chemistry Department, Panjab University, Chandigarh-3, India.*

hexane–benzene (4:1, 1:1) and benzene eluates on crystallization from ether–hexane afforded 121 mg of cubic crystals of 12-methyleneprogesterone, VIII*a*,[7] m.p. 104–105° (yield 27%). Two recrystallizations from ether–hexane raised the melting point to 105–106°, $[\alpha]_D^{27}$ 189° (*c* 0.92 in $CHCl_3$), λ_{max}^{EtOH} 240 mμ (ε 18,500). $\nu_{max}^{CCl_4}$ 3070 cm^{-1}, 1643 cm^{-1}, 890 cm^{-1} (>CH=CH$_2$); 1707 cm^{-1} (20-ketone); 1675 cm^{-1}, 1617 cm^{-1} (Δ^4-3-ketone). Calc. for $C_{22}H_{30}O_2$: C 80.91, H 9.25; found: C 80.70, H 9.05.

The benzene–ether eluates afforded 210 mg of an oil which resisted crystallization. Its infrared spectrum showed absorption bands at 1727 cm^{-1} (12-acetate); 1705 cm^{-1} (20-ketone); 1675 cm^{-1}, 1617 cm^{-1} (Δ^4-3-ketone). It was tentatively assigned the 12β-methyl-12α-acetoxyprogesterone configuration VIII*b* on the basis of its infrared spectrum, and from the analogous reaction that 12β-methyl-12α-hydroxypregnan-3,20-dione with acetic acid, acetic anhydride, and *p*-toluene sulphonic acid gives 12β-methyl-12α-acetoxypregnan-3,20-dione as the minor product of the reaction (2).

ACKNOWLEDGMENTS

We wish to express our thanks to the National Research Council, and Messrs. Ayerst, McKenna and Harrison Ltd. for generous financial assistance.

1. G. Just and R. Nagarajan. Can. J. Chem. **39**, 548 (1961).
2. R. Nagarajan and G. Just. Can. J. Chem. **39**, 1274 (1961).
3. E. Schwenk, B. Riegel, R. B. Moffett, and E. Stahl. J. Am. Chem. Soc. **65**, 549 (1943). M. Sorkin and T. Reichstein. Helv. Chim. Acta, **29**, 1218 (1946).
4. Ch. R. Engel and W. W. Huculak. Can. J. Chem. **37**, 2031 (1959).
5. G. I. Poos, G. E. Arth, R. E. Beyler, and L. H. Sarett. J. Am. Chem. Soc. **75**, 422 (1953).
6. P. Bladon and W. McMeekin. J. Chem. Soc. 2191 (1960).
7. S. G. Levine and M. E. Wall. J. Am. Chem. Soc. **82**, 3391 (1960).
8. P. Hegner and T. Reichstein. Helv. Chim. Acta, **26**, 715 (1943). J. von Euw and T. Reichstein. Helv. Chim. Acta, **29**, 654 (1946).
9. T. Reichstein and E. v. Arx. Helv. Chim. Acta, **23**, 747 (1940).
10. R. B. Turner. J. Am. Chem. Soc. **75**, 3489 (1953).
11. L. J. Bellamy. The infrared spectra of complex molecules. John Wiley and Sons, Inc., New York. 1958. p. 34.
12. H. Vanderhaeghe, E. R. Katzenellenbogen, K. Dobriner, and T. F. Gallagher. J. Am. Chem. Soc. 74, 2810 (1952).
13. P. Z. Bedoukian. J. Am. Chem. Soc. **67**, 1430 (1945). C. W. Marshall, T. H. Kritchevsky, S. Lieberman, and T. F. Gallagher. J. Am. Chem. Soc. **70**, 1837 (1948).

Received October 20, 1961.
Department of Chemistry,
McGill University,
Montreal, Quebec.

PREPARATION OF ALUMINUM *tert*-ALKOXIDES

M. S. Bains*

The alcohol interchange method for the preparation of aluminum alkoxides has been mentioned by various workers (1, 2) and was used elegantly by Mehrotra (3, 4) in preparing pure primary and secondary aluminum alkoxides for studying their physical properties. It was claimed that repeated attempts to obtain aluminum *tert*-butoxide and aluminum *tert*-amyloxide from aluminum isopropoxide by the interchange method failed since the third isopropoxide group did not interchange. Steric hindrance was considered the main cause for this failure of complete interchange and consequently for steric reasons the dimeric nature of these mixed alkoxides was proposed through isopropoxide bridges as

[7]*The progesterone derivative VIIIa was obtained in another polymorphic modification as needles, m.p. 135–136°.*

**National Research Council of Canada Postdoctoral Fellow. Present address: Chemistry Department, Panjab University, Chandigarh-3, India.*

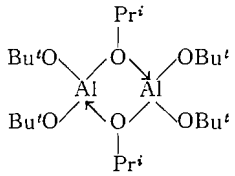

(I)

and

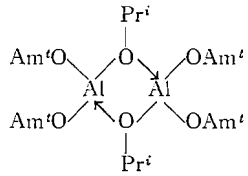

(II)

However, aluminum *tert*-butoxide could be prepared by direct action of *tert*-butanol on aluminum (5), but aluminum *tert*-amyloxide could not be obtained by this method.

Nevertheless, in the present research, attempts to prepare aluminum monoisopropoxide di-*tert*-butoxide, $Al(OPr^i)(OBu^t)_2$, by the interchange method resulted in the formation of aluminum tri-*tert*-butoxide and it was very difficult to prepare the pure mixed alkoxide in one operation. Found: Al, 10.91, 10.90%; $Al(OBu^t)_3$ requires: Al, 10.95%.

The interchange of aluminum isopropoxide with *tert*-amyl alcohol or diethylmethyl carbinol gave the hitherto unknown aluminum *tert*-amyloxide, $Al(OAm^t)_3$, or aluminum diethylmethylcarbinoloxide, $Al(OCMeEt_2)_3$, respectively. The former compound was sublimed at 130–135° C bath temperature under 0.02–0.03 mm pressure and the latter was sublimed at 155° C under the same pressure. The analysis for aluminum was as follows:

	Aluminum analysis		
Compound	Found		Calculated
$Al(OAm^t)_3$	9.3	9.35	9.37
$Al(OCMeEt_2)_3$	8.3	8.4	8.20

Since the higher tertiary alcohols are extremely sensitive to acids it is important that the reagents should be freed from acidic impurities. The apparatus should be washed with alkali and rinsed with distilled water before it is dried and used. The temperature of the heating bath for reflux purposes should be kept as low as possible and under no circumstances should a heating mantle be used since it may cause overheating.

A careful study of the literature (4, 6, 7) shows that in the preparation of aluminum *tert*-alkoxides by transesterification there is no evidence that the interchange of the third alkoxide group is hindered. Even Mehrotra's own results (4) show that in one of his interchange reactions, the ratio of Pr^iO:Al is 0.81 in the unsublimed material. Still he seems to draw a parallelism in his publications (4, 6) with previous work on zirconium alkoxides (9) and believes that the shielding effect of *tert*-alkoxide groups (I and II) hindered the co-ordination of *tert*-butanol for further interchange. In fact, it appears that, in his experiments, insufficient time was allowed for interchange to reach completion. Some preliminary experiments on alcohol interchange have further shown that even at a lower temperature (36° C) the interchange was approaching completion in the case of aluminum isopropoxide and *tert*-butyl alcohol.

Furthermore, the proton magnetic resonance spectrum (8) of the mixed alkoxide, $Al(OPr^i)(OBu^t)_2$, revealed resonances corresponding to two distinguishable isopropoxide groups and two *tert*-butoxide groups, quantitatively in accordance with the participation of both alkoxide groups in bridging. This indicates that the steric factors involved are not strong enough to prevent the *tert*-butoxide groups from bridging. Moreover, the fact that aluminum *tert*-butoxide is dimeric supports this conclusion since, in this compound, the bridging must of necessity involve the *tert*-butoxide groups.

The details of this work will be published in due course.

ACKNOWLEDGMENTS

The author is indebted to Professor D. C. Bradley for valuable discussion and wishes to thank the National Research Council (Canada) for supporting this research.

1. H. Adkins and F. W. Cox. J. Am. Chem. Soc. **60**, 1151 (1938).
2. C. Tischenko. J. Russ. Phys. Chem. Soc. **31**, 694, 784 (1899).
3. R. C. Mehrotra. J. Ind. Chem. Soc. **31**, 85 (1954).
4. R. C. Mehrotra. J. Ind. Chem. Soc. **30**, 585 (1953).
5. W. Wayne and H. Adkins. Org. Syntheses. **21**, p. 8 (1941).
6. R. C. Mehrotra. J. Am. Chem. Soc. **76**, 2266 (1954).
7. R. H. Baker. J. Am. Chem. Soc. **60**, 2673 (1938).
8. M. S. Bains, D. C. Bradley, and J. B. Stothers. Unpublished results.
9. D. C. Bradley, R. C. Mehrotra, and W. Wardlaw. J. Chem. Soc. 4204 (1952).

Received October 20, 1961.
Chemistry Department,
The University of Western Ontario,
London, Ontario.

FURANOCOUMARINS OF PHELLOPTERUS LITTORALIS*

Chao-Hwa Yang† and Stewart A. Brown

Phellopterus littoralis Benth. has been reported by Noguchi and Kawanami (1) to contain the furanocoumarin pheleopterin (I*a*) in the fruit. Our interest in the biosynthesis of coumarins led us to initiate a preliminary extraction study of the coumarins in this species. This note reports the identification of bergapten (I*b*) and the tentative identification of imperatorin (I*c*) in extracts of greenhouse-grown plants, as well as the presence

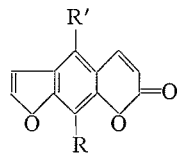

Structure I

(*a*) R = $OCH_2CH{=}C(CH_3)_2$; R′ = OCH_3
(*b*) R = H; R′ = OCH_3
(*c*) R = $OCH_2CH{=}C(CH_3)_2$; R′ = H

of still-unidentified coumarins, but the failure to confirm the presence of phellopterin. The first two coumarins have not been found previously in this species. Evidence for the presence of imperatorin in *Phellopterus* plants up to the early fruiting stage was found, but when an attempt was made to confirm its presence in older plants imperatorin could not be detected, and instead the fruits, and probably the roots as well, contained bergapten. The Japanese authors gave no information about their source plants except the location of collection, but the present observations suggest that the stage of growth is an important factor controlling the nature of the coumarin pattern in this species.

The tentative identification of imperatorin is based on paper chromatographic behavior and on the fact that all absorption maxima of the unknown coumarin and authentic

*Issued as N.R.C. No. 6641.
†National Research Council Postdoctorate Fellow, 1959–60. Present address: University of Oklahoma Research Institute, Norman, Okla., U.S.A.

ACKNOWLEDGMENTS

The author is indebted to Professor D. C. Bradley for valuable discussion and wishes to thank the National Research Council (Canada) for supporting this research.

1. H. Adkins and F. W. Cox. J. Am. Chem. Soc. **60**, 1151 (1938).
2. C. Tischenko. J. Russ. Phys. Chem. Soc. **31**, 694, 784 (1899).
3. R. C. Mehrotra. J. Ind. Chem. Soc. **31**, 85 (1954).
4. R. C. Mehrotra. J. Ind. Chem. Soc. **30**, 585 (1953).
5. W. Wayne and H. Adkins. Org. Syntheses. **21**, p. 8 (1941).
6. R. C. Mehrotra. J. Am. Chem. Soc. **76**, 2266 (1954).
7. R. H. Baker. J. Am. Chem. Soc. **60**, 2673 (1938).
8. M. S. Bains, D. C. Bradley, and J. B. Stothers. Unpublished results.
9. D. C. Bradley, R. C. Mehrotra, and W. Wardlaw. J. Chem. Soc. 4204 (1952).

Received October 20, 1961.
Chemistry Department,
The University of Western Ontario,
London, Ontario.

FURANOCOUMARINS OF PHELLOPTERUS LITTORALIS*

Chao-Hwa Yang† and Stewart A. Brown

Phellopterus littoralis Benth. has been reported by Noguchi and Kawanami (1) to contain the furanocoumarin pheleopterin (I*a*) in the fruit. Our interest in the biosynthesis of coumarins led us to initiate a preliminary extraction study of the coumarins in this species. This note reports the identification of bergapten (I*b*) and the tentative identification of imperatorin (I*c*) in extracts of greenhouse-grown plants, as well as the presence

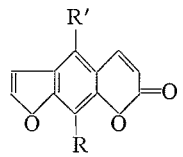

Structure I

(*a*) R = $OCH_2CH{=}C(CH_3)_2$; R′ = OCH_3
(*b*) R = H; R′ = OCH_3
(*c*) R = $OCH_2CH{=}C(CH_3)_2$; R′ = H

of still-unidentified coumarins, but the failure to confirm the presence of phellopterin. The first two coumarins have not been found previously in this species. Evidence for the presence of imperatorin in *Phellopterus* plants up to the early fruiting stage was found, but when an attempt was made to confirm its presence in older plants imperatorin could not be detected, and instead the fruits, and probably the roots as well, contained bergapten. The Japanese authors gave no information about their source plants except the location of collection, but the present observations suggest that the stage of growth is an important factor controlling the nature of the coumarin pattern in this species.

The tentative identification of imperatorin is based on paper chromatographic behavior and on the fact that all absorption maxima of the unknown coumarin and authentic

*Issued as N.R.C. No. 6641.
†National Research Council Postdoctorate Fellow, 1959–60. Present address: University of Oklahoma Research Institute, Norman, Okla., U.S.A.

imperatorin are identical over the range of 220–340 mμ. Insufficient material was available for rigorous purification, and as authentic phellopterin was not obtainable, the possibility that the unknown is phellopterin has not been strictly eliminated. Imperatorin and phellopterin both melt at 102°.

The demonstration of bergapten, and probably imperatorin, in this species is of interest from the biosynthetic point of view because of the structural similarities of both these coumarins to phellopterin. However, any attempt to suggest definite pathways of biosynthesis on the basis of existing data would be premature.

EXPERIMENTAL

Coumarins of Roots

In the late summer of 1959 young *Phellopterus* plants, grown from seed, were transplanted to coarse quartz sand which was irrigated at intervals from below with "California" nutrient medium (2). The temperature of the greenhouse was maintained at 25.5° during the day and 17° at night. Toward the end of January, 1960, three plants were harvested and dried under reduced pressure below 40° to give a total of ca. 20 g of powdered roots and 40 g of powdered shoots. After separate ether extractions of the root and shoot residues in Soxhlet extractors, a lactone fraction was prepared from each extract by the method of Baerheim Svendsen and Ottestad (3), which involved successive removal of acidic, phenolic, and unsaponifiable fractions from the ether extracts. Paper-chromatographic study of the lactone fractions indicated the absence of coumarins in the shoot extract, but the root extract contained small amounts of coumarin-like compounds. Several weeks later a second extraction representing 120 g of dried plant yielded an additional lactone fraction, but this was contaminated with oily material. The oil was largely distilled onto a cold finger by several hours' heating at 90° at a pressure below 1 mm Hg, and the residue was passed through an alumina column with benzene as the eluent. Coumarins moved off the column in two bands which fluoresced yellow when viewed under ultraviolet light (3660 Å), each band yielding a very small amount of a white solid upon solvent removal. Characterization was carried out by chromatographic comparison on paper with authentic samples of furanocoumarins. The material in the major band closely resembled imperatorin in its chromatographic behavior and its appearance under ultraviolet illumination after being sprayed with 1% alcoholic potassium hydroxide.

Coumarins of Fruits

At the end of March, 1960, fresh green fruits (160 g) were extracted by disintegration with a convenient volume of hot ethanol in a Waring blendor, and filtered. After two additional extractions of the residue with hot 80% ethanol, the combined extracts were concentrated *in vacuo* and the aqueous residue submitted to continuous ether extraction. The lactone fraction from the ether extract was isolated as described above. Chromatography of the coumarin fraction on alumina (Woelm, Grade II, non-alkaline) with benzene effected a separation of three major bands. The fastest gave 2 mg of crystals which were recrystallized from ether as long, colorless needles with an ultraviolet absorption spectrum in ethanol identical with that of authentic imperatorin (maxima at 249 and 300 mμ, shoulders at 243 and 264 mμ). The R_f values and other behavior of these two compounds checked very well when they were compared in 15% acetic acid and in isopropanol–water (1:4) on paper. The unknown had, however, a melting range of 90–95° (imperatorin melts at 102°), and as too little remained for further purification, the identification must be considered only tentative.

The compound from the second band gave 14 mg of colorless crystals after two recrystallizations from ether, m.p. 64–65°. In ethanol it gave a simple absorption spectrum with only two maxima, at 246 and 287 mμ. Its identity was not established, but its low melting point and simple spectrum suggest that it may be a furanocoumarin with a long aliphatic chain joined to the nucleus in an ether linkage. The last band from the column yielded only 3 mg of colorless solid, which was not purified.

In an attempt to obtain the additional material necessary for unequivocal identification, fresh fruits totalling 2 kg were collected over a 2-month period (May–July), and stored in the frozen state until used. The isolation procedure was modified to avoid heating *in vacuo*, which has been reported (4) to cause migration of the aliphatic chain of imperatorin to form an artifact, alloimperatorin. Oily material was removed from the lactone fraction by passage through a cellulose column in 20% isopropanol. The isopropanol in the eluate was removed by concentration *in vacuo*, and the coumarins in the aqueous residue were recovered by continuous ether extraction. The individual coumarins were separated in benzene solution on an alumina column (Woelm, Grade III, non-alkaline). Contrary to the assumption that it would be imperatorin, the material from the fast-moving band in this experiment gave colorless crystals which melted sharply at 185°. Its ultraviolet absorption spectrum closely resembled that of bergapten. When mixed with authentic bergapten, it caused no lowering of the melting point. The root coumarin fraction isolated at this growth stage also showed evidence of the presence of bergapten.

ACKNOWLEDGMENTS

Seeds of *Phellopterus littoralis* were generously donated by the Kusakabe Experimental Station, Saitama, Japan. We wish to thank Dr. Gerhard Billek of the University of Vienna, Dr. Asima Chatterjee of the University College of Science and Technology, Calcutta, and Dr. Giovanni Rodighiero of Padova University for various authentic coumarin samples used in this study.

1. T. NOGUCHI and M. KAWANAMI. J. Pharm. Soc. Japan, **60**, 57 (1940).
2. C. ELLIS and M. W. SWANEY. Soilless growth of plants. 2nd ed. *Revised and enlarged by* T. EASTWOOD. Reinhold Publishing Corp., New York. 1947.
3. A. BAERHEIM SVENDSEN and E. OTTESTAD. Pharm. Acta Helv. **32**, 457 (1957).
4. T. NOGUCHI and M. KAWANAMI. J. Pharm. Soc. Japan, **61**, 77 (1941); Chem. Abstr. **36**, 464 (1942).

RECEIVED OCTOBER 30, 1961.
NATIONAL RESEARCH COUNCIL,
PRAIRIE REGIONAL LABORATORY,
SASKATOON, SASK.

THE THERMOSIPHON AS A SIMPLE CIRCULATING PUMP FOR GASES*

D. VAN DER AUWERA† AND R. A. BACK

In gas kinetics and related fields, there is often a need for an efficient means of circulating gases in a closed system. Most pumps used in the past have been of either a piston-and-valve or a rotary-impeller type. While these pumps are reasonably satisfactory for most purposes, they suffer certain disadvantages, such as low flowrates (limited by displacement), intermittent action (piston pumps), mechanical failure, and an almost complete loss of efficiency at pressures below 1 mm Hg. For the past 2 years we have been using a thermosiphon as a circulating pump in this laboratory, and it appears to have some advantages in these respects. We thought it worth while to describe its characteristics, and to point out some of its advantages and limitations.

The thermosiphon consisted of two parallel Pyrex tubes, 25-mm i.d. and 2.1 m long, mounted vertically, and joined at the top in a smooth U-bend. One tube could be heated electrically, while the other was cooled by tap water passing through a jacket. The lower ends of the thermosiphon were joined to the components completing the circulation system, which in this case comprised two U-traps about 30 cm long and a cylindrical photolysis cell of about 200-cc capacity. The traps and all connecting tubing were of 20-mm i.d.

Flowrates were measured by injecting a small quantity of a second gas into the system and following its passage around the circuit by means of a thermistor mounted in the gas stream and linked through a suitable bridge to a chart recorder. The mixing of the added gas was slow enough so that from 10 to 20 complete passages around the circuit, each marked by a sharp deflection of the recorder pen, were easily observed, and the volume flowrate calculated.

Issued as N.R.C. No. 6635.
†*N.R.C. Postdoctorate Fellow 1959–61.*

ACKNOWLEDGMENTS

Seeds of *Phellopterus littoralis* were generously donated by the Kusakabe Experimental Station, Saitama, Japan. We wish to thank Dr. Gerhard Billek of the University of Vienna, Dr. Asima Chatterjee of the University College of Science and Technology, Calcutta, and Dr. Giovanni Rodighiero of Padova University for various authentic coumarin samples used in this study.

1. T. NOGUCHI and M. KAWANAMI. J. Pharm. Soc. Japan, **60**, 57 (1940).
2. C. ELLIS and M. W. SWANEY. Soilless growth of plants. 2nd ed. *Revised and enlarged by* T. EASTWOOD. Reinhold Publishing Corp., New York. 1947.
3. A. BAERHEIM SVENDSEN and E. OTTESTAD. Pharm. Acta Helv. **32**, 457 (1957).
4. T. NOGUCHI and M. KAWANAMI. J. Pharm. Soc. Japan, **61**, 77 (1941); Chem. Abstr. **36**, 464 (1942).

RECEIVED OCTOBER 30, 1961.
NATIONAL RESEARCH COUNCIL,
PRAIRIE REGIONAL LABORATORY,
SASKATOON, SASK.

THE THERMOSIPHON AS A SIMPLE CIRCULATING PUMP FOR GASES*

D. VAN DER AUWERA† AND R. A. BACK

In gas kinetics and related fields, there is often a need for an efficient means of circulating gases in a closed system. Most pumps used in the past have been of either a piston-and-valve or a rotary-impeller type. While these pumps are reasonably satisfactory for most purposes, they suffer certain disadvantages, such as low flowrates (limited by displacement), intermittent action (piston pumps), mechanical failure, and an almost complete loss of efficiency at pressures below 1 mm Hg. For the past 2 years we have been using a thermosiphon as a circulating pump in this laboratory, and it appears to have some advantages in these respects. We thought it worth while to describe its characteristics, and to point out some of its advantages and limitations.

The thermosiphon consisted of two parallel Pyrex tubes, 25-mm i.d. and 2.1 m long, mounted vertically, and joined at the top in a smooth U-bend. One tube could be heated electrically, while the other was cooled by tap water passing through a jacket. The lower ends of the thermosiphon were joined to the components completing the circulation system, which in this case comprised two U-traps about 30 cm long and a cylindrical photolysis cell of about 200-cc capacity. The traps and all connecting tubing were of 20-mm i.d.

Flowrates were measured by injecting a small quantity of a second gas into the system and following its passage around the circuit by means of a thermistor mounted in the gas stream and linked through a suitable bridge to a chart recorder. The mixing of the added gas was slow enough so that from 10 to 20 complete passages around the circuit, each marked by a sharp deflection of the recorder pen, were easily observed, and the volume flowrate calculated.

Issued as N.R.C. No. 6635.
†*N.R.C. Postdoctorate Fellow 1959–61.*

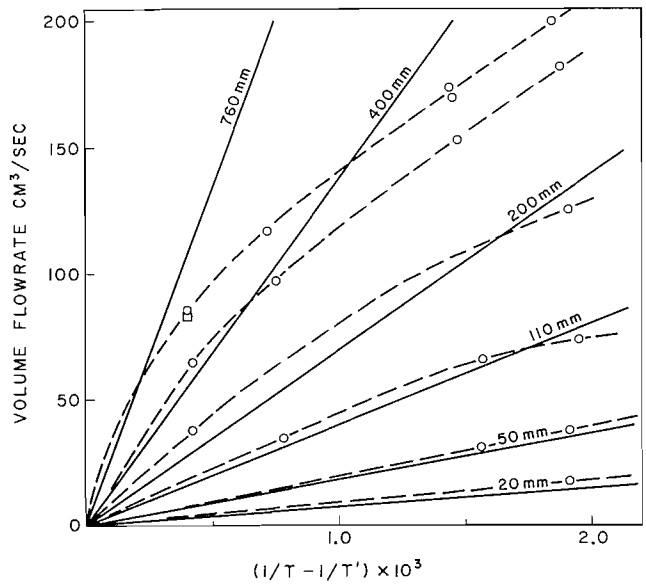

Fig. 1. Volume flowrates in thermosiphon. Solid lines are calculated, dashed curves are measured values. ○ = nitrogen, □ = methane.

Figure 1 shows measured flowrates of nitrogen and methane at various pressures, plotted against $(1/T-1/T')$, where T and T' are the absolute temperatures of the cold and hot arms of the thermosiphon respectively. It is interesting to compare these observed flowrates with those predicted by simple theory. The difference in density of the gas in the two arms introduces a force which drives the gas through the system at a volume flowrate (assuming simple viscous flow) given by

$$F = \frac{(\pi g/128R)(M/\eta)hP(1/T-1/T')}{r_I+r_E},$$

where g = gravitational acceleration, R = gas constant, M = molecular weight, η = coefficient of viscosity, h = height of thermosiphon, P = pressure, and r is a "flow resistance" defined as $\sum (L_i/d_i^4)$ where L_i and d_i are the length and diameter respectively of each component of the flow circuit. The term r_I is the "internal" flow resistance of the thermosiphon itself, while r_E is that of the "external" components of the system.

Flowrates calculated from this equation are shown as the solid lines in Fig. 1. At low pressures and flowrates, the measured values lie somewhat above the calculated ones, perhaps due to error in estimating r_I and r_E. The linear dependence of F upon P and upon $(1/T-1/T')$ is approximately confirmed by experiment at low pressures and flowrates, but F falls off rather badly at flowrates greater than 100 cc/sec. This is probably due to the failure of the gas to attain the temperature of the walls immediately upon entering each arm of the siphon. An increase in either pressure or flowrate enhances this effect and reduces the average temperature difference between the arms. This was, in fact, observed with a thermocouple mounted in the gas stream.

The relative flowrates obtained with nitrogen ($M/\eta = 1.57$) and methane ($M/\eta = 1.48$), shown in Fig. 1, are in approximate agreement with a linear dependence of F upon M/η.

Using experimentally practical values of h, P, T, and T', the absolute value of ΔP generated is very small, so that the flow resistance must be minimized in order to achieve

high flowrates. This is the most serious limitation of the thermosiphon, and makes it quite impractical as a means of forcing a gas through a constricted system. Furthermore, the need for large-bore tubing, since r varies as d^4, results in a rather large volume. Within these limitations, however, the thermosiphon is remarkably flexible, as the four parameters h, P, $(1/T-1/T')$, and r may be varied almost independently.* Thus, for example, if experimental conditions dictate certain values of P, T, and T', then h and r may be adjusted to give the desired flowrate, etc. In practice, T' is the most conveniently controlled parameter, permitting wide variation in F from 0 up to a maximum value dependent on the other parameters and upon the thermal stability of the gas.

The dependence of F upon d^4 permits, in theory, the achievement of very high flowrates where d is not limited by other factors. The observed fall-off in F (Fig. 1), probably due to the time lag in heating and cooling the gas in the two arms, could be at least partially eliminated by suitable preheating and precooling, and by increasing h. With its inability to operate against an appreciable pressure gradient or flow resistance, and its high flowrates, limited in theory only by d, the thermosiphon is seen to be the converse of the piston pump, in which the flowrate is fixed by the displacement, but which will operate against a large and variable pressure head.

The dependence of F upon pressure also deserves some comment. Although F decreases linearly with decreasing pressure, there should be no sudden loss of efficiency at low pressures, as observed with piston and impeller pumps, and in fact, F should increase somewhat as viscous flow gives way to molecular flow. Thus, if large enough values of h, T', and d can be used, the thermosiphon should operate well at pressures from 1 mm to 10^{-3} mm.

Finally, it should be noted that the thermosiphon has no moving parts or electronic components, and is thus completely reliable and trouble-free in operation.

Received October 25, 1961.
Division of Pure Chemistry,
National Research Council,
Ottawa, Canada.

NUCLEAR MAGNETIC RESONANCE STUDIES OF HYDROGEN BONDING IN ETHANOL AND 2,2,2-TRIFLUOROETHANOL

B. D. Nageswara Rao,[1] Putcha Venkateswarlu,[1,2] A. S. N. Murthy,[3] and C. N. R. Rao[3,4]

Liddel and Becker (1) have measured the infrared spectra of methanol, ethanol, and *t*-butanol in carbon tetrachloride at several temperatures. They assumed that the decrease in the band intensity of the free O—H stretching vibration near 3630 cm^{-1} could be taken as a measure of the dimerization in dilute solutions, and from the temperature coefficient of this effect they obtained the apparent ΔH values. The ΔH of these three alcohols was in the order methanol > ethanol > *t*-butanol. The shift of the hydroxyl

*h and r are only independent if $r_E \gg r_I$. If h is increased until $r_I \gg r_E$, further increase in h does not increase F, since $r_I \propto h$, and the effects cancel.

[1]Department of Physics, Muslim University, Aligarh, India.
[2]Present address: Department of Physics, Indian Institute of Technology, Kanpur, India.
[3]Department of Inorganic and Physical Chemistry, Indian Institute of Science, Bangalore 12, India.
[4]To whom all the correspondence should be addressed.

high flowrates. This is the most serious limitation of the thermosiphon, and makes it quite impractical as a means of forcing a gas through a constricted system. Furthermore, the need for large-bore tubing, since r varies as d^4, results in a rather large volume. Within these limitations, however, the thermosiphon is remarkably flexible, as the four parameters h, P, $(1/T-1/T')$, and r may be varied almost independently.* Thus, for example, if experimental conditions dictate certain values of P, T, and T', then h and r may be adjusted to give the desired flowrate, etc. In practice, T' is the most conveniently controlled parameter, permitting wide variation in F from 0 up to a maximum value dependent on the other parameters and upon the thermal stability of the gas.

The dependence of F upon d^4 permits, in theory, the achievement of very high flowrates where d is not limited by other factors. The observed fall-off in F (Fig. 1), probably due to the time lag in heating and cooling the gas in the two arms, could be at least partially eliminated by suitable preheating and precooling, and by increasing h. With its inability to operate against an appreciable pressure gradient or flow resistance, and its high flowrates, limited in theory only by d, the thermosiphon is seen to be the converse of the piston pump, in which the flowrate is fixed by the displacement, but which will operate against a large and variable pressure head.

The dependence of F upon pressure also deserves some comment. Although F decreases linearly with decreasing pressure, there should be no sudden loss of efficiency at low pressures, as observed with piston and impeller pumps, and in fact, F should increase somewhat as viscous flow gives way to molecular flow. Thus, if large enough values of h, T', and d can be used, the thermosiphon should operate well at pressures from 1 mm to 10^{-3} mm.

Finally, it should be noted that the thermosiphon has no moving parts or electronic components, and is thus completely reliable and trouble-free in operation.

Received October 25, 1961.
Division of Pure Chemistry,
National Research Council,
Ottawa, Canada.

NUCLEAR MAGNETIC RESONANCE STUDIES OF HYDROGEN BONDING IN ETHANOL AND 2,2,2-TRIFLUOROETHANOL

B. D. Nageswara Rao,[1] Putcha Venkateswarlu,[1,2] A. S. N. Murthy,[3] and C. N. R. Rao[3,4]

Liddel and Becker (1) have measured the infrared spectra of methanol, ethanol, and *t*-butanol in carbon tetrachloride at several temperatures. They assumed that the decrease in the band intensity of the free O—H stretching vibration near 3630 cm^{-1} could be taken as a measure of the dimerization in dilute solutions, and from the temperature coefficient of this effect they obtained the apparent ΔH values. The ΔH of these three alcohols was in the order methanol > ethanol > *t*-butanol. The shift of the hydroxyl

*h and r are only independent if $r_E \gg r_I$. If h is increased until $r_I \gg r_E$, further increase in h does not increase F, since $r_I \propto h$, and the effects cancel.

[1]Department of Physics, Muslim University, Aligarh, India.
[2]Present address: Department of Physics, Indian Institute of Technology, Kanpur, India.
[3]Department of Inorganic and Physical Chemistry, Indian Institute of Science, Bangalore 12, India.
[4]To whom all the correspondence should be addressed.

proton resonance frequency with concentration of alcohol has also been associated with the hydrogen bonding between alcohol molecules (2). Davis, Pitzer, and Rao (2) have recently studied the proton magnetic resonance spectra of solutions of methanol, ethanol, *i*-propanol, and *t*-butanol in carbon tetrachloride and have calculated the apparent ΔH values. The trend in ΔH values was found to be methanol > ethanol > *i*-propanol > *t*-butanol. Although the uncertainties in the ΔH values are rather large, it is possible that the trend in ΔH with the structure of the alcohol may reflect either steric or electronegativity effects on the strength of the hydrogen bond. The monomer chemical shifts, δ_M, obtained by extrapolation to infinite dilution, also showed variation in the order methanol > ethanol > *i*-propanol $\cong$ *t*-butanol (3). In order to determine the importance of steric or (and) electrical effects in deciding the hydrogen bonding in alcohols, we have now studied the proton magnetic resonance spectra of trifluoroethanol and ethanol in benzene solution.

The proton magnetic resonance spectra of solutions of anhydrous ethanol and trifluoroethanol in benzene were recorded on a Varian high-resolution n.m.r. spectrometer operated at a fixed frequency of 40 Mc/sec. Sample tubes of 4.5-mm outer diameter were used and the measurements were made while the tubes were spinning. The chemical shifts of the hydroxyl proton have been calculated with respect to benzene signal. The error in the δ values varies between ± 0.3 and ± 1.7 cycles/sec. Each observation is an average of at least six independent measurements. All experiments were conducted at room temperature ($31 \pm 1°$ C).

The variation of δ with mole fraction of alcohol for trifluoroethanol and ethanol is shown in Fig. 1. It is clear from the figure that the δ at infinite dilution, δ_M, is lower for trifluoroethanol (246 cycles/sec, 6.015 p.p.m.) than for ethanol (292 cycles/sec, 7.03 p.p.m.). Further, the slope of the curve at low concentrations (<0.04 mole fraction) is greater for ethanol. It may be noted in this connection that the free O—H stretching frequency of trifluoroethanol has been found by earlier workers (4) to be slightly lower than that of ethanol. But the free O—H stretching band persists even in the pure liquid in trifluoroethanol, indicating appreciable concentration of monomeric species (4). Apparently, the equilibrium constant for dimer formation is lower for trifluoroethanol compared to ethanol. This probably explains the greater slope of the curve (Fig. 1) for ethanol. The lower δ_M for trifluoroethanol is understandable since a more electronegative group should lessen the shielding of the hydroxyl proton. The greater acidity of trifluoroethanol compared to ethanol should result in a decreased shielding of the hydroxyl proton. It would appear as though steric effects are important in view of the decrease in δ_M with the increase in the bulk of the alkyl group. There is no reason why steric effects should affect δ_M, while they may be important in determining the equilibrium constant and ΔH of dimerization. Apparently, a strict comparison of δ_M values is possible only if the alcohols are structurally very similar.

Our observation that trifluoroethanol is less associated than ethanol at low concentrations due to the electronegativity of the CF_3 group is further supported by the recent infrared (5) and n.m.r. (6) studies on chloroethanols. Chloroethanols also show greater concentration of monomeric species compared to ethanol. The δ_M of trichloroethanol has also been found to be about 40 cycles/sec lower than that of ethanol (7). It is interesting to note that decrease in δ_M in trichloroethanol and trifluoroethanol are of the same magnitude. The polarities of the CF_3 and CCl_3 groups are also very similar (8).

Recently it has been found that trifluoroethanol causes a much greater solvent blue-shift on the $n \rightarrow \pi^*$ transition of the carbonyl group than ethanol (9), indicating that trifluoroethanol is a better hydrogen-bond donor than ethanol. Thus, the $n \rightarrow \pi^*$ band

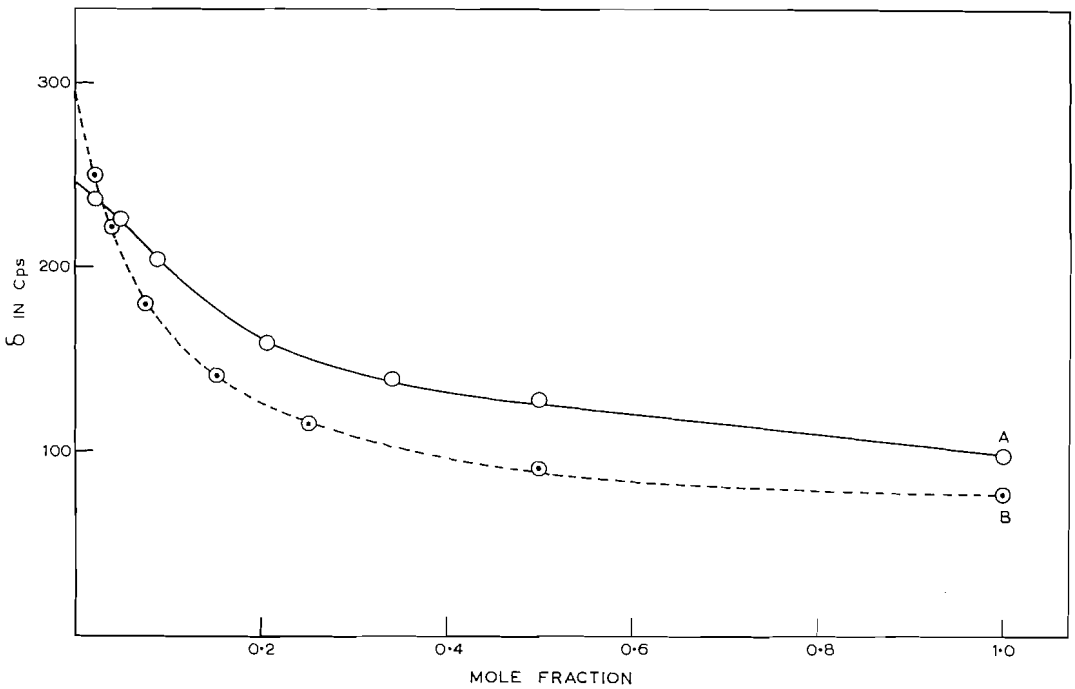

FIG. 1. Chemical shift of the OH proton resonance, δ in cycles/sec versus mole fraction of alcohol x: (A) trifluoroethanol, (B) ethanol.

maximum of acetone found at 277 mμ in heptane is shifted to 270 mμ and 265 mμ in ethanol and trifluoroethanol respectively. This may also be partly related to the higher concentration of monomeric species in trifluoroethanol. Mukherjee and Grunwald (10) have also concluded that trifluoroethanol is a better donor than ethanol, from their numerous physical measurements.

The authors are thankful to Professor M. R. A. Rao for his keen interest in the work and to Pennsalt Chemicals Corporation, Philadelphia, Pa., U.S.A., for a gift sample of trifluoroethanol.

1. U. LIDDEL and E. D. BECKER. Spectrochim. Acta, **10**, 70 (1957).
2. J. C. DAVIS, JR., K. S. PITZER, and C. N. R. RAO. J. Phys. Chem. **64**, 1714 (1960).
3. J. C. DAVIS, JR. NMR studies of hydrogen bonding. Ph.D. thesis. University of California, Berkeley, Calif., U.S.A. 1959.
4. C. G. CANNON and B. C. STACE. Spectrochim. Acta, **13**, 253 (1958).
5. M. L. JOSIEN and P. PINEAU. Compt. rend. **250**, 2559 (1960).
6. J. CANTACUZENE, J. GASSIER, Y. LHERMITTE, and M. MARTIN. Compt. rend. **251**, 866 (1960).
7. T. M. CONNOR and C. REID. J. Mol. Spectroscopy, **7**, 32 (1961).
8. R. W. TAFT, JR. *In* Steric effects in organic chemistry. *Edited by* M. S. Newman. John Wiley & Sons, New York. 1956.
9. C. N. R. RAO, G. K. GOLDMAN, and A. BALASUBRAMANIAN. Can. J. Chem. **38**, 2508 (1960).
10. L. M. MUKHERJEE and E. GRUNWALD. J. Phys. Chem. **62**, 1311 (1958).

RECEIVED OCTOBER 25, 1961.
DEPARTMENT OF PHYSICS,
MUSLIM UNIVERSITY,
ALIGARH, INDIA,
AND
DEPARTMENT OF INORGANIC AND PHYSICAL CHEMISTRY,
INDIAN INSTITUTE OF SCIENCE,
BANGALORE 12, INDIA.

IONIZATION POTENTIALS OF SOME PERFLUOROALKYL ARSINES[1]

W. R. CULLEN AND D. C. FROST

Measurements of the first ionization potentials of derivatives of the group V elements have been mainly confined to compounds of nitrogen (1), and little attempt has been made to study the effects of systematic substitution of the hydrogens of the parent hydrides by other groups. Derivatives of arsenic are especially suitable for such studies because of the availability of a large number of simple volatile compounds, and in this investigation the first ionization potentials of a number of arsines containing methyl, trifluoromethyl, and chloro groups have been measured.

EXPERIMENTAL

Compounds

The compounds shown in Table I were prepared by standard methods from the literature except for the arsenic trichloride where a commercial sample was used.

Apparatus and Method

The ionization potentials were obtained by electron impact mass spectrometry, and were derived by treating the relevant ionization efficiency curve and a standard (Xe^+ or Kr^+) with the Warren extrapolation method (2). The results, although reproducible to 0.1 ev, may well be slightly greater than the adiabatic values; however, this is not expected to unduly influence the trends shown within the groups of similar molecular species dealt with here.

Results

The new results are shown in Table I, together with some other values for comparison.

TABLE I

First ionization potentials

Compound	I.P. (ev)	Compound	I.P. (ev)
$(CF_3)_3As$	11.0	NH_3	10.15*
$(CF_3)_2AsCH_3$	10.5	CH_3NH_2	8.97*
$CF_3As(CH_3)_2$	9.2	$(CH_3)_2NH$	8.24*
$As(CH_3)_3$	8.3	$(CH_3)_3N$	7.82*
$P(CF_3)_3$	11.3	$P(CH_3)_3$	No parent ion
$(CF_3)_2AsH$	10.9	$(CH_3)_2AsH$	9.0
CF_3AsH_2	—	CH_3AsH_2	9.7
AsH_3	10.6		
$(CF_3)_2AsCl$	11.0	$(CH_3)_2AsCl$	9.9
CF_3AsCl_2	—	CH_3AsCl_2	10.4
$AsCl_3$	11.7		

*See reference 9.

DISCUSSION

In the series of compounds containing CH_3, H, and As, a progressive decrease in ionization potential is found as the number of CH_3 groups is increased. This corresponds to a decrease of about 0.7 ev per CH_3 group substituted for a hydrogen in the parent arsine. In the case of ammonia a similar though less regular decrease is observed (Table I). It is generally felt that the parent ion of ammonia is formed by removal of an electron

[1]*Research supported by the National Research Council of Canada.*

from the lone pair on the nitrogen atom (3). It is not certain, however, that the parent ions of the methyl amines are also formed by the same process, though it is likely that this is so (4).

In the series $(CH_3)_xAsCl_{3-x}$ an irregular decrease in ionization potential occurs as the number of CH_3 groups is increased. This can be attributed to the inductive effect of the CH_3 groups and the electron-withdrawing effect of the chloro groups raising or lowering the energy of the arsenic lone pair. Similarly in the series $(CF_3)_xAsH_{3-x}$ and $(CF_3)_xAs(CH_3)_{3-x}$ an increase in ionization potential would be expected as the number of CF_3 groups is increased, owing to the strong electron-withdrawing power of this group. However, in the series $(CF_3)_xAsCl_{3-x}$ the substitution of CF_3 seems to result in a small but significant lowering of the ionization potential, a result which could indicate that to a first approximation the electron-withdrawing power of the CF_3 group is less than that of the chloro group. This conclusion is the reverse of that expressed by other workers (5).

Qualitatively the results of the present investigation for the series $(CF_3)_xAs(CH_3)_{3-x}$ can be compared with the ease of complex formation and ease of hydrolysis of these compounds. The ease of forming donor–acceptor complexes, e.g. with silver iodide, and onium complexes, e.g. with CH_3I, decreases as the number of CF_3 groups is increased (6). Haszeldine and West have attributed this effect to the ability of the CF_3 group to lower the energy of the lone-pair electrons to such an extent as to make complex formation difficult. The degree of difficulty would depend on the number of CF_3 groups present. The reverse tendency is found with respect to ease of solvolysis of these compounds to eliminate the CF_3 group as CF_3H. Thus, the rate of solvolysis increases as the number of CF_3 groups is increased. This has been interpreted (6) in terms of the solvolysis occurring by nucleophilic attack on the arsenic atom which, formally, becomes more positive as the number of electron-withdrawing CF_3 groups attached to it is increased. The ionization potential variation found for these compounds reflects the same trends.

Quantitative tests of these ionization potential values are more difficult to find, and only one source of such a test seems to be available. Certain of the electronic transitions of the aryl arsines have recently been assigned as being due to intramolecular charge transfer involving excitation of an electron from the non-bonding lone pair to an antibonding π-orbital of a phenyl group (7). The energy of such a transition is given to a first approximation by the expression (8) $I_D - E_A - C$, where I_D is the ionization potential of the donor (presumably the arsenic lone pair), E_A the electron affinity of the acceptor (the phenyl group), and C the mutual electrostatic energy of D^+ and A^- relative to that of D and A.

Therefore, for the compounds $C_6H_5As(CH_3)_2$ and $C_6H_5As(CH_3)(CF_3)$, assuming that the configuration around the arsenic is essentially the same in both cases, the energy difference in the charge-transfer bands should be approximately equal to the difference in ionization potential of the arsenic lone pair. From Table I it is seen that substitution of a CF_3 for a CH_3 should increase the energy of the transition by about 0.7 ev. The experimental difference is 0.34 ev, but this value is probably lower than it would otherwise be because of interaction between the CF_3 group and the C_6H_5 group (7). Unfortunately, interactions of this sort prohibit similar comparisons being made with the spectra of other arsines so far investigated.

If similar calculations are made for the phenyl amines then very much worse agreement is found; however, in this case there is probably less charge-transfer character in the excited state (8).

1. F. H. FIELD and J. L. FRANKLIN. Electron impact phenomena. Academic Press, Inc., New York. 1957.
2. J. W. WARREN. Nature, **165**, 810 (1950).
3. A. D. WALSH and P. A. WARSOP. Trans. Faraday Soc. **57**, 345 (1961).
4. J. COLLIN. Can. J. Chem. **37**, 1053 (1959).
5. J. J. LAGOWSKI. Quart. Revs. (London), **13**, 233 (1959). E. A. ROBINSON. Can. J. Chem. **39**, 247 (1961).
6. R. N. HASZELDINE and B. O. WEST. J. Chem. Soc. 3880 (1957).
7. W. R. CULLEN and R. M. HOCHSTRASSER. J. Mol. Spectroscopy, **5**, 118 (1960).
8. J. N. MURRELL. Quart. Revs. (London), **15**, 191 (1961).
9. K. WATANABE. J. Chem. Phys. **26**, 542 (1957).

RECEIVED NOVEMBER 6, 1961.
THE CHEMISTRY DEPARTMENT,
UNIVERSITY OF BRITISH COLUMBIA,
VANCOUVER 8, B.C.

Canadian Journal of Chemistry

Issued by THE NATIONAL RESEARCH COUNCIL OF CANADA

VOLUME 40 MARCH 1962 NUMBER 3

CHEMISTRY OF THE TRIFLUOROMETHYL GROUP

PART V. INFRARED SPECTRA OF SOME PHOSPHORUS COMPOUNDS CONTAINING CF_3

M. A. A. BEG* AND H. C. CLARK

The Department of Chemistry, University of British Columbia, Vancouver, British Columbia

Received November 20, 1961

ABSTRACT

The infrared spectra of several series of trifluoromethyl–phosphorus compounds are correlated, the compounds examined being the iodides CF_3PI_2 and $(CF_3)_2PI$, the methyl-trifluoromethyl-phosphines of the general formula $(CH_3)_nP(CF_3)_{3-n}$, where $n = 1$, 2, or 3, and the analogous phenyl-trifluoromethyl-phosphines. Satisfactory assignments are made for the majority of absorption bands in the 650–4000 cm^{-1} region. The infrared spectra of some phosphine – boron trifluoride adducts are also examined and assignments of the principal bands are made.

INTRODUCTION

Although in the past 12 years, a large number of perfluoroalkyl-metallic and -metalloidal compounds have been prepared, few attempts have been made to correlate their infrared spectra. This is surprising since the infrared technique has proved extremely valuable in the characterization of these compounds, largely because of the intense, characteristic C—F absorption in the 1000–1300 cm^{-1} region. However, it is only very recently that correlations have been formulated for such simple perfluoro compounds as the trifluoromethyl (1, 2) and pentafluoroethyl halides (3) and there is only one other detailed report dealing with the infrared spectra of perfluoro-organometallic compounds (4). In earlier papers of this series (5, 6) we have described the preparations of the phenyl-trifluoromethyl-phosphines and a number of their complex derivatives. Since the analogous methyl-trifluoromethyl compounds have been described previously (7–9), a wide range of trifluoromethyl–phosphorus derivatives is now available and it seemed useful to examine in some detail their infrared spectra.

EXPERIMENTAL

The preparations of the compounds have been described in detail elsewhere (5–9).

Infrared absorption spectra were recorded in the 650–4000 cm^{-1} range, using a Perkin–Elmer model 21 double-beam spectrophotometer fitted with NaCl optics, and operated at a slit program setting of 927. Gas spectra were recorded using a 9-cm gas cell fitted with NaCl plates, and were measured at a number of pressures so as to obtain complete resolution. The spectra of liquids were recorded using liquid films between NaCl plates. Most spectra were calibrated against known peaks of a polystyrene film, and frequencies are considered accurate to ±0.3%. Relative intensities and band characteristics are described in terms of the usual notation, as indicated by Stafford and Stone (4).

**Present address: Central Laboratories, Pakistan Council of Scientific & Industrial Research, Karachi, Pakistan.*

DISCUSSION

Before discussing the spectra of the trifluoromethyl–phosphorus compounds, some consideration should first be given to the CF_3 group itself, which gives rise to four fundamental vibrations. These are composed of two A_1 type vibrations, the symmetrical CF_3 stretching at about 1100 cm^{-1}, and the symmetrical CF_3 deformation at about 700 cm^{-1}; and two degenerate E type vibrations, the antisymmetrical CF_3 stretching at about 1180 cm^{-1} and the antisymmetrical CF_3 deformation at about 520 cm^{-1}. The atom or group bonded to the CF_3 group will give rise to two vibrations, symmetrical stretching of CF_3—X and the rocking of CF_3 against X. Edgell and May (10), from a study of CF_3—X vibrations, conclude that interaction between the CF_3 and CF_3—X vibrations is small and that the spectra are therefore best interpreted in terms of the behavior of the CF_3 group as a stiff or rigid group. This implies that the fundamental vibrations due to a CF_3 group should not differ greatly from molecule to molecule, although some small shifts in frequency may be expected as the electronegativity of X is changed (1).

Trifluoromethyliodophosphines

In considering the infrared spectra of trifluoromethyl–phosphorus compounds, it seems best to consider first the compounds CF_3PI_2 and $(CF_3)_2PI$ since the P—I stretching vibration lies outside the frequency range being studied. The observed frequencies and suggested assignments are listed in Table I, using the frequencies reported by earlier workers (11).

TABLE I

Vibrational frequencies in CF_3PI_2 and $(CF_3)_2PI$

CF_3PI_2	$(CF_3)_2PI$	Assignment
	2252 m	Comb. (2×1131?)
	2217 s	Comb. (2×1119?)
1272 m	1273 m	Comb. (2×P—C symm. stretch.?)
	1256 w	
	1203 s	Antisymm. and symm. CF_3 stretch.
	1183 m	
1157 s	1162 s	
1142 s	1131 s	
1111 s	1119 m	
1072 m		
	1029 m	
	951 w	
	854 w	
	798 m	
737 s	748 s	Symm. CF_3 deform.
	714 w	Antisymm. P—C stretch.

In CF_3PI_2, the absorption at 1111 cm^{-1} is assigned to the symmetrical CF_3 stretching corresponding to the 1073 cm^{-1} band in CF_3I (10), while those at 1142 and 1157 cm^{-1} arise from the doubly degenerate antisymmetrical CF_3 stretching, this being observed at 1185 cm^{-1} in CF_3I. The absorption at 737 cm^{-1} is probably the symmetrical CF_3 deformation frequency, found at 741 cm^{-1} in CF_3I. However, the P—C asymmetric stretching might also be expected about here, since it is observed at 717, 707 cm^{-1} in $P(CH_3)_3$ (12). This assignment of the 737 cm^{-1} is therefore only tentative.

When more than one CF_3 group is attached to the phosphorus atom, splitting of the characteristic C—F frequencies occurs, as would be expected from the presence of two

equivalent groups (14). Hence in the spectrum of $(CF_3)_2PI$ there are five resolved absorptions in 1100–1220 cm^{-1} region. These are actually observed as three main bands with submaxima at 1119 and 1183 cm^{-1}. When three CF_3 groups are attached to the same atom, as in $(CF_3)_3P$, four main absorption frequencies with submaxima are observed. The number of main absorption bands in this region is therefore sometimes taken as an indication of the number of CF_3 groups present; however, without detailed mathematical treatment no detailed assignments can be made. The symmetrical CF_3 deformation mode in $(CF_3)_2PI$ is observed at 748 cm^{-1} in support of the assignment of the 737 cm^{-1} band of CF_3PI_2. Possibly the 714 cm^{-1} absorption may be attributed to the P—C antisymmetrical stretching vibration, particularly since the splittings of the CF_3 deformation band are not likely to be greater than 15 to 20 cm^{-1}.

Methyl-trifluoromethyl-phosphines

It is now possible to make similar correlations of the spectra of $(CH_3)_3P$, $(CH_3)_2PCF_3$, $CH_3P(CF_3)_2$, and $P(CF_3)_3$. The vibrational frequencies of $(CH_3)_3P$ have recently been studied in detail (12) and while use is made below of these assignments, the present results also offer some confirmation of them. The observed absorption frequencies and their suggested assignments are given in Table II, which makes use of Halmann's (12)

TABLE II

Vibrational frequencies of methyl-trifluoromethyl-phosphines

$(CH_3)_3P$	$(CH_3)_2PCF_3$	$CH_3P(CF_3)_2$	$P(CF_3)_3$*	Assignment
2970 m	2995 m	2985 w		CH antisymm. stretch.
2920 m	2934 m	2934 w		CH symm. stretch.
2850 m	2840 m	2825 w		CH symm. stretch.
	2290 w	2290 w	2298 m	Comb. (2×CF stretch.)
	2240 w		2242 m	
1430 m	1440 m	1465 m		CH antisymm. bend.
1417 m	1425 w			CH antisymm. bend.
	1378 w	1375 m	1390 m	Comb. ($2\times CF_3$ deform.)
1310 m	1310 w	1307 m		CH symm. bend.
		(1307 m?)	1308 m	Comb. (see ref. 17)
1298 w	1295 w			CH symm. bend.
		1283 m	1277 m	Comb. (2×P—C symm. stretch.?)
		1203 vs	1230 vs	
	1175 vs	1167 vs	1183 vs	Symm. and antisymm. C—F stretch.
	1125 vs	1143 s	1153 vs	
	1118 vs	1115 vs	1127 vs	
1067 m				CH_3 rock.
			1041 m	
			1023 m	
960 m	955 m	912 m		CH_3 rock.
947 w	906 m	892 m		CH_3 rock.
			966 m	
			923 m	
	876 m	855, 862 w	844 w	
			797 w	
	755, 745 w	750, 745 m	754 s	CF_3 symm. deform.
717, 707 s	725, 701 m	725 m	726 m	Antisymm. P—C stretch.
652 m	680 w			Symm. P—C stretch.

*A number of weak absorptions are reported in the 1400–2200 cm^{-1} region.

assignments for $(CH_3)_3P$, and the reported frequencies of $P(CF_3)_3$ (11).

The assignments for C—F stretching and CF_3 deformation follow those discussed earlier. In $(CH_3)_2PCF_3$ the bands at 1175 and 1125 cm^{-1} are the antisymmetric stretching vibrations and that at 1118 cm^{-1}, the symmetric vibration, but detailed assignments cannot be made when more than one CF_3 group is present. Three points require further

comment. Firstly, there seems to be good agreement, in all cases, for vibrations involving the CH_3 group. There are two exceptions where expected bands are not observed for $CH_3P(CF_3)_2$ but this is probably due to their very low intensity. Secondly, for $(CH_3)_3P$, $(CH_3)_2PCF_3$, and $CH_3P(CF_3)_2$, there are marked similarities in band shapes in the 890–975 cm^{-1} region, these being quite different from the 966 and 923 cm^{-1} vibrations observed for $(CF_3)_3P$. For the former compounds, absorption in this region is attributed to CH_3 rocking. Thirdly, the moderately intense absorption observed for all compounds in the 700–730 cm^{-1} region is assigned to the antisymmetrical P—C stretching. If this is correct, it appears that this vibration is unaffected by the stepwise replacement of CF_3 for CH_3.

Phenyl-trifluoromethyl-phosphines

The infrared spectra of phosphorus compounds containing both phenyl and trifluoromethyl groups are much more complex than those already discussed, largely due to the numerous vibrations associated with the phenyl group. The observed frequencies for three such compounds are listed in Table III.

TABLE III

Vibrational frequencies in phenyl–trifluoromethyl–phosphorus compounds

$(C_6H_5)(CF_3)PI$	$(C_6H_5)_2PCF_3$	$C_6H_5P(CF_3)_2$	Assignment
3060 w	3060 w	3080 w	Symm. and antisymm. C—H stretch.
	3000 w		
2900 w	2910 vw	2920 w	
2340 w		2320 w	Comb. (2×1170)
	2240 vw	2220 vw	Comb. (2×1105)
	1965 w	1980 w	
1880 vw	1880 w	1870 w	
		1835 vw	
1800 vw	1810 w	1810 vw	
1660 w	1660 w	1660 w	
1585 w	1585 w	1590 w	Skeletal C—C vibrations
1490 m	1485 m	1490 m	
1440 m	1440 m	1445 m	
1385 w	1385 w	1390 vw	Comb. (2×690) ?
1335 w	1325 w	1330 w	
1310 w	1310 w		
1270 w	1275 w	1265 w	
(1210) m		1190 vs	Symm. and antisymm. C—F stretch.
		1170 s	
1150 vs	1150 vs	1140 vs	
1115 vs	1105 vs	1100 vs	
1070 m	1070 m	1070 m	Ring vibration ?
1025 m	1027 m	1030 m	
1000 m	1000 m	1000 m	Phenyl—P
	970, 915 w		
	875 w	875 w	
830 w	845 w		Out-of-plane C—H bend.
	800 w	805 w	
745 s	745 s	750, 745 s	(See text)
715 w	720 w	700 m(sh)	Antisymm. P—C stretch.
690 s	695 s	690 s	Out-of-plane C—H bend.

Although all frequencies cannot be assigned, the similarities in the three spectra are very striking. In phenyl compounds, the skeletal C—C vibrations usually occur at 1440–1625 cm^{-1}. In these phosphorus compounds, they are invariably found at 1440–45 cm^{-1} in the form of an intense sharp band, and accompanied by two other sharp absorptions of lesser intensity at 1490 and 1590 cm^{-1}. The ring vibration thought to be very sensitive to the substituent on the phenyl ring is said to occur at 1045–1185 cm^{-1} (15), and is observed at 1088 cm^{-1} for $(C_6H_5)_3P$. Since all the compounds of Table III show

a medium intensity band at 1070 cm^{-1}, it is assigned this vibration. Similarly, all three compounds show a well-resolved absorption at 1000 cm^{-1} which has been observed (13) in a large number of other compounds containing the phenyl—P grouping.

Other characteristic absorptions of the phenyl group are also observed. Thus the strong bands at 690 cm^{-1}, accompanied by another strong absorption at 745–750 cm^{-1}, and perhaps the weak absorption at 800–810 cm^{-1} are due to out-of-plane C—H bending vibrations and this particular combination of bands is characteristic of monosubstituted phenyl groups (16). The strong band at 750 cm^{-1} presumably overlaps the CF_3 deformation frequency observed in other CF_3 compounds. We again tentatively assign the weak 700–715 cm^{-1} band to the P—C antisymmetrical stretching vibration.

The C—F stretching vibrations are again observed in the 1100–1200 cm^{-1} regions; for $(C_6H_5)(CF_3)PI$ and $(C_6H_5)_2PCF_3$, only two such vibrations are observed in each case, those at 1150 cm^{-1} being due to the asymmetric mode, and those at 1115 cm^{-1} and 1105 cm^{-1} being assigned as symmetrical stretching. In $(C_6H_5)P(CF_3)_2$, coupling occurs between the CF_3 modes and an increased number of bands is observed.

Phosphine – Boron Trifluoride Adducts

As part of our studies of the donor properties of trifluoromethyl-phosphines, a number of their boron trifluoride adducts were prepared. In Table IV are listed the important maxima observed in their infrared spectra.

TABLE IV

Principal vibrational frequencies for phosphine–BF_3 adducts

$(CH_3)_3P.BF_3$	$(CH_3)_2PCF_3.BF_3$	$(C_6H_5)_2PCF_3.BF_3$	$(C_6H_5)_3P.BF_3$	Assignment
		3150 w	3250 m	
3000 w	3100 w	3050 w	3150 w	C—H stretch.
2900 w	3000 w	2950 w	3050 w	
	2300 w	2300 w		Comb.
		1590 w	1575 w	
		1475 w	1475 w	Skeletal C—C
		1440 w	1435 m	vibrations
1425 w	1430 w			CH bend.
1300 w	1320 m			CH bend.
		1220 m	1235 w	
	1175–1025 vs (br)	1175 m	1180 w	
		1150 s		
1125 s		1125 s		C—F and B—F
1085 s		1095 s(br)	1075–1085 vs	stretch.
1060 s		1070 s	1030–1050 s	
1037 s		1030 m		
		995 m	1000 m	Phenyl—P
970 m	970 m			CH_3 rock.
		900 m	910 m	
		870–835 m(br)	885 m	
785 m	780 w	790 w	770 s	See text
	750 s	745 s	740 s	
705 w	705 m	700 m	715 m, 695 s	See text
675 w	675 m	690 s	680 m	

Most of the frequencies found to be characteristic of the free phosphines are also observed in the spectra of their BF_3 adducts; however, the characteristic absorptions of boron trifluoride are not found. Instead of the intense B—F stretching vibrations at 1454 and 1505 cm^{-1} (18), there is a wide region of intense absorption at 1030–1180 cm^{-1}. Although the bands are broad and good resolution is impossible, it is clear from a consideration of the spectra of $(C_6H_5)_2PCF_3.BF_3$, $(C_6H_5)_2P.BF_3$, and $(C_6H_5)_3P.BF_3$ that absorption in this region is due to B—F vibrations (1030–1090 cm^{-1}) and also C—F

stretching vibrations (1125–1175 cm^{-1}). This shift in the B—F stretching vibrations to lower frequency results from the change of symmetry accompanying complex formation, and has been observed for other BF_3 adducts (19). Also, the spectra do not reveal any absorption due to water, so hydrolysis of the adducts to give BF_4^- cannot have occurred. A number of bands are observed in the 670–750 cm^{-1} region but it is impossible to make definite assignments. The P—C stretching vibrations should no longer be found in this region, but the phenyl C—H out-of-plane vibrations, the B—F bending vibrations, and the CF_3 deformation modes may cause absorption. In all four of the BF_3 adducts, a band is found at 770–790 cm^{-1}. The origin of this is uncertain, although a very weak band is observed here for fluoroborates (20) and has been assigned as the symmetrical breathing vibration of the B—F bonds. However, in the present instances, the intensities of these bands are much greater than observed in fluoroborates.

In conclusion, the examination of the infrared spectra of these trifluoromethyl–phosphorus compounds not only shows the usefulness of infrared spectroscopy in the characterization of organophosphorus compounds but also provides further information concerning C—F and P—C absorption in the infrared region of the spectrum. For a complete understanding of these absorptions, many other related compounds will have to be prepared and examined.

ACKNOWLEDGMENTS

We gratefully acknowledge the support of the National Research Council, and M. A. A. B. expresses thanks for a scholarship received from C.S.I.R. (Pakistan) under the auspices of the Colombo Plan.

REFERENCES

1. R. McGee, F. F. Cleveland, A. G. Meister, C. E. Decker, and S. I. Miller. J. Chem. Phys. **21**, 242 (1953).
2. W. B. Person and S. R. Polo. Spectrochim .Acta, **17**, 101 (1961).
3. O. Risgin and R. C. Taylor. Spectrochim. Acta, **15**, 1036 (1959).
4. S. L. Stafford and F. G. A. Stone. Spectrochim. Acta, **17**, 412 (1961).
5. M. A. A. Beg and H. C. Clark. Can. J. Chem. **39**, 564 (1961).
6. M. A. A. Beg and H. C. Clark. Can. J. Chem. **40**, 283 (1962).
7. R. N. Haszeldine and B. O. West. J. Chem. Soc. 3631 (1956).
8. R. N. Haszeldine and B. O. West. J. Chem. Soc. 3880 (1957).
9. M. A. A. Beg and H. C. Clark. Can. J. Chem. **38**, 119 (1960).
10. W. F. Edgell and C. E. May. J. Chem. Phys. **22**, 1808 (1954).
11. F. W. Bennett, H. J. Emeleus, and R. N. Haszeldine. J. Chem. Soc. 1565 (1953).
12. M. Halmann. Spectrochim. Acta, **16**, 407 (1960).
13. L. W. Daasch and D. C. Smith. Anal. Chem. **23**, 853 (1951).
14. G. Herzberg. Infra-red and raman spectra of polyatomic molecules. D. Van Nostrand Co., New York. 1945.
15. R. D. Kross and V. A. Passell. J. Am. Chem. Soc. **77**, 5858 (1955).
16. L. J. Bellamy. The infra-red spectra of complex molecules. 2nd ed. Methuen and Co. Ltd., London. 1958. p. 76.
17. S. N. Nabi and N. Sheppard. J. Chem. Soc. 3439 (1959).
18. J. Vanderryn. J. Chem. Phys. **30**, 331 (1959).
19. P. Chalandon and B. P. Susz. Helv. Chim. Acta, **41**, 697 (1958).
20. G. L. Coté and H. W. Thompson. Proc. Roy. Soc. (London), A, **210**, 217 (1951).

IONIZATION OF ORGANIC COMPOUNDS

II. THIOACETAMIDE IN AQUEOUS SODIUM HYDROXIDE. THE H_- ACIDITY FUNCTION[1]

J. T. EDWARD AND I. C. WANG

The Department of Chemistry, McGill University, Montreal, Que.

Received November 7, 1961

ABSTRACT

The ionization ratio of thioacetamide in aqueous sodium hydroxide, determined spectrophotometrically, is proportional to the concentration of hydroxide ion up to a concentration of about 1 M, and indicates a pK_{HA} of 13.4. For more concentrated solutions the ionizing power increases more rapidly than the hydroxide ion concentration; from the experimentally determined ionization ratios the values of the h_- acidity function for 1–6 M sodium hydroxide have been calculated. The relation of h_- values to the salting-out parameters and water activities of concentrated sodium hydroxide solutions is discussed.

INTRODUCTION

It has been customary to represent the ionization in aqueous alkaline solution of a weak uncharged acid HA by

$$HA + OH^- \rightleftarrows A^- + H_2O \qquad [1]$$

and its ionization ratio ($[A^-]/[HA]$) by

$$[A^-]/[HA] = K_{HA}[OH^-]f_{HA}f_{OH^-}/K_Wf_{A^-}, \qquad [2]$$

the quantities in square brackets representing molar concentrations, the f's molar activity coefficients, K_{HA} the ionization constant of the acid, and K_W the ionic product of water. It has been recognized that the various molecules and ions are hydrated to different extents, but for dilute enough solutions no explicit account needs to be taken of these effects; in such solutions the f terms approach unity, and equation [2] becomes

$$[A^-]/[HA] = K_{HA}[OH^-]/K_W. \qquad [3]$$

This equation holds as a reasonable approximation for the ionization of various weak organic acids in concentrations of up to about 0.5 M sodium or potassium hydroxide (1), changes in the activity coefficient terms with concentration cancelling out to a large extent. However, in more concentrated solutions of alkali the ionization ratio begins to increase much more rapidly than the hydroxide ion concentration. Accordingly, an acidity function, h_-, defined by

$$[A^-]/[HA] = K_{HA}/h_-, \qquad [4]$$

has been devised to measure the proton-abstracting power of strongly alkaline solutions (1, 2). By definition h_- approaches $[H^+]$ and H_- ($= -\log h_-$) approaches pH as a limit in dilute aqueous solution. This acidity function may be expected to prove useful in distinguishing between possible reaction mechanisms from kinetic results in strongly alkaline solution (3).

Schwarzenbach and Sulzberger (1) used substituted indigos as indicators, and obtained H_- values (which they preferred to term pH values) for aqueous sodium and potassium

[1]*The paper by H. J. Campbell and J. T. Edward, Can. J. Chem. 38, 2109 (1960), is to be considered as Part I of this retitled series.*

hydroxide solutions varying in strength from 0.1 M to saturated. They also tried variously substituted glutacondialdehyde dianils as indicators, and obtained ionization ratios (and hence H_- values) increasing more rapidly with hydroxide ion concentration than those obtained with substituted indigos. They rejected these H_- values and suggested that the glutacondialdehyde derivatives did not ionize by losing a proton according to equation [1], but instead added a hydroxide ion. No convincing reason was advanced for this mode of ionization, which in fact would not be expected to lead to the color changes observed with these indicators in strong alkali; an alternative explanation for the divergence of the two H_- scales is given later in this paper.

Both types of indicators were strongly salted out of the aqueous solutions by the concentrated alkali, so that an immiscible organic solvent was present as a second phase for reasons of solubility. Other investigators have avoided the salting out of indicators by using aqueous organic (4) or organic solvents (3), or by using bases such as hydrazine (5), ethylene diamine (6), or ethanolamine (7). However, small polar molecules are not salted out to the same extent as large dyestuff molecules, and in certain instances are salted in (8). In the present work we have studied the ionization in aqueous sodium hydroxide of the small, highly polar thioacetamide molecule.

EXPERIMENTAL

Thioacetamide was recrystallized from ether to a constant melting point of 112.6–113.9° C (reported m.p. 114° (9)) and dissolved in distilled water to give solutions of accurately known concentration, varying between about 0.2 M and 0.002 M, according to the region of the spectrum being investigated. Sodium hydroxide solutions were prepared by dilution of concentrated aqueous solutions from which sodium carbonate had settled, with the usual precautions to exclude carbon dioxide, were standardized by titration, and were shown to be substantially free from carbonate (10, 11). The solutions were brought to 25.0±0.1° C, and then 0.100 ml of thioacetamide solution was mixed quickly with 3.00 ml of sodium hydroxide solution in a stoppered quartz cell of 1-cm light path. The absorption of the solution was measured in a Beckmann DU spectrophotometer against a blank of the same hydroxide concentration, the cell compartment being maintained at 25.0±0.1° C by thermospacers. Hydrolysis of thioacetamide in the more alkaline solutions led to a progressive drop in absorption (cf. ref. 12); the absorption at the moment of mixing was obtained by measuring the absorption at different times after mixing and extrapolation. The reproducibility of measurements was found to be ±1%. The concentration of sodium hydroxide in the sample solution was determined by titration; it was shown that following the above procedure no significant amount of carbonate was formed.

RESULTS AND DISCUSSION

Effect of Ionization on Spectrum of Thioacetamide

The absorption spectra of thioacetamide in water (Fig. 1) and in buffer solutions of pH 9.71, 10.41, 10.73, and 11.87 are practically identical, and are evidently due to the unionized molecule (I). However, in solutions of more alkaline pH the spectrum changes, becoming finally constant again with concentrations of sodium hydroxide above about 4 M. The absorption curve for strongly alkaline solutions (Fig. 1) must represent the spectrum of the conjugate base (II); the fact that all curves go through an isobestic point at 250 mμ supports this interpretation of the spectral changes (13).[2]

[2]*A referee has suggested that the failure of the spectrum to change appreciably with increase of sodium hydroxide concentration above about 4 M may be explained by a levelling off of the basicity of the medium in the region 4 M–8 M, so that thioacetamide may be still incompletely ionized in 8.45 M hydroxide. While this is a theoretical possibility, we consider it most improbable in view of the strong increase in basicity with increase of hydroxide concentration from 4 M to 8 M found by Schwarzenbach and Sulzberger (1). (Admittedly, the* extent *of the increase is dependent on the choice of indicator, but it seems unlikely that thioacetamide should differ greatly from the substituted indigos.) Furthermore, the good agreement of spectral results in the more dilute hydroxide solutions with those expected from equations [3] and [5] indicates that the correct value of* ϵ_{A^-} *has been used in these equations; i.e., that ionization in 8.45 M hydroxide is essentially complete.*

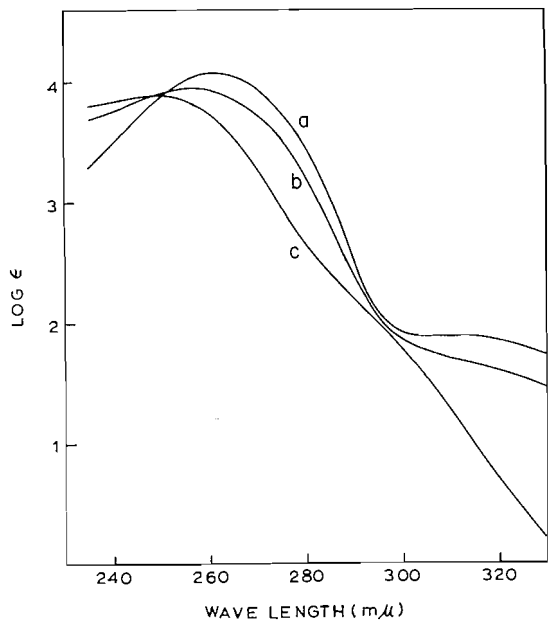

FIG. 1. Ultraviolet absorption of thioacetamide in (*a*) water; (*b*) 0.235 *N* sodium hydroxide; (*c*) 8.45 *N* sodium hydroxide.

Janssen (14) showed that thioacetamide in ethanol has a weak absorption peak at 327 mμ and a strong peak at 266 mμ, which he attributed to $n \rightarrow \pi^*$ and $n \rightarrow \sigma^*$ transitions respectively of the thiocarbonyl group. As expected for such transitions (15), both peaks undergo blue shifts when the solvent is changed from ethanol to water (Table I). The

TABLE I

Absorption peaks of thioacetamide in aqueous solution

Solvent	$n \rightarrow \pi^*$ transition		$n \rightarrow \sigma^*$ transition	
	λ_{max} (mμ)	ϵ_{max}	λ_{max} (mμ)	ϵ_{max}
Water	310	76.6	260	11,960
Conc. sulphuric acid	—	—	237[a]	8,800[a]
8.45 *N* sodium hydroxide	—[b]	—	248	7,700

[a]Reference 14.
[b]Inflection at 290 mμ (cf. Fig 1).

further blue shifts in alkaline or acid solution (Table I), which cause the $n \rightarrow \pi^*$ peak to be submerged in the more intense $n \rightarrow \sigma^*$ peak, are in accord with the structures II and III for the conjugate base and acid respectively of thioacetamide; the ionic charge in both cases would be expected to oppose $n \rightarrow \pi^*$ or $n \rightarrow \sigma^*$ transitions, which involve the shift of an electron from sulphur towards carbon. As already pointed out by Janssen, the ultraviolet spectrum of the conjugate acid does not support the formulation IV advocated by Spinner (16).

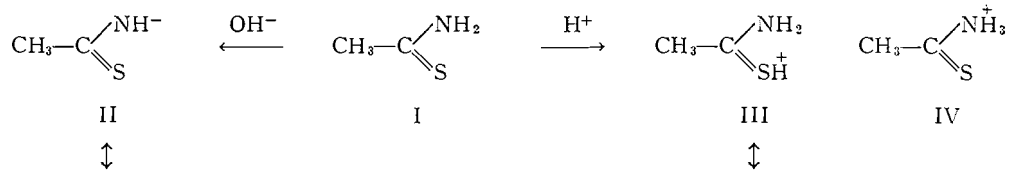

Dissociation Constant of Thioacetamide

The ionization ratios of thioacetamide in various strengths of alkali were computed from the equation

$$[A^-]/[HA] = (\epsilon_{HA} - \epsilon)/(\epsilon - \epsilon_{A^-}), \qquad [5]$$

where ϵ_{HA}, ϵ_{A^-}, and ϵ are the molecular extinction coefficients at 310 or 260 mμ in water, in 8.45 *M* sodium hydroxide, and in the test solution respectively. A plot of log ([A$^-$]/[HA]) against log [OH$^-$] (Fig. 2) fits reasonably well a straight line of unit slope over the

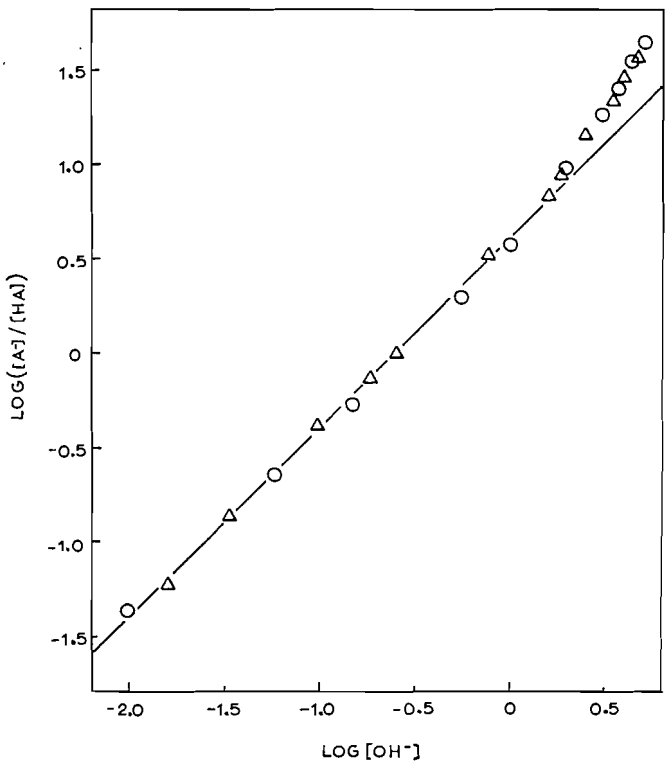

FIG. 2. Relation between hydroxide ion concentration and ionization ratio ([A$^-$]/[HA]) of thioacetamide, as determined by measurements of ultraviolet absorption at 260 mμ (○) and 310 mμ (△).

range 0.01–1 *M* sodium hydroxide (log [OH$^-$] of −2.0 to 0), as required by equation [3]. The intercept of this curve indicates $pK_{HA} = 13.4$ for thioacetamide, since $pK_W = 14.00$ at 25° (17, p. 481). Dissociation constants of about this order of magnitude have been reported for some amides (18, 19, 20), although acetamide shows no appreciable ionization

in 1 *M* sodium hydroxide (21). However, it seems likely that thioamides in general will prove more acidic than amides (cf. hydantoin and thiohydantoin (22)).

Experimental H_- Values of 1–6 M Sodium Hydroxide Solutions

The present work indicates that for the ionization of thioacetamide in 0.01–1 *M* sodium hydroxide, H_- is given by

$$H_- = pK_w + \log [OH^-]. \qquad [6]$$

(Previous work has shown the identity of H_- with pH for less alkaline aqueous solutions (5, 6).) However, for sodium hydroxide concentrations above 1 *M* the relationship given by equations [3] and [6] breaks down. The H_- values calculated for various concentrations of sodium hydroxide from the experimentally observed ionization ratios according to equations [4] and [5] are given in Table II, and shown as experimental points in Fig. 3.

TABLE II

H_- values for different molar concentrations of aqueous sodium hydroxide

[NaOH]	ϵ_{260}	H_-	[NaOH]	ϵ_{310}	H_-
0	11,960	—	0	76.6	—
0.0097	11,700	12.03	0.015	73.3	12.17
0.058	10,800	12.75	0.033	69.6	12.53
0.147	9,770	13.12	0.095	59.7	13.01
0.556	7,780	13.69	0.184	51.7	13.27
1.011	7,000	13.97	0.252	47.2	13.40
1.97	6,250	14.37	0.761	31.6	13.90
3.04	5,980	14.65	1.57	25.7	14.22
3.75	5,890	14.79	1.83	23.9	14.34
4.32	5,680	15.04	2.49	21.8	14.55
8.45	5,640	—	3.44	20.5	14.73
			3.98	19.9	14.85
			4.59	19.5	14.95
			8.45	17.9	—

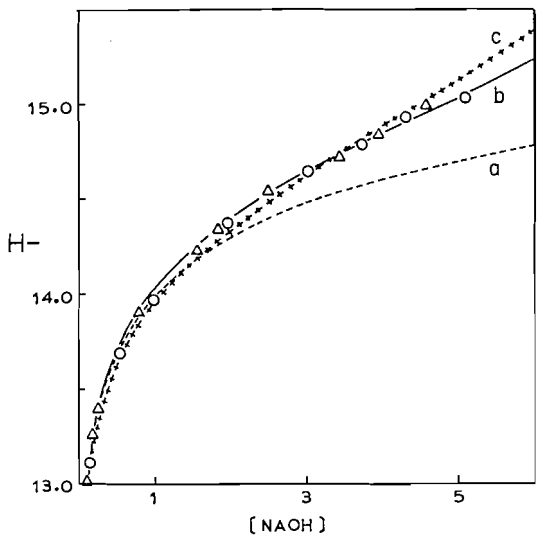

FIG. 3. Relation between molar concentration of sodium hydroxide and H_-. Points: experimental values calculated from ionization ratio of thioacetamide, determined from ultraviolet absorption at 260 mμ (○) and at 310 mμ (△). Curves: (*a*) theoretical for eq. [6]; (*b*) theoretical for eq. [13] with $v+y-p-1 = 3.2$; (*c*) Schwarzenbach and Sulzberger's experimental curve.

These values agree fairly well with those obtained by Schwarzenbach and Sulzberger (1) using substituted indigos as indicators, although the presentation by these authors of their results in graphical form only precludes a detailed comparison with our results.

Calculation of H_- Values for 1–6 M Sodium Hydroxide

The H_- values of 1–6 M solutions of sodium hydroxide may be calculated by a method developed essentially from that of Bascombe and Bell (23) for calculating H_0 values of solutions of mineral acids. We take account of the fact that the hydroxide ion, because of its small size and localized charge, is almost certainly more heavily hydrated than the usual organic conjugate base A^- with a charge dispersed by resonance. Consequently, equation [1] must be replaced by

$$HA + OH^- \rightleftarrows A^- + (p+1)H_2O, \qquad [7]$$

where HA, OH^-, and A^- represent the *hydrated* species, and p the difference in hydration numbers of (HA + OH^-) and of A^-. Equation [2] must then be replaced by

$$[A^-]/[HA] = K_{HA}[OH^-]f_{HA}f_{OH^-}/K_W a_W^{p+1} f_{A^-}, \qquad [8]$$

where a_W is the water activity of the sodium hydroxide solutions (24, p. 510). (For very dilute hydroxide solutions $a_W \rightarrow 1$ and equation [8] reduces to equation [2].) From the definition of H_- in terms of ionization ratios (equation [4]) we then obtain

$$H_- = pK_W + \log [OH^-] + \log f_{HA} + \log (f_{OH^-}/f_{A^-}) - (p+1) \log a_W. \qquad [9]$$

The possibility of using this equation to calculate the change in H_- with changing hydroxide ion concentration depends on whether or not some estimate of the change due to the activity coefficient terms can be made. Unfortunately, there is no satisfactory theoretical treatment for these changes in concentrated electrolyte solutions (8; 17, p. 379; 24, p. 223). However, it is known that for the salting out of neutral molecules $\log \gamma$ (where γ is the molal activity coefficient) is generally a linear function of the ionic strength of the electrolyte solution (8; 17, p. 379); while the ionic strength in turn is related to a_W. Consequently, it seems likely that as a first approximation

$$\log f_{HA} \approx v \log a_W. \qquad [10]$$

Such a relation is supported by the data shown in Fig. 4 for the molar activity coefficients f of the neutral molecules benzene (25), oxygen (26), and hydrogen (26) in aqueous sodium hydroxide, f being obtained from solubilities and defined as unity in pure water. Comparable data for thioacetamide are not available, but it would be expected that the slope (v) of a similar plot would be smaller than the slopes in Fig. 4, and possibly even of opposite sign, because of the polar character of the molecule (8). In such a case the deviation from linearity might be less serious than in the plots of Fig. 4.

It seems likely that the values of $\log f-$ for the anions of 1–1 electrolytes are also approximately linear functions of $\log a_W$ over the concentration range (1–6 M) being considered, so that

$$\log (f_{OH^-}/f_{A^-}) \approx y \log a_W. \qquad [11]$$

Starting with an infinitely dilute solution ($\log a_W = 0$), an increase in electrolyte concentration up to about 1 M (i.e. a decrease in $\log a_W$) leads to a decrease from unity (i.e. from $\log f\pm = 0$) in the molar mean activity coefficient $f\pm$, due to the interionic forces described in the Debye–Hückel treatment. However, further increase in concentration may lead to an increase in $f\pm$ because of the opposing effect of ion–solvent interactions

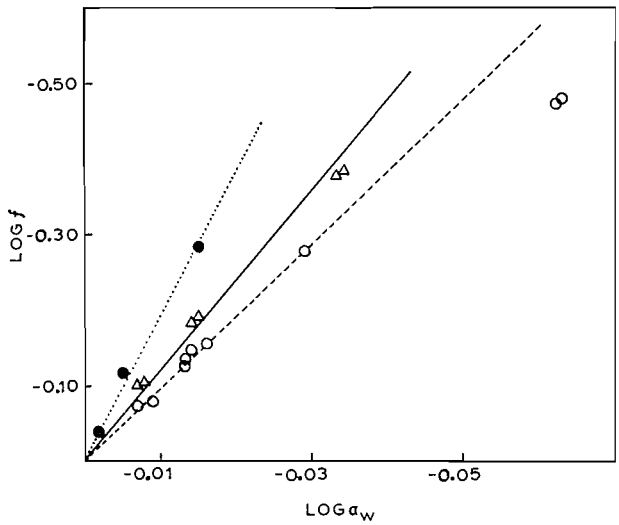

FIG. 4. Variation of molar activity coefficients (f) of hydrogen (○), oxygen (△), and benzene (●) in aqueous sodium hydroxide with the activity of the water (a_W).

(24, p. 223). This is shown in Fig. 5 for various concentrations (up to the highest for which data are available) of sodium chloride (up to 6 M), sodium hydroxide (up to 6 M),

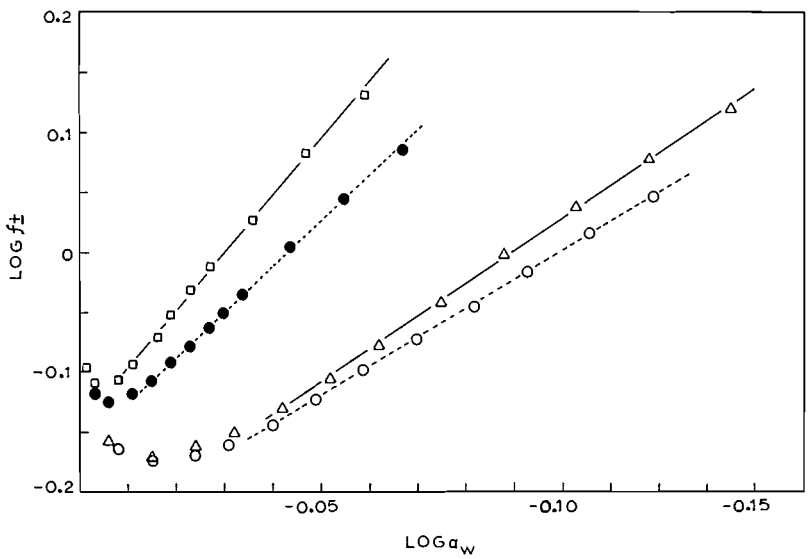

FIG. 5. Relation between molar mean activity coefficient ($f\pm$) and water activity (a_W) for aqueous solutions of sodium chloride (○), sodium hydroxide (△), sodium acetate (●), and sodium propionate (□).

sodium acetate (up to 3.5 M), and sodium propionate (up to 3 M). The $f\pm$ values for this figure were computed in the usual way (24, p. 32) from mean *molal* activity coefficients tabulated in the literature (24, p. 492) by taking account of the densities of the solutions (27). Water activities for various concentrations of sodium chloride (24, p. 476) and

sodium hydroxide (24, p. 510) are recorded, while those for various concentrations of sodium acetate and sodium propionate may be calculated from isopiestic data (28). It is evident from this figure that for concentrations of these electrolytes above about 1 M, $\log f\pm$ is an approximately linear function of $\log a_W$. Such a relationship is compatible with the relationship given in equation [11], if it is assumed that activity coefficients of both anions and cations are altering in the same way with increase in total electrolyte concentration.

Accepting equations [10] and [11], equations [8] and [9] may be transformed into

$$[A^-]/[HA] = K_{HA}[OH^-]a_W^{v+y-p-1}/K_W, \quad [12]$$

$$H_- = pK_W + \log [OH^-] + (v+y-p-1)\log a_W. \quad [13]$$

A plot of $\{\log ([A^-]/[HA]) - \log [OH^-]\}$ against $\log a_W$ for thioacetamide in sodium hydroxide gives an approximately straight-line curve (Fig. 6),[3] in accordance with

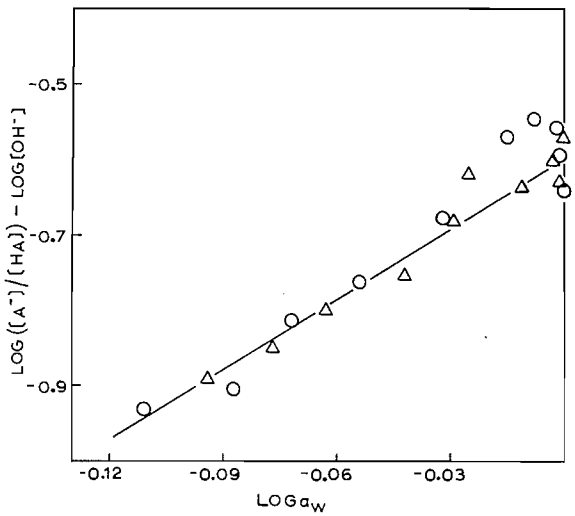

FIG. 6. Relation of ionization ratio ($[A^-]/[HA]$) and hydroxide ion concentration to the water activity of sodium hydroxide solutions. Experimental points: ionization ratio obtained from ultraviolet absorption at 260 mμ (○) and at 310 mμ (△).

equation [12]. The slope of the curve indicates $v+y-p-1 = 3.2$. Using this value, the H_- curve (6) shown in Fig. 3 has been calculated from equation [13]. The agreement with experimental values is reasonably satisfactory over the range of sodium hydroxide concentrations investigated.

Generality of H_- Scale for Sodium Hydroxide Solutions

The success of this treatment raises doubts as to whether any H_- scale for aqueous sodium hydroxide solutions is likely to have the generality of the H_0 scale for the common mineral acids. The success of the latter depends on the fact that the activity coefficients of different neutral molecules and their conjugate acids change only slightly with change of acid concentration (29). Consequently, the change of H_0 with acid concentration is

[3]*The scatter of points for the most dilute solutions, where* $\log a_W \to 0$, *is to be expected, since the points are based on the differences between small values, so that the effects of experimental error are magnified.*

determined chiefly by the differing degree of hydration of H_3O^+ and of the conjugate acids of the Brønsted bases being investigated (23); it seems likely that the failure of the ionization of a substance to follow H_0 can be ascribed to a degree of hydration of the conjugate acid differing from that of the conjugate acid of the Hammett indicator used to establish that portion of the H_0 scale (30). However, it is known that the activity coefficients of neutral molecules (and probably of ions) change very greatly, and in individual fashion, with change of concentration of sodium hydroxide, as shown by the strong but variable salting-out effects of this electrolyte (8). Additionally, it seems unlikely that different conjugate bases will be hydrated to the same extent. Hence it seems unlikely that $(v+y-p-1)$ of equation [13] should be the same for compounds of different type. This would explain the systematic differences observed by Schwarzenbach and Sulzberger (1) in the ionization of substituted indigos and of glutacondialdehyde dianils, while the similarity in the H_- scales established with thioacetamide and with substituted indigos would appear to be a chance coincidence. Obviously, a study of the ionization in sodium hydroxide of many widely varied indicators would be desirable. The success of the H_- scale in aqueous solutions of hydrazine (5) and organic bases (6, 7) with many different types of indicators may be ascribed to the weakly ionic nature of these bases, which causes them to have only minor salting-out effects.

ACKNOWLEDGMENTS

We are grateful to Professor R. Stewart for discussion, and to the National Research Council for financial assistance.

REFERENCES

1. G. SCHWARZENBACH and R. SULZBERGER. Helv. Chim. Acta, **27**, 348 (1944).
2. L. P. HAMMETT. Physical organic chemistry. McGraw-Hill Book Co., Inc., New York. 1940. p. 269. M. A. PAUL and F. A. LONG. Chem. Revs. **57**, 1 (1957).
3. J. H. RIDD. Chem. & Ind. (London), 1268 (1957). M. F. L. ALLISON, C. BAMFORD, and J. H. RIDD. Chem. & Ind. (London), 718 (1958).
4. C. H. LANGFORD and R. L. BURWELL. J. Am. Chem. Soc. **82**, 1503 (1960).
5. N. C. DENO. J. Am. Chem. Soc. **74**, 2039 (1952).
6. R. SCHAAL. Compt. rend. **238**, 2156 (1954); J. chim. phys. **52**, 784, 796 (1955).
7. F. MAURE and R. SCHAAL. Bull. soc. chim. France, 1138 (1956).
8. F. A. LONG and W. F. MCDEVIT. Chem. Revs. **51**, 119 (1952).
9. W. F. KOHLRAUSCH and J. WAGNER. Z. physik. Chem. B, **45**, 235 (1940).
10. A. I. VOGEL. Quantitative inorganic analysis. 2nd ed. Longmans Green, London. 1951. p. 242.
11. W. J. BLAEDEL and H. V. MALMSTADT. Anal. Chem. **24**, 455 (1952).
12. D. ROSENTHAL and T. I. TAYLOR. J. Am. Chem. Soc. **79**, 2684 (1957).
13. L. A. FLEXSER, L. P. HAMMETT, and A. DINGWALL. J. Am. Chem. Soc. **57**, 2103 (1935).
14. M. J. JANSSEN. Rev. trav. chim. **79**, 454, 464 (1960).
15. M. KASHA. Discussions Faraday Soc. **9**, 14 (1950). H. M. MCCONNELL. J. Chem. Phys. **20**, 700 (1952).
16. E. SPINNER. Spectrochim. Acta, **11**, 95 (1959).
17. H. S. HARNED and B. B. OWEN. The physical chemistry of electrolytic solutions. 2nd ed. Reinhold Publishing Corpn., New York. 1950.
18. P. A. LEVENE, L. W. BASS, R. E. STEIGER, and I. BENCOWITZ. J. Biol. Chem. **72**, 815 (1927).
19. S. S. BIECHLER and R. W. TAFT. J. Am. Chem. Soc. **79**, 4927 (1957).
20. E. W. WESTHEAD and H. MORAWETZ. J. Am. Chem. Soc. **80**, 237 (1958).
21. J. T. EDWARD and K. A. TERRY. Unpublished researches.
22. J. T. EDWARD and S. NIELSEN. J. Chem. Soc. 5075 (1957).
23. R. P. BELL and K. N. BASCOMBE. Discussions Faraday Soc. **24**, 158 (1957).
24. R. A. ROBINSON and R. H. STOKES. Electrolyte solutions. 2nd ed. Butterworths, London, 1959.
25. W. F. MCDEVIT and F. A. LONG. J. Am. Chem. Soc. **74**, 1773 (1952).
26. G. GEFFECKEN. Z. physik. Chem. **49**, 257 (1904).
27. INTERNATIONAL CRITICAL TABLES. Vol. III. 1st ed. McGraw-Hill Book Co., New York. 1928. pp. 79, 83. G. AKERLOF and G. KEGELES. J. Am. Chem. Soc. **61**, 1027 (1939).
28. R. A. ROBINSON. J. Am. Chem. Soc. **57**, 1165 (1935). E. R. B. SMITH and R. A. ROBINSON. Trans. Faraday Soc. **38**, 70 (1942).
29. N. C. DENO and C. PERIZZOLO. J. Am. Chem. Soc. **79**, 1245 (1957).
30. R. W. TAFT. J. Am. Chem. Soc. **82**, 2962 (1960).

ON ELECTRODEPOSITED THALLIC OXIDE

WILLIAM T. FOLEY
The Chemistry Department, St. Francis Xavier University, Antigonish, Nova Scotia
Received November 1, 1961

ABSTRACT

Thallium oxide, electrolytically deposited at the anode, has a defective oxide structure and the thallium (I) content is about 1% by weight. The conductivity of the oxide is $(1.54 \pm 0.04) \times 10^3$ ohm^{-1} cm^{-1} and the conductivity is of the *n*-type. The oxide contains variable amounts of water, which it retains very tenaciously.

The composition of thallium oxide formed on a platium anode by oxidation of aqueous thallium (I) solutions has been the subject of many research papers and a few names from an extensive literature will be mentioned. Gallo and Ceuni (1) reported the formation of Tl_2O_5 and Tzentnershver and Trebaczkiewicz (2) asserted that the oxide was Tl_2O_4. Skanavi-Grigor'eva and Starovera (3) found the oxide to contain substantial amounts of anions. This report deals with the composition and with some properties of the oxide.

Thallium oxide may be plated on the anode from a solution buffered to pH 9.5 by an NH_4NO_3–NH_4OH buffer and containing silver ion as a cathodic depolarizer. The electrochemical reactions occur with 100% current efficiencies (4) so that the weight of silver deposited affords a very precise measure of the electrochemical equivalent weight of the oxide. The equivalent weight based on the formula Tl_2O_3 is 114.2 but the experimental value varies from 116.1 to 116.8, with a mean value of about 116.3 for electrolysis conducted at room temperature and at a current density of 0.03 amp/cm^2. The deposit is jet-black and it is very adherent. The samples were dried for 20 minutes at 110° C; drying for prolonged periods of time yielded the same results as were obtained by drying for 20 minutes.

We have found that the oxide contains an appreciable quantity of thallium (I). The oxide dissolves readily in cold dilute solutions of hydrochloric acid by virtue of the high stability of the chloride complex of thallium (III). As the oxide dissolves, one may see on the electrode, traces of the bright yellow salt which one obtains on mixing solutions of thallium (I) chloride with thallium (III) chloride. The dissolved oxide may be analyzed for thallium (I) coulometrically with electrogenerated chlorine (5) and with the detection of the end point amperometrically. The possibility existed that the thallium (I) could have been formed in the process of solution by a redox reaction between thallium (III) and chloride. This point was checked by titrating with EDTA, at pH 5, with xylenol orange as indicator, the solution which had been used in the coulometric titration. The amount of thallium (III) calculated from the weight of silver and from the coulometric measurement checked beautifully with that calculated from the EDTA titration. Representative data are given in Table I.

The first column shows the weight of oxide and the second shows the number of microfaradays based on the weight of the cathode deposit. If we divide the number in the first column by the number of faradays we obtain the electrochemical equivalent. The fourth column indicates the volume of 0.1 *M* EDTA calculated from one-half of the total number of microfaradays.

TABLE I
Thallium (I) and (III) in oxide

Oxide (grams)	Silver (microfaradays)	From coulometer (microfaradays)	EDTA (ml)	
			Calc.	Meas.
0.5246	4499	52.6	22.76	22.74
0.5080	4341	65.4	22.03	22.04
0.6077	5203	69.7	26.36	26.32
0.3937	3373	45.9	17.10	17.10

The microfaradays for thallium (I) varied from run to run, but the average of 30 runs was 1.33% of the total number of microfaradays. There was a possibility that the thallium was present as thallium (II) rather than thallium (I) and that the latter was formed by dismutation of thallium (II) during the process of solution. A powdered sample was tested for paramagnetism by suspending in a magnetic field of 4.3 kilogauss, with a silk thread, a tiny capillary containing the oxide. The capillary lined up smartly at right angles to the field and thus displayed its diamagnetic character and showed the absence of thallium (II).

In an effort to show that the thallium (I) was not present in the compound as a result of adsorption, some electrolyses were performed at temperatures of 25°, 50°, and 75° C and also at current densities as low as 2×10^{-4} amp/cm^2. In all cases the thallium (I) content was independent of the current density and the temperature. At the highest temperature the weight of oxide based on the sum of the thallium (I) oxide and the thallium (III) oxide was much closer to the actual weight of the oxide than was true of an electrolysis carried out at room temperature. As will be shown later, this means that the water content of oxide samples prepared at 75° C and at low current densities was lower than the water content of oxide samples prepared at lower temperatures.

The conductivity of the oxide was next measured. A platinum anode 0.25 mm thick and 50 cm^2 in area was polished to a mirror finish and it was then plated with oxide at a current density of 6×10^{-4} amp/cm^2 until it was about 2.5 mm thick. The sample was dried for an hour at 110° C and, after cooling, it was given a heavy coating of collodian. The deposit was cut carefully with a razor blade near the perimeter of the electrode so that the main sheet of oxide could be removed readily from the platinum. The side which had been adjacent to the platinum had a metallic luster. Fairly large areas of the oxide would be free from cracks and such sections were removed and glued to glass slides with plastic cement. A block of this oxide was now cut to uniform size with a razor blade and was prepared for the conductivity measurement.

The four-terminal method was used to measure the conductivity. Since a pressure-laden contact would fracture the specimen, silver paint, such as is used to make printed circuits, was used to make the contacts. The current leads were made from No. 22 copper wire, whose ends were flattened by hammering, and they were painted to the ends of the oxide block with the silver paint. The potential leads were made from No. 44 copper wire, which was fastened to the oxide with silver paint that was applied through a narrow stencil. The current leads were connected to a regulated high-voltage supply through a 50,000-ohm resistor in order that a constant current would be had even though there might be minor changes in the contact resistances. In series also with these was a precision resistor across which was placed an L and N Type K2 potentiometer to provide a means of measuring the current. The potential leads were attached to a Keithly Model 610A

electrometer and, since no current was flowing, the contact resistance of the potential leads played no significant role. From the formula

$$\text{conductivity} = l/RA,$$

where l is the length, R the resistance in ohms, and A the cross-sectional area in cm^2, the conductivity of the oxide was found to be $(1.54 \pm 0.04) \times 10^3$ ohm^{-1} cm^{-1}. This order of magnitude is typical of a semiconductor.

The question of whether the defective oxide was a p or an n-type was answered by measurement of the sign of the Hall coefficient. A slab of oxide was prepared for such a measurement by attaching current leads as before and by spotting on it three Hall probes (two on one side and one on the opposite side) of No. 40 wire. The two probes on one side were centered electrically by means of a potentiometer while current was flowing. The specimen was placed in a magnetic field of 11.3 kilogauss. The magnetic field, acting on the current-bearing slab, gave rise to a transverse potential gradient, known as the Hall e.m.f. and a measurement of the sign of the Hall e.m.f. agreed with the conclusion that the conductivity was of the n-type. Apparently the oxide has a defective oxide lattice. The X-ray studies of Scatturin and Torrati (6) on the oxide of thallium prepared by oxidizing thallium sulphate with hydrogen peroxide suggested that their oxide had a defective oxide structure also.

A consideration of the data of Table I will show that the sum of the weights of thallium (III) oxide and thallium (I) oxide does not account for the electrochemical equivalent weight. Peltier and Duval (7) have found from a thermogravimetric study that the thallium oxide prepared by chemical means is distinctly different from that prepared by electrolytic means: the electrolytic oxide retains water very tenaciously and its pyrolysis curve beyond 677° C differs greatly from that of the other oxide.

In a study of the effect of temperature on the stability of thallium (III) oxide, samples of oxide were heated for a half hour at 190° under a pressure of 5 microns and these samples were sealed off and placed in a furnace at 300° C for several hours. When cooled, the ampules had droplets of water clinging to their inner walls. Samples of thallium oxide, which had been powdered and dried at 110° C, were heated in a tube furnace in a current of oxygen to minimize decomposition of the oxide–sesquioxide. In this way it has been possible to account quantitatively for the equivalent weight of the oxide. A typical result is given in Table II.

TABLE II

Analysis of thallium oxide

Equivalent weight of oxide	116.5_5
Wt. of Tl_2O_3 based on formula	114.22
Loss of water on heating to 340° C	0.81
Wt. of Tl_2O	1.48
Total	116.5_1

The oxide which had been dried for 1 hour at 340° C was analyzed for thallium (I) and it was found that, despite the atmosphere of oxygen, the thallium (I) content had increased to 1.95%. When this value of the thallium (I) oxide was added to 98.05%, the corrected value of the thallium (III) oxide, there was perfect accounting for everything in the moisture-free oxide. If the oxide is heated to 340° C in the air, the thallium (I) content is increased to a much higher value. The tendency of the oxide to decompose

when it is heated to render it anhydrous has been responsible for the confusion in the literature on the composition of the oxide.

How is the water retained by the oxide that is heated to constant weight at 110° C? The water seems to have its usual specific volume because the density of the electrodeposited oxide varies from 9.720 to 9.775 and these values have been determined by the buoyancy method and also by the pyonometer method. Thus the measured density of 9.730 for a sample of oxide whose equivalent weight was 116.2 agrees well with a value calculated on the assumption that the deposit is made up of thallium oxide with an X-ray density of 10.38 and of water present to the extent of 0.72%. An X-ray investigation of the oxide, using filtered copper radiation and large powder cameras, showed that the oxide dried at 110° C gave a pattern measured with a diffractometer identical with that of a sample which had been dried at 340° C in a current of oxygen. These findings do not invalidate the view that the water present in the oxide dried at 110° C is not in the crystal lattice. The powder pattern agreed almost perfectly with that reported by Swanson and Fuyat (8), who show that the crystal is cubic with space group $I2_13$, having 16 molecules to the unit cell. It might be mentioned here that a powder X-ray pattern was obtained for thallium oxide formed at the anode in the presence of ammonium fluoride and it showed that the lattice constants for this oxide, which contains fluoride, are distinctly different from those obtained for thallium oxide. The replacement of fluoride for oxygen in the lattice likely caused serious distortion of the crystal. Had the water been incorporated in the crystal it is likely that it would also have caused a change in the lattice constants.

If the water was mechanically trapped or occluded in the crystal lattice, one would expect to find traces of silver in the solution formed on dissolving the oxide: none was found. If the water was mechanically trapped, one would expect that freezing the sample would cause a change in the forces of attachment so that the water could then be removed readily on heating. A sample of oxide which had been dried at 110° C was immersed in liquid nitrogen for an hour. The electrode was then heated to 110° C for an hour and then was reweighed. There was no decrease in the weight of the oxide. This suggests that the water is not occluded.

It has been found in this laboratory that when the oxide is plated with the potential of the anode controlled by a potentiostat the plot of the logarithm of the current against the time did not give a straight line. According to Lingane (9) such a plot should yield a straight line when the electrode reaction occurs at 100% efficiency and when the rate of the reaction is controlled by the diffusion of the electroreactive species to the surface of the electrode. This suggests that the oxidation reaction is complex. Workers in kinetics of reactions, for example Vetter and Thiemke (10), have postulated the existence of Tl (II) as an intermediate in the oxidation of Tl (I). Perhaps the source of the defect structure of the oxide might be similarly explained.

ACKNOWLEDGMENTS

The author acknowledges with gratitude the technical assistance of Miss J. M. Osyany in making the conductivity measurements, and also the financial assistance of the Defence Research Board in making this work possible with Grant No. 9510-12.

REFERENCES

1. G. Gallo and G. Ceuni. Gazz. chim. ital. **39**, 285 (1908).
2. M. Tzentnershver and T. Trebaczkiewicz. Z. physik. Chem. A, **165**, 367 (1933).
3. M. S. Skanavi-Grigor'eva and V. I. Starovera. Zhur. Obscheĭ Khim. **28**, 1689 (1958).

4. W. T. FOLEY. J. Electrochem. Soc. **104**, 638 (1957).
5. R. P. BUCK, P. S. FARRINGTON, and E. H. SMITH. Anal. Chem. **24**, 1195 (1952).
6. V. SCATTURIN and M. TORRATI. Ricera Sci. **23**, 1805 (1953).
7. S. PELTIER and C. DUVAL. Anal. Chim. Acta, **2**, 210 (1948).
8. H. E. SWANSON and R. K. FUYAT. Natl. Bur. Standards Circ. No. 539, **2**, 28 (1953).
9. J. J. LINGANE. J. Am. Chem. Soc. **67**, 1916 (1945).
10. K. J. VETTER and G. THIEMKE. Z. Electrochem. **64**, 805 (1960).

ELECTRON PARAMAGNETIC RESONANCE STUDIES ON FREE RADICALS PRODUCED BY Tβ-PARTICLES IN FROZEN H_2O AND D_2O MEDIA AT LIQUID NITROGEN TEMPERATURE

J. KROH,[1] B. C. GREEN, and J. W. T. SPINKS
The Department of Chemistry, University of Saskatchewan, Saskatoon, Saskatchewan
Received August 24, 1961

ABSTRACT

Samples of H_2O and D_2O and solutions of H_2O_2, $HClO_4$, HF, etc., in light and heavy water, were tritiated with T_2O to activities of from 0.1 to 1 c/ml.

The paramagnetic resonance spectra recorded at liquid nitrogen temperature and interpreted as representing H(D) atoms and OH(OD), $HO_2(DO_2)$ free radicals were compared with those induced under analogous conditions by Co^{60} γ-rays.

The lower radical yields observed in the present work have been ascribed to the difference in linear energy transfer between Tβ-particles and more penetrating radiations.

INTRODUCTION

As reported previously in several communications (1–3), the tritium technique of inducing electron paramagnetic resonance (EPR) spectra at low temperatures has several advantages. First of all, even for high doses of radiation (of the order of 10^{21} ev/ml) no spectral background due to irradiated glass or quartz (of the samples tubes) is produced. Secondly, the method may be used fairly universally in EPR studies of various systems, including organic materials not miscible with water (3). Lastly, the high density of ionization of Tβ particles allows one to examine the effects of linear energy transfer (LET) on the formation and trapping of free radicals.

The present work was undertaken to provide quantitative information on the production of radicals in tritiated H_2O and D_2O ice, as well as in some tritiated H_2O and D_2O solutions.

EXPERIMENTAL

Materials

Double-distilled H_2O, or D_2O (99.8% purity), was refluxed for several hours immediately before using, in a closed-circuit Pyrex apparatus, provided with a column 30 cm long and packed with glass Fenske helices. All materials present in the solutions ($HClO_4$, HF, H_2O_2, etc.) were of analytical grade and were used without further purification. A solution of T_2O, with an activity of 5 c/ml, provided by Merck and Co. Ltd., was used for tritiation of the samples.

Preparation of the Samples

The required activity of the sample was obtained by micropipetting and mixing the calculated volumes of T_2O solution and the experimental material directly in the sample tube. The tubes, Pyrex or quartz, were 4 mm in outside diameter and approximately 22 cm long. Some solutions were degassed by using the freeze–pump–thaw technique. This procedure was carried out in a small bulb, about 1 cm in diameter, blown onto the end of the sample tube.

Irradiation and Recording of the Spectra

The samples were kept in liquid nitrogen over the whole period of the experiment, in some cases up to 4×10^3 hours.

All electron spin resonance spectra were drawn with a Varian Associates V 4500 EPR spectrometer, equipped with an X band microwave bridge. The tip of a quartz Dewar flask containing the sample was inserted into the resonant cavity. A 6-inch Varian magnet system was used. The magnetic field modulation amplitude (frequency of 200 cycles/sec) was chosen for maximum signal strength at optimum resolution. The spectra are essentially "first derivative" curves.

[1]*Lodz, w. Zwirki 36, Politechnika, Poland.*

The magnetic field sweep in the region of $g = 2.00$ was calibrated by drawing spectra for the semi-quinone ion. Microcrystalline α,α-diphenyl-β-picrylhydrazyl (DPPH) was included with a sample when it was desired to mark the position of the DPPH peak on a spectrum.

Estimates of the quantity of spins in the samples were simplified by using the same size of tubing for all samples and by using sufficient material in the tubing to occupy fully the active region of the cavity. When the shape and width of spectra were identical, the heights of maxima on the curves were used for comparisons of relative numbers of spins. If shape and width differences were apparent, double integrations of the spectral curves were used when comparing relative concentrations. Estimates of absolute quantities of "spins" were obtained through indirect comparisons of the spectra of the samples and the spectra of freshly prepared solutions of DPPH, of known concentration, in benzene. Spectra which were compared for quantitative information were drawn under identical operating conditions and conditions for which power-saturation effects were absent. Indirect comparisons of the DPPH solutions and the samples were made through the use of the gamma-irradiated barium salt of dichloroacetic acid or a dispersion of charcoal in lactose. This technique was used because the DPPH solutions were found to be unstable, because the width of their spectra narrows greatly at liquid nitrogen temperatures, and because the homogeneity of the frozen "solution" is questionable.

The accuracies of estimates of relative "spin" concentrations are probably of the order of a few per cent. The estimates of absolute values of "spin" concentrations involve various uncertainties. The values obtained in this work appear to be reasonable and are considered to be well within 50% of the true values.

Warming Experiments

The thermal stability of the free radicals was examined in the following manner. The sample was placed in a hole 2 cm deep and 5.5 mm in diameter drilled along the axis in the upper end of a brass rod 30 cm long and 2.5 cm in diameter. The lower part of this rod was immersed in liquid nitrogen, and the temperature of the sample was regulated by the depth of the immersion. Two iron–constantin thermocouples, located near the sample, were used for recording the temperature. The measuring system was calibrated with several "freezing systems", and it allowed one to read the temperature to within 2 to 3 degrees.

The warming of the sample and recording of the spectrum, the latter always at liquid nitrogen temperature, were performed alternately. During the warming of a sample the temperature was raised from −196° C (liquid nitrogen temperature) to a required value in a period of about 8–10 minutes. This time was kept approximately constant by controlling the distance between the upper end of the brass rod and the level of the liquid nitrogen in which the lower end was immersed.

H_2 Analysis

The production of molecular hydrogen in the tritiated samples was examined by a gas chromatography method. After the samples were degassed and sealed up in the break-seal containers, they were kept in liquid nitrogen until the required dose of radiation was absorbed. Then, after the sample was thawed, the evolved gas was introduced, using helium as a carrier, into the gas chromatography system. The chromatograph was equipped with a silica gel column, and it operated at room temperature.

The system was calibrated with hydrogen produced in degassed water by Co^{60} γ-rays applied in doses varying from 4.8×10^{18} to 2×10^{19} ev/ml. In plotting the calibration curve (recorded signal vs. amount of H_2) the value of $G(H_2) = 0.45$ (4) for γ-irradiated water was used.

RESULTS

Irradiation of H_2O and D_2O Ice

The EPR spectra of degassed, tritiated H_2O, D_2O, and H_2O+D_2O ice are shown in Fig. 1A, 1B, and 1C, respectively. The location of spectra in the magnetic field is marked by a vertical line indicating the position of the center of the DPPH spectrum. In all diagrams, the magnetic field increases to the right.

The spectra in Fig. 1A and 1B have been interpreted (see discussion) as representing OH and OD radicals, respectively.

The spectrum of OH radicals (1A) consists of a doublet with a separation of about 40 gauss and $g = 2.01$. OD radicals (1B) are represented by a triplet with approximately the same g and separation of 6 gauss between neighboring lines.

The spectrum in Fig. 1C is that of the sample containing D_2O and H_2O in the volumetric ratio 4:1. The central OD triplet is located between two peaks ascribed to the OH doublet. The latter is just noticeable in the spectrum of Fig. 1B, since the amount of

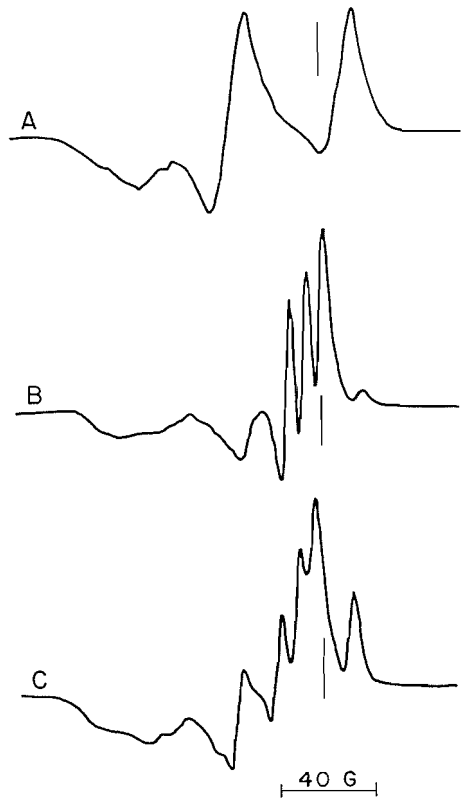

FIG. 1. EPR spectra of tritiated H_2O (A), D_2O (B), and H_2O+D_2O (C) ice.

H_2O unavoidably introduced into the sample with T_2O does not exceed, in this case, 2%.

The concentration of OH and OD radicals, as measured in the samples irradiated at a dose rate of 7.6×10^{17} ev/ml hr, are plotted against the total absorbed dose in Fig. 2.

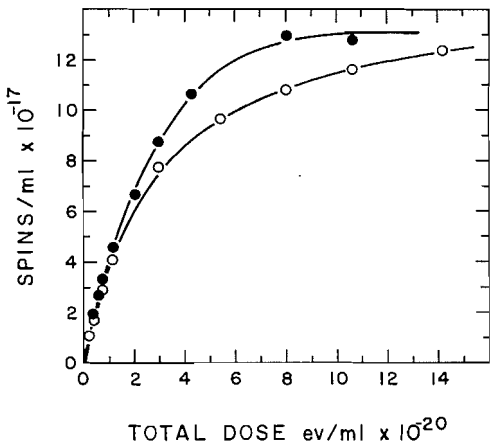

FIG. 2. Formation of OH (O) and OD (●) radicals in tritiated H_2O and D_2O ice.

Both types of radicals seem to reach their stationary concentrations at a level of about 1.3×10^{18} spins/ml.

To examine the dose-rate dependence at the initial radical yields, several samples were tritiated to lower activity and irradiated at a dose rate of 10^{17} ev/ml hr. The initial stage of the formation of OH radicals in one such sample is shown in Fig. 3, curve 1.

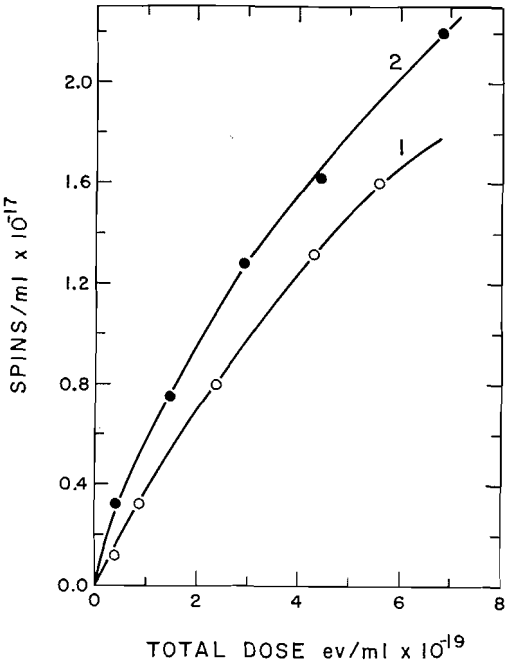

FIG. 3. Formation of OH radicals, as determined immediately after tritiation (1) and after melting and refreezing the sample (2).

Some of the samples were thawed, frozen in liquid nitrogen, irradiated, and examined again. It was found that such procedure results in increased radical yields. This may be seen in Fig. 3, where curve 2 represents the formation of OH radicals in the thawed and refrozen sample.

The yields of OH and OD radicals, as found under various experimental conditions, are as follows:

TABLE I

Radical yields in H_2O and D_2O Ice (G values)

	OH radical		OD radical	
Dose rate (ev/ml hr)	Immediately after tritiation	After second freezing	Immediately after tritiation	After second freezing
7.85×10^{16}	—	—	0.36	0.50
8.95×10^{16}	0.32	0.85	—	—
7.6×10^{17}	0.32	—	0.45	—

In the H_2O ice samples an interesting orientation effect was observed. Both the height of the OH doublet and its shape were found to depend on the position of the sample in the cavity. Turning the sample around its vertical axis changed the height of the OH

peaks. This passed through four successive maxima in a 360° rotation. Neighboring maxima were spaced approximately 90° apart. Moreover, of the two pairs of "opposite" maxima, spaced 180° apart, one was particularly pronounced. Effects on spectra of orientation with respect to the magnetic field for irradiated single ice crystals were reported by McMillan, Matheson, and Smaller (5) and by Livingston, Zeldes, and Taylor (6). It appears probable that a net crystallite alignment in our samples was responsible for the observed orientation effects. To ensure reproducibility, all OH spectra are recorded with the sample placed in its "maximum" position. A similar but less marked effect existed in the D_2O ice.

On warming of the sample, both OH and OD radicals seem to disappear in the same temperature range. As shown in Fig. 4, a rapid drop in the concentration of radicals

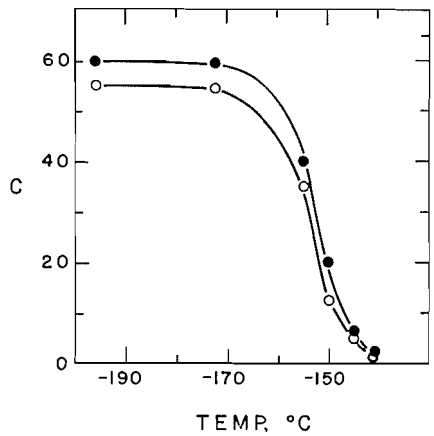

FIG. 4. Thermal decay curves of OH (○) and OD (●) radicals in H_2O and D_2O ice. The concentration (C) of free radicals is given in relative units.

occurs between −160 and −150° C. The weak EPR signal left after removal of OH radicals, i.e., at about −140° C, is shown in Fig. 5A. The concentration of the radical

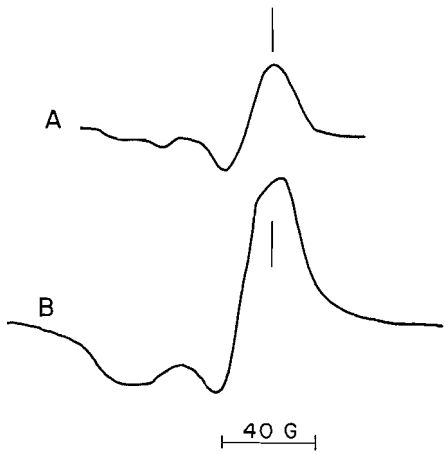

FIG. 5. EPR spectra of tritiated H_2O ice warmed from liquid nitrogen temperature to about −140° C (A) and tritiated H_2O_2 at −196° C (B).

represented by this spectrum for the sample with activity 1 c/ml irradiated with a total dose of 1.4×10^{21} ev/ml amounts to about 5% of the initial (before warming) concentration of OH radicals. The analogous spectrum recorded at $-140°$ C for D_2O ice was found to be much less intense.

In order to determine the nature of the radicals surviving in warmed H_2O ice, a 20% aqueous solution of H_2O_2 was tritiated to the activity 0.33 c/ml, degassed, and frozen in liquid nitrogen. The EPR spectrum of the radicals formed under these conditions is shown in Fig. 5B. The radical is formed with a very high yield, $G = 4$, and its concentration increases linearly with the time of irradiation up to doses of the order of 10^{21} ev/ml (see Discussion).

No H(D) atoms were found in tritiated $H_2O(D_2O)$ ice even in the samples subjected to large doses of the order of 10^{21} ev/ml.

Irradiation of Acidified and Alkaline H_2O and D_2O

Guided by the experiments of Livingston and Weinberger, several tritiated samples of $HClO_4+H_2O$ (I) and $HClO_4+H_2O+D_2O$ (II) mixtures were examined. In both types (I and II) of samples the activity was 0.5 c/ml, equivalent to the dose rate of 3.8×10^{17} ev/ml hr.

In samples I the molar ratio of $HClO_4$ was 1:7, whereas in samples II the molar ratio $HClO_4$:H_2O:D_2O was 1:3:4. Thus, in samples II the total numbers of H and D atoms were approximately equal. In all samples containing perchloric acid, H and D "atoms" were readily produced. The EPR spectra showed also the presence of other paramagnetic species, represented by absorption in the $g = 2$ region.

This "central" part of the spectrum could be almost completely eliminated by recording at the very low power necessary for the prevention of the saturation of the H and D lines. In contrast to this, by using high microwave power, the central spectrum was enhanced, whereas H and D signals were found to be strongly saturated and weakened.

The relative heights of the three deuterium lines changed extensively when the microwave power was altered at saturation levels. The "true" height of the center line is uncertain at higher-power levels, due to admixture with other absorption in the $g = 2.00$ region. It appears at these powers to be equal in height to or slightly shorter than the low-field deuterium line. The ratio of the peak height of the low-field line to the peak height of the high-field line changed from more than 5 to 1 as the microwave power was decreased. Jens, Foner, Cochran, and Bowers (8) reported the center line higher than *either* the low- or high-field line for condensed discharge products in deuterium at 4° K.

The low-field hydrogen line was *slightly* higher than the high-field line under power-saturation conditions. This difference reversed at lower microwave powers. The deuterium appears to show saturation effects more readily than the hydrogen.

The low-power spectrum of sample II is shown in Fig. 6. The spectrum consists of two hydrogen lines with separation of about 500 gauss and three D lines with separation of about 80 gauss.

Satellites were observed on both the H and D lines at microwave-power-saturation levels and in the earlier stages of the irradiations. They were not observed in the later stages. Zeldes, Livingston, and co-workers have reported satellites in similar systems (6, 9, 10).

Figure 7 shows the concentrations of H atoms in sample I (curve 1) and H and D atoms in sample II (curves 2 and 3) as plotted against the total dose of radiation.

FIG. 6. "Low-power" EPR spectrum of tritiated $HClO_4+H_2O+D_2O$ mixture at liquid nitrogen temperature. The spectrum consists of two H and three D lines.

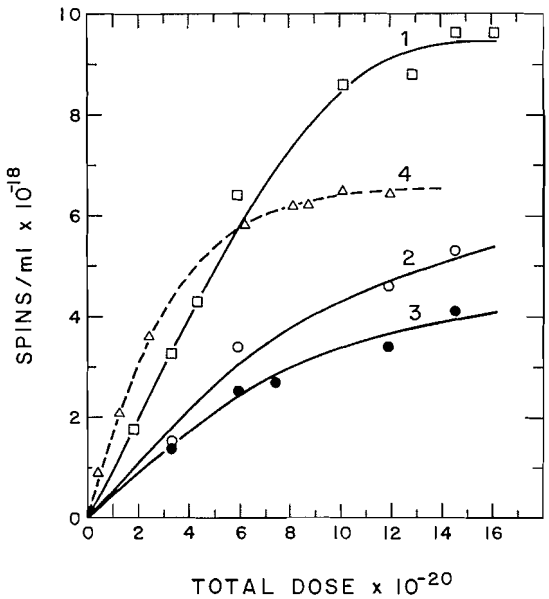

FIG. 7. Formation of stabilized atomic hydrogen and deuterium in $HClO_4$ solutions. Curve 1 shows hydrogen production in sample I ($HClO_4+H_2O$). Curve 2 shows the hydrogen production in sample II ($HClO_4+H_2O+D_2O$). Curve 3 shows the production of atomic deuterium in sample II. Curve 4 shows the formation of H atoms in sample I, as calculated on the basis of line height. The difference between the results of integration and determining line heights may be seen by comparing curve 1 and 4.

The initial yield rate of H radicals in sample I is $G(H) = 1$, and the saturation concentration of H atoms is of the order of 10^{19} spins/ml. In sample II the initial yield rates were $G(H) \approx G(D) = 0.5$, but the concentration of H atoms seems to increase faster than that of D atoms.

The width of the H and D lines increases noticeably with concentration, especially when the latter approaches the stationary level. This can be seen in Fig. 8, showing H lines corresponding to two different concentrations. Line-width changes with increased radiation dosage have been reported by Livingston and co-workers (6, 7). Thus, an estimate of H concentration based on the line height would be misleading. This is demonstrated in Fig. 7, in which the broken curve 4 represents the "concentrations" of H atoms in sample I, as calculated from the line heights.

The central "high-power" spectra of samples I and II are shown in Fig. 9A and 9B, respectively. The spectrum of the tritiated $HClO_4+H_2O+D_2O$ mixture (sample II)

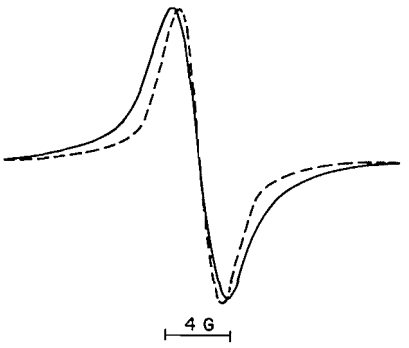

FIG. 8. Two hydrogen lines recorded for $HClO_4+H_2O$ sample after the dosage of 6×10^{20} ev/ml (broken) and 14.5×10^{20} ev/ml (continuous).

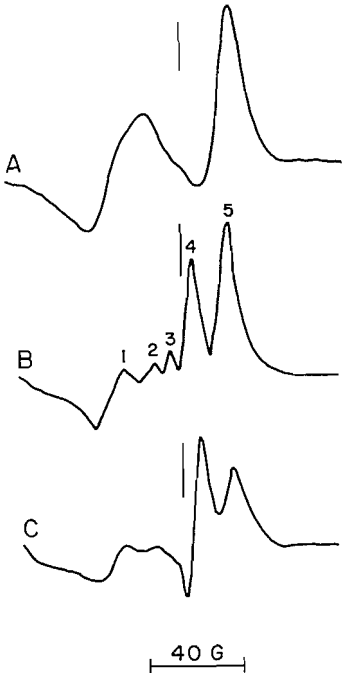

FIG. 9. "High-power" EPR spectra of $HClO_4+H_2O$ (A) and $HClO_4+H_2O+D_2O$ (B) samples. Spectrum (B) changes into (C) after subjecting the sample to large doses of radiation.

changes its shape in the course of irradiation. This can be seen by comparing spectra 9B and 9C, induced by low and high doses of radiation, respectively.

On warming sample II, the concentration of H and D atoms falls, as shown in Fig. 10. Curves denoted by "OH" and "OD+D" were determined by examining the decrease of the high-field peak in spectrum 9A and peak 4 in spectrum 9B, respectively.

At about $-150°$ C a new spectrum appears in both samples I and II. The broken curve in Fig. 10 represents the increase in intensity of this new, unidentified spectrum with temperature. Among the other members of this series, the simplest spectrum in the central, $g = 2$ region was obtained by irradiation of hydrofluoric acid (Fig. 11). On warming the acid, this spectrum disappears in a temperature range very close to that of the disappearance of "OH" radicals in $HClO_4$ samples (Fig. 10), but the deformation

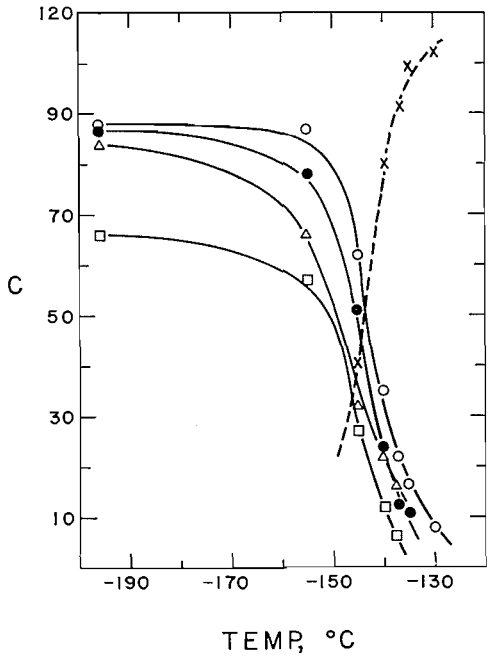

FIG. 10. Thermal decay curves of free radicals produced in tritiated $HClO_4$ samples: OH (□), OD+D (△), D (●), H (○). The broken curve represents the formation of a new radical, appearing on warming.

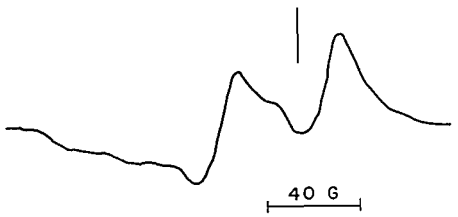

FIG. 11. High-power EPR spectrum of tritiated HF sample.

of the spectrum and the production of new species occurs to a much less extent than in perchloric acid. However, the formation of stable H atoms at −196° C is much lower in the HF medium than in $HClO_4$. In 16% HF, tritiated to 0.33 c/ml, the initial hydrogen yield was found to be 0.06. Moreover, the concentration of H atoms reaches the stationary state at about 2×10^{17} spins/ml, a much lower concentration than that found for $HClO_4$.

In other acidified and alkaline solutions which were examined, the concentration of atomic hydrogen was even lower. In 24% HCl solution, tritiated to 0.33 c/ml, H lines, though easily detectable, could not be used for any reliable quantitative measurements. In concentrated 10 *M* NaOH solution with the same activity, atomic hydrogen was produced with slightly higher yield, though still lower by one order of magnitude than in HF. Following the last observation, diluted (0.1 *M*) and concentrated (5 *M*) aqueous solutions of LiOH, NaOH, KOH, and $Ba(OH)_2$ were irradiated at liquid nitrogen temperature with Co^{60} γ-rays. In all concentrated solutions, small quantities of hydrogen were found. The most favorable conditions for the production of H atoms seem to exist in NaOH solutions.

Most of the tritiated materials became strongly colored in the course of irradiation. $HClO_4$ solutions acquired yellowish coloring; HCl, bright green; NaOH, dark blue.

Production of Molecular Hydrogen

Tritiated samples of water and 35% $HClO_4$, each 10 ml in volume, were degassed and frozen in liquid nitrogen. After they had absorbed the total dose of 2.55×10^{18} ev/ml at a dose rate of 1.52×10^{16} ev/ml hr, the samples were thawed and examined chromatographically. The whole analytical procedure was carried out under exactly the same conditions as in the calibration experiments, with γ-irradiated samples. The yields of molecular hydrogen in ice and frozen $HClO_4$ solution were found to have G values of 0.1 and 0.31, respectively.

In the identical H_2O and $HClO_4$ samples irradiated at room temperature to the total dose of 1.96×10^{19} ev/ml, the respective yields in water and perchloric acid had G values of 0.59 and 0.30.

DISCUSSION

The EPR spectra of tritiated H_2O and D_2O ice (Fig. I, A and B) have been assumed to represent OH and OD radicals, respectively. Such an interpretation seemed to be supported by recent reports of other authors. The EPR spectra found for Co^{60} γ-irradiated ice by Siegel (12) and his colleagues, and ascribed by them to OH and OD radicals, are identical with those reported here.* Very similar spectra were found by Piette *et al.* (13) for ice irradiated by fast electrons, and by McMillan *et al.* (5) for γ-irradiated single crystals of ice.

Results of ultraviolet irradiations of dilute H_2O_2 solutions at liquid nitrogen temperature, reported by us (11) recently, also support the above interpretation. The EPR spectrum recorded at liquid nitrogen temperature after prolonged ultraviolet irradiation of 10^{-3} to 10^{-2} M H_2O_2 becomes identical with that in Fig. 1, A. Photolysis of H_2O_2 most likely results only in OH formation, and in the dilute medium any secondary processes are of low probability.

The increase in radical yields after melting and refreezing (Table I and Fig. 3) is of considerable interest. Melting of the tritiated H_2O ice results in OH recombination and production of small quantities of H_2O_2. The concentration of the latter may be calculated from the specific activity of the sample and the duration of the experiment; in the case of the samples referred to in Table I as "after second freezing", this is of the order of 10^{-3} M. It is difficult to make any quantitative estimate of the probable effect of this amount of H_2O_2 on OH yield since, as indicated in ref. 11, the yield of OH on irradiation of H_2O_2 is strongly dependent on the H_2O_2 concentration. However, it has been pointed out (11) that the yield of HO_2 radicals in H_2O_2 is greater than that of OH radicals in ice by a factor of about 10, leading to G_{HO_2} in H_2O_2 of about 4. If HO_2 is formed by $OH + H_2O_2 \rightarrow HO_2 + H_2O$, it follows that the initial G_{OH} in H_2O_2 solutions must also be about 4. Thus, a small percentage of H_2O_2, say 1%, could give a 10% increase in OH yield, and it is therefore not unreasonable to attribute a good fraction of the observed 25% or so increase to H_2O_2 produced in the irradiation prior to thawing and refreezing.

The spectrum in Fig. 5A, left after warming H_2O ice to about $-140°$ C, is thought to represent the HO_2 radical. The spectrum is very similar to that obtained by irradiation

**Our attention has been drawn to a very recent paper by Flournoy and Siegel (given at the International Free Radical Symposium in Uppsala in June 1961) in which radical formation in tritium-enriched ice is reported. They give a curve for* OH *buildup similar to ours and then proceed to discuss the rate of disappearance of* OH *at 100° K.*

of concentrated H_2O_2, both with Tβ-particles (Fig. 5, B) and ultraviolet rays. In concentrated hydrogen peroxide most of the OH radicals are thought to be scavenged in the reaction $OH + H_2O_2 \rightarrow H_2O + HO_2$, resulting in the formation of HO_2 radicals. The thermal stability of the radical represented by spectrum 5A is the same as the stability of radicals produced in concentrated H_2O_2.

Of particular interest is the comparison of radical yields for various types of radiation. The corrected (14) value of $G(OH)$ reported by Siegel and colleagues (12) for γ-irradiated ice is about 0.6. The values for tritiated ice, given in the first column of Table I, are lower almost by half. An analogous situation occurs in the production of atomic hydrogen in $HClO_4$ solutions.

Several experiments were carried out in order to compare directly the yields of stabilized atomic hydrogen for Co^{60} γ-rays ($G(H)_\gamma$) and Tβ-particles ($G(H)_\beta$). Tritiated $HClO_4$ samples, used previously for the determination of $G(H)_\beta$ were melted, refrozen in liquid nitrogen, irradiated by Co^{60} γ-rays at a dose rate of 4.8×10^{18} ev/ml hr, and then immediately subjected to EPR examination. Under such conditions, atomic hydrogen was mainly produced by γ-radiolysis, the dose rate for γ-rays being more than one order of magnitude higher than that for Tβ-particles. However, the results $G(H)_{\gamma+\beta}$ were corrected by subtracting the small contribution of Tβ-particles. The value of $G(H)_\gamma$ in sample I was found to be very close to 2, in good agreement with the value of about 2.1 reported by Livingston and Weinberger for $HClO_4$ (0.125 mole fraction). Hence, by reference to Table II the ratio $G(H)_\gamma/G(H)_\beta$ may be assumed to be about 2.

The above differences between Tβ- and γ-radiolysis are most likely due to the higher LET of Tβ-particles, resulting in greater density of radicals and eventually in a larger fraction of radicals undergoing recombination.

The comparison of stationary concentrations of H and OH radicals in γ- and Tβ-irradiated samples is inconclusive. The stationary concentrations of H atoms in $HClO_4 + H_2O$ mixture (mole ratio 1:7) for γ-rays (5) and Tβ-particles are 2.9×10^{19} atoms/g and 10^{19} atoms/ml, respectively. However, for OH radicals produced in H_2O ice these values show a reversed order of magnitude and are 0.36×10^{18} * and 1.3×10^{18} spins/ml, respectively.

The spectra induced in $HClO_4$ and shown in Fig. 9 most likely represent some species produced by radiolysis of perchloric acid, superimposed on an OH doublet and OD triplet, respectively. This conclusion may be drawn by comparing the g values and separations of the spectra in Figs. 9 and 1. Neglecting the deformation of the spectrum by an unidentified component due to the presence of the acid, the spectrum in 9A may be treated as essentially representing an OH doublet, whereas in spectrum 9B, peaks 1 and 5 correspond to the OH doublet and peaks 2, 3, and 4 to the OD triplet. Moreover, peak 4 coincides with the central D line. Consequently, in the warming experiments (Fig. 10) the high-field peak in spectrum 9A and peak 4 in spectrum 9B are denoted as "OH" and "OD+D", respectively.

The difference in shape between the low-dose spectrum in 9B and the high dose spectrum in 9C may be explained by referring to Figs. 2 and 7, and assuming that the kinetics of OH(OD) formation, as determined for ice, remains approximately unchanged in $HClO_4$.

The above-mentioned figures show that the stationary concentration of OH and OD radicals in ice is approached at a much lower dosage than that of D atoms in $HClO_4$

**This value was estimated by applying to the stationary concentration reported by Siegel and colleagues (12) the same correction (14) given by the authors in reference to G values.*

(sample II, curve 3 in Fig. 7). Consequently, after prolonged irradiation, peak 5 in spectrum 9B reaches a constant height, whereas peak 4, representing OD radicals and D atoms, still increases.

The kinetics of formation and thermal stabilities of the H and OH and the D and OD radicals produced in H_2O and D_2O media are essentially the same. According to Fig. 2 and Table I, $G(OD) \geq G(OH)$, as in liquid water. However, in view of the limited accuracy of the quantitative results reported here, any theoretical discussion of the comparative mechanism of the H_2O and D_2O radiolysis would not be justified.

Some further conclusions, concerning the final fate of radicals disappearing on warming and to some extent in the course of irradiation, may be drawn on the basis of Table II.

TABLE II

Some radical and molecular yields (G values) of Tβ-radiolysis of H_2O and $HClO_4$

Product	Medium	
	$HClO_4$ (0.125 mole fraction)	H_2O
Stabilized H	1.0	0
Stabilized OH	—	0.32
H_2 After irradiating the sample at liq. N_2 temperature and melting	0.31	0.1
H_2 After irradiation at room temperature	0.30	0.59

According to Siegel *et al.* (12), OH radicals in γ-irradiated ice undergo mainly an H+OH reaction. Livingston and Weinberger (7) claim that the predominant process in the disappearance of H atoms in irradiated acids is H+H combination. Our results seem to be in agreement with both opinions.

The basic difference between conditions of radical recombination in H_2O and $HClO_4$ medium is that in the latter the concentration of stabilized H atoms is building up in the course of irradiation. Consequently, when the radicals are liberated by warming, the reaction H+H may successfully compete with other recombination processes. In ice at $-196°$ C, no stabilized atomic hydrogen is produced and most of the H atoms probably combine immediately after formation with OH radicals, the H+H process being negligible because of the very low concentration of hydrogen atoms.

The predominance of the H+H reaction in $HClO_4$ medium, and of the H+OH reaction in ice, may be seen by comparing $G(H_2)$ values in both media. The yield of molecular hydrogen in $HClO_4$ (Table II) is higher than in ice by a factor of 3 and accounts for almost two thirds of the hydrogen which could be theoretically produced by H+H combination. All samples prepared for gas analysis were irradiated with low doses so that during the irradiation, the concentration of radicals may be assumed to increase linearly with the dose. In this stage of irradiation the recombination of radicals is negligible.

The stationary concentrations of stabilized OH radicals in H_2O and $HClO_4$ matrix are hardly comparable. If, however, both values are of the same order, then, according to Figs. 2 and 7, the values of [H] would, after prolonged irradiation, reach a much higher level than the value [OH]. Thus, it is possible that as the irradiation progresses the conditions for H+H combination become even more favorable, as compared with the H+OH reaction.

The figures given in Table II show that the ratio $G(H_2)^{HClO_4}/G(H_2)^{H_2O}$ is about six times higher at liquid nitrogen temperature than at room temperature. This again seems to indicate that the accumulation of stabilized H atoms occurring only at liquid nitrogen temperature in $HClO_4$ is a main factor contributing to high H_2 yield in this medium.

Finally, comparison of Figs. 4 and 10 shows that OH radicals in ice disappear at about 10° lower temperature than OH radicals in $HClO_4$. Thus, the presence of stabilized atomic hydrogen does not facilitate the removal of OH radicals. On the contrary, the OH radicals are less mobile in $HClO_4$ matrix, possibly being more strongly hydrogen bonded or in complexes with the acid.

The yields of molecular hydrogen in $HClO_4$ (0.316 in 0.125 mole fraction solution) and in ice (0.1) given in Table II, are in very good agreement with those found by Livingston and Weinberger (7) for γ-irradiated acid and ice. However, the ratio $G(H_2)/G(H)$ is twice as high in tritiated acid as in γ-irradiated material. This may be, at least partly, accounted for by the different LET of these types of radiation.

It is worth mentioning that in $HClO_4$ medium, H atoms (and OH radicals) may also be removed by combining with some other species formed by irradiation of perchloric acid. This might explain the appearance of a new spectrum, when the sample is warmed, which is represented by a broken curve in Fig. 10, corresponding to the same temperature range in which H atoms rapidly disappear.

ACKNOWLEDGMENTS

We are grateful to the National Research Council of Canada for continued support.

REFERENCES

1. J. KROH, J. W. T. SPINKS, and B. C. GREEN. Nature, **189**, 655 (1961).
2. J. KROH, J. W. T. SPINKS, and B. C. GREEN. Science, **133**, 1082 (1961).
3. J. KROH and J. W. T. SPINKS. J. Chem. Phys. **35**, 760 (1961).
4. C. J. HOCHANADEL and S. C. LIND. Ann. Rev. Phys. Chem. **7**, 91 (1956).
5. J. A. MCMILLAN, M. S. MATHESON, and B. SMALLER. J. Chem. Phys. **33**, 609 (1960).
6. R. LIVINGSTON, H. ZELDES, and E. H. TAYLOR. Discussions Faraday Soc. **19**, 166 (1955).
7. R. LIVINGSTON and A. J. WEINBERGER. J. Chem. Phys. **33**, 499 (1960).
8. C. K. JEN, S. N. FONER, E. L. COCHRAN, and V. A. BOWERS. Phys. Rev. **112**, 1169 (1958).
9. G. T. TRAMMEL, H. ZELDES, and R. LIVINGSTON. Phys. Rev. **110**, 630 (1958).
10. H. ZELDES and R. LIVINGSTON. Phys. Rev. **96**, 1702 (1954).
11. J. KROH, J. W. T. SPINKS, and B. C. GREEN. J. Am. Chem. Soc. **83**, 2201 (1961).
12. S. SIEGEL, L. H. BAUM, S. SKOLNIK, and J. M. FLOURNOY. J. Chem. Phys. **32**, 1249 (1960). S. SIEGEL, J. M. FLOURNOY, and L. H. BAUM. J. Chem. Phys. **34**, 1782 (1961).
13. L. H. PIETTE, R. C. REMPEL, H. E. WEAVER, and M. FLOURNOY. J. Chem. Phys. **30**, 1623 (1959).
14. ERRATUM TO REFERENCE 7. J. Chem. Phys. **34**, 339 (1961).

PERFLUOROALKYL ARSENICALS

PART IV. SOME REACTIONS OF TRIFLUOROIODOMETHANE WITH ALKYL ARSINES

W. R. CULLEN
The Chemistry Department, University of British Columbia, Vancouver, British Columbia
Received October 31, 1961

ABSTRACT

Trifluoroiodomethane reacts with triethyl- and tri-*n*-butylarsine, and tri-*n*-butylphosphine to give products of the type R_2MCF_3. Heptafluoroiodopropane reacts similarly with trimethylarsine. Trifluoroiodomethane also reacts with the compounds $(CH_3)_2AsX$ (X = C_6H_5, Cl, I) and CH_3AsI_2 to give $CH_3As(CF_3)_2$; and in most of these reactions the compound $CH_3As(CF_3)I$ is also formed, which is converted to the compound $CH_3As(CF_3)Cl$ by reaction with silver chloride.

DISCUSSION AND RESULTS

Alkyl-trifluoromethyl-arsines and -phosphines can best be obtained by exchange reactions using the compounds $(CF_3)_3M$ and $(CH_3)_3M$ (1, 2, 3):

$$(CF_3)_3M + CH_3I \rightarrow (CF_3)_2MCH_3 + CF_3I$$
$$2(CH_3)_3M + CF_3I \rightarrow (CH_3)_2MCF_3 + (CH_3)_4MI$$

or in the case of the arsines by the reaction of alkyl-iodo-arsines with trifluoroiodomethane in the presence of mercury (4), for example,

$$(CH_3)_2AsI + Hg + ICF_3 \rightarrow (CH_3)_2AsCF_3 + HgI_2.$$

However, it has recently been found (5) that the main products from the reactions of diethyl- and di-*n*-butyl-iodoarsine with trifluoroiodomethane in the presence of mercury are ethylbistrifluoromethylarsine and *n*-butylbistrifluoromethylarsine respectively. No di-*n*-butylbistrifluoromethylarsine was isolated from these reactions and only a little diethyltrifluoromethylarsine was found. These results suggest that an exchange reaction takes place between the initially formed dialkyltrifluoromethylarsine and trifluoroiodomethane, producing the alkylbistrifluoromethylarsine.

It has now been found that neither triethylarsine nor tri-*n*-butylarsine reacts with trifluoroiodomethane at 20°, and at 100° the major products (in good yield) of the reaction is the dialkyltrifluoromethylarsine. Only small yields of the corresponding alkylbistrifluoromethylarsines are obtained. Thus some other explanation must be sought for these apparently contradictory results. The reaction of trifluoroiodomethane with tri-*n*-butylphosphine occurs more readily than with the corresponding arsine. Thus at 20° di-*n*-butyltrifluoromethylphosphine is formed in low yield. When the reaction is carried out at 100° the yield is not much improved. There is no indication that further exchange to produce *n*-butylbistrifluoromethylphosphine takes place in this reaction. This result agrees with the findings of Haszeldine and West (3), who report that dimethyltrifluoromethylphosphine is stable to trifluoroiodomethane even at 240°, whereas the corresponding arsine at 240° is converted by trifluoroiodomethane to methylbistrifluoromethylarsine. Thus the result of the present investigation, that further reaction of dialkyl trifluoromethyl arsines takes place to a limited extent at 100° to give alkyl bistrifluoromethyl arsines, is not unexpected.

It is very difficult to recover the unreacted trifluoroiodomethane from reactions with tri-*n*-butylphosphine, suggesting that, on mixing, a moderately stable phosphonium

complex is formed. Mixtures of triphenylphosphine and trifluoroiodomethane behave similarly. Such a complex has been suggested as an intermediate for exchange reactions (2) and its stability in the case of the reaction of tri-*n*-butylphosphine could account for the low yield of the trifluoromethylphosphine.

Heptafluoroiodopropane has also been found to react in exchange reactions. Thus heptafluoropropyldimethylarsine is obtained in moderate yield from the reaction of trimethylarsine and heptafluoroiodopropane at 100°:

$$C_3F_7I + (CH_3)_3As \rightarrow C_3F_7As(CH_3)_2 + (CH_3)_4AsI.$$

The reaction in this case is slower than the one in which trifluoroiodomethane is used (2).

The effect of changing the basicity of the arsine in reactions of this sort has been investigated by reacting the compounds $(CH_3)_2AsX$ (X = C_6H_5, Cl, I) and CH_3AsI_2 with trifluoroiodomethane. In no case does reaction occur below 100°, a result which could be expected if the reaction proceeds through the formation of a quaternary iodide (2), since the basicity of these compounds must be considerably lower than that of trimethylarsine. However, reaction does occur at higher temperatures and a large number of products is obtained from a given reaction, for example,

$$(CH_3)_2AsI + CF_3I \rightarrow CF_3H + CH_3I + CH_3As(CF_3)_2 + CH_3As(CF_3)I + (CH_3)_4AsI_3 + ?$$

$$(CH_3)_2AsC_6H_5 + CF_3I \rightarrow CF_3H + CH_3I + C_6H_5CF_3 + CH_3As(CF_3)_2 + C_6H_5As(CF_3)CH_3 + C_6H_5As(CF_3)_2 + C_6H_5As(CH_3)_3I_3 + ?$$

Both methylbistrifluoromethylarsine and iodomethyltrifluoromethylarsine are amongst the products of the reaction of trifluoroiodomethane with chlorodimethylarsine and diiodomethylarsine. The reaction of triphenylphosphine and chlorodiphenylphosphine with trifluoroiodomethane has recently been found to give diphenyltrifluoromethylphosphine together with a number of other products (7). In all these reactions the nature and variety of the products suggest that a radical mechanism is involved. Such a mechanism has been suggested by many workers (e.g. ref. 8) for the reaction of arsenic metal (or arsenic triiodide) with trifluoroiodomethane, a reaction which yields the compounds $(CF_3)_nAsI_{3-n}$ (n = 1, 2, 3). On this basis a radical reaction could be expected to produce iodomethyltrifluoromethylarsine from the reaction of trifluoroiodomethane with the compounds $(CH_3)_2AsX$ (X = Cl, I) and CH_3AsI_2, though it would be difficult to account for the formation of this product using a mechanism based on an arsonium intermediate. However, in the reactions of the alkylarsines with trifluoroiodomethane there is no evidence for the formation of tristrifluoromethylarsine, a likely product from a radical reaction. The results of Haszeldine and West (3) suggest that in the presence of trifluoroiodomethane and iodomethane the most stable arsenic compound containing methyl and trifluoromethyl groups is methylbistrifluoromethylarsine, so the formation of this compound even in reactions with a free radical mechanism could be expected.

The new compound iodomethyltrifluoromethylarsine attacks mercury and has only been provisionally characterized on the basis of its infrared spectrum, which shows the presence of CH_3, and only one CF_3 group since there are only two strong bands in the C—F stretch region. This feature is present in the spectra of other reported trifluoromethyl-arsines and -phosphines (9, 10, 11), and in the spectra of the other new compounds prepared in this investigation, namely, di-*n*-butyltrifluoromethylphosphine, b.p. ca. 160° (760 mm), 115° (83 mm); di-*n*-butyltrifluoromethylarsine, b.p. 186° (760 mm), 110°

(60 mm); and chloromethyltrifluoromethylarsine, b.p. 76° (760 mm). The last compound is obtained by reacting the corresponding iodo-arsine with silver chloride, a result which confirms the identification of the iodo-arsine. The chloro-arsine has a boiling point midway between chlorobistrifluoromethylarsine (46° (12)) and chlorodimethylarsine (107° (13)), and other chemical and physical properties are expected to show the same trend. Further work is in progress on this interesting compound.

Dimethyltrifluoromethylarsine is sufficiently basic to form an arsonium iodide at 20° when reacted with iodomethane (2). However, diethyltrifluoromethylarsine does not react with iodomethane at 20° or with iodoethane at 100°; and at 150° reaction with iodoethane take place, producing fluoroform, trifluoroiodomethane, and tetraethylarsonium triiodide. The rate of hydrolysis of the ethyl-trifluoromethyl-arsines is faster than that of the corresponding methyl-trifluoromethyl-arsines (6), indicating that the ethyl compounds are less basic than the corresponding methyl compounds (2). Thus, formation of arsonium compounds by reaction with alkyl iodides would be expected to be less easy in the case of the ethyl-trifluoromethyl-arsines.

EXPERIMENTAL

The techniques used for this investigation were the same as have been described in previous papers in this series. Descriptions of the methods of preparation of starting materials are included only for those compounds not previously used in this series of investigations.

Reaction of Triethylarsine with Trifluoroiodomethane

Triethylarsine was prepared from arsenic trichloride and ethylmagnesium bromide (14). The arsine (14.0 g) and trifluoroiodomethane (99.0 g) in a sealed tube (100 ml) were left at 20° for 5 months. Only a small amount of white solid was produced and trap-to-trap distillation gave a quantitative recovery of trifluoroiodomethane (99.0 g). The white solid (<10 mg) was shown to be mainly tetraethylarsonium iodide by means of its infrared spectrum and X-ray powder photograph. When triethylarsine (6.563 g) and trifluoroiodomethane (10.760 g), in a sealed tube (50 ml), were left for 2 weeks at 20° no solid appeared, but after it was heated at 100° for 5 days a colorless solid was produced. Trap-to-trap distillation of the volatile contents of the tube gave two fractions. Infrared examination of the least volatile fraction showed it to be mainly diethyltrifluoromethylarsine together with a little ethylbistrifluoromethylarsine (5). The fraction was distilled in a nitrogen atmosphere (760 mm) and 3.2 g (78% yield) of diethyltrifluoromethylarsine was obtained, b.p. 110–114° (lit. value 111° (5)). The arsine was also identified by its infrared spectrum and gas phase molecular weight of 198 (calc. 204). The colorless solid remaining in the reaction tube was dissolved in ethanol (100 ml). The solution was filtered, and the solid was precipitated by the addition of a large excess of ether. This was repeated and the product was identified as tetraethylarsonium iodide (5.3 g, 82% yield) by means of its infrared spectrum and X-ray powder photograph. In another experiment triethylarsine (3.8 g) and trifluoroiodomethane (23.7 g) were heated to 100° for 18 days. The reaction mixture darkened in color but no solid was produced. Trap-to-trap distillation gave a less volatile fraction (2.5 g) which was found to contain a much greater proportion of ethylbistrifluoromethylarsine than was obtained from the reaction described above.

Reaction of Tri-n-butylarsine with Trifluoroiodomethane

Tri-*n*-butylarsine was prepared by the appropriate Grignard reaction (14). The arsine (7.8 g) and trifluoroiodomethane (17.7 g) were heated to 100° for 20 days. The mixture slowly darkened in color but no solid was deposited. Trap-to-trap distillation of the volatile contents of the tube gave 13.2 g of trifluoroiodomethane which contained some fluoroform, and a less volatile fraction (2.4 g) which when distilled in a nitrogen atmosphere at reduced pressure gave two fractions: one, b.p. 46–48° (50 mm), which was identified as *n*-butylbistrifluoromethylarsine (0.7 g) by its infrared spectrum (5); the other, b.p. 111° (60 mm), which was similarly identified as di-*n*-butyltrifluoromethylarsine (1.5 g) (q.v.). The residue in the reaction tube, a viscous red oil (5 g), was extracted with ether. Distillation of the ether extracts in a nitrogen atmosphere (760 mm) gave more *di-n-butyltrifluoromethylarsine* (1.0 g), b.p. 186°. Anal. Calc. for $C_9H_{18}AsF_3$: C, 41.8; H, 6.98; As, 29.1; F, 22.1%; mol. wt., 258. Found: C, 41.5; H, 7.10; As, 29.1; F, 22.4%; mol. wt., 250. The infrared spectrum showed the following absorption bands (liquid film): 2910 (s), 2885 (s), 2835 (m), 1460 (m), 1452 (m), 1411 (w), 1377 (m), 1340 (w), 1285 (w), 1251 (w), 1185 (m), 1133 (vs), 1092 (vs), 1035 (sh)(m), 885 (w), 765 (w), 710 (m). The ether-insoluble residue from the reaction tube was soluble in alcohol. Infrared examination of this oil showed that trifluoromethyl groups were absent. It decomposed on attempted distillation at 10^{-3} mm.

Reaction of Trimethylarsine with Heptafluoroiodopropane

Trimethylarsine was prepared by the Grignard method (15). There was no obvious sign of reaction at 20° between the arsine (3.3 g) and the heptafluoroiodopropane (20.3 g); however, at 100° immediate reaction occurred and after 3 days at this temperature a copious colorless precipitate had formed. The volatile contents of the tube were removed and distilled in a nitrogen atmosphere (760 mm) to give unreacted heptafluoroiodopropane and heptafluoropropyldimethylarsine (1.3 g), b.p. 89–90 (lit. value 93° (4)). The infrared spectrum of this sample was identical with that of the pure compound (4). The solid reaction product (2.4 g) was recrystallized from alcohol and was identified as tetramethylarsonium iodide by means of its infrared spectrum and X-ray powder photograph.

Reaction of Dimethylphenylarsine with Trifluoroiodomethane

Dimethylphenylarsine was prepared by the reaction of phenylmagnesium bromide on iododimethylarsine (16). The arsine (6.3 g) and trifluoroiodomethane (11.6 g) did not react after 3 weeks at 20° or after 4 days at 100°. The arsine (2.2 g) and trifluoroiodomethane (16.0 g) were heated to 170° for 12 hours. The reaction mixture became dark brown. Trap-to-trap distillation isolated the following volatile fractions (identified by their infrared spectra): 0.92 g of a mixture of fluoroform and trifluoroiodomethane; 12.9 g of trifluoroiodomethane; 1.05 g of a mixture containing iodomethane, methylbistrifluoromethylarsine, and benzotrifluoride; and 1.1 g of a mixture of phenylbistrifluoromethylarsine and methylphenyltrifluoromethylarsine. A reddish violet solid (0.8 g) was left in the reaction tube. The solid, after recrystallization from alcohol, melted at 93–98° and was probably impure phenyltrimethylarsonium triiodide (lit. value, m.p. 103° (17)).

Reaction of Tri-n-butylphosphine with Trifluoroiodomethane

Commercial tri-*n*-butylphosphine (7.2 g) and trifluoroiodomethane (11.7 g) were left at 20° for 3 days. After 1 day a considerable amount of pale yellow precipitate had formed. The tube was opened to the vacuum system and only trifluoroiodomethane (1.6 g) was recovered, with difficulty, from the viscous yellow oil remaining in the tube. The tube and contents were not warmed above room temperature. The oil was extracted with ether, leaving a pale yellow solid. The ether extract was distilled in a nitrogen atmosphere (760 mm) and gave 0.3 g of di-*n*-butyltrifluoromethylphosphine, b.p. ca. 160°, and an involatile gummy residue. The trifluoromethylphosphine was provisionally identified by its infrared spectrum, which showed the presence of *n*-butyl groups and only one trifluoromethyl group (only two strong C—F stretching vibrations). In a second experiment the phosphine (6.1 g) and trifluoroiodomethane (13.3 g) were heated to 100° for 2 days. Again the volatile contents of the tube were difficult to remove from the viscous residue; however, after the tube was heated to 60° for 3 hours, 7.6 g of impure trifluoroiodomethane and 0.7 g of di-*n*-butyltrifluoromethylphosphine were obtained. The trifluoromethylphosphine fractions from both experiments were combined and distilled in a nitrogen atmosphere at 83 mm, all the material boiled at 115°, and analysis confirmed the identification. Calc. for $C_9H_{18}F_3P$: C, 50.4; H, 8.34; F, 26.6; P, 14.5%; mol. wt., 214. Found: C, 50.7; H, 8.58; F, 26.4; P, 14.5%; mol. wt., 229. The infrared spectrum showed the following absorption bands (liquid film): 2980 (s), 2950 (s), 2885 (s), 2200 (vw), 1470 (s), 1420 (m), 1384 (s), 1348 (w), 1297 (w), 1274 (w), 1215 (m), 1162 (vs), 1103 (vs), 1051 (w), 1007 (w), 968 (s), 897 (w), 781 (w), 727 (sh)(m), 717 (s). In an attempt to improve the yield of the trifluoromethylphosphine, tri-*n*-butylphosphine (6.3 g) and trifluoroiodomethane (18.3 g) were heated to 100° for 2 weeks, but only 0.6 g of the trifluoromethylphosphine was isolated in the vacuum system.

Reaction of Iododimethylarsine with Trifluoroiodomethane

The iodo-arsine (4.8 g) and trifluoroiodomethane (11.8 g) did not react at 100° (2 days) since 11.8 g of trifluoroiodomethane were recovered. When the same reactants were heated to 170° for 1 day a dark solid formed. Trap-to-trap distillation gave 0.04 g of a mixture of fluoroform and trifluoroiodomethane, 9.3 g of trifluoroiodomethane, and 1.5 g of methylbistrifluoromethylarsine containing some iodomethane. These fractions were identified by their infrared spectra. A slightly volatile pale yellow liquid (0.37 g) was also obtained. This fraction reacted with mercury; its infrared spectrum showed the presence of methyl groups and only one trifluoromethyl group (only two strong bands in the C—F stretching region); and the fraction was provisionally identified as iodomethyltrifluoromethylarsine. The solid residue in the reaction tube (4.6 g) contained 0.4 g of an unidentified acetone-insoluble substance. The acetone-soluble solid consisted mainly of tetramethylarsonium triiodide on the evidence of its X-ray powder photograph.

Reaction of Diiodomethylarsine with Trifluoroiodomethane

Diiodomethylarsine (9.2 g) and trifluoroiodomethane (12.1 g) were immiscible at 20° and at 100°. No reaction took place after 20 hours at 100°. The same reactants after 18 hours at 170° had produced a dark solid. Trap-to-trap distillation of the volatile contents of the tube gave trifluoroiodomethane (10.4 g) containing a trace of fluoroform, methylbistrifluoromethylarsine (0.97 g) containing a little iodomethane, and 0.63 g of iodomethyltrifluoromethylarsine. The fractions were identified by their infrared spectra. The solid residue in the reaction tube (7.9 g) was identified as being mainly arsenic triiodide on the evidence of its X-ray powder photograph.

Reaction of Chlorodimethylarsine with Trifluoroiodomethane

There was no reaction between the arsine (11.3 g) and trifluoroiodomethane (11.5 g) after 1 day at 20°. Similarly the arsine (2.19 g) and trifluoroiodomethane (4.267 g) did not react when heated to 85° for 3 days. When the same reactants were heated to 240° for 10 hours an orange solid was formed. Trap-to-trap distillation gave fluoroform (0.88 g), a mixture of trifluoroiodomethane and chloromethane (1.911 g, mol. wt., 117), 1.091 g of a mixture of methylbistrifluoromethylarsine containing a little iodomethane, and 0.4 g of iodomethyltrifluoromethylarsine.

Preparation of Chloromethyltrifluoromethylarsine

The iodomethyltrifluoromethylarsine produced in the above reactions was condensed onto dry silver chloride and left for 1 week at 20°. Silver iodide was formed. The colorless product attacked mercury, contained only one trifluoromethyl group, and boiled at 76° in an atmosphere of nitrogen; it was identified as *chloromethyltrifluoromethylarsine*. Anal. Hydrolysis with 10% aqueous sodium hydroxide at 100° for 2 days gave fluoroform equivalent to a CF_3 content of 35.1%. The vapor phase molecular weight was 295. Calc. for $C_2H_3AsClF_3$: CF_3, 35.4%; mol. wt., 295. The infrared spectrum showed the following absorption bands (vapor phase): 3010 (w), 2930 (w), 2810 (vw), 2310 (w), 2260 (w), 2215 (w), 1880 (w), 1842 (w), 1420 (m), 1262 (m), 1205 (sh)(s), 1156 (vs), 1111 (vs), 1060 (m), 1049 (m), 1000 (vw), 900 (vw), (860 (sh), 855, 848, 844, 837) (s), 795 (vw), (735, 724, 720) (s).

Reaction of Diethyltrifluoromethylarsine with Iodoethane and Iodomethane

The arsine (0.5 g) and a large excess of iodoethane (5 ml) were left for 6 weeks at 20°. No solid product was formed. The same reactants were heated to 100° for 2 weeks; again no solid was formed, and trap-to-trap distillation showed that no fluoroform or trifluoroiodomethane had been produced. When the reactants were heated to 150° for 1 day, reaction occurred with the formation of a low-melting solid. The most volatile product of the reaction was found to be a mixture of fluoroform, ethylene, and trifluoroiodomethane (0.35 g, mol. wt., 64.0). The mixture was identified by its infrared spectrum. The violet solid was twice recrystallized from alcohol and the final product was identified as tetraethylarsonium triiodide, m.p. 56–57° (lit. value 54° (17)). The infrared spectrum of the crude solid showed the presence of ethyl groups and the absence of trifluoromethyl. Diethyltrifluoromethylarsine did not react with excess iodomethane after 1 month at 20°.

ACKNOWLEDGMENTS

The author wishes to acknowledge financial assistance from the National Research Council of Canada. He is also indebted to Mr. M. M. Baig for assistance with the reaction involving phenyldimethylarsine. Microanalyses were carried out by Dr. Alfred Bernhardt.

REFERENCES

1. H. J. Emeléus, R. N. Haszeldine, and E. G. Walachewski. J. Chem. Soc. 1552 (1953).
2. R. N. Haszeldine and B. O. West. J. Chem. Soc. 3631 (1956).
3. R. N. Haszeldine and B. O. West. J. Chem. Soc. 3880 (1957).
4. W. R. Cullen. Can. J. Chem. **38**, 439 (1960).
5. W. R. Cullen. Can. J. Chem. **39**, 2486 (1961).
6. W. R. Cullen. Unpublished observations.
7. M. A. Beg and H. C. Clark. Can. J. Chem. **40**, 283 (1962).
8. E. G. Walachewski. Ber. **86**, 272 (1953).
9. F. W. Bennett, H. J. Emeléus, and R. N. Haszeldine. J. Chem. Soc. 1565 (1953).
10. W. Mahler and A. B. Burg. J. Am. Chem. Soc. **80**, 6161 (1958).
11. W. R. Cullen. Can. J. Chem. **38**, 445 (1960).
12. W. R. Cullen. Can. J. Chem. **39**, 1855 (1961).
13. E. Krausse and A. von Grosse. Die Chemie der metal-organischen verbindungen. Borntraeger, Berlin. 1937.
14. W. J. C. Dyke and W. J. Jones. J. Chem. Soc. 2426 (1930).
15. F. G. Mann and A. F. Wells. J. Chem. Soc. 702 (1932).
16. G. J. Burrows and E. E. Turner. J. Chem. Soc. 1373 (1920).
17. W. Steinkopf and G. Schwenn. Ber. **54**, 1437 (1921).

THE PROTON MAGNETIC RESONANCE SPECTRUM OF 1-FLUORO-2,4-DINITROBENZENE

T. SCHAEFER
Department of Chemistry, University of Manitoba, Winnipeg, Manitoba
Received November 23, 1961

ABSTRACT

A reliable analysis of the proton resonance spectrum of 1-fluoro-2,4-dinitrobenzene is described. Solvent effects were used to obtain this analysis and a possible source of error in a previous analysis is indicated. Spectra parameters are also derived for 1,5-difluoro-2,4-dinitrobenzene. The spectrum of the latter compound confirms the assignment of peaks in the spectrum of the former.

INTRODUCTION

A recent publication presents the results of an analysis of the high-resolution nuclear magnetic resonance spectrum of 1-fluoro-2,4-dinitrobenzene (1). In the course of an as yet unpublished study in this laboratory of solvent effects on such spectra we have had occasion to measure the proton magnetic resonance spectrum of this compound in acetone and benzene. The results indicate a certain inaccuracy of the analysis in reference 1. By comparing the spectra in the two solvents a possible reason for this inaccuracy was found and a better set of coupling constants has been derived.

EXPERIMENTAL AND RESULTS

The proton magnetic resonance spectra were measured as 5 mole% solutions in acetone and benzene using a Varian spectrometer operating at 60 Mc/sec. The external reference was chloroform, and calibration of spectra was done by the sideband technique. Figures 1(*b*) and 2 show the spectra of 1-fluoro-2,4-dinitrobenzene in acetone and benzene, respectively. Figure 1(*a*) gives the spectrum of 1,5-difluoro-2,4-dinitrobenzene in acetone.

ANALYSIS OF SPECTRA

Proton Spectrum of 1-Fluoro-2,4-dinitrobenzene in Benzene

This spectrum can clearly be regarded as the *ABR* part of an *ABRX* spectrum, as indicated in the molecular diagram in Fig. 2 (2). The analysis of the *ABRX* case is straightforward and, in fact, the possible transitions and their intensities can be immediately written down in a concise manner in the notation developed by Pople and Schaefer (3). The calculated spectrum appears in Fig. 2 and it is clear that the spectrum is very nearly a first-order one.* Values of the parameters determined are given in Table I.

Proton Spectrum of 1-Fluoro-2,4-dinitrobenzene in Acetone

It is tempting to analyze the spectrum in acetone as the *ABR* part of an *ABRX* spectrum with the protons assigned as indicated in Fig. 1(*b*). However, the attempt soon results in the realization that the correct assignment would be that of an *ABC* part

**Perhaps it should be pointed out that in order to prevent some of the peaks from appearing high on the shoulder of the intense solvent line a very slight amount of u-mode was introduced into the signal input at the phase detector. This trick may have introduced some distortion of peak intensities near the solvent line. It is also true that coupling to C^{13} nuclei in the solvent results in weak, unwanted signals in the extreme regions of the recorded spectrum. These may have distorted some of the lines in those regions.*

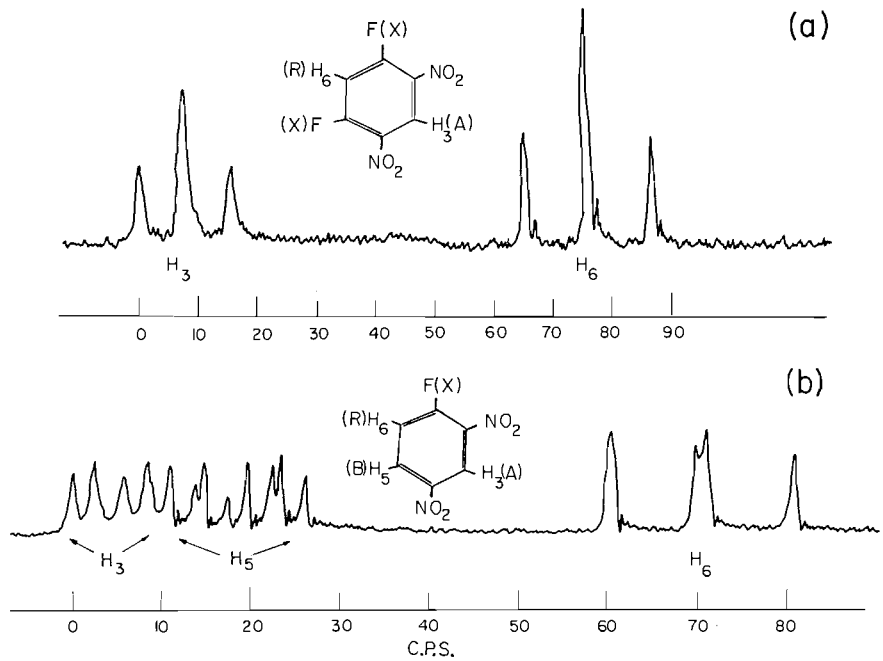

FIG. 1. (*a*) The proton resonance spectrum of 5 mole% 1,5-difluoro-2,4-dinitrobenzene in acetone at 60 Mc/sec. (*b*) The proton resonance spectrum of 5 mole% 1-fluoro-2,4-dinitrobenzene in acetone at 60 Mc/sec.

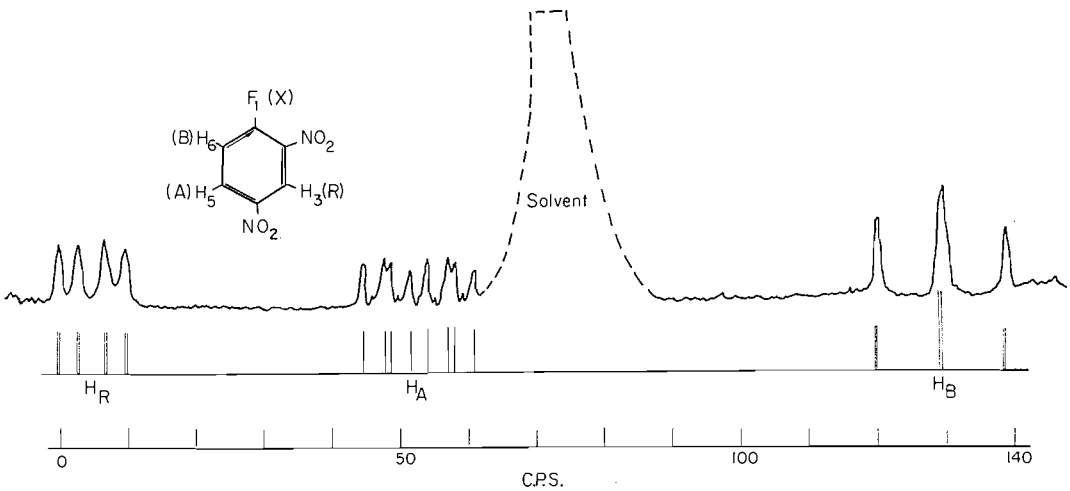

FIG. 2. The proton resonance spectrum of 5 mole% 1-fluoro-2,4-dinitrobenzene in benzene at 60 Mc/sec.

of an *ABCX* spectrum. The parameters obtained from an *ABRX* analysis are given in Table I. The large error in these values appears because of alternate choices for these values in an approximate analysis. From the chemical shift dependence of the relative positions in the high-field group of peaks it can be concluded that J_o^{HH} and J_o^{HF} have the same sign.

TABLE I

Parameters in c.p.s. obtained from the proton spectra of 1-fluoro-2,4-dinitrobenzene at 60 Mc/sec

	5 mole% in benzene	5 mole% in acetone*	Reference 1
J_o^{HH}	9.5±0.1	9.3±0.4	8.7±0.3
J_m^{HH}	3.0±0.1	3.0±0.1	2.9±0.2
J_p^{HH}	0.1±0.1	0.2±0.4	0.6±0.3
J_o^{HF}	9.5±0.1	10.1±0.4	10.4±0.2
J_m^{HF}†	6.4±0.1	6.7±0.1	6.5±0.3
J_m^{HF}‡	3.9±0.1	3.6±0.3	3.8±0.3
$\nu_6-\nu_5$	77.3±0.3	49.6±2	
$\nu_5-\nu_3$	47.6±0.3	14.5±1	
$\nu_3-\nu_{CHCl_3}$§	−26.3±0.5	−90.4±1	

*From an *ABRX* approximation.
†Proton situated between the nitro groups.
‡Proton situated next to one nitro group.
§External chloroform reference value corrected for bulk susceptibility.

Proton Spectrum of 1,5-Difluoro-2,4-dinitrobenzene in Acetone

The spectrum is the *AR* part of an ARX_2 spectrum and is therefore first order. This is clearly a consequence of the symmetry of the molecule and of the vanishingly small value of J_p^{HH}. The parameters obtained are $J_o^{HF} = 10.2\pm0.1$, $J_m^{HF} = 7.5\pm0.1$, $J_p^{HH} < 0.2$ cycles/sec, $\nu_6-\nu_3 = 67.9\pm0.2$ cycles/sec; $\nu_6-\nu_{CHCl_3\ ext} = -27.2\pm0.5$ cycles/sec, corrected for bulk susceptibility effects.

The peaks from proton 3 between the nitro groups are broadened by interactions depending on the quadrupole moment of the N^{14} nuclei in the nitro groups. This circumstance assures a correct assignment and also indicates the correct assignment in the spectra of 1-fluoro-2,4-dinitrobenzene, where the corresponding proton peaks are similarly broadened.

DISCUSSION

Since the proton spectrum of 1-fluoro-2,4-dinitrobenzene in benzene is very nearly first order its analysis yields the most reliable values of the parameters. The analysis of the spectrum of this compound in acetone illustrates the need for care in fixing probable errors of parameters obtained from an approximate analysis. Once again the spectra in different solutions indicate the great help solvent effects can give in spectra analysis. One assumption inherent in the use of different solvents is that the coupling constants in the solute do not change from solvent to solvent. In unpublished work we have found this assumption justified in the closely related molecule 1,5-difluoro-2,4-dinitrobenzene. If the molecule under investigation can exist in different conformations whose stability can be influenced by the polarity of the solvent the above assumption can be wrong (4).

Solvent effects in these compounds and related ones are very large. They reach 2 p.p.m. for some ring protons and will be reported later.

ACKNOWLEDGMENTS

This work was supported by the National Research Council and by the Research Corporation.

REFERENCES

1. B. D. Nageswara Rao and Putcha Venkateswarlu. Proc. Indian Acad. Sci. A, **52**, 109 (1960); Chem. Abstr. **55**, 4154*c* (1961).
2. J. A. Pople, W. G. Schneider, and H. J. Bernstein. High resolution nuclear magnetic resonance. McGraw-Hill Book Co., New York, N.Y. 1959.
3. J. A. Pople and T. Schaefer. Mol. Phys. **3**, 547 (1960).
4. E. B. Whipple, J. H. Goldstein, and G. R. McClure. J. Am. Chem. Soc. **82**, 3811 (1960).

PHOTOLYSIS OF NITRATE ESTERS

PART I. PHOTONITRATION OF DIPHENYLAMINE

L. D. Hayward, R. A. Kitchen, and D. J. Livingstone
Department of Chemistry, University of British Columbia, Vancouver, British Columbia

Received November 22, 1961

ABSTRACT

The photolysis of nitrate esters dissolved in benzene or ethanol or absorbed on filter paper occurred readily under illumination in the 265 mμ to 334 mμ spectral region. Equimolar amounts of 1,4;3,6-dianhydro-D-glucitol-2,5-dinitrate and diphenylamine dissolved in absolute ethanol or benzene did not react in the dark at 25°. Irradiation of the nitrogen-purged solutions for 2 hours at 15° with a mercury arc followed by chromatographic separation yielded 2-nitro-, 4-nitro-, N-nitroso-, and 4-nitroso-diphenylamine together with about 4% unreacted diphenylamine and an unidentified mixture of more polar compounds. In a partial fractionation of the aromatic photoproducts approximately 80% of the original diphenylamine was recovered in the form of the monosubstituted derivatives which contained about 37% of the original ester nitrogen as C-nitro groups and 2 to 3% as C- and N-nitroso groups.

Possible mechanisms of the photonitration are discussed.

INTRODUCTION

It was suggested by Gray and Williams in 1959 that photolysis of nitrate esters would be a useful method for the preparation of alkoxyl radicals provided that the nitrogen dioxide concurrently formed could be rapidly removed from the system (1). In this laboratory it was recently discovered that the photolysis of covalent nitrates in the presence of diphenylamine produced colored compounds useful for detecting the esters on paper chromatograms (2, 3). The yellow to orange photoproducts resembled those obtained by Coldwell and McLean (4, 5) by irradiation of nitrate ion and diphenylamine. These authors identified 2- and 4-nitrodiphenylamine as the major organic products and found no evidence for the formation of nitroso derivatives (5). In view of the well-known scavenging action of diphenylamine in both the solid state and in solution for nitrogen dioxide (6–9) it seemed probable that irradiation of nitrate esters in organic solvents containing diphenylamine would provide a system in which alkoxyl radical reactions might be conveniently studied.

We have been unable to find in the literature any detailed report of the products of photolysis of nitrate esters in solution. Photolysis of methyl and ethyl nitrates in the gas phase yielded hydrogen, nitromethane, formaldehyde, and acetaldehyde in addition to nitrogen, carbon, and their oxides (1, 10, 11). Bands attributed to ethoxyl radicals were detected in fluorescence when ethyl nitrate was irradiated in the Schumann region (12). The reactions postulated to account for the photoproducts paralleled those invoked for thermal decomposition where the initial, rate-determining step has been established as homolytic alkoxy–nitro bond fission (1, 13, 14). Photolysis of polynitrate esters in the condensed state also caused evolution of nitrogen and the oxides of carbon and nitrogen; the thermal stability of the explosive compounds was reduced and, for cellulose nitrate, depolymerization and oxidation occurred (15–21).

The present work was concerned with establishing the scope and conditions for the photoreaction of covalent nitrates with diphenylamine in solution and with the isolation and identification of the major aromatic products.

EXPERIMENTAL

Chromatography

Mixtures of nitrate esters, diphenylamine, and diphenylamine derivatives were separated by thin-layer chromatography (TLC) on glass plates coated with a mixture of silicic acid (Mallinckrodt, 100 mesh, for chromatography) and plaster of Paris (70:30 w/w) (22). Separation on a preparative scale was made on 1×1×18-in. chromatobars cast from the same mixture and developed by the ascending method (23). No separation of diphenylamine derivatives could be obtained with untreated or silicic-acid-impregnated paper (24); the hydrophobic compounds ran with the solvent front in each case.

Chromatograms were developed with mixtures of anhydrous solvents in the following volume ratios: S1: benzene – petroleum ether (1:1); S2: ether – petroleum ether (3:39); S3: ether–benzene (1:19). The purified petroleum ether fraction employed distilled over the range 85° to 110°.

Colorless compounds were detected with spray reagents as follows:

R1: A 5% solution of concentrated nitric acid in concentrated sulphuric acid (22). Diphenylamine and its derivatives gave characteristic colors at 25° and all organic components appeared as charred spots on heating the sprayed plates.

R2: A 1% solution of diphenylamine in 95% ethanol, followed by exposure to a shortwave ultraviolet lamp for 10 minutes. Nitrate esters appeared as yellow-green spots on a colorless background (3).

R3: A 5% solution of calcium nitrate in 95% ethanol, followed by ultraviolet irradiation. Diphenylamine produced yellow-green spots as for R2.

Materials

1,4;3,6-Dianhydro-D-glucitol-2,5-dinitrate (isosorbide dinitrate) was prepared by the method of Jackson and Hayward (14). The stable form of the compound was obtained (m.p. 69.2–70.0°), which showed the same elemental analyses, specific rotation, infrared spectrum, and chromatographic behavior as the labile form (m.p. 50.5–51.5°) (14). The ultraviolet spectrum of a 10^{-4} *M* solution of the dinitrate in absolute ethanol showed no absorption above 250 mμ and no inflection in the rapidly increasing absorption curve which commenced at an indefinite point around 250 mμ and continued beyond 210 mμ (Fig. 1). Similar

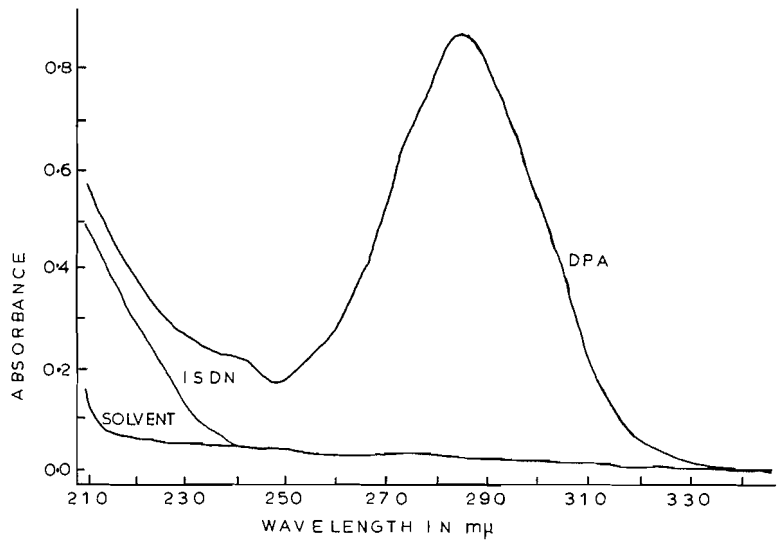

FIG. 1. Ultraviolet absorption spectra in absolute ethanol solution of 1,4;3,6-dianhydro-D-glucitol-2,5-dinitrate (ISDN, 10^{-4} *M*) and diphenylamine (DPA, 4×10^{-5} *M*).

curves were obtained at concentrations of 10^{-2} and 10^{-6} *M*. These spectra were distinctly different from those of open-chain, secondary aliphatic nitrate esters, which showed a characteristic inflection at 270 mμ (25), but agreed well with those of other polynitrate esters (31). The other nitrate esters employed have been described elsewhere (26–29, 34).

Diphenylamine, 2-nitrodiphenylamine, 4-nitrodiphenylamine, N-nitrosodiphenylamine, and 4-nitrosodiphenylamine were recrystallized to constant melting points (7) and then chromatographed on silicic acid until homogeneous. 4-Nitrosodiphenylamine required further purification by sublimation *in vacuo*. The corrected melting points and ultraviolet spectra of these compounds are shown in Table I, together with the reported values. The infrared spectra of 5% solutions of diphenylamine, 2-nitrodiphenylamine, and N-nitrosodiphenylamine in carbon tetrachloride closely matched the published spectra (30).

Irradiation of Solutions

Absolute ethanol or benzene solutions, 0.02 or 0.04 *M* in both isosorbide dinitrate and diphenylamine, were irradiated in quartz test tubes cooled to 15.0±0.5° by impinging streams of water. Nitrogen gas was introduced through thin glass capillaries for stirring and purging of air while the tubes were exposed at a distance of 20 cm to the unfiltered emission from a quartz capillary mercury arc lamp (Mineralite Model V43, Ultraviolet Products, Inc., Los Angeles). Aliquots of the solutions were removed from time to time for examination by TLC. The photoproducts were isolated on a preparative scale by concentration of the solutions in the dark followed by separation on chromatobars.

Photochemical Spot Tests

To determine the effective wavelength range for the photolysis, partially overlapped spots, 1 cm in diameter, of nitrate ester and diphenylamine (4) were deposited from ethanol solutions on 7-cm circles of Whatman No. 1 filter paper in a darkroom. A spotted and air-dried paper was exposed at 25° to each of the 10 major groups of lines between 250 mμ and 400 mμ in the medium-pressure mercury arc spectrum isolated by means of a 250-mm grating monochromator with quartz optics (Bausch and Lomb Optical Co., Rochester). The relative intensities of the lines were calculated from tables of emission spectra and transmission efficiencies of the monochromator and the irradiations were timed for intervals inversely proportional to these intensities. The colors developed in the overlapped and non-overlapped regions of the spots on the irradiated papers were compared visually in daylight with those of non-irradiated spots immediately after exposure and again after standing for several hours in the dark. Attempts to separate the photoproducts by irradiation of mixtures of nitrate ester and diphenylamine *in situ* as spots on chromatoplates or filter paper followed by direct chromatography were unsuccessful, probably because the penetration of the light into the solids was insufficient to produce detectable amounts of products.

TABLE I

Melting points and ultraviolet spectra of diphenylamine and derivatives

			Ultraviolet spectra* (mμ)			
	M.p. (°C)		Observed		Reported (31)	
Compound	Observed	Reported (7)	Max.	Min.	Max.	Min.
Diphenylamine	52.7–53.5	53	285†	247–249†	285	249
2-Nitrodiphenylamine	72.5–73.3	74.9–76.0	423–424	324–330	422–423	323–327
			254–258	243–244	251–259	238–239
			223–224		221–222	214–215
4-Nitrodiphenylamine	133.5–134.3	135.0–135.5	390	300–310	390	305–306
			255–257		257	
N-Nitrosodiphenylamine	66.5–66.9	66.2–66.8	286–296	259–260	295–296	259–260
4-Nitrosodiphenylamine	146.0–146.5	145.4–146.6	401–403‡	271–277‡	405–407‡	279–281‡
			260		258–260	237–240

*In absolute ethanol.
†See Fig. 1.
‡Two drops of 6 *N* hydrochloric acid were added to 100 ml of the ethanol solution.

RESULTS

A series of 25 crystalline nitrate esters containing from 1 to 8 nitrate groups per molecule produced greenish-yellow- to orange-colored products in the irradiation spot test with diphenylamine. No regular change in the color intensity of the developed spots with number of nitrate groups per molecule was apparent, although diastereoisomeric compounds such as the 1,2,4,5,6-pentanitrate derivatives of D-mannitol and D,L-glactitol (27, 28) differed in this respect. 1,4;3,6-Dianhydro-D-glucitol-2,5-dinitrate (isosorbide dinitrate) was selected for more detailed study as the simplest and most readily accessible crystalline aliphatic nitrate ester with known configuration and conformation. A difference in rate of reaction of the exo and endo nitrate ester groups in this optically active compound was demonstrated in an earlier research (14) and offered the possibility of detecting any stereospecificity in the photolysis.

Compounds containing oxy-nitrogen groups other than the nitrate ester group were also examined in the photochemical spot test with diphenylamine. Negative results were obtained with nitromethane, 2-nitropropane, 6-nitrosothymol, N-methyl-N-nitroso-

p-toluenesulphonamide, and the 1-oxides (32) of 5,5-dimethyl-Δ^1-pyrroline and 2,4,4-trimethyl-Δ^1-pyrroline. Isoamyl nitrite developed a pale yellow color which may have been caused by thermal rather than photolytic decomposition (33). Coldwell found (2) that aromatic C-nitro groups in 2,4-dinitrotoluene and 2,4,6-trinitrotoluene and N-nitro groups in trimethylenetrinitramine and 2,4,5-trinitrophenylmethylnitramide did not respond to the test.

Irradiation with light from the monochromator of isosorbide dinitrate and diphenylamine as partially overlapped spots established that the lines of the mercury arc spectrum lying between 265 mμ and 334 mμ produced a bright yellow color in the mixture. At shorter wavelengths the unmixed portions of the spots darkened, indicating more extensive photodecomposition of both diphenylamine and nitrate ester. At longer wavelengths no color appeared on the filter paper and this result was confirmed by absence of color in an alcohol solution of the reactants irradiated at 365 mμ.

Exposure to the unfiltered mercury arc spectrum of 0.04 *M* solutions of isosorbide dinitrate in absolute ethanol or benzene produced no apparent coloration. Examination of the solutions by TLC after irradiation for 3 hours indicated that, in addition to unchanged dinitrate, a highly polar product was present, which, like isosorbide, did not migrate on the chromatoplate with solvent S1. No other organic compounds could be detected on the developed plates with spray reagent R1. After irradiation for 21 hours the ethanol solution was evaporated to a colorless sirup which weighed 17.7% less than the original dinitrate and did not crystallize on seeding with isosorbide or its mono- and di-nitrate derivatives. The calculated weight loss for replacement of one NO_2 group by hydrogen in isosorbide dinitrate was 19.0%.

Solutions 0.02 *M* in both isosorbide dinitrate and diphenylamine in ethanol or benzene remained colorless on standing at room temperature for 24 hours in the dark; TLC showed only the original solutes to be present. After standing for a further 24 hours in closed Pyrex containers in the ordinary laboratory light, both solutions were very faintly yellow but the concentration of the photoproducts was too low to be detected by chromatography. When the nitrogen-purged solutions were exposed in quartz containers to the mercury arc at 15° they developed increasing intensity of yellow color with time of irradiation. After 20 minutes isosorbide dinitrate could no longer be detected in the ethanol solution by TLC, and spots corresponding to the colored reaction products began to appear. After irradiation for 2 hours six organic components of the reaction mixture were separated on the chromatoplates. Five of these products migrated with R_f values corresponding to unreacted diphenylamine, 2-nitrodiphenylamine, N-nitrosodiphenylamine, 4-nitrodiphenylamine, and 4-nitrosodiphenylamine in three different solvents (S1, S2, S3); the colorless sixth component did not move from the point of application on the plates. Similar patterns of spots were obtained from the photoreaction mixture and from a synthetic mixture of the nitro- and nitroso-diphenylamine compounds plus diphenylamine and isosorbide when chromatographed in the same solvents. When each of the diphenylamine derivatives in turn was added to an aliquot of the reaction mixture the developed chromatogram showed enrichment of a spot already present; the area and intensity of the original spot was increased in each case. The same pattern of spots was obtained also from the irradiated benzene solution and from ethanol solutions in which isosorbide dinitrate was replaced by D-mannitol hexanitrate (27) or meso-hydrobenzoin dinitrate (34).

The photoproduct from a 2-hour irradiation of an ethanol solution containing 170 mg of isosorbide dinitrate and 122 mg of diphenylamine was fractionated on a chromatobar and the central portion of each of the six separated zones was removed, powdered, and

eluted with acetone in subdued light. The weights of the six crude fractions obtained on evaporation of the acetone are shown in Table II. Fractions 2 and 4 were further purified

TABLE II

Fractions isolated from an irradiated solution of 1,4;3,6-dianhydro-D-glucitol-2,5-dinitrate and diphenylamine in absolute ethanol*

Fraction†	Major component	Weight (mg)	Ultraviolet spectra (mμ)‡ Max.	Min.
1	Diphenylamine	5.11	285, 255	270, 250
2	2-Nitrodiphenylamine	89.19	423, 257, 226	324, 238
3	N-Nitrosodiphenylamine	4.97	333, 283	292, 270
4	4-Nitrodiphenylamine	26.51	390, 256	305
5	4-Nitrosodiphenylamine	2.59	390, 287	255
6	Unknown	13.95	General absorption between 450 and 350, increasing rapidly beyond 350	

*Irradiated for 2 hours at 15° in a quartz vessel under nitrogen with unfiltered mercury arc; the initial concentration was 7.20×10^{-4} mole of each solute in 16 ml of solution.
†Center portion of each zone from chromatobar in order of decreasing R_f values.
‡Spectra were taken on rechromatographed fractions in absolute ethanol.

on chromatobars to yield 21.0 mg of pure 2-nitrodiphenylamine (m.p. 72.0–73.0°) and 6.95 mg of pure 4-nitrodiphenylamine (m.p. 132.5–133.2°) respectively. The identities of these compounds were confirmed by their ultraviolet spectra (Tables I and II), infrared spectra, and R_f values when compared with authentic samples.

Because of the small amounts of material available fractions 1, 3, 5, and 6 were rechromatographed from streaks applied to chromatoplates. The developed bands corresponding to the original fractions were scraped from the plates and worked up as before. The recovered fractions 1, 3, and 5 were not completely pure but the major components were identified from the R_f values and ultraviolet spectra (Tables I and II). Fraction 6 did not migrate and appeared to be a mixture.

DISCUSSION

The results showed clearly that an oxy-nitrogen group was transferred from nitrate esters to diphenylamine in the photolysis reaction in solution. Since the emphasis in working up the reaction mixture was primarily on isolation and identification of the aromatic products the fractionation results were only semiquantitative. The total weight of the separated fractions amounted to 49% of the weight of the original reactants. Based on the weights of the crude fractions (Table II), the identified products accounted for approximately 84% of the original diphenylamine, 80% in the form of the nitro and nitroso derivatives and the remainder in unchanged form. Thirty-seven percent of the original ester nitrogen was recovered as C-nitro groups in the diphenylamine derivatives and a further 2 to 3% could be accounted for as N- and C-nitroso groups. The apparent ortho to para ratio of 3 in the major products, 2- and 4-nitrodiphenylamine, could not be considered as significant, however, since the separations were not strictly quantitative.

The absence of a "dark reaction" between isosorbide dinitrate and diphenylamine at 25° and the slow reaction of the stronger base pyridine with the dinitrate at 115° (14) ruled out nucleophilic attack of unexcited diphenylamine on the ester from consideration in the mechanism of the photonitration. A comparison of the ultraviolet spectra of the reactants (Fig. 1) showed that diphenylamine absorbed far more of the incident light than the nitrate ester in the effective spectral region (265 to 334 mμ). This suggested

the possibility that the photoproducts resulted from attack on the ester by diphenylnitrogen radicals formed in a photodissociation of the diphenylamine. However, Tarutina has shown that irradiation of diphenylamine in benzene solution under similar conditions caused only slight decomposition of the N—H bonds unless an active radical was supplied simultaneously in the irradiated solution (35). This fact, taken together with the weight loss suffered by isosorbide dinitrate when irradiated alone in ethanol solution, indicated that a true photolytic cleavage of the nitrate ester group probably preceded the photonitration.

Among the seven other oxy-nitrogen functional groups which have been tested only the nitrite ester appeared to undergo a similar photolytic fission. Photolysis of nitrite esters with alkoxy–nitroso bond fission was reported recently by Barton and co-workers (36–38) as a preparative procedure. Yunker and Higuchi (33) showed that diphenylamine stabilized isoamyl nitrite by combining with the thermal decomposition products to form the same nitro derivatives of diphenylamine obtained in the well-known stabilization of nitrate ester explosives (6–9).

One pathway suggested by Coldwell and McLean (24) for the photonitration of diphenylamine was that the nitrodiphenylamine derivatives were formed by direct N-nitrosation of diphenylamine followed by rearrangement to the C-nitroso compound and subsequent oxidation. This mechanism appeared unlikely to predominate in the photoreaction in benzene solution in the present case. Molecular oxygen was continuously purged from the system during irradiation and the recent work of Kemula and Gabrowska on the photochemical reaction of benzene with oxygen (39) indicated that any atomic oxygen formed from nitrate ester would combine rapidly and irreversibly with the excited benzene solvent. The similarity of the products obtained in the two solvents would rule out this mechanism for the ethanol solutions also.

An alternative pathway for the photonitration, also suggested by Coldwell and McLean, was direct nitration of the phenyl rings. This seemed the more plausible, especially in the light of the recent work of Barnes and Hickinbottom on the thermal rearrangement of N-methyl-N-*p*-nitrophenylnitramine (40). These authors found that the migration of the nitro groups, brought about thermally, was not intramolecular but involved homolytic rupture of the N—NO_2 bond and the form of the nitro group thus created nitrated suitably activated phenyl rings. We believe a similar intermediate may be involved in the nitrate ester photolysis and further studies of the reaction are in progress.

ACKNOWLEDGMENTS

We thank Drs. C. Reid and P. Gray for helpful discussions and Dr. R. Bonnett for samples of pyrroline oxides. This work was supported by a research grant from the Defence Research Board of Canada.

REFERENCES

1. P. GRAY and A. WILLIAMS. Chem. Revs. **59**, 239 (1959).
2. B. B. COLDWELL. Analyst, **84**, 665 (1959).
3. M. JACKSON and L. D. HAYWARD. J. Chromatog. **5**, 166 (1961).
4. B. B. COLDWELL and S. R. MCLEAN. Can. J. Chem. **36**, 652 (1958).
5. B. B. COLDWELL and S. R. MCLEAN. Can. J. Chem. **37**, 1637 (1959).
6. T. L. DAVIS. The chemistry of powder and explosives. Vol. II. John Wiley and Sons, Inc., New York. 1943.
7. W. A. SCHROEDER, E. W. MALMBERG, L. L. FONG, K. N. TRUEBLOOD, J. D. LANDERL, and E. HOERGER. Ind. Eng. Chem. **41**, 2818 (1949).
8. H. MURAOUR. Bull. soc. chim. France, **3** (5), 2240 (1936).
9. V. R. GRASSIE, L. MITCHELL, J. M. PEPPER, and C. B. PURVES. Can. J. Research, B, **28**, 468 (1950).

10. J. A. GRAY and D. W. G. STYLE. Trans. Faraday Soc. **49**, 52 (1953).
11. P. GRAY and G. T. ROGERS. Trans. Faraday Soc. **50**, 28 (1954).
12. D. W. G. STYLE and J. C. WARD. Trans. Faraday Soc. **49**, 999 (1953).
13. R. BOSCHAN, R. T. MERROW, and R. W. VANDOLAH. Chem. Revs. **55**, 485 (1955).
14. M. JACKSON and L. D. HAYWARD. Can. J. Chem. **38**, 496 (1960).
15. T. URBANSKI, W. MALENDOWICZ, and K. DYBOWICZ. Compt. rend. **209**, 103 (1939).
16. T. URBANSKI. Roczniki Chem. **21**, 120 (1947).
17. H. B. DEVORE, A. H. PFUND, and V. COFMAN. J. Phys. Chem. **33**, 1836 (1929).
18. S. OGURI, M. TAKEI, and N. FUJITA. J. Soc. Chem. Ind. (Japan), **42**, Suppl. binding 54 (1939).
19. G. BETTI and P. MERLI. Ann. chim. appl. **31**, 197 (1941); Chem. Abstr. **35**, 6794 (1941).
20. T. S. LAWTON, JR. and H. K. NASON. Ind. Eng. Chem. **36**, 1128 (1944).
21. S. MINC. Przeglad Chem. **6**, 83 (1948); Chem. Abstr. **43**, 2427 (1949).
22. N. ALLENTOFF and G. F WRIGHT. Can. J. Chem. **35**, 900 (1957).
23. J. M. MILLER and J. G. KIRCHNER. Anal. Chem. **23**, 428 (1951).
24. G. V. MAVINETTI, J. ERBLAND, and J. KOCHEN. Federation Proc. **16** (3), 837 (1957).
25. A. E. GILLAM and E. S. STERN. Introduction to electronic absorption spectroscopy. 2nd ed. Edward Arnold Ltd., London. 1957. p. 66.
26. E. P. SWAN and L. D. HAYWARD. Can. J. Chem. **34**, 856 (1956).
27. L. D. HAYWARD. J. Am. Chem. Soc. **73**, 1974 (1951).
28. G. G. MCKEOWN and L. D. HAYWARD. Can. J. Chem. **33**, 1392 (1955).
29. L. D. HAYWARD and C. B. PURVES. Can. J. Chem. **32**, 19 (1954).
30. F. PRISTERA. Anal. Chem. **25**, 844 (1953).
31. W. A. SCHROEDER, P. E. WILCOX, K. N. TRUEBLOOD, and A. O. DEKKER. Anal. Chem. **23**, 1740 (1951).
32. R. BONNETT, R. F. C. BROWN, V. M. CLARK, I. O. SUTHERLAND, and A. TODD. J. Chem. Soc. 2094 (1959).
33. M. H. YUNKER and T. HIGUCHI. J. Am. Pharm. Assoc., Sc. Ed. **47**, 621 (1958).
34. I. G. CSIZMADIA and L. D. HAYWARD. To be published.
35. L. I. TARUTINA. Primenenie Metodov Spektroskopii v Prom. Prodovol'stven. Tovarov i Sel'sk. Khoz., Leningrad. Gosudarst. Univ. im. A. A. Zhdanova, Materialy Soveshchaniya, Leningrad. **1955**, 170 (Pub. 1957); Chem. Abstr. **53**, 21094 (1959).
36. D. H. R. BARTON, J. M. BEATON, L. E. GELLER, and M. M. PECHET. J. Am. Chem. Soc. **82**, 2640 (1960).
37. A. L. NUSSBAUM, F. E. CARLON, E. P. OLIVETO, E. TOWNLEY, P. KABASAKALIAN, and D. H. R. BARTON. J. Am. Chem. Soc. **82**, 2973 (1960).
38. C. H. ROBINSON, O. GNOJ, A. MITCHELL, R. WAYNE, E. TOWNLEY, P. KABASAKALIAN, E. P. OLIVETO, and D. H. R. BARTON. J. Am. Chem. Soc. **83**, 1771 (1961).
39. W. KEMULA and A. GRABOWSKA. Bull. acad. polon. sci. Classe (III), **8**, 525 (1960).
40. T. J. BARNES and W. J. HICKINBOTTOM. J. Chem. Soc. 2616 (1961).

ORGANIC PEROXIDES

III. REACTIONS OF DIALKYL PEROXIDES WITH ORGANOLITHIUM AND ORGANOMAGNESIUM COMPOUNDS[1]

G. A. Baramki, H. S. Chang, and J. T. Edward
Department of Chemistry, McGill University, Montreal, Que.

Received November 10, 1961

ABSTRACT

Optimum conditions for obtaining arylalkyl ethers from the reactions of aryl-lithium or -magnesium compounds with dialkyl peroxides have been investigated. The reactions are considered to take place by ionic or four-center mechanisms.

Gilman and Adams (1) found that, while di-(triphenylmethyl) peroxide is inert to phenylmagnesium bromide, diethyl peroxide reacts with it to give a 34% yield of phenetole. Di-*t*-butyl peroxide does not react with this Grignard reagent (2), even at 80° (3), but reacts at ordinary temperatures with the less-hindered Grignard reagents derived from primary and secondary bromides to give low yields of *t*-butyl ethers.

Because of the possible usefulness of this method for synthesizing certain otherwise inaccessible ethers, we have studied the reactions of four dialkyl peroxides with phenyllithium and the phenyl Grignard reagent (Table I), as well as the reaction of dimethyl peroxide with some other organo-lithium and -magnesium compounds (Table II). Best

TABLE I

Yields of ethers from reactions of dialkyl peroxides with phenyllithium and phenylmagnesium bromide

Peroxide	Reaction temp. (°C)	Yield (%) from PhLi	Yield (%) from PhMgBr
Dimethyl	15–20	80	77
Methyl *t*-butyl	15–20	63	20
Methyl *t*-butyl	35	72	38
Diethyl	15–20	38	30*
Di-*t*-butyl	0–5	3.3	—
Di-*t*-butyl	15–20	19	—
Di-*t*-butyl	35	39	0†
Di-*t*-butyl	80	38	0‡

*Gilman and Adams (1) report a 34% yield.
†Compare ref. 2.
‡Compare ref. 3.

TABLE II

Yields of methyl ethers (ROMe) from reactions of dimethyl peroxide with RLi and RMgBr at 15–20° C

R	Yield (%) with RLi	Yield (%) with RMgBr
p-Anisyl	45	47
p-Biphenylyl	65	53
β-Naphthyl	21	—

[1]*The papers by J. T. Edward, J. Chem. Soc, 1464 (1954), 222 (1956), are considered Parts I and II of this series.*

yields were obtained with dimethyl peroxide, which reacted equally well with both lithium and magnesium compounds. However, this peroxide is explosive and capricious, and the much safer methyl *t*-butyl peroxide gave with phenyllithium (but not with phenylmagnesium bromide) almost the same yields of anisole. No phenyl *t*-butyl ether was obtained from these reactions. With the more highly hindered di-*t*-butyl peroxide the superiority of phenyllithium was more marked (Table I), but even so the reaction was still incomplete after 12–14 hours at 15–20°, 45% of the peroxide being recovered. Reaction was complete in this time at 35°, but the yield was inferior to that obtained in the reaction of phenylmagnesium bromide with *t*-butyl perbenzoate, recently described by Lawesson and Yang (3). It would seem that the latter reaction will prove, in some instances, the method of choice for preparing *t*-butyl ethers, while the reaction of organolithium compounds with methyl *t*-butyl peroxide will prove perferable for preparing methyl ethers.

Gilman and Adams (1) isolated a 30% yield of biphenyl, along with phenetole, from the reaction of diethyl peroxide with phenylmagnesium bromide. We also obtained 10–30% yields of biaryls from the mixtures after reaction of the peroxides. However, it was shown in several cases (and seems likely for the others) that the biaryl was formed during the preparation of the organometallic compound.

Organometallic compounds sometimes react by free-radical mechanisms (4). However, while triphenylmethylsodium reacted with dimethyl peroxide to give a methyl ether, triphenylmethyl radical failed to react. Consequently, the reaction of triphenylmethylsodium is most plausibly explained by an ionic mechanism involving an S_N2 attack on oxygen:

$$Ph_3C^- \overset{R_1}{\curvearrowright} O\text{—}OR_2 \longrightarrow Ph_3C\text{—}OR_1 + {}^-OR_2.$$

A similar mechanism appears likely for the reactions of phenyllithium. The decreased rate of reaction as R_1 is changed from methyl to *t*-butyl finds a parallel in the decreasing facility of S_N2 attacks on the carbon atom of alkyl halides as the neighboring alkyl group becomes more highly branched (5); the lesser effect of the nature of R_2 is also in harmony with this mechanism. On the other hand, the much greater sensitivity to steric effects, particularly to the nature of R_2, observed in the reactions of Grignard reagents, is best explained by a four-center mechanism of the type generally postulated for the reactions of these compounds (6). The recent work of Dessy (7) indicates the phenyl Grignard reagent to be a complex of Ph_2Mg and $MgBr_2$, with only a negligible amount of PhMgBr. A four-center reaction of this complex with the peroxide linkage would require a conformational change (I → II)[2] of the peroxide which becomes progressively more difficult as the bulk of *both* R_1 and R_2 increases. The effect of such conformational equilibria on reaction rates is now well established (10). Further, it would be expected that the more stable transition state (III) would be that one in which the R_1 was the less bulky of the two alkyl groups, because of bulk of the phenyl group. This accords with the exclusive formation of anisole (IV; R_1 = Me) from methyl *t*-butyl peroxide (I; R_1 = Me, R_2 = Bu^t).

EXPERIMENTAL

Materials

Dimethyl peroxide, prepared according to Rieche and Brumshagen (11), was not isolated as a pure liquid but was passed in a stream of nitrogen through a long column of Drierite and then into dry peroxide-free

[2]*It seems likely that neither I nor II are planar molecules (8, 9) but that attainment of the transition state (III) requires the movement of* R_1 *and* R_2 *towards each other.*

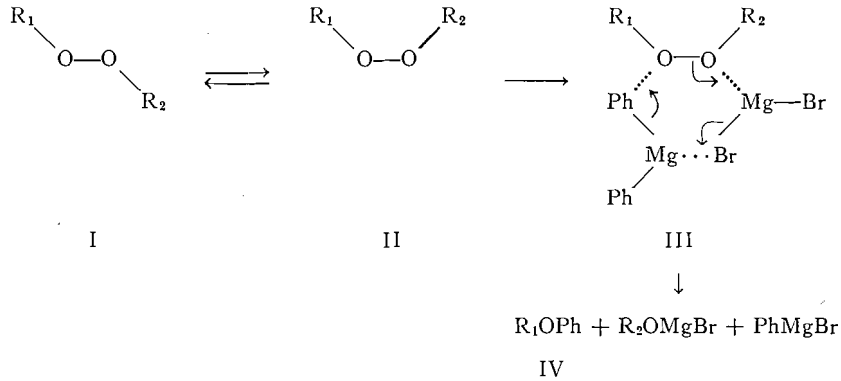

ether cooled to −70° (yield, about 70%). This ether solution was reasonably safe to handle and could be stored in the refrigerator without apparent deterioration; however, twice it exploded during addition to a solution of organometallic compound. It was analyzed for peroxide by a modification of Rieche and Brumshagen's method (11). Ten milliliters of the solution was mixed with standard aqueous stannous chloride solution (5 ml) in a tightly stoppered flask, and the mixture was stirred magnetically for 2 hours. The ether layer was then separated, washed quickly with two 10-ml portions of water, and the washings added to the stannous chloride solution. Excess standard iodine solution was added to this solution, which was then back-titrated with standard sodium thiosulphate solution.

Methyl *t*-butyl peroxide, b.p. 23° at 119 mm, d^{20} 0.811 g/ml, n_D^{24} 1.3770, was prepared by the procedure of Rust *et al.* (12), and diethyl peroxide, b.p. 22° at 90 mm, n_D^{22} 1.3862, by the method of Baeyer and Villiger (13) as modified by Harris and Egerton (14). Commercial grade di-*t*-butyl peroxide, b.p. 112° at 760 mm, n_D^{20} 1.3890, was used without purification.

General Procedure

Ether solutions of the Grignard reagent or aryllithium were prepared under nitrogen in the usual way, filtered, and the concentration of organometallic compound determined by addition of a 2-ml aliquot to an excess of standard hydrochloric acid and back-titration with standard sodium hydroxide. To aliquots of these solutions the dialkyl peroxide, diluted with an equal volume of anhydrous ether, was added under nitrogen over 1- to 2-hour periods with stirring at the temperatures indicated (Tables I and II). The reaction mixture was left overnight (12–14 hours) at this temperature, and then worked up in the usual manner, except that the ether solution was washed with aqueous sodium hydroxide to remove a trace of phenol formed by oxidation of the organometallic compound by molecular oxygen. The products, when liquid, were isolated by careful distillation through a Nester and Faust spinning-band column, and identified by boiling point, refractive index, and infrared spectrum. Solid products were identified by melting point, mixed melting point, and infrared spectrum. Yields are based on the quantity of peroxide, a 10–20% excess of organometallic compound being used.

Further details of some reactions are given below.

(a) Reaction of methyl t-butyl peroxide with phenyllithium.—*t*-Butanol, b.p. 79°, was isolated in 46% yield from the reaction carried out at 15–20° C.

(b) Reaction of methyl t-butyl peroxide with phenylmagnesium bromide.—The *t*-butanol (52% yield) isolated from this reaction carried out at 15–20° contained a small amount of unreacted peroxide, as shown by an additional strong band at 875 cm^{-1} (15, pp. 120–121) in its infrared spectrum.

(c) Reaction of di-t-butyl peroxide with phenyllithium.—From the reaction carried at 0–5° C, 89% of peroxide, b.p. 50–54° at 145 mm, was recovered; at 15–20°, 45%; at 35°, 0%.

(d) Reaction of dimethyl peroxide with p-anisylmagnesium bromide and p-anisyllithium.—The ether solution from reaction of the Grignard reagent was distilled through a short Vigreux column to give *p*-dimethoxybenzene, b.p. 88–96° at 6 mm, which solidified in the receiver. Similar treatment of the ether solution from reaction of phenyllithium gave an oil, b.p. 86–96° at 6 mm, which contained *p*-bromoanisole, and which partially crystallized only by chilling to 0°. *p*-Dimethoxybenzene was removed by repeated chilling and quick filtration.

(e) Reaction of dimethyl peroxide with 2-naphthyllithium.—After reaction, 2,2′-binaphthyl (30% yield) separated from the ether solution and was recrystallized from benzene as white flakes, m.p. 180° (reported m.p. 187° (16)). The residue from the ether solution was chromatographed on neutral alumina. Elution with petroleum ether (b.p. 67–69°) yielded naphthalene, while elution with benzene – petroleum ether, 40:60, yielded 2-methoxynaphthalene, m.p. 72°.

(f) Reaction of dimethyl peroxide with triphenylmethylsodium.—Dimethyl peroxide (0.08 mole) was added to triphenylmethylsodium (17) prepared from triphenylchloromethane (0.114 mole) and sodium amalgam (0.25 g-atom). After the addition (20 minutes), the triphenylmethylsodium had been largely consumed,

as shown by the change in color of the reaction mixture from red to yellow. The syrup remaining on evaporation of the ether, after dissolution in petroleum ether, afforded crystals of triphenylmethane, but only intractable gums were obtained on evaporation of the mother liquors. However, the presence of methoxytriphenylmethane in the gum was shown by an infrared peak of medium intensity at 2825 cm^{-1} characteristic of the methoxyl group (18) and found in an authentic specimen of methoxy-triphenylmethane prepared by the method of Straus and Hüssy (19). The gum also showed a peak at 2880 cm^{-1} corresponding to the C—H stretching vibration of triphenylmethane (20).

(g) Reaction of diethyl peroxide with triphenylmethylsodium.—This reaction also yielded an uncrystallizable gum, in which the presence of an ethyl ether was shown by a strong infrared peak at 1085 cm^{-1}, as well as by aliphatic C—H stretching frequencies at 2980 and 2940 cm^{-1} (medium intensity) (15, p. 13). A C—H stretching peak for triphenylmethane was observed at 2880 cm^{-1}.

Attempted Reaction of Dimethyl Peroxide with Triphenylmethyl Radical

Dimethyl peroxide (0.08 mole) in benzene solution was added with stirring under nitrogen to a solution of hexaphenylethane in benzene, prepared from triphenylchloromethane (0.066 mole) and zinc dust (0.63 g-atom) (21). After a further 30 minutes under nitrogen, air was bubbled through the reaction mixture to change any unreacted hexaphenylethane into the insoluble di-(triphenylmethyl) peroxide. The peroxide was removed by filtration and identified by melting point and infrared spectrum (peak at 895 cm^{-1} for peroxide linkage (15, pp. 120–121)). The benzene solution on evaporation gave a residue which had an infrared spectrum identical with that of triphenylchloromethane, and showed no absorption in the region 3000–2800 cm^{-1}, indicating the absence of any methoxytriphenylmethane. Recrystallization of the residue from benzene gave colorless plates, m.p. 108–110°, undepressed by admixture with authentic triphenylchloromethane.

ACKNOWLEDGMENTS

We are grateful to Dr. A. Taurins for assistance with infrared measurements, to the Ford Foundation for a special fellowship during 1957–1959 (to G. A. B.), and to the National Research Council for financial support.

REFERENCES

1. H. Gilman and C. H. Adams. J. Am. Chem. Soc. **47**, 2816 (1925).
2. T. W. Campbell, W. Burney, and T. L. Jacobs. J. Am. Chem. Soc. **72**, 2735 (1950).
3. S. Lawesson and N. C. Yang. J. Am. Chem. Soc. **81**, 4230 (1959).
4. M. S. Kharasch and O. Reinmuth. Grignard reactions of non-metallic substances. Prentice-Hall Inc., New York. 1954. pp. 116–132.
5. C. K. Ingold. Structure and mechanism in organic chemistry. Bell, London. 1953. p. 403.
6. J. Miller, G. Gregoriou, and H. S. Mosher. J. Am. Chem. Soc. **83**, 3966 (1961). R. E. Dessy and R. M. Salinger. Abstracts of 140th Meeting of American Chemical Society, Chicago. Sept. 1961. 9 Q.
7. R. E. Dessy and G. S. Handler. J. Am. Chem. Soc. **80**, 5824 (1958).
8. A. D. Walsh. Progress in stereochemistry. Vol. I. *Edited by* W. Klyne. Butterworths, London. 1954. p. 1.
9. J. A. Barltrop, P. M. Hayes, and M. Calvin. J. Am. Chem. Soc. **76**, 4348 (1954). G. Claeson, G. Androes, and M. Calvin. J. Am. Chem. Soc. **83**, 4357 (1961).
10. E. L. Eliel. J. Chem. Educ. **37**, 126 (1960).
11. H. Rieche and W. Brumshagen. Ber. **61**, 951 (1928).
12. F. F. Rust, F. H. Seubold, and W. E. Vaughan. J. Am. Chem. Soc. **72**, 338 (1950).
13. A. Baeyer and V. Villiger. Ber. **33**, 3387 (1900).
14. E. J. Harris and A. C. Egerton. Proc. Roy. Soc. A, **168**, 1 (1938).
15. L. J. Bellamy. The infra-red spectra of complex molecules. Wiley, New York. 1958.
16. R. L. Shriner, R. C. Fuson, and D. Y. Curtin. The systematic identification of organic compounds. Wiley, New York. 1956. p. 313.
17. W. B. Renfrow and C. R. Hauser. Organic syntheses. Collective Vol. II. *Edited by* A. H. Blatt. Wiley, New York. 1943. p. 607.
18. H. B. Henbest, G. D. Meakins, B. Nicholls, and A. A. Wagland. J. Chem. Soc. 1462 (1957).
19. F. Straus and W. Hüssy. Ber. **42**, 2168 (1909).
20. J. J. Fox and A. E. Martin. Proc. Roy. Soc. A, **175**, 208 (1940).
21. A. I. Vogel. Practical organic chemistry. Longman, Green and Co., London. 1951. p. 822.

THE INTERACTION OF FRIEDEL–CRAFTS CATALYSTS WITH ORGANIC MOLECULES

II. BORON TRIFLUORIDE WITH BENZOIC ANHYDRIDE[1]

DENYS COOK
Exploratory Research Laboratory, Dow Chemical of Canada, Limited, Sarnia, Ontario
Received November 24, 1961

ABSTRACT

The complex of boron trifluoride with benzoic anhydride has been prepared. One molecule of anhydride coordinates three molecules of boron trifluoride. The infrared spectrum shows that coordination takes place at the carbonyl groups, whose frequency is lowered some 200 cm^{-1}. There is no trace of the benzoylium cation, $C_6H_5CO^+$. Although the spectra are complex, tentative assignments are made.

INTRODUCTION

Recent work has shown the existence of the acetylium cation, CH_3CO^+, in mixtures of acid halides and strong Lewis acids (1, 2). This ion is thought to be an intermediate in the Friedel–Crafts ketone synthesis. There is strong evidence, however, that acid halides and Lewis acids can interact, giving stable complexes without ionization (2, 3). The complex formation is thought to be due to a donor–acceptor interaction between the carbonyl lone pair electrons and the vacant orbital of the Lewis acid. This complex presumably is also active in ketone synthesis.

Besides acid halides, acid anhydrides have been used in acylation reactions (4). Benzoic anhydride, for example, contains the structural elements of benzoylium benzoate, $C_6H_5CO^+OCOC_6H_5^-$, into which it could conceivably ionize under the influence of a strong Lewis acid. The purpose of the investigation was to see if any ionic species was present in the complex, thus identifying a possible common acylating agent in all Friedel–Crafts ketone syntheses, or, if not, to speculate on the constitution of the complex.

RESULTS AND DISCUSSION

Benzoic Acid – Boron Trifluoride Complex

The structure of anhydrides is probably as shown in I. Other structures derived from I

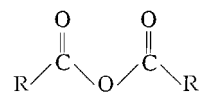

I

by rotation of the acyl group around the C—O bond are far more sterically hindered than I, even when R = CH_3. If R = C_6H_5 or any bulky alkyl groups, I is the only structure that can accommodate such groups without angular distortion. I is presumably planar, and therefore contains a plane of symmetry which bisects the C—O—C angle at right angles to the molecular plane.

The splitting of the carbonyl group frequency, observed in all anhydrides, has been ascribed to coupling of an in-phase and an out-of-phase motion of the two carbonyl

[1]*Contribution No. 57.*

groups, resulting in a low- and high-frequency band (5, 6). This explanation has been tacitly accepted, but has been held with some reservations. Certainly both bands at 1799 cm^{-1} and 1738 cm^{-1} (doublets) are connected with the carbonyl group. (See Table I.)

TABLE I

Bands in spectrum of $(C_6H_5CO)_2O$ and the BF_3 complex

$(C_6H_5CO)_2O{:}3BF_3$, solid in nujol and fluorolube	1620m,sh, 1610s, 1601s, 1568s, 1561s, 1503m, 1463m,sh, 1458s, 1448s, 1434s, 1428m,sh, 1308w, 1272m, 1240s, 1208m, 1170s, 1153s, 1148s, 1065m,sh, 1044s,sh, 1032vs, 988s, 946w, 901w, 870m, 832vw, 810m, 770m, 721s, 695w, 681m
$(C_6H_5CO)_2O$, solution in CCl_4 and CS_2	1799vs, 1790vs, 1738s, 1733s, 1696w, 1603m, 1589m, 1494w, 1452s, 1402w, 1305w, 1270m, 1240m, 1203vs, 1168s, 1072m, 1034vs, 1012vs, 996vs, 935w, 872w, 780m, 702vs, 688m

In the complex both of these two bands have disappeared. To account for this it is suggested that each carbonyl group complexes with one BF_3 molecule as shown in II,

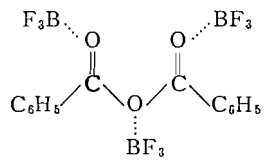

II

and a further BF_3 molecule coordinates at the bridge oxygen. This is in accord with the stoichiometry of the complex (see experimental section) requiring three BF_3 units per molecule of benzoic anhydride.

Having postulated BF_3 coordination at the carbonyl group, and with the knowledge that such coordination can lower carbonyl frequencies by a few hundred cm^{-1}, it is then proper to look for perturbed carbonyl frequencies in the region 1650 to 1450 cm^{-1}. There is, in fact, an abundance of bands, which makes the task somewhat difficult. Seven bands can be seen at 1610, 1601, 1568, 1503, 1458, 1448, and 1434 cm^{-1}. The last band would represent a shift of 366 cm^{-1} between anhydride and complex, and this seems rather a high value. Other fundamentals in this region would be ring modes of the aromatic nucleus, but the 1458 cm^{-1} band seems too intense for these. It is thought reasonable, therefore, to assign the 1601 cm^{-1} band to the perturbed high-frequency carbonyl vibration, and the 1458 cm^{-1} band to the low-frequency one. The 1610, 1568, 1503, and 1448 bands would then be assigned to ring modes or combinations. Their high intensity would be borrowed from the two carbonyl bands. The only other donor site in the benzoic anhydride molecule is the bridge oxygen which coordinates one BF_3 molecule. In the anhydride a very strong band is located at 1203 cm^{-1} and is generally thought to be associated with the C—O—C grouping. It has the character of an asymmetric C—O stretch. In acetic anhydride the band is at 1118 cm^{-1}. (It is doubtful if these frequencies can be designated as group frequencies, as, for example, carbonyl frequencies can. Variations in these frequencies do not have the significance that other group frequencies have.)

In the complex there are a number of bands in the 1000–1300 cm^{-1} region, but one of the bands near 1153 cm^{-1} could be approximately described as due to a C—O asymmetric stretching vibration. Vibrational interactions will be prevalent in the complex, and the free anhydride, in the C—C—O—C—C framework, so that it becomes difficult to

characterize each band as due to a specific vibration. However, the lower frequency in the complex compared with the anhydride is in keeping with known behavior of complex formation. This assignment seems a little arbitrary at the moment, but will be strengthened by subsequent assignment of other bands in the 1000–1300 cm^{-1} region to other vibrations.

In all boron trifluoride complexes the originally trigonally planar arrangement around the boron atom gives way to an approximately tetrahedral one. The three B—F bonds lengthen considerably and the donor atom makes the fourth bond at a distance closely approaching that of covalent organic compounds. Thus, in the complexes, one would expect two B—F stretching frequencies, one symmetric, the other asymmetric, in the region 900 to 1300 cm^{-1}. Furthermore, since boron has two isotopes of mass 10 and 11, in the natural ratio of 1:4, each of these B—F stretching frequencies should be doublets with a high-frequency component having about one fourth the intensity of the lower-frequency component. These doublets should be infrared active since it is only in the totally symmetric modes like ν_1 in BF_4^-, ν_1 in BF_3 that no isotope splitting occurs. It seems very unlikely that there would be no motion of the B atom in the B—F stretching modes in the complexes. The separation of the isotopic bands would be about 40 to 50 cm^{-1}.

Two bands which qualify extremely well for the asymmetric B—F stretch are located at 1272 and 1240 cm^{-1}. When rough corrections are made for band overlap these two bands have intensities in a ratio quite close to 1:4. For the symmetric B—F stretch the bands at 1065 and 1032 cm^{-1} seem very appropriate. They have the right frequency separation and intensity ratio.

One strong band is still unassigned in this region, at 988 cm^{-1}. This can be assigned to a B—O ligand bond. This is a good deal lower in frequency than a purely covalent B—O stretching vibration, as, for example, in methoxyboranes (7), 1250–1400 cm^{-1}, reflecting the weaker nature of the coordinate link. It is, however, consistent with other B—X stretching frequencies in various BF_3 complexes, for example, BF_3:pyridine, 1095 cm^{-1} (8).

While the complex nature of the spectra precludes a complete assignment at this stage, two very important incontrovertible facts are clear. First, there are no bands in the spectra near 2200 cm^{-1} associated with the ionic species ($C_6H_5CO^+SbF_6^-$, 2193 cm^{-1}) (9). Since these species give rise to intense bands it can be categorically stated that they are absent in gross amounts. Fractions of a percent could not be detected by present methods. Secondly, coordination of BF_3 occurs at both carbonyl groups and the bridge oxygen. It is clearly probable that whatever ability these complexes have in acylation does not come from any ionic species formed in the complex.

Acetic Anhydride – Boron Trifluoride Complex

Many similar features have been found in a complex of acetic anhydride with 2 moles of boron trifluoride. Total absence of absorption in the 2200–2300 cm^{-1} region indicates the absence of the acylium ion, CH_3CO^+. The absence of strong bands in the 1700–1800 cm^{-1} region also indicates an alteration in the C=O bond character. A structure similar to II is tentatively suggested, though some irreversible reaction cannot, at this stage, be ruled out. Further work is progressing with this material.

EXPERIMENTAL

The Spectra

A Perkin–Elmer 221 prism-grating spectrometer was used to record the spectra. Emulsions of the solid in nujol and fluorolube pressed between sodium chloride plates gave very good spectra. Since the compounds were somewhat sensitive to moisture the samples were prepared in a dry box.

The Compounds

Benzoic anhydride (Distillation Product Industries, white label grade), 22.6 g (0.1 mole), was dissolved in 450 g dry carbon tetrachloride, then saturated with BF_3, when a slowly developing white precipitate was observed. After filtration, and further treatment with BF_3, more solid was observed. No attempt was made to obtain a quantitative yield. The substance was slowly attacked by water, yielding benzoic acid and boric acid. A quantitative determination of the composition of the material by gravimetric methods showed that one anhydride molecule coordinated three BF_3 molecules.

ACKNOWLEDGMENT

The assistance of Miss C. D. Anderson in recording the spectra is gratefully acknowledged.

REFERENCES

1. B. P. Susz and J.-J. Wuhrmann. Helv. Chim. Acta, **40**, 971 (1957).
2. D. Cook. Can. J. Chem. **37**, 48 (1959).
3. D. Cassimatis, P. Gagneaux, and B. P. Susz. Helv. Chim. Acta, **43**, 424 (1960).
4. P. H. Given and D. L. Hammick. J. Chem. Soc. 1327 (1947).
5. L. J. Bellamy. The infrared spectra of complex molecules. 2nd ed. Methuen and Co. Ltd., London. 1958. p. 127.
6. R. N. Jones and C. Sandorfy. Chemical applications of spectroscopy. *Edited by* W. West. Interscience Publishers, New York. 1956. p. 496.
7. L. J. Bellamy, W. Gerrard, M. F. Lappert, and R. L. Williams. J. Chem. Soc. 2412 (1958).
8. A. R. Katritzky. J. Chem. Soc. 2049 (1959).
9. D. Cook. Unpublished data.

METALLO-ORGANIC COMPOUNDS CONTAINING METAL–NITROGEN BONDS

PART II. SOME DIALKYLAMINO DERIVATIVES OF Nb(V) AND Nb(IV)[1]

D. C. BRADLEY AND I. M. THOMAS[2]
Department of Chemistry, University of Western Ontario, London, Ontario

Received October 26, 1961

ABSTRACT

Reactions involving niobium pentachloride and lithium dialkylamides ($LiNR_2$, where R = Me, Et, Pr^n, Bu^n) led to considerable reduction of niobium to Nb(IV) as the length of the alkyl chains increased. $Nb(NMe_2)_5$ was isolated by sublimation but distillation of the other products gave tetrakis-(dialkylamino)-niobium(IV) compounds. Steric factors are apparently responsible for the low stability of pentakis-(dialkylamino)-niobium(V) compounds. The smaller steric effects of —$NMeBu^n$ and piperidino groups allowed the isolation of pentakis derivatives. The thermal decomposition of $Nb(NMeBu^n)_5$ gave mainly $Nb(NMeBu^n)_4$ with some $Bu^nN{=}Nb(NMeBu^n)_3$. Steric effects were also revealed in the replacement of —NMe_2 groups in $Nb(NMe_2)_5$ by —NEt_2 groups and in replacement of —NEt_2 groups in $Nb(NEt_2)_4$ by piperidino groups.

In a previous communication (1) we reported that tetrakis-dialkylamino derivatives $M(NR_2)_4$ of titanium and zirconium could be prepared by the action of the appropriate lithium dialkylamide and the metal tetrachloride. These new compounds were thermally stable insofar as they survived distillation under reduced pressure, although they were readily hydrolyzed or alcoholized. Aminolysis reactions revealed that very powerful steric effects came into play and it appeared in most cases that steric hindrance was sufficient to prevent polymerization through intermolecular metal–nitrogen coordinate bonds.

We now report some results obtained from the reactions involving lithium alkylamides with niobium pentachloride. When the lithium di-*n*-alkylamides, $LiNR_2$ (where R = Me, Et, Pr^n, and Bu^n), were used, reduction of the niobium to the quadrivalent state occurred to an extent which increased with the length of the *n*-alkyl chains in the amine, i.e. Me, 9%; Et, 69%; Pr^n, 85%; Bu^n, 91%. Only in the case of the dimethylamino derivative was it possible to isolate a pentakis compound, $Nb(NMe_2)_5$. This was obtained as a brown solid by sublimation at 100° at 0.1 mm. With the higher amines distillation of the reaction products led to the isolation of the tetrakis-dialkylamino-niobium(IV) compounds as red or brown liquids, as shown in Table I.

It is important to understand the factors which control the degree of reduction of the niobium in reactions involving lithium dialkylamides and niobium pentachloride. An obvious possibility is the opposition by steric factors to formation of stable pentakis compounds, and it is clear that the order of steric effects is: $Bu^n{}_2N > Pr^n{}_2N > Et_2N \gg Me_2N$. This order of steric effects is nicely in line with the observed order of degrees of reduction in the $LiNR_2$–$NbCl_5$ reactions. However, it is also possible that electronic factors may play an important part. Here we are on less certain ground but it seems reasonable to suppose that reduction involves the uncoupling of electrons in a metal–nitrogen bond, with the formation of an NR_2 radical. Assuming that the inductive effect (electron release) of the alkyl groups tends to stabilize the —NR_2 radical this would lead

[1]*For Part I, see ref. 1.*
[2]*Present address: Anderson Chemical Division, Stauffer Chemical Corporation, Weston, Michigan, U.S.A.*

TABLE I

Properties of dialkylamino-niobium compounds

Compound	Appearance	Volatility* (0.1 mm pressure)
$Nb(NMe_2)_5$	Brown solid	100° C†
$Nb(NEt_2)_4$	Brown liquid	120° C
$Nb(NMe_2)_3(NEt_2)_2$	Pale brown solid	110° C‡
$Nb(NMe_2)(NEt_2)_3$	Red liquid	120° C
$Nb(NPr^n_2)_4$	Red liquid	155° C
$Nb(NBu^n_2)_4$	Red liquid	175° C
$Nb(NMeBu^n)_5$	Red liquid	150° C‡
$Nb(NMeBu^n)_4$	Red liquid	150° C
$Nb(NC_5H_{10})_5$	Yellow crystals	~170° C‡
$Nb(NC_5H_{10})_4$	Brown liquid	~170° C‡
$Nb(NEt_2)_3(NC_5H_{10})$	Brown liquid	170° C
$Nb(NEt_2)_2(NC_5H_{10})_2$	Viscous brown liquid	170° C‡

*These figures are not true boiling points.
†Sublimes.
‡Decomposes.

to the following ease of formation of radicals: $NBu^n_2 > NPr^n_2 > NEt_2 > NMe_2$, which is also in line with the observed degrees of reduction of the niobium. In an attempt to resolve this problem we have investigated some reactions of $NbCl_5$ with other lithium alkylamides. In the reaction involving the lithium derivative of N-methyl-*n*-butylamine, $MeBu^nNH$, no reduction occurred and the pentakis compound $Nb(NMeBu^n)_5$ was obtained. However, attempts to distill the compound led to extensive reduction of the niobium and the volatile product was substantially the tetrakis compound $Nb(NMeBu^n)_4$. We will defer discussion on the details of this interesting decomposition until later and point out at this stage that our success in obtaining $Nb(NMeBu^n)_5$ strongly supports the view that steric factors play a predominant role in the reduction of niobium alkylamides. This is because the relatively small N-methyl group will allow the bulky *n*-butyl group in Nb—$NMeBu^n$ groups to bend back and away from the center of intramolecular congestion. Further evidence in support of the stereochemical hypothesis resulted from the reaction involving lithium piperidide and $NbCl_5$. In this reaction only 15% reduction of niobium occurred. Moreover, by aminolysis of $Nb(NMe_2)_5$ with piperidine the pure pentakis-piperidino-niobium $Nb(NC_5H_{10})_5$ was obtained as a bright yellow crystalline compound. Since the piperidino-group has a steric effect very similar to that of the dimethylamino group but an inductive effect nearer to the diethylamino or di-*n*-propylamino group we conclude it must be steric effects which prevent the formation of stable pentakis-dialkylamino compounds of the higher di-*n*-alkylamino groups.

Some interesting results were obtained from the aminolysis reactions involving $Nb(NMe_2)_5$ and excess diethylamine under various conditions. In a reaction lasting 2 hours at the temperature of boiling diethylamine no reduction of niobium occurred and disubstitution was effected. However, attempts to distill the tris-(dimethylamino)-bis-(diethylamino)-niobium(V) $Nb(NMe_2)_3(NEt_2)_2$ so obtained led to decomposition. In another experiment, continued until it appeared that all of the dimethylamino groups had been replaced (9 days), reduction occurred (30%) and analysis showed that dimethylamino groups were still present. Distillation of the product gave a volatile quadrivalent niobium mixed alkylamide, $Nb(NMe_2)(NEt_2)_3$. From these experiments it is clear that steric effects are very powerful in preventing substitution of Me_2N groups by Et_2N groups. In addition, it appears that the niobium can accommodate three dimethylamino and two diethylamino groups but that the introduction of the third or fourth diethylamino group leads to instability.

The niobium(IV) compounds obtained in this research were similar in volatility to the tetrakis-dialkylamino-titanium compounds prepared before (1) and they should provide valuable starting materials for the synthesis of other Nb(IV) compounds. For example, we have prepared tetrakis-piperidino-niobium(IV) by aminolysis involving tetrakis-diethylamino-niobium(IV). Even in this system it was clear that steric hindrance was important because in a preliminary experiment conducted in boiling benzene for over 4 hours only disubstitution occurred. However, the $Nb(NEt_2)_2(NC_5H_{10})_2$ thus formed disproportionated when heated and a small amount of the volatile $Nb(NEt_2)_3(NC_5H_{10})$ was obtained. Complete replacement of diethylamino groups was effected by a reaction lasting 6 days, but the low volatility of $Nb(NC_5H_{10})_4$ precluded its purification by distillation. This feature of $Nb(NC_5H_{10})_4$ calls to mind the abnormally low volatility of $Ti(NC_5H_{10})_4$. From considerations of molecular size and organic content it would be expected that the tetrakis-piperidino derivatives would have volatilities intermediate between the tetrakis-diethylamino derivatives (Ti, 110° at 0.05 mm; Nb, 120° at 0.1 mm) and the tetrakis-di-*n*-propylamino derivatives (Ti, 150° at 0.1 mm; Nb, 155° at 0.1 mm). In fact they are considerably less volatile (Ti, 180° at 0.1 mm; Nb, decomposes at 170° at 0.1 mm). Since the piperidino groups will exert less steric hindrance than either NEt_2 or NPr^n_2 groups it was thought that the piperidino compounds might be polymeric in nature. Nevertheless, determination of the molecular weight of $Ti(NC_5H_{10})_4$ in boiling benzene showed that this compound was monomeric (1) and the reason for its abnormally low volatility is obscure.

Let us now return to the thermal decomposition of $Nb(NMeBu^n)_5$ mentioned earlier in the paper. About 90% of the niobium originally in the pentakis compound was recovered in the form of a deep red liquid which distilled at 150° at 0.1 mm. Analysis of the distillate showed that it was substantially tetrakis-(N-methyl-*n*-butylamino)-niobium(IV) but the N:Nb ratio of 4:1 and the average valency of 4.25 for the niobium showed that a quinquevalent niobium compound with N:Nb = 4:1 and a volatility similar to $Nb(NMeBu^n)_4$ must also be present. Our experience with tantalum compounds (2) suggested that the quinquevalent niobium compound might be $Bu^nN{=}Nb(NMeBu^n)_3$. This was confirmed by gas chromatography of the volatile products of alcoholysis by which means primary *n*-butylamine was identified in addition to N-methyl-*n*-butylamine. It appears that the thermal decomposition of $Nb(NMeBu^n)_5$ involves some novel reactions since besides practically quantitative recovery of niobium as $Nb(NMeBu^n)_4 + Bu^nN{=}Nb(NMeBu^n)_3$ there was obtained a more volatile product consisting of substantially N-methyl-*n*-butylamine. Further work on this interesting reaction is in progress. Special attention was paid to the possibility that compounds of the type $RN{=}Nb(NR_2)_3$ might also be formed in the thermal decomposition of the other $Nb(NR_2)_5$ compounds but no evidence for this was forthcoming.

EXPERIMENTAL

1. General

All reactions were carried out in carefully dried glass apparatus under an atmosphere of dry oxygen-free nitrogen.

Amines were stored over sodium wire and fractionally distilled over fresh sodium immediately prior to use. The purity of the amines was checked by gas chromatographic analysis.

The niobium analyses were obtained by weighing samples directly into weighed platinum crucibles, hydrolyzing cautiously with water, and igniting carefully to Nb_2O_5. The nitrogen content (as basic nitrogen) was determined by steam distillation and subsequent titration of the amine produced by hydrolysis in alkaline solution. The valency of the niobium was determined by the following chemical method. A sample of the compound was added to a 10-cc aliquot of a solution of anhydrous ferric chloride (15 g) and sulphuric acid (15 cc, conc.) in ethanol (150 cc). When a clear solution was obtained (usually within 10 seconds) the aliquot was added to dilute sulphuric acid and titrated against standard ceric sulphate solution. A blank determination was carried out on the ferric chloride – sulphuric acid – ethanol reagent.

2. Preparation of Lithium Dialkylamides

In order to remove lithium chloride by filtration from the products of the lithium dialkylamide – $NbCl_5$ reaction it was necessary to prepare a solution of $LiNR_2$ in pentane free from lithium halides. The following method proved to be satisfactory. Normal-butyl chloride (theoretical amount) in twice its volume of pentane was slowly added to a suspension of finely cut lithium ribbon in pentane. The rate of addition was adjusted to maintain the pentane at a moderate rate of reflux. The mixture was stirred until cool and then kept at room temperature for several hours. The clear solution of butyllithium was decanted from the insoluble lithium chloride and the concentration of butyllithium was determined by titration against standard acid. The dialkylamine (10% excess over theoretical) was then added dropwise to the stirred solution of butyllithium at a rate sufficient to maintain the pentane in a state of reflux. The lithium dialkylamide was precipitated and in all cases appeared to be practically insoluble. After completing the addition of the dialkylamine the system was stirred for a further 30 minutes and was then ready for use.

3. Reactions Involving $NbCl_5$ and Lithium Dialkylamides

(i) Lithium Dimethylamide

Niobium pentachloride (11.5 g) was added to a stirred suspension of lithium dimethylamide (0.215 g-equiv) in pentane. A slow reaction occurred with the development of an orange color. The mixture was kept stirred at room temperature for 20 hours and was then filtered to remove insoluble lithium salts. Evaporation of pentane from the filtrate left a light brown solid (13.8 g; calc. for $Nb(NMe_2)_5$, 13.3 g). Found: Nb, 27.4; NMe_2, 63.7; valency of Nb, 4.90, 4.93; Cl, trace; Li, trace; ratio N: Nb, 4.90:1. $Nb(NMe_2)_5$ requires: Nb, 29.7; NMe_2, 70.3%.

A sample of the foregoing product (11.0 g) was heated under 0.1 mm Hg pressure and sublimed at 100° C, giving a dark brown solid (6.33 g; 58% yield) which proved to be pentakis-(dimethylamino)-niobium(V). Found: Nb, 29.6; NMe_2, 70.0%; valency of Nb, 5.00, 4.98. The non-volatile residue (3.73 g) was also a brown solid. Found: Nb, 28.9; NMe_2, 38.8%; valency of Nb, 4.53, 4.54; ratio N: Nb, 2.83:1.

(ii) Lithium Diethylamide

Niobium pentachloride (10.1 g) and lithium diethylamide (0.195 g-equiv) were caused to react as in the previous experiment. The niobium product, isolated as before, was a red viscous liquid (16.4 g; calc. for $Nb(NEt_2)_4$, 14.29). Found: Nb, 20.4; NEt_2, 73.8; valency of Nb, 4.31, 4.32; Cl, trace; Li, absent; ratio N:Nb, 4.65:1. $Nb(NEt_2)_4$ requires: Nb, 24.4; NEt_2, 75.6%. Distillation of this product (13.7 g) gave tetrakis-(diethylamino)-niobium(IV) as a brown liquid product (9.0 g; 76% yield; b.p. 120° C at 0.1 mm). Found: Nb, 24.5; NEt_2, 76.3%; valency of Nb, 3.98.

(iii) Lithium Di-n-propylamide

Niobium pentachloride (13.2 g) was added to a stirred suspension of lithium di-*n*-propylamide (0.255 g-equiv) in pentane over a period of 30 minutes and a deep red color developed. After being stirred for 6 hours the mixture was filtered and the filtrate evaporated under reduced pressure, leaving a deep red liquid product (25.5 g; calc. for $Nb(NPr_2)_4$, 24.1 g). Found: Nb, 17.2; N, 10.9; valency of Nb, 4.16, 4.15; Cl, absent; Li, absent; ratio N:Nb, 4.22:1. $Nb(NPr_2)_4$ requires: Nb, 18.8; N, 11.36%. Distillation of this product afforded tetrakis-(di-*n*-propylamino)-niobium(IV) as a dark red liquid (17.9 g; 81% yield; b.p. 155° C at 0.1 mm). Found: Nb, 19.0; N, 11.4%; valency of Nb, 4.04, 4.07. A sample of this compound was allowed to react with *n*-butanol and the volatile products were subjected to gas chromatographic analysis. Only di-*n*-propylamine was identified as the volatile product of alcoholysis.

(iv) Lithium Di-n-butylamide

Niobium pentachloride (11.0 g) was added to a stirred suspension of lithium di-*n*-butylamide in pentane over a period of 45 minutes. The dark brown mixture was stirred at room temperature for 5 hours, then filtered, and the filtrate evaporated under reduced pressure. The product remaining after drying for 2 hours at 40° C at 0.1 mm was a dark red liquid (30.0 g; calc. for $Nb(NBu_2)_4$,Bu_2NH, 29.9 g). Found: Nb, 12.1; N, 9.53%; valency of Nb, 4.08, 4.10; Li, absent; Cl, trace; ratio N:Nb, 5.22:1. A sample (26.8 g) of this product was distilled under reduced pressure but due to the high temperature involved, decomposition was considerable. The product was redistilled and finally gave tetrakis-(di-*n*-butylamino)-niobium(IV) as a deep red liquid (4.05 g; b.p. 175° C at 0.1 mm). Found: Nb, 15.6; N, 9.17; valency of Nb, 4.25, 4.28; ratio N:Nb, 3.90:1. $Nb(NBu_2)_4$ requires: Nb, 15.3; N, 9.25%. The valency determination suggested that an appreciable proportion of a quinquevalent niobium compound was also present but the only reasonable possibility would be $Bu^nN{=}Nb(NBu^n)_3$ since this has the same N:Nb ratio as $Nb(NBu_2)_4$ and would have a similar volatility. Since $BuN{=}Nb(NBu_2)_3$ requires: Nb, 16.9; N, 10.2%, this would also explain the fact that the product was a slightly higher Nb% than $Nb(NBu_2)_4$ but it is not consistent with the lower N%. However, gas chromatographic analysis of the volatile products of *n*-butanolysis showed that di-*n*-butylamine was the only amine liberated, and this result rules out the possibility that the compound was contaminated with $Bu^nN{=}Nb(NBu^n_2)_3$.

(v) Lithium Piperidide

Niobium pentachloride (8.8 g) was added to a stirred suspension of lithium piperidide (0.165 g-equiv) in petrol (boiling range, 35–60° C). A slow reaction occurred and after the addition the brown mixture was refluxed for 6 hours and then left stirred at room temperature for a further 20 hours. The final product

obtained after filtration and evaporation of the solvent was a red viscous liquid (15.3 g; calc. for $Nb(NC_5H_{10})_5$, 16.4 g). Found: Nb, 15.6; NC_5H_{10}, 58.4; valency of Nb, 4.85; Cl, trace; Li, absent; ratio N:Nb, 4.14:1. $Nb(NC_5H_{10})_5$ requires: Nb, 18.1; NC_5H_{10}, 81.9%. Attempts to purify the crude product by means of crystallization from petrol or by distillation at 0.1 mm pressure were unsuccessful. At temperatures above 170° C, decomposition to a black solid (found: Nb, 27.2; NC_5H_{10}, 23.7%; valency of Nb, 4.16; ratio N:Nb, 0.96:1) occurred.

(vi) Lithium N-Methyl-n-butylamide

Niobium pentachloride (13.5 g) was added to a stirred suspension of lithium N-methyl-*n*-butylamide (0.252 g-equiv) in pentane over a period of 45 minutes and the mixture became orange. After being stirred for 6 hours at room temperature this mixture was filtered, and the filtrate evaporated under reduced pressure, leaving a dark brown liquid product (25.9 g; calc. for $Nb(NMeBu^n)_5$, 26.1 g). Found: Nb, 17.5; N, 12.7; valency of Nb, 4.96; ratio N:Nb, 4.82:1. $Nb(NMeBu^n)_5$ requires: Nb, 17.76; N, 13.4%. The pentakis-(N-methyl-*n*-butylamino)-niobium(V) (24.1 g) was heated under reduced pressure and a product was distilled over accompanied by considerable decomposition. Redistillation gave a deep red liquid distillate (17.0 g; yield 86%; b.p. 150° at 0.1 mm). Found: Nb, 21.5; N, 12.75; valency of Nb, 4.27, 4.24; ratio N:Nb, 3.94:1. $Nb(NMeBu)_4$ requires: Nb, 21.25; N, 12.82. $BuN{=}Nb(NMeBu)_3$ requires: Nb, 22.0; N, 13.26%. The analytical data on this substance suggested that it was a mixture of $Nb(NMeBu^n)_4$ and $Bu^nN{=}Nb(NMeBu^n)_3$. A sample (3.45 g) of the substance was treated with *n*-butanol (5.0 g) and refluxed until the solution became colorless (ca. 3 minutes). The volatile products and excess *n*-butanol were evaporated off under reduced pressure and the residue distilled under reduced pressure to give niobium pentabutoxide (3.37 g; 93% yield; b.p. 200° C at 0.1 mm). Found: Nb, 20.4; N, absent. $Nb(OBu)_5$ requires: Nb, 20.3%. Gas chromatographic analysis of the butanolic condensate revealed the presence of primary *n*-butylamine in addition to N-methyl-*n*-butylamine. The presence of $Bu^nN{=}Nb(NMeBu^n)_3$ in the original substance was thus confirmed. It is also interesting to note that oxidation of the niobium from quadrivalent to quinquevalent occurred during the butanolysis and it is clear that niobium tetraalkoxides are very unstable. In addition to the red substance produced by heating $Nb(NMeBu^n)_5$ there was obtained by condensation at ca. −78° C a volatile product (5.2 g) which was predominantly N-methyl-*n*-butylamine (about 90% as estimated by gas chromatography). Acidimetric titration gave an equivalent weight of 96 compared with the calculated 87 for $MeBu^nNH$ and this also suggested the presence of about 10% of non-basic component in the mixture.

4. Aminolysis of Dialkylamino-niobium Compounds

(i) Piperidine and $Nb(NMe_2)_5$

Piperidine (8 ml) was caused to react with $Nb(NMe_2)_5$ (3.19 g) in petrol (boiling range 35–60° C; 50 ml) at the boiling point. When no more dimethylamine appeared to be evolved (after 3 days) the solvent and excess piperidine were evaporated off under reduced pressure and a light brown solid was left. This was crystallized from petrol and gave the pentakis-(piperidino)-niobium(V) as a bright yellow solid (1.6 g; 31% yield). Found: Nb, 18.3; NC_5H_{10}, 81.0. $Nb(NC_5H_{10})_5$ requires: Nb, 18.1; NC_5H_{10}, 81.9%.

(ii) Piperidine and $Nb(NEt_2)_4$

Piperidine (10 ml) and $Nb(NEt_2)_4$ (3.93 g) were caused to react in boiling benzene (30 ml) in an apparatus fitted with a fractionation column in order to take off the diethylamine liberated. After 4 hours reaction the solvent and excess piperidine were evaporated off under reduced pressure and a dark brown viscous liquid (4.32 g) was left. Found: Nb, 22.8; N, 13.7; valency of Nb, 4.05; ratio N:Nb, 3.99:1. $Nb(NEt_2)_2(NC_5H_{10})_2$ requires: Nb, 22.9; N, 13.8%. A sample (2.8 g) of this product was distilled to give a brown liquid distillate (0.5 g; b.p. 170° C at 0.1 mm). Found: Nb, 23.6; N, 14.35; ratio N:Nb, 4.03. $Nb(NEt_2)_3(NC_5H_{10})$ requires: Nb, 23.6; N, 14.25%.

In an attempt to force the completion of the aminolysis another sample of $Nb(NEt_2)_4$ (2.58 g) was caused to react with piperidine (20 ml) in boiling benzene (70 ml) and the liberated diethylamine was fractionated off during 6 days. At this stage it appeared from gas chromatographic analysis of the distillate that the liberation of diethylamine was complete. After evaporating off the solvent and excess piperidine a dark brown liquid (3.1 g; calc. for $Nb(NC_5H_{10})_4$, 2.9 g) remained. Found: Nb, 20.1; NC_5H_{10}, 79.8; valency of Nb, 4.02, 4.05; N:Nb, 4.38:1. $Nb(NC_5H_{10})_4$ requires: Nb, 21.6; NC_5H_{10}, 78.4%. Gas chromatographic analysis of the volatile products of butanolysis showed that the only base present was piperidine. The analytical results suggested that some piperidine was coordinated to the tetrakis-(piperidino)-niobium(IV). Attempts to distill the compound under reduced pressure were unsuccessful since it decomposed at temperatures above 170° C.

(iii) Diethylamine and $Nb(NMe_2)_5$

Diethylamine (25 ml) was added to $Nb(NMe_2)_5$ (3.0 g) and refluxed for 2 hours during which time some dimethylamine was liberated. After evaporating off the excess diethylamine a light brown solid (3.33 g) remained. Found: Nb, 25.5; N, 18.8; valency of Nb, 4.95, 4.97; ratio N:Nb, 4.90:1. $Nb(NMe_2)_3(NEt_2)_2$ requires: Nb, 25.2; N, 19.0%. A sample of the tris-(dimethylamino)-bis-(diethylamino)-niobium(V) (2.6 g) was heated under 0.1 mm pressure, and at 110° C a red liquid distilled over (0.5 g). Found: Nb, 32.2; N, 13.6; valency of Nb, 4.39; ratio N:Nb, 2.80:1.

In another experiment $Nb(NMe_2)_5$ (3.92 g) was refluxed with diethylamine (50 cc) and the liberated dimethylamine fractionated off over a period of 9 days. At this stage it was apparent from gas chromatographic analysis of the distillate that liberation of dimethylamine had ceased. A red liquid product (3.86 g) remained after the evaporation of excess diethylamine. Found: Nb, 27.9; N, 14.7; valency of Nb, 4.70; ratio N:Nb, 3.5:1. That this product was a mixed alkylamide was shown by the gas chromatographic analysis of the volatile products of butanolysis, which revealed the presence of both diethylamine and dimethylamine. A sample (2.38 g) of the mixed alkylamide was heated to 120° C at 0.1 mm when a red liquid distilled over (1.0 g). Found: Nb, 26.0; N, 15.45; ratio N:Nb, 3.94:1. $Nb(NMe_2)(NEt_2)_3$ requires: Nb, 26.2; N, 15.9%.

ACKNOWLEDGMENT

The authors are indebted to the Wright Air Development Division of the Air Research and Development Command, United States Air Force, for sponsoring this research.

REFERENCES

1. D. C. Bradley and I. M. Thomas. J. Chem. Soc. 3857 (1960).
2. D. C. Bradley and I. M. Thomas. Proc. Chem. Soc. 225 (1959).

THE ALKALOIDS OF STEMONA SESSILIFOLIA[1]

O. E. EDWARDS, G. FENIAK,[2] AND K. L. HANDA[3]
Division of Pure Chemistry, National Research Council, Ottawa, Canada

Received November 21, 1961

ABSTRACT

The alkaloids tuberostemonine, oxotuberostemonine, and the new base tuberostemonine-A have been isolated from the rhizomes of *Stemona sessilifolia*. Tuberostemonine has been oxidized to oxotuberostemonine and tuberostemonine-A has been related to tuberostemonine through common oxidation products. Study of transformation products of tuberostemonine has enabled assignment of partial structure V to the alkaloid.

The work of Schild (1) and a group of Japanese chemists* has resulted in an array of transformation products of the alkaloid tuberostemonine. Their efforts have indicated the presence of an N-substituted pyrrolidine, a C-ethyl group, and two γ-lactones in the molecule. In the hope of obtaining other members of this interesting group of alkaloids for complementary investigation, we examined the bases from the rhizomes of *Stemona sessilifolia* Miq. (1). However, the main alkaloid proved to be tuberostemonine, the main alkaloid of *Stemona tuberosa*,† with a much smaller quantity of a new base and traces of oxotuberostemonine (4).

We hence commenced a thorough examination of the reactions of the nitrogen-containing ring of tuberostemonine. Oxidation of the sodium salt of partially hydrolyzed tuberostemonine with permanganate gave, as reported earlier (1), a lactam ($\nu_{max}^{CHCl_3}$ 1677 cm^{-1}) which still contained a γ-lactone ring ($\nu_{max}^{CHCl_3}$ 1770 cm^{-1}). This analyzed correctly for $C_{17}H_{25}NO_3$ and hence had lost a five-carbon group containing one lactone ring. Since no new oxygen function other than the lactam carbonyl appeared in the C_{17} compound, the C_5 unit must have been attached to one of the carbons α to the nitrogen. The formation of *l*-methylsuccinic acid was observed during an analogous oxidation (1, 2), suggesting that this represented the C_5 unit lost.

Further insight into the nature of the C_5 unit came from a dehydrogenation of the pyrrolidine ring. We were able to obtain an approximately 40% yield of the previously described bisdehydro compound by silver oxide oxidation of tuberostemonine (1, 5). The ultraviolet spectrum (λ_{max}^{EtOH} 236 mμ (ϵ 9200)), the positive Ehrlich test (1), and coupling with diazonium salts were all consistent with this being a pyrrole. We were able to confirm Schild's observation (1) that this underwent hydrogenolysis involving 1 mole of hydrogen, to give an acid. The latter was characterized for the first time. The hydrogenolysis and formation of the C_{17} lactam require that the pyrrole ring and one lactone have the relationship expressed in I.

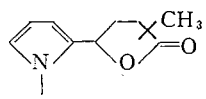

I

[1]*Issued as N.R.C. No. 6676.*
[2]*National Research Council Postdoctorate Fellow.*
[3]*Visiting scientist under Colombo plan sponsorship.*
**See reference 2 for a summary of the observations of the ITSUU group.*
†*See reference 3 for a review of isolation studies and early work on tuberostemonine.*

Examination of the n.m.r. spectrum of the bisdehydro compound (Fig. 1) disclosed the presence of one vinyl hydrogen which, in view of the absence of evidence for the presence

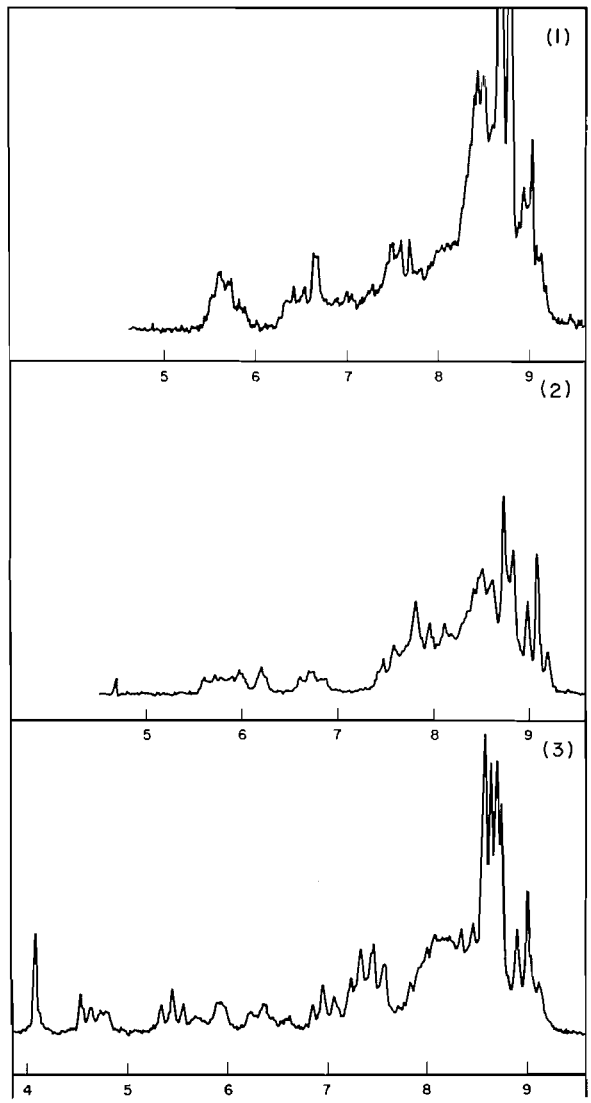

FIG. 1. The n.m.r. spectra of (1) tuberostemonine (V), (2) C_{17} lactam (III), and (3) bisdehydrotuberostemonine (II) in chloroform solution at 60 Mc/s with tetramethylsilane as an internal reference.

of a double bond in tuberostemonine, was probably on the pyrrole ring. This was confirmed by its smooth replacement with bromine on treatment with N-bromosuccinimide. The product had no vinyl hydrogen.

The pyrrole hydrogen had a chemical shift (τ 4.1)* which showed it to be on a β position on the ring (7). Finally, this hydrogen and the lactone side chain were proved to be vicinal by cyclization of the hydrogenolysis acid to give a ketone. The environment of the pyrrole ring in the bisdehydro compound could now be expanded to II, since the

**The chemical shifts are given in τ values following Tiers (6).*

methyl group n.m.r. signal was still at low field (τ 8.5) in the above ketone (Fig. 1) and the signal for the starred hydrogen in the bisdehydro compound II (τ 4.7) showed

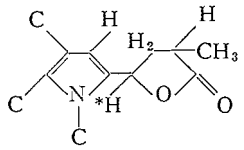

II

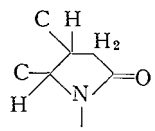

III

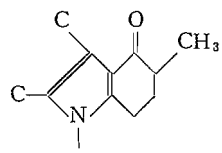

IV

complex coupling. The C_{17} lactam hence contained the structure III and the ketone structure IV.

The presence of a second C-methyl group was demonstrated by the doublet centered at τ 8.7 in the C_{17} lactam (Fig. 1) and a similar doublet at τ 8.8 in the ketone IV. From the chemical shift and relative constancy of position of this signal, the methyl group must be on the carbon α to the carbonyl, or on the one carrying the "ether" oxygen of the second γ-lactone ring. A clean triplet centered at τ 5.45 in the spectrum of the bisdehydro compound and near τ 5.2 in the spectrum of ketone IV must be due to a tertiary hydrogen on the carbon holding the "ether" oxygen of this lactone. The coupling pattern of this hydrogen and the methyl group precludes their being on the same carbon, hence the latter must be α to the lactone carbonyl. In addition the C-ethyl group observed by Kaneko (2) was discernible as an irregular triplet at τ 9.05 in the spectra of tuberostemonine and the transformation products (Fig. 1). Since its position is constant in these compounds it is not attached directly to the pyrrolidine ring in the alkaloid.

Attempts to find volatile aldehyde, acid, or ketone from mild permanganate oxidation of tuberostemonine, or volatile amine from hydrolysis of the bisdehydro compound failed. This is good but not decisive evidence that the nitrogen is common to two rings. Finally, the presence of only three hydrogen signals below τ 7.0 in the n.m.r spectrum of the C_{17} lactam requires that there is only one hydrogen on each of the carbons attached to the nitrogen. We can thus write the partial structure V for tuberostemonine. The empirical

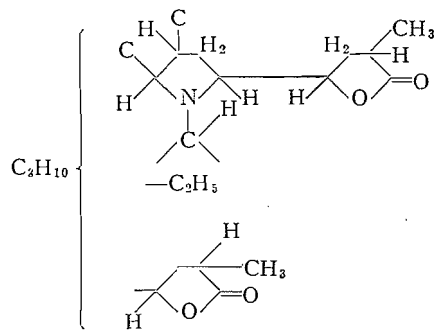

V

formula of tuberostemonine requires the presence of seven double bond equivalents, hence it contains two rings more than are present in formula V.

It seemed probable from the earlier observations (4) that oxotuberostemonine was a product of air oxidation of tuberostemonine. We have now shown that it can be produced in ca. 9% yield from tuberostemonine by mercuric acetate oxidation, thus establishing a definite connection between the two compounds. The empirical formula $C_{22}H_{31}NO_5$

showed the introduction of a double bond and an oxygen function. The infrared spectrum contained an OH stretching band (3540 cm^{-1}, $CHCl_3$) and the two lactone rings (ν_{max} 1742, 1780 cm^{-1}, mull; 1770 cm^{-1}, $CHCl_3$). It was a weak base (pK_a' 4.5 in 80% methanol), and in rough agreement with the spectrum described earlier (8), it had λ_{max}^{EtOH} 243 mμ (ϵ 8600). Its origin by mercuric acetate oxidation made it likely that it was a combined enamine and carbinolamine. The system shown,

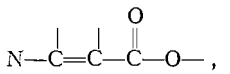

was considered incompatible with the ultraviolet absorption (λ_{max} for N,N-dialkyl-β-aminoacrylic esters (9) is 274 mμ) and the unperturbed lactone frequencies in chloroform. We hence consider oxotuberostemonine to contain the system VI. The tetrasubstituted

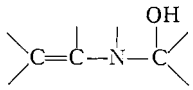

VI

character of the double bond follows from the absence of vinyl hydrogens in its n.m.r. spectrum. Although oxotuberostemonine steadily consumes permanganate in slightly acidic acetone, much of it is recovered after reduction of the equivalent of 1.5 atoms of oxygen, and very little lactam is formed. From this, and the absence of a hydrogen signal below τ 6 in its n.m.r. spectrum, we conclude that the hydroxyl is on a fully substituted carbon, as illustrated in VI.

Oxotuberostemonine is not readily dehydrated, but after 0.5 hour in refluxing acetic anhydride only 20% was recovered unchanged (see also ref. 4). The balance was neutral, and gave a positive Ehrlich test. It would not crystallize however and had different ultraviolet absorption (λ_{max} 224 mμ) from the bisdehydro compound. This seems to eliminate from consideration the arrangement of functions shown in VII.

The product of hydrolysis of oxotuberostemonine using 2 moles of alkali gave an infrared spectrum showing the presence of a little residual γ-lactone but no ketone carbonyl. We hence also eliminate VIII as a possible partial structure. Insufficient evidence is available to distinguish between the remaining possibilities.

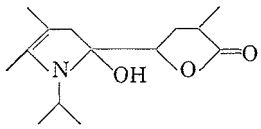

VII

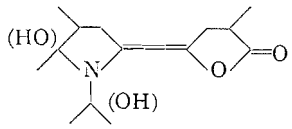

VIII

The weak basicity of oxotuberostemonine was not readily predictable on the basis of combined enamine and carbinolamine character. With no steric restriction to immonium salt formation either one alone is base strengthening (10, 11). We can only conclude that the inductive effect of one group is sufficient to destabilize the immonium salt formed from the other, i.e.,

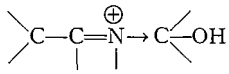

or

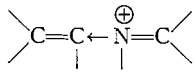

The bromo derivative mentioned above must contain partial structure IX, but the diazonium coupling product had lost one lactone group, and we hence consider it to contain partial structure X. The displacement of alkyl groups and carboxyl groups from the

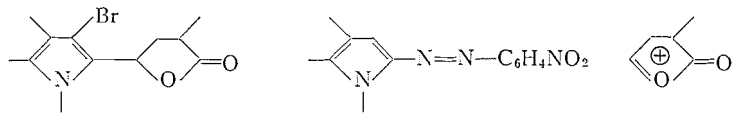

IX X XI

pyrrole ring by the diazonium ion has been reported (12). The lactone unit is probably displaced relatively easily because of a moderate stability of the oxonium ion XI.

It was found possible, after some experimentation, to produce what the Japanese workers designated as tuberostemonine (regenerated) (13) by prolonged exposure of tuberostemonine to hydrogen in the presence of platinum. This isomer of tuberostemonine gave very similar infrared and n.m.r. spectra to those of tuberostemonine, hence was probably a stereoisomer formed by a dehydrogenation–hydrogenation process. To test this we attempted to oxidize it with silver oxide in the hope that the same bisdehydro compound (II) would be obtained as from the original base. However, it proved inert to the reagent. Permanganate oxidation of the sodium salt gave a C_{17} lactam different from that described above.

From the mother liquors remaining from crystallization of tuberostemonine we were able to separate, by countercurrent distribution, oxotuberostemonine and an isomer of tuberostemonine which we have called tuberostemonine-A (m.p. 118°; $[\alpha]_D$ −65° (ethanol)). By silver oxide oxidation and action of permanganate on its sodium salt the latter gave the same bisdehydro compound and C_{17} lactam respectively as tuberostemonine. It is hence epimeric to tuberostemonine at the carbon on the pyrrolidine ring carrying the C_5 lactone unit. The new base showed a mixed melting point depression with a sample of isotuberostemonine (14) (which may be a third stereoisomer of tuberostemonine) kindly provided by Dr. T. Kaneko.

EXPERIMENTAL

Isolation of the Alkaloids

Freshly ground dried root of *Stemona sessilifolia* (44 lb), obtained from Mikuni and Co. Ltd., Tokyo, was percolated at room temperature with ethanol until little alkaloid was being extracted. The ethanol was removed under reduced pressure, leaving a thick syrup. This was diluted with water, made basic with sodium carbonate, and extracted with chloroform. The residue left after evaporation of the chloroform was dissolved in 10% sulphuric acid and the solution extracted with ether, which removed neutral material. The aqueous layer was made basic with sodium carbonate and the alkaloids extracted into benzene. The benzene was distilled, then the residue dissolved in the minimum quantity of methanol. On standing at 5° C the solution deposited crystalline tuberostemonine (137 g, 0.68%). The dark brown mother liquor was concentrated and acidified with hydrochloric acid. Fourteen grams of the hydrochloride of tuberostemonine-A, m.p. 136–140°, crystallized.

The final mother liquor was concentrated, made basic, and the alkaloids extracted into ether. The residue from evaporation of the ether would not crystallize. It was adsorbed from benzene onto 600 g of silica gel and separated into benzene-eluted and chloroform-eluted fractions. These were separately submitted to countercurrent distribution between benzene and buffer of pH 3.5 (upper phase moving). After 100 transfers the benzene eluate gave 500 mg of oxotuberostemonine (tubes 70–100) and 120 mg of tuberostemonine-A, m.p. 116–118° (tubes 60–70). The chloroform eluate gave 700 mg of oxotuberostemonine (tubes 70–100) and 1.5 g of tuberostemonine (tubes 25–40). The remaining tubes yielded nothing crystalline.

Tuberostemonine

This crystallized as needles from ethanol, m.p. 86–88°. After distillation at 150°, 1×10^{-4} mm it had ν_{max}^{film} 1770 cm^{-1}.

Oxotuberostemonine

Yield 1.2 g (0.006%). It crystallized as flat, shimmering needles from methanol, m.p. 217° undepressed when mixed with an authentic sample kindly provided by Dr. T. Kaneko. It had λ_{max}^{EtOH} 243 mμ (ε 8600) and $\nu_{max}^{CHCl_3}$ 3540 cm^{-1} (OH), 1770 cm^{-1} (γ-lactone), 1685 cm^{-1} (C=C).

Tuberostemonine-A

Yield 14 g (0.07%). The hydrochloride was recrystallized to a constant melting point of 140–141°. Found: C, 61.09; H, 8.59; N, 3.18. Calc. for $C_{22}H_{34}ClNO_4.H_2O$: C, 61.47; H, 8.38, N, 3.26. It had ν_{max}^{nujol} 2400, 1780 cm^{-1}. The salt was dissolved in water, the base liberated using ammonia, and then extracted into ether. It crystallized from methanol as needles, m.p. 118–120°, with pK_a' (5.45 in 80% methanol) and $[\alpha]_D$ −65° (*c*, 1.0). Found: C, 70.06; H, 8.79; N, 3.74; molecular weight by nonaqueous titration, 371. Calc. for $C_{22}H_{33}O_4N$: C, 70.36; H, 8.86; N, 3.73; molecular weight, 375. Its ultraviolet spectrum showed only end absorption. It had $\nu_{max}^{CHCl_3}$ 1765 cm^{-1} and an n.m.r. spectrum very similar to that of tuberostemonine. A mixture of the base with authentic isotuberostemonine showed a marked depression of melting point. No other crystalline salt of tuberostemonine-A was obtained.

Tuberostemonine-A (0.20 g) was oxidized in ethanol with silver oxide from 0.75 g of silver nitrate, as described for oxidation of tuberostemonine. A solution of the product in benzene was extracted twice with 10-ml portions of 2 *N* sulphuric acid, then with water. The material remaining in the benzene was adsorbed onto 2 g of neutral alumina, activity IV. The substance eluted with benzene crystallized from methanol, giving a 32% yield, m.p. 172–174°. Found: C, 71.58; H, 8.22. Calc. for $C_{22}H_{29}O_4N$: C, 71.13; H, 7.87. This did not depress the melting point of authentic bisdehydrotuberostemonine.

Tuberostemonine-A (0.5 g) was dissolved by being heated in 50 ml of 10% aqueous potassium hydroxide. The solution was cooled to −2° and carbon dioxide bubbled through it until the pH reached 8.5. After addition of 50 ml of methylene chloride 40 ml of 2% aqueous potassium permanganate was added during 1 hour to the stirred mixture. The neutral product was isolated as described for tuberostemonine oxidation, then adsorbed from benzene onto 150 mg of neutral alumina, activity III. Benzene, benzene–chloroform (1:1), and chloroform were used to elute the material. The last two solvents gave eluates which crystallized from acetone–heptane. Yield 25 mg, m.p. 127–130°. This did not depress the melting point of the C_{17} lactam from tuberostemonine.

Mild Permanganate Oxidation of Tuberostemonine

During a period of an hour, 75 ml of 4% aq. potassium permanganate was added to a stirred solution of 0.61 g of tuberostemonine in 20 ml of 5% aq. acetic acid. A gentle stream of nitrogen was passed through the mixture, and the effluent gas was passed through 2,4-dinitrophenylhydrazine reagent. There was no evidence of hydrazone formation.

No significant quantity of volatile acid was formed during an oxidation similar to the one described above in which phosphoric acid was used in place of acetic acid. (The pH was maintained at 5–7 during the course of the reaction.)

Oxidation of Tuberostemonine with Alkaline Potassium Permanganate

A mixture of 1.00 g of tuberostemonine (m.p. 82–84°) and 50 ml of 10% aq. potassium hydroxide was stirred and heated to reflux in an atmosphere of nitrogen until it was homogeneous. It was cooled in ice and a stream of carbon dioxide was passed through until the pH was between 9 and 10. Dichloromethane (50 ml) was added, the temperature was adjusted to −1°, and during a period of 45 minutes a total of 80 ml of 2% aq. potassium permanganate was added to the vigorously stirred mixture. The reaction mixture was made acid to Congo red by the careful addition of 10% aq. sulphuric acid, and sulphur dioxide was passed through until the manganese dioxide had dissolved. The organic layer was separated and the aqueous layer was extracted with dichloromethane (3×25 ml). The combined extracts were washed with water (2×25 ml), 2% aq. sodium carbonate (2×25 ml), and again with water (2×25 ml). They were filtered through anhyd. sodium sulphate and concentrated under reduced pressure. The residual viscous yellow oil (0.32 g) was chromatographed on neutral alumina, activity III. The fractions eluted with benzene–chloroform were crystallized from acetone–heptane, giving 0.165 g, m.p. 129–133°. This material seemed to be solvated; after it was distilled at 145° and 10^{-3} mm pressure, it melted at 139–141.5°; $[\alpha]_D$ −72° (*c*, 1.53 in $CHCl_3$); $\nu_{max}^{CHCl_3}$ 1770, 1677 cm^{-1}. Found: C, 70.05; H, 8.54; N, 4.87. Calc. for $C_{17}H_{25}NO_3$: C, 70.08; H, 8.65; N, 4.81.

Bisdehydrotuberostemonine

Freshly precipitated silver oxide from 7.5 g of silver nitrate was washed free of alkali and then washed with ethanol. Tuberostemonine (2 g) was dissolved in 100 ml of ethanol, then 20 ml of water was added. The silver oxide was added to this, and the suspension stirred in a nitrogen atmosphere for 12 hours. After filtration the solvent was removed under reduced pressure. The residue was dissolved in 100 ml of benzene, then the base extracted into two 20-ml portions of 3 *N* sulphuric acid. The benzene layer was washed with water, dried, and distilled, leaving 1.3 g of residue. This was adsorbed onto 6 g of alumina, activity IV. The material eluted with benzene was recrystallized from methanol three times, giving 0.8 g (40%) of bisdehydro compound, m.p. 172–174°. It had λ_{max}^{EtOH} 236 mμ (ε 9200).

Diazo Coupling of Bisdehydrotuberostemonine

A slight excess of *p*-nitrophenyldiazonium chloride was added dropwise to a stirred solution of 0.093 g of bisdehydrotuberostemonine in 10 ml of glacial acetic acid at 15° during 30 minutes. It was filtered and the filtrate was diluted with an equal volume of water. The resulting voluminous precipitate was collected by

filtration, washed well with water, and triturated with ethanol (2×5 ml). The amorphous brick red solid began to darken at 160° and decomposed at 166°. $\lambda_{max}^{CHCl_3}$ 471 mμ, ν_{max}^{nujol} 1757, 1602, 1588, 1517 cm^{-1}. Found: C, 64.95; H, 6.47; N, 13.19. Calc. for $C_{23}H_{26}N_4O_4$: C, 65.38; H, 6.20; N, 13.26.

Hydrogenation of Bisdehydrotuberostemonine

Bisdehydrotuberostemonine (0.131 g) was hydrogenated in ethanol over 30% palladium on charcoal at room temperature and atmospheric pressure. The uptake of hydrogen was 8.9 ml during 30 minutes. The catalyst was removed by filtration and the filtrate was concentrated under reduced pressure. The residue was a colorless, acidic glass; pK_a 5.7 (in 1:1 ethanol–water); λ_{max}^{EtOH} 224 mμ (ε 7600). It was analyzed as the methyl ester, which was prepared by treating it with an excess of ethereal diazomethane. The ester distilled at 170° at 10^{-3} mm; $[\alpha]_D$ +27.5° (*c*, 0.72 in $CHCl_3$); λ_{max}^{EtOH} 224 mμ (ε 7600); ν_{max}^{film} 1770, 1735 cm^{-1}. Found: C, 70.96; H, 8.34; N, 3.52. Calc. for $C_{23}H_{33}NO_4$: C, 71.29; H, 8.58; N, 3.61. The material gave a positive Ehrlich test.

Ketone IV

A solution of 0.222 g of the hydrogenated bisdehydrotuberostemonine in a mixture of 5 ml glacial acetic acid and 5 ml of acetic anhydride was allowed to stand at room temperature for 15 hours. Water (5 ml) was added, the solution was allowed to stand for an additional hour at room temperature and then was warmed on the steam bath for 5 minutes. It was diluted with 25 ml of water and extracted with benzene (4×10 ml). The benzene extracts were combined and washed with water (2×10 ml), 1% aq. sodium carbonate (until the washings were alkaline), and then again with water (2×10 ml). The benzene solution was filtered through anhyd. sodium sulphate and concentrated under reduced pressure. The tan-colored residue was recrystallized from ethanol, giving 0.135 g, m.p. 236–240°. After two additional recrystallizations from ethanol, white prisms melting at 245.5–248° were obtained; $[\alpha]_D$ +140° (*c*, 2.22 in $CHCl_3$); λ_{max}^{EtOH} 214 mμ (ε 13,500), 255 mμ (ε 10,200), 280 mμ (ε 5800); $\nu_{max}^{CHCl_3}$ 1644, 1757 cm^{-1}. Found: C, 74.18; H, 8.20; N, 4.08. Calc. for $C_{22}H_{29}NO_3$: C, 74.33; H, 8.22; N, 3.94.

Attempted Hydrolysis of Bisdehydrotuberostemonine

A mixture of 0.093 g of bisdehydrotuberostemonine, 0.084 g of anhyd. sodium bicarbonate, 0.105 g of hydroxylamine hydrochloride, and 2 ml of ethanol was heated in a sealed tube at 95° for 18 hours. The contents of the tube were cooled, made strongly alkaline with 10% aq. potassium hydroxide, and distilled to dryness. The distillate was titrated with hydrochloric acid and concentrated to dryness under reduced pressure. The infrared spectrum of the residue was identical with that of ammonium chloride.

Treatment of bisdehydrotuberostemonine with 25% ethanolic phosphoric acid in a sealed tube at 140° for 18 hours did not result in the formation of any volatile amine.

Bromination of Bisdehydrotuberostemonine

Two hundred milligrams of bisdehydrotuberostemonine was dissolved in 5 ml of dry chloroform. To this was added 100 mg of N-bromosuccinimide in 5 ml of dry chloroform. When the reagent had disappeared (starch–iodide test) the reaction mixture was washed with 2 *N* sodium hydroxide, then water. The product crystallized from methanol, giving 165 mg (64%), m.p. 120–125° (decomp.). Found: C, 58.70; H, 6.36; Br, 17.95. Calc. for $C_{22}H_{28}BrNO_4$: C, 58.53; H, 6.43; Br, 17.71. It had ν_{max}^{nujol} 1770 cm^{-1}.

Mercuric Acetate Oxidation of Tuberostemonine

Pure tuberostemonine (3 g), m.p. 86–88°, was dissolved in 20 ml of 10% acetic acid. A solution of 4 g of mercuric acetate in 40 ml of 10% acetic acid was added, then the solution warmed to 50° for ca. 5 minutes. Mercurous acetate which precipitated was collected by filtration. The residual mercuric ion was precipitated using hydrogen sulphide. After filtration the filtrate was extracted with ether but nothing was removed. The aqueous solution was made basic with ammonia and extracted with ether. The base recovered from the ether was dissolved in benzene and passed through a short column containing 4.5 g of alumina, activity IV. The benzene eluate crystallized from methanol, giving 250 mg (9%) of oxotuberostemonine, m.p. 217–218°. This did not depress the melting point of a sample of oxotuberostemonine kindly supplied by Dr. T. Kaneko. The more strongly adsorbed products did not crystallize.

Action of Acetic Anhydride on Oxotuberostemonine

A solution of 30 mg of oxotuberostemonine in 5 ml of acetic anhydride was refluxed for 0.5 hour. The solvent was removed under reduced pressure and the residue separated into neutral and basic products by distribution between benzene and 6 *N* hydrochloric acid. The 11 mg of neutral material was adsorbed from benzene on 40 mg of alumina, activity IV. Benzene eluted 7 mg of amorphous substance giving a positive Ehrlich test and having λ_{max} 224 mμ in ethanol. Its infrared spectrum ($CHCl_3$) contained only the γ-lactone band at 1760 cm^{-1} in the carbonyl region. The basic product gave 6 mg of unchanged oxotuberostemonine, m.p. 215–218°.

Oxidation of Tuberostemonine (Regenerated) with Alkaline Potassium Permanganate

The method described above for the preparation of the C_{17} lactam was used. The crude product was purified as follows. A benzene solution of the mixture was adsorbed onto a column of neutral alumina,

activity III. The fractions that were eluted with benzene–chloroform were crystallized twice from acetone–heptane and then distilled at 160° and 10^{-3} mm. The yield was 12% of the theoretical; m.p. 132–134.5°; $\nu_{max}^{CHCl_3}$ 1764, 1673 cm^{-1}. Found: C, 69.87; H, 8.39; N, 4.80. Calc. for $C_{17}H_{25}NO_3$: C, 70.08; H, 8.65; N, 4.81. A mixed melting point with the C_{17} lactam was depressed to 95–110°. The infrared spectra of the two compounds were quite different in the region between 900 and 1500 cm^{-1}.

ACKNOWLEDGMENTS

We wish to thank Mr. A. Knoll for the extractions and preliminary separations, Mr. H. Seguin for the analyses, Mr. J. Nicholson for the n.m.r. spectra, and Mr. R. Lauzon for the infrared spectra. We are grateful to Dr. T. Kaneko for reference samples.

REFERENCES

1. H. SCHILD. Ber. **69**, 74 (1936).
2. T. KANEKO. Ann. Rep. ITSUU Lab. (Tokyo), **11**, 45 (1960).
3. T. A. HENRY. The plant alkaloids. J. and A. Churchill Ltd., London. 1949. p. 766.
4. H. KONDO, M. SATOMI, and T. ODERA. Ann. Rep. ITSUU Lab. (Tokyo), **5**, 99 (1954).
5. H. KONDO, SUZUKI, and M. SATOMI. J. Pharm. Soc. Japan, **59**, 177 (1939); Chem. Zentr. **1940**, I, 1841.
6. G. D. TIERS. J. Phys. Chem. **62**, 1151 (1958).
7. R. J. ABRAHAM and H. J. BERNSTEIN. Can. J. Chem. **37**, 1056 (1959). R. J. ABRAHAM, E. BULLOCK, and S. S. MITRA. Can. J. Chem. **37**, 1859 (1959).
8. H. KONDO, M. SATOMI, and T. KANEKO. Ann. Rep. ITSUU Lab. (Tokyo), **6**, 63 (1955).
9. S. A. GLICKMAN and A. C. COPE. J. Am. Chem. Soc. **67**, 1017 (1945).
10. R. ADAMS and J. E. MAHON. J. Am. Chem. Soc. **64**, 2588 (1942).
11. O. E. EDWARDS, F. H. CLARKE, and B. DOUGLAS. Can. J. Chem. **32**, 235 (1954).
12. A. TREIBS and H. DERRA-SCHERER. Ann. **589**, 196 (1954).
13. H. KONDO, M. SATOMI, and T. KANEKO. Ann. Rep. ITSUU Lab. (Tokyo), **8**, 51 (1957).
14. H. KONDO, M. SATOMI, and T. KANEKO. Ann. Rep. ITSUU Lab. (Tokyo), **7**, 64 (1956).

ON THE MECHANISM OF DISSOLUTION OF MAGNESIUM IN AQUEOUS MAGNESIUM CHLORIDE SOLUTIONS

PART II[1]

E. J. CASEY, R. E. BERGERON,[2] AND G. D. NAGY[3]

The Defence Research Chemical Laboratories, Ottawa, Ontario

Received July 4, 1961

ABSTRACT

Measurements have been made of the effect of pressure on the rate of dissolution of Mg at pH 2.0 in two concentrations of aqueous $MgCl_2$. Over the pressure range 0.026–2.5 atmospheres, the rates in 0.3 and 3.0 molal solutions have, respectively, the pressure dependences

$$v \propto 1/P_{H_2}^{1/2} \text{ and } v \propto P_{H_2}.$$

The induction period of the reaction was studied in detail with a sensitive gas-measuring technique. Hydrogen enters the metal in the early stages, to about 1 cc per cc Mg at 27° C. Its rate of release after the specimen is dried is about five times higher than the rate at which it enters the magnesium.

X-Ray diffraction patterns of insoluble reaction products formed on the metal surface after prolonged reaction were examined. Magnesium and magnesium hydroxide are formed in both solutions, while a substantial amount of still unidentified extra solid material (not one of the hydrated hydroxy chlorides) is formed in the 3 molal solution.

A mechanism is proposed which describes the pressure measurements quantitatively and is consistent with the other known facts. It involves univalent magnesium as an essential intermediate, the rate being controlled by H_2 bubble growth through the gelatinous $Mg(OH)_2$ film, which remains on and protects the surface in 0.3 molal solution, and by bubble nucleation in 3 molal solution, in which the film is complexed away.

INTRODUCTION

In a paper a few years ago (1) we presented experimental results which showed that the corrosion of magnesium in aqueous magnesium chloride differed markedly from that in KCl and KNO_3. Although at low concentration (ionic strength <3) the initial rate of dissolution of the metal in these three salts is about the same, beyond ionic strength 3 of $MgCl_2$ the rate increases rapidly with increasing concentration and reaches a maximum value slightly before saturation. In this high-concentration region not only is the rate abnormally high but it is independent of pH and has an activation energy of 11.4 kcal, much higher than that found for dissolutions under transport control. Yet in the low concentrations the rate follows the solubility of MgO in the electrolyte, passing through a maximum value at 0.3 molal, the rates being just about the same as in KCl or KNO_3 at the same pH, and being proportional to hydrogen ion activity. The activation energy in acidic KCl was found to be 3 kcal/mole.

In both the high- and low-concentration regions the corrosion was found to be under cathodic control, the hydrogen electrode being polarized at least 1.8 volts and the magnesium about 0.4 volts.

The initial rates were measured as rates of gas evolution, and were confirmed by weight measurements in those cases in which no film was left on the surface. The measurements of volumes of H_2 evolved as a function of time all had a slight induction period, which, at the time, was ignored. The sensitivity of the measurements was about 0.1 cc.

Since the rate of dissolution of the metal in the early stages of the reaction is apparently controlled by the cathodic reactions of H_2 evolution, in the work now to be reported the

[1]*Condensed from D.R.C.L. Report No. 158.*
[2]*Present address: Labatt's Ltd., Montreal, Que.*
[3]*Present address: Department of Chemistry, University of Toronto, Ontario.*

effect of pressure on rate was measured in both high and low concentrations. The induction period was then studied with a more sensitive (~0.005 cc) gas-measuring technique and the activation energy in 0.3 molal $MgCl_2$ (i.e. in the low concentration region) accurately measured. The results have led to a better understanding of the mechanism of the early stages of the dissolution process.

EXPERIMENTAL METHODS AND RESULTS

The magnesium specimens used for the experiments were short ($\frac{1}{4}$ in.) cylinders of $\frac{5}{8}$-in. diameter, turned from commercially pure, distilled magnesium ingot obtained from Dominion Magnesium Ltd. All but one flat face was covered with stop-off lacquer. The surface to be studied was prepared as described previously (1), by being filed, etched in 0.5 *N* HCl for 1 minute, washed in distilled water, and dried on an absorbent material (Webril) immediately before introduction into the reaction chamber.

The electrolytes were prepared from reagent grade $MgCl_2$. Since it is hygroscopic, it was first dried at 80° C, the solutions were made up approximately, and the pH was adjusted to 2.0 with HCl before analysis. The final concentrations were set to 0.30 and 3.0 molal, at pH = 2.0. Samples were saturated with H_2, with O_2, with N_2, and with air, but no differences were found either in the ultraviolet spectra or the rate of reaction. Apparently the reaction proceeds fast enough at pH = 2 that any foreign gas, even if it could have an effect, is displaced by H_2.

Effects of Pressure on Rate of Dissolution

Corrosion occurred in 20-ml portions of solution in a reaction chamber thermostated at 25° C. The remainder of the apparatus (see Fig. 1)—namely the filling device and

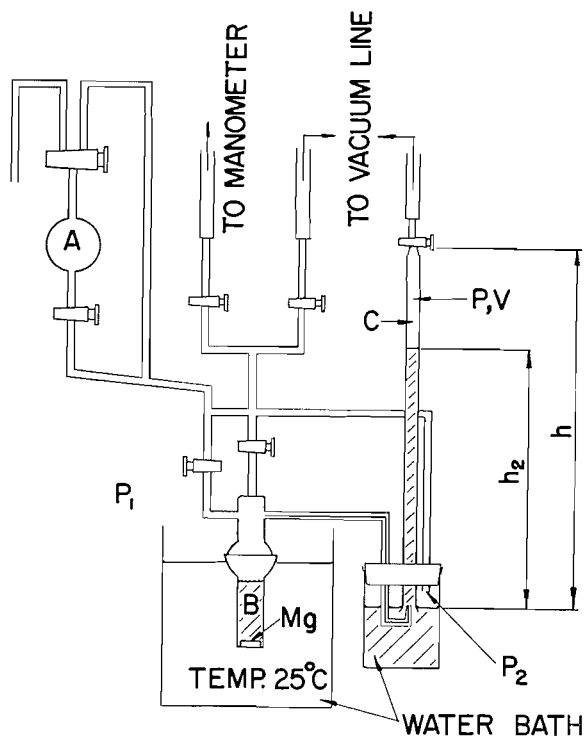

FIG. 1. Schematic diagram of apparatus used to measure rate as a function pressure. A = filling device, B = reaction chamber, C = gas collector, P_1 = atmospheric pressure.

the leads to the manifold, to the vacuum pump to the manometer, and to the gas-measuring unit—was not temperature controlled. However, the room temperature was about 25° C and since the longest test runs were not more than 2 hours, the problem of temperature deviation was not serious. In a typical run the electrolyte was added to the filling chamber A by first reducing the pressure in A and then allowing the air pressure to force liquid up and in through the tube at the left. With the stopcocks properly set, the air could be pumped from both the solution and the specimen, before the pressure at which reaction to occur was set, usually simply by admitting air. When reaction was to begin, the stopcocks under A were opened and the electrolyte flowed evenly down the delivery tube into the reaction chamber B. These cocks were then closed, the one to the manometer was closed, and collection of gas began in chamber C. The gas was collected in an inverted burette by the water displacement method, and the volume of gas collected was measured as a function of time of corrosion. The rate of gas production v'' was determined from the initial slope of the volume–time curve. In cases in which an induction period occurred, reasonably satisfactory initial rates could be obtained after the induction period was finished. The value of v'' determined by the slope of the volume–time curve at the same value of the volume for different runs was found to give reproducible results, and this method of analysis was adopted.

For the apparatus depicted in Fig. 1 a hydrostatics argument has been developed by which the rates of change of gas volume in the measuring burette ($dV^P/dt \equiv v''$) can be converted into rates ($dV^{760}/dt \equiv v'$) in terms of volume at 25° C and 1 atm pressure. Thus, it can be seen from Fig. 1 that since

$$P_2 = P + h_2/\rho$$

and

$$P = P^{\text{vap}} + P^{\text{H}_2},$$

then

$$\frac{V^{760}}{V^P} = \frac{P_2 - h_2/\rho - P^{\text{vap}}}{760}, \qquad [a]$$

where ρ is the density of mercury, and all pressures are in mm Hg, P^{vap} is the vapor pressure of water, P^{H_2} the pressure of the hydrogen gas in chamber C.

Differentiation with respect to time gives:

$$\frac{dV^{760}}{dt} = \frac{1}{760}\left[(P_2 - h_2/\rho - P^{\text{vap}})\frac{dV^P}{dt} + V^P(-dh_2/dt)/\rho\right]. \qquad [b]$$

Since

$$V^P = \pi r^2(h - h_2),$$

$$dh_2/dt = -(1/\pi r^2)dV^P/dt.$$

Letting v'' be dV^P/dt and v' be dV^{760}/dt, insertion of expressions for V^P and (dh_2/dt) into equation [b] gives

$$v' = (1/760)(P_2 - 2h_2/\rho - P^{\text{vap}} + h/\rho)v''. \qquad [c]$$

Conversions of the measured rates (v'') into the reduced rates (v') were made by means of this expression. Conversion of v' into rate v (in terms of weight of magnesium dissolved) was made assuming mole-for-mole reaction of Mg for H_2.

With the apparatus in this form (Fig. 1), it was possible to conduct experiments at atmospheric and at reduced pressures. For work at pressures greater than atmospheric it was necessary to seal off all leads from the reaction chamber, and as a result it became impossible to use the gas evolution method. Hence, at higher pressures only weight loss determinations could be obtained, and these could be relied upon only in cases where no insoluble products were accumulated on the surface over an extended period of time. For this reason measurements at higher pressures were made only in 3 molal $MgCl_2$.

The results of measurements in 0.3 molal $MgCl_2$ are contained in Table I, and the

TABLE I

Rate of dissolution at various pressures in 0.3 molal $MgCl_2$
(h = 410 mm; P^{vap} = 25 mm Hg)

P_2 (mm Hg)	$v''\times10^3$ (ml cm^{-2} sec^{-1})	h_2 (mm)	$v'\times10^3$ (ml cm^{-2} sec^{-1})	$v\times10^3$ (mg cm^{-2} sec^{-1})
758	0.174	33	0.162	0.163
	0.110	33	0.102	0.103
	0.163	33	0.151	0.152
	0.156	33	0.145	0.146
	0.148	33	0.137	0.138
	0.151	33	0.140	0.141
607	0.198	33	0.145	0.146
595	0.227	33	0.163	0.164
502	0.264	33	0.158	0.159
491	0.333	33	0.194	0.195
488	0.350	33	0.203	0.204
390	0.430	30	0.197	0.198
300	0.565	33	0.189	0.190
256	0.750	32	0.209	0.210
200	1.27	30	0.267	0.268
180	1.76	33	0.313	0.315
157	2.01	30	0.308	0.310
114	3.05	21	0.351	0.351
102	2.51	21	0.349	0.351
100	3.37	21	0.326	0.328
93	4.80	21	0.421	0.423

results of measurements in 3.0 molal $MgCl_2$ are contained in Table II. In summary, the rate (converted to mg cm^{-2} sec^{-1}) in 0.3 molal $MgCl_2$ decreases with increasing pressure; in 3.0 molal $MgCl_2$ the rate increases slightly with increasing pressure. The latter dependence is linear (Fig. 2). By contrast, a plot of log rate vs. log P for the 0.3 molal results (Fig. 3) shows

$$v \propto P^{-0.5}.$$

Examination of the Induction Period

Corrosion experiments were carried out in 46 ml of 0.3 molal $MgCl_2$. The gas-measuring apparatus was simply a horizontal capillary tube of cross-sectional area 0.04 cm^2 with a 0.5-cm Hg bubble connected to the reaction vessel by about 16 in. of fine capillary tubing with short tygon connecting tubes. The measuring device was thermostated at 27.4°±0.1° C, while the reaction vessel was in a water–glycol bath which could be thermostated to ±0.03° from 0–45° (see Fig. 4). After the surface had been prepared, the Mg sample was dropped into the electrolyte in the reaction chamber, which had previously been allowed to come to thermal equilibrium with the bath, and the connections quickly made. The first reading was usually taken about 100 seconds after the sample

TABLE II

Rate of dissolution at various pressures in 3.0 molal $MgCl_2$
(h = 455 mm; P^{vap} = mm Hg)

P_2 (mm Hg)	$v'' \times 10^3$ (ml cm^{-2} sec^{-1})	h_2 (mm)	$v' \times 10^3$ (ml cm^{-2} sec^{-1})	$v \times 10^3$ (mg cm^{-2} sec^{-1})
1790				1.90*
1350				1.82*
758	1.84	32	1.74	1.73
	2.06	35	1.94	1.93
	1.80	32	1.71	1.70
	1.71	26	1.64	1.63
	1.76	32	1.67	1.66
	1.71	29	1.63	1.62
	1.73	29	1.65	1.64 (1.63*)
500	2.74	28	1.69	1.68
380	3.71	28	1.70	1.69
	3.64	21	1.71	1.70
	3.11	23	1.45	1.44 (1.79*)
290	4.08	23	1.42	1.41
248	5.80	19	1.74	1.73 (1.62*)
200	7.26	31	1.56	1.55
100	14.7	15	1.67	1.66
	14.4	13	1.69	1.68
	14.2	13	1.67	1.66
91	13.5	15	1.40	1.39
	15.5	9	1.36	1.75
	14.5	15	1.44	1.43
				1.49*
65	24.1	15	1.63	1.62
				1.59*
23				1.57*

*Initial rate determined by weight loss method.

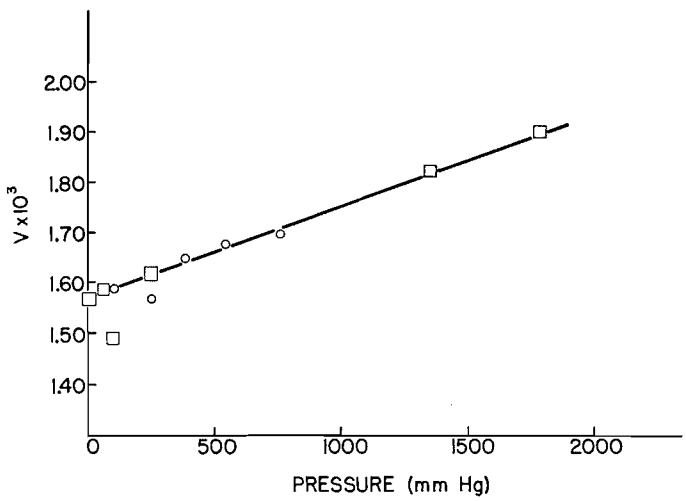

FIG. 2. Dependence of rate on pressure in 3.0 molal $MgCl_2$ (pH 2.0, 25° C): ○ from gas evolved, □ from weight loss.

had hit the electrolyte. Since the mercury bubble sometimes stuck, the capillary was tapped sharply a few times before a reading until the equilibrium position was reached. Since the bubble position in the capillary could be read to ±0.02 cm, the sensitivity was about 0.001 cm, but being limited by temperature control, was found to be reliable to about ±0.005 cc.

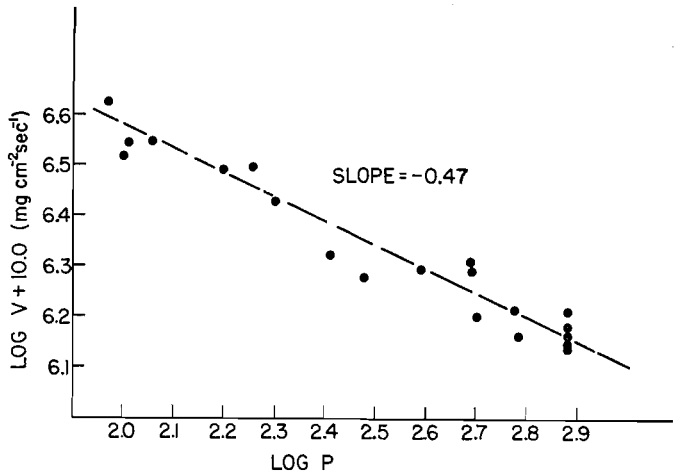

FIG. 3. Dependence of rate on pressure in 0.3 molal $MgCl_2$ (pH 2.0, 25° C).

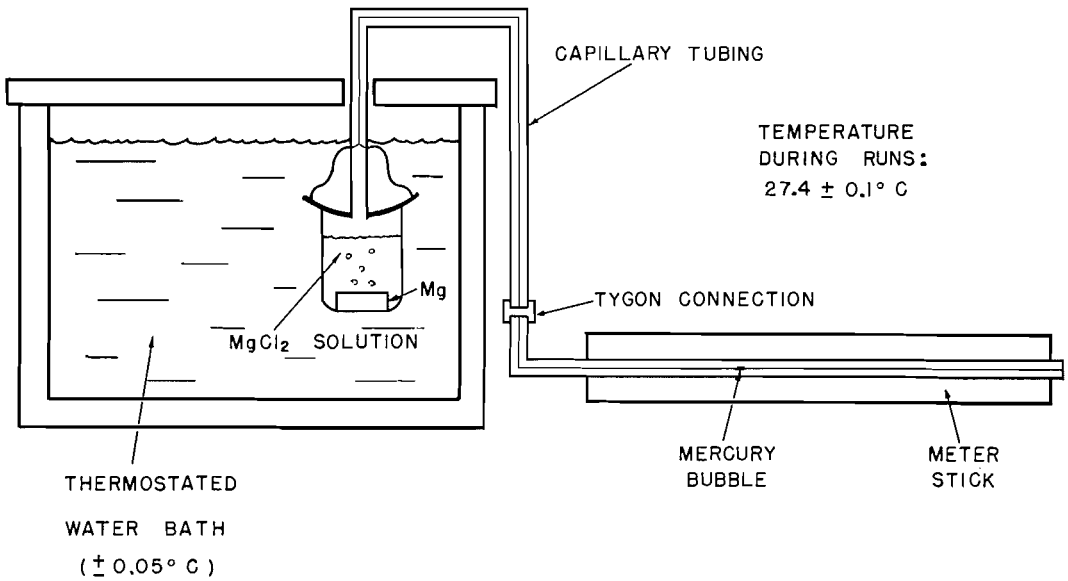

FIG. 4. Schematic diagram of capillary tube apparatus for studying induction period.

Figures 5 and 6 show typical results obtained at 0, 12, 18, 25, 30, 35, and 45°. Below 35° the "induction period" was usually, but not always, linear, and its slope (v_1) easily distinguished from the "true" rate (v). The break from v_1 to v occurs at a value of volume evolved which decreases with increasing temperature.

The rates at various temperatures are collected in Arrhenius plots in Figs. 7(*a*) and 7(*b*) (a duplicate set of experiments with fresh materials), from which the activation energy for both v_1 and v is seen to be 12.2 ± 0.6 kcal/mole. This fact is an indication that the rate-controlling step of the induction period is not different from that of the main corrosion period. In fact it was next shown that during the induction period hydrogen

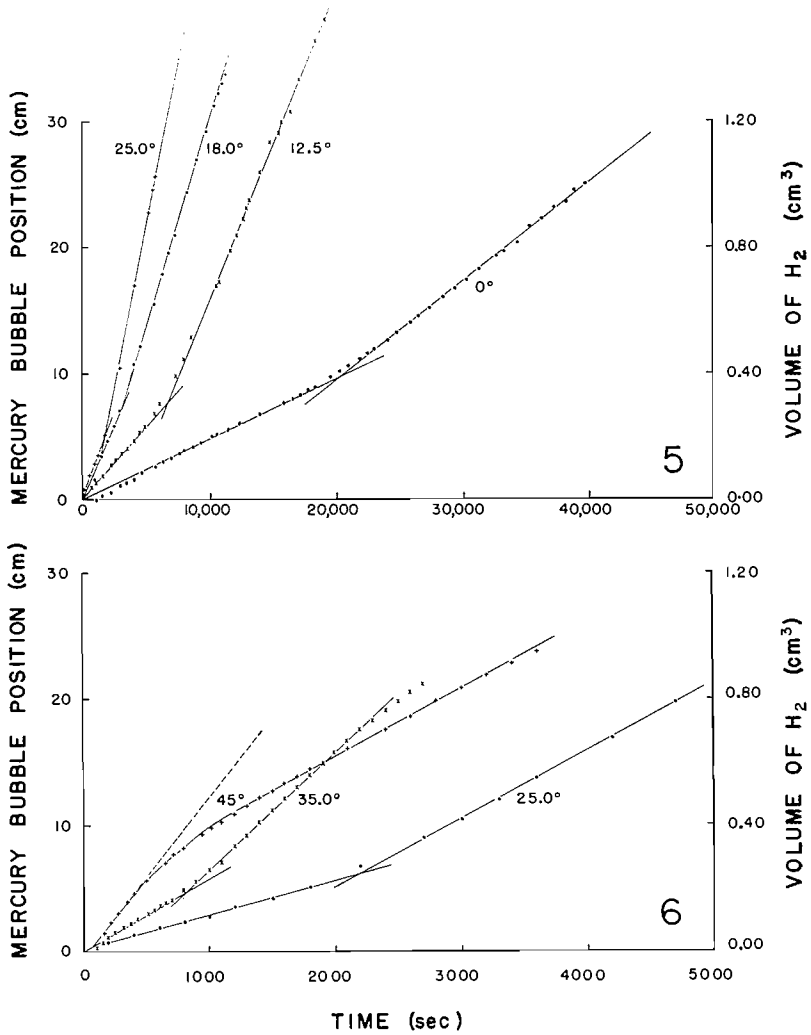

FIG. 5. Typical results of volume measured as function of time, at 0°, 12°, 18°, 25° C.
FIG. 6. Typical results of volume measured as function of time, at 25°, 35°, 45° C.

gas enters not only the electrolyte but also the metal itself to a rather astonishing amount, approximately 1 cc H_2 per cc Mg at 27°. The experimental procedures are described in the remainder of this section.

As a preliminary a *fresh* Mg specimen was allowed to react in *fresh* electrolyte to beyond the break from v_1 to v. Thus *used*, the specimen was then allowed to react in *fresh* electrolyte and the *used* electrolyte fitted with a *fresh* specimen of Mg. In the latter case the solution had been already saturated with H_2 from the preliminary part of the experiment. However, the results consistently showed the rate to be less than the final rate of the preliminary experiment (for example, see Fig. 8).

Optical stereomicroscopic examination of a used specimen, following rapid washing and dehydration in absolute alcohol and mounting under degassed mineral oil, disclosed the liberation of gas bubbles from the magnesium, rapidly at first and then more slowly,

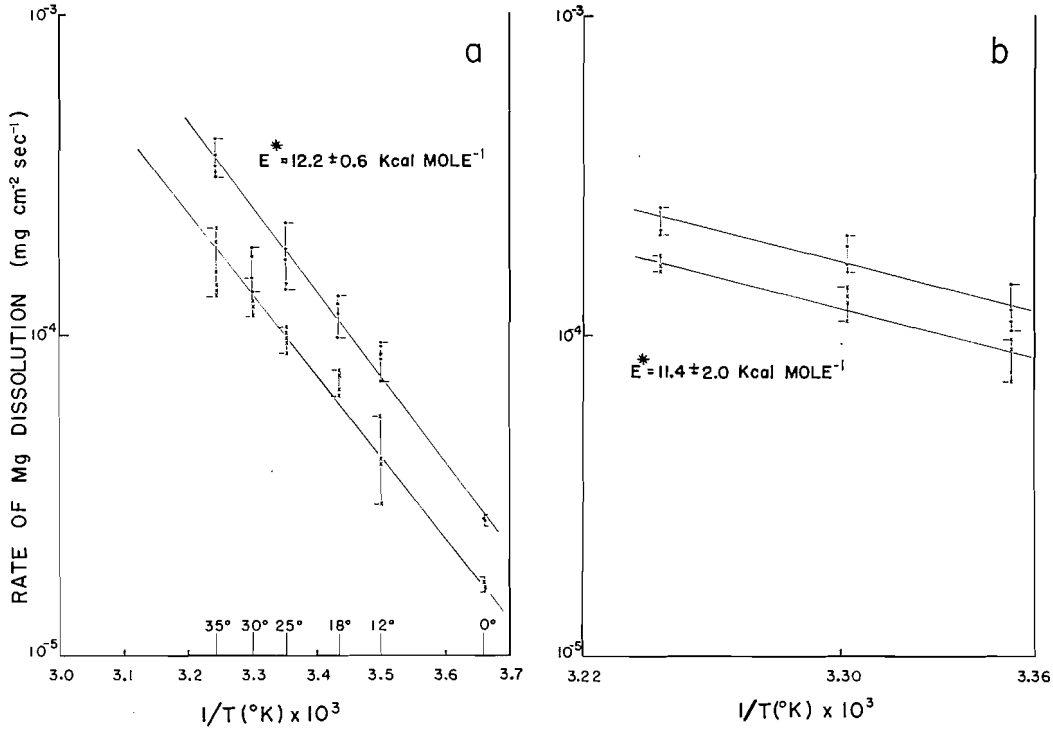

FIG. 7. Arrhenius plots for rate as function of temperature for 0.3 molal $MgCl_2$ solutions: (*a*) No. 1, (*b*) No. 2. Upper curve v; lower curve v_i; pH 2.0.

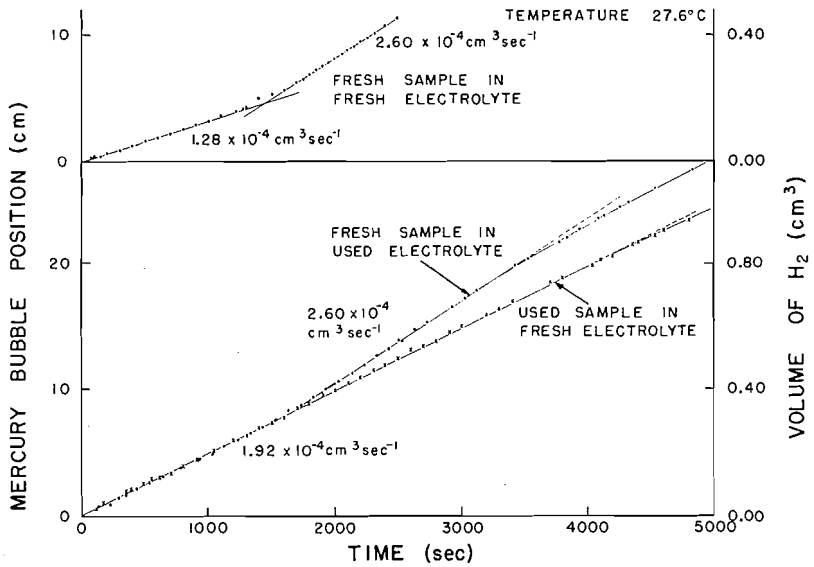

FIG. 8. Dissolution of freshly prepared magnesium in electrolyte already saturated with hydrogen; and dissolution of H_2-saturated magnesium in fresh electrolyte.

but continuing over several hours. At the same time, there was no indication that hydrogen had been stored in the plastic which coated the magnesium.

Figure 9 shows the results of measurement of the gas liberated at 27.6° C from a specimen corroded at the same temperature. Following the corrosion step, the specimen

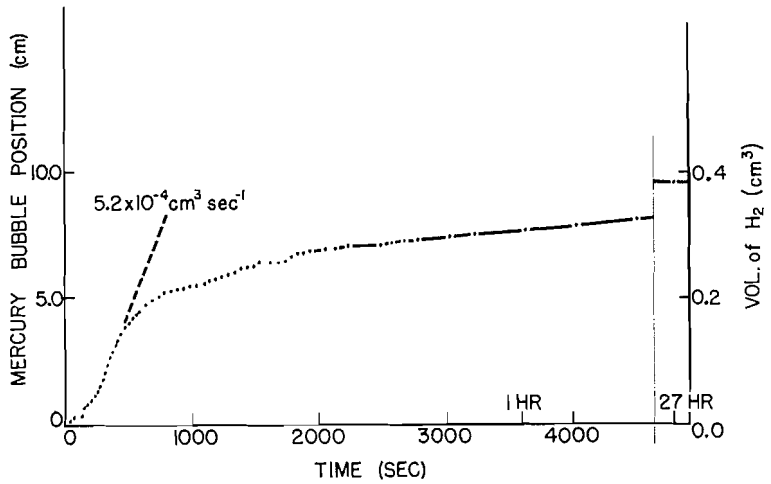

FIG. 9. Liberation of hydrogen stored in magnesium during corrosion in 0.3 molal $MgCl_2$. Volume vs. time after drying in cold absolute alcohol and mounting, under CCl_4, in small capillary measuring apparatus at 27.6° C.

(area 1.14 cm^2, 0.4 cm high) was washed with distilled water for 5 seconds at room temperature, then in cold (−20° C) absolute alcohol for 40 seconds before being mounted in the measuring chamber under 20 ml of CCl_4. Experience had shown that CCl_4 could be used to prevent O_2 from reaching the active surface, to float away any residual water contained in cracks and fissures, and yet to assist the release of gas bubbles as soon as they formed on the surface. Any side reaction adversely affects the measurement; for example, under absolute alcohol, a slow but detectable corrosion of Mg continued for hours and was measured superimposed on the stored H_2 which was being released. The possibility that some of this prolonged H_2 production is due to acid forced into cracks and fissures and not removed by the alcohol wash cannot be ruled out.

In the example considered in Fig. 9, v_i was 1.16×10^{-4} cm^3/sec and v was 2.38×10^{-4}. The break occurred at about 1500 seconds. If it is assumed that the difference is the rate at which H_2 penetrates the magnesium, it can be calculated that 0.18 cc is lost to the Mg sample in the induction period, and remains there during the steady state of the dissolution process. However, the measured value of the amount released was 0.38 cm^3. The difference is presently assumed to be that which entered during the preparation of the sample. (It will be recalled that the sample was etched for 1 minute in 0.5 *N* HCl prior to the dissolution experiment with a possible small contribution from acid left in the fissure.) The initial rate of escape of H_2, following a short induction period (which must exist because the Mg entered the chamber directly from alcohol at −20° C), was 5.2×10^{-4} cm^3/sec, nearly five times the rate at which it entered during corrosion in the aqueous $MgCl_2$.

Absorption and X-Ray Diffraction Spectra

The X-ray diffraction spectrum was taken of each of several samples of the product built up by extended reaction of Mg with $MgCl_2$ solutions. Spectra formed by precipitation reactions were taken for comparison. Table III lists lattice spacings obtained from reaction in 0.3 and in 3.0 molal $MgCl_2$.

TABLE III

Lattice spacings (Å) for corrosion products

Mg	Reaction Mg + 0.3 molal $MgCl_2$	$Mg(OH)_2$	Reaction Mg + 3.0 molal $MgCl_2$	Mg(OH)Cl
			11.6 W^+	
			5.80 S	5.75 (100)
	4.77 S	4.76 (80)	4.83 S	
	4.19 W		4.17 S^-	
			3.80 W	
			3.39 W	
			2.97 W	
				2.84 (20)
2.77 (30)	2.72 W		2.72 W	2.76 (40)
2.60 (25)			2.64 W^+	
2.45 (100)	2.42 S^+		2.44 S	
	2.36 S^+	2.37 (100)	2.38 S	
			2.20 W^-	2.22 (28)
			1.98 M^-	1.92(3); 2.04 (8)*
1.90 (20)				
	1.80 M	1.79 (80)	1.80 M	1.87 (8)
				1.68 (36)
1.60 (20)	1.60 M^+	1.57 (70)	1.57 M	1.60 (8)
			1.55 W^-	
1.47 (20)	1.50 M^-	1.49 (60)	1.50 W	
				1.43 (8)
1.38 (18)	1.38 W	1.37 (60)	1.38 W^-	
1.34 (13)				
1.30 (3)	1.31 W	1.31 (60)	1.32 W	1.33 (4)
1.23 (3)				
1.18 (3)	1.19 W	1.18 (50)		
1.08 (3)				
1.03 (7)		1.03		
		1.01		

*Two ASTM cards.

The product formed in 0.3 molal $MgCl_2$, after being scraped from the surface, washed, dried, and mounted on a quartz fiber under vaseline, had a spectrum which was attributable to $Mg(OH)_2$ plus a small amount of Mg metal.

The product formed in 3 molal $MgCl_2$ was more difficult to handle, being hygroscopic, but, after desiccation at 25° and mounting, gave a spectrum which contained at least two components. One was definitely $Mg(OH)_2$. None of the reported spectra of the hydrated magnesium hydroxy chlorides (2), either singly or superimposed, could account for the rest of the spectrum, although three of the five most prominent lines said* to be characteristic of Mg(OH)Cl appear, and this material may be a second part of the product. If so, a third part is still unidentified. The two prominent spacings of the remainder are at 11.6 and 4.17 Å, the former indicating a heavily hydrated, very basic hydroxy chloride.†

Before and after certain corrosion experiments ultraviolet absorption spectra were taken on solutions saturated with N_2 or O_2 or air. If oxygen was present, the characteristic absorption of OCl^- at 3800 Å was present, but its presence did not seem to have any effect on rate of H_2 evolution.

*ASTM cards. However, Bianco (Ann. de Chim. **3**, 370 (1958)) more recently ascribes this spectrum to be anhydrous $Mg_2(OH)_3Cl$.

†See Y. Bianco, Ann. de Chim. **3**, 370 (1958), for recent X-ray and chemical analyses of hydroxychlorides; and P. M. de Wolff and L. Walter-Lévy, Acta Cryst. **6**, 40 (1953), for spectrum and structural analysis of the most common hydrate, $Mg_2(OH)_3Cl.4H_2O$.

DISCUSSION

A Mechanism Which Describes Pressure Measurements

The simplest formulation which, in principle, describes the results obtained at low concentration is the following:

$$Mg + H^+ \underset{k_{-1}}{\overset{k_1}{\rightleftharpoons}} Mg^+ + 1/2H_2, \qquad \text{fast} \qquad [1]$$

$$Mg^+ + H_2O \xrightarrow{k_2} Mg^{++} + 1/2H_2 + OH^-, \qquad \text{slow} \qquad [2]$$

for which a steady-state argument readily shows:

$$v = \frac{C_1[H^+]}{P_{H_2}^{1/2} + C_2},$$

where

$$C_1 = \frac{k_1 k_2}{k_{-1}}[H_2O][Mg] \text{ and } C_2 = \frac{k_2}{k_{-1}}[H_2O].$$

Further, if reaction [1] is in labile equilibrium, i.e. if $k_{-1} \gg k_2$,

$$v = C_1 \frac{[H^+]}{P_{H_2}^{1/2}}.$$

A more explicit mechanism, which is easy to envisage, and which does not differ in principle with the one above, is the hydrogen molecule–ion mechanism illustrated in Fig. 10 and described below:

$$Mg + H_2O = MgOH_{2\,ads} \qquad \text{fast} \qquad [1a]$$

$$MgOH_{2\,ads} + H^+_{ads} \underset{k_{-2}}{\overset{k_2}{\rightleftharpoons}} MgOH_{ads} + H_2^+{}_{ads} \qquad \text{fast} \qquad [1b]$$

$$MgOH_{ads} + H^+_{ads} \xrightarrow{k_3} MgOH^+ + 1/2H_2 \qquad \text{slow} \qquad [2]$$

or $MgOH_{soln}$

$$2H_2^+{}_{ads} \underset{k_{-4}}{\overset{k_4}{\rightleftharpoons}} H_{2\,gas} + 2H^+_{ads}. \qquad [3]$$

From this it follows, as before, from a steady-state argument that

$$v = \frac{C_3[H^+]}{P_{H_2}^{1/2} + C_4},$$

where $C_3 = K_1(k_2/k_{-2})k_3K_4[Mg][H_2O]$; $C_4 = k_3(K_4/k_{-2})$; and $K_4 = k_4/k_{-4}$. Similar to the first case, if equilibrium obtains in reaction [2] (i.e. if $k_{-2} \gg k_3$), then:

$$v = \frac{C_3[H^+]}{P_{H_2}^{1/2}}.$$

Note that in this model the rate decreases with increasing P_{H_2} because of the increase in the number of adsorbed H_2^+ ions which react with and reduce the steady-state concentration of $MgOH_{ads}$. Thus the rate is controlled by the concentration of hydrogen molecule–ions adsorbed on the surface.

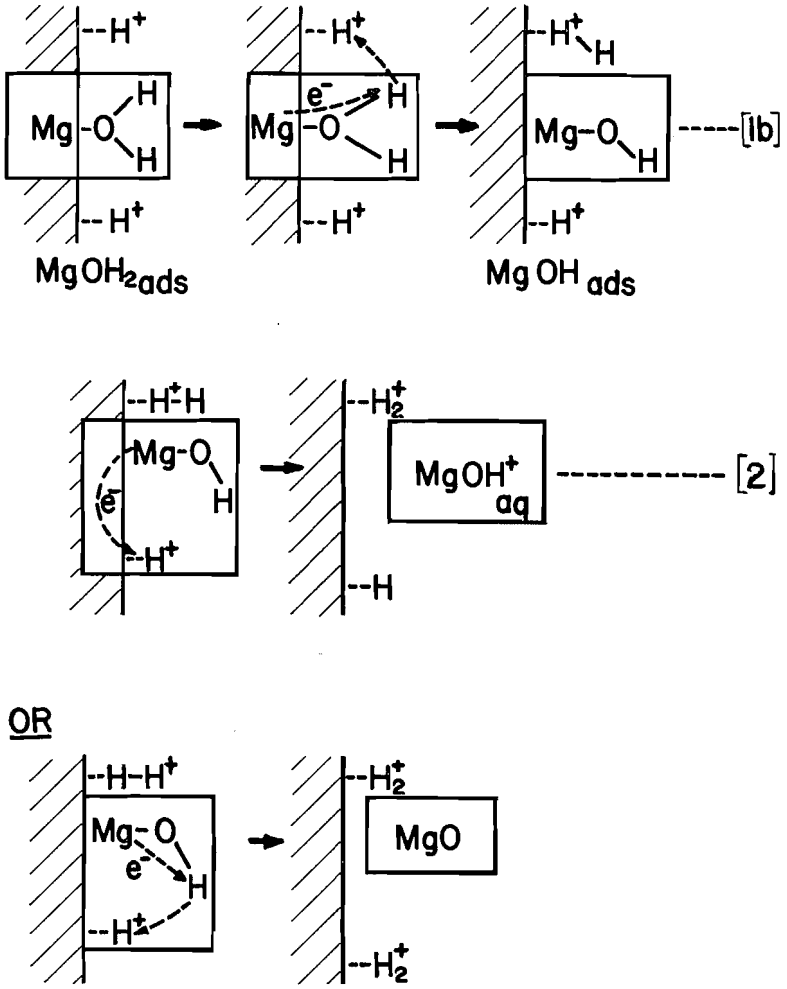

FIG. 10(*a*). Pictorial representation of reactions [1*b*] and [2].

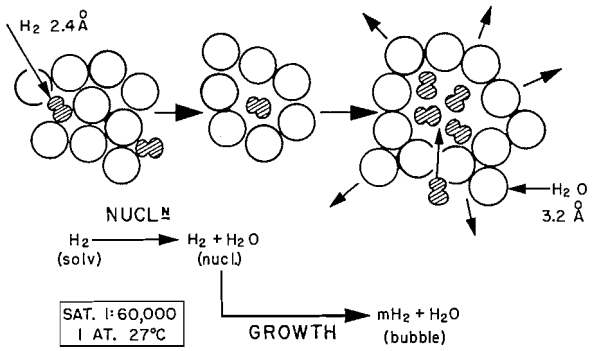

FIG. 10(*b*). Bubble formation.

Now consider the steps of reaction [3]:

$$2H^+_{2\,ads} = H_{2\,ads} + 2H^+ \qquad [3a]$$

$$H_{2\,ads} + nH_2O = H_{2\,aq} + S \text{ (S=surface site)} \qquad [3b]$$

$$S + H_{2\,aq} \underset{\text{collapse}}{\overset{\text{nucleation}}{\rightleftharpoons}} N + nH_2O \qquad [3c]$$

$$mN \underset{}{\overset{\text{growth}}{\rightleftharpoons}} \text{bubble} \qquad [3d]$$

$$\text{bubble} = H_2 \text{ gas.} \qquad [3e]$$

If the growth step, reaction [3*d*], is slow because of the high viscosity of the medium, say, then step [3*c*] is in equilibrium. Then reaction [3] is in equilibrium, and the derived rate $v \propto [H^+]/P_{H_2}^{1/2}$ applies. This is the observed fact in the dissolution of Mg in the low-concentration region (0.3 molal $MgCl_2$, pH = 2.0).

If, however, the growth step is rapid, step [3*d*] is not in equilibrium; and the rate is limited by the rate of nucleation [3*c*]. Then $v \propto P_{H_2}$, independent of $[H^+]$. This is the result obtained in the high-concentration region (3.0 molal $MgCl_2$, pH = 2.0).

Whether [3*d*] or [3*c*] is the slowest step in the hydrogen removal process, the elementary process—viz. H_2 molecule entering the elementary gas pocket—is the same; this is consistent with the fact that activation energy for the overall process is the same in both cases, about 12 kcal/mole.

A Further Test: Effects of X Irradiation on Rate

The subtle difference between equilibrium (0.3 molal) and lack of it (3 molal $MgCl_2$) in reaction [3*c*] has fostered the notion that any experimental variation which would disturb slightly the amount of adsorbed hydrogen molecule-ions in the steady state should affect the rate in the first case but not the second. Hence, corroding specimens in both solutions were subjected to 300 kv X rays and to a magnetic field of 15,000 gauss.

Ionizing radiation is now well known* to lead to increased adsorption of H atoms on noble metal surfaces provided they are at a potential positive to that of the hydrogen electrode. In the present case the potential is about 1.8 volts negative, and photodesorption would be anticipated. A result of photodesorption of H_2^+ ions would be (see reaction [1*b*]) increased concentration of $MgOH_{ads}$, and hence increased rate of dissolution for the case in which bubble growth is rate determining. Figure 11 is a composite of six experiments in which the specimen and reaction chamber were irradiated with X and gamma rays. The lower curve shows that the rate in 0.3 molal $MgCl_2$ is increased during irradiation by X rays and that the rate returns to the normal value after irradiation has ceased. The upper curves show not only that the irradiation must be very intense before the rate in 3 molal $MgCl_2$ is affected, but also the important fact that the rate remains enhanced after irradiation has ceased. After 3 Mev gamma irradiation, the solution gave strong visible and ultraviolet absorptions due to Cl_2 and OCl^- and perhaps some H_2 was produced by γ-ray absorption; but it is difficult to understand how either of these could enhance the rate after the radiation had ceased. It seems more probable that the absorbed radiation induced faults in the metal which enhanced subsequent nucleation of bubbles on the "activated" surface.

The effect of a 15,000 gauss magnetic field was explored for a slightly different reason. Since the postulated intermediates, Mg^+ and H atom, are both paramagnetic because of an unpaired electron, our analysis suggests that the rate might be altered in 0.3 molal $MgCl_2$, where rate $\propto [MgOH_{ads}]$, but not in 3 molal $MgCl_2$, where nucleation is rate determining.

After proper temperature control of the reaction chamber (when placed between the poles of the electromagnet) had been achieved, several experiments were done at both

*See I. Henderson, E. G. Lovering, R. L. Haines, and E. J. Casey, Can. J. Chem. **37**, 164 (1959); and F. S. Feates, Trans. Faraday Soc. **56**, 1671 (1960), for discussion and references to earlier work, particularly that of Veselovsky et al. in the period 1954–1956.*

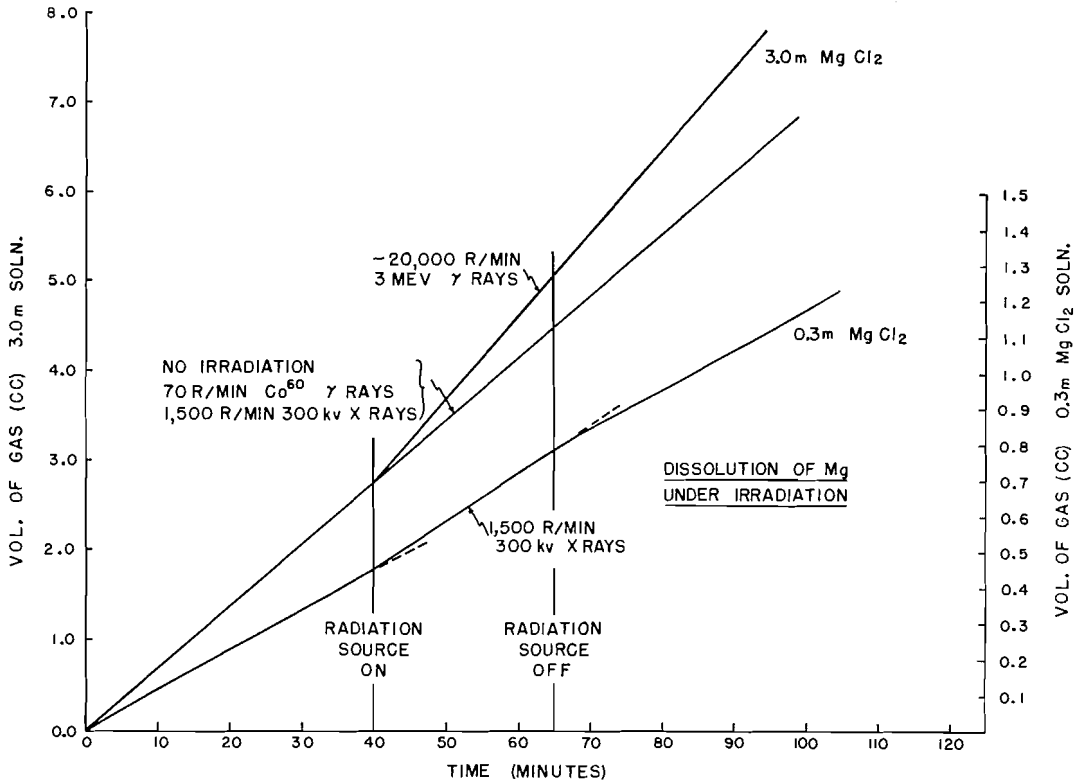

FIG. 11. Effect of X rays on rate of dissolution.

27° and at 1.5°. However, each experiment turned up a new difficulty, and sufficient sensitivity had not been achieved when the magnet had to be returned to its normal use. An indication of increased rate in 0.3 molal $MgCl_2$ was obtained, but the effect was not reliably demonstrated, and more work needs to be done.

Some Peculiarities of the Induction Period

If the rate following the induction period is the true initial rate of dissolution, then a fraction of the hydrogen liberated is not being measured in the early stages. The amount of H_2 needed to saturate 46 cc of distilled water at 27° is calculated, from the solubility, to be 0.6 cc. Because the gas is salted out by 0.3 molal $MgCl_2$, the solubility in the electrolyte would be much less, and can be estimated from the activity to be <0.1 cc. No pertinent solubility data could be found reported in the literature.

The induction period is not always linear, but is sometimes more or less sigmoid, as if it were an adsorption curve. Actually the induction probably is due to two processes: the sorption of gaseous hydrogen in small pores and crystal defects in the magnesium, and the "pouring" of two-dimensional liquid (i.e. adsorbed) hydrogen from the reaction surface into the larger cracks and fissures. It is currently assumed that "liquid pouring" predominates when the induction period is linear and that gas adsorption predominates when the induction period is sigmoid. The measured rate during the induction period v_i is the difference between the true rate v and the superimposed "storing" rates: (*a*) the "liquid" pouring rate, $v_{Mg}^{H_2\ liq}$; (*b*) the gas adsorption rate, $v_{Mg}^{H_2\ gas}$; and (*c*) the rate of solution of H_2 in the electrolyte, $v_{soln}^{H_2\ gas}$. Thus:

$$v_i = v - [v_{Mg}^{H_2\ liq} + v_{Mg}^{H_2\ gas}] - v_{soln}^{H_2\ gas}.$$

Figure 8 also shows (the result typical of triplicate experiments) that

$$v_{soln}^{H_2\ gas} \cong v_{Mg}^{H_2},$$

where

$$v_{Mg}^{H_2} = [v_{Mg}^{H_2\ liq} + v_{Mg}^{H_2\ gas}],$$

and discloses further the rather puzzling indication that a magnesium sample presaturated with H_2 corrodes in fresh electrolyte at a *constant* and significantly lower rate, as though the fresh electrolyte cannot receive hydrogen at any appreciable rate unless some of it at the same time penetrates the metal.

Other Comments on the Proposed Mechanism

The postulates concerning mechanism raise interesting questions about the nature of the activated complex in the gas liberation process. An analysis has been done which shows that the inverse half-power dependence of rate on pressure is mathematically consistent with a very large value (11.7 liters/mole, STP) for the volume of activation defined by absolute rate theory. This value seems intuitively to be of the right order of magnitude for a H_2 molecule divesting itself of water and pushing back water molecules as it forms the nucleus of a gas bubble. Yet, since the energy required to make a hole the size of a water molecule is approximately equal (4) to the latent heat of vaporization (10.4 cal/mole for pure water), and since the activation energy was found to be 12.2 cal/mole, the radius of the activated complex must be just a few angstroms. However, from the Kelvin equation derived in a form suitable to express surface energy as a function of radius of a bubble, and the volume of activation, the radius of the stable bubble nucleus can be estimated to be about 2×10^{-4} cm. This value can be compared with the estimate of Plesset *et al.* (3) of 10^{-3} cm obtained from a different approach; this riddle about the nature of the early stages of bubble formation has not been solved.

It is now well established (5) that the overvoltage for hydrogen evolution increases with decreasing hydrogen pressure. However, increased rate of hydrogen evolution with increased hydrogen pressure, as was found in the studies in high $MgCl_2$ concentration, is uncommon. The only other case of which we are aware is inferred to have existed in the experiments of Webb and Linford (6). They measured current efficiencies of electroplating of copper. The values of hydrogen evolution rate at different pressures are replotted in Fig. 12, and show that the rate increased with increased pressure. Common to their results and to ours are the conditions of very high overpotential ($\sim$1.8 volts in our case!) and continued renewal of surface.

Figure 10 depicts a mechanism by which Mg can leave the metal as either Mg^+ or Mg^{++}. Either is possible in our experiments, because the essential feature of the proposed mechanism is only that $v_{[1b]} \gg v_{[2]}$. However, in anodic dissolution in which external current flows, there is much controversial evidence* concerning whether the ion leaves the surface as Mg^+ or as Mg^{++}, or as both simultaneously: the number of coulombs passed to effect a given weight loss may vary by a factor of 2. The work described in this report throws no light on the anodic problem *per se*, although it does provide the following alternative mechanisms: the second electron from $MgOH_{ads}$ has the alternative of passing into the metal, leaving $MgOH^+$ (i.e. divalent magnesium) to desorb; or $MgOH_{ads}$ can itself desorb (i.e. as univalent magnesium) and reduce water by electron transfer out in the solution.

**For discussion of this question see reference 7.*

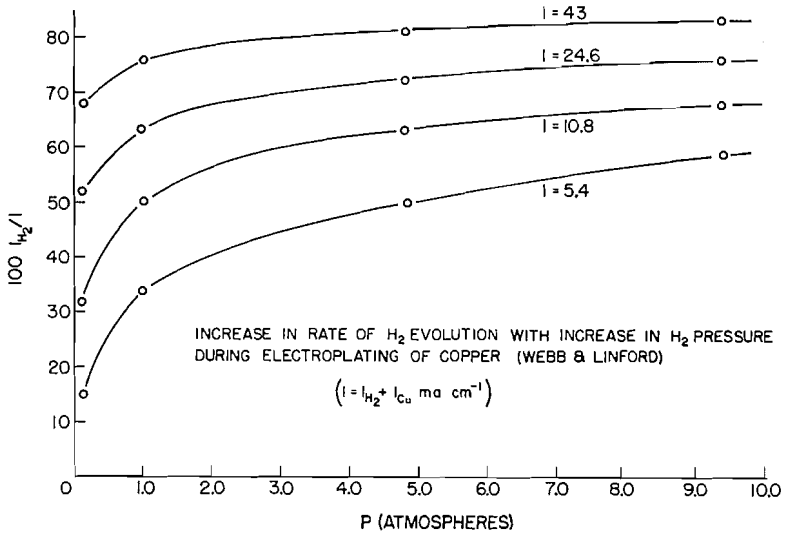

FIG. 12. Percent of total electroplating current which is due to hydrogen evolution.

Glicksman (8) has used our earlier (1) proposal, that the rate of dissolution is controlled by transport through gelatinous reaction product ($Mg(OH_2)$?), to explain why the hydrogen evolution reaction rate increases with increasing anodic current; thus higher anodic currents cause increased acid attack of the covering layer and therefore decrease the protection offered by it. The elaboration of the mechanism by the present work offers another simple explanation: more univalent magnesium is desorbed from the surface at higher currents. Since both the anodic and the dissolution reactions are highly exothermic, there probably exists at the metal–solution interface a high local temperature, which should favor the desorption of $MgOH_{ads}$.

SUMMARY

(1) The following table summarizes the facts, new and old, which are known about this reaction at pH = 2.

Concn. <1 molal $MgCl_2$	Concn. >1 molal $MgCl_2$
(*a*) v low, as in acidic KCl or KNO_3	v abnormally high
(*b*) $v \propto a_{H^+}^n$, where $n \simeq 1$	v independent of a_{H^+}
(*c*) $v \propto$ solubility of MgO in electrolyte	$v \propto$ solubility of Mg(OH)Cl?
(*d*) $E^* = 12.2 \pm 0.6$ kcal/mole	$E^* = 11.4 \pm 1.0$ kcal/mole
(*e*) Mg wet by Hg in electrolyte	Mg not wet by Hg in electrolyte
(*f*) Cathodic control	Cathodic control
(*g*) Dried reaction product: $Mg(OH)_2$ + Mg	Dried reaction product: $Mg(OH)_2$ + Mg(OH)Cl (possibly) + unidentified component
(*h*) $v \propto 1/P^{1/2}$ when $n = 1$	$v \propto P$
(*i*) $v_i = v - v_{Mg}^{H_2} - v_{soln}^{H_2\ gas}$ and $v_{Mg}^{H_2} \cong v_{soln}^{H_2\ gas}$	
(*j*) v increased by X rays, during irradiation only	v increased permanently by high-intensity radiation

(2) A kinetic analysis of the results indicates that bubble growth is rate determining in the low-concentration region, and that bubble nucleation is rate determining in the high-concentration region. The postulate of univalent magnesium ion (Mg^+) as an intermediate is essential to describing the results quantitatively.

(3) During the early stages of the reaction, hydrogen enters the magnesium metal to an amount ~1 cc per cc Mg at 27° C, decreasing with increasing temperature.

REFERENCES

1. E. J. CASEY and R. E. BERGERON. Can. J. Chem. **31**, 849 (1953).
2. W. FEITKNECHT *et al.* Helv. Chim. Acta, **27**, 1480 (1944); Fortschr. Chem. Forsch. **2**, 670 (1953), translated in full by British Atomic Energy Research Establishment, Lib./Trans 622, 1956; Chimia (Switz.), **13**, 113 (1959).
3. P. S. EPSTEIN and M. S. PLESSET. J. Chem. Phys. **18**, 1505 (1950). M. S. PLESSET and S. A. ZWICK. J. Appl. Phy. **25**, 493 (1954).
4. S. GLASSTONE, K. J. LAIDLER, and H. EYRING. The theory of rate processes. McGraw-Hill Book Co., Inc., New York. 1941. p. 477.
5. S. SCHULDINER. J. Electrochem. Soc. **106**, 891 (1959); **107**, 452 (1960).
6. R. E. WEBB and H. B. LINFORD. J. Electrochem. Soc. **94**, 261 (1948).
7. J. L. ROBINSON and P. F. KING. J. Electrochem. Soc. **108**, 36 (1961). I. EPELBOIN and M. FROMENT. J. Electrochem. Soc. **104**, 395 (1957).
8. R. GLICKSMAN. J. Electrochem. Soc. **106**, 83 (1959).

THE INTERACTION OF FRIEDEL–CRAFTS CATALYSTS WITH ORGANIC MOLECULES

III. THE $CH_3COCl:GaCl_3$ SYSTEM[1]

DENYS COOK
Exploratory Research Laboratory, Dow Chemical of Canada, Limited, Sarnia, Ontario
Received November 24, 1961

ABSTRACT

The equimolar complex of acetyl chloride and gallium trichloride has been prepared and its infrared spectrum, both in the pure state and in nitrobenzene solution, has been recorded. In the pure complex a strong band at 2300 cm^{-1}, hitherto attributed to the acetylium ion, has been observed. In solution in nitrobenzene, the 2300 cm^{-1} band is almost completely replaced by one at 2200 cm^{-1}, while undissociated CH_3COCl is present. Certain bands in this spectrum are consistent with the presence of the nitrobenzene – gallium chloride complex. A re-evaluation of the assignments of the acetylium ion suggests that a more complicated ionic species may be present in the solid state, possibly $[CH_3CO \ldots GaCl_3]^+Cl^-$.

INTRODUCTION

In the last 4 years many infrared spectroscopic investigations of acid halide – Lewis acid systems have been published by Susz and his colleagues (1)* in Geneva. Several communications from this laboratory have dealt with similar topics (2–4), while a brief comment on one system was made by Terenin and his collaborators (5).

There has been general agreement that a strong band at 2300 cm^{-1} in the spectra of acetyl halides with Lewis acids was due to the acetylium ion, CH_3CO^+, formed by the process [1]:

$$CH_3COX + MX_n = CH_3CO^+ + MX_{n+1}^- \qquad [1]$$

I

Similarly, aromatic acid halide complexes have given spectra containing a strong band at ~2200 cm^{-1}, indicating the presence of a (substituted) benzoylium cation, as in equation [2]:

$$R_xC_6H_{(5-x)}COX + MX_n = R_xC_6H_{(5-x)}CO^+ + MX_{n+1}^- \qquad [2]$$

II

The lower frequency of the benzoylium cation compared with the acetylium cation was attributed to conjugation of the CO group with the ring, a familiar situation in infrared spectroscopy.

In certain complexes two bands in the triple bond region have been observed for acetylium salts, viz. 2300 and 2200 cm^{-1} (2, 5), for which no adequate explanation has been offered. The present paper will examine possible causes of these two bands.

Greenwood and Wade showed the gallium chloride – acetyl chloride complex to be an excellent acetylating agent and an investigation of the liquid–solid phase diagram of the system revealed a dystectic point at 86° C (decomp.) with an equimolar ratio (6).

[1]*Contribution No. 58.*
**This paper is number XIII in the series and contains previous references.*

The investigation of the complex by infrared spectroscopy was therefore undertaken, in order to establish the active species in Friedel–Crafts ketone synthesis.

EXPERIMENTAL

Materials

Acetyl chloride (2.23 g, 0.0285 mole) was mixed with 5.0 g $GaCl_3$ (0.0285 mole) in a vacuum system similar to that described previously (2). All handling of the materials prior to mixing was done in a dry box. The $GaCl_3$ was supplied by the Eagle-Picher Co. and the acetyl chloride was from the J. T. Baker Co. The mixture was heated to about 80° C to allow complete interaction; it did not solidify on cooling to room temperature but remained as a light brown viscous liquid. This behavior has been observed previously by other workers (6). When allowed to react with excess benzene, acetophenone was found in good yield.

Spectra

A Perkin–Elmer 221G prism-grating spectrometer was used to record the spectra. The liquid spectrum was obtained as a film between BaF_2 plates (NaCl plates were attacked) and all preparative work was done in a dry box. The nitrobenzene solution was prepared by making a solution of 0.6 g complex in 1.5 g nitrobenzene. A sodium chloride sealed cell was used for this solution, and a variable path cell of similar thickness containing nitrobenzene was placed in the reference beam of the spectrometer. No damage was done to the sodium chloride sealed cell, as shown by the absence of window bands, or etching, after the run.

RESULTS AND DISCUSSION

Figure 1 shows a spectrum of the gallium trichloride – acetyl chloride complex as a liquid film. The bands from this spectrum are collected in Table I with those of the complex in nitrobenzene and compared with other spectra.

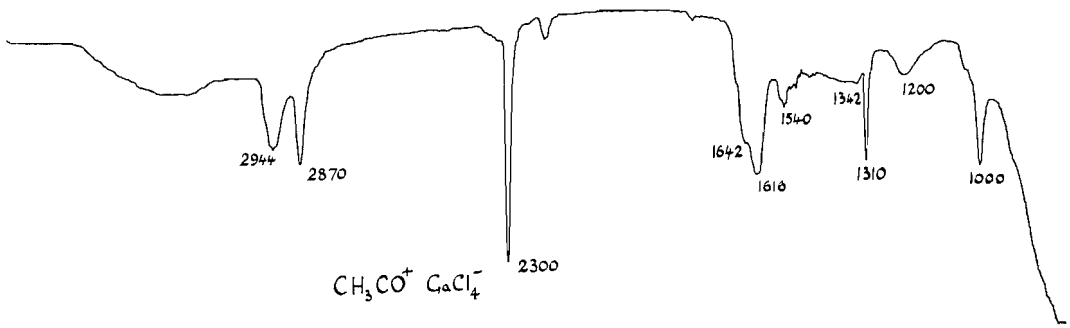

FIG. 1. Spectrum of the gallium trichloride – acetyl chloride complex as a liquid film.

The strong sharp band at 2300 cm^{-1} is typical of the acetylium ion: the weak band at 2199 cm^{-1} should also be noted. The two bands at 2944 and 2870 cm^{-1} are undoubtedly the asymmetric and symmetric CH stretching vibrations, and the expected deformation frequencies are present at 1342 and 1310 cm^{-1}. The 1000 cm^{-1} band has been regarded as a C—C stretching vibration. No vibration of the anion has been observed, since they are outside the range of a spectrometer using a sodium chloride prism-grating combination (7). The band of medium strength at 1616 cm^{-1} is associated with the presence of a small amount of the donor–acceptor complex (III). The spectrum of the complex in nitro-

$$CH_3COX + MX_n = CH_3—C(=O\ldots MX_n)X \qquad [3]$$

III

TABLE I

Infrared bands and assignments in complexes

	CH_3COCl $AlCl_3$†	CH_3COCl $AlCl_3$‡	CH_3COF BF_3§	CH_3COCl $SbCl_5$‖	CH_3COF SbF_5‖	CH_3COCl $GaCl_3$* ¶
ν_5, e**	2950m	2941m	2960s	2920m	2976s	2944m
ν_1, a_1		2874m	2890s	2857m	2911s	2870m
ν_2, a_1	2305s	2307s	2299s	2283s	2294s	2300s
	2200sh	2203vs	2220w			
$\nu_{C=O} \cdots MX_n$	1639m	1637vs	1619m	1709m	1621w	1616m
	1560m	1567s	1560w	1587w	1554w	1540w
	1485m	1497s				
			1402m	1385w	1418vw	
ν_6, e		1379s,b	1372m	1364m	1469m	1342w
ν_3, a_1	1312m	1348s	1329m	1317s	1335s	1310m
		1321s				
		1305s	1293w			
ν_7, e?		1236m		1236w	1235vw	1200w
	1154w	1159m	1134sh	1139s		
		1117m				
		1018m,sh				
ν_4, a_1	1000vs	1006vs	993s	1000s,b	1018s	1000m
		969m				
	893w			920w	898w	
	844w		848sh	829w		
	719m	716m	716w		720w,sh	
		662m,sh				
		649m				
ν_8, e		390s				

*In solution in nitrobenzene the following bands were recorded: 2960w, 2905w, 2300vw, 2195m, 1796m, 1610m,b, 1500m,b, 1244s, 1170m, 1088m, 1000m.
†Ref. 20.
‡Ref. 2.
§Ref. 19.
‖Unpublished work.
¶Present work.
**Assignments based on CH_3CO^+ ion using standard notation.

benzene shows some unusual features. The 2300 cm^{-1} band is reduced greatly in intensity and a new band is seen at 2195 cm^{-1}. The strong band at 1796 cm^{-1} obviously belongs to acetyl chloride. Two bands, one at about 1500 cm^{-1}, which is very broad and without structure, the other at 1244 cm^{-1}, which is fairly sharp, are to be identified with nitrobenzene complexed with gallium trichloride. Susz showed that the asymmetric NO_2 stretching vibration altered little on complex formation of nitrobenzene with $AlCl_3$, $AlBr_3$, and $TiCl_4$ (8). The symmetric NO_2 stretching vibration, however, decreased from about 1350 cm^{-1} in nitrobenzene to 1250–1260 cm^{-1} in the complexes. A shoulder on the high-frequency side of the 1550 cm^{-1} band, at about 1610 cm^{-1} recalls the 1616 cm^{-1} band in the primary complex.

On dissolution, therefore, of the primary complex in nitrobenzene, several different species are formed according to scheme [4]:

$$\text{primary complex} \rightarrow \begin{cases} CH_3COCl & 1796\ cm^{-1}, \\ CH_3C(Cl)=O \ldots GaCl_3 & 1610\ cm^{-1}, \\ C_6H_5N(=O)=O \ldots GaCl_3 & 1550 \text{ and } 1244\ cm^{-1}, \\ ? & 2200\ cm^{-1}. \end{cases} \quad [4]$$

It is proper, then, at this time, to consider more closely the nature of the species responsible for the absorption at 2200 cm^{-1} just discussed, and see what bearing this might have

on the structure of the primary complex. Originally (2) it was supposed that the 2200 cm^{-1} band in the $CH_3COCl:AlCl_3$ complex was due either to an ion pair of the type IV or a complex of the acetylium ion with $AlCl_3$ (V). Both of these explanations now seem

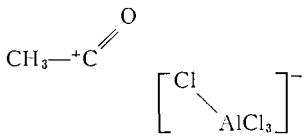

IV

$CH_3CO^+ \ldots AlCl_3 \equiv [CH_3CO \ldots AlCl_3]^+$

V

inadequate, the first since the central carbon atom is still trigonally hybridized, the second for a much more fundamental reason, which will now be considered.

The key to the problem will be stated first. Whenever a *linear* molecule such as CH_3CO^+ forms a complex with an electron deficient material the CO stretching frequency would be *raised* to a higher value than in the free ion. This viewpoint is diametrically opposed to that put forward earlier (2) and its justification is fundamental to the problem. The argument of a lowered CO frequency in the complex was made by analogy with the lowering of carbonyl frequencies when complexed with Lewis acids. Susz has recently summarized many experimental details (9) and in the $CH_3COCl:TiCl_4$ system which is of type III he found a decrease of some 3 md/Å in the force constant of the CO bond (10). The extrapolation to a linear model, however, is unjustified, since it does not take into account mechanical factors which become of great significance.

The rise in frequency when linear molecules form complexes with Lewis acids is best illustrated by a consideration of the vibrational spectra of some nitrile complexes, several of which are listed in Table II (11–14). The complex dimethylnitrilium hexachloroantimonate should be particularly noted (13). In every case, the complex has a higher CN stretching frequency than the free nitrile. Gerrard *et al.* (14), correctly discounting coupling or mass (of the ligand) effects, concluded that the bond order (and force constant, presumably) of the CN bond was higher in the complex than in the free nitrile. Such a conclusion is neither necessary nor realistic, for the correct explanation is implicit in the work of Overend and Scherer (15) on the vibrational frequencies and force constants of the carbonyl halides. The rather surprising result was established that, in COF_2, $COCl_2$, $COBr_2$, and several mixed halides, the force constant K_{CO} is virtually the same at about 12.7 md/Å, though there is about 100 cm^{-1} difference in the carbonyl frequencies. The

TABLE II

CN stretching frequencies in acetonitrile complexes

Compound	Frequency (cm^{-1})	$\Delta\nu$ (cm^{-1})
CH_3CN	2253*	
$CH_3CN:BF_3$	2359†	116
$CH_3CN:AlBr_3$	2335*	82
$CH_3CN:AlCl_3$	2330*	77
$CH_3CN:SnCl_4$	2330*	77
$CH_3CN:BCl_3$	2325†	72
$CH_3CN:BBr_3$	2320	67
$2CH_3CN:TiCl_4$	2304†	51
$2CH_3CN:SnCl_4$	2303†	50
$[CH_3CNCH_3]^+SbCl_6^-$	2416‡	163

*Ref. 11.
†Ref. 12.
‡Ref. 13.

explanation lies in the fact that in COF_2 only 84% of the potential energy of the CO vibration resides in the CO bond. Significant percentages come from the CX stretching mode and the XCX angular deformation. Alternatively, one can say that as the CO bond stretches it compresses the CX bond and deforms the XCX angle, and this resistance forces the vibrational frequency higher. The larger the force constant of the CX bond the larger will be this effect.

Naturally, as the XCX angle becomes smaller this effect becomes larger, which is the reason why small rings have elevated carbonyl frequencies (16). In the limit, therefore, a linear molecule results, such as the nitrile complexes or the acetylium ion complexes. Even a small force constant for the D—M bond in $CH_3C{\equiv}D{-}MX_n$ (D stands for donor) should produce a large rise in frequency for the CD stretching vibration in the complex compared with that in the free $CH_3C{\equiv}D$.

This effect is probably quite universal and seems to account for variations in acetylenic triple bond stretching frequencies, as shown in Table III. Although the changes in ν_{CC}

TABLE III

Triple bond stretching frequencies and force constants in some acetylenes*

		Force constant (md/Å)		
XC≡CY	Frequency (cm^{-1})	K_{XC}	K_{CC}	K_{CY}
HCCH	1974			
CH_3CCH	2146	5.13	15.80	5.00
CH_3CCI	2197		15.80	3.57
CH_3CCBr	2230		15.80	4.35
CH_3CCCl	2263		15.80	5.30
CH_3CCCH_3	2313	5.29	15.60	5.29

*A. G. Meister, J. Chem. Phys. **16**, 950 (1948).

from HCCH to CH_3CCH are probably due to a combination of mass and force constant effect, from CH_3CCI on it would seem to be due solely to the force constant effect, since ν_{CC} parallels K_{CY} and all the masses are greater than 15. This mass is probably close to the limiting value, as found by Halford (17) for carbonyl vibrations, and by Whiffen (18) for XCN molecules.

Returning now to the constitution of the complex, the foregoing arguments are quite in accord with the reversal of the assignments previously considered. The complex ion $(CH_3CO \ldots MX_n)^+$ would have a CO vibration at 2300 cm^{-1} and the uncomplexed acetylium ion, CH_3CO^+, a CO vibration at 2200 cm^{-1}. The reaction expressing the formation of the complex would then be [5]:

$$CH_3COX + MX_n = [CH_3CO \ldots MX_n]^+X^- \qquad [5]$$

V

It now remains to be seen whether the other bands in the spectra can be adequately assigned to the complex ion V. The CH_3 asymmetric and symmetric stretching and deformation frequencies fit the new structure reasonably well. In fact, the variations observed in these four frequencies in different complexes are easier to understand if the CH_3 group is in a slightly different environment in different complexes. That is to say, small differences in the MX_n portion of the complex might produce slight variations in the fundamentals. If the acetylium ion itself were subject to such variations one would have to invoke some kind of environmental interaction, which might be difficult to justify.

One of the difficulties with the assignments of the bands to the acetylium ion has been the lack of a suitable band for the methyl rocking vibration. A weak band at 1200 cm^{-1} in the $CH_3COCl:GaCl_3$ complex and at 1235 cm^{-1} in the $CH_3COF:SbF_5$ complex had been tentatively assigned to this vibration, but not even a weak band showed in the spectrum of $CH_3COF:BF_3$ (19), or $CH_3COCl:AlCl_3$ (20).

If now the assignments for the dimethylnitrilium ion (13) are kept in mind then the 1000 cm^{-1} band is more acceptably assigned to the CH_3 rocking vibration, and the medium to weak band at 716 cm^{-1} becomes the C—C stretching vibration. In several of the complexes with strong absorption bands near 700 cm^{-1}, due to metal–fluorine stretching vibrations, the C—C stretching vibration may be submerged. The M . . . O stretching vibration has not been observed, and it may be in the low-frequency region outside the range of NaCl optics. Many of the metal–halogen stretching vibrations, too, will lie outside this range.

The dissociation of the primary complex in solution now becomes quite understandable since the Lewis acid now just has to shift from a weak base, CH_3CO^+, to a stronger base, $C_6H_5NO_2$. This does then not involve the dissociation of a stable species MX_{n+1}^-, such as BF_4^-, $AlCl_4^-$, $GaCl_4^-$, etc., into $MX_n + X^-$, followed by recombination of the MX_n with nitrobenzene, and is therefore more plausible energetically.

ACKNOWLEDGMENTS

The assistance of Miss C. D. Anderson in recording the spectra is gratefully acknowledged, and Dr. S. J. Kuhn and Dr. G. A. Olah are warmly thanked for their preparation of the SbF_5 complex.

REFERENCES

1. B. P. Susz and D. Cassimatis. Helv. Chim. Acta, **44**, 395 (1961).
2. D. Cook. Can. J. Chem. **37**, 48 (1959).
3. D. Cook. Abstracts, International Congress of Pure and Applied Chemistry, Montreal, Que. August 11, 1961. Paper A 107.
4. E. B. Baker and G. A. Olah. Abstracts, International Congress of Pure and Applied Chemistry, Montreal, Que. August 11, 1961. Paper A 106.
5. A. N. Terenin, V. N. Filiminov, and D. S. Bistrov. Izvest. Akad. Nauk U.S.S.R. Phys. Chem. Sect. **22**, 1100 (1958).
6. N. N. Greenwood and K. Wade. J. Chem. Soc. 1527 (1956).
7. L. A. Woodward and A. A. Nord. J. Chem. Soc. 3721 (1956).
8. P. Gagneaux, D. Janjic, and B. P. Susz. Helv. Chim. Acta, **41**, 1322 (1958).
9. B. P. Susz. Compt. rend. **248**, 2569 (1959).
10. D. Cassimatis and B. P. Susz. Helv. Chim. Acta, **44**, 943 (1961).
11. A. Terenin, W. Filimonov, and D. Bystrov. Z. Elektrochem. **62**, 180 (1958).
12. H. J. Coerver and C. Curran. J. Am. Chem. Soc. **80**, 3522 (1958).
13. G. C. Turrel and J. E. Gordon. J. Chem. Phys. **30**, 895 (1958).
14. W. Gerrard, M. F. Lappert, H. Pyszora, and J. W. Wallis. J. Chem. Soc. 2182 (1960).
15. J. Overend and J. R. Scherer. J. Chem. Phys. **32**, 1296 (1960).
16. D. Cook. Can. J. Chem. **39**, 31 (1961).
17. J. O. Halford. J. Chem. Phys. **24**, 830 (1956).
18. D. H. Whiffen. Chem. & Ind. (London), 193 (1957).
19. B. P. Susz and J.-J. Wuhrmann. Helv. Chim. Acta, **40**, 722 (1957).
20. B. P. Susz and J.-J. Wuhrmann. Helv. Chim. Acta, **40**, 971 (1957).

THE REACTION OF OXYGEN ATOMS WITH CARBON TETRACHLORIDE[1]

A. Y-M. UNG[2] AND H. I. SCHIFF
Upper Atmosphere Chemistry Group, McGill University, Montreal, Que.

Received November 22, 1961

ABSTRACT

The homogeneous reaction between O atoms and CCl_4 was studied in a flow system under conditions of complete consumption of atoms, in the presence and in the absence of molecular oxygen. The only products of the reaction are Cl_2, CO, CO_2, and $COCl_2$. No compounds containing more than one carbon atom were detected. The dependence of the products on CCl_4 concentration suggests that the primary reactions are

$$O + CCl_4 \rightarrow [O.CCl_4] \rightarrow COCl_2 + Cl_2$$
$$\rightarrow CO + 2Cl_2,$$

which are too slow to consume all the atoms. Carbon dioxide is produced by secondary reactions which are fast enough to consume all the atoms, the most important of which is

$$O + COCl_2 \rightarrow CO_2 + Cl_2.$$

However, the dependence of the ratio $(CO_2 + COCl_2)/CO$ on CCl_4 concentration in the presence of O_2 indicates other reactions also produce CO_2. The rapid disappearance of O atoms in the systems containing O_2 suggests a chain mechanism in which Cl_2 is mainly converted to the atomic form. Carbon dioxide can then be produced by the sequence

$$CO + Cl \rightleftharpoons COCl$$
$$COCl + O \rightarrow CO_2 + Cl$$
$$COCl + O_2 \rightarrow CO_2 + ClO.$$

The rate constant for the primary process was found to be independent of O, O_2, and CCl_4 concentration and could be represented by the equation

$$k = 3.3\times10^{-14} \exp(-4500/RT) \text{ cm}^3 \text{ molecule}^{-1} \text{ sec}^{-1}.$$

INTRODUCTION

The initial attack of an oxygen atom on a hydrocarbon molecule may occur in a variety of ways. Thus Avramenko *et al.* (1) have concluded that the atom may abstract one or two hydrogen atoms, rupture a C—C or a C=C bond, or insert itself into the C—H bond to form an alcohol. On the other hand, Cvetanović (2, 3) in a systematic investigation of the reaction of atomic oxygen with olefins finds that the atom first adds to the double bond to form a biradical. This biradical can then either undergo a triplet–singlet transition to form an epoxide, or rearrange to form a carbonyl compound.

The reaction of O atoms with CCl_4 was chosen for the present study, since none of these initial modes of attack is possible. The absolute rate constant for the initial reaction was also measured as a function of temperature, since only relative rate constants and activation energies are currently available for most oxygen atom reactions.

EXPERIMENTAL

Materials

A cylinder of oxygen was selected from a number supplied by the Imperial Oxygen Company, on the basis of its low nitrogen content, and used throughout the course of this work.

[1]*This work received financial assistance from the Defence Research Board of Canada and the U.S.A.F. Cambridge Research Laboratories.*

[2]*Present address: National Research Council, Ottawa, Canada.*

Reagent grade CCl_4, obtained from the Fisher Scientific Company, and Cl_2, $COCl_2$, CO, and CO_2, obtained from the Matheson Company, were further purified by trap-to-trap distillation.

Nitric oxide, a Matheson product, was freed from acidic impurities by passage through Ascarite. Nitrogen dioxide was prepared by oxidation of NO and distilled until the solid was colorless. It was stored with a small amount of O_2.

Apparatus

The reaction vessel and flow system were similar to those used previously in this laboratory (4). Atomic oxygen was formed by a microwave discharge operating at 2450 mc. This produced a few percent of atomic oxygen in a large excess of molecular oxygen. Alternately, O atoms could be produced in the absence of O_2 by the titration of N atoms with NO (5).

Flow rates of gases were controlled by fine needle valves and measured with calibrated flowmeters. The pressure was measured at both ends of the reaction vessel with McLeod gauges. Care was taken to exclude Hg vapor from the apparatus.

Procedure

In one set of experiments, the products of the reaction were studied as a function of the partial pressure of CCl_4 for several values of the total pressure, partial pressure of O atoms, and temperature. The CCl_4 flow rate was always a small fraction of the total gas flow to prevent its variation affecting the reaction time, but sufficiently large to consume all the atoms in the reaction tube. This condition was necessary to prevent O_3 formation in the traps. A metallic catalyst for recombining the atoms before the trap could not be used in the presence of CCl_4 without inducing heterogeneous reactions.

The initial atom concentration was determined by the NO_2 'clean-up' method (5). A relatively large excess of NO_2 was added through the inlet jet and the amount of NO produced by the rapid reaction $NO_2 + O \rightarrow NO + O_2$ determined. Carbon tetrachloride was then added through the jet and permitted to flow for at least half an hour to reach a steady condition before products were trapped. During this stabilization period the effluent gases were made to bypass the traps. Condensable products were then collected for a sufficient time to obtain analyzable samples. The products were identified mass spectrometrically and subsequently analyzed by conventional methods. Chlorine gas was absorbed by HgS; CO_2 and $COCl_2$ were separated with a Le Roy still and measured by a gas burrette. A mass spectrometric analysis of the non-condensable gas showed CO to be its only product component. Carbon monoxide was subsequently analyzed by conversion to CO_2 in a CuO-filled combustion column located downstream from the traps.

In the experiments designed to determine the rate constants for the initial reaction, O atom concentrations were measured as a function of time by the photometric method described by Elias and Schiff (4). The glow resulted from the small amount of NO produced in the discharge from the N_2 impurity in the oxygen. A small correction for these concentrations was made for the slight dilution caused by the introduction of the CCl_4.

Since the reaction is highly exothermic and also possesses an appreciable activation energy, the experiments were performed with low concentration of both reactants. Temperature measurements made with a thermocouple encased in a movable, thin-walled tube indicated that nowhere in the reaction vessel was the temperature more than 1° C above that of the walls.

RESULTS AND DISCUSSION

The reaction proceeded with no visible reaction flame. The products of the reaction were found to be $COCl_2$, CO, CO_2, and Cl_2 exclusively. A series of experiments designed to test the mass balance showed that, on the average, these products accounted for 98% of the CCl_4 reacted. No compounds containing more than one carbon atom were formed. Nor were there any liquid or solid deposits formed on the walls, a conclusion supported by the fact that the walls retained a constant catalytic activity towards atom recombination. This is in contrast to the deposits found by Sobering and Winkler (6) in the reaction of CCl_4 with N atoms. No solid deposits were formed even when CCl_4 was intentionally introduced in large excess or when the system was free of molecular oxygen.

Table I, and Figs. 1 to 3, show the products as a function of CCl_4 flow rate at three different temperatures and two different pressures. The total chlorine content in the products will be seen to be twice the total carbon within experimental error, which again indicates that no major product escaped detection. Chlorine gas shows initially a rapid and then a slower, approximately linear rise, as do CO and $COCl_2$. This behavior is consistent with these products being formed in the primary reaction, which is therefore

TABLE I

Dependence of products on reactant concentration

CCl_4, 10^{-6} mole sec^{-1}	Products, 10^{-8} mole sec^{-1}						% total carbon			$\frac{CO_2+COCl_2}{CO}$
	Cl_2	CO	CO_2	$COCl_2$	Total Cl_2	Total C	CO	CO_2	$COCl_2$	
(A) O_2 flow: 5.5×10^{-5} mole sec^{-1}; O atom flow: 9.31×10^{-7} mole sec^{-1}; T = 4° C; $P \simeq 2$ mm; reaction time $\simeq$ 0.45 sec										
0.34	0.82	0.098	0.280	0.098	0.92	0.48	20	59	20	3.84
0.39	0.97	0.115	0.301	0.129	1.05	0.55	20	55	23	3.74
1.43	1.47	0.230	0.386	0.214	1.69	0.53	29	47	26	2.60
1.90	1.55	0.242	0.435	0.243	1.79	0.92	26	47	26	2.80
2.25	2.05	0.311	0.448	0.235	2.29	0.99	32	45	24	2.20
2.55	1.93	0.320	0.516	0.280	2.21	1.12	29	46	25	2.48
2.72	2.55	0.363	0.511	0.299	2.85	1.17	32	43	26	2.23
3.42	2.56	0.427	0.542	0.342	2.91	1.31	32	41	26	2.06
3.83	2.56	0.487	0.570	0.485	3.05	1.54	32	37	31	2.16
4.13	2.91	0.515	0.515	0.458	3.37	1.49	34	34	31	1.89
(B) O_2 flow; 5.5×10^{-5} mole sec^{-1}; O atom flow: 2.67×10^{-7} mole sec^{-1}; T = 100° C; $P \simeq 2.1$ mm; reaction time = 0.44 sec										
1.52	1.76	0.313	0.427	0.342	2.11	1.08	29	39	32	2.45
1.85	2.07	0.341	0.457	0.371	2.44	1.17	29	39	32	2.43
2.33	2.20	0.430	0.451	0.430	2.63	1.31	33	34	32	2.05
3.05	2.57	0.494	0.472	0.536	3.11	1.50	33	32	35	2.04
3.45	2.94	0.560	0.512	0.634	3.57	1.71	33	30	37	2.05
3.61	2.82	0.575	0.533	0.640	3.46	1.75	33	30	37	2.00
3.71	3.19	0.640	0.533	0.660	3.85	1.83	35	29	36	1.87
4.08	—	0.710	0.490	0.782	—	1.98	36	26	39	1.80
4.42	3.65	0.734	0.514	0.757	4.41	2.01	36	25	39	1.74
4.45	3.77	0.742	0.514	0.800	4.50	2.01	36	25	39	1.77
(C) O_2 flow: 1.71×10^{-4} mole sec^{-1}; O atom flow: 1.99×10^{-6} mole sec^{-1}; T = 10° C; $P \simeq 4.1$ mm; reaction time $\simeq$ 0.29 sec										
0.28	0.84	0.164	0.269	0.096	0.94	0.53	31	51	18	2.22
2.46	1.56	0.322	0.406	0.214	1.77	0.94	34	43	23	1.92
2.91	1.93	0.386	0.470	0.214	2.15	1.07	36	44	20	1.77
3.23	1.94	0.363	0.533	0.235	2.18	1.31	32	47	21	2.12
3.42	—	0.455	0.556	0.193	—	1.20	38	46	16	1.64
3.76	2.29	0.515	0.480	0.235	2.53	1.23	42	39	19	1.39
(D) N_2 flow: 5.5×10^{-5} mole sec^{-1}; O atom flow: 5×10^{-7} mole sec^{-1}; T = 4° C; $P \simeq 2$ mm; reaction time $\simeq$ 0.45 sec										
4.90	3.38	0.62	0.91	0.33	3.71	1.86	33	49	18	1.98
3.56	2.55	0.47	0.68	0.30	2.85	1.45	33	47	21	2.07
3.20	2.57	0.47	0.66	0.26	2.83	1.39	34	47	19	1.93

too slow to consume all the atoms under these conditions. On the other hand, CO_2 levels off after its initial rise, which suggests that it is not formed in the primary reaction. The secondary reactions must be sufficiently fast to consume all the atoms in the system.

Primary Reactions

The abstraction reaction

$$CCl_4 + O \rightarrow CCl_3 + ClO \qquad [1]$$

cannot be the sole primary reaction, since the CCl_3 radicals would react rapidly with the excess O_2 (7):

$$CCl_3 + O_2 \rightarrow COCl_2 + ClO, \qquad [2]$$

and there would be no reasonable way of forming CO. The same objection can be raised against the reaction

$$CCl_4 + O \rightarrow CCl_2 + Cl_2O, \qquad [3]$$

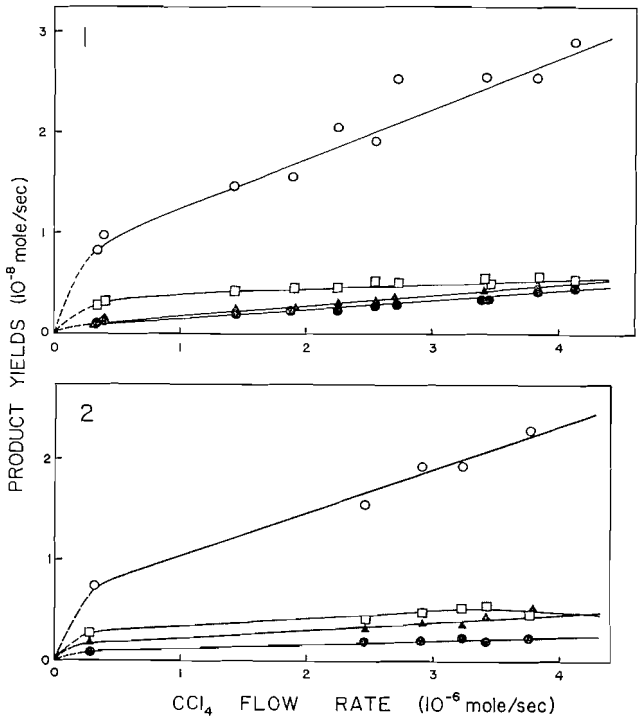

FIG. 1. Product yields as a function of CCl_4 flow rate: ○ Cl_2; ● $COCl_2$; ▲ CO; □ CO_2. $T = 4°$ C, $P = 2$ mm.

FIG. 2. Product yields as a function of CCl_4 flow rate: ○ Cl_2; ● $COCl_2$; ▲ CO; □ CO_2. $T = 10°$ C, $P = 4$ mm.

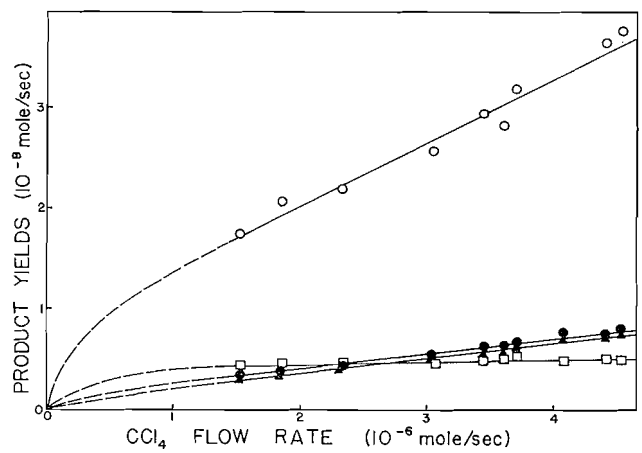

FIG. 3. Product yields as a function of CCl_4 flow rate: ○ Cl_2; ● $COCl_2$; ▲ CO; □ CO_2. $T = 100°$ C, $P = 2$ mm.

which would also be highly endothermic. Moreover, reactions [1] and [3] cannot even be significant primary processes since they should lead to radical recombination products (8) under conditions of large CCl_4 excess or in an O_2-free system.

It is actually unlikely that any free radical is formed in the primary process. Sato and Cvetanović (3) have shown that the presence of O_2 in atomic oxygen–olefin reactions has a marked effect on the products because of the reactions of free radicals with O_2,

most of which have appreciable activation energies. However, in the present studies, the products did not change appreciably when the O_2 content or the temperature was varied.

In view of the electrophylic nature of O atoms (2) and the electron density in CCl_4, it is likely that a reasonably stable collision complex is formed. The primary products could then be accounted for by two alternate decomposition modes of the complex:

$$O + CCl_4 \rightarrow [CCl_4.O] \rightarrow COCl_2 + Cl_2 \quad [4]$$

$$\rightarrow CO + 2Cl_2. \quad [5]$$

To account for the overall change in spin, one may suggest that the complex is initially formed in the triplet state. However, a considerable stereochemical rearrangement is required, which could be aided if the O atom inserts into the C—Cl bond. This would bring the two Cl atoms into proper bonding distance. Such insertion reactions have been suggested in explaining the formation of alcohols in atomic oxygen – paraffin reactions (1). Since reaction [4] is 97 kcal/mole exothermic, it might be suggested that the $COCl_2$ molecule is formed with excess internal energy and subsequently dissociates into $CO + Cl_2$. But if this occurred, the ratio $CO/COCl_2$ should decrease with pressure, while the converse was observed.

In the reaction of N atoms with CCl_4, Sobering and Winkler (6) postulated an atom attack on the complex

$$N + [CCl_4.N] \rightarrow N_2 + CCl_3 + Cl$$

to explain the formation of CCl_3 polymers in their system. The absence of such deposit in the present study mitigates against the analogous O-atom reaction.

Secondary Reactions

Some of the secondary reactions capable of producing CO_2 include:

$$CO + O + M \rightarrow CO_2 + M \quad [6]$$

$$CO + O \rightarrow CO_2^* \rightarrow CO_2 + h\nu \quad [7]$$

$$COCl_2 + O \rightarrow CO_2 + Cl_2. \quad [8]$$

The reaction of CO with O atoms has been found by several authors (9, 10) to be slow, and also, in the present study, to have a large temperature coefficient. Mahan (11) has recently reported that the reaction of O atoms with CO proceeds by [7] rather than [6], with a change in multiplicity and a rate constant of $1.5\times10^{-14}\exp(-4300/RT)$ $cm^3molecule^{-1}sec^{-1}$. It would therefore be far too slow to be important in the present investigation. Moreover, it would produce an increase in the CO_2/CO ratio with temperature, which is contrary to observation.

Reaction [8] probably does not proceed in a single step since it would be spin disallowed and would require the simultaneous rupture and formation of two bonds. Nevertheless, in separate experiments, O atoms were found to react rapidly with $COCl_2$ to form CO_2 and Cl_2, and reaction [8] can be used to represent this overall reaction. From these experiments the rate of this reaction can be estimated to be approximately 10^{-14} $cm^3molecule^{-1}sec^{-1}$, while the rate of the initial reaction was found to be 2×10^{-17} cm^3-$molecule^{-1}sec^{-1}$. The $COCl_2$ concentration should therefore be of the order of 10^{-3} times the CCl_4 concentration, in agreement with the results shown in Table I. The decrease in the $CO_2/COCl_2$ ratio with CCl_4 flow is explicable in terms of the corresponding decrease in the O atom concentration and the decreased rate of reaction [8]. However, this reaction cannot be the sole source of CO_2 in the system. If it were, the ratio $(CO_2 + COCl_2)/CO$ would be independent of CCl_4 concentration. This ratio is constant for the O_2-free system but decreases with CCl_4 flow rate in the systems containing molecular oxygen.

An explanation for this is suggested by an independent observation. It was possible to measure simultaneously the rate of CCl_4 consumption and the rate of O atom disappearance.[3] It was found that at 4° C and 2.1 mm, 40 oxygen atoms disappeared for each CCl_4 molecule consumed; this increased to 135 when the O_2 pressure was doubled, and decreased to 10 when the temperature was increased to 100° C. However, in the O_2-free system, only 2.5 oxygen atoms disappeared per CCl_4 molecule. The actual stoichiometry of the reaction corresponded to an average of 1.5 oxygen atoms appearing in the products per CCl_4 reacting.

Kaufman found (9) Cl_2 to be an extremely good catalyst for O atom recombination in the presence of O_2—some 10 oxygen atoms being recombined per Cl_2 molecule present. He proposed the following chain mechanism to account for his observations:

$$O + Cl_2 \rightarrow ClO + Cl \qquad [9]$$
$$O + ClO \rightarrow O_2 + Cl \qquad [10]$$
$$Cl + O_2 + M \rightarrow ClOO + M \qquad [11]$$
$$ClOO + O \rightarrow ClO + O_2. \qquad [12]$$

Such a chain might also occur in the present system and account for the catalyzed recombination of O atoms in the presence of molecular oxygen. The recombination would then be faster at higher O_2 pressure, and less important at higher temperature, since reactions [4] and [5] have a higher activation energy than reaction [9]. The excess consumption of atoms relative to stoichiometry in the O_2-free system could then be due to reactions [9] and [10], or to CCl_4 or the reaction products being more efficient third bodies in the normal atom recombination.

Such catalyzed atom recombination can also account for the shapes of the curves in Figs. 1–3. At low CCl_4 flow rates very little Cl_2 is present, the atom concentration will remain relatively high, and the rate of reactions [4] and [5] will be relatively fast. As the amount of Cl_2 produced increases, the atom concentration will decrease and the slope of the product curve will decrease. The increased O_2 pressure decreases the atom concentration and consequently the slope in Fig. 2. An increase in temperature increases the slope in Fig. 3 because $E_{4,5} > E_9$. The absence of such a chain in the O_2-free system means that the O atom concentration remains higher and this accounts for the large amount of CO_2 produced in the secondary reactions.

If reactions [9] to [12] are indeed operative in the present system, the fate of the new reactive species must be considered. Because of the relative rapidity of reactions [10] and [12], steady-state considerations show that the concentrations of ClO and ClOO are too small to be significant. On the other hand, this mechanism predicts that under the present experimental conditions more than half the chlorine will be present in atomic form.

The reaction of Cl atoms with CCl_4 and with $COCl_2$ are endothermic and have both been found to be slow at room temperature (12, 13). However, the following reactions may be significant in the present system:

$$Cl + CO \rightleftharpoons COCl \qquad [13]$$
$$COCl + Cl_2 \rightarrow COCl_2 + Cl \qquad [14]$$
$$COCl + O_2 \rightarrow CO_2 + ClO \qquad [15]$$
$$COCl + O \rightarrow CO_2 + Cl \qquad [16]$$
$$COCl + Cl \rightarrow CO + Cl_2. \qquad [17]$$

[3]*The rate of* O*-atom disappearance is corrected for the normal three-body recombination of the atoms in the absence of* CCl_4.

The equilibrium reaction [13] has been studied by Bodenstein and co-workers (15) and more recently by Burns and Dainton (16), who give for the equilibrium constant $\log K = -6310/4.571T+2.806$. Although objections may be raised against reaction [15] on steric grounds, Rollefson (17) claims that both [14] and [15] are required to explain the chlorine-catalyzed photooxidation of CO and gives $E_{14}-E_{15} = 3$ kcal and $A_{14}/A_{15} = 30\pm5$.

Reactions [13], [15], and [16] catalytically convert CO into CO_2, and provide an explanation for the change in the $(CO_2 + COCl_2)/CO$ with CCl_4 flow rate in the systems containing O_2. The decrease in the O atom concentration with CCl_4 flow rate results in a decrease in the Cl/Cl_2 ratio and consequently in the conversion of CO to CO_2. In the absence of O_2 the value of the ratio may still be augmented by the sequence of reactions [9], [10], [13], and [16]. But, since there is no chain mechanism for O atom recombination in this system, the value of the ratio will not vary with CCl_4 flow to the same degree as in the systems containing O_2. However, the fact that in all the systems the ratio tends assymptotically at high CCl_4 flows to a value slightly less than 2 suggests that the ratio k_4/k_5 is probably also close to this value.

Rate Constant of the Primary Reaction

Since CCl_4 is neither reformed nor consumed by any of the secondary reactions, the rate of its disappearance can be represented by the simple bimolecular equation

$$\frac{d[CCl_4]}{dt} = -k[O][CCl_4]$$

which, upon integration between times t_1 and t_2, becomes

$$\ln \frac{[CCl_4]_1}{[CCl_4]_2} = k\int_{t_1}^{t_2}[O]dt.$$

To determine the rate constant k, it is only necessary to know the CCl_4 concentration at two times and the O atom concentration as a function of time over this interval. Since all the atoms were consumed in the reaction tube, no explicit knowledge of t_2 was necessary; $[CCl_4]_1$ was then taken as the known initial concentration at the inlet jet, and $[CCl_4]_2$ the amount of unreacted reagent recovered in the trap. Since only a small percentage of the CCl_4 reacted, greater accuracy was obtained when $[CCl_4]_2$ was determined by subtraction of the product equivalents from the value of $[CCl_4]_1$. The time scale used in evaluating the integral was obtained from the calibrated flow rates and the diameter of the reaction tube. Axial and radial photometry measurements indicated that diffusion corrections in these directions are negligible and that streamlined flow conditions were closely approximated.

Rate constants were determined at several temperatures over a considerable range of reagent concentrations and are shown in Table II. The value of k at 19° C is seen to be constant within experimental error over a 13-fold change in CCl_4 concentration, which provides ample justification for the method. The small amount of NO produced in the discharge did not affect the value of k. This was proved by the experiments (marked with an asterisk in the table) in which additional NO was deliberately introduced. The presence of NO will increase the rate of O atom consumption but this is automatically accounted for in the evaluation of the integral. The independence of the rate constant on total pressure confirms that the reaction is homogeneous and agrees with Cvetanović's conclusion that the presence of molecular oxygen does not affect the rate of the initial reaction.

TABLE II

Rate constant of primary process

CCl_4 flow$\times10^6$, mole sec^{-1}	$[O]_0\times10^{-15}$, molecule cc^{-1}	$\log\frac{[CCl_4]_1}{[CCl_4]_2}\times10^3$	$\int_1^2[O]dt\times10^{-11}$, molecule cc^{-1} sec	$k\times10^{17}$, cc $molecule^{-1}$ sec^{-1}
(A) T = 4° C; average total pressure = 2.12 mm; average total flow = 5.87×10^{-5} mole sec^{-1}				
3.23	1.16	1.72	3.55	1.11
3.44	1.16	1.69	3.15	1.10
3.74	1.16	1.63	3.24	1.16
4.03	1.16	1.59	3.15	1.16
4.76*	1.16	1.31	3.03	1.00
4.76	1.16	1.33	2.93	1.05
				1.10±0.04
(B) T = 10° C; average total pressure = 4.2 mm; average total flow = 1.76×10^{-4} mole sec^{-1}				
2.68	1.61	1.62	2.34	1.60
3.12	1.61	1.54	2.18	1.62
3.16	1.61	1.54	2.16	1.65
4.02	1.61	1.42	1.98	1.67
				1.64±0.03
(C) T = 19° C; average total pressure = 3.05 mm; average total flow = 6.2×10^{-5} mole sec^{-1}				
0.38	0.942	2.10	2.47	1.95
0.68	0.935	1.94	2.33	1.91
1.04	0.930	1.78	2.12	1.93
1.50	0.924	1.55	1.95	1.83
1.58	0.920	1.55	1.98	1.80
2.43	0.925	1.36	1.73	1.81
2.56	0.923	1.32	1.70	1.81
3.42	0.926	1.26	1.56	1.92
4.21	0.944	1.21	1.46	1.90
4.56	0.954	1.19	1.49	1.84
4.91	0.948	1.18	1.40	1.93
				1.88±0.05
(D) T = 56° C; average total pressure = 2.22 mm; average total flow = 6.4×10^{-5} mole sec^{-1}				
1.88	1.23	8.34	4.97	3.85
3.98	1.24	6.59	4.13	3.67
4.79	1.24	5.94	3.72	3.65
4.89	1.24	5.81	3.77	3.67
				3.71±0.08
(E) T = 100° C; average total pressure = 2.18 mm; average total flow = 5.95×10^{-5} mole sec^{-1}				
3.16	0.254	2.49	0.587	9.75
3.46	0.255	2.19	0.531	9.50
4.41*	0.255	2.05	0.500	9.45
4.93	0.252	1.95	0.497	9.03
				9.43±0.25

*NO added.

Figure 4 is an Arrhenius plot of the rate constant which can be represented by the equation

$$k = (3.3\pm1.5)\times10^{-14}\exp\left(\frac{-4500\pm300}{RT}\right)\ \text{cm}^3\ \text{molecule}^{-1}\ \text{sec}^{-1}.$$

The small pre-exponential factor indicates the difficulty of the O atom attack on the carbon atom of the molecule.

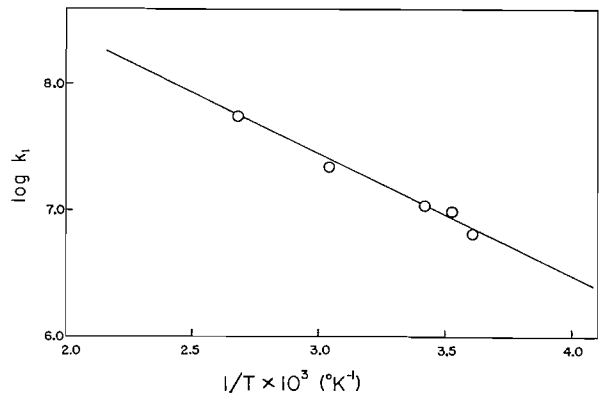

FIG. 4. Arrhenius plot of log k vs. $1/T$ (k in cm^3 mole^{-1} sec^{-1} units).

Acknowledgment is gratefully made for the assistance of Dr. L. Elias throughout the course of this work.

REFERENCES

1. L. I. AVRAMENKO and R. V. KOLESNIKOVA. Doklady Akad. Nauk S.S.S.R. **89**, 1037 (1953); **91**, 107 (1953); **92**, 349 (1953); Zhur. Fiz. Khim. **30**, 581 (1956).
2. R. J. CVETANOVIĆ. J. Chem. Phys. **25**, 376 (1956); Can. J. Chem. **36**, 623 (1958).
3. S. SATO and R. J. CVETANOVIĆ. Can. J. Chem. **37**, 953 (1959).
4. L. ELIAS and H. I. SCHIFF. Can. J. Chem. **38**, 1657 (1960).
5. J. E. MORGAN, L. ELIAS, and H. I. SCHIFF. J. Chem. Phys. **27**, 1141 (1960).
6. S. E. SOBERING and C. A. WINKLER. Can. J. Chem. **36**, 1223 (1958).
7. W. FRANKE and H. J. SCHUMACHER. Z. physik. Chem. B, **42**, 297 (1939).
8. H. W. MELVILLE, J. C. ROBB, and R. C. TUTTON. Discussions Faraday Soc. **10**, 154 (1951).
9. F. KAUFMAN. Proc. Roy. Soc. A, **247**, 123 (1958).
10. P. HARTECK and U. KOPSCH. Z. physik. Chem. B, **12**, 327 (1931).
11. B. H. MAHAN. St. Louis Meeting A.C.S. March 1961.
12. G. M. SCHWAB. Z. physik. Chem. A, **178**, 123 (1936).
13. G. M. SCHWAB and U. HEYDE. Z. physik. Chem. B, **8**, 147 (1930).
14. H. J. SCHUMACHER and K. WOLFF. Z. physik. Chem. B, **25**, 161 (1934).
15. M. BODENSTEIN, W. BRENSCHEDE, and H. J. SCHUMACHER. Z. physik. Chem. B, **40**, 121 (1938).
16. W. G. BURNS and F. S. DAINTON. Trans. Faraday Soc. **48**, 39 (1952).
17. G. K. ROLLEFSON. J. Am. Chem. Soc. **55**, 148 (1933).

LE SPECTRE INFRAROUGE ET LA STRUCTURE MOLÉCULAIRE DE L'ACIDE PERCHLORIQUE ABSOLU

PAUL A. GIGUÈRE ET RODRIGUE SAVOIE[1]
Département de Chimie, Université Laval, Québec, Qué.

Reçu le 8 Novembre 1961

RÉSUMÉ

Les spectres d'absorption de l'acide perchlorique absolu dans les trois états physiques ainsi que ceux de l'acide deutéré $DClO_4$ solide et gazeux ont été étudiés en infrarouge de 5000 à 300 cm^{-1}. Toutes les bandes peuvent s'interpréter selon une structure quasi-tétraédrale de la molécule covalente de symétrie C_s. Les bandes OH dans le cristal révèlent des liaisons hydrogène sensiblement plus faibles que dans l'acide sulfurique (énergie moyenne, 3 kcal). Les fréquences mesurées conduisent indirectement aux longueurs de liaisons 1.70 Å pour Cl—OH et 1.45 Å pour Cl—O en bon accord avec les rayons covalents des atomes et la structure des perchlorates alcalins. La torsion interne dans la molécule libre est gênée par un seuil de potentiel de 1.6 kcal $mole^{-1}$. À partir de ces données on calcule les valeurs suivantes pour les fonctions d'état de la molécule $HClO_4$ à l'état standard à 25° C: $-(F^0-E^0)/T = 58.9$ et $S^0 = 70.7$ cal deg^{-1} $mole^{-1}$.

INTRODUCTION

On possède relativement peu de données sur la structure moléculaire de l'acide perchlorique anhydre $HClO_4$ contrairement au cas du monohydrate. En effet, ce dernier offre un intérêt particulier du fait de l'ion H_3O^+; aussi a-t-il été l'objet de nombreux travaux au moyen des méthodes spectroscopiques et de diffraction. (Voir référence 1 pour revue de la question.) Jusqu'ici l'acide absolu n'a été étudié qu'en effet Raman (2–6) où l'on a observé quelque neuf bandes (Tableau I) facilement identifiables avec

TABLEAU I

Spectre Raman de l'acide perchlorique liquide
(Fréquences en cm^{-1})

(Réf. 2)	(Réf. 4)	(Réf. 5)	(Réf. 6)	Modes (réf. 7)		
	284*	277*	284*	Torsion?		(a′)
	424	425	424	Déformation	$\widehat{OClOH}$	(a″)
570	577	572	577	Déformation	$\widehat{OClO}$	(a′)
		585		Déformation	$\widehat{OClO}$	(a″)
730	740	738	740	Valence	Cl—OH	(a′)
1026	1031	1032	1001	Valence	Cl—O	(a′)
1190	1210	1182	1210	Déformation	$\widehat{ClOH}$	(a′)
		1312		Valence	Cl—O	(a″)
	3243 3425		3300	Valence	O—H	(a′)

*Bande due à Cl_2O_7.

les vibrations normales de la molécule (5, 7). Pour l'infrarouge, le caractère corrosif et fortement oxydant de l'acide perchlorique pose des problèmes d'ordre technique. Un premier travail avec l'acide solide (p.f. −112° C) n'a pas permis de déchiffrer complètement le spectre à cause du chevauchement de certaines bandes. Heureusement l'acide

[1]*Boursier du Conseil national des Recherches.*

perchlorique est assez volatil et assez stable (en l'absence d'agents réducteurs) pour permettre d'observer sans trop de difficultés le spectre de la vapeur. Enfin, grâce à l'étude d'un échantillon d'acide fortement deutéré on a pu compléter l'identification des fréquences fondamentales.

PARTIE EXPÉRIMENTALE

L'acide pur a été obtenu par la méthode de Smith (8), i.e. en distillant sous pression réduite (environ 3 mm Hg) une solution aqueuse à 72% de $HClO_4$ commercial ("Reagent Grade", The Nichols Chemical Co.) additionnée d'oléum à 20% ("Technical Grade", Anachemia Chemicals Ltd.). L'appareil en Pyrex était assemblé au moyen de rodages non lubrifiés; pour assurer l'étanchéité ces derniers étaient enveloppés à l'extérieur de bandes de caoutchouc sous tension (Cenco "Para Rubber Tape"). La présence d'un excès d'oléum assurait un produit strictement anhydre; effectivement les spectres ne montraient aucune indication de la forte bande de l'ion ClO_4^- vers 940 cm^{-1} (9). L'acide deutéré a été préparé en distillant sous pression réduite à environ 65° C un mélange 1:5 de $KClO_4$ et de D_2SO_4 à 97% d'acide. Ce dernier provenait de la condensation ménagée de vapeurs de SO_3 (par évaporation d'un oléum à 30%) dans un petit volume d'eau lourde (à 99.7% de deutérium) refroidie dans un mélange réfrigérant approprié. Le produit ainsi obtenu était de nouveau distillé pour le débarrasser des traces d'impuretés, entre autre D_2SO_4 décelé par sa bande d'absorption caractéristique à 1360 cm^{-1} (10). Les deux acides sulfurique et perchlorique concentrés étant fortement hygroscopiques, il était presque impossible de prévenir toute contamination par l'humidité atmosphérique au cours des manipulations. D'après l'intensité relative des bandes OH dans les spectres de $DClO_4$ on peut évaluer le degré de contamination de ce dernier à quelque 15 ou 20%.

Autant que possible les échantillons étaient fraîchement préparés; autrement il fallait les garder à l'obscurité et dans la neige carbonique pour ralentir la décomposition. En effet, à température ordinaire l'acide anhydre se décompose pour donner des oxydes de chlore, dont Cl_2O_7, qui sont explosifs (8).

Pour le spectre de l'acide cristallin on pressait une goutte du liquide entre deux disques de chlorure d'argent fraîchement polis et montés ensuite dans une cellule à vide conventionnelle (11). En refroidissant avec l'azote liquide le film d'acide se solidifiait facilement. À en juger par l'allure des spectres les échantillons étaient surtout cristallins. Contrairement à son monohydrate (12) l'acide perchlorique absolu n'existe que sous une seule forme allotropique, du moins dans l'intervalle de température couvert ici. Pour le spectre de l'acide liquide les disques de chlorure d'argent portant l'échantillon étaient simplement entourés d'une mince bande de Teflon pour arrêter l'humidité atmosphérique. Comme le chlorure d'argent est opaque au-delà de 400 cm^{-1} il a fallu utiliser pour la région s'étendant jusqu'à 300 cm^{-1} des feuilles de polyéthylène d'environ 1 mm d'épaisseur. Des essais préliminaires ont révélé que ce matériau n'est que légèrement attaqué par l'acide perchlorique absolu pourvu qu'il soit d'abord refroidi suffisamment (en pratique à −70° C). De toute façon le spectre d'absorption des plaques de polyéthylène était enregistré par après pour fin de correction.

Enfin pour l'étude de la vapeur on a employé une cellule d'absorption de 12 cm d'épaisseur en Pyrex fermée par des fenêtres de chlorure d'argent ou de Téflon, selon la région, et maintenues contre le tube de verre par un dispositif à ressort. Un bouchon rodé et une tubulure latérale permettaient de remplir la cellule d'air sec et d'y introduire l'échantillon d'acide liquide. Malgré que cette dernière opération fut effectuée en atmosphère sèche il se formait toujours dans la cellule une légère fumée blanche qui se condensait finalement sur les parois et les fenêtres. Cependant il ne semblait pas en résulter d'absorption notable. Dans le cas des bandes les plus fortes les vapeurs d'acide étaient diluées avec de l'azote sec afin d'obtenir une absorption raisonnable.

Un spectrophotomètre de Beckman, modèle IR-4 à double faisceau, et un appareil de Perkin-Elmer, modèle 112-C, muni de prismes de chlorure de sodium ou de bromure de césium ont été utilisés. Avec ce dernier on a toujours enregistré le fond avec la cellule d'absorption sous vide et à la température de l'azote liquide, car la limite de transmission du chlorure d'argent est sensiblement déplacée vers les basses fréquences à basse température.

DISCUSSION DES RÉSULTATS

On sait qu'à l'état anhydre l'acide perchlorique existe essentiellement sous la forme covalente. En effet, bien que cet acide soit l'un des plus forts connus en milieu aqueux, ses propriétés physiques, et en particulier sa très basse conductivité électrique (4, 13), prouvent que l'autodissociation selon les schémas possibles

$$2HClO_4 \rightleftharpoons H_2ClO_4^+ + ClO_4^- \qquad [1]$$

et

$$2HClO_4 \rightleftharpoons HCl_2O_7^+ + OH^- \qquad [2]$$

est extrêmement faible, en sorte que le spectre moléculaire ne saurait montrer aucune indication d'espèces ioniques. Aussi bien toutes les fréquences observées tant en infrarouge qu'en Raman peuvent s'interpréter sans ambiguité selon la structure prévue pour la molécule covalente (5, 7). À noter que les quatre atomes situés dans le plan de symétrie C_s de la molécule peuvent se trouver dans la configuration *cis* ou *trans* ainsi:

A priori la première semble plus probable étant donné l'attraction entre l'atome d'hydrogène et l'un des atomes d'oxygène du groupe ClO_3. (Voir cependant le cas un peu analogue de HNO_2 (14, 15) où les deux formes coexistent même dans la vapeur.)

Des 12 vibrations fondamentales de $HClO_4$ 8 sont symétriques (a') et 4 asymétriques (a'') par rapport au plan C_s. L'identification des bandes observées (Tableau II) est relativement facile si on se refère au spectre déjà bien étudié (7) d'une molécule assez semblable spectroscopiquement, $FClO_3$. Les fréquences fondamentales de cette dernière devraient se retrouver dans $HClO_4$ à peu près inchangées, sauf que trois seront dédoublées. En outre on y observera les trois vibrations de l'atome d'hydrogène. La plus élevée de ces dernières, la vibration de valence O—H, apparaît dans la vapeur à 3560 cm^{-1} (Fig. 1).

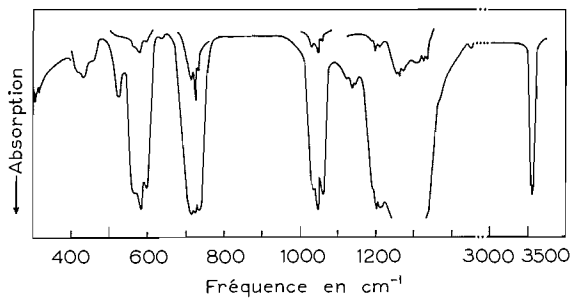

FIG. 1. Spectre infrarouge de $HClO_4$ à l'état gazeux.

Le décalage isotopique de cette fréquence dans $DClO_4$ (Fig. 2) est à peu près dans le rapport prévu, soit 1.36. Par ailleurs dans les phases condensées (Figs. 3 et 4) ces fréquences sont notablement abaissées du fait des liaisons hydrogène (Tableau II).

La fréquence de déformation OH est moins évidente car elle tombe dans la région des vibrations de valence du groupe ClO_3 vers 8 μ. La plus élevée de celles-ci à 1326 cm^{-1} appartient sans aucun doute à la vibration asymétrique ν_9 par analogie avec la vibration correspondante dans $FClO_3$ à 1315 cm^{-1} (Fig. 5). Des deux vibrations Cl—O symétriques l'une doit se trouver assez près de ν_9; on peut donc lui assigner avec certitude la forte bande à 1263 cm^{-1}. Quant à la seconde, ν_4, totalement symétrique par rapport à l'axe Cl—OH, on la trouve à 1050 cm^{-1} (comparé à 1061 cm^{-1} dans $FClO_3$). Effectivement ces trois fréquences demeurent presque identiques dans les spectres des phases condensées aussi bien que dans ceux de $DClO_4$. Il reste donc pour le mode de déformation OH la bande d'intensité moyenne à 1200 cm^{-1} dans la vapeur qui montre bien le décalage isotopique attendu (à 928 cm^{-1}) dans $DClO_4$. Cette fois les liaisons hydrogène causent

TABLEAU II

Spectres infrarouges de $HClO_4$ et $DClO_4$
(Fréquences en cm^{-1})

$HClO_4$			$DClO_4$		Vibrations		
Vapeur	Liquide	Solide	Vapeur	Solide			
4750					$\nu_1+\nu_2$	(A')	
3576, 3560, 3551	3275	3260			ν_1	(a')	valence O—H
			2626	2400	ν_1	(a')	valence O—D
2450							
			1925				
1450							
1336, 1326, 1310	1315	1315	1336, 1325, 1315	1320	ν_9	(a'')	valence Cl—O
1303					$\nu_5+\nu_{10}$	(A'')	
1288					$\nu_5+\nu_6$	(A')	?
1274, 1263, 1254		1283	1284, 1268, 1255	1261	ν_2	(a')	valence Cl—O
1210, 1200, 1188	1245	1245	1208, 1198, 1182	1200	ν_3	(a')	déformation OH
	1215	1200			$\nu_6+\nu_{12}$	(A'')	
1145, 1134, 1122					$2\nu_{10}$	(A')	
1062, 1050, 1039	1041	1033	1033	1033	ν_4	(a')	valence Cl—O
1059, 1047, 1035					ν_4	$(HCl^{37}O_4)$	
			939, 928, 915	965			déformation OD
737, 725, 716	743	740, 760		740, 763	ν_5	(a')	valence Cl—OH
734, 721, 712					ν_5	$(HCl^{37}O_4)$	
632		603		600			
595, 579, 567	582	585	585	583	ν_{10}	(a'')	déformation $\widehat{OClO}$
560	571	566	574	554	ν_6	(a')	déformation $\widehat{OClO}$
526	?	?					
519					ν_7	(a')	déformation $\widehat{OClO}$
450, 430, 415	440	428		417	ν_{11}	(a'')	déformation $\widehat{OClOH}$
390		371, 346			ν_8	(a')	déformation $\widehat{OClOH}$
318, 307	480	478		310	ν_{12}	(a')	torsion OH

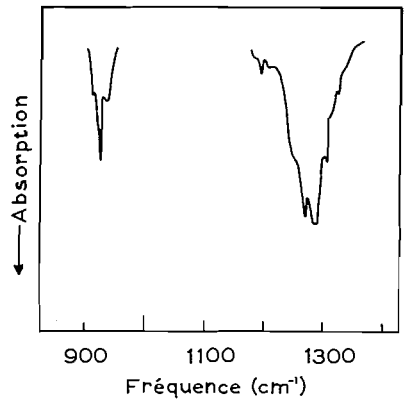

FIG. 2. Bandes d'absorption infrarouge de $DClO_4$ à l'état gazeux entre 7 et 12 μ.

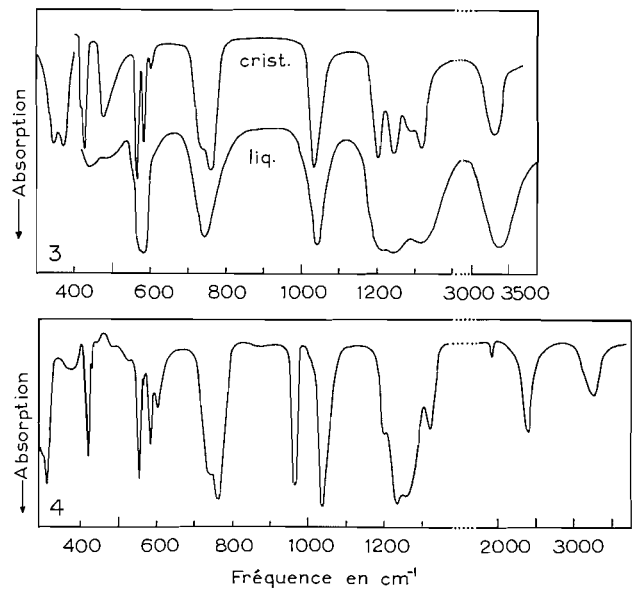

FIG. 3. Spectres infrarouges de l'acide perchlorique anhydre dans les états condensés.
FIG. 4. Spectre d'absorption de $DClO_4$ solide en infrarouge.

une légère élévation de fréquence, soit à 1245 cm^{-1} dans $HClO_4$ et à 965 cm^{-1} dans $DClO_4$ à l'état solide. Il faut noter ici que la présence d'une forte bande exactement à 1200 cm^{-1} dans le spectre du cristal est une coïncidence. En effet, à cause du décalage vapeur–solide déjà mentionné, il faut attribuer cette bande non pas à la déformation OH mais plutôt à des harmoniques ou combinaisons de fondamentales.

Enfin la troisième fréquence OH dite de torsion doit naturellement être assez basse. Lide et Mann (7) ont suggéré de lui attribuer provisoirement la bande à 284 cm^{-1} dans le spectre Raman de l'acide liquide (Tableau I). Cette valeur conviendrait bien pour la molécule libre, mais elle est certainement trop basse pour l'acide liquide à cause des liaisons hydrogène. De toute façon il semble maintenant évident que la bande à 284 cm^{-1} n'appartient pas à $HClO_4$ mais bien plutôt à Cl_2O_7 (3, 16), un produit de la décomposition de l'acide anhydre, sans doute sous l'influence de la radiation excitatrice Raman. Nous croyons plus logique d'assigner au mode de torsion interne la large bande centrée autour

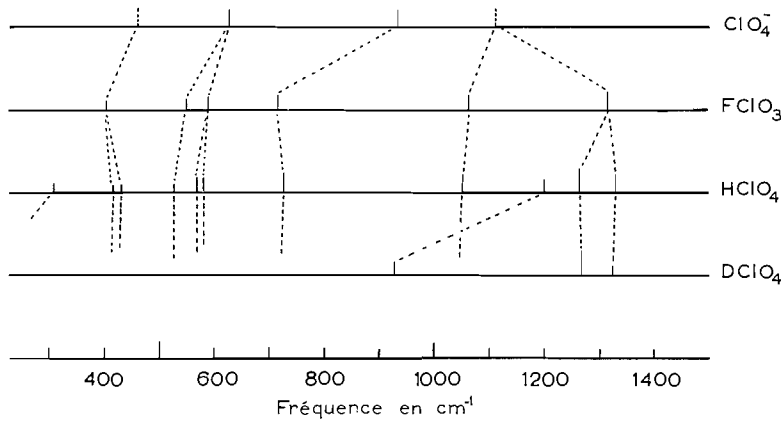

FIG. 5. Corrélation entre les fréquences normales de $HClO_4$ et autres molécules analogues.

de 310 cm^{-1} dans le spectre de la vapeur (Fig. 1) qu'on retrouve décalée à 480 cm^{-1} dans les phases condensées (Fig. 3). Pour $DClO_4$ dont seul le solide a été étudié dans cette région, la bande à 310 cm^{-1} est de fréquence appropriée pour le rapport isotopique, même si elle paraît un peu mince pour une vibration de ce genre.

Il est intéressant de comparer les fréquences de valence OH dans l'acide perchlorique gazeux et solide avec les quantités correspondantes dans d'autres composés apparentés. (Tableau III). Il ressort clairement de ces données que les liaisons hydrogène dans

TABLEAU III

Vibrations de valence OH dans diverses molécules
(Fréquences en cm^{-1})

	ν_v	ν_s	Réf.		$\nu_v - \nu_s$	Réf.
$HClO_4$	3560	3260	—	$HClO_4$	300	—
HNO_3	3560	3226	17	H_2O_2	430	18
H_2SO_4	—	2970	10	CH_3OH	450	19
				H_2O	500	18

$HClO_4$ anhydre (aussi bien que dans HNO_3) sont nettement plus faibles que dans H_2SO_4 et même que dans H_2O, H_2O_2 et les alcools. Des corrélations empiriques (20) permettent d'évaluer l'énergie de ces liaisons dans $HClO_4$ à quelque 3 kcal et les distances interatomiques O—H et O—H . . . . O à environ 1.0 Å et 2.85 Å respectivement. La faiblesse relative des liaisons hydrogène dans cet acide est due en partie à la répulsion entre les groupes ClO_4 fortement électronégatifs. Ces observations rejoignent des conclusions antérieures sur le faible degré d'association moléculaire de l'acide perchlorique absolu basées, entre autre, sur la faible viscosité et la grande volatilité du liquide (6) et le point de fusion relativement bas (−112° C) du solide. Pour la même raison on doit écarter la suggestion faite autrefois (21) de molécules dimères

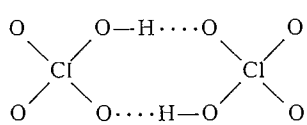

comme dans les acides gras.

La connaissance de toutes les fréquences normales de $HClO_4$ permet le calcul de ses fonctions d'état. Cependant, vu l'absence de détermination expérimentale directe des distances et des angles interatomiques, la contribution des niveaux de rotation ne peut être évaluée avec grande précision. Les paramètres utilisés à cette fin (Tableau IV) ont

TABLEAU IV

Données structurales et thermodynamiques de $HClO_4$

Distances (Å)	Angles	Moments d'inertie (g cm²)	Modes	$-\frac{(F^0-E^0)}{T}$ (cal deg^{-1} mole^{-1})	S^0 (cal deg^{-1} mole^{-1})
Cl—O = 1.45	$\widehat{OClO}$ = 114°	$I_A = I_B = 1.72\times10^{-38}$	Translation	34.76	39.73
Cl—OH = 1.70	$\widehat{OClOH}$ = 105°	$I_C = 1.59\times10^{-38}$	Rotation	22.37	25.36
O—H = 0.97	$\widehat{ClOH}$ = 105°	$I_{torsion} = 1.47\times10^{-40}$	Vibration	1.06	4.80
		Seuil, V_0 = 1.6 kcal	Torsion	0.71	1.81
			Total	58.9	70.7

été choisis comme suit: Les distances Cl—O dans l'acide doivent être à peu près les mêmes que dans l'ion ClO_4^-. Malheureusement les données existantes pour celles-ci dans les perchlorates alcalins (22) se situent entre des limites assez larges, soit de 1.42 à 1.49 Å. Par ailleurs la règle de Badger appliquée aux vibrations Cl—O ν_2 et ν_9 conduit à une valeur moyenne de 1.45 Å. Cette même règle donne, à partir de $\nu_5 = 725$ cm^{-1}, une longueur de 1.71 Å pour la liaison simple Cl—OH, soit à peu près la somme des rayons covalents simples des atomes Cl et O, 1.69 Å (23); d'où notre choix de la valeur intermédiaire, 1.70 Å. Pour la longueur et l'angle de la liaison OH des valeurs assez voisines de celles dans H_2O sont à prévoir. Quant aux angles dans le tétraèdre ClO_4, il est raisonnable de supposer que l'orbitale de l'unique liaison simple occupera moins d'espace que les orbitales des trois autres liaisons essentiellement doubles.

Mentionnons enfin que la contribution des degrés de liberté de translation a été calculée pour l'espèce isotopique $HCl^{35}OH$, et que la torsion, ou rotation interne, a été traitée par la méthode de Pitzer (24). De la fréquence $\nu_{12} = 307$ cm^{-1} dans la molécule libre on déduit pour le seuil de potentiel de symétrie $n = 3$ une valeur, 1.6 kcal, beaucoup plus faible que celle acceptée pour la molécule HNO_3, 7 kcal (25). La raison principale de cette différence tient sans doute à la plus grande distance entre les atomes H et O dans $HClO_4$, environ 2.3 Å, comparée à 1.7 Å dans HNO_3 (22).

REMERCIEMENT

Pour l'exécution de ce travail les auteurs ont bénéficié d'une généreuse subvention du Conseil national des Recherches du Canada.

SUMMARY

The infrared spectra of anhydrous $HClO_4$ and $DClO_4$ in the three physical states were measured between 300 and 5000 cm^{-1}. All the fundamental frequencies of the covalent molecule of C_s symmetry were obtained. The OH frequencies in the crystal indicate hydrogen bonds appreciably weaker (3 kcal) than those in sulphuric acid. From empirical correlations the following bond lengths are deduced: 1.70 Å for the Cl—OH and 1.45 Å for the Cl—O bonds. In the free $HClO_4$ molecule internal rotation is hindered by a threefold potential barrier of some 1.6 kcal. The measured vibrational frequencies were

used in conjunction with probable values of the structural parameters to calculate the following thermodynamic quantities for $HClO_4$ in the standard state at 25° C: $-(F^0 - E^0)/T = 58.9$ and $S^0 = 70.7$ cal deg^{-1} mole^{-1}.

BIBLIOGRAPHIE

1. F. S. Lee et G. B. Carpenter. J. Phys. Chem. **63**, 279 (1959).
2. R. Fonteyne. Nature, **138**, 886 (1936).
3. R. Fonteyne. Natuurw. Tijdschr. (Ghent), **20**, 112, 275 (1938); **21**, 6 (1939).
4. A. Simon, H. Reuther et G. Kratzsch. Z. anorg. u. allgem. Chem. **239**, 329 (1938).
5. O. Redlich, E. K. Holt et J. Bigeleisen. J. Am. Chem. Soc. **66**, 13 (1944).
6. A. Simon et M. Weist. Z. anorg. u. allgem. Chem. **268**, 301 (1952).
7. D. R. Lide, Jr. et D. E. Mann. J. Chem. Phys. **25**, 1128 (1956).
8. G. F. Smith. J. Am. Chem. Soc. **75**, 184 (1953).
9. F. A. Miller et C. H. Wilkins. Anal. Chem. **24**, 1253 (1952).
10. P. A. Giguère et R. Savoie. Can. J. Chem. **38**, 2467 (1960).
11. E. L. Wagner et D. F. Hornig. J. Chem. Phys. **18**, 296 (1950).
12. R. C. Taylor et G. L. Vidale. J. Am. Chem. Soc. **78**, 5999 (1956).
13. R. J. Gillespie. Communication personnelle.
14. L. M. Jones, R. M. Badger et G. E. Moore. J. Chem. Phys. **19**, 1599 (1951).
15. L. D'Or et P. Tarte. Bull. soc. roy. sci. Liège, **8–10**, 478 (1951).
16. R. Savoie. Résultats inédits.
17. S. A. Stern, J. T. Mulhaupt et W. B. Kay. Chem. Revs. **60**, 185 (1960).
18. P. A. Giguère et K. B. Harvey. J. Mol. Spectroscopy, **3**, 36 (1959).
19. M. Falk et E. Whalley. J. Chem. Phys. **34**, 1554 (1961).
20. E. R. Lippincott et R. J. Schroeder. J. Chem. Phys. **23**, 1099 (1955).
21. A. Hantzsch. Ber. **60**, 1940 (1927).
22. L. E. Sutton (*Editeur*). Tables of interatomic distances. Special Publication No. 11. The Chemical Society, London. 1958.
23. V. Schomaker et D. P. Stevenson. J. Am. Chem. Soc. **63**, 37 (1941).
24. K. S. Pitzer. J. Chem. Phys. **5**, 469 (1937).
25. W. R. Forsythe et W. F. Giauque. J. Am. Chem. Soc. **64**, 48 (1942).

THE SYNTHESIS OF ACETAMIDO-DEOXY KETOSES BY ACETOBACTER SUBOXYDANS

PART III

J. K. N. JONES, M. B. PERRY, AND J. C. TURNER
The Department of Organic Chemistry, Queen's University, Kingston, Ontario

Received November 14, 1961

ABSTRACT

1-Acetamido-1-deoxy-D-arabinitol, 1-acetamido-1-deoxy-D-ribitol, and 1-acetamido-1-deoxy-D-mannitol were synthesized and characterized. Microbiological oxidation of 1-acetamido-1-deoxy-D-arabinitol and 1-acetamido-1-deoxy-D-ribitol gave the crystalline acyclic 2-pentuloses 5-acetamido-5-deoxy-D-*threo*-pentulose and 5-acetamido-5-deoxy-L-*erythro*-pentulose respectively.

RESULTS AND DISCUSSION

Crude 1-amino-1-deoxy-D-arabinitol, 1-amino-1-deoxy-D-ribitol, and 1-amino-1-deoxy-D-mannitol were prepared by the method of Holly *et al.* (1) and purified via the salicylidene Schiff's bases by the method of Kagan *et al.* (2). *N*-Acetylation of the pure amino-deoxy polyhydric alcohols with aqueous acetic anhydride (3) then gave 1-acetamido-1-deoxy-D-arabinitol (I), 1-acetamido-1-deoxy-D-ribitol (II), and 1-acetamido-1-deoxy-D-mannitol (III) respectively, which were characterized by periodate oxidation studies, elemental analyses, and infrared spectra.

The microbiological oxidation of acetamido-deoxy polyhydric alcohols by *Acetobacter suboxydans* has recently been investigated in this laboratory (4, 5). We now wish to report the microbiological oxidation of 1-acetamido-1-deoxy-D-arabinitol (I) to 5-acetamido-5-deoxy-D-*threo*-pentulose (IV) and of 1-acetamido-1-deoxy-D-ribitol (II) to 5-acetamido-5-deoxy-L-*erythro*-pentulose (V). Both oxidation products (IV, V) were obtained as strongly reducing crystalline solids which gave absorptions in the infrared corresponding to OH, NH, the amide linkage, and the saturated carbonyl group. Periodate oxidation studies yielded almost identical results in each case (periodate uptake 2.75 moles, formic acid 1.1 moles, formaldehyde 0.75 mole) and indicated that the compounds possessed a primary alcohol group. The results also indicate that approximately 0.2 mole glycollic acid was formed during the oxidation, which was then stable to further attack by periodate ion (6). It was concluded that the carbonyl group was located at carbon 2 in both cases and that cleavage by periodate ion was more rapid between carbons 1 and 2 than between carbons 2 and 3. Since both compounds were therefore probably 2-ketoses, the formation of furanose rings would be prohibited and the acyclic zigzag conformation would be adopted. The hydroxyl groups at carbons 3 and 4 of ketose IV would then be favorably situated for the formation of an isopropylidene derivative. Ketose IV, on reaction with acidified acetone, gave a strongly reducing syrupy isopropylidene derivative (VI) which gave absorptions in the infrared corresponding to OH, NH, the amide linkage, the saturated carbonyl group, and the isopropylidene group. The compound, on periodate oxidation, consumed 0.75 mole periodate, with the liberation of 0.63 mole titratable acid and 0.67 mole formaldehyde, indicating that carbons 1 and 2 were not involved in ketal formation and that the compound was the 3,4-*O*-isopropylidene derivative (VI). Ketose V under similar reaction conditions also gave a syrupy isopropylidene derivative (VII).

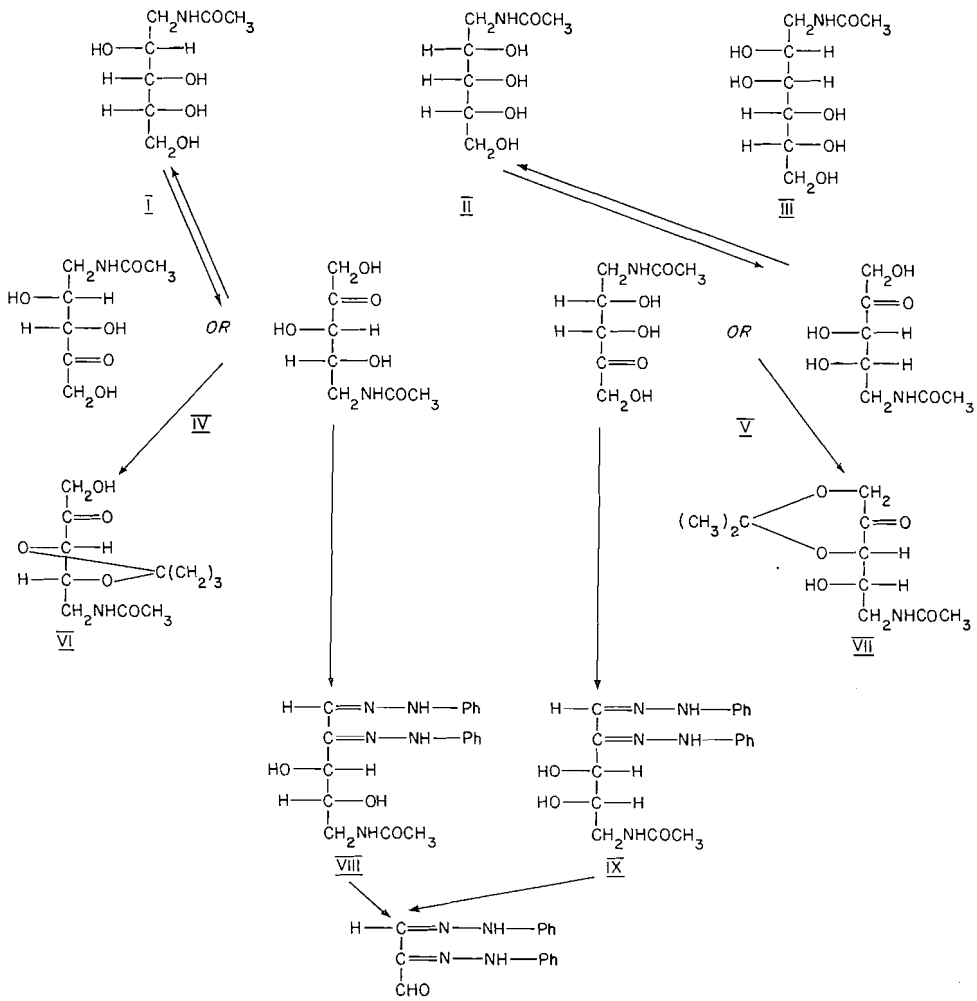

The infrared spectrum was similar to that of the 3,4-*O*-isopropylidene derivative (VI) except that the saturated carbonyl absorption was much stronger. However, the isopropylidene derivative VII was only weakly reducing and on periodate oxidation consumed 0.36 mole periodate, liberating 0.1 mole titratable acid and 0.1 mole formaldehyde, which suggested that hydrolysis to ketose V was occurring before oxidation. It was concluded that compound VII was probably the 1,3-*O*-isopropylidene derivative, which was possible since the carbonyl group distorted the carbon chain sufficiently to bring the primary alcohol group near carbon 3.

Ketose IV gave a crystalline phenylosazone (VIII) which, when oxidized with periodate by the method of Hough, Powell, and Woods (7), consumed 1.18 moles of periodate and released no formic acid or formaldehyde. A rapid formation of the 1,2-bisphenylhydrazone of mesoxalaldehyde (8) occurred. These results indicated that the phenylosazone (VIII) possessed free hydroxyl groups at carbons 3 and 4 and that the ketose (IV) from which it was derived was a 2-ketose. Ketose V also gave a crystalline phenylosazone (IX), which on periodate oxidation gave results closely similar to those

obtained from the oxidation of phenylosazone VIII, and the same conclusions were reached regarding the structure of phenylosazone IX and its parent ketose (V). In the case of IX, however, the precipitation of the 1,2-bisphenylhydrazone of mesoxalaldeh de occurred more slowly, which indicated that the free hydroxyl groups at carbons 3 and 4 of phenylosazone IX were less favorably situated for cleavage by periodate ion than those in the other phenylosazone (VIII), in agreement with the finding for the ketal formation of the free ketoses (IV and V).

Ketose IV on reduction with sodium borohydride gave crystalline 1-acetamido-1-deoxy-D-arabinitol (I), which indicated that the hydroxyl groups at carbons 3 and 4 of ketose IV were in the D-*threo* configuration, since the position of the carbonyl group had been fixed at carbon 2 by previous evidence. Ketose V on reduction with sodium borohydride gave a syrup which could not be satisfactorily crystallized, although paper chromatography and paper electrophoresis indicated the presence of a single compound. However, the syrup, when acetylated, gave a syrupy acetate which had infrared spectrum and retention time on gas–liquid chromatographic analysis identical with the syrupy acetate prepared from 1-acetamido-1-deoxy-D-ribitol (II), although the optical rotation was different. This indicated that some 1-acetamido-1-deoxy-D-ribitol (II) was present in the sodium borohydride reduction product and that the hydroxyl groups at carbons 3 and 4 of ketose V were in the L-*erythro* configuration, since the position of the carbonyl group had been fixed at carbon 2 by previous evidence.

The above evidence indicated that the biological oxidation product from 1-acetamido-1-deoxy-D-arabinitol (I) was the acyclic 2-pentulose 5-acetamido-5-deoxy-D-*threo*-pentulose (IV) and that the biological oxidation product from 1-acetamido-1-deoxy-D-ribitol (II) was the acyclic 2-pentulose 5-acetamido-5-deoxy-L-*erythro*-pentulose (V), in accordance with the Bertrand–Hudson rules for oxidation by *Acetobacter suboxydans* (9, 10).

Studies on the biological oxidation product from 1-acetamido-1-deoxy-D-mannitol (III) are in progress and will be the subject of a later communication.

EXPERIMENTAL

Solutions were concentrated under reduced pressure (ca. 15 mm) below 40° C. Melting points are uncorrected and optical rotations were measured at 23±3° C in water unless otherwise stated. Paper chromatography was carried out by the descending method (11) using Whatman No. 1 paper in the following solvent systems (v/v):

(A) butan-1-ol/ethanol/water, 9:3:3;
(B) ethyl acetate/acetic acid/formic acid/water, 18:3:1:4;
(C) butan-1-ol/pyridine/water, 5:3:2.

Rates of movements of compounds on paper chromatograms are given relative to that of rhamnose (R_{rh} value). Ketose sugars were detected on paper chromatograms with the orcinol – trichloroacetic acid spray reagent (12), other reducing compounds with the *p*-anisidine hydrochloride spray reagent (13), and non-reducing compounds with the alkaline silver nitrate spray reagent (14). Infrared spectra were measured in chloroform solution or as a dispersion in a potassium bromide pellet, using a Perkin–Elmer Model 21 spectrophotometer. Formaldehyde produced in periodate oxidations was determined by the chromotropic acid method (15).

Preparation of 1-Acetamido-1-deoxy Polyhydric Alcohols

1-Amino-1-deoxy polyhydric alcohols were prepared by the method of Kagan *et al.* (2) in which the free aldose sugar was dissolved in liquid ammonia and hydrogenated with Raney nickel catalyst at 2000 p.s.i. and 85° C for 2.5 hours. The 1-amino-1-deoxy polyhydric alcohols were isolated from the crude reaction mixture as the crystalline salicylidene Schiff's bases. Hydrolysis of the Schiff's bases with dilute hydrochloric acid then gave the corresponding 1-amino-1-deoxy polyhydric alcohol hydrochlorides which were deionized in aqueous solution on columns of Amberlite IRA 400 anion-exchange resin to yield the pure 1-amino-1-deoxy polyhydric alcohols. Physical constants of products and intermediates are listed in Table I.

TABLE I

Physical constants of products and intermediates in the preparation of 1-amino-1-deoxy polyhydric alcohols
(Literature values are given in parentheses (2))

Compound	M.p. (°C)	$[\alpha]_D$
Salicylidene 1-amino-1-deoxy-D-arabinitol	188–190 (187–188)	
Salicylidene 1-amino-1-deoxy-D-ribitol	125–127 (126–128)	
Salicylidene 1-amino-1-deoxy-D-mannitol	199–201	
1-Amino-1-deoxy-D-arabinitol hydrochloride	136.5–137.5	+15°
1-Amino-1-deoxy-D-ribitol hydrochloride	132.5–134	−8°
1-Amino-1-deoxy-D-mannitol hydrochloride	163–165	+5°
1-Amino-1-deoxy-D-arabinitol	114–120 (decomp.)	+4°
1-Amino-1-deoxy-D-ribitol	syrup	+5°
1-Amino-1-deoxy-D-mannitol	134–135 (decomp.)	+1°

1-Acetamido-1-deoxy polyhydric alcohols were prepared by *N*-acetylation in aqueous acetic anhydride (3) of the corresponding pure 1-amino-1-deoxy polyhydric alcohols. Yields, physical constants, and elemental analyses are listed in Table II, and infrared data and the results of periodate oxidation studies are listed in Table III.

TABLE II

1-Acetamido-1-deoxy polyhydric alcohols

Compound	% yield after three recrystallizations	M.p. (°C)	$[\alpha]_D$	R_{rh} Solvent: A	B	C	Analysis (%) Calc. C	H	N	Found C	H	N
1-Acetamido-1-deoxy-D-arabinitol	59	146.5–147.5	+23°	0.83	0.94	0.76	43.5	7.8	7.3	43.6	7.9	7.2
1-Acetamido-1-deoxy-D-ribitol	57	91.5–92	−24°	0.89	1.07	0.82	43.5	7.8	7.3	43.4	7.7	7.1
1-Acetamido-1-deoxy-D-mannitol	59	152.5–153	+13°	0.70	0.77	0.65	43.1	7.6	6.3	43.0	7.7	6.1

TABLE III

Infrared data and results of periodate oxidation studies on 1-acetamido-1-deoxy polyhydric alcohols

Compound	Absorptions in the infrared (cm^{-1})	Periodate oxidation (unbuffered aqueous solution) Time (hours)	Periodate uptake (moles/mole)	Formic acid (moles/mole)
1-Acetamido-1-deoxy-D-arabinitol	OH(3400), NH(3300), amide I (1630), amide II (1600)	0.08 1.00 20	3.03 3.04 3.05	1.98 1.98 1.98
1-Acetamido-1-deoxy-D-ribitol	OH and NH (3340), amide I (1610), amide II (1570)	0.08 1.0 3.25	3.04 3.01 3.02	1.93 1.97 1.97
1-Acetamido-1-deoxy-D-mannitol	OH and NH (3350), amide I (1635), amide II (1555)	0.08 1.00 3.00	3.94 3.97 3.97	2.91 2.94 2.94

SECTION A. STUDIES ON 5-ACETAMIDO-5-DEOXY-D-*threo*-PENTULOSE

5-Acetamido-5-deoxy-D-threo-*pentulose*

1-Acetamido-1-deoxy-D-arabinitol (10 g), sorbitol monohydrate (0.5 g), potassium dihydrogen phosphate (0.05 g), and yeast extract powder (0.5 g) were dissolved in tap water (100 ml), sterilized, and innoculated with *Acetobacter suboxydans* in the usual way (4). After 10 days, when Somogyi estimations (16) of the copper-reducing power of the medium indicated an 81% conversion to ketose sugar, the medium was poured into 2 volumes of ethanol, filtered, and the filtrate was deionized by rapid passage through small columns of Amberlite IR 120 (H^+) and Duolite A4 (OH^-) resins at 5° C and concentrated to dryness. The syrup obtained was fractionated on a cellulose column, butan-1-ol half-saturated with water being used as irrigant, and 5-acetamido-5-deoxy-D-*threo*-pentulose was obtained as a chromatographically pure syrup which crystallized after desiccation for 1 month. The ketose was recrystallized from ethanol/ether to give needles, m.p. 105–106° C, $[\alpha]_D$ +34°, which reduced Fehling's solution immediately at room temperature. Absorptions in the infrared were recorded at 3340 cm^{-1} (OH and NH), 1720 cm^{-1} (saturated carbonyl group), 1640 cm^{-1} (amide I), and 1580 cm^{-1} (amide II). The ketose had R_{rh} 0.94 (solvent A), 1.12 (solvent B), and 0.97 (solvent C), and gave an immediate intense spot with the alkaline silver nitrate spray reagent. Anal. Calc. for $C_7H_{13}O_5N$: C, 44.0%; H, 6.8%; N, 7.3%. Found: C, 43.8%; H, 6.9%; N, 7.5%.

Periodate Oxidation of 5-Acetamido-5-deoxy-D-threo-*pentulose*

The ketose was oxidized with an approximately twofold excess of sodium metaperiodate in unbuffered aqueous solution. The results are recorded in Table IV.

TABLE IV

Periodate oxidation of 5-acetamido-5-deoxy-D-*threo*-pentulose

Time (hours)	Periodate uptake (moles/mole)	Formic acid (moles/mole)	Formaldehyde (moles/mole)
0.08	2.20	1.09	0.73
2	2.74	1.11	0.73
3	2.75	1.11	—
4	2.75	1.11	0.73

5-Acetamido-5-deoxy-3,4-O-isopropylidene-D-threo-*pentulose*

5-Acetamido-5-deoxy-D-*threo*-pentulose (300 mg) was shaken at room temperature with dry acetone (150 ml) containing concentrated sulphuric acid (4 drops) for 18 hours. The solution was then neutralized with barium carbonate, filtered, and evaporated to dryness. The residual syrup was separated from a trace of unreacted ketose by chromatography on Whatman No. 3 MM paper in solvent A overnight, and obtained as a chromatographically pure syrup (180 mg), $[\alpha]_D$ +17° (*c*, 1.75 in ethanol), R_{rh} 2.3 (solvent A), 1.84 (solvent B), 1.54 (solvent C). The syrup reduced Fehling's solution rapidly at room temperature and gave the following infrared absorptions: 3460 cm^{-1} (OH), 3360 cm^{-1} (NH), 1725 cm^{-1} (saturated carbonyl group), 1665 cm^{-1} (amide I), 1525 cm^{-1} (amide II), 1390, 1380 cm^{-1} (CH of isopropylidene group).

Periodate Oxidation of 5-Acetamido-5-deoxy-3,4-O-isopropylidene-D-threo-*pentulose*

The isopropylidene ketose was oxidized in 50% aqueous ethanol solution (unbuffered) with a twofold excess of sodium metaperiodate. The results are recorded in Table V. (A fourfold excess of periodate was used for the estimation of formaldehyde.)

TABLE V

Periodate oxidation of 5-acetamido-5-deoxy-3,4-*O*-isopropylidene-D-*threo*-pentulose

Time (hours)	Periodate uptake (moles/mole)	Formic acid (moles/mole)	Formaldehyde (moles/mole)
0.08	0.14	0.07	0.19
1.17	0.29	0.29	0.40
5	0.42	0.38	0.51 (4 hours)
26	0.62	0.56	0.59 (22.5 hours)
52	0.75	0.63	0.67 (70 hours)

5-Acetamido-5-deoxy-D-threo-*pentose Phenylosazone*

The phenylosazone was prepared by the usual method, using freshly distilled phenylhydrazine and glacial acetic acid. Several recrystallizations from aqueous ethanol gave bright yellow needles, m.p. 197–199° C. The phenylosazone gave absorptions in the infrared at 3260 cm^{-1} (OH and NH), 3080 cm^{-1} (aromatic CH), 1660 cm^{-1} (amide I), 1640 cm^{-1} (amide II), and 1605, 1500, 745, 685 cm^{-1} (aromatic ring). Anal. Calc. for $C_{19}H_{23}O_3N_5.H_2O$: C, 58.9%; H, 6.5%; N, 18.1%. Found: C, 59.6%; H, 6.5%; N, 18.1%.

Periodate Oxidation of 5-Acetamido-5-deoxy-D-threo-*pentose Phenylosazone*

The phenylosazone was oxidized in 50% aqueous ethanol by the method of Hough, Powell, and Woods (7). The results of the oxidation are shown in Table VI. One minute after oxidation had started, yellow

TABLE VI

Periodate oxidation of 5-acetamido-5-deoxy-D-*threo*-pentose phenylosazone

Time (hours)	Periodate uptake (moles/mole)	Formic acid (moles/mole)	Formaldehyde (moles/mole)
0.33	1.18	0.00	0.00
1	1.16	0.00	0.00
2.5	1.15	0.00	—

needles separated from the solution. The crystals were centrifuged off and the supernatant was returned to the flask for oxidation studies. The crystals were recrystallized from aqueous ethanol and had m.p. 187–189° C. An authentic specimen of the 1,2-bisphenylhydrazone of mesoxalaldehyde had m.p. 194° C, and the mixed m.p. was 189–191° C. The infrared spectra of the authentic and derived specimens of the 1,2-bisphenylhydrazone of mesoxalaldehyde were identical over the range 4000–600 cm^{-1}.

Sodium Borohydride Reduction of 5-Acetamido-5-deoxy-D-threo-*pentulose*

5-Acetamido-5-deoxy-D-*threo*-pentulose (200 mg) was reduced with an equal weight of sodium borohydride in aqueous solution at 0° C for 3 hours. After removal of sodium borohydride and sodium borate the product was obtained as a clear syrup (200 mg). The syrup was dissolved in ethanol, cooled, and seeded with 1-acetamido-1-deoxy-D-arabinitol. Crystallization occurred and the crystals were filtered off, dried, and recrystallized from ethanol and had m.p. 145–147° C (47 mg). 1-Acetamido-1-deoxy-D-arabinitol had m.p. 146.5–147.5° C, and the mixed m.p. was 145–147° C. The infrared spectra of the authentic and derived specimens were identical over the range 4000–600 cm^{-1}. The derived specimen had $[\alpha]_D$ +22.6° and the authentic specimen had $[\alpha]_D$ +23°.

Section B. Studies on 5-Acetamido-5-deoxy-L-*erythro*-pentulose

5-Acetamido-5-deoxy-L-erythro-*pentulose*

1-Acetamido-1-deoxy-D-ribitol was oxidized by *Acetobacter suboxydans* using exactly the same procedure as that described for 1-acetamido-1-deoxy-D-arabinitol (Section A) to give an 83% conversion to ketose sugar after 10 days. After 21 days the medium was worked up in the usual way and the syrup obtained was fractionated on a cellulose column using butan-1-ol half-saturated with water as irrigant. 5-Acetamido-5-deoxy-L-*erythro*-pentulose was obtained as a chromatographically pure syrup which crystallized after desiccation for 1 week. The ketose was recrystallized from aqueous ethanol to give prisms, m.p. 160–164° C (decomp.), $[\alpha]_D$ +7°, which reduced Fehling's solution immediately at room temperature. Absorptions in the infrared were recorded at 3480 cm^{-1} (OH), 3310 cm^{-1} (NH), 1725 cm^{-1} (saturated carbonyl group), 1630 cm^{-1} (amide I), 1565 cm^{-1} (amide II). The ketose had R_{rh} 1.0 (solvent A), 1.15 (solvent B), 1.02 (solvent C), and gave an immediate intense spot with the alkaline silver nitrate spray reagent. Anal. Calc. for $C_7H_{13}O_5N$: C, 44.0%; H, 6.8%; N, 7.3%. Found: C, 43.8%; H, 6.9%; N, 7.5%.

Periodate Oxidation of 5-Acetamido-5-deoxy-L-erythro-*pentulose*

The ketose was oxidized with an approximately twofold excess of sodium metaperiodate in an unbuffered aqueous solution. The results are recorded in Table VII.

5-Acetamido-5-deoxy-1,3(?)-O-isopropylidene-L-erythro-*pentulose*

5-Acetamido-5-deoxy-L-*erythro*-pentulose (200 mg) was shaken with dry acetone (150 ml) containing concentrated sulphuric acid (4 drops), at room temperature, for 18 hours. The reaction mixture was neutralized with barium carbonate and filtered, the filtrate was evaporated to dryness, and the residue was examined on paper chromatograms. The orcinol – trichloroacetic acid spray reagent revealed three components, the major one having R_{rh} 2.74 (solvent A), 1.72 (solvent C), and this was separated by chromatography on Whatman No. 3 MM paper in solvent A. The material was obtained on elution as a

TABLE VII

Periodate oxidation of 5-acetamido-5-deoxy-L-*erythro*-pentulose

Time (hours)	Periodate uptake (moles/mole)	Formic acid (moles/mole)	Formaldehyde (moles/mole)
0.08	2.16	1.07	0.76
1.25	2.73	1.08	0.77
2.5	2.72	1.08	—
3.75	2.74	1.09	0.74

yellow syrup (83 mg). The optical rotation could not be measured due to the color of the solution. The syrup gave absorptions in the infrared at 3450 cm^{-1} (OH), 3350 cm^{-1} (NH), 1740 cm^{-1} (saturated carbonyl group), 1660 cm^{-1} (amide I), 1525 cm^{-1} (amide II), 1390, 1380 cm^{-1} (CH of the isopropylidene group). The syrup did not reduce Fehling's solution at room temperature but did so when heated; it gave a slow, weak reaction with the alkaline silver nitrate spray reagent.

*Periodate Oxidation of 5-Acetamido-5-deoxy-1,3(?)-O-isopropylidene-*L-erythro-*pentulose*

The isopropylidene ketose was oxidized in 50% aqueous ethanol solution (unbuffered) with a twofold excess of sodium metaperiodate. The results are recorded in Table VIII.

TABLE VIII

Periodate oxidation of 5-acetamido-5-deoxy-1,3(?)-*O*-isopropylidene-L-*erythro*-pentulose

Time (hours)	Periodate uptake (moles/mole)	Formic acid (moles/mole)	Formaldehyde (moles/mole)
0.17	0.05	0.02	0.00
1.42	0.09	0.05	0.08 (1.58 hours)
4	0.12	0.05	0.08
23.5	0.36	0.11	0.10 (22.5 hours)

*5-Acetamido-5-deoxy-*L-erythro-*pentose Phenylosazone*

The phenylosazone was prepared by the usual method, using freshly distilled phenylhydrazine and glacial acetic acid. Several recrystallizations of the product from ethanol gave bright yellow needles, m.p. 180–182° C. The phenylosazone gave absorptions in the infrared at 3550 cm^{-1} (OH), 3310 cm^{-1} (NH), 3080 cm^{-1} (aromatic CH), 1650 cm^{-1} (amide I), 1630 cm^{-1} (amide II) and 1605, 1495, 745, 690 cm^{-1} (aromatic ring). Anal. Calc. for $C_{19}H_{23}O_3N_5$: C, 61.8%; H, 6.2%; N, 19.0%. Found: C, 61.2%, 61.7%; H, 6.5%, 7.0%; N, 19.7%, 19.4%. Good analyses were not obtained despite repeated recrystallizations.

*Periodate Oxidation of 5-Acetamido-5-deoxy-*L-erythro-*pentose Phenylosazone*

The phenylosazone was oxidized under the same conditions as those used for 5-acetamido-5-deoxy-D-*threo*-pentose phenylosazone (Section A). The results of the oxidation are shown in Table IX. Fifteen

TABLE IX

Periodate oxidation of 5-acetamido-5-deoxy-L-*erythro*-pentose phenylosazone

Time (hours)	Periodate uptake (moles/mole)	Formic acid (moles/mole)	Formaldehyde (moles/mole)
0.17	1.24	0.00	0.00
1.17	1.15	0.00	0.00
2.5	1.14	0.00	—
4	1.14	0.00	—

minutes after oxidation had commenced, a precipitate of the 1,2-bisphenylhydrazone of mesoxalaldehyde appeared and was isolated as described in Section A. It had m.p. 185–187° C and an authentic specimen had m.p. 192–193° C; mixed m.p. was 185–187° C. The infrared spectra of the authentic and derived specimens of the 1,2-bisphenylhydrazone of mesoxalaldehyde were identical over the range 4000–600 cm^{-1}.

Sodium Borohydride Reduction of 5-Acetamido-5-deoxy-L-erythro-*pentulose*

5-Acetamido-5-deoxy-L-*erythro*-pentulose (300 mg) was reduced with an equal weight of sodium borohydride in aqueous solution at 0° C for 4 hours. After removal of sodium borohydride and sodium borate the product was obtained as a pale yellow syrup (315 mg) which was dissolved in ethanol, seeded with 1-acetamido-1-deoxy-D-ribitol, and cooled. Crystallization occurred but on attempted filtration the crystals immediately liquefied, and repeated attempts to isolate the material failed. The syrup gave one spot on paper chromatograms R_{rh} 0.91 (solvent A), 1.0 (solvent B), 0.83 (solvent C). Paper electrophoresis in pH 9.2 sodium borate buffer at 500 volts for 5 hours gave one spot with a rate of movement slightly less than that of 1-acetamido-1-deoxy-D-ribitol. The syrup was acetylated with acetic anhydride in pyridine solution and gave a syrupy product (466 mg) which had $[\alpha]_D$ −15° (*c*, 3.78 in chloroform). Acetylation of 1-acetamido-1-deoxy-D-ribitol gave a syrupy acetate which had $[\alpha]_D$ +3° (*c*, 4.1 in chloroform). When subjected to gas–liquid chromatographic analysis (column packing D, reference 17) at a flow rate of 100 ml/minute and temperatures of 213° C or 225° C, the two acetates had identical retention times and a mixture of the two gave a single symmetrical peak. The two acetates had practically identical infrared spectra and gave absorptions at 3440 cm^{-1} (NH), 1740 cm^{-1} (carbonyl group of *O*-acetate), 1680 cm^{-1} (amide I), and 1520 cm^{-1} (amide II). It was concluded that the sodium borohydride reduction product from 5-acetamido-5-deoxy-L-*erythro*-pentulose contained mainly 1-acetamido-1-deoxy-D-ribitol and an isomeric 1-acetamido-1-deoxy pentitol.

ACKNOWLEDGMENTS

We wish to thank the National Research Council for financial assistance (N.R.C. 706 and T-39) and Queen's University for the award of a scholarship to one of us (J. C. T.). We would also like to thank Mr. J. Mackintosh for technical assistance, and the Royal Military College, Kingston, Ontario, for the use of a high-pressure hydrogenator.

REFERENCES

1. F. W. Holly, E. W. Peel, R. Mozingo, and K. Folkers. J. Am. Chem. Soc. **72**, 5416 (1950).
2. F. Kagan, M. A. Rebenstoff, and R. V. Heinzelman. J. Am. Chem. Soc. **79**, 3541 (1957).
3. G. A. Levvy and A. McAllan. Biochem. J. **73**, 127 (1959).
4. J. K. N. Jones, M. B. Perry, and J. C. Turner. Can. J. Chem. **39**, 965 (1961).
5. J. K. N. Jones, M. B. Perry, and J. C. Turner. Can. J. Chem. **39**, 2400 (1961).
6. P. Fleury, J. Courtois, R. Perles, and L. DeDizet. Bull. soc. chim. France, 347 (1954).
7. L. Hough, D. B. Powell, and B. W. Woods. J. Chem. Soc. 4799 (1956).
8. E. Chargaff and B. Magasanik. J. Am. Chem. Soc. **69**, 1459 (1947).
9. R. M. Hann, E. B. Tilden, and C. S. Hudson. J. Am. Chem. Soc. **60**, 1201 (1938).
10. G. Bertrand. Ann. chim. (Paris), **3** (8), 209, 287 (1904).
11. S. M. Partridge. Biochem. J. **42**, 238 (1948).
12. R. Klevstrand and A. Nordal. Acta. Chem. Scand. **4**, 1320 (1950).
13. L. Hough, J. K. N. Jones, and W. H. Wadman. J. Chem. Soc. 1702 (1950).
14. W. E. Trevelyan, D. P. Proctor, and J. S. Harrison. Nature, **166**, 444 (1950).
15. J. F. O'Dea and R. A. Gibbons. Biochem. J. **55**, 580 (1953).
16. M. Somogyi. J. Biol. Chem. **160**, 61, 69 (1945).
17. S. W. Gunner, J. K. N. Jones, and M. B. Perry. Can. J. Chem. **39**, 1892 (1961).

THE SYNTHESIS OF MERCAPTOINDOLES

E. PIERS, V. B. HAARSTAD, R. J. CUSHLEY, AND R. K. BROWN
Department of Chemistry, University of Alberta, Edmonton, Alberta

Received December 4, 1961

ABSTRACT

The 4-, 5-, 6-, and 7-mercaptoindoles have been prepared via the Reissert condensation of the isomeric benzylthio-*o*-nitrotoluenes. The latter were synthesized by diazotization of the corresponding 2-nitrotoluidines or by direct displacement of the halogen atom in monobrominated *o*-nitrotoluenes with the benzylmercapto group using dimethylformamide as solvent.

INTRODUCTION

Interest in the preparation of 4-mercaptoindole arose from the observation that the structurally analogous 6-mercaptopurine has been used successfully in the treatment of some forms of cancer (1, 2).

Apart from attempts to prepare 3-mercaptoindole, which oxidizes extremely easily to the diindolyl disulphide (3, 4), to our knowledge, no report exists in the literature concerning the remaining isomeric mercaptoindoles. Hence it was thought of interest to prepare the 4-, 5-, 6-, and 7-mercaptoindoles.

DISCUSSION

Attempts at direct replacement of nuclear bromine or chlorine in the benzene ring portion of indole by the mercapto group using potassium hydrogen sulphide or thiourea in various solvents met with failure, although similar procedures were successful when applied to 2-bromopyridine or to several chloropurines (5–7). Preparation of the mercaptophenylhydrazones which could be converted to the indole structure by Fischer's method (8) was quite unsatisfactory. However, since methoxy-*o*-nitrotoluenes and ethyl oxalate had been condensed and cyclized to methoxyindoles (9) via the Reissert procedure (10), the same approach was investigated in the present case and was found to be quite successful. Accordingly the isomeric 4-, 5-, 6-, and 7-benzylthio-2-nitrotoluenes were synthesized for this purpose.

The intermediate 4-benzylthio-2-nitrotoluene was prepared in 32% yield from 2-nitro-*p*-toluidine (11) by converting the latter to 4-mercapto-2-nitrotoluene via diazotization (12, 13) followed by treatment with base and benzyl chloride. The 5-benzylthio-2-nitrotoluene was obtained by nitration of aceto-*m*-toluidide according to the general method given by Fieser (14) and then conversion of the amine to the thioether as in the case of the 4-isomer.

The compound 6-nitro-*o*-toluidine required for the preparation of 2-benzylthio-6-nitrotoluene via the route indicated above could not be made satisfactorily by published procedures. Selective reduction of trinitrotoluene, reported to give 4-amino-2,6-dinitrotoluene (17), in our hands produced a substance which could be deaminated (18) only in very low yield. The crude 2,6-dinitrotoluene obtained from this reaction failed to reduce satisfactorily to 6-nitro-*o*-toluidine either with ammonium sulphide (19) or by electrolytic means (20). A more direct route to 6-benzylthio-2-nitrotoluene became available when it was found that the more nucleophylic potassium benzyl mercaptide displaced the halogen (21) in 2-bromo-6-nitrotoluene, especially if the reaction was carried out in dimethylformamide (22), yielding 26% of the thioether.

The fourth isomer, 3-benzylthio-2-nitrotoluene, necessary for the synthesis of 7-mercaptoindole, was obtained by two routes. The first involved the conversion of *m*-toluic acid to 2-nitro-*m*-toluic acid (23), which was then subjected to the Schmidt reaction (24), yielding 2-nitro-*m*-toluidine. This amine was converted to 3-benzylthio-2-nitrotoluene, in 19% yield, by the same method employed for the preparation of the 4- and 5-benzylthio-2-nitrotoluenes (12, 13). In the second route, the displacement of the halogen atom of 3-bromo-2-nitrotoluene (25) by treatment with potassium benzyl mercaptide in dimethylformamide gave the 3-benzylthio-2-nitrotoluene in 86% yield.

Although potassium ethoxide is a more effective base in the Reissert reaction of nitrotoluenes with ethyl oxalate (15), the cheaper sodium ethoxide was found to be quite satisfactory for the condensation of both 4- and 5-benzylthio-2-nitrotoluene with the ester. These conditions, when applied to the 3- and 6-benzylthio-2-nitrotoluenes, gave only small amounts of the pyruvate. However, use of potassium ethoxide as base and ether as solvent (15), along with extended reaction times of several days at room temperature, permitted the isolation of the potassium enolates of ethyl 3- and 6-benzylthio-2-nitrophenylpyruvate. The 6-benzylthio-2-nitrotoluene required, at the maximum, 6 days at room temperature to produce the enolate in 94% yield while the 3-benzylthio-2-nitrotoluene gave the condensation product in only 68% yield even after 16 days' reaction time. The greater difficulty which the 3- and 6-isomers find in undergoing the Reissert condensation might be attributed to the lower degree of activation which the methyl group experiences due to the ortho nitro group. If coplanarity of the nitro group with the ring is responsible, at least in part, for the activation of the methyl group and subsequent removal of a proton by base to form the carbanion, it is readily seen that the groups in the two positions ortho to the nitro substituent in 3-benzylthio-2-nitrotoluene (structure I) and the buttressing effect of the benzylthio group upon the methyl substituent in the 6-benzylthio-2-nitrotoluene (structure II) would indeed cause a marked restriction to the coplanarity of the nitro group with the ring as compared with that attainable in the 4- (and 5-) benzylthio-2-nitrotoluene (structure III). In support of this view it has been found that the position of the characteristic absorption bands in the infrared spectrum of the nitro group in these nitrotoluenes resemble those for the aliphatic nitro group in nitromethane to a progressively greater degree in the order 3-benzylthio-2-nitrotoluene > 6-benzylthio-2-nitrotoluene > 4-benzylthio-2-nitrotoluene (Table I). The order of the apparent ease of condensation of these toluenes with ethyl oxalate is 4-benzylthio-2-nitrotoluene > 6-benzylthio-2-nitrotoluene > 3-benzylthio-3-nitrotoluene.

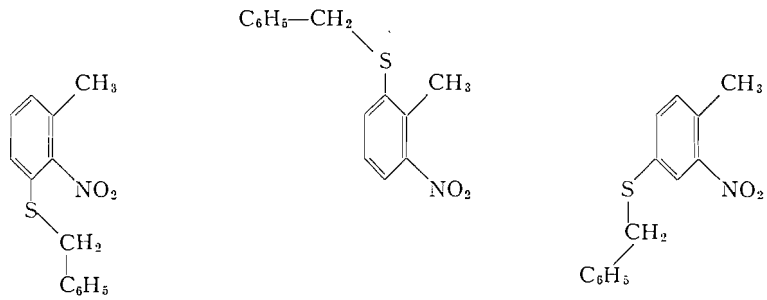

I II III

It is also possible that the greater difficulty in the formation of the pyruvate in the case of the 3- and 6-benzylthio-2-nitrotoluenes than for the 4- and 5-isomers may be due to an unfavorable shift in the equilibria indicated below.

TABLE I

Stretching bands of the nitro group in the infrared*
(Calibrated with polystyrene, 6.238 μ)

Compound	Stretching bands, μ	
	Asymmetric	Symmetric
o-Nitrotoluene	6.54	7.40
4-Benzylthio-2-nitrotoluene	6.53	7.40
6-Benzylthio-2-nitrotoluene	6.52	7.37
3-Benzylthio-2-nitrotoluene	6.50	7.29
Nitromethane	6.38	7.18

*Compare the data given for the infrared spectra of nitro compounds by R. N. Jones and C. Sandorfy in A. Weissburger's *Chemical applications of spectroscopy* (Interscience Publishers, Inc., New York. 1956. p. 540).

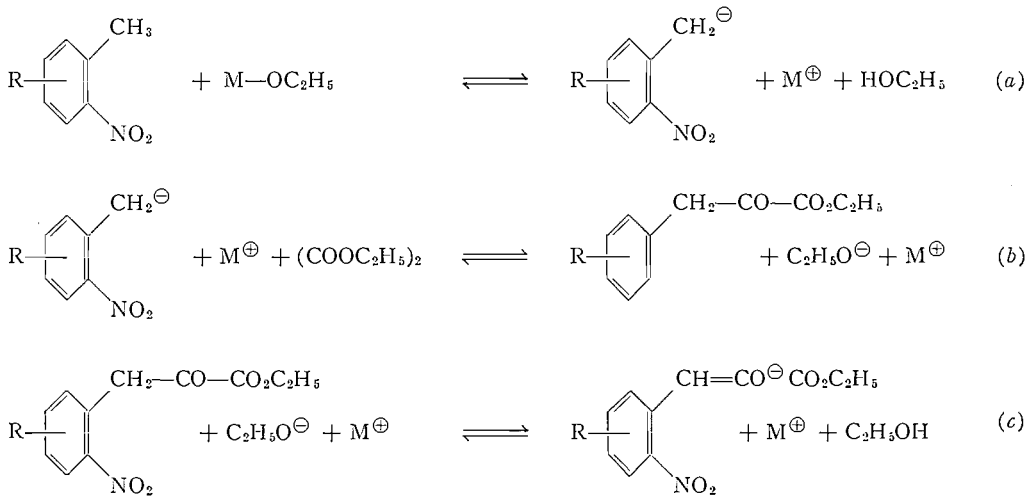

The requirement of a stronger base to shift the equilibrium to the right in equation (*c*) as well as solvent conditions which cause the precipitation of the enolate (step *c*) is therefore understandable. It has been found that in attempts at converting the potassium enolate of ethyl 6-benzylthio-2-nitrophenylpyruvate to the pyruvic acid by treatment with aqueous base some 6-benzylthio-2-nitrotoluene was obtained. Hence, for best results, the potassium enolate was used directly for the next step in the synthesis of the indole. In fact when pure 4-benzylthio-2-nitrophenylpyruvic acid was left in a solution of 95% ethanol (from which the acid could be crystallized) for a period of 4 weeks at room temperature, the bulk of the pyruvic acid reverted to 4-benzylthio-2-nitrotoluene. This clearly demonstrates the reversible nature of the Reissert reaction. The Reissert condensation appears to resemble the Claisen condensation in many respects (26). A detailed study of the Reissert reaction is at present under way in this laboratory.

The 4- and 5-benzylthio-2-nitrophenylpyruvic acids were reductively cyclized in the usual way with ferrous ammonium sulphate (9, 16). In the case of the potassium enolates of ethyl 3- (and 6-) benzylthio-2-nitrophenyl pyruvate, best results were obtained when a hot solution of the salt in dilute ammonium hydroxide was added to a boiling suspension of ferrous hydroxide. Following elimination of contaminating sulphate ion (16), decarboxylation of both 5- and 6-benzylthioindole-2-carboxylic acid was readily accomplished according to directions in the literature using a copper chromite catalyst (16). This

method, however, when applied to the 4- and 7-benzylthioindole-2-carboxylic acids gave low yields of products which were quite difficult to purify. In addition, considerable sulphur was lost as H_2S. A modified method of decarboxylation, recently described (27), using as catalyst a small amount of the copper salt of the respective indolecarboxylic acid, gave excellent yields of easily purified 4- and 7-benzylthioindoles.

Cleavage of the thioethers with sodium in liquid ammonia to the respective mercaptoindoles followed published directions with some slight modifications (28, 29).

EXPERIMENTAL

All melting points are uncorrected.

4-Benzylthio-2-nitrotoluene

Fifty-four grams (0.355 mole) of 2-nitro-*p*-toluidine, prepared by the method of Cohen and Dakin (11), was diazotized and converted to the xanthogenic ester according to Bennett and Berry (12, 13). The crude ester was hydrolyzed in a refluxing solution made from 20 g of sodium in 200 ml of ethanol to which 40 ml of water was added. An atmosphere of oxygen-free nitrogen was employed to minimize oxidation of the mercaptan to the disulphide. After 1 hour's reflux the solution was diluted with an equal volume of boiled distilled water (N_2) and poured into a separatory funnel previously flushed out with nitrogen. After the addition of 50 g of benzyl chloride, the mixture was shaken vigorously for 5 minutes. A further addition of 10 g of benzyl chloride was made and the mixture again shaken for 5 minutes. During this time enough 6 *N* sodium hydroxide was introduced periodically to maintain an alkaline condition. Combined ether extracts of the cooled solution were washed with water and dried (Na_2SO_4). Removal of the ether left an oil which was fractionally distilled under vacuum to yield 29 g (32%) of 4-benzylthio-2-nitrotoluene, b.p. 143° at 0.2 mm, m.p. 78°. The thioether crystallized well from 95% ethanol. Calc. for $C_{14}H_{13}O_2NS$: S, 12.37. Found: S, 12.23.

6-Nitro-m-toluidine

m-Toluidine was acetylated (ref. 14, p. 165) and the resulting *m*-acetotoluidide nitrated by the general method given by Fieser (ref. 14, p. 170). The crude product obtained proved to be a mixture of acetylated and unacetylated 6-nitro-*m*-toluidine. This material, without further purification, was hydrolyzed in 20-gram batches by refluxing with 1200 ml of a 1:1 mixture of concentrated hydrochloric acid and water containing enough ethanol to dissolve the solid when hot. Following a 1-hour reflux period, the solution was cooled and neutralized with solid sodium carbonate. The precipitate was removed and extracted with boiling dilute hydrochloric acid. (Any solid not soluble in the hot dilute acid was subjected to further hydrolysis as above.) The precipitate obtained from basification of the combined extracts was washed with water and air dried. The crude material melted at 129–130° (lit. 133–134° (30)) and was quite satisfactory for the next reaction.

5-Benzylthio-2-nitrotoluene

By the same method employed above 54 g of 6-nitro-*m*-toluidine was converted to 26.5 g (29%) of 5-benzylthio-2-nitrotoluene, m.p. 55.5–57°. Calc. for $C_{14}H_{13}O_2NS$: S, 12.37. Found: S, 12.28.

2-Bromo-6-nitrotoluene

o-Nitrotoluene was brominated by published procedures (32). The 2-bromo-6-nitrotoluene was separated from the 4-bromo-2-nitrotoluene by fractionation under reduced pressure with a meter-length column containing a stainless steel packing. The 2-bromo-6-nitrotoluene distilled over first and the product solidified in the receiver. The next fraction came over as an oil and proved to be a mixture of the two isomers. Recrystallization of the solid 2-bromo-6-nitrotoluene from ethanol containing a small amount of water gave a 26% yield of pure product. B.p. 108–110° at 3.3 mm; m.p. 41–42°, lit. 42° (19).

6-Benzylthio-2-nitrotoluene

Powdered potassium carbonate (38.8 g, 0.28 mole) was stirred into 50 ml of dimethylformamide containing 55 g (0.25 mole) of 2-bromo-6-nitrotoluene. To this was added 31.3 g (0.25 mole) of benzyl mercaptan (33) all at once. The stirred reaction mixture, kept under nitrogen, was heated for 4 hours at 50–55° and then stirred at room temperature for 14 hours. The addition of an equal volume of water, followed by cooling to 0°, produced a yellow solid which was triturated with dilute sodium hydroxide and then with water. Crystallization from ethanol gave 17.5 g (26%) of yellow needles, m.p. 102–103°. Calc. for $C_{14}H_{13}O_2NS$: C, 64.86; H, 5.02; N, 5.41; S, 12.35. Found: C, 64.72; H, 5.27; N, 5.38; S, 12.42.

3-Benzylthio-2-nitrotoluene

Following the same procedure outlined above, 17.0 g (0.079 mole) of 3-bromo-2-nitrotoluene (25) afforded 17.5 g (86%) of 3-benzylthio-2-nitrotoluene melting at 53–54°. Anal. Found: C, 64.56; H, 5.48; N, 5.27; S, 12.47.

4-Benzylthio-2-nitrophenylpyruvic Acid

To a solution of 6.9 g (0.30 mole) of sodium in 170 ml of anhydrous ethanol were added 44 g (0.30 mole) of diethyl oxalate and 77 g (0.30 mole) of 4-benzylthio-2-nitrotoluene. The reaction mixture, which rapidly became dark red, was refluxed for 1 hour, cooled, diluted with twice its volume of water, and then thrice extracted with ether. The aqueous layer was acidified to Congo red with concentrated hydrochloric acid. Air was blown through the solution to remove residual ether, whereupon crystallization occurred. The solid was separated, dissolved in dilute ammonium hydroxide, and again reprecipitated with hydrochloric acid. Crystallization from an alcohol–water mixture gave 66 g of 4-benzylthio-2-nitrophenylpyruvic acid which melted at 166–167° with decomposition. From the ethereal extract was recovered 9 g of unchanged 4-benzylthio-2-nitrotoluene. Yield, based upon the thioether consumed, 75%.

5-Benzylthio-2-nitrophenylpyruvic Acid

By the same method described above, 5-benzylthio-2-nitrotoluene afforded an oil which failed to solidify. It was therefore purified further by solution in cold dilute ammonium hydroxide followed by precipitation with concentrated hydrochloric acid. An ether extract of the oil was dried (Na_2SO_4), freed of solvent, and the residual oil subjected to the reductive cyclization step in the synthesis.

Potassium Enolate of Ethyl 3-Benzylthio-2-nitrophenylpyruvate

Potassium (4.7 g, 0.12 mole) was dissolved in 20 ml of anhydrous ethanol. To this solution, diluted with 150 ml of dry ether, was added 17.5 g (0.12 mole) of diethyl oxalate, followed 15 minutes later by an anhydrous ether solution of 3-benzylthio-2-nitrotoluene (26 g, 0.10 mole). A deep orange solution resulted which, when left at room temperature for 16 days, slowly deposited the potassium enolate as an orange precipitate. The solid, collected and washed thoroughly with anhydrous ether and then air dried, weighed 27.0 g (68% crude yield). This salt was used directly in the reductive cyclization step.

Potassium Enolate of Ethyl 6-Benzylthio-2-nitrophenylpyruvate

This salt was obtained in 94% yield from 6-benzylthio-2-nitrotoluene by the method described above. The reaction time required in this case was 6 days rather than 16.

6-Benzylthioindole-2-carboxylic Acid

The reductive cyclization of 4-benzylthio-2-nitrophenylpyruvic acid was accomplished according to published procedures (9). The resulting 6-benzylthioindole-2-carboxylic acid was freed from sulphate ion and purified according to Rydon and Tweddle (16). The solid acid obtained after removal of the ether was taken up in cold dilute ammonium hydroxide. Upon acidification (HCl) and cooling, the solution deposited a solid which was air dried. From 15 g of the pyruvic acid there was obtained 8 g (62%) of the indolecarboxylic acid, m.p. 215°. Calc. for $C_{16}H_{13}O_2NS$: S, 11.35. Found: S, 11.32.

5-Benzylthioindole-2-carboxylic Acid

The same method of reductive ring closure converted the crude, oily 5-benzylthio-2-nitrophenylpyruvic acid to 5-benzylthioindole-2-carboxylic acid, m.p. 210–211° (decomp.). Calc. for $C_{16}H_{13}O_2NS$: S, 11.35. Found: S, 11.40. Yield, based upon 45 g of 5-benzylthio-2-nitrotoluene used in the Reissert condensation reaction from which 19 g of the toluene was recovered unchanged, 15.2 g (54%).

7-Benzylthioindole-2-carboxylic Acid

For best results, the usual reductive cyclization (9, 16) was modified as follows. A solution of the potassium enolate of ethyl 3-benzylthio-2-nitrophenylpyruvate (10.0 g, 0.025 mole) in hot (80°) 4 *N* ammonium hydroxide (250 ml) was added slowly with stirring to a boiling suspension of ferrous hydroxide. (The latter was obtained by the addition of 25 ml of ammonium hydroxide, $d = 0.90$, to a boiling solution of ferrous sulphate heptahydrate, 45 g, 0.16 mole, in 300 ml of water.) The resulting mixture was boiled for 90 minutes and then filtered. The ferric oxide sludge was repeatedly extracted with boiling 2 *N* ammonium hydroxide until acidification of an aliquot of the extract failed to precipitate the indolecarboxylic acid. The combined extracts were cooled to 5°, filtered, and washed several times with ether. Upon acidification a solid appeared which when dried gave 2.2 g (31%) of 7-benzylthioindole-2-carboxylic acid melting at 165–166°. Calc. for $C_{16}H_{13}O_2NS$: C, 67.84; H, 4.59; N, 4.95; S, 11.31. Found: C, 67.59; H, 4.75; N, 5.05; S, 11.54.

4-Benzylthioindole-2-carboxylic Acid

This compound was prepared similarly in 56% yield from the potassium enolate of ethyl 6-benzylthio-2-nitrophenylpyruvate. Purification as above gave a brown solid melting at 185–186°. Anal. Found: C, 67.84; H, 4.63; N, 4.96; S, 11.22.

6-Benzylthioindole

Decarboxylation was carried out essentially according to published directions (16) using quinoline and copper chromite (31). Thirty-two grams of 6-benzylthioindole-2-carboxylic acid in 320 ml of distilled quinoline containing 5 g of copper chromite catalyst was heated 16 hours at 200°. The crude indole obtained from this reaction was dissolved in ethanol and clarified with charcoal. Three crops of product were obtained

by successive reductions in the volume of the solvent. The combined precipitates, crystallized from an alcohol–water mixture, afforded 18 g (67%) of 6-benzylthioindole, m.p. 106.5–107°. Calc. for $C_{15}H_{13}NS$: S, 13.41. Found: S, 13.32.

5-Benzylthioindole

5-Benzylthioindole-2-carboxylic acid (15 g) was similarly decarboxylated by heating for 11 hours at 200–210° and gave 6.6 g (52%) of 5-benzylthioindole melting sharply at 74–75°. Calc. for $C_{15}H_{13}NS$: S, 13.41. Found: S, 13.62.

7-Benzylthioindole

Since decarboxylation of 7-benzylthioindole-2-carboxylic acid by the usual procedure (16), employed successfully for the 5- and 6-isomers, proved to be quite unsatisfactory, giving poor yields even after extended times of reaction and also causing some loss of sulphur as H_2S, a modified procedure recently described (27) which avoids these difficulties was employed. From 2.83 g (0.01 mole) of the acid there was obtained 2.05 g (85%) of 7-benzylthioindole melting at 52–53° (from skellysolve B). Calc. for $C_{15}H_{13}NS$: C, 75.27; H, 5.47; N, 5.85; S, 13.40. Found: C, 75.36; H, 5.42; N, 5.93; S, 13.71.

4-Benzylthioindole

This compound was prepared in 80% yield from the corresponding indolecarboxylic acid as described above. It melted at 35–36° (from ethanol). Anal. Found: C, 75.49; H, 5.42; N, 5.98; S, 13.36.

6-Mercaptoindole

This compound was prepared by a modification of the procedure reported by du Vigneaud *et al.* (28, 29). Commercial anhydrous liquid ammonia (125 ml) was placed in a 50×150 mm test tube supported in a Dewar flask by means of a cork ring. To the ammonia was added 5 g (0.02 mole) of 6-benzylthioindole. Small pieces of freshly cut sodium metal were stirred into the ammonia until a blue color of 5–10 minutes' duration was obtained. Excess sodium was then destroyed by ammonium iodide, added until the blue color just disappeared. The reaction tube was then removed from the Dewar flask and the ammonia driven off under a blanket of purified nitrogen. Distilled water (125 ml), previously boiled and cooled, was added to the tube, along with sufficient 3 *N* hydrochloric acid to acidify the solution. The solid which appeared when the solution was cooled was removed and taken up in dilute sodium hydroxide and again precipitated with acid. When washed with water and dried in a desiccator over P_2O_5 (N_2) it melted sharply at 70–71°. Yield, 1.5 g (47%). Calc. for C_8H_7NS: S, 21.49. Found: S, 21.30.

5-Mercaptoindole

Debenzylation of 4 g of 5-benzylthioindole as above afforded 1.5 g (60%) of the mercaptan, which melted at 75–76°. Anal. Found: S, 21.48.

4-Mercaptoindole

Debenzylation of 3.57 g (0.15 mole) of 4-benzylthioindole followed the procedure described above but with the following changes. The ammonia was kept in an Erlenmeyer flask surrounded by dry ice. The flask was kept stoppered throughout the reaction as much as possible to minimize absorption of CO_2 by the liquid ammonia. Following the removal of ammonia, and addition of water to the ammonium salt of the mercaptan, the resulting aqueous solution was washed several times with ether to remove unreduced material. Acidification at 0° gave a solid which was dried in a desiccator under vacuum over dry calcium chloride. The substance was an oil at room temperature, but was readily crystallized from Skellysolve B at dry ice temperatures. Yield 1.5 g (68%). Calc. for C_8H_7NS: C, 64.39; H, 4.73; N, 9.39; S, 21.49. Found: C, 64.37; H, 4.93; N, 9.49; S, 21.08.

7-Mercaptoindole

Debenzylation of 3.3 g (0.014 mole) of 7-benzylthioindole by the same procedure as employed for the 4-benzylthioindole gave 1.8 g (87%) of the pure mercaptan melting at 57–58° (from Skellysolve B). Anal. Found: C, 64.25; H, 4.69; N, 9.31; S, 21.45.

ACKNOWLEDGMENTS

The authors wish to thank the Hercules Powder Company for the donation of a quantity of *m*-toluic acid. Grateful acknowledgment is made to the National Cancer Institute of Canada and to the National Research Council of Canada for continued financial support during the course of this work.

REFERENCES

1. J. H. Burchenal, D. A. Karnofsky, M. L. Murphy, and R. R. Ellison. Proc. Am. Assoc. Cancer Research, **1**, 7 (1953).
2. D. A. Clark, F. S. Phillips, S. S. Sternberg, C. C. Stock, and G. B. Elion. Proc. Am. Assoc. Cancer Research, **1**, 9 (1953).

3. B. ODDO and Q. MINGOIA. Gazz. chim. ital. **62**, 299 (1932).
4. M. S. GRANT and H. R. SNYDER. J. Am. Chem. Soc. **82**, 2742 (1960).
5. J. A. JOHNSON, H. J. SHAEFFER, and H. J. THOMAS. J. Am. Chem. Soc. **80**, 699 (1958).
6. M. A. PHILLIPS and H. SHAPIRO. J. Chem. Soc. 584 (1942).
7. J. R. THIRTLE. J. Am. Chem. Soc. **68**, 342 (1946).
8. E. FISCHER. Ber. **19**, 1563 (1886).
9. K. G. BLAIKIE and W. H. PERKIN. J. Chem. Soc. 296 (1924).
10. A. REISSERT. Ber. **30**, 1030 (1897).
11. J. B. COHEN and H. D. DAKIN. J. Chem. Soc. 1333 (1902).
12. G. M. BENNETT and W. A. BERRY. J. Chem. Soc. 1666 (1927).
13. D. S. TARBELL and D. K. FUKUSHIMA. Organic syntheses. Coll. Vol. III. John Wiley & Sons, Inc., New York, N.Y. 1955. p. 809.
14. L. F. FIESER. Experiments in organic chemistry. 2nd ed. D. C. Heath and Co., New York. 1941.
15. W. WISLICENUS and E. THOMA. Ann. **436**, 42 (1924).
16. H. N. RYDON and J. C. TWEDDLE. J. Chem. Soc. 3499 (1955).
17. R. J. FOSTER, F. G. ROSICKY, and C. NIEMANN. J. Am. Chem. Soc. **72**, 3959 (1950).
18. N. KORNBLUM and D. C. IFFLAND. J. Am. Chem. Soc. **71**, 2137 (1949).
19. C. S. GIBSON and J. D. A. JOHNSON. J. Chem. Soc. 1244 (1929).
20. K. BRAND and H. ZÖLLER. Ber. **40**, 3324 (1907).
21. H. J. SCHAEFFER and H. J. THOMAS. J. Am. Chem. Soc. **80**, 4896 (1958).
22. T. P. JOHNSTON, L. B. HOLUM, and J. A. MONTGOMERY. J. Am. Chem. Soc. **80**, 6265 (1958).
23. E. MÜLLER. Ber. **42**, 430 (1909).
24. K. F. SCHMIDT. Ber. **57**, 704 (1924).
25. B. E. LEGGETTER and R. K. BROWN. Can. J. Chem. **38**, 1467 (1960).
26. C. K. INGOLD. Structure and mechanism in organic chemistry. Cornell University Press, Ithaca, New York. 1953. pp. 788–796.
27. E. PIERS and R. K. BROWN. Can. J. Chem. This issue.
28. V. DU VIGNEAUD, L. F. AUDRIETH, and H. S. LORING. J. Am. Chem. Soc. **52**, 4500 (1930).
29. R. H. SIFFERD and V. DU VIGNEAUD. J. Biol. Chem. **108**, 753 (1935).
30. J. B. COHEN and H. D. DAKIN. J. Chem. Soc. 331 (1903).
31. W. A. LAZIER and H. R. ARNOLD. Organic syntheses. Coll. Vol. II. John Wiley & Sons, Inc., New York, N.Y. 1943. p. 142.
32. W. GLUUD. Ber. **48**, 432 (1915).
33. G. G. URQUHART, J. W. YATES, JR., and R. CONNOR. Organic syntheses. Vol. 21. John Wiley & Sons, Inc., New York, N.Y. 1941. p. 36.

THE DISCRETENESS-OF-CHARGE EFFECT IN ELECTRIC DOUBLE LAYER THEORY[1]

S. LEVINE[1,2]
Division of Applied Chemistry, National Research Council, Ottawa, Canada
G. M. BELL
Department of Mathematics, Manchester College of Science and Technology, Manchester, England
AND
D. CALVERT
Department of Mathematics, University of Manchester, Manchester, England
Received July 19, 1961

ABSTRACT

The Stern–Grahame–Devanathan theory of the electrical double layer in aqueous systems is modified to include the so-called discreteness-of-charge effect of Esin and Shikov and Ershler. This provides an explanation of a number of phenomena which are at variance with the Stern theory. A simple method of incorporating the above effect into the Stern theory is suggested by the work of Grahame and is equivalent in principle to the discrete-ion approximation employed by the Russian authors. It is shown that the effect can be interpreted in terms of a 'self-atmosphere' potential at the counterions adsorbed in the Stern layer. This provides a new term in the energy of an adsorbed ion, which is very nearly proportional to the surface density of these ions and which had hitherto been included in the specific adsorption potential in the Stern adsorption isotherm. This energy is not small and accounts for the conclusion reached by Grahame that the adsorption potential varies strongly with the surface charge. Grahame found that the potential at the plane separating the compact and diffuse parts of the double layer in the solution phase (i.e. the outer Helmholtz plane) at the mercury – aqueous electrolyte interface displays a maximum as the potential across the interface is varied, and this property is reproduced by the theory. The effect of ion size on the adsorption isotherm is also considered.

1. INTRODUCTION

In the course of his extensive investigations of the properties of the electric double layer at the interface between mercury and aqueous electrolyte, Grahame (1) demonstrated a number of properties which are at variance with the Stern theory (2). One anomaly is that if the original Stern theory be accepted then the specific adsorption energy of an anion (e.g. chloride ion) adsorbed by the mercury surface is not constant, as had been previously assumed, but exhibits a marked increase as the surface charge becomes more positive. Grahame suggested that this variation of the specific adsorption energy is due to a covalent bond between the anion and the mercury surface, the strength of which increases as the mercury charge becomes more positive. Such a hypothesis seems inconsistent with the usual theory of chemical valency. The outer electron shell of the adsorbed anion is completed by the process of ionization, and although some electron sharing and anion polarization are likely, it is difficult to understand how such strong dependence of binding on surface charge can occur. In the present paper a simple explanation, based on distinguishing the mean electrostatic potential at any point in the plane of the centers of the adsorbed anions from the mean potential at the center of an adsorbed ion occupying this point will be developed. The difference between

[1]*Issued as N.R.C. No. 6696.*
[2]*Visiting Scientist, Division of Applied Chemistry, National Research Council, Ottawa. On leave of absence from Department of Mathematics, University of Manchester, England, from March 1960 to January 1961.*

these two potentials can be regarded as originating in the so-called discreteness-of-charge effect, which has been investigated by a number of Russian scientists (3–5) and by Grahame (6). The approach adopted here, first suggested by Grahame (6), is simpler but equivalent in principle.

In his modification of the original Stern picture of the region in the electrolyte solution adjacent to the mercury surface, Grahame (1) distinguished between the plane of centers of the layer of specifically adsorbed ions and the limit of the diffuse layer. These were designated as the inner Helmholtz plane (to be abbreviated to I.H.P.) and the outer Helmholtz plane (O.H.P.) respectively. In the Stern theory, the O.H.P. is identical with the I.H.P., and the mean potential at this common plane increases uniformly with the potential drop across the mercury–electrolyte interface. Assuming that the Gouy–Chapman theory applies to the diffuse layer, Grahame and Soderberg (7–9) were able to determine the variation with interfacial potential of the potential at the O.H.P. at a specified electrolyte concentration. They obtained the rather striking result that if specific adsorption takes place, the magnitude of the potential at the O.H.P. passes through a maximum. This behavior will be reproduced in the theory presented below. The discreteness-of-charge effect was originally proposed to explain the variation of mercury wall potential with electrolyte concentration at the electrocapillary maximum. This aspect has been treated by the Russian workers (3–5, 10, 11) and others (12), and will therefore not be discussed here.

Current interest in the region between the mercury wall and the O.H.P. is directed into two main channels, its dielectric and electrostrictive properties (13–15) and discrete-ion effects. The present paper is concerned with the second topic and for this purpose, any variation in the dielectric constant and thickness of this region with interfacial potential will be ignored, except for a brief discussion of certain aspects at the end of the paper. In this connection it is important to note that as well as the discreteness-of-charge effect there is another discrete-ion effect which is due to short range forces, i.e. to the size of each adsorbed ion. Such an ion will occupy at least one adsorption site and if it is large or if it retains part of its hydration shell it may occupy more than one. The occupied sites are not available to the other adsorbed ions and this affects the entropy of distribution and hence the chemical potential of the adsorbed ions. These ion-size effects have received inadequate attention up to now but they are incorporated in the present theory and it will be shown that they explain the large discrepancies between the results of two different methods used by Grahame (8) and Grahame and Parsons (9) to determine the ratio of the distances of the I.H.P. and the O.H.P. from the wall. As a result it seems likely that these distances vary much less with changes in the physical conditions of the system than these authors believed.

Since the discreteness-of-charge and ion-size effects are likely to be of importance in a number of colloidal phenomena, we shall not confine our attention to the mercury – aqueous electrolyte interface, but shall consider the more general case of a plane colloidal surface in contact with an aqueous electrolyte. Such a surface, for example, may be the wall of a plate-like particle immersed in a dispersion medium containing coagulating electrolytes. Recently the authors (16, 17) incorporated the discrete-charge effect into the theory of colloid stability of Derjaguin and Landau (18) and Verwey and Overbeek (19). This leads to an explanation of the dependence of coagulating electrolyte concentration on the surface potential of the particles, a property which had hitherto been inconsistent with the stability theory.

2. THE STERN–GRAHAME–DEVANATHAN MODEL OF THE DOUBLE LAYER

Employing the electric double layer model of Grahame (1) and Devanathan (20) for a single plate-like particle it is assumed that there is an 'inner region' of oriented water dipoles, of thickness d (~5 Å) and dielectric constant ϵ_1 (~10–20), lying between the plate wall and O.H.P. The volume density in the dispersion medium of the potential-determining ions, which constitute the original charge on the plate surface, is small compared with the corresponding density n (number of ions of either type per unit volume) of the coagulating electrolyte, which is a $z-z$ valency type. The centers of a layer of adsorbed counterions, of valency z_β, where z_β may be $+z$ or $-z$, are situated on the I.H.P. inside the inner region at a distance β from the plate wall. The I.H.P. thus divides the inner region into two parts, which will be called the inner and outer zones and which are of thicknesses β and $\gamma = d-\beta$ (Fig. 1). All the charge is assumed

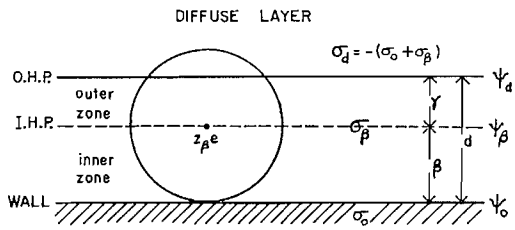

FIG. 1. Model of the electric double layer.

to be situated in the plane of the particle wall, in the I.H.P., or in the diffuse layer. Hence the two zones act as condensers of capacities dK/β and dK/γ per unit area, where $K = \epsilon_1/4\pi d$. The mean electrostatic potentials at the particle wall, the I.H.P., and the O.H.P. are denoted by ψ_0, ψ_β, and ψ_d respectively. Also, σ_0 and σ_β are the mean surface densities at the particle wall and I.H.P. and σ_d is the total charge contained in a column of the diffuse layer of unit cross section. Within each zone the potential distribution function satisfies Laplace's equation and therefore we have a linear variation in potential. Assuming the electric field in the particle interior to be zero, it follows from electrostatics that

$$\psi_0-\psi_\beta = \beta\sigma_0/dK \tag{2.1}$$

and

$$\psi_\beta-\psi_d = \gamma(\sigma_0+\sigma_\beta)/dK. \tag{2.2}$$

Applying the Gouy–Chapman theory to the diffuse layer,

$$\sigma_d = -\frac{\epsilon\kappa}{2\pi}\frac{kT}{ze}\sinh(ze\psi_d/2kT), \tag{2.3}$$

where k is Boltzmann's constant, T the absolute temperature, e the electronic charge, and κ the Debye–Huckel parameter defined by

$$\kappa^2 = 8\pi nz^2e^2/\epsilon kT. \tag{2.4}$$

Also, the condition of electrical neutrality reads

$$\sigma_0+\sigma_\beta+\sigma_d = 0. \tag{2.5}$$

For a given ψ_0 and n one more relation is required to determine the potential distribution, and this has the form of a modified Stern adsorption isotherm, which is obtained

by equating the chemical potential of an adsorbed ion, μ_β say, to that of an ion of the same type in the electrolyte interior. Let ν be the number of adsorbed ions per unit area and $g(\nu)$ the number of configurations per unit area available to these ions. Then the contribution to the chemical potential of an adsorbed ion from $g(\nu)$ is

$$\mu_\beta^c = -kTd \log_e g(\nu)/d\nu. \tag{2.6}$$

If each adsorbed counterion still retains a portion of its hydration shell and therefore occupies more than one adsorption site, say p sites, then a simple expression for $g(\nu)$ is obtained by adapting to surfaces the zero-order approximation to the entropy of mixing molecules of different sizes, which is provided by the volume fraction statistics of Flory (21) and Huggins (22). Suppose that N_s is the density of adsorption sites on the plate surface so that each occupied site spans an area $1/N_s$ and each ion an area p/N_s. Then the formula for $g(\nu)$ corresponding to Flory–Huggins' is

$$\log_e g(\nu) = -\nu \log_e (p\nu/N_s) - (N_s - p\nu) \log_e [(N_s - p\nu)/N_s]. \tag{2.7}$$

Differentiating with respect to ν and writing $\sigma_\beta = z_\beta e\nu$, (2.6) becomes

$$\mu_\beta^c = A + kT \log_e [\sigma_\beta (N_s z_\beta e)^{p-1}/(N_s z_\beta e - p\sigma_\beta)^p], \tag{2.8}$$

where A is a constant.

To determine the electrostatic contribution to μ_β, the Guntelberg–Muller (23) charging process in the theory of electrolytes is employed and it is imagined that the charge on a specified adsorbed ion is e', which is varied from 0 to its full value $z_\beta e$. Let Ψ_β be the mean potential at the center of the given adsorbed ion carrying the charge e', due to the Coulomb interaction of all the ions. Following Loeb (24) the potential is conveniently written as

$$\Psi_\beta = \psi_\beta + \phi_\beta, \tag{2.9}$$

where ψ_β is the mean potential at any point on the I.H.P. and ϕ_β is the "perturbation" potential due to the "self-atmosphere" of the adsorbed ion and its induced image in the plate wall. The electrostatic contribution to μ_β now reads

$$\mu_\beta^e = \int_0^{z_\beta e} \Psi_\beta de' = z_\beta e\psi_\beta + \int_0^{z_\beta e} \phi_\beta de', \tag{2.10}$$

noting that ψ_β may be assumed independent of e'. We may therefore write the chemical potential of an adsorbed ion as

$$\mu_\beta = \xi_\beta + kT \log_e [\sigma_\beta (N_s z_\beta e)^{p-1}/(N_s z_\beta e - p\sigma_\beta)^p] + z_\beta e\psi_\beta + \int_0^{z_\beta e} \phi_\beta de', \tag{2.11}$$

where ξ_β depends on temperature and pressure. There are other terms in μ_β which do not occur in ordinary electrolyte theory, in particular, the energy of polarization of the adsorbed ion in the electric field of the double layer. This will be considered briefly at the end of the paper.

The chemical potential of an ion in the electrolyte interior may be expressed as

$$\mu_0 = \xi_0 + kT \log_e nf/(2n + n_0), \tag{2.12}$$

where ξ_0 is a function of temperature and pressure only, n_0 is the number of water molecules per unit volume, and f is the activity coefficient. Equating the two chemical potentials (2.11) and (2.12) and assuming $n_0 \gg n$, it is easily seen that

$$\frac{\sigma_\beta}{nf} = \frac{(N_s z_\beta e - p\sigma_\beta)^p}{n_0 (N_s z_\beta e)^{p-1}} \exp [(\Phi_\beta + z_\beta e\psi_\beta)/kT], \tag{2.13}$$

where

$$\Phi_\beta = \xi_0 - \xi_\beta - \int_0^{z_\beta e} \phi_\beta de'. \tag{2.14}$$

The relation (2.13) becomes the Stern adsorption isotherm if $p = 1$, $f = 1$, and Φ_β is identified with the specific adsorption isotherm. It will be shown, however, that the last term on the right of (2.14) is a function of σ_β and this property is absent in the classical Stern theory.

3. SELF-ATMOSPHERE POTENTIAL AT AN ADSORBED ION

The mean potential ψ_β at a point on the I.H.P. is so defined that all ions are undergoing thermal motion, i.e. no ion is permanently located at this point. Thus ψ_β is the potential at any point in the I.H.P. when a uniform surface charge distribution σ_β is situated on the plane. Suppose now that the center of a specified adsorbed ion carrying the charge e', where $0 < |e'| < |z_\beta e|$, is situated at a point on the I.H.P. (Fig. 2). The

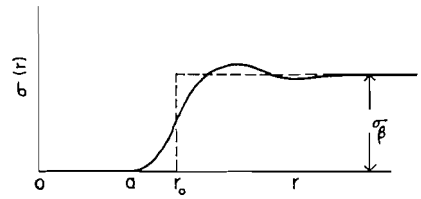

FIG. 2. Distribution of surface charge density in the inner Helmholtz plane surrounding an adsorbed ion.

mean charge distribution on the I.H.P. surrounding this charge will no longer be uniform but will be given by some function $\sigma(r)$, where r is the distance from the specified ion to an arbitrary point on the I.H.P. If $W(r)$ is the potential of the mean force acting between the specified ion e' and any other ion (charge $z_\beta e$) in the I.H.P. at distance r, then

$$\sigma(r) = \sigma_\beta f(r), \qquad f(r) = \exp\,[-W(r)/kT]. \tag{3.1}$$

At large r, the surface charge density should not be affected by the fixed ion at $r = 0$ and so $\sigma(r) \to \sigma_\beta$, which means $W(r) \to 0$, as $r \to \infty$; and if a is the nearest distance of approach between ion e' and a second adsorbed ion, $W(r) = \infty$ for $r < a$. The total charge on the I.H.P. defined by the charge distribution $\sigma(r)$ differs by an amount e' from that defined by the uniform distribution σ_β, since one ion of charge e' has been removed from the distribution. If the I.H.P. is assumed infinitely large, we obtain the relation

$$2\pi \int_0^\infty r[\sigma_\beta - \sigma(r)]dr = 2\pi\sigma_\beta \int_0^\infty r[1-f(r)]dr = e' \tag{3.2}$$

or, noting that $f(r) = 0$ for $r < a$,

$$2\pi\sigma_\beta \int_a^\infty r[1-f(r)]dr = e' - \pi a^2\sigma_\beta. \tag{3.3}$$

It is convenient to consider the following limiting case: (i) the dielectric constant is uniform right up to the plate surface and equal to ϵ, (ii) the electrolyte concentration

is vanishingly small, which means that the diffuse layer may be ignored. There will then be two terms in the perturbation potential of an adsorbed ion. One is the ordinary electrostatic image term in the wall of the colloidal plate, namely

$$\phi_\beta' = \left(\frac{\epsilon-\epsilon_p}{\epsilon+\epsilon_p}\right)\frac{e'}{2\beta\epsilon}, \tag{3.4}$$

where ϵ_p is the dielectric constant of the plate medium, which is assumed to be infinitely thick. The other term is due to the departure of the surface charge density on the I.H.P. from the uniform value and can therefore be expressed in terms of the difference in densities $\sigma_\beta - \sigma(r)$. It reads

$$\phi_\beta'' = -\frac{2\pi\sigma_\beta}{\epsilon}\int_0^\infty\left[\frac{1}{r}+\left(\frac{\epsilon-\epsilon_p}{\epsilon+\epsilon_p}\right)\frac{1}{(r^2+4\beta^2)^{\frac{1}{2}}}\right][1-f(r)]rdr, \tag{3.5}$$

where the second term in the square brackets is due to the corresponding image of the charge difference $\sigma_\beta - \sigma(r)$. An accurate determination of $\sigma(r)$ is difficult, but two approximations to it have been suggested. The first is the 'discrete-ion' model of Esin and Shikov (3) and Ershler (4), who consider the case of $\epsilon_p = \infty$. The distribution $\sigma(r)$ and its image in the plate wall* are replaced by an infinite hexagonal array of discrete ionic charges (each equal to $z_\beta e$) in the I.H.P. and a parallel array of opposite charges ($-z_\beta e$) at a distance 2β. The above authors make the further approximation of replacing each ion-image pair by an equivalent electric point dipole. If s is the distance between nearest-neighboring ions in the I.H.P. and $\epsilon_p = \infty$ then (3.5) becomes very nearly

$$\phi_\beta'' = -\frac{4\pi\sigma_\beta\beta}{\epsilon}+\frac{22\beta^2 z_\beta e}{\epsilon s^3} = -\frac{4\pi\sigma_\beta\beta}{\epsilon}\left(1-\frac{11\sqrt{3}}{4\pi}\frac{\beta}{s}\right) \tag{3.6}$$

since the area allotted to each ion in the hexagonal array is $(\sqrt{3}/2)s^2$ and the corresponding charge density is $\sigma_\beta = 2z_\beta e/\sqrt{3}s^2$. We shall employ a simpler method, which is equivalent in principle and may be termed the cutoff approximation. Each adsorbed ion is regarded as the center of a circular area in the I.H.P. from which the uniform charge density σ_β is removed. Thus

$$\sigma(r) = \begin{cases}0\\ \sigma_\beta\end{cases} \quad \text{or} \quad f(r) = \begin{cases}0, & r < r_0\\ 1, & > r\ r_0\end{cases} \tag{3.7}$$

where the radius r_0 of the area is determined by the condition (3.2) or (3.3) (Fig. 2). This yields

$$\pi r_0^2\sigma_\beta = e'. \tag{3.8}$$

Substitution of (3.7) into (3.5) yields

$$\phi_\beta'' = -\frac{2\pi\sigma_\beta}{\epsilon}\left[r_0+\left(\frac{\epsilon-\epsilon_p}{\epsilon+\epsilon_p}\right)\left\{(r_0^2+4\beta^2)^{\frac{1}{2}}-2\beta\right\}\right]. \tag{3.9}$$

When $r_0 \gg 2\beta$, this simplifies to

$$\phi_\beta'' = \frac{4\pi\sigma_\beta}{\epsilon}\left[\left(\frac{\epsilon-\epsilon_p}{\epsilon+\epsilon_p}\right)\beta-\frac{\epsilon r_0}{(\epsilon+\epsilon_p)}-\frac{\beta^2}{r_0}\left(\frac{\epsilon-\epsilon_p}{\epsilon+\epsilon_p}\right)+\ldots\right] \tag{3.10}$$

which, in the limiting case of $\epsilon_p = \infty$, reduces to

$$\phi_\beta'' = -\frac{4\pi\sigma_\beta\beta}{\epsilon}\left(1-\frac{\beta}{r_0}+\ldots\right). \tag{3.11}$$

**These authors actually put $\epsilon = \infty$ and introduced images in the O.H.P.*

On substituting $\pi r_0^2 = (\sqrt{3}/2)s^2$, the 'discrete-ion' approximation (3.6) reads

$$\phi_\beta'' = -\frac{4\pi\sigma_\beta\beta}{\epsilon}\left(1-0.80\frac{\beta}{r_0}+\ldots\right), \tag{3.12}$$

which does not differ much from the 'cutoff' approximation (3.11).

Suppose now that the adsorbed counterions are embedded in the inner region of thickness d and dielectric constant ϵ_1 at distance β from the plate wall. Then the self-atmosphere potential ϕ_β'' is conveniently written as

$$\phi_\beta'' = -\frac{4\pi\sigma_\beta\beta\gamma}{\epsilon_1 d}\,g = -\frac{\beta\gamma}{d^2K}\,\sigma_\beta g, \tag{3.13}$$

where g is a factor depending on r_0, γ, d, the dielectric constants, and the electrolyte concentration. The determination of g in the general case is difficult but certain limiting cases have been considered and these indicate the general behavior of g. Firstly suppose that the particle medium is conducting ($\epsilon_p = \infty$), $\epsilon \gg \epsilon_1$ so that effectively $\epsilon = \infty$, and $\beta = \gamma$. Then it is shown in the Appendix that

$$\phi_\beta'' = -\frac{\pi\sigma_\beta d}{\epsilon_1}\left[1-\frac{8\tau}{\pi}\sum_{m=1}^{\infty}\frac{1}{(2m-1)}K_1(\sqrt{2m-1}\;\pi\tau)\right], \tag{3.14}$$

where $\tau = r_0/d$ and K_1 is the Bessel function of the second kind with imaginary argument and of order 1. For $\tau > 1$ corresponding to $|\sigma_\beta| < 16$ μcoulombs/cm^2 when $z = 1$ and $d = 5$ Å, the first term only in the series need be considered and as shown in Table I, even this term is small. It is possible to extend the analysis to the case where the I.H.P. is no longer midway between the mercury wall and the O.H.P., and the corresponding leading term in ϕ_β'' becomes simply (3.13) with $g = 1$.

TABLE I

τ	1	2	3
$K_1(\pi\tau)$	0.34×10^{-2}	0.99×10^{-4}	0.34×10^{-5}

This is the limiting form for ϕ_β'' when $r_0 = \infty$ and $g = 1$ and it may be derived quite simply in the following way. Consider a sheet of charge of density $-\sigma_\beta$ situated at the I.H.P. between two equipotential planes A' and B' (the plate wall and O.H.P.) at zero potential and at distances β and γ. This sheet is imagined to have two sides with charge distributed as shown in Fig. 3. A and B are the image planes. The electric field between

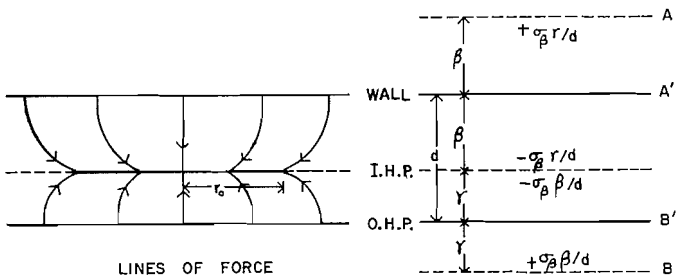

FIG. 3. Model of the inner region yielding the limiting expression (3.15) for the self-atmosphere potential when $r_0 = \infty$, $\epsilon = \infty$, and $\epsilon_p = \infty$ ($g = 1$).

A′ and the I.H.P. is $4\pi\sigma_\beta\gamma/d\epsilon_1$, and hence the potential drop from A′ to the I.H.P. is $4\pi\sigma_\beta\beta\gamma/d\epsilon_1$. This must also be the potential difference between the plane B′ and the I.H.P. Since A′ and B′ are at zero potential, the potential at the I.H.P. is

$$\phi_\beta'' = -\frac{4\pi\sigma_\beta\beta\gamma}{\epsilon_1 d}, \tag{3.15}$$

which is the required result. The higher terms in (3.14) and in the corresponding formula when $\beta \neq \gamma$ are small because the lines of force near the center of the circle of radius r_0 are practically normal to the I.H.P.; in other words, the edge effects are small for $r_0 > d$ ($\tau > 1$).

The drop in mean potential across the outer zone $\psi_\beta - \psi_d$ is designated the macropotential by Ershler (4). Also, if we exclude the self-image term ϕ_β' the true potential at the center of the adsorbed ion is

$$\psi_A = \psi_\beta + \phi_\beta'' = \psi_\beta - \beta\gamma\sigma_\beta g/d^2K \tag{3.16}$$

and Ershler refers to the difference $\psi_A - \psi_d$ as the macropotential. Putting $g = 1$ we readily derive from (2.1), (2.2), and (3.16),

$$\psi_A - \psi_d = \frac{\gamma}{(\gamma+\beta)}(\psi_0 - \psi_d). \tag{3.17}$$

This linear relation is already given by Grahame (6). In their rigorous mathematical treatment of a hexagonal array of discrete point charges situated on the I.H.P., with perfectly conducting colloidal wall and O.H.P., Levich, Kiryanov, and Filinovsky (5) also obtain (3.17) provided the coverage of adsorption sites by counterions does not exceed 25–30%. The Russian authors quite correctly maintain that the micropotential and not the macropotential should be introduced in the Stern adsorption isotherm. In our present notation, this means that in the exponential term on the right-hand side of (2.13) we should write

$$\Phi_\beta - z_\beta e\psi_\beta = \Phi_\beta' - z_\beta e\psi_A, \tag{3.18}$$

where

$$\Phi_\beta' = \xi_0 - \xi_\beta - \int_0^{z_\beta e} \phi_\beta' de', \tag{3.19}$$

which is independent of the charge densities σ_0 and σ_β and may be identified with the specific adsorption potential (apart from an additive constant). We note that ϕ_β'' is independent of e' and that the self-image term ϕ_β', which is proportional to e', is obtained in the usual manner by considering multiple image reflections in the O.H.P. and the plate wall, but we shall not require its explicit formula (5).

In the introduction we commented on Grahame's conclusion that the energy Φ_β exhibits a marked increase as the surface charge σ_0 becomes more positive in the case of chloride ion adsorbed at the mercury – aqueous electrolyte interface. Writing $\Phi_\beta = -eU_\beta$ ($z_\beta = -1$), Grahame (1) estimated that U_β increases by about 0.18 volts as σ_0 varies from -4 to 18 μcoulombs/cm^2 for 0.3 N NaCl solution. The corresponding variation of the charge density σ_β of adsorbed chloride ions is from -1 to about -28 μcoulombs/cm^2. In the present theory the variation in U_β is attributed to the term $-e\phi_\beta''$. An increase in the magnitude $|\Delta\sigma_\beta|$ of σ_β of 27 μcoulombs/cm^2 corresponds to an increase in U_β of

$$|\Delta U_\beta| = \frac{\beta\gamma}{d^2K}|\Delta\sigma_\beta| = 27\frac{\beta\gamma}{d^2K} \text{ volts},$$

where K is in μfarads/cm^2. According to Grahame and Parsons (9), $K \approx 30$ μfarads/cm^2 and $\gamma/d \approx \frac{1}{4}$, so that $|\Delta U_\beta| = 0.17$ volts, which is in excellent agreement with Grahame's estimate.

The dielectric constants ϵ_p of silver halide crystals are in the range 11–15 and are perhaps not very different from the dielectric constant ϵ_1 of the inner region. Thus for such colloidal media, a first approximation is obtained by putting $\epsilon_p = \epsilon_1$. If we assume $\epsilon = \infty$, then it follows from (3.11) that

$$\phi_\beta'' = -\frac{4\pi\sigma_\beta\gamma}{\epsilon_1}\left(1 - \frac{\gamma}{r_0} + \ldots\right). \tag{3.20}$$

When $\gamma/r_0 \ll 1$, this becomes identical with (3.13) provided $g = d/\beta$. For small coverages of the adsorption sites, g increases from 1 to d/β as ϵ_p decreases from ∞ to ϵ_1. In the limiting case of $r_0 = \infty$, it is easily shown that ϕ_β'' is given by the leading term in (3.20) for any (finite) value of the dielectric constant ϵ_p. As in the derivation of (3.15) we imagine a sheet of density $-\sigma_\beta$ situated at the I.H.P., but now the colloidal wall has a dielectric constant ϵ_p. The dielectric displacement within the colloidal medium may be assumed to vanish, since otherwise the I.H.P. would be at infinite potential with respect to the colloidal interior. This means that the dielectric displacement in the inner zone vanishes, differing from zero only in the outer zone. There is now one image plane at B (Fig. 4) and the electric field between the I.H.P. and B′ is $4\pi\sigma_\beta/\epsilon_1$. Since B′ is at zero

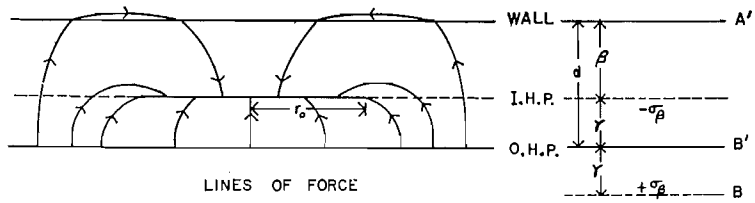

FIG. 4. Model of the inner region yielding the limiting expression $\phi_\beta'' = -4\pi\sigma_\beta\gamma/\epsilon_1$, for the self-atmosphere potential when $r_0 = \infty$, $\epsilon = \infty$, and $\epsilon_p < \infty$.

potential, the potential at the I.H.P. is given by the first term in (3.20). The plot of g as a function of r_0/d for various values of the ratio $f = (\epsilon_p - \epsilon_1)/(\epsilon_p + \epsilon_1)$ and for $\beta = \gamma$ and $\epsilon = \infty$, is shown in Fig. 5. (The mathematical details are omitted from the present

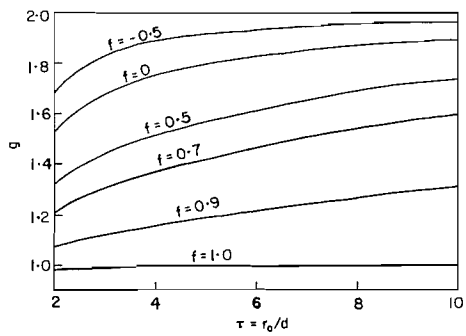

FIG. 5. Plot of g as a function of r_0/d for various values of the ratio $f = (\epsilon_p - \epsilon_1)/(\epsilon_p + \epsilon_1)$ and for $\beta = \gamma$ and $\epsilon = \infty$.

f	1.0	0.9	0.7	0.5	0	−0.5
ϵ_p/ϵ_1	∞	19	17/3	3	1	1/3

paper.) The convergence to the limiting value $g = 2$ at $r_0 = \infty$ is seen to be rather slow. This is due to the lack of symmetry on the two sides of the I.H.P., as illustrated in Fig. 4, leading to a much larger 'edge effect' than in the 'two-conductor' case of Fig. 3.

For fixed r_0/d and $\epsilon = \infty$, the magnitude of ϕ_β'' increases as the ratio ϵ_p/ϵ_1 diminishes. This behavior can be understood as follows. The potential ϕ_β'' at the center of a circular disk, situated on the I.H.P., is due to a uniform charge density $-\sigma_\beta$ on the disk and to the infinite set of induced images of this charge distribution in the two boundary planes of the inner region (Fig. 6). When these planes are perfectly conducting ($f = 1$),

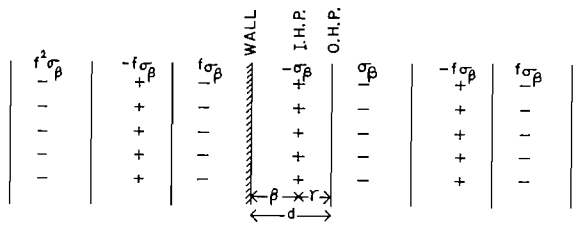

FIG. 6. Infinite set of images in the mercury wall and the outer Helmholtz plane; $f = (\epsilon_p - \epsilon_1)/(\epsilon_p + \epsilon_1)$, $\epsilon = \infty$.

the first-order image in each plane has a charge density σ_β and since these exert a greater influence than the higher-order images, the net effect of the images is to reduce the magnitude of ϕ_β''. If now the colloidal wall is a dielectric, the charge density in its first-order image drops to $f\sigma_\beta$ and the reduction in the magnitude of ϕ_β'' is correspondingly smaller. Thus ϕ_β'' increases in magnitude as f decreases.

Suppose now that the O.H.P. is no longer assumed to be an equipotential plane and that the electrolyte concentration is very small. The charge density of the first-order image in this plane will be $f'\sigma_\beta$ very nearly, where $f' = (\epsilon - \epsilon_1)/(\epsilon + \epsilon_1)$. For typical values of $\epsilon_1 = 16$ and $\epsilon = 80$, $f' = 0.80$, so that the reduction from the case of the perfect conductor is not large. The effect of the factor f' is again to increase the magnitude of ϕ_β''. However, with increase in electrolyte concentration, ϕ_β'' will approach the value corresponding to an equipotential O.H.P. Ershler (4) has given the following explanation for assuming an equipotential O.H.P. at large electrolyte concentrations. A single adsorbed ion in the I.H.P. induces an oppositely charged ionic cloud in the diffuse layer extending into this layer a distance comparable with $1/\kappa$, where κ is the Debye–Huckel parameter characteristic of the local ionic concentration. At large electrolyte concentrations or large values of ψ_d, the local value of $1/\kappa$ will be small and as first approximation we may assume that all the charge in the cloud lies in the O.H.P. The distribution of the charge in this plane must be such that the potential beyond the plane in the electrolyte solution is zero at every point. Such a distribution of potential is obtained when the solution side is a perfect conductor at zero potential.

The general conclusion is that g will not differ much from d/β when ϵ_p/ϵ_1 is of the order of 1, provided the coverage of adsorption sites is less than, say 10%. For smaller values of ϵ_p/ϵ_1 and at low coverage, g may exceed d/β.

The simple expression (3.13) for ϕ_β'', which applied at small σ_β, is a two-dimensional analogue of the Debye–Huckel self-atmosphere potential in the limit of small electrolyte concentrations. The two potentials differ in that ϕ_β'' is proportional to the surface concentration of adsorbed ions whereas the Debye–Huckel potential is proportional to the square root of the volume electrolyte concentration, and we shall demonstrate that

this different dependence on concentration is essential. It is well known that the self-atmosphere of an ion in the electrolyte interior should satisfy a certain condition of self-consistency (23) and it is readily shown that ϕ_β'' obeys a corresponding condition. The adsorbed layer of ions is treated as a separate phase, and an electrostatic free energy per unit area, which is associated with ϕ_β'', can be defined as follows. Introducing the Debye–Huckel charging process suppose that all the adsorbed ions carry a fraction λ of their normal charge and that a specified adsorbed ion is assigned a charge e′, which is varied independently. Then the self-atmosphere potential at this ion will depend on λ, e', and the density of adsorbed ions ν; thus we may write $\phi_\beta'' = \phi_\beta''(\lambda, \nu, e')$. The electrostatic free energy per unit area takes the form

$$f_{e1}(\nu) = \nu z_\beta e \int_0^1 \phi_\beta''(\lambda, \nu, z_\beta \lambda e) d\lambda, \tag{3.21}$$

where it is imagined that ν is held fixed during the charging from $\lambda = 0$ to 1. Then the condition of self-consistency that ϕ_β'' should satisfy takes the form

$$\int_0^{z_\beta e} \phi_\beta''(1, \nu, e') de' = \frac{df_{e1}(\nu)}{d\nu}. \tag{3.22}$$

From (3.13), the dependence of ϕ_β'' on the relevant parameters λ, ν, and e' takes the form $\phi_\beta'' = C\lambda\nu$, where C is a constant. It is seen that ϕ_β'' satisfies the condition (3.22) and we conclude that a linear dependence on σ_β requires that ϕ_β'' be independent of e'.

It is rather striking that the 'discrete-ion' and 'cutoff' approximations lead to the same linear relation (3.17) which is valid for perfectly conducting walls of the inner region and small coverage of adsorption sites. This must mean that the two methods of approximation give identical results under these conditions, but they may differ when ϵ_p is finite. The presence of a term in the adsorption energy which is proportional to the surface density of ions is not new in adsorption energy. It occurs in the theory of adsorption of gases on solids whenever the interaction of adsorbed molecules occupying adjacent sites on the solid surface is taken into account. An entirely different approach to the problem of the self-atmosphere effect and therefore to the determination of $\sigma(r)$ is suggested by the theory of adsorption of gases on solids, when dipole interactions between adsorbed molecules are considered. This involves the Bethe or some similar method designed to treat the immediate environment of a lattice site occupied by a molecule (see Miller (25)). Such an approach should help to decide which of the two approximations to $\sigma(r)$, the 'discrete-ion' or 'cutoff' model, provides a better estimate of ϕ_β'', but this will not be investigated here.

There is one inconsistency in the use of the cutoff approximation (3.7) which requires some explanation. Whereas the distances between the ions is fixed, independent of e' in the discrete-ion approximation, the radius r_0, defined by (3.8), is a function of e' in the cutoff approximation. In the Guntelberg process employed in (2.10), we imagine that the charge e' of an adsorbed ion varies from 0 to its full value $z_\beta e$, and by (3.8) the radius r_0 also increases from zero to its corresponding final value. However, it is easily shown that the cutoff model violates the formula (3.3) when $|e'| < \pi a^2 |\sigma_\beta|$. Suppose that z_β and therefore σ_β are positive. Since $\sigma(r)$ is either 0 or σ_β in the cutoff model, $\sigma_\beta - \sigma(r)$ and therefore the left-hand side of (3.3) cannot be negative, whereas for such small e', the right-hand side of (3.3) is negative. At small e', $\sigma(r)$ cannot be approximated by the cutoff formula (3.7); it is seen from (3.3) that $f(r) > 1$ (and thus $|\sigma(r)| > |\sigma_\beta|$) for some part of the range $r > a$. However, at small coverage the dominant term in ϕ_β'', which is independent of e', satisfies the condition of self-consistency (3.22) and is not affected by this correction to $\sigma(r)$ at small e'.

Instead of allowing r_0 to tend to zero, it would be more realistic to regard the 'exclusion diameter' a as the minimum value of r_0 and to suppose that $r_0 = a$ when $|e'| < \pi a^2|\sigma_\beta|$. For such small values of e', the relation (3.3) is satisfied if it is imagined that a ring of charge $\pi a^2\sigma_\beta - e'$, distributed uniformly round the circle of radius a, is superposed on the cutoff form (3.7). This is equivalent to assuming that when e' is so small that the charge in the area occupied by the ion on the I.H.P. is actually less than the average, then a compensating charge accumulates in the region immediately surrounding the ion (Fig. 2). For this crude but simple correction to the cutoff charge density (3.7), there will be a new term in the self-atmosphere potential of an adsorbed ion carrying the charge e'. It is sufficient to consider the simple case where $\epsilon_p = \epsilon_1$ and $\epsilon = \infty$. Then this new term reads

$$\phi_\beta''' = \frac{(\pi a^2\sigma_\beta - e')}{\epsilon_1}\left[\frac{1}{a} - \frac{1}{(a^2+4\gamma^2)^{\frac{1}{2}}}\right], \tag{3.23}$$

which contributes to the chemical potential μ_β of an adsorbed ion an amount

$$\int_0^{\pi a^2\sigma_\beta} \phi_\beta''' de' = \frac{(\pi a^2\sigma_\beta)^2}{2\epsilon_1}\left[\frac{1}{a} - \frac{1}{(a^2+4\gamma^2)^{\frac{1}{2}}}\right]. \tag{3.24}$$

This should be compared with the corresponding contribution from (3.20), which for $\gamma/r_0 \ll 1$ reads $-4\pi\sigma_\beta\gamma z_\beta e/\epsilon_1$. Choosing $a = 2\gamma$ and substituting $\pi r_0^2\sigma_\beta = z_\beta e$, the ratio of these two terms becomes $-0.073(a/r_0)^2$. This is small even for coverage of adsorption sites as high as 30% and we may conclude that the inconsistency in the cutoff approximation at small e' is unimportant.

In a paper dealing with the double layer free energy of soap micelles, Overbeek and Stigter (26) have suggested another method of correcting for the self-atmosphere of an adsorbed ion. It is imagined that the charge of an adsorbed ion is smeared out over a circular area of radius r_0, and the electrical work required to assemble this continuous charge distribution on the circle is determined. This is not equivalent to the corresponding energy of charging which is given by the integral in (2.10) and consequently the method of these authors cannot be correct.

4. VARIATION OF POTENTIAL AT O.H.P. WITH PLATE POTENTIAL

We proceed to investigate the effect of the self-atmosphere potential at an adsorbed ion on the double layer properties of a single plate. It is convenient to introduce the dimensionless quantities

$$\eta_0 = e\psi_0/kT, \qquad \eta_\beta = e\psi_\beta/kT, \qquad \eta_d = e\psi_d/kT \tag{4.1}$$

and also

$$Q = \frac{\epsilon_1 d}{4\pi\beta\gamma}\frac{kT}{e} = \frac{d^2K}{\beta\gamma}\frac{kT}{e}, \tag{4.2}$$

which has the dimensions of charge per unit area. Then (2.1) and (2.2) become respectively

$$\eta_0 - \eta_\beta = \frac{d}{\gamma}\frac{\sigma_0}{Q} \tag{4.3}$$

and

$$\eta_\beta - \eta_d = \frac{d}{\beta}\frac{(\sigma_0+\sigma_\beta)}{Q}. \tag{4.4}$$

Also, substituting (3.16) into (3.18), the equilibrium condition (2.13) can be expressed as

$$z_\beta\eta_\beta = \log_e \frac{nf}{n_0} + \log_e\left[\frac{(N_s z_\beta e - p\sigma_\beta)^p}{\sigma_\beta (N_s z_\beta e)^{p-1}}\right] + \frac{g z_\beta \sigma_\beta}{Q} + \frac{\Phi_\beta'}{kT}. \tag{4.5}$$

Eliminating σ_0 from (4.3) and (4.4),

$$\eta_d = \frac{d}{\beta}\eta_\beta - \frac{\gamma}{\beta}\eta_0 - \frac{d}{\beta}\frac{\sigma_\beta}{Q}, \tag{4.6}$$

and now eliminating η_β from (4.5) and (4.6),

$$\eta_d = \frac{d}{\beta}\left[\frac{1}{z_\beta}\log_e\frac{nf}{n_0} + \frac{1}{z_\beta}\log_e\left[\frac{(N_s z_\beta e - p\sigma_\beta)^p}{\sigma_\beta (N_s z_\beta e)^{p-1}}\right] - \frac{\gamma}{d}\eta_0 + \frac{(g-1)\sigma_\beta}{Q} + \frac{\Phi_\beta'}{kT}\right], \tag{4.7}$$

which expresses η_d in terms of σ_β and η_0. From (4.3) and (4.4) we can also eliminate η_β to obtain

$$\eta_0 = \eta_d + \frac{(\sigma_0+\sigma_\beta)}{Q}\frac{d^2}{\beta\gamma} - \frac{d}{\gamma}\frac{\sigma_\beta}{Q}. \tag{4.8}$$

It is convenient to introduce

$$\sigma_\beta^0 = Q/z_\beta g,\ x = \sigma_\beta/\sigma_\beta^0,\ b = \sigma_\beta^0/N_s z_\beta e. \tag{4.9}$$

Then, making use of (2.3), (2.4), (2.5), (4.1), and (4.2), the relation (4.8) can be written as

$$\eta_0 = \eta_d + \frac{\kappa\epsilon}{2\pi K z}\sinh\frac{1}{2}z\eta_d - \frac{dx}{\gamma g z_\beta} \tag{4.10}$$

and (4.7) as

$$x - \log_e x + p\log_e(1-pbx) = z_\beta\eta_d + \frac{z_\beta}{z}\frac{\kappa\epsilon}{2\pi K}\frac{\gamma}{d}\sinh\frac{1}{2}z\eta_d + C, \tag{4.11}$$

where

$$C = \alpha - \log_e nf. \tag{4.12}$$

Here α is a constant involving the specific adsorption potential Φ_β', the number of adsorption sites N_s, and the distances β and γ. The two relations (4.10) and (4.11) yield η_d as a function of η_0 in terms of the parameter x. We can also write (4.5) as

$$z_\beta\eta_\beta = x - \log_e x + p\log_e(1-pbx) - C, \tag{4.13}$$

thus expressing η_β in terms of x.

Suppose we vary the potential ψ_0 at the wall by changing the concentration of potential-determining ions in the dispersion medium, while the concentration n of the coagulating electrolyte is unaltered. It is assumed that K, β, and γ do not vary with ψ_0. For the mercury – aqueous electrolyte system, ψ_0 is the potential across the interface and this is varied externally. The density of adsorbed ions σ_β, and therefore the ratio x, will change with ψ_0. Differentiating (4.13) with respect to η_0, we find that

$$\frac{d\eta_\beta}{d\eta_0} = \frac{d\eta_\beta}{dx}\frac{dx}{d\eta_0} = 0 \tag{4.14}$$

when

$$1 - \frac{1}{x} - \frac{p^2 b}{1-pbx} = 0. \tag{4.15}$$

We shall find that $pb \ll 1$ and the root of the quadratic equation (4.15) in which we are interested is that in the neighborhood of $x = 1$; the discarded root is approximately $1/(pb)$. Differentiating (4.10) and (4.11) with respect to η_0,

$$\frac{dx}{d\eta_0} = \frac{\gamma g z_\beta}{d}\left[1-\left(1+\frac{\kappa\epsilon}{4\pi K}\cosh\frac{1}{2}z\eta_d\right)\frac{d\eta_d}{d\eta_0}\right] \tag{4.16}$$

$$\left[1-\frac{1}{x}-\frac{p^2b}{1-pbx}\right]\frac{dx}{d\eta_0} = z_\beta\left[1+\frac{\kappa\epsilon}{4\pi K}\frac{\gamma}{d}\cosh\frac{1}{2}z\eta_d\right]\frac{d\eta_d}{d\eta_0}. \tag{4.17}$$

It follows that at the value of x defined by (4.15)

$$dx/d\eta_0 = \gamma g z_\beta/d \tag{4.18}$$

and

$$d\eta_d/d\eta_0 = 0. \tag{4.19}$$

It is readily verified that the magnitudes of ψ_β and ψ_d have maxima at the root of (4.15). Thus differentiating (4.17) again and substituting (4.18),

$$\frac{d^2\eta_d}{d\eta_0^2} = \left(\frac{\gamma g}{d}\right)^2 z_\beta\left[\frac{1}{x}-\frac{p^3b^2}{(1-pbx)^2}\right]\Big/\left[1+\frac{\kappa\epsilon}{4\pi K}\frac{\gamma}{d}\cosh\frac{1}{2}z\eta_d\right], \tag{4.20}$$

evaluated at this root. When $z_\beta > 0$, the right-hand side of (4.20) is positive, so that we have a minimum in ψ_d. Assuming the plate wall to be negatively charged and ψ_d to be negative, this means that the magnitude of ψ_d has a maximum. When $z_\beta < 0$, we assume ψ_d is positive and again the magnitude of ψ_d has a maximum. Similar considerations apply to ψ_β.

The physical basis for the maxima can be understood on examining the potential ψ_A which is given by (3.16). The electrostatic work gained when an ion of valency z_β is adsorbed on the I.H.P. is not $z_\beta e\psi_\beta$ but $z_\beta e\psi_A$, and by (3.16) and (4.9),

$$z_\beta\eta_A = z_\beta\eta_\beta - x, \tag{4.21}$$

where $\eta_A = e\psi_A/kT$. It follows from (4.13) and (4.18) that at the maxima,

$$\frac{d(z_\beta\eta_A)}{d\eta_0} = -\frac{\gamma g z_\beta}{d}\left(\frac{1}{x}+\frac{p^2b}{1-pbx}\right), \tag{4.22}$$

which does not vanish. This implies that ψ_A increases steadily in magnitude with the plate potential. However, by (3.16),

$$\frac{d\psi_\beta}{d\psi_0} = \frac{d\psi_A}{d\psi_0} - \frac{d\phi_\beta''}{d\psi_0} \tag{4.23}$$

and the two terms on the right have opposite signs. At small coverages, $\psi_\beta \approx \psi_A$ and the first term dominates. At the value of x defined by (4.15), the two terms in (4.23) cancel one another and for larger coverages, the second (self-atmosphere) term is the larger. The classical Stern theory is obtained by putting $g = 0$ and $p = 1$ in equation (4.5). This means that the self-atmosphere term on the right of (4.23) is absent and therefore $d\psi_\beta/d\psi_0$ is always positive.

Making use of (4.2) and (4.9), it is readily verified that the self-atmosphere term (3.13) is given by

$$z_\beta e\phi_\beta''/kT = -x. \tag{4.24}$$

At the maximum in $|\psi_d|$, $x \approx 1$ and by (4.9) the fraction of sites occupied by adsorbed ions is conveniently obtained from values of Q. In Fig. 7, we have plotted Q in μcoulombs/cm^2 for various values of the relative position γ/d of the I.H.P. in the inner region and

of the dielectric constant ϵ_1, choosing $T = 25°$ C and $d = 5$ Å. These values are symmetrical about $\gamma/d = 0.5$. The fraction of adsorption sites occupied at the maximum is approximately $Q/|z_\beta|gN_s e$. For a density of adsorption sites $N_s = 5\times10^{14}$, $N_s e = 80$ μcoulombs/cm^2, and it is seen from Fig. 7 that for $|z_\beta| = 1$ and a typical range $g = 1$

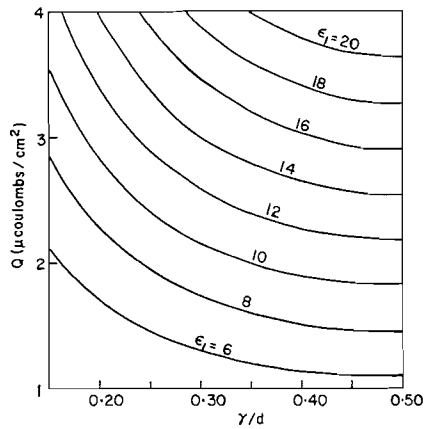

FIG. 7. Plot of Q against γ/d; $Q/z_\beta g$ equals approximately the charge density of adsorbed ions at the maximum in $|\psi_d|$.

to 2, the coverage of sites at the maximum is less than 5%. Furthermore, this coverage is reduced by the factor $1/|z_\beta|$, when $|z_\beta| > 1$.

From their measurements on the rate of change of differential capacity with the chemical potential of the electrolyte at the mercury – aqueous electrolyte interface, Grahame and Soderberg (7), Grahame (8), and recently Grahame and Parsons (9) determined the variation of ψ_d with ψ_0 and obtained a maximum in $|\psi_d|$ when univalent anions are adsorbed by the mercury surface. Comparison of the theory developed in this paper with the experimental results of Grahame (8) on the adsorption of iodide ions in the mercury – KI electrolyte system at 25° C will now be made. Since the plate wall is metallic, we shall assume $g = 1$. There is one difficulty encountered in the interpretation of these experiments which is relevant to our comparison and which concerns the value to be chosen for the ratio γ/d. Two methods of determining γ/d have been devised and it would appear that these disagree. In one method a relation which is obtained by adding (2.1) and (2.2) is employed, namely

$$\psi_0 - \psi_d = \frac{\sigma_0}{K} + \frac{\sigma_\beta}{K_2}, \tag{4.25}$$

where

$$K_2 = dK/\gamma \tag{4.26}$$

is the capacity of the outer zone. It is possible to determine all the quantities in (4.25) except K and K_2 and these can be calculated from the experimental data. We should mention that the experimentally determined potential at the mercury wall includes the so-called Lange χ-potential which may be regarded as originating in the dipole layers at the interface. Grahame (1) corrects for this by subtracting a potential difference of 0.488 volts, which is observed at the electrocapillary maximum (when $\sigma_0 = 0$) of an unadsorbed electrolyte and in this way obtains a value for the potential which can be

attributed to the true charge distributed and will be identified with the potential ψ_0 introduced in this paper. The relation (4.25) now yields $\gamma/d = 0.4$, which varies very little with σ_β.

The alternative method of calculating γ/d, which is simplified by Grahame and Parsons (9), involves the equation (4.5) for $g = 1$ and $z_\beta = -1$. Making use of (4.6), we may express (4.5) as

$$(4.27)\quad \log_e(|\sigma_\beta|/nf) - e\psi_d/kT - p\log_e(1 - p\sigma_\beta/N_s z_\beta e) = B + (\gamma/d)e(\psi_0 - \psi_d)/kT,$$

where B is a constant characteristic of the adsorbed ion and the adsorbing surface. The above authors omit the last term on the left-hand side of (4.27) and on examining the variation of $\psi_0 - \psi_d$ with the left-hand side of (4.27) at fixed σ_0 find that both B and γ/d depend on σ_0. For example, with KI, γ/d increases from 0.4 to 0.8 as σ_0 changes from -4 to 18 μcoulombs/cm^2. However, such a variation in γ/d is most unlikely since it would imply distances of the adsorbed I ion from the mercury surface smaller than its radius (2.18 Å). In Table II, we have substituted Grahame's data for electrolyte concentrations $c = 0.05$, 0.25 and 1.0 N KI into equation (4.27), assuming that γ/d has

TABLE II

(KI at 25° C, $\gamma/d = 0.4$, $p = 1.83$, $N_s e = 80.1$ μcoulombs/cm^2)

c (mole/l.)	f	σ_0 (μcoulombs/cm^2)	$-\sigma_\beta$ (μcoulombs/cm^2)	$-\psi_0$ (volts)	$-\psi_d$ (volts)	B	B^*
		-4	4.00	0.2995	0.0930	11.60	11.41
0.05	0.820	4	14.16	0.1979	0.1054	11.48	10.76
		14	27.23	0.0349	0.1183	11.60	9.92
		-4	8.90	0.3570	0.0785	11.70	11.29
0.25	0.720	4	20.18	0.2194	0.0705	11.35	10.21
		14	33.04	0.0898	0.0753	11.45	8.87
		-4	14.21	0.4177	0.0628	11.78	11.06
1.0	0.646	4	25.69	0.2731	0.0705	11.19	9.58
		14	38.10	0.1343	0.0753	11.67	7.92

the fixed value 0.4. The parameter p is determined by choosing the same value for B when $\sigma_0 = -4$ and 14 μcoulombs/cm^2 at $c = 0.05$ N KI. B^* is the value of B when the co-area term is omitted. The results in this table demonstrate that the insertion of the Flory–Huggins co-area term on the left of (4.27) largely removes the anomalies of strongly varying B and γ/d and so the two methods of determining γ/d are in reasonable agreement.

Most recently Mott and Watts-Tobin (15) arrived at the result (3.17) by arguing that for small concentrations of adsorbed counterions the lines of force are approximately normal to the mercury wall in the inner region. They also introduced an additional term in the adsorption energy of the counterion which is proportional to the 3/2th power of the surface density of adsorbed ions and which, in our notation, reads

$$\frac{2\pi z_\beta \sigma_\beta e \gamma^2}{\epsilon_1 r_0}.$$

This term is intended to serve the same purpose as our co-area term, namely to correct for varying B and γ/d. However, it resembles the second-order term in the expansion (3.11) and will therefore be practically eliminated when the multiple image reflections in the O.H.P. and mercury wall are properly introduced.

The equation (4.27) directly involves the co-area and discrete-ion effects but not the dielectric constant ϵ_1, of the inner region. However, the polarization energy of an absorbed ion has been omitted in the expression (2.11) for the chemical potential μ_β and therefore in (4.27). This energy is related to the dependence of ϵ_1 on the density ν of adsorbed ions and is usually regarded in colloid theory as the source of the apparent increase of specific adsorption potential with the polarizability of the ion, e.g. from F^- to I^-. A simple expression for this energy term can be obtained by assuming that the adsorbed ion is embedded in a homogeneous medium of dielectric constant ϵ_1. According to the linear relation (3.17), the electric field acting on the ion is equal to $(\psi_0-\psi_d)/d$ and hence its polarization energy is given approximately by (27)

$$\mu_\beta^{p} = -\frac{d}{8\pi}\left(\frac{\psi_0-\psi_d}{d}\right)^2\frac{\partial\epsilon_1}{\partial\nu} = -\left(\frac{kT}{e}\right)^2\frac{1}{8\pi d}(\eta_0-\eta_d)^2\frac{\partial\epsilon_1}{\partial\nu}, \tag{4.28}$$

making use of (2.1) and (2.2) and ignoring any 'natural' or 'residual' field when $\sigma_0 = \sigma_\beta = 0$. When μ_β^{p} is added to the expression (2.11) for μ_β, there is a corresponding new term on the right-hand side of (4.11) given by μ_β^{p}/kT and $\eta_0-\eta_d$ is expressed in terms of η_d and r by (4.10). This term should also be added to the left-hand side of equation (4.27). However, little is known about the magnitude of the derivative $\partial\epsilon_1/\partial\nu$. Grahame and Parsons (8, 9) have found that for KI and KCl electrolyte – mercury systems, K and therefore ϵ_1, depend only slightly on ν and this is consistent with the small variation in B demonstrated in Table II. The insertion of the polarization term in (4.27) should affect somewhat the value of p but since an independent estimate of $\partial\epsilon_1/\partial\nu$ is not known, we shall not pursue this further.

Let the experimental values of σ_0, σ_β, ψ_d, and ψ_0 at the maximum in $|\psi_d|$ be $\sigma_0^{(m)}$, $\sigma_\beta^{(m)}$, $\psi_d^{(m)}$, and $\psi_0^{(m)}$ respectively. Putting $z_\beta = -1$, and making use of (4.9), the relation (4.15) becomes

$$x = 1 - \frac{p^2\sigma_\beta^{(m)}/N_s e}{1+p\sigma_\beta^{(m)}/N_s e} = 1+h, \text{ say.} \tag{4.29}$$

Also, putting $g = 1$, $\gamma/d = 0.4$, $d = 5$ Å, and $p = 0$ and 2, we can determine $\sigma_\beta^0 = \sigma_\beta^{(m)}/x$ at the maximum and hence, from (4.2) and (4.9), the capacity K and the dielectric constant ϵ_1 of the inner region. Finally, the value of $\psi_0^{(m)}$ is calculated from (4.10) at a given electrolyte concentration c. Comparison with the experimental values for $\psi_0^{(m)}$ obtained by Grahame (8) for three electrolyte concentrations of KI are shown in Table III. Since the properties of the inner region are expressed in terms of the parameters γ/d and K only, ϵ_1 is proportional to the value chosen for d. The experimental values for K correspond to an empty inner region, i.e. $\sigma_\beta = 0$, and are assumed to depend on σ_0 only. We have also plotted (Fig. 8) the variation of ψ_0 with ψ_d in the case of 0.05 N KI for $p = 0$ and 2, $\gamma/d = 0.4$, and the fixed (theoretical) values of K given in Table III ($K = 25.2$ and 22.0 μfarads/cm^2 respectively). In the comparison with the experimental points of Grahame (8) it is convenient to choose the same value for $\psi_0^{(m)}$. When $p = 0$ and $g = 1$, it is possible to eliminate x from the equations (4.10) and (4.11) and so obtain a single equation relating η_0 and η_d. Putting $z_\beta = -1$, this reads

$$\eta_d + \frac{\kappa\epsilon}{2\pi Kz}\sinh\tfrac{1}{2}z\eta_d = \frac{\beta\eta_d+\gamma\eta_0}{d} - \exp\left[\frac{\beta\eta_d+\gamma\eta_0}{d} - C\right]. \tag{4.30}$$

We see from Table III that if K is assumed independent of ψ_0 at a given concentration c, its theoretical value at the maximum in $|\psi_d|$ is less than the experimental value for $\sigma_\beta = 0$ and the same σ_0. The dependence of K on ψ_0 at a given c is probably the

TABLE III

Values of parameters at maximum in $|\psi_d|$
(KI at 25° C, $\gamma/d = 0.4$, $d = 5$ Å; c in mole/l., $\sigma_0^{(m)}$, $\sigma_\beta^{(m)}$ in μcoulombs/cm², $\psi_d^{(m)}$, $\psi_0^{(m)}$ in volts, K in μfarads/cm²)

Experimental data

c	$-\sigma_0^{(m)}$	$-\sigma_\beta^{(m)}$	$-\psi_d^{(m)}$	$-\psi_0^{(m)}$	K ($\sigma_\beta = 0$)
0.1	7.0	2.3	0.085	0.39	25.0
0.05	5.0	2.7	0.092	0.33	26.4
0.025	3.9	3.0	0.100	0.28	27.4

Theoretical values

		$p = 0$ ($h = 0$)			$p = 2$			
c	$(1/K)(dK/d\eta_0)$	K	ϵ_1	$-\psi_0^{(m)}$	K	ϵ_1	$-\psi_0^{(m)}$	h
		K independent of ψ_0 at specified c						
0.1		21.5	12.1	0.45	19.1	10.8	0.49	0.122
0.05		25.2	15.8	0.33	22.0	12.5	0.37	0.145
0.025		28.0	17.6	0.26	24.1	13.6	0.29	0.162
		K dependent on ψ_0 at specified c						
0.1	0.024	30.1		0.35	27.6		0.37	
0.05	0.022	31.7		0.28	28.3		0.31	
0.025	0.024	34.0		0.23	29.7		0.25	

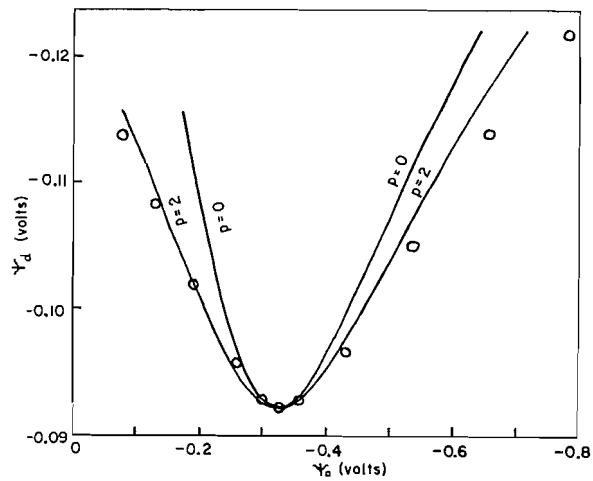

FIG. 8. Plot of ψ_d against ψ_0: O = experimental points. Mercury–electrolyte interface, 0.05 N KI.

main source of the difference, a secondary factor being the neglect of the polarization term (4.28). Introducing this dependence, the maximum in $|\psi_d|$ is no longer defined by (4.15), but, from (4.10) and (4.11), by

$$\left(\frac{1}{x} + \frac{p^2 b}{1-pbx}\right)\left(1 + \frac{\kappa\epsilon t}{2\pi K z}\sinh \tfrac{1}{2} z\eta_d\right) = 1 + \frac{dt}{\gamma g z_\beta}\frac{p^2 bx}{1-pbx}, \tag{4.31}$$

where $t = (1/K)(dK/d\eta_0)_c$. Putting $g = 1$ and $z_\beta = -1$, this may be written as

$$K = -\frac{\kappa\epsilon t}{2\pi z}\sinh \tfrac{1}{2} z\eta_d^{(m)} - \frac{1-(d/\gamma)ht}{1+h}\frac{e\beta\gamma}{kTd^2}\sigma_\beta^{(m)}, \tag{4.32}$$

where h is defined in (4.29) and $\eta_d^{(m)} = e\psi_d^{(m)}/kT$. The values of t can be estimated

from Grahame's data at $\sigma_\beta = 0$ if K is assumed independent of σ_β. It is seen from Table III that the theoretical values of K now exceed the experimental ones, although the agreement is somewhat closer for $p = 2$. The difference between the theoretical and experimental values of $\psi_0^{(m)}$ is greatly reduced at $c = 0.1$ and $p = 2$ but poorer agreement is obtained at $c = 0.025$ mole/l. Also, it readily follows from (4.11) that on the cathodic side of the maximum, where $x \approx 0$, the difference between the theoretical curves and the experimental points in Fig. 8 can be attributed to a drop in K with increase in $|\psi_0|$. However, the experimental decrease in K from 26.4 to 21 μfarads/cm^2 when σ_0 varies from -5 to -14 μcoulombs/cm^2 and $\sigma_\beta = 0$ is found to overcorrect for $p = 2$. A more detailed comparison seems unwarranted without the inclusion of the polarization energy and other factors, such as electrostriction, which have been ignored in the simple model of the inner region employed in this paper.

ACKNOWLEDGMENT

The authors are indebted to Dr. I. E. Puddington, Division of Applied Chemistry, National Research Council, Ottawa, for helpful discussions.

APPENDIX

Suppose that the inner region, of dielectric constant ϵ_1 and thickness d, is bounded by two perfectly conducting walls and that the I.H.P. coincides with the median plane, i.e. $\beta = \gamma = d/2$. In the cutoff approximation, ϕ_β'' is the potential at the center of a circular disk, situated in the I.H.P. and having radius r_0, due to a uniform charge density $-\sigma_\beta$ on this disk. We need to consider an infinite set of images associated with multiple reflections between two equipotential surfaces ($f = 1$) at separation d. (The array of images is illustrated in Fig. 6 in the more general case where $f \neq 1$ and $\gamma \neq \beta$.) The expression (3.5) is replaced by

$$\text{(A.1)} \qquad \phi_\beta'' = -\frac{2\pi\sigma_\beta}{\epsilon_1}\left[r_0 + 2\sum_{n=1}^{\infty}(-1)^n\{\sqrt{(r_0^2+n^2d^2)} - nd\}\right]$$

$$= -\frac{2\pi\sigma_\beta d}{\epsilon_1}\left[\tau + 2\sum_{n=1}^{\infty}(-1)^n\{\sqrt{(\tau^2+n^2)} - n\}\right].$$

When $\tau > 1$, it is possible to replace the series by a much more rapidly converging series by applying the Poisson summation formula in the following way.* Let $F(x)$ be a function which is integrable in the range $(-\infty, \infty)$ and is defined as $\frac{1}{2}\{F(x+0)+F(x-0)\}$ at points of discontinuity. Then, putting

$$\text{(A.2)} \qquad G(y) = \int_{-\infty}^{\infty} F(x)\exp(-2\pi i y x)dx,$$

the Poisson summation formula reads

$$\text{(A.3)} \qquad \sum_{x=-\infty}^{\infty} F(x) = \sum_{y=-\infty}^{\infty} G(y),$$

where the summation is taken over integral values of x and y only. If this is applied to the function

$$\text{(A.4)} \qquad F(x) = \begin{cases} \{\sqrt{(\tau^2+x^2)} - x\}\exp(\pi i x), & x > 0 \\ \frac{1}{2}\tau, & x = 0 \\ 0, & x < 0 \end{cases}$$

The authors are indebted to Professor G. E. H. Reuter of Durham University, for bringing this method to their attention.

then (A.1) becomes

$$\phi_\beta'' = -\frac{4\pi\sigma_\beta d}{\epsilon_1}\sum_{-\infty}^{\infty} F(x) = -\frac{4\pi\sigma_\beta d}{\epsilon_1}\sum_{-\infty}^{\infty} G(y). \tag{A.5}$$

Now

$$G(y) = \int_0^\infty \{\sqrt{(\tau^2+x^2)}-x\}\exp\{-2\pi i(y-\tfrac{1}{2})x\}dx \tag{A.6}$$

$$= \frac{\tau}{\pi i(2y-1)} + \frac{1}{\pi^2(2y-1)^2} - \frac{\tau^2}{\pi^2(2y-1)^2}\int_0^\infty \frac{\exp\{-2\pi i(y-\frac{1}{2})x\}}{(\tau^2+x^2)^{3/2}}dx,$$

integrating by parts twice. Noting that

$$\sum_{y=-\infty}^{\infty}\frac{1}{(2y-1)} = 0, \qquad \sum_{y=-\infty}^{\infty}\frac{1}{(2y-1)^2} = \frac{\pi^2}{4}$$

it follows that

$$\sum_{-\infty}^{\infty} G(y) = \frac{1}{4} - \sum_{-\infty}^{\infty} G_1(y) = \frac{1}{4} - \sum_{y=1}^{\infty}\{G_1(y)+G_1(1-y)\}, \tag{A.7}$$

where

$$G_1(y) = \frac{\tau^2}{\pi^2(2y-1)^2}\int_0^\infty \frac{\exp\{-2\pi i(y-\frac{1}{2})x\}}{(\tau^2+x^2)^{3/2}}dx$$

and so*

$$G_1(y)+G_1(1-y) = \frac{2\tau^2}{\pi^2(2y-1)^2}\int_0^\infty \frac{\cos(2y-1)\pi x}{(\tau^2+x^2)^{3/2}}dx = \frac{\pi(2y-1)}{\tau}K_1\{(2y-1)\pi\tau\}. \tag{A.8}$$

Thus, writing m instead of y, we obtain (3.14).

REFERENCES

1. D. C. GRAHAME. Chem. Revs. **41**, 441 (1947).
2. O. STERN. Z. Elektrochem. **30**, 508 (1924).
3. O. A. ESIN and V. M. SHIKOV. Zhur. Fiz. Khim. **17**, 236 (1943).
4. B. V. ERSHLER. Zhur. Fiz. Khim. **20**, 679 (1946).
5. V. G. LEVICH, V. A. KIRYANOV, and V. YU. FILINOVSKY. Doklady Akad. Nauk S.S.S.R. **135**, 1475 (1960).
6. D. C. GRAHAME. Z. Elektrochem. **62**, 264 (1958).
7. D. C. GRAHAME and B. A. SODERBERG. J. Chem. Phys. **22**, 449 (1954).
8. D. C. GRAHAME. J. Am. Chem. Soc. **80**, 4201 (1958); Technical Report No. 5 (second series) to the Office of Naval Research. Aug. 1, 1957. Contract No. N-onr-2309(01).
9. D. C. GRAHAME and R. PARSONS. J. Am. Chem. Soc. **83**, 1291 (1961).
10. O. ESIN and B. F. MARKOV. Zhur. Fiz. Khim. **13**, 318 (1939).
11. Z. A. IOFA and A. FRUMKIN. Zhur. Fiz. Khim. **18**, 268 (1944).
12. R. PARSONS. *In* Modern aspects of electrochemistry I. *Edited by* O'M. Bockris. Butterworths, London. 1954; Proc. 2nd Intern. Congr. of Surface Activity, **3**, 38 (1958).
13. J. R. MACDONALD. J. Chem. Phys. **22**, 1857 (1954). J. R. MACDONALD and C. A. BARLOW. To be published.
14. R. J. WATTS-TOBIN. Phil. Mag. **6**, 133 (1961).
15. N. F. MOTT and R. J. WATTS-TOBIN. Electrochim. Acta, **4**, 79 (1961).
16. S. LEVINE, G. M. BELL, and D. CALVERT. Nature, **191**, 699 (1961).
17. S. LEVINE and G. M. BELL. J. Colloid Sci. In press.
18. B. V. DERJAGUIN and L. LANDAU. Acta Physicochim. U.R.S.S. **14**, 633 (1941).
19. E. J. W. VERWEY and J. TH. G. OVERBEEK. Theory of the stability of lyophobic colloids. Elsevier Press, Inc., New York. 1948.

Bassett's integral for K_1 is used here (Watson, reference 28), namely

$$K_1(xz) = \frac{2z\Gamma(\frac{3}{2})}{x\Gamma(\frac{1}{2})}\int_0^\infty \frac{\cos xu}{(u^2+z^2)^{3/2}}du.$$

20. M. A. V. DEVANATHAN. Trans. Faraday Soc. **50**, 373 (1954).
21. P. J. FLORY. J. Chem. Phys. **10**, 51 (1942).
22. M. L. HUGGINS. J. Phys. Chem. **46**, 151 (1942); Ann. N. Y. Acad. Sci. **43**, 1 (1942).
23. K. H. FOWLER and E. A. GUGGENHEIM. Statistical thermodynamics. Cambridge University Press. 1949. Chap. 9.
24. A. L. LOEB. J. Colloid Sci. **6**, 75 (1951).
25. A. R. MILLER. The adsorption of gases on solids. Cambridge University Press. 1949. Chap. 7.
26. J. TH. G. OVERBEEK and D. STIGTER. Rec. trav. chim. **75**, 1263 (1956).
27. M. J. SPARNAAY. Rec. trav. chim. **77**, 872 (1958).
28. G. N. WATSON. Theory of Bessel functions. Cambridge University Press. 1932.

ELEMENTARY PROCESSES IN THE DECOMPOSITION OF OZONE

D. J. McKENNEY AND K. J. LAIDLER
The Department of Chemistry, University of Ottawa, Ottawa, Canada

Received June 2, 1961

ABSTRACT

Potential-energy surfaces are considered for the O_4 complex, treated as the three-body complex O . . . O . . . O_2. By means of these it is shown that $O(^3P)$ reacting with O_3 may give rise to a molecule of O_2 in its ground state and one in any of the states $^3\Sigma_g^-$ (ground), $^1\Delta_g$, and $^1\Sigma_g^+$; $^3\Sigma_u^+$ cannot be produced. Most of the oxygen molecules produced are expected to be in the ground electronic state, but will be vibrationally excited. Such molecules are readily deactivated and unlikely to lead to energy chains by the reaction

$$O_2^* + O_3 \rightarrow 2O_2 + O.$$

Such chains are therefore unlikely in the thermal decomposition and in that initiated by visible radiation. In ultraviolet light $O(^1D)$ atoms are produced and the potential-energy surfaces show that these give rise very efficiently to $O(^1D) + O_3 \rightarrow O_2 + O_2(^3\Sigma_u^-)$; the latter have 141 kcal in excess of the ground state. It is suggested that the subsequent radiative process

$$O_2(^3\Sigma_u^-) \rightarrow O_2(^3\Sigma_g^-) + h\nu$$

is responsible for sustaining the population of vibrationally excited oxygen molecules in the ground state and that these propagate energy chains, as postulated by McGrath and Norrish (1). The significance of these conclusions is discussed with reference to the experimental evidence.

INTRODUCTION

Recent papers (2, 3) have been concerned with the evidence for and against the existence of energy chains in the thermal and photochemical decomposition of ozone. There is general agreement that, in the thermal reaction and that brought about by visible (red) radiation, there is production of oxygen atoms in their ground (^3P) states, and that in ultraviolet light, excited (^1D) atoms are produced. An important question is whether these two types of atoms can give rise to energy chains by reacting with O_3 and producing excited oxygen molecules which can regenerate oxygen atoms by reaction with O_3. Benson (3) and McGrath and Norrish (1) have argued that the experimental evidence supports the conclusion that $O(^3P)$ atoms cannot give rise to chains, but that $O(^1D)$ atoms do; in other words, there are energy chains in the ultraviolet reaction, but not in the thermal reaction or in the reaction brought about by red light. These authors, however, have postulated quite different mechanisms for the reaction in the ultraviolet.

In the present paper we examine the question from the standpoint of potential-energy surfaces, and arrive at conclusions that are essentially the same as Benson's. It is suggested, however, that a modified McGrath and Norrish mechanism is probably correct for the ultraviolet reaction.

POTENTIAL-ENERGY SURFACES

The course of a reaction between oxygen atoms and ozone molecules may be considered with reference to the potential-energy surfaces for the O_4 system. Figure 1 shows that this requires six parameters for its complete description, but for convenience it may be considered as the three-body system O . . . O . . . O_2, and energy plotted as a function of the two distances r_1 and r_2. Such a potential-energy surface, shown as Fig. 2, may be regarded as a section through the complete seven-dimensional diagram required for a tetratomic complex, this section relating to a particular interatomic distance r' and to particular values for θ_1 and θ_2 and for the torsional angle ϕ.

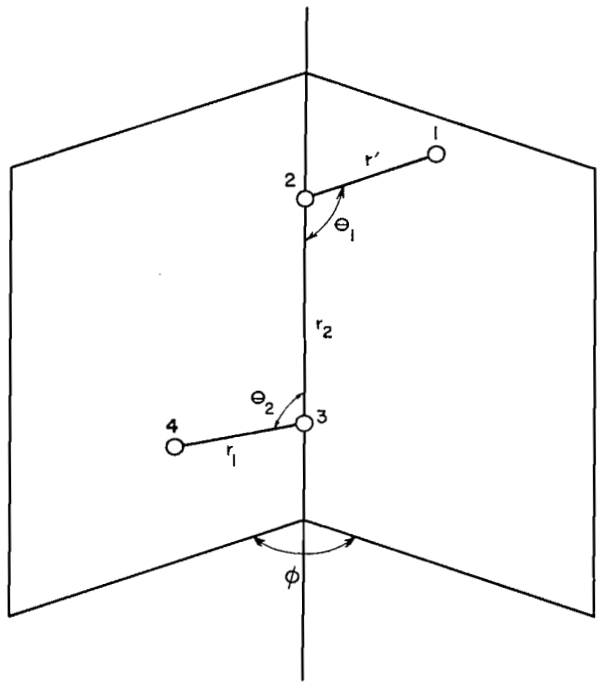

FIG. 1. The O_4 species.

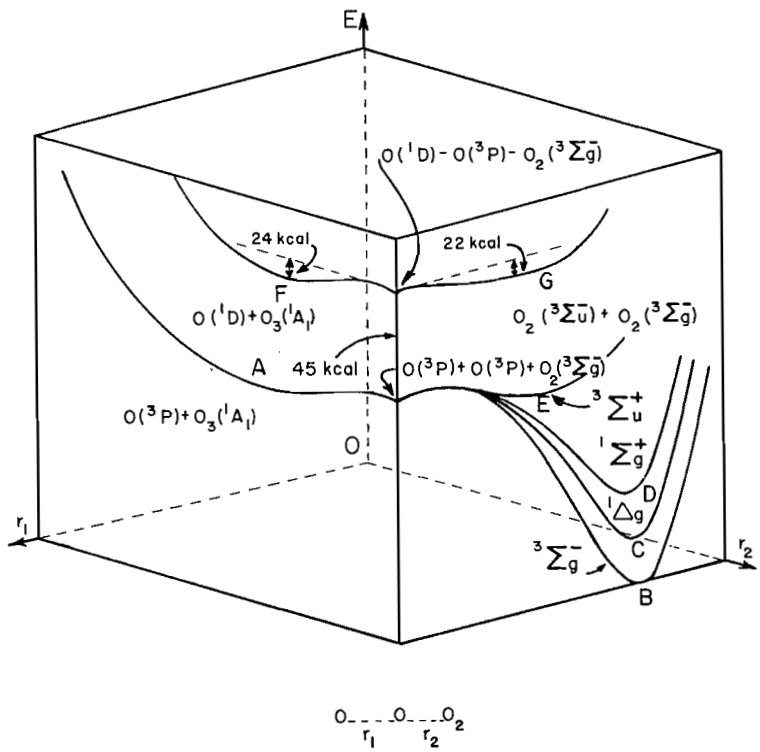

FIG. 2. Potential-energy surfaces for O_4, treated as the three-body system O . . . O . . . O_2.

Figure 2 shows two sets of curves, one for r_1 very large (i.e. for $O + O_3$) and the other for r_2 very large (for $O_2 + O_2$). These curves are connected by surfaces within the diagram, and reactions must involve motion along a potential-energy surface, possibly with a jump at a suitable crossing point.

The initial state of the reaction $O(^3P) + O_3$ is represented by point A in the diagram, and points B, C, and D represent the possible final states; experimentally (4) the activation energy is 6 kcal, so that the production of $O_2(^3\Sigma_g^-) + O_2(^3\Sigma_u^+)$ is excluded on energetic grounds since the final state E lies 8 kcal higher than the initial state. The reaction paths connecting A with B, C, and D are represented schematically in Fig. 3.

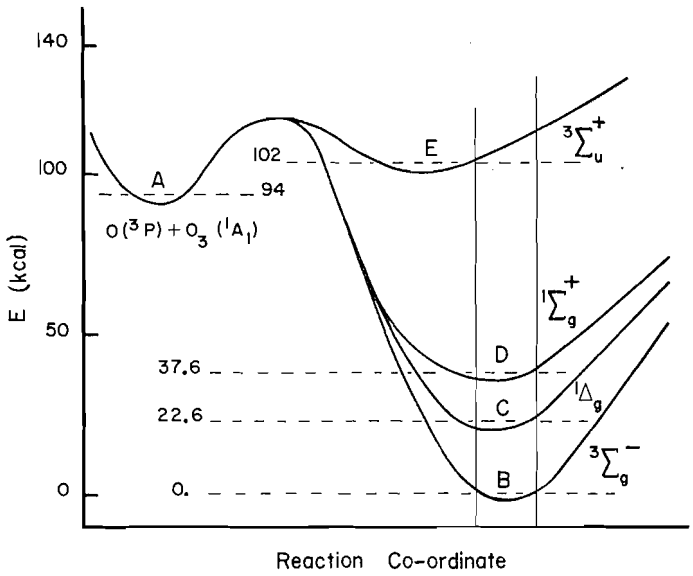

FIG. 3. Section through Fig. 2, showing the possible reaction paths.

If the splitting of the surfaces occurs after the activated state the probabilities of forming the $^3\Sigma_g^-$, $^1\Delta_g$, and $^1\Sigma_g^+$ states will be respectively 1/2, 1/3, and 1/6, corresponding to the multiplicities. (The $^1\Delta_g$ state is doubly degenerate.) It is also possible for the activated complex for the formation of $^1\Sigma_g^+$ to be higher than that for $^1\Delta_g$, which may be higher than that for $^3\Sigma_g^-$; in this case the probability of forming $O_2(^3\Sigma_g^-)$ is greater than 1/2. Most of the energy released in the reaction will therefore pass into non-electronic forms, and will be readily dissipated on collisions.

For energy chains to be set up the reaction

$$O_2^* + O_3 \rightarrow 2O_2 + O \qquad [1]$$

must occur. The ΔH for this reaction (5) is $25.7 - E_e$, where E_e is the excitation energy for the O_2 molecule, so that for the reaction to be exothermic E_e must be at least 25.7 kcal. This condition is only satisfied by the $^1\Sigma_g^+$ state or by the lower ($^1\Delta_g$ and $^3\Sigma_g^-$) states if they have sufficient vibrational energy. Since, however, the $^1\Sigma_g^+$ state is formed with, at the most, a probability of 1/6, and vibrational energy is readily dissipated, it is clear that the formation of oxygen atoms by reaction [1] will occur only with low efficiency. Energy chains cannot, therefore, be of any importance when $O(^3P)$ atoms are involved, i.e. in the thermal decomposition and in the photochemical decomposition induced by visible radiation.

Point F in Fig. 2 represents the system $O(^1D) + O_3$; it is connected by a surface to the curve passing through G and corresponding to the formation of $O_2(^3\Sigma_g^-) + O_2^*(^3\Sigma_u^-)$. The latter species has an energy of 141 kcal in excess of the ground state. Schumacher (2) has pointed out, as evident from Fig. 2 also, that this reaction is endothermic, the difference in energy between the initial and the final state being 2 kcal. One would expect, therefore, that this reaction should have an appreciable activation energy. Benson (3) has answered this objection by taking into account the fact that the O atoms can have excess translational energies, which are dissipated relatively slowly, and hence the production of $O_2^*(^3\Sigma_u^-)$ molecules can be quite fast at high O_3 concentrations. The nature of the surface does not permit the formation of the second molecule of oxygen in any lower excited state, except with very low probability. The highly excited $^3\Sigma_u^-$ molecules have a short life of 2.5×10^{-9} second (6) due to the radiative process $O_2(^3\Sigma_u^-) \rightarrow O_2(^3\Sigma_g^-) + h\nu$, which gives rise to the Schumann–Runge emission bands of O_2. The ground-state oxygen molecules produced by this process will, according to the Frank–Condon principle, give vibrationally excited O_2 molecules in exactly those levels observed in the ozone photolysis by McGrath and Norrish. This can be readily seen by reference to Fig. 4.

It is perhaps significant that these workers (8) observed a maximum value around $v'' = 13$ (53.5 kcal/mole) in the vibrational energy distribution. There is no explanation for this maximum given in their paper, and one would expect that if vibrationally excited O_2 molecules were produced solely by the endothermic process

$$O(^1D) + O_3(^1A) \rightarrow O_2^*(^3\Sigma_g^-) + O_2(^3\Sigma_g^-),$$

the population of these vibrational levels should be a maximum at the lower energy levels. The fact that there is a maximum at $v'' = 13$, however, strongly suggests that the population of these vibrational energy levels is a result of the process

$$O_2(^3\Sigma_u^-) \rightarrow O_2^*(^3\Sigma_g^-) + h\nu.$$

As can be seen from Fig. 4, the transition from the minimum of the $^3\Sigma_u^-$ state would produce O_2 molecules in the ground state ($^3\Sigma_g^-$) in roughly the 12th or 13th vibrational level. This should then be a maximum, as is the case. The radiation given off in the process is of very short wavelength (2000 Å) (2) and consequently would be absorbed by undecomposed ozone.

DISCUSSION

The above conclusions are consistent with the experimental results of the aforementioned authors. Some specific remarks about the decomposition mechanism may now be made.

McGrath and Norrish (1, 8) flash photolyzed, using ultraviolet radiation, a mixture of O_3, H_2O, and N_2 in the ratio 1:3:100, and obtained strong OH absorption. This is attributed to the occurrence of the exothermic reaction

$$O(^1D) + H_2O \rightarrow 2OH + 29.2 \text{ kcal.}$$

Hydroxyl radicals could not be obtained with $O(^3P)$ atoms, owing to the endothermicity of the reaction

$$O(^3P) + H_2O \rightarrow 2OH - 16.8 \text{ kcal.}$$

In agreement with this the addition of water has little or no effect on the thermal decomposition of ozone (3, 9).

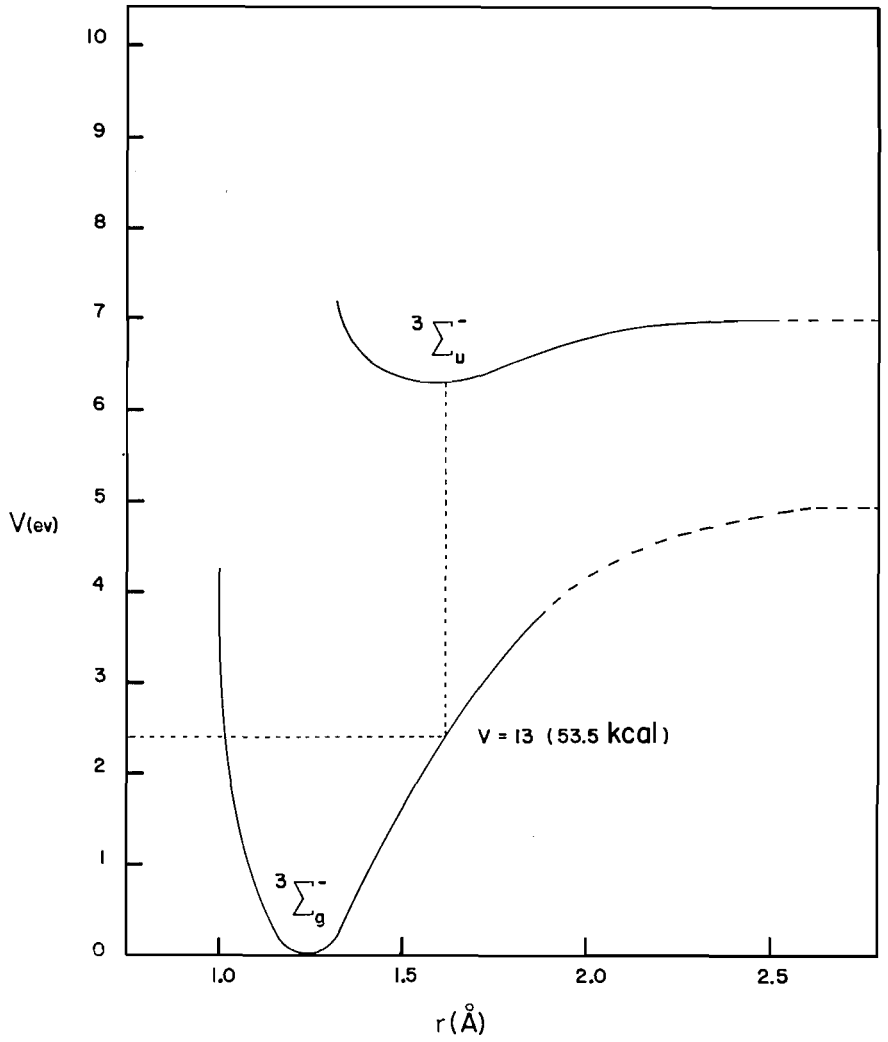

FIG. 4. Potential-energy curves (7) for the O_2 molecule, showing that a maximum in the vibrational energy distribution is expected for $v = 13$ for $^3\Sigma_u^- \rightarrow {}^3\Sigma_g^-$.

The most likely mechanism for the thermal decomposition of ozone (where only $O(^3P)$ atoms can be produced) is that of Benson and Axworthy (10), which is

$$O_3 + M \rightleftarrows O + O_2 + M \quad [2]$$

$$O + O_3 \rightarrow 2O_2. \quad [3]$$

At the ordinary pressures the first reaction will be in its second-order region (11). The probability of forming electronically excited $O_2(^1\Sigma_g^+)$ is very low, as was pointed out above, and therefore the possibility of energy chains in the thermal reaction is excluded. If, however, energy chains were involved, the following reactions would have to be added:

$$O + O_3 \rightarrow O_2 + O_2^* \quad [4]$$

$$O_2^* + O_3 \rightarrow 2O_2 + O, \quad [5]$$

but Benson and Axworthy (4, 10) showed that this led to a kinetic scheme which is inconsistent with experiment.

Similar comments apply to the work with visible radiation, which produces $O(^3P)$ atoms. The quantum yields are probably (3) always less than 2, so that there is no evidence for energy chains.

The most probable mechanism in ultraviolet light involves as the initiating step

$$O_3 + h\nu \rightarrow O_2 \text{ (singlet)} + O(^1D). \quad [6]$$

The oxygen molecules must be in a singlet state for spin conservation; it may be the $^1\Sigma_g^+$ state, which requires that the wavelength is less than 3100 Å. Reaction [6] will be followed by

$$O(^1D) + O_3 \rightarrow O_2(^3\Sigma_g^-) + O_2(^3\Sigma_u^-), \quad [7]$$

as discussed above, and this is followed by the rapid transition

$$O_2(^3\Sigma_u^-) \rightarrow O_2^*(^3\Sigma_g^-) + h\nu. \quad [8]$$

The propagation of the chain then takes place by the vibrationally excited $O_2^*(^3\Sigma_g^-)$ molecules of excitation energy > 69 kcal reacting with ozone, i.e.,

$$O_2^*(^3\Sigma_g^-) + O_3(^1A) \rightarrow 2O_2(^3\Sigma_g^-) + O(^1D). \quad [9]$$

The latter reaction is the essential feature in the McGrath and Norrish mechanism. The termination steps are probably

$$\begin{aligned} O + O + M &\rightarrow O_2 + M \\ O + O_2 + M &\rightarrow O_3 + M \\ O_2^* + M &\rightarrow O_2 + M, \end{aligned} \quad [10]$$

where M represents a molecule of oxygen, ozone, or an inert gas.

REFERENCES

1. W. D. McGrath and R. G. W. Norrish. Proc. Roy. Soc. (London), A, **254**, 317 (1960).
2. H. J. Schumacher. J. Chem. Phys. **33**, 938 (1960).
3. S. W. Benson. J. Chem. Phys. **33**, 939 (1960).
4. S. W. Benson. Foundations of chemical kinetics. McGraw-Hill Book Company, New York. 1960. pp. 400–408.
5. E. K. Gill and K. J. Laidler. Can. J. Chem. **36**, 79 (1958).
6. D. W. O. Heddle. J. Chem. Phys. **32**, 1889 (1960).
7. J. T. Vanderslice, E. A. Mason, and W. G. Maisch. J. Chem. Phys. **32**, 515 (1960).
8. W. D. McGrath and R. G. W. Norrish. Proc. Roy. Soc. (London), A, **242**, 265 (1957).
9. J. A. Zaslowsky, H. B. Urback, F. Leighton, R. J. Wnuk, and J. A. Wojtowicz. J. Am. Chem. Soc. **82**, 2682 (1960).
10. S. W. Benson and A. E. Axworthy. J. Chem. Phys. **26**, 1718 (1957).
11. E. K. Gill and K. J. Laidler. Trans. Faraday Soc. **55**, 753 (1959).

HIGH-PRECISION VOLUME TITRIMETRY

G. A. DEAN[1]
Department of Chemistry, Dalhousie University, Halifax, Nova Scotia
Received July 31, 1961

ABSTRACT

Ways in which the ultimate limit of volume titrimetry may be reached are analyzed: the most suitable approach, based essentially upon the use of a bulb burette, allows, in theory, a mechanical precision better than that of the best weight techniques to be obtained, and the various factors influencing this precision are detailed. Several end-point systems potentially sensitive to considerably better than 1 part per million (p.p.m.) are discussed. An attempt at high precision with the iron(II)/dichromate titration, using refined equipment and an amperometric end point, is described: the observed precision was 0.7–1.1 p.p.m. for two experiments of about eight titrations each; the calculated precision, estimated from the resultant of the component precisions, was about 0.9 p.p.m. The ultimate limit of precision of any titrimetric operation, whether by weight or by volume, is shown to be about 0.1 p.p.m.

INTRODUCTION

Accounts of attempts to use titrimetric apparatus at the limit of their precision have appeared fairly frequently over the past 50 years. One of the most recent is that of Bishop (1), who has determined the attainable limits of weight titrimetry using refined apparatus and techniques: under the most favorable circumstances, and by working under "atomic weight" conditions, the highest precision obtained by him was ±13 parts per million (p.p.m.) for five titrations of arsenious oxide with potassium bromate. The overall mechanical precision was shown to be about ±2 p.p.m.; consequently, the greater part of the previous value would appear to be due to uncertainty in the location of the (graphical potentiometric) end point. This view is corroborated by reference to the work of Richards and Forbes (2), who, in their classic atomic-weight experiments involving the conversion of silver to silver nitrate, obtained a precision for the ratio $Ag:AgNO_3$ of ±2.7 p.p.m. in six determinations, or about the same as the estimated overall precision of the weighings. An interesting combination of techniques was used by Baxter and Hale for their determination of the atomic weight of iodine (3): weighed amounts of iodine pentoxide and sodium carbonate were allowed to react in solution and the neutralization completed volumetrically using bromothymol blue as indicator. The indicator exhibited a complete color change over the range 10 p.p.m., and an overall precision of ±13 p.p.m. for seven determinations was attained.

The attainable limits of volume titrimetry using conventional apparatus have been determined (4–7); minor changes in the apparatus allow improvements to be made, as exemplified by refs. 5 and 8; the present work discusses ways in which the ultimate limit may be reached and describes an attempt to reach this limit with refined equipment.

In the following account it is understood that the levels of precision being considered are often considerably better than the accuracy and consequently may be of diminished value. Aspects of accuracy have been fully discussed by Bishop (1) and will not be considered here.

PRECISION OF VOLUME TITRIMETRY

The ultimate precision of any titration is limited by the precision of the mechanical measurements and by the sensitivity of the end point. For the purpose of the present

[1]*National Research Council of Canada Postdoctorate Fellow, 1959–61. Present address: Soil Bureau, P.O. Box 8001, Wellington, New Zealand.*

work the system to be considered is that of a simple titration of one reagent with another. For maximum precision, 50 ml and 0.1 *N* are adopted as the nominal optimum volume and concentration, respectively, of each reagent. In the following account all values of precision are expressed as a standard deviation.

Mechanical Limit of Volumetric Measurements—Pipettes

A constant temperature is an inherent requirement of any precise volumetric operation. This means that, in practice, the volumetric apparatus has to be immersed in a liquid bath suitably thermostatted. Because of this immersion, and because the degree of temperature control required (see later) and the need for preventing evaporation prohibit the transfer of liquid in the usual manner, a conventional pipette is unsuitable and something akin to a burette must be used.

Mechanical Limit of Volumetric Measurements—Burettes

Other things being equal, the precision of a burette is a function of the tube diameter (5). Bulb or chamber burettes, in which the capacity is divided between a bulb and a finely divided graduated section, are often used to secure a moderate increase in precision at the expense of a restriction in range, and the carrying through of this principle to its logical conclusion allows the ultimate in precision to be obtained.*

The various factors influencing the precision of a burette have received detailed attention (5). Given adequate control of temperature and pressure, the mechanical precision of a bulb burette will be limited only by

(1) precision of the initial setting,
(2) precision of the volume of liquid remaining on the walls after delivery (the wall film),
(3) precision of the drainage,
(4) precision of the final setting.

To achieve maximum precision of the initial setting, the top of the bulb can be fitted either with a short graduated section, when similar considerations as for (4) would apply (see below), or with an "automatic zero". Of the various types of automatic zero currently in use, one similar to that shown in Fig. 1 is to be preferred. The internal diameter of the inner tip may be made as fine as required, since it is not subject to the same limitations as a graduated section (see below), and consequently the variability of the automatic zero may be rendered negligible. This factor, together with the automatic zero's positive, convenient, and unambiguous operation, renders it indispensable for precise work.

The variability of the wall film should not be a significant factor provided that the burette is not exposed to vibration (6). Unfortunately, the outflow rates for delivery from the bulb and from the graduated section, as determined by consideration of (2) and (3), see below, are not the same; hence provision must be made for changing the rate of outflow as the meniscus passes from the bulb to the graduated section. The decrease in the wall film owing to the decreased rate of delivery while setting to the mark, and the effect of this upon the overall precision, may be rendered negligible by an adequately long delivery time.

**Syringe burettes, in which the movement of a piston inside a precision-bore tube is controlled by a micrometer head, have found increasing use over the past few years (4, 9). However, apart from the difficulty of thermostatting such a burette, purely mechanical considerations preclude its use here. For example, the typical minimum division of a good micrometer head is 0.001 cm; assuming that 0.1 of this division is to be equivalent to, say, 0.00001 ml, then the maximum syringe diameter is about 0.3 cm, and would require a length of 5 m to contain a 50-ml volume. Conversely, a syringe 10 cm in length and 5 cm² in cross section would require a micrometer head sensitive to 20 mμ. Clearly, syringe burettes are impractical for high-precision work.*

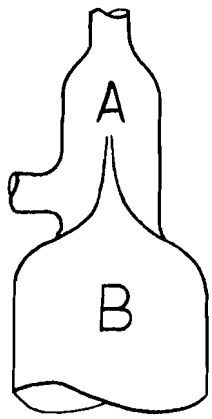

FIG. 1. Automatic zero. With B filled, the level in A is allowed to rise above the inner tip. The zero is then set by withdrawing liquid through the side arm until the level has fallen below that of the inner tip.

The influence of drainage over the time required for a titration may be prevented by an adequately long delivery time (6).

The variability of the final setting may, in theory, be made smaller indefinitely by reducing the internal diameter of the graduated section (5). In practice, however, there is a lower limit of between 0.5 and 1.0 mm, depending on the design of the burette, below which the outflow time becomes inconveniently long.

Consequently, of the four contributing precisions, the last is likely to set the overall limit. Using the results of Dean and Herringshaw (5), and the most accurate setting that can be expected with small tubes (i.e., between settings 1 and 2 of ref. 5), values of (4)

TABLE I

Calculated precision of the final setting

Bore of graduated section (mm)	Calculated precision of setting (ml)	Precision referred to 50 ml (p.p.m.)
1.25	0.00002	0.4
1.00	0.00001	0.2
0.75	0.000004	0.08
0.50	0.0000015	0.03

can be calculated, and are presented in Table I. By comparison, it is unlikely that a weight burette plus 50 g of liquid could be weighed *reliably* to better than ± 5 μg, or to about ± 0.1 p.p.m. (1).

Limiting Sensitivity of the End Point

Hitherto, the sensitivity of the end point has proved to be the limiting factor in the quest for high precision (see, e.g., ref. 1). As the sensitivity of the end point is largely subjective it is not possible to quote exact values; Table II summarizes some values for sensitive end points which have been reported in precise work. While even the best values of Table II are still approximately two orders of magnitude greater than the practical limit of mechanical precision, it is possible to achieve considerably better sensitivity by careful selection of the reagents and method. Two such methods are outlined in Table III

TABLE II

Observed sensitivity of some sensitive end points

Method of locating end point	Titration	Sensitivity* (p.p.m.)	Ref.
Visual	Oxalate/permanganate	100	10
	Fe(II)/dichromate/barium diphenylamine sulphonic acid	200	11
	Iodine/thiosulphate/starch	20	12
	Borax/hydrochloric acid	260	1
	Ferrocyanide/Ce(IV)/Victoria Green	240	7
	$As_2O_3/KBrO_3$	180	1
Photometric	Borax/hydrochloric acid	50	1
	Ferrocyanide/Ce(IV)/Victoria Green	80	7
	$As_2O_3/KBrO_3$	30	1
Graphical potentiometric	$As_2O_3/KBrO_3$	15	1
	$KBr/AgNO_3$	30	1
	$KI/KMnO_4$	50	13

*For titrations involving 50 ml of 0.1 *N* reagent, or equivalent, except for borax/hydrochloric acid (0.5 *N*).

TABLE III

Calculated sensitivity of two sensitive methods of detection

Method	Reagent	Minimum detectable change in concentration, $N \times 10^8$	Minimum detectable change in concentration, referred to 0.1 *N* (p.p.m.)
Spectrophotometric	$KMnO_4$	100*	10
	Ce(IV)	8*	0.8
	Iodine	4*	0.4
Amperometric ("dead-stop")	Fe(II)	0.1†	0.01
	Ce(IV)	~0.1‡	~0.01
	Iodine	~0.01‡	~0.001
	Bromine	0.5§	0.05

*The minimum detectable change in concentration, ΔN, was calculated from $\Delta N = \Delta d/\epsilon l$, where Δd = minimum detectable change in optical density = 0.002; l = path length ~ 4–5 cm; and ϵ = *normal* extinction coefficient = 450 at 520 mμ (14), 5,000 at 320 mμ (15), and 13,000 at 353 mμ (16) for $KMnO_4$, Ce(IV), and iodine, respectively.

†Experiments involving [Fe(II)] from 0.1 *N* to 0.0002 *N* in both macro- and micro-titrations, and with various amperometric pairs, have shown that in solutions *N* to sulphuric acid and 0.5 *M* to orthophosphoric acid the change in [Fe(II)] required to produce a change in current of 1 μa/cm² of electrode area (based on one electrode, both electrodes equal) under an applied potential difference of 300 mv is fairly constant at 2×10^{-6} *N*. The minimum detectable change in concentration was calculated by assuming electrodes each 1 cm² in area, a galvanometer of f.s.d. = 0.1 μa, and a minimum reliable change in deflection of 1% f.s.d., or about 0.001 μa. (Even this value can be exceeded by at least one order of magnitude by the sensitivity of some commercially available instruments (see, e.g., ref. 17).) Note that, for Fe(II), and under similar conditions of electrode area and galvanometer sensitivity, the method is more sensitive than the "sensitive end point procedure" of Cooke, Reilley, and Furman (18).

‡Estimated from the value for Fe(II) by comparison with the results of Stone and Scholten (19).

§From the results of Sease *et al.* (20) and corrected to the same conditions as for Fe(II).

and show that, in favorable cases, and provided that the conditions are carefully chosen to enable the full sensitivity to be realized, the limiting sensitivity of the end point can be made to equal or even exceed the limiting mechanical precision.

AN ATTEMPT AT HIGH PRECISION WITH THE IRON(II)/DICHROMATE TITRATION USING AN AMPEROMETRIC END POINT

The iron(II)/dichromate titration was chosen because the exceptionally low background and completeness of reaction at the end point allow the full sensitivity of the amperometric end point to be realized. The basis of the apparatus was a pair of 50-ml bulb burettes

with a 0.5-ml graduated section, designed in accordance with the previous considerations, and made of Kimble KG 33 borosilicate glass to special order by Ace Glass Inc., Vineland, New Jersey. The completed apparatus is shown diagrammatically in Fig. 2. It was situated in a basement laboratory, free from vibration and excessive variation in temperature.

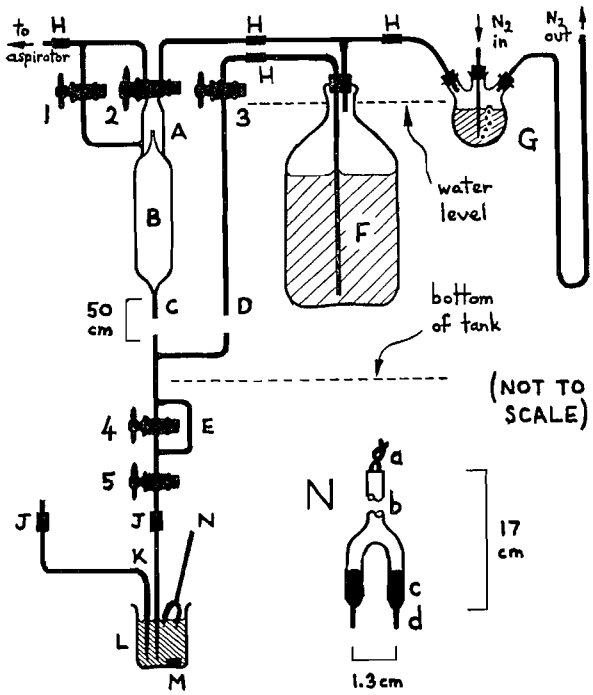

FIG. 2. Apparatus for high-precision volume titrimetry.

1–5 = Kimble stopcocks with Teflon plugs (For clarity, stopcocks 1–3, and E, have been turned through 90°; 4 and 5 through 180°, about the vertical; 4 and 5 are of 1-mm bore.)
A = automatic zero (see Fig. 1)
B = bulb, ~50 ml
C = graduated stem, 0.5 ml in 0.001-ml divisions, of precision-bore capillary tubing
D = side arm of 2-mm capillary tubing
E = capillary bypass: a slower rate of delivery is obtained by closing tap 4
F = 9-liter "serum" bottle of Pyrex glass
G = source of nitrogen at atmospheric pressure (used with the F-burette only) (The 250-ml 3-necked flask contains a solution of Fe(II) similar to that in F. The long U-tube of 7-mm tubing (capacity ~20 ml) guards against momentary overloads.)
H = silicone-rubber connections secured with tubing clamps (not shown)
J = 0.25-in. wall Tygon connections secured with tubing clamps (not shown)
K = 1-mm capillary tubing with finely drawn-out tip
L = 150-ml beaker
M = Teflon-sheathed stirring bar
N = amperometric pair: *a*, insulated solid copper wire; *b*, 7-mm soft-glass tubing; *c*, mercury; *d*, ~0.5-mm platinum wire.

(The D-burette etc. (not shown) are identical with the F-burette etc., except for the omission of G.)

EXPERIMENTAL

Temperature Control

A volume precision of 0.1 p.p.m. requires that a temperature constant to 0.0005° be maintained. To avoid the considerable difficulty of thermostatting to this level directly, a "tandem" arrangement was used: the whole apparatus was immersed in a large tank fitted with a Perspex window and filled with distilled water stirred slowly at constant speed, and this was immersed, in turn, in a larger tank also filled with distilled water and fitted with a similar window. Both tanks were equipped with covers.

The larger tank was thermostatted at 23° (about 1° higher than the maximum annual laboratory temperature) to ±0.005° (measured in the least favorable position between the Perspex windows) using a powerful

stirrer and a 500-watt immersion heater controlled by a "Red Top" mercurial thermoregulator via an electronic relay, with a minimum heating cycle of 1 minute. When a temperature difference of 1° was artificially maintained between the two tanks, the inner tank varied by about 0.03° per minute; consequently, the inner tank should be constant to $\pm 0.03 \times 0.005° = 0.00015°$. The total volume of water involved was just over 0.5 m^3, to which a few grams of thymol were added to prevent marine growths.

The lower burette taps protruded from the bottom of the tank: the exposed "dead space" was kept to a minimum (about 0.3 ml) to minimize the effect of any changes in room temperature. Owing to the difference in length between the two burette tips (Fig. 2) there was a difference in dead space of about 0.15 ml; during a titration, the observed change in temperature near the burette tips was never more than 0.2°, corresponding to a maximum difference of 0.000005 ml with respect to 0.15 ml. The difference in thermal expansion between the two reagents (see later), and referred to the remaining dead space, would tend to reduce this figure.

The burettes were viewed through the Perspex windows, and the upper taps manipulated by rods passing through seals in the windows. It was intended that the inner tank should be completely immersed, but owing to the failure of some of the seals the tanks could be filled only to the level shown in Fig. 2, and consequently the inner tank was not completely isolated from changes in room temperature. Fortunately, owing to the favorable location of the tank, room-temperature fluctuations were very small: short-term fluctuations in the inner tank could not be detected with an E-Mil GS 10300 Differential Thermometer (Beckmann type), minimum division 0.002°, and any temperature drift was never more than 0.001° per hour.

Stopcocks

Kimble stopcocks with Teflon plugs were used in preference to conventional stopcocks in order to avoid the use of grease. Taps 3 and 5 (Fig. 2), in particular, were required to be exceptionally leakproof, and those finally supplied* had to be very tight before a satisfactory performance was achieved: under these conditions their operation remained smooth, but the lockwashers were ineffective and the threads were in danger of stripping. However, by rotating the plug in one direction only, or by manipulating with both hands, a satisfactory performance was achieved. Under constant temperature conditions, the tendency to stick, which is often encountered with these stopcocks (due to the grossly dissimilar thermal expansion coefficients of glass and Teflon), was never observed. A small incision with a razor blade was made at right angles to the plug axis across the ends of the hole in the plug of tap 5; this allowed very fine control of the delivery.

Preparation of the Apparatus

The whole apparatus was cleaned with permanganic–sulphuric acid cleaning mixture (prepared by adding powdered potassium permanganate to concentrated sulphuric acid, with stirring, until the solution is deep green in color; the preparation and use of this solution is without hazard) followed by thorough rinsing with dilute acidified hydrogen peroxide to remove any traces of manganese dioxide, and then with water redistilled from dilute alkaline permanganate in an all-Pyrex-glass still fitted with splash guards; the bottles and connecting tubes were then steamed with steam evolved from boiling dilute alkaline permanganate. The rubber bungs and silicone–rubber connections were cleaned by immersion in boiling 3 *N* aqueous sodium hydroxide for two 1-hour periods followed by thorough rinsing in distilled water.

After conditioning the assembled apparatus for 1 month with the appropriate reagents, it was again thoroughly cleaned, as before. Finally, the bottles were filled with freshly redistilled water and the appropriate reagents added to approximately 0.1 *N* strength. After reassembly, the apparatus was allowed to condition itself for 8 weeks before the titrations of Table IV were performed.

Reagents

It was observed that solutions of reagent-grade potassium dichromate, of various manufacture, in redistilled water and contained in bottles treated as previously, had a strong tendency to become "greasy", as shown by incomplete wetting of the walls. On recrystallizing the dichromate four times from redistilled water according to the recommended procedure (21) it no longer showed this tendency, even on allowing the solution to stand for 3 months; consequently, such recrystallized dichromate was used.

Reagent-grade ferrous sulphate and sulphuric acid were found to be satisfactory with respect to "greasiness" and were used without further purification. However, the former (like most solid reagents) was found to contain minute quantities of dust and foreign matter, and a concentrated solution in dilute sulphuric acid was filtered through sintered glass and used for the preparation of the final solution. This final solution was deoxygenated by bubbling nitrogen through it for 7 days and was subsequently stored under nitrogen, as shown in Fig. 2.

"Titration acid" was prepared by adding 100 ml of reagent-grade concentrated sulphuric acid to 100 ml of reagent-grade orthophosphoric acid and 200 ml of redistilled water. Ten milliliters of titration acid per titration produced a better end point than 5 ml, while 20 ml produced little improvement over 10 ml; therefore 10 ml was used per titration, giving at the end point $[H_2SO_4] \sim 0.9$ *N* and $[H_3PO_4] \sim 0.45$ *M*.

**Messrs. Ace Glass Inc. reported having great difficulty in finding specimens of the required standard.*

Amperometric Apparatus

An amperometric "pair" (N, Fig. 2) was constructed of smooth platinum wire ~0.5 mm in diameter, sealed in soft glass, with ~0.7 cm or ~0.1 cm^2 exposed. The latter was deliberately small to avoid significant oxidation of iron(II) by the oxide film (22). A potential difference of 300 mv was applied across the pair by the circuit shown in Fig. 3. The pair was normally left exposed to the atmosphere (no improvement

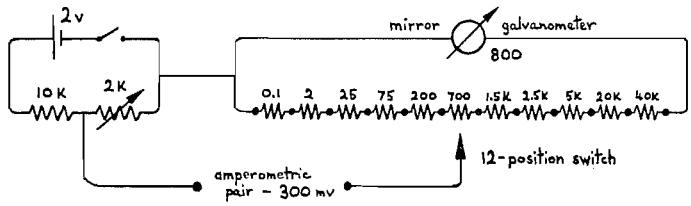

FIG. 3. Amperometric circuit. Resistances in ohms; total shunt resistance = 70 K = critical damping resistance of the Leeds and Northrup mirror-galvanometer type 2285f.

was noted on storing in water) except in between titrations, when the platinum was immersed in chromic–sulphuric acid cleaning mixture (prepared by grinding concentrated sulphuric acid with an excess of anhydrous chromium trioxide) in order to maintain a sensitive response.

A Leeds and Northrup mirror-galvanometer type 2285f (maximum sensitivity 0.025 μa for full-scale deflection (f.s.d.) = 50 cm) was used in conjunction with a special shunt (Fig. 3), similar in principle to that used by Cooke, Reilley, and Furman (15), constructed from high-stability resistors and which presented a constant resistance to the galvanometer independent of the sensitivity. The galvanometer was carefully checked for linearity by replacing the pair with a resistor and measuring the potential difference with a Beckmann model GS pH meter sensitive to 0.1% f.s.d.

At the fairly slow stirring rates required to avoid loss of solution through splashing, the limiting current (9) is not attained, and a constant rate of stirring is essential if steady currents are to be obtained. Ordinary variable-speed magnetic stirrers were found to exhibit random (and sometimes very pronounced) fluctuations in speed, and so a specially constructed synchronous magnetic stirrer was used together with a small Teflon-sheathed stirring bar.

Diffusion of reagent from the very fine, drawn-out capillary tips of the burettes could not be detected over the period required for the determination of the end point.

Reading the Burette

The graduated section was of Ace Glass "Trubore" precision-bore capillary tubing, about 0.12 cm in internal diameter (manufacturers tolerance ±0.002 cm), and 8 mm in external diameter. (Since the outcome of the experiments could not be anticipated, the higher potential precision afforded by the use of a smaller-diameter tube was sacrificed for the sake of a greater range in delivery.)

The minimum division was 0.001 ml and occupied ~1 mm. All graduations were deliberately confined to the front. To avoid parallax, a strip of "Vitrolite" (milk-white glass) carrying similar graduations was placed behind the tube at such a distance (~4 cm) that the situation depicted in Fig. 4A was obtained. In accurate work, the need for making all readings at a mark has been described (5). However, if the meniscus was inadvertently stopped between graduations, or if the setting was not exact, then an exact reading using an "optical-lever" vernier could be obtained: the eye was moved until the meniscus and the graduation were brought into the required relationship, when the correct position could be read off from the graduated backing, as illustrated in Fig. 4B. The method was sensitive to 0.01 of the minimum division, i.e., to 0.00001 ml, which corresponds well with the value previously calculated (Table I) despite the absence of a suitable background (which could not be provided owing to the immersion of the burettes).

Initial Adjustment of Concentration

Because of the restricted range of the burettes, the concentrations of the solutions had to be adjusted to suit: a solution could easily be concentrated without dismantling any part of the apparatus by blowing dry nitrogen through the solution via the tip of the burette. Minute bubbles of air or nitrogen that remained subsequently in the capillary network were easily removed by connecting an aspirator to the burette tip and manipulating the appropriate stopcocks. By this means a solution could be concentrated by up to 0.1% per hour. The final concentrations of reagents were: $K_2Cr_2O_7$, 0.101 *N*; $FeSO_4$, 0.100 *N* in 0.48 *N* H_2SO_4.

Titration Procedure

In the following account, the burette containing ferrous iron or dichromate is designated as the F-burette or D-burette, respectively.

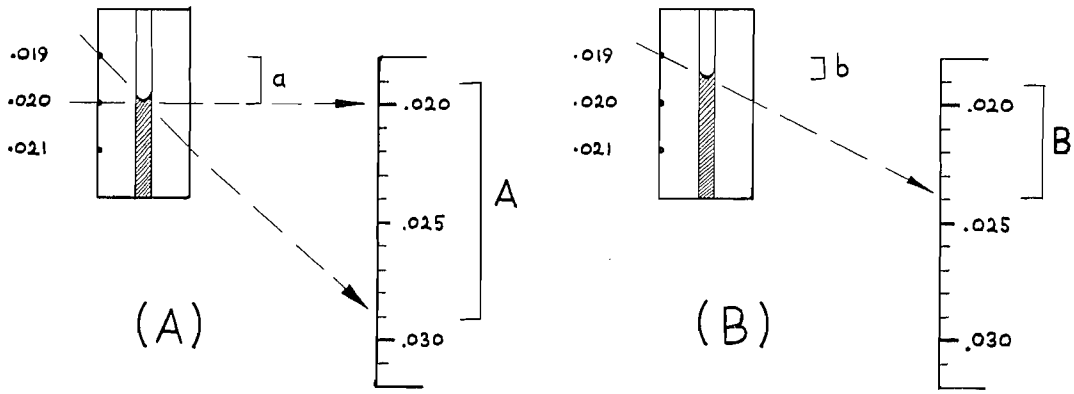

FIG. 4. Burette reading by "optical-lever" vernier.

(A) Correct relationship between burette scale and backing scale with the meniscus on a mark (the diagram is *not to scale*).

(B) Determination of reading when the meniscus is between marks. For the example shown, reading = 0.019 $+b$. Since $b/a = b/0.001 = B/A = (0.0238-0.019)/(0.029-0.019) = 0.0048/0.01$, or $b = 0.00048$, reading = 0.01948.

Both burettes were filled simultaneously, as follows: taps 1, 4, and 5 were closed, 3 was opened, 2 turned to connect A with the aspirator, and solution allowed to flow in until the inner tip of the automatic zero was covered. (A slow rate of filling was maintained to ensure that the heating due to kinetic effects (5) was negligible.) Tap 2 was then closed, 4 and 5 were opened, and a few milliliters of solution allowed to flow out, when 5 and 3 were closed and the outside of the tips rinsed with water. The beaker and stirring bar were placed in position and 2 turned to connect A with G. Tap 1 of the D-burette was manipulated until the level in the automatic zero had fallen well below that of the inner tip and was then closed. Finally, tap 5 of the D-burette was opened and the burette allowed to deliver.

After about three quarters of the volume had been delivered, as measured by a mark on the bulb, 10 ml of titration acid was added from a 10-ml graduated cylinder (the close timing involved did not permit a pipette to be used), and the stirrer started. The zero on the F-burette was adjusted, and the burette allowed to deliver as for the D-burette. When the meniscus in the D-burette reached a mark on the lower shoulder of the bulb, tap 4 was closed, and delivery allowed to continue at the slower rate until the meniscus entered the graduated section, when it was adjusted to the zero by manipulating tap 5. The amperometric pair was then thoroughly rinsed in running distilled water and placed in the solution. The F-burette was treated similarly to the D-burette, except that delivery was continued to the end point.

Very near the end point the reaction was somewhat slow, and at least 1 minute was allowed after each addition before the current was recorded. The maximum galvanometer sensitivity that could be used was $\sim$0.2 μa/f.s.d. or about one tenth of its maximum sensitivity. Some typical end points are given in Fig. 5.

RESULTS

Titrations without Temperature Control

To investigate the importance of temperature control, initial titrations were made *without* thermostatic control or water in the tanks. In two separate experiments of five and seven titrations each, in which the air temperature around the burettes increased by about 1° over 3 hours, the net titer increased by about 0.005 ± 0.001 ml/deg. (A decrease of a few seconds in the delivery time was also observed, but was too small to be significant here; the burettes were too similar for differences in volume to be significant: D-bulb, volume = 50.38 ml, F-bulb, volume = 50.25 ml.) Although the figure for this increase may be somewhat misleading, since the temperatures of the *solutions* were not determined, it compares fairly well with the value 0.003 ml/deg calculated on the basis of the difference in thermal expansion between water and 0.5 N sulphuric acid (23), and emphasizes the appreciable magnitude of this effect, which seldom receives consideration in volumetric work (24).

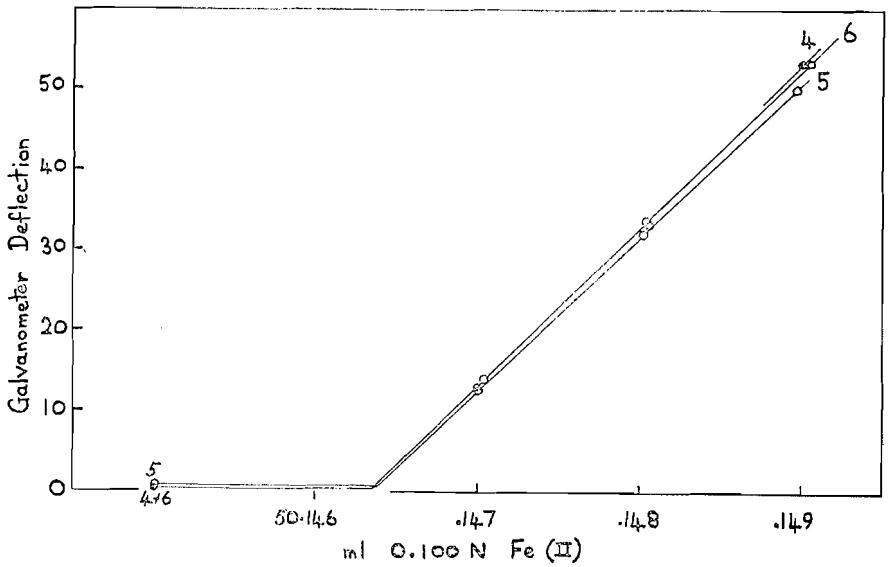

FIG. 5. Typical amperometric end points (titer uncorrected and f.s.d. = 0.18 μa). The values are taken from run II: 4, 50.14638 ml; 5, 50.14639 ml; 6, 50.14636 ml.

Air Oxidation of the Iron(II)

Owing to the presence of a few percent of oxygen in the nitrogen used (but which was not discovered until after the experiments had been completed), very gradual oxidation of the ferrous sulphate was observed. Over a period of 3 weeks, which included the titrations of Table IV, the rate of oxidation (calculated from the variation in titer from day to day) was constant and was equivalent to an increase in titer of 0.0000805 ±0.0000015 ml per hour, or about 0.0038% per day. (A value of 0.15% per day was observed without the use of nitrogen.)

As each titration occupied about 25 minutes, the overall change in titer over a series of titrations was significant; however, by recording the time at which each titration took place, and using the above value for the rate of oxidation, an accurate correction was easily made. This correction has been made for all titrations carried out in any one run. No correction has been made for the change in titer *between* runs.

Observed Precision

With the burettes properly thermostatted, and observing all precautions, the results given in Table IV were obtained. For some reason, possibly through evaporation within the body of the stopcock or at the silicone–rubber connections, the first few titrations were always considerably different (±20 p.p.m. average) from later ones, and consequently these have been omitted from Table IV. Three titrations with abnormal delivery times have also been omitted from Table IV. The results of Table IV show that a precision of about 1 p.p.m. for eight to nine titrations has been achieved, with a maximum precision of 0.7 p.p.m. for eight titrations (run II).

Calculated Precision

Some of the contributions to the overall precision have been evaluated previously. The remainder are detailed below, and the whole summarized in Table V.

TABLE IV

Observed precision of the iron(II)/dichromate titration using the apparatus of Fig. 2

	Run I (23.6.61)		Run II (30.6.61)		Run III (8.7.61)	
	Expt.	Titer	Expt.	Titer	Expt.	Titer
	4	50.13243	3	50.14676	4	50.16295
	5	41	4	71	5	86
	6	56	5	66	6	83
	7	55	6	61	8	92
			7	70	9	84
	(Without using "optical-lever" vernier)		8	69	10	80
			9	65	11	78
			11	62	13	89
			12	67	14	81
Mean		50.132488		50.146674		50.162853
Precision (ml)		0.000078		0.000047*		0.000057*
Precision (p.p.m.)		1.6		0.9		1.1
No. of titrations		4		9		9

*If the first result is omitted the precision is 0.000033 ml (0.7 p.p.m.) and 0.000047 ml (0.9 p.p.m.) for runs II and III, respectively.

TABLE V

Individual contributions to the overall precision

Source of error	Precision (ml)	Remarks
Imperfect graduation	0.00000	Assumed
Non-uniformity of bore	00	Assumed
Automatic zero (diameter of inner tip = 0.5 mm)	00	From Table I
Setting to mark, D-burette	01	From p. 551
Uncertainty in graphical location of end point	02	—
Titration-acid blank	015	From p. 555
Variability of wall film	~03	From p. 554
Fluctuations of temperature:		
inside tank	<01	<0.0005°
outside tank	<005	From p. 550
Leakage of taps	<01	Over 5 minutes
Air oxidation correction	<01	—
Total precision (ml)	~0.000045	
Total precision (p.p.m.)	~0.9	

NOTE: Owing to the compressibility of water, a change of only 1 mm in atmospheric pressure alters the volume by 0.06 p.p.m. (26). Fortunately, if the change is assumed to affect both solutions equally, the effect is self-cancelling.

Precision of the Wall Film

The precision of the wall film may be calculated from consideration of the delivery time (6). Observed values of the latter, together with the calculated wall-film precision, are given in Table VI.

Because of the significant personal error, the overall contribution to the total titration precision caused by variability of the wall film cannot be calculated accurately, but is estimated to be about 0.00003 ml, and is the same whether calculated directly from the results of Table VI or from the aspect of a variable error in the changeover position.

Titration-acid Blank

The titration acid was found to contain very small amounts of reducible impurities: the observed decrease in titer produced by a further addition of 10 ml of titration acid was: titration acid A, 0.0015 ml; titration acid B, 0.0017 ml (A and B were from different batches). Independent tests showed that about four fifths of this was due to impurities

TABLE VI

Observed delivery time (DT) and the calculated wall film

	D-burette	F-burette
DT, bulb, zero to mark (sec)	294	307
Precision (sec)	1.0	0.9
No. of determinations	(11+5+12)	(14+6)
Calculated wall film (ml)	0.0233	0.0229
Precision (ml)	0.000039	0.000034
DT, shoulder, mark to zero (sec)	170	64
Precision (sec)	3.0	2.5
No. of determinations	(4+9)	(16+18)
Estimated wall film (ml)	<0.0005	<0.0005
Precision (ml)	<0.000006	<0.000010
DT, graduated section, 0–0.1 ml (sec)	44	25
Calculated wall film, 0–0.1 ml (ml)	0.00066	0.00088

NOTE: The rate of meniscus descent at the mark was low, and a personal error of about 0.5 second was unavoidable; bulb deliveries timed to the zero of the graduated section showed a much better precision of about 0.2 second. No significant effect of small changes (0.5°) in room temperature upon the delivery time was observed.

in the orthophosphoric acid. These levels of impurities are equivalent to about 1 p.p.m. and 4 p.p.m. of SO_2 in the sulphuric and orthophosphoric acids, respectively, and are in good agreement with those found by Meites (25). The level of impurities was but little affected by boiling of the titration acid for an hour with a large excess of persulphate or peroxide, thus confirming the observations of Meites (25). Since the volume delivered by the 10-ml graduated cylinder was estimated to be precise to ± 0.1 ml, the variability caused by the titration acid was about ± 0.000015 ml.

Calculated Overall Precision of the Titration

The individual contributions to the total precision are summarized in Table V. As all these components are independent, the overall precision may be calculated in the usual manner, and the calculated precision for the titration is seen to be about 0.9 p.p.m., in good agreement with the observed precision of 0.7–1.1 p.p.m.

CONCLUSION

It has been shown that, with properly designed apparatus, a precision of 1 p.p.m. in volume titrimetry can be readily achieved. Further refinements are possible, and would lead to further improvements, but ± 0.1 p.p.m. is probably the maximum precision which can be achieved. The latter is of the same order as that of the best high-precision balances.

Consequently, the limiting precision of any titrimetric operation, whether by weight or by volume, is likely to be 0.1 p.p.m.; although even this is exceeded by the sensitivity of certain favorable end-point systems, it is still approximately three orders of magnitude better than the average accuracy of present atomic weights (27).

Although, from the aspect of accuracy, the volumetric technique described offers no advantage over weight techniques (a sensitive balance and calibrated weights are still required for calibration purposes and for the preparation of solutions), its convenience makes it an attractive proposition where purely comparative investigations are being made.

ACKNOWLEDGMENT

Grateful acknowledgment is made to the National Research Council for financial support.

REFERENCES

1. E. BISHOP. Anal. Chim. Acta, **20**, 405 (1959).
2. T. W. RICHARDS and G. S. FORBES. J. Am. Chem. Soc. **29**, 808 (1907).
3. G. P. BAXTER and A. H. HALE. J. Am. Chem. Soc. **56**, 617 (1934).
4. E. J. CONWAY. Microdiffusion analysis and volumetric error. 4th revised ed. Crosby Lockwood and Son Ltd., London. 1957.
5. G. A. DEAN and J. F. HERRINGSHAW. Analyst, **86**, 434 (1961).
6. G. A. DEAN and J. F. HERRINGSHAW. Analyst, **86**, 440 (1961).
7. E. BISHOP. Anal. Chim. Acta, **20**, 315 (1959).
8. W. M. THORNTON. Ind. Eng. Chem., Anal. Ed. **16**, 50 (1944).
9. J. J. LINGANE. Electroanalytical chemistry. 2nd ed. Interscience. 1958.
10. R. S. MCBRIDE. J. Am. Chem. Soc. **34**, 393 (1912).
11. P. J. HARDWICK. Analyst, **75**, 10 (1950).
12. E. W. WASHBURN. J. Am. Chem. Soc. **30**, 43 (1908).
13. I. M. KOLTHOFF, H. A. LAITINEN, and J. J. LINGANE. J. Am. Chem. Soc. **59**, 430 (1937).
14. R. H. MULLER. Ind. Eng. Chem., Anal. Ed. **7**, 361 (1935).
15. C. E. BRICKER and P. B. SWEETSER. Anal. Chem. **24**, 409 (1952).
16. A. D. AUTREY and R. E. CONNICK. J. Am. Chem. Soc. **73**, 1842 (1951).
17. W. D. COOKE, C. N. REILLEY, and N. H. FURMAN. Anal. Chem. **24**, 205 (1952).
18. W. D. COOKE, C. N. REILLEY, and N. H. FURMAN. Anal. Chem. **23**, 1662 (1951).
19. K. G. STONE and H. G. SCHOLTEN. Anal. Chem. **24**, 671 (1952).
20. J. W. SEASE, C. NIEMANN, and E. H. SWIFT. Anal. Chem. **19**, 199 (1947).
21. P.V.S. REAGENTS PURIFIED FOR VOLUMETRIC STANDARDISATION. Hopkin and Williams Ltd., Chadwell Heath, Essex, England.
22. I. M. KOLTHOFF and N. TANAKA. Anal. Chem. **26**, 632 (1954).
23. SUTTON'S VOLUMETRIC ANALYSIS. 13th ed. *Revised by* J. GRANT. Butterworth. 1955. p. 72.
24. M. G. MELLON. Ind. Eng. Chem., Anal. Ed. **2**, 260 (1930).
25. L. MEITES. Anal. Chem. **24**, 1058 (1952).
26. R. E. GIBSON and O. H. LOEFFLER. J. Am. Chem. Soc. **63**, 898 (1941).
27. E. WICHERS. *In* Treatise on analytical chemistry. Vol. I. *Edited by* I. M. Kolthoff and P. J. Elving. Interscience. 1959. p. 171.

NOTES

OCCURRENCE OF LARGE NORMAL SECONDARY INTERMOLECULAR KINETIC ISOTOPE EFFECTS IN NON-EQUILIBRIUM SYSTEMS[1]

B. S. RABINOVITCH[2] AND J. H. CURRENT[3]

Recently it has been pointed out (1) that large *inverse* secondary isotope effects may occur in the low-pressure, non-equilibrium region of thermal unimolecular reactions. We wish to call attention to the existence also of large *normal* secondary kinetic isotope effects in non-equilibrium systems produced by non-thermal methods of activation.

Consider an equilibrium thermal unimolecular system in the RRKM formulation (1), then

$$k_\infty = \int_{\epsilon \geqslant \epsilon_0} k_\epsilon K(\epsilon) d\epsilon = \int_{\epsilon \geqslant \epsilon_0} \frac{I_r \sum_{\epsilon_v^+ \leqslant \epsilon^+} P^+_{\epsilon_v} N^*_\epsilon e^{-\epsilon/kT} d\epsilon}{hN^*_\epsilon} \frac{}{Q_v}, \qquad [1]$$

where $K(\epsilon)$ is a Boltzmann distribution factor, $P^+_{\epsilon_v}$ is the degeneracy of active energy states of the activated complex at the level ϵ_v^+, N^*_ϵ is the density of active energy states of the energized molecule at internal energy ϵ, Q_v is the corresponding partition function, and I_r is a residue of other partition functions for adiabatic degrees of freedom. It is evident that factors of N^*_ϵ cancel in equation [1]. For a non-thermal mode of excitation, e.g. light absorption, electron impact, radiolysis, chemical activation, etc., such cancellation need not occur and the average rate constant for activated molecules is

$$k = \int_{\epsilon \geqslant \epsilon_0} k_\epsilon f(\epsilon) d\epsilon,$$

where $f(\epsilon)$ is a non-equilibrium distribution of energized molecules. Then for two isotopically labelled species, say H and D,

$$k_H/k_D = \int k_{\epsilon H} f(\epsilon)_H d\epsilon \Big/ \int k_{\epsilon D} f(\epsilon)_D d\epsilon, \qquad [2]$$

where $f(\epsilon)_D$ may or may not equal $f(\epsilon)_H$, depending on the characteristics of the technique. In the special case that $f(\epsilon)_H = f(\epsilon)_D \sim \delta(\epsilon')$, we have

$$k \simeq k_{\epsilon'} = I_r \sum_{\epsilon_v^+ = 0}^{(\epsilon' - \epsilon_0)} P^+_{\epsilon_v}/hN^*_{\epsilon'}, \qquad [3]$$

and for the limiting case $\epsilon' \to \epsilon_0$, then

$$\sum P^+_{\epsilon_v H} \simeq \sum P^+_{\epsilon_v D} \simeq 1,$$

[1]*Work supported by the Office of Naval Research in part.*
Issued as N.R.C. No. 6669.
[2]*Visiting Scientist, National Research Council, from the University of Washington. John Simon Guggenheim Fellow, 1961–62, and International Award Fellow, Petroleum Research Fund, American Chemical Society, 1961–62.*
[3]*N.S.F. Predoctoral Co-operative Fellow, University of Washington.*

and

$$k_H/k_D \simeq \frac{I_{rH}N^*_{\epsilon'D}}{I_{rD}N^*_{\epsilon'H}}, \qquad [4]$$

where the I_r ratio is very close to unity but the density ratio may be a large number (2); for example, it has the approximate value 40 for C_3H_6 and C_3D_6 at 70 kcal mole^{-1} in the harmonic oscillator approximation (1, 2). Equation [4] gives the maximum effect; in general the $P^+_{\epsilon_v}$ ratio will not be unity and will partially compensate the density ratio. As seen further below, the $f(\epsilon)$ functions may also have compensatory character.

The correspondence between this case and the thermal, low-pressure, inverse secondary isotope effect is worth remarking on, and may be seen from the explanation previously given (1) for the latter. There, the collision probability replaces the specific decomposition probability k_ϵ, so

$$k_0 = \omega \int_{\epsilon \geqslant \epsilon_0} N^*_\epsilon e^{-\epsilon/kT} d\epsilon / Q_v,$$

and

$$k_{0H}/k_{0D} = \frac{\omega_H Q_{vD} R}{\omega_D Q_{vH}},$$

where the ω ratio is close to unity, and the integral ratio R is $\ll 1$, and no term in $\Delta\epsilon_0$ has been written for a purely secondary isotope effect. Since R strongly outweighs the Q_v ratio (which here has an effect similar to that of the $\sum P^+_{\epsilon_v}$ terms previously mentioned) a large inverse effect was found.[4]

The decomposition of chemically activated ethyl-d_x radicals provides an example of the new *normal* effect:

$$H_2C{=}CH_2 + D \rightarrow H_2\dot{C}{-}CH_2D^* \rightarrow H_2C{=}CHD + H, \qquad [d_1]$$

$$\textit{trans}\text{-}DHC{=}CHD + D \rightarrow DH\dot{C}{-}CHD_2^* \rightarrow DHC{=}CD_2 + H. \qquad [d_3]$$

The characteristics and energetics of a closely related system, *trans*-DHC=CHD + H → DHC—CH_2D^*, have been previously described (3). A large absolute effect is not to be expected in this case for several reasons: only two H atoms are replaced by D between the reacting species; also, $f(\epsilon)$ is by no means a delta function located just above ϵ_{0H}, since both radicals are produced by C—D bond formation and possess a minimum excess energy with respect to C—H rupture of ~1.8 kcal; finally, $f(E)$ for reaction $[d_3]$ is relatively broadened a little (4), which further tends to reduce the kinetic isotope ratio below the maximum limiting value.

The limiting observed average values per C—H bond for these systems studied at 195° and 300° K, and extrapolated to zero pressure,[5] is $(k_{d_1}/k_{d_3})_0 \simeq 2.2$. An expected small variation of the ratio, as between 195° and 300° K, was obscured by large experimental error. The accuracy of the determination is not high but the experimental effect is unequivocal.

A recent summary of secondary isotope effects for equilibrium thermal unimolecular systems gives an average value of 1.12 per D atom (5). The present quantum statistical effects are essentially unrelated to the mechanistic effects (6), which are of greatest

[4]*This effect has been explicitly confirmed for the* CH_3NC—CD_3NC *isomerization system by F. W. Schneider and B. S. Rabinovitch (unpublished results).*

[5]*This extrapolation gives* $\langle 1/k \rangle k^{-1}$ *(see reference 3).*

importance in the examples of the summary, and can be orders of magnitude larger than those that arise in such equilibrium unimolecular systems (7)—approaching as a limit in favorable cases, the ratio of the products of frequencies of the two species.

Investigation of other systems is continuing.

1. B. S. RABINOVITCH, D. W. SETSER, and F. W. SCHNEIDER. Can. J. Chem. **39**, 2609 (1961).
2. B. S. RABINOVITCH and J. H. CURRENT. J. Chem. Phys. **35**, 2250 (1961).
3. B. S. RABINOVITCH, D. H. DILLS, W. H. MCLAIN, and J. H. CURRENT. J. Chem. Phys. **32**, 493 (1960).
4. J. H. CURRENT and B. S. RABINOVITCH. To be published.
5. S. SELTZER. J. Am. Chem. Soc. **83**, 2625 (1961).
6. N. C. LI, A. KAGANOVE, H. L. CRESPI, and J. J. KATZ. J. Am. Chem. Soc. **83**, 3040 (1961).
7. M. WOLFSBERG. J. Chem. Phys. **33**, 2 (1960).

RECEIVED NOVEMBER 17, 1961.
DEPARTMENT OF CHEMISTRY,
UNIVERSITY OF WASHINGTON,
SEATTLE, WASH., U.S.A.,
AND
DIVISION OF APPLIED CHEMISTRY,
NATIONAL RESEARCH COUNCIL,
OTTAWA, CANADA.

THE DECARBOXYLATION OF RING-SUBSTITUTED INDOLE-2(AND 3)-CARBOXYLIC ACIDS

E. PIERS AND R. K. BROWN

The synthesis of indoles by the Reissert method (1) or by Fischer cyclization (2) of pyruvic acid phenylhydrazone requires a final removal of carbon dioxide from the indole-2-carboxylic acid formed in these reactions.

Such decarboxylations have been accomplished in the case of 4-, 5-, 6-, and 7-fluoroindole-2-carboxylic acids in yields of 80, 52, 51, and 48% respectively by simply heating the substances above the melting point (3). The 4- and 6-chloroindole-2-carboxylic acids required more vigorous treatment but readily gave the decarboxylated product in 73 to 78% yield when they were heated with cuprous chloride in refluxing quinoline (4, 5). However, Barletrop and Taylor (6) were unsuccessful in their attempts to remove the carboxyl group from 4- or 6-bromoindole-2-carboxylic acid by heating these compounds in refluxing quinoline with or without catalysts such as cuprous bromide, cupric oxide, or copper powder.

The variable and frequently poor results obtained in decarboxylation of the benzene-ring-halogenated indole-2-carboxylic acids by Uhle's method (4, 5) was found by Rydon and Tweddle (7) to be due to contamination of the acid by sulphate ion stemming from the ferrous ammonium sulphate reductive cyclization step. These authors, by careful elimination of the sulphate ion as well as replacement of the usual cuprous chloride catalyst by copper chromite, were able to obtain consistently good yields of the 4-, 5-, 6-, and 7-chloroindoles.

Plieninger *et al.* (8) reported 60% yields of the 4- and 6-bromoindoles from the corresponding 2-carboxylic acids by mixing the acids with molten cuprous bromide followed by heating the fusion mixture in refluxing quinoline. Snyder and co-workers (9) obtained a 21–24% yield of 5-bromoindole by heating 5-bromoindole-2-carboxylic acid with a mixture of copper bronze and copper chromite, but only a very small yield of product

importance in the examples of the summary, and can be orders of magnitude larger than those that arise in such equilibrium unimolecular systems (7)—approaching as a limit in favorable cases, the ratio of the products of frequencies of the two species.

Investigation of other systems is continuing.

1. B. S. RABINOVITCH, D. W. SETSER, and F. W. SCHNEIDER. Can. J. Chem. **39**, 2609 (1961).
2. B. S. RABINOVITCH and J. H. CURRENT. J. Chem. Phys. **35**, 2250 (1961).
3. B. S. RABINOVITCH, D. H. DILLS, W. H. MCLAIN, and J. H. CURRENT. J. Chem. Phys. **32**, 493 (1960).
4. J. H. CURRENT and B. S. RABINOVITCH. To be published.
5. S. SELTZER. J. Am. Chem. Soc. **83**, 2625 (1961).
6. N. C. LI, A. KAGANOVE, H. L. CRESPI, and J. J. KATZ. J. Am. Chem. Soc. **83**, 3040 (1961).
7. M. WOLFSBERG. J. Chem. Phys. **33**, 2 (1960).

RECEIVED NOVEMBER 17, 1961.
DEPARTMENT OF CHEMISTRY,
UNIVERSITY OF WASHINGTON,
SEATTLE, WASH., U.S.A.,
AND
DIVISION OF APPLIED CHEMISTRY,
NATIONAL RESEARCH COUNCIL,
OTTAWA, CANADA.

THE DECARBOXYLATION OF RING-SUBSTITUTED INDOLE-2(AND 3)-CARBOXYLIC ACIDS

E. PIERS AND R. K. BROWN

The synthesis of indoles by the Reissert method (1) or by Fischer cyclization (2) of pyruvic acid phenylhydrazone requires a final removal of carbon dioxide from the indole-2-carboxylic acid formed in these reactions.

Such decarboxylations have been accomplished in the case of 4-, 5-, 6-, and 7-fluoroindole-2-carboxylic acids in yields of 80, 52, 51, and 48% respectively by simply heating the substances above the melting point (3). The 4- and 6-chloroindole-2-carboxylic acids required more vigorous treatment but readily gave the decarboxylated product in 73 to 78% yield when they were heated with cuprous chloride in refluxing quinoline (4, 5). However, Barletrop and Taylor (6) were unsuccessful in their attempts to remove the carboxyl group from 4- or 6-bromoindole-2-carboxylic acid by heating these compounds in refluxing quinoline with or without catalysts such as cuprous bromide, cupric oxide, or copper powder.

The variable and frequently poor results obtained in decarboxylation of the benzene-ring-halogenated indole-2-carboxylic acids by Uhle's method (4, 5) was found by Rydon and Tweddle (7) to be due to contamination of the acid by sulphate ion stemming from the ferrous ammonium sulphate reductive cyclization step. These authors, by careful elimination of the sulphate ion as well as replacement of the usual cuprous chloride catalyst by copper chromite, were able to obtain consistently good yields of the 4-, 5-, 6-, and 7-chloroindoles.

Plieninger *et al.* (8) reported 60% yields of the 4- and 6-bromoindoles from the corresponding 2-carboxylic acids by mixing the acids with molten cuprous bromide followed by heating the fusion mixture in refluxing quinoline. Snyder and co-workers (9) obtained a 21–24% yield of 5-bromoindole by heating 5-bromoindole-2-carboxylic acid with a mixture of copper bronze and copper chromite, but only a very small yield of product

when they attempted to decarboxylate the ammonium salt of the acid in glycerol. Harvey later found that 5,6-dimethoxyindole-2-carboxylic acid heated in glycerol gave 97% yield of decarboxylated product (10).

The successful removal of carbon dioxide from 5-iodoindole-2-carboxylic acid (11) by the quinoline – copper chromite procedure of Rydon and Tweedle (7) indicates that to date this is the most generally satisfactory method reported in the literature for the decarboxylation of substituted indole-2-carboxylic acids.

In this laboratory a number of benzene-ring-substituted indoles were prepared from the corresponding 2-carboxylic acids. Plieninger's method (8) was found, in our hands, to be unsatisfactory as well as somewhat tedious, whereas the copper chromite – quinoline technique (7) gave quite unsatisfactory results in several instances (see Table I). Use

TABLE I

Indole compound	Method of decarboxylation	Temperature of decarboxylation	Time required (hours)	Yield of pure decarboxylated product (%)
5-Br; 2-CO_2H	*b*	Refluxing quinoline	36	22
	c	210–215°	4	63
6-Br; 2-CO_2H	*b*	Refluxing quinoline	36	25
	c	210–220°	5	74
7-Br; 2-CO_2H	*b*	Refluxing quinoline	48	48 (ref. 12)
	c	215–220°	5	61
4-$C_6H_5CH_2S$—; 2-CO_2H	*b*	Refluxing quinoline	24	Insignificant
	c	205–210°	2.5	80
7-$C_6H_5CH_2S$—; 2-CO_2H	*b*	Refluxing quinoline	24	15
	c	210–215°	5	85
6-NO_2; 3-CO_2H (ref. 14)	*a*	145–150°	3	90
	c	125–130°	1.5	86

(*a*) Method involved heated quinoline with no added catalyst.
(*b*) Method was that devised by Rydon and Tweddle (7) and modified as in ref. 12.
(*c*) Method is the present method involving hot quinoline, the acid, and catalytic amounts of its copper salt.

of this latter procedure on 7-bromoindole-2-carboxylic acid (12) required frequent additions of small amounts of copper chromite catalyst to the hot quinoline solution during the reaction for successful removal of carbon dioxide (48% yield). However, the 4- and 6-benzylmercaptoindole-2-carboxylic acids were decarboxylated in very poor yield with simultaneous loss of some of the sulphur as H_2S. Accordingly a route was sought which would provide not only improved yields but also avoid loss of substituent in the case of the more sensitive sulphur-containing compounds.

It has long been known that a carboxylic acid, heated with catalytic amounts of its copper salt, undergoes facile decarboxylation (13). When this method was applied to the decarboxylation of the substituted indole-2(and 3)-carboxylic acids in hot quinoline, a marked improvement in yield and quality of product was experienced. Generally, temperatures necessary to effect elimination of carbon dioxide were lower, and the times to complete the reaction were less, than those found for other methods employed. Furthermore, the thioethers did not lose sulphur during the decarboxylation. This procedure appears to be of wider applicability than those previously reported in the literature. The results are shown in Table I, in which the copper chromite and copper salt methods are compared.

Preparation of the Copper Salt

A stirred mixture of the acid (0.01 mole), sodium carbonate (0.005 mole), and water (100 ml) was heated until the acid dissolved. Upon the addition of a solution of cupric sulphate pentahydrate (0.005 mole) in 50 ml of water, the blue cupric salt of the indole-2-carboxylic acid precipitated. The solid was washed thoroughly with water, air-dried, and then given a final drying in a vacuum desiccator over calcium chloride.

The Procedure for Decarboxylation

A mixture of the indole-2-carboxylic acid (0.01 mole) and its copper salt (0.0004 mole) in 10 ml of synthetic quinoline was heated until carbon dioxide began to evolve. The mixture was kept at this temperature until gas evolution ceased (1.5–5 hours). The cooled solution was taken up in ether and the ether solution was washed several times with 1 *N* hydrochloric acid, once with water, twice with sodium carbonate solution, and finally with water. When the dried (Na_2SO_4) ether solution was freed from solvent a solid was obtained. This was further purified, if necessary, by passage through a short column of neutral alumina, using methylene dichloride as eluant.

ACKNOWLEDGMENT

The authors wish to thank the National Research Council of Canada for their financial support during the course of this work.

1. A. Reissert. Ber. **30**, 1030 (1897).
2. E. Fischer. Ann. **236**, 126 (1886).
3. F. L. Allen, J. C. Brunton, and H. Suschitzky. J. Chem. Soc. 1283 (1955).
4. F. C. Uhle. J. Am. Chem. Soc. **71**, 761 (1949).
5. S. W. Fox and M. W. Bullock. J. Am. Chem. Soc. **73**, 2754 (1951).
6. J. A. Barletrop and D. G. H. Taylor. J. Chem. Soc. 3399 (1954).
7. H. N. Rydon and J. C. Tweddle. J. Chem. Soc. 3499 (1955).
8. H. Plieninger, F. Suehiro, K. Suhr, and M. Desker. Ber. **88**, 370 (1955).
9. H. R. Snyder, S. M. Parmerter, and L. Katz. J. Am. Chem. Soc. **70**, 222 (1948).
10. D. G. Harvey. J. Chem. Soc. 2536 (1955).
11. D. G. Harvey. J. Chem. Soc. 3760 (1958).
12. B. E. Leggetter and R. K. Brown. Can. J. Chem. **38**, 1467 (1960).
13. G. Dougherty. J. Am. Chem. Soc. **50**, 571 (1928).
14. R. Majima and M. Kotake. Ber. **63**, 2237 (1930).

Received October 4, 1961.
Department of Chemistry,
University of Alberta,
Edmonton, Alberta.

N,N-BRIDGED DERIVATIVES OF ADENINE[1]

Sumner H. Burstein and H. J. Ringold

The reaction of 6-bis(2-hydroxyethyl)aminopurine (I*a*) with thionyl chloride was reported in 1957 by DiPaco and Tauro (1) to yield the adenine mustard derivative (II). Huber (2) in an earlier publication reported that the identical reaction gave an ionic halogen-containing product to which he assigned the dimeric piperazinium chloride structure (III). A 1960 United States patent of Lyttle and Petering (3) stated that the product derived from I*a* and thionyl chloride contained 1 equivalent of ionic halogen and

[1]*This work was aided by Grant No. T-185 from the American Cancer Society.*

Preparation of the Copper Salt

A stirred mixture of the acid (0.01 mole), sodium carbonate (0.005 mole), and water (100 ml) was heated until the acid dissolved. Upon the addition of a solution of cupric sulphate pentahydrate (0.005 mole) in 50 ml of water, the blue cupric salt of the indole-2-carboxylic acid precipitated. The solid was washed thoroughly with water, air-dried, and then given a final drying in a vacuum desiccator over calcium chloride.

The Procedure for Decarboxylation

A mixture of the indole-2-carboxylic acid (0.01 mole) and its copper salt (0.0004 mole) in 10 ml of synthetic quinoline was heated until carbon dioxide began to evolve. The mixture was kept at this temperature until gas evolution ceased (1.5–5 hours). The cooled solution was taken up in ether and the ether solution was washed several times with 1 *N* hydrochloric acid, once with water, twice with sodium carbonate solution, and finally with water. When the dried (Na_2SO_4) ether solution was freed from solvent a solid was obtained. This was further purified, if necessary, by passage through a short column of neutral alumina, using methylene dichloride as eluant.

ACKNOWLEDGMENT

The authors wish to thank the National Research Council of Canada for their financial support during the course of this work.

1. A. Reissert. Ber. **30**, 1030 (1897).
2. E. Fischer. Ann. **236**, 126 (1886).
3. F. L. Allen, J. C. Brunton, and H. Suschitzky. J. Chem. Soc. 1283 (1955).
4. F. C. Uhle. J. Am. Chem. Soc. **71**, 761 (1949).
5. S. W. Fox and M. W. Bullock. J. Am. Chem. Soc. **73**, 2754 (1951).
6. J. A. Barletrop and D. G. H. Taylor. J. Chem. Soc. 3399 (1954).
7. H. N. Rydon and J. C. Tweddle. J. Chem. Soc. 3499 (1955).
8. H. Plieninger, F. Suehiro, K. Suhr, and M. Desker. Ber. **88**, 370 (1955).
9. H. R. Snyder, S. M. Parmerter, and L. Katz. J. Am. Chem. Soc. **70**, 222 (1948).
10. D. G. Harvey. J. Chem. Soc. 2536 (1955).
11. D. G. Harvey. J. Chem. Soc. 3760 (1958).
12. B. E. Leggetter and R. K. Brown. Can. J. Chem. **38**, 1467 (1960).
13. G. Dougherty. J. Am. Chem. Soc. **50**, 571 (1928).
14. R. Majima and M. Kotake. Ber. **63**, 2237 (1930).

Received October 4, 1961.
Department of Chemistry,
University of Alberta,
Edmonton, Alberta.

N,N-BRIDGED DERIVATIVES OF ADENINE[1]

Sumner H. Burstein and H. J. Ringold

The reaction of 6-bis(2-hydroxyethyl)aminopurine (I*a*) with thionyl chloride was reported in 1957 by DiPaco and Tauro (1) to yield the adenine mustard derivative (II). Huber (2) in an earlier publication reported that the identical reaction gave an ionic halogen-containing product to which he assigned the dimeric piperazinium chloride structure (III). A 1960 United States patent of Lyttle and Petering (3) stated that the product derived from I*a* and thionyl chloride contained 1 equivalent of ionic halogen and

[1]*This work was aided by Grant No. T-185 from the American Cancer Society.*

had probably undergone internal cyclization to the 1- or to the 7-nitrogen position. We have had occasion to prepare what appears to be the same product obtained by the three groups enumerated above and wish to record our observations and conclusions regarding its structure.

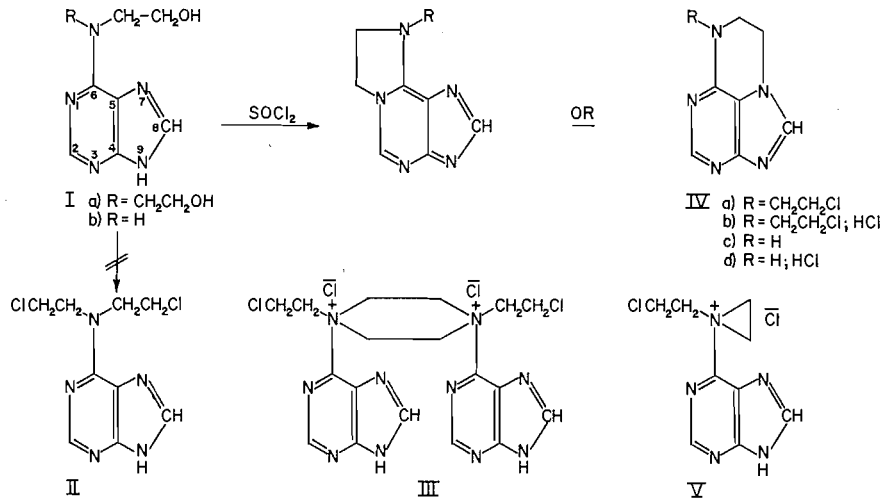

The reaction of 6-bis(2-hydroxyethyl)aminopurine (I*a*) with thionyl chloride, either at room temperature or under reflux, gave a product (IV*b*) of melting point 254–256° (decomp.) analyzing for $C_9H_{11}Cl_2N_5$. The compound, which was readily soluble in water, reacted instantaneously with excess silver nitrate, forming 1 equivalent of silver chloride. Titration with 0.1 *N* aqueous sodium hydroxide demonstrated a pK_a of 6.8 and when alkali was added to a pH of 12, followed by retitration with 0.1 *N* HCl, the titration curve did not show any major deviation. This behavior appeared to be indicative of a hydrochloride. When IV*b* was treated at room temperature with sodium acetate a product (IV*a*), which had lost a mole of hydrogen chloride, was isolated. The latter was readily reconverted to IV*b* by treatment with anhydrous hydrogen chloride in ethanol. This conclusively establishes that IV*b* is a hydrochloride and therefore eliminates the piperazinium structure (III), the conventional nitrogen mustard structure (II), as well as the quaternary aziridine structure (V). The latter could have been considered a structural possibility on the basis of ionic halogen content.

Thus it is evident that IV*b* is, in fact, a product that has undergone self-alkylation[2] on either the 1- or 7-nitrogen function and that IV*a* is simply the cyclized hydrogen-chloride-free product.

Before discussing the attempt to resolve the question of 1- or 7-cyclization, the behavior of the "one-armed" compound (I*b*) is pertinent at this point. When 6-(2-hydroxyethyl)-aminopurine (I*b*) (2, 4) (prepared by the reaction of 6-chloropurine with ethanolamine) was reacted with thionyl chloride a product, $C_7H_8ClN_5$ (IV*d*), was obtained. This compound exhibited an acidity parallel to IV*b*, the pK_a being 7.0. Further, the titration curve of IV*d* was very similar to that of IV*b* and neutralization with sodium acetate or alkali resulted in the loss of hydrogen chloride and formation of a halogen-free product (IV*c*). The latter was readily reconverted to the original hydrochloride. From these character-

[2]*W. T. Caldwell and S. Toukan, Temple University, have reached similar conclusions in an independent study (private communication from Professor Caldwell).*

istics as well as from the similar ultraviolet spectral curves of the two series of compounds, it may be concluded that the same type of cyclization has occurred with both the "one-armed" and "two-armed" substances. Further, the cyclization of I*b* establishes that a quaternary aziridine, V, is not an intermediate in the formation of IV*b*.

The n.m.r. of IV*a* in deuterochloroform solution showed adenine ring hydrogen peaks at $\tau = 1.79$ and 2.21, while N-benzyltriacanthine (5), a γ,γ-dimethylallyl 7-substituted adenine derivative, showed ring hydrogens at $\tau = 2.05$ and 2.23 (5). Assignment of the 2.21–2.23 position to the unperturbed 2-proton would be consistent with cyclization to the 7-position, the 8-proton being shifted various degrees by the different substituents attached to the 7-nitrogen.

The ultraviolet spectra of our products, however, are not in accord with that expected for a 7-substituted adenine. Triacanthine and 7-D-ribofuranosidoadenine (6) are reported to exhibit $\lambda_{max}^{neutral}$ 273 mμ, ϵ 13,000 and a $\lambda_{max}^{pH\ 1}$ for triacanthine of 277 mμ, ϵ 18,000. Compounds IV*a* and IV*c* respectively exhibit $\lambda_{max}^{H_2O}$ 264 mμ and 270 mμ and undergo a hypsochromic displacement of 2 mμ rather than a bathochromic shift in going from water to 0.1 *N* hydrochloric acid. It is possible that the presence of the third ring in IV is modifying the spectrum but at the present time neither the 1- nor 7-cyclized structure can be discarded. In this connection it should be noted that Ramage and Trappe (7) reported the cyclization of 2-chloro-4-methyl-5-amino-6(2-chloroethyl)aminopyrimidine to a five- rather than to a six-membered ring, while Chu, Harris, and Mautner (8) prepared 8-bis-(β-chloroethyl)-aminoadenine hydrochloride without internal cyclization having occurred, although self-alkylation to either the 7- or 9-position would have led to a new five-membered ring.

Compounds IV*a* and IV*c* were found to be non-toxic in the mouse at a daily dose of 500 mg/kg for a period of 1 week[3] and have not demonstrated any significant antitumor activity.[4]

EXPERIMENTAL

Melting points are uncorrected and ultraviolet spectral determinations were made with a Carey model 14 recording spectrophotometer. We are grateful to Mr. T. A. Wittstruck for the n.m.r. determination. Elementary analyses were performed by Midwest Microlab, Inc., 7838 Forest Lane, Indianapolis 20, Indiana.

6-Bis(2-hydroxyethyl)aminopurine (Ia)

A mixture of 6-chloropurine[5] (5.0 g), diethanolamine (10 ml), and absolute ethanol (50 ml) was heated for 8 hours under reflux and then cooled overnight at 0°, yielding 6.5 g of I*a*, m.p. 219–221° (reported 205° (1), 216–218° (2), 228–231° (3)); $\lambda_{max}^{H_2O}$ 213 and 276 mμ, ϵ 16,500 and 18,300; $\lambda_{max}^{0.1\ N\ HCl}$ 284 mμ, ϵ 16,400. The constants were unchanged after further crystallization from 95% ethanol. Anal. Calc. for $C_9H_{13}N_5O_2$: C, 48.42; H, 5.87; N, 31.37. Found: C, 48.28; H, 5.99; N, 31.23.

Reaction of Ia with Thionyl Chloride – Preparation of IVb

(a) With Heating

The bis-hydroxyethyl derivative (I*a*) (5.0 g) was heated for 16 hours, with stirring, in boiling, freshly distilled thionyl chloride (100 ml). The solvent was removed *in vacuo* and the residue stirred with absolute ethanol (50 ml). The product, 5.0 g, exhibited m.p. 250° (decomp.) while the analytical specimen from absolute ethanol melted at 254–256° (decomp.); $\lambda_{max}^{H_2O}$ 215 and 268 mμ, ϵ 18,500 and 13,100; $\lambda_{max}^{0.1N\ HCl}$ 215 and 268 mμ, ϵ 18,500 and 13,400. (Reported m.p. 245° (1), 243–247° (2), 253–255° (3).) Titration with 0.1 *N* sodium hydroxide gave pK_a 6.8. Anal. Calc. for $C_9H_{11}Cl_2N_5$: C, 41.56; H, 4.26; N, 26.93; Cl, 27.26. Found: C, 41.53; H, 4.34; N, 27.04; Cl, 27.29.

(b) Without Heating

A suspension of I*a* (480 mg) in thionyl chloride (15 ml) was stirred for 14 hours at room temperature. The precipitate was filtered through a sintered-glass funnel and washed with benzene and then absolute

[3]*Toxicity studies by Dr. R. I. Dorfman of this foundation.*
[4]*Antitumor assays by the Cancer Chemotherapy National Service Center.*
[5]*We wish to thank Burroughs Wellcome and Co. for a generous gift of material.*

ethanol, yielding 600 mg of IV*b*, m.p. 246–248°, whose ultraviolet and infrared spectra were identical with the product obtained in (*a*). Recrystallization from absolute ethanol gave 453 mg of product, m.p. 254° (decomp.), whose infrared spectrum was unchanged.

Reaction of IVb with Silver Nitrate

A solution of IV*b* (65 mg) in water (10 ml) was reacted with silver nitrate solution (2.0 equiv. in 5 ml of water) containing a drop of nitric acid, causing instantaneous formation of a precipitate. The silver chloride was rapidly filtered and then washed with ethanol–acetone and dried. Weight 32 mg (0.89 equiv.).

Neutralization of IVb – Preparation of IVa

Sodium acetate trihydrate (500 mg) was added to a solution of hydrochoride IV*b* (500 mg) in water (5 ml). The solvent was removed at room temperature *in vacuo* and the residue extracted with chloroform and crystallized several times from chloroform–hexane to yield an analytical specimen of IV*a*, m.p. 310–315°; $\lambda_{max}^{H_2O}$ 214 and 270 mμ, ε 18,300 and 12,700; $\lambda_{max}^{0.1N\,HCl}$ 215 and 268 mμ, ε 19,700 and 14,200; n.m.r. ($CDCl_3$) 1.79, 2.21, 5.50, 5.61, 5.71, 5.78, 5.97, and 6.06 τ. Anal. Calc. for $C_9H_{10}ClN_5$: C, 47.79; H, 4.69. Found: C, 47.92; H, 4.81.

Reconversion of IVa to IVb

Hydrogen chloride was bubbled for 30 minutes through a stirred suspension of IV*a* (50 mg) in absolute ethanol (5 ml). Ether was added and the precipitate was filtered, washed with ether, and recrystallized from methanol, yielding the hydrochloride IV*c*, m.p. 254° (decomp.), whose infrared spectrum was identical with the product described above.

6-(2-Hydroxyelhyl)aminopurine (Ib)

A mixture of 6-chloropurine (5.0 g) and 2-aminoethanol (10 ml) in absolute ethanol (50 ml) was heated for 3 hours under reflux and then cooled, yielding 5.14 g of I*b*, m.p. 250–252°. An analytical specimen obtained from ethanol exhibited m.p. 255–257° (reported 247–249° (2)); $\lambda_{max}^{H_2O}$ 267 mμ, ε 15,000, $\lambda_{max}^{0.1N\,HCl}$ 273 mμ, ε 14,500. Anal. Calc. for $C_7H_9N_5O$: C, 46.91; H, 5.06. Found: C, 46.73; H, 5.20.

Reaction of Ib with Thionyl Chloride – Preparation of IVd

A stirred suspension of I*b* (2.0 g) in freshly distilled thionyl chloride (50 ml) was boiled for 16 hours under anhydrous conditions. The thick paste was cooled, filtered, and the precipitate washed with benzene and then suspended in absolute ethanol and stirred for a few minutes. The collected precipitate of IV*d* weighed 1.7 g and exhibited m.p. 305–309° (decomp.). Crystallization from methanol gave an analytical sample, m.p. 306–310°, whose pK_a (titration with 0.1 *N* aqueous sodium hydroxide) was 7.0. Anal. Calc. for $C_7H_8ClN_5$: C, 42.54; H, 4.08; N, 35.45; Cl, 17.95. Found: C, 42.87; H, 4.08; N, 35.70; Cl, 17.93.

Reaction of IVd with Silver Nitrate

A solution of IV*d* (200 mg) in water (20 ml) was treated with silver nitrate (180 mg, 1.05 equiv.) in 5 ml of water. A few drops of dilute nitric acid were added and the precipitate, which had formed immediately after the silver nitrate addition, was removed by centrifugation, washed, and dried, yielding 137 mg (0.95 equiv.) of silver chloride.

Neutralization of IVd – Preparation of IVc

Solid sodium bicarbonate (200 mg) was added to a clear ice-cold solution of 200 mg of IV*d* in water (2 ml). Carbon dioxide was liberated and a crystalline product deposited. Collection of V*a* and recrystallization from methanol yielded 102 mg of pure product, m.p. 295–296°. When sodium acetate (400 mg) was substituted for bicarbonate the identical product was obtained. $\lambda_{max}^{H_2O}$ 212 and 264 mμ, ε 17,500 and 10,400. $\lambda_{max}^{0.1N\,HCl}$ 211 and 262 mμ, ε 18,900 and 11,600. Anal. Calc. for $C_7H_7N_5$: C, 52.16; H, 4.38; N, 43.46. Found: C, 51.94; H, 4.43; N, 43.27.

Reconversion of IVc to IVd

Treatment of IV*c* with hydrogen chloride exactly as described above for IV*a* to IV*b*, gave the hydrochloride, m.p. 305–309° (decomp.), identical with the original sample.

1. G. DiPaco and C. S. Tauro. Ann. Chim. (Rome), **47**, 698 (1957); Chem. Abstr. **52**, 1179 (1958).
2. G. Huber. Angew. Chem. **68**, 706 (1956).
3. D. A. Lyttle and H. G. Petering. U.S. Patent No. 2,957,875 (1960).
4. H. G. Windmueller and N. O. Kaplan. Abstracts Division of Biological Chemistry, New York Meeting of the American Chemical Society, Sept. 1960. p. 28c.
5. N. J. Leonard and J. A. Deyrup. J. Am. Chem. Soc. **82**, 6202 (1960).
6. W. Friedrich and K. Bernhauer. Chem. Ber. **89**, 2507 (1956).
7. G. R. Ramage and G. Trappe. J. Chem. Soc. 4410 (1952).
8. S. H. Chu, J. E. Harris, and H. G. Mautner. J. Org. Chem. **25**, 1759 (1960).

Received October 10, 1961.
Worcester Foundation
for Experimental Biology,
Shrewsbury, Massachusetts, U.S.A.

ADSORPTION OF CHROMIC ACID ON SILICA

H. P. DIBBS

INTRODUCTION

A chromic acid – sulphuric acid mixture is frequently used as a cleaning agent for glassware and silica ware and is widely recommended for this purpose in texts on quantitative analysis (1) and elsewhere (2). However, when precise measurements are involved, the use of this mixture is suspect, because of the possibility of etching the glass surface and the difficulty of removing final traces of chromium from the surface (3, 4). In order to investigate the amount of chromium left on fused quartz after chromic acid cleaning, a number of quartz rods, cleaned in this way, were irradiated with thermal neutrons and the amount of chromium remaining estimated with the aid of gamma-ray spectrometry.

EXPERIMENTAL DETAILS

The quartz used in this work was manufactured by the General Electric Company, Willoughby, Ohio, and had a specified purity of 99.97% SiO_2. It was in the form of 1-mm diameter rods which were cut into 3-cm lengths. Four batches, each containing 40 pieces, were prepared. Each batch was first cleaned in a detergent solution, with an ultrasonic generator, to remove superficial grease and dirt. After repeated rinsing in distilled water, the rods were dried at 110° C. One batch was then put aside to act as a standard. The remaining three groups were soaked overnight in a chromic acid – sulphuric acid mixture (35 ml of saturated sodium dichromate solution made up to 1 liter with concentrated sulphuric acid). Each batch of rods was then washed at least 20 times with distilled water and dried at 110° C. Two batches of these rods were taken and given further treatment. One group was placed in 10% hydrofluoric acid for 10 minutes and the other group in a 50/50 nitric acid – sulphuric acid mixture for 3 hours. After washing in distilled water they were dried as before.

For reactor irradiation, the four batches of rods were sealed into separate polythene bags, which in turn were wrapped in superpure aluminum foil. Fifty milligrams of potassium dichromate, sealed in a Vycor vial, was irradiated in the same irradiation can as the rods, to act as a chromium reference standard. Approximately 2 weeks after irradiation, the batches of rods were examined on a 100-channel gamma-ray spectrometer. Chromium was identified by half-life measurements and by the 0.32 Mev photo peak of chromium-51. The amount of chromium present was calculated by dissolving the potassium dichromate reference standard in water and counting a suitable aliquot of the solution in a position of geometry comparable to that of the quartz rods.

RESULTS

The amount of chromium found on the batches of rods is given in Table I.

TABLE I

Amounts of chromium detected

Batch	Treatment	Wt. of Cr/batch (μg)
S	None	0
1	Cleaned in chromic acid	7.7
2	Cleaned in chromic acid followed by HF	5.2
3	Cleaned in chromic acid followed by HNO_3/H_2SO_4	3.3

The geometrical surface area of the rods was approximately 40 cm^2. Therefore, for group 1, which had no treatment following the chromic acid – sulphuric acid cleaning, about 0.2 μg of chromium per apparent square centimeter of area remained after washing. Treatment with HF or the HNO_3/H_2SO_4 mixture, after the chromic acid – sulphuric acid cleaning (batches 2 and 3), resulted in a decrease in the amount of chromium on the quartz surface, but did not remove it all.

From these results it is apparent that a chromic acid – sulphuric acid cleaning mixture, although satisfactory for routine operations, should not be used in circumstances where minor traces of chromium are deleterious.

Adsorption behavior similar to that of quartz would be expected with laboratory glassware cleaned in a chromic acid – sulphuric acid mixture. However, most glassware now in common use is of the borosilicate type and it is not practical to use reactor irradiation to ascertain the amount of chromium remaining after cleaning because of the very high thermal neutron cross section of boron.

ACKNOWLEDGMENTS

The author wishes to express his thanks to Mr. J. L. Horwood for performing the gamma-ray spectrometer analysis. This paper is published by permission of the Director, Mines Branch, Department of Mines and Technical Surveys, Ottawa, Canada.

1. A. I. VOGEL. A textbook of quantitative inorganic analysis. Longmans, Green and Co., London. 1948. p. 240.
2. J. C. HUGHES. National Bureau of Standards Circular 602. 1959. p. 9.
3. J. C. W. FRAZER, W. A. PATRICK, and H. E. SMITH. J. Phys. Chem. **31**, 897 (1927).
4. J. R. PARTINGTON. An advanced treatise on physical chemistry. Vol. 2. Longmans, Green and Co., New York. 1950. p. 281.

RECEIVED OCTOBER 19, 1961.
MINERAL SCIENCES DIVISION,
MINES BRANCH,
DEPARTMENT OF MINES AND TECHNICAL SURVEYS,
OTTAWA, CANADA.

THE X-RAY ANALYSIS OF HETISINE HYDROBROMIDE*

MARIA PRZYBYLSKA

The crystals of hetisine hydrobromide, $C_{20}H_{27}O_3N.HBr$, were prepared and crystallized from absolute methanol by Dr. G. Feniak. They were found to belong to the space group $P2_1$. The unit cell dimensions are: $a = 9.75$, $b = 10.84$, $c = 9.46$ Å, $\beta = 114°40'$; $Z = 2$.

Three-dimensional data were collected from Weissenberg films, and the number of observed reflections, out of all those possible within the range given by the Cu radiation, amounted to 86%. The determination of space group was confirmed and the bromine atom was located at $x = 0.063$ and $z = 0.257$, by means of two Patterson syntheses, carried out with the $(h0l)$ and $(hk0)$ data. The y coordinate of bromine was taken as 0.250 and a three-dimensional Fourier synthesis, based on phases calculated only for the heavy atom, was computed for sections perpendicular to the b axis.

An examination of models of this synthesis led to the complete solution of the molecular structure of this compound. The choice of correct atomic positions and the elimination of their mirror image peaks was based solely on consideration of the interatomic distances and valency angles. In addition to mirror images, three spurious peaks were found along the b axis, directly above the bromine atom. Since the data were collected from levels normal to the b axis and the temperature factor is unusually low (2 Å^2), there was no doubt that they were diffraction effects caused by the termination of the Fourier series.

Issued as N.R.C. No. 6670.

From these results it is apparent that a chromic acid – sulphuric acid cleaning mixture, although satisfactory for routine operations, should not be used in circumstances where minor traces of chromium are deleterious.

Adsorption behavior similar to that of quartz would be expected with laboratory glassware cleaned in a chromic acid – sulphuric acid mixture. However, most glassware now in common use is of the borosilicate type and it is not practical to use reactor irradiation to ascertain the amount of chromium remaining after cleaning because of the very high thermal neutron cross section of boron.

ACKNOWLEDGMENTS

The author wishes to express his thanks to Mr. J. L. Horwood for performing the gamma-ray spectrometer analysis. This paper is published by permission of the Director, Mines Branch, Department of Mines and Technical Surveys, Ottawa, Canada.

1. A. I. VOGEL. A textbook of quantitative inorganic analysis. Longmans, Green and Co., London. 1948. p. 240.
2. J. C. HUGHES. National Bureau of Standards Circular 602. 1959. p. 9.
3. J. C. W. FRAZER, W. A. PATRICK, and H. E. SMITH. J. Phys. Chem. **31**, 897 (1927).
4. J. R. PARTINGTON. An advanced treatise on physical chemistry. Vol. 2. Longmans, Green and Co., New York. 1950. p. 281.

RECEIVED OCTOBER 19, 1961.
MINERAL SCIENCES DIVISION,
MINES BRANCH,
DEPARTMENT OF MINES AND TECHNICAL SURVEYS,
OTTAWA, CANADA.

THE X-RAY ANALYSIS OF HETISINE HYDROBROMIDE*

MARIA PRZYBYLSKA

The crystals of hetisine hydrobromide, $C_{20}H_{27}O_3N.HBr$, were prepared and crystallized from absolute methanol by Dr. G. Feniak. They were found to belong to the space group $P2_1$. The unit cell dimensions are: $a = 9.75$, $b = 10.84$, $c = 9.46$ Å, $\beta = 114°40'$; $Z = 2$.

Three-dimensional data were collected from Weissenberg films, and the number of observed reflections, out of all those possible within the range given by the Cu radiation, amounted to 86%. The determination of space group was confirmed and the bromine atom was located at $x = 0.063$ and $z = 0.257$, by means of two Patterson syntheses, carried out with the $(h0l)$ and $(hk0)$ data. The y coordinate of bromine was taken as 0.250 and a three-dimensional Fourier synthesis, based on phases calculated only for the heavy atom, was computed for sections perpendicular to the b axis.

An examination of models of this synthesis led to the complete solution of the molecular structure of this compound. The choice of correct atomic positions and the elimination of their mirror image peaks was based solely on consideration of the interatomic distances and valency angles. In addition to mirror images, three spurious peaks were found along the b axis, directly above the bromine atom. Since the data were collected from levels normal to the b axis and the temperature factor is unusually low (2 Å^2), there was no doubt that they were diffraction effects caused by the termination of the Fourier series.

**Issued as N.R.C. No. 6670.*

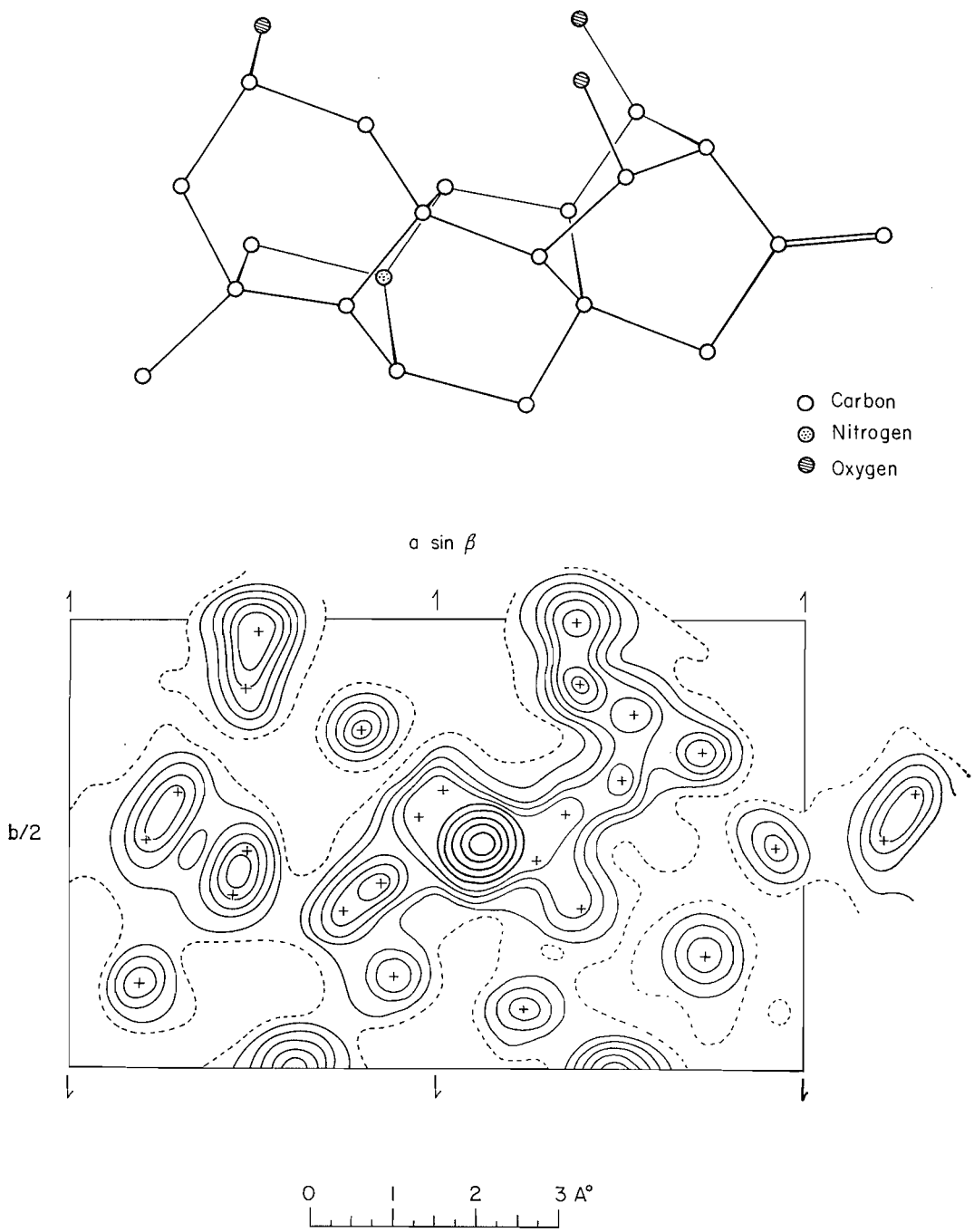

FIG. 1. A projection of the structure of hetisine hydrobromide along the c axis, with the corresponding diagram of the molecule. Light atom contours are at intervals of 2 e Å^{-2}, starting with a broken line at 2 e Å^{-2}. The bromine atom contours above 10 e Å^{-2} are at 10 e Å^{-2} and are drawn with heavier lines. The centers of all light atoms are marked by crosses.

This original molecular structure was later established as the correct one, but the first set of atomic coordinates consisted of only 21 atoms, all of which were treated as carbon atoms for the structure factor calculations. It is interesting that the $C{=}CH_2$ bond length was found even at this early stage of investigation to be 1.29 Å, and therefore in good agreement with the theoretical value. The ρ_o and $\rho_o - \rho_c$ maps for the three axial zones had confirmed the position of the additional three atoms and made possible the identification of the oxygen atoms. The nitrogen atom was identified by taking into account the chemical work on hetisine. Two structures have been postulated for hetisine (1) on the basis of limited chemical evidence. While the carbon–nitrogen skeleton proposed by Wiesner and Valenta (2) proves to be correct, the substituents were found to be located differently than in either of these structures.

The (001) Fourier projection of hetisine hydrobromide, together with the corresponding schematic drawing of the molecule, is given in Fig. 1.

A three-dimensional Fourier synthesis which was subsequently evaluated left no doubt as to the reliability of the structure, as all the false mirror image peaks had disappeared and the electron density values at the atomic centers were found to be in excellent agreement with the positions of the nitrogen and oxygen atoms.

The values of the discrepancy factor, R, omitting the unobserved reflections, are at present: 0.23, 0.18, and 0.14 for the $h0l$, $hk0$, and $0kl$ spectra, respectively. The overall R factor for the hkl data is 0.22. The refinement of atomic parameters is still in progress, and a detailed report of this work will be published later.

ACKNOWLEDGMENTS

I am indebted to Dr. F. R. Ahmed for computational assistance and for the use of his IBM 650 and 1620 programs. I wish to express my gratitude to Dr. O. E. Edwards for suggesting this investigation, for valuable discussions, and for providing the pure specimen of the alkaloid, and to Dr. Léo Marion for his full support and unfailing encouragement. I wish to thank also Mrs. C. Mackey for her help throughout the course of this work.

1. S. W. Pelletier. Tetrahedron, **14**, 76 (1961).
2. K. Wiesner and Z. Valenta. Progress in the chemistry of organic natural products. Vol. XVI. Springer-Verlag, Vienna. 1958. p. 26.

Received December 13, 1961.
Division of Pure Chemistry,
National Research Council,
Ottawa, Canada.

RING CONTRACTION IN THE MERCURY-PHOTOSENSITIZED DECOMPOSITION OF CYCLOPENTENE

W. A. Gibbons, W. F. Allen, and H. E. Gunning

Flowers and Frey (1) have recently reported that in the thermal isomerization of vinyl cyclopropane at 339–390° C, cyclopentene is the principal product (98%). In a current study of the mercury-photosensitized reactions of cyclopentene, we have found

This original molecular structure was later established as the correct one, but the first set of atomic coordinates consisted of only 21 atoms, all of which were treated as carbon atoms for the structure factor calculations. It is interesting that the C=CH_2 bond length was found even at this early stage of investigation to be 1.29 Å, and therefore in good agreement with the theoretical value. The ρ_o and $\rho_o - \rho_c$ maps for the three axial zones had confirmed the position of the additional three atoms and made possible the identification of the oxygen atoms. The nitrogen atom was identified by taking into account the chemical work on hetisine. Two structures have been postulated for hetisine (1) on the basis of limited chemical evidence. While the carbon–nitrogen skeleton proposed by Wiesner and Valenta (2) proves to be correct, the substituents were found to be located differently than in either of these structures.

The (001) Fourier projection of hetisine hydrobromide, together with the corresponding schematic drawing of the molecule, is given in Fig. 1.

A three-dimensional Fourier synthesis which was subsequently evaluated left no doubt as to the reliability of the structure, as all the false mirror image peaks had disappeared and the electron density values at the atomic centers were found to be in excellent agreement with the positions of the nitrogen and oxygen atoms.

The values of the discrepancy factor, R, omitting the unobserved reflections, are at present: 0.23, 0.18, and 0.14 for the $h0l$, $hk0$, and $0kl$ spectra, respectively. The overall R factor for the hkl data is 0.22. The refinement of atomic parameters is still in progress, and a detailed report of this work will be published later.

ACKNOWLEDGMENTS

I am indebted to Dr. F. R. Ahmed for computational assistance and for the use of his IBM 650 and 1620 programs. I wish to express my gratitude to Dr. O. E. Edwards for suggesting this investigation, for valuable discussions, and for providing the pure specimen of the alkaloid, and to Dr. Léo Marion for his full support and unfailing encouragement. I wish to thank also Mrs. C. Mackey for her help throughout the course of this work.

1. S. W. Pelletier. Tetrahedron, **14**, 76 (1961).
2. K. Wiesner and Z. Valenta. Progress in the chemistry of organic natural products. Vol. XVI. Springer-Verlag, Vienna. 1958. p. 26.

Received December 13, 1961.
Division of Pure Chemistry,
National Research Council,
Ottawa, Canada.

RING CONTRACTION IN THE MERCURY-PHOTOSENSITIZED DECOMPOSITION OF CYCLOPENTENE

W. A. Gibbons, W. F. Allen, and H. E. Gunning

Flowers and Frey (1) have recently reported that in the thermal isomerization of vinyl cyclopropane at 339–390° C, cyclopentene is the principal product (98%). In a current study of the mercury-photosensitized reactions of cyclopentene, we have found

vinyl cyclopropane to be a major product. In sharp contrast with early work on the thermal decomposition of cyclopentene (2, 3) where hydrogen and cyclopentadiene were the principal products, we found only small yields of hydrogen, no cyclopentadiene, a number of C_{10} products, and some liquid polymer, especially at low pressures. Typical quantum yields for a 10-minute run, at 27° C and 30 mm pressure of substrate, are: vinyl cyclopropane (0.24); H_2 (0.034); $C_{10}H_{14}$ (0.16); $C_{10}H_{16}$ (0.22); and $C_{10}H_{18}$ (0.05).

Preliminary results show that the quantum yields of all major products decrease gradually with increasing substrate pressure, and that the formation of C_{10} products is completely inhibited by 6% NO, whereas hydrogen and vinyl cyclopropane production remains unaffected.

Cyclopentene and vinyl cyclopropane have valence tautomeric structures, i.e. only carbon–carbon bond shifts are involved in isomerization. Similar valence tautomerism has been shown to occur with a number of cyclic dienes and trienes (4–7).

EXPERIMENTAL

Phillips Research grade cyclopentene, with a stated purity of 99.72%, was used. Gas chromatographic analysis with a silica gel column showed the presence of 0.15% cyclopentane and 0.05% cyclopentadiene. The nitric oxide was Matheson C.P. grade, distilled from a liquid-oxygen trap, the middle fraction being used. The propane for actinometry was Matheson "Instrument Grade" with a stated purity of 99.9%. After trap-to-trap distillation, the middle fraction was taken for the measurements.

A conventional high-vacuum apparatus was used, with 50-mm quartz cells. The lamp was an air-cooled, Hanovia 87A45 low-pressure mercury lamp (Vycor 7910 body).

The products condensable in liquid nitrogen were separated by gas–liquid chromatography, using silica gel columns to isolate a C_5 fraction and the three C_{10} products. The C_5 fraction was further partitioned into unreacted substrate, and the individual C_5 products on an oxydipropionitrile column. The non-condensable gas was shown to be hydrogen by mass spectrometry.

Parent peak analysis on a mass spectrometer indicated the principal products to be C_5H_8, $C_{10}H_{14}$, $C_{10}H_{16}$, and $C_{10}H_{18}$. The infrared spectrum of the C_5H_8 product showed that methyl groups were absent (i.e. no absorption at 1385 ± 10 cm^{-1}). In addition, the n.m.r. spectrum, using tetramethylsilane as an internal standard, revealed two bands, between 9.2 τ and 9.8 τ, which could be ascribed to a cyclopropyl group. The infrared spectrum was identical with that reported by Van Volkenburgh (8) for vinyl cyclopropane.

Selective absorption on a sulphuric acid:firebrick column (9) established that the $C_{10}H_{14}$ and $C_{10}H_{16}$ products were unsaturated while the $C_{10}H_{18}$ was not. The $C_{10}H_{18}$ had the same retention times as bicyclopentyl on two chromatographic columns. The products are believed to be a cyclopentenyl cyclopentene, a cyclopentyl cyclopentene, and bicyclopentyl.

A detailed study of the cyclopentene reaction will be submitted to this journal at a later date.

ACKNOWLEDGMENTS

This work was partially supported by a grant from Imperial Oil Limited, which assistance is gratefully acknowledged.

1. M. C. Flowers and H. M. Frey. J. Chem. Soc. 3547 (1961).
2. F. O. Rice and M. T. Murphy. J. Am. Chem. Soc. **64**, 896 (1942).
3. D. W. Vanas and W. D. Walters. J. Am. Chem. Soc. **70**, 4035 (1948).
4. D. H. R. Barton. Helv. Chim. Acta, **42**, 2604 (1959).
5. R. Srinivasan. J. Am. Chem. Soc. **83**, 2806 (1961).
6. O. L. Chapman and D. J. Pasto. Chem. & Ind. (London), 53 (1961).
7. W. G. Dauben and R. L. Cargill. Tetrahedron, **12**, 186 (1961).
8. R. Van Volkenburgh, K. W. Greenlee, I. M. Derfer, and C. E. Boord. J. Am. Chem. Soc. **71**, 3595 (1949).
9. G. D. Lutwick. Ph.D. Thesis, University of Alberta, Edmonton, Alberta. 1961.

Received December 11, 1961.
Department of Chemistry,
University of Alberta,
Edmonton, Alberta.

DIMETHYLPHENYLBENZYLAMMONIUM CHLORIDE AS A REAGENT FOR PLATINUM

D. E. RYAN

The use of dimethylphenylbenzylammonium chloride as a reagent for the gravimetric determination of platinum was recommended by Ryan (1). Westland and Westland (2), in a critical examination of the method, suggested a revised procedure to correct deficiencies they had found in the original method; unfortunately, their comments are based upon the use of impure reagent and are only valid in that instance. Their reagent was prepared by mixing commercial dimethylaniline and benzyl chloride with no intermediate purification of these materials; aqueous solutions of their reagent developed a blue coloration within 2 weeks. Dimethylphenylbenzylammonium chloride prepared from purified reactants is a white, stable compound; aqueous solutions, as stated in the original paper, may be kept for several months in a dark bottle with no signs of discoloration, and the platinum complex, under prolonged heating, shows no tendency to darken or tar.

H. M. Whitehead, in view of the Westland and Westland paper, recently prepared some dimethylphenylbenzylammonium chloride in this laboratory and reinvestigated the precipitation of platinum by this reagent. Determinations were carried out using both the original (1) and revised (2) procedures; no difference in results, as shown below, was evident.

	Pt recovered, mg	
Pt taken, mg	Original method	Modified method
21.08	21.08	21.07
13.72	13.73	13.72

The results show that washing with cyclohexane and dioxane are unnecessary when pure reagent is available. The losses in weight by the platinum precipitate, as recorded by Westland and Westland, are undoubtedly due to contamination by reagent impurities; washing by organic solvents gives good results by removal of these impurities. The thermal graphs given in the Westlands' paper confirm this rather than support the suggestion of decomposition of the platinum complex; 226.7 mg of complex decreased to 225.6 mg (by less than 0.5%) after 10 hours' heating.

1. D. E. RYAN. Can. J. Chem. **34**, 1683 (1956).
2. A. D. WESTLAND and L. WESTLAND. Talanta, **3**, 364 (1960).

RECEIVED NOVEMBER 14, 1961.
DEPARTMENT OF CHEMISTRY,
DALHOUSIE UNIVERSITY,
HALIFAX, NOVA SCOTIA.

A SYNTHESIS OF ISOASPARAGINE FROM β-BENZYL ASPARTATE

LEO BENOITON

In the course of the preparation of some aspartic acid peptides, ample supplies of β-benzyl aspartate and β-benzyl *N*-carbobenzoxyaspartate were required. The methods available for the synthesis of these compounds are lengthy. The latter is prepared by the

selective saponification of carbobenzoxyaspartic acid dibenzyl ester (1, 2), which in turn is decarbobenzoxylated with hydrogen bromide to provide the β-benzyl aspartate hydrobromide (3). We therefore sought a simplified synthesis for these intermediates.

β-Benzyl L-aspartate was prepared directly from aspartic acid by benzylation of the ω-carboxyl group in the manner used for glutamic acid (4). Subsequent carbobenzoxylation provided the β-benzyl *N*-carbobenzoxy-L-aspartate in good yield.

The ready accessibility of these intermediates permits a simple and unequivocal synthesis of isoasparagine, analogous to that already described for isoglutamine (5). β-Benzyl *N*-carbobenzoxy-L-aspartate was amidated using the mixed anhydride procedure (6), and the product, benzyl *N*-carbobenzoxy-L-isoasparagine,[1] was subsequently catalytically hydrogenated to give isoasparagine which is free of asparagine, the usual contaminating by-product in most isoasparagine syntheses.[2]

EXPERIMENTAL

β-Benzyl L-*Aspartate*

Sulphuric acid (10 ml) was added to anhydrous ether (100 ml) followed by benzyl alcohol (100 ml). The ether was removed under vacuum and finely ground L-aspartic acid (13.4 g) was added, in several portions, while the mixture was magnetically stirred. The ensuing solution was left at room temperature for 24 hours, 95% ethanol (200 ml) was added, followed by pyridine (50 ml), which was added dropwise while the solution was vigorously stirred. The mixture was cooled overnight, the deposit was filtered off and washed by trituration with ether. Recrystallization from water containing a few drops of pyridine afforded pure β-benzyl L-aspartate (8.9–9.9 g, 40–45%), m.p. 218–220° C, $[\alpha]_D^{25}$ +28.1° (*c*, 1; *N* HCl). (Found: C, 58.9; H, 5.7; N, 6.2. $C_{11}H_{13}NO_4$ requires: C, 59.2; H, 5.9; N, 6.3%.)

*β-Benzyl N-Carbobenzoxy-*L-*aspartate*

β-Benzyl L-aspartate (4.46 g, 20 mmoles) was dissolved in hot water (300 ml) and the solution was allowed to cool. When the temperature reached 60° C (the compound begins to crystallize at 55° C) sodium bicarbonate (3.5 g, 50 mmoles) and carbobenzoxy chloride (4.1 g, 24 mmoles) were added and the solution was stirred vigorously for 3 hours. The solution was then extracted twice with ether, and acidified to congo red with hydrochloric acid. The mixture was cooled for several hours (if the product is an oil it soon crystallizes), filtered, and the product was dried at 50° under vacuum. One recrystallization from benzene gave 5.3 g (75%), m.p. 107–108° C, $[\alpha]_D^{25}$ +11.9° (*c*, 10; acetic acid) (lit. m.p. 108°, $[\alpha]_D^{25}$ +12.1° (1)). (Found: N, 4.0. Calc. for $C_{19}H_{19}NO_6$: N, 3.9%.)

*Benzyl N-Carbobenzoxy-*L-*isoasparagine*

β-Benzyl *N*-carbobenzoxy-L-aspartate (1.79 g, 5 mmoles) was dissolved in purified dioxane (10 ml) containing tributylamine (1.2 ml, 5 mmoles). The solution was cooled to 10° and ethyl chloroformate (0.49 ml, 5 mmoles) was added. The solution was kept at 10° for 20 minutes after which anhydrous ammonia was bubbled through for 15 minutes. After an additional 15 minutes, the dioxane was removed under vacuum with a water-bath temperature under 45°. To the residue was added carbon tetrachloride (20 ml) and water (20 ml), and the mixture was shaken vigorously. The white product was filtered off, dried in a vacuum desiccator, and recrystallized from ethanol to give 1.1 g (62%), m.p. 103° C, $[\alpha]_D^{21}$ −12.8° (*c*, 2; dimethylformamide). (Found: C, 65.1; H, 5.5; N, 7.9. $C_{19}H_{20}N_2O_5$ requires: C, 64.0; H, 5.7; N, 7.9%.)

L-*Isoasparagine*

Benzyl *N*-carbobenzoxy-L-isoasparagine (0.89 g) was hydrogenated over palladized charcoal for 24 hours in 50% aqueous ethanol containing a few drops of acetic acid. The catalyst was filtered off, the solution was evaporated to dryness, the residue was dissolved in water, and three volumes of ethanol were added. After cooling, the product was recrystallized from water–ethanol to give needles (0.56 g, 75%), $[\alpha]_D^{25}$ +14.8° (*c*, 1.5; 0.1 *N* HCl) (lit. $[\alpha]_D^{20}$ +14.9° (8); $[\alpha]_D^{18}$ +15.5° (9)). (Found: C, 31.8; H, 6.6; N, 18.5. Calc. for $C_4H_8N_2O_3 \cdot H_2O$: C, 32.0; H, 6.7; N, 18.7%.) The material is free of asparagine, as evidenced by paper chromatography in *n*-butanol – acetic acid – water (12:3:5) (R_f isoasparagine 0.18; R_f asparagine 0.12).

1. A. Berger and E. Katchalski. J. Am. Chem. Soc. **73**, 4084 (1951).
2. P. M. Bryant, R. H. Moore, P. J. Pimlott, and G. T. Young. J. Chem. Soc. 3868 (1959).
3. D. Ben Ishai and A. Berger. J. Org. Chem. **17**, 1564 (1952).
4. S. Guttmann and R. A. Boissonnas. Helv. Chim. Acta, **41**, 1852 (1958).

[1]*Bernhardt has reported the preparation of this compound (7) but to our knowledge no details have been published.*
[2]*See reference 8 for most of the pertinent references.*

5. M. KRAML and L. P. BOUTHILLIER. Can. J. Chem. **33**, 1630 (1955).
6. R. A. BOISSONNAS. Helv. Chim. Acta, **34**, 874 (1951).
7. S. A. BERNHARDT. J. Cellular Comp. Physiol. **54**, supplement I, 195 (1959).
8. C. RESSLER. J. Am. Chem. Soc. **82**, 1641 (1960).
9. M. BERGMANN and L. ZERVAS. Ber. B, **65**, 1192 (1932).

RECEIVED DECEMBER 5, 1961.
DEPARTMENT OF BIOCHEMISTRY,
SCHOOL OF MEDICINE,
UNIVERSITY OF OTTAWA,
OTTAWA, ONTARIO.

FURFURALDEHYDE FROM THE ALDOBIURONIC ACID 2-*O*-(4-*O*-METHYL-α-D-GLUCOPYRANOSYL URONIC ACID)-D-XYLOPYRANOSE

S. K. SEN AND P. C. DAS GUPTA

It has been found by many workers (1) that uronic acids give 33–45% of the theoretical value of furfuraldehyde when distilled with 12% hydrochloric acid. Norris and Resch (2) have shown that glucuronic acid in combination gives 21.48% of its weight of furfuraldehyde. It has been suggested from time to time that the yield of furfuraldehyde for uronic acids be corrected before interpreting the results for pentosans. Wise and Ratliff (3) assumed that the uronic acids present in wood would evolve 35% of the theoretically possible amount of furfural and corrected their pentosan values accordingly. Hemicellulose from plant material generally contains 4-*O*-methyl-D-glucuronic acid as the major uronic acid component. The aldobiuronic acid 2-*O*-(4-*O*-methyl-α-D-glucopyranosyl uronic acid)-D-xylopyranose has been isolated from the partial hydrolysis product of many plant materials. It was thought that the yield of furfuraldehyde from this compound would correspond more closely with the yield to be expected from the acidic component of the parent polysaccharide.

The aldobiuronic acid used here was isolated by partial acid hydrolysis of the hemicellulose from Mesta fiber (*Hibiscus cannabinus*) (4) by column chromatography (5). Further purification by paper chromatography with the solvent system butanol–pyridine–water (10:3:3) removed small amounts of xylose. The aldobiuronic acid was extracted from the paper with water and the solution was treated with Amberlite resin IR-120(H), filtered, and concentrated to a syrup. The syrup was dried to a powder in a vacuum desiccator over P_2O_5. The aldobiuronic acid had $[\alpha]_D^{32}$ +96.6° (*c*, 1.07 in water) (found: OMe 9.25%, uronic anhydride 51.04%, equivalent weight 337.5; calc. for $C_{12}H_{20}O_{11}$: OMe 9.1%, uronic anhydride 51.76%, equivalent weight 340). The aldobiuronic acid was characterized as 2-*O*-(4-*O*-methyl-α-D-glucopyranosyl uronic acid)-D-xylopyranose by conversion to methyl 2-*O*-[methyl(2,3-di-*O*-acetyl-4-*O*-methyl-α-D-glucopyranosyl)uronate]-3,4-di-*O*-acetyl-D-xylopyranoside (6) having m.p. 201° C and $[\alpha]_D^{25}$ +99.6° (*c*, 0.6 in chloroform). Furfuraldehyde was estimated as phloroglucide according to the TAPPI method (7) and calculated from the weight of phloroglucide using Krober's table. In actual experiment 86.97 mg of aldobiuronic acid gave 50.7 mg furfural-phloroglucide. Thus after the xylose portion of the aldobiuronic acid is accounted for, it appears that 4-*O*-methyl-glucuronic acid residue evolves 15.04% of its weight of furfural. On glucuronic anhydride the yield is 16.24%, which is 29.77% of the theoretical value. The precipitate of furfural-phloroglucide did not contain any methoxyl group.

DIMETHYLPHENYLBENZYLAMMONIUM CHLORIDE AS A REAGENT FOR PLATINUM

D. E. RYAN

The use of dimethylphenylbenzylammonium chloride as a reagent for the gravimetric determination of platinum was recommended by Ryan (1). Westland and Westland (2), in a critical examination of the method, suggested a revised procedure to correct deficiencies they had found in the original method; unfortunately, their comments are based upon the use of impure reagent and are only valid in that instance. Their reagent was prepared by mixing commercial dimethylaniline and benzyl chloride with no intermediate purification of these materials; aqueous solutions of their reagent developed a blue coloration within 2 weeks. Dimethylphenylbenzylammonium chloride prepared from purified reactants is a white, stable compound; aqueous solutions, as stated in the original paper, may be kept for several months in a dark bottle with no signs of discoloration, and the platinum complex, under prolonged heating, shows no tendency to darken or tar.

H. M. Whitehead, in view of the Westland and Westland paper, recently prepared some dimethylphenylbenzylammonium chloride in this laboratory and reinvestigated the precipitation of platinum by this reagent. Determinations were carried out using both the original (1) and revised (2) procedures; no difference in results, as shown below, was evident.

	Pt recovered, mg	
Pt taken, mg	Original method	Modified method
21.08	21.08	21.07
13.72	13.73	13.72

The results show that washing with cyclohexane and dioxane are unnecessary when pure reagent is available. The losses in weight by the platinum precipitate, as recorded by Westland and Westland, are undoubtedly due to contamination by reagent impurities; washing by organic solvents gives good results by removal of these impurities. The thermal graphs given in the Westlands' paper confirm this rather than support the suggestion of decomposition of the platinum complex; 226.7 mg of complex decreased to 225.6 mg (by less than 0.5%) after 10 hours' heating.

1. D. E. RYAN. Can. J. Chem. **34**, 1683 (1956).
2. A. D. WESTLAND and L. WESTLAND. Talanta, **3**, 364 (1960).

RECEIVED NOVEMBER 14, 1961.
DEPARTMENT OF CHEMISTRY,
DALHOUSIE UNIVERSITY,
HALIFAX, NOVA SCOTIA.

A SYNTHESIS OF ISOASPARAGINE FROM β-BENZYL ASPARTATE

LEO BENOITON

In the course of the preparation of some aspartic acid peptides, ample supplies of β-benzyl aspartate and β-benzyl *N*-carbobenzoxyaspartate were required. The methods available for the synthesis of these compounds are lengthy. The latter is prepared by the

5. M. KRAML and L. P. BOUTHILLIER. Can. J. Chem. **33**, 1630 (1955).
6. R. A. BOISSONNAS. Helv. Chim. Acta, **34**, 874 (1951).
7. S. A. BERNHARDT. J. Cellular Comp. Physiol. **54**, supplement I, 195 (1959).
8. C. RESSLER. J. Am. Chem. Soc. **82**, 1641 (1960).
9. M. BERGMANN and L. ZERVAS. Ber. B, **65**, 1192 (1932).

RECEIVED DECEMBER 5, 1961.
DEPARTMENT OF BIOCHEMISTRY,
SCHOOL OF MEDICINE,
UNIVERSITY OF OTTAWA,
OTTAWA, ONTARIO.

FURFURALDEHYDE FROM THE ALDOBIURONIC ACID 2-*O*-(4-*O*-METHYL-α-D-GLUCOPYRANOSYL URONIC ACID)-D-XYLOPYRANOSE

S. K. SEN AND P. C. DAS GUPTA

It has been found by many workers (1) that uronic acids give 33–45% of the theoretical value of furfuraldehyde when distilled with 12% hydrochloric acid. Norris and Resch (2) have shown that glucuronic acid in combination gives 21.48% of its weight of furfuraldehyde. It has been suggested from time to time that the yield of furfuraldehyde for uronic acids be corrected before interpreting the results for pentosans. Wise and Ratliff (3) assumed that the uronic acids present in wood would evolve 35% of the theoretically possible amount of furfural and corrected their pentosan values accordingly. Hemicellulose from plant material generally contains 4-*O*-methyl-D-glucuronic acid as the major uronic acid component. The aldobiuronic acid 2-*O*-(4-*O*-methyl-α-D-glucopyranosyl uronic acid)-D-xylopyranose has been isolated from the partial hydrolysis product of many plant materials. It was thought that the yield of furfuraldehyde from this compound would correspond more closely with the yield to be expected from the acidic component of the parent polysaccharide.

The aldobiuronic acid used here was isolated by partial acid hydrolysis of the hemicellulose from Mesta fiber (*Hibiscus cannabinus*) (4) by column chromatography (5). Further purification by paper chromatography with the solvent system butanol–pyridine–water (10:3:3) removed small amounts of xylose. The aldobiuronic acid was extracted from the paper with water and the solution was treated with Amberlite resin IR-120(H), filtered, and concentrated to a syrup. The syrup was dried to a powder in a vacuum desiccator over P_2O_5. The aldobiuronic acid had $[\alpha]_D^{32}$ +96.6° (*c*, 1.07 in water) (found: OMe 9.25%, uronic anhydride 51.04%, equivalent weight 337.5; calc. for $C_{12}H_{20}O_{11}$: OMe 9.1%, uronic anhydride 51.76%, equivalent weight 340). The aldobiuronic acid was characterized as 2-*O*-(4-*O*-methyl-α-D-glucopyranosyl uronic acid)-D-xylopyranose by conversion to methyl 2-*O*-[methyl(2,3-di-*O*-acetyl-4-*O*-methyl-α-D-glucopyranosyl)uronate]-3,4-di-*O*-acetyl-D-xylopyranoside (6) having m.p. 201° C and $[\alpha]_D^{25}$ +99.6° (*c*, 0.6 in chloroform). Furfuraldehyde was estimated as phloroglucide according to the TAPPI method (7) and calculated from the weight of phloroglucide using Krober's table. In actual experiment 86.97 mg of aldobiuronic acid gave 50.7 mg furfural-phloroglucide. Thus after the xylose portion of the aldobiuronic acid is accounted for, it appears that 4-*O*-methyl-glucuronic acid residue evolves 15.04% of its weight of furfural. On glucuronic anhydride the yield is 16.24%, which is 29.77% of the theoretical value. The precipitate of furfural-phloroglucide did not contain any methoxyl group.

1. B. L. BROWNING. *In* Wood chemistry. *Edited by* L. E. Wise and E. C. Jahn. 2nd ed. Reinhold Publishing Corp., New York. 1952. p. 1163.
2. F. W. NORRIS and C. E. RESCH. Biochem. J. **29**, 1590 (1935).
3. L. E. WISE and E. K. RATLIFF. Anal. Chem. **19**, 459 (1947).
4. S. K. SEN. Ph.D. Thesis, University of Calcutta, Calcutta, India. 1961.
5. R. L. WHISTLER, H. E. CONRAD, and L. HOUGH. J. Am. Chem. Soc. **76**, 1668 (1954).
6. T. E. TIMELL. Can. J. Chem. **37**, 827 (1959).
7. TESTING METHODS of the Technical Association of the Pulp and Paper Industry. T 19m-50, 1958 (July).

RECEIVED SEPTEMBER 19, 1961.
DEPARTMENT OF CHEMISTRY,
TECHNOLOGICAL RESEARCH LABORATORIES,
INDIAN CENTRAL JUTE COMMITTEE,
CALCUTTA-40, INDIA.

Canadian Journal of Chemistry

Issued by THE NATIONAL RESEARCH COUNCIL OF CANADA

VOLUME 40 APRIL 1962 NUMBER 4

PERFLUOROALKYL ARSENICALS

PART V. SOME SOLVOLYSIS STUDIES

W. R. CULLEN

Chemistry Department, University of British Columbia, Vancouver, British Columbia

Received November 17, 1961

ABSTRACT

The ammonolysis of tetrakistrifluoromethyldiarsine probably proceeds through solvolytic fission of the As—As bond. Solvolysis of the diarsine by sodium methoxide in methanol does not seem to proceed by this mechanism. Chlorobistrifluoromethylarsine is stable to ethanol and ethanethiol below 110° but reacts violently with solid sodium alcoholates to give only decomposition products. With solid sodium mercaptide chlorobistrifluoromethylarsine yields ethylmercaptobistrifluoromethylarsine. This mercapto-arsine is also obtained by reacting iodobistrifluoromethylarsine with mercuric mercaptide. Ammonolysis and hydrolysis studies of the compounds R_2AsCF_3 and $RAs(CF_3)_2$ ($R = C_2H_5$, C_4H_9) indicate that the mechanism of solvolysis could be S_N2.

DISCUSSION AND RESULTS

Alkaline hydrolysis of trifluoromethyl arsenicals to fluoroform is usually rapid and quantitative, though trifluoromethylarsine, bistrifluoromethylarsine, and tetrakistrifluoromethyldiarsine hydrolyze to fluoroform and fluoride (1, 2). The postulated mechanism for the hydrolysis of the diarsine involves hydrolytic fission of the As—As bond:

$$(CF_3)_2As—As(CF_3)_2 \xrightarrow{H_2O} (CF_3)_2AsH + (CF_3)_2AsOH.$$

Ammonolysis of trifluoromethyl arsenicals seems to parallel hydrolysis, though the diarsine and ammonia do not give fluoride (3). In this paper further solvolysis reactions of the diarsine and other trifluoromethyl arsenicals are described.

Ammonolysis of tetrakistrifluoromethyldiarsine gives 89% of the trifluoromethyl as fluoroform (3). Ammonolysis of bistrifluoromethylarsine under similar conditions gives 76% of the trifluoromethyl as fluoroform and no fluoride. Thus if the ammonolysis of the diarsine also proceeds through solvolylic fission of the As—As bond,

$$(CF_3)_2As—As(CF_3)_2 \xrightarrow{NH_3} (CF_3)_2AsNH_2 + HAs(CF_3)_2,$$

the yield of fluoroform would be expected to be 50% (from the $(CF_3)_2AsNH_2$ (3)) plus 76% of 50% (from the $(CF_3)_2AsH$): a total of 88%, in good agreement with the experimental result. Furthermore the experimental observations during the ammonolysis of the diarsine and bistrifluoromethylarsine correspond very well. The diarsine is stable to methanol at 20° (4 days) but is decomposed by methanolic sodium methoxide to give fluoroform (90%) but no fluoride. Bistrifluoromethylarsine under similar conditions gives

fluoroform (67%) and no fluoride. If the solvolysis of the diarsine occurred by fission of the As—As bond,

$$(CF_3)_2As—As(CF_3)_2 \xrightarrow{CH_3OH} (CF_3)_2AsOCH_3 + (CH_3)_2AsH,$$

then the expected yield of fluoroform would be 50% (from the $(CF_3)_2AsOCH_3$) plus 67% of 50% (from the $(CF_3)_2AsH$): a total of 83.5%, which is less than the experimental result. Methanolysis of $(CF_3)_2AsOCH_3$ would be expected to be complete since tris-trifluoromethylarsine, although slowly attacked by ethanol at 20°, is at least 98% solvolyzed to fluoroform by methanolic sodium methoxide. Methanolysis of both the diarsine and bistrifluoromethylarsine produces a green solution, but a water-insoluble product is obtained from methanolysis of the arsine. In view of this and the discrepancy between the expected and found yields of fluoroform it seems that methanolysis of the diarsine does not proceed through solvolytic fission of the As—As bond. The hydrolysis of tetrakistrifluoromethyldiphosphine is also believed to proceed through fission of the P—P bond, and part of the evidence offered for this is that bistrifluoromethylphosphine and fluoroform are produced by the reaction of the diphosphine with dilute hydrochloric acid at 100° (4). It has now been found that tetrakistrifluoromethyldiarsine is stable under the same conditions. The diphosphine is unstable to liquid ammonia and 48% of the trifluoromethyl is lost as fluoroform after 28 days. Thus the extent of ammonolysis of the diphosphine is less than that of the diarsine. Similar results have been found for tristrifluoromethyl-phosphine and -arsine (3).

Chlorobistrifluoromethylphosphine reacts with ethanol below 20° to give ethoxybistrifluoromethylphosphine (5), and when warmed with ethanethiol the corresponding mercapto-phosphine is obtained (6). Chlorobistrifluoromethylarsine is stable to ethanol below 120° and to ethanethiol below 110°. In an attempt to prepare alkoxybistrifluoromethylarsines chlorobistrifluoromethylarsine was reacted with sodium methoxide and ethoxide. A violent reaction takes place and only decomposition products can be isolated. In a more controlled reaction using sodium methoxide bistrifluoromethylarsine oxide was produced. The reaction of chlorobistrifluoromethylarsine with sodium mercaptide is less violent and ethylmercaptobistrifluoromethylarsine is obtained. The same product

$$(CF_3)_2AsCl + NaSC_2H_5 \rightarrow NaCl + (CF_3)_2AsSC_2H_5$$

$$(CF_3)_2AsI + Hg(SC_2H_5) \rightarrow C_2H_5HgI + (CF_3)_2AsSC_2H_5$$

is obtained from the reaction of mercury mercaptide with iodobistrifluoromethylarsine. The use of solid sodium and mercury mercaptides for reactions of this sort has not previously been reported, though the lead(II) derivatives have recently been used to prepare mercapto-silanes (7).

Chlorobistrifluoromethyl-arsine and -phosphine react readily with ammonia (3, 8), yet the phosphine does not react with sodamide (8). A similar result has now been found for the arsine. The arsine is also stable to formamide at 20°.

The rates of hydrolysis of the compounds $(CH_3)_xAs(CF_3)_{3-x}$ have been found to increase as the number of trifluoromethyl groups is increased (2, 9). A similar result has been found for the rates of hydrolysis and ammonolysis of the compounds $(C_3H_5)_xAs(CF_3)_{3-x}$ (10). It has now been found that the compounds $R_xAs(CF_3)_{3-x}$ (R = C_2H_5, n-C_4H_9) show this same trend with respect to ammonolysis and hydrolysis. Comparison of the details of these experiments with those of Haszeldine and West (9) suggests that for a particular number of trifluoromethyl groups the rate of hydrolysis decreases in the order $CH_3 > C_2H_5 > C_4H_9$. Ammonolysis of the ethyl compounds also seems to

be faster than ammonolysis of the corresponding *n*-butyl compounds. Heptafluoropropyldimethylarsine is also slowly attacked by ammonia, giving heptafluoropropane. These results are consistent with the idea that solvolysis involves nucleophylic attack at the arsenic atom (9), and suggest that mechanism could well be S_N2.

Tristrifluoromethylarsine is stable to liquid sulphur dioxide at 20°.

EXPERIMENTAL

The trifluoromethyl arsenicals were prepared by recorded methods. Techniques used were similar to those previously described. Most compounds solvolyzed to give fluoroform, the identity and purity of which was checked spectroscopically and, where possible, by molecular weight measurement.

Solvolysis of Chlorobistrifluoromethylarsine

Chlorobistrifluoromethylarsine (0.870 g) and dry ethanol (0.259 g) did not react after 3 days at 83° or 13 hours at 120°. Similarly no reaction occurred between the arsine (0.296 g) and ethanethiol (7.5 g) after 44 hours at 110°, or between the arsine (0.510 g) and formamide (0.34 g) after 3 days at 20°. Chlorobistrifluoromethylarsine (0.663 g) and excess sodium methoxide reacted violently on being warmed quickly from −196° to 20° to give fluoroform (0.142 g, 97% of the trifluoromethyl); methanol was identified in the remaining volatile fraction by its infrared spectrum. The water-insoluble solid product contained elemental arsenic, identified by its X-ray powder photograph. In a second experiment the chloro-arsine (1.457 g) and sodium methoxide (1.2 g) were allowed to warm up from −196° to 20° over 16 hours, a vigorous reaction took place at −10° and some charring occurred. The volatile products were fluoroform (0.331 g, 40%) and a fraction (0.434 g; molecular weight (M), 352) whose infrared spectrum was almost identical with that of a sample of bistrifluoromethylarsine oxide. Excess sodium ethoxide and chlorobistrifluoromethylarsine reacted violently, giving ethylene, fluoroform, ethanol, and arsenic metal, but no ethoxybistrifluoromethylarsine was formed. Chlorobistrifluoromethylarsine (1.325 g) and excess sodium mercaptide reacted vigorously on being warmed to 20° to give, amongst other unidentified products, ethylene and a slightly impure sample of *ethylmercaptobistrifluoromethylarsine* (1.107 g). Anal. Found: CF_3, 49.5%; M, 277. $C_4H_5AsF_6S$ requires: CF_3, 50.5%; M, 274. The infrared spectrum of this fraction was consistent with that expected for the mercapto-arsine. Found: liquid film: 2965 (m), 2925 (m), 2870 (w), 2220 (w), 1650 (vw), 1465 (m), 1434 (w), 1383 (w), 1264 (s), 1167 (vs), 1133 (vs), 1100 (vs), 1057 (m), 1043 (m), 966 (w), 758 (w), 726 (s). The same compound was produced in 90% yield from the reaction of iodobistrifluoromethylarsine with excess mercury mercaptide at 20° (4 days). Chlorobistrifluoromethylarsine (0.814 g) and sodamide (5 g) did not react at 20° (9 days) (93% recovery). Found: M, 250. Calc. for C_2AsClF_6: M, 249.

Solvolysis of Tristrifluoromethylarsine

Tristrifluoromethylarsine (0.924 g) and dry ethanol (1 g) at 20° (12 days) gave fluoroform (0.053 g, 7.7% of the trifluoromethyl). The arsine (0.765 g) and 5 ml of a 10% solution of sodium methoxide in methanol after 3 days at 20° gave fluoroform (0.548 g) equivalent to 98% of the trifluoromethyl. Tristrifluoromethylarsine (1.689 g) and sulphur dioxide (14.98 g) did not react after 7 days at 20°.

Solvolysis of Tetrakistrifluoromethyldiarsine

The diarsine (0.327 g) and dilute hydrochloric acid (10 ml) did not react after 24 hours at 100°. No reaction occurred between the diarsine (0.308 g) and dry methanol (10 ml) after 4 days at 20°. The diarsine (0.353 g) and 6 ml of a 5% solution of sodium methoxide in methanol gave, on being warmed to 20°, a green solution which slowly became colorless then brown after 12 hours. After 6 days fluoroform (0.209 g; 90% of the trifluoromethyl) was obtained. The solid remaining in the tube contained at least two phases and was completely soluble in water. This solution contained arsenite but no fluoride.

Solvolysis of Bistrifluoromethylarsine

Bistrifluoromethylarsine (0.306 g) and ammonia (4.40 g) gave a green solution and a white precipitate at low temperature. The color gradually faded from the solution as it was warmed to 20° and the solid became red-brown. After 28 days fluoroform (0.152 g; 76% of the trifluoromethyl) was obtained. Arsenite but no fluoride was produced. Bistrifluoromethylarsine (0.185 g) and 4 ml of a 5% solution of sodium methoxide in methanol gave a transient green solution on being warmed to 20°. After 12 hours a copious brown precipitate had formed. After 5 days fluoroform (0.081 g) equivalent to 67% of the available trifluoromethyl was isolated. The brown solid remaining in the reaction tube contained arsenite but no fluoride and was partly insoluble in water and acetone. The infrared spectrum of this solid indicated the presence of C—F groups.

Reaction of Tetrakistrifluoromethyldiphosphine with Ammonia

The diphosphine (0.264 g) and ammonia (1.79 g) gave a colorless solution at 20° which slowly deposited a white solid. After 14 hours the solid was red-brown. After 28 days fluoroform (0.105 g) equivalent to 48% of the trifluoromethyl was obtained. No fluoride was produced.

Solvolysis of Trifluoromethyl Arsenicals containing Ethyl and n-Butyl Groups

The results can be summarized as follows:

Compound	mmoles	Solvolysis reagent	Time	Temp. (°C)	Yield of fluoroform (%)
$C_2H_5As(CF_3)_2$	0.912	10% NaOH (10 ml)	4 days	100	100
	1.52	Liquid NH_3 (3.9 g)	10 days	20	36
$(C_2H_5)_2AsCF_3$	2.29	20% NaOH (10 ml)	3 days	20	1
	1.37	10% NaOH (10 ml)	12 hours	100	34
	1.67	Liquid NH_3 (6.9 g)	14 days	20	7
n-$C_4H_9As(CF_3)_2$	1.63	20% NaOH (10 ml)	5 days	20	2
	1.55	10% NaOH (10 ml)	11 hours	100	38
	1.83	Liquid NH_3 (6.3 g)	11 days	20	14
$(n$-$C_4H_9)_2AsCF_3$	1.43	10% NaOH (10 ml)	12 hours	100	10
	1.29	Liquid NH_3 (5.3 g)	13 days	20	<0.5
$(CH_3)_2AsC_3F_7$	0.722	Liquid NH_3 (1.2 g)	9 days	20	11 (C_3F_7H)*

*The excess ammonia was removed with hydrochloric acid.

ACKNOWLEDGMENTS

The author wishes to acknowledge financial assistance from the National Research Council of Canada for part of this work. He is also grateful to Professor H. J. Emeléus for the help and encouragement given him while some of the work was done at Cambridge University.

REFERENCES

1. G. R. A. Brandt, H. J. Emeléus, and R. N. Haszeldine. J. Chem. Soc. 2552 (1952).
2. H. J. Emeléus, R. N. Haszeldine, and E. G. Walachewski. J. Chem. Soc. 1552 (1953).
3. W. R. Cullen and H. J. Emeléus. J. Chem. Soc. 372 (1959).
4. F. W. Bennett, H. J. Emeléus, and R. N. Haszeldine. J. Chem. Soc. 3886 (1954).
5. H. J. Emeléus and J. D. Smith. J. Chem. Soc. 375 (1959).
6. G. S. Harris. Ph.D. Thesis, Cambridge. 1958.
7. E. W. Abel. J. Chem. Soc. 4406 (1960).
8. G. S. Harris. J. Chem. Soc. 512 (1958).
9. R. N. Haszeldine and B. O. West. J. Chem. Soc. 3880 (1957).
10. W. R. Cullen. Can. J. Chem. **38**, 445 (1960).

DERIVATIVES OF MONOGERMANE

PART I. THE VIBRATION–ROTATION SPECTRA OF GERMYL FLUORIDE AND BROMIDE[1]

J. E. GRIFFITHS[2]
Bell Telephone Laboratories, Incorporated, Murray Hill, New Jersey, U.S.A.

AND

T. N. SRIVASTAVA[3] AND M. ONYSZCHUK
Inorganic Chemistry Laboratory, McGill University, Montreal, Que.

Received December 12, 1961

ABSTRACT

The vibration–rotation infrared absorption spectra of germyl fluoride and bromide have been observed. All of the fundamentals in GeH_3F were located, and the rotational structure of the *E*-type bands were resolved and analyzed. The low-frequency band, $\nu_3(a_1)$, in GeH_3Br was not observed but an estimate of its position was made from the frequencies of the combination band $\nu_3+\nu_6$ and of ν_6. The rotational constant A'' and the Coriolis constants ζ_4, ζ_5, and ζ_6 were calculated for both molecules, and agreement with microwave A'' values was satisfactory. Thermodynamic functions based upon a rigid-rotator, harmonic-oscillator model have been evaluated for germyl fluoride and bromide.

INTRODUCTION

The infrared vibrational spectra of only six compounds containing the germyl (GeH_3—) group have been reported. These are germane (1), monodeuterogermane (2), digermane (3), chlorogermane and chlorogermane-d_3 (4), and vinylgermane (5). The molecular structure of the fluoride (6), chloride (7), and bromide (8) have been determined by microwave spectroscopy, the results of which were subsequently confirmed in the case of the chloride by an analysis of the rotational structure of its perpendicular infrared absorption bands (4). In the course of an investigation of tetracovalent germanium compounds, in which the germyl derivatives were of particular interest, we prepared a series of GeH_3X compounds, where X is F, Cl, Br, I, CN, NCO, NCS, and CH_3, and measured their infrared vibrational spectra under medium dispersion. A detailed treatment of the vibration–rotation spectra of the fluoride and the bromide is presented here.

EXPERIMENTAL

All volatile compounds were manipulated in a glass high-vacuum apparatus in which the stopcocks were lubricated with a chlorofluorocarbon stopcock lubricant.

Germyl bromide was obtained by the reaction of germane with bromine, using a method similar to that described for the preparation of silyl bromide (9). Bromine (7.9 mmoles), in small portions, was condensed into a tube fitted with a stopcock in which a sample of germane (8.1 mmoles) had been cooled to −196° C. After each addition of bromine, the mixture was warmed slowly until the color of bromine had just disappeared. The products were separated from unconsumed germane by fractional condensation and vaporization in a trap cooled to −160° C before proceeding to the next addition of bromine. Germyl bromide was recovered from the product mixture by several distillations at −78° C (91% yield; found: molecular weight (M) 156.0, v.p. 25.7 mm at −23° C; calc. for GeH_3Br: M 155.5, v.p. 25.0 mm at −23° C (10)).

Germyl fluoride was prepared by the interaction of excess silver(I) fluoride with germyl bromide (11). The bromide (2.0 mmoles) was passed slowly through a sample of glass wool and powdered silver fluoride contained in a U-tube which was cooled to −22.9° C. The monofluoride (1.67 mmoles; found: M 94.7;

[1]*This work was presented in part at the Eighth Ottawa Symposium on Applied Spectroscopy, Ottawa, Ontario, September 18–20, 1961.*

[2]*Holder of N.R.C. Studentships, 1956–58.*

[3]*Holder of a N.R.C. Postdoctorate Research Fellowship, 1959–61. Present address: Department of Chemistry, University of Lucknow, Lucknow, India.*

calc. for GeH_3F: M 94.6) was separated from the difluoride (0.151 mmoles; found: M 112.8; calc. for GeH_2F_2: M 112.6) by passing a mixture of the two through a trap cooled to −95° C, at which temperature the difluoride is involatile. It is particularly important to ensure complete removal of the difluoride, since there are several very intense absorption bands in its infrared spectrum (12) which occur in the same spectral regions as absorptions due to the monofluoride.

Spectra were recorded in the range of 4000 to 625 cm^{-1} with a Perkin–Elmer Model 221-G spectrophotometer using a NaCl prism-grating optical system and with a Perkin–Elmer Model 21 instrument equipped with CaF_2 and NaCl prisms. These instruments were calibrated using CO_2, CO, and NH_3 so that an absolute accuracy of about 1 cm^{-1} is claimed. Small frequency differences, however, as encountered in the analysis of the rotational structure of the perpendicular bands, are expected to be accurate to about ±0.2 cm^{-1}. The ν_6 vibration in the spectrum of the bromide was observed with a Perkin–Elmer Infracord instrument equipped with a KBr prism. The resolution (ca. 4 cm^{-1}) was adequate to distinguish between successive peaks in this absorption band. This instrument was calibrated with polyethylene, and an accuracy of ±3 cm^{-1} was obtained. The measured separation of successive Q branches is expected to be accurate to about ±0.3 cm^{-1}.

Measurements were made on compounds in the gas phase contained in a 7.5-cm cell fitted with KBr windows at pressures of 5.5, 10.0, and 17.0 mm for the fluoride and 17.0 and 25.0 mm for the bromide.

RESULTS

The frequencies and assignments of the fundamental bands for germyl fluoride and bromide are listed in Table I and the vibrational spectra are shown in Figs. 1 and 2. The

TABLE I

Fundamental frequencies of GeH_3F and GeH_3Br

Vibration	Vibration number	Species	Frequency (cm^{-1})	
			GeH_3F	GeH_3Br
Ge—H stretch	1	A_1	2118.9	2113.3
Ge—H_3 bend	2	A_1	859.0	831.5
Ge—X stretch	3	A_1	689.2	(319)*
Ge—H stretch	4	E	2128.6	2124.4
GeH_3 bend	5	E	874.2	872.3
GeH_3 rock	6	E	663.7	578.9

*Estimated from $\nu_3+\nu_6$.

individual fundamental bands, observed under higher resolution than that used to obtain Figs. 1 and 2, of the fluoride are shown in Figs. 3–7 and of the bromide in Figs. 8–11. Assignments of the subband peaks in the perpendicular absorption bands are listed in Table II for the fluoride, and in Table III for the bromide.

DISCUSSION

The rotational structure of the perpendicular-type bands and the band contours of the parallel-type bands confirm the microwave studies, which indicate that the fluoride and bromide are symmetric tops of C_{3v} symmetry. Monohalogermanes, GeH_3X, have three symmetric vibrations of species A_1 and three doubly degenerate perpendicular vibrations of species E. These, as well as all overtones and combinations, are infrared and Raman active.

Vibrational assignments for the A_1-type fundamentals were made on the basis of band contours which show a PQR structure, and for the E-type fundamentals on the basis of the s,w,w,s intensity alteration in the subband peaks arising from the nuclear spins of the protons and the C_{3v} symmetry of the molecule. Location of the centers of the P, Q, and R branches of the parallel bands was not always apparent because of the strong overlap with less intense perpendicular bands. Thus, vibrations ν_1 and ν_4, ν_2 and

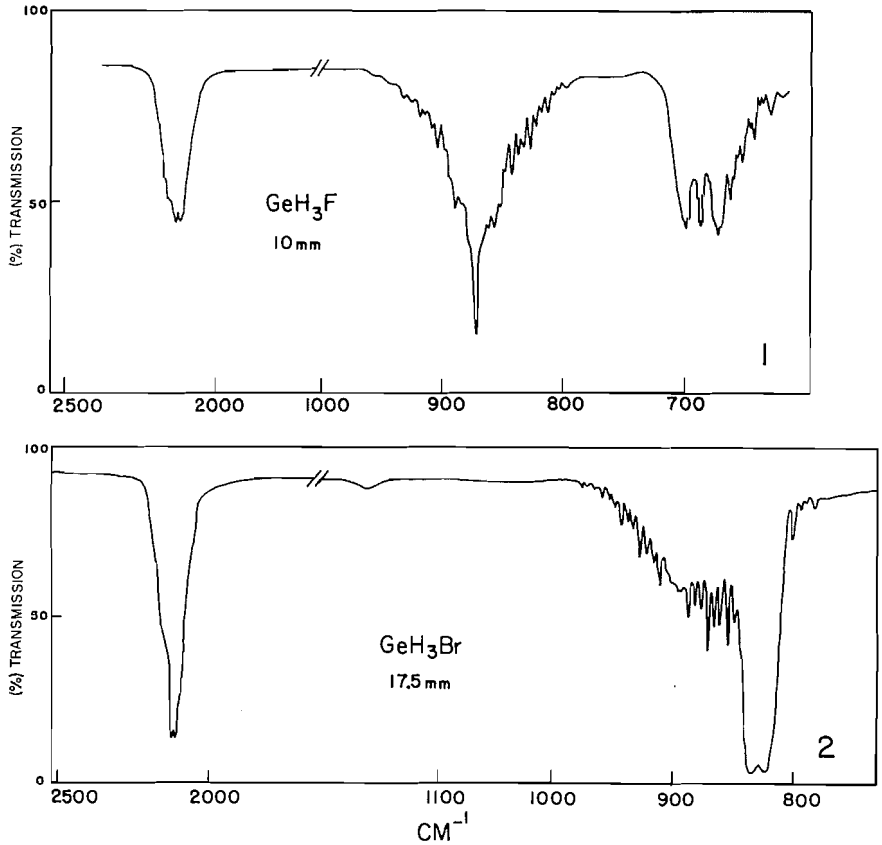

FIG. 1. The infrared spectrum of GeH_3F.
FIG. 2. The infrared spectrum of GeH_3Br.

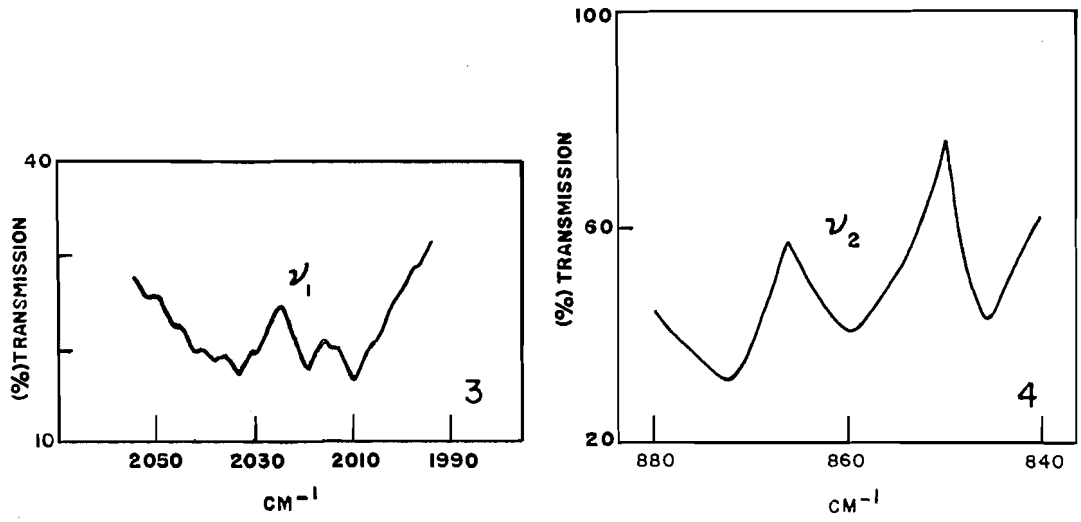

FIG. 3. The ν_1 band in GeH_3F.
FIG. 4. The ν_2 band in GeH_3F.

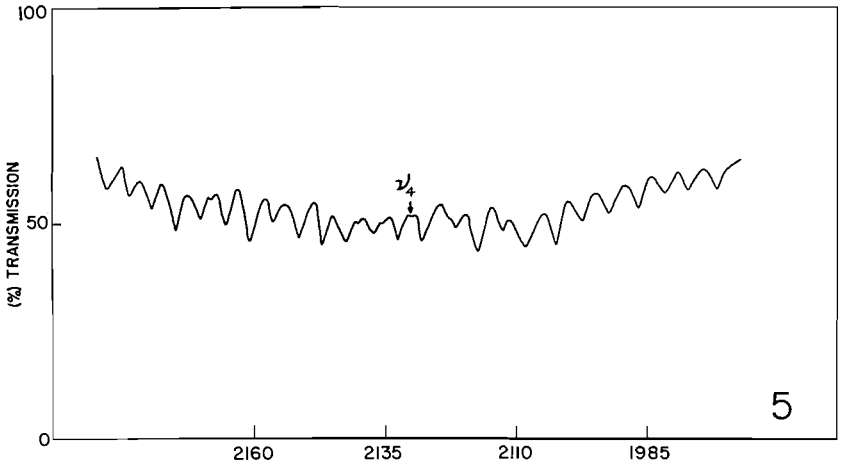

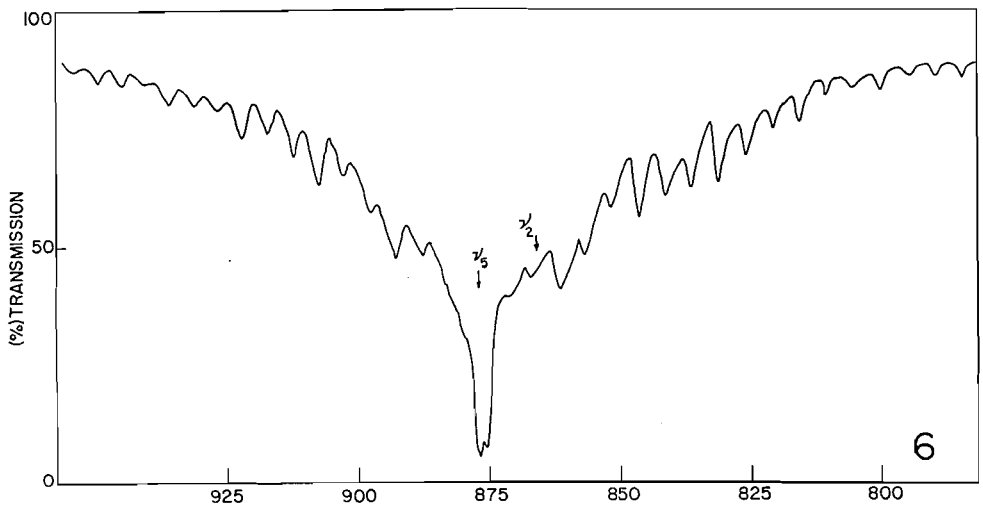

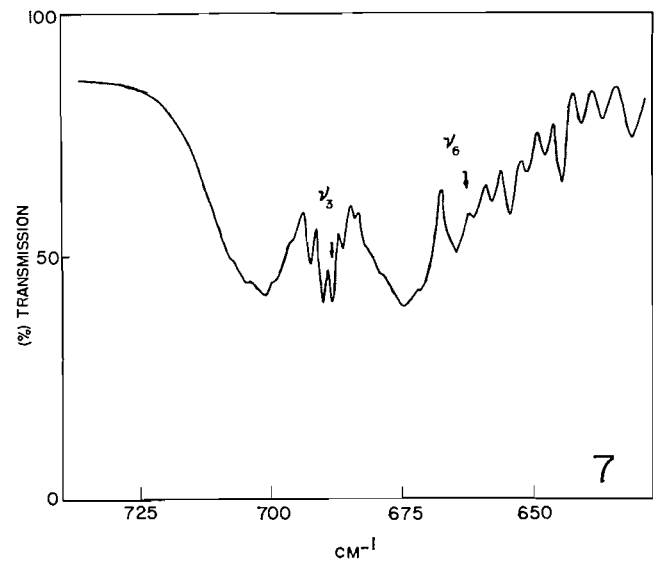

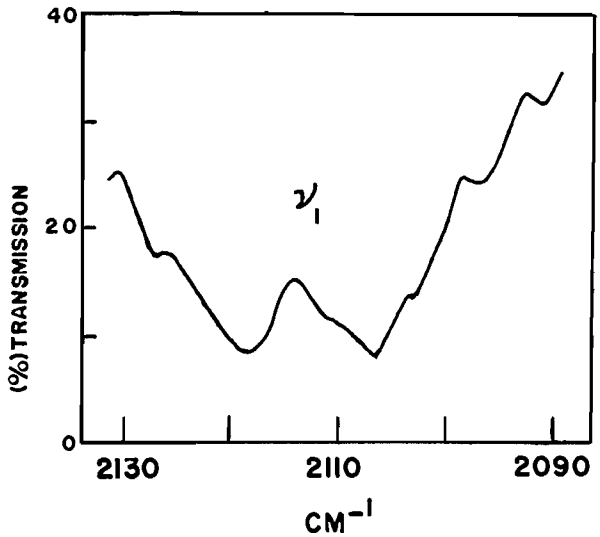

FIG. 8. The ν_1 band in GeH_3Br.

ν_5, and ν_3 and ν_6 in the spectrum of the fluoride, and ν_1 and ν_4, and ν_2 and ν_5 in the spectrum of the bromide, overlapped. When it was not obvious, the structures of the parallel bands were estimated by subtracting the contributions of the perpendicular bands from the overall band contours as described by Lord and Steese (4). In this way, the frequencies of the P, Q, and R branches and the P–R separations were determined.

Non-degenerate (A_1) Vibrations

The fine structure in the parallel bands was not observed in the fluoride and bromide spectra because the resolution in our spectrometers was not high enough. The rotational constants, B_0, which are known from microwave investigations to be 0.335 cm^{-1} for the fluoride and 0.079 cm^{-1} for the bromide, determine the line spacings in the parallel bands. These values are so small that individual lines of separation $2B$ were not resolved. Parallel bands of the fluoride showed well-defined PQR triplet structure, since the ratio of rotational constants, B/A, is high and controls the relative intensity ratio of the Q to the P and R branches. This ratio is very small in the bromide so that the Q branch could not be resolved and only the P–R doublet structures were observed. The P–R spacings for germyl fluoride and bromide were calculated from the formulas of Gerhard and Dennison (13) and are compared with the observed values in Table IV. The agreement between observed and calculated spacings is considered to be reasonable in view of the overlapping parallel and perpendicular bands and the large number of germanium isotopes.

Degenerate (E) Vibrations

The rotational structure of the E-type bands was easily resolved since the rotational constants A and the ratios A/B are large in the fluoride and bromide. Analysis of the spectrum was facilitated by assigning appropriate K values to the ${}^RQ_K$ and ${}^PQ_K$ subbands of comparable intensity at high values of K, where there was negligible absorption

FIG. 5. The ν_4 band in GeH_3F.
FIG. 6. The ν_2 and ν_5 bands in GeH_3F.
FIG. 7. The ν_3 and ν_6 bands in GeH_3F.

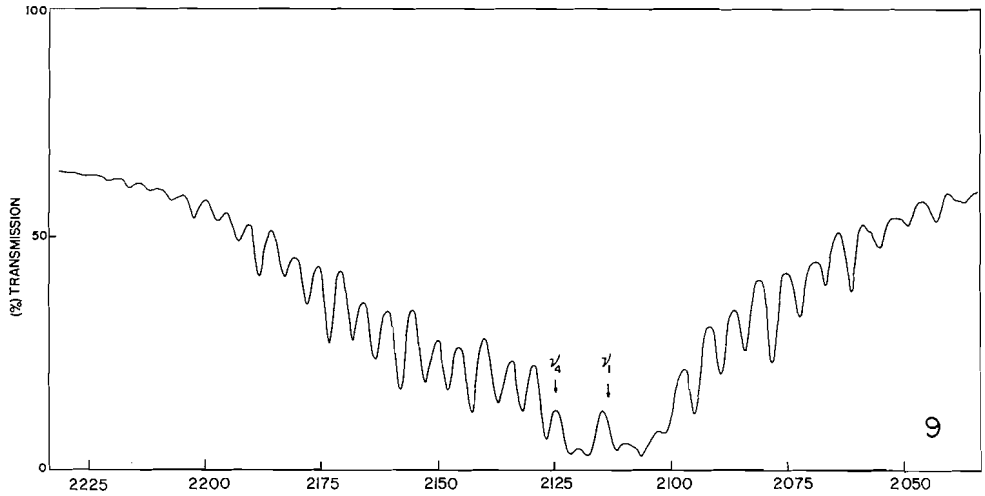

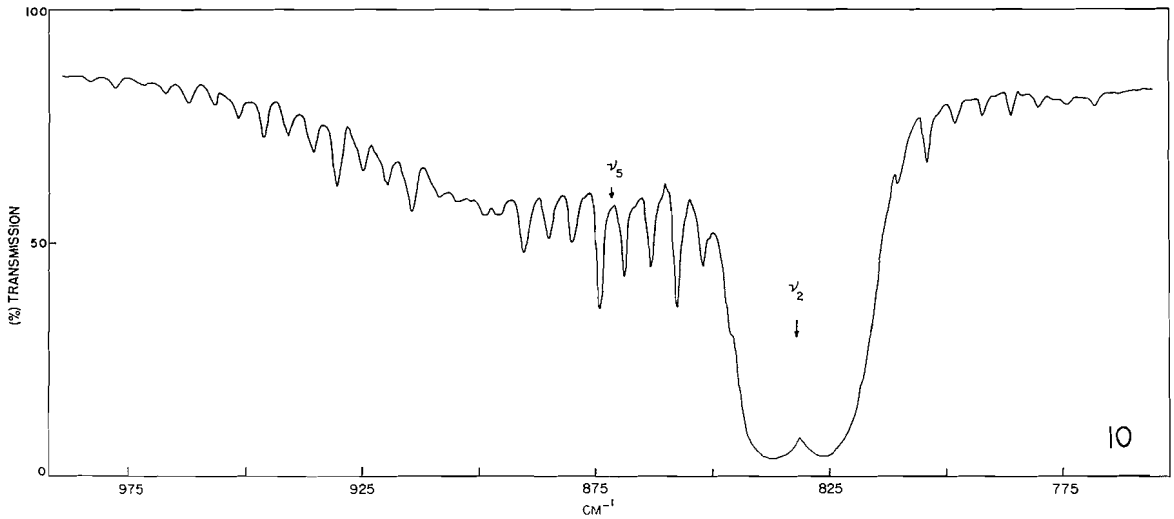

FIG. 9. The ν_1 and ν_4 bands in GeH_3Br.
FIG. 10. The ν_2 and ν_5 bands in GeH_3Br.

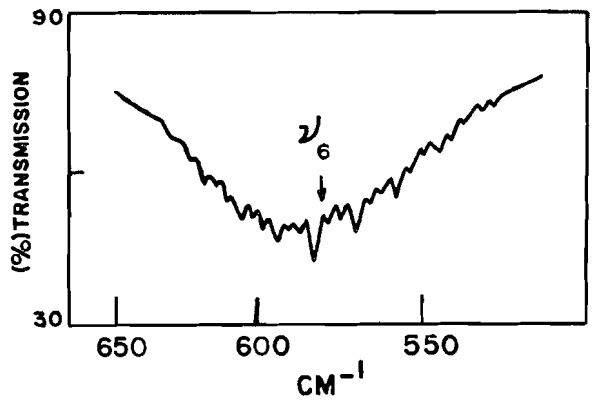

FIG. 11. The ν_6 band in GeH_3Br.

TABLE II

Frequencies (cm^{-1}, vac.) of subbands in GeH_3F

	Subbands of ν_4					Subbands of ν_5					Subbands of ν_6				
K	^RQ_K	^PQ_K	Intensity	$^RQ_K-{}^PQ_K$	$^RQ_K+{}^PQ_K$	^RQ_K	^PQ_K	Intensity	$^RQ_K-{}^PQ_K$	$^RQ_K+{}^PQ_K$	^RQ_K	^PQ_K	Intensity	$^RQ_K-{}^PQ_K$	$^RQ_K+{}^PQ_K$
0	2133.2	—	s	—	—	876.9	—	s	—	—	664.9	—	s	—	—
1	2137.9	2128.4	w	9.5	4266.3	882.2	871.5	w	10.7	1753.7	—	661.9	w	—	—
2	2142.9	2123.5	w	19.4	4266.4	887.5	866.8	w	20.7	1754.3	671.8	658.6	w	13.2	1330.4
3	2147.7	2118.5	s	29.2	4266.2	892.8	861.1	s	31.3	1753.9	—	654.9	s	—	—
4	2151.9	2113.2	w	38.7	4265.1	897.2	856.6	w	40.6	1753.8	—	651.7	w	—	—
5	2156.3	2108.3	w	48.0	4264.6	902.6	851.6	w	51.0	1754.2	681.8	648.0	w	33.8	1329.8
6	2161.4	2103.2	s	58.2	4264.6	907.5	846.3	s	61.2	1753.8	684.7	644.9	s	39.8	1329.6
7	2166.1	2098.1	w	68.0	4264.2	912.4	841.3	w	71.1	1753.7	687.0	641.4	w	45.6	1328.4
8	2171.1	2093.1	w	78.0	4264.2	917.4	836.3	w	81.1	1753.7	690.9	637.1	w	53.8	1328.0
9	2175.6	2087.9	s	87.7	4263.5	922.2	831.2	s	91.0	1753.4	693.3	—	s	—	—
10	2180.2	2082.6	w	97.6	4262.8	926.9	826.2	w	100.7	1753.1	696.5	—	w	—	—
11	2184.4	2077.4	w	107.0	4261.8	931.3	820.8	w	110.5	1752.1	699.8	—	w	—	—
12	2188.6	2072.4	s	116.2	4261.0	936.1	815.6	s	120.5	1751.7					
13						—	810.6	w	—	—					
14						—	805.6	w	—	—					
15						—	800.3	s	—	—					
16						—	794.3	w	—	—					
17						—	789.8	w	—	—					
18						—	784.4	s	—	—					

TABLE III

Frequencies (cm^{-1}, vac.) of subbands in GeH_3Br

	Subbands of ν_4					Subbands of ν_5					Subbands of ν_6				
K	^RQ_K	^PQ_K	Intensity	$^RQ_K-{}^PQ_K$	$^RQ_K+{}^PQ_K$	^RQ_K	^PQ_K	Intensity	$^RQ_K-{}^PQ_K$	$^RQ_K+{}^PQ_K$	^RQ_K	^PQ_K	Intensity	$^RQ_K-{}^PQ_K$	$^RQ_K+{}^PQ_K$
0	2126.6	—	s	—	—	873.3	—	s	—	—	580.9	—	s	—	—
1	2131.8	—	w	—	—	880.0	868.9	w	11.1	1748.9	584.7	576.4	w	8.3	1161.1
2	2137.0	—	w	—	—	884.9	863.4	w	21.5	1748.3	588.9	572.1	w	16.8	1161.0
3	2142.5	—	s	—	—	890.6	857.6	s	33.0	1748.2	592.8	568.0	s	24.8	1160.8
4	2147.8	—	w	—	—	(897.3)	852.2	w	—	—	597.0	563.7	w	33.3	1160.7
5	2152.7	—	w	—	—	(907.0)	847.0	w	—	—	600.6	560.3	w	40.3	1160.9
6	2158.0	2094.9	s	63.1	4252.9	914.3	—	s	—	—	604.9	556.1	s	48.8	1161.0
7	2163.4	2089.1	w	74.3	4252.5	919.4	—	w	—	—	609.4	552.4	w	57.0	1161.8
8	2168.3	2084.0	w	84.3	4252.3	924.7	—	w	—	—	613.5	548.4	w	65.1	1161.9
9	2173.3	2078.5	s	94.8	4251.8	930.3	—	s	—	—	618.0	544.1	s	73.9	1162.1
10	2178.1	2072.3	w	105.8	4250.4	935.3	815.7	w	119.6	1751.0	622.1	—	w		
11	2182.9	2066.8	w	116.1	4249.7	940.7	810.2	w	130.5	1750.9					
12	2188.2	2061.3	s	126.9	4249.5	946.2	804.2	s	142.0	1750.4					
13	2192.8	2055.1	w	137.7	4247.9	951.5	798.3	w	153.2	1749.8					
14	2197.5	2049.2	w	148.3	4246.7	956.8	792.3	w	164.5	1749.1					
15	2202.5	2043.5	s	159.0	4246.0	962.1	786.4	s	175.7	1748.5					
16	2208.3	2037.5	w	170.8	4245.8	967.4	780.4	w	187.0	1747.8					
17	2212.0	—	w	—	—	972.4	774.2	w	198.2	1746.6					
18	2216.5	—	s	—	—	978.0	768.3	s	209.7	1746.3					

TABLE IV

P–R separations in the parallel bands

Vibration number		*P–R* separations (cm^{-1})	
		GeH_3F	GeH_3Br
1		23.9	12.1
2		26.2	11.8
3		26.6	—
	Average	25.6	12.0
	Calculated	26.4	12.1

of the more intense overlapping parallel bands. The *s,w,w,s* intensity alteration of these subbands was helpful in this analysis, for the band centers lie between strong ${}^RQ_0$ and the weak ${}^PQ_1$ subbranches.

With the exception of ν_5 in the spectrum of GeH_3Br, the analysis of the rotational structure of the perpendicular bands was straightforward. The ${}^RQ_K$ subband peaks in ν_5 were strongly perturbed near $K = 4$, due to Fermi resonance with the combination band $\nu_3+\nu_6$. Thus, the ${}^RQ_4$ and the ${}^RQ_5$ subbands were each split into two lines, the separation of which should theoretically allow an evaluation of the constants of the perturbation. The details of these splittings, however, were rather poorly defined; therefore, the constants were not evaluated. Although ν_3 in GeH_3Br was not observed directly, it was possible to estimate its position from the difference $(\nu_3+\nu_6)-(\nu_6) = 319\ cm^{-1}$. Since the origin of the combination band is not known precisely and the effects of anharmonicity were ignored, the frequency of ν_3 is probably not accurate to better than $\pm 10\ cm^{-1}$. Because of the perturbation of ν_5 at small K and the overlapping of ν_5 by ν_2 at $K = 6$–9, the subband peaks were analyzed using only the frequencies of ${}^RQ_K$ subbands having $K > 10$. The general method used in the rotational analysis is as follows.

Subband frequencies may be represented (14) by the equation

$$[1]\quad \nu_i = \nu_0+[A_v'(1-2\zeta_i)-B_v']\pm 2[A_v'(1-\zeta_i)-B_v']K+[(A_v'-B_v')-(A_v''-B_v'')]K^2,$$

where ν_0 is the band origin, A (or B) $= h/8\pi^2 I_A$ (or $h/8\pi^2 I_B$), ζ is the Coriolis coupling coefficient, and the single and double primes refer to the upper and lower vibration states, respectively. Thus, the fundamental frequency of an E-type band occurs $(A_v'(1-2\zeta_i)-B_v')\ cm^{-1}$ below the strongest subband peak, ${}^RQ_0$. The coefficient of the K term was obtained by plotting $({}^RQ_K-{}^PQ_K)/2$ versus K, the slope being equal to the coefficient, while the slope and intercept of the straight line resulting from a plot of $({}^RQ_K+{}^PQ_K)/2$ against K^2 gave the coefficient of K^2 and the constant term, respectively. A least-squares treatment of the points gave the following equations for the subband frequencies of E-type bands in germyl fluoride and bromide.

For germyl fluoride,

$$[2]\quad \nu_4 = 2131.2\pm 4.85K-0.018K^2$$

$$[3]\quad \nu_5 = 877.0\pm 5.11K-0.004K^2$$

$$[4]\quad \nu_6 = 664.7\pm 3.32K-0.002K^2.$$

For germyl bromide,

$$[5]\quad \nu_4 = 2127.1\pm 5.29K-0.018K^2$$

[6] $$\nu_5 = 875.6 \pm 5.88K - 0.006K^2$$

[7] $$\nu_6 = 580.4 \pm 4.10K + 0.008K^2.$$

For XYZ_3 molecules, the ζ sum rule is

[8] $$\sum_{i=4}^{6} \Delta\nu_i = 6(A' - B') - 2A' \sum_{i=4}^{6} \zeta_i,$$

where

[9] $$\sum_{i=4}^{6} \zeta_i = B'/2A'$$

and

$$\Delta\nu_i = ({}^{R}Q_K - {}^{P}Q_K)/2K;$$

therefore,

[10] $$\sum_{i=4}^{6} \Delta\nu_i = 6A' - 7B'$$

if the variation of A' and B' with the vibrational state is neglected (see eq. [1]). Using the B_0 value from microwave studies for B', A' is readily obtained and represents an average $A' = (A_4' + A_5' + A_6')/3$. By assuming $B' = B''$ for ν_4, ν_5, and ν_6, the coefficients of K^2 in eqs. [2–7] allow an evaluation of A'' and of the various A_i', which then may be substituted in eq. [1] to yield values of ζ_i. The results are listed in Table V.

TABLE V

Rotational constants of GeH_3F and GeH_3Br

Constant	GeH_3F	GeH_3Br
A''	2.612±0.02	2.642±0.03
A'' (microwave)	2.700±0.10	2.532±0.20
A_4'	2.594±0.02	2.624±0.02
A_5'	2.608±0.02	2.636±0.02
A_6'	2.610±0.02	2.650±0.02
B (microwave)	0.335	0.079
ζ_4	−0.064±0.005	−0.038±0.007
ζ_5	−0.108±0.010	−0.145±0.012
ζ_6	0.236±0.005	0.197±0.007

Table VI summarizes the various structural parameters determined by microwave spectroscopy for the fluoride, chloride, and bromide. The microwave A'' constants all

TABLE VI

Structural parameters of GeH_3F, GeH_3Cl, and GeH_3Br

Parameter	GeH_3F	GeH_3Cl	GeH_3Br
d(Ge—H)*	1.52±0.03	1.52±0.03	1.55±0.05
d(Ge—X)*	1.73±0.01	2.148±0.003	2.297±0.001
θ(H—Ge—H)*	109°54′±90′	110°54′±90′	112°±1°
A''*	2.700±0.10	2.667±0.07	2.532±0.2
A''	2.612±0.02	2.603±0.006	2.642±0.03

*Microwave results.

agree within experimental error with those determined by infrared methods, although the former tend to have somewhat higher values than the latter. This is not unexpected

since the microwave values were calculated for the ground state and the infrared constants were determined on the assumption that $B_v' = B_v''$ for all perpendicular vibrations.

Thermodynamic Functions

The thermodynamic values listed in Table VII for germyl fluoride and bromide,

TABLE VII

Thermodynamic functions* of GeH_3F and GeH_3Br

Temperature (° K)	GeH_3F				GeH_3Br			
	$-(F°-E_0°)/T$	$(H°-E_0°)/T$	$S°$	$C_p°$	$-(F°-E_0°)/T$	$(H°-E_0°)/T$	$S°$	$C_p°$
200	47.52	8.23	55.77	9.50	52.09	8.78	60.88	10.81
298.16	50.96	9.10	60.08	12.23	55.80	9.89	65.71	13.42
400	53.80	10.21	64.03	14.63	58.88	11.07	69.96	15.52
500	56.20	11.29	67.50	16.45	61.47	12.12	73.61	17.11
600	58.35	12.27	70.64	17.90	63.77	13.07	76.85	18.41
700	60.31	13.17	73.49	19.09	65.85	13.91	79.78	19.49
800	62.12	13.97	76.11	20.08	67.76	14.67	82.44	20.39
900	63.81	14.70	78.53	20.89	69.53	15.35	84.89	21.14
1000	65.40	15.35	80.77	21.56	71.18	15.96	87.16	21.77

*Units are cal $deg^{-1}mole^{-1}$.

respectively, were calculated on a rigid-rotator, harmonic-oscillator approximation and are given for the ideal gas state and 1 atm pressure (14).

ACKNOWLEDGMENTS

We are grateful to the National Research Council for Studentships (to J. E. G.), a Postdoctorate Fellowship (to T. N. S.), and an Annual Grant (to (M. O.). We thank Dr. D. Edelson of the Bell Telephone Laboratories, Incorporated, for writing the program for computation of the thermodynamic functions on an IBM 7090 computer.

REFERENCES

1. D. F. Heath, J. W. Linnett, and P. J. Wheatley. Trans. Faraday Soc. **46**, 137 (1950).
2. L. P. Lindeman and M. K. Wilson. J. Chem. Phys. **22**, 1723 (1954).
3. D. A. Dows and R. M. Hexter. J. Chem. Phys. **24**, 1029 (1956).
4. R. C. Lord and C. M. Steese. J. Chem. Phys. **22**, 542 (1954).
5. F. E. Brinckman and F. G. A. Stone. J. Inorg. & Nuclear Chem. **11**, 24 (1959).
6. J. E. Griffiths and K. B. McAfee, Jr. Proc. Chem. Soc. 456 (1961).
7. B. P. Dailey, J. M. Mays, and C. H. Townes. Phys. Rev. **76**, 136 (1949).
8. A. H. Sharbaugh, B. S. Pritchard, V. G. Thomas, J. M. Mays, and B. P. Dailey. Phys. Rev. **79**, 189L (1950).
9. S. Sujishi and S. Witz. J. Am. Chem. Soc. **76**, 4631 (1954).
10. L. M. Dennis and P. R. Judy. J. Am. Chem. Soc. **51**, 2321 (1929).
11. T. N. Srivastava and M. Onyszchuk. Proc. Chem. Soc. 205 (1961).
12. T. N. Srivastava, J. E. Griffiths, and M. Onyszchuk. Unpublished work.
13. S. L. Gerhard and D. M. Dennison. Phys. Rev. **43**, 197 (1933).
14. G. Herzberg. Infrared and raman spectra. D. Van Nostrand Co., Inc., New York. 1945. pp. 429, 501.

ARSENIDES OF THE TRANSITION METALS

VI. ELECTRICAL AND MAGNETIC PROPERTIES OF THE TRIARSENIDES[1]

C. M. PLEASS[2] AND R. D. HEYDING

Division of Applied Chemistry, National Research Council, Ottawa, Canada

Received November 29, 1961

ABSTRACT

Homogeneity limits at 750° C of the ternary DO_2 triarsenides $(Ni,Co)As_3$, $(Fe,Co)As_3$, and $(Fe,Ni)As_3$ have been established. The electrical and magnetic properties of these systems and the triarsenides of cobalt, rhodium, and iridium have been examined. The results are:

System	Limits	Magnetic properties	Electrical properties
$CoAs_3$	—	$\chi_g^{25°} = -0.158\times10^{-6}$	Semiconductor
$RhAs_3$	—	$\chi_g^{25°} = -0.219\times10^{-6}$	Semiconductor
$IrAs_3$	—	$\chi_g^{25°} = -0.253\times10^{-6}$	—
$Ni_xCo_{1-x}As_3$	$0 \leqslant x \leqslant 0.65$	$p_{eff} = 0.8$–$1.2\ \mu_B$/Ni	Ni donor atom
$Fe_xCo_{1-x}As_3$	$0 \leqslant x \leqslant 0.16$	$p_{eff} = 1.9$–$2.7\ \mu_B$/Fe	Fe donor atom
$Fe_xNi_{1-x}As_3$	$0.25 \leqslant x \leqslant 0.46$	Weak paramagnetism	Semi- to metallic

These data are discussed with reference to the bonding model proposed by Dudkin and Abrikosov. The model is satisfactory for the binary compounds and the Ni/Co system, but not for the Fe/Co and Fe/Ni systems.

INTRODUCTION

Skutterudite ($CoAs_3$, DO_2) type structures are found among the phosphides, arsenides, and antimonides of cobalt, rhodium, and iridium, as well as the phosphides of nickel and palladium (1). In this lattice each metal atom is surrounded octahedrally by six pnigogens,[3] while each of the latter is shared by two metal atoms and has two other pnigogens as nearest neighbors, forming a distorted tetrahedral environment. These compounds and the pyrite-type diarsenides $PtAs_2$ and $PdAs_2$ are the only transition metal pnictides in which the metal atoms are entirely surrounded by pnigogens, precluding direct metal–metal interaction.

Dudkin and Abrikosov (2–5) have proposed an electronic model for $CoSb_3$ which they have used with considerable success in describing the electrical properties of doped and undoped specimens. They have assumed that the bonds in these compounds are semiconducting bonds as defined by Mooser and Pearson (6, 7). In this model each antimony atom forms single covalent bonds with its two nearest antimony neighbors, and half bonds with the two metal neighbors, as indicated in Fig. 1. The antimony $5s$ and $5p$ orbitals are completely occupied, and are assumed to form sp^3 l.c.a.o. orbitals in accord with the distorted tetrahedral environment of the antimony atoms. Each metal atom in turn forms half bonds with the six pnigogen atoms which surround it, the three valence electrons required occupying octahedral d^2sp^3 hybrid orbitals. Although the metal bonding orbitals are only partially occupied they do not overlap other metal orbitals and metallic conduction would not be expected to occur.

[1]*Issued as N.R.C. No. 6697.*
[2]*N.R.C. Postdoctorate Fellow. Present address: Bell Telephone Laboratories, Murray Hill, N.J., U.S.A.*
[3]*Group VA elements:* N, P, As, Sb, Bi.

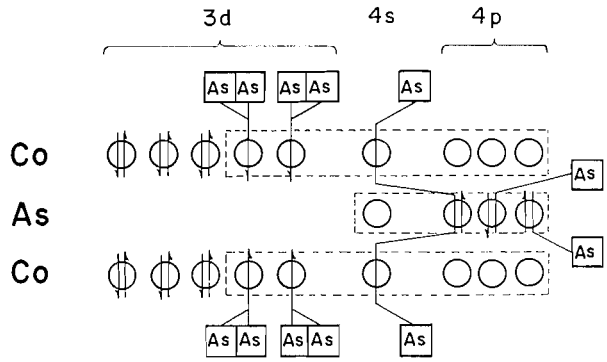

FIG. 1. Bonding model of $CoAs_3$ according to Dudkin and Abrikosov (5).

If this model is correct, certain predictions can be made concerning the magnetic and electrical properties of these compounds. The cobalt family of tripnictides, Co(Rh,Ir)P_3, Co(Rh,Ir)As_3, Co(Rh,Ir)Sb_3, should be diamagnetic and semiconducting. Indeed, both $CoSb_3$ (5) and $CoAs_3$ (8) are semiconductors, the latter having an energy gap of approximately 0.25 ev. Very recently Kjekshus and Pedersen have reported that $IrAs_3$ and $IrSb_3$ are diamagnetic (9). Similarly, the iron family analogues, with one less *d* electron, should be paramagnetic and semiconducting. In the nickel family analogues, the additional metal electron cannot be accepted by the *d* orbitals, which are completely occupied, and must be assumed to occupy a higher energy level, possibly within the conduction band; consequently these compounds should be weakly paramagnetic and metallic conductors.

With the exception of NiP_3 and PdP_3 (10), the iron and nickel analogues have not been prepared synthetically, nor do they exist in nature. However, cobalt is often partially replaced by nickel and iron in natural skutterudites (11), and Dudkin has established the substitutional solid solution limits of iron and nickel in $CoSb_3$ (2, 5). We have determined the substitution limits in the systems $Fe_xCo_{1-x}As_3$, $Ni_xCo_{1-x}As_3$, and $Fe_xNi_{1-x}As_3$ at 750° C in the presence of excess arsenic. Unit cell dimensions, magnetic susceptibilities, electrical conductances, and thermal e.m.f. polarities of these solid solutions and of the binary compounds $CoAs_3$, $RhAs_3$, and $IrAs_3$ have been determined for their intrinsic interest and as a measure of the validity of Dudkin's model.

EXPERIMENTAL

1. *Sample Preparation*

Alloys were prepared by the direct interaction of arsenic and metal powders in sealed, evacuated tubes. Iron, cobalt, and nickel sponges were supplied by Johnson, Matthey and Co., with the following spectroscopic analyses in p.p.m.:

	Mn	Fe	Co	Ni	Cu	Other
Fe	3	X	—	2	—	4
Co	—	—	X	1	2	5
Ni	—	2	2	X	—	8

Rhodium and iridium sponge supplied by Baker and Co. were found by spectroscopic analysis to contain slight traces of Ca, Cu, Si, and Fe and Sb, Si, and Ca, respectively. The sponge was reduced in purified hydrogen at 600° C prior to use.

Cominco high-purity arsenic, containing Ca, Cu, Pb, Mg, and S, each less than 0.1 p.p.m., and Si less than 0.2 p.p.m., was sublimed *in vacuo* at 450° C (i.e. converted to an amorphous form) to facilitate grinding, and stored *in vacuo*.

Specimens were prepared in 5- to 10-g quantities by weighing calculated quantities of metal and arsenic powders in air and sealing in pyrex tubes under high vacuum with 5–10% excess arsenic to suppress dissociation. After the specimen was heated for 24 hours at 400–450° C the product was removed, ground, and resealed in vycor or clear quartz for a series of 6- to 7-day annealing periods at 750° C. At the end of each annealing period the alloy was slow-cooled in the furnace, reground, and sampled for a Debye–Scherrer pattern. Annealing was repeated until all diffraction lines due to extraneous phases had been eliminated and consecutive photographs showed no change in lattice parameters. At temperatures below 750° C equilibrium was attained only slowly, and at higher temperatures most of the alloys suffered peritectic decomposition.

The excess arsenic was removed by maintaining a very small temperature gradient along the sample tube during annealing, thus causing the arsenic to crystallize in the void space away from the bulk of the sample.

Debye–Scherrer patterns were obtained in 11.46-cm Norelco cameras using Co K_α radiation.

Resistivity and Seebeck coefficient specimens were prepared by slow sintering at 750° C in the presence of excess arsenic. Finely ground partially reacted alloy was tamped firmly into 4-mm I.D. heavy wall vitreosil tubing, forming a rod 5–12 cm in length. Excess arsenic was added above the specimen, and the tube evacuated, sealed, and sintered for 6–7 days at 750° C. The rod was pushed from the capillary, sampled for diffraction pattern, and resealed in a standard annealing tube. Annealing then followed the course previously outlined.

2. Magnetic Susceptibilities

Susceptibilities were determined by the Curie method using Henry pole-caps and the experimental arrangement described in an earlier paper (10). The atmosphere in the temperature control system and balance was dry, purified nitrogen at 770 mm pressure. Powdered specimens of about 1 g were held in a quartz bucket for study in the temperature region 83° to 670° K. Under these experimental conditions the susceptibility of crystalline arsenic was determined with no tarnishing of the crystal faces or detectable loss in weight due to vaporization of As_2O_3 or arsenic itself. For higher temperatures the bucket was replaced by a sealed, flat-bottomed quartz ampoule of sufficient length that it could be opened and resealed in a region exposed to negligible field. The force on the specimen was determined at three magnet currents, the minimum field to which any part of the specimen was subjected being ca. 8000 gauss. The apparent susceptibilities were plotted against $1/(H_{max}+H_{min})$ for specimens showing field dependence, and the data extrapolated to infinite field strength to eliminate the effect of ferromagnetic impurities.

3. Electrical Properties

The resistivity of sintered specimens was determined in a simple d-c. circuit over the temperature range 80°–670° K. Current from a storage cell was passed through the specimen in series with a standard resistance, and the potential drop across a known length of sample measured using null-point probes. The direction of the current was reversed at each experimental point and the mean potential drop determined to eliminate stray contact and thermal voltages. Measurements were made with the specimen under vacuum above room temperature and under a small nitrogen pressure below room temperature.

The Seebeck coefficients of these compounds versus copper were determined for $CoAs_3$ specimens only. Calibrated copper/constantan thermocouples silver-soldered into pure copper hemispheres of ca. 0.35-mm D. made spring-loaded contact with the ends of the sintered specimen. The sample was held by a boron nitride sleeve which also served to support small differential heaters at each end of the specimen. The whole was sealed *in vacuo* and thermostated for measurements from 80° to 670° K. A minimum of 12 hours was allowed for the apparatus to come to equilibrium under any given set of conditions.

A very simple apparatus showing the polarity of the hot junction of the specimen/copper couple was used to determine the type of conduction occurring in the iron- and nickel-substituted semiconductors.

RESULTS AND DISCUSSION

1. Limits of Solid Solution Regions and Stoichiometry

The limits to which iron and nickel can be substituted for cobalt in $CoAs_3$, and iron for nickel in the hypothetical compound $NiAs_3$ at 750° C, as determined by Debye–Scherrer patterns, are given in Table I. In this table comparison is made with the limits and unit cell dimensions observed by Holmes in naturally occurring skutterudites (8). The unit cell dimensions of the solid solutions are, within experimental error, linear functions of the composition (Fig. 2).

TABLE I

Substitution limits at 750° C, and room-temperature lattice dimensions in iron- and nickel-substituted $CoAs_3$

System	Observed limits	Mineral limits (Holmes (11))	Specimen	Unit cell, obs. (Å)	Mineral (11)
$Fe_xCo_{1-x}As_3$	$0 \leqslant x \leqslant 0.16$	$0 \leqslant x \leqslant 0.25$	$CoAs_3$	8.206±2	8.187
$Ni_xCo_{1-x}As_3$	$0 \leqslant x \leqslant 0.65$	$0 \leqslant x \leqslant 0.50$	$Ni_{0.25}Co_{0.75}As_3$	8.236±2	8.207
$Fe_xNi_{1-x}As_3$	$0.25 \leqslant x \leqslant 0.46$	—	$Fe_{0.46}Ni_{0.54}As_3$	8.256±2	8.235

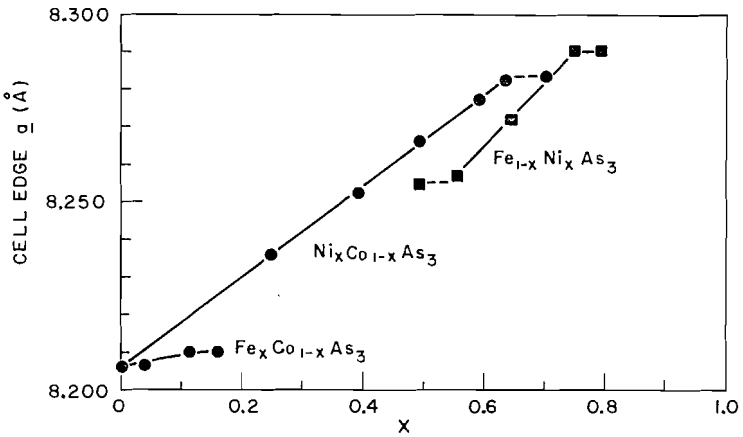

FIG. 2. Cubic unit cell dimensions of substituted triarsenides as a function of composition.

Throughout this study total analyses have indicated persistent deviations from stoichiometry. Indeed, specimens annealed at 750° C are more properly represented by the formula $(M_xM'_{1-x})As_{3-y}$, with $0 \leqslant y \leqslant 0.20$. The deviation from stoichiometry does not appear to be a function of the degree of substitution, nor is there any detectable variation in lattice dimensions with arsenic content. Analyses of some 40 alloys do indicate, however, that departure from ideality in the $(Fe,Co)As_3$ system is significantly greater than in the other three systems (Table II). In all systems the deviations are considerably less than have been observed in natural skutterudites (11).

TABLE II

Departure from stoichiometry

(Specimens annealed at 750° C in the presence of excess As)

System	$(3-y)_{min}$	$(3-y)_{max}$	$(3-y)_{mean}$
$CoAs_{3-y}$	2.946	2.962	2.955
$(Ni,Co)As_{3-y}$	2.91	2.99	2.95
$(Fe,Co)As_{3-y}$	2.66	2.94	2.87
$(Fe,Ni)As_{3-y}$	2.91	2.98	2.94

We were unable to devise a satisfactory technique for density determinations on these compounds; consequently it is not possible to say whether or not arsenic vacancies in the lattice are occupied by metal atoms.

Stoichiometric $CoAs_3$ can be prepared by prolonged annealing at 650° C in the presence of excess arsenic. The properties of stoichiometric $CoAs_3$ discussed below were obtained on specimens prepared at this lower temperature.

2. Magnetic and Electrical Properties

(a) $CoAs_3$, $RhAs_3$, and $IrAs_3$

The binary triarsenides are diamagnetic, as predicted by Dudkin's model. Room temperature (296° K) susceptibilities at infinite field strength are:

$$CoAs_3: \quad \chi_g^\infty = -0.158 \pm 0.002 \times 10^{-6} \text{ e.m.u./g};$$
$$RhAs_3: \quad \chi_g^\infty = -0.219 \pm 0.002 \times 10^{-6} \text{ e.m.u./g};$$
$$IrAs_3: \quad \chi_g^\infty = -0.253 \pm 0.002 \times 10^{-6} \text{ e.m.u./g}.$$

The susceptibilities of all three compounds are slightly temperature dependent, as shown in Fig. 3. The susceptibilities of $IrAs_3$ reported by Kjekshus and Pedersen (9) have

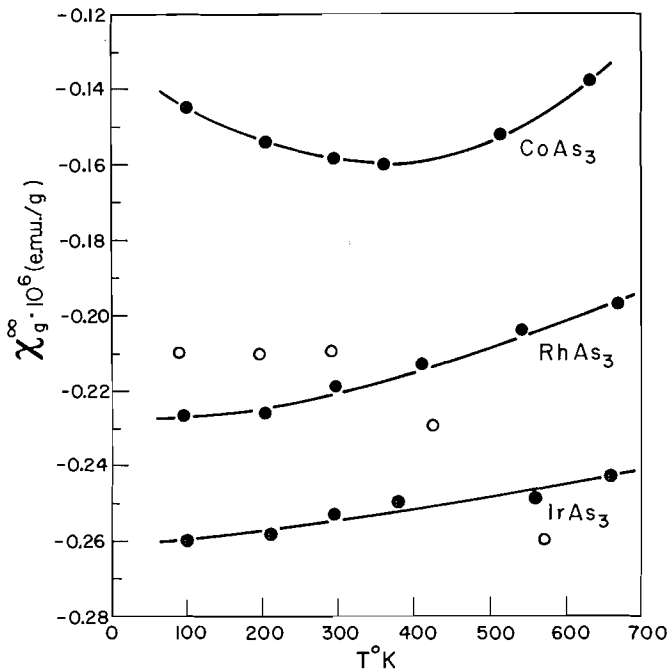

FIG. 3. Mass susceptibilities of $CoAs_3$, $RhAs_3$, and $IrAs_3$ at infinite field strength in c.g.s. e.m.u./g. Open points are the susceptibilities of $IrAs_3$ recorded by Kjekshus and Pedersen (9).

been included in this figure. Since the Gouy method was used by these authors and extrapolation of experimental susceptibilities to infinite field strength could not have been made, agreement with our values is not unsatisfactory.

Typical temperature/resistivity curves are shown in Fig. 4(*a*). The data represented were obtained on a stoichiometric specimen of $CoAs_3$, although deviations from stoichiometry did not affect the resistivity within experimental uncertainty. All three compounds were found to be *p*-type semiconductors. The thermal e.m.f. of $CoAs_3$ measured against copper increases from 10 μv/°C at 100° K to a maximum of 140 μv/°C at 320° K, and then decreases to 85 μv/°C at 600° K.

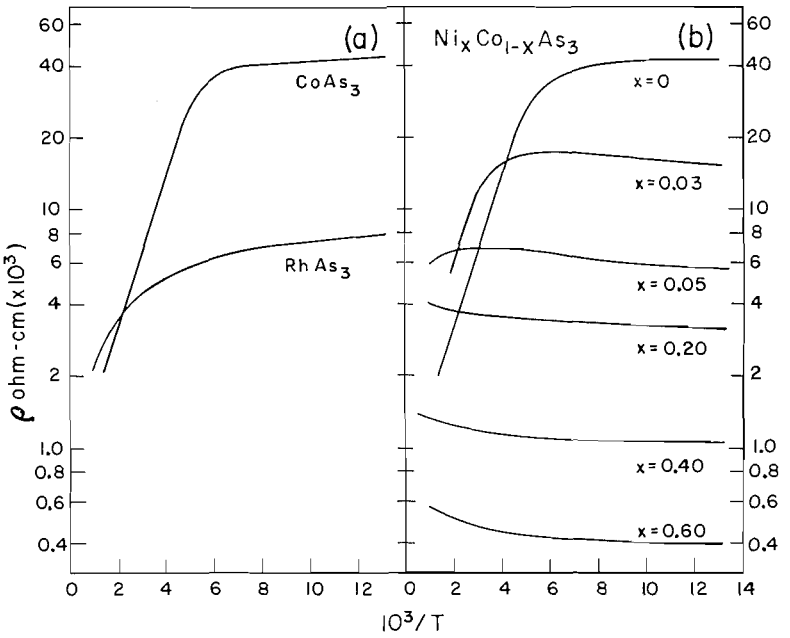

FIG. 4. (*a*) Resistivity of stoichiometric binary triarsenides as a function of temperature. (*b*) Resistivity of nickel-substituted cobalt triarsenide as a function of temperature and composition.

The decrease in diamagnetic susceptibilities observed at higher temperatures is consistent with the electrical behavior of these compounds. With increasing temperature, the number of electrons in the conduction band increases, and consequently the conductivity and the paramagnetic contribution due to the conduction electrons also increase.

(b) The System $Ni_xCo_{1-x}As_{3-y}$

The effect of nickel substitution on the electrical resistivity of $CoAs_3$ is illustrated in Fig. 4(*b*). In agreement with the model, nickel behaves as a donor impurity. At appreciable nickel concentrations semiconducting properties are lost and the system becomes metallic in character. Conduction becomes *n* type with 1% substitution of nickel for cobalt.

Susceptibilities of three specimens with 3, 20, and 40% substitution are given in Table III. At 3% substitution the triarsenide is weakly diamagnetic except at low temperatures; at higher concentrations the paramagnetic contribution of the conduction electrons is sufficient to make the overall susceptibility positive. Reciprocal susceptibilities are plotted as a function of temperature in Fig. 5. At 20% substitution the effective moment per nickel atom is 0.804 μ_B with a Weiss constant of $-290°$ K, while at 40% substitution $p_{eff} = 1.24\ \mu_B$, and $\theta_w = -1200°$ K.

(c) The System $Fe_xCo_{1-x}As_{3-y}$

Susceptibilities of three specimens in this system are given in Table IV. Observed susceptibilities are the sum of individual paramagnetic contributions due to conduction and unpaired electrons (if any), and diamagnetic contributions due to the arsenic, cobalt, and iron cores. At low iron concentrations the diamagnetic terms will be of the same order of magnitude as the paramagnetic terms, and to recognize the temperature

TABLE III

Mass susceptibilities of $Ni_xCo_{1-x}As_3$ (c.g.s. e.m.u./g)

$x = 0.03$		$x = 0.20$		$x = 0.40$	
T (°K)	$\chi_g^\infty \times 10^6$	T (°K)	$\chi_g^\infty \times 10^6$	T (°K)	$\chi_g^\infty \times 10^6$
106	0.0073	96	0.118	89	0.215
198	−0.056	132	0.106	201	0.196
255	−0.067	189	0.0941	250	0.189
350	−0.079	225	0.0856	380	0.172
472	−0.095	256	0.0832	499	0.160
590	−0.105	366	0.0708	602	0.152
		442	0.0638	665	0.148
		497	0.0568		

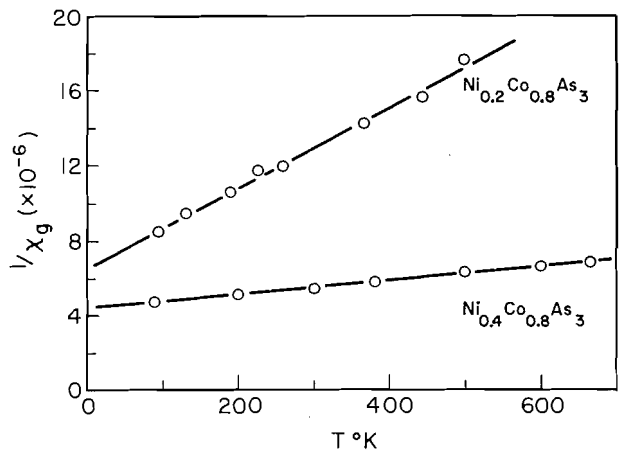

FIG. 5. Reciprocal susceptibility of nickel-substituted cobalt triarsenide as a function of temperature and composition.

dependence of the paramagnetic terms some correction for diamagnetic susceptibility must be made. As a first approximation we have assumed the diamagnetic terms in $Fe_xCo_{1-x}As_3$ to equal the diamagnetic susceptibility of $CoAs_3$ itself. The corrected or paramagnetic susceptibilities, χ_p, given in Table IV were obtained by subtracting the mass susceptibilities of $CoAs_3$ at the appropriate temperatures (cf. Fig. 3).

TABLE IV

Mass susceptibilities of $Fe_xCo_{1-x}As_3$ (c.g.s. e.m.u./g)

$x = 0.059$			$x = 0.107$			$x = 0.151$		
T	$\chi_g^\infty \times 10^6$	$\chi_p^\infty \times 10^6$	T	$\chi_g^\infty \times 10^6$	$\chi_p^\infty \times 10^6$	T	$\chi_g^\infty \times 10^6$	$\chi_p^\infty \times 10^6$
97	0.259	0.399	141	0.766	0.907	93	0.785	0.929
194	0.098	0.252	181	0.671	0.830	152	0.545	0.695
271	0.056	0.212	216	0.593	0.750	191	0.432	0.585
360	0.023	0.183	260	0.524	0.679	246	0.356	0.512
598	0.000	0.143	400	0.375	0.528	371	0.250	0.410
688	0.000	0.128	615	0.265	0.412	501	0.183	0.337
						653	0.160	0.295

The reciprocals of these paramagnetic susceptibilities are plotted as a function of temperature in Fig. 6. Effective moments per iron atom obtained from this graph are given in Table V.

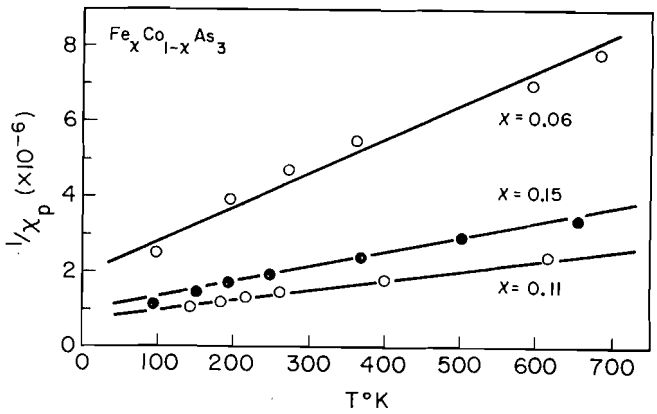

FIG. 6. Reciprocal of 'paramagnetic' susceptibility of iron-substituted cobalt triarsenides as a function of temperature and composition.

TABLE V

Effective moments per iron atom in $Fe_xCo_{1-x}As_{3-y}$

x	$3-y$	C	θ_w (°K)	p_{eff} (μ_B)
0.0592	2.915	0.542	−215	2.06
0.1070	2.890	0.935	−290	2.71
0.1508	2.890	0.480	−250	1.88

These data are consistent with an unpaired electron in Fe and an appreciable conduction electron contribution. This is in agreement with the model which requires an unpaired electron in a non-bonding d orbital. The model predicts that no appreciable change in semiconducting character should occur on the substitution of iron for cobalt. In fact, substitution of iron has a profound effect on the resistivity, as shown in Fig. 7(a). Metallic behavior results with the substitution of as little as 1% of the cobalt by iron, and additional substitution increases the resistivity. At 1% substitution conduction is p type, and at higher concentrations, n type.

Two possible explanations of this behavior can be considered. If the distribution of electrons in bonding and non-bonding levels is correct, conduction may occur via d band interaction. This implies that the Mooser–Pearson rules cannot be applied to these systems, and refutes the basic assumption in Dudkin's model. Alternatively, if d^3 hybrids rather than d^2sp^3 hybrids are the prominent bonding nodes about the iron atom, there will be two fully occupied non-bonding d orbitals, and the eighth electron may occupy the 4s level within the conduction band. One would expect the moment of this electron to be partially quenched and the effective moment to be less than has been observed; some decrease in effective moment with increasing iron concentration is indicated, but only after substitution of one iron atom in each unit cell has been made.

(d) The System $Fe_xNi_{1-x}As_{3-y}$

The model predicts that these compounds should be strongly paramagnetic due to the unpaired spin in Fe, and metallic in conduction due to the conduction electron in

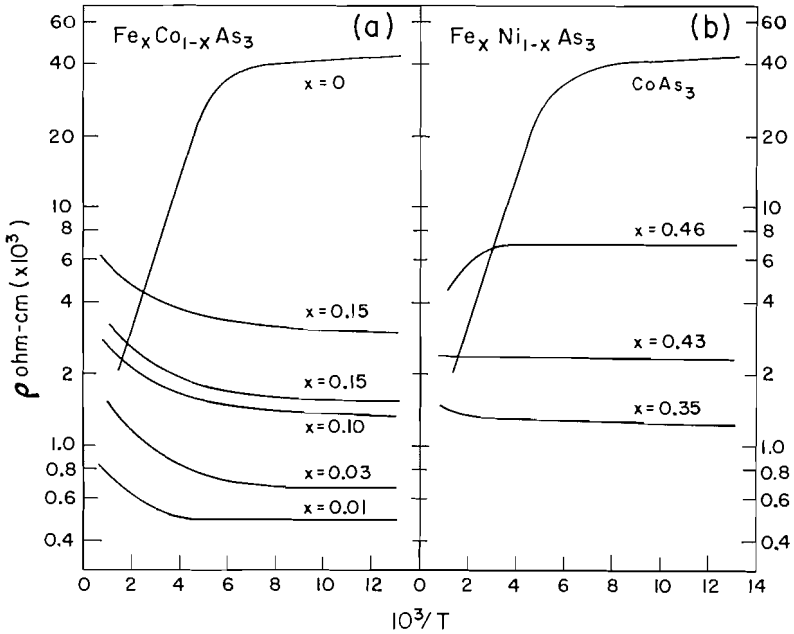

FIG. 7. (*a*) Resistivity of iron-substituted cobalt triarsenide as a function of temperature and composition; data for $x = 0.15$ were obtained with two separate alloys. (*b*) Resistivity of iron/nickel triarsenides as a function of composition and temperature.

Ni. Here again the model is not supported by experimental evidence. The compound with 46% Fe (i.e., at the iron-rich limit of the solid solution region) exhibits semiconducting character (cf. Fig. 7(*b*)). Conduction is *n* type. With increasing substitution of nickel for iron the resistivity decreases and the system becomes metallic.

The mass susceptibilities (Table VI) are small, and the moment per metal atom is much less than one might expect in comparison with the Fe/Co system. In Fig. 8 the

TABLE VI

Mass susceptibilities of $Fe_xNi_{1-x}As_3$ (c.g.s. e.m.u./g)

$x = 0.45$		$x = 0.35$		$x = 0.25$	
T (°K)	$\chi_g^{\infty} \times 10^6$	T (°K)	$\chi_g^{\infty} \times 10^6$	T (°K)	$\chi_g^{\infty} \times 10^6$
102	0.0664	89	0.146	96	0.164
158	0.0512	179	0.131	158	0.147
207	0.0425	197	0.127	196	0.142
230	0.0395	246	0.118	245	0.137
258	0.0363	342	0.118	348	0.133
296	0.0322	495	0.115	515	0.130
364	0.0307	591	0.115	568	0.130
473	0.0305	659	0.115	659	0.131
592	0.0344	693	0.120		
685	0.0368				

susceptibilities are compared with Ni/Co and Fe/Co alloys and with $CoAs_3$. The temperature dependence has the same form as that of $CoAs_3$ and the Ni/Co compounds; indeed, nickel and iron appear to form pairs which are equivalent in magnetic behavior

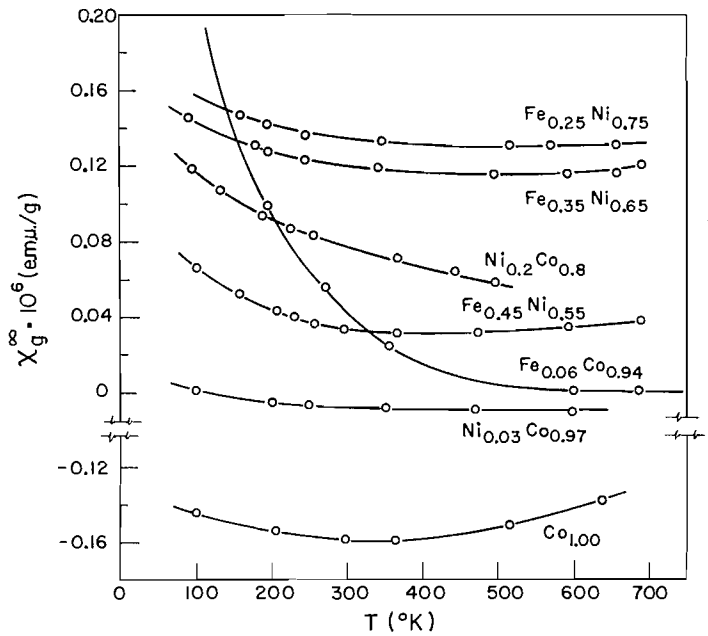

FIG. 8. Comparison of mass susceptibilities of $M_xM'_{1-x}As_3$ alloys as a function of temperature.

to cobalt in the nickel/cobalt system. Writing the general formula $Fe_xNi_{1-x}As_3$ in the form $Ni_{1-2x}(Fe,Ni)_{2x}As_3$, paramagnetic susceptibilities increase in the order $Ni_{0.03}Co_{0.97}$, $Ni_{0.1}(Fe,Ni)_{0.9}$, $Ni_{0.2}Co_{0.8}$, $Ni_{0.3}(Fe,Ni)_{0.7}$, with $(Fe,Ni)_{2x}$ roughly equivalent to Co_{2x}.

Even allowing that conductance measurements on sintered powders do not give reliable values of the resistivity, the same analogy can be drawn in the electrical properties of the Ni/Fe and Ni/Co alloys. There is a gradual transition from semiconducting to metallic behavior, and a decrease in resistivity, in the order $Ni_{0.03}Co_{0.97}$, $Ni_{0.05}Co_{0.95}$, $Ni_{0.08}(Fe,Ni)_{0.92}$, $Ni_{0.2}Co_{0.8}$, $Ni_{0.14}(Fe,Ni)_{0.86}$, $Ni_{0.3}(Fe,Ni)_{0.7}$, $Ni_{0.4}Co_{0.6}$ (cf. Figs. 4(*b*) and 7(*b*)).

It is tempting to propose that electron transfer occurs, and that (Fe^-Ni^+) pairs are formed. In terms of Dudkin's model, this simply requires that the conduction electron in Ni occupy the unpaired non-bonding *d* orbital in Fe. We feel that there is not sufficient evidence to support such a proposal. If it could be shown that an $Fe_{0.5}Ni_{0.5}$ tripnictide is diamagnetic, and that in an iron-rich region magnetic and electrical properties are analogous to those of an iron-substituted cobalt series, some form of electron transfer might be accepted as the basis of a model.

SUMMARY

1. The DO_2 triarsenides $CoAs_3$, $RhAs_3$, and $IrAs_3$ are diamagnetic semiconductors.

2. Substitution of Ni for Co in $CoAs_3$ causes a linear increase in unit cell dimensions. Nickel acts as a donor impurity. With nickel substitution greater than ca. 10%, conductance is metallic in nature. The effective moment per nickel atom is equivalent to less than one unpaired electron, and the Weiss constant in nickel-rich specimens is large and negative. In electrical and magnetic properties nickel behaves like cobalt with an additional electron in the conduction band.

3. Substitution of Fe for Co in $CoAs_3$ increases unit cell dimensions. Iron acts as a donor impurity, with less than 1% substitution leading to metallic character. The effective moment per iron atom is equivalent to between one and two unpaired electrons, and the Weiss constant is relatively small and negative. Iron in this system does not behave as cobalt with one less electron in a non-bonding orbital.

4. In the DO_2 $(Fe,Ni)As_3$ ternary system, iron appears to be in a different state than in the $(Fe,Co)As_3$ system. The effective moment per iron atom is less than one unpaired electron. The properties of this system are comparable to those of the $(Ni,Co)As_3$ system, implying that iron/nickel interaction results in behavior very similar to that exhibited by cobalt.

5. The model proposed by Dudkin describes adequately the electrical and magnetic properties of the binary triarsenides and the nickel/cobalt triarsenides. It is less satisfactory when applied to the iron/cobalt and iron/nickel triarsenides.

ACKNOWLEDGMENTS

We are indebted to Mr. G. J. G. Despault for assistance in preparing specimens, Miss M. McLellan for assistance in obtaining Debye–Scherrer patterns, and Mr. S. L. Bennett for much of the resistivity data.

REFERENCES

1. R. D. Heyding and L. D. Calvert. Can. J. Chem. **39**, 955 (1961).
2. L. D. Dudkin. Soviet Phys.–Tech. Phys. **3**, 216 (1958).
3. L. D. Dudkin and N. Kh. Abrikosov. Zhur. Neorg. Khim. **1**, 2096 (1956).
4. L. D. Dudkin and N. Kh. Abrikosov. Zhur. Neorg. Khim. **2**, 212 (1957).
5. L. D. Dudkin and N. Kh. Abrikosov. Soviet Phys., Solid State, **1**, 126 (1959).
6. E. Mooser and W. B. Pearson. Phys. Rev. **101**, 1608 (1956).
7. E. Mooser and W. B. Pearson. J. Electronics, **1**, 629 (1956).
8. F. Hulliger. Thesis E.T.H., Zurich. 1959. p. 636.
9. A. Kjekshus and G. Pedersen. Acta Cryst. **14**, 1065 (1961).
10. S. Rundqvist. Acta Chem. Scand. **15**, 451 (1961).
11. R. J. Holmes. Bull. Geol. Soc. Am. **58**, 299 (1947).

THERMAL CONDUCTION IN A TIAN–CALVET MICROCALORIMETER[1]

L. BENJAMIN[2] AND G. C. BENSON
Division of Pure Chemistry, National Research Council, Ottawa, Canada
Received November 30, 1961

ABSTRACT

The transfer of heat in a Tian–Calvet microcalorimeter is treated theoretically. Although quantitative agreement between predicted behavior and experimental observation is not obtained, the qualitative features brought out by the considerations should be helpful in the design and use of this type of calorimeter.

INTRODUCTION

Several microcalorimeters of the Tian–Calvet type have been described in the literature and are being used to study small heat effects and reaction rates in both chemical and biological systems (for a survey and bibliography see Calvet and Prat (1) or Rossini (2)). Equations relating to the use of such instruments have been derived (3) on the basis of thermal conduction theory and applied to experiment (4, 5) by the empirical fitting of constants in the equations. A description is here given of a somewhat different approach to the same problem in which an attempt is made to calculate a priori the behavior of a microcalorimeter from the geometry and physical properties of the materials, using certain integrals tabulated recently (6). Although such a theory is necessarily approximate, the results should be helpful in the design of microcalorimeters with specified time constants and in the use of such instruments. Results of the theory are compared with experimental curves obtained with a microcalorimeter in operation in this laboratory.

CONDUCTIVITY THEORY

Detailed accounts of the construction of microcalorimeters of the Tian–Calvet type have been given elsewhere (1, 2, 7). For the purpose of the present treatment only brief reference will be made to the principal features of the calorimeter in this laboratory since the design of this equipment follows closely that described by Attree *et al.* (7). A Dural block with tapered holes to accommodate four thermopile units is held at a constant temperature inside five concentric cans contained in an air thermostat. Each thermopile is constructed between a silver thimble and a set of Dural rings separated by teflon spacers, the resulting unit fitting snugly into one of the holes in the block. The photograph (Fig. 1) shows one of these units, inverted, with 4 of the 12 rings in position; there are 12 rows of 6 junctions and an additional junction at the bottom of the thimble. Two such units are placed in diametrically opposite holes in the block and the thermopiles connected in opposition. The resulting e.m.f. and its integral with time are amplified and recorded as in reference 7.

For the purposes of the theory, heat effects of interest are considered to occur in one of the thimbles. In Fig. 2 the temperature of the thimble, $V(t)$, is assumed uniform, as would be the case with a well-stirred fluid content or if the thimble were a perfect conductor; a is the inner radius of the Dural rings and $v(r,t)$ is the temperature at a distance r

[1]*Issued as N.R.C. No. 6692.*
[2]*National Research Council of Canada Postdoctorate Fellow 1958–60. Present address: Miami Valley Laboratories, The Procter and Gamble Company, Cincinnati 39, Ohio, U.S.A.*

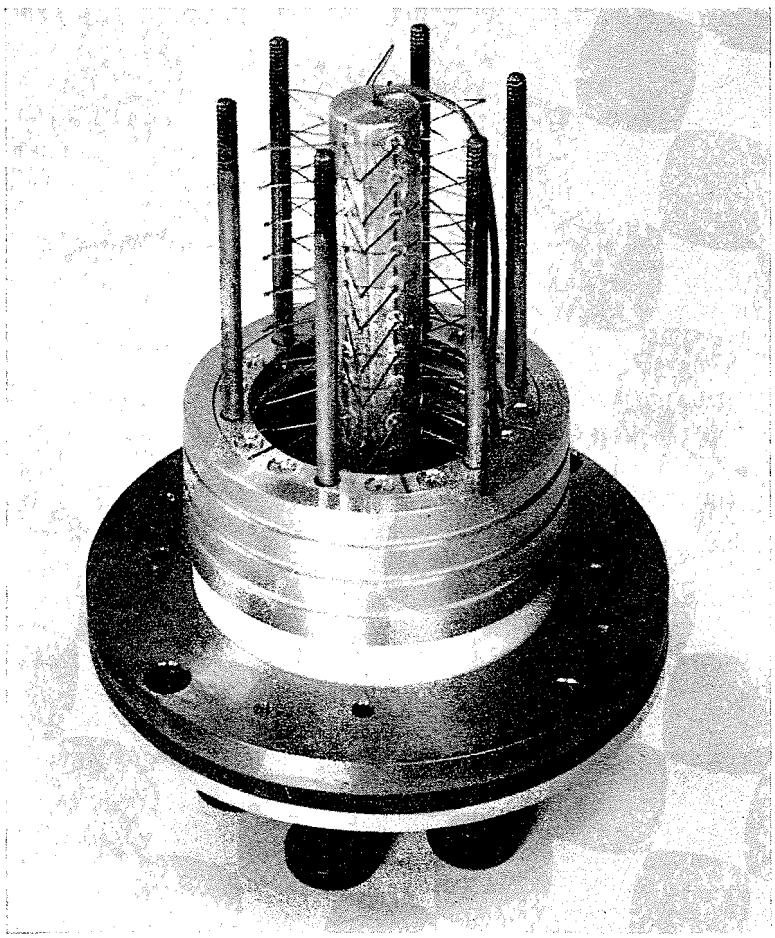

FIG. 1. Photograph of one of the partially assembled thermopiles.

from the center of the thimble at time t. The problem then reduces to that of predicting the following quantities:

(i) $V(t)-v_s(t)$, the temperature difference recorded by the thermopile, where $v_s(t) = v(a,t)$; this difference will be designated by E_t;

(ii) $\int_0^t [V(u)-v_s(u)]du$, which is proportional to the heat transferred to the block in time t and is referred to as I_t;

(iii) $v_s(t)$, the change in block surface temperature with time.

If the assumption is made that the block is infinite in both the axial and radial directions, then we can consider the calorimeter assembly as approximating to a region bounded internally by a circular cylinder of a perfect conductor (radius a) having a thermal resistance $1/H$ per unit area at the surface. This problem has been considered for certain heating conditions by Jaeger (8); in general, solutions are obtained by the Laplace transform method (9). Three dimensionless parameters are used to describe the thermal characteristics of the assembly:

$$h = K(aH)^{-1} \qquad [1]$$

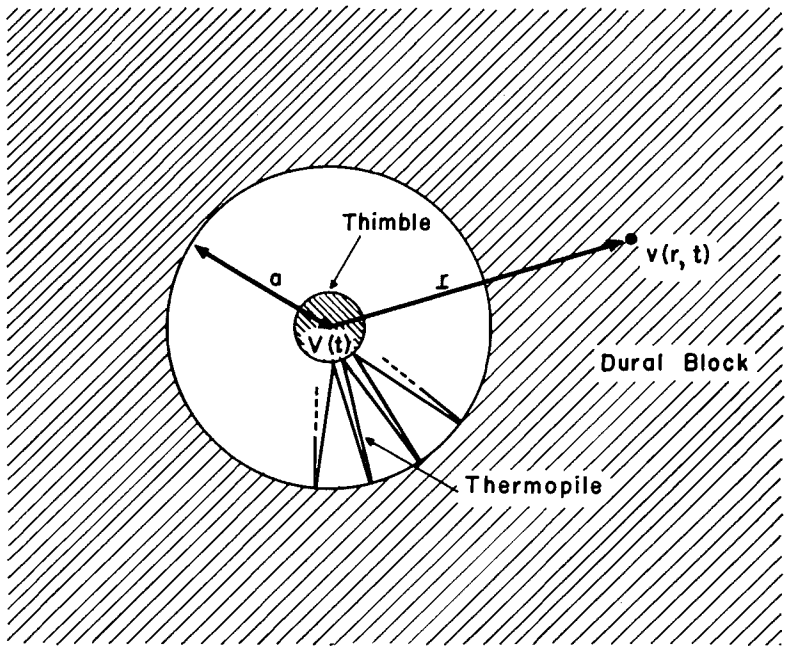

FIG. 2. Diagram of the cylindrically symmetric model used in calculating heat conduction in the microcalorimeter.

[2] $$\alpha = 2\pi a^2 \rho c S^{-1}$$

[3] $$\tau = \kappa t a^{-2},$$

where K, ρ, c, and κ are the thermal conductivity, density, specific heat, and diffusivity in the infinite region; S is the heat capacity of unit length of the internal cylinder; and t is the time. A heating condition frequently used in the microcalorimeter is as follows: at zero time the block and reaction thimble are at the same uniform temperature (taken to be zero) and heat is then supplied for a time t^* at a constant rate Q calories per second per unit length of the thimble. Using the method of the Laplace transformation it can be shown that for $t \leqslant t^*$,

[4a] $$V(t) = \frac{Q}{K} G(h,\alpha,\tau)$$

[5a] $$v_s(t) = \frac{Q}{K}\left[G(h,\alpha,\tau) - \frac{h}{2\pi}\{1-F(h,\alpha,\tau)\} \right]$$

[6a] $$V(t) - v_s(t) = \frac{Q}{K}\frac{h}{2\pi}[1-F(h,\alpha,\tau)]$$

[7a] $$\int_0^t [V(u)-v_s(u)]du = \frac{Q}{K}\frac{a^2 h}{\kappa}\left[\frac{\tau}{2\pi} - \frac{1}{\alpha} G(h,\alpha,\tau) \right]$$

and for $t \geqslant t^*$,

[4b] $$V(t) = \frac{Q}{K}[G(h,\alpha,\tau) - G(h,\alpha,\tau-\tau^*)]$$

$$[5b] \qquad v_s(t) = \frac{Q}{K}\left[G(h,\alpha,\tau)-G(h,\alpha,\tau-\tau^*) + \frac{h}{2\pi}\{F(h,\alpha,\tau)-F(h,\alpha,\tau-\tau^*)\}\right]$$

$$[6b] \qquad V(t)-v_s(t) = \frac{Q}{K}\frac{h}{2\pi}[F(h,\alpha,\tau-\tau^*)-F(h,\alpha,\tau)]$$

$$[7b] \qquad \int_0^t [V(u)-v_s(u)]du = \frac{Q}{K}\frac{a^2h}{\kappa}\left[\frac{\tau^*}{2\pi} - \frac{1}{\alpha}\{G(h,\alpha,\tau)-G(h,\alpha,\tau-\tau^*)\}\right].$$

In these equations the functions $F(h,\alpha,\tau)$ and $G(h,\alpha,\tau)$ are integrals which have been tabulated for certain values of h, α, and τ by Jaeger (8) and by Bullard (10). Values of $F(h,\alpha,\tau)$ and $G(h,\alpha,\tau)$ suitable for use in the present context have recently been computed (6), together with values of a third function, $E(h,\alpha,\tau)$, defined by the equation

$$[8] \qquad E(h,\alpha,\tau) = -\frac{\partial}{\partial\tau}F(h,\alpha,\tau).$$

This function can be used to determine the rate of change of $v_s(t)$ with time through differentiated forms of eqns. [5*a*] and [5*b*].

COMPARISON WITH EXPERIMENT

The theory as outlined above is approximate when applied to experiment in as much as the assumptions which have been made are not strictly valid for the following reasons:

(*a*) $V(t)$ is not uniform since very little stirring of the cell contents can take place in practise. However, $V(t)$ will not vary appreciably over the surface of the thimble because of the high thermal conductivity of silver and the uniform distribution of the thermocouple junctions over the surface. Within the cell a thermal gradient will be present but this radial variation should be small except for very low values of h.

(*b*) The calorimeter assembly does not have perfect cylindrical symmetry. The approximation introduced by neglecting the finite size of the block in directions normal to the axis of the thimble is probably quite good except for small h values. The presence of end effects associated with the finite length of the assembly may cause more serious errors in the use of the theory.

The total heat capacity calculated by summing the heat capacities of the thimble and its contents is about 20 cal (deg. C)$^{-1}$. This ignores contributions from the glass and plastic connections to the cell, which are difficult to estimate. A value near 35 cal (deg. C)$^{-1}$ is indicated by analysis of heating curves as described in reference 2 (see pp. 247–250). For the present calculations we have therefore used a value of $S = 3$ cal (deg. C)$^{-1}$, the length of the thimble being about 10.5 cm. The corresponding value of α is 9.39, which is taken as 9 for convenience.

The radiation constant H, defined as the heat transferred per second per unit temperature difference across unit area, will be made up mainly from conduction along the thermocouple wires H_{tc}, radiation from the thimble H_{rad}, and air convection (including air conduction) H_{air}.

H_{tc} is estimated to be 3.21×10^{-5} cal sec^{-1} cm^{-2} (deg. C)$^{-1}$. There must also be a considerable contribution to thermal conduction from connections to the cell and thimble, although these are made of poorly conducting materials where possible.

H_{rad} is less readily calculated since the emissivity of the silver thimble and thermocouple wires varies greatly, being 0.02 for polished silver and 0.2 for a dull surface. Using a value of 0.1, H_{rad} is found to be 0.6×10^{-5} cal sec^{-1} cm^{-2} (deg. C)$^{-1}$.

Both conduction and convection are possible in the air space separating the thimble and block. Convection in an enclosed vertical space is discussed by McAdams (11) and Jakob (12), who describe experimental results with air which show that no appreciable convection occurs between two surfaces as long as $x^3\Delta T < 11.4$ cm^3 deg. C, where x is the separation of the surfaces and ΔT the temperature difference between them. In the present case this corresponds to $V(t)-v_s(t)$ being less than 2° C, a condition which will be satisfied for heat inputs up to about 60 calories. Conduction in air leads to a value of 2.0×10^{-5} cal sec^{-1} cm^{-2} (deg. C)$^{-1}$ for H_{air}.

From the above considerations it appears that a minimum value of H is 6×10^{-5} cal sec^{-1} cm^{-2} (deg. C)$^{-1}$, corresponding to $h = 2200$, while larger values are to be expected due to conduction along cell connections.

The silver thimble containing a reaction cell is heated by means of an electrical heater wire and $E_t = V(t)-v_s(t)$ reaches a maximum value E_{t^*} at time t^*, decaying slowly to zero thereafter.[3] A convenient way of expressing this variation is by plotting the ratio E_t/E_{t^*} against time. This is done in Fig. 3 for curves calculated from theory and from

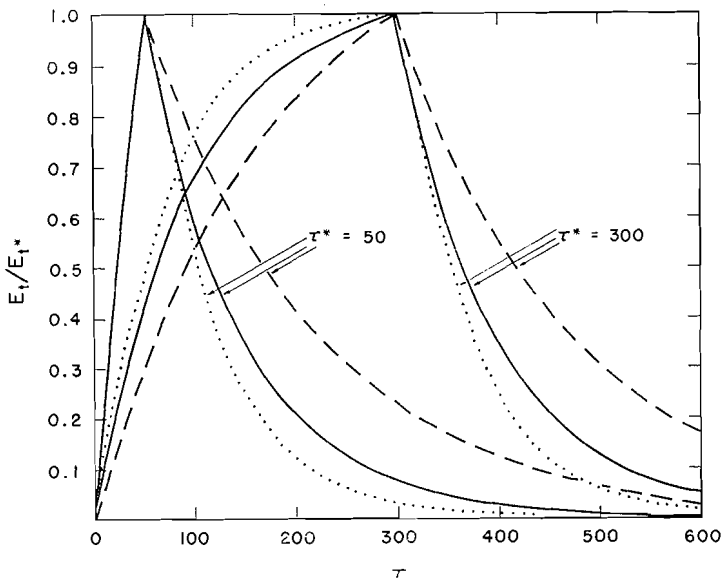

FIG. 3. Comparison of experimental and theoretical curves of the ratio E_t/E_{t^*}: · · · $\alpha = 9$, $h = 600$; — — $\alpha = 9$, $h = 1500$; —— experimental.

experimental observations and for two τ^* values (note $t = 0.202\tau$ minutes). The theoretical curves for two different values of h were obtained from eqns. [6a] and [6b] using the table in reference 6. It appears that using $\alpha = 9$ a value of h near 1000 would fit the experimental curves. The effect of variation of α can be judged from Fig. 4, where it may be seen that an increase in α leads to a lower time constant for the decay curve. A close fit of the experimental curve in Fig. 3 could therefore also be obtained with a somewhat higher α value (10–12) and a value of h more in keeping with that estimated (2200). This implies that a lower value of S should have been used in estimating α, as was indicated by a priori calculations.

[3]*In the absence of convection, heating and cooling result in reciprocal behavior and only heating will generally be referred to in this discussion.*

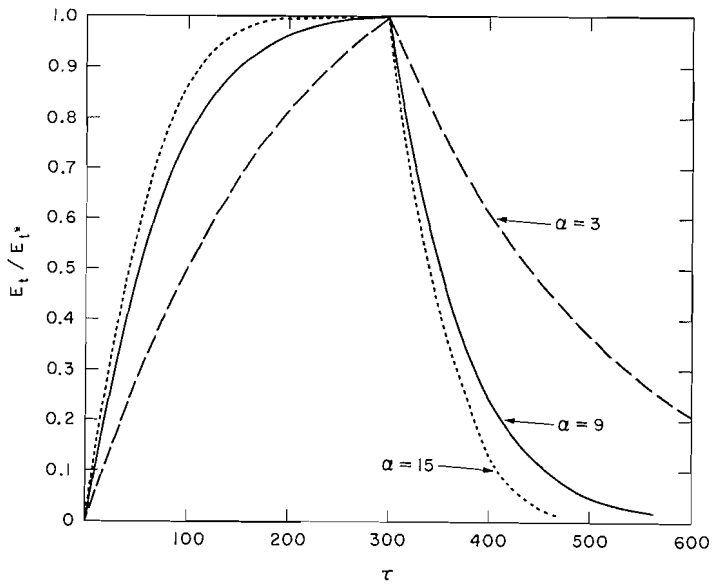

FIG. 4. Plots showing the effect on the ratio E_t/E_t^* of varying the parameter α ($\tau^* = 300$, $h = 600$).

The integrated temperature difference I_t is compared with theory in Fig. 5. The ordinates plotted in this graph are values of $1-I_t/I_\infty$, where I_∞ is the value I_t approaches in the limit as t goes to infinity.

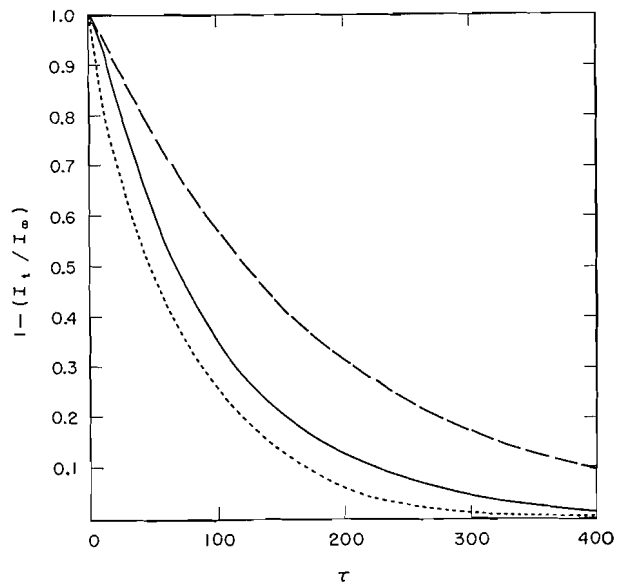

FIG. 5. Comparison of experimental and theoretical curves of $1-(I_t/I_\infty)$ ($\tau^* = 10$): - - - $\alpha = 9$, $h = 600$; — — $\alpha = 9$, $h = 1500$; —— experimental.

The block surface temperature $v_s(t)$ is found to have a maximum value near $t = t^*$ and decays to zero in a manner similar to $V(t)-v_s(t)$ but the curve is more drawn out.

This is illustrated in Fig. 6, where $v_s(t)$ is compared with the maximum temperature difference E_{t^*}. As τ^* increases, the variation during heating approaches a limiting curve

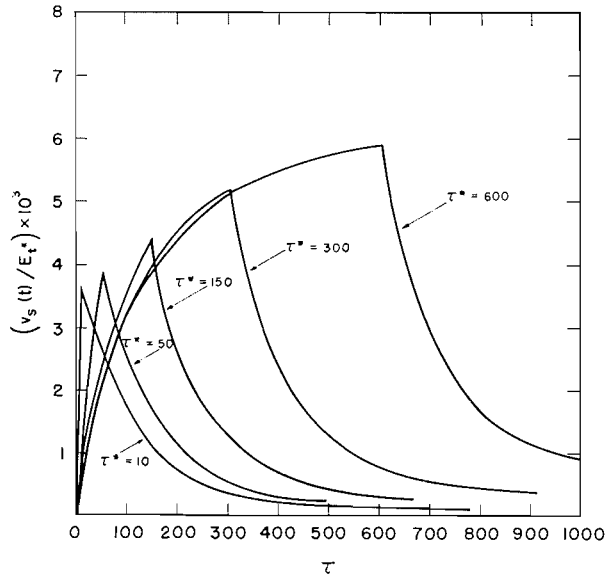

FIG. 6. Plots showing the effect on the ratio $v_s(t)/E_{t^*}$ of varying τ^* ($\alpha = 9$, $h = 600$).

which is not sensitive to changes in α but is more dependent on h. Increasing τ^* results in slower decay of the curves.

DISCUSSION

Prediction of the experimental behavior as outlined appears to be correct within a factor of two and is dependent on the values of the parameters h and α. Differences between experiment and theory are consistent with the probable errors in the estimated values of these parameters, requiring that smaller h and larger α be used.

Somewhat better agreement between the estimated value of α and that found by experiment might have been expected and the difference is no doubt due to neglect of contributions of the cell connections in calculating α. The method used to obtain α by experiment must take account of such contributions since it involves setting up a steady-state condition in which the heat loss from the cell equals the heat input and this will only be true when the temperature in all parts of the assembly is independent of time. Since there exists no large heat sink, similar to the metal block, in good thermal contact with the upper cell connections, considerable heating of the latter over a relatively large distance may pertain in the steady-state condition, resulting in a smaller value. Because of the time necessary to attain thermal equilibrium in these relatively poorly conducting components of the assembly, the value of the total heat capacity will lie between that calculated for the cell ($\sim$20 cal (deg. C)$^{-1}$) and that found for steady-state conditions ($\sim$35 cal (deg. C)$^{-1}$), depending on whether t^* is relatively small or very large. A value near 28 cal (deg. C)$^{-1}$ is indicated from the temperature rise found for t^* equal to 2 minutes; the corresponding α value would probably give better agreement of the theory with experiment. This variation of the heat capacity of the system is discussed by Calvet (1, 2), who, in a typical case, finds a 10% increase in heat capacity when t^* is increased

from 1 minute to 24 hours. An even larger increase is to be expected in the present calorimeter since it would appear to have a lower H value than that used by Calvet.[4]

In any heated cell which is not a perfect conductor, thermal disequilibrium will exist and may be characterized by a constant D for the particular cell together with its contents (2). This disequilibrium will also result in an increased apparent heat capacity but the effect is generally much smaller than that due to contributions of the cell connections.

In view of these considerations it is apparent that a straightforward estimate of the heat capacity neglecting cell connections may be in error by nearly 100% and the actual value depends on the time of heating, t^*. The 40% increase necessary to match this estimate with experimental values for small t^* in the present assembly may serve as an empirical guide to other applications of the theory described. An even greater increase would be necessary for very large t^* values.

Despite this variation in α (and also presumably small changes in h) with t^*, I_∞, the total area under the temperature difference – time curve, is found experimentally to be proportional to the heat input for t^* values of from 2 minutes to 1 hour and for heats up to 2–3 cal. At greater heat inputs, this proportionality, even for t^* values constant at 2 minutes, no longer holds, with I_∞ becoming increasingly lower than that expected as more heat is introduced during a heating period. Temperature rises in this region are not large (0.1–0.5° C) and any transfer of heat, other than by convection, should still be proportional to the temperature difference between the block and cell. As stated earlier, air convection would not be expected to be present in this range of temperature rise. Convection in the liquid contents of the cell may, however, become important at this stage and account for part of this non-linear variation of I_∞ with heat input. A further reason may be due to an increase in thermal disequilibrium in this range. The accuracy of the microcalorimeter for estimating heat effects in this region is less than in the range 0.05–2 cal, where optimum performance is found. This is to be expected if heat transfer is no longer linear, since I_∞ will then depend on the thermogenetic curve.

As can be seen in Fig. 6, v_s decays to zero very slowly and this has the effect of causing tailing of the temperature difference and I_t curves. Thus, accumulation of the last few percent of the heat effect may be somewhat prolonged and often it would be advantageous to stop a run at this point and reload the cells. This could be done by applying a correction to the I_t value at, say, 95% I_∞ on the basis of curves of the type shown in Fig. 5: little loss of accuracy should result in this way, particularly if a good fit of the experimental and theoretical curves is used.

ACKNOWLEDGMENTS

We are indebted to Dean P. R. Gendron, Professor K. J. Laidler, and Dr. H. M. Papée for supplying us with details of the calorimetric equipment at the University of Ottawa and to the late Dr. R. W. Attree and to Mr. L. Cushing for discussions of the calorimeter at A.E.C.L. Chalk River. The construction of our own calorimeter was undertaken in association with Dr. P. White and his collaboration in this phase of the work is gratefully acknowledged.

REFERENCES

1. E. CALVET and H. PRAT. Microcalorimetrie. Masson et Cie, Paris. 1956.
2. F. D. ROSSINI. Experimental thermochemistry. Interscience Publishers, New York. 1956. Chap. 12.
3. G. LAVILLE. Compt. rend. **240**, 1060 (1955).

[4]*A convenient measure of the thermal decay time of a microcalorimeter is the time taken for the temperature of the cell to fall to half its value in the steady-state condition. In the present calorimeter this time is approximately 15 minutes.*

4. G. LAVILLE. Compt. rend. **240**, 1195 (1955).
5. E. CALVET and F. CAMIA. J. chim. phys. **55**, 818 (1958).
6. G. C. BENSON and L. BENJAMIN. Can. J. Phys. **40**, 317 (1962).
7. R. W. ATTREE, R. L. CUSHING, J. A. LADD, and J. J. PIERONI. Rev. Sci. Instr. **29**, 491 (1958).
8. J. C. JAEGER. Australian J. Phys. **9**, 167 (1956).
9. H. S. CARSLAW and J. C. JAEGER. Conduction of heat in solids. 2nd ed. Clarendon Press, Oxford. 1959.
10. E. BULLARD. Proc. Roy. Soc. (London), A, **222**, 408 (1954).
11. W. H. MCADAMS. Heat transmission. 3rd ed. McGraw-Hill, New York. 1954. p. 181.
12. M. JAKOB. Heat transfer. Vol. I. 1st ed. John Wiley and Sons, New York. 1949. pp. 534–542.

CYCLIZATION OF AROMATIC PHENYLHYDRAZONES WITH CARBON MONOXIDE TO YIELD SUBSTITUTED PHTHALIMIDINES*

ALEX ROSENTHAL AND MARY R. S. WEIR
Department of Chemistry, University of British Columbia, Vancouver, British Columbia

Received December 5, 1961

ABSTRACT

The reaction of benzophenone phenylhydrazone with carbon monoxide at 230° and 3800 p.s.i. to give 3-phenylphthalimidine-*N*-carboxyanilide, and at lower temperatures (190–220°) to give a mixture of 3-phenylphthalimidine-*N*-carboxyanilide and 3-phenylphthalimidine has been studied. An independent synthesis of 3-phenylphthalimidine-*N*-carboxyanilide is described. 4-Methylbenzophenone phenylhydrazone reacted with carbon monoxide to give a mixture of two isomers, 3-phenyl-6-methylphthalimidine-*N*-carboxyanilide and 3-(*p*-tolyl)-phthalimidine-*N*-carboxyanilide, whose infrared spectra are described. An independent synthesis of 3-(*p*-tolyl)phthalimidine-*N*-carboxyanilide has also been carried out.

When aromatic nitrogen-containing compounds (having a $\rangle C{=}N-$ or a $-N{=}N-$ group) are treated with carbon monoxide in the presence of dicobalt octacarbonyl catalyst, ring-closure reactions have, in several instances (1–4), been observed. The present work deals with the reaction of carbon monoxide with benzophenone phenylhydrazone and 4-methylbenzophenone phenylhydrazone.

Benzophenone phenylhydrazone reacted with carbon monoxide at 3800 p.s.i. and at 230–240° in the presence of preformed dicobalt octacarbonyl catalyst to give 3-phenylphthalimidine-*N*-carboxyanilide (I) in about 70% yield. The structure determination of the latter was as follows: (I) was subjected to hydrolysis by 75% sulphuric acid and two products were isolated: aniline, identified as tribromoaniline, and a yellow solid of melting point 230° whose molecular formula was $C_{14}H_{10}O_2$. The latter was identical with the hydrolysis product of 3-phenylphthalimidine. Refluxing (I) in 99% deuterium oxide gave material whose infrared spectrum indicated the presence of an N—D grouping (see experimental section). These observations suggested that the carbonylation product contained the 3-phenylphthalimidine ring structure, an N—H group, and a group capable of yielding aniline on hydrolysis. Infrared and elemental analysis established the presence of two carbonyl groups. The work of Murahashi and Horiie (4) on azobenzene (see Chart II) suggested that the second carbonyl group (the first being incorporated into the 3-phenylphthalimidine ring) might well be situated between the two nitrogen atoms, forming an *N*-carboxyanilide side chain, which contains the required N—H group and which would give aniline an acid hydrolysis. The structure of (I) was then established by direct comparison (infrared analysis and mixed melting point) with an authentic sample of 3-phenylphthalimidine-*N*-carboxyanilide. The characteristic infrared absorption peaks of this carboxyanilide are listed in the experimental section.

When the reaction temperature was reduced to 210–220° the product was a mixture which separated on fractional crystallization from benzene into 3-phenylphthalimidine (II) (50%) and 3-phenylphthalimidine-*N*-carboxyanilide (12%). On further reduction of the temperature to 190–200° only 3-phenylphthalimidine (25%) was isolated. The structure of (II) was established by direct comparison with an authentic sample of 3-phenylphthalimidine, prepared by the method of Rose (8), and by the preparation of the monoacetyl derivative by treatment with sodium acetate and acetic anhydride (8).

**Presented at the 140th A.C.S. Meeting, Chicago, September 1961.*

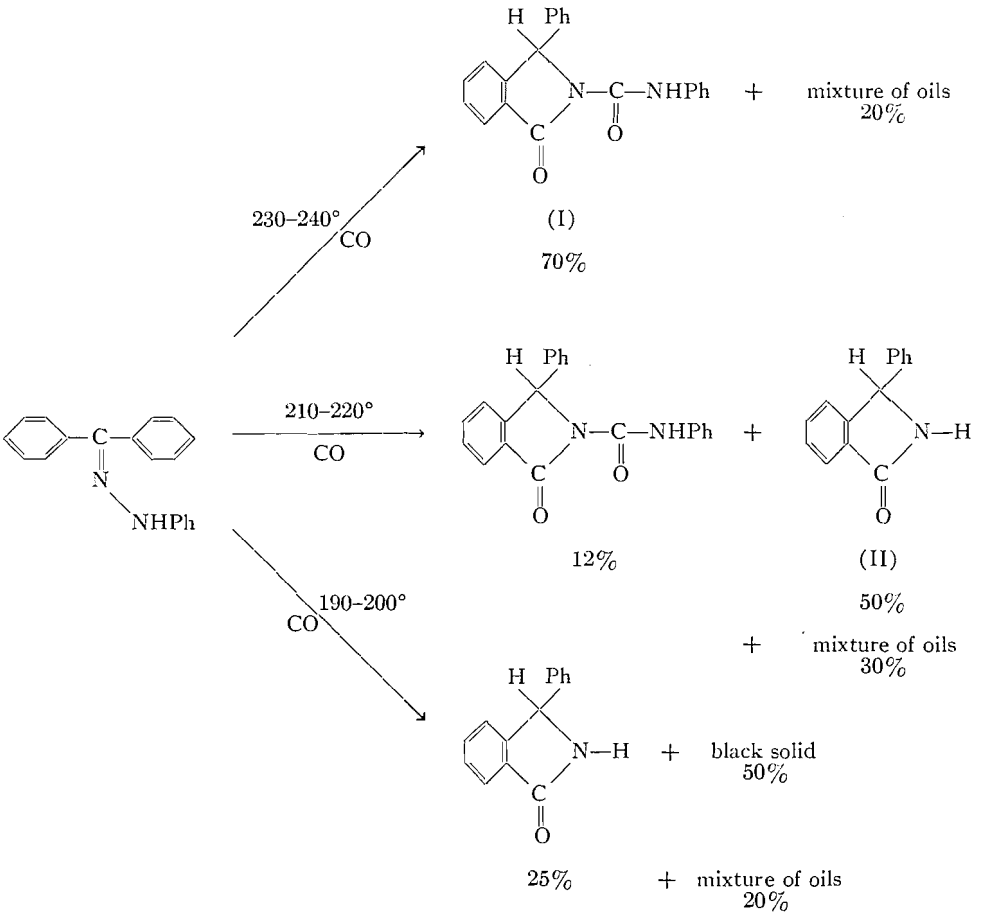

CHART I

The same temperature dependence of the number of carbon monoxide entities incorporated into the product was observed by Murahashi and Horiie (4), whose results are illustrated in Chart II.

When 4-methylbenzophenone phenylhydrazone was treated with carbon monoxide at 230° under the same conditions a mixture of two isomers, 3-(*p*-tolyl)phthalimidine-*N*-carboxyanilide (III) and 3-phenyl,6-methylphthalimidine-*N*-carboxyanilide (IV), of melting points 183–186° and 226–227° respectively, was obtained (Chart III). Both were present in about 20% yield, and were isolated from the reaction mixture in pure form by fractional crystallization from benzene. Structures (III) and (IV) are based on infrared analyses and elemental analyses, and, in the case of (III), on direct comparison with an authentic sample of 3-(*p*-tolyl)phthalimidine-*N*-carboxyanilide, prepared by the condensation (6) of 3-(*p*-tolyl)phthalimidine (7, 8) with phenyl isocyanate. The infrared spectra of (III) and (IV) differ only slightly from each other and from that of 3-phenylphthalimidine-*N*-carboxyanilide (I), the carbonyl peaks at 5.86 and 5.92 μ, and the other characteristic phthalimidine-*N*-carboxyanilide bands at 6.25, 6.42, 6.90, 7.40, and 8.10 μ, being present in the spectra of all three compounds. The strong band at 6.70 μ present in (I) and in (IV) is considerably weakened in (III), and a strong band at 8.54 μ in (IV) is absent in (I) and (III). Differences in the 11-, 12- ,and 13-μ regions of the spectra of these compounds were also observed.

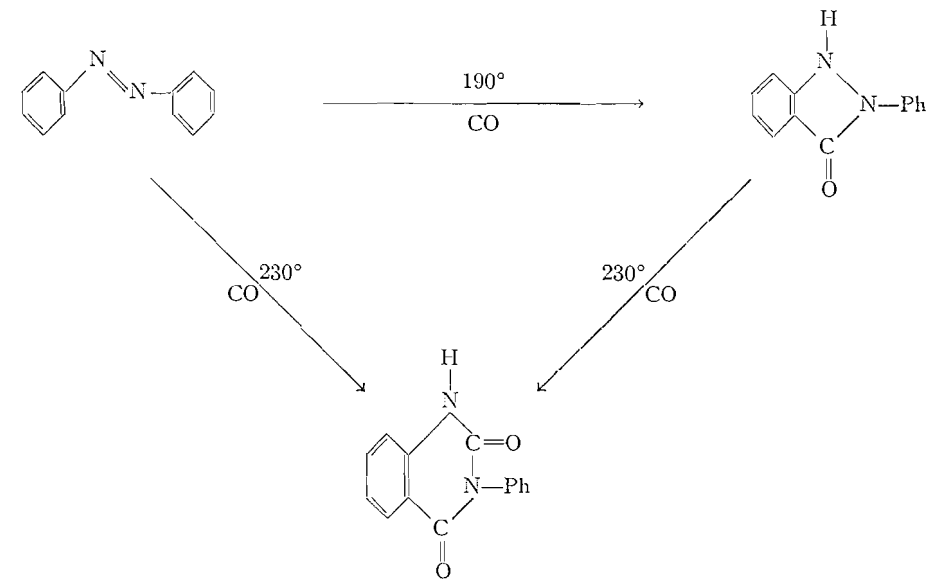

CHART II

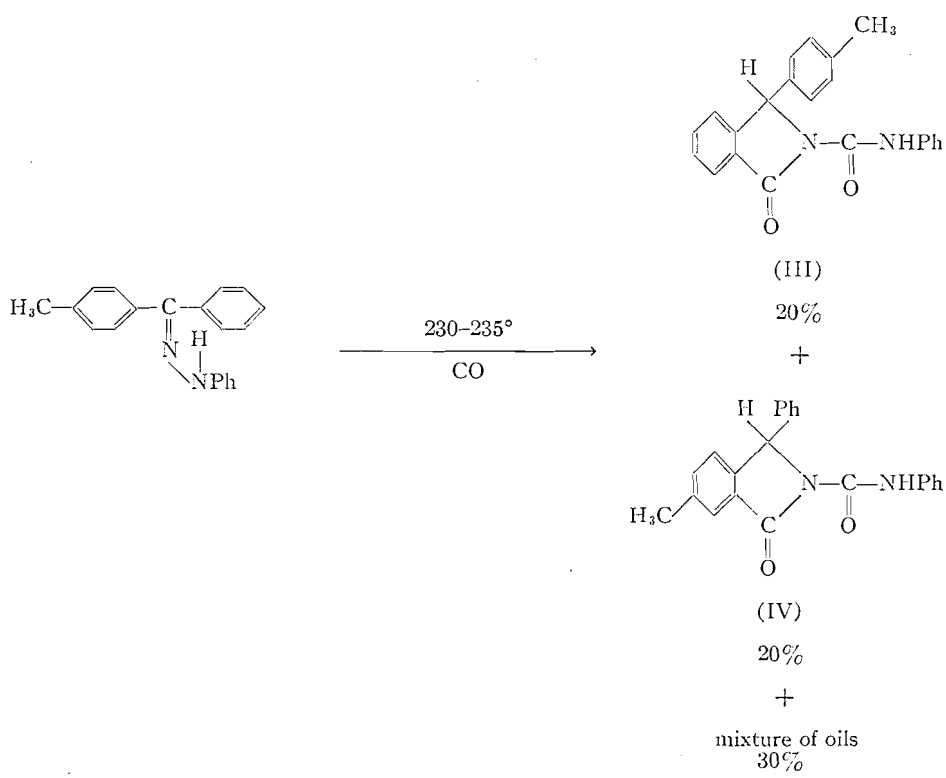

CHART III

Thus, having established by direct comparison structure (III), and it being apparent from infrared analysis that (III) and (IV) varied only slightly, it was concluded that (IV) must be 3-phenyl,6-methylphthalimidine-*N*-carboxyanilide.

This result differs from previous observations (4) on the effect of substituents on carbon monoxide ring-closure reactions in substituted azobenzenes; here the cyclization always occurred on the substituted ring.

EXPERIMENTAL

General Considerations

(*a*) The high-pressure equipment has been described previously (1).

(*b*) In every carbonylation run 2 g (0.006 mole) of dicobalt octacarbonyl catalyst was used, and carbon monoxide was added to an initial pressure of 2000 p.s.i. at room temperature.

(*c*) The reaction products listed include only those observed to be present in greater than 5%.

(*d*) The mixtures of oils obtained in all the runs after separation of the crystalline reaction products were shown by chromatography on alumina to be composed of at least five components. Further investigation of these mixtures was not pursued at this stage.

(*e*) The black solid (see Chart I) appeared to be an organo-cobalt complex which was insoluble in organic solvents.

Preparation of Benzophenone Phenylhydrazone

A mixture of 4 g (0.022 mole) of benzophenone, 4 g (0.034 mole) of freshly distilled phenylhydrazine, and 0.05 g of zinc chloride was heated to reflux, with stirring, for 30 minutes. On cooling of the mixture the material solidified to a pale yellow mass, which was washed with dilute acetic acid and then water, and was recrystallized from 95% ethanol; 4.7 g (78%) of white, needle crystals was obtained, m.p. 137–138° (5).

Preparation of 4-Methylbenzophenone Phenylhydrazone

To a solution of 6 g (0.033 mole) of 4-methylbenzophenone (prepared by a minor modification of the method of Bachmann (9)) in the minimum amount of glacial acetic acid was added 4.2 g (0.036 mole) of freshly distilled phenylhydrazine. The mixture was left overnight in the refrigerator and the brown oil thus obtained was washed free of acetic acid and dissolved in 95% ethanol. Allowing the ethanolic solution to stand at room temperature for 48 hours resulted in the formation of white crystals of m.p. 107–109° (yield, 63%) (10).

Carbonylation Reaction

A typical carbonylation run was as follows:

To a solution of 7 g (0.023 mole) of benzophenone phenylhydrazone in 50 ml of dry benzene was added 2 g (0.006 mole) of dicobalt octacarbonyl catalyst and 2000 p.s.i. of carbon monoxide (Matheson, C.P. gas). The mixture was heated to 230–240° with shaking for 190 minutes. The bomb was then cooled overnight and vented. The reaction product consisted of a dark brown liquid and 6 g (71%) of yellow solid. The solid was crystallized twice from 75% acetic acid, giving white needles of m.p. 211–214°. The infrared spectrum of this material in a KBr pellet showed strong carbonyl bands at 5.86 and 5.92 μ, and also strong bands at 6.25, 6.42, 6.70, 6.90, 7.40, 7.68, and 8.10 μ. Anal. Found: C, 76.51; H, 4.96; N, 8.41; O, 9.97; mol. wt. (Rast), 314. Calc. for $C_{21}H_{16}N_2O_2$: C, 76.80; H, 4.88; N, 8.50; O, 9.76; mol. wt., 328.

Sulphuric Acid (75%) Hydrolysis of 3-Phenylphthalimidine-N-carboxyanilide

3-Phenylphthalimidine-*N*-carboxyanilide (0.2 g) was dissolved in 40 ml of 75% sulphuric acid solution and refluxed for 4 hours. The mixture was then poured into 100 ml of water, the small amount of brown solid was filtered, and the remaining acidic solution was extracted with ether and dried over anhydrous sodium sulphate. Bromine water was added to 15 ml of the residual aqueous solution and a white precipitate was obtained of m.p. 120°; mixed m.p. with an authentic sample of 2,4,6-tribromoaniline, 121°. The infrared spectrum of the material was identical with that of 2,4,6-tribromoaniline.

Exchange Reaction of 3-Phenylphthalimidine-N-carboxyanilide with D_2O

3-Phenylphthalimidine-*N*-carboxyanilide (0.1 g) was refluxed for 6 hours in 10 ml of 99% D_2O containing 0.05 g of K_2CO_3. The solid was then filtered, washed with a small quantity of ethanol, and dried. The infrared spectrum showed a strong N—D band at 4.18 μ, and a weakening of the amide II band at 6.25 μ and the amide III band at 8.10 μ, these changes being in accord with those reported by Bellamy (11).

Synthesis of 3-Phenylphthalimidine-N-carboxyanilide (6)

A mixture of 0.3 g (0.0014 mole) of 3-phenylphthalimidine, 0.2 g (0.0017 mole) of phenyl isocyanate, and 20 ml of toluene (the latter dried over calcium chloride, filtered, and then stored over sodium) was refluxed for 24 hours. The solution was then cooled, and the resulting solid precipitate was filtered, washed with toluene, dried, and weighed; 0.45 g (95%), m.p. 212–215°, was obtained; mixed m.p. (with the product (1) of the carbonylation reaction) 213–215°. The infrared spectrum of this compound was identical with that of the carbonylation reaction product.

Carbonylation of Benzophenone Phenylhydrazone at 210–220°

The product obtained from the carbonylation of benzophenone phenylhydrazone at 210–220° consisted of 3.3 g of a greyish, granular solid and a brown benzene solution. On recrystallization from ethanol the solid had a m.p. of 211–214°. After purification by chromatography on alumina, using chloroform as eluent, the melting point was 223–225°, and the mixed melting point with an authentic sample of 3-phenylphthalimidine 223–226°. The brown benzene solution was boiled to destroy remaining catalyst and the solvent removed. This gave 1.6 g of a bluish solid, which, on washing with benzene and recrystallization from ethanol, gave white needles of m.p. 212–215°. The mixed melting point with an authentic sample of 3-phenylphthalimidine-*N*-carboxyanilide was 211–214°.

Carbonylation of 4-Methylbenzophenone Phenylhydrazone

The clear, brown benzene solution obtained from the carbonylation of 4-methylbenzophenone phenylhydrazone was boiled for 30 minutes to destroy any remaining catalyst, was filtered, and was concentrated to a volume of about 25–30 ml and then was left in the refrigerator overnight. This gave 1.9 g of white crystals, which on recrystallization from ethanol had m.p. 226–227°. (The purity of this material was checked by chromatography on both alumina and silicic acid columns, and no change in melting point was observed in the chromatographed material.) The residual benzene solution was reconcentrated to about 10 ml and was again cooled. A second 2-g fraction of white solid was thus obtained. Recrystallization from ethanol gave white crystals of m.p. 183–186°. Anal. Found: isomer of m.p. 226–227°: C, 76.93; H, 5.33; N, 8.20; isomer of m.p. 183–186°: C, 77.30; H, 5.20; N, 8.16. Calc. for $C_{22}H_{18}N_2O_2$: C, 77.20; H, 5.30; N, 8.19.

Preparation of 3-(p-Tolyl)phthalimidine

The method used here was an adaptation of that described by Rose (8) for the preparation of 3-phenylphthalimidine.

To a solution of 56 g (1.00 mole) of potassium hydroxide in 200 ml of water was added 24.5 g (0.10 mole) of *p*-toluyl-*o*-benzoic acid, prepared by the method of Fieser (7), and 16 g (0.19 mole) of hydroxylamine hydrochloride in concentrated aqueous solution. The reaction mixture was boiled for 20 minutes, with stirring, and was then allowed to stand for 12 hours at room temperature. The solution was cooled in ice, and the product anhydro-oxime was precipitated by the addition of concentrated hydrochloric acid, and was recrystallized from 95% ethanol. It was then dissolved in the minimum amount of glacial acetic acid, a large excess of zinc dust was added, and the mixture was heated with vigorous stirring for several hours. It was then cooled and poured into ice water, and the resulting white precipitate was filtered, and then recrystallized from 75% acetic acid, m.p. 216–219°. The infrared spectrum of this material was very similar to that of 3-phenylphthalimidine, with bands at 5.96, 6.22, 6.91, 7.38, 5.58, 7.70, and 8.80 μ. Anal. Found: C, 80.80; H, 5.91; N, 5.95. Calc. for $C_{15}H_{13}NO$: C, 80.80; H, 5.84; N, 6.28.

Preparation of 3-(p-Tolyl)phthalimidine-N-carboxyanilide (6)

A mixture of 0.7 g (0.0031 mole) of 3-(*p*-tolyl)phthalimidine and 1 g (0.0084 mole) of phenyl isocyanate in 40 ml of benzene was refluxed for 24 hours. The solution was then concentrated and cooled, and the resulting solid was crystallized from 95% ethanol, m.p. 187–188.5°; mixed m.p. of this compound with material (III) from the carbonylation reaction was 183–186°. Anal. Found: C, 77.37; H, 5.41; N, 8.05. Calc. for $C_{22}H_{18}N_2O_2$: C, 77.30; H, 5.27; N, 8.19.

ACKNOWLEDGMENTS

Grateful acknowledgment is made to the National Research Council for financial support of this work.

This research was also supported in part by a grant from the Petroleum Research Fund administered by the American Chemical Society. Grateful acknowledgment is made to the donors of this fund.

REFERENCES

1. A. Rosenthal, R. F. Astbury, and A. Hubscher. J. Org. Chem. **23**, 1037 (1958).
2. A. Rosenthal and A. Hubscher. J. Org. Chem. **25**, 1562 (1960).
3. S. Murahashi. J. Am. Chem. Soc. **77**, 6403 (1955).
4. S. Murahashi and S. Horiie. J. Am. Chem. Soc. **78**, 4816 (1956).
5. G. Reddelin. Ann. **388**, 165 (1912).
6. P. F. Wiley. J. Am. Chem. Soc. **71**, 1310 (1949).
7. L. F. Fieser. Organic syntheses. Coll. Vol. I. John Wiley & Sons, Inc., New York. 1941. p. 517.
8. R. E. Rose. J. Am. Chem. Soc. **33**, 388 (1911).
9. W. E. Bachmann, E. Carlson, Jr., and J. C. Moran. J. Org. Chem. **13**, 916 (1948).
10. B. Overton. Ber. **26**, 26 (1893).
11. L. J. Bellamy. The infra-red spectra of complex molecules. 2nd ed. John Wiley & Sons, Inc., New York. 1958. p. 207.

THE INFRARED SPECTRA AND PHASE TRANSITIONS OF SOLID PIPERIDINIUM HALIDES

A. CABANA AND C. SANDORFY
Department of Chemistry, University of Montreal, Montreal, Que.
Received November 27, 1961

ABSTRACT

The infrared spectra of solid films of piperidinium halides were measured at both room temperature and low temperatures. The spectra of the chloride and the bromide are not appreciably affected by cooling, but the spectrum of the iodide exhibits spectacular changes. These changes are explained by assuming the occurrence of a phase transition at about −15° C. The possibility of a "chair" → "boat" interconversion is also discussed.

INTRODUCTION

Substituted ammonium halides often undergo crystalline phase changes at low temperatures. In this laboratory we have been investigating these phase changes by means of infrared spectra. Piperidinium halides exhibit some special features which are presented here. No attempt will be made to assign all the bands in the infrared spectra of the piperidinium halides; rather, the emphasis will be put on the comparison of room- and low-temperature spectra in order to investigate the occurrence and nature of changes in the crystal or molecular structure. The room-temperature spectra of piperidinium halides have already been discussed in the literature (1–4).

EXPERIMENTAL

Piperidinium chloride, bromide, and iodide were prepared and purified by standard methods; the spectra are those of solid films prepared by sublimation *in vacuo*. A Perkin–Elmer model 21 spectrometer was used, mounted with a sodium chloride prism. The spectra presented in this paper were measured at room temperature, 25° C, and at liquid-air temperature, −190° C. They were also measured at −72° C but these spectra are not given since, in all cases, they showed no significant differences from those measured at −190° C. The low-temperature cell was essentially a brass Dewar in which the sample was cooled by direct metallic conduction, dry ice plus alcohol and liquid air being the two refrigerants.

RESULTS

The NH_2^+ group does not have any degenerate vibrations. There is a group of strong bands between 3000 and 2800 cm^{-1} which contains the two NH_2^+ stretching bands and the two CH_2 stretching bands followed by a few combination bands. The complexity of the 2800 and 1400 cm^{-1} regions is probably partly due to the fact that CH_2 groups linked directly to the nitrogen have stretching and deformation frequencies slightly different from those of the other CH_2 groups. The NH_2^+ bending band lies near 1600 cm^{-1} and is split into two in the spectra of both the chloride and the bromide.

The differences between the room- and low-temperature spectra of the chloride and the bromide (Figs. 1 and 2) are slight, with the usual sharpening of the bands and resolution of some of the shoulders being evident at the low temperature: no indication of a change in the crystal structure can be discerned.

The iodide behaves differently. The spectrum measured at −190° C contains about twice as many bands as the one at 25° C (Fig. 3); and shows an appreciable increase in scattered light, a phenomenon often accompanying phase transitions. Some of the bands

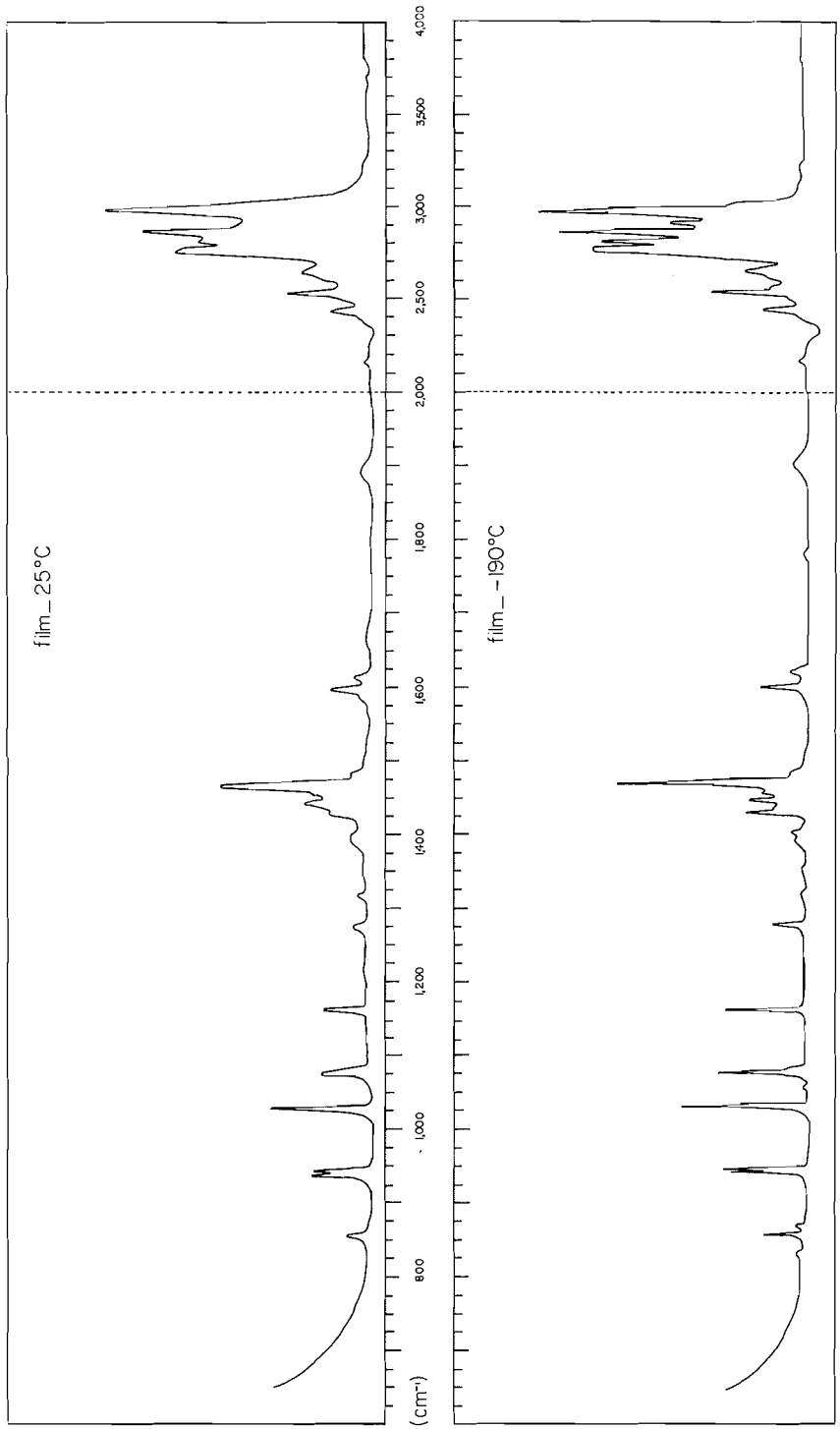

FIG. 1. The infrared spectra of piperidinium chloride at 25° C and −190° C. The ordinate is linear in % absorption.

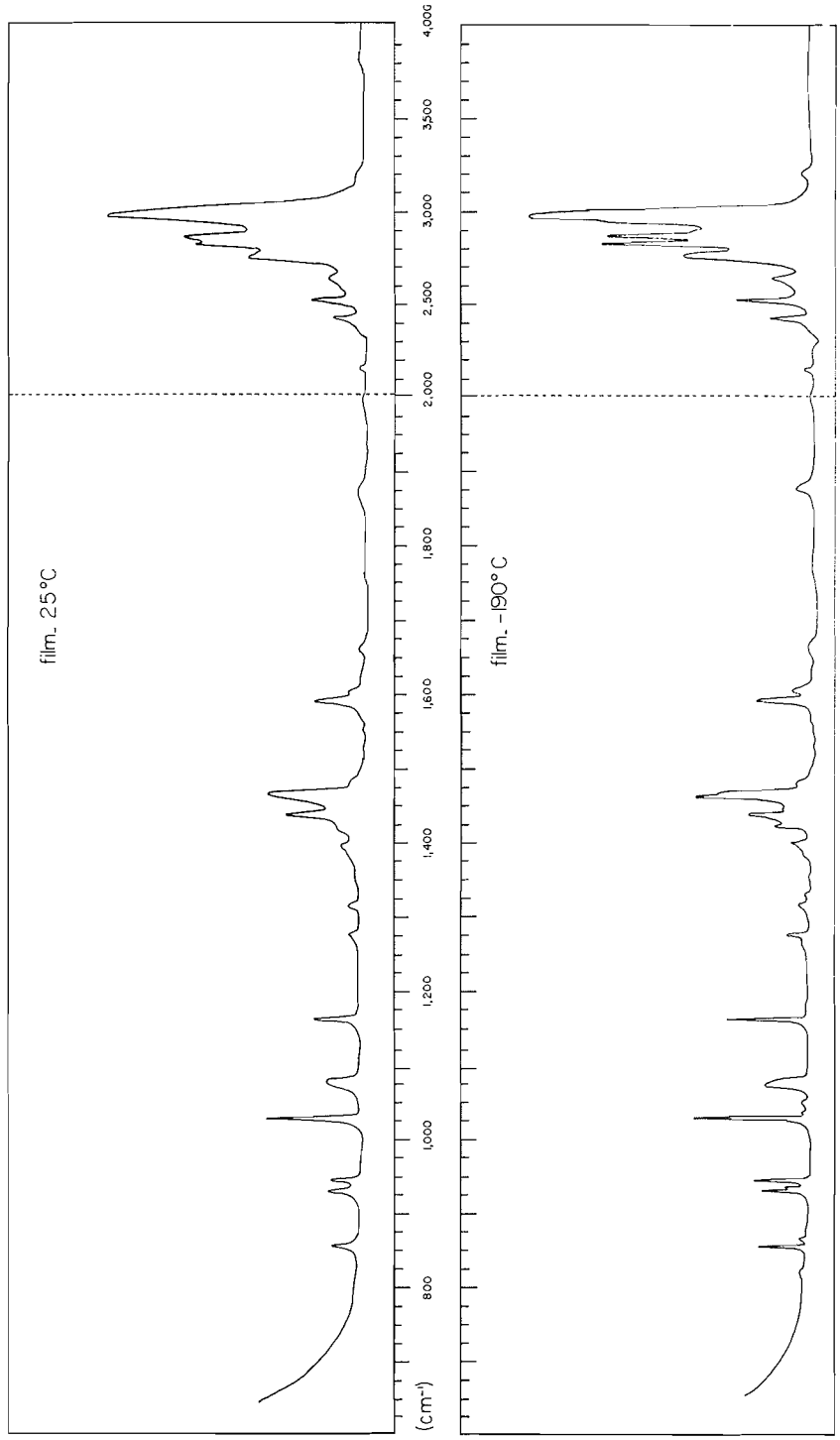

FIG. 2. The infrared spectra of piperidinium bromide at 25° C and −190° C. The ordinate is linear in % absorption.

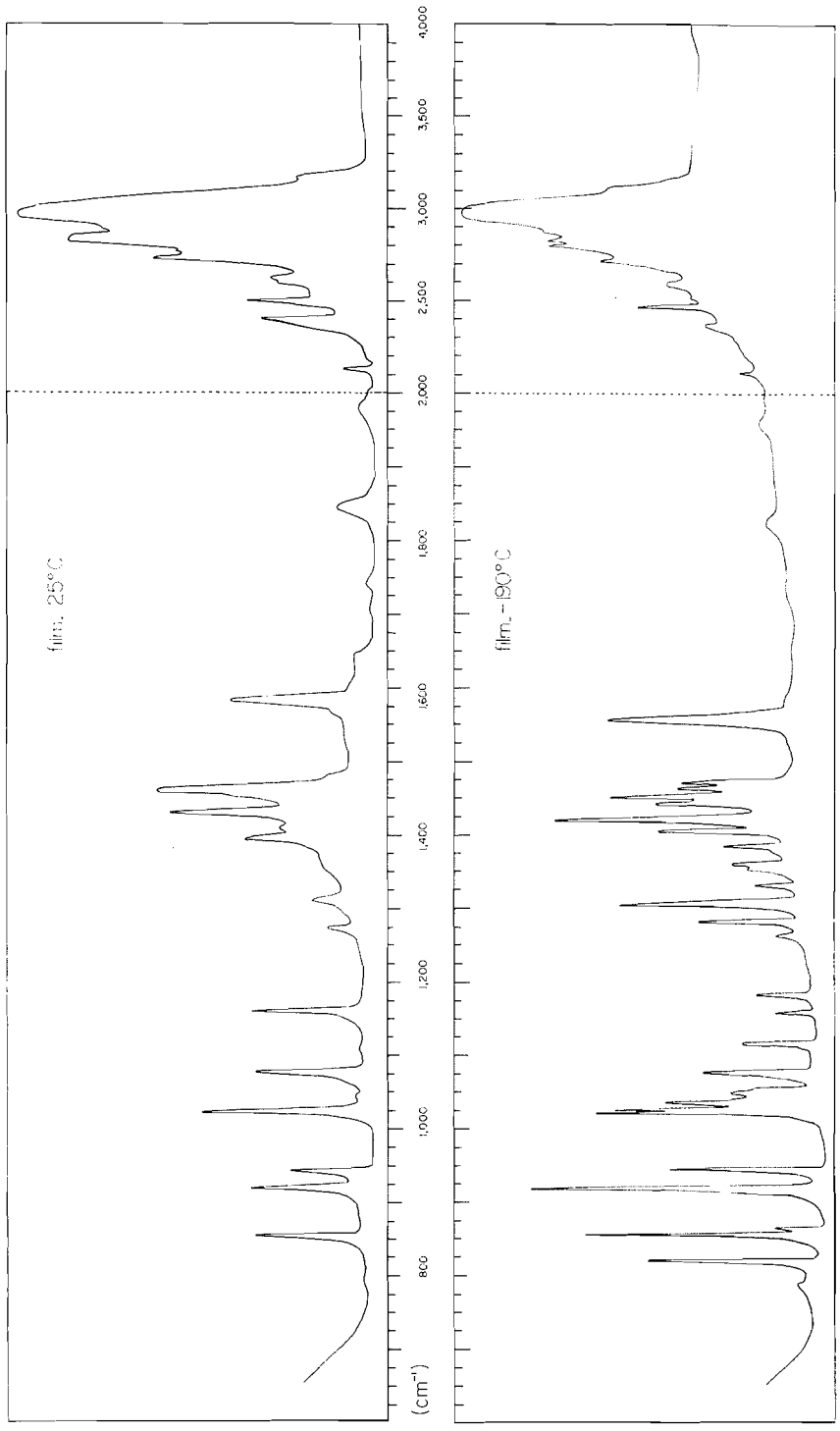

FIG. 3. The infrared spectra of piperidinium iodide at 25° C and −190° C. The ordinate is linear in % absorption.

in the low-temperature spectrum are obviously new, e.g. the bands near 817, 1046, 1114, 1180, and 1350 cm^{-1}. Some other bands are in almost exactly the same places in both the room- and low-temperature spectra, e.g. those at 854, 917, and 943 cm^{-1}. Some band splitting occurs at −190° C, e.g. at 1023 and 1455 cm^{-1}. The NH_2^+ stretching and bending vibrations do not yield new bands at −190° C, but they shift slightly.

DISCUSSION

Recently Rérat (5) examined the crystal structure of piperidinium chloride at room temperature using X-ray techniques. He found that the structure is orthorhombic (space group: D_{2h}^{11}—*Pcmb*) with four molecules per unit cell, and that the piperidinium ion has the "chair" form. From this alone we can conclude, on the basis of the close similarity between their spectra, that at room temperature all three halides have a similar crystal structure and the "chair" form. The same conclusion is valid at low temperature for the chloride and the bromide, but not the iodide, which must change its crystal structure and perhaps even its conformation.

The spectacular change in the spectrum of piperidinium iodide occurs suddenly at a temperature between −10° C and −20° C; further cooling does not radically change the spectrum. This seems to exclude the possibility of a mixture of "boat" and "chair" being present or in fact any other kind of mixture. Further evidence against the mixture contention is the fact that the NH_2^+ bending band shifts from 1580 cm^{-1} at 25° C to 1565 cm^{-1} at −190° C, remaining a single band throughout; if a mixture were present, two well-separated bands would be seen. The wealth of bands found in the low-temperature spectrum shows that a number of bands which are forbidden at room temperature become allowed at low temperature (the "new" bands). Some splitting of bands is also observed, e.g. at 1023 and 1455 cm^{-1}, and may be linked to coupling between molecules in the same unit cell or to removal of degeneracy.

The piperidinium ion is isoelectronic with cyclohexane. Therefore, assuming that the perturbation caused by the replacement of one carbon by a positively charged nitrogen is slight, the "chair" form must have approximately D_{3d} symmetry. Since in this symmetry group many bands are forbidden or degenerate, this explains the relatively low number of bands found in the room-temperature spectra. The problem is very similar to the one of cyclohexane which has been treated in detail by Ramsay and Sutherland (6). The low-temperature spectrum of the iodide can then be understood if we suppose that a phase transition has occurred, and that the symmetry of the crystalline environment has been decisively lowered around the piperidinium ion. This would explain, in a general way, the appearance of new bands and the observed splittings. The bands which are allowed anyway might not shift appreciably.

Table I compares the observed frequencies in the infrared and Raman spectra of cyclohexane, taken from Ramsay and Sutherland, and those in the infrared spectra of piperidinium iodide at 25° C and at −190° C. There is a close similarity between the spectra of the two compounds. It can be seen that at room temperature the piperidinium ion has an (approximate) center of symmetry in the crystal, and that at low temperature this is lost and the originally Raman-active or inactive (the one near 1110 cm^{-1}) fundamentals appear.

"Chair" → "boat" interconversion would explain the increase in the number of bands at the low temperature equally well, since the symmetry of the "boat" form is much lower than that of the "chair" form. It would be surprising, however, if the "chair" form were stable at higher temperatures and the "boat" form at lower temperatures,

TABLE I

The infrared and Raman frequencies (in cm^{-1}) of cyclohexane (6) and the infrared frequencies of piperidinium iodide from 1500 to 700 cm^{-1} *

Cyclohexane		Piperidinium iodide	
Infrared (vapor)	Raman (liquid)	Infrared, 25° C (solid)	Infrared, −190° C (solid)
	802 (10)		817 (5)
864 (6)		852 (6)	854 (6)
903 (5)		917 (6)	917 (9)
		940 (4)	943 (4)
1015 (1)	1029 (6)	1022 (8)	1020 (7), 1026
1042 (3)			1032 (3)
			1046 (2)
		1075 (6)	1075 (4)
			1114 (3)
	1157 (3)	1158 (6)	1157 (2)
			1180 (3)
			1261 (1)
1261 (5)	1267 (6)	1271 (2)	1281 (5)
		1308 (2)	1302 (7)
			1329 (2)
	1348 (2)		1350 (2), 1358
		(1358)	
		1392 (3)	1382 (3)
		1407 (1)	1402 (4)
	1426 (½)	1430 (7)	1418 (9)
			1440 (4)
	1444 (6)		1450 (6)
1456 (10)	1465 (½)	1460 (10)	1461 (3), 1470 (3)

*Approximate intensities are in parentheses, with 10 corresponding to the strongest band of a spectrum.

although the replacement of one carbon atom by N^+ and the hydrogen bonds make the case somewhat different from that of cyclohexane. There is also a spectral argument against this interpretation. As we stated earlier, some bands are in almost exactly the same places in both the room- and low-temperature spectra. This is very unlikely to happen if "chair" → "boat" interconversion actually does occur, except for some highly localized CH_2 bands, which are certainly not the observed non-shifting bands below 1300 cm^{-1}.

The question arises as to why the chloride and the bromide do not exhibit the same phenomenon as the iodide. In this respect it may be pointed out that although there is a close similarity between the spectra of all three halides at 25° C, the spectra of the chloride and the bromide are much more nearly identical with each other than with the spectrum of the iodide. In particular, the positions of the NH_2^+ stretching and bending bands show that the hydrogen bonds are weaker in the latter compound.

CONCLUSION

The changes that occur in the spectrum of piperidinium iodide on cooling are probably due to a phase transition, the symmetry around the piperidinium ion being considerably lowered thereby. The interesting possibility of a "chair" → "boat" transformation seems to be unlikely.

The room-temperature spectra of the three halides, and the low-temperature spectra of the chloride and the bromide, are all well in accord with a "chair" configuration for the piperidinium ion and a relatively high crystal symmetry.

Further X-ray and Raman investigations would be expected to throw more light on these problems.

ACKNOWLEDGMENTS

We acknowledge financial support from the National Research Council of Canada. We are indebted to Mr. David Davies for correcting the English of our manuscript.

REFERENCES

1. K. NAKANISHI, T. GOTO, and M. OHASHI. Bull. Chem. Soc. Japan, **30**, 403 (1957).
2. R. A. HEACOCK and L. MARION. Can. J. Chem. **34**, 1782 (1956).
3. B. CHENON and C. SANDORFY. Can. J. Chem. **36**, 1181 (1958).
4. C. BRISSETTE and C. SANDORFY. Can. J. Chem. **38**, 34 (1960).
5. C. RÉRAT. Acta Cryst. **13**, 72 (1960).
6. D. A. RAMSAY and G. B. B. M. SUTHERLAND. Proc. Roy. Soc. (London), A, **190**, 245 (1947).

INFRARED SPECTRA AND PHASE CHANGES OF SOLID ANILINIUM HALIDES

A. CABANA AND C. SANDORFY
Department of Chemistry, University of Montreal, Montreal, Que.

Received November 27, 1961

ABSTRACT

The infrared spectra of anilinium chloride, bromide, and iodide, measured at 22° C and at −190° C, are presented. The spectrum of the chloride is essentially the same at both temperatures but the spectra of both the bromide and the iodide exhibit changes indicating a crystalline phase transition, in accordance with recent X-ray determinations of the crystal structures of these compounds.

INTRODUCTION

The crystal structure of methylammonium chloride was investigated by Hughes and Lipscomb (1), who found that at room temperature it is tetragonal, with the C—N axis coinciding with the fourfold crystallographic axis (space group: D_{4h}^{7}—$P4/nmm$), every nitrogen atom being surrounded by four chloride ions and there being two molecules per unit cell. The space group, along with the number of molecules per unit cell, indicates that the ions must be on sites of symmetry D_{2d} or C_{4v}. In order to reconcile the threefold symmetry of the ion with one of these site symmetries, the ion must randomize its orientation either by rotation or by orientational disorder. King and Lipscomb (2) have shown that *n*-propylammonium chloride and bromide have crystal structures similar to that of methylammonium chloride at room temperature (also space group D_{4h}^{7}—$P4/nmm$ with two molecules per unit cell). Again the NH_3^+ group must randomize its orientation. Taguchi (3) in a recent publication summarized our present knowledge of the crystal structures of primary amine hydrohalides, and divided them into two groups: In the first group he placed those with crystal structures similar to that of methylammonium chloride and having the aforementioned characteristics. In the second group the crystals are monoclinic or orthorhombic, every nitrogen atom is surrounded by three (not four) halogen ions, and there are four molecules per unit cell. Typical of the second group are cyclohexylammonium chloride and bromide, which were studied by Shimada, Okaya, and Nakamura (4), using X-ray techniques (space group: C_2^5—$Pca2_1$). The space group of the crystal along with the number of molecules per unit cell indicates that the molecules in the crystal lie on general positions. Therefore there is no longer any contradiction between the symmetries of the crystal and the NH_3^+ group: the atoms are in fixed positions. The crystals belonging to the first group undergo phase changes at lower temperatures. The resulting phases were studied by X-ray techniques by King and Lipscomb (5) for *n*-propylammonium chloride (space group: C_{2h}^3—$C2/m$), by infrared techniques by Waldron (6) for methylammonium chloride, and by the authors (7) for all four methylammonium halides. It turns out that the low-temperature phases of the halides belonging to the first group have crystal structures similar to those of the halides belonging to the second group,* which do not undergo phase changes at all (3).

Anilinium halides exhibit some unexpected features which have recently aroused renewed interest among crystallographers. They also constitute a good test of the usefulness of infrared spectra in detecting phase changes. We measured their spectra at different temperatures and we shall now discuss the cases of the three halides one by one.

**See, however, the δ-phases of methylammonium bromide and iodide (7).*

ANILINIUM CHLORIDE

Brown (8) determined the crystal structure of anilinium chloride at room temperature using X-ray techniques. It is monoclinic with three chlorine ions surrounding the NH_3^+ group and has four molecules per unit cell (space group: C_s^4—Cc). Thus, it is similar to the crystal structure of the amine hydrohalides of the second group. Accordingly it has never been reported to undergo phase changes at lower temperatures, and it has an infrared spectrum very similar to the spectrum of cyclohexylammonium chloride (Figs. 1 and 2).

The broad complex band centered at about 2810 cm^{-1} for anilinium chloride contains the NH_3^+ stretching vibrations overlapped and followed by a number of combination bands. The strong band at 2570 cm^{-1} has also been shown to be a combination band (9). The sharp band at about 2040 cm^{-1} has an appearance very similar to that of the band at 2062 cm^{-1} and 2080 cm^{-1} in the low-temperature phases (γ- and β-phases respectively) of methylammonium chloride. Waldron (6) assigned this band to the sum of the torsional oscillation frequency of the NH_3^+ group (ν_6) and its asymmetrical bending frequency (ν_9). It was shown by the authors (7) to be a good indicator of less than threefold symmetry around the NH_3^+ group; it is invariably also present in the spectra of solid primary amine hydrohalides whose crystal structure belongs to the second group—cyclohexylammonium chloride is a good example (Fig. 1). The asymmetrical and symmetrical bending vibrations of the NH_3^+ group give bands near 1600 cm^{-1} and 1500 cm^{-1} respectively, very close to the two well-known bands of the phenyl ring. The band at 1470 cm^{-1} is very probably the first overtone of the out-of-plane CH bending vibration near 740 cm^{-1}, its intensity being increased by Fermi resonance. The degenerate NH_3^+ rocking band is probably the one near 1100 cm^{-1} and the C—N stretching band the one at 1020 cm^{-1}. The comparatively lower frequency of the NH_3^+ stretching band in the spectra of anilinium chloride (2810 cm^{-1} compared to 2980 cm^{-1}) shows that the hydrogen bonds in anilinium chloride are stronger than in cyclohexylammonium chloride.

The main point to emphasize, as regards the present investigation, is that the spectrum of anilinium chloride is practically the same at 25° C as at −190° C. At the low temperature the normal sharpening of the bands in the spectra of crystals occurs to give a somewhat better resolution of overlapping bands, with a few shoulders becoming separate bands; but no differences indicating a change of phase are observable. This is in complete agreement with the crystallographic results.

ANILINIUM BROMIDE

While cyclohexylammonium bromide and iodide have spectra very similar to that of the chloride, anilinium bromide has a spectrum exhibiting significant differences from that of anilinium chloride (Fig. 3). At 25° C the NH_3^+ stretching region near 2860 cm^{-1} is very broad and structureless, as also are the NH_3^+ asymmetrical bending band near 1570 cm^{-1} and the NH_3^+ rocking band near 1110 cm^{-1}. They all belong to degenerate vibrations. At lower temperatures all these bands become much sharper, the extent of the sharpening being clearly much greater than in cases where no change of crystal structure occurs. The ($\nu_6+\nu_9$) band near 2040 cm^{-1} is absent from the spectra. These changes indicate a crystal structure at room temperature with a symmetry not very different from that of the α-phase of methylammonium chloride, and higher than that of cyclohexylammonium chloride or anilinium chloride.

This conclusion is in excellent agreement with the recent X-ray work of Taguchi (3). According to his measurements the higher-temperature phase is orthorhombic (space

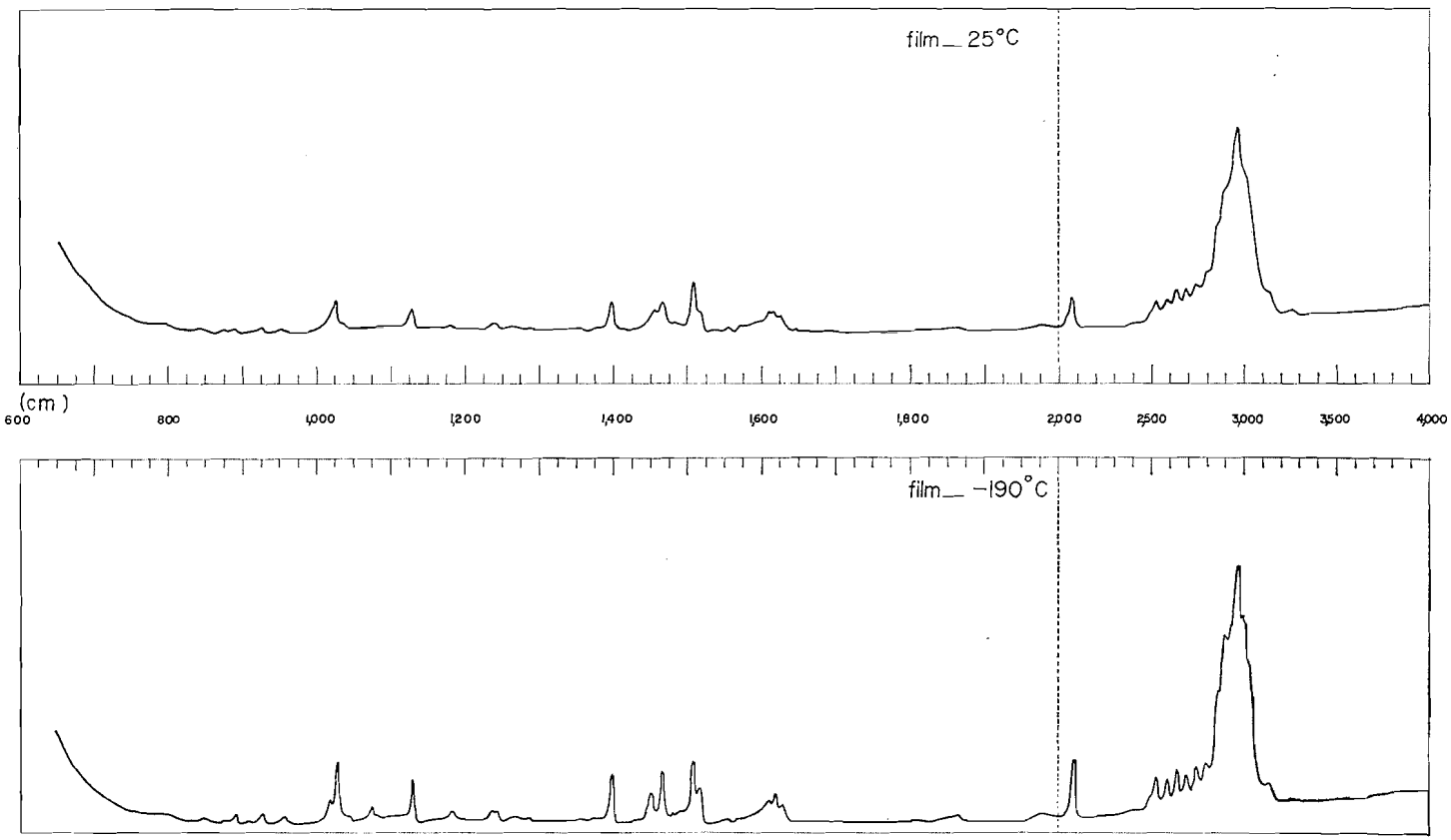

FIG. 1. The infrared spectrum of cyclohexylammonium chloride at 25° C (above) and −190° C (below). The ordinate is linear in percent absorption.

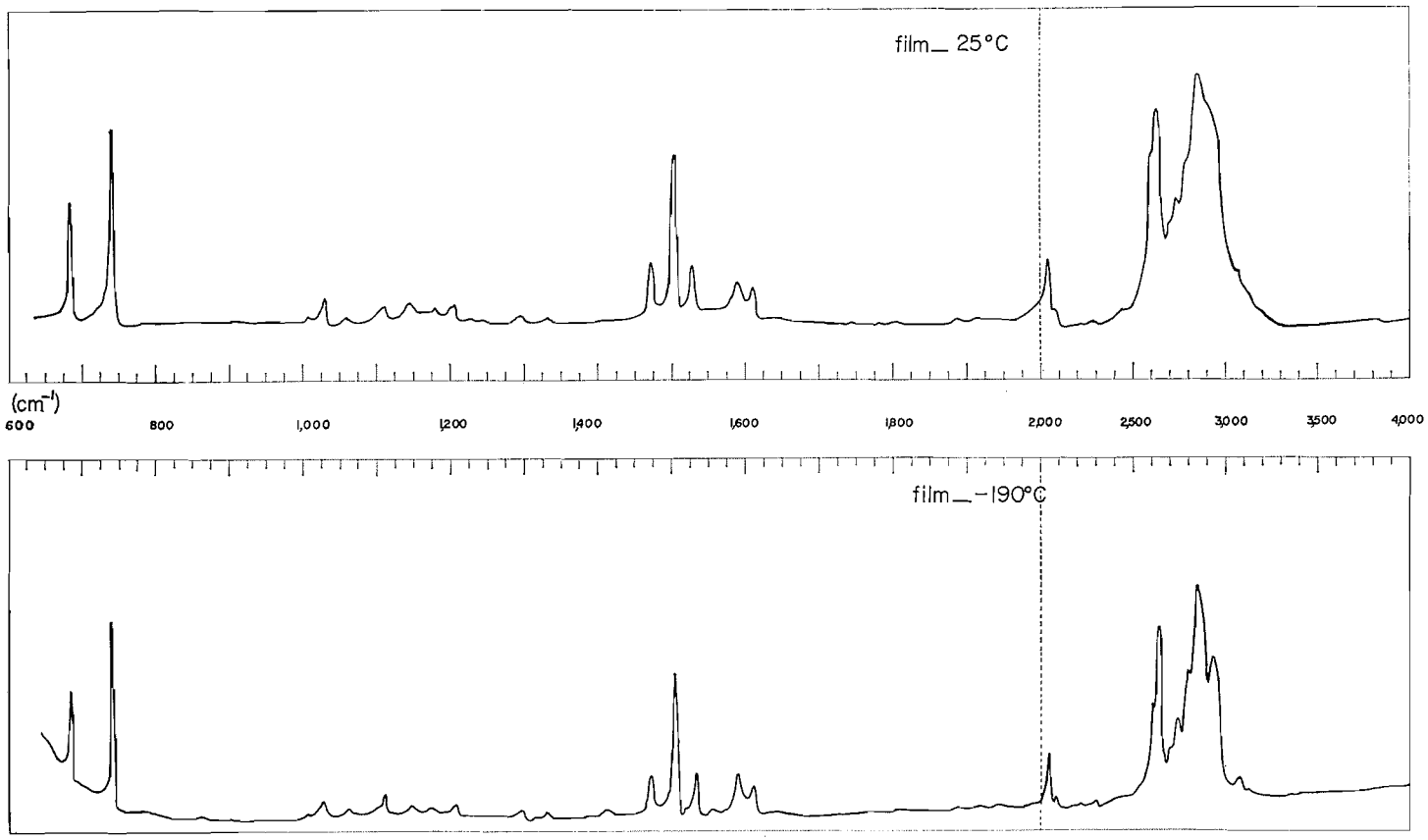

FIG. 2. The infrared spectrum of anilinium chloride at 25° C (above) and −190° C (below). The ordinate is linear in percent absorption.

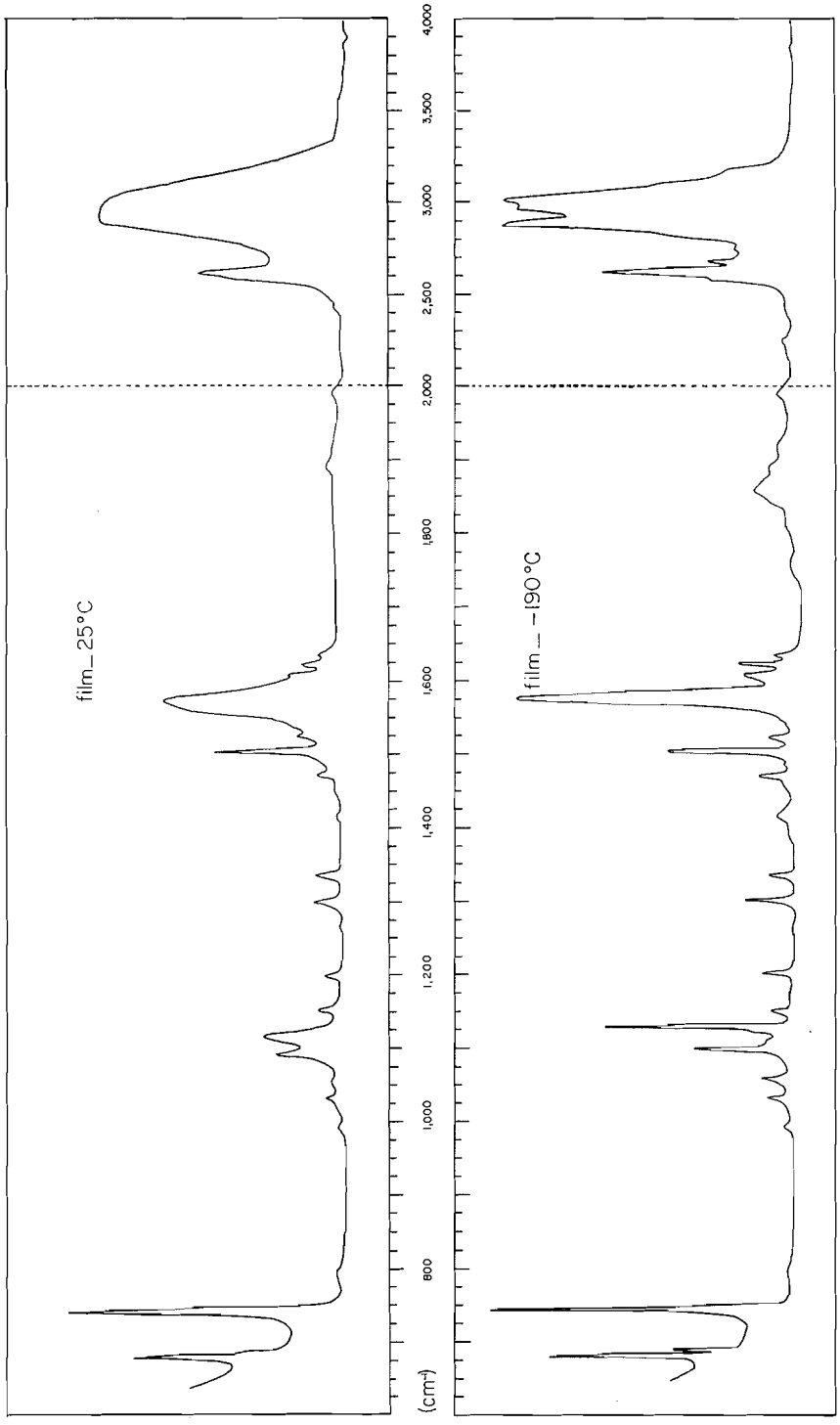

FIG. 3. The infrared spectrum of anilinium bromide at 25° C (above) and −190° C (below). The ordinate is linear in percent absorption.

group: D_{2h}^{10}—*Pnaa*) and the low-temperature phase monoclinic (space group: C_{2h}^{5}—$P2_1/a$), with both phases having four molecules per unit cell. The crystal symmetry of the higher-temperature phase requires that the N—C_1 – – – C_4 axis should lie on a digonal axis. Thus, the NH_3^+ group, which has threefold symmetry with respect to the same axis, must randomize its orientation with respect to this axis. According to Taguchi this is achieved by a disordering whereby the NH_3^+ group "assumes two (or a multiple of two) equally stable orientations with respect to the N—C_1 – – – C_4 axis, or may be flipping among different orientations". This ceases at lower temperatures since then the symmetry of the crystal is lower, the ions lie on general positions in the crystal, and the atoms can take up fixed positions. Suga (10), who has studied the thermal properties of anilinium bromide, has shown that the transition is a typical order–disorder transition with a critical temperature of 22° C. This well explains the broadness of the bands mentioned in the preceding paragraph.

A weak broad band appears in the low-temperature spectrum at 1850 cm^{-1} which may be due to a combination between the asymmetrical bending vibration and a lattice vibration at about 300 cm^{-1}. It may seem surprising that the ($\nu_6+\nu_9$) combination band, which was fairly prominent in the spectra of the chloride, does not appear in the low-temperature spectrum. This may indicate a lesser departure from threefold symmetry around the NH_3^+ group than in the chloride (cf. the δ-phase of methylammonium bromide (7)).

Concluding this section we can say that again there is excellent agreement between X-ray and infrared data.

ANILINIUM IODIDE

To the authors' knowledge the crystal structure of anilinium iodide has not been studied using X-ray techniques. Since, however, both room- and low-temperature spectra (Fig. 4) are very similar to the corresponding spectra of the bromide, it is probably safe to predict that the iodide has two phases with crystal structures similar to those of the corresponding phases of the bromide, and that a similar order–disorder transition must take place between them. Confirmation of this deduction by X-ray techniques or by a study of the thermal properties of the crystal would be most welcome.

EXPERIMENTAL

The salts were prepared and purified by standard methods. The spectra are those of solid films prepared by sublimation *in vacuo* under moderate heating. A Perkin–Elmer model 21 spectrometer was used mounted with a sodium chloride prism. The spectra given in Figs. 1–4 were measured at 25° C and −190° C. We also measured them at −70° C but in all cases they were similar to those measured at −190° C except for the greater degree of band sharpening at the lower temperature.

DISCUSSION

Infrared spectra are not an absolute means of discerning crystalline phase changes. There are normal changes which occur when the temperature is lowered: the bands become sharper, shoulders are often resolved as bands, and changing conditions for band overlap may alter the relative intensities of close-lying bands. If these are the only spectral differences observed, then the spectroscopist must conclude that no change in crystal structure has been detected. In the other extreme, spectacular changes in the spectrum, band splittings, and major changes in intensities and band positions accompany phase changes when these imply the loss of high-symmetry elements (such as threefold or higher axis), or a change in the number of molecules per unit cell. Such spectacular changes are observed in the case of the methylammonium halides.

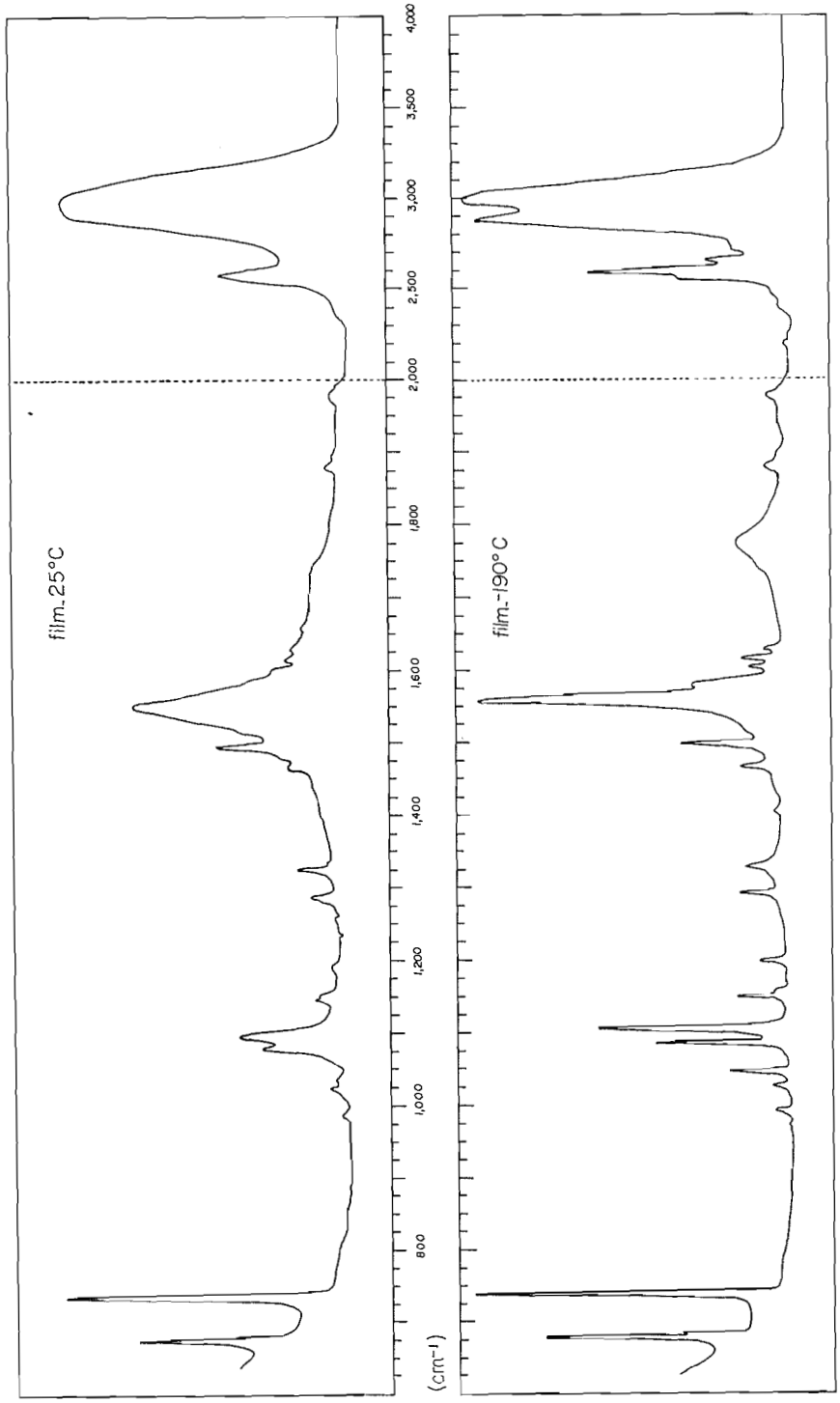

FIG. 4. The infrared spectrum of anilinium iodide at 25° C (above) and −190° C (below). The ordinate is linear in percent absorption.

Anilinium bromide and iodide appear to be intermediate cases: a moderate change in crystal symmetry is accompanied by an order–disorder transition. Correspondingly there are changes in the spectrum which are less spectacular but still significant—they concern the intensity and especially the broadness of the bands. This case constitutes a good illustration of the power of infrared spectra in the detection of phase transitions. Care should be taken not to discount relatively minor changes in the spectra when looking for phase transitions.

ACKNOWLEDGMENTS

We enjoyed the privilege of a conversation with Professor S. Seki from Osaka University, Japan.

We acknowledge financial support from the National Research Council of Canada.

We are indebted to Mr. David Davies for correcting the English of our manuscript.

REFERENCES

1. E. W. HUGHES and W. N. LIPSCOMB. J. Am. Chem. Soc. **68**, 1970 (1946).
2. M. V. KING and W. N. LIPSCOMB. Acta Cryst. **3**, 222 (1950).
3. I. TAGUCHI. Bull. Chem. Soc. Japan, **34**, 392 (1961).
4. A. SHIMADA, Y. OKAYA, and M. NAKAMURA. Acta Cryst. **8**, 819 (1955).
5. M. V. KING and W. N. LIPSCOMB. Acta Cryst. **3**, 227 (1950).
6. R. D. WALDRON. J. Chem. Phys. **21**, 734 (1953).
7. A. CABANA and C. SANDORFY. In press.
8. C. J. BROWN. Acta Cryst. **2**, 228 (1949).
9. C. BRISSETTE and C. SANDORFY. Can. J. Chem. **38**, 34 (1960).
10. H. SUGA. Bull. Chem. Soc. Japan, **34**, 426 (1961).

NITROGEN-FREE DERIVATIVES OF ATISINE: AN EXTREMELY HINDERED CARBOXYLIC ACID[1]

J. W. ApSimon,[2] O. E. Edwards, and R. Howe[2]
Division of Pure Chemistry, National Research Council, Ottawa, Canada

Received December 8, 1961

ABSTRACT

The action of nitrous acid on azomethines derived from the alkaloid atisine gave a good yield of nitrogen-free hemiacetal, thus providing the first means of removing the nitrogen from the diterpenoid alkaloids. Transformation products of the hemiacetal, including the most hindered carboxylic acid hitherto known, are described. The internal oxidation–reduction reactions encountered in this and related work are discussed.

The early work on the chemistry of atisine, the main alkaloid of *Aconitum heterophyllum*, was done by Jacobs and his colleagues (1). A structure for dihydroatisine was postulated by Wiesner and co-workers (2) and elaborated by addition of the oxazolidine ring to structure I for the alkaloid (3). The oxidation studies and selenium dehydrogenations at 340° which formed the basis for this assignment did not rigorously prove the structure, and left the stereochemistry unknown.

Recent work on atisine, however, has confirmed the presence of the bicyclo[2,2,2]octane system substituted as in I (4, 5); work on ajaconine has given strong support to the remaining features of the proposed skeleton (6(*a*)), and the Garrya alkaloids and atisine have been interrelated (7). Evidence has also been produced for the relative and absolute

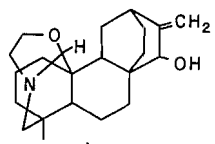

I

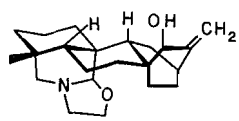

II

stereochemistry illustrated in II (4–6, 8–10). In order to test these conclusions by interrelation of atisine with diterpenes of known structure and stereochemistry, a method was developed of removing the nitrogen from the alkaloid. We now amplify our preliminary report on this deamination (11).

Our early attempts to open the hetero ring centered on methods of raising both carbons flanking the nitrogen to aldehyde or carboxyl oxidation levels, when hydrolytic removal of the nitrogen should be possible. It seemed desirable to have C-16 and C-17 at different oxidation levels in the deamination product, so that C-17 could be selectively deoxygenated to the angular methyl while leaving a labelling function on C-16.

If immonium ions are intermediate in most oxidations of carbon attached to nitrogen (12), then it should not be possible to directly oxidize azomethine III to the lactam IV. Indeed, preliminary experiments using N-bromosuccinimide and potassium permanganate showed little promise.[3] An obvious way to surmount this difficulty was to oxidize the N-methyl carbinolamine V or its methyl ether in basic media. On the basis

[1]*Issued as N.R.C. No. 6735.*
[2]*National Research Council Postdoctorate Fellow.*
[3]*Unpublished experiments by Dr. D. Dvornik.*

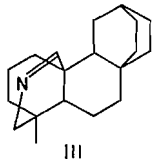
III

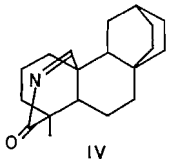
IV

of the stereochemistry shown in V the 17-hydrogen is inaccessible to oxidizing agents; hence attack should be on the N-methyl or on C-16.

The carbinolamine V and the isocarbinolamine VI were prepared as illustrated. The

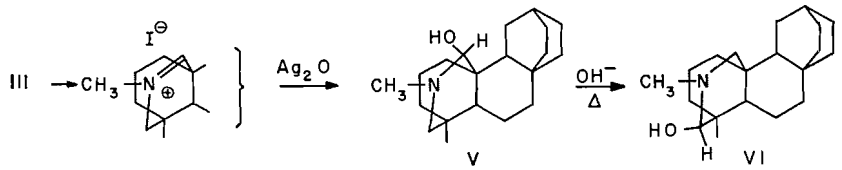
V VI

isocarbinolamine was characterized as its anhydronium iodide VII (the isomethiodide). Again, oxidation of V with alkaline ferricyanide, N-bromosuccinimide following by permanganate, and alkaline permanganate was not encouraging. The only crystalline neutral product isolated was the lactam VIII, which could also be prepared by chromium trioxide – pyridine oxidation of IX or permanganate oxidation of the isocarbinolamine VI. This implies a ready interchange of oxidation levels between C-16 and C-17, a point which will be discussed further in the sequel.

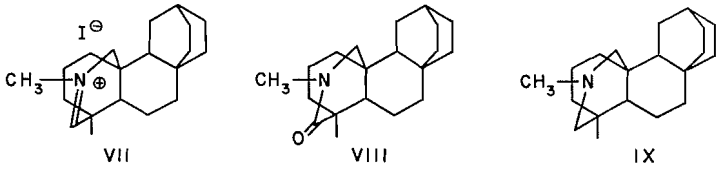
VII VIII IX

Two other possible methods of achieving the objective were attempted. One, the reaction of the azomethine with acetic anhydride, led to an unusual product[4] but little, if any, of the desired N-acetyl carbinolamine acetate. The second was the attractive possibility that the azomethine III was in slight but significant equilibrium with the hydrated form, the secondary aminocarbinolamine. If this could be trapped by nitrous acid, or if nitrous acid reacted directly with the azomethine, giving the N-nitroso carbinolamine X, we expected that an irreversible sequence would ensue, leading at least formally through the primary carbonium ion XI to products with the hetero ring open.

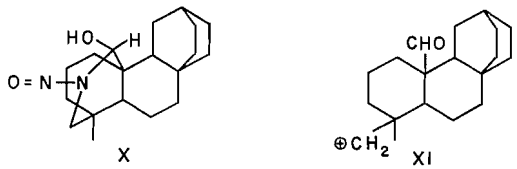
X XI

The reaction of III with nitrous acid was carried out in aqueous dioxane containing sodium acetate. The latter was added to provide a generous supply of nucleophilic anions, with the thought of trapping the primary carbonium ion before it could rearrange. However, a yield of up to 78% of hemiacetal was obtained from the reaction,

[4]*This work will be the subject of a separate communication.*

with no appreciable amount of aldehyde acetate. This indicated that the aldehyde oxygen was participating in the deamination as illustrated, forestalling any rearrangement, and that a cyclic oxonium ion was the primary product:

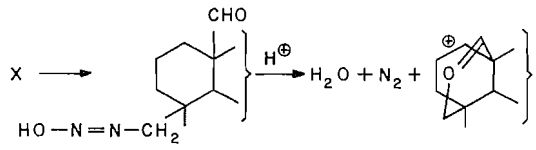

We at first believed the structure of the hemiacetal to be XII (11), but subsequent work provides convincing evidence that it is in fact XIII.[5] The evidence for this assignment will now be considered.

The hemiacetal analyzed correctly for $C_{19}H_{30}O_2$. Its infrared spectrum contained hydroxyl absorption at 3350 cm^{-1} and an ether band in the correct hemiacetal range (1050 cm^{-1}). It could be oxidized to a δ-lactone (XIV) (ν_{max} 1725 cm^{-1}) and reduced by lithium aluminum hydride to a diol. Wolff–Kishner reduction converted it to a primary alcohol. This could be oxidized with sodium dichromate to an aldehyde and the latter

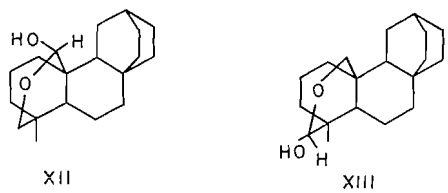

converted to a carboxylic acid (XV) by Kiliani reagent (14). On the basis of XIII these changes can be formulated as shown:

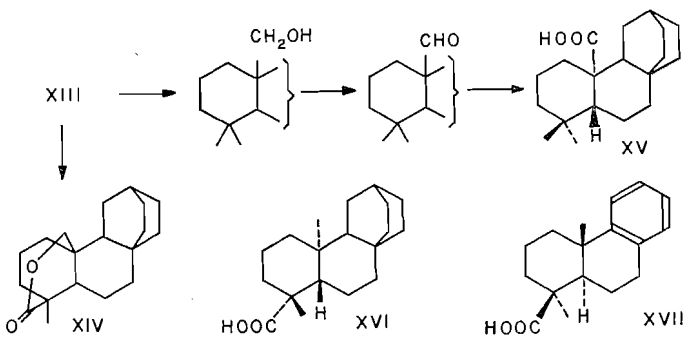

Had the hemiacetal been XII the acid would have been XVI. The problem lay in distinguishing between these two possibilities.

The formation of the lactone would have favored XIII rather than XII if one could guarantee that the hemiacetal was oxidized as such, since as noted above, the 17-hydrogen of XII would have been inaccessible. However, since the hydroxy aldehyde could be the species being oxidized this argument is weak. The lactone, aldehyde, and acid had their C=O stretching vibrations at abnormally low frequencies (ν_{max} 1725, 1696, and

[5]*Djerassi and Vorbrüggen have recently carried out a parallel set of reactions in the Garrya series (9) and have obtained the hemiacetal analogous to XII. We are grateful to them for keeping us informed of the progress of their work. Recently also, Schaffner, Arigoni, and Jeger (13) have used an analogous deamination reaction in conessine chemistry.*

1690 cm^{-1} respectively), a phenomenon most probably associated with steric compression of the chromophore. Similarly the ultraviolet absorption of the acid (λ_{max} 222 mμ) occurred at longer wavelength than any known acid (Table I), an effect which can be

TABLE I

Ultraviolet data in 95% ethanol

	λ_{max}	ϵ
Trans-anti-trans acid (XXI)	204.5	226
Trans-anti-cis acid (XVIII)	202	350
Tetrahydropimaric acid	203.5	135
Tetrahydroisopimaric acid	203.5	178
Unknown acid	222	80

correlated with the extent of alkyl substitution near a carboxyl (15).[6] However, the most unusual property of the acid was its very low acidity. In 70% ethanol its pK_a' was 9.6 and in 80% methyl cellosolve[7] its pK_a' was 9.2, compared to 7.1 and 7.8 for pimaric and isopimaric acid respectively in 75% ethanol. Our suspicion that the acid had structure XV rather than XVI was aroused when a sample of desoxypodocarpic acid XVII, kindly supplied by Professor E. Wenkert, was found to have a pK_a' of 8.25 (75% ethanol). This made it clear that the shielding of the axial carboxyl by the angular methyl was not sufficient to account for the weak acidity of the unknown. However, desoxypodocarpic acid is a poor model due to the flattened aromatic ring C. We hence decided to compare

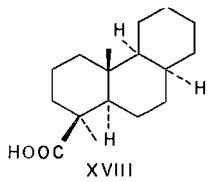

XVIII

the unknown with acid XVIII, which we hoped could be produced from agathenedicarboxylic acid (17) as illustrated:

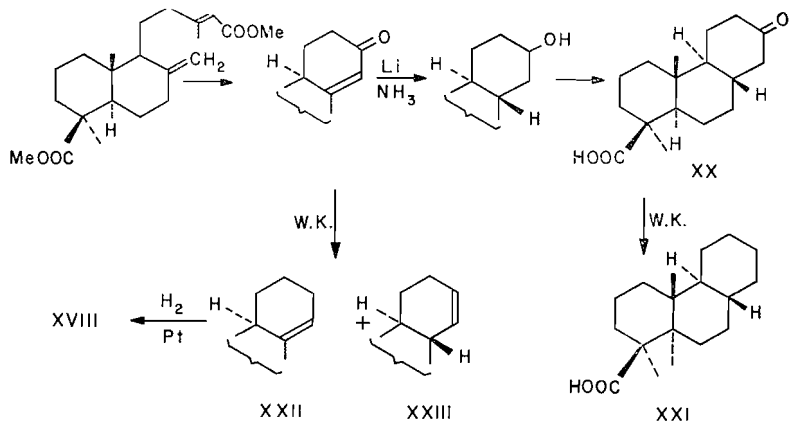

[6]*The values reported in our preliminary communication were determined on an old Beckman ultraviolet spectrophotometer. The new values, determined on a Carey Model 11 spectrophotometer with fused quartz optics, are more accurate. They cast doubt on the wavelengths of the maxima reported in reference 15.*

[7]*We are grateful to Dr. W. P. Arya, who determined this value. The calculated value (16) is 8.91.*

We were able to prepare the trans-anti-trans acid XXI in a pure state by the route shown. The optical rotatory dispersion curve[8] of XX was almost identical with that of cholestane-3-one (18), thus proving the configuration to be as illustrated. However, the Wolff–Kishner reduction of the α,β unsaturated ketone gave a mixture of olefins, presumably XXII and XXIII, from which, on hydrogenation, a mixture of XVIII and XXI resulted. A generous gift of ketones XXIV and XXV by Dr. R. H. Bible (derived from podocarpic acid (19)) enabled us to prepare XXI as a check on the assigned

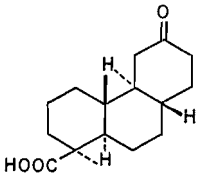

XXIV

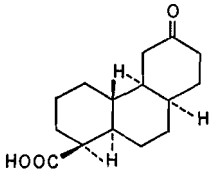

XXV

structures,[9] and to prepare XVIII in a pure state.

The pK_a' (75% alcohol) of these acids was 8.2 and 8.4 respectively, again much stronger than the unknown. Since XVIII most probably has the conformation illustrated in XXVI ring C should simulate the branch of the bicyclooctane ring 'cis' to the carboxyl in the unknown acid. Thus it is an excellent model for XVI, making it unlikely that the unknown had this structure.

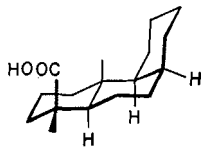

XXVI

Convincing evidence for structure XV for the unknown acid came from comparison of its n.m.r. spectrum with those of the model acids (Table II). Methyl groups attached

TABLE II

Chemical shifts of methyl groups in τ (CCl_4)

Acid	C-15	C-16	C-17
Tetrahydropimaric	—	8.84	9.26
XXI	8.78	—	9.27
XVIII	8.75	—	9.03
Unknown	9.20	9.10	—

to the same carbon as a carboxyl should resonate at considerably lower field than isolated methyls. However, trans-spatial deshielding of the angular methyl by an axial carboxyl on C-1 would introduce some ambiguity unless its magnitude were known.[10]

[8]*We are grateful to Dr. A. V. Robertson for determining this property.*

[9]*The identity of XXI from the two sources, incidentally, provides a direct steric correlation between podocarpic and agathenedicarboxylic acid (for correlation of podocarpic acid with abietic acid see ref. 20(a); for correlation of agathenedicarboxylic acid with abietic acid see ref. 20(b)).*

[10]*We are grateful to Dr. P. de Mayo, who suggested the use of this method of distinguishing between XV and XVI, and to Dr. F. A. L. Anet, who drew our attention to the trans-spatial factor. At that time (1959) good reference acids were not available.*

The chemical shift of C-17 in XXI is practically identical with that for the same carbon in the pimaric acids (Table II and ref. 21). However, in the case of XVIII C-17 resonates at considerably lower field[11] (9.03), indicative of steric pressure forcing it close to the axial carboxyl. This must represent close to the maximum possible transspatial deshielding for the system.

The effect of an equatorial carboxyl on the methyl attached to the same carbon in the resin acids results in a chemical shift for the group of around 8.84 (Table II and ref. 21). An axial carboxyl, however, gives a methyl on the same carbon a shift near 8.75. The chemical shift of the methyls in the unknown acid are incompatible with either of the above situations, but the signal at 9.10 corresponds well with that expected for a methyl in close proximity in space to a carboxyl. Hence of the two possible structures for the unknown acid, XV must be the correct one.

A further test of this assignment became possible when it was observed that oxidation by dichromate of the diol obtained by lithium aluminum hydride reduction of the hemiacetal XIII gave two lactones. The one produced in lesser amount proved to be identical with the lactone from bromine water or dichromate oxidation of the hemiacetal. The major lactone was isomeric with it, and should hence have structure XXVII. Comparison of the n.m.r. spectra of the two lactones showed that the lone methyl signal in the new lactone was at higher field (9.1) than that in the lactone from the hemiacetal (8.9), in agreement with the assigned structure.[12]

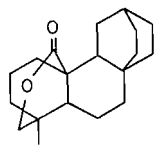

XXVII

In order to complete the comparison of physical properties attempts were made to prepare acid XVI. We were unable to open the lactone ring of XIV, hence a route to XVI via the hydroxy and aldehydo acids was closed.[13] It seemed possible that the lactones could be partially reduced to the hemiacetals, thus providing a method of going from XXVII via XII to acid XVI. In fact reduction with a limited amount of lithium aluminum hydride XIV was converted to XIII in good yield. However, comparable reductions of lactone XXVII gave mixtures of unchanged lactone, the diol, and hemiacetal XIII. Hence, once again, a possible promising route to acid XVI was not realized. We believe, however, that the above evidence is adequate to prove the deamination product to have structure XIII and the highly abnormal acid to be XV.

The acid XV could not be extracted from ether by dilute sodium hydroxide solution, a further indication of its abnormal character. All the unusual properties of this acid must be associated with shielding of the carboxyl by the angular methyl group and one branch of the dicyclooctane system. We attribute its very low acidity, the weakest hitherto reported (see also footnote 5), to steric hindrance of solvation of the anion derived from it.

The slower $LiAlH_4$ reduction of lactone XXVII than of lactone XIV is not surprising, since normal reduction leading first to the alkoxide XXVIII is prohibited by the extreme

[11] *Chemical shifts are given in τ values (22).*

[12] *We are unable to account for the larger yield of XXVII, unless steric compression of the hydrogens on C-17 accelerates their elimination in the oxidation.*

[13] *We thank Dr. A. Nicolson for some of these attempts.*

crowding of the side of C-17 facing the bicyclooctane ring (see XXIX). Internal hydride

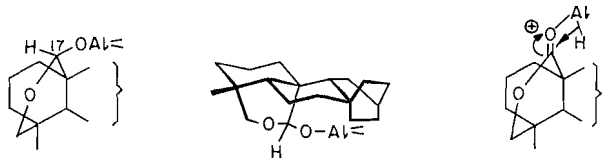

XXVIII XXIX XXX

transfer shown in XXX is possible but again subject to extreme hindrance. The most likely possibility is that the reaction proceeds mainly as shown:

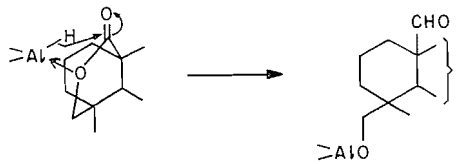

This relieves the serious interactions at once, and since the aldehyde would be rapidly reduced, accounts for the fact that little hemiacetal survives, in contrast to the reduction of the isomeric lactone (XIV).

In the above work three new instances were encountered in which an exchange of oxidation level between C-16 and C-17 took place: the original deamination, the oxidation of carbinolamine V, and the reduction of lactone XXVII. Three other phenomena of this type have been observed in the simpler diterpenoid alkaloids: (*a*) The atisine-to-isoatisine conversion exemplified in the present work by the rearrangement of V to VI. The mechanism of this strong base-catalyzed reaction is probably the following:

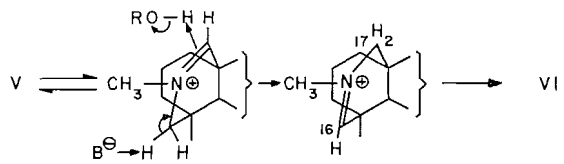

The driving force for the nearly complete conversion seems to be the 17-oxygen:5-hydrogen interaction (6(*a*)). (*b*) The thermal conversion of isoatisine salts to atisine salts in hot acetic anhydride (23), for which possible mechanism is a 1:3 hydrogen shift as illustrated:[14]

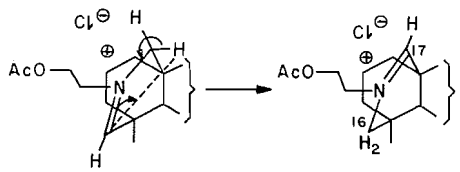

(*c*) The formation of the Δ^{17}-azomethine from isoatisine diacetate, when the Δ^{16}-azomethine was expected. This rearrangement took place in boiling carbon tetrachloride (24), i.e. in

[14]*A bimolecular process seems prohibited by the extremely crowded environment of the nitrogen.*

a relatively non-polar medium (but some water present) with possible base catalysis:

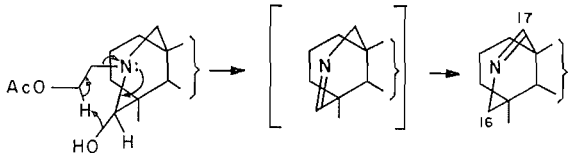

The driving force in the case of (*b*) and (*c*) appears to be the relief of 10:17:19 hydrogen interactions (6(*a*), 24).

The dismutation in (*c*) and in the three cases in the present work are remarkable for the mild conditions under which they take place. The species undergoing the dismutation in the deamination reaction could be the azomethine, the azomethine salt, the N-nitroso carbinolamine, or the hemiacetal. The reaction cited in (*c*) provides strong evidence that the azomethine double bond is mobile in the presence of organic base in hot carbon tetrachloride. It is tempting to think that the equilibrium is set up in the deamination, and that the Δ^{16} isomer reacts much faster with nitrous acid. However, the reaction takes place in acid medium, and despite the low pK_a' of the azomethine (6.0 in 80% alcohol) it must be largely in the form of its salt. Thus the base catalysis, which seems necessary for the isomerization, is absent and we consider it unlikely that any appreciable amount of the unstable azomethine is formed. Similarly the isomerization of immonium salts is negligible at 80° (24), hence even more so at room temperature. Even if equilibrium were set up, in each case almost exclusively on the Δ^{17} side, it seems very unlikely that the rate of reaction with nitrous acid would be sufficiently different to make the product arise exclusively from the Δ^{16} isomer.

A more likely entity to equilibrate is the N-nitroso carbinolamine X. The 5-hydrogen: oxygen repulsion and 10:17:19 hydrogen interactions should force this into equilibrium with the immonium ion XXXI. This, however, would be a high-energy state because

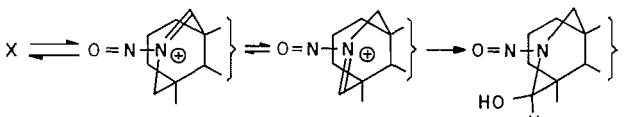

XXXI XXXII XXXIII

of the proximity of the positive nitrogen to the positive end of the N=O dipole. It thus might rearrange with greater facility than ordinary immonium salts by 1,3-hydride transfer or proton exchange with solvent to XXXII. The latter would hydrate nearly irreversibly to XXXIII, which would then give rise to hemiacetal XIII. However, if this were correct it is difficult to account for the fact that no product derived from X is isolated since opening of X to the N-nitroso aldehyde would also relieve the non-bonded interactions.

We are thus forced to the conclusion that part, if not all, of the dismutation takes place between the hemiacetals, XII going to XIII via the oxonium ions:

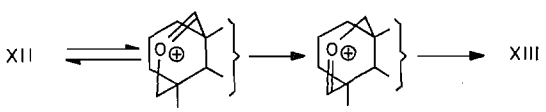

This also seems to be the best explanation of the formation of XIII on the reduction of lactone XXVII by lithium aluminum hydride. This would be acid catalyzed at least to the oxonium ion stage and also probably take place on the surface of alumina during chromatography. An attempt was made to generate a mixture of the two hemiacetals by the action of acid on XIII, but only unchanged XIII and amorphous products were obtained.

Finally, the deamination of the C_{20}-azomethine alcohol XXXIV (24) gave a good yield of a hemiacetal, presumably XXXV, characterized as the methyl acetal. This now had substituents on ring C, making possible conversion to known diterpenes. However, the conversion of ring C to a phenol in related work (4) proved very expensive, hence

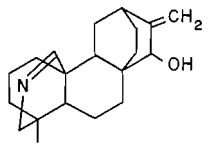

XXXIV

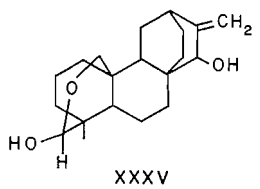

XXXV

an interrelation with podocarpane derivatives by this route did not seem practical. Removal of the nitrogen from the Garrya alkaloids has recently enabled correlation with the diterpene kaurene and rotatory dispersion comparison with other members of the phyllocladene family (9, 10). This has provided confirmation of the absolute stereochemistry suggested for these and the atisine group of alkaloids (4, 6(*a*)).[15]

EXPERIMENTAL

Rotations of absolute ethanol solutions, ultraviolet spectra of 95% ethanol solutions, infrared spectra of nujol mulls, unless otherwise stated, were determined. The pK_a' values are the pH's at half titration in the indicated solvent mixture. Melting points were taken on a Kofler hot stage. Alumina activities are on the Brockmann scale (25).

Methiodide of C_{19}-Azomethine

C_{19}-Azomethine (54 mg) in acetone was treated with excess methyl iodide in acetone. The product, after three crystallizations from acetone, formed needles, m.p. 326–328°; $[\alpha]_D$ −27° (*c*, 1.19); $[M]_D$ −112°; pK_a ~12.5 (95% EtOH). Found: C, 58.01; H, 7.62. Calc. for $C_{20}H_{32}NI$ (413): C, 58.11; H, 7.75. Infrared spectrum: ν_{max} 1685 cm^{-1} ($>C=\overset{+}{N}<$).

Isomethiodide VII from the C_{19}-Azomethine

C_{19}-Azomethine (70 mg) was converted to methiodide as above, and the solvent evaporated. The crystalline residue was refluxed for 7 hours under nitrogen with 5 ml of a solution of 400 mg of potassium hydroxide in 7 ml of methanol. (The conversion was not complete after 3 hours.) The methanol was removed under reduced pressure, the residue taken up in water and extracted into ether which was washed and dried. The pale yellow gum from the ether was dissolved in methanol and exactly neutralized with hydriodic acid in methanol. The solvent was removed under reduced pressure and the residue taken up in methanol to which charcoal was added. The solution was filtered through a short celite column and the methanol evaporated. The crystalline residue was recrystallized four times from acetone–hexane and formed needles, m.p. 273° (evacuated capillary); $[\alpha]_D$ −24° (*c*, 1.43); $[M]_D$ −99°; pK_a 10.65 (95% EtOH). Found: C, 57.87; H, 7.45. Calc. for $C_{20}H_{32}NI$ (413): C, 58.11; H, 7.75. Infrared spectrum: ν_{max} 1697 cm^{-1} ($>C=\overset{+}{N}<$).

Lactam VIII from Isocarbinolamine VI

The isomethiodide (85 mg) was dissolved in 4 ml of dioxane–water (3:1) and treated with an excess of freshly precipitated silver oxide. After 1 hour the material was filtered and the residue washed with a little

[15]*Further proof of the correctness of the structure and stereochemistry has now been provided (J. ApSimon and O. E. Edwards, in preparation) by partial synthesis from podocarpic acid of the mirror image of an N-acetyl phenol derived from atisine (4).*

dioxane–water. (There appeared to have been some reduction of the silver oxide.) A solution of potassium permanganate (22 mg, 1 equiv.) in 3 ml of water was added dropwise to the filtrate. The first few drops were decolorized slowly but then decolorization became more rapid and manganese dioxide separated. After half of the permanganate solution had been added, the purple color persisted for 0.5 hour and so the addition was stopped. Sodium bisulphite was added to decolorize the solution, which was then percolated through celite to remove manganese dioxide. The filtrate was evaporated to dryness *in vacuo* and the residue taken up in ether. The ether solution was washed with 6 *N* sulphuric acid to remove any basic material, and then with water. The ether extract furnished 30 mg of neutral material of which 22.7 mg was pentane soluble and crystalline with m.p. 129–132°. Recrystallization from pentane gave the lactam VIII as prisms, m.p. 134.5–136°; $[\alpha]_D$ −56° (*c*, 0.81); $[M]_D$ −170°. Found: C, 79.91; H, 10.20. Calc. for $C_{20}H_{31}ON$ (301): C, 79.67; H, 10.37. Infrared spectrum: ν_{max} 1649 cm^{-1} (δ-lactam).

The lactam was recovered quantitatively after 2 hours at 200° in a solution of potassium hydroxide in trimethylene glycol.

N-Methyl Base IX

Azomethine methiodide (220 mg) was dissolved in aqueous methanol (80%, 10 ml) and a large excess of sodium borohydride (130 mg) was added. The solution became cloudy and an oil was gradually precipitated. After 3 hours the solvent was evaporated and the residue taken up in ether, washed with aqueous sodium carbonate, then water, and the ether dried with sodium sulphate. The ether extract was evaporated to give a clear gum (163 mg) which solidified. After four recrystallizations from acetone the product formed prisms, m.p. 59–60°; $[\alpha]_D$ −71° (*c*, 0.93); $[M]_D$ −211°. Found: C, 83.74; H, 11.36. Calc. for $C_{20}H_{33}N$ (287): C, 83.56; H, 11.57.

Lactam VIII from N-Methyl Base IX

A solution of the N-methyl base (85 mg) in pyridine (4 ml) was added to a solution of chromic oxide (138 mg) in pyridine (4 ml) and kept for 20 hours at room temperature. Sulphur dioxide was passed in with cooling until the solution was clear blue-green. The solvent was removed under reduced pressure, and the residue taken up in ether and washed with dilute aqueous hydrochloric acid, then water. The dried ether extract was evaporated to give a clear gum (51 mg) which solidified easily on seeding with the isolactam. The gum was chromatographed on neutral alumina (Grade IV, 1.5 g) and eluted with hexane (20 ml) to give 31 mg of crystalline lactam as prisms from pentane, m.p. 134–136°; $[\alpha]_D$ −57° (*c*, 0.69); $[M]_D$ −171°. It did not depress the melting point of the lactam from the isocarbinolamine and their infrared spectra (mulls) were identical.

Oxidation of N-Methyl Carbinolamine V

The methiodide from 108 mg of azomethine was dissolved in aqueous dioxane and stirred with excess freshly prepared silver oxide. The solid was removed by filtration. A solution of 0.7 g of sodium hydroxide in 4 ml of water was added to the filtrate, followed by dropwise addition over 20 minutes of a solution of 90 mg of potassium permanganate in 8 ml of water. The manganese dioxide was removed by filtration and the filtrate was acidified with dilute sulphuric acid and extracted with methylene chloride. The methylene chloride solution yielded 52 mg of neutral product. This was adsorbed from pentane solution onto 500 mg of alumina (Grade II). One component of the mixture was rapidly eluted with pentane. Chloroform then eluted a fraction from which was obtained, after recrystallization, 15 mg of lactam, m.p. 134.5–136°. This did not depress the melting point of lactam VIII, and their infrared spectra were identical.

Action of Nitrous Acid on the C_{19}-Azomethine III

A solution of azomethine (250 mg), sodium acetate (625 mg), and sodium nitrite (625 mg) in a mixture of dioxane (37.5 ml) and water (25 ml) was treated dropwise with a solution of acetic acid (1.25 ml) in dioxane (2.5 ml) over 6 hours. Nitrogen was passed over the solution continuously and during the addition of the acid the mixture was agitated vigorously. After standing for a further 12 hours, the solvents were evaporated at 30° and the residue taken up in ether. The ether extract was washed with aqueous potassium carbonate, water, 6 *N* sulphuric acid, and then again with water. On evaporation of the dried ether extract, 265 mg of a neutral yellow gum was obtained, $[\alpha]_D$ −48° (*c*, 1.05, $CHCl_3$). Adsorption on alumina (Grade III neutral, 8 g) and eluting with hexane gave the following fractions:

(1) mobile liquid (7.2 mg),
(2) material which crystallized from pentane (17.3 mg),
(3) non-crystalline yellow gum,
(4) yellowish solid, very soluble in pentane (20 mg).

Benzene and benzene–chloroform (3:2) eluted 208 mg of nearly pure hemiacetal (78%) which crystallized spontaneously.

This yield of hemiacetal was exceptional, and on repetition under apparently identical conditions the yield could drop to 60% or less of hemiacetal. The sodium acetate was added with the thought of trapping the primary carbonium ion before it could rearrange. However, no acetate ester was formed, and it appears that this may be useless.

Hemiacetal XIII and its Reduction

After recrystallization from pentane the hemiacetal had m.p. 164–165°, $[\alpha]_D$ −56° (*c*, 1.09). Its infrared spectrum had ν_{max} 3350 (OH) and 1050 (O—C—O—C) cm^{-1}. Found: C, 78.83; H, 10.37. Calc. for $C_{19}H_{30}O_2$: C, 78.57; H, 10.41.

The hemiacetal was inert to sodium borohydride in aqueous methanol. However, in a refluxing solution of lithium aluminum hydride in ether it was quantitatively converted in 1 hour to the corresponding diol. This crystallized from aqueous alcohol as fine needles, m.p. 169°. For analysis this was sublimed at 140° at 5×10^{-4} mm. Found: C, 78.11; H, 11.08. Calc. for $C_{19}H_{32}O_2$: C, 78.03; H, 11.03.

Oxidation of Hemiacetal XIII to a Lactone

(*a*) Hemiacetal (20 mg) in dioxane (3 ml) was treated dropwise with bromine water. The first few drops were decolorized rapidly. The reaction mixture containing a small excess of bromine was left overnight. The solvent was evaporated and the white solid taken up in ether, washed with water, and dried. Evaporation of the ether gave the lactone as a white solid (19 mg). This was purified by percolating a benzene solution through neutral alumina (Grade III). Recrystallization from methanol–water afforded plates, m.p. 162.5–164°, $[\alpha]_D$ −37° (*c*, 0.91). Found: C, 79.03; H, 9.77. Calc. for $C_{19}H_{28}O_2$ (288): C, 79.12; H, 9.79%. Infrared spectrum: ν_{max} 1725 cm^{-1} (δ-lactone).

(*b*) A solution of 80 mg of hemiacetal in 4 ml of acetic acid was oxidized during 0.5 hour by 31 mg of sodium dichromate dihydrate in 1.25 ml of acetic acid. The excess reagent was destroyed by sodium sulphite, then the acetic acid removed under reduced pressure. The residue was taken up in methylene chloride, and this washed with dilute acid and sodium carbonate solution. The 79 mg of product was chromatographed on 1.7 g of neutral alumina (Grade II). Benzene and 1:1 benzene–ether eluted 55 mg of lactone. After recrystallization from aqueous methanol this melted at 163°; mixed m.p. with the lactone from oxidation by bromine–water 164°. The lactone was reduced by lithium aluminum hydride in refluxing ether to the same diol, m.p. 169°, obtained on reduction of the hemiacetal.

Primary Alcohol from XIII

Hemiacetal XIII (150 mg) and hydrazine (95%, 2 ml) in triethylene glycol (4 ml) were warmed overnight on a water bath. A further portion of hydrazine (1 ml) was added and the mixture refluxed at 140° for 1 hour. Potassium hydroxide pellets (1 g) were added gradually and the temperature raised to 200° for 6 hours. Water was added to the cooled mixture, which was then extracted with ether, washed with water, and dried. Evaporation of the ether gave a white solid (138 mg). Chromatography on neutral alumina (Grade III, 5 g) and elution with hexane–benzene mixtures gave a pentane-soluble solid (122 mg) which when crystallized from methanol gave prisms, m.p. 96°, $[\alpha]_D$ −38° (*c*, 1.00). Found: C, 82.30; H, 11.50. Calc. for $C_{19}H_{32}O$: C, 82.54; H, 11.66%. Infrared spectrum: ν_{max} 3260, 1017 cm^{-1} (OH).

Oxidation of Primary Alcohol to Aldehyde

The primary alcohol (88 mg) in acetic acid (4 ml) was treated dropwise with a solution of sodium dichromate dihydrate (31 mg) in acetic acid (1 ml). A small excess of reagent was present for 3 hours. Excess reagent was destroyed with sodium bisulphite and the solvents were evaporated. The solid was taken up in ether, washed with dilute aqueous sodium hydroxide (1%), water, and then dried. Evaporation of the ether gave a neutral solid (81 mg) which was chromatographed on neutral alumina (Grade III, 2 g). Elution with pentane gave the aldehyde, which crystallized from methanol as plates, m.p. 129–131°, $[\alpha]_D$ −94° (*c*, 0.84). Found: C, 82.99; H, 10.75. Calc. for $C_{19}H_{30}O$ (274): C, 83.15; H, 11.02%. Infrared spectrum: ν_{max} 2760, 2680, 1696 cm^{-1} (—CHO).

Oxidation of Aldehyde to Acid XV

Aldehyde (45 mg) in acetic acid (8 ml) was kept with a slight excess of a modified Kiliani reagent (600 mg of sodium dichromate, 800 mg of concentrated H_2SO_4, 1.35 g of water, and 1.35 g of acetic acid) for 2 hours. Excess reagent was decomposed with methanol and a small amount of sodium bicarbonate was added to neutralize the sulphuric acid. The solvents were evaporated and the solid was taken up in ether. The ether solution was extracted with aqueous sodium hydroxide (5%), washed with water, and dried. On evaporation the ether layer gave 37 mg of 'neutral' material. The alkaline extract, on acidification and extraction with ether, afforded 3 mg of gummy material. The 'neutral' material was chromatographed on neutral alumina (Grade III, 1 g). Hexane eluted a trace of aldehyde, while chloroform–methanol eluted the acid (32 mg), which crystallized from methanol–water as plates, m.p. 217°, $[\alpha]_D$ −45° (*c*, 1.43). Found: C, 78.63; H, 10.26. Calc. for $C_{19}H_{30}O_2$: C, 78.57; H, 10.41%. Its pK_a' in 70% alcohol was 9.6 and in 80% dimethyl cellosolve was 9.42 (16). Its infrared spectrum (nujol mull) had peaks at 1695 cm^{-1} (medium) and 1675 cm^{-1} (strong) and a characteristic band for carboxylic acids at 1256 cm^{-1} (medium). In rather concentrated chloroform solution (9.7 mg/ml) its infrared absorption had peaks at 3560, 3480 cm^{-1} (OH) and 1730 (medium), 1690 (strong) cm^{-1} (C=O). In dilute solution in chloroform a new band appeared at 1715 cm^{-1} and the 1730 cm^{-1} band increased in intensity at the expense of the one at 1690 cm^{-1}.

The sodium salt of the acid was prepared in methanol. After removal of the solvent under reduced pressure the residual solid was washed with dry ether. Its infrared spectrum (nujol mull) had no absorption between 1600 and 1800 cm^{-1}, but had typical carboxylate anion absorption at 1565 (medium) and 1545 (strong) cm^{-1}.

1β-Methoxycarbonyl-1α,12β-dimethyl-7-hydroxy-trans-anti-trans-perhydrophenanthrene (XIX)

The α,β-unsaturated ketone from agathenedicarboxylic acid (17) (200 mg) in dry ether was slowly added to a vigorously stirred solution of lithium (300 mg) in liquid ammonia (100 ml). After 40 minutes the stirring was stopped, ammonium chloride (1 g) was carefully added, and the ammonia allowed to evaporate. Water (50 ml) was added to the residual slurry and the mixture was continuously ether-extracted for 36 hours. The extract was dried and evaporated, yielding a yellow oil (170 mg), which was distilled under reduced pressure. The main fraction (120 mg) distilled at 130–140° at 10^{-3} mm and crystallized on treatment with ethyl acetate. Recrystallization from the minimum volume of ethyl acetate yielded colorless prisms (95 mg), m.p. 107–108°, $[\alpha]_D$ +55.5° (*c*, 0.46). Found: C, 73.41; H, 10.30. Calc. for $C_{18}H_{30}O_3$: C, 73.43; H, 10.27. Infrared spectrum: ν_{max} 3550 cm^{-1} (hydroxyl), 1710 cm^{-1} (ester).

1β-Methoxycarbonyl-1α,12β-dimethyl-trans-anti-trans-perhydro-7-phenanthrone (XX)

The above alcohol (100 mg) in benzene (10 ml) and acetic acid (5 ml) was mixed with a solution of sodium dichromate dihydrate (75 mg) in acetic acid (10 ml) and allowed to stand at room temperature for 4 hours. The mixture was poured into water (50 ml) and the benzene layer separated. The aqueous layer was further extracted with benzene (3×25 ml) and the combined extracts washed well with 2 *N* sodium carbonate solution and water. The extract was dried and evaporated, yielding a pale yellow oil (83 mg) which crystallized on treatment with ether. Sublimation at 155° at 5×10^{-4} mm yielded colorless needles, m.p. 196°. Found: C, 73.64; H, 9.42. Calc. for $C_{18}H_{28}O_3$: C, 73.93; H, 9.65. Infrared spectrum: ν_{max} at 1720 cm^{-1}, strong and broad (ketone and ester). Its optical rotatory dispersion curve showed a single positive Cotton effect, λ_{max} 306 mμ, $[\alpha]_{max}$ +1000°; λ_{min} (approx.) 272 mμ, $[\alpha]_{min}$ −625°.

1β-Carboxyl-1α,12β-dimethyl-trans-anti-trans-perhydrophenanthrene (XXI)

The keto ester XX (50 mg) in hydrazine hydrate (100%) (1.5 ml) and triethylene glycol (2 ml) was heated to 140° during 1 hour, potassium hydroxide (600 mg) was added, and the temperature was raised to 200°±5° for a further 4 hours. The reaction mixture was cooled, acidified with 2 *N* sulphuric acid, and ether-extracted. The ether extract was washed well with water, dried, and evaporated to yield a pale yellow oil (35 mg). The product was chromatographed on silica (3 g) in pentane–benzene (50:50) to yield colorless needles, m.p. 130–140°. Sublimation at 120° at 10^{-4} mm yielded the analytical sample (20 mg), m.p. 150–154°, $[\alpha]_D$ +34° (*c*, 0.36). Found: C, 77.07; H, 10.74. Calc. for $C_{17}H_{28}O_2$: C, 77.22; H, 10.67. Infrared spectrum: ν_{max} 1697 cm^{-1} (—COOH); pK_a in 80% ethanol 8.4.

The same acid (XXI) (mixed melting point, infrared, and n.m.r. spectra) was also obtained by a similar Wolff–Kishner reduction of 1β-carboxyl-1α,12β-dimethyl-*trans*-anti-*trans* perhydro-6-phenanthrone (XXIV), kindly supplied by Dr. R. H. Bible, Jr.

1β-Carboxyl-1α,12β-dimethyl-trans-anti-cis-perhydrophenanthrene (XVIII)

1β-Carboxyl-1α,12β-dimethyl-*trans*-anti-*cis*-perhydro-6-phenanthrone (510 mg) (kindly supplied by Dr. R. H. Bible, Jr.), 100% hydrazine hydrate (4 ml), and triethylene glycol (4 ml) were heated to 140° during 1 hour. Potassium hydroxide (4 g) was added and the temperature raised to 200°±5° for a further 4 hours. The reaction mixture was cooled, acidified with 2 *N* sulphuric acid, and ether-extracted. The ether extract was washed well with water, dried, and evaporated to yield a colorless crystalline product (415 mg), m.p. 140–158°. Sublimation at 118° at 10^{-4} mm yielded colorless prisms of the acid XVIII, m.p. 171°, $[\alpha]_D$ +89° (*c*, 0.33). Found: C, 77.31; H, 10.84. Calc. for $C_{17}H_{28}O_2$: C, 77.22; H, 10.67. Infrared spectrum: ν_{max} 1695 cm^{-1} (—COOH); pK_a in 80% ethanol 8.2.

Attempted Synthesis of XVIII from Agathenedicarboxylic Acid

The α,β-unsaturated ketone from agathenedicarboxylic acid (600 mg) in triethylene glycol (5 ml) and hydrazine hydrate (100%) (3 ml) were heated to 140° during 1 hour. Potassium hydroxide (3 g) was added and the temperature raised to 200° for 5 hours. The mixture was cooled, acidified with 2 *N* H_2SO_4, and thoroughly ether-extracted. Drying and evaporation yielded a semicrystalline oil (650 mg) which was chromatographed on silica (10 g). Elution with pentane removed triethylene glycol while benzene–pentane (50:50) gave colorless prisms, m.p. ca. 140°. Recrystallization from *n*-pentane yielded colorless prisms, m.p. 140–145°, $[\alpha]_D$ +128° (*c*, 0.47). Found: C, 77.67; H, 9.76. Calc. for $C_{17}H_{26}O_2$: C, 77.82; H, 9.99. Infrared spectrum: ν_{max} 1698 cm^{-1} (—COOH). Proton resonance was observed at 8.80, 9.16, and 9.35. More than one vinyl hydrogen signal was present, indicating contamination with XXIII.

Hydrogenation of Wolff–Kishner Product

The acid produced above (25 mg) in acetic acid (10 ml) was hydrogenated in the presence of prereduced platinum oxide (24 mg). In 1 hour the uptake of 2.4 ml of hydrogen was observed (calc. for 1 mole 2.3 ml). The solution was filtered and the catalyst washed well with alcohol. Removal of the solvents under vacuum left a colorless oil (25 mg) which crystallized on treatment with ethyl acetate, m.p. 118–132°. Sublimation at 120° at 10^{-4} mm yielded colorless prisms, m.p. 130–136°, $[\alpha]_D$ +32° (*c*, 0.42). Found: C, 77.35; H, 10.54. Calc. for $C_{17}H_{29}O_2$: C, 77.22; H, 10.67. Infrared spectrum: ν_{max} at 1695 cm^{-1} (—COOH). Proton resonance observed at 8.78, 9.025, 9.27, corresponding to a mixture of XVIII and XXI.

The 16,17-Diol

To a solution of 493 mg of hemiacetal XII in 25 ml of dry ether was added 490 mg of lithium aluminum hydride. The solution was refluxed for 2 hours, then the excess reagent destroyed using ethyl acetate. Dilute sulphuric acid was cautiously added, the layers separated, and the aqueous layer extracted three times with ether. The spontaneously crystalline product weighed 540 mg. It was recrystallized from acetone–hexane to a constant melting point of 169°, then sublimed at 110° at 5×10^{-4} mm for analysis. It had $[\alpha]_D$ −28° (*c*, 1.25). Found: C, 78.11; H, 11.08. Calc. for $C_{19}H_{32}O_2$: C, 78.03; H, 11.03. Under less vigorous conditions some hemiacetal remained unreduced.

Lactone XXVII

The 16,17-diol (171 mg) was dissolved in 3 ml of acetic acid. To this was added, with stirring, a solution of 160 mg of sodium dichromate dihydrate in 2 ml of acetic acid. The oxidation was rapid until nearly the equivalent of two atoms of oxygen had been added. After completion of the addition (2 minutes) the reaction mixture was left for 0.5 hour at room temperature. The excess reagent was reduced with sodium bisulphite solution, then the solvent removed under reduced pressure. The residue was taken up in dilute acid and methylene chloride. The methylene chloride was washed with dilute sodium carbonate solution, dried, and the solvent evaporated. The 159 mg of neutral product was adsorbed from hexane on 5 g of neutral alumina (Grade II). After a small non-crystalline forerun (4 mg), hexane and benzene eluted 64 mg of pure lactone. Benzene–ether, 1:1, eluted a mixture of lactones (50 mg), and ether and methanol in ether eluted hydroxylic product. The combined early eluates were crystallized to a constant melting point of 168°, $[\alpha]_D^{25}$ −16° (*c*, 1.49), then sublimed for analysis. Found: C, 78.99; H, 9.94. Calc. for $C_{19}H_{28}O_2$: C, 79.12; H, 9.79. The more strongly adsorbed lactone mixture was separated by careful chromatography into the above lactone and a lactone identical with the one from oxidation of the hemiacetal. The hydroxylic products could not be resolved into pure substances by further chromatography.

Reduction of Lactone XIV to Hemiacetal

Pure lactone (32 mg) was dissolved in 2 ml of dry ether. To this was added a solution of approximately 4 mg of lithium aluminum hydride in 2 ml of ether. After 12 minutes at room temperature the reagent was destroyed with one drop of methanol. The solvent was removed under reduced pressure, and the residue distributed between methylene chloride and dilute acid. The 32 mg of product gave 27 mg of pure hemiacetal XIII.

Reduction of Lactone XXVII

The lactone was inert to sodium borohydride in hot aqueous dioxane. A solution of 14 mg of the lactone in dry ether containing 40 mg of lithium aluminum hydride was completely reduced to the 16,17-diol, m.p. and mixed m.p. 165°, in 15 minutes at room temperature.

A solution of 31 mg of the lactone, m.p. 167°, in 5 ml of ether was prepared. To this was added 2 ml of ether containing approximately 3 mg of lithium aluminum hydride. After 3 minutes at room temperature the excess reagent was destroyed with two drops of methanol and the solvent removed under reduced pressure. The residue was taken up in methylene chloride and dilute sulphuric acid. The methylene chloride layer and washings yielded 31 mg of product. This was dissolved in ca. 2 ml of hexane. After standing overnight the solution had deposited 8 mg of diol. The soluble product was adsorbed from hexane onto 530 mg of neutral alumina, activity II. Hexane, benzene, and ether eluted unchanged lactone (11 mg). Methanol in ether and ethanol in chloroform eluted 10 mg of a mixture of hemiacetal and diol, which were separated by crystallization from hexane. The hemiacetal after three recrystallizations from hexane melted at 164° (crystal form fine matted needles changing slowly to tiny cubes). It did not depress the melting point of hemiacetal XIII, and their infrared spectra (nujol mull of fine needles) were identical.

A reduction for 10 minutes of 48 mg of lactone in 6 ml of ether containing 7 mg of lithium aluminum hydride gave 35 mg of diol, 9 mg of unchanged lactone, and 2 mg of hemiacetal.

Action of Nitrous Acid on the C_{20}-Azomethine Acetate (XXXIV)

A solution of azomethine acetate (500 mg), sodium acetate (1.3 g), and sodium nitrite (1.25 g) in a mixture of dioxane (75 ml) and water (50 ml) was treated dropwise with a solution of acetic acid (2.5 ml) in dioxane (5.0 ml) during 5 hours. Nitrogen was passed over the solution continuously and during the addition of the acid, the mixture was agitated vigorously. The mixture was allowed to stand at room temperature overnight and the solvents were then removed at 50° under reduced pressure. The residue was dissolved in ether and washed with potassium carbonate, water, 6 *N* sulphuric acid, and then again with water. The dried extract was then evaporated, yielding a yellow gum (470 mg) which could not be induced to crystallize. It had infrared absorption at 3400 (OH), 1735 (acetate), and 1640 ($\rangle C{=}CH_2$) cm^{-1}.

The above oil was warmed with methanol and evaporated to small bulk and diluted with water, yielding colorless needles (390 mg). The analytical sample was sublimed at 160° at 10^{-3} mm, m.p. 175°, $[\alpha]_D^1$ −78.5° (*c*, 0.96). Infrared maximum at 1730 cm^{-1} (acetate), 1657 cm^{-1} ($\rangle C{=}CH_2$), and complex ether absorption in the region 1000–1100 cm^{-1}. Found: C, 73.47; H, 9.36; OMe, 8.25. Calc. for $C_{23}H_{36}O_4$: C, 73.36; H, 9.64; OMe, 8.07.

ACKNOWLEDGMENTS

We thank Mr. A. Knoll for the technical assistance, Mr. R. Lauzon for the infrared spectra, and Mr. J. Nicholson for the n.m.r. spectra. We are grateful to Dr. R. Bible for generous gifts of podocarpic derivatives.

REFERENCES

1. W. A. JACOBS. J. Org. Chem. **16**, 1593 (1951).
2. K. WIESNER, R. ARMSTRONG, M. F. BARTLETT, and J. A. EDWARDS. Chem. & Ind. (London), 132 (1954).
3. S. W. PELLETIER and W. A. JACOBS. J. Am. Chem. Soc. **76**, 4496 (1954).
4. D. DVORNIK and O. E. EDWARDS. Chem. & Ind. (London), 623 (1958).
5. S. W. PELLETIER. Chem. & Ind. (London), 1116 (1958).
6. (*a*) D. DVORNIK and O. E. EDWARDS. Tetrahedron, **14**, 54 (1961).
   (*b*) S. W. PELLETIER. Tetrahedron, **14**, 76 (1961).
7. S. W. PELLETIER. J. Am. Chem. Soc. **82**, 2398 (1960).
8. K. WIESNER and J. A. EDWARDS. Experientia, **11**, 255 (1955).
9. H. VORBRÜGGEN and C. DJERASSI. Tetrahedron Letters, No. 3, 119 (1961).
10. C. DJERASSI, E. MOSETTIG, R. C. CAMBIE, P. S. RUTLEDGE, and L. H. BRIGGS. J. Am. Chem. Soc. **83**, 3720 (1961).
11. O E. EDWARDS and R. HOWE. Proc. Chem. Soc. 62 (1959).
12. N. J. LEONARD, A. S. HAY, R. W. FULMER, and V. W. GASH. J. Am. Chem. Soc. **77**, 439 (1955).
13. K. SCHAEFFNER, D. ARIGONI, and O. JEGER. Experientia, **16**, 169 (1960).
14. H. KILIANI and B. MERCK. Ber. **34**, 3562 (1901).
15. J. CASON and G. SUMRELL. J. Org. Chem. **16**, 1177 (1951).
16. P. F. SOMMER, V. P. ARYA, and W. SIMON. Tetrahedron Letters, No. 20, 18 (1960).
17. L. RUZICKA, E. BERROLD, and A. TALLICHET. Helv. Chim. Acta, **24**, 223 (1941).
18. C. DJERASSI, W. CLOSSON, and A. E. LIPPMAN. J. Am. Chem. Soc. **78**, 3163 (1956).
19. R. H. BIBLE and R. R. BURTNER. J. Org. Chem. **26**, 1174 (1961).
20. (*a*) W. P. CAMPBELL and D. TODD. J. Am. Chem. Soc. **64**, 928 (1942).
    (*b*) L. RUZICKA, R. ZWICKY, and O. JEGER. Helv. Chim. Acta, **31**, 2143 (1948).
21. J. C. W. CHIEN. J. Am. Chem. Soc. **82**, 4762 (1960).
22. G. D. TIERS. J. Phys. Chem. **62**, 1151 (1958).
23. O. E. EDWARDS and T. SINGH. Can. J. Chem. **33**, 448 (1955).
24. D. DVORNIK and O. E. EDWARDS. Can. J. Chem. **35**, 860 (1957).
25. H. BROCKMANN and H. SCHODDER. Ber. **74**, 73 (1941).

THE RAMAN SPECTRA OF SULPHURIC, DEUTEROSULPHURIC, FLUOROSULPHURIC, CHLOROSULPHURIC, AND METHANESULPHONIC ACIDS AND THEIR ANIONS

R. J. GILLESPIE AND E. A. ROBINSON[1]
Department of Chemistry, McMaster University, Hamilton, Ontario
Received October 27, 1961

ABSTRACT

The Raman spectra of sulphuric acid, deuterosulphuric acid, chlorosulphuric acid, and methanesulphonic acid have been redetermined, and the spectrum of fluorosulphuric acid measured for the first time. The spectra of fluorosulphuric acid – sulphuric acid, chlorosulphuric acid – sulphuric acid, and fluorosulphuric acid – arsenic trifluoride mixtures have also been measured. The spectra of the hydrogen sulphate, deutero sulphate, fluorosulphate, chlorosulphate, and methanesulphonate anions have been obtained in various solvents. Frequencies are assigned to the normal modes of vibration of all these acids and their anions and the assignments are compared with those of previous workers.

During the investigation of the Raman spectra of the systems H_2SO_4–SO_3, D_2SO_4–SO_3, HSO_3F–SO_3, and HSO_3Cl–SO_3 reported in the following papers it became clear that the spectra of the acids H_2SO_4, D_2SO_4, HSO_3F, HSO_3Cl and their anions were not all known with certainty, either because all the expected lines had not been observed or because no complete assignment of the observed frequencies to the normal modes of vibration had been made. Therefore the Raman spectra of these acids and their anions, and the spectra of methanesulphonic acid and the methanesulphonate ion, were redetermined and in each case the observed frequencies have been assigned to the normal modes of vibration.

SULPHURIC ACID AND DEUTEROSULPHURIC ACID

The results of our measurements of the Raman spectra of H_2SO_4 and D_2SO_4 and the infrared spectrum of H_2SO_4 in the sodium chloride region are given in Table I together with the results of some of the earlier workers (1–5). Our Raman spectra are also shown in Fig. 1. Table I does not include the results of all the previous studies since there is generally good agreement between the various sets of measurements and much of the earlier work has recently been discussed by Walrafen and Dodd (2) and by Giguère and Savoie (4). Some workers have observed additional Raman shifts at 740 and 1050 cm^{-1} and additional weak bands in the infrared at 332, 675, 1050, and 1240 cm^{-1} that we did not observe in our Raman spectrum of H_2SO_4. Also, lines at 711 and 1050 cm^{-1} and at 305 and 475 cm^{-1} have been reported in the Raman and infrared spectra of D_2SO_4 that were not observed by us.

The 1050 cm^{-1} line, which increases in intensity on addition of water to sulphuric acid, is undoubtedly due to the HSO_4^- ion. Giguère and Savoie (4) observed this line in their infrared spectrum of sulphuric acid and claimed that it was due to HSO_4^- ions formed in the autoprotolysis of sulphuric acid,

$$2H_2SO_4 \rightleftarrows H_3SO_4^+ + HSO_4^-.$$

However, it has been shown by other methods that the concentrations of the autoprotolysis ions in 100% sulphuric acid are very small (e.g. at 25° $[H_3SO_4^+] = 0.013$ molal; $[HSO_4^-]$

[1]*Present address: Department of Chemistry, University of Toronto, Toronto 5, Ontario.*

= 0.018 molal (6)), and it is therefore most unlikely that any frequencies due to these ions could be detected in the pure acid by either infrared or Raman spectroscopy. Giguère and Savoie's observation of the 1050 cm^{-1} line in their infrared spectrum was undoubtedly due to HSO_4^- ions formed by the ionization of water impurity in their sample. The same explanation doubtless applies in other cases where the 1050 cm^{-1} has been reported as a line of sulphuric acid. The line observed by Leckie (3) at 740 cm^{-1} is probably due to H_3O^+ impurity since lines near this frequency have been observed in the infrared spectra of hydroxonium salts (7).

In the H_2SO_4 molecules, nine of the normal modes can be described approximately as a symmetric and an asymmetric stretch and a bending mode of the SO_2 group, three similar vibrations of the $S[OH(D)]_2$ group, SO_2 and $S[OH(D)]_2$ rocking modes, and a torsion. In addition there are six vibrations of the OH(D) groups. A reasonably complete assignment of the frequencies to the fundamental modes of H_2SO_4 has been given by Giguère and Savoie (4) and a partial assignment has also been suggested by Walrafen and Dodd (2).

TABLE I

The vibrational spectra of H_2SO_4, D_2SO_4, HSO_3Cl, HSO_3F, and CH_3SO_3H (frequencies in cm^{-1})

H_2SO_4							
Raman				Infrared			
(*a*)	(*b*)	(*c*)	(*d*)	(*a*)	(*e*)	(*f*)	(*c*)
—	—	—	—	—	332	—	—
392(4)dp?	384–434p?	381p?	387(2)	—	372	—	380
422(4)dp		417dp	424(m)	—	420	—	420
563(10)d?	564p?	564dp	560(m)	—	549	—	564
—	—	—	741(w)	—	675	—	675
910(10)p	916p	905p	913(s)	910m	907	903m	905
976(2)dp	970dp	965dp	975(w)	953s	967	967s	965
—	1045p*	—	—	—	1050*	—	—
1137(10)p	1140p	1140p	1140(m)	—	—	—	—
1195(5)p	—	1195dp	1195(w)	1162s	1170	1171s	1175–1250
—	—	—	—	—	1240	—	—
1368dp	1364	1370dp	1360(w)	1360s	1365	1364s	1370
—	—	—	—	—	—	—	1800
—	—	—	—	—	2450	2430w	2490
—	—	—	—	—	2970	3000s	3090

D_2SO_4				HSO_3Cl			
Raman		Infrared		Raman			
(*a*)	(*d*)	(*e*)	(*c*)	(*a*)	(*g*)	(*h*)	(*i*)
—	—	—	305	200(2)p	200(2)?	200(2)	194
356(4)dp?	—	—	—	—	298(7)dp	298(7)	—
395(4)dp	412	—	380	312(8)dp	313(7)	313(7)dp	300
—	—	—	475	416(10)p	416(10)p	416(15)p	410
522(4)p	—	—	—	482(1)dp	482(1)?	482(1)	498
560(6)dp?	550	—	562	513(6)dp	513(4)dp	513(4)	—
—	711	—	—	625(8)p	623(3)dp	623(3)p	606
906(10)p	902	—	900	920(6)p	916(3)p	916(3)p	920
980(2)dp	—	—	985	1150(10)p	1153(3)p	1153(3)p	—
—	1050†	—	—	1209(6)p	—	1213(4)p	1183
—	1133	—	—	1408(4)dp	1396(3)dp	1396(3)dp	1430
1170(10)p	1192	—	1195				
1340(3)dp	1330	—	1350				
—	—	1860	1820				
—	—	2280	2230				

TABLE I (*Concluded*)

HSO_3F		CH_3SO_3H			
Raman	Infrared	Raman			
(*a*)	(*a*)	(*a*)	(*j*)	(*k*)	(*l*)
391	—	338(4)?	335(5)	335(3)	335(4)p?
405(8)dp	—	420(1)	—	—	425(0)
555	—	480(2)p?	479(2)	—	476(2)
560(10)p?	—	506(3)dp	505(3)	502(2)	504(3)dp
850(10)p	840	535(5)p	538(6)	535(4)	534(10)p
960(6)p	960	—	—	—	576?
1178(8)	1145	—	—	—	718(2)p
1230(6)p	1220	772(7)p	774(8)	769(6)	769(2)p
1445(3)dp	1440	—	—	—	810(0)
		904(3)p?	905(2)	895(1)	897(3)dp
		985(1)	986(2)	—	976(3)dp?
		—	—	—	1051(1)dp?
		1123(4)p	1128(4)	—	1112(8)p
		1174(2)p	1174(1)	1179(4)	1170(4)dp
		1265(1)	—	—	1266(2)
		1350(2)	1374(2)	—	1369(4)dp
		1420(4)	1425(2)	1413(3)	1418(10)
		2945(6)	2944(7)	2945(5)	2943(20)
		3032(3)	3033(3)	3030(3)	3034(8)
		—	—	3125(3)	

NOTE: (*a*) Present results; (*b*) Venkateswaren (1); (*c*) Walrafen and Dodd (2); (*d*) Leckie (3); (*e*) Giguère and Savoie (4); (*f*) Marcus and Fresco (5); (*g*) Simon, Kriegsmann, and Dutz (24); (*h*) Matossi and Aderhold (26); (*i*) Vogel-Högler (27); (*j*) Simon and Kriegsmann (11); (*k*) Sandemann (28); (*l*) Gerding and Maarsen (10).
*Due to HSO_4^-.
†Due to DSO_4^-.

Our assignments for the SO_2 stretching and bending modes and the $S(OH)_2$ stretches (Table II) agree with those given by Giguère and Savoie but the remaining assignments

TABLE II

Assignment of the fundamental vibrations of H_2SO_4 and D_2SO_4 (frequencies in cm^{-1})

Species	H_2SO_4			D_2SO_4			Approximate description*
	(*a*)	(*b*)	(*c*)	(*a*)	(*b*)	(*c*)	
a_1	1195	1170	1140	1170	—	—	SO_2 sym. stretch
	910	907	905	907	—	—	$S[OH(D)]_2$ sym. stretch
	563	549	741	522	—	—	SO_2 bend
	392	332?	381	356	—	—	$S[OH(D)]_2$ bend
a_2	392	—	417	356	—	—	Torsion
b_1	973	967	1370	980	—	—	$S[OH(D)]_2$ asym. stretch
	563	420?	1190	560	—	—	SO_2 rock
b_2	1368	1365	965	1340	—	—	SO_2 asym. stretch
	422	372?	564	395	—	—	$S[OH(D)]_2$ rock
a_1	2450	2450	2430	—	1860	1820	O—H(D) sym. stretch
	1137	1170?	1170–1240	—	—	—	O—H(D) bend
a_2	—	740	420	—	—	305	O—H(D) wag
b_1	2970	2970	3000	—	2280	2230	O—H(D) asym. stretch
	—	1240	1800	—	—	—	O—H(D) bend
b_2	—	675?	675	—	—	475	O—H(D) wag

NOTE: (*a*) This work; (*b*) Giguère and Savoie (4); (*c*) Walrafen and Dodd (2).
*Walrafen and Dodd gave a different description of the normal modes of the sulphuric acid molecule based on the four modes of the sulphate ion.

differ from those given by these authors. In the spectrum of SO_2F_2 the SO_2 bend and SO_2 rock have approximately the same frequency of 545 cm^{-1} and are not resolved in the Raman spectrum of the liquid (8). Similarly, in the spectrum of H_2SO_4 it appears that the SO_2 bend and SO_2 rock have approximately the same frequency of 563 cm^{-1}

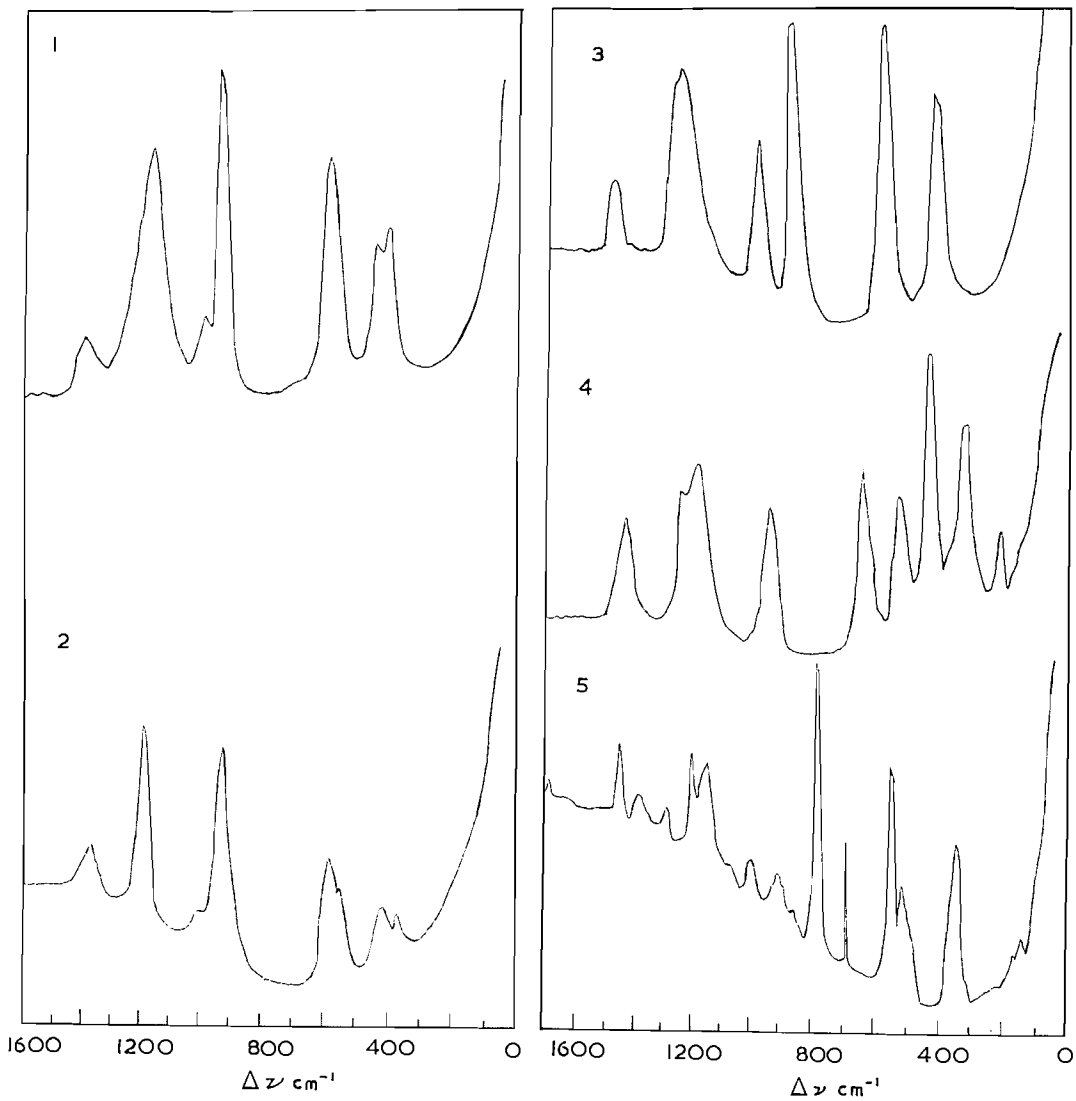

FIG. 1. Raman spectra: (1) H_2SO_4, (2) D_2SO_4, (3) HSO_3F, (4) HSO_3Cl, (5) CH_3SO_3H.

and are not resolved in the Raman spectrum. We agree with Venkateswaren (1) in finding that this line is weakly polarized whereas Walrafen and Dodd (2) found it to be depolarized. If it is indeed weakly polarized this is consistent with it actually consisting of two lines, one of which is polarized and one of which is depolarized. In the spectrum of D_2SO_4 the two lines expected in this region of the spectrum are in fact observed at 560 cm^{-1} (depolarized?) and 522 cm^{-1} (polarized). The latter is assigned to the SO_2 bend and the 560 cm^{-1} line to the SO_2 rock.

In the Raman spectra of H_2SO_4 and D_2SO_4 the lines at 422 and 395 cm^{-1}, respectively, are assigned to the $S(OH)_2$ and $S(OD)_2$ rocking modes and the lines at 392 and 356 cm^{-1}, respectively, to the $S(OH)_2$ and $S(OD)_2$ bending modes. The 392 cm^{-1} line has been reported by Venkateswaren (1) and by Walrafen and Dodd (2) to be weakly polarized.

Although we failed to observe any polarization of either the 392 or the 356 cm^{-1} line it seems probable that both lines are very weakly polarized. The apparent weak polarization of the 392 cm^{-1} line may be due to the depolarized line arising from the torsional mode also having a frequency of approximately 392 cm^{-1} in both H_2SO_4 and D_2SO_4 (cf. 360 cm^{-1} for the torsional mode in SO_2F_2 (8)). It seems probable that the line due to the torsional mode is in fact coincident with some other line in the spectrum since the torsional mode (a_2) should be active in the Raman and inactive in the infrared spectrum and no lines are observed in the Raman spectrum which do not have their counterparts in the infrared spectrum.

It is difficult to make any comparison of our assignment with that of Walrafen and Dodd (2) since these authors assume that the spectrum of sulphuric acid may be related to that of the sulphate ion in crystalline calcium sulphate, for which nine frequencies have been observed. Although they admit that the interactions which remove the degeneracies of the four fundamental frequencies of the sulphate ion to give the nine observed frequencies, are probably considerably different from those arising from the formation of S—OH bonds they assume that the frequencies of crystalline $CaSO_4$ may be used as a guide to the assignment of the frequencies of sulphuric acid, and of the HSO_4^- ion. This does not seem to us to be as reasonable a basis for making assignments as our comparison with other SO_2X_2 molecules and SO_3X^- ions.

Of the six vibrational frequencies (two stretches, two bends, and two wagging or torsional modes) which are theoretically expected to be associated with the O—H(D) groups we have only observed one, a bend at 1137 cm^{-1}, for sulphuric acid. The rather high frequency of this vibration is presumably to be attributed to strong hydrogen bonding between the O—H groups and other oxygen atoms. The O—H(D) stretches were not observed in our Raman spectra presumably due to the insensitivity of the photographic plates in the 1800–3000 cm^{-1} region. However, Giguère and Savoie (4) observed bands in the spectrum of H_2SO_4 at 2450 and 2970 cm^{-1} and in the infrared spectrum of D_2SO_4 at 1860 and 2200 cm^{-1}, which they assigned as the symmetric and asymmetric O—H(D) stretches, respectively. Similar bands were also reported by Walrafen and Dodd (2). Other very weak and somewhat doubtful lines in the infrared spectrum at 1240, 675, and 332 cm^{-1} for H_2SO_4 and at 475 and 305 cm^{-1} for D_2SO_4 may possibly be due to other OH(D) bending or torsional modes.

FLUOROSULPHURIC, CHLOROSULPHURIC, AND METHANESULPHONIC ACIDS

The results of our measurements of the Raman and infrared spectra of HSO_3F, HSO_3Cl, and CH_3SO_3H are given in Table I and Fig. 1. The Raman spectra of HSO_3Cl and $MeSO_3H$ have been reported previously by other workers but there has been no previous study of fluorosulphuric acid. Our measurements are in good agreement with the earlier work except for a few details which are discussed later. The Raman spectra of the systems HSO_3F–H_2SO_4 and HSO_3Cl–H_2SO_4 were also studied and the results are given in Table III. The spectra contain only the lines of the component acids, indicating that there is no extensive ionization or any other reaction in these systems (9).

The nine fundamental vibrations of a molecule of the type SO_2XY may be approximately described as SO_2 symmetric and asymmetric stretches, an SO_2 bending mode, SX and SY stretches, an SO_2 rock, an S—X wag, and S—Y wag, and a torsion. In the molecules HSO_3F, HSO_3Cl, and CH_3SO_3H there are, in addition, three vibrations of the O—H group and in the latter compound nine vibrations of the CH_3 group. Our assignments for these molecules are given in Table IV.

TABLE III

Raman spectra of the H_2SO_4–HSO_3F and H_2SO_4–HSO_3Cl systems (frequencies in cm^{-1})

H_2SO_4–HSO_3F					H_2SO_4–HSO_3Cl				
Percentage of H_2SO_4:					Percentage of H_2SO_4:				
100.0	50.4	28.4	17.2	0.0	100.0	68.2	48.2	25.4	0.0
392	389	390	389	391	—	—	206	208	200
422	420	419	400	405	—	310	319	315	312
—	—	—	550	555	392	385	386	—	—
563	565	562	562	560	422	418	420	418	416
—	849	853	848	850	—	—	—	490	482
910	910	910	906	—	—	506	512	512	513
976	970	970	966	960	563	560	562	560	—
1137	1139	1150	1153	1178	—	620	625	625	625
1195	1202	1205	1190	—	910	915	915	910	—
—	—	1240	1230	1230	—	—	—	925	920
1368	1367	1370	1365	—	976	970	970	970	—
—	1445	1450	1442	1445	1137	1140	1145	1145	1150
					1195	1185	1178	1190	—
					—	1206	1209	1209	1209
					1368	1398	1405	1402	1408

TABLE IV

Assignment of the fundamental vibrations of the acids HO—SO_2—X (frequencies in cm^{-1})

Approximate description of vibration	Species	HSO_3F	HSO_3Cl			CH_3SO_3H		
		(*a*)	(*a*)	(*b*)	(*c*)	(*a*)	(*d*)	(*e*)
SO_2 sym. stretch	(*a'*)	1230	1209	1153	1153	1174	1112	1128
SO_2 asym. stretch	(*a''*)	1445	1408	1396	1396	1350	1369	1354
SO_2 bend	(*a'*)	560	623	623	—	535	534	538
SO_2 rock	(*a''*)	555	513	513	—	506	335	505
S—X stretch	(*a'*)	850	416	416	—	772	769	774
S—OH stretch	(*a'*)	960	920	916	—	904	718	905
S—W wag	(*a'*)	405	200	200	—	338	504	335
S—O wag	(*a'*)	560	482	482	—	480	—	479
Torsion	(*a''*)	391	312	298 313	—	420	—	—
O—H bend	(*a''*)	1178	1150	—	—	1123	1170	1174

NOTE: (*a*) Present work; (*b*) Simon, Kriegsmann, and Dutz (25); (*c*) Vogel-Högler (27); (*d*) Gerding and Maarsen (10); (*e*) Simon and Kriegsmann (11).

The assignment of the line at 1174 cm^{-1} to the SO_2 symmetric stretch in CH_3SO_3H differs from the assignment of previous workers (10, 11) who assigned this frequency to the O—H wag and gave 1128 cm^{-1} as the SO_2 symmetric stretch. Our assignment of the SO_2 symmetric stretch in HSO_3Cl also differs from that given previously by Simon *et al.* (25). These authors did not observe a separate line at 1209 cm^{-1} but only a broad band centered at 1153 cm^{-1}, which they assigned to the SO_2 symmetric stretch. In our spectrum two separate lines were observed in this region at 1209 and 1150 cm^{-1}. The former is assigned to the SO_2 symmetric stretch and the latter to an O—H bend. In sulphuric acid we have assigned the analogous vibrations at 1195 and 1137 cm^{-1}, respectively. Two lines are also observed at similar frequencies in the spectrum of fluorosulphuric acid; one at 1230 cm^{-1} is assigned to the SO_2 symmetric stretch and the other at 1178 cm^{-1} to an O—H wag. In the spectrum of a 50 mole% solution of HSO_3F in AsF_3 the band at 1178 cm^{-1} is absent, although that at 1230 cm^{-1} appears strongly (Fig. 2); this supports the assignment of the 1178 cm^{-1} line as an O—H bend. Presumably

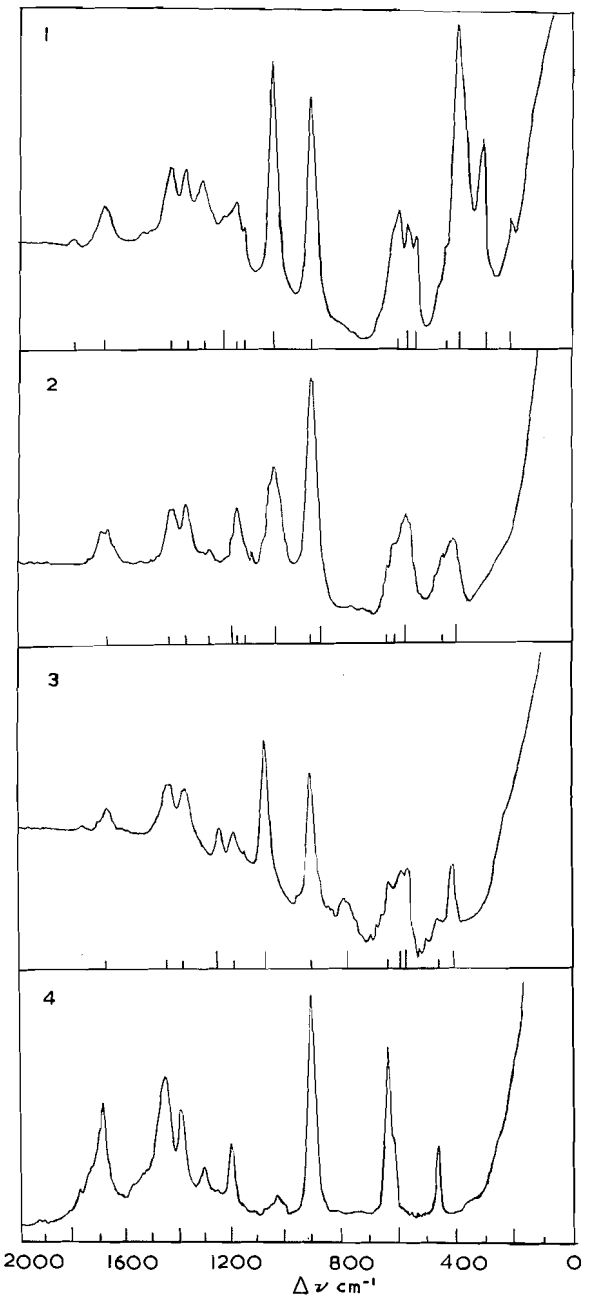

FIG. 2. Raman spectra of 1:1 mixtures of some acids with acetic acid: (1) HSO_3Cl–CH_3CO_2H, (2) H_2SO_4–CH_3CO_2H, (3) HSO_3F–CH_3CO_2H, (4) CH_3CO_2H. ¦ anion lines, | solvent lines.

the change in the nature and extent of hydrogen bonding caused by diluting the HSO_3F with AsF_3 shifts this band to some other region of the spectrum, probably to a lower frequency where it is obscured by another line. In other respects this spectrum is simply a superposition of the Raman spectra of arsenic trifluoride and fluorosulphuric acid, showing that there is no appreciable reaction or ionization in this system. This result is

in agreement with conductimetric measurements on dilute solutions of arsenic trifluoride in fluorosulphuric acid which show that AsF_3 is only slightly ionized (12).

It is interesting to note that the S—OH stretching frequencies HSO_3F, 960 cm^{-1}; HSO_3Cl, 920 cm^{-1}; CH_3SO_3H, 904 cm^{-1} decrease in the order of decreasing acid strength (9). The frequency of the O—H bend also apparently decreases as the acid strength decreases.

The assignments of the SO_2 bend and rocking vibration in these molecules were made by comparison with the assignment of the similar modes of SO_2Cl_2 and SO_2F_2 (8) and they are also consistent with the assignments made above for H_2SO_4 and D_2SO_4.

In fluorosulphuric acid the SF stretch is identified as the line at 850 cm^{-1} by comparison with the frequency of the similar vibration in related molecules. The remaining lines in the Raman spectrum of HSO_3F at 405 and 395 cm^{-1} can be reasonably assigned to the S—F wag and to the torsional mode. The only remaining vibration to which a frequency has to be assigned is the S(OH) bend. We presume that this also contributes to the band at 560 cm^{-1} on the grounds that the frequency of this vibration is probably greater than 482 cm^{-1}, which we assign below to the analogous vibration in HSO_3Cl, since the S(OH) stretch has a higher frequency in HSO_3F than in HSO_3Cl.

In the spectrum of HSO_3Cl the strong polarized band at 416 cm^{-1} is assigned to the S—Cl stretch and the low-frequency line at 200 cm^{-1} to the S—Cl wag. The line at 312 cm^{-1} is assigned as the torsion as this is the only low-frequency depolarized line. This assignment is also reasonably consistent with the frequencies assigned to this torsion in other related molecules. Only the S—OH wag remains to be considered and the weak line at 482 cm^{-1} must be assigned to this vibration.

In the spectrum of methanesulphonic acid the line at 772 cm^{-1} can without doubt be assigned to the C—S stretch. The frequency of 338 cm^{-1} (polarized) then seems reasonable for the S—CH_3 wag, leaving the line at 420 cm^{-1} as the torsion and that at 480 cm^{-1} (polarized) as the S—OH wag. The frequency of the S(OH) bend is very similar to that in HSO_2Cl, which is consistent with the similarity of the frequencies of the S(OH) stretches of these two molecules. The remaining lines may be assigned to C—H vibrations: 985 cm^{-1} as a CH_3 wag, 1265 and 1420 cm^{-1} as CH_3 bends, and 3032 and 2945 cm^{-1} as CH_3 stretches (11). The O—H stretch has apparently not been observed.

THE ANIONS HSO_4^-, DSO_4^-, SO_3F^-, SO_3Cl^-, $CH_3SO_3^-$

These ions have all been studied previously, although, in some cases, only a few of the strongest lines were observed or a limited region of the spectrum only was investigated, especially in the case of infrared studies. The results obtained in the present work are shown in Table V together with those of other investigators.

Siebert studied the Raman spectrum of a solution of sodium fluorosulphate in water (13). The infrared spectra of solid alkali metal, ammonium, silver, and triphenyl carbonium fluorosulphates have been investigated by Sharpe (14). A single line at 1080 cm^{-1} due to the fluorosulphate ion was observed by Millen (15) in the Raman spectrum of solid nitronium fluorosulphate. In the present work the following solutions containing the fluorosulphate ion were examined:

(i) Sodium fluorosulphate in water.

(ii) Solutions of sodium chloride and of sodium sulphate in fluorosulphuric acid. In these solutions fluorosulphate ion is formed according to the equations

$$Na_2SO_4 + 2HSO_3F = 2Na^+ + 2SO_3F^- + H_2SO_4,$$

$$NaCl + HSO_3F = Na^+ + SO_3F^- + HCl.$$

TABLE V

The vibrational spectra of the ions HSO_4^-, DSO_4^-, SO_3F^-, SO_3Cl^-, and $CH_3SO_3^-$
(frequencies in cm^{-1})

HSO_4^-					SO_3F^-					
(*a*)	(*b*)	(*c*)	(*d*)	(*e*)	(*f*)	(*g*)	(*h*)	(*i*)	(*j*)	(*k*)
440	420	—	429	420	409	409	408	408	—	—
608	595	590	594	593	566	566	562	562	565	—
902	890	895	887	885	592	592	600	608	583	—
—	—	—	982	—	786	786	782	808	732	710
1036	1042	1040	1051	1050	—	—	—	—	970	—
1195	1191	1195	1200	1230	1082	1082	1080	1083	1073	1070
—	—	—	—	1341	1250	1287	1225	1235	1277	1289
					—	—	—	—	1299	—
					—	—	—	—	1656	1643
					—	—	—	—	2347	2320

$CH_3SO_3^-$					DSO_4^-	SO_3Cl^-				
(*l*)	(*m*)	(*n*)	(*o*)	(*p*)	(*q*)	(*r*)	(*s*)	(*t*)	(*u*)	(*v*)
344	—	346	345	348	411	215	220	220	—	—
533	—	522	524	533	572	390	392	400	—	—
560	—	552	556	560	632	540	535	538	535	540
778	789	785	784	789	910	563	567	570	565	562
960	964	962	965	970	1050	—	—	—	585	580
1050	1060*	1049	1049	1054	1194	1050	1052	1050	1044	1044
1177	1200	1182	1185	1184	—	—	—	—	1150	1160
1268	1254	1238	1238	1225	—	1195	1191	1200	1275	1250
1368	1330	1362	1362	—						
1435	1417	1421	1425	1429						
—	1433	—	—	—						
—	2340	—	—	—						
2943	2945	2943	2943	2944						
3020	3020	3021	3022	3024						

NOTE: (*a*) Present results, water in sulphuric acid (85% H_2SO_4) (Raman).
(*b*) Present results, sulphuric acid in acetic acid (Raman). Lines due to CH_3COOH and $CH_3COOH_2^+$ observed at 452, 629, 914, 1179, 1283, 1370, 1425, and 1676 cm^{-1}.
(*c*) Present results, $KHSO_4$ in sulphuric acid (Raman).
(*d*) $NaHSO_4$ in water (Raman) (Siebert (13)).
(*e*) Water in sulphuric acid (infrared) (Walrafen and Dodd (2)).
(*f*) Present results, $KFSO_3$ in water (Raman).
(*g*) $KFSO_3$ in water (Raman) (Siebert (13)).
(*h*) Present results, fluorosulphuric acid in acetic acid (Raman). Lines also appear in the spectrum at 461, 671, 908, 1192, 1380, 1448, and 1678 cm^{-1} due presumably to CH_3COOH and $CH_3COOH_2^+$.
(*i*) Present results, water in HSO_3F (Raman). Lines also appear in the spectrum at 844, 970, 1185, and 1408 cm^{-1} due to non-ionized HSO_3F, and at 910 cm^{-1} due to H_2SO_4.
(*j*) $KFSO_3$ (infrared) (Sharpe (14)).
(*k*) $Ph_3C^+.SO_3F^-$ (infrared) (Sharpe and Sheppard (29)).
(*l*) Present results, water in menthanesulphonic acid. Lines which were observed at 484 and 912 cm^{-1} are presumably due to non-ionized CH_3SO_3H.
(*m*) $CH_3SO_3.Na$ (infrared) (Siebert (13)).
(*n*) $CH_3SO_3.K$ (infrared) (Gerding and Maarsen (10)).
(*o*) $CH_3SO_3.Na$ (infrared) (Gerding and Maarsen (10)).
(*p*) $CH_3SO_3.Na$ (infrared) (Simon and Kriegsmann (19)).
(*q*) Present results, deuterium oxide in D_2SO_4 (12% D_2O) (Raman).
(*r*) Present results, $NaSO_3Cl$ in dimethyl sulphoxide (Raman). Lines due to the solvent were observed at 311, 337, 384, 602, 671, 703, 901, 931, 955, 1043, 1149, 1228, 1312, 1335, and 1420 cm^{-1}.
(*s*) Present results, KSO_3Cl in dimethyl sulphoxide (Raman). Lines due to the solvent were observed at 309, 384, 602, 671, 703, 901, 931, 953, 1044, 1149, 1230, 1314, 1340, and 1422 cm^{-1}.
(*t*) Present results, HSO_3Cl dissolved in acetic acid (Raman). Lines due to CH_3COOH and $CH_3COOH_2^+$ were observed at 603, 910, 1159, 1303, 1370, 1430, and 1676 cm^{-1}. The line observed at 313 cm^{-1} is presumably due to non-ionized chlorosulphuric acid.
(*u*) $PCl_5.SO_3$ (infrared) (Waddington and Klanberg (16)).
(*v*) $[(CH_3)_4N]Cl.SO_3$ (infrared) (Waddington and Klanberg (16)).
*Actually observed as a triplet at 1050, 1060, and 1073 cm^{-1}.

The hydrogen chloride was removed by warming the solutions. In the Raman spectra of these solutions only one new Raman shift, a strong line at 1080 cm^{-1}, was observed, and the intensity of the solvent line at 1230 cm^{-1} was enhanced. Other lines due to the fluorosulphate ion are obscured by the spectrum of the solvent.

(iii) Mixtures of acetic acid and fluorosulphuric acid. In addition to the lines due to the component acids several new lines which could be attributed to the SO_3F^- ion were observed (Fig. 3).

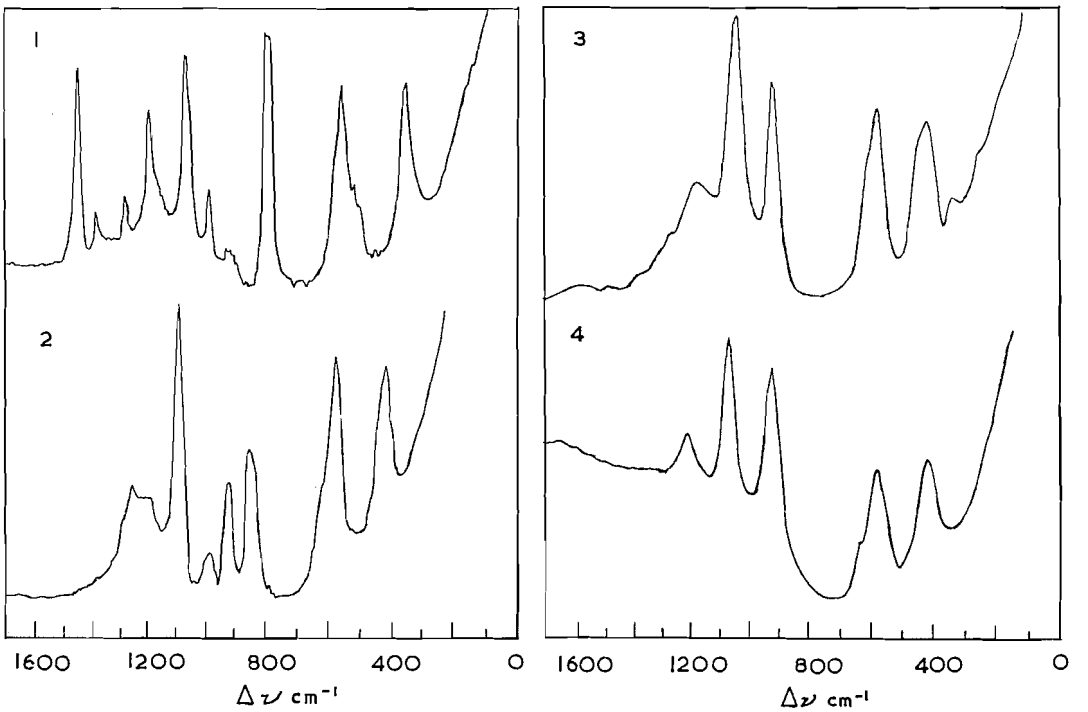

FIG. 3. Raman spectra of solutions of water in some acids: (1) 15% H_2O in CH_3SO_3H, (2) 10% H_2O in HSO_3F, (3) 15% H_2O in H_2SO_4, (4) 12% D_2O in D_2SO_4.

(iv) Solutions of water in fluorosulphuric acid. Fluorosulphate ion is formed by the ionization

$$H_2O + HSO_3F \rightleftharpoons H_3O^+ + SO_3F^-,$$

although there is also slow hydrolysis,

$$HSO_3F + H_2O \rightleftharpoons HF + H_2SO_4.$$

Lines due to the FSO_3^- ion and the 910 cm^{-1} line of sulphuric acid were observed in addition to those of fluorosulphuric acid (Fig. 2).

Simple metal chlorosulphates have not been studied previously, although Waddington and Klanberg (16) have attributed some of the bands of the infrared spectra of the 1:1 complexes of $[(CH_3)_4N]Cl$ and PCl_5 with sulphur trioxide, which they formulated as the chlorosulphates $(CH_3)_4N^+SO_3Cl^-$ and $PCl_4^+SO_3Cl^-$, to the chlorosulphate ion.

The following solutions containing the chlorosulphate ion were studied:

(i) Solutions of sodium and potassium chlorosulphates in dimethyl sulphoxide.

(ii) Mixtures of acetic acid and chlorosulphuric acid. In addition to the lines due to the component acids several new lines which could be attributed to the SO_3Cl^- ion were observed (Fig. 3).

(iii) Solutions of potassium chloride and potassium sulphate in chlorosulphuric acid in which the chlorosulphate ion is formed by the reactions

$$K_2SO_4 + 2HSO_3Cl = 2K^+ + 2SO_3Cl^- + H_2SO_4,$$
$$KCl + HSO_3Cl = K^+ + SO_3Cl^- + HCl.$$

The spectrum of the SO_3Cl^- ion is partially obscured by that of the acid. However, a strong line is observed at 1054 cm^{-1}, the 1209 cm^{-1} line of the acid is enhanced, and a weak line is found at 538 cm^{-1}.

The vibrational spectrum of HSO_4^- has been obtained previously from studies of solutions of water in sulphuric acid (e.g. ref. 2), from an aqueous solution of sodium hydrogensulphate (13), and from infrared studies of crystalline ammonium, sodium, and potassium hydrogensulphates (17). In the present work the Raman spectrum of the hydrogensulphate ion was obtained from the spectrum of three different solutions:

(i) Solutions of water in sulphuric acid in which hydrogensulphate ion is formed according to the equation

$$H_2O + H_2SO_4 = H_3O^+ + HSO_4^-.$$

The spectra obtained (Fig. 3) were somewhat more complex than would be expected from this equation and a detailed interpretation of the spectra gives evidence for some additional species, probably the hydrogen-bonded "ion-pair" $H_3O^+.HSO_4^-$. These measurements will be discussed in more detail in a later paper.

(ii) A solution of sulphuric acid in acetic acid (Fig. 2). The low intensities of the characteristic lines of sulphuric acid in the spectrum of an approximately equimolal mixture of sulphuric and acetic acids shows that ionization is extensive:

$$CH_3CO_2H + H_2SO_4 = CH_3CO_2H_2^+ + HSO_4^-.$$

This is consistent with the conclusion from previous cryoscopic and conductimetric measurements that ionization is essentially complete in dilute solutions of acetic acid in sulphuric acid (18).

(iii) A solution of potassium sulphate in sulphuric acid.

There is generally good agreement between our different sets of measurements and earlier work with respect to the frequencies that may be attributed to the hydrogensulphate ion. The infrared spectra of solid hydrogen sulphates (17) are rather more complex than the spectra of the ion in solution: this is presumably to be attributed to crystal-field splitting of the three degenerate modes of the HSO_4^- ion. Because of their complexity these spectra have not been given in Table V; they lend general support to our assignment of the six fundamentals.

The fundamental frequencies of the deuterosulphate ion were obtained from the spectra of solutions of D_2O in D_2SO_4. Similar measurements have previously been reported by Leckie (3), although he did not interpret his spectra in detail.

The spectrum of the methanesulphonate ion was obtained similarly from measurements on solutions of water in methanesulphonic acid. The infrared spectra of some salts of methanesulphonic acid have been reported previously by Gerding and Maarsen (10), by Siebert (13), and by Simon and Kriegsmann (19). The present spectrum is in good agreement with the previous work.

The ions XSO_3^- have tetrahedral structures and belong to the C_{3v} point group. They therefore have six normal modes of vibration which should all be active in both the Raman and the infrared spectrum. It is convenient to describe the three totally symmetric (a) vibrations as an SO_3 symmetric stretch, an SX stretch, and an SO_3 symmetric bend, and the asymmetric (e) vibrations as an SO_3 asymmetric stretch, an SX wag (or XSO_3 deformation), and an SO_3 asymmetric bend. Our assignments and those of previous workers are given in Table VI.

TABLE VI

Assignment of the fundamental vibrations of the anions XSO_3^- (frequencies in cm^{-1})

Approximate description	HSO_4^-*		DSO_4^-	SO_3Cl^-		SO_3F^-			$CH_3SO_3^-$			
	(*a*)	(*b*)	(*a*)	(*a*)	(*c*)	(*a*)	(*b*)	(*d*)	(*a*)	(*e*)	(*b*)	(*f*)
SO_3 sym. stretch (*a*)	1040	1051	1050	1050	1044	1082	1082	1073	1050	1054	1055	1049
SX stretch (*a*)	895	887	907	416	540	786	786	732	778	789	790	785
SO_3 sym. bend (*a*)	594	594	572	535	565	566	566	565	560	533	562	554
SO_3 asym. stretch (*e*)	1195	1200	1194	1195	1275	1230	1287	1277	1177	1200	1200	1183
SO_3 asym. bend (*e*)	594	594	632	585	583	592	592	583	532	560	532	523
SX wag (*e*)	411	429	411	220	—	405	409	—	344	346	348	346

NOTE: (*a*) Present results; (*b*) Siebert (13); (*c*) Waddington and Klanberg (16); (*d*) Sharpe (14); (*e*) Simon and Kriegsmann (11); (*f*) Gerding and Maarsen (10).
*Walrafen and Dodd (2) also assign the frequencies of HSO_4^- to normal vibrations of the ion but only group them as (*a*) or (*e*) vibrations, i.e. 1341, 1050, and 885 cm^{-1} (*a*); 1230, 593, and 417 cm^{-1} (*e*).

The SO_3 symmetric and asymmetric stretches and bends are easily assigned by comparison with the frequencies of the corresponding SO_2 vibrations. It is found that frequencies of the symmetric and asymmetric stretching modes fit the same linear relationship that has been shown to hold for the SO_2 symmetric and asymmetric stretches of sulphuryl compounds (20). They have lower frequencies than the corresponding SO_2 stretches in the parent acids, which is consistent with the reduced double-bond character of the SO bonds.

The SX stretches have frequencies that are very similar to those of the SX stretching modes in the parent acids. The somewhat lower frequency of the SF stretch in the fluorosulphate ion compared with that for the analogous vibration in fluorosulphuric acid is interesting and probably indicates that the partial double-bond character of the S—F bond in the fluorosulphate ion is appreciably less than in fluorosulphuric acid.

The spectrum of the SO_3F^- ion is very similar to that of the isoelectronic species perchloryl fluoride, ClO_3F, for which the Raman spectrum has been obtained by Powell and Lippincott (21) and the infrared spectrum by Lide and Mann (22). The assignment for SO_3F^- given in Table VI receives strong support from the fact that it is closely paralleled by Powell and Lippincott's assignment for ClO_3F, as is shown in Table VII.

TABLE VII

Comparison of the Raman spectra of ClO_3F and SO_3F^- (frequencies in cm^{-1})

SO_3F^-	ClO_3F		
	Assignment (21)		
408	405	Cl—F rock	$\nu_6(e)$
566	549	ClO_3 deformation	$\nu_3(a_1)$
592	589	ClO_3 deformation	$\nu_5(e)$
786	704, 714*	Cl—F stretch	$\nu_2(a_1)$
1082	1061	ClO_3 symmetric stretch	$\nu_1(a_1)$
1230	1315 or 1175	ClO_3 asymmetric stretch	$\nu_4(e)$

NOTE: ν_4 was assigned the frequency of 1315 cm^{-1} by Powell and Lippincott (21). It could be reassigned the frequency of 1175 cm^{-1}, which was interpreted by these workers as $2\nu_6$, in which case the 1312 cm^{-1} line could be reassigned to $\nu_2+\nu_6$.
*Two lines due to $Cl^{37}F$ and $Cl^{35}F$ respectively.

Waddington and Klanberg (16) did not observe the lines at 220 and 416 cm^{-1} in the spectrum of SO_3Cl^-, since their measurements did not extend to this region of the

spectrum. They assigned 540 cm^{-1} as the S—Cl stretch, 1275 cm^{-1} (in $(CH_3)_4N.SO_3Cl$) as the SO_3 asymmetric stretch, and 1150 cm^{-1} as a combination of the S—Cl stretch and asymmetric SO_3 bend ($\nu_2(a_1)+\nu_5(e)$ = 580+540 = 1120). We reassign the band at 1150 cm^{-1} in their spectrum, which corresponds to the line at 1195 cm^{-1} in our spectrum, to the SO_3 asymmetric stretch in which case the line at 1275 cm^{-1} in their infrared spectrum can be interpreted as a combination of the symmetric SO_3 stretch and S—Cl wag ($\nu_1(a_1)+\nu_6(e)$ = 1050+220 = 1270 cm^{-1}). We assume that the line at 565 cm^{-1} in the infrared spectrum, which we did not observe in the Raman spectrum, is due to the removal of degeneracy by the crystal field.

The line at 960 cm^{-1} in the spectrum of the methanesulphonate ion may be assigned as a CH_3 wag and those at 1268 and 1435 cm^{-1}, and 2943 and 3020 cm^{-1}, as CH_3 bends and CH_3 stretches by comparison with the similar lines in the spectrum of methanesulphonic acid. The line at 1368 cm^{-1} is presumably also a CH_3 wag and an analogous line may be present in the spectrum of methanesulphonic acid but it almost coincides with the line at 1350 cm^{-1}, which is the SO_2 symmetric stretch in this molecule. It is of interest to note that the frequencies of the CH_3 vibrations are very similar in both the acid and its anion.

EXPERIMENTAL

Sulphuric acid was prepared by adjustment of the freezing point of A.R. grade acid to 10.37° (30) by addition of A.R. grade oleum. Fluorosulphuric acid and chlorosulphuric acid were purified by distillation of the commercial products in a dry atmosphere, and had b.p.'s 161–162° and 152°, respectively. Methanesulphonic acid (Eastman Kodak) was purified by fractional crystallization (m.p. = 19.6°). Deuterosulphuric acid was prepared by slowly distilling sulphur trioxide into cooled deuterium oxide (ca. 97% D_2O) until the increase in weight indicated that a weak deutero-oleum had been produced. Then deuterium oxide was added to the weak oleum until the maximum freezing point of 14.2° was reached (23). Potassium fluorosulphate was prepared by the reaction between potassium chloride and fluorosulphuric acid. Fluorosulphuric acid was distilled onto the chloride and then the mixture heated under reflux until the reaction was complete. Excess fluorosulphuric acid was removed under reduced pressure. Sodium and potassium chlorosulphates were prepared by a similar method except that in this case only slightly more than the stoichiometric amount of chlorosulphuric acid was used and the excess removed by washing with acetonitrile and nitromethane. Acetic acid was purified by fractional crystallization. Dimethyl sulphoxide was 99.9% pure "Baker analyzed" solvent.

The Raman spectrometer and the method for obtaining depolarization factors have been described previously (24). Specimens for infrared spectra were thin films of liquid pressed between silver chloride disks. The infrared spectra were obtained with a Perkin-Elmer (model 21) spectrometer.

ACKNOWLEDGMENTS

We thank Dr. Sharda Dasgupta for carrying out the infrared measurements and Dr. R. H. Tomlinson for a gift of deuterium oxide.

The National Research Council and the Ontario Research Foundation are thanked for financial assistance.

REFERENCES

1. C. S. Venkateswaren. Proc. Indian Acad. Sci. A, **4**, 174 (1936).
2. G. E. Walrafen and D. M. Dodd. Trans. Faraday Soc. **57**, 1286 (1961).
3. A. H. Leckie. Trans. Faraday Soc. **32**, 1700 (1936).
4. P. A. Giguère and R. Savoie. Can. J. Chem. **38**, 2467 (1960).
5. R. A. Marcus and J. M. Fresco. J. Chem. Phys. **27**, 564 (1957).
6. R. J. Gillespie and E. A. Robinson. *In* Advances in inorganic chemistry and radiochemistry. Vol. I. 1959. p. 387.
7. C. C. Ferriso and D. F. Hornig. **23**, 1464 (1955).
8. R. J. Gillespie and E. A. Robinson. Can. J. Chem. **39**, 2171 (1961).
9. J. Barr, R. J. Gillespie, and E. A. Robinson. Can. J. Chem. **39**, 1266 (1961).
10. H. Gerding and J. W. Maarsen. Rec. trav. chim. **77**, 374 (1958).
11. A. Simon and H. Kriegsmann. Ber. **89**, 238 (1956).

12. J. BARR and R. J. GILLESPIE. Unpublished results.
13. H. SIEBERT. Z. anorg. u. allgem. Chem. **289**, 15 (1957).
14. D. W. A. SHARPE. J. Chem. Soc. 376 (1957).
15. D. J. MILLEN. J. Chem. Soc. 2606 (1950).
16. T. C. WADDINGTON and F. KLANBERG. J. Chem. Soc. 2339 (1960).
17. F. A. MILLER, A. L. CARLSON, F. F. BENTLEY, and W. H. JONES. Spectrochim. Acta, **16**, 135 (1960). F. A. MILLER and C. H. WILKINS. Anal. Chem. **26**, 1253 (1952).
18. R. J. GILLESPIE. J. Chem. Soc. 2473 (1950). R. J. GILLESPIE and S. WASIF. J. Chem. Soc. 221 (1953).
19. A. SIMON and H. KRIEGSMANN. Ber. **89**, 1718 (1956).
20. E. A. ROBINSON. Can. J. Chem. **39**, 247 (1961).
21. F. X. POWELL and E. R. LIPPINCOTT. J. Chem. Phys. **32**, 1883 (1960).
22. D. R. LIDE and D. E. MANN. J. Chem. Phys. **25**, 1138 (1956).
23. R. H. FLOWERS, R. J. GILLESPIE, and J. V. OUBRIDGE. J. Chem. Soc. 667 (1958).
24. R. J. GILLESPIE and E. A. ROBINSON. Can. J. Chem. **39**, 2179 (1961).
25. A. SIMON, H. KRIEGSMANN, and H. DUTZ. Ber. **89**, 2378 (1956).
26. F. MATOSSI and H. ADERHOLD. Z. physik, **68**, 683 (1931).
27. R. VOGEL-HÖGLER. Acta Phys. Austriaca, **1**, 323 (1948).
28. I. SANDEMANN. J. Chem. Soc. 1135 (1953).
29. D. W. A. SHARPE and N. SHEPPARD. J. Chem. Soc. 674 (1957).
30. J. E. KUNZLER and W. F. GIAUQUE. J. Am. Chem. Soc. **74**, 5271 (1952).

RAMAN SPECTRA OF THE H_2SO_4–SO_3 AND D_2SO_4–SO_3 SYSTEMS: EVIDENCE FOR THE OCCURRENCE OF POLYSULPHURIC ACIDS

R. J. GILLESPIE AND E. A. ROBINSON[1]
Department of Chemistry, McMaster University, Hamilton, Ontario

Received October 27, 1961

ABSTRACT

The Raman spectra of oleums, i.e. mixtures of sulphur trioxide and sulphuric acid, have been re-examined. Similar measurements on the sulphur trioxide – deuterosulphuric acid (D_2SO_4) system are also reported. The experimental results and conclusions of previous similar work on oleums are discussed. By comparison of the spectra of oleums with those of the polysulphuryl halides it is shown that the polysulphuric acids $H_2S_2O_7$ and $H_2S_3O_{10}$ are present in this system. The increase in the frequency of the SO_2 stretching vibrations with increasing concentration of sulphur trioxide gives evidence for the existence of higher polysulphuric acids such as $H_2S_4O_{13}$ at high concentrations of sulphur trioxide. In relatively concentrated oleum, sulphur trioxide monomer and trimer are also present. It is shown that the self-dissociation of liquid $H_2S_2O_7$ gives mainly molecular $H_2S_2O_{10}$ and H_2SO_4 and not ionic species. The conclusions reached from the interpretation of the Raman spectra of the D_2SO_4–SO_3 system are similar to those arrived at for sulphuric acid oleums. The spectra of solutions of $NaHSO_4$ in oleums were also examined, and are discussed.

INTRODUCTION

The constitution of oleum solutions has been examined by several workers using Raman spectroscopy. The early work is surveyed by Millen (1) and more recently the system has been examined by Walrafen and Young (2). The infrared spectra of oleums have also been reported very recently by Giguère and Savoie (3). The previous workers are agreed that the spectra give evidence for the formation of $H_2S_2O_7$. Millen (1) claimed that the spectra also provide evidence for the formation of higher polysulphuric acids such as $H_2S_3O_{10}$ and $H_2S_4O_{13}$. The occurrence of such species in the H_2SO_4–SO_3 system has been disputed by Walrafen and Young (2), who claim that the Raman spectra can be explained in terms of H_2SO_4, $H_2S_2O_7$, ions derived from $H_2S_2O_7$ (e.g. $HS_2O_7^-$ and $H_3SO_4^+$), SO_3 monomer, and SO_3 polymer only. Giguère and Savoie (3) claim that their spectra also indicate the formation of higher polysulphuric acids such as $H_2S_3O_{10}$ in addition to $H_2S_2O_7$. In fact neither Millen's interpretation of the earlier Raman spectra (1) nor the work of Giguère and Savoie (3) gives direct proof for the existence of polyacids higher than $H_2S_2O_7$ and their arguments are not conclusive. Thus, although salts such as $K_2S_3O_{10}$ (4) and $(NO_2)_2S_3O_{10}$ (5) are well established, the existence of the parent acid has been less certain. The present work provides conclusive evidence for the occurrence of $H_2S_3O_{10}$ and strong evidence for higher acids such as $H_2S_4O_{13}$, although it is not possible to deduce the exact chain lengths of the higher polyacids. By comparison of the Raman spectra of oleums with those of $S_2O_5F_2$ and $S_3O_8F_2$, which have been shown to be linear acyclic polymers (6), the occurrence of $H_2S_2O_7$ and $H_2S_3O_{10}$, which are isoelectronic with $S_2O_5F_2$ and $S_3O_8F_2$, respectively, is proved. Although comparison of the oleum spectra with that of $S_4O_{11}F_2$ (7), with which $H_2S_4O_{13}$ is isoelectronic, is inconclusive, the variation of the frequency of the SO_2 symmetric stretching vibration with SO_3 concentration gives strong evidence for higher polysulphuric acids, such as $H_2S_4O_{13}$, at high sulphur trioxide concentrations.

SOLUTIONS OF SULPHUR TRIOXIDE IN SULPHURIC ACID

The Raman spectra of 14 oleum solutions with compositions intermediate between H_2SO_4 and SO_3 are given in Table I and some of the spectra are shown in Fig. 1, together

[1]*Present address: Department of Chemistry, University of Toronto, Toronto 5, Ontario.*

TABLE I

Raman shifts in oleums (frequencies in cm^{-1})

100% H_2SO_4	7.2	11.6	20.9	26.6	34.0	41.2	45.9	51.2	56.5	60.3	68.8	73.1	82.2	92.2	100.0% SO_3
—	—	—	—	140(1)	137(1)	135(2)	145(2)	142(2)	148(2)	140(2)	—	—	—	—	120(2)
—	155(1)	152(1)	148(2)	154(1)	—	—	—	—	—	—	160(2)	165(3)	165(3)	—	147(2)
—	—	—	—	—	176(1)	173(1)	175(1)	160(2)	174(2)	170(2)	—	—	—	—	—
—	—	—	—	—	—	250(1)	252(1)	249(2)	249(2)	256(2)	246(2)	250(2)	243(2)	232(1)	243(1/2)
—	305(1)	302(2)	300(3)	300(4)	298(6)	296(6)	298(6)	298(6)	294(6)	292(6)	292(4)	295(4)	290(4)	290(4)	290(5)
—	327(3)	323(4)	322(5)	325(6)	325(8)	325(8)	328(6)	325(8)	325(8)	320(8)	322(8)	328(5)	322(5)	320(3)	322(2)
—	—	—	—	—	—	—	—	—	—	—	—	—	—	—	337(1)
—	—	—	—	—	—	—	350(1/2−)	352(1)	355(2)	360(3)	358(4)	360(5)	368(6)	368(5)	368(6)
392(5)	388(5)	385(4)	386(2)	388(1)	382(1/2−)	—	—	—	—	—	—	—	—	—	—
422(5)	419(5)	422(4)	419(2)	415(1)	415(1/2)	415(1/2)	415(1/2)	410(1/2−)	409(1/2−)	—	417(1)	400(1/2)	401(1/2)	410(1/2)	410(2)
—	474(1/2)	472(1)	471(2)	470(3)	470(4)	470(5)	470(5)	470(5)	473(4)	470(4)	470(4)	470(3)	477(2)	477(1)	480(2)
—	517(1/2)	506(1)	506(2)	520(3)	522(4)	504(4)	504(5)	500(5)	593(4)	490(4)	493(4)	495(3)	—	—	—
—	—	—	—	—	—	528(6)	528(6)	526(6)	529(6)	530(6)	529(6)	536(5)	532(4)	533(6)	534(4)
563(8)	563(8)	557(8)	559(8)	563(7)	560(8)	562(5)	562(5)	560(4)	566(3)	562(3)	562(3)	574(2)	575(1/2)	—	560(1)
—	—	—	—	—	—	—	—	—	—	—	—	—	—	—	600(1/2)
—	—	—	—	—	—	—	—	—	—	—	—	—	—	—	—
—	—	—	633(1/2)	641(1/2)	630(1/2)	631(1/2)	630(1/2)	630(1/2)	630(1/2)	630(1/2)	632(1/2)	—	—	650(1)	657(4)
—	—	—	—	—	—	—	—	—	—	—	—	—	660(3)	665(1)	—
—	—	—	685(1/2−)	682(1/2)	682(1)	688(2)	690(2)	684(3)	687(4)	685(4)	687(4)	690(4)	697(4)	700(2)	698(3)
—	731(2)	729(4)	730(5)	732(6)	730(8)	735(10)	735(10)	735(8)	735(8)	734(7)	735(6)	740(5)	726(2)	729(1)	—
—	810(1/2)	800(1)	813(1)	810(1)	810(1)	812(1)	809(1)	812(1)	812(1/2)	810(1/2)	809(1/2)	—	—	—	804(1)
—	—	—	—	—	—	—	850(1/2)	855(1/2)	855(1/2)	860(1/2)	858(1/2)	—	854(1)	—	860(2)
—	—	—	—	—	—	—	—	—	—	—	—	—	—	—	881(1)
910(10)	910(9)	912(9)	911(7)	900(6)	903(2)	903(2)	900(2)	906(1)	900(1/2)	—	—	—	—	—	—
976(2)	980(2)	977(3)	970(3)	968(4)	967(4)	965(5)	960(5)	960(5)	963(5)	963(5)	957(5)	960(4)	950(2)	957(1/2−)	—
—	—	—	—	—	—	—	—	—	1020(1/2−)	—	1020(1/2−)	1020(1/2−)	1020(1/2−)	1020(1/2−)	1020(1/2)
—	—	—	—	1075(1/2)	1075(1)	1075(2)	1075(2)	1075(2)	1075(3)	1075(3)	1075(4)	1073(5)	1072(6)	1072(10)	1073(8)
1137(10)	1130(10)	1132(10)	1132(10)	1145(10)	1148(6)	1175(7)	1175(7)	1178(6)	1174(5)	1170(4)	1178(4)	1182(2)	1170(1)	1170(1)	1162(1)
1195(3)	1225(4)	1215(4)	1220(5)	1218(6)	1215(10)	1224(10)	1224(10)	1232(10)	1227(10)	1230(10)	1232(10)	—	—	1224(1)	1224(4)
—	—	—	—	—	—	—	—	—	—	—	—	1250(7)	1256(4)	1260(2)	—
—	—	—	—	—	—	—	—	—	1270(1/2)	1270(1/2)	1270(1)	1275(1)	1270(2)	1270(3)	1270(10)
1368(2)	1370(2)	1370(2)	1360(1)	1357(1)	1356(1/2)	—	—	—	—	—	—	—	1385(2)	1385(3)	1390(3)
—	1422(1/2)	1422(1)	1424(2)	1415(2)	1417(2)	1430(3)	1425(3)	1432(4)	1429(4)	1430( )	1432(1)	1430(3)	1410(2)	—	—
—	—	—	1450(1/2)	1452(1/2)	1450(2)	1469(4)	1458(4)	1470(1)	1465(1)	1460(3)	1480(3)	1480(2)	1450(2)	—	—
—	—	—	—	—	—	—	—	—	—	—	—	—	1480(2)	1486(1)	1489(5)
—	—	—	—	—	—	—	—	—	—	1492(1)	—	1515(1)	1515(1)	1520(1/2)	1515(3)

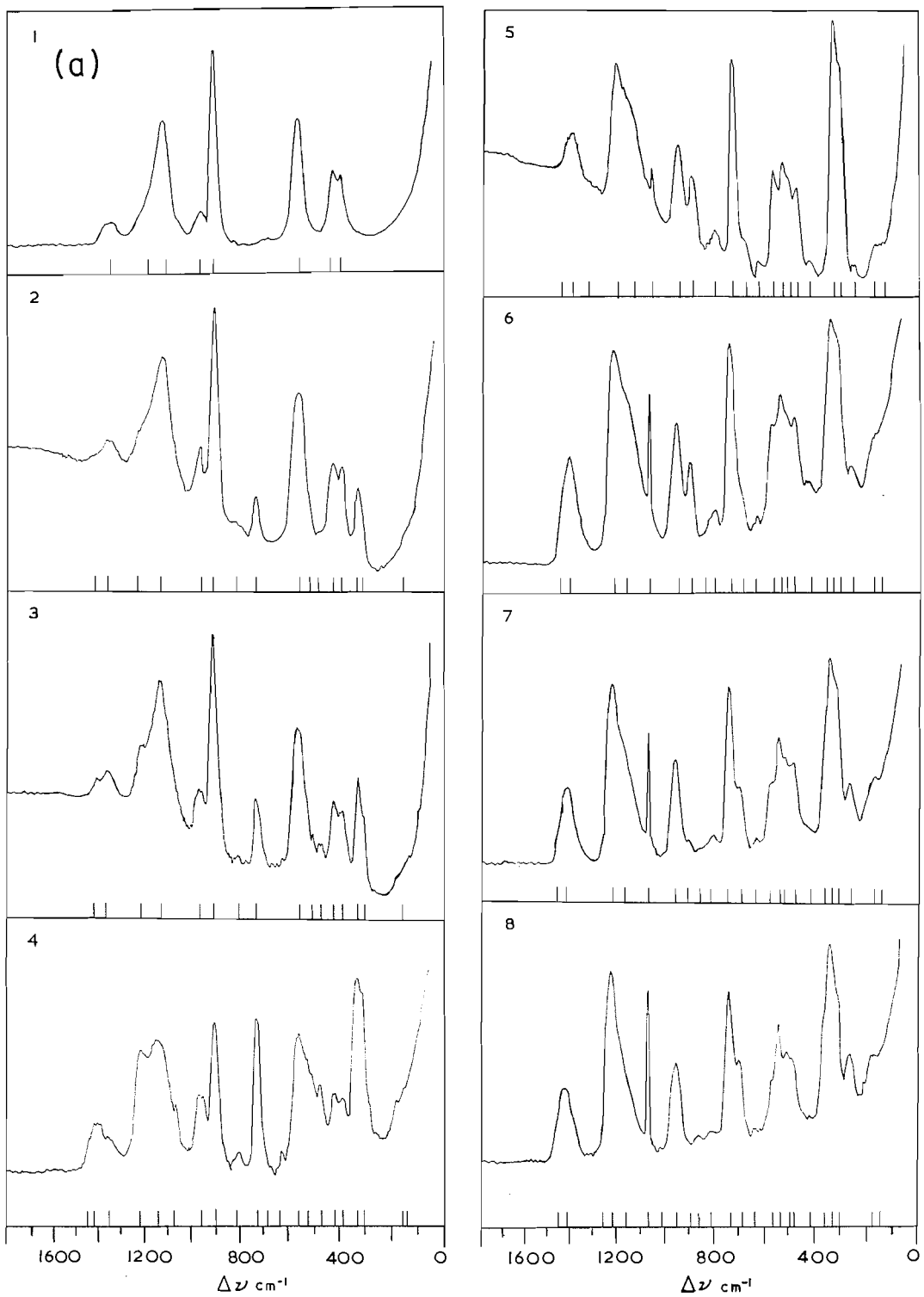

FIG. 1(*a*).

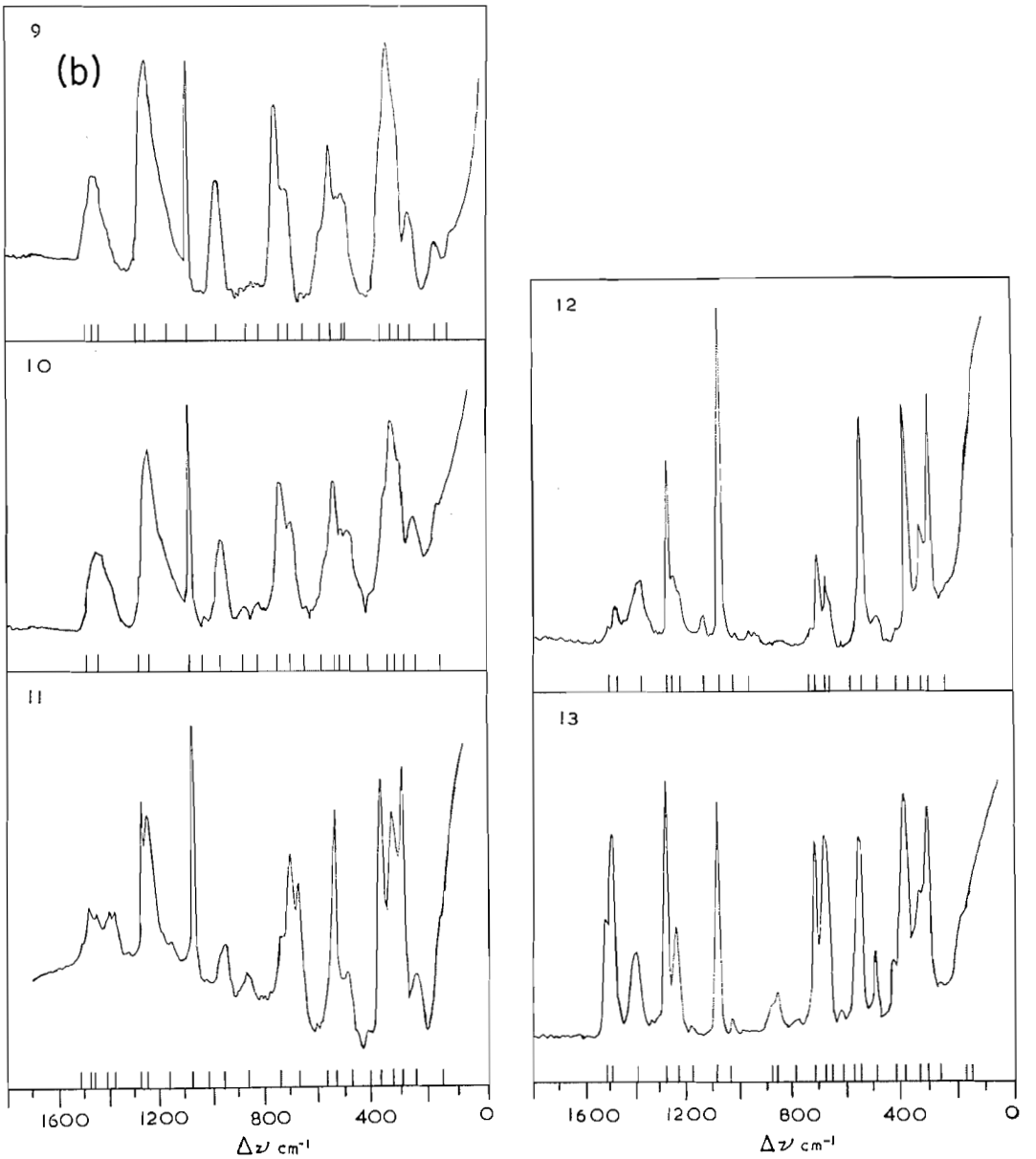

FIG. 1(*b*).

FIG. 1 (*a* and *b*). Raman spectra of oleums: (1) H_2SO_4, (2) 7.2% SO_3, (3) 11.1% SO_3, (4) 26.6% SO_3, (5) 35.8% SO_3, (6) 45.9% SO_3 ($H_2S_2O_7$), (7) 51.2% SO_3, (8) 56.5% SO_3, (9) 60.3% SO_3, (10) 68.8% SO_3, (11) 82.2% SO_3, (12) 92.2% SO_3, (13) 100% SO_3.

with the spectra of H_2SO_4 and liquid sulphur trioxide taken from previous publications (8, 9). These spectra are in good agreement with those obtained by previous workers except that we observed a number of additional lines and some lines were found in less concentrated oleums than previously.

Region 0 to 11.6% SO_3

When sulphur trioxide is added to 100% sulphuric acid several new frequencies appear in the Raman spectra of the solutions which are not observed in the spectrum of sulphuric acid itself and most of the lines due to sulphuric acid begin to diminish in intensity. New lines are observed at 152, 302, 323, 472, 506, 729, 800, and 1422 cm^{-1}. The sulphuric acid line at 563 cm^{-1} shifts slightly (to approximately 557 cm^{-1}) but does not change appreciably in intensity as the stoichiometric concentration of SO_3 increases, and the lines at 976 cm^{-1} and 1137 cm^{-1} increase in intensity while the sulphuric acid frequency at 1195 cm^{-1} gradually shifts to 1215 cm^{-1}. The new lines in the oleum spectra have their counterparts at very similar frequencies in the spectrum of $S_2O_5F_2$ except for the lines at 977, 1215, and 1422 cm^{-1} (Table II). This provides strong evidence that $H_2S_2O_7$ has a structure similar to that of $S_2O_5F_2$, i.e. $HO.SO_2.O.SO_2.OH$.

The lines at 1215 and 1422 cm^{-1} are obviously due to stretching vibrations of the SO_2 group and their occurrence at lower frequencies in the spectrum of $S_2O_5(OH)_2$ than the corresponding vibrations in disulphuryl fluoride but at higher frequencies than in sulphuric acid (8) is consistent with the established correlation of the SO_2 stretching frequencies with the electronegativities of the attached groups (10). A pair of symmetric stretching frequencies and a pair of asymmetric stretching frequencies are expected theoretically but it appears that the two lines expected for the symmetric stretches are not resolved. The expected separation of the two lines is approximately 20 cm^{-1}, which is of the same order as the width of the observed line at 1215 cm^{-1}. The slight change in the position of the sulphuric acid line at 1137 cm^{-1}, which has been assigned as an O—H bend (8) is consistent with the similar vibration in $H_2S_2O_7$ having a similar frequency. This also explains why its intensity changes little in *dilute* oleums, since on adding SO_3 to sulphuric acid the concentration of O—H bonds changes only slowly at low concentrations of sulphur trioxide.

In the Raman spectrum of $S_2O_5F_2$ an SF stretching vibration gives a strong line at 872 cm^{-1} and no analogous line is observed in the oleum spectra as expected. However, as the line at 977 cm^{-1} in the oleum spectrum is not present in the spectrum of $S_2O_5F_2$ it is reasonable to assign this line to the S—OH stretch of $S_2O_5(OH)_2$. At low concentrations of sulphur trioxide in sulphuric acid this line is at 977 cm^{-1}, and is not resolved from the asymmetric $S(OH)_2$ stretching frequency due to sulphuric acid, but in stronger oleums where sulphuric acid is no longer present its frequency can be more accurately determined as 968 cm^{-1}. In fluorosulphuric acid, which has been shown to be a stronger acid than sulphuric acid (11), the S(OH) stretch has been observed at 960 cm^{-1} (8). The shift of the SO_2 vibrations in $H_2S_2O_7$ to higher frequencies as compared to the SO_2 vibrations in H_2SO_4 is also consistent with $H_2S_2O_7$ being a stronger acid than H_2SO_4 (10). The other vibrations are assigned frequencies by comparison with the spectra of sulphuric acid (8) and disulphuryl fluoride (4), as shown in Table II.

The freezing-point depressions and conductivities of dilute solutions of SO_3 in sulphuric acid are consistent with the formation of $H_2S_2O_7$, which behaves as a weak acid of the sulphuric acid solvent system (11),

$$K_1 = [H_3SO_4^+][HS_2O_7^-]/[H_2S_2O_7][H_2SO_4] = 0.0014.$$

Thus a 1 molal solution of $H_2S_2O_7$ in sulphuric acid (7% SO_3) is only 12% ionized, and a 5 molal solution (21% SO_3) is only 5% ionized. It is shown later that a strong line at 1080 cm^{-1} is diagnostic of the $HS_2O_7^-$ ion, and no line at this frequency is detected in the oleum spectra, which is consistent with the concentration of $HS_2O_7^-$ being small.

TABLE II

Comparison of the spectra of oleums with the spectra of $S_2O_5F_2$ and $S_3O_8F_2$ (frequencies in cm^{-1})

		Percentage of SO_3:									
$S_2O_6F_2$	$S_3O_8F_2$	11.6	12.5		45.5	46.5		73.4	69.0		Approximate description of vibration
Raman (6)	Raman (6)	Raman	I.R. (3)		Raman	I.R. (3)		Raman	I.R. (3)		
157	145	152	—	$H_2S_2O_7$	145	—	$H_2S_2O_7$*	—	—		Skeletal bend
—	165	—	—		175	—	$H_2S_3O_{10}$	165	—	$H_2S_3O_{10}$*	Skeletal bend
—	195	—	—		—	—		—	—		
—	226	—	—		—	—		—	—		
—	245	—	—		252	—	$H_2S_3O_{10}$*	250	—	$H_2S_3O_{10}$*	Skeletal bend
290	288	302	—	$H_2S_2O_7$	298	—	$H_2S_2O_7$*	295	—	$H_2S_2O_7$*	Torsion
323	318	323	—	$H_2S_2O_7$	328	—	$H_2S_2O_7$*	328	—	$H_2S_2O_7$*	Skeletal stretch
—	324	—	—		350	—	$H_2S_3O_{10}$*	360	—	$H_2S_3O_{10}$*	Skeletal stretch
350	350	—	—		—	—		400	—	$H_2S_3O_{10}$*	Torsion?
366	359	—	—		—	—		—	—		
—	—	385	—	H_2SO_4	—	—		—	—		
—	—	422	—	H_2SO_4	415	—	H_2SO_4	—	—		
435	403	—	—		—	—		—	—		
455	468	472	475	$H_2S_2O_7$	470	472	$H_2S_2O_7$*	470	476	$H_2S_2O_7$*	SO_2 rock
487	—	—	—		504	513	$H_2S_2O_7$*	495	516	$H_2S_2O_7$*	SO_2 bend
518	528	506	—	$H_2S_2O_7$	528	538	SO_3, $H_2S_3O_{10}$*	536	540	SO_3, $H_2S_3O_{10}$*	SO_2 bend
540	—	557	555	H_2SO_4, $H_2S_2O_7$	562	552	H_2SO_4, $H_2S_2O_7$*	574	—		SO_2 bend
560	—	—	618	$H_2S_2O_7$	—	619	$H_2S_2O_7$*	—	618	$H_2S_2O_7$*	SO_2 rock
630	—	—	655	$H_2S_2O_7$	630	640	$H_2S_2O_7$*	—	640	$H_2S_2O_7$*	SO_2 rock
—	699	—	—		690	688	$H_2S_3O_{10}$*	690	688	$H_2S_3O_{10}$*	SO_2 rock
733	724	729	732	$H_2S_2O_7$	735	732	$H_2S_2O_7$*	740	728	$H_2S_2O_7$*	SO_2 rock
—	761	—	—		—	—		—			
814	835	800	807	$H_2S_2O_7$	809	806	$H_2S_2O_7$*	—	806	$H_2S_2O_7$*	Skeletal stretch
—	—	—	—		850	—	$H_2S_3O_{10}$*	—	—		Skeletal stretch
872	876	—	—		—	—		—	—		
—	—	912	908	H_2SO_4	900	(905)	H_2SO_4	—	—		
—	—	980	970	H_2SO_4, $H_2S_2O_7$	960	969	$H_2S_2O_7$*	960	965	$H_2S_2O_7$*	S—OH stretch
—	—	—	—					1020	—		
—	—	—	—		1075	1075	SO_3	1073	1075	SO_3	
—	—	1132	—	H_2SO_4, $H_2S_2O_7$	1175	—	H_2SO_4, $H_2S_2O_7$*	1182	—	$H_2S_2O_7$*	O—H wag
—	1198	1215	1185	H_2SO_4, $H_2S_2O_7$	1224	1200	H_2SO_4, $H_2S_2O_7$*	1250	1200	$H_2S_2O_7$*	SO_2 symmetric stretch
1249	1241	—	—		—	—		—	—		
1264	1268	—	—		—	—		—	—		
—	—	—	—		—	—		1275	—	S_3O_9	
—	—	1370	1365	H_2SO_4	—	1370	SO_3	—	1370	SO_3	
—	1468	1422	—	$H_2S_2O_7$	1425	1430	$H_2S_2O_7$*	1430	1430	$H_2S_2O_7$*	SO_2 asymmetric stretch
1490	1490	—	—		1458	—	$H_2S_3O_{10}$*	1460	—	$H_2S_3O_{10}$*	SO_2 asymmetric stretch
1511	1515	—	—		—	—		—	—		
—	—	—	—		—	—		1515	—	S_3O_9	

*These lines are probably also common to higher polysulphuric acids.

There are in fact no lines which can be assigned to any of the ions $H_3SO_4^+$, $HS_2O_7^-$, and $S_2O_7^=$. The sulphuryl stretches of the anions of the acids $XSO_2.OH$ have frequencies in the range 1030 to 1090 cm^{-1} (8), and in the oleum spectra the only lines which occur in this range are the very sharp line at 1075 cm^{-1}, which is diagnostic of SO_3 monomer, and a weak line at 1020 cm^{-1}, which is found only at very high concentrations of SO_3 and is due to SO_3 trimer (9).

Region 11.6 to 41.2% SO_3

In this region the lines assigned to the species $H_2S_2O_7$ increase in intensity and those due to H_2SO_4 decrease in intensity. At 20.9% SO_3 new lines appear at 633 cm^{-1}, 685 cm^{-1}, and 1450 cm^{-1}. At a slightly higher concentration a new line appears at 140 cm^{-1} and at 35.8% SO_3 further low-frequency lines are observed at 176 cm^{-1} and 257 cm^{-1}. Also, in 26.6% SO_3 a sharp line appears at 1075 cm^{-1} and in 35.8% SO_3 a further line is found at 530 cm^{-1}. These latter lines are due to monomeric SO_3 (9), although the 530 cm^{-1} line is probably common to other species as well. The presence of free sulphur trioxide is also indicated by the high SO_3 vapor pressure of these solutions. The weak line at 630 cm^{-1} can be attributed to an SO_2 rocking mode of $H_2S_2O_7$, by comparison with the assignment of a line of the same frequency in the spectrum of $S_2O_5F_2$ (4).

It has been shown that the line at 150 cm^{-1} in the spectra of the disulphuryl halides, which has been assigned to the S—O—S bend, is replaced by several (theoretically five) lines in the spectra of trisulphuryl halides which are also due to skeletal bends (4). Thus the replacement in the most dilute oleums of the single line at 155 cm^{-1}, which is assigned to the S—O—S bend of $H_2S_2O_7$, by lines at 140, 176, and 257 cm^{-1} in the more concentrated oleums is considered to be due to the formation of trisulphuric acid, $H_2S_3O_{10}$. The line at approximately 700 cm^{-1} in the spectra of the disulphuryl halides (4) is replaced by two lines at approximately this frequency in the spectra of the trisulphuryl halides (699 and 724 cm^{-1} in the spectrum of $S_3O_8F_2$). Hence the appearance of a new line at 685 cm^{-1} in stronger oleums in addition to the 730 cm^{-1} line which occurs in weaker oleums also is ascribed to the formation of $H_2S_3O_{10}$. It has similarly been observed that a peak near 730 cm^{-1} in the infrared spectra of diphosphates is replaced by two peaks near 680 and 730 cm^{-1} in the infrared spectra of triphosphates and this has been used as a diagnostic test for these compounds (12).

The new line at 1450 cm^{-1} is interpreted as the SO_2 asymmetric stretch of $H_2S_3O_{10}$. As expected, it is weak and the non-appearance of the symmetric stretch as a separate line, which according to the straight-line relationship between SO_2 symmetric and asymmetric stretching frequencies (10) should occur near 1230 cm^{-1}, is probably due to overlap with the 1215 cm^{-1} line of $H_2S_2O_7$. In fact the band assigned to the symmetric stretch in $H_2S_2O_7$ gradually shifts to higher frequencies as the concentration of SO_3 increases.

The spectrum of dilute oleum is very similar to that of $S_2O_5F_2$, which is isoelectronic with $H_2S_2O_7$, but with increasing concentration of SO_3 the spectra become more similar to those of $S_3O_8F_2$, which is isoelectronic with $H_2S_3O_{10}$.

Liquid Disulphuric Acid (45.9% SO_3)

Cryoscopic studies have shown that $H_2S_2O_7$ undergoes extensive self-dissociation (13, 14). In the spectrum of liquid $H_2S_2O_7$ we assign the line at 900 cm^{-1} to the S—OH symmetric stretch in H_2SO_4 and the line at 965 cm^{-1} to the S—OH stretch in $H_2S_2O_7$. The two lines at 690 and 735 cm^{-1} and the low-frequency lines at 145, 175, and 252 cm^{-1} are all diagnostic of $H_2S_3O_{10}$. The line at 1075 cm^{-1} is due to sulphur trioxide monomer.

In addition the SOS symmetric stretch of $H_2S_2O_7$ at 328 cm^{-1} is accompanied by a weak line at 350 cm^{-1} and the SOS asymmetric stretch of $H_2S_2O_7$ at 809 cm^{-1} is accompanied by a weak line at 850 cm^{-1}. It has been shown previously that each of the two lines in the spectra of disulphuryl halides that are due to skeletal stretches splits into two lines in the spectra of the trisulphuryl halides (4). Thus we attribute the weak lines at 350 and 850 cm^{-1} in the spectrum of liquid $H_2S_2O_7$ to the species $H_2S_3O_{10}$. We conclude that the main self-dissociation process in liquid disulphuric acid is

$$2H_2S_2O_7 = H_2S_3O_{10} + H_2SO_4. \quad [1]$$

Since the strong sharp line at 1075 cm^{-1}, which is diagnostic of SO_3 monomer, is also present in the spectrum, the dissociation

$$H_2S_2O_7 = H_2SO_4 + SO_3 \quad [2]$$

must be of some importance. No lines are present in the spectrum of liquid disulphuric acid which can be attributed to ionic species. The low specific conductance of liquid $H_2S_2O_7$ ($\kappa = 3.7\times10^{-3}$ ohm^{-1} cm^{-1}) is consistent with the absence of appreciable concentrations of self-dissociation ions (15).

Region 45.9% to 100% SO_3

Comparison of the Raman spectra of concentrated oleums with the spectrum of $S_4O_{11}F_2$ (7) does not give conclusive evidence for the occurrence in the oleum system of higher polysulphuric acids such as $H_2S_4O_{13}$. Further splitting of lines in the spectrum of a trisulphuryl compound is to be expected on going to a tetrasulphuryl compound but these were not resolved in the spectrum of $S_4O_{11}F_2$ (7), presumably due to extensive overlapping of the lines resulting from the 45 normal vibrations of this molecule. Thus we have not been able to find characteristic diagnostic frequencies for tetrasulphuryl compounds. However, the SO_2 symmetric stretch, which has a frequency of 1195 cm^{-1} in H_2SO_4, 1224 cm^{-1} in oleum of the composition $H_2S_2O_7$, and 1230 cm^{-1} at the composition $H_2S_3O_{10}$, gradually moves to even higher frequencies as the concentration of SO_3 in oleum increases until at very high stoichiometric concentrations of SO_3, e.g. 92.2% SO_3, it is at 1260 cm^{-1}. The weak line attributed to the SO_2 asymmetric stretch also shifts to higher frequencies, although its low intensity makes this shift more difficult to observe. We interpret the continuous shift of the SO_2 stretching frequencies with increasing SO_3 concentration to the presence of increasing amounts of higher polysulphuric acids such as $H_2S_4O_{13}$. It is noteworthy that the SO_2 symmetric stretch has a frequency of 1260 cm^{-1} in the solid, acyclic, polymeric, α, and β forms of sulphur trioxide. The 1260 cm^{-1} line that is observed in 92.2% oleum cannot be due to S_3O_9 since this has symmetric SO_2 stretching frequencies at 1230 and 1270 cm^{-1} (9) and lines are observed at 1224 and 1270 cm^{-1} in the spectrum of 92.2% oleum *in addition* to the well-resolved line at 1260 cm^{-1}. This latter line also cannot be due to monomeric SO_3, which has SO stretching frequencies of 1070 and 1390 cm^{-1} (16). It is, moreover, not likely that the shift in frequency from 1220 to 1260 cm^{-1} is merely a solvent shift since over the same composition range the symmetric SO stretch of monomeric SO_3 has a constant frequency of 1070 cm^{-1}. We conclude therefore that the polysulphuric acids $HO.SO_2.(SO_3)_nOH$ have SO_2 symmetric stretching frequencies of 1230 cm^{-1} for $n = 1$, and higher frequencies for higher values of n up to a limiting value of 1260 cm^{-1} when n becomes rather large.

The 1270 cm^{-1} line which first appears in the 56.5% oleum and increases in intensity up to 100% SO_3 has been previously assigned as the in-phase symmetric SO_2 stretch of S_3O_9 (9). As it is the strongest line of this species none of the other lines in the spectrum of 56.5% oleum can be due to S_3O_9; they would be too weak to be observed.

Discussion of Previous Work

Millen (1) attributed lines in the oleum spectra at 480 and 530 cm^{-1} to $H_2S_3O_{10}$ and at 245 and 688 cm^{-1} to $H_2S_4O_{13}$ on the grounds that the first two appeared in the spectra at higher concentrations of SO_3 (36%) than other lines attributed to $H_2S_2O_7$, and the latter two at still higher concentrations (51%). However, we find a line at 471 cm^{-1} even in the weakest oleum studied (7.2%), and as there is a line at 487 cm^{-1} in the spectrum of $S_2O_5F_2$ the 471 cm^{-1} line can be assigned with some certainty to $H_2S_2O_7$. Similarly we find a line at 257 cm^{-1} in a 35.8% oleum and a line at 685 cm^{-1} in a 20.9% oleum. Comparison with the spectrum of $S_3O_8F_2$ shows that these lines can in fact be attributed with some certainty to $H_2S_3O_{10}$ rather than uniquely to $H_2S_4O_{13}$, although they are likely to occur in its spectrum also. The appearance of a new Raman line as the concentration of SO_3 is increased cannot be reliably correlated with the appearance of a new species at that concentration since it may arise from a line of weak intensity of a species that is present at considerably lower concentrations but not in sufficient amount to give an observable line.

Giguère and Savoie's interpretation of their infrared spectra (3) agrees reasonably well with our interpretation of the Raman spectra. Thus they assigned lines at 550, 970, 1185, and 1368 cm^{-1} as being common to both H_2SO_4 and $H_2S_2O_7$ while lines at 732 and 806 cm^{-1} were regarded as characteristic of $H_2S_2O_7$ and higher polysulphuric acids and were assigned to SOS skeletal vibrations. We assign the 806 cm^{-1} line to a skeletal vibration but according to our assignment the 732 cm^{-1} line is due to an SO_2 rocking mode. Using the same type of argument as Millen (1), Giguère and Savoie (3) have assigned a line at 688 cm^{-1}, which they first observed in a 25% oleum, and a line at 1430 cm^{-1}, which they first observed in a 23% oleum, to $H_2S_3O_{10}$. This is in agreement with our assignment for the 688 cm^{-1} line, but we find a line at 1420 cm^{-1}, which we assign to $H_2S_2O_7$, in the most dilute oleums studied that gradually shifts to higher frequencies in the higher polysulphuric acids. In agreement with the present work these authors were unable to find any conclusive evidence for the ions $H_3SO_4^+$ and $HS_2O_7^-$ in the oleums studied nor did they find any infrared bands that could be unambiguously assigned to $H_2S_4O_{13}$ or higher polysulphuric acids. The frequencies of the lines observed in the infrared spectra generally agree well with those observed in the Raman spectra. The infrared spectra contain two lines at approximately 618 and 640 cm^{-1} that are not observed in the Raman spectra.

Our conclusions are in more serious disagreement with the recent work of Walrafen and Young (2), who used a photoelectric method in an attempt to obtain estimates of the concentrations of species in the H_2SO_4–SO_3 system. Unfortunately, although the relative intensities of the lines that they observed are undoubtedly more accurate than could be obtained from our photographic work, they obtained many fewer lines and several closely spaced groups of lines are very poorly, if at all, resolved in their spectra. Because they found that the only lines in the Raman spectra of oleums that were not present in the spectra of either H_2SO_4 or liquid sulphur trioxide reached a maximum intensity at approximately the composition $H_2S_2O_7$ they assumed that this acid and its ions are the only new species formed in H_2SO_4–SO_3 mixtures. However, we find a number of lines that cannot be attributed to either H_2SO_4 or to SO_3 and its polymers that continue to increase in intensity in solutions containing more SO_3 than corresponds to the composition $H_2S_2O_7$ and which by comparison with the spectra of the polysulphuryl halides may be assigned to $H_2S_3O_{10}$ and higher polysulphuric acids. Young and Walrafen's quantitative interpretation of their results rests on their assumption that the only poly-

sulphuric acid that is formed is $H_2S_2O_7$ and on the further assumption that this acid is extensively ionized. This latter assumption is in direct contradiction to evidence from the results of extensive studies of the freezing points (11), conductivities (11), and acidity functions (17) of the H_2SO_4–SO_3 system, which show that $H_2S_2O_7$ is only a rather weak acid of the sulphuric acid system and is only very incompletely ionized even in the most dilute oleum studied in the Raman work.

Walrafen and Young found, as we have, that the intensity of the 910 cm^{-1} line does not decrease in intensity in proportion to the expected decrease in the concentration of H_2SO_4. They assumed therefore that one of the ions formed in the ionization of $H_2S_2O_7$ (i.e. $H_3SO_4^+$ or $HS_2O_7^-$) must also contribute to the intensity of the 910 cm^{-1} line. Our explanation for the persistence of this frequency at concentrations of SO_3 greater than that required for the stoichiometric formation of $H_2S_2O_7$ is, however, that free H_2SO_4 is in fact still present in the system as a consequence of the self-dissociation of $H_2S_2O_7$ into H_2SO_4 and $H_2S_3O_{10}$. Moreover, as is discussed later, it is unlikely that either of the ions $H_3SO_4^+$ or $HS_2O_7^-$ could contribute to the 910 cm^{-1} line.

Walrafen and Young also make the arbitrary assumption that "Raman radiation having a frequency of 300–325 cm^{-1} contains energy from two sources, $H_2S_2O_7$ and $HS_2O_7^-$". Our results on the other hand show two distinct lines in this region of the spectrum at 302 and 323 cm^{-1} which have been assigned to a torsional mode and a skeletal stretch, respectively, of $H_2S_2O_7$ and the higher polysulphuric acids.

It is unfortunate that the inadequate sensitivity and resolution of the photoelectric method used by Walrafen and Young and the unjustified assumptions made in the interpretation of their spectra and also the inaccuracy of their titration method of determining the concentrations of their oleums invalidate what would otherwise be useful information on the concentrations of the various species present in oleums. Although the present work establishes the nature of the species present with some certainty it gives only qualitative information on their relative concentrations.

SOLUTIONS OF SODIUM SULPHATE IN OLEUM

An important point in Walrafen and Young's discussion of their results is the assumption that the $HS_2O_7^-$ ion contributes to the intensity of the 910 cm^{-1} line. We have suggested above that this ion is not present in sufficient concentration in oleums to give rise to any characteristic lines in the spectrum. It seemed important therefore to attempt to obtain the spectrum of the $HS_2O_7^-$ ion and accordingly the Raman spectra of solutions of sodium sulphate in some oleums of different strengths were measured. The results of these measurements are given in Table III and Fig. 2. Some similar measurements have been reported previously by Millen (1). The compositions of the solutions are expressed in terms of the ratio $n_b/n_a{}^i$ where n_b is the number of moles of $NaHSO_4$ added to $n_a{}^i$ moles of $H_2S_2O_7$. The $HS_2O_7^-$ ion is formed in these solutions by the reaction

$$H_2S_2O_7 + NaHSO_4 = Na^+ + HS_2O_7^- + H_2SO_4. \quad [3]$$

At high concentrations of $NaHSO_4$ substantial quantities of $S_2O_7^=$ are also formed according to the equation

$$HS_2O_7^- + NaHSO_4 = Na^+ + S_2O_7^= + H_2SO_4. \quad [4]$$

The concentrations of all the species in a solution for various values of $n_b/n_a{}^i$ may be calculated from the following data (11) using a similar method to that outlined in a previous publication (18):

TABLE III

Raman shifts for solutions of $NaHSO_4$ in oleum (frequencies in cm^{-1})

	7.2% oleum					11.1% oleum					26.6% oleum			41.2% oleum	
n_b/n_a[i]:	0.00	0.29	0.56	1.00	2.00	0.00	0.29	0.56	1.00	1.44	0.00	0.56	1.00	00.0	0.29
	—	—	—	—	—	—	—	—	—	—	140(1)	—	—	135(2)	140(2)
	155(1)	145(1)	148(1)	145(1)	145(1)	155(1)	145(1)	145(1)	145(1)	148(1)	154(1)	145(1)	150(1)	173(1)	178(1)
	—	—	—	—	—	—	—	—	—	—	—	—	—	250(1)	—
	305(1)	310(2)	308(2)	315(3)	—	302(2)	313(3)	311(3)	311(3)	308(2)	300(4)	301(3)	301(4)	296(6)	300(6)
	327(3)	329(3)	325(3)	328(3)	325(3)	327(4)	325(4)	326(4)	324(4)	324(4)	325(6)	326(5)	325(5)	325(8)	325(8)
	388(5)	392(3)	389(5)	390(5)	394(5)	391(4)	385(4)	385(4)	390(4)	390(4)	388(1)	389(1)	389(1)	—	392(1)
	419(5)	420(5)	420(5)	520(5)	420(4)	418(4)	418(4)	420(4)	420(4)	420(4)	415(1)	420(1)	420(1)	415(1/2)	423(1/2)
	474(1/2)	470(?)	470(?)	—	—	474(1)	481(1)	481(1)	483(1)	480(1/2)	470(3)	460(2)	462(1)	470(5)	480(5)
	517(1/2)	529(1/2)	529(1/2)	—	—	510(1)	510(1/2)	520(1/2)	530(1/2)	540(1)	520(3)	506(1)	506(1/2)	504(4)	505(3)
	—	—	—	—	—	—	—	—	—	—	—	—	—	528(6)	530(5)
	563(8)	559(8)	562(8)	559(6)	562(6)	563(8)	559(8)	556(8)	559(8)	559(8)	563(7)	559(7)	556(7)	562(5)	560(5)
	—	612(1/2)	615(1/2)	—	—	—	590(1/2)	590(1/2)	—	—	641(1/2)	629(1/2+)	629(1/2−)	631(1/2)	632(1/2)
	—	—	—	—	—	—	—	—	—	—	682(1/2)	700(1)	690(1/2−)	688(2)	695(1)
	731(2)	731(1/2)	735(1)	728(1/2)	—	735(4)	728(4)	730(3)	730(2)	728(1)	732(6)	730(4)	739(4)	735(10)	733(9)
	810(1/2)	825(1/2)	825(1/2)	823(1/2)	—	806(1)	820(1)	823(1)	826(1)	829(1)	810(1)	815(1/2)	818(1)	812(1)	810(1)
	—	—	885(1/2)	882(1)	882(1)	—	882(1/2)	890(1/2)	895(1/2)	895(1)	—	—	—	—	—
	910(9)	912(9)	912(9)	910(9)	910(9)	911(9)	912(9)	911(9)	911(9)	908(9)	900(6)	908(6)	903(6)	903(2)	904(2)
	—	—	—	—	—	—	—	—	—	—	—	955(1)	—	—	943(1)
	980(2)	971(2)	973(2)	968(2)	968(1)	980(3)	966(2)	966(3)	966(3)	966(3)	968(4)	975(3)	970(2)	965(5)	980(3)
	—	—	—	1049(1)	1052(2)	—	—	—	1040(1/2)	1040(1)	—	—	1040(1/2)	—	—
	—	1084(1)	1083(3)	1082(4)	1090(3)	—	1082(1)	1082(3)	1082(6)	1082(8)	1075(1/2)*	1083(4)	1082(6)	1075(2)*	1083(5)
	1130(10)	1118(6)	1144(6)	1152(5)	1158(4)	1135(10)	1150(10)	1150(10)	1155(8)	1158(8)	1145(10)	1160(10)	1155(6)	1175(7)	1168(3)
	1225(4)	1205(4)	1210(3)	1210(2)	1205(1)	1215(4)	1212(4)	1210(3)	1213(4)	1215(3)	1218(6)	1230(7)	1230(6)	1224(10)	1226(4)
	1370(2)	1365(2)	1365(2)	1365(2)	1364(1)	1375(2)	1375(2)	1365(2)	1365(2)	1365(2)	1357(1)	1350(1)	1340(1)	—	—
	1422(1/2)	1420(1)	1450(1)	1420(1/2)	—	1422(1)	1430(1)	1420(1)	1420(1)	1420(1/2)	1415(2)	1421(2)	1425(2)	1430(3)	1420(2)
	—	—	—	—	—	—	—	—	—	—	1452(1/2)	—	—	1469(4)	—

*Due to SO_3 monomer.

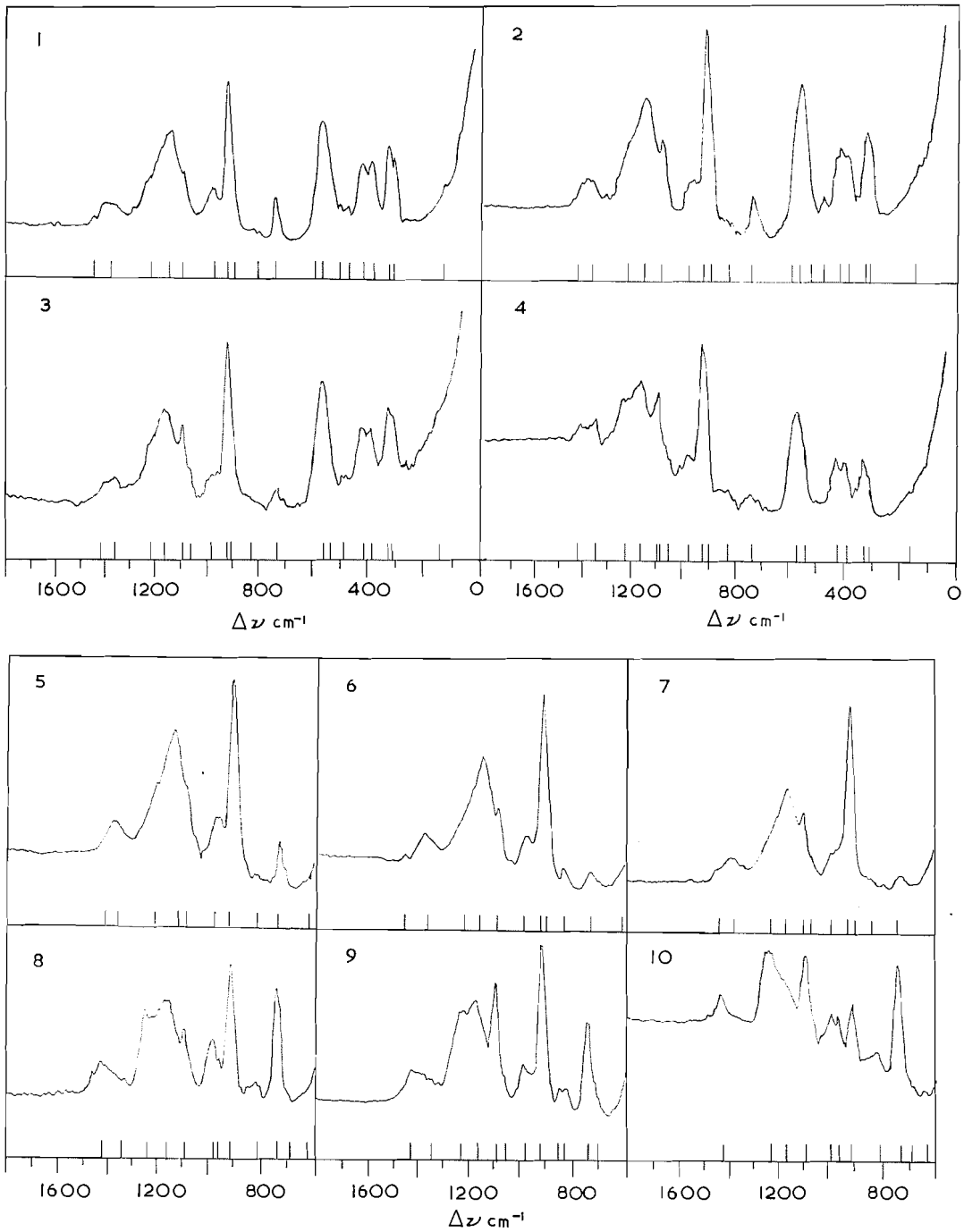

FIG. 2. Raman spectra of solutions of sodium sulphate in oleums.

	(1)	(2)	(3)	(4)	(5)	(6)	(7)	(8)	(9)	(10)
% SO_3	11.1	11.1	11.1	11.1	7.2	7.2	7.2	26.6	29.6	41.2
n_b/n_a	0.29	0.56	1.00	1.49	0.29	0.56	1.00	0.56	1.00	0.28

$$K_{ap}' = [H_3SO_4^+][HSO_4^-][H_2SO_4]^2 = 2.4\times10^{-6}$$
$$K_1 = [H_3SO_4^+][HS_2O_7^-]/[H_2S_2O_7][H_2SO_4] = 1.4\times10^{-3}$$
$$K_2 = [H_3SO_4^+][S_2O_7^=]/[HS_2O_7^-][H_2SO_4] = 1\times10^{-4}.$$

This value of K_2 is an estimate based on the assumption that $K_1/K_2 = 10$, as is the case for the first two dissociation constants of diphosphoric acid in water for which $K_1 = 1.4\times10^{-1}$ and $K_2 = 1.1\times10^{-2}$. The results of these calculations are shown in Fig. 3. No allowance has been made for probable non-ideal behavior of the solutions

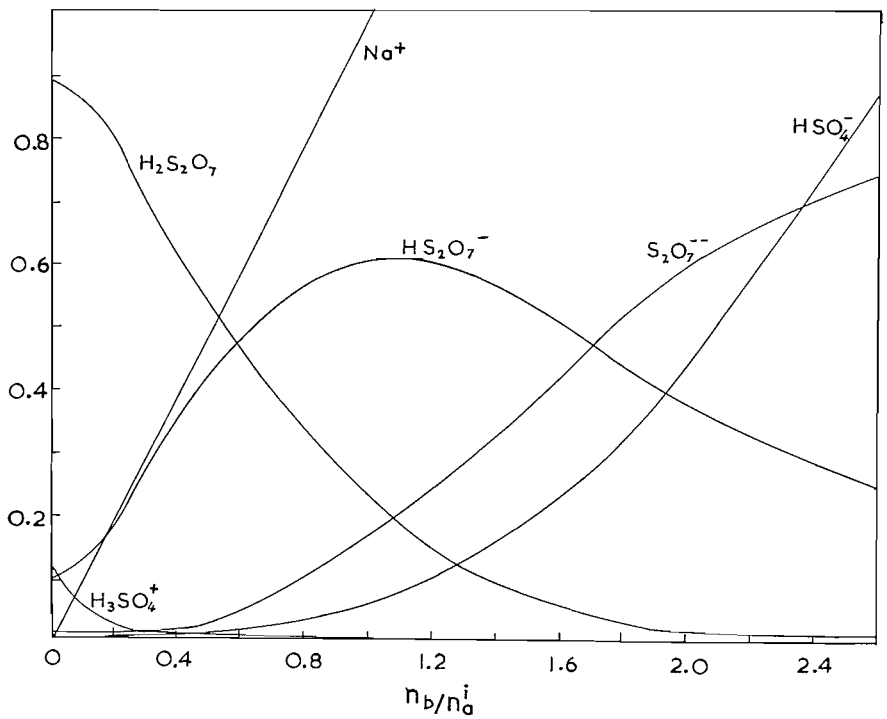

FIG. 3. Approximate concentrations of species in solutions of $NaHSO_4$ in oleum (1 molal $H_2S_2O_7$ in H_2SO_4).

or for the possibility of the conversion of the $HS_2O_7^-$ and $S_2O_7^=$ ions to higher polymeric forms such as $S_3O_{10}^=$ but Fig. 3 indicates at least approximately the manner in which the relative concentrations of species change as $NaHSO_4$ is added to an oleum, which is adequate for our present purpose.

It is possible to predict frequencies for some of the more important characteristic vibrations of $HS_2O_7^-$ and $S_2O_7^=$ by utilizing correlations derived from observations on related molecules and ions (8). Thus the following frequencies have been found for the S—OH stretching mode: HSO_4^-, 895 cm^{-1}; H_2SO_4, $(\nu_{sym}+\nu_{asym})/2$ = 944 cm^{-1}; HSO_3F, 960 cm^{-1}; $H_2S_2O_7$, 968 cm^{-1}. There seems to be an increase in the frequency of this vibration with increasing acid strength, and a frequency of between 944 and 968 cm^{-1}, probably close to 968 cm^{-1}, would be expected for the S—OH stretching frequency in the $HS_2O_7^-$ ion. It is rather unlikely that this vibration (or any other vibration of the $HS_2O_7^-$ ion) could contribute to the intensity of the 910 cm^{-1}, as was assumed by

Walrafen and Young (2). The SO_2 stretching vibrations also show a similar increase in frequency with increasing acid strength. Thus the following frequencies have been found for the SO_2 symmetric stretch: HSO_4^-, 1040 cm^{-1}; SO_3F^-, 1080 cm^{-1}; H_2SO_4, 1195 cm^{-1}; $H_2S_2O_7$, 1224 cm^{-1}; HSO_3F, 1230 cm^{-1}; and for the SO_2 asymmetric stretch: HSO_4^-, 1195 cm^{-1}; SO_3F^-, 1228 cm^{-1}; H_2SO_4, 1368 cm^{-1}; $H_2S_2O_7$, 1425 cm^{-1}; HSO_3F, 1445 cm^{-1}. The close similarities in the frequencies of the SO_2 stretching vibrations for HSO_3F and $H_2S_2O_7$ make it very probable that the vibrations of the —O.SO_3^- part of the $HS_2O_7^-$ ion will have frequencies close to those in SO_3F^-, i.e. 1080 and 1230 cm^{-1}, while the frequencies for the HO.SO_2.O— part of the ion should be close to those in $H_2S_2O_7$ itself, i.e. 1225 and 1425 cm^{-1}.

Sodium hydrogensulphate was added to 1 molal $H_2S_2O_7$, (7% SO_3) to give solutions with $n_b/n_a{}^i = 0.29$, 0.56, 1.00, and 2.00. There is little change in the spectrum compared with that of the original oleum until the composition $n_b/n_a{}^i = 0.56$ is reached. A solution of this composition has a minimum conductivity, the concentrations of $H_3SO_4^+$ and HSO_4^- are very small, and the most important ionic species are Na^+ and $HS_2O_7^-$ (19). At this composition a new, relatively sharp line is observed at 1080 cm^{-1} and its intensity increases as further $NaHSO_4$ is added. We therefore attribute this line, as Millen (1) did, to the $HS_2O_7^-$ ion, and we assign it to the SO_2 symmetric stretch of the O.SO_3^- part of the ion: its frequency agrees well with that predicted above. The corresponding asymmetric stretch is not observed as a separate line as it almost certainly has a very similar frequency to the symmetric SO_2 stretch of $H_2S_2O_7$. Although at the composition $n_b/n_a{}^i = 1.00$, molecular $H_2S_2O_7$ has been substantially replaced by $HS_2O_7^-$ ions the intensities of the lines at approximately 1210 and 1420 cm^{-1} do not diminish very greatly and therefore we assign these frequencies to the SO_2 stretching vibrations in the HO.SO_2.O— part of the ion in addition to the similar vibrations in the $H_2S_2O_7$ molecule.

At the composition $n_b/n_a{}^i = 2.00$, $HS_2O_7^-$ ion has been substantially converted to $S_2O_7^=$. Since the 1080 cm^{-1} remains in the spectrum with about the same intensity it must also be a frequency of the $S_2O_7^=$ ion: this is reasonable as not much change in the SO_2 symmetric stretch of the —O.SO_3^- part of $HS_2O_7^-$ would be expected when the second hydrogen is ionized to give $S_2O_7^=$.

The S—OH stretch of the $HS_2O_7^-$ ion is difficult to detect in the spectra because the S—OH stretch of $H_2S_2O_7$ and the asymmetric S—OH stretch of H_2SO_4 give lines at 960 cm^{-1}. However, in the 7% and 11% oleums solutions with $n_b/n_a{}^i = 1.00$ a new line may be present in the spectra at 940–950 cm^{-1}, since the line at 960 cm^{-1} appears to broaden and to merge into the 910 cm^{-1} line due to the symmetric S—OH stretch of sulphuric acid, whereas in the spectra of the original oleums and also of solutions containing larger quantities of $NaHSO_4$ the 960 cm^{-1} line is well resolved from the 910 cm^{-1} line. The above conclusions are confirmed by the spectra of solutions of $NaHSO_4$ in 26% and 45% oleum.

The spectra of these solutions are difficult to interpret in detail because of the considerable overlapping of the lines due to different molecular and ionic species. However, it seems clear that the 1080 cm^{-1} line is diagnostic of the $HS_2O_7^-$ and probably the $S_2O_7^=$ ions as well and the fact that this line is not observed in oleums, but appears and increases in intensity on the addition of $NaHSO_4$, is consistent with other strong evidence that disulphuric acid is a rather weak acid of the sulphuric acid system and not a strong acid as assumed by Walrafen and Young. It is unlikely therefore that the $HS_2O_7^-$ ion

contributes substantially to the intensity of the 910 cm^{-1} line in oleums as claimed by these authors, particularly as the S—OH stretch of this ion almost certainly has a frequency in the range 940–960 cm^{-1} and this is the only vibration that is likely to give rise to a line in this region of the spectrum.

SOLUTIONS OF SULPHUR TRIOXIDE IN DEUTEROSULPHURIC ACID

We have not studied the D_2SO_4–SO_3 system as extensively as the H_2SO_4–SO_3 system but the Raman spectra (Table IV) are very similar to the spectra of protosulphuric

TABLE IV

Raman spectra of solutions of sulphur trioxide in deuterosulphuric acid (frequencies in cm^{-1})

	Percentage of SO_3:					
D_2SO_4	6.2	16.4	27.1	56.9	82.1	100.0
—	142(2)	143(2)	145(3)	145(3)	144(?)	147(2)
—	193(1)	196?(1)	190?(1)	190(1)	—	—
—	—	—	—	240(1/2)	230(1/2)	—
—	—	—	—	—	—	243(1/2)
—	—	—	274(1)	260(1/2)	290(5)	290(5)
—	300(1/2)	300(3)	305(4)	300(6)	310	—
—	326(1/2)	325(4)	325(5)	325(8)	320(5)	322(2)
—	—	—	—	—	—	337(1)
356(1)	351(1/2)	352(1/2)	355(1/2)	354(4)	369	368(6)
395(2)	400(1)	404(1)	—	—	373	—
—	—	—	431(1)	449(1)	406(1/2)	410(2)
—	—	—	—	479(2)	478(2)	480(2)
—	475(1/2)	482(1/2)	490(1)	499(1)	495	—
—	500(1)	500(2)	—	—	—	—
522(4)	525(3)	525(2)	525(3)	530(3)	535(8)	534(4)
560(6)	650(6)	565(2)	560(3)	563(1)	—	560(1)
—	—	583(2)	—	612(1/2)	596(1/2−)	600(1/2)
—	—	—	—	—	661(4)	657(4)
—	—	—	706(1/2)	685(3)	694(6)	698(3)
—	731(1)	730(3)	730(4)	730(6)	723(3)	—
—	—	—	—	—	844(1/2)	844(1)
—	—	—	—	—	872(1/2)	860(2)
—	—	—	—	—	—	881(1)
906(10)	906(10)	906(6)	903(4)	—	940(2)	—
980(1)	982(2)	980(2)	975(3)	960(6)	962(1)	—
—	—	—	—	—	1014(1/2)	1020(1/2)
—	—	—	1075(1/2−)	1075(4)	1070(8)	1073(8)
1170(10)	1170(8)	1178(5)	1183(5)	1205(3)	—	1162(1)
—	1230(1)	1230(3)	1235(4)	1230(10)	1220(3)	1224(4)
—	—	—	—	1255(2)	1254(8)	—
—	—	—	—	—	1275(6)	1270(10)
1344(2)	1340(2)	1350(1)	—	—	1385(2)	1390(3)
—	—	—	1420(1/2)	1416(3)	1408(2)	—
—	—	—	—	1444(3)	1460(2)	—
—	—	—	—	—	1474(3)	1489(5)
—	—	—	—	—	1515(1)	1515(3)

acid oleums. The observed lines may be assigned by comparison of the spectra with the spectra of the polysulphuryl fluorides and the protosulphuric acid oleums as shown in Table V. This comparison clearly demonstrates the formation of $D_2S_2O_7$. Earlier cryoscopic and conductimetric measurements on the D_2SO_4–SO_3 system have been interpreted in terms of the formation of $D_2S_2O_7$, which behaves as a very weak acid (20). The absence of any lines in the Raman spectra which can be assigned to ions confirms the behavior of $D_2S_2O_7$ as a weak acid in D_2SO_4.

TABLE V

Assignments of frequencies in the Raman spectra of solutions of sulphur trioxide in deuterosulphuric acid

16.4% SO_3			56.9% SO_3		
Frequency (cm^{-1})	Assignment		Frequency (cm^{-1})	Assignment	
143	$D_2S_2O_7$	SOS bend	145	$D_2S_2O_7$, $D_2S_3O_{10}$*	Skeletal bend
			190	$D_2S_3O_{10}$*	Skeletal
300	$D_2S_2O_7$	Torsion	260	$D_2S_3O_{10}$	Skeletal
325	$D_2S_2O_7$	SOS stretch, s	300	$D_2S_2O_7$, $D_2S_2O_{10}$*	Torsion
352	D_2SO_4		325	$D_2S_2O_7$, $D_2S_3O_{10}$*	Skeletal stretch
404	D_2SO_4		354	$D_2S_3O_{10}$*	Skeletal stretch
482	$D_2S_2O_7$	SO_2 rock	449	$D_2S_3O_{10}$*	Torsion?
500	$D_2S_2O_7$	SO_2 rock	479	$D_2S_2O_7$, $D_2S_3O_{10}$*	SO_2 rock
525	D_2SO_4, $D_2S_2O_7$	SO_2 bend	499	$D_2S_2O_7$, $D_2S_3O_{10}$*	SO_2 bend
565	D_2SO_4		530	$D_2S_2O_7$, $D_2S_3O_{10}$*	SO_2 bend
583	$D_2S_2O_7$	SO_2 rock	563	D_2SO_4, $D_2S_2O_7$*	SO_2 bend
			612	$D_2S_3O_{10}$*	SO_2 rock?
730	$D_2S_2O_7$	SO_2 rock	685	$D_2S_3O_{10}$*	SO_2 rock
906	D_2SO_4		730	$D_2S_2O_7$, $D_2S_3O_{10}$*	SO_2 rock
980	D_2SO_4, $D_2S_2O_7$	S—OD stretch	960	$D_2S_2O_7$, $D_2S_3O_{10}$*	S—OD stretch
1175	D_2SO_4		1075	SO_3	SO stretch, s
			1205	$D_2S_2O_7$	SO_2 stretch, s
1230	$D_2S_2O_7$	SO_2 stretch, s	1230	$D_2S_2O_7$	SO_2 stretch, s
1340	D_2SO_4		1255	$D_2S_3O_{10}$*	SO_2 stretch, s
(1420)	$D_2S_2O_7$	SO_2 stretch, a	1416	$D_2S_2O_7$	SO_2 stretch, a
			1444	$D_2S_3O_{10}$*	SO_2 stretch, a
			1515	High polymer	SO_2 stretch, a

*These lines are probably also common to higher polyacids.

As the concentration of sulphur trioxide increases most of the Raman frequencies of D_2SO_4 (8) diminish in intensity and those due $D_2S_2O_7$ increase in intensity. The strong diagnostic frequency at 1075 cm^{-1} due to monomeric SO_3 is first observed in a relatively dilute oleum (27.1% SO_3) and this line grows in intensity as the concentration of the oleum increases. The band at 1270 cm^{-1}, which is diagnostic of the trimer S_3O_9, does not appear until the strength of the oleum is increased to approximately 80% SO_3. The formation of higher deuteropolysulphuric acids, e.g. $D_2S_3O_{10}$, is indicated both by the splitting of the 730 cm^{-1} line into two lines at 685 and 730 cm^{-1} and by the shift of the SO_2 symmetric stretch to higher frequencies with increasing stoichiometric concentration of SO_3. In dilute oleums the line at 1230 cm^{-1} is attributed to an SO_2 symmetric stretch of $D_2S_2O_7$. This line shifts to 1225 cm^{-1} in the strongest oleums and this is attributed to the formation of higher polyacids such as $D_2S_3O_{10}$ and $D_2S_4O_{13}$.

EXPERIMENTAL

Sulphuric acid (100%) was prepared, as has been described elsewhere (21), from analytical grade concentrated sulphuric acid and 30% oleum, by adjustment to the maximum freezing point of 10.37°. Deuterosulphuric acid was prepared by distilling sulphur trioxide into cooled deuterium oxide until there was a slight excess of sulphur trioxide. The 100% acid was then obtained by adjustment of the freezing point to 14.42° by addition of small amounts of deuterium oxide (20). The oleum solutions were prepared by weight by distillation of pure sulphur trioxide into the 100% acid. Sulphur trioxide was obtained by distillation of 65% commercial oleum to which potassium persulphate had been added to oxidize any sulphur dioxide present to the trioxide.

In the recent work of Giguère and Savoie (3) and of Walrafen and Young (2) the compositions of the oleums studied were obtained by titration with sodium hydroxide solution. As the latter workers point out this method of determining the compositions of solutions of sulphur trioxide in sulphuric acid is very inaccurate, particularly for strong oleums. Our method of preparing oleums of known composition is simple and the concentrations of the solutions were obtained very accurately.

The Raman spectra were measured with the photographic apparatus described previously using exposures of approximately 2 to 4 minutes. The spectra were measured by comparison with a standard iron arc using a Leeds and Northrup microphotometer (4). The frequencies of the lines reported are probably accurate to ± 5 cm^{-1}.

ACKNOWLEDGMENTS

Dr. R. H. Tomlinson is thanked for a gift of deuterium oxide, and the National Research Council and the Ontario Research Foundation for financial support.

REFERENCES

1. D. J. MILLEN. J. Chem. Soc. 2589 (1950).
2. G. E. WALRAFEN and T. F. YOUNG. Trans. Faraday Soc. **56**, 1419 (1960).
3. P. A. GIGUÈRE and R. SAVOIE. Can. J. Chem. **38**, 2467 (1960).
4. P. BAUMGARTEN and E. THILO. Ber. **71**, 2596 (1938).
5. D. R. GODDARD, E. D. HUGHES, and C. K. INGOLD. J. Chem. Soc. 2559 (1950). K. ERIKS and C. H. MACGILLAVERY. Acta Cryst. **7**, 430 (1954).
6. R. J. GILLESPIE and E. A. ROBINSON. Can. J. Chem. **39**, 2179 (1961).
7. R. J. GILLESPIE, J. V. OUBRIDGE, and E. A. ROBINSON. Proc. Chem. Soc. 428 (1961). R. J. GILLESPIE and E. A. ROBINSON. Unpublished results.
8. R. J. GILLESPIE and E. A. ROBINSON. Can. J. Chem. **40**, 644 (1962).
9. R. J. GILLESPIE and E. A. ROBINSON. Can. J. Chem. **39**, 2189 (1961).
10. E. A. ROBINSON. Can. J. Chem. **39**, 247 (1961).
11. R. J. GILLESPIE and E. A. ROBINSON. Advances in inorganic chemistry and radiochemistry. Vol. I. Academic Press, New York. 1959. p. 385.
12. D. E. C. CORBRIDGE and E. J. LOWE. J. Chem. Soc. 493 (1954).
13. J. R. BRAYFORD and P. A. H. WYATT. Trans. Faraday Soc. **52**, 642 (1956).
14. B. DACRE and P. A. H. WYATT. Proc. Chem. Soc. 18 (1960).
15. R. J. GILLESPIE and R. W. CHILD. Unpublished results.
16. H. GERDING and N. F. MOERMAN. Z. physik. Chem. B, **35**, 216 (1935).
17. J. C. D. BRAND, A. W. P. JARVIE, and W. C. HORNIG. J. Chem. Soc. 3844 (1959).
18. S. J. BASS, R. J. GILLESPIE, and E. A. ROBINSON. J. Chem. Soc. 821 (1960).
19. R. H. FLOWERS, R. J. GILLESPIE, and E. A. ROBINSON. Can. J. Chem. **38**, 1363 (1960).
20. R. H. FLOWERS, R. J. GILLESPIE, J. V. OUBRIDGE, and C. SOLOMONS. J. Chem. Soc. 1363 (1960).
21. R. J. GILLESPIE, J. V. OUBRIDGE, and C. SOLOMONS. J. Chem. Soc. 1804 (1957).

SOLUTIONS OF SULPHUR TRIOXIDE IN FLUOROSULPHURIC ACID AND CHLOROSULPHURIC ACID: RAMAN AND N.M.R. SPECTROSCOPIC EVIDENCE FOR THE FORMATION OF HALOGENOPOLYSULPHURIC ACIDS

R. J. GILLESPIE AND E. A. ROBINSON[1]
Department of Chemistry, McMaster University, Hamilton, Ontario
Received October 27, 1961

ABSTRACT

The Raman spectra of solutions of sulphur trioxide in fluorosulphuric acid and chlorosulphuric acid have been examined. By comparing the spectra with those of the polysulphuryl halides and the polysulphuric acids the formation of the halogen-substituted polysulphuric acids HS_2O_6F, HS_3O_9F, HS_2O_6Cl, and HS_3O_9Cl is proved and some evidence is obtained for higher polyacids such as $HS_4O_{12}F$ and $HS_4O_{12}Cl$. The fluorine n.m.r. spectra of solutions of sulphur trioxide in fluorosulphuric acid have also been investigated: they provide supporting evidence for the formation of fluoropolysulphuric acids. Vibrational frequencies diagnostic of the ions $S_2O_6F^-$ and $S_2O_6Cl^-$ have been obtained from the Raman spectra of fluorosulphuric acid solutions containing both sulphur trioxide and sodium fluorosulphate, and chlorosulphuric acid solutions containing both sodium chlorosulphate and sulphur trioxide.

The preceding paper gives an analysis of the spectra of solutions of sulphur trioxide in sulphuric acid in terms of the formation of the polysulphuric acids $H_2S_2O_7$, $H_2S_3O_{10}$, and higher polyacids (1). This paper presents the results of a similar investigation of the Raman spectra of solutions of sulphur trioxide in fluorosulphuric acid and chlorosulphuric acid.

THE FLUOROSULPHURIC ACID – SULPHUR TRIOXIDE SYSTEM

Raman Spectra

Cryoscopic and conductimetric measurements have shown (2) that sulphur trioxide behaves as a non-electrolyte in dilute solution in fluorosulphuric acid. There has been no previous Raman spectroscopic investigation of this system. Our results are shown in Table I and Fig. 1.

The spectrum of the most dilute solution studied (4.6% SO_3) has new lines at 300, 311, 325, 458, 721, 1074, 1202, 1394, 1412, and 1489 cm^{-1}, which are not present in the spectrum of fluorosulphuric acid (3). The lines at 1074 and 1394 cm^{-1} can be assigned to sulphuric trioxide monomer (4). The five lines from 300 to 721 cm^{-1} may be compared with similar lines in the spectrum of $S_2O_5F_2$ at 290, 301, 323, 455, and 733 cm^{-1} (5). The spectra of relatively dilute solutions of SO_3 in fluorosulphuric acid are also very similar to the spectra of dilute solutions of sulphur trioxide in sulphuric acid (Table II), in which the formation of the compound $H_2S_2O_7$ (I) is well established. The new lines in the spectra are thus consistent with the formation of a disulphuryl compound. The high-frequency lines at 1212, 1243, 1412, and 1489 cm^{-1} are undoubtedly due to SO_2 valency vibrations. For a disulphuryl compound of the type $S_2O_5X_2$ or S_2O_5XY four valency vibrations of the SO_2 groups are expected (5) (two symmetric stretches and two asymmetric stretches), and thus the above lines may be assigned to two symmetric stretches (1212 and 1241 cm^{-1}), and two asymmetric stretches (1412 and 1489 cm^{-1}), of a disulphuryl compound. By comparison with the SO_2 valency vibrations in the spectrum of $S_2O_5F_2$ at 1249, 1264, 1490, and 1511 cm^{-1} it is clear that the high-frequency lines

[1]*Present address: Department of Chemistry, University of Toronto, Toronto 5, Ontario.*

TABLE I

Raman spectra of solutions of sulphur trioxide in fluorosulphuric acid (frequencies in cm^{-1})

Percentage of SO_3:							
0.0	4.6	7.9	23.3	37.7	52.6	80.0	89.4
—	—	140(1/2)	138(1)	144(2)	141(3)	160(2)	154(1)
—	—	—	215(1/2−)	220(1/2)	235(1)	232(2)	238(1)
—	—	—	232(1/2)	243(1/2)	243(1)	242(1)	—
—	—	—	—	—	—	—	270(1)
—	300(1/2)	302(1)	294(3)	294(4)	295(5)	287(3)	290(2)
—	311(1)	314(2)	307(4)	307(5)	310(6)	—	—
—	325(1)	327(2)	322(5)	322(6)	325(7)	320(5)	322(3)
—	—	—	352(1/2)	349(1/2)	352(1)	365(1)	365(1)
—	—	—	—	364(1/2)	370(1/2)	368(1)	370(1)
391(4)	392(3)	390(2)	395(1/2)	390(1/2)	385(1/2)	—	390(1)
405(4)	402(4)	403(2)	405(1/2)	406(1/2)	407(1/2)	—	—
—	458(1/2)	461(1/2)	450(1)	452(1)	458(1)	450(1)	460(1)
—	—	—	505(1/2)	494(1/2)	497(1)	480(2)	477(2)
—	—	—	530(1)	530(2)	530(5)	533(6)	533(7)
550(5)	550(5)	550(4)	550(2)	540(3)	540(4)	—	—
562(5)	562(5)	556(4)	554(3)	563(3)	563(3)	—	—
—	—	—	—	—	—	—	650(1/2)
—	—	—	—	—	—	662(1/2)	665(1)
—	—	—	705(1/2)	704(1)	703(3)	700(2)	703(1)
—	721(1)	727(2)	724(4)	724(6)	727(5)	729(3)	729(2)
—	—	—	—	—	794(1/2)	—	794(1/2)
850(8)	850(7)	850(7)	850(6)	850(6)	852(4)	856(2)	852(1)
960(6)	960(6)	960(5)	962(4)	958(4)	966(2)	—	—
—	—	973(1)	970(1)	970(2)	975(2)	970(2)	970(1)
—	1074(1/2−)	1072(1)	1075(2)	1072(3)	1075(4)	1072(6)	1072(10)
1160(2)	1160(2)	1170(2)	1180(2)	1183(1)	1170(1/2)	1162(1/2)	1162(1/2−)
1230(5)	1241(5)	1248(3)	1250(5)	1250(5)	1254(5)	1258(3)	1258(1)
—	—	—	—	—	1268(1/2)	1268(2)	1270(3)
—	—	1394(1/2−)	1394(1/2)	1390(1/2)	1393(1/2)	1392(1)	1392(2)
—	1412(1)	1411(1)	1410(1)	1424(1)	1415(1/2)	—	—
1445(2)	1439(2)	1439(2)	1447(2)	1457(1)	1460(1/2)	—	—
—	1489(1)	1489(1)	1488(2)	1489(1)	1488(1)	1488(2)	1486(2)
—	—	—	—	—	—	1510(1)	1510(1)

observed in the spectrum of the $HFSO_3$–SO_3 system are not due to $S_2O_5F_2$ (II), although this might have been formed by the reaction

$$2HFSO_3 + SO_3 = S_2O_5F_2 + H_2SO_4.$$

Moreover, none of the characteristic vibrational frequencies of H_2SO_4 are found in these spectra.

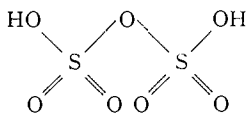

I

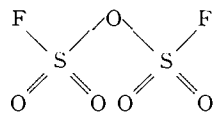

II

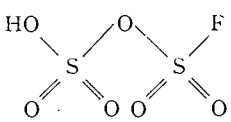

III

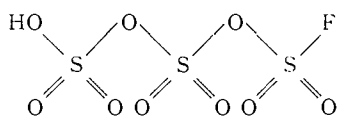

IV

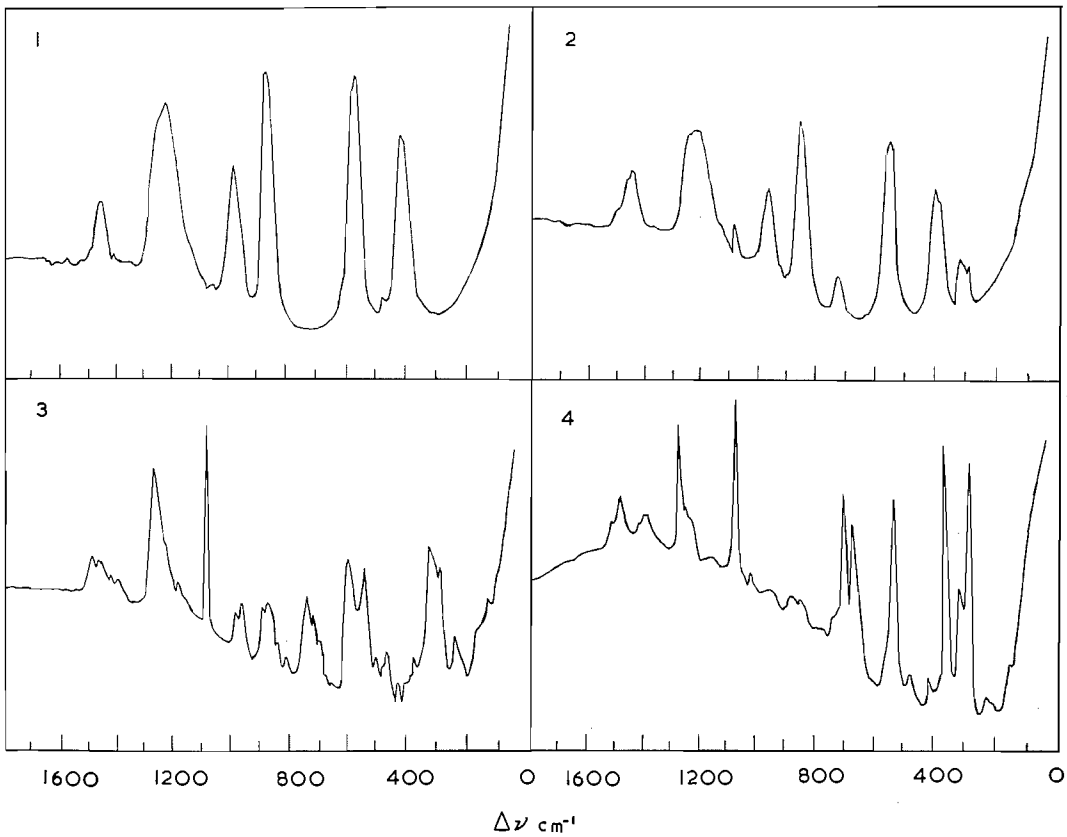

FIG. 1. Raman spectra of the HSO_3F–SO_3 system: (1) HSO_3F, (2) HSO_3F – 4.8% SO_3, (3) HSO_3F – 32.6% SO_3, (4) HSO_3F – 89.4% SO_3.

We conclude therefore that sulphur trioxide reacts with fluorosulphuric acid to form fluorodisulphuric acid, $S_2O_5F(OH)$ (III), in much the same manner as SO_3 reacts with sulphuric acid to form disulphuric acid. The comparison in Table III of the frequencies of the SO_2 stretching vibrations observed in the SO_3–HSO_3F system with those of $S_2O_5F_2$, S_2O_5FCl, $S_2O_5Cl_2$, and $S_2O_5(OH)_2$ provides strong support for attributing them to the new species $S_2O_5F(OH)$.

The S—OH stretch of $S_2O_5F(OH)$ would be expected to have a frequency close to 960 cm^{-1}, the frequency of the analogous vibration in fluorosulphuric acid. Therefore the new line which first appears at 973 cm^{-1} in the spectrum of the 7.9% SO_3 solution may be assigned to the S—OH stretch of fluorodisulphuric acid. In the spectrum of this solution another new line appears at 140 cm^{-1}, which can be assigned to the S—O—S bend of HFS_2O_6 by comparison with the line at 157 cm^{-1} in the spectrum of $S_2O_5F_2$. At slightly higher concentrations of stoichiometric sulphur trioxide further new lines appear in the spectra at 215, 232, 352, 364, 505, 530, and 705 cm^{-1}. The multiplicity of lines at low frequencies and in particular the replacement of the line at approximately 724 cm^{-1} by two lines at 724 and 705 cm^{-1} is diagnostic of a trisulphuryl compound (4) and thus we conclude that as the concentration of SO_3 increases the higher polyacid $S_3O_8F(OH)$ (IV) is also present in the system. At relatively high concentrations of sulphur trioxide

TABLE II

Comparison of the spectra of HSO_3F–SO_3 solutions with the spectra of $S_2O_5F_2$, $S_3O_8F_2$, $H_2S_2O_7$, and $H_2S_3O_{10}$ (frequencies in cm^{-1})

		% SO_3 in HSO_3F:		Assignment				% SO_3 in HSO_3F:	
$S_2O_6F_2$	$H_2S_2O_7$	4.6	7.9	Species	Vibration	$S_3O_8F_2$	$H_2S_3O_{10}$	52.6	89.4
157	145	—	140	HS_2O_6F	SOS bend	145	145	140	154
290	298	301	302	HS_2O_6F	Torsion	165	175	—	—
301	—	311	314	HS_2O_6F	SF wag	195	—	—	—
323	328	325	327	HS_2O_6F	SOS stretch	226	—	235	238
350	—	—	—			245	252	243	270
366	—	—	—			288	298	295	290
—	—	392	390	HSO_3F		318	—	310	—
—	—	402	403	HSO_3F		324	328	325	322
435	—	—	—			350	350	352	365
455	—	458	461	HS_2O_6F	SF wag	359	—	370	370
487	470	—	—			—	—	385	390
518	504	550	550	HSO_3F, HS_2O_6F	SO_2 bend	403	400	407	—
540	562	562	556	HSO_3F, HS_2O_6F	SO_2 bend	468	470	458	460
560	619	—	—	—		—	504	497	497
630	640	—	—	—		528	528	530	553
733	735	721	727	HS_2O_6F	SO_2 rock	—	—	540	—
814	809	—	—	—		—	562	563	—
872	—	850	850	HSO_3F, HS_2O_6F	SF stretch	—	619	—	650
—	—	960	960	HSO_3F		—	640	—	665
—	960	—	973	HS_2O_6F	S(OH) stretch	699	690	703	703
—	—	1074	1072	SO_3		724	735	727	729
—	1175	1160	1150	HSO_3F, HS_2O_6F	OH wag	761	—	794	794
1249		1212	1213	HS_2O_6F	SO_2 stretch	835	809	—	—
1264	1224	1241	1248	HSO_3F, HS_2O_6F		—	850	—	—
—		—	1394	SO_3		876	—	852	852
1490	1425	1412	1441	HS_2O_6F	SO_2 stretch	—	—	966	—
1511		1439	1439	HSO_3F		—	960	975	970
		1489	1489	HS_2O_6F	SO_2 stretch	—	—	1075	1072
						—	1175	1170	1162
						1198	—	—	—
						1241	1224	1213	1225
						1268	1250	1254	1258
						—	—	1268	1270
						—	—	1393	1392
						1468	1425	1415	—
						1490	1458	1460	1486
						1515		1488	1510

TABLE III

SO_2 stretching vibrations in disulphuryl compounds

$S_2O_5F_2$	1249	1490	$S_2O_5F_2$	1249	1490	$S_2O_5Cl_2$	1189	1442
	1264	1511		1264	1511		1209	1462
S_2O_5FCl	1205	1453	$S_2O_5F(OH)$	1210	1410	$S_2O_5Cl(OH)$	1209	1408
	1248	1487		1250	1489		1235	1452
$S_2O_5Cl_2$	1189	1442	$S_2O_5(OH)_2$	1220	1420*	$S_2O_5(OH)_2$	1220	1420*
	1209	1462						

*Mean frequency of two unresolved lines.

in fluorosulphuric acid only a few new lines appear in the spectra. However, as was found to be the case for solutions of sulphur trioxide in sulphuric acid (1) at very high concentrations of SO_3, a line appears at 1270 cm^{-1} which is indicative of the presence of sulphur trioxide trimer, S_3O_9, in these solutions. The SO_2 symmetric stretch at 1250 cm^{-1} (which is well resolved from the adjacent line due to sulphur trioxide trimer) shifts slightly to approximately 1258 cm^{-1}. This small but real shift in frequency may possibly be ascribed to the formation of higher polysulphuric acids such as $S_4O_{11}F(OH)$. Table II gives our assignment of the observed spectral lines of two dilute solutions of sulphur trioxide in fluorosulphuric acid.

N.M.R. Spectra

Further evidence for the formation of fluoropolysulphuric acids in this system was obtained from a study of the variation of the chemical shift in the fluorine n.m.r. spectra of the fluorosulphuric acid – sulphur trioxide system (Fig. 2). As the stoichiometric concentration of sulphur trioxide increases the single fluorine resonance peak shifts to lower field. The fact that a separate resonance is not observed for each polyacid indicates that there is some rapid exchange process which averages the chemical environment of

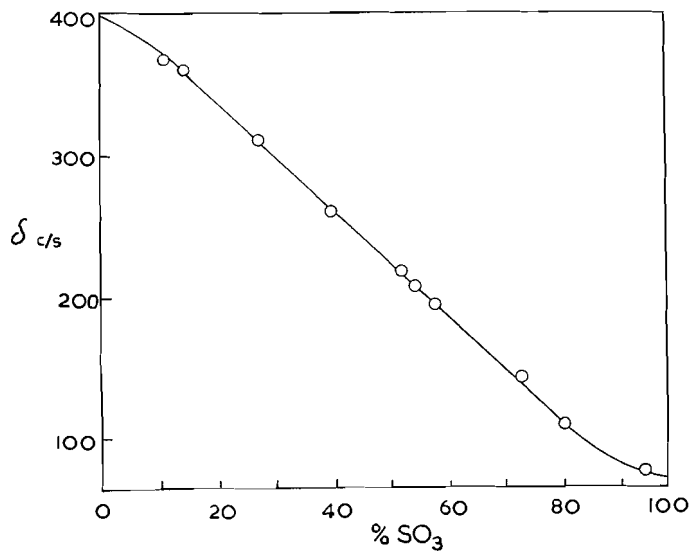

FIG. 2. F^{19} chemical shifts in the HSO_3F–SO_3 system. δ, chemical shift from internal $S_2O_5F_2$ (c/s at 56.4 Mc).

the fluorine atoms. Since the presence of free SO_3 in the system is indicated by the occurrence of the 1074 cm^{-1} line even at low SO_3 concentrations, the exchange process is most probably the exchange of SO_3 between the various polyacids:

$$H(SO_3)_nF + SO_3 \rightleftharpoons H(SO_3)_{n+1}F.$$

It is of interest to compare the relative chemical shifts in the fluorosulphuric acid – sulphur trioxide system with the corresponding shifts of the polysulphuryl fluorides (6). Figure 3 shows such a comparison for the purpose of which we have interpolated the

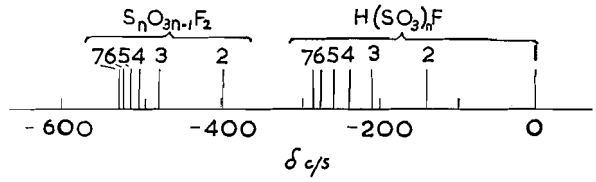

FIG. 3. Comparison of the F^{19} chemical shifts of the fluoropolysulphuric acids and the polysulphuryl fluorides. δ, chemical shift from internal $S_2O_5F_2$ (c/s at 56.4 Mc).

chemical shifts in the $HFSO_3$–SO_3 system at the stoichiometric compositions corresponding to complete formation of the acids HS_2O_6F, HS_3O_9F, $HS_4O_{12}F$, $HS_5O_{15}F$, etc., although, in fact, at these compositions the system undoubtedly contains several of these species in equilibrium. There is a striking similarity between the spectrum of the polysulphuryl fluoride resonances and those of the fluoropolysulphuric acids.

Addition of a polysulphuryl fluoride such as $S_2O_5F_2$ to a solution of SO_3 in fluorosulphuric acid gave an additional line in the n.m.r. spectrum, showing that these species were not present in the original system—a conclusion which agrees with our deduction from the Raman spectra that polysulphuryl fluorides are not formed from the reaction between fluorosulphuric acid and sulphur trioxide at room temperature. Polysulphuryl fluorides were formed, however, when sulphur trioxide and fluorosulphuric acid were heated to 100° in sealed tubes for several hours (Fig. 4).

The Raman and n.m.r. spectra of solutions of sulphur trioxide in fluorosulphuric acid at room temperature therefore indicate the formation of the fluoropolysulphuric acids HS_2O_6F, HS_3O_9F, and perhaps higher polyacids such as $HS_4O_{12}F$, although at higher temperatures polysulphuryl fluorides are also formed.

The $S_2O_6F^-$ Ion

When potassium fluorosulphate was added to a dilute solution of sulphur trioxide in fluorosulphuric acid the only marked change in the spectrum was the appearance of a strong line at 1080 cm^{-1}. The frequency of this line is the same as that of a characteristic frequency of the hydrogen disulphate ion (1). This is consistent with the formation of the fluorodisulphate ion, $FS_2O_6^-$, according to the equation

$$KFSO_3 + HFS_2O_6 = FS_2O_6^- + HFSO_3.$$

No line is observed at 1080 cm^{-1} in the spectrum of the fluorosulphuric acid – sulphur trioxide system. We conclude that the ion $FS_2O_6^-$ is not present in solutions of SO_3 in $HFSO_3$ and that therefore the acid HFS_2O_6 is a very weak acid of the fluorosulphuric acid system. This is in agreement with cryoscopic and conductimetric measurements (2) which show that SO_3 is a non-electrolyte in fluorosulphuric acid, although these measurements do not distinguish between the possibilities that the solution contains monomeric SO_3 or the non-ionized acid HS_2O_6F.

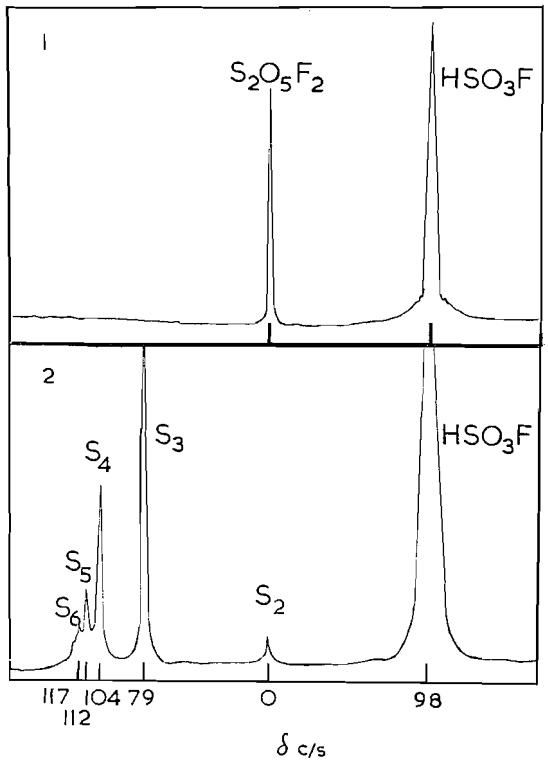

FIG. 4. Nuclear magnetic resonance spectra illustrating the formation of polysulphuryl fluorides in the HSO_3F–SO_3 system at elevated temperatures: (1) HSO_3F – 37% SO_3 at room temperature ($S_2O_5F_2$ was added to provide a reference signal); (2) HSO_3F – 37% SO_3 after 4 hours at 100° (S_n denotes the polysulphuryl fluoride $S_nO_{3n-1}F_2$).

Complexes are known between ionic fluorides and sulphur trioxide, e.g. $KF.2SO_3$ (7); these compounds may be formulated as salts of fluorodisulphuric acid.

THE CHLOROSULPHURIC ACID - SULPHUR TRIOXIDE SYSTEM

Solutions of sulphur trioxide in chlorosulphuric acid have received some attention previously due to their use in aromatic sulphonation and as smoke gases in war. The densities and viscosities of solutions of sulphur trioxide in chlorosulphuric acid have been examined by McCallum and Tollefson (8), who also found that no solid phase exists in such solutions up to 60% SO_3 by weight at room temperature. Vapor pressure measurements have been reported by Balson and Adam (9), and the Raman spectrum of a 1:1 mixture of SO_3 and chlorosulphuric acid has been discussed by Gerding (10), who did not report the spectrum but only his conclusion that a complex is formed, which he regarded as a loosely bound addition compound $SO_3.HSO_3Cl$.

The Raman spectra of several solutions of SO_3 in chlorosulphuric acid are shown in Table IV and Fig. 5. The analysis of these spectra follows very much the same pattern as that given above for solutions of sulphur trioxide in fluorosulphuric acid.

At relatively low concentrations of sulphur trioxide in chlorosulphuric acid, e.g. 12.8% SO_3, many new lines appear in the spectrum which cannot be attributed to either component. These occur at 148, 218, 232, 275, 289, 301, 360, 595, 720, 803, 950, 1075, 1235, and 1452 cm^{-1} in the spectrum of the 12.8% SO_3 solution. The line at 1075 cm^{-1}

TABLE IV

Raman spectra of solutions of sulphur trioxide in chlorosulphuric acid (frequencies in cm^{-1})

Percentage of SO_3:						
0	12.8	19.8	25.1	36.7	70.0	92.8
—	148(1)	145(2)	142(2)	148(2)	145(2)	153(3)
200(2)	205(2)	208(2)	208(2)	208(2)	208(2)	208(1/2)
—	218(1)	218(2)	220(2)	218(1)	218(1)	—
—	232(2)	234(3)	239(3)	237(2)	234(1/2)	235(1/2)
—	275(1/2)	278(1/2)	278(1/2)	278(1)	—	—
—	289(2)	289(4)	289(5)	289(6)	286(6)	288(8)
—	301(4)	310(5)	303(5)	300(6)	310(3)	—
312(8)	319(4)	323(5)	320(5)	320(6)	320(2)	320(2)
—	—	—	—	350(2)	350(5)	337(1/2−)
—	360(2)	364(1)	360(1)	360(3)	370	365(8)
—	—	395(2)	398(2)	395(3)	395(1)	—
416(10)	419(10)	418(10)	419(9)	415(8)	415(5)	410(2)
—	494(1)	494(2)	489(2)	484(1)	484(1)	483(1/2−)
—	—	—	—	494(1)	—	—
513(6)	514(6)	517(3)	514(3)	520(1)	527(3)	533(5)
—	—	—	573(1)	572(1/2)	—	—
—	595(4)	598(5)	596(6)	598(3)	602(1/2)	608(1/2)
623(10)	625(6)	623(5)	625(5)	622(4)	624(3)	—
—	—	—	—	—	663(2)	657(3)
—	—	—	—	—	685(2)	665(4)
—	—	—	700(1/2−)	685(1)	696(3)	700(5)
—	720(3)	720(4)	723(4)	721(5)	723(2)	723(1/2)
—	803(1)	790(1)	800(1)	800(1)	780(1)	—
—	—	—	—	—	852(2)	854(1)
920(8)	920(8)	918(4)	920(4)	920(1)	—	—
—	950(1/2)	958(1)	960(2)	960(2)	960(1)	—
—	—	—	—	—	—	—
—	1075(1/2)	1073(1)	1075(1)	1075(2)	1071(8)	1072(10)
1150(10)	1155(8)	1152(6)	1160(5)	1150(4)	1163(1)	1138(1/2−)
1209(6)	1205(8)	1204(6)	1200(6)	1200(6)	1207(3)	1224(2)
—	1235(1)	1235(2)	1235(3)	1235(4)	1241(6)	1258(2)
—	—	—	—	—	1270(2)	1270(6)
1408(3)	1408(3)	1408(3)	1408(2)	1400(2)	1408(1)	1390(3)
—	1452(2)	1452(2)	1448(2)	1442(3)	1450(3)	1460(2)
—	—	—	—	—	1479(2)	1486(3)
—	—	—	—	—	1520(1)	1512(1/2)

is due to SO_3 monomer (4) and the other lines are to be compared with lines in the spectrum of $S_2O_5Cl_2$ (5) at 147, 235, 273, 298, 370, 593, 716, 760, 1189, 1209, 1442, and 1462 cm^{-1} (Table V). This comparison clearly indicates the formation of a disulphuryl compound in the $HClSO_3$–SO_3 system. The spectra are also very similar to those of dilute solutions of SO_3 in sulphuric acid, where the formation of disulphuric acid (I) is well established. Again it is necessary to distinguish between the possible formation of chlorodisulphuric acid (V) or disulphuryl chloride (VI). The spectra support the forma-

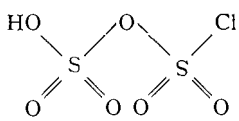

V

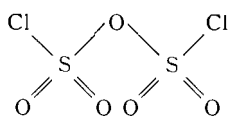

VI

tion of the former rather than the latter since the new line at 950 cm^{-1} can be assigned to the S—OH stretch in this species (compare 920 cm^{-1} for the S—OH stretch in chlorosulphuric acid (3), and 960 cm^{-1} for the S—OH stretch in $H_2S_2O_7$ (1)). The new lines

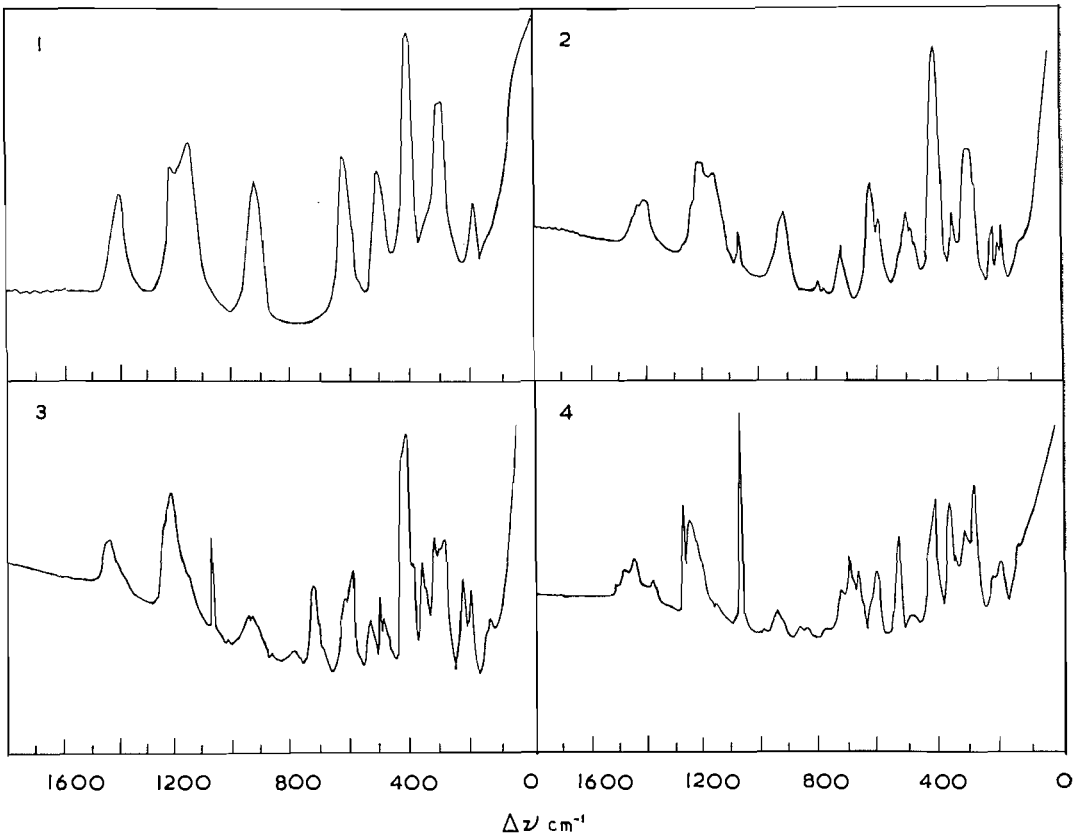

FIG. 5. Raman spectra of the HSO_3Cl–SO_3 system: (1) HSO_3Cl, (2) HSO_3Cl – 12.8% SO_3, (3) HSO_3Cl – 36.7% SO_3, (4) HSO_3Cl – 70% SO_3.

at 1235 and approximately 1450 cm^{-1} can be assigned, respectively, as a symmetric and an asymmetric stretching frequency of the SO_2 group. Since the intensities of the lines at approximately 1209 and 1408 cm^{-1}, which are the symmetric and asymmetric SO_2 vibrations of chlorosulphuric acid, change little even in solutions of high SO_3 content we conclude that these lines are also common to the spectrum of the new disulphuryl compound. Thus the new species has two symmetric stretches at approximately 1209 and 1235 cm^{-1} and two asymmetric stretches at approximately 1408 and 1452 cm^{-1}. The comparison of these frequencies with those of the SO_2 stretches of the other disulphuryl compounds shown in Table III strongly suggests that the new species is $S_2O_5Cl(OH)$.

As the concentration of SO_3 in chlorosulphuric acid increases, the spectra become increasingly similar to the spectrum of a trisulphuryl compound. In particular the line at 720 cm^{-1} is replaced by two lines in the same region of the spectrum at approximately 700 and 723 cm^{-1}. This is diagnostic of the formation of a trisulphuryl compound (5), i.e. $S_3O_8Cl(OH)$. As the concentration of SO_3 increases the symmetric stretch originally at 1235 cm^{-1} moves to higher frequencies, e.g. in 92.8% SO_3 the symmetric stretch is at 1258 cm^{-1}. There is also a line at approximately 1480 cm^{-1} which can be assigned as the corresponding SO_2 asymmetric stretch. This may be taken as evidence for the formation of higher polysulphuric acids such as $HS_4O_{12}Cl$.

TABLE V

Comparison of the spectra of HSO_3Cl–SO_3 solutions with the spectra of $S_2O_5Cl_2$, $S_3O_8Cl_2$, $H_2S_2O_7$, and $H_2S_3O_{10}$ (frequencies in cm^{-1})

		% SO_3 in HSO_3Cl:		Assignment				% SO_3 in HSO_3Cl:	
$S_2O_5Cl_2$	$H_2S_2O_7$	12.8	19.8	Species	Vibration	$S_3O_8Cl_2$	$H_2S_3O_{10}$	70.0	92.8
147	145	148	145	HS_2O_6Cl	SOS bend	136	145	145	153
—	—	205	208	HSO_3Cl		169	175	—	—
200	—	218	218	HS_2O_6Cl	SCl wag	200	—	208	208
235	—	232	234	HS_2O_6Cl	SCl wag	226	—	218	—
273	298	275	278	HS_2O_6Cl	Torsion	—	—	234	235
298	328	289	289	HS_2O_6Cl	SOS stretch	275	252	286	288
—	—	301	310	HS_2O_6Cl	S—OH wag	291	298	310	—
—	—	319	323	HSO_3Cl	—	308	328	320	320
326	—	—	—	—	—	342	—	350	337
353	—	—	—	—	—	362	350	370	365
370	—	360	364	HS_2O_6Cl	Torsion	—	400	395	—
—	—	—	395	HS_3O_9Cl?	—	415	—	415	410
412	—	419	418	HSO_2Cl, HS_2O_6Cl	SCl stretch	440	—	—	—
427	—	—	—	—	—	485	470	484	483
—	470	494	494	HSO_3Cl, HS_2O_6Cl	SO_2 rock	512	504	—	—
490	504	514	517	HSO_3Cl, HS_2O_6Cl	SO_2 bend	—	528	527	533
560	—	—	—	—	—	595	562	602	608
593	562	595	598	HS_2O_6Cl	SO_2 bend	—	619	624	—
607	—	—	—	—	—	650	640	663	657
621	630	625	623	HSO_3Cl, HS_2O_6Cl	SO_2 rock	686	690	685	665
716	735	720	720	HS_2O_6Cl	SO_2 rock	—	—	696	700
760	809	803	790	HS_2O_6Cl	SOS stretch	723	735	723	723
—	—	920	918	HSO_3Cl	—	770	809	780	—
—	960	950	958	HS_2O_6Cl	S—OH stretch	870	850	852	854
—	—	1075	1073	SO_3	—	—	960	960	—
—	1175	1155	1152	HSO_3Cl, HS_2O_6Cl	O—H wag	—	—	1071	1072
1189	—	1205	1204	HSO_3Cl, HS_2O_6Cl	SO_2 stretch	—	1175	1163	—
1209	1224	1235	1235	HS_2O_6Cl		1193	—	—	—
1442	—	1408	1408	HSO_3Cl, HS_2O_6Cl	SO_2 stretch	1208	1224	1207	1224
1462	1425	1452	1452	HS_2O_6Cl		1220	1250	1241	1258
						—	—	1270	1270
						1450	1425	1408	1390
						1480	1458	1450	1460
						—	—	1479	1486
						—	—	1520	1512

On addition of sodium chlorosulphate to a dilute solution of SO_3 in chlorosulphuric acid the principal change in the spectrum is the appearance of a new line at 1080 cm^{-1}. Since this frequency is very similar to that of one of the SO_2 stretches of the $HS_2O_7^-$ ion we assign it to one of the SO_2 vibrations of the $ClS_2O_6^-$ ion. As this line is not present in the original chlorosulphuric acid oleum solutions we conclude that chlorodisulphuric acid is very little ionized in solution in chlorosulphuric acid.

The Raman spectra of solutions of sulphur trioxide in chlorosulphuric acid are consistent with the formation of the chloropolysulphuric acids HS_2O_6Cl, HS_3O_9Cl, and probably $HS_4O_{12}Cl$ and higher polyacids. As was the case for the corresponding fluoroacids the sharp line in the spectra at 1075 cm^{-1} indicates the presence of some free sulphur trioxide even at low stoichiometric concentrations of SO_3 and there is probably rapid exchange according to the equation

$$H(SO_3)_nCl + SO_3 \rightleftharpoons H(SO_3)_{n+1}Cl.$$

It is known that simple ionic chlorides such as sodium chloride form addition compounds with sulphur trioxide, e.g. $NaCl.SO_3$, $NaCl.2SO_3$, $NaCl.3SO_3$ (11). These compounds may be formulated as the salts of chlorosulphuric acid and the chloropolysulphuric acids, i.e. $NaClSO_3$, $NaClS_2O_6$, and $NaClS_3O_9$.

EXPERIMENTAL

Fluorosulphuric acid and chlorosulphuric acid were purified by distillation of the commercial products and had boiling points of 161° and 153°, respectively. Solutions were made up by weight by distilling sulphur trioxide into the acid. Sulphur trioxide was obtained by distillation from 65% fuming sulphuric acid or from commercial stabilized sulphur trioxide "Sulfan B".

The Raman spectroscopic measurements were carried out as has been described previously (5) using a Hilger E 612 spectrometer in conjunction with a water-cooled "Toronto" mercury arc lamp. The spectra were recorded photographically and measured by means of a Leeds and Northrup microphotometer.

The n.m.r. measurements were carried out using a Varian Associates n.m.r. spectrometer, operating at 56.4 Mc/sec. The spectra were calibrated using the side-band technique and shifts were measured with respect to disulphuryl fluoride as an internal reference.

ACKNOWLEDGMENTS

Dr. J. V. Oubridge is thanked for preliminary work on the n.m.r. spectra and Mr. J. Bacon for experimental assistance. The Ontario Research Foundation, the Defence Research Board, and the Allied Chemical Company are thanked for financial support.

REFERENCES

1. R. J. GILLESPIE and E. A. ROBINSON. Can. J. Chem. **40**, 658 (1962).
2. R. J. GILLESPIE, J. BARR, and R. C. THOMPSON. Unpublished results.
3. R. J. GILLESPIE and E. A. ROBINSON. Can. J. Chem. **40**, 644 (1962).
4. R. J. GILLESPIE and E. A. ROBINSON. Can. J. Chem. **39**, 2189 (1961).
5. R. J. GILLESPIE and E. A. ROBINSON. Can. J. Chem. **39**, 2179 (1961).
6. R. J. GILLESPIE, J. V. OUBRIDGE, and E. A. ROBINSON. Proc. Chem. Soc. 428 (1961).
7. P. BAUMGARTEN. Chemie, Die, **55**, 117 (1942). H. A. LEHMANN and L. KOLDITZ. Z. anorg. u. allgem. Chem. **272**, 69 (1953).
8. K. J. MCCALLUM and E. L. TOLLEFSON. Can. J. Research, F, **26**, 241 (1948).
9. E. W. BALSON and N. K. ADAM. Trans. Faraday Soc. **44**, 412 (1948).
10. H. GERDING. J. chim. phys. **46**, 118 (1949).
11. A. W. HIXSON and A. H. TENNEY. Ind. Eng. Chem. **33**, 1472 (1941). W. TRAUBE. Ber. **46**, 2522 (1913).

THE KINETICS OF THE REACTION OF ACTIVE NITROGEN WITH ETHYLENE[1]

E. M. LEVY[2] AND C. A. WINKLER

Upper Atmosphere Chemistry Research Group, Physical Chemistry Laboratory, McGill University, Montreal, Que.

Received December 1, 1961

ABSTRACT

A comparison has been made of five methods for terminating the reaction of active nitrogen with ethylene in the temperature range 295° to 673° K. These were based on deactivating the active nitrogen by low-temperature trapping, by addition of nitric oxide, and by passing it over copper oxide or cobalt catalysts. With the nitric oxide and cobalt catalyst techniques, which appeared to be the most reliable of those used, an activation energy of 400 ± 200 cal/mole, with a P factor of about 10^{-5}, have been determined for the reaction.

INTRODUCTION

Although the reactions of active nitrogen with a large number of organic and inorganic compounds have been studied, most of the earlier investigations were of a semiquantitative nature, in which the extents of product formation were determined as functions of reactant flow rates, and plausible mechanisms suggested on the basis of this formation. In some cases, rate constants, of doubtful reliability, were calculated from such data, while, in one study, the rate constant of the active nitrogen – ethylene reaction was roughly determined by a diffusion flame technique (1). Recently, rate constants have been reported for the reactions of active nitrogen with atomic oxygen (2), molecular oxygen (3, 4), ozone (5), nitric oxide (4, 6), nitrogen dioxide (6), ethylene (7, 8, 9), and hydrogen bromide (8), but, with one exception (7), reaction time has not been a controlled parameter in these investigations.

In the present study, a comparison has been made of several experimental techniques by which the reaction of active nitrogen with ethylene might be terminated, so as to enable the reaction time, and hence the rate constant, to be estimated. By comparing the techniques for a range of reaction temperatures between 295° K and 673° K, it has been possible to select two methods that appear to be reliable for terminating such reactions, and it is now intended to apply these to evaluating the kinetic constants for other active nitrogen reactions.

EXPERIMENTAL

Materials

"Bone-dry" nitrogen was obtained from the Linde Company, and passed over copper turnings at 425° C, and through a liquid air trap to remove traces of oxygen, water, and carbon dioxide.

U.S.P. ethylene was obtained from the Ohio Chemical Company, and was subjected to two trap-to-trap distillations, only the middle two-thirds of each distillate being retained.

Nitric oxide, obtained from the Matheson Chemical Company Ltd., was purified by condensing it into a bulb containing Caroxite, which adsorbed the nitrogen dioxide. The nitric oxide was then allowed to evaporate from a dry ice – acetone bath which retained the N_2O_3, and the whole procedure was repeated.

Apparatus and Experimental Methods

The apparatus differed significantly from that previously described (10) and is shown in Fig. 1.

Nitrogen was passed through the dibutyl phthalate manostat, H, through a furnace, F, containing copper

[1]*Financial assistance was received from National Research Council.*

[2]*Holder of National Research Council Studentships 1959–1960 and 1960–1961. Present address: Atlantic Regional Laboratory, National Research Council, Halifax.*

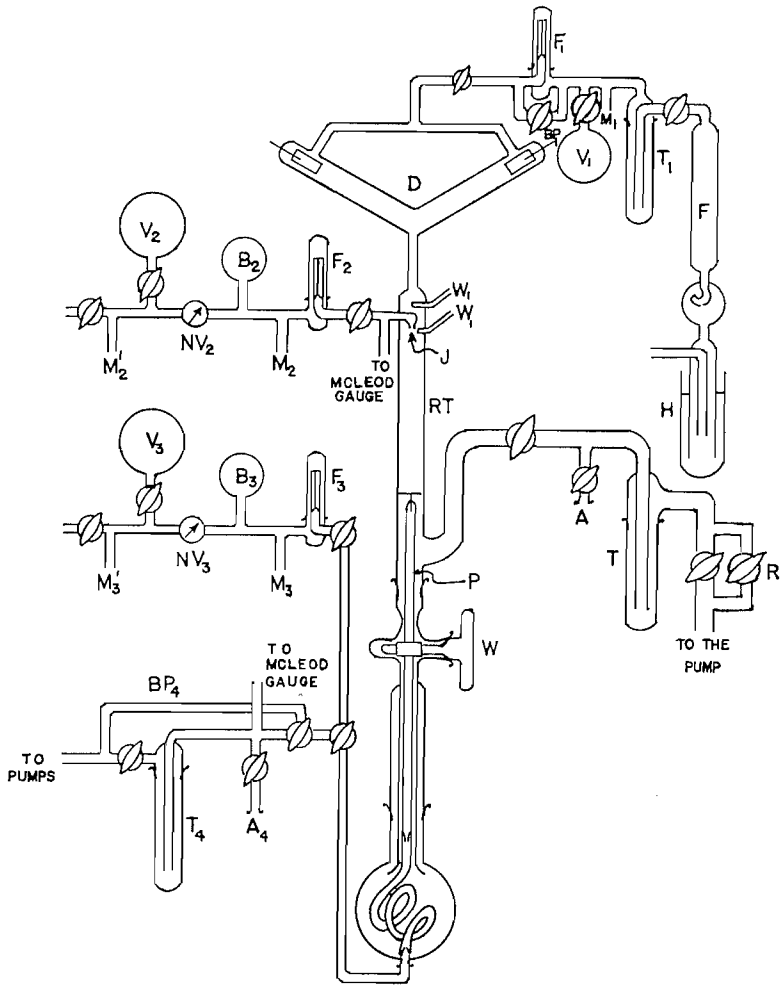

FIG. 1. Diagram of the apparatus.

turnings, and a trap, T_1, into the capillary flowmeter, F_1, which had been previously calibrated by the rate of evacuation, through it, of the known volume, V_1. The gas then entered the discharge tube, D, the construction and operation of which were similar to those described previously.

The reactant was metered by a flow system (subscripts 2) consisting of a known volume, V_2, a ballast volume, B_2, manometers, M_2 and M_2', a fine control needle valve, NV_2, and a capillary flowmeter, F_2. The reactant entered the reaction tube, RT, through the fixed reactant jet, J. Thermocouple wells, W_1, were placed 1 cm above and below the reactant jet. The reactions occurred in a Pyrex U-tube with an internal diameter of 22 mm. From there, the gas stream passed through a large liquid air trap, T, in which the condensable gases were retained. Continuous pumping was provided by a Cenco Hypervac 23 rotary oil pump.

In several of the techniques used to terminate the reactions, the reaction tube was provided with a movable probe mechanism, P (11), constructed from 10-mm Pyrex tubing, and sufficiently long to explore the entire length of the reaction tube. Its upper tip carried various contrivances to terminate the reaction. It was raised or lowered, under vacuum, by rotating the ground-glass joint, W. A friction drive between the probe and the projection of the joint was provided by a sleeve of rubber tubing. The bottom of the probe was connected with rubber tubing to either a second flow system (subscripts 3), or to a pumping system (subscripts 4). Through the former arrangement, gases were introduced into the reaction tube at any desired position, whereas the latter permitted the removal of samples of the reaction mixture after various reaction times.

Briefly, the experimental procedures were as follows:

(*a*) In a low-temperature technique for terminating the reaction between active nitrogen and ethylene, the reaction was stopped by immersing the U-shaped reaction tube in liquid air. (No probe mechanism was needed in these experiments.) The recombination of the nitrogen atoms was greatly enhanced (12), and the ethylene was condensed, at the low temperature, to deprive both reactants of their abilities to react.

In these experiments, the inner surface of the reaction tube was coated with disodium hydrogen phosphate (13), to retard the recombination of the nitrogen atoms on the walls of the reaction tube, and to stabilize the wall conditions. The reaction tube was heated to 400° C.

With the reaction tube immersed to the desired level in liquid air, purified nitrogen was passed through the apparatus, and the discharge operated until the temperature attained a constant and reproducible value, as an indication of a constant and reproducible initial active-nitrogen flow rate. Ethylene was then admitted, at a constant flow rate, to the stream of active nitrogen for a period of 100 seconds. The discharge and the flows of gases were stopped, the apparatus evacuated and isolated from the pump, and the condensable gases transferred to an absorber at A containing frozen, degassed water, where the hydrogen cyanide was later titrated with standard silver nitrate.

Experiments were made with flow rates of ethylene ranging from 0.9 to 14.8 μmoles per second, at a constant initial active-nitrogen flow rate, and with liquid air levels maintained at distances of 18.0, 23.5, and 29.0 cm from the fixed reactant jet, corresponding to reaction times of 19, 24, and 30 mseconds respectively. Experiments were also made, in which the reaction was permitted to proceed to completion, over a distance of 140 cm, as a basis for estimating the total initial active-nitrogen flow rate (7), which proved to be 14.0 μmoles per second.

(*b*) In a second technique for terminating the reaction between active nitrogen and ethylene, unreacted nitrogen atoms in the reaction mixture were consumed rapidly by flooding the reaction mixture with nitric oxide (7), introduced through the movable probe at any desired level. For this purpose, the probe was equipped with a 14-mm hemispherical bulb containing six small holes in its periphery, in a plane perpendicular to the gas stream in the reaction tube. Nitric oxide, at a flow rate in excess of that required to consume the active nitrogen completely, was passed into the reaction tube through this bulb, with the conditions of pressure and linear velocity of the gases selected so that the nitric oxide emerged radially from the bulb with no diffusion upstream, and a sharp plane of demarcation between the Lewis–Rayleigh afterglow and the nitric oxide reaction flame was obtained. Ethylene was passed into the stream of active nitrogen through the fixed reactant jet for a period of 100 seconds, and the products were trapped and analyzed as before. The nitrogen atom flow rate in these experiments was 7.0±0.3 μmoles per second, the ethylene flow rates were in the range 2.8 to 4.6 μmoles per second, the reaction times ranged from 2.1 to 55.8 mseconds, and reaction temperatures from 295° K to 671° K.

(*c*) A third method for studying the reaction of active nitrogen with ethylene was to remove a portion of the reaction mixture through the movable probe. The reaction was stopped at the tip of the probe by a small amount of oxidized copper turnings, an efficient catalyst for the recombination of nitrogen atoms (14). After a 2-minute period, during which the probe was flushed through the bypass, BP_4, the aliquot was diverted to the trap, T_4, for a period of 30 minutes. The hydrogen cyanide was treated as before. The extent of the reaction as a function of time was established by taking aliquots at various positions along the axis of the reaction tube. Separate experiments were made to determine the fraction of the total gases in the aliquot, from which the total extent of reaction was readily calculated. Nitrogen atom flow rates of 4.2 and 8.8 μmoles per second were used, with flow rates of ethylene between 1.1 and 3.0 μmoles per second, and reaction times that ranged from 1.6 to 40.2 mseconds. Reaction temperatures were 297° K and 543° K.

(*d*) The catalytic properties of copper oxide were utilized in still another way to promote the recombination of the nitrogen atoms, and hence to terminate the reaction of active nitrogen with ethylene. A fresh layer of copper was electrodeposited from a copper sulphate solution upon 45-mesh copper gauze, and a 21-mm disk of this gauze fastened with silver solder to a platinum wire, which was sealed into the end of the probe. The copper was oxidized by heating it in an oxygen-rich flame. The Lewis–Rayleigh afterglow was completely extinguished at the surface of the target, which was in a plane perpendicular to the flow of gases in the reaction tube. Again, the experiments were of 100 seconds' duration, and were made in the manner described previously. The nitrogen atom flow rate was 6.1 μmoles per second, the ethylene flow rate was 3.6 μmoles per second, the reaction time ranged from 3 to 45.5 mseconds, and the temperatures used were 295° K and 536° K.

(*e*) In a variation of the target procedure of section (*d*), above, the probe was equipped with a circular piece of 45-mesh platinum gauze which was electroplated with a black, spongy layer of cobalt, from an ammoniacal cobalt sulphate solution (15). In addition, three small holes were blown in the tube of the probe at a distance of 3 cm downstream from the cobalt target. This permitted "blank" experiments to be made, in which ethylene was passed into the gas stream after the active nitrogen had impinged on the target. The hydrogen cyanide from these experiments was limited entirely by the amount of active nitrogen that failed to be deactivated by the target, and provided a convenient means for checking the efficiency of the catalyst for deactivating the active nitrogen. In practice, it was found that reproducible results could be obtained only if the experiments were made at progressively shorter reaction times. Moving the cobalt target along the reaction tube apparently left behind traces of the catalyst on the walls. By working at

successively shorter reaction times, i.e. always moving the probe upward, the wall of the reaction tube in the region where the reaction occurred did not come in contact with the catalyst prior to the reaction, and contamination of it was thereby avoided.

For these experiments the ranges of conditions were: nitrogen atom flow rate, 2.9 to 9.8 μmoles per second; ethylene flow rate, 1.9 to 8.8 μmoles per second; reaction time, 5.2 to 47.6 mseconds; temperature, 298° K to 672° K.

RESULTS AND DISCUSSIONS

Rate constants were calculated on the assumption that the rate-determining step is a second-order process of the type

$$N + C_2H_4 \rightarrow HCN + \text{other products}$$

followed by fast reactions between nitrogen atoms and the free radicals formed in the initial step. The consumption of nitrogen atoms by the homogeneous and heterogeneous recombination of nitrogen atoms was neglected, since it was expected that these reactions would be insignificant in competition with the ethylene reaction. Rate constants for the disappearance of hydrocarbon may then be evaluated from the usual second-order rate expression

$$k = \frac{2.303}{t(a-2b)} \log \frac{b}{a} \frac{(a-2x)}{(b-x)},$$

where x = the concentration of ethylene consumed, which was found, for the flow rates used, to be approximately 1/2 of the HCN produced;
t = the duration of the reaction;
a = the initial active-nitrogen concentration, determined from the maximum production of HCN in the reaction with ethylene;
b = the initial ethylene concentration.

The reaction times were calculated from the linear velocity of the gas, and the distance between the point of injection of the reactant and the plane of termination of the reaction. Flow rates were converted to concentrations in the customary manner. The effect of temperature was considered in both these calculations.

Typical values of the second-order rate constant are shown in Table I, and the averages of a number of determinations of the rate constant at various temperatures, and by the various experimental methods, are listed in Table II.

In the low-temperature technique for terminating the active nitrogen – ethylene reaction, the main experimental uncertainty lies in the effectiveness of the low temperature for stopping the reaction, and the time required for the transfer of heat. These would tend to yield a conical, rather than a planar, region of termination, with a corresponding uncertainty in the calculation of the reaction time, and hence in the rate constants.

In the aliquot and copper oxide target techniques, the main uncertainty was in the behavior of the catalyst. At temperatures above 536° K, the copper oxide appeared to undergo some reduction, either by thermal decomposition at the low pressure, or by a reaction with one or more components of the gas stream that passed over the catalyst. As a consequence, rate constants determined by this method, at the higher temperatures, are uncertain. At the lower temperatures, however, where the catalyst was stable, the method seemed to be satisfactory, and the rate constants should be reliable.

The rate constants obtained by termination with nitric oxide and by the cobalt target are in close agreement. Such good agreement of the rate constants, over such a wide range

TABLE I

Typical second-order rate constants for the reaction of active nitrogen with ethylene

Method of termination	NO		CuO target		Co target	
Temp. (°K)	295		295		298	
N atom flow (mole/sec×10^6)	6.8		6.1		6.7	
C_2H_4 flow (mole/sec×10^6)	4.6		3.7		2.6	
	t (sec)	k*	t (sec)	k	t (sec)	k
	13×10^{-3}	1.9×10^{-14}	3×10^{-3}	1.5×10^{-14}	14×10^{-3}	2.0×10^{-14}
	18	2.1	6	1.4	19	2.0
	22	2.3	12	1.5	24	1.6
	47	1.4	18	1.8	28	1.8
	56	1.4	30	1.8	31	1.4
			45	1.5	33	1.8
					48	1.8
		Av. 1.8×10^{-14}		Av. 1.6×10^{-14}	57	1.5
						Av. 1.7×10^{-14}

Method of termination	NO		Co target	
Temp. (°K)	672		672	
N atom flow (mole/sec×10^6)	7.0		2.9	
C_2H_4 flow (mole/sec×10^6)	2.8		8.8	
	t (sec)	k	t (sec)	k
	2.0×10^{-3}	3.2×10^{-14}	5.2×10^{-3}	3.6×10^{-14}
	4.2	2.4	6.2	3.5
	5.2	1.8	8.3	3.1
	6.2	2.1	10.4	2.5
	8.3	1.8	12.5	2.2
		Av. 2.3×10^{-14}		Av. 3.0×10^{-14}

*Units of k are cc molecule^{-1} sec^{-1}.

TABLE II

Average rate constants for the reaction of active nitrogen with ethylene

Technique for termination	Temperature (°K)	Pressure (mm)	Rate constant (cc/molecule sec)
Low temperature	673	1.50	1.9×10^{-14}
Nitric oxide	295	2.90	1.8×10^{-14}
	400	2.90	2.0
	528	3.17	2.2
	671	3.00	2.3
Aliquot	297	1.75	2.2×10^{-14}
	297	3.10	2.4
	543	1.75	3.8
	543	3.10	7.5
CuO target	295	2.50	1.6×10^{-14}
	536	2.80	2.6
Co target	298	2.60	1.7×10^{-14}
	542	2.60	2.8
	672	3.00	3.0

of temperature, seems quite improbable unless these methods not only terminate the active nitrogen–ethylene reaction with some precision, but also do not interfere appreciably with the production or recovery of hydrogen cyanide from the reaction. The cobalt target method has some advantage over the nitric oxide method, in that a check can be

made on the efficiency of the catalyst for stopping the reaction. By introducing ethylene through the probe, below the target, it was shown that deactivation of the active nitrogen, hence the termination of the reaction with ethylene, was virtually complete at the surface of the cobalt target (not more than 0.20% of the total initial active nitrogen ever survived its encounter with the target). Using this as a basis for comparison, it might then be concluded that the nitric oxide method was equally effective for terminating the reaction.

The rate constants for the active nitrogen–ethylene reaction, obtained with the nitric oxide and cobalt target techniques, are in reasonable agreement with those obtained by Greenblatt and Winkler (1) in their application of a diffusion flame technique, but are only about 1/10th as large as the value determined by Milton and Dunford (8), who also used a diffusion flame method. In view of the different experimental techniques employed, and the errors involved in each, this discrepancy is probably of the order to be expected. Similarly, the factor of about 5 between the present results and those obtained by mass spectrometry by Herron (9) is probably due mainly to experimental errors, since, for the conditions used, the N atom concentrations estimated by HCN production and by the NO titration differ by a factor of less than 2 (6). More significant than the difference between the data from these two studies is their similarity in showing practically no effect of temperature on the rate constant for the ethylene reaction, corresponding to a very low activation energy. The present value, 2.0×10^{-14} cc molecule^{-1} sec^{-1}, at 400° K, is in good agreement with a value of 3.0×10^{-14} cc molecule^{-1} sec^{-1}, at 423° K, obtained by Wright and Winkler (7) with the nitric oxide method for terminating the reaction.

From the data obtained with the nitric oxide and cobalt target techniques, activation energies of 250 and 600 cal/mole, respectively, may be calculated. It would seem reasonable, therefore, to assume a value of 400 ± 200 cal/mole for the activation energy of this reaction. This gives a P factor of the order of 10^{-5} for the reaction. The low steric factor is probably associated with the spin-disallowed reaction previously assumed (16) for the initial attack,

$$N + C_2H_4 \rightarrow HCN + CH_3.$$

Since it would appear that confidence may be placed in terminating the active nitrogen–ethylene reaction by the nitric oxide and the cobalt target techniques, these two techniques are now being used to evaluate the kinetic constants for the reactions of active nitrogen with other hydrocarbons and hydrocarbon derivatives.

REFERENCES

1. J. H. GREENBLATT and C. A. WINKLER. Can. J. Research, B, **27**, 732 (1949).
2. C. MAVROYANNIS and C. A. WINKLER. Can. J. Chem. **39**, 1601 (1961).
3. C. MAVROYANNIS and C. A. WINKLER. International Symposium on Chemical Reactions in the Lower and Upper Atmosphere, San Francisco. April, 1961.
4. M. A. A. CLYNE and B. A. THRUSH. Nature, **189**, 56 (1961).
5. M. C. CHEN and H. A. TAYLOR. J. Chem. Phys. **34**, 1344 (1961).
6. G. J. VERBEKE and C. A. WINKLER. J. Phys. Chem. **64**, 319 (1960).
7. A. N. WRIGHT and C. A. WINKLER. Can. J. Chem. In press.
8. E. R. V. MILTON and H. B. DUNFORD. J. Chem. Phys. **34**, 51 (1961).
9. J. T. HERRON. J. Chem. Phys. **33**, 1273 (1960).
10. P. A. GARTAGANIS and C. A. WINKLER. Can. J. Chem. **34**, 1457 (1956).
11. A. Y. UNG. Ph.D. Thesis, McGill University, Montreal, Que. 1961.
12. LORD RAYLEIGH. Proc. Roy. Soc. (London), A, **176**, 1 (1940).
13. R. A. BACK, W. DUTTON, and C. A. WINKLER. Can. J. Chem. **37**, 2059 (1959).
14. R. J. STRUTT. Proc. Roy. Soc. (London), A, **85**, 219 (1911).
15. J. E. MORGAN. Private communication.
16. J. H. GREENBLATT and C. A. WINKLER. Can. J. Research, B, **27**, 721 (1949).

THE EFFECT OF ADDED ELECTROLYTE ON HYDROGEN-BONDING EQUILIBRIUM IN DILUTE SOLUTIONS OF *t*-BUTYL ALCOHOL IN CARBON TETRACHLORIDE[1]

J. B. HYNE AND R. M. LEVY[2]
Department of Chemistry, University of Alberta, Calgary, Alberta

Received December 11, 1961

ABSTRACT

The effect of added tetra-*n*-butyl ammonium bromide on the hydrogen-bonding equilibrium of *t*-butyl alcohol in 0.0 to 0.08 *M* solution in carbon tetrachloride has been studied by infrared investigation of the spectral range 2.5–3.5 μ. The observations have been interpreted in terms of specific interaction between the alcohol and the more polar species of the salt which are present in the complex electrolyte equilibria (for example, ions and ion pairs). It is suggested that these species function as nucleation centers for aggregates of alcohol molecules, the enhanced degree of hydrogen bonding permitted in these aggregates being reflected in the infrared spectral response.

INTRODUCTION

It has been repeatedly demonstrated that the equilibrium between monomeric and polymeric forms of alcohols in non-polar solvents is very sensitive to concentration. Systems of alcohols in benzene or carbon tetrachloride have been extensively studied in recent years by both infrared (1–6) and n.m.r. techniques (7–11), all results being consistent with the predicted increase in association of the monomeric alcohol to higher *n*-mers with increasing concentration. In the infrared spectral studies, the increasing association is reflected in increased absorption in the region of 2.9 to 3.0 μ, normally assigned to a hydrogen-bonded hydroxyl, with a concomitant decrease in absorption at lower wavelengths characteristic of unassociated hydroxyl. In such binary systems, the problem is now one of establishing the distribution among various associated species (dimers, trimers, tetramers, etc.) rather than establishing the existence of the association phenomenon.

Recently Bufalini and Stern reported (12) that addition of tetra-*n*-butyl ammonium salts to methanol solutions in benzene resulted in a marked enhancement of the infrared absorption characteristic of associated hydroxyl over that corresponding to free hydroxyl. In their brief report these authors suggested that these results might be indicative of specific interaction between the added electrolyte and the alcohol component of the binary solvent mixture. In connection with our studies of specific solvation phenomena, we have carried out a preliminary quantitative investigation of the effect of added tetra-*n*-butyl ammonium bromide on the infrared spectral response of the hydroxyl function of *t*-butyl alcohol in dilute solution in carbon tetrachloride. Our choice of this system was based on the fact that detailed studies have been made of association in the binary *t*-butyl alcohol – carbon tetrachloride system (7, 4, 11) and on the electrical (13) and dielectric (14, 15) properties of tetra-*n*-butyl ammonium bromide in low dielectric solvents.

EXPERIMENTAL

Materials

Carbon tetrachloride: Matheson, Coleman, and Bell spectral grade used without further purification. *t*-Butyl alcohol: stock material purified as reported previously (7). Tetra-*n*-butyl ammonium bromide: prepared by the method of Accasina, Petrucci, and Fuoss (16).

[1]*Work was done largely at Dartmouth College, Hanover, N.H.*
[2]*Present address: Department of Chemistry, University of California, Berkeley, California.*

Solution

Stock solutions of various concentrations of salt in carbon tetrachloride were prepared and *t*-butyl alcohol added volumetrically to obtain various concentrations over the range studied. Each salt solution was freshly prepared before each run and *t*-butyl alcohol dilutions made sequentially for each set of points at a given salt concentration.

Spectra

All spectra were run on a Perkin–Elmer Model 21 double beam spectrometer with scale expansion. Solvent compensation was made in matched 1-mm sodium chloride cells.

RESULTS

The spectra presented in Figs. 1(*a*) and 1(*b*) illustrate the effect of added tetra-*n*-butyl ammonium bromide(0.04 *M*) on the hydroxyl absorption region of various concentrations

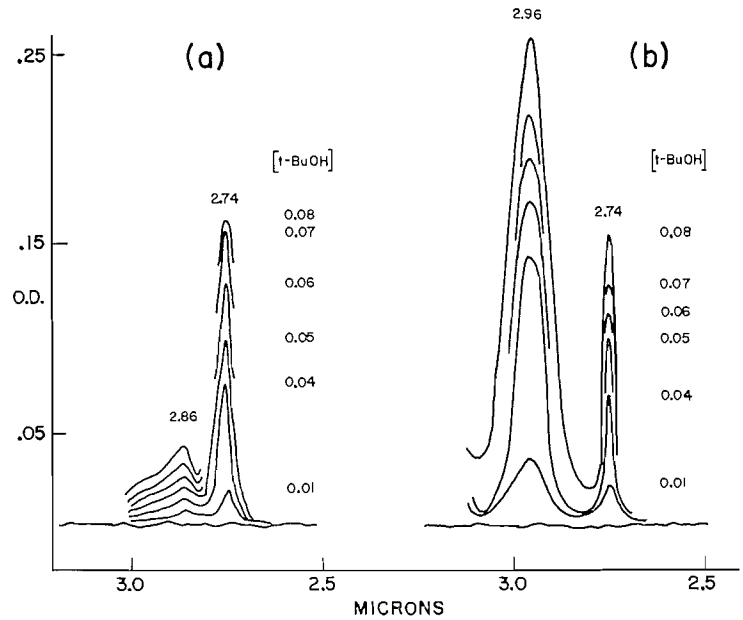

FIG. 1. The 2.5–3.5 μ region for various concentrations of *t*-butyl alcohol in carbon tetrachloride (*a*) without salt, (*b*) with added 0.04 *M* tetra-*n*-butyl ammonium bromide.

(0.0 to 0.08 *M*) of *t*-butyl alcohol in carbon tetrachloride. In the absence of salt (Fig. 1(*a*)), the two principal absorptions are at 2.74 μ and 2.86 μ, with an indication of the development of a peak at 2.96 μ at higher alcohol concentrations. These absorptions have been previously assigned (1) to various free and hydrogen-bonded hydroxyl O—H stretching vibrations as indicated below.

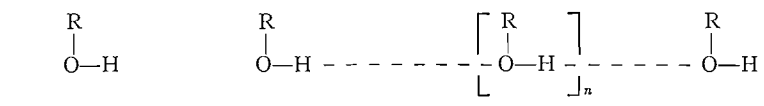

As a consequence of these assignments, the 2.74 μ absorption may be associated with monomer alcohol species, the 2.86 μ principally with dimeric species and the 2.96 μ absorption of the internal hydrogen-bonded hydroxyl groups with higher polymeric

alcohol species. The spectra in Fig. 1(*a*) indicate that the degree of polymerization to higher *n*-mers in the concentration range 0.0 to 0.08 *M* alcohol is very small, and it was with the intention of avoiding complications due to this polymer absorption that the alcohol concentration in this work was restricted to the range below 0.08 *M*. It is also noteworthy that over this same concentration range the change in n.m.r. chemical shift

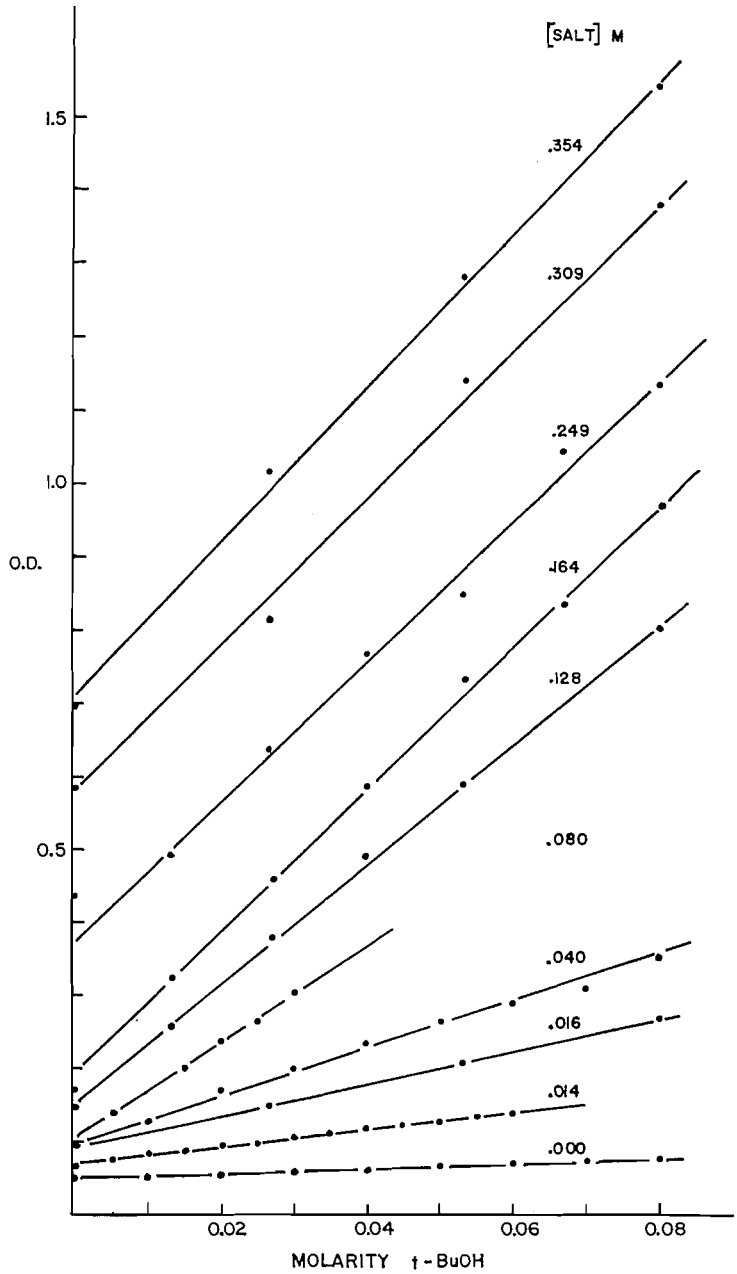

FIG. 2. Optical density at 2.96 μ versus *t*-butyl alcohol concentration for various fixed concentrations of added tetra-*n*-butyl ammonium bromide.

associated with the hydroxyl hydrogen has been found (7, 11) to be small, an observation in keeping with the assumption that higher polymer formation is minimal in this concentration range.

A very marked enhancement of the absorption at 2.96 μ is seen in Fig. 1(*b*) for the same concentration range of alcohol but in the presence of a fixed concentration (0.04 M) of tetra-*n*-butyl ammonium bromide. One of the most significant facts revealed by the comparison of Figs. 1(*a*) and 1(*b*) is that the dependence of absorption at 2.74 μ (free hydroxyl) on total concentration of alcohol is not as sensitive to the presence of salt as the absorption at 2.96 μ.

The dependence of the 2.96 μ absorption on alcohol concentration (0.0 to 0.08 M) has also been studied as a function of added salt concentration. Sets of spectra similar to that in Fig. 1(*b*) were obtained for various fixed salt concentrations (0.0 to 0.35 M). These data are presented in Fig. 2 as a plot of $\Delta \log I_0/I$ (2.96 μ) versus concentration of alcohol (total); $\Delta \log I_0/I$ represents the difference between absorbance at 2.96 μ at that particular alcohol concentration and the absorbance at 2.96 μ with no alcohol present. The optical density scale is an arbitrary one for the sake of clarity. The scale for any line can be reconstructed, however, by taking the intercept at zero alcohol concentration as the zero of the optical density scale.

DISCUSSION

Two important features are apparent in the comparison of Figs. 1(*a*) and 1(*b*). The absorption at 2.86 μ, characteristic of the terminal hydrogen-bonded hydroxyl in the dilute alcohol solutions without salt, is completely swamped by the very intense absorption at 2.96 μ, which characterizes the spectra with salt added. However, the intense absorption at 2.96 μ does not *appear* to occur at the expense of the absorption at 2.74 μ since this absorption differs only slightly, as a function of total alcohol concentration, from that in the system without added salt. In Fig. 3, the optical density of the various wavelengths for both systems (with and without salt) is plotted against the total alcohol concentration. Within the experimental uncertainty of the points, there is only a small difference between the dependence of the 2.74 μ absorption on total alcohol concentration in the two systems. This difference, however, is in the correct sense, indicating slight depletion of the 2.74 μ absorption in the system with salt as a result of the appearance of high absorption at 2.96 μ. The explanation which suggests itself is that the extinction coefficient associated with the 2.96 μ absorption is very much larger than that for the 2.74 μ absorption, the ratio indicated by the data in Fig. 2 being of the order of 20 to 1.

The similarity between the wavelength of the intense absorption with salt added (2.96 μ) and that associated with the higher polymeric alcohol forms in more concentrated alcohol solutions (2.96 μ) raises the question of whether the effect of the added salt is merely one of stabilizing the higher polymeric forms. That is to say, the 2.96 μ absorption with added salt is due to the same molecular vibration as is observed in higher concentration alcohol solutions without salt. Liddel and Becker (4) have reported integrated molar absorption coefficients per OH bond for the monomer and polymer forms of *t*-butyl alcohol in carbon tetrachloride as being in the ratio of 1:16. This ratio is sufficiently close to the required 1:20 ratio predicted from Fig. 2 to support an argument that the 2.96 μ absorption observed with added salt is due to a polymeric form similar to that found at higher alcohol concentrations without salt. If this argument is valid, however, it implies that the association equilibrium constant for monomers to polymers is very much higher in the presence of salt compared with the value in the absence of salt. This is

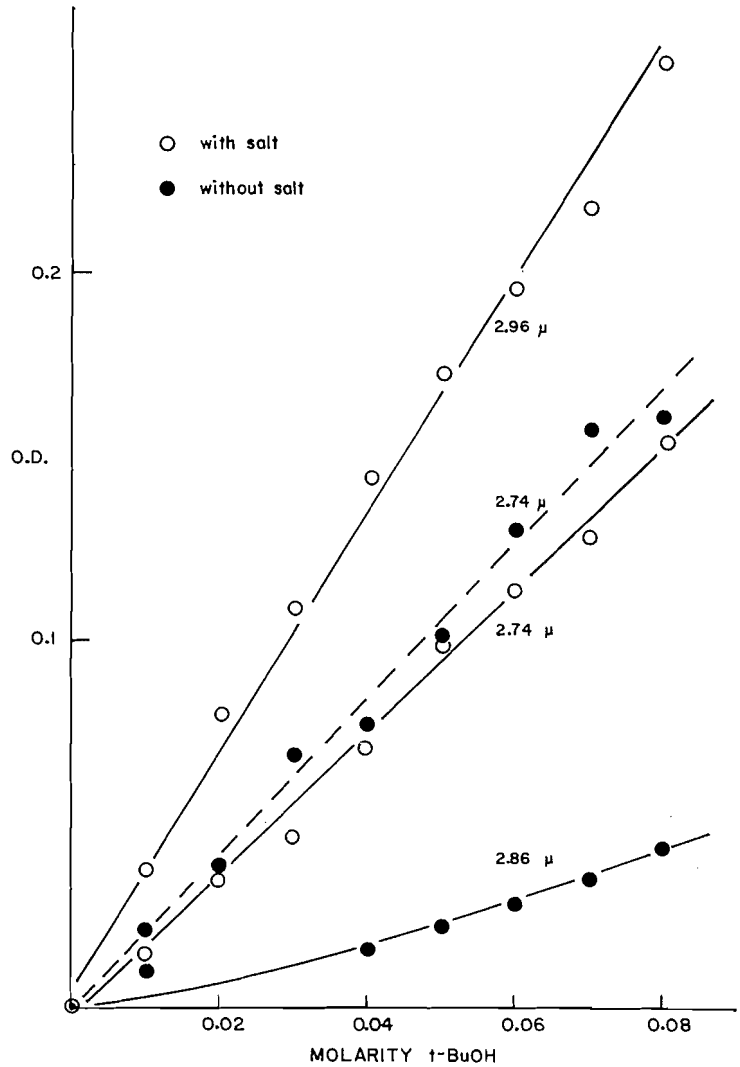

FIG. 3. Comparison of optical density dependence on alcohol concentration at various wavelengths for *t*-butyl alcohol in carbon tetrachloride with and without added salt.

tantamount to the statement made above that the polymeric form is more stable in the presence of the salt. An approximate calculation based on the optical densities of Fig. 1 and the 1:16 ratio for molar absorption coefficients indicates that the association constant for monomer to polymer association is a factor of 10 greater in the presence of salt compared with that in the absence of salt.

It must be emphasized, however, that it is only on the basis of similar λ_{max} values and similar absorption coefficient ratios that the conclusion is drawn that the same type of polymer OH vibration makes a major contribution to the absorption at 2.96 μ in the two cases.

The higher value of the association constant in the presence of salt can be rationalized by a model envisaging specific organization of the alcohol molecules about polar salt

entities in the solution. It is not unreasonable to assume that salt ions or ion pairs will favor the more polar alcohol hydroxyl groups in their immediate solvation shell with the low polarity methyl groups turned outward toward the non-polar carbon tetrachloride bulk solvent. In such a structure, there will exist a very favorable opportunity for internal hydrogen bonding of the type generally assigned a $\lambda_{max} = 2.96\ \mu$ (1). The polar salt species therefore serve as a nucleation center for the aggregation of alcohol molecules into a "micellar" structure in which hydrogen bonding will be favored. A difference of a factor of 10 in the monomer–polymer association constant is not unreasonable in the presence of such a polymer structure stabilizer as the salt species. It should also be noted, however, that in the proposed model there exists an equally favorable situation for hydrogen bonding of the type R—O—H---Br^-. It is not unreasonable to assume that the molar absorption coefficient of a hydroxyl group bonded in this manner will also be high and could be close to the same λ_{max} as that for internal hydrogen bonding (2.96 μ). The total absorption at 2.96 μ may therefore be due to both types of hydrogen-bonded hydroxyl. Since both phenomena are conditional upon specific interaction between the alcohol hydroxyl and the polar salt entities the breakdown into one form of bonding or the other is not critical at this stage of the argument.

The equilibrium proposed to account for the dramatic effect of added salt may be formalized as:

$$\mathrm{ROH} + (\mathrm{salt}) \overset{K}{\rightleftharpoons} \mathrm{R\overline{OH}}\ (\mathrm{salt}) \qquad [1]$$

where $\mathrm{R\overline{OH}}$ (salt) represents a hydrogen-bonded alcohol molecule in the aggregation around the salt species. Therefore

$$[\mathrm{ROH}] = \frac{1}{[(\mathrm{salt})].K} \cdot [\mathrm{R\overline{OH}(salt)}] \qquad [2]$$

or

$$(\mathrm{O.D.})_{2.96\,\mu} = C.K[(\mathrm{salt})].[\mathrm{ROH}], \qquad [3]$$

where the constant C contains the various constants of the Beer's law relationship. At a fixed concentration of salt a plot of [ROH] versus $(\mathrm{O.D.})_{2.96\mu}$ should therefore be linear, as is found in the plots of experimental data in Fig. 2. If the effect of the added salt was simply a medium effect then the slope of the plots of equation [3] should be a linear function of the salt concentration as this is varied for each set of points since

$$\text{slope [3]} = \frac{(\mathrm{O.D.})_{2.96\,\mu}}{[\mathrm{ROH}]} = C.K[(\mathrm{salt})]\ . \qquad [4]$$

In Fig. 4, it is seen that this linear relationship does not hold, indicating that the total salt concentration is not a direct linear measure of the effect of the salt on the hydrogen-bonding equilibrium. The curvature of the plot suggests that some particular species of the salt in solution, the concentration of which is determined by the total salt concentration, is primarily responsible for the observed effect of the added salt on the hydrogen-bonding equilibrium.

It is only to be expected that, in such low dielectric media as carbon tetrachloride, the salt will be present very largely as ionic aggregates. Although the bulk dielectric constant of the medium will change as alcohol is added, the change will be very small. The difference

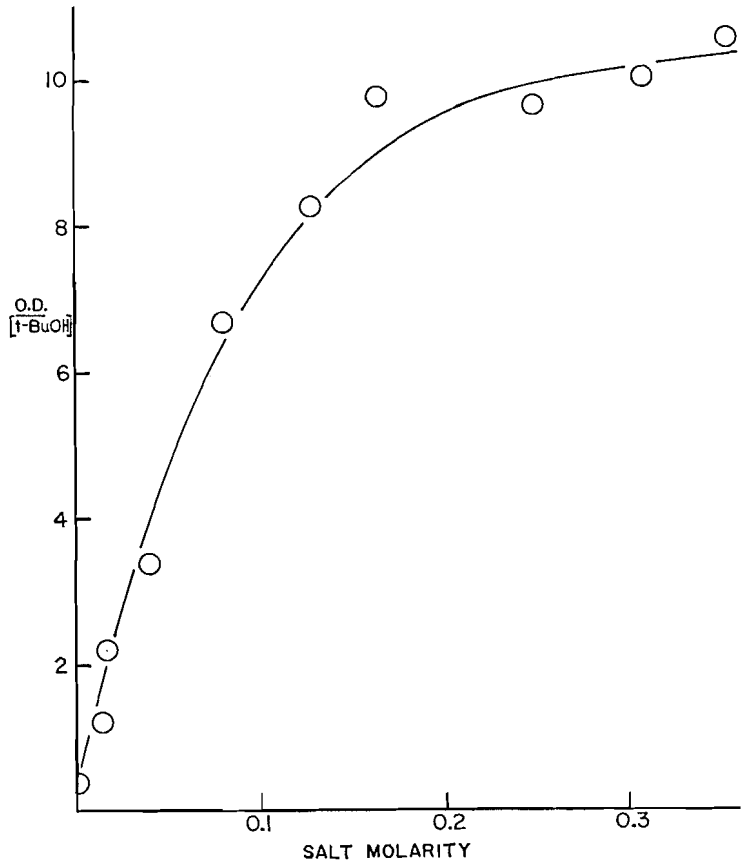

Fig. 4. Plot of slope of equation [3] versus concentration of tetra-*n*-butyl ammonium bromide.

between the bulk dielectric constant of pure carbon tetrachloride and carbon tetrachloride with 0.08 *M* added *t*-butyl alcohol cannot be greater than 0.5 (see, for example, ref. 14). It may therefore be assumed that there can be little if any *bulk* effect on the electrolyte equilibria as a result of varying the *t*-butyl alcohol concentration. The electrolyte equilibria involved may be represented as

$$(n\mathrm{Bu})_4\mathrm{N}^+ + \mathrm{Br}^- \overset{K_{ip}}{\rightleftharpoons} (n\mathrm{Bu})_4\mathrm{N}^+\mathrm{Br}^- \overset{K_{qp}}{\rightleftharpoons} (n\mathrm{Bu})_4\mathrm{N}^+\ \mathrm{Br}^- \cdots \mathrm{Br}^-\mathrm{N}^+(n\mathrm{Bu})_4$$

Ions — Ion pairs — Ion quadrupoles and higher aggregates

As the total salt concentration is increased, the coupled equilibria shown above will lead to a limiting value for the fraction of salt present as ions or ion pairs. Accordingly the concentration of these species in solution will not be a linear function of the total salt concentration. If the observed effect of added salt on the hydrogen-bonding equilibrium is due in large part to the nucleating action of the ions and ion pairs, this would account for the curvature in the plot of Fig. 4. It is furthermore reasonable to assume that the ions and ion pairs will have the greatest effect in terms of specifically solvating them-

selves with alcohol molecules. In the higher electrolyte aggregates, the bulky *n*-butyl groups provide the hydrocarbon shell between the charged nitrogen and bromine atoms and the carbon tetrachloride solvent. Indeed, it might be said that the formation of these electrolyte aggregates is itself a manifestation of specific solvation, one ion pair being specifically solvated by another. In the case of ion pairs, the bromide end of the ion pair is not well shielded by the four *n*-butyl groups of the ammonium ion and hence will tend to orient around itself *t*-butyl alcohol molecules with the polar hydroxyl group in the immediate vicinity of the charged center. In the case of the very few free ions present in such low dielectric solvents, the bromide ion would exert a highly specific ordering effect on the alcohol and would be expected to surround itself with a screen of alcohol molecules oriented with the polar hydroxyl groups pointing inward toward the bromide ion. The ammonium ion carries its own hydrocarbon low polarity screen and would probably be less effective as a nucleating center for specific alcohol aggregations. It is of interest to note that Bufalini and Stern (12, 17) reported considerable dependence of the hydrogen-bonding equilibrium response in the infrared on the nature of the salt *anion*.

A detailed quantitative analysis of the form of the plot shown in Fig. 4 does not appear to be possible at this time. Although Sadek and Fuoss (13) have reported the dissociation constants for tetra-*n*-butyl ammonium bromide in alcohol – carbon tetrachloride solvent mixtures, the limitations of the conductance method they used dictated a minimum dielectric constant for the solvent of 15. This is far above the bulk dielectric constant of the carbon tetrachloride – alcohol mixtures used in this work. However, using Sadek and Fuoss's results we can extrapolate to lower dielectric constant to obtain an approximate value for K(dissoc.) = 10^{-5} in carbon tetrachloride. It should be noted that this value is for the dissociation of ion pairs to free ions and does not take into account the equilibrium between ion pairs and higher aggregates. Furthermore, the value 10^{-5} would appear to be the upper limit for the dissociation constant in view of the considerably lower values of K found by Fuoss and Kraus (18) for alkylammonium nitrates in dioxane–water mixtures of low dielectric constant. A dissociation constant of this order of magnitude or less predicts a levelling off in the fractional dissociation to ions at concentrations below 0.2 M. This is qualitatively in keeping with the observed form of the plot in Fig. 4. Even if an accurate value for the ion-pair dissociation constant were available, however, the problem is complicated by the sensitivity of the ion quadrupole – ion pair equilibrium to alcohol concentration. Richardson and Stern (14, 15) have recently reported the results of dielectric studies on tetra-*n*-butyl ammonium bromide in benzene–methanol mixtures. These authors interpret their results as indicative of the great sensitivity of the quadrupole–pair equilibrium to added small amounts of the more polar alcohol. Although the bulk dielectric constant of the solvent changes by only 0.04 on adding 0.01 mole fraction of methanol to benzene, the quadrupole–pair equilibrium constant changes by a factor of 200 in favor of the ion pairs. Clearly the role of the alcohol molecules is highly specific and this may indeed be further evidence of the specific solvation role of the polar alcohol molecules in stabilizing the ion pairs. Since the experimental data presented in Fig. 2 are for fixed salt concentrations but over a range of 0.0 to 0.08 M *t*-butyl alcohol, the observed linear increase in optical density with alcohol concentration may be due to both increasing alcohol concentration and changes in the relative distribution of the total salt in the form of ions, ion pairs, and quadrupoles.

In the very recent paper of Bufalini and Stern (17), similar findings with a series of tetra-*n*-butyl ammonium salts in several alcohol–benzene systems are reported. Although these results differ in detail from those reported here, there is little question that both sets

of evidence support the concept of selective solvation of the electrolyte species by the more polar alcohol component of the binary solvent mixture. Comparison of Bufalini and Stern's data in benzene with those reported here in carbon tetrachloride indicates some significant differences in the stability of monomeric alcohol species relative to associated forms and also in the relative values of apparent extinction coefficients. Although it is somewhat premature to attempt a detailed explanation of the effect of changing the "inert" low dielectric component of the solvent, it is not surprising that replacing benzene with carbon tetrachloride should bring about significant changes in the quantitative aspects of the phenomenon. Davis, Pitzer, and Rao have reported (11) an n.m.r. study of hydrogen bonding of ethanol in both carbon tetrachloride and benzene at 22° C. The dependence of the hydroxyl proton shift on alcohol concentration is quite different in these two systems. These authors also point out that the presence of a minimum in the molar polarization curve for ethanol in carbon tetrachloride and the absence of such a minimum in the ethanol–benzene system may be interpreted as a reflection of significantly different distributions among possible associated structures in the two "inert" solvents. Bufalini and Stern's data on several electrolytes with varying cation provide some evidence in favor of the alcohol-to-cation hydrogen bond rather than the alcohol-to-alcohol hydrogen bonding in the alcohol aggregates around the electrolyte. As suggested previously in this paper, the precise molecular nature of the vibration responsible for the enhancement of absorption in the 3 μ region is not critical to the specific solvation argument and further work will be needed to elucidate this point. It is worth noting, however, that in benzene, Bufalini and Stern report the absorption maximum at 3.03 μ while, in carbon tetrachloride, the value observed was 2.96 μ. This difference may be significant in terms of structural changes between the two systems.

ACKNOWLEDGMENT

The authors are indebted to Dr. P. J. Krueger of this department for his helpful comments on, and discussion of, this work.

REFERENCES

1. W. C. Coburn and E. Grunwald. J. Am. Chem. Soc. **80**, 1318 (1958).
2. R. Mecke. Discussions Faraday Soc. **9**, 161 (1950).
3. F. A. Smith and E. C. Creitz. J. Research Natl. Bur. Standards, **46**, 145 (1951).
4. U. Liddel and E. D. Becker. Spectrochim. Acta, **10**, 70 (1957).
5. Inskeep, Kelleher, McMahon, and Somers. J. Chem. Phys. **28**, 1033 (1958).
6. N. D. Coggeshall and E. L. Soier. J. Am. Chem. Soc. **73**, 5414 (1951).
7. M. Saunders and J. B. Hyne. J. Chem. Phys. **29**, 1319 (1958).
8. E. D. Becker, U. Liddel, and J. M. Schoolery. J. Mol. Spectroscopy, **2**, 1 (1958).
9. C. M. Huggins, G. C. Pimentel, and J. N. Schoolery. J. Phys. Chem. **60**, 1311 (1956).
10. C. A. Cohen and C. Reid. J. Phys. Chem. **61**, 790 (1957).
11. J. C. Davis, Jr., K. S. Pitzer, and C. N. R. Rao. J. Phys. Chem. **64**, 1744 (1960).
12. J. Bufalini and K. H. Stern. Science, **130**, 1249 (1959).
13. H. Sadek and R. M. Fuoss. J. Am. Chem. Soc. **76**, 5902, 5905 (1954); **72**, 5902 (1950).
14. E. A. Richardson and K. H. Stern. J. Am. Chem. Soc. **82**, 1296 (1960).
15. K. H. Stern and E. A. Richardson. J. Phys. Chem. **64**, 1901 (1960).
16. F. Accascina, S. Petrucci, and R. M. Fuoss. J. Am. Chem. Soc. **81**, 1301 (1959).
17. J. Bufalini and K. H. Stern. J. Am. Chem. Soc. **83**, 4362 (1961).
18. R. M. Fuoss and C. A. Kraus. J. Am. Chem. Soc. **55**, 1019 (1933).

DEUTERIUM ISOTOPE EFFECTS IN ABSTRACTION OF HYDROGEN ATOMS FROM PHENOLS

R. A. BIRD, G. A. HARPELL, AND K. E. RUSSELL
Department of Chemistry, Queen's University, Kingston, Ontario
Received December 11, 1961

ABSTRACT

The effect of six deuterated phenols on the rate and degree of polymerization of styrene has been studied. The rate and degree of polymerization are decreased by deuterated phenols to a much less extent than by the corresponding phenols. Approximate transfer constants are estimated, and it is found that the transfer constant for hydrogen abstraction from the deuterated phenol is less than 0.2 of the transfer constant for the normal phenol. The rates of reaction of 2,2-diphenyl-1-picrylhydrazyl with three deuterated phenols have been determined. The rate constants for deuterated 2,6-di-*t*-butylphenol and 4-bromophenol are less than 0.15 of those for the corresponding phenols, but the isotope effect appears to be small with 4-nitrophenol.

In a recent study (1) it was shown that phenols lower both the rate and degree of polymerization of styrene and that the magnitude of the decrease depends on the nature and position of substituents in the phenol. The results are interpreted in terms of an attack by polystyryl radicals on the OH group of the phenol. Support for this suggestion comes from the observation that certain O-methyl phenols do not significantly alter the rate and degree of polymerization of styrene. In an attempt to obtain more positive evidence, the effect of six deuterated phenols on the polymerization of styrene has been determined, and the derived transfer constants compared with those estimated for the normal phenols.

In a separate study (2) the rates of reaction of 2,2-diphenyl-1-picrylhydrazyl (DPPH) with a wide range of substituted phenols were obtained. The rate-determining step was considered to be the abstraction by DPPH of a hydrogen atom from the OH group of the phenol since O-methyl phenols are relatively weak hydrogen donors, and deuteration of 2,6-di-*t*-butyl-4-methylphenol decreases the rate constant for hydrogen abstraction at 20° by a factor of 1.95 (3). Strong supporting evidence has now been obtained using deuterated 2,6-di-*t*-butylphenol and 4-bromophenol as donors. A surprisingly small isotope effect was observed with 4-nitrophenol.

EXPERIMENTAL

Styrene, a gift of Dow Chemical of Canada, Ltd., was distilled at reduced pressure and then degassed and subjected to two distillations on the vacuum line. It was stored at −78.5°. The phenols were normally recrystallized twice and dried in a vacuum desiccator. Deuteration was effected by adding about 4 g of heavy water or deuterated methanol to 1.5 g of the phenol and leaving overnight at 60° or refluxing for 2 hours. The water and methanol were removed on the vacuum line and the procedure was twice repeated. The extent of deuteration was estimated by taking infrared spectra of the deuterated phenols in chloroform solution. The purified chloroform was dried over calcium chloride and the sodium chloride cells were filled in a dry box. The general experimental procedure for studying the effect of phenols on the polymerization of styrene at 60° has been described elsewhere (1).

For the DPPH reactions the normal procedure was followed (2) except for the making up of the reaction mixtures. Benzene was stirred with calcium chloride on the vacuum line and distilled into a reaction tube containing weighed amounts of DPPH and the phenol. The tube was sealed and the rate of disappearance of DPPH determined at 30°. Concentrations of phenols were in the range 0.04–0.08 *M*

RESULTS AND DISCUSSION

Infrared analysis of the deuterated phenols showed that deuterium was substituted only at the OH group, and the extent of deuteration varied from 85% to 93%. These are probably minimum values since exchange may occur during the preparation of the chloroform solutions and in the filling of the sodium chloride cells. No attempt has been made to correct for undeuterated material in the samples used in this work. Table I

TABLE I

Extent of retardation and transfer constants at 60°

Phenol	Retardation		k_{tr}/k_p	
	Phenol	Deuterated phenol	Phenol*	Deuterated phenol
1-Naphthol	28% (0.2 *M*)	3% (0.2 *M*)	0.048±0.017	0.007
4-Benzyloxyphenol	20% (0.2 *M*)	2% (0.2 *M*)	0.029±0.014	0.001
2,3,4,6-Tetramethylphenol	39% (0.2 *M*)	2% (0.2 *M*)	0.058±0.024	0.002
Catechol	53% (0.2 *M*)	5% (0.2 *M*)	0.13 ±0.058	0.026
4-*t*-Butylcatechol	23% (0.02 *M*)	26% (0.2 *M*)	0.36 ±0.19	0.037
Pyrogallol	37% (0.006 *M*)	9% (0.006 *M*)	1.04 ±0.47	0.16

*Mean values. The limits shown are the standard deviations of six estimated values.

shows the effect of ordinary and deuterated phenols on the rate of polymerization of styrene at 60°. The results are given as the decrease in rate of polymerization for a 0.2 *M* solution of the phenol in styrene except for ordinary 4-*t*-butyl catechol where a 0.02 *M* solution was used and for ordinary and deuterated pyrogallol where 0.006 *M* solutions were used. It is seen that at equivalent concentrations the deuterated phenols all lower the rate of polymerization to a far less extent than the corresponding phenols. A similar conclusion applies to the effect of deuterated phenols on the degree of polymerization of the polystyrene. These qualitative conclusions can be explained if the phenols react with polystyryl radicals in the transfer step of reaction [1].

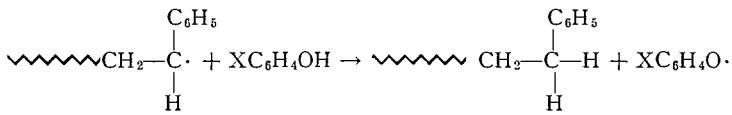

[1]

The phenoxy radical may cause retardation of polymerization by reacting with a polystyryl radical or with another phenoxy radical, and if the rate of formation of phenoxy radicals by reaction [1] is lower with the deuterated phenols, the extent of retardation will be smaller. Similarly the effect of the deuterated phenol on the degree of polymerization is smaller than with the normal phenol if reaction [1] proceeds at a relatively low rate.

Quantitative analysis of both the rate and degree of polymerization data leads to estimates of the transfer constant k_{tr}/k_p, where k_{tr} is the rate constant of reaction [1] and k_p is the rate constant for propagation of the polymerization of styrene. Since k_p is probably independent of the added phenol, the transfer constants are proportional to the rate constants for hydrogen abstraction, k_{tr}. Transfer constants for retarders may be estimated from rate data by the method of Jenkins (4). Three values of the transfer constant were obtained for each phenol assuming (*a*) that all phenoxy radicals disappear by cross termination with polystyryl radicals, or (*b*) that all phenoxy radicals disappear by mutual termination with other phenoxy radicals, or (*c*) that the rate constant for

cross termination is the geometric mean of rate constants for mutual termination of polystyryl and phenoxy radicals. Transfer constants were also estimated from the degree of polymerization data. For the retarders, three values of the transfer constant were obtained using (*a*) the simple chain transfer equation developed for non-retarders, (*b*) an equation developed on the assumption that the geometric mean assumption applies to the termination reactions of phenoxy and polystyryl radicals, and (*c*) an equation developed on the assumption that mutual termination of phenoxy radicals can be neglected (1). In the absence of reliable information concerning the exact fate of the phenoxy radicals, mean values of the six estimates for each retarding phenol were determined. These mean values for the retarders are given in Table I. The individual values vary by an average of about 40% from the mean. For those deuterated phenols which show no significant retardation, the transfer constants were obtained using the simple chain transfer equation. The transfer constants for deuterated 4-benzyloxyphenol and 2,3,4,6-tetramethylphenol may be low because the method of analysis tends to give low results for weakly retarding phenols (1). The values for the catechols and pyrogallol are calculated from the total effects which they and their reaction products exert on the rate and degree of polymerization.

The transfer constants given in Table I show that the rate constant for abstraction of deuterium from a deuterated phenol is probably less than 0.2 of the rate constant for abstraction of hydrogen from the corresponding phenol. The ratio of rate constants calculated on the assumption of a simple zero-point energy effect (5) with $\nu_{O-H} = 3620$ cm^{-1} and $\nu_{O-D} = 2660$ cm^{-1} is 0.126 at a temperature of 60°.

The rate-determining step in the reaction of DPPH with phenols is assumed to involve the abstraction of a hydrogen atom from the phenol (2):

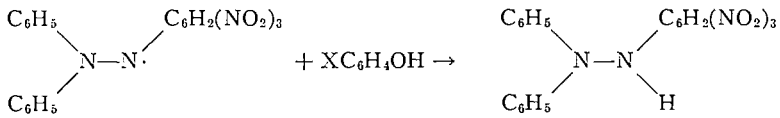

[2]

Rate constants k_2 for reaction [2] are obtained from the rate of loss of DPPH and the stoichiometry of the overall reaction. The rate constants at 30° for normal and deuterated di-*t*-butylphenol, 4-bromophenol, and 4-nitrophenol are given in Table II. In the first

TABLE II

Rate constants k_2 for reaction [2] at 30°

Phenol	k_2 (cc/mole sec)	
	Phenol	Deuterated phenol
2,6-Di-*t*-butylphenol	19.8	2.44
4-Bromophenol	41.8	5.94
4-Nitrophenol	0.43	0.28

two cases, the ratios of rate constants for deuterated and normal phenols are 0.123 and 0.143. These results compare with a value of 0.102 calculated for a temperature of 30° on the assumption of a simple zero-point energy effect. The experimental ratio for 4-nitrophenol is 0.66 but it is not certain whether the small isotope effect is real or is due to difficulties in working with this particular phenol. Fairly high concentrations of the three relatively unreactive phenols were used in these studies so that any exchange

which occurred between the deuterated phenols and reactive impurities, such as water, would have a small effect. However, at these relatively high concentrations, some phenols do not show a simple kinetic behavior; there is frequently a rapid initial drop in optical density of the solution and the overall rate of reaction is not proportional to the concentration of phenol. 4-Nitrophenol behaves in this manner and the so-called second-order rate constant is dependent on the concentration of the nitrophenol. It is possible that the smaller isotope effect observed with 4-nitrophenol is connected with this complex behavior.

The observed ratios of rate constants for deuterated and normal phenols are presumably maximum values, because any normal phenol present in the deuterated phenol would increase the observed rate constant. The isotope effects strongly support the suggestion that hydrogen is abstracted from the O—H group of the phenol in the rate-determining step of the reaction with DPPH. McGowan, Powell, and Raw (6) suggest that DPPH abstracts a hydride ion rather than a hydrogen atom as in reaction [2], but a radical mechanism is probably to be preferred. Boozer, Hammond, Hamilton, and Sen (7) have concluded that the reaction of alkyl-peroxy radicals with phenols proceeds through an intermediate complex between radical and phenol and that an isotope effect should not necessarily be observed. Caldwell and Ihrig (8) have interpreted the kinetics of polymerization of methyl methacrylate in the presence of phenols in terms of a complex between a polymethyl methacrylate radical and a phenol molecule. Intermediate complexes may possibly be formed in the reactions of DPPH with phenols, or less likely of polystyryl radicals with phenols, but, if so, they do not prevent the observation of large kinetic isotope effects in most of the reactions studied.

ACKNOWLEDGMENTS

The authors are grateful to the National Research Council for generous financial help. They acknowledge the assistance of Mr. John Myher in the kinetic experiments involving DPPH.

REFERENCES

1. M. P. Godsay, G. A. Harpell, and K. E. Russell. J. Polymer Sci. In press.
2. J. S. Hogg, D. H. Lohmann, and K. E. Russell. Can. J. Chem. **39**, 1588 (1961).
3. A. F. Bickel and E. C. Kooyman. J. Chem. Soc. 2415 (1957).
4. A. D. Jenkins. Trans. Faraday Soc. **54**, 1885 (1958).
5. L. Melander. Isotope effects on reaction rates. Ronald Press, New York. 1960. p. 20.
6. J. C. McGowan, T. Powell, and R. Raw. J. Chem. Soc. 3103 (1959).
7. C. E. Boozer, G. S. Hammond, C. E. Hamilton, and J. N. Sen. J. Am. Chem. Soc. **77**, 3238 (1955).
8. R. G. Caldwell and J. L. Ihrig. J. Polymer Sci. **46**, 507 (1960).

THE CRYSTAL STRUCTURE OF Ag_3Ca_5[1]

R. P. RAND AND L. D. CALVERT
Division of Applied Chemistry, National Research Council, Ottawa, Canada

Received November 30, 1961

ABSTRACT

Ag_3Ca_5 is tetragonal, $a = 8.039 \pm 5$ Å, $c = 15.011 \pm 15$ Å, $c/a = 1.87$, space group $I4/mcm$. The structure is of the $D8_l$ type with 4 Ag_I in 4(*a*); 8 Ag_{II} in 8(*h*), $x = 0.378 \pm 5$; 4 Ca_I in 4(*c*); and 16 Ca_{II} in 16(*l*), $x = 0.164 \pm 5$ and $z = 0.150 \pm 5$. The structure is characterized by sheets of closely linked Ag and Ca atoms parallel to (001). An indexed powder pattern is given. $NH_4Pb_2Br_5$, $RbPb_2Br_5$, and KPb_2Br_5 also have the same structure and should be included together with B_3Cr_5, Ge_3Ta_5, Si_3Ta_5, and Si_3Nb_5 in the $D8_l$ group.

INTRODUCTION

Little is known about the binary compounds of the relatively inert metals of Group IB with the strongly electropositive elements of Group IIA but they are of interest because of the possibility of forming strongly directed bonding systems or showing charge transfer effects. The Ag–Ca phase diagram has been studied by Baar (1) using thermal techniques exclusively. He reported a compound tentatively given the formula $AgCa_2$ in the region 66–71 at.% Ca. Subsequently Degard (2) examined alloys of the compositions of all the compounds and eutectics reported by Baar. He reported only mixtures of AgCa and Ca in the region 50–100 at.% Ca.

EXPERIMENTAL

Ag_3Ca_5 has been obtained as small fragments chipped from ingots prepared by Dr. W. A. Alexander for use in a cooling curve apparatus. The metals were of high purity. Spectrographic analysis of the silver showed the following impurities (in p.p.m.): Pb 10, Fe 4, Si 5, Cd 20, Ca < 1, Mg < 1; Cu, Sn, Na not visible. The calcium was six times distilled before use and analysis gave Mg 2, Fe 2.5, Mn 1, Si 2, Ba 2.5, Sr 2.5 p.p.m.; Cu, Pb, Zn, Cd, Ni, Sb, Li, Cr, Al, Ag all not visible. Typical analyses for nitrogen in the calcium ranged from 140 to 260 p.p.m. To avoid air contamination of the alloys the calcium was distilled from a side arm of the mild steel cooling curve apparatus directly onto the silver at 950–960° C. The X-ray samples were taken after the cooling curves had been observed. Tests of impurity pickup in the alloys after the cooling curves had been observed showed Fe 110–200 p.p.m., and N_2 in the range 100–110 p.p.m. for an alloy that had been melted six times. It is believed that the iron is largely mechanically included in the ingots and that this accounts for the variation in the analyses. The three ingots from which Ag_3Ca_5 was obtained ranged in nominal composition from 62 to 70 at.% Ca. The best chemical analysis for Ag_3Ca_5 was made on a 0.5-mg sample ($D_m = 3.6 \pm 1$ g/cm^3) used for recording a major portion of the X-ray data. This sample had only a few weak powder lines corresponding to some surface decomposition. The analysis gave 59.0 wt.% Ag, 37.3 wt.% Ca, which on correcting to 100%, assuming the difference to be O_2 or H_2O, gives Ag 61.3 wt.% and Ca 38.7 wt.%; calculated for Ag_3Ca_5: 38.2 wt.% Ca. The empirical formula was established from the structure analysis before the chemical analysis was available.

Ag_3Ca_5 is a silver-white, brittle compound, stable in an inert atmosphere. It decomposes moderately quickly in dry air and rapidly in moist air. Since the formula of the compound was unknown, samples were taken from all ingots as they became available. Likely looking fragments (1–50 mg) were selected and their densities were determined on a microbalance. While most of the density values lay randomly between the possible limits, a few clustered near certain modal values. X-Ray photographs of these were then taken in a powder camera. Eight samples were found to be single crystals and were examined using a precession camera; four were examined in some detail. The samples were handled under liquids dried over sodium and protected during exposure by a coating of an acetone-soluble vinylidene chloride copolymer (Saran Resin F220, Dow Chemical Co., Sarnia, Ontario) or by sealing into glass capillaries. The reflections *hk*0, *hk*1, *hk*2, *hk*3, *hhl*, *h*0*l*, and those in the [3$\bar{1}$0] zone were recorded using Mo radiation.

[1]*Issued as N.R.C. No. 6715.*

CRYSTALLOGRAPHIC DATA

The crystals were tetragonal with good to excellent cleavage parallel to (001), diffraction symbol $4/mmm$. I—c—, $a = 8.039 \pm 5$ Å, $c = 15.011 \pm 15$ Å, $c/a = 1.87$, $D_m = 3.6 \pm 1$ g/cm³, $D_x = 3.59$ g/cm³, $V = 970.1$ Å³, F.W. = 524.04, $Z = 4$, $Fooo = 964$, μ_l for Mo $K_\alpha = 90.7$ cm^{-1}, $B = 1.23$ Å². Within the limits of the precession method there were no variations in the axial lengths of the samples examined. The complete X-ray powder pattern is given in Table I. The indexing is listed only to $d = 1.6$ Å since beyond this

TABLE I

Powder diffraction pattern of Ag_3Ca_5

($I4/mcm$, $a = 8.039 \pm 5$ Å, $c = 15.011 \pm 15$ Å, Ni-filtered Cu radiation, $\lambda\alpha_1 = 1.54050$ Å, temp. 22° C, camera diam. 11.46 cm, cutoff 14 Å, intensities by comparison with a logarithmic scale, b = broad)

I_{obs}	hkl	d_{obs}	d_{calc}	I_{obs}	d_{obs}	I_{obs}	d_{obs}
5	002	7.3	7.51	25	1.555	12	1.030
25	112	4.4	4.53	5	1.536	10	1.021
1	020	3.9	4.02	50	1.499	12	1.011
5	004	3.7	3.75	25	1.442	10	1.002
5	121	3.5	3.50	20b	1.416	15	0.9767
2	114	3.1	3.13	5	1.364	15	.9668
100	123	2.88	2.92	10	1.349	15	.9438
8	220	2.81	2.84	15b	1.326	10	.9367
15	024	2.71	2.74	5	1.288	10	.9308
4	222	2.63	2.66	15	1.269	12	.9161
35	130	2.51	2.54	5	1.245	12	.9024
10	006	2.48	2.50	5	1.224	10	.8887
25	125	2.28	2.30	18	1.200	5	.8762
12	231	2.18	2.21	5	1.187	5	.8671
17	134	2.09	2.10	10	1.158	15	.8552
12	233	2.02	2.04	12	1.128	10	.8430
17	042	1.92	1.94	12	1.118	12	.8334
12	226 008	1.86	1.88 1.88	10	1.106	12	.8239
2	127	1.83	1.84	5	1.095	$\alpha_1$15	.8050
2	143	1.80	1.82	5	1.085	$\alpha_1$15	.7962
20	235	1.78	1.79	5	1.063	α_1 8	.7831
10	334	1.68	1.69	12	1.050	$\alpha_1$12	.7816
7	244	1.61	1.62	5	1.041	$\alpha_1$10	.7782

there are too many ambiguities. It should be noted that powder patterns of this material may show strong absorption effects with the larger d-values, in error by 1–2% if the samples are unduly large. This pattern was obtained from samples having nominal compositions close to Ag_3Ca_5, whereas samples on either side of this composition showed mixed patterns.

STRUCTURE DETERMINATION

The original attempts to solve this structure were based on partial data obtained from two crystals extracted from a diffusion couple. One crystal, on chemical analysis, gave the formula $Ag_2Ca_{5.06}$; the other decomposed before being analyzed. No satisfactory solution for the structure was achieved by simple trial and error methods so fresh samples were obtained from the cooling curve ingots which had just become available. Care was taken to examine a number of samples in order to avoid possible difficulties due to twinning or other sample variations. The intensities for the reflections $hk0$ and hhl were obtained from timed precession photographs and corrected for Lorentz-polarization effects. The appropriate temperature factor and absolute scaling factor were obtained by Wilson's method (3). The possible space groups are $I4cm$ (C_{4v}^{10}), $I\bar{4}c2$ (D_{2d}^{10}), and $I4/mcm$ (D_{4h}^{18}). A comparison of the average intensities of the axial rows with those of the axial zones and the general zones (4) indicated the space group $I4/mcm$ as the most

probable. The fact that all zones were centric was taken to confirm this hypothesis. A consideration of atomic volumes together with the possible space group positions gave Ag_3Ca_5 as a likely formula and a trial structure of the $D8_l$-type was readily established. The optimum values for the individual parameters were obtained by varying each parameter systematically and calculating $R = \sum |F_{obs}| - |F_{calc}| / \sum |F_{obs}|$ for selected groups of planes particularly sensitive to the parameter in question. Shifts of 0.005 from the optimum positions gave markedly worse values of R. The reflections $00l$, $33l$, and $44l$ were used for the Ca_{II} z parameter; $11l$, $55l$, and a group of eight $hk0$ reflections were used to derive the Ag_{II} x parameter. The final structure has 4 Ag_I in 4(a), $0,0,\frac{1}{4}$; 8 Ag_{II} in 8(h), $x,\frac{1}{2}+x,0$ with $x = 0.378\pm5$; 4 Ca_I in 4(c) 0,0,0; and 16 Ca_{II} in 16(l), $x,\frac{1}{2}+x,z$ with $x = 0.164\pm5$ and $z = 0.150\pm5$. This structure gave $R = 0.07$ for all observed $hk0$ and $R = 0.20$ for all observed hhl planes. As a final check calculations of a few hkl reflections from the $[3\bar{1}0]$ zone gave $R = 0.09$. Subject to the limitations involved a rough estimate of the accuracy of the coordinates may be obtained from Luzzati's formula (12). This gives $|\overline{\Delta r}| \approx 0.05$ Å, corresponding to 0.003 for z and 0.006 for x. The agreement is generally good except for 004 where $F_c = 326$. Extinction may perhaps account for this disagreement. The crystals used were mostly multiple, with the various portions having the c-axis parallel. For the $hk0$ reflections the multiple spots were spread out but in the hhl reflections they are overlapped to an unknown degree and it is assumed that this accounts for the larger R value for these reflections (Table II).

TABLE II

Observed and calculated structure factors

$hk0$	F_o	F_c	hhl	F_o	F_c	hkl	F_o	F_c
020	94	+101	004	220	+326	550	0	+ 3
220	265	+263	114	129	+114	552	163	−119
130	390	+446	220	241	+261	448	315	+275
040	187	−175	222	128	−103	554	33	+ 4
330	165	−135	006	274	+347	00,14	230	+199
240	216	+202	224	171	+149	33,12	0	+ 32
150	219	+219	116	190	−257	11,14	166	−140
440	364	+372	226	37	− 48	556	101	−130
350	101	+100	008	422	+507	44,10	76	+ 66
060	253	+252	330	181	−134	22,14	0	− 22
260	63	+ 58	332	168	−151	558	0	+ 13
170	25	0	118	0	+ 19	660	171	+174
370	221	+223	334	239	+201	662	77	− 62
080	202	+183	228	171	+167	44,12	186	+206
280	110	+112	336	315	−238	33,14	154	−189
660	177	+174	00,10	0	− 2	55,10	77	− 82
570	128	+124	440	388	+376	44,14	76	+ 96
480	0	− 21	11,10	114	−133	668	131	+114
190	79	+ 60	442	160	+122	770	0	− 3
390	64	+ 54	22,10	86	− 88	772	104	− 81
770	0	− 2	444	355	+272	66,10	130	−100
2,10,0	85	+ 83	338	58	− 60	55,14	71	− 93
590	135	+147	00,12	247	+287	776	95	− 87
4,10,0	79	+ 80	11,12	0	+ 32	213	329	−377
1,11,0	90	+ 91	44, 6	179	+139	413	129	+124
3,11,0	38	+ 40	33,10	0	− 20	613	128	+130
112	266	−245	22,12	122	+107			

DISCUSSION

The $D8_l$ structure was reported by Bertaut and Blum in 1953 for B_3Cr_5 (5). It has since been observed for Ge_3Ta_5 (6), Si_3Ta_5, and Si_3Nb_5 (7). Not previously noted is the fact that the same structure was reported for the ionic compounds $NH_4Pb_2Br_5$, $RbPb_2Br_5$, and KPb_2Br_5 by Powell in 1937 (8). (The origin used by Powell is removed $\frac{1}{2},\frac{1}{2},0$ from

that used in this paper.) All these compounds, although isostructural, are not isomorphous in the sense that their powder patterns are directly comparable since the wide variations in atomic sizes and scattering power obscure the fundamental similarity.

This structure can be most conveniently discussed in terms of slabs of atoms parallel to (001). Fig. 1(*a*), which is a full cell projection onto (010), shows the atoms arranged in layers at $z = 0$ (A), 0.15 (B), 0.25 (C), 0.35 (B), 0.50 (A), and so on. The interatomic distances corresponding to contacts are listed in Table III, and representative pairs of

TABLE III

Calculated interatomic distances (Å) for Ag_3Ca_5

Ag_I—$8Ca_{II}$	3.36	Ag_{II}—$1Ag_{II}$	2.77	Ca_{II}—$2Ag_{II}$	3.24
		—$2Ca_I$	3.19	—$1Ag_{II}$	3.32
Ca_I—$4Ag_{II}$	3.19	—$4Ca_{II}$	3.24	—$2Ag_I$	3.36
—$8Ca_{II}$	3.76	—$2Ca_{II}$	3.32	—$1Ca_{II}$	3.58
				—$1Ca_{II}$	3.73
				—$2Ca_I$	3.76

atoms corresponding to these distances are indicated by dotted lines in Fig. 1. The atoms lying in layers BCB are shown projected onto (001) in Fig. 1(*b*). This arrangement is the Al_2Cu structure (C16 type). The Ag_I atom lies in the center of eight Ca_{II} atoms arranged at the vertices of a square antiprism, 3.36 Å away from the Ag. For a coordination of eight the Ag—Ca distance is calculated to be 3.37 Å on the basis of the radii observed in the metals corrected for eight coordination.

The short Ca_{II}—Ca_{II} distance of 3.58 Å deserves attention. A calculation of the interatomic distance between the same pair of atoms in the 20 or so known C16-type structures shows that some apparent contraction occurs frequently but that it is most marked when the large atom is relatively "open", i.e. with a small ion core in respect to its metallic radius. For example, in Na_2Au the ratio rAu/rNa is 0.73 and the observed Na—Na distance is 3.30 Å as compared to 3.80 Å in the metal; in the present case rAg/rCa is 0.75 and the observed Ca—Ca distance is 3.58 Å as compared to 3.96 Å for the metal. The position marked H in Fig. 1(*b*) is at the center of a tetrahedral hole of radius 2.39 Å, about the size of a carbon or nitrogen atom.

The atoms in the layers BAB are projected onto (001) in Fig. 1(*c*). This layer, which forms the most striking feature of the structure, is identical with the structures of Th_3Al_2 (9) and U_3Si_2 (10). The Ca_I atoms are linked to four Ag_{II} atoms (3.19 Å) at the corners of a square while each Ag_{II} atom is linked to two Ca_I and one Ag_{II} (2.77 Å), the whole array forming a sheet of closely linked atoms parallel to (001). The relatively tight linkage in this layer probably accounts for the observed cleavage on (001). In addition to the contacts within the layer each Ca_I is connected to eight Ca_{II} (3.76 Å) at the corners of a square prism while each Ag_{II} is connected to six Ca_{II} at the vertices of a right triangular prism (four at 3.24 Å plus two at 3.32 Å). The Ca_I—Ag_{II} distance of 3.19 Å within the layer corresponds to a value somewhat larger than that calculated for 4-fold coordination but on the other hand the Ca_I—Ca_{II} distance of 3.76 Å is somewhat less than that calculated for CN = 8 (3.92 Å) or CN = 12 (3.96 Å), so that the coordination around Ca_I is intermediate in character between 4- and 12-fold. Similarly the short Ag_{II}—Ag_{II} distance (2.77 Å) and Ag_{II}—Ca_I distance (3.19 Å) are actually rather longer than that estimated for 3-fold coordination (~2.5 Å, ~3.0 Å), whereas the average Ag—Ca distance (3.25 Å) is somewhat shorter than that calculated for total 8-fold coordination (3.37 Å), leading to the conclusion that the bonding shows some evidence of an "electrochemical" effect, i.e. some degree of ionic character.

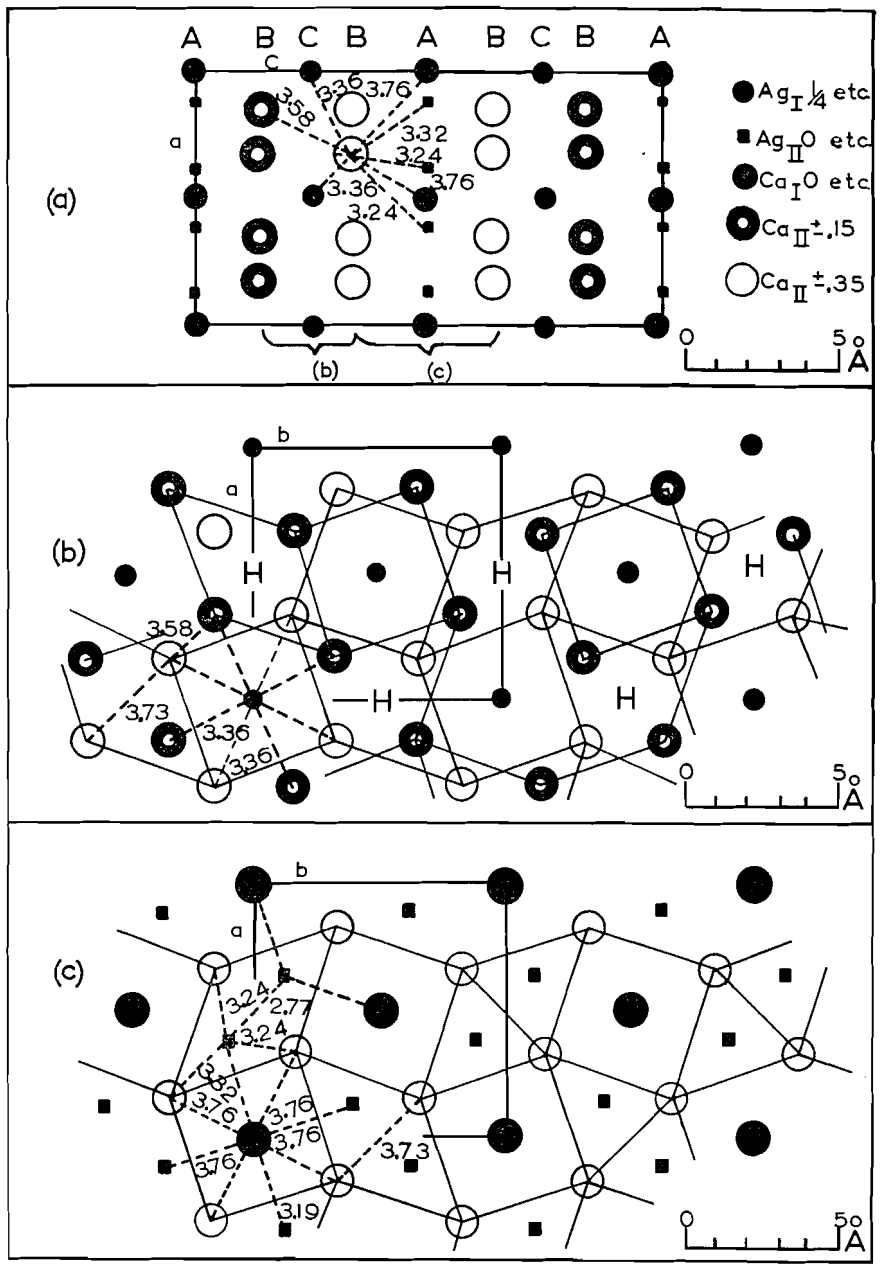

FIG. 1. Projections of the Ag_3Ca_5 structure. (*a*) Full cell projection onto (010); (*b*) layers BCB projected onto (001); (*c*) layers BAB projected onto (001).

The coordination of the Ca_{II} atom is complex and not easily pictured. The interatomic distances corresponding to contacts are indicated in Fig. 1(*a*) by dotted lines. The average of the nine distances is 3.48 Å whereas a weighted average of Ag—Ca (CN = 8) is ~3.6 Å.

This structure may be considered as being primarily determined by the relative sizes of the atoms concerned and not by their normal group valencies, metallic nature, or

electron/atom ratio, as may be seen by studying the formulae and radius ratios of the isostructural compounds listed in Table IV, in which metallic radii for CN = 12 have

TABLE IV

Compounds crystallizing with the $D8_l$ structure

Compound	Radius ratio	Compound	Radius ratio
Ag_3Ca_5	0.76	Ge_3Ta_5	0.90
B_2Cr_5	0.72	$RbPb_2Br_5$	0.77
KPb_2Br_5	0.68 (0.8?)	Si_3Ta_5	0.79
$NH_4Pb_2Br_5$	0.77 (0.8?)	Si_3Nb_5	0.77

been compared except for $NH_4Pb_2Br_5$, KPb_2Br_5, and $RbPb_2Br_5$, where the appropriate ionic radii have been used. A similar conclusion with respect to the Al_2Cu (C16) structure which comprises layers BCB (Fig. 1(*b*)) of the present structure has been proposed by Raynor (11). Secondly, the average interatomic distances are somewhat shorter and the average coordination numbers are somewhat smaller than might be expected on a purely metallic basis. This suggests that the bonding, although primarily metallic, is modified by a noticeable "electrochemical" effect. A more detailed discussion of the bonding is reserved until the results from other Ag–Ca compounds are available.

REFERENCES

1. N. Baar. Z. anorg. Chem. **70**, 352 (1911).
2. C. Degard. Z. Krist. **90**, 399 (1935).
3. A. J. C. Wilson. Nature, **150**, 152 (1942).
4. International Tables for X-Ray Crystallography. Vol. II. The Kynoch Press, Birmingham, England. 1959. p. 355.
5. F. Bertaut and P. Blum. Compt. rend. **236**, 1055 (1953).
6. H. Nowotny, A. W. Searcy, and J. E. Orr. J. Phys. Chem. **60**, 677 (1956).
7. E. Parthé, B. Lux, and H. Nowotny. Monatsch. Chem. **86**, 859 (1955).
8. H. M. Powell and H. S. Tasker. J. Chem. Soc. 119 (1937).
9. J. R. Murray. J. Inst. Metals, **84**, 91 (1955–1956). P. B. Braun and J. H. N. van Vucht. Acta Cryst. **8**, 117 (1955).
10. W. H. Zachariasen. Acta Cryst. **2**, 94 (1949).
11. G. V. Raynor. Progr. in Metal Phys. **1**, 33 (1950).
12. V. Luzzati. Acta Cryst. **5**, 802 (1952).

STEREOCHEMICAL STUDIES

IV. ACID-CATALYZED EQUILIBRATION OF α- AND β-FORMS OF 3-ALKOXY-4-OXA-5α-CHOLESTANES. THE ANOMERIC EFFECT

J. T. EDWARD AND I. PUSKAS[1]
Department of Chemistry, McGill University, Montreal, Que.

Received November 28, 1961

ABSTRACT

The α- and β-anomers of 3-methoxy-, 3-isopropoxy-, 3-cyclohexyloxy-, and 3-phenoxy-4-oxa-5α-cholestane were separated by chromatography on alumina. The configurations of the anomers were assigned from a consideration of their optical rotations. Acid-catalyzed equilibration of the 3-alkoxy anomers favored formation of the axial isomer, the proportions of α- to β-forms being about 7:3. 2α-Phenoxy-4-oxa-5α-cholestane in acid solution was in equilibrium with phenol and 4-oxa-5α-cholest-2-ene.

The reaction of benzyl alcohol with 3α-chloro-4-oxa-5α-cholestane in the presence of base, or with 4-oxa-5α-cholestan-3α-ol in the presence of acid, has been shown to yield a mixture from which 3α- and 3β-benzyloxy-4-oxa-5α-cholestane could be separated by chromatography on alumina. On the other hand, the corresponding reactions of methanol yielded mixtures from which only 3α-methoxy-4-oxa-5α-cholestane could be isolated in a pure state (1).

We have now found that by using a larger chromatographic column it is possible to separate 3β-methoxy-4-oxa-5α-cholestane from these mixtures. This chromatographic method was also used to separate the isomeric 3-isopropoxy-, 3-cyclohexyloxy-, and 3-phenoxy-4-oxa-5α-cholestanes, produced by reaction of 3α-chloro-4-oxa-5α-cholestane with the appropriate alcohol or phenol.

For each pair of isomers, the configuration at the 3-position was determined by a comparison of molecular rotations. According to Hudson's rules of isorotation (2), for aldopyranosides the molecular rotation of an α-D-glycoside should be about 350–400° more positive than that of the β-D-anomer. This rule has been rationalized by Whiffen (3) and Brewster (4) in their more general treatments of the effect of structure upon optical rotation. Since 3-substituted 4-oxa-5α-cholestanes have the C-1 conformation of the majority of D-pyranosides (5), about the same difference between the molecular rotations of α- and β-anomers should be observed. The results in Table I show this expectation to be confirmed. As anticipated, the molecular rotation difference is significantly greater for α- and β-forms of 3-phenoxy-4-oxa-5α-cholestane (+678°); phenyl α-D-glycopyranosides generally differ from phenyl β-D-glycopyranosides in molecular rotation by about +600° (6, 7).

According to these configurational assignments, the isomer more strongly adsorbed on alumina is in every case that having an equatorial alkoxy group. This is in line with the effect on adsorption of the configuration of the hydroxyl groups of steroidal alcohols (8). The differences in melting points of the pairs of isomers (Table II) are also those expected from their configurations. While the melting points of methyl α- and β-D-glycopyranosides vary in an irregular fashion, the melting points of phenyl (7) and higher alkyl (9) β-D-glycopyranosides are generally above those of the α-anomers, probably because of the better packing in the crystal possible for molecules with the bulky anomeric group equatorial.

[1]*Holder of N.R.C. Studentship, 1959–1961.*

TABLE I

Molecular rotation $[M]_D$ values (in deg) of 3-substituted 4-oxa-5α-cholestanes

3-Substituent	Solvent*	$[M]_D$ of α-Form	$[M]_D$ of β-Form	$\Delta[M]_D$
Methoxy	$CHCl_3$	+451	+64	+387
Methoxy	THF–MeOH, 1:1	+468	+73	+395
Isopropoxy	$CHCl_3$	+485	+54	+431
Isopropoxy	Pr^iOH	+498	+61	+437
Cyclohexyloxy	$CHCl_3$	+488	+40	+448
Cyclohexyloxy	THF–Cyc, 2:3	+511	+38	+473
Phenoxy	$CHCl_3$	+755	+77†	+678
Phenoxy	THF–PhOH	+792		

*THF = tetrahydrofuran; Cyc = cyclohexanol; ratios of solvent mixtures in v/v.
†Not rigorously purified because of lack of material.

TABLE II

Melting points of 3-substituted 4-oxa-5α-cholestanes

3-Substitutent	α-Anomer m.p. (°C)	β-Anomer m.p. (°C)
Methoxy	98–99.5 (1)	78
Isopropoxy	Syrup	90
Cyclohexyloxy	Syrup	109–110
Benzyloxy	42–51 (1)*	131–132 (1)
Phenoxy	112–117*	141

*Melting points of slightly impure compounds.

Both α- and β-forms of the 3-alkoxy-4-oxa-5α-cholestanes underwent mutarotation in acid solution, the same equilibrium value of the optical rotation being obtained starting with either isomer. Some typical results are shown in Fig. 1. Previously this type of change had been observed with 3α- and 3β-benzyloxy-4-oxa-5α-cholestane, and shown to be due to the formation of an equilibrium mixture of the α- and β-isomer (1). The same is true for the changes now under consideration. In the case of the 3-methoxy derivatives,

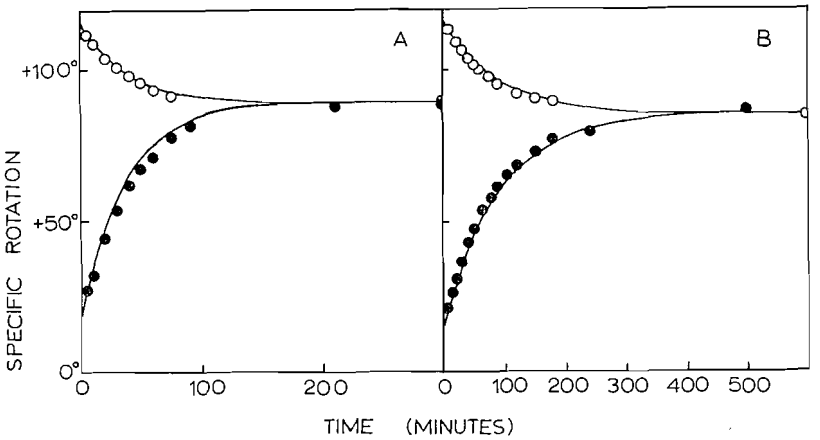

FIG. 1. Mutarotation of 3-alkoxy-4-oxa-5α-cholestanes; experimental values shown as points, and theoretical values for first-order reactions (having rate constant k) as curves. (A) 3α- (○) and 3β- (●) methoxy compounds in absolute methanol – tetrahydrofuran, 1:1 (v/v), 0.013 N with respect to hydrogen chloride, at 27±1.5° C; k = 0.027 min^{-1} (natural logs). (B) 3α- (○) and 3β- (●) isopropoxy compounds in absolute isopropanol, 0.084 N with respect to hydrogen chloride, at 22±0.5° C; k = 0.0115 min^{-1}.

the equilibrium mixture was recovered from solution and separated by chromatography into the 3α- and 3β-isomers; in the case of the 3-isopropoxy and 3-cyclohexyloxy derivatives, the equilibrium mixture was shown by qualitative infrared spectroscopy to be made up practically completely of 3α- and 3β-isomers. The equilibrium distributions of the isomers obtained from polarimetric measurements at 25±4°, assuming the equilibrium mixture to be made up solely of the 3α- and 3β-isomers, are shown in Table III.

TABLE III

Anomeric equilibrium of 3-substituted 4-oxa-5α-cholestanes

	By polarimetry		By chromatography	
3-Substituent	Solvent	% α-form	Solvent	% α-form
Methoxy	MeOH	73±2	MeOH	67
Isopropoxy	Pr^iOH	71±2	Pr^iOH	75
Cyclohexyloxy	Cyc–THF, 3:2	69±2	Cyc	66
Benzyloxy (1)	$PhCH_2OH$–THF, 3:2	73±3	$PhCH_2OH$	85

These distributions are in rough agreement with those obtained by actual chromatographic separation of equilibrium mixtures (Table III). (The values for the isopropoxy and cyclohexyloxy derivatives in this table are derived from the experiments in which 3α-chloro-4-oxa-5α-cholestane was solvolyzed in the appropriate alcohol to give the alkoxy derivative and hydrogen chloride.) Better agreement could not be expected, because of the possibility of changes in composition during the removal of the solvent from the mixtures at reduced pressures and slightly elevated temperatures prior to chromatography; this (in part) may account for the presence of small amounts of 4-oxa-5α-cholest-2-ene and of other unidentified products in the chromatographic fractions.

The equilibrium distribution of isomeric 3-alkoxy-4-oxa-5α-cholestanes are about the same, regardless of the nature of the alkyl group, the axial (α) isomer being favored (Table III). Evidently the "anomeric effect" (1, 10, 11) outweighs the effect of steric interactions between an axial oxygen atom and the axial hydrogen atoms at the 1- and 5-positions; the latter effect is apparently approximately independent of the size of the alkyl group, as would be expected if the alkoxyl group has the conformation shown in formula I. The equilibrium constants K (= concentration of α-isomer/concentration of

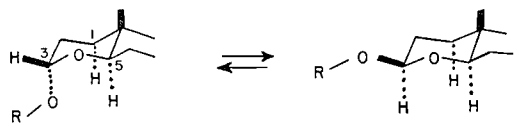

(I) (II)

β-isomer) of 2.4±0.2 for the four isomerization reactions correspond to free energy differences (ΔF) of 520±50 cal/mole between the α- and β-isomers. This compares with a ΔF of 715 cal/mole between the corresponding α- and β-anomers of methyl D-glucoside (77% α-anomer at equilibrium in acidic methanol (12)). For all of these compounds ΔF may be considered as made up of the difference between the anomeric effect and the interaction energy for an axial oxygen and two axial hydrogen atoms. The greater ΔF for the sugar may be due in part to a greater value of the anomeric effect in this compound because of the inductive effects of the many hydroxyl groups (1, 11). However, it may

also be due in part to differing values of interaction energies of axial groups in glucosides and in 4-oxa-5α-cholestanes because of a stiffening of ring A in the latter through fusion with ring B (13). Thus ΔF between axial and equatorial hydroxyl groups of 4-*t*-butylcyclohexanol in isopropanol at 90° is 0.96 kcal/mole (14), and of cholestan-3-ol in boiling propanol is 2.0 kcal/mole (13).* Consequently, any attempt to estimate the separate contributions to ΔF made by the anomeric effect and by non-bonded repulsions in these compounds must be regarded as highly speculative until independent estimates of the interaction energies are available.

In any one equilibration experiment the changes in rotation followed the expected first-order kinetics with reasonable accuracy, as shown by the examples in Fig. 1. However, while the equilibrium constants obtained in different experiments were reasonably reproducible, the rate constants differed sometimes by factors of 2–3. Similar difficulties in reproducing rate constants for the acid-catalyzed mutarotation of glycosides have been reported, and attributed to the effect of traces of water in the alcohol (11).

In acidic solution in the presence of a large molar excess of phenol, 3α-phenoxy-4-oxa-5α-cholestane eliminated phenol by a first-order reaction (Fig. 2) to give an equili-

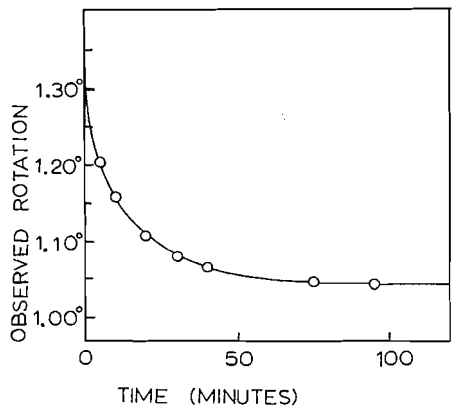

FIG. 2. Change in rotation, on standing, of a solution of 3α-phenoxy-4-oxa-5α-cholestane in acidic phenol–tetrahydrofuran, 1:4 (v/v) at 28.5±0.5° C. Circles: experimental values; curve: theoretical for a first-order reaction having rate constant = 0.054 min^{-1}.

brium mixture made up of about 2 moles of the phenoxy compound per mole of 4-oxa-5α-cholest-2-ene. This indicates a much smaller thermodynamic stability for the 3-phenoxy as compared with 3-alkoxy compounds: the latter may also be in equilibrium with 4-oxa-5α-cholest-2-ene in acidic alcohol (see above), but the quantity of the latter at equilibrium must be very much smaller, and not enough to affect appreciably the calculated equilibrium distributions shown in Table III. The lesser thermodynamic stability of the 3α-phenoxy compound was shown more directly in an equilibration experiment starting with 3α-methoxy-4-oxa-5α-cholestane and a large excess of phenol in acidic tetrahydrofuran. The products (3α-methoxy-, 3α-phenoxy-, 3β-phenoxy-4-oxa-5α-cholestane, etc.) were isolated by chromatography on alumina. Bearing in mind the limitations of such a method, discussed above, the constants calculated from these results can be considered only very approximate. However, for the reaction

3α-methoxy-4-oxa-5α-cholestane + phenol $\rightleftarrows$ 3α-phenoxy-4-oxa-5α-cholestane + methanol

an equilibrium constant ≈ 0.05 may be calculated, and for the equilibrium between 3α- and 3β-phenoxy-4-oxa-5α-cholestane, $K > 6$.

**We are grateful to a referee for bringing this point to our attention.*

EXPERIMENTAL

Intensities of infrared absorption are indicated after the frequencies either by the semiquantitative notation used previously (15) or by molecular extinction coefficients (in parentheses). Chromatography was on Woelm alumina; Brockmann activity grades shown. Melting points are uncorrected.

3β-Methoxy-4-oxa-5α-cholestane

3α-Methoxy-4-oxa-5α-cholestane (1) (235 mg) was dissolved by gentle warming in a solvent prepared previously by addition of acetyl chloride (0.5 ml) to absolute methanol (20 ml) and absolute tetrahydrofuran (5 ml). After solution was complete, excess silver carbonate (about 3 g) (16) was added with stirring. The insoluble silver salts were removed by filtration and washed with anhydrous ether. The filtrate and washings evaporated at reduced pressure left a solid which was chromatographed on alumina (50 g, basic, grade III). Elution with ligroin (200 ml) brought down the starting material (156 mg), identified by infrared spectrum and mixed melting point, while ligroin–benzene, 4:1, v/v (140 ml) washed down the *3β-methoxy isomer* (76 mg), m.p. 74–76° C. Recrystallization from methanol raised the m.p. to 78° C, depressed by admixture with the α-isomer; $[\alpha]_D^{26}$ +15.8° (*c*, 1.35 in chloroform); $[\alpha]_D^{26}$ +18.6° (*c*, 1.26 in tetrahydrofuran–methanol, 1:1, v/v); $\nu_{max}^{CCl_4}$ in cm^{-1}: 2920 (525), 2842 (288), 2725 (23), 2620 (17), 1469 (160), 1457 (138), 1448 (152), 1387 (180), 1368 (77), 1345 (71), 1326 (42), 1203 (50), 1169 (192), 1142 (115), 1132 (109), 1123 (132), 1098 (124), 1093 (120), 1072 (400), 1048 (230), 1027 (90), 936 (106), 928 (sh 65), 902 (48), 865 (34). Calc. for $C_{27}H_{48}O_2$: C, 80.20; H, 11.95; OMe, 7.68%. Found: C, 80.30; H, 11.90; OMe, 7.65%.

In a similar experiment in which 3α-methoxy-4-oxa-5α-cholestane (155 mg) was isomerized in acidic absolute ether – absolute methanol (1:1, v/v), 108 mg of α- and 47 mg of β-methoxy isomer were isolated by chromatography.

3α- and 3β-Isopropoxy-4-oxa-5α-cholestane

A solution of 3α-chloro-4-oxa-5α-cholestane (325 mg) in isopropanol (7 ml, spectro grade, water content less than 0.5%) was refluxed for 3 hours. The solvent was removed under reduced pressure and the residual syrup (342 mg) chromatographed on alumina (32 g, basic, grade III). Elution with the volumes of ligroin shown below afforded the following fractions:

(*a*) 30 ml: nothing;

(*b*) 10 ml: crystals of 4-oxa-5α-cholest-2-ene (6 mg), identified by m.p. and infrared spectrum;

(*c*) 50 ml: a syrup (202 mg) which proved to be 3α-isopropoxy-4-oxa-5α-cholestane, shown by its infrared spectrum to be contaminated with carbonyl-containing impurities;

(*d*) 60 ml: nothing;

(*e*) 35 ml: sticky crystals (14 mg) of an unidentified material; $\nu_{max}^{CCl_4}$ in cm^{-1}: 2950 (vs), 2870 (s), 1470 (s), 1450 (s), 1382 (s), 1370 (m), 1335 (w), 1261 (w), 1126 (m), 1101 (s), 1087 (s), 1049 (m), 1023 (s), 952 (w), 933 (w), 907 (w), 870 (w);

(*f*) 200 ml: impure crystals (67 mg) of 3β-isopropoxy-4-oxa-5α-cholestane.

Further elution with 25 ml benzene–ether (1:1, v/v) brought down a glassy solid (47 mg) which could not be identified, and with 25 ml benzene–methanol (3:2, v/v), crystals of 4-oxa-5α-cholestan-3α-ol (3 mg).

Chromatographic fraction *c* was dissolved in hot methanol and filtered under suction on a hot funnel. The solvent was evaporated from the filtrate, and the residual syrup stirred with small amount of hot methanol. The methanol was decanted from the syrup. Repetition of this process removed the carbonyl-containing impurities, although with an appreciable loss of the main product. The residual syrupy liquid, which appeared to be *3α-isopropoxy-4-oxa-5α-cholestane*, resisted all attempts at crystallization; $n_D^{22.8}$ 1.4938; $[\alpha]_D^{21}$ +112.3° (*c*, 1.42 in chloroform); $[\alpha]_D^{22}$ +115° (*c*, 1.51 in isopropanol); $\nu_{max}^{CCl_4}$ in cm^{-1}: 2925 (608), 2860 (337), 1470 (188), 1449 (135), 1382 (185), 1369 (148), 1335 (84), 1129 (214), 1098 (123), 1080 (67), 1038 (319), 956 (70), 932 (98), 899 (61), 873 (35). Calc. for $C_{29}H_{52}O_2$: C, 80.49; H, 12.11%. Found: C, 80.41; H, 12.00%.

Fraction *e* was dissolved in hot methanol and filtered under suction through a hot funnel. The precipitate separating in the filtrate redissolved on warming. On slow cooling, a syrup separated. The solution was decanted from the syrup, and on standing at 4° C deposited crystals which, on recrystallization from methanol, gave pure *3β-isopropoxy-4-oxa-5α-cholestane* (16 mg), m.p. 90° C; $[\alpha]_D^{23}$ +12.5° (*c*, 1.085 in chloroform); $[\alpha]_D^{23}$ +14° (*c*, 1.37 in isopropanol); $\nu_{max}^{CCl_4}$ in cm^{-1}: 2935 (595), 2680 (330), 1470 (192), 1458 (149), 1450 (146), 1384 (208), 1372 (160), 1337 (104), 1313 (55), 1192 (66), 1166 (255), 1138 (180), 1121 (225), 1093 (155), 1066 (470), 1045 (314), 944 (76), 933 (106), 902 (53). Calc. for $C_{29}H_{52}O_2$: C, 80.49; H, 12.11%. Found: C, 80.57; H, 12.05%.

On concentration of the combined mother liquors a further 24 mg of slightly impure crystals of 3β-isopropoxy-4-oxa-5α-cholestane was obtained (total yield 11.5%).

3α- and 3β-Cyclohexyloxy-4-oxa-5α-cholestane

A solution of 3α-chloro-4-oxa-5α-cholestane (167 mg) in cyclohexanol (3 ml, m.p. 22–24°) was heated to 120° C for 2 hours. The solvent was then removed under reduced pressure and the residual syrup chromatographed on alumina (32 g, basic, grade III). Elution with the solvents indicated gave the following fractions:

(*a*) 25 ml ligroin: nothing;
(*b*) 15 ml ligroin: crystals of 4-oxa-5α-cholest-2-ene (7 mg), identified by m.p. and infrared spectrum;
(*c*) 40 ml ligroin: syrup (123 mg), shown below to be 3α-cyclohexyloxy-4-oxa-5α-cholestane;
(*d*) 30 ml ligroin–benzene, 9:1, v/v: syrup (13 mg) having characteristic absorption peaks in CCl_4 at 1103, 1089, 1062, 1049, and 1024 cm^{-1} which are absent in the spectrum of both 3α- and 3β-cyclohexyloxy isomers (see below); the fraction must be a mixture of at least two compounds, since in another run the corresponding fraction showed the 1103 and 1089 cm^{-1} peaks only;
(*e*) 45 ml ligroin–benzene, 3:2, v/v: crystals (62 mg) shown below to be impure 3β-cyclohexyloxy-4-oxa-5α-cholestane.

Fraction *c* was dissolved in 20 ml hot methanol, treated with charcoal, and filtered, but all attempts to obtain crystals from the filtrate failed. Removal of the solvent left a syrup which appeared to be *3α-cyclohexyloxy-4-oxa-5α-cholestane*; $[\alpha]_D^{20}$ +103° (*c*, 1.23 in chloroform); $[\alpha]_D^{26}$ +108° (*c*, 1.78 in cyclohexanol–tetrahydrofuran, 3:2, v/v); $\nu_{max}^{CCl_4}$ in cm^{-1}: 2920 (780), 2845 (400), 1468 (166), 1450 (186), 1374–1379 (110), 1368 (114), 1233 (52), 1120 (202), 1098 (100), 1057 (182), 1035 (410), 931 (102), 910 (66), 888 (50). Calc. for $C_{32}H_{56}O_2$: C, 81.29; H, 11.94%. Found: C, 81.34; H, 11.94%.

Fraction *e* was dissolved in ligroin and decolorized with charcoal. The crystals left by evaporation of the solvent dissolved partially in hot methanol – ethyl acetate (9:1, v/v), leaving behind some undissolved syrup. On cooling, the solution gave colorless prisms of *3β-cyclohexyloxy-4-oxa-5α-cholestane* (22 mg), micro m.p. 108–110° C, unchanged by further recrystallization from methanol; $[\alpha]_D^{25}$ +8.5° (*c*, 1.34 in chloroform); $[\alpha]_D^{25}$ +8.1° (*c*, 1.15 in cyclohexanol–tetrahydrofuran, 3:2, v/v); $\nu_{max}^{CCl_4}$ in cm^{-1}: 2920 (685), 2840 (397), 1468 (164), 1454 (186), 1385 (120), 1368 (136), 1343 (82), 1166 (211), 1137 (175), 1120 (172), 1092 (159), 1068 (365), 1044 (330), 932 (100). Calc. for $C_{32}H_{56}O_2$: C, 81.29; H, 11.94%. Found: C, 81.08; H, 11.84%.

3α- and 3β-Phenoxy-4-oxa-5α-cholestane

(*a*) *From 3α-Chloro-4-oxa-5α-cholestane*

A solution of 3α-chloro-4-oxa-5α-cholestane (120 mg) and freshly distilled phenol (94 mg) in absolute tetrahydrofuran (4 ml) was refluxed gently overnight. The solvent was removed under reduced pressure and the residual syrup stirred with distilled water. The water was decanted and the syrup dried in a vacuum desiccator and chromatographed on alumina (20 g, basic, grade III) to give the following fractions:
(*a*) 20 ml ligroin: 4-oxa-5α-cholest-2-ene (2 mg);
(*b*) 25 ml ligroin: crystals (25 mg);
(*c*) 25 ml ligroin: unidentifiable syrup (11 mg);
(*d*) 20 ml ligroin; sticky crystals (19 mg);
(*e*) more ligroin, followed by more polar solvents: differing syrupy, foamy, and glassy fractions (60 mg).

Fraction *b*, twice recrystallized from ethyl acetate – ethanol (1:1, v/v), gave shining needles of *3α-phenoxy-4-oxa-5α-cholestane* (17 mg), m.p. 141° C; $[\alpha]_D^{25}$ +162° (*c*, 1.38 in chloroform); $\lambda\lambda_{max}$ 264, 270, 276 mμ; $\epsilon\epsilon_{max}$ 1120, 1590, 1360 (in cyclohexane); $\nu_{max}^{CCl_4}$ in cm^{-1}: 3053 (24), 3025 (29), 2926 (565), 2850 (304), 1597 (130), 1495 (255), 1469 (159), 1462 (125), 1448 (128), 1383 (124), 1367 (117), 1290 (49), 1226 (278), 1175 (76), 1160 (172), 1112 (202), 1102 (139), 1078 (82), 1038 (360), 963 (156), 948 (308), 935 (174), 921 (220), 890 (54), 690 (96). Calc. for $C_{32}H_{50}O_2$: C, 82.35; H, 10.80%. Found: C, 82.28; H, 10.61%.

Fraction *d*, recrystallized from ethyl acetate – ethanol at 0° C, gave colorless needles on the side of the flask and a syrup on the bottom. The crystals (2.8 mg) were separated, washed with methanol, and dried, and appeared to be slightly impure *3β-phenoxy-4-oxa-5α-cholestane*; micro m.p. 112–117° C; $[\alpha]_D^{25}$ +8.2° (*c*, 0.766 in chloroform); $\lambda\lambda_{max}$ 263, 269, 276 mμ; $\epsilon\epsilon_{max}$ 830, 1140, 975 (in cyclohexane; values of extinction coefficients uncertain because of weighing errors with small sample used); ν_{max}^{KBr} in cm^{-1}: 3050 (w, sh), 3030 (w, sh), 2925 (vs), 2845 (s), 1600 (m), 1582 (m), 1497 (s), 1468 (m), 1455 (m), 1446 (sh), 1393 (m), 1384 (m), 1367 (w), 1244 (s), 1227 (m), 1205 (w), 1179 (w), 1162 (w), 1139 (w), 1104 (w), 1070 (vs), 1051 (m), 1028 (w), 1001 (w), 994 (w), 960 (w), 939 (m), 910 (w), 904 (w), 885 (m), 832 (m), 819 (m), 755 (vs), 690 (s).

(*b*) *From 3α-Methoxy-4-oxa-5α-cholestane*

3α-Methoxy-4-oxa-5α-cholestane (140 mg) and freshly distilled phenol (2 g) were dissolved in absolute tetrahydrofuran (15 ml), and some dry hydrogen chloride was blown into the solution. The flask was stoppered and left to stand at room temperature for 2 hours. The acid was then neutralized by the addition of freshly prepared silver carbonate. The insoluble inorganic salts were removed by filtration and washed with ether. The combined filtrate and washings were concentrated *in vacuo*, and the residual syrup was dissolved in ether. The ether solution was washed with 5% sodium hydroxide solution and with water, and partially dried by washing with saturated sodium chloride solution. The ether was removed under vacuum and the residual syrup (163 mg) chromatographed on alumina (30 g, basic, grade III) to give the following fractions, identified by infrared spectroscopy:
(*a*) 40 ml ligroin: crystals of 4-oxa-5α-cholest-3-ene (10 mg);
(*b*) 35 ml ligroin: crystals of 3α-phenoxy-4-oxa-5α-cholestane (92 mg);
(*c*) 35 ml ligroin: crystals of 3α-methoxy-4-oxa-5α-cholestane (21 mg);
(*d*) 25 ml ligroin–benzene, 4:1, v/v: differing syrupy fractions, containing aromatic groups as revealed by their spectra (14 mg);
(*e*) 25 ml ligroin–benzene, 4:1, v/v: impure crystals of 3β-methoxy-4-oxa-5α-cholestane (14 mg).

Fraction *b* was purified by recrystallization from ethyl acetate – ethanol (1:1, v/v) to give pure needles of 3α-phenoxy-4-oxa-5α-cholestane, m.p. 141°, mixed m.p. 141°.

In fraction *d* there was infrared evidence for the presence of 3β-phenoxy-4-oxa-5α-cholestane accompanied by much impurity.

Acid-catalyzed Equilibration of 3α- and 3β-Alkoxy-4-oxa-5α-cholestanes

A solution of hydrogen chloride in the requisite alcohol was prepared by addition of a small amount of acetyl chloride, and the acid concentration determined by titration. An aliquot (0.02–0.06 ml) of this solution was added (at zero time) to a solution of 3-alkoxy-4-oxa-5α-cholestane (14–18 mg) in about 0.9 ml of the alcohol or alcohol–tetrahydrofuran mixture (Table III) contained in a 1.00-ml volumetric flask. The solution was made up to 1.00 ml and mixed, and polarimetric measurements were made as quickly as possible.

Acid-catalyzed Elimination of Phenol from 3α-Phenoxy-4-oxa-5α-cholestane

An aliquot (0.02 ml) of 0.0186 *N* hydrogen chloride in tetrahydrofuran was added to 3α-phenoxy-4-oxa-5α-cholestane (15.55 mg) in about 0.9 ml of phenol–tetrahydrofuran (20%, v/v). The solution was made up to 100 ml with the same solvent and mixed, and polarimetric measurements were taken (Fig. 2). After reaction the solution was treated with anhydrous sodium carbonate and the solvent removed under reduced pressure. The residue in ether was extracted with water, 5% aqueous sodium carbonate, and water, and dried. The solid, after removal of the ether, was analyzed by infrared spectroscopy and found to contain 3α-phenoxy-4-oxa-5α-cholestane and 4-oxa-5α-cholest-2-ene in approximately 2:1 ratio. The ratio from polarimetric measurements (Fig. 2) at equilibrium was 1.87:1, assuming only 3α-phenoxy-4-oxa-5α-cholestane and 4-oxa-5α-cholest-2-ene (and no 3β-phenoxy-4-oxa-5α-cholestane) to be present, and the specific rotation of 4-oxa-5α-cholest-2-ene to be the same in the present solvent as in chloroform (1): both assumptions are only approximately true (cf. Table I).

ACKNOWLEDGMENTS

Helpful comments from Dr. J. C. P. Schwarz, and the financial assistance of the National Research Council, are gratefully acknowledged.

REFERENCES

1. J. T. EDWARD, P. F. MORAND, and I. PUSKAS. Can. J. Chem. **39**, 2069 (1961).
2. C. S. HUDSON. J. Am. Chem. Soc. **31**, 66 (1909).
3. D. H. WHIFFEN. Chem. & Ind. (London), 964 (1956).
4. J. H. BREWSTER. J. Am. Chem. Soc. **81**, 5475, 5483 (1959).
5. R. E. REEVES. J. Am. Chem. Soc. **72**, 1499 (1950).
6. F. J. BATES and ASSOCIATES. Polarimetry, saccharimetry and the sugars. U.S. Government Printing Office, Washington. 1942. pp. 704–760.
7. J. CONCHIE, G. A. LEVVY, and C. A. MARSH. Advances in Carbohydrate Chem. **12**, 180 (1957).
8. K. SAVARD. J. Biol. Chem. **202**, 457 (1953). R. V. BROOKS, W. KLYNE, and E. MILLER. Biochem. J. **54**, 212 (1953).
9. B. LINDBERG. Acta Chem. Scand. **3**, 151 (1949).
10. J. T. EDWARD. Chem. & Ind. (London), 1102 (1955).
11. R. U. LEMIEUX and P. CHU. Abstracts of Papers, the American Chemical Society Meeting, San Francisco, Calif. April 13–18, 1958. 31N. N. J. CHU. Ph.D. Thesis, University of Ottawa, Ottawa, Ontario. 1959. p. 97.
12. C. J. JUNGIUS. Z. physik. Chem. **52**, 97 (1905).
13. R. C. COOKSON. Ann. Repts. on Progr. Chem. (Chem. Soc. London), **54**, 172 (1957).
14. E. L. ELIEL and R. S. RO. J. Am. Chem. Soc. **79**, 5992 (1957).
15. J. T. EDWARD and P. F. MORAND. Can. J. Chem. **38**, 1316 (1960).
16. C. M. MCCLOSKEY and G. H. COLEMAN. *In* Organic syntheses. Vol. 25. *Edited by* W. E. Bachmann. John Wiley & Sons, New York. 1945. p. 54.

DETERMINATION OF THE ACTIVITIES OF MAGNESIUM IN LIQUID MAGNESIUM–TIN ALLOYS BY VAPOR PRESSURE MEASUREMENTS[1]

S. ASHTAKALA[2] AND L. M. PIDGEON[3]

Department of Metallurgical Engineering, University of Toronto, Toronto, Ontario

Received December 4, 1961

ABSTRACT

The vapor pressure of liquid magnesium–tin alloys has been measured between 780° C and 1010° C using the isopiestic method.

Activities of magnesium were obtained at 800° C, 910° C, and 940° C. Activities of tin showed a negative departure from ideality, and those of magnesium, both negative and a slight positive departure.

Partial heats and entropies of mixing were calculated, and values are negative for most of the composition range. Partial free energies of mixing for the entire composition range showed negative values. Integral heats, entropies, and free energies were calculated from the partial quantities. These values were negative, indicating an ordered liquid alloy.

INTRODUCTION

The measurement of vapor pressures in reactive metal systems presents special difficulties owing to the reactivity of the volatile metal, and many established techniques are unsuitable. Static isopiestic methods offer advantages which more than offset the objection that the results must be based on the work of others. The method is particularly applicable to systems consisting of but one volatile component. This paper describes measurement of the vapor pressure of magnesium over liquid magnesium–tin alloys using an elaboration of the method of Herasymenko (7). The changes adapted the technique to the treatment of liquid alloys, and at the same time achieved a more reliable system for the measurement of alloy temperature.

DESCRIPTION OF METHOD

Metallic magnesium was heated at a constant temperature T_1 at one end of a long tube. The magnesium vapor was allowed to come to equilibrium with the samples of tin kept at different temperatures, along the length of the tube, the temperature of the alloys being higher than that of magnesium. The composition of the alloys reached at equilibrium is established by quenching and subsequent analysis. Knowing the vapor pressure of magnesium from published data (1), and the temperature of the alloy, the activity of magnesium could be calculated from the formula

$$a_{Mg} = P^\circ/P_1^\circ,$$

where P° is the vapor pressure of pure magnesium at the temperature of the magnesium chamber, and P_1° is the vapor pressure of pure magnesium at the temperature of the alloy.

The basic limitation of this method is that the vapor pressures of the volatile component should be known accurately, and its accuracy is dependent on the accuracy of the work of others. On the other hand, the values obtained can easily be recalculated, if different values are subsequently accepted for the vapor pressure data of the volatile component.

[1]*Constructed from a thesis presented by S. Ashtakala in partial fulfillment of the requirements for the degree of Doctor of Philosophy in the Department of Metallurgical Engineering, University of Toronto.*

[2]*Present address: c/o B. Sitaramaiah Advocate No. 11, Uttaradi Mutt Road, Bangalore-4, Mysore State, India.*

[3]*Professor and Head of the Department of Metallurgical Engineering, University of Toronto.*

EXPERIMENTAL PROCEDURE

(1) Assembly of the Reaction Tube

The reaction tube consisted of two parts—the magnesium chamber and the alloy chamber, connected by a small diameter tube, as shown in Fig. 1. The reaction tube was made of mild steel.

The magnesium chamber contained about 55 g of pure magnesium. The alloy chamber contained 10 thermocouple wells at equal distances. Inside the alloy chamber, the thermocouple wells were fitted with high-temperature porcelain tubes.

Tin samples were placed in graphite boats which were placed on the thermocouple wells. The boats were prevented from touching the steel tube by porcelain insulators. After positioning the tin boats, the assembly was connected to the vacuum system by a small tube and pumped down to about 0.001 mm Hg. The vacuum offtake was then "hot pressure welded" and sealed.

The furnace was provided with silicon carbide resistors controlled in two sections so that a suitable temperature gradient could be produced. It contained an inner "Inconel" tube, as shown in Fig. 2, in which the reaction tube was placed. The thermocouple wires were passed through the water-cooled copper end plate to the outside of the furnace, sealed by means of Pliocene cement. The end plate was made vacuum-tight by means of an O-ring.

The materials used in the experiments consisted of zone-refined tin of 99.999% Sn and silico-thermic magnesium of 99.96% Mg (courtesy of Dominion Magnesium Limited).

The "Inconel" tube was placed under slight vacuum in order to minimize the pressure differential inside and outside the reaction tube. The two sections of the furnace were heated and controlled separately, and power input was so manipulated that the temperatures of the alloys were always higher than that of magnesium.

At the end of the run, argon was introduced into the "Inconel" tube, the end plate was removed, and the reaction tube pulled out on rails and quenched by means of water sprayed on all the sides of the tube. The whole operation took about a minute.

(2) Precision and Accuracy of Experiments

(a) Temperature Measurement

The temperature of the chamber containing the magnesium "boiler" was constant to $\pm 0.5°$, and an exploratory thermocouple in the boiler itself indicated barely detectable changes.

In the part of the system containing the deliberate temperature gradient, it is of utmost importance that temperature of the alloy chambers be constant longitudinally and radially, and that the temperature as read by the thermocouple be that of the liquid alloy.

At the beginning of the experiments, the temperatures of the magnesium and alloy chambers, as read by thermocouples inside the thermocouple wells, were compared with a second set of thermocouples inserted into the melt directly.

As a result of these experiments, the shape and size of the graphite boats for the alloys and that of the magnesium chamber were established. It was also observed that, as long as the temperature difference between the hot and cold ends of the alloy chamber was less than 120° C and above a minimum of 750° C, the temperature as recorded by thermocouples in the wells agreed with the temperature inside the melt within $\pm 0.5°$ C.

(b) Alloy Analysis

Alloy analysis indicated an accuracy of $\pm 0.5\%$ by weight of magnesium. This resulted in an error of ± 1 mole% Mg in the lowest magnesium concentrations and ± 0.2 mole% Mg in the highest magnesium concentrations.

In most cases, each magnesium chamber was used for one experiment and occasionally for two experiments. At the end of the run, magnesium in the chamber was analyzed for tin content, which was found to be negligible.

(c) Quenching

Care is taken to quench the magnesium chamber faster than the rest of the tube. If the magnesium pressure is high during quenching, magnesium would condense on the relatively colder reaction tube than in the alloy. If the alloy pressure is high, magnesium would also condense on the tube. At no time was a condensate in evidence. It is considered that this effect, if any, was of a negligible proportion.

(d) Equilibrium

It would be expected that the time taken to reach equilibrium would be longest for an alloy of high magnesium content at the lowest magnesium pressure. Once the time required for such an alloy to come to equilibrium is established, all other alloys can safely be assumed to reach equilibrium in this time.

Experiments were conducted at low pressures for different periods of time, between 48 and 72 hours, and they showed similar results within the experimental error. In one experiment, instead of using pure tin in the alloy chambers, alternate samples were mixed with magnesium such that the equilibrium was approached from opposite sides in alternate cases, and results were within the accepted error. The various experimental points plotted on the log P vs. $1/T$ curves were obtained from different experiments, and all fell on a straight line within the experimental error, indicating that the equilibrium had been established. All experiments were conducted for 2 days or more.

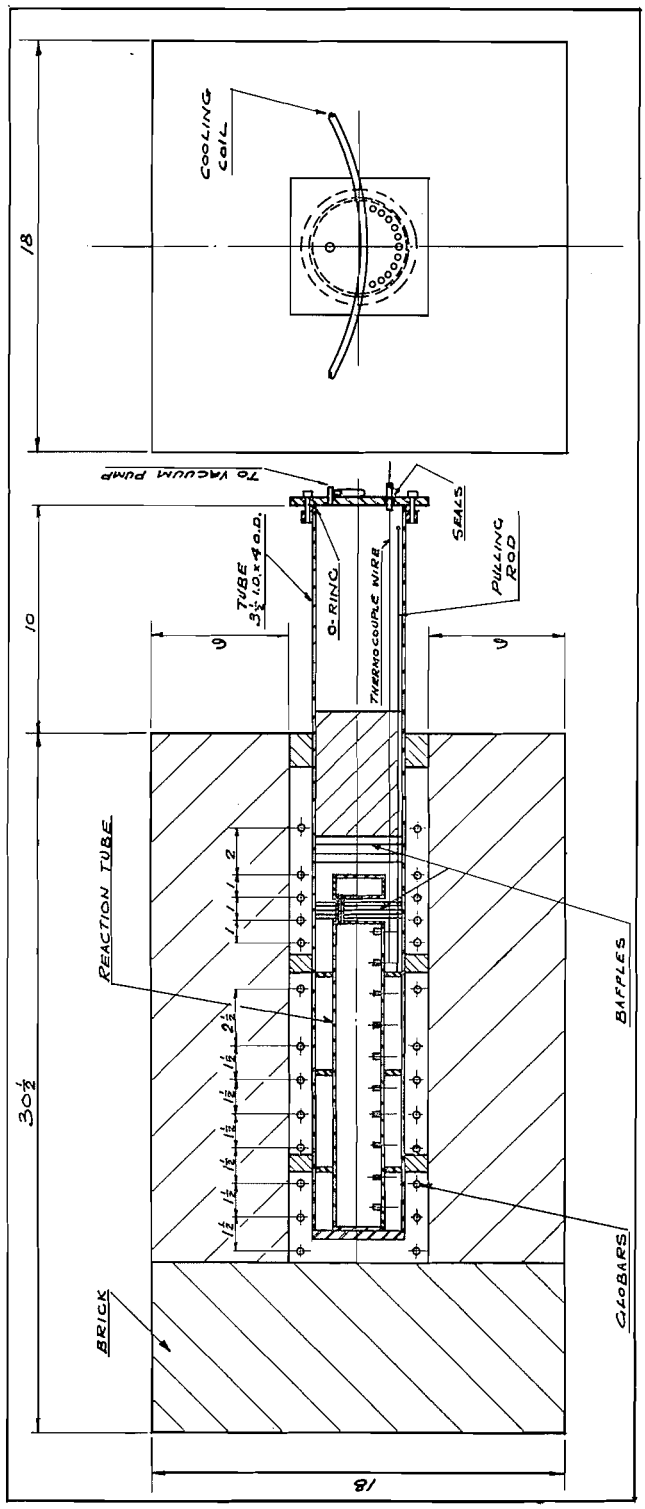

FIG. 1. Furnace and assembly (dimensions are in inches).

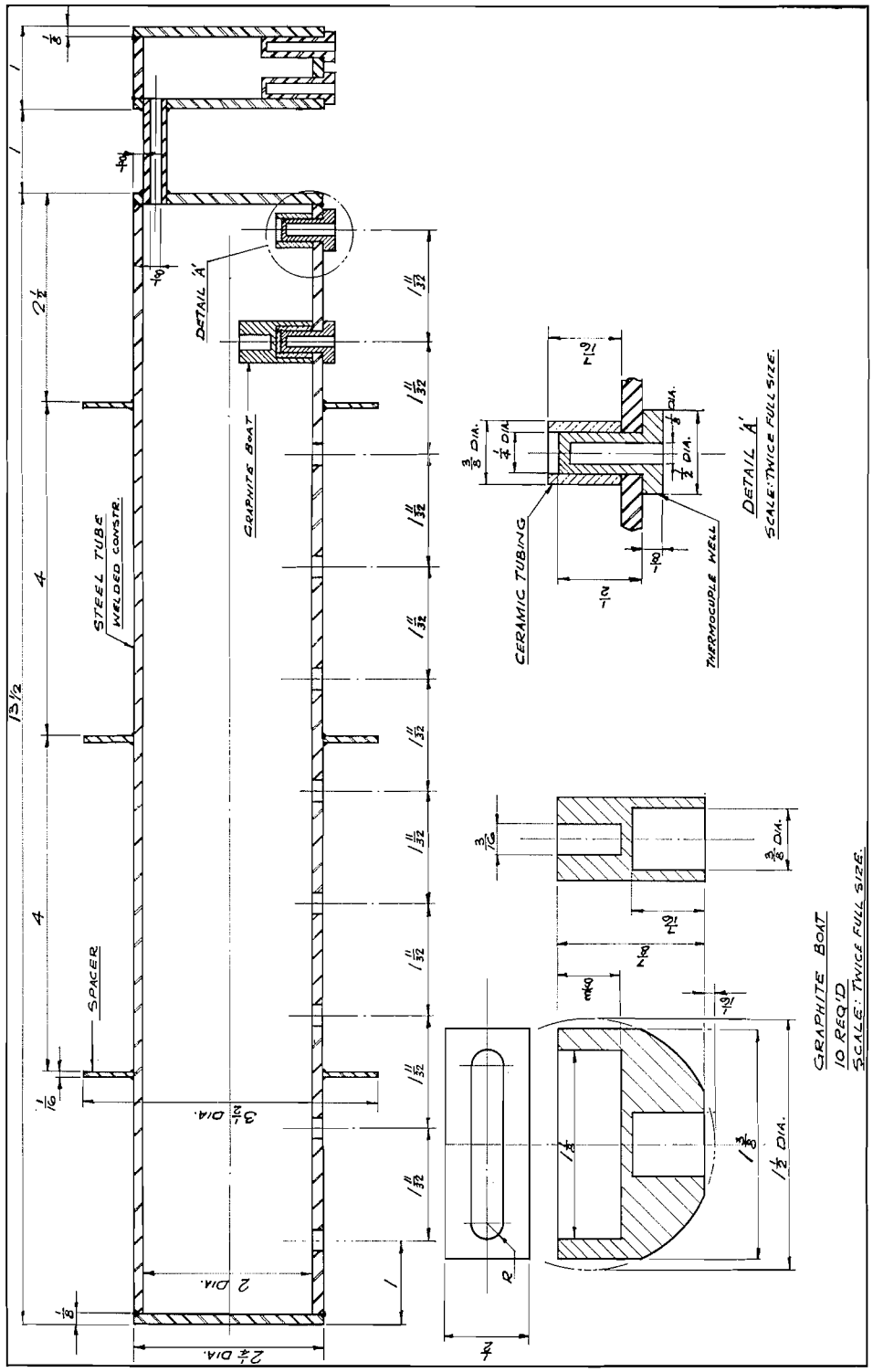

FIG. 2. Reaction tube (dimensions are in inches).

EXPERIMENTAL RESULTS AND DISCUSSION

For the calculation of the vapor pressure of liquid magnesium, the data of Kubaschewski (1) were employed; the vapor pressures are given by the formula

$$[1] \qquad \log P_{Mg}\ (\text{mm Hg}) = -7550/T - 1.41 \log T + 12.79.$$

The magnesium content of the tin–magnesium alloys was measured as a function of temperature at various pressures of magnesium. The experimental results are shown in Table I.

At the pressures used, it was only possible to obtain a variation in composition ranging from about 0.9 N_{Mg} to 0.3 N_{Mg}. In order to measure the activities at 910° C below this limit, the temperature gradient between the hot and the cold ends of the reaction tube would have to be about 300° C, well above the 120° C limit of the apparatus. Hence, activities below 0.3 N_{Mg} were not obtained.

(1) Magnesium Pressure Over the Alloys

From the results obtained, log P vs. $1/T$ curves were plotted for different compositions of Sn–Mg alloys, as shown in Fig. 3.

The magnesium pressures of these alloys are expressed in the form

$$[2] \qquad \log P_{Mg} = -A/T + B,$$

where the pressures are expressed in atmospheres and the temperature in degrees absolute. The vapor pressures of magnesium given in equation [1] are also expressed in this form for the same temperature range. The values obtained for the constants A and B are shown in Table II.

(2) Activities of Magnesium

The activities of magnesium at three temperatures, i.e., 880° C, 910° C, and 940° C, were calculated from the experimental data and shown in Fig. 4. The curve is extrapolated below 0.3 N_{Mg}. The α function of magnesium is expressed by the following formula:

$$[3] \qquad \alpha_i = \frac{\ln \gamma_i}{(1-N_i)^2},$$

where γ_i is the activity coefficient of component i and N_i is the mole fraction of the same component. The α function of magnesium is plotted against N_{Sn}, and the linear segment thus obtained from 0.7 N_{Sn} to 0.3 N_{Sn} is extrapolated to higher concentrations of tin. The calculated activities of magnesium from the α function gave added confidence to the extrapolation of the activity curve.

P_{Mg} values at low concentrations of magnesium were calculated from the activities thus obtained at the three temperatures. From plots of P_{Mg} vs. $1/T$ the values of the constants A and B in equation [2] were calculated and are shown in Table II.

(3) Activities of Tin

The activities of tin at the three temperatures 880° C, 910° C, and 940° C are calculated by the graphical integration of Gibbs–Duhem equation,

$$[4] \qquad \ln \gamma_{Sn} = \int_{N_{Sn}=1}^{N_{Sn}} \frac{N_{Mg}}{N_{Sn}}\, d \ln \gamma_{Mg}.$$

TABLE I

Composition of the Sn–Mg alloy at various temperatures and vapor pressures of Mg

Magnesium pressure in mm of Hg:															
209.8		111.1		79.25		66.05		39.6		26.31		25.58		16.05	
t, °C	N_{Mg}	t, °C	N_{Mg}	t, °C	N_{Mg}	t, °C	N_{Mg}	t, °C	N_{Mg}	t, °C	N_{Mg}	t, °C	N_{Mg}	t, °C	N_{Mg}
973	0.892	912	0.890	886	0.845	875	0.793	837	0.787	820	0.715	811	0.730	770	0.763
975	0.850	914	0.849	903	0.720	887	0.711	848	0.730	840	0.630	824	0.68	781	0.717
977	0.841	924	0.768	918	0.641	913	0.595	868	0.671	863	0.550	837	0.611	796	0.660
978	0.801	933	0.741	936	0.55	931	0.499	888	0.560	881	0.485	853	0.561	814	0.595
990	0.711	959	0.587	955	0.475	950	0.420	908	0.480	901	0.410	874	0.488	834	0.511
1,005	0.642	968	0.540	980	0.42	966	0.375	927	0.444			890	0.445	852	0.476
1,014	0.562	984	0.501	1,001	0.34	983	0.33					909	0.375	869	0.421
		1,015	0.401			1,000	0.31					928	0.329	888	0.370

TABLE II

Magnesium pressures (in atmospheres) expressed by $\log P_{Mg} = -A/T+B$ of various alloy compositions, and partial heats and entropies of solution per gram atom of Mg

N_{Mg}	Phase	A	B	Temp. range, °C	$\Delta\bar{H}_{Mg}$, cal	$\Delta\bar{S}_{Mg}$, cal	$\Delta\bar{F}_{Mg}$* at 910° C, cal	$\Delta\bar{F}_{Mg}$† at 910° C, cal
0.9	Liq.	6,760	4.875	1,020–750	+412	+0.476	−151	−164
0.8	Liq.	6,940	4.980	1,011–766	−412	−0.0045	−407	−445
0.7	Liq.	7,190	5.120	992–784	−1,556	−0.645	−793	−803
0.6	Liq.	7,750	5.472	1,011–811	−4,118	−2.256	−1,450	−1,463
0.5	Liq.	8,160	6.05	1,029–838	−8,053	−4.901	−2,255	−2,274
0.4	Liq.	9,380	6.475	1,012–876	−11,577	−6.845	−3,480	−3,492
0.3	Liq.	10,950	7.50	1,019–920	−18,761	−11.536	−5,114	−5,118
0.2	Liq.	12,570	8.461	910–880	−26,174	−15.93	−7,326	−7,354
0.1	Liq.	14,800	9.73	910–880	−36,379	−21.74	−10,661	−10,712
Pure Mg	Liq.	6,850	4.979	910–880				

NOTE: The A and B values are obtained from equations $\Delta\bar{H}_{Mg} = 4.576\ (A°-A)$ and $\Delta\bar{S}_{Mg} = 4.576\ (B°-B)$, where $A°$ and $B°$ correspond to pure magnesium.
*$\Delta\bar{F}_{Mg} = \Delta_M\bar{H}_R - T\Delta\bar{S}_{Mg}$.
†$\Delta\bar{F}_{Mg} = RT \ln a_{Mg}$.

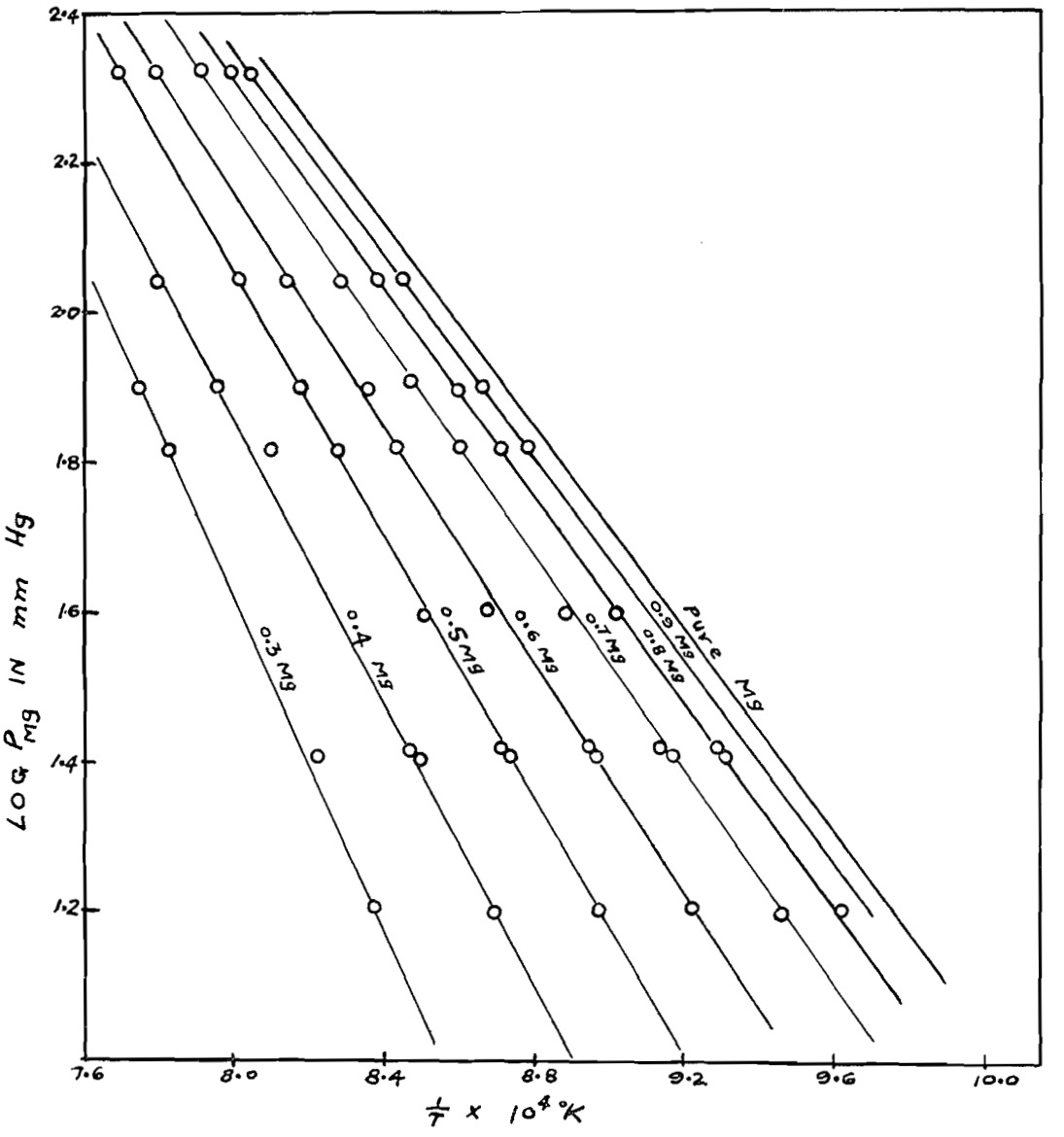

FIG. 3. Log P_{Mg} vs. $1/T$ magnesium–tin alloys.

The results obtained are shown in Fig. 4.

It can be seen from Fig. 4 that, for the most part, the activity curve of magnesium has a negative deviation from ideality, as can be expected in a system exhibiting intermetallic compounds. (The magnesium–tin system has an intermetallic compound, Mg_2Sn.) A negative departure is associated with a tendency for one atom to group with the other type, and a positive departure indicates a tendency for each type of atom to group with similar atoms. If this reasoning is pursued in the present case, it must be concluded that such tendencies change with the composition, since a positive departure exists above 0.7 N_{Mg}.

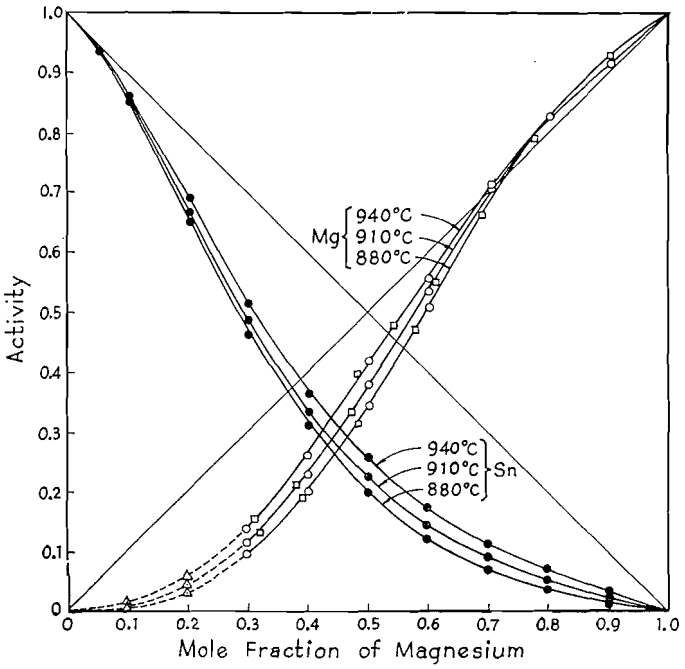

FIG. 4. Activity vs. mole fraction of magnesium: □, experimental data; ○, interpolated from Fig. 3; △, extrapolated from plot of α function; ●, calculated from tables.

It is of interest to note that the composition at which the deviation changes from positive to negative occurs at about the composition of the intermetallic compound Mg_2Sn.

Unlike magnesium, the activities of tin are negative throughout the composition range. The activity measurements of the magnesium–tin system were carried out by Schneider and Esch (2) using boiling point methods. In the range 93.9–66.7 mole% of magnesium at 1100° C, it was found to behave ideally. As can be seen from the present work, the activities of magnesium are approaching ideality in this range of composition. It can also be seen that the curves approach ideality at the higher temperatures. The maximum deviation from ideality in this range, even at 910° C, is of the order of 0.2 N_{Mg}. These observations of Schneider and Esch corroborate the present work.

(4) Partial Molal Properties

From the values of the constants A and B shown in Table II, it can be shown that

$$\Delta\bar{H}_{Mg} = 4.576\ (A^\circ - A) \quad [5]$$

$$\Delta\bar{S}_{Mg} = 4.576\ (B^\circ - B), \quad [6]$$

where A° and B° refer to pure magnesium and A and B refer to different alloys. The partial free energies are calculated from the activities of magnesium from the formula

$$\Delta\bar{F}_{Mg} = RT \ln a_{Mg}. \quad [7]$$

The values of the three partial molal quantities thus obtained at 910° C are shown in Table II.

(5) Integral Quantities

The integral quantities can be calculated from the partial quantities by the graphical

TABLE III

Heats, free energies, and entropies of formation of magnesium–tin alloys at 910° C

N_{Mg}	(1) ΔF^M, kcal	(2) ΔH^M, kcal	(3) ΔH^M, kcal	(4) ΔS^M, e.u.	(5) ΔS^M, e.u.	(6) ΔF^{id}, kcal	(7) ΔS^{id}, e.u.	(8) ΔS^{Ex}, e.u.
0.9	−0.95	−2.38		−1.2	−1.32	−0.27	+0.23	−1.43
0.8	−1.64	−4.9	−2.75	−2.75	−2.87	−1.17	+0.99	−3.74
0.7	−2.18	−7.06	−3.25	−4.12	−4.25	−1.43	+1.21	−5.33
0.6	−2.75	−8.6	−3.40	−4.94	−5.22	−1.58	+1.33	−6.27
0.5	−2.79	−9.28	−3.25	−5.48	−5.65	−1.62	+1.37	−6.85
0.4	−2.78	−9.13	−2.65	−5.36	−5.47	−1.58	+1.33	−6.69
0.3	−2.56	−8.0	−2.00	−4.59	−5.28	−1.43	+1.21	−5.8
0.2	−1.47	−6.6		−4.33	−4.12	−1.17	+0.99	−5.32
0.1	−1.18	−3.37		−1.85	−2.2	−0.27	+0.23	−2.08

NOTE: (1) Obtained from graphical integration of $\Delta F = N_{Sn} \int_0^{N_{Mg}} \bar{F}_{Mg} d(N_{Mg}/N_{Sn})$.

(2) Obtained by graphical integration of $\Delta H = N_{Sn} \int_0^{N_{Mg}} \bar{H}_{Mg} d(N_{Mg}/N_{Sn})$.

(3) Results of Kawakami (38) at 880° C.

(4) Obtained from the equation $\Delta F = \Delta H - T\Delta S$.

(5) Obtained by graphical integration of $\Delta S = N_{Sn} \int_0^{N_{Mg}} \Delta\bar{S}_{Mg} d(N_{Mg}/N_{Sn})$.

(6) Obtained from the equation $\Delta F_{ideal} = RT(N_1 \ln N_1 + N_2 \ln N_2)$.

(7) Obtained from the equation $\Delta S_{ideal} = -R\,(N_1 \ln N_1 + N_2 \ln N_2)$.

(8) Obtained from the equation $\Delta S^M = \Delta S^{id}_{ideal} + \Delta S^{Ex}_{excess}$.

integration of the Duhem–Margules equation. For a two component system, the integral quantities can be expressed as

$$[8] \qquad \Delta X^{M} = N_B \int_0^{N_A} \Delta \bar{X}_A d\frac{N_A}{N_B},$$

where ΔX^{M} may be the heat, entropy, or free energy of formation.

Each of the three integral quantities are obtained by graphical integration of the above equation.

The integral values thus obtained are shown in Table III, along with the ideal entropies and free energies of mixing.

The ideal entropies and free energies are expressed by the equation

$$\Delta S^{id} = -R(N_1 \ln N_1 + N_2 \ln N_2),$$

$$\Delta F^{id} = RT(N_1 \ln N_1 + N_2 \ln N_2).$$

The values of excess entropies are also tabulated in Table III, obtained from the equation

$$\Delta S^{M} = \Delta S^{id} + \Delta S^{Ex}.$$

From the results obtained, it can be seen that the magnesium–tin system does not behave as a regular solution. It may be said that the magnitude of the integral quantities thus obtained indicates that the liquid magnesium–tin alloy forms non-ideal solutions and that some degree of order is present.

It is of interest to note here that Boltaks (3) concluded from electrical and magnetic studies of Mg_2Sn that the bonding must be a mixture of metallic and polar types.

(6) Comparison of Heats of Formation with Literature Values

Heats of formation of liquid Mg–Sn system at 800° C were obtained by Kawakami (4) by direct combination of the constituent metals at various compositions in a calorimeter. His results are shown in Table III. It can be seen that his results are less negative than those obtained in the present work. The heat of formation of solid Mg_2Sn is given by Kubaschewski (5) as -6100 ± 400 cal/g-atom at 20° C. Biltz and Holverschiet (6) also measured the heat of formation of solid Mg_2Sn at 20° C calorimetrically from the heats of solution in HCl $FeCl_3$/aq., and reported a value of $-20{,}000$ cal/g-atom. Kawakami's results give a value of -3.3 kcal for the formation of liquid Mg_2Sn at 800° C. From the values of Kubaschewski for the heat of formation of solid Mg_2Sn and that of Kawakami for liquid Mg_2Sn, the value of heat of transformation of solid Mg_2Sn to liquid Mg_2Sn at 800° C can be calculated to be $+2.6$ kcal.

Using Biltz's results, a heat of formation of liquid Mg_2Sn of -17.4 kcal is found. The present work shows a value of -7.5 kcal for the heat of formation of liquid Mg_2Sn at 910° C. Thus, the present value lies between that of Kawakami and Biltz.

It is estimated that the ΔF_{Mg} values are correct to about ± 100 cal at low concentrations of magnesium to ± 50 cal at high concentrations. ΔH_{Mg} values are correct to ± 600 cal at low concentrations of magnesium to ± 100 calories at high concentrations. The error in ΔS_{Mg} values is of the order of ± 0.5 to ± 0.05 cal/deg mole.

ACKNOWLEDGMENT

The authors gratefully acknowledge financial support from the Advisory Committee on Scientific Research of the University of Toronto.

REFERENCES

1. O. KUBASCHEWSKI and E. LL. EVANS. Metallurgical thermochemistry. Pergamon Press. 1955. p. 326.
2. A. SCHNEIDER and E. K. STOLL. Z. Elektrochem. **47**, 519 (1941).
3. B. I. BOLTAKS. Zhur. Tekh. Fiz. **20**, 180 (1950).
4. M. KAWAKAMI. Sci. Repts. Tôhoku Imp. Univ. First Ser. **192**, 521 (1930).
5. O. KUBASCHEWSKI and CATTERALL. Thermochemical data of alloys. Pergamon Press, London. Sp. 32.
6. W. BILTZ and F. MAYER. Z. anorg. aveg. chem. **176**, 23 (1928).
7. P. HERASYMENKO. Acta Met. **4**, 1 (1956).

OXYGEN EVOLUTION FROM SODIUM HYPOCHLORITE SOLUTIONS

M. W. LISTER
Department of Chemistry, University of Toronto, Toronto, Ontario

AND

R. C. PETTERSON[1]
Research Department, Purex Corporation Ltd., South Gate, Calif., U.S.A.

Received September 21, 1961

ABSTRACT

The rates of oxygen evolution from carefully purified solutions of sodium hypochlorite have been measured. Methods of purification are described, and it is found that substantially the same rate is observed regardless of the method of purification. The rate of oxygen evolution is proportional to the square of the concentration of hypochlorite ions. The effect of temperature and ionic strength are examined. The rate constant is 7.5×10^{-6} $(\text{g-mol/l.})^{-1}(\text{min})^{-1}$ at 60° C and an ionic strength of 3.5; the activation energy is 26.6 kcal/g-mol. These results are compared with the corresponding quantities for the reaction of hypochlorite ions to form chlorite and chloride ions, and some tentative explanations are offered.

In an earlier paper (1), one of the present authors examined the decomposition of aqueous sodium hypochlorite solutions, particularly the rate of decomposition to sodium chlorate and chloride. The accompanying reaction giving sodium chloride and oxygen was examined more superficially. Rates of oxygen evolution were observed on a number of solutions at that time, but it was never proved that the oxygen evolution could not be ascribed to the presence of traces of catalyst. The reasons for this uncertainty were as follows. Firstly, measurements on the catalyzed reaction (2) showed that the observed rates could be accounted for by the presence of copper in concentrations of the order of a μg/l. Secondly, the rates were somewhat variable. Thirdly, it was found that the observed rates were roughly proportional to the concentration of hypochlorite, and it is difficult to suggest a simple first-order mechanism for the uncatalyzed reaction. However, relatively low orders of dependence on hypochlorite concentration are observed for the catalyzed reaction, which suggests that these earlier solutions contained traces of catalyst. Finally, and perhaps the most convincing reason for believing some catalyst to be present, it was found that the apparent activation energy for oxygen evolution was 21 kcal/g-mol, less than the 24.8 kcal/g-mol found for the reaction giving chlorate and chloride; yet the latter is the predominant reaction.

Other workers have also examined this decomposition, though they usually did not separate the rates of the two reactions. Giordani (3) found a second-order gas evolution; but his conclusions about the reaction to chlorate had not been confirmed, so it seemed worth while to investigate the reaction in more detail.

EXPERIMENTAL PART

The main problem was to obtain sodium hypochlorite free from traces of catalyst. At present only cobalt, nickel, and copper are known to catalyze this decomposition, so that the methods of purification were directed towards the removal or complexing of these metals. It seemed much more promising to purify the sodium hypochlorite solution as opposed to the chlorine and sodium hydroxide solution from which it was made. The following general methods of purification, or at least of removal of catalyst, were employed:

(1) precipitation of a compound in the solution in the hope that any catalyst would coprecipitate with it;

[1]*Present address: Department of Chemistry, Massachusetts Institute of Technology, Cambridge, Mass., U.S.A.*

(2) deactivation of the catalyst by means of a complexing agent;
(3) a combination of these methods, by precipitation of sodium periodate.
The details of the methods were as follows:

(1) Coprecipitation.—It was already known that precipitation of calcium carbonate in a sodium hypochlorite solution would carry down a considerable fraction of any copper, nickel, or cobalt present. In a typical run, 10 ml of 1.0 *M* sodium carbonate solution was added to about 1 liter of sodium hypochlorite solution, and an equivalent amount of calcium chloride solution was then added slowly with vigorous stirring. After standing of the solution for a short time, the precipitate was filtered off on a sintered-glass filter. In many runs this procedure was repeated, usually five times in all. Other precipitates were examined: magnesium hydroxide, lanthanum hydroxide, calcium fluoride, and barium sulphate. In each case the metal ion (i.e. barium, etc.) was added last. The amounts used were much the same as described above for calcium carbonate; i.e. 10 ml of 1.0 *M* solution of the metal being precipitated was added to 1 liter of sodium hypochlorite. Magnesium and lanthanum hydroxides were chosen because they might be similar to the chemical form of the catalytic metals; calcium fluoride and barium sulphate because they are very insoluble salts of fairly simple structure. In fact, magnesium hydroxide and lanthanum hydroxide were fairly efficient, but none of them was superior to calcium carbonate.

(2) Complexing agents.—A number of organic complexing agents were examined, the substances chosen all having the stability constant for the copper (II) complex greater than 10^4, and having chemical structures which would not be too easily attacked by hypochlorite ions. The complexing agents were tested by adding about 4 g to 1 liter of sodium hypochlorite. As it turned out, few resisted attack by the sodium hypochlorite for long, particularly if the solution was not very alkaline. Most of these compounds generate acid on oxidation, and as the pH fell the rate of gas evolution rose. Sulphosalicyclic acid acted as a moderately efficient complexing agent as long as the solution was alkaline. O-Phenanthroline behaved similarly. Salicyclic acid, ethylenediaminetetraacetic acid, acetylacetone, and 8-hydroxyquinoline were tested, but found to be useless. Consequently none of these provide a satisfactory method of purifying the solution.

(3) Precipitation of sodium periodate.—Since periodate ions form stable complex salts with copper, nickel, and cobalt, and since sodium periodate is relatively insoluble, the following method of purification was tried. Sodium iodate solution (containing some sodium hydroxide) was added to the sodium hypochlorite solution. This was then rapidly warmed to 80° C, when sodium periodate precipitated. The solution was cooled and filtered. This procedure could be repeated for more efficient purification. It was found that the solutions so treated gave relatively low rates of gas evolution, showing that this was an effective method. In a typical run 10 ml of 0.25 *M* sodium iodate was added to about 1 liter of approximately 1.5 *M* sodium hypochlorite, to which had been added enough sodium hydroxide to replace that used up in the precipitation of sodium periodate, $Na_2H_3IO_6$. The solution was heated, cooled, and filtered, as described above. This was done five times in all; however, the sodium hydroxide was only added once, but in sufficient quantity to keep the solution alkaline throughout.

Measurement of Oxygen Evolution

The rates of evolution of gas were measured simply by keeping a weighed amount (about 900 ml) of the solution at constant temperature, and measuring the rate of evolution of gas in a gas burette. This held up to 50 ml, and could be read to 0.05 ml. In calculating the rate of oxygen evolution, it was assumed that the gas was always saturated with water vapor at the temperature of the water jacket of the gas burette. The concentration of sodium hypochlorite was found at intervals by analysis of samples, and the initial solutions were completely analyzed so that the ionic strength could be computed. The methods of analysis were the same as those given in an earlier paper (4). The solution was stirred throughout the run, and no readings of gas volume were used in the calculations until the gas had been found to be coming off at a constant rate. The solutions had been largely freed of dissolved gas during the filtrations, and oxygen must build up to a certain degree of supersaturation before a steady rate is reached. This took a surprisingly long time, usually several hours, or even a day at lower temperatures. This initial retention of oxygen in the solution can lead to results which make the oxygen evolution appear to be first order, at least approximately, since the gas rate is lower than it should be in the early part of a run when the concentration of hypochlorite ions is high.

The results are given in Tables I and II. The results are presented in the form of the calculated rate constants. The second-order rate constant is obtained from the equation

$$d[O_2]/dt = 1/2K_0[OCl^-]^2$$

and the first-order constant from

$$d[O_2]/dt = 1/2K_0^*[OCl^-].$$

The factor of one half arises, as two hypochlorite ions produce one oxygen molecule. It is evident from an examination of Table I that the second-order rate constant stays constant, while the first-order does not. The rate constants quoted in Tables I and II are slightly approximate since it is impossible to obtain, in practice, an instantaneous value of the rate of gas evolution. The oxygen must be collected over a period

TABLE I

Runs at 60° C and ionic strength about 3.5

Run	Mean [ClO^-], g-mol/l.	[NaOH], g-mol/l.	Purified by	$K_0 \times 10^6$ (2nd order), $(g\text{-}mol/l.)^{-1}min^{-1}$	$K_0^* \times 10^6$ (1st order), min^{-1}
1	1.430	0.051	$CaCO_3$	7.70	11.01
2	1.427	0.072	"	8.16	11.61
3	1.344	0.036	"	7.76	10.43
4	1.365	0.041	"	7.79	11.44
5	1.102	0.029	"	7.12	7.85
6	0.972	0.031	"	7.39	7.18
7	1.285	0.040	"	7.14	9.17
8	1.265	0.020	"	7.22	9.13
9	1.426	0.024	"	7.71	10.99
10	1.548	0.109	$Mg(OH)_2$	7.27	11.25
	1.478			7.81	11.54
	1.164			7.67	8.93
11	1.471	0.044	$La(OH)_3$	7.21	10.61
12	1.309	0.030	"	8.01	10.49
13	1.353	0.040	$Na_2H_3IO_6$	7.25	9.81
14	1.450	0.024	CaF_2	7.35	10.66
15	1.042	0.057	$Na_2H_3IO_6$	7.35	7.66
	0.946			7.90	7.47
16	1.153	0.008	$Na_2H_3IO_6$	8.04	9.27
17	1.168		$CaCO_3$	7.68	8.97
	1.006			8.23	8.27
	0.837			7.88	6.60
	0.702			7.74	5.43
	0.529			8.43	4.46
	0.484			8.33	4.03
18	1.221		$CaCO_3$	7.85	9.58
	0.819			7.61	6.23
	0.694			7.96	5.52
	0.657			7.96	5.23

TABLE II

(All solutions purified by calcium carbonate treatment)

Run	Temp., °C	Ionic strength	Mean [ClO^-], g-mol/l.	$K_0^* \times 10^6$ (2nd order), $(g\text{-}mol/l.)^{-1}min^{-1}$
19	50	3.5	1.149	2.19
			1.054	2.18
			0.985	2.23
			0.918	2.34
			0.860	2.37
20	50	"	1.068	2.21
			1.000	2.21
			0.930	2.25
			0.873	2.38
21	40	"	0.812	0.635
			0.784	0.631
22	40	"	0.825	0.609
			0.796	0.593
23	40	"	1.123	0.671
			1.088	0.621
			1.074	0.644
			1.047	0.672
24	40	"	1.122	0.670
			1.061	0.747
			1.031	0.596
25	40	"	1.395	0.645
			1.281	0.637
			1.233	0.621
			1.184	0.655

TABLE II (*Concluded*)

Run	Temp., °C	Ionic strength	Mean [ClO⁻], g-mol/l.	$K_0^* \times 10^6$ (2nd order), (g-mol/l.)$^{-1}$min^{-1}
26	40	3.5	1.448	0.725
			1.324	0.675
			1.266	0.669
			1.215	0.687
27	60	1.8	0.695	4.01
28	60	1.8	0.713	4.97
29	60	1.8	0.720	4.28
30	60	1.8	0.651	4.32
31	60	2.7	0.996	5.86
			0.849	6.35
			0.743	6.44
32	60	2.7	0.992	6.04
			0.846	6.13
			0.736	6.47
33	60	0.9	0.351	6.15
			0.333	4.55
			0.315	5.16
34	60	0.9	0.345	6.41
			0.333	4.65
			0.325	5.45
			0.309	6.29
35	40	1.8	0.623	0.255
36	40	1.8	0.633	0.260
37	50	1.8	0.565	1.07
38	50	1.8	0.576	1.04

of time so that an average rate is obtained. The concentration of hypochlorite used in the calculation was obtained by plotting $[ClO^-]^{-1}$ against time, which gives a linear plot, and by using the value of $[ClO^-]^{-1}$ at the midpoint of the period of gas collection. It follows from the rate equations that the approximate value of K_0 (2nd order) is related to the true value by the equation

$$K_0(\text{approx.}) = K_0.\frac{[1+(3K_1/4+K_0/2)X_0t]^2}{[1+2(3K_1/4+K_0/2)X_0t]},$$

where t is the time interval during which gas was collected, K_1 is the rate constant of the reaction giving sodium chlorate, and X_0 is the initial concentration of hypochlorite ions. In no run did this approximation cause an error of more than 0.07%.

DISCUSSION OF RESULTS

The first point to note from Table I, as mentioned above, is that gas evolution from carefully purified sodium hypochlorite is in fact second order in hypochlorite ions. The method of purification is indicated in Table I, and purification by calcium carbonate or by sodium periodate precipitation gave the same result. The average value of K_0 at 60° C and 3.5 ionic strength is 7.5×10^{-6} (g-mol/l.)$^{-1}$min^{-1}. The concentrations of sodium hydroxide are given in Table I. These varied from about 0.1 M to 0.01 M, and within these limits there is no drift of rate with hydroxide ion concentration. This indicates that the reaction is one of hypochlorite ions, and not hypochlorous acid.

Measurements were made at other ionic strengths and other temperatures and these are given in Table II. The effect of ionic strength is as would be expected: it causes little change in K_0 at low ionic strengths, but a rise at high ionic strengths. A plot of log K_0 against $1/T$ is reasonably linear, and gives an activation energy of 26.6 kcal/g-mol at an ionic strength of 3.5. A slightly higher value is obtained at lower ionic strengths. This value (26.6 kcal) is larger than the activation energy of 24.8 kcal/g-mol found for the reaction

$$2ClO^- \rightarrow ClO_2^- + Cl^-.$$

If K_1 is the rate constant of this reaction, then

$$K_1 = 1.76 \times 10^{12} e^{-24,800/RT},$$
$$K_0 = 2.10 \times 10^{12} e^{-26,600/RT}, \text{ time in minutes.}$$

This is equivalent to saying that the entropy of activation of the two reactions is much the same (for K_0, $\Delta S^{\ddagger} = -12.5$ cal/deg, and for K_1, $\Delta S^{\ddagger} = -12.8$ cal/deg). This presumably indicates that the activated complex for the two reactions is somewhat the same sort of species in both cases: one might speculate that it consists of two ions close together but differently oriented; i.e.

[1] reaction to chlorite: $O^-—Cl—O^-—Cl$

[2] reaction to oxygen: $Cl—O^-—O^-—Cl$.

If the negative charge on the hypochlorite ion resides chiefly on the oxygen atom, this would make the second species less stable, as is required by experiment; in fact a simple model like this could account for a much larger difference in activation energy than is observed.

Another possibility is that the activated complex might have a cyclic structure and

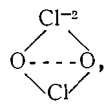

this in fact could be the intermediate for either reaction. This would imply that the very small difference in the entropies of activation was due to experimental error. However, a compact structure like this seems less probable than one in which the atoms have not had to come so close together.

Some tentative calculations were also made on the relative energies of $OClOCl^{-2}$ and $ClOOCl^{-2}$ as intermediates. If it is assumed that the four electrons that previously formed the bonds in the two ions have become delocalized in σ-bonds extending over all four atoms, then application of Hückel's molecular orbital method (5) makes $OClOCl^{-2}$ more stable than $ClOOCl^{-2}$: the difference, using plausible values for the electronegativities of the atoms, is 0.35β. This difference will be offset to some extent by the greater proximity of the larger effective nuclear charges on the chlorines in $OClOCl^{-2}$. This conclusion is not dependent on the exact choice of values for the electronegativities, and hence for the Coulomb integrals for these atoms; provided chlorine and oxygen are different in this respect, $OClOCl^{-2}$ will be more stable. Consequently, if this picture of the activated intermediate state is correct, it explains the preferential formation of chlorite and chloride ions, as opposed to chloride ions and oxygen.

REFERENCES

1. M. W. Lister. Can. J. Chem. **34**, 465 (1956).
2. M. W. Lister. Can. J. Chem. **34**, 479 (1956).
3. F. Giordani. Gazz. chim. ital. **54**, 844 (1924).
4. M. W. Lister. Can. J. Chem. **30**, 879 (1952).
5. E. Hückel. Z. Physik, **70**, 204 (1931).

HEATS OF DILUTION OF POLYISOBUTYLENE SOLUTIONS

M. SENEZ[1] AND H. DAOUST
Department of Chemistry, University of Montreal, Montreal, Que.

Received December 18, 1961

ABSTRACT

The measurements of heats of dilution of polyisobutylene solutions in benzene, toluene, and chlorobenzene have been carried out with a Tian–Calvet microcalorimeter at 25° C. The dilution technique previously described has been improved and the extrapolated enthalpy parameter κ_1^* for each system has been corrected for the excluded volume effect using the Krigbaum–Carpenter–Kaneko–Roig formulation for the second virial coefficient A_2. No detectable variation in κ_1^* was found for high molecular weights ($\geqslant$43,000); but a definite increase in κ_1^* was found for very low molecular weights.

INTRODUCTION

In a preceding paper (1), a comparative study was made of the different treatments dealing with the effect of polymer–solvent interaction on viscosity. In this paper, statistical thermodynamic theory will be applied to calorimetric data of heats of dilution of the same systems.

It is now well known that lattice theories of polymer solutions fail to represent the behavior of thermodynamic functions, particularly for dilute solutions, where, contrary to experiment, they predict the chemical potential of the solvent to be practically independent of molecular weight; the necessary microscopic discontinuity of polymer concentration at high dilution is, of course, primarily responsible for this. The agreement is also not perfect in the case of concentrated solutions due to the inadequacy of a rigid lattice as a model for polymer solution theory.

Flory (2) was the first to propose a statistical mechanical calculation for the variation of the second virial coefficient A_2 with molecular weight, while Zimm (3), using the molecular distribution function formalism and Gaussian statistics for the configuration of a single chain, was able to calculate the molecular weight dependent double contact term in the expansion of the integral for A_2. Calculations of the higher-order contact terms of the series, taking into account the departure from purely Gaussian statistics, have been attempted (4, 5), and the results show that the series is slowly converging. Thus, several authors (6, 7) have tried to improve the original model of a uniform density equivalent sphere first used by Flory to represent the interacting molecules. Recently, a rather simple but ingenious theory was given by Krigbaum *et al.* (8) and was shown to predict very well the variation of A_2 with molecular weight.

Unfortunately, the calculation of the higher virial coefficients is not feasible. Fixman, in his recent theory (9), makes the parameters in the Gaussian potential of Flory and Krigbaum agree with the exact coefficient of the double contact term of A_2 and uses it to calculate the variation of osmotic pressure with concentration. This theory is certainly an improvement, but it is not in very good agreement with experiments (10), except with very good solvents. At present, it is rather difficult to predict the values of the thermodynamic functions except in infinitely dilute solutions. Also, it must not be forgotten that the theory is applicable only to high-polymer and not to short-chain solutions, although an important increase of the heat of dilution is observed in going from a high polymer to the dimer (see below).

[1]*Present address: Department of Chemistry, University of Manchester, Manchester, England.*

In this paper, we shall present our calorimetric data and show that the application of the new Krigbaum dilute solution theory gives results which are in good agreement with those of the intrinsic viscosity theory of Kurata and Yamakawa (5).

EXPERIMENTAL

The Tian–Calvet microcalorimeter and the dilution cell used have been previously described in the literature (11, 12). Originally, the partition cell was designed to have no vapor space and has been used accordingly as such at first. However, in this way the solution in the cell is stirred only in the bottom compartment and an important part of the heat of dilution is lost due to an incomplete dilution. To improve the mixing process, it is preferable to fill only half of the solution and solvent compartments. Since the variation of solvent activity is not rapid for polymer concentrations below 50%, the effect of vapor space is far less important than that of an incomplete dilution. The vapor pressure of the solvent above a high-polymer solution can be approximately calculated with the semiempirical Flory–Huggins equation

$$p_1/p_1^0 = \phi_1 \exp(\phi_2+\chi_1\phi_2^2), \qquad [1]$$

where p_1 and p_1^0 are the vapor pressures of the solvent above the solution and the pure solvent respectively, ϕ_1 and ϕ_2 are the volume fractions of solvent and polymer, and χ_1, an interaction parameter. The limits of the vapor phase correction, $\Delta H'$, are given by

$$K[(a_1'-1)V_U + (a_1'-a_1)V_L] < \Delta H' < K(1-a_1)V_L,$$

where $K = L_v^0 p_1^0/RT$, L_v^0 being the molar heat of vaporization of the pure solvent, V_U and V_L are the vapor phase volumes above the solvent and the solution respectively, and a_1 and a_1', the solvent activities before and after dilution. Since $V_U = V_L$ and $(a_1'-1) \cong -(a_1'-a_1)$, we have simply

$$0 < \Delta H' < K(1-a_1)V_L.$$

For example, in diluting a benzene solution from $\phi_2 = 0.4$ to 0.2, with $K = 0.042$ cal cm^{-3}, $V_L = 2$ cm^3, and $\chi_1 = 0.5$, we find $\Delta H' < 0.0006$ cal, whereas the heat of dilution is about 0.5 cal. Thus the vapor phase correction is not only small (for ϕ_2 below 0.5, of course) but also insensitive to the exact value of χ_1, so that it is necessary to have only a rough idea of the values of the solvent activities. That correction is evidently still smaller for less volatile solvents.

The heat of stirring is the most important correction, being of the order of 50% of the measured heat effect, but can be determined with surprising precision. Measurements were also performed using a stainless steel mesh cage, by a method previously described (13).

Materials

The polymer fractions used were obtained by a double fractional precipitation using the benzene–acetone pair at 25° C and originated from samples of "Vistanex" supplied by Enjay Co. Inc. Molecular weights were determined from viscosity measurements of their cyclohexane solutions.

The solvents used were reagent grade, which were distilled in a 30-theoretical-plate column and kept over "Drierite".

RESULTS AND DISCUSSION

If one assumes that the heat of dilution can be expressed as a power series of the volume fraction

$$\Delta\bar{H}_1 = RT\kappa_1^*\phi_2^2+RT\kappa_2^*\phi_2^3+\ldots, \qquad [2]$$

where the κ^*'s are the uncorrected enthalpy parameters for the chosen temperature (and molecular weight), then the integral heat of dilution is given by

$$\Delta H_d = (RTm_2\bar{v}_2/V_1)\,[\kappa_1^*(\phi_2-\phi_2')+\kappa_2^*(\phi_2^2-\phi_2'^2)/2+\ldots], \qquad [3]$$

where m_2 is the mass of polymer, $\bar{v}_2$ its specific volume, and V_1 the molar volume of the solvent. It is customary (12) to rewrite equation [3] and plot the results in terms of an apparent enthalpy parameter κ_a^* as a function of the average concentration $\bar{\phi}_2$:

$$\kappa_a^* = \Delta H_d V_1/RT\bar{v}_2 m_2(\phi_2-\phi_2') = \kappa_1^*+\kappa_2^*\bar{\phi}_2+\ldots. \qquad [4]$$

The third and higher coefficients of the power series in $\bar{\phi}_2$ are slightly higher than those defined in equation [2], the difference being greater the greater is $(\phi_2-\phi_2')$.

According to the dilute solution theory of Krigbaum *et al.* (8), the second virial coefficient can be given by the following equation:

$$A_2 = (\bar{v}_2/V_1)\psi_1(1-\theta/T)F(X,\rho), \qquad [5]$$

where ψ_1 and $\psi_1\theta/T$ are entropy and enthalpy parameters respectively. The factor $F(X,\rho)$ is related to the excluded volume effect, ρ^3 being the ratio of the number of long-range contacts to the total number of intramolecular contacts. It can be shown from equation [5] that κ_1^*, as actually extrapolated from heats of dilution measurements carried out at definite concentrations, is related to the real enthalpy parameter κ_1, by

$$\kappa_1^* = \kappa_1[F(X,\rho)+(T-\theta)(T/\theta)\partial F(X,\rho)/\partial T]. \qquad [6]$$

It can be seen from the results shown in Fig. 1 that, in concentrated solutions, κ_a^* is practically independent of molecular weight (if it is sufficiently large) in accordance with calorimetric measurements of heats of mixing on the same systems (14) and also

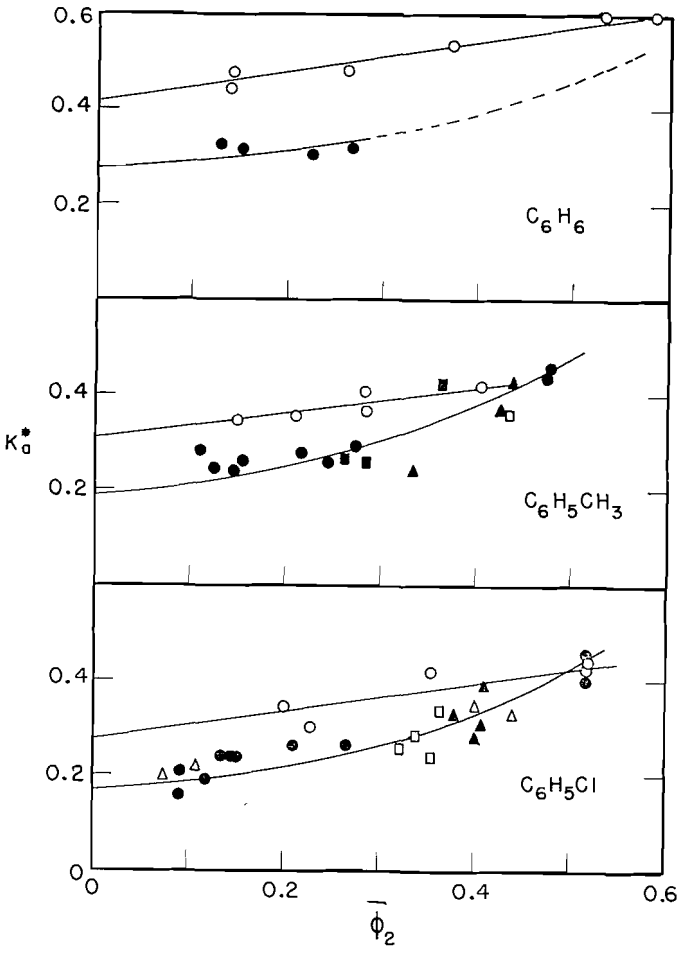

FIG. 1. The variation of the apparent heat parameter with the average volume fraction of polyisobutylene at 25° C. (Molecular weights: ○ 8,000; ● 43,000; △ 157,000; ▲ 270,000; □ 440,000; ■ 780,000.) The broken part of the curve for benzene has been drawn through the data obtained by the cage method; the data were taken from ref. 12.

with the predictions of the lattice theory. However, lattice theories cannot account quantitatively for the observed variation of thermodynamic functions. For instance, if one looks at the results covering the whole concentration range, the ratio $(\Delta\bar{S}_1 - R\phi_2/x)/\phi_2^2$ for polyisobutylene–benzene system obtained from the combined osmotic pressure data of Flory and Daoust (15) and vapor pressure data of Bawn and Patel (16), one sees that it is impossible to fit the results, because for small ϕ_2, the coordination number is smaller than 6 and for ϕ_2 larger than 0.5, it goes up to infinity. This is no doubt due to some kind of "melting" process in either component, and this has been observed before (17). Similarly, the enthalpy function cannot be fitted with a constant value for the coordination number. In dilute solution, a value of $\Delta\bar{S}_1$ or $\Delta\bar{H}_1$ corresponding to a coordination number smaller than 6 has been ascribed to back-coiling of the chain (18), but, since the theory ignores the important feature of discontinuity in polymer concentration in dilute solution (where it claims to apply), it cannot explain satisfactorily the thermodynamic functions. Fixman's theory predicts a variation of κ_a^* with concentration, but with a curvature in opposite sign to the observed one.

Turning now to the dilute solution theory, we observe first that the experimental value of κ_1^* for polyisobutylene–benzene at 25° C is around 0.28 and that it is equal to κ_1 or ψ_1 since the θ-temperature is 24.5° C and $F(X,\rho) = 1$ at θ. There is certainly a significant difference between the value 0.21 found previously (12) with no vapor space but insufficient stirring and the value 0.28 actually reported. This revised value 0.28 for ψ_1 agrees better than the value of 0.34 from osmotic measurements of Flory and Krigbaum (19) near the θ-temperature and also with that estimated from the Kurata–Yamakawa theory of viscosity (1). The value of κ_1 at the θ-temperature for polyisobutylene–benzene system can also be evaluated from the osmotic data of Flory and Daoust (15) at 25° C and 50° C. The calculated value at 37.5° C is 0.19 and it can be shown (20) that $d\kappa_1^*/dT$ for that system near the θ-temperature is given by

$$d\kappa_1^*/dT = -2\times10^{-5}M^{\frac{1}{2}}. \qquad [7]$$

With $M = 84{,}000$, $d\kappa_1^*/dT = 0.006$; then $\kappa_1^* = 0.26$ at 25° C, a value in agreement with those given above.

The General Case: Polyisobutylene in Chlorobenzene and in Toluene at 25° C

It has been shown in the preceding paper (1) that for these two systems θ and ψ_1 are almost the same. Since at 25° C, these systems are 37° C above θ, κ_1 should be estimated through the use of equation [6]. For weak interactions, i.e. for temperature ranging from θ to $\theta+16°$, $F(X,\rho)$ can be replaced by the $F(z)$ factor given by the Kurata–Yamakawa theory where $z = X\alpha^3/3^{3/2}$, but in the present case, it is better to use the tabulated values of $F(X,\rho)$ of Krigbaum *et al.* with $\rho = 0.3$ and X being computed according to a semiempirical method described previously (1). The estimated calorimetric values for κ_1 are 0.29 and 0.31 for PIB–chlorobenzene and PIB–toluene respectively.

Variation of κ_1^* with Molecular Weight

Since $F(X,\rho)$ is molecular weight dependent, κ_1^* should decrease with increasing molecular weight. However, it is difficult to detect this variation experimentally because of the difficulty of using molecular weights higher than about 2×10^5 in the calorimetric method due to the rapid increase in the viscosity of the solutions. For instance, the theoretically predicted decrease in κ_1^* for molecular weights between 43,000 and 157,000 is 0.02 and that variation is comparable with the experimental error in κ_1^*. However, Fig. 1 and Table I show that κ_1^* really increases when one goes to very low molecular weights and to the dimer.

TABLE I

Heat of dilution parameters κ_1* for polyisobutylene solutions at 25° C

Molecular wt.	Benzene	Toluene	Chlorobenzene
Dimer*	1.18	0.77	0.83
8,000	0.42	0.31	0.28
$\geqslant$43,000	0.28	0.19	0.17

*Values determined at only one concentration (ϕ_2 = 0.3).

ACKNOWLEDGMENTS

We wish to thank Professor Marcel Rinfret for his constructive suggestions concerning the use of the microcalorimeters of this department. We also wish to thank the National Research Council of Canada for the generous financial assistance in this investigation. M. S. wishes to express his gratitude to Canadian Industries Limited for the award of a bursary for the last two years of his Ph.D. residence.

REFERENCES

1. H. DAOUST and M. SENEZ. Polymer, **2**, 393 (1961).
2. P. J. FLORY. J. Chem. Phys. **13**, 453 (1945).
3. B. H. ZIMM. J. Chem. Phys. **14**, 164 (1946).
4. A. C. ALBRECHT. J. Chem. Phys. **27**, 1002 (1957).
5. M. KURATA and H. YAMAKAWA. J. Chem. Phys. **29**, 311 (1958).
6. P. J. FLORY and W. R. KRIGBAUM. J. Chem. Phys. **18**, 1086 (1950).
7. A. ISIHARA and R. KOYAMA. J. Chem. Phys. **25**, 712 (1956).
8. W. R. KRIGBAUM, D. K. CARPENTER, M. KANEKO, and A. ROIG. J. Chem. Phys. **33**, 921 (1960).
9. M. FIXMAN. J. Chem. Phys. **33**, 370 (1960); J. Polymer Sci. **47**, 91 (1960).
10. J. LEONARD and H. DAOUST. J. Polymer Sci. In press (1962).
11. E. CALVET and H. PRAT. Microcalorimetrie. Applications physico-chimiques et biologiques. Masson, Paris. 1956.
12. M. A. KABAYAMA and H. DAOUST. J. Phys. Chem. **62**, 1127 (1958).
13. H. DAOUST and M. RINFRET. Can. J. Chem. **32**, 492 (1954).
14. C. WATTERS, H. DAOUST, and M. RINFRET. Can. J. Chem. **38**, 1087 (1960).
15. P. J. FLORY and H. DAOUST. J. Polymer Sci. **25**, 429 (1957).
16. C. E. H. BAWN and R. D. PATEL. Trans. Faraday Soc. **52**, 1664 (1956).
17. W. R. KRIGBAUM and D. O. GEYMER. J. Am. Chem. Soc. **81**, 1859 (1959).
18. A. J. STAVERMAN. Rec. trav. chim. **69**, 183 (1950).
19. P. J. FLORY and W. R. KRIGBAUM. J. Am. Chem. Soc. **75**, 5254 (1953).
20. M. SENEZ. Ph.D. Thesis, Montreal. 1961.

DERIVATIVES OF MONOGERMANE

PART II. PREPARATION AND PROPERTIES OF GERMYL PSEUDOHALIDES AND RELATED COMPOUNDS[1, 2]

T. N. SRIVASTAVA,[3] J. E. GRIFFITHS,[4] AND M. ONYSZCHUK
Inorganic Chemistry Laboratory, McGill University, Montreal, Que.

Received December 27, 1961

ABSTRACT

Germyl isocyanate, isothiocyanate, and acetate have been prepared in almost quantitative yield by the interaction of germyl bromide with silver cyanate, thiocyanate, and acetate, respectively. Some of the physical properties of these new germyl derivatives are reported, and their thermal decompositions at moderate temperatures are described. The reaction of germyl bromide with silver oxide or carbonate produces germanium(II) hydride and water instead of digermoxane. Germyl bromide reacts with silver nitrite, forming germane, nitrous oxide, and nitric oxide as the only volatile products.

INTRODUCTION

Only 24 volatile compounds containing the germyl group (GeH_3—) have been reported up to the present time. These are of three main types: (i) binary hydrides, Ge_nH_{2n+2}, with $n = 1$ up to 5 (1–5), (ii) monohalides GeH_3X, with X = F, Cl, Br, I (6–9), and (iii) monoalkylgermanes (10–12). Vinylgermane (13), germyl cyanide (14), and digermthian (8) have also been prepared. By contrast, about 50 silyl (SiH_3—) compounds were known up to 1956 when MacDiarmid (15) reviewed their chemistry. Several of these were first obtained by the action of silyl halides on silver salts. In this paper we describe the reactions of germyl chloride and bromide with some silver salts. Our object has been the preparation of new compounds containing the germyl group and to compare their properties with analogous silyl derivatives.

RESULTS AND DISCUSSION

Preparation of Germyl Derivatives

In our attempts to prepare new germyl compounds we followed the pattern suggested by the following silver salt conversion series for silyl compounds, as proposed by MacDiarmid (15):

$$(SiH_3)_2Te \rightarrow SiH_3I \rightarrow (SiH_3)_2Se \rightarrow (SiH_3)_2S \rightarrow SiH_3Br \rightarrow$$
$$SiH_3Cl \rightarrow SiH_3CN \rightarrow SiH_3NCS \rightarrow SiH_3NCO \rightarrow (SiH_3)_2O \rightarrow SiH_3F.$$

By reaction with the appropriate silver salt, any compound in this series can be converted into any other following it but not into one preceding it. This conversion series is similar to those described earlier for trialkylsilyl (16) and trialkylgermyl (17) compounds.

Contrary to the above series, we found that neither germyl chloride nor germyl bromide reacted with silver carbonate or oxide to yield digermoxane, $(GeH_3)_2O$. However, this

[1]*Financial assistance for this work was received from the National Research Council. Parts of this work were described at the 42nd Annual Conference of the Chemical Institute of Canada, Halifax, N.S., May 25–27, 1959, and at the Annual Meeting of the Royal Society of Canada, Montreal, June 3–7, 1961.*

[2]*Part I: J. E. Griffiths, T. N. Srivastava, and M. Onyszchuk. Can. J. Chem. This issue.*

[3]*Holder of an N.R.C. Postdoctorate Research Fellowship at McGill University, 1959–61; on leave from the Department of Chemistry, University of Lucknow, Lucknow, India.*

[4]*Holder of N.R.C. Studentships, 1956–58. Present address: Bell Telephone Laboratories, Incorporated, Murray Hill, New Jersey, U.S.A.*

compound might have been an unstable intermediate in the following observed reactions:

$$2GeH_3Br + Ag_2CO_3 \rightarrow [(GeH_3)_2O] + 2AgBr + CO_2$$
$$\downarrow$$
$$2GeH_2 + H_2O$$
$$\uparrow$$
$$2GeH_3Br + Ag_2O \rightarrow [(GeH_3)_2O] + 2AgBr.$$

Sujishi (8) reported that germyl iodide reacts with silver oxide or mercuric oxide to produce digermoxane, but it decomposes during purification into germane and water as the only volatile products. More recently, Sujishi and Goldfarb (18) claimed the detection of digermoxane by infrared spectral measurements on the hydrolysis products of germyl cyanide, but they could not isolate pure digermoxane. The apparent instability of germyl ethers containing Ge—H bonds is further evident from the recent observations that (i) hydrolysis of *n*-butylbromogermane does not yield the expected 1,1′-di-*n*-butyldigermoxane (19) and (ii) interaction of methylbromogermane with silver carbonate does not give 1,1′-dimethyldigermoxane (20). By contrast, stable silyl ethers with Si—H bonds are easily obtained by the reaction of silyl halides with either water or silver carbonate (15, 21, 22).

In agreement with the silyl conversion series, we found that germyl bromide reacted with silver cyanide to produce germyl cyanide, GeH_3CN. However, we could not isolate a pure sample due to its decomposition at 25° in the presence of an unidentified impurity. Sujishi and Keith (14) obtained pure germyl cyanide from the reaction of germyl bromide with silver cyanide. The infrared spectrum of pure germyl cyanide reveals that, like silyl cyanide (23), it exists mainly in the normal form at room temperature (24, 25).

The fact that germyl bromide is more reactive than the chloride toward silver salts is evident from our observation that germyl bromide but not germyl chloride reacted with silver cyanate to produce germyl isocyanate, GeH_3NCO. The iso structure, confirmed by its infrared spectrum (24), is not surprising because cyanic acid and its esters have the iso structure. Covalent normal cyanates have not yet been detected, presumably because they are thermodynamically unstable with respect to their iso forms. Interestingly, silyl isocyanate, SiH_3NCO, has not yet been isolated, though MacDiarmid tried to prepare it by the reaction of silyl iodide with silver cyanate; he obtained silicon tetraisocyanate instead (26).

As expected, germyl bromide reacted with silver thiocyanate to form germyl isothiocyanate, GeH_3NCS, in high yield. This is similar to the preparation of silyl isothiocyanate from silyl iodide and silver thiocyanate. Infrared spectra of germyl and silyl isothiocyanates confirm their iso structures (24, 27).

We found that other silver salts, such as silver acetate and nitrite, reacted with germyl bromide. Thus, germyl acetate was obtained conveniently by the reaction of germyl bromide with silver acetate. Germyl nitrite was probably an unstable intermediate in the reaction between germyl bromide and silver nitrite which produced germane, nitrous oxide, and nitric oxide as the only volatile products.

Thermal Decomposition of Germyl Derivatives

Germyl isocyanate, isothiocyanate, and acetate were stable at ambient temperatures, but they decomposed at higher temperatures (50–200°) into polymeric germanium(II) hydride and the corresponding hydroacid, as represented by the equation

$$xGeH_3X \rightarrow (GeH_2)_x + xHX,$$

where X = NCO, NCS, or $OCOCH_3$. Germanium(II) hydride decomposes in a complex manner, yielding hydrogen, germane, germanium, and $(GeH)_x$, in amounts which depend on the temperature and duration of heating (28, 29). Germyl fluoride, like silyl halides (15), disproportionates at 25°, yielding germane and difluorogermane in equimolar quantities (6):

$$2GeH_3F = GeH_4 + GeH_2F_2.$$

Germyl chloride, however, decomposes at room temperature as follows (7):

$$2GeH_3Cl = GeH_4 + 2HCl + Ge.$$

As yet there is no quantitative data for the thermal decomposition of germyl bromide and iodide.

The fact that germyl halides and pseudohalides are less stable than the corresponding silyl compounds might be attributed to a difference in the polarities of the Ge—H and Si—H bonds in these compounds. Germanium and silicon have almost identical electronegativities, 1.90 and 2.00 respectively (30, 31), and their tetracovalent radii are not appreciably different, 1.17 and 1.22 Å, respectively (32). In spite of these similarities, the dipole moments of germyl chloride (2.12 D) and silyl chloride (1.30 D) differ significantly (33). These values suggest that the Ge—Cl bond is more polar than the Si—Cl bond. This might be due, in part, to the lesser tendency of germanium to use its vacant 4*d*-orbitals in d_π–p_π partial double bonding with the chlorine atom. If this is true, the electron-withdrawing effect of the chlorine atom might make the hydrogen atoms, also bonded to germanium, electropositive with respect to germanium and hence more susceptible to nucleophilic attack than the hydrogen atoms bonded to silicon, which are electronegative with respect to silicon. We believe that this protonic (or acidic) nature of the hydrogen atoms in germyl halides and pseudohalides accounts for their lesser thermal stability compared with their silicon analogues. Replacement of all hydrogen atoms in germyl halides and pseudohalides with electron-releasing methyl groups gives trimethylgermyl halides and pseudohalides which are known to be more stable thermally than the corresponding germyl derivatives (34, 24).

EXPERIMENTAL

Apparatus and Methods

The apparatus, techniques, and measurements of vapor pressure, molecular weight (M), and melting point have been described in a previous paper (20). In each reaction of germyl chloride or bromide with a silver salt, the vapor of the halide was passed slowly through a column loosely packed with a mixture of the dry salt and powdered glass wool.

Materials

Germane was prepared by the reduction of an aqueous acidic solution of germanium dioxide with sodium borohydride. Piper and Wilson (35), who first described this method, reported yields of germane in the range 60–75%. We obtained yields of 90–95% by allowing the reduction to occur at 35° instead of at 0°.

Germyl chloride was obtained by the reaction of germane with hydrogen chloride in the presence of aluminum(III) chloride as catalyst (7). It was separated from the mixture of products by several distillations at −96° (20% yield). (Found: M, 110.5; v.p. 69.7 mm at −23.6°; lit. (7) v.p. 70.2 mm at −23.6°. Calc. for GeH_3Cl: M, 111.1.)

Germyl bromide can be prepared by the reaction of germane with hydrogen bromide using aluminum(III) bromide as catalyst (7), but the yield is usually less than 10%. Yields of 60–90% were obtained by the reaction of germane with bromine, using a method similar to that described by Sujishi and Witz (36) for the preparation of silyl bromide. In one of our typical preparations bromine (7.9 mmole) was condensed in successive small portions onto germane (8.1 mmole) cooled to −196°. After each addition of bromine the mixture was warmed slowly until the color of bromine just disappeared, then the mixture was frozen again before the next addition of bromine. Germyl bromide was recovered from the product mixture by several distillations at −78° (91% yield). (Found: M, 156.0; v.p. 25.7 mm at −23°; lit. (7) v.p. 25.0 mm at −23°. Calc. for GeH_3Br: M, 155.5.)

The silver salts Ag_2O, Ag_2CO_3, AgOCN, and AgSCN were prepared by treating aqueous solutions of silver nitrate with equivalent amounts of aqueous NaOH, Na_2CO_3, KOCN, and NH_4SCN, respectively. Commercial samples of AgCN, $AgC_2H_3O_2$, and $AgNO_2$ were used. All silver salts were dried in a high vacuum for several days before they were used.

Reactions of Germyl Chloride

(a) With Silver Cyanide

Upon reaction with germyl chloride (1.50 mmole) at 25°, silver cyanide changed from white to brown, and a volatile material, which sublimed without melting, resulted. This volatile product was separated by distillation at −80° into: (i) a distillate (0.78 mmole) (found: M, 49.2) which was mainly hydrogen cyanide (calc. M, 27.0), as evident from its infrared spectrum and (ii) a residue which was crude germyl cyanide (0.62 mmole) (found: M, 100.1; calc. for GeH_3CN: M, 101.6). The molecular weight of the crude germyl cyanide decreased from 100.1 to 48.4 after it had been kept at 25° for 16 hours, and its vapor pressure became 89.1 mm at −22.9°, slightly higher than that of pure hydrogen cyanide (lit. (37) v.p. 85.2 mm at −22.9°). A non-volatile, yellow amorphous powder, undoubtedly germanium(II) hydride, remained on the walls of the storage bulb after the hydrogen cyanide had been removed. Evidently the crude germyl cyanide contained impurities, probably germyl chloride and hydrogen cyanide, which catalyzed its decomposition at 25° into hydrogen cyanide and germanium(II) hydride, as represented by

$$x\mathrm{GeH_3CN} \rightarrow (\mathrm{GeH_2})_x + x\mathrm{HCN}.$$

(b) With Silver Carbonate

Silver carbonate changed gradually from greenish-yellow to black when it reacted with germyl chloride (1.91 mmole). The condensable products consisted of carbon dioxide (0.28 mmole) (found: M, 44.3; calc. for CO_2: M, 44.0) and unchanged germyl chloride (1.43 mmole) (found: M, 106.9; calc. for GeH_3Cl: M, 111.1). Digermoxane $(GeH_3)_2O$, the expected product, was not obtained. The ratio of consumed germyl chloride to carbon dioxide produced was 1.72:1, rather than 2:1, as would be expected if the reaction

$$2\mathrm{GeH_3Cl} + \mathrm{Ag_2CO_3} \rightarrow \mathrm{GeH_2} + \mathrm{H_2O} + \mathrm{Ag_2O} + \mathrm{CO_2}$$

had occurred exclusively. Additional carbon dioxide probably resulted from thermal decomposition of some silver carbonate.

(c) With Silver Oxide

There was no noticeable change when germyl chloride (2.18 mmole) was passed 12 times through a column of dry silver oxide. Hydrogen was not produced and the recovery of germyl chloride (2.07 mmole) was almost quantitative. Therefore, no reaction occurred between germyl chloride and silver oxide.

Reactions of Germyl Bromide

(a) With Silver Cyanate

An exothermic reaction between germyl bromide (2.63 mmole) and dry silver cyanate produced germyl isocyanate in almost quantitative yield (2.43 mmole, 93% yield). (Found: M, 116.7; v.p. 27.7 mm at 0°. Calc. for GeH_3NCO: M, 117.6.) This new compound melts at $-44.0\pm0.5°$ and its vapor pressures in the range −23° to 23° are given by $\log_{10} p_{mm} = 8.369-(1891/T)$, which gives an extrapolated boiling point of 71.5°, a latent heat of vaporization of 8651 cal mole^{-1}, and a Trouton constant of 25.1.

Germyl isocyanate (2.24 mmole) did not decompose when heated for 40 hours at 110°, but after 12 hours at 200–220°, a lustrous silvery mirror of metallic germanium appeared uniformly on the walls of the flask. The volatile products were: (i) hydrogen (0.20 mmole), (ii) cyanic acid (0.21 mmole) (found: M, 44.1; v.p. 18.7 mm at −45°; lit. (38) v.p. 18.4 mm at −45°; calc. for HNCO: M, 43.0), and (iii) unchanged germyl isocyanate (1.99 mmole). Only 10% of the original germyl isocyanate decomposed and the ratio of hydrogen to cyanic acid was approximately 1:1; the ratio of decomposed germyl isocyanate to either hydrogen or cyanic acid was also about 1:1. These facts indicate that decomposition of germyl isocyanate occurred according to the equation

$$\mathrm{GeH_3NCO} \rightarrow \mathrm{Ge} + \mathrm{H_2} + \mathrm{HNCO}.$$

(b) With Silver Thiocyanate

Germyl bromide (2.08 mmole) and dry silver thiocyanate gave an exothermic reaction which yielded germyl isothiocyanate almost quantitatively (2.01 mmole, 97% yield). (Found: NCS, 43.6%. Calc. for GeH_3NCS: NCS, 43.33%.) This new germyl derivative has a melting point of $18.6\pm0.3°$ and its vapor pressures in the range 19 to 50° are given by $\log_{10} p_{mm} = 8.268-(2280/T)$, which indicates a latent heat of vaporization of 10.4 kcal mole^{-1}, an extrapolated boiling point of 150°, and a Trouton constant of 24.6. After germyl isothiocyanate (3.13 mmole) was heated for 20 hours at 55°, it decomposed completely into germane (1.07 mmole) (found: M, 77.2; calc. for GeH_4: M, 76.6) and a yellow, non-volatile residue. This residue did not dissolve in carbon disulphide, indicating that it did not contain free sulphur. The residue was non-homogeneous and could not be analyzed. It probably consisted of polymeric thiocyanic acid and solid germanium hydrides.

The ratio of decomposed germyl isothiocyanate to germane was approximately 3:1, as one might expect if decomposition had occurred according to the following scheme:

$$GeH_3NCS \rightarrow GeH_2 + HNCS,$$
$$3GeH_2 \rightarrow GeH_4 + 2GeH,$$
$$xHNCS \rightarrow (HNCS)_x.$$

(c) With Silver Oxide

Germyl bromide (4.20 mmole) reacted completely with silver oxide, producing carbon dioxide (0.27 mmole) (found: M, 44.7; calc. for CO_2: M, 42.0) and water (2.63 mmole) (found: M, 19.0; v.p. 12.6 mm at 15°; lit. (39) v.p. 12.8 mm at 15°; calc. for H_2O: M, 18.0), but no digermoxane. Evidently the main reaction was

$$2GeH_3Br + Ag_2O \rightarrow 2GeH_2 + 2AgBr + H_2O,$$

and the additional water (0.53 mmole) probably came from the silver oxide, which may not have been completely dry even though it had been evacuated for several days.

(d) With Silver Carbonate

Germyl bromide (2.31 mmole) was completely consumed in a highly exothermic reaction with silver carbonate. Digermoxane, the expected product, was not found among the products, which were carbon dioxide (7.46 mmole) and water (2.01 mmole). The reaction appeared to be

$$2GeH_3Br + Ag_2CO_3 \rightarrow 2GeH_2 + 2AgBr + CO_2 + H_2O.$$

The excess carbon dioxide undoubtedly resulted from the thermal decomposition of silver carbonate and the additional water probably came from the incompletely dry silver carbonate.

In another experiment the reaction between germyl bromide (1.84 mmole) and silver carbonate was allowed to occur at −28° for 5 hours. Again carbon dioxide (2.36 mmole) and water (0.90 mmole) were the only products. This time, the ratio of consumed germyl bromide to water was almost exactly 2:1, in accord with the above equation for the overall reaction.

(e) With Silver Acetate

Germyl bromide (3.20 mmole) reacted completely with dry silver acetate to form germyl acetate (3.07 mmole, 96% yield). (Found: M, 136.1; $C_2H_3O_2$, 43.6%; v.p. 9.7 mm at 0°. Calc. for $GeH_3C_2H_3O_2$: M, 134.7; $C_2H_3O_2$, 43.85%.) This new compound has a melting point of 12.8±0.1° and vapor pressures in the range −10 to 40° expressed by $\log_{10} p_{mm} = 9.227 - (2256/T)$, which gives a latent heat of vaporization of 10.3 kcal mole^{-1}, an extrapolated boiling point of 82.4°, and a Trouton constant of 30.0.

The yellow deposit which appeared after germyl acetate (1.80 mmole) was heated for only 10 minutes at 100–110° became orange-red after 16 hours of heating. The volatile products were: (i) hydrogen (1.09 mmole) and (ii) a mixture (1.38 mmole) (found: M, 95.6) of acetic acid (calc. M, 60.0) and germyl acetate (calc. M, 134.7) which could not be separated by fractional distillation. Assuming ideal gaseous behavior, we estimated that this mixture contained 0.72 mmole acetic acid and 0.66 mmole undecomposed germyl acetate. These results indicate that decomposition occurred to an extent of about 60%, probably according to the following scheme:

$$GeH_3C_2H_3O_2 \rightarrow GeH_2 + HC_2H_3O_2,$$
$$2GeH_2 \rightarrow 2GeH + H_2.$$

(f) With Silver Nitrite

The interaction of germyl bromide (1.87 mmole) with dry silver nitrite for 5 hours at −28° resulted in darkening of the silver nitrite and in complete consumption of germyl bromide. The volatile product mixture consisted of: (i) a fraction (0.69 mmole) (found: M, 65.4) which was shown by infrared measurements to be a mixture of germane (calc. M, 76.6) and nitrous oxide (calc. M, 44.0), (ii) nitric oxide (1.31 mmole) (found: M, 31.5; calc. for NO: M, 30.0), and (iii) water (0.88 mmole). There was no evidence of the expected germyl nitrite.

ACKNOWLEDGMENTS

We thank the National Research Council for a Postdoctorate Fellowship (to T. N. S.), two Studentships (to J. E. G.), and an Annual Grant (to M. O.). We are grateful to Mrs. P. Hayden (née Hilary Thomas) for technical assistance.

REFERENCES

1. R. B. Corey, A. W. Laubengayer, and L. M. Dennis. J. Am. Chem. Soc. **47**, 112 (1925).
2. L. M. Dennis, R. B. Corey, and R. W. Moore. J. Am. Chem. Soc. **46**, 657 (1924).
3. L. P. Lindeman and M. K. Wilson. J. Chem. Phys. **24**, 1723 (1954).
4. E. Amberger. Angew. Chem. **71**, 372 (1959).
5. K. Borer and C. S. G. Phillips. Proc. Chem. Soc. 189 (1959).
6. T. N. Srivastava and M. Onyszchuk. Proc. Chem. Soc. 205 (1961).

7. L. M. DENNIS and P. R. JUDY. J. Am. Chem. Soc. **51**, 2321 (1929).
8. S. SUJISHI. Abstracts of the XVIIth International Congress of Pure and Applied Chemistry, Munich. 1959. p. 53.
9. R. C. LORD and C. M. STEESE. J. Phys. Chem. **22**, 542 (1954).
10. G. K. TEAL and C. A. KRAUS. J. Am. Chem. Soc. **72**, 4706 (1950).
11. O. H. JOHNSON and L. V. JONES. J. Org. Chem. **17**, 1172 (1952).
12. J. SATGÉ, R. MATHES-NOËL, and M. LESBRE. Compt. rend. **249**, 131 (1959).
13. F. E. BRINCKMAN and F. G. A. STONE. J. Inorg. & Nuclear Chem. **11**, 24 (1959).
14. S. SUJISHI and J. N. KEITH. Abstracts of the 134th Meeting of the American Chemical Society, Div. Inorg. Chem. 1958. p. 44N.
15. A. G. MACDIARMID. Quart. Revs. (London), **10**, 208 (1956).
16. C. EABORN. J. Chem. Soc. 3077 (1950).
17. H. H. ANDERSON. J. Am. Chem. Soc. **78**, 1692 (1956).
18. S. SUJISHI and T. D. GOLDFARB. Abstracts of the 140th Meeting of the American Chemical Society, Div. Inorg. Chem. 1961. p. 35N.
19. H. H. ANDERSON. J. Am. Chem. Soc. **82**, 3016 (1960).
20. J. E. GRIFFITHS and M. ONYSZCHUK. Can. J. Chem. **39**, 339 (1961).
21. H. J. EMELÉUS and M. ONYSZCHUK. J. Chem. Soc. 604 (1958).
22. H. J. EMELÉUS and L. E. SMYTHE. J. Chem. Soc. 609 (1958).
23. H. R. LINTON and E. R. NIXON. Spectrochim. Acta, **10**, 299 (1958).
24. T. N. SRIVASTAVA, J. E. GRIFFITHS, and M. ONYSZCHUK. Unpublished results.
25. T. D. GOLDFARB. Symposium on molecular structure and spectroscopy. Ohio State University, Columbus. 1961. Paper P4.
26. A. G. MACDIARMID. J. Inorg. & Nuclear Chem. **2**, 88 (1956).
27. A. G. MACDIARMID and A. G. MADDOCK. J. Inorg. & Nuclear Chem. **1**, 411 (1955).
28. P. ROYEN and R. SCHWARZ. Z. anorg. u. allgem. Chem. **211**, 412 (1933); **215**, 288, 295 (1933).
29. L. M. DENNIS and N. A. SKOW. J. Am. Chem. Soc. **52**, 2369 (1930).
30. A. L. ALLRED and E. G. ROCHOW. J. Inorg. & Nuclear Chem. **5**, 269 (1958).
31. R. S. DRAGO. J. Inorg. & Nuclear Chem. **15**, 237 (1960).
32. L. PAULING. The nature of the chemical bond. 3rd ed. Cornell University Press, Ithaca, New York. 1960. p. 224.
33. J. M. MAYS and B. P. DAILEY. J. Chem. Phys. **20**, 1695 (1952).
34. D. SEYFERTH and N. KAHLEN. J. Org. Chem. **25**, 809 (1960).
35. T. S. PIPER and M. K. WILSON. J. Inorg. & Nuclear Chem. **4**, 22 (1957).
36. S. SUJISHI and S. WITZ. J. Am. Chem. Soc. **16**, 4631 (1954).
37. W. F. GIAQUE and R. A. RUEHRWEIN. J. Am. Chem. Soc. **61**, 2626 (1939).
38. M. LINHARD. Z. anorg. u. allgem. Chem. **236**, 200 (1958).
39. HANDBOOK OF PHYSICS AND CHEMISTRY. 41st ed. Chemical Rubber Publishing Co., Cleveland, Ohio. 1959. p. 2326.

COMPLEXES BETWEEN LAMELLAR STRUCTURES AND BROMINE, IODINE CHLORIDE, AND CHROMYL CHLORIDE[1]

J. G. HOOLEY

Department of Chemistry, University of British Columbia, Vancouver, British Columbia

Received May 12, 1961

ABSTRACT

Isotherms of Br_2 on four sizes of natural graphite crystals were measured with a recording vacuum balance. For 0.02- to 2-mm crystals, capillary condensation near saturation was small but significant, surface adsorption was negligible, and the composition $C_{16}Br_2$ was independent of pressure from 0.9 to 0.5. For the 0.002- to 0.01-mm crystals capillary condensation near saturation and surface adsorption were much greater, there was less intercalation than in the larger crystals, and there were no pressure-independent compositions. These effects of crystal size on the isotherm are believed to account for many of the variations in the reported compositions of lamellates in general and show that the complete isotherm on natural crystals at least 0.02 mm across should be determined. When this was done, there were pressure-independent compositions of $C_{16}Br_2$, $C_{16}ICl$, C_8ICl, and about $C_{40}CrO_2Cl_2$. In the latter case the longer the intercalated material remained in the structure the less of it diffused out on reducing the pressure to zero, until finally, none left. For these three adducts there were threshold partial pressures below which no intercalation occurred of 0.05 for Br_2, 0.03 for ICl, and 0.25 for CrO_2Cl_2 at 20° C. The adsorption curves above these pressures gave isosteric heats of 11, 12, and 13 kcal mole^{-1}. For a mixture of 0.02- to 2-mm crystals the rate of absorption of Br_2 or ICl at saturation was inversely proportional to composition for the first third of the reaction and was reproduced in subsequent runs on the same sample. The diffusion coefficient for this initial portion for ICl was three times the value for Br_2.

Isotherms of the three adducts on BN and MoS_2 showed no conclusive evidence for intercalation.

INTRODUCTION

Various workers have reported the intercalation of graphite by these three materials. The evidence for separation of the carbon layers has been X-ray data and exfoliation on rapid heating of the "compound" or lamellate. Compositions are usually reported as atomic ratios and these will be used in the following discussion although it is realized that proof of compound formation is often lacking. The reported composition in the saturated vapor varies. Thus, in Br_2 the usual value is C_8Br (1) but Herold (2) reports $C_{10}Br$ with an Acheson artificial graphite and Reyerson (3) reports 33% bromine (same as in $C_{13}Br$) with a purified natural graphite. Intercalation by ICl was first reported by Hennig (4), who found a 73% weight increase in Acheson pitch bonded artificial graphite suspended in vapor over the liquid at room temperature. He did not report it as an atomic ratio because the ICl was probably not stoichiometric. Rüdorff (5) reported $C_{5.4}ICl$ in graphite powder in saturated vapor at 30° C. Intercalation by CrO_2Cl_2 was first reported by Croft (6, 7), who heated the liquid with 65–100 mesh natural graphite for 4 hours at 100° C and obtained $C_{17}CrO_2Cl_2$, which exfoliated on heating. This was confirmed by Rüdorff (5), who found a maximum composition of $C_{12}CrO_2Cl_2$ if liquid were used but only $C_{130}CrO_2Cl_2$ for the vapor.

The purpose of the present work was to study the complete isotherms of these three adducts on graphite crystals of various sizes in the hope that variations of the above sort could be explained. These results were then to be applied to the interpretation of the isotherms on two other lamellar structures—BN and MoS_2. Thus, Croft (7) reported intercalation of BN by $FeCl_3$ and certain other compounds but not by Br_2 at 75° C. Rüdorff (8) was unable to verify any of these intercalations and confirmed the non-

[1]*Financial assistance from the National Research Council of Canada was received for this work.*

intercalations by Br_2. Rüdorff (9) has reported intercalation of MoS_2 by alkali metals.

Finally, rate measurements of some of the above processes were planned to help interpret the mechanism of intercalation.

MATERIALS

Natural graphite.—The four sizes will be designated.

Gr I—flakes of 1–2 mm from a deposit near Willsboro, N.Y., U.S.A.;

Gr II—spectroscopic carbon SP–1 from the National Carbon Co., Cleveland, Ohio. These are purified natural flakes 0.02–0.10 mm across;

Gr III—Gr II ball milled 37 hours in air to flakes of 0.01 mm;

Gr IV—Gr II ball milled 112 hours in air to flakes of 0.002 mm.

The porcelain mill contained a single flint pebble rolling in a groove of the same size. The flake sizes are those of the specks in a slurry with ethanol between two slide covers viewed through a microscope with a 0.01-mm scale.

Carbon blacks.—These were from G. Cabot Inc., Cambridge, Mass., U.S.A. Spheron 6 2700°—80-Å crystals in 300-Å blocks. Sterling MT 3100°— >200-Å crystals in 5000-Å blocks. The crystal sizes were estimated from X-ray line broadening and the sizes of the blocks of crystals from electron microscopy by the supplier (10).

Boron nitride.—A white powder supplied by the Norton Co. of Niagara Falls, Canada, with the following data (11) was used: a bulk density of 0.1 g ml^{-1} with particles 0.001 mm in average diameter plus some thin plates up to 0.026 mm across and rods 0.0005 mm in diameter×0.020 mm long. It had been fired at 2000° C and was 98% BN by their N analysis.

Molybdenum disulphide.—A powder, designated Moly-Paul No. 3, was supplied by K. S. Paul Ltd. of London, England, with the following analysis: Mo 59.0%, S 39.3%, plus less than 0.1% of each of Fe, Cu, and SiO_2. The particle size was determined in ethanol suspension to be 0.002 mm. Also, 3-cm chunks from Climax Molybdenum Co., New York, U.S.A., were used.

Bromine.—Reagent grade bromine was used and the middle fraction from a distillation was redistilled under vacuum into the balance reservoir.

Iodine chloride.—Commercial material was distilled and the middle 50%, which came over at 101° C at 760 mm, was redistilled under vacuum into the balance reservoir.

Chromyl chloride.—Chromyl chloride was supplied by the Allied Chemical and Dye Corp. of New York. It was distilled, the middle 50% being collected at 116° C and 760 mm and redistilled under vacuum into the balance reservoir. Its measured vapor pressure at 20° C was 1.7 cm and at −1.2° C, 0.45 cm. The reported m.p. is −96.5° C.

METHOD

The recording vacuum thermobalance and spoon gauge developed in this laboratory (12, 13) were used to determine the isotherms and rates of absorption. The sensitivities used were 1 to 5 mv mg^{-1} for weight and 50 mv cm^{-1} for pressure. The sample weight was chosen so that the expected change would be within the 300 mv linear output range of the balance and was therefore usually about 0.2 g for graphite. The weighed sample was sealed in the balance, the system was evacuated with a mercury diffusion pump, and liquid N_2 was placed around the trap next to the pump. After several hours or when the weight was steady the tap between the balance and the trap was closed and adduct was admitted to the desired pressure from the reservoir. Pressure was reduced at any stage by opening the tap to the trap. At the end of a run this trap, which was connected

by a tapered joint, was removed and cleaned. All taps in contact with adduct were greased with Kel F and held a vacuum of 10^{-5} cm for at least a week.

For temperatures above 20° C the reactor tube was immersed in an oil bath thermostated to 0.1° C. For temperatures from 20 to −27° C a special reactor tube was used with a jacket through which ethylene glycol was pumped from an Aminco low-temperature thermostated bath, again 0.1° C. An improved method of quickly damping spring oscillations was developed. It consisted of an arc-shaped glass fiber attached to a small glass tube resting in a side arm. An iron core was sealed in this glass tube so that an external magnet would move the fiber horizontally to or from the vertical suspension fiber to the sample bucket.

Because CrO_2Cl_2 is said to be light sensitive the whole apparatus was shielded with black cloth when used with that substance. After 2 months of use no decomposition products could be seen inside the system.

The graphite chromyl chloride lamellates were analyzed for Cl by first oxidizing the sample with pure O_2 in a 500-ml Schoniger flask (14) using 10 ml H_2O, 1 ml 2 *N* NaOH, and 3 drops 30% H_2O_2 as an adsorbent. Combustion was complete for samples less than 20 mg. The solution was boiled, acidified to Methyl Red with HNO_3, and boiled with 0.2 g $CaCO_3$. The cold solution plus 1.5 ml 1 *M* K_2CrO_4 was titrated with 0.01 *N* $AgNO_3$. The observation of the red end point in the yellow solution was found to be much easier if a pair of glassblower's goggles was worn during the titration. The didymium glass absorbs the yellow only. All runs were in triplicate.

RESULTS AND DISCUSSION

I. Bromine

1. Graphite and Carbon Black

a. High Relative Pressure

Previous workers refer to compositions in a vapor close to or at saturation without specifying all the experimental conditions. Accordingly, the following studies were made to evaluate the various factors that determine partial pressures near unity. Reproducible high partial pressures that could be roughly estimated were obtained by suspending the sample 1 cm from the bottom of a 2-cm diameter reaction tube which was thermostated over the bottom 12 cm at some temperature between 20° C and −27° C in a room at 22 to 24° C. The system was evacuated to 10^{-5} cm and bromine was admitted until a layer of liquid was present. Now although liquid is present only 1 cm below the sample, the partial pressure of vapor in the sample is not necessarily unity. The following data are presented to show the extent to which it approaches this value when the temperature differential between the room and the jacket is decreased or when the length of the jacketed portion is increased or when visible radiation is excluded. These are all variations that decrease the heat transfer to the bromine or to the sample and which therefore increase the partial pressure in the sample.

Temperature differential.—For the usual 12 cm of jacket length and with the reactor tube in darkness, the bromine uptake is plotted in Fig. 1 against jacket temperature for two carbon blacks and graphite Gr I. The measured bromine pressure is also marked along the abscissa. The degree of saturation at the lower temperatures can be estimated by reference to the actual isotherms of the two carbon blacks at 20° C, assuming that at a given partial pressure the uptake is the same at 20° as at, say, −10° C. These approximate values are marked on the abscissa. Although they are not known precisely,

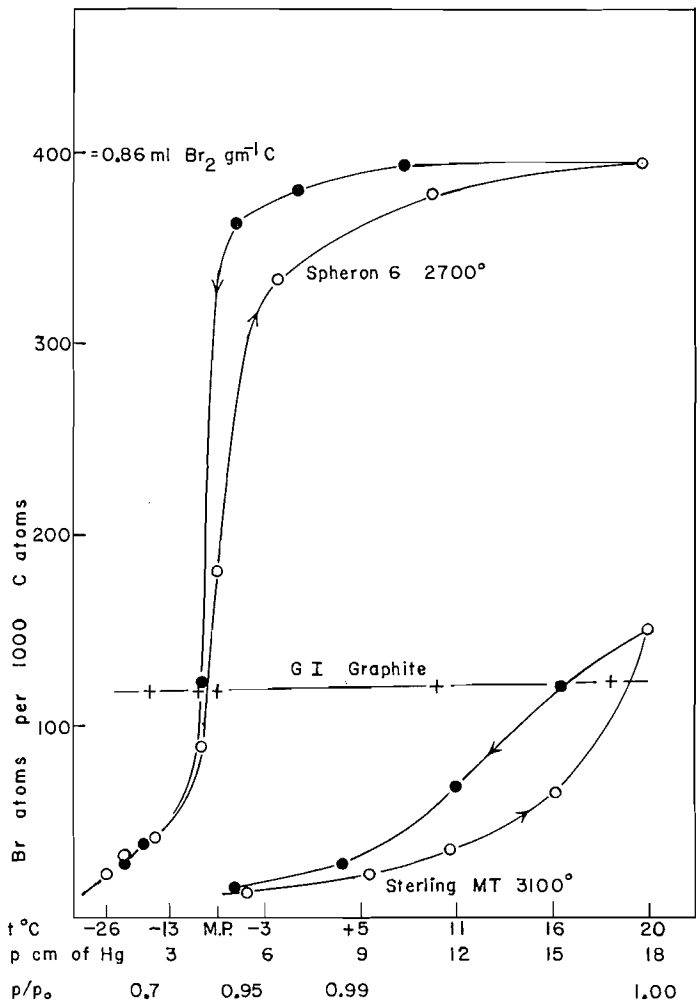

FIG. 1. Absorption of Br_2 near saturation.

they can be exactly reproduced by controlling the three conditions listed above. In practice, room temperature remains close to 22° C, so that the differential is controlled by the jacket temperature. If that is 20° C the vapor is as close to saturation as is feasible. Above that, condensation may occur in the balance system when bromine is admitted from the reservoir.

The compositions in Fig. 1 are believed to be equilibrium values. They were reached in 24 hours or less and many were shown to remain constant for an additional 48 hours. The hysteresis loops for the two carbon blacks were reproducible and show much more hysteresis than in the pressure range 0 to 0.9 of previous work (15). The small hysteresis at those lower pressures, which does not show up on the scale of Fig. 1, was believed to be the result of intercalation in some of the small graphite crystals of the carbon black (15). The large hysteresis at high pressure is believed to be the result of capillary condensation of bromine in the interparticle voids for the following reasons. First, it is known (10) that the carbon black particles are approximately spheres of nonuniform size, and de Boer (16) has shown that the voids in such a system will condense vapor

below saturation and give rise to hysteresis of the kind observed. Furthermore, the small voids in the fine Spheron 6 should and do condense a greater proportion of liquid at a low partial pressure than do the larger voids in the coarser Sterling MT 3100°. Finally, the range of particle sizes is known to be less for Spheron 6 (10) and so it should and does condense its bromine over a shorter pressure range than does Sterling MT 3100°.

The case of graphite Gr I is of special interest because it is a natural graphite of the sort used in lamellar studies. In Fig. 1 the loss of 0.005 Br/C units in going from a partial pressure of 1 to 0.9 is believed to be loss of bromine condensed between the crystals. The amount is considerably less than from the carbon blacks because of the very different shape and size distribution of the particles. For the smaller crystals of Gr II—also a natural graphite—the loss is 0.020 in the same pressure range (Fig. 2). For these two

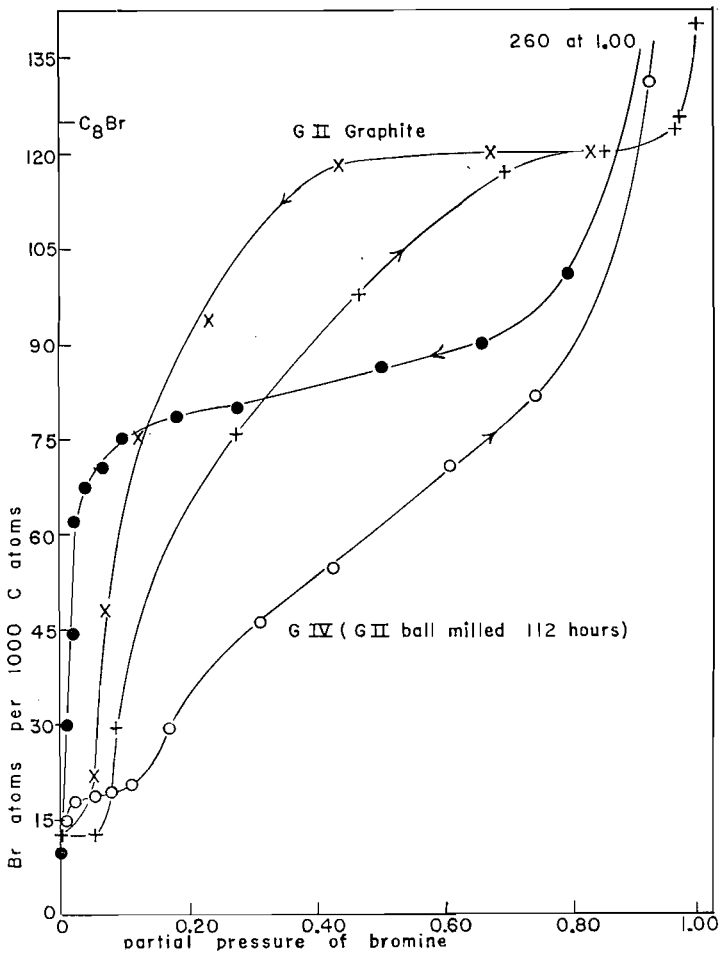

FIG. 2. Isotherms of Br_2 for two particle sizes of graphite.

graphites then, the composition near saturation is governed partly by the size distribution of the interparticle voids. This could be the cause of some of the variations in reported compositions of lamellates in general and shows that only from the complete isotherm can the existence of stoichiometric compounds be postulated.

Length of thermostated jacket.—This was held constant at 12 cm in the above experiments. In one run, however, when 38 cm was thermostated the amount absorbed by Sterling MT 3100° was the same as in Fig. 1 at 20° C but was 100 at 0° C. This increase by a factor of four in the amount condensed at 0° C when the jacket length was increased is caused by a higher partial pressure in the sample. This in turn is caused by a decreased heat leak to the sample along the suspension fiber and through the vapor. If the heat leak was reduced still further by using a longer tube the pressure would become still closer to unity and the amount condensed would approach that at 20° C. The fact that the change in jacket length did not change the absorption at 20° C shows that within experimental error the heat leak was zero at 20° C and that the partial pressure was unity for both lengths of jacket at that temperature.

Visible radiation.—This was held constant at zero in the above experiments by wrapping the reactor tube and section above it in opaque cloth. The following observations were made of the effect of visible radiation on the amount absorbed. A 60-watt bulb 22 cm from the jacketed tube lowered the value for Spheron 6 2700° at 20° C from 400 down to 100. Daylight or even the rather weak ceiling lights also decreased the value below that for a darkened tube. The effect is believed to be a decrease in partial pressure caused by the rise in temperature of the bromine vapor as it absorbs visible light. It could be the cause of some of the variations in reported compositions at high partial pressure.

b. Isotherms for Various Sizes of Graphite Crystals

For the 0.02- to 0.10-mm crystals of graphite Gr II surface adsorption is negligible with the techniques used, and capillary condensation occurs only above a partial pressure of 0.9. Hence below that pressure only lamellar absorption is being measured in the 20° C isotherm for Gr II in Fig. 2. This isotherm is reproducible and starts with the so-called residue compound (17) which remains after the first run to saturation and back to zero pressure. The initial adsorption curve from zero composition lies below the one shown and reaches the same composition at saturation. Both it and the one in Fig. 2 show the threshold pressure for intercalation of 0.05 (1 cm at 20° C), which has been observed in previous work (15). The desorption branch shows a lamellar composition of 0.120 or C_8Br persisting from a pressure of 0.9 to 0.5. This refutes the statement one sometimes sees that this compound or lamellate is stable only in saturated vapor.

The 1- to 2-mm crystals of Gr I show the same general shape of isotherm as do the smaller crystals of Gr II, although the residue composition is twice as great and capillary condensation at saturation is less. The critical pressure for intercalation and the maximum lamellar composition were, however, the same.

The 0.002-mm crystals of Gr IV made by grinding Gr II show a very different isotherm. In Fig. 2 adsorption begins at the lowest pressure used and continues until a monolayer is formed with a composition about 0.010 above that of the residue. The area calculated from this is 26 $m^2 g^{-1}$ (15). Then the isotherm levels off somewhat until the threshold pressure is reached, and although the exact value cannot be read off as precisely as for Gr II, it is close to the Gr II value. At high pressure there is much more capillary condensation and on the desorption branch there is no indication of any lamellate, even at C_8Br. The steepness of the final desorption to zero pressure is curious and no explanation is offered.

The 0.01-mm flakes of Gr III show the same isotherm as for Gr IV except that the residue composition is half as great and the saturation value is 6% less.

It thus appears that variations in the size of the graphite crystals used by different workers could explain some of the discrepancies in composition and in the reported

existence of lamellates in general. The above results show that crystals larger than 0.02 mm give a uniform composition with Br_2.

c. Rates of Absorption

These were measured in saturated vapor at 20° C by admitting bromine to the darkened, evacuated, and thermostated system until liquid condensed in the reactor. The resultant spring oscillations were then stopped as described under Method. The whole procedure required about 1 minute, after which a smooth record of weight versus time was available. It was found that for the first 25 to 50% of the absorption the composition was proportional to the square root of time. Hence, in that region the rate is inversely proportional to the composition and the rate or diffusion constants in Table I were calculated from the

TABLE I

Bromine diffusion coefficient D, $(Br_2/C)^2\ min^{-1} \times 10^4$

Sample	Temp., °C	Pressure, cm	D
Gr I graphite	20	17.6	0.062, 0.062
Gr II graphite	20	17.6	0.65, 0.65, 0.60
"	9.4	10.0	0.60
"	9.4	10.0	0.65, 0.60
"	0.3	6.0	0.55
"	−12.0	3.5	0.40, 0.40
Gr IV graphite	20	17.6	0.72
Sterling MT 3100°	20	17.6	0.025 then 0.045
Spheron 6 2700°	20	17.6	0.55 then 0.90
"	0	5.9	0.020 then 0.21

initial slopes of plots such as Figs. 3 and 4. These coefficients are really the averages for a variety of crystal sizes and hence they cannot be interpreted in terms of a reaction mechanism. In the following two sections, however, certain conclusions are drawn from other aspects of the data.

Particle type and reproducibility.—Two kinds of behavior were observed and found to depend on the type of particle in the powder. In the first kind, the diffusion coefficient D decreases after the initial linear portion and finally becomes zero, as in Fig. 3. This occurs for those powders in which the individual particle is a graphite crystal. Gr I is in this category and shows an initial D of 0.062 both for the original sample and for subsequent runs on the residue compound formed from it. This reproducibility shows that the residual bromine does not interfere with diffusion into the crystal and is therefore probably trapped toward the center of the crystal. It also shows that the formation and decomposition of the lamellate C_8Br does not change the lattice or edges in any way that would affect diffusion into the structure. Similar results were obtained with the smaller crystals of Gr II, the D being about 10 times as large and reproducible with the same or different samples. For the even smaller Gr IV the initial D was 0.72—about the same as for the coarser Gr II. However, in Gr IV considerable condensation occurs along with the intercalation and it was not possible to separate the two processes.

In the second kind of behavior, D increases after the initial linear portion and later falls to zero, as in Fig. 4. This occurs for carbon blacks in which the particles are aggregates of graphite crystals and for which nearly all of the absorption is by capillary condensation. The increase in D may mark the establishment of a continuous liquid layer after which spreading and therefore condensation can occur more rapidly. Whereas the D for a graphite was reproducible and independent of sample weight over a factor

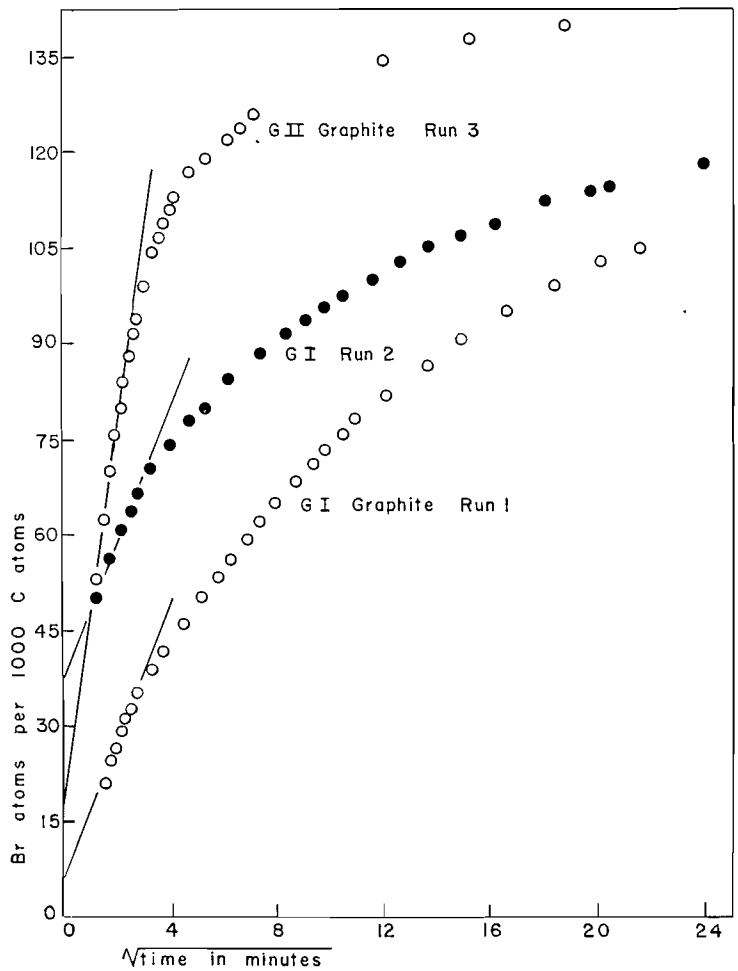

FIG. 3. Rate of absorption of Br_2 in graphite.

of at least three, that for a carbon black was not. This could be the result of variations in packing.

Rate as a function of temperature.—The above rates were all measured at 20° C and the final composition was that for the saturated vapor. At lower temperatures, however, the partial pressure is less than 1 even though liquid is present in the reactor. The effect on the final composition can be seen in Fig. 1. It is negligible for Gr I and Gr II but not for a carbon black. It will be noticed, however, that for Spheron 6 2700° at 0° C the final composition is only about 20% less than at 20° C. The rate for this black at 0° C was therefore determined along with rates at even lower temperatures for Gr II. The general behavior was the same as at 20° C. The lower values of D are listed in Table I and give for Gr II an energy of activation of 2.4 kcal mole^{-1}. For the carbon blacks, D was much more temperature dependent than for graphite and even less reproducible than at 20° C.

2. Boron Nitride

This powder resembles graphite Gr IV in particle size but its isotherm in Fig. 5 is very different. The only evidence for intercalation is the hysteresis to low pressure. However,

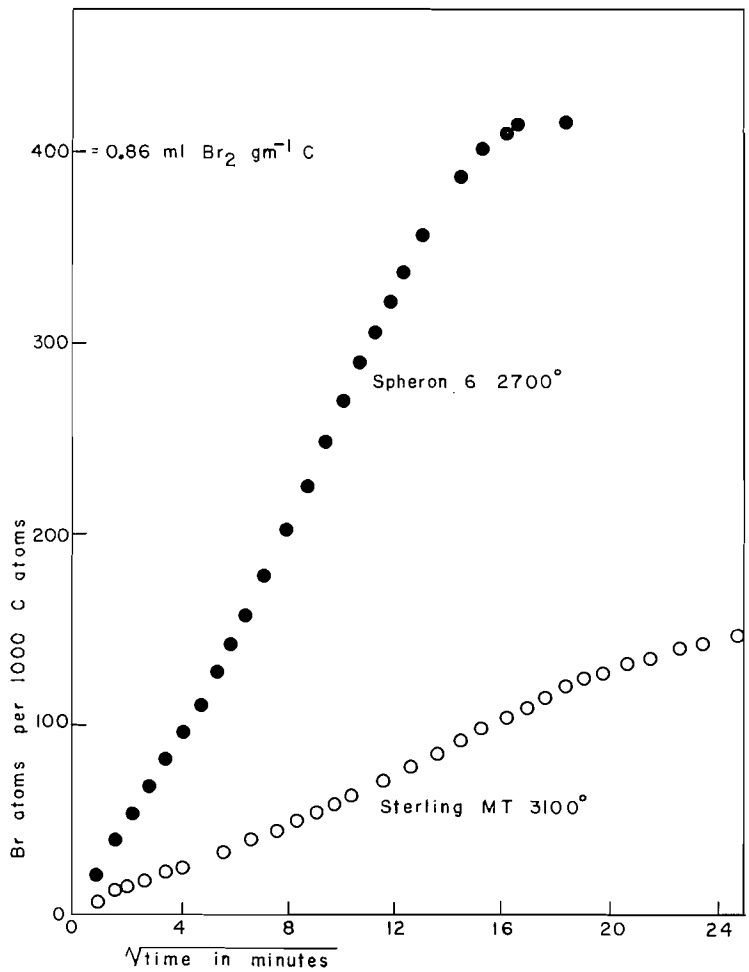

FIG. 4. Rate of absorption of Br_2 in carbon black.

the amount of hysteresis and of absorption at, say, a pressure of 0.5 is only about 5% as much as for Gr IV and there is no bromine residue at zero pressure. The isotherm could be accounted for by capillary condensation between platelets of BN.

3. Molybdenum Disulphide

The isotherm on Moly Paul No. 3 powder is shown in Fig. 6 and a run was also made on 1-mm flakes of MoS_2 shaved from a chunk. The latter absorbed no Br_2 at 20° C until the pressure reached saturation, at which point 0.020 ml g^{-1} condensed and, on slight reduction of pressure, evaporated, leaving no residue at zero pressure. There was apparently only capillary condensation between the flakes. The MoS_2 powder for Fig. 6 resembled graphite Gr IV in particle size and the isotherms of the two in Figs. 6 and 2 have certain features in common. Thus, there is hysteresis, a steep desorption curve at low pressure, a residue at zero pressure, and the amounts absorbed at an intermediate pressure, say 0.4, differ only by a factor of two when expressed in atomic ratio units. These features of Fig. 6 are, however, not necessarily caused by intercalation. Thus, the hysteresis and absorption at low pressure could be the result of condensation between

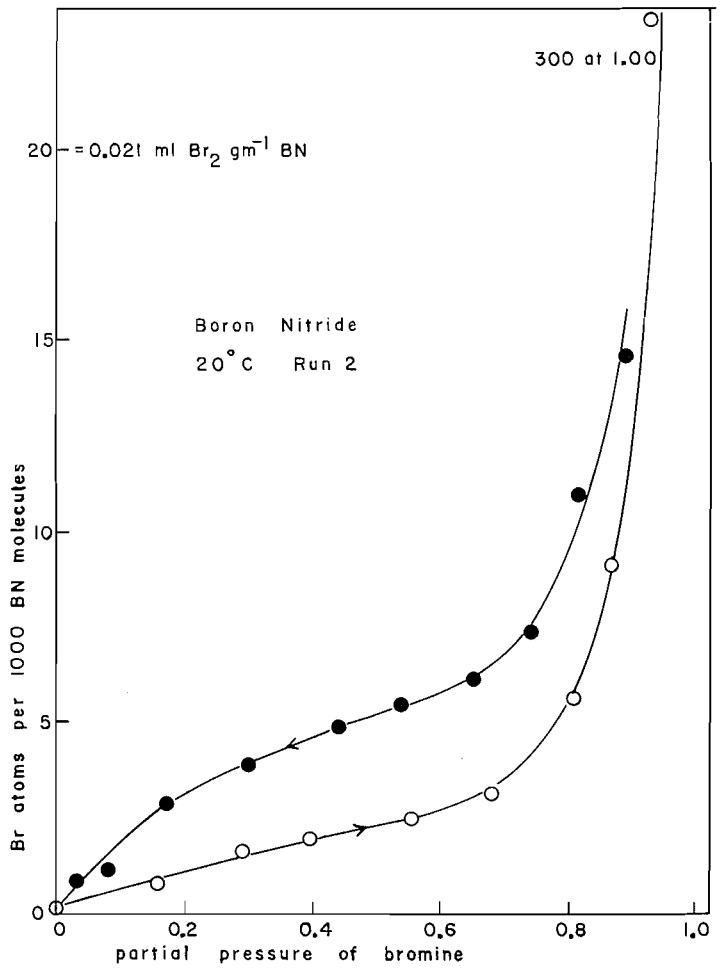

FIG. 5. Isotherm of Br_2 on BN powder.

MoS_2 platelets. The amount involved at a pressure of 0.4 is only 0.006 ml g^{-1}. This is the same as for the BN powder in which intercalation is very unlikely. The residue at zero pressure could be the result of edge atom reaction with bromine. In view of the non-intercalation of large MoS_2 crystals this latter interpretation of Fig. 6 is preferred.

II. Iodine Chloride

1. Graphite Gr II

In the 20° C isotherm of Fig. 7 those points above a partial pressure of 0.65 scattered badly in spite of several attempts to obtain a reproducible curve. At saturation, four values varied from 0.150 to 0.195. Below that pressure, however, the values were reproduced in subsequent runs on the same or different samples. Compositions that were nearly independent of pressure occurred at $C_{16}ICl$ for both adsorption and desorption and at C_8ICl for desorption. The only indication of Rüdorff's lamellate (5) is at saturation. Thus, if the maximum value of 0.195 is reduced by the amount condensed between the particles, one obtains 0.184 or $C_{5.4}ICl$—exactly his composition. The amount condensed is assumed to be 0.045 ml g^{-1}—the same as for Br_2.

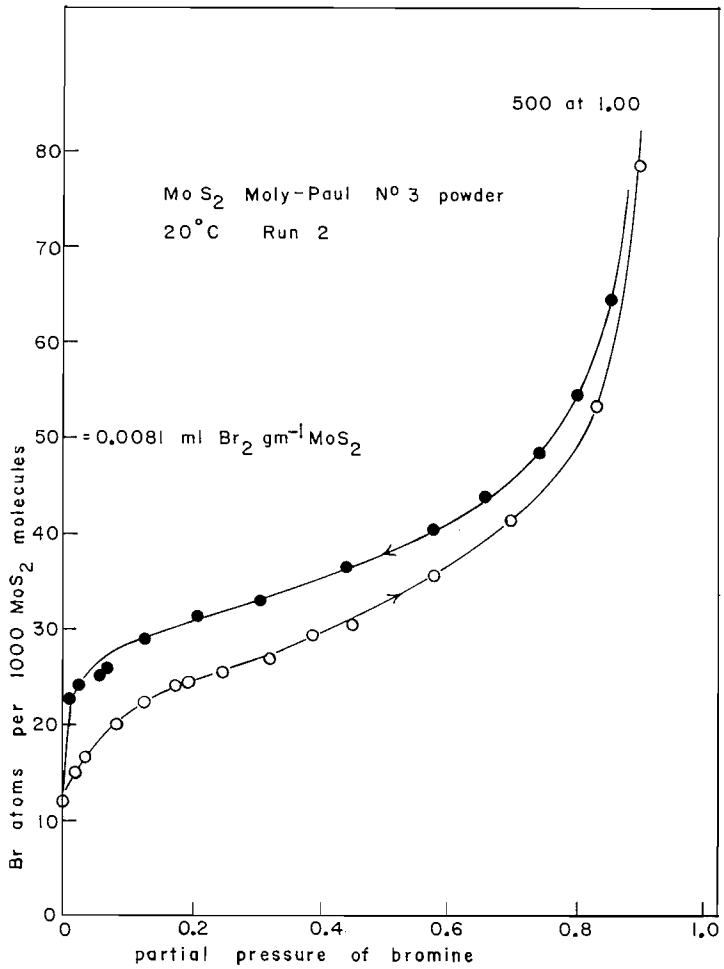

FIG. 6. Isotherm of Br_2 on MoS_2 powder.

Isotherms at 35 and 50° C were also determined, although the maximum partial pressures attainable were 0.5 and 0.3 respectively. The adsorption curves approached $C_{16}ICl$ as at 20° and on desorption there was hysteresis. From the adsorption curves at the three temperatures Arrhenius plots at compositions 0.03, 0.04, and 0.05 were made. Linearity was excellent and the three slopes gave an isosteric heat of 11.6 ± 0.5 kcal $mole^{-1}$.

For the isotherms at 35° and 50°, a threshold pressure of about 0.03 was noted below which no absorption occurred. If there was a similar critical pressure at 20° it was missed and would be below the 0.15 cm of the first point in Fig. 7.

The kinetic behavior in saturated vapor resembled that in bromine. Thus, in the plot of ICl/C against the square root of time at 20° C the initial linear portion extended to 0.050 and from its slope a diffusion coefficient D of 1.8×10^{-4} $(ICl/C)^2$ min^{-1} was calculated. This is about three times the value for bromine in the same graphite at the same temperature.

Finally, there was a residue "compound" whose composition reached a steady 0.010 after several days in saturated vapor. This is about the same as for bromine.

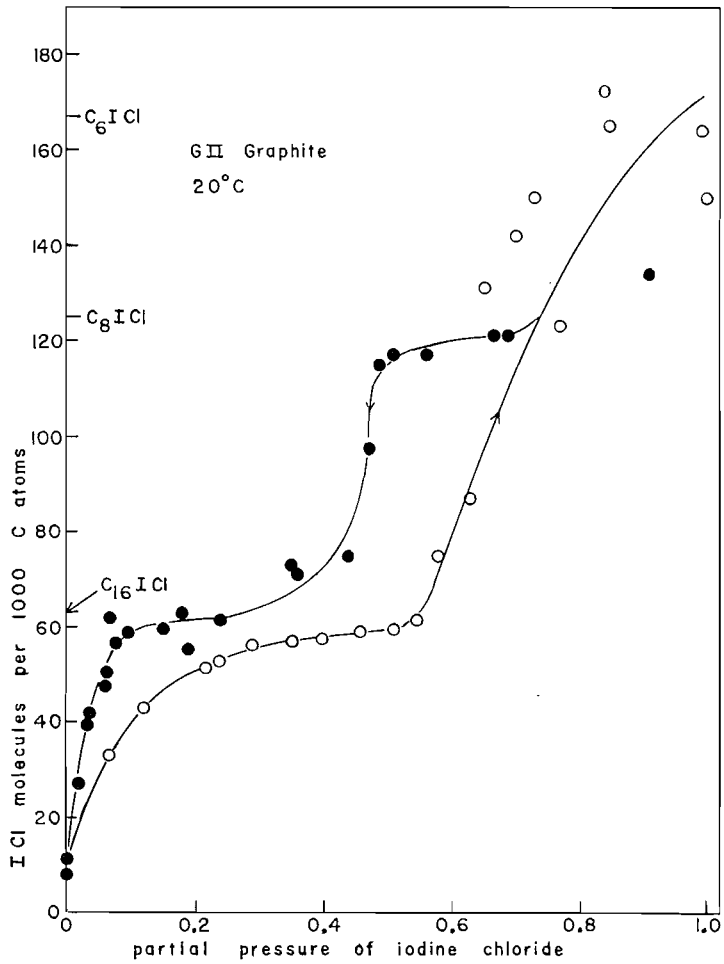

FIG. 7. Isotherm of ICl on graphite.

2. Carbon Black—Spheron 6 2700°

The 20° isotherm in Fig. 8 resembles that for Br_2, although the amount of hysteresis is about 15 times as great. Now it has been shown for Br_2 that hysteresis increases with the size of the graphite crystal in the black (15). If ICl behaves similarly, its isotherms would be more useful than those of Br_2 in estimating crystal size.

3. Boron Nitride

For the isotherm at 20° in Fig. 9 adsorption always occurred along path I. Desorption followed path II if there had been no previous desorption and path I if there had been. Furthermore, the effect of a previous desorption could be wiped out if the reactor tube was opened and the powder stirred and shaken down with a few sharp taps to the holder. Then path II would be followed during the next desorption. The desorption of ICl therefore affects the packing of this particular powder in such a way as to eliminate hysteresis. There is apparently no intercalation of ICl.

4. Molybdenum Disulphide

The 20° isotherm on Moly Paul No. 3 powder in Fig. 10 was reproducible although the values are somewhat scattered. As in the case of the Br_2 isotherm on this powder

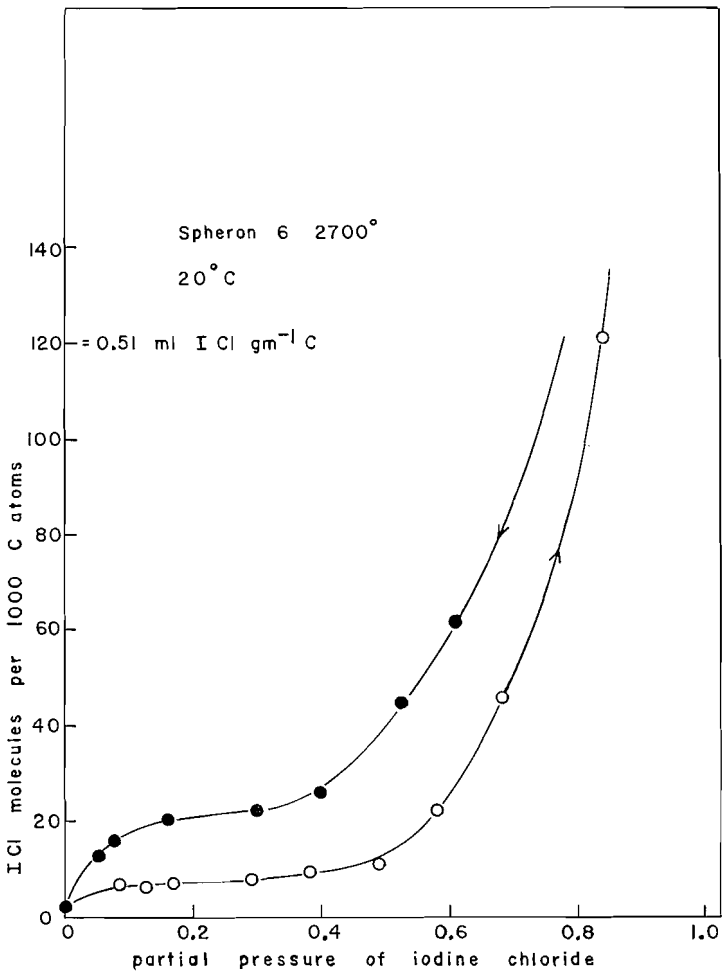

FIG. 8. Isotherm of ICl on a carbon black.

there are certain features compatible with intercalation. Thus the atomic ratio at an intermediate pressure—say 0.4—is comparable with that for Br_2 in graphite Gr IV and there is hysteresis to a low pressure and a residue. The first two features, however, can be explained by capillary condensation and the third by edge atom reaction, as in the case of Br_2. The amount of condensation at pressure 0.4 is 0.022 ml g^{-1}—the same as for ICl in the initial desorption from BN powder. In this latter case there was only condensation and the data proves no more than this for ICl on MoS_2 powder.

III. Chromyl Chloride

1. Graphite

The 20° isotherm for the 0.02- to 0.10-mm crystals of Gr II is shown in Fig. 11. The threshold pressure below which no absorption occurs is 0.4 cm or a partial pressure of 0.25, whereas for Br_2 and ICl the values were 0.05 and 0.03 respectively. Above that pressure the adsorption branch resembles that for Br_2 but levels off at $C_{37}CrO_2Cl_2$ as compared with $C_{16}Br_2$. The steep rise just below saturation was also noted in the Br_2 isotherm and is interparticle condensation. On lowering the pressure to 0.9 this condensed

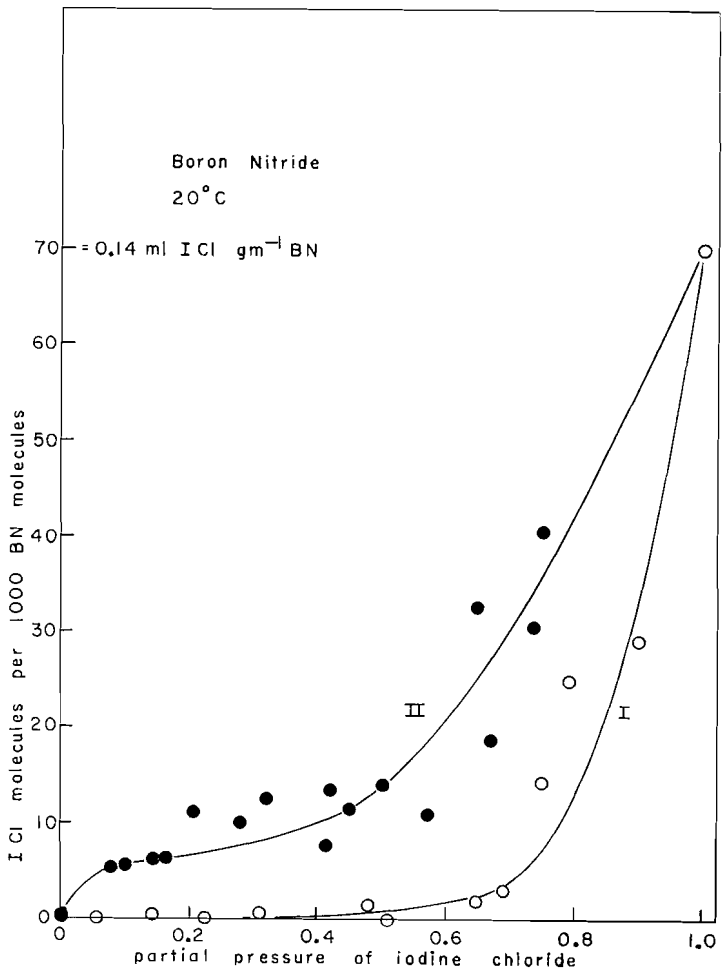

FIG. 9. Isotherm of ICl on BN powder.

material was lost and from there to zero pressure there was no further weight change. A repeat run to saturation and back duplicated the horizontal line and steep rise above pressure 0.9. The 1- to 2-mm crystals of Gr I graphite behaved similarly, although there was less condensation at saturation and the final CrO_2Cl_2 content was somewhat less. That the weight increase on forming these residues may be represented as CrO_2Cl_2 was shown by the fact that the Cl content calculated on this assumption is nearly the same as the analytical value. Thus for three samples the Cl percentages calculated from the weight increases were 10.7, 10.9, and 7.9 and from analysis 10.5 ± 0.6, 10.1 ± 0.2, and 7.1 ± 0.2 respectively.

After one of the runs on Gr II in which 0.261 g of graphite formed 0.353 g of residue, the latter was heated in a vacuum with a liquid N_2 trap in the line. The weight first changed at 300° C and after 1 hour at 330° had dropped to a steady 0.327 g and remained constant even after 2 hours at 500° C. This final product contained $5.7\pm0.2\%$ Cl, whereas the value would be 9.2% if pure CrO_2Cl_2 had been lost during heating. If, however, only Cl was lost and the amount was 1 atom per molecule of CrO_2Cl_2, the Cl content would have dropped to 6.3%. Loss of somewhat more chlorine per molecule

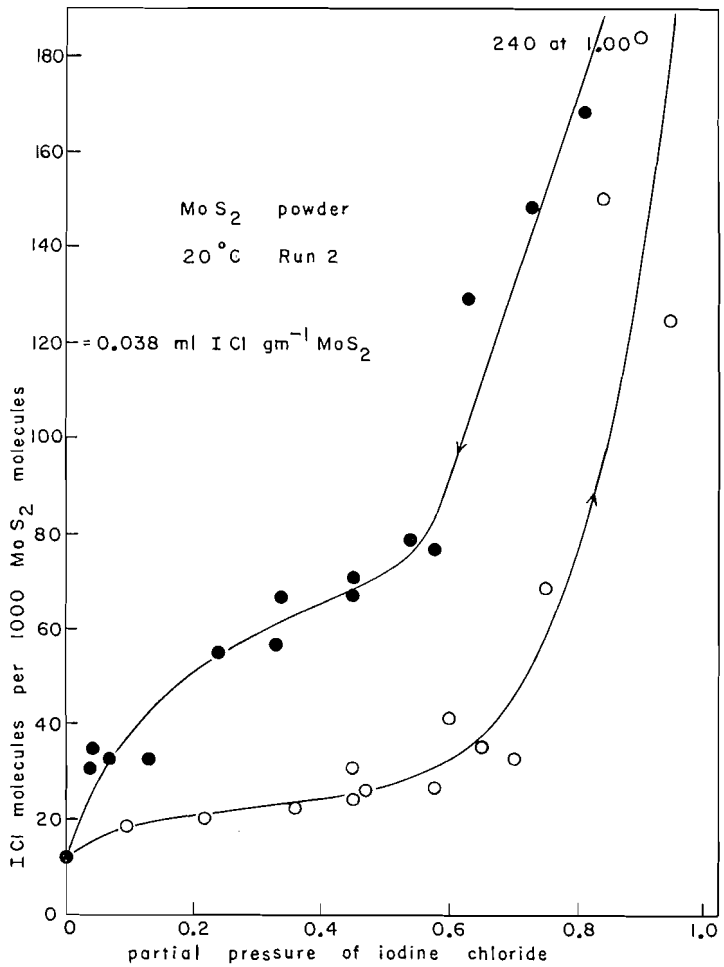

FIG. 10. Isotherm of ICl on MoS_2 powder.

has been reported when CrO_2Cl_2 is heated in a sealed tube (18). The reaction claimed is

$$3CrO_2Cl_2 \rightarrow (CrO_2)_3Cl_2 + 2Cl_2.$$

If this were the amount lost in the above case, the final Cl content would have been 4.3%. It therefore appears that graphite retains the intercalated material as CrO_2Cl_2 unless heated above 300° C, in which case about half the chlorine is lost to give a product that is not volatile at 500° C.

The small crystals of Gr IV, which are Gr II ground to 0.002 mm, gave an entirely different isotherm. The one shown in Fig. 11 is for the second run on a given sample. In the first run the desorption rose from 0 to 0.002 at a pressure of 0.2 and then gradually approached the curve shown, reaching it near saturation. The features to be explained are the small residue, the hysteresis, and the large absorption near saturation. Now in the case of Br_2 on Gr IV (Fig. 2) there was much less intercalation than in the large Gr II crystals. In the present case of CrO_2Cl_2 this is apparently also true. Furthermore, if the smaller amount intercalated behaves as it did in Gr II it will not be lost at zero pressure and will therefore account for the smaller residue of 0.004. The isotherm on this residue exhibits hysteresis which must be associated with the capillary condensation

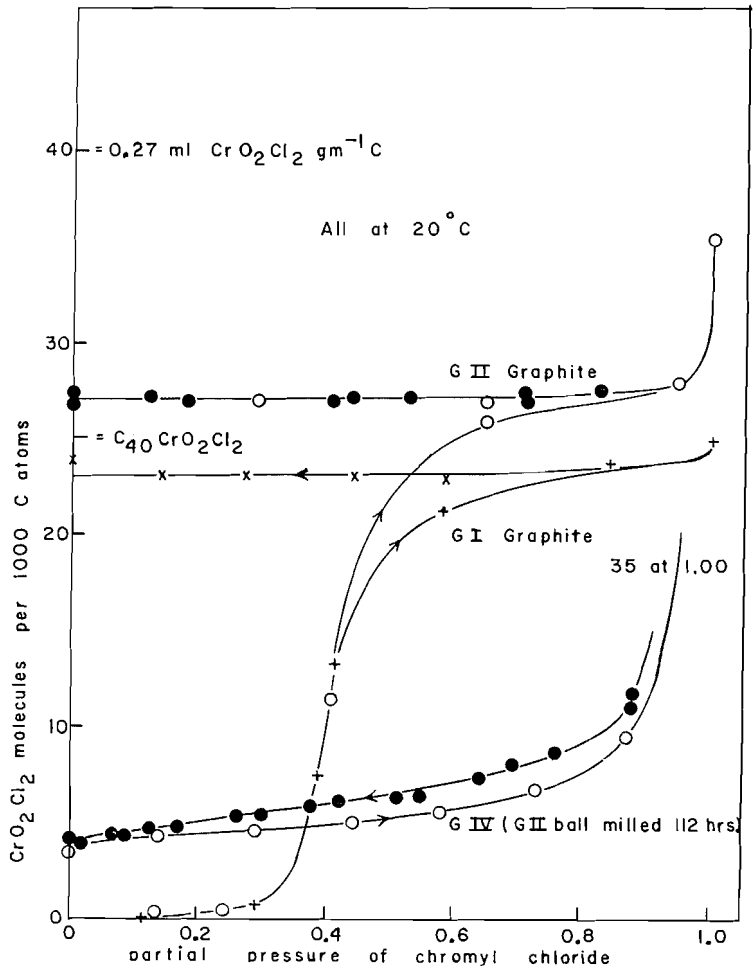

FIG. 11. Isotherms of CrO_2Cl_2 on graphite.

between crystals. In the case of the coarser Gr II there was less condensation at saturation and any hysteresis associated with it was too small to be observed.

There is an interesting time and temperature effect for Gr II that does not show up in Fig. 11 but which is illustrated in Fig. 12. It is that the residue composition increases with the time spent in CrO_2Cl_2 vapor and finally reaches the composition observed in the vapor at a pressure of about 0.9. The increase with time is much slower at the $-1.2°$ C of Fig. 12 than at 20° and so the residue composition is still below the high-pressure value after three runs—a total of 3 days in saturated vapor. The reason for the slight decrease in the high-pressure value after the first run is unknown. Again, at higher temperature the rate of fixing of CrO_2Cl_2 is higher, as shown by the three runs in Fig. 13. For the initial one at 44° C the desorption is horizontal after only 1 hour at 1.7 cm—a partial pressure of 0.45. For the next run, which uses this residue but at 30° C, the desorption is horizontal after 12 hours or less at 1.7 cm. An additional run at the same temperatures duplicated the horizontal desorption line. In the third run at 20° C the desorption branch did fall off toward zero pressure because only 4 hours was spent at saturation. The above behavior could be explained by the production of a nonvolatile

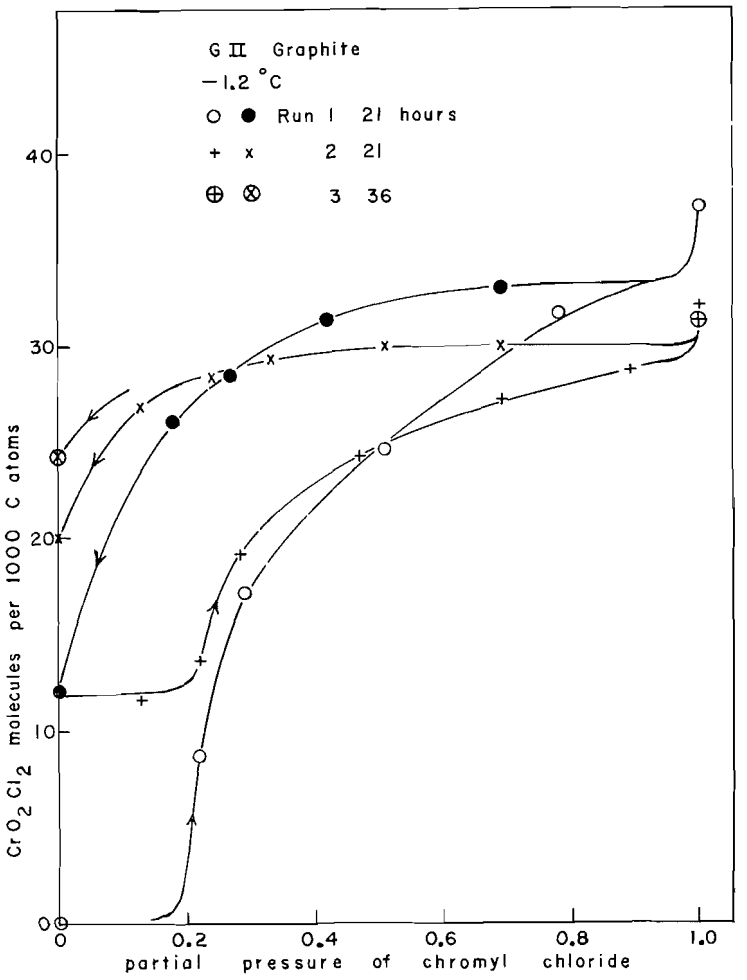

FIG. 12. Isotherm showing increased retention of CrO_2Cl_2 with time.

product either by a slow reaction of CrO_2Cl_2 with the carbon layers or by a slow polymerization of the intercalated CrO_2Cl_2.

From the three initial adsorption curves on Gr II at −1.2, 8.6, and 20° C Arrhenius plots at six compositions from 0.005 to 0.030 were made. Linearity was excellent and from the slope an isosteric heat of intercalation of 13±0.9 kcal mole^{-1} was calculated.

2. Carbon Black

The 20° C isotherm for Spheron 6 2700° resembled that for graphite Gr IV in Fig. 11. It showed the same amount of hysteresis and the same residue composition. The saturation composition was 0.81 ml g^{-1}—about the same as for Br_2.

3. Boron Nitride

The 20° C isotherm showed negligible adsorption and no hysteresis below a pressure of 0.6 and capillary condensation with some hysteresis at high pressure. The saturation absorption of 0.34 ml g^{-1} equals the value for Br_2. There was no residue and no evidence for intercalation.

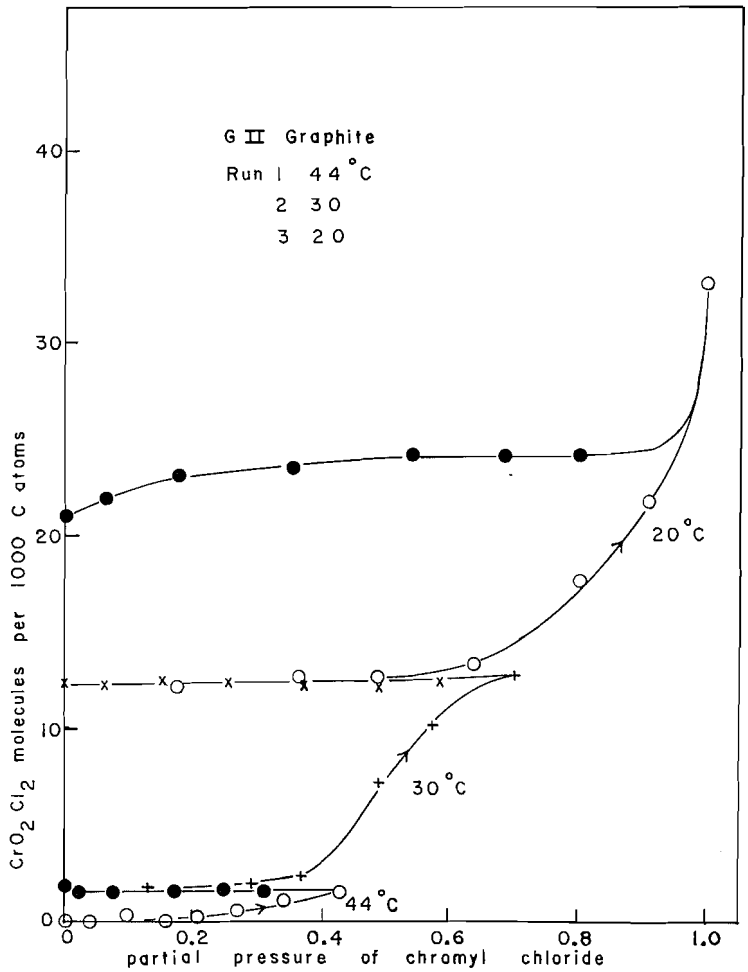

FIG. 13. sotherms showing effect of temperature on retention of CrO_2Cl_2.

4. Molybdenum Disulphide

The 20° C isotherm of the Moly Paul powder resembled that for graphite Gr IV in Fig. 11. There was even less hysteresis, a residue of 0.008, and a saturation absorption of 0.07 ml g^{-1}. There is therefore no definite evidence for intercalation.

CONCLUSIONS

The work with Br_2 on the four sizes of natural graphite crystals shows that measurement of the composition while in the vapor above liquid Br_2 is insufficient for reporting the stoichiometric ratios of lamellar compounds. Not only must the complete isotherm be determined with special attention to experimental conditions at saturation but also the effect of particle size on the isotherm must be studied. Thus, surface adsorption is negligible only for crystals over about 0.05 mm across. Capillary condensation is also less for larger crystals but even for the 0.1- to 2-mm range is not negligible at saturation and for 0.002-mm crystals it is greater than the amount intercalated. Indeed, for these small crystals the amount intercalated is, for some unknown reason, considerably less

than for the 0.02- to 2-mm range. Hence, in studying intercalation it is necessary to determine the complete isotherm for natural crystals over about 0.02 mm across.

When this is done, it is evident that there is a threshold partial pressure for intercalation at 20° C in graphite which is 0.05 for Br_2, about 0.03 for ICl, and 0.25 for CrO_2Cl_2. When more of these are known their significance may become apparent.

The 20° isotherms of Br_2 and ICl show the following compositions to be independent of partial pressure over the ranges indicated: $C_{16}Br_2$ (1.00 to 0.5), $C_{16}ICl$ (0.3 to 0.1), and C_8ICl (0.7 to 0.5). The isotherm of CrO_2Cl_2 was different in that the desorption curve was time dependent. That is, the amount leaving on pressure reduction decreased for longer times spent in the saturated vapor until, finally, none left even at zero pressure. This could be the result of a slow polymerization of intercalated CrO_2Cl_2 to produce a nonvolatile product. The limiting composition was about $C_{40}CrO_2Cl_2$, which is about three times as much as Rüdorff (5) found in the vapor and one third as much as he found in the liquid.

The rate of intercalation in the saturated vapor of Br_2 or ICl was inversely proportional to composition for about the first third of the process and had an energy of activation of about 2 kcal $mole^{-1}$. The significance of this relationship is lost, however, because the graphite used was a mixture of crystal sizes. The fact that the rate was, however, reproduced in subsequent runs on a sample is interesting because it shows that neither the process of intercalation and its reverse nor the existence of residual Br_2 or ICl in the graphite affects the initial rate. The residual material is therefore probably stored near the center of the crystal. The initial diffusion rate for ICl was three times as great as for Br_2. The lower threshold pressure and the existence of the more concentrated C_8ICl also show that this adduct enters graphite more readily than does Br_2.

If one considers hysteresis to be one of the characteristics of intercalation then the isotherms on BN and MoS_2 powders can, with one exception, be explained either by a small amount of intercalation or by a combination of surface adsorption and capillary condensation. The exception is ICl on BN for which only the initial cycle shows hysteresis. Subsequent cycles show negligible absorption below saturation and no hysteresis. This and the fact that hysteresis could be restored by stirring the powder show that it must have been associated with the packing of the powder and not with intercalation. Although this curious effect was not observed for the other isotherms on BN and MoS_2, it does show that the hysteresis to low pressures in those cases could be the result of capillary condensation and is not proof of intercalation. Another characteristic of intercalation, in graphite at least, is a residue at zero pressure. Now BN powder does not show this characteristic but MoS_2 powder does for all three adducts. Neither result is conclusive of course but they do suggest that BN powder is not intercalated and that MoS_2 powder either is intercalated or reacts at its edges with adduct to give a nonvolatile product. The latter conclusion is in agreement with the behavior of massive MoS_2. These large crystals absorb adduct only at saturation and leave no residue. This definitely shows capillary condensation and no intercalation. The residue formed by reaction of adduct with the relatively smaller number of edge atoms in this case was apparently too small to be detected. The conclusion, then, is that BN and MoS_2 are not intercalated by these three adducts.

ACKNOWLEDGMENTS

Grateful acknowledgment is made to Professor R. M. Barrer and his staff for their hospitality during my study leave at Imperial College, London, where this was written.

REFERENCES

1. W. RÜDORFF. Z. anorg. u. allgem. Chem. **245**, 383 (1941).
2. A. HEROLD. Compt. rend. **239**, 591 (1954).
3. L. H. REYERSON, J. E. WERTZ, W. WELTNER, and H. WHITEHURST. J. Phys. Chem. **61**, 1334 (1957).
4. G. R. HENNIG. J. Chem. Phys. **20**, 1443 (1952).
5. W. RÜDORFF, V. SILS, and R. ZELLER. Z. anorg. u. allgem. Chem. **283**, 299 (1956).
6. R. C. CROFT and R. G. THOMAS. Nature, **168**, 32 (1951).
7. R. C. CROFT. Australian J. Chem. **9**, 184 (1956).
8. W. RÜDORFF and E. STUMPP. Z. Naturforsch. Pt. b, **13b**, 459 (1958).
9. W. RÜDORFF. Angew. Chem. **71**, 487 (1959).
10. CABOT CARBON BLACKS UNDER THE ELECTRON MICROSCOPE. G. Cabot, Inc., Boston, Mass., U.S.A. 1953. pp. 59, 89.
11. G. R. FINLAY and G. H. FETTERLEY. Ceram. Bull. **31**, 141 (1952).
12. J. G. HOOLEY. Can. J. Chem. **35**, 374 (1957).
13. J. G. HOOLEY. Can. J. Chem. **35**, 1414 (1957).
14. W. SCHONIGER. Mikrochim. Acta, 123 (1955).
15. J. G. HOOLEY. Can. J. Chem. **37**, 899 (1959).
16. J. H. DE BOER. The structure and properties of porous materials. *Edited by* D. H. Everett and F. S. Stone. Butterworths, London. 1958. p. 68.
17. G. HENNIG. J. Chem. Phys. **20**, 1438 (1952).
18. T. E. THORPE. J. Chem. Soc. **23**, 31 (1870).

A CALCULATION OF THE H_2O_2 MOLECULE BY THE LCAO–MO–SCF METHOD

YOSHITO AMAKO[1] AND PAUL A. GIGUÈRE
Department of Chemistry, Laval University, Québec, Que.

Received October 16, 1961

ABSTRACT

The electronic structure of the hydrogen peroxide molecule in three different configurations, namely the cis, the trans, and the non-planar or skew forms, were calculated according to the LCAO–MO–SCF approximation. All the electrons were considered except those of the K-shell of the oxygen atoms. The orbitals of these atoms are essentially of the sp^3 hybrid type. It was shown that the skew form of the molecule with an azimuthal angle Φ of about 120° is the most stable, due mainly to conjugation of the σ_5 and σ_6 orbitals of the oxygen atoms with the other molecular orbitals. On the contrary, in the cis and trans forms these two orbitals are non-bonding. Because of the approximate nature of the treatment, especially as regards the screening effect of the K-electrons, the calculated orbital energies are definitely too large. However, the heights found for the cis and the trans barriers are in a reasonable mutual ratio. Numerical values were also obtained for the ionization potentials and the dipole moment of the skew model; the latter result, 2.05 D, agrees well with the experimental data.

INTRODUCTION

The first computation of the electronic structure of the H_2O_2 molecule was done in 1934 by Penney and Sutherland (1, 2) using the electron pair method and taking into account only the $2p$ electrons of the oxygen atoms. This first approximation was sufficient to prove that, somewhat contrary to expectation, a skew configuration of the molecule (Fig. 1*c*) with an azimuthal (or dihedral) angle Φ of the order of 100° should be more stable than either the trans or the cis configurations. Because of interaction of the unshared electron pairs on the oxygen atoms, free rotation of the OH groups about the O—O bond is opposed presumably by a high cis and a low trans energy barrier (Fig. 2). The same conclusion was reached later by Lassettre and Dean (3) from calculation of the electrostatic forces between various electron configurations of the molecule. Depending on the assumed values for the quadrupole moments, they arrived at azimuthal angles Φ ranging from 94° to 113°, but their barrier heights were appreciably different from those of Penney and Sutherland. In fact a wide variety of estimates have been made so far for these energy barriers, based either on calculations or on experimental data (Table I). It was thought that a treatment of this molecule after the molecular

TABLE I

Previous estimates of energy barriers to internal rotation in H_2O_2

Trans	Cis	Method	Reference
~6 kcal	~10 kcal	Calculation (electron pairs)	1
~0.5 ev	~1 ev	" " "	2
2.3–10 kcal	12–20 kcal	" quadrupole moments	3
1.8 kcal	6.9 kcal	" (Fourier coefficients)	4
*6 kcal		Infrared spectra	5
*4.7 kcal		" "	6
*3.5 kcal		Low-temperature calorimetry	7
113 cm^{-1}		Microwave spectra	8
590 cal	1290 cal	Calculation	9
300 cm^{-1}	1300 cm^{-1}	Infrared spectra (rotational)	10

*Average value for a symmetrical twofold barrier. 1 ev = 23.06 kcal; 1 cm^{-1} = 2.8 cal.

[1]*Postdoctorate Fellow of the National Research Council for 1960–1961.*

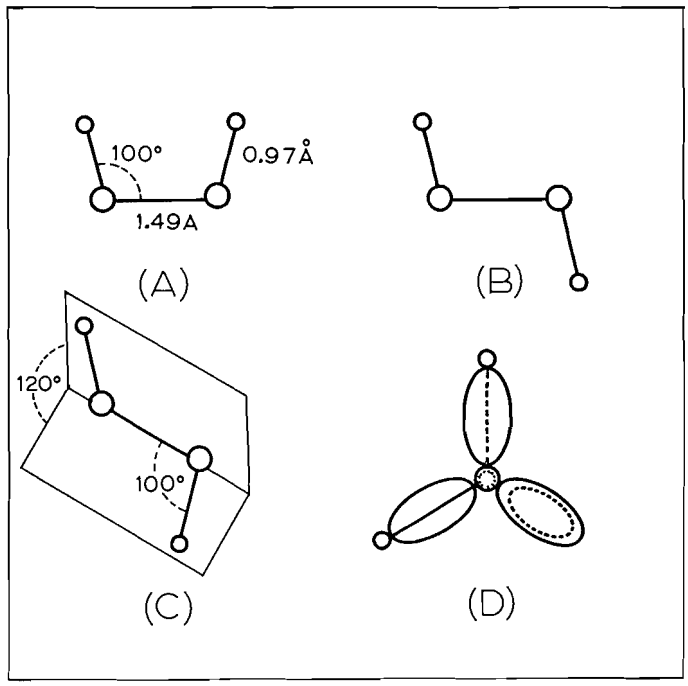

FIG. 1. Possible configurations for the H_2O_2 molecule: (A) cis, (B) trans, (C) skew, (D) projection of the latter along the O–O axis showing the lone pair orbitals of the oxygen atoms.

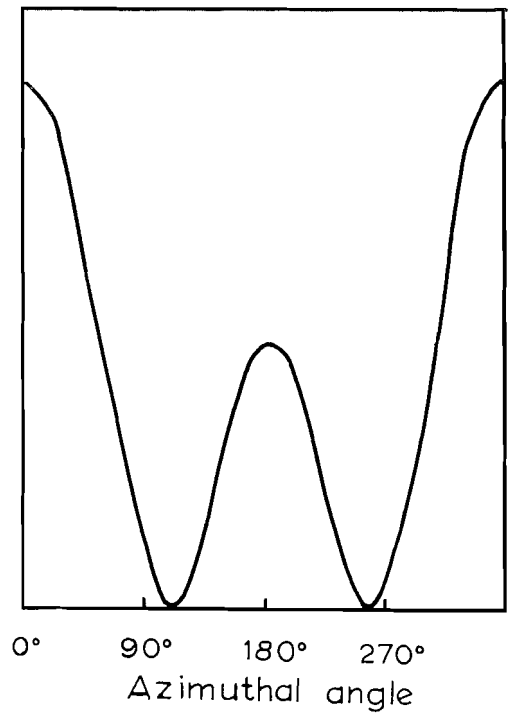

FIG. 2. Potential barriers hindering internal rotation in the H_2O_2 molecule.

orbital approximation—more precisely, the one known as "linear combination of atomic orbitals, molecular orbitals, self-consistent field"—would add to our knowledge, particularly on the type of hybridization of the oxygen atom orbitals and the true configuration of the ground state. Because of limited time and computation facilities, numerous approximations had to be made, the most serious of which was the neglect of the K-shell electrons of the oxygen atoms. Largely because of that, the calculated orbital energies turned out to be too large. Nevertheless, it is of interest that the MO method places the three possible forms of the H_2O_2 molecule not only in the correct order of stability, namely skew > trans > cis, but also on a plausible relative scale.

DETAILS OF THE CALCULATIONS

The method followed here was first outlined by Roothan (11). Throughout the calculations Slater's atomic wave functions were used:

$$h_1, h_2 = \frac{1}{\sqrt{\pi}} \exp(-Z_1 r_{1,2}),$$

$$s_{1,2} = \sqrt{\frac{Z_2^5}{3\pi}}\, r_{1,2} \exp(-Z_2 r_{1,2}),$$

$$x_{1,2} = \sqrt{\frac{Z_2^5}{\pi}}\, r_{1,2} \sin\theta_{1,2} \cos\phi_{1,2} \exp(-Z_2 r_{1,2}),$$

$$y_{1,2} = \sqrt{\frac{Z_2^5}{\pi}}\, r_{1,2} \sin\theta_{1,2} \sin\phi_{1,2} \exp(-Z_2 r_{1,2}),$$

$$z_{1,2} = \sqrt{\frac{Z_2^5}{\pi}}\, r_{1,2} \cos\theta_{1,2} \exp(-Z_2 r_{1,2}),$$

where h_1, h_2 indicate the $1s$ atomic orbitals of the two hydrogen atoms, $s_{1,2}$, $x_{1,2}$, $y_{1,2}$, and $z_{1,2}$, the $2s$, $2p_x$, $2p_y$, and $2p_z$ atomic orbitals of the oxygen atoms. $Z_{1,2}$ corresponds to the Slater effective nuclear charge, namely $Z_1 = 1$ and $Z_2 = 2.257$.

The three structural parameters, $r_{O-O} = 1.49$ Å, $r_{O-H} = 0.97$ Å, and $\theta_{OOH} = 100°$ (Fig. 1), selected for these calculations were taken from a critical compilation (12) of all the experimental data available at the time. The latest investigations (10, 13) seem to indicate a trend towards slightly smaller values for both bond lengths as well as for the angle θ. Since the same parameters were used for the three configurations, it follows that the results for the cis and trans forms are less correct than those for the skew form. As for the azimuthal angle Φ, its value had to be assumed a priori because it was not feasible to repeat the calculations for more than one skew model. The original estimate of Penney and Sutherland, namely 90° from interaction of the lone pair electrons plus some 5° or 10° due to repulsion of the hydrogen atoms, was based on the premise of pure p orbitals for the oxygen atoms. However, by analogy with the case of H_2O, it is more likely that the orbitals of the oxygen atoms in H_2O_2 are of the sp^3 hybrid type. Therefore, the major interaction between the two OH groups in that molecule should have near-threefold symmetry and, accordingly, the azimuthal angle was taken as 120°.

For simplicity the y axis was chosen as coincident with the O—O bond and one of the OH groups was considered as fixed in space. (Cf. Fig. 3 for the coordinate system.) Then the atomic wave functions for the skew and the trans forms were written down as follows, for example,

$$[1] \qquad (z_2)_{skew} = -\cos(\pi - \Phi) \cdot (z_2)_{cis} + \sin(\pi - \Phi) \cdot (x_2)_{cis},$$

$$[2] \qquad (z_2)_{trans} = -(z_2)_{cis},$$

so that the integrals for these two forms could be derived from those for the cis form.

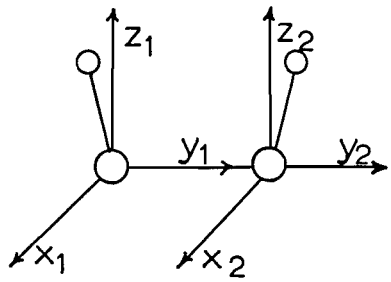

FIG. 3. System of coordinates used for the calculations.

Symmetry Orbitals

It was convenient to transform each atomic wave function into symmetry orbitals according to the point-group symmetry of the three forms of the molecule considered here, these being C_{2v} for the cis, C_2 for the skew, and C_{2h} for the trans forms. These symmetry orbitals can be classified as follows:

I. Cis form (C_{2v})

$$A_1: \quad \sigma_1 = \frac{1}{\sqrt{2}}(h_1+h_2),$$

$$\sigma_2 = \frac{1}{\sqrt{2}}(s_1+s_2),$$

$$\sigma_3 = \frac{1}{\sqrt{2}}(y_1-y_2),$$

$$\sigma_4 = \frac{1}{\sqrt{2}}(z_1+z_2);$$

$$A_2: \quad \sigma_5 = \frac{1}{\sqrt{2}}(x_1-x_2);$$

$$B_1: \quad \sigma_6 = \frac{1}{\sqrt{2}}(x_1+x_2);$$

$$B_2: \quad \sigma_7 = \frac{1}{\sqrt{2}}(h_1-h_2),$$

$$\sigma_8 = \frac{1}{\sqrt{2}}(s_1-s_2),$$

$$\sigma_9 = \frac{1}{\sqrt{2}}(y_1+y_2),$$

$$\sigma_{10} = \frac{1}{\sqrt{2}}(z_1-z_2).$$

II. Skew form (C_2)

$$A: \quad \sigma_1, \sigma_2, \sigma_3, \sigma_4, \sigma_5;$$

$$B: \quad \sigma_7, \sigma_8, \sigma_9, \sigma_{10}, \sigma_6.$$

III. Trans form (C_{2h})

$$A_g\colon\ \sigma_1, \sigma_2, \sigma_3, \sigma_4;$$

$$A_u\colon\ \sigma_5;$$

$$B_g\colon\ \sigma_6;$$

$$B_u\colon\ \sigma_7, \sigma_8, \sigma_9, \sigma_{10}.$$

These symmetry orbitals made it possible to reduce the 10×10 determinant into smaller ones, namely, two 4×4 and two 1×1 for each of the cis and the trans forms, and two 5×5 for the skew form of the molecule. The general procedure followed was the same as used by Mulligan (14) for his study of the CO_2 molecule. In the present case the bare nuclear field potentials are written thus:

$$[3] \qquad H = -\frac{\nabla^2}{2} - \frac{1}{r_{H_1}} - \frac{1}{r_{H_2}} - \frac{6}{r_{O_1}} - \frac{6}{r_{O_2}},$$

the nuclear charge on the oxygen atoms being arbitrarily taken as 6 because of exclusion of the K-shell electrons. Therefore, the energy values calculated refer to that hypothetical state.

DISCUSSION

Molecular Orbitals and Energies

The various orbital energies found for each form of the molecule are shown schematically in Fig. 4 and are listed below along with the corresponding wave functions. Each MO is denoted by the symbol of irreducible representation to which it belongs preceded by a running number which identifies the orbitals of the same symmetry. The σ_n terms are the symmetry orbitals defined above.

One obvious conclusion from these results is the fact that the s orbitals of the oxygen atoms share in the bonding in each and every MO. Therefore, the valence state of oxygen in H_2O_2 must be nearer to the sp^3 hybrid than to the pure p state, as we assumed originally by analogy with the case of H_2O, and the electron distribution must be approximately tetrahedral. Another significant conclusion relates to the behavior of the σ_5 and σ_6 orbitals, which are non-bonding in the cis and trans forms, but take part in conjugation with the other MO in the skew form. The increased stability of the latter stems mainly from this unique property. Recently, Pauling (15) has assumed sp hybridization for the oxygen atoms in H_2O_2 which, as in the treatment of Penney and Sutherland, leads to an azimuthal angle Φ close to 90°.

The Azimuthal Angle

Since in the MO approximation the interaction of the non-bonding orbitals of oxygen with the hydrogen orbitals is the major factor in stabilizing the skew form of H_2O_2, it follows that maximum overlap between them will occur for an azimuthal angle of about 120° as shown in Fig. 1*d*. A number of values have been found or proposed for this parameter following the original estimate of Penney and Sutherland (Table II). The first pertinent spectroscopic evidence (16) showed that the H_2O_2 molecule is in fact a slightly asymmetric top; from this it was predicted that Φ could not be in the range 85°–95°. Because it is unlikely a priori that Φ be much smaller than a right angle, a larger value seemed favored. In a recent neutron diffraction study of the H_2O_2 single crystal (13) where the hydrogen atoms could be located, Φ was found nearly equal to

Energy (ev)	Wave function
	Cis form
− 68.282	$\psi(1\,a_1) = 0.0644\,\sigma_1 - 0.9642\,\sigma_2 + 0.0169\,\sigma_3 - 0.1104\,\sigma_4$
− 65.003	$\psi(1\,b_2) = 0.0722\,\sigma_7 - 1.1154\,\sigma_8 + 0.0062\,\sigma_9 - 0.0081\,\sigma_{10}$
− 17.122	$\psi(2\,b_2) = 0.6499\,\sigma_7 - 0.2937\,\sigma_8 - 0.2119\,\sigma_9 + 0.6938\,\sigma_{10}$
− 16.405	$\psi(2\,a_1) = 0.2045\,\sigma_1 + 0.0316\,\sigma_2 - 0.8916\,\sigma_3 - 0.1029\,\sigma_4$
− 10.499	$\psi(3\,a_1) = 0.5469\,\sigma_1 - 0.3628\,\sigma_2 + 0.0874\,\sigma_3 + 0.6423\,\sigma_4$
− 6.119	$\psi(b_1) = 0.9670\,\sigma_6$
− 4.084	$\psi(3\,b_2) = 0.4298\,\sigma_7 - 0.3883\,\sigma_8 - 0.9644\,\sigma_9 - 0.5432\,\sigma_{10}$
− 0.623	$\psi(a_2) = 1.0366\,\sigma_5$
12.008	$\psi(4\,a_1) = 0.9804\,\sigma_1 - 0.4870\,\sigma_2 + 0.2092\,\sigma_3 - 0.8246\,\sigma_4$
29.796	$\psi(4\,b_2) = 1.2185\,\sigma_7 - 0.3535\,\sigma_8 + 0.6307\,\sigma_9 - 0.7019\,\sigma_{10}$
	Skew form
− 65.391	$\psi(1a) = 0.1128\,\sigma_1 + 0.8508\,\sigma_2 + 0.0478\,\sigma_3 + 0.0546\,\sigma_4 + 0.0526\,\sigma_5$
− 61.863	$\psi(1b) = 0.1697\,\sigma_7 + 0.9846\,\sigma_8 - 0.0496\,\sigma_9 + 0.0244\,\sigma_{10} + 0.0681\,\sigma_6$
− 22.875	$\psi(2a) = 0.5158\,\sigma_1 - 0.2941\,\sigma_2 - 0.3335\,\sigma_3 + 0.6023\,\sigma_4 - 0.3641\,\sigma_5$
− 21.745	$\psi(2b) = 0.6033\,\sigma_7 - 0.3762\,\sigma_8 + 0.1121\,\sigma_9 + 0.6424\,\sigma_{10} - 0.0564\,\sigma_6$
− 12.537	$\psi(3a) = 0.1399\,\sigma_1 + 0.0572\,\sigma_2 - 0.7260\,\sigma_3 - 0.3133\,\sigma_4 + 0.5306\,\sigma_5$
− 12.447	$\psi(3b) = 0.1788\,\sigma_7 - 0.0282\,\sigma_8 - 0.0339\,\sigma_9 - 0.2613\,\sigma_{10} - 0.9920\,\sigma_6$
− 6.431	$\psi(4a) = 0.1510\,\sigma_1 - 0.2537\,\sigma_2 + 0.3646\,\sigma_3 + 0.4075\,\sigma_4 + 0.7435\,\sigma_5$
11.703	$\psi(4b) = 0.2678\,\sigma_7 - 0.4526\,\sigma_8 - 1.0999\,\sigma_9 - 0.1540\,\sigma_{10} + 0.0873\,\sigma_6$
23.036	$\psi(5a) = 1.0882\,\sigma_1 - 0.6953\,\sigma_2 + 0.2716\,\sigma_3 - 0.7517\,\sigma_4 - 0.0444\,\sigma_5$
40.774	$\psi(5b) = 1.1106\,\sigma_7 - 0.4782\,\sigma_8 + 0.3781\,\sigma_9 - 0.8261\,\sigma_{10} + 0.2042\,\sigma_6$
	Trans form
− 64.972	$\psi(1a_g) = 0.1015\,\sigma_1 + 0.8691\,\sigma_2 - 0.0054\,\sigma_3 + 0.0633\,\sigma_4$
− 60.976	$\psi(1\,b_u) = 0.1131\,\sigma_7 + 1.0372\,\sigma_8 + 0.0249\,\sigma_9 + 0.0052\,\sigma_{10}$
− 19.956	$\psi(2\,b_u) = 0.6962\,\sigma_7 - 0.4219\,\sigma_8 - 0.1109\,\sigma_9 + 0.5412\,\sigma_{10}$
− 17.673	$\psi(2\,a_g) = 0.5477\,\sigma_1 - 0.3512\,\sigma_2 - 0.3463\,\sigma_3 + 0.6508\,\sigma_4$
− 16.263	$\psi(b_g) = 1.0366\,\sigma_6$
− 12.689	$\psi(a_u) = 0.9670\,\sigma_5$
− 6.766	$\psi(3\,a_g) = 0.0345\,\sigma_1 + 0.1411\,\sigma_2 - 0.8075\,\sigma_3 - 0.4977\,\sigma_4$
15.235	$\psi(3\,b_u) = 0.3780\,\sigma_7 - 0.3841\,\sigma_8 - 0.9941\,\sigma_9 - 0.4837\,\sigma_{10}$
21.769	$\psi(4\,a_g) = 0.0818\,\sigma_1 + 0.0644\,\sigma_2 - 0.8671\,\sigma_3 - 0.3411\,\sigma_4$
40.973	$\psi(4\,b_u) = 1.0333\,\sigma_7 - 0.3742\,\sigma_8 + 0.6062\,\sigma_9 - 0.8025\,\sigma_{10}$

a right angle. However, this result in no way conflicts with the present conclusion since the two correspond in fact to different physical states of the molecule. In the crystal, packing conditions and intermolecular forces are sufficient to distort the azimuthal angle appreciably from its value in the free molecule, because the restoring force involved is certainly small (low barriers to internal rotation). This is borne out by the rather wide range of values reported for Φ (from 90° to 130°) in various crystals (Table II). A high-dispersion study of the rotational structure of several infrared bands of H_2O_2 has been carried out lately (10) from which it was possible to get very accurate rotational constants of the molecule. It is gratifying that the azimuthal angle thus found agrees exactly with our conclusion.

Ionization Potentials

The above results for the ionization potentials refer to an hypothetical energy state since the *K*-shell electrons were not included in the calculations. In order to translate these data into the actual state of the molecule, we assume that the energy of the highest filled orbital is equal to the one experimentally known ionization potential, 11.26 ev (20). Addition of this *ad hoc* constant, 4.83 (= 11.26 − 6.43), yields the values shown in Fig. 4. Experimental data with which to compare the above are lacking unfortunately. Nevertheless, it is of interest that they agree nicely with the theoretical estimates of Mulliken (21) for levels 3 and 2 (Fig. 4, last column).

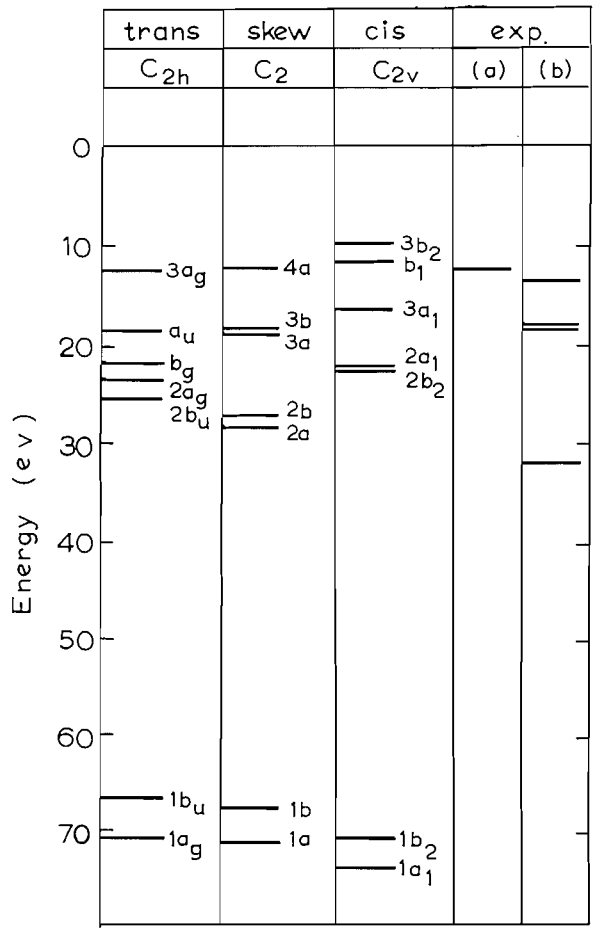

FIG. 4. Schematic energy levels for the three configurations of the H_2O_2 molecule. Experimental data: (*a*) Lindeman and Guffy (20), (*b*) Mulliken's estimates (21).

TABLE II

Previous estimates of the azimuthal angle in H_2O_2

Method	Φ	Reference
Calculation (valence bond approximation)	~100°	1
" (electrostatic forces)	94°–113°	3
Infrared spectra (rotational)	>95°	16
X-ray diffraction of crystalline $CO(NH_2)_2 \cdot H_2O_2$	106°	17
" " " H_2O_2	93.5°	18
" " " $H_2O_2 \cdot 2H_2O$	130°	19
Neutron diffraction of crystalline H_2O_2	90.8°	13
Infrared spectra (rotational)	119.8°	10

Dipole Moment

Using the well-known equation

$$\mu = \int \psi_\epsilon \sum_i r_i \psi dv \qquad [4]$$

the dipole moment of the skew form of H_2O_2 with $\Phi = 120°$ was calculated to be 2.05 D. The necessary integrals, listed below in Table III, refer to the C_2 axis of the molecule.

TABLE III

Dipole moment integrals

$(h_1 z_m h_1)$ =	0.85951	$(h_1 z_m s_2)$ =	0.02047
$(h_1 z_m s_1)$ =	0.06310	$(h_1 z_m y_2)$ =	0.00187
$(h_1 z_m z_1)$ =	0.13595	$(h_1 z_m z_2)$ =	0.00107
$(h_1 z_m y_1)$ =	−0.02397	$(h_1 z_m x_2)$ =	−0.00093

Experimental values of 2.13 D for dilute solutions in dioxane and, more recently, of 2.26 D from the Stark effect in the microwave spectrum of the vapor, have been reported in the literature (12).

Total Energy

The total electronic energy is given by the equation

$$E_n = \sum_{i}^{\text{occup}} 2H_i + \sum_{i}^{\text{occup}} \sum_{j=1} (2J_{ij} - K_{ij}) \qquad [5]$$

and the orbital energy, by

$$\epsilon_i = H_i + \sum_{j=1}^{\text{occup}} (2J_{ij} - K_{ij}). \qquad [6]$$

Then the total energy is expressed as

$$E_n = \sum_{i}^{\text{occup}} (H_i + \epsilon_i) \qquad [7]$$

where

$$H_i = \int \psi_i H \psi_i dv$$

and

$$\psi_i = \sum b_{ip} \chi_p.$$

The calculated values of H_i are listed in Table IV from which the relative stability of the three forms of the H_2O_2 molecule appear in the expected order, namely, skew > trans > cis. The differences between them are in the ratio 3 to 1, which seems quite

TABLE IV

Total energy of the H_2O_2 molecule*

	Cis	Skew	Trans
H_1	− 18.0694	− 17.6835	− 17.6262
H_2	− 17.7574	− 17.3762	− 17.6454
H_3	− 13.1030	− 13.8647	− 12.3882
H_4	− 14.8231	− 12.7954	− 13.3904
H_5	− 12.5929	− 14.7582	− 14.5890
H_6	− 13.9370	− 14.4826	− 14.1643
H_7	− 13.9745	− 13.3801	− 14.3353
ΣH_i	−104.2573	−104.3407	−104.1388
$\Sigma \epsilon_i$	− 13.7828	− 14.9423	− 14.6487
Total electronic energy	−118.0401	−119.2830	−118.7875
Nuclear repulsion energy	45.9336	45.7813	45.7552
Total molecular energy	− 72.1065	− 73.5017	− 73.0323

*In atomic units. Contribution of the *K*-shell electrons not included.

plausible, although the actual figures are certainly too large for the corresponding barrier heights. As pointed out above these exceedingly large orbital energies are due mainly to the exclusion from our calculation of the K-electrons of the oxygen atoms, and the uncertainty as to their screening effect on the outer electrons. Indeed, for lack of a more reliable estimate a screening factor of one was assumed. This, and a number of other approximations, had to be resorted to in evaluating the many integrals involved, nearly one thousand in all.

ACKNOWLEDGMENTS

The authors are grateful to the National Research Council for a generous research grant, to the "Centre de Calcul de l'Université Laval", and to the IBM Company for assistance in carrying out the computations.

RÉSUMÉ

On présente les résultats de calculs par la méthode LCAO–MO–SCF de la structure électronique de la molécule H_2O_2 dans trois configurations possibles, soit cis, trans et oblique. On prouve que cette dernière, dans laquelle l'angle dièdre est d'environ 120°, est plus stable que les deux autres à cause de la conjugaison des orbitales σ_5 et σ_6 des atomes d'oxygène avec les autres orbitales moléculaires. Au contraire, dans les formes cis et trans ces deux orbitales demeurent non-liantes. On montre que les orbitales de l'oxygène sont dans l'état hybride sp^3 et on calcule les potentiels d'ionisation et le moment dipolaire de la molécule. Les résultats sont en bon accord avec les données de la littérature. Par contre les différences entre l'énergie totale calculée pour les trois formes conduisent à des valeurs trop fortes pour les barrières de potentiel qui gênent la rotation libre dans la molécule H_2O_2.

REFERENCES

1. W. G. Penney and G. B. B. M. Sutherland. Trans. Faraday Soc. **30**, 898 (1934).
2. W. G. Penney and G. B. B. M. Sutherland. J. Chem. Phys. **2**, 492 (1934).
3. E. N. Lassettre and L. B. Dean. J. Chem. Phys. **17**, 317 (1949).
4. N. W. Luft. J. Chem. Phys. **22**, 1814 (1954).
5. I. D. Liu. Ph.D. Thesis, Laval University, Quebec, Que. 1954.
6. O. Bain and P. A. Giguère. Can. J. Chem. **33**, 527 (1955).
7. P. A. Giguère, I. D. Liu, J. S. Dugdale, and J. A. Morrison. Can. J. Chem. **32**, 117 (1954).
8. J. T. Massey and D. R. Harris. J. Chem. Phys. **22**, 442 (1954).
9. E. Hirota. J. Chem. Phys. **28**, 839 (1958).
10. R. L. Redington, W. B. Olson, and P. C. Cross. J. Chem. Phys. In press.
11. C. C. J. Roothan. Revs. Modern Phys. **23**, 69 (1951).
12. W. S. Schumb, C. N. Satterfield, and R. L. Wentworth. Hydrogen peroxide. Reinhold Publishing Corp., New York. 1955.
13. W. R. Busing and H. A. Levy. Chem. Ann. Prog. Rep. Oak Ridge National Laboratory. June 20, 1959.
14. J. F. Mulligan. J. Chem. Phys. **19**, 347 (1951).
15. L. Pauling. The nature of the chemical bond. 3rd ed. Cornell University Press, Ithaca, N.Y. 1960. p. 134.
16. L. R. Zumwalt and P. A. Giguère. J. Chem. Phys. **9**, 458 (1941).
17. C. S. Lu, E. W. Hughes, and P. A. Giguère. J. Am. Chem. Soc. **63**, 1507 (1941).
18. S. C. Abrahams, R. L. Collin, and W. N. Lipscomb. Acta Cryst. **4**, 15 (1951).
19. I. Olovsson and D. H. Templeton. Acta Chem. Scand. **14**, 1325 (1960).
20. L. P. Lindeman and J. C. Guffy. J. Chem. Phys. **29**, 246 (1958).
21. R. S. Mulliken. J. Chem. Phys. **3**, 506 (1935).

APPENDIX

The calculations for the cis and the trans forms were made manually but for the skew model an IBM 605 computer was used. For the program of the latter, the secular determinant is written as follows

$$|(H+G)-S\epsilon| \equiv 0, \qquad [8]$$

where the terms containing the energy parameters appear in the non-diagonal elements. These terms are usually missing in the eigenvalue problems for which programs are available at present. Therefore a special program had to be set up, which required finding out the inverse matrix S^{-1}

$$S^{-1}S = \delta. \qquad [9]$$

Through multiplication of the above secular determinant by the inverse matrix

$$|S^{-1}(H+G)-\delta\epsilon| \equiv 0 \qquad [10]$$

we revert to the usual eigenvalue problem.

MANGANESE(III) COMPLEXES WITH ETHYLENEDIAMINETETRAACETIC ACID[1]

Y. YOSHINO, A. OUCHI, Y. TSUNODA, AND M. KOJIMA[2]
Department of Chemistry, The College of General Education, University of Tokyo, Meguro-ku, Tokyo, Japan

Received December 28, 1961

ABSTRACT

Manganese(III) ethylenediaminetetraacetic acid complex has been prepared by various methods. The solid having a composition of $KMnY.2.5H_2O$ is obtained as deep red crystals when the manganese dioxide suspension reacts with free ethylenediaminetetraacetic acid (H_4Y). The manganese was shown to be trivalent from its redox equivalent in its reaction with acidified iodide solution, and its magnetic moment, which was 4.89 Bohr magnetons, corresponding to four unpaired electron spins. The complex ion has an absorption maximum at 500 mμ ($\log \epsilon = 2.67$) in a slightly acidic medium. The variation of the visible spectra with pH has been studied by the spectrophotometric method, the value $pK \simeq 5.3$ being obtained between the red and the yellow species. Observations have been made on the type of bond between the metal and carboxylate groups by the infrared spectral method. From its ion-exchange and pH titration behavior a formula, $K[Mn(OH_2)EDTA].1.5H_2O$, was suggested.

INTRODUCTION

The formation of manganese(III)–EDTA complex in solution was utilized by Přibil *et al.* for the photometry and redox titration of manganese (1, 2, 3). They oxidized divalent manganese to the trivalent state by means of lead dioxide, sodium bismuthate, etc. in the presence of excess EDTA. However, since the manganese(III)–EDTA complex solution thus obtained contains reaction products of the oxidizing agents, their methods for the formation of the manganese(III)–EDTA complex was found to be unsuitable for studying the nature of the complex. In the course of study on the stabilization of less familiar oxidation states of metals by coordination (4, 5), the present authors have found that the manganese(III)–EDTA complexes could be formed by the reaction of EDTA with manganese compounds of higher oxidation states, such as manganese dioxide or potassium permanganate. The critical examination of stoichiometry of the complex formation reaction revealed that the manganese dioxide or permanganate ion was reduced by EDTA itself, giving a reddish-purple solution of the manganese(III)–EDTA complex. After a number of attempts, we have been able to prepare a crystalline solid. The present paper describes the preparation and properties of the complex of this sort.

EXPERIMENTAL

Materials

Inorganic salts, acids, and bases were all the JIS[3] special-class grade. Free acid (H_4Y) and disodium salt ($Na_2H_2Y.2H_2O$) of ethylenediaminetetraacetic acid were also the JIS special-class grade. Fe(III)–EDTA chelate, $NaFe(C_{10}H_{12}N_2O_8).2H_2O$, purchased from Daiichi Pure Chemicals Co., was of reagent grade. Co(III)–EDTA chelate, $KCo(C_{10}H_{12}N_2O_8).2H_2O$, was prepared according to the method of Dwyer *et al.* (6). Organic solvents of the JIS first-class grade were used after distillation.

As ion-exchange resins, strongly acidic cation-exchange resin Diaion SK-1 of 100–200 mesh (sulphonated polystyrene-divinyl-benzene copolymer, purchased from Mitsubishi Kasei Co., Tokyo) and strongly basic anion-exchange resin, Dowex 1-X8, 100–200 mesh, were employed in a column method.

[1]*Presented in part at the 14th Annual Conference of the Chemical Society of Japan in Tokyo in April, 1961. Preliminary paper was published in the Bull. Chem. Soc. Japan,* ***34****, 1194 (1961).*
[2]*Present address: Government Chemical Industrial Research Institute, Tokyo.*
[3]*Japanese Industrial Standard.*

Instruments

Magnetic measurements were made on the solid complex using a Goüy apparatus of conventional type. An X-ray diffractometer, "Geigerflex" of Rigaku Denki Co., was used for examining powder diffraction patterns of the chelate using Cu K_{α_1} ray. For thermal analysis, the "Tokoshi type" thermobalance was used. The infrared spectra were recorded with a recording spectrophotometer of Nihon Bunko Co., type DS-301, equipped with a sodium chloride prism. As the sample, which was handled as a potassium bromide pellet, decomposed gradually, a Nujol mull technique was employed. Visible and ultraviolet spectra were measured with the EPS II recording spectrophotometer and the EPU II spectrophotometer, both from Hitachi Co. The pH of the solution was measured by a glass electrode pH-meter of Iio Denki Co., model 43.

PREPARATION OF COMPLEXES

(i) Formation of Manganese(III)–EDTA Complex in Solution

In preliminary attempts, various methods for the preparation of the manganese(III)–EDTA complex in solution were tried.

(*a*) Freshly prepared manganese dioxide suspended in water was mixed with solid EDTA (H_4Y) under vigorous stirring. The resultant reddish purple complex in the filtrate was determined by both spectrophotometry and iodometric titration. The relation between the mole ratio EDTA to MnO_2 and that of produced Mn(III)–EDTA complex was shown in Fig. 1. During the reaction the evolution of carbon dioxide was observed

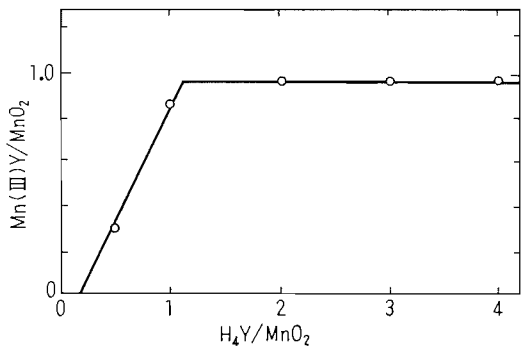

FIG. 1. Relation between the mole ratio of EDTA to manganese dioxide and the mole ratio of produced Mn(III)Y to manganese dioxide (MnO_2: 2.69×10^{-3} mole).

and a little of EDTA was lost; this may be due to the oxidation of EDTA by manganese dioxide. However, the mole ratio of Mn(III) to EDTA in the complex was found to be close to 1:1.

(*b*) In the above-mentioned case, H_4Y could be replaced by a mixed solution of Na_2H_2Y and acetic acid (pH 2.5–3). In this case, however, the yield, i.e., the ratio of Mn(III)–EDTA to MnO_2, showed a maximum at EDTA/$MnO_2 \simeq 1$, and then gradually decreased as the ratio EDTA/MnO_2 was increased. This is presumably ascribed to the partial decomposition of Mn(III)–EDTA by the excess of EDTA in the solution.

(*c*) It was also found that potassium permanganate could be used in place of manganese dioxide. The maximum yield was obtained at the point where the mole ratio EDTA/MnO_4^- was a little larger than 1, although the reaction sometimes did not proceed smoothly, depending upon the conditions employed, and the yield and the purity of the products were not always high.

(*d*) The manganese(III)–EDTA complex was also formed by oxidizing manganese(II)–EDTA complex with manganese dioxide. The relation between the obtained Mn(III)–EDTA and the used Mn(II)–EDTA is illustrated in Fig. 2. For a fixed amount of MnO_2, the amount of Mn(III)–EDTA increased until Mn(II)–EDTA/MnO_2 reached ca. 1.7,

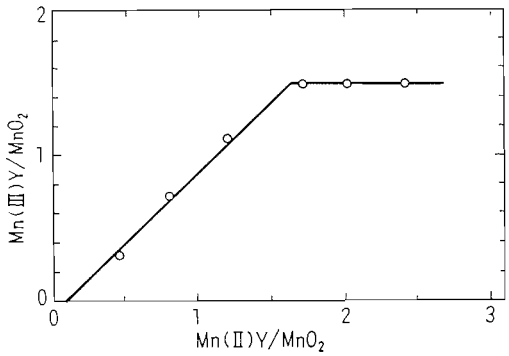

FIG. 2. Relation between the mole ratio of Mn(II)Y to manganese dioxide and the mole ratio of produced Mn(III)Y to manganese dioxide (MnO_2: 2.69×10^{-3} mole).

and then the yield remained nearly constant (Mn(III)–EDTA/$MnO_2 \simeq 1.5$). It seems that the EDTA chelated to Mn(II) is easily decomposed by oxidation, but, in the above case, the main reaction may be

$$2Mn(II)Y + Mn(IV) \rightarrow 2Mn(III)Y + Mn(II).$$

(ii) Preparation of Solid Complex

After a number of attempts, it was found that an extension of the method described above in (*a*) was most suitable for preparing a solid complex. One of the typical methods of preparation of potassium salt is as follows:

Six grams of finely powdered potassium permanganate were added to a mixed solution of 40 ml of water and 10 ml of ethanol. The mixture was shaken and then carefully warmed. After the vigorous reaction had ended, the mixture was warmed repeatedly in order to expell the excess ethanol and aldehyde. To the mixture of manganese dioxide and potassium hydroxide so obtained, 10 g of EDTA (H_4Y) was added. With vigorous stirring, a reaction took place, evolving carbon dioxide, and a deep cherry-red solution was obtained. After the excess manganese dioxide was filtered off with a glass filter, an equal volume of cold ethanol was added to the filtrate. The mixture was allowed to stand for 3–4 hours in a cold, dark place. The precipitated crystals were then filtered off with a glass filter and washed with 90%, then absolute ethanol and ether. Finally they were dried in the air in a cold, dark place. The yield based on the used EDTA (H_4Y) was 45–60%.

When more diluted solution of manganese(III)–EDTA was mixed with an equal volume of ethanol, large, needle-like crystals were obtained after standing of the solution for 1 or 2 days in a refrigerator.

(iii) Analysis

The manganese was separated as hydroxides by the addition of sodium hydroxide and hydrogen peroxide to the complex solution. After the hydroxides were dissolved in dilute sulphuric acid with the aid of sodium sulphite, the manganese was weighed as manganese sulphate, or back-titrated with EDTA and zinc chloride solutions at pH 10 using Eriochrome Black T as indicator. A check on the manganese content was made by iodometric titration: the sample was added to acidified potassium iodide solution, and then liberated iodine was titrated with thiosulphate solution. The results of these separate determinations were in good agreement, and this means that the

manganese in the complex is in a trivalent state. To determine potassium, the solid sample was ignited at red heat and the residue was dissolved in hydrochloric acid. From the solution so obtained, potassium was determined gravimetrically by its weight as potassium sulphate after separation from other constituents. Carbon and hydrogen were determined through microchemical analysis, with special care being taken for the presence of potassium by the addition of tungsten trioxide to the sample. The nitrogen analysis was made by micro-Dumas method.

The results of a typical analysis follow: Found: K, 9.41%; Mn, 12.70%; C, 28.73%; H, 3.85%; N, 6.67%. Calculated for $KMn(III)(C_{10}H_{12}O_8N_2).2.5H_2O$: K, 9.14%; Mn, 12.88%; C, 28.13%; H, 3.91%; N, 6.56%.

That the solid has a 1:1 mole ratio of manganese to EDTA was checked by the EDTA titration method after reducing the complex with ascorbic acid.

PROPERTIES OF COMPLEX

The potassium salt of the manganese(III)–EDTA complex is a deep red crystal. Its X-ray diffraction pattern is shown in Fig. 3. It is very soluble in water, slightly soluble

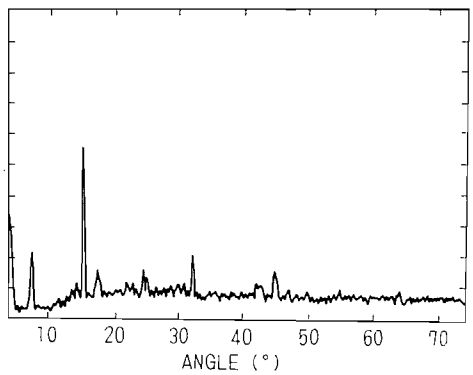

FIG. 3. X-Ray powder diffraction pattern of potassium salt of Mn(III)–EDTA complex (Cu K_{α_1}, λ = 1.54050 Å).

in glacial acetic acid, but insoluble in most organic solvents, such as absolute ethanol, ethyl ether, or acetone. At 0° C, in dark and dry air, the complex can be preserved even after a month, but at room temperature and especially in the daylight, it decomposes rapidly, leaving a colorless mass (probably Mn(II)–EDTA). Such characteristics are quite similar to those of oxalate complexes of trivalent manganese (7).

(i) Magnetic Measurement

As is to be expected the complex is paramagnetic, and the observed susceptibility was 9996×10^{-6} at 21° C. After allowing for the diamagnetic susceptibility of the various atoms the magnetic moment was calculated as 4.89 Bohr magnetons. The calculated value for "spin only" atom with four unpaired electron spins is 4.90. Hence these results support a formula with Mn(III).

(ii) Thermal Analysis

The thermal decomposition behavior of the solid complex was examined from 20° C to 300° C by using a thermobalance. The result is illustrated in Fig. 4. At about 80° C, the weight loss equivalent to ca. 0.5 mole of water per mole of the complex was observed

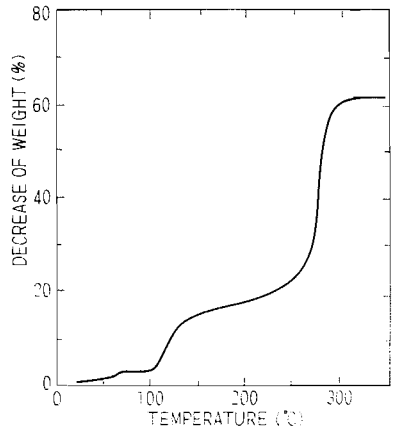

FIG. 4. The thermal analysis of potassium salt of Mn(III)–EDTA complex.

but the oxidation power of the products remained almost unchanged in this range. Hence the decrease of weight at this stage may correspond to the water of crystallization or some form of loosely bound water. At 100–200° C, 12–13% of the weight loss took place. The products at this state were still soluble in water, but the mole ratio of manganese to EDTA was greater than 1. Therefore, the decrease in weight at 100–200° C may correspond to the sum of the weight of the coordinated water and that of decomposed EDTA. The remaining EDTA was completely decomposed at 260–300° C; the residue, ca. 38% of the original sample, is probably a mixture of potassium carbonate and a compound similar to manganese oxycarbonate($MnO.MnCO_3$).

(iii) Infrared Spectra

A typical spectrum of the solid complex was shown in Fig. 5. As is seen in many trivalent transition metal – EDTA chelates (8), a characteristic strong absorption of

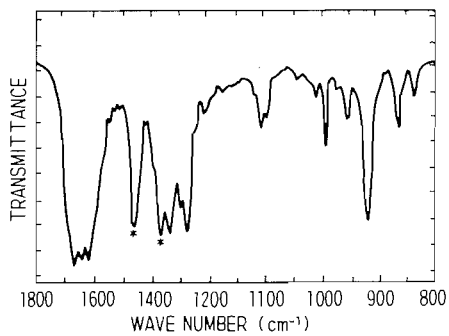

FIG. 5. Infrared spectra of potassium salt of Mn(III)–EDTA complex by Nujol method (*: absorption of Nujol).

the carboxylate group was observed in the 1600–1700 cm^{-1} region, but its fine structure was rather complicated; the complex exhibited three peaks due to antisymmetric vibration of carboxylate group at 1660, 1640, and 1600 cm^{-1}. Assignments for these frequencies would not be easy, but according to the extensive studies by Sawyer *et al.* (8), one possible interpretation would be that at least one of the COO^- groups is not bonded

to the manganese ion. Another factor which should be taken into consideration is a stereochemical one. It has been known that the distortion of octahedron of Mn^{3+} ion gives four short bonds and two long ones (9). In view of this, four carboxylate groups may be bonded to the metal in two ways.

(iv) Visible and Ultraviolet Spectra

Visible absorption spectra of the complex in acetic acid – sodium acetate buffer solutions of various pH were measured, and the results are shown in Fig. 6. Between

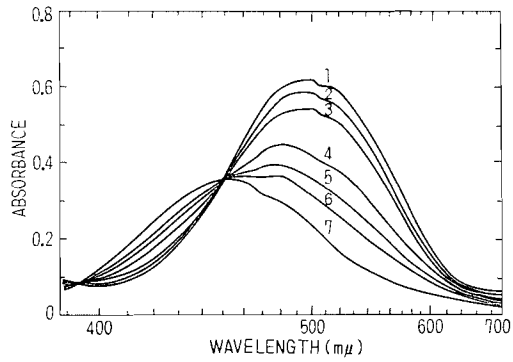

FIG. 6. The absorption spectra of Mn(III)–EDTA complexes in acetic acid – sodium acetate buffer solutions (μ = 0.1, Mn(III)Y: 9.34×10^{-4} mole/l.). The pH values of the solutions are: (1) 2.70, (2) 4.53, (3) 5.00, (4) 5.50, (5) 6.07, (6) 6.57, (7) 9.71.

pH 2.5–4.0 the maximum absorptions were observed at 500 mμ (log ϵ = 2.67), while in the higher pH region the color turned yellow and the maximum shifted to 450 mμ (log ϵ = 2.41). The spectra of the red species are very similar to those of manganese-(III)–trioxalato complex (λ_{max} at 500 mμ, log ϵ = 2.41) (7). As has been interpreted by some authors (10, 11), the absorption at 500 mμ may be due to $t_{2g} \rightarrow e_g$ transition for one 3*d* electron of the Mn^{3+} ion. In the series of these spectra isosbestic points were observed at about 390 mμ and 450 mμ.

Figure 7 illustrates the relation between the extinction at 500 mμ and the pH of the solutions. From this, the p*K* value between red and yellow species was evaluated as 5.3.

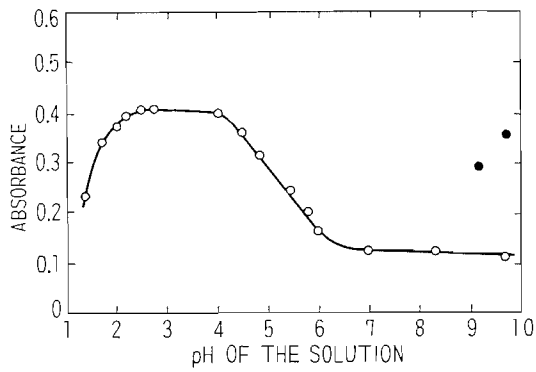

FIG. 7. The absorbance of Mn(III)–EDTA complexes at 500 mμ in acetic acid – sodium acetate buffer solutions (μ = 0.1, Mn(III)Y: 5.90×10^{-4} mole/l.) (●: absorbance of MnO_2 colloidal solution).

The yellow species was more unstable and readily decomposed in aqueous solution, giving manganese dioxide precipitation. However, when its solution was acidified immediately after its formation, the spectra and oxidation equivalent of the reproduced red species was nearly the same as those of the original red species. Yet, the attempts to produce the yellow species directly from manganese dioxide and alkaline EDTA solution or to obtain the solid yellow species have not been successful.

In the ultraviolet region, no remarkable absorption maximum was recognized but the absorption increased rapidly as the wavelength decreased.

(v) Acid–Base Titrations and Ion-exchange Behavior

Although the Mn(III)–EDTA complex is not stable enough in alkaline solution, it was found possible to follow its general behavior in acid–base titrations. Curve (A) in Fig. 8 was obtained when an aqueous solution of the solid complex was titrated with

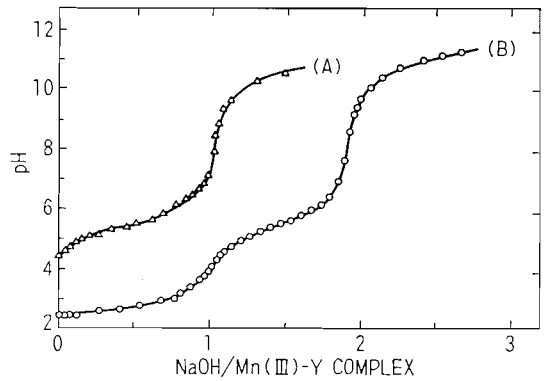

FIG. 8. Titration curves of Mn(III)–EDTA complexes with 0.1 *N* sodium hydroxide at 4±1° C. (A) 1.09×10^{-3} mole of KMn(III)Y; (B) 4.02×10^{-3} mole of HMn(III)Y.

standard sodium hydroxide solution. The curve has a single inflection point at a neutralization point (pH = 8.0) with approximately 1 mole of sodium hydroxide per mole of the complex. The pH of the half-neutralized solution is 5.5, which agrees fairly well with the pK value obtained from the spectral measurement.

In another run, a solution of the free complex acid was prepared by passing the potassium salt through the hydrogen form of a cation-exchange resin. On titration of the free acid with sodium hydroxide the curve (B) in Fig. 8 was obtained. This has inflection at 1 mole and ca. 1.9 mole of sodium hydroxide added per mole of the complex. The deviation of the second inflection point from 2 moles of NaOH may be due to the partial decomposition of the complex throughout the process.

For the purpose of comparison, similar acid–base titrations were carried out using Fe(III)–EDTA (Na salt) and Co(III)–EDTA (K salt). These results are plotted in Figs. 9 and 10. In the case of Co(III)–EDTA chelate in which EDTA is covalently bonded to the metal as a sexadentate ligand (12, 13), the pH of the solution of the potassium salt rises rapidly, showing no inflection point, while the free complex acid acts as a fairly strong monobasic acid. On the other hand, Fe(III)–EDTA complex behaves just in the same way as Mn(III)–EDTA complex, giving a single inflection point for sodium salt and two inflection points for its free acid. As was pointed out

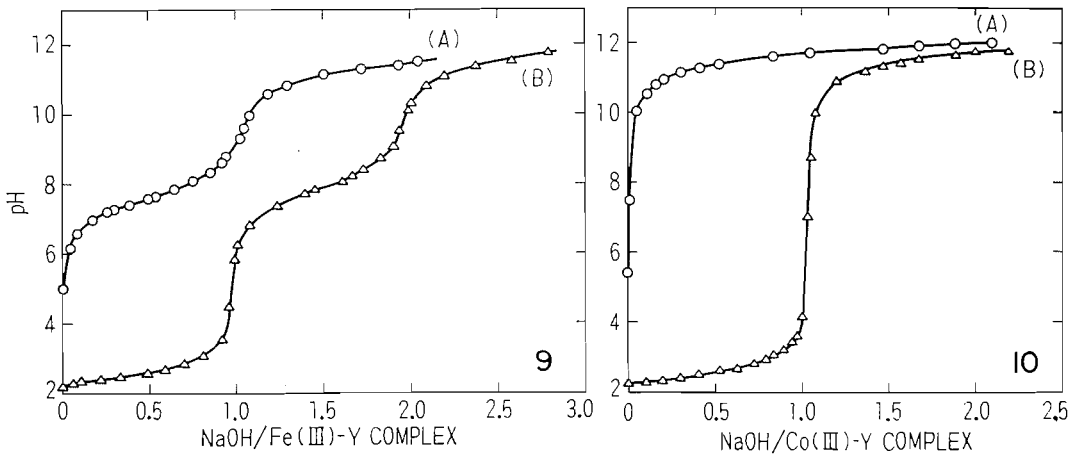

FIG. 9. Titration curves of Fe(III)–EDTA complexes with 0.1 *N* sodium hydroxide at 25±1° C. (A) 4.00×10^{-4} mole of $Na[Fe(OH_2)Y]$; (B) 4.00×10^{-4} mole of $H[Fe(OH_2)Y]$.

FIG. 10. Titration curves of Co(III)–EDTA complex with 0.1 *N* sodium hydroxide at 25±1° C. (A) 5.10×10^{-4} mole of K[Co(III)Y]; (B) 5.10×10^{-4} mole of H[Co(III)Y].

by Schwarzenbach (14), the Fe(III)–EDTA complex hydrolyzes strongly in higher pH region, forming a hydroxo complex, thus

$$[Fe(OH_2)EDTA]^- \rightleftarrows [Fe(OH)EDTA]^{2-} + H^+. \quad \text{(i)}$$

Analogously, the pH behavior of the free acid of Mn(III)–EDTA complex may be conveniently expressed in the following way:

$$H[Mn(OH_2)EDTA] \rightleftarrows H^+ + [Mn(OH_2)EDTA]^-, \; pK_1 \simeq 2.7 \quad \text{(ii)}$$

$$[Mn(OH_2)EDTA]^- \rightleftarrows H^+ + [Mn(OH)EDTA]^{2-}, \; pK_2 \simeq 5.5. \quad \text{(iii)}$$

That the Mn(III)–EDTA complex resembles the Fe(III)–EDTA rather than the Co(III)–EDTA complex could be checked by an anion-exchange experiment. When a solution of potassium salt of Co(III)–EDTA complex was passed into a column of Dowex 1-X8 in its chloride form, the complex anion displaces the chloride ion into the effluent. By the use of 4.08×10^{-4} mole of the complex it was found that 4.25×10^{-4} mole of chloride was displaced by the complex (Cl^-/complex = 1.04). However, similar experiments gave a displacement ratio Cl^-/complex of 1.4 for the Fe(III)–EDTA and 1.3 for the Mn(III)–EDTA complex. Moreover, by further washing of the columns with water the chloride ions continued to appear in the effluents and the flow rate became extremely slow. Such behavior for Fe(III)–EDTA and Mn(III)–EDTA complexes may be interpreted by assuming that the Fe(III)–EDTA and Mn(III)–EDTA complexes hydrolyze partially in the resin phase, as represented by equations (i) and (iii), and this hydrolysis is followed by a subsequent increase in the negative charges of complex anions.

(vi) General Remarks

From the results described above, there can be little doubt that the solid is a 1:1 chelate of the trivalent manganese with EDTA, but it is not yet possible to write a detailed formula for the potassium salt of the manganese(III) complex. At the present state, the following two formulae would fit the experimental facts:

(A) $K[Mn(III)(C_{10}H_{12}O_8N_2)(H_2O)].1.5H_2O$

(B) $K[Mn(III)(C_{10}H_{12}O_8N_2)(H_2O)_2].0.5H_2O$.

The result of the thermal analysis, which suggests the presence of $0.5H_2O$, supports the formula (B). Recently Hoard *et al.* (15) reported on the X-ray evidence for the seven coordination for $[Fe(III)(OH_2)Y]^-$ and $[Mn(II)(OH_2)Y]^{2-}$. In view of the close resemblance between the Fe(III) and Mn(III) ions there might also be a possibility of seven coordination for the Mn(III)–EDTA complex, but at present we do not have any direct evidence for it.

ACKNOWLEDGMENTS

The authors would like to express their thanks to their colleagues, to Dr. K. Imahori for infrared measurements, to Dr. Y. Takano for X-ray measurements, to Mr. M. Kinoshita for magnetic measurements, to Mr. S. Masuda for elementary analyses, and to Professor D. McCoy of the Sophia University for helping with the manuscript.

REFERENCES

1. R. Přibil and J. Horacek. Collection Czechoslov. Chem. Commun. **14**, 626 (1949).
2. R. Přibil and V. Sumon. Collection Czechoslov. Chem. Commun. **14**, 454 (1949).
3. R. Přibil and E. Hornychova. Chem. listy, **40**, 101 (1950).
4. M. W. Lister and Y. Yoshino. Can. J. Chem. **38**, 1291 (1960).
5. A. Ouchi, H. Matsumoto, and Y. Yoshino. Nippon Kagaku Zasshi. In press.
6. F. P. Dwyer, E. C. Gyarfas, and E. C. Mellor. J. Phys. Chem. **59**, 296 (1955).
7. G. H. Cartledge and W. P. Bricks. J. Am. Chem. Soc. **58**, 2061, 2065 (1936).
8. D. T. Sawyer and J. M. Mckinnie. J. Am. Chem. Soc. **82**,, 4191 (1960).
9. L. E. Orgel. An introduction to transition-metal chemistry. Methuen & Co. Ltd., London. 1960. p. 60.
10. C. Furlani and A. Ciana. Ann. chim. (Rome), **48**, 286 (1958).
11. C. K. Jørgensen. Energy levels of complexes and gaseous ions. Jul. Gjelleraps Forlag, Copenhagen. 1957. p. 34.
12. D. H. Busch and J. C. Bailar, Jr. J. Am. Chem. Soc. **75**, 4574 (1953).
13. H. A. Weakliem and J. L. Hoard. J. Am. Chem. Soc. **81**, 549 (1959).
14. G. Schwarzenbach and W. Biedermann. Helv. Chim. Acta, **31**, 459 (1948).
15. J. L. Hoard, M. Lind, and J. V. Silverton. J. Am. Chem. Soc. **83**, 2770, 3533 (1961).

THE RAMAN SPECTRUM OF THE SULPHURIC ACIDIUM ION: THE CONSTITUTION OF CONCENTRATED SOLUTIONS OF TETRA(HYDROGENSULPHATO)BORIC ACID IN SULPHURIC ACID

R. J. Gillespie and E. A. Robinson[1]
Department of Chemistry, McMaster University, Hamilton, Ontario
Received December 15, 1961

ABSTRACT

The Raman spectra of sulphuric acid solutions of tetra(hydrogensulphato)boric acid and its sodium and hydronium salts have been examined. Frequencies are assigned to some of the vibrations of the sulphuric acidium ion, $H_3SO_4^+$, and are compared with the frequencies of the analogous vibrations of H_2SO_4 and HSO_4^-. Evidence is presented that elimination of disulphuric acid occurs between molecules of $HB(HSO_4)_4$ to give polymers containing B—O—B linkages.

No frequencies have been observed in either the infrared or Raman spectra of sulphuric acid oleums that can be attributed to the $H_3SO_4^+$ ion (1, 2), presumably because disulphuric acid and the higher polysulphuric acids are not strong enough acids to give a concentration of the $H_3SO_4^+$ ion that is sufficiently large to be detected by these methods (3). It was decided, therefore, to examine the Raman spectra of solutions of the relatively strong tetra(hydrogensulphato)boric acid, $HB(HSO_4)_4$, in the hope of obtaining frequencies for some of the vibrations of the $H_3SO_4^+$ ion.

When boric acid is dissolved in dilute sulphuric acid oleum, tetra(hydrogensulphato)-boric acid, $HB(HSO_4)_4$, is formed:

$$H_3BO_3 + 3H_2S_2O_7 = HB(HSO_4)_4 + 2H_2SO_4. \quad [1]$$

The conductivities of this acid in sulphuric acid show that it is a relatively strong acid of the sulphuric acid solvent system ($K_a = 0.2$ mole kg^{-1} (3)). Cryoscopic measurements on solutions of the acid (4), conductimetric titrations with various bases (5), and measurements of the Hammett acidity function, H_0 (6), all confirm the extensive ionization of tetra(hydrogensulphato)boric acid in sulphuric acid:

$$HB(HSO_4)_4 + H_2SO_4 = H_3SO_4^+ + B(HSO_4)_4^-. \quad [2]$$

In order to interpret the Raman spectra it was necessary to also have information on the spectra of solutions of the salts $NaB(HSO_4)_4$ and $H_3O.B(HSO_4)_4$; these were obtained by neutralizing the acid with an equivalent amount of the base $NaHSO_4$, and by dissolving boric acid in sulphuric acid:

$$H_3BO_3 + 6H_2SO_4 = 3H_3O^+ + B(HSO_4)_4^- + 2HSO_4^-. \quad [3]$$

The Raman spectra are given in Table I. In the spectrum of a 0.35 molal solution of $HB(HSO_4)_4$ in sulphuric acid most of the observed frequencies are due to the solvent sulphuric acid but, in addition, new lines were observed at 730, 985, 1100, 1260, and 1480 cm^{-1}.

In the spectrum of a 0.4 molal solution of H_3BO_3 in sulphuric acid all the observed frequencies can be assigned to sulphuric acid except for a strong line at 1040 cm^{-1} and a line at 588 cm^{-1}, both of which are undoubtedly due to the hydrogen sulphate ion

[1]*Present address: Department of Chemistry, University of Toronto, Toronto 5, Ontario.*

TABLE I

Raman spectra of solutions of H_3BO_3, $HB(HSO_4)_4$, and $NaB(HSO_4)_4$ in H_2SO_4 (frequencies in cm^{-1})

(a)		(b)		(c)	
396	H_2SO_4	393	H_2SO_4	395	H_2SO_4
422	H_2SO_4	412	H_2SO_4	420	H_2SO_4
564	H_2SO_4	563	H_2SO_4	560	H_2SO_4
588	HSO_4^-	—	—	590	HSO_4^-
—	—	—	—	625	$B(HSO_4)_4^-$
—	—	—	—	700	$B(HSO_4)_4^-$
—	—	730	$B(HSO_4)_4^-$	730	$B(HSO_4)_4^-$
911	H_2SO_4	913	H_2SO_4	910	H_2SO_4
973	H_2SO_4	973	H_2SO_4	975	H_2SO_4
—		985	$H_3SO_4^+$	—	—
1040	HSO_4^-	—	—	1040	HSO_4^-
1100	$B(HSO_4)_4^-$	1100	$B(HSO_4)_4^-$	1100	$B(HSO_4)_4^-$
1148	H_2SO_4	1140	H_2SO_4	1150	H_2SO_4
1195	H_2SO_4, HSO_4^-	1195	H_2SO_4	1195	H_2SO_4, HSO_4^-
1260	$B(HSO_4)_4^-$	1260	$B(HSO_4)_4^-$, $H_3SO_4^+$	1260	$B(HSO_4)_4^-$
1370	H_2SO_4	1365	H_2SO_4	1370	H_2SO_4
—	—	1480	$H_3SO_4^+$	—	—

NOTE: (*a*) 0.4 molal H_3BO_3 in H_2SO_4; (*b*) 0.35 molal $HB(HSO_4)_4$ in H_2SO_4; (*c*) 0.35 molal $NaB(HSO_4)_4$ in H_2SO_4.

(8), and a relatively weak line at 1100 cm^{-1}, which also occurs in solutions of the acid. This latter line is assigned to the symmetric stretch of the SO_2 group in the $B(O.SO_2.OH)_4^-$ ion. The corresponding asymmetric stretch, according to the linear relationship between SO_2 symmetric and asymmetric stretches (9), should occur at ~1260 cm^{-1}. A very weak line of this frequency appears to be present in the spectrum. The frequency of 1100 cm^{-1} for the SO_2 symmetric stretch in the $B(HSO_4)_4^-$ ion seems reasonable in view of the frequency of ~1200 cm^{-1} for this vibration in the acids $X.SO_2.OH$ and of ~1050 cm^{-1} in their anions $X.SO_2.O^-$ (8).

Although the SO_2 asymmetric stretch of the $B(HSO_4)_4^-$ ion probably contributes to the line at 1260 cm^{-1} in the spectrum of the 0.35 molal solution of $HB(HSO_4)_4$, the intensity of this line is much greater than in the spectrum of the 0.4 molal solution of H_3BO_3 in sulphuric acid. Thus we assign the frequency 1260 cm^{-1} also to the SO_2 symmetric stretch of the sulphuric acidium cation. The very weak line at 1480 cm^{-1} in the spectrum of the acid can then be assigned to the asymmetric SO_2 stretch of the $H_3SO_4^+$ ion: the pair of frequencies 1260 and 1480 cm^{-1} fit the straight-line relationship reasonably well. The new line at 985 cm^{-1} can be very reasonably assigned to the S—OH symmetric stretch of the $H_3SO_4^+$ ion, by comparison with the frequencies of this vibration in H_2SO_4 and HSO_4^- (Table II), and the 730 cm^{-1} line assigned to the $B(HSO_4)_4^-$ ion, probably to an SO_2 rocking mode.

In the molecules XSO_2OH the frequencies of the SO_2 and S(OH) stretching vibrations have been found to increase with increasing electronegativity of the group X (8). The

TABLE II

Comparison of the SO_2 and S—OH stretching frequencies of HSO_4^-, H_2SO_4, and $H_3SO_4^+$ (frequencies in cm^{-1})

Species	SO_2 (sym.)	SO_2 (asym.)	S—OH
HSO_4^-	1040	1195	895
H_2SO_4	1195	1368	910
$H_3SO_4^+$	1260	1480	985

frequencies which we have assigned to the stretching vibrations of the $H_3SO_4^+$ ion are compared in Table II with the frequencies of these vibrations in H_2SO_4 and HSO_4^- (8). It may be seen that the frequencies increase in the order $\nu_{HO.SO_2.O^-} > \nu_{HO.SO_2.OH} > \nu_{HO.SO_2.OH_2^+}$, which is quite consistent with the increasing electronegativity of the groups $-O^-$, $-OH$, and $-OH_2^+$.

When a 0.35 molal solution of $HB(HSO_4)_4$ was neutralized with an equivalent amount of $NaHSO_4$,

$$HB(HSO_4)_4 + NaHSO_4 = NaB(HSO_4)_4 + H_2SO_4, \quad [4]$$

the lines at 985 and 1480 cm^{-1} disappeared from the spectrum but the lines at 730, 1100, and 1260 cm^{-1}, which are assigned to the $B(HSO_4)_4^-$ ion, remained. Additional weak lines were also observed at 590, 625, 700, and 1040 cm^{-1}. The lines at 590 and 1040 cm^{-1} are due to the HSO_4^- ion (8), and the lines at 625 and 700 cm^{-1} may be due to vibrations of the $B(HSO_4)_4^-$ ion. Lines at these frequencies are also found in the more concentrated solutions of $HB(HSO_4)_4$.

The spectra of the concentrated solutions of $HB(HSO_4)_4$ in sulphuric acid are rather complex (Table III). Apart from the frequencies that can be reasonably assigned to

TABLE III

Raman spectra of concentrated solutions of $HB(HSO_4)_4$ in H_2SO_4 (frequencies in cm^{-1})

(*a*)	(*b*)	Assignment*
—	145 (2)	$H_2S_2O_7$
—	259 (1)	$H_2S_3O_{10}$
310 (4)	303 (6)	$H_2S_2O_7$
330 (6)	327 (10)	$H_2S_2O_7$
—	369 (1)	$H_2S_3O_{10}$
388 (2)	395 (1/2)	H_2SO_4
420 (2)	420 (2)	H_2SO_4
474 (1)	471 (3)	$H_2S_2O_7$
—	507 (4)	$H_2S_2O_7$
—	527 (3)	$H_2S_2O_7$
550 (10)	559 (2)	H_2SO_4
630 (1)	635 (1)	$H_2S_2O_7$, $B(HSO_4)_4^-$
661 (1/2−)	657 (1/2)	$B(HSO_4)_4^-$
703 (1)	702 (2)	$B(HSO_4)_4^-$
733 (4)	735 (6)	$H_2S_2O_7$, $B(HSO_4)_4^-$
805 (1/2)	802 (1)	$H_2S_2O_7$
909 (8)	906 (6)	H_2SO_4
970 (2)	966 (4)	H_2SO_4, $H_2S_2O_7$
985 (2)	983 (3)	$H_3SO_4^+$
—	1075 (1/2)	SO_3
1100 (3)	1100 (4)	$B(HSO_4)_4^-$
1140 (6)	1170 (6)	H_2SO_4
1210 (4)	1226 (8)	H_2SO_4, $H_2S_2O_7$
1265 (2)	1260 (2)	$H_3SO_4^+$, $B(HSO_4)_4^-$
1375 (2)	1360 (2)	H_2SO_4
1425 (1)	1421 (4)	$H_2S_2O_7$
1452 (1)	1461 (3)	$H_2S_3O_{10}$
1480 (1)	1480 (2)	$H_3SO_4^+$

NOTE: (*a*) 1.4 molal $HB(HSO_4)_4$ in H_2SO_4; (*b*) 5 molal $HB(HSO_4)_4$ in H_2SO_4.
*Many of the lines assigned to $H_2S_2O_7$ are probably common also to $H_2S_3O_{10}$ (1).

H_2SO_4 and $B(HSO_4)_4^-$ there are many other lines, some of which are obviously due to $H_2S_2O_7$ and $H_2S_3O_{10}$ (1). Tentative assignments are given in Table III. In a 5 molal solution of $HB(HSO_4)_4$ the intensities of the H_2SO_4 lines, in particular the 910 cm^{-1} line, relative to the lines of $H_2S_2O_7$, in particular the 327 cm^{-1} line, are approximately

the same as in a 20% oleum (1) in which the mole ratio $H_2S_2O_7/H_2SO_4 = 0.3$. Although some $H_2S_2O_7$ is formed by the reaction

$$H_3SO_4^+ + H_2SO_4 = H_3O^+ + H_2S_2O_7, \qquad [5]$$

this occurs only to the extent of a few percent in a 5 molal solution (7). Evidently the concentration of $H_2S_2O_7$ is much greater than can be accounted for in this way.

The most reasonable explanation for the occurrence of relatively large concentrations of disulphuric acid in concentrated solutions of $HB(HSO_4)_4$ is that it is eliminated in a condensation process between $B(HSO_4)_4^-$ ions giving polymeric anions containing B—O—B linkages. Evidence is presented in a following paper that these B—O—B linkages are generally contained in a six-membered ring which also contains a sulphate group, e.g.

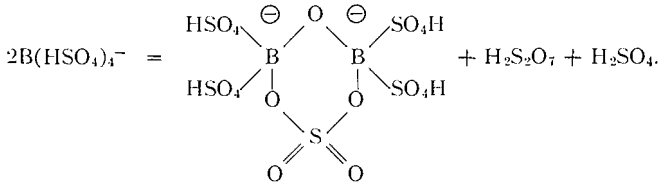

Quantitative elimination of $H_2S_2O_7$ according to the above equation would in the case of a 5 molal solution of $HB(HSO_4)_4$ give a solution in which the mole ratio of $H_2S_2O_7$ to H_2SO_4 is equal to 0.3. This agrees with the estimate given above from the comparison of the spectrum with that of a 20% oleum. Evidently this polymerization reaction is extensive if not complete.

EXPERIMENTAL

The Raman spectra were obtained as previously described (10). The preparation of solutions of tetra-(hydrogensulphato)boric acid has been described in a previous publication (4).

ACKNOWLEDGMENTS

Financial support from the National Research Council and the Ontario Research Foundation is gratefully acknowledged.

REFERENCES

1. R. J. GILLESPIE and E. A. ROBINSON. Can. J. Chem. **40**, 658 (1962).
2. P. A. GIGUÈRE and R. SAVOIE. Can. J. Chem. **38**, 2476 (1960).
3. J. BARR, R. J. GILLESPIE, and E. A. ROBINSON. Can. J. Chem. **39**, 1286 (1961).
4. R. H. FLOWERS, R. J. GILLESPIE, and J. V. OUBRIDGE. J. Chem. Soc. 1925 (1956).
5. R. H. FLOWERS, R. J. GILLESPIE, and E. A. ROBINSON. Can. J. Chem. **38**, 1363 (1960).
6. J. BARR, R. J. GILLESPIE, and E. A. ROBINSON. Unpublished results.
7. R. H. FLOWERS, R. J. GILLESPIE, E. A. ROBINSON, and C. SOLOMONS. J. Chem. Soc. 4327 (1960).
8. R. J. GILLESPIE and E. A. ROBINSON. Can. J. Chem. **40**, 644 (1962).
9. E. A. ROBINSON. Can. J. Chem. **39**, 273 (1961).
10. R. J. GILLESPIE and E. A. ROBINSON. Can. J. Chem. **39**, 2179 (1961).

TERPENOIDS

I. THE CONSTITUTION AND STEREOCHEMISTRY OF CEANOTHIC ACID[1]

P. DE MAYO AND A. N. STARRATT
Department of Chemistry, University of Western Ontario, London, Ontario
Received November 27, 1961

ABSTRACT

Ceanothic acid, a substance previously isolated by Julian, Pikl, and Dawson (J. Am. Chem. Soc. **60**, 77 (1938)), has been shown to be a triterpenoid related to the lupeol–betulin group, but in which ring A is five-membered. It has been degraded to the keto ester A norbetulonic acid methyl ester, a substance of defined constitution and stereochemistry. The hydroxyl and carboxyl groups attached to ring A have been shown by spectroscopic studies to be trans, the stereochemistry of ceanothic acid being that represented by (XII).

By the extraction of the root bark of *Ceanothus americanus* (Jersey Tea) Julian, Pikl, and Dawson (2) isolated a crystalline acid which was termed ceanothic acid. This substance, which had not been reported by other investigators of the root bark (3), was characterized by the American workers as a hydroxy dicarboxylic acid and attributed the formula $C_{29}H_{44}O_5$. It was characterized by the preparation of a dimethyl ester and of a dimethyl ester acetate.

They reported, further, that on heating to the melting point 1 mole each of water and carbon dioxide were evolved. The major fragment they concluded, for unspecified reasons, but probably on the basis of alkaline non-solubility, was a lactone, and hence proposed that ceanothic acid was a γ-hydroxy acid.

Attempted repetition of the method of isolation used by Julian, Pikl, and Dawson did not lead, in our hands, to the isolation of any ceanothic acid. These authors remark on the variability of the plant, and subsequent workers (4) have also made similar observations. A modified procedure was evolved and is described in the experimental section of this paper. The acid so isolated had the properties ascribed to it by the early workers, but, as will be seen in the sequel, the empirical formula requires modification to $C_{30}H_{46}O_5$, a point difficult of determination from analyses alone.

The infrared spectra of ceanothic acid and of its dimethyl ester showed bands at 833 (nujol mull) and 889 cm^{-1}, respectively, indicative of the presence of an exo methylene group. This interpretation was supported by the disappearance of this band on catalytic hydrogenation both of the acid and of the ester to their respective saturated dihydro compounds. The n.m.r. spectrum of the ester showed a doublet at τ 5.37 ($J \sim 7.7$ c.p.s.) (2 hydrogens) attributed to the methylene group and a singlet (3 hydrogens) at τ 8.36 attributed to a vinylic methyl group (5, p. 61). These observations, in the absence of any other double bond, indicated the presence of an isopropenyl group.

The n.m.r. spectrum, further, showed singlets (1 hydrogen) at τ 5.98 and τ 7.51. It thus seemed probable that both the hydroxyl group and one of the carboxyl groups were attached to carbon atoms bearing one hydrogen atom: these bands are in appropriate places for the respective methine hydrogens (5, pp. 55, 57).

Evidence for the proximity of the hydroxyl group and the secondary carboxyl group was obtained by an examination of the "lactone" obtained by Julian, Pikl, and Dawson (2). This substance was, in fact, an unsaturated acid, as evinced by its conversion, with

[1]*Part of the material reported herein formed the substance of a preliminary communication (1).*

diazomethane, to the corresponding ester. In addition to the bands at τ 5.40 and τ 8.46 in the n.m.r. spectrum, indicative of the continuing presence of the isopropenyl group, two hydrogens producing an AB pattern (doublets at τ 4.16 and τ 4.66; $J_{AB} \sim 5.4$ c.p.s.) were present. The formation of this pattern is evidence for the transformation indicated in the conversion of (I) to (II), that is, the dehydration–decarboxylation of a β-hydroxy acid.

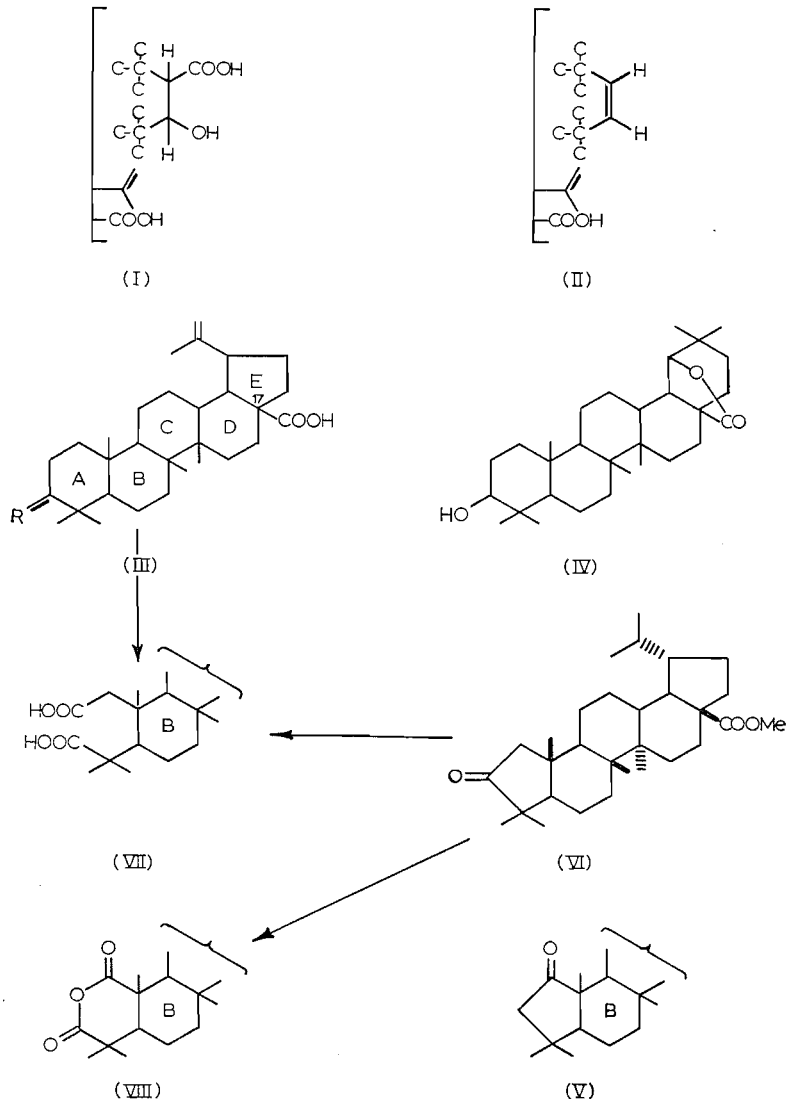

This was confirmed, as follows. Dimethyl ceanothate was converted into the benzoate (isolated only as an oil) and the latter pyrolyzed at 330° to eliminate benzoic acid. The isolated anhydroacid showed the expected ultraviolet end absorption for an isolated isopropenyl group and an α,β-unsaturated ester. Furthermore, a band (singlet, 1 hydrogen) at τ 3.9 in the n.m.r. spectrum indicated the presence of the expected vinyl hydrogen in addition to those of the isopropenyl group (5, p. 61).

Since dihydroceanothic acid and its dimethyl ester showed no absorption in the ultraviolet spectrum in the 200–210 mμ region, they were, presumably, saturated. It followed that ceanothic acid was, therefore, pentacarbocyclic. Some relationship to the lupeol – betulin – betulinic acid (III, R = H, OH) series seemed probable in view of the presence of the isopropenyl group and this view was strengthened by the presence of betulinic acid itself amongst the root constituents.

One of the characteristic transformations of the lupeol–betulin group of substances is the ready acid-catalyzed expansion of the terminal, E, ring to give derivatives of the β-amyrin series (6). In those substances having a carboxyl function at C_{17} concomitant lactonization occurs: betulinic acid (III, R = H, OH), for instance, is converted into (IV). When subjected to suitable conditions—refluxing formic acid for 3 hours—ceanothic acid was converted into a γ lactone (bands at 1696 (carboxyl) and 1762 cm^{-1} (γ lactone)) with the simultaneous disappearance of the isopropenyl group. The resulting monocarboxylic acid lactone was further characterized as the acetate, indicating the nonparticipation of the hydroxyl group in the lactonization process, and as the methyl ester.

Some modification of the betulinic acid skeleton in ceanothic acid was, however, necessary since the functions indicated in (I) cannot otherwise be accommodated. The grouping in (I) was suggestive of the occurrence of a 'biogenetic' pinacolic rearrangement at some stage in the genesis of ceanothic acid, such as may take place in the formation of gibberellic acid (7) and of the aldehyde in magnamycin (8).

Oxidation of methyl dihydroceanothate with sodium dichromate gave the corresponding ketone. Alkaline hydrolysis resulted in the loss of carbon dioxide expected of a β-keto ester and the formation of a ketonic monoester. This substance showed an unresolved band in the infrared spectrum (at 1738 cm^{-1}) for the cyclopentanone and ester, while its precursor showed bands (CCl_4) at 1750 (cyclopentanone) and 1727 cm^{-1} (ester).

Two possible structures, (V) and (VI), were possible for this ketone, but its properties suggested that it was (VI), a substance previously prepared by Ruzicka *et al.* (9, 15) from betulonic acid by hydrogenation, nitric acid oxidation to (VII), followed by pyrolysis and esterification. Direct preparation of this substance from methyl dihydrobetulonate and comparison of it, the derived 2:4-dinitrophenylhydrazone, and anhydride (VIII) (obtained by selenium dioxide oxidation) showed them to be identical in every respect. Four possible structures, (IX), (X), (XI), and (XII), followed for ceanothic acid.

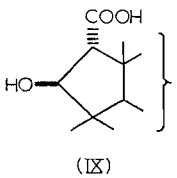

(IX)

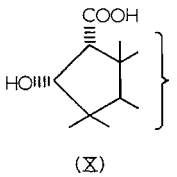

(X)

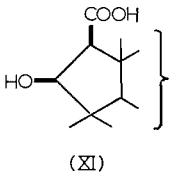

(XI)

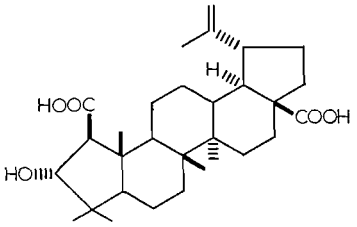

(XII)

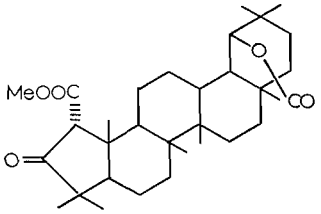

(XIII)

It has already been noted that, in dimethyl ceanothate, the methine hydrogens adjacent to the carbomethoxyl and hydroxyl groups were singlets; that is, although the hydrogens were on contiguous carbon atoms, the coupling constant was close to zero. In contrast, the ketone (XIII), derived from methyl ceanothate lactone, on reduction with sodium borohydride gave an epimeric alcoholic lactone, methyl isoceanothate lactone. This substance showed, in its n.m.r. spectrum, a doublet at τ 7.0, the methine hydrogens being coupled, and a quartet at τ 5.9 (5, pp. 55, 57), the hydrogen on the carbon bearing oxygen being split by the adjacent methine hydrogen and by the hydroxyl hydrogen. This would suggest that in dimethyl ceanothate the hydrogen atoms are at an angle of about 90° (10, 11) and, therefore, in the trans relationship.

Further evidence supporting this view was obtained from a study of infrared spectra. Treatment of methyl dehydroceanothate lactone, (XIII), with sodium methoxide resulted in a rapid epimerization of the carbomethoxyl group—which must, therefore, be in the unstable configuration—and the formation of the isomeric methyl dehydroepiceanothate lactone. Reduction of this with sodium borohydride then gave methyl epiceanothate lactone. Three of the four epimeric hydroxy esters were now in hand. The infrared spectra of these substances in solution were determined in the carbonyl and hydroxyl regions. The results are recorded in Table I. Methyl dihydroceanothate shows a normal

TABLE I

Compound	ν_{ester} (cm^{-1})*	$\nu_{hydroxyl}$ (cm^{-1})*	Concentration (%)†
Dimethyl dihydroceanothate	1733	3634 (sharp), ~3510 (broad)	2.5
		3634 (sharp)	1.2
		3640 (sharp)	0.2
Methyl isoceanothate lactone	1718	3582 (sharp)	0.7
		3580 (sharp)	0.1
Methyl epiceanothate lactone	1717	3632 (sharp), 3508 (broad)	1.9 ($CHCl_3$)‡
		3634 (sharp), 3508 (broad)	0.3

*Spectra taken in CCl_4 (Fisher Spectranalyzed) unless specified otherwise.
†Maximum concentration limited by compound solubility.
‡Chloroform washed and dried to remove alcohol.

unbonded ester and, in agreement, the hydroxyl group shows bonding (intermolecular) only in the most concentrated solution. In contrast, the epimeric methyl isoceanothate lactone shows a bonded ester group and a bonded hydroxyl band even in dilute solution. These results support the trans and cis configurations, respectively, allocated. It seems probable that methyl epiceanothate lactone is, also, cis.

Structures (IX) and (XII) remain for ceanothic acid, and inspection of models suggests that the β-carbomethoxyl group is under more severe non-bonded interaction than the α epimer. In view of the ready epimerization of methyl dehydroceanothate lactone, stereostructure (XII) is preferred for ceanothic acid.[2]

An attempt was made to confirm this from optical rotatory dispersion measurements. An amplitude of 200, 203, and 228 for methyl dehydroepiceanothate lactone, methyl dehydroceanothate lactone, and (VI) respectively was recorded. The differences are too small to be interpretable, particularly since slight changes in the conformation of the cyclo-

[2]*We understand that Dr. J. J. H. Simes (University of New South Wales) has independently arrived at the same stereochemical conclusions with regards to ceanothic acid. We wish to thank Dr. Simes for this information.*

pentanone ring are likely to be of considerable significance (12). It is interesting, however, that the proposed stereochemistry of the keto esters is that predicted by Bose's empirical rule (13).

The substance emmolic acid, recently isolated by Boyer, Eade, Locksley, and Simes (14) from *Emmenospermum alphitonioides* F. Muell. has constants comparable with those of ceanothic acid, and, where the same derivatives have been prepared, there is good agreement. We have been informed[3] that these substances are identical: the name used by Julian, Pikl, and Dawson (2) should therefore be that retained.

After the preparation of this manuscript a recent publication (16) by Mechoulam became available. This author concurs in the allocation of the β configuration to the carboxyl group of ceanothic acid, but concludes that the hydroxyl group is cis. The reasons advanced are that, first, lithium aluminum hydride reduction of the ketone derived from dimethyl ceanothate and of dimethyl ceanothate itself gives the same triol. It is proposed that the hydroxyl produced by ketonic reduction is that which is more hindered, i.e. β, and that this configuration is, therefore, that present in ceanothic acid itself. Secondly, it is reported that in dilute (unspecified) solution in carbon tetrachloride the triol exhibits hydrogen bonding of the hydroxyl group, again apparently supporting the cis allocation of configuration.

We do not find these results persuasive. The prediction of the configuration of the hydroxyl produced by ketonic reduction is quite uncertain in the presence of a nearby function with which the lithium aluminum hydride can chelate and direct the stereochemical course of reduction. It cannot thence be concluded that the alcohol produced is the more hindered. The assignment of the configuration rests solely, therefore (assuming no epimerization of the carbomethoxyl group during the reduction), on a single observation with regard to hydrogen bonding. We believe that such observations are only relevant if the appropriate epimer is available for comparison. Since, in the triol, the situation is complicated by a third (primary) hydroxyl group, the conclusion is rendered yet more dubious.

EXPERIMENTAL

Infrared spectra and rotations were determined in chloroform solution and ultraviolet spectra in ethanol unless otherwise stated. Melting points were uncorrected and determined on the Köfler hot stage. Nuclear magnetic resonance spectra were determined at 60 Mc/s on the Varian V-4304 spectrometer in carbon tetrachloride solution with 1% tetramethylsilane as an internal reference. Alumina was Woelm neutral, standardized according to Brockmann. Light petroleum refers to the fraction of b.p. 60–80°.

Extraction of Ceanothus americanus

Extraction and isolation in the manner described by Julian, Pikl, and Dawson (2) was not successful in our hands. By different procedures, different proportions of the various acid constituents were obtained. That leading to ceanothic acid is described below; other procedures will be described in a forthcoming publication.

The ground root bark (2 kg, supplied by S. B. Penick and Co.) was extracted continuously with ether in a Soxhlet apparatus for 33 hours. The residue (35 g) was extracted with light petroleum under reflux for 3 hours, the light petroleum then being replaced, and the process repeated four times. The residue, in ethereal solution, was extracted exhaustively with potassium hydroxide solution (2%). A solid (A), which separated at the interface, was removed by filtration. Acidification of the alkaline solution and isolation with ether gave the crude acid mixture (11 g), which was further defatted by extraction with light petroleum.

The acid mixture (10.4 g) was added, in benzene solution, to a column of silica (B.D.H.; 300 g). Elution with benzene–ether (20:1) gave an *acid* (538 mg), which, after recrystallization from ether–methanol, had melting point 350–354° (decomp.), $[\alpha]_D$ +39° (*c*, 1.23; pyridine). Found: C, 76.45; H, 9.23; O, 14.43%.[4]

[3]*We wish to thank Dr. T. G. Halsall (Oxford) for this information.*

[4]*Further work on this substance, ceanothenic acid, and better methods of isolation will be reported in due course.*

Further elution with the same solvent mixture then gave betulinic acid (232 mg), m.p. 270–285°, identified as described below. Elution with benzene–ether (10:1) then gave material which after two crystallizations from ether–benzene gave ceanothic acid (350 mg), m.p. 330–340° (with evolution of gas). Further recrystallization from ether–methanol gave pure ceanothic acid, m.p. 356–357° (gas evolution), $[\alpha]_D$ +38°: (*c*, 1.20; ethanol). Julian, Pikl, and Dawson (2) report m.p. 354°. The substance showed ν_{max} at 3480, 1720, 1641, and 883 cm^{-1} (nujol mull).

Identification of Betulinic Acid

The salt (A) was acidified and the acid isolated with ether. It was identical with the crude betulinic acid isolated during chromatography. It was reduced in ethereal solution with excess lithium aluminum hydride, the crude diol acetylated, and the diacetate, m.p. 215–216°, $[\alpha]_D$ +14° (*c*, 0.90) was identical in infrared spectrum and gave no melting point depression on admixture with an authentic specimen of betulin diacetate.

Dimethyl Ceanothate

Methylation with diazomethane gave the dimethyl ester, m.p. 221–223° (Julian, Pikl, and Dawson (2) report 223°), $[\alpha]_D$ +41° (*c*, 1.00). Acetylation gave the acetate, m.p. 157–160° (Julian, Pikl, and Dawson (2) report 157°), $[\alpha]_D$ +29° (*c*, 1.07).

Dimethyl Dihydroceanothate

Dimethyl ceanothate (53 mg) in ethanolic solution was hydrogenated over palladized charcoal (35 mg, 5%). After chromatography on alumina the material eluted with benzene–ether (20:1) was crystallized from ether–methanol, when the dimethyl dihydroceanothate obtained had m.p. 262–263°, $[\alpha]_D$ +21° (*c*, 1.36). Calc. for $C_{32}H_{52}O_5 . 0.5MeOH$: C, 73.31; H, 10.15%. Found: C, 73.06; H, 9.91%.

The same substance was obtained by hydrogenation in glacial acetic acid solution over platinum oxide catalyst; 1.0 mole hydrogen was absorbed.

Dihydroceanothic Acid

Ceanothic acid (199 mg) was hydrogenated in acetic acid solution over platinum oxide. Crystallized from ether–methanol, the acid had melting point above 350°, $[\alpha]_D$ +11° (*c*, 0.97; ethanol). Calc. for $C_{30}H_{48}O_5$: C, 73.73; H, 9.90%. Found: C, 73.94; H, 10.04%.

Pyrolysis of Dimethyl Ceanothate Benzoate

Dimethyl ceanothate (89 mg) was converted into the benzoate (benzoyl chloride – pyridine). After extensive chromatography it was obtained only as an oil (77 mg). This oil (69 mg) was heated at 330° under a slow stream of nitrogen. The crude product was refluxed for 1 hour with methanolic potassium hydroxide (5%) and the neutral material was isolated with ether and chromatographed on alumina (Grade 1; 2 g). Elution with light petroleum – benzene (1:1) and crystallization from ether–methanol gave dimethyl anhydroceanothate (19 mg), m.p. 166–168°, $[\alpha]_D$ −16° (*c*, 1.51), λ_{inf} 215 mμ (ϵ 7500). Calc. for $C_{32}H_{48}O_4$: C, 77.37; H, 9.74; OMe, 12.5%. Found: C, 77.65; H, 9.63; OMe, 12.39%.

On catalytic hydrogenation in acetic acid solution over platinum oxide 2 moles of hydrogen were absorbed.

Ceanothic Acid Lactone

Ceanothic acid (60 mg) was refluxed in formic acid (98%) for 3 hours, the formic acid removed *in vacuo*, and the residue refluxed with methanolic potassium hydroxide (5%) for 30 minutes. Isolation with ether and crystallization from ether – light petroleum gave the lactone, m.p. 190–205° and 303–305°, $[\alpha]_D$ +90° (*c*, 0.91), ν_{max} 1760, 1695 cm^{-1}. Calc. for $C_{30}H_{46}O_5 . 0.5H_2O$: C, 72.72; H, 9.49%. Found: C, 72.24; H, 9.55%.

The acid lactone, on methylation with ethereal diazomethane, gave the methyl ester, m.p. 256–257°, $[\alpha]_D$ +90° (*c*, 0.98). Calc. for $C_{31}H_{48}O_5$: C, 74.36; H, 9.66%. Found: C, 74.08; H, 9.66%. The lactone, prepared from ceanothic acid (296 mg), was acetylated (acetic anhydride – pyridine) and the crude acetate chromatographed on silica gel (15 g). Elution with benzene–ether (20:1) afforded, after crystallization from ether–methanol, the acetate, m.p. 309–311° (decomp.), $[\alpha]_D$ +70° (*c*, 1.19). Calc. for $C_{32}H_{48}O_6$: C, 72.69; H, 9.15%. Found: C, 72.64; H, 9.16%.

Methyl Dehydroceanothate Lactone

Methyl ceanothate lactone (70 mg) in acetic acid (6 ml) containing sodium dichromate (44 mg) was allowed to stand overnight at room temperature. Isolation in the usual way gave, after crystallization from chloroform–methanol, the ketone, m.p. 220–225° and 319–324°, $[\alpha]_D$ +178° (*c*, 0.63). Calc. for $C_{31}H_{46}O_5$: C, 74.66; H, 9.30%. Found: C, 74.76; H, 9.25%.

Decarboxyanhydroceanothic Acid

Ceanothic acid (47 mg) was heated in a Wood's metal bath under nitrogen until the temperature rose to 350°. The product was taken up in ether, washed with dilute potassium hydroxide solution, and, after evaporation of the ether, was crystallized from ether – light petroleum, when it has m.p. 238–244° (Julian, Pikl, and Dawson (2) record 234°), $[\alpha]_D$ +27° (*c*, 0.79), ν_{max} 1697, 1643, 881 cm^{-1} (CCl_4). Calc. for $C_{29}H_{44}O_2$: C, 82.02; H, 10.44%. Found: C, 81.97; H, 10.62%.

Methyl Dehydrodihydroceanothate

Methyl dihydroceanothate (45 mg) in acetic acid (5 ml) containing sodium dichromate (18 mg) was allowed to stand overnight at room temperature. Isolation and crystallization from ether–methanol gave the keto ester, m.p. 183–184°, $[\alpha]_D$ +94° (*c*, 1.25), ν_{max} 1750 cm^{-1}. Calc. for $C_{32}H_{50}O_5 . 0.5MeOH$: C, 73.59; H, 9.81%. Found: C, 73.77; H, 9.45%.

Methyl Decarboxydehydrodihydroceanothate

Methyl dehydrodihydroceanothate (59 mg) was refluxed 2 hours in methanolic potassium hydroxide (10 ml; 10%). Isolation and crystallization from ether–methanol afforded the decarboxy ester, m.p. 180.5–181.5°, $[\alpha]_D$ +72° (*c*, 1.11). Calc. for $C_{30}H_{48}O_3$: C, 78.89; H, 10.59%. Found: C, 78.32; H, 10.67%. The melting point was undepressed on admixture with A-nor-dihydrobetulonic acid methyl ester of the same melting point prepared as described by Ruzicka and Isler (15). Ruzicka, Brenner, and Rey (9) record $[\alpha]_D$ +84.6°. It was also prepared as described below. The infrared spectra were superposable. The 2:4-dinitrophenylhydrazone, crystallized from chloroform–methanol, had melting point 261–263° and gave no depression in melting point on admixture. Calc. for $C_{36}H_{52}N_4O_6$: C, 67.89; H, 8.23; N, 8.80%. Found: C, 67.94; H, 8.19; N, 9.03%.

The ceanothic keto ester (28 mg) was heated in a sealed tube with selenium dioxide (120 mg) and dioxan (4 ml) at 200° for 11½ hours. The anhydride, isolated as described by Ruzicka and Isler (15), had m.p. 271–272°, $[\alpha]_D$ +40° (*c*, 1.32), ν_{max} 1800, 1755, 1720 cm^{-1}. These authors report m.p. 269–270° (cor.), $[\alpha]_D$ +42.5°.

The Oxidation of Methyl Dihydrobetulonate

The keto ester (255 mg) was added to a precooled mixture of fuming nitric acid (11 ml; 90%) and glacial acetic acid (10 ml), and stirred for ¾ hour at 0°, when the ester had dissolved, and allowed to stand for a further ¾ hour. After dilution with water the collected material was chromatographed on silica gel (11 g). Elution with benzene afforded some starting material after which elution with benzene–ether (20:1) gave A-secodihydrobetulinic acid tricarboxylic acid monomethyl ester, m.p. 160–163°, $[\alpha]_D$ +8° (*c*, 1.08). Calc. for $C_{31}H_{50}O_6 . 0.5H_2O$: C, 70.59; H, 9.67%. Found: C, 70.72; H, 9.46%. Methylation (diazomethane) gave the known trimethyl ester, m.p. 147–149°, $[\alpha]_D$ −18° (*c*, 1.2). Ruzicka and Isler report 145° (15).

Pyrolysis of the diacid ester at 260° (12 mm Hg) gave a mixture of anhydride and cyclopentanone. Hydrolysis with alcoholic potassium hydroxide (5%) and isolation of the neutral material gave the A-nor ketone identical in melting point and mixed melting point with the material described above.

Epimerization of Methyl Dehydroceanothate Lactone

The lactone (13.6 mg) in methanol (5 ml) had $[\alpha]_D$ +153°. Methanolic sodium methoxide (5%; 0.5 ml) was added and the rotation redetermined immediately and found to be $[\alpha]_D$ +113°. It was not changed on further standing. Repetition of the above experiment on a larger scale (101 mg) on isolation of the product gave, after crystallization from chloroform–methanol, methyl dehydroepiceanothate lactone, m.p. 328–330° (decomp.), $[\alpha]_D$ +117° (*c*, 0.71). Calc. for $C_{31}H_{46}O_5$: C, 74.66; H, 9.30%. Found: C, 74.83; H, 9.33%.

Methyl Epiceanothate Lactone

To methyl dehydroepiceanothate lactone (40 mg) in dioxan (5 ml), methanol (5 ml), and water (1 ml) was added sodium borohydride (40 mg). After 45 minutes the product was isolated with ether and, after evaporation of the solvent, chromatographed on alumina (Grade 3; 2 g). Elution with benzene – light petroleum (1:1) followed by crystallization of the product from chloroform–methanol gave the alcohol, m.p. 301–303°, $[\alpha]_D$ +31° (*c*, 1.19). Calc. for $C_{31}H_{48}O_5$: C, 74.36; H, 9.66%. Found: C, 74.44; H, 9.47%.

Methyl Isoceanothate Lactone

Methyl dehydroceanothate lactone (129 mg) in dioxan (13 ml), methanol (15 ml), and water (4 ml) was treated with sodium borohydride (50 mg). After 35 minutes the product was isolated and chromatographed on alumina (Grade 3; 12 g). Elution with benzene – light petroleum (1:1) gave, after crystallization from chloroform–methanol, the alcohol, m.p. 239–240°, $[\alpha]_D$ +85° (*c*, 0.84). Calc. for $C_{31}H_{48}O_5$: C, 74.36; H, 9.66%. Found: C, 74.17; H, 9.52%.

ACKNOWLEDGMENTS

We wish to thank Dr. J. B. Stothers for the n.m.r. spectra, Dr. J. E. D. Levisalles, Miss H. Herrmann, and Miss L. Ohnimus (Strasbourg) for the optical rotatory dispersion measurements, and Dr. C. J. W. Brooks (Glasgow) for an informative discussion. We also wish to thank Dr. R. A. Abramovitch (Saskatoon) for a generous supply of crude acids.

The authors are indebted to the National Research Council of Canada and to the Research Corporation for financial support.

REFERENCES

1. P. DE MAYO and A. N. STARRATT. Tetrahedron Letters, No. 7, 259 (1961).
2. P. L. JULIAN, J. PIKL, and R. DAWSON. J. Am. Chem. Soc. **60**, 77 (1938).
3. A. BERTHO and W. S. LIANG. Arch. Pharm. **271**, 273 (1933).
4. R. A. ABRAMOVITCH and G. TERTZAKIAN. Can. J. Chem. **39**, 1733 (1961).
5. L. M. JACKMAN. Applications of nuclear magnetic resonance spectroscopy in organic chemistry. Pergamon Press. 1959.
6. G. S. DAVY, T. G. HALSALL, and E. R. H. JONES. J. Chem. Soc. 2696 (1951).
7. P. W. BRIAN, J. F. GROVE, and J. MACMILLAN. Fortschre. Chem. org. Naturstoffe, **18**, 350 (1960).
8. R. B. WOODWARD. Festschrt. Arthur Stoll, 524 (1957).
9. L. RUZICKA, M. BRENNER, and E. REY. Helv. Chim. Acta, **24**, 515 (1941).
10. M. KARPLUS. J. Chem. Phys. **30**, 11 (1959).
11. F. A. L. ANET. Can. J. Chem. **39**, 789 (1961).
12. W. KLYNE. Tetrahedron, **13**, 29 (1961).
13. A. K. BOSE. Tetrahedron Letters, No. 14, 461 (1961).
14. J. P. BOYER, R. A. EADE, H. LOCKSLEY, and J. J. H. SIMES. Australian J. Chem. **11**, 236 (1958).
15. L. RUZICKA and O. ISLER. Helv. Chim. Acta, **19**, 506 (1936).
16. R. MECHOULAM. Chem. & Ind. (London), 1835 (1961).

A KINETIC STUDY OF THE METATHETICAL AND ADDITION REACTIONS CHARACTERISTIC OF ALLYL POLYMERIZATION

A. C. R. Brown and D. G. L. James
Department of Chemistry, University of British Columbia, Vancouver, British Columbia
Received September 25, 1961

ABSTRACT

The rate constants of the reactions

$$CH_3CH_2\cdot + CH_2{=}CH{-}CH_2OH \rightarrow CH_3CH_2{-}CH_2{-}\dot{C}H{-}CH_2OH, \quad [7]$$

$$CH_3CH_2\cdot + CH_2{=}CH{-}CH_2OH \rightarrow CH_3CH_3 + CH_2{=}CH{-}\dot{C}H{-}OH \quad [6]$$

have been measured in the gas phase between 50° and 142° C:

$$k_7/k_2^{1/2} = (5.5\pm2.7)\times10^{-8}\exp(-7750\pm350)/RT \text{ cm}^{3/2}\text{ molecule}^{-1/2}\text{ sec}^{-1/2},$$

$$k_6/k_2^{1/2} = (2.5\pm1.0)\times10^{-8}\exp(-7600\pm300)/RT \text{ cm}^{3/2}\text{ molecule}^{-1/2}\text{ sec}^{-1/2},$$

where k_2 is the (known) rate constant for the reaction

$$2CH_3CH_2\cdot \rightarrow C_4H_{10}. \quad [2]$$

The significance of these values is discussed in relation to the propagation and chain transfer processes in the polymerization of allyl alcohol. A consideration of the rates of addition of free radicals to a series of monomers of diverse reactivity reveals that a correlation exists between the rate constants for the addition of the ethyl radical in the gas phase and of certain polymer radicals in the liquid phase.

An application of the general equation proposed by Bamford, Jenkins, and Johnston for radical reactivity leads to the conclusion that $k_p \approx 2k_7$ and that $k_p/k_f \approx k_7/k_6 = 1.8$ for allyl alcohol at 60° C. Predictions based upon these relationships are compared with experimental data for the propagation and degree of homopolymerization of allyl alcohol and for inhibition and propagation in copolymerization; reasonable agreement is found in all cases.

INTRODUCTION

The polymerization of allyl alcohol appears to offer the clearest example of allylic kinetics (1); but the kinetic study is rendered difficult by the low reactivity of the monomer (2). In this paper we offer a new approach to problems of this kind, and suggest that our method may be of general use in the study of the energetics of the elementary reactions of polymerization.

Allyl polymerization owes its distinctive character to a delicate balance between the rates of two competing reactions: addition and metathesis. Each of these alternatives involves the same reactants: a growing polymer radical, vinylic in nature, and an allylic monomer molecule:

$$M_j\cdot + CH_2{=}CH{-}CH_2X \rightarrow M_j{-}CH_2{-}\dot{C}H{-}CH_2X \text{ (addition)},$$

$$M_j\cdot + CH_2{=}CH{-}CH_2X \rightarrow M_jH + CH_2{=}CH{-}\dot{C}HX \text{ (metathesis)}.$$

Addition forms another vinylic polymer radical, equal in reactivity to its parent, and is thereby a step in the propagation of polymerization. Metathesis produces a new class of radical, the allylic radical $CH_2{=}CH{-}CHX\cdot$. The allylic radical is stabilized by resonance (3) and has a reactivity decisively lower than the vinylic radical (4); indeed, the allylic radical is characteristically too unreactive to add to the monomer molecule, and so cannot propagate the chain (5). Instead, it may terminate the chain by combining with a growing polymer radical, or it may be removed by dimerization. In either case, metathesis results in both structural and kinetic chain termination, whereas addition is the

essential reaction of propagation in both allyl and vinyl polymerization. The experimental evidence for these views has been derived largely from kinetic studies of the polymerization of allyl acetate (5–8), and a comprehensive kinetic scheme has been proposed by Litt and Eirich (7).

The ideal allyl monomer for this study is one which reveals most clearly the competition between metathesis and addition. Certain allyl monomers are unsuitable because they display either vinylic reactivity (allyl chloride (9)), effective chain transfer (allyl acetate (10, 11)), or radical displacement reactions (allyl trimethyl acetate (10)). Allyl alcohol was chosen for this study because the OH group is neither reactive in itself nor does it confer abnormal reactivity upon the double bond (12). Thus, allyl alcohol can be polymerized very slowly by peroxidic catalysts, but only an oil with a degree of polymerization of five is obtained, and fresh catalyst must be added frequently to the system (13, 14).

Our aim is the comparison of the rates of the metathetical and addition reactions of allyl alcohol, chosen as a typical allylic monomer. To eliminate inessentials, we have chosen the simplest vinylic radical, $CH_3CH_2\cdot$, to attack the monomer, and have studied the reaction in the gas phase. In this way we avoid the variable influences of chain length and configuration of the vinylic polymer radical, and other problems arising from interactions in the liquid phase.

EXPERIMENTAL METHODS

The apparatus and method have been described in two earlier papers (15, 16). Certain improvements in the techniques of purification of reactants and analysis of products have been adopted in this investigation. The diethyl ketone and the allyl alcohol, both White Label grade materials of the Eastman Kodak Company, were purified by gas chromatography, using the 6-ft "Ucon polar" column of the Beckmann Megachrom instrument at 110° C. The 2,3-dimethyl butadiene-1,3, the cyclohexadiene-1,3 and the 2,5-dimethyl hexadiene-2,4 were purified in the same way.

The analysis followed the original pattern of fractionation into CO, C_2, and C_4 samples, supplemented by analysis by gas chromatography. The CO fraction was found to be pure and free from traces of hydrogen and methane. The C_2 fraction was analyzed in a stream of helium at 80° C on a 2-m silica gel column, and consisted entirely of C_2H_4 and C_2H_6. Mixtures of C_2H_4 and C_2H_6 of known composition were used to calibrate the apparatus for the analysis of the C_2 fractions. The C_2H_4/C_2H_6 ratio could then be measured by a comparison of peak areas, if the area of the C_2H_4 peak was multiplied by 1.08. For reaction temperatures below 145° C it was found that the C_4 fraction sometimes contained a trace of 1-pentene, but this did not exceed 0.5% of the butane, and was usually much less than this. The proportion of 1-pentene formed was greater for reactions above 145° C and consequently this temperature was not exceeded in quantitative studies.

THE KINETICS OF THE REACTIONS OF THE ETHYL RADICAL

The photolysis of pure diethyl ketone conforms to the established mechanism (17–20):

$$CH_3CH_2—CO—CH_2CH_3 + h\nu \rightarrow 2CH_3CH_2\cdot + CO \quad [1]$$

$$2CH_3CH_2\cdot \rightarrow C_4H_{10} \quad [2]$$

$$2CH_3CH_2\cdot \rightarrow C_2H_6 + C_2H_4 \quad [3]$$

$$CH_3CH_2\cdot + CH_3CH_2—CO—CH_2CH_3 \rightarrow CH_3CH_3 + CH_3\dot{C}H—CO—CH_2CH_3. \quad [4]$$

At higher light intensities and below 250° C the pentanonyl radical is removed by the reaction

$$CH_3CH_2\cdot + CH_3\dot{C}H—CO—CH_2CH_3 \rightarrow CH_3CH(CH_2CH_3)—CO—CH_2CH_3. \quad [5]$$

One molecule of carbon monoxide is equivalent to two ethyl radicals and hence to one molecule of either ethane or butane. The material balance may be defined by the ratio

$$M = \frac{R_{C_2H_6} + R_{C_4H_{10}}}{R_{CO}},$$

where the symbol R_Z represents the rate of formation of the product Z in molecule sec^{-1} cm^{-3} of illuminated volume. The quantity M was found to have the value 0.997 ± 0.03 over a wide range of temperature and light intensity, showing that reactions [1] to [5] account for all the products (15).

If a gaseous mixture of allyl alcohol and diethyl ketone is illuminated, the metathetical and addition reactions of the ethyl radical with allyl alcohol will take place. At higher light intensities the metathetical reaction will take the course

$$CH_3CH_2\cdot + CH_2{=}CH{-}CH_2OH \rightarrow CH_3CH_3 + CH_2{=}CH{-}\dot{C}HOH, \qquad [6]$$

$$CH_3CH_2\cdot + CH_2{=}CH{-}\dot{C}HOH \rightarrow CH_2{=}CH{-}CH(CH_2CH_3)OH. \qquad [6a]$$

The rate of reaction [6] is given by the following equation, which remains valid even if [6*a*] does not represent the exclusive fate of the allylic radical:

$$\frac{k_6}{k_2^{1/2}} = \left(\frac{R_{C_2}}{R_{C_4}} - \frac{2k_3}{k_2}\right)\frac{R_{C_4}^{1/2}}{[B]} - \frac{[D]}{[B]}\frac{k_4}{k_2^{1/2}},$$

where [D] and [B] represent the concentration of diethyl ketone and allyl alcohol, respectively, in molecule cm^{-3}.

The addition of the ethyl radical to allyl alcohol will form a vinylic radical:

$$CH_3CH_2\cdot + CH_2{=}CH{-}CH_2OH \rightarrow CH_3CH_2{-}CH_2{-}\dot{C}H{-}CH_2OH. \qquad [7]$$

The adduct will react with a second ethyl radical, either directly,

$$CH_3CH_2\cdot + CH_3CH_2{-}CH_2{-}\dot{C}H{-}CH_2OH \rightarrow CH_3CH_2{-}CH_2{-}CH(CH_2CH_3){-}CH_2OH, \qquad [7a]$$

or through some intermediate process (such as metathesis with diethyl ketone followed by reaction [5]).

In all such cases ethyl radicals disappear from the system without the formation of C_2H_6 or C_4H_{10}, and so the value of M falls below unity. Since two ethyl radicals are equivalent to one allyl alcohol molecule in the addition reaction, the rate equation is given by

$$\frac{k_7}{k_2^{1/2}} = \frac{R_{CO} - (R_{C_2H_6} + R_{C_4H_{10}})}{[B](R_{C_4H_{10}})^{1/2}} = \frac{(1-M)}{[B]}\frac{R_{CO}}{(R_{C_4H_{10}})^{1/2}}.$$

The rate equation for addition is not rigorous if ethane or ethylene is formed by reactions of the type

$$CH_3CH_2\cdot + CH_2{=}CH{-}\dot{C}HOH \rightarrow CH_2{=}CH_2 + CH_2{=}CH{-}CH_2OH \qquad [6b]$$

or

$$CH_3CH_2\cdot + CH_3CH_2{-}CH_2{-}\dot{C}H{-}CH_2OH \rightarrow CH_3CH_3 + CH_3CH_2{-}CH{=}CH{-}CH_2OH. \qquad [7b]$$

These reactions would lead to an increase in M and erroneously small values of k_7. We have shown elsewhere on the basis of experimental evidence that such reactions will have no more than a negligible effect upon the validity of the rate equation (16).

RESULTS

The results obtained from the photolysis of diethyl ketone in the presence of allyl alcohol are presented in Fig. 1.

Statistical analysis of the data give us the results of Table I; values for 1-heptene (16) and for vinyl acetate (22) have been added for comparison. Allyl alcohol is significantly more reactive than 1-heptene at 100° C with respect to both addition and metathesis. The greater reactivity of allyl alcohol may be attributed to the greater electrophilic

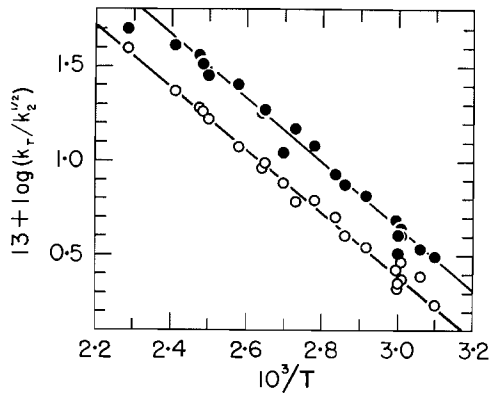

FIG. 1. Addition and metathetical reactions of the ethyl radical with allyl alcohol: ●, addition, $E_7 - \frac{1}{2}E_2 = 7.8$ kcal mole^{-1}; ○, metathesis, $E_6 - \frac{1}{2}E_2 = 7.6$ kcal mole^{-1}.

character of the OH group—considerably mitigated by its distance from the double bond.

The 1-pentene found in the butane fraction for reactions above 145° C may arise from a radical displacement reaction:

$$CH_3CH_2\cdot + CH_2{=}CH{-}CH_2OH \rightarrow CH_3CH_2{-}CH_2{-}CH{=}CH_2 + OH\cdot. \quad [8]$$

This is equivalent to stating that the product of addition is unstable, and may decompose in the period normally elapsing between its formation and its combination with an ethyl radical. By the nature of the rate equations we would expect k_7 to be affected at a lower temperature than k_6, and in Fig. 1 the point corresponding to k_7 at the highest temperature employed shows a negative deviation from the straight line.

The values of $k_4/k_2^{1/2}$ calculated from preliminary photolyses with pure diethyl ketone were in full agreement with the earlier values (15). The ratio of the disproportionation and combination constants of the ethyl radical, k_3/k_2, was found to be 0.134 ± 0.01 in this study, indistinguishable from the value of 0.136 ± 0.02 reported previously (15), and of 0.135 in the most recent work (20). This concordance establishes a basis for comparing the results of this study with the earlier data.

DISCUSSION

The Relevance of k_6 and k_7 to Polymerization Kinetics

Allyl polymerization owes its distinctive quality to the restriction of the values of k_p/k_t to a narrow range of about 2 to 20. We have found that $k_7/k_6 = 1.8$ for allyl alcohol at 60° C, but this ratio is relevant to the polymerization of allyl alcohol only if $k_p/k_t \approx k_7/k_6$. Here we shall present the evidence for this equation, and we begin by showing that k_p and k_7 are of the same order of magnitude, and, indeed, that $k_p \approx 2k_7$ for allyl alcohol at 60° C.

The value of the addition constant k_7 may be calculated using the value of k_2 measured by Shepp and Kutschke (21): $k_2 = 5.06 \times 10^{-10} \exp(-2000 \pm 1000)/RT$ cm^3 molecule^{-1} sec^{-1}. Values of k_7 are compared with k_p for vinyl acetate at 60° C, and for this monomer $k_p = 1.8\, k_7$:

allyl alcohol:	$k_7 = 2.2 \times 10^{-18}$ cm^3 molecule^{-1} sec^{-1},
vinyl acetate (22):	$k_7 = 3.5 \times 10^{-18}$ cm^3 molecule^{-1} sec^{-1},
vinyl acetate (23):	$k_p = 6.3 \times 10^{-18}$ cm^3 molecule^{-1} sec^{-1}.

TABLE I

Reactions of the ethyl radical with unsaturated molecules

Substrate	Nature of reaction	Number of runs	C	B	$13+\log (A_r/A_2^{1/2})$	$E_r-\frac{1}{2}E_2$ (kcal mole^{-1})	$13+\log (k_r/k_2^{1/2})$ (at 100° C)
Allyl alcohol	Addition	18	5.739	1.695	5.7±0.2	7.75±0.35	1.20
1-Heptene (16)	Addition	34	5.156	1.530	5.2±0.1	7.0±0.2	1.06
Vinyl acetate (22)	Addition	22	5.300	1.485	5.3±0.3	6.8±0.4	1.32
Allyl alcohol	Metathesis	17	5.385	1.665	5.4±0.2	7.6±0.3	0.92
1-Heptene (16)	Metathesis	22	5.605	1.825	5.6±0.3	8.3±0.5	0.71

NOTE: The constants B and C are the coefficients of the straight lines $13+\log (k_r/k_2^{1/2}) = C-10^3B/T$ fitted to the experimental results. The symbol k_r represents either k_6 or k_7, expressed in units of cm^3 molecule^{-1} sec^{-1}. The limits of error are calculated at the 5% probability level.

TABLE II

Correlation of the rate constants for the addition of the ethyl radical to certain substrates in the gas phase with monomer reactivity ratios of copolymerization (r_1), each at 60° C

Substrate	$13+\log (k_7/k_2^{1/2})$	$\log (1/r_1)$ (M_1:CH_2=CHOAc)	$\log (1/r_1)$ (M_1:CH_2=CHCN)	q_2 (kcal mole^{-1})	$10^{10}\epsilon_2$ (e.s.u.)	M_2 (24)
1-Heptyne (16)	0.25	−0.42	−0.51	−0.25	−0.34	1-Hexyne
1-Heptene (16)	0.57	−0.36	−0.31	−0.4	−0.4	1-Hexene
Allyl alcohol (25)	0.65	—	−0.60	—	—	Allyl alcohol
Allyl alcohol (25)	0.65	−0.14	−0.33	−0.64	−0.29	Allyl acetate
Vinyl butyl ether (26)	0.77	−0.20	−0.35	−0.68	−0.55	Vinyl isobutyl ether
Vinyl acetate (22)	0.84	0.00	−0.57	−0.72	−0.11	Vinyl acetate
2,4,4-Trimethyl 1-pentene (16)	0.93	−0.24	−0.15	−0.6	−0.42	Isobutene
Styrene (22)	2.26	+1.49	+1.20	−3.10	−0.24	Styrene
2,3-Dimethyl butadiene-1,3 (25)	2.66	+1.82	+1.52	−3.6	−0.24	Butadiene
Acrylonitrile (26)	2.86	+1.53	0.00	−2.7	+0.34	Acrylonitrile

Vinyl acetate has been introduced because it resembles allyl alcohol both in its reactivity towards the ethyl radical, and also in degree of resonance stabilization and electron-donor power in polymerization. In Fig. 2 we demonstrate the correlation between the rate

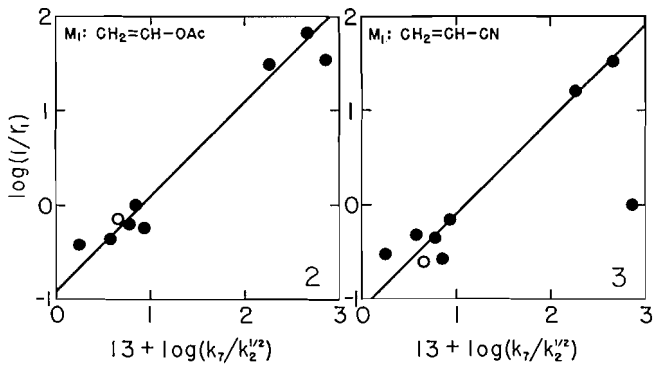

FIGS. 2 and 3. Correlation of rate constants for addition: of the ethyl radical in the gas phase and (2) the polyvinyl acetate radical, or (3) the polyacrylonitrile radical, in solution. The open circle represents allyl alcohol.

constants for the addition of the ethyl and polyvinyl acetate radicals respectively to a series of monomers. The diversity of these monomers is evident from the range of the values (24) of q and ϵ given in Table II. A reference line of unit slope has been drawn; the small degree of scatter about this line supports the validity of the correlation. The values of the reactivity ratios r_1 were calculated from the revised equation of Schwan and Price (24):

$$RT \ln (1/r_1) = (q_1 - q_2) + 7.23 \times 10^{20} \epsilon_1(\epsilon_1 - \epsilon_2);$$

unfortunately their data do not include allyl alcohol, but the point for the closely related monomer allyl acetate is shown by the open circle. Figure 3 is the corresponding correlation diagram for the ethyl and polyacrylonitrile radicals; here allyl alcohol is marked by an open circle. This is a far more severe test of correlation, as the polyacrylonitrile radical differs markedly from the ethyl radical in its resonance stabilization and its electrophilic nature (27); yet the scatter of points about the line of unit gradient is small, the only significant deviation being for acrylonitrile monomer. As the ethyl and polyvinyl acetate radicals are much more nearly matched in reactivity, it seems reasonable to assume that the point for allyl alcohol would lie close to the straight line of Fig. 2. On this basis we may estimate that $k_p \approx 2k_7$ for allyl alcohol, giving $k_p = 4 \times 10^{-18}$ cm^3 molecule^{-1} sec^{-1} at 60° C, similar to the value of k_p for vinyl acetate.

In support of the proposition that $k_p/k_t \approx k_7/k_6$ for allyl alcohol we shall apply the general equation proposed by Bamford, Jenkins, and Johnston for radical reactivity (28):

$$\log k_S = \log k_T + \alpha\sigma + \beta.$$

The rate constants k_S and k_T refer respectively to the reaction of a given radical $R.CH_2CHX\cdot$ with a substrate S and to metathesis of the same radical with toluene; σ is the Hammett constant for the group X, and α and β are constants for the substrate S. The parameter σ is zero for the ethyl radical and very small for the polyallyl alcohol radical; it therefore follows that

$$\log \left(\frac{k_p}{k_t} \Big/ \frac{k_7}{k_6} \right) = (\alpha_A - \alpha_M)\sigma_X,$$

where the subscripts A, M, and X refer to addition, metathesis, and the polymer radical respectively. Since α gives a measure of the intrinsic polarity of the reaction, which is small in each case, it follows that the difference $(\alpha_A - \alpha_M)$ is very small, and the product $(\alpha_A - \alpha_M)\sigma_X$ is negligible. We may therefore write $k_p/k_t \approx k_7/k_6$, and expect the latter ratio to predict the behavior of allyl alcohol in polymerizing systems. In the next section we shall show that this expectation is fulfilled.

The Application of k_6 and k_7 to the Polymerization of Allyl Alcohol

High polymer is readily formed from both vinyl acetate and methyl acrylate by the action of a trace of free radical catalyst; whereas allyl alcohol is so unreactive that Staudinger originally believed that no polymer could be obtained from this monomer (29). This reluctance to polymerize is not due to the low reactivity of the double bond of allyl alcohol. It is clear from the following rate constants, from Table I, and from the relationship $k_p \approx 2k_7$, that the double bond of vinyl acetate is only slightly more reactive:

allyl alcohol: $k_7 = 12.4\times10^{-13} \exp(-8800/RT)$ cm^3 molecule^{-1} sec^{-1},
vinyl acetate (23): $k_p = 4.0\times10^{-13} \exp(-7300/RT)$ cm^3 molecule^{-1} sec^{-1},
methyl acrylate (30): $k_p = 1.7\times10^{-13} \exp(-7100/RT)$ cm^3 molecule^{-1} sec^{-1}.

The essential difference is the presence of a site for rapid metathesis in allyl alcohol, which causes degradative chain transfer to dominate the polymerization. No such site exists in vinyl acetate (22) and its polymerization proceeds unchecked by significant chain transfer.

The number-average molecular weight of polyallyl alcohol may be estimated from our results. This quantity is given by k_p/k_t, the ratio of the propagation and transfer constants (31), and therefore approximately by k_7/k_6, which has the value of 1.9 at 100° C. This is considerably lower than the value of 5 reported for a mixture of 155 parts of allyl alcohol and 2 parts of hydrogen peroxide, held at 100° C for 116 hours with frequent replenishment of the hydrogen peroxide (13). However, in such a system we may expect extensive reactivation of the "dead" polymer by metathesis with the hydroxyl radicals present. By this means new reactive polymer radicals would be formed, and, in principle, the degree of polymerization could be increased indefinitely.

The approximate equality of k_6 and k_7 for allyl alcohol explains the powerful inhibiting action of this substance upon the polymerization of certain other monomers. Allyl alcohol inhibits the polymerization of butadiene so effectively that the corresponding copolymer must be prepared indirectly (1). Reactivity in this system rapidly becomes transferred to the $CH_2{=}CH{-}\dot{C}HOH$ radical, which is too unreactive to add to allyl alcohol or to the stabilized butadiene ($q = -3.6$ kcal mole^{-1}) (24).

In contrast, allyl alcohol does form high copolymer with acrylonitrile (14); clearly it must be possible for the $CH_2{=}CH{-}\dot{C}HOH$ radical to add to the double bond of acrylonitrile. This difference in behavior may be explained in terms of the lowering of the energy of activation for the addition by contribution of ionic forms to the stability of the activated complex (27). The $CH_2{=}CH{-}\dot{C}HOH$ radical will behave as a weak electron donor. Acrylonitrile ($\epsilon = +0.34\times10^{-10}$ e.s.u. (24)) is strongly electrophilic; it is reduced at the dropping mercury electrode at the low half-wave potential of -1.94 volt (S.C.E.) (32), and is very readily polymerized by an anionic chain mechanism by such catalysts as butyl lithium (33) and a solution of sodium and naphthalene in tetrahydrofuran (34). The polar effect should therefore be pronounced for acrylonitrile and very weak for butadiene ($\epsilon = -0.24\times10^{-10}$ e.s.u. (24)). This situation closely resembles

that of Fig. 3, where the apparently anomalous behavior of acrylonitrile is also due to its electrophilic nature.

CONCLUSIONS

We have tested the relevance of values of k_6 and k_7 to the study of the polymerization of allyl alcohol in such varied aspects as the magnitude of the propagation constant, the competition between propagation and chain transfer, the degree of polymerization, and propagation and inhibition in copolymerization. In each case the observed behavior of the propagating system is consistent with predictions based upon the values of k_6 and k_7. The measure of success renders it probable that the polymerization of other monomers may be interpreted in terms of the reactions of the monomer with the ethyl radical in the gas phase (22).

ACKNOWLEDGMENTS

We wish to thank the National Research Council of Canada for the financial support of this work, and also for a studentship to one of us (A. C. R. B.).

REFERENCES

1. R. C. LAIBLE. Chem. Revs. **58**, 807 (1958).
2. N. G. GAYLORD and F. R. EIRICH. J. Am. Chem. Soc. **73**, 4981 (1951).
3. D. J. RUZICKA and W. A. BRYCE. Can. J. Chem. **38**, 827 (1960).
4. N. N. SEMENOV. Some problems in chemical kinetics and reactivity. Vol. I. Pergamon Press, London. 1958. p. 37.
5. P. BARTLETT and R. ALTSCHUL. J. Am. Chem. Soc. **67**, 816 (1945).
6. N. G. GAYLORD and F. R. EIRICH. J. Am. Chem. Soc. **74**, 334 (1952).
7. M. LITT and F. R. EIRICH. J. Polymer Sci. **45**, 379 (1960).
8. P. BARTLETT and F. TATE. J. Am. Chem. Soc. **75**, 91 (1953).
9. N. G. GAYLORD. J. Polymer Sci. **7**, 575 (1951).
10. N. G. GAYLORD. J. Polymer Sci. **22**, 71 (1956).
11. I. SAKURADA and G. TAKAHASHI. Chem. High Polymers (Tokyo), **11**, 266 (1954).
12. SHELL CHEMICAL CORPORATION. Allyl alcohol. Technical publication Sc46-32. 1946. p. 26.
13. D. ADELSON and H. GRAY. U.S. Patent No. 2,555,775 (June 5, 1951); Chem. Abstr. **45**, 8270*h* (1951).
14. G. OSTER and Y. MIZUTANI. J. Polymer Sci. **22**, 173 (1956).
15. D. G. L. JAMES and E. W. R. STEACIE. Proc. Roy. Soc. (London), A, **244**, 289 (1958).
16. D. G. L. JAMES and E. W. R. STEACIE. Proc. Roy. Soc. (London), A, **244**, 297 (1958).
17. L. M. DORFMANN and Z. D. SHELDON. J. Chem. Phys. **17**, 511 (1949).
18. K. O. KUTSCHKE, M. H. J. WIJNEN, and E. W. R. STEACIE. J. Am. Chem. Soc. **74**, 714 (1952).
19. R. K. BRINTON and E. W. R. STEACIE. Can. J. Chem. **33**, 1840 (1955).
20. D. S. WEIR. J. Am. Chem. Soc. **83**, 2629 (1961).
21. A. SHEPP and K. O. KUTSCHKE. J. Chem. Phys. **26**, 1020 (1957).
22. D. G. L. JAMES and D. MACCALLUM. Proc. Chem. Soc. 259 (1961).
23. M. S. MATHESON, E. E. AUER, E. B. BEVILACQUA, and E. J. HART. J. Am. Chem. Soc. **71**, 2610 (1949).
24. T. C. SCHWAN and C. C. PRICE. J. Polymer Sci. **40**, 457 (1959).
25. A. C. R. BROWN and D. G. L. JAMES. Unpublished results.
26. D. G. L. JAMES and D. MACCALLUM. Unpublished results.
27. F. R. MAYO. J. Chem. Educ. **36**, 157 (1959).
28. C. H. BAMFORD, A. D. JENKINS, and R. JOHNSTON. Trans. Faraday Soc. **55**, 418 (1959).
29. H. STAUDINGER and T. FLEITMANN. Ann. **480**, 92 (1930).
30. M. S. MATHESON, E. E. AUER, E. B. BEVILACQUA, and E. J. HART. J. Am. Chem. Soc. **73**, 5395 (1951).
31. C. H. BAMFORD, W. G. BARB, A. D. JENKINS, and P. F. ONYON. The kinetics of vinyl polymerization by radical mechanisms. Butterworths Scientific Publications, London. 1958. pp. 15, 270.
32. T. FUENO, K. ASADA, K. MOROKUMA, and J. FURUKAWA. J. Polymer Sci. **40**, 511 (1959).
33. M. FRANKEL, A. OTTOLENGHI, M. ALBECK, and A. ZILKHA. J. Chem. Soc. 3858 (1959).
34. M. SZWARC, M. LEVY, and R. MILKOVITCH. J. Am. Chem. Soc. **78**, 2656 (1956).

ORGANIC PEROXIDES

IV. CATALYSIS OF AROYL PEROXIDE REACTIONS BY ALUMINUM CHLORIDE: THE DIRECT INTRODUCTION OF *O*-AROYL GROUPS INTO AROMATIC NUCLEI

J. T. EDWARD, H. S. CHANG, AND S. A. SAMAD[1]
Department of Chemistry, McGill University, Montreal, Que.

Received December 13, 1961

ABSTRACT

In inert solvents in the presence of aluminum chloride, aroyl peroxides decompose to esters and carbon dioxide. In highly nucleophilic solvents such as anisole or mesitylene, *p,p'*-dinitrobenzoyl peroxide effects a Friedel–Crafts type of substitution of the solvent molecule. Both decomposition and substitution reactions probably depend on a heterolytic fission of the peroxide linkage catalyzed by aluminum chloride.

Reynhart (1) claimed that in the presence of aluminum chloride benzoyl peroxide reacted with benzene at 0° C to give a 90% yield of phenyl benzoate and 92% yield of benzoic acid:

$$ArH + (ArCO_2)_2 \rightarrow ArCO_2Ar + ArCO_2H. \quad [1]$$

At higher temperatures the yield of ester was said to drop, and the amounts of diphenyl formed to increase (1, 2).

In a reinvestigation of this reaction we obtained much lower yields of phenyl benzoate, which did not seem to be much affected by temperature. Furthermore, the compound was obtained when solvents other than benzene were used, seemingly from the overall reaction

$$(ArCO_2)_2 \rightarrow ArCO_2Ar + CO_2, \quad [2]$$

as shown by the concomitant formation of carbon dioxide (Table I). This mode of decomposition had already been observed by Reynhart (1) when benzoyl peroxide in

TABLE I

$AlCl_3$-catalyzed decomposition of benzoyl peroxide in different solvents

Solvent	Temp. (°C)	Yields (%)		
		Carbon dioxide	Phenyl benzoate	Benzoic acid*
Methylene chloride	8–10	—†	26	27
Benzene	0–5	29	29	30
Benzene	50	74	28	12
Nitrobenzene	0–5	46	49	16
Nitrobenzene	50	31	23	18
Toluene	50	44	41	25‡
1,3-Dimethoxy benzene	0–5	—†	0	66§
Mesitylene	0–5	—†	0	29
Nitrobenzene–toluene, 1:1 (v/v)	0–5	—†	21	42
Nitrobenzene–anisole, 1:1 (v/v)	0–5	—†	0	76–79‖

*Based on $(PhCO_2)_2 \rightarrow 2PhCO_2H$.
†Not investigated.
‡Trace of phenol also formed.
§2,4-Dimethoxyphenyl benzoate (3% yield) also formed.
‖4,4'-Dimethoxy diphenyl (22–23% yield) also formed.

[1]*Holder of Colombo Plan Fellowship, 1957–1960.*

petroleum ether was treated with antimony pentachloride. However, the peroxide may be diverted from this mode of decomposition by suitable solvents. Thus from a reaction in a mixture of nitrobenzene and anisole, 4,4′-dimethoxydiphenyl was isolated in 22–23% yield; other bianisyls were also probably formed, but not obtained crystalline. From a reaction in 1,3-dimethoxybenzene a very small amount of 2,4-dimethoxyphenyl benzoate was isolated. This was the only crystalline product resulting from a Friedel–Crafts attack on solvent following equation [1]; it is possible that mesitylene also reacted partially in this fashion, but no crystalline benzoate could be isolated.

With boron trifluoride etherate in place of aluminum chloride, no decomposition of the peroxide in benzene took place.

It seems likely that aluminum chloride, like Brønsted acids (3), promotes the ionic fission of the peroxide linkage of aroyl peroxides. The electron deficiency of the developing oxygen cation may then be relieved either by synchronous migration of an aryl group (4) (route *a*, Scheme I) to give the aryloxyformyl cation (III), or by synchronous electron donation from an external aromatic nucleus (II) (route *b*), after the fashion of many Friedel–Crafts acylations (5). Evidently the latter route is possible only with highly reactive aromatic nuclei such as 1,3-dimethoxybenzene. The ions III and IV

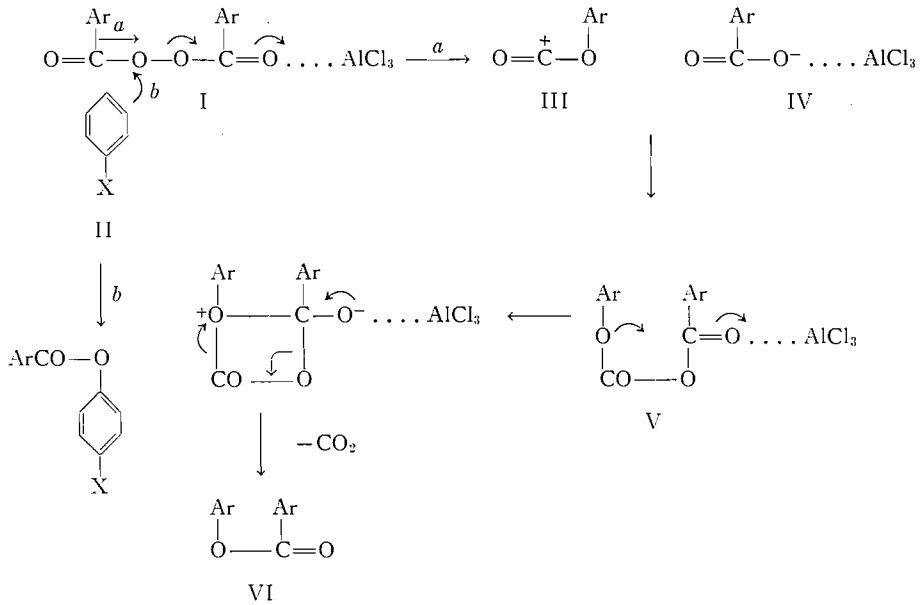

SCHEME I

formed by route *a* can recombine to form the carboxylic–carbonic anhydride (V): Leffler (3) has already obtained an anhydride of this type by rearrangement of *p*-methoxy-*p*′-nitrobenzoyl peroxide in thionyl chloride. Benzoic–phenylcarbonic anhydride (V; Ar = Ph) was reported by Windholz (6) to decompose to give a 10% yield of phenyl benzoate (equation [3]) and 80% yields of benzoic anhydride and diphenyl carbonate (equation [4]):

$$PhCO.O.CO.OPh \rightarrow PhCOOPh + CO_2 \quad [3]$$

$$2PhCO.O.CO.OPh \rightarrow (PhCO)_2O + CO(OPh)_2 + CO_2. \quad [4]$$

However, it seems likely that in the presence of aluminum chloride, decomposition

would take place mainly according to equation [3]. Thus benzoic–ethylcarbonic anhydride, which is stable at room temperature, decomposes at 175–185° to give 50% of ethyl benzoate and 50% of benzoic anhydride; however, in the presence of boron trifluoride etherate, decomposition takes place at room temperature to give ethyl benzoate almost exclusively (6). Similarly we have found benzoic–ethylcarbonic anhydride in benzene decomposes at room temperature in the presence of aluminum chloride to give a 48% yield of ethyl benzoate and 14% yield of benzoic acid (presumably from benzoic anhydride). The mechanism for the catalyzed decomposition of benzoic–phenylcarbonic anhydride (V; Ar = Ph) shown in Scheme I is suggested by the fact that the uncatalyzed decomposition is greatly facilitated by electron-withdrawing groups in the acyl portion of the anhydride (6–9).

An alternative mechanism was considered in which the phenoxyformyl cation (III; Ar = Ph) lost carbon dioxide to form the phenyl cation (a reaction for which analogies exist (9–11)), followed by union of the latter with benzoate ion (IV; Ar = Ph) to give phenyl benzoate. However, the reaction of the phenyl cation with $PhCO_2^- \ldots . AlCl_3$ would be expected to give also some chlorobenzene; none of this compound could be detected by gas chromatography in the products of the aluminum-chloride-catalyzed decomposition of benzoyl peroxide in toluene.

The heterolysis of the peroxide linkage leading to phenyl benzoate (route *a*) probably receives anchimeric assistance from the migrating phenyl group. It was expected that *p,p'*-dinitrobenzoyl peroxide would rearrange by this route less readily than benzoyl peroxide because of the lesser migratory aptitude of the *p*-nitrophenyl group (12), so that in this case route *b* might compete successfully with route *a*. This expectation was realized when sufficiently reactive aromatic compounds were used as solvents in the reaction, direct substitution of *p*-nitrobenzoyloxy groups into solvent molecules taking place. The results are listed in Table II. It is obvious from the 54–77% yields of *p*-nitrobenzoic acid that competing reactions are taking place, since the maximum yield of this acid can be only 50% if the reaction path is defined by equation [1]. Oxidation of solvent molecules to biaryls could give *p*-nitrobenzoic acid in a maximum yield of 100%; however, in no case were biaryls isolated.

TABLE II

Products of $AlCl_3$-catalyzed reactions of *p,p'*-dinitrobenzoyl peroxide in aromatic solvents

	p-Nitrobenzoate		*p*-Nitrobenzoic acid
Solvent	Aryl group	Yield (%)	Yield (%)*
m-Xylene	2,4-Dimethylphenyl	5	72
Mesitylene	Mesityl	34	68
Anisole	*o*-Methoxyphenyl	7	57
	p-Methoxyphenyl	21	
Phenetole	*o*-Ethoxyphenyl	10	54
	p-Ethoxyphenyl	12	
Veratrole	3,4-Dimethoxyphenyl?	trace	77
1,3-Dimethoxybenzene	2,4-Dimethoxyphenyl	20	59

*Based on $(O_2N.C_6H_4.CO_2)_2 \rightarrow 2O_2N.C_6H_4.CO_2H$.

Except for *o*- and *p*-methoxyphenyl *p'*-nitrobenzoates, the esters of Table II are new compounds. The identities of the compounds obtained from *m*-xylene, anisole, and phenetole were established by comparison with authentic specimens prepared from the appropriate phenols. The ester obtained from 1,3-dimethoxybenzene was shown to be 2,4-dimethoxyphenyl *p'*-nitrobenzoate because it differed from the other two possible isomers,

3,5-dimethoxyphenyl and 2,6-dimethoxyphenyl *p'*-nitrobenzoates, both of which were synthesized. The orientation of the substitution reaction revealed by the products in Table II is in accord with an electrophilic attack on the aromatic nucleus, as postulated in Scheme I.

Without fairly strongly electron-releasing substituents, the benzene ring is insufficiently reactive to effect this type of Friedel–Crafts reaction. A suspension of *p,p'*-dinitrobenzoyl peroxide in benzene in the presence of aluminum chloride reacted only very slowly at room temperature, 21% of *p*-nitrobenzoic acid and 70% of recovered peroxide being obtained after 48 hours. The neutral residue after removal of benzene showed weak absorption at 1748 cm^{-1} indicative of a *p*-nitrobenzoyl group, but no crystalline product could be isolated. On the other hand, in methylene dichloride a 65% yield of the rearrangement product, *p*-nitrophenyl *p'*-nitrobenzoate, was obtained after reaction overnight at 0°. The more rapid reaction in this solvent may be due to the greater solubility of aluminum chloride and the peroxide in it.

A serious limitation on the usefulness of this Friedel–Crafts method for introducing the *p*-nitrobenzoyloxy group directly into aromatic nuclei lies in the fact that no suitable solvent for the reaction has been found. Attempts to bring about the reaction of naphthalene with *p,p'*-dinitrobenzoyl peroxide in nitrobenzene or nitromethane solvents gave only gummy and intractable products. Even 1,3-dimethoxybenzene gave an intractable product when the reaction was carried out in methylene chloride solution. It is to be expected that the bimolecular reaction of peroxide with an aromatic compound (route *b*), as compared with unimolecular decomposition of the peroxide (route *a*), will be disfavored by dilution with an inert solvent. However, it was not possible to isolate any *p*-nitrophenyl *p'*-nitrobenzoate (from route *a*) from the reaction with 1,3-dimethoxybenzene in methylene chloride, so that the course of the reaction in this solvent mixture remains unknown.

Finally, the aluminum-chloride-catalyzed decomposition of the unsymmetrical *p*-nitrobenzoyl peroxide was studied. This reaction was of interest because the nature of the product should be determined by the rates of two competing reactions *a* and *b* (Scheme II). Reaction *a* should be favored by the greater basicity of the benzoyl carbonyl group,

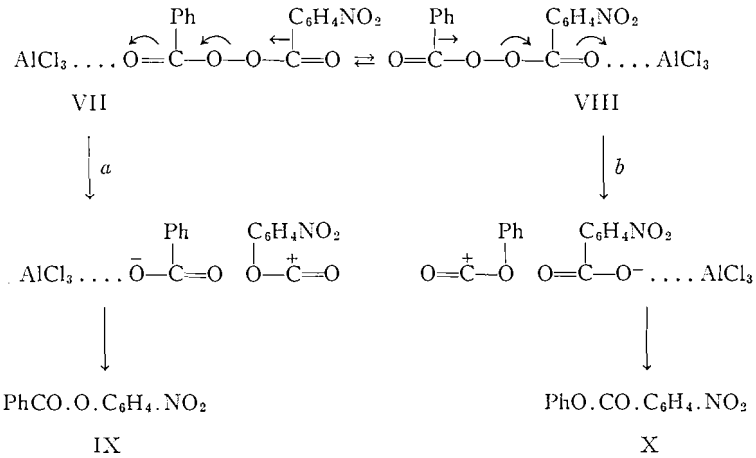

SCHEME II

and hence by a greater concentration of the complex VII than of VIII; on the other hand, the heterolysis of the latter should take place more readily because the anchimeric

assistance of a phenyl group is superior to that of a *p*-nitrophenyl group. In the event, the latter effect is predominant, as evidenced by the isolation in 81% yield of phenyl *p*-nitrobenzoate (X), but of no *p*-nitrophenyl benzoate (IX), when the reaction was carried out in methylene chloride. The aluminum-chloride-catalyzed decomposition thus follows the rearrangement pattern found by Leffler (3, 7) for the uncatalyzed decomposition of unsymmetrical peroxides. A small yield (12%) of *p*-nitrobenzoic acid probably came from the anhydride, produced by a reaction similar to that of equation [4]. In benzene and in nitrobenzene the catalyzed decomposition of this peroxide followed a less clear-cut path. The yield of *p*-nitrobenzoic acid was considerably larger, and of neutral material considerably smaller. From the latter a gummy material was obtained which appeared from its infrared spectrum to contain phenyl *p*-nitrobenzoate, but which could not be purified further.

EXPERIMENTAL

Materials

Commercial benzoyl peroxide was crystallized by addition of methanol to a concentrated solution of the peroxide in chloroform, and dried by several days standing at room temperature in an evacuated desiccator. *p,p'*-Dinitrobenzoyl peroxide was prepared from *p*-nitrobenzoyl chloride and sodium peroxide by the method of Price and Krebs (13). *p*-Nitrobenzoyl peroxide was prepared according to Wieland and Rasuwajew (14), and crystallized from ethanol, m.p. 113° (decomp.).

Reactions of Benzoyl Peroxide

Benzoyl peroxide dissolved in about four times its weight of organic solvent was added under nitrogen slowly with stirring to an equimolar quantity of aluminum chloride suspended in about the same volume of the same solvent. The nitrogen passing slowly over the reaction mixture was led through a known volume of standard alkali, which was subsequently titrated for carbon dioxide (15). Reaction was allowed to proceed for 7 hours or more, except for the reaction in nitrobenzene (4 hours at 0°, 5 hours at 50°: Table I). The reaction mixture was then treated with dilute aqueous hydrochloric acid and filtered from a solid residue. The solid residue and the organic layer in the filtrate were both extracted with aqueous sodium bicarbonate to remove benzoic acid. The neutral organic solution was then washed with water, dried, and distilled: phenyl benzoate came over at 162° at 13 mm and solidified, m.p. and mixed m.p. 69°. A considerable amount of intractable resinous solid was left behind in the distillation flask (about 30% of weight of peroxide; b.p. > 230° at 0.5 mm).

For the reactions in nitrobenzene–toluene and nitrobenzene–anisole, benzoyl peroxide (24.2 g; 0.1 mole) dissolved in toluene or anisole (125 ml) was added to aluminum chloride (13.5 g; 0.1 mole) dissolved in nitrobenzene (125 ml). From the latter experiment 4,4'-dimethoxydiphenyl (5.0 g; 23%) was isolated by distillation of the organic layer obtained as described above, b.p. 154° at 0.5 mm. Crystallized from ethanol, it had m.p. 169°, undepressed by admixture with an authentic specimen.

From the reaction in 1,3-dimethoxybenzene, the neutral fraction on distillation gave no phenyl benzoate but a gum (2.1 g), b.p. 195° at 1 mm, having strong absorption at 1743 cm^{-1}. The gum was chromatographed on alumina, using petroleum ether as eluent, to give an oily solid which crystallized from petroleum ether in colorless rods (0.24 g), m.p. 89° (reported m.p. 2,4-dimethoxyphenyl benzoate 90° (16)); $\nu_{max}^{CCl_4}$ in cm^{-1}: 3030 (m), 2960 (m), 2840 (m), 1740 (s), 1600 (s), 1470 (s), 1443 (s), 1318 (s), 1270–1245 (s, broad), 1180 (s), 1162 (s), 1125 (s), 1080 (s), 1062 (s), 1030 (s), 925 (m). Calc. for $C_{15}H_{14}O_4$: C, 69.76; H, 5.42%. Found: C, 69.95; H, 5.50%.

From the reaction of benzoyl peroxide (4.82 g) in mesitylene, the neutral fraction gave a liquid (2.5 g), b.p. 156–166° at 1 mm, having strong absorption at 1740 cm^{-1}.

Reactions of p,p'-Dinitrobenzoyl Peroxide

Because of its very small solubility in most organic solvents, this peroxide was slowly added as a solid to a suspension of aluminum chloride in an organic solvent at room temperature. The reaction mixture was kept overnight at 0° C unless otherwise noted, and then worked up in the general fashion described above for benzoyl peroxide reactions. Results with the different solvents are given in Table II and below.

(a) Methylene Dichloride

Evaporation of the neutral fraction gave a solid which crystallized from ethanol as colorless needles, m.p. 159°, identified as *p*-nitrophenyl *p'*-nitrobenzoate by mixed melting point (recorded m.p. 159° (17)).

(b) Benzene

To a stirred suspension of aluminum chloride (1.35 g; 0.01 mole) in benzene (75 ml) was added the peroxide (3.32 g; 0.01 mole) at 22°. The mixture was left at room temperature for 48 hours and then worked

up in the usual way to give 0.69 g (21%) of *p*-nitrobenzoic acid. The residue of insoluble material was unreacted peroxide; further crops were obtained from the neutral benzene solution on concentration, giving a total recovery of 2.30 g (70%). Complete evaporation of the benzene gave a tar (0.57 g), which was chromatographed on alumina using light petroleum (b.p. 66–75°) and benzene as eluents. No crystalline product was obtained, but several fractions showed a weak infrared peak at 1748 cm^{-1}.

(c) m-Xylene

Removal of xylene from the neutral fraction left a gum, which was chromatographed on alumina using petroleum ether (b.p. 66–75°) and benzene as eluents. A few semisolid fractions were obtained which were triturated with ethanol and then recrystallized from this solvent (charcoal) as colorless needles of 2,4-dimethylphenyl *p*-nitrobenzoate, m.p. 112°. The same compound (m.p. and mixed m.p.) was obtained from 2,4-dimethylphenol and *p*-nitrobenzoyl chloride in pyridine. Calc. for $C_{15}H_{13}NO_4$: C, 66.42; H, 4.79; N, 5.16%. Found: C, 66.21; H, 4.92; N, 5.11%.

(d) Mesitylene

The gummy residue from the neutral fraction was chromatographed as above to give a few solid fractions, obtained on crystallization from ethanol as slightly brownish plates, m.p. 122°, of mesityl *p*-nitrobenzoate. Calc. for $C_{16}H_{15}NO_4$: C, 67.37; H, 5.26; N, 4.91%. Found: C, 67.30; H, 5.33; N, 5.00%. Infrared spectrum: $\nu_{max}^{CCl_4}$ in cm^{-1}: 3030 (m, sh), 2940 (s), 2870 (m), 1743 (s), 1610 (s), 1525 (m), 1487 (s), 1350 (s), 1322 (m), 1275–1240 (s), 1195 (m), 1140 (s), 1080 (s), 1010 (w), 870 (m), 695 (w, sh).

(e) Anisole

A stirred suspension of aluminum chloride (1.35 g) and peroxide (3.32 g) in anisole (35 ml) was allowed to react at 22° for 7 hours. From the neutral fraction anisole was removed by distillation at 15 mm. The gummy residue (0.87 g) was chromatographed on alumina using, successively, petroleum ether (b.p. 66–75°), benzene, and ether as eluents. The first few fractions gave pale yellowish needles of *o*-methoxyphenyl *p'*-nitrobenzoate (0.19 g; 7%), m.p. 102° alone or admixed with an authentic specimen (recorded m.p. 102° (18)). Later fractions gave almost colorless needles of *p*-methoxyphenyl *p'*-nitrobenzoate (0.57 g; 21%), m.p. 112° alone or admixed with an authentic specimen (recorded m.p. 113–115° (18)).

(f) Phenetole

This reaction was carried out under the same conditions as described above for anisole. Removal of phenetole from the neutral fraction at 44° at 1 mm left a residue (1.15 g), which was chromatographed on alumina. The solid from the first few fractions, after crystallization from ethanol, was obtained as yellowish plates (0.31 g; 10%), m.p. 114°, and was identified as *o*-ethoxyphenyl *p'*-nitrobenzoate by comparison (m.p. and mixed m.p.) with the compound prepared by reaction of *o*-ethoxyphenol with *p*-nitrobenzoyl chloride in pyridine. Calc. for $C_{15}H_{13}O_5N$: C, 62.72; H, 4.53; N, 4.88%. Found: C, 62.90; H, 4.66; N, 4.82%. Infrared spectrum: $\nu_{max}^{CCl_4}$ in cm^{-1}: 3040 (w), 2980 (m), 2925 (m), 2872 (w), 1740 (s), 1700 (w), 1600 (s), 1490 (s), 1470 (s), 1450 (m), 1405 (m), 1340 (s), 1275–1225 (s), 1175 (s), 1110 (m), 1060 (s), 1035 (m), 920 (w), 835 (m).

The next few fractions (0.31 g) had unsharp melting points (ca. 92–99°) and were evidently mixtures. However, later fractions could be crystallized from ethanol to give plates (0.37 g; 12%) melting sharply at 118°. This compound was identified as *p-ethoxyphenyl p-nitrobenzoate* by comparison (m.p. and mixed m.p.) with the compound prepared from *p*-ethoxyphenol and *p*-nitrobenzoyl chloride in pyridine. Found: C, 62.63; H, 4.56; N, 4.98%. Infrared spectrum: $\nu_{max}^{CCl_4}$ in cm^{-1}: 3055 (w), 2985 (m), 2940 (w), 1740 (s), 1478 (m), 1345 (s), 1275–1225 (s), 1185 (m), 1105 (w), 1070 (m), 1042 (m).

(g) Veratrole

From a reaction using 3.32 g of peroxide, the neutral fraction on distillation gave a very small quantity of solid product, b.p. 150° at 1 mm, which crystallized from ethanol in colorless rods, m.p. 135°. Infrared spectrum: $\nu_{max}^{CCl_4}$ in cm^{-1}: 3030 (w), 2960 (m), 2840 (m), 1742 (s), 1605 (m), 1495 (s), 1475 (m), 1347 (s), 1275–1225 (s), 1165 (m), 1090 (s), 1000 (w), 870 (m), 690 (w).

(h) 1,3-Dimethoxybenzene

The neutral fraction on distillation gave a solid, b.p. 225° at 1 mm, which crystallized from ethanol as colorless rods of *2,4-dimethoxyphenyl p'-nitrobenzoate*, m.p. 128°. Calc. for $C_{15}H_{13}NO_6$: C, 59.41; H, 4.29; N, 4.63%. Found: C, 59.65; H, 4.39; N, 4.65%. The melting point was depressed by admixture of the compound with 3,5-dimethoxyphenyl *p'*-nitrobenzoate and with 2,6-dimethoxyphenyl *p'*-nitrobenzoate (see below). Infrared spectrum: $\nu_{max}^{CHCl_3}$ in cm^{-1}: 3030 (w), 2940 (m), 2840 (m), 1740 (s), 1609 (s), 1495 (w), 1460 (m), 1350 (s), 1320 (m), 1157 (m), 1120 (m), 1070 (s), 1015 (w), 865 (w).

2,6-Dimethoxyphenyl *p'*-nitrobenzoate, prepared from 2,6-dimethoxyphenol, crystallized from ethanol as pale yellowish needles, m.p. 164°. Found: C, 59.57; H, 4.33; N, 4.55%. 3,5-Dimethoxyphenyl *p'*-nitrobenzoate, prepared from 3,5-dimethoxyphenol, crystallized from ethanol as pale yellowish needles, m.p. 141°. Found: C, 59.51; H, 4.26; N, 4.59%.

(i) 1,3-Dimethoxybenzene in Methylene Chloride

From a mixture of aluminum chloride (1.35 g; 0.01 mole), *p,p'*-dinitrobenzoyl peroxide (3.32 g; 0.01 mole), and 1,3-dimethoxybenzene (4 ml; 0.03 mole) in methylene chloride (50 ml), mixed at 20° and left overnight at 0°, *p*-nitrobenzoic acid (1.04 g; 31%) was obtained by the usual work-up. The methylene

chloride solution was washed and dried. On slow concentration of the solution *p*-nitrobenzoic anhydride separated and was recrystallized from benzene as colorless flakes (0.5 g; 16%), m.p. and mixed m.p. 191° (recorded m.p. 189–190° (19)). The mother liquor on further concentration afforded a gum which did not distill at temperatures up to 270° at 1 mm, and which did not give any crystalline fraction on chromatography on alumina.

Reactions of p-Nitrobenzoyl Peroxide in Different Solvents

(a) Methylene Chloride

To a stirred suspension of aluminum chloride (1.35 g) in methylene chloride (50 ml), the peroxide (2.87 g) was added at 8–10°. The mixture was stirred a further 2 hours, left overnight at 0°, and then worked up as usual. After removal of *p*-nitrobenzoic acid (0.35 g; 12%), m.p. 236–237°, the methylene chloride solution was washed with water, dried, and evaporated. The residue on crystallization from petroleum ether (b.p. 55–75°) gave colorless flakes of phenyl *p*-nitrobenzoate (1.97 g; 81%), m.p. and mixed m.p. 129–130°.

(b) Benzene

This experiment was carried out as in the previous one, except that benzene (60 ml) was used in place of methylene chloride. Extraction with bicarbonate, in the usual work-up, removed a mixture (0.83 g) of *p*-nitrobenzoic and benzoic acids, m.p. 227–232°. The residue from the neutral fraction, after removal of solvent, was chromatographed on alumina. Elution with petroleum ether (b.p. 65–75°) and benzene gave a series of fractions of impure solid (0.41 g), which crystallized from ethanol as colorless flakes melting over the range 100–115°. The range was not diminished by further crystallization.

(c) Nitrobenzene

A similar experiment using nitrobenzene (50 ml) as solvent gave a mixture (0.82 g) of *p*-nitrobenzoic and benzoic acids, m.p. 230–234°, and a neutral product (0.36 g), m.p. 100–120°, similar to the neutral product of the previous experiment.

Decomposition of Benzoic–Ethylcarbonic Anhydride by Aluminum Chloride in Benzene

To aluminum chloride (4.05 g; 0.03 mole), suspended in dry benzene (50 ml) under a nitrogen atmosphere, was added with constant stirring at room temperature benzoic–ethylcarbonic anhydride (5.82 g; 0.03 mole) prepared according to Tarbell and Leister (20). The mixture was left overnight, and then worked up in the usual way to yield benzoic acid (0.51 g; 14%). The neutral solution was washed, dried, and distilled. A liquid (2.26 g; 48%), b.p. 78–80° at 1 mm, was collected and identified as ethyl benzoate by comparison of its refractive index (n_D^{23} 1.5046) and infrared spectrum with those from an authentic specimen.

ACKNOWLEDGMENTS

We are grateful to Professors D. H. R. Barton, D. J. Cram, and D. L. de Tar for helpful comments, to Dr. W. F. Hemmens for preliminary experiments, to Dr. T. Vrbaski for gas chromatographic analyses, and to the National Research Council for financial support.

REFERENCES

1. A. F. A. Reynhart. Rec. trav. chim. **46**, 54, 62 (1927).
2. H. Gelissen and P. H. Hermans. Ber. **58**, 479 (1925).
3. J. E. Leffler. J. Am. Chem. Soc. **72**, 67 (1950).
4. D. B. Denney. J. Am. Chem. Soc. **78**, 590 (1956).
5. H. C. Brown and F. R. Jensen. J. Am. Chem. Soc. **80**, 2291 (1958).
6. T. B. Windholz. J. Org. Chem. **25**, 1703 (1960).
7. J. E. Leffler and C. C. Petropoulos. J. Am. Chem. Soc. **79**, 3068 (1957).
8. R. Boschan. J. Am. Chem. Soc. **81**, 3341 (1959). M. Green. Chem. & Ind. (London), 435 (1961).
9. E. J. Longosz and D. S. Tarbell. J. Org. Chem. **26**, 2161 (1961).
10. E. J. Corey, N. L. Bauld, R. T. Lande, J. Casanova, and E. T. Kaiser. J. Am. Chem. Soc. **82**, 2645 (1960).
11. P. S. Skell and I. Starer. J. Am. Chem. Soc. **81**, 4118 (1959).
12. P. D. Bartlett and J. O. Cotman. J. Am. Chem. Soc. **72**, 3095 (1950).
13. C. C. Price and E. Krebs. Org. Syntheses, **23**, 65 (1943).
14. H. Wieland and G. Rasuwajew. Ann. **480**, 157 (1930).
15. A. I. Vogel. A text-book of quantitative inorganic analysis. 2nd ed. Longmans Green, New York. 1939. p. 242.
16. E. Späth, M. Pailev, and G. Gergely. Ber. **73**, 795 (1940).
17. E. B. Barnett and I. G. Nixon. Chem. News, **129**, 190 (1924).
18. J. Forrest, S. H. Tucker, and M. Whalley. J. Chem. Soc. 303 (1951).
19. I. M. Heilbron and H. M. Bunbury. Dictionary of organic compounds. Vol. III. Eyre and Spottiswoode, London. 1934. p. 100.
20. D. S. Tarbell and N. A. Leister. J. Org. Chem. **23**, 1149 (1958).

NOTES

SOME PROPERTIES OF BETA-NITROPROPIONIC ACID

A. M. UNRAU

Beta-nitropropionic acid is one of the three naturally occurring organic nitro compounds. In a recent review, Pailer (1) has presented a thorough discussion of the chemistry of chloramphenicol (chloromycetin) and aristolochic acid I and II, and of the occurrence of beta-nitropropionic acid, either as the free acid or in the form of a glycoside, in a number of plants and fungae. The significance of the occurrence of this nitro acid in plants is not understood and up to this time, very little has been reported regarding its chemical properties. In a recent communication, Birch *et al.* (2) have presented evidence that beta-nitropropionic acid may be formed from aspartic acid in a *Penicillium* species.

Beta-nitropropionic acid may be prepared by the reaction of nitrite with beta-iodopropionic acid and beta-iodopropionitrile or in a 30–40% yield by treating beta-propiolactone with sodium nitrite (3). Treatment of the nitro acid with aqueous alkali (saturated sodium borate or sodium bicarbonate) in an autoclave at 15-lb pressure yields relatively small quantities of nitrite ion which, however, can be quantitatively determined (4). A possible mechanism for the formation of relatively small quantities of nitrite ion rests in the observation that homologous nitroparaffins yield trialkylisoxazoles upon reaction with alkali (5). Lippincott (6) has proposed that the nitro group in an intermediate shown below is lost to yield a dioxime which was isolated when an organic base was used.

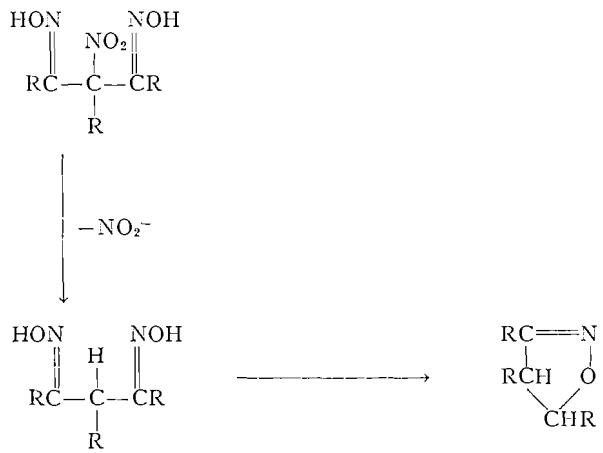

Hydrolysis of the dioxime gave the final cyclic compound. In the above sequence, one nitro group per 3 moles of original nitroparaffin is lost as nitrite ion.

The observation was made that the alkali-catalyzed condensation of formaldehyde (7) with beta-nitropropionic acid resulted, upon alkaline hydrolysis, in a 3- to 4-fold increase in nitrite ion formation. Vanderbilt and Hass (8) have shown that a variety of bases may be used to catalyze this aldol-type condensation involving primary nitroparaffins. The condensation of beta-nitropropionic acid with 2 moles of formaldehyde apparently

results in the formation of 3-nitro-3,3-dihydroxymethyl propionic, acid which cannot react with base as illustrated for the unsubstituted nitro compound. It is postulated that the nitro group may be lost by a beta elimination, as illustrated.

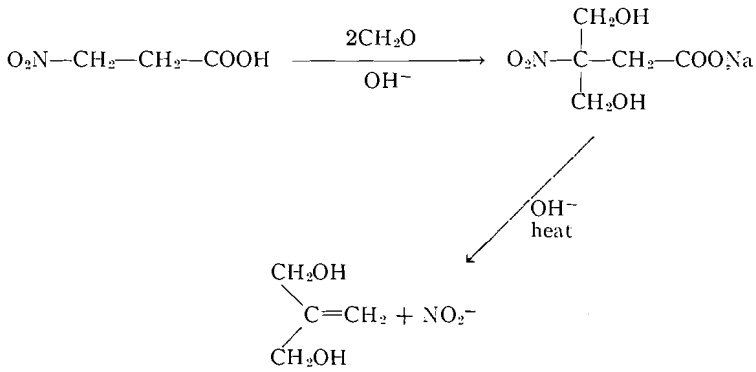

An alternative mechanism whereby the nitro group may be eliminated from the substituted nitro acid finds its analogy in the reaction of halohydrins with alkali to yield epoxides.

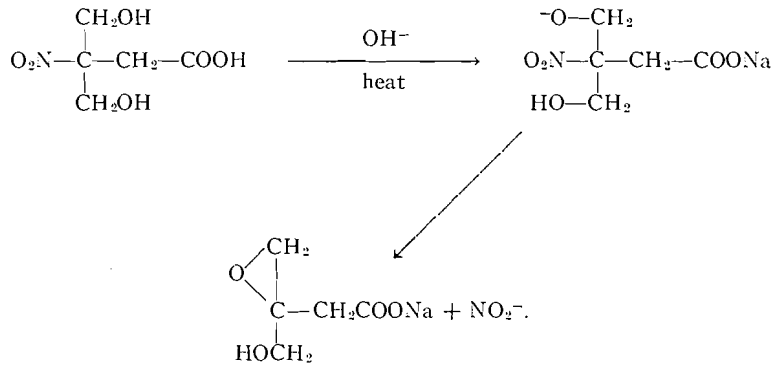

When the reaction sequence was applied to nitropropane, approximately three to four times as much nitrite ion was detected in the reaction mixture compared to the case in which no formaldehyde was added. In this case, a beta elimination of the type suggested for the fully substituted beta-nitropropionic acid is not possible and the elimination of the nitro group is believed to proceed by the formation of epoxides.

In both instances when beta-nitropropionic acid and nitropropane were subjected to the reaction series, a very marked dependence was observed with respect to nitrite ion formation on the strength of the alkali used. Hass and Riley (5) have stressed that the addition of aldehydes to nitroparaffins must compete with at least two other reactions, namely (*a*) aldol condensation of the aldehyde with itself and (*b*) the conversion of the nitroparaffin to the isoxazole. Since low yields of nitrite ion were observed when strong (8–25%) solutions of NaOH were used, one or both of the above reactions was dominant. The greatest removal of the nitro group from beta-nitropropionic acid was observed when sodium bicarbonate or sodium borate buffers were used. Organic bases have not been tried.

Since primary aliphatic nitro compounds are known to give hydroxylamine in high yield when boiled with 88% sulphuric acid or concentrated hydrochloric acid (9), an

attempt was made to utilize this reaction as an analytical method for the determination of beta-nitropropionic acid. The reaction was entirely unsuccessful regardless of how vigorously the nitro acid was treated. It is believed that the reaction proceeds normally to give, in this case, the carboxyhydroxamic acid but that the latter probably forms an anhydride, as represented in reaction B.

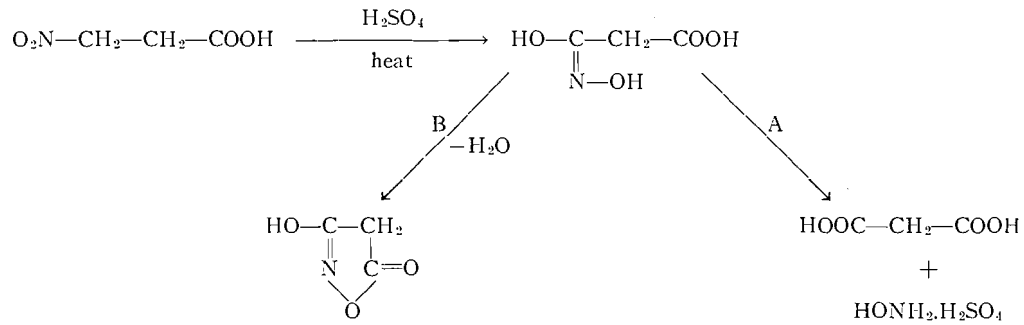

Whereas the usual red solutions of the corresponding nitrolates were obtained when nitropropane and nitroethane were treated with nitrous acid and alkali in that order, beta-nitropropionic acid gave instead a pale yellow color. Using the procedure described by Altschuler and Cohen (10) which involves the above reaction sequence, a prominent absorption maximum was observed at 333 to 335 mμ. Preliminary trials indicated that in the absence of interfering substances microamounts of the nitro acid may be detected in this manner.

EXPERIMENTAL

Reagents

(1) Sulphanilic acid: to a 1:2 (v/v) mixture of water and concentrated hydrochloric acid was added 0.5 g sulphanilic acid;

(2) naphthylamine: naphthylamine hydrochloride (0.5 g) was dissolved in ethanol (20 ml), and water (75 ml) and concentrated hydrochloric acid (5 ml) were added;

(3) formaldehyde: 8–9% aqueous solution;

(4) sodium acetate buffer: 2 *M*;

(5) buffers for alkaline hydrolysis: (A) sodium borate, 0.2 *M*, (B) sodium bicarbonate, 2 *M*, (C) sodium hydroxide, 2, 5, and 10% solutions;

(6) standard solutions: (A) beta-nitropropionic acid, 0.05 mg per ml (aqueous solution), (B) 1-nitropropane, 0.5 mg per ml (aqueous solution);

(7) sulphuric acid: 88%;

(8) sodium nitrite solution, approximately 7%.

Alkaline Hydrolysis of Nitro Compounds

Into beakers or Erlenmeyer flasks (150 ml) were transferred standard solutions of nitro compound (1 ml) and sodium borate buffer (5 ml). The mixture was autoclaved at 15 p.s.i. pressure for 1 hour. After the solutions were cooled in an ice bath, water (10 ml) and sulphanilic acid (3 ml) were added. After about 4 minutes, naphthylamine reagent (3 ml) and 95% ethanol (10 ml) were added and the pH of the solution adjusted to about 2.5 with sodium acetate buffer. The solutions were made to volume (50 ml) and the absorbance determined in a colorimeter at 520 mμ.

In a similar manner, alkaline hydrolyses of the two nitro compounds were performed using alkaline buffers B and C. Alternative procedure: Into matched borosilicate glass colorimeter tubes were transferred (1 ml) standard solutions of nitrocompounds and alkaline buffers A, B, or C (5 ml). The tubes were capped with aluminum foil and placed in a boiling-water bath for 1.5 hours. After the tubes were cooled in an ice bath, sulphanilic acid (3 ml) was added and the contents mixed. After the mixture had stood for about 4 minutes, naphthylamine (3 ml) and 95% ethanol (10 ml) were added, the contents mixed, and without adjusting the pH, the absorbance of the solutions measured at 520 mμ.

Addition of formaldehyde:—To a mixture of alkaline buffer and nitro compound as described above was added (1 ml) 8–9% aqueous formaldehyde, and the solutions were treated as above.

Acid Hydrolysis of Compounds

Into a 50-ml round-bottomed flask fitted with a condenser was transferred an aliquot (1 ml) of standard solution of nitro compound and 88% sulphuric acid (10 ml). The solution was refluxed for 3.5–4 hours, after which time the extent of formation of hydroxylamine was determined colorimetrically by a standard procedure (4).

Conversion of Nitro Compounds to Nitrolates

To an aliquot (2 ml) of the nitro compound was added (3 ml) sodium nitrite solution and concentrated hydrochloric acid (2 ml) in that order. The solutions were made alkaline with 10% sodium hydroxide solution and the color formation observed. Nitropropane gave the expected red-colored solution while beta-nitropropionic acid gave a pale yellow solution with an absorption maximum at 334–340 mμ.

Helpful discussions with Dr. H. Larson, University of Hawaii, are gratefully acknowledged.

1. M. Pailer. Fortschr. Chem. org. Naturstoffe, **18**, 55 (1960).
2. A. T. Birch, B. J. McLaughlin, H. Smith, and J. Winter. Chem. & Ind. (London), 840 (1960).
3. A. R. Cook. Arch. Biochem. Biophys. **55**, 114 (1955).
4. A. O. A. C. Methods of analysis. 8th ed. 1955. p. 127.
5. H. B. Hass and Elizabeth F. Riley. Chem. Revs. **32**, 373 (1943).
6. S. B. Lippincott. J. Am. Chem. Soc. **62**, 2604 (1940).
7. L. Henry. Compt. rend. **120**, 1265 (1895).
8. B. M. Vanderbilt and H. B. Hass. Ind. Eng. Chem. **32**, 34 (1940); U.S. Patent No. 2,139,120 (Dec. 6, 1938).
9. V. Meyer and C. Wurster. Ber. **6**, 1168 (1893). E. Bomberger and E. Rust. Ber. **35**, 45 (1902). S. B. Lippincott and H. B. Hass. Ind. Eng. Chem. **31**, 119 (1939).
10. A. P. Altschuler and J. R. Cohen. Anal. Chem. **32**, 881 (1960).

Received September 14, 1961.
Department of Plant Science,
University of Manitoba,
Winnipeg, Manitoba.

TRANSITION METAL ARSENIDES

V. A NOTE ON THE RHODIUM/ARSENIC SYSTEM AND THE MONOCLINIC DIARSENIDES OF THE COBALT FAMILY*

J. Claire Quesnel and R. D. Heyding

Identification of the compounds Rh_2As, RhAs, $RhAs_2$, and $RhAs_3$ in the rhodium/arsenic system was reported in an earlier note (1). Using sealed quartz tube techniques to prepare the specimens, phase relations in this system have been examined in the temperature region 300° to 1000° C. Powdered specimens were allowed to approach equilibrium for 3 months at 300° C, and progressively shorter times at higher temperatures, to 24 hours at 1000° C. The samples were quenched in ice water and examined by Debye–Scherrer patterns obtained in 11.46-cm cameras with Cu K_α radiation.

Two additional compounds have been recognized, the first at $Rh_{1.7}As$, and the second in a homogeneous field from $Rh_{1.6}As$ to $Rh_{1.3}As$. The homogeneity limits of the latter phase are only slightly temperature dependent. The patterns of both of these compounds are comparatively complex, and as yet no symmetry elements have been recognized. Apparently neither is isostructural with known transition metal pnictides.

No liquid phases were observed in the system to 1000° C in the metal-rich region, or to 900° C in the arsenic-rich region. From 300° to 1000° C the phase diagram is featureless except for a polymorphic transition in Rh_2As. The low-temperature modification described earlier (α-Rh_2As) with the cubic C1 (Ir_2P, Rh_2P) structure transforms at 650–700°

*Issued as N.R.C. No. 6702.

Acid Hydrolysis of Compounds

Into a 50-ml round-bottomed flask fitted with a condenser was transferred an aliquot (1 ml) of standard solution of nitro compound and 88% sulphuric acid (10 ml). The solution was refluxed for 3.5–4 hours, after which time the extent of formation of hydroxylamine was determined colorimetrically by a standard procedure (4).

Conversion of Nitro Compounds to Nitrolates

To an aliquot (2 ml) of the nitro compound was added (3 ml) sodium nitrite solution and concentrated hydrochloric acid (2 ml) in that order. The solutions were made alkaline with 10% sodium hydroxide solution and the color formation observed. Nitropropane gave the expected red-colored solution while beta-nitropropionic acid gave a pale yellow solution with an absorption maximum at 334–340 mμ.

Helpful discussions with Dr. H. Larson, University of Hawaii, are gratefully acknowledged.

1. M. Pailer. Fortschr. Chem. org. Naturstoffe, **18**, 55 (1960).
2. A. T. Birch, B. J. McLaughlin, H. Smith, and J. Winter. Chem. & Ind. (London), 840 (1960).
3. A. R. Cook. Arch. Biochem. Biophys. **55**, 114 (1955).
4. A. O. A. C. Methods of analysis. 8th ed. 1955. p. 127.
5. H. B. Hass and Elizabeth F. Riley. Chem. Revs. **32**, 373 (1943).
6. S. B. Lippincott. J. Am. Chem. Soc. **62**, 2604 (1940).
7. L. Henry. Compt. rend. **120**, 1265 (1895).
8. B. M. Vanderbilt and H. B. Hass. Ind. Eng. Chem. **32**, 34 (1940); U.S. Patent No. 2,139,120 (Dec. 6, 1938).
9. V. Meyer and C. Wurster. Ber. **6**, 1168 (1893). E. Bomberger and E. Rust. Ber. **35**, 45 (1902). S. B. Lippincott and H. B. Hass. Ind. Eng. Chem. **31**, 119 (1939).
10. A. P. Altschuler and J. R. Cohen. Anal. Chem. **32**, 881 (1960).

Received September 14, 1961.
Department of Plant Science,
University of Manitoba,
Winnipeg, Manitoba.

TRANSITION METAL ARSENIDES

V. A NOTE ON THE RHODIUM/ARSENIC SYSTEM AND THE MONOCLINIC DIARSENIDES OF THE COBALT FAMILY*

J. Claire Quesnel and R. D. Heyding

Identification of the compounds Rh_2As, RhAs, $RhAs_2$, and $RhAs_3$ in the rhodium/arsenic system was reported in an earlier note (1). Using sealed quartz tube techniques to prepare the specimens, phase relations in this system have been examined in the temperature region 300° to 1000° C. Powdered specimens were allowed to approach equilibrium for 3 months at 300° C, and progressively shorter times at higher temperatures, to 24 hours at 1000° C. The samples were quenched in ice water and examined by Debye–Scherrer patterns obtained in 11.46-cm cameras with Cu K_α radiation.

Two additional compounds have been recognized, the first at $Rh_{1.7}As$, and the second in a homogeneous field from $Rh_{1.6}As$ to $Rh_{1.3}As$. The homogeneity limits of the latter phase are only slightly temperature dependent. The patterns of both of these compounds are comparatively complex, and as yet no symmetry elements have been recognized. Apparently neither is isostructural with known transition metal pnictides.

No liquid phases were observed in the system to 1000° C in the metal-rich region, or to 900° C in the arsenic-rich region. From 300° to 1000° C the phase diagram is featureless except for a polymorphic transition in Rh_2As. The low-temperature modification described earlier (α-Rh_2As) with the cubic C1 (Ir_2P, Rh_2P) structure transforms at 650–700°

*Issued as N.R.C. No. 6702.

C to an orthorhombic C23 (Co_2P, Re_2P) high-temperature modification (β-Rh_2As). The powder diffraction patterns of these two structures are given in Tables I and II.

TABLE I

Powder diffraction pattern of α-Rh_2As (stable below 650° C)
(Cubic C1 (O_h^5, $Fm3m$) antifluorite; $a = 5.678 \pm 0.002$ Å;
11.46-cm Debye–Scherrer camera, Cu K_α radiation)

I	d_{obs}	d_{calc}	hkl	I	d_{obs}	d_{calc}	hkl
8.6	3.25	3.28	111	4.4	1.091	1.093	333
21	2.82	2.84	200				511
2.8	2.33	2.32	211	33	1.002	1.004	440
100	2.00	2.01	220	7	0.9594	0.9597	531
8.6	1.705	1.712	311	41	0.9455	0.9464	600
8.6	1.634	1.639	222	51	0.8976	0.8978	620
21	1.414	1.420	400	2.8	0.8660	0.8659	533
4.6	1.298	1.303	331	8.6	0.8559	0.8560	622
11	1.266	1.270	420	17	0.8192	0.8195	444
0.7	1.221	1.211	332	11	0.7947	0.7951	711
64	1.156	1.159	422	21	0.7871	0.7874	640

TABLE II

Powder diffraction pattern of β-Rh_2As (stable above 700° C)
(Orthorhombic C23 (D_{2h}^{16}, $Pnma$) $PbCl_2$; $a = 5.89 \pm 0.01$, $b = 3.89 \pm 0.01$, $c = 7.32 \pm 0.01$ Å;
11.46-cm Debye–Scherrer camera, Cu K_α radiation)

I	d_{obs}	d_{calc}	hkl	I	d_{obs}	d_{calc}	hkl
80	2.424	2.431	112	13	1.487	1.485	222
41	2.343	2.349	210	21	1.475	1.474	123
21	2.289	2.295	202	13	1.445	1.447	214
21	2.248	2.255	103	13	1.423	1.424	313
100	2.232	2.237	211	13	1.374	1.377	410
41	2.071	2.069	013			1.374	015
80	1.947	1.947	020	26	1.358	1.359	321
21	1.894	1.897	301	13	1.337	1.339	304
21	1.878	1.880	203			1.335	415
17	1.832	1.831	004	13	1.314	1.311	205
5	1.751	1.748	104	33	1.296	1.301	124
21	1.731	1.731	302	33	1.268	1.266	314
13	1.703	1.705	311	8.6	1.247	1.249	131
17	1.692	1.693	213	5	1.216	1.215	224
5	1.598	1.595	114	17	1.201	1.200	413

With the structure determinations of RhP_2 and IrP_2 by Rundqvist (2), and of $CoSb_2$, $RhSb_2$, and $IrSb_2$ by Zhuravlev *et al.* (3), the existence of a new class of monoclinic MX_2 pnictides has been established. Obviously the diarsenides of cobalt, rhodium, and iridium would be expected to be isostructural with the diphosphides and diantimonides. We have compared the powder diffraction patterns of the arsenides with those of RhP_2 and $RhSb_2$. Rundqvist recorded the pattern of the phosphide, but none has been published for the antimonide. Accordingly $RhSb_2$ was synthesized and its powder diffraction pattern indexed using, initially, the unit cell dimensions given by Zhuravlev.

Diffraction patterns for $RhAs_2$, $IrAs_2$, and $RhSb_2$ were obtained in a Guinier – de Wolff focusing camera with Cu K_α radiation using As_2O_3 as an internal standard. The pattern of $CoAs_2$ was obtained with a 19-cm Debye–Scherrer camera with Co K_α radiation, again using As_2O_3 as an internal standard.

The patterns were indexed by direct comparison of the five or six most intense reflections with those of the phosphide and antimonide. Refinement gave the monoclinic unit

cell dimensions recorded in Table III. The diffraction patterns of the arsenides and of $RhSb_2$ are given in Tables IV–VII.

TABLE III

Unit cell dimensions of the cobalt family dipnictides

(Monoclinic C_{2h}^5, $P2_1/c$)

Compound	a (Å)	b (Å)	c (Å)	β	Ref.
$CoAs_2$	5.805±0.005	5.885±0.002	5.853±0.005	114°11′	Q & H
$CoSb_2$	6.52	6.38	6.55	118°10′	3
RhP_2	5.743	5.794	5.837	112°55′	2
$RhAs_2$	6.041±0.005	6.082±0.002	6.126±0.005	114°20′	Q & H
$RhSb_2$	6.604±0.005	6.557±0.002	6.668±0.005	116°38′	Q & H
	6.57	6.52	6.66	116°05′	3
α-$RhBi_2$	6.7	6.8	6.9	117°	3
IrP_2	5.746	5.791	5.850	111°36′	2
$IrAs_2$	6.060±0.005	6.071±0.002	6.158±0.005	113°16′	Q & H
$IrSb_2$	6.58	6.53	6.68	115°30′	3

TABLE IV

Powder diffraction pattern of $CoAs_2$

(Monoclinic RhP_2; a = 5.805, b = 5.885, c = 5.853 Å, β = 114°11′; 19-cm Debye–Scherrer camera, As_2O_3 standard, Co K_α radiation)

I	d_{obs}	d_{calc}	hkl	I	d_{obs}	d_{calc}	hkl
6.6	2.939	2.937	020	49	1.660	1.660	131
31	2.670	2.670	002	20	1.638	1.638	$12\bar{3}$
31	2.650	2.655	$11\bar{2}$			1.637	$13\bar{2}$
		2.650	200	20	1.628	1.628	$32\bar{1}$
100	2.539	2.539	$12\bar{1}$	31	1.618	1.618	$31\bar{3}$
49	2.432	2.431	012	16	1.578	1.580	032
49	2.415	2.415	210	16	1.575	1.575	320
25	2.318	2.321	$21\bar{2}$	25	1.564	1.564	$20\bar{2}$
10	2.046	2.046	102	5.3	1.551	1.548	$23\bar{2}$
5.3	1.973	1.976	022	5.3	1.476	1.477	$40\bar{2}$
5.3	1.962	1.968	220	5.3	1.468	1.469	040
20B	1.915	1.918	$30\bar{2}$	5.3	1.459	1.461	$32\bar{3}$
		1.915	$22\bar{2}$	20	1.334	1.335	004
31	1.870	1.870	$11\bar{3}$			1.334	123
31	1.857	1.856	$31\bar{1}$	20	1.329	1.329	$32\bar{1}$
5.3	1.830	1.832	$21\bar{3}$	10	1.326	1.327	$22\bar{4}$
25	1.826	1.826	$13\bar{1}$				

TABLE V

Powder diffraction pattern of $RhAs_2$

(Monoclinic RhP_2; a = 6.041, b = 6.082, c = 6.126 Å, β = 114°20′; Guinier – de Wolff focusing camera, As_2O_3 standard, Cu $K\alpha$ radiation)

I	d_{obs}	d_{calc}	hkl	I	d_{obs}	d_{calc}	hkl
64	3.934	3.931	$11\bar{1}$	13	1.873	1.876	$21\bar{3}$
41	3.039	3.039	020	4.4	1.778	1.779	013
64	2.791	2.789	002	3.5	1.755	1.757	310
64	2.753	2.753	200			1.756	122
5.5	2.731	2.733	$11\bar{2}$	64	1.724	1.726	131
2.8	2.67	2.66	120	11	1.693	1.694	$12\bar{3}$
100	2.612	2.617	$12\bar{1}$			1.690	$13\bar{2}$
41	2.535	2.536	012	11	1.675	1.674	$32\bar{1}$
41	2.507	2.507	210	41B	1.646	1.651	$31\bar{3}$
13	2.365	2.368	$21\bar{2}$			1.644	202
8.6	2.151	2.151	102	7	1.637	1.639	032
13	2.055	2.055	022	7	1.631	1.632	230

TABLE V (*Concluded*)

I	d_{obs}	d_{calc}	hkl	I	d_{obs}	d_{calc}	hkl
13	2.040	2.040	220	5.5	1.589	1.587	023
3.5	2.017	2.017	211			1.588	212
21	1.962	1.955	$30\bar{2}$	2.8	1.575	1.571	320
51	1.934	1.936	$11\bar{3}$	8.6	1.397	1.396	004
64	1.907	1.910	$31\bar{1}$	8.6	1.388	1.388	321
51	1.885	1.886	$13\bar{1}$				

TABLE VI

Powder diffraction pattern of $IrAs_2$
(Monoclinic RhP_2; $a = 6.060$, $b = 6.071$, $c = 6.158$ Å, $\beta = 113°16'$;
Guinier – de Wolff focusing camera, As_2O_3 standard, Cu $K\alpha$ radiation)

I	d_{obs}	d_{calc}	hkl	I	d_{obs}	d_{calc}	hkl
4.4	5.569	5.562	100	41	2.051	2.051	220
6	4.133	4.137	011			2.051	$21\bar{1}$
7	4.092	4.107	110	33	1.951	1.952	$22\bar{2}$
100	3.904	3.904	$11\bar{1}$	41	1.940	1.943	$30\bar{2}$
4	3.052	3.056	$10\bar{2}$			1.941	$11\bar{3}$
33	3.033	3.033	020	51B	1.910	1.912	$31\bar{1}$
9	2.942	2.938	111			1.905	$03\bar{1}$
51	2.827	2.827	002	33	1.882	1.881	$13\bar{1}$
51	2.783	2.783	200	17	1.865	1.866	$21\bar{3}$
1	2.728	2.730	$11\bar{2}$	13	1.801	1.800	013
1	2.670	2.665	120	7	1.779	1.779	122
33	2.611	2.609	$12\bar{1}$			1.774	310
11	2.564	2.563	$01\bar{2}$	51	1.734	1.734	$13\bar{1}$
7*	2.543	2.549	$20\bar{2}$	4	1.697	1.698	$12\bar{3}$
17	2.528	2.529	210	11	1.680	1.679	$20\bar{2}$
9	2.352	2.352	$21\bar{2}$			1.678	$32\bar{1}$
9	2.196	2.195	$10\bar{2}$	2	1.646	1.646	032
4	2.151	2.153	$12\bar{2}$	33	1.636	1.636	$23\bar{0}$
21	2.069	2.070	022			1.636	$31\bar{3}$

*Overlap with As_2O_3 standard.

TABLE VII

Powder diffraction pattern of $RhSb_2$
(Monoclinic RhP_2; $a = 6.604$, $b = 6.557$, $c = 6.668$ Å, $\beta = 116°38'$;
Guinier – de Wolff focusing camera, As_2O_3 standard, Cu K_α radiation)

I	d_{obs}	d_{calc}	hkl	I	d_{obs}	d_{calc}	hkl
26	4.288	4.279	$11\bar{1}$	3.3	1.872	1.874	122
17	3.280	3.280	020	51	1.853	1.853	$13\bar{1}$
17	3.078	3.078	111	17	1.831	1.832	$12\bar{3}$
51	2.982	2.982	$00\bar{2}$	33	1.815	1.817	$32\bar{1}$
	2.978	2.968	$11\bar{2}$	11	1.762	1.764	032
51	2.953	2.951	200	11	1.756	1.758	230
100	2.838	2.838	$12\bar{1}$	21	1.742	1.743	202
64	2.715	2.715	012	8.6	1.701	1.701	023
64	2.691	2.691	210	5.5	1.689	1.687	320
33	2.600	2.595	$21\bar{2}$	8.6	1.636	1.633	$32\bar{3}$
13	2.279	2.282	$10\bar{2}$	5.5	1.538	1.536	$23\bar{3}$
13	2.207	2.207	022	21	1.488	1.491	004
13	2.193	2.194	220	33	1.418	1.420	$24\bar{2}$
21	2.143	2.142	$30\bar{2}$	5.5	1.343	1.346	420
41	2.094	2.092	$11\bar{3}$	7	1.327	1.328	133
41	2.073	2.071	$31\bar{1}$	5.5	1.322	1.322	331
33	2.052	2.052	130	33	1.279	1.279	$51\bar{3}$
41	2.040	2.040	$13\bar{1}$	13	1.250	1.248	$51\bar{1}$
8.6	1.903	1.903	013				

Since these patterns were indexed we have learned of an independent single-crystal study by Kjekshus, showing $IrAs_2$ and $IrSb_2$ to be monoclinic (4).

We are indebted to Dr. J. E. Gillott, and to Miss M. McLellan, for assistance in obtaining Guinier and Debye–Scherrer patterns, respectively.

1. R. D. Heyding and L. D. Calvert. Can. J. Chem. **39**, 955 (1961).
2. S. Rundqvist. Acta Chem. Scand. **15**, 451 (1961).
3. N. N. Zhuravlev, G. S. Zhdanov, and R. N. Kuz'min. Soviet Phys. Cryst. **5**, 532 (1961).
4. A. Kjekshus. University of Oslo, Norway. Private communication.

Received November 6, 1961.
Division of Applied Chemistry,
National Research Council,
Ottawa, Canada.

STEROIDAL 3-CHLORO-3,5-DIENES

R. Deghenghi and R. Gaudry

In some cases the modification of the Δ^4-3 ketone moiety (I) of the natural steroidal hormones has led to biologically active analogues, particularly in the anabolic–androgenic field (1, 2).

The 3-enol-ether analogues (3), for instance, (II) R = O-alkyl, of methyltestosterone

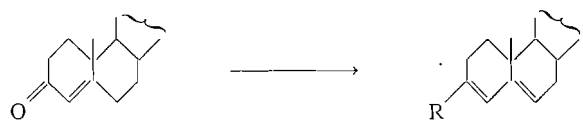

I II

were found to be more active, by the oral route, than their parent compound (4).

We chose to modify the Δ^4-3 keto portion of the molecule by forming a 3-chloro-3,5-diene (II, R = Cl), which thus had the same geometry (II) of ring A and B, with concomitant increased stability of the diene system.[1]

Previous examples of steroidal 3-chloro-3,5 dienes were one prepared by Ruzicka by the action of benzoyl chloride at 100° C (5,6) on 4-cholestene-3-one and a 3-chloro-3,5-androstadien-17-one that was described in 1937 by Kuwada (7), but was not completely characterized and was without any mention of its biological activity.

The observation (8) that the action of oxalyl chloride on some Δ^4-3-keto-etianic acids in order to form the corresponding acid chlorides, according to the method of Wilds (9), resulted, in absence of pyridine, in an attack of the Δ^4-3-keto moiety, with the formation of a 3-chloro-3,5-diene,[2] prompted us to employ this reagent to transform a number of steroidal Δ^4-3 ketones into new analogues (II, R = Cl).

The acid-catalyzed reaction proceeds smoothly at room temperature and in most cases is completed in 1 hour in yields of 50–70% of theory.

[1]*The 3-enol-ether analogues were assumed to be active "per se" and not as precursors of the conjugated 3-keto steroids by endogenous hydrolysis (4).*

[2]*Reichstein et al. (10) have noted a decrease in the yield of a similar reaction from 83% to 75% when pyridine was omitted. They could isolate minor unidentified by-products which, in our opinion, may well be the corresponding chlorodienes. Oxalic acid is, of course, a product of the reaction and was therefore chosen by us to catalyze our transformations.*

Since these patterns were indexed we have learned of an independent single-crystal study by Kjekshus, showing $IrAs_2$ and $IrSb_2$ to be monoclinic (4).

We are indebted to Dr. J. E. Gillott, and to Miss M. McLellan, for assistance in obtaining Guinier and Debye–Scherrer patterns, respectively.

1. R. D. Heyding and L. D. Calvert. Can. J. Chem. **39**, 955 (1961).
2. S. Rundqvist. Acta Chem. Scand. **15**, 451 (1961).
3. N. N. Zhuravlev, G. S. Zhdanov, and R. N. Kuz'min. Soviet Phys. Cryst. **5**, 532 (1961).
4. A. Kjekshus. University of Oslo, Norway. Private communication.

Received November 6, 1961.
Division of Applied Chemistry,
National Research Council,
Ottawa, Canada.

STEROIDAL 3-CHLORO-3,5-DIENES

R. Deghenghi and R. Gaudry

In some cases the modification of the Δ^4-3 ketone moiety (I) of the natural steroidal hormones has led to biologically active analogues, particularly in the anabolic–androgenic field (1, 2).

The 3-enol-ether analogues (3), for instance, (II) R = O-alkyl, of methyltestosterone

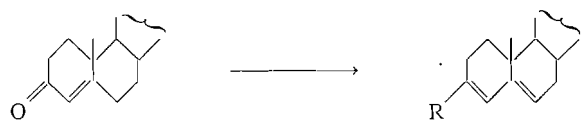

I II

were found to be more active, by the oral route, than their parent compound (4).

We chose to modify the Δ^4-3 keto portion of the molecule by forming a 3-chloro-3,5-diene (II, R = Cl), which thus had the same geometry (II) of ring A and B, with concomitant increased stability of the diene system.[1]

Previous examples of steroidal 3-chloro-3,5 dienes were one prepared by Ruzicka by the action of benzoyl chloride at 100° C (5,6) on 4-cholestene-3-one and a 3-chloro-3,5-androstadien-17-one that was described in 1937 by Kuwada (7), but was not completely characterized and was without any mention of its biological activity.

The observation (8) that the action of oxalyl chloride on some Δ^4-3-keto-etianic acids in order to form the corresponding acid chlorides, according to the method of Wilds (9), resulted, in absence of pyridine, in an attack of the Δ^4-3-keto moiety, with the formation of a 3-chloro-3,5-diene,[2] prompted us to employ this reagent to transform a number of steroidal Δ^4-3 ketones into new analogues (II, R = Cl).

The acid-catalyzed reaction proceeds smoothly at room temperature and in most cases is completed in 1 hour in yields of 50–70% of theory.

[1]*The 3-enol-ether analogues were assumed to be active "per se" and not as precursors of the conjugated 3-keto steroids by endogenous hydrolysis (4).*

[2]*Reichstein et al. (10) have noted a decrease in the yield of a similar reaction from 83% to 75% when pyridine was omitted. They could isolate minor unidentified by-products which, in our opinion, may well be the corresponding chlorodienes. Oxalic acid is, of course, a product of the reaction and was therefore chosen by us to catalyze our transformations.*

Progesterone, testosterone acetate, methyltestosterone acetate, and cortisone acetate were readily transformed by this method. A hindered alcoholic function (like the 17-hydroxyl group in cortisone) was not affected by the reagent.

The resulting chlorodienes were stable, crystalline substances, with a characteristic ultraviolet absorption at 242 mμ with two shoulders at 236 and 250 mμ and a log ε of 4.4. The infrared absorption in chloroform reveals a single $\Delta^{3,5}$ band at 1621 cm^{-1}. The molecular change in the rotation from the parent Δ^4-3 keto steroid is −850.

The 3-chlorodiene IV, obtained from cortisone, was devoid of appreciable glucocorticoid activity (liver glycogen deposition) but caused sodium excretion; the adduct III from progesterone was inactive in the Clauberg test. 17β-Acetoxy-3-chloro-3,5-androstadiene V (from testosterone acetate) showed a favorable anabolic–androgenic activity ratio (levator ani and seminal vescicles weight test).

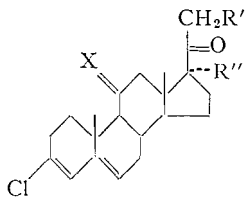

III, R′ = R″ = H, X = H_2
IV, R′ = OAc, R″ = OH
X = O

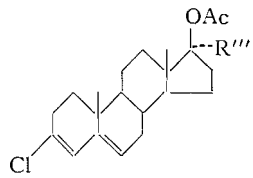

V, R‴ = H
VI, R‴ = CH_3

EXPERIMENTAL[3]

3-Chloro-3,5-pregnadiene-20-one III

A solution of 10 g of progesterone in 100 ml of dry benzene was stirred at room temperature for 2 hours in the presence of 30 cc oxalyl chloride and 0.5 g oxalic acid. The organic solvent was evaporated at reduced pressure and the residue was taken up in ether, washed with $NaHCO_3$ solution, and water. The solvent was dried and evaporated to give crude 3-chloro-3,5-pregnadiene-20-one, 10 g, which was recrystallized from ether. Colorless needles, m.p. 126–128° C, $[\alpha]_D$ −61°, λ_{max} 242 mμ, log ε 4.4. Calc. for $C_{21}H_{29}OCl$ (332.9): C, 75.77; H, 8.78; Cl, 10.65%. Found: C, 75.86; H, 8.76; Cl, 10.56%.

3-Chloro-3,5-androstadiene-17β-ol Acetate V

A quantity of 1 g of testosterone acetate was dissolved in 25 cc dry benzene and stirred with 5 cc oxalyl chloride and 0.1 g oxalic acid for 1 hour. The usual working up gave 0.6 g *17β-acetoxy-3-chloro-3,5-androstadiene*, m.p. 148–152° C, $[\alpha]_D$ −172°, λ_{max} 242 mμ, log ε 4.4. Calc. for $C_{21}H_{29}O_2Cl$ (348.9): C, 72.29; H, 8.38; Cl, 10.16%. Found: C, 72.19; H, 8.30; Cl, 10.10%.

17α-Methyl-3-chloro-3,5-androstadiene-17β-ol Acetate VI

A quantity of 6 g of 17α-methyltestosterone acetate was dissolved in 100 ml dry benzene and stirred with 20 ml of oxalyl chloride and 0.3 g oxalic acid at room temperature for 1½ hours. The reaction mixture was worked up as in the previous examples to give 3.5 g *17α-methyl-17β-acetoxy-3-chloro-3,5-androstadiene*, m.p. 127–128° C after crystallization from methanol, $[\alpha]_D$ −148°, λ_{max} 242 mμ, log ε 4.4. Calc. for $C_{22}H_{31}O_2Cl$ (362.9): C, 72.80; H, 8.61; Cl, 9.77%. Found: C, 73.01; H, 8.45; Cl, 9.90%.

21-Acetoxy-17α-hydroxy-3-chloro-3,5-pregnadiene-11,20-dione IV

A quantity of 3 g of cortisone acetate in 100 ml dry benzene was stirred with 0.4 g oxalic acid and 20 cc oxalyl chloride for 18 hours at room temperature. The usual working up gave needles of *21-acetoxy-17α-hydroxy-3-chloro-3,5-pregnadiene-11,20-dione*, 1.6 g, m.p. 195–197° C from methanol–water, $[\alpha]_D$ ±0, λ_{max} 242 mμ, log ε 4.4. Calc. for $C_{23}H_{29}O_5Cl$ (420.9): C, 65.63; H, 6.94; Cl, 8.42%. Found: C, 65.29; H, 6.76; Cl, 8.43%.

[3]*Melting points were determined in evacuated capillaries and corrected. Rotations measured at 23° C in 1%* $CHCl_3$ *solution.*

ACKNOWLEDGMENTS

We are indebted to Drs. C. Revesz, G. Rochefort, and C. I. Chappel for the biological assays, to Dr. G. Papineau-Couture, Mr. M. Boulerice, Mr. W. Turnbull, and their associates for the analytical data, and to Mr. A. Philipp for technical assistance.

REFERENCES

1. ANON. Brit. Med. J. 1245 (1961).
2. A. ERCOLI and R. GARDI. J. Am. Chem. Soc. **82**, 746 (1960).
3. E. SCHWENK, G. FLEISCHER, and B. WHITMAN. J. Am. Chem. Soc. **60**, 1702 (1938).
4. A. ERCOLI, G. BRUNI, G. FALCONI, R. GARDI, and A. MELI. Endocrinology, **67**, 521 (1960).
5. L. RUZICKA and W. H. FISCHER. Helv. Chim. Acta, **19**, 806, 1371 (1936).
6. W. BERGMANN. J. Org. Chem. **4**, 40, 46 (1939).
7. S. KUWADA, M. MIYASAKI, and S. HOSHIKI. J. Pharm. Soc. Japan, **57**, 234 (1937).
8. R. DEGHENGHI. Unpublished results.
9. A. L. WILDS. J. Am. Chem. Soc. **70**, 2427 (1948); U.S. Patent No. 2,538,611 (Jan. 16, 1951).
10. F. REBER, A. LARDON, and T. REICHSTEIN. Helv. Chim. Acta, **37**, 45 (1954).

RECEIVED NOVEMBER 7, 1961.
AYERST RESEARCH LABORATORIES,
P.O. BOX 6115,
MONTREAL, QUE.

A PHOTOCHEMICAL PREPARATION OF SOME HALOGENATED CYCLOPROPANES

EDWARD L. DEDIO, PETER J. KOZAK, SERGE N. VINOGRADOV, AND HARRY E. GUNNING

The photochlorination of cyclopropane was first reported by Gustavson (1). Roberts and Dirstine (2) attempted a flow photochlorination in their investigation of the thermal chlorination of cyclopropane. Using high flow rates, of the order of moles per hour, and a 4:1 ratio of cyclopropane to chlorine, they obtained a yield of monochlorocyclopropane of only 7.6% of the cyclopropane consumed, even with partial recycling of the reaction mixture. Slabey (3), using essentially the same apparatus as Roberts and Dirstine, and similar conditions, but without recycling of the cyclopropane, obtained a yield of about 10%.

In our investigations of the formation and behavior of cycloalkyl radicals in the gas phase, in particular, of the photolysis and mercury-photosensitized decomposition of monohalocyclopropanes, we were led to explore means of preparing these compounds quickly and conveniently. It has been found that cyclopropane can be photochlorinated and photobrominated in a simple flow system without recycling the cyclopropane. In the former case, we were able to obtain yields of monochlorocyclopropane up to 20–30% of the cyclopropane consumed, with flow rates much lower than those used by previous investigators. In the case of photobromination, nitrogen was used as the carrier of bromine, and chlorine served to initiate the photobromination. The yields of monobromocyclopropane were correspondingly lower, usually not exceeding 10% of the cyclopropane consumed. Photobromination, in the absence of chlorine, resulted in the opening of the cyclopropane ring. Attempts to photoiodinate cyclopropane, again with nitrogen as the carrier gas, and chlorine as the initiator, were unsuccessful.

Table I shows some representative results of the photochlorination of cyclopropane. It is seen that the ratio of monochlorocyclopropane to 1,1-dichlorocyclopropane varies directly, while the total yield varies inversely, with the cyclopropane-to-chlorine ratio.

ACKNOWLEDGMENTS

We are indebted to Drs. C. Revesz, G. Rochefort, and C. I. Chappel for the biological assays, to Dr. G. Papineau-Couture, Mr. M. Boulerice, Mr. W. Turnbull, and their associates for the analytical data, and to Mr. A. Philipp for technical assistance.

REFERENCES

1. ANON. Brit. Med. J. 1245 (1961).
2. A. ERCOLI and R. GARDI. J. Am. Chem. Soc. **82**, 746 (1960).
3. E. SCHWENK, G. FLEISCHER, and B. WHITMAN. J. Am. Chem. Soc. **60**, 1702 (1938).
4. A. ERCOLI, G. BRUNI, G. FALCONI, R. GARDI, and A. MELI. Endocrinology, **67**, 521 (1960).
5. L. RUZICKA and W. H. FISCHER. Helv. Chim. Acta, **19**, 806, 1371 (1936).
6. W. BERGMANN. J. Org. Chem. **4**, 40, 46 (1939).
7. S. KUWADA, M. MIYASAKI, and S. HOSHIKI. J. Pharm. Soc. Japan, **57**, 234 (1937).
8. R. DEGHENGHI. Unpublished results.
9. A. L. WILDS. J. Am. Chem. Soc. **70**, 2427 (1948); U.S. Patent No. 2,538,611 (Jan. 16, 1951).
10. F. REBER, A. LARDON, and T. REICHSTEIN. Helv. Chim. Acta, **37**, 45 (1954).

RECEIVED NOVEMBER 7, 1961.
AYERST RESEARCH LABORATORIES,
P.O. BOX 6115,
MONTREAL, QUE.

A PHOTOCHEMICAL PREPARATION OF SOME HALOGENATED CYCLOPROPANES

EDWARD L. DEDIO, PETER J. KOZAK, SERGE N. VINOGRADOV, AND HARRY E. GUNNING

The photochlorination of cyclopropane was first reported by Gustavson (1). Roberts and Dirstine (2) attempted a flow photochlorination in their investigation of the thermal chlorination of cyclopropane. Using high flow rates, of the order of moles per hour, and a 4:1 ratio of cyclopropane to chlorine, they obtained a yield of monochlorocyclopropane of only 7.6% of the cyclopropane consumed, even with partial recycling of the reaction mixture. Slabey (3), using essentially the same apparatus as Roberts and Dirstine, and similar conditions, but without recycling of the cyclopropane, obtained a yield of about 10%.

In our investigations of the formation and behavior of cycloalkyl radicals in the gas phase, in particular, of the photolysis and mercury-photosensitized decomposition of monohalocyclopropanes, we were led to explore means of preparing these compounds quickly and conveniently. It has been found that cyclopropane can be photochlorinated and photobrominated in a simple flow system without recycling the cyclopropane. In the former case, we were able to obtain yields of monochlorocyclopropane up to 20–30% of the cyclopropane consumed, with flow rates much lower than those used by previous investigators. In the case of photobromination, nitrogen was used as the carrier of bromine, and chlorine served to initiate the photobromination. The yields of monobromocyclopropane were correspondingly lower, usually not exceeding 10% of the cyclopropane consumed. Photobromination, in the absence of chlorine, resulted in the opening of the cyclopropane ring. Attempts to photoiodinate cyclopropane, again with nitrogen as the carrier gas, and chlorine as the initiator, were unsuccessful.

Table I shows some representative results of the photochlorination of cyclopropane. It is seen that the ratio of monochlorocyclopropane to 1,1-dichlorocyclopropane varies directly, while the total yield varies inversely, with the cyclopropane-to-chlorine ratio.

TABLE I

The photochlorination of cyclopropane

Flow rate (moles/hr)		Molar ratio	Total yield		%yield*
$\widehat{C_3H_6}$	Cl_2	$\frac{\widehat{C_3H_6}}{Cl_2}$	(g/hr)	$\frac{\widehat{C_3H_5Cl}}{\widehat{C_3H_4Cl_2}}$	$\widehat{C_3H_5Cl}$
0.26	0.05	4.3	2.7	2.7	9.8
0.13	0.03	4.3	1.3	1.9	8.5
0.42	0.12	3.5	4.0	0.8	5.5 (4.9)
0.31	0.13	2.4	4.0	0.7	6.8 (6.2)
0.15	0.08	2.0	4.5	0.6	14
0.13	0.07	1.9	4.5	0.8	20
0.11	0.07	1.6	4.5	0.6	20
0.13	0.11	1.2	7.0	0.8	31
0.13	0.17	0.8	6.6	0.7	27
0.07	0.13	0.5	10.0	0.2	29 (22)
0.07	0.34	0.2	12.0	0.05	11

*Calculated as mole % of the $\widehat{C_3H_6}$ consumed using the values given in column 5. The values in parentheses were calculated, taking into consideration the areas of the remaining peaks in the chromatograms.

It is seen that, contrary to expectations, the best yield of monochlorocyclopropane is obtained when the molar ratio of cyclopropane to chlorine in near unity.

Table II shows some typical results of the photobromination of cyclopropane. Here, as in the case of the photochlorination, there was no difficulty in separating the monobrominated cyclopropane from the rest of the products by distillation. While the yields

TABLE II

The chlorine-initiated photobromination of cyclopropane

Flow rate (moles/hr)			Total yield	% of total yield		Moles $\widehat{C_3H_5Br}$
$\widehat{C_3H_6}$	Cl_2	Br_2*	(g/hr)	$\widehat{C_3H_5Cl}$	$\widehat{C_3H_5Br}$	Moles $\widehat{C_3H_6}$
0.27	0.14	0.036	9.7	8	39	0.12
0.27	0.14	0.025	7.8	15	23	0.06
0.27	0.14	0.020	6.4	17	28	0.06
0.27	0.18	0.036	12.3	12	24	0.09
0.27	0.18	0.025	9.4	18	21	0.06
0.27	0.18	0.020	6.6	22	20	0.04

*Using nitrogen as carrier. The amount of bromine was determined in separate experiments by condensing it at dry-ice temperature and weighing.

of the monobromocyclopropane were only about 10% of the cyclopropane consumed, the simplicity of the method presents some advantage over the conventional method of preparing the monobromo derivative from the silver salt of the cyclopropylcarboxylic acid (4). It should also be stressed that, in both cases, the photochemical method produced, albeit in small quantities, several higher halogenated cyclopropanes which can be isolated by temperature-programed gas–liquid partition chromatography (G.L.P.C.). It is thus a convenient method of simultaneously preparing several related compounds.

EXPERIMENTAL

The flow apparatus is shown in Fig. 1. The spiral cells were of pyrex tubing and 100 to 200 cm long, the diameter of each loop being about 10 cm. The lamp was a General Electric, H85-C3, medium-pressure mercury arc. The flow was regulated by needle valves on each cylinder, and measured with a soap-bubble flowmeter, prior to each photohalogenation. Total flow rates varied between 50 and 200 ml/min at S.T.P. The collector was kept immersed in ice during a run.

The cyclopropane (U.S.P. Ohio Chemical Co., and The Matheson Co.), chlorine (The Matheson Co.), bromine (reagent grade, Allied Chemical Co.), and nitrogen (purified grade, The Matheson Co.) were used

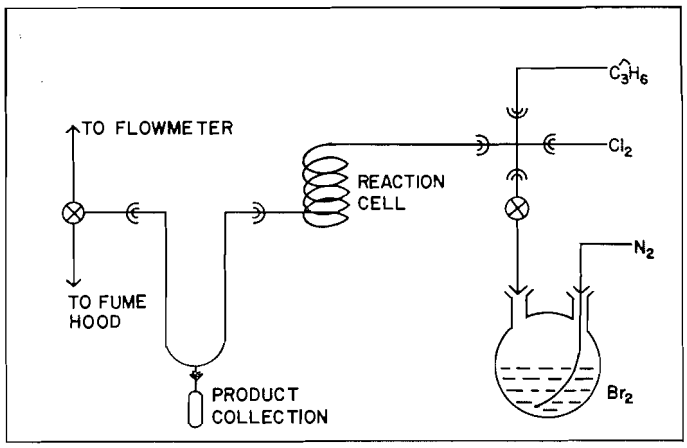

FIG. 1. Diagram of flow photohalogenation of cyclopropane.

without purification. The liquid products were washed twice with equal volumes of aqueous sodium sulphite solution (8%) and twice with equal volumes of aqueous sodium carbonate solution (8%). Initial separation of the products was performed by distillation and the final purification achieved with temperature-programed gas–liquid partition chromatography in columns packed with di-(2-ethyl)-hexyl sebacate or silicone rubber on firebrick.

The total yield of crude products was obtained by weighing, while estimates of individual yields were calculated from the G.L.P.C. data.

The monochlorocyclopropane, 1,1-dichlorocyclopropane, and the monobromocyclopropane were identified by their physical properties, and by comparison of their infrared spectra to previously published results (2–5). In addition, the following microanalyses were obtained.

Monochlorocyclopropane: Found: C, 46.3%; H, 7.1%; Cl, 45.1%. Calc.: C, 47.0%; H, 6.5%; Cl, 46.3%.
1,1-Dichlorocyclopropane: Found: C, 31.6%; H, 3.5%; Cl, 64.9%. Calc.: C, 32.5%; H, 3.6%; Cl, 63.9%.
Monobromocyclopropane: Found: C, 29.7%; H, 4.9%; Br, 64.8%. Calc.: C, 29.8%; H, 4.1%; Br, 66.1%.

Finally, in the case of the monohalocyclopropanes, the formation of cyclopropane during a photolytic decomposition in the presence of a saturated hydrocarbon was considered as additional evidence that the compound was a cyclopropane derivative.

ACKNOWLEDGMENTS

The investigation was supported in part by the National Research Council under Grant No. N.R.C. T 162 (Gunning). This assistance is gratefully acknowledged.

1. G. GUSTAVSON. J. prakt. Chem. **42**, 495 (1890).
2. J. D. ROBERTS and P. H. DIRSTINE. J. Am. Chem. Soc. **67**, 1281 (1945).
3. V. A. SLABEY. J. Am. Chem. Soc. **74**, 4928 (1952).
4. J. D. ROBERTS and J. C. CHAMBERS. J. Am. Chem. Soc. **73**, 3176 (1951).
5. J. D. ROBERTS and J. C. CHAMBERS. J. Am. Chem. Soc. **73**, 5030 (1951).

RECEIVED DECEMBER 28, 1961.
CHEMISTRY DEPARTMENT,
UNIVERSITY OF ALBERTA,
EDMONTON, ALBERTA.

COORDINATION COMPOUNDS OF NICKEL (II)
PART III. FURTHER MAGNETIC STUDIES OF SOLUTIONS

H. C. CLARK, K. MACVICAR, AND R. J. O'BRIEN

There has recently been much interest in the so-called "magnetically anomalous" complexes of nickel (II). Apart from recent work on some aminotroponeimine-nickel (II) chelates (1), attention has been centered on the behavior of substituted nickel (II)

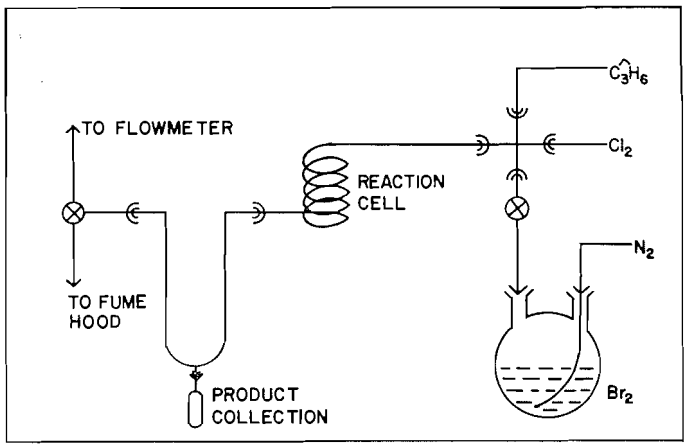

FIG. 1. Diagram of flow photohalogenation of cyclopropane.

without purification. The liquid products were washed twice with equal volumes of aqueous sodium sulphite solution (8%) and twice with equal volumes of aqueous sodium carbonate solution (8%). Initial separation of the products was performed by distillation and the final purification achieved with temperature-programed gas–liquid partition chromatography in columns packed with di-(2-ethyl)-hexyl sebacate or silicone rubber on firebrick.

The total yield of crude products was obtained by weighing, while estimates of individual yields were calculated from the G.L.P.C. data.

The monochlorocyclopropane, 1,1-dichlorocyclopropane, and the monobromocyclopropane were identified by their physical properties, and by comparison of their infrared spectra to previously published results (2–5). In addition, the following microanalyses were obtained.

Monochlorocyclopropane: Found: C, 46.3%; H, 7.1%; Cl, 45.1%. Calc.: C, 47.0%; H, 6.5%; Cl, 46.3%.
1,1-Dichlorocyclopropane: Found: C, 31.6%; H, 3.5%; Cl, 64.9%. Calc.: C, 32.5%; H, 3.6%; Cl, 63.9%.
Monobromocyclopropane: Found: C, 29.7%; H, 4.9%; Br, 64.8%. Calc.: C, 29.8%; H, 4.1%; Br, 66.1%.

Finally, in the case of the monohalocyclopropanes, the formation of cyclopropane during a photolytic decomposition in the presence of a saturated hydrocarbon was considered as additional evidence that the compound was a cyclopropane derivative.

ACKNOWLEDGMENTS

The investigation was supported in part by the National Research Council under Grant No. N.R.C. T 162 (Gunning). This assistance is gratefully acknowledged.

1. G. GUSTAVSON. J. prakt. Chem. **42**, 495 (1890).
2. J. D. ROBERTS and P. H. DIRSTINE. J. Am. Chem. Soc. **67**, 1281 (1945).
3. V. A. SLABEY. J. Am. Chem. Soc. **74**, 4928 (1952).
4. J. D. ROBERTS and J. C. CHAMBERS. J. Am. Chem. Soc. **73**, 3176 (1951).
5. J. D. ROBERTS and J. C. CHAMBERS. J. Am. Chem. Soc. **73**, 5030 (1951).

RECEIVED DECEMBER 28, 1961.
CHEMISTRY DEPARTMENT,
UNIVERSITY OF ALBERTA,
EDMONTON, ALBERTA.

COORDINATION COMPOUNDS OF NICKEL (II)
PART III. FURTHER MAGNETIC STUDIES OF SOLUTIONS

H. C. CLARK, K. MACVICAR, AND R. J. O'BRIEN

There has recently been much interest in the so-called "magnetically anomalous" complexes of nickel (II). Apart from recent work on some aminotroponeimine-nickel (II) chelates (1), attention has been centered on the behavior of substituted nickel (II)

salicylaldimine complexes. Current views on possible interpretations of the magnetic and spectroscopic behavior of these complexes have been summarized in the previous paper of this series (2) and by Ferguson (3). It now seems clear that the appearance of paramagnetism in solutions of these complexes (e.g. bis-N-methyl-salicylaldimine nickel (II)) in non-coordinating solvents such as chloroform, carbon tetrachloride, etc. is due to association of the solute, rather than to solvent perturbation. Such solute interaction must give some type of distorted octahedral configuration about the nickel atoms, thereby decreasing the singlet–triplet separation so as to make the triplet state thermally accessible. There is, however, no evidence which indicates the mode of association and, indeed, two different models for association are required in view of the very different properties of the two paramagnetic species of bis-N-methyl-5-chloro-salicylaldimine nickel (II) (2). Although earlier magnetic measurements (4–6) of solutions of these salicylaldimine complexes gave little indication of concentration dependence of the magnetic susceptibility, such dependence must clearly occur in those cases where solute association takes place. To clarify this point and in an attempt to gain information concerning the associated species, we have made a further series of magnetic measurements.

EXPERIMENTAL

The compounds studied were bis-N-methyl-salicylaldimine nickel (II) and bis-N-*n*-butyl-salicylaldimine nickel (II); their preparations are described elsewhere (4, 7). Solvents were carefully purified and dried by standard methods, and magnetic measurements were made using the apparatus described previously (2). The results obtained are shown in Table I and Figs. 1 and 2.

TABLE I

(A) Concentration and temperature variation of the molar susceptibility ($\times 10^3$) of bis-N-methyl-salicylaldimine nickel (II) in $CHCl_3$ solution

Temperature (°K)	221	239	253	263	273	283	294
3.1% (w/w) ≡ 0.146 *M*	5.285	4.426	3.662	3.267	2.810	2.381	2.123
Temperature	220.5	239	254	264	271.5	283	293
2.00% (w/w) ≡ 0.0936 *M*	4.448	3.731	2.920	2.550	2.146	1.845	1.402
Temperature	218	237	253	263	272	281.5	294
1.00% (w/w) ≡ 0.0468 *M*	3.800	3.146	2.336	1.797	1.127	0.866	0.601

(B) Solvent dependence of the molar susceptibility ($\times 10^3$) of bis-N-*n*-butyl-salicylaldimine nickel (II)

Temperature	215	239	253	263	271	282	293
3.00% (w/w) ≡ 0.113 *M* in 100% $CHCl_3$	2.986	1.893	1.228	0.883	0.686	0.509	0.219
Temperature	231	245	258	279	291		
9.0% (w/w) ≡ 0.37 *M* in 10% pyridine – 90% $CHCl_3$	4.451	4.194	4.014	3.742	3.532		

(C) Concentration dependence of the magnetic susceptibility ($\times 10^3$) of bis-N-*n*-butyl-salicylaldimine nickel (II) in chloroform and pyridine–chloroform at 298° K

Concentration (*M*)	0.407	0.371	0.318	0.269	0.233
$\chi_M \times 10^3$ in 100% $CHCl_3$	0.464	0.306	0.216	0.176	0.150
$\chi_M \times 10^3$ in 10% C_5H_5N – 90% $CHCl_3$	3.370	3.380	3.420	3.350	3.510

Molecular weights were determined cryoscopically in benzene solution; the following results (Table II) were obtained.

DISCUSSION

Contrary to earlier reports, the present results show that the magnetic susceptibilities are in fact concentration dependent except for solutions where a strongly coordinating base, such as pyridine, is present. This concentration dependence, giving a greater degree

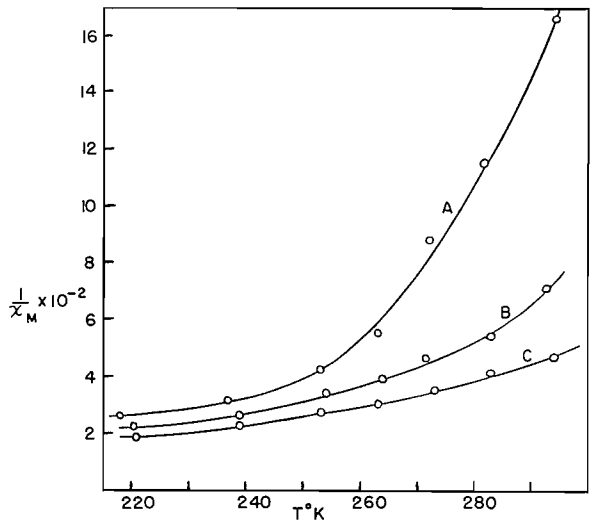

FIG. 1. Magnetic susceptibility of the N-methyl complex in $CHCl_3$ solution: A, 1.0%; B, 2.0%; C, 3.1%

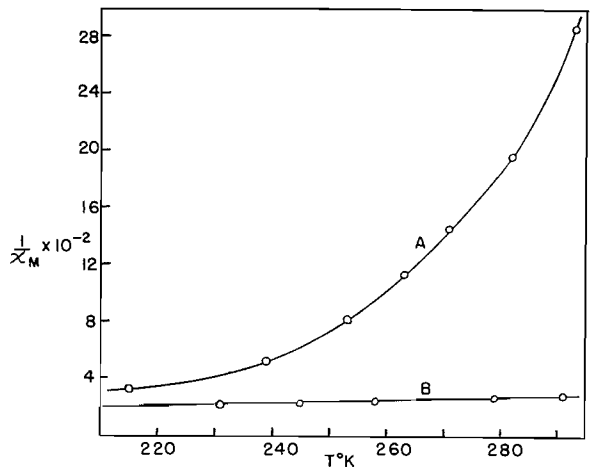

FIG. 2. Magnetic susceptibility of the N-butyl complex: A, in $CHCl_3$; B, in 10% pyridine – 90% $CHCl_3$.

TABLE II

Molecular weight determinations

Concentration (% by weight)	0.50	0.75	1.0	2.0	3.0	4.0
N-Methyl complex	357	415	540			
N-*n*-Butyl complex		447	465	512	570	683

of paramagnetism with increasing concentration, together with the observed increases in molecular weight with increasing concentration, provides excellent evidence that solute association occurs in these solutions of both the complexes. Since our measurements were made, the results of similar experiments by Holm have been published (8). Our results are in general agreement with Holm's in that both confirm the suggestion, originally made by Ferguson (3), as to the occurrence of association. However, the

present extension of measurements to low temperatures allows an important difference in interpretation to be made. Holm considers the low paramagnetism at room temperature of all the *n*-alkyl complexes (other than methyl) to be insignificant and he hence concludes (9) that these complexes are monomeric in solution. The measurements of Holm and McKinney were, however, made at only one concentration, or over a very restricted concentration range, and at only one temperature. The present magnetic measurements show clearly, when examined over the temperature and much wider concentration ranges, and particularly below room temperature, that there is ample evidence for association of the *n*-butyl complex. This is also supported by the molecular weight measurements. We therefore conclude that association occurs in non-coordinating solvents for all substituted salicylaldimine nickel (II) complexes so far investigated. When a strong base, such as pyridine, is present rapid solvation to octahedral, paramagnetic ($\mu \sim 3.2$ B.M.), dipyridine adducts (5, 10) occurs. The magnetic susceptibility then follows the Curie–Weiss law, as shown by Fig. 2.

Of the possible modes of solute association, that involving Ni—O intermolecular interactions to give an approximately octahedral arrangement about each nickel atom has been considered previously (2, 8, 11). An obvious alternative is that involving Ni—N intermolecular interactions to give the same type of arrangement. Miller and Sharpe (12) have rejected the possibility of coordination of the benzene rings of one molecule of bis-salicylaldehyde nickel (II) to the nickel atoms of adjacent molecules. An examination of the infrared spectra of the various forms of bis-N-methyl-5-chloro-salicylaldimine nickel (II) (2) likewise makes this type of interaction unlikely for the salicylaldimine complexes, since no frequency shifts are observed for absorptions associated with the phenyl groups (13).

Holm (8) has interpreted his results as indicating that, for the *n*-alkyl complexes (other than methyl), rotational motion of the alkyl groups must introduce a definite steric barrier so as to strongly inhibit association. Since our present results show that appreciable association occurs for these higher alkyl complexes, it seems that such steric effects are probably not the factors determining the occurrence or non-occurrence of association, although they apparently influence the degree of association. Detailed crystallographic studies are probably necessary to gain any reliable indication of the manner of association.

ACKNOWLEDGMENTS

The support of the National Research Council and Research Corporation are gratefully acknowledged.

1. W. D. Phillips and R. E. Benson. J. Chem. Phys. **33**, 607 (1960).
2. H. C. Clark and R. J. O'Brien. Can. J. Chem. **39**, 1030 (1961).
3. J. Ferguson. J. Chem. Phys. **34**, 611 (1961); Spectrochim. Acta, **17**, 316 (1961).
4. J. B. Willis and D. P. Mellor. J. Am. Chem. Soc. **69**, 1237 (1947).
5. H. C. Clark and A. L. Odell. J. Chem. Soc. 3431 (1955).
6. S. Fujii and M. Sumitani. Sci. Repts. Tôhoku Univ. First Ser. **37**, 49 (1953).
7. L. Sacconi, P. Paoletti, and G. Del Re. J. Am. Chem. Soc. **79**, 4062 (1957).
8. R. H. Holm. J. Am. Chem. Soc. **83**, 4683 (1961).
9. R. H. Holm and T. M. McKinney. J. Am. Chem. Soc. **82**, 5506 (1960).
10. F. Basolo and W. R. Matoush. J. Am. Chem. Soc. **75**, 5663 (1953).
11. C. M. Harris, S. H. Lenzer, and R. L. Martin. Australian J. Chem. **11**, 331 (1958).
12. J. R. Miller and A. G. Sharpe. J. Chem. Soc. 2594 (1961).
13. H. C. Clark. Unpublished observations.

Received December 11, 1961.
Department of Chemistry,
University of British Columbia,
Vancouver 8, B.C.

THE SYNTHESIS OF ACETAMIDO-DEOXY KETOSES BY ACETOBACTER SUBOXYDANS. PART IV

J. C. TURNER

Methyl 6-amino-6-deoxy-α-D-glucoside (I) was prepared by the method of Cramer *et al.* (1) and *N*-acetylated with aqueous acetic anhydride (2) to give methyl 6-acetamido-6-deoxy-α-D-glucoside (II). Acid hydrolysis of the methyl glucoside (II) then gave 6-acetamido-6-deoxy-D-glucose (III) (1,3), from which a crystalline phenylosazone (IV) was prepared.

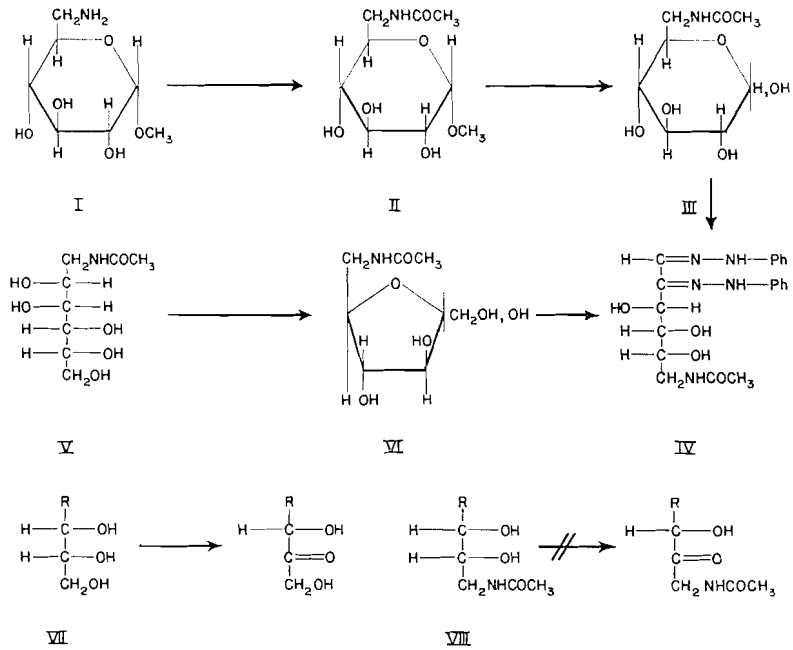

1-Acetamido-1-deoxy-D-mannitol (V) (4) was oxidized by *Acetobacter suboxydans* under conditions described in a previous publication (5) to give an 84% yield of a syrupy ketose sugar (VI). The ketose (VI) gave a crystalline phenylosazone (IV) which was identical with that obtained from 6-acetamido-6-deoxy-D-glucose (III). The ketose (VI) was therefore epimeric with 6-acetamido-6-deoxy-D-glucose (III) and thus possessed the D-fructose or D-*arabo*-hexulose configuration, and was therefore 6-acetamido-6-deoxy-D-*arabo*-hexulose.

As no other ketose was detected in the oxidation medium, it was concluded that oxidation of a polyhydric alcohol possessing the D-*erythro* configuration of hydroxyl groups according to the Bertrand–Hudson rules (VII) (6, 7) does not occur when the hydroxyl group of the primary alcohol group is replaced by an acetamido-deoxy group (VIII).

EXPERIMENTAL

Methyl 6-amino-6-deoxy-α-D-glucoside

Methyl 6-*O*-*p*-toluenesulphonyl-α-D-glucoside (5 g) (m.p. 116–118° C, $[\alpha]_D$ +106° (*c*, 2.2 in ethanol); lit. values: m.p. 124° C, $[\alpha]_D$ +98.5° (ethanol) (1)) was dissolved in absolute methanol (180 ml) and cooled

to 0° C. The solution was saturated with anhydrous ammonia, then heated in an autoclave at 120° C for 16 hours. After cooling, the dark solution was boiled with charcoal and filtered, and the filtrate was passed through Amberlite IRA 400 (OH^-) anion-exchange resin. The eluate was evaporated to dryness to give syrupy methyl 6-amino-6-deoxy-α-D-glucoside (3 g) (1).

Methyl 6-acetamido-6-deoxy-α-D-glucoside

Syrupy methyl 6-amino-6-deoxy-α-D-glucoside (3 g) was *N*-acetylated with aqueous acetic anhydride (2) to give crystalline methyl 6-acetamido-6-deoxy-α-D-glucoside. The product was recrystallized three times from methanol–ether to give needles (2.0 g) which had m.p. 163–164° C, $[\alpha]_D$ +133° (*c*, 2.0 in water) and gave absorptions in the infrared (potassium bromide disk) at 3500 cm^{-1} (OH), 3300 cm^{-1} (NH), 1640 cm^{-1} (amide I), and 1565 cm^{-1} (amide II).

Anal. Calc. for $C_9H_{17}O_6N$: C, 46.0%; H, 7.2%; N, 6.0%. Found: C, 46.0%; H, 7.7%; N, 6.2%.

6-Acetamido-6-deoxy-D-glucose

Methyl 6-acetamido-6-deoxy-α-D-glucoside (600 mg) was hydrolyzed with *N* sulphuric acid (15 ml) at 100° C for 3.5 hours. The solution was cooled to room temperature and passed through Duolite A4 (OH^-) anion-exchange resin and the eluate was evaporated to dryness. The residue was *N*-acetylated with aqueous acetic anhydride (2) as some de-*N*-acetylation had been observed in trial experiments under the same hydrolysis conditions. The product, which was obtained as a pale yellow syrup, contained unhydrolyzed methyl 6-acetamido-6-deoxy-α-D-glucoside and 6-acetamido-6-deoxy-D-glucose. The latter was separated by chromatography on Whatman 3MM paper using butan-1-ol–ethanol–water, 3:1:1, as solvent, and obtained as a clear, colorless syrup (100 mg), which crystallized on the addition of ethanol. When recrystallized from aqueous ethanol the 6-acetamido-6-deoxy-D-glucose (65 mg) had m.p. 203–205° C (decomp.), $[\alpha]_D$ +35±3° → +44±4° (18 hours) (*c*, 0.7 in water). (Lit. values: m.p. 182–183° C (decomp.), $[\alpha]_D$ +42° (in water, after 2 hours) (1) and m.p. 196–198° C (decomp.), $[\alpha]_D$ +44° → +35° (in water, after 24 hours) (3).)

6-Acetamido-6-deoxy-D-glucose gave absorptions in the infrared (potassium bromide disk) at 3300 cm^{-1} (OH and NH), 1625 cm^{-1} (amide I), and 1570 cm^{-1} (amide II).

*6-Acetamido-6-deoxy-*D-arabo-*hexose Phenylosazone*

The phenylosazone was prepared by the usual method using freshly distilled phenylhydrazine and glacial acetic acid. The phenylosazone was recrystallized from aqueous ethanol to give needles, m.p. 207–209° C (decomp.). The phenylosazone gave absorptions in the infrared (potassium bromide disk) at 3300 cm^{-1} (OH, NH) 3040 cm^{-1} (aromatic CH), 2900 cm^{-1} (aliphatic CH), 1635 cm^{-1} (amide I), 1580 cm^{-1} (amide II), and 1600, 1495, 745, 690 cm^{-1} (phenyl group).

*6-Acetamido-6-deoxy-*D-arabo-*hexulose*

1-Acetamido-1-deoxy-D-mannitol was oxidized by *Acetobacter suboxydans* under conditions described in a previous publication (5) and oxidation was complete after 21 days. The oxidation product was separated by chromatography on a cellulose column using butan-1-ol half-saturated with water as irrigant, and was obtained as a pale yellow syrup, $[\alpha]_D$ −8±2° (*c*, 1.94 in water). The ketose gave one spot on paper chromatography in several different solvent systems and gave a pink color with the orcinol – trichloroacetic acid spray reagent (8), changing to green on prolonged heating. The ketose gave absorptions in the infrared at 3300 cm^{-1} (OH, NH), 1725 cm^{-1} (saturated carbonyl group), 1640 cm^{-1} (amide I), and 1565 cm^{-1} (amide II). The infrared spectrum was obtained by smearing a little of the syrupy ketose on the surface of a potassium bromide disk.

The carbonyl peak at 1725 cm^{-1}, which was very weak, indicated that some of the ketose (ca. 5%) existed in the acyclic form and this was also suggested by the fact that the ketose slowly reduced Fehling's solution at room temperature (4).

*6-Acetamido-6-deoxy-*D-arabo-*hexose Phenylosazone*

The phenylosazone was prepared from the ketose under the same conditions as those used for 6-acetamido-6-deoxy-D-glucose. The phenylosazone was obtained as needles, m.p. 211–215° C (decomp.) and had a mixed melting point with the phenylosazone from 6-acetamido-6-deoxy-D-glucose of 206–209° C (decomp.). The infrared spectra of the two phenylosazones were identical over the range 4000–600 cm^{-1} and the two phenylosazones moved at identical rates on paper chromatograms in several different solvents.

Anal. Calc. for $C_{20}H_{25}O_4N_5$: C, 60.1%; H, 6.3%; N, 17.6%. Found: C, 60.3%; H, 6.9%; N, 17.5%.

*Periodate Oxidation of 6-Acetamido-6-deoxy-*D-*glucose and 6-Acetamido-6-deoxy-*D-arabo-*hexulose*

6-Acetamido-6-deoxy-D-glucose and 6-acetamido-6-deoxy-D-*arabo*-hexulose were each oxidized with an excess of sodium metaperiodate in unbuffered aqueous solution. The oxidation solutions were allowed to stand for 2 hours at room temperature, then tested for formaldehyde using the chromotropic acid method (9). 6-Acetamido-6-deoxy-D-glucose gave no formaldehyde, while 6-acetamido-6-deoxy-D-*arabo*-hexulose gave a strongly positive test for formaldehyde.

ACKNOWLEDGMENTS

The author wishes to thank the National Research Council for financial assistance (N.R.C. 706 and T-39) and for the award of a studentship.

1. F. CRAMER, H. OTTERBACH, and H. SPRINGMAN. Chem. Ber. **92**, 384 (1959).
2. G. A. LEVVY and A. MCALLAN. Biochem. J. **73**, 127 (1959).
3. M. J. CRON *et al.* J. Am. Chem. Soc. **80**, 2342 (1958).
4. J. K. N. JONES, M. B. PERRY, and J. C. TURNER. Can. J. Chem. In press (1962).
5. J. K. N. JONES, M. B. PERRY, and J. C. TURNER. Can. J. Chem. **39**, 965 (1961).
6. G. BERTRAND. Ann. Chim. (Paris), **3**, (8) 209, 287 (1904).
7. R. M. HANN, E. B. TILDEN, and C. S. HUDSON. J. Am. Chem. Soc. **60**, 1201 (1938).
8. R. KLEVSTRAND and A. NORDAL. Acta Chem. Scand. **4**, 1320 (1950).
9. J. F. O'DEA and R. A. GIBBONS. Biochem. J. **55**, 580 (1953).

RECEIVED DECEMBER 27, 1961.
DEPARTMENT OF ORGANIC CHEMISTRY,
QUEEN'S UNIVERSITY,
KINGSTON, ONTARIO.

HYPERFINE STRUCTURE IN THE ELECTRON SPIN RESONANCE SPECTRUM OF THE DIPHENYLENE RADICAL ANION

C. A. MCDOWELL AND K. F. PAULUS

The electron spin resonance spectra of the positive and negative radical ions of diphenylene were previously studied by McDowell and Rowlands (1). In that work it was mentioned that the observed five-line spectra could not be further resolved into the expected complete spectra of 25 lines. We now wish to report that we have been able to resolve completely the e.s.r. spectrum of the diphenylene radical anion. The radical anion was prepared by reacting the parent hydrocarbon with metallic potassium in purified, degassed, 1,2-dimethoxyethane as a solvent. The solvent had previously been carefully dried by allowing it to stand in contact with excess sodium anthracenide.

The spectra were recorded on a Varian e.s.r. spectrometer with 100 kc/s modulation and using a 12-in. Varian magnet. All the spectra were run at very low concentrations ($\sim 10^{-4}$ molar). The magnetic field calibrations were obtained by measuring the field with a proton resonance magnetometer, a 3-mm probe coil containing glycerol being inserted in the magnet gap. The associated marginal oscillator was frequency-modulated at 20 c/s and the proton resonance signal was displayed on an oscilloscope. A signal generator was loosely coupled and tuned for zero beat on the oscilloscope; the generator frequency and also the kystron frequency were measured with a Hewlett Packard 524/525/540 frequency counter which was standardized periodically against the WWV radio station.

Figure 1 shows the typical e.s.r. spectrum observed for the diphenylene radical anion in dimethoxyethane. The complete spectrum is shown in the upper portion of the figure while the detail of one of the five main bands is shown in the lower portion of the diagram. From the spectra we obtain the coupling constants for the two types of protons in diphenylene (see Fig. 2) to be $a^{H}_{(2)} = 2.76 \pm 0.01$ gauss, and $a^{H}_{(1)}$ to be 0.206 ± 0.008 gauss.

As is well known, the coupling constants for hyperfine splitting, a^{H}_{i}, due to protons are related to the average spin density, ρ_i, on the adjacent carbon atoms by the equation $a^{H}_{i} = Q\rho_i$. Q is a constant, negative in sign, which has been given various values such as

ACKNOWLEDGMENTS

The author wishes to thank the National Research Council for financial assistance (N.R.C. 706 and T-39) and for the award of a studentship.

1. F. CRAMER, H. OTTERBACH, and H. SPRINGMAN. Chem. Ber. **92**, 384 (1959).
2. G. A. LEVVY and A. MCALLAN. Biochem. J. **73**, 127 (1959).
3. M. J. CRON *et al.* J. Am. Chem. Soc. **80**, 2342 (1958).
4. J. K. N. JONES, M. B. PERRY, and J. C. TURNER. Can. J. Chem. In press (1962).
5. J. K. N. JONES, M. B. PERRY, and J. C. TURNER. Can. J. Chem. **39**, 965 (1961).
6. G. BERTRAND. Ann. Chim. (Paris), **3**, (8) 209, 287 (1904).
7. R. M. HANN, E. B. TILDEN, and C. S. HUDSON. J. Am. Chem. Soc. **60**, 1201 (1938).
8. R. KLEVSTRAND and A. NORDAL. Acta Chem. Scand. **4**, 1320 (1950).
9. J. F. O'DEA and R. A. GIBBONS. Biochem. J. **55**, 580 (1953).

RECEIVED DECEMBER 27, 1961.
DEPARTMENT OF ORGANIC CHEMISTRY,
QUEEN'S UNIVERSITY,
KINGSTON, ONTARIO.

HYPERFINE STRUCTURE IN THE ELECTRON SPIN RESONANCE SPECTRUM OF THE DIPHENYLENE RADICAL ANION

C. A. MCDOWELL AND K. F. PAULUS

The electron spin resonance spectra of the positive and negative radical ions of diphenylene were previously studied by McDowell and Rowlands (1). In that work it was mentioned that the observed five-line spectra could not be further resolved into the expected complete spectra of 25 lines. We now wish to report that we have been able to resolve completely the e.s.r. spectrum of the diphenylene radical anion. The radical anion was prepared by reacting the parent hydrocarbon with metallic potassium in purified, degassed, 1,2-dimethoxyethane as a solvent. The solvent had previously been carefully dried by allowing it to stand in contact with excess sodium anthracenide.

The spectra were recorded on a Varian e.s.r. spectrometer with 100 kc/s modulation and using a 12-in. Varian magnet. All the spectra were run at very low concentrations ($\sim 10^{-4}$ molar). The magnetic field calibrations were obtained by measuring the field with a proton resonance magnetometer, a 3-mm probe coil containing glycerol being inserted in the magnet gap. The associated marginal oscillator was frequency-modulated at 20 c/s and the proton resonance signal was displayed on an oscilloscope. A signal generator was loosely coupled and tuned for zero beat on the oscilloscope; the generator frequency and also the kystron frequency were measured with a Hewlett Packard 524/525/540 frequency counter which was standardized periodically against the WWV radio station.

Figure 1 shows the typical e.s.r. spectrum observed for the diphenylene radical anion in dimethoxyethane. The complete spectrum is shown in the upper portion of the figure while the detail of one of the five main bands is shown in the lower portion of the diagram. From the spectra we obtain the coupling constants for the two types of protons in diphenylene (see Fig. 2) to be $a^{H}_{(2)} = 2.76 \pm 0.01$ gauss, and $a^{H}_{(1)}$ to be 0.206 ± 0.008 gauss.

As is well known, the coupling constants for hyperfine splitting, a^{H}_{i}, due to protons are related to the average spin density, ρ_i, on the adjacent carbon atoms by the equation $a^{H}_{i} = Q\rho_i$. Q is a constant, negative in sign, which has been given various values such as

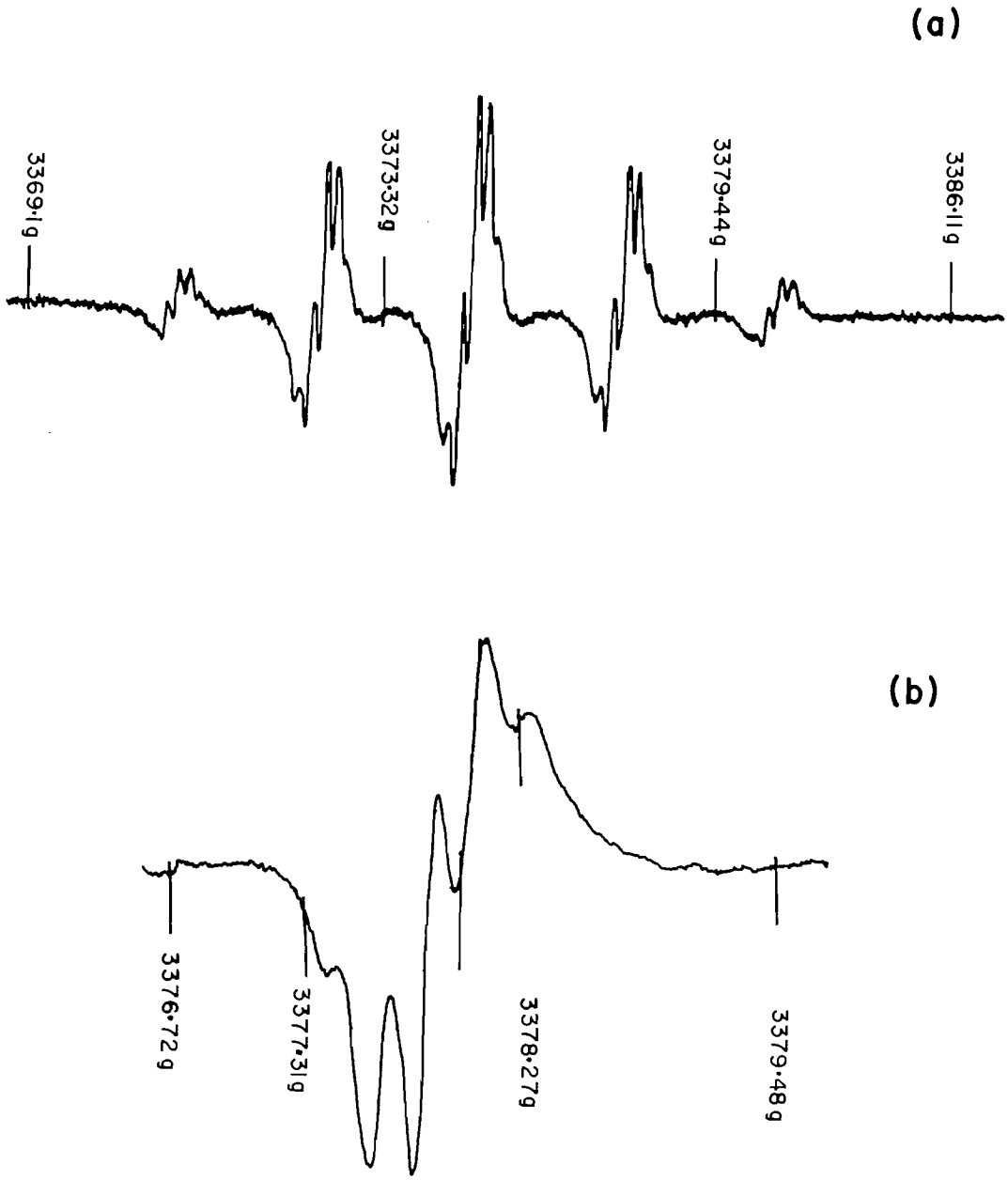

FIG. 1. A typical electron spin resonance spectrum for the diphenylene radical anion in dimethoxyethane; (*a*) complete spectrum, (*b*) one of the main bands shown in greater detail.

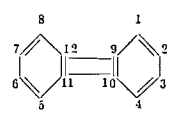

FIG. 2. Numbering system for the diphenylene molecule.

-22.5 gauss for the benzene negative ion (2), -25.67 gauss for the cyclooctatetraenyl radical anion (3), and values of about -30, which are necessary to fit the observed electron spin resonance spectra of polynuclear hydrocarbon radical ions, assuming the electron densities are given by the simple Hückel LCAO approximation (4). McLachlan (5) has analyzed most of the accurate data on these radical ions and concluded that the best value was $Q = -24.2$ gauss. Karplus and Fraenkel (6) have recently used a variation-perturbation method to calculate for the CHC_2 fragment, a value of $Q = -23.72$ gauss. Because of the success of McLachlan's treatment of the e.s.r. spectra of polynuclear hydrocarbon radical ions we shall adopt his value of $Q = -24.2$ gauss. Our experimental values for the hyperfine interaction constants then give the spin densities at carbon atoms 1 and 2 in the diphenylene radical anion to be $\rho_1 = 0.0085$, and $\rho_2 = 0.1140$. It also follows that the spin densities at carbon atoms 9, 10, 11, and 12 are $\rho_9 = \rho_{10} = \rho_{11} = \rho_{12} = 0.1275$. These values may be compared with those predicted by the simple Hückel LCAO approximation as given in Table I of reference 1. There it is shown that the Hückel theory gives $\rho_1 = 0.0269$, $\rho_2 = 0.0873$, and $\rho_9 = 0.1360$. However, altering the Coulombic integral for the four central carbon atoms so that it becomes equal to the normal carbon Coulombic integral *plus one-fifth* the carbon–carbon resonance integral, i.e. we take $\alpha_{C_9} = \alpha_C + 1/5\beta$, we obtain the following results: $\rho_1 = 0.032$, $\rho_2 = 0.0853$, and $\rho_9 = 0.1274$. For this latter set of parameters the calculated values for ρ_1 and ρ_2 do not agree well with the experimental values, but there is remarkably good agreement between the calculated and experimental values for ρ_9.

Because of the high spin density at the two sets of four equivalent carbon atoms C_9, C_{10}, C_{11}, and C_{12}, and also C_2, C_3, C_6, and C_7, and the nature of the spectrum shown in Fig. 1, it seemed that it might be possible to observe the hyperfine splittings due to C^{13}. The magnitude of this C^{13} hyperfine splitting can be calculated from two recent theories of C^{13} hyperfine interactions (6, 7). We choose to follow the more recent theory of Karplus and Fraenkel (6) as it seems to be somewhat more complete and gives good agreement with the known experimental values. The expected hyperfine splitting constants for $a^{C^{13}_{(2)}}$ was calculated to be 2.35 gauss and this would lie beneath the main lines in the spectrum of the diphenylene radical anion. For C_{11}, etc. the value calculated from the Karplus and Fraenkel theory for the case of the diphenylene radical anion depends on the nature of the interactions chosen. If the interaction parameters are chosen to represent C_1, C_9, and C_{10} the value calculated for $a^{C^{13}_{(9)}}$ is 2.64 gauss. If, however, the interaction path is taken to be C_9, C_{10}, C_{12}, C_1, then there results the value of 0.98 gauss for $a^{C^{13}_{(6)}}$. None of these C^{13} hyperfine interactions would be observable for the natural abundance of C^{13} in the diphenylene radical anion.

We wish to thank the National Research Council of Canada for generous grants in aid of this research work.

1. C. A. McDowell and J. R. Rowlands. Can. J. Chem. **38**, 503 (1960).
2. S. I. Weissman, T. R. Tuttle, and E. de Boer. J. Phys. Chem. **61**, 28 (1957).
3. T. J. Katz and H. L. Strauss. J. Chem. Phys. **32**, 1873 (1960).
4. E. de Boer and S. I. Weissman. J. Am. Chem. Soc. **80**, 4549 (1958).
5. A. D. McLachlan. Mol. Phys. **3**, 233 (1960).
6. M. Karplus and G. K. Fraenkel. J. Chem. Phys. **35**, 1312 (1961).
7. A. D. McLachlan, H. H. Dearman, and R. Lefebre. J. Chem. Phys. **33**, 65 (1960).

Received November 27, 1961.
Department of Chemistry,
University of British Columbia,
Vancouver 8, B.C.

5-BROMOPENTANOIC ACID AND 2,5-DIBROMOPENTANOIC ACID

N. ISENBERG, J. B. LEIBSOHN, AND V. E. MEROLA

We wish to report a convenient synthesis of 5-bromopentanoic acid and 2,5-dibromopentanoic acid from cyclopentanone. 5-Bromopentanoic acid has been synthesized from diethyl phenoxypropylmalonate (1), from 5-phenoxypentanoic acid (1), and from dihydropyran (2) in reasonable yields. Attempts to convert cyclopentanone to δ-valerolactone with hydrogen peroxide and to obtain 5-bromopentanoic acid from the lactone with hydrobromic acid (3) resulted in a low yield (18%). Using the method of Sager and Duckworth (4) we were able to prepare 5-bromopentanoic acid from cyclopentanone in 49% yield.

5-Bromopentanoic acid was also prepared from pentanediol in 25% yield by converting the diol to the lactone in the presence of copper chromite (5). The crude lactone was then treated with hydrobromic acid.

2,5-Dibromopentanoic acid was prepared from 5-bromopentanoic acid according to the method of Merchant, Wickert, and Marvel (1) in 85% yield.

EXPERIMENTAL

Synthesis from Cyclopentanone

Cyclopentanone (37.5 g) was oxidized with peroxytrifluoroacetic acid (4) to yield 42.8 g of crude δ-valerolactone. The crude material was refluxed with 100 ml of 48% hydrobromic acid for 3 hours and the two layers were separated. The upper aqueous layer was diluted with 200 ml of water and was extracted with several portions of ether. The organic layers were combined and dried over anhydrous sodium sulphate. The ether was removed by distillation and the product was distilled at reduced pressure. 5-Bromopentanoic acid was obtained (39.4 g; 49%).

Synthesis from 1,5-Pentanodiol

1,5-Pentanodiol (52 g) was heated under reflux in the presence of copper chromite to yield 35 g of crude δ-valerolactone. The crude material was refluxed with 100 ml of 48% hydrobromic acid for 3 hours and the product was separated and purified as described before. 5-Bromopentanoic acid was obtained (22.5 g; 25%).

5-Bromopentanoic Acid.—Neutralization equivalent: 181.48; found, 181; melting point: 38°–39° (1); observed, 38°–39°; boiling point: 142°–145° at 13 mm (1); observed, 104°–106° at 1.5 mm.

Synthesis of 2,5-Dibromopentanoic Acid from 5-Bromopentanoic Acid

5-Bromopentanoic acid (10 g) was converted to 2,5-dibromopentanoic acid with bromine and phosphorus tribromide (1). 2,5-Dibromopentanoic acid was obtained (12.2 g; 85%). The overall yield starting with cyclopentanone is 42%.

2,5-Dibromopentanoic Acid.—Neutralization equivalent: 260.40; found, 261; boiling point: 150°–152° at 5 mm (1); observed, 134°–136° at 2 mm; n_D^{25}, 1.5347 (1); observed, 1.5338.

ACKNOWLEDGMENT

We are indebted to the National Science Foundation for financial support under grant NSF-G12705 (Undergraduate Science Education Program).

1. R. MERCHANT, J. N. WICKERT, and C. S. MARVEL. J. Am. Chem. Soc. **49**, 1828 (1927).
2. R. GAUDRY and L. BERLINGUET. Can. J. Research, B, **27**, 282 (1949).
3. M. FLING, F. MINARD, and S. FOX. J. Am. Chem. Soc. **69**, 2466 (1947).
4. W. F. SAGER and A. DUCKWORTH. J. Am. Chem. Soc. **77**, 188 (1955).
5. L. E. SCHNIEPP and H. H. GELLER. J. Am. Chem. Soc. **69**, 1545 (1947).

RECEIVED JANUARY 9, 1962.
DEPARTMENT OF CHEMISTRY,
SKIDMORE COLLEGE,
SARATOGA SPRINGS, N.Y., U.S.A.

Canadian Journal of Chemistry

Issued by THE NATIONAL RESEARCH COUNCIL OF CANADA

VOLUME 40 MAY 1962 NUMBER 5

THE HALF-LIFE OF Ca^{41} [1]

J. R. S. DROUIN[2] AND L. YAFFE

Department of Chemistry, McGill University, Montreal, Que.

Received November 22, 1961

ABSTRACT

Ca^{41}, a nuclide decaying by orbital electron capture, has been again identified and its half-life measured. The activity of the source, a highly irradiated sample of calcium carbonate, had decayed for 10 years so that competing activities were non-existent. The measurement was made with a gas-flow proportional counter with well-determined characteristics. A value of $(7.5\pm1.1)\times10^4$ years has been obtained.

INTRODUCTION

The nuclide Ca^{41} has previously been prepared and measured by only one group of workers, viz. Brown, Hanna, and Yaffe (1). Richards, Smith, and Browne (2) had shown by measurements on the threshold of the reaction $K^{41}(p,n)Ca^{41}$ that an energy of only 0.44 ± 0.02 Mev is available for the decay of Ca^{41}. Thus the decay to K^{41} would be by electron capture with the simultaneous emission of potassium X rays.

Brown, Hanna, and Yaffe prepared Ca^{41} by a 15-week irradiation, in a high neutron flux, of calcium depleted 200-fold in the isotope of mass 44. The material was subjected to a rigorous chemical purification and the X rays emitted by the source measured by an argon-filled proportional counter equipped with a thin window.

The identification of the nuclide and the measurement of its half-life were both rendered exceedingly difficult because of the β^--activity due to Ca^{45} (153 days), produced by the reaction $Ca^{44}(n,\gamma)Ca^{45}$, even in this highly depleted source. This caused the production of calcium X rays by ionization of the material in the source. Hence a composite X-ray peak composed of the fluorescent calcium X rays and potassium X rays due to Ca^{41} was superimposed over a background of the same intensity as the composite peak. The use of a potassium 'critical' absorber helped to discriminate against the calcium X rays. The rigid chemical purification, and the fact that the potassium X-ray activity being detected was proportional to neutron flux in several samples, ruled out possibilities other than Ca^{41}.

The half-life determination rested on the resolution of a composite peak and was found to be $(1.1\pm0.3)\times10^5$ years.

We were fortunate in having available a highly irradiated sample of calcium,* the activity of which had decayed for about 10 years, so that the Ca^{45} contribution was now negligible. This communication reports the remeasurement of the half-life of Ca^{41} under more favorable conditions and reaffirms its identity.

[1]*This work received financial assistance from the National Research Council of Canada.*

[2]*Present address: CARDE, P.O. Box 1427, Quebec City, Que.*

**We wish to express our appreciation to Dr. R. H. Betts, Chemistry Branch, Atomic Energy of Canada Limited, Chalk River, Ontario, who helped greatly in making this sample available to us.*

EXPERIMENTAL AND RESULTS

(a) Irradiation

A sample of 'spec-pure' calcium carbonate was irradiated in the NRX nuclear reactor at Chalk River for a period of about 10 months, along with a small amount of cobalt wire, which was used as a flux monitor. Measurement of the monitor showed that the sample had been subjected to a total integrated flux of 8.1×10^{20} neutrons cm^{-2}. The activity of the calcium sample was allowed to decay for about 10 years, after which time it showed no activity measurable by highly sensitive β- and γ-counters.

(b) Determination of Calcium Content

The calcium carbonate was purified, evaporated to dryness with nitric acid, and made up to volume with distilled water. The calcium content of the 'master solution' was determined by a method described by Welcher (3) which consisted of an EDTA titration using an indicator made of *o*-cresolphthalein complexes. The EDTA solution was standardized against a standard calcium nitrate solution. The calibration curve is shown in Fig. 1.

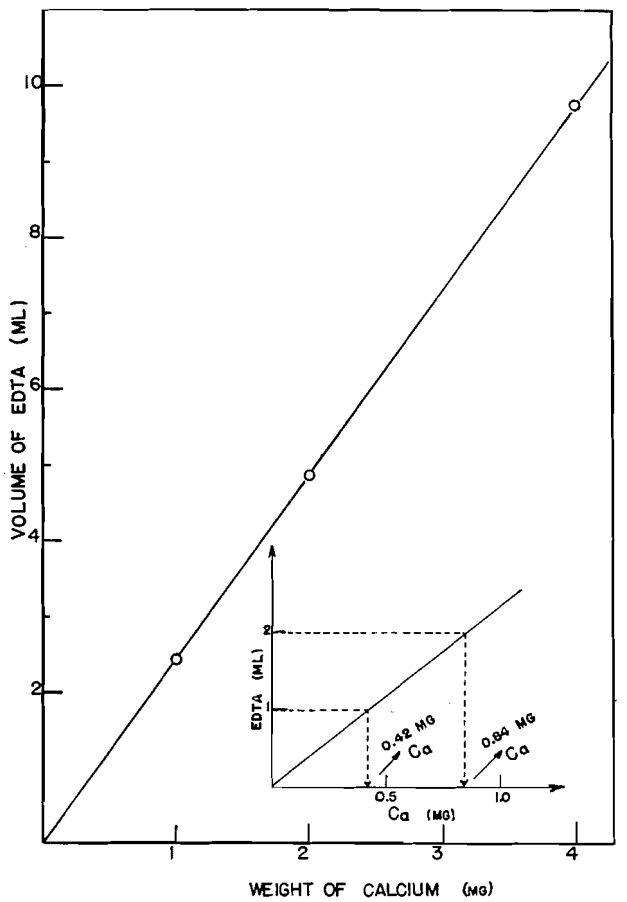

FIG. 1. Analysis of calcium 'master solution'.

Two aliquots, namely 100 and 200 μl, were withdrawn from the solution and analyzed. The results are shown in the bottom of Fig. 1, giving a value of $0.42 \pm .01$ mg of Ca per 100 μl of the solution. A great deal of care was taken with the above analysis, since, in the previous measurement, the determination of the Ca content of the source introduced an error of $\pm 15\%$.

(c) Specific Activity Determination

The disintegration rate of the sample was determined using a gas-flow proportional counter. A sketch of this is shown in Fig. 2. The counter pulses were fed into a cathode follower, amplifier, and pulse height analyzer. A detailed description of the operating characteristics of such a counter has been given previously (4).

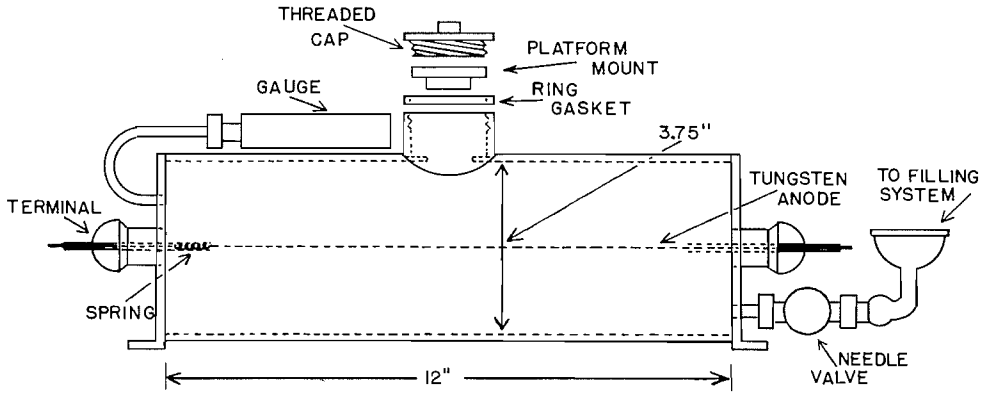

FIG. 2. Gas-flow proportional counter.

The sample was mounted internally in the counter on a platform. The source mount, prior to the evaporation of the sample, was treated with a 5% insulin solution which was removed as completely as possible. A sample of 100 μl was deposited on an area of 1 cm^2. During the process of evaporation the mounted source was continually rocked in order to keep all parts of the area, originally covered, wet until the last possible moment. When the sample was completely dry, it was covered with an aluminum absorber thick enough (0.8 μ) to absorb all the Auger electrons emanating from the source (5).

The source was placed in the counter, and characteristic K X rays of potassium were identified as shown in Fig. 3. The characteristic K X rays from Cr^{51}, Fe^{55}, and Zn^{65} were used to calibrate the energy response of the counter as shown in this figure and verify that the measured activity corresponded to potassium K X rays.

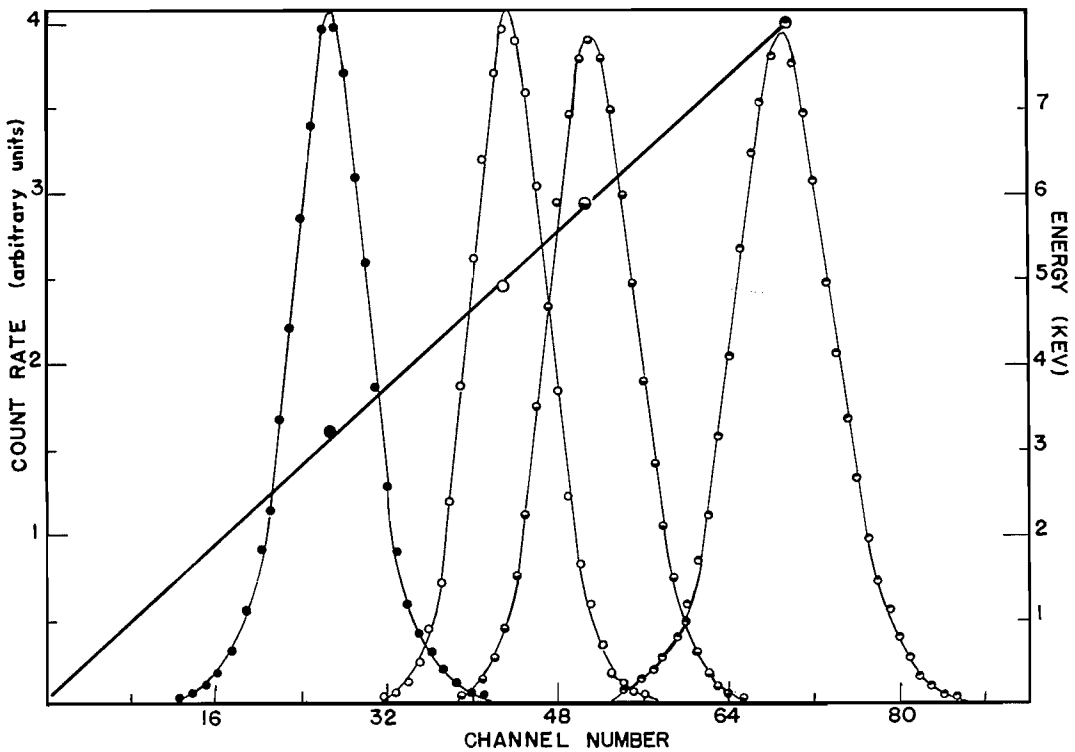

FIG. 3. Energy calibration of the counter: ● Ca^{41}, ○ Cr^{51}, ◒ Fe^{55}, ◓ Zn^{65}.

In Fig. 4 is shown the photopeak due to the potassium K X rays from which the half-life measurement data were taken. The background during this measurement was slightly less than 1 count per minute per channel

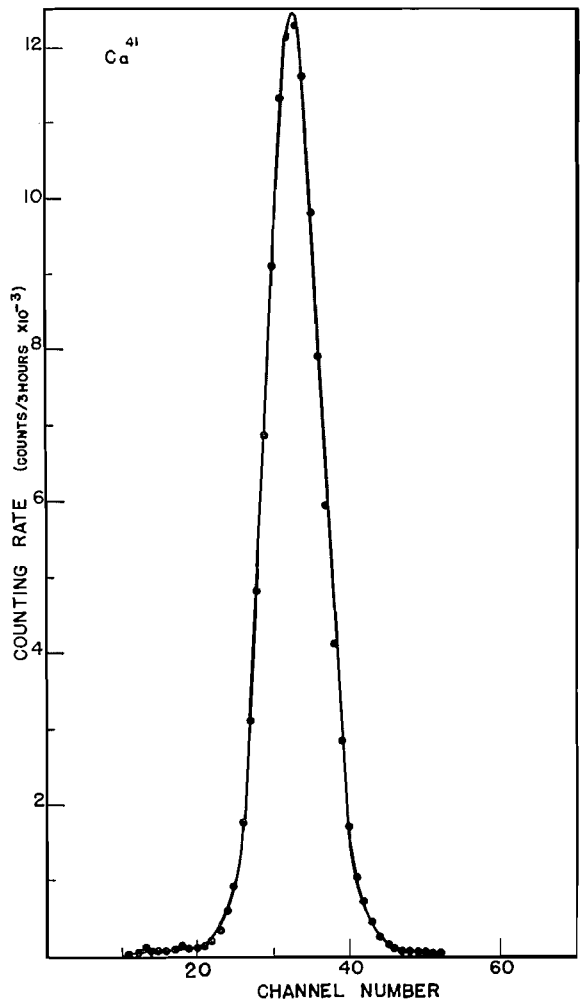

FIG. 4. Photopeak due to Ca^{41}.

and of course no calcium fluorescent X rays were detectable. The instrumental arrangement enabled the background to be subtracted automatically.

When the counter was operated at pressures of 1 and 2 atm, the counting rates were reproducible within the standard deviation, showing that the X rays were completely absorbed in the counter.

To change the measured counting rate into a disintegration rate, the following corrections had to be employed:

(i) Self-absorption: This factor is exceedingly important for such low-energy X rays (3.2 Kev). This was determined experimentally in the following way. The source was diluted with known amounts of inactive calcium nitrate and the counting rate measured. The area of the source was kept constant. The results are shown in Fig. 5. From this the decrease in count rate due to self-absorption was determined to be 14% for the sample used.

(ii) Transmission of the characteristic X rays by the Auger electron absorber: The transmission of the potassium K X rays was obtained by inserting into an equation derived by Campion and Merritt (6) the proper mass absorption coefficient and thickness for the aluminum absorber (7). The above equation is applicable in the present case, i.e. an uncollimated beam of radiation. The Auger electron absorber was found to transmit 67% of the potassium K X rays.

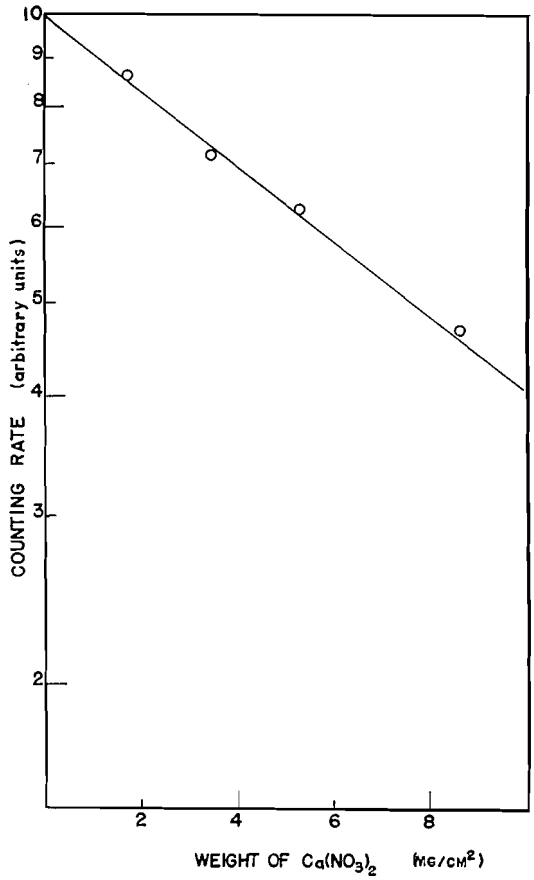

FIG. 5. Self-absorption of potassium K X rays in calcium nitrate.

(iii) Fluorescence yield: The K-fluorescence yield of potassium, W_k, has been semiempirically calculated by Hagedoorn and Wapstra (8) to be 0.120, and this value has been used. Brown *et al.* used an interpolated value of 0.13 ± 0.01, which agrees very well with the recent work quoted above.

(iv) L-capture contributions: From the theoretical results of Brysk and Rose (9), the L/K capture (including L_{II}- and L_{III}-capture contributions) was evaluated as 0.089.

(v) Geometrical efficiency of the counter: The geometrical efficiency of the counter has previously (4) been determined to be 50%.

From Fig. 4, the number of potassium K X rays beneath the peak was manually integrated and found to be 594 ± 6 counts min^{-1} for 0.42 mg Ca.

From the irradiation data and the cross section, one obtained the number of Ca^{41} atoms, N_{41}, formed by irradiating a known number of Ca^{40} atoms, N_{40}, as follows:

$$N_{41} = N_{40}\sigma(nv)t,$$

where nv = integrated neutron flux = 8.07×10^{20} neutrons cm^{-2}, σ = cross section = 0.22 barns (10). Therefore, in 1 mg of naturally occurring Ca (97% Ca^{40}), there were produced

$$N_{41} = \frac{6.02\times10^{20}}{40}\times0.97\times0.22\times10^{-24}\times8.07\times10^{20} = 2.59\times10^{15} \text{ atoms.}$$

The disintegration rate, obtained by applying the corrections discussed above, is

$$594\times\frac{1}{0.86}\times\frac{1}{0.67}\times\frac{1}{.12}\times1.089\times2$$

$$= 1.87\times10^{4} \text{ disintegrations } min^{-1} \text{ for 0.42 mg Ca}$$
$$= 4.45\times10^{4} \text{ disintegrations } min^{-1} mg^{-1} \text{ Ca.}$$

The disintegration rate = $N_{41}\lambda$, where

$$\lambda = \frac{0.693}{\text{half-life}}.$$

Therefore

$$\text{half-life} = \frac{2.59\times10^{15}\times0.693}{4.45\times10^{4}\times365\times1440}$$

$$= 76{,}700 \text{ years.}$$

The errors involved in the actual measurement itself are small (~1%). Other errors in the absorption corrections, flux determination, etc., impose limits of ±15% on the measurement, yielding a final value of $(7.7\pm1.1)\times10^{4}$ years.

This agrees remarkably well, within the errors quoted, with the value of Brown, Hanna, and Yaffe. The latter calculated theoretically the half-life one would predict assuming that this is an α-type first-order forbidden transition. This is possible since the ft values of β-emitters of this type are closely grouped. Their results gave an upper limit of 6×10^{4} years, just outside the experimental limits of error. Our value brings this half-life into closer agreement with the prediction.

REFERENCES

1. F. Brown, G. C. Hanna, and L. Yaffe. Proc. Roy. Soc. (London), A, **220**, 103 (1953).
2. H. T. Richards, R. V. Smith, and C. P. Browne. Phys. Rev. **80**, 524 (1950).
3. F. J. Welcher. The analytical uses of EDTA. D. Van Nostrand Co., Inc., Toronto. 1957.
4. J. R. S. Drouin and L. Yaffe. Can. J. Chem. **39**, 717 (1961).
5. A. T. Nelms. Natl. Bur. Standards Circ. No. 577. 1958.
6. P. J. Campion and W. P. Merritt. Atomic Energy of Canada Limited Rept. CRP-745. 1957.
7. G. W. Grodstein. Natl. Bur. Standards Circ. No. 583. 1957.
8. H. L. Hagedoorn and A. H. Wapstra. Nuclear Phys. **15**, 146 (1960).
9. H. Brysk and M. E. Rose. Revs. Modern Phys. **30**, 1169 (1958).
10. H. Pomerance. Phys. Rev. **88**, 412 (1952).

CONDUCTANCES OF AQUEOUS SOLUTIONS OF SODIUM OCTANOATE AT 25° AND 35° AND THE LIMITING CONDUCTANCE OF THE OCTANOATE ION

A. N. CAMPBELL, E. M. KARTZMARK, AND G. R. LAKSHMINARAYANAN
Chemistry Department, University of Manitoba, Winnipeg, Manitoba

Received January 3, 1962

ABSTRACT

Equivalent conductances, densities, and viscosities of aqueous solutions of sodium octanoate have been determined at 25° and 35° C, at concentrations ranging from 0.0002 *M* to 2.8 *M*. The limiting equivalent conductances of the octanoate ion have been determined as 23.08 mhos and 29.09 mhos, at 25° and 35° C respectively.

Comparison has been made of our experimental conductances with those calculated, using the equations of Robinson–Stokes, of Falkenhagen–Leist, and of Fuoss.

No evidence has been found of micelle formation in solutions of sodium octanoate.

The work here described on the conductance of sodium octanoate is part of our general project of measuring the electrical conductance of sodium salts of higher fatty acids over a wide range of concentration. It might be supposed a progressive increase of anion size would eventually lead to an anion so large that it would be virtually motionless and non-conducting but it is known that, after a certain number of carbon atoms in the chain is reached, micelle formation occurs and it is known that micelles are conducting. Why this should be so is not immediately obvious, since though the charge is increased the mass is increased in the same ratio, but presumably some alignment occurs after the manner of liquid crystals, so that the resistance to movement is reduced.

We continue to endeavor to fit the conductance equations of Wishaw–Stokes (1) and Falkenhagen–Leist (2) to our experimental results, although we now admit that these equations must be considered to be empirical in the concentrated range. We have also used Fuoss' latest equation (3) for the same purpose.

EXPERIMENTAL PROCEDURE

n-Octanoic acid, otherwise known as caprylic acid, obtained from the Eastman Kodak Company, was redistilled. The acid was neutralized with the equivalent quantity of sodium hydroxide, dissolved in alcohol, and the solution concentrated by slow evaporation. A mixture of acetone and alcohol, in the ratio of 2 to 1, was added to the concentrated solution, when the sodium salt was thrown out of solution. The filtered salt was dried in a vacuum oven, ground, and stored over barium oxide.

The salt was analyzed by conversion to sodium sulphate, a method given in Stock, Staehler, Patnode, and Dennis (4). The method, the only one available, is somewhat crude. Four analyses gave the purity as 99.5%. The presence of alkali, as an impurity, would give a high, not a low, result. Direct pH measurements on the aqueous solution of the salt gave a value in good agreement with that calculated for the hydrolysis of sodium octanoate.

Conductance water, having a specific conductance at 25° C of $2\text{–}3\times10^{-7}$ mhos, was obtained by bubbling nitrogen through distilled water. We have found this method to be more satisfactory than more complicated methods. The more concentrated solutions were prepared by direct weighing of salt and solution, the very dilute solutions by the technique of Shedlovsky (5), using a duplicate of his large silica conductance cell. In calculating the constant of this cell we used the equation of Fuoss (6) for the equivalent conductance of potassium chloride solutions of varying concentration, at 25° C.

The methods of measuring viscosity and density require no description. The method of Campbell and Bock (7) was used to correct the equivalent conductance for the effect of hydrolysis. The ionization constant of octanoic acid was obtained from the data given by Dippy (8).

EXPERIMENTAL RESULTS

The experimental results are given in Tables I and II.

TABLE I

Densities, viscosities, and conductances of sodium octanoate at 25° C

Concentration (mole/liter)	Density (g/ml)	Relative viscosity	Specific conductance (mhos/cm $\times 10^4$)	Equivalent conductance (mhos)	Conductance viscosity product
0.000237			0.17186	72.21	72.21*
0.000647			0.46317	71.49	71.57*
0.001233			0.87750	70.91	71.18*
0.001624			1.1485	70.58	70.81*
0.002088			1.4687	70.22	70.25*
0.002858			2.0010	69.91	70.30*
0.01086	0.99731	1.022	7.2143	66.38	68.82
0.07416	0.99935	1.071	44.706	60.27	64.65
0.1043	1.0024	1.095	60.652	58.17	63.70
0.1977	1.0046	1.182	107.06	54.40	63.10
0.3484	1.0084	1.332	169.64	48.69	63.53
0.5099	1.0128	1.537	220.23	42.87	65.89
0.6245	1.0159	1.723	258.71	41.42	71.35
0.8409	1.0210	2.222	320.16	38.07	85.47
1.1332	1.0277	3.460	397.01	35.04	122.60
1.6338	1.0386	8.311	491.38	30.07	249.89
2.1137	1.0495	26.027	520.35	24.62	640.78
2.8287	1.0659	65.069	501.36	17.72	1153.02

*The viscosities corresponding to the first six low concentrations were not determined experimentally: they were obtained by linear interpolation.

TABLE II

Densities, viscosities, and conductivities of sodium octanoate at 35° C

Concentration (mole/liter)	Density (g/ml)	Relative viscosity	Specific conductance (mhos/cm $\times 10^4$)	Equivalent conductance (mhos)	Conductance viscosity product
0.000236			0.21265	89.51	89.51*
0.000646			0.57321	88.66	88.77*
0.001232			1.0868	87.93	88.14*
0.001619			1.4189	87.40	87.67*
0.002081			1.8189	87.19	87.53*
0.002850			2.4738	86.58	87.05*
0.01082	0.99418	1.020	8.9059	82.31	85.26
0.07395	0.99642	1.069	55.245	74.71	79.87
0.1040	0.99742	1.092	74.902	72.03	79.44
0.1970	1.0001	1.165	133.231	67.63	77.33
0.3472	1.0041	1.323	211.48	60.91	78.94
0.5079	1.0079	1.521	274.45	54.04	83.09
0.6223	1.0108	1.701	322.81	51.87	88.23
0.6373	1.0155	2.192	403.14	48.15	105.53
1.1280	1.0225	3.409	500.84	44.41	151.43
1.6255	1.0342	8.159	620.03	38.16	311.34
2.1021	1.0445	25.350	661.49	31.47	797.76
2.8213	1.0603	54.149	645.31	22.87	1238.39

*The viscosities corresponding to the first six low concentrations were not determined experimentally: they were obtained by linear interpolation.

DISCUSSION OF RESULTS

The overall error in the equivalent conductance measurements amounts to 0.1%. The first six measurements in the dilute region were used to calculate the limiting conductance. The methods of Kohlrausch, of Shedlovsky (5), and of Fuoss (3) were used.

The value of Λ_0 obtained by the three methods, at 25° and at 35°, are as follows:

	Λ_0 at 25° (mhos)	Λ_0 at 35° (mhos)
Kohlrausch	73.18	90.63
Shedlovsky	73.30	90.90
Fuoss	73.34	90.92

Using the Kohlrausch values for Λ_0 and the values 50.10 mhos at 25° and 61.54 mhos at 35° for the ionic conductance of the sodium ion (9), the ionic conductances of octanoate ion at 25° and 35° respectively result as 23.08 mhos and 29.09 mhos.

The Arrhenius equation applied to the conductance figures at the two temperatures, and to the corresponding viscosities (fluidities), for the same concentrations and temperatures, yielded the figures of Table III, for the activation energies of conductance and of viscosity, respectively.

TABLE III

Activation energy of conductance and viscosity between 25° C and 35° C

Concentration (mole/liter)	Activation energy of conductance (kcal/mole)	Activation energy of fluidity (kcal/mole)
0.0	3.897	3.880
0.25	4.103	4.027
0.50	4.110	4.080
1.00	4.116	4.016
1.50	4.228	4.162
2.00	4.439	4.339
2.50	4.721	6.080

As usual, the figures of activation energies of conductance and of viscosity are very similar, suggesting a fundamental resemblance between the mechanisms of the two processes in aqueous solution. The sudden increase in the energy of viscosity at the highest concentration indicates a change in the nature of the flow, perhaps on approach to micelle formation. In anhydrous melts, the activation energies of conductance and of viscosity are generally far from equal.

It is well known that Walden's rule does not apply to different concentrations of the same electrolyte in the same solvent but it is always interesting to work out the values of Λ_η and to plot these values against concentration in the form of $\sqrt{c}$. This has been done in Fig. 1.

As usual, we applied the Robinson–Stokes and the Falkenhagen–Leist equations to our work. To these we have now added the Fuoss equation. The method of using this latest equation is detailed in Chap. XV of "Electrolytic Conductance" by Fuoss and Accascina (10).

As with sodium hexanoate (11), we found that the agreement with the equations of Robinson–Stokes and Falkenhagen–Leist was not good. We therefore reproduce here only the calculations for dilute solution (Tables IV and V). Although the experimental values agree in general within 0.65 mhos in the case of the Robinson–Stokes and Falkenhagen–Leist equations up to a concentration of nearly 0.1 M at 25° C and 0.075 M at

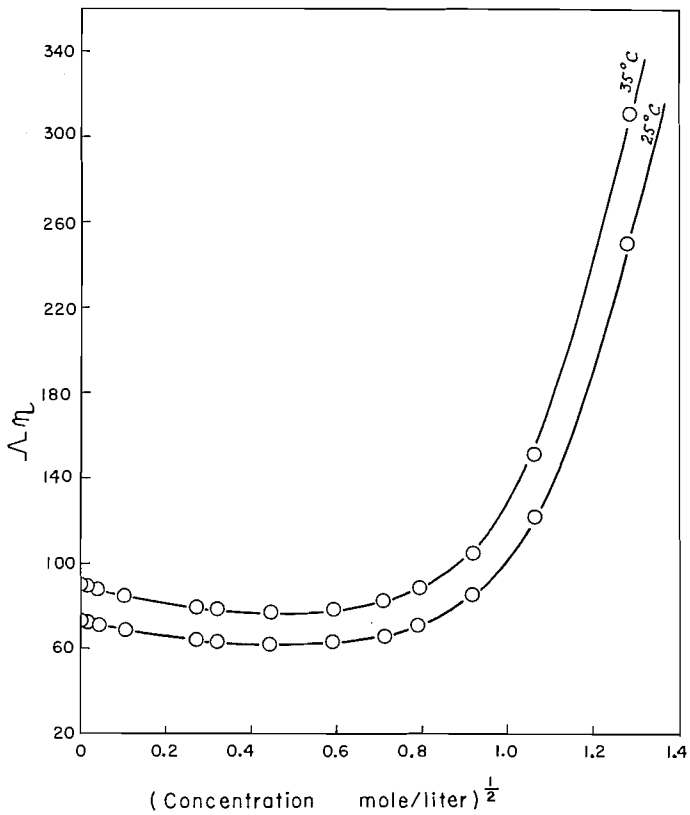

FIG. 1. $\Lambda\eta$ vs. $\sqrt{c}$.

TABLE IV

Calculated equivalent conductances at 25° C

Concentration (mole/liter)	Equivalent conductance (mhos)	Calculated equivalent conductances (mhos)				
		Robinson–Stokes		Falkenhagen–Leist		Fuoss–Onsager
		$\mathring{a}$ = 15.0 Å	$\mathring{a}$ = 23.0 Å	$\mathring{a}$ = 11.0 Å	$\mathring{a}$ = 13.5 Å	$\mathring{a}$ = 7.0 Å
0.000237	72.21	72.11	72.12	72.08	72.11	72.20
0.000647	71.49	71.36	71.43	71.34	71.44	71.51
0.001233	70.91	70.66	70.86	70.66	70.73	70.83
0.001624	70.58	70.37	70.58	70.31	70.40	70.58
0.002088	70.22	70.04	70.28	69.96	70.07	70.27
0.002858	69.91	69.54	69.87	69.47	69.59	69.85
0.01086	66.38	66.41	67.30	66.18	66.56	67.81
0.07416	60.27	59.79	61.38	59.46	60.49	70.55
0.1043	58.17	57.82	59.67	57.53	58.96	—
0.1977	54.40	52.36	53.81	52.28	53.61	—
0.3484	48.69	45.49	47.49	45.69	47.04	—

35° C, the very high $\mathring{a}$ value, necessary for agreement, seems to be unrealistic, particularly when there is no evidence of micelle formation. On the other hand the Fuoss–Onsager equation reproduces the data very well within 0.15 mhos at 25° C and 0.1 mhos at 35° C in the very dilute region, though the agreement is limited to a narrow region

TABLE V
Calculated equivalent conductances at 35° C

Concentration (mole/liter)	Equivalent conductance (mhos)	Calculated equivalent conductance (mhos)				
		Robinson–Stokes		Falkenhagen–Leist		Fuoss–Onsager
		$\mathring{a}$ = 13.5 Å	$\mathring{a}$ = 19.0 Å	$\mathring{a}$ = 9.0 Å	$\mathring{a}$ = 10.5 Å	$\mathring{a}$ = 7.8 Å
0.000236	89.51	89.52	89.56	89.23	89.27	89.51
0.000646	88.66	88.33	88.51	88.28	88.30	88.67
0.001232	87.93	87.37	87.73	87.41	87.47	87.91
0.001619	87.40	87.09	87.27	86.77	87.03	87.53
0.002081	87.19	86.62	87.02	86.50	86.59	87.13
0.002850	86.58	86.03	86.44	85.84	85.96	86.67
0.01082	82.31	82.09	82.33	81.62	81.95	84.45
0.07395	74.71	73.55	75.38	72.45	73.40	90.53
0.1040	72.03	71.07	73.08	69.93	71.04	—
0.1970	67.63	64.90	67.02	63.93	65.26	—
0.3472	60.91	55.93	58.28	55.14	56.23	—

of concentration. It is claimed that the Fuoss equation can reproduce the experimental results as long as $K\mathring{a} < 0.2$; because of the high $\mathring{a}$ value (7–8 Å) this corresponds to a concentration not greater than 0.01 *M*.

Admitting that the equations of Robinson–Stokes and Falkenhagen–Leist are to some extent empirical, it is still surprising that, for example, in the case of lithium chlorate (12), the agreement between calculated and observed results is so good. Perhaps the "distance of closest approach" cannot be expressed in terms of a single parameter when dealing with a long-chain ion.

It has been stated by Smith and Robinson (13) that micelle formation occurs in solutions of sodium octanoate but, judging by the behavior of the conductance and viscosity curves, we think it unlikely. Certainly, micelle formation must set in when a certain number of carbon atoms in the ion has been attained but we think this number is greater than eight. To investigate this point we determined the apparent molecular weight at different concentrations by the vacuum flask freezing point depression techniques. In this method finely shaved ice and a solution of sodium octanoate are thoroughly stirred until equilibrium is established. The temperature is noted and an analysis then made by evaporation of water from a sample. The results are contained in Table VI. They show no evidence of enhanced molecular weight.

TABLE VI

Concentration (g of salt/100 g H_2O)	Apparent molecular weight
2.464	100.4
5.496	96.5
7.553	93.1
10.575	88.7

Work is continuing on the acid containing 10 carbon atoms.

REFERENCES

1. B. F. Wishaw and R. H. Stokes. J. Am. Chem. Soc. **76**, 2065 (1954).
2. H. Falkenhagen, M. Leist, and G. Kelbg. Ann. Physik, **11**, 51 (1952).
3. R. M. Fuoss. J. Am. Chem. Soc. **80**, 3163 (1958).
4. A. Stock, A. Staehler, W. Patnode, and L. M. Dennis. Quantitative chemical analysis. 1st ed. McGraw-Hill Book Co., Inc., New York and London. 1935. p. 95.

5. T. SHEDLOVSKY. J. Am. Chem. Soc. **54**, 1405 (1932).
6. J. E. LIND, JR., J. J. ZWELENIK, and R. M. FUOSS. J. Am. Chem. Soc. **81**, 1557 (1959).
7. A. N. CAMPBELL and E. BOCK. Can. J. Chem. **36**, 330 (1958).
8. J. F. J. DIPPY. J. Chem. Soc. 1222 (1938).
9. G. C. BENSON and A. R. GORDON. J. Chem. Phys. **13**, 473 (1945).
10. R. M. FUOSS and F. ACCASCINA. Electrolytic conductance. Interscience Pub., New York. 1959. Chap. XV.
11. A. N. CAMPBELL and J. I. FRIESEN. Can. J. Chem. **38**, 1939 (1960).
12. A. N. CAMPBELL, E. M. KARTZMARK, and W. PATERSON. Can. J. Chem. **36**, 1004 (1958).
13. E. R. B. SMITH and R. A. ROBINSON. Trans. Faraday Soc. **38**, 70 (1942).

THE HETEROGENEOUS AND HOMOGENEOUS THERMAL DECOMPOSITIONS OF NICKEL CARBONYL[1]

R. K. CHAN[2] AND R. MCINTOSH[3]
Department of Chemistry, University of Toronto, Toronto, Ontario
Received January 5, 1962

ABSTRACT

The homogeneous thermal decomposition of $Ni(CO)_4$ between 35° C and 80° C and over a pressure range of 15 mm to 80 mm of Hg has been distinguished from the heterogeneous reaction occurring on the freshly deposited nickel surface. The activation energy of the homogeneous reaction was found to be 19.1 kcal $mole^{-1}$ and of the heterogeneous reaction, 14.3 kcal $mole^{-1}$. The activated complex for the heterogeneous reaction is $Ni(CO)_4$, which is physically adsorbed. The heat of adsorption of $Ni(CO)_4$ is 7.4 kcal $mole^{-1}$. Carbon monoxide is also adsorbed upon the same sites with a heat of adsorption of 13.3 kcal $mole^{-1}$, which is much greater than its latent heat of vaporization. The homogeneous reaction may be inhibited by a surface of sodium chloride. Nickel deposited upon rutile behaves in the same way catalytically as nickel deposited upon glass wool.

INTRODUCTION

The thermal decomposition of $Ni(CO)_4$ was first reported by Mittasch (1). Mechanisms have been suggested for the homogeneous reaction by Bawn (2) and Garrat and Thompson (3). Bawn noted that the reaction was partially heterogeneous, about 20% of the decomposition occurring by a heterogeneous mechanism under some conditions. Tonosaki and Suginuma (4), on the other hand, concluded that the reaction was completely heterogeneous. As the heterogeneous reaction would be similar to those reported by Taylor and his associates in the studies of the decomposition of germane, arsine, and stibine (5), in the sense that reaction occurs upon a freshly deposited, and hence clean, metallic surface, an attempt has been made to examine the reaction more fully, and to pay particular attention to the heterogeneous reaction. The heterogeneous part of the reaction was exaggerated by packing the vessel with glass wool (up to the amount of 1 g). This procedure sufficed to permit the separation of the composite reaction into its two parts. The homogeneous part was found to obey the mechanism proposed by Bawn (2) and by Garrat and Thompson (3). The heterogeneous part was explicable if the rate was assumed proportional to adsorbed $Ni(CO)_4$, which competes for adsorption sites with CO. The $Ni(CO)_4$ is physically adsorbed, while the CO has a sufficiently high heat of adsorption to suggest chemisorption.

Additional experiments were performed with finely divided rutile suspended in glass wool, and with finely divided sodium chloride. The latter substance could not be effectively dispersed throughout the glass wool. These experiments showed two things: first, the rate of the heterogeneous reaction is not dependent upon the substrate upon which the nickel layer forms; second, a salt surface of appreciable area will reduce the initial composite rate very substantially below the rate for the homogeneous reaction. This is explained by assuming that the intermediate $Ni(CO)_3$ is adsorbed and recombination with CO occurs on the ionic surface. Further study of the influence of polar and non-polar surfaces is thus warranted.

[1]*Based on a thesis submitted as partial fulfillment of the requirements for the degree of Doctor of Philosophy in the School of Graduate Studies, University of Toronto.*
[2]*Present address: Division of Applied Chemistry, National Research Council, Ottawa, Ontario.*
[3]*Present address: Department of Chemistry, Queen's University, Kingston, Ontario.*

EXPERIMENTAL

The experimental assembly was conventional except for the pressure gauge (see Fig. 1). As Mittasch (1) had shown that the presence of Hg accelerated the reaction, and as this was confirmed in preliminary experiments, a metal bellows gauge was constructed which had a sensitivity of 0.15 mm of Hg per mm

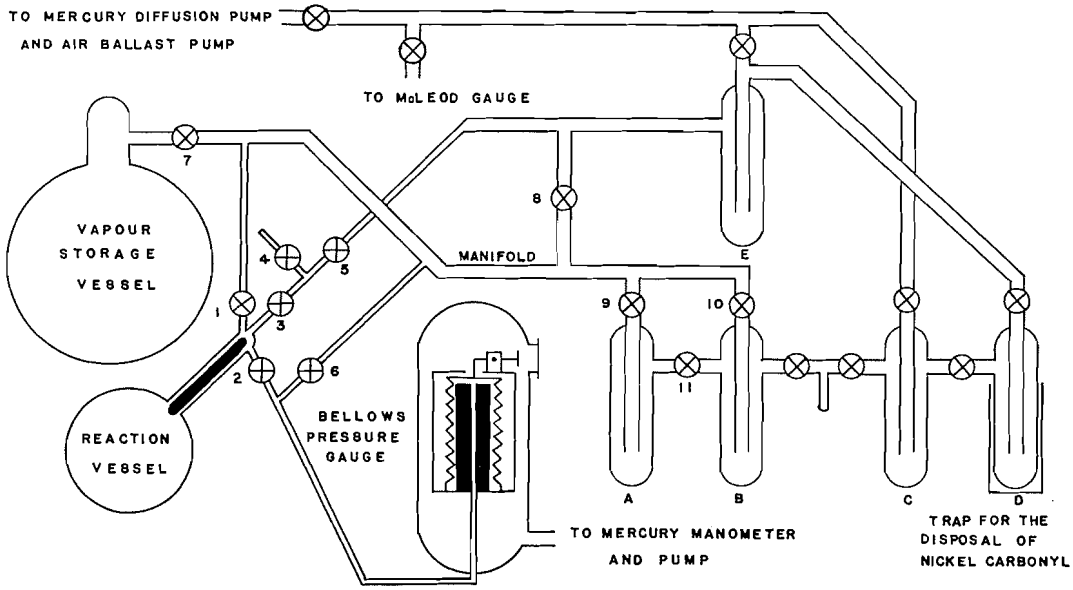

FIG. 1. Apparatus for decomposing nickel carbonyl: A and B, traps for vacuum distillation; C and B, liquid air traps.

deflection. The temperature range studied was 35° C to 80° C, and the pressure range about 15 mm to 80 mm. The $Ni(CO_4)$ was obtained from the City Chemical Corporation of New York. It was freed of dissolved air by trap-to-trap distillation and by vigorous pumping of the frozen material. Dry ice was used as the refrigerant as Mittasch and Kuss (6) have reported violent explosions when liquid air was used as the coolant.

The reaction vessel was pumped at 100° C for, at least, 5 hours before use. Several decompositions had to be carried out before the reaction rate became reproducible. The rate was then reproducible for many runs until the thickness of the deposited nickel was estimated to be 5000 layers of nickel. Thereafter the rate began to accelerate and the nickel was no longer deposited as a coherent metallic film but as an apparently fine powder. The reaction vessel was then cleaned and the surface again conditioned for further experiments.

The glass fibers used to increase the surface were obtained from the Corning Glass Works, Corning, New York. The average diameter of the fibers was reported as $8.6\pm0.7\times10^{-4}$ cm on the basis of an examination of 24 fibers (7). The surface area per gram was thus taken to be 0.2 m^2. The estimated area of the quartz reaction vessel was 200 cm^2. (Quartz was employed because the removal of nickel films by washing with dilute nitric acid brought about changes of the rate of reaction in a clean vessel.)

Rutile powder having a specific surface of 80 m^2/g was also used, dispersed in a known amount of glass wool. Only amounts below about 15 mg could be suspended in the glass wool. Similarly, sodium chloride of specific surface up to 90 m^2/g was employed. The preparation of the sodium chloride has been described in earlier publications (8–10).

PROCEDURES FOR EVALUATING THE RATE OF DECOMPOSITION AT $t = 0$

As the time of admission of the $Ni(CO)_4$ to the reaction vessel is finite, and because some oscillation of the gauge was observed initially, care was exercised in the evaluation of the initial composite rate. Three procedures were tested and compared. These were:

(*a*) A plot of x/t versus $1/t \ln p/(p-x)$ was made arising from the equation

$$\frac{x}{t} = \frac{1+pb_c}{b_c}\frac{1}{t}\ln\frac{p}{p-x} - \frac{k_c}{b_c},$$

which is the integrated form of the assumed rate equation

$$\frac{dx}{dt} = \frac{k_c(p-x)}{1+b_c x}.$$

This method is sensitive to the value of the gauge reading at zero time.

(*b*) A cubic equation of the form $x = \alpha_0+\alpha_1 t+\alpha_2 t^2+\alpha_3 t^3$ was fitted to the experimental data. The coefficient α_1 gives the initial composite rate. α_0 gives the value of the gauge reading at zero time required in (*a*) above.

(*c*) A solution of the equation $1/t = (\alpha/x)-\beta$ for α,β was made on the basis of the finding that an expression of the form $x = (\alpha t)/(1+\beta t)$ fitted the experimental data quite well.

These three procedures were made into a program suitable for the I.B.M. 650 computer. The results were within $\pm 2\%$ for the three methods of expressing the data.

The uncertainty caused by an error in selecting zero time was also examined. The timer was normally started at a value of -2 seconds as the $Ni(CO)_4$ was admitted to the vessel, since Bawn (2) had established that this was a reasonable time for the admission and warming of the gas to be completed. The value of zero time was then arbitrarily shifted between -2 seconds and $+2$ seconds and several values of the initial rate of decomposition were re-evaluated. The error introduced was always less than $\pm 5\%$, depending upon the temperature and initial pressure. The choice of the origin for the time axis was, therefore, relatively unimportant because the pressure increase in the first few seconds was almost linear with time.

EVALUATION OF THE CONSTANTS OF THE RATE EQUATIONS OF THE HOMOGENEOUS AND HETEROGENEOUS REACTIONS

The rate of the homogeneous reaction was assumed to obey the equation given by Garratt and Thompson (3), namely:

$$\left(\frac{dx}{dt}\right)_{\text{homo}} = \frac{K_1(p-x)}{1+4(K_3/K_2)x} = \frac{k_2(p-x)}{1+b_2 x},$$

where p is the initial pressure of $Ni(CO)_4$, the amount decomposed at time t is x (in units of pressure), and K_1, K_2, K_3 are the respective specific rate constants of the reactions

$$Ni(CO)_4 \xrightarrow{K_1} Ni(CO)_3 + CO,$$

$$Ni(CO)_3 \xrightarrow{K_2} Ni + 3CO,$$

$$Ni(CO)_3 + CO \xrightarrow{K_3} Ni(CO)_4.$$

The rate of the heterogeneous reaction was assumed to be given by

$$\left(\frac{dx}{dt}\right)_{\text{heter}} = \frac{k_1 A b(p-x)}{1+b(p-x)+b_1 x},$$

based upon the view that the rate depends upon the surface area and the fraction of the surface covered by reactant molecules. It is implicit also in the expression that CO competes with $Ni(CO)_4$ for adsorption sites. The constant $b_1/4$ is the Langmuir constant for adsorption of CO and the constant b that for $Ni(CO)_4$.

The observed composite rate was then assumed to be formed according to the relation

$$\left(\frac{dx}{dt}\right)_{\text{comp}} = \left(\frac{dx}{dt}\right)_{\text{homo}} + \left(\frac{dx}{dt}\right)_{\text{heter}} = \frac{k_2(p-x)}{1+b_2 x} + \frac{k_1 A b(p-x)}{1+b(p-x)+b_1 x}.$$

Moreover, the composite rate was found, by observation, to be suitable for representation in the form

$$\left(\frac{dx}{dt}\right)_{\text{comp}} = \frac{k_c(p-x)}{1+b_c x}.$$

At $t = 0$

$$\left(\frac{dx}{dt}\right)_{\substack{\text{comp}\\ t=0}} = k_c p = \frac{k_1 A b p}{1+bp} + k_2 p.$$

A plot of initial composite rate versus surface area for fixed temperature and initial pressure should yield $(k_1 bp)/(1+bp)$ from its slope and $k_2 p$ from its intercept (see Fig. 2).

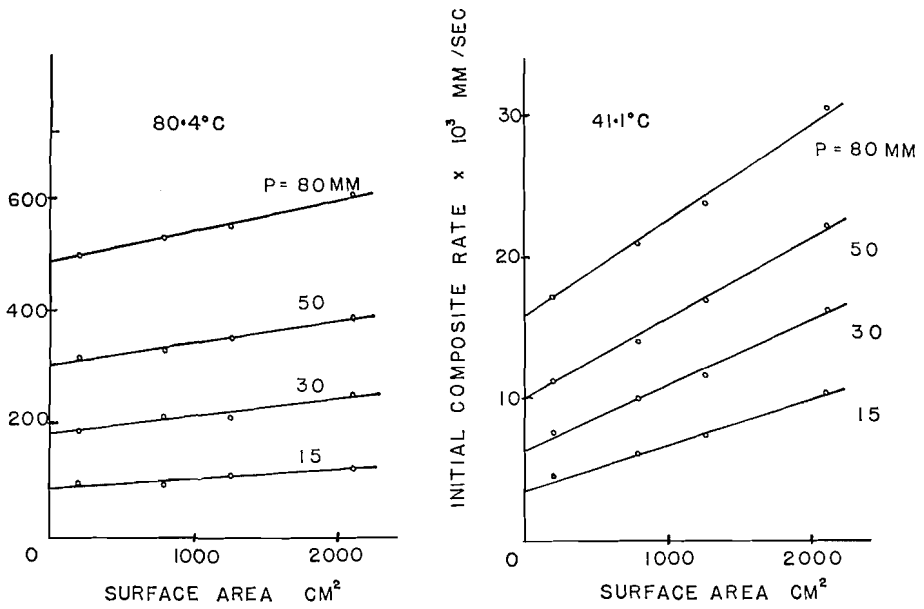

FIG. 2. Initial composite rate versus surface area.

Intercepts of similar plots for a given temperature but different initial pressures give the initial homogeneous rates from which k_2 may be obtained.

The heterogeneous rate constant k_1 and b may be solved in the following way:

$$k_c p - k_2 p = \frac{k_1 A b p}{1+bp} = \left(\frac{dx}{dt}\right)_{\substack{\text{heter}\\ t=0}}$$

and

$$1 \Big/ \left(\frac{dx}{dt}\right)_{\substack{\text{heter}\\ t=0}} = \frac{1}{k_1 A b}\frac{1}{p} + \frac{1}{k_1 A}.$$

Thus, from the appropriate plot, $k_1 A$ and $k_1 A b$ are obtained, and so a value of b, since A is known. Thus far, k_1, k_2, and b are known. The remaining constants, b_1 and $4K_3/K_2 = b_2$, are obtained in the following way. Since the observed composite rate equation is to

be accounted for on the assumption of the homogeneous and heterogeneous equations for all values of x and t, it can be shown that

$$k_c = \frac{k_1 A b}{1+bp} + k_2$$

and

$$b_1 = b_c(1+bp)+b$$
$$b_2 = b_c.$$

Because $b_1/4$ and b are constants in Langmuir's adsorption isotherm, they are expected to be constant for a given temperature. In order to fulfill this requirement b_c must increase as p decreases. Experiment confirms this prediction. However, it is not clear why b_2 should also increase with decreasing p, and this question will be discussed later.

Thus all five constants can be evaluated for a given temperature, provided A is known.

CHARACTERISTICS OF THE HOMOGENEOUS REACTION

On the basis of the mechanism outlined above, and first given by Garratt and Thompson (3), it follows that the homogeneous reaction at zero time should be first order in the pressure of $Ni(CO)_4$. This is adequately demonstrated in Fig. 3 for the entire range of

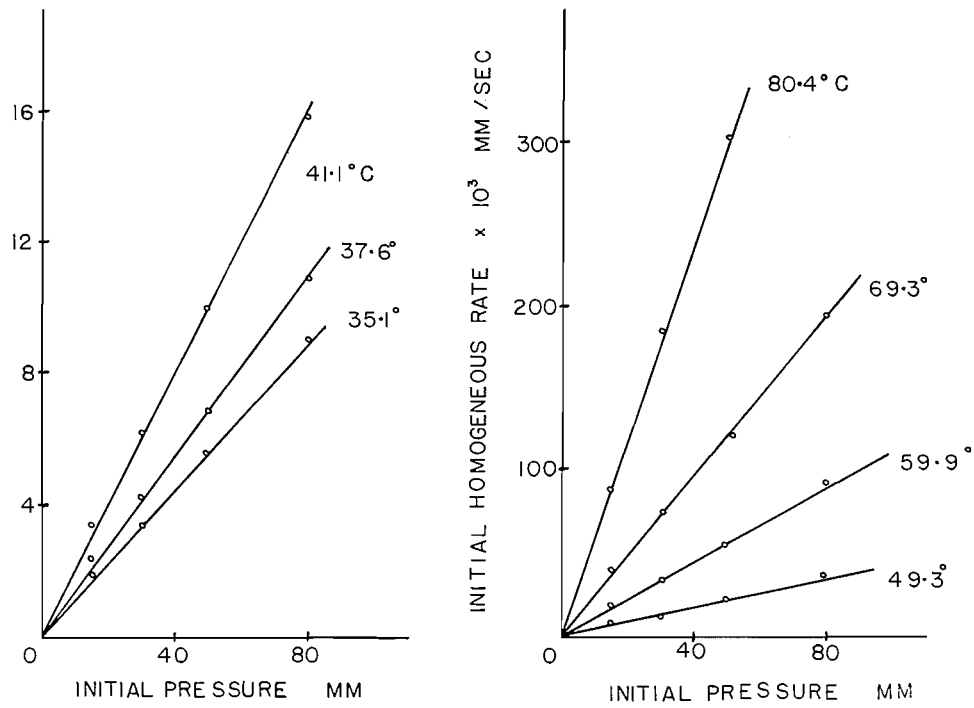

FIG. 3. Initial homogeneous rate versus initial pressure.

temperature. The initial homogeneous rate and the specific rate constant k_2 are given in Table I. From the variation of k_2 with temperature, plotted in the usual way in Fig. 4, the activation energy of this primary step was determined to be 19.1 kcal mole^{-1}. The

TABLE I

Initial homogeneous rate and homogeneous rate constant

	Temp. (°C)	Initial pressure of $Ni(CO)_4$ (mm Hg) 15	30	50	80
$k_2p\times10^3$	35.1	1.8	3.4	5.5	9.1
$k_2\times10^4$		1.20	1.13	1.10	1.14
$k_2p\times10^3$	37.6	2.4	4.1	6.8	11.0
$k_2\times10^4$		1.60	1.37	1.36	1.38
$k_2p\times10^3$	41.1	3.4	6.2	10.0	15.9
$k_2\times10^4$		2.27	2.06	2.00	1.99
$k_2p\times10^3$	49.3	6.5	12.5	21.0	35.5
$k_2\times10^4$		4.33	4.16	4.20	4.40
$k_2p\times10^3$	59.9	17.0	34.5	55.0	92.0
$k_2\times10^4$		11.3	11.5	11.0	11.5
$k_2p\times10^3$	69.3	38	76	123	196
$k_2\times10^4$		25.4	25.3	24.6	24.5
$k_2p\times10^3$	80.4	88	184	305	487
$k_2\times10^4$		58.7	61.3	61.0	60.8

NOTE: k_2p in mm/sec and k_2 in sec^{-1}.

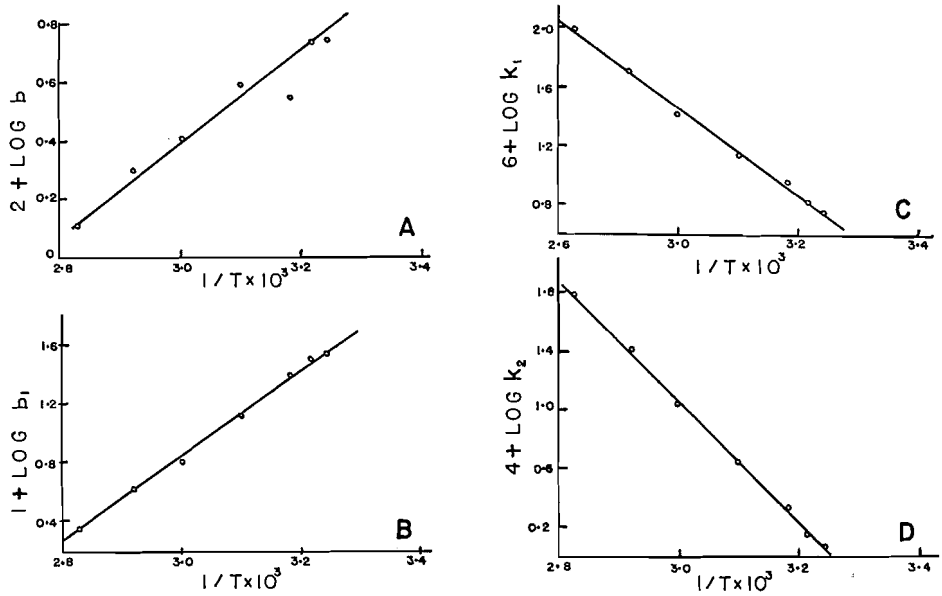

FIG. 4. (A) Heat of adsorption of $Ni(CO)_4$ = 7.4 kcal $mole^{-1}$; (B) heat of adsorption of CO = 13.3 kcal $mole^{-1}$; (C) activation energy of heterogeneous reaction = 14.3 kcal $mole^{-1}$; (D) activation energy of homogeneous reaction = 19.1 kcal $mole^{-1}$.

activation energy determined by Garratt and Thompson (3) was 12 kcal $mole^{-1}$, and by Bawn 10.3 kcal $mole^{-1}$ (2) for temperatures in the neighborhood of 100° C and on the assumption that the reaction is essentially homogeneous at this and higher temperatures. (This assumption is supported by our observations.) Tonosaki and Suginuma (4) give a value of 18.7 kcal $mole^{-1}$. They employed a rate expression identical with Bawn's and also with Garratt's and Thompson's, although the reaction was considered to be entirely heterogeneous. Their value cannot be compared directly with the values obtained

in this work for the individual reactions, but a comparison was made for the activation energy of the composite reaction in an unpacked vessel at 50 mm pressure. The apparent activation energy for this set of conditions was 18.9 kcal mole^{-1}. This is practically indistinguishable from the value given by Tonosaki and Suginuma, but considerably higher than those reported by the other authors.

CHARACTERISTICS OF THE HETEROGENEOUS REACTION

Since the initial heterogeneous rate is proportional to the surface area, its value per unit surface should be the same for all amounts of glass wool. Somewhat serious errors occur for the empty vessel because of the small contribution of the heterogeneous reaction. Thus, in Fig. 5, only the data involving glass wool are plotted.

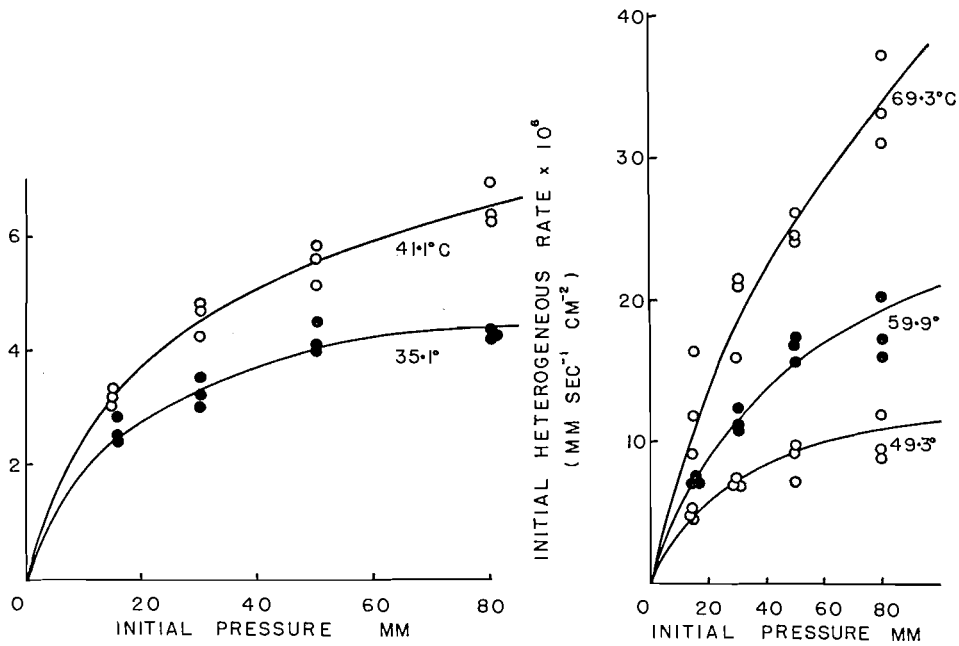

FIG. 5. Initial heterogeneous rate per unit surface area versus initial pressure.

The two constants k_1 and b were evaluated from these data and are given in Table II. Included are values given by employment of the equation $b = 3.52\times10^{-7} \exp(7400/RT)$.

TABLE II

Heterogeneous rate constant and Langmuir's adsorption isotherm constants for $Ni(CO)_4$ and CO

Temperature (°C)	$k_1\times10^6$ (mm sec^{-1}cm^{-2})	$b\times10^2$ (mm^{-1})	b (calc)$\times10^2$ (mm^{-1})	b_1 (mm^{-1})
35.1	5.52	5.51	6.28	3.44
37.6	6.41	5.38	5.70	3.11
41.1	8.85	3.49	5.00	2.49
49.3	13.6	3.91	3.72	1.32
59.9	26.3	2.57	2.57	0.646
69.3	51.3	2.00	1.91	0.414
80.4	100	1.28	1.35	0.226

(This equation was utilized to provide values of b required to obtain b_1.) From the variations of these constants with temperature the activation energy of the heterogeneous reaction, E_{heter}, and the heat of adsorption of $Ni(CO)_4$ upon the fresh nickel surface were obtained (see Fig. 4). E_{heter} is 14.3 kcal mole^{-1} and $Q_{Ni(CO)_4}$ is 7.4 kcal mole^{-1}. The latter figure may be compared with the reported value of 6.5 kcal mole^{-1} given by Dewar and Jones for the latent heat of vaporization of $Ni(CO)_4$ (11). The agreement is sufficiently close to warrant the conclusion that the $Ni(CO)_4$ is physically adsorbed upon the nickel films. This view is also consistent with the entropy of the activated complex, which is recorded in a later section.

It has been assumed in the equation describing the course of the heterogeneous reaction that carbon monoxide is also adsorbed upon the nickel film and uses up sites which would otherwise be available for the adsorption of $Ni(CO)_4$. The Langmuir constant for the adsorption of carbon monoxide is $b_1/4$, and its variation with temperature provides a value of the heat of adsorption. These data are also recorded in Fig. 4 and Table II, from which a value of Q_{CO} = 13.3 kcal mole^{-1} is obtained. This value is so greatly in excess of the latent heat of vaporization, 1.44 kcal mole^{-1}, at its normal boiling point (12), that the CO is chemisorbed upon the nickel. Tonosaki and Suginuma (4) were also of the view that CO is strongly adsorbed compared with $Ni(CO)_4$.

If b_1 has the significance attributed to it, b_c must, according to the equation $b_1 = b_c(1+bp)+b$, increase with diminishing pressure. The trend is illustrated in Fig. 6.

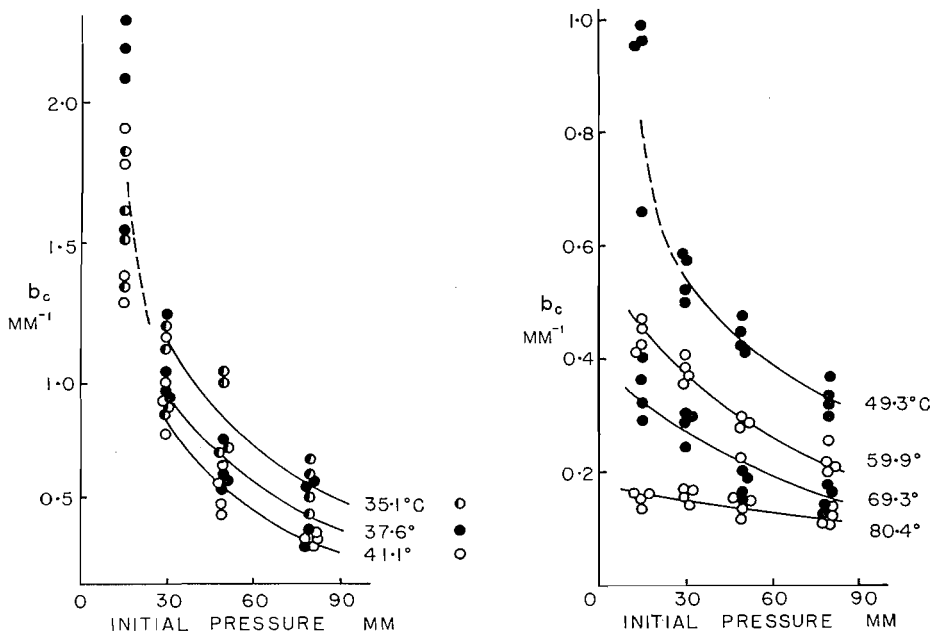

FIG. 6. Variation of b_c with pressure of $Ni(CO)_4$ at different temperatures.

THE VARIATION OF b_2 WITH PRESSURE

On the basis of the equations resulting from the assumed mechanisms, it has been shown that $b_2 = b_c$, and that b_c increases with diminishing pressure of $Ni(CO)_4$. This finding presents difficulties which require discussion. In the first place, if b_c is a function

of pressure of $Ni(CO)_4$, then it should not be possible to represent the course of a reaction by means of the equation

$$\left(\frac{dx}{dt}\right)_{comp} = \frac{k_c(p-x)}{1+b_c x}.$$

In the second place, b_2 is $4K_3/K_2$, and there is no obvious reason why this ratio should vary with pressure.

The answer appears to be that b_c becomes less dependent upon pressure as the temperature is increased. For a low-temperature run, say in the vicinity of 40° C, the rate of decomposition is slow, and an experiment was normally concluded when about 5% of the $Ni(CO)_4$ had decomposed. The variation of b_c would not be easily detected in this circumstance. At a high temperature, say 80° C, the decomposition was carried to about 10%, but for this temperature the variation of b_c with pressure is small. Thus the empirical equation appeared valid under all the experimental conditions employed. A more complicated expression of the composite rate would presumably remove the contradictions.

EXPERIMENTS USING RUTILE AND SODIUM CHLORIDE PACKINGS

The experiments in which these powders were employed need not be described extensively. Rutile could be dispersed and suspended to the extent of about 15 mg in a small amount of glass wool. Up to this amount of suspended rutile, the heterogeneous reaction rate increased linearly with amount of rutile. The absolute value of the rate agreed with expectation on the basis of the known behavior of the nickel film formed upon glass wool when the respective surface areas of rutile and glass wool were taken into account. Thus one concludes that the surface properties of the nickel deposited upon rutile are the same as those of nickel deposited upon glass wool.

In the course of these experiments with rutile, it was further established that exposure of the deposited nickel film to oxygen decreases the rate of the heterogeneous reaction. After the deposition of further layers of nickel (only a few partial decompositions are required), the rate was re-established. Thus oxygen inhibits the heterogeneous reaction, contrary to its effect on a germanium surface when germane is thermally decomposed (13). Its effect also differs in that the inhibition is eliminated on further deposition of nickel, whereas the oxygen had a persistent effect with germanium films and was therefore considered to diffuse to the surface on addition of further germanium.

The experiments with sodium chloride were less informative. The powder could not be satisfactorily dispersed, and showed little specific surface due to clumping. An attempt to avoid this clumping led to the deposition of sodium chloride upon the quartz wall by allowing a smoke of salt to deposit on the flask. After the usual pumping procedure, it was found that reaction was slow, appreciably less than that of the homogeneous reaction at the same temperature. This finding was established conclusively in repeated experiments.

To rationalize this result, it was postulated that $Ni(CO)_3$ is readily adsorbed upon the polar surface, and there reacts with CO to reform $Ni(CO)_4$. Therefore, two extra steps have to be added to the mechanism offered by Garratt and Thompson (3):

$$Ni(CO)_3 + S \xrightarrow{K_4} Ni(CO)_3\text{-}S$$

$$Ni(CO)_3\text{-}S + CO \xrightarrow{K_5} Ni(CO)_4 + S,$$

where S is adsorption site on the salt surface and $Ni(CO)_3$-S represents the adsorbed

$Ni(CO)_3$. The modified homogeneous decomposition may be expressed through the equation

$$\frac{-dNi(CO)_4}{dt} = \frac{K_1 Ni(CO)_4}{1+\frac{K_3}{K_2}CO+\frac{K_4}{K_2}S}.$$

If the term $(K_4/K_2)S$ is large as compared to $1+(K_3/K_2)CO$, the rate can be reduced appreciably. The effect has not been extensively investigated, but it is clear that a study of this inhibition, and inhibition by other surfaces, is warranted.

ENTROPIES OF THE ACTIVATED COMPLEXES

On the basis of the reaction rates which have been determined experimentally and the theory of absolute reaction rates of Glasstone, Laidler, and Eyring (14), the entropy of activation of the homogeneous reaction is found to be −16.2 e.u. From this the effective collision frequency is determined to be about 10^{10} per second. This is abnormally low. Even lower results would be obtained using the activation energies reported by Bawn (2) and by Garratt and Thompson (3). From this standpoint the decomposition reaction is somewhat unusual.

On the other hand, the entropy change on formation of the activated complex of the heterogeneous reaction, assumed to be adsorbed $Ni(CO)_4$, is calculated to be −16.7 e.u. at 40° C. The standard state for the gaseous $Ni(CO)_4$ is 1 atm and that for the adsorbed $Ni(CO)_4$ is taken as $\theta = \frac{1}{2}$ (15). The entropy change is about what would be expected if one degree of translational freedom had been lost, but no appreciable change had been suffered in the rotational and vibrational freedom (−18.3 e.u.). This is consistent with the statement made earlier that $Ni(CO)_4$ is physically adsorbed upon the nickel films.

SUMMARY

The activation energy of the homogeneous decomposition of $Ni(CO)_4$ has been shown to be 19.1 kcal mole^{-1}, and the reaction is first order in $Ni(CO)_4$. In the presence of an ionic surface such as sodium chloride, the intermediate postulated in the homogeneous reaction, namely $Ni(CO)_3$, appears to be adsorbed, and recombines with CO, so that the rate of reaction is appreciably reduced.

The activation energy of the heterogeneous reaction has been determined to be 14.3 kcal mole^{-1}. The activated complex is adsorbed $Ni(CO)_4$, which is physically adsorbed and mobile. The heat of adsorption upon the nickel substrate is 7.4 kcal mole^{-1}. The sites of the nickel surface also adsorb CO, which is more firmly bound. The heat of adsorption of CO is 13.3 kcal mole^{-1}, which suggests chemical rather than physical binding.

ACKNOWLEDGMENTS

It is a pleasure to acknowledge financial support of this investigation by the National Research Council and the Advisory Committee on Research of the University of Toronto.

REFERENCES

1. A. Mittasch. Z. physik. Chem. **40**, 1 (1902).
2. C. H. E. Bawn. Trans. Faraday Soc. **31**, 440 (1935).
3. A. P. Garratt and H. W. Thompson. J. Chem. Soc. 1822 (1934).
4. K. Tonosaki and B. Suginuma. Bull Inst. Phys. Chem. Research (Tokyo), **22**, 1012, 1026 (1943).
5. H. Taylor. Can. J. Chem. **33**, 838 (1955).
6. A. Mittasch and E. Kuss. Chem. Ztg. **50**, 125 (1926).
7. M. E. Nordberg. Private communication.

8. A. CRAIG and R. McINTOSH. Can. J. Chem. **30**, 448 (1952).
9. D. M. YOUNG and J. A. MORRISON. J. Sci. Instr. **31**, 90 (1954).
10. F. W. THOMPSON, G. S. ROSE, and J. A. MORRISON. J. Sci. Instr. **32**, 325 (1955).
11. J. DEWAR and H. O. JONES. Proc. Roy. Soc. (London), A, **71**, 427 (1903).
12. HANDBOOK OF CHEMISTRY AND PHYSICS. 40th ed. Chemical Rubber Publishing Co., Ohio. 1958–59.
13. K. TAMARU, M. BOUDART, and H. TAYLOR. J. Phys. Chem. **59**, 801 (1955).
14. S. GLASSTONE, K. J. LAIDLER, and H. EYRING. The theory of rate processes. McGraw-Hill. 1941.
15. C. KEMBALL. Advances in catalysis and related subjects. Vol. 2. Academic Press Inc., New York. 1952.

BIOSYNTHESIS OF SUGARS FOUND IN BACTERIAL POLYSACCHARIDES

PART I. BIOSYNTHESIS OF L-RHAMNOSE

J. K. N. JONES, M. B. PERRY, AND R. J. STOODLEY
Department of Chemistry, Queen's University, Kingston, Ontario

Received November 30, 1961

ABSTRACT

Azotobacter indicum was grown on media which contained D-glucose-1-C^{14}, D-glucose-2-C^{14}, D-glucose-6-C^{14}, D-mannose-1-C^{14}, or D-galactose-1-C^{14}. The radioactive polysaccharides produced were hydrolyzed and the specific activities of the isolated D-glucose and L-rhamnose were measured. The sugars were degraded and the distribution of activity in the individual carbon atoms was determined.

The results suggest that some L-rhamnose is formed from D-glucose by a pathway which involves the breakdown of the glucose carbon skeleton.

INTRODUCTION

The conversion of D-glucose to deoxy sugars of the L-series has received considerable attention. For example, using isotopic tracer techniques the biosynthesis of L-fucose has been studied in bacteria (1–3) and in man (4). The results favor a direct conversion of D-glucose to L-fucose. A similar conclusion (5) has been reached in the case of colitose (3-deoxy-L-fucose). The biosynthesis of L-rhamnose has been investigated in bacteria (6–9) and in plants (10), and again a direct conversion of D-glucose to L-rhamnose is indicated.

Bacterial extracts can transform guanosine diphosphate D-mannose to guanosine diphosphate L-fucose (11) and thymidine diphosphate D-glucose to thymidine diphosphate L-rhamnose (12–14). Intermediates in these interconversions have recently been characterized (15, 16) and they provide strong evidence for the existence of direct pathways, although they do not preclude the existence of alternative pathways in vivo.

Azotobacter indicum produces an extracellular polysaccharide when grown in suitable media containing sugar substrates (17, 18). Studies in this department (19) have shown that, when a peptone medium is used, the polysaccharide contains D-*glycero*-D-*manno*-heptose, D-glucose, D-mannose, D-glucuronic acid, L-rhamnose, and arabinose.

In the present paper the results of growing the organism in a peptone medium, containing a variety of C^{14}-labelled hexoses, are reported. The polysaccharides were hydrolyzed and the distribution of activity in the carbon atoms of D-glucose and L-rhamnose was determined. The possible origin of the heptose sugar will be discussed in a future communication.

EXPERIMENTAL

Materials

The radioactive sugars were purchased from Merck and Co., Montreal, Que. *A. indicum*-446 was kindly supplied from the Culture Collection of the National Research Laboratories, Ottawa, Ontario.

Determination of Radioactivity

Carbon dioxide was precipitated as barium carbonate. Hydrazones, dimedon derivatives, iodoform, and barium carbonate were plated in triplicate on sintered-glass planchets (6–12 mg per plate). The samples were counted in a proportional methane gas flow counter. The barium carbonate self-absorption curve was used to correct all solid samples to their activity at "infinite thickness" (20).

Liquid samples containing radioactive sugars were evaporated on aluminum plates and counted at "infinite thinness". The activity was converted to microcuries (μc), assuming 50% counting efficiency. The values are not absolute and should not be directly compared with the activities of solid samples.

Growth of A. indicum and Isolation of Polysaccharide

The culture medium contained dipotassium hydrogen phosphate (12 mg), magnesium sulphate (5 mg), calcium carbonate (500 mg), peptone (25 mg), sugar (1.00 g with 100 μc activity), and distilled water (25 ml). The suspension was autoclaved and inoculated with *A. indicum*, growing in a similar liquid medium. Sterile, carbon dioxide free air was slowly drawn through the medium; the evolved carbon dioxide was collected in a trap containing 2 *N* sodium hydroxide (200 ml). The specific activity of the carbon dioxide was determined.

Generally, the medium became quite viscous after 7–10 days. After about 2 weeks the medium was diluted with water (25 ml) and shaken to dissolve the slime which accumulated on the flask wall. The suspension was centrifuged (12,000 r.p.m. for 90 minutes) and the clear supernate was poured into ethanol (2 vol.). The gel-like precipitate was collected by centrifugation, washed with 60% ethanol (4×), absolute ethanol (2×), acetone, and ether, and dried in a vacuum desiccator containing silica gel. The supernate and ethanol washings were combined and evaporated to a syrup, which was dried.

In a control experiment radioactive glucose was added to a non-radioactive solution of polysaccharide. When the polysaccharide was isolated in the above manner it contained no appreciable activity.

The yields of extracellular polysaccharide and carbon dioxide produced, when *A. indicum* was grown in media containing C^{14}-labelled sugars, are shown in Table I.

TABLE I

Yields of extracellular polysaccharide and evolved carbon dioxide

Sugar substrate	Weight of sugar (g)	Time of growth (days)	Weight of polymer isolated (g)	Weight of substrate recovered (g)	Yield of polymer (%)	Yield of CO_2 (%)
D-Glucose-U-C^{14}	1.00	12	0.149	0.585	36	65
D-Glucose-1-C^{14}	1.00	22	0.150	0.480	29	58
D-Glucose-2-C^{14}	1.00	14	0.095	0.591	23	85
D-Glucose-6-C^{14}	1.00	18	0.174	0.461	32	74
D-Mannose-1-C^{14}	1.00	14	0.224	0.415	38	65
D-Galactose-1-C^{14}	1.00	14	0.156	0.507	32	73

The specific activities of the sugar substrates and evolved carbon dioxide are shown in Table II.

TABLE II

Specific activities of evolved carbon dioxide, hydrolyzates, and isolated sugars

Sugar substrate	Specific activity of sugar (μc/mmole C)	Specific* activity of CO_2 (μc/mmole C)	Specific activity of hydrolyzate (μc/mmole C)	Specific activities of sugars (μc/mmole C)	
				Glucose	Rhamnose
D-Glucose-U-C^{14}	3.00	1.73	2.36	—	—
D-Glucose-1-C^{14}	3.00	1.46	1.80	3.12	2.73
D-Glucose-2-C^{14}	3.00	1.42	1.88	3.09	2.80
D-Glucose-6-C^{14}	3.00	1.08	1.94	2.89	2.05
D-Mannose-1-C^{14}	3.00	1.60	2.05	3.03	2.93
D-Galactose-1-C^{14}	3.00	1.62	2.09	3.04	2.86

*The average molecular weight of the sugars in the hydrolyzate was taken to be 180.

Hydrolysis of Polysaccharide

The polysaccharide was hydrolyzed with 90% formic acid for 7.5 hours at 100° C in a sealed tube. After evaporation, *N* sulphuric acid was added to the syrup. The solution was heated on a boiling-water bath for 5 hours, neutralized (barium carbonate), filtered, and passed through Amberlite IR 120 (H^+) ion-exchange resin. The eluate was evaporated to a syrup, which was dried in a vacuum desiccator containing silica gel. Usually 50–60% by weight of the polysaccharide was recovered as monosaccharides. The specific activity of the hydrolyzate was measured and is shown in Table II.

Isolation of Radioactive Sugars

The No. 3 MM Whatman paper on which the hydrolyzates were fractionated was prewashed with the developing solvent—butan-1-ol–pyridine–water (10:3:3, v/v). Sugars were fractionated by multiple development (21) using developing times of 16, 12, 12, and 17 hours. The chromatograms were placed in contact with X-ray films for 8 days and the areas containing radioactive sugars were eluted with water. The eluates

which contained glucose and rhamnose were diluted to known volumes. The concentration of these sugars was estimated on triplicate samples by the phenol – sulphuric acid method (22). The specific activities of these sugars are recorded in Table II.

"Carrier" D-glucose and L-rhamnose were added to their respective solutions, which were then evaporated to syrups. Glucose was crystallized from aqueous ethanol, and rhamnose from moist acetone.

Degradation of L-*Rhamnose*

L-Rhamnose was degraded by the reactions outlined in Fig. 1.

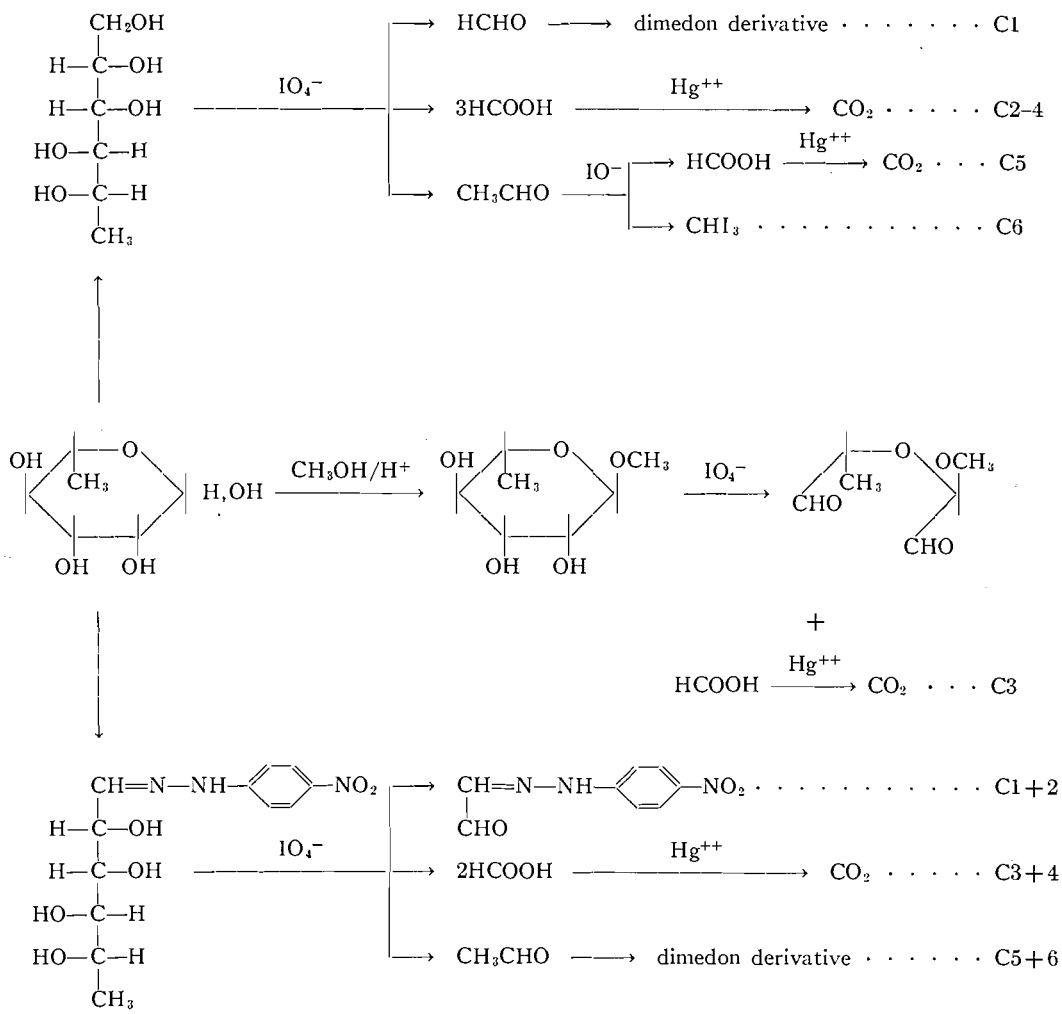

FIG. 1. Degradation of L-rhamnose-C^{14}.

Determination of C^{14} *in C1, C2–4, C5, and C6*

L-Rhamnitol was prepared *in situ* by reducing L-rhamnose (20 mg) with 1% sodium borohydride (2 ml). Excess borohydride was destroyed after 12 hours by the addition of 2 *N* sulphuric acid. The rhamnitol was oxidized by the procedure developed by Nicolet and Shinn (23). Phosphate buffer at pH 8 (10 ml) was added to the solution together with glycine (200 mg) and 0.3 *M* sodium metaperiodate (1.5 ml). Nitrogen was bubbled through the solution to remove acetaldehyde (C5+6), which was collected in 2% sodium metabisulphite. The bisulphite solution was concentrated *in vacuo* to a small volume and potassium carbonate (1.0 g) was added (24) followed by 9 *N* potassium hydroxide (0.05 ml) and 0.1 *M* iodine in 20% potassium iodide (2 ml). The iodoform (C6) was collected by filtration after 15 minutes, washed well with water,

and plated. The plates were dried *in vacuo* over silica gel and their specific activities determined. The material, m.p. 117–118° C, was obtained in 30–35% yield. The filtrate and washings were acidified with 2 *N* sulphuric acid and iodine was destroyed by the addition of dilute sodium thiosulphate. The solution was neutralized and the formic acid (C5) was oxidized to carbon dioxide with mercuric acetate (25) in about 30% yield.

The solution obtained after removal of acetaldehyde contained formaldehyde (C1) and formic acid (C2–4); it was acidified with acetic acid, and dimedon was added. The formaldehyde dimedon was collected after 20 hours and was obtained in about 70% yield, after recrystallization from aqueous ethanol; m.p. 188° C. The derivative was dried in a vacuum desiccator containing silica gel and its specific activity determined. The formic acid in the filtrate was oxidized to carbon dioxide (25) in about 70% yield, and its specific activity was determined.

Determination of C^{14} in C1–6

L-Rhamnose *p*-nitrophenylhydrazone was prepared in the usual manner in yields of 80–85%; m.p. 190–192° C. Portions of the hydrazone (ca. 8 mg) were ground to a fine powder in ether and the suspensions were plated. The plates were dried in an oven at 100° C for 15 minutes and their specific activities were determined.

Determination of C^{14} in C1+2 and C5+6

The *p*-nitrophenylhydrazone (50 mg) was dissolved in pH 8 phosphate buffer (8 ml), and 0.3 *M* sodium metaperiodate (1.5 ml) was added to the chilled solution. Glyoxal *p*-nitrophenylhydrazone (C1+2), which precipitated within a few seconds, was removed by centrifugation and recrystallized from aqueous acetone. The material was obtained in 50–60% yield; m.p. 198–200° C; it was plated and dried in a vacuum desiccator prior to the determination of its specific activity.

Nitrogen was bubbled through the supernate and the acetaldehyde was collected in an ice-cold solution of dimedon at pH 4.3 (26). The precipitated derivative was collected after 20 hours by filtration, and, after recrystallization from aqueous ethanol, was obtained in 30–40% yield; m.p. 139–140° C. The specific activity of C5+6 was determined.

Determination of C^{14} in C3

L-Rhamnose (50–100 mg) was dissolved in methanolic hydrogen chloride (2 ml concentrated hydrochloric acid in 100 ml methanol) and the solution refluxed for 10 hours. The solution was diluted with water and passed through Duolite A4 (OH^-) resin. The eluate was concentrated to a syrup and fractionated chromatographically on Whatman No. 3 MM paper using a neutral solvent—butan-1-ol–ethanol–water (3:1:1, v/v). End strips of the chromatogram were sprayed with silver nitrate (27) and the area of paper containing methyl α-L-rhamnopyranoside was eluted with water. The solution was concentrated, and the syrup allowed to crystallize. When a sufficient quantity of glycoside was available it was recrystallized from ethyl acetate; m.p. 100–101° C.

The glycoside (30–40 mg) was dissolved in water (1 ml) and oxidized with 0.3 *M* periodic acid (1 ml). After 2.5 hours the solution was passed through Duolite A4 (OH^-) resin, which was then washed with water (100 ml). The column was washed with 0.2 *M* barium hydroxide (15 ml) and water (30 ml). The eluate was neutralized with 3 *N* sulphuric acid and the formic acid (C3) oxidized to carbon dioxide in the usual manner (25).

Degradation of D-*Glucose*

Determination of C^{14} in C1+6 and C2–5

D-Glucitol was prepared *in situ* by reducing D-glucose (15 mg) with 1% sodium borohydride (2 ml). Excess borohydride was destroyed after 12 hours by the addition of 2 *N* sulphuric acid. Phosphate buffer at pH 8 was added to the solution together with 0.3 *M* sodium metaperiodate (1.5 ml). Barium acetate was added after 2 hours and the insoluble barium salts were removed by filtration. The solution was acidified with acetic acid and dimedon was added. The formaldehyde dimedon was collected after 20 hours and recrystallized from aqueous ethanol; m.p. 188° C. The material was obtained in 70% yield and was used to determine the specific activity of C1+6. The specific activity of C2–5 was measured by oxidizing the formic acid in the filtrate to carbon dioxide (25).

Determination of C^{14} in C1–6

Glucose (4–6 mg) was oxidized to carbon dioxide by Van Slyke's procedure (28) and its specific activity determined. Glucose *p*-nitrophenylhydrazone was prepared in 70–75% yield; m.p. 188–189° C. The specific activity of C1–6 was determined by directly counting the hydrazone.

Determination of C^{14} in C1+2 and C6

Glucose *p*-nitrophenylhydrazone was oxidized in a manner similar to that described for rhamnose *p*-nitrophenylhydrazone. Glyoxal *p*-nitrophenylhydrazone (C1+2) was recrystallized from aqueous acetone and its specific activity was determined. Dimedon was added to the filtrate and the formaldehyde dimedon was collected after 20 hours. The derivative, after recrystallization from aqueous ethanol, was obtained in about 50% yield; it was used to determine the specific activity of C6.

The specific activities of the fragments obtained during the degradation of rhamnose are recorded in Table III.

TABLE III

Specific activities of rhamnose fragments (c.p.m./mmole C)

Rhamnose carbons	Sugar substrate				
	G-1-C^{14}	G-2-C^{14}	G-6-C^{14}	M-1-C^{14}	Gal-1-C^{14}
C1–6	10,170	20,010	19,380	22,060	18,940
C1+2	23,780	46,900	5,250	45,670	39,080
C5+6	4,350	6,560	46,170	12,460	5,490
C1	44,610	13,780	13,610	91,840	—
C2–4	1,310	31,540	0	1,860	2,570
C5	2,300	—	0	2,300	3,120
C6	6,230	0	97,250	24,270	8,690
C3	1,970	7,870	—	2,460	3,940

NOTE: G = glucose, M = mannose, Gal = galactose.

The specific activities of the fragments obtained during the degradation of glucose are shown in Table IV.

TABLE IV

Specific activities of glucose fragments (c.p.m./mmole C)

Glucose carbons	Sugar substrate				
	G-1-C^{14}	G-2-C^{14}	G-6-C^{14}	M-1-C^{14}	Gal-1-C^{14}
C1–6*	8,730	18,600	25,440	31,590	13,320
C1–6†	—	19,140	26,100	29,250	11,970
C1+2	21,960	50,760	6,390	80,100	34,020
C6	4,140	2,340	159,840	32,000	13,500
C1+6	21,690	7,200	79,020	84,060	36,720
C2–5	1,000	25,250	590	2,570	2,610

NOTE: G = glucose, M = mannose, Gal = galactose.
*Determined by Van Slyke oxidation (28) of glucose.
†Determined by directly counting glucose *p*-nitrophenylhydrazone.

The percentage distribution of activity in the carbon atoms of L-rhamnose and D-glucose is shown in Table V. The specific activities shown in Tables III and IV were multiplied by the number of carbon atoms they represented to give total activities. The total activity of the rhamnose molecule was calculated by summing the activities of C1, C2–4, C5, and C6. Generally, this value corresponded (±7%) with the activity of C1–6, determined by an independent method. The total activity of the glucose molecule was calculated by summing the activities of C1+6 and C2–5. The value corresponded (±7%) with the activity of C1–6, determined by two independent methods. When D-glucose-6-C^{14} was the substrate the value obtained for C6 was slightly greater than that of C1+6. In this case the total activity was compounded from the sum of the activities of C1+2, C2–5, and C6.

TABLE V

Distribution of C^{14} in individual carbon atoms of isolated sugars

Sugar substrate	Sugar isolated	C^{14} as % total in monosaccharide					
		C1	C2	C3	C4	C5	C6
G-1-C^{14}	Rhamnose	78	←——	7	—→	4	11
	Glucose	83	←————	8	———→		9
G-2-C^{14}	Rhamnose	11	66	7	5	11	0
	Glucose	10	77	←———	11	——→	2
G-6-C^{14}	Rhamnose	12	←————	0	———→		88
	Glucose	7	←————	1	———→		91
M-1-C^{14}	Rhamnose	74	←——	4	—→	2	20
	Glucose	76	←————	6	———→		18
Gal-1-C^{14}	Rhamnose	80	←——	8	—→	3	9
	Glucose	72	←————	12	———→		16

NOTE: G = glucose, M = mannose, Gal = galactose.

DISCUSSION

A. indicum was grown in aerated, buffered media which contained C^{14}-labelled sugar substrates. Generally about 30% of the sugar utilized was converted to extracellular polysaccharide and most of the remainder was oxidized to carbon dioxide.

The specific activity of the evolved carbon dioxide was substantially lower than that of the sugar substrate, even when D-glucose-U-C^{14} was the substrate. This isotope dilution may be due to peptone in the medium serving as an additional carbon source. Also, acidic materials may be liberated into the medium by the bacteria, displacing inactive carbon dioxide from calcium carbonate. Furthermore an exchange reaction between metabolic carbon dioxide and inactive carbonate may occur. Nevertheless, the specific activity of carbon dioxide evolved during the D-glucose-6-C^{14} growth was noticeably lower than in the other cases, indicating that the hexose monophosphate shunt is probably operating in the organism.

The isolated polysaccharides were hydrolyzed and usually 50–60% of their weight was recovered. However, although the specific activities of the hydrolyzates were quite similar, they were lower than those of the original substrates, indicating that they contained inactive materials.

The specific activities of the isolated glucose and rhamnose were determined. They were usually quite similar to each other and to the specific activities of the original substrates. However, the specific activity of L-rhamnose isolated from the D-glucose-6-C^{14} growth was approximately 30% lower than in the other cases. This result is believed to be significant and indicates that C6 of D-glucose contributes only about 70% as much to the L-rhamnose skeleton as does C1 or C2 of D-glucose or C1 of D-mannose and D-galactose.

A number of degradations of L-rhamnose have been reported in the literature. In this work rhamnose of low specific activity was occasionally isolated and it was necessary to devise a procedure which required less than 1 mmole of sugar. Quite often the majority of the activity is found in the terminal carbon atoms and it is then unnecessary and time consuming to use a procedure which gives the activity of each carbon atom. It is an advantage, therefore, to use a procedure which initially gives the activity of the terminal carbon atoms.

Hauser and Karnovsky (6) oxidized potassium rhamnonate to carbon dioxide (C1), formic acid (C2–4), and acetaldehyde (C5+6). However, about 0.5 mmole of rhamnose is required for this degradation, and in one case (8) poor recoveries of activity were reported. The same information can be readily obtained by oxidation of rhamnitol, using the procedure of Nicolet and Shinn (23), and only about 0.12 mmole of sugar is required.

Rhamnose phenylosazone has been used (6) to determine the activity of C1–3, C4, and C5+6. However, on a 0.5-mmole scale the present authors were unable to obtain better than 25% yield of recrystallized osazone. Rhamnose *p*-nitrophenylhydrazone could be prepared in over 80% yield and was therefore used to determine the specific activities of C1+2 and C5+6.

The isotope content of C3 was determined by periodate oxidation of methyl α-L-rhamnopyranoside. Watkin and Neish (10) have recently described a method for degrading rhamnose which involves the periodate oxidation of its glycopyranosides. The specific activities of C2, C3, C4, C5, and C6 were determined directly while that of C1 was calculated by difference, about 1 mmole of rhamnose being required for the degradation.

The degradative studies revealed that about $77 \pm 6\%$ of the activity was retained in C1 of the isolated monosaccharides, when D-glucose-1-C^{14}, D-mannose-1-C^{14}, or D-galactose-1-C^{14} were substrates. The majority of the remaining radioactivity was located in C6 of the hexoses.

When D-glucose-6-C^{14} served as substrate most of the activity was recovered in C6 of the hexoses (90±2%). The remaining activity was found in C1 of these sugars.

Approximately 72±6% of the activity was recovered in C2 and 10% in C5 of D-glucose and L-rhamnose, when D-glucose-2-C^{14} was substrate. In addition about 10% of the activity was found in C1 of these sugars. The latter result further indicates that C1 decarboxylation is occurring and suggests that some of the pentose formed by the hexose monophosphate shunt is reutilized for hexose synthesis. Apparently about 10% of hexose is resynthesized by this route and it can presumably equilibrate with substrate hexose.

About 10% of activity was detected in C6, C5, or C1 of D-glucose and L-rhamnose, when D-glucose-1-C^{14}, D-glucose-2-C^{14}, or D-glucose-6-C^{14} were the respective substrates.

These results suggest that there is a hexose pool which at equilibrium contains about 20% of hexose resynthesized from equilibrated trioses (formed from D-fructose 1,6-diphosphate via the Embden–Meyerhof pathway) and about 10% of hexose resynthesized from pentose (produced by the hexose monophosphate shunt) by the action of transketolase.

The specific activity of L-rhamnose derived from D-glucose-6-C^{14} was about 30% lower than that derived from 1-C^{14}-labelled precusors, and so it will be assumed that 70% of L-rhamnose is synthesized directly from D-glucose. This transformation probably proceeds via the thymidine diphosphate derivatives (12–14) and requires three epimerizations and a reduction of $—CH_2OH$ to $—CH_3$. An intermediate in this interconversion, the thymidine diphosphate derivative of 6-deoxy-4-oxo-D-glucose, has recently been isolated from a cell-free enzyme system of *Pseudomonas aeruginosa* (16). Presumably a second pathway, involving scission of the glucose carbon skeleton, contributes to rhamnose biosynthesis in *A. indicum*. A possible route, which has not been demonstrated experimentally, may involve the transfer of a dihydroxy acetone unit from D-fructose 6-phosphate to L-pyruvaldehyde (produced by glycolysis) by the action of transaldolase. The resultant 6-deoxy-L-sorbose might then be converted to L-rhamnulose.

It is interesting to note that the same sugar can form different nucleotides. For example, glucose can form uridine diphosphate glucose and thymidine diphosphate glucose, which presumably results in a channelling of the sugar to different metabolic pathways. If glucose 1-phosphate and the glucose nucleotides can act as glycosyl donors in polysaccharide synthesis, then different linkages may be produced in the polysaccharide chain.

There are a number of other studies on the biosynthesis of L-rhamnose using isotopic tracer techniques. Hauser and Karnovsky (6, 7) have studied the biosynthesis of the rhamnolipide produced by *P. aeruginosa*. They found that glycerol and propanediol could serve equally well for L-rhamnose synthesis. Degradation of L-rhamnose indicated that it was formed by the combination of two triose units. When D-glucose-6-C^{14} in the presence of inactive glycerol was the substrate, the rhamnose contained 35% of its activity in C1 and 48% in C6. On the other hand, with D-fructose-6-C^{14} as substrate, 83% of the activity was recovered in C6 of L-rhamnose. These results presumably reflect fundamental metabolic differences of the two sugars. Although the results indicate that L-rhamnose is formed from two triose units, it is possible that a hexose precursor is first formed which is then directly transformed to L-rhamnose.

Southard and co-workers (8) have investigated the conversion of D-glucose-1-C^{14} and D-glucose-6-C^{14} to L-rhamnose of streptococcal cell walls. Although only 60–80% of the total activity was recovered in their degradations, the majority of activity was retained in the terminal carbon atoms. However, the specific activity of the L-rhamnose isolated

from D-glucose-6-C^{14} was about 30% higher than that derived from D-glucose-1-C^{14}. It would be necessary to isolate and degrade bacterial glucose to determine the significance of this result.

Taylor and Juni (9) have studied the biosynthesis of D-glucose and L-rhamnose in a bacterial capsular polysaccharide. Unlabelled polysaccharide was isolated when D-glucose-1-C^{14} and D-glucose-2-C^{14} were the substrates. However, with D-glucose-6-C^{14}, the isolated D-glucose and L-rhamnose contained twice the initial specific activity. The bacterial D-glucose was not degraded but the L-rhamnose contained 50% of its activity in C1 and 43% in C6. The results indicated that the polysaccharide was derived only from C4, C5, and C6 of D-glucose. It was not possible to decide whether L-rhamnose arose directly from trioses or from a six-carbon sugar which was synthesized from the trioses.

Recently, Watkin and Neish have studied the biosynthesis of L-rhamnose from D-glucose in buckwheat (10). These authors showed that the isolated D-glucose and L-rhamnose possessed similar specific activities and distributions of activity, suggesting a direct conversion of D-glucose to L-rhamnose.

Whatever interpretation is placed upon the results presented in this paper, there appears to be a pathway for L-rhamnose biosynthesis which involves the breakdown of the glucose carbon skeleton.

ACKNOWLEDGMENTS

The authors are grateful to Dr. G. B. Krotkov and Dr. C. D. Nelson of the Biology Department of Queen's University for making available the counting apparatus. They are indebted to the National Research Council for grants (T-39 and N.R.C. 706) and for the award of a Studentship (to R. J. S.).

REFERENCES

1. S. SEGAL and Y. J. TOPPER. Biochim. et Biophys. Acta, **25**, 419 (1957).
2. E. C. HEATH and S. ROSEMAN. J. Biol. Chem. **230**, 511 (1958).
3. J. F. WILKINSON. Nature, **180**, 995 (1957).
4. S. SEGAL and Y. J. TOPPER. Biochim. et Biophys. Acta, **42**, 147 (1960).
5. M. A. CYNKIN and G. ASHWELL. Bacteriol. Proc. (Soc. Am. Bacteriologists), 161 (1960).
6. G. HAUSER and M. L. KARNOVSKY. J. Biol. Chem. **224**, 91 (1957).
7. G. HAUSER and M. L. KARNOVSKY. J. Biol. Chem. **233**, 287 (1958).
8. W. H. SOUTHARD, J. A. HAYASHI, and S. S. BARKULIS. J. Bacteriol. **78**, 79 (1959).
9. W. H. TAYLOR and E. JUNI. J. Biol. Chem. **236**, 1231 (1961).
10. J. E. WATKIN and A. C. NEISH. Phytochem. **1**, 52 (1961).
11. V. GINSBURG. J. Biol. Chem. **235**, 2196 (1960).
12. S. KORNFELD and L. GLASER. Biochim. et Biophys. Acta, **42**, 548 (1960).
13. J. H. PAZUR and E. W. SHUEY. J. Am. Chem. Soc. **82**, 5009 (1960).
14. N. L. BLUMSOM and J. BADDILEY. Biochem. J. **81**, 114 (1961).
15. V. GINSBURG. J. Biol. Chem. **236**, 2389 (1961).
16. S. KORNFELD and L. GLASER. J. Biol. Chem. **236**, 1795 (1961).
17. J. P. MARTIN. J. Bacteriol. **50**, 349 (1945).
18. C. QUINNELL, S. KNIGHT, and P. W. WILSON. Can. J. Microbiol. **3**, 277 (1957).
19. W. SOWA. Personal communication.
20. M. L. KARNOVSKY, J. M. FOSTER, L. I. GIDEZ, V. D. HAGERMAN, C. V. ROBINSON, A. K. SOLOMON, and C. A. VILLEE. Anal. Chem. **27**, 852 (1955).
21. A. JEANES, C. S. WISE, and R. J. DIMLER. Anal. Chem. **23**, 415 (1951).
22. M. DUBOIS, K. A. GILLES, J. K. HAMILTON, P. A. REBERS, and F. SMITH. Anal. Chem. **26**, 350 (1956).
23. B. H. NICOLET and L. A. SHINN. J. Am. Chem. Soc. **63**, 1456 (1941).
24. G. EHRENSVARD, L. REIO, E. SALUSTE, and R. STJERNHOLM. J. Biol. Chem. **189**, 93 (1951).
25. H. D. WIEKE and B. JACOBS. Ind. Eng. Chem., Anal. Ed. **8**, 44 (1936).
26. M. BRIN and R. E. OLSON. J. Biol. Chem. **199**, 475 (1952).
27. W. E. TREVELYAN, D. P. PROCTOR, and J. S. HARRISON. Nature, **166**, 444 (1950).
28. D. D. VAN SLYKE, J. PLAZIN, and J. R. WEISIGER. J. Biol. Chem. **192**, 299 (1951).

TRYPTAMINES, CARBOLINES, AND RELATED COMPOUNDS

PART X. AN ALTERNATIVE SYNTHESIS, AND THE NITRATION, OF δ-CARBOLINE[1]

R. A. ABRAMOVITCH AND K. A. H. ADAMS
Department of Chemistry, University of Saskatchewan, Saskatoon, Saskatchewan

Received January 10, 1962

ABSTRACT

δ-Carboline, together with β-carboline, has been synthesized in reasonably good yield by the Fischer cyclization of cyclohexanone 3-pyridylhydrazone followed by dehydrogenation of the separated tetrahydro derivatives. The isomer ratios of products formed in this and similar reactions are discussed. Nitration of δ-carboline gives a mixture of the 6- and 8-nitro derivatives, the latter being the predominant product. The magnitude of the dipole moment of δ-carboline is appreciably higher than that predicted from molecular orbital calculations (15).

The first unambiguous synthesis of δ-carboline* (I) was described in Part VIII of this series (1), in which the cyclization of 3-azido-2-phenylpyridine was reported to give variable yields of (I). In order to study the substitution reactions of this ring system a synthesis giving more reproducible yields was required. An alternative method of obtaining the δ-carboline ring system was sought and found in the Fischer cyclization of cyclohexanone 3-pyridylhydrazone (II).

The Fischer cyclization of pyridylhydrazones has been found by a number of workers to take place with greater difficulty than the cyclization of the corresponding phenylhydrazones. Perkin and Robinson were unable to effect the cyclization of acetone 2-quinolylhydrazone (2), and Fargher and Furness (3) and Okuda and Robison (4) obtained similar negative results using a number of 2-pyridylhydrazones. Clemo and Holt prepared 1-methyl-5,6,7,8-tetrahydro-β-carboline in low yield from cyclohexanone 2-methyl-3-pyridylhydrazone and zinc chloride (5). A moderate yield of 5,6,7,8-tetrahydro-α-carboline was obtained by heating cyclohexanone 2-pyridylhydrazone with polyphosphoric acid (4). Ficken and Kendall have recently examined the cyclization of the pyridylhydrazones of isopropylmethyl ketone to give the corresponding azaindole derivatives (6). They found that heating with zinc chloride to a relatively high temperature (210–250°) was necessary to effect ring closure. It is interesting to note, as well, that isopropylmethyl ketone 3-pyridylhydrazone was reported by these authors to give exclusively 2,3,3-trimethyl-3H-4-azaindole; i.e. cyclization had occurred at the α-position of the pyridine ring only. Similarly, Takahashi, Saikachi, Goto, and Shimamura (7) obtained 5-chloro-2-methyl-4-azaindole from acetone 2-chloro-5-pyridylhydrazone.

3-Hydrazinopyridine reacted with cyclohexanone to give the required cyclohexanone 3-pyridylhydrazone (II), which was somewhat unstable in air but could be kept for long periods in a closed container in the refrigerator. Cyclization was effected by fusion of (II) with zinc chloride at 250° and gave a high yield (94%) of a mixture of 6,7,8,9-tetrahydro-δ-carboline (III) (63%) and 5,6,7,8-tetrahydro-β-carboline (IV) (37%). The structures of (III) and (IV) were established by dehydrogenation to the corresponding fully aromatic structures. The dehydrogenations were carried out by heating the compound with 10% palladium–charcoal in boiling mesitylene; the catalyst became poisoned

[1]*Part IX: R. A. Abramovitch and K. A. H. Adams. Can. J. Chem.* **39**, *2516 (1961).*

**The trivial names α-, β-, and δ-carboline have been used throughout this paper and in previous papers in this series. They are acceptable according to the Definitive I.U.P.A.C. 1957 Rules for Nomenclature, and refer to 9H-pyrido[2,3-b]indole, 9H-pyrido[3,4-b]indole, and 5H-pyrido[3,2-b]indole (Ring Index), respectively.*

after about half the reaction had occurred and a second batch had to be added. The mixture of tetrahydro derivatives could be separated by chromatography on a column of alumina, when the δ-carboline derivative was eluted first, followed by the β-compound. The order of elution is similar to that reported by Abramovitch (8) for the separation of mixtures of *ind-N*-methyl-δ-carboline and *ind-N*-methyl-β-carboline. The cyclization of cyclohexanone 3-pyridylhydrazone was found to give very reproducible yields, thus providing a good route to the δ-carboline ring system.

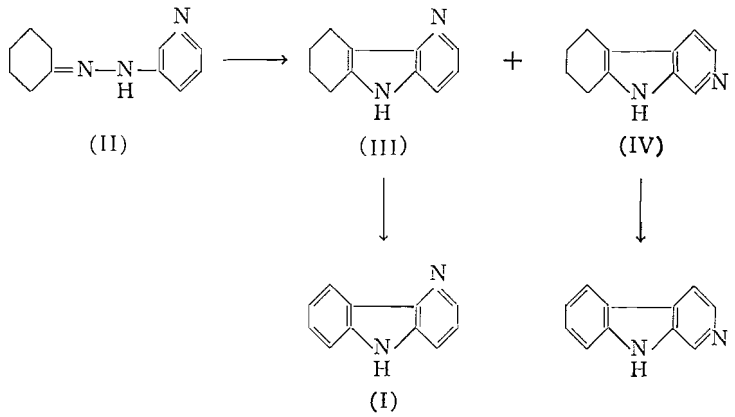

The observation that ring closure at the 2-position of the pyridine ring predominates is in agreement with the results of Ficken and Kendall (6) but differs in that these authors did not observe any cyclization to the 4-position of the pyridine nucleus. In pyridine derivatives possessing an electron-releasing group in the 3-position electrophilic attack generally leads to substitution in the 2-, rather than the 4-, position (9). This has been discussed by Schofield (10), who suggested that protonation and some form of chelation may be responsible. In the present study, attack at C_2 was favored over attack at C_4 to the extent of about 2:1. In contrast, the Graebe–Ullmann cyclization of 1-β-pyridylbenztriazole apparently results in exclusive substitution at C_4 of the pyridine nucleus (11). Molecular orbital calculations on the pyridine ring itself indicate that the π-electron density in the ground state is greater at the 4- than at the 2-position whereas the atom localization energies (A_e) for a Wheland-type transition state indicate (for pyridine but not pyridinium salts) that electrophilic substitution should be easier at the 2- than at the 4-position (12). A 3-amino substituent may well activate the 2- and 4-positions to different extents. Also, in the case of the Fischer cyclization, particularly that catalyzed by zinc chloride, there is no doubt that the pyridine nitrogen is coordinated with the metal atom. It would seem safe to suggest, however, that "strong" electrophilic reagents which do not make a large electron demand upon the substrate could well substitute into the pyridine ring according to the order of the ground-state π-electron densities at the nuclear carbons, whereas "weak" electrophilic reagents would probably follow the pattern suggested by the atom localization energies, with various shades possible in between, depending upon whether the transition state resembled more the starting materials or a Wheland-type intermediate structure.

The nitration of α- and β-carboline has already been studied. Thus, in the case of α-carboline it has been reported that 6-nitro-α-carboline is obtained exclusively (13), whereas mononitration of β-carboline gives mainly 6-nitro-β-carboline together with a

lesser amount of what was suggested to be the 8-nitro derivative (14). Paoloni (15) has carried out some simple Hückel molecular orbital calculations of the ground-state π-electron densities for the four carbolines. These indicate that, in all cases, C_8 has the highest π-electron density, with C_6 the next highest.* As it is believed that in nitrations the transition state is somewhat closer in electron distribution to the unperturbed ground state than to the Wheland-type intermediate (16) it might have been expected from Paoloni's calculations that substitution at the 8-position* would have been favored (17), which is not the case. The nitration of δ-carboline with concentrated nitric acid has now been studied, and was found to lead to a mixture of two isomeric mononitro derivatives. The major product (56% after recrystallization) separated from the reaction mixture in the form of its salt. The free base did not melt below 360°. The second nitro compound (17% yield) had m.p. 232–233°.

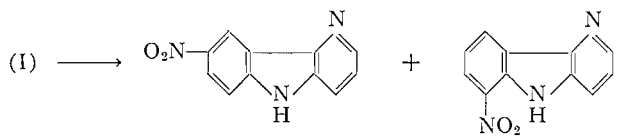

(V) (VI)

By analogy with the nitration of carbazole (18) and of α- and β-carboline, it was initially assumed that the high-melting major product was probably 8-nitro-δ-carboline† (V) while the low-melting isomer was 6-nitro-δ-carboline† (VI). Tentative confirmation of the assignment of structure (VI) to the low-melting isomer was obtained from a study of its infrared and ultraviolet absorption spectra. It was hoped, in particular, that the infrared spectrum would show evidence of the hydrogen bonding possible between the nitro group and the indolic N—H group. The N—H group of the low-melting isomer absorbed at 3420 cm^{-1} (dilute $CHCl_3$ solution), which is a lower frequency than is the N—H stretching band of δ-carboline (3450 cm^{-1}, $CHCl_3$ solution). The N—H group of *N*-methyl-*o*-nitroaniline absorbs at 3415 cm^{-1}. Unfortunately, the extreme insolubility in solvents suitable for infrared studies of the high-melting isomer made it impossible to determine its N—H stretching frequency under the same conditions. Spectra of the nitro compounds measured by the KBr disk technique did not give sharp N—H bands, so that the frequencies could not be accurately determined. The asymmetric and symmetric NO_2 frequencies could, however, be compared in this way. The bands for the low-melting isomer were at 1518 and 1320 cm^{-1} respectively, whereas the corresponding ones for the high-melting isomer appeared at 1528 and 1328 cm^{-1}. The lower frequencies for the low-melting nitro compound could be due to hydrogen bonding, a conclusion similar to that drawn by Hathway and Flett, who studied the infrared spectra of some *o*-nitronaphthylamines (20). It has been reported that *o*-nitroaniline absorbs at longer

Numbering here applies to the α- and β-carbolines. See also the following footnote.

†*Note that the numbering in the γ- and δ-carboline ring systems is different from that in the α- and β-isomers (19).*

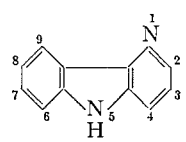

(I)

wavelengths in the ultraviolet than do the para and meta isomers (21). Also, 1-nitrocarbazole absorbs in the visible region at 403 mμ (22). The ultraviolet absorption spectrum of the low-melting nitro-δ-carboline has a band at 385 mμ which tails into the visible region, whereas the high-melting compound does not absorb appreciably in the visible. Finally, the hydrogen-bonded structure is supported by the *relatively* low melting point of (VI).

The structure of the high-melting nitro-δ-carboline as (V) was confirmed by reducing it to the corresponding amine, which gave a positive test for a *p*-phenylenediamine with a primary amino group (23).

An attempt was made to study the pattern of nucleophilic substitution in δ-carboline. When (I) was treated with phenyllithium an insoluble *ind-N*-lithium salt was formed and no further reaction occurred. The reaction was repeated using the very small quantity of *ind-N*-methyl-δ-carboline on hand instead of (I); a low yield of a basic product exhibiting bands at 690 and 765 cm^{-1} (monosubstituted phenyl) was obtained, but in insufficient quantities to permit characterization. Reduction of δ-carboline with sodium and butanol proved to be difficult and in most cases starting material was recovered. Under more vigorous conditions over half of the δ-carboline was unchanged but the crude mixture (from which no other product could be isolated in a pure state) gave a positive Ehrlich test. Acetylation of the crude reaction mixture did not lead to the isolation of any pure reduction product. Catalytic reduction of δ-carboline was also attempted using 5% ruthenium on charcoal at 100° and 1350 p.s.i. of hydrogen; unchanged δ-carboline was recovered. It is not clear why δ-carboline should be more difficult to reduce than the other carbolines.

Paoloni (15) has estimated the dipole moments of the four carbolines from his molecular orbital calculations. His predicted value for δ-carboline is 3.90 D. The dipole moment of δ-carboline in benzene at 20° was kindly determined for us by Dr. G. F Wright and found to be 4.92 D, slightly more than 1 D greater than the calculated value. This result, together with the fact that there is a lack of correspondence between the calculated (15) and measured (1) ultraviolet absorption bands of δ-carboline, point to the limitations of the simple molecular orbital calculations in this case.

EXPERIMENTAL

Melting points are uncorrected. Infrared spectra were measured with a Perkin–Elmer Model 21 instrument equipped with sodium chloride optics. Ultraviolet absorption spectra were measured on a Cary Model 14 recording spectrometer.

Cyclohexanone 3-Pyridylhydrazone

3-Hydrazinopyridine (3.91 g) was heated under reflux with a solution of cyclohexanone (2.8 ml) and pyridine (4 ml) in ethanol for 4 hours. The reaction mixture was poured into water and the crystalline precipitate filtered. Recrystallization of the crude product (4.82 g) from aqueous ethanol (charcoal) gave the *hydrazone* as pale yellow-brown crystals, m.p. 139–141° (decomp.). Calc. for $C_{11}H_{15}N_3$: C, 69.81; H, 7.99. Found: C, 69.73; H, 7.88.

Fischer Cyclization of Cyclohexanone 3-Pyridylhydrazone—6,7,8,9-Tetrahydro-δ-carboline and 5,6,7,8-Tetrahydro-β-carboline

Cyclohexanone 3-pyridylhydrazone (2 g) was intimately mixed with zinc chloride dihydrate (7 g) and the mixture heated in a metal bath at 250–260° (bath temperature) with occasional stirring. After the initial vigorous reaction was over (6 minutes) heating was continued for an additional 5 minutes. The cooled melt was dissolved in 10% hydrochloric acid, filtered to remove a small amount of brown solid, basified with 2 *N* sodium hydroxide, and extracted with ether. The dried (Na_2SO_4) ether solution was evaporated and left behind a brown oil which solidified (1.7 g).

The crude mixture (3.1 g) was chromatographed on a column of neutral alumina. Elution with benzene – light petroleum (b.p. 60–80°) (5:1) gave *6,7,8,9-tetrahydro-δ-carboline* (1.66 g) which, after recrystallization from benzene or from aqueous ethanol, melted at 199–200°. Calc. for $C_{11}H_{12}N_2$: C, 76.71; H, 7.02. Found:

C, 76.71; H, 7.16. λ_{max} 230, 260, 290 mμ; $\epsilon \times 10^{-3}$ 28.30, 9.54, 9.32. Elution with ether–benzene (1:1) gave a brown solid (1 g) which, on recrystallization from aqueous alcohol, gave *5,6,7,8-tetrahydro-β-carboline* as white leaflets, m.p. 197–198°. Found: C, 76.86; H, 7.17. λ_{max} 229, 267, 300 mμ; $\epsilon \times 10^{-3}$ 29.00, 7.45, 5.85.

δ-Carboline

6,7,8,9-Tetrahydro-δ-carboline (1.43 g) was dissolved in hot mesitylene (15 ml), and 10% palladium–charcoal (225 mg) added. The suspension was boiled under reflux for 8 hours, a second lot of catalyst (225 mg) was added, and heating was continued for an additional 10 hours. The reaction mixture was diluted with benzene, the catalyst filtered, and the cooled filtrate saturated with dry hydrogen chloride. The crystalline hydrochloride was filtered, washed with ether, dissolved in water, and the solution made alkaline to give δ-carboline (1.2 g), m.p. 207–208°, after recrystallization from benzene. The melting point was not depressed on admixture with an authentic sample (1) of δ-carboline. The infrared spectra of the two samples were identical. The melting point of the methiodide (249–250°) was not depressed on admixture with an authentic sample of *py-N*-methyl-δ-carbolinium iodide (1).

β-Carboline

Prepared similarly from 5,6,7,8-tetrahydro-β-carboline (300 mg), β-carboline (290 mg) was obtained as fine white needles, m.p. 197–198°. The melting point of the methiodide was not depressed on admixture with an authentic sample (1) of *py-N*-methyl-β-carbolinium iodide.

Nitration of δ-Carboline

δ-Carboline (0.570 g) was stirred with concentrated nitric acid (6 ml) at room temperature for 2 hours, during which time the color of the solution changed to greenish-yellow and a precipitate separated. The precipitate was filtered, washed with water, and stirred with concentrated ammonium hydroxide. The solid was filtered, washed with water and with methanol, and recrystallized from pyridine to give *8-nitro-δ-carboline* (410 mg), m.p. above 360°. An analysis sample was purified by sublimation at 250° at 0.07 mm and recrystallization from pyridine. Calc. for $C_{11}H_7N_3O_2$: C, 61.97; H, 3.31. Found: C, 61.94; H, 3.50.

The acidic filtrate from the nitration mixture was basified with ammonia and extracted with chloroform. The dried (Na_2SO_4) chloroform solution was evaporated to give a bright yellow solid (202 mg), which was purified by chromatography on a column of alumina. Elution with benzene – light petroleum (b.p. 60–80°) gave *6-nitro-δ-carboline* (122 mg) which, after recrystallization from methanol, had m.p. 232–233°. Calc. for $C_{11}H_7N_3O_2$: C, 61.97; H, 3.31. Found: C, 61.66; H, 3.44. The compound was initially obtained in the form of yellow needles. On being kept under cold methanol these gradually changed to prisms having the same melting point.

8-Amino-δ-carboline

8-Nitro-δ-carboline (410 mg) was suspended in concentrated hydrochloric acid (4 ml), and a solution of stannous chloride dihydrate (2.15 g) in concentrated hydrochloric acid (6 ml) was added. The mixture was heated on the steam bath with stirring for 1.5 hours, cooled, and basified. Extraction with ether gave the crude amine (347 mg), which was difficult to purify and which was discolored on standing. It gave a blue-black precipitate when oxidized with potassium persulphate in the presence of aniline, a test characteristic of a *p*-phenylenediamine derivative with a free primary amino group (23). Attempted acetylation of the amine using a procedure described in Vogel's "Practical organic chemistry" (24) led, instead, to the analytically pure *amine monohydrochloride*, m.p. above 300° (from methanol). Calc. for $C_{11}H_9N_3$,HCl: C, 60.14; H, 4.56. Found: C, 60.22; H, 4.20.

ACKNOWLEDGMENTS

This work was carried out during the tenure (by K. A. H. A.) of a C.I.L. Scholarship (1960–1961). Financial support from the National Research Council is gratefully acknowledged. The authors wish to thank Dr. G. F Wright (Toronto) for the determination of the dipole moment of δ-carboline.

REFERENCES

1. R. A. Abramovitch, K. A. H. Adams, and A. D. Notation. Can. J. Chem. **38**, 2152 (1960).
2. W. H. Perkin, Jr. and R. Robinson. J. Chem. Soc. 1973 (1913).
3. R. G. Fargher and R. Furness. J. Chem. Soc. 688 (1915).
4. S. Okuda and M. M. Robison. J. Am. Chem. Soc. **81**, 740 (1959).
5. G. R. Clemo and R. J. W. Holt. J. Chem. Soc. 1313 (1953).
6. G. E. Ficken and J. D. Kendall. J. Chem. Soc. 3202 (1959).
7. T. Takahashi, H. Saikachi, H. Goto, and S. Shimamura. J. Pharm. Soc. Japan, **64**, 7 (1944).
8. R. A. Abramovitch. Can. J. Chem. **38**, 2273 (1960).
9. A. Albert. Heterocyclic chemistry. University of London, Athlone Press, London. 1959. p. 64.
10. K. Schofield. Quart. Revs. (London), **4**, 387 (1950).
11. E. Späth and K. Eiter. Ber. **73**, 719 (1940).

12. R. A. BARNES. *In* The chemistry of heterocyclic compounds. Pyridine and its derivatives. Part I. *Edited by* A. WEISSBERGER. Interscience Publishers, Inc., New York. 1960. pp. 14–16.
13. R. R. BURTNER. U.S. Patent No. 2,690,441 (1954); Chem. Abstr. **49**, 13,297 (1955).
14. H. R. SNYDER, S. M. PARMERTER, and L. KATZ. J. Am. Chem. Soc. **70**, 222 (1948).
15. L. PAOLONI. Gazz. chim. ital. **90**, 1530 (1960).
16. P. B. D. DE LA MARE and J. H. RIDD. Aromatic substitution, nitration and halogenation. Butterworths, London. 1959. pp. 224–225.
17. R. D. BROWN and R. D. HARCOURT. J. Chem. Soc. 3451 (1959).
18. W. FREUDENBERG. *In* Heterocyclic compounds. Vol. III. *Edited by* R. C. ELDERFIELD. John Wiley and Sons, New York. 1952. p. 319.
19. A. M. PATTERSON, L. T. CAPPELL, and D. F. WALKER. The ring index. 2nd ed. American Chemical Society, Washington. 1960. pp. 372–373.
20. D. E. HATHWAY and M. ST. C. FLETT. Trans. Faraday Soc. **45**, 818 (1949).
21. A. BURAWOY, M. CAIS, J. T. CHAMBERLAIN, F. LIVERSEDGE, and A. R. THOMPSON. J. Chem. Soc. 3721 (1955).
22. W. A. SCHROEDER, P. E. WILCOX, K. N. TRUEBLOOD, and A. O. DEKKER. Anal. Chem. **23**, 1740 (1951).
23. F. FEIGEL. Spot tests, organic applications. Vol. II. Elsevier Pub. Co., Amsterdam. 1954. p. 296.
24. A. I. VOGEL. Practical organic chemistry. 3rd ed. Longmans, Green and Co., London. 1957. p. 652.

ENERGY BARRIERS AND STRUCTURE OF *cis*-, MUCO-, AND ALLO-INOSITOL HEXAACETATES IN SOLUTION[1]

S. BROWNSTEIN
Division of Applied Chemistry, National Research Council, Ottawa, Canada
Received September 29, 1961

ABSTRACT

The proton resonance spectra of *cis*-, muco-, and allo-inositol hexaacetates as a function of temperature yield enthalpies of activation and Arrhenius factors for some of the skeletal oscillations of the six-membered ring.

INTRODUCTION

When the location of substituents on a cyclohexane ring is such that one conformation is strongly favored, proton resonance spectroscopy may often be used to determine axial and equatorial substituents and the conformation of the ring (1–4). In those cases where rapid inversion of the chair form of the cyclohexane ring exchanges the substituents between axial and equatorial positions only an averaged signal is observed. However, by lowering the temperature to reduce the rate of inversion it is often possible to observe the individual conformations and determine the rate of inversion (5–9). When the rate of exchange of a substituent between an axial and equatorial position is comparable to the difference in chemical shift between them, the spectral lines corresponding to the individual positions merge to a single averaged line. This yields a single rate measurement, and an Arrhenius factor of 10^{13} has been assumed to obtain the enthalpy of activation. Quantitative calculations of line shape as a function of exchange rate have been made (10–12), enabling exchange rates to be determined over a temperature range. In the cyclohexane system for those cases where the Arrhenius factor was obtained by nuclear magnetic resonance methods values of $10^{10.1}$, $10^{14.3}$, and $10^{16.6}$ were found (6, 9).

The results obtained in the present study also indicate that the "normal" Arrhenius factor may be a poor approximation in the cyclohexane system.

An investigation of ring inversions for some monosubstituted cyclohexanes by ultrasonic relaxation yields "normal" Arrhenius factors (13). The activation energies are in agreement with those obtained by proton resonance measurements (7). From the limited results available it is difficult to determine under what circumstances "normal" Arrhenius factors may be assumed. It is also proposed that the ring inversion may occur via a chair–planar–chair pathway analogous to the Alg vibrational mode in cyclohexane (13). The limited data presently available suggest that a solution of the problem of ring inversions in the cyclohexane system will require careful examination of many more compounds. The results for a few compounds are presented in this paper.

DISCUSSION

The geometrical relationship of the substituents in *cis*-, allo-, and muco-inositol hexaacetate as a planar model and in the chair forms is shown in Fig. 1. The acetate groups are shown but the protons attached to the cyclohexane ring are not indicated. In these three isomers an inversion of the chair form of the cyclohexane ring causes the three

[1]*Issued as N.R.C. No. 6742.*

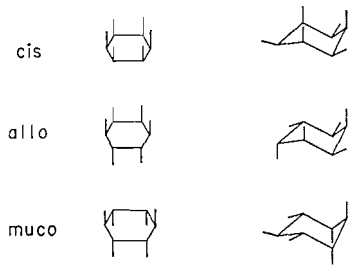

FIG. 1. The relationship of the substituents in *cis*-, allo-, and muco-inositol hexaacetates.

axial substituents to become equatorial and vice versa, resulting in an identical conformation. Therefore changes in the proton resonance spectrum with temperature will only reflect a change in the inversion rate since contributions from varying amounts of two conformations cannot occur.

In Fig. 2 some representative spectra of these compounds are shown. The rate constants are obtained by fitting the observed spectra with those theoretically calculated in the

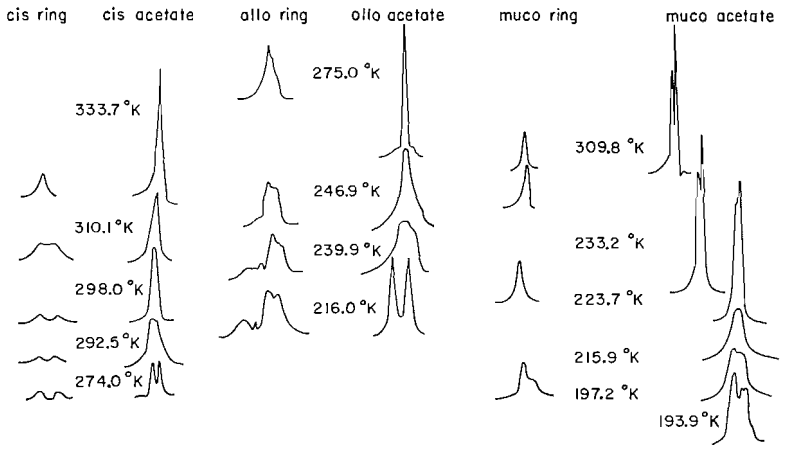

FIG. 2. Proton resonance spectra of inositol hexaacetates.

case of the cis and allo isomers (12, 14). For the muco isomer two magnetic averaging mechanisms are occurring. The one which is observed at low temperatures yields a complex pattern of overlapping lines which cannot be rigorously analyzed. However, the rate of this averaging process can be estimated as 12.5 sec^{-1} at 197.2° K from the coalescence of the individual peaks at this temperature. If the assumption is made that the Arrhenius factor for this averaging process is the mean of those observed for the cis and allo isomers an enthalpy of activation of 4.7 kcal/mole is obtained. There will be considerable uncertainty in this value because of the approximate nature of the rate and the assumption of a value for the Arrhenius factor. The magnetic averaging which is observed at high temperatures causes the merging of the two sharp peaks due to the acetate protons.

It was not possible to obtain sufficiently high temperatures to cause complete merging of the separate acetate peaks in the muco isomer. The rates were calculated from the decrease in separation of the lines, assuming they had a negligible width (15). The results

are plotted in Fig. 3 and the thermodynamic quantities are listed in Table I. These were derived from a least-squares fit of the experimental points except for the low-temperature

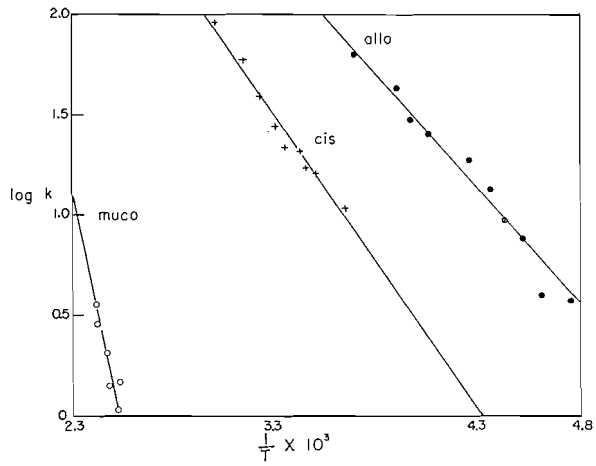

FIG. 3. Temperature dependence of the inversion rate.

TABLE I

Activation enthalpies and Arrhenius factors for ring oscillations of some inositol hexaacetates

Isomer	ΔH^*	log A
cis	6.60±0.05	6.24
allo	5.48±0.05	6.26
muco	4.7	6.25
	20.2±2	11.2

averaging for the muco isomer, as described previously. The greater uncertainties for the high-temperature averaging for the muco isomer are readily explained by the error inherent in measuring the separation of two lines which are at most 1.91 cycles apart. The assumption of negligible line width may also be expected to introduce an error.

In the chair form of the cis isomer there are two groups of three geometrically identical acetate substituents and a similar arrangement of hydrogens attached to the cyclohexane ring. The proton resonance spectrum, when inversion is sufficiently slow, has two peaks of equal intensity for both the acetate groups and the ring protons, which agrees with this structure. For the chair form of the allo isomer there are three equatorial and three axial acetate groups but all those in a given group are no longer identical. Nevertheless two peaks of equal intensity may be observed for the acetate protons. A complex trace is obtained for the ring protons which indicates the variety of environments. This too agrees with the chair structure for the allo isomer.

In the chair form of the muco isomer there are also three equatorial and three axial acetate groups, with those in a given group not identical. Therefore when inversion is slow one would expect either two peaks of equal intensity or more than two peaks. Similarly for the ring protons a complex trace might be expected. If inversion between the two chair forms of the cyclohexane ring is rapid this still does not average all the acetate groups. In a given conformation there is one equatorial acetate group which has an

equatorial acetate on each side of it. There is also an axial group with axial acetate groups on each adjacent ring carbon atom. When inversion to the other chair conformation occurs these two groups exchange environments and appear in an average magnetic environment if the rate of exchange is sufficiently rapid. Similarly there are two equatorial and two axial acetate groups, each of which is situated between an axial and an equatorial group. Inversion of the cyclohexane ring can also average the environment of these four acetate groups. However, the environments of the two and the four acetate groups remain unique. This can be visualized by inspection of the chair conformation of muco-inositol hexaacetate shown in Fig. 1.

The observed spectra agree with this interpretation. At the lowest temperature a complex spectrum containing at least three peaks is observed, as shown in Fig. 2. A total of four peaks with intensity ratio 1:2:2:1 might occur. However, overlap of two of these would give rise to the observed spectrum. As the temperature is raised a two-line pattern is eventually obtained, with intensity ratio of 2:1. This corresponds to rapid inversion of the chair form of the cyclohexane ring. At still higher temperatures the separation between the lines decreases from 1.9 to 1.4 cycles at the highest temperature reached. This requires an additional averaging mechanism. Conversion to the boat form might possibly be such a mechanism.

In Fig. 4 are shown four possible conformations when the ring is in a boat configuration.

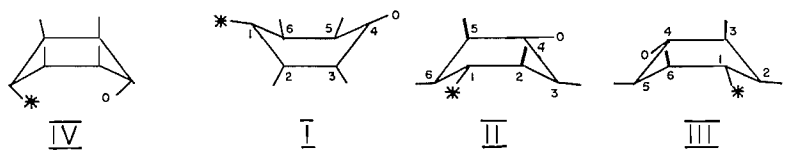

FIG. 4. Boat conformations of muco-inositol hexaacetate.

In conformation I all six acetate groups are in a pseudoequatorial location. However, the two distinguished by marks are not equivalent to the other four. If the ring inverts conformation IV is obtained. This is not equivalent to conformation I since now all six acetate groups are in pseudoaxial positions. A great deal of steric repulsion may reasonably be expected between the acetate groups, causing this conformation to have a much higher energy than conformation I. The ring protons in conformation I will all be axial and will have the same configuration as shown for the acetate groups in conformation IV. Another mode of motion for the boat form of the cyclohexane ring allows an infinite number of intermediate configurations without altering the carbon–carbon bond angles (16). When substituents are placed on the cyclohexane ring to give the stereochemistry of muco-inositol hexaacetate the possibilities are reduced to those shown by conformations I–III. Conformation II may be generated from conformation I by a rotation about all the carbon–carbon bonds of the cyclohexane ring. Atoms 3 and 6 are now at the prows of the boat instead of 1 and 4. By a further rotation atoms 2 and 5 take up this position as shown in conformation III. Conformations II and III are identical, except for a mirror image transformation because labels are on two of the acetate groups. However, they are not the same as conformation I.

The two acetate groups which are averaged by chair–chair inversion of the cyclohexane ring correspond to those at the prows of the boat. They will still be different from the other four acetate groups. Even though the same groups of two and four remain non-equivalent

during a chair–boat conversion magnetic averaging will still occur provided that the magnetic environment of the two acetate groups is different in the boat conformation I than in the average of the two chair conformations. A similar situation will apply for the four equivalent acetate groups. An averaging of all six acetate groups could occur by transformations among conformations I, II, and III. Since conformations II and III contain two axial acetate groups they might be of higher potential energy than conformation I and the extent of this type of magnetic averaging is difficult to estimate.

In the chair–chair inversion of *cis*-inositol hexaacetate all six acetate groups have to pass by each other. In the allo isomer four pairs are adjacent during inversion and in the muco isomer only two pairs. The observed enthalpies of activation also decrease in this order. Since a chair–chair inversion is presumably involved in all three of these averaging processes it may be safe to assume a similar Arrhenius factor for the muco isomer. The magnetic averaging observed at high temperatures for the muco isomer must occur by a different mechanism, resulting in a very different Arrhenius factor.

EXPERIMENTAL

The proton resonance spectra were obtained on a Varian Associates high-resolution nuclear magnetic resonance spectrometer operating at 56.4 Mc/sec. The spectra were calibrated using side-band modulation, with the modulating frequency altered during recording of the spectra. The modulating frequencies were determined to 0.1 cycle/sec by counting with a Hewlett Packard Model 521C frequency counter. By averaging many determinations peak positions were determined to an accuracy of 0.1 cycle/sec for muco-inositol hexaacetate. This accuracy was not necessary for the other isomers since line shapes rather than peak positions were used to calculate the inversion rates. Since the widths of the resonance lines due to the inositol acetates were often temperature dependent they could not be used as a criterion of instrument resolution. The width at half height of a modulation sideband from the solvent signal was used to determine resolution. This width was between 0.5 and 1.1 cycle/sec in all the measurements.

The thermostated probe assembly has been described previously, but was modified by using polyurethane-foam-jacketed glass tubes to introduce the thermostating gas, and by attaching the outlet to a water aspirator to increase the pressure differential across the probe assembly (17). A temperature range of $\pm 140°$ C could be obtained. Chloroform solutions of the acetates were used. Purity of the inositol acetates was determined by vapor phase chromatography to be 97% for the allo isomer, 99% for the cis isomer, and 99.8% for the muco isomer.

ACKNOWLEDGMENTS

The author is indebted to Professor S. J. Angyal for kindly supplying the inositol hexaacetates and a description of their purity. A referee suggested the low-temperature measurements of the muco isomer.

REFERENCES

1. R. U. Lemieux, R. K. Kullnig, H. J. Bernstein, and W. G. Schneider. J. Am. Chem. Soc. **79**, 1005 (1957); **80**, 6098 (1958).
2. R. U. Lemieux, R. K. Kullnig, and R. Y. Moir. J. Am. Chem. Soc. **80**, 2237 (1958).
3. S. Brownstein. J. Am. Chem. Soc. **81**, 1606 (1959).
4. E. L. Eliel. Chem. & Ind. (London), 568 (1959).
5. F. R. Jensen, D. S. Noyce, C. H. Sederholm, and A. J. Berlin. J. Am. Chem. Soc. **82**, 1256 (1960).
6. G. V. D. Tiers. Proc. Chem. Soc. 389 (1960).
7. L. W. Reeves and K. O. Stromme. Trans. Faraday Soc. **57**, 390 (1961).
8. W. B. Moniz and J. A. Dixon. J. Am. Chem. Soc. **83**, 1671 (1961).
9. G. Claeson, G. Androes, and M. Calvin. J. Am. Chem. Soc. **83**, 4357 (1961).
10. H. S. Gutowsky and C. H. Holm. J. Chem. Phys. **25**, 1228 (1956).
11. E. Grunwald, A. Loewenstein, and S. Meiboom. J. Chem. Phys. **27**, 630 (1957).
12. S. Meiboom. Tables of exchange broadened nmr multiplets. ASTIA No. AD-213-032.
13. J. E. Piercy. J. Acoust. Soc. Am. **33**, 198 (1961).
14. A. Loewenstein and S. Meiboom. J. Chem. Phys. **27**, 831 (1957).
15. S. Brownstein and A. E. Stillman. J. Phys. Chem. **63**, 2061 (1959).
16. P. Hazebroek and L. J. Oosterhoff. Discussions Faraday Soc. **10**, 87 (1951).
17. S. Brownstein. Can. J. Chem. **37**, 1119 (1959).

THE PROTON MAGNETIC RESONANCE SPECTRA OF CHRYSANTHEMUM ETHYL ESTER AND THE RELATED *cis*- AND *trans*-CHRYSANTHEMUMIC ACIDS

H. M. Hutton and T. Schaefer
Department of Chemistry, University of Manitoba, Winnipeg, Manitoba
Received November 24, 1961

ABSTRACT

The high-resolution proton magnetic resonance spectra of a mixture of the cis and trans isomers of chrysanthemum monocarboxylic acid ethyl ester have been studied. The *cis*-chrysanthemumic and *trans*-chrysanthemumic acids spectra were obtained to facilitate the interpretation of the complex spectra of the ester. The percentage of the trans isomer in the chrysanthemum ester was measured to be 62.0±1.1%. The cyclopropane proton spin coupling constants were found to be $J_{cis} = 8.7$ c.p.s. and $J_{trans} = 5.4$ c.p.s., in reasonable agreement with Karplus' calculations of the dependence of coupling constants on the dihedral angle.

INTRODUCTION

There have been no unequivocal measurements of the cis and trans proton coupling constants in the cyclopropane ring. In the present work the analyses of the *cis*- and *trans*-chrysanthemum ester and the corresponding acids were used to obtain these values. The chrysanthemum ester sample was a mixture of both the cis and the trans isomers, making a complete assignment of spectra lines difficult. It was found more convenient to analyze the *cis*- and *trans*-chrysanthemumic acids separately in order to identify the resonance peaks. Since the two ring protons interact only with the isobutenyl proton the analysis was that of an ABX-type system.

It was necessary to use solvents which preferentially shifted the proton signals in such a manner that the resonance peaks of the ring protons were not obscured by the other peaks. Carbon disulphide was used for the *cis*-chrysanthemumic acid and benzene for the trans acid.

EXPERIMENTAL

The spectra were obtained on a Varian V4302 DP 60 Mc/s spectrometer at room temperature. The line separations were measured by the side-band technique, using a Hewlitt and Packard 521c frequency counter. The chrysanthemum ester (min. 95%), the *cis*-chrysanthemumic acid (99.9%), and the *trans*-chrysanthemumic acid (100%) were of known purity as supplied by Benzol Products Co., and were not purified further. Since the acids were of limited solubility saturated solutions were used; the ester concentrations were approximate by volume since the solvents were only used to obtain preferential proton shifts. Internal benzene was used as the reference point in the measurement of the shifts.

ANALYSIS

I. cis-Chrysanthemumic Acid in CS_2

The spectrum of the *cis*-chrysanthemumic acid is shown in Fig. 1 together with the calculated spectrum for the ring protons corresponding to the AB part of an ABX system. The X part of the spectrum, at 114 c.p.s. with respect to internal benzene, consists of two doublets whose components are further split by the two isobutenyl methyl groups. The peaks of the latter occur at 324 c.p.s. and 328 c.p.s. The methyl groups attached to the cyclopropane ring have the same shift and occur at 357 c.p.s. The carboxyl proton peak is situated at −287 c.p.s. and is not shown in Fig. 1. The results of the ABX analysis gave J_{AB} (cis) = 8.7 c.p.s., $J_{AX} = 8.1$ c.p.s., $J_{BX} \approx 0$ c.p.s. The coupling constant of the X proton to the isobutenyl methyl group protons was about 1.4 c.p.s.

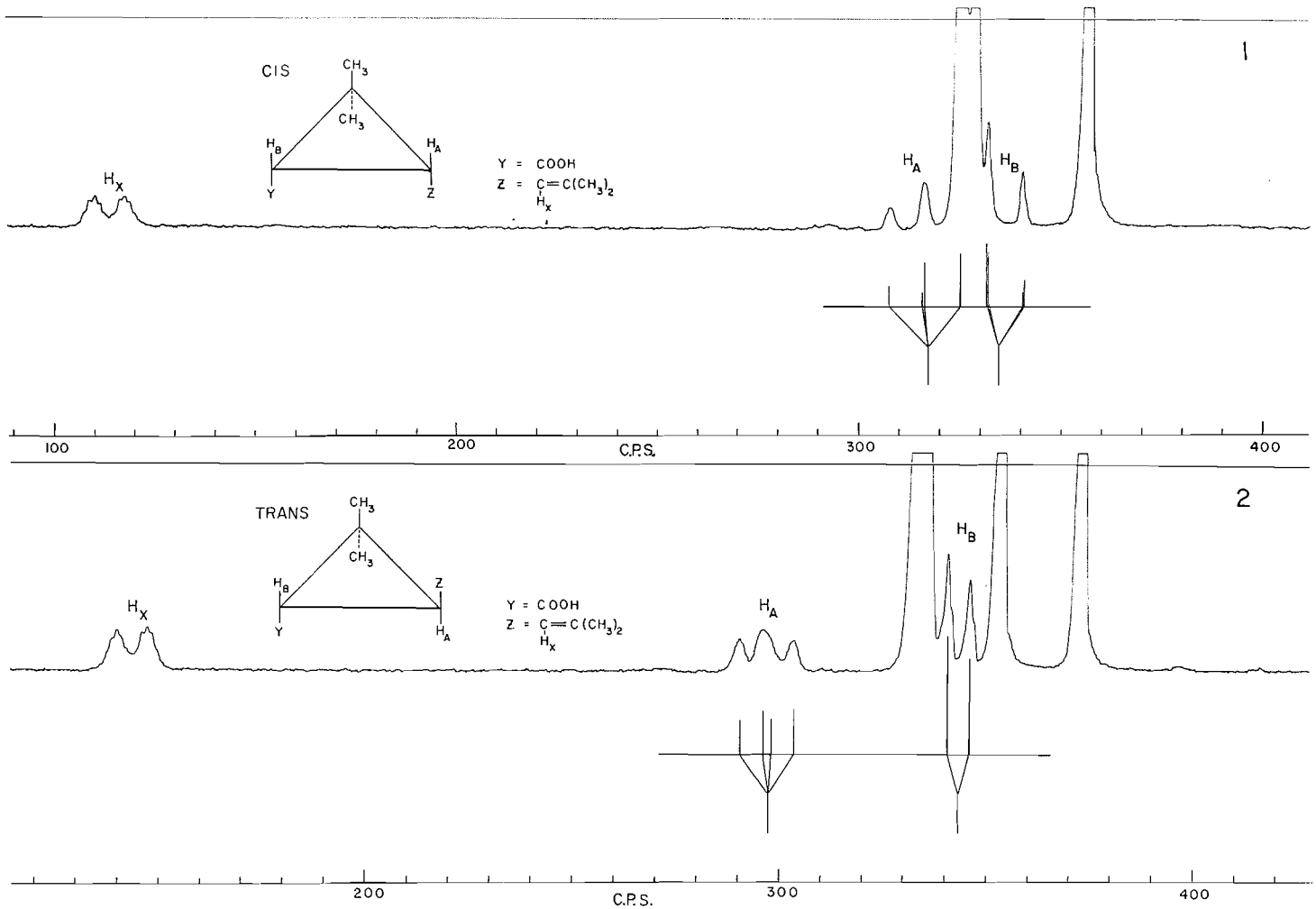

FIG. 1. Proton resonance spectrum at 60 Mc/s of *cis*-chrysanthemumic acid saturated in CS_2; calibration is with respect to internal benzene.
FIG. 2. Proton resonance spectrum at 60 Mc/s of *trans*-chrysanthemumic acid saturated in benzene; calibration is with respect to internal benzene.

II. Trans-Chrysanthemumic Acid in Benzene

The proton spectrum is shown in Fig. 2 together with the calculated spectrum for the ring protons corresponding to the AB part of an ABX system. The X part of the spectrum, at 144 c.p.s. from internal benzene, consists of two doublets whose components are further split by the isobutenyl methyl groups by about 1.4 c.p.s. The isobutenyl methyl group peaks occur at 335 c.p.s. The two methyl group peaks attached to the ring occur at 353 c.p.s. and 373 c.p.s. The results of the ABX analysis gave J_{AB} (trans) = 5.4 c.p.s., J_{AX} = 7.6 c.p.s., $J_{BX} \approx 0$ c.p.s.

III. Chrysanthemum Ester

The spectra of the chrysanthemum ester is given in Fig. 3 with the interpretation and the assignment of peaks relative to internal benzene in Table I. The coupling constants have been included in Table II.

TABLE I

Assignment of peaks of the chrysanthemum ester*

Resonance peak	Neat ester (c.p.s.)	1:1 benzene (c.p.s.)	1:6 CS_2 (c.p.s.)
H_X group (cis)	112	94	111
H_X group (trans)	142	141	136
—CH_2 ester (trans)	185	182	174
	192	189	181
	199	196	188
	206	203	195
—CH_2 ester (cis)	187	185	176
	194	192	183
	201	199	190
	208	206	197
H_A (trans)	313	297	299
	321	302	304
	321	304	307
	329	309	—
H_A (cis)	332	316	—
	—	325	—
CH_3 isobutenyl (cis)	341	333	318
	—	337	—
CH_3 isobutenyl (trans)	341	337	318
H_B (cis)	351	—	323
	—	—	332
H_B (trans)	358	345	—
	—	351	—
CH_3 ring (trans)	372	356	347
	377	373	352
CH_3 ring (cis)	370	373	345
CH_3 ester (trans)	363	365	338
	370	372	345
	377	379	352
CH_3 ester (cis)	365	367	340
	372	374	347
	379	381	354

*Measurements are with respect to internal benzene.

Since the ethyl group in the cis isomer is in a different magnetic environment than the ethyl group in the trans isomer, the cis and trans CH_3 resonance peaks are slightly shifted from each other. Similarly the —CH_2 peaks are displaced from each other as is shown in Fig. 3. From spectra of the ester mixture the percentage of the *trans-* and *cis-*chrysanthemum isomers was readily calculated by taking advantage of this displacement of the CH_2 lines in the cis and trans esters. A comparison of the heights of corresponding

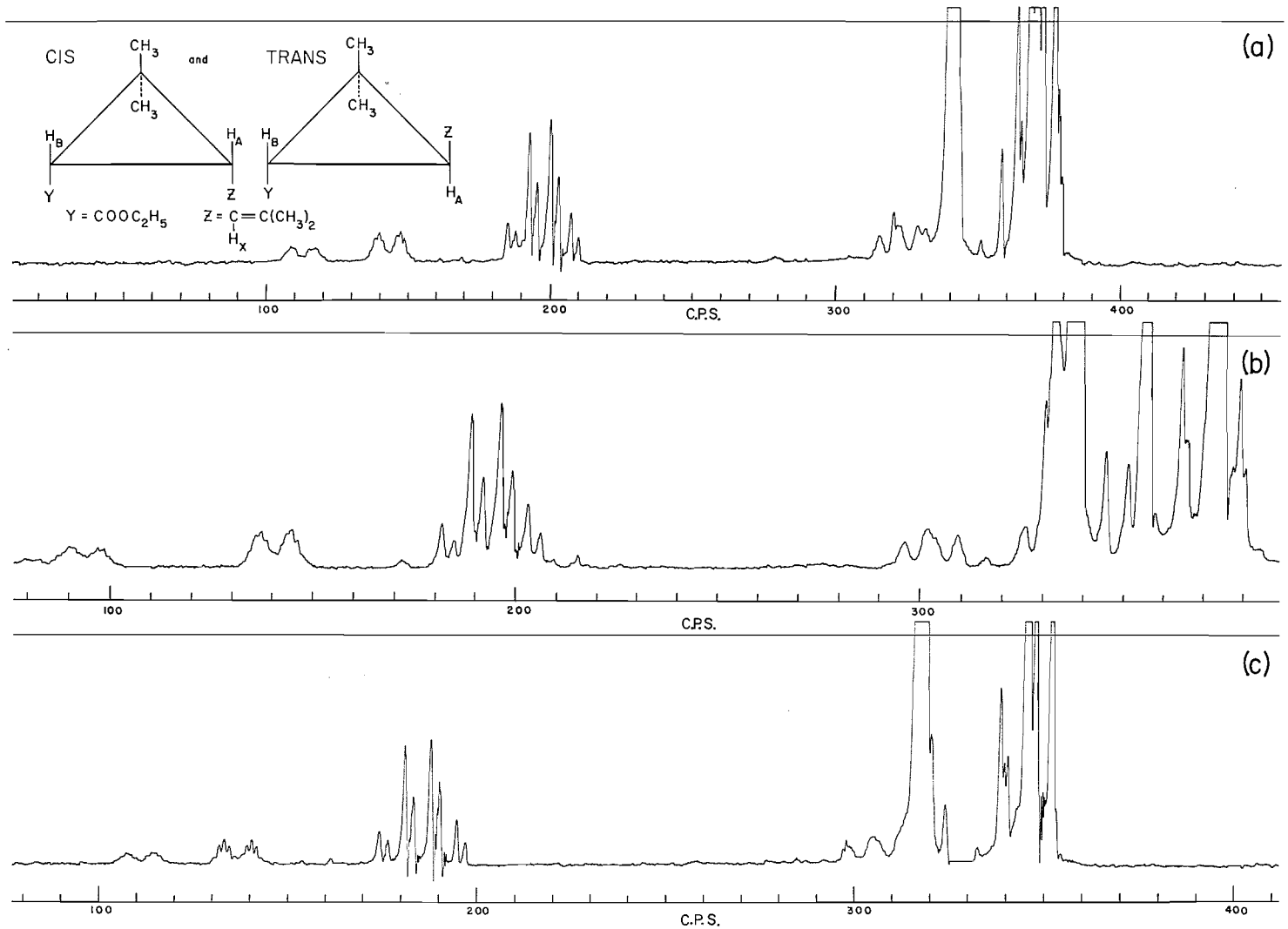

FIG. 3. Proton resonance spectra of chrysanthemum monocarboxylic acid ethyl ester at 60 Mc/s: (*a*) neat; (*b*) 1:1 in benzene; (*c*) 1: 6 in CS_2.

TABLE II

Chrysanthemum ester coupling constants in c.p.s.

	Neat	1:1 benzene	1:6 CS_2
J_{AB} (cis)	—	8.7±0.2	8.7±0.1
J_{AB} (trans)	5.7±0.2	5.5±0.1	—
J_{AX} (cis)	8.2±0.3	8.0±0.3	7.9±0.3
J_{AX} (trans)	8.1±0.1	7.7±0.1	7.9±0.1
J_{BX} (cis)	0	0	0
J_{BX} (trans)	0	0	0
$J_{X\text{-}CH_3}$ (cis)	—	1.2±0.1	1.4±0.2
$J_{X\text{-}CH_3}$ (trans)	—	1.4±0.1	1.5±0.2
$J_{CH_2\text{-}CH_3\ (ester)}$ (cis)	7.2±0.1*	7.1±0.1*	7.2±0.1*
$J_{CH_2\text{-}CH_3\ (ester)}$ (trans)	7.1±0.1*	7.1±0.1*	7.2±0.1*

*A first-order analysis value.

resonance peaks gave the percentage of the trans isomer. A more accurate method would be the comparison of peak areas but since the peak widths are no doubt very nearly the same this first method was thought to be sufficient for our purpose. Within experimental error the same percentage, 62.0±1.1% trans isomer, was obtained for the ester neat, in benzene, and in carbon disulphide. A previous infrared study gave 65% trans ester (1).

DISCUSSION

(a) Cyclopropane

Karplus has expressed the coupling constant between protons *a* and *b* in the fragment H_a—C—C—H_b as a squared cosine function of the dihedral angle (2). A consideration of the electron-diffraction results of Hassel and Viervoll for cyclopropane yield 0° and about 147° for the dihedral angle between the cis-vicinal and trans-vicinal protons, respectively (3). Karplus then predicts 8.2 c.p.s. and 6.4 c.p.s. for the cis and trans coupling constants, respectively, compared to 8.7 c.p.s. and 5.4 c.p.s. found experimentally. It is not impossible that the large groups in our substituted cyclopropanes distort the dihedral angles somewhat. It is, however, gratifying to see a rough agreement between calculated and observed values.

It had been thought that Karplus' calculation did not apply to the cyclopropane ring (4). Jackman found $J_{cis} = J_{trans} = 6.3$ c.p.s. from an analysis of *trans*-1,2-dibromocyclopropane (4). The triplet proton resonances observed for the CHBr groups in this A_2X_2 system was taken as evidence that J_{cis} and J_{trans} are equal. It is perhaps possible that J_{gem} is large enough to obscure differences in J_{cis} and J_{trans} and that the value of 6.3 c.p.s. actually represents an average of J_{cis} and J_{trans}. There may also be a small effect depending on the electronegativity of the substituent. Small effects have been observed in substituted ethanes for which the H—C—C—H coupling constant is given by $8.4-0.4\,E$, where E is the electronegativity of the substituent (5). The smaller value of 6.3 c.p.s. found by Jackman as compared to our average of 7.0 c.p.s. is in the right direction. From data on over 100 substituted ethylenes a definite correlation has been established between the electronegativity of the *atom in the substituent group attached to the vinyl carbon* and the values of the proton coupling constants (6, 7). Such electronegativity effects are larger for unsaturated systems such as the ethylenes than for the ethanes.

The proton coupling constants for cyclopropane itself have been measured from the C^{13} satellites of its proton spectrum (8). The value of 7.5±0.5 c.p.s. quoted for both the

cis and trans coupling constants is, no doubt, an average value for reasons which are now well known (9).

A recent publication gives the proton spectrum of thujopsene and hinokiic acid (10). Only the X part of the spectrum is visible and one obtains only the sum of J_{cis} and J_{trans}. This is 14.0 c.p.s., a value entirely in keeping with our sum of 14.1 c.p.s.

(b) Comparison with Other Ring Systems

In Table III there are collected the calculated and observed proton coupling constants for eight different values of the dihedral angle. They are taken from data given for

TABLE III

Calculated and observed proton coupling constants in c.p.s. for some ring compounds

Angle	Coupling constants		Reference
	Calculated	Observed	
0°	8.2	7.7–8.7	11 and this paper
ca. 44°	4.1	4.0–4.4	11
ca. 60°	1.7	2–4	12
ca. 79°	0	0	11
ca. 90°	0	0	11 and references therein
ca. 120°	2.1	2.2	11
ca. 147°*	6.4	5.4	This paper
ca. 180°	9.2	5–8	12

*We thank a referee for pointing out an error in our previous estimate of this angle.

three-, five-, and six-membered rings and include the judicious measurements of Anet (11, 12). The six-membered rings are assumed to exist in one conformation only (12). A certain amount of distortion from the assumed dihedral angle is possible for most of these rings but the overall agreement between theory and experiment is encouraging.

On the other hand, values of proton coupling constants in three-membered rings containing the heteroatoms oxygen, nitrogen, and sulphur do not agree very well with Karplus' predictions (13, 14) although the ratios of cis to trans coupling constants are roughly those predicted by Karplus. It is interesting to note that the deviation from the predicted values increases with the difference in electronegativity between the heteroatoms and carbon. The deviation is in the same direction as for the substituted ethylenes mentioned above. For sulphur, with an electronegativity similar to that of carbon, the coupling constants are close to the value we have found for our cyclopropanes. The geometries of these molecules show relatively small changes (13), and it seems reasonable to assume that the couplings in these heterocyclic propanes depend not only on angular factors but also on the electronegativity of the heteroatom.

CONCLUSION

Unequivocal values for cis and trans proton coupling constants in the same cyclopropane ring have been observed. They fall reasonably well into the scheme devised by Karplus. A consideration of the proton coupling constants in heterocyclic propanes suggests that both angular factors and electronegativities are important in determining their magnitudes. It was also shown that the measurements of relative concentrations of geometrical isomers of substituted cyclopropanes can be measured rapidly in favorable cases by n.m.r. methods. Further work is needed to determine the gem coupling constant in cyclopropane derivatives. This is being done and a knowledge of all these types of couplings constant will facilitate the interpretation of quite complex spectra.

ACKNOWLEDGMENTS

We thank Dr. W. F. Ringk of Benzol Products Company for the compounds used in this work. One of us (H. H.) would like to thank Canadian Industries Limited for fellowship support. This work was supported by the National Research Council and the Research Corporation.

REFERENCES

1. W. F. RINGK. Private communication.
2. M. KARPLUS. J. Chem. Phys. **30**, 13 (1959).
3. O. HASSEL and J. H. VIERVOLL. Acta Chem. Scand. **1**, 149 (1947).
4. L. M. JACKMAN. Applications of NMR spectroscopy in organic chemistry. Pergamon Press, New York. 1959. p. 86.
5. R. E. GLICK and A. A. BOTHNER-BY. J. Chem. Phys. **25**, 362 (1956).
6. T. SCHAEFER. Can. J. Chem. **40**, 1 (1962).
7. J. S. WAUGH and S. CASTELLANO. J. Chem. Phys. **35**, 1900 (1961).
8. N. MULLER and D. E. PRITCHARD. J. Chem. Phys. **31**, 768 (1959).
9. T. SCHAEFER and W. G. SCHNEIDER. Can. J. Chem. **37**, 2078 (1959).
10. S. FORSEN and T. NORIN. Acta Chem. Scand. **15**, 592 (1961).
11. F. A. L. ANET. Can. J. Chem. **39**, 789 (1961).
12. R. V. LEMIEUX, R. K. KULLNIG, H. G. BERNSTEIN, and W. G. SCHNEIDER. J. Am. Chem. Soc. **80**, 6098 (1958).
13. F. S. MORTIMER. J. Mol. Spectroscopy, **5**, 199 (1960).
14. C. A. REILLY and J. D. SWALEN. J. Chem. Phys. **34**, 980 (1961).

THE BASE-CATALYZED REARRANGEMENT OF N-ALKYL TRIPHENYLISOXAZOLIUM SALTS

J. F. KING AND T. DURST[1]
Department of Chemistry, University of Western Ontario, London, Ontario
Received January 17, 1962

ABSTRACT

The action of base on trisubstituted N-alkyl isoxazolium salts, first described by Kohler and co-workers (1, 2), has been reinvestigated. On the basis of photochemical and spectroscopic studies it is concluded that the reaction of the N-methyl triphenylisoxazolium ion (I*a*) with aqueous sodium hydroxide leads to 4,5,6-triphenyl-2*H*-1,3-oxazine (III), a derivative of a heterocycle previously known only in benz-fused systems.

In 1928, Kohler and Blatt (1) described the action of alkali on N-methyl triphenylisoxazolium "ferric chloride double salt" (I*a*). Among the materials produced was one obtained most readily by shaking the isoxazolium salt with dilute aqueous alkali and

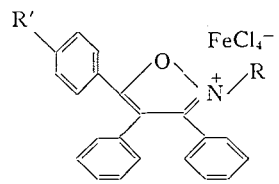

I*a*, R = CH_3; R′ = H
I*b*, R = CH_2CH_3; R′ = Br

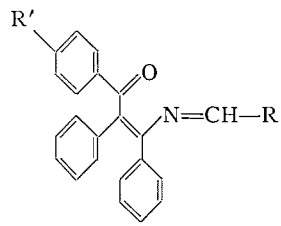

II*a*, R, R′ = H
II*b*, R = CH_3; R′ = Br

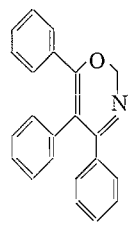

III

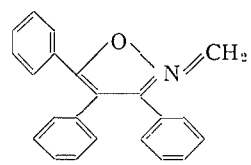

IV

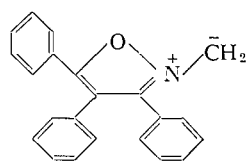

V

ether for a few minutes and then separating and evaporating the ether layer. This they called the "anhydro compound" because of a presumed relation with some hydrated "pseudo bases". As possible representations of the "anhydro compound" they discussed structures II*a*, III, and IV, tentatively adopting II*a*; later Kohler and Richtmyer (2) considered II*a* as "definitely established". In the final communication of the series, Kohler and Bruce (3) described the preparation of an "anhydro compound" from the benzisoxazolium salt VI*c*, and assigned structure VII*c* to this compound.

Aliphatic Schiff bases are known to be reactive species readily undergoing polymerization and other addition reactions (4, 5). Those derived from formaldehyde are, in fact, apparently unstable under the usual conditions of their formation and only

[1]*Holder of a National Research Council Bursary.*

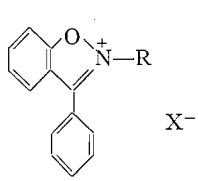

VI*a*, R = CH_3
VI*b*, R = $CH_2\phi$
VI*c*, R = CH_2CH_3

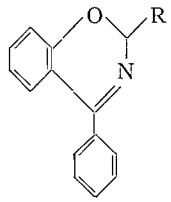

VII*a*, R = H
VIII*b*, R = ϕ
VII*c*, R = CH_3

hydrolysis or—in the absence of water—trimerization products have been isolated. It seemed to us that the comparative stability of the "anhydro compound" from the triphenylisoxazolium ferrichloride (I*a*) was not compatible with structure II*a* and, further, it was felt that the nature of this and the other "anhydro compounds" could be shown by the use of modern physical and chemical methods not available to Kohler and his co-workers.

Accordingly, we have prepared compounds I*a*, VI*a*, and VI*b* (as the ferric chloride or perchlorate salts) and obtained crystalline "anhydro compounds" by what is essentially Kohler's procedure. In Table I are listed the ultraviolet maxima, infrared peaks in the

TABLE I

The "anhydro compounds" and model compounds: spectroscopic data

	ν_{max} (cm^{-1})	$\lambda\lambda_{max}$ (mμ) (ϵ, in parentheses)	δ (p.p.m.) from tetramethylsilane
"Anhydro compound" from I*a*	1626	239 (15,700) 338 (6,200)	5.58
"Anhydro compound" from VI*a*	1616	238 (10,900) 325 (1,700)	5.54
"Anhydro compound" from VI*b*	1610	240 (12,400) 329 (1,700)	6.39
Benzalaniline	1628	—	8.35
Benzophenone anil	1623	—	—
Benzyliminobenzophenone	1626	—	—
"Methanol adduct" (X)	1575, 1550	238 (9,300) 350 (12,500)	4.36*
Propyliminoacetaldehyde (XI)	1673	—	7.63†
2-Phenyl-2*H*-1,3-benzoxazin-4-one (XII)	—	—	6.22
Formaldehyde 2,4-dinitrophenylhydrazone	—	—	6.73, 7.12‡

*Doublet, j = 9 cycles/sec.
†Quartet, j = 4 cycles/sec.
‡*AB* quartet, j = 11 cycles/sec.

carbonyl region, and the chemical shifts of hydrogens attached to the non-aromatic carbon atoms; unless otherwise noted the n.m.r. peaks are singlets.

In addition to structures II*a*, VII*a*, and VII*b*, which correspond to Kohler's proposals, structures III, VIII*a*, and VIII*b* for these three "anhydro compounds" are a priori possible. Structure IV in which the nitrogen has 10 valence electrons is, of course, not possible and the related ylide (V) would be much too unstable to be isolated under these conditions.

The single infrared maximum around 1620 cm^{-1} shown by each of the compounds is in accord with the cyclic structures III, VII*a*, and VII*b* being well within the range 1660–1480 cm^{-1} quoted by Bellamy (6) and similar to the C=N maxima of benzophenone anil (1623 cm^{-1}) and benzyliminobenzophenone (1626 cm^{-1}). The open-chain structures II*a*, VIII*a* and VIII*b*, on the other hand, would be expected to show two bands in this region.

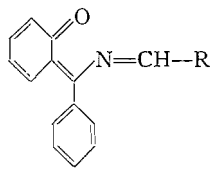

VIII*a*, R = H

VIII*b*, R = ϕ

The observation of only one band can be rationalized only by assuming that the carbonyl and azomethine absorptions coincide, an assumption that is extremely tenuous since the absorption occurs outside the normal range of carbonyl groups not involved in hydrogen bonding.

The ultraviolet data also agree well with the cyclic structures. The long wavelength bands of the "anhydro compounds" derived from the benzisoxazoles (at 325 and 329 mμ, respectively) are very close to that of benzylimino-*o*-hydroxybenzophenone (IX), which is found at 328 mμ. The close similarity between the ultraviolet spectra of the two

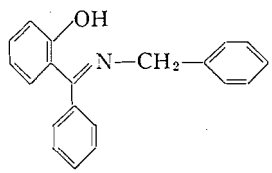

IX

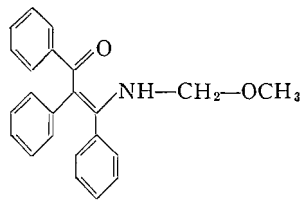

X

"anhydro compounds" derived from the benzisoxazole also argues in favor of the cyclic structures. In the open-chain structure VIII*b*, the "new" phenyl group is conjugated with the main chromophoric system, which would be expected to result in distinct differences in the spectrum. The ultraviolet spectrum of the "methanol adduct" (X) (the formation of which is discussed below) is of interest in connection with the structure of the triphenyl "anhydro compound". The long wavelength of band X is found at *longer* wavelengths (by 12 mμ) than the corresponding band in the "anhydro compound". Though on the basis of the cyclic structure (III) for the "anhydro compound" this is unremarkable, on the basis of structure II*a* it would mean that the conjugation of another double bond with the chromophore of X yields a distinct hypsochromic shift.

Though the nuclear magnetic resonance spectra of comparatively few model systems have been reported, again the cyclic structures are much more satisfactory for their interpretation than the acyclic. Protons bonded to an azomethine carbon evidently absorb at rather low field. Aliphatic aldoximes have been found at 6.3–7.0 p.p.m. (7), aliphatic aldehyde semicarbazones at 7.4–7.8 p.p.m. (8), and aliphatic aldehyde 2,4-dinitrophenylhydrazones at 6.8–7.2 p.p.m. (8). We have found that the azomethine proton of propyliminoacetaldehyde (XI) absorbs at 7.63 p.p.m and the corresponding protons of formaldehyde 2,4-dinitrophenylhydrazone at 6.73 and 7.12 p.p.m. The methylene protons of the "anhydro compounds" derived from the N-methyl isoxazolium salts (I*a* and VI*a*), however, are found at 5.58 and 5.54 p.p.m. The corresponding methine proton of the "anhydro compound" from the N-benzyl isoxazolium salt (VI*b*) absorbs at 6.39 p.p.m.; the azomethine proton of benzalaniline absorbs at 8.35 p.p.m.; the methine proton of the model compound XII (9) on the other hand is found at 6.22 p.p.m.

$CH_3CH{=}NCH_2CH_2CH_3$

XI

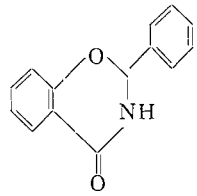

XII

It is evident that the n.m.r., infrared, and ultraviolet data individually agree—on the basis of expectations derived from the study of model systems—far better with the cyclic structures III, VII*a*, and VII*b* for the "anhydro compounds" than with the open-chain structures II, VIII*a*, and VIII*b*. In addition the data show a measure of agreement with one another which, independent of the model systems, strongly supports the same conclusion. The C=N bands in the infrared are in the same region, the ultraviolet spectra of the two benz-fused compounds are very similar, and the chemical shift of the methylene protons of the two "anhydro compounds" derived from N-methyl isoxazolium salts are virtually identical; the shift to lower field accompanying the replacement of one proton by a phenyl group is as expected.

Following the conclusions from the physical data just discussed and anticipating those of the discussion of the chemical reactions of the compounds, we shall, for simplicity, describe the reactions in terms of the cyclic structures III, VII*a*, and VII*b*, and shall refer to the compounds by the corresponding names.

Kohler and Blatt (1) reported that the triphenyloxazine (III), on being refluxed with methanol for an hour, was converted to a "methanol adduct" to which he ascribed structure X. We have prepared this compound and have measured its infrared, ultraviolet, and n.m.r. spectra, which, coupled with Kohler's observation that the "methanol adduct" (like the oxazine (III) itself) hydrolyzes readily to dibenzoylphenylmethane, comprise good support for the structure (X) proposed by Kohler. The formation of X from the "anhydro compound" is readily rationalized on the basis of the oxazine structure (III) by assuming that under the conditions of the reaction the oxazine (III) is reversibly converted into the open-chain compound (II*a*); such a transformation is, formally at least, merely a variant on the familiar ring–chain tautomerism of oxazolidines, tetrahydrooxazines, and similar compounds.

Kohler and Blatt also reported (1) that the oxazine (III) reacts with phenyl magnesium bromide, giving the vinylamine XIII. Again this reaction probably proceeds via an open-chain intermediate, though it is likely that the ring opening is accelerated by complexing with the metal. The action of Grignard reagents on carbinolamine ethers to yield products derived from the corresponding Schiff bases has been frequently observed (10).

Kohler and co-workers (1, 2) described the action of ozone on the triphenyl "anhydro compounds"; most notably, ozonolysis of the "anhydro compound" from I*b* (in ethyl bromide solution at room temperature) gave *p*-bromobenzil and benzamide. They considered that the results of these experiments established the open-chain structures (II*a* and II*b*) for these compounds. It has already been shown, however, that structure II*a* for the "anhydro compound" derived from I*a* is far from satisfactory in explaining the spectroscopic data, and since ozone is a highly reactive species which may yield so-called abnormal products by a number of different mechanisms (11, 12), it is much more reasonable to propose that the root of the apparent anomaly lies with the ozonolysis rather than the physical data. The double bond in III bears an oxygen and a carbon–nitrogen

double bond; it is notable that a formally similar system in 2,3,6-trimethyl-4-pyrone (XIV) leads to "abnormal" ozonolysis products, methylglyoxal and biacetyl (13). The process XV → XVI (or its one-step equivalent) illustrates a possible mode of ozone addition which would yield abnormal cleavage products. It is, of course, also conceivable that the ozone is reacting with the small equilibrium concentration of the open-chain tautomer under the conditions of the reaction.

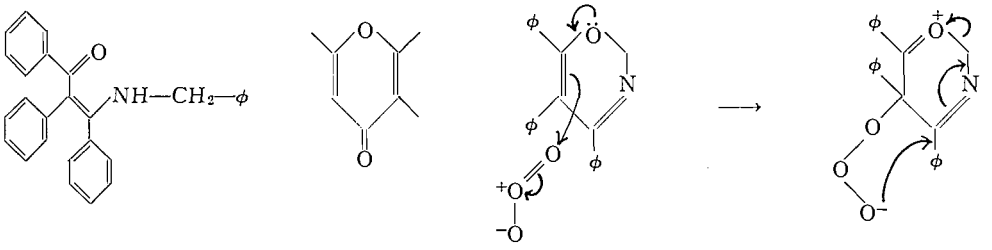

XIII XIV XV XVI

To provide further information about the nature of the "anhydro compounds" we have investigated some photochemical reactions of these compounds. Barton (14) has recently suggested that it is a general property of any ring of $2n$ members containing $(n-1)$ conjugated double bonds, when irradiated with light of the appropriate wavelength, to form an open-chain compound having n conjugated double bonds. It would be expected then that ultraviolet irradiation of III would yield II*a* and that if formation of the methanol adduct takes place via II*a*, the reaction might be accelerated by ultraviolet irradiation. We have, in fact, found that irradiation of a solution of the oxazine (III) in methanol at −60° leads to complete conversion to the methanol adduct (X) within 2 hours. The thermal reaction, which takes place rapidly in refluxing methanol and slowly at room temperature, is completely suppressed at −60°. These results are in accord with Scheme 1.

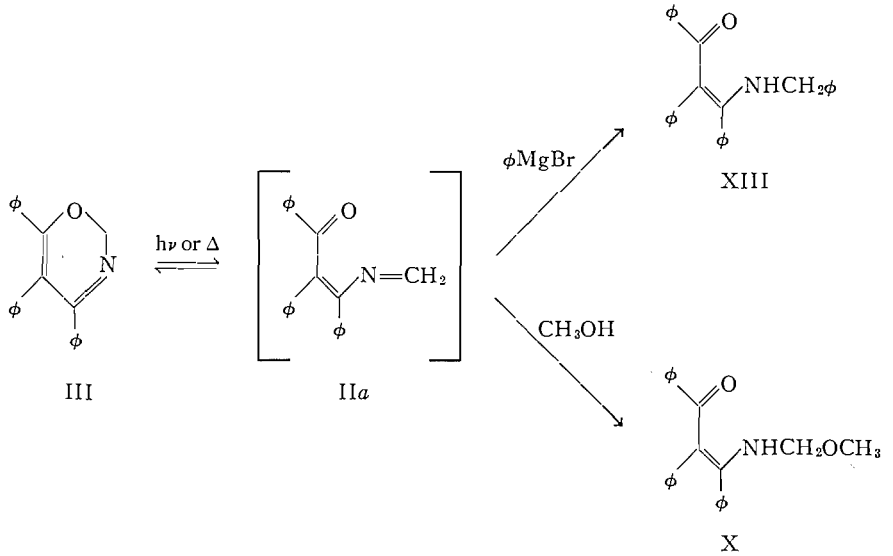

III II*a* XIII X

SCHEME 1

Irradiation of VII*a* and VII*b* would also be expected to yield the open-chain species VIII*a* and VIII*b*, respectively, though since the ring opening disrupts the aromatic system, it would be anticipated that these compounds would cyclize very readily, giving back starting materials. When a solution of VII*a* in dry methanol was irradiated, only starting material was isolated. When irradiated in methanol–ether (reagent grades) *o*-hydroxybenzophenone was obtained. Irradiation in dry methanol in the presence of aniline yielded the anil of *o*-hydroxybenzophenone. Without irradiation no reaction was observed either after refluxing with methanol–ether or on standing in the methanol–aniline mixture. These results agree with Scheme 2, analogous to Scheme 1.

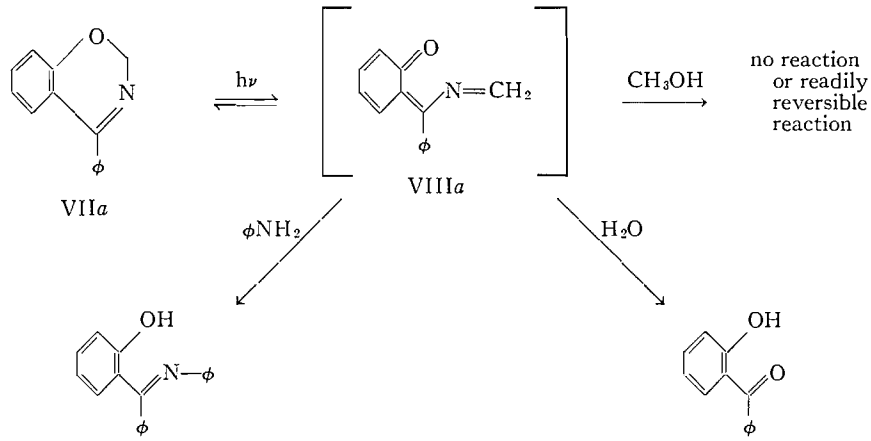

SCHEME 2

In addition to allowing ready rationalization and correct prediction of the thermal and photochemical addition reactions, the oxazine structures predict that the triphenyl compound (III) should be more reactive than the benz-fused compounds (VII*a* and VII*b*). On the other hand, reactions involving additions to structures VIII*a* and VIII*b* would lead to aromatic systems and hence should proceed more readily than the corresponding reactions with II*a*. The observed order of reactivity is that predicted on the basis of the oxazine structures III, VII*a*, and VII*b*.

From this study of the spectroscopic properties and a number of chemical reactions of Kohler's "anhydro compounds", we conclude that they are best represented by the oxazine structures III, VII*a*, and VII*b*. It appears that a "bare" (i.e. not fused to a benzene ring) 2*H*-1,3-oxazine, though a simple heterocyclic system, has not been reported previously; the "anhydro compound" (III) is evidently the first example of this type of heterocycle.

As reasonable mechanisms for the formation of the oxazine we suggest that an ylide (V), formed by abstraction of a proton by base, may either rearrange as indicated by the arrows in structure XVII (a process which is formally analogous to the Stevens rearrangement) or, alternatively, the ring of the ylide (V) may open to form II*a*, which then equilibrates with III.

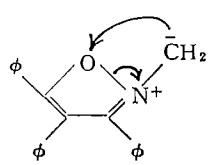

XVII

EXPERIMENTAL

Infrared and nuclear magnetic resonance spectra were determined in dilute carbon tetrachloride solution using, respectively, a Beckman IR-7 grating spectrophotometer equipped with sodium chloride optics, and a Varian DP-60 spectrometer. Chemical shifts are reported in parts per million from internal tetramethylsilane. Ultraviolet spectra were determined in cyclohexane solution using a Beckman DK-1 instrument. Petroleum ether refers to the fraction of b.p. 35–60°. Melting points were determined on a Kofler block and are uncorrected.

*4,5,6-Triphenyl-2*H*-1,3-oxazine (III)*

This compound was prepared from N-methyl triphenylisoxazolium ferrichloride (I*a*) (m.p. 161–162°) as described by Kohler and Blatt (1) and melted at 140–141°; reported m.p. 140–141° (1).

3-Phenyl-1,2-benzisoxazole

The following procedure was found to be more satisfactory than that of Kohler and Richtmyer (2). *o*-Chlorobenzophenone oxime (15) (4.42 g) was dissolved in a mixture of 50% aqueous potassium hydroxide solution (30 ml) and ethylene glycol monomethyl ether (10 ml). The solution was refluxed and after about 1 hour had separated into two phases. After being heated for a further 6 hours, the mixture was cooled, yielding a crystalline product. Recrystallization from methanol gave 3.1 g (80%) of material melting at 82–83°.

N-Methyl-3-phenyl-1,2-benzisoxazolium Ferrichloride (VIa)

3-Phenyl-1,2-benzisoxazole (3.3 g) was added to freshly distilled dimethyl sulphate (15 ml) and heated at 125° for 24 hours. The solution was cooled and treated with 6 *N* hydrochloric acid. Ferric chloride solution (2 parts $FeCl_3$ to 1 part water) was added until the yellow salt precipitated; yield 6.25 g (90%); m.p. 117–119°. Calculated for $C_{12}H_{12}ONFeCl_4$: C, 41.22%; H, 2.97%; N, 3.35%. Found: C, 41.36%; H, 3.12%; N, 3.43%.

*3-Phenyl-2*H*-1,3-benzoxazine (VIIa)*

N-Methyl-3-phenyl-1,2-benzisoxazolium ferrichloride (5.25 g) was shaken for 15 minutes with ether (15 ml) and a 5% aqueous solution of sodium hydroxide (15 ml). The ether layer was washed with water, dried over anhydrous sodium sulphate, and evaporated, yielding a yellow oil (1.35 g, 50%). Addition of a solution of picric acid in ether gave a dimorphous yellow picrate, m.p. 103–104° (from methylene chloride – ether) and 158–160° (from glacial acetic acid). A solution of the picrate in methylene chloride was poured onto a column of basic alumina (Woelm, grade I); on elution with benzene a white solid was obtained which recrystallized from ether – petroleum ether as white needles, m.p. 49–50°. The infrared spectra of the crystalline and crude oily materials were virtually identical. Calculated for $C_{14}H_{11}ON$: C, 80.37%; H, 5.30%; N, 6.81%. Found: C, 80.64%; H, 5.28%; N, 6.69%.

N-Benzyl-3-phenyl-1,2-benzisoxazolium Perchlorate (VIb)

3-Phenyl-1,2-benzisoxazole (440 mg) was dissolved in benzyl chloride (3 ml), and a saturated solution of silver perchlorate (500 mg) in ether added. A white precipitate formed immediately, which was filtered off and triturated with methylene chloride. The mixture was filtered (to remove the silver chloride) and the filtrate evaporated to about 2 ml. Addition of ether gave white crystals (275 mg, 30%) which, after four recrystallizations from methylene chloride – ether, melted at 164–165°. Calculated for $C_{20}H_{16}O_5NCl$: C, 62.26%; H, 4.18%; N, 3.63%. Found: C, 61.86%; H, 4.26%; N, 3.41%.

*2,4-Diphenyl-2*H*-1,3-benzoxazine (VIIb)*

The perchlorate (VI*b*) (145 mg) was dissolved in methanol (5 ml) and a 5% aqueous sodium hydroxide solution (15 ml) added with stirring during 15 minutes. On work-up a crystalline material (89 mg, 84%) was obtained which recrystallized from methylene chloride – petroleum ether as white needles melting at 97–99°. Calculated for $C_{20}H_{15}ON$: C, 84.18%; H, 5.30%; N, 4.91%. Found: C, 83.87%; H, 4.90%; N, 5.19%.

*Irradiation of 4,5,6-triphenyl-2*H*-1,3-oxazine*

4,5,6-Triphenyl-2*H*-1,3-oxazine (III) (50 mg) was dissolved in a mixture of ether (20 ml) and methanol (2 ml). The solution was divided into two equal portions and each half placed in a glass-stoppered, 50-ml round-bottomed Pyrex flask. One flask was wrapped carefully with aluminum foil to allow as little light as possible to reach the inside, the other flask was not wrapped. The flasks were immersed in cold methanol contained in a stainless steel beaker cooled in a dry ice – methanol bath. The temperature of the methanol surrounding the reaction flasks was kept at $-60\pm5°$ during the experiment. A Hanovia C-H-3 ultraviolet lamp was placed in a Pyrex test tube and immersed in the methanol bath so that the light source was the same distance (ca. 2 cm) from each flask. After 90 minutes' irradiation both samples were removed from the bath and the solvent removed *in vacuo*. The infrared spectrum of the crude irradiated material indicated that it consisted largely of the "methanol adduct" (X); recrystallization gave X (17 mg), identified by comparison of the melting point and infrared spectrum with that of an authentic sample obtained by Kohler and Blatt's procedure (1). The infrared spectrum of the crude material from the shielded sample indicated it to be almost pure starting material, which, after recrystallization, was identified as III by melting point and infrared spectrum.

In a second experiment ultraviolet spectroscopy showed that the irradiated sample was converted to the methanol adduct in less than 2 hours and that no significant change took place with the shielded sample in 6 hours.

*Irradiation of 4-phenyl-2*H*-1,3-benzoxazine (VIIa)*

(a) In Methanol–Ether

4-Phenyl-2*H*-1,3-benzoxazine (450 mg) was dissolved in a mixture of ether (Mallinckrodt anhydrous, 85 ml) and methanol (Fisher Spectranalyzed, 85 ml), and the solution irradiated for 10 hours in a quartz immersion apparatus (16) using a Hanovia C-H-3 lamp. The solvent was evaporated and the material soluble in ether chromatographed on silica gel. Elution with petroleum ether – benzene (20:1) gave a yellow oil (200 mg), identified by its infrared and n.m.r. spectra as *o*-hydroxybenzophenone.

(b) In Dry Methanol

When the irradiation was carried out under the same conditions as in (*a*) but using as solvent methanol carefully dried by the magnesium methoxide procedure, only starting material was obtained.

(c) In Methanol–Aniline

4-Phenyl-2*H*-1,3-benzoxazine (450 mg) and freshly distilled aniline (1 ml) were dissolved in methanol dried by the magnesium methoxide procedure (170 ml), and the solution irradiated in the immersion apparatus. After about 10 minutes the solution began to redden and within ½ hour was a dark red. The irradiation was continued for 10 hours. The solvent was then evaporated and the residue triturated with methylene chloride. The methylene chloride solution was filtered through a silica gel column and the solvent evaporated, leaving yellow needles (205 mg), identified by melting point, mixed melting point, and infrared spectrum as the anil of *o*-hydroxybenzophenone (17). The proton magnetic resonance spectrum of the anil showed a singlet (due to hydrogen-bonded O—H) at 13.80 p.p.m. and a broad absorption at 6.7 to 7.3 p.p.m. due to the aromatic hydrogens.

*Treatment of 4-Phenyl-2*H*-1,3-benzoxazine (VIIa) with Methanol–Ether*

4-Phenyl-2*H*-1,3-benzoxazine (25 mg) was dissolved in a mixture of methanol (Fisher Spectranalyzed, 5 ml) and ether (Mallinckrodt anhydrous, 5 ml), and the solution refluxed for 12 hours. The solvent was evaporated; the infrared spectrum of the residue showed it to be unchanged starting material.

*Treatment of 4-Phenyl-2*H*-1,3-benzoxazine (VIIa) with Methanol–Aniline*

Aniline (0.2 ml) was added to a solution of 4-phenyl-2*H*-1,3-benzoxazine (10 mg) in dry methanol (15 ml), and the solution allowed to stand at room temperature for 16 hours. The infrared spectrum of the product showed it to be unchanged starting material.

ACKNOWLEDGMENTS

Valuable preliminary experiments in this study were carried out by Mr. R. S. Bernier. The n.m.r. spectrum of 4,5,6-triphenyl-2*H*-1,3-oxazine was obtained through the courtesy of Professor K. Wiesner, University of New Brunswick, Fredericton, N.B. Other n.m.r. spectra were determined in this department by Mr. R. E. Klinck and Dr. J. B. Stothers; we are especially grateful to Dr. Stothers for aid in the interpretation of the n.m.r. spectra.

The National Research Council of Canada has supported this work by grants-in-aid and a bursary.

REFERENCES

1. E. P. Kohler and A. H. Blatt. J. Am. Chem. Soc. **50**, 1217 (1928).
2. E. P. Kohler and N. K. Richtmyer. J. Am. Chem. Soc. **50**, 3092 (1928).
3. E. P. Kohler and W. F. Bruce. J. Am. Chem. Soc. **53**, 644 (1931).
4. M. M. Sprung. Chem. Revs. **26**, 297 (1940).
5. R. Tiollais. Bull. soc. chim. France, 708 (1947).
6. L. J. Bellamy. The infra-red spectra of complex molecules. 2nd ed. Wiley, New York. 1958. p. 263.
7. W. D. Phillips. Ann. N.Y. Acad. Sci. **70**, 817 (1958).
8. D. Y. Curtin, J. A. Gourse, W. H. Richardson, and K. L. Rinehart. J. Org. Chem. **24**, 93 (1959).
9. C. A. Keane and W. M. S. Nicholls. J. Chem. Soc. **91**, 264 (1907).
10. R. Schröter. *In* Methoden der organischen Chemie (Houben–Weyl). Vol. 11. Part 1. 4th ed. Georg Thieme Verlag, Stuttgart. 1957. pp. 815–816.
11. P. S. Bailey. Chem. Revs. **58**, 925 (1958).
12. P. S. Bailey, S. B. Mainthia, and C. J. Abshire. J. Am. Chem. Soc. **82**, 6136 (1960).
13. J. P. Wibaut. Festschr. Arthur Stoll. 227 (1957).
14. D. H. R. Barton. Helv. Chim. Acta, **42**, 2604 (1959).
15. K. von Auwers, M. Lechner, and H. Bundesmann. Ber. **58**, 36 (1925).
16. P. de Mayo. Ultraviolet photochemistry of simple unsaturated systems. *In* Advances in organic chemistry. Vol. II. Interscience. 1960. p. 367.
17. C. Graebe and F. Keller. Ber. **32**, 1683 (1899).

THE CONDUCTANCE OF MOLTEN LITHIUM CHLORATE AND THE EFFECT OF ADDITIONS OF TRACES OF NONELECTROLYTES ON THE CONDUCTANCE

A. N. CAMPBELL, E. M. KARTZMARK, AND D. F. WILLIAMS[1]
Chemistry Department, University of Manitoba, Winnipeg, Manitoba
Received November 30, 1961

ABSTRACT

The specific conductance of pure molten lithium chlorate between 130 and 145° C was determined and an activation energy of conductance deduced. Additions of substances having various dielectric constants were made to molten lithium chlorate and the conductances determined. These additions were: (*a*) water, 0–6% by weight; (*b*) nitrobenzene, 0–0.4% by weight; (*c*) methyl alcohol, 0–1.25% by weight. The results are discussed.

Although much experimental work has emanated from this and other laboratories on the conductance and viscosity of concentrated aqueous solutions, over the last dozen or so years, a satisfactory theoretical treatment is still lacking. It is contended by many that the Debye–Hückel–Onsager treatment has been pushed to its limit when κa $(= (50.29\mathring{a}\sqrt{c})/(\epsilon T)^{1/2})$ becomes greater than 0.2, corresponding in most cases to a concentration not greater than 0.05 *M*. According to Fuoss, "It therefore seems futile to look for a solution to the problem of higher concentrations by an extension of the present theory which is, however, valid for low concentrations." (1)

Since the original great advances in the theory of conductance were made by the study of what has been called "slightly impure distilled water", it seemed to us that interest might now well shift to the study of molten salts, to which traces of impurity were added, more especially as we had at our disposal, in the form of lithium chlorate, a very low melting salt. The melting point of this salt lies at 127.8° C, and this is about 150° lower than that of any other simple salt. The present paper deals with the conductance of molten lithium chlorate, at a temperature slightly above its melting point, both pure and in the presence of trace addition. The theoretical treatment of the problem of conductance in melts is extensive, though somewhat inconclusive; it therefore seems to us best to limit this paper largely to an account of results obtained.

The electrical conductivities of aqueous solutions of lithium chlorate, ranging in concentration from dilute aqueous solutions to molten salt, were most recently determined by Campbell, Kartzmark, and Paterson (2), but for experimental reasons, there was a gap in the measurements between 90 and 100% lithium chlorate. This gap has now been filled.

EXPERIMENTAL

Lithium chlorate was prepared by the method of Kraus and Burgess (3), as modified by Campbell and Griffiths (4). Lithium chlorate is extremely hygroscopic and must be handled in a nitrogen-filled dry box. We used barium oxide to dehydrate the dry-box atmosphere. The final product ($LiClO_3$) was heated at 100° C, under high vacuum, for 6–8 weeks. The melting point obtained was 127.8° C.

Since we intended to admit, at first, only traces of water to the lithium chlorate, it was important that the lithium chlorate should be truly anhydrous. After abortive attempts at detection of water by infrared absorption, we were finally successful with gas chromatography. The method was as follows:

[1]*Holder of a Cominco Fellowship*, 1960–61.

A Precision Chromofrac VP-7 instrument was used: argon was the carrier gas. The instrument was calibrated for water by injecting samples of 0.01 ml ethyl alcohol containing known amounts of water. The lower limit of detection was found to be 1 part of water in 500 parts of alcohol, by volume. Lithium chlorate (31.101 g), mixed with dry sand, was heated in a hard-glass tube. Under the catalytic action of the sand, the lithium chlorate decomposed to chloride. The evolved oxygen, together with any moisture it might contain, was trapped in liquid nitrogen. A test of the residual showed that decomposition was complete.

The trapped gases were allowed to warm up slowly to 0° C and a measured quantity of ethyl alcohol then added. The solution was then allowed to warm up to room temperature and then passed through the chromatograph. The result showed that our preparation of lithium chlorate contained less than 0.006% water by weight.

For the conductance determinations we used a large double-jacketed thermostat containing 18 gal of Marcol GX oil. The temperature of the thermostat was 131.8° C±0.06° C; this fluctuation occurred over a cycle of steady rise and fall, as the heater went on and off. Temperatures were read on a Beckmann thermometer which had been calibrated against a platinum resistance thermometer. The method of conductance determination was identical with that used in dilute solution work. It is sufficient to say that the bridge used was a Leeds and Northrup Jones conductivity bridge. The input signals were provided by an audio oscillator. The output from the bridge was coupled through a three-stage amplifier to an oscilloscope. This circuit proved capable of detecting changes of less than 0.1 ohm in 3000 ohms. The conductance cell is represented in Fig. 1. Powdered anhydrous lithium chlorate was introduced into the weighed cell, in the dry box, and

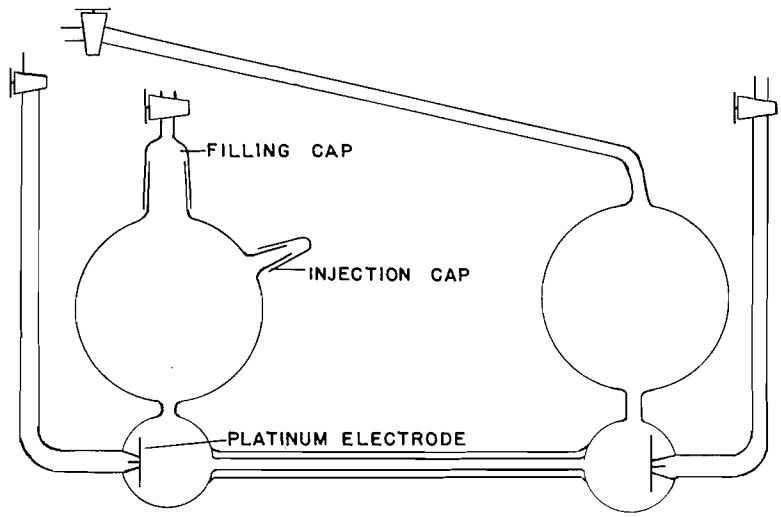

FIG. 1. The conductance cell.

the whole reweighed. When the cell was placed in the thermostat, the salt melted, leaving air bubbles along the capillary and attached to the electrodes. These were removed by causing the melt to flow into the bulbous compartments. After thermal equilibrium had been reached, the resistance of the cell was measured at the maximum and minimum temperatures of the bath fluctuation, using signal frequencies of 1,000, 5,000, and 10,000 cycles/sec. An oscilloscope was used as null point detector. A graph of temperature against resistance was then plotted for each of the frequencies used and the resistance corresponding to 131.8° C was then plotted against $1/\sqrt{(\text{frequency})}$ (Fig. 2). Extrapolation of this graph to infinite frequency gave the resistance of the cell in the absence of ionic polarization.

A calibrated syringe was used to introduce the addition reagents. The cell constant was determined after the completion of each experiment: no change was detectable.

In addition to the isothermal experiments at 131.8° C, the conductance of pure (molten) lithium chlorate was determined over the range of temperature 130°–140° C. The activation energy was obtained from a plot of $\log_{10} \kappa_{sp}$ vs. $1/T$. The slope of this straight line is equal to $-\Delta E_\kappa/R$.

EXPERIMENTAL RESULTS

The experimental results are summarized in Tables I and II. The activation energy derived from the data in Table I is 6.3 kcal/mole, between 130 and 140° C.

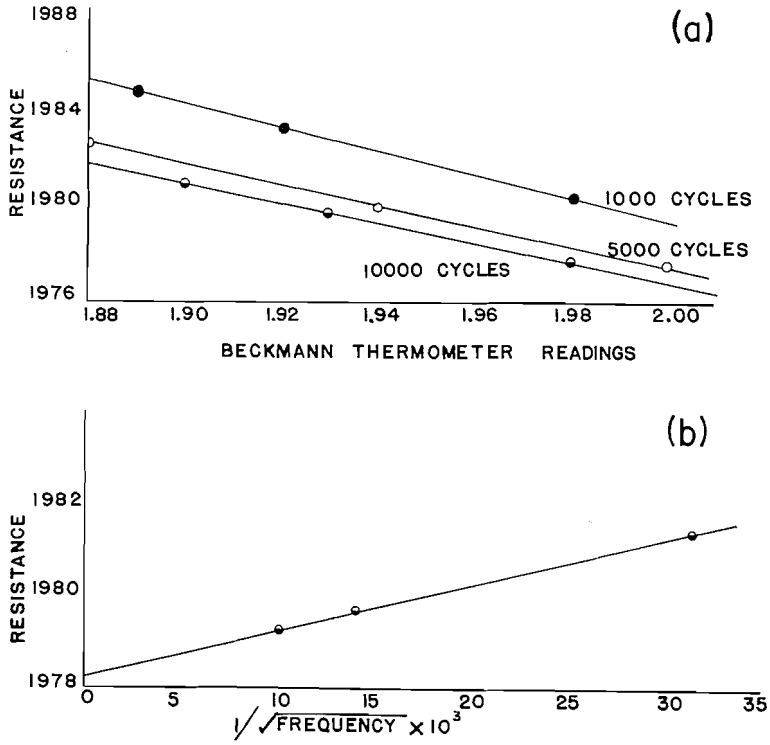

FIG. 2. (*a*) Resistance vs. Beckmann temperature. (*b*) Resistance at 131.8° C vs. $(1/\sqrt{F})\times 10^3$: an example showing the calculation of a resistance at infinite frequency.

TABLE I

Temperature, resistance, and specific conductance of pure molten lithium chlorate

Temperature (°C)	Resistance at infinite frequency (Ω)	Specific conductance	$(1/T)\times 10^4$	$\log_{10} \kappa_{sp}$
131.80	2350.0	0.1150	24.70	−0.9389
143.01	1903.0	0.1420	24.04	−0.8477
140.78	1973.0	0.1370	24.17	−0.8623
136.49	2149.0	0.1258	24.42	−0.8993
135.69	2222.8	0.1231	24.47	−0.9098
131.80	2347.4	0.1152	24.70	−0.9385

DISCUSSION OF RESULTS

The conductances with small additions of water are in good agreement with the figures of Campbell, Kartzmark, and Paterson (2), for solutions of 93.98 and 100 weight% lithium chlorate.

Nitrobenzene Additions

Nitrobenzene was found to have a very limited solubility in molten lithium chlorate. The maximum amount of nitrobenzene in a one-phase system at 131.8° was only 0.4 weight%.

TABLE II

Effect of small amounts of additive on conductance

Moles additive	Moles lithium chlorate	Percentage by weight additive	Resistance at infinite frequency (Ω)	Specific conductance
Water				
—	1.0	—	2350.0	0.1150
0.013	1.0	0.261	2308.2	0.1171
0.026	1.0	0.520	2248.6	0.1202
0.0394	1.0	0.779	2202.1	0.1227
0.0527	1.0	1.04	2174.6	0.1243
0.0656	1.0	1.29	2132.4	0.1268
0.0785	1.0	1.54	2075.3	0.1302
0.0922	1.0	1.80	2038.3	0.1326
0.1313	1.0	2.55	1977.4	0.1368
0.1445	1.0	2.80	1935.5	0.1397
0.2121	1.0	4.02	1812.8	0.1492
0.2758	1.0	5.21	1695.3	0.1594
0.3157	1.0	5.92	1657.1	0.1631
Nitrobenzene (density 1.19867)				
—	1.0	—	2353.8	0.1148
0.001335	1.0	0.1815	2359.2	0.1145
0.002667	1.0	0.362	2367.5	0.1142
Methyl alcohol (density 0.7928)				
—	1.0	—	2351.5	0.1149
0.06587	1.0	0.223	2358.2	0.1146
0.1218	1.0	0.43	2368.9	0.1141
—	1.0	—	2353.8	0.1148
0.1789	1.0	0.63	2373.0	0.1139
0.2686	1.0	0.94	2417.6	0.1118
0.3580	1.0	1.25	2474.7	0.1092

NOTE: Dielectric constants of additives: water, 78.54 at 25°; nitrobenzene, 34.82 at 25°; methyl alcohol, 32.63 at 25°.

Methyl Alcohol Additions

The solubility of methyl alcohol in lithium chlorate is large but a practical limit is set, at 131.8° C, by the fact that chemical decomposition of the methyl alcohol occurs at a concentration of methyl alcohol greater than 5% by weight; at least, gas bubbles are evolved, which adhere to the electrodes and block the capillary, rendering the resistance readings uncertain.

In order to compare the conductance of lithium chlorate in methyl alcohol as solvent with a corresponding concentration in water, a value of the specific conductance, at 25° C, of a solution of lithium chlorate in methyl alcohol, containing 55.8 weight% lithium chlorate, was determined. The value found was $\kappa_{sp} = 0.00939$. This should be compared with the corresponding figure for 55.71 weight% lithium chlorate in water of 0.1189 (2).

The specific conductance, related to the mole ratio of additive to lithium chlorate, is given in Table III. (The results are represented graphically in Fig. 3.)

The Arrhenius equation, when applied to the present results, gives:

$$\kappa_{sp} = A_\kappa \exp(-\Delta E_\kappa/RT).$$

Over the small temperature range of 130–140° C, the graph of $\log_{10} \kappa_{sp}$ vs. $1/T$ is essentially linear, giving an activation energy of 6.3 kcal/mole. This value is rather high and is comparable with those of mercuric chloride (5) and mercuric bromide (6), viz. 6.15 and 6.2 kcal respectively, but in the latter cases complex ion formation is known

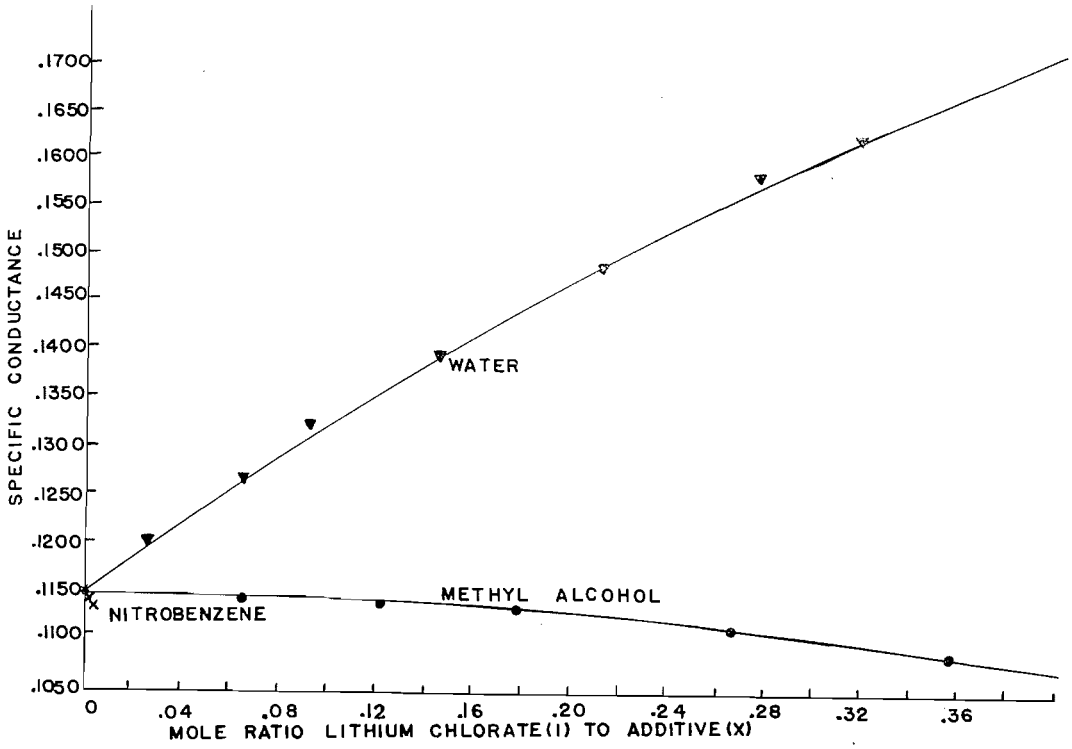

FIG. 3. Specific conductance vs. mole ratio of additive.

to occur. Yaffe and van Artsdalen (7) have shown that the value of ΔE increases considerably as the melting point is approached from a higher temperature, and it may be that the value of ΔE for lithium chlorate between 130° and 140° should not be considered as the true activation energy. Further experiments will determine the activation energy at higher temperatures.

The addition of a small amount of water increased the specific conductance considerably. The conductance of the pure melt at 131.8° C is 0.1150 ± 0.0002 mhos. The addition of 2% of water increases the specific conductance to 0.1336, an increase of 16%. This initial rate of increase of conductance is slightly greater than that found for additions of water between 2 and 6% (12%). This may indicate that the role played by the initial water molecules is not entirely the same as that of water molecules entering the system at higher dilution. It is possible that the effect of the addition of water is twofold, on the one hand causing an increase in the number of Li^+ ions available for conduction, on the other an increase in the effective size of the lithium ion, caused by its combination with water molecules. The first effect will increase the conductivity, whereas the latter will do the reverse. It can be assumed that the effect of the chlorate ion on conductance, under these conditions, is small and constant, because of its large size and consequent small mobility, compared with that of the (naked) lithium ion.

The second additive investigated was methyl alcohol. Little change in the conductivity is noticed until a mole ratio of 1:0.18 or 0.63% by weight of methyl alcohol is present. The tendency is towards a slow decrease in specific conductance. Thus a methyl alcohol/lithium chlorate solution of mole ratio 1:0.26 has a specific conductance of 0.1125 whereas

a comparable water/lithium chlorate solution has a specific conductance of 0.1560. The difference is presumably due to the much greater ionizing power of water; a fact substantiated when the conductance of a 55.8% lithium chlorate solution in methyl alcohol, specific conductance at 25° C 0.0094, is compared to an equivalent aqueous solution, specific conductance 0.115. Partial ionization of the lithium chlorate by the methyl alcohol present can be seen when the comparison is made with the effects of the third additive investigated, nitrobenzene. Though only a small addition is possible, the more rapid decrease in conductance for comparable mole ratios is immediately noticed.

These results suggest that in the case of lithium chlorate the predominating influence exerted by traces of nonelectrolytes upon the conductance may be that affecting the degree of ionization. Further experiments, which will involve determinations of density, viscosity, and conductance, will furnish us with a more complete study of the thermodynamic principles involved.

REFERENCES

1. R. M. Fuoss and F. Accascina. Electrolytic conductance. Interscience Publishers Inc., New York. 1959.
2. A. N. Campbell, E. M. Kartzmark, and W. G. Paterson. Can. J. Chem. **36**, 1004 (1958).
3. C. A. Kraus and W. M. Burgess. J. Am. Chem. Soc. **49**, 1226 (1957).
4. A. N. Campbell and J. E. Griffiths. Can. J. Chem. **34**, 1647 (1958).
5. J. O. M. Bockris, E. H. Crook, H. Bloom, and N. E. Richards. Proc. Roy. Soc. (London), A, **255**, 558 (1960).
6. G. J. Janz and J. D. E. McIntyre. Ann. N.Y. Acad. Sci. **79**, 790 (1960).
7. I. S. Yaffe and E. R. van Artsdalen. J. Phys. Chem. **60**, 1125 (1956).

A NEW PHOTOCHEMICAL REACTION: THE STRUCTURE AND ABSOLUTE STEREOCHEMISTRY OF ATISINE[1]

J. W. ApSimon[2] and O. E. Edwards
Division of Pure Chemistry, National Research Council, Ottawa, Canada

Received February 5, 1962

ABSTRACT

Irradiation of azides of diterpenoid acids with 1α- and 1β-carboxyl groups gave the corresponding isocyanates and ca. 25% yields of lactams. The azide of hexanoic acid under comparable conditions gave 8% of hexanamide. The reaction has been used to convert podocarpic acid to the enantiomer of the phenol III derived from atisine. This completes the structure proof of the atisine family of alkaloids, the Garrya alkaloids, and related diterpenes, and proves the absolute stereochemistry of these substances.

There is extensive evidence that the alkaloid atisine contains the features shown in rings B, C, and D of formula I (2, 3, 4). The evidence for the structure of ring A and the nitrogen-containing bridge was indirect, resting on the products of selenium dehydrogenation and superficial oxidation (3, 4) and on interpretation of n.m.r. spectra (3). Considerable evidence had been obtained for the relative and absolute stereochemistry shown in I (2, 3, 4). Very recently interrelation of the Garrya alkaloids, steviol, and kaurene, and extensive rotatory dispersion observations have provided confirmation of this absolute stereochemistry (5). However, since the structure of steviol and kaurene have not been rigorously proved, the ring A and hetero ring structure needed confirmation. We have now provided very direct proof of the correctness of the structure and absolute stereochemistry shown in I by partial synthesis of the N-acetyl phenol II from podocarpic acid. This proved to be the mirror image of the N-acetyl phenol III,

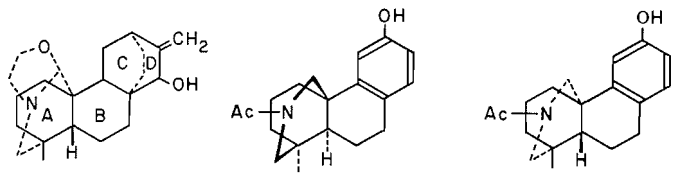

which had been prepared earlier from atisine (2).

For partial synthesis of II a method was sought of substituting the angular methyl (C-17) of resin acid derivatives. A very direct possibility of doing this and immediately forming the heterocyclic system IV common to all diterpenoid alkaloids of known structure suggested itself. Thermal decomposition of acid azides leads via electron-deficient nitrogen to the isocyanate. It seemed possible that if the intermediate were generated in close proximity to a saturated carbon the nitrene or diradical might substitute this carbon. We were encouraged in this conception by the report of attack of thermally generated nitrenes from aryl azides on methyl groups, giving rise to heterocyclic rings (6), i.e. V → VI (after oxidative aromatization).

[1]*Issued as N.R.C. No. 6791.*
A preliminary report of some of this work has been published (1).
[2]*N.R.C. Postdoctorate Fellow 1960–1962.*

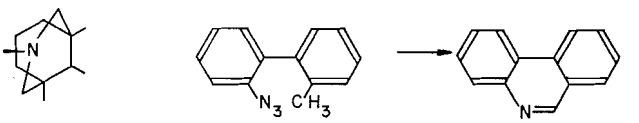

IV V VI

It seemed probable that the chance of attack on saturated carbon in the case of acid azides would be increased if the energy for decomposition was supplied by ultraviolet irradiation. Not only might the electron-deficient nitrogen then be more energetic, but it might be in a different electronic state (triplet rather than singlet), thus enabling the substitution reaction to compete favorably with the rearrangement.[3]

Previous work on the photolysis of acid azides had shown that isocyanates were produced as in the thermal reaction (7). It thus appeared imperative to have the saturated carbon exceptionally close to the electron-deficient nitrogen if we were to observe the desired reaction. We hence chose for study the azide of the trans-anti-cis acid VII available to us from other work (8). In this acid, ring C should provide steric compression of the angular methyl group, forcing it unusually close to the axial carboxyl.

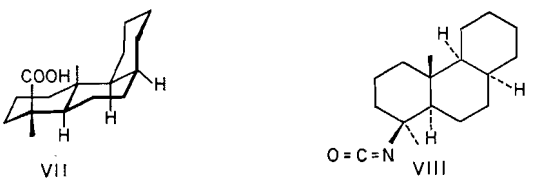

VII VIII

The azide of VII was prepared via the acid chloride and hydrazide. Because of its sensitivity it was not isolated, but merely characterized by its infrared absorption at 2145 and 1700 cm^{-1}. When a dry hexane solution of this was refluxed for 1 hour only the corresponding isocyanate VIII was produced. When the same solution was irradiated in a 1-cm quartz cell using a Hanovia ultraviolet lamp, at room temperature, there was steady evolution of nitrogen. After completion of the reaction the products were separated using chromatography on alumina. The isocyanate VIII, which was the main product (65%), was very readily eluted. The more strongly adsorbed products were a δ-lactam (9) ($\nu_{max}^{CHCl_3}$ 1665 cm^{-1}), in 25% yield, and a trace of γ-lactam (10) ($\nu_{max}^{CHCl_3}$ 1685 cm^{-1}), both of which gave correct analyses for $C_{18}H_{27}NO$. The δ-lactam could unambiguously be assigned the desired structure IX since the n.m.r. signal for the angular methyl group (C-17) which appeared at $\tau = 9.03$ in the spectrum of the parent acid and $\tau = 9.09$ in that of the hydrazide was missing from its spectrum (n.m.r. spectra of carbon tetrachloride solutions with tetramethylsilane as internal standard). The γ-lactam was either

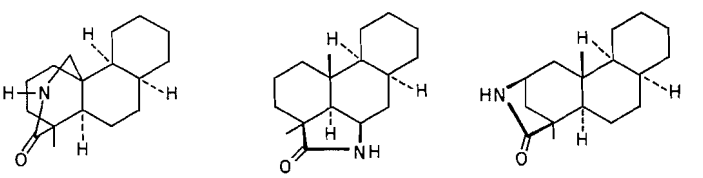

IX X XI

[3]*The rearrangement most likely involves migration of the alkyl group with its full complement of electrons, and hence requires a singlet state of nitrogen (nitrene).*

X or XI, but insufficient evidence was available to distinguish between these possibilities.

In order to pursue the potentialities of the substitution and to assess the importance of the steric compression discussed above we next examined the azide of the methyl ether of podocarpic acid (XII). With the flattened ring C, this should have the methyl and carboxyl functions at a more normal 1,3 diaxial distance. The photolysis of XII in hexane proceeded smoothly. To our surprise a 25% yield of a mixture of lactams was

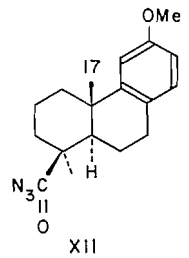

XII

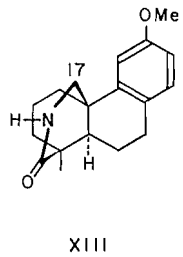

XIII

again produced. The δ-lactam which predominated crystallized on the walls of the photolysis cell. It analyzed for $C_{18}H_{23}NO_2$ and had ν_{max}^{nujol} 1655 cm^{-1}. Since the high-field signal expected for an angular methyl group (C-17) was absent from its n.m.r. spectrum it clearly had structure XIII. A 5% yield of γ-lactam (ν_{max}^{nujol} 1695 cm^{-1}) was also produced.

In order to examine the reaction under conditions where only secondary carbon could be substituted the azide (XIV) from dihydropimaric acid was prepared. When this was irradiated in hexane a lactam again crystallized on the walls. This analyzed for $C_{20}H_{31}NO$ and had $\nu_{max}^{CHCl_3}$ 1685 (γ-lactam). In view of the geometric limitations this can only be XV. The yield was similar (26%) to that in the methyl substitution. The

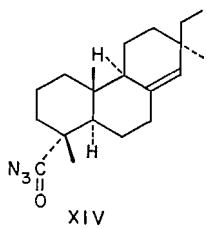

XIV

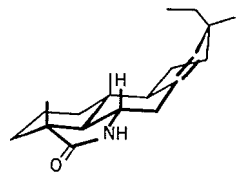

XV

reaction thus provides a new[4] and potentially valuable method for introducing substituents on ring B of the resin acids.

Finally, in an attempt to observe the proportion of γ- and δ-lactams formed when equivalent methylenes were available for substitution, the azide of hexanoic acid was irradiated. An 8% yield of hexanamide was produced, probably by hydrogen abstraction from the solvent. The other products besides isocyanate were a complex mixture, which will be the object of further study.

As discussed by Smolinsky for the thermal decomposition of aryl azides (4, 11) the photolysis of acid azides could involve the singlet nitrene XVI or the corresponding

[4]*Chromic acid oxidation has been used to place oxygen on ring B of resin acids with an aromatic ring C (12), and in the case of one pimaric acid isomer (Ukita's acid) (13) selenium dioxide has been used to introduce oxygen on* C-9.

triplet diradical XVII (unpaired spins of two of the unshared electrons). He produced evidence for the triplet character of the nitrogen in the thermal reaction (11).

XVI XVII

We consider that the formation of the hexanamide from the azide proves the diradical nature of the nitrogen doing the hydrogen abstraction in this photolysis. Had the nitrene state done the hydrogen abstraction the first stage would be as in (*a*):

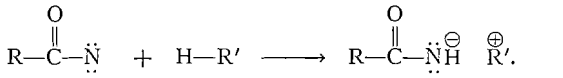

(*a*)

The charged particles in the non-polar solvent would form an ion pair which would collapse to uncharged RCONHR′. While it seems probable by analogy that the lactam formation also involves a triplet nitrogen as shown:

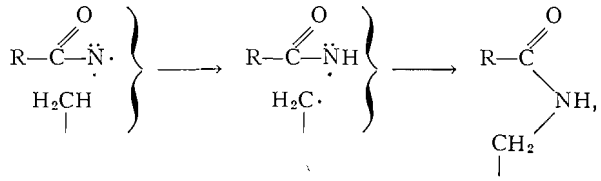

the product could equally well arise from nitrene as in (*a*) or by insertion of nitrene into the C—H bond. An attempt to decompose the azide of dihydropimaric acid by energy transfer from triplet benzophenone (14), and hence get information about the mechanism, produced no change in product ratio or yield over photolysis without the benzophenone.

This reaction takes its place with the Hofmann–Loffler–Freytag reaction (15, 16) and the recently developed photolysis of aliphatic azides (17) as a means of forming nitrogen-containing rings by substitution on saturated carbon. The latter two reactions seem to preferentially form pyrrolidine rather than piperidine rings (six-membered cyclic transition state for hydrogen abstraction). The formation predominantly of piperidone in the compounds with a 1β-carboxyl when two possibilities for pyrrolidone formation were present is remarkable. This is particularly so if hydrogen is abstracted as hydride ions or hydrogen atoms, since this should be easier from secondary than from primary carbon. The proximity of the 1β-carboxylic function and the angular methyl is the most probable cause of this preferential δ-lactam formation.

With lactam XIII readily available we were now in a position to synthesize phenol II. Hydrolysis of XIII with hot constant-boiling hydrobromic acid gave the phenolic lactam, which was then reduced by lithium aluminum hydride in refluxing dioxane to the secondary aminophenol. This was acetylated, then partially hydrolyzed to the N-acetyl phenol II. This melted at 279–280° and its infrared spectrum (nujol mull) was identical with that of the N-acetyl phenol from atisine (2). However, its rotation was +112°, compared to −105° for the atisine degradation product. This proves decisively that the latter is correctly represented by III and that atisine has the structure and

stereochemistry illustrated in I. Since podocarpic acid has been synthesized (18), this work opens a way to total synthesis of the mirror images of diterpenoid alkaloids.

EXPERIMENTAL

Rotations were of ethanol solutions, infrared spectra were of Nujol mulls, unless otherwise stated, and melting points were taken on a Kofler hot stage.

Azide of VII

1β-Carboxy-1α,12β-dimethyl-*trans*-anti-*cis*-perhydrophenanthrene (8) (850 mg) in dry ether (25 ml) and pyridine (3 drops) was allowed to react with thionyl chloride (2 ml) for 2 hours at room temperature. The precipitated pyridine hydrochloride was removed by filtration and the solution evaporated *in vacuo*, yielding a pale yellow oil (870 mg) which crystallized on standing. This product showed infrared absorption at 1795 cm^{-1} (acid chloride) but none at 1695 cm^{-1} (COOH). The acid chloride was readily hydrolyzed to the parent acid.

The acid chloride (800 mg) in ether (50 ml) was added to 100% hydrazine hydrate (2 ml) in absolute ethanol (10 ml) at 0° C. The mixture was vigorously shaken for 3 minutes, poured into water, and extracted with ether. The ether extract was washed well with water, dried, and evaporated, yielding a crystalline product forming colorless needles (780 mg) from ether/*n*-hexane, m.p. 160°, $[\alpha]_D$ +47° (*c*, 0.34). Found: C, 73.14; H, 10.71; N, 10.28. Calc. for $C_{17}H_{30}N_2O$: C, 73.33; H, 10.86; N, 10.06. Infrared spectrum: ν_{max} 3400 cm^{-1}, 1600 cm^{-1} (amide).

The above hydrazide (500 mg) was dissolved in acetic acid (20 ml) and cooled to 0° C. A saturated solution of sodium nitrite (250 mg) in water was added and the mixture vigorously shaken for 1 minute. The mixture was diluted with water and extracted several times with *n*-hexane. The extract was washed with ice-cold water, 5% sodium bicarbonate, and water again, then dried with anhydrous sodium sulphate. The infrared spectrum of this hexane solution showed absorption at 2145 cm^{-1} and 1700 cm^{-1} (acid azide).

Photolysis of the Azide of VII

The hexane solution of the azide was irradiated using a Hanovia ultraviolet lamp, at room temperature, in a 1-cm quartz cell. The photolysis cell had a capacity of ca. 150 ml and was fitted with a circulating device. A similar quartz cell, through which cold water was passed, was placed between the light source and the photolysis cell to keep the reaction cool. A steady evolution of nitrogen was observed and the disappearance of the azide bands in the infrared spectrum was complete after 6 hours. The reaction mixture was evaporated, yielding a pale yellow oil (260 mg) which was chromatographed on alumina (Grade IV, 7 g) in hexane. The following fractions were obtained.

Eluant	Fraction No.	Wt. (mg)	Infrared indicates
Hexane	1, 2	163	Isocyanate
Hexane/benzene (70/30)	3–5	5	γ-Lactam
Benzene/chloroform (30/70)	10–15	62	δ-Lactam

The isocyanate (VIII) was sublimed at 90° at 10^{-4} mm, yielding colorless prisms, m.p. 64–66°, $[\alpha]_D$ +36°, (*c*, 1.07). Found: C, 78.26; H, 10.39; N, 5.56. Calc. for $C_{17}H_{27}NO$: C, 78.11; H, 10.41; N, 5.36. Infrared spectrum: ν_{max} 2250 cm^{-1} (isocyanate).

The next eluted product was the γ-lactam (X or XI), m.p. 182°, $[\alpha]_D$ +27° (*c*, 0.33), forming colorless needles from ethanol. Sublimation at 170° at 10^{-4} mm yielded the analytical sample. Found: C, 78.38; H, 10.13. Calc. for $C_{17}H_{27}ON$: C, 78.11; H, 10.41. Infrared spectrum: ν_{max} 1680 cm^{-1} (γ-lactam). The more strongly absorbed δ-lactam (IX) was crystallized twice from ether/pentane and sublimed at 120° at 10^{-3} mm to yield colorless needles, m.p. 183°, $[\alpha]_D$ +23° (*c*, 2.02). Found: C, 78.37; H, 10.13; N, 5.25. Calc. for $C_{17}H_{27}NO$: C, 78.11; H, 10.41; N, 5.36. Infrared spectrum: ν_{max} 3200 cm^{-1} (>NH), 1650 cm^{-1} (δ-lactam); 1665 cm^{-1} in CCl_4.

Thermal Rearrangement of the Azide of VII

The hexane solution of the azide from a comparable run was refluxed for 1 hour, cooled, and evaporated to yield quantitatively the isocyanate (VIII) described above.

Photolysis of O-Methyl Podocarpic Acid Azide (XII)

A hexane solution of this azide (XII) was readily prepared using the previous procedure. The hydrazide prepared during this sequence readily crystallized from ethyl acetate as colorless needles, m.p. 166°, $[\alpha]_D$ +124° (*c*, 0.38). Found: C, 71.39; H, 8.62; N, 9.51. Calc. for $C_{18}H_{26}O_2N_2$: C, 71.49; H, 8.67; N, 9.26. Infrared spectrum: ν_{max} 3350 cm^{-1} (>NH), 1615 cm^{-1} (amide), 1600 cm^{-1} and 1560 cm^{-1} (aromatic).

A hexane solution of XII (ν_{max} 2150 cm^{-1} and 1700 cm^{-1}) from 1 g of hydrazide was irradiated as described for VII. After 2 hours a colorless crystalline product was observed forming on the windows of the photolysis cell. After 16 hours the disappearance of the azide absorption was observed in the infrared spectrum of the solution. The hexane solution was decanted and chromatographed on alumina (Grade IV). The isocyanate was eluted with hexane as a colorless oil (500 mg) which slowly crystallized. Sublimation at 80° at 10^{-3} mm gave colorless prisms, m.p. 62°, $[\alpha]_D$ +89° (*c*, 1.32). Found: C, 75.93; H, 8.10; N, 5.05. Calc. for $C_{18}H_{23}NO_2$: C, 75.75; H, 8.12; N, 4.91. Infrared spectrum: ν_{max} 2260 cm^{-1} (isocyanate), 1600 cm^{-1} and 1560 cm^{-1} (aromatic). Elution with benzene/hexane (1/1) yielded a crystalline product (45 mg) forming needles from acetone, m.p. 284°. This was too insoluble for a rotation determination. Found: C, 75.92; H, 8.08; N, 4.88. Calc. for $C_{18}H_{23}NO_2$: C, 75.75; H, 8.12; N, 4.91. Infrared spectrum: ν_{max} 1695 cm^{-1} (γ-lactam), 1600 cm^{-1} and 1560 cm^{-1} (aromatic).

The product which crystallized on the window of the photolysis cell was collected and recrystallized from ethanol, yielding colorless prisms of XIII (190 mg), m.p. 274°, $[\alpha]_D$ +41° (*c*, 0.33). Found: C, 76.03; H, 8.14; N, 4.96; OMe, 10.80. Calc. for $C_{17}H_{20}NO(OMe)$: C, 75.75; H, 8.12; N, 4.91; OMe, 10.88. Infrared spectrum: ν_{max} 3300 cm^{-1} (>NH), 1655 cm^{-1} (δ-lactam), 1600 cm^{-1} and 1560 cm^{-1} (aromatic).

Thermal Rearrangement of XII

The hexane solution of the acid azide (XII) was refluxed for 1 hour and evaporated to yield quantitatively the isocyanate, $[\alpha]_D$ +89° (*c*, 0.73), described above.

Synthesis of Phenol II

A solution of the lactam (XIII) (200 mg), obtained from O-methyl podocarpic acid, in acetic acid (3 ml) and 48% hydrobromic acid (10 ml) was refluxed for 3 hours. The cooled mixture was evaporated to dryness *in vacuo*, yielding a colorless product (160 mg) which was crystallized from ethanol to yield needles, m.p. 347°. This was too insoluble for a rotation determination. Found: C, 74.97; H, 7.82. Calc. for $C_{17}H_{21}NO_2$: C, 75.24; H, 7.80. Infrared spectrum, ν_{max} 3300 cm^{-1} (>NH), 3140 cm^{-1} (—OH), 1650 cm^{-1} (amide), 1600 cm^{-1} and 1560 cm^{-1} (aromatic).

The phenolic lactam (150 mg) was dissolved in hot dioxane (75 ml), and lithium aluminum hydride (100 mg) in ether (10 ml) was added at such a rate that the ether distilled off. The mixture was refluxed for 2 hours, cooled, and the excess lithium aluminum hydride was decomposed with ethereal methanol. Evaporation to dryness *in vacuo* yielded a colorless product, which was extracted several times with warm ethanol. The ethanol extract yielded a secondary amine (110 mg) which exhibited no infrared absorption in the carbonyl region but complex absorption in the 3500 cm^{-1}–3300 cm^{-1} region (amine + phenol).

This amine was dissolved in pyridine (5 ml) and acetic anhydride (5 ml). The solution was refluxed for 40 minutes, cooled, and poured into 2 *N* hydrochloric acid (50 ml). The product was extracted into ether. The ether solution was washed well with water and 2 *N* hydrochloric acid, dried, and evaporated, yielding a pale yellow oil (91 mg) which showed no absorption in the hydroxyl region of its infrared spectrum but had absorption at 1738 cm^{-1} (acetate) and 1610 cm^{-1} (amide). This product was dissolved in methanol (15 ml) and water (5 ml). Potassium hydroxide (10 ml, 5%) was added and the mixture refluxed for 3 minutes. The solution was cooled and extracted with ether. The aqueous layer was acidified with 2 *N* hydrochloric acid and extracted with chloroform. The chloroform extract was dried and evaporated to yield a crystalline residue (53 mg). Recrystallization from acetone gave small colorless prisms, m.p. 279–280°, $[\alpha]_D$ +112° (*c*, 0.45). Found: C, 76.40; H, 8.34. Calc. for $C_{19}H_{25}NO_2$: C, 76.22; H, 8.42. The infrared spectrum of this N-acetyl phenol (II) was identical with that of the phenol (III) obtained from the degradation of atisine.

Photolysis of Dihydropimaric Acid Azide (XIV)

A hexane solution of the above azide (XIV) was prepared using the described procedure. The hydrazide formed colorless needles from aqueous ethanol (900 mg), m.p. 156–157°, $[\alpha]_D$ 7° (*c*, 0.76). Found: C, 75.64; H, 10.60; N, 8.88. Calc. for $C_{20}H_{34}N_2O$: C, 75.42; H, 10.76; N, 8.80. Infrared spectrum: ν_{max} 3380 cm^{-1} (>NH), 1620 cm^{-1} and 1590 cm^{-1} (amide). The hexane solution of the acid azide prepared from this hydrazide (850 mg), which showed infrared absorption at 2130 cm^{-1} and 1700 cm^{-1}, was irradiated as described for VII. After 12 hours the disappearance of azide absorption was observed and the solution was then evaporated to dryness and chromatographed on alumina (Grade IV). Hexane eluted the isocyanate (520 mg) as a colorless oil, b.p. 130–140° at 10^{-1} mm. Found: C, 79.82; H, 10.48. Calc. for $C_{20}H_{31}NO$: C, 79.67; H, 10.37. Infrared spectrum: ν_{max} 2245 cm^{-1} (isocyanate). The benzene eluates yielded a crystalline product, XV (153 mg), forming needles from aqueous methanol with m.p. 209°. The analytical sample sublimed at 162° at 10^{-4} mm as colorless prisms, m.p. 210°, $[\alpha]_D$ 7° (*c*, 0.9). Found: C, 79.82; H, 10.51; N, 4.81. Calc. for $C_{20}H_{31}NO$: C, 79.67; H, 10.37; N, 4.65. Infrared spectrum: ν_{max} 3250 cm^{-1} (>NH), 1690 cm^{-1} and 1640 cm^{-1} (γ-lactam), 1685 cm^{-1} (in $CHCl_3$, γ-lactam). Dihydropimaric acid (250 mg) in hexane (150 ml) was unchanged after photolysis for 12 hours.

Photolysis of Hexanoic Azide

Hexanoyl chloride (2 g) in dioxane (25 ml) and sodium azide (2.5 g) in water (10 ml) were vigorously shaken for 5 minutes and extracted with cyclohexane. The organic layer was well washed with water, 5% sodium bicarbonate, and water again, then dried with anhydrous sodium sulphate. This solution, which exhibited infrared absorption at 2130 cm^{-1} and 1710 cm^{-1} (acid azide), was irradiated as described for VII during 12 hours. The only product that could be readily separated from the resulting mixture was the amide of hexanoic acid (230 mg), m.p. and mixed m.p. 99–100° after sublimation at 70° at 10^{-4} mm and having the requisite infrared spectrum. Found: C, 62.90; H, 11.23; N, 12.09. Calc. for $C_6H_{13}ON$: C, 62.57; H, 11.38; N, 12.16.

REFERENCES

1. J. W. ApSimon and O. E. Edwards. Proc. Chem. Soc. 461 (1961).
2. D. Dvornik and O. E. Edwards. Chem. & Ind. (London), 623 (1958); Can. J. Chem. In preparation.
3. D. Dvornik and O. E. Edwards. Tetrahedron, **14**, 54 (1961).
4. S. W. Pelletier. Tetrahedron, **14**, 76 (1961).
5. C. Djerassi, P. Quitt, E. Mosettig, R. C. Cambie, P. S. Rutledge, and L. H. Briggs. J. Am. Chem. Soc. **83**, 3720 (1961).
6. G. Smolinsky. J. Am. Chem. Soc. **82**, 4717 (1960).
7. A. Schönberg. Präparative organische Photochemie. Springer Verlag, Berlin. 1958. p. 192.
8. J. W. ApSimon, O. E. Edwards, and R. Howe. Can. J. Chem. **40**, 630 (1962).
9. O. E. Edwards and T. Singh. Can. J. Chem. **32**, 683 (1954).
10. O. E. Edwards, M. Chaput, F. H. Clarke, and T. Singh. Can. J. Chem. **32**, 785 (1954).
11. G. Smolinsky. J. Am. Chem. Soc. **83**, 2489 (1961).
12. E. Wenkert and B. G. Jackson. J. Am. Chem. Soc. **80**, 211 (1958).
13. O. E. Edwards and R. Howe. Can. J. Chem. **37**, 760 (1959).
14. G. S. Hammond. Abstracts of the 17th Organic Chemistry Symposium, American Chemical Society. June 25–29, 1961. p. 48.
15. E. J. Corey and W. R. Hertler. J. Am. Chem. Soc. **81**, 5209 (1959).
16. K. Schaffner, D. Arigoni, and O. Jeger. Experientia, **16**, 169 (1960).
17. D. H. R. Barton and L. R. Morgan. Proc. Chem. Soc. 206 (1961).
18. E. Wenkert and A. Tahara. J. Am. Chem. Soc. **82**, 3229 (1960).

KINETICS OF FORMATION OF ANODIC OXIDE FILMS ON BISMUTH

L. MASING[1] AND L. YOUNG
British Columbia Research Council, University of British Columbia, Vancouver, British Columbia
Received January 3, 1962

ABSTRACT

The steady-state and transient kinetics of formation of thin insulating anodic oxide films on bismuth have been investigated. The thickness of the films was determined by the spectrophotometric method. No dependence on the crystal face of the substrate was detected (sensitivity better than 1% with thicker films). The transient behavior was found to be somewhat different from that of tantalum. The activation distances were found to be unusually large. The dielectric properties were also investigated.

INTRODUCTION

Anodic polarization of bismuth electrodes immersed, for example, in dilute sodium hydroxide solution produces uniform, insulating oxide films which show bright interference colors, and which behave, in many ways, analogously with anodic oxide films on tantalum, aluminum, titanium, and similar more reactive metals (1, 2). Bismuth was chosen for the present study because it was thought that the comparison of the behavior of bismuth with that of materials which are so different in most other respects might be expected to help to show which aspects of the kinetics of anodic film growth are essentially characteristic of the process and which are special to the particular metal. In addition there is, of course, the possibility that some application may be found for the films, particularly since there have been only two or three papers on the subject since the exploratory work of Güntherschulze and Betz in 1931. Bismuth is obtainable in rather pure state, single crystals are easily grown, and, though this technique was not used, it is of interest, in view of recent trends, that thin layers of the metal are easily fabricated by evaporation.

EXPERIMENTAL PROCEDURES

The metal was obtained from the Consolidated Mining and Smelting Co. of Canada and was of 99.999% purity. Spherical single crystals about 2 cm in diameter were grown for us by K. G. Davis of the Physical Metallurgy Department of the University of British Columbia. Faces corresponding to (100), (110), and (111) on the pseudocubic description were prepared. These were abraded with metallurgical papers down to 4×0 paper and were then electropolished in a bath due to Hare and Mallon (3) containing 10 volumes ethanol, 10 volumes orthophosphoric acid (S.G. 1.75), and 3 volumes concentrated hydrochloric acid (S.G. 1.19) at a current density of approximately 100 ma cm^{-2} and cell voltage of around 2.5 volt using a tubular tantalum cathode. The bath was stirred. It was at an initial temperature of about 20° C. The specimens were washed in ethanol and water. They were then dipped into a 1:4 mixture by volume of concentrated hydrochloric acid and water and, finally, washed again in water before placing in the cell. Anodic oxide films were removed in the above acid solution and the specimens were reused several times before repolishing.

Electrical contact to the specimens was made with a metal rod screwed into the bismuth crystals and insulated with apiezon-type waxes or epoxy resin. Various other stopping-off materials were tried in preliminary work. The technique was also tried of using a tantalum rod as connector, anodized to provide insulation and screwed in tightly either with or without a Teflon gasket.

Various cells were used. The kinetic work reported here was obtained with a cell similar to that used previously with tantalum (4). The reference electrode in the work quoted was a hydrogen electrode in the same solution. The whole cell was immersed in a water thermostat. It was not practical to bring the tip of the Luggin capillary very close to the specimen. In some experiments no capillary was used. In most of the

[1]*Present address: Sprague-T.C.C. (Canada) Ltd., 50 Bertal Road, Toronto 15, Ontario.*

work the ohmic drop of potential in the solution did not matter since it was independent of the thickness of the film at constant current and was eliminated in calculating such quantities as $\Delta V/\Delta D$. When it was necessary to correct for it, the electrolyte resistance R_e between anode and cathode was determined by extrapolating plots of series equivalent resistance against reciprocal frequency to infinite frequency; the ohmic fall was then taken as IR_e, where I denotes the total current.

The electrolyte used in the work quoted was 0.1 M sodium hydroxide in distilled water. The specimen was immersed for 5 minutes before starting formation in order to let it take up the temperature of the bath. The solution was circulated rapidly during formation.

The formation was at constant current and was controlled using the automatic electronic device used previously for tantalum (e.g., ref. 4). This terminates the current when a preset voltage is reached with respect to the reference electrode, and exhibits the times required to traverse successive 1- or 10-volt intervals during formation. Other equipment, such as the a-c. bridge and the spectrophotometric apparatus, were also as previously described.

RESULTS

General Behavior

The initial questions to which answers should be sought were clear from previous work on tantalum (e.g., refs. 4–8). The difficulty is, of course, that bismuth does not behave as ideally as does tantalum. With tantalum, for example, the current efficiency for the production of oxide is very close to 100% over a wide range of current density and temperature in a wide variety of solutions. With bismuth, oxygen evolution occurs more readily. However, under favorable conditions, the reduction in current efficiency due to this side reaction is not excessive. Numerical values are given later. Another difference from tantalum is that the film material is appreciably soluble. The films are also shown to be unstable by increases in the dielectric losses with time on standing in the solution. Possibly, as with aluminum (9), a non-aqueous or partly non-aqueous solution could be found that would give more ideal behavior, but experiments made with various common non-aqueous solvents that have been used for anodizing did not uncover any preferable alternative. In preliminary experiments various forms of non-ideal behavior were encountered. In the final experiments, quoted here, the behavior was very reasonably reproducible. The chief limitation was that we were able to obtain accurate kinetic data only over a rather limited range of temperature.

The field in the oxide required to produce a given ionic current density of the order of a few ma cm^{-2} is roughly of the order of one sixth of the value for tantalum. In other words, films formed at a few ma cm^{-2} to 10 volt on bismuth are of the same order of thickness as films formed to 60 volt on tantalum. However, the total maximum thickness that can be produced before breakdown occurs is of the same order as with tantalum. This is perhaps not without significance. Under the conditions of the present experiments the current efficiency fell off quickly at a little over 50 volt, more or less, according to whether the current density was higher or lower.

Except following breakdown, the films were structureless under the light microscope. They can be removed by attaching adhesive tape and pulling.

The experimental results to be presented are as follows. First, the dielectric properties of the film are discussed. The determination of thickness and derived quantities is then reviewed. The kinetic results are then described, first for steady-state conditions and then for transient conditions. The significance of the results in deciding the mechanism of the process is dealt with in the discussion section.

Dielectric Properties of the Oxide Film

Since the size of the specimens used for the kinetic studies gave capacitances that were too high for the accurate measurement of their frequency dependence, measurements were made with a smaller polycrystalline specimen of 99.999% material, about 0.86 cm^2

in area, of dimensions about 6 mm×3 mm×3 mm. This was stopped off with picien wax and etched in 70% nitric acid. It was immersed symmetrically in a large platinum tube electrode.

Figure 1 shows the reciprocal of the series equivalent capacity C_s (normalized to unity at 1 kc/s), and the loss tangent (tan δ) plotted against the logarithm of the frequency f

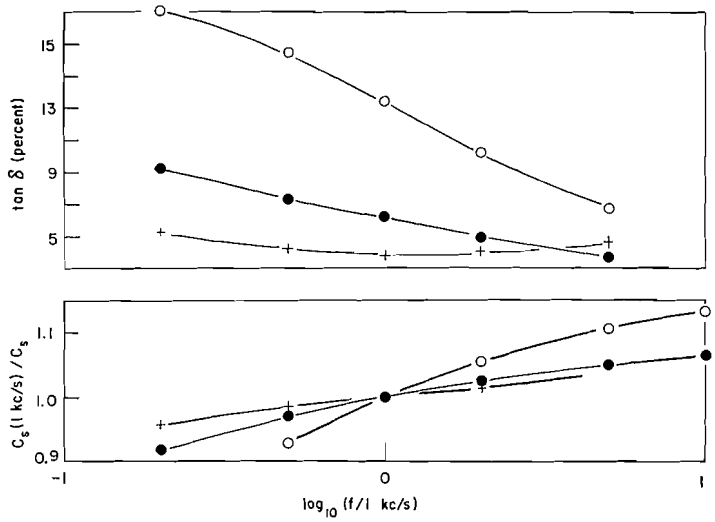

FIG. 1. Loss tangent (tan δ) and reciprocal series equivalent capacity (normalized) for three thicknesses of oxide (formed to voltages of 30 v (○), 10 v (●), and 3 v (+) at 2 ma cm^{-2} and 1.4° C) as function of frequency f of measurement.

for a series of films formed to 3, 10, and 30 volt respectively at 2.0 ma cm^{-2} and 1.4° C. To eliminate the time dependence, the measurements at the various frequencies were made first in order of increasing frequency and then back. The plotted values are the means. The figure shows that the dielectric losses are very much larger than would be found with non-porous films on tantalum or aluminum. The losses increase with increasing thickness of oxide.

Similar high dielectric losses with anodic oxide films on zirconium (10) may satisfactorily be explained by assuming that the films contain a comparatively high density of microfissures. The alternative would be that the dielectric losses of the flawless film material were unusually high. The electrolyte solution is supposed to penetrate into these cracks and to provide a parallel leakage conductance. The theory may be tested by varying the conductivity of the electrolyte. Figure 2 shows the effects with bismuth of reducing the concentration of the solution. The losses were, as expected, markedly decreased.

The increase in the losses with increasing thickness is also typical of films on zirconium and other metals. It appears that as the film thickens, stresses accumulate which cause cracking.

Reciprocal Capacity and Formation Potential

Figure 3 shows the reciprocal capacity at 1 kc/s plotted against the successive potentials to which the specimen was formed at the indicated current densities. The film was removed after each separate formation (see Experimental Procedure), and the next film then formed starting from the "bare" metal. The significance of such plots is as follows.

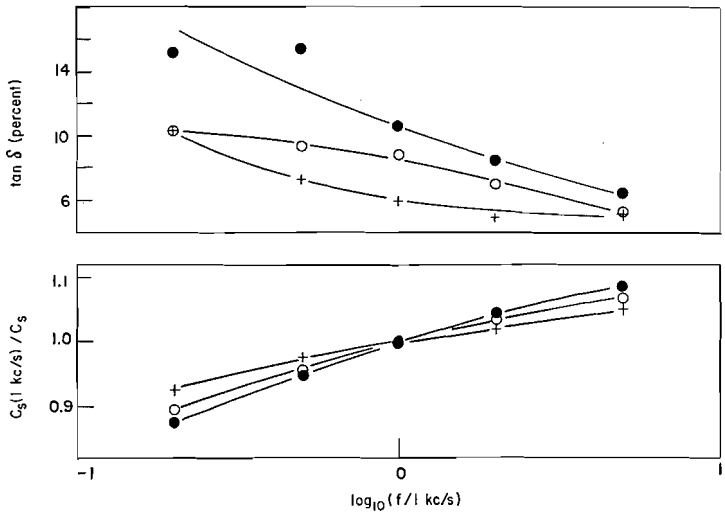

FIG. 2. Loss tangent and reciprocal capacity for a single film measured in 0.1 *M* NaOH (○), in 0.01 *M* NaOH (+), and remeasured in 0.1 *M* NaOH (●).

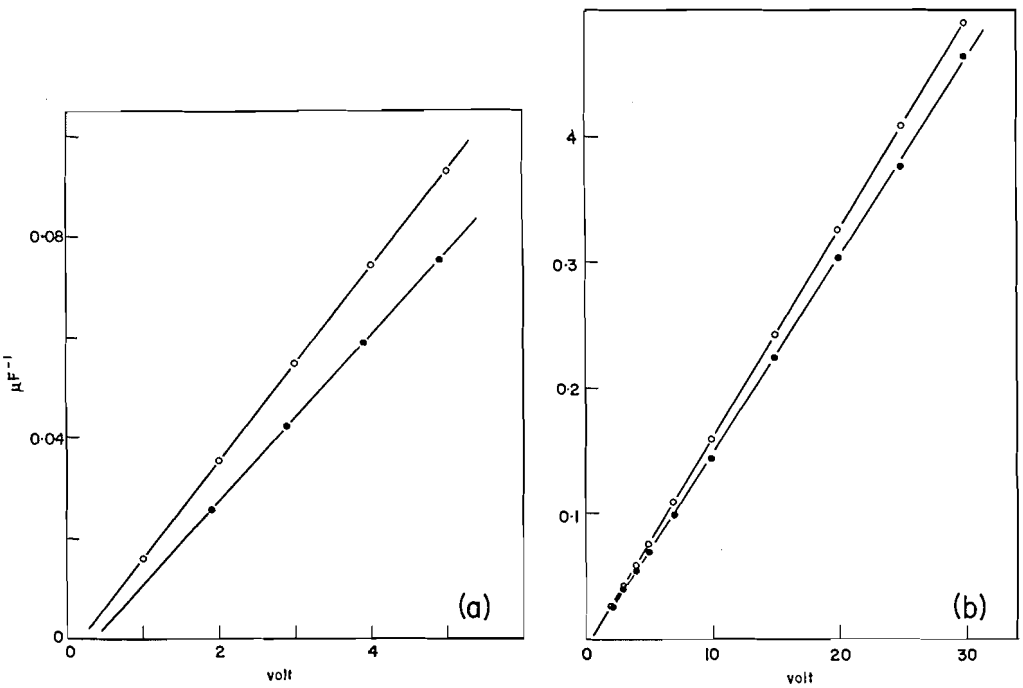

FIG. 3. (*a*) Reciprocal series equivalent capacity at 1 kc/s versus potential against hydrogen electrode in same solution to which the specimen was formed in 0.1 *M* NaOH at 0° C with current densities 0.2 ma cm^{-2} (○) and 2 ma cm^{-2} (●).
(*b*) Reciprocal capacity at 100 c.p.s. (●) and at 1 kc/s (○) versus potential (larger scale than (*a*)), for film formed at 2 ma cm^{-2} and 0° C.

The E.M.F. which causes the electrochemical formation of oxide is the oxide overpotential, defined as the actual potential of the electrode with respect to some reference electrode less the reversible potential for the oxide-producing reaction (in this case

assumed to be $2Bi + 3H_2O = Bi_2O_3 + 3H_2$, $E^0 = 0.37$ volt). The overpotential V may formally be considered to be made up of a possible contribution V_i from the interfaces oxide/metal and oxide/solution plus a term ED, where E is the mean overfield in the oxide (defined analogously with the overpotential) and D is the thickness of the film. The interfacial contribution will be expected to be independent of D but possibly to be dependent on the current density and the temperature. Thus

$$\begin{aligned} V &= ED + V_i \\ &= E\epsilon A/4\pi C + V_i, \end{aligned}$$

where ϵ is the dielectric constant, A is the area, and C is the capacity. Thus the slope of the plots is a measure of the field E and its constancy indicates either that ϵ and E are inversely correlated, or, more probably, that ϵ and E are independent of D. The deviation of the intercept on the voltage axis at zero $1/C$ from the calculated reversible potential is a measure of V_i. Clearly, V_i was of the same order as the experimental error, the observed deviation being within about 0.2 volt. Thus we expect differential measures of the field strength (of the form $\Delta V/\Delta D$) to equal integral measures (of the form V/D).

Thickness, Dielectric Constant, and Related Quantities

Principles of Method

There are several types of measurement that purport to give a measure of the thickness of the films. Each type involves one or more parameters, such as the density of the oxide, the refractive index, or the dielectric constant. By comparing the data from the various types of measurement, first a check is obtained that thickness is indeed being measured and that the films are uniform, and, secondly, various relations are obtained among the parameters. If sufficient of these may be taken as known, the values of the others may be deduced. The charge to form an increment of thickness x is expected to be

$$Q = xA\rho 6F/M, \qquad [1]$$

where A denotes true area; ρ, the density; F, the Faraday; M, the molecular weight (the oxide being presumed to be Bi_2O_3). The consequent change in reciprocal capacity is expected to be

$$\Delta(1/C) = x4\pi/\epsilon A, \qquad [2]$$

where ϵ denotes the dielectric constant. Minima in the specular reflectivity at a wavelength λ are expected to occur with successive increments of thickness,

$$x = \lambda/2n\cos\theta, \qquad [3]$$

where n is the refractive index, assumed constant, and θ is the angle of refraction. In previous work with tantalum and niobium, it was shown that it was not necessary to assume that the true area is equal to the measured macroscopic area, since the area may be eliminated between [1] and [2]. With bismuth, however, it seemed preferable to assume that the true area was equal to the apparent area. The calculation was done by first determining the field strength at various temperatures and current densities in terms of the optical thickness (involving n). Values of the fields were also obtained with the thickness calculated from the charge to form the films, using a method by which it was hoped to allow for current efficiencies below 100%. Comparison gave n/ρ. A similar procedure using the capacity to estimate the thickness gave ϵn. The refractive index here was for $\lambda = 4000$ Å. By also determining the field at one current density and temperature only in terms of n for $\lambda = 5890$ Å, the ratio of the refractive indices at these two

wavelengths was determined. Finally, a value of the index in sodium light was assumed. Corresponding numerical values for ϵ, ρ, and the field strengths could then be deduced. If a preferable value of any of these should later become available, it would be a simple matter to recalculate the data given here to fit the new value.

Optical Thickness

Figure 4 shows tracings of the spectrophotometer records of the minima in reflectivity, shown as maxima in "optical density," for specimens giving destructive interference at

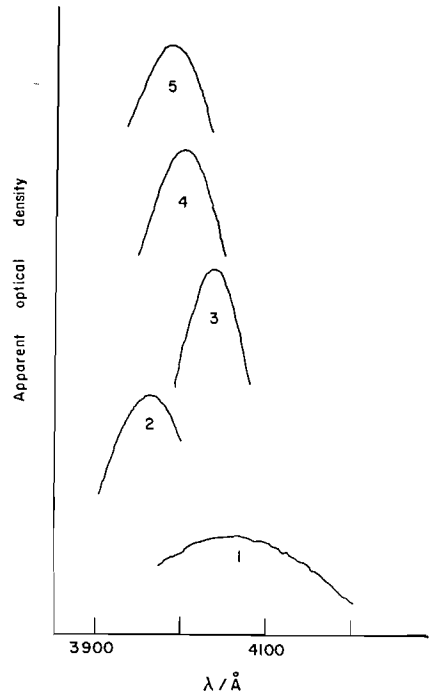

FIG. 4. Tracings of spectrophotometer recordings (apparent optical density) of minima in specular reflectivity (maximum in optical density) at near-normal incidence for films giving minima near 4000 Å in successive orders of interference.

successive orders at wavelengths near 4000 Å. The peaks are flattest in the first order, but are then the most sensitive to the thickness of oxide (cf. Fig. 5). The wavelength (λ) of the peak may be determined (excluding calibration errors of the instrument) to about 10 Å with thin films and 5 Å with thick films, giving a thickness (D) sensitivity of a few Å of oxide (see Table IV for $dD/d\lambda$).

Figure 5 shows plots of the wavelengths of the peaks versus voltage for specimens formed at a given current density and temperature. Such plots were interpolated to obtain estimates of the potentials corresponding to the thicknesses giving interference in successive orders at precisely 4000 Å for each current density and temperature. Numerical data are given in Table I. In all such experiments, each film was formed on "bare" metal, the previous film being first dissolved away.

Figure 6 shows the voltages giving interference at successive orders at 4000 Å plotted against order of interference (i.e., thickness in units of $\lambda/2n\cos\theta$ with arbitrary zero) for formation at a given current density and temperature. The plot is linear. This was

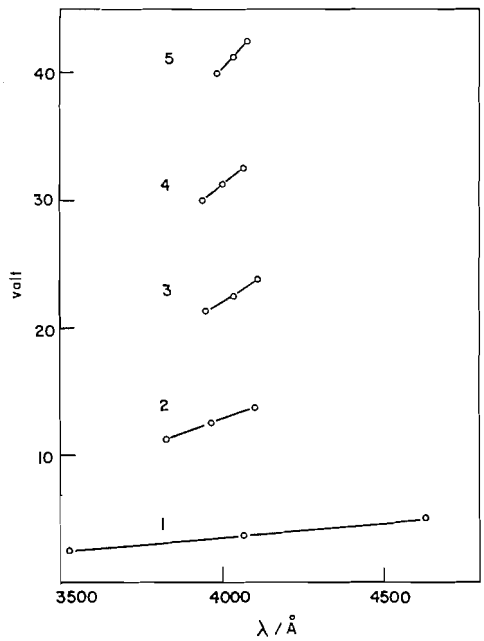

FIG. 5. Potential (against hydrogen electrode in the same solution) to which film was formed at 2 ma cm^{-2} and 25° C plotted against wavelength of interference for films giving interference at wavelengths close to 4000 Å in successive orders.

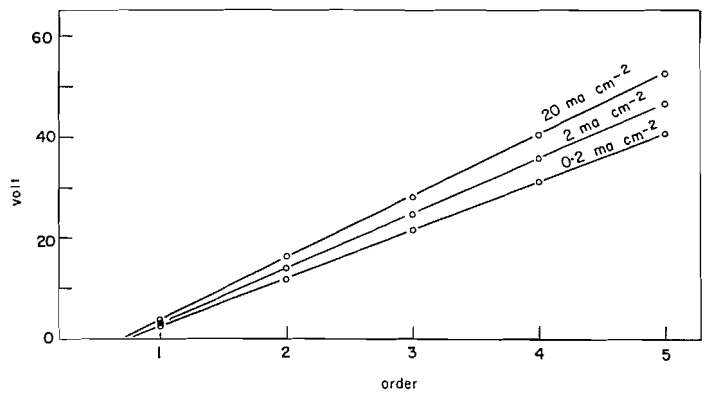

FIG. 6. Oxide overpotential (formation at 0.2, 2, and 20 ma cm^{-2} and 0° C) for films giving interference at 4000 Å in successive orders plotted against order of interference (i.e., thickness in arbitrary units with arbitrary zero).

typical and indicates the absence of detectable variation of field with thickness at constant current.* The slope of such plots, estimated graphically, was taken as a measure of the field strength for the conditions of the plot.

To obtain the dispersion of the refractive index between 4000 Å and 5890 Å, the slopes of two such plots were compared, one plot for each wavelength of interference. The ratio of the refractive indices was $n(4000\ \text{Å})/n(5890\ \text{Å}) = 1.19$ (estimated accuracy, ± 0.02). Thus if the (rather old) published (11) value of the index for white light is assumed as

*The unlikely alternative is that compensation occurs in that the various methods suggest constant field but that parameters such as the refractive index vary to compensate for an actual change in field.

TABLE IA

Potentials (in volts) against hydrogen electrode in the same solution (ohmic p.d. eliminated) corresponding to the thicknesses D_1, D_2, . . . giving interference at 4000 Å in successive order for various current densities and temperatures

	Total current density (ma cm^{-2}):					
D	0.2	0.63	2.0	6.3	20.0	20.9
At 0° C						
1	3.0		3.6		4.4	
2	12.4		14.3		16.7	
3	21.9		25.3		29.0	
4	31.5		36.3		40.9	
5	40.9		47.0		52.8	
At 25° C						
1	2.5	2.6	2.8	3.0	3.5	
2	10.1	10.8	12.2	13.0	14.3	
3	17.7	19.0	21.5	23.2	24.0	
4	25.7	27.7	30.9	32.9	35.5	
5	33.5	36.4	40.2	42.7	46.0	
At 50° C						
1						2.8
2						12.1
3						21.6
4						30.9
5						40.2

TABLE IB

Increases (rounded to nearest 0.1 volt) in potential corresponding to increase in thickness from D_1 to D_2, D_2 to D_3, etc. (i.e., by $\lambda/2n \cos\theta$) for various current densities and temperatures (this is a measure of the field in the oxide)

	Total current density (ma cm^{-2}):					
D	0.2	0.63	2.0	6.3	20.0	20.9
At 0° C						
2–1	9.3		10.8		12.2	
3–2	9.5		11.0		12.2	
4–3	9.6		11.0		12.0	
5–4	9.4		10.8		12.0	
At 25° C						
2–1	7.6	8.2	9.4	10.0	10.8	
3–2	7.6	8.2	9.3	10.1	10.8	
4–3	8.0	8.8	9.4	9.7	10.4	
5–4	7.8	8.7	9.3	9.9	10.6	
At 50° C						
2–1						9.4
3–2						9.5
4–3						9.3
5–4						9.2

n(5890 Å) = 1.91, we have n(4000 Å) = 2.27. The value 1.91 was obtained using a prism of metal converted to oxide by heating in air and cannot be considered reliable though it is the same as the mean of one pair of values tabulated by Larsen (12) for bismite. It is assumed quite arbitrarily and all the other numerical values of field, etc. are derived from this value. Furthermore, it is assumed that the refractive index is independent of the current density and temperature of formation.

Data on the capacities at 1 kc/s of films formed at 2 ma cm^{-2} at 0° C gave $\epsilon n = 140$, i.e. $\epsilon = 62$ for n(4000 Å) = 2.27.

The Charge to Form the Films

Figure 7 shows statistical plots illustrating the variations of the charge required to increase the potential by 1 volt during formation at a given current density and temperature. The individual values are grouped into successive 5-volt ranges. The plots are of the

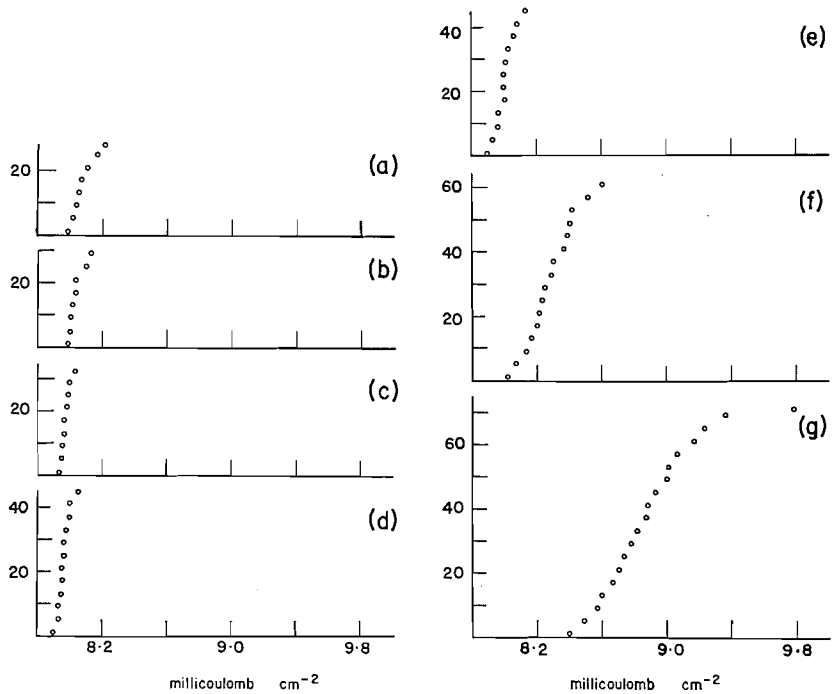

FIG. 7. The ordinate shows the number of specimen trials in which less than the charge/cm² indicated in the abscissa was required to form through 1 volt in the voltage intervals indicated at 2 ma cm⁻² and 25° C. The abscissa scale is common to the whole set of plots. (*a*) 31–36 v, (*b*) 26–31 v, (*c*) 21–26 v, (*d*) 16–21 v, (*e*) 11–16 v, (*f*) 6–11 v, (*g*) 1–6 v.

integrated type (13) instead of the usual distribution function type. The number of specimen trials which required less than a given amount of charge is plotted against the charge.

To use these plots, we rely on the principle that the charge can never be less than corresponds to 100% current efficiency* but that it can exceed this amount without limitations. Thus the estimated values of the charge can be less than the theoretical minimum only by the small measuring error.

To obtain an estimate of the theoretical charge, the plots of Fig. 7 are extrapolated to zero specimens and the intercept on the charge axis is taken as the required value. This gives an estimate of

$$\frac{dQ}{dV} = \frac{dQ}{dD}\cdot\frac{dD}{dV} = \frac{(A\rho 6F)}{M}\frac{1}{E}.$$

**To avoid misunderstandings, we note that references are occasionally made in the literature to current efficiencies greater than 100%. Such statements usually mean that the actual reaction was not that being assumed. In some cases the experimental result was really that the weight increase had been found to be greater than expected. This can occur, for example, if components of the solution have been absorbed by the oxide.*

Figure 8 shows how the results tended to vary with the potential. The charge was in all cases high at the beginning of the formation, then decreased as the thickness increased,

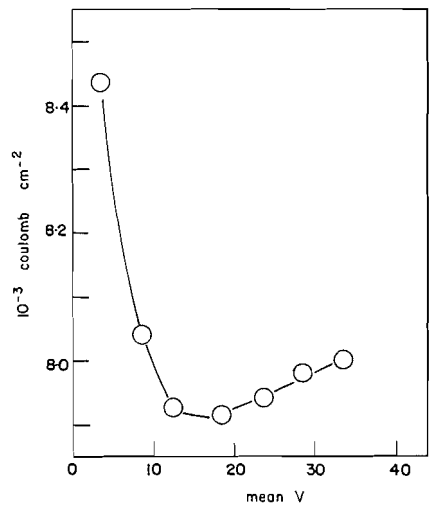

FIG. 8. Estimated minimum charge/cm² to form through 1 volt at 2 ma cm^{-2} and 25° C plotted against mean voltage (from intercepts in Fig. 7).

and finally rose slowly with further increase in thickness. Since the field calculated from the optical thickness showed no such variation over the same range of thickness, these variations appear to be without significance. A mean was taken of the values for each current density and temperature, excluding the values for voltages less than 10. The scatter of the data was least for the conditions of Fig. 8, i.e., 2 ma cm^{-2} and 25° C. Other data are given in Fig. 9.

Together with the fields from the optical thickness, the data gave an overall mean value of $n/\rho = 0.333$ (accuracy believed to be a few percent). With $n(4000\ \text{Å}) = 2.27$, this gives $\rho = 6.8$ g cm^{-3}. Published values of the bulk density fall in the range 8.2–8.9 g cm^{-3}. Evidently if the assumed index is correct, the films differ somewhat in properties from chemically prepared Bi_2O_3.

Current Efficiency

The field strengths obtained from the optical thickness refer to total applied current density. To estimate the ionic current density a mean was taken of the times required to traverse the last 1 volt (or 10 volt at the highest current density) before the current was terminated for all the specimens in the various orders of interference which were used to determine the field at a given applied current and temperature. This gave a mean dV/dt for these conditions. The ionic current density i was calculated from

$$i = \frac{1}{E}\frac{dV}{dt}\frac{6F\rho}{M},$$

where E was the optically determined field. A value of n/ρ is required and the value determined above was used. A value of n itself is not required. This gave the results for the current efficiency reproduced in Table II.

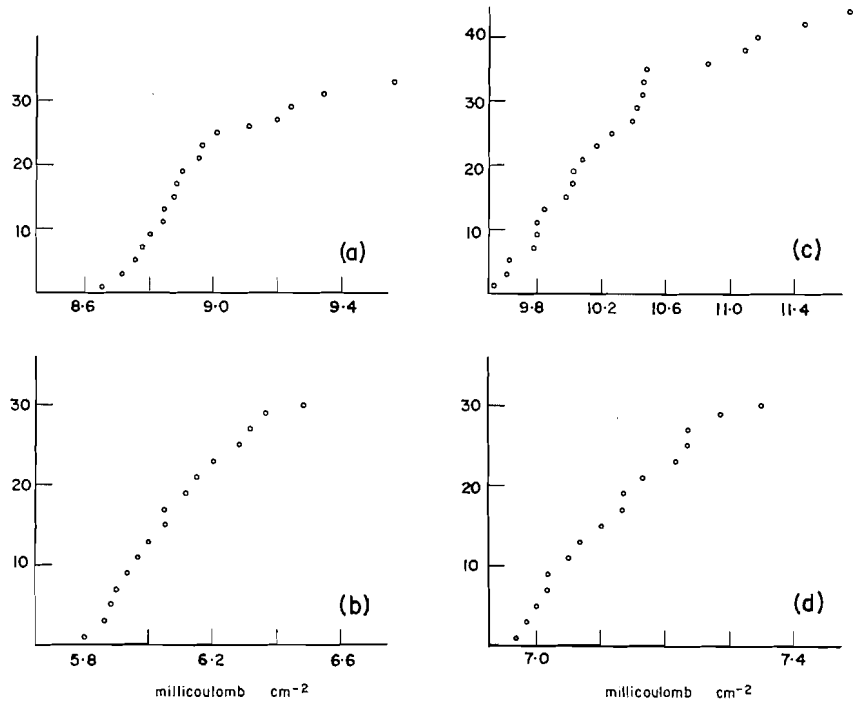

FIG. 9. Similar data to Fig. 7 for conditions shown. (*a*) 0.2 ma cm^{-2}, 0° C, 11–16 v; (*b*) 20 ma cm^{-2}, 0° C, 4–55 v; (*c*) 0.2 ma cm^{-2}, 25° C, 11–16 v; (*d*) 20 ma cm^{-2}, 25° C, 2–48 v.

TABLE II

Current efficiency for the formation of oxide calculated from rate of rise of potential (see text)

Total current density (ma cm^{-2})	Temperature (°C): 0	25	50
20	97	99	101
2	97	96	—
0.2	86	92	—

Zero of Thickness

Unless values of the optical constants of the metal are assumed, the spectrophotometric method gives a measure of increments of thickness rather than of absolute thickness. Three methods may be used to obtain a zero point. First, as shown above, the plots of reciprocal capacity versus potential (Fig. 3) suggest that if a plot is made of thickness with unknown zero against oxide overpotential (for a given current density and temperature), the intercept at zero overpotential would indicate the zero of thickness. Thus, in Fig. 6, this would give the thickness D_1 (say) of the film giving first-order interference at 4000 Å as a fraction 0.29 ($\pm 10\%$ spread) of the increment between orders (i.e., of $\lambda/2n \cos\theta = 884$ Å if $n(4000 \text{ Å}) = 2.27$). This gives $D_1 = 255$ ($\pm 10\%$ or more) Å. The second method is to plot the charge-to-form against the order of interference. This neglects the film present before anodization (with tantalum the thickness of this preexisting film can be estimated from the charge-to-form, with certain assumptions). The

plot shown in Fig. 10 is for 2 ma cm^{-2} at 25° C and, clearly, gave good agreement within the accuracy of the data. Thirdly, the increase in voltage that is required to produce a

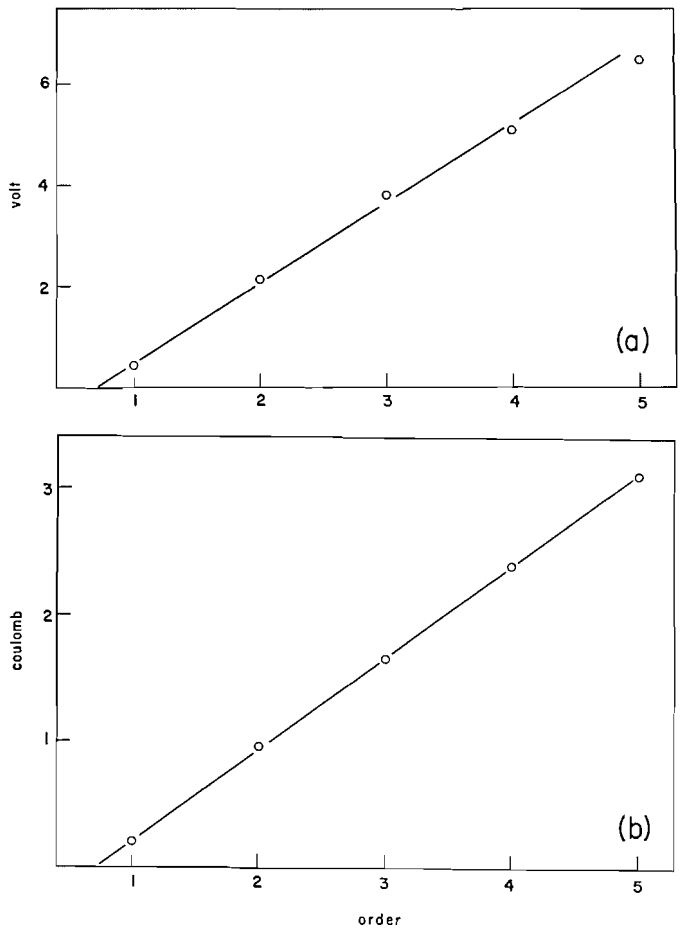

FIG. 10. (*a*) Increase in potential required to increase steady-state current density at 25° C by a factor of 10 plotted against order of interference. Mean values using all points available at each thickness.
(*b*) Total charge required to form at 2 ma cm^{-2} and 25° C to thicknesses giving destructive interference at 4000 Å in successive orders plotted against order of interference.

10-fold increase in current may also be plotted against the order of interference, as shown in Fig. 10. In drawing the line shown, the zero has been taken in agreement with that given by the above methods. This method involves fewer assumptions but is less precise.

Steady-State Kinetics

Figure 11 shows data on the field from the optical thickness versus $\log_{10}$ (ionic current density). The field and the ionic current density were determined as explained in previous sections. The difference between the total and the ionic current density is quite small on the logarithmic plot. The plots are linear within experimental error, but it is perhaps doubtful whether small deviations from linearity of the type observed with tantalum would have been detected, the accuracy being less than with tantalum.

With tantalum and niobium a mean value of $dE/d \log_e i$ (the equivalent of the Tafel slope in the kinetics of non-film-forming electrode processes) over a fixed range of i has

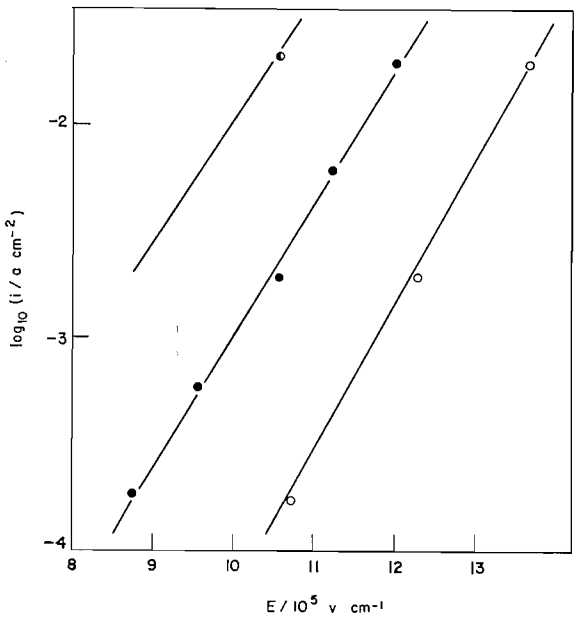

FIG. 11. Log_{10} (ionic current density) versus field strength at 0° C (○), 25° C (●), and 50° C (◐) in 0.1 *M* NaOH. The points are experimental, the continuous lines are calculated from the fitted equation (see text). The ionic current density was derived from dV/dt. The fields are differential values ($\Delta V/\Delta D$) derived from the slopes of plots such as Fig. 6.

been found to be nearly independent of temperature instead of proportional to temperature as expected on simple theory. With bismuth, as with aluminum, it has not proved possible to obtain accurate results over a wide enough range of temperature to obtain a real test of the temperature dependence of $dE/d \log_e i$. We, therefore, have chosen to fit the data with the expression $i = i_0 \exp \{-(W-qaE)/kT\}$. The constants are given with the number of digits needed to reproduce closely the experimental data. They are, of course, individually known to much lower accuracy. The values are $\log_{10} (i_0/\text{a cm}^{-2}) = 10.09$, $W = 1.14$ ev, and $a = 12.2$ Å, q being assumed to be $3e$, where e is the charge on the proton. The lines in Fig. 10 are calculated from the above expression with these values of the constants.

Transient Kinetics

As with other "valve metals," the system adjusts slowly to a sudden change in field or current. The field–current relations that have been reported above refer to the situation where a constant current has been applied for a long enough time to achieve steady-state conditions. Two types of experiment were made under transient conditions.

The first type of experiment consisted in applying a constant current until a steady state was set up and then suddenly changing the potential (i.e., the field). The current immediately after the change was determined by the method (4) described elsewhere (involving cathode ray oscilloscope photography). The "transient" Tafel slope defined as $\Delta E/\Delta \log_e i$ was then calculated. Results are given in Fig. 12 and Table III.

In the second kind of experiment, the current was recorded during the period after the field had been suddenly increased to a new value. Tracings of photographs are given in Fig. 13, which also contains the result of a similar experiment with tantalum. With

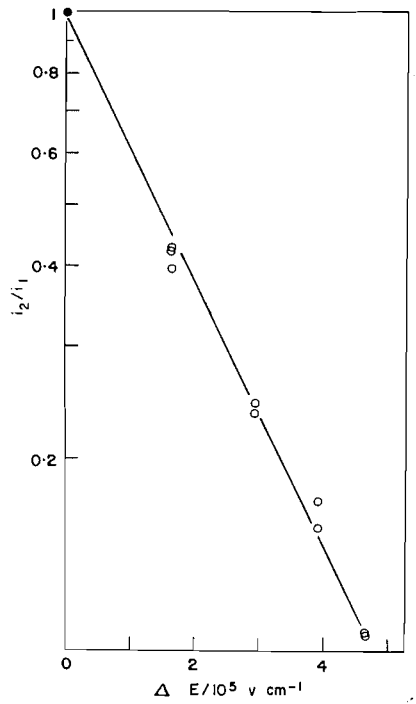

FIG. 12. Change in $\log_{10} i$ (shown as ratio i_2/i_1 of final to initial current with logarithmic scale) for sudden decrease ΔE in field (50° C, initial current $i_1 = 20.9$ ma cm^{-2}).

TABLE III

Transient Tafel slope and derived activation distance for mobility of ions (a_2)

Temperature (°C)	Initial total current density (ma cm^{-2})	$\Delta E/\Delta \log_e i$ (10^5 v cm^{-1})	a_2 (Å)
0	2.0	2.34	3.35
0	20.9	2.19	3.59
50	20.9	2.08	4.46

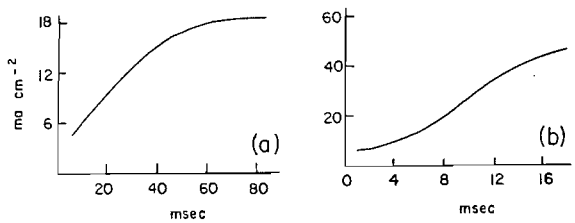

FIG. 13. (*a*) Tracing of oscilloscope photograph showing current versus time following sudden change as potential reached 20 volt from formation at constant current density (2 ma cm^{-2}) to formation at constant voltage (28 volt) for bismuth. Temperature 4° C.
(*b*) Similar but not identical experiment with tantalum. Initial formation at 4 ma cm^{-2} to 90 volt. After 1 minute on open circuit, 100 volt was suddenly applied.

tantalum (4), the current (after its initial sudden jump) increased slowly at first and then more rapidly. With bismuth, the current increased rapidly at first and then more slowly. It would have been preferable to have been able to check this result by working at lower

fields with specimens with a very low initial concentration of mobile ions. This experiment, however, is difficult because of the lower current efficiencies at lower current densities.

Dependence of Kinetics on Crystal Face

With tantalum no variation with crystal face of the substrate metal in the field required to produce a given ionic current has been detected. Probably a variation of 1% would have been found. On the other hand, with indium antimonide a difference was found by Dewald (14), though only at the low end of the range of field studied. Differences occur with titanium (15) and with zirconium and hafnium (16, 17), but only under circumstances that are not fully established. Differences have been found with thin anodic films on cadmium (18), but these are probably a special case, since the oxide is crystalline and epitaxial.

With spherical single crystals of bismuth, no variation in interference color could be seen by eye. To obtain numerical data, films were prepared on a single crystal on which three contiguous faces ((100), (111), and (110)) had been prepared. The specimen was formed at 0.2 ma cm^{-2} in one set of experiments, and at 20 ma cm^{-2} in another set, to a series of potentials giving interference near 4000 Å in successive orders. The wavelengths of the peaks were measured on the three crystal faces. The wavelengths of interference for the films on the three crystal faces were not entirely consistently in the same order but showed some tendency to be so. The maximum difference between any two faces at each formation voltage was calculated. The quantities $dD/d\lambda$ (i.e., the variation in film thickness corresponding to unit change of wavelength) were determined from the data of Fig. 5 for the successive thicknesses (say D_1, D_2, D_3, D_4) giving interference at 4000 Å. From the differences in λ and the $dD/d\lambda$, the corresponding maximum variation in oxide thickness between any two faces was calculated. The results are given in Table IV. The

TABLE IV

Test of possible variation of kinetics with crystal face of substrate metal

Order of interference	Maximum difference in λ between any two faces (Å)	$dD/d\lambda$	Maximum difference in D (Å)	D (Å)	Maximum percent variation in field
Formation at 20 ma cm^{-2} and 25° C					
1	67	0.18	12	250	5
2	19	0.66	12	1170	1
3	11	1.0	11	2080	0.5
4	7	1.4	10	2910	0.3
Formation at 0.2 ma cm^{-2} and 25° C					
1	19	0.17	3	190	2
2	28	0.67	19	990	2

maximum percentage change in field was about 5% at D_1, falling to 0.3% at D_4. Probably the small differences observed were due to slight variation between crystal faces in the ohmic potential fall in the solution. Variations in optical constants of the metal from face to face will not affect the above test.

Although no appreciable change was detected between crystal faces, the kinetic data given here were, as a precaution, obtained for a specific face, (111). It should be mentioned that in preliminary work with polycrystalline material, different crystal faces were sometimes found to show different colors. The reason for this was not discovered—possibly the effect is due to some variation in the state of the surface produced during its preparation prior to anodization, perhaps because the etching process was sensitive to the crystal face.

DISCUSSION

The discussion of the significance of the results as regards the fundamental mechanisms involved can only be tentative. The experimental results do not provide answers to all the questions that one would wish to ask and the possible alternative theories cannot be said to have been fully explored. Despite the recent intensive study of tantalum, the behavior even of this metal is not well understood.

As a preliminary point, we note that the evidence seems consistent with a uniform film though, of course, narrow transitional layers near the interfaces are not excluded.

The constancy of the field with thickness does not mean, as is sometimes stated, that there is no space charge present. It may mean either that the films are so thin and the space charge density so small that the change in field across the film is negligible or it may mean that the films are so thick that the space charge layers required to adjust the rate of entry of ions to the rate of passage through the oxide are complete and yet occupy only a small fraction of the total thickness. The second case means that we have the same conditions as with macroscopic-sized conductors. The first case is that dealt with by the theory of Cabrera and Mott. In this case, the field required to give a particular ionic current is entirely determined by the properties of the metal/oxide interface. It is not wholly certain but it appears likely that in this case the kinetics should depend to a detectable extent on the crystal face of the substrate metal. Since no such dependence was found and since, also, it is difficult to explain convincingly the transients on this theory, one is led to conclude that the results refer to the second case, that is to ionic conduction by an electrically neutral slab of oxide, the interfaces playing no part.

The most striking difference from tantalum, aluminum, zirconium, and similar metals is that the field strengths required to give the observable range of ionic currents are comparatively very low, though still sufficiently high to give "high-field conduction" (i.e., an exponential dependence of current on field). It has been suggested in connection with work on niobium (19) that an inverse correlation seems possible between the dielectric constant and the ionic resistivity. The present results are in accord with this idea.

One might expect that the lowness of the fields would lead to differences in mechanism, but this is no more than an expectation since the fields are low only because ionic movement is relatively easy, so that effects requiring high fields with tantalum might well be expected at lower fields with bismuth.

The best approach to the explanation of the transients involves the idea that the concentration of mobile ions is a function of the field but adjusts only slowly to a sudden change in the field. Since electroneutrality is being postulated, this must be taken to mean that a background of negative space charge is a function of the field and only adjusts slowly to change in the field. The concentration of mobile ions is supposed to be in itself variable, but to take up the value giving electroneutrality. It is perhaps difficult to envisage that electroneutrality should be maintained at all times, even after a sudden change in the field, but this simplifying assumption has been made in several recent papers and is difficult to avoid if one is to have a simple mathematical treatment of the model to be discussed. Space charge effects would be more in line with the usual, rather vague, explanations of similar effects with bulk materials.

An idea first proposed by Bean, Fisher, and Vermilyea (20) to account for certain reported features of the steady-state kinetics with tantalum was applied by Vermilyea (5) and by Dewald (6) to the transients with this and other metals with some initial success. The idea is that the high fields directly produce Frenkel defects. (A Frenkel

defect is the electrically neutral combination of vacant lattice site and interstitial metal ion.) The process is equivalent to the ordinary process of ionic mobility except that here the ion moves from a lattice to an interstitial site rather than from one interstitial site to the next. The interstitial ions are supposed to be mobile but (to avoid complications) the vacant sites are supposed to be immobile. The rate of production of defects was supposed to be given by the usual form of expression for ionic mobility, $N\nu_1 \exp\{-(W_1 - qa_1E)/kT\}$, where N = concentration of filled cation sites, ν_1 = vibration frequency, W_1 = activation energy at zero field, q = charge on ions, a_1 = activation distance, and the rate of destruction is given by $i\sigma m$, where i = current, σ = cross section for the capture of interstitial ions by vacant sites, and m = concentration of vacant lattice sites. Thus,

$$dm/dt = N\nu_1 \exp\{-(W_1 - qa_1E)/kT\} - i\sigma m$$
$$i = 2a_2\nu_2 m \exp\{-(W_2 - qa_2E)/kT\}.$$

Thus for a sudden increase in field, $(\Delta E/\Delta \log_e i) = kT/qa_2$, and for steady-state conditions, $dE/d \log_e i = 2kT/q(a_2+a_1)$. Furthermore, on suddenly increasing the field, the current after the initial sudden change should increase rapidly at first and then more slowly. With tantalum (4), the current actually builds up slowly and then more rapidly, thus suggesting the existence of some sort of cascade process involving the production of Frenkel defects by the moving ions instead of by the field alone. With bismuth, on the other hand, the behavior found is qualitatively as expected.

With tantalum and niobium, which are the only metals which behave sufficiently ideally for it, so far, to have been proved possible to obtain unequivocal evidence on the point, the Tafel slope, for steady-state conditions, shows an unexpected form of temperature dependence. With tantalum the Tafel slope for transient conditions has been shown to exhibit a similar anomalous temperature dependence. According to the most recent work (4), which happens to be by one of us, the behavior may be explained by the necessity to include a higher power of the field, so that $(\alpha - \beta E)$ replaces a in the above equations. With the lower fields with which we are here concerned one might anticipate that, if the explanation is correct, the simple form of temperature dependence would be shown. Unfortunately, we were not able to obtain experimental data over a wide enough range of temperature to settle the point. The data on the transient Tafel slope (Table III) obtained at 0° C and 50° C (with initial current about 20 ma cm^{-2}) show the same absence of the expected temperature dependence as would be found with tantalum (with fixed initial current). The data are probably statistically significant on this point but we do not consider them to be decisive. Significant values of the steady-state Tafel slope could be obtained at 0° C and 25° C only. They were, as it happens, consistent with proportionality to temperature.

The values of the activation distances (obtained from the Tafel slopes, see earlier) are unusually large. Thus with tantalum a_2 is of the order of 1 Å and a_1 of the order 5 Å (varying with temperature and current density). With bismuth a_2 is of the order 4 Å and a_1 of the order 22 Å.

ACKNOWLEDGMENT

This work was supported by the Defence Research Board of Canada and is published with their permission.

REFERENCES

1. A. Günterschulze and H. Betz. Z. Elektrochem. **37**, 726 (1931).
2. V. Čupr and E. Dvořáková. Collection Czechoslov. Chem. Commun. **22**, 305 (1957).
3. G. A. Hare and H. D. Mallon. Private communication.

4. L. YOUNG. Proc. Roy. Soc. (London), A, **263**, 395 (1961).
5. D. A. VERMILYEA. J. Electrochem. Soc. **104**, 427 (1957).
6. J. F. DEWALD. J. Phys. Chem. Solids, **2**, 55 (1957).
7. F. WINKEL, C. A. PISTORIUS, and W. CH. VAN GEEL. Philips Research Repts. **13**, 277 (1958).
8. L. YOUNG. Anodic oxide films. Academic Press. 1961.
9. W. J. BERNARD. J. Electrochem. Soc. **108**, 446 (1961).
10. L. YOUNG. Trans. Faraday Soc. **55**, 842 (1959).
11. A. KUNDT. Ber. Berlin Akad. **1**, 255 (1888).
12. E. S. LARSEN. U.S. Geol. Survey Bull. **679**, 48 (1921).
13. U. R. EVANS. Metallic corrosion, passivity and protection. 2nd ed. Arnold. 1946. p. 797.
14. J. F. DEWALD. J. Electrochem. Soc. **104**, 230 (1957).
15. B. RIVOLTA. Met. ital. **50**, 255 (1958).
16. R. D. MISCH and E. S. FISHER. Acta Met. **4**, 222 (1956).
17. R. D. MISCH and W. E. RUTHER. J. Electrochem. Soc. **100**, 531 (1953).
18. P. E. LAKE and E. J. CASEY. J. Electrochem. Soc. **105**, 52 (1958).
19. L. YOUNG. Can. J. Chem. **38**, 1141 (1960).
20. C. P. BEAN, J. C. FISHER, and D. A. VERMILYEA. Phys. Rev. **101**, 551 (1956).

STEROIDS AND RELATED PRODUCTS

XVII. THE SYNTHESIS OF 3,9,12,20-TETRAOXYGENATED 9,12-*seco*-STEROIDS. PART II[1,2,3,4]

CH. R. ENGEL[5]

Collip Medical Research Laboratory, University of Western Ontario, London, Ontario, and Department of Chemistry, Laval University, Quebec, Que.

AND

S. RAKHIT[6]

Department of Chemistry, Laval University, Quebec, Que.

AND

W. W. HUCULAK

Department of Chemistry, University of Western Ontario, London, Ontario

Received January 26, 1962

ABSTRACT

It is shown that the ozonolysis of $\Delta^{9(11)}$-12-keto steroids with a trans fusion of rings A and B proceeds in better yields than the corresponding opening of ring C in the sterically more hindered A/B-cis series. The syntheses of 23ξ-bromo-3β-hydroxy-9-oxo-9,12-*seco*-25-iso-5α,22β-spirostan-12-oic acid and some of its derivatives as well as of 3β,20α-dihydroxy-9-oxo-9,12-*seco*-12-pregnanoic acid and some of its ester derivatives are reported. It is demonstrated that the reduction with lithium aluminum hydride in tetrahydrofuran of a 12,20-diketone leads predominantly to a 12β,20α-dihydroxy derivative, in contradistinction to the reduction of a 12α-acetoxy-20-ketone, which affords mostly the 20β-alcohol.

In Part I of this study (1), we described an opening of ring C of the steroid nucleus, in the presence of protected alcohol functions in positions 3 and 20, leading to a 9-oxo-9,12-*seco*-12-acid derivative of type II. The fission of ring C was effected by ozonolysis of a $\Delta^{9(11)}$-12-ketone (compare I), a reaction which gave only a low yield of the desired *seco* product.

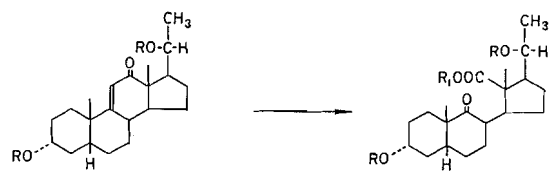

I, R = acyl

II, R = H, acyl
R_1 = H, alkyl

An inspection of models (compare Fig. 1) suggests that this reaction should proceed in better yields in the case of steroids with a trans fusion of rings A and B. It can be

[1]*Part of the results reported in this paper were the subject of a communication presented before the 40th Annual Conference of the Chemical Institute of Canada, Vancouver, B.C., June 1957, others before the 29th Congress of the French Canadian Association for the Advancement of Science, Ottawa, October 1961.*

[2]*Part of this paper is abbreviated from a portion of the M.Sc. thesis of W. W. Huculak, accepted by the School of Graduate Studies of the University of Western Ontario, 1959.*

[3]*For Part I of this study see reference 1.*

[4]*For the previous paper of this series see reference 2.*

[5]*Correspondence should be addressed to this author at the Faculty of Science, Laval University, Quebec, Que.*

[6]*N.R.C. Postdoctorate Fellow, 1960–62.*

seen that even though a 9,11-double bond is also shielded in the case of an A/B-trans fused system (Fig. 1*b*), particularly by the hydrogen substituents of carbon atom 1, the attack, especially from the α-side of the molecule, is far more hindered in the case of a cis fusion of rings A and B. In that instance, ring A (which is perpendicular to the plane of the rest of the ring system), the equatorial hydrogen atom in position 1, and the axial 2α- and 4α-hydrogen atoms protect the double bond in a cage-like manner (see Fig. 1*a*). In this publication we endeavor to show that the stereochemistry of the fusion of rings A and B indeed influences the yield of ozonolysis of a 9,11-unsaturated 12-keto steroid.

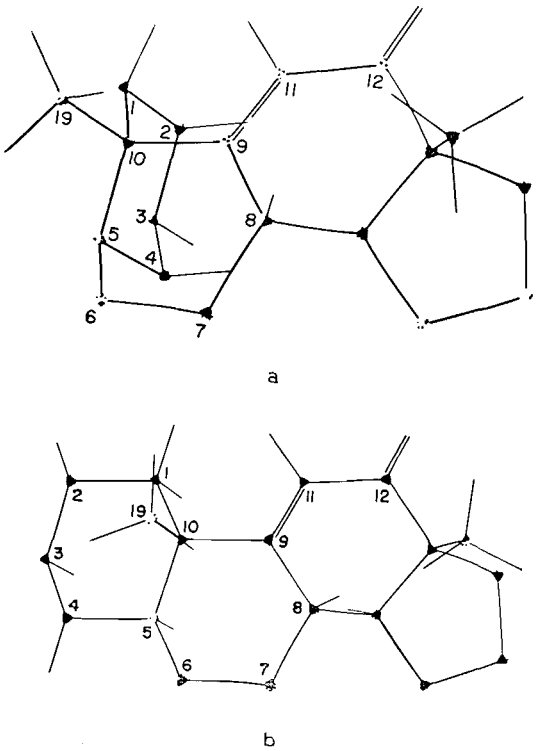

FIG. 1. Models of $\Delta^{9(11)}$-12-keto steroids: (*a*) with cis fusion of rings A and B; (*b*) with trans fusion of rings A and B.

In a first series of experiments, we transformed hecogenin acetate (III*a*), according to Djerassi's method (3), to 23ξ-bromo-9(11)-dehydrohecogenin acetate (IV), which we ozonized under conditions similar to those employed in our experiments in the A/B-cis series (1). The usual working up of the ozonide with aqueous hydrogen peroxide gave a 52% yield of acidic material. Methylation and reacetylation afforded a product which gave, upon chromatography, crystalline acetoxy methyl ester V*b* in an overall yield of 13% (from III*a*). Reozonization of the neutral fraction isolated from the ozonolysis product gave a 71% yield of acidic material from which a further 14% of pure ester V*b* was obtained. These yields are significantly higher than those achieved in the A/B-cis series (1). The structure of the *seco* derivatives (V, V*a*, V*b*) was ascertained by infrared and elemental analyses of the acetoxy methyl ester V*b*.

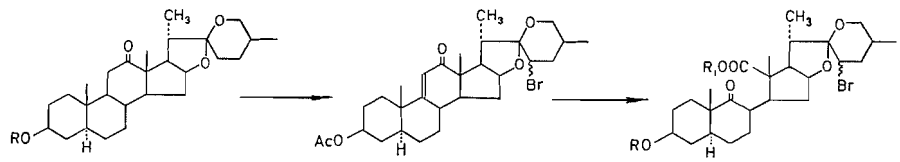

III, R = H
IIIa, R = Ac

IV

V, R = R$_1$ = H
Va, R = H; R$_1$ = CH$_3$
Vb, R = Ac; R$_1$ = CH$_3$

After this preliminary set of experiments, which already seemed to confirm our assumption of a more facile opening of the 9,11-double bond in the A/B-trans series, we wished to compare the yield of the formation of a 9-oxo-9,12-*seco*-12-acid of the A/B-trans series in the instance of a compound truly analogous to the derivatives which we had studied in the A/B-cis series. This endeavor was of particular interest to us since our goal was the synthesis of 3,20-dioxygenated 9-oxo-9,12-*seco*-12-acids (compare ref. 1).

We chose hecogenin (III) as starting material and degraded its acetate III*a*, according to the experimental procedure of Wall and co-workers (4, compare also refs. 5 and 6), to Δ^{16}-5α-pregnen-3β-ol-12,20-dione (VI), which we isolated as the acetate VI*a* (6, 7). The unsaturated diketone VI*a* was reduced in the usual fashion, with palladium on charcoal, to the saturated acetoxy diketone VII (6).

We decided to transform the 3β-acetoxy-12,20-diketone VII to the 3,20-diacetoxy-12-keto derivative IX (and thence to the unsaturated 12-ketone VIII) by metal hydride reduction of the keto functions with concomitant hydrolysis at position 3 (compare X), followed by partial esterification of the 3- and 20-hydroxy groups (compare X*a*), and by subsequent oxidation of the unprotected 12-hydroxy function.[7]

The reduction of the diketo acetate VII with lithium aluminum hydride in tetrahydrofuran gave a crystalline product from which a homogenous trihydroxy adduct was isolated in high yield; we assign to this compound the structure of 3β,12β,20α-trihydroxy-5α-pregnane (X).

Indeed, the diacetate obtained by careful selective acetylation of the triol must be a 3,20-diacetate (compare X*a*), since its oxidation yields a keto diacetate (compare IX), which can be readily dehydrogenated with selenium dioxide to an α,β-unsaturated ketone; such a reaction is possible in the case of a 12-ketone but not in the case of a 20-ketone. Furthermore, the infrared carbonyl absorption of the α,β-unsaturated ketone (ν_{max}^{KBr} 1675 and 1604 cm^{-1}) is in accord with structure VIII but not with that of a Δ^{16}-20-ketone.[8] Upon diacetylation of the trihydroxy derivative X to the hydroxy diacetate X*a*, a decrement of molecular rotation of 45° is observed. A compilation of data from the literature (compare also ref. 8) indicates that the decrement due to acetylation of a 3β-alcohol of the A/B-trans series averages 30°. Hence, acetylation of the 20-hydroxy function of triol X resulted in a decrement of rotation of approximately 15° (or, in the case of an exceptionally strong negative contribution of the acetylation in position 3, in a

[7] *Another pathway will be described in a subsequent paper of this series.*

[8] *The diacetate cannot be a 12,20-diacetate since a 3β-hydroxy function is esterified faster than hydroxy functions in 12 and 20. Also, the ultraviolet absorption maximum of the above-mentioned α,β-unsaturated ketone (compare VIII) (λ_{max}^{EtOH} 238 mμ) agrees with that of a $\Delta^{9(11)}$-12-ketone but not with that of a Δ^{1}-3-ketone, which would have been formed if a 12,20-diacetoxy-3-hydroxy derivative of the A/B-trans series had been subjected to the above-described sequence of transformations.*

very small increment). This is in excellent agreement with an α-configuration of the 20-hydroxy function, but not with a β-configuration, which results invariably in a marked increment of molecular rotation (9).

The β-configuration of the 12-hydroxy group of compound X follows from the facile triacetylation of this product, at room temperature; under analogous conditions a 12α-hydroxy group is not acetylated. Furthermore, the molecular rotation of the resulting triacetate X*b* exceeds that of the diacetate X*a* by 15° only; acetylation of a 12α-alcohol results invariably in a strong increment (averaging 150–190°) of molecular rotation (compare refs. 10, p. 179; 11–15, and, for extreme values, 16–18).

The predominant formation of a 20α-alcohol (compare X) by reduction of the acetoxy diketone VII with lithium aluminum hydride in tetrahydrofuran is of interest. In the majority of cases (compare ref. 10, pp. 568, 622, and the relevant references therein) metal hydride reduction of a 20-ketone leads mainly to 20β-alcohols. As we reported in the first part of this study (1), reduction of 3α,12α-diacetoxypregnan-20-one with lithium aluminum hydride affords predominantly the 20β-alcohol. However, Just and Nagarajan (19) showed recently that reduction of the corresponding 3α,12α-dihydroxy-20-ketone, with the same reagent, gives a high yield of the 20α-alcohol; these authors suggest that this is due to a bridging of the 12- and 20-oxygen functions by an intermediate complex with the aluminum hydride ion; the formation of this complex would force the side chain into a conformation inducive to reduction to a 20α-alcohol. The reduction of the 20-ketone to a 20α-alcohol in the presence of a 12-keto function could be explained in a similar manner.[9]

The formation in high yield of the equatorial 12β-alcohol (compare X) by metal hydride reduction of the 12-ketone VII is in accord with conformational and configurational expectations and confirms the results obtained by Hirschmann *et al.* (20) in the reduction of hecogenin acetate (III*a*) with lithium aluminum hydride; according to these authors, the 12α- and 12β-alcohols are formed in approximate yields of 25 and 75%, respectively.[10] Reduction of an 11α-halo-12-ketone (compare for instance ref. 21) and of a 9,11-unsaturated 12-ketone (22) with metal hydrides also yields predominantly the 12β-alcohols. Only Pataki, Meyer, and Reichstein (23) report that reduction of methyl 3α-acetoxy-12-oxoetianate with sodium borohydride affords the two 12α- and 12β-epimeric alcohols in 41 and 31% yields, respectively.

As mentioned above, 3β,12β,20α-dihydroxy-5α-pregnane (X) can be partially acetylated in positions 3 and 20. Treatment of the triol with approximately three equivalents of acetic anhydride in pyridine, at 0°, gave a 50% yield of diacetate X*a*. The remainder of the product consisted mainly of triacetate X*b*. After separation of the diacetate X*a* from the reaction product, the rest of the mixture was hydrolyzed, with methanolic potassium hydroxide, to the triol X. Thus, the effective yield of diacetylation could be raised to approximately 80%. Oxidation of the hydroxy diacetate X*a* with chromic acid in acetic acid gave the diacetoxy ketone IX in over 80% yield. Conversion of this product

[9]*We shall discuss the stereochemical course of the reduction of 20-keto steroids with metal hydrides, in relation to the conformation of the side chain, in more detail in a forthcoming paper of this series.*

[10]*In their discussion of the stereochemical course of the reduction of steroid ketones with metal hydrides, Fieser and Fieser (10, pp. 268–270) indicate that the reduction of a 12-ketone gives a 1:1 ratio of the two 12-hydroxy epimers; they refer to the above-quoted article by Hirschmann et al. (20). These authors mention indeed that after methylsuccinylation of the reduction product the two 12-epimeric 3β-monomethylsuccinates were isolated in approximately equal amounts; but they also indicate that there remained, after the separation of the crystalline epimers from the crude reaction product, an amorphous mixture, amounting to more than 50% of the total product; this amorphous material was largely succinylated in both the 3- and 12-positions and afforded, upon hydrolysis, rockogenin, the 12β-hydroxy epimer. Thus, the actual yield of the 12β-alcohol amounts approximately to 75% and the yield of the 12α-epimer to approximately 25%, as indicated above.*

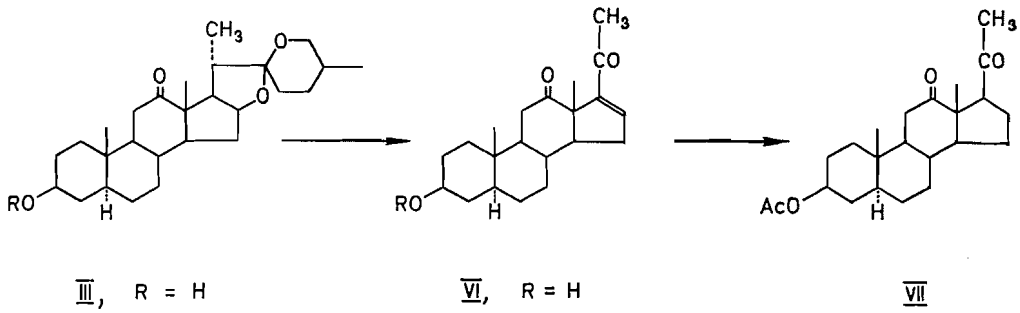

III, R = H
IIIa, R = Ac

VI, R = H
VIa, R = Ac

VII

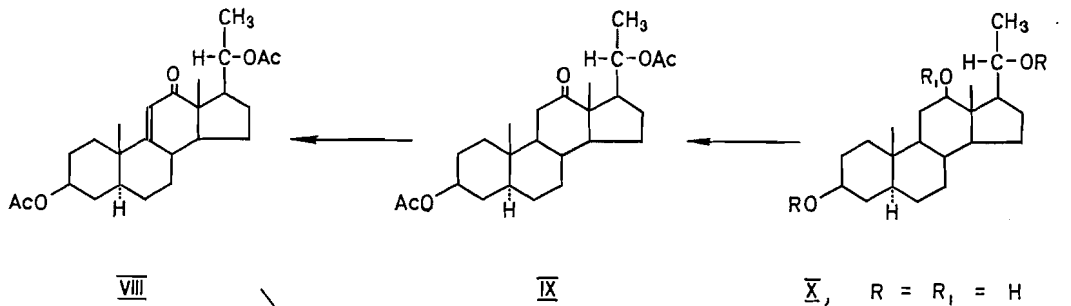

VIII

IX

X, R = R$_1$ = H
Xa, R = Ac; R$_1$ = H
Xb, R = R$_1$ = Ac

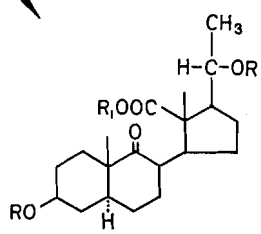

XI, R = R$_1$ = H
XIa, R = H; R$_1$ = CH$_3$
XIb, R = Ac; R$_1$ = CH$_3$

to the 9,11-unsaturated diacetoxy ketone VIII, with selenium dioxide (24, 25), proceeded in almost 70% yield.

Ozonolysis of the 9,11-unsaturated 12-ketone VIII under conditions equivalent to those described in the first part of this investigation (1) gave a 63% yield of acidic material (compare XI), which afforded upon methylation (compare XI*a*) and acetylation, in an overall yield (from VIII) of 11%, crystalline methyl 3β,20α-diacetoxy-9-oxo-9,12-*seco*-5α-pregnan-12-oate (XI*b*), characterized by elemental analysis and by its infrared and ultraviolet absorption spectra, as well as by the spectra of the intermediates XI and XI*a*. Reozonization of the neutral fraction isolated from the product of ozonolysis gave a 47% yield of an acid fraction which afforded another 7% of pure diacetoxy methyl ester XI*b*. The yields of both the crude acid fractions (compare XI) and of pure diacetoxy methyl ester XI*b* were significantly higher than those obtained with the 3,20-diacetoxy-9,11-unsaturated 12-ketone of the A/B-cis series (1). The yield of crude acid material obtained upon ozonolysis was raised from 25–30% to 50–60%, the yield of pure diacetoxy methyl ester (XI*b*), after reozonization of the neutral ozonolysis fraction, from 5 to 18%. Thus, the results of both the ozonolysis of 23ξ-bromo-9-dehydrohecogenin acetate (IV) and of $\Delta^{9(11)}$-3β,20α-diacetoxy-5α-pregnen-12-one (VIII) confirm our postulate that the 9,11-double bond of an A/B-trans steroid is opened more readily than that of a product with an A/B-cis configuration.

EXPERIMENTAL[11, 12, 13]

Methyl 23ξ-Bromo-3β-acetoxy-9-oxo-9,12-seco-25-iso-5α,22β-spirostan-12-oate (Vb) from 23ξ-Bromo-9(11)-dehydrohecogenin Acetate (IV)

A quantity of 900 mg of 23ξ-bromo-9(11)-dehydrohecogenin acetate (IV), prepared from hecogenin acetate (III*a*), according to the method of Djerassi *et al.* (3), was dissolved in a mixture of 13.5 cc of acetic acid and 13.5 cc of ethyl acetate. At −10°, a stream of oxygen, containing 8% of ozone and flowing at an approximate rate of 160 cc per minute, was passed through the solution for the period of 4.5 hours (approximately 85 equivalents of ozone). Water (3.5 cc) and 30% hydrogen peroxide (0.35 cc) were added and the mixture was stored for 18 hours at room temperature. The product was dissolved in 2 l. of ether and the solution was washed with water and extracted with a 1.5 *N* sodium hydroxide solution. The ethereal solution was washed until neutral and dried over sodium sulphate; evaporation of the solvent gave 451 mg of neutral product.

The aqueous alkaline solution was acidified with sulphuric acid to the Congo-blue reaction and the resulting mixture was extracted with chloroform. The organic layer was washed until neutral and dried over sodium sulphate and the solvent was removed. Thus, 458 mg (52%) of crude *hydroxy keto acid V* was obtained. This product could not be crystallized. The material was dissolved in 5 cc of absolute methanol and treated at 0° with 26 cc of a 2.7% ethereal diazomethane solution. After 10 minutes the solution was allowed to warm to room temperature and was stored at 25° for another 16 hours. The excess diazomethane was destroyed with acetic acid and the solvent was removed *in vacuo*. The residue (454 mg), representing crude *hydroxy keto methyl ester Va*, could not be crystallized. The material was acetylated in the usual fashion with 4 cc of acetic anhydride in 7 cc of pyridine and the resulting crude acetoxy keto ester V*b* (461 mg) was dissolved in 4 cc of benzene and absorbed on 14 g of slightly alkaline aluminum oxide. Benzene–ether mixtures (4:1 and 1:1) eluted 122 mg (12.7%) of crystalline methyl *23ξ-bromo-3β-acetoxy-9-oxo-9,12-seco-25-iso-5α,22β-spirostan-12-oate (Vb)*, which melted after one recrystallization from methanol–water at 99–101°. The bromine-containing product was recrystallized twice from methanol–water for analysis; short prisms, m.p. 100–101°, $[\alpha]_D^{22}$ 5° (*c*, 0.985 in $CHCl_3$), λ_{max}^{EtOH} 282 mμ, ν_{max}^{KBr} 1720 cm^{-1} (broad ester band), 1707 cm^{-1} (9-ketone), 1251 and 1242 cm^{-1} (double ester band). Anal. Calc. for $C_{29}H_{43}O_7Br$: C, 59.68; H, 7.43. Found: C, 59.43; H, 7.46.

The neutral fraction of the ozonolysis experiment (451 mg) was dissolved in 14 cc of a 1:1 mixture of acetic acid and ethyl acetate and treated at −10° with ozone for 2.5 hours, as described above. The ozonide

[11] *The melting points were taken in evacuated capillaries and the temperatures were corrected.*

[12] *We are indebted to Mr. J. F. Alicino, Metuchen, N.J., and to Mr. A. Bernhardt, Mülheim (Ruhr), Germany, for the microanalyses, and we extend to them our sincere appreciation.*

[13] *If not otherwise stated, Merck's aluminum oxide was used for chromatography. The alkaline reagent was treated as described in footnote 18 of reference 26. We sincerely thank Merck and Company, Montreal, for the generous gift of this material.*

was decomposed with 2 cc of water and 0.2 cc of a 30% hydrogen peroxide solution. The usual working up (see above) gave 118 mg of neutral product and 304 mg (71%) of acidic material. The acid fraction was methylated and acetylated according to the method described above. Chromatography of the resulting product gave 113 mg (13.9%) of crystalline acetoxy methyl ester V*b*, which yielded, after one recrystallization from methanol–water, 98 mg of ester V*b*, melting at 99–100°.

Δ^{16}-3β-Acetoxy-5α-pregnene-12,20-dione (VIa)

A quantity of 25 g of hecogenin acetate (III*a*) was converted according to the procedure of Wall *et al.* (4) to *Δ^{16}-3β-hydroxy-5α-pregnene-12,20-dione (VI)*. The crude amorphous product (21.3 g) was dissolved in 80 cc of pyridine and treated for 16 hours with 40 cc of acetic anhydride, at room temperature. The usual working up afforded 21.5 g of a yellow oil which was chromatographed on 650 g of aluminum oxide Woelm (activity II–III). Petroleum ether – benzene (1:1 and 1:4) and benzene eluted 12.2 g (58.6%) of *Δ^{16}-3β-acetoxy-5α-pregnene-12,20-dione (VIa)*, m.p. 169–173°. Recrystallization from ether–ethanol afforded 10.4 g (45%) of pure acetate VI*a*; m.p. 178–180°, $[\alpha]_D^{25}$ 126° (*c*, 1.00 in $CHCl_3$), λ_{max}^{EtOH} 227 mμ (log ε 3.94). Recrystallization from ether gave a product melting between 176 and 177°, $[\alpha]_D^{25}$ 128° (*c*, 1.00 in $CHCl_3$), λ_{max}^{EtOH} 227 mμ (log ε 3.92). Anal. Calc. for $C_{23}H_{32}O_4$: C, 74.16; H, 8.66. Found: C, 74.02; H, 8.60.

3β-Acetoxy-5α-pregnane-12,20-dione (VII)

A solution of 9.5 g of Δ^{16}-3β-acetoxy-5α-pregnene-12,20-dione (VI*a*), m.p. 174–174.5°, in 500 cc of 95% ethanol was hydrogenated with 1 molecular equivalent of hydrogen over 950 mg of 5% palladium on charcoal at room temperature and at atmospheric pressure. The solution was filtered over sodium sulphate and taken to dryness. Recrystallization of the crude product (9.55 g) from ethanol gave 9.3 g (97% yield) of crystalline acetoxy diketone VII, m.p. 183–184°. The product showed no ultraviolet absorption at 227 mμ. A sample was recrystallized twice from ethanol, for analysis; prisms, m.p. 186–187°, $[\alpha]_D^{22}$ 138° (*c*, 0.981 in $CHCl_3$). Anal. Calc. for $C_{23}H_{34}O_4$: C, 73.76; H, 9.15. Found: C, 73.69; H, 9.00.

3β,12β,20α-Trihydroxy-5α-pregnane (X)

A solution of 1.0 g of 3β-acetoxy-5α-pregnane-12,20-dione (VII) in 80 cc of absolute tetrahydrofuran was added over a period of 15 minutes to a slurry of 1.23 g of lithium aluminum hydride in 80 cc of absolute tetrahydrofuran. The mixture was refluxed for 1 hour and was kept at room temperature for another 16 hours. The excess lithium aluminum hydride was decomposed with ethyl acetate and ice, and the product was poured into iced 2 *N* sulphuric acid. The mixture was extracted with ether, the ethereal solution was washed with iced dilute sulphuric acid, cold sodium bicarbonate solution, and water and was dried over sodium sulphate. Removal of the solvent afforded 950 mg of a semicrystalline solid, m.p. 205–210°, which showed no carbonyl absorption in the infrared. Recrystallization from ethanol afforded 820 mg (91%) of 3β,12β, 20α-trihydroxy-5α-pregnane (X), m.p. 219–221°. A sample was recrystallized three times from ether–methanol, for analysis; prisms, m.p. 225–226°, $[\alpha]_D^{24}$ 1.1° (*c*, 1.000 in $CHCl_3$), $[\alpha]_D^{22}$ 0.7° (*c*, 0.991 in methyl cellusolve). Anal. Calc. for $C_{21}H_{36}O_3$: C, 74.95; H, 10.78. Found: C, 75.04, 74.98; H, 10.65, 10.88.

Diacetate (Xa)

A solution of 10 g of 3β,12β,20α-trihydroxy-5α-pregnane (X) in 28 cc of pyridine was treated at 0° with 9 cc of acetic anhydride. The mixture was kept for 16 hours at 0° and was worked up in the usual manner. The resulting amorphous product (12.964 g) was dissolved in 25 cc of benzene and chromatographed on 370 g of aluminum oxide (activity II–III). Petroleum ether – benzene (1:1 and 1:4), benzene, and benzene–ether (4:1) gave 3.44 g of crystalline *triacetate Xb* (see below); benzene–ether (1:1) eluted an oil, and ether washings afforded 6.264 g (50.1%) of crystalline *diacetate Xa*, m.p. 181–185°. Ethyl acetate and methanol eluted oils. Recrystallization of the diacetate X*a* from ether – petroleum ether gave 4.011 g of fluffy, long needles, m.p. 188–190°. A sample was recrystallized three times for analysis; m.p. 192–193°, $[\alpha]_D^{22}$ −9.2° (*c*, 0.649 in $CHCl_3$).[14] Anal. Calc. for $C_{25}H_{40}O_5$: C, 71.39; H, 9.59. Found: C, 71.40; H, 9.56.

The mother liquors of the crystallization of X*a* (1.831 g) were combined with the amorphous chromatogram fractions and with the crude triacetate X*b*, isolated from the chromatogram (see above). This product (8.641 g) was dissolved in 455 cc of methanol and refluxed for 6 hours with 282 cc of an 8.1% methanolic potassium hydroxide solution. The mixture was kept for another 16 hours at room temperature, and was subsequently poured into 3 l. of water. The precipitate was extracted with ether, the organic solution was washed until neutral and dried over sodium sulphate. Evaporation of the solvent gave 7.03 g of a crude product, which yielded upon crystallization from acetone 6.09 g of starting material, *3β,12β,20α-trihydroxy-5α-pregnane (X)*, m.p. 217.5–219°. Considering this recovery of the triol X, the yield of diacetate X*a* was 82%.

In another run, 750 mg of the triol X was acetylated to 647 mg of crude diacetate X*a*, m.p. 170–180° (69% yield, not taking into account the recovery of starting material).

[14]*We sincerely thank Professor G. Just and Dr. G. R. Nagarajan, McGill University, Montreal, for taking this rotation in their microtube.*

Triacetate Xb

A solution of 150 mg of 3β,12β,20α-trihydroxy-5α-pregnane (X) in 2 cc of pyridine was treated at room temperature for 16 hours with 0.8 cc of acetic anhydride. The usual working up gave 215 mg of a foam which afforded, upon filtration over aluminum oxide, 195 mg (95% yield) of crystalline triacetate X*b*, m.p. 162–164°. A sample was recrystallized three times from acetone–hexane and was subsequently sublimed for analysis in high vacuum, at 110°; small prisms, m.p. 167–169°, $[\alpha]_D^{24}$ −4.9° (*c*, 1.000 in $CHCl_3$). Anal. Calc. for $C_{27}H_{42}O_6$: C, 70.09; H, 9.15. Found: C, 69.84; H, 9.23.

3β,20α-Diacetoxy-5α-pregnan-12-one (IX)

To a solution of 500 mg of 3β,20α-diacetoxy-5α-pregnan-12β-ol (X*a*), m.p. 191–192°, in 21 cc of acetic acid, a solution of 131 mg of chromic oxide in 1.25 cc of 90% acetic acid was added, at 17°. The mixture was kept at the same temperature for 17 hours, was then treated with 3 cc of methanol, and was finally poured into 250 cc of water. The product was extracted with ether and worked up in the usual fashion. Thus, 496 mg of crystals, m.p. 148–154°, were obtained. Recrystallization from ether–hexane gave 385 mg of diacetoxy ketone IX, m.p. 164–167°. Chromatography of the mother liquors afforded another 35 mg of the diacetoxy ketone IX, m.p. 164.5–166.5° (total yield 84%). A sample was recrystallized twice from ether–hexane for analysis; fine needles, m.p. 168–170°, $[\alpha]_D^{22}$ 58.2° (*c*, 1.00 in $CHCl_3$). Anal. Calc. for $C_{25}H_{38}O_5$: C, 71.74; H, 9.15. Found: C, 71.72; H, 9.09.

$\Delta^{9(11)}$-3β,20α-Diacetoxy-5α-pregnen-12-one (VIII)

To a solution of 600 mg of 3β,20α-diacetoxy-5α-pregnan-12-one (IX) in 8.04 cc of 0.0006 *N* hydrogen chloride in acetic acid, 450 mg of selenium dioxide was added. The mixture was refluxed for 20 hours, cooled, and poured into 500 cc of ether. After filtration over sodium sulphate, the solution was washed with water, cold dilute hydrochloric acid, iced sodium bicarbonate solution, and again with water and was dried over sodium sulphate. Removal of the solvent gave 605 mg of a product which crystallized from ether–hexane. A solution of this material in 3 cc of benzene was absorbed on 18 g of aluminum oxide. Benzene–ether (4:1) eluted crystalline $\Delta^{9(11)}$-3β,20α-diacetoxy-5α-pregnen-12-one (VIII), m.p. 174–179°, which gave upon one recrystallization from ether–hexane 409 mg (67.5%) of the unsaturated ketone VIII, m.p. 184–185°, $[\alpha]_D^{23}$ 42.5°(*c*, 0.99 in $CHCl_3$), λ_{max}^{EtOH} 238 mμ (log ε 4.1), ν_{max}^{KBr} 1740 and 1254 cm^{-1} (3β,20α-diacetate), 1685 and 1604 cm^{-1} ($\Delta^{9(11)}$-12-keto doublet). Anal. Calc. for $C_{25}H_{36}O_5$: C, 72.08; H, 8.71. Found: C, 72.19; H, 8.57.

Methyl 3β,20α-Diacetoxy-9-oxo-9,12-seco-5α-pregnan-12-oate (XIb)

At −10°, a stream of oxygen, containing 7.8% of ozone, was passed through a solution of 1.5 g of $\Delta^{9(11)}$-3β,20α-diacetoxy-5α-pregnen-12-one (VIII) in 29.7 cc of acetic acid and 29.7 cc of ethyl acetate, at a flow rate of 140 cc per minute, for the period of 105 minutes. There was added 7 cc of water and 0.7 cc of a 30% hydrogen peroxide solution, and the mixture was allowed to stand overnight at room temperature. The product was extracted with 2 l. of ether, the ethereal solution was washed with water, six times with iced 1.5 *N* sodium hydroxide solution, and again with water and was dried over sodium sulphate. Removal of the solvent gave 603 mg of a neutral product.

The alkaline washings were combined and acidified with sulphuric acid to the Congo-blue reaction. The product was extracted with chloroform and the organic solution was washed until neutral and was dried. Removal of the solvent gave 803 mg (63%) of amorphous acid (compare XI) which resisted all attempts of crystallization.

A solution of this acid (803 mg), in 4 cc of absolute methanol and 8 cc of absolute ether, was treated at 0° with 43 cc of a 1.5% ethereal diazomethane solution. The product was kept for 20 hours at room temperature and the excess diazomethane was destroyed with acetic acid. Evaporation of the solvent *in vacuo* gave 820 mg of an amorphous neutral product (compare XI*a*). Acetylation at room temperature with 4 cc of acetic anhydride in 10 cc of pyridine gave 843 mg of amorphous material, which was dissolved in 5 cc of benzene and absorbed on 24 g of aluminum oxide. Benzene–ether (4:1 and 1:1) eluted crystalline fractions contaminated with oils. Recrystallization from aqueous methanol gave 182 mg (11.2%, from VIII) of colorless, fine, short needles, m.p. 147–148°, representing the diacetoxy keto methyl ester XI*b*. A sample was recrystallized four times for analysis; m.p. 153–154°, $[\alpha]_D^{22}$ 101° (*c*, 1.060 in $CHCl_3$), λ_{max}^{EtOH} 280 mμ. Anal. Calc. for $C_{25}H_{38}O_7$: C, 66.64; H, 8.50. Found: C, 66.47; H, 8.50.

The neutral fraction (603 mg) isolated after ozonolysis (see above) was dissolved in 12 cc of acetic acid and 12 cc of ethyl acetate and reozonized at −10° with a 7.9% ozone stream, for 67 minutes (flow rate 180 cc per minute). The product was treated as described above with 2.8 cc of water and 0.28 cc of a 30% hydrogen peroxide solution. The material was worked up as described above and there was obtained 286 mg of a neutral fraction and 301 mg (47%) of an acid fraction (compare XI) which was methylated in 1.5 cc of absolute methanol and 3 cc of absolute ether with excess diazomethane (16.5 cc of a 1.5% ethereal solution). The reaction product (307 mg) was acetylated in the usual fashion. Chromatography of the amorphous material thus obtained (314 mg) afforded 111 mg (13.6% yield from the neutral product of the first ozonolysis, 6.9% yield calculated from the total starting material) of *seco* ester XI*b*, m.p. 147.5–148.5°. The total yield of the *seco* ester XI*b*, after one reozonization, amounted to 18%.

ACKNOWLEDGMENTS

We extend sincere thanks to Mr. R. W. White, Science Service Laboratory, London, Ontario, for a number of infrared analyses, and to Mrs. J. Capitaine and Mr. D. Capitaine for their valuable assistance. We are greatly indebted to The National Research Council of Canada, The Federal–Provincial Departments of Health and Welfare, Ottawa and Toronto, to Ayerst, McKenna and Harrison, Ltd., Montreal, the Schering Corporation, Bloomfield, N.J., the Schering Corporation Ltd., Montreal, and to the Canadian Life Insurance Officers Association, for financial support. We appreciated the kind encouragement of Dean J. B. Collip and of Professor J. A. Gunton, in whose departments part of this work was carried out at the University of Western Ontario, and the cooperation of the authorities of Laval University, in particular of Director P. A. Giguère.

REFERENCES

1. Ch. R. Engel and W. W. Huculak. Can. J. Chem. **37**, 2031 (1959).
2. Ch. R. Engel, G. Just, and R. Buttery. Can. J. Chem. **39**, 1805 (1961).
3. C. Djerassi, H. Martinez, and G. Rosenkranz. J. Org. Chem. **16**, 303 (1951).
4. M. E. Wall, H. E. Kenney, and E. S. Rothman. J. Am. Chem. Soc. **77**, 5665 (1955).
5. R. E. Marker, R. B. Wagner, P. R. Ulshafer, E. L. Wittbecker, D. P. J. Goldsmith, and C. H. Ruof. J. Am. Chem. Soc. **69**, 2167 (1947).
6. G. P. Mueller, R. E. Stobaugh, and R. S. Winniford. J. Am. Chem. Soc. **75**, 4888 (1953).
7. R. B. Wagner, J. A. Moore, and R. F. Forker. J. Am. Chem. Soc. **72**, 1856 (1950).
8. D. H. Barton and W. Klyne. Chem. & Ind. (London), 755 (1948).
9. L. H. Sarett. J. Am. Chem. Soc. **71**, 1175 (1945).
10. L. F. Fieser and M. Fieser. Steroids. Reinhold Publishing Corp., New York, and T. Chapman and Hall, Ltd., London. 1960.
11. T. Reichstein and M. Sorkin. Helv. Chim. Acta, **25**, 797 (1942).
12. V. Burckhardt and T. Reichstein. Helv. Chim. Acta, **25**, 821 (1942).
13. A. V. McIntosh, A. M. Searcy, E. M. Meinzer, and R. H. Levin. J. Am. Chem. Soc. **71**, 3317 (1949).
14. M. Sorkin and T. Reichstein. Helv. Chim. Acta, **26**, 2097 (1943).
15. Ch. Meystre and A. Wettstein. Helv. Chim. Acta, **32**, 1978 (1949).
16. Pl. A. Plattner and H. Heusser. Helv. Chim. Acta, **27**, 748 (1944).
17. T. Reichstein and E. v. Arx. Helv. Chim. Acta, **23**, 747 (1940).
18. C. W. Shoppee and T. Reichstein. Helv. Chim. Acta, **24**, 351 (1941).
19. G. Just and R. Nagarajan. Can. J. Chem. **39**, 548 (1961).
20. R. Hirschmann, C. S. Snoddy, Jr., C. F. Hiskey, and N. L. Wendler. J. Am. Chem. Soc. **76**, 4013 (1954).
21. J. W. Cornforth, J. M. Osbond, and G. H. Phillipps. J. Chem. Soc. 907 (1954).
22. A. Bowers, E. Denot, M. B. Sanchez, F. Neumann, and C. Djerassi. J. Chem. Soc. 1859 (1961).
23. S. Pataki, K. Meyer, and T. Reichstein. Helv. Chim. Acta, **36**, 1295 (1953).
24. E. Schwenk and E. Stahl. Arch. Biochem. **14**, 125 (1947).
25. B. F. McKenzie, V. R. Mattox, L. L. Engel, and E. C. Kendall. J. Biol. Chem. **173**, 271 (1948).
26. Ch. R. Engel and G. Just. J. Am. Chem. Soc. **76**, 4909 (1954).

THE THERMAL DECOMPOSITION OF HEXAFLUOROAZOMETHANE[1]

ELIZABETH LEVENTHAL, CHARLES R. SIMONDS,[2] AND COLIN STEEL[3]
Chemistry Department, University of Toronto, Toronto, Ontario

Received December 18, 1961

ABSTRACT

The pyrolysis of hexafluoroazomethane has been studied in a static system between 0.3 mm and 73 mm and 572° K and 634° K by measuring the rate of nitrogen formation. The rate constant of the high-pressure homogeneous reaction is given by $k = 10^{16.17\pm0.15} \exp(-55{,}200 \pm 400/RT)$ sec^{-1}.

INTRODUCTION

There has recently been interest in the thermal decomposition of azo compounds in connection with the problem of frequency factors in unimolecular reactions (1, 2). Most azo compounds possess high-frequency factors and the reported data for the simple members are shown in Table I. Hexafluoroazomethane appeared to be somewhat out of

TABLE I
Decomposition of azo compounds in the gas phase

Compound	Reference	log A (sec^{-1})	E (kcal mole^{-1})
$CF_3N{=}NCF_3$	3	13.9	48.5
$CF_3N{=}NCF_3$	This work	16.2	55.2
$CH_3N{=}NCH_3$	6	15.7	51.2
$C_2H_5N{=}NC_2H_5$	9	15.7	48.5
i-$C_4H_9N{=}N$$i$-$C_4H_9$	13	16.3	42.8

line, since the entropy of activation is significantly lower than the entropy of activation of the other compounds. The decomposition of hexafluoroazomethane has been studied by the toluene carrier technique (3), and as has been emphasized elsewhere (1, 2), this method gives low results for the high-pressure frequency factor A_∞, and for the high-pressure activation energy E_∞, if the system is in the pressure-dependent region. For these reasons we have reinvestigated the reaction using a static system similar to the one used for the pyrolysis of azomethane.

EXPERIMENTAL

Materials

Hexafluoroazomethane was prepared after the manner of Ruff and Willenberg (4). Gas chromatographic and mass spectrometric analyses showed the presence of 3% of higher-boiling impurities, which were probably perfluorotetramethylhydrazine and perfluorohexamethyltetrazine (5). The propylene was Phillips Research Grade.

Apparatus

A 460-ml Pyrex reaction vessel was contained in an electric furnace kept constant to ±0.05° C by means of a platinum resistance thermometer proportional controller. The output from the bridge was amplified and fed onto a recorder so that a record of the temperature variation throughout the reaction was obtained. The temperature was read to 0.05° C by means of a two-junction thermocouple contained within an axial well in the reaction vessel.

[1]*We are pleased to acknowledge support of this work by the National Research Council.*
[2]*Present address: Royal Military College, Kingston, Ontario.*
[3]*To whom inquiries should be sent. Present address: Information Technology Laboratories, Maguire Road, Lexington, Massachusetts.*

Procedure

In the experiments with hexafluoroazomethane alone the reactant was measured in a gas burette and the gas transferred quantitatively to the reaction vessel by freezing it into a small side thimble which was attached to the vessel. For the runs with added gas (propylene), the latter was quickly added to the vessel immediately after the azo compound had been flash-vaporized from the thimble, the positive propylene pressure ensuring that no hexafluoroazomethane diffused out of the reaction vessel. At the end of the run the products were pumped through two liquid nitrogen traps, by means of a diffusion pump and a Toepler pump working in series, into calibrated volumes where the pressure and volume of the non-condensable fraction were measured. The sample was then analyzed by gas chromatography or mass spectrometry. In the experiments with hexafluoroazomethane alone analyses showed that the non-condensable sample was pure nitrogen. In the runs with excess propylene, however, impurities were detected. A typical analysis was: N_2, 97½%; CH_4, 2½%; ethane, ½%; propylene, ½%.

RESULTS AND DISCUSSION

Variation in the Experimental First-order Rate Constant with Percentage Decomposition

The first step in the decomposition is undoubtedly

$$CF_3N{=}NCF_3 \rightarrow 2CF_3 + N_2. \qquad [1]$$

The trifluoromethyl radicals will then add to the parent compound so that the latter can no longer undergo reaction [1]. These addition reactions have been observed by Young and Dacey (5). Thus we should expect the experimental first-order rate constant to decrease with increasing percentage reaction. This can be seen from the data given in Fig. 1. In the subsequent experiments, therefore, we limited the decomposition to not

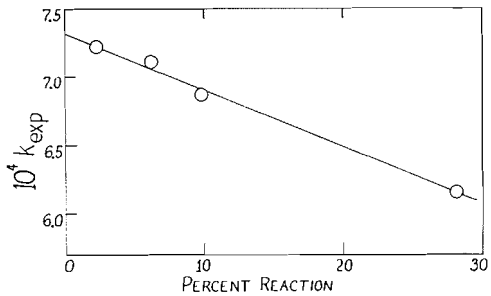

FIG. 1. Variation in experimental first-order rate constant (sec^{-1}) with percentage decomposition. Pressure of hexafluoroazomethane 4.9±0.5 cm Hg; temperature 594.8° K.

more than 20% (it was in fact generally less than 10%) and corrected all the rates to 0% decomposition. Such corrected rate constants are designated k to distinguish them from the original experimental rate constants $k_{expt.}$

Effect of Packing and Seasoning the Reaction Vessel

The pyrolysis of azomethane has been shown to be complicated by a surface effect which could be effectively removed by seasoning the surface of the reaction vessel with allyl bromide for 12 hours at 500° C (6). The results given in Table II for the decomposition of hexafluoroazomethane show that there is no significant difference between the rates obtained using packed and unpacked vessels. Furthermore, seasoning had no effect on the reaction. We may conclude that the decomposition proceeds homogeneously in the gas phase.

Effect of Pressure on the Reaction

Slater's theory (7, 8) indicates that the various vibrational modes contribute to different extents to the reaction coordinate. Thus, for example, the fast motions associated with

TABLE II

Effect of packing and seasoning the reaction vessel

No. of runs	10^4k (sec^{-1})	P_{azo} (cm Hg)	$\frac{\text{Surface area}}{\text{volume}}$ (cm^{-1})
7	1.60±0.10	0.20±0.01	8.27*
4	1.61±0.20	0.15±0.02	0.98†
4	1.54±0.15	0.17±0.02	0.98*

NOTE: All rate constants corrected to 611.0° K.
*Unseasoned surface.
†Surface seasoned with allyl bromide at 500° C for 12 hours.

light hydrogen atoms can have little effect on the slower motion associated with a C—N stretching vibration. If we therefore substitute fluorine for hydrogen in azomethane we should expect the number of effective normal mode vibrations to increase. In terms of the Kassel model we should expect hexafluoroazomethane to be associated with a larger value of s (the number of effective oscillators) than is azomethane. Thus the pressure-dependent region should be shifted towards lower pressures, and for any pressure range the variation in rate constant with pressure should be less for hexafluoroazomethane than for azomethane. This can be seen in Fig. 2; here we have compared the results for both

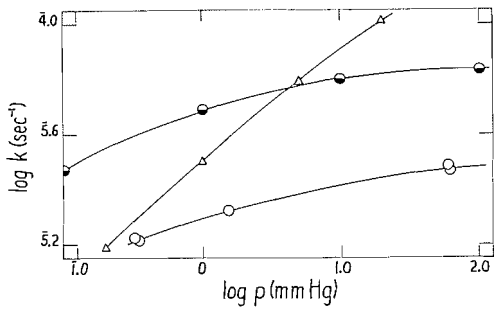

FIG. 2. Variation in rate constant with pressure: △ azomethane 563° K (6); ◒ azoethane 533° K (9); ○ hexafluoroazomethane 584° K.

systems. We have also added the curve for azoethane for comparison (9). The limited rate–pressure curve obtained here for hexafluoroazomethane was fitted by a Kassel (10) model having $s = 23\pm3$. The apparatus used was incapable of yielding data for higher or lower pressures. However, we hope to investigate the pressure dependence over a wide range using a newly designed apparatus. Tentatively we may state that the rates at very high pressures will not be very much greater than those obtained at 6–7 cm Hg, so that the latter results, to a good approximation, give the limiting high-pressure rates.

The Effect of Propylene on the Reaction

In the thermal decomposition of azomethane, propylene acted both as an energy transfer agent and as a chain inhibitor. In the former role it tended to increase the rate of reaction, in the latter it decreased the rate of reaction. As can be seen from Fig. 3 and from equations (*a*) and (*c*) below, for hexafluoroazomethane, propylene acts simply as an energy transfer agent, there being no evidence of any chain inhibition.

Arrhenius Parameters

In Fig. 3 we have given Arrhenius plots for three sets of experimental conditions.

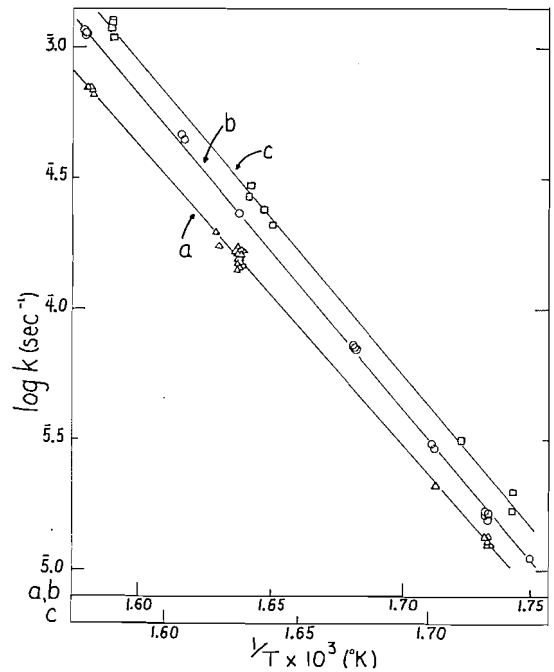

FIG. 3. Arrhenius plots for the thermal decomposition of hexafluoroazomethane. (*a*) P_{azo} 1.7±0.2, P_{prop} 0; (*b*) P_{azo} 63±7, P_{prop} 0; (*c*) P_{azo} 1.7±0.2, P_{prop} 66±7 mm Hg.

The corresponding equations determined by the method of least mean squares are:

$$k_{1.5\text{ mm}} = 10^{15.1\pm0.20} \exp(-52{,}700\pm600/RT)\ (\text{sec}^{-1}) \qquad (a)$$

$$k_{63\text{ mm}} = 10^{16.17\pm0.15} \exp(-55{,}200\pm400/RT)\ (\text{sec}^{-1}) \qquad (b)$$

$$k_{1.5\text{ mm, prop}} = 10^{15.93\pm0.20} \exp(-54{,}600\pm600/RT)\ (\text{sec}^{-1}) \qquad (c)$$

CONCLUSION

This study indicates that hexafluoroazomethane decomposes by a homogeneous non-chain mechanism with a frequency factor which is similar to those of the other simple azo compounds. Thus the reactivity of these compounds is governed by their activation energies. This can be seen in Table I. Azoisopropane affords an apparent exception to this regular trend, since Ramsperger (11) has reported that the rate constants are best fitted by the equation $k = 10^{13.7} \exp(-40{,}900/RT)$ sec^{-1}. However, Cohen and Zand (12) have recently reinvestigated the reaction and have shown that the decomposition is complicated by rearrangement to the isomeric hydrazone. The decomposition of azoisopropane, which merits more detailed study, is a complex process, accounting for the exceptional entropy and energy of activation.

ACKNOWLEDGMENT

The authors wish to thank Dr. J. R. Dacey for his generous provision of materials and facilities for the preparation of hexafluoroazomethane.

REFERENCES

1. C. STEEL. J. Chem. Phys. **31**, 899 (1959).
2. C. STEEL and K. J. LAIDLER. J. Chem. Phys. **34**, 1827 (1961).
3. D. CLARK and H. O. PRITCHARD. J. Chem. Soc. 2136 (1956).
4. O. RUFF and W. WILLENBERG. Ber. B, **73**, 724 (1940).
5. J. R. DACEY and D. M. YOUNG. J. Chem. Phys. **23**, 1302 (1955).
6. C. STEEL and A. F. TROTMAN-DICKENSON. J. Chem. Soc. 975 (1959).
7. N. B. SLATER. Theory of unimolecular reactions. Cornell University Press. 1959. pp. 180–184.
8. A. F. TROTMAN-DICKENSON. Gas kinetics. Butterworths. 1955. p. 68.
9. W. D. CLARK. Ph.D. Dissertation, University of Oregon, Eugene, Oregon. June 1959.
10. L. S. KASSEL. Kinetics of homogeneous gas reactions. Chemical Catalog Co., New York. 1932. Chap. 1, 5.
11. H. C. RAMSPERGER. J. Am. Chem. Soc. **50**, 714 (1928).
12. S. G. COHEN and R. ZAND. Private communication.
13. J. B. LEVY and B. K. W. COPELAND. J. Am. Chem. Soc. **82**, 5314 (1960).

STUDIES ON THE STABILITY OF THE DIMER OF 2,4-TOLYLENE DIISOCYANATE

PRITAM SINGH
Department of Chemistry, Laval University, Quebec, Que.

AND

JEAN L. BOIVIN
Chemistry Section, Canadian Armament Research and Development Establishment, Valcartier, Que.

Received February 9, 1962

ABSTRACT

A series of carbamates of the dimer of 2,4-tolylene diisocyanate was prepared from different alcohols, leaving the uretidine-dione ring unaffected. Di-*sec*-butylamine and dibenzylamine did not affect the dimer ring and reacted only with the two free isocyanate groups. However, di-*n*-propylamine, di-*n*-butylamine, and di-*n*-amylamine ruptured the ring, and diureas of the monomer were obtained. Alkaline reduction changed the dimer ring into a ureylene link and a N-substituted amide was formed by the Leuckart reaction. Hydrazine hydrate gave an unsymmetrical monosubstituted urea whereas hydroxylamine broke the ring and gave the corresponding oxime of the formamide.

INTRODUCTION

In the manufacture of polyurethanes, polymeric diols are chain-extended with diisocyanates such as 2,4-tolylene diisocyanate (TDI) (1). Since commercial TDI contains a dimer it is of interest to study the stability of the uretidine-dione ring of the dimer (TDID), which shows isocyanate activity at relatively higher temperatures than the monomer. This property is being used to modify elastomers, plastics, and foams (2).

RESULTS

When the dimer of 2,4-tolylene diisocyanate was reacted with alcohols at about 90°, the corresponding diurethanes were formed, giving only traces of allophanates. The diurethanes prepared are listed in Table I. Higher temperatures in the range of 125 to 160° and catalysts such as triethylamine and N-methyl morpholine appeared to be necessary for the formation of allophanates (3) and triphenyl isocyanates (4).

TDID did not react with the *tert*-butyl alcohol probably because of its easy dehydration. Benzyl alcohol gave a reaction product which analyzed for a compound made from 1 mole of TDI and 2 moles of benzoic acid. However, this compound could not be prepared from TDI and benzoic acid. Under milder conditions only 1 mole of benzoic acid reacted with the isocyanate group in para position, which was due to the high reactivity of the para group compared to the ortho group (5).

The failure to dimerize 3-methylcarbamyl-2-isocyanatotoluene in pyridine was probably due to the fact that the *o*-isocyanate is hindered (6). Heating under reflux with benzene or ethyl acetate in excess changed TDID to an amorphous powder which was insoluble in all common organic solvents, but soluble in dimethylformamide. On heating the product to 215° for 45 minutes a yellow, hard-setting resin was obtained which was soluble in dimethylformamide.

Some of the dialkylamines used, such as di-*n*-propyl, di-*n*-butyl, and di-*n*-amylamines, ruptured the uretidine-dione rings of TDID very easily (Table II). In *o*-dichlorobenzene, the dimer ring was found to react with di-*n*-butylamine at an appreciable rate even at

TABLE I

1,3-Bis(4′-methyl-3′-R-carbamylphenyl) uretidine-2,4-dione

R	Yield (%)	M.p. (°C)	Crystallization solvent	Reflux time (hr)	Formula	C		H	
						Calc. (%)	Found (%)	Calc. (%)	Found (%)
Methyl	90	207–208	$HCON(CH_3)_2$	3	$C_{20}H_{20}O_6N_4$	58.2	58.3	4.85	4.92
Ethyl	95	205	Dioxane	4	$C_{22}H_{24}O_6N_4$	60.0	59.9	5.46	5.46
n-Propyl	85	197	$HCON(CH_3)_2$	3	$C_{24}H_{28}O_6N_4$	61.5	61.4	6.00	5.91
Isopropyl	84	215	"	3	$C_{24}H_{28}O_6N_4$	61.5	61.9	6.00	6.27
n-Butyl	98	197.5	Cellosolve	4	$C_{26}H_{32}O_6N_4$	62.9	62.9	6.45	6.54
Isobutyl	98	205	"	3	$C_{26}H_{32}O_6N_4$	62.9	63.3	6.45	6.57
n-Amyl	90	197	"	4	$C_{28}H_{36}O_6N_4$	64.1	63.7	6.87	6.72
Isoamyl	87	199	$HCON(CH_3)_2$	3	$C_{28}H_{36}O_6N_4$	64.1	63.9	6.87	7.10
3-Pentyl	90	198	Cellosolve	3	$C_{28}H_{36}O_6N_4$	64.1	63.5	6.87	6.77
n-Hexyl	80	186	$HCON(CH_3)_2$	3	$C_{30}H_{40}O_6N_4$	65.2	65.0	7.24	7.24
n-Heptyl	99	185	"	4	$C_{32}H_{44}O_6N_4$	66.2	65.8	7.65	7.77
n-Octyl	98	185	"	$4\frac{1}{2}$	$C_{34}H_{48}O_6N_4$	67.1	67.1	8.00	7.99
Capryl	98	186	"	5	$C_{34}H_{48}O_6N_4$	67.1	67.5	8.00	8.56
n-Dodecyl	70	180 (softens at 170)	Benzene and dioxane	5	$C_{42}H_{64}O_6N_4$	70.0	69.9	8.88	8.82

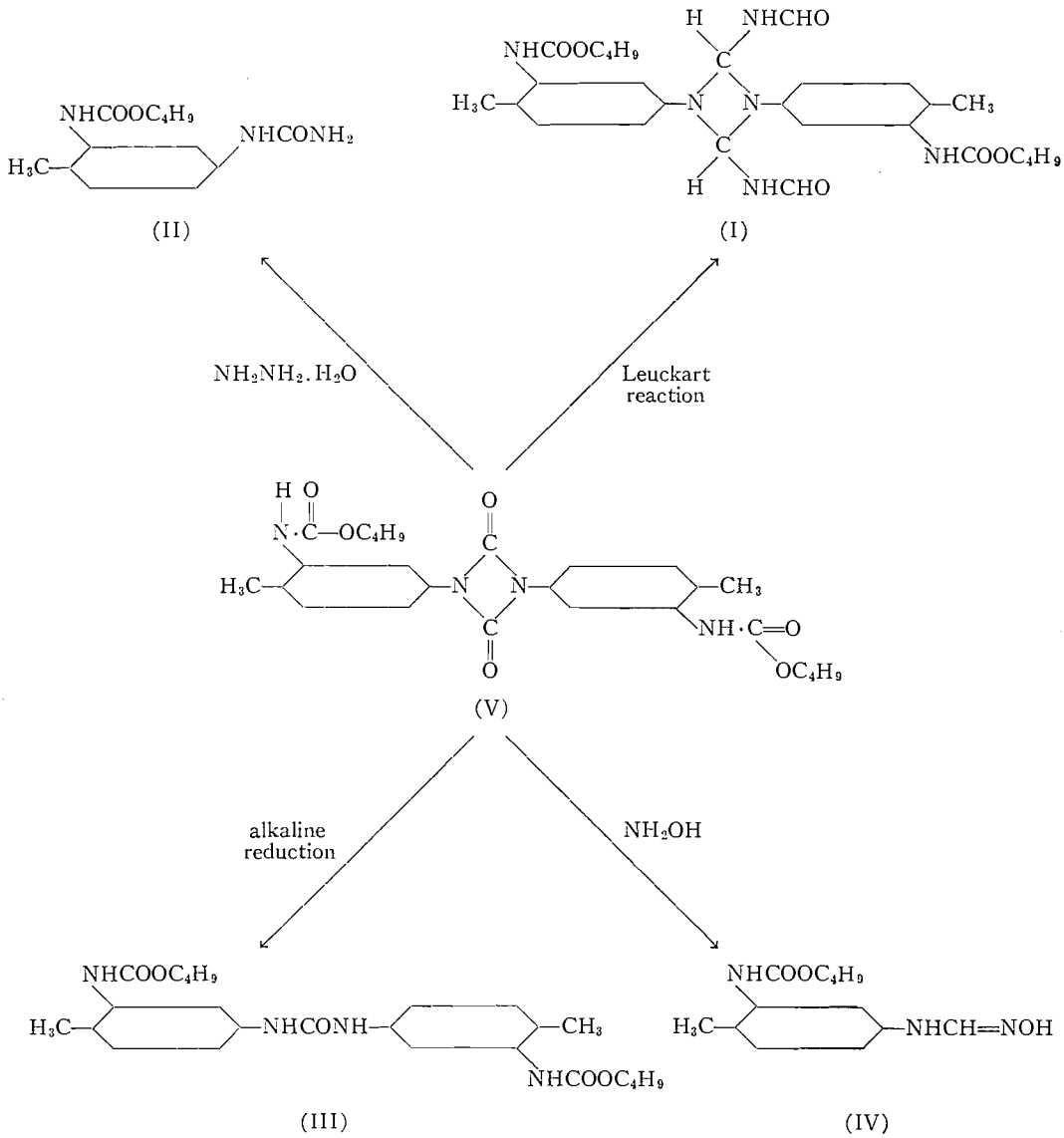

50° (7, 8). Diisobutylamine and dibenzylamine, however, left the ring unaffected and reacted with the *o*-isocyanate groups to yield substituted ureas (Table III). Both compounds showed characteristic infrared absorption bands for CO stretching frequency of the four-membered uretidine-dione ring.

For the oxidation, reduction, and carbonyl activity studies the two free isocyanate groups in TDID were blocked by forming the *n*-butyl urethanes (V). The structure of the new diurethane derivative of TDID was derived from its analysis and infrared spectrum. The blocking of the two isocyanate groups seemed to enhance the stability of the uretidine-dione ring. Heating a solution of the compound in benzene or ethyl acetate under reflux did not affect the ring, which was found to be moderately stable toward oxidation by potassium persulphate, lead tetraacetate, and selenium dioxide in dioxane.

TABLE II

2,4-Bis(N′,N′-di-R-ureido) toluene

R	Yield (%)	M.p. (°C)	Crystallization solvent	Reflux time (hr)	Formula	C		H	
						Calc. (%)	Found (%)	Calc. (%)	Found (%)
Di-*n*-propyl	60	124	Pet. ether	4½	$C_{21}H_{36}O_2N_4$	67.0	67.0	9.57	9.63
Di-*n*-butyl	80	111	"	4	$C_{25}H_{44}O_2N_4$	69.4	69.4	10.18	9.88
Di-*n*-amyl	50	98	"	3	$C_{29}H_{52}O_2N_4$	71.3	71.7	10.66	10.70

TABLE III

1,3-Bis(4′-methyl-3′-(N′,N′-di-R-ureido)phenyl) uretidine-2,4-dione

R	Yield (%)	M.p. (°C)	Crystallization solvent	Reflux time (hr)	Formula	C		H	
						Calc. (%)	Found (%)	Calc. (%)	Found (%)
Di-*sec*-butyl	70	176	Dioxane	3	$C_{34}H_{50}O_4N_6$	67.3	66.8	8.38	8.32
Di-benzyl	80	197	$HCON(CH_3)_2$	9½	$C_{46}H_{42}O_4N_6$	74.4	74.6	5.66	6.16

Alkaline reduction by various reagents such as sodium methylate, magnesium methylate, ammonium sulphide, or zinc and alcoholic ammonia all readily changed the ring into the ureylene link, with the appearance of CO and NH absorption bands at 1630 and 1602 cm^{-1} respectively. In alkaline medium, it seems that the ring was dissociated and that one of the isocyanate groups was hydrolyzed to amino group, which in turn reacted with the other isocyanate group to give symmetrical ureas. Hydrazine hydrate, on the other hand, reduced the ring to form an unsymmetrical monosubstituted urea.

The Leuckart reaction seems to give the corresponding N,N-substituted amide, according to infrared spectra determination. The new absorption for CO stretching (formyl group) at 1662 cm^{-1} (m) coupled with the appearance of free NH stretching vibration at 3410 cm^{-1} (m) and 3010 cm^{-1} (w) provide evidence for the presence of formyl derivatives of the primary amine (9). The failure to isolate any carbamate from the alcoholic solvent further lent credence to the conclusion that the uretidine-dione ring was intact. There was evidence that the CO group in the uretidine-dione ring acted as a true carbonyl, since hydroxylamine gave the oxime in poor yield. The elemental analysis corresponded to that of a N-substituted formamide oxime obtained from the monomer. This was also supported by the appearance of C—N and N—OH absorption bands and the absence of —N=C=N— absorption bands.

EXPERIMENTAL

General

The reactions with alcohols and diamine were performed in a 100-ml three-necked flask fitted with a mercury sealed stirrer. The condenser carried a $CaCl_2$ tube. Alcohols and diamines were taken in excess (2–3 ml) for 0.001 mole (1.0 g) of the dimer. The solvent used for the reactions was petroleum ether, A.R. (B.D.H.), b.p. 80–100° (40 ml). After the reaction was over the mixture was cooled, the compound filtered, washed, and dried in vacuum before crystallization.

All the melting points reported are uncorrected and most of them depend on the rate of heating. The infrared spectra were recorded with a Beckman IR–4 spectrophotometer using KBr pellets containing 0.5% by weight of sample, and reported spectra are all calibrated. Ultraviolet spectra were all recorded with a Beckman DK1-A spectrophotometer using 95% ethanol as solvent. Analyses were performed by Micro Tech Laboratories, Skokie, Ill.

2-Isocyanato-4-benzoylcarbamyl Toluene

A solution of 2,4-tolylene diisocyanate (5.0 g, 0.03 mole) and benzoic acid (3.65 g, 0.03 mole) in petroleum ether (100 ml, b.p. 80–100° C) was heated on a steam bath for half an hour. The solution was stirred with a stream of nitrogen to exclude moisture. On cooling of the solution, a compound melting at 84–85° C was obtained which upon crystallizing twice from petroleum ether (b.p. 80–100° C) gave an analytical sample of m.p. 85° C. Yield, 5.8 g (67%). If an excess of benzoic acid was used, the same compound was obtained under the same experimental conditions. Calc. for $C_{16}H_{12}O_4N_2$: C, 64.8%; H, 4.05%. Found: C, 64.8%; H, 4.09%.

2,4-Bis(benzylcarbamyl) Toluene

The dimer of 2,4-tolylene diisocyanate (1.0 g, 0.003 mole) and benzyl alcohol (2 ml) were heated under reflux in petroleum ether (40 ml, b.p. 80–100° C) for 5 hours. The reaction mixture was cooled and the solid filtered, washed with petroleum ether, and dried. The solid was crystallized twice from cellosolve to give an analytical sample of m.p. 217.5° C. Yield, 0.8 g (50%). Ultraviolet absorption spectrum in dimethyl formamide: λ_{max}: 2650 Å, E_{max}: 10,323; inflection point: 2780 Å. The infrared absorption spectrum showed two carbonyl absorption bands of the mixed anhydride at 1775 cm^{-1} (s), 1697 cm^{-1} (s) and C—O—C stretching vibration at 1065 cm^{-1} (s). Calc. for $C_{23}H_{18}O_6N_4$: C, 66.0%; H, 4.30%. Found: C, 66.7%; H, 4.43%.

Attempted Dimerization of 2-Isocyanato-4-methylcarbamyl Toluene

A solution of 2-isocyanato-4-methylcarbamyl toluene (2.0 g, 0.009 mole) in pyridine (10 ml) was kept at room temperature for 24 to 240 hours. No dimer was obtained. A drop of triethyl phosphate as catalyst at elevated temperature (80–100° C) did not give any dimer either.

1,3-Bis(4-methyl-3-n-butyl-carbamylphenyl)-2,4-bis(N-formamido) Uretidine (I)

To a stirred solution of ammonium formate (3.0 g) in ethanol (30 ml), 1,3-bis(4-methyl-3-*n*-butylcarbamylphenyl) uretidine-2,4-dione (1.0 g), m.p. 197°, was added. The mixture was refluxed for 2 hours

with constant stirring. The clear solution obtained on vacuum evaporation and dilution gave a precipitate, which was filtered and washed with water. Yield, 0.8 g; m.p. 160–162°. Two crystallizations from ethanol gave the analytical sample with a melting point of 164–165°, molecular weight (Rast) 525. λ_{max}: 2250 Å, E_{max}: 8310. Free NH stretching modes, 3410 cm^{-1} (m), 3050 cm^{-1} (w); amide I band, 1720 cm^{-1} (s); amide II band, 1662 cm^{-1} (m). Calc. for $C_{28}H_{38}O_6N_6$: C, 60.6%; H, 6.85%; N, 15.1%. Found: C, 60.5%; H, 6.62%; N, 14.9%.

N-(4-Methyl-3-n-butyl-carbamylphenyl) Urea (II)

To a solution of 1,2-bis(4-methyl-3-*n*-butyl-carbamylphenyl) uretidine-2,4-dione (1.0 g), m.p. 197°, in 95% ethanol (30 ml) was added hydrazine hydrate (85%, 5 ml). After the reaction mixture was refluxed for half an hour with constant stirring, alcohol (20 ml) was removed *in vacuo*. The residue on cooling gave a compound melting at 201–202°. Yield, 0.7 g. Three crystallizations from acetonitrile gave a pure compound of m.p. 208–209°. λ_{max}: 2830 Å, E_{max}: 13,515; λ_{max}: 2400 Å, E_{max}: 11,130; λ_{max}: 2180 Å, E_{max}: 1325. CO and NH absorptions of the monosubstituted ureas are 1692 cm^{-1} (s), 1610 cm^{-1} (s) respectively. Calc. for $C_{13}H_{19}O_3N_3$: C, 58.8%; H, 7.16%; N, 15.8%. Found: C, 58.7%; H, 6.88%; N, 16.0%.

N,N'-Di(4-methyl-3-n-butyl-carbamylphenyl) Urea (III)

To a stirred suspension of 1,3-bis(4-methyl-3-*n*-butyl-carbamylphenyl) uretidine-2,4-dione (2.0 g), m.p. 197°, in absolute methanol (50 ml), magnesium turnings (1.0 g) were added in small portions while temperature was maintained at 60° for 40 minutes. The reaction mixture was filtered through glass wool and evaporated under reduced pressure. Hydrochloric acid (10%, 50 ml) was then added and the mixture warmed, cooled, filtered, and washed free from acid with water. Crystallization from ethanol–water gave the compound of m.p. 180–181°. Yield 1.6 g. λ_{max}: 2180 Å. E_{max}: 35,720; λ_{max}: 2590 Å, E_{max}: 38,070; inflection point: 2950 Å. CO and NH absorption for disubstituted urea partial structure, 1630 cm^{-1} (m), 1602 cm^{-1} (m) respectively. Calc. for $C_{25}H_{34}O_5N_4$: C, 63.8%; H, 7.23%; N, 11.9%. Found: C, 63.5%; H, 7.23%; N, 12.1%. Reduction with sodium and methanol or with hydrazine hydrate plus 5% solution of sodium in methanol gave the above compound in identical yield. Alkaline reduction with ammonium sulphide at 60° for 4 hours or by zinc and alcoholic ammonia likewise gave the same compound in excellent yields of 80–90%. Mixed melting point determinations showed no depression and the infrared spectra were superimposable.

N-(4-Methyl-3-n-butyl-carbamylphenyl) Formamide Oxime (IV)

To a suspension of 1,3-bis(4-methyl-3-*n*-butyl-carbamylphenyl) uretidine-2,4-dione (m.p. 197°, 1.0 g) in a mixture of ethanol (25 ml) and water (25 ml), hydroxylamine hydrochloride (2.5 g) and sodium acetate (4.0 g) were added, and the reaction mixture refluxed with stirring for 1 hour. After the reaction mixture was evaporated to 30 ml and cooled, a precipitate was obtained, m.p. 169–170° C. Yield, 0.40 g. Two crystallizations from acetonitrile gave the analytical sample of m.p. 170–171°. λ_{max}: 2850 Å, E_{max}: 2630; λ_{max}: 2400 Å, E_{max}: 23,670; λ_{max}: 2180 Å, E_{max}: 31,560. C—N absorption of oxime, 1660 cm^{-1} (s). Free OH stretching frequencies for N—OH group, 3460 cm^{-1} (s) and 3400 cm^{-1} (s). Calc. for $C_{13}H_{19}O_3N_3$: C, 58.8%; H, 7.16%; N, 15.9%. Found: C, 58.7%; H, 7.0%; N, 16.4%.

REFERENCES

1. L. A. Dickinson. Rubber Age, (N.Y.), **82**, 96 (1957).
2. A-G. Fabriken Bayer. Brit. Patent No. 783,564 (September 25, 1956).
3. I. C. Kogen. 130th Meeting of the American Chemical Society. September, 1956. Paper No. 33.
4. W. J. Balon, E. Barthel, C. L. Kehr, E. O. Langerak, R. L. Pelley, D. M. Simons, K. Smeltz, and O. Stallman. 130th Meeting of the American Chemical Society. September, 1956. Paper No. 40.
5. M. Morton and M. A. Deisz. 130th Meeting of the American Chemical Society. September, 1956. Paper No. 34.
6. J. H. Saunders. Rubber Chem. and Technol. **32**, 337 (1959).
7. J. H. Saunders and E. E. Hardy. J. Am. Chem. Soc. **75**, 5439 (1953).
8. R. L. Craven. 130th Meeting of the American Chemical Society. September, 1956. Paper No. 32.
9. L. J. Bellamy. The infrared spectra of complex molecules. John Wiley and Sons, Inc., New York. 1959.

HYDRODESULPHURIZATION OF THIOPHENE

II. REACTIONS OVER A CHROMIA CATALYST[1, 2]

P. J. OWENS[3] AND C. H. AMBERG
Division of Applied Chemistry, National Research Council, Ottawa, Canada

Received November 17, 1961

ABSTRACT

The hydrodesulphurization of thiophene to butane and H_2S over chromia has been studied by flow and microreactor techniques. The sulphided, i.e. mixed oxide–sulphide, catalyst showed improved desulphurization activity compared to pure chromia, while butene hydrogenation activity was reduced by a factor of at least 10^3. The apparent activation energy of the flow reaction was 24–25 kcal/mole. No organosulphur compounds were found among the products. The reaction proceeded predominantly via butadiene and butene intermediates, with a preference for 1-butene; their rates of hydrogenation as well as the rates of isomerization of the butenes have been compared as a function of temperature. The reaction also partly went to completion at the original desulphurization site, without the desorption of intermediates, presumably by a series of analogous steps on the surface.

INTRODUCTION

In a previous publication (1) a microreactor method first described by Kokes, Tobin, and Emmett (2) was further developed to study the desulphurization of thiophene over a presulphided cobalt molybdate catalyst supported on alumina. With hydrogen acting as both reactant and carrier gas, continuous flow as well as pulse techniques showed that the reaction to butane and H_2S proceeds, in the main, in steps through butadiene and butene and not, as has also been suggested, through butyl mercaptan, thiolane, or other sulphur compounds. Approximate relative rates were assigned to the various steps.

By making use of the catalyst bed also as a gas–solid partition column it was possible to examine adsorption–desorption behavior of reactants and products under reaction conditions, and hence the influence of the adsorbates on the course of the reaction. Thus, for instance, it was found that adsorbed H_2S modifies the surface so as to suppress butene hydrogenation in contrast to its much weaker effect on thiophene conversion.

Some preliminary data using an unsupported chromia catalyst, again in a presulphided state, were also presented. These have now been extended by a more thorough search for reaction intermediates as well as by measurements of the relative rates of the reaction steps over a range of temperatures. Pertinent adsorption studies will be submitted as Part III of this series.

EXPERIMENTAL

The microreactor and associated apparatus have already been described (1). The reactor was operated only at atmospheric pressure. The catalyst employed was an unsupported chromia, prepared by the method of Burwell *et al.* (3) and activated by heating slowly to 400° in hydrogen. It was then stabilized as a desulphurization catalyst by passage of a thiophene–hydrogen mixture over it for several hours at 400°. The catalyst tended to oxidize and was resulphided from time to time whenever injected H_2S samples showed, by generating water peaks observable on the chromatogram, that such oxidation had occurred. The freshly sulphided catalyst contained 14.2% sulphur, and was therefore a mixed oxide–sulphide. In this it is similar to catalysts made from supported cobalt molybdate (1) and the oxides of iron (4) and molybdenum (5). The sulphided chromia was amorphous to X rays. It had a B.E.T. surface area of 118 m^2/g, decreased from 223 m^2/g for freshly prepared chromia.

[1]*Issued as N.R.C. No. 6751.*
[2]*For Part I, see reference 1.*
[3]*National Research Council Postdoctorate Fellow 1959–1961, now with the Heavy Organic Chemicals Division, I.C.I. Ltd., Billingham, England.*

RESULTS AND DISCUSSION

Effect of Temperature

The effect of temperature on catalyst activity for both the shot and flow reactions is shown in Fig. 1. The activity per square meter of catalyst surface was nearly identical in

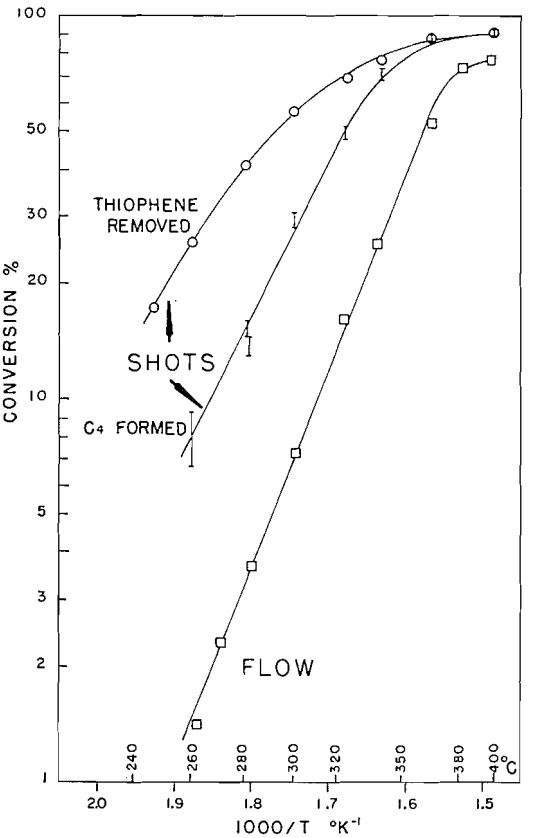

FIG. 1. Effect of temperature on thiophene conversion for flow and shot reactions (2.5 g chromia; 5.7 l./hr H_2; thiophene used: shots 5μl, flow 6.6% in H_2).

both cases with that of cobalt molybdate, provided allowance is made for the lower thiophene-to-hydrogen ratio used in the earlier flow experiment.

The apparent activation energy of the flow reaction was 24–25 kcal/mole, the same value that was obtained on supported cobalt molybdate (1) and supported chromia (6). The shot experiments gave two different curves, C_4 formed and thiophene removed (Fig. 1), due presumably to irreversible adsorption or polymerization of one of these, as discussed before (1). The lines are closer together in this case, probably because the weight of catalyst used was smaller and therefore the losses reduced. In both the flow and shot reactions the apparent rate constant fell off at high-percentage conversions, as one might expect from this type of plot.

Shot conversions were higher than flow conversions at the same temperature (Fig. 1), but were found to vary considerably with sample size. There is no a priori reason to

suppose that the reaction pattern in flow and shot experiments was fundamentally different. This is supported by the fact that the temperature coefficients for C_4 formation from shots and in steady flow appear to be nearly the same (see slopes, Fig. 1), though the former can only be measured approximately.

Reaction Products

The reaction products were examined for traces of butyl mercaptan or tetrahydrothiophene, but neither could be found. In addition, the rate of reaction of each of these compounds was checked at 400°. The conversion obtained using tetrahydrothiophene was only twice the conversion of thiophene at this temperature, so that if any had been formed almost all of it should have been present in the products. We conclude that none was formed. Butyl mercaptan was approximately 30 times as reactive as thiophene, but as little as 0.03% in the reaction products would have been clearly visible on the chromatogram. This is the amount that should have remained if 5% of the thiophene which reacted had done so by the mercaptan route.

The reaction scheme already presented (1), which involves intermediate formation of butadiene and the *n*-butenes as well as stepwise hydrogenation of these to butane, was further investigated by measuring the rates of the various hydrogenation and isomerization steps over a range of temperatures, using pure C_4 shots in hydrogen carrier gas. The results are shown in Figs. 2 and 3, and Arrhenius coefficients calculated from the slopes are listed in Table I.

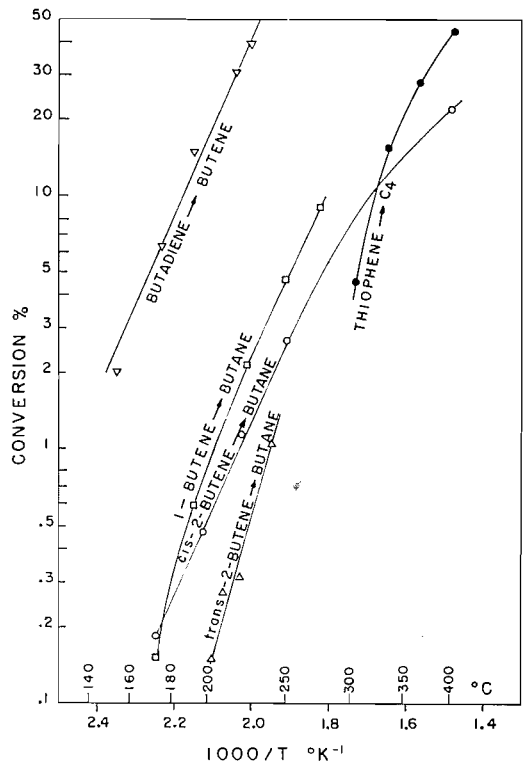

FIG. 2. Hydrogenation rates (0.113 g chromia; 1.3 l./hr H_2; shots 0.2 cc at N.T.P., or 0.7 μl).

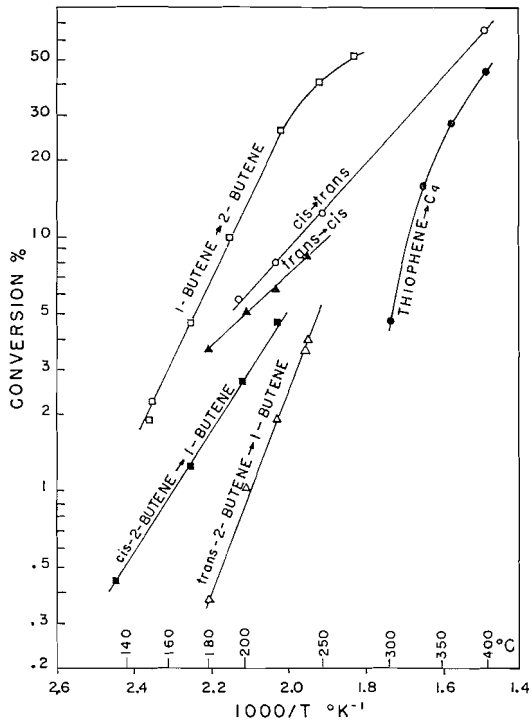

FIG. 3. Isomerization rates (0.113 g chromia; 1.3 l./hr H_2; shots 0.2 cc at N.T.P.; data on conversion of 0.7 μl thiophene shots included for comparison).

TABLE I

Apparent activation energies of various reactions

Reaction	Temp. range (°C)	E (kcal/mole)
Thiophene → C_4	260–330	24
Butadiene → butene	170–230	16
1-Butene → butane	190–270	15.5
cis → butane	170–250	15.5
trans → butane	310–360	15.5
	200–250	~25
1-Butene → 2-butene	150–225	14.5
trans → 1-butene	180–280	~17
cis → 1-butene	135–220	~11
trans → *cis*	180–240	6.5
cis → *trans*	250–400	8.5
	190–250	6.5
	120–180	0

At low temperatures (i.e. at 150° and below) the reactions were relatively simple (see Table II). 1-Butene isomerized to a mixture of *trans*- and *cis*-2-butene (about 64% *cis*-2-butene); pure *cis*-2-butene isomerized almost exclusively to *trans*-2-butene, and vice versa. Butadiene hydrogenation yielded all three isomers, but with a high preponderance of 1-butene.

Above 200° these were still the dominant reactions, but isomerization of 2-butene to 1-butene and hydrogenation of all three butene isomers to butane also occurred. There

TABLE II

Products formed, in moles/100 moles of reactant converted, in low-temperature* reactions of C_4's

	Reactant:							
	Butadiene		1-Butene		*trans*-2-Butene		*cis*-2-Butene	
Products	Below 150°†	220°	Below 150°†	220°	Below 180°†	220°	Below 120°†	220°
n-Butane	0	3	2	8	0	4	0	9
1-Butene	68	53	—	—	0	22	0	34
trans-2-Butene	20	23	34	40	—	—	100	58
cis-2-Butene	12	21	64	52	100	74	—	—
Conversion (%)	0	41	0	29	0	8	0	14

*Temperatures are given in °C.
†Results extrapolated to zero conversion.

was no evidence of a simple reaction scheme (for example with a single intermediate in isomerization and hydrogenation of all the isomers) even though there was a tendency of the catalyst to yield excess *cis*-2-butene. The ratio of *cis*- to *trans*-2-butene in the products of 1-butene was high, and similar to that obtained by Cvetanović and Foster with KOH-impregnated chromia (7), but different from the ratio they obtained with pure chromia. It is tempting to speculate that the initial sulphiding treatment of our catalyst had an effect on its acidity similar to that of KOH impregnation.

The sulphided catalyst was different from pure chromia also in its olefin hydrogenation activity. Though its activity for olefin isomerization was similar to that of pure chromia activated at the same temperature (8), its hydrogenation activity was less than that of pure chromia (8) by a factor of 10^3–10^4. Littlewood and Burwell (8) have presented evidence to show that isomerization and hydrogenation occur on different sites on pure chromia. If this is so, it suggests that sulphiding of the catalyst practically eliminates one of these two types of site. It is noteworthy, however, that the activity of chromia for thiophene desulphurization rose appreciably during sulphiding, so that while catalyst activity was destroyed for one reaction it increased for another. The effect of H_2S on subsequent butene hydrogenation over sulphided chromia was small (see Part III); therefore the hydrogenation rates in Fig. 2 and Table I, unlike those in the earlier work, were not measured in the presence of H_2S.

Initial Products from Thiophene at 400°

The C_4 products obtained from thiophene at 400° showed a non-equilibrium distribution of isomers when small amounts of catalyst were used. Isomerization and hydrogenation of the individual pure hydrocarbons were found to be incomplete at this temperature. Now if one assumes the same changes to occur in a hydrocarbon formed from thiophene as occur in the hydrocarbon injected as such, then the composition of the initial C_4 mixture formed from thiophene can be calculated. (This assumption would not be strictly correct if large concentration gradients were set up in the catalyst pores; however, we consider this to be unlikely.) The result of such a calculation is shown in Table III, together with the composition actually found. A comparison of the butane figures in the table shows that the reaction is only partially stepwise via intermediates free in the gas phase, and to the extent of 27.8%, goes to completion at the original desulphurization site. Furthermore, the data probably correspond to a low hydrogen-to-thiophene ratio; with smaller shot sizes (higher H_2/thiophene ratio) no butadiene at all

TABLE III

Composition of C_4 product from thiophene at 400° C
(2 μl shot over 0.113 g chromia; H_2 flow: 2.4 cc/sec)

	Found (%)	Corrected for subsequent reaction (%)
n-Butane	33.9	27.8
1-Butene	21.6	30.3
trans-2-Butene	23.9	15.5
cis-2-Butene	18.4	18.3
Butadiene	2.2	8.1

was found, even at the highest flow rates used. It is conceivable that in flow reactions using a high hydrogen-to-thiophene ratio about half the butane product is formed directly at the desulphurization site, and the other half via the hydrogenation of butene.

In consequence, the most plausible picture of the reaction is that of a series of hydrogenation steps on the surface, in which the sulphur atom is eliminated first and desorption is possible at any subsequent stage, i.e. as butadiene, butene, or butane. The second of these surface steps, butadiene hydrogenation, must be relatively fast if such a reaction is to yield the product distribution shown in Table III; from Fig. 2 it seems likely that this is so.

CONCLUSIONS

The activity of sulphided chromia for desulphurization was similar to that of sulphided cobalt molybdate when compared on a surface area basis. Initial sulphiding of the chromia increased its desulphurization activity, but decreased its activity for butene hydrogenation by a factor of 10^3–10^4. Neither reaction was much affected by H_2S, in contrast to the earlier results (1). Butene isomerization activity was probably not altered by sulphiding.

The apparent activation energy for the continuous flow reaction between thiophene and hydrogen over chromia was 24–25 kcal/mole, the same value that applies to cobalt molybdate and supported chromia catalysts.

Conversion of thiophene to butane was essentially a stepwise reaction. The only intermediates free in the gas phase were butadiene and the three butenes, especially 1-butene; there was no evidence for the formation of organosulphur compounds at any stage of the reaction. To a considerable extent butane formation occurred at the original desulphurization site. The butadiene hydrogenation step was very rapid compared with any of the others at all temperatures.

REFERENCES

1. P. J. Owens and C. H. Amberg. Advances in Chem. Ser. No. 33, 182 (1961).
2. R. J. Kokes, H. Tobin, Jr., and P. H. Emmett. J. Am. Chem. Soc. **77**, 5860 (1955).
3. R. L. Burwell, Jr., A. B. Littlewood, M. Cardew, G. Pass, and C. T. H. Stoddart. J. Am. Chem. Soc. **82**, 6272 (1960).
4. F. P. Ivanovskiĭ, R. S. Kalvarskaya, G. S. Beskova, and N. P. Sokolova. Zhur. Fiz. Khim. **30**, 1860 (1956).
5. E. H. M. Badger, R. H. Griffith, and W. B. S. Newling. Proc. Roy. Soc. (London), A, **197**, 184 (1949).
6. H. van Looy and G. Limido. Compt. rend. congr. intern. chim. ind., 31e, Liège, 1958 (Ind. chim. belge, Suppl.), **1**, 645 (1959).
7. R. J. Cvetanović and N. F. Foster. Discussions Faraday Soc. No. 28, 201 (1959).
8. A. B. Littlewood and R. L. Burwell, Jr. J. Am. Chem. Soc. **82**, 6287 (1960).

HYDRODESULPHURIZATION OF THIOPHENE

III. ADSORPTION OF REACTANTS AND PRODUCTS ON CHROMIA[1, 2]

P. J. OWENS[3] AND C. H. AMBERG
Division of Applied Chemistry, National Research Council, Ottawa, Canada

Received November 17, 1961

ABSTRACT

The adsorption of thiophene, butene, hydrogen, and H_2S on sulphided chromia was studied by a chromatographic method. Results were similar to those obtained earlier with a cobalt molybdate catalyst (P. J. Owens and C. H. Amberg, Advances in Chem. Ser. No. 33, 182 (1961)), showing strong interaction of the surface with H_2 and H_2S at reaction temperatures and weaker interaction with thiophene and butene. The main difference lay in the effect of adsorbed H_2S on butene hydrogenation, the suppression being far less marked on chromia. Thiophene adsorption or product desorption are unlikely to be rate controlling in the desulphurization reaction, but neither hydrogen adsorption nor surface reaction could be ruled out as possible slow steps.

INTRODUCTION

A grasp of the relevant adsorption processes is essential to an understanding of either the mechanism or the kinetics of a catalytic process. High-temperature adsorption is difficult to study with conventional volumetric apparatus where reaction occurs, so that until the recent introduction of chromatographic adsorption studies little such knowledge had accumulated (1). The present work surveys the interactions of thiophene, hydrogen, butene, and H_2S with a modified chromia catalyst, alone and in various combinations, and also attempts to draw some conclusions regarding the possible effect of such interactions on the overall reaction rate.

EXPERIMENTAL

Adsorption was studied mainly by the chromatographic techniques already described (2). The catalyst column was connected straight to the katharometer in all experiments, so that eluted bands were recorded directly and peak retardation occurred only on the catalyst. The flow rates of the various carrier gases were measured at the katharometer exit by water displacement. A small amount of tracer—helium, argon, or nitrogen—was added to the sample shot, and the separation between the peak maxima was taken as a measure of the delay time of the adsorbed gas.

RESULTS

Adsorption of Thiophene and Butene

The retention volumes of product butene and thiophene on sulphided chromia were similar to those measured earlier on cobalt molybdate, but had slightly different temperature coefficients (Fig. 1). The values obtained from the slopes in Fig. 1, after making appropriate corrections for the temperature at which flow rates were measured, were 7.0 and 8.0 ± 0.5 kcal/mole for thiophene and butene respectively, compared with 9.5 ± 1.0 and 8.5 ± 0.5 on cobalt molybdate. In this temperature range, the retention volumes on chromia were exactly the same in both helium and hydrogen carrier gases, and as before (2), the effect of adsorbed H_2S on the retention volume was slight.

[1] *Issued as N.R.C. No. 6752.*
[2] *For Parts I and II, see references 2 and 5 respectively.*
[3] *National Research Council Postdoctorate Fellow 1959–1961, now with the Heavy Organic Chemicals Division, I.C.I. Ltd., Billingham, England.*

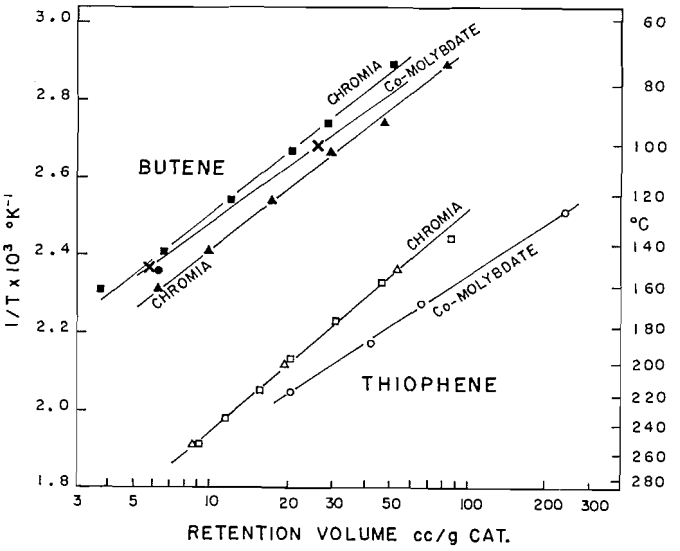

FIG. 1. Thiophene and butene adsorption. Peak retention volumes vs. temperature. Open symbols for thiophene, others for butene: □ chromia, 0.35 cc/g catalyst shots, H_2 carrier gas; △ chromia, He carrier gas; ○ cobalt molybdate, 0.40 cc/g catalyst shots, H_2 carrier gas; ■ chromia, 0.34 cc/g catalyst shots, H_2 carrier gas; ● chromia, He carrier gas; ▲ chromia, 0.031 cc/g catalyst shots, H_2 carrier gas; × cobalt molybdate, 0.39 cc/g catalyst shots, H_2 carrier gas.

The method of peak integration recently suggested by Cremer (3) was used to construct the isotherms shown in Fig. 2 from the chromatograms, and these were then used to

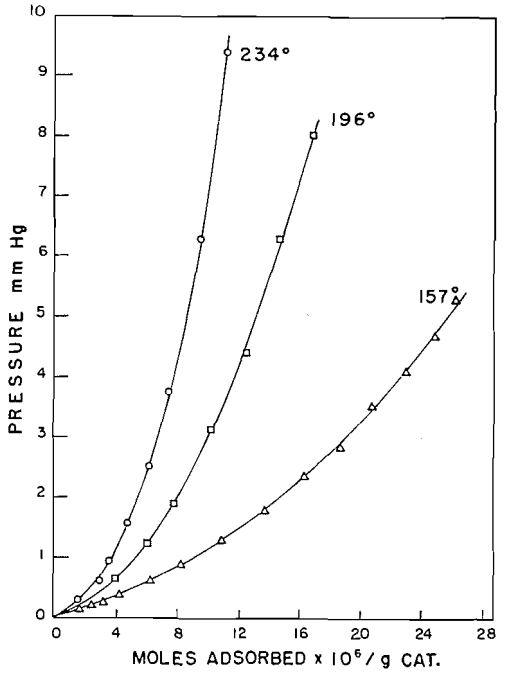

FIG. 2. Adsorption isotherms of thiophene on chromia catalyst. Estimated from the chromatograms in H_2 carrier gas by the method of Cremer (3), allowing for diffusion.

calculate isosteric heats of adsorption for thiophene. The results were in the range 8–11 kcal/mole, but were somewhat uncertain, because a small amount of irreversible adsorption as well as peak tailing always took place. Nevertheless, the figures are interesting as approximate values to compare with the temperature coefficients obtained above, which under ideal conditions should equal heats of adsorption. Chromatographic theory cannot strictly be applied to systems with curved isotherms, and even at very small shot sizes may give low results (4); however, the results taken together reinforce the view that high-temperature thiophene adsorption on chromia is relatively weak and rapid when compared, for example, with hydrogen adsorption (see below).

Another effect of irreversible adsorption can be seen in Fig. 3, where it causes the thiophene retention volumes to tend to infinity at small shot sizes. The amount of

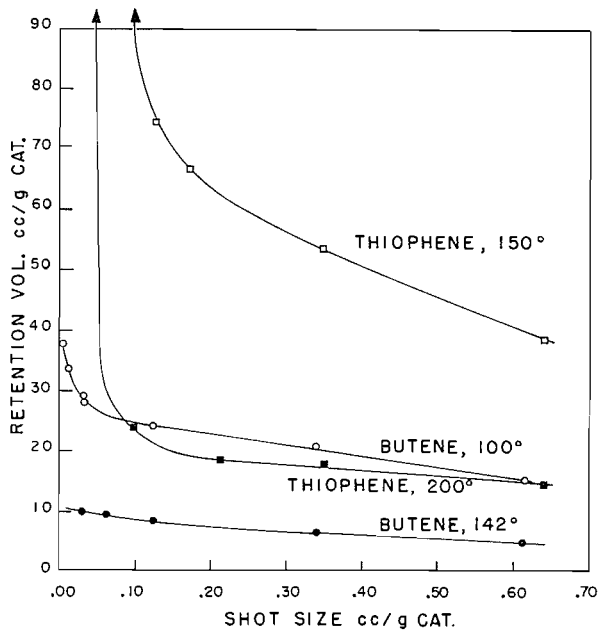

FIG. 3. Effect of sample size on retention volume. Thiophene and butene on chromia catalyst, in H_2 carrier gas.

thiophene irreversibly adsorbed varied, but was seldom more than 0.5 μl, and it appeared to be independent of shot size or catalyst temperature. It could have been due to some side reaction, such as polymerization or carbon formation; it was apparently unconnected with the main reaction and small compared with the amount of thiophene converted at high temperature. The phenomenon could be the explanation for the discrepancy in thiophene converted and products eluted over both cobalt molybdate and chromia catalysts (2, 5).

At lower temperatures (e.g. 250°) it is unlikely that the relatively weak, reversible thiophene adsorption could be rate controlling. It is unfortunately not possible to calculate a rate of adsorption from the chromatographic data to compare with the measured rate of reaction. On the other hand it is possible to find from the chromatogram the minimum number of adsorption–desorption steps that a thiophene molecule undergoes in travelling through the column; this is given by the plate number. (The true number of steps on a

porous catalyst is presumably much higher.) At 250°, approximately 5% conversion occurred per plate or equilibrium stage, so that less than 5%—and probably very much less—would have converted at each of the actual adsorption steps. Thiophene adsorption is thus rapid compared with the overall rate of reaction at least up to 250°. However, with a temperature coefficient of only 7 kcal/mole it increases in rate much more slowly than the overall process, which has a temperature coefficient of approximately 25 kcal/mole (5); so that without knowing the number of adsorption steps which occur within the catalyst pores in each equilibrium stage, one cannot be certain that adsorption remains relatively rapid at higher temperatures. The only indication that it does so is given by the temperature coefficient of the flow reaction, which remains at 25 kcal/mole up to at least 360–370° (5); any change in the rate-controlling step would have caused a change in the overall temperature coefficient.

From Fig. 1, the adsorption–desorption process is an order of magnitude faster for butene than it is for thiophene, at all temperatures. This makes it extremely unlikely that butene desorption could be the slowest step at any temperature, unless it desorbed from reaction sites in an entirely different way from that observed at 80–160°. This also is unlikely, because over cobalt molybdate, butene formed from thiophene had a retention volume between those of butene alone and thiophene, as might be expected (2), and there is no reason to suspect that it would behave differently over chromia.

There is one important reservation to be made, however, about the conclusions drawn from the above results. At present we are unable to calculate the number of adsorption–desorption steps made by the average molecule within one plate of the catalyst. If this number was very large, and if the proportion of the surface occupied by "active" sites was small, it would be quite possible for most of the thiophene or butene adsorptions to occur on inactive parts of the surface and for the observed conversion per plate to occur on only a few sites. In this case the above measurements would reflect the inactive rather than the active adsorption steps, and the possibility of the significant thiophene adsorption or butene desorption being slow would remain.

Hydrogen

Hydrogen chemisorption has been extensively studied on pure chromia, but never, so far, on sulphided chromia. On the former it occurs at all temperatures from −195° (6) up to at least 500° (7), and in amounts up to 0.1 cc/m² of surface at the higher temperatures (7). Activation energies of 13–21 kcal/mole have been reported for adsorption (8–10), as well as an increase in the activation energy of desorption from 15 to 45 kcal/mole with decreasing coverage (10). The rate of adsorption increases with temperature (11) and pressure (10); it decreases with amount adsorbed according to the Elovich equation (9).

Our results suggest that hydrogen chemisorption on sulphided chromia is similar. In chromatographic experiments using helium carrier gas, hydrogen peaks behaved in the same way as on cobalt molybdate. The first few shots were adsorbed rapidly and completely, until the catalyst reached a certain hydrogen content. Thereafter the peak height and delay obtained depended both on shot size and on the time interval between shots, i.e. on the amount of hydrogen still adsorbed on the catalyst. As before, curves of peak height or delay vs. shot size could be corrected for hydrogen already adsorbed, so that all the data lay on one line.

During the further course of a series of constant-volume injections the peak heights gradually tended to increase; this was attributed to slow adsorption at high coverages.

Large shot sizes seemed to increase both the rate of this drift and the rate of attainment of equilibrium: in other words the rate of the slow chemisorption was increased by pressure as in static experiments on pure chromia (10).

The peaks had very small delay times and plate numbers, showing again that equilibrium was not reached during the time of passage of one shot. As the temperature rose, the peak heights for a given shot size dropped, demonstrating that adsorption was more rapid at higher temperatures.

Variations in the rate of adsorption with coverage, pressure, and temperature were thus seen to be in the same direction as on pure chromia. However, it was not convenient to measure the extent of chemisorption chromatographically; therefore a few static measurements were made using a conventional volumetric apparatus (see Fig. 4). The amount

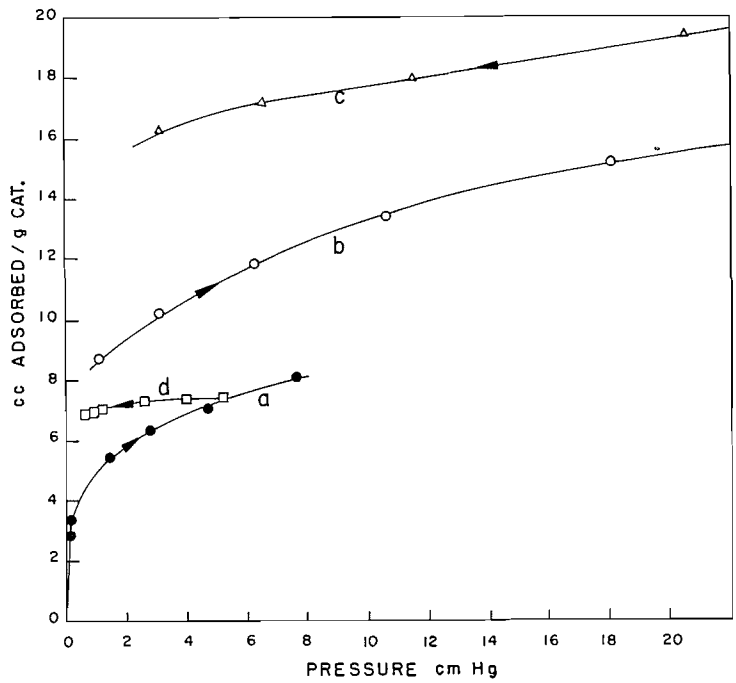

FIG. 4. Hydrogen adsorption, curves *a–c* at 330°, curve *d* at 350°.
a. Adsorption on chromia catalyst outgassed 18 hours at 400°; points at ½-hour intervals.
b. Adsorption after same treatment and 5 hours in 1 cm H_2; points at 1-hour intervals.
c. Desorption following adsorption at 36 cm H_2; points at 1-hour intervals.
d. Rapid desorption measured chromatographically; points at approximately 10-second intervals.

of hydrogen chemisorbed is seen to be similar to or larger than the amount adsorbing on pure chromia (7), with the extreme slowness of approach to equilibrium being quite evident.

One of the hydrogen chromatograms was used to calculate an isotherm by the Cremer method (3); this is also shown in Fig. 4 as curve *d*. It was obtained on a catalyst which had been brought apparently to equilibrium by repeated hydrogen injections at a point in the peak tail corresponding to 4.2 mm hydrogen pressure. For that reason it is drawn, somewhat arbitrarily, through a static point obtained after 2 hours' adsorption at a similar pressure. The amount of hydrogen adsorbed during passage of a shot which

raised the hydrogen pressure to at least 5.5 cm is clearly small (~0.28 cc/g) compared with equilibrium adsorption at 5.5 cm (4–5 cc/g). This is a measure of departure from equilibrium under chromatographic conditions, and shows again the relative slowness of hydrogen adsorption.

Since hydrogen chemisorption occurs at so low a rate, it is natural to ask whether it might be rate controlling in the desulphurization reaction. The hydrogen consumption in the flow reaction at 333° was 1.8 cc at N.T.P. min^{-1} (g catalyst)$^{-1}$. It is possible to make only very rough estimates of the rate of chemisorption at 76 cm pressure from the data in Fig. 4. If one uses for this purpose Kubokawa's result (10) that the rate of chemisorption is proportional to pressure to the power 0.8, the calculated rates of chemisorption appear to be of the right order of magnitude. An independent estimate from the amount of hydrogen completely adsorbed during the time of passage of a chromatographic peak gave a figure of 11 cc min^{-1} (g catalyst)$^{-1}$. Without a precise knowledge of the dependence of chemisorption rate on pressure and coverage even this higher estimate must be considered close enough to the reaction rate not to exclude hydrogen chemisorption as a possible rate-determining step.

Strongly (and more rapidly) chemisorbed hydrogen has been found relatively inactive in desulphurization and butene hydrogenation on cobalt molybdate (2) and in low-temperature exchange reactions on chromia (7). In the present work, conversions of butene and thiophene shots reacted with preadsorbed hydrogen were found to fall off very rapidly as the hydrogen eluted from the catalyst. In Fig. 5, *a* and *b*, these conversions are plotted against the partial pressure of hydrogen in the helium carrier gas leaving the

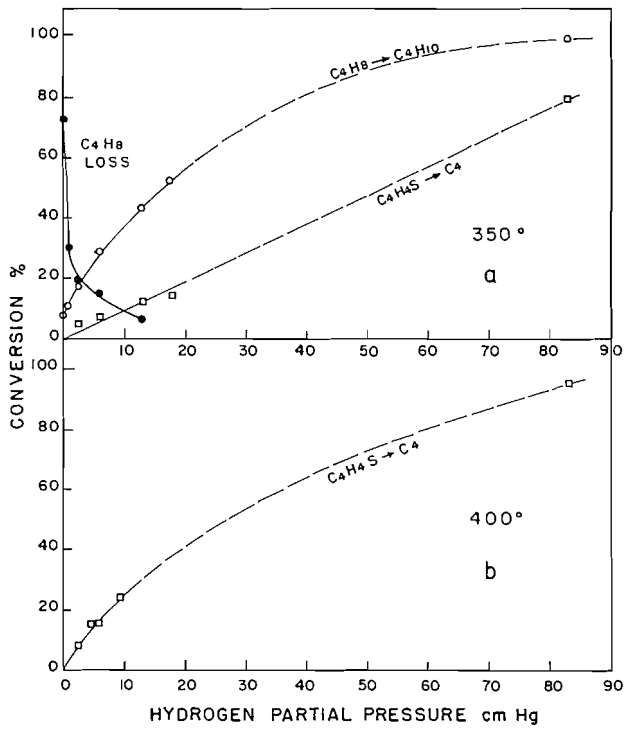

FIG. 5. Reaction of thiophene and butene with preadsorbed hydrogen. Shots injected at various points (i.e. partial pressures) in the tail of a desorbing hydrogen band, helium carrier gas.

catalyst. Conversions in hydrogen carrier gas at 83 cm are included. It is obvious from Fig. 4 (curve *d*) that the total amount of hydrogen chemisorbed would have changed very little during this rapid elution, so that the conversion was determined not by the total amount of hydrogen chemisorbed, but apparently by the partial pressure of hydrogen free in the gas phase. This means that strongly chemisorbed hydrogen is not reactive and that a much smaller amount of weakly sorbed hydrogen, which can establish equilibrium with the gas phase more rapidly, is solely responsible for the reaction.

The considerable loss from butene shots at low hydrogen partial pressures is interesting (Fig. 5*a*). It suggests that rapid carbon formation, which is well known to occur at low hydrogen partial pressures, might come about largely by the polymerization and coking of product butene rather than of thiophene itself. These large losses did not arise during the measurement of retention volumes (e.g. Figs. 1 and 3), no matter whether hydrogen or helium was used as a carrier gas, because of the lower temperatures involved.

Hydrogen Sulphide

Hydrogen sulphide adsorption was investigated by the chromatographic method only. The same type of behavior occurred as on cobalt molybdate (2): the peak shapes obtained were similar and the delay times at 300° were almost the same when corrected for catalyst weight and carrier gas velocity.

Both peak delay and peak height were found to depend largely on the total H_2S on the chromia, i.e. shot size plus preadsorbed H_2S. A typical result is shown in Fig. 6. Peak delays were longer at 400° than at 300°, and as before, there was an apparent change in base level of adsorbed H_2S with temperature. For example, catalyst heated to 400° in hydrogen adsorbed approximately 2.0 cc H_2S/g irreversibly at 300° before desorption commenced. The base level also appeared to be different in hydrogen and helium carrier

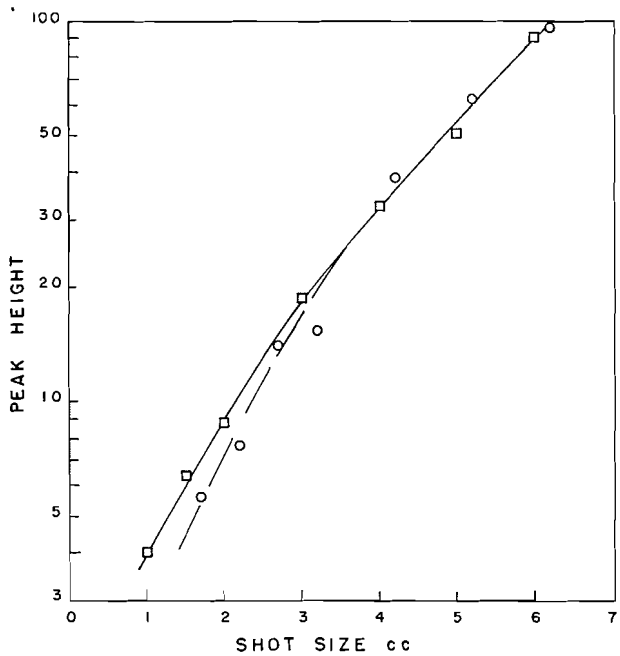

FIG. 6. Peak heights (arbitrary units) for H_2S shots injected while preadsorbed H_2S was emerging at different desorption rates: □ 0.20 cc/min; ○ 0.64 cc/min, shot sizes corrected by the 1.2 cc H_2S still present on the catalyst.

gases. Thus chromia saturated with H_2S and then flushed in a helium stream for 10 minutes (i.e. until desorption became very slow) released a total of 3.2 cc H_2S upon injection of three successive 3-cc hydrogen shots. Also, the low rate of removal of H_2S from the surface, as measured by the amount subsequently readsorbed, was higher in hydrogen than in helium (Table I), in contrast to the results with butene and thiophene, and the inverse delay time vs. shot size plots were quite different (Fig. 7). Hydrogen thus displaces H_2S, as well as eluting it, presumably by adsorbing on the same sites.

TABLE I

Slow H_2S desorption between 2.5 and t minutes in hydrogen and helium carrier gases (1.6 g chromia at 400°, 5.3 l./hr H_2 or He)

	Time t (minutes):		
	5	60	180
cc desorbed in H_2	1.2	3.1	4.6
in He	0.38	1.2	1.8

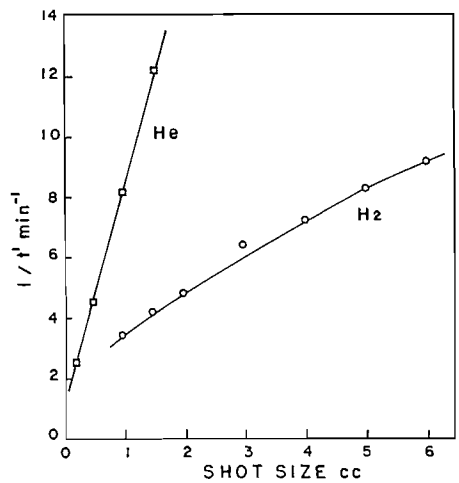

FIG. 7. Hydrogen sulphide breakthrough rates in H_2 and He carrier gases at 400°.

The hydrogenation of butene shots was reduced by preadsorbed H_2S to the small extent shown in Fig. 8, in sharp contrast to the earlier results (2). Similar amounts of H_2S had a similar effect on thiophene conversion. It has already been suggested (2) that H_2S acts on cobalt molybdate by poisoning fast hydrogenation sites, leaving only sites capable of both desulphurization and slow hydrogenation. It now seems likely (5) that the fast hydrogenation sites on chromia are permanently eliminated during presulphiding, so that further poisoning with H_2S has little effect.

Using the data for shot conversions of thiophene in the presence of H_2S over chromia, the percentage drop in conversion in a flow reaction due to H_2S produced was estimated to be 20, 10, and 0% at 400, 350, and 300° respectively. A similar calculation using our published data for cobalt molybdate indicated that conversion at 300° was 30% lower than it might have been in the absence of an H_2S effect. Adsorbed H_2S thus affects the overall reaction appreciably, but does not exert a controlling influence.

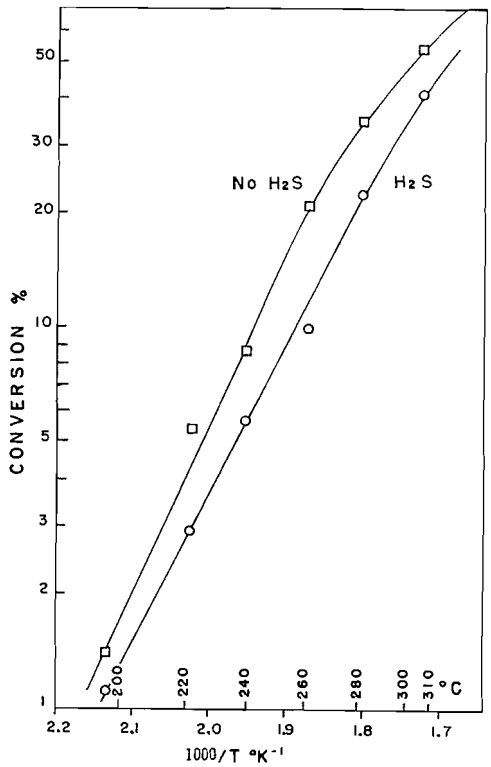

FIG. 8. Effect of H_2S on butene hydrogenation over chromia catalyst.

To calculate the effect of H_2S on flow conversion it was necessary to assume that the peak heights obtained from various samples of H_2S approximated the instantaneous desorption rates corresponding to the total H_2S contents of the catalyst (i.e. preadsorbed plus sample). Since data obtained at two different catalyst contents correlated tolerably well together (Fig. 6), there was some basis for this assumption. The rates of formation of H_2S in a flow experiment were known (5); these gave the H_2S desorption rates at various temperatures in a steady-state experiment; from this together with Fig. 6 the catalyst H_2S contents could be calculated. Then, by comparing the slug conversions in the absence of H_2S and in the presence of the amount calculated, the effect of H_2S on conversion in a steady-state experiment could be estimated.

Olefins

The effect of adding olefins to thiophene shots was investigated briefly, to gain some idea whether product butene was likely to have an inhibiting effect on the flow reaction by occupying desulphurization sites. Gaseous butene could not readily be handled in the same syringe as liquid thiophene. Therefore the liquid olefins hexene and cyclohexene were used; these had retention volumes intermediate between those of butene and thiophene. Adding 2 μl hexene to a 2-μl thiophene shot produced a negligible effect; adding 6 μl reduced thiophene conversion by 10–15%. The effects of cyclohexene and cyclohexane were slightly weaker, in that order; it is noteworthy in that connection that cyclohexene consumed as much hydrogen as thiophene itself. However, 15 μl of hexene

was found to cut the thiophene retention volume by 100%. We conclude that hydrocarbons are unable to compete for desulphurization sites, so that the butene produced should not inhibit the reaction significantly. Nevertheless, in the desulphurization of, say, low-sulphur cracked feedstocks the large proportion of hydrocarbons present could be expected to inhibit thiophene removal to an appreciable extent.

CONCLUSIONS

In view of the obvious chemical differences between chromia and supported cobalt molybdate catalysts, the close similarity in adsorption phenomena is striking. Moreover, Griffith, Marsh, and Newling (12) have shown that extensive hydrogen chemisorption and weaker thiophene adsorption occur also on sulphided molybdenum oxide and on pure nickel and molybdenum sulphides at high temperatures, so that this type of adsorption behavior appears to have some generality among desulphurization catalysts. (Hydrogen sulphide and butene adsorption were not included in this earlier study (12).) On the other hand, supported chromia is probably somewhat different, kinetic studies having shown that thiophene adsorption is more extensive than hydrogen adsorption on a catalyst of this type (13). Further work along these lines is being planned at present. The main difference between chromia and cobalt molybdate lay in the marked effect of adsorbed H_2S on butene hydrogenation over the latter.

The observed adsorption of thiophene and butene on chromia was relatively rapid and weak, and the effect of adsorbed H_2S on desulphurization was small, so that it appears unlikely that adsorption of thiophene, desorption of butene, or desorption of H_2S could constitute rate-determining steps under any conditions. Hydrogen adsorption on the other hand was slow and could be rate controlling, particularly since the strongly and more rapidly adsorbed hydrogen did not take part in the reaction, but the results do not exclude the possibility that the surface reaction might also be slow.

ACKNOWLEDGMENTS

The authors wish to thank Mr. D. Kulawic for technical assistance.

REFERENCES

1. E. H. M. Badger, R. H. Griffith, and W. B. S. Newling. Proc. Roy. Soc. (London), A, **197**, 184 (1949).
2. P. J. Owens and C. H. Amberg. Advances in Chem. Ser. No. 33, 182 (1961).
3. E. Cremer. Monatsh. Chem. **92**, 112 (1961).
4. J. J. Carberry. Nature, **189**, 391 (1961).
5. P. J. Owens and C. H. Amberg. Can. J. Chem. This issue.
6. D. S. MacIver and H. H. Tobin. J. Phys. Chem. **64**, 451 (1960).
7. S. W. Weller and S. E. Voltz. J. Am. Chem. Soc. **76**, 4695 (1954).
8. J. Howard and H. S. Taylor. J. Am. Chem. Soc. **56**, 2259 (1934).
9. R. L. Burwell, Jr. and H. S. Taylor. J. Am. Chem. Soc. **58**, 697 (1936).
10. Y. Kubokawa. Bull. Chem. Soc. Japan, **33**, 747 (1960).
11. H. W. Kohlschütter. Z. anorg. u. allgem. Chem. **220**, 370 (1934).
12. R. H. Griffith, J. D. F. Marsh, and W. B. S. Newling. Proc. Roy. Soc. (London), A, **197**, 194 (1949).
13. H. van Looy and G. Limido. Compt. rend. congr. intern. chim. ind., 31e, Liège, 1958 (Ind. chim. belge, Suppl.), **1**, 645 (1959).

THE NUMBER-AVERAGE AND WEIGHT-AVERAGE MOLECULAR WEIGHT OF SOME NONIONIC SURFACE-ACTIVE AGENTS*

A. F. Sirianni, J. M. G. Cowie, and I. E. Puddington
Division of Applied Chemistry, National Research Council, Ottawa, Canada

Received January 12, 1962

ABSTRACT

Further evidence for the existence of large differences between the weight- and number-average molecular weight for nonionic surface-active substances in nonaqueous solvents has been found when the property is assessed by light-scattering and vapor-pressure-lowering measurements. Equilibrium ultracentrifuge measurements support the results obtained by vapor-pressure-lowering determinations. Sorbitan and glycerol monostearates have been examined in benzene solution.

INTRODUCTION

It has been noted by Debye (1) that number-average ($\bar{M}_n$) and weight-average ($\bar{M}_w$) molecular weights of nonionic detergents in nonaqueous solvents may differ considerably. Some of the difference may be due to the existence of heterogeneous clusters of molecules in solution (1). In the case of α-monoglycerides the presence of free fatty acid as an impurity magnified the difference by increasing the value obtained from light-scattering and decreasing the value obtained from vapor-pressure-lowering measurements.

In a previous communication it was indicated that solutions of pure hexaoxyethyleneglycol monoethers having an alkyl chain of 12 or of 14 carbon atoms consisted of monomers and dimers when examined by vapor pressure lowering in benzene at about 30° C (3). Light-scattering measurements on solutions of pure hexaoxyethylene *n*-tridecanol in benzene at 25° C indicated a micelle consisting of 99 monomers (4). This compound differs from the previous two by only one carbon atom in the alkyl chain, and the results suggest the probability of the two methods of examination yielding quite different answers for the state of aggregation of a number of dissolved polar molecules.

The present investigation was undertaken to assess the behavior of sorbitan monostearate (span 60†) in which the existence of nonequilibrium states in benzene solutions was reported by Becher using light scattering (5). Solutions were examined by light scattering at 25° and 45° C and by two methods depending on vapor pressure lowering in solution. Benzene was used as a solvent in most instances. Solution properties of a commercial sample of glycerylmonostearate are also included.

EXPERIMENTAL

The light-scattering measurements were carried out with a Brice–Phoenix light-scattering photometer using blue light at 436 mμ and a small semioctagonal cell in conjunction with a small slit system. The usual precautions to exclude dust and other foreign matter were taken.

The sample of commercial sorbitan monostearate was obtained purified to the extent that the free polyol had been removed by extraction rendering the detergent completely soluble in benzene. Solutions were made with reagent grade benzene freshly distilled over CaH_2. A commercial sample of glycerylmonostearate (Aldo 33, Glyco Product Company) was used without further purification other than evacuation at room temperature in order to remove volatile matter.

*Issued as N.R.C. No. 6787.

†*Obtained through the courtesy of Dr. Paul Becher, Chemical Research Department, Atlas Powder Co., Wilmington, Delaware.*

The experimental technique and the apparatus used to carry out differential vapor pressure measurements between pure solvent and solutions have been described elsewhere (6). Apparent molecular weights were calculated from Raoult's Law.

Some determinations were also carried out with a Mechrolab vapor pressure osmometer Model 301 at 37° C. Samples were prepared as described for the light-scattering experiments. The instrument was calibrated with solutions of recrystallized sucrose octaacetate (mol. wt. = 678), triphenylmethane (mol. wt. = 244), and benzil (mol. wt. = 210) over a concentration range of 0.01 to 0.1 molal. These limits are optimal since at higher and at lower concentrations reproducibility is considerably reduced (7). The solutions were shaken periodically and allowed to equilibrate by standing overnight prior to use. The syringes employed to feed the thermistor beads were thoroughly cleaned with benzene, then rinsed 8–10 times with the appropriate solution. ΔR readings for each solution were taken at 1-minute intervals for 5 minutes. Fresh drops of solvent and solution were then placed on the thermistors and the measurements repeated. Usually three to four sets of measurements were taken for each concentration. Although the readings were virtually constant after 1 minute, the average value after 3 minutes was used in the calculation.

The apparent molecular weight of an unknown was calculated using the molar constant from the calibration curve. Calibration solutions should not deviate from the ideal behavior over the concentration range used. The data obtained with benzene solutions used fitted very closely a common straight line having a slight negative slope when $\Delta R/C$ is plotted against ΔR, where ΔR = dial reading in ohms and C = molal concentration. Caution is necessary, however, when taking molar constants from a portion of the calibration curve lying beyond the last experimental points, particularly if a slight amount of curvature is indicated in the plot. A detailed account of the operating procedure of the Mechrolab osmometer is given in the instruction manual (7), and the theory by Brady, Huff, and McBain (8).

RESULTS AND DISCUSSION

The variation of the apparent molecular weight with solute concentration (g solute/100 g solvent) for sorbitan monostearate in benzene using the Mechrolab osmometer and in benzene and alcohol using a differential mercury micromanometer is shown in Fig. 1.

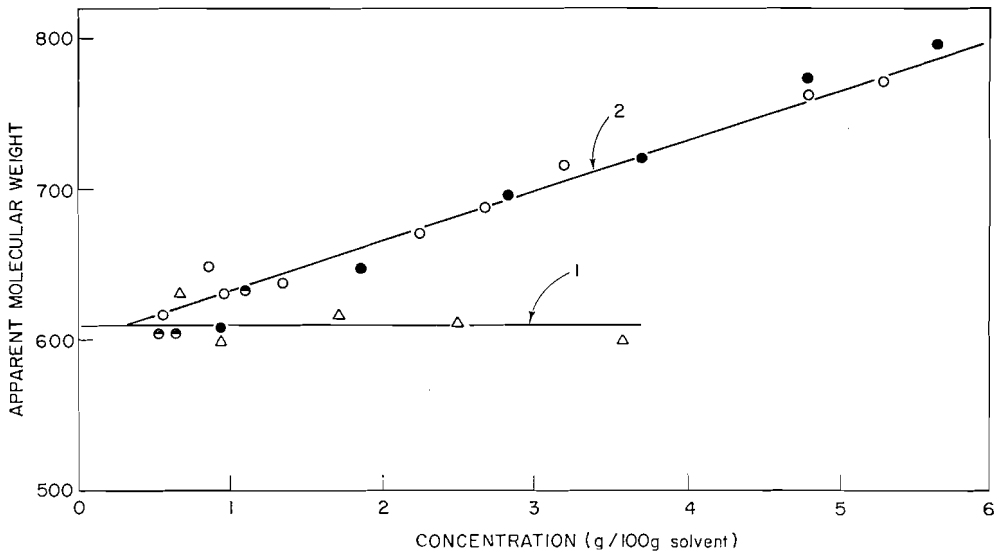

FIG. 1. Apparent molecular weight versus solute concentration for sorbitan monostearate. Curve 1, in alcohol. Curve 2, in benzene. The filled circles were obtained with the osmometer at 37° C. The open and semifilled circles were obtained by static vapor pressure determinations at 35 and 45° C respectively.

Curve 1 was obtained with alcohol at about 44° C and the molecular weight is virtually independent of concentration over the range examined. The sample contains about 5% free fatty acid of average molecular weight 275. The ester portion has a molecular weight of about 628. Thus the value of 610 indicated in alcohol is in good agreement with the analytical data for the compound (9). Curve 2 indicates the behavior in benzene. The

filled circles were obtained with the osmometer at 37°. The open and semifilled circles were obtained from static differential vapor pressure determinations in benzene at 35° C and 45° C respectively. In the concentration range 1–5% no large differences in apparent molecular weights are observed between these two methods of measurement. Below about 1% solute concentration, however, some deviation appears and the molecular weight obtained employing the osmometer is somewhat lower. The reason for this is not too clear but it might be caused by increases in the surface concentration of the unstirred drops due to slight surface activity of the solute or perhaps to insufficient lagging of the thermostat resulting in excessive evaporation from the drops. The tendency with the differential micromanometer is in the reverse direction and the apparent molecular weight can be slightly higher in the very dilute region, possibly owing to adsorption of solute on the container walls. In the static measurements the solutions are made with anhydrous solvents that are carefully freed from permanent gases and are continually stirred. This is not possible with the osmometer however.

The results of the light-scattering measurements on benzene solutions of sorbitan monostearate, summarized in Table I, are shown by Fig. 2. Curve 1 is obtained at 25° C

TABLE I

Summary of results indicated from light scattering on solutions of sorbitan monostearate

Concentration (%)	$\tau \times 10^{-3}$	$Hc/\tau \times 10^{5}$
At 25° C; refractive index increment = −0.0515 ml/g		
1.996	1.41	1.30
1.522	0.96	1.46
1.250	0.62	1.58
1.006	0.59	1.57
0.740	0.43	1.85
0.416	0.20	1.91
$\bar{M}_w$ = 48,500, second virial coefficient—negative		
At 45° C; refractive index increment = −0.0420 ml/g		
1.943	0.89	1.33
1.560	0.75	1.27
1.229	0.61	1.23
1.003	0.52	1.18
0.719	0.36	1.22
0.408	0.21	1.18
$\bar{M}_w$ = 89,300, second virial coefficient—positive		

and the data fit a line having a slight upward curvature. Curve 2 is obtained at 45° C and the experimental points fall on a curved line concave downwards. A micellar weight of about 48,500 is obtained at 25° C, which is in good agreement with the value calculated from the results reported by Becher with the same system (5). The critical micelle concentration (c.m.c.) is about 0.1 g/100 ml. A micellar weight of about 89,000 is indicated at 45° C. The larger aggregates at the higher temperature are consistent with the behavior of a number of surface-active materials in aqueous solution.

The large difference in micellar weight indicated between light scattering and vapor pressure lowering is similar to the observations with the hexaoxyethyleneglycol ethers (3). The latter method suggests slight association only, while agglomerates containing about 80 monomers are indicated by light-scattering measurements. It is unlikely that the low values from the vapor pressure measurements are due to small quantities of water in the benzene, since agreement between the static and the osmometric results,

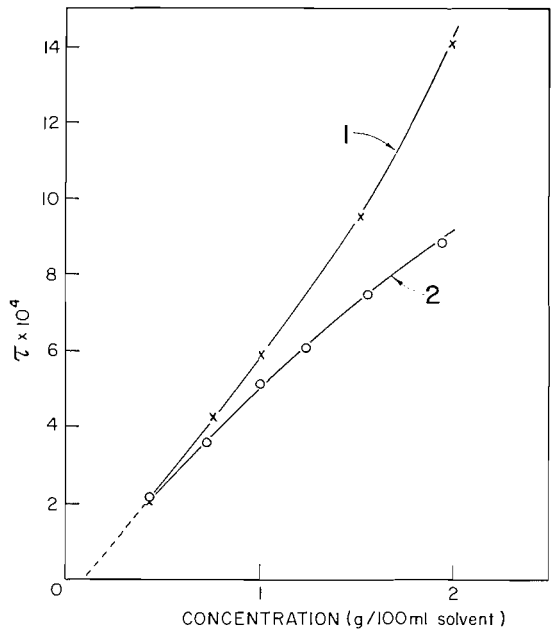

FIG. 2. Turbidity–concentration curves for sorbitan monostearate in benzene solution. Curve 1 and curve 2 were obtained at 25 and 45° C respectively.

where conditions are much less rigorously controlled, is good. It seems more probable that the micelle structure is sufficiently weak to allow the components to act individually in their effect on the vapor pressure of the solvent, while it behaves as a unit in scattering light.

The size of the sorbitan monostearate micelle was also estimated by measuring its molecular weight in the ultracentrifuge using the equilibrium method. A Spinco model E ultracentrifuge equipped with phase plate Schlieren optics and a rotor temperature control unit was used. A 2% solution of the material in benzene was examined in an Epon-filled, 12-mm double-sector cell which allows simultaneous photographing of the solvent base line and the solution pattern. The length of the solution column was 3 mm, and 0.05 ml of mercury was placed in the solution sector to provide the correct curvature at the cell bottom, thus reducing the possibility of convective disturbances. Rotor speeds were 50,740 r.p.m. and the temperature was controlled at 25° C.

Photographs were taken at a bar angle of 40° and magnified ×20 prior to measurements. The molecular weight at equilibrium was calculated from the equation (10)

$$M_w = \frac{1}{\bar{x}C_0}\left(\frac{dc}{dx}\right)_{x=\bar{x}} \frac{RT}{\omega^2(1-\bar{V}\rho)},$$

where (dc/dx) is the concentration gradient at the point $\bar{x}$ defined as $\bar{x} = (a+b)/2$. Here a and b are the distances from the center of rotation to the meniscus and base of the solution and C_0 is the initial concentration and was measured by means of a synthetic boundary cell.

The value of M_w obtained for a 2% solution was approximately 800. While this is somewhat higher than the 660 indicated by vapor pressure depression at this concentration,

it is far smaller than the micellar size suggested by light scattering. Since a point of inflection is frequently observed in the density vs. concentration relation at the c.m.c. for solutions of surface-active materials, some significance may be attached to the fact that the sample is under considerable pressure during the ultracentrifugal measurements. It seems unlikely, however, that heterogeneity in the sample can be affecting the light-scattering results seriously.

The commercial sample of glycerylmonostearate yielded no conclusive results when benzene solutions up to 1% concentration were examined by light scattering. However, an $\bar{M}_w$ of 4730 was estimated from measurements below 0.5% concentration for a pure α-glycerylmonostearate by Robinson, although the light scattered was so small that a c.m.c. was not measurable (11). Debye and Prins (2) obtained an $\bar{M}_w$ of 4000 and a c.m.c. of 0.14 g/100 ml for a similar pure compound in benzene at about room temperature.

The apparent molecular weight of the sample of glyceryl monostearate assessed by static vapor pressure lowering is indicated by Fig. 3. The filled circles were obtained with

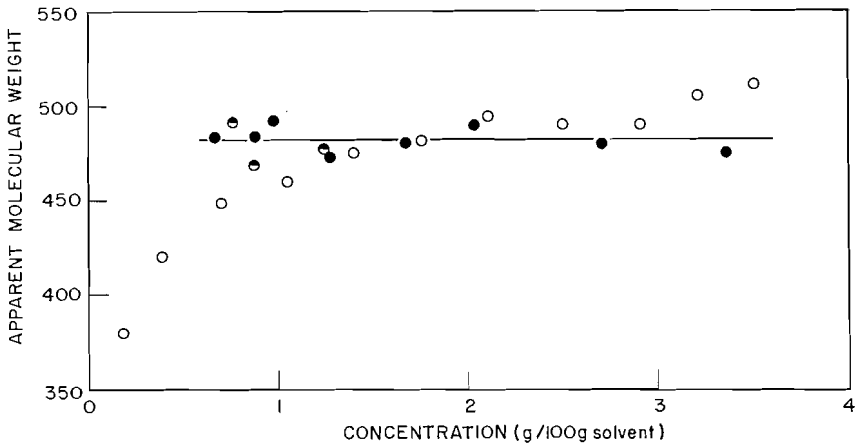

FIG. 3. Apparent molecular weight versus solute concentration for glycerylmonostearate. Filled and semifilled circles were obtained with alcohol at 39 and 45° C respectively by static vapor pressure measurements. Open circles with benzene at 37° C using the osmometer.

ethanol at 39°. A few of the measurements were made at 45° C (semifilled circles). Again the molecular weight appears reasonably constant over the concentration range examined. It is 35% higher than the calculated value for the pure compound. The open circles were obtained with solutions in benzene at 37° C employing the osmometer. The apparent molecular weight increases quickly with increasing solute concentration, reaching a nearly constant value at about 1.5%. Assuming a monomer weight of 358, solute aggregation does not appear to proceed beyond an equilibrium mixture of monomers and dimers. A c.m.c. of 0.12 g/100 g solvent agrees well with the value 0.14 g/100 ml obtained for the pure α-monostearin from light-scattering determinations by Debye and Prins (2). Considering that some impurities may be present in the commercial substance it is difficult to ascribe too much significance to the c.m.c. indicated by our measurements. However, the ratio of the size of the solute units indicated by light scattering and by vapor pressure depression is again large and suggests that quite different properties of the units are being measured by the two procedures.

REFERENCES

1. P. DEBYE and H. COLL. Technical Report No. 2 Contract Nunr-401 (17), Task No. 051-360. Office of Naval Research. 1959.
2. P. DEBYE and W. PRINS. J. Colloid Sci. **13**, 86 (1958).
3. A. F. SIRIANNI and B. A. GINGRAS. Can. J. Chem. **39**, 331 (1961).
4. P. BECHER. J. Phys. Chem. **64**, 1221 (1960).
5. P. BECHER and N. K. CLIFTON. J. Colloid Sci. **14**, 519 (1959).
6. A. F. SIRIANNI and I. E. PUDDINGTON. Can. J. Chem. **33**, 755 (1955).
7. INSTRUCTION MANUAL Mechrolab Vapor Pressure Osmometer Model 301, Mechrolab Inc.
8. A. P. BRADY, H. HUFF, and J. W. MCBAIN. J. Phys. & Colloid Chem. **55**, 304 (1951).
9. P. BECHER. Private communication.
10. D. A. YPHANTIS. Ann. N.Y. Acad. Sci. **88**, 586 (1960).
11. N. ROBINSON. J. Pharm. Pharmacol. **12**, 685 (1960).

HYDROGEN BONDING IN PHENOL, ANILINE, AND THIOPHENOL BY NUCLEAR MAGNETIC RESONANCE SPECTROSCOPY AND CRYOSCOPY

B. D. NAGESWARA RAO AND PUTCHA VENKATESWARLU[1]
Department of Physics, Muslim University, Aligarh, India

AND

A. S. N. MURTHY AND C. N. R. RAO[2]
Department of Inorganic and Physical Chemistry, Indian Institute of Science, Bangalore 12, India

Received December 27, 1961

ABSTRACT

Hydrogen bonding in phenol, aniline, and thiophenol has been investigated by n.m.r. spectroscopy and cryoscopy. While phenol shows evidence for the presence of monomer–dimer–polymer equilibrium, thiophenol only indicates low monomer–dimer equilibrium. The extent of association in these three systems decreases in the order phenol, aniline, thiophenol.

Hydrogen bonding in hydroxy compounds has been investigated in great detail by infrared (1–3) and n.m.r. (4–6) spectroscopy. Recently, association of phenol has also been investigated by ultraviolet spectroscopy (7–9). The hydrogen bonding of some heterocyclic amines has been investigated by Fuson *et al.* (10) by infrared spectroscopy. Although the hydrogen bonding in aniline has been studied by several workers (10–14) by infrared spectroscopy, the situation is not very clear (15). Fuson *et al.* (10) have concluded that the shift to lower frequencies in the NH stretching bands of aniline with increase in concentration is due to N—H - - - N bond formation. Recent ultraviolet spectroscopic studies show that hydrogen bonding in aniline is not very considerable (8). However, there has been no n.m.r. investigation on aniline. Hydrogen bonding in liquid thiols has been indicated by infrared studies (16, 17), but no n.m.r. studies have been reported. We have now studied hydrogen bonding in phenol, aniline, and thiophenol by n.m.r. spectroscopy. In addition, molecular weights of these compounds have also been determined as functions of concentration.

EXPERIMENTAL

The proton magnetic resonance spectra of solutions of anhydrous phenol, aniline, and thiophenol in carbon tetrachloride were recorded on a Varian high-resolution n.m.r. spectrometer operated at a fixed frequency of 40 Mc/sec. Sample tubes of 4.5-mm outer diameter were used. The chemical shifts have been calculated using the para ring proton (18) as the reference. The standard deviation in the chemical shifts varies between 0.5 and 2 cycle/sec.

Molecular weights of the compounds were determined in benzene solution as a function of concentration by the cryoscopic method.

Phenol, aniline, and thiophenol of high purity were used, care being taken to see that they were completely anhydrous. All the solvents were purified and fractionated before use.

RESULTS AND DISCUSSION

The chemical shifts of —OH, —NH_2, and —SH proton magnetic resonance of phenol, aniline, and thiophenol are shown as functions of concentration in Fig. 1. It can be clearly seen that there is considerable hydrogen bonding in the case of phenol and the results can be interpreted in terms of monomer–dimer–polymer equilibrium (5, 6). The

[1]*Presently at Department of Physics, Indian Institute of Technology, Kanpur, India.*
[2]*To whom all the correspondence should be addressed at the Department of Inorganic and Physical Chemistry, Indian Institute of Science, Bangalore 12, India.*

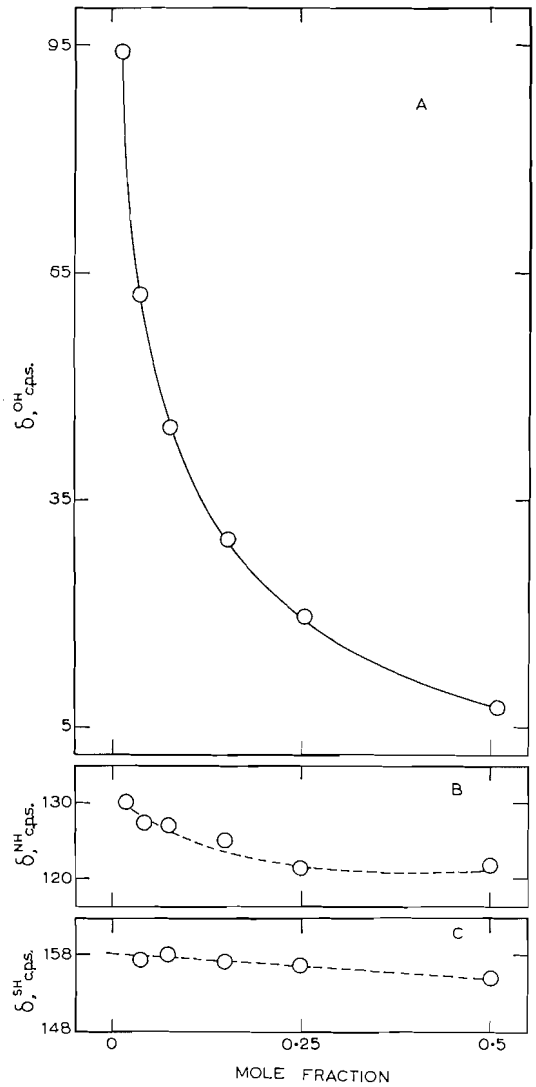

FIG. 1. Plots of proton chemical shifts versus mole fraction: A, phenol; B, aniline; C, thiophenol.

variation in the chemical shift in the case of aniline is considerably less than that of phenol, suggesting lower equilibrium constants for the monomer–dimer–polymer equilibrium in aniline. It might be expected that N—H - - - N hydrogen bonds are energetically less favorable than O—H - - - O hydrogen bonds.

The variation of δ_{SH} with concentration of thiophenol is nearly linear and is probably due to weak hydrogen bonding. It is also possible that the small changes in δ_{SH} may simply be due to solvent effects. It seems likely, however, that the linearity is due to a monomer–dimer equilibrium present over the entire range of concentrations. Monomer–dimer equilibrium in phenol can be realized only at very low concentrations. Our conclusion with regard to the monomer–dimer equilibrium in thiophenol is in agreement with the infrared studies of Spurr and Byers (17). The observation that there is negligible self-association in thiophenol compared to phenol is also consistent with the fact that thiophenol is a stronger acid than phenol.

In Fig. 2, the molecular weights of phenol, aniline, and thiophenol are shown as functions of concentration. It can be seen that phenol approaches the theoretical molecular

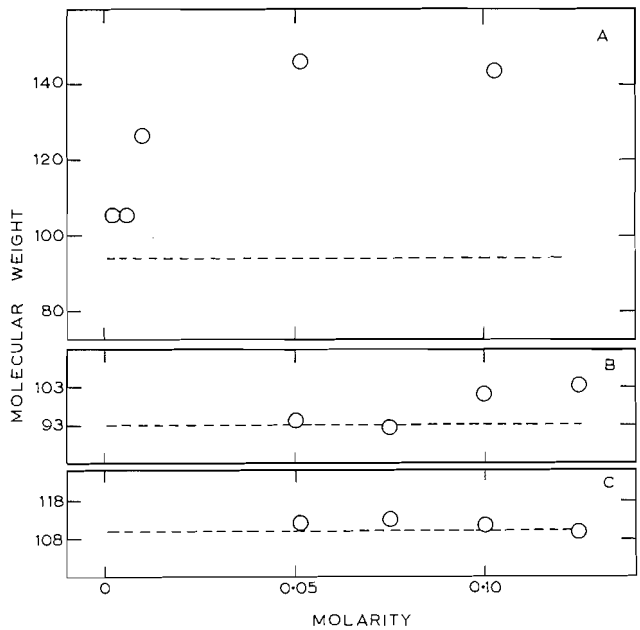

FIG. 2. Cryoscopic molecular weights as a function of concentration: A, phenol; B, aniline; C, thiophenol. Dotted lines represent theoretical molecular weights.

weight only at very low concentrations, while thiophenol gives the theoretical molecular weight throughout the range studied. Aniline falls in between these two cases. These results clearly point out that association due to hydrogen bonding decreases in the order phenol, aniline, thiophenol. Since the theoretical molecular weight of thiophenol is found throughout the range of concentrations investigated, it may be concluded that the equilibrium constant for dimerization (as indicated by n.m.r. studies) must be very low.

ACKNOWLEDGMENT

The authors are thankful to Professor M. R. A. Rao for his interest.

REFERENCES

1. U. LIDDEL and E. D. BECKER. Spectrochim. Acta, **10**, 70 (1957).
2. W. C. COBURN and E. GRUNWALD. J. Am. Chem. Soc. **80**, 1318 (1958).
3. F. A. SMITH and E. C. CREITZ. J. Research Natl. Bur. Standards, **46**, 145 (1956).
4. M. SAUNDERS and J. B. HYNE. J. Chem. Phys. **29**, 1319 (1958).
5. E. D. BECKER. J. Chem. Phys. **31**, 269 (1959).
6. J. C. DAVIS, JR., K. S. PITZER, and C. N. R. RAO. J. Phys. Chem. **64**, 1744 (1960).
7. M. ITO. J. Mol. Spectroscopy, **4**, 125 (1960).
8. J. C. DEARDEN and W. F. FORBES. Can. J. Chem. **38**, 896 (1960).
9. C. N. R. RAO and A. S. N. MURTHY. J. Sci. Ind. Research (India), **20B**, 290 (1961).
10. N. FUSON, M. L. JOSIEN, R. L. POWELL, and E. UTTERBACK. J. Chem. Phys. **20**, 145 (1952).
11. A. N. BUSWELL, J. R. DOWNING, and W. H. RODEBUSH. J. Am. Chem. Soc. **62**, 2759 (1940).
12. E. L. KINSEY and J. W. ELLIS. J. Chem. Phys. **5**, 399 (1937).
13. W. GORDY. J. Chem. Phys. **7**, 167 (1939).
14. E. WILLIAMS, R. HOFSTADTER, and R. C. HERMAN. J. Chem. Phys. **7**, 802 (1939).
15. R. N. JONES and C. SANDORFY. *In* Chemical applications of spectroscopy. Interscience, New York. 1956. Chap. IV.
16. M. L. JOSIEN, P. DIZABO, and P. SAUMAGNE. Bull. soc. chim. France, 423 (1957).
17. R. A. SPURR and H. F. BYERS. J. Phys. Chem. **62**, 425 (1958).
18. J. A. POPLE, W. G. SCHNEIDER, and H. J. BERNSTEIN. High resolution nuclear magnetic resonance. McGraw Hill, New York. 1959.

IONIZATION OF ORGANIC COMPOUNDS

III. BASICITIES OF PROPIONIC ACID AND PROPIONAMIDE

J. T. EDWARD AND I. C. WANG
Department of Chemistry, McGill University, Montreal, Que.

Received February 9, 1962

ABSTRACT

Protonation constants (pK_{BH^+}) of −6.8 and −0.9 have been determined for propionic acid and propionamide, respectively, from measurements of their ultraviolet absorption in various concentrations of sulphuric acid. The ionization ratio of propionamide and of other amides increases more slowly than the Hammett acidity function, h_0, with increase in acid concentration. This may be explained by assuming that in a given concentration of sulphuric acid the protonated amide is more heavily hydrated than the protonated Hammett indicator used to establish the h_0 scale for this region of acid concentrations.

The equilibria in aqueous sulphuric acid of many types of aromatic compounds (B) (1–4), assumed to ionize according to the equation

$$BH^+ \rightleftarrows B + H^+, \qquad [1]$$

have been investigated by Hammett's method (5) in which the ionization ratio $[BH^+]/[B]$ is determined spectrophotometrically. Ionizations of this type are assumed to follow the Hammett acidity function h_0 (6, 7), so that the protonation constants K_{BH^+} of the compounds, defined as

$$K_{BH^+} = [B]h_0/[BH^+] \qquad [2]$$

(the quantities in brackets being molar concentrations), may be calculated from the spectrophotometric results.

Aliphatic compounds absorb much more feebly in the spectral regions accessible with most spectrophotometers, and perhaps for this reason their ionizations have not been much studied by Hammett's method. Most investigations of the basicities of aliphatic amides have been carried out by titration (8) or indicator (9) methods using solutions in acetic or formic acids. However, it is not certain that the relative strengths of different Brønsted bases are the same in these solvents as in water (10). In one of the rare applications of Hammett's method, Goldfarb, Mele, and Gutstein (11) determined the basicities of a number of aliphatic amides by observing the change in their absorption at 200–210 mμ with changing acidity. The absorption curves of aliphatic amides have a shoulder or inflection in this region (12), due to a weak peak casued by an $n \rightarrow \pi^*$ transition (13, 14) buried in the edge of a more intense peak at about 190 mμ which has been attributed to a $\pi \rightarrow \pi^*$ transition (14, 15). Protonation of the amide group, if it takes place, as is now believed (16, 17), on the carbonyl oxygen, should cause a large blue shift of the $n \rightarrow \pi^*$ peak (18). In fact, Goldfarb *et al.* observed a decrease in absorption at 200–210 mμ with increasing acidity of the medium. However, the spectral data, according to their method of calculation, indicated two equilibria and two ionization constants. Since even in absolute sulphuric acid aliphatic amides are only monoprotonated (19), the interpretation of these results has remained puzzling.

Goldfarb and his co-workers (11) also calculated a pK_{BH^+} of −6.10 for acetic acid from the change with acidity of the $n \rightarrow \pi^*$ peak at about 203 mμ (12, 20).

In the present work we have studied, by Hammett's method, the ionization of propionamide and of propionic acid (whose pK_{BH^+} values were required in another connection) using a spectrophotometer which enabled us to measure absorption down to wavelengths of about 186 mμ. Attention was given to the interpretation of the spectral data in an attempt to discover whether it necessitated two pK_{BH^+} values for the amide. In the event, it was found that the calculation of two protonation constants was probably an error arising from the assumption (now known to be invalid (21)) that the ionization of *all* monoprotonated Brønsted bases must follow the h_0 acidity function according to equation [2].

EXPERIMENTAL

Materials

Propionamide (Eastman) was recrystallized from aqueous ethanol to a constant melting point of 80.7–82.0° (lit. m.p. 79.5° (22)). Propionic acid was distilled through a Vigreux column, the middle fraction boiling at 140–142°, n_D^{24} 1.3852, being taken (lit. b.p. 140.8°, n_D^{25} 1.3843 (23)). Sulphuric acid solutions were prepared and standardized as described previously (18).

Apparatus

A Unicam SP 500 spectrophotometer was used. There was no temperature control in the cell compartment, and the temperature of the solutions was 24±3° during measurements. Sulphuric acid of 10–30% concentration absorbs very strongly below 200 mμ, presumably because of the presence of sulphate ion (whose concentration is at a maximum in about 17% acid (24)), and consequently for solutions of this concentration matched silica cells having a 1-mm light path were used. For other concentrations of sulphuric acid quartz cells of 1-cm light path were used.

Procedure

Aliquots (1.00 ml) of an aqueous solution of propionamide or propionic acid of known concentration were diluted with aqueous acid to 25.00 ml in a volumetric flask. Extinction coefficients at different wavelengths were measured within 4–5 minutes; reproducibility of the measurements was within ±1%. Hydrolysis of propionamide in this time was negligible, as expected (11, 25); even after 15 minutes no change in absorption could be observed. Beer's law was valid for all the concentration ranges studied.

The concentration of acid in the solutions was determined by titration using phenolphthalein as an indicator, and correcting, where necessary, for the propionic acid present. Corresponding H_0 values were obtained from large-scale plots of H_0 against acid concentration constructed from the data of Paul and Long (7).

RESULTS AND DISCUSSION

Protonation of Propionic Acid

Propionic acid in aqueous solution has absorption peaks at 203 mμ (ε 46) and 189 mμ (ε 59). However, the latter peak is due to propionate ion, as shown by the absorption of sodium propionate in water (λ_{max} 188 mμ, ϵ_{max} 1410).[1] In 0.8% sulphuric acid, in which ionization to propionate is effectively suppressed, propionic acid has only one peak, at 206 mμ (ε 43.5).

As the sulphuric acid concentration is increased to 62.5%, this peak undergoes a progressive blue shift to 196 mμ (Fig. 1), which must be due to a medium effect. However, with further increase of acid concentration to 95.4% this peak disappears, presumably because of protonation of the carbonyl group (3). In absolute sulphuric acid propionic acid is known to be monoprotonated (27). While the spectral changes must be due mainly to protonation as the sulphuric acid concentration is increased from 62.5% to 95.4%, they must also be due in part to medium effects, as shown by the failure of the absorption curves (see Fig. 1) to pass through an isobestic point (5).

[1]*The maxima reported for acetic acid (10, 18) and other aliphatic acids (e.g., ref. 26) in water are probably very slightly in error because of a failure to take account of ionization.*

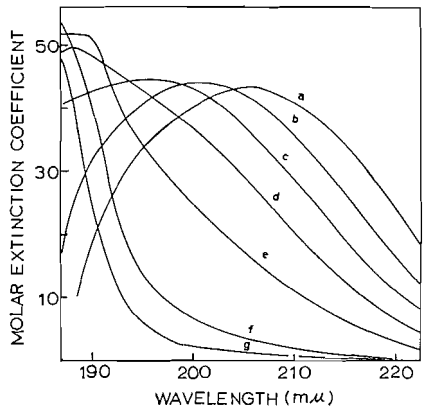

FIG. 1. Ultraviolet absorption of propionic acid in the following concentrations of aqueous sulphuric acid: *a*, 0.8; *b*, 50.2; *c*, 62.5; *d*, 72.1; *e*, 78.6; *f*, 86.8; *g*, 95.4%.

The $n \rightarrow \pi^*$ peaks of aliphatic ketones change with increasing acidity of medium in a very similar fashion; the reasons given for the medium effect as the acid concentration is raised to 65% (18) may apply in the present instance also.

Plots of the molar extinction coefficient ϵ at different wavelengths against the H_0 values of the solutions gave sigmoid curves, from which the inflection points were obtained by the graphical method of Stewart and Yates (2). The H_0 value at the inflection point then gave the pK_{BH^+} (method A, Table I). The experimental sigmoid curves were moderately close to those theoretically required by equation [3], derived from equation [2] by a consideration of Beer's law:

TABLE I

Protonation constants (pK_{BH^+}) of propionic acid and propionamide from absorption measurements at different wavelengths (λ)

	$-pK_{BH^+}$ of propionic acid		$-pK_{BH^+}$ of propionamide
λ(mμ)	Method A	Method B	Method A
190	—	—	0.7
192	—	—	0.8
194	—	—	0.9
196	7.1	—	0.9
198	7.1	7.0	1.0
200	6.9	6.8	0.8
203	6.6	7.0	—
205	6.8	6.9	—
210	6.6	—	—
215	6.5	—	—

$$pK_{BH^+} = H_0 - \log (\epsilon_{BH^+} - \epsilon)/(\epsilon - \epsilon_B), \quad [3]$$

ϵ_B, ϵ_{BH^+}, and ϵ being the molar extinction coefficients of the unprotonated acid, the protonated acid, and the mixture of protonated and unprotonated forms in a solution of acidity function H_0, respectively. This is shown in Fig. 2, in which the points represent experimental values and the curve has been calculated from equation [3] assuming $pK_{BH^+} = -7.0$, $\epsilon_B = 44.0$, and $\epsilon_{BH^+} = 3.0$.

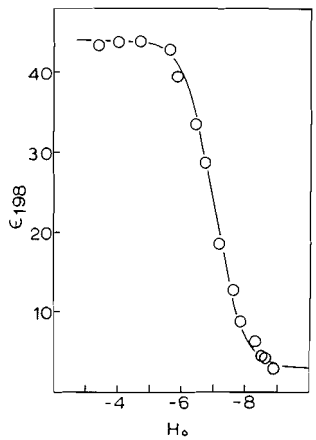

FIG. 2. Ionization of propionic acid in sulphuric acid.

Method A takes no account of the medium effect. It was thought that the pK_{BH^+} values obtained from measurements at different wavelengths might agree better if this effect were corrected by Hammett's method (5) of shifting absorption curves laterally to varying extents to make them all pass through an isobestic point, in this case at $\lambda = 192.5$ mμ, $\epsilon = 44.2$. The corrected values of ϵ, read from such a graph, were plotted against H_0, and pK_{BH^+} values obtained as before from such plots (method B, Table I). This method did not lead to significantly improved agreement of pK_{BH^+} values. It may be remarked that Hammett's assumption (5) about the medium effect—that it causes a lateral shift in absorption curves but no change in intensity—remains unproved.

By averaging the results in Table I, a pK_{BH^+} of -6.8 ± 0.3 is obtained for propionic acid.

Effect of Acidity on Spectrum of Propionamide

Aliphatic ketones exhibit three absorption peaks: a weak peak at about 280 mμ, a more intense peak at about 190 mμ, and a still more intense peak at about 150 mμ. These peaks have been assigned by McMurry (13), largely on the basis of their intensities, to $n \rightarrow \pi^*$, $n \rightarrow \sigma^*$, and $\pi \rightarrow \pi^*$ transitions respectively. The substitution of an amino for an alkyl group alters the energies of the orbitals of the ground state and the excited states, so that the weak peak of amides at about 220 mμ is attributed to a $n \rightarrow \pi^*$ transition and the intense peak at about 190 mμ to a $\pi \rightarrow \pi^*$ transition (14, 15).

The absorption curve for propionamide in water (Fig. 3) conforms to the general pattern in showing a shoulder at about 215 mμ ($\epsilon \sim 130$) which disappears in 33% sulphuric acid (Fig. 3B) presumably because of protonation of the carbonyl group (17, 28). However, the intense peak at 187 mμ (ϵ 6350) shows a shoulder at about 190 mμ (Fig. 3A),[2] and is most plausibly explained as being made up of two overlapping peaks: a peak at about 187 mμ ($\epsilon \sim 4500$) due to a $n \rightarrow \sigma^*$ transition and a peak at about 190 mμ ($\epsilon \sim 2800$) due to a $\pi \rightarrow \pi^*$ transition. This composite nature of the observed peak would explain the spectral changes observed as the solvent is changed from water to 33% sulphuric acid (Fig. 3A). Protonation of the carbonyl oxygen would be expected to cause a large blue shift of the $n \rightarrow \sigma^*$ peak (29), and a small red shift of the $\pi \rightarrow \pi^*$ peak (14, 30). The peak at 188 mμ remaining in 33% acid is accordingly attributed to a

[2]*We find, in agreement with Ley and Arends (12), that the absorption curve of acetamide in aqueous solution does not show a shoulder in this region.*

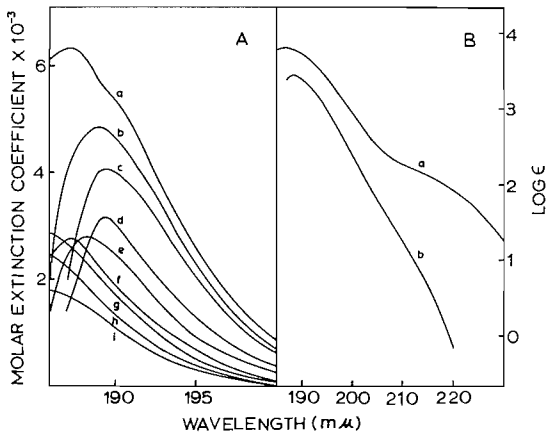

FIG. 3. Ultraviolet absorption of propionamide in the following concentrations of aqueous sulphuric acid: A: *a*, 0; *b*, 4.9; *c*, 11.3; *d*, 23.8; *e*, 33.0; *f*, 35.1; *g*, 55.2; *h*, 72.0; *i*, 96.4%; B: *a*, 0; *b*, 33.0%.

$\pi \rightarrow \pi^*$ transition of the protonated amide, and the shift of this peak to shorter wavelengths with further increase of acid concentration to a medium effect. The causes of shifts due to medium effects are often obscure.

This analysis of the absorption peak at 187 mμ is admittedly contentious and other interpretations of the changes in spectra with altering acidity are possible. Further work on the effect of solvents on the absorption of amides is planned.

Calculation of Protonation Constants of Propionamide

From plots of ϵ against H_0 (Fig. 4), the protonation constant of propionamide may be

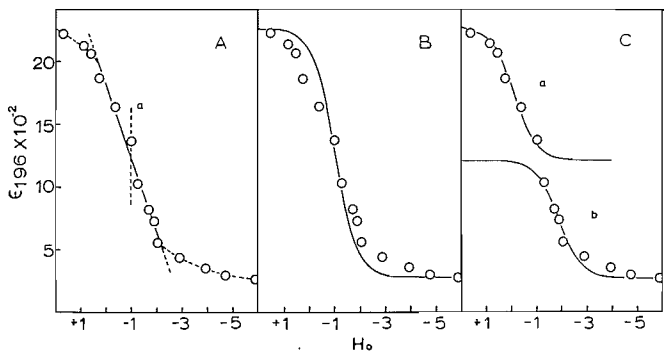

FIG. 4. Ionization of propionamide in sulphuric acid.

obtained by three different procedures:

1. The inflection point of the experimental sigmoid curve, and thence the pK_{BH^+} value, may be found by the method of Stewart and Yates (2). This is illustrated in Fig. 4A: the line *a* indicates the midpoint of the straight-line portion of the curve, and hence the inflection point.

For reasons made apparent in the sequel, we consider this the best method available. Values of the protonation constant obtained from measurements at different wavelengths are given in Table I, and indicate a pK_{BH^+} of -0.9 ± 0.1.

2. The theoretical curve is calculated from equation [3] using different values of ϵ_B, ϵ_{BH^+}, and pK_{BH^+}, the curve giving the best fit being found by trial and error. This is illustrated in Fig. 4B, in which the curve has been calculated assuming $pK_{BH^+} = -1.0$, $\epsilon_B = 2260$, and $\epsilon_{BH^+} = 260$.

It is found that the experimental points for propionamide deviate from the theoretical curve in a manner which is characteristic for all amides so far studied (4, 25, 31): in the neighborhood of the inflection point, the slope of the experimental curve is always less than theoretical (i.e. increase of h_0 produces a smaller increase in the ionization ratio than predicted by equation [2]). This has also been shown in plots of log $\{(\epsilon_{BH^+}-\epsilon)/(\epsilon-\epsilon_B)\}$ against H_0 for seven substituted benzamides having pK_{BH^+} ranging from -2.00 to -3.11 (32). According to equation [3], these plots should give straight-line curves of slope = 1; in fact, straight-line curves having slopes of 0.58–0.70 were obtained.

These discrepancies have hitherto been attributed to medium effects (25, 32). However, the deviation is always in the same direction regardless of the type of amide or of electronic transition ($n \rightarrow \pi^*$, $\pi \rightarrow \pi^*$, etc.) being considered, and it seems likely that it is due to a general failure of equation [2] when applied to the ionization of amides. This equation has been found inapplicable to the ionization of other types of Brønsted bases also (31), and the reason for its failure is given in the last section of this paper.

3. A better fit of theoretical values with the experimental results is obtained by assuming two equilibria and hence two curves calculated from equation [3]. This has been done in Fig. 4C, assuming $pK_{BH_1^+} = 0.1$, $\epsilon_B = 2260$, and $\epsilon_{BH_1^+} = 1200$ to calculate curve *a* and $pK_{BH_2^+} = -1.9$ and $\epsilon_{BH_2^+} = 260$ to calculate curve *b*. However, the two pK_{BH^+} values are not uniquely defined in this procedure: a reasonably satisfactory fit is obtained with two other pK_{BH^+} values (for example, $+0.2$ and -1.7 for Fig. 4C, with $\epsilon_{BH_1^+} = 1500$).

This procedure is the graphical equivalent of the method of calculation followed by Goldfarb, Mele, and Gutstein (11). Its only justification lies in the procrustean assumption that the experimental data for all compounds must fit equation [3]. Since we have grounds for rejecting this assumption, we may also reject this procedure because there is no evidence for the two equilibria which it postulates. If so, the pK_{BH^+} should lie somewhere between the $pK_{BH_1^+}$ and $pK_{BH_2^+}$ values of Goldfarb *et al.* On the assumption that the inflection point (i.e. the midpoint of the central straight-line portion of the experimental sigmoid curve (2)) lies somewhere on the straight-line curve between $H_0 = pK_{BH_1^+}$ and $H_0 = pK_{BH_2^+}$, pK_{BH^+} can be shown to be given by the equation

$$pK_{BH^+} = pK_{BH_1^+} + (pK_{BH_2^+} - pK_{BH_1^+})(\epsilon_{BH_1^+} - \epsilon_{BH^+})/(\epsilon_B - \epsilon_{BH_2^+}). \quad [4]$$

In Table II are given the values thus calculated from the recorded data of Goldfarb *et al.*

TABLE II
Protonation constants calculated from the experimental data of Goldfarb *et al.* (9)

Compound	$-pK_{BH^+}$	Compound	$-pK_{BH^+}$
Acetamide	0.59	N-*i*-Butylacetamide	0.61
N-Methylacetamide	1.25	Glycinamide	4.91
N-*n*-Butylacetamide	0.40	Aceturic acid	3.06

The value for acetamide is in good agreement with the protonation constant (-0.50) for aqueous solution recorded by Hall (8). It would appear, consequently, that propionamide is a weaker base than acetamide, and propionic acid a weaker base than acetic

acid. This may indicate that hyperconjugation is more important than inductive effects in stabilizing protonated amide and carboxylic acid groups.

Failure of the H_0 Acidity Function to Apply to the Protonation of Amides

The failure of equation [2] when applied to the protonation of amides may be attributed to the neglect of hydration effects in deriving this equation. The importance of these effects was first pointed out by Taft (21). The reasonable consistency of the H_0 scale as determined by Hammett using different indicators and different mineral acids (6, 7) was probably in part fortuitous: almost all the indicators used in the more dilute acid regions were substituted anilines, the conjugate acids of which should be hydrated to the same extent in a given acid solution (21). This is less than the hydration of the hydrogen ion (33), so that the ionization of a Hammett indicator (In) is given by

$$InH^+ + nH_2O \rightleftarrows In + H^+, \qquad [5]$$

the formulae representing the hydrated ions or molecules. The equilibrium constant K_{InH^+} for this equilibrium is

$$K_{InH^+} = ([In]a_{H^+}f_{In})/([InH^+]a_{H_2O}{}^n f_{InH^+}), \qquad [6]$$

where the a's represent activities and the f's molar-concentration activity coefficients. Operationally the acidity function h_0 of an acid solution is defined (6, 7) by

$$K_{InH^+} = ([In]h_0)/[InH^+] \qquad [7]$$

and hence

$$h_0 = (a_{H^+}f_{In})/(a_{H_2O}{}^n f_{InH^+}). \qquad [8]$$

This equation, differing from the original equation of Hammett (6) by taking account of water activities, has already been derived in slightly different form by Bascombe and Bell (33), who showed that for 0–8 M hydrochloric, sulphuric, and perchloric acid solutions $n \approx 4$.

The ionization of an acid BH^+ in a given concentration of aqueous mineral acid will also involve a number of water molecules, differing possibly from the number involved in the ionization of InH^+:

$$BH^+ + mH_2O \rightleftarrows B + H^+. \qquad [9]$$

The equilibrium constant K'_{BH^+} is then given by

$$K'_{BH^+} = ([B]a_{H^+}f_B)/([BH^+]a_{H_2O}{}^m f_{BH^+}), \qquad [10]$$

which combined with equation [8] gives

$$K'_{BH^+} = ([B]h_0 f_B f_{InH^+})/([BH^+]a_{H_2O}{}^{m-n} f_{In} f_{BH^+}). \qquad [11]$$

It is usually assumed (6, 7, 21) that the term $(f_B f_{InH^+})/(f_{In} f_{BH^+})$ is reasonably invariant with change of acidity; this assumption is supported by the work of Deno and his collaborators on the solubilities of neutral organic compounds (34) and of organic salts (34, 35) in different concentrations of sulphuric acid. Accepting this assumption, equation [11] becomes

$$K'_{BH^+} = ([B]h_0)/([BH^+]a_{H_2O}{}^h), \qquad [12]$$

where $(m-n)$, the difference in hydration numbers of InH^+ and BH^+, is termed the hydration parameter h.

This last equation reduces to equation [2] when $h = 0$, i.e. when BH^+ and InH^+ are hydrated to the same extent, if B and In are (as assumed by Bascombe and Bell (33)) unhydrated. This case is represented for a hypothetical base having $pK_{BH^+} = -2$ by curve *a* in Fig. 5, which gives the percentage protonation of the base for different H_0

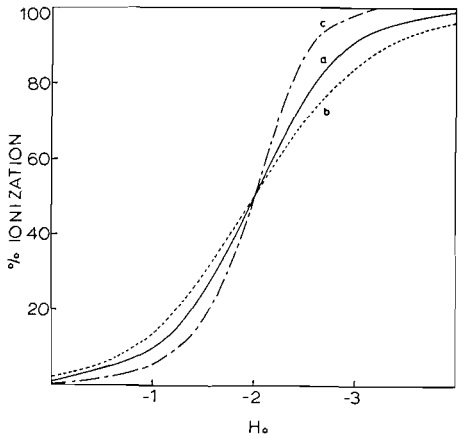

FIG. 5. Theoretical curves according to equation [12] for ionization of a base having $pK_{BH^+} = -2.0$ and *a*, $h = 0$; *b*, $h = -2$; *c*, $h = +2$.

values. When BH^+ has a greater hydration number than InH^+, $h < 0$ and the ionization ratio according to equation [12] is then proportional to $h_0 a_{H_2O}^{-h}$. Since a_{H_2O} (and hence $a_{H_2O}^{-h}$) decreases as the acid concentration (and h_0) increases (33), the ionization ratio will increase more slowly with increase of h_0 than indicated by equation [2]. This is the situation we have already found for amides. In curve *b* of Fig. 5 it is illustrated for a hypothetical base having $pK_{BH^+} = -2$ and $h = -2$; the curve has been calculated for ionization in aqueous sulphuric acid using the H_0 (7) and a_{H_2O} (36) values recorded in the literature for various concentrations of this acid. Similarly, the curve *c* has been calculated for the ionization in sulphuric acid of a base having $pK_{BH^+} = -2$ and $h = +2$. Curves of this last type have been found characteristic of the ionization of certain substituted thioureas (31); the significance of the positive value of h will be discussed in a later communication.

It should be noted that according to this treatment K_{BH^+} is not a true equilibrium constant except when $h = 0$ and $K_{BH^+} = K'_{BH^+}$. K_{BH^+} may be regarded as a constant operationally defined by equation [2], i.e. it is equal to the h_0 value at which the base is half ionized. K'_{BH^+} may then be calculated from K_{BH^+} by the equation

$$K'_{BH^+} = K_{BH^+}/a_{H_2O}{}^h, \qquad [13]$$

the a_{H_2O} in this case being the water activity of the acid solution of $H_0 = pK_{BH^+}$.

The hydration parameter required in equation [13] may be obtained from the slope of the plot of $\log\{(\epsilon_B - \epsilon)/(\epsilon - \epsilon_{BH^+})\} + H_0$ against $\log a_{H_2O}$, since equation [12] may be rewritten in the form

$$\log\{(\epsilon_B - \epsilon)/(\epsilon - \epsilon_{BH^+})\} + H_0 = -h \log a_{H_2O} + pK'_{BH^+}. \qquad [14]$$

Such a plot for propionamide is shown in Fig. 6. Unfortunately, it is seen that h is continually decreasing as a_{H_2O} decreases, i.e. as the acid becomes more concentrated (Table

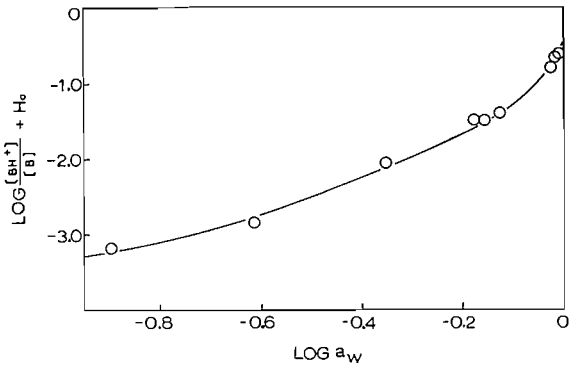

FIG. 6. Plot of {log (ionization ratio)$+H_0$} against log (water activity) for solutions of propionamide in aqueous sulphuric acid.

III). This trend, which has been noted by us for other amides (31) and by Taft (21) for other bases, greatly reduces the practical usefulness of equation [12]. It is to be expected,

TABLE III

Hydration parameter (h) of propionamide in sulphuric acid solutions of different acidities

$-H_0$	$-\log a_{H_2O}$	h
—	0	16.4
0.90	0.048	8.1
1.5	0.10	5.1
2.7	0.30	2.9
3.6	0.50	2.5
4.2	0.70	1.9
4.7	0.90	0.5

since with decreasing water activity the hydration numbers of all ions will tend towards zero. Consequently the difference in hydration numbers of InH^+ and BH^+, which defines h, should decrease.

The fact that in general h will be very small for ionizations in very strong acids means that in these acids the deviation of the ionization ratio from that given by equation [2] will be small. This is exemplified for propionic acid in Fig. 2. Furthermore, the continuous decrease in h with increase in acidity indicates that curve b of Fig. 5, calculated on the assumption of a constant h, is unrealistic. If $h = -2$ at $H_0 = -2$, then at lower acidities $h < -2$ and curve b should diverge more from curve a; at higher acidities $h > -2$ and curve b should be closer to curve a. However, in all cases (curves a, b, and c of Fig. 5) the inflection points of the curves indicate the H_0 value for half-ionization of the bases. Consequently, we consider the graphical method of Stewart and Yates (2) the best one for determining pK_{BH^+}, as redefined above.

ACKNOWLEDGMENTS

We are grateful to Professors N. C. Deno and R. Stewart for access to unpublished material, to Professors G. C. B. Cave and C. Sandorfy for the use of equipment, and to the National Research Council for financial assistance.

REFERENCES

1. K. YATES and R. STEWART. Can. J. Chem. **37**, 664 (1959).
2. R. STEWART and K. YATES. J. Am. Chem. Soc. **80**, 6355 (1958).
3. R. STEWART and K. YATES. J. Am. Chem. Soc. **82**, 4059 (1960).
4. J. T. EDWARD, H. S. CHANG, K. YATES, and R. STEWART. Can. J. Chem. **38**, 1518 (1960).
5. L. A. FLEXSER, L. P. HAMMETT, and A. DINGWALL. J. Am. Chem. Soc. **57**, 2103 (1935).
6. L. P. HAMMETT. Physical organic chemistry. McGraw-Hill, New York. 1940. p. 267.
7. M. A. PAUL and F. A. LONG. Chem. Revs. **57**, 1 (1957).
8. N. F. HALL. J. Am. Chem. Soc. **52**, 5115 (1930). R. HUISGEN and H. BRADE. Chem. Ber. **90**, 1432, 1437 (1957).
9. L. P. HAMMETT and A. DEYRUP. J. Am. Chem. Soc. **54**, 4239 (1932). H. LEMAIRE and H. J. LUCAS. J. Am. Chem. Soc. **73**, 5198 (1951). R. HUISGEN, I. UGI, H. BRADE, and E. RAUENBUSCH. Ann. **586**, 30 (1954).
10. D. P. N. SATCHELL. J. Chem. Soc. 3524 (1957); 1916 (1958).
11. A. R. GOLDFARB, A. MELE, and N. GUTSTEIN. J. Am. Chem. Soc. **77**, 6194 (1955).
12. H. LEY and B. ARENDS. Z. physik. Chem. B, **17**, 177 (1932). W. HEROLD. Z. physik. Chem. B, **18**, 265 (1932).
13. H. L. MCMURRY and R. S. MULLIKEN. Proc. Natl. Acad. Sci. U.S. **26**, 312 (1940). H. L. MCMURRY. J. Chem. Phys. **9**, 231, 241 (1941).
14. J. W. SIDMAN. Chem. Revs. **58**, 689 (1958).
15. H. D. HUNT and W. T. SIMPSON. J. Am. Chem. Soc. **75**, 4540 (1953). D. L. PETERSON and W. T. SIMPSON. J. Am. Chem. Soc. **79**, 2375 (1957).
16. A. R. KATRITZKY and R. A. Y. JONES. Chem. & Ind. (London), 722 (1961).
17. R. STEWART, L. J. MUENSTER, and J. T. EDWARD. Chem. & Ind. (London), 1906 (1961).
18. H. J. CAMPBELL and J. T. EDWARD. Can. J. Chem. **38**, 2109 (1960).
19. A. HANTZSCH. Ber. **64**, 667 (1931). J. L. O'BRIEN and C. NIEMANN. J. Am. Chem. Soc. **72**, 5348 (1950).
20. G. BRIEGLEB and W. STROHMEYER. Naturwiss. **33**, 344 (1946).
21. R. W. TAFT. J. Am. Chem. Soc. **82**, 2965 (1960).
22. H. A. TAYLOR and T. W. DAVIS. J. Phys. Chem. **32**, 1470 (1928).
23. R. R. DREISBACH and S. A. MARTIN. Ind. Eng. Chem. **41**, 2875, 2879 (1949).
24. T. F. YOUNG, L. F. MARANVILLE, and H. M. SMITH. *In* The structure of electrolytic solutions. *Edited by* W. J. Hamer. John Wiley, New York. 1959. p. 35.
25. J. T. EDWARD and S. C. R. MEACOCK. J. Chem. Soc. 2000 (1957).
26. M. PESTEMER and A. ASLEV-KLINKER. Z. Electrochem. **53**, 387 (1949).
27. G. ODDO and A. CASALINO. Gazz. chim. ital. **47** (2), 200 (1917).
28. M. KASHA. Discussions Faraday Soc. **9**, 14 (1950).
29. M. J. JANSSEN. Rec. trav. chim. **79**, 464 (1960).
30. H. MCCONNELL. J. Chem. Phys. **20**, 700 (1952).
31. J. T. EDWARD and I. C. WANG. Unpublished researches.
32. H. S. CHANG. M.Sc. Thesis, McGill University, Montreal, Que. 1960. p. 43.
33. K. N. BASCOMBE and R. P. BELL. Discussions Faraday Soc. **24**, 158 (1957).
34. N. C. DENO and C. PERIZZOLO. J. Am. Chem. Soc. **79**, 1345 (1957).
35. N. C. DENO, H. E. BERKHEIMER, W. L. EVANS, and H. J. PETERSON. J. Am. Chem. Soc. **81**, 2344 (1959).
36. R. A. ROBINSON and R. H. STOKES. Electrolyte solutions. Butterworths, London. 1955. p. 462.

THE PHOSPHORYLATION OF 2-METHYL-Δ^2-OXAZOLINE*

R. GREENHALGH

Defence Research Chemical Laboratories, Ottawa, Canada

Received January 5, 1962

ABSTRACT

In common with other acylating agents, diisopropyl phosphorochloridate reacts with 2-methyl-Δ^2-oxazoline in aqueous and ethereal media to yield N-phosphoryl derivatives. In both media, phosphorylation is followed by ring opening between positions 1 and 5, as shown by the isolation of diisopropyl N-acetyl-N-2-chloroethylphosphoramidate and diisopropyl N-acetyl-N-2-hydroxyethylphosphoramidate. The latter compound undergoes further rearrangement, being slowly converted to diisopropyl N-2-acetoxyethylphosphoramidate in aqueous bicarbonate solution.

Nuclear magnetic resonance studies of 2-methyl-Δ^2-oxazoline in aqueous bicarbonate solution (pH 8.5) reveal that it is all transformed to N-acetylethanolamine within 23 hours. This short lifetime allows speculation regarding the origin of 2-acetamidoethyl diisopropyl phosphate isolated from the reaction of the base with diisopropyl phosphorofluoridate.

The normal products resulting from the action of acylating agents with 2-substituted-Δ^2-oxazolines in anhydrous or aqueous media are N-acyl derivatives (1, 2). The reaction of diisopropyl phosphorofluoridate (DFP) with 2-methyl-Δ^2-oxazoline (methyl oxazoline) appears to be an exception in that Porter *et al.* (3) obtained 2-aminoethyl dihydrogen phosphate.

Repetition of this reaction under their conditions (4) confirmed the result, since 2-aminoethyl diisopropyl phosphate and 2-acetamidoethyl diisopropyl phosphate were isolated in small yields. The isolation procedure was modified to avoid acidic conditions, under which N $\rightarrow$ O migration of phosphoryl groups is known to occur (5). This precaution eliminated one possible mode of formation of the O-phosphoryl derivatives.

In order to determine whether phosphorylation and acetylation of methyl oxazoline proceed by different mechanisms the reaction between the chloro analogue of DFP, diisopropyl phosphorochloridate (DClP), and methyl oxazoline was studied. Wagner-Jauregg *et al.* (6) have shown that DClP is more reactive than DFP, readily reacting with primary and secondary amines to give N-phosphoryl derivatives.

Methyl oxazoline, when treated with DClP at room temperature for 24 hours in sodium bicarbonate solutions (pH 8.2), gave a 51% yield of diisopropyl N-2-acetoxyethylphosphoramidate together with a little N-acetylethanolamine. This reaction clearly indicates that phosphorylation of methyl oxazoline, like acylation, gives an N-acyl derivative. If the reaction was stopped after 1 hour, a neutral oily product was obtained which appeared to be isomeric with diisopropyl N-2-acetoxyethylphosphoramidate, having the same elemental analysis, including one acetyl group, but a different infrared spectrum. No N—H or C=O (ester) absorption was apparent; instead the compound showed absorption at 3400 cm^{-1}, 1690 cm^{-1}, and 1050 cm^{-1}, which were tentatively assigned to the O—H, C=O (amide I), and C—OH stretching vibrations (7). The existence of an hydroxyl group in the molecule was confirmed by acetylation, which gave a quantitative yield of an oil whose infrared spectrum showed no absorption at 3400 cm^{-1} and 1050 cm^{-1} but two new bands appeared at 1740 cm^{-1} and 1230 cm^{-1}, which were assigned to the C=O (ester) and C—OC (ester) stretching vibrations. The only location remaining for the acetyl group, to which the band at 1690 cm^{-1} is ascribed, is on the nitro-

**Issued as D.R.C.L. Report No. 363.*

gen atom, the lack of any N—H and amide II absorption being in keeping with a tertiary amide structure. The high frequency of the C=O stretching vibration is in agreement with the nitrogen atom being substituted with a diisopropyl phosphoryl group, since electrophilic groups substituted on the amide nitrogen increase the C=O frequency (8).

On the basis of these results, the product isolated from the reaction of methyl oxazoline with DClP after 1 hour was assigned structure I, with which the n.m.r. spectrum is in agreement. If this material is allowed to remain on an alumina column (ca. 1 hour) prior to elution, it is quantitatively converted to diisopropyl N-2-acetoxyethylphosphoramidate (II). The migration can also be effected by allowing the compound to stand overnight in aqueous sodium bicarbonate at pH 8.2.

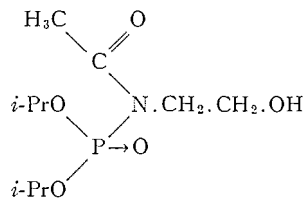

I

Treatment of methyl oxazoline with DClP in anhydrous ether in the absence of a base gives an oily product whose infrared spectrum, apart from absorption at 3400 cm^{-1} and 1050 cm^{-1}, is identical with that of I. Since elemental analysis revealed the presence of chlorine and an acetyl group the material was thought to be the chloro analogue of I, namely diisopropyl N-2-chloroethylphosphoramidate (III). Replacement of the hydroxyl by the chloro group stabilized the molecule to the extent that it could be chromatographed on alumina without undergoing migration.

Fry (1) considers the acylation of Δ^2-oxazolines to proceed by formation of a salt-like intermediate, followed by ring opening between positions 1 and 5 in ether and 2 and 3 in aqueous bicarbonate solution. This work elaborated the previous explanation by Goldberg and Kelly (9) of the ring opening of oxazolinium salts. They compared the 1/5 ring opening of phenyl oxazoline hydrochloride to give N-2-chloroethylbenzamide with the similar degradation of imidate hydrohalides to alkyl chlorides and amides. This decomposition of imidate hydrohalides was later shown to be first order with respect to the halide ion (10). Stevens *et al.* (11) confirmed the bimolecular nature of the reaction by isolating *sec*-butyl chloride with inverted configuration from the thermal decomposition of optically active *sec*-butyl acetimidate hydrochloride.

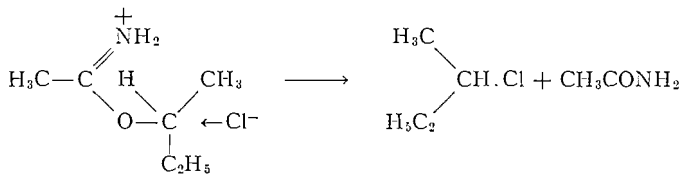

By analogy, the mode of phosphorylation of methyl oxazoline can be considered to give first a salt-like intermediate which cleaves between positions 1 and 5 under both anhydrous acidic and aqueous basic conditions. The last stage in aqueous bicarbonate is the migration of the acetyl group from the N to the O atom.

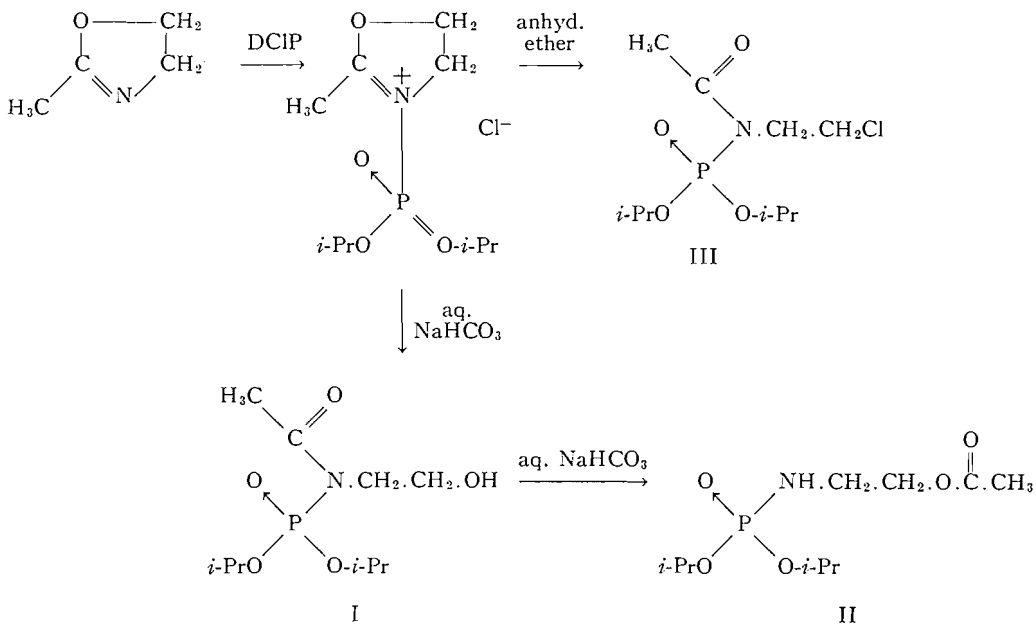

The transformation of methyl oxazoline in aqueous solution has been studied by Porter *et al.* (12) and very recently by Martin and Parcell (13). The first authors studied unbuffered solutions having initial pH values of 4.8, 5.4, and 6.2 whilst the latter employed buffered solutions in the pH range −1 to 7. Other work (14), which will be reported elsewhere, indicated that the expressions derived (12, 13) for the rate of disappearance of methyl oxazoline could not be extrapolated to higher pH values as used in our phosphorylation experiments (pH 8.5–9). This work involved a study of an aqueous solution of methyl oxazoline (2.5%) at controlled pH values in the range 0 to 10. Our results give excellent agreement with those of Martin and Parcell from pH 0 to 6, but discrepancies appear outside this range. Nuclear magnetic resonance spectroscopy was used to follow the reaction since it readily differentiates between the methyl protons of methyl oxazoline, O-acetylethanolamine, N-acetylethanolamine, and acetic acid. When this technique was applied to a control of methyl oxazoline (1% in 6% sodium bicarbonate), the triplet at 2.724, 2.746, and 2.770 p.p.m. up field from water resulting from methyl oxazoline disappeared in 23 hours. The only other signal detected was a single peak at 2.698 p.p.m. corresponding to N-acetylethanolamine (O-acetylethanolamine 2.563 p.p.m.). An infrared study (thin film, CaF_2 plates) of a similar solution of methyl oxazoline but in D_2O and using deuterated sodium bicarbonate confirmed the result.

Since methyl oxazoline is readily converted to N-acetylethanolamine under the conditions employed in the reaction of methyl oxazoline and DFP, a separate experiment was carried out with DFP and N-acetylethanolamine, and 2-acetamidoethyl diisopropyl phosphate was isolated.

It would therefore appear likely that under the conditions used for the phosphorylation of methyl oxazoline with DFP, 2-acetamidoethyl diisopropyl phosphate arises from the reaction of N-acetylethanolamine with DFP. However, the isolation of 2-aminoethyl diisopropyl phosphate remains unexplained.

EXPERIMENTAL

Infrared spectra were recorded on a Perkin–Elmer 221G spectrophotometer and the nuclear magnetic resonance spectra on a Varian V4300 spectrometer. Paper chromatograms were run on Whatman No. 1 paper using butanol:acetic acid:water, 4:1:5, as the developer.

2-Methyl-Δ^2-oxazoline was prepared by the method of Wenker (15), b.p. 109–110°.

Diisopropyl phosphorochloridate was prepared according to McIvor *et al.* (16), b.p. 74° at 10 mm.

Diisopropyl phosphorofluoridate was prepared by the method of Goldwhite and Saunders (17), b.p. 63° at 1 mm.

N-Acetylethanolamine was prepared according to Wenker (15), b.p. 140° at 0.1 mm.

Diisopropyl N-2-hydroxyethylphosphoramidate was prepared according to Plapinger and Wagner-Jauregg (5) and distilled at 95–98° at 0.1 mm. Infrared (film): 3375 cm^{-1}, OH; 3280 cm^{-1}, NH; 1230 cm^{-1}, P → O; 1178, 1140, 1107 cm^{-1}, C—OP (isopropyl); 1061 cm^{-1}, C—OH; 1018, 989 cm^{-1}, P—OC.

Diisopropyl N-2-Acetoxyethylphosphoramidate

Diisopropyl N-2-hydroxyethylphosphoramidate (800 mg) and triethylamine (395 mg) were dissolved in anhydrous ether, and acetyl chloride (305 mg) was slowly added. After standing for 72 hours, the solution was filtered and the filtrate evaporated to give an oil (845 mg) which distilled at 95–98° at 0.05 mm, n_{21}^{D} 1.435 (yield 86%). Calc. for $C_{10}H_{22}O_5NP$: N, 5.28; P, 11.68%. Found: N, 5.57; P, 11.34%. Infrared (film): 3250 cm^{-1}, NH; 1740 cm^{-1}, C=O (ester); 1232 cm^{-1}, P → O and C—OC (ester); 1170, 1135, 1108 cm^{-1}, C—OP (isopropyl); 1015, 985 cm^{-1}, P—OC.

Reaction of DClP with 2-Methyl-Δ^2-oxazoline in Aqueous Bicarbonate Solution

(*a*) DClP (1.71 g) was added over a period of 2 hours to a stirred solution of methyl oxazoline (500 mg) and sodium bicarbonate (1.5 g) in water (17 ml). The solution was stirred for 20 hours and then ether-extracted to give 823 mg (52%) of oil which distilled at 95–99° at 0.1 mm, n_{21}^{D} 1.434. Calc. for $C_{10}H_{22}O_5NP$: C, 45.2; H, 8.37; N, 5.28; P, 11.68%. Found: C, 45.36; H, 8.58; N, 5.04; P, 11.78%. Infrared (film): 3250 cm^{-1}, NH; 1740 cm^{-1}, C=O (ester); 1232 cm^{-1}, P → O and C—OC (ester); 1170, 1135, 1108 cm^{-1}, C—OP (isopropyl); 1015, 985 cm^{-1}, P—OC. The infrared spectrum was identical with that of an authentic sample of diisopropyl N-2-acetoxyethylphosphoramidate.

(*b*) Using the quantities of reactants mentioned above, DClP was added to the solution in 15 minutes and after an hour the solution was extracted with chloroform. The chloroform extract gave diisopropyl N-acetyl-N-2-hydroxyethylphosphoramidate, 910 mg (58%), as a yellowish oil, which was distilled at 95–100° at 0.01 mm. Calc. for $C_{10}H_{22}O_5NP$: C, 45.2; H, 8.37; N, 5.28; P, 11.68; CH_3CO, 16.22%. Found: C, 45.51; H, 8.34; N, 5.08; P, 11.82; CH_3CO, 16.01%. Infrared (film): 3400 cm^{-1}, OH; 1685 cm^{-1}, C=O (amide I); 1270 cm^{-1}, P → O; 1170, 1135, 1108 cm^{-1}, C—OP (isopropyl); 1050 cm^{-1} (sh), C—OH; 1010, 985 cm^{-1}, P—OC.

(*c*) A mixture of methyl oxazoline (2 g), DClP (11.49 g), sodium bicarbonate (12 g), and isopropanol (75 ml) was made up to 200 ml with water, maintained at 37° for 4 days, and then extracted with ether followed by chloroform. The ether extract contained 2.1 g of oil, of which 500 mg was chromatographed on Woelm IV neutral alumina; the main products were diisopropyl N-2-acetoxyethylphosphoramidate (289 mg), which was eluted with 2:1 benzene:ether, and N-acetylethanolamine (25 mg), eluted with 50:1 chloroform:methanol. All the chloroform extract (102 mg) was chromatographed on the same type of alumina; diisopropyl N-2-acetoxyethylphosphoramidate (59 mg) was eluted with 8:1 benzene:chloroform; diisopropyl N-2-hydroxyethylphosphoramidate (20 mg) was eluted with 20:1 chloroform:methanol and N-acetylethanolamine (16 mg) was eluted with 100:1 chloroform:methanol. The fractions were identified by comparison of the infrared spectra with those of authentic samples.

The total yields of diisopropyl N-2-acetoxyethylphosphoramidate and diisopropyl N-2-hydroxyethylphosphoramidate were 1.28 g (20%) and 20 mg (0.4%) respectively.

Reaction of DClP with 2-Methyl-Δ^2-oxazoline in Anhydrous Ether

DClP (1.16 g) in anhydrous ether was added to a stirred solution of methyl oxazoline (500 mg) in anhydrous ether. After the solution was stirred for 18 hours the solvent was removed and the residue freed of volatiles by pumping at 0.3 mm, yielding 1.62 g of yellow oil. A 500-mg aliquot was chromatographed on Woelm neutral alumina grade III and two main fractions were obtained. Elution with 4:1 benzene:pentane gave a colorless oil (340 mg) which distilled at 85–90° at 0.1 mm. Yield 68%. Calc. for $C_{10}H_{12}O_4NPCl$: N, 4.89; P, 11.19; Cl, 12.42%. Found: N, 4.61; P, 10.98; Cl, 12.65%. Infrared (film): 1690 cm^{-1}, C=O (amide I); 1270 cm^{-1}, P → O; 1174, 1138, 1095 cm^{-1}, C—OP (isopropyl); 1010 (sh), 986, 970 (sh) cm^{-1}, P—OC. From the n.m.r., infrared, and analytical data this compound was concluded to be diisopropyl N-acetyl-N-2-chloroethylphosphoramidate. A second fraction (128 mg) was eluted with 1:1 benzene:ether as a clear oil and had an infrared spectrum identical with that of N-2-chloroethyl-N-acetylethylamine. Infrared (film): 3280 cm^{-1}, NH; 1650 cm^{-1}, C=O (amide I); 1565 cm^{-1}, OCNH (amide II); 1260 cm^{-1} (amide III).

Acetylation of Diisopropyl N-Acetyl-N-2-hydroxyethylphosphoramidate

Acetyl chloride (300 mg) was slowly added to a solution of triethylamine (388 mg) and diisopropyl N-acetyl-N-2-hydroxyethylphosphoramidate (850 mg) in anhydrous ether. After the solution had stood overnight, the white precipitate of triethylamine hydrochloride was filtered off; evaporation of the ethereal filtrate gave 890 mg of yellow oil which distilled at 87–90° at 0.1 mm, giving diisopropyl N-acetyl N-2-acetoxyethylphosphoramidate (92%) as a clear oil. Calc. for $C_{12}H_{24}O_5NP$: N, 4.53; P, 10.02; CH_3CO, 23.90%. Found: N, 4.66; P, 9.75; CH_3CO, 23.66%.

Reaction of DFP with 2-Methyl-Δ^2-oxazoline

A solution of methyl oxazoline (2 g), DFP (11 g), and sodium bicarbonate (12 g) in water was homogenized by the addition of isopropanol (75 ml), and the volume was made up to 200 ml. The reaction was carried out in a fume hood, and the solution kept at 37° for 4½ days. After this time, the reaction mixture was extracted with ether and chloroform, which yielded 758 mg and 45 mg of oil, respectively.

A portion (500 mg) of the ether extract was chromatographed on Woelm neutral alumina grade IV (15 g) and three main fractions were obtained. The first fraction eluted was DFP (27 mg), with 2:1 benzene: pentane; followed by N-acetylethanolamine (110 mg), eluted with 80:1 chloroform:methanol; and finally sodium diisopropyl phosphate (221 mg), eluted with methanol. All the chloroform extract was chromatographed on 2 g alumina, giving two main fractions: N-acetylethanolamine (10 mg), eluted with 90:1 chloroform: methanol, and sodium diisopropyl phosphate (22 mg), eluted with 100:1 methanol:acetic acid. All these compounds were identified by comparison of their infrared spectra with those of authentic samples. Two small fractions from the chloroform extract eluted with 1:1 chloroform:ether showed positive ninhydrin and Hanes–Isherwood (18) spots at R_F 0.72 and 0.73 respectively, and also Hanes–Isherwood-positive spots at R_F 0.89 and 0.92 respectively.

These two fractions were combined (10 mg), and 5 mg streaked on a sheet of Whatman No. 3 paper 18×18 in. and separated electrophoretically in an E.C. Model 40 apparatus, using 1N formic acid as the buffer at 900 v for 1 hour. Three Hanes–Isherwood-positive bands were detected at −6, −1.5, and +2.6 cm using the print method (19). After air drying the paper, the bands were cut out and eluted with water (2 ml). The eluate was passed through a millipore filter and in the case of band 1, through 1 cc IRA 400 (OH^-) before evaporating to dryness. Band 1 gave 1.1 mg of oil, band 2, 2.5 mg, and band 3, 1.3 mg. These oils were shown to be pure by re-examination of chromatographic and electrophoretic properties. These values, together with the spectral data, are given in Table I.

TABLE I

Paper chromatographic, paper electrophoretic, and infrared absorption data of the three fractions from the chloroform extract

			Chromogenic reaction			
Band	R_F	Mobility* (cm)	Ninhydrin	Hanes–Isherwood	Chlorine (20)	Infrared spectra ($CHCl_3$) (cm^{-1})
1	0.72	−7.9	+	+	+	3470, 3200, 1580, 1250, 1178, 1150, 1105, 1000, 800
2	0.92	−1.4		+	+	3450, 3350, 1670, 1520, 1180, 1150, 1105, 1015
3	0.81	+3.3		+		2700, 2100, 1650, 1210, 1170, 1150, 1180, 1020

*Mobility is measured as the distance moved from the start line, and the sign denotes the electrode towards which migration occurred.

On the basis of these properties being identical with those of 2-aminoethyl diisopropyl phosphate in the case of band 1, 2-acetamidoethyl diisopropyl phosphate for band 2, and diisopropyl dihydrogen phosphate for band 3, the compounds were assigned these structures. The yield of 2-aminoethyl diisopropyl phosphate was 0.07% and 2-acetamidoethyl diisopropyl phosphate 0.08%.

Reaction of DFP with N-Acetylethanolamine

N-Acetylethanolamine (2.45 g) was mixed with DFP (11 g), sodium bicarbonate (12 g), and isopropanol (75 ml) and made up to 200 ml. The reaction was maintained at 37° for 4 days.

After 4 days at 37° the reaction was extracted with ether and chloroform. The ether extract gave a brown oil (908 mg), of which 500 mg was chromatographed on Woelm neutral alumina grade IV (15 g). The products isolated in order of elution were DFP (233 mg), triisopropylphosphate (7 mg), 2-acetamidoethyl diisopropyl phosphate (12 mg), N-acetylethanolamine (87 mg), and diisopropyl dihydrogen phosphate (141 mg). The chloroform extract gave 43 mg of oil which yielded on chromatography 2-acetamidoethyl

diisopropyl phosphate (9 mg) and N-acetylethanolamine (15 mg). All the products were identified by paper chromatography and infrared spectra by comparison with known samples. The main product was 2-acetamidoethyl diisopropyl phosphate, 30 mg (0.47%).

ACKNOWLEDGMENTS

The author is indebted to Mr. J. Legari for technical assistance and to Dr. M. A. Weinberger for interpretation of the n.m.r. spectra. Microanalyses were carried out by Mr. J. Helie, infrared absorption spectra by Mr. R. Gravelle, and n.m.r. spectra by Mr. K. Oikawa.

REFERENCES

1. E. M. FRY. J. Org. Chem. **15**, 802 (1950).
2. B. M. TRYON. U.S. Patent No. 2,410,318 (1946).
3. G. R. PORTER, H. N. RYDON, and J. A. SCHOFIELD. Nature, **182**, 927 (1958).
4. H. N. RYDON. Private communication.
5. R. E. PLAPINGER and T. WAGNER-JAUREGG. J. Am. Chem. Soc. **75**, 5757 (1953).
6. T. WAGNER-JAUREGG, J. J. O'NEILL, and W. H. SUMMERSON. J. Am. Chem. Soc. **73**, 5202 (1951).
7. L. J. BELLAMY. The infrared spectra of complex molecules. Methuen, London. 1958.
8. R. E. RICHARDS and H. W. THOMSON. J. Chem. Soc. 1248 (1947).
9. A. A. GOLDBERG and W. KELLY. J. Chem. Soc. 1919 (1948).
10. S. M. MCELVAIN and B. E. TATE. J. Am. Chem. Soc. **72**, 2233 (1951).
11. C. L. STEVENS, D. MORROW, and J. LAWSON. J. Am. Chem. Soc. **77**, 2341 (1955).
12. G. R. PORTER, H. N. RYDON, and J. A. SCHOFIELD. J. Chem. Soc. 2686 (1960).
13. R. B. MARTIN and A. PARCELL. J. Am. Chem. Soc. **83**, 4835 (1961).
14. R. GREENHALGH and M. A. WEINBERGER. To be published.
15. H. WENKER. J. Am. Chem. Soc. **57**, 1079 (1935).
16. R. A. MCIVOR, G. D. MCCARTHY, and G. A. GRANT. Can. J. Chem. **34**, 1819 (1956).
17. H. GOLDWHITE and B. C. SAUNDERS. J. Chem. Soc. 2040 (1955).
18. C. S. HANES and F. A. ISHERWOOD. Nature, **164**, 1107 (1949).
19. H. H. BROWNELL, J. G. HAMILTON, and A. A. CASSELMAN. Anal. Chem. **28**, 550 (1957).
20. H. N. RYDON and P. W. G. SMITH. Nature, **169**, 922 (1952).

TOTAL SYNTHESIS OF STEROIDAL DERIVATIVES

I. SYNTHESIS OF HYDROCHRYSENE ANALOGUES AND RELATED COMPOUNDS

JAMES P. KUTNEY, WM. MCCRAE,[1] AND ARNOLD BY
Department of Chemistry, University of British Columbia, Vancouver, British Columbia
Received December 6, 1961

ABSTRACT

A synthetic sequence leading to the total synthesis of several hydrochrysene derivatives is described. It is noted that these derivatives may provide entry into the synthesis of various interesting steroidal analogues.

Recently a considerable effort has been put forth to study the effect of substituents attached to the steroid skeleton on the biological properties of these compounds. Indeed, dramatic effects have been obtained for substitutents such as methyl, hydroxyl, and halogen, particularly fluorine, when these groups are situated at rather specific positions on the nucleus. Related to these studies, the removal of angular methyl groups, as in 18-nor and 19-nor steroids, or of methylene groups from the ring skeleton to generate ring-contracted steroidal nuclei has also been accompanied with very important alterations in the biological activity of these molecules (1, 2).

All of the above studies have involved the use of the naturally occurring steroids as starting materials, and although these are obviously the logical choice in most cases, they offered certain limitations in synthesizing some of the steroidal derivatives which were of interest in our studies between structure and biological activity. For this reason, we initiated investigations directed toward the total synthesis of steroidal analogues, with particular emphasis on intermediates which would readily lend themselves to the introduction of substituents or alterations of the actual skeleton not conveniently possible from the natural steroids. This paper outlines the total synthesis of hydrochrysene derivatives which fulfill this aim.

Of the various approaches which were available, the one utilizing the Robinson–Mannich base reaction originally developed by Robinson and co-workers (3) and so successfully applied in the elegant researches of Johnson and co-workers (4) was selected. Condensation of 6-methoxy-2-tetralone (I) with 1-diethylamino-3-pentanone methiodide, in the presence of sodium methoxide, provided an isomeric mixture of the tricyclic ketones (II and III). The arrangement of the double bond in the tricyclic ketone permits its migration into conjugation with either the aromatic ring or with the carbonyl function (II $\rightleftarrows$ III). It was not surprising, therefore, to find that our product was an oily mixture of both isomers. The ultraviolet spectrum of this mixture indicated a broad band in the 250–260 mμ region and the infrared spectrum indicated the presence of saturated and unsaturated carbonyl functions (5.86 and 6.05 μ). Careful chromatography of this mixture, first on alumina and then on silica gel, allowed the separation into the two respective isomers, II (λ_{max} 253 mμ, infrared 6.05 μ) and III (λ_{max} 275 mμ, infrared 5.85 μ). In general, this separation involved considerable losses, and for preparative purposes, in the subsequent condensation, the isomeric mixture was employed. It is pertinent to point out that a similar mixture was encountered by Johnson and co-workers in a similar reaction (5).

[1]*Holder of N.R.C. Postdoctorate Fellowship, 1960–1961.*

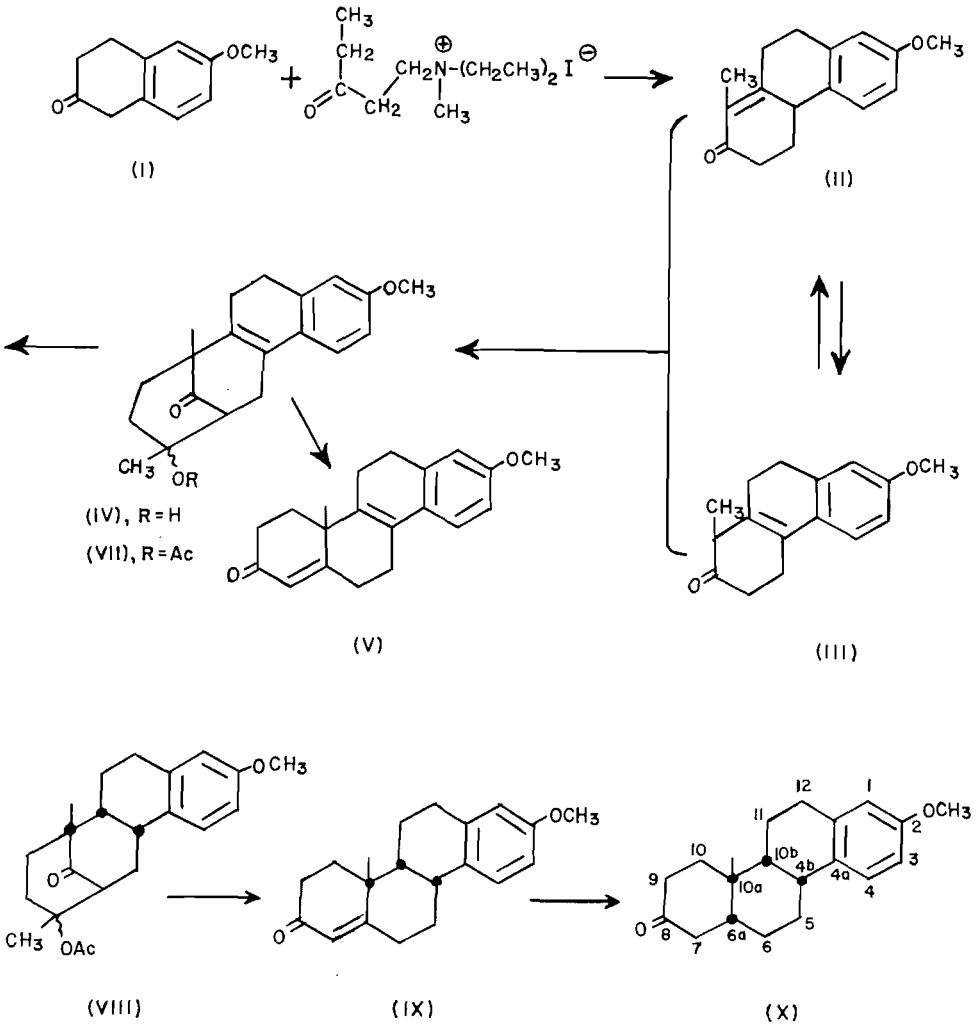

The common anion derived from either isomer II or III made it unnecessary to isolate each isomer in a pure state for the second Robinson–Mannich cyclization. Consequently, the tricyclic ketone mixture was treated with either 1-diethylamino-3-butanone methiodide or methyl vinyl ketone and the condensation was allowed to proceed, in the presence of sodium methoxide, to yield a tetracyclic product. In our hands, the use of methyl vinyl ketone instead of the Mannich base was more convenient and provided better results and we have utilized it in most of our condensations. It should be noted that a similar preference for the use of the parent ketone instead of the Mannich base methiodide is indicated by Woodward and co-workers in a related reaction (6). The nature of the tetracyclic product depended on the reaction conditions—the hydroxy ketone (IV) was formed at lower temperatures whereas the tetracyclic ketone (V) was the major product at refluxing methanol temperature. Since ketone V was readily obtained from the hydroxy ketone by treatment with base, and since the ketol IV allowed us to obtain some of the desired hydrochrysene derivatives, we concentrated our efforts on developing optimum conditions for the sequence II, III $\rightarrow$ IV $\rightarrow$ V.

The nature of the ketol structure deserves some comment since at the outset, two formulations (IV or VI) are possible depending on the manner of the final cyclization. The structure IV was anticipated, since Johnson and co-workers (8) have recently

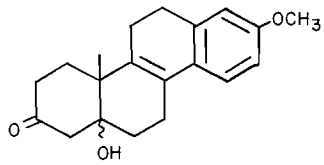

(VI)

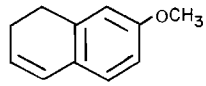

(XII)

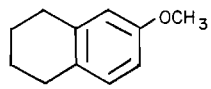

(XIII)

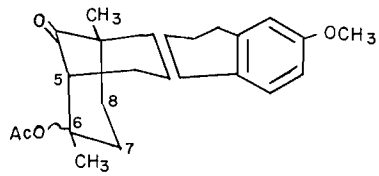

(XI)

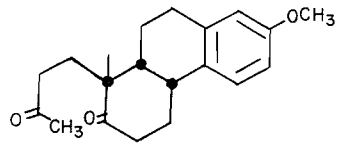

(XIV)

published a detailed paper indicating that the correct structure for their ketols, obtained in an analogous sequence, is represented by a formulation of type IV and not VI as originally proposed. Indeed, our hydroxy ketone, m.p. 216–218°, could be readily assigned the bridged structure IV on the basis of the following evidence. The infrared spectrum of the substance indicated the presence of a saturated carbonyl chromophore (5.88 μ) and a hydroxyl function, and the ultraviolet spectrum (λ_{max} 274 mμ; λ_{min} 236 mμ) was characteristic of a *p*-methoxystyrene chromophore. Subsequent comparison with the model compound, 3,4-dihydro-6-methoxynaphthalene (XII) (λ_{max} 269 mμ; λ_{min} 237 mμ), indicated that the ultraviolet spectra were virtually superimposable except for a slight shift of the maximum in IV, as expected for more substitution on the chromophore. This spectral data is obviously consistent for both IV or VI, but when we turned to consider the n.m.r. data, we could exclude VI very easily. The n.m.r. spectrum, run in pyridine (7), showed *two* sharp signals at high applied magnetic field characteristic of proton resonance from methyl groups (9.38 τ, $-\overset{|}{\underset{|}{C}}-CH_3$ and 9.22 τ, $HO-\overset{|}{\underset{|}{C}}-CH_3$)—a situation clearly consistent with structure IV but not VI. In addition the characteristic signals for the methoxyl group and the aromatic protons were present (see experimental portion). Acetylation of IV with isopropenyl acetate provided a good yield of the expected acetate, VII, m.p. 150–150.5°. Apart from the usual carbonyl absorption characteristic of the ketone and acetate functions (5.78, 5.85 μ) in the infrared, the n.m.r. spectrum of this substance, run in pyridine, also indicated some interesting features. Firstly, the presence of two high-field signals (9.42, 8.98 τ) confirmed the presence of two methyl groups. In addition it is to be noted that one of these signals is shifted downfield upon acetylation and this is expected in such a structure as IV. This evidence allows us to assign, with certainty, the highest-field signal to the angular methyl group. It is well known (7) that pyridine exerts a considerable solvent shift in the n.m.r. and in order to see what effect is noticed in this series of compounds, we also ran the acetate VII, under identical conditions with deuteriochloroform as the solvent. In general all the signals were shifted

downfield with some signals being shifted much more than others. For example, the high-field signals now occurred at 8.80 and 8.35 τ. In addition the resolution in pyridine was far superior to that in deuteriochloroform so that pyridine appears to be an excellent solvent for compounds of this type.

It has been known for some time (8) that catalytic hydrogenation of the acetates of ketols of type IV effects stereoselective reduction of the styrene double bond, with the hydrogen being absorbed from the β face of the molecule. This stereochemical course can be rationalized if one considers the conformational expression for the acetate VII (see XI). It becomes clear that β-side hydrogenation would be expected because approach of the catalyst to the α-side of the double bond is seriously hindered by the bridge containing carbons 6, 7, and 8. When the ketol VII was catalytically reduced by the use of palladium hydroxide on strontium carbonate, a good yield of the reduction product (VIII) was obtained. The ultraviolet spectrum of this substance (λ_{max} 278 and 286 mμ) was virtually superimposable upon the spectrum of an authentic sample of 1,2,3,4-tetrahydro-6-methoxynaphthalene (XIII), indicating that complete reduction had occurred. The infrared spectrum still retained the typical saturated carbonyl chromophore, and the acetate group (5.86, 5.80 μ) and the n.m.r. spectrum, with signals at high field (8.90 τ, $-\overset{|}{\underset{|}{C}}-CH_3$; 8.47 τ, $-\overset{|}{\underset{OAc}{C}}-CH_3$), were entirely consistent with the above formulation.

When the above reduction product (VIII) was refluxed in benzene in the presence of sodium methoxide, an excellent yield of the expected tetracyclic ketone IX was obtained. This substance, m.p. 158–159°, now exhibited a conjugated carbonyl absorption in the infrared spectrum (6.04 μ) and a new absorption occurred at 233 mμ in the ultraviolet apart from the usual aromatic absorption already mentioned in VIII. The n.m.r. spectrum of this substance was completely different from that of the starting material and, apart from a detailed description given in the experimental portion, may be mentioned the presence of only *one* signal at high field (8.53 τ, $-\overset{|}{\underset{|}{C}}-CH_3$) and a weak signal in the olefinic proton region (4.16 τ), which is clearly in support of structure IX. This interesting reaction, previously observed by Johnson and his co-workers, (8) may be rationalized as taking place via a reverse aldol reaction to give, in this case, the diketone XIV, followed by recyclization to the ketol structure XV, which then undergoes a base-catalyzed elimination of water to provide the product IX.

In order to provide further desirable derivatives in this series, the unsaturated ketone IX was catalytically reduced by the use of palladium on charcoal containing a trace of concentrated hydrobromic acid—reaction conditions known to provide ring A/B cis

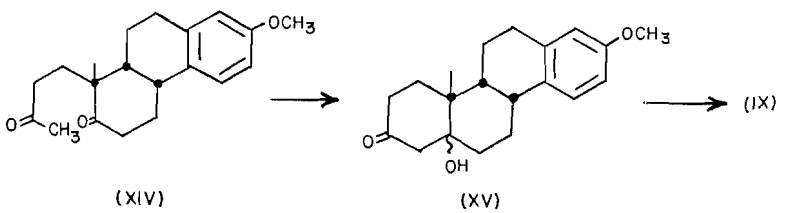

fusions in compounds of this type (9). The reduction product, m.p. 76.5–77.5°, was assigned the cis-syn-cis structure X. The completeness of the reduction was indicated by the infrared spectrum of the product (5.86 μ) and its ultraviolet spectrum, which now showed a complete disappearance of the conjugated carbonyl chromophore and a retention of the typical aromatic absorption, making the spectrum superimposable on that of the methoxy tetralin, XIII. The n.m.r. spectrum was also instructive, indicating absence of olefinic signals and the presence of a sharp peak at 8.85 τ, attributable to one $-\overset{|}{\underset{|}{C}}-CH_3$ function. It is interesting to note that in X, where there are no ring olefinic bonds present to create a deshielding effect on the methyl signal, the peak now occurs at higher fields and in the region more normally attributable to methyl protons.

Finally, in the hope of providing hydrochrysene derivatives with different stereochemistry at the ring junctures, we have subjected the ketol IV to a more drastic methoxide treatment and have obtained, in high yield, the expected tetracyclic ketone, V. This material, m.p. 142–143°,* exhibited a strong carbonyl absorption in the infrared due to the conjugated chromophore in ring A (6.01 μ), and the ultraviolet spectrum of the material indicated two maxima (235 mμ (broad) and 270 mμ). The n.m.r. spectrum had, among its important features, a single band at high field (8.52 τ, $-\overset{|}{\underset{|}{C}}-CH_3$) and a weak signal due to the olefinic proton (4.13 τ). Other n.m.r. signals appearing in the spectrum are given in the experimental portion. The mode of formation of V is analogous to the one already given for IX.

It is pertinent to point out that although the substances described herein differ from the ones previously prepared only in the nature of the aromatic nucleus, this difference represents an important modification for the synthesis of many steroidal substances. The aromatic system in the above compounds lends itself readily to numerous interesting variations not conveniently obtainable previously. Indeed, Nagata and co-workers (11) have very recently described the preparation of various C-18-substituted steroids and related substances, utilizing such intermediates as V. We hope to present other interesting modifications in a forthcoming publication.

EXPERIMENTAL

All melting points were determined on a Fischer–Johns apparatus and are uncorrected. The ultraviolet spectra were recorded in 95% ethanol on a Cary 11 recording spectrophotometer. Infrared spectra were recorded as potassium bromide pellets on a Perkin–Elmer Model 21 spectrophotometer. The n.m.r. spectra were taken at 60 megacycles on a Varian A 60 instrument. In all cases tetramethylsilane was the external standard set at 0 c.p.s. In all cases integration of areas under the signals was carried out and the number of protons corresponding to each signal indicated in parentheses. The positions of the signals are recorded in the Tiers τ scale. The analyses were performed by Dr. A. Bernhardt and his associates, Mulheim (Ruhr) Germany, and by Mrs. Aldridge, University of British Columbia.

Reaction of 6-Methoxy-2-tetralone (I) with 1-Diethylamino-3-pentanone Methiodide

We have performed numerous experiments in order to obtain optimum reaction conditions. We have found that maximum yields are only obtainable if the reactions are conducted under absolutely anhydrous conditions and in the complete absence of oxygen. The apparatus described in *Org. Syntheses* (12) was used throughout the entire sequence.

**This substance has been independently mentioned in a recent communication (10). We found the ultraviolet data presented for this substance to be incorrect. We are very grateful to Dr. W. Nagata for providing us with a comparison sample and thereby allowing us to establish, beyond doubt, that their material is identical with ours.*

To a 250-ml 3-necked flask fitted with a drying tube, a dropping funnel, and a source of dry nitrogen, 1-diethylamino-3-pentanone (28.5 g) dissolved in dry benzene (83 ml) was added. The solution was chilled (ice bath) and dry nitrogen was passed into the flask over a period of 20 minutes. With nitrogen still passing into the flask, methyl iodide (13.5 g) was added dropwise, over a period of 1 hour, to the stirred pentanone solution. The temperature of the reaction mixture was kept at 0° during the addition, and after addition was complete, the reaction mixture was stirred at 0° for a further 3 hours, with a slow passage of nitrogen being maintained. In order to complete the reaction, the mixture was kept at 0° overnight and was then ready for use. This stock solution, containing the gummy methiodide, could be used for several condensations. Just before use, dry methanol (30 ml) was added to dissolve the methiodide and while still cold, aliquots of this solution were used in the various condensations.

A 1-liter 3-necked flask was equipped with a pressure-equalized dropping funnel, a stirrer, and a reflux condenser which was connected at the top through a 3-way stopcock to a vacuum source (water aspirator) and dry nitrogen (12). The system was evacuated, and with a rapid escaping stream of nitrogen passing through, the apparatus was flame dried. Anhydrous methanol (105 ml) was put into the flask and sodium (4.43 g) was added through an escaping stream of dry nitrogen. After the metal had dissolved, the methoxide solution was cooled to 0°, the system evacuated until the solvent began to boil, then filled with dry nitrogen, and the procedure repeated once more. To this stirred, cold basic solution, a solution of 6-methoxy-2-tetralone (23.11 g) in dry benzene (51 ml) was added rapidly through the dropping funnel. The dropping funnel was then charged with an aliquot (0.73 parts of the above stock solution) of the cold Mannich base methiodide (in an escaping stream of nitrogen) and the methiodide was then added over a period of 40 minutes with stirring and cooling to 0°. The reaction mixture gradually became green and stirring was continued for 1.75 hours at 0° in an atmosphere of nitrogen. Finally, the mixture was refluxed for 1 hour, during which time the solution developed an orange color. After cooling to 0°, the reaction was treated with 2 *N* sulphuric acid (147 ml) and then diluted with water (90 ml). The mixture was extracted with several portions of ether, the ethereal layer dried over anhydrous magnesium sulphate, and solvent evaporated *in vacuo* to yield a crude oily product. This oily product was partially distilled to yield a fraction (2.14 g) distilling in the range 100–119° at 0.1 mm which proved to be unreacted tetralone. The residual oil (28.42 g, 89.5% yield) consisted almost entirely of the desired tricyclic ketone mixture, although the infrared spectrum of this material showed the presence of a hydroxy-containing material. Chromatography of this oil on silica gel (330 g) and elution with benzene yielded the desired product as an isomeric mixture: II, III (23.3 g, 81% yield). Finally, elution with ether removed the hydroxy-containing material, which was not further characterized.

A small aliquot of the 23.3-g fraction was distilled at 230–250° (bath temp.) at 0.15 mm to yield an analytical sample of the tricyclic ketone. The ultraviolet spectrum indicated λ_{max} 225 (log ϵ 3.93), 254 mμ (log ϵ 4.06), λ_{min} 235 mμ (log ϵ 3.85); and the infrared spectrum showed 5.86 and 6.05 μ. Found: C, 78.97; H, 7.50; O, 13.65. Calc. for $C_{16}H_{18}O_2$: C, 79.31; H, 7.49; O, 13.22.

In one experiment, a small portion (1 g) of the tricyclic ketone mixture was chromatographed on deactivated alumina (grade II–III). Elution with benzene and benzene–ether mixture yielded a poor recovery (600 mg) of a yellow gum. This gum was then further rechromatographed on silica gel (6 g). Elution with benzene – petroleum ether (1:1) yielded, in the initial fractions, a small amount of the isomer III, λ_{max} 275 mμ (log ϵ 3.93), λ_{min} 242 mμ (log ϵ 3.45); infrared 5.85 μ. Found: C, 79.10; H, 7.54; O, 13.31. Continued elution with the same solvent yielded a small amount of isomer II, λ_{max} 253 mμ (log ϵ 4.10); infrared 6.05 μ. Found: C, 79.24; H, 7.41; O, 13.12. Due to the poor recovery encountered in this experiment, this separation was abandoned.

For the subsequent condensation with methyl vinyl ketone, the tricyclic ketone mixture, as obtained from the silica gel chromatography, was always distilled immediately before reaction so as to remove traces of water etc.

Reaction of Tricyclic Ketone with Methyl Vinyl Ketone—Preparation of Ketol (IV)

In numerous experiments attempted wherein we used 1-diethylamino-3-butanone methiodide or methyl vinyl ketone we found the latter reagent to be much more convenient and better yields were realized. Consequently only the procedure with this reagent is outlined here.

A 250-ml 3-necked flask was fitted with a stirrer, a dropping funnel, etc., exactly as already indicated in the first condensation above. After any moisture or oxygen was eliminated from the system as above, the flask was charged with a solution of the tricyclic ketone mixture (15.33 g) in anhydrous methanol (28 ml) (in an escaping stream of nitrogen). The dropping funnel was now filled with a sodium methoxide solution prepared from sodium metal (1.09 g) in dry methanol (28 ml) and the entire system was evacuated until the solvent began to boil. Dry nitrogen was then admitted, the system evacuated, and the procedure repeated again. The sodium methoxide solution was now added (in an escaping stream of nitrogen) rapidly to the stirred tricyclic ketone mixture, kept at 0°. To this reaction mixture, kept at 0°, a solution of dry methyl vinyl ketone (6.66 g, obtained from Matheson, Coleman and Bell, dried over anhydrous potassium carbonate, and freshly distilled) in anhydrous methanol (20 ml) was added dropwise over a period of 25 minutes, with a slow nitrogen stream being maintained. During the addition, the reaction mixture gradually attained a dark green color and after the addition was complete, the mixture was stirred for a further 2

hours at 0°. During this period a precipitate started to form. To complete the reaction, the ice bath was removed and the stirring was continued for 18 hours at room temperature under a nitrogen atmosphere. The reaction mixture was cooled to 0° and glacial acetic acid (7 ml) was added. The solid product was filtered off, washed with a small amount of ethyl ether, cold water, a small amount of ethanol, and then dried. The yield of this white solid was 13.72 g (69.5%) and it had a melting point of 200–206°. On one or two occasions, the melting started as low as 180°.

A small portion of this product was recrystallized several times from methanol to yield the analytical sample, m.p. 216–218° (with some decomposition). λ_{max} 274 mμ (log ϵ 4.07), λ_{min} 236 mμ (log ϵ 3.24); infrared 5.88 μ; n.m.r. signals (pyridine): 9.38 (—C(—CH$_3$)—, area = 3 H), 9.22 (HO—C(—CH$_3$)—, area = 3 H), 6.92 (OCH$_3$, area = 3 H), 4.44 (OH, area = 1 H), remaining signals in region 7.0–9.0 τ (area = 11 H) due to ring CH$_2$'s etc. The aromatic region is masked by the solvent. Found: C, 76.76; H, 8.09; O, 15.61; mol. wt. (Rast) 310. Calc. for $C_{20}H_{24}O_3$: C, 76.89; H, 7.74; O, 15.36; mol. wt. 312.

Acetylation of Ketol

A mixture of the ketol IV (5.25 g), *p*-toluenesulphonic acid monohydrate (33.7 mg), and isopropenyl acetate (27 ml) was heated on a steam bath for 5 hours. The solid which was present at the beginning of the reaction dissolved after about 1 hour. The reaction mixture was cooled to room temperature, 2 drops of pyridine were added, and the solvent was removed in a current of air. The residue was dissolved in a small amount of hot 95% ethyl alcohol, the solution was filtered and then concentrated to a volume of 30 ml. Upon cooling of the solution, the first crop of crystals (4.56 g) separated and had a melting point of 146–149°. An additional 0.53 g (total 5.09 g, 85.4%) was recovered as a second crop, m.p. 139–146°. Recrystallization of a small portion from aqueous ethanol provided a pure sample of the acetate VII, m.p. 150–150.5°. λ_{max} 275 mμ (log ϵ 4.16), λ_{min} 237 mμ (log ϵ 3.54); infrared 5.78, 5.85 μ; n.m.r. signals (pyridine): 9.42 (—C(—CH$_3$)—, area = 3 H), 8.98 (—C(=O)—O—C(—CH$_3$)—, area = 3 H), 8.70 (O—C(=O)—CH$_3$, area = 3 H), 6.95 (OCH$_3$, area = 3 H), remaining signals in region 7.0–8.6 τ (area = 11 H) due to ring CH$_2$'s etc.; n.m.r. signals (deuteriochloroform): 8.80 (—C(—CH$_3$)—, area = 3 H), 8.35 (—C(=O)—O—C(—CH$_3$)—, area = 3 H), 8.02 (—C(=O)—CH$_3$, area = 3 H), 6.19 (OCH$_3$, area = 3 H), remaining signals in region 6.5–8.0 (area = 11 H) due to ring CH$_2$'s etc., multiplet centered at 3.05 τ (aromatic H, area = 3 H). Found: C, 74.06; H, 7.66; O, 18.04. Calc. for $C_{22}H_{26}O_4$: C, 74.55; H, 7.39; O, 18.06.

Catalytic Hydrogenation of Unsaturated Tetracyclic Acetate

A solution of the unsaturated acetate VII (4.56 g) in 95% ethanol (170 ml, the alcohol was pretreated with Raney nickel) was hydrogenated over 30% palladium hydroxide on strontium carbonate (1.47 g) at hydrogen pressure of 40 lb/in^2 and room temperature for 20 hours. The catalyst was removed by filtration and the clear filtrate was concentrated to a small volume. The first crop (3.5 g) of crystals which separated melted at 148–150°. An additional 0.14 g (total, 3.64 g) was recovered from the mother liquors. A small portion was recrystallized twice from aqueous ethanol to yield the desired syn-cis product, VIII, m.p. 152.5–153.5°. λ_{max} 277 (log ϵ 3.39), 286 (log ϵ 3.39), 226 mμ (log ϵ 3.96); λ_{min} 248 (log ϵ 2.79), 283 mμ (log ϵ 3.20) virtually identical with the ultraviolet spectrum of XIII, which shows λ_{max} 278 (log ϵ 3.38), 287 (log ϵ 3.32), 223 mμ (log ϵ 3.97); λ_{min} 247 (log ϵ 2.58), 284 mμ (log ϵ 3.30).

The infrared spectrum of VIII shows bands at 5.80 and 5.86 μ; n.m.r. signals (deuteriochloroform): 8.90 (—C(—CH$_3$)—, area = 3 H), 8.47 (—C(=O)—O—C(—CH$_3$)—, area = 3 H), 8.05 (—C(=O)—CH$_3$), 6.24 (OCH$_3$, area = 3 H), remaining signals in region 6.6–8.2 (area = 16 H, including 3 H of acetate), multiplet centered at 3.08 τ (aromatic H, area = 3 H). Found: C, 74.00; H, 7.86; O, 17.87. Calc. for $C_{22}H_{28}O_4$: C, 74.13; H, 7.92; O, 17.96.

Synthesis of syn-cis-2-Methoxy-8-keto-10a-methyl-4b,5,6,8,9,10,10a,10b,11,12-decahydrochrysene (IX)

The apparatus used in this experiment was set up exactly as in the tricyclic ketone preparation in order to maintain anhydrous conditions and a nitrogen atmosphere at all times.

Into the 250-ml 3-necked flask, which was flame-dried and evacuated as before, dry methanol (70 ml) was added and then sodium (1.37 g) was added gradually in small pieces. After the sodium had reacted, the methoxide solution was cooled and the entire apparatus evacuated until the solvent began to boil; dry nitrogen was then admitted, the system evacuated, and the entire process repeated several times. To the stirred methoxide solution, a solution of the acetate VIII (3.5 g) in dry benzene (20 ml) was added through

a dropping funnel under a flow of escaping nitrogen. After the addition was complete, the system was evacuated again, dry nitrogen admitted, etc. to ensure complete removal of oxygen. The reaction mixture was then refluxed for 5 hours in this inert atmosphere. At the end of the refluxing period the reaction was cooled in ice, glacial acetic acid (4 ml) was added, and the mixture was swirled for several minutes. Some water and benzene were added to the reaction flask, the layers were then separated, and the aqueous layer was extracted with ether. The combined organic solutions were washed with a saturated solution of sodium chloride and dried over anhydrous magnesium sulphate. Concentration of the solvent under reduced pressure provided a first crop (1.83 g) of pale yellow needles, m.p. 155.5–158.5°. An additional 0.91 g (total 2.74 g, 94%) was recovered from the mother liquors. Two recrystallizations from ethanol provided an analytical sample of IX, m.p. 158–159°. λ_{max} 233 (log ϵ 4.23), 277 (log ϵ 3.35), 287 mμ (log ϵ 3.29); λ_{min} 274 (log ϵ 3.32), 284 mμ (log ϵ 3.24); infrared 6.04 μ; n.m.r. signals (deuteriochloroform): 8.53 (—C(CH$_3$)—, area = 3 H), 6.22 (OCH_3, area = 3 H), remaining signals in region 6.6–8.4 (area = 14 H), 4.16 (O=C—C(H)=C<, area = 1 H), multiplet centered at 3.12 τ (aromatic H, area = 3 H). Found: C, 80.68; H, 8.21; O, 10.84; Calc. for $C_{20}H_{24}O_2$: C, 81.04; H, 8.16; O, 10.80.

Synthesis of cis-syn-cis-2-Methoxy-8-keto-10a-methyl-4b,5,6,6a,7,8,9,10,10a,10b,11,12-dodecahydrochrysene (X)

A solution of the unsaturated tetracyclic ketone IX (2.6 g) in a 4:1 mixture of benzene – 95% ethanol (82 ml, benzene was refluxed with sodium, then with Raney nickel, while the ethanol was refluxed with Raney nickel) was treated with 10% palladium on carbon (0.33 g) and 1 drop of 48% hydrobromic acid. This mixture was hydrogenated at room temperature and atmospheric pressure for 5 hours, after which time 1 mole of hydrogen had been absorbed. The catalyst was removed by filtration and the solvent removed *in vacuo*, whereby a yellow gum was obtained. This gum was dissolved in benzene (10 ml) and chromatographed on deactivated alumina (29 g, approx. activity II–III). Elution with benzene yielded 2.38 g of a gum which crystallized nicely from a small volume of aqueous ethanol. Two further recrystallizations from the same solvent yielded pure X, as plates, m.p. 76.5–77.5°. λ_{max} 287 (log ϵ 3.15), 280 (log ϵ 3.16), 226 mμ (log ϵ 3.87); λ_{min} 284 (log ϵ 3.15), 248 mμ (log ϵ 2.14); infrared 5.86 μ; n.m.r. signals (deuteriochloroform): 8.85 (—C(CH$_3$)—, area = 3 H), 6.28 (OCH_3, area = 3 H), remaining signals in region 7.0–8.7 (area = 17 H), multiplet centered at 3.16 τ (aromatic H, area = 3 H). Found: C, 80.60; H, 8.98; O, 10.49. Calc. for $C_{20}H_{26}O_2$: C, 80.49; H, 8.78; O, 10.73.

Synthesis of 2-Methoxy-8-keto-10a-methyl-5,6,8,9,10,10a,11,12-octahydrochrysene (V)

(a) From the Ketol IV

Again the apparatus used was exactly the same as in the previous condensations wherein anhydrous and oxygen-free conditions are maintained.

Anhydrous methanol (280 ml) was put into a 1-liter 3-necked flask which had been previously dried and evacuated to remove air. Sodium (2.07 g) was then added gradually in small pieces, in an escaping stream of nitrogen. The apparatus was evacuated until the solvent began to boil, dry nitrogen admitted, etc., and to this methoxide solution, the dry ketol IV (17.7 g) was added. The mixture was refluxed for about 4 hours in this inert atmosphere. The ketol, which was not entirely soluble at the beginning, dissolved completely after about 2 hours and the solution attained a yellow coloration. The reaction mixture was cooled to 0°, glacial acetic acid (7 ml) was added, and the resulting pale yellow crystalline product was removed by filtration. This solid was washed with a small amount of ether, water, a small volume of ethanol, and then dried to yield crude tetracyclic ketone V (13.7 g), m.p. 140–142.5°. The filtrate was diluted with water and the aqueous layer extracted with ether. The ethereal layer was washed with a saturated solution of sodium chloride and dried over anhydrous magnesium sulphate. Evaporation of the solvent yielded a residual gum which upon seeding provided an additional 2.3 g (total 16 g) of the desired product. Several recrystallizations of the product from dimethyl cellosolve provided analytically pure V, m.p. 142–143°. λ_{max} 235 (broad, log ϵ 4.26), 270 mμ (log ϵ 4.25); λ_{min} 252 mμ (log ϵ 4.17); infrared 6.01 μ; n.m.r. signals (deuteriochloroform): 8.52 (—C(CH$_3$)—, area = 3 H), 6.19 (OCH_3, area = 3 H), remaining signals in region 6.5–8.0 (area = 12 H), 4.13 (O=C—C(H)=C<, area = 1 H), multiplet centered at 3.09 τ (aromatic H, area = 3 H). Found: C, 81.30; H, 7.30; O, 10.89; mol. wt. (Rast) 312. Calc. for $C_{20}H_{22}O_2$: C, 81.60; H, 7.53; O, 10.87; mol. wt. 294.

This preparation of V was, in our hands, superior to the one described in part (*b*) and we have used it in most of our preparations.

(b) Directly from Tricyclic Ketone

As before, the reaction was run under anhydrous conditions and in an inert atmosphere.

The methiodide of 1-diethylamino-3-butanone was prepared crystalline in the manner already described for the corresponding pentanone from 1-diethylamino-3-butanone (1.11 g) and methyl iodide (1.2 g). A solution of this methiodide (2.16 g) in anhydrous methanol (5 ml) was added dropwise over a period of 1 hour to the ice-cold mixture of the tricyclic ketone (1.9 g) in dry benzene (30 ml) and a sodium methoxide solution (from 0.278 g sodium in 10 ml methanol). After the addition was complete, stirring was continued for a further 30 minutes at 0°, and then the mixture was refluxed for 40 minutes. The reaction mixture was cooled, treated with 2 *N* sulphuric acid (15 ml), and extracted with benzene. The benzene layer was washed with water and dried over anhydrous magnesium sulphate. The solvent was evaporated *in vacuo* to yield a gummy product (2.5 g). This oil could not be conveniently crystallized, so it was then purified by chromatography on silica gel. Elution with benzene – petroleum ether (6:4) yielded a small amount of semicrystalline gum (0.7 g) which crystallized from dimethyl cellosolve. Several more recrystallizations from this solvent yielded the desired product, V, m.p. 142–143°. This product was shown to be identical with the one obtained in part (*a*).

ACKNOWLEDGMENTS

Financial aid from the National Research Council of Canada and the National Institutes of Health, Grant No. CY-5037, is very gratefully acknowledged.

REFERENCES

1. C. DJERASSI, L. MIRAMONTES, G. ROSENKRANZ, and F. SONDHEIMER. J. Am. Chem. Soc. **76**, 4092 (1954). D. A. MCGINTY and C. DJERASSI. Ann. N.Y. Acad. Sci. **71**, 500 (1958). V. A. DRILL and B. RIEGEL. Recent Progr. in Hormone Research, **14**, 29 (1958).
2. M. RAJIC, T. RULL, and G. OURISSON. Bull. soc. chim. France, 1213 (1961).
3. H. M. E. CARDWELL, J. W. CORNFORTH, S. R. DUFF, H. HOLTERMANN, and R. ROBINSON. J. Chem. Soc. 361 (1953).
4. W. S. JOHNSON. J. Am. Chem. Soc. **78**, 6278 (1956) and subsequent papers.
5. W. S. JOHNSON, J. SZMUSZKOVICZ, E. R. ROGIER, H. I. HADLER, and H. WYNBERG. J. Am. Chem. Soc. **78**, 6285 (1956).
6. R. B. WOODWARD, F. SONDHEIMER, D. TAUB, K. HEUSLER, and W. H. MCLAMORE. J. Am. Chem. Soc. **74**, 4223 (1952).
7. G. SLOMP and F. MACKELLAR. J. Am. Chem. Soc. **82**, 999 (1960).
8. W. S. JOHNSON, J. J. KORST, R. A. CLEMENT, and J. DUTTA. J. Am. Chem. Soc. **82**, 614 (1960).
9. W. S. JOHNSON, J. ACKERMAN, J. F. EASTHAM, and H. A. DEWALT. J. Am. Chem. Soc. **78**, 6302 (1956).
10. W. NAGATA, T. TERASAWA, S. HIRAI, and K. TAKEDA. Tetrahedron Letters, No. 17, 27 (1960).
11. W. NAGATA, T. TERASAWA, S. HIRAI, and K. TAKEDA. Tetrahedron, **13**, 295 (1961).
12. W. S. JOHNSON and W. P. SCHNEIDER. Org. Syntheses, **30**, 18 (1950).

LE SPECTRE INFRAROUGE DE L'ANHYDRIDE PERCHLORIQUE Cl_2O_7

RODRIGUE SAVOIE[1] ET PAUL A. GIGUÈRE
Département de Chimie, Université Laval, Québec, Qué.

Reçu le 15 février 1962

RÉSUMÉ

Le spectre infrarouge de l'anhydride perchlorique gazeux mesuré entre 220 et 1500 cm^{-1} a révélé une dizaine de bandes. Dans le cristal on a observé jusqu'à 17 bandes distinctes. Ces spectres concordent bien avec le spectre Raman et la structure proposée par Fonteyne, soit deux groupes ClO_3 reliés par un pont d'oxygène. Des diverses configurations possibles selon cette structure celle qui contient la chaîne

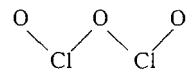

dans un plan de symétrie semble la plus probable.

L'anhydride perchlorique a été isolé pour la première fois par Michael et Conn (1) par déshydratation de l'acide perchlorique. Quoique plus stable que les autres oxydes de chlore, et d'un pouvoir oxydant moindre, il peut cependant exploser violemment sous l'effet d'un choc ou d'un brusque changement de température. De plus, sa préparation entraîne parfois la formation d'autres oxydes de chlore, dont Cl_2O, ClO_2 ou Cl_2O_6, qui peuvent provoquer une explosion.

On sait peu de chose sur la structure moléculaire de ce composé. Fonteyne (2) a d'abord mesuré le spectre Raman d'une solution à 40% dans CCl_4. D'après la ressemblance avec le spectre de l'acide perchlorique, il en a déduit que la molécule doit contenir deux groupes ClO_3 reliés par un pont d'oxygène. Il a ensuite déterminé le moment dipolaire, 0.72 ± 0.02 debye, et il a évalué à 128° l'angle entre les valences Cl—O—Cl du pont central (3).

Au cours d'un travail récent sur le spectre infrarouge de l'acide perchlorique absolu (4) nous avons observé à quelques reprises des bandes d'absorption qui ne pouvaient appartenir à cet acide, mais qui, par contre, concordaient bien avec le spectre Raman de l'anhydride. Aussi, il nous a semblé à propos d'étudier systématiquement le spectre moléculaire de ce composé.

MÉTHODE EXPÉRIMENTALE

On trouve dans la littérature (5) plusieurs méthodes de préparation de l'anhydride perchlorique. Les échantillons employés ici ont été obtenus comme suit: quelque quatre ou cinq gouttes d'acide perchlorique anhydre (4) préalablement refroidi à −70° C étaient ajoutées à du pentoxyde de phosphore dans un petit ballon également refroidi dans de la glace sèche. En laissant réchauffer le mélange lentement jusqu'à la température ambiante l'anhydride gazeux se dégageait, et il était entraîné par un courant d'azote sec à travers trois colonnes de purification. La première et la dernière étaient remplies de pentoxyde de phosphore sur de la laine de verre afin de compléter la déshydratation de l'acide perchlorique, tandis que celle du centre contenait des tournures de cuivre fraîchement réduit en vue d'éliminer le chlore et ses autres oxydes. Le courant d'anhydride était ensuite introduit directement dans la cellule à absorption.

L'appareil, tout en verre, était assemblé au moyen de rodages normalisés. La lubrification de ces derniers, ainsi que des robinets, a posé un problème épineux. Les graisses du type "Fluorocarbon" (Halocarbon Products) conviennent bien à pression ordinaire, mais elles sont trop volatiles pour le travail sous vide. Dans ce cas, nous avons utilisé une quantité minimum de lubrifiant à base de silicone (Dow Corning) qui était légèrement attaqué au cours des expériences. Avant chaque préparation l'appareil était nettoyé avec un oxydant énergique (acide sulfurique fumant) puis assemblé et séché sous vide. Il fallait remplacer chaque fois le pentoxyde de phosphore sans quoi un peu de chlore était entraîné avec l'anhydride, ce qui avait un effet marqué sur le spectre du solide, en particulier.

[1]*Boursier du Conseil national des Recherches.*

Pour prendre le spectre du gaz, la cellule à absorption consistait en un tube de verre de 12 cm de long et 5 cm de diamètre fermé par des fenêtres de chlorure d'argent ou de Teflon selon la région à couvrir. En cas d'explosion la cellule était montée dans une cage de Plexiglass. Quant au solide, il a été étudié au moyen d'une cellule à vide conventionnelle munie de fenêtres de bromure de césium. Le gaz était condensé sous pression réduite à la température de l'air liquide, soit sur un disque de chlorure d'argent, soit—pour la région des basses fréquences au-delà de 400 cm^{-1}—sur une plaque de polythène. Les spectres ont été enregistrés sur spectrophotomètres de Perkin–Elmer: l'un (modèle 112-C) muni de prismes de chlorure de sodium ou de bromure de césium, l'autre, à réseaux (modèle 201-C) pour les basses fréquences (de 320 à 220 cm^{-1}).

DISCUSSION DES RÉSULTATS

De façon générale, les bandes infrarouges de Cl_2O_7 gazeux sont d'apparence un peu diffuse (Fig. 1) tant à cause de chevauchements multiples qu'à cause de la faible séparation

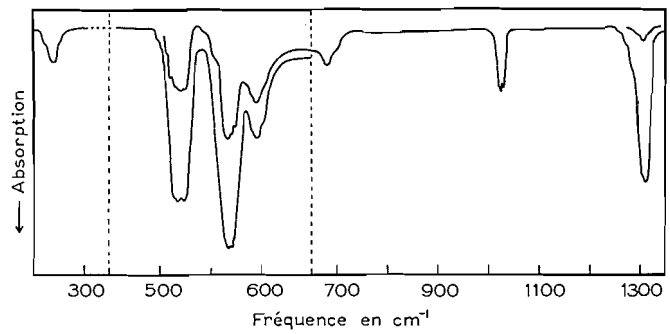

FIG. 1. Spectre d'absorption infrarouge de Cl_2O_7 gazeux.

(environ 8 cm^{-1}) des branches P, Q et R. En outre, il y a dans certains cas possibilité de décalages isotopiques appréciables, puisque les espèces $Cl^{35}OCl^{35}$, $Cl^{35}OCl^{37}$ et $Cl^{37}OCl^{37}$ sont présentes dans des concentrations relatives de 5:2:1. Dans le cristal (Fig. 2) les

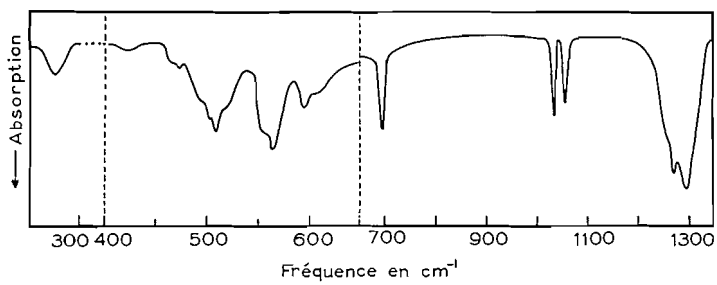

FIG. 2. Spectre infrarouge de Cl_2O_7 à l'état cristallin.

forces intermoléculaires conduisent à une séparation parfois assez marquée des modes semblables. Ces spectres confirment bien la structure proposée par Fonteyne; en particulier la présence des bandes caractéristiques du groupe ClO_3, comme dans l'acide perchlorique (4), ne laisse aucun doute à ce sujet.

Cependant, cette structure comporte plus d'une configuration spatiale selon l'orientation mutuelle des deux groupes ClO_3, laquelle peut être symétrique ou non. Dans le premier cas (formes *cis*, I*a* et I*b*, Fig. 3) la molécule aura deux plans de symétrie (C_{2v}), et 4 de ses 21 vibrations fondamentales (classe A_2) seront inactives en infrarouge. Dans

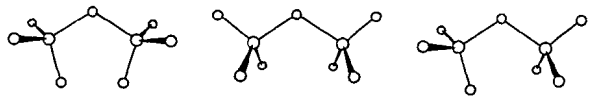

Ia Ib II

FIG. 3. Configurations possibles pour la molécule $ClO_3—O—ClO_3$.

le cas contraire (forme *trans*, II, Fig. 3) on n'aura qu'un plan de symétrie (C_s) et toutes les fondamentales seront actives. Les données actuelles ne permettant pas de trancher la question, nous avons choisi d'interpréter nos résultats d'après le modèle I*b* (Fig. 3) qui, comme nous le verrons plus loin, est le plus probable. La classification des divers modes de vibration de ce modèle est reproduite dans le Tableau I d'après la notation adoptée

TABLEAU I

Classification des fréquences fondamentales de Cl_2O_7

	A_1	A_2	B_1	B_2
ClO_3 valence asym.	ν_1	ν_8	ν_{12}	ν_{18}
ClO_3 valence sym.	ν_2	—	ν_{13}	—
Cl_2O valence asym.	—	—	ν_{14}	—
ClO_3 déform. asym.	ν_3	ν_9	ν_{15}	ν_{19}
ClO_3 déform. sym.	ν_4	—	ν_{16}	—
Cl_2O valence sym.	ν_5	—	—	—
ClO_3 balancement $\perp$	—	ν_{10}	—	ν_{20}
ClO_3 balancement $\parallel$	ν_6	—	ν_{17}	—
Cl_2O déform.	ν_7	—	—	—
ClO_3 torsion	—	ν_{11}	—	ν_{21}

par Herzberg (6) pour décrire une molécule analogue, $CH_3—O—CH_3$. Ici les indications symétriques et asymétriques pour les groupes ClO_3 se rapportent à leur axe ternaire, tandis que les notations $\parallel$ et $\perp$ se réfèrent au plan Cl—O—Cl (xz) de la molécule.

Les fréquences fondamentales

Les fréquences les plus élevées appartiennent naturellement aux vibrations de valence ClO_3. Des cinq modes actifs, les trois asymétriques ν_1, ν_{12} et ν_{18} coïncident aux environs de 1310 cm^{-1} dans le spectre du gaz (Tableau II), mais dans le cristal on peut les distinguer à 1260, 1272 et 1294 cm^{-1}. De même, les deux vibrations symétriques ν_2 et ν_{13} qui se superposent à 1025 cm^{-1} dans le gaz, sont largement séparées dans le solide (1034 et 1057 cm^{-1}). On s'attendrait à une distribution assez semblable pour les modes de déformation des groupes ClO_3. En pratique on observe trois régions de forte absorption vers 600, 570 et 520 cm^{-1} respectivement. La première, que nous attribuons à la vibration asymétrique ν_{19}, se résout en deux bandes distinctes (595 et 612 cm^{-1}) dans le solide. Il s'agit ici, croyons-nous, d'un dédoublement dû au champ de force du cristal plutôt que de deux modes distincts appartenant à une molécule de symétrie C_s.

Les deux autres fréquences de déformation asymétrique, ν_3 et ν_{15}, qui se situent probablement à 554 et 565 cm^{-1} dans le solide, se recouvrent en partie vers 560–570 cm^{-1} dans le gaz. Enfin, il reste pour les deux modes symétriques de ce groupe, ν_4 et ν_{16}, la bande à 510 cm^{-1} qui s'accompagne dans le cristal de deux pics satellites à 501 et 523 cm^{-1}. Comme le premier a son équivalent dans le spectre Raman, nous l'attribuons au mode totalement symétrique ν_4. Le second peut provenir, soit du dédoublement de ν_{16}, soit de quelque impureté; en effet son intensité semblait varier quelque peu d'un échantillon à l'autre.

TABLEAU II

Spectres moléculaires de Cl_2O_7
(Fréquences en cm^{-1})

Infrarouge			
Gaz	Solide	Raman	Modes
1317 1309 1300	1294	1295 (0.5)*	ν_{18} (b_2)
1280 1271 1260	1272 1260	1270 (0.5)	ν_1 (a_1) ν_{12} (b_1)
1030 1025 1021	1057 1034	1348 (4) P	ν_{13} (b_1) ν_2 (a_1)
696 680	695	695 (2) P	ν_{14} (b_1)
613 600 592	612 595	595 (0.5)	ν_{19} (b_2)
577 571 568	565		ν_{15} (b_1)
559 (546)?	554		ν_3 (a_1)
	523		?
526 521 516 512 509	510		ν_{16} (b_1)
506 501	501 495	501 (1)	ν_4 (a_1) ν_5 (a_1)
(472)?	472 464		ν_{20} (b_2)
		429 (1) P	ν_6 (a_1)
	(423)?		ν_{17} (b_1)
(281) 271 (261)	278	280 (2) P	ν_7 (a_1)

NOTE: P = polarisée.
*Intensités relatives entre parenthèses.

La molécule possède encore quatre modes de balancement (rocking) des groupes ClO_3, et deux de torsion interne (twisting), ν_{11} et ν_{21}. Ces derniers sont certainement de très basse fréquence, donc au-delà de la région couverte ici. Quant aux premiers, les deux de type $\perp$ devraient normalement être de fréquence un peu plus élevée que dans $HClO_4$, soit aux environs de 440 cm^{-1}, vu la double force de rappel sur l'oxygène médian. En fait un examen soigné de cette région n'a révélé qu'une très faible absorption vers 472 cm^{-1} dans la vapeur, tandis que dans le cristal, un doublet distinct apparaît à 464 et 472 cm^{-1} que nous assignons provisoirement à la vibration ν_{20}. Les deux autres modes, dits $\parallel$, ν_6 et ν_{17}, sont encore plus imprécis. La bande polarisée à 429 cm^{-1} dans le spectre Raman conviendrait bien pour le premier, et la faible bande infrarouge à 423 cm^{-1} pour le second.

Enfin il reste à identifier les trois vibrations caractéristiques du pont Cl—O—Cl. Fonteyne avait attribué au mode asymétrique ν_{14} l'une des deux fréquences 501 et 595 cm^{-1} plutôt que celle à 695 cm^{-1}, parce que cette dernière est polarisée en Raman. Cependant la comparaison avec le spectre infrarouge de l'acide perchlorique nous conduit à rejeter cette interprétation. La vibration de valence symétrique ν_5 est plus difficile à

localiser car elle tombe vraisemblablement dans une région de forte absorption due aux groupes ClO_3 vers 500 cm^{-1}. Pour le mode de déformation Cl—O—Cl la fréquence 280 cm^{-1} en Raman s'accorde parfaitement avec les fréquences infrarouges 270 cm^{-1} dans le gaz et 278 cm^{-1} dans le solide.

Structure moléculaire de Cl_2O_7

Vu la proximité de plusieurs fréquences fondamentales de Cl_2O_7 et de $HClO_4$ on peut conclure que les paramètres correspondants sont presque les mêmes dans les deux molécules (4), soit des longueurs de 1.70 Å et 1.45 Å respectivement pour les liaisons Cl—O simples et doubles, et des angles ∠OClO d'environ 105° entre liaisons doubles et 115° entre une liaison simple et une double. Quant à l'angle ∠ClOCl du pont d'oxygène, Fonteyne l'avait évalué à 128°, mais en se basant sur des fréquences de vibration incorrectes (501 et 429 cm^{-1}). Cette valeur est certainement trop grande; en fait on doit s'attendre ici à un angle de l'ordre de 111° comme dans la molécule triatomique Cl_2O (7).

Reste à choisir entre les trois configurations possibles (Fig. 3). La première, I*a*, est sans doute à rejeter car elle rapproche deux des oxygènes sur les groupes ClO_3 adjacents à une distance beaucoup moindre (quelque 2 Å) que le double du rayon de van der Waals de cet atome, 1.4 Å d'après Pauling (8). Des deux autres, la configuration symétrique I*b* nous paraît la plus probable parce que l'orientation de chaque groupe ClO_3 y est décalée par rapport à l'axe ternaire O—Cl de l'autre groupe. Cette orientation alternée, qui est la plus fréquente, assure un meilleur équilibre des forces de répulsion entre les groupes ClO_3 ainsi qu'entre les doublets libres sur l'oxygène médian (hybridation sp^3 ?). Notons en outre, bien que des corrélations de ce genre ne soient pas tellement probantes, que dans les molécules analogues CH_3—O—CH_3 (9) et CH_3—S—CH_3 (10) c'est la forme I*b* qui est la plus stable. De toute façon il serait bon d'étudier la molécule Cl_2O_7 par quelque méthode directe pour trancher cette question.

REMERCIEMENTS

Ce travail a été rendu possible grâce à une subvention du Conseil national des Recherches.

SUMMARY

The infrared spectra of chlorine heptoxide Cl_2O_7 have been measured between 220 and 1500 cm^{-1}. In the gas 10 absorption bands, rather diffuse, were observed, and in the solid, some 17 bands. The frequencies, together with those of the Raman spectra, confirm the structure proposed by Fonteyne of two ClO_3 groupes linked by an oxygen bridge. From the spectroscopic data it cannot be decided which of the various configurations possible for such a structure is the correct one, although an arrangement with the chain

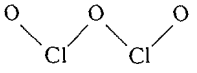

in one plane of symmetry seems the most likely.

BIBLIOGRAPHIE

1. A. Michael et W. T. Conn. Am. Chem. J. **23**, 444 (1900); **25**, 89 (1901).
2. R. Fonteyne. Natuurw. Tijdschr. (Ghent), **20**, 112 (1938).
3. R. Fonteyne. Natuurw. Tijdschr. (Ghent), **20**, 275 (1938).
4. P. A. Giguère et R. Savoie. Can. J. Chem. **40**, 495 (1962).
5. P. Pascal. Nouveau traité de chimie minérale. Masson et Cie, Paris. 1960. Tome XVI, p. 298.

6. G. HERZBERG. Infrared and Raman spectra of polyatomic molecules. D. Van Nostrand Co., Inc., New York. 1945. p. 353.
7. J. D. DUNITZ et K. HEDBERG. J. Am. Chem. Soc. **72**, 3108 (1950).
8. L. PAULING. The nature of the chemical bond. 3rd ed. Cornell University Press, Ithaca, N.Y. 1960. p. 260.
9. K. KIMURA et M. KUBO. J. Chem. Phys. **30**, 151 (1959).
10. L. PIERCE et M. HAVASKI. J. Chem. Phys. **35**, 479 (1961).

THE FORMATION AND THE THERMODYNAMIC PROPERTIES OF K_2TiCl_6 IN KCl–LiCl MELTS[1]

J. H. MUI[2] AND S. N. FLENGAS[3]

Department of Metallurgical Engineering, University of Toronto, Toronto, Ontario

Received October 5, 1961

ABSTRACT

The reaction between gaseous titanium tetrachloride and the eutectic melt of potassium and lithium chlorides was investigated at various temperatures and pressures. It was found that, at an optimum temperature of 370° C, titanium tetrachloride vapor at a pressure of 1 atm reacts with the potassium chloride in the eutectic to yield K_2TiCl_6 as a solid mixture with lithium chloride.

The solubilities of K_2TiCl_6, and the partial molar properties of the solutions of K_2TiCl_6, and of potassium chloride, in the eutectic melt of potassium and lithium chlorides were obtained by vapor pressure measurements. It was found that the solubility of titanium tetrachloride increases from 1.5 weight% at 420° C to 5 weight% at 500° C. The activities of K_2TiCl_6, and of potassium chloride, indicate positive deviations from ideality.

INTRODUCTION

Many existing methods for the production of titanium metal involve the electrolytic reduction of titanium tetrachloride in solution in various molten salt mixtures of alkali chlorides or alkaline earth chlorides. However, in spite of the recent promising developments in this field (1, 2), the solubilities and the other thermodynamic properties of the solutions of titanium tetrachloride in molten salts are virtually unknown.

In a previous investigation (3), it was found that the solubility of titanium tetrachloride in the equimolar mixture of potassium and sodium chlorides at 690° C is 14% by weight. This solubility was attributed to the formation of the compound K_2TiCl_6. The thermal stability (4) and crystal structure (5) of K_2TiCl_6 prepared in the pure state were also determined.

The present work was undertaken to provide further information concerning the thermodynamic properties of K_2TiCl_6 in solution in the eutectic melt of potassium and lithium chlorides over the temperature range 350° C to 550° C.

Specifically, the problems investigated were (*a*) the extent of the chemical reaction between titanium tetrachloride vapor and the eutectic melt of potassium and lithium chlorides, and (*b*) the solubilities of K_2TiCl_6 in the melt. These two problems are closely associated with the recovery of titanium metal by fused salt electrolysis in a "low-temperature" cell that would employ titanium tetrachloride as the feed material, and would operate at temperatures of 500° C or less.

I. THE FORMATION OF K_2TiCl_6 IN THE KCl–LiCl EUTECTIC MELT

EXPERIMENTAL

The titanium tetrachloride for use in the experiments was obtained by purification of the commercially pure material. This was achieved by refluxing in the presence of copper filings for about 2 hours and by fractional distillation in a dry atmosphere. The front and end tailings of the distillate were rejected, and the middle portion was stored in sealed containers.

[1]*Paper presented at the 18th International Congress of Pure and Applied Chemistry, August 6–12, 1961, Montreal, Que.*

[2]*Present address: Department of Mining and Metallurgy, University of British Columbia, Vancouver, British Columbia.*

[3]*Department of Metallurgical Engineering, University of Toronto, Toronto 5, Ontario.*

The eutectic mixture of potassium and lithium chlorides was prepared from the reagent grade materials (41 mole% KCl, and 59 mole% LiCl). The melt was purified by using anhydrous hydrogen chloride following the method of Boston and Smith (6). The purified melt was transferred in Pyrex ampoules and was sealed under an argon atmosphere.

The reaction between titanium tetrachloride vapor and the eutectic melt of potassium and lithium chlorides was investigated by using the quartz spring balance apparatus described in a previous investigation (3). The method involved the direct measurement of the increase of the weight of a given quantity of the melt exposed to an atmosphere of titanium tetrachloride vapor at a given pressure.

Results and Discussion

The changes of length of the quartz spring, i.e., the corresponding change in weight of the sample, were measured as a function of time at various furnace temperatures and different pressures of titanium tetrachloride vapor.

From these measurements the percentage reaction of the initial potassium chloride in the eutectic, as a function of time, was calculated using the equation

$$2KCl + TiCl_4 = K_2TiCl_6.$$

The reaction between solid lithium chloride and titanium tetrachloride vapor was also investigated and, under similar experimental conditions, there was no evidence of any chemical reaction.

The results of these measurements at various temperatures and pressures are shown in Fig. 1.

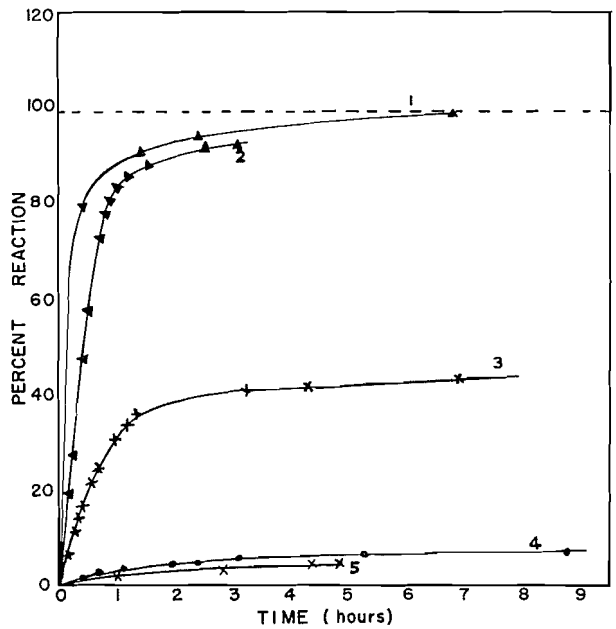

FIG. 1. Reaction between $TiCl_4$ vapor and the eutectic melt of KCl–LiCl at various temperatures and pressures:

Run No.	Temp. (°C)	P_{TiCl_4} (atm)
1	355	0.9
2	373	0.5
3	388	1.0
4	400	0.9
5	448	0.5

It is seen that at temperatures between 355° C and 375° C, the reaction is relatively slow and reaches completion within 7 hours. At higher temperatures, that is, between 390° C and 450° C, the apparent reaction rate decreases further, and the reaction does not reach equilibrium within the time of observation. By comparing curves 1 and 2 with curves 4 and 5 in Fig. 1, it becomes apparent that the reaction is not pressure dependent to any significant extent. On the contrary, the main controlling factor is temperature.

In an attempt to explain the anomalous behavior of the system, the course of the reaction was also investigated by a method involving the visual observation of the reaction site during the formation of K_2TiCl_6. The very simple apparatus consisted of a Pyrex tube of 1-in. diameter, bent at right angles and closed at one end. Purified titanium tetrachloride was introduced into the vertical closed-end arm, and was frozen with liquid air. A silica boat containing about 10 g of solid eutectic mixture was placed in the horizontal arm and the apparatus was evacuated and sealed under vacuum; the titanium tetrachloride was then heated to 136° C using a silicone oil bath, and the eutectic mixture was heated to 400° C using a tubular furnace fitted with an observation window.

The qualitative observations from the experiment may be described as follows: initially, titanium tetrachloride vapor dissolved into the transparent and colorless melt, and the solution acquired a deep yellow color. Subsequently, a solid layer gradually formed on the surface of the melt, this layer then thickened and eventually covered the entire surface. No liquid was found to remain after about 20 hours, and the reaction product was a yellow solid mass of uniform appearance. The solid was analyzed by X rays and the diffraction pattern indicated that K_2TiCl_6 and unreacted lithium chloride were the major components.

It is evident that the reaction takes place at the surface of a saturated solution of K_2TiCl_6 in the eutectic melt of potassium and lithium chlorides. The insoluble reaction products adhere to the surface of the melt by surface tension or density effects, and lithium chloride is codeposited as the eutectic mixture becomes depleted of its potassium chloride. Although the data available at present are quite insufficient to explain the kinetic mechanism of this reaction, it appears that the decrease of the overall reaction rate must be associated with the formation of the solid surface layer of K_2TiCl_6 + LiCl, which essentially separates the reactants. The study of the kinetic mechanism of this reaction is beyond the scope of the present investigation and will be the object of further study. However, these experiments indicate that titanium tetrachloride vapor reacts with the potassium chloride in the eutectic mixture of potassium and lithium chlorides. At about 400° C, the reaction is a driven one and the product K_2TiCl_6 has a limited solubility in the melt.

II. SOLUBILITIES AND PARTIAL MOLAR PROPERTIES OF K_2TiCl_6 IN THE KCl–LiCl EUTECTIC MELT

The solubilities of K_2TiCl_6, and the partial molar properties of the solutions of K_2TiCl_6 and of potassium chloride, in the eutectic melt of potassium and lithium chlorides, were investigated by measuring the pressure of titanium tetrachloride vapor in equilibrium with a melt containing K_2TiCl_6.

Experimental

Pure K_2TiCl_6 (99.9%) was prepared by the method described previously (4), and was analyzed both chemically and by means of its X-ray diffraction pattern.

The apparatus for the vapor pressure measurements, as shown in Fig. 2, consisted of a tubular furnace B fitted with an observation window, the reaction cell A, the pressure gauge D, and the pressure control train.

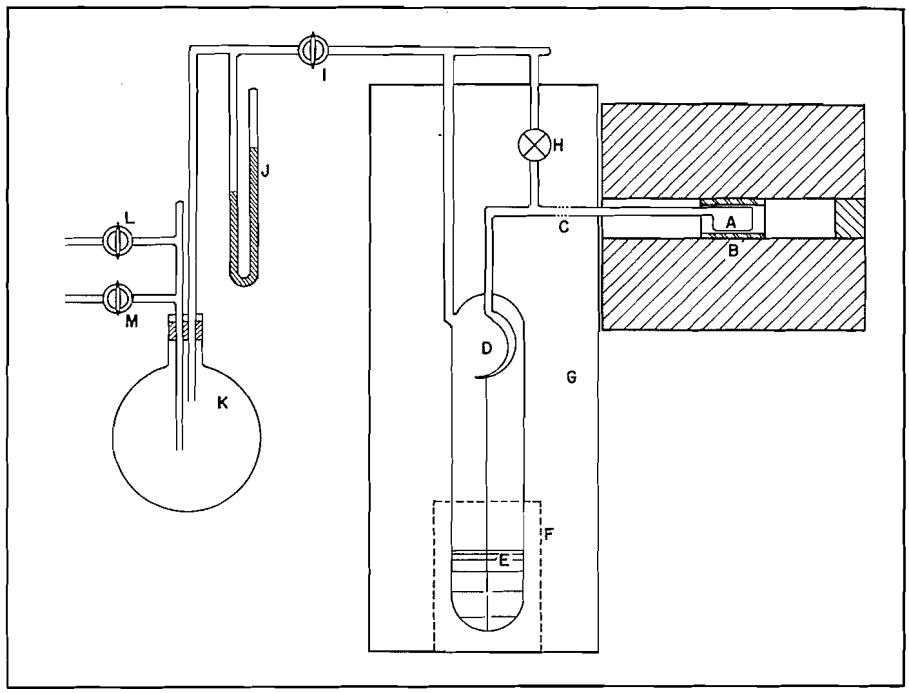

FIG. 2. Apparatus for the vapor pressure measurements.

A = sample cell	H = metal valve
B = furnace	I = stopcock
C = graded seal	J = mercury manometer
D = spoon gauge	K = air reservoir
E = damping fluid	L = to vacuum pump
F = observation window	M = to oxygen or air
G = air bath	

The reaction cell was heated in the tubular furnace, the temperature of which was kept constant to within ∓1° C by a thermocouple set in a well just beside the sample, and connected with a Honeywell proportional temperature controller. The quartz cell, $\frac{3}{4}$-in. diameter and $1\frac{1}{2}$-in. length, was connected to the spoon gauge through a quartz-to-Pyrex graded seal. The pressure gauge was a modified Bourdon "sickle" or "spoon gauge" constructed from thin Pyrex glass and having a sensitivity of about ∓1 mm of mercury. A glass pointer, about 8 in. long, attached to the tip of the spoon was used as a zero-point indicator. The gauge was enclosed in a glass tube closed at one end, and a small amount of silicone oil, Dow Corning Fluid 550, was also added to damp out the vibrations of the pointer and to act as a diffracting medium. The reaction cell and the gauge were connected to the pressure control train by using a Kovar, Pyrex-to-metal joint, and a stainless steel valve. The pressure control train included an air reservoir and the closed-end mercury manometer. The pressure in the system was regulated by manipulating the valves leading to the vacuum pump and to the air reservoir. During measurements, the gauge was used only as a "zero-point" indicator, and the reaction pressure at all times was balanced by changing the pressure in the outside jacket. A three-point technique was used to observe the neutral position, and the reaction pressure was read directly on the closed-end mercury manometer.

To avoid any condensation of titanium tetrachloride, all parts of the main apparatus outside the furnace were enclosed in an air bath at a temperature of about 145° C.

At the beginning of a run, 5 to 10 g of the various mixtures of K_2TiCl_6, and of the solid eutectic, were transferred into the quartz cell in a dry box. The cell was immediately connected to the apparatus, and the entire system evacuated. In order to melt the eutectic, the cell was heated to about 360° C, the system was then closed and allowed to stand for about 6 hours; the valve leading to the vacuum pump was then opened, and the system was evacuated for about 5 minutes at that temperature.

The decomposition pressures were measured at equilibrium as a function of temperature and composition of the melt. At temperatures up to 450° C, equilibrium was reached in about 2 to 3 hours, but the readings were taken after about 8 hours. At temperatures above 450° C, equilibrium was established in about 1 hour, but readings were taken after at least 5 hours. Equilibrium readings were taken for increasing and decreasing temperatures.

Thermodynamic Considerations

The thermal decomposition of (*a*) pure solid K_2TiCl_6, and (*b*) K_2TiCl_6 in solution in the eutectic melt of potassium and lithium chlorides may be represented by the following equilibria:

K_2TiCl_6 solid:

$$K_2TiCl_6\,(s) \rightleftharpoons 2KCl\,(s) + TiCl_4\,(g). \qquad [1]$$

K_2TiCl_6 in solution:

$$K_2TiCl_6\,(s) \rightleftharpoons (K_2TiCl_6)_{eut} \qquad [2]$$

and

$$(K_2TiCl_6)_{eut} \rightleftharpoons 2(KCl)_{eut} + TiCl_4\,(g). \qquad [2a]$$

By choosing as the standard states pure K_2TiCl_6 and pure potassium chloride at the temperature of the experiments, the activity equation may be readily derived as

$$\frac{a^2_{KCl}}{a_{K_2TiCl_6}} = \frac{P^0}{P}. \qquad [3]$$

For a "saturated" solution, the activity of K_2TiCl_6 in the solid phase is equal to the activity of K_2TiCl_6 in solution and this, by convention, may be taken as equal to unity. Therefore

$$a_{K_2TiCl_6} = 1,$$

and the activity of potassium chloride in the eutectic melt may be calculated. Thus, at a given temperature, equation [3] becomes

$$a^2_{KCl} = \frac{P^0}{P_1}, \qquad [4]$$

where P^0 is the pressure of titanium tetrachloride vapor in equilibrium with solid K_2TiCl_6, and P_1 is its pressure in equilibrium with a saturated solution of K_2TiCl_6 in the melt.

For a completely miscible system, the activity of K_2TiCl_6 may be calculated directly from equation [3], in the form

$$a_{K_2TiCl_6} = a^2_{KCl}\cdot(P_2/P^0), \qquad [5]$$

where P_2 is the pressure of titanium tetrachloride in equilibrium with a completely miscible system, P^0 has the same significance as before, and a_{KCl} is the activity of potassium chloride in the saturated solution at the same temperature. In making the above calculation, it is assumed that small amounts of K_2TiCl_6 of the order of 1 mole% would not have any significant effect on the activity of potassium chloride in the eutectic.

Results and Discussion

The decomposition pressures of solid K_2TiCl_6 at equilibrium have been measured previously by Flengas and Ingraham (4), and by Morozov and Toptygin (7). The equilibrium pressures reported in both these investigations were, however, significantly different. It was, therefore, decided to redetermine the equilibrium pressures of the system over the temperature range 350° C to 550° C.

The results, along with those of the previous two investigations, plotted as log P versus $1/T$, are shown in Fig. 3.

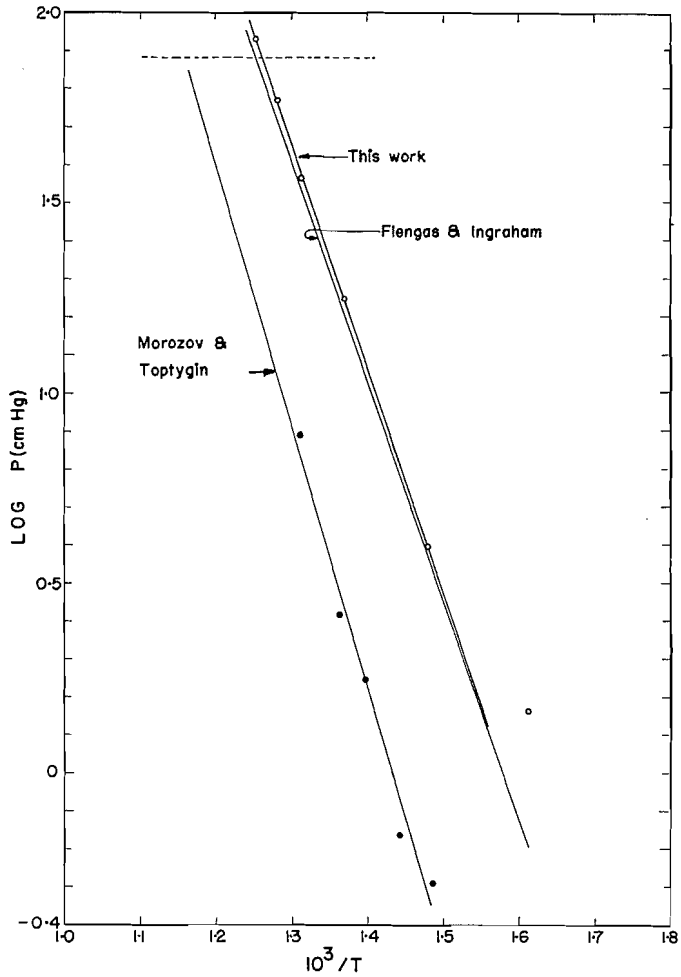

FIG. 3. Equilibrium decomposition pressures of solid K_2TiCl_6.

It is seen that these results are in good agreement with the original data of Flengas and Ingraham (4).

The pressures of titanium tetrachloride vapor in equilibrium with pure solid K_2TiCl_6 are represented by the equation

$$\log P^0_{(\text{cm of Hg})} = \frac{-5930}{T} + 9.3636, \qquad [6]$$

which is valid for the temperature range between 350° C and 550° C.

The heat of formation of K_2TiCl_6 from solid potassium chloride and titanium tetrachloride vapor can be calculated from the slope of the pressure curve by using the van't Hoff equation, and is -27.1 ± 0.4 kcal/mole, which is in good agreement with -26.4 ± 1.3 kcal/mole obtained previously (4).

The pressures of titanium tetrachloride in equilibrium with various mixtures of K_2TiCl_6, and of the eutectic melt, were then measured at temperatures between 350° C and 525° C. The results are given in Fig. 4.

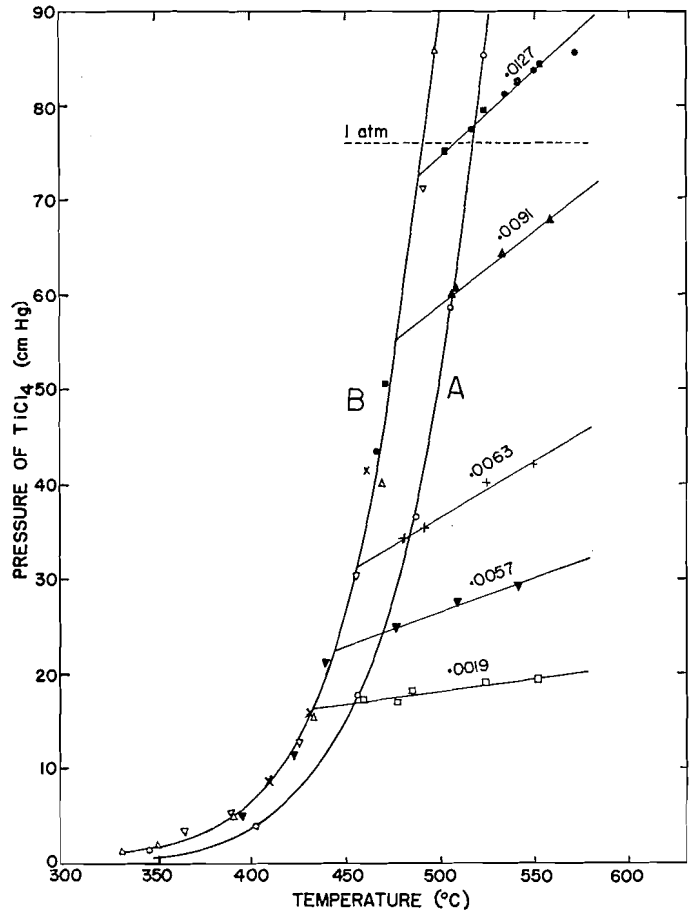

FIG. 4. Equilibrium decomposition pressures of K_2TiCl_6 in KCl–LiCl eutectic melts:

Symbol	Run No.	$N_{K_2TiCl_6}$
○	1	1
△	2	.2100
▽	3	.0796
×	4	.0440
■	5	.0124
●	6	.0130
▲	7	.0091
▼	8	.0057
□	9	.0019
+	10	.0063

For the purpose of comparison, curves A and B represent respectively the results with pure K_2TiCl_6 and with the various mixtures. The decomposition pressures of the saturated solutions of K_2TiCl_6 in the eutectic melt are given by the continuous part of curve B. The horizontal branches of curve B represent the completely miscible systems. The corresponding mole fractions of K_2TiCl_6 are given also in the diagram.

The temperature of complete miscibility, that is, the liquidus temperature of the ternary, is found from the intercept of the horizontal and the vertical parts of curve B,

and the composition of the mixture at this temperature is the liquidus composition. The region to the left of curve B thus represents the two-phase systems of constant activity, and the region to the right of curve B represents the completely miscible one-phase system of changing activity. The pronounced change in slope between any two parts of the same curve reflects the sharp decrease of the activity of K_2TiCl_6 with increase in temperature, when K_2TiCl_6 becomes completely soluble.

From Fig. 4, it is seen that at a given temperature a saturated solution of K_2TiCl_6 has a higher decomposition pressure of titanium tetrachloride than the corresponding pure solid. Solutions, on the other hand, in the range of complete miscibility have lower decomposition pressures than pure solid K_2TiCl_6.

The pressures of titanium tetrachloride in equilibrium with the saturated solutions are well represented by the linear equation

$$\log P_{1(\text{cm of Hg})} = \frac{-6006}{T} + 9.7328, \qquad [7]$$

which is valid for the temperature range between 350° C and 500° C.

The behavior of the system of the eutectic melt in contact with titanium tetrachloride vapor can also be predicted from the pressure curves in Fig. 4. Thus, at a given temperature of the melt, it should be expected that titanium tetrachloride would dissolve until the decomposition pressure of the solution becomes equal to the applied pressure of the vapor. If the applied pressure is maintained constant while the temperature of the melt is reduced below the corresponding liquidus temperature of the ternary, then solid K_2TiCl_6 should be precipitated. The reaction under these conditions should be a driven reaction, and should continue indefinitely, provided that the composition of the eutectic does not change and that the supply of melt is unlimited. When the available amount of eutectic melt is limited, the formation of K_2TiCl_6 should take place and the composition of the melt should change until it reaches the liquidus composition of the binary mixture of potassium and lithium chlorides at the temperature of the experiment. Any further precipitation of K_2TiCl_6 would then be followed by the codeposition of solid lithium chloride and the composition of the melt would thus remain unchanged until the completion of the reaction. These conditions have been simulated in the experiments described in the first part of this paper.

The solubilities of titanium tetrachloride at various temperatures were obtained from the intercepts of the horizontal and the vertical parts of curve B in Fig. 4. The results are given in Fig. 5 as weight percent soluble titanium tetrachloride against temperature.

For the purpose of calculation, the composition of the melt was corrected for the amount of titanium tetrachloride in the gas phase, assuming that the system obeys the ideal gas laws. The correction factor was particularly significant for mixtures containing less than 1% titanium tetrachloride, and the solubilities in this range could not be obtained accurately. It was also found that, at temperatures above 500° C, the decomposition pressures of the more concentrated solutions exceeded 1 atm and could not be measured with the existing apparatus. However, the results obtained within the temperature and the composition ranges allowed by the system were well reproducible, and the average deviations which are shown in Fig. 5 represent the expected error which is introduced when the composition of the melt is corrected for the amount of titanium tetrachloride present in the gas phase of the non-isothermal system.

It is seen in Fig. 5 that the solubility of titanium tetrachloride in the eutectic melt of potassium and lithium chlorides is rather limited and increases with temperature from

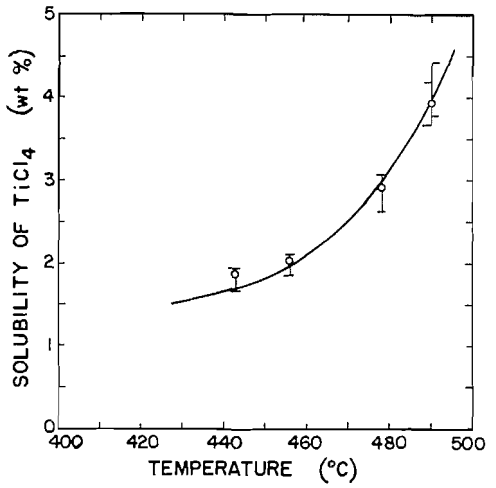

FIG. 5. Solubilities of $TiCl_4$ in KCl–LiCl eutectic melt.

about 1.5% at 420° C to 5% at 500° C. These results are much higher than the solubilities found by Smolinski and Leach (8) by the chemical analysis of a melt that had been previously saturated with titanium tetrachloride.

Activity Calculations

The activities of potassium chloride in the melt of potassium and lithium chlorides at the eutectic composition (0.41 mole% KCl, and 0.59 mole% LiCl) were calculated using equation [4], and the pressure data given by equations [6] and [7]. The results obtained regarding the activities are given in Fig. 6, and the experimental data are summarized in Table I. The excess partial molar properties of the solutions which are calculated from the data are given in Table II.

It is seen that, in the temperature range between 350° C and 500° C, the activity coefficients demonstrate slight positive deviations from ideality. However, the existence of a rather large excess partial molar entropy of mixing also indicates that the system cannot be treated as a regular solution. These results are in disagreement with the activities calculated by Aukrust *et al.* (9) from the phase diagram of the binary system of potassium and lithium chlorides. The latter calculations indicated rather small negative deviations from ideality, and that at the eutectic composition the system approaches regularity.

The derivation of activities from phase diagrams has been criticized by Kubaschewski and Evans (10) on the grounds of the many assumptions involved in the calculation, and the present work supports this view.

The activities, and the other thermodynamic properties of the solutions of K_2TiCl_6 in the eutectic melt of potassium and lithium chlorides, were calculated by using equation [5], and the data given in Table I. In order to calculate the activities of K_2TiCl_6 for temperatures as high as 550° C, for which the pressure data were available, it was necessary to extrapolate the activities of potassium chloride for about 50° C, as shown in Fig. 4. The results of the calculations are given in Fig. 7, and the excess partial molar properties of the solutions are listed in Table III. Despite the scatter of the points in Fig. 7, the activity coefficients are reasonably constant for each temperature. Also, due

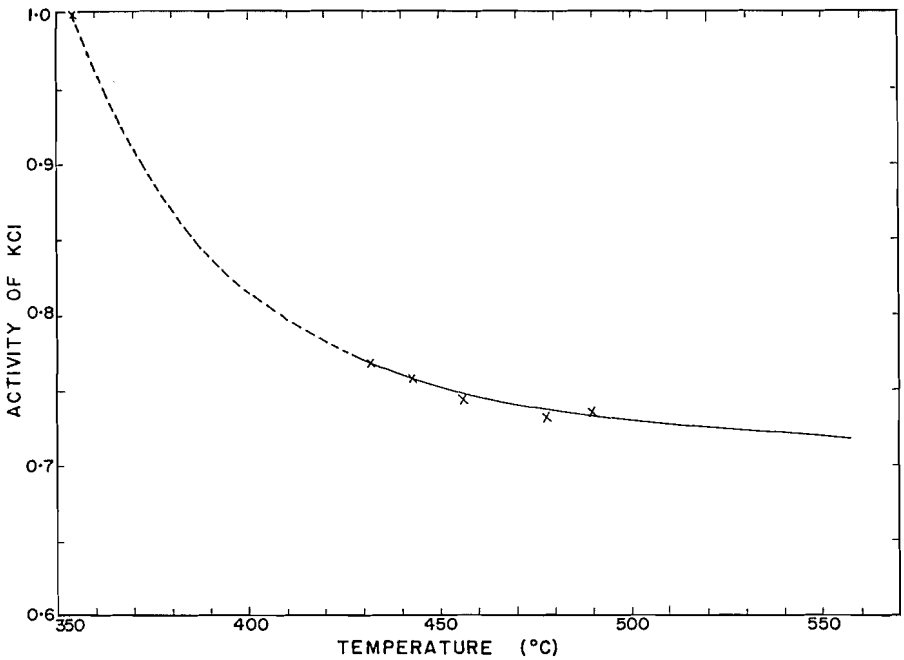

FIG. 6. Activities of KCl in the eutectic melt of KCl–LiCl.

TABLE I

Summary of data

Temp. (°C)	Solubility		Equilibrium pressures of $TiCl_4$ (cm Hg)		Activities	
	Wt% $TiCl_4$	Mole% K_2TiCl_6	$(K_2TiCl_6)_{eut}$	K_2TiCl_6 (s)	a_{KCl}	$a_{K_2TiCl_6}$
354*	—	—	—	—	1.000	—
443	1.86	0.57	22.3	12.8	0.758	1.0
450	1.86	0.57	22.8	15.0	0.750	0.856
500	1.86	0.57	26.4	50.6	0.730	0.278
525	1.86	0.57	28.2	85.6	0.723	0.172
550	1.86	0.57	30.1	144.1	0.718	0.108
456	2.04	0.63	31.2	17.2	0.744	1.0
500	2.04	0.63	36.4	50.6	0.730	0.383
525	2.04	0.63	39.3	85.6	0.723	0.240
550	2.04	0.63	42.1	144.1	0.718	0.151
478	2.91	0.91	55.3	29.4	0.731	1.0
500	2.91	0.91	58.8	50.6	0.730	0.619
525	2.91	0.91	62.7	85.6	0.723	0.383
550	2.91	0.91	66.7	144.1	0.718	0.239
490	3.99	1.27	72.6	40.0	0.736	1.0
500	3.99	1.27	74.4	50.6	0.730	0.784
525	3.99	1.27	78.9	85.6	0.723	0.482
550	3.99	1.27	83.5	144.1	0.718	0.299

*Melting point of the eutectic mixture of KCl, LiCl.

to the limited amount of data available, the excess partial molar properties cannot be regarded as particularly accurate. An estimate of the error in the excess partial molar heat of solution of K_2TiCl_6 is ± 2.0 kcal/mole. The data in Table III indicate pronounced

TABLE II

Excess partial molar properties of potassium chloride in the eutectic melt of KCl–LiCl

t (°C)	γ_{KCl}	$\overline{\Delta F}^{XS}$ (cal/mole)	$\overline{\Delta H}$ (cal/mole)	$\overline{\Delta S}^{XS}$ (e.u.)
354	2.44	+1180	−1000	−3.47
432	1.87	+878	−1000	−2.67
443	1.85	+875	−1000	−2.62
456	1.81	+863	−1000	−2.55
478	1.78	+862	−1000	−2.48
490	1.80	+895	−1000	−2.48

TABLE III

Excess partial properties of K_2TiCl_6 in the eutectic melt of KCl–LiCl

t (°C)	$\gamma_{K_2TiCl_6}$	$\overline{\Delta F}^{XS}$ (cal/mole)	$\overline{\Delta H}$ (cal/mole)	$\overline{\Delta S}^{XS}$ (e.u.)
500	63.3	6,370	24,200	23.1
525	40.0	5,840	24,200	23.1
550	24.2	5,220	24,200	23.1

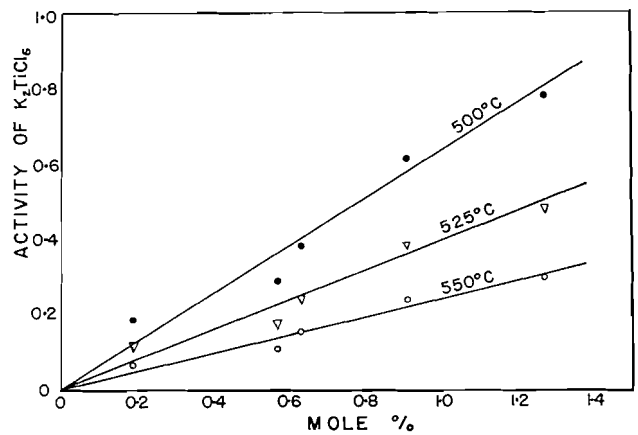

FIG. 7. Activities of K_2TiCl_6 in the eutectic melt of KCl–LiCl.

positive deviations from ideality, as expected from the tendency of the system to form saturated solutions. The large excess partial molar entropy of mixing, which is usually associated with the vibrational energy of the system, indicates a change in the bond type of the titanium ion in the melt. The change could be interpreted either in terms of a decrease of the coordination number of titanium or in terms of a weakening of the chemical bond. The decrease of the activity coefficients with increasing temperature indicates the tendency of the system to approach ideality at higher temperatures. At constant temperature, the activity is proportional to the mole fraction, which indicates that Henry's law is applicable to the system.

CONCLUSIONS

The results obtained in this investigation may be discussed with reference to electrolytic cells used for the recovery of titanium metal by fused salt electrolysis. The operation of experimental titanium cells in the region of 500° C has already been reported in the

literature (2). The common features of these cells were, the low operating temperatures of about 500° C, the use of potassium and lithium chlorides as the solvent melt, and the use of titanium tetrachloride vapor as the feed material.

The prerequisite of any high-temperature electrolytic reduction should be the existence of a suitable ionic solution. The properties of titanium tetrachloride, as determined in the present investigation, however, exclude the possibility of a true electrolytic process, at least on a large scale.

At low temperatures, that is, at or below 400° C, it should be possible to prepare relatively stable solutions of titanium tetrachloride, but the solubilities are extremely low. Under these conditions, any electrolytic cell would reach its limiting current densities at very low currents. Any attempt to increase the electrolytic current would lead to the buildup of a concentration overvoltage, and eventually to the reduction of the alkali metals in the solvent.

At temperatures higher than 500° C, it should be possible to prepare concentrated solutions of titanium tetrachloride. However, at such temperatures, the decomposition pressures are quite high, and "stable" solutions can only be realized in a completely closed or even a pressurized system by controlling the pressure of titanium tetrachloride vapour over the solutions.

It is felt that the various titanium cells which have been operated so far have not satisfied the conditions imposed by the system. In all probability, the primary step was the reduction of the alkali metal ions, the titanium metal being recovered as a by-product of the overall cell reaction.

ACKNOWLEDGMENTS

This work was carried out with financial assistance from the National Research Council of Canada. The authors wish also to thank N.R.C. for a maintenance grant to one of us (J. H. M.). The assistance in the analysis of the samples provided by the analytical section, Mineral Sciences Division, Mines Branch, Department of Mines and Technical Surveys, Ottawa, is also gratefully acknowledged.

REFERENCES

1. W. R. Opie and K. A. Svanstrom. Trans. AIME. **215**, 253 (1959).
2. U.S. Patent No. 2,780,593 (1957). New Jersey Zinc Co., New York.
3. S. N. Flengas. Ann. N.Y. Acad. Sci. **79**, 853 (1960).
4. S. N. Flengas and T. R. Ingraham. Can. J. Chem. **38**, 813 (1960).
5. J. A. Bland and S. N. Flengas. Can. J. Phys. **39**, 941 (1961).
6. C. R. Boston and G. P. Smith. J. Phys. Chem. **62**, 409 (1958).
7. I. S. Morozov and D.Ya. Toptygin. Russ. Y. Inorg. Chem. **5**, 42 (1960).
8. J. Smolinski and L. A. Leach. Technical Note No. Met. 247, Ministry of Supply, London. 1957.
9. A. Aukrust, B. Bjorge, H. Flood, and T. Forland. Ann. N. Y. Acad. Sci. **79**, 830 (1960).
10. O. Kubaschewski and E. LL. Evans. Metallurgical thermochemistry. Pergamon Press. 1958. p. 47.

THE SULPHURIC ACID SOLVENT SYSTEM

PART III. THE PREPARATION AND STRUCTURES OF SOME COMPLEX SULPHATOBORATES

R. J. GILLESPIE
Department of Chemistry, McMaster University, Hamilton, Ontario

AND

E. A. ROBINSON
Department of Chemistry, University of Toronto, Toronto, Ontario

Received February 8, 1962

ABSTRACT

By neutralizing sulphuric acid solutions of tetra(hydrogensulphato)boric acid with various metal hydrogensulphates, sodium, potassium, ammonium, and strontium salts have been prepared. From the compositions of these salts, and from the results of cryoscopic and conductimetric measurements on their solutions in sulphuric acid, it is concluded that they are best formulated as polysulphatoborates containing the six-membered ring

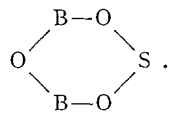

It is shown that previously described sulphato compounds of boron can also be satisfactorily formulated on this basis.

Cryoscopic and conductimetric measurements on dilute solutions of boric acid and boric oxide in 100% sulphuric acid and in dilute oleums have been interpreted in terms of the formation of tetra(hydrogensulphato)boric acid, $HB(HSO_4)_4$, and its hydronium salt (1). Conductimetric titrations (2) and a comparison of the electrical conductivities of sulphuric acid solutions of $HB(HSO_4)_4$ with those of disulphuric acid (3) show that $HB(HSO_4)_4$ is a rather strong acid of the sulphuric acid solvent system which is extensively ionized in dilute solution according to the equation

$$HB(HSO_4)_4 + H_2SO_4 = H_3SO_4^+ + B(HSO_4)_4^-.$$

Further confirmation of this ionization has been obtained from the observation of lines in the Raman spectra of solutions of $HB(HSO_4)_4$ in sulphuric acid that may be assigned to the $H_3SO_4^+$ ion (4). The Raman spectra also showed that in concentrated solutions of $HB(HSO_4)_4$ disulphuric acid is formed.

The earlier work (1) showed that the hydronium salt of tetra(hydrogensulphato)boric acid is formed when boric acid is dissolved in 100% sulphuric acid:

$$B(OH)_3 + 6H_2SO_4 = 3H_3O^+ + B(HSO_4)_4^- + 2HSO_4^-,$$

and solutions of other salts were obtained by titrating the acid with various hydrogen sulphates (2), e.g.,

$$HB(HSO_4)_4 + KHSO_4 = KB(HSO_4)_4 + H_2SO_4.$$

It was the object of the present work to attempt to isolate solid tetra(hydrogensulphato)-borates from such solutions.

EXPERIMENTAL

Preparations

Solutions of tetra(hydrogensulphato)boric acid were prepared by dissolving the calculated quantity of recrystallized "Analar" boric acid in an oleum which had been prepared by distilling a weighed quantity of sulphur trioxide into 100% acid:

$$B(OH)_3 + 3H_2S_2O_7 = HB(HSO_4)_4 + 2H_2SO_4.$$

These solutions were neutralized by adding a sulphuric acid solution containing the equivalent quantity of a metal sulphate (K_2SO_4, Na_2SO_4, $(NH_4)_2SO_4$, $BaSO_4$, $SrSO_4$), or an organic base (2:4-dinitroaniline). White solids separated after a few hours from the solutions neutralized with K_2SO_4 and $(NH_4)_2SO_4$ but in the case of those neutralized with Na_2SO_4 and $SrSO_4$ precipitation did not occur until after several days and even then in some cases only when the solution was heated to 100° to 200°. It was not found possible to precipitate salts of barium, lead, or 2:4-dinitroaniline.

The salts were filtered in a dry box through a sintered-glass filter and washed with dry nitromethane to remove the last traces of sulphuric acid. Nitromethane was then removed by drawing dry air through the filter. The compounds were stored over sulphuric acid in a vacuum desiccator. The salts were white and slightly hydroscopic: they evolved sulphur trioxide on heating.

Analysis

The salts were hydrolyzed completely to metal sulphate, sulphuric acid, and boric acid on dissolving in water. Sulphuric acid was determined by titration with standard sodium hydroxide solution. Boric acid was determined by neutralizing the sulphuric acid with the required amount of sodium hydroxide and then continuing the titration after the addition of a large excess of mannitol (5). The results of the volumetric determinations are expressed in terms of the ratio, $r = n_{H_2SO_4}/n_{H_3BO_3}$, of the number of moles of sulphuric acid to the number of moles of boric acid produced on hydrolysis, e.g., $2KB(HSO_4)_4 + 6H_2O = K_2SO_4 + 2H_3BO_3 + 7H_2SO_4$, $r = 3.5$. Ammonium and strontium were determined by standard methods. The analytical results are given in Table I.

Cryoscopic and Conductimetric Measurements

The salts obtained were generally not very soluble in sulphuric acid but in some cases appreciable freezing-point depressions and electrical conductivities were obtained. The freezing-point depressions and conductivities were measured by methods that have been described previously (6, 7). A cryoscopic equivalent weight, defined as the weight of substance which, when dissolved in 1000 g of sulphuric acid, gives the molal freezing-point depression for a non-electrolyte of 6.12°, was calculated from the cryoscopic results (8). A conductimetric equivalent weight, defined as the weight of substance which, when dissolved in 1000 g of sulphuric acid, produces 1 mole of hydrogensulphate ion, was obtained by comparing the observed conductivities with the conductivities of potassium and hydronium hydrogensulphates (9). For example,

$$M_2B_2O(SO_4)(HSO_4)_4 + 4H_2SO_4 = 2M^+ + H_3O^+ + 2B(HSO_4)_4^- + HSO_4^-,$$

cryoscopic equivalent weight = (molecular weight)/6, conductimetric equivalent weight = molecular weight.

DISCUSSION

Comparison of the analytical results with the calculated values given in Table II for the tetra(hydrogensulphato)borates, $MB(HSO_4)_4$, and the corresponding sulphates, $MB(SO_4)_2$, shows that in no case did the salts obtained have either of these simple compositions. The observed cryoscopic equivalent weights are smaller than the values required for compounds with these compositions and the conductimetric equivalent weights are much smaller than the infinite values predicted for $MB(HSO_4)_4$ or $MB(SO_4)_2$. The analytical results are also not consistent with those expected for any polymeric compound of intermediate composition formed by the elimination of H_2SO_4 molecules between $B(HSO_4)_4^-$ ions.

Recently several authors (10) have discussed the principles underlying the structures of the hydrated polyborates. It appears that the basic structure is the six-membered ring I in which one, or at most two, of the boron atoms has a tetrahedral four-coordinated configuration, while the remainder have a trigonal three-coordinated configuration. Thus the ions II and III and condensed forms in which one or two boron atoms are shared between two rings, e.g. IV, V, VI, and VII, have been postulated to account for the

TABLE I

Comparison of analytical results and calculated compositions for some sulphatoborates

		Analytical results					Calculated compositions				Cryoscopic equiv. wt.		Conductimetric equiv. wt.	
Salt	Cation	r	% B	% SO_4*	% cation	n†	r	% B	% SO_4*	% cation	Exptl.	Theor.	Exptl.	Theor.
1	K	1.64	4.14	59.0	—	6	1.66	4.05	59.9	—	98	89	—	—
2	K	1.88	3.57	61.1	—	2–4	2.00–1.75	3.61–3.93	61.0–64.0	—	—	—	—	—
3	K	1.88	3.65	61.3	—	2–4	2.00–1.75	3.61–3.93	61.0–64.0	—	—	—	—	—
4	K	1.65	4.02	58.0	—	6	1.66	4.05	59.9	—	101	89	580	535
5	K	1.83	3.78	56.8	—	2–4	2.00–1.75	3.61–3.93	61.0–64.0	—	99	89–93	—	—
6	K	1.83	3.30	51.2	—	2–4	2.00–1.75	3.61–3.93	61.0–64.0	—	—	—	—	—
7	K	2.00	3.51	61.7	—	2	2.00	3.61	64.0	—	—	—	—	—
8	K	1.88	3.71	61.8	—	2–4	2.00–1.75	3.61–3.93	61.0–64.0	—	—	—	—	—
9	K	1.75	3.96	57.9	—	4	1.75	3.93	61.0	—	—	—	—	—
10	Na	1.60	4.71	61.8	—	8	1.62	4.69	63.3	—	—	—	711	496
11	NH_4	1.75	4.35	68.6	7.38	4	1.75	4.25	66.1	7.18	—	—	—	—
12	NH_4	1.70	4.23	70.1	7.21	4	1.75	4.25	66.1	7.18	—	—	—	—
13	NH_4	1.78	4.39	69.8	7.15	4	1.75	4.25	66.1	7.18	88	85	570	509
14	Sr	2.00	3.77	63.6	14.20	2	2.00	3.55	63.0	14.37	124	122	820	610
15	Sr	1.90	3.94	63.7	14.59	2–4	2.00–1.75	3.55–3.86	63.0–60.0	14.37–15.63	—	—	—	—

*This value includes only the sulphate which can be titrated as H_2SO_4 after hydrolysis.
†n refers to the general formula $M_nB_nO_{n/2}(SO_4)_{(3n-4)/2}(HSO_4)_{n+2}$.

TABLE II

Calculated compositions for some sulphatoborates

Formula	Structure of anion	r	% B	% SO_4*	% NH_4^+	Cryoscopic equiv. wt.	Conductimetric equiv. wt.
$KB(SO_4)_2$	—	1.50	4.47	59.53	—	121.0	∞
$NH_4.B(SO_4)_2$	—	1.50	4.92	65.49	8.18	110.0	∞
$KB(HSO_4)_4$	—	3.50	2.47	76.72	—	219.1	∞
$NH_4.B(HSO_4)_4$	—	3.50	2.59	80.59	4.32	208.6	∞
$K_2B_2O(SO_4)(HSO_4)_4$	XI	2.00	3.61	64.02	—	100.0	600.2
$(NH_4)_2B_2O(SO_4)(HSO_4)_4$	XI	2.00	3.88	68.85	6.47	93.0	558.1
$K_4B_4O_2(SO_4)_3(HSO_4)_6$	XVIII	1.75	3.93	61.00	—	91.9	551.2
$(NH_4)_4B_4O_2(SO_4)_3(HSO_4)_6$	XVIII	1.75	4.25	66.05	7.78	84.9	509.1
$K_6B_6O_3(SO_4)_5(HSO_4)_8$	XIX	1.66	4.05	59.87	—	89.1	534.8
$(NH_4)_6B_6O_3(SO_4)_5(HSO_4)_8$	XIX	1.66	4.39	64.98	7.32	82.1	492.7
$K_8B_8O_4(SO_4)_7(HSO_4)_{10}$	—	1.62	4.11	59.30	—	87.8	526.7
$(NH_4)_8B_8O_4(SO_4)_7(HSO_4)_{10}$	—	1.62	4.47	64.44	7.45	80.7	484.5
$K_nB_nO_{n/2}(SO_4)_{(3n-4)/2}(HSO_4)_{n+2}$†	—	1.50	4.64	57.40	—	83.7	502.1
$(NH_4)_nB_nO_{n/2}(SO_4)_{(3n-4)/2}(HSO_4)_{n+2}$†	—	1.50	4.70	62.65	7.84	76.7	460.0
$KB_2O(SO_4)(HSO_4)_3$	X	1.75	4.66	72.46	—	116.0	∞
$NH_4.B_2O(SO_4)(HSO_4)_3$	X	1.75	4.88	75.91	4.07	110.7	∞
$K_2B_4O_2(SO_4)_3(HSO_4)_4$	—	1.50	5.21	69.45	—	105.0	∞
$(NH_4)_2B_4O_2(SO_4)_3(HSO_4)_4$	—	1.50	5.59	73.16	4.58	97.5	∞
$K_3B_6O_3(SO_4)_5(HSO_4)_5$	—	1.42	5.43	68.28	—	99.6	∞
$(NH_4)_3B_6O_3(SO_4)_5(HSO_4)_5$	—	1.42	5.73	72.09	4.78	94.4	∞
$K_4B_8O_4(SO_4)_7(HSO_4)_6$	—	1.38	5.54	67.66	—	97.6	∞
$(NH_4)_4B_8O_4(SO_4)_7(HSO_4)_6$	—	1.38	5.86	71.52	4.88	92.3	∞
$K_{n/2}B_nO_{n/2}(SO_4)_{n-1}(HSO_4)_{(n/2)+2}$†	—	1.25	5.91	65.64	—	91.5	∞
$(NH_4)_{n/2}B_nO_{n/2}(SO_4)_{n-1}(HSO_4)_{(n/2)+2}$†	—	1.25	6.27	69.63	5.23	86.2	∞

*This value includes only the sulphate which can be titrated as H_2SO_4 after hydrolysis.
†The values given are the limiting values when n becomes very large.

compositions of a large number of borates. These complex ions either occur as discrete units in the crystal or as larger polymeric structures in which these basic units are joined by oxygen bridges formed by the elimination of water between —OH groups. X-Ray diffraction and nuclear magnetic resonance studies have provided evidence for the existence of some of the postulated anions (10, 11).

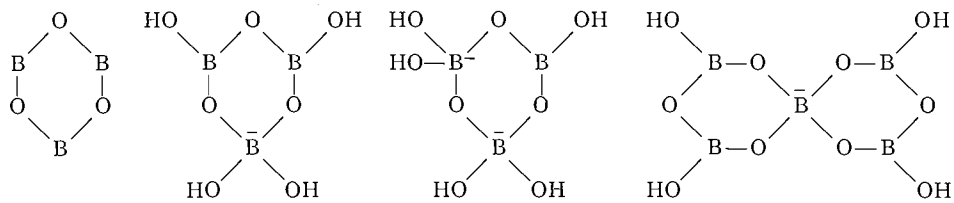

I II III IV

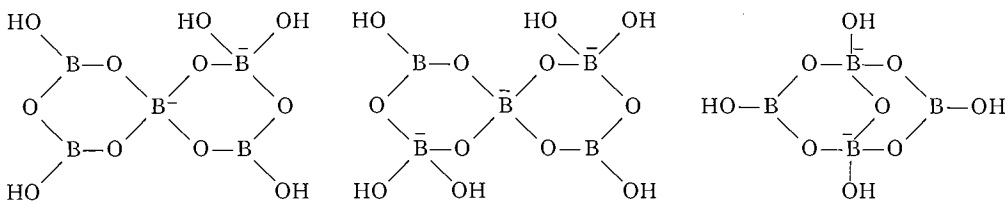

V VI VII

It seemed reasonable, therefore, to attempt to explain the compositions of the sulphatoborates in terms of similar structures.

We first considered as possibilities structures corresponding to II to VII but with OH groups replaced by $—HSO_4$ groups (designated II′ to VII′ in Table III) and with SO_4

TABLE III

Calculated values of the titration ratio r

Structure	Formula	r	Structure	Formula	r
II′	$MB_3O_3(HSO_4)_4$	1.17	II″	$MB_3O_3(SO_4)_2$	0.50
III′	$M_2B_3O_3(HSO_4)_5$	1.33	III″	$M_4B_6O_6(SO_4)_5$	0.66
IV′	$MB_5O_6(HSO_4)_6$	0.70	IV″	$MB_5O_6(SO_4)_3$	0.30
V′	$M_2B_5O_6(HSO_4)_5$	0.80	V″	$M_4B_{10}O_{12}(SO_4)_5$	0.30
VI′	$M_3B_5O_6(HSO_4)_6$	0.70	VI″	$M_3B_5O_6(SO_4)_3$	0.10
X	$MB_2O(SO_4)(HSO_4)_3$	1.75	X′	$M_2B_4O_3(SO_4)_5$	1.00
XI	$M_2B_2O(SO_4)(HSO_4)_4$	2.00	XI′	$M_2B_2O(SO_4)_3$	1.00
XII	$MB_3O_2(SO_4)_2(HSO_4)_2$	1.17	XII′	$MB_3O_2(SO_4)_3$	0.82
XIII	$M_2B_3O_2(SO_4)_2(HSO_4)_3$	1.25	XIII′	$M_4B_6O_4(SO_4)_7$	0.82
XIV	$M_3B_3O_2(SO_4)_2(HSO_4)_4$	1.50	XIV′	$M_3B_3O_2(SO_4)_4$	0.82
XVI	$MB_2O(SO_4)_2(HSO_4)_4$	1.25	XVI′	$M_2B_4O_3(SO_4)_5$	1.00
XVII	$M_2B_2O(SO_4)_2(HSO_4)_2$	1.50	XVII′	$M_2B_2O(SO_4)_3$	1.00

groups forming bridges between rings (designated II″ to VII″ in Table III). These polymers may be imagined as being formed by elimination of disulphuric acid from simple $B(HSO_4)_4^-$ anions, e.g.,

$$3B(HSO_4)_4^- \rightarrow B_3O_3(HSO_4)_4^- + H_2S_2O_7 + 2HS_2O_7^- + 2H_2SO_4.$$

II′

The corresponding values of the hydrolysis ratio r, the ratio of the number of moles of sulphuric acid to the number of moles of boric acid produced on complete hydrolysis of the salt, are given in Table III: in all cases they are smaller than the observed values. Consequently we next considered the possibility that the six-membered ring unit is retained but that one boron atom is replaced by a sulphur atom to give the basic ring structure VIII.

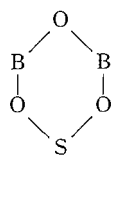

VIII

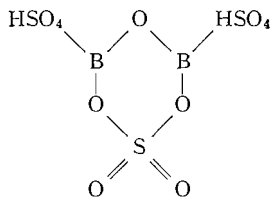

IX

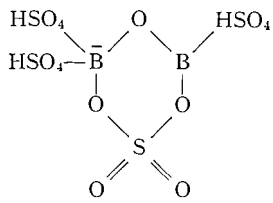

X

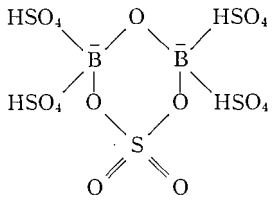

XI

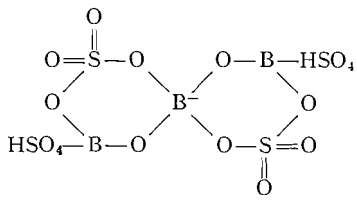

XII

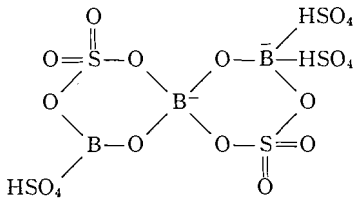

XIII

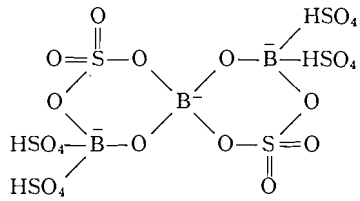

XIV

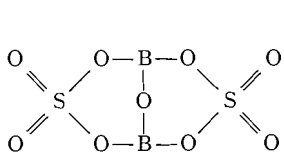

XV

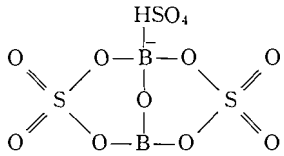

XVI

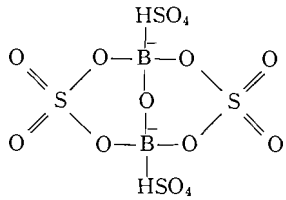

XVII

It may be seen from Table III that, of these structures, only X and XI have r values which agree reasonably well with the observed values. However, in order to account for r values as low as 1.6 it is necessary to postulate that, in some cases, further polymerization occurs by elimination of sulphuric acid between the $-SO_4H$ groups of the anions X or XI to form chains or other complex structures with sulphate bridges between six-membered rings. Titration ratios, r, for salts containing fully condensed polymeric anions in which elimination of sulphuric acid between all the $-SO_4H$ groups has taken place (X′–XVII′) are given in Table III. All the observed values of r fall between the limiting values for the simple anion XI and its fully condensed form XI′ but many of the observed values fall outside the limiting values for X and its fully condensed form X′. Since the observed r values are generally considerably larger than are required by the fully condensed form XI it seems reasonable to suppose that the salts consist mainly of polymers that contain only a few of the six-membered ring units, e.g. the "dimer" XVIII and the "trimer" XIX.

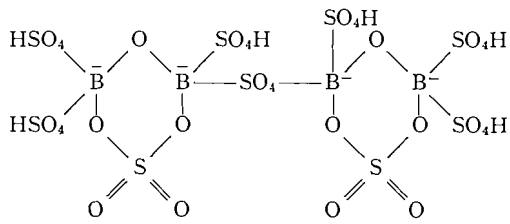

XVIII

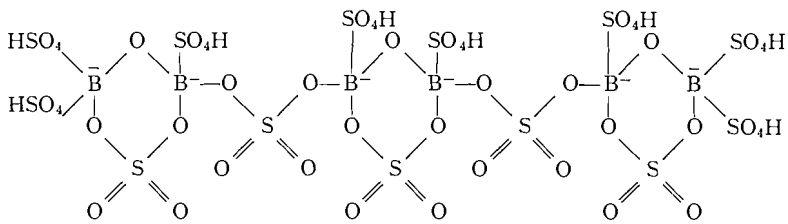

XIX

Calculated composition for the potassium and ammonium salts of these anions are given in Table II together with similar values for the corresponding "tetramer" and infinite polymer ($n = 8$ and $n = \infty$ in the general formula $M_nB_nO_{n/2}(SO_4)_{(3n-4)/2}(HSO_4)_{n+2}$). The analytical data for each of the salts can be explained by assuming that they contain the simple anion XI or its condensed forms such as XVIII and XIX with $n = 2$, 4, 6, or 8. For comparison the calculated compositions for X and some of its condensed forms are also given in Table II: the agreement between the observed and calculated compositions is not very good. We conclude, therefore, that the salts described in Table I are best considered as containing the anion XI and its condensed forms such as XVIII and XIX. However, it is probable that none of the products obtained was actually a pure salt containing a single anion, rather it is most likely that they were mixtures of salts of the simple anion XI and/or one or more of its condensed forms.

It seems more reasonable to formulate the condensed structures with bridging sulphate groups as in XVIII and XIX rather than with bidentate sulphate groups because of the very small size of the boron atom. In this connection it is of interest to compare the present structures with that of methylene sulphate, which has been shown (12) to be dimeric in benzene and therefore to have structure XX rather than XXI.

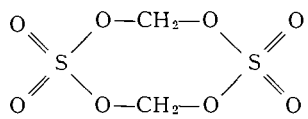

XX

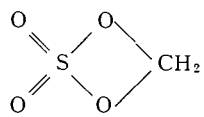

XXI

Comparison with trimethylene sulphate is also appropriate. This is monomeric in benzene (12) and can therefore presumably be formulated as in XXII with a six-membered ring analogous to VIII.

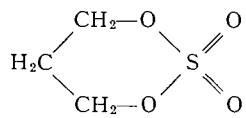

XXII

Early workers have reported several compounds as products of the reactions between boric acid or boric oxide and sulphuric acid, oleum, or sulphur trioxide. The reaction of BCl_3 with SO_3 has been reported (12) to give sulphuryl chloride and a boron compound having the composition $B_2O_3.SO_3$. A product of the same composition is also given by the reaction between BBr_3 and SO_3. The compounds $B_2O_3.SO_3$ and $B_2O_3.2SO_3$ were obtained by Pictet and Karl (14) by heating boric oxide and sulphur trioxide in sealed tubes at 115° and 250°, respectively. Merz (13) obtained a transparent glass having the composition $5B_2O_3.2SO_3.2H_2O$ and Schultz and Sellac (13) report a compound which their analysis showed to have the composition $B_2O_3.3SO_3.H_2O$, which they obtained by treating a solution of boric acid in sulphuric acid with SO_3 or by dissolving boric acid in sulphuric oleum and then evaporating to dryness. These compounds can all be formulated in terms of the six-membered ring VIII as the basic unit. The proposed structure for $B_2O_3.SO_3$ is based on structure IX and is formed by elimination of $H_2S_2O_7$ between such units to give the infinite polymer XXIII. The compound $B_2O_3.2SO_3$ may be formulated

as XV or as the infinite polymer XXIV with sulphate bridges between the following rings:

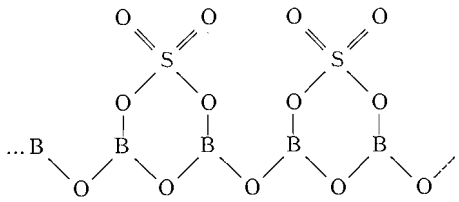

XXIII

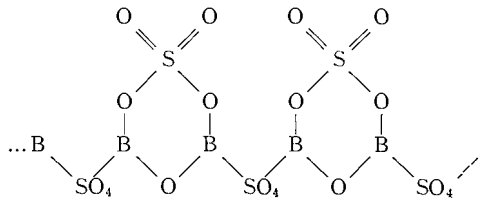

XXIV

The compound $B_2O_3.3SO_3.H_2O$ or $B_2O(SO_4)(HSO_4)_2$ probably has structure IX, and the compound $5B_2O_3.2SO_3.2H_2O$ can be formulated as the complex borate–sulphatoborate XXV.

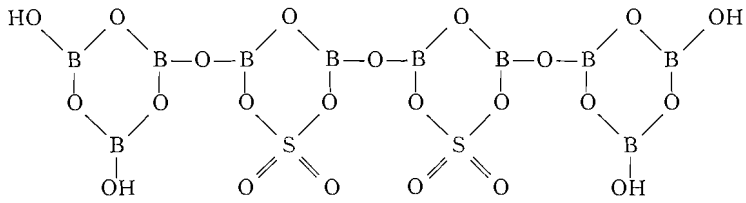

XXV

By heating potassium or sodium hydrogen sulphates with boric acid at 500° or by heating a mixture of sodium borate, sodium sulphate, and sulphuric acid, compounds corresponding to the composition $M(BO).SO_4$ have been obtained (13). These may be formulated as the salts of XXVI or XXVII.

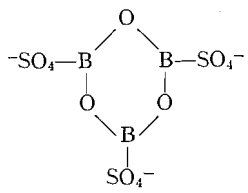

XXVI

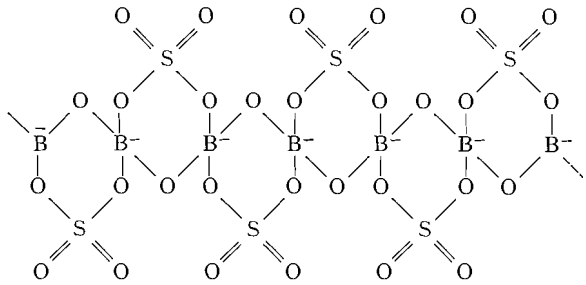

XXVII

d'Arcy (15) prepared a compound with composition $H_3BO_3.3SO_3$ or $B(HSO_4)_3$ from the reaction of sulphur trioxide with boric acid. We have also obtained a white, very hygroscopic compound corresponding very closely in composition to $B(HSO_4)_3$ by dissolving boric oxide in excess sulphur trioxide and then removing excess sulphur trioxide under vacuum. Greenwood and Thompson (16) obtained a similar compound from the reaction of boron trichloride with sulphuric acid:

$$BCl_3 + 3H_2SO_4 = B(HSO_4)_3 + 3HCl.$$

They also claim to have obtained the acid $HB(HSO_4)_4$ as a wet solid by the reaction between 1 mole of BCl_3 and 4 moles of sulphuric acid:

$$BCl_3 + 4H_2SO_4 = HB(HSO_4)_4 + 3HCl.$$

In view of the evidence from the Raman spectra of concentrated solutions of this acid in sulphuric acid that elimination of $H_2S_2O_7$ occurs to give B—O—B links (4) and in view of the complex structures of the salts discussed in this paper it seems unlikely that this wet solid was in fact the pure acid $HB(HSO_4)_4$. It is more likely that the product of this reaction is a mixture of polysulphatoboric acids with sulphuric acid and disulphuric acid with the overall composition $HB(HSO_4)_4$.

ACKNOWLEDGMENT

We thank the National Research Council for financial assistance.

REFERENCES

1. R. H. FLOWERS, R. J. GILLESPIE, and J. V. OUBRIDGE. J. Chem. Soc. 1925 (1956).
2. R. H. FLOWERS, R. J. GILLESPIE, and E. A. ROBINSON. Can. J. Chem. **38**, 1363 (1960).
3. J. BARR, R. J. GILLESPIE, and E. A. ROBINSON. Can. J. Chem. **39**, 1266 (1961).
4. R. J. GILLESPIE and E. A. ROBINSON. Can. J. Chem. **40**, 784 (1962).
5. M. HOLLANDER and W. RIEMANN. Ind. and Eng. Chem., Anal. Ed. **17**, 602 (1945).
6. R. J. GILLESPIE, J. V. OUBRIDGE, and C. SOLOMONS. J. Chem. Soc. 1804 (1957).
7. R. J. GILLESPIE, E. D. HUGHES, and C. K. INGOLD. J. Chem. Soc. 2473 (1950).
8. R. J. GILLESPIE. J. Chem. Soc. 1851 (1954).
9. S. J. BASS, R. H. FLOWERS, R. J. GILLESPIE, E. A. ROBINSON, and C. SOLOMONS. J. Chem. Soc. 4315 (1960).
10. J. O. EDWARDS and V. ROSS. J. Inorg. & Nuclear Chem. **15**, 326 (1960). J. DALE. J. Chem. Soc. 922 (1961). C. L. CHRIST. Am. Mineralogist, **45**, 334 (1960).
11. F. HOLUJ and H. E. PETCH. Can. J. Phys. **38**, 515 (1960). P. J. BRAY, J. O. EDWARDS, J. G. O'KEEFE, V. F. ROSS, and I. TATSUZAKI. J. Chem. Phys. **35**, 435 (1961).
12. W. BAKER and F. B. FIELD. J. Chem. Soc. 86 (1932).
13. J. W. MELLOR. A comprehensive treatise on inorganic and theoretical chemistry. Vol. **5**. Longmans, London. 1924.
14. A. PICTET and E. KARL. Bull. soc. chim. France, **3**, 1114 (1908).
15. R. F. D'ARCY. J. Chem. Soc. **55**, 159 (1889).
16. N. N. GREENWOOD and A. THOMPSON. J. Chem. Soc. 3643 (1959).

THE ACTION OF ANHYDROUS ACIDS ON ATP:CREATINE PHOSPHOTRANSFERASE*

FLORANTE A. QUIOCHO AND FELIX FRIEDBERG
Department of Biochemistry, Howard University Medical School, Washington, D.C.

Received December 19, 1961

ABSTRACT

Treatment of ATP:creatine phosphotransferase with anhydrous sulphuric acid permits transposition of 24% of the threonine residues and 69% of the serine residues. Treatment with anhydrous phosphoric acid yields similar results: 41% of the threonine residues and 60% of the serine residues are rearranged. Anhydrous formic acid does not induce an N- to O-acyl migration in the protein.

Non-specific hydrolysis of peptide bonds or destruction of certain amino acids that might have occurred simultaneously with rearrangement during the anhydrous sulphuric or anhydrous phosphoric acid appears to be very slight. When the protein is treated with anhydrous sulphuric acid, however, phenylalanine "disappears" almost completely from the chromatogram.

Following the suggestion by Bergmann and Miekeley (1) that serine displays a distinctive chemical reactivity through N-acyl to O-acyl transformation, Elliott (2) rearranged C-peptide bonds involving the beta-hydroxy amino acids serine and threonine with 97.5% anhydrous sulphuric acid. Such a N–O acyl migration frees the α-amino groups of the serine and threonine residues involved. Since nitrous acid reacts with these amino groups the difference in amino acid content after nitrous acid treatment in protein exposed to anhydrous acid and protein not exposed can be taken as a measure of transposition. In the experiments reported here this method was applied to ATP:creatine phosphotransferase (EC 2.7.3.2.).† A study was made of the comparative efficiency of anhydrous concentrated sulphuric acid, phosphoric acid, and formic acid. In addition, information was sought on the effect of these reagents on the other amino acids of the protein.

EXPERIMENTAL PROCEDURE

ATP:creatine phosphotransferase prepared by procedure B of Kuby *et al.* (3), crystallized twice, and lyophilized, showed a single peak on ultracentrifugation.

Treatment with Sulphuric Acid

To 100 mg of enzyme dried over P_2O_5 *in vacuo* at 60°, 4 ml of cold concentrated sulphuric acid were added. The flask was securely stoppered to prevent entry of moisture, gently shaken until the protein was dissolved, and then allowed to stand for 72 hours in a desiccator. The solution which was originally pale yellow turned somewhat darker. At the end of the specified time, the flask was cooled well below −40°, anhydrous ether, previously cooled below −40°, was added, and the mixture was thoroughly shaken. The resulting protein precipitate was washed several times with cold ether until the washings were free from $SO_4^=$ (as tested with $BaCl_2$) and then dissolved in distilled water (6 ml).

Treatment with Phosphoric Acid

ATP:creatine phosphotransferase (100 mg) was dried over P_2O_5 *in vacuo* at 60° and transferred to a glass-stoppered flask. H_3PO_4 (4g, 85%) and P_2O_5 (about 400 mg) were added. After incubation at 40° for

*This work was supported by a grant-in-aid (G-14363) from the National Science Foundation and an equipment grant from the Charles F. Kettering Foundation.

†*According to the "Report of the Commission on Enzymes of the International Union of Biochemistry", Pergamon Press, 1961, page 98, the name of the enzyme is ATP:creatine phosphotransferase. The associated trivial name is creatine kinase. The official number of the enzyme is 2.7.3.2.*

We believe that it will be useful to follow these recommendations in the Report of the Enzyme Commission, in order to achieve a common terminology among authors.

72 hours, a mixture of crushed ice and ice water was added to the flask to bring the total volume to approximately 100 ml, followed by a small excess of $CaCO_3$ to precipitate the phosphate. The supernatant liquid was dialyzed against distilled water and then lyophilized. The dry material was resuspended in 6 ml of distilled water.

Treatment with Formic Acid

To 100 mg of ATP:creatine phosphotransferase dried over P_2O_5 *in vacuo* at 60° and placed into a glass-stoppered flask 10 ml of 98% formic acid was added. After incubation for 72 hours at room temperature, the resulting solution was lyophilized. The dried protein was dissolved in 6 ml of distilled water.

Nitrous Acid Treatment of Proteins

The aqueous solution obtained as described above was dialyzed against 0.5 *N* acetate buffer (pH 4.0). It was then treated with 414 mg $NaNO_2$ and incubated for 16 hours at room temperature. The resulting solution was dialyzed against distilled water and lyophilized.

Hydrolysis and Amino Acid Analysis

Some of the dried material (10 mg) was hydrolyzed with 2 ml 6 *N* HCl for 22 hours at 110° in evacuated and sealed tubes. The hydrolyzate was taken to dryness *in vacuo* over NaOH pellets, dissolved in sodium citrate buffer, pH 2.2, and analyzed in the Spinco Amino Acid Analyzer (4).

Control runs were performed on ATP:creatine phosphotransferase hydrolyzed by 6 *N* HCl without prior treatment by anhydrous concentrated acid both with and without nitrous acid exposure.

RESULTS AND DISCUSSION

Table I shows that treatment of ATP:creatine phosphotransferase with anhydrous sulphuric acid permits transposition of 24% of the threonine residues and 69% of the serine residues. This limited conversion is in agreement with Elliott's study in silk fibroin, where 60% of the serine residues was rearranged (2). (There are few threonine residues in silk fibroin.) In lysozyme, however, he found nearly all serine residues affected, but only one-third of the threonine residues were converted (5). The extent of the induced

TABLE I

Amino acid composition of ATP:creatine phosphotransferase after treatment with anhydrous acids (g amino acid/100 g of protein)*

Amino acid	Untreated†	HONO	H_2SO_4	H_3PO_4	HCOOH
Lysine	10.60	0.45	0.36	0.65	0.83
Histidine	6.06	5.40	5.80	5.28	6.05
NH_3‡	1.41	1.58	2.36	1.92	1.74
Arginine	7.86	7.43	6.16	5.13	7.45
Aspartic acid	12.96	13.45	12.92	12.25	13.25
Threonine	4.63	4.76	3.64	2.82	4.63
Serine	4.54	4.60	1.45	1.83	4.24
Glutamic acid‡	14.28	15.28	15.63	16.31	14.52
Proline	5.96	5.32	6.02	5.30	5.30
Glycine	6.28	6.45	6.24	5.74	5.98
Alanine	2.89	2.96	2.49	2.42	2.87
Valine	6.93	7.25	7.09	6.80	7.02
Methionine	3.40	3.07	2.41	2.81	3.11
Isoleucine	3.75	3.93	3.95	4.04	4.27
Leucine	11.34	11.39	11.42	10.67	11.60
Tyrosine	4.11	0.27	0.31	0.11	0.22
Phenylalanine	5.93	6.50	0.75	6.86	6.66

*Values given are averages of two determinations.

†The data here agree with those previously reported (12) except for the amino acids glycine and phenylalanine, which are considerably higher in the present paper. We believe that the automatic assay allows better separation of the glycine–alanine and phenylalanine–tyrosine pairs and yields more accurate results. Since the amino acid analyses were performed only after a single period of hydrolysis (22 hours) the absolute values for such amino acids as threonine, serine, or valine are not quantitatively reliable. The amount of cystine is small (about 3 moles/molecule), is destroyed by hydrolysis, and can only be determined by special means.

‡The large ammonia content in the hydrolyzates of the acid-treated protein might be due to ammonia in the mineral acids carried through to the hydrolysis stage. We have, however, no explanation for the high values of glutamic acid. The ratios of the height of the glutamic acid peaks yielded by the 570 and 440 mμ tracings remain constant. There is no evidence for another substance under the glutamic acid peak.

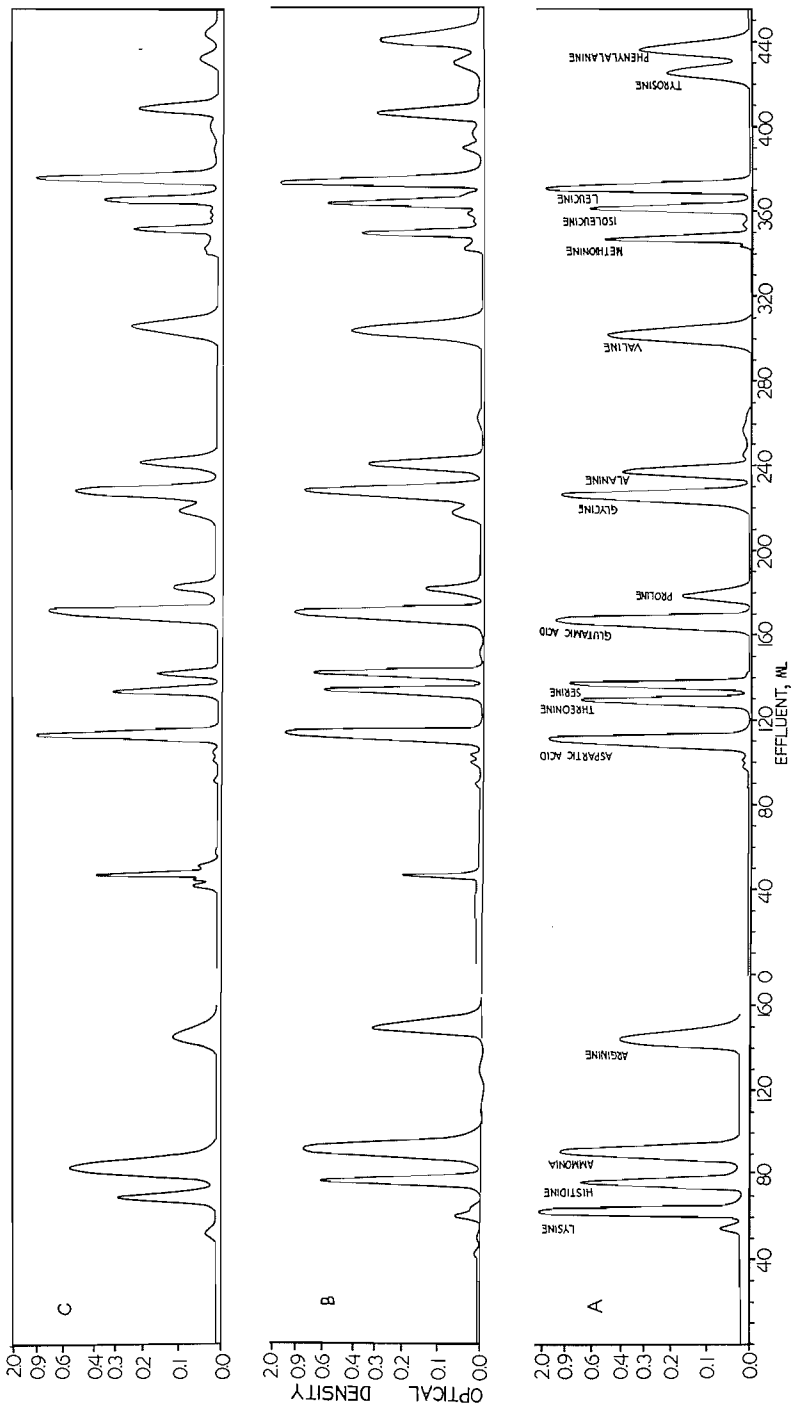

FIG. 1. Chromatograms for: A. Untreated ATP:creatine phosphotransferase. B. HONO-treated ATP:creatine phosphotransferase. C. H_2SO_4–HONO-treated ATP:creatine phosphotransferase. D. HONO-treated poly-L-lysine (upper curve), HONO-treated poly-L-tyrosine (lower curve). Leucine was added as a marker. There were no other peaks on the entire chromatogram. The lower curve is included because it shows that the peak midway between leucine and phenylalanine cannot be the result of a reacted tyrosine.

The basic amino acids and ammonia were separated on a 15-cm column operated at 50° and with the pH 5.28, 0.35 *N* sodium citrate buffer. The acidic and neutral amino acids were separated on a 150-cm column, which was also operated at 50°, starting with the pH 3.25, 0.2 *N* sodium citrate buffer, with a change to the pH 4.25, 0.2 *N* sodium citrate buffer at 260 ml (8 hours and 40 minutes). Since amounts of materials used in loading the columns varied, the table should be consulted for quantitative data.

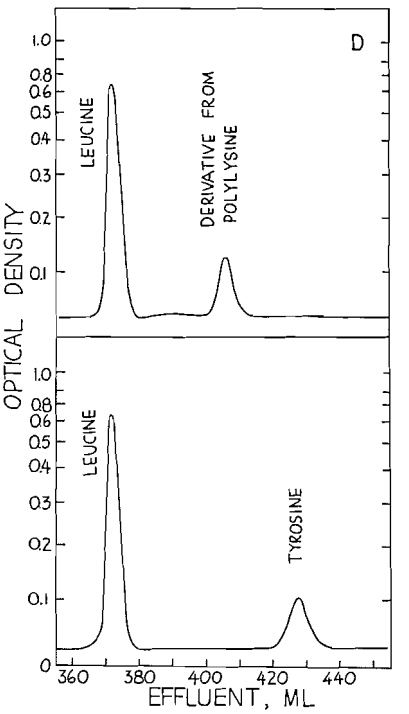

FIG. 1D.

shift was not increased on further standing of the reaction mixture. Wiseblatt *et al.* (6), who applied the method to wheat gluten also observed the preferential release of the amino groups of serine and Ramachandran and McConnell (7) reported 60–70% transposition of the peptide bonds of serine but none of those of threonine in gliadin. Hence, one may conclude that such transpositions are usually not complete and that threonine residues are more resistant than serine residues. The results for the treatment of ATP: creatine phosphotransferase by anhydrous phosphoric acid are similar: 60% of the serine residues and 41% of the threonine residues are rearranged (Table I). Fasman (8) demonstrated that concentrated sulphuric acid causes poly-DL-serine to rearrange to the polyester, to the extent of 70% of the original number of amide bonds. The remaining hydroxyls of the serine residues become sulphonated. Upon hydrolysis of serine-O-sulphate under the conditions of our experiments (22 hours hydrolysis) we observed 80% recovery of the free serine. Even though this incomplete hydrolysis of serine-O-sulphate could conceivably increase our values obtained for the transposition of the peptide bond of serine and probably also threonine, such an error should be slight. Whereas Josefsson and Edman (9) postulated that the increase in amino nitrogen during the reaction of ribonuclease with anhydrous formic acid is due to N-, O-acyl migration, more recent studies invalidate such a hypothesis (10, 11). Our results support the conclusion that anhydrous formic acid does not bring about an N- to O-acyl migration at the hydroxy-amino acid residues of ATP:creatine phosphotransferase.

That some non-specific hydrolysis of peptide bonds or destruction of certain amino acids might have occurred simultaneously with the rearrangement during the sulphuric or phosphoric acid treatment, but only to a very slight extent, is indicated by the lower

values for the amino acids arginine, alanine, and methionine after sulphuric acid treatment, and for alanine and arginine after phosphoric acid treatment. Only one major alteration in amino acid patterns can be deduced from the data: When the protein is treated with anhydrous sulphuric acid, phenylalanine "disappears" almost completely from the chromatogram (Fig. 1C). The sulphonated phenylalanine, migrating very rapidly on the Dowex resin, would be expected to emerge in front of the aspartic acid (the first amino acid in the effluent). Tyrosine-O-sulphate, for example, moves ahead of the aspartic acid. Anhydrous phosphoric acid treatment has no such effect.

Nitrous acid, itself, under the conditions employed in this study, induces nitrosation of tyrosine, besides deamination of the epsilon-amino group of lysine. In the chromatograms tyrosine and lysine are almost completely absent (Fig. 1B). A new peak appears in the effluent midway between leucine and phenylalanine which can also be obtained by exposing poly-L-lysine to the nitrous acid treatment (Figs. 1B and 1D). In addition there is a pronounced unidentified shoulder to the right of glycine (Fig. 1B).

REFERENCES

1. M. Bergmann and A. Miekeley. Hoppe-Seyler's Z. physiol. Chem. **140**, 128 (1924).
2. D. F. Elliot. Biochem. J. **50**, 542 (1952).
3. S. A. Kuby, L. Noda, and H. A. Lardy. J. Biol. Chem. **209**, 191 (1954).
4. S. Moore, D. H. Spackman, and W. H. Stein. Anal. Chem. **30**, 1185 (1958).
5. D. F. Elliot. The chemical structure of proteins. *In* Ciba Foundation Symposium. *Edited by* G. E. E. Wolstenholme and M. P. Cameron. Churchill Ltd., London, England. 1953.
6. L. Wiseblatt, L. Wilson, and W. B. McConnell. Can. J. Chem. **33**, 1295 (1955).
7. L. K. Ramachandran and W. B. McConnell. Can. J. Chem. **23**, 1638 (1955).
8. G. D. Fasman. Science, **131**, 420 (1960).
9. L. Josefsson and P. Edman. Biochem. Biophys. Acta, **25**, 614 (1957).
10. L. Smillie and H. Neurath. J. Biol. Chem. **234**, 355 (1959).
11. J. Rabinowitz. Compt. rend. trav. lab. Carlsberg. Sér. chim. **31**, 483 (1960).
12. F. Friedberg. Arch. Biochem. Biophys. **61**, 263 (1956).

NOTES

NEAR-INFRARED SPECTRA OF ALIPHATIC ALDEHYDES

J. F. KING AND B. VIG

It has been known for many years that numerous functional groups show characteristic absorption in the near-infrared region of the electromagnetic spectrum and that these absorption bands are most commonly overtones or combination bands involving hydrogen (see reference 1). Their use for the purposes of structural elucidation has been proposed in review articles on near-infrared spectra (1, 2), but remarkably few practical applications have been made to date. We have investigated the spectra of a number of aldehydes and wish to point out the utility of measurements in this region of the spectrum for confirming the presence of the aldehyde grouping and for providing information concerning its environment.

The bands arising from combination of the carbonyl stretching mode (around 1700 cm^{-1}) with each of the formyl C—H bands (around 2800 and 2700 cm^{-1}) would be expected to appear around 4500 and 4400 cm^{-1} respectively. It has previously been reported (1, 3) that aldehydes absorb in these regions, though except for a recent study of aromatic aldehydes (3), the specific basis of this generalization has not been disclosed. We have measured the near-infrared spectra of more than 30 aldehydes and find that all of the compounds show the two expected combination bands. These peaks are normally comparatively strong ($\epsilon \approx 1$) and in some of the simplest compounds are the strongest bands in the near-infrared spectrum. (Chloral, a possible exception, shows two bands but the low-frequency absorption, like the corresponding band in the infrared region, is of much lower intensity than the other: it is not certain that this band is due to the aldehyde function.) Examination of the near-infrared spectra of a substantial number of other compounds shows that absorption due to other functional groups (including saturated hydrocarbon units) may obscure the low-frequency band but that the region around 4500 cm^{-1} is comparatively free of absorption by other functions. What interference there is stems from double bonds bearing hydrogen, though these usually absorb at somewhat higher frequencies.

Though other carbonyl functions may absorb in the region of the C=O stretching mode of aldehydes, and other groups (e.g. certain other C—H groups, N-methyl groups, etc.) in the region of the formyl C—H bands, the combination band is unique to aldehydes. It would appear that the presence of the 4400 and 4500 cm^{-1} bands together with the 1700, 2700, and 2800 cm^{-1} absorptions is good circumstantial—if not absolute—proof of the presence of an aldehyde. In addition, the absence of the combination bands—notwithstanding the presence of bands at 1700, 2700, and 2800 cm^{-1}—would appear to exclude the possibility of the presence of an aldehyde.

In Table I are listed the aldehyde bands of a number of "α,β-saturated" and α,β-unsaturated aldehydes. The combination bands of the saturated aldehydes (excepting chloral) were found in the regions 4415–4445 cm^{-1} and 4525–4550 cm^{-1} and those of the α,β-unsaturated aldehydes in the regions 4360–4415 cm^{-1} and 4480–4510 cm^{-1}, respectively. The lower limit of the low-frequency band of the α,β-unsaturated compounds is

TABLE I

Infrared and near-infrared absorption of aldehydes

Aldehyde	Formyl C—H bands (A), cm^{-1}	C=O band (B), cm^{-1}	Sum (A)+(B), cm^{-1}	Observed near-infrared bands, cm^{-1}	Extinction coefficient (ϵ)
(*a*) "α,β-Saturated"					
1. Acetaldehyde	2723	1730	4453	4445	0.8
	2834		4564	4550	0.7
2. Propionaldehyde	2715	1737	4452	4435	1.3
	2813		4550	4540	0.8
3. Butyraldehyde	2719	1731	4450	4435	1.2
	2815		4546	4535	0.9
4. Caprylaldehyde (octanal)	2713	1729	4442	4440	1.3
	2816		4545	4535	1.0
5. Lauraldehyde (dodecanal)	2713	1729	4442	4440	0.9
	2817		4546	4535	1.0
6. Cyclohexanecarboxaldehyde	2698	1729	4427	4430	1.1
	2798		4527	4525	0.8
7. 2,2,4-Trimethyl-3-pentenal	2696	1727	4423	4415	2.3
	2795		4522	4525	1.1
8. Citronellal				4440	1.7
				4540	1.1
9. Chloral	2680	1765	4445	4435	0.2
	2850		4615	4615	1.9
10. Phenylacetaldehyde	2715	1728	4443	4445	0.8
	2809		4537	4540	0.8
(*b*) α,β-Unsaturated					
1. Crotonaldehyde	2725	1699	4424	4415	1.3
	2805		4504	4490	1.0
2. Tiglaldehyde	2708	1691	4399	4415	2.3
	2809		4500	4491	1.2
3. Cinnamaldehyde	2735	1686	4421	4415	1.0
	2807		4493	4480	1.9
4. 1-Cyclohexene-1-carboxaldehyde	2708, 2722	1690	4398, 4412	4360	3.8
	2806		4496	4505	2.2
5. 1-Cycloheptene-1-carboxaldehyde	2706, 2720	1690	4396, 4416	4360	4.1
	2815		4496	4510	1.7
6. 2,4-Hexadienal	2725	1688	4413	4410	1.3
	2801		4489	4485	1.0
7. Citral				4415	1.9
				4510	1.2
8. β-Methoxy-α-phenylcinnamaldehyde (II)	2756	1662	4418	4422	1.2
	2850		4512	4501	0.7
9. Aldehyde (I) from helminthosporal*				4400	3.4
				4485	1.8

*Determined in chloroform solution. Control experiments indicate that the position of the aldehyde peaks is not significantly different in chloroform and carbon tetrachloride solutions.

uncertain because absorption in this region due to other groups makes it difficult to determine the precise position of the aldehyde peak; the comparatively high extinction coefficient of these bands is almost certainly due to the presence of other absorption in this region. Included in the table also are the fundamental C=O and C—H frequencies and the sum obtained by adding the C=O frequency to each of the formyl C—H frequencies. Agreement between the near-infrared bands and the sums of the infrared frequencies is good, what differences there are being readily ascribable to anharmonicity and, to some extent, experimental uncertainty. Recently, Powers *et al.* (3) have confirmed the assignment of the 4500 and 4400 cm^{-1} bands in benzaldehyde as the combination of the C=O and C—H bands, by measuring the spectrum of benzaldehyde deuterated on the α-carbon. These authors also report the near-infrared frequencies of 11 other aromatic aldehydes. We have measured most of these compounds and a few other aromatic

aldehydes as well and find that all show the two combination bands. Our values for these compounds are in acceptable agreement with those of Powers *et al.*, and need not be duplicated here.

The usefulness of the near-infrared spectra of aldehydes has been shown in the study of the fungal sesquiterpene helminthosporal (4). This compound on oxidation yielded an acid in which the nature of the third oxygen was not clear. The absorption of the carboxyl group obscured the 2700 and 1700 cm^{-1} regions of the infrared spectrum, and attempts to remove this interference by esterification of the carboxyl group or to establish the nature of the oxygen by classical means led to intractable materials. The near-infrared spectrum, however, showed bands at 4480 and 4400 cm^{-1}, clearly indicating an α,β-unsaturated aldehyde as in I. The proton magnetic resonance spectrum confirmed the presence of the aldehyde group.

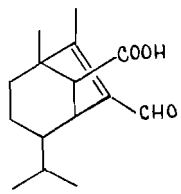

I

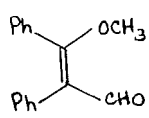

II

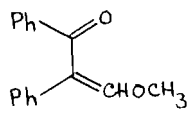

III

The near-infrared spectrum has been used in determining the structure of the crystalline product (m.p. 128°) obtained by methylating formyldesoxybenzoin with diazomethane (5). The near-infrared and infrared data (see Table I) together with the n.m.r. peak at 9.36 p.p.m. from tetramethylsilane show the structure to be II rather than III.

EXPERIMENTAL

The near-infrared spectra were determined with a Beckman DK-1 spectrophotometer using approximately 5% solutions in carbon tetrachloride in 1-cm quartz cells. With conventional cells, about 3 ml of solution is required; use of a semimicrocell reduces the volume necessary to less than 1 ml. Calibration indicates the error of the measurements to be less than ± 10 cm^{-1}. The values quoted represent the average of three or more measurements rounded to the nearest 5 cm^{-1}.

The infrared spectra were determined on a Beckman IR-7 grating spectrophotometer equipped with sodium chloride optics. The spectrum of each compound in carbon tetrachloride solution was determined using 0.1-mm sodium chloride cells.

Most of the compounds used in this study were commercial materials purified, in the case of solids, by recrystallization, and in the case of liquids, by washing with aqueous sodium bicarbonate, drying with Drierite, and distilling.

We are indebted to Dr. J. B. Stothers and Mr. R. E. Klinck for samples of 1-cyclohexene-1-carboxaldehyde and 1-cycloheptene-1-carboxaldehyde, and to Mr. Tony Durst for the spectrum of β-methoxy-α-phenylcinnamaldehyde.

This work was supported by the National Research Council.

1. W. Kaye. Spectrochim. Acta, **6**, 257 (1954).
2. O. H. Wheeler. Chem. Revs. **59**, 629 (1959).
3. R. M. Powers, J. L. Harper, and Han Tai. Anal. Chem. **32**, 1287 (1960).
4. P. de Mayo, E. Y. Spencer, and R. W. White. Can. J. Chem. **39**, 1608 (1961).
5. J. F. King and T. Durst. Unpublished observations.

Received January 17, 1962.
Department of Chemistry,
University of Western Ontario,
London, Ontario.

THE ISOLATION OF A REPRESENTATIVE LIGNIN FRACTION FROM WOOD AND STRAW MEALS

J. M. PEPPER AND P. D. S. WOOD

Previous publications (1–3) have described the isolation of a representative lignin fraction by the acidolysis in a dioxane–water medium of spruce and aspen wood meals. The application of this procedure gave rise, in good yields, to a readily obtained lignin product, which on preliminary examination appeared to be only moderately changed from the protolignin of the original plant substance and hence quite amenable to fundamental chemical studies. This report deals with a study of the generality of the application of this procedure to the isolation of a lignin fraction from the sapwood of 11 deciduous and coniferous trees and from the straw of four cereals. The "dioxane-lignins" so obtained, were examined according to their yield (based on the original Klason lignin content of the plant materials), methoxyl content, and fundamental carbon and hydrogen analysis for representative samples of each group.

SOURCE AND PREPARATION OF PLANT MATERIAL

Deciduous woods.—The sapwood of aspen (*Populus tremuloides* Michx.), mountain ash (*Sorbus aucuparia* L.), willow (*Salix* sp.), and cherry (*Prunus* sp.) were separately cut first into small chips and then ground in a Wiley mill (ca. 20 mesh).* The milled wood meal was air-dried, then extracted continuously for 48 hours with a benzene – ethyl alcohol (95%, 1:1) mixture in a large Soxhlet extractor to remove the extractives. The resultant wood meal was air-dried before storage.

Coniferous woods.—The sapwood of each of alpine larch (*Larix laricina* (Du Roi) Koch), western red cedar (*Thuja plicata* D. Donn), black spruce (*Picea mariana* (Mill.) B. S. P.), white spruce (*Picea glauca* (Moench) Voss), jack pine (*Pinus banksiana* Lamb), and balsam fir (*Abies balsamea* (L.) Mill.) was treated as described for the deciduous woods.

Cereal straws.—Clean, hand-picked samples of straw, dry but in a slightly green condition, of wheat (*Triticum vulgare* (Thatcher variety)), oats (*Avena sativa* (Exeter variety)), barley (*Hordeum vulgare* (Parlsland variety)), and rye (*Secale cereale* (Prolific variety)) were first hammer-milled and then extracted and treated in the same fashion as were the wood meals.

EXTRACTION OF LIGNIN

Pre-extracted, air-dry wood or cereal meal (25 g) was used in each case. The general procedure of lignin extraction was that reported earlier by Pepper and Siddiqueullah (2) and modified by the same authors (3).

EXPERIMENTAL RESULTS

The lignin sample isolated from each of the 15 plant materials was examined for its yield (based on the original Klason lignin content), color, and methoxyl content. Samples of the lignin representative of each of the three plant divisions were analyzed for their carbon and hydrogen content. These data are summarized in Table I.

**For one sample of aspen, grinding was continued to pass 50 mesh but on subsequent extraction no significant increase in lignin yield was obtained.*

TABLE I

Analytical data on products of acidolysis of wood and straw meals*

Plant substances	Klason lignin (%)	Residual meal		Isolated lignin			
		Weight (g)	Recovery (%)	Weight (g)	Percentage of Klason lignin	Color	Methoxyl content (%)†
Aspen	17.7	16.3	65.2	1.480‡	35.4	Pale tan	22.0
Mountain ash	19.7	14.7	58.8	1.303	28.5	Pink	22.4
Cherry	18.2	14.9	59.6	0.920	21.8	Maroon	21.1
Willow	23.2	16.9	67.6	1.64§	30.4	Pale tan	21.0
Alpine larch	28.9	18.8	75.2	0.696	10.3	Pink-grey	15.3
Balsam fir	28.4	20.1	80.4	0.695	10.6	Pale tan	15.6
Black spruce	28.1	19.1	76.4	0.814‖	12.7	Pale tan	15.4
Jack pine	27.0	19.5	78.0	0.688¶	11.2	Tan	15.4
Tamarack	25.7	19.3	77.2	0.707	11.7	Pale tan	15.5
Western red cedar	31.3	19.5	78.0	1.331	18.3	Tan	15.1
White spruce	26.4	19.3	77.2	0.844**	13.9	Pale tan	14.6
Barley	17.9	13.5	54.0	1.965	48.2	Dark tan	16.4
Oats	19.0	14.1	56.4	1.914††	43.9	Pale tan	16.7
Rye	19.8	14.3	57.2	2.034	44.3	Pale tan	16.6
Wheat	21.0	13.3	53.2	2.492‡‡	51.7	Dark tan	15.6

*Based on 25 g of air-dried wood or straw meal.
†Average of duplicate analyses.
‡Found: C, 58.31; H, 5.61%.
§Found: C, 59.48; H, 6.20%.
‖Found: C, 63.41; H, 6.27%.
¶Found: C, 62.58; H, 6.34%.
**Found: C, 63.91; H, 6.27%.
††Found: C, 59.26; H, 5.71%; N, nil%.
‡‡Found: C, 59.50; H, 5.61%; N, nil%.

It is interesting to note that during the acidolysis of cherry and mountain ash wood meal, bright red dioxane–water solutions were formed compared with the yellow-brown solutions normally obtained; the residual meal was red instead of the usual tan color. The precipitated lignin was also red, the color increasing in intensity by adsorption from the supernatant solution. On treatment with sodium hydroxide or sodium carbonate the red color of the solution or the precipitate was changed reversibly to bright green.

Presumably in these two species leucoanthocyanins were present in the sapwood used, and were not removed by the 48-hour benzene–ethanol extraction. On treatment with the acid dioxane–water solution, conversion to the colored anthocyanidins occurred, the color being in part adsorbed on the lignin precipitate. The red color of the washed and dried lignin persisted, though the centrifugate faded to a yellow-brown color after a few days, even in the dark.

DISCUSSION

This study has indicated the applicability of the acidolysis procedure for the isolation of a representative lignin fraction from the three divisions of lignified material studied, namely the deciduous and coniferous woods and cereal straws. By this method it is apparent that lignin is most easily isolated from the cereal straws (40–50% yield) and least easily from the conifers (10–20% yield), with the deciduous woods occupying an intermediate position (20–35% yield). The known difference in the composition of these three species of lignin is supported by the analytical data of Table I. The deciduous woods and cereal straws give rise to similar yields (18–23%) of Klason lignin as opposed to the

much higher yields (25–31%) obtained from the conifers, and the former group has a carbon and hydrogen content of about 59 and 5.5% respectively as apposed to about 63 and 6.3% respectively for the latter group. There is, too, a slight but significant difference in the methoxyl content of the deciduous and straw lignins, the latter being about 1% greater than the former.

ACKNOWLEDGMENTS

The authors wish to express their thanks to Dr. C. Riley of the Canadian Agriculture Research Station, Saskatoon, and to Mr. H. Gerrie, Department of Field Husbandry, University of Saskatchewan, Saskatoon, for their assistance in the provision of various wood and straw samples. Acknowledgment is also made of the financial assistance given by the Saskatchewan Research Council in support of this research.

1. J. M. PEPPER, P. E. T. BAYLIS, and E. ADLER. Can. J. Chem. **37**, 1241 (1959).
2. J. M. PEPPER and M. SIDDIQUEULLAH. Can. J. Chem. **39**, 1454 (1961).
3. J. M. PEPPER and M. SIDDIQUEULLAH. Can. J. Chem. **39**, 390 (1961).

RECEIVED DECEMBER 20, 1961.
DEPARTMENT OF CHEMISTRY,
UNIVERSITY OF SASKATCHEWAN,
SASKATOON, SASKATCHEWAN.

UREA AND SODIUM CHLORIDE WHISKERS*

L. D. CALVERT, A. F. SIRIANNI, AND I. E. PUDDINGTON

INTRODUCTION

The growth of molybdena whiskers on a molybdenum trioxide – silicon dioxide substrate was reported by Callahan, Petrucci, and Brown (1). Sodium chloride whiskers possessing a visible twist and having a mean length of 180 mm and a thickness of 1–30 μ were obtained by Jeszenszky and Hartmann (2). Sodium chloride whiskers have also been reported by Fells and Firth (3). Alumina, zirconia, and silica whiskers have been observed by Cunningham (4). Twists on alumina whiskers have been described by Sears, De Vries, and Huffine (5).

While the behavior of finely divided silica in hydrocarbon oil was being investigated, an accidental observation led to the experiments described below in which urea whiskers of the order of 25 cm in length and very thin sodium chloride crystals of 2–3 cm in length were obtained. A few casual experiments suggested that other salts might be prepared in whisker form by similar procedures but this was not pursued.

EXPERIMENTAL

The silica aquagel was obtained by electrodialyzing solutions of N grade sodium silicate produced by the Philadelphia Quartz Co. containing 4–5% silicon dioxide. The system was dialyzed to a pH of about 5. On standing, the silica sol sets to a hard, almost transparent silica aquagel.

About 25 g of urea was added to 500 g of silica aquagel containing about 30 g of SiO_2, and thoroughly mixed until a syrupy texture was obtained. About 10 g of a semirefined hydrocarbon oil of 174 SUS viscosity at 210° F diluted with about 10 g of varsol was added, and a uniform emulsion prepared. About 50% of the water was boiled off at atmospheric pressure while the slurry was being stirred. The powdery residue

**Issued as N.R.C. No. 6733.*

much higher yields (25–31%) obtained from the conifers, and the former group has a carbon and hydrogen content of about 59 and 5.5% respectively as apposed to about 63 and 6.3% respectively for the latter group. There is, too, a slight but significant difference in the methoxyl content of the deciduous and straw lignins, the latter being about 1% greater than the former.

ACKNOWLEDGMENTS

The authors wish to express their thanks to Dr. C. Riley of the Canadian Agriculture Research Station, Saskatoon, and to Mr. H. Gerrie, Department of Field Husbandry, University of Saskatchewan, Saskatoon, for their assistance in the provision of various wood and straw samples. Acknowledgment is also made of the financial assistance given by the Saskatchewan Research Council in support of this research.

1. J. M. PEPPER, P. E. T. BAYLIS, and E. ADLER. Can. J. Chem. **37**, 1241 (1959).
2. J. M. PEPPER and M. SIDDIQUEULLAH. Can. J. Chem. **39**, 1454 (1961).
3. J. M. PEPPER and M. SIDDIQUEULLAH. Can. J. Chem. **39**, 390 (1961).

RECEIVED DECEMBER 20, 1961.
DEPARTMENT OF CHEMISTRY,
UNIVERSITY OF SASKATCHEWAN,
SASKATOON, SASKATCHEWAN.

UREA AND SODIUM CHLORIDE WHISKERS*

L. D. CALVERT, A. F. SIRIANNI, AND I. E. PUDDINGTON

INTRODUCTION

The growth of molybdena whiskers on a molybdenum trioxide – silicon dioxide substrate was reported by Callahan, Petrucci, and Brown (1). Sodium chloride whiskers possessing a visible twist and having a mean length of 180 mm and a thickness of 1–30 μ were obtained by Jeszenszky and Hartmann (2). Sodium chloride whiskers have also been reported by Fells and Firth (3). Alumina, zirconia, and silica whiskers have been observed by Cunningham (4). Twists on alumina whiskers have been described by Sears, De Vries, and Huffine (5).

While the behavior of finely divided silica in hydrocarbon oil was being investigated, an accidental observation led to the experiments described below in which urea whiskers of the order of 25 cm in length and very thin sodium chloride crystals of 2–3 cm in length were obtained. A few casual experiments suggested that other salts might be prepared in whisker form by similar procedures but this was not pursued.

EXPERIMENTAL

The silica aquagel was obtained by electrodialyzing solutions of N grade sodium silicate produced by the Philadelphia Quartz Co. containing 4–5% silicon dioxide. The system was dialyzed to a pH of about 5. On standing, the silica sol sets to a hard, almost transparent silica aquagel.

About 25 g of urea was added to 500 g of silica aquagel containing about 30 g of SiO_2, and thoroughly mixed until a syrupy texture was obtained. About 10 g of a semirefined hydrocarbon oil of 174 SUS viscosity at 210° F diluted with about 10 g of varsol was added, and a uniform emulsion prepared. About 50% of the water was boiled off at atmospheric pressure while the slurry was being stirred. The powdery residue

*Issued as N.R.C. No. 6733.

was packed into crystallizing dishes with a spatula and the remaining water was evaporated under the following experimental conditions:

(*a*) at room temperature from open containers,
(*b*) in an oven at 110° C,
(*c*) under reduced pressure at room temperature,
(*d*) at a variety of constant relative humidities at room temerature.

The details of the whisker growth observed are given below. Sodium chloride whiskers were produced by substituting salt for urea in the silica aquagel – hydrocarbon oil mixture.

RESULTS

Extremely fine urea whiskers of the order of 10–12 cm in length appeared in various areas perpendicular to the surface of the packed substrate while it was left to stand overnight at room temperature. After about 6 days, a large number of fibers grew to a length of about 25 cm. Meanwhile, a very dense fibrous growth of short crystals swelled the substrate into a thick soft mat of about eight times its original volume. No further obvious change occurred on longer standing. The fibrous growth in the substrate and the appearance of the urea whiskers can be seen in Fig. 1. Short intertwined urea fibrils were produced by heating the mixture at 110° C. A somewhat similar type of growth appeared upon evacuating a warm suspension.

A longer time was required for crystal growth to occur in an enclosed system at a constant relative humidity at room temperature. Portions of the urea substrate were packed in Petri dishes to a depth of about 1 cm and placed in desiccators containing supersaturated solutions of zinc chloride, calcium nitrate, and ammonium chloride to give respective relative humidities of about 10, 51, and 79%. Each system was closed under a slight vacuum. After about 14 days, a sudden fibrous growth intermingled with a large number of longer crystals appeared in the desiccator over the $ZnCl_2$ solution. This is shown in Fig. 2. The elongated column of fibrous crystals shown in the right-hand side of the photograph was obtained by raising the temperature overnight to about 40° C. The upper portion of the column was contaminated with some silica and oil. When growth was resumed at room temperature the center portion remained white, and virtually free of contaminants. There was no evidence of crystal growth in the desiccator at about 79% relative humidity even after 4 months. After about 3 weeks, short, rather thick crystals appeared where the relative humidity was maintained at 51%. These were less voluminous than those which appeared at 10% relative humidity.

It was found that the long white crystals melted at 131° C, contained no ash, and gave a positive test for amine. An infrared spectrum identified the material as urea. X-Ray diffraction photographs corresponded to the known urea pattern. When the surface was coated with a dye and growth encouraged by raising the temperature of the material about 15° C above room temperature, dyed portions were completely lifted upwards by the growing fibers. There was no visible evidence of crystal growth above the dye level. Some fibers which had bent ends were noted to be at different angular positions during their early period of growth.

Morphology of the Whiskers

Urea

The rapidly grown silky fibrils (100–200 μ diam.) were found to be loosely connected bundles of heavily notched, "ribbon-like" fibers, as frequently curved as straight. Individual fibers showed perfect cleavage parallel and perpendicular to the fiber direction. The broken ends usually presented a stepped appearance with the cleavage faces perpendicular to each other. These faces are probably (011) and (001) since these are the

known cleavage faces for urea. The X-ray results show that the cleavage perpendicular to the fiber must be on (001). X-Ray rotation photographs of the silky fibrils gave typical fiber diagrams with the fiber axis as [001]; the arcing on the photographs corresponded to a variation of $\pm 15°$ from the mean fiber direction for individual fibers. A similar rotation photograph of a single 20-μ fiber, typical of the slowly grown fibers, showed it to be a single crystal with (001) as its fiber axis. Such individual fibers, which are typically uniform in diameter along their length, show extinction parallel to the fiber when examined in a microscope under crossed polars; if the fiber has a bend in it the direction of extinction follows the bend. Examination in an optical goniometer usually reveals continuous or streaky reflections extending over many degrees with maxima separated by 90°. The external appearance of these fibers is deceptive but most appear as spiral "ribbons". Goniometric measurement of the twist gives values in the range 12–20°/mm for long, straight fibers. One spiral "ribbon" with a twist of 12°/mm over a 10-mm length was found to be roughly triangular in cross section, rounded at the corners, with a single re-entrant right-angled notch on one side. The spiralling of this notch was apparently sufficient to create the observed spiral ribbon-like appearance. It is probable that the flat faces bounding the notches are responsible for the observed goniometer signals 90° apart while the rounded corners yield the continuous or streaky reflections. Such a cross section, though observed a number of times, was not as common as a strongly notched cross section, much wider in one cross dimension than the other. In no case was a central hole observed in a cross section, although many fibers appeared to be hollow on casual inspection.

Sodium Chloride

Very thin sodium chloride whiskers of the order of 2–3 cm in length were observed growing on the surface of a substrate after it had stood at room temperature for about 6 days. Many shorter fibrous crystals swelled the substrate to a thick soft mat. The longer crystals lying almost flat on the surface of the mat can be seen from Fig. 3. These fibers were identified as sodium chloride from their X-ray diffraction photographs.

The fibers of sodium chloride were generally fine (20 μ), with the thinnest bending easily in the draughts present in the room. While generally similar to the urea fibers, they were not so ribbon-like (diameters seldom differing by more than 3:2) and much more regular in form. They were distinguished by frequent kinks at right angles. One such fiber was observed with four kinks in a short distance forming a rectangular "spiral". X-Ray rotation photographs showed the fibers to be single crystals with [001] (i.e. any cubic axis) as the fiber axis. Optical goniometry usually gave faces separated by 90°, the most likely form being {011}. An exceptionally good fiber gave four reflections, tentatively identified as coming from the faces (110), ($1\bar{1}0$), ($\bar{3}\bar{2}0$), and ($\bar{3}20$). Many fibers showing a slight spiral twist were so fine that no satisfactory observations of their form could be made.

CONCLUSIONS

Although no final conclusions can be given at the present time, the evidence suggests that the growth proceeds from the base and that the conditions defining the diameter and twist of the fiber persist over fairly long periods of time. The formation of the whiskers seems to be dependent on some feature of the substrate and the rate of loss of water. Curiously, whiskers grew in relative humidities of 10 and 51% but not of 79%. As the total amount of water is depleted many surface imperfections occur and crystal growth can take place relatively unrestricted in many directions. The type of

FIG. 1. Urea whiskers and fibrous crystals grown at room temperature.
FIG. 2. Urea whiskers and fibrous crystals grown at 10% relative humidity at room temperature.

PLATE II

FIG. 3. Sodium chloride whiskers and fibrous crystals grown at room temperature.

hydrocarbon oil seems to have little influence since very thin urea whiskers of the order 5–6 cm in length were obtained using medicinal oil instead of the less refined hydrocarbon oil.* Whiskers could not be produced using urea and oil alone. It may be remarked that needle growth of crystals is favored when crystallization is rapid and requires the dissipation of a large amount of energy. The factors governing the growth of these fibers are not yet understood and a series of experiments to define them is planned (6).

ACKNOWLEDGMENT

The authors wish to thank Miss M. McLellan for making the measurements reported here.

1. J. L. CALLAHAN, R. H. PETRUCCI, and C. A. BROWN. J. Colloid Sci. **15**, 418 (1960).
2. B. JESZENSZKY and C. E. HARTMANN. Nature, **189**, 213 (1961).
3. H. A. FELLS and J. B. FIRTH. Proc. Roy. Soc. (London), A, **112**, 468 (1926).
4. A. L. CUNNINGHAM. Report on Contract No. Nonr-2619(00). April 14, 1960.
5. G. W. SEARS, R. C. DE VRIES, and C. HUFFINE. J. Chem. Phys. **34**, 2142 (1961).
6. R. H. DOREMUS, B. W. ROBERTS, and D. TURNBULL. Growth and perfection of crystals. John Wiley and Sons, Inc., New York. 1958. p. 68.

RECEIVED DECEMBER 9, 1961.
DIVISION OF APPLIED CHEMISTRY,
NATIONAL RESEARCH COUNCIL,
OTTAWA, CANADA.

THE DECOMPOSITION OF *n*-PENTANE SENSITIZED BY ALLYL RADICALS

W. A. BRYCE AND M. S. HARDIMAN

The inhibition of the thermal decomposition of paraffin hydrocarbons by propylene has for many years been ascribed to the removal, from the system, of chain-propagating radicals such as CH_3 and C_2H_5 by hydrogen abstraction from the inhibitor (1, 2). It was assumed that the allyl radical formed was not sufficiently reactive to serve as a chain propagator and hence the rate of the overall decomposition was substantially reduced compared with the rate in the absence of propylene. The residual rate of the so-called "fully inhibited" reaction has, in the past, been ascribed to non-radical molecular processes.

Interest in the reactivity of the allyl radical has developed during the past few years. A reconsideration of its role in organic decompositions inhibited by propylene has been made necessary by the results of recent investigations (3–6) which have established that allyl radicals are capable of abstracting hydrogen at temperatures above 400° C. It can therefore no longer be argued that inhibition by propylene at these temperatures is a consequence of the inability of allyl to propagate decomposition chains. The role of allyl and of nitric oxide in the mechanism of inhibited decompositions has been discussed in general terms by McNesby and Gordon (5) and by Bryce and Ruzicka (6) and has been supported by recent results (7) on the pyrolysis of normal butane. Detailed theoretical treatments of the kinetics of inhibited decompositions have been presented recently by Laidler and Wojciechowski (8) and by Eyring (9). It is assumed in both of these discussions that molecular mechanisms play no significant part.

**Bundles of crystals 3–4 cm in length, thick at the base and tapering to a point at the tips, were obtained from silica aquagel alone after about 1 month's time.*

hydrocarbon oil seems to have little influence since very thin urea whiskers of the order 5–6 cm in length were obtained using medicinal oil instead of the less refined hydrocarbon oil.* Whiskers could not be produced using urea and oil alone. It may be remarked that needle growth of crystals is favored when crystallization is rapid and requires the dissipation of a large amount of energy. The factors governing the growth of these fibers are not yet understood and a series of experiments to define them is planned (6).

ACKNOWLEDGMENT

The authors wish to thank Miss M. McLellan for making the measurements reported here.

1. J. L. CALLAHAN, R. H. PETRUCCI, and C. A. BROWN. J. Colloid Sci. **15**, 418 (1960).
2. B. JESZENSZKY and C. E. HARTMANN. Nature, **189**, 213 (1961).
3. H. A. FELLS and J. B. FIRTH. Proc. Roy. Soc. (London), A, **112**, 468 (1926).
4. A. L. CUNNINGHAM. Report on Contract No. Nonr-2619(00). April 14, 1960.
5. G. W. SEARS, R. C. DE VRIES, and C. HUFFINE. J. Chem. Phys. **34**, 2142 (1961).
6. R. H. DOREMUS, B. W. ROBERTS, and D. TURNBULL. Growth and perfection of crystals. John Wiley and Sons, Inc., New York. 1958. p. 68.

RECEIVED DECEMBER 9, 1961.
DIVISION OF APPLIED CHEMISTRY,
NATIONAL RESEARCH COUNCIL,
OTTAWA, CANADA.

THE DECOMPOSITION OF *n*-PENTANE SENSITIZED BY ALLYL RADICALS

W. A. BRYCE AND M. S. HARDIMAN

The inhibition of the thermal decomposition of paraffin hydrocarbons by propylene has for many years been ascribed to the removal, from the system, of chain-propagating radicals such as CH_3 and C_2H_5 by hydrogen abstraction from the inhibitor (1, 2). It was assumed that the allyl radical formed was not sufficiently reactive to serve as a chain propagator and hence the rate of the overall decomposition was substantially reduced compared with the rate in the absence of propylene. The residual rate of the so-called "fully inhibited" reaction has, in the past, been ascribed to non-radical molecular processes.

Interest in the reactivity of the allyl radical has developed during the past few years. A reconsideration of its role in organic decompositions inhibited by propylene has been made necessary by the results of recent investigations (3–6) which have established that allyl radicals are capable of abstracting hydrogen at temperatures above 400° C. It can therefore no longer be argued that inhibition by propylene at these temperatures is a consequence of the inability of allyl to propagate decomposition chains. The role of allyl and of nitric oxide in the mechanism of inhibited decompositions has been discussed in general terms by McNesby and Gordon (5) and by Bryce and Ruzicka (6) and has been supported by recent results (7) on the pyrolysis of normal butane. Detailed theoretical treatments of the kinetics of inhibited decompositions have been presented recently by Laidler and Wojciechowski (8) and by Eyring (9). It is assumed in both of these discussions that molecular mechanisms play no significant part.

**Bundles of crystals 3–4 cm in length, thick at the base and tapering to a point at the tips, were obtained from silica aquagel alone after about 1 month's time.*

In an attempt to demonstrate directly the ability of allyl radicals to initiate the decomposition of paraffin hydrocarbons an investigation has been made of the pyrolysis of *n*-pentane in the presence of varying amounts of diallyl (1,5-hexadiene). The latter compound decomposes at a temperature substantially lower than that required for the pyrolysis of *n*-pentane and the kinetic and analytical evidence (5, 6) indicates that the primary dissociation results in the formation of two allyl radicals:

$$CH_2{=}CH{-}CH_2{-}CH_2{-}CH{=}CH_2 \rightarrow 2CH_2{=}CH{-}CH_2\cdot.$$

The effect of the allyl radicals thus generated on the rate of decomposition of *n*-pentane was observed by following the pressure change in the system and by obtaining a complete analytical mass balance for the components of the reaction mixture at the specified reaction time. All analyses were done by gas chromatography using conventional techniques.

The overall effect of the addition of diallyl to *n*-pentane is illustrated by the pressure–time curves presented in Fig. 1. It is recognized that there are limitations to the reliance

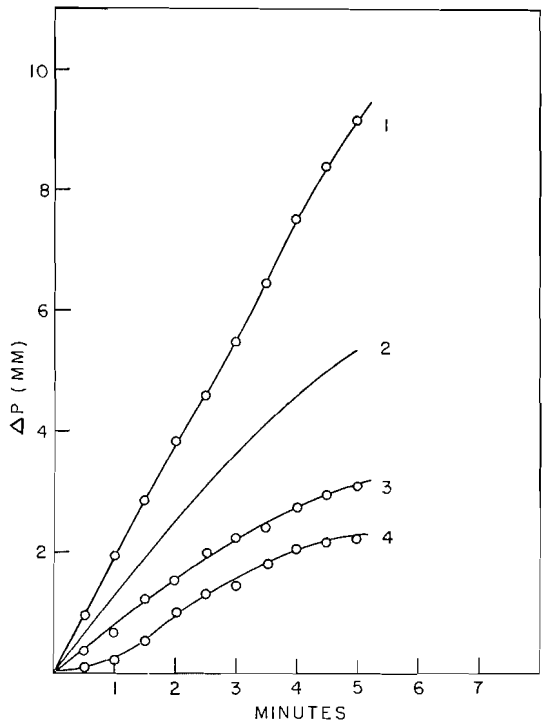

FIG. 1. The effect of the addition of diallyl on the rate of decomposition of *n*-pentane at 480° C: (1) 90 mm *n*-pentane plus 10 mm diallyl; (2) calculated assuming independent decomposition of *n*-pentane and diallyl; (3) 90 mm *n*-pentane; (4) 10 mm diallyl plus 90 mm Kr.

one can place on pressure measurements as a means of following gas-phase reactions, particularly when polymerizable materials are involved. However, this technique does provide a measure of reaction rate where the main process involves the decomposition of a paraffin. It is apparent from a comparison of curves 1 and 3 that the decomposition of *n*-pentane at 90 mm pressure is significantly accelerated by the addition of 10 mm of diallyl. The pressure change versus time curve for 10 mm of diallyl to which 90 mm

of krypton was added to maintain a total pressure of 100 mm is given in curve 4. The more rapid decomposition of diallyl than of *n*-pentane can be seen from the fact that the pressure increase for 10 mm of diallyl plus 90 mm Kr at 3 minutes is 22% while the corresponding figure for *n*-pentane alone is only 2.4%. If one were to make the extreme assumption that the *n*-pentane and diallyl were decomposing independently the total pressure increase would be merely the sum of curves 3 and 4. The resultant, curve 2, falls well below the results shown in curve 1. The effect of the diallyl in initiating the decomposition of *n*-pentane thus appears to be established.

Further indication of the initiation of *n*-pentane decomposition by allyl radicals is revealed by the analytical results for propylene and ethylene. These two compounds, which are formed in roughly the same proportions in the pyrolysis of *n*-pentane, together constitute about half of the decomposition products under normal conditions. In Fig. 2,

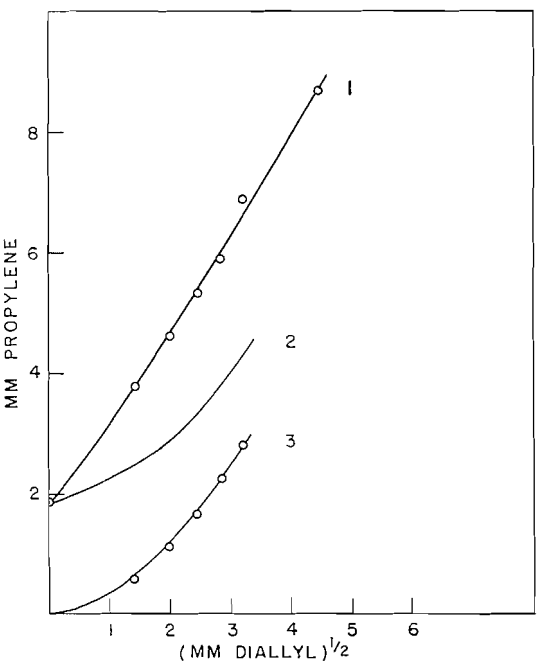

FIG. 2. Propylene yield at 5 minutes as a function of square root of diallyl pressure: (1) *n*-pentane plus diallyl; (2) calculated assuming independent decomposition of *n*-pentane and diallyl; (3) diallyl plus krypton. Total pressure, 100 mm.

curve 1, the partial pressure of propylene in the reaction mixture is plotted against the square root of the diallyl partial pressure for a reaction time of 5 minutes. The total initial pressure was kept constant at 100 mm. The temperature was again 480° C. The propylene pressure was plotted as a function of $(P_{\text{diallyl}})^{1/2}$ on the assumption that the latter quantity was a measure of allyl radical concentration in accordance with an equilibrium dissociation of diallyl:

$$\text{diallyl} \rightleftharpoons 2\text{allyl};$$

$$P_{\text{allyl}} = (KP_{\text{diallyl}})^{1/2}.$$

Curve 3 in Fig. 2 shows the variation of the partial pressure of propylene in the reaction mixture at 5 minutes' reaction time for the decomposition of diallyl in the presence of

krypton for the range of partial pressures of diallyl used in this investigation. If again one were to make the assumption that *n*-pentane and diallyl were decomposing independently in the pentane–diallyl mixtures, the partial pressure of propylene would be merely the sum of the propylene produced by each compound. The variation of this sum with square root of diallyl concentration is presented in curve 2. The fact that this curve falls well below curve 1 establishes that the decomposition of the diallyl sensitizes the decomposition of *n*-pentane to propylene and other products. The overall dependence of propylene production on the square root of the diallyl pressure is slightly greater than linear.

Results of the same kind for the production of ethylene are given in Fig. 3. The production of ethylene, which must involve secondary decomposition processes, is much

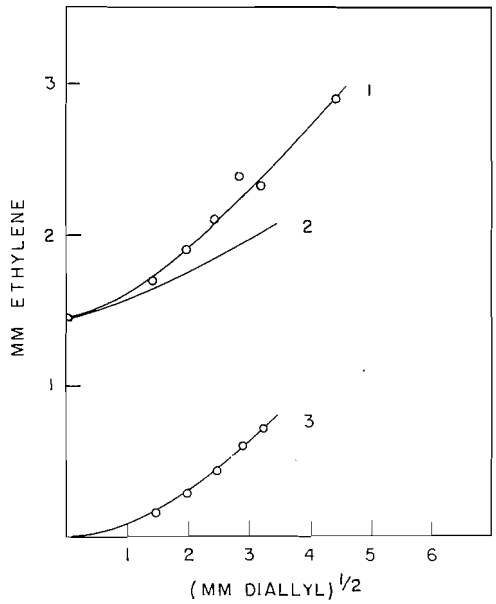

FIG. 3. Ethylene yield at 5 minutes as a function of square root of diallyl pressure: (1) *n*-pentane plus diallyl; (2) calculated assuming independent decomposition of *n*-pentane and diallyl; (3) diallyl plus krypton. Total pressure, 100 mm.

less dependent on the square root of the diallyl pressure than is the production of propylene, as is revealed by a comparison of the slopes of curves in Figs. 3 and 2. The production of ethylene by the decomposition of diallyl in the presence of krypton is shown in curve 3. The C_2H_4 which would be produced assuming the independent decomposition of *n*-pentane and diallyl is given by curve 2. It is thus apparent that the decomposition of diallyl has sensitized those processes in the *n*-pentane decomposition which result in the formation of ethylene.

A more complete account of this work will be published at a later date.

We are grateful to the National Research Council for financial support.

1. E. W. R. STEACIE. Atomic and free radical reactions. Reinhold, New York. 1954. Chap. IV.
2. N. N. SEMENOV. Some problems of chemical kinetics and reactivity. Vol. 1. Pergamon, London. 1958. p. 244.
3. J. R. MCNESBY and A. S. GORDON. J. Am. Chem. Soc. **79**, 4593 (1957).

4. W. A. BRYCE and P. KEBARLE. Trans. Faraday Soc. **54**, 1660 (1958).
5. D. J. RUZICKA and W. A. BRYCE. Can. J. Chem. **38**, 827 (1960).
6. W. A. BRYCE and D. J. RUZICKA. Can. J. Chem. **38**, 835 (1960).
7. J. H. PURNELL and C. P. QUINN. Nature, **189**, 656 (1961).
8. K. J. LAIDLER and B. W. WOJCIECHOWSKI. Can. J. Chem. **38**, 1027 (1960).
9. H. EYRING. Abstracts of Papers, XVIIth International Congress I.U.P.A.C., Montreal, Que. 1961. Paper A1-64.

RECEIVED JANUARY 22, 1962.
DEPARTMENT OF CHEMISTRY,
UNIVERSITY OF BRITISH COLUMBIA,
VANCOUVER, BRITISH COLUMBIA.

THE SYSTEM LITHIUM SULPHATE – MAGNESIUM SULPHATE – WATER AT 30° C

G. ARAVAMUDAN[1]

INTRODUCTION

The equilibrium relationships were studied in the system lithium sulphate – magnesium sulphate – water at 30° C and below in order to find out whether lithium sulphate would behave as the other alkali metal sulphates and ammonium sulphate, which are well known to form double salts with the magnesium salt. The binary system of the two salts is of the simple eutectic type and is devoid of any compounds, according to Bergman and Golubova (1).

EXPERIMENTAL

The complexes, comprised of the three components, were prepared by several different methods at 30° C so that the complete nature of the isotherm, inclusive of the metastable regions, if any, and of the kinetics of approach to equilibrium could be ascertained. In general, the complexes were prepared by the admixture of pairs of solid and liquid phases as follows: (i) lithium sulphate monohydrate and concentrated or supersaturated solutions of magnesium sulphate, (ii) anhydrous lithium salt and liquid phase as in (i), (iii) magnesium sulphate heptahydrate and saturated solutions of lithium salt, (iv) partially desiccated magnesium sulphate heptahydrate (containing 13–15% water by weight) and liquid phase as in (iii), (v) mixtures of $Li_2SO_4.H_2O$ and $MgSO_4.7H_2O$ crystals and water, and (vi) anhydrous lithium salt and solutions containing lithium and magnesium sulphate. Besides the above methods, controlled evaporation at 30° C of solutions containing various proportions of the lithium and magnesium salts was also carried out. The complexes were well agitated at 30±0.02° C for varying periods of time, after which the saturated solutions were quickly separated from the wet solid phase by conventional methods. Equilibrium was found to be attained within 24 hours in most cases. However, much longer periods of about 15 days or more were required in cases where the complexes were made by the method (iv). The scheme of analysis adopted in all cases consisted of the determination of the percentage of total anhydrous salt by drying to constant weight and of percentage of magnesium by the oxine method, which was found to give values accurate to 0.1%.

RESULTS AND DISCUSSION

A representative set of results of the experiments obtained under equilibrium conditions at 30° C is set forth in Table I. Extrapolation of tie lines in Fig. 1 shows clearly that three solid phases exist at 30° C, namely, $Li_2SO_4.H_2O$, $MgSO_4.7H_2O$, and $MgSO_4.6H_2O$, the last of which appears under metastable conditions only. Addition of lithium sulphate, in anhydrous or hydrated state, to supersaturated solutions of magnesium sulphate resulted in the crystallization of the magnesium sulphate hexahydrate in most cases. Two invariant points were realized, the first related to the cosaturation

[1]*Present address: Department of Chemistry, Indian Institute of Technology, Madras-36, India.*

4. W. A. BRYCE and P. KEBARLE. Trans. Faraday Soc. **54**, 1660 (1958).
5. D. J. RUZICKA and W. A. BRYCE. Can. J. Chem. **38**, 827 (1960).
6. W. A. BRYCE and D. J. RUZICKA. Can. J. Chem. **38**, 835 (1960).
7. J. H. PURNELL and C. P. QUINN. Nature, **189**, 656 (1961).
8. K. J. LAIDLER and B. W. WOJCIECHOWSKI. Can. J. Chem. **38**, 1027 (1960).
9. H. EYRING. Abstracts of Papers, XVIIth International Congress I.U.P.A.C., Montreal, Que. 1961. Paper A1-64.

RECEIVED JANUARY 22, 1962.
DEPARTMENT OF CHEMISTRY,
UNIVERSITY OF BRITISH COLUMBIA,
VANCOUVER, BRITISH COLUMBIA.

THE SYSTEM LITHIUM SULPHATE – MAGNESIUM SULPHATE – WATER AT 30° C

G. ARAVAMUDAN[1]

INTRODUCTION

The equilibrium relationships were studied in the system lithium sulphate – magnesium sulphate – water at 30° C and below in order to find out whether lithium sulphate would behave as the other alkali metal sulphates and ammonium sulphate, which are well known to form double salts with the magnesium salt. The binary system of the two salts is of the simple eutectic type and is devoid of any compounds, according to Bergman and Golubova (1).

EXPERIMENTAL

The complexes, comprised of the three components, were prepared by several different methods at 30° C so that the complete nature of the isotherm, inclusive of the metastable regions, if any, and of the kinetics of approach to equilibrium could be ascertained. In general, the complexes were prepared by the admixture of pairs of solid and liquid phases as follows: (i) lithium sulphate monohydrate and concentrated or supersaturated solutions of magnesium sulphate, (ii) anhydrous lithium salt and liquid phase as in (i), (iii) magnesium sulphate heptahydrate and saturated solutions of lithium salt, (iv) partially desiccated magnesium sulphate heptahydrate (containing 13–15% water by weight) and liquid phase as in (iii), (v) mixtures of $Li_2SO_4.H_2O$ and $MgSO_4.7H_2O$ crystals and water, and (vi) anhydrous lithium salt and solutions containing lithium and magnesium sulphate. Besides the above methods, controlled evaporation at 30° C of solutions containing various proportions of the lithium and magnesium salts was also carried out. The complexes were well agitated at 30±0.02° C for varying periods of time, after which the saturated solutions were quickly separated from the wet solid phase by conventional methods. Equilibrium was found to be attained within 24 hours in most cases. However, much longer periods of about 15 days or more were required in cases where the complexes were made by the method (iv). The scheme of analysis adopted in all cases consisted of the determination of the percentage of total anhydrous salt by drying to constant weight and of percentage of magnesium by the oxine method, which was found to give values accurate to 0.1%.

RESULTS AND DISCUSSION

A representative set of results of the experiments obtained under equilibrium conditions at 30° C is set forth in Table I. Extrapolation of tie lines in Fig. 1 shows clearly that three solid phases exist at 30° C, namely, $Li_2SO_4.H_2O$, $MgSO_4.7H_2O$, and $MgSO_4.6H_2O$, the last of which appears under metastable conditions only. Addition of lithium sulphate, in anhydrous or hydrated state, to supersaturated solutions of magnesium sulphate resulted in the crystallization of the magnesium sulphate hexahydrate in most cases. Two invariant points were realized, the first related to the cosaturation

[1]*Present address: Department of Chemistry, Indian Institute of Technology, Madras-36, India.*

TABLE I

The system Li_2SO_4–$MgSO_4$–H_2O at 30° C

Amount contained in 100 g saturated solution		Amount contained in 100 g wet residue		Composition of solid phase
Li_2SO_4	$MgSO_4$	Li_2SO_4	$MgSO_4$	
25.39				$Li_2SO_4.H_2O$
23.87	2.52	73.58	0.494	"
21.93	5.69	72.80	1.178	"
20.81	7.55	71.60	1.660	"
19.25	10.16	70.80	2.306	"
17.90	12.48	71.32	2.683	"
15.81	15.76	69.56	3.641	"
13.47	19.88	68.67	4.692	"
12.10	22.45	69.02	5.164	"
	28.10			$MgSO_4.7H_2O$
2.70	26.20	0.41	45.47	"
5.11	24.77	0.94	44.45	"
7.65	23.33	1.46	44.07	"
9.61	22.24	1.93	43.41	"
12.18	20.99	2.36	43.49	"
13.18	20.39	41.69	21.08	$MgSO_4.7H_2O$ $+Li_2SO_4.H_2O$
	31.02			$MgSO_4.6H_2O$
2.32	29.32	0.47	48.02	"
5.02	27.44	0.95	47.94	"
7.61	25.69	1.60	47.15	"
10.23	24.07	1.99	47.27	"
11.12	23.44	2.16	46.98	"
11.70	23.20	42.97	21.43	$MgSO_4.6H_2O$ $+Li_2SO_4.H_2O$

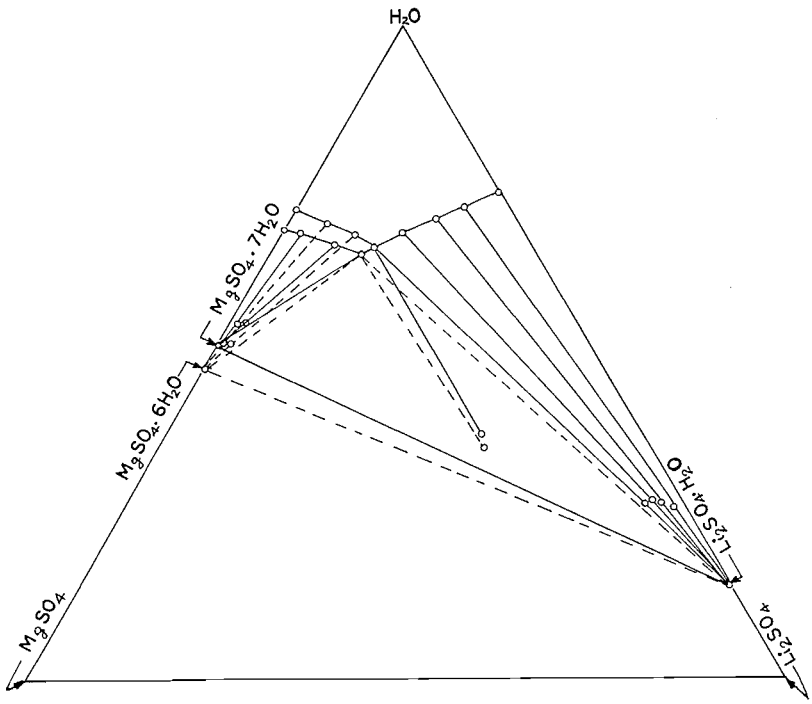

FIG. 1. The system Li_2SO_4–$MgSO_4$–H_2O at 30° C.

of the phases $Li_2SO_4.H_2O$ and $MgSO_4.7H_2O$ and the second of the phases $Li_2SO_4.H_2O$ and $MgSO_4.6H_2O$. Experiments carried at lower temperatures down to 0° C did not reveal any new phases apart from the above ones. While this study was in progress, results on the ternary system at 25° C and 75° C were reported by Lepeshkov and Romashova (2, 3). The authors have missed the metastable existence of the hexahydrate at 25° C.

ACKNOWLEDGMENTS

The author wishes to thank Professor K. R. Krishnaswami for his keen interest in the work and the Government of India for financial assistance.

1. A. G. Bergman and M. S. Golubova. Doklady Akad. Nauk S.S.S.R. **89**, 471 (1953).
2. I. N. Lepeshkov and N. N. Romashova. Russ. J. Inorg. Chem. (Chem. Soc. London), **4**, 1301 (1959).
3. I. N. Lepeshkov and N. N. Romashova. Russ. J. Inorg. Chem. (Chem. Soc. London), **5**, 1216 (1960).

Received December 18, 1961.
Department of Inorganic and Physical Chemistry,
Indian Institute of Science,
Bangalore-12, India.

SECONDARY ISOTOPE EFFECT IN THE ADDITION OF HYDROGEN ATOMS TO PROPYLENE-d_6[1]

M. Takahasi[2] and R. J. Cvetanović

In several recent studies the magnitudes and direction of the secondary deuterium isotope effects on reaction rates have been interpreted in terms of the configuration of the reaction centers in the transition complex (1–3). In particular Matsuoka and Szwarc (3) have found an increase of 7 to 11% in the rate of addition of methyl radicals to α,α,β-styrene-d_3 relative to styrene containing no deuterium, both carried out in isooctane solution. Although in the expected direction, the magnitude of the isotope effect was much smaller than that calculated (82%) on the assumption of a tetrahedral transition state. In view of this the authors concluded that the configuration of the transition state deviated only slightly from that of the initial state.

Recent work in this laboratory and elsewhere has shown important differences in the trends in reactivities of some free radicals. These are at least partly explainable in terms of the differences in the electron-seeking properties of the free radicals. The relative rates of addition of hydrogen atoms to a number of olefins in the gas phase have been recently determined in this laboratory (4, 5) and the trends in the rates are similar to those of methyl radicals in the corresponding reactions, although both are vastly different from the trends shown by oxygen atoms. Neither hydrogen atoms nor methyl radicals are likely to exhibit an appreciable electrophilic character and a similarity in their behavior is not unexpected. At the same time, besides a broad similarity, some significant quantitative differences in the reactivity trends of these two radical species have also been found. The latter are perhaps due to different steric requirements of the two reagents, although

[1]*Issued as N.R.C. No. 6746.*
[2]*National Research Council Postdoctorate Fellow 1960–61.*

of the phases $Li_2SO_4.H_2O$ and $MgSO_4.7H_2O$ and the second of the phases $Li_2SO_4.H_2O$ and $MgSO_4.6H_2O$. Experiments carried at lower temperatures down to 0° C did not reveal any new phases apart from the above ones. While this study was in progress, results on the ternary system at 25° C and 75° C were reported by Lepeshkov and Romashova (2, 3). The authors have missed the metastable existence of the hexahydrate at 25° C.

ACKNOWLEDGMENTS

The author wishes to thank Professor K. R. Krishnaswami for his keen interest in the work and the Government of India for financial assistance.

1. A. G. Bergman and M. S. Golubova. Doklady Akad. Nauk S.S.S.R. **89**, 471 (1953).
2. I. N. Lepeshkov and N. N. Romashova. Russ. J. Inorg. Chem. (Chem. Soc. London), **4**, 1301 (1959).
3. I. N. Lepeshkov and N. N. Romashova. Russ. J. Inorg. Chem. (Chem. Soc. London), **5**, 1216 (1960).

Received December 18, 1961.
Department of Inorganic and Physical Chemistry,
Indian Institute of Science,
Bangalore-12, India.

SECONDARY ISOTOPE EFFECT IN THE ADDITION OF HYDROGEN ATOMS TO PROPYLENE-d_6[1]

M. Takahasi[2] and R. J. Cvetanović

In several recent studies the magnitudes and direction of the secondary deuterium isotope effects on reaction rates have been interpreted in terms of the configuration of the reaction centers in the transition complex (1–3). In particular Matsuoka and Szwarc (3) have found an increase of 7 to 11% in the rate of addition of methyl radicals to α,α,β-styrene-d_3 relative to styrene containing no deuterium, both carried out in isooctane solution. Although in the expected direction, the magnitude of the isotope effect was much smaller than that calculated (82%) on the assumption of a tetrahedral transition state. In view of this the authors concluded that the configuration of the transition state deviated only slightly from that of the initial state.

Recent work in this laboratory and elsewhere has shown important differences in the trends in reactivities of some free radicals. These are at least partly explainable in terms of the differences in the electron-seeking properties of the free radicals. The relative rates of addition of hydrogen atoms to a number of olefins in the gas phase have been recently determined in this laboratory (4, 5) and the trends in the rates are similar to those of methyl radicals in the corresponding reactions, although both are vastly different from the trends shown by oxygen atoms. Neither hydrogen atoms nor methyl radicals are likely to exhibit an appreciable electrophilic character and a similarity in their behavior is not unexpected. At the same time, besides a broad similarity, some significant quantitative differences in the reactivity trends of these two radical species have also been found. The latter are perhaps due to different steric requirements of the two reagents, although

[1]*Issued as N.R.C. No. 6746.*
[2]*National Research Council Postdoctorate Fellow 1960–61.*

this point necessitates further study. In view of some difference in the behavior of hydrogen atoms and methyl radicals it was thought necessary to determine experimentally[3] the secondary isotope effect in the addition of hydrogen atoms to an olefinic double bond. For this purpose propylene and propylene-d_6 have been chosen as a representative pair of a light and a heavy olefin. With some modification in the design of the reaction vessel, the technique developed previously (4, 5) has been used for determination of the relative rate constants.

Hydrogen atoms are produced by mercury-photosensitized decomposition of *n*-butane and abstract another hydrogen atom from the *n*-butane to produce H_2 (reaction 1). When smaller amounts of an olefin are added, hydrogen atoms may also add to it (reaction 2) or abstract from it (reaction 3). Reactions have to be carried out with rigorously purified *n*-butane and at very small conversions. Under such conditions (4, 5),

$$[1] \qquad f(H_2) = \frac{R_{H_2}[1+\{q_2(Ol)/q_1(B)\}]}{R_{H_2}{}^* - R_{H_2}[1+\{q_2(Ol)/q_1(B)\}]} = \frac{k_3}{k_2} + \frac{k_1}{k_2}\frac{(B)}{(Ol)},$$

where $R_{H_2}{}^*$ and R_{H_2} are the rates of hydrogen formation in the absence and presence of the added olefin, respectively, (B) stands for *n*-butane and (Ol) for the olefin, and q_2/q_1 is the ratio of the quenching efficiencies of the olefin and *n*-butane. Since butane is always present in huge excess, q_2/q_1 does not have to be known too accurately and the previously employed (5) q_2/q_1 value of 8.2 has been also used in the present work. The same value was adopted for both C_3H_6 and C_3D_6 but even an appreciable difference in the quenching efficiencies of the two compounds could not have a significant effect on the results. The experimental $f(H_2)$ values are plotted against (B)/(Ol) and the slope of the linear plot gives k_1/k_2 and the intercept k_3/k_2.

The reaction system consisted of a 13.2-l. pyrex flask with a quartz window 5 cm in diameter attached to it through a large graded seal. The flask was provided with a glass stirrer on teflon bearings operated by an external rotating magnet and the gases were continuously stirred in the course of the reaction. The reactants were introduced through mercury cutoffs; they were then thoroughly degassed by repeated condensation and evaporation and saturated with mercury vapor by circulating with an all-glass plunger-type pump through a mercury saturator.

Phillips research grade *n*-butane was further purified to remove traces of olefin contaminants by passage through three wash bottles of concentrated H_2SO_4, over KOH pellets and through an activated silica gel column, followed by degassing and bulb-to-bulb distillation under reduced pressure. Phillips research grade propylene and propylene-d_6 obtained from Merck, Sharp & Dohme were thoroughly degassed in the usual manner. Mass spectrometric analysis of the deuteropropylene indicated 96% propylene-d_6 and 4% propylene-d_5. Reactions were carried out at 25±1° C, using 450 mm *n*-butane and varying small amounts of the olefin. The mercury resonance radiation was obtained from a low-pressure mercury vapor lamp, operated at a constant current of 100 ma supplied through a transformer from a voltage stabilizer. Exposure times of 20 minutes were used and the fluctuations in the lamp current remained less than 1% in these intervals. Hydrogen was collected through two liquid nitrogen traps by means of two mercury diffusion pumps and was measured on a constant volume burette.

The results of the measurements are given in Table I, where "Ratio" represents the ratio of the concentrations of *n*-butane and the added olefin, (B)/(Ol), and $f(H_2)$ is

[3]*No attempt has been made in the present work to estimate the expected theoretical values of the secondary isotope effects for different configurations of the transition state. The experimental value obtained is compared with the values reported in reference 3 for methyl radicals.*

TABLE I

The values of $f(H_2)$ at various n-butane/propylene ratios

Propylene							
Ratio	689	597	433	294	108		
$f(H_2)$	1.030	0.908	0.669	0.469	0.193		
Propylene-d_6							
Ratio	758	654	587	497	374	284	104
$f(H_2)$	1.108	0.955	0.828	0.660	0.578	0.464	0.209

defined in equation [1]. In the present work $R_{H_2}{}^*$ has not been corrected for finite conversion and residual olefin impurity (5). The values of the slopes and the intercepts of the plots of $f(H_2)$ vs. (B)/(Ol) have been calculated by the method of least mean squares and the k_2/k_1 and k_3/k_2 values thus obtained and their probable errors (6) are summarized in Table II. For comparison the previously determined (5) value for C_3H_6 is also given in the table and the agreement with the present result is seen to be satisfactory.

TABLE II

The values of k_2/k_1 and k_3/k_2

	k_2/k_1	k_3/k_2	Note
Previous result with propylene (5)	695±16	0.033±0.015	Circulating reaction system
Present result with propylene	692.3±3.8	0.0410±0.0037	Static reaction system (stirred reactor)
Present result with propylene-d_6	746±25	0.063±0.023	Static reaction system (stirred reactor)

The magnitude of the secondary isotope effect in the addition of H atoms to C_3D_6 and C_3H_6 is, on the basis of the results in Table II, $k_2(D)/k_2(H) = 1.078\pm0.037$. Thus the secondary isotope effect seems to be in the same direction as in the case of methyl radical addition to styrene and styrene-d_3 (3) and, as in this latter case, it is quite small.

The values of k_3/k_2 given in Table II indicate that $k_3(D)/k_3(H)$ is between 0.9 and 2.1. However, in view of the large extrapolations that have to be made, the intercepts of the $f(H_2)$-vs.-(B)/(Ol) plots may be considerably more uncertain than is suggested by the estimated limits of error in k_3/k_2 values in Table II. Consequently, much quantitative significance cannot be attached to these values. In agreement with this, direct mass spectrometric determinations of the HD-to-H_2 ratio in the hydrogen collected from the mixtures of n-butane and C_3D_6 give for $k_3(D)/k_1$ values of only 0.8–2.2. This would indicate some 20 times smaller rates of abstraction of D atoms from C_3D_6 than would have to be assumed on the basis of the mean value of the intercept of the $f(H_2)$-vs.-(B)/(C_3D_6) plot. The discrepancy may be entirely due to the large experimental uncertainties of the values of the intercepts. An alternative possibility is that a very small fraction (α) of the initial interaction of n-butane with the excited mercury atoms results in direct formation of H_2 (by molecular detachment) rather than giving H atoms and butyl radicals. In view of the experimental uncertainties and the smallness of this effect further, more extensive work is necessary to establish with certainty the cause of the apparent discrepancy. However, even if it should turn out that a small amount of molecular detachment of H_2 does occur in the mercury-photosensitized decomposition of n-butane, i.e. $\alpha > 0$, the present and the previously determined (5) relative rates of addition of hydrogen atoms to olefins will not be affected. The slope of the $f(H_2)$-vs.-(B)/(Ol) plots would in

this case be equal to $(1/1-\alpha)k_1/k_2$ and therefore the ratios of k_2 values for various olefins would remain unchanged.

The authors are grateful to Dr. A. W. Tickner for the mass spectrometric analysis.

1. A. STREITWIESER, JR. and R. C. FAHEY. Chem. & Ind. (London), 1417 (1957). A. STREITWIESER, JR., R. H. JAGOW, R. C. FAHEY, and S. SUZUKI. J. Am. Chem. Soc. **80**, 2326 (1958).
2. S. SELTZER. J. Am. Chem. Soc. **83**, 1861 (1961).
3. M. MATSUOKA and M. SZWARC. J. Am. Chem. Soc. **83**, 1260 (1961).
4. R. J. CVETANOVIĆ, W. E. FALCONER, and K. R. JENNINGS. J. Chem. Phys. **35**, 1225 (1961).
5. K. R. JENNINGS and R. J. CVETANOVIĆ. J. Chem. Phys. **35**, 1233 (1961).
6. H. MARGENAU and G. M. MURPHY. The mathematics of physics and chemistry. 2nd ed. D. Van Nostrand Co., Inc., Princeton, N.J. 1956. pp. 515, 519.

RECEIVED NOVEMBER 17, 1961.
DIVISION OF APPLIED CHEMISTRY,
NATIONAL RESEARCH COUNCIL,
OTTAWA, ONTARIO.

A RADIOCHEMICAL METHOD FOR THE ESTIMATION OF THE SULPHYDRYL-TO-DISULPHIDE RATIO IN WHEAT GLUTEN

C. C. LEE AND E. R. SAMUELS

Considerable interest has been shown in our earlier note (1) on S-(N-ethylsuccinimido)-L-cysteine (I), the adduct formed between L-cysteine and N-ethylmaleimide (NEM), and the possible use of I as a carrier for the estimation of the relative amounts of sulphydryl and disulphide groups in proteins containing S^{35}. Since some unchanged I can be recovered from an acid hydrolyzate after hydrolysis of peptide bonds (1), if a S^{35}-labelled protein were allowed to react with NEM and then hydrolyzed, any sulphydryl groups originally present as cysteine residues would give rise to S^{35}-labelled I, which could then be isolated with the aid of ordinary I as carrier. The present communication reports some preliminary results on the application of this technique in a study with gluten of wheat flour in which S^{35} has been incorporated.

Gluten was chosen for investigation because of the possible involvement of sulphydryl groups in the action of flour improvers (2–4). Minute amounts of oxidizing agents, such as bromate or iodate, are known to have the capability of improving the bread-making quality of flour. Suggestions have been made that such an improver action may be due to the formation of disulphide cross-linkages from oxidation of sulphydryl groups of the gluten (2), or the inhibition of interchange reactions in the protein network between disulphide bonds and sulphydryl groups, presumably through the oxidative destruction of the sulphydryls (3, 4). Because of the very low sulphydryl contents of flour, it has been difficult to obtain a clearcut demonstration of a direct oxidation of flour sulphydryls by flour improvers (5). The application of the sensitive tracer technique may be of advantage; hence the present study was undertaken.

Carrier-free S^{35} as sulphate was injected into the stems of maturing wheat plants of the Thatcher variety about 20 days before harvest. The resulting kernels were milled to provide a radioactive flour. Fractionation studies (6, 7) showed that the protein fractions obtained do contain S^{35}. Dough samples were prepared, each from 15 g of active flour, 7 ml of distilled water, and no improver, 50 p.p.m.* potassium bromate, or 50 p.p.m.

**Throughout this note, p.p.m. refers to parts per million based on the weight of flour.*

this case be equal to $(1/1-\alpha)k_1/k_2$ and therefore the ratios of k_2 values for various olefins would remain unchanged.

The authors are grateful to Dr. A. W. Tickner for the mass spectrometric analysis.

1. A. STREITWIESER, JR. and R. C. FAHEY. Chem. & Ind. (London), 1417 (1957). A. STREITWIESER, JR., R. H. JAGOW, R. C. FAHEY, and S. SUZUKI. J. Am. Chem. Soc. **80**, 2326 (1958).
2. S. SELTZER. J. Am. Chem. Soc. **83**, 1861 (1961).
3. M. MATSUOKA and M. SZWARC. J. Am. Chem. Soc. **83**, 1260 (1961).
4. R. J. CVETANOVIĆ, W. E. FALCONER, and K. R. JENNINGS. J. Chem. Phys. **35**, 1225 (1961).
5. K. R. JENNINGS and R. J. CVETANOVIĆ. J. Chem. Phys. **35**, 1233 (1961).
6. H. MARGENAU and G. M. MURPHY. The mathematics of physics and chemistry. 2nd ed. D. Van Nostrand Co., Inc., Princeton, N.J. 1956. pp. 515, 519.

RECEIVED NOVEMBER 17, 1961.
DIVISION OF APPLIED CHEMISTRY,
NATIONAL RESEARCH COUNCIL,
OTTAWA, ONTARIO.

A RADIOCHEMICAL METHOD FOR THE ESTIMATION OF THE SULPHYDRYL-TO-DISULPHIDE RATIO IN WHEAT GLUTEN

C. C. LEE AND E. R. SAMUELS

Considerable interest has been shown in our earlier note (1) on S-(N-ethylsuccinimido)-L-cysteine (I), the adduct formed between L-cysteine and N-ethylmaleimide (NEM), and the possible use of I as a carrier for the estimation of the relative amounts of sulphydryl and disulphide groups in proteins containing S^{35}. Since some unchanged I can be recovered from an acid hydrolyzate after hydrolysis of peptide bonds (1), if a S^{35}-labelled protein were allowed to react with NEM and then hydrolyzed, any sulphydryl groups originally present as cysteine residues would give rise to S^{35}-labelled I, which could then be isolated with the aid of ordinary I as carrier. The present communication reports some preliminary results on the application of this technique in a study with gluten of wheat flour in which S^{35} has been incorporated.

Gluten was chosen for investigation because of the possible involvement of sulphydryl groups in the action of flour improvers (2–4). Minute amounts of oxidizing agents, such as bromate or iodate, are known to have the capability of improving the bread-making quality of flour. Suggestions have been made that such an improver action may be due to the formation of disulphide cross-linkages from oxidation of sulphydryl groups of the gluten (2), or the inhibition of interchange reactions in the protein network between disulphide bonds and sulphydryl groups, presumably through the oxidative destruction of the sulphydryls (3, 4). Because of the very low sulphydryl contents of flour, it has been difficult to obtain a clearcut demonstration of a direct oxidation of flour sulphydryls by flour improvers (5). The application of the sensitive tracer technique may be of advantage; hence the present study was undertaken.

Carrier-free S^{35} as sulphate was injected into the stems of maturing wheat plants of the Thatcher variety about 20 days before harvest. The resulting kernels were milled to provide a radioactive flour. Fractionation studies (6, 7) showed that the protein fractions obtained do contain S^{35}. Dough samples were prepared, each from 15 g of active flour, 7 ml of distilled water, and no improver, 50 p.p.m.* potassium bromate, or 50 p.p.m.

**Throughout this note, p.p.m. refers to parts per million based on the weight of flour.*

potassium iodate. The dough was allowed to stand 3 hours, then thoroughly mixed with a solution of 400 p.p.m. NEM in 2 ml of distilled water, and then allowed to stand one more hour. The gluten was separated by washing off the starch (8) and dried at 100° C. A 1-g sample of pulverized, dry gluten was hydrolyzed by refluxing (100–103° C) for 18 hours in 50 ml of 6 *N* hydrochloric acid. The hydrolyzate was concentrated under reduced pressure, filtered, and made up to a volume of 25 ml. Twenty-five milligrams of ordinary NEM–cysteine adduct (I) was then added as carrier to aid in the subsequent development and separation of I by paper chromatography.

Although one-dimensional ascending paper chromatography was effective in separating I from cystine (1), it was necessary to use two-dimensional ascending paper chromatography, run at right angles to each other, in order to separate I from cystine and methionine. The solvent systems employed were 1-butanol, pyridine, acetic acid, water (BPAW) at the volume ratio of 30:20:6:24 and water-saturated phenol (WSP) (454 g phenol and 113.5 ml water). A number of 5-λ aliquots of each hydrolyzate were chromatographed on Whatman No. 1 filter paper, first in the BPAW system for about 18 hours, air dried, and then in the WSP system for about 20 hours. After air drying again, the chromatograms were developed with 0.1% ninhydrin in acetone. The spots corresponding to cystine, methionine, and adduct I were the only ones that showed activities significantly above background. The activity of the spot corresponding to cystine was of the order of 5000 c.p.m. The average values for the ratio of the activity of adduct I to the activity of cystine were 4.02:100, 3.67:100, and 0.86:100, respectively, for the chromatograms derived from doughs treated with no improver, with 50 p.p.m. potassium bromate, and with 50 p.p.m. potassium iodate. These decreases in the ratios of the activity of I to that of cystine indicate that some of the cysteine residues of the gluten were destroyed, likely by oxidation, after treatment with bromate or iodate. The data showed that under the conditions of the present experiments, the destruction of sulphydryls amounted to about 10% and 80%, respectively, when the dough was treated with 50 p.p.m. potassium bromate and with 50 p.p.m. potassium iodate.

For an absolute quantitative determination of the sulphydryl content of a protein by the measurement of the activity of I, it would be essential to have a complete recovery of I from the reaction of NEM with all of the sulphydryl groups of the protein. The use of an excess of NEM in the present experiments should facilitate its reaction with all the available sulphydryl groups of the dough. However, it is uncertain whether complete recovery of I from the gluten hydrolyzate was achieved because some decomposition of I might have occurred during the protein hydrolysis. On the other hand, if the fraction of I lost, if any, during protein hydrolysis were constant, as might be expected for hydrolyses carried out under identical conditions, relative comparisons of sulphydryl contents, as reported in this note, should still be valid. In order to demonstrate that the recovery of I after hydrolysis was constant, the following experiments were carried out. Radioactive adduct I was prepared from reaction of N-ethylmaleimide-1-C^{14} * with L-cysteine. It showed a single active spot after paper chromatography. This adduct was subjected to 10 replicate hydrolytic treatments in 6 *N* hydrochloric acid for 18 hours at 100–103° C, either with or without the presence of some ordinary gluten. Each hydrolyzate was chromatographed in the usual manner and the spot corresponding to adduct I was counted. The recovery of activity was essentially constant, amounting to 81±1% of the activity of I before hydrolysis. Thus the loss of I during hydrolysis under our experimental conditions is constant and the relative activities of I recovered after hydrolysis can be used as a measure of the sulphydryl content.

**Obtained from Schwarz Bio Research Inc., Mount Vernon, New York.*

To further establish the applicability of this radiochemical method, 1.0, 0.7, or 0.5 mmole of reduced glutathione in 10 ml of water was treated with 10 ml of solution containing 2.0 mmoles of C^{14}-labelled NEM. The resulting mixture was allowed to stand overnight, concentrated to a small volume, hydrolyzed in 6 *N* hydrochloric acid, and then chromatographed in the usual way. The spot corresponding to the recovered adduct I showed activities of 293, 211, and 150 c.p.m., respectively, for the original glutathione content of 1.0, 0.7, and 0.5 mmole. The activity ratio of 293:211:150 corresponds to 1.00:0.72:0.51, in excellent agreement with the known glutathione contents.

ACKNOWLEDGMENTS

The financial support given by the National Research Council of Canada and the award of a Province of Saskatchewan Graduate Research Scholarship to one of us (E. R. S.) are gratefully acknowledged.

1. C. C. Lee and E. R. Samuels. Can. J. Chem. **39**, 1152 (1961).
2. B. Sullivan. J. Agr. Food Chem. **2**, 1231 (1954).
3. S. Goldstein. Mitt. Gebiete Lebensm. u. Hyg. **48**, 87 (1957).
4. R. Frater, F. J. R. Hird, H. J. Moss, and J. R. Yates. Nature, **186**, 451 (1960).
5. H. A. Sokol, D. K. Mecham, and J. W. Pence. Cereal Chem. **37**, 151 (1960).
6. W. B. McConnell and L. K. Ramachandran. Can. J. Biochem. Physiol. **34**, 180 (1956).
7. E. Bilinski and W. B. McConnell. Cereal Chem. **35**, 66 (1958).
8. E. C. Swanson (*Editor*). Cereal laboratory methods. 6th ed. American Association of Cereal Chemists, Inc., St. Paul. 1957. p. 191.

Received October 10, 1961.
Department of Chemistry,
University of Saskatchewan,
Saskatoon, Saskatchewan.

Canadian Journal of Chemistry

Issued by THE NATIONAL RESEARCH COUNCIL OF CANADA

VOLUME 40 JUNE 1962 NUMBER 6

THIN LAYER CHROMATOGRAPHY OF CARBOHYDRATE ACETATES[1]

M. E. TATE[2] AND C. T. BISHOP

Division of Applied Biology, National Research Council, Ottawa, Canada

Received February 19, 1962

ABSTRACT

Thin layer chromatography on silica gel G with benzene–methanol mixtures is a rapid method for the analytical or semimicro preparative separation of low molecular weight carbohydrate acetates. Some mixtures of inositol acetates are also resolved by the same procedure. A sensitive spray reagent has been developed for the analytical detection of acetates on the chromatographic plates and is based on the formation of the ferric hydroxamate of acetic acid. Oligosaccharide acetates are easily detected on a semimicro preparative scale by spraying the chromatographic plates with water, a general, non-destructive method for detection of hydrophobic compounds. The chromatograms can be run in 40 minutes and multiple development can be carried out to improve resolution when necessary.

Thin layer chromatography has been reviewed in several recent articles (1–4). Its application to carbohydrates has so far been limited to the free sugars (5), which are strongly polar and, with the exception of certain specific conditions, are more conveniently separated by paper chromatography. The most spectacular applications of thin layer chromatography have been to the separation of slightly polar compounds, which are resolved only poorly or not at all by paper chromatography. The readily available carbohydrate acetates fall into this category and a study of their behavior on thin layer chromatograms was therefore undertaken and is described in the present paper.

This work constitutes an extension to thin layer chromatography of the separation of carbohydrate acetates on columns of Magnesol–Celite as described by McNeely, Binkley, and Wolfrom (6). The substitution of silica gel G for Magnesol–Celite was indicated when preliminary experiments showed the presence of ghost spots from pure, fully acetylated monosaccharides on thin layers of Magnesol–Celite after multiple development. Behavior of acid–base indicators on thin layer chromatograms of Magnesol–Celite showed that the adsorbent was alkaline. It was likely, therefore, that the ghost spots were a result of partial deacetylation of the compounds during the drying of plates between developments.

Good separations of carbohydrate acetates were obtained on thin layers of silica gel G using benzene–methanol mixtures containing 2–10% (v/v) of methanol. The mobilities of the various components were dependent on the concentration of methanol, within the above limits, and were presumably related to the strength of hydrogen bonding between the silicic acid and the compounds concerned. For example, with two developments, 4% of methanol in benzene is sufficient to resolve the acetylated lower members of the polymer homologous series of $1 \rightarrow 3$ linked β-D-glucose units obtained from laminarin.

[1]*Issued as N.R.C. No. 6799.*

[2]*National Research Council of Canada Postdoctorate Fellow 1960–1962.*

However, again with two developments, 10% of methanol in benzene is necessary to separate the acetates of a similar series of $1 \rightarrow 4$ linked β-D-N-acetylglucosamine units obtained from chitin.

Figure 1 shows the separation of the anomeric acetates of D-glucose, maltose, and cellobiose, and of the β-acetates of the polymer homologous series of oligosaccharides obtained from laminarin. These separations serve to illustrate the resolving power of this technique; the relative mobilities of anomeric pairs ($\beta > \alpha$) were the same as given by the Magnesol–Celite procedure (6) for the compounds used.

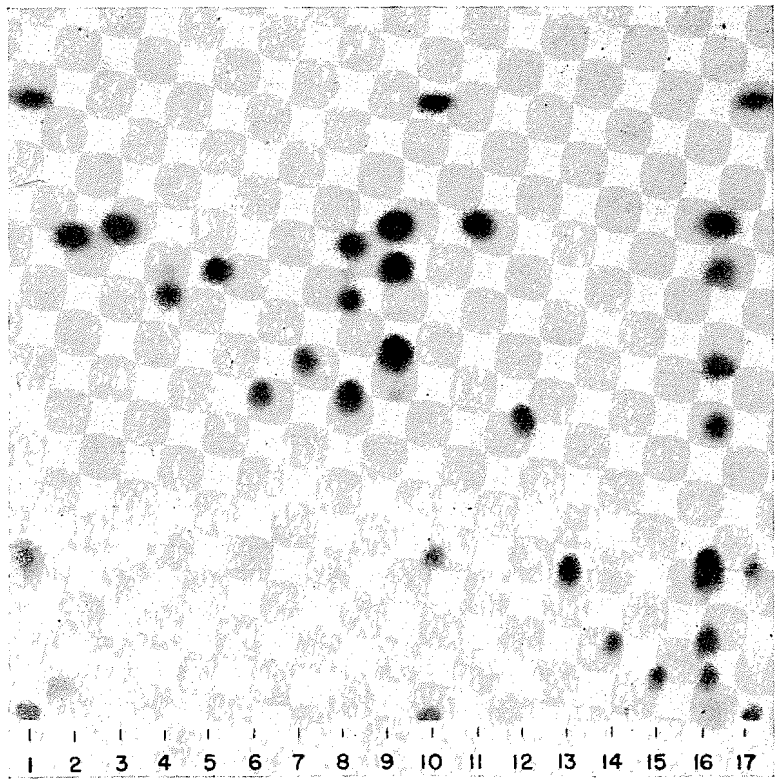

FIG. 1. Thin layer chromatogram of various carbohydrate acetates.*
Adsorbent: silica gel G; solvent: 4% methanol in benzene (v/v); double development (2×17 cm).
Components in decreasing order of mobility:

1, 10, 17. (Dyes as controls) Sudan III, methyl red, methyl orange
2. α-D-Glucopyranose pentaacetate
3, 11. β-D-Glucopyranose pentaacetate
4. α-Maltose octaacetate
5. β-Maltose octaacetate
6. α-Cellobiose octaacetate
7. β-Cellobiose octaacetate
8. Compounds 2, 4, and 6
9. Compounds 3 (11), 5, and 7
12. β-Laminaribiose octaacetate
13. β-Laminaritriose undecaacetate
14. β-Laminaritetraose tetradecaacetate
15. β-Laminaripentaose heptadecaacetate
16. Compounds 3 (11), 5, 7, 12–15

Figure 2 shows the separation of the inositol hexaacetates, four of which were completely resolved. *scyllo*-Inositol hexaacetate showed anomalous behavior and gave only

Trace impurities in 4 and 7 were anomers of the compounds cited.

a weak spot that was not resolved from either *allo-* or *muco*-inositol. The weak intensity of the *scyllo*-inositol hexaacetate spot was caused, at least partially, by the low solubility of this compound; heavier applications merely resulted in a streak running to the origin. With the exception of *scyllo*-inositol hexaacetate, the order of mobilities of the inositol hexaacetates was remarkably similar to the inverse order of electrophoretic mobilities of the inositol–borate complexes reported by Angyal and McHugh (7). These data are shown in Table I and indicate that a complex formation similar to that in the borate complexes may be responsible for the adsorption of inositol hexaacetates in thin layer chromatography.

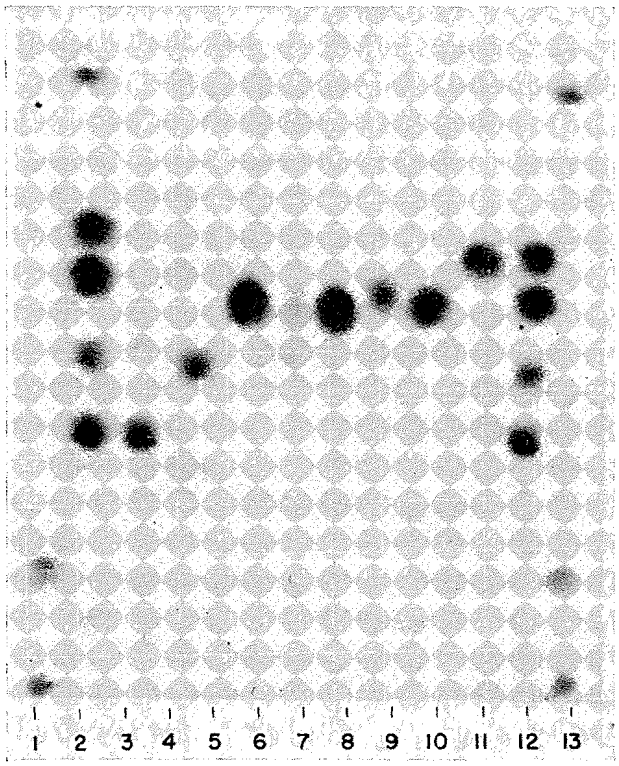

FIG. 2. Thin layer chromatogram of inositol hexaacetates.
Adsorbent: silica gel G; solvent: 4% methanol in benzene (v/v); double development (2×17 cm).
Components in decreasing order of mobility:

1, 13. (Dyes as controls) Sudan III,* methyl red, methyl orange
2, 12. *dl-*, *myo-*, *epi-*, and *cis*-Inositol hexaacetates
3. *cis*-Inositol hexaacetate
4. Blank
5. *epi*-Inositol hexaacetate
6. *muco*-Inositol hexaacetate
7. *scyllo*-Inositol hexaacetate (weak)
8. *allo*-Inositol hexaacetate
9. *neo*-Inositol hexaacetate
10. *myo*-Inositol hexaacetate
11. *dl*-Inositol hexaacetate

Figure 3 shows the separation of a mixture of oligosaccharide acetates on a semimicro preparative scale; this particular mixture of oligosaccharides was obtained by partial acid hydrolysis of a commercial dextran. The bands were detected by a spray of water

**This dye is displaced from position 1 toward position 2 because of irregular development at the edge of the plate.*

TABLE I

Relative mobilities of inositol–borate complexes on paper electrophoresis and of inositol hexaacetates on thin layer chromatograms

Inositol	M_G values in 0.012 M sodium tetraborate (7)	Distance moved (cm) from origin as hexaacetate*
cis-	1.6	5.8
epi-	1.5	7.5
muco-	0.87	8.9
allo-	0.54	8.8
myo-	0.30	9.1
neo-	0.30	9.2
dl-	0.28	10.0
scyllo-	0.02	8.9

*Double development (2×17 cm) of thin layer chromatogram on silica gel G using 4% methanol in benzene (v/v).

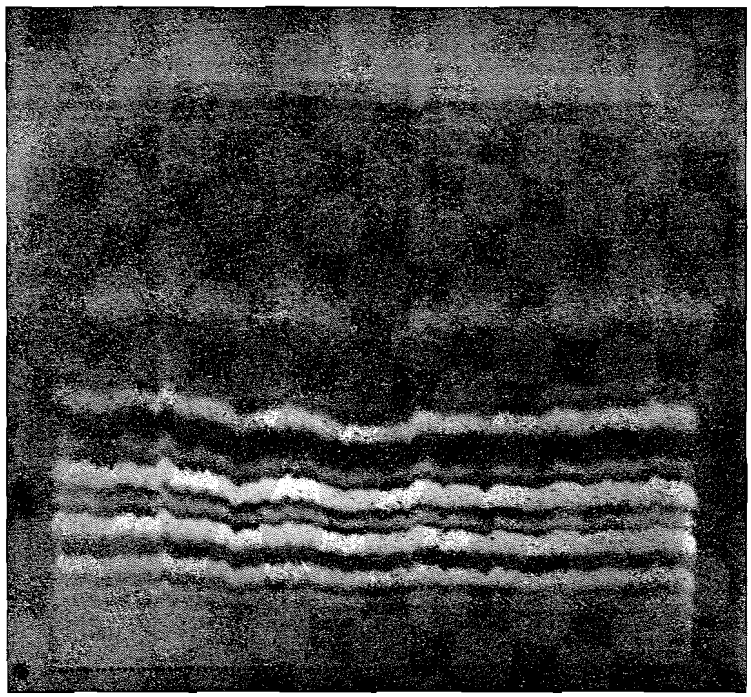

FIG. 3. Semimicro preparative thin layer chromatogram.
Adsorbent: silica gel G; solvent: 4% methanol in benzene (v/v); double development (2×17 cm).
Components: β-oligosaccharide acetates obtained by acetylation of partial acid hydrolysis products from commercial dextran.

applied until the plates were saturated; at that stage the background became translucent and the hydrophobic compounds appeared as white bands. This method of detection offers considerable advantages over other procedures, such as spraying guide strips or applying an indicating reagent as a streak. First, no material is sacrificed for detection purposes because the water spray is non-destructive. Second, the separated products can be recovered completely and with no mixing of closely neighboring components because the full bands are visible and any minor irregularities can be traced. The maximum load of the mixture of oligosaccharide acetates that could be resolved was 25 mg on a

20-cm plate. When an oligosaccharide acetate was run as a spot the minimum amount detectable by the water spray was 100 γ. Monosaccharide acetates are not sufficiently hydrophobic to be detectable by this technique, which is, however, applicable to any strongly hydrophobic compound and has also been applied to lipids in these laboratories.

High concentrations of carbohydrate acetates may also be detected on thin layer chromatograms by iodine vapor but the sensitivity is of the same order as the water spray, i.e. 100 γ. Detection of carbohydrate acetates in the range 5–100 γ required the development of a more sensitive procedure. Demole (1) has mentioned application of the ferric hydroxamate reaction to volatile esters and this has now been extended to the non-volatile acetates. Factors involved in this reaction have been thoroughly investigated by Goddu *et al.* (8) and have been developed for paper chromatographic procedures by other workers (9, 10). The procedures developed for paper chromatography were not directly applicable to thin layer chromatography and were therefore modified as described in the experimental section.

Thin layer chromatography thus offers a rapid and convenient method for analyzing hydrophobic derivatives of carbohydrates. Other procedures for the analysis of carbohydrate acetates include reverse phase chromatography on acetylated paper (11), paper chromatography in two-phase organic solvent systems (12), and the Magnesol–Celite column procedures (6). The present method offers advantages in speed, simplicity, and sensitivity over these other procedures. The method should prove useful for following the course of a reaction involving hydrophobic carbohydrates, e.g. acetolysis of polysaccharides or molecular rearrangements in the monosaccharide series, and for isolating identifiable amounts of closely related products.

EXPERIMENTAL

Analytical Separations

Smooth glass plates (20×20×0.37 cm) were coated with a uniform layer (250 microns thick) of silica gel G* (a standardized mixture of silicic acid and gypsum) using a commercial applicator.* The applicator was loaded with a well-mixed slurry prepared by addition of silica gel G (30 g) to distilled water (60 ml) with stirring. After application of the thin layer the plates were dried in an oven at 110° C for 30 minutes and allowed to cool. Samples were applied from a thin wire loop (ca. 1-mm diameter) with the aid of a numbered plastic template. Standard solutions of the carbohydrate acetates were made at 2% (w/v) concentration in chloroform. Spots were applied in a line 2 cm from one edge of the plate and were spaced at intervals of 1 cm. Marker dyes of Sudan III, methyl red, and methyl orange were applied to each plate as controls. Under the conditions used methyl orange remained at the origin, Sudan III moved near the solvent front, and, depending upon the methanol content of the solvent system, methyl red moved to an intermediate position approximating the mobility of a fully acetylated trisaccharide.

Chromatograms were developed by the ascending technique in rectangular tanks (25×25×7 cm) lined with filter paper for good equilibration and containing the solvent system to a depth of 1 cm. The edge of the plate along which the samples had been applied was placed in the solvent, the tank was closed, and the solvent was allowed to rise to within 2 cm of the top of the plate; this required approximately 40 minutes. Multiple development was used when high resolution was desired and was especially necessary for the separation of anomeric acetates. To do this, the developed chromatograms were removed from the tank, dried in a current of air, and replaced in the tank for a second development. This process could, of course, be repeated as many times as necessary.

The solvent system used must be varied in methanol content according to the compounds under investigation. Thus, the separations shown in Figs. 1, 2, and 3 were obtained with 4% of methanol in benzene. Separation of more-polar compounds, such as fully acetylated amino sugars, required an increase in methanol concentration to 10% but resolution of non-polar, low molecular weight acetates required only 2% of methanol in the solvent system. Solvent in the tank was replaced each day because the methanol content was gradually depleted by adsorption onto the silicic acid.

Detection of Acetates by the Ferric Hydroxamate Reaction

The solutions used were:

(A) 10% (w/v) aqueous hydroxylamine hydrochloride;

**Desaga–Brinkman, Brinkman Instruments Incorp., Great Neck, New York.*

(B) 20% (w/v) aqueous sodium hydroxide;
(C) ferric nitrate.$9H_2O$ (40 g), distilled water (600 ml), glacial acetic acid (400 ml);
(D) concentrated hydrochloric acid.

After the final development with solvent the plates were dried in a current of air and sprayed with a mixture containing equal volumes of solutions A and B until the surface was uniformly moistened. The plates were then heated in an oven at 100–110° C for 10 minutes, cooled to room temperature, and then sprayed with the ferric nitrate reagent (45 ml of solution C plus 6 ml of solution D). The acetates appeared as dark purple spots on a yellow background; a speckled, pink background indicated that further spraying with the ferric nitrate reagent was necessary. The spots remain visible for at least 1 week but gradually diminish in intensity after the first hour. For permanent records the plates may be photographed or traced on glassine paper. The spray reagents are stable for approximately 48 hours but for best results should be mixed just prior to use. *R* values have not been recorded because they have no valid significance when multiple development is used.

Semimicro Preparative Separation

The chromatographic plates were prepared as described for the analytical procedure. The crude mixture of acetates in chloroform (10–30%, w/v) was applied from a capillary or a wire loop as a band of contiguous spots 2 cm from one edge of the plate; each spot was approximately 2 mm in diameter. The plate was developed twice (2×17 cm) in benzene containing 4% (v/v) of methanol. After the second development the plate was dried and sprayed with water (see Fig. 3) and the bands were circumscribed with a sharp scalpel. The plate was then allowed to dry and individual bands were removed by holding the plate vertically on glassine paper and scraping the bands from the surface with a scalpel. The silica gel containing a single component was then transferred from the glassine paper to a numbered glass tube which had been constricted and plugged with cotton wool to form a miniature column. The product was then eluted with a mixture of methanol:chloroform (1:1, v/v) and the eluate was evaporated in a stream of air. The plate depicted in Fig. 3 yielded the following quantities: bands are numbered in order of decreasing mobility: band (1) 0.5 mg; (2) 0.3 mg; (3) 1.0 mg; (4) 0.6 mg; (5+6) 1.7 mg; (7) 1.8 mg; (8) 1.2 mg; (9) 0.9 mg. The homogeneity of each band was verified by deacetylation and examination of the products by paper chromatography in ethyl acetate:pyridine:water, 10:4:3. Under these conditions, components in the weaker bands were not resolved from those in the immediately following stronger bands. This result indicated that the pairs of weak and strong bands were perhaps anomers, although the possibility exists that they were different oligosaccharides that were not resolved by paper chromatography.

The mixture of acetylated oligosaccharides was obtained by hydrolysis of a commercial dextran according to the method of Barker *et al.* (13) and acetylation of the products by acetic anhydride and sodium acetate. The maximum load of this mixture of oligosaccharide acetates was 25 mg/20 cm of plate. The maximum volume of solution which can be spotted in a single application was approximately 0.06 ml, i.e. 3 μl/cm.

ACKNOWLEDGMENTS

The authors wish to thank Professor S. J. Angyal, The University of New South Wales, Broadway, N.S.W., Australia, for samples of the inositol hexaacetates. We are grateful to Dr. W. J. Whelan for the polymer homologous series of acetylated oligosaccharides from laminarin.

REFERENCES

1. E. Demole. Chromatog. Revs. **1**, 1 (1958).
2. E. Demole. J. Chromatog. **6**, 2 (1961).
3. E. G. Wollish, M. Schmall, and M. Hawrylyshin. Anal. Chem. **33**, 1138 (1961).
4. E. Stahl. Angew. Chem. **73**, 646 (1961).
5. E. Stahl and U. Kaltenbach. J. Chromatog. **5**, 351 (1961).
6. W. H. McNeely, W. W. Binkley, and M. L. Wolfrom. J. Am. Chem. Soc. **67**, 527 (1945).
7. S. J. Angyal and D. J. McHugh. J. Chem. Soc. 1423 (1957).
8. R. F. Goddu, N. F. LeBlanc, and C. M. Wright. Anal. Chem. **27**, 1251 (1955).
9. M. Abdel-Akher and F. Smith. J. Am. Chem. Soc. **73**, 5859 (1951).
10. S. Hajdu, H. Weiss, and E. Titus. J. Pharmacol. Exptl. Therap. **120**, 99 (1957).
11. F. Micheel and H. Schweppe. Mikrochim. Acta, 53 (1954).
12. B. Wickberg. Acta Chem. Scand. **12**, 615 (1958).
13. S. A. Barker, E. J. Bourne, A. E. James, W. B. Neely, and M. Stacey. J. Chem. Soc. 2096 (1955).

POTENTIAL CYTOSTATIC CARBOHYDRATE DERIVATIVES

PART II. N-MUSTARD PHOSPHATES

KITTY M. VAGI, VINCENT W. ADAMKIEWICZ, AND THOMAS NOGRADY[1]

Department of Physiology, University of Montreal, Montreal, Que.

Received January 22, 1962

ABSTRACT

2,3,4,6-Tetra-O-acetyl-D-glucosyl-(N-bis-β-chloroethyl)-phosphoramidate and ethyl-D-fructopyranoside-1-(N-bis-β-chloroethyl)-phosphoramidate have been synthesized. The first compound inhibited Adenocarcinoma 755 to 40–50%.

Many attempts were recently undertaken in the field of experimental chemotherapy of malignant tumors to enhance the selectivity of the chemotherapeutic agents, particularly that of the N-mustards. Many types of carriers were used, among them carbohydrates (cf. refs. 1–3). Other transport forms of "hidden" or "toxagenic" N-mustards were also designed, one of the most successful among them the phosphoramidate esters of the Cytoxan type, by Arnold and collaborators (4).

It seemed promising to combine the favorable transport characteristics of carbohydrates and phosphoramidate esters, particularly, because the carbohydrate phosphates are metabolites, with an already existing phosphatase and phosphoramidase enzyme system. It might be expected that the same enzyme system would be capable of splitting the sugar phosphate – N-mustard combination, liberating the N-mustard from its inactive transport form.

Therefore several series of carbohydrate-(N-bis-β-chloroethyl)-phosphoramidates were synthesized.

By reacting 2,3,4,6-tetra-O-acetyl-β-D-glucose (I) (5) with bis-(β-chloroethyl)-phosphoramidic dichloride (6) in the presence of triethylamine, 2,3,4,6-tetra-O-acetyl-1-glucosyl-(N-bis-β-chloroethyl)-phosphoramidic chloride (II) was obtained, either in 15 hours at room temperature or 45 minutes at 80°. Usually without isolating the chloride (II), it was then esterified with benzyl alcohol to III in a quantitative yield. This consumed the theoretical amount of H_2 on hydrogenation in ethanolic solution with Pd–C catalyst, yielding 2,3,4,6-tetra-O-acetyl-(α,β?)-D-glucopyranosyl-N-bis-(β-chloroethyl)-phosphoramidate (IV), an almost colorless, water-soluble, and strongly acidic syrup.

This behaved, however, quite peculiarly. It failed to crystallize, and could not be distilled. No salt formation could be achieved without splitting off the bis-(β-chloroethyl)-amine group. Organic bases such as cyclohexylamine, norephedrine, or even the weak novocain (pK_b 5.15) were able to decompose the molecule, and bis-(β-chloroethyl)-amine hydrochloride could be isolated. This was surprising, because according to known facts (7), the P—N bond in phosphoramidates is acid sensitive and alkali stable, although some diesters of phosphoric acid are known to be very unstable in alkali. This sensitivity towards bases in polar solvents was, however, a general characteristic in our series. Chromatography on acid-washed alumina caused the same splitting, basic ionic exchange resins in alcoholic solution even more so, as well as attempted catalytic deacetylation with sodium methylate.

[1]*Present address: Department of Chemistry, Loyola College, Montreal 28, Que.*

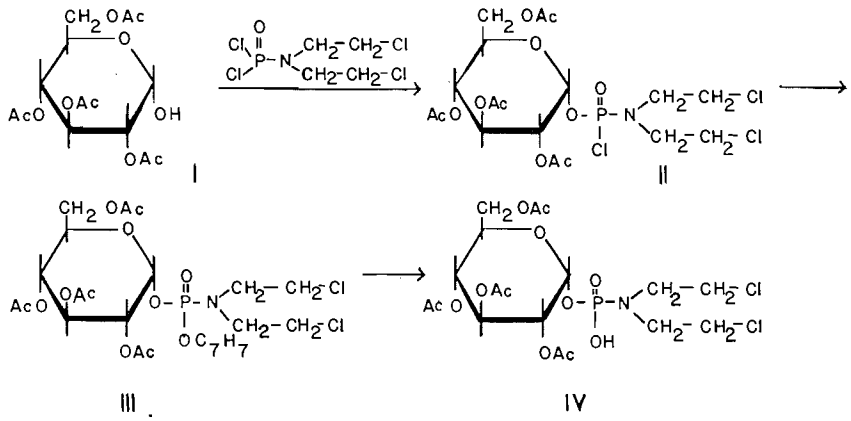

Deacetylation of IV was therefore attempted with cold ethanolic hydrochloric acid, which gave a crude, dark oil, with the approximate analysis. Not being able to purify it satisfactorily, we submitted the acetylated compound (IV) for cancerostatic screening, which did not show any activity against Sarcoma 180. It inhibitied, however, Adenocarcinoma 755 in doses of 250 mg per kg per day (for 7 days) to an extent of 40–50%.

The whole reaction sequence, starting from 2,3:4,5-di-O-isopropylidene-β-D-fructopyranose (V) (8), was repeated. The phosphoramidic chloride (VI) was obtained, and subsequent esterification with benzyl alcohol yielded the benzyl-phosphoramidate (VII), which, on catalytic hydrogenolysis, furnished the free phosphoramidate (VIII).

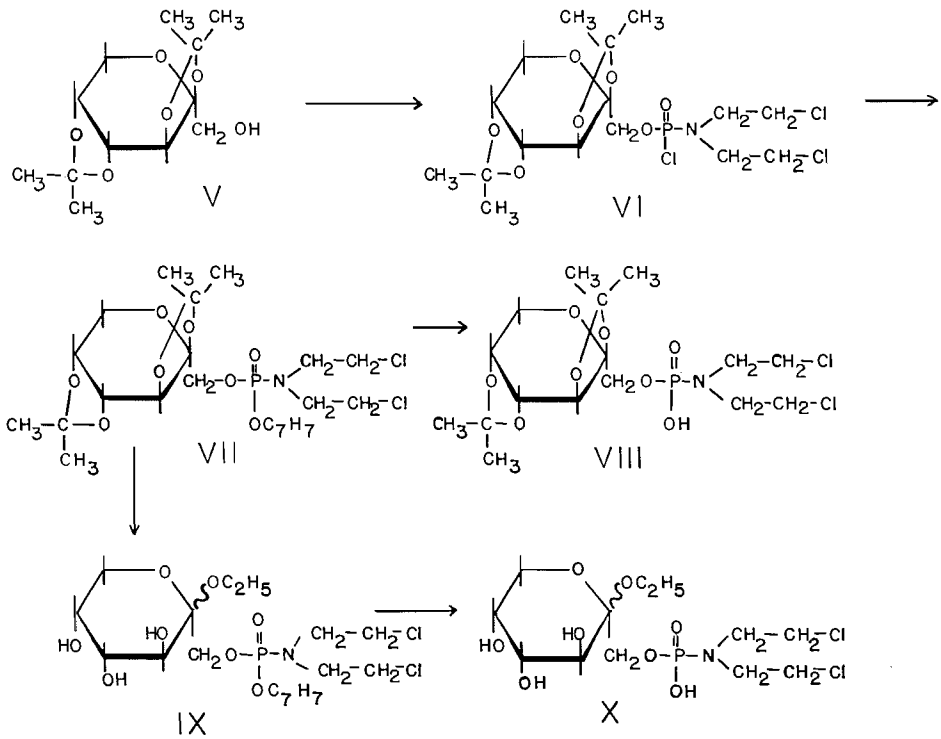

Attempted removal of the isopropylidene groups with ethanolic hydrochloric acid from VII gave a dark syrup, presumably IX. This, when hydrogenated, gave ethyl-(α,β?)-D-fructopyranoside-1-(N-bis-β-chloroethyl)-phosphoramidate (X) as a yellow oil, which, however, darkened in a matter of hours, and gave inconsistent analyses. The compound exhibited the same base sensitivity as the glucose derivatives II–IV, and presented the same difficulties regarding purification.

EXPERIMENTAL*

2,3,4,6-Tetra-O-acetyl-(α,β?)-D-glucopyranosyl-(N-bis-β-chloroethyl)-phosphoramidic Chloride (II)

N-Bis-(β-chloroethyl)-phosphoramidic dichloride (1.30 g) (8) and 2,3,4,6-tetraacetyl-glucopyranose (1.74 g) (7) stood with 0.72 ml triethylamine in 20 ml benzene at room temperature, until the theoretical amount of triethylamine hydrochloride precipitated, and the reaction mixture became neutral (15 hours). After the triethylamine hydrochloride was filtered off, the benzene solution was washed once with ice water, dried, and evaporated to dryness under reduced pressure, affording 2.85 g (100%) of yellow syrup. $[\alpha]_D^{20}$: +47.0°; n_D^{25}: 1.4791. Anal. Calc. for $C_{18}H_{27}Cl_3NO_{11}P$: C, 37.88; H, 4.77; N, 2.45. Found: C, 37.41; H, 4.93; N, 2.36.

2,3,4,6-Tetra-O-acetyl-(α,β?)-D-glucopyranosyl-(N-bis-β-chloroethyl)-benzyl-phosphoramidate (III)

Freshly prepared II (2.85 g) and 0.54 ml benzyl alcohol were refluxed with 0.72 ml triethylamine in 30 ml benzene for 40–60 minutes, until the reaction mixture became neutral. Then, the triethylamine hydrochloride was filtered off, and the benzene solution was washed once with ice water, dried, and evaporated under reduced pressure, yielding 3.2 g (100%) of yellow syrup. $[\alpha]_D^{20}$: +32.0°; n_D^{25}: 1.4959. Anal. Calc. for $C_{25}H_{34}Cl_2NO_{12}P$: C, 46.74; H, 5.33; N, 2.18. Found: C, 46.16; H, 5.38; N, 2.26.

2,3,4,6-Tetra-O-acetyl-(α,β?)-D-glucopyranosyl-(N-bis-β-chloroethyl)-phosphoramidate (IV)

Compound III (1.28 g), dissolved in 20 ml ethanol, was hydrogenated in the presence of 0.2 g of 5% Pd–C catalyst. It consumed the theoretical 48 ml of H_2 in 1 hour. After filtration and evaporation, 0.95 g (85%) of an almost colorless viscous syrup was obtained. $[\alpha]_D^{20}$: +42.9°; n_D^{25}: 1.4730. Anal. Calc. for $C_{18}H_{28}Cl_2NO_{12}P$: C, 39.14; H, 5.11; N, 2.54. Found: C, 39.60; H, 5.16; N, 2.62.

2,3:4,5-Di-O-isopropylidene-β-D-fructopyranose-1-(N-bis-β-chloroethyl)-phosphoramidic Chloride (VI)

N-Bis-(β-chloroethyl)-phosphoramidic dichloride (1.30 g) and 2,3:4,5-di-O-isopropylidene-β-D-fructopyranose (1.30 g) were refluxed with 0.72 ml triethylamine in 20 ml toluene for 6–8 hours, until the reaction mixture was neutral. The precipitated triethylamine hydrochloride was filtered off and washed with toluene. The combined toluene solutions were washed once with ice water, dried, and evaporated under reduced pressure, resulting in 2.35 g (97.5%) of yellow syrup. $[\alpha]_D^{20}$: −18.0°; n_D^{20}: 1.4900. Anal. Calc. for $C_{16}H_{27}Cl_3NO_7P$: C, 39.81; H, 5.64; N, 2.90. Found: C, 39.3; H, 5.8; N, 2.90.

2,3:4,5-Di-O-isopropylidene-β-D-fructopyranose-1-(N-bis-β-chloroethyl)-benzyl-phosphoramidate (VII)

Compound VI (7.42 g) and 1.67 ml benzyl alcohol were refluxed with 2.22 ml triethylamine in 40 ml toluene for 20–24 hours. After working up as above, the yield was 6.32 g (75%) of a yellow syrup. $[\alpha]_D^{20}$: −16.2°; n_D^{25}: 1.4982. Anal. Calc. for $C_{23}H_{34}Cl_2NO_8P$: C, 49.83; H, 6.18; N, 2.53. Found: C, 49.32; H, 6.26; N, 2.73.

2,3:4,5-Di-O-isopropylidene-β-D-fructopyranose-1-(N-bis-β-chloroethyl)-phosphoramidate (VIII)

Compound VII (1.1 g) was dissolved in 15 ml ethanol and hydrogenated in the presence of 0.2 g of 5% Pd–C catalyst. It consumed 46 ml hydrogen (calc. 48 ml) in 50 minutes. After filtration, it was evaporated under reduced pressure. The residue was a yellow syrup, 0.90 g (93%). $[\alpha]_D^{20}$: −18.0°; n_D^{25}: 1.4830. Anal. Calc. for $C_{16}H_{28}Cl_2NO_8P$: C, 41.39; H, 6.08; N, 3.02. Found: C, 41.8; H, 6.7; N, 3.10.

Ethyl-(α,β?)-D-fructopyranoside-1-(N-bis-β-chloroethyl)-phosphoramidate (XI)

Compound VII (1.05 g) was dissolved in 3 ml of 16% ethanolic hydrochloric acid. After standing for 2.5 hours at room temperature, the red reaction mixture was evaporated to dryness under reduced pressure, dissolved again in 10 ml ethanol, and hydrogenated in the presence of Pd–C catalyst. Worked up as usual, the resulting yellow syrup weighed 0.67 g (72.5%). $[\alpha]_D^{20}$: −8.3°; n_D^{25}: 1.493. Anal. Calc. for $C_{12}H_{24}Cl_2NO_8P$: C, 34.96; H, 5.87; N, 3.40. Found: C, 35.61; H, 6.04; N, 3.39.

ACKNOWLEDGMENTS

This investigation was supported by the U.S. Department of Health and Welfare, National Institutes of Health (Grant No. 2260), the National Cancer Institute of Canada,

**All optical rotations were measured in methanol, c = 2. Microanalyses by Dr. C. Daesslé Laboratory, Montreal.*

and the National Research Council of Canada (Grant No. MA 640). The cancerostatic screening was done by the Sloan-Kettering Institute for Cancer Research, Rye, New York. We thank Dr. C. C. Stock for making the data available to us.

REFERENCES

1. T. F. NOGRADY. J. Org. Chem. **26**, 4177 (1961).
2. L. VARGHA, L. TOLDY, Ö. FEHER, and S. LENDVAI. J. Chem. Soc. 810 (1957).
3. E. REIST, R. R. SPENCER, and B. R. BAKER. J. Am. Chem. Soc. **82**, 2025 (1960).
4. H. ARNOLD, F. BOURSEAUX, and N. BROCK. Arzneimittel-Forsch. **11**, 143 (1961).
5. S. B. HENDRICKS, O. R. WULF, and U. LIDDEL. J. Am. Chem. Soc. **58**, 1998 (1936).
6. O. M. FRIEDMAN and A. M. SELIGMAN. J. Am. Chem. Soc. **76**, 655 (1954).
7. F. CRAMER. Angew. Chem. **72**, 245 (1960).
8. M. L. WOLFROM, W. L. SHILLING, and W. W. BINKLEY. J. Am. Chem. Soc. **72**, 4544 (1950).

THE PREPARATION OF SOME THIOSEMICARBAZONES AND THEIR COPPER COMPLEXES

PART III[1]

B. A. GINGRAS, T. SUPRUNCHUK, AND C. H. BAYLEY
Division of Applied Chemistry, National Research Council, Ottawa, Canada

Received February 7, 1962

ABSTRACT

Reactions of some diketones with thiosemicarbazide have been studied under various conditions. Monothiosemicarbazones, dithiosemicarbazones, and cyclization products can be obtained. It was found that dithiosemicarbazones form 1:1 complexes with Cu(II) but failed to react with Cu(I). Dithiosemicarbazones in which the N^2-hydrogen atom has been replaced by Me do not form complexes, confirming our views about the importance of this hydrogen atom in the thione ↔ thiol tautomerism necessary for complex formation. 4,4-Dimethyldithiosemicarbazones behave like the unsubstituted parent compounds in forming 1:1 complexes with Cu(II). Infrared spectra provide evidence for the structure of a cyclization product, 5,6-diphenyl-3-thio-1,2,4-triazine, which had been erroneously described by various authors as the thiol tautomer, 5,6-diphenyl-3-mercapto-1,2,4-triazine.

In previous publications (1, 2), the reactions of thiosemicarbazones (tscs) with Cu(I) and Cu(II) ions were reported. A polymeric structure was suggested for the insoluble 1:1 complexes obtained from these reactions (2), and the antifungal activity of both free tscs and their copper complexes was also reported (3). The present work describes the reactions of mono- and di-tscs with a number of metals. It was found that monotscs which form complexes readily with copper in alkaline or neutral solution fail to react similarly with the following metals: Ag(I), Hg(II), Ni(II), Mn(II), Zn(II), Sn(II), Co(II), Fe(II), and Fe(III). Guha-Sircar *et al.* (4) obtained solid precipitates from tscs and several of these metals at pH from 3 to 7, and suggested that this reaction could be used for the quantitative determination of cations. In the present work, precipitates were obtained with the cations mentioned above but no definite products were isolated. The high metal content (approx. 50%) indicated that these solid materials were mostly inorganic, consisting probably of the metal sulphides.

The fact that tscs form definite complexes with copper only, coupled with our previous finding that antifungal activity is usually limited to the free tscs, the complexes being inactive (3), is believed to be quite significant in the study of the mechanism of antifungal action of these compounds. The role and the nature of the metal in biological processes involving metal-binding substances is of great importance (5) and work is currently being carried out along this line and will be reported elsewhere.

A number of dithiosemicarbazones (ditscs) were prepared from dicarbonyl compounds in order to examine their reaction with metals and eventually to study their antifungal properties. The reaction of dicarbonyl compounds with thiosemicarbazide is not simple and mixtures of products are usually obtained. The separation of these mixtures is complicated by the low solubility of the various components and the discrepancies encountered in the literature concerning their melting points.

Glyoxal (I) (R = R′ = H) and diacetyl (I) (R = R′ = CH_3) gave readily the ditscs (III), but benzil (I) (R = R′ = C_6H_5) afforded a mixture of monotscs (II), ditscs (III), and the cyclization product 5,6-diphenyl-3-thio-1,2,4-triazine (IV) (R = R′ = C_6H_5).

[1]*Issued as N.R.C. No. 6795.*

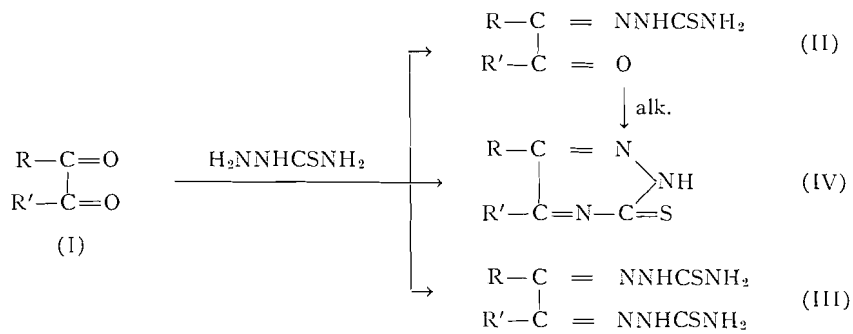

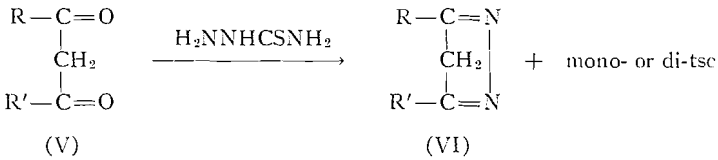

In the case of 1,3-diphenyl-1,3-propanedione (V) (R = R′ = C_6H_5), the monotsc and a cyclization product, 3,5-diphenyl pyrazole (VI) (R = R′ = C_6H_5), were obtained, while many attempts to isolate the ditsc were unsuccessful. Pyrazoles are usually obtained from reaction of 1,3-dicarbonyl compounds with hydrazine or semicarbazides (6), so it is not surprising that thiosemicarbazide should give rise to similar compounds. 1-Phenyl-1,3-butanedione (V) (R = CH_3, R′ = C_6H_5) gave the expected ditsc plus an unidentified product, $C_{20}H_{19}N_5S$. 2,5-Hexanedione, 2,3-heptanedione, and 2,3-octanedione gave the expected ditscs and no other tractable products. We failed to isolate the mono- or di-tsc from acetyl acetone, and part of the diketone must have been broken down since acetyl thiosemicarbazide was identified from the reaction mixture.

The preparation of Cu(II) and Ni(II) complexes with a few ditscs (diacetyl, 2,3-pentanedione, 2,3-hexanedione, 1-phenyl-1,2-propanedione ditscs) has been previously described (7–9). Later, Górski *et al.* (10) obtained metal complexes with the ditsc of the diethyl ester of 2,3-dioxobutane-1,4-dicarboxylic acid, but did not isolate the compounds. We found that ditscs examined in this work formed 1:1 complexes readily with Cu(II)* but no definite products were obtained using Cu(I) in ammoniacal solution, or with Fe(II), Fe(III), Zn(II), Sn(II), Co(II), Hg(II), or Ag(I) in neutral or alkaline solution.

Substituted ditscs were prepared from 2-methyl and 4,4-dimethyl thiosemicarbazide with glyoxal, and their reaction with copper was studied. The 2-methyl derivative did not form a complex, confirming our previous findings (2) that the N^2-hydrogen atom is a requirement of the tautomeric equilibrium illustrated below, which is necessary for the formation of complexes.

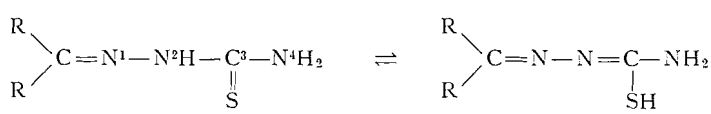

**2,5-Hexanedione and 2,3-heptanedione ditscs gave solid precipitates with Cu(II) but no definite products could be identified.*

On the other hand, both glyoxal and diacetyl di(4,4-dimethyl)tscs readily formed 1:1 copper complexes, as did the unsubstituted ditscs. Considering that ditscs contain two thiosemicarbazide residues, the 1:1 complexes described here may be regarded as 2:1 with respect to the thiosemicarbazide–copper ratio, for the important species here is the thiosemicarbazide residue, $=N—NH—CS—NH_2$, which alone is responsible for complex formation. On this basis, ditsc–copper complexes are quite different from monotsc–copper complexes, in which the ratio of thiosemicarbazide to copper is unity. The structure of ditsc–copper complexes is probably best represented by the conventional formula (VII), previously suggested by Bähr (7).

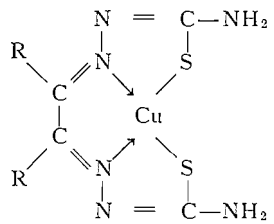

(VII)

The compounds discussed in this work are listed in Table I together with their infrared spectra. Only two regions of the spectrum are of particular interest, the 3500–3000 cm^{-1}

TABLE I

Compounds and their infrared spectra in two regions

Compounds		3500–3000 cm^{-1}	1700–1500 cm^{-1}
Glyoxal ditsc		3380 m, 3230 m, 3130 m	1650 w, 1605 s
Glyoxal di(2-methyl)tsc		3420 s, 3240 s, 3120 m	1685 w, 1675 w
Glyoxal di(4,4-dimethyl)tsc		3425 s, 3200 m, 3045 w	1575 m, 1550 m
Glyoxal ditsc-Cu(II)		3440 w, 3390 m, 3250 w	1655 m, 1630 m, 1570 m
Glyoxal di(4,4-dimethyl)tsc-Cu(II)		3420 m	1625 w, 1570 w
Diacetyl ditsc		3425 s, 3200 s, 3260 w, 3160 w	1695 w, 1600 w
Diacetyl di(4,4-dimethyl)tsc		3280 m	1525 s
Diacetyl ditsc-Cu(II)		3400 s, 3290 s, 3140 s	1630 s, 1595 s
Diacetyl di(4,4-dimethyl)tsc-Cu(II)		3410 m	1500 s
2,5-Hexanedione ditsc		3400 s, 3200 s, 3140 w	1585 s, 1515 s
2,3-Heptanedione ditsc		3440 m, 3280 m, 3160 m	1600 s
2,3-Octanedione ditsc		3400 m, 3240 w, 3140 w	1690 w, 1600 s
2,3-Octanedione ditsc-Cu(II)		3290 w, 3140 m	1615 m, 1585 m, 1530 m
1-Phenyl-1,3-butanedione ditsc		3410 w, 3220 m, 3120 w	1585 s, 1540 w
1,3-Diphenyl-1,3-propanedione monotsc		3440 m, 3300 s, 3150 w	1590 s, 1575 w
3,5-Diphenyl pyrazole		—	1610 w, 1590 w, 1575 w
Benzil monotsc		3150–3120 b	1555 s, 1500 w
Benzil ditsc		3420 w, 3220 m, 3140 m	1660 s, 1600 s
5,6-Diphenyl-3-thio-1,2,4-triazine	(KBr)	3120 m	1585 w, 1565 m, 1540 s
	(Soln.)	3380 m	1585 w, 1550–1500 b
5-6-Diphenyl-3-oxy-1,2,4-triazine	(KBr)	3400 m	1680–1650 b, 1600 m, 1585 m, 1565 s
	(Soln.)	3400 m	1700–1650 b, 1590 s, 1565 s
5,6-Diphenyl-3-thio-1,2,4-triazine-Cu(II)		3400 m, 3060 w	1625 w, 1600 m

NOTE: s, strong; m, medium; w, weak; b, broad. Unless otherwise noted, the spectra were taken from KBr pellets.

(N—H stretching) and the 1700–1500 cm^{-1} (double-bond region). The spectra of ditscs resemble those of monotscs discussed earlier (2). Due to the overlapping of the bands in the N—H region, it has not been possible to ascribe the various absorptions to definite vibrations. It can be seen that the copper complexes have one more band in the double-bond region than the original compounds and this is in agreement with the suggested formula for the complexes.

As can be seen from the table, the spectrum of benzil monotsc shows a broad NH absorption at 3120–3150^{-1} and the band at 1555 cm^{-1} is a little low for the free carbonyl group. Considering the spectrum of benzil ditsc, which has no carbonyl, the bands in the double-bond region due to C=N are at 1660 and 1600 cm^{-1}. The lack of a carbonyl absorption in the case of benzil monotsc can be explained by a conjugate chelation between the carbonyl and the NH group of the thiosemicarbazide residue:

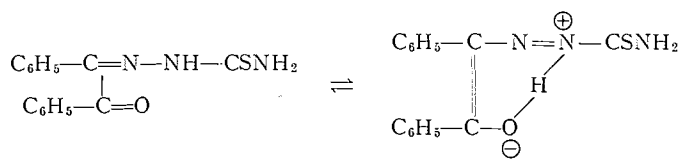

This phenomenon has been observed before with dicarbonyl compounds (11) and the presence of the broad NH band, due to the hydrogen bridge, lends support to this theory. This agrees with the findings of Sadler (12) that in α-diketone monotscs, strong intramolecular NH·····O=C bonds predominate.

The spectrum of 5,6-diphenyl-3-thio-1,2,4-triazine (IV*a*) is particularly interesting in that it shows one sharp NH band at 3120 cm^{-1} (KBr), 3380 cm^{-1} (chloroform solution), and no SH band could be observed in either media. This triazine has been described before (8, 13, 14) and its structure was assumed to be (IV*b*) and not (IV*a*). On the basis

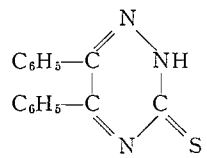

(IV*a*)

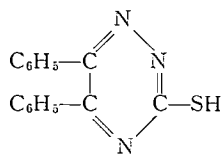

(IV*b*)

of its infrared spectrum, structure (IV*a*) is to be preferred and the tautomer (IV*b*) probably does not exist in the solid state nor in solution in chloroform. This is in agreement with similar findings that open-chain tscs exist only in the thiono form in the solid state (15), and 3-mercapto-5-oxo-1,2,4-triazines were recently shown to exist in the keto and thiono forms in neutral solution (16). However, there is little doubt that in the presence of a base, the thione ↔ thiol tautomerism takes place since both tscs and thiotriazine dissolve in alkali, and the S-Na salt of acetone tsc has already been described (17). As a comparison, the analogous 3-oxy-1,2,4-triazine (VIII) was prepared and its infrared

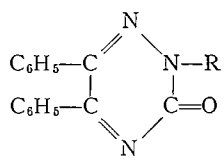

(VIII) R = H
(IX) R = CH_3

spectrum taken both in the solid state and in chloroform solution. The same behavior was found in this case and no OH bands were detected. The weak peak at 3450 cm^{-1} (KBr) and 3350 cm^{-1} (chloroform) is due to N—H stretching. Furthermore, there is no doubt about the strong carbonyl absorption at 1685 cm^{-1}, both in KBr and chloroform.

Chemical evidence also supports the ketonic structure of the oxytriazine, since all attempts to methylate the O atom failed, the product being the N-CH_3 derivative (IX) (18).

The structure of 3,5-diphenyl pyrazole (VI) (R = R′ = C_6H_5) is confirmed by its infrared spectrum, which is of requisite character, the lack of NH bands being its most significant feature.

EXPERIMENTAL

The diketones and thiosemicarbazide were reagent grade material. Glyoxal was a 30% aqueous solution. 2-Methyl and 4,4-dimethyl thiosemicarbazides were prepared in this laboratory as previously described (19, 20). All melting points were taken on a Fisher-John apparatus and are corrected.

Glyoxal ditsc

Glyoxal (30% aq. soln.) (20 g, 0.1 mole) was dissolved in ethyl alcohol (250 ml) and the solution heated on a steam bath. To this was added a solution of thiosemicarbazide (18.2 g, 0.2 mole) in water (600 ml) containing acetic acid (40 ml). A solid precipitated out and heating was continued for 15 minutes. The mixture was cooled and the solid was collected by filtration and washed with hot alcohol and hot acetone; m.p. > 300° C decomp.; lit. m.p. > 300° C (1), 17.2 g, 84.6%.

Glyoxal Di(2-methyl)tsc

Glyoxal (30% aq. soln.) (20 g, 0.1 mole) was added dropwise to a solution of 2-methyl thiosemicarbazide (4.75 g, 0.045 mole) in water (150 ml), and the mixture heated at 50° C for 10 minutes. A yellow solid precipitated out which, after cooling of the mixture, was separated by filtration, washed, and dried; m.p. 276° C, 1.83 g, 35%. Calc. for $C_6H_{12}N_6S_2$: C, 31.00; H, 5.17; N, 36.2; S, 27.6%. Found: C, 31.20; H, 5.11; N, 36.00; S, 27.6%.

Glyoxal Di(4,4-dimethyl)tsc

Glyoxal di(4,4-dimethyl)tsc was prepared similarly using glyoxal (11.83 g, 0.025 mole) in alcohol (100 ml) and 4,4-dimethyl thiosemicarbazide (5.95 g, 0.05 mole) in water (100 ml) containing acetic acid (10 ml). A yellow precipitate was collected and washed with boiling alcohol; m.p. 203° C, 5.05 g, 77%. Calc. for $C_8H_{16}N_6S_2$: C, 36.9; H, 6.16; N, 32.3; S, 24.6%. Found: C, 36.83; H, 6.13; N, 32.45; S, 25.0%.

Glyoxal ditsc-Cu(II)

To a gently refluxing solution of glyoxal ditsc (2 g, 0.01 mole) in N,N-dimethylformamide (100 ml) was added dropwise, with stirring, a hot solution of cupric acetate (2 g, 0.01 mole) in 40 ml of aqueous alcohol (50%). Heating was continued for 15 minutes and the black precipitate was collected; m.p. 236° C, 1.9 g, 71.4%. Calc. for $C_4H_6N_6S_2 \cdot Cu$: C, 18.07; H, 2.26; N, 31.62; S, 24.1; Cu, 23.96%. Found: C, 18.77; H, 2.87; N, 30.90; S, 24.3; Cu, 23.96%.

Glyoxal Di(4,4-dimethyl)tsc-Cu(II)

Cupric acetate (3.4 g, 0.017 mole) in alcohol (100 ml) was added to a hot solution of glyoxal di(4,4-dimethyl)tsc (4 g, 0.017 mole) in dimethyl sulphoxide (450 ml), and heating on the steam bath was continued for 15 minutes. The resulting purple solution was allowed to cool, and after addition of water, the crystals that formed were collected, washed with water and hydrochloric acid (3%), and recrystallized from alcohol. The 1:1 copper complex had m.p. 244° C, 3.86 g, 70%. Calc. for $C_8H_{14}N_6S_2 \cdot Cu$: C, 29.78; H, 4.65; N, 26.05; S, 19.84; Cu, 19.7%. Found: C, 30.12; H, 4.36; N, 26.10; S, 19.78; Cu, 19.9%.

Diacetyl ditsc

This was prepared by adding a warm solution of thiosemicarbazide (3.6 g, 0.04 mole) in water (120 ml) containing 6 ml of acetic acid to a warm solution of diacetyl (1.72 g, 0.02 mole) in ethyl alcohol (200 ml). The yellow precipitate obtained was collected and washed with boiling alcohol and acetone; m.p. 272° C, lit. m.p. 255° C (9), 4.5 g, 97%. Calc. for $C_6H_{12}N_6S_2$: C, 31.05; H, 5.18; N, 36.2; S, 27.6%. Found: C, 31.50; H, 5.35; N, 36.05; S, 27.24%.

Diacetyl Di(4,4-dimethyl)tsc

This was prepared as above using diacetyl (1.72 g, 0.02 mole) in ethyl alcohol (100 ml) and 4,4-dimethyl thiosemicarbazide in water (100 ml) and acetic acid (8 ml). The compound obtained had m.p. 198° C, 1.9 g, 32.9%. Calc. for $C_{10}H_{20}N_6S_2$: C, 41.7; H, 6.95; N, 29.2; S, 22.2%. Found: C, 42.3; H, 7.5; N, 28.8; S, 22.15%.

Diacetyl ditsc-Cu(II)

To a hot solution of diacetyl ditsc (2.4 g, 0.01 mole) in dimethylformamide (240 ml) was added copper acetate (2 g, 0.01 mole) in water (50 ml), and the mixture was heated and stirred for an additional 15 minutes. A dark colored precipitate was formed which, after cooling of the mixture, was collected and washed with hydrochloric acid (3%), water, hot alcohol, and acetone; m.p. 267° C decomp., 2.09 g, 71%. Calc. for $C_6H_{10}N_6S_2 \cdot Cu$: C, 24.55; H, 3.41; N, 28.63; S, 21.8; Cu, 21.6%. Found: C, 24.04; H, 3.59; N, 28.7; S, 21.8; Cu, 21.2%.

Diacetyl Di(4,4-dimethyl)tsc-Cu(II)

A solution of cupric acetate (1.04 g, 0.005 mole) in alcohol (100 ml) was added dropwise to a refluxing solution of diacetyl di(4,4-dimethyl)tsc (1.5 g, 0.005 mole) in chloroform (150 ml) and heating was continued for 15 minutes, during which time a solid precipitated out. After cooling of the mixture, the precipitate was collected, washed, and crystallized from acetone; m.p. 300° C, 0.32 g, 17.4%. Calc. for $C_{10}H_{19}N_6S_2 \cdot Cu$: C, 34.25; H, 5.43; N, 23.95; S, 18.25; Cu, 18.12%. Found: C, 35.17; H, 5.25; N, 24.2; S, 18.6; Cu, 17.93%.

2,5-Hexanedione ditsc

This was prepared by adding a warm solution of thiosemicarbazide (3.6 g, 0.04 mole) in water (120 ml) containing acetic acid (16 ml) to a solution of 2,5-hexanedione (2.28 g, 0.02 mole) in alcohol (200 ml). The white precipitate obtained had m.p. 272° C, 4.5 g, 86.5%. Calc. for $C_8H_{16}N_6S_2$: C, 36.95; H, 6.15; N, 32.3; S, 24.6%. Found: C, 37.13; H, 6.54; N, 32.0; S, 24.5%.

2,3-Heptanedione ditsc

This was obtained as above using 2,3-heptanedione (12.8 g, 0.1 mole) in alcohol (200 ml) and thiosemicarbazide (18.2 g, 0.2 mole) in water (600 ml) containing acetic acid (40 ml). The product, after recrystallization from aqueous ethyl cellosolve, had m.p. 218° C; lit. m.p. 222° C (9), 10.5 g, 40%.

2,3-Octanedione ditsc

This was made by the usual method starting with 2,3-octanedione (4.26 g, 0.03 mole) in alcohol (200 ml) and thiosemicarbazide (5.47 g, 0.06 mole) in water (200 ml) and acetic acid (10 ml). The product, 4.75 g, 55%, had m.p. 230° C. Calc. for $C_{10}H_{20}N_6S_2$: C, 41.7; H, 6.94; N, 29.15; S, 22.20%. Found: C, 41.93; H, 7.28; N, 28.6; S, 22.10%.

2,3-Octanedione ditsc-Cu(II)

Copper acetate (2 g, 0.01 mole) in water (80 ml) was added dropwise to a refluxing solution of 2,3-octanedione ditsc (2.88 g, 0.01 mole) in N,N-dimethylformamide (100 ml). The mixture was stirred and heating was continued for 15 minutes, during which time a brown precipitate was formed. This was collected, washed with water, and recrystallized from alcohol; m.p. 225° C, 0.65 g, 18.6%. Calc. for $C_{10}H_{18}N_6S_2 \cdot Cu$: C, 34.38; H, 5.16; N, 24.01; S, 18.3; Cu, 18.17%. Found: C, 34.81; H, 5.75; N, 23.95; S, 17.92; Cu, 17.9%.

1-Phenyl-1,3-butanedione ditsc

The usual procedure of adding an aqueous solution of thiosemicarbazide to the diketone in alcohol afforded only an unidentified product of m.p. 106° C: $C_{20}H_{19}N_5S$. The required ditsc was obtained by using the following method:

Thiosemicarbazide (1.9 g, 0.02 mole) in boiling alcohol (150 ml) was added to the previously molten 1-phenyl-1,3-butanedione (1.62 g, 0.01 mole). The resulting solution was refluxed for 30 minutes and allowed to cool. The ditsc crystallized out and, after recrystallization from *n*-hexane, had m.p. 131° C, 0.39 g, 12.6%. Calc. for $C_{12}H_{16}N_6S_2$: C, 46.7; H, 5.2; N, 27.28; S, 20.78%. Found: C, 46.85; H, 5.23; N, 27.20; S, 20.40%.

Reaction of 1,3-Diphenyl-1,3-propanedione with Thiosemicarbazide

A solution of thiosemicarbazide (1.8 g, 0.02 mole) in water (60 ml) and acetic acid (8 ml) was added to the diketone (4.49 g, 0.02 mole) in alcohol (110 ml), and the resulting mixture was heated for 15 minutes on the steam bath and allowed to cool. 3,5-Diphenyl pyrazole crystallized out, and after filtration, it was recrystallized from benzene–hexane; m.p. 197° C, 1.55 g, 35.4%; lit. m.p. 197–200° C (21). Calc. for $C_{15}H_{12}N_2$: C, 81.8; H, 5.45; N, 12.7%. Found: C, 82.0; H, 5.45; N, 12.55%.

The mother liquor, after addition of water, yielded the monotsc (0.85 g, 14.3%), which, after recrystallization from benzene–hexane, and from alcohol, had m.p. 128° C. Calc. for $C_{16}H_{15}N_3OS$: C, 64.6; H, 5.05; N, 14.13; S, 10.78%. Found: C, 64.57; H, 5.38; N, 14.78; S, 10.58%.

Reaction of Benzil with Thiosemicarbazide

As the conventional method of condensation gave mixtures of products, the following modified procedure was used:

Benzil (2.1 g, 0.01 mole) and thiosemicarbazide (1.8 g, 0.02 mole) were dissolved in N,N-dimethylformamide, and concentrated hydrochloric acid (3 ml) was added. After being heated on the steam bath for 4 hours, the solution was allowed to evaporate slowly until benzil ditsc had precipitated out. The product

was collected and washed with water followed by hot alcohol. It had m.p. 217° C, 1.15 g, 42.4%. Calc. for $C_{16}H_{16}N_6S_2$: C, 53.9; H, 4.49; N, 23.6; S, 17.99%. Found: C, 52.98; H, 4.58; N, 23.4; S, 17.40%.

5,6-Diphenyl-3-thio-1,2,4-triazine was obtained in a 67% yield by a method described previously (22). The compound, after recrystallization from acetone, had m.p. 220° C; lit. m.p. 233° C (22), 226° C (23). Calc. for $C_{15}H_{11}N_3S$: C, 67.9; H, 4.15; N, 15.84; S, 12.08%. Found: C, 67.31; H, 3.92; N, 16.12; S, 12.28%.

A small amount of benzil monotsc was identified as a by-product, and after recrystallization from acetone, had m.p. 190° C; lit. m.p. 188° C (23). Calc. for $C_{15}H_{13}N_3OS$: C, 63.7; H, 4.6; N, 14.84; S, 11.3%. Found: C, 64.14; H, 5.48; N, 14.50; S, 10.93%.

5,6-Diphenyl-3-thio-1,2,4-triazine-Cu(II)

A small amount (200 mg) of copper complex was obtained from the addition of copper acetate (10 g, 0.05 mole) in water (200 ml) to a boiling solution of the triazine (13.8 g, 0.05 mole) in a large excess of acetone (500 ml). The complex precipitated out and was separated by filtration, washed successively with water, hydrochloric acid (3%), alcohol, acetone, and finally recrystallized from pyridine, m.p. 302° C. There was not sufficient material for further purification, but the elementary analysis is in fair agreement with the calculated values. Calc. for $C_{15}H_{10}N_3S \cdot Cu$: C, 54.9; H, 3.06; N, 12.82; S, 9.77; Cu, 19.38%. Found: C, 53.2; H, 3.12; N, 13.19; S, 10.02; Cu, 18.1%.

ACKNOWLEDGMENTS

Our thanks are due Mr. E. C. Goodhue and Mr. R. Ironside, both of the Analytical Section, for carrying out the metal analyses and for taking the infrared spectra respectively.

REFERENCES

1. B. A. GINGRAS, R. W. HORNAL, and C. H. BAYLEY. Can. J. Chem. **38**, 712 (1960).
2. B. A. GINGRAS, R. L. SOMORJAI, and C. H. BAYLEY. Can. J. Chem. **39**, 973 (1961).
3. B. G. BENNS, B. A. GINGRAS, and C. H. BAYLEY. Appl. Microbiol. **8**, 353 (1960).
4. S. S. GUHA-SIRCAR and S. SATPATHY. J. Indian Chem. Soc. **31**, 6, 451 (1954). S. S. GUHA-SIRCAR and G. N. MITRA. J. Indian Chem. Soc. **32**, 7, 435 (1955).
5. A. ALBERT. Selective toxicity. Methuen & Co. Ltd., London. 1960.
6. E. H. RODD (*Editor*). Chemistry of carbon compounds. Elsevier Publishing Co., Amsterdam. 1957. p. 246.
7. G. BÄHR. Z. anorg. u. allgem. Chem. **268**, 351 (1952).
8. G. BÄHR. Z. anorg. u. allgem. Chem. **273**, 325 (1953).
9. G. BÄHR and E. SCHLEITZER. Z. anorg. u. allgem. Chem. **278**, 136 (1955).
10. W. GÓRSKI, M. ZOLNIEROWICZ, and T. LIPIEC. Chem. Anal. (Warsaw), **3**, 647 (1958).
11. L. J. BELLAMY. The infra-red spectra of complex molecules. Methuen & Co. Ltd., London. 1954. p. 123.
12. P. W. SADLER. J. Chem. Soc. 957 (1961).
13. M. POLONOVSKI and M. PESSON. Compt. rend. **232**, 1260 (1951).
14. M. PESSON, G. POLMANSS, and S. DUPIN. Compt. rend. **248**, 1677 (1959).
15. S. G. BOGOMOLOV, E. A. POSTOVSKI, and U. H. SCHEINKER. Doklady Akad. Nauk S.S.S.R. **91**, 1111 (1953).
16. M. TIŠLER and Ž. URBAŠKI. J. Org. Chem. **25**, 770 (1960).
17. F. J. WILSON and R. BURNS. J. Chem. Soc. 870 (1922).
18. M. POLONOVSKI, M. PESSON, and P. RAJZMAN. Bull. soc. chim. France, 240 (1955).
19. A. H. GREER and G. B. L. SMITH. J. Am. Chem. Soc. **72**, 874 (1950).
20. K. A. JENSEN. J. prakt. Chem. **159**, 189 (1941).
21. A. DORNOW and W. BORTSCH. Ann. **602**, 23 (1957).
22. E. FISCHER. Belgian Pat. No. 503980 (December, 1951).
23. P. W. SADLER. J. Chem. Soc. 243 (1961).

ELECTRON SPIN RESONANCE OF X-RAY-IRRADIATED SINGLE CRYSTALS OF *dl*-ALANINE HYDROCHLORIDE

W. C. LIN AND C. A. MCDOWELL
Department of Chemistry, University of British Columbia, Vancouver, British Columbia
Received January 18, 1962

ABSTRACT

The electron spin resonance of an X-ray-irradiated single crystal of *dl*-alanine hydrochloride indicates that the radical formed is probably the same as that produced by X- and γ-ray irradiation of alanine. The components of the hyperfine interaction tensor for the radical have been evaluated.

INTRODUCTION

The electron spin resonance (e.s.r.) spectra of X-ray-irradiated single crystals of α-alanine was first studied in detail by Miyagawa and Gordy (1). They identified the radical as CH_3—$\dot{C}$H—R. The odd electron was found to have a nearly isotropic hyperfine interaction with the three methyl protons, and an anisotropic hyperfine interaction with the α-proton.

Alanine crystals have orthorhombic symmetry and the unit cell contains four molecules. There are, therefore, four non-equivalent molecular sites for each crystal orientation. Only when the external field is parallel to a crystal axis do the four site spectra become coincident. This means that for the principal element, say A_1 of the hyperfine interaction tensor **A**, there are four different sets of values for the direction cosines. Neither the signs of these direction cosines nor those of principal values of **A** can be determined conveniently from the experimental data. Miyagawa and Gordy (1) made use of observed second-order effects to analyze their spectra, and calculated values for the components of the interaction tensor, which have been corrected recently by Morton and Horsfield (2), who made further studies on single crystals of alanine.

We here report the results we have obtained in studies of the e.s.r. spectra of irradiated single crystals of *dl*-alanine hydrochloride. The advantage of studying this compound is that the crystals are monoclinic and there are not so many complications as in the case of alanine. There are only two non-equivalent sites in such crystals. When the *b* axis of this type of crystal is placed vertical in the magnetic field, the two sites become equivalent.

EXPERIMENTAL

The crystals of *dl*-alanine hydrochloride were grown from aqueous solution. An idealized diagram of the monoclinic crystals of *dl*-alanine hydrochloride is shown in Fig. 1. The relevant crystallographic data (Dr. J. Trotter, personal communication) are: monoclinic, space group $P2_1/c$, $a = 9.20 \pm 0.02$ Å, $b = 9.04 \pm 0.02$ Å, $c = 7.31 \pm 0.02$ Å, $\beta = 95°21' \pm 5'$. There are four molecules per unit cell. Suitable specimens were irradiated at room temperature with 50 kv X rays for several hours. After irradiation the crystals were studied in our 9 Gc/sec e.s.r. spectrometer with 10 kc/sec modulation and using a 6-in. Varian magnet with pole shims to provide a homogeneous magnetic field (3). The error in measuring the angular rotation of the crystals was about ±2°, and the hyperfine splitting constants are probably correct to about ±0.5 gauss.

RESULTS AND DISCUSSION

The energy levels of an oriented radical in a single crystal (with orbitally quenched electron angular momentum) in external field can be calculated from the Hamiltonian

$$\mathcal{H} = g\beta\mathbf{H}.\mathbf{S} + \mathbf{S}.\mathbf{A}.\mathbf{I} - g_n\beta_n\mathbf{H}.\mathbf{I} \qquad [1]$$

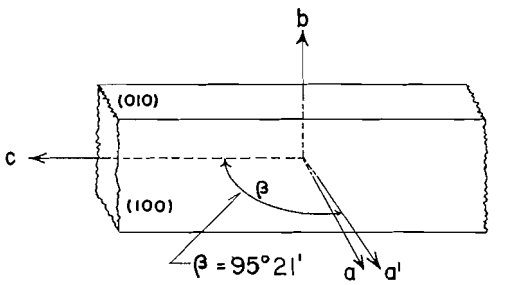

FIG. 1. An idealized sketch showing the relation of the form of the monoclinic crystals of *dl*-alanine hydrochloride to the crystal axes and the experimental reference axes.

and our data have been interpreted in terms of these levels.

The spectra observed were very similar to those of X-ray-irradiated alanine except for certain rather minor differences. In the example shown in Fig. 2 it will be seen that there is a further splitting of the lines into triplets with intensity ratios of 1:2:1. The main pattern in Fig. 2 is regarded as being a five-line spectrum with intensity ratios of 1:4:6:4:1, and that in Fig. 3 an eight-line spectrum with intensity ratios of 1:1:3:3:3:3:1:1. In Fig. 4 is shown a spectrum corresponding to the *c* axis $\perp \mathbf{H}_0$ and an orientation with direction cosines of $\sqrt{3}/2,1/2,0$, with respect to $\mathbf{H}_0$. This illustrates the separation of the two separate spectra due to the two non-equivalent radicals in the unit cell.

Using the hyperfine interactions measured from the spectra we have calculated the π-electron – σ-proton interaction tensor $\mathbf{A}_\sigma$ and the π-electron – methyl proton interaction tensor $\mathbf{A}_m$ with respect to an orthogonal system of axes *a*, *b*, *c*. The crystallographic *b* axis has been taken as our *b* axis but the *a* and *c* axes are chosen arbitrarily. Our *c* axis is along the elongated direction of the crystal. The components of the calculated tensors, in gauss, are:

$$\mathbf{A}_\sigma = \begin{bmatrix} 15.3 & \pm 5.4 & 2.5 \\ \pm 5.4 & 28.3 & 0 \\ 2.5 & 0 & 18.5 \end{bmatrix} \qquad \mathbf{A}_m = \begin{bmatrix} 23.7 & 0 & 0 \\ 0 & 28.3 & 0 \\ 0 & 0 & 21.8 \end{bmatrix} \qquad [2]$$

The direction cosines of the principal values of these tensors with respect to the *a*,*b*,*c* system of axes are given in Table I. In recording these data the principal values of the $\mathbf{A}_\sigma$ tensor have been written with the correct negative sign (4); the $\mathbf{A}_m$ tensor is known to be positive in sign (5).

TABLE I

Direction cosines of principal values of interaction tensors $\mathbf{A}_\sigma$ and $\mathbf{A}_m$ with respect to the *a*,*b*,*c*, system of axes

$\mathbf{A}_\sigma$				$\mathbf{A}_m$			
Principal values	Direction cosines			Principal values	Direction cosines		
	l	*m*	*n*		*l*	*m*	*n*
−12.4	∓0.880	+0.300	±0.360	+28.3	0	1	0
−19.4	∓0.316	+0.191	∓0.930	+23.7	1	0	0
−30.4	∓0.348	−0.934	∓0.074	+21.8	0	0	1

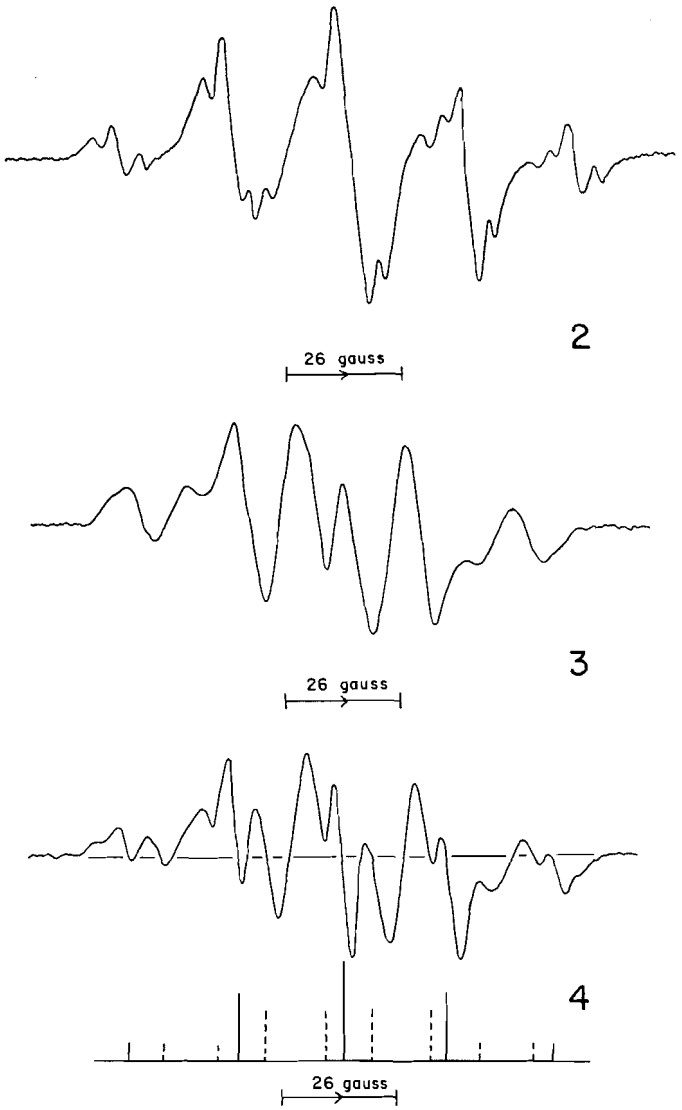

FIG. 2. Electron spin resonance spectrum of an X-ray-irradiated single crystal of *dl*-alanine HCl (H direction cosines: 0,1,0).
FIG. 3. Electron spin resonance spectrum of an X-ray-irradiated single crystal of *dl*-alanine HCl (H direction cosines: $1/2,0,-\sqrt{3}/2$).
FIG. 4. Electron spin resonance spectrum of an X-ray-irradiated single crystal of *dl*-alanine HCl (H direction cosines: $\sqrt{3}/2,1/2,0$).

The values in Table I agree well with those given for the radical produced by X-ray irradiation of alanine (2). The principal values for $\mathbf{A}_\sigma$ are quite similar to those for the $\cdot CH(COOH)_2$ radical (4) and indicate that the unpaired electron density at the α-carbon atom in the radical is approximately 0.9. The values resulting for the electron – methyl protons interaction tensor give an isotropic contribution of 24.6 gauss, which is quite close to the value of 25 gauss estimated for a freely rotating methyl group (5).* The

**This value also agrees well with the recently reported result for a freely rotating methyl group in the* $CH_3 \cdot C(COOH)_2$ *radical (see C. Heller, J. Chem. Phys. 36, 175 (1962)).*

principal values for anisotropic portion of $\mathbf{A}_m$, namely, +3.7, −0.9, −2.8 gauss, are not axially symmetric. Plotting the angular variation of the hyperfine splitting constants for the methyl group on polar diagrams indicates that they are nearly symmetrical (see Table I). There may be a small asymmetry; but in this crystal it is extremely difficult to resolve the small differences between the two nearly isotropic methyl proton hyperfine splittings corresponding to two non-equivalent sites and so one cannot readily determine the degree of anisotropy. This means that calculations of the angle between the C—CH_3 bond and the C—H bond are subject to large errors and for these reasons such calculations are not given here.

Earlier we mentioned that where the lines could be resolved, triplets with intensity ratios of 1:2:1 were found to have a separation of up to 4 gauss. It is likely that this triplet splitting is caused by interaction with protons belonging to a neighboring molecule in the host crystal.

ACKNOWLEDGMENTS

We wish to thank the National Research Council of Canada and the Defense Research Board for generously providing grants in aid of this work.

REFERENCES

1. I. MIYAGAWA and W. GORDY. J. Chem. Phys. **32**, 255 (1960).
2. J. R. MORTON and A. J. HORSFIELD. J. Chem. Phys. **35**, 1142 (1961).
3. W. C. LIN and C. A. McDOWELL. Mol. Phys. **4**, 333, 343 (1961).
4. H. M. McCONNELL, C. HELLER, T. COLE, and R. W. FESSENDEN. J. Am. Chem. Soc. **82**, 766 (1960).
5. A. D. McLACHLAN. Mol. Phys. **1**, 233 (1958).

THE PHOTOIONIZATION OF NITROGEN DIOXIDE

D. C. Frost, D. Mak, and C. A. McDowell
Department of Chemistry, University of British Columbia, Vancouver, British Columbia
Received February 2, 1962

ABSTRACT

The ionization of nitrogen dioxide by photons has been studied using a photoionization mass spectrometric technique and also by the ordinary electron impact method. The photoionization results show a large variation in the relative ionization efficiency within the energy range 9–14 ev, and help to explain the differences between previously reported values for the first ionization potential of this compound. The photoionization efficiency curve indicates the first ionization potential to lie at 9.8 ev and inner ionization potentials to lie at about 11.1 and 12.7 ev.

The electron impact ionization efficiency curve for the NO_2^+ ion exhibits a low ion intensity near the threshold. This confirms the viewpoint that previous determinations of the first ionization potential have employed threshold energy measuring techniques not properly suited for the type of molecule such as nitrogen dioxide which radically changes symmetry on ionization.

INTRODUCTION

The values reported in the literature for the first ionization potential of nitrogen dioxide show a remarkable variation. Electron impact studies have led to the values of 11 ev (1), 11.3 ev (2), and 11.0 ev (3). Kandel (4) deduced a value of 9.91 ev from his studies on the ionization and dissociation of nitromethane. Spectroscopic studies by Price and Simpson (5) led to a value of 12.3 ev for an inner ionization potential based on the extrapolation of two probable Rydberg bands in the far-ultraviolet absorption spectrum of nitrogen dioxide. Further work by Weissler, Sampson, Ogawa, and Cook (6) using a combination of a photoionization monochromator and a mass spectrometer yielded a value of 11.3 ev for the first ionization potential. More recently, photoionization studies carried out by Nakayama, Kitamura, and Watanabe (7) have yielded a value of 9.78 $\pm$0.05 ev for the first ionization potential of nitrogen dioxide, and suggested the occurrence of a second ionization potential at 11.62 ev. It should be pointed out that Weissler *et al.* did not investigate the region below 11 ev in much detail and for this reason missed the first ionization potential of this compound. The work to be described, which included both electron impact and photoionization studies using a mass spectrometer, confirms the previous value obtained from photoionization measurements for the first ionization potential of nitrogen dioxide and also indicates why the other workers may have obtained some of the results quoted.

EXPERIMENTAL

The apparatus, to be fully described elsewhere, basically consists of a 60-deg sector field 6-in. magnetic radius mass spectrometer designed so that it can be used with an electron or a photon ionizing source. The light source was a gas discharge tube, containing mixtures of rare gases and H_2 or D_2, excited at a microwave frequency of 2460 Mc/s. A Seya–Namioka type monochromator was used to provide ionizing radiation. The resolution of the monochromator is about 6 Å, which means the photon energy spread is 0.07 ev at 12 ev. After traversing the mass spectrometer ion chamber, the radiation strikes a sodium-salicylate-coated photomultiplier, the output of which is taken to be proportional to the radiation intensity. The optical system is windowless, and the pressure is kept low through efficient differential pumping. An ion–electron multiplier is used to measure the resolved ion currents. The ratio of ion current to photon intensity is determined at as many wavelengths as possible and then plotted against photon energy (see refs. 6 and 8 for a description of similar instruments). The NO_2 was prepared by reacting oxygen with nitric oxide which had been purified by low-temperature distillation.

DISCUSSION

As mentioned in the Introduction, values reported in the literature for the first ionization potential of NO_2 show remarkable disagreements, and it is the purpose of this paper to present new measurements which help to explain the apparent discrepancies.

Figure 1 shows the photoionization efficiency curve for NO_2^+. It is seen that the threshold energy (9.80 ± 0.05 ev) agrees with the adiabatic value (7). However, the ion intensity

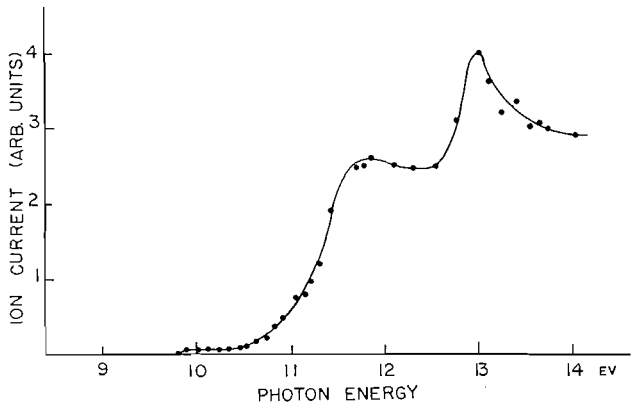

FIG. 1. Photoionization efficiency curve for nitrogen dioxide.

remains low (compared with that at much higher energies) and fairly constant up to about 10.5 ev. Here, an inner adiabatic ionization potential is indicated since the curve begins to rise. The photon energy at the point of greatest slope in this region, about 11.1 ev, should equal the corresponding vertical ionization potential provided ionization is occurring only through this second process. The electron impact measurements of Steuckelberg and Smyth (1), and Collin (2), seem to be associated with our vertical ionization potential at 11.1 ev.

Figure 2 shows the electron impact ion efficiency curves for NO_2^+ and Kr^+, which we obtained using a conventional ion source. Clearly the curved portion of the NO_2^+ ionization efficiency curve extends over a much greater energy range than that of Kr^+, and it

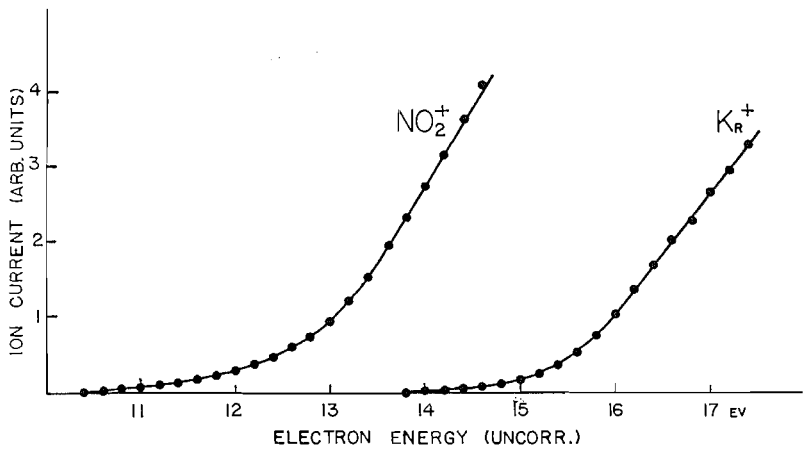

FIG. 2. Electron impact ionization efficiency curve for nitrogen dioxide.

is difficult to decide the threshold energy for NO_2^+ formation. It would seem therefore that in the case of nitrogen dioxide there is likely to be considerable uncertainty as to the interpretation of the first ionization potential from electron impact studies. We find this value to be about 10.5 ev, using the initial upward break method, and, since it lies between the first and second adiabatic ionization potentials, it should decrease as the ion current detector sensitivity is increased.

At photon energies greater than 12 ev the ion efficiency for NO_2^+ shows a slight decrease. Why this should be so is not clear, unless preionization is responsible for the maximum. The ionization increase at about 12.4 ev can be correlated with Price and Simpson's Rydberg series limit at 12.3 ev. The vertical ionization potential here would normally correspond to the photon energy where the photoionization curve has the greatest slope, but it is difficult to account for the peak at 13 ev unless preionization is involved.

We find no evidence to support the proposed ionization potential which Nakayama *et al.* claim to have observed at 11.62 ev. In view of the marked increase in ion current which we observe just below 11 ev, it may well be that the rise in total ionization seen by Nakayama *et al.* at 10.83 ev is only partially due to formation of the ion pair $NO^+ + O^-$ (theoretically formed at a minimum energy at 10.89 ev). We attempted to clarify this point by studying the formation of NO^+ from nitrogen dioxide by photoionization. It was extremely difficult, however, to obtain satisfactory results. Even with very pure nitrogen dioxide as a starting material there seemed to be more NO^+ present than would have been expected from the process under discussion. This extra nitric oxide could probably have been produced by the photolysis of the nitrogen dioxide in the ion chamber. Light of wavelength less than 4000 Å is well known (9) to cause the following reaction:

$$2NO_2 + h\nu = 2NO + O_2. \qquad [1]$$

It is possible that the occurrence of this reaction caused our experiments to be indefinite on this particular point.

Closer examination of the basis on which Nakayama *et al.* evaluated the second ionization potential of 11.62 ev makes it apparent that it may not be so well established as it might at first sight appear. Those authors assigned six absorption bands as Rydberg bands and fitted them to the Rydberg series

$$\nu_m = 93{,}695 - 2/(n+0.21)^2,$$

with $n = 3$, (?), 4, 5, 6, 7, 8 . . . . In Table 2 of their paper they compare the calculated and observed positions of the bands. The agreements for bands with $n = 4$ to 8 are fairly good but in the case of the band with $n = 3$ a discrepancy of 6334 cm^{-1} was found between the observed and the calculated frequencies. Presumably for this reason the authors labelled this band, $n = 3$, as being doubtfully assigned.

The electronic structure of the nitrogen dioxide molecule has been considered by many authors (9–14). Recent work has confirmed the earlier views that the unpaired electron can be regarded as being localized mainly on the nitrogen atom. This would mean that the first ionization potential at 9.8 ev would refer to the removal of an electron from the $4a_1$ molecular orbital. As the nitrogen dioxide molecule is bent in its ground state, it is expected that on ionizing to form NO_2^+ by the removal of an electron from the $4a_1$ orbital, this ion would be formed in its linear ground state. There is evidence that the NO_2^+ ion is, in fact, linear (15). None of the theoretical values for the ionization potentials

agree well with the experimental results. In this connection we may note that McEwen (12) has pointed out that the NO_2^+ ion can be formed in singlet and triplet excited states. It is important to realize that both the radical (NO_2) ground state and the three lowest singlet configurations of the positive ion are strongly stabilized by interaction with low-energy doubly excited configurations. The corresponding interactions with the $^3B_2$ and $^3A_2$ triplet configurations of the ion are much smaller. The difficulty in adequately taking these factors into account in the calculations makes the theoretical results less satisfactory than might have been expected.

ACKNOWLEDGMENTS

We wish to thank the National Research Council of Canada for grants in aid of this work. In earlier phases of this work we were greatly assisted by support from the Geophysical Research Directorate of the U.S. Air Force, Cambridge Research Centre, and we wish to extend our thanks to that body for its generosity.

REFERENCES

1. E. C. G. Steuckelberg and H. D. Smyth. Phys. Rev. **36**, 478 (1930).
2. R. W. Kiser and I. C. Hisatsune. J. Phys. Chem. **65**, 1444 (1961).
3. J. Collin and F. P. Lossing. J. Chem. Phys. **28**, 900 (1958).
4. R. J. Kandel. J. Chem. Phys. **23**, 84 (1955).
5. W. C. Price and D. M. Simpson. Trans. Faraday Soc. **37**, 106 (1941).
6. G. L. Weissler, J. A. R. Sampson, M. Ogawa, and G. R. Cook. J. Opt. Soc. Am. **49**, 338 (1959).
7. T. Nakayama, M. Y. Kitamura, and K. Watanabe. J. Chem. Phys. **30**, 1180 (1959).
8. H. Hurzeler, M. G. Inghram, and J. D. Morrison. J. Chem. Phys. **28**, 76 (1958).
9. R. G. W. Norrish. J. Chem. Soc. 1158 (1929).
10. R. S. Mulliken. Revs. Modern Phys. **14**, 204 (1942).
11. A. D. Walsh. J. Chem. Soc. 2260 (1953).
12. K. L. McEwen. J. Chem. Phys. **32**, 1801 (1960).
13. M. Green and J. W. Linnett. Trans. Faraday Soc. **57**, 1 (1961).
14. J. Serre. Mol. Phys. **4**, 269 (1961).
15. R. J. Gillespie and D. J. Miller. Quart. Revs. (London), **2**, 277 (1948).

LYCOPODIUM ALKALOIDS

XII. FLABELLIFORMINE

M. CURCUMELLI-RODOSTAMO AND D. B. MACLEAN
Department of Chemistry, McMaster University, Hamilton, Ontario
Received February 13, 1962

ABSTRACT

Evidence is furnished which establishes the structure of a new alkaloid isolated from *Lycopodium flabelliforme.*

In the present publication we wish to report evidence which enables the assignment of structure I to a new alkaloid obtained from *Lycopodium flabelliforme.*

The alkaloid, for which the name flabelliformine seems appropriate, is sparingly soluble in cold ether. Advantage was taken of this property in its isolation from the bases obtained, after the separation of lycopodine from the crude alkaloid mixture.

Analysis of flabelliformine, I, fits the formula $C_{16}H_{25}O_2N$. The infrared spectrum of the alkaloid, measured in chloroform solution, shows ketonic carbonyl absorption at 1705 cm^{-1} and a hydroxyl band at 3560 cm^{-1}. Reduction of the carbonyl group with sodium borohydride affords the diol II, $C_{16}H_{27}O_2N$. The hydroxyl group appears to be attached to a tertiary carbon atom, since flabelliformine is recovered unchanged after treatment with chromium trioxide and its n.m.r. spectrum shows no absorption below a τ-value of 6.5.

Treatment of the alkaloid with hydrogen iodide replaces the hydroxyl group with hydrogen; the reaction product is identical with lycopodine, III (1–4). Flabelliformine, therefore, is formally derived from lycopodine by replacement of a methine hydrogen by a hydroxyl group.

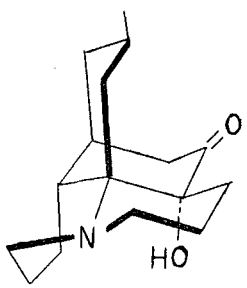

I

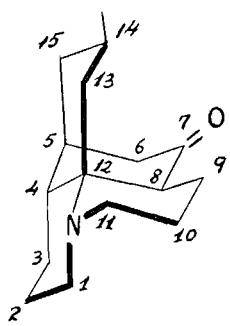

III

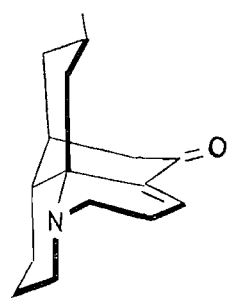

IV

Dehydration of I, effected by both phosphoric acid and *p*-toluenesulphonic acid, affords a non-crystalline product, IV, which was converted to a crystalline methiodide, V, $C_{17}H_{26}ONI$. Compound IV has the properties of an α,β-unsaturated ketone. The ultraviolet spectrum of this substance shows maximum absorption at 245 mμ and the infrared spectrum, measured in carbon tetrachloride solution, has bands of equal intensity at 1685 and 1617 cm^{-1}. The n.m.r. spectrum of IV has a triplet at a τ-value of 3.01 which is attributed to a proton on the β-carbon of the α,β-unsaturated carbonyl system (5, 6).

Compound IV is formed without alteration of the carbon skeleton present in the alkaloid, since on hydrogenation, over a platinum catalyst, it yields lycopodine. The double bond must occupy the 8,9 position, as shown. A double bond in the alternative conjugated position would result in a very large distortion of bond angles. The hydroxyl group in I is therefore attached to C_8.

The conversion of flabelliformine, I, to lycopodine, III, proves that both alkaloids have the same configuration at C_4, C_5, C_{12}, and C_{14}.

The configuration at C_8 can be deduced from spectral data. The absorption at 3560 cm^{-1}, in the spectrum of flabelliformine, shows that the hydroxyl group is hydrogen bonded. The bonding is intramolecular, for the peak is not displaced on dilution. A comparison of the infrared and ultraviolet spectra of lycopodine and flabelliformine indicates that the hydroxyl is not hydrogen bonded with the carbonyl oxygen. The infrared spectrum of lycopodine (chloroform solution) shows carbonyl absorption at 1693 cm^{-1}, while that of flabelliformine has a band at 1705 cm^{-1}. Their ultraviolet spectra have maxima at 284 and 303 mμ respectively (7). The hydrogen bonding appears, therefore, to involve the nitrogen lone pair. Structure I, alone, fulfills the spatial requirements for such an interaction.

EXPERIMENTAL

Isolation of Flabelliformine

The crude alkaloid mixture was obtained from *L. flabelliforme* by the method of Manske and Marion (8). Lycopodine was isolated by column chromatography as described by Barclay and MacLean (9). The other, more strongly adsorbed, alkaloids were eluted with chloroform and combined. The mixture of bases was shaken with cold ether and the ether-insoluble residue crystallized from acetone–methanol. The material obtained was dissolved in acetone and treated with 48% hydrobromic acid. Flabelliformine hydrobromide separated immediately. From the mother liquors dihydrolycopodine (2, 10) was obtained. Recrystallization of the hydrobromide from acetone, containing a small quantity of water, gave crystals melting over 337° with decomposition. The alkaloid (I) liberated from the hydrobromide salt melts at 210–211°. A change in crystalline form occurs at 150°. Calc. for $C_{16}H_{25}O_2N$: C, 72.96; H, 9.57; N, 5.32%. Found: C, 73.04; H, 9.68; N, 5.33%.

The infrared spectrum of flabelliformine, determined in chloroform, shows hydroxyl absorption at 3560 cm^{-1}, carbonyl absorption at 1705 cm^{-1}, and a band at 1415 cm^{-1} attributed to a methylene group adjacent to the carbonyl. The ultraviolet spectrum has $\lambda_{max}^{CH_3OH}$ at 303 mμ (ϵ, 50). The n.m.r. spectrum of the alkaloid shows no absorption below a τ-value of 6.5, indicating the absence of the group $\rangle$CH—OH.

Flabelliformine, when treated with methyl iodide in acetone solution, gave a crystalline methiodide which melted over 335° with decomposition. Calc. for $C_{17}H_{28}O_2NI$: C, 50.37; H, 6.96; N, 3.45%. Found: C, 50.75; H, 7.08; N, 3.35%.

Preparation of Compound II

A solution of sodium borohydride (0.20 g) in ethanol was added slowly to a stirred ethanolic solution of flabelliformine (0.15 g). After addition of the hydride solution, the mixture was stirred for 2 hours and then left to stand overnight. Excess reagent was destroyed with acetone and the reaction mixture evaporated to dryness. Water was added to the residue. The mixture was acidified with hydrochloric acid and heated briefly on a steam bath. It was then basified with ammonia and extracted with chloroform. From the chloroform extract a crystalline product (compound II) was obtained (0.12 g) which, on recrystallization from ether, afforded crystals melting at 217–217.5°. Calc. for $C_{16}H_{27}O_2N$: C, 72.41; H, 10.26; N, 5.28%. Found: C, 72.41; H, 10.28; N, 5.28%.

The infrared spectrum (Nujol mull) of compound II shows no carbonyl-group absorption but has two bands in the hydroxyl region at 3610 and 3460 cm^{-1}.

Treatment of Flabelliformine with Chromium Trioxide

A solution of chromium trioxide (0.10 g) in water was added dropwise over a period of 1 hour to a stirred solution of flabelliformine (0.040 g) in 10% aqueous acetic acid. The temperature was maintained at −5 to −10° during the addition, and the mixture was stirred at this temperature for a further 5 hours. The oxidant was destroyed with methanol and the reaction mixture kept in a refrigerator overnight. The solution was then concentrated, made strongly acidic with hydrochloric acid, and extracted with chloroform. It was then basified with ammonia and again extracted with chloroform. From the last extract flabelliformine (0.033 g) was recovered.

Treatment of Flabelliformine with Hydriodic Acid

Flabelliformine (0.05 g) was dissolved in hydriodic acid (4 ml, 47%). The solution was refluxed for 17 hours, then made basic with ammonia and extracted with chloroform. The compound isolated (0.03 g) from the chloroform extract was found to be identical with lycopodine: the melting point of the product was not depressed on admixture with an authentic sample of lycopodine and the infrared spectra of the two samples, measured both in Nujol mull and carbon tetrachloride, were superimposable.

Dehydration of I by Treatment with Phosphoric Acid

A solution of flabelliformine (I) (0.11 g) in 88% aqueous phosphoric acid (7 ml) was heated on a steam bath for 12 hours. The mixture was cooled, made basic with potassium hydroxide, and extracted with chloroform. Evaporation of the chloroform left an oil (IV) (0.09 g) which could not be induced to crystallize.

The infrared spectrum (film) of compound IV shows absorption at 1614 cm^{-1} (conjugated double bond) and 1678 cm^{-1} (conjugated carbonyl); the two bands are situated at 1617 and 1685 cm^{-1} when the spectrum is measured in carbon tetrachloride solution. Compound IV has $\lambda_{max}^{CH_3OH}$ at 245 mμ. The n.m.r. spectrum (in $CDCl_3$) exhibits a triplet at a τ-value of 3.01.

Dissolution of compound IV in acetone and treatment with an excess of methyl iodide afforded a crystalline methiodide, V, which melted over 285° with decomposition. Calc. for $C_{17}H_{26}ONI$: C, 52.71; H, 6.77; N, 3.62%. Found: C, 52.40; H, 6.86; N, 3.55%.

The infrared spectrum (Nujol mull) of compound V shows bands at 1620 and 1688 cm^{-1}.

Dehydration of I by Treatment with p-Toluenesulphonic Acid

A solution of flabelliformine and *p*-toluenesulphonic acid in *o*-xylene was heated under reflux for 12 hours. The reaction mixture was extracted with water. The extract was shaken with ether to remove completely the xylene, basified with ammonia, and extracted with chloroform. The product obtained from the chloroform solution was identical with compound IV described in the preceding section.

Hydrogenation of Compound IV

A solution of compound IV in methanol was shaken with hydrogen (35 p.s.i.g.) and platinum oxide for 16 hours.

The catalyst was removed by filtration and the solvent evaporated. The residue was dissolved in acetone and treated with methyl iodide. A crystalline methiodide separated which melted with decomposition at 315–318°. The methiodide was shown to be identical with lycopodine methiodide by a mixed melting point determination and comparison of infrared spectra.

ACKNOWLEDGMENTS

We wish to express our thanks to the National Research Council of Canada, and to the Ontario Research Foundation, for financial assistance. We are indebted to Mr. J. C. F. Young, who isolated the flabelliformine.

REFERENCES

1. W. A. HARRISON and D. B. MACLEAN. Chem. & Ind. (London), 261 (1960).
2. W. A. HARRISON, M. CURCUMELLI-RODOSTAMO, D. F. CARSON, L. R. C. BARCLAY, and D. B. MACLEAN. Can. J. Chem. **39**, 2086 (1961).
3. F. A. L. ANET. Tetrahedron Letters, No. 20, 13 (1960).
4. K. WIESNER, J. E. FRANCIS, J. A. FINDLAY, and Z. VALENTA. Tetrahedron Letters, No. 5, 187 (1961).
5. R. R. FRASER. Can. J. Chem. **38**, 549 (1960).
6. W. N. FRENCH. Ph.D. Thesis, McMaster University, Hamilton, Ontario. September, 1960.
7. R. C. COOKSON and S. H. DANDEGAONKER. J. Chem. Soc. 352 (1955).
8. R. H. F. MANSKE and L. MARION. Can. J. Research, B, **20**, 87 (1942).
9. L. R. C. BARCLAY and D. B. MACLEAN. Can. J. Chem. **34**, 1519 (1956).
10. D. B. MACLEAN, R. H. F. MANSKE, and L. MARION. Can. J. Research, B, **28**, 460 (1950).

NUCLEAR MAGNETIC RESONANCE STUDIES

PART I. THE CHEMICAL SHIFT OF THE FORMYL PROTON IN AROMATIC ALDEHYDES[1]

R. E. KLINCK AND J. B. STOTHERS
Department of Chemistry, University of Western Ontario, London, Ontario

Received February 7, 1962

ABSTRACT

Chemical shift data for the formyl proton in some 30 aromatic aldehydes are reported. It was found that meta- and para-substituted benzaldehydes exhibited this peak in the range 9.65–10.20 δ, while ortho-substituted compounds appear at lower field, 10.20–10.50 δ; the former shifts show an approximate correlation with the Hammett sigma parameter. Evidence for steric inhibition of resonance is presented for some ortho-substituted compounds and some interesting solvent effects are discussed.

INTRODUCTION

Although it is well known (1, 2) that the aldehyde proton absorbs in a characteristic region of the N.M.R. spectrum (i.e., 9–11 p.p.m. from tetramethylsilane), no extensive survey of its resonance position has so far been reported. The present study was undertaken to determine those structural features which influence the chemical shift of this proton. While our investigation has included examples from the aliphatic, alicyclic, and aromatic series, only the latter is discussed in this paper. The results from the other series will be reported in the near future.

On the basis of the present theories of magnetic shielding (3) one can suggest the major structural features which would be expected to contribute to the chemical shift of the formyl proton in an aromatic aldehyde. The shielding of a specific nucleus is considered to be determined by two major factors: (*a*) the electron density about that nucleus, and (*b*) the presence of magnetically anisotropic groupings within the molecule. In this series of compounds, the anisotropic carbonyl group and the aromatic ring would be expected to have pronounced effects on the chemical shifts, as would variations in the electron density about the formyl proton.

For protons, the electron distribution about the nucleus is essentially isotropic and the local effect, (*a*) above, is diamagnetic and directly dependent on the electron density. Therefore, the greater the electron density, the greater will be the shielding, due to the circulations of the electrons surrounding a specific proton. In an aldehyde molecule, the electrophilic character of the carbonyl carbon will tend to polarize the C—H and C—C bonds attached thereto. The polarization of the C—H bond will reduce the electron density about the formyl proton and so must contribute to the low shielding observed for it. Electron-releasing groups bonded to the carbonyl group will reduce the electrophilic nature of the carbonyl carbon and so decrease the polarization of the C—H bond. Thus, it is suggested that formyl protons in conjugated systems would be shielded relative to those in analogous saturated cases. Support for this hypothesis is provided by the observation that, as a rule, carbonyl groups conjugated with ethylenic or phenyl groups are less reactive towards nucleophiles than are simple carbonyl compounds. The

[1]*These results were presented as part of a paper at the 44th Annual Conference of the Chemical Institute of Canada, Montreal, August 3–5, 1961.*

C^{13} chemical shifts of the carbonyl carbon in a number of aldehydes also furnish evidence for this view, since the carbonyl carbons in aromatic and α,β-unsaturated aldehydes appear at significantly higher field than those in related saturated cases (4). This shift is presumably due to the increased electron density about the carbon atom in the conjugated systems. Similar correlations have been presented for C^{13} chemical shifts and electron densities in aromatic molecules (5–7). Similarly, any other factors which affect the polarization of the carbonyl carbon could be expected to be reflected in the chemical shift of the formyl proton.

Pople (8) has shown that a major contribution to the low shielding observed for the formyl proton in aldehydes arises from the anisotropy of the carbonyl grouping. It has been shown that this group has a large diamagnetic anisotropy arising from electron circulations occurring when the applied field is normal to the plane of the trigonal carbon atom (9, 10). Since a detailed discussion of the influence of this grouping on neighboring nuclei has appeared (2) in terms of the point dipole approximation due to McConnell (11), it is sufficient to note that protons in the plane of the trigonal carbon would be subjected to a strong deshielding effect. The orientation of the proton in the formyl grouping cannot change relative to the carbonyl bond in any aldehyde, and so it seems reasonable to assume that this strong effect will be approximately constant in a series of aldehydes.

A third important factor in this series of compounds will be the contribution to the shielding by the aromatic nucleus whose ring current effects are well established (12–15). The anisotropy of the aromatic ring is such that the field induced by the circulation of the π electrons around the ring serves to accentuate the applied field in the plane of the ring and thus to deshield nuclei in this plane. This effect is maximal in the plane of, and close to, the ring and decreases as the orientation of a specific nucleus is changed therefrom. In the aromatic series, it is evident that the formyl proton will not be far removed from this plane at any time and so would experience a strong deshielding effect. In the case of polycyclic aromatics, this effect will be enhanced since the ring current contributions are larger (13).

From these considerations, it is suggested that the important factors which determine the chemical shift of a formyl proton in an aromatic aldehyde include the contributions by the anisotropic carbonyl bond and aromatic ring and the degree of polarization of the formyl C—H bond. It is found that this rather simple model accounts qualitatively for the observed results, although a quantitative evaluation of the relative contributions of these factors is not yet possible because of their interdependence.

EXPERIMENTAL

A Varian V-4302 spectrometer operating at 60 Mc/sec was employed for all measurements. The peak positions were determined using the usual audio side-band technique (16) by interpolation between two side bands of the reference signal placed on either side of the desired peak. An audio oscillator whose output was continuously monitored with a Hewlett-Packard 522B frequency counter was used throughout. In most instances, the compounds were examined in 20, 10, and 5% (w/v) solutions in carbon tetrachloride. If the compound was sparingly soluble in this solvent, a similar range of concentrations in deuterochloroform was measured. A few aldehydes were studied in both solvents to determine the effect of changing the solvent. Some substituted benzaldehydes were examined in acetone, methanol, cyclohexane, and benzene solutions as well. The tabulated data are those obtained for the most dilute solutions (5%) and are given in p.p.m. (δ) relative to internal tetramethylsilane with an estimated precision of ± 0.01 p.p.m. Each value is the mean of at least 10 separate measurements.

The compounds used in this study are commercially available and were purified by distillation or recrystallization before use. Spectrograde carbon tetrachloride (Fisher Scientific) was used throughout and the deuterochloroform was obtained from Merck, Sharpe and Dohme (min. 99% D).

RESULTS

The chemical shift data are collected in tabular form as follows: Table I, meta- and para-substituted benzaldehydes; Table II, ortho-substituted benzaldehydes and polycyclic aromatic aldehydes. For comparative purposes, the data for a few other aldehydes are given in the text below.

TABLE I

Chemical shifts of the formyl proton in some meta- and para-substituted benzaldehydes (in p.p.m. from tetramethylsilane; 5% solution (w/v))

Aldehyde	CCl_4*	$CDCl_3$*
Benzaldehyde	9.96 (+0.02)	10.02 (+0.02)
m-Tolualdehyde	9.90 (+0.03)	9.98 (+0.03)
p-Tolualdehyde	9.89 (+0.03)	9.96 (+0.03)
p-Anisaldehyde	9.81 (+0.02)	—
m-Nitrobenzaldehyde	—	10.13 (−0.03)
p-Nitrobenzaldehyde	—	10.18 (−0.01)
m-Hydroxybenzaldehyde	—	9.91 (—)
p-Hydroxybenzaldehyde	—	9.86 (—)
m-Chlorobenzaldehyde	9.94 (+0.02)	—
p-Chlorobenzaldehyde	9.94 (0.00)	—
3,4-Dichlorobenzaldehyde	9.91 (—)	—
m-Bromobenzaldehyde	9.91 (+0.01)	—
p-Dimethylaminobenzaldehyde	9.65 (+0.05)	—
m-Fluorobenzaldehyde	9.95† (+0.02)	—
p-Fluorobenzaldehyde	9.92 (+0.01)	—
p-Cyanobenzaldehyde	—	10.08 (−0.04)
m-Benzyloxybenzaldehyde	9.88 (+0.05)	—
p-Acetamidobenzaldehyde	—	9.89 (—)
3,5-Dimethoxybenzaldehyde	9.82 (+0.04)	—
3,4,5-Trimethoxybenzaldehyde	9.73 (+0.02)	—
Piperonal	9.74 (+0.02)	—
Vanillin	—	9.82 (+0.02)

*The bracketed quantity is the shift (in p.p.m.) observed upon dilution of 20% solutions.
†This is the center of the observed doublet, $J = 1.8$ cycles/sec.

TABLE II

Chemical shift data for the formyl proton in some ortho-substituted benzaldehydes and some polycyclic aldehydes (5% solutions (w/v) in p.p.m. from tetramethylsilane)

Aldehyde	CCl_4*	$CDCl_3$*
Salicylaldehyde	9.86 (+0.05)	9.89 (+0.03)
Benzaldehyde	9.96 (+0.02)	10.02 (+0.02)
o-Tolualdehyde	10.18 (+0.03)	—
o-Nitrobenzaldehyde	10.37 (+0.03)	10.43 (+0.03)
o-Anisaldehyde	10.39† (+0.01)	—
o-Chlorobenzaldehyde	10.45 (+0.04)	—
Mesitylaldehyde	10.49 (+0.04)	—
1-Naphthaldehyde	10.31 (+0.07)	10.38 (+0.07)
2-Naphthaldehyde	—	10.14 (+0.05)
9-Anthraldehyde	—	11.51‡ (+0.24)
Phenanthrene-9-carboxaldehyde	—	10.39‡ (+0.17)

*Bracketed quantity is dilution shift for 20–5% solution.
†This is the center of the observed doublet, $J = 0.8$ cycle/sec, due to coupling with one of the ring protons. This splitting has been noted previously (17).
‡2.5% solutions.

Although spin coupling of aldehydic hydrogen with the ring protons has been observed in a number of heterocyclic cases (17), it can be noted that, in general, the aromatic

formyl protons appear as singlets and spin coupling with the benzenoid protons is not resolved. In the present series, two exceptions were found: *o*-anisaldehyde exhibits a coupling constant of 0.8 cycles/sec for the formyl proton while *m*-fluorobenzaldehyde shows a splitting of 1.8 cycles/sec, but which other nucleus is involved was not established in either case.

DISCUSSION

General Considerations

For aromatic aldehydes, it has been suggested above that the chemical shift of the formyl proton will be determined by the relative magnitudes of two opposing factors since it may be assumed that the deshielding effect of the carbonyl group will be approximately the same in all cases. The local shielding contribution which depends on the polarization of the C—H bond will be opposed by the deshielding influence of the aromatic ring current. Since acetaldehyde absorbs at 9.73 δ and benzaldehyde at 9.96 δ (both in CCl_4 solution), it appears that the ring current effect outweighs the conjugative shielding. For comparative purposes, it may be noted that acrolein and crotonaldehyde absorb at 9.53 and 9.43 δ, respectively. In these two compounds, a conjugative effect would be opposed by the deshielding due to the anisotropic olefinic bond which tends to deshield in its plane, and since the shifts are to higher field relative to acetaldehyde one can conclude that the effect of conjugation is the stronger. Other evidence in support of a shielding effect by conjugation is provided by the C^{13} results mentioned above.

A further indication that the ring current contribution is a major factor affecting the shielding of the formyl proton in benzaldehyde is provided by the chemical shift of this proton in cinnamaldehyde, which absorbs at 9.64 δ (i.e., 0.32 p.p.m. to high field relative to benzaldehyde). There should be a substantial reduction in the ring current effect since the formyl proton is farther removed from the aromatic nucleus and, to a first approximation, the conjugative contribution may be considered to be comparable to that in benzaldehyde. Although this view may be oversimplified, the observed shift is consistent with the argument.

In a series of substituted benzaldehydes changes in the magnitudes of each of the shielding factors could be expected. As a first approximation, however, it seems reasonable to assume that the ring current effect remains virtually constant. Abraham (18) has suggested that the magnitude of the ring current in a given system is related to the resonance energy of that system and since large changes in the resonance energies of the members of this series are not expected, this assumption would appear to be rational. Variations in the polarization of the C—H bond therefore should be more important and the electronic effects of substituents should influence the formyl shifts in a predictable manner. Similar correlations have been discussed for a number of other systems (7, 19–22). Since an electron-releasing substituent would tend to decrease the positive nature of the carbonyl, the shift of the formyl proton in such a system would be expected to be towards higher field, while electron-withdrawing groups would tend to produce the opposite effect. One can consider the results in detail on the basis of these assumptions.

Meta- and Para-substituted Benzaldehydes

The data in Table I show that the formyl proton in this series absorbs in the region 9.65–10.18 δ, and that these shifts depend markedly on the substituent. Qualitatively the trend is as expected for the simple model and the observed shifts appear to be a measure of the electron supply to, or withdrawal from, the carbonyl grouping. Thus, one might

expect a linear correlation between the chemical shifts and the Hammett sigma parameter of the various substituents. Only a rough correlation, however, is observed, as shown in Fig. 1, which was plotted using the sigma values listed by McDaniel and Brown

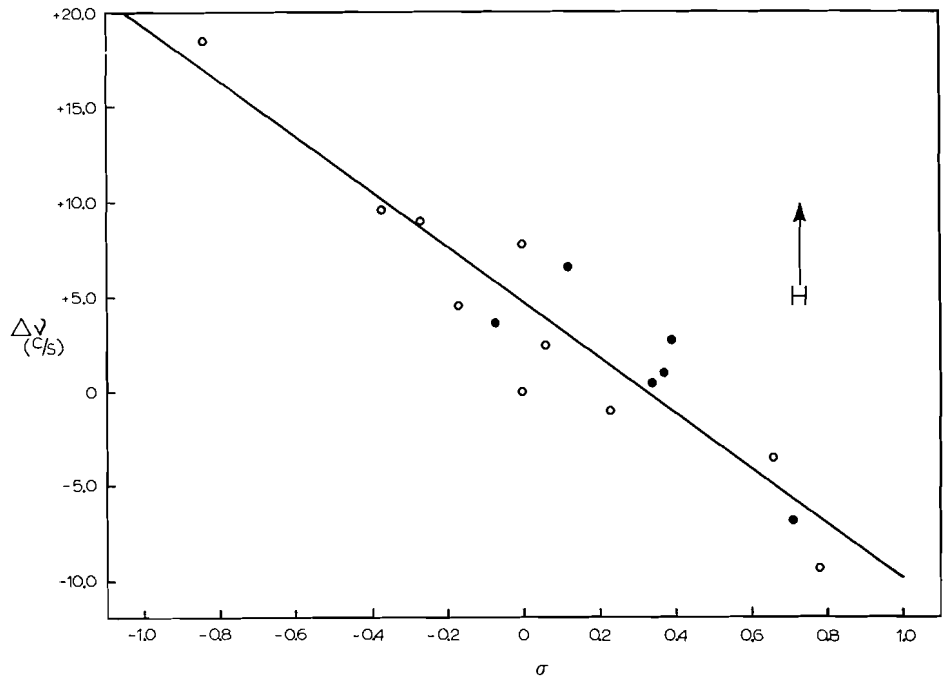

FIG. 1. Correlation of the formyl proton chemical shifts of *m*- and *p*-substituted benzaldehydes by Hammett's σ. The shifts are given in cycles/sec (at 60 Mc/sec) from the peak position of the formyl proton in benzaldehyde. (○ indicates *p*-isomer; ● indicates *m*-isomer.)

(23) and the chemical shifts relative to benzaldehyde. Since some of the samples are insufficiently soluble in carbon tetrachloride to allow measurements over the usual concentration range, the values obtained in deuterochloroform solution were compared to the chemical shift of benzaldehyde in that solvent. No better linear correlation could be obtained using the Taft parameters, σ_R and σ_I (24). The line indicated in Fig. 1 was obtained by a least-squares analysis of the data, considering the shift of benzaldehyde no more reliable than the others.

The largest deviation (ca. 5 cycles/sec) was found for benzaldehyde while other significant deviations (ca. 3.5 cycles/sec) are evident for the *m*-hydroxy-, *m*-bromo, and *p*-acetamido derivatives. It is interesting to find that the para-substituted examples appear to give the closest approach to a linear relation. This could be an indication that the meta substituents exert a small effect through space on the formyl proton. Since rather precise linear free-energy correlations have been obtained for fluorine chemical shifts in *m*- and *p*-substituted fluorobenzenes (19, 20), these results suggest that formyl protons, owing to their lack of inner shell electrons and hence a more exposed nucleus, are more susceptible to the effects of anisotropic meta substituents.

The influence of inductive effects on the chemical shift of the formyl proton is clearly demonstrated by the strong electron-withdrawing cyano and nitro groups, both of which

produce significant shifts to lower field. Presumably this is a result of polarization of the C—H bond via the strong inductive effect on the carbonyl carbon atom.

Ortho-substituted Benzaldehydes

The formyl proton in ortho-substituted benzaldehydes appears at lower field (10.18–10.49 δ) than the *m*- and *p*-substituted examples, with one exception, salicylaldehyde. This compound is a special case because of intramolecular hydrogen bonding of the ortho-hydroxyl group with the carbonyl oxygen atom. The observed shift for the aldehydic proton at 9.89 δ may be compared to that of the *p*-substituted isomer at 9.86 δ. In these two compounds the conjugative effect and the ring current contributions would be similar and, thus, it appears that the effect of hydrogen bonding is small. (It can be noted that a change in solvent from CCl_4 to $CDCl_3$ results in a smaller shift (2 cycles/sec) than in other examples.) It would appear, therefore, that hydrogen bonding involving the formyl oxygen produces a small shift to lower field, which is in the expected direction. (The effect on the chemical shift of the carbonyl carbon, however, is significant and is also to lower field.) Another factor which will contribute to the shielding of the formyl proton but which is difficult to estimate is the effect of the anisotropic hydroxyl group itself. This could conceivably mask the effect of hydrogen bonding (however, see below).

The other examples in this series do not show any correlation of chemical shift with substituent polarity. These observations indicate that the conjugative effect is markedly reduced. Other evidence bearing on this point has been provided by Wolfenden and Jencks (26) from a comparison of the reactivities of a series of ortho- and para-substituted benzaldehydes. These authors have concluded that electron donation by resonance is more effective from the para position than from the ortho for the methoxyl, methyl, and chloro groups. In the present series, since the shifts are all to *lower* field than benzaldehyde itself, the results indicate that the conjugative shielding contribution by the ring is also reduced. These observations suggest that the ortho substituents force the formyl group out of the plane of the ring and thus reduce the shielding effect due to conjugation. This would result in an increased polarization of the C—H bond and a reduction in the local shielding contribution. The net effect would be a shift to lower field. Since the formyl proton cannot be far from the plane of the aromatic ring even in the extreme (ca. 1 Å), the ring current effect would still be relatively strong. Inductive effects could still be operative and so the relative shifts of *o*-tolualdehyde and *o*-nitrobenzaldehyde appear to be reasonable. Again, the effect of the anisotropic substituents would be difficult to estimate, but it is interesting that these ortho-substituted compounds absorb over a rather narrow range.

An alternative explanation for these shifts would invoke a possible hydrogen bonding of the formyl proton with the polar ortho substituents. In fact, this interpretation has been advanced to account for the observed infrared absorption maxima for a number of ortho-substituted benzaldehydes (27, 28). One would have considerable difficulty, however, defending this view as a rational explanation for the observed chemical shifts for both *o*-tolualdehyde and mesitylaldehyde, which absorb at 10.18 and 10.49 δ, respectively. Since hydrogen bonding would be comparable in these cases, one would expect the chemical shifts to be similar. For comparison, *p*-tolualdehyde appears at 9.89 δ.

Polycyclic Aromatic Aldehydes

Four polycyclic compounds were included in this survey and the data are given in Table II. It is to be expected that the ring current effects of these larger aromatic systems would be greater than in the benzaldehydes, and the observed shifts are in qualitative

agreement with this expectation. Bernstein, Schneider, and Pople (13) have shown the effect of larger ring systems in a series of polycyclic aromatic hydrocarbons and were able to account for the enhanced shifts in a quantitative fashion. More recently, Abraham has applied the method to an analysis of the chemical shifts in porphyrins (18). In the present series, a similar approach appears worthwhile.

As a model for the evaluation of the ring current effect first used by Pople (12, 13) and since modified by Waugh and Fessenden (14) and, more recently, by Johnson and Bovey (15), the aromatic nucleus is considered to provide a closed loop around which the π electrons circulate under the influence of an applied field, H_0, normal to the plane of the ring. The circulation of these electrons produces an induced magnetic field which accentuates H_0 in the plane of the ring (i.e., deshields nuclei in this orientation) and opposes H_0 over the ring (i.e., a shielding effect). Between these two extremes the effect is intermediate. Johnson and Bovey have provided tables of the magnitude of this effect calculated for all orientations about a benzene nucleus (29), in terms of the distances a given nucleus is from the center of, and from the plane of, the ring. Using Dreiding models, these distances were measured for the formyl protons in benzaldehyde, 1- and 2-naphthaldehydes, 9-anthraldehyde, and phenanthrene-9-carboxaldehyde. As a first approximation, only planar conformations were considered and, in those cases in which there are two, equal populations in each were assumed. Furthermore, only the effect of the ring(s) in addition to that to which the formyl group is bonded is considered in order to compare the enhanced ring current with that of benzaldehyde. The additional deshielding contributions for the four examples are found to be (p.p.m.): +0.15, 2-naphthaldehyde; +0.38, 1-naphthaldehyde; +0.53, phenanthrene-9-carboxaldehyde; +0.75, 9-anthraldehyde, while the observed shifts relative to benzaldehyde are +0.12, +0.36, +0.37, and +1.51 p.p.m., respectively. A direct comparison of these figures, of course, assumes that the relative shifts are due entirely to the larger ring current. Differences in the electron-releasing characteristics of these aromatic groupings at the various points of attachment of the formyl groups will also be a factor which would tend to oppose the ring current contribution. This probably accounts in part for the differences observed in the first three examples. Furthermore, since the contributions of the additional ring(s) is not necessarily equal for both conformations, a difference in populations could also be reflected in the observed shifts. In the case of 9-anthraldehyde, however, the observed shift is much larger than that calculated. A steric effect of the two *peri*-hydrogens could be responsible for this result. If the formyl group were hindered from attaining coplanarity with the anthracene nucleus, the deshielding influence of the aromatic system would not be greatly reduced while the conjugative shielding factor would be substantially diminished.

Although evidence for steric inhibition of resonance in the case of 1-naphthaldehyde has been reported (25), the N.M.R. data do not definitely substantiate this point since the relative contributions of the various operative factors cannot be established.*

It is interesting that the contribution calculated for the aromatic nucleus by the method of Johnson and Bovey is +0.58 p.p.m. and since benzaldehyde absorbs at 0.23 p.p.m. to low field relative to acetaldehyde the conjugative contribution may be estimated to be −0.35 p.p.m. for this molecule. For comparative purposes, the value for the ring current effect on a formyl proton for a conformation in which the plane of the carbonyl

**It can be noted that the proton spectra could be used as an analytical method for mixtures of 1- and 2-naphthaldehydes since the formyl protons are well separated (0.24 p.p.m. in $CDCl_3$), whereas the carbonyl stretching modes are reported (30) to absorb at 1700 and 1702 cm^{-1}, respectively.*

group is at 90° to the ring is estimated, as above, to be +0.44 p.p.m., which indicates that the deshielding effect is still strong, while a conjugative effect would be markedly reduced.

Solvent Effects

As the data in Tables I and II show, there are no large shifts observed on dilution in either carbon tetrachloride or deuterochloroform solutions for most of the aldehydes. Usually the dilution shift is less than 2 cycles/sec (ca. 0.03 p.p.m.). Since some of the aldehydes could not be studied in CCl_4 solution, a few were examined in both solvents to determine whether or not an association was involved in $CDCl_3$. There is a small, but significant, shift to lower field of ca. 0.07 p.p.m., which is presumably due to hydrogen bonding of the carbonyl group with the solvent. Support for this conclusion is provided by the observation that salicylaldehyde exhibits a smaller shift to low field for this solvent change (0.03 p.p.m.). The effect of hydrogen bonding on the formyl shifts, therefore, appears to be small.

In two cases, however, the shift on dilution is marked. Both of the tricyclic aromatic examples undergo shifts to lower field upon dilution in $CDCl_3$ in the following way: 9-anthraldehyde: 30% solution, 11.18 δ; 20%, 11.27 δ; 10%, 11.41 δ; 5%, 11.47 δ; 2.5%, 11.51 δ; 1.25%, 11.53 δ; phenanthrene-9-carboxaldehyde: 30%, 10.15 δ; 20%, 10.22 δ; 10%, 10.31 δ; 5%, 10.37 δ; 2.5%, 10.39 δ. These results indicate that the tricyclic aldehydes tend to associate with each other in chloroform solution. It is interesting to note that the dilution shifts for these compounds in acetone or in benzene solution are much smaller (ca. 4 cycles/sec for a concentration range of 20–5%) and are comparable to the results discussed above. Further work is required to clear up the question of self-association in these two cases and this study is in hand.

To investigate solvent effects on the chemical shifts of formyl protons in more detail, a few substituted benzaldehydes were examined in cyclohexane, methanol, acetone, and benzene solutions as well. These results are presented in Fig. 2. For comparative purposes, propionaldehyde and crotonaldehyde were included in this series of experiments. The shifts are presented relative to those obtained in CCl_4 solution and a correction of −0.07 p.p.m. has been used for the nitro derivatives which were examined in $CDCl_3$. A slight inaccuracy in this correction would be without effect on the conclusions drawn below.

From these results, the following important general features can be noted: (1) Relative to carbon tetrachloride, the signals are shifted to lower field in acetone and higher field in benzene solution. (2) The solvent shifts in acetone are virtually independent of the substituent on the aromatic ring, while those in benzene are markedly dependent on it. (3) Methanol solutions do not exhibit appreciable shifts relative to carbon tetrachloride solutions. This observation provides further evidence that hydrogen-bonding effects are small. (4) Steric hindrance of the formyl group by bulky ortho substituents does not appear to produce a significant change in the solvent effects, as shown by the data for mesitylaldehyde. Points (1) and (2) are similar to observations reported by Schaefer and Schneider (31) from a study of solvent effects on aromatic proton shifts in some substituted toluenes and fluorobenzenes. Since these authors have presented a detailed discussion of the various factors involved it is sufficient to note that strong evidence for a specific solute–solvent association was presented for these two solvents. A similar conclusion appears to be justified in the present series.

The most striking effects are observed in benzene solution. For most cases the shift is to higher field and, in contrast to the trend observed in acetone, is markedly dependent on

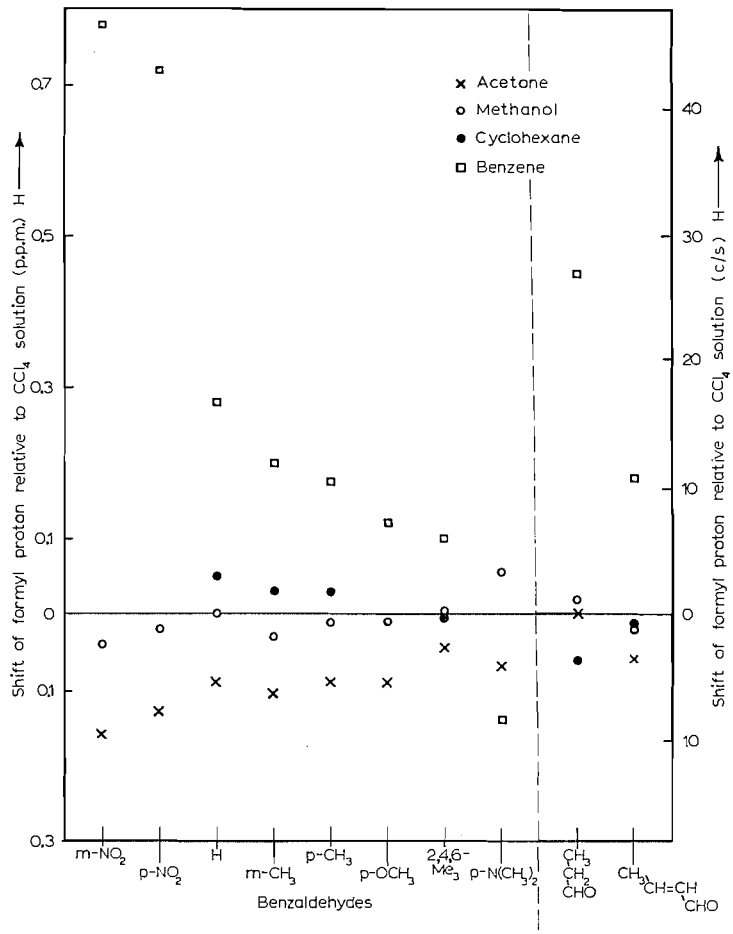

FIG. 2. Shifts of the formyl proton of various aldehydes in dilute benzene, acetone, methanol, and cyclohexane solutions relative to their resonance position for a dilute carbon tetrachloride solution. The shifts are given in p.p.m. and in cycles/sec for a fixed radio frequency of 60 Mc/sec.

the substituent. It is interesting that the shifts to higher field decrease with change in the substituent in the order NO_2, H, CH_3, CH_3O, $(CH_3)_2N$. These data indicate that the substituted benzaldehydes are associated with solvent molecules in a rather specific manner. It appears that this interaction depends markedly on the polarization of the molecule, such that the solvating benzene molecule(s) is most strongly associated with the relatively electron-deficient portion of the aldehyde molecule. One possible interpretation of these results is that the solvating molecule(s) tends to lie over the relatively planar solute molecule, as indicated in Fig. 3(*a* and *b*) and the variations in chemical shifts may be interpreted in terms of the benzene ring anisotropy, as discussed above. For example, in the case of *p*-nitrobenzaldehyde, it is suggested that the interaction involves the formyl grouping (Fig. 3(*a*)) while in the case of the *p*-dimethylamino derivative, the association involves the substituent (Fig. 3(*b*)). Further tests of this suggestion include a study of the solvent dependence of the chemical shifts of all protons in the solute molecule and this approach is being actively pursued.

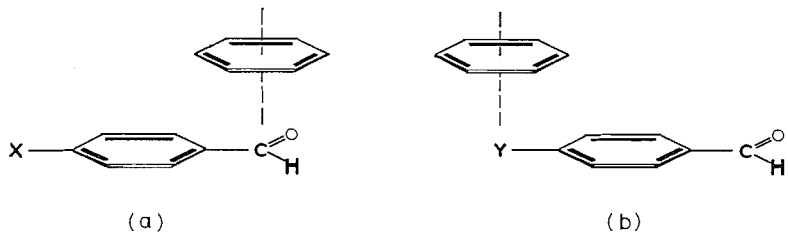

FIG. 3. Schematic representations of a possible solute–solvent interaction for substituted benzaldehydes in benzene: (*a*) electron-withdrawing substituent, (*b*) electron-releasing substituent.

CONCLUSIONS

The results of this survey indicate that, in addition to the strong deshielding effect of the carbonyl group, contributions by the aromatic ring current effect and change in the polarization of the carbonyl group constitute the major factors controlling the chemical shift of the formyl proton in aromatic aldehydes. At this stage, however, only a qualitative discussion of these effects is possible in the absence of quantitative evaluations of these various factors and since some of the assumptions may be valid only as first approximations. A knowledge of the chemical shift of the formyl proton, however, could assist in a structural elucidation, particularly for distinguishing ortho-substituted aldehydes.

Relatively minor effects are noted in hydrogen-bonded systems, and anisotropic meta substituents appear to affect the chemical shift of this proton slightly. In a number of cases in which a bulky ortho substituent could hinder the formyl group from attaining coplanarity with the ring, evidence for a steric inhibition of resonance was obtained for *o*-methyl, *o*-methoxyl, *o*-chloro, and *o*-nitro groups. Solute–solvent interactions are observed in acetone and benzene solutions and, in the latter case, depend upon the substitution of the aromatic ring.

ACKNOWLEDGMENT

We wish to express our thanks to the National Research Council of Canada for the financial assistance which made this project possible.

REFERENCES

1. L. H. MEYER, A. SAIKA, and H. S. GUTOWSKY. J. Am. Chem. Soc. **75**, 4567 (1953).
2. L. M. JACKMAN. Applications of NMR in organic chemistry. Pergamon, New York. 1959.
3. J. A. POPLE, W. G. SCHNEIDER, and H. J. BERNSTEIN. High-resolution nuclear magnetic resonance. McGraw-Hill, New York. 1959. Chap. 7.
4. J. B. STOTHERS. Unpublished observations.
5. H. SPIESECKE and W. G. SCHNEIDER. Tetrahedron Letters, No. 14, 468 (1961).
6. P. C. LAUTERBUR. J. Am. Chem. Soc. **83**, 1838 (1961).
7. P. C. LAUTERBUR. Tetrahedron Letters, No. 8, 274 (1961).
8. J. A. POPLE. Proc. Roy. Soc. (London), A, **239**, 550 (1957).
9. L. M. JACKMAN and R. H. WILEY. J. Chem. Soc. 2881 (1960).
10. P. T. NARASIMHAN and M. T. ROGERS. J. Phys. Chem. **63**, 1388 (1959).
11. H. M. MCCONNELL. J. Chem. Phys. **27**, 226 (1957).
12. J. A. POPLE. J. Chem. Phys. **24**, 1111 (1956); Proc. Roy. Soc. (London), A, **239**, 541 (1957); Mol. Phys. **1**, 175 (1958).
13. H. J. BERNSTEIN, W. G. SCHNEIDER, and J. A. POPLE. Proc. Roy. Soc. (London), A, **236**, 515 (1956).
14. J. S. WAUGH and R. W. FESSENDEN. J. Am. Chem. Soc. **79**, 846 (1957).
15. C. E. JOHNSON and F. A. BOVEY. J. Chem. Phys. **29**, 1012 (1958).
16. J. T. ARNOLD and M. E. PACKARD. J. Chem. Phys. **19**, 1608 (1951).
17. S. GRONOWITZ and R. A. HOFFMAN. Acta Chem. Scand. **13**, 1687 (1959).
18. R. J. ABRAHAM. Mol. Phys. **4**, 145 (1961).
19. H. S. GUTOWSKY, D. W. MCCALL, B. R. MCGARVEY, and L. H. MEYER. J. Am. Chem. Soc. **74**, 4809 (1952).
20. (*a*) R. W. TAFT. J. Am. Chem. Soc. **79**, 1045 (1957).
(*b*) R. W. TAFT, R. E. GLICK, I. C. LEWIS, I. FOX, and S. EHRENSON. J. Am. Chem. Soc. **82**, 756 (1960).

21. R. R. FRASER. Can. J. Chem. **38**, 2226 (1960).
22. H. SPIESECKE and W. G. SCHNEIDER. J. Chem. Phys. **35**, 731 (1961).
23. D. H. MCDANIEL and H. C. BROWN. J. Org. Chem. **23**, 420 (1958).
24. R. W. TAFT, N. C. DENO, and A. S. SKELL. Ann. Rev. Phys. Chem. **9**, 292 (1958).
25. W. REEVE and E. L. COMPERE. J. Am. Chem. Soc. **83**, 2755 (1961).
26. R. WOLFENDEN and W. P. JENCKS. J. Am. Chem. Soc. **83**, 2763 (1961).
27. S. PINCHAS. Anal. Chem. **27**, 2 (1955); **29**, 334 (1957); Chem & Ind. (London), 1451 (1959).
28. B. C. CURRAN. J. Am. Chem. Soc. **67**, 1835 (1945).
29. F. A. BOVEY. Personal communication. October, 1961.
30. L. J. BELLAMY. Infra red spectra of complex molecules. Methuen, London. 1958.
31. T. SCHAEFER and W. G. SCHNEIDER. J. Chem. Phys. **32**, 1218 (1960).

THE REACTIVE SPECIES IN ACTIVE NITROGEN[1]

A. N. WRIGHT,[2] R. L. NELSON,[3] AND C. A. WINKLER
Upper Atmosphere Chemistry Research Group, McGill University, Montreal, Que.

Received November 9, 1961

ABSTRACT

A study has been made of the discrepancy between the N-atom content of active nitrogen as inferred from the maximum HCN production from the reaction of many hydrocarbons, and that indicated by the extent of NO destruction. The HCN production from several hydrocarbons was similar at high reaction temperatures in a spherical reaction vessel, and was independent of reaction temperature in a cylindrical reaction vessel. The ratio (NO destroyed)/(HCN produced) was found to be independent of the mode of excitation of the molecular nitrogen and of the N-atom concentration, and to be unaffected by the addition, upstream, of N_2O or CO_2. Although NH_3 was found to be a minor product of the hydrocarbon reactions, HCN accounted for at least 96% of the N-atom content of the products under conditions where its formation is considered a measure of the N-atom concentration. The NO "titration" value, the maximum extent of HCN production from C_2H_4, and the destruction of NH_3 after different times of decay of active nitrogen gave evidence that part of the NO reaction occurred, as does the NH_3 reaction, with excited nitrogen molecules. The long lifetime of the N_2^* species capable of reaction with NO or NH_3, as calculated from the above data, strongly favors its identification as low vibrational levels of the $N_2(A^3\Sigma_u^+)$ molecule. A consideration of the values for the NO/HCN, NH_3/HCN, and NH_3/NO ratios, after different times of decay, for poisoned and unpoisoned systems, suggested that the N_2^* responsible for the NH_3 reaction is formed only during homogeneous recombination of N atoms, while the N_2^* responsible for reaction with NO might be produced by wall recombination as well. Possible reactions of excited molecules present in the active nitrogen – NO system that might lead to decomposition of NO without consumption of N atoms are discussed.

INTRODUCTION

Although the chemical activity of active nitrogen appears to be due mainly to ground-state atoms (1), recent work indicates that excited molecules (2–5) might be important in at least some active nitrogen reactions. For example, there seems little doubt that the reaction of active nitrogen with NH_3 involves excited molecules (6–8). Verbeke and Winkler have also suggested (9) that the greater nitrogen atom content of active nitrogen indicated by the NO titration (10), in comparison with that inferred from the maximum production of HCN from ethylene, may be due to reaction of NO with excited nitrogen molecules, in addition to its very rapid reaction with nitrogen atoms. On the other hand, the discrepancy between the two estimates of nitrogen-atom concentration has been attributed (11, 12) to the complexity of the hydrocarbon reaction.

The destruction of NH_3 in measurable amounts has only been detected in active nitrogen produced by a condensed discharge (6, 9, 13) and it has been suggested (14) that this reaction occurs with a species that is produced only by this mode of excitation of the molecular nitrogen. It has been reported (14) that, in active nitrogen produced by a microwave discharge, the maximum yield of HCN and the NO titration technique both indicate the same nitrogen-atom concentration.

The purpose of the present work was twofold: (i) to examine more closely the discrepancy between the two chemical methods of estimating the nitrogen-atom concentration of active nitrogen, (ii) to study the relative extents of reaction of active nitrogen, after

[1]*This work received financial assistance from the Geophysics Research Directorate of the Air Force Cambridge Research Laboratories, Air Force Research Division; the Defence Research Board of Canada; and the National Research Council of Canada.*

[2]*Postdoctoral Fellow.*

[3]*Postdoctoral Fellow. Present address: Department of Chemistry, Brandeis University, Boston, Mass., U.S.A.*

different times of decay, with reactants that appear to involve mainly nitrogen atoms (e.g. C_2H_4), excited molecules (e.g. NH_3), or both (e.g. NO). Some of these interrelations have been examined previously as a function of pressure (13) and, in a preliminary way, as a function of decay of active nitrogen (9), but not as a function of time of decay of active nitrogen under controlled reaction conditions.

An investigation was first made of the effect of the shape of the reaction vessel on the temperature dependence of HCN production from hydrocarbons, in the region where this was independent of flow rate of the hydrocarbon, in active nitrogen produced by a condensed discharge and by a microwave system. Many of the preliminary results of the present investigation were reported at the Symposium on Some Fundamental Aspects of Atomic Reactions held at McGill University, Montreal, September 6 and 7, 1960.

EXPERIMENTAL

Nitrogen, nitric oxide, ammonia, and the hydrocarbons used were purified by methods similar to those described in previous papers from this laboratory. Nitrous oxide and carbon dioxide were freed from water by distillation at $-78°$ C.

The products of the reactions with hydrocarbons were trapped at liquid air temperature and distilled into an absorber that contained ice at liquid air temperature, and the aqueous solution analyzed after the absorber had been allowed to warm to room temperature. The amount of NH_3 in the products was estimated by titration with standard sulphuric acid, and this was followed by analysis for hydrogen cyanide by standard silver nitrate titration, in the presence of added ammonia, with potassium iodide as indicator. Ammonia was also qualitatively identified among the reaction products by infrared spectroscopy. Cyanogen has been shown, by previous workers, to be present in relatively insignificant quantities.

Excess NH_3 from the ammonia reaction was analyzed in the same way as the ammonia content of the products from the hydrocarbon reactions.

The products from the nitric oxide reaction consisted of nitric oxide and nitrogen dioxide (generally present as N_2O_3) and these were trapped quantitatively at about $-210°$ C, using liquid nitrogen under reduced pressure. Nitric oxide was separated, with a Toepler pump, from the nitrogen dioxide, maintained at $-64°$ C, and the amount of each gas was measured by pressure–volume methods at constant temperature. This technique gave good agreement with that used by Verbeke and Winkler (9). The reaction of nitric oxide with active nitrogen was also followed by the gas phase titration method (10).

The reactions of active nitrogen with nitrous oxide and carbon dioxide were followed by trapping unreacted nitrous oxide, or carbon dioxide, at liquid air temperatures and estimating their amounts by pressure–volume methods at constant temperature. No other products were observed, even with a trap at $-210°$ C.

The experiments described in this paper were made in two different types of apparatus, (I) and (II). To increase the reproducibility in the experiments, both types of apparatus were equipped with a stopcock between the reaction vessel and products trap. This minimized contamination of the reaction vessel and discharge regions by reaction products. Kel-F stopcock grease was used and was unaffected by active nitrogen. To obtain reproducible results, it was also necessary to operate the condensed discharge, in either apparatus, for at least 15 minutes prior to initiating a reaction.

Apparatus (I) was similar to that used by previous workers (6, 9, 13). The reaction vessels were of unpoisoned pyrex and the dimensions were varied in several of the experiments. Condensed and microwave discharges were used as alternative methods of obtaining active nitrogen. The condensed discharge operated between aluminum electrodes, 45 cm apart, and at a flash rate of about 10 sec^{-1}. The microwave discharge operated at 2450 Mc/sec and was supplied from a Raytheon 125-watt generator. The flow rate of molecular nitrogen, at a pressure of 2.45 mm Hg, was 133×10^{-6} mole/sec.

Apparatus (II) utilized a condensed discharge to produce a high concentration of nitrogen atoms, to facilitate the study of possible reactions of excited nitrogen molecules, which are probably produced by the recombination of nitrogen atoms (13). A large bulb was incorporated into the center of the discharge tube to reduce "pulsing" in the active nitrogen stream. The reaction vessel was a straight, pyrex tube of 25-mm diameter, which contained two fixed reactant jets, about 14 and 14.5 cm below the discharge tube. It was also provided with a mobile reactant jet that could be moved from 0.1 to 45 cm below the lower of the two fixed jets, by a stopcock arrangement (15) that provided a friction drive on the lower part of the mobile jet column. This column contained a glass-encased thermocouple, which permitted a measurement of temperature 3.0 cm below the outlet of the mobile jet. Both the fixed upper jets, and the mobile jet, contained six small holes placed symmetrically around their bulbous ends to produce an even flow of reactant into the active nitrogen stream.

All experiments in apparatus (II) were made in an unheated reaction vessel and at a pressure of 3 mm of Hg. The flow rate of molecular nitrogen was 378×10^{-6} mole/sec, corresponding to a linear flow rate of

478 cm/sec. Experiments were made in both an unpoisoned reaction vessel, and in the reaction vessel poisoned by water vapor ($<0.03\times10^{-6}$ mole/sec), introduced through a capillary leak into the molecular nitrogen before the discharge. This minute amount of vapor apparently has no measurable effect (16) on the course of the active nitrogen reactions but does poison the walls of the apparatus effectively against the decay of nitrogen atoms.

RESULTS

A Comparison of the Maximum Extent of Reaction of Active Nitrogen with Nitric Oxide and with Hydrocarbons

The extent of the reaction with NO was taken as the initial flow rate of NO minus the flow rate of total nitrogen oxides (i.e. $NO+NO_2$) analyzed in the products. Hydrogen cyanide production was taken as a measure of the reaction of nitrogen atoms with ethylene, ethane, *n*-butane, and but-2-ene. At the maximum extent of these reactions, the total of ammonia and cyanogen in the products never exceeded 4% of the hydrogen cyanide.

In Table I are shown the data obtained, using apparatus (I), when variations were made in reaction temperature, dimensions of the reaction vessel, and type of discharge

TABLE I

Reaction of active nitrogen with nitric oxide compared with production of HCN from hydrocarbons

Reaction vessel	Discharge	Total press., mm Hg	Temp., °C	Hydrocarbon	Max. HCN produced, mole/sec ($\times10^6$)	Max. NO consumed, mole/sec ($\times10^6$)	Ratio NO/HCN
A. Sphere, 85 mm i.d.	Condensed	2.45	50	C_2H_4, *n*-C_4H_{10}, C_4H_8	5.0	12.4	2.5
			440	" " "	7.75	12.4	1.6
Sphere, 85 mm i.d.	"	2.45	50	C_2H_6	2.2*	12.4	5.6
			440	"	7.4	12.4	1.7
B. Cylinder, 20 mm i.d.	"	2.45	40	C_2H_4, *n*-C_4H_{10}	6.8	11.2	1.7
			400	" "	7.2	11.2	1.6
C. Sphere, 110 mm i.d.	"	2.45	50	C_2H_4	2.2	4.0	1.8
			440	"	2.6	4.0	1.5
D. Sphere, 110 mm i.d.	"	2.45	50	C_2H_4	1.5	2.6	1.7
			440	"	1.5	2.6	1.7
E. Sphere, 85 mm i.d.	Microwave	2.45	80	C_2H_4	1.4	2.4	1.7
			440	C_2H_4, C_2H_6	1.4	2.4	1.7
F. Cylinder, 20 mm i.d.	"	2.45	80	C_2H_4	1.3	2.2	1.7
			440	"	1.3	2.2	1.7
G. Cylinder, 20 mm i.d.	"	3.70	110	C_2H_4	1.9	3.8	2.0
			440	"	1.9	3.8	2.0

*The HCN yield from ethane at 50° C never reached a true limiting value.

used to produce the active nitrogen. Values for NO consumption obtained by product analysis agreed well with results obtained by the gas phase titration with NO at the lower atom concentrations, but at higher atom concentrations (systems A and B) the titration gave results that were 10–20% lower than those reported in the table.

The Production of Ammonia from the Reaction of Active Nitrogen with Ethylene and Ethane

The relative amounts of HCN and NH_3 produced in these reactions in a spherical, unpoisoned reaction vessel, with a condensed discharge, are shown in Table II. Production of ammonia from *n*-butane and but-2-ene was found to be similar to that from ethylene at both temperatures.

TABLE II

Production of NH_3 in the reaction of active nitrogen with C_2H_4 and C_2H_6

Reactant flow rate	Reaction of ethylene				Reaction of ethane			
	at 50° C		at 440° C		at 50° C		at 440° C	
	HCN	NH_3	HCN	NH_3	HCN	NH_3	HCN	NH_3
1.0*	1.3	0.02	1.3	0.18	0.6	0.02	0.9	0.15
2.2	2.4	0.03	—	—	0.9	0.04	—	—
2.8	—	—	3.0	0.26	—	—	3.2	0.18
4.0	2.8	0.03	—	—	—	—	—	—
6.9	—	—	4.1	0.05	—	—	3.9	0.05
14 8	3.0	0.03	4.2	0.04	1.1	0.05	4.2	0.03
22.7	3.0	0.03	4.2	0.03	1.3	0.05	4.2	0.03

*All units are mole/sec$\times 10^{-6}$.

The Influence of Nitrous Oxide and Carbon Dioxide on the Reactions of Active Nitrogen with Nitric Oxide and Ethylene

Apparatus (I) was used, with a reaction vessel consisting of two spherical bulbs, connected by a 10-cm pyrex tube of 20-mm i.d. Nitrous oxide or CO_2 entered the active nitrogen in the upper bulb (85-mm i.d.), while NO or C_2H_4 was admitted to the lower bulb (110-mm i.d.). A condensed discharge activated the nitrogen, and the vessel walls were not poisoned.

The admission of either N_2O or CO_2 to the active nitrogen in the upper vessel caused no significant change in the heat given off at any position in the system. Both N_2O and CO_2 were destroyed to a minor extent; the N_2O destruction appeared to increase with reaction temperature. The addition of these gases to the active nitrogen resulted in an increase in the maximum extents of reaction of both NO and C_2H_4, but the ratio $NO_{consumed}/HCN_{produced}$ remained essentially unchanged over a range of flow rates of N_2O or CO_2 from 2×10^{-6} to 30×10^{-6} mole/sec. Typical results, for a flow rate of N_2O or CO_2 of 6.7×10^{-6} mole/sec, are shown in Table III.

TABLE III

Effect of N_2O and CO_2 on the reactions of active nitrogen with NO and C_2H_4

	Maximum extent of HCN production from ethylene, mole/sec ($\times10^6$)	Maximum extent of decomposition of NO, mole/sec ($\times10^6$)	Ratio NO/HCN
Without N_2O	3.7	6.3	1.7
With N_2O	4.2	7.1	1.7
Without CO_2	3.6	6.4	1.8
With CO_2	4.4	7.7	1.7

A Comparison of the Plateau Values for HCN Production from C_2H_4 and of NH_3 Destruction and NO Destruction, after Different Times of Decay of Active Nitrogen

Apparatus (II) permitted the accurate determination of these plateau values (maximum extents of reaction) at four different levels, spaced 15 cm apart, of the mobile jet under otherwise similar conditions. These levels corresponded to 31.4, 62.7, and 94.3 milliseconds of decay of active nitrogen after the reference level, 0.1 cm below the lowest fixed jet. The temperature increases in the active nitrogen stream at these same positions were also determined before the reactant was introduced. The extent of NO destruction was estimated, at the different levels, by a visual gas phase titration (10). Since the results

obtained in apparatus (I) indicate that the HCN plateau values are independent of reaction temperature in a cylindrical vessel, and this has recently been confirmed by other workers (17) for the ethylene reaction, these values are considered to be a measure of the maximum HCN production from ethylene. Good linear relations, of which those in Fig. 1 are typical, were obtained between the plateau values for the reactions and the

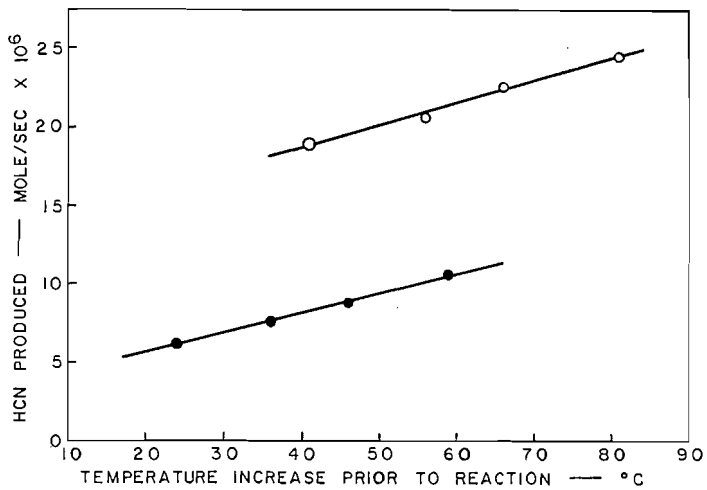

FIG. 1. Plot of HCN produced from ethylene against the temperature of the active nitrogen, above room temperature: ○, poisoned system; ●, unpoisoned system.

temperature increases in the active nitrogen in both the poisoned and unpoisoned systems. Unfortunately, the possibility of estimating the relative concentrations of active nitrogen from such relative temperature increases is applicable only to a given apparatus and given operating conditions. For example, for a temperature increase of 46° C prior to reaction, the destruction of NH_3, or production of HCN from C_2H_4, in the poisoned system, was more than double, while NO destruction was slightly less than double that observed in the unpoisoned system. Presumably, the condition of the system determines the N-atom concentration upstream, hence the extent of formation of excited nitrogen molecules, and both of these, in turn, may be reflected in the observed temperature increases and plateau values for the reactions.

A plot of NH_3 destroyed against HCN produced from C_2H_4, at the different levels in the reaction tube, is linear for both the poisoned and unpoisoned systems (Fig. 2). Extrapolation of the line for the unpoisoned system to zero HCN production gives an intercept on the axis of NH_3 destruction of 0.2×10^{-6} mole/sec, while a similar extrapolation of the line for the poisoned system gives an intercept on the axis of HCN production of 11×10^{-6} mole/sec.[4]

The ratios (NH_3 decomposed/HCN produced), (NO decomposed/HCN produced), and (NH_3 decomposed/NO decomposed), more simply referred to hereafter as the ratios NH_3/HCN, NO/HCN, and NH_3/NO, all decrease, at constant pressure, with time of decay of the active nitrogen in the poisoned system, while in the unpoisoned system the ratio NO/HCN increases markedly, and the ratio NH_3/HCN increases slightly. Verbeke

[4]*Extrapolation to zero value of* HCN *production yields values corresponding to reaction conditions where the* N*-atom concentration has fallen to a very low value, i.e., to long distances downstream. Of course, the extrapolated values are applicable only to the present system, wherein a large* N*-atom concentration existed upstream, and a relatively high concentration of excited nitrogen molecules may then exist at a distant position downstream, as a result of* N*-atom recombination upstream.*

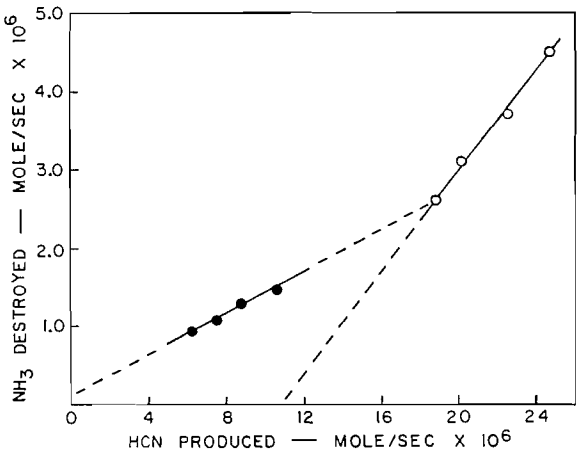

FIG. 2. Plot of NH_3 destroyed against HCN produced from C_2H_4 at the different levels: ○, poisoned system; ●, unpoisoned system.

and Winkler (9) had some indication of an increase in the NO/HCN ratio with decay time in a poisoned system.

Reasonably good straight lines are obtained if plots are made of NH_3/HCN against HCN (Fig. 3A), NO/HCN against HCN (Fig. 3B), and NH_3/NO against NO (Fig. 4)

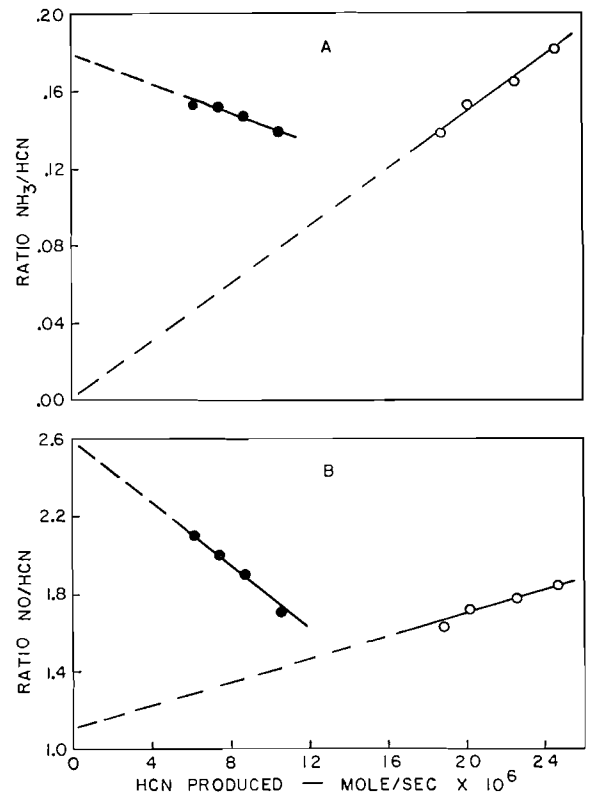

FIG. 3. (A) Plot of ratio NH_3 destroyed/HCN produced; (B) plot of ratio NO destroyed/HCN produced: ○, poisoned system; ●, unpoisoned system.

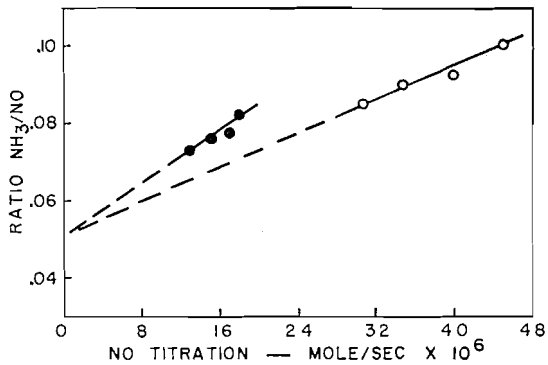

FIG. 4. Plot of ratio NH_3 destroyed/NO destroyed against NO titration value at the different levels: ○, poisoned system; ●, unpoisoned system.

for different levels in the reaction tube. Extrapolation of these, as indicated in the figures, are certainly not accurate, but it is apparent that the lines of Fig. 3 are of opposite slopes for the poisoned and unpoisoned systems, and extrapolate to widely different intercepts, while the lines in Fig. 4 are of similar slope and extrapolate to similar values for the two systems. The significance of these relations will be discussed later.

Effect of Adding NH_3 Upstream from NO, C_2H_4, or NH_3; and C_2H_4 above NH_3

The experiments were made in apparatus (II).

(a) Effect of Adding NH_3 above NO

Since both the reactions of NO and NH_3 may be due, at least in part, to the reaction of excited nitrogen molecules, the addition of one upstream might be expected to decrease the extent of the reaction of the other. However, when NH_3 was introduced at a flow rate of 4.0×10^{-6} mole/sec through the fixed upper jet, the change in the end point of the NO titration was negligible in the poisoned system at all levels down to 45 cm. If anything, there was a slight increase in the end point, especially at the 45-cm level. In the unpoisoned system, the increase in the end point was more significant, e.g., 3.7×10^{-6} mole/sec at the 30-cm level, when NH_3 was added at a flow rate of 2.2×10^{-6} mole/sec.

(b) Effect of Adding NH_3 above C_2H_4

If the reaction of NH_3 with active nitrogen involves N atoms in any way, the HCN production from C_2H_4 might be expected to decrease when NH_3 is added upstream. In fact, addition of NH_3 at the fixed upper jet slightly *increased* the HCN production from C_2H_4 over that obtained at the various levels and flow rates when no NH_3 was added upstream. This increase was larger in the unpoisoned system. The results are given in Table IV.

In the poisoned system, the C_2H_4 reaction temperature at the 45-, 30-, and 15-cm levels, in the presence of NH_3, was about 3° C higher than in its absence, while, in the unpoisoned system, the corresponding increase was about 8° C at all three levels. In the unpoisoned system, an increase in the intensity of active nitrogen afterglow was observed at the lower levels, upon the introduction of the NH_3.

The addition of C_2H_4 downstream from NH_3 was found to decrease the extent of NH_3 decomposition and this decrease became larger as the C_2H_4 was added closer to the NH_3 jet. Since the addition of an excess of C_2H_4 below NH_3 appeared to terminate the NH_3 active nitrogen reaction, this method has been used (18) to obtain a rate constant for the NH_3 reaction.

TABLE IV

Effect of addition of NH_3 on HCN production from C_2H_4

Level at which C_2H_4 added, cm	C_2H_4 flow rate, mole/sec ($\times 10^6$)	NH_3 flow rate, mole/sec ($\times 10^6$)	Increase in HCN production, mole/sec ($\times 10^6$)
	Poisoned system		
45	52	2.5	2.1
45	60	"	2.4
30	52	2.5	1.4
30	60	"	1.4
15	52	2.5	1.5
15	60	"	0.4
15	60	8.0	2.7
0	46	2.5	0.4
0	60	"	1.7
0	60	11.7	2.1
	Unpoisoned system		
45	46	2.5	3.9
45	"	7.7	4.2
30	46	2.5	4.5
15	46	2.8	2.6

(c) Effect of Adding C_2H_4 above NH_3

In the poisoned system, no decomposition of NH_3 was observed, after accounting for the slight NH_3 production from the C_2H_4 reaction, when 8.0×10^{-6} mole/sec of NH_3 was added at the 15- and 30-cm levels and 46×10^{-6} mole/sec of C_2H_4 added at the fixed upper jet. The extent of HCN production from the C_2H_4 reaction was slightly decreased. It may be noted that, at the 15-cm level, NH_3 was added in the region of the active nitrogen – C_2H_4 reaction flame, while at the 30-cm level, no reaction flame was visible.

(d) Effect of Adding NH_3 above NH_3

Ammonia was added through the fixed upper jet at flow rates lower than those corresponding to the plateau for destruction of NH_3. Most of the NH_3 that was added was therefore destroyed above the 30-cm level. If excited molecules, capable of destroying NH_3, were formed only during the decay of nitrogen atoms, in the presence of NH_3, the addition of excess NH_3 at the lower positions should result in a total NH_3 destruction almost equal to that obtained when the excess is added at the fixed upper jet. However, for successive additions in the poisoned system, the combined extent of NH_3 destruction was 0.5×10^{-6} mole/sec less at the 30-cm level, and 1.0×10^{-6} mole/sec less at the 45-cm level, than when a flow rate of NH_3 in the plateau region, e.g., 8.0×10^{-6} mole/sec, was added at the fixed upper jet. In the unpoisoned system, the total extent of NH_3 destruction was approximately the same (1.5×10^{-6} mole/sec) whether the reactant was introduced at the upper level only, or at both upper and lower levels.

DISCUSSION

Essentially equal yields of HCN from hydrocarbons have been obtained in apparatus (I), as follows: ethylene, *n*-butane, but-2-ene, and ethane at elevated temperatures in a spherical reaction vessel, and ethylene and *n*-butane in an unheated cylindrical reaction vessel. The maximum HCN production from the hydrocarbons, except from C_2H_6, does not vary, to any extent, with reaction temperature in a cylindrical vessel, with active nitrogen produced by either a condensed or microwave discharge. Consequently, any

uncertainty about having reached an HCN plateau that is independent of reaction temperature is eliminated, and there appears to be added justification for assuming that this value of HCN production corresponds to the N-atom concentration in the system. The reasons for the temperature dependence of HCN production observed in the present work, and in many previous studies (see, for example, ref. 13), in a spherical reaction vessel are not obvious, and further study of this problem is in progress.

The observed discrepancy between the estimations of active nitrogen concentration from NO destruction and from maximum HCN production, as reflected in the NO/HCN ratios of Table I, agrees well with that obtained previously (9) at similar reaction pressures, for active nitrogen produced by a microwave discharge: a value of about 1.7 at 2.45 mm, compared with a previous value of 1.6 at 2 mm, and a value of 2.0 at 3.7 mm, compared with the earlier value of 1.9 at 4.0 mm. Contrary to recent assumptions (19), the present data confirm the previous conclusion (9) that the NO/HCN ratio does not change appreciably with active nitrogen concentration at a constant total pressure, nor does it depend upon the mode of excitation of the nitrogen.

The lower N-atom concentration indicated by the extent of HCN production from hydrocarbons apparently cannot be due to the formation of N-containing products, other than HCN, in these reactions, since the total content of N atoms in the form of NH_3 or $(CN)_2$ recovered from the hydrocarbon reactions, under conditions of maximum HCN production, is less than 4% of that recovered as HCN.[5]

Similarly, it seems unlikely that the discrepancy between the NO and HCN estimates of atomic nitrogen concentration is due to catalyzed recombination of N atoms on the parent hydrocarbon, after initial formation of a complex of relatively long life (20),

$$N + N\cdot C_2H_4 \rightarrow N_2 + C_2H_4, \qquad [1]$$

since the NO/HCN ratio would then be temperature dependent, and possibly also dependent on the N-atom concentration (13). No dependence of the ratio on temperature was observed in a cylindrical reaction vessel (Table I), while, in the unpoisoned system of apparatus (II), the ratio *increased* (Fig. 3B) with decreasing N-atom concentrations after longer decay times of the active nitrogen.

Again, the suggestion of Zinman (11) that the formation of a complex of a substantial lifetime might explain the pressure dependence (9) of the NO/HCN ratio also appears untenable. In modified form, his scheme may be represented by

$$N + RH \rightarrow [N\cdot RH]^* \qquad [2]$$

$$[N\cdot RH]^* \rightarrow HCN + R' + --- \qquad [3]$$

$$R' + N \rightarrow HCN + --- \qquad [3']$$

$$[N\cdot RH]^* \xrightarrow{M} [N\cdot RH] \rightarrow \tfrac{1}{2}N_2 + RH. \qquad [4]$$

Reaction [3'] is necessary since the reaction of N atoms with free radicals, which may conserve spin, is probably faster (21) than the N-atom reaction with the parent hydrocarbon. If it is assumed that the NO titration measures the N-atom concentration, this mechanism gives

$$\frac{[\text{NO consumed}]}{[\text{HCN produced}]} = \frac{[N]}{[HCN]} = \frac{nk_3 + k_4[M]}{nk_3}, \qquad [5]$$

[5] *The yield of* NH_3 *from the* C_2H_6 *reaction in the unheated spherical reaction vessel (Table II) was a considerable fraction of the slight* HCN *yield. However, there is considerable evidence, as will be discussed in a later paper, that this reaction involves excited nitrogen molecules at low reaction temperatures.*

where n = number of carbon atoms in the hydrocarbon. On this basis, the NO/HCN ratio should depend on the molecular weight of the hydrocarbon, which is not borne out by the experiments described in Table I. Furthermore, experiments in apparatus (II) indicated that the NO/HCN ratio increased with time of decay of the active nitrogen in the unpoisoned system. Since the ratios involved plateau values for HCN production at the various levels for constant pressure conditions, an explanation for the discrepancy represented by the NO/HCN ratio must involve more than its pressure dependence.

Finally, it should be emphasized, perhaps, that a discrepancy, similar to that given by the NO/HCN ratio, has been observed when the active nitrogen concentration, estimated by the NO titration, was compared with the extent of reaction of active nitrogen with NO_2 (9) and, more recently, by the extent of its reaction with O_2, as given by the production of O atoms (22).[6] Among the widely different chemical methods studied, therefore, the NO reaction, whether followed by gas phase titration or by analytical methods, appears to be unique in indicating an exceptionally high atomic nitrogen concentration.

The observation that the NO/HCN ratio does not have a fixed value, even at a given pressure, but depends on the time of decay of the active nitrogen, suggests (since the HCN data are based on plateau values) that the extent of the NO reaction does not vary directly with the N-atom concentration, but involves excited molecules derived from atom recombination or directly from the discharge tube. This is suggested also by the similarity in the plots of NH_3/HCN and NO/HCN against HCN yield for the poisoned and unpoisoned systems (Fig. 3), since the NH_3 reaction is known to involve excited molecules. Again, the similarities in slopes of the NH_3/NO plots against NO (Fig. 4), for both the poisoned and unpoisoned systems, and in the extrapolation of the lines to a similar low value, strongly suggest that both reactions occur, at least in part, with species produced by a similar mechanism.

Since the NO/HCN ratio may increase with time of decay of the active nitrogen, it is not likely that NO reacts with some species of long life, other than N atoms, that may be produced in a particular type of discharge. Moreover, most of the excited species that might be produced during the excitation process are known to be of short life (2, 23), and can be expected to decay rapidly with time. If an excited molecular species is responsible for part of the NO reaction, it is probably formed during the recombination of $N(^4S)$ atoms. The decrease in the NO/HCN ratio with decay of the active nitrogen in the poisoned system may then be explained if the disappearance of N atoms in this system, which occurs at about twice the rate of the homogeneous recombination, is considerably slower than that of any N_2^* which might have been produced, mostly upstream in the region of relatively high N-atom concentration.[7] The same seems also to be true for the N_2^* that reacts with NH_3 in a poisoned system, since it appears, from the extrapolation in Fig. 2, that the decomposition of NH_3 falls to zero at rather high values of the N-atom concentration in such a system. In contrast, in the unpoisoned system, the extrapolated value for NH_3 destruction at zero HCN production suggests a considerable concentration of N_2^* in this system, even under conditions where the N-atom concentration has fallen to a low value. The small limiting extent of NH_3 destruction suggests further that N_2^* is produced during the relatively small homogeneous part of the overall decay of N atoms in the unpoisoned system.

[6]*It might be noted, however, that the analysis of* O*-atom concentration in this reaction by the* NO_2 *titration recently indicated a* N*-atom concentration similar to that inferred from the* NO *titration* (12).

[7]*This explanation suggests that a system poisoned with metaphosphoric acid (9) corresponds more closely with an unpoisoned system than with a system poisoned with* H_2O *vapor. For* O *atoms, at least, small amounts of water vapor have been shown (24) to be a most effective poison against surface recombination.*

The difference in slopes and intercepts (Fig. 3A) when the NH_3/HCN ratios are plotted against HCN, for the poisoned and unpoisoned systems, may also be explained if the N_2^* responsible for NH_3 decomposition is formed by homogeneous recombination and persists in significant concentrations, in the unpoisoned system, into the regions where the N-atom concentration has fallen to low values. The much higher extrapolated value of 2.6 for the plot of NO/HCN against HCN (Fig. 3B) in the unpoisoned system suggests that some N_2^* capable of NO destruction may be formed by wall decay of N atoms. The corresponding extrapolated value of 1.1 in the poisoned system indicates that the concentration of N_2^* responsible for NO destruction becomes negligible when the N-atom concentration has decreased to a very low value in this system.

In view of the preceding discussion, it seems reasonable to conclude that NO is destroyed not only by N atoms, but also by an excited molecular species of considerable lifetime produced by both homogeneous and surface decay of N atoms. The destruction of NH_3, on the other hand, appears to be due only to an excited molecule produced during homogeneous decay.

Nature of the Excited Molecular Species that might React with NO

A vibrationally excited, ground-state nitrogen molecule might contain sufficient energy to cause dissociation of NO during a collision process, and, at least in the lower vibrational levels, would be expected to be of long life (23, 25, 26). Quite high vibrational levels of the ground state may be populated directly by homogeneous recombination of N atoms, as pointed out by Polanyi (27) for atomic association reactions of this type. To contain sufficient energy to cause dissociation of NO after a collision of the Second Kind, the molecule would have to be in at least the 27th vibrational level (9). There is some experimental evidence (28) for the presence, in active nitrogen, of $N_2(X^1\Sigma_g^+)$ in vibrational levels as high as the 27th, but they would presumably be deactivated readily by collision processes because of their small vibrational level spacing. It is improbable, therefore, that such molecules would be present in sufficient concentration to account for the NO/HCN ratios.

Another possibility is that such molecules are *produced* in the excitation process. Kaufman and Kelso (25) found that the addition of N_2O or CO_2 removed energy from certain species, probably ground-state molecules in low vibrational levels, in active nitrogen emanating from a microwave discharge. In the present studies, the addition of either gas to discharged nitrogen made little difference to the NO/HCN ratio (Table III). Moreover, there was negligible temperature increase when these gases were introduced into active nitrogen formed in a condensed discharge, compared with that observed (25) in active nitrogen from a microwave discharge. This suggests that microwave excitation may be more effective than a condensed discharge in producing excited ground-state molecules of low-energy content, and that, if NO reacts with excited nitrogen molecules, as well as atoms, the N_2^* are certainly of higher energy than those removed by collision with N_2O or CO_2.

Production of vibrationally excited, ground-state molecules might be expected to be favored, through spin coupling (29) with the paramagnetic NO molecule, in the reaction

$$N(^4S) + NO(X^2\Pi) \rightarrow N_2(X)\dagger + O(^3P) \qquad [6]$$

in a manner analogous to that found for other reactions of atoms with molecules (e.g. ref. 30). In fact, there is evidence that this reaction does produce nitrogen in low-lying levels of the ground state (25). However, it is exothermic only to the extent of about 75 kcal, and the maximum energy that might be expected to remain as vibrational energy

in the newly formed bond would be between about 53 kcal, corresponding to $v = 8$ (31), and 75 kcal, corresponding to $v = 12$ (27). Hence, although reaction [6] occurs at almost the bimolecular collision rate (12, 32), and would provide vibrationally excited molecules almost immediately after the introduction of NO, such molecules could not directly decompose NO.

On the other hand, $N_2(A^3\Sigma_u^+)$, in the first or second vibrational levels, would have sufficient energy to decompose NO in a collision of the Second Kind. Such a molecule may be formed directly by recombination of N atoms, or by a cascade process after the N atoms recombine into a higher state. Since its transition to the ground state, the only lower-energy state available, involves a change in spin (the forbidden Vegard–Kaplan bands), it has a relatively long radiative lifetime, recently estimated (33) to be between 0.24 and 50 second. It has also been shown (23) that, although vibrational levels of the A state higher than $v = 1$ lose their energy in a number of collisions much less than 10^8, the $v = 1$ level can survive 10^9 collisions. Moreover, there is the possibility of a resonance energy transfer between low vibrational levels of the A-state molecule and NO, as pointed out previously (9). For these several reasons, it is suggested that NO might be decomposed in the following process, which may conserve spin:

$$N_2(A^3\Sigma_u^+)_{v = \text{low values}} + NO(X^2\Pi) \rightarrow N_2(X^1\Sigma_g^+) + N(^4S) + O(^3P). \quad [7]$$

It should be noted that, although the A-state molecule has recently been observed in absorption (34, 35), no direct evidence is available that its concentration in active nitrogen is sufficient to account for the NO/HCN discrepancy. There is little question, however, that its concentration is much greater than that of the B-state molecule, or other triplet-state molecules such as the precursor of the 'Y' bands in active nitrogen (36, 37), the $Y^3\Sigma_u^-$ (perhaps better referred to as the $B'^3\Sigma_u^-$ (38, 39)) state, or of the $^3\Delta_u$ state, all of which probably have very short lifetimes (33, 8). Process [7] is therefore favored over the analogous process, for which evidence has been obtained by Heath (40),

$$N_2(B^3\Pi_g) + NO(X^2\Pi) \rightarrow N_2(X^1\Sigma_g^+) + NO(^2\Sigma^-). \quad [8]$$

Heath observed that the active nitrogen afterglow, especially transitions from $v = 5$, 6, and 7 levels of the B state, was weakened at higher pressures (10 to 760 mm) in the presence of NO. He suggested, therefore, a resonance energy transfer in process [8], which conserves spin and may lead to the dissociation of NO, to explain the disappearance of the First Positive group in high-pressure air discharges. The $^4\Sigma^-$ state for NO correlates with the dissociation limit (41, 42) for NO into $N(^4S) + O(^1D)$.

The Lifetimes of the Excited Molecules Involved in the NO and NH_3 Reactions

The plateau values for NO and NH_3 destruction, after different times of decay of the active nitrogen, permit calculation of lifetimes for the excited molecular species that appear to be involved in these reactions, provided the rate constant of surface decay of the N atoms is known for the given experimental conditions. This was obtained, for the present study, from the equation

$$-d[N]/dt = k_1[N] + k_2[N]^2P, \quad [9]$$

where $k_1[N]$ represents the rate of heterogeneous decay, and $k_2[N]^2P$ represents the rate of homogeneous decay of N atoms. The value of k_2 may be taken to be 3×10^{-33} cc^2 molecule^{-2} sec^{-1} (43, 44).[8] Values of [N] were inferred from maximum HCN yields in the

[8]*This value was based on a* N*-atom concentration deduced from* HCN *production from* C_2H_4 *or* C_2H_6 *at high reaction temperatures, and consequently could be too high if values of* [N] *so obtained were too low.*

C_2H_4 reaction at various levels, and values of $d[N]/dt$ were obtained as slopes of the straight-line plots of HCN production against decay time of the active nitrogen at the 0-, 15-, and 30-cm levels (-1.57×10^{16} and -1.00×10^{16} molecules cc^{-1} sec^{-1} respectively in the poisoned and unpoisoned systems). The following reasonable values of k_1 (sec^{-1}) were obtained:[9]

Level, cm	Poisoned system	Unpoisoned system
0	1.4	3.5
15	1.7	4.4

The rate of decay of the N_2^* species, assumed capable of causing the decomposition of NO in reaction [7], may be represented by

$$d[N_2^*]/dt = \tfrac{1}{2}ak_2[N]^2P+\tfrac{1}{2}bk_1[N]-k_3[N_2^*], \qquad [10]$$

from which,

$$k_3 = \frac{k_1[N]}{2[N_2^*]} + \frac{k_2[N]^2P}{2[N_2^*]} - \frac{d\ln[N_2^*]}{dt}. \qquad [11]$$

The first term on the right-hand side of equation [10] represents the rate of production of N_2^* by homogeneous recombination, the second term its rate of possible production by heterogeneous recombination, and the last term its decay. The concentration of molecular nitrogen is approximated by the total pressure, P, in the system. Equation [11] is derived by arbitrarily taking the values of the constants a and b to be unity. This is a reasonable value for a if, for example, N_2^* represents the A state of nitrogen, since this state may be populated directly during the volume decay of N atoms, as well as from the end result of light emission in the First Positive system. Although the value of b is much more uncertain, the recent work of Harteck, Reeves, and Mannella (4, 48) supports the possibility that an excited molecular species may be formed during surface recombination.

Values of $d\ln[N_2^*]/dt$ were obtained from plots of $\ln\frac{1}{2}(NO-HCN)$ against time, on the assumption that $[N_2^*] = \frac{1}{2}(NO_{reacted}-HCN_{produced})$. Values of k_1, k_2, and [N] were taken as outlined previously, and the following values for k_3 were obtained:

$k_3 = 7.9$ sec^{-1}, poisoned system at 0-cm level;
$= 9.7$ sec^{-1}, poisoned system at 15-cm level;
$= 8.3$ sec^{-1}, unpoisoned system at 15-cm level.

Accordingly, the excited state of N_2, assumed capable of reacting with NO, is calculated to have a half-life, assuming its decay to be a first-order process, of about 8.4×10^{-2} second. This value is somewhat higher than the minimum lifetime of 10^{-2} second observed by Lichtin (49) and the value of 2.6×10^{-2} second recently observed by Wilkinson and Mulliken (50), but less than the value of 0.15 second inferred by Carleton (34), for the $v = 0$ level of the $N_2(A^3\Sigma_u^+)$ molecule. (The A state contains 142 kcal/mole of excess energy and low-lying vibrational levels of this electronic state would contain sufficient energy, 150 kcal/mole, to cause reaction [7].)

[9]*If values for k_1 are similarly calculated from the* NO *data, it is found that the value for the unpoisoned system (2.1 sec^{-1}) agrees well with that (2.5 sec^{-1}) previously reported (45) for such a system, but a larger, not a smaller, value is obtained for the poisoned system. If the larger value of k_2 obtained by other investigators (46, 47) from the* NO *titration are substituted into equation [9], along with the present* NO *data, the anomaly is accentuated. This suggests that the* N*-atom concentrations inferred from the* NO *titration are too high.*

The extents of NH_3 destruction at different levels enable a similar calculation of the rate constant, k_4, for the decay of the N_2^* species capable of destroying NH_3. However, recent measurements (18) on the rate of the active nitrogen – NH_3 reaction have given further indication that the N_2^* responsible for the NH_3 reaction is formed only during homogeneous decay of N atoms, in which case $b = 0$ in equations [10] or [11]. The values obtained for k_4 (sec^{-1}) are then:

Level, cm	Poisoned system	Unpoisoned system
0	10.6	6.7
15	9.6	7.3

The average value in the poisoned system of 10.1 sec^{-1} indicates a half-life for the N_2^* species of 6.9×10^{-2} second.

It is interesting, perhaps, that there is a definite trend towards higher values of the ratio of N_2^* responsible for NO destruction, given by $\frac{1}{2}(NO-HCN)$, to N_2^* responsible for NH_3 reaction, given by the extent of NH_3 destruction, at greater times of decay of the active nitrogen in the unpoisoned system:

Level, cm	Poisoned system	Unpoisoned system
0	2.24	2.52
15	2.35	3.15
30	2.32	3.24
45	2.23	3.58

This gives further evidence that NO may react with a N_2^* species produced at the wall as well as in volume decay of N atoms.

The Behavior of Reactions in the Presence of NH_3, N_2O, and CO_2

Herron *et al.* (14) have observed that the addition of NH_3 to active nitrogen produced by a microwave discharge, in which the destruction of NH_3 was immeasurably small, did not affect the value of the NO titration. The significant *increase* in the NO titration, observed in the present studies, when NH_3 was added to the unpoisoned system, may be attributed to a slower decay of N atoms in the presence of the polar NH_3 molecule, which may serve as a poison against the wall recombination of N atoms. Consequently, if NO reacts with N_2^*, it would seem that the N_2^* involved is different from that responsible for the decomposition of NH_3, *or*, that the products of the NH_3 decomposition react rapidly with NO. The latter alternative is quite possible, since Bamford has shown (51) that NO rapidly scavenges NH_2 radicals, even at room temperature, according to

$$NO + NH_2 \rightarrow N_2 + ---. \qquad [12]$$

Moreover, the reaction

$$NH_2 + NO \rightarrow N_2 + H_2O \qquad [12']$$

occurs (52) during the photolysis of NH_3 in the presence of NO, and in NH_3 flames (53), together, perhaps, with the reaction

$$NH + NO \rightarrow N_2 + OH. \qquad [13]$$

Since the addition of NH_3 upstream from C_2H_4 did not decrease the extent of HCN production (Table IV), the reaction of NH_3 with active nitrogen apparently does not consume N atoms. The slight increase in HCN production in the poisoned system is

difficult to explain, but might be due to additional wall poisoning by NH_3. The greater increase, proportionately, in HCN production in the unpoisoned system is almost certainly due to the efficient wall poisoning by small amounts of NH_3 in this system. The increased temperature of the C_2H_4 reaction, in both systems, in the presence of added NH_3, may then be explained by more extensive reaction in the presence of the higher N-atom concentration promoted by the poisoning effect of NH_3. The poisoning effect of NH_3 might also account for the visual increase in the afterglow intensity *downstream* when small amounts of NH_3 were added upstream in the unpoisoned system. A decrease in light intensity in the region where a low flow rate of NH_3 is added, accompanied by an increase at points further downstream in the unpoisoned system, has recently been confirmed quantitatively by measurements (54) with a photomultiplier tube. Since the total destruction of NH_3 was not affected by addition of small amounts of NH_3 upstream in the unpoisoned system, the slower decay of N atoms, due to NH_3 absorption on the walls, appears to compensate for any loss of N_2^* effective for the NH_3 reaction resulting from a low NH_3 concentration in the region between the fixed and mobile jets.

The small increase in HCN production from C_2H_4, and in the extent of NO decomposition, in the presence of N_2O or CO_2 (Table III), might also be attributed to poisoning of the walls against atom recombination by these molecules in the unpoisoned system of apparatus (I). This wall effect might also provide an explanation for the enhanced afterglow intensity observed downstream by Kaufman and Kelso (25) when N_2O was added upstream. These authors attributed the higher N-atom concentration downstream to a decreased rate of homogeneous recombination of N atoms in the region of higher temperature produced upstream by the absorption of energy by N_2O from excited nitrogen molecules of relatively low energy content. However, the rate of homogeneous recombination of N atoms has a small temperature dependence (14), and, although the temperature coefficient of this association reaction has generally been considered to have a negative value (55), there have been some indications (43, 44) that it may even have a small positive value.

Since no NH_3 decomposition was observed when C_2H_4 was added upstream, it is apparent that C_2H_4 may remove the N_2^* responsible for the NH_3 reaction. This is not surprising, in view of the many degrees of freedom of the ethylene molecule. However, although an excited C_2H_4 molecule formed during a collision of the Second Kind with N_2^* might suffer some decomposition, such fragments would consume N atoms (1) before producing HCN. In the opinion of the authors, the direct formation of HCN from hydrocarbons through chemical reaction with N_2^* is considerably less probable than the decomposition of NO induced by N_2^*.

REFERENCES

1. H. G. V. Evans and C. A. Winkler. Can. J. Chem. **34**, 1217 (1956).
2. G. E. Beale, Jr. and H. P. Broida. J. Chem. Phys. **31**, 1030 (1959).
3. U. H. Kurzweg and H. P. Broida. J. Mol. Spectroscopy, **3**, 388 (1959).
4. P. Harteck, R. R. Reeves, and G. Mannella. Can. J. Chem. **38**, 1648 (1960).
5. R. A. Young and K. C. Clark. J. Chem. Phys. **32**, 604 (1960).
6. G. R. Freeman and C. A. Winkler. J. Phys. Chem. **59**, 371 (1955).
7. G. B. Kistiakowsky and G. G. Volpi. J. Chem. Phys. **28**, 665 (1958).
8. K. D. Bayes and G. B. Kistiakowsky. J. Chem. Phys. **32**, 992 (1960).
9. G. J. Verbeke and C. A. Winkler. J. Phys. Chem. **64**, 319 (1960).
10. (*a*) G. B. Kistiakowsky and G. G. Volpi. J. Chem. Phys. **27**, 1141 (1957).
    (*b*) F. Kaufman and J. R. Kelso. J. Chem. Phys. **27**, 1209 (1957).
11. W. C. Zinman. J. Phys. Chem. **64**, 1343 (1960).
12. M. A. A. Clyne and B. A. Thrush. Proc. Roy. Soc. (London), A, **261**, 259 (1961).
13. R. Kelly and C. A. Winkler. Can. J. Chem. **38**, 2514 (1960).
14. J. T. Herron, J. C. Franklin, P. Bradt, and V. H. Dibeler. J. Chem. Phys. **30**, 879 (1959).

15. A. UNG. Ph.D Thesis, McGill University, Montreal, Que. 1961.
16. R. A. BACK and C. A. WINKLER. Unpublished results.
17. E. R. V. MILTON and H. B. DUNFORD. J. Chem. Phys. **34**, 51 (1961).
18. A. N. WRIGHT and C. A. WINKLER. Can. J. Chem. **40**, 5 (1962).
19. K. R. JENNINGS. Quart. Revs. (London), **15**, 237 (1961).
20. W. FORST, H. G. V. EVANS, and C. A. WINKLER. J. Phys. Chem. **61**, 320 (1957).
21. H. G. V. EVANS, G. R. FREEMAN, and C. A. WINKLER. Can. J. Chem. **34**, 1271 (1956).
22. C. MAVROYANNIS and C. A. WINKLER. International Symposium on the Chemistry of the Lower and Upper Atmosphere, San Francisco, Calif. April 1961.
23. J. NOXON. Active nitrogen at high pressures. Thesis, Harvard University, Cambridge, Mass. 1957.
24. C. B. KRETSCHMER and H. C. PETERSEN. J. Chem. Phys. **33**, 948 (1960).
25. F. KAUFMAN and J. R. KELSO. J. Chem. Phys. **28**, 510 (1958).
26. J. S. LUKASIK and J. E. YOUNG. J. Chem. Phys. **27**, 1149 (1957).
27. J. C. POLANYI. J. Chem. Phys. **31**, 1338 (1959).
28. M. BROOK and J. KAPLAN. Phys. Rev. **96**, 1540 (1954).
29. J. P. SIMONS. Nature, **186**, 551 (1960).
30. N. BASCO and R. G. W. NORRISH. Can. J. Chem. **38**, 1769 (1960).
31. F. T. SMITH. J. Chem. Phys. **31**, 1352 (1959).
32. J. T. HERRON. J. Chem. Phys. **35**, 1139 (1961).
33. R. A. YOUNG. J. Chem. Phys. **33**, 1112 (1960); **34**, 339 (1961).
34. N. P. CARLETON. Final Report to AFCRC, Contract AF 19(604)-1041. 1959.
35. P. G. WILKINSON. J. Chem. Phys. **30**, 773 (1959).
36. G. B. KISTIAKOWSKY and P. WARNECK. J. Chem. Phys. **27**, 1417 (1957).
37. F. LEBLANC, Y. TANAKA, and A. JURSA. J. Chem. Phys. **28**, 979 (1958).
38. G. H. DIEKE and D. F. HEATH. J. Chem. Phys. **33**, 432 (1960).
39. P. F. WILKINSON. J. Chem. Phys. **32**, 1061 (1960).
40. D. F. HEATH. New data on the emission spectrum of air. Los Alamos Scientific Laboratory of the University of California. January 6, 1960.
41. R. S. MULLIKEN. Revs. Modern Phys. **4**, 1 (1932).
42. J. T. VANDERSLICE, E. A. MASON, and W. G. MIASCH. J. Chem. Phys. **31**, 738 (1959).
43. R. KELLY and C. A. WINKLER. Can. J. Chem. **37**, 62 (1959).
44. R. A. BACK, W. DUTTON, and C. A. WINKLER. Can. J. Chem. **37**, 2059 (1959).
45. C. MAVROYANNIS and C. A. WINKLER. Can. J. Chem. **39**, 1601 (1961).
46. P. HARTECK, R. R. REEVES, and G. MANNELLA. J. Chem. Phys. **29**, 608 (1958).
47. J. T. HERRON, J. L. FRANKLIN, P. BRADT, and V. H. DIBELER. J. Chem. Phys. **29**, 230 (1958).
48. P. HARTECK, R. R. REEVES, and G. MANNELLA. J. Chem. Phys. **32**, 946 (1960); **33**, 636 (1960).
49. W. LICHTIN. J. Chem. Phys. **26**, 306 (1957).
50. P. G. WILKINSON and R. S. MULLIKEN. J. Chem. Phys. **31**, 674 (1959).
51. C. H. BAMFORD. Trans. Faraday Soc. **35**, 568 (1939).
52. A. SEREWICZ and W. A. NOYES, JR. J. Phys. Chem. **63**, 843 (1959).
53. G. K. ADAMS, W. G. PARKER, and H. G. WOLFHARD. Discussions Faraday Soc. **14**, 97 (1953).
54. A. N. WRIGHT and C. A. WINKLER. Unpublished results.
55. LORD RAYLEIGH. Proc. Roy. Soc. (London), A, **176**, 1 (1940).

A PROTECTED ANGIOTENSIN II

ROBERT H. MAZUR
Division of Chemical Research, G. D. Searle & Co., Skokie, Ill., U.S.A.

Received November 27, 1961

ABSTRACT

The preparation of an octapeptide, carbobenzoxy-(β-benzyl ester)-L-aspartyl-nitro-L-arginyl-L-valyl-L-tyrosyl-L-isoleucyl-(im)benzyl-L-histidyl-L-prolyl-L-phenylalanine methyl ester, a derivative of angiotensin II, is described.

We would like to report the synthesis of a protected angiotensin II, carbobenzoxy-(β-benzyl ester)-L-aspartyl-nitro-L-arginyl-L-valyl-L-tyrosyl-L-isoleucyl-(im)benzyl-L-histidyl-L-prolyl-L-phenylalanine methyl ester (VIII). The octapeptide was built up one

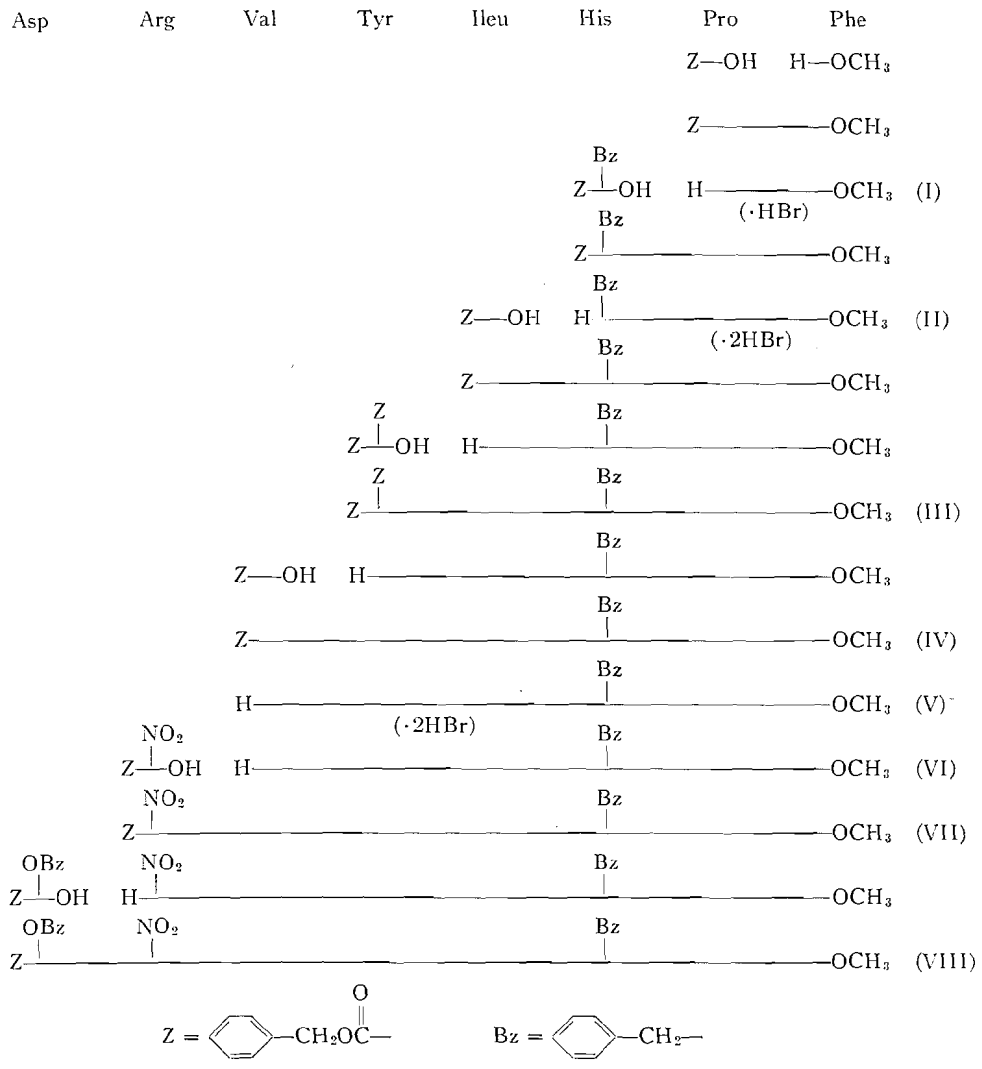

unit at a time beginning from the C-terminal end in order to minimize racemization (1). The ready purification of the intermediates and the final product indicated the absence of any substantial quantity of diastereomers. At each stage dicyclohexylcarbodiimide (2) was used to effect coupling. The synthesis was not carried through to angiotensin II itself as this material has already been reported (3, 4, 5) and also because our choice of protecting groups proved not to be especially felicitous from the standpoint of ready removal. Thus, we had expected to be able to debenzylate the imidazole ring of histidine by hydrogenation and, in fact, the reaction has been recently reported (6). In our hands, however, hydrogenolysis was erratic and unpredictable and usually stopped after partial debenzylation. Removal with sodium in liquid ammonia is undesirable as the powerful reducing system seems to cause side reactions with complex peptides (7, 8).

It might be anticipated that the C-terminal methyl ester would be difficult to remove without rearrangement in the presence of N-terminal aspartic acid. α-Aspartyl peptides in the presence of either strong acid or base gave mixtures containing varying amounts of β-aspartyl peptides,* presumably through a succinimide intermediate. This difficulty has been largely overcome recently by the introduction of the *p*-nitrobenzyl ester (10, 11, 12), which is reasonably stable to hydrogen bromide in acetic acid and can be removed by catalytic hydrogenation.

The structure of our angiotensin II derives from the method of synthesis and was confirmed by total hydrolysis of the product.

EXPERIMENTAL

We would like to thank R. T. Dillon and associates for analyses, rotations, and spectra. The rotations were carried out at 25±2° C. We are especially grateful to S. Eich and D. Malik for determination of the amino acid ratios. Certain peptide derivatives seemed to hold solvent tenaciously. The analytical samples were dried initially overnight at room temperature and approximately 100 mm pressure. When water of crystallization was indicated, the analysis was repeated after drying 4 hours at 100° under high vacuum.

L-Prolyl-L-phenylalanine Methyl Ester Hydrobromide (I)

L-Phenylalanine methyl ester hydrochloride (13) (54.0 g, 0.25 mole) and carbobenzoxy-L-proline (14) (61.5 g, 0.247 mole) were suspended in 600 ml methylene chloride, and 35.0 ml (0.25 mole) triethylamine was added. The clear solution was stirred in an ice bath and 53.5 g (0.26 mole) dicyclohexylcarbodiimide in 200 ml methylene chloride added. The mixture was allowed to stand overnight at 5°. The dicyclohexylurea was removed by filtration and the methylene chloride washed successively with 1 *N* hydrochloric acid, 10% sodium sulphate, and 1 *N* potassium bicarbonate. The organic phase was dried over sodium sulphate and concentrated to give 109 g of a viscous liquid.

The crude product was dissolved in 400 ml 2 *N* hydrobromic acid in acetic acid and allowed to stand 1½ hours at room temperature. The solution was concentrated to a small volume at 45° and the ester hydrobromide precipitated with ether. Purification was effected by dissolving the ester hydrobromide in 75 ml methanol and 750 ml ethyl acetate and concentrating until crystallization began. L-Prolyl-L-phenylalanine methyl ester hydrobromide was obtained as rectangular prisms, 57.7 g (66%), m.p. 171–172°, $[\alpha]_D^{25}$ −36° (*c* 2, water) (lit. (6), m.p. 169.5–170.5°, $[\alpha]_D^{19}$ −37° (*c* 2, water)).

Anal. Calc. for $C_{15}H_{21}BrN_2O_3$: N, 7.84; Br, 22.37. Found: N, 7.84; Br, 22.26.

(Im)Benzyl-L-histidyl-L-prolyl-L-phenylalanine Methyl Ester Dihydrobromide (II)

Carbobenzoxy-(im)benzyl-L-histidine (15, 16, 17) (31.0 g, 0.0815 mole) was dissolved in 100 ml dimethylformamide containing 11.6 ml (0.083 mole) triethylamine and the solution diluted with 300 ml methylene chloride. Finely powdered I (29.4 g, 0.082 mole) was added, followed by 17.3 g (0.084 mole) dicyclohexylcarbodiimide in 100 ml methylene chloride. The mixture was stirred in an ice bath for 1 hour and allowed to stand overnight at 5°. After removal of the dicyclohexylurea by filtration, the methylene chloride was washed successively with 1 *N* hydrochloric acid, 10% sodium sulphate, and 1 *N* potassium bicarbonate, dried over sodium sulphate, and the solvents distilled under vacuum.

The residual oil was dissolved in 300 ml 2 *N* hydrobromic acid in acetic acid and allowed to stand 1 hour at room temperature. The solution was concentrated nearly to dryness at 45° and the residue slurried with ethyl acetate to yield 48.9 g (90.5%) tripeptide, m.p. 211–214°. Crystallization from methanol – ethyl

**For a recent review of the problems associated with the synthesis of aspartyl and glutamyl peptides, see reference 9.*

acetate gave (im)benzyl-L-histidyl-L-prolyl-L-phenylalanine methyl ester dihydrobromide as long silky needles, m.p. 217–219°; $[\alpha]_D^{23}$ +26° (*c* 1, methanol), $[\alpha]_D^{26}$ +28° (*c* 1, water) (lit. (6), m.p. 199–201°, $[\alpha]_D^{21}$ −23° (*c* 3, water)).

Anal. Calc. for $C_{23}H_{28}Br_2N_4O_3$: N, 9.86; Br, 28.12. Found: N, 10.22; Br, 27.98.

O,N-Dicarbobenzoxy-L-tyrosyl-L-isoleucyl-(im)benzyl-L-histidyl-L-prolyl-L-phenylalanine Methyl Ester (III)

Compound II (53.2 g, 0.080 mole) was dissolved in 100 ml water, layered with 250 ml ethyl acetate, and 8.9 g (0.16 mole) potassium hydroxide in 15 ml water added, followed by 500 ml cold 50% potassium carbonate. The mixture was shaken vigorously, the ethyl acetate layer separated, the aqueous layer extracted with 100 ml ethyl acetate, and the combined extracts dried over sodium sulphate and concentrated. The total crude ester in 300 ml methylene chloride was added to 20.9 g (0.079 mole) carbobenzoxy-L-isoleucine (3) in 150 ml methylene chloride. The solution was stirred in an ice bath and 17.1 g (0.083 mole) dicyclohexylcarbodiimide in 100 ml methylene chloride added. The mixture was allowed to stand overnight at 5°. The usual work-up yielded 55.0 g (93%) carbobenzoxy-L-isoleucyl-(im)benzyl-L-histidyl-L-prolyl-L-phenylalanine methyl ester, a glass-like material.

The above crude protected tetrapeptide (15.02 g, 0.02 mole) in 80 ml 2 *N* hydrogen bromide in acetic acid was allowed to stand 1½ hours at room temperature and the solution concentrated to dryness at 45°. The residue was dissolved in 15 ml water and the solution extracted with ether to remove benzyl bromide. The aqueous layer was neutralized with 2 equivalents of 40% potassium hydroxide, basified with 200 ml 50% potassium carbonate, and the crude ester extracted into ethyl acetate. The ethyl acetate was dried over sodium sulphate and distilled to yield 12.40 g (100%) L-isoleucyl-(im)benzyl-L-histidyl-L-prolyl-L-phenylalanine methyl ester, a glass-like material.

The above crude ester (0.02 mole) and 11.20 g (0.025 mole) O,N-dicarbobenzoxy-L-tyrosine (18, 19) in 150 ml methylene chloride were stirred in an ice bath and treated with 5.15 g (0.025 mole) dicyclohexylcarbodiimide in 50 ml methylene chloride. The mixture was allowed to stand overnight at 5° and, on working up as usual, gave 30.0 g of an oily residue. The total material was purified by countercurrent distribution in methanol – water – chloroform – carbon tetrachloride 37:10:26:27, 40 ml phases, 136 transfers. The peaks were located by ultraviolet absorption at 278 mμ. The main product had a partition coefficient $K = 0.09$. A by-product with $K = 0.37$ was also present. From tubes 3–25 was isolated 15.2 g (72%) of amorphous O,N-dicarbobenzoxy-L-tyrosyl-L-isoleucyl-(im)benzyl-L-histidyl-L-prolyl-L-phenylalanine methyl ester, sinter from 90°, liquefy 146–151°. Crystallization from methanol gave circular plates, lose shape 89–90°, liquefy above 160°, $[\alpha]_D^{24}$ −43° (*c* 1, methanol).

Anal. Calc. for $C_{59}H_{65}N_7O_{11}$: C, 67.60; H, 6.25; N, 9.36. Calc. for $C_{59}H_{65}N_7O_{11}\cdot H_2O$: C, 66.46; H, 6.33; N, 9.20. Found: C, 66.57; H, 6.53; N, 9.05. After drying at 100°, found: C, 66.91; H, 6.18.

Carbobenzoxy-L-valyl-L-tyrosyl-L-isoleucyl-(im)benzyl-L-histidyl-L-prolyl-L-phenylalanine Methyl Ester (IV)

Compound III (21.0 g, 0.02 mole) in 150 ml 2 *N* hydrogen bromide in acetic acid was allowed to stand 1½ hours at room temperature. The solution was concentrated to dryness at 45°, the residue dissolved in 150 ml 33% methanol, benzyl bromide removed by ether extraction, and the aqueous layer treated with 50 ml each of saturated potassium bicarbonate and saturated potassium carbonate. The basic ester was taken up in ethyl acetate, the ethyl acetate dried over sodium sulphate and distilled to yield 15.6 g (100%) L-tyrosyl-L-isoleucyl-(im)benzyl-L-histidyl-L-prolyl-L-phenylalanine methyl ester, a glass-like material.

Total crude base (0.02 mole) and 5.78 g (0.023 mole) carbobenzoxy-L-valine (14) in 100 ml methylene chloride were stirred in an ice bath and 4.75 g (0.023 g) dicyclohexylcarbodiimide in 50 ml methylene chloride was added. The mixture was allowed to stand overnight at 5°. The usual work-up yielded 18.8 g of a glass which was purified by countercurrent distribution in methanol – water – chloroform – carbon tetrachloride 37:10:26:27, 40 ml phases, 250 transfers. The peaks were located by ultraviolet absorption at 278 mμ. Two materials ($K_1 = 0.16$ and $K_2 = 0.50$) proved to be present. The desired product was the one with the lower partition coefficient, and from tubes 20–55 was obtained 13.4 g (66%) of carbobenzoxy-L-valyl-L-tyrosyl-L-isoleucyl-(im)benzyl-L-histidyl-L-prolyl-L-phenylalanine methyl ester as a white powder, m.p. 188–191°. Crystallization from methanol – ethyl acetate by concentration to the cloud point gave circular plates, m.p. 192–194°, $[\alpha]_D^{23}$ −66° (*c* 1, methanol), λ_{max}^{MeOH} 252, 258, 264, 268, 278.5 mμ, $\epsilon_{278.5}$ 1490. The amino acid composition (except for (im)benzyl-histidine) was determined by Stein–Moore (20) analysis. Found: Val, 1.04; Tyr, 0.98; Ileu, 1.03; Pro, 1.00; Phe, 1.10.

Anal. Calc. for $C_{56}H_{68}N_8O_{10}$: C, 66.38; H, 6.77; N, 11.06. Calc. for $C_{56}H_{68}N_8O_{10}\cdot H_2O$: C, 65.22; H, 6.84; N, 10.87. Found: C, 65.08; H, 6.58; N, 10.61. After drying at 100°, found: C, 66.06; H, 6.80.

Carbobenzoxy-L-valyl-L-tyrosyl-L-isoleucyl-(im)benzyl-L-histidyl-L-prolyl-L-phenylalanine

Compound IV (5.15 g, 0.005 mole) in 45 ml methanol was cooled in an ice bath and 5.0 ml 4 *N* lithium hydroxide added. The solution was allowed to stand ½ hour at room temperature and treated with an amount of ca. 4 *N* hydrochloric acid exactly equivalent to the alkali present. The mixture was diluted with 50 ml water, the product filtered, washed with water, and dried to yield 5.05 g (98%) of the carbobenzoxy-hexapeptide acid, m.p. 171–174°. Crystallization from methanol – ethyl acetate by concentration to the cloud point gave a white powder, m.p. 176–179°, $[\alpha]_D^{26}$ −50° (*c* 1, methanol).

Anal. Calc. for $C_{55}H_{66}N_8O_{10}$: C, 66.11; H, 6.66; N, 11.22. Calc. for $C_{55}H_{66}N_8O_{10}\cdot H_2O$: C, 64.94; H, 6.74; N, 11.02. Found: C, 64.32; H, 6.72; N, 11.19. After drying at 100°, found: C, 64.72; H, 6.54.

L-*Valyl*-L-*tyrosyl*-L-*isoleucyl-(im)benzyl*-L-*histidyl*-L-*prolyl*-L-*phenylalanine Methyl Ester Dihydrobromide (V)*

Compound IV (1.03 g, 0.001 mole) in 10 ml 2 *N* hydrobromic acid in acetic acid was allowed to stand 1 hour at room temperature and concentrated to dryness at 50°. The residue was precipitated from methanol with ethyl acetate and gave the desired hexapeptide ester dihydrobromide as a white powder, 0.79 g (76%), m.p. 220–223°. Crystallization from methanol – ethyl acetate by concentration to the cloud point raised the melting point to 224–225°, $[\alpha]_D^{25}$ −20° (*c* 1, methanol).

Anal. Calc. for $C_{48}H_{64}Br_2N_8O_8$: C, 55.36; H, 6.20; N, 10.77. Calc. for $C_{48}H_{64}Br_2N_8O_8 \cdot H_2O$: C, 54.44; H, 6.28; N, 10.58. Found: C, 53.83; H, 6.24; N, 10.44. After drying at 100°, found: C, 54.02; H, 5.98.

L-*Valyl*-L-*tyrosyl*-L-*isoleucyl-(im)benzyl*-L-*histidyl*-L-*prolyl*-L-*phenylalanine Methyl Ester (VI)*

Crude dihydrobromide, obtained as described above from 6.56 g compound IV, was dissolved in 25 ml water and the solution washed with ethyl acetate. Addition of saturated potassium carbonate solution resulted in a precipitate, which was removed by filtration and washed thoroughly with water and ethyl acetate. The white powder proved to be hexapeptide ester, 3.45 g (61%), m.p. 216–219°, $[\alpha]_D^{26}$ −52° (*c* 1, methanol).

Anal. Calc. for $C_{48}H_{62}N_8O_8$: C, 65.58; H, 7.11; N, 12.75. Calc. for $C_{48}H_{62}N_8O_8 \cdot H_2O$: C, 64.26; H, 7.19; N, 12.49. Found: C, 63.85; H, 7.33; N, 12.50. After drying at 100°, found: C, 65.06; H, 7.29.

Carbobenzoxy-nitro-L-*arginyl*-L-*valyl*-L-*tyrosyl*-L-*isoleucyl-(im)benzyl*-L-*histidyl*-L-*prolyl*-L-*phenylalanine Methyl Ester (VII)*

Compound VI (3.25 g, 0.0037 mole) and 2.12 g (0.006 mole) carbobenzoxynitro-L-arginine (21) were dissolved in 17 ml dimethylformamide, the solution was cooled in an ice bath, and 1.36 g (0.0066 mole) dicyclohexylcarbodiimide was added with stirring. The mixture was allowed to stand overnight at 5°. The dicyclohexylurea was filtered, washed with methanol, and the combined filtrates were diluted with a large volume of water. The resulting white solid was purified by countercurrent distribution in methanol – water – chloroform – carbon tetrachloride 37:10:26:27, 40 ml phases, 200 transfers. The peaks were located by ultraviolet absorption at 270 mμ. The major product had $K = 0.34$ with an impurity at $K = 0.92$. Fractions 24–82 yielded the desired protected heptapeptide, 4.43 g (98%), m.p. 220–221°. Crystallization from methanol gave a granular solid, m.p. 224–225°, $[\alpha]_D^{25}$ −67° (*c* 1, methanol), λ_{max}^{MeOH} 270 mμ, ε 16,700.

Anal. Calc. for $C_{62}H_{79}N_{13}O_{13}$: C, 61.32; H, 6.56; N, 15.00. Found: C, 60.80; H, 6.80; N, 14.96.

Dibenzyl-L-*Aspartate p-Toluenesulphonate*

L-Aspartic acid (13.3 g, 0.1 mole) and 20.9 g (0.11 mole) *p*-toluenesulphonic acid monohydrate were dissolved in 108 g (1.0 mole) benzyl alcohol and the solution diluted with 200 ml carbon tetrachloride. The solution was heated overnight under reflux (continuous water separator). Dilution of the cooled solution with 1 l. ether precipitated the dibenzyl ester toluenesulphonate as white needles, 47.8 g (98%), m.p. 156–158°. Crystallization from 1:1 isopropanol – ethyl acetate raised the melting point to 159–161°, $[\alpha]_D^{26}$ −2° (*c* 1, methanol) (lit. (22), m.p. 158–160°).

Anal. Calc. for $C_{25}H_{27}NO_7S$: C, 61.84; H, 5.61; N, 2.89. Found: C, 61.88; H, 5.52; N, 2.73.

Dibenzyl Carbobenzoxy-L-*aspartate*

Dibenzyl aspartate toluenesulphonate (41.6 g, 0.0858 mole) was suspended in 400 ml chloroform, the mixture stirred in an ice bath and treated successively with 215 ml (50% excess) 1 *M* potassium carbonate and 19.3 ml (0.0945 mole) 4.9 *M* carbobenzoxy chloride in toluene. The mixture was stirred very vigorously for 2 hours at 0°. The chloroform layer was washed with 1 *N* hydrochloric acid and 10% sodium sulphate, dried over sodium sulphate, and the chloroform distilled. The residue was crystallized from cyclohexane to yield, in two crops, 36.7 g (96%) dibenzyl carbobenzoxy-L-aspartate, m.p. 67–68.5° (lit. (23), m.p. 66.5°).

β-Benzyl Carbobenzoxy-L-*aspartate*

The procedure of Bryant *et al.* (24) was followed. From 22.4 g (0.05 mole) diester was obtained 11.8 g (66%) of the desired monoester, thick needles from 1:1 benzene–cyclohexane, m.p. 107–109°; $[\alpha]_D^{26}$ 0° (*c* 1, methanol), +10° (*c* 1, acetic acid) (lit. (24), m.p. 107–109°).

Carbobenzoxy-(β-benzyl ester)-L-*aspartyl-nitro*-L-*arginyl*-L-*valyl*-L-*tyrosyl*-L-*isoleucyl-(im)benzyl*-L-*histidyl*-L-*prolyl*-L-*phenylalanine Methyl Ester (VIII)*

Heptapeptide VII (1.95 g, 0.0016 mole) in 20 ml 2 *N* hydrobromic acid in acetic acid was allowed to stand 1 hour at room temperature. The solution was concentrated at 45° to about 10 ml and diluted with 200 ml dry ether. The resulting precipitate was isolated by filtration, redissolved in 10 ml dry methanol, and precipitated with 200 ml dry ether, yielding 2.24 g (slightly over theory) of a non-hygroscopic white powder, decomp. above 195°, no m.p.

The above product was suspended in 4 ml dimethylformamide, and 0.50 ml triethylamine added and the mixture stirred until the peptide dissolved. The mixture was cooled in an ice bath, the precipitate filtered and washed with 4 ml cold dimethylformamide to yield 0.50 g (100%) triethylamine hydrobromide.

The filtrate was stirred in an ice bath and treated successively with 0.71 g (0.002 mole) β-benzyl-carbobenzoxy-L-aspartate and 0.45 g (0.0022 mole) dicyclohexylcarbodiimide. The mixture was allowed to stand overnight at 5°, dicyclohexylurea removed by filtration, and the filtrate diluted with water and extracted

with chloroform. The product which remained suspended in the aqueous dimethylformamide was filtered, washed with ethyl acetate, and dried to yield 2.06 g of a white powder, m.p. 168–173°. Reprecipitation from methanol – ethyl acetate yielded 0.87 g (39%) of the protected octapeptide VIII, m.p. 193–196°. Slow evaporation of a solution of this material from methanol – ethyl acetate gave circular plates, m.p. 206–208°, $[\alpha]_D^{26}$ −65° (*c* 0.5, methanol), λ_{max}^{MeOH} 270 mμ, ε 17,700.

Anal. Calc. for $C_{73}H_{90}N_{14}O_{16}$: C, 61.76; H, 6.39; N, 13.82. Found: C, 61.27; H, 6.51; N, 13.82.

A sample (5.0 mg) in 6 ml acetic acid and 0.1 ml conc. hydrochloric acid was hydrogenated overnight over 50 mg palladium on barium sulphate (25) in order to remove the protecting groups from aspartic acid and arginine. The residue, after removal of the catalyst, was analyzed for amino acid ratio (except for (im)-benzyl-histidine) by the Stein–Moore method (20).

Found: Asp, 1.15; Arg, 0.96; Val, 1.17; Tyr, 0.95; Ileu, 0.94; Pro, 1.00; Phe, 1.24.

REFERENCES

1. H. SCHWARZ and F. M. BUMPUS. J. Am. Chem. Soc. **81**, 890 (1959).
2. J. C. SHEEHAN and G. P. HESS. J. Am. Chem. Soc. **77**, 1067 (1955).
3. W. RITTEL, B. ISELIN, H. KAPPELER, B. RINIKER, and R. SCHWYZER. Helv. Chim. Acta, **40**, 614 (1957).
4. H. SCHWARZ, F. M. BUMPUS, and I. H. PAGE. J. Am. Chem. Soc. **79**, 5697 (1957).
5. K. ARAKAWA and F. M. BUMPUS. J. Am. Chem. Soc. **83**, 728 (1961).
6. E. BRICAS and C. NICOT-GUTTON. Bull. soc. chim. France, 466 (1960).
7. R. SCHWYZER, W. RITTEL, H. KAPPELER, and B. ISELIN. Angew. Chem. **72**, 915 (1960).
8. K. HOFMANN and H. YAJIMA. J. Am. Chem. Soc. **83**, 2289 (1961).
9. J. RUDINGER. *In* Proceedings of the Symposium on Methods of Peptide Synthesis. Collection Czechoslov. Chem. Commun. **24**, 95 (1959). K. MEDZIHRADSZKY. *In* Proceedings of the Symposium on Methods of Peptide Synthesis. Collection Czechoslov. Chem. Commun. **24**, 107 (1959).
10. R. SCHWYZER and P. SIEBER. Helv. Chim. Acta, **42**, 972 (1959).
11. H. SCHWARZ and K. ARAKAWA. J. Am. Chem. Soc. **81**, 5691 (1959).
12. J. E. SHIELDS, W. H. MCGREGOR, and F. H. CARPENTER. J. Org. Chem. **26**, 1491 (1961).
13. R. A. BOISSONNAS, S. GUTTMANN, P. A. JAQUENOUD, and J. P. WALLER. Helv. Chim. Acta, **39**, 1421 (1956).
14. W. GRASSMANN and E. WÜNSCH. Chem. Ber. **91**, 462 (1958).
15. A. H. COOK, I. HEILBRON, and A. P. MAHANDERAN. J. Chem. Soc. 1061 (1949).
16. B. G. OVERELL and V. PETROW. J. Chem. Soc. 232 (1955).
17. D. THEODOROPOULOS. J. Org. Chem. **21**, 1550 (1956).
18. E. KATCHALSKI and M. SELA. J. Am. Chem. Soc. **75**, 5284 (1953).
19. R. SCHWYZER, M. FEURER, B. ISELIN, and H. KÄGI. Helv. Chim. Acta, **38**, 80 (1955).
20. S. MOORE, D. H. SPACKMAN, and W. H. STEIN. Anal. Chem. **30**, 1185 (1958).
21. K. HOFMANN, W. D. PECKHAM, and A. RHEINER. J. Am. Chem. Soc. **78**, 238 (1956).
22. L. ZERVAS, M. WINITZ, and J. P. GREENSTEIN. J. Org. Chem. **22**, 1515 (1957).
23. A. BERGER and E. KATCHALSKI. J. Am. Chem. Soc. **73**, 4084 (1951).
24. P. M. BRYANT, R. H. MOORE, P. J. PIMLOTT, and G. T. YOUNG. J. Chem. Soc. 3868 (1959).
25. R. KUHN and J. HAAS. Angew. Chem. **67**, 785 (1955).

COORDINATION COMPOUNDS OF OLEFINS WITH SOLID COMPLEX SILVER SALTS

I. COORDINATION COMPOUNDS WITH ANHYDROUS SILVER FLUOBORATE[1]

H. W. QUINN AND D. N. GLEW
Exploratory Research Laboratory, Dow Chemical of Canada, Limited, Sarnia, Ontario

Received February 15, 1962

ABSTRACT

Interaction of solid silver fluoborate with the gaseous olefins ethylene, propylene, and the four butenes has been observed to provide 12 new stoichiometric solid coordination compounds (silver fluoborate – olefin complexes) of high stability. Experimental investigation of the univariant pressure–temperature stability lines for the complexes has been made and the thermodynamic functions calculated: the heat content change for complex dissociation is between 9 and 13 kcal/mole of olefin liberated. Infrared spectra of the complexed olefins indicate that the strength of the silver–olefin bond is primarily dependent upon the basicity of the olefin and a comparison of the thermodynamics of dissociation shows anomalous behavior on the part of isobutylene and *trans*-2-butene as compared with the regularity displayed by the other four olefins.

INTRODUCTION

Although a number of studies have been reported on the argentation of olefins in solution (1–10), there are relatively few data on the corresponding solid silver salt – olefin complexes, probably since these are not readily formed on exposure of the silver salts to the olefin. Of those silver salts which complex directly with olefins, silver perchlorate forms complexes with cyclohexene and the pinenes which are solids at room temperature containing 2 moles of olefin per mole of silver perchlorate, whilst silver nitrate forms with cyclohexene a complex which is a liquid at room temperature, crystallizing at 0° C (11). Presently, no structural data have been reported for the silver salt – monoolefin complexes, although the structures are available for the related silver salt – cyclic polyolefin complexes $AgClO_4.C_6H_6$ (12) and $AgNO_3.C_8H_8$ (13).

The lower olefin complexes of silver salts are apparently not readily formed and generally exert high dissociation pressures, as observed by Francis (14), who formed the liquid complexes silver nitrate – propylene and silver nitrate – 1-butene, using the olefins under pressure, but was unable to obtain similar complexes with ethylene, isobutylene, and 2-butene. Similar solid complexes of the cuprous halides with the lower olefins $CuCl.C_2H_4$, $CuCl.C_3H_6$, $CuCl.iso\text{-}C_4H_8$, and $CuBr.C_2H_4$ (15), which probably involve copper–olefin interactions analogous to those of the silver–olefin complexes, are relatively unstable, $CuCl.C_3H_6$ decomposing at 20° C and $CuCl.iso\text{-}C_4H_8$ at −18° C. Surprisingly, no reference has yet been made to solid complexes between silver perchlorate and the lower olefins.

In marked contrast to the difficulty of formation and lack of stability of the known silver and copper salt – lower olefin complexes, silver fluoborate readily absorbs ethylene, propylene, and the four butenes at low pressures at room temperature to yield stable solid silver fluoborate – olefin complexes, for which the stoichiometries, pressure–temperature stability lines, and infrared absorption spectra are reported. Also included for comparison is a limited investigation of the solid propylene complexes of silver perchlorate (this salt being isomorphous with silver fluoborate) and of silver hexafluoroantimonate (which has a similar, but larger, perfluorinated anion).

[1]*Contribution No. 41.*

EXPERIMENTAL

Anhydrous silver fluoborate was prepared from silver fluoride and boron trifluoride according to the method of Olah and Quinn (16).

Anhydrous silver hexafluoroantimonate was prepared by reaction of antimony pentafluoride with silver fluoride in anhydrous liquid hydrogen fluoride; the solid silver hexafluoroantimonate was precipitated and the hydrogen fluoride removed by pumping. Both salts were very hygroscopic and were stored under normal pentane until required, when the paraffin was removed by pumping.

Anhydrous silver perchlorate, purchased from A. S. LaPine and Co., was ground in a mortar under pentane to give a smaller particle size.

Ethylene, propylene, *cis*-2-butene, and *trans*-2-butene were Matheson C.P. Grade with a 99.5% minimum purity.

1-Butene and isobutylene were Phillips Pure Grade materials of 99% minimum purity. Before use, all olefins were dried by passage through a column containing phosphorus pentoxide and were freeze-degassed at liquid nitrogen temperatures.

Determination of Complex Stoichiometry

The stoichiometry of the silver salt – olefin complexes was determined by measurement of the weight increase attending complex formation of 250–400 mg of silver salt contained in a quartz bucket suspended from a quartz spiral of sensitivity 5.577 mg/mm, after admission of the gaseous olefin to the thermostated spiral chamber. The spiral extension was measured to ±0.02 mm with a cathetometer by observing the displacement of the tip of the lower hook of the spiral. Temperature control was maintained to ±0.1° C by pumping fluid from a thermostat through an outer jacket of the spiral chamber.

In order to detect all the stoichiometric complexes, the olefin pressures applied to the silver salt were gradually increased and the temperature of the spiral chamber gradually lowered. When olefin ceased to be taken up under a given set of conditions, more pressing conditions were applied until, with the exception of ethylene, the olefin attained its liquid saturation value.

Complex Dissociation Pressure Measurement

Although the approximate locations of the pressure–temperature stability lines for the various silver salt – olefin equilibria were obtained from the stoichiometric studies using the quartz spiral, these olefin pressure data were insufficiently precise for determination of the corresponding thermodynamic functions. A more accurate determination of the complex stability lines (complex dissociation pressures) was therefore conducted as follows. Approximately 2 g of silver salt contained in a 25-ml glass vapor pressure cell was evacuated and then exposed to the olefin at 650 mm Hg pressure at between 20 and 30° C until no further pressure decrease was observed. The temperature of the cell was then decreased to between −5 and 0° C and the system allowed to react until no further pressure drop was detectable; in this manner, the complex with the highest olefin content was obtained. The cell system containing the complex was then allowed to equilibrate with its lower complex or solid silver salt at a series of preselected temperatures, and the equilibrium olefin pressures were measured on a mercury manometer to ±0.01 mm using a cathetometer. After measurement of the pressure–temperature equilibrium line for decomposition of the highest olefin complex, gaseous olefin was removed from the system to furnish the complex of next-lower olefin content, which in turn was investigated in the same manner. Temperatures between −5 and 55° were controlled to ±0.1° C by immersing the vapor pressure cell in a liquid thermostat, while lower temperatures were maintained using freezing monochlorobenzene and chloroform baths.

Infrared Spectra

Samples were prepared by exposing the silver salts to the olefin at pressures such that only the silver salt:2 olefin complex was produced. Nujol and fluorolube mulls of these 1:2 complexes were prepared in a dry box and the infrared spectra recorded with a Perkin–Elmer 221 spectrophotometer equipped with NaCl optics.

RESULTS

Complex Stoichiometry

In Table I are presented the experimental values for the stoichiometry of the silver fluoborate – olefin complexes as determined by the quartz spiral method, together with the integral ratios considered to represent their exact stoichiometry.

Of the olefins studied, ethylene is exceptional in forming complexes with silver fluoborate:ethylene ratios of 1:1, 2:3, 1:2, and 1:3, of which the 1:1 and 2:3 complexes are peculiar to ethylene alone. Furthermore, it is observed (*vide infra Dissociation Pressure Data*) that the 2:3 and 1:2 ethylene complexes undergo phase transitions to yield two

TABLE I

Stoichiometry of solid silver fluoborate olefinates

Olefin	Observed stoichiometry	Exact stoichiometry
Ethylene	$AgBF_4.0.960\pm0.022C_2H_4$	$AgBF_4.C_2H_4$
	$AgBF_4.1.489\pm0.014C_2H_4$	$AgBF_4.1.5C_2H_4$
	$AgBF_4.1.993\pm0.011C_2H_4$	$AgBF_4.2C_2H_4$
	$AgBF_4.2.989\pm0.007C_2H_4$	$AgBF_4.3C_2H_4$
Propylene	$AgBF_4.1.996\pm0.007C_3H_6$	$AgBF_4.2C_3H_6$
	$AgBF_4.2.964\pm0.005C_3H_6$	$AgBF_4.3C_3H_6$
1-Butene	$AgBF_4.1.968\pm0.009C_4H_8$	$AgBF_4.2C_4H_8$
	$AgBF_4.2.914\pm0.006C_4H_8$	$AgBF_4.3C_4H_8$
Isobutene	$AgBF_4.1.986\pm0.008C_4H_8$	$AgBF_4.2C_4H_8$
cis-2-Butene	$AgBF_4.1.948\pm0.009C_4H_8$	$AgBF_4.2C_4H_8$
	$AgBF_4.2.927\pm0.006C_4H_8$	$AgBF_4.3C_4H_8$
trans-2-Butene	$AgBF_4.1.859\pm0.009C_4H_8$	$AgBF_4.2C_4H_8$

higher-temperature modifications, giving a total of six distinct silver fluoborate – ethylene complexes. For propylene and the four butenes the lowest complexes, yielding solid silver fluoborate and olefin on decomposition, maintain a 1:2 silver fluoborate:olefin ratio, as reported for the silver perchlorate complexes of cyclohexene and the pinenes (11). The 1:2 complexes of isobutene and *trans*-2-butene were observed not to form 1:3 complexes even at high olefin pressures and low temperatures, which behavior contrasts with that of the other olefins.

The striking one-to-one correspondence of the silver fluoborate:ethylene complex formulae with the 1:1, 2:3, 1:2, and 1:3 series of silver iodide ammoniates observed by Biltz and Stollenwerk (17) suggests isomorphism with similar volume ratios for ethylene molecule:fluoborate lattices and ammonia molecule:iodide lattices. It is, therefore, suggested that the ability of ethylene to form a graded series of silver fluoborate complexes, as opposed to the higher olefins which form, at most, only two complexes, is dependent mainly upon its small size, which permits its incorporation into lattices with only small lattice energy differences. The fewer complexes formed by the other olefins would indicate that in order to incorporate the larger olefins, the necessary lattice expansions are such that only specifically oriented sites can be occupied by olefin molecules to stabilize the complex lattice. The lack of stability of any 1:3 complex between silver fluoborate and isobutylene or *trans*-2-butene probably arises from a blocking of the sites available for such complex formation by the alkyl groups of those olefin molecules already complexed.

Dissociation Pressure Data

In Table II are presented the series of solid silver salt – olefin complexes, values of the constants A and B, with standard errors, for the dissociation pressure equation $\log P$ (mm) $= A - B/(273.16 + t°\ \mathrm{C})$ for complex dissociation to a lower complex or to the silver salt and gaseous olefin, the temperature ranges of experimental investigation, and the complex dissociation pressure (International mm of Hg) computed at 25° C. The constants A and B, together with their standard errors, were derived from the least-squares fit of four to nine experimental pressure–temperature measurements over the indicated temperature ranges. Investigation of the solid $AgBF_4.2$(1-butene) complex was limited to an upper temperature of 37.5° C by fusion of the complex, whilst the $AgBF_4.3$ olefin complexes were necessarily investigated at temperatures below 10° C where the complex dissociation pressures were less than 1 atm.

TABLE II

Dissociation pressure equations for silver salt olefinates

Complex	Vapor pressure constants		Temperature range (°C)	Vapor pressure at 25° C (mm Hg)
	A	*B*		
$AgBF_4.C_2H_4$	8.8835±0.0015	2,319.1±9.9	9.8–49.8	12.75±0.12
$AgBF_4.1.5C_2H_4$ (α)	6.4963±0.0013	1,455.1±19.9	9.8–25.3	41.32±0.29
$AgBF_4.1.5C_2H_4$ (β)	8.8755±0.0010	2,165.1±14.2	25.3–49.8	
$AgBF_4.2C_2H_4$ (α)	6.7095±0.0003	1,309.3±6.6	5.2–27.3	208.10±0.60
$AgBF_4.2C_2H_4$ (β)	7.3226±0.0004	1,493.5±5.3	27.3–50.3	
$AgBF_4.3C_2H_4$	10.8567±0.0001	2,250.7±2.1	−0.3– 8.0	2032.5±0.8*
$AgBF_4.2C_3H_6$	9.2396±0.0020	2,398.4±10.4	0.0–50.3	15.69±0.21
$AgBF_4.3C_3H_6$	10.6762±0.0023	2,168.1±7.1	−46.8– 3.0	2538.8±26.9*
$AgSbF_6.3C_3H_6$	10.7311±0.0031	2,452.4±20.9	0.0–32.3	320.6±4.6
$AgClO_4.2C_3H_6$	7.4016±0.0001	1,551.5±0.2	0.0–25.4	157.78±0.02
$AgBF_4.2C_4H_8$-1	9.7898±0.0013	2,628.5±14.8	14.7–35.4	9.42±0.06
$AgBF_4.3C_4H_8$-1	11.2211±0.0005	2,466.6±10.6	−0.8– 9.0	887.9±2.2*
$AgBF_4.2i$-C_4H_8	9.1134±0.0024	2,435.2±16.2	14.9–51.6	8.83±0.10
$AgBF_4.2cis$-C_4H_8-2	10.0602±0.0022	2,818.1±19.5	24.6–54.6	4.06±0.04
$AgBF_4.3cis$-C_4H_8-2	11.5610±0.0018	2,597.5±27.9	−4.1–10.5	706.7±8.7*
$AgBF_4.2trans$-C_4H_8-2	10.6698±0.0016	2,788.5±10.5	14.5–54.8	20.77±0.17

*Vapor pressures at 25° C from equation.

The relative positions of the linear log P vs. $1/T$ dissociation lines for the six silver fluoborate – ethylene complexes are illustrated in Fig. 1, in which the lines represent the higher complex undergoing dissociation to the next lower complex and gaseous ethylene, the lowest complex yielding silver fluoborate and ethylene. The complexes $AgBF_4.1.5C_2H_4$ and $AgBF_4.2C_2H_4$ are observed to display breaks in their dissociation lines occurring at 25.3 and 27.3° C respectively, indicating phase transitions from a lower-temperature α form to a higher-temperature β modification in each case; the dissociation equation constants, A and B, for both α and β forms of each complex are included in Table II.

A comparison of the propylene dissociation pressures at 25° C for the pairs of complexes $AgClO_4.2C_3H_6$–$AgBF_4.2C_3H_6$ and $AgBF_4.3C_3H_6$–$AgSbF_6.3C_3H_6$ indicates increasing propylene complex stability with these salts in the order $AgClO_4 < AgBF_4 < AgSbF_6$. Since the silver salt – olefin complexes, as represented by Dewar (18), result from direct interaction of olefin with the silver ion and do not involve any large olefin–anion interactions, it is suggested that these observed differences in propylene complex stability arise from differences between the lattice structures of the complexes due to the changing silver ion – anion interactions with changes of anion composition, size, and geometry. The considerably increased stability of the silver fluoborate – propylene complex over that of the perchlorate is unexpected since fluoborate and perchlorate salts are generally isomorphous with similar lattice spacings (19, 20); we are, therefore, forced to conclude that although these complexes may be isomorphous, the energy required for lattice expansion permitting incorporation of propylene is greater for the perchlorates. The even greater stability of the silver hexafluoroantimonate complex most probably arises from the larger radius of the SbF_6^- anion, which increases lattice spacings (21), reduces cation–anion crystal energy terms, and leads to reduction of repulsive energy attending the relatively smaller lattice expansion for incorporation of propylene into the complex.

Thermodynamic Data

In Table III are presented values for the changes of the standard thermodynamic functions with standard errors at 25° C for complex dissociation to the next-lower complex

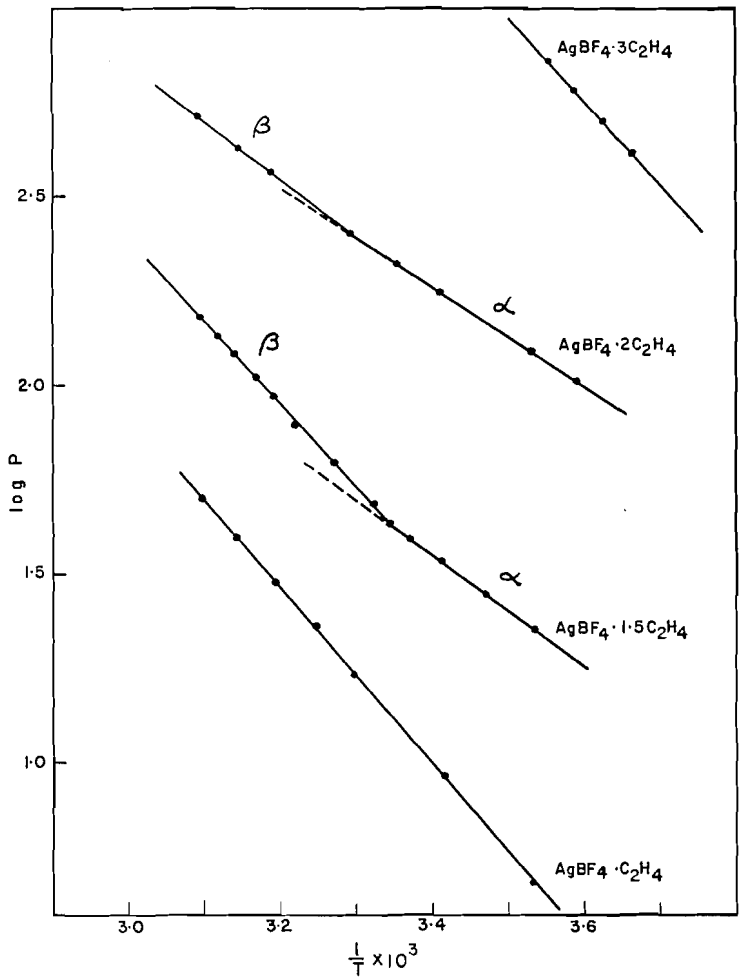

FIG. 1. Stability lines for the solid silver fluoborate – ethylene complexes.

and 1 mole of gaseous olefin at 1 International atm pressure, as represented, for example, by the equation

$$2(AgBF_4.1.5C_2H_4) \rightarrow 2(AgBF_4.C_2H_4) + C_2H_4.$$

These thermodynamic functions, designated by the subscript E, have been derived from the dissociation equation constants in Table II and are expressed in thermochemical calories (1 cal = 4.1840 joules).

In Table IV values are presented for the standard thermodynamic functions at 25° C, designated by subscript D, which represent complex dissociation to solid silver salt and 1 mole of gaseous olefin at 1 International atm pressure, as exemplified by the equation

$$\tfrac{2}{3}(AgBF_4.1.5C_2H_4) \rightarrow \tfrac{2}{3}AgBF_4 + C_2H_4.$$

The occurrence of transitions at so nearly the same temperature in both the $AgBF_4.1.5C_2H_4$ and $AgBF_4.2C_2H_4$ complexes, for which the enthalpy change differences ΔH_D^0 $(1.5\beta) - \Delta H_D^0$ $(1.5\alpha) = +1083$ and ΔH_D^0 $(2\beta) - \Delta H_D^0$ $(2\alpha) = +1023$ cal/mole of ethylene are both positive of the same magnitude, is indicative of similar constitutional

TABLE III

Thermodynamic functions for silver salt olefinate equilibria at 25° C

Complex	ΔH_E^0 (cal/mole)	ΔS_E^0 (cal/mole deg)	ΔF_E^0 (cal/mole)
$AgBF_4.C_2H_4$	10,611±45	27.466±0.007	2,422±6
$AgBF_4.1.5C_2H_4$ (α)	6,658±91	16.543±0.006	1,726±4
$AgBF_4.1.5C_2H_4$ (β)	9,907±65	27.429±0.005	
$AgBF_4.2C_2H_4$ (α)	5,991±30	17.518±0.001	768±2
$AgBF_4.2C_2H_4$ (β)	6,834±24	20.324±0.002	
$AgBF_4.3C_2H_4$	10,299±9	36.494±0.000	−582±0
$AgBF_4.2C_3H_6$	10,974±47	29.095±0.009	2,299±8
$AgBF_4.3C_3H_6$	9,921±32	35.669±0.010	−714±6
$AgSbF_6.3C_3H_6$	11,221±96	35.920±0.014	511±8
$AgClO_4.2C_3H_6$	7,099±1	20.685±0.000	932±0
$AgBF_4.2C_4H_8$-1	12,027±68	31.613±0.006	2,601±4
$AgBF_4.3C_4H_8$-1	11,286±49	38.162±0.002	−92±1
$AgBF_4.2i$-C_4H_8	11,143±74	28.518±0.011	2,640±7
$AgBF_4.2cis$-C_4H_8-2	12,895±89	32.850±0.010	3,100±6
$AgBF_4.3cis$-C_4H_8-2	11,885±127	39.717±0.008	43±7
$AgBF_4.2trans$-C_4H_8-2	12,759±48	35.640±0.007	2,133±5

TABLE IV

Thermodynamic functions for silver salt olefinate dissociation at 25° C

Complex	ΔH_D^0 (cal/mole)	ΔS_D^0 (cal/mole deg)	ΔF_D^0 (cal/mole)
$AgBF_4.C_2H_4$	10,611	27.466	2,422
$AgBF_4.1.5C_2H_4$ (α)	9,293	23.825	2,190
$AgBF_4.1.5C_2H_4$ (β)	10,376	27.454	
$AgBF_4.2C_2H_4$ (α)	8,468	22.248	1,835
$AgBF_4.2C_2H_4$ (β)	9,491	25.671	
$AgBF_4.3C_2H_4$	9,078	26.997	1,029
$AgBF_4.2C_3H_6$	10,974	29.095	2,299
$AgBF_4.3C_3H_6$	10,623	31.286	1,295
$AgBF_4.2C_4H_8$-1	12,027	31.613	2,601
$AgBF_4.3C_4H_8$-1	11,780	33.796	1,703
$AgBF_4.2i$-C_4H_8	11,143	28.518	2,640
$AgBF_4.2cis$-C_4H_8-2	12,895	32.850	3,100
$AgBF_4.3cis$-C_4H_8-2	12,558	35.139	2,081
$AgBF_4.2trans$-C_4H_8-2	12,759	35.640	2,133

changes occurring in both complexes at the transition points and of probable isomorphism of the ionic lattices of the 1.5α and 2α forms and of the 1.5β and 2β forms. This conclusion is supported by the good correlation with the $\Delta S_D^0/\Delta H_D^0$ regression line for the 1:2 complexes (*vide infra*) shown by the ΔS_D^0 and ΔH_D^0 functions of both the 1.5β and 2β ethylene complexes and the almost equal deviations from that regression line exhibited by the functions for the 1.5α and 2α modifications.

In Fig. 2 are shown the two linear $\Delta S_D^0/\Delta H_D^0$ correlations furnished by the thermodynamic functions for the silver salt.2 olefin and silver salt.3 olefin complexes, from which it is seen that the 1:3 complexes invariably present higher ΔS_D^0 and slightly lower ΔH_D^0 values than the corresponding 1:2 complexes. The $\Delta S_D^0/\Delta H_D^0$ regression line for the 1:2 complexes, if meaningful, extending over the wide stability range from $AgClO_4.2C_3H_6$, $AgBF_4.2C_2H_4$ (β), $AgBF_4.1.5C_2H_4$ (β) to $AgBF_4.2$ *cis*-2-butene suggests a similar ionic lattice type for all these complexes with sufficient spatial extension to accommodate

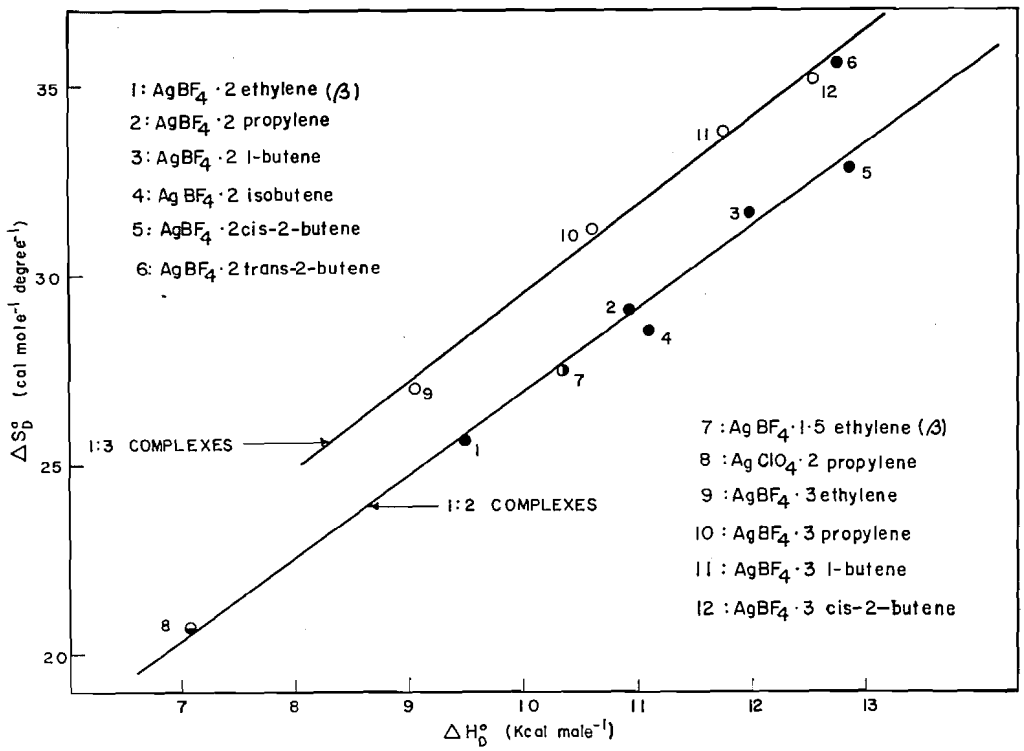

FIG. 2. Entropy–enthalpy plot for the silver salt olefinates.

olefins as large as 1-butene and *cis*-2-butene. The generally increasing ΔS_D^0 and ΔH_D^0 values exhibited by the larger olefins arise from increasing Ag^+–olefin attractive energies, which progressively limit the olefin freedom. *trans*-2-Butene, however, with a normal ΔH_D^0 value equal to that of *cis*-2-butene, presents an anomalously high ΔS_D^0 value, which is most reasonably attributed to its geometrical incompatability with its lattice environment leading to additional severe configurational restrictions. The lower values of ΔS_D^0 and ΔH_D^0 for $AgClO_4.2C_3H_6$, compared with the isomorphous $AgBF_4.2C_3H_6$, arise from increased repulsive perchlorate ion – olefin interactions (as compared with fluoborate ion – olefin interactions) which diminish the attractive orienting constraint of the silver ion – olefin bond. The source of these increased perchlorate lattice repulsions, leading to the enthalpy change reduction of 4000 cal/mole propylene, probably lies in the increased energy of perchlorate lattice expansion and anion displacement required to extend or break the donor–acceptor contacts of the perchlorate oxygen atoms with the electrophilic silver cation. This explanation is similar to that proposed by Sharp and Sharpe (21) for the aromatic complexes of silver fluoborate and perchlorate, except that the donor–acceptor bonding suggested by us is considered to approximate energetically more nearly to hydration and ammination (17) rather than to strong covalent bond formation.

The $\Delta S_D^0/\Delta H_D^0$ regression line for the 1:3 complexes is indicative of a common lattice type in which increases of silver ion – olefin bond strength, reflected in higher ΔH_D^0 values, are associated with increasing olefin restrictions and increased ΔS_D^0 values. The general displacement to higher entropy values of the $\Delta S_D^0/\Delta H_D^0$ line for the 1:3 complexes almost certainly results from the more severe orientation limitations of the olefin imposed

by the higher coordination of the silver cation; the lack of 1:3 complexes with isobutylene and *trans*-2-butene reflects their geometrical inability to pack within the space adjacent to the silver ion.

Infrared investigation of the fluorolube mulls of the $AgBF_4$.2 olefin complexes revealed absorption bands perturbed to lower frequencies for the olefin double-bond stretch vibrations in all complexes from ethylene to *trans*-2-butene. Although the band intensity for the ethylene complex was very low, that for the other olefins, including *trans*-2-butene, was moderate, indicating a small perturbation from central symmetry for complexed ethylene, but considerable non-central distortion of the complexed *trans*-2-butene, with non-symmetric ion fields at the double bond in both cases.

In Fig. 3 is illustrated the linear correlation of $\Delta\nu$ ($\nu_{\text{uncomplexed}} - \nu_{\text{complexed}}$), the olefin double-bond stretch frequency perturbation due to complex formation, with the olefin

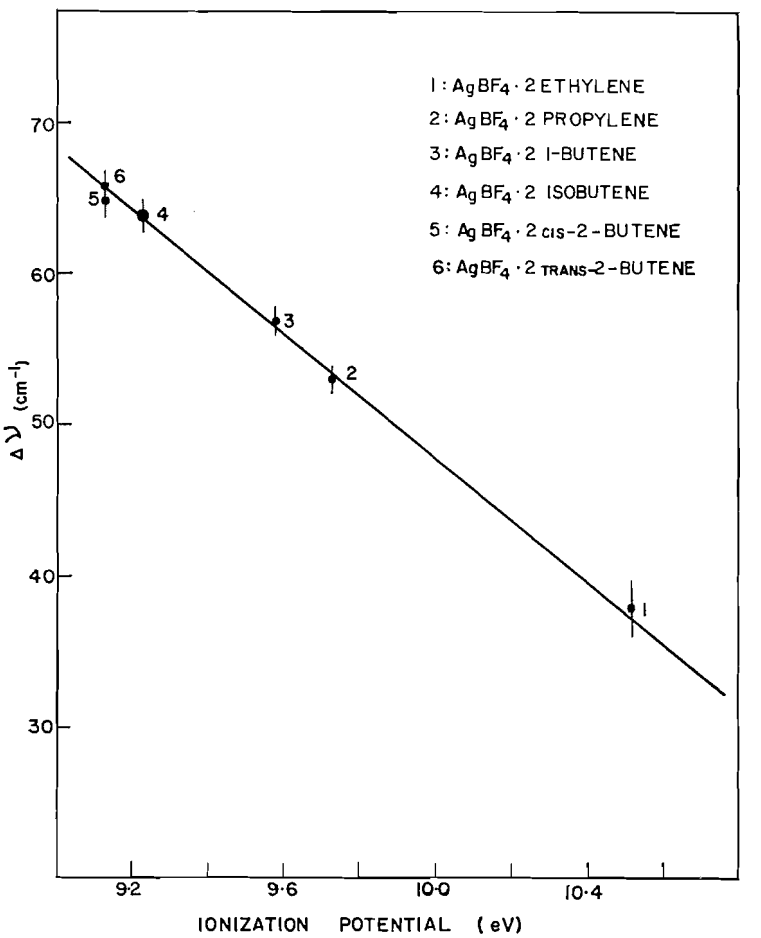

FIG. 3. Complexed olefin double-bond stretch perturbation – olefin ionization potential correlation.

ionization potential for the six solid 1:2 complexes. Values for $\nu_{\text{uncomplexed}}$ were determined from the infrared stretch frequencies of the olefins dissolved in carbon tetrachloride, except for the infrared-inactive ethylene and *trans*-2-butene, for which the Raman values

were used (22). The ionization potentials were taken from the work of Watanabe (23). The correlation shows that, with decreasing ionization potential, i.e. with increasing olefin basicity, the electrophilic silver cation effects increasingly larger perturbations of the olefin double-bond stretch frequency through the formation of stronger Ag^+–olefin bonds. This remarkably smooth linear correlation, involving the stretch frequency perturbation of olefins complexed in a solid ionic lattice and the ionization potentials in the unperturbed gaseous state, indicates that the silver ion – olefin bonds within the complexes must be fully formed or saturated and that other steric and lattice factors dependent upon olefin geometry are smaller and do not sensibly affect the Ag^+–olefin bonds. This point is further supported by the substantial agreement of the infrared shifts 65 and 66 cm^{-1} for *cis*- and *trans*-2-butene in the solid silver fluoborate complexes with the 62 and 65 cm^{-1} Raman shifts (24) for complex formation of these same olefins in aqueous silver nitrate solution, for which the silver cation environment differs considerably.

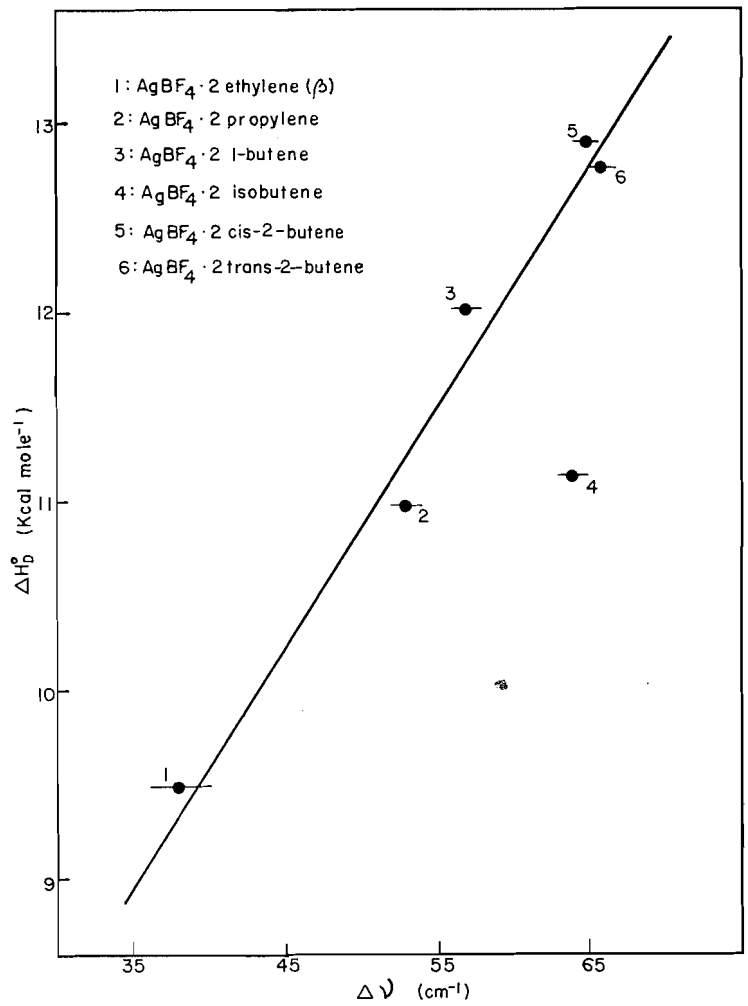

FIG. 4. Enthalpy – double-bond stretch perturbation plot for silver fluoborate.2 olefinates.

Since the Ag^+–olefin interaction energy in the solid silver fluoborate.2 olefin complexes will be some continuous function of $\Delta\nu$, and the correlation of Fig. 3 indicates that geometrical and steric factors little effect $\Delta\nu$, and thus the Ag^+–olefin bond energy, it is to be expected that the value of ΔH_D^0 for complex formation would be predominately determined by the Ag^+–olefin bond energy and should, therefore, correlate with the observed $\Delta\nu$ values. That this is so is illustrated in Fig. 4, where the ΔH_D^0 values for the 1:2 complexes are seen to be linearly related to the corresponding $\Delta\nu$ values. The ΔH_D^0 functions for the ethylene, propylene, 1-butene, and *cis*- and *trans*-2-butenes deviate from the regression line by less than 250 cal/mole of olefin, which is within the 95% confidence limit of error for the ΔH_D^0 values, whilst the ΔH_D^0 for the isobutylene complex deviates significantly by some 1500 cal/mole of olefin below that predicted from its $\Delta\nu$ value. In so far as isobutylene exhibits no deviation in Fig. 3, the low ΔH_D^0 value must be considered a real effect resulting from steric repulsions between the ionic lattice and the isobutylene molecule in its particular geometrical configuration. Since the ΔH_D^0 and ΔS_D^0 for the isobutylene complex correlate in Fig. 2, the reduced ΔH_D^0 value due to lattice repulsion must arise in such a manner that the complexed isobutylene is less severely restricted by the repulsion; this behavior sharply contrasts with that of the *trans*-2-butene complex, which presents a normal ΔH_D^0 but a large ΔS_D^0.

X-Ray diffraction studies now being pursued should aid in the elucidation of the difference between the various solid complexes since a knowledge of the lattice structures could permit a better estimation of the contribution to ΔH_D^0 effected by lattice changes.

ACKNOWLEDGMENTS

The contribution of D. Cook and C. D. Anderson, who have determined the infrared spectra of the complexes, is gratefully acknowledged by the authors.

REFERENCES

1. W. F. EBERZ, H. J. WELGE, D. M. YOST, and H. J. LUCAS. J. Am. Chem. Soc. **59**, 45 (1937).
2. S. WINSTEIN and H. J. LUCAS. J. Am. Chem. Soc. **60**, 836 (1938).
3. H. J. LUCAS, R. S. MOORE, and D. PRESSMAN. J. Am. Chem. Soc. **65**, 227 (1943).
4. H. J. LUCAS, F. W. BILLMEYER, JR., and D. PRESSMAN. J. Am. Chem. Soc. **65**, 230 (1943).
5. F. R. HEPNER, K. N. TRUEBLOOD, and H. J. LUCAS. J. Am. Chem. Soc. **74**, 1333 (1952).
6. K. N. TRUEBLOOD and H. J. LUCAS. J. Am. Chem. Soc. **74**, 1338 (1952).
7. R. M. KEEFER, L. J. ANDREWS, and R. E. KEPNER. J. Am. Chem. Soc. **71**, 3906 (1949).
8. J. G. TRAYNHAM and M. F. SEHNERT. J. Am. Chem. Soc. **78**, 4024 (1956).
9. J. G. TRAYNHAM and J. R. OLECHOWSKI. J. Am. Chem. Soc. **81**, 571 (1959).
10. P. BRANDT. Acta Chem. Scand. **13**, 1639 (1959).
11. A. E. COMYNS and H. J. LUCAS. J. Am. Chem. Soc. **79**, 4339 (1957).
12. H. G. SMITH and R. E. RUNDLE. J. Am. Chem. Soc. **80**, 5075 (1958).
13. F. S. MATHEWS and W. N. LIPSCOMB. J. Phys. Chem. **63**, 845 (1959).
14. A. W. FRANCIS. J. Am. Chem. Soc. **73**, 3709 (1951).
15. E. R. GILLILAND, J. E. SEEBOLD, J. R. FITZHUGH, and P. S. MORGAN. J. Am. Chem. Soc. **61**, 1960 (1939).
16. G. A. OLAH and H. W. QUINN. J. Inorg. & Nuclear Chem. **14**, 295 (1960).
17. W. BILTZ and W. STOLLENWERK. Z. anorg. u. allgem. Chem. **114**, 174 (1920).
18. M. J. S. DEWAR. Bull. soc. chim. France, **18**, C79 (1951).
19. L. J. KLINKENBERG and J. A. A. KETELAAR. Rec. trav. chim. **54**, 959 (1935).
20. L. J. KLINKENBERG. Rec. trav. chim. **56**, 36 (1937).
21. D. W. A. SHARP and A. G. SHARPE. J. Chem. Soc. 1855 (1956).
22. K. W. F. KOHLRAUSCH. Ramanspectrum. Akademische Verlagsgesellschaft Becker and Eiler, Leipzig. 1943. pp. 119, 314.
23. K. WATANABE, T. NAKAYAMA, and J. MOTTL. Final report on ionization potential of molecules by a photoionization method. University of Hawaii, Honolulu, Hawaii. 1959.
24. H. J. TAUFEN, M. J. MURRAY, and T. F. CLEVELAND. J. Am. Chem. Soc. **63**, 3500 (1941).

STEREOCHEMISTRY OF ARSENIC

PART III. *o*-PHENYLENEDIARSINE OXYCHLORIDE[1]

W. R. CULLEN AND J. TROTTER

Department of Chemistry, University of British Columbia, Vancouver, British Columbia

Received February 1, 1962

ABSTRACT

Crystals of *o*-phenylenediarsine oxychloride, $C_6H_4As_2Cl_2O$, are monoclinic with four molecules in a unit cell of dimensions $a = 14.50$, $b = 8.38$, $c = 7.66$ Å, $\beta = 105.8°$, space group $C2/c$. The structure has been determined from projections along the b and c axes. Each molecule is situated on a 2-fold symmetry axis and is planar except for the chlorine atoms, which lie one on either side of the plane of the other atoms. The values of the bond lengths and valency angles have been obtained. Abnormal valency angles at the arsenic and oxygen atoms are the result of their presence in the five-membered ring, and the unusual stability of the molecule in spite of these angles can be interpreted in terms of aromatic character, involving $d\pi-p\pi$ bonding. The intermolecular separations correspond to normal van der Waals interactions.

EXPERIMENTAL

o-Phenylenediarsine oxychloride (Fig. 1) was prepared by reducing a solution of *o*-phenylenediarsonic acid in concentrated hydrochloric acid with sulphur dioxide (1). The diarsonic acid was prepared by the reaction

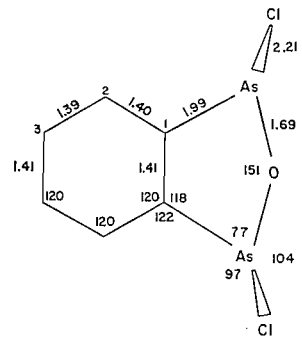

FIG. 1. Measured bond lengths (Å) and valency angles (degrees).

of sodium arsenite solution with diazotized *o*-aminophenylarsonic acid. The crude oxychloride was purified with charcoal and by recrystallization from carbon disulphide. The final product consisted of colorless plates, m.p. 146–149° (lit. value, 148°), with the (100) face developed.

The unit cell dimensions and space group were determined from rotation and oscillation photographs of crystals rotating about the *b*- and *c*-axes, and *h*0*l*, *h*1*l*, and *hk*0 Weissenberg films. The density was determined by displacing carbon tetrachloride from a density bottle.

The crystal data are: $C_6H_4As_2Cl_2O$; M, 312.8; m.p. 146–149°. Monoclinic, $a = 14.50\pm0.05$, $b = 8.38\pm0.02$, $c = 7.66\pm0.02$ Å, $\beta = 105.8\pm0.5°$. Volume of the unit cell = 896 Å^3. d_c (with $Z = 4$) = 2.31, $d_m \sim 2.4$ g cm^{-3}. Absorption coefficient for X rays: $\lambda = 1.542$ Å, $\mu = 143$ cm^{-1}. Total number of electrons per unit cell = $F(000) = 592$. Absent spectra: *hkl* when $(h+k)$ is odd, *h*0*l* when l is odd. Space group is either C_s^4—Cc or C_{2h}^6—$C2/c$.

The intensities of the *h*0*l* and *hk*0 reflections were recorded on Weissenberg films for a crystal rotating in turn about the *b*- and *c*-axes, with Cu K_α radiation, the multiple-film technique being used to correlate strong and weak reflections. The range of intensities measured was about 5000 to 1, the estimates being made visually. The crystal cross sections perpendicular to the rotation axes were 0.5×0.1 mm, but no absorption

[1]*Part I: W. R. Cullen and J. Trotter. Can. J. Chem.* **39**, *2602 (1961). Part II: J. Trotter. J. Chem. Soc. In press.*

corrections were applied; there may, therefore, be some inaccuracies in the measured structure factors as a result of absorption errors. The structure amplitudes were derived by the usual formulae for a mosaic crystal, the absolute scale being established later by correlation with the calculated structure factors. Sixty-three independent $h0l$ reflections and 70 $hk0$ reflections were observed, representing 91% and 83% respectively of the possible numbers observable with Cu K_α radiation.

Structure Analysis

Projection down [010]

Space group $C2/c$ requires that the *o*-phenylenediarsine oxychloride molecule possesses a 2-fold symmetry axis which is coincident with the space group symmetry axis, while Cc imposes no restrictions on the molecular symmetry. The As–As vector was clearly resolved on the *b*-axis Patterson map, coordinates were obtained for the As atoms, and structure factors were calculated with the origin taken midway between two arsenic atoms. A Fourier series was then summed, using as coefficients measured structure amplitudes and calculated signs. Since the phases were based on arsenic contributions only, the resulting electron-density map was necessarily centrosymmetric. Good resolution of the chlorine atoms indicated that space group $C2/c$ was the correct one (absence of a center of symmetry would have resulted in four half-chlorine peaks, the true ones and another two centrosymmetrically related ones). Coordinates were obtained for all the atoms in the molecule, those for the carbon atoms by assuming C—C = 1.40 Å, and structure factors were calculated for all the $h0l$ reflections, using the scattering factors for arsenic, carbon, and oxygen of Berghuis *et al.* (2), that for arsenic being corrected for anomalous dispersion (3), and Tomiie and Stam's (4) scattering curve for chlorine. A second F_o synthesis was computed, and the resulting electron-density map (Fig. 2) indicated small shifts in some of the atomic coordinates. Structure factors were recalculated, and

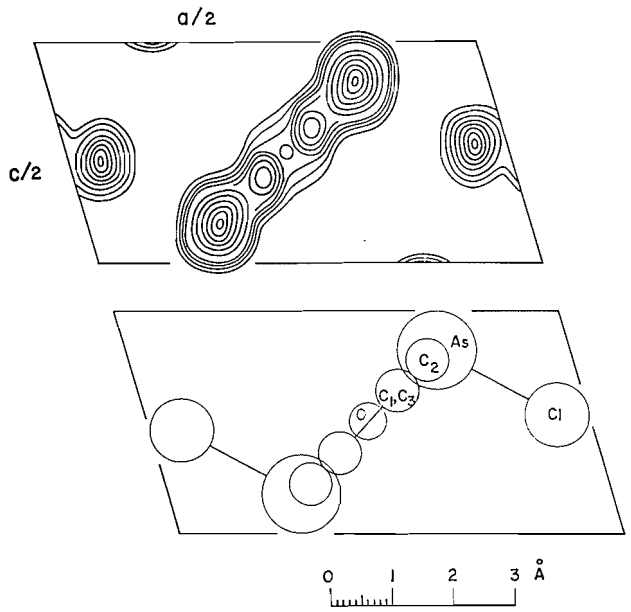

FIG. 2. Electron-density projection along the *b*-axis, with contours at intervals of 2 e Å^{-2}, starting at 4 e Å^{-2}, except at the arsenic atom, where contours above 10 are at intervals of 5 e Å^{-2}.

as no reflections had changed sign refinement was complete. Best agreement between measured and calculated structure factors (discrepancy factor = 0.16 for the observed reflections) was obtained by using a temperature factor of the form

$$\exp -\{3.7 \sin^2\theta/\lambda^2 + 0.0152l^2\}.$$

This corresponds to anisotropic thermal vibrations with the direction of maximum vibration parallel to the *c*-axis. This is probably a real effect, which does not appear to be due to the omission of a correction for absorption, as no thermal anisotropy was indicated for the $hk0$ zone, although the crystal cross sections for both zones were similar. Measured and calculated structure factors are listed in Table I.

Projection down [001]

Coordinates for the As atom were derived from the Patterson projection, and further analysis proceeded by successive F_o syntheses. The final electron-density projection along the *c*-axis is shown in Fig. 3, and

TABLE I

Measured and calculated structure factors

$h\ k\ l$	F_o	F_c	$h\ k\ l$	F_o	F_c	$h\ k\ l$	F_o	F_c	$h\ k\ l$	F_o	F_c
2 0 0	72	+ 79	0 0 4	29	− 28	7 1 0	20	− 16	7 5 0	40	− 48
4	69	− 62	2	9	+ 6	9	62	+ 74	9	42	+ 57
6	136	−152	4	87	+107	11	34	+ 26	11	25	+ 12
8	43	+ 17	6	24	− 22	13	<7	− 1	13	8	− 11
10	127	+119	8	41	− 45	15	<7	− 9	15	14	− 18
12	10	− 12	10	20	− 19	17	5	− 2	0 6 0	140	+139
14	15	− 20	12	8	+ 9	0 2 0	183	−177	2	7	− 1
16	37	− 37	$\overline{14}$	10	+ 29	2	8	+ 22	4	56	+ 42
$\overline{18}$	<5	+ 14	$\overline{16}$ 0 6	22	+ 15	4	44	+ 32	6	67	− 64
$\overline{18}$ 0 2	28	+ 21	$\overline{14}$	15	+ 10	6	55	+ 58	8	13	+ 9
$\overline{16}$	11	+ 23	$\overline{12}$	<9	+ 1	8	10	− 15	10	50	+ 57
$\overline{14}$	64	− 64	$\overline{10}$	72	− 63	10	59	− 57	12	<6	− 6
$\overline{12}$	<9	− 15	$\overline{8}$	23	− 15	12	10	+ 15	14	<5	− 9
$\overline{10}$	25	+ 13	$\overline{6}$	15	− 15	14	11	+ 11	1 7 0	7	+ 5
$\overline{8}$	131	+138	$\overline{4}$	43	+ 46	16	20	+ 21	3	7	− 1
$\overline{6}$	36	− 29	$\overline{2}$	23	+ 6	1 3 0	151	−158	5	8	0
$\overline{4}$	280	−295	0	50	− 56	3	120	+111	7	7	+ 1
$\overline{2}$	166	−178	2	<9	+ 1	5	91	+ 90	9	8	+ 6
0	70	− 69	4	8	+ 10	7	78	+ 79	11	<6	+ 4
2	201	+252	6	18	+ 36	9	104	−122	13	<5	+ 1
4	18	− 20	8	13	− 7	11	61	− 56	0 8 0	75	− 65
6	65	− 75	$\overline{10}$	26	− 19	13	<7	− 2	2	13	+ 1
8	49	− 61	$\overline{14}$ 0 8	11	+ 14	15	15	+ 23	4	27	+ 25
10	18	+ 21	$\overline{12}$	11	+ 9	17	14	+ 14	6	31	+ 36
12	71	+ 72	$\overline{10}$	6	+ 6	0 4 0	89	− 79	8	7	− 3
14	11	− 11	$\overline{8}$	23	− 22	2	8	− 25	10	30	− 30
$\overline{16}$	11	− 9	$\overline{6}$	9	− 2	4	14	− 16	12	<3	+ 5
$\overline{18}$ 0 4	7	+ 11	$\overline{4}$	9	+ 10	6	<6	+ 5	1 9 0	27	− 27
$\overline{16}$	24	+ 17	$\overline{2}$	7	+ 10	8	15	− 7	3	15	+ 21
$\overline{14}$	7	+ 14	0	<8	+ 1	10	9	− 14	5	16	+ 17
$\overline{12}$	75	− 72	2	15	− 21	12	<8	+ 10	7	17	+ 20
$\overline{10}$	6	− 1	4	5	+ 2	14	8	− 1	9	10	− 25
$\overline{8}$	58	+ 46	6	<5	+ 4	16	<5	+ 5	0 10 0	7	+ 5
$\overline{6}$	162	+148	1 1 0	39	+ 29	1 5 0	83	+ 71	2	6	0
$\overline{4}$	63	+ 45	3	64	− 68	3	43	− 55	4	<5	+ 1
$\overline{2}$	131	−126	5	4	− 5	5	54	− 45	6	<4	+ 1

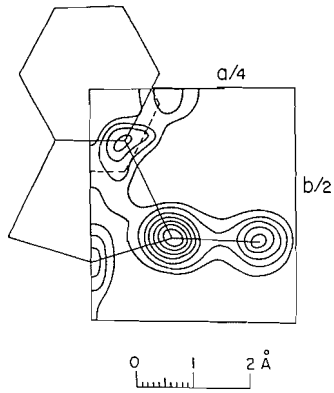

FIG. 3. Electron-density projection along the *c*-axis; contours at arbitrary intervals.

measured and calculated structure factors are included in Table I. No thermal anisotropy was indicated, an isotropic temperature factor with $B = 3.7$ Å^2 giving a discrepancy factor of 0.16 for the observed reflections.

Coordinates and Molecular Dimensions

The final positional parameters are listed in Table II, x, y, and z being fractions of the unit cell edges.

TABLE II

Final positional parameters

Atom	x	y	z
As	0.1004	0.1766	0.4125
Cl	0.2138	0.1742	0.2687
O	0	0.127	0.250
C1	0.043	0.387	0.320
2	0.086	0.531	0.389
3	0.043	0.674	0.320

The bond distances and valency angles in the molecule, calculated from the coordinates of Table II, are shown in Fig. 1. The best plane through the As, O, and C atoms has equation

$$0.5178X' - 0.8555Z' + 1.6383 = 0,$$

where X' and Z' are coordinates in Å units referred to orthogonal axes a', b, and c, and there are no significant deviations of As, O, and C atoms from this plane (maximum $\Delta = 0.01$ Å). The chlorine atoms, however, lie one above and one below the plane at perpendicular distances from it of 2.14 Å.

The standard deviations of the atomic positions (5) are $\sigma(x) = \sigma(y) = \sigma(z) = 0.006$ Å for As, 0.014 Å for Cl, and 0.04 Å for C. For the oxygen atom, the x- and z-parameters are fixed by symmetry, and $\sigma(y) = 0.03$ Å.

Intermolecular Distances

All the intermolecular contacts correspond to normal van der Waals interactions. The perpendicular distance between molecular planes is 3.28 Å, but no atoms overlap directly, the shortest contacts being C—C = 3.87, As—Cl = 4.04, O—O = 4.38 Å. In the b-direction, the shortest separation is O—C = 3.86 Å.

DISCUSSION

The molecule is completely planar within the limits of experimental error, except for the chlorine atoms, which lie one on either side of the plane of the other atoms.

Differences between chemically equivalent bond lengths and valency angles are not significant, the mean values being (with standard deviations):

$$\begin{aligned} \text{As—Cl} &= 2.21 \pm 0.01_5 \text{ Å} \\ \text{As—O} &= 1.69 \pm 0.01 \text{ Å} \\ \text{As—C} &= 1.99 \pm 0.04 \text{ Å} \\ \text{C—C} &= 1.40 \pm 0.03 \text{ Å} \end{aligned}$$

$$\begin{aligned}
\angle \text{Cl—As—O} &= 104\pm\tfrac{1}{2}^\circ \\
\angle \text{Cl—As—C} &= 97\pm1^\circ \\
\angle \text{O—As—C} &= 77\pm1\tfrac{1}{2}^\circ \\
\angle \text{As—O—As} &= 151\pm1^\circ \\
\angle \text{As—C—C} &= 120\pm4^\circ \\
\angle \text{C—C—C} &= 120\pm3^\circ.
\end{aligned}$$

The As—Cl bond distances are only slightly greater than those reported for arsenic trichloride (6) (2.16 Å), and chlorodimethylarsine (7) (2.18 Å) and the As—C distances are very similar to those in trimethylarsine (8) (1.98 Å) and bromodiphenylarsine (9) (1.99 Å). The only As—O distances which are available for comparison are those in arsenic trioxide, As_4O_6 (10, 11) (1.78 Å), and in the arsenate ion (11, 12) (1.75 Å); the corresponding bond lengths in *o*-phenylenediarsine oxychloride are shorter than these.

The general configuration around the arsenic atoms is similar to the arrangement in other trivalent arsenic compounds, with three bonds directed pyramidally, and the lone pair completing a tetrahedron. The angles between the bonds are usually in the range 95–105°, and in *o*-phenylenediarsine oxychloride the angles which are external to the five-membered ring have values in this range, ∠ Cl—As—O = 104° and Cl—As—C = 97°. The formation of the five-membered ring, however, results in a considerable reduction in the ∠ O—As—C valency angle (77°). In addition, the oxygen valency angle (151°) is very much larger than the normal value of 105° (in As_4O_6 the As—O—As angle is 128°). These abnormal valency angles are made more remarkable by the fact that the compound is unusually stable, the As—O—As unit being unattacked by hot concentrated acid, although the bonds can be broken by thionyl chloride to give tetrachloro-*o*-phenylenediarsine (13). The stability, planarity, and unusual valency angles of the five-membered ring suggest that this system might have some degree of aromatic character. The large oxygen valency angle suggests that the oxygen is approaching a state of *sp* hybridization, and that the two lone pairs on the oxygen are in approximately $p\pi$ orbitals. If this is the case, then $d\pi$–$p\pi$ bonding could occur using unoccupied 4*d* orbitals on the arsenic atoms, accounting for the shorter As—O distance in the oxychloride in comparison with the oxide and with the arsenate ion. This $d\pi$–$p\pi$ bonding might also be expected to occur between the arsenic atoms and the phenylene π-electrons, resulting in an extended aromatic system. No shortening of the As—C bonds below normal values has been observed, but these distances have been determined with rather less precision than the As—O length.

We are indebted to the National Research Council of Canada for financial support.

REFERENCES

1. L. Kalb. Ann. **423**, 39 (1921).
2. J. Berghuis, IJ. M. Haanappel, M. Potters, B. O. Loopstra, C. H. MacGillavry, and A. L. Veenendaal. Acta Cryst. **8**, 478 (1955).
3. C. H. Dauben and D. H. Templeton. Acta Cryst. **8**, 841 (1955).
4. Y. Tomiie and C. H. Stam. Acta Cryst. **11**, 126 (1958).
5. D. W. J. Cruickshank. Acta Cryst. **2**, 65 (1949).
6. P. Kisliuk and C. H. Townes. J. Chem. Phys. **18**, 1109 (1950).
7. H. A. Skinner and L. E. Sutton. Trans. Faraday Soc. **40**, 164 (1944).
8. H. D. Springall and L. O. Brockway. J. Am. Chem. Soc. **60**, 996 (1938).
9. J. Trotter. J. Chem. Soc. In press.
10. C. S. Lu and J. Donohue. J. Am. Chem. Soc. **66**, 818 (1944).
11. Tables of interatomic distances and configurations in molecules and ions. Chem. Soc. Special Publ. No. 11. 1958.
12. L. Helmholz and R. Levine. J. Am. Chem. Soc. **64**, 354 (1942).
13. J. Chatt and F. G. Mann. J. Chem. Soc. 610 (1939).

THE CHEMICAL COMPOSITION OF THE WOOD EXTRACTIVES OF SORBUS DECORA (SARG.) SCHNEID.[1]

N. NARASIMHACHARI[2] AND E. VON RUDLOFF
National Research Council of Canada, Prairie Regional Laboratory, Saskatoon, Saskatchewan
Received February 27, 1962

ABSTRACT

The wood of the showy mountain ash was found to contain about 3% acetone-soluble material. The major constituents of the extract were a polymorphous xyloside of (+)-dimethoxyisolariciresinol, the recently discovered hydroxy diphenyls aucuparin and methoxy-aucuparin, and fatty acid esters of β-sitosterol, another phytosterol, and of untractable phenolic material. Small amounts of free β-sitosterol and a mixture of hydrocarbons as well as traces of an unknown leucoanthocyanidin were also isolated. The xyloside predominated in the sapwood, whereas the aucuparins were found mainly in the heartwood. Gas–liquid chromatography was instrumental in the detection and separation of the aucuparins.

The wood extractives of the showy mountain ash (*Sorbus decora* (Sarg.) Schneid.) have been investigated as part of a continuing study of the chemical composition of the wood and bark of trees and shrubs found in the Prairie provinces. It is a small- to medium-sized tree found from the Atlantic coast westward into Manitoba. The wood is not used commercially and the literature has no references to its chemical composition. Professor H. Erdtman (1) is studying the heartwood constituents of the European mountain ash (*Sorbus aucuparia* L.) and it was at his suggestion that the North American species was investigated. Recently, Erdtman *et al.* (2) have isolated from *S. aucuparia* two new hydroxy diphenyls, aucuparin (4-hydroxy-3,5-dimethoxy diphenyl, m.p. 101° C) and methoxy aucuparin (4-hydroxy-3,5,2′-trimethoxy diphenyl, m.p. 122° C). The two aucuparins, and a xyloside* of melting point 163.5–164° C, $[\alpha]_D$ +41°, obtained from the same wood, were kindly given to us and were instrumental in the identification of the same constituents in *S. decora*.

The freshly milled wood of *S. decora* was found to contain about 3% of acetone-soluble material. The extract was fractionated into petrol-, ether-, ethyl-acetate-, and water-soluble constituents. When further fractionation was carried out, considerable difficulty was encountered because the hydroxy diphenyls could not be extracted quantitatively into aqueous alkali and were present in all but the water-soluble portion. A sparingly soluble sodium salt was obtained from which the two aucuparins were obtained as a mixture. Chromatography gave only partial separations and distillation *in vacuo* also gave only a mixture. The two diphenyls could be separated by fractional crystallization, but since their mixed melting points did not show a true depression it was difficult to determine their degree of purity. Therefore, their separation by means of gas–liquid chromatography (GLC) was investigated, when it was found that the free phenols, their methyl ethers, or their acetates could be separated on a 3-ft SE-30 silicone polymer column at 230° C. This technique was used in all subsequent work to analyze the various fractions for their content of the aucuparins and also to isolate small amounts of the pure compounds. The properties of the pure compounds thus obtained agreed in all respects with those reported by Erdtman *et al.* (2).

[1]*Issued as N.R.C. No. 6826.*
[2]*National Research Council of Canada Postdoctorate Fellow, 1960–1961. Present address: Hindustani Antibiotics Ltd., Pimpri, Poona, India.*
*ADDED IN PROOF: *β-xyloside of (+)-dimethoxyisolariciresinol (H. Erdtman et al. Acta Chem. Scand. In press).*

The neutral components of the petrol- (and ether-) soluble fractions were found to consist mainly of a mixture of fatty acid esters and free β-sitosterol. The ester fraction was saponified and from the non-saponifiable portion β-sitosterol, a small amount of a phytosterol, m.p. 162–163° C, and a hydrocarbon mixture were isolated. The saponifiable portion was acidified, methylated, and analyzed by GLC (3). Peaks corresponding to myristic, palmitic, palmitoleic, stearic, oleic, and linoleic acids in the area ratio of 1:9.2:1.0:1.8:2.8:1.4 were recorded.

The water-soluble portion deposited white crystals on standing. Recrystallization gave a product, m.p. 164–165° C, $[\alpha]_D$+41°. The mixed melting point with the xyloside sent by Erdtman was undepressed and hydrolysis with dilute acid gave an amorphous aglycone and xylose (paper chromatography). The infrared spectrum of the aglycone corresponded to those of lignans. When the wood extract from an immature tree having no heartwood was fractionated, a xyloside of melting point 120–121° C, $[\alpha]_D$+41°, was isolated, but by seeding with the xyloside, m.p. 165° C, it was converted to the higher-melting modification. Recently, Freudenberg and Weinges (4) reported the isolation of the xyloside of (+)-dimethoxyisolariciresinol (I), m.p. 122° C, $[\alpha]_D^{25}$+38°, from the wood of *Alnus glutinosa*, and this compound, kindly made available by Dr. Weinges, did not depress the melting point of the low-melting modification. The aglycones of these xylosides had infrared spectra which agreed in all respects. The polymorphous xyloside from the *Sorbus* species is, therefore, (+)-dimethoxyisolariciresinol xyloside. The xyloside lyoniside, isolated recently by Yasue and Kato (5) from the wood of *Lyonia ovafolia* Sieb. et Zucc. var. *elliptica* Hand.-Mass, is also polymorphous (m.p. 123.5/165.1° C, $[\alpha]_D$+26.7°), which these authors believed to be identical with the above compound. This has been confirmed by Weinges (6), and more recently by Erdtman (1), who has determined the configuration of the xyloside linkage.

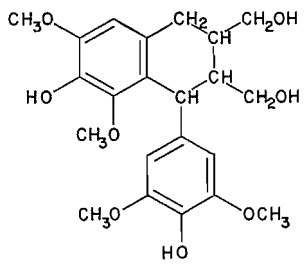

I

Besides the two aucuparins, the phenolic or acidic fractions were found to contain traces of leucoanthocyanidin and an amorphous phenolic ester fraction. The spectra and chromatographic behavior of the former showed it to be different from either leucocyanidin or leucopelargonidin. The amount isolated was insufficient for characterization by alkali degradation. The amorphous ester gave, on saponification, a mixture of long-chain fatty acids and a mixture of phenolic alcohols. The phenolic material was not obtained pure. Thin-layer and paper chromatography gave two spots differing from either dimethoxyisolariciresinol or coniferyl alcohol.

The substitution pattern found in ring A of the aucuparins is the same as that in dimethoxyisolariciresinol, and this suggests a close biogenetic relationship. The finding of these three compounds in both the European and the North American mountain ash is of interest in taxonomic correlations. Other *Sorbus* species are being investigated to determine whether these compounds are characteristic constituents of the mountain ash.

EXPERIMENTAL

Known compounds were identified by mixed melting point and comparison of infrared spectra with those of authentic specimens. Melting points were measured on a Leitz hot-stage microscope. Molecular weights were determined by means of a thermometric vapor pressure osmometer (Model 301 Mechrolab Inc.). The GLC experiments were carried out with an instrument of conventional design which was built in this laboratory (7, 8). It has a thermal conductivity cell and helium was used as carrier gas. The 3 ft×¼ in. O.D. (91×0.6 cm) stainless steel column was packed with SE-30 silicone polymer (Dow Corning) on Chromosorb W (40–60 mesh) in the ratio of 1 to 6. The column temperature was 230° C, that of the injector 260–270° C, and the flow rate was 120 ml per minute. The analysis of the methyl esters of the fatty acid mixture was carried out on a 6 ft×¼ in. O.D. poly(ethyleneglycol phthalate) column at 215° C and 60 ml He per minute. The percentage compositions of mixtures were obtained by measuring the area under the peaks by the triangulation method. Retention times (RT) were measured at the initial emergence of the peaks.

The wood of a mature tree of *S. decora* was obtained from the Kenora district, northern Ontario. The wood was cut and separated into sap and heartwood. The milled heartwood (4.0 kg) was extracted with acetone in a Soxhlet extractor for 24 hours. The acetone extract was evaporated to dryness. The residue (120 g) was extracted with petrol (b.p. 40–60° C, 1 liter) under reflux. The clear extract was decanted from the viscous residue. The residue was then similarly extracted with ether. The insoluble residue was taken up in boiling water (1 liter) to give a turbid solution and this was extracted under reflux with three portions (0.5 liter) of ethyl acetate. The aqueous residue was reduced in volume by evaporation on a rotary evaporator and kept at 2–5° C for several weeks. In other experiments the sapwood and wood of a young tree were milled and extracted in the same manner.

Petrol-soluble Fraction (15% of Total Extract)

Evaporation of the petrol solution gave a viscous oil (18 g). An aliquot (10 g) was chromatographed on silicic acid (100 g) using petrol (b.p. 40–60° C), petrol–ether (9:1), chloroform, and chloroform – 2-butanone (9:1) as eluants. The fractions collected (100 ml) were tested for homogeneity by thin-layer chromatography (TLC) on silica gel G with benzene–ether (7:3) as developing solvent.

Fatty Acid Esters and Hydrocarbons (6.0 g)

The fractions eluted by petrol showed on TLC two fast-moving and overlapping yellow spots. The infrared spectra showed a strong carbonyl absorption (1740 cm^{-1}). The combined fractions were saponified with potassium hydroxide (10%) in aqueous ethanol (50%), and the non-saponifiable components (3.0 g) were extracted with petrol ether. The saponifiable portion was worked up in the usual manner to give the free acids (3.0 g). An aliquot was methylated with diazomethane and analyzed by GLC (polyester column), when peaks corresponding in retention time to myristic, palmitic, palmitoleic, stearic, oleic, and linoleic acids were recorded with areas in the ratio of 1:9.2:1.0:1.8:2.8:1.4.

A small aliquot of the non-saponifiable portion was analyzed by TLC, using β-sitosterol (R_f = 0.28) as reference standard. Three distinct spots with R_f values of 0.95, 0.28, and 0.26 respectively were obtained. The mixture was chromatographed on a column of silicic acid. Petrol eluted a yellow band (R_f 0.95) which, on evaporation of the solvent, gave an oily residue (0.6 g). The infrared spectrum corresponded to that of hydrocarbons. The material was distilled *in vacuo* (3 mm Hg), when practically all distilled at about 180° C (air bath). Found: C, 86.50%; H, 12.58%; molecular weight, 309. Analysis by GLC (SE-30 column, 230° C) showed it to be a mixture of at least six components (relative retention time 0.8–2.0, *n*-docosane 1.00) which could not be resolved.

Further elution of the silicic acid column with petrol–ether (9:1) gave impure β-sitosterol (2.1 g). Recrystallization from methanol gave crystalline β-sitosterol, m.p. 138–139° C, R_f 0.28. Elution with chloroform gave a small amount (0.1 g) of an oily residue (R_f 0.26) which crystallized from methanol, m.p. 162–163° C. The infrared spectrum was similar to that of β-sitosterol. The compound could thus be α-sitosterol.

β-Sitosterol (0.5 g)

The fractions eluted with petrol–ether (9:1) from the original column was composed mainly of β-sitosterol (TLC). The pooled fractions were evaporated to dryness and the residue was crystallized from methanol to give β-sitosterol, m.p. 138–139° C.

Aucuparin and Methoxyaucuparin (3.2 g)

The fractions eluted with chloroform gave a viscous oily residue on evaporation, which solidified slowly. The material was triturated with a little methanol and filtered, when crude crystals of m.p. 112–114° C were obtained (3.0 g). Fractional crystallization from methanol gave a small amount (0.1 g) of colorless crystals, m.p. 118–120° C, corresponding in all respects with methoxyaucuparin. The residual material was a mixture of aucuparin and methoxyaucuparin (1:1, GLC, RT = 2.1 and 2.9 minutes) from which the pure components were obtained in mg amounts by preparative GLC (see below). Aliquots of the mixture were methylated and acetylated in the usual manner and GLC analysis gave peaks corresponding to the derivatives of authentic aucuparin and methoxyaucuparin (see below).

Ether-soluble Fraction (21%)

The ether-soluble material (25 g) was taken up in ether (1 liter) and then extracted with aqueous sodium hydroxide (10%, 50 ml). A copious precipitate of an insoluble sodium salt formed, which was filtered off and washed with cold water. The aqueous and ether layers were separated and the alkali extraction of the

ether solution was repeated. Evaporation of the ether layer gave only a trace of residue which, on GLC analysis, gave only peaks corresponding to the two aucuparins. The combined aqueous alkaline solutions (A) were investigated further (see below).

Aucuparin and Methoxyaucuparin (10 g)

The insoluble sodium salt was suspended in cold water, acidified with dilute hydrochloric acid, and extracted with ether. The pale brown residue from the ether extract failed to crystallize from methanol or ethanol. Distillation of an aliquot *in vacuo* (3 mm Hg) gave a distillate, b.p. about 140° C, which crystallized on standing. TLC, using chloroform containing 10% acetic acid, and paper chromatography (*n*-butanol – acetic acid – water, 4:1:1.8) showed only one spot (ultraviolet light, permanganate spray). However, GLC once again showed the two peaks of aucuparin and methoxyaucuparin in a 1:1 ratio (RT = 2.1 and 2.9 minutes respectively). Preparative runs on a mg scale on the same column (glass traps cooled in acetone – dry ice mixture) gave as the first fraction crude crystals, m.p. 95–98° C, which on recrystallization had m.p. 100–101° C. Its properties agreed with those of aucuparin in all respects. The second fraction had m.p. 116–118° C, recrystallized from methanol, m.p. 119–120° C, and was identical with methoxyaucuparin.

Larger amounts of the two diphenyls were obtained by chromatographing the mixture (1.0 g) on a silicic acid column (30 g), eluting with chloroform (25 ml fractions), and checking the contents of each fraction, after evaporation to a low volume, by GLC. The fractions containing mainly aucuparin were pooled, acetylated (acetic anhydride – pyridine method), and the acetate fractionally crystallized. The pure acetate (GLC, RT = 2.3 minutes) formed thick, rhombohedral plates, m.p. 148–149° C. Found: C, 70.34%; H, 5.95%. Calculated for $C_{16}H_{16}O_4$: C, 70.57%; H, 5.92%. Deacetylation with alcoholic hydrochloric acid (1:1) gave pure aucuparin, m.p. 100–101° C. Found: C, 72.72%; H, 6.24%. Calculated for $C_{14}H_{14}O_3$: C, 73.02%; H, 6.13%. Methylation with dimethyl sulphate and potassium carbonate in anhydrous acetone gave the methyl ether as a colorless liquid, b.p. 110° C at 3 mm pressure (RT = 1.5 minutes), which crystallized on standing for a long time, m.p. 68–70° C.

In the same manner, from the pooled fractions containing mainly methoxyaucuparin, the acetate was obtained pure (GLC, RT = 3.4 minutes), m.p. 119° C. Found: C, 67.48%; H, 6.09%; OAc, 15.50%. Calculated for $C_{17}H_{18}O_5$: C, 67.54%; H, 6.00%; OAc, 14.3%. Deacetylation gave pure methoxyaucuparin (GLC, RT = 2.9 minutes), m.p. 120–121° C. Found: C, 69.44%; H, 6.22%; OCH_3, 31.55%. Calculated for $C_{15}H_{16}O_4(3\times OCH_3)$: C, 69.21%; H, 6.20%; OCH_3, 34.20%. The methyl ether crystallized on standing for a long time, m.p. 65–66° C (RT = 2.2 minutes). Found: C, 69.88%; H, 6.37%; OCH_3, 42.30%. Calculated for $C_{16}H_{18}O_4(4\times OCH_3)$: C, 70.05%; H, 6.61%; OCH_3, 45.26%.

Other Phenols from the Ether-soluble Fraction

The ether-extracted aqueous alkaline solution A was acidified with dilute hydrochloric acid and extracted with ether. The ether extract gave a dark brown viscous material (14 g). An aliquot (5 g) was chromatographed on a silicic acid column. Elution with chloroform gave first impure aucuparin, m.p. 100–101° C, and then impure methoxyaucuparin, m.p. 119–120° C. Elution with chloroform – 2-butanone (4:1) gave a dark brown viscous material which solidified into a glass. Extensive drying gave an amorphous powder which could not be crystallized. The material (4.0 g) was dissolved in methanol (25 ml) and placed onto a polyamide powder column (9). Elution with water removed most of the material as a brown, turbid solution, which did not yield any crystalline material. Elution with aqueous methanol (50%) gave a brown, amorphous solid on evaporation to a small volume. It was filtered off and washed with water. The compound gave a positive ferric chloride reaction (green), was soluble in aqueous alkali, and its infrared spectrum had strong adsorption bands in the hydroxyl (3420 cm^{-1}) and carbonyl (1700 cm^{-1}) region. Attempts to obtain it crystalline, or to prepare a crystalline methyl ether or acetate, failed.

Saponification gave a mixture of fatty acids and phenols, but only traces of neutral alcohols. The free fatty acids were separated from the phenols by chromatography on silicic acid and elution with petrol (b.p. 40–60° C). These were methylated with diazomethane (in ether) and then analyzed by GLC. Peaks corresponding to lauric, myristic, two unknown, palmitic, palmitoleic, stearic, linoleic, and linolenic acids were recorded in a ratio of 5:1.4:1:2.8:24:2:1.6:10.7:25.2:1. The phenolic fraction was eluted with chloroform, when a brown solid material was obtained. The phenolic character was confirmed by the infrared spectrum, which also showed a strong CH_2 band in the 2900 cm^{-1} range, and by a positive ferric chloride reaction. TLC analysis gave two partially separated spots R_f 0.66 and 0.72 (coniferyl alcohol 0.37) when chloroform – acetic acid (9:1) was used. Paper chromatography gave two overlapping spots R_f 0.87 and 0.91 (dimethoxyisolariciresinol 0.44) with *n*-butanol – acetic acid – water (4:1:1.8) as solvent. Further attempts at separation failed to yield pure components.

Ethyl acetate soluble Fraction (29%)

Evaporation of the ethyl acetate under reduced pressure gave a viscous material (35 g) which did not crystallize. It gave a positive leucoanthocyanidin color reaction (violet) with *n*-butanol and hydrochloric acid. GLC showed the presence of aucuparin and methoxyaucuparin. When the mixture (0.2 g) was methylated with dimethyl sulphate in the presence of anhydrous potassium carbonate and anhydrous acetone a product was obtained which gave four individual peaks on GLC analysis (RT 0.8, 1.5, 2.0, 2.2 minutes). Three components (RT 0.8, 1.5, 2.2 minutes) could be isolated in mg amounts, two of which corresponded to the methyl ethers of aucuparin and methoxyaucuparin (RT 1.5 and 2.2 minutes respectively). Attempts to isolate the unknowns and the leucoanthocyanidin in larger amounts failed.

Water-soluble Fraction (33%)

The aqueous solution was concentrated *in vacuo* to about 250 ml and was extracted exhaustively with ethyl acetate. On leaving the aqueous solution at 0 to 3° C for several weeks, a crystalline white solid (4.0 g) separated. It was filtered off and recrystallized twice from methanol to give colorless needles, m.p. 164–165° C, $[\alpha]_D$+41.0° (*c*, 0.7%, acetone–water), undepressed melting point in admixture with the xyloside sent by Professor H. Erdtman. Found: C, 57.01%; H, 6.79%; OCH_3, 20.77%; loss on drying, 3.06%. Calculated for $C_{27}H_{36}O_{12}.H_2O$: C, 56.84%; H, 6.60%; OCH_3, 21.77%; H_2O, 3.16%. The xyloside was hydrolyzed enzymatically with hemicellulase (commercial sample) and the hydrolyzate was analyzed by paper chromatography (xylose as reference standard), when a spot corresponding to xylose was obtained. The xyloside was methylated with dimethyl sulphate and anhydrous potassium carbonate in anhydrous acetone to give the dimethyl xyloside, m.p. 58–60° C. Found: OCH_3, 31.47%. Calculated for $C_{29}H_{40}O_{12}$-$(6\times OCH_3)$: OCH_3, 32.08%. This was hydrolyzed with methanolic sulphuric acid (4%) and the methylated aglycone was isolated in the usual manner, m.p. 158–160° C, $[\alpha]_D$+31.9° (*c*, 1.14%, acetone). Yasue and Kato (5) report m.p. 158–160° C, $[\alpha]_D$+30.1°, whereas Weinges (6) reports m.p. 152° C. Found, after drying *in vacuo* at 100° C: C, 60.04%; H, 7.19%; OCH_3, 41.11%; molecular weight, 449. Calculated for $C_{24}H_{32}O_8$: C, 64.27%; H, 7.19%; OCH_3, 41.52%; molecular weight, 448.5. An aliquot of the mother liquors from which the xyloside was obtained was hydrolyzed with sulphuric acid (4%). A deep red solution resulted which, on boiling, deposited a deeply colored polymeric amorphous solid. The material was not investigated further.

In other experiments the sapwood and the wood of the young tree were extracted with acetone and the residual extracts were fractionated by solvent segregation as above. The major portion of the extract was water soluble, and from this fraction the same xyloside crystallized to give a low-melting modification, m.p. 121–122° C, $[\alpha]_D^{25}$+41.0°. The melting point was not depressed with the xyloside of (+)-dimethoxyisolariciresinol, m.p. 122–124° C, sent by Dr. K. Weinges. Found for the vacuum-dried sample: C, 58.60%; H, 6.55%; OCH_3, 21.9%. Calculated for $C_{27}H_{36}O_{12}$: C, 58.74%; H, 6.57%; OCH_3, 22.49%. Methylation and hydrolysis gave the same aglycone, m.p. 158–160° C, as described above. When a solution of this xyloside was seeded with the high-melting form, crystals of m.p. 163–164° C were obtained. An equal mixture of the low- and high-melting modification dissolved in a little water deposited crystals of m.p. 163–165° C. Thus, the high-melting modification appears to be the more stable form.

ACKNOWLEDGMENTS

The authors wish to thank Professor H. Erdtman for his very helpful suggestions and the gift of the aucuparins and xyloside. Thanks are also due to Dr. K. Weinges for the gift of (+)-dimethoxyisolariciresinol xyloside and to Mr. F. E. Sider, district forester, Kenora, Ontario, for having procured the wood of the showy mountain ash. The microanalyses were carried out by Mr. M. Mazurek and the infrared spectra were recorded by Mr. W. C. Haid. We also would like to thank Mr. M. Granat for technical assistance.

REFERENCES

1. H. ERDTMAN. Private communication.
2. H. ERDTMAN, G. ERIKSSON, and T. NORIN. Acta Chem. Scand. **15**, 1796 (1961).
3. B. M. CRAIG and N. L. MURTY. J. Am. Oil Chemists' Soc. **36**, 1124 (1959).
4. K. FREUDENBERG and K. WEINGES. Tetrahedron Letters, No. 17, 19 (1959).
5. M. YASUE and Y. KATO. J. Pharm. Soc. Japan, **80**, 1013 (1960).
6. K. WEINGES. Chem. Ber. **94**, 2522 (1961).
7. B. M. CRAIG and N. L. MURTY. Can. J. Chem. **36**, 1297 (1958).
8. B. M. CRAIG and N. L. MURTY. J. Am. Oil Chemists' Soc. **36**, 549 (1959).
9. H. ENDRES. Z. anal. Chem. **181**, 331 (1961).

GAS–LIQUID CHROMATOGRAPHY OF SOME FLAVONOID COMPOUNDS AND HYDROXY DIPHENYLS[1]

N. NARASIMHACHARI[2] AND E. VON RUDLOFF
National Research Council of Canada, Prairie Regional Laboratory, Saskatoon, Saskatchewan

Received February 19, 1962

ABSTRACT

Gas–liquid chromatography of the methyl ethers of 36 flavones, flavanones, isoflavones, and chalkones, 2 chromones, and 9 hydroxy diphenyls was carried out, using SE-30 silicone polymer as liquid phase. The results obtained show that this technique can be used for the separation, isolation, and identification of milligram amounts of these compounds. The influence of methylation, acetylation, and hydrogen bonding was demonstrated and is discussed. Dehydration of a 2-hydroxyisoflavanone to the corresponding isoflavone and isomerization between some flavanones and chalkones were encountered. No linear relationship between the number of substituents and retention time was obtained, indicating that substituents at different positions of a flavonoid nucleus influence the retention characteristics in a different manner. This was especially noticeable with some 3- and 5-substituted flavones, but in other instances the difference in retention times was also sufficient to differentiate between position isomers.

INTRODUCTION

The successful separation of simple phenols by means of gas–liquid chromatography (GLC) has been reported by several authors (1–12), but does not appear to have been achieved with more complex phenols. Recently the authors (13) were able to separate and isolate the two hydroxy diphenyls aucuparin and methoxyaucuparin (4-hydroxy-3,5-dimethoxy- and 4-hydroxy-2′,3,5-trimethoxy-diphenyl) and their methyl ethers and acetates by GLC. It was of considerable interest for our studies of wood extractives to determine whether flavonoid compounds could also be chromatographed satisfactorily. Since most flavonoids, or at least their methyl ethers and acetates, can be distilled *in vacuo*, this seemed possible in principle. This paper describes the results obtained with a representative variety of flavones, flavonols, isoflavones, chalkones, flavanones, flavanonols, chromones, and hydroxy diphenyls, or their methylated and acetylated derivatives.

As the flavonoid compounds have high boiling points, only liquid phases suitable for use above 200° C could be considered. Polyesters of the Craig type and bis-(*m*-phenoxyphenoxy)benzene had been used by one of us (12) for the separation of eugenol, isoeugenol, and anisole. These liquid phases proved to be unsuitable for the chromatography of flavonoids. However, as with the hydroxy diphenyls aucuparin and methoxyaucuparin, many flavonoids could be eluted as fairly symmetrical peaks from a 3-ft column containing SE-30 silicone polymer as liquid phase. This substrate was first used in the successful separation of steroids (at 220–265° C) by VandenHeuvel *et al.* (14). Columns containing this liquid phase in 15, 10, and 5% amounts on Chromosorb W, and in 0.5% amount on micro glass beads, were made up and with these columns satisfactory chromatography of the flavonoids and diphenyls listed in Tables I and II was obtained. The first three columns allowed the separation and isolation of milligram amounts, which proved particularly useful for identifying the isomerization products of chalkones and flavanones.

[1]*Issued as N.R.C. No. 6800.*
[2]*National Research Council of Canada Postdoctorate Fellow, 1960–1961.*

TABLE I

Relative retention times (with respect to 7-methylflavone) of hydroxy diphenyls and simpler flavonoids at 235° C

Group	Substitution	15% SE-30*	0.5% SE-30†
Diphenyl	2-Hydroxy	0.04	—
	2,2′-Dihydroxy	0.05	—
	4,4′-Dihydroxy	0.31	—
	4-Hydroxy-3,5-dimethoxy‡	0.25	—
	3,4,5-Trimethoxy	0.19	—
	4-Acetoxy-3,5-dimethoxy	0.28	—
	4-Hydroxy-3,5,2′-trimethoxy§	0.27	—
	3,4,5,2′-Tetramethoxy	0.42	—
Phenyl benzyl ketone	2-Hydroxy-4,6-dimethoxy	0.50	—
Chromone	3,5,7-Trimethoxy-2-methyl	0.33	—
	Khellin (furano chromone) (32)	0.40	—
Flavone	None	0.40	0.42
	3-Hydroxy	0.47	0.48
	3-Methoxy	0.42	0.45
	3-Acetoxy	0.57	0.62
	7-Methoxy	*1.00*	*1.00*
	5-Hydroxy-7-methoxy	1.15	1.20
	5,7-Dimethoxy	1.95	2.05
	5,7-Diacetoxy	2.55	2.60
	5-Hydroxy-3,7-dimethoxy	1.25	1.27
	3,5,7-Trimethoxy	2.40	2.35
	5,7-Diacetoxy-2′-methoxy	3.95	4.00
Isoflavone	5-Hydroxy-7-methoxy	0.99	—
	5,7-Dimethoxy	1.50	1.55
	5-Hydroxy-7-methoxy-2-methyl	1.55	—
	5,7-Dimethoxy-2-methyl	1.65	—
	5,7-Diacetoxy-2-methyl	1.70	1.75
Flavanone	7-Methoxy	0.47+0.80	0.45+0.75
	5-Hydroxy-7-methoxy	0.65	0.65
	5,7-Dimethoxy	1.10	1.10
	7,4′-Dimethoxy	1.13+2.00	—
	5,6,7-Trimethoxy	1.30+1.60	—
	5-Hydroxy-7,4′-dimethoxy	1.60	—
	7-Methoxy-5,4′-dihydroxy	—	2.1
Chalkones	2′-Hydroxy-4′-methoxy	0.47+0.79	0.45+0.75
	2′-Hydroxy-4,4′-dimethoxy	1.15+2.06	—
	2′-Hydroxy-4′,6′-dimethoxy	1.07	—
Isoflavanones	5,7-Dimethoxy	0.90	0.60
	2-Hydroxy-5,7-dimethoxy‖	1.57	1.55

*Flow rate: 120 ml helium/min; RT 7-methoxyflavone: 8.1 minutes.
†Flow rate: 150 ml helium/min; RT 7-methoxyflavone: 1.1 minutes.
‡Aucuparin.
§Methoxyaucuparin.
‖Dehydrated to 5,7-dimethoxyisoflavone.

It is common practice to report the retention times (RT) of individual compounds as relative retention time (RRT) with respect to a suitable standard substance. Initially flavone itself was used for this purpose, but this was found to have too low a retention time on the 0.5% column to give accurate RRT values. Therefore, 7-methoxyflavone was chosen, being readily synthesized and more suitable as regards retention characteristics.

EXPERIMENTAL

The gas-chromatographic unit was of conventional design and built in this laboratory (15, 16). The column and thermal conductivity cell were controlled at the same temperature. The injector could be heated separately by means of a variac control. The columns were constructed of 3-ft lengths of $\frac{1}{4}$-in O.D. stainless steel tubing, which was coiled (5- to 8-in diameter) to fit into the heating oven. In preparative runs the exit

TABLE II

Relative retention times of tetra- and penta-substituted flavonoids on the 3-ft 0.5% SE-30 column at 235° C

Group	Substitution	RRT
Flavone	7-Methoxy	1.00
	3,5,7,4′-Tetramethoxy	5.90
	3,7,3′,4′-Tetramethoxy	4.72
	3,5,7,3′,4′-Pentamethoxy	9.90
	5-Hydroxy-3,7,4′-trimethoxy	3.82
	5-Hydroxy-3,7,3′,4′-tetramethoxy	7.10
Isoflavone	5,7,4′-Trimethoxy-2-methyl	4.65
	5-Hydroxy-7,4′-dimethoxy-2-methyl	2.70
Flavanone	5-Hydroxy-7,3′,4′-trimethoxy	3.4
	5,4′-Dihydroxy-7-methoxy	2.1
Chalkone	2′-Hydroxy-4,6′,4′-trimethoxy	3.3

gases were led into glass traps which were externally cooled in a dry ice – acetone mixture. Chromatograms were recorded on a 1-mv Honeywell recorder using a chart speed of 6 min/in. The carrier gas was helium, which was introduced at 40 to 60 p.s.i. at the column inlet. The outlet was at atmospheric pressure and the gas flow rate was measured by means of a moving soap bubble. Samples were introduced as solutions (0.5 to 2 μl, 30–50% in acetone or chloroform) with a hypodermic syringe. Retention times were measured at the initial emergence of peaks (12) and these were reproducible within ±0.1 minute for individual compounds. The peaks were of regular shape and no sign of decomposition was detected. Recovery of isolated samples was not quantitative (approx. 50 to 75%).

MATERIALS

The simple hydroxy diphenyls were commercial samples. Aucuparin and methoxy-aucuparin were isolated from the wood of *Sorbus decora* (13); the methyl ethers and acetates were prepared by standard procedures.

Flavones

7-Methoxyflavone, m.p. 110–111° C, was prepared by dehydrogenation with selenium dioxide of 2′-hydroxy-4′-methoxychalkone (17). Flavone, 3-hydroxyflavone, kaempferol, fisetin, and quercetin were commercial samples (chromatographically pure), from which the fully methylated derivatives were obtained by methylation with excess dimethyl sulphate and anhydrous potassium carbonate in anhydrous acetone: 3-methoxyflavone, m.p. 107° C (18); kaempferol tetramethyl ether, m.p. 165–166° C (19); fisetin tetramethyl ether, m.p. 150° C; quercetin pentamethyl ether, m.p. 144–145° C (20). Chrysin dimethyl ether, m.p. 75–76° C, was similarly obtained from chrysin (21). Galangin trimethyl ether, m.p. 195–197° C, was obtained from galangin-3-methyl ether prepared according to the method of Kalff and Robinson (22).

The partial methyl ethers with the 5-hydroxyl group free were prepared by methylation with diazomethane in methanol–ether: galangin-3,7-dimethyl ether, m.p. 145–146° C (22); kaempferol trimethyl ether, m.p. 154–155° C (23); quercetin tetramethyl ether, m.p. 156–157° C (24). Tectochrysin was obtained from natural sources (21).

Isoflavones and Isoflavanones

2-Hydroxy-5,7-dimethoxyisoflavanone, 5,7-dimethoxy- and 5-hydroxy-7-methoxy-isoflavones

2-Hydroxy-4,6-dimethoxy phenyl benzyl ketone (25) (1 g) was dissolved in ethyl formate (10 ml) and the cooled solution was added to ice-cold powdered sodium (1 g). After being left at 0° C for 24 hours the mixture was poured into ice water. The solution

was acidified to pH 2–3 with cold dilute hydrochloric acid and the sticky solid which separated out was filtered, washed with water, and crystallized from methanol to give rectangular prisms, m.p. 145–146° C. It agreed in its properties with those reported for 2-hydroxy-5,7-dimethoxyisoflavanone as reported by Narasimhachari *et al.* (26). Dehydration with acetic anhydride (26) gave 5,7-dimethoxyisoflavone, m.p. 121° C (26). 5-Hydroxy-7-methoxyisoflavone was obtained by controlled demethylation of the dimethoxy compound with hydroiodic acid at 120° C according to Aghoramurti *et al.* (27).

5,7-Dihydroxy-2-methylisoflavone, m.p. 228–229° C, and 5,7-dihydroxy-4′-methoxy-2-methylisoflavone, m.p. 208–209° C, were prepared according to the method of Baker and Robinson (28). Partial methylation of these dihydroxy compounds with 1 mole of dimethyl sulphate and anhydrous potassium carbonate in anhydrous acetone gave 5-hydroxy-7-methoxy-2-methylisoflavone, m.p. 186–187° C (28), and 5-hydroxy-4′,7-dimethoxy-2-methylisoflavone, m.p. 197–199° C (28). Complete methylation with excess dimethyl sulphate gave the corresponding fully methylated derivatives, m.p. 98–100° C and 175–176° C respectively.

5,7-Dimethoxyisoflavanone

5,7-Dimethoxyisoflavone (0.2 g) was hydrogenated in the presence of palladium-on-charcoal catalyst (25 mg) for 24 hours (29). The product was crystallized from ethyl acetate containing petrol, m.p. 151–152° C. Found: C, 71.73%; H, 5.72%. Calculated for $C_{17}H_{16}O_4$: C, 71.82%; H, 5.67%.

Chalkones and Flavanones

The 2′-hydroxychalkones were obtained by the standard procedure. The appropriate *o*-hydroxyacetophenone (1 mole equivalent) and the substituted benzaldehyde (1.5 mole equivalent) were dissolved in alcohol and to the mixture was added potassium hydroxide (2 g/g ketone). The mixture was left in a stoppered flask at room temperature for 48 hours. It was then diluted with water and extracted with ether. The aqueous layer was separated and acidified, when the chalkone was precipitated. It was filtered, washed with dilute aqueous sodium carbonate solution and water, and crystallized from alcohol. 2′-Hydroxy-4′-methoxychalkone, m.p. 104–106° C; 2′-hydroxy-4′,4-dimethoxychalkone, m.p. 110° C; 2′-hydroxy-4′,6′-dimethoxychalkone, m.p. 91–92° C; 2′-hydroxy-4,4′,6′-trimethoxychalkone, m.p. 113–114° C were thus obtained.

The fully methylated flavanones were obtained from these 2′-hydroxychalkones by heating under reflux with alcoholic sulphuric acid (4%). These could also be obtained practically pure from the ether extract of the chalkone condensation (see above) by silicic acid chromatography. 7-Methoxyflavanone, m.p. 89° C; 7,4′-dimethoxyflavanone, m.p. 95° C; 5,7-dimethoxyflavanone, m.p. 144–145° C; 4′,5,7-trimethoxyflavanone, m.p. 128° C were obtained.

Naringenin-7,4′-dimethyl ether, m.p. 114–116° C, and hesperetin-7,3′-dimethyl ether, m.p. 136–137° C, were obtained by partial methylation of naringenin and hesperetin (commercial samples) respectively according to the method of Narasimhachari and Seshadri (30). Similarly, pinocembrinmonomethyl ether, m.p. 110–112° C, was obtained from pinocembrin (21). Sakuranetin was a sample from natural sources (31).

GLC of some of the flavanones and chalkones gave two peaks in varying proportions. Each component was isolated in preparative runs (10 mg) and identified by mixed melting point and comparison of ultraviolet spectra. Re-injection of each component confirmed that thermal isomerization between these flavanones and chalkones took place. The amounts of each formed were determined by measuring the area under the peak (error = ±3% to 10%).

Chromones

Khellin (32) was obtained from commercial sources. Complete methylation of 3-methoxy-5,7-dihydroxy-2-methylchromone (33) gave 3,5,7-trimethoxy-2-methylchromone.

RESULTS AND DISCUSSION

The relative retention times of the hydroxy diphenyls and the simpler flavonoids with reference to 7-methoxyflavone as obtained on the 15% and 0.5% SE-30 columns are shown in Table I. No noteworthy difference in these RRT values was obtained on the 10% and 5% columns, although the actual retention times decreased accordingly. Thus, the RT values for 7-methoxyflavone were 8.1, 5.3, 3.8, and 1.1 minutes on the 15, 10, 5, and 0.5% column respectively. As expected, a fairly regular increase in the RT was observed when the number of substituents in the parent compound was increased. Conversion of a free hydroxyl group to the methyl ether decreased the RT, whereas acetylation increased it to a value above that of the free phenol. These findings hold only for compounds in which no intramolecular hydrogen bonding of free hydroxyl groups can take place. Where hydrogen bonding can occur, the RT of the free phenol is very much lower than expected for a corresponding non-hydrogen bonded compound. Thus the value obtained for 2,2′-dihydroxy diphenyl is practically that of a monohydroxy diphenyl. 4,4′-Dihydroxy diphenyl gave a retention time expected for the dihydroxy analogue. The effect of hydrogen bonding is especially noticeable with 5-hydroxy-flavones, -flavanones, and -isoflavones; e.g., the 5-hydroxy-7-methoxy compound has a much lower RT than the corresponding 5,7-dimethoxy derivative (see Table I). This marked effect was also found with the higher-substituted compounds (see Table II).

Compounds with more than two free hydroxyl groups or three methoxyl groups were not eluted within practical times from the 15, 10, or 5% SE-30 columns at 230–235° C. The use of higher temperatures to shorten the RT values seemed undesirable, not only because of shorter column life, but because the chance of thermal decomposition of injected compounds would be very much enhanced. Decomposition of hydroxy and acetoxy steroids at 220–260° C on the SE-30 substrate was reported by VandenHeuvel *et al.* (13) (see also below). Therefore, 0.5% SE-30 polymer on micro glass beads at 230° C was used for the chromatography of the higher-substituted flavonoids. The relative retention times of tetra- and penta-substituted flavonoids with respect to 7-methoxyflavone are shown in Table II.

Substitution at the various positions of the flavonoid nucleus appears to affect the retention characteristics differently. Thus, 3-methoxyflavone has a much lower retention time than 7-methoxyflavone. The finding that even 3-hydroxyflavone has a lower retention time than the standard indicates that substituents at this position are somehow shielded and do not increase the retention time by an expected increment. Such increases are obtained by substitution at the various positions of the aromatic nuclei (except for the 5-hydroxy and other hydrogen-bonding substituents), but the increments were not regular for each additional group added. This is fortunate, since it leads to different retention times for position isomers and thus facilitates their separation; e.g., 3,5,7,4′- and 3,7,3′,4′-tetramethoxyflavone had RRT 5.90 and 4.72 respectively. Whether the lower value for the latter compound is due to the proximity of the 3′ and 4′ substituent or a markedly different behavior between 3′- and 5-substituted flavones cannot be deduced from the present data. 5-Hydroxy-7,3′,4′-trimethoxyflavanone (Table II) had a considerably higher RRT than 5-hydroxy-7,4′-dimethoxyflavanone (Table I). This suggests again that no general conclusion in this direction can be drawn.

The differences in retention times between the various groups of compounds studied are sufficient to be of value in their separation and isolation. For example, 5,7-dimethoxy-flavone, -isoflavone, -flavanone, and -isoflavanone had RRT 1.95, 1.50, 1.10, and 0.90 (0.60) respectively. The double bond in the heterocyclic ring of the flavones causes a longer retention on the SE-30 columns, and the iso compounds are retained a noticeably shorter time than the corresponding flavones or flavanones. The conjugation of the B-ring with the double bond and carbonyl group in flavones may account for the higher RRT values. The different retention times of different groups of compounds with the same substitution pattern is especially useful in view of the co-occurrence of such groups in plants.

The increase in retention times with increasing number of substituents is much more marked with flavones than with isoflavones (see Table I). A similar conclusion could not be drawn for flavanones and isoflavanones because too few of the latter group were available for study. In general, the RRT values obtained on the 0.5% column were the same or slightly higher than those recorded with the 15% column. However, the value of 5,7-dimethoxyisoflavanone was much lower on the former column (0.6 as against 0.9). Repeated runs at different times, or in consecutive runs, did not change this result. Possibly some minor influence due to the solid support Chromosorb W plays a more significant role in the chromatography of this particular compound.

Two chemical reactions due to the high temperatures necessary for chromatography were encountered. Several of the flavanones and chalkones gave two distinct peaks on the chromatogram (see Table I). The former usually gave a large peak followed by a smaller one whereas some of the chalkones gave two peaks in the reverse order of size. When the RRT values obtained for 7-methoxyflavanone, for example, are compared with those for 2′-hydroxy-4′-methoxychalkone these were found to be the same (within an error ± 0.03) for both peaks. These effects were shown to be due to isomerization between flavanones and the corresponding chalkones by isolating both components and comparing the ultraviolet spectra with the starting materials. The component with lower RRT invariably corresponded to the flavanone and that with higher RRT to the chalkone. On re-injecting 7-methoxyflavanone the two peaks were obtained in the ratio of 7 to 1, whereas with 2′-hydroxy-4′-methoxychalkone it was 1 to 3. This shows that an equilibrium mixture is not obtained during chromatography and different operating conditions may result in different ratios. The finding that 2′-hydroxy-4′,6′-dimethoxy- and 5,7-dimethoxy-flavanone gave only a single peak corresponding to the flavanone structure indicates that certain substituents may stabilize the flavanone structure.

Another type of reaction was encountered with 2-hydroxy-5,7-dimethoxyisoflavanone. This compound gave on chromatography the retention time of 5,7-dimethoxyisoflavone (see Table I). Isolation confirmed that the 2-hydroxyisoflavanone had been dehydrated completely to the isoflavone. This is to be expected, since this dehydration is obtained by chemical means (26, 34, 35). Whalley (35) proposes a trans configuration (2(*a*)-hydroxyl, 3(*a*)-hydrogen) for the eliminated elements. On the other hand, for unimolecular thermal decompositions giving rise to olefins, Barton (36) proposes cis elimination. This aspect requires further study. During the preparation of 5,7-dimethoxyisoflavone it was noted that with sodium and ethyl formate the reaction product was the 2-hydroxyisoflavanone. The formation of this intermediate was reported earlier by Narasimhachari *et al.* (26), methyl formate being used, by Whalley (34, 37) in the synthesis of 2′-substituted isoflavones, and by Baker *et al.* (38) in the condensation of phenyl benzyl ketones with ethyl oxalyl chloride. The infrared spectrum confirms the 2-hydroxyisoflavanone

structure assigned to the intermediate. 2-Hydroxy-4,6-dimethoxy phenyl benzyl ketone was also chromatographed (cf. Table I) to demonstrate that GLC can be readily used to identify unreacted starting material.

Since GLC permits the isolation of practically pure compounds in milligram amounts, and thus allows confirmation of identity by infrared and ultraviolet spectroscopy, this technique appears to be eminently suited for the investigation of mixtures of complex phenols found in plant extractives. This should prove especially useful in surveys of related species for the occurrence of the same, or closely related, flavonoid constituents. The technique is now being applied to current investigations of phenolic fractions in wood and other plant extractives. The results described above also show that GLC can be used with success in the study of chemical changes and reactions of flavonoid compounds.

ACKNOWLEDGMENTS

The authors wish to express their gratitude to Professor H. Erdtman for the gift of chrysin, tectochrysin, and pinocembrin. The infrared and ultraviolet spectra were recorded by Mr. W. C. Haid.

REFERENCES

1. L. IRVINE and T. J. MITCHELL. J. Appl. Chem. (London), **8**, 3, 425 (1958).
2. W. CARRUTHERS, R. A. W. JOHNSTONE, and J. R. PLIMMER. Chem. & Ind. (London), 331 (1958).
3. S. H. LANGER, P. PANTAGES, and I. WENDER. Chem. & Ind. (London), 1664 (1958).
4. C. KARR, P. M. BROWN, P. A. ESTEP, and G. L. HUMPHREY. Anal. Chem. **30**, 1413 (1958).
5. I. SOBOLEV and C. SCHUERCH. Tappi, **41**, 447 (1958).
6. G. BERGMANN and D. JENTZSCH. Z. anal. Chem. **164**, 10 (1958).
7. A. KREYENBUHL and H. WEISS. Bull. soc. chim. France, 1880 (1959).
8. J. S. FITZGERALD. Australian J. Appl. Sci. **10**, 169 (1959).
9. J. JÁNAK, R. KOMERS, and J. SIMA. Collection Czechoslov. Chem. Commun. **24**, 1492 (1959).
10. J. JÁNAK and R. KOMERS. Collection Czechoslov. Chem. Commun. **24**, 1960 (1959).
11. D. S. PAYN. Chem. & Ind. (London), 1090 (1960).
12. E. VON RUDLOFF. Can. J. Chem. **38**, 631 (1960).
13. N. NARASIMHACHARI and E. VON RUDLOFF. Can. J. Chem. This issue.
14. W. J. A. VANDENHEUVEL, C. C. SWEELEY, and E. C. HORNING. J. Am. Chem. Soc. **82**, 3481 (1960).
15. B. M. CRAIG and N. L. MURTY. Can. J. Chem. **36**, 1297 (1958).
16. B. M. CRAIG and N. L. MURTY. J. Am. Oil Chemists' Soc. **36**, 549 (1959).
17. H. S. MAHAL, H. S. RAI, and K. VENKATARAMAN. J. Chem. Soc. 866 (1935).
18. S. HATTORI. Acta Phytochim. (Japan), 4, 44 (1928).
19. P. R. RAO and T. R. SESHADRI. Proc. Indian Acad. Sci. A, 24, 456 (1946).
20. N. NARASIMHACHARI, S. NARAYANASWAMI, and T. R. SESHADRI. Proc. Indian Acad. Sci. A, **37**, 103 (1953).
21. H. ERDTMAN. Svensk Kem. Tidskr. **56**, 2, 26 (1944).
22. J. KALFF and R. ROBINSON. J. Chem. Soc. 181 (1925).
23. A. C. JAIN and T. R. SESHADRI. J. Sci. Ind. Research (India), B, **12**, 564 (1953).
24. A. S. GOMM and M. NIERENSTEIN. J. Am. Chem. Soc. **53**, 4408 (1931).
25. G. G. BADCOCK, G. W. K. CAVILL, A. ROBERTSON, and W. B. WHALLEY. J. Chem. Soc. 2961 (1950).
26. N. NARASIMHACHARI, D. RAJAGOPALAN, and T. R. SESHADRI. J. Sci. Ind. Research (India), B, **12**, 287 (1953).
27. K. AGHORAMURTI, N. NARASIMHACHARI, and T. R. SESHADRI. Proc. Indian Acad. Sci. A, **31**, 257 (1951).
28. W. BAKER and R. ROBINSON. J. Chem. Soc. 1984 (1925); 2713 (1926).
29. F. E. KING and K. G. NEILL. J. Chem. Soc. 4752 (1952).
30. N. NARASIMHACHARI and T. R. SESHADRI. Proc. Indian Acad. Sci. A, **22**, 223 (1948).
31. N. NARASIMHACHARI and T. R. SESHADRI. Proc. Indian Acad. Sci. A, **30**, 271 (1949).
32. E. SPÄTH and W. GRUBER. Ber. **71**, 106 (1938).
33. J. KALFF and R. ROBINSON. J. Chem. Soc. 1968 (1925).
34. W. B. WHALLEY. J. Am. Chem. Soc. **75**, 1059 (1953).
35. W. B. WHALLEY. Chemistry of natural tannins symposium. 1956. p. 155.
36. D. H. R. BARTON. J. Chem. Soc. 2174 (1949).
37. W. B. WHALLEY. J. Chem. Soc. 3366 (1953).
38. W. BAKER, J. CHADDERTON, J. B. HARBORNE, and W. D. OLLIS. J. Chem. Soc. 1852 (1953).

REARRANGEMENT STUDIES WITH C^{14}

XII. THE REACTION OF NITROUS ACID WITH 2-α- OR 2-β-NAPHTHYLETHYLAMINE-1-C^{14}

A. G. FORMAN[1] AND C. C. LEE
Department of Chemistry, University of Saskatchewan, Saskatoon, Saskatchewan

Received February 20, 1962

ABSTRACT

On treatment with sodium nitrite, 2-α-naphthylethylamine-1-C^{14} in aqueous hydrochloric acid or glacial acetic acid gives rise to the corresponding alcohol, which shows rearrangement of C^{14} from the C-1 to the C-2 positions to the extent of 32–35%; the 2-β-naphthyl isomer exhibits 26–28% rearrangement. The significance of these results is discussed.

INTRODUCTION

Isotope position rearrangement in the reaction of 2-phenylethylamine-1-C^{14} with nitrous acid in both aqueous and non-aqueous media has been reported and the results discussed in terms of possible reaction mechanisms (1, 2). The percentage of rearrangement was approximately 20%, considerably more than the 1.5% rearrangement observed for the reaction of nitrous acid with ethylamine-1-C^{14} (3), thus strongly suggesting anchimeric assistance by the phenyl group and the probable involvement of the non-classical ethylenephenonium ion I[2] for at least part of the reaction. This paper reports the degree of rearrangement during the same reaction of the analogous naphthyl derivatives.

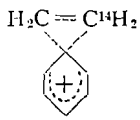

I

RESULTS AND DISCUSSION

2-β-Naphthylethylamine-1-C^{14} was prepared from β-naphthoic acid by reduction to the corresponding carbinol, which was converted to the chloride by means of thionyl chloride; the resulting β-chloromethylnaphthalene was treated with potassium cyanide-C^{14} to give the nitrile, which was reduced with lithium aluminum hydride to give the desired amine. Analogously, 2-α-naphthylethylamine-1-C^{14} was prepared starting from α-chloromethylnaphthalene. That no rearrangement had occurred during any step of the syntheses was demonstrated by permanganate oxidation of either of the amines to give the corresponding inactive α- or β-naphthoic acid.

The reaction of the amines with nitrous acid was carried out in dilute hydrochloric acid and in glacial acetic acid, yielding, respectively, 2-α- or 2-β-naphthylethanol and 2-α- or 2-β-naphthylethyl acetate. The acetates were saponified with sodium ethoxide in 95% ethanol. To demonstrate that the saponification of the acetates did not affect the

[1]*Holder of a National Research Council of Canada Studentship, 1961–1962; on leave from the Department of Chemistry, Carleton University, Ottawa, Ontario.*

[2]*Previously we have used "ethylphenonium" as the name of this ion. In analogy with other "onium" ions, such as "ethyleneoxonium" ion, we will use the terms "ethylenephenonium" and "ethylenenaphthonium" in this paper. Instead of "phenonium" ion, the name "benzenocarbonium" ion has also been recorded in the literature.*

degree of rearrangement, 2-α-naphthylethyl acetate was isolated in one experiment and this ester was treated with lithium aluminum hydride to give the alcohol. The purified alcohols were assayed for radioactivity and then oxidized with alkaline permanganate to the corresponding naphthoic acids. A comparison of the molar activities of the alcohol and corresponding acid gave a direct measure of the degree of rearrangement of C^{14} from the C-1 to the C-2 positions. The results are tabulated in Table I.

TABLE I

Rearrangements in the reaction between nitrous acid and 2-α- or 2-β-naphthylethylamine-1-C^{14}

Reaction medium	Compound assayed	Activity* (c.p.m./mmole) Run I	Activity* (c.p.m./mmole) Run II	% rearrangement Run I	% rearrangement Run II
H_2O–HCl	α-$C_{10}H_7CH_2CH_2OH$	54.1	23.8		
	α-$C_{10}H_7COOH$	18.4	7.6	34	32
HOAc	α-$C_{10}H_7CH_2CH_2OH$	223	222 (219)†		
	α-$C_{10}H_7COOH$	78.3	78.2 (76.8)†	35	35 (35)†
H_2O–HCl	β-$C_{10}H_7CH_2CH_2OH$	126	45		
	β-$C_{10}H_7COOH$	34.6	12.7	27	28
HOAc	β-$C_{10}H_7CH_2CH_2OH$	131	125		
	β-$C_{10}H_7COOH$	34.1	32.4	26	26

*Radioactivity was measured in a liquid scintillation counter. Each sample, weighing about 10 mg, was dissolved in 20 ml of toluene containing 4g/l. of DPO and 100 mg/l. of POPOP and then counted for sufficient length of time to give at least 10,000 counts. Under these conditions, use of toluene-C^{14} as an internal standard showed that there was no quenching by the compounds assayed.

†In this experiment, the acetate was treated with $LiAlH_4$ to give the alcohol.

From Table I, it may be noted that practically the same degrees of rearrangement were observed in both aqueous and acetic acid media. Similar observations were made by investigators of the reaction of nitrous acid with 2-phenylethylamine-1-C^{14} (1, 2). Several attempts were made to carry out the reaction of the naphthylethylamines in anhydrous formic acid in order to determine whether a greater amount of rearrangement would result in this more ionizing medium. However, these attempts were unsuccessful due to the rapid formation of a polymeric tar. Even when the temperature of the reaction mixture was maintained at the freezing point of formic acid, no ester could be isolated.

The observed rearrangements may be regarded as the result of some net 1,2-naphthyl shifts in these reactions. Possibly, one may visualize these reactions as proceeding to some extent through the bridged α- and β-ethylenenaphthonium ions II and III, and the remainder through the classical naphthylethyl ions IV and V. On the other hand,

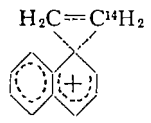

II

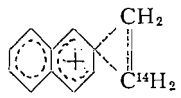

III

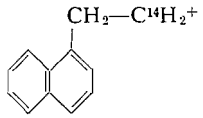

IV

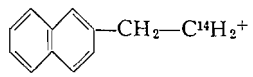

V

it may be more accurate to consider II and IV or III and V as contributing structures of the actual transition states. Should IV be formed during the reaction, one might predict the possible formation of some acenaphthene through internal electrophilic substitution, i.e.

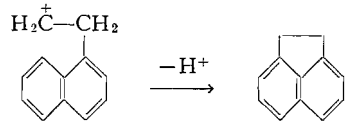

The crude products from reaction of the α-isomer were examined by gas–liquid chromatography and compared with known acenaphthene. No trace of the hydrocarbon was found.

The average degree of rearrangement for the reaction with 2-α-naphthylethylamine-1-C^{14} was 34%. Should the reaction proceed via the ethylenenaphthonium ion II, this higher degree of rearrangement, as compared to about 20% rearrangement for the reaction with the phenylethyl derivative (2), may be due to greater positive-charge delocalization in II as compared to I. The somewhat lower extent of rearrangement of about 27% for the β-naphthyl isomer is to be expected because of less electron localization at the β-position of the naphthalene nucleus, as evidenced by the well-known preference for formation of the α-isomer in electrophilic substitution, and as predicted by valence bond and molecular orbital theory (4).

EXPERIMENTAL

Preparation of 2-α-Naphthyl- and 2-β-Naphthyl-ethylamine-1-C^{14}

β-Naphthoic acid was reduced with lithium aluminum hydride according to the general method of Nystrom and Brown (5). Average yield of β-naphthylcarbinol, m.p. 79.5–80.5° C (lit. (6) m.p. 80–81° C), was 91%. This product was converted to β-chloromethylnaphthalene, m.p. 46–47° C (lit. (7) m.p. 47.5–48.5° C), in 77% yield by the method of Gilman and Kirby (8). The α- and β-chloromethylnaphthalenes were converted to the corresponding nitriles according to Wislicenus and Elvert (9) in 80% yield. 2-α-Naphthylacetonitrile-1-C^{14} was obtained as an oil, b.p. 165–170° C at 2 mm (lit. (9) 183–187° C at 13 mm); 2-β-naphthylacetonitrile-1-C^{14} crystallized from cyclohexane as a pale yellow solid, m.p. 85–86° C (lit. (10) m.p. 85.5–86° C). The nitriles were reduced to 2-α-naphthylethylamine-1-C^{14} and 2-β-naphthylethylamine-1-C^{14}, respectively, by means of lithium aluminum hydride, according to the method of Amundsen and Nelson (11). The yields were about 45%. The acetyl derivatives of the α- and β-isomers melted at 90–91° C and 109–110° C, respectively (lit. (12) m.p. 91° C and 110° C).

Reaction of Amines with Nitrous Acid in Acetic Acid

Sodium nitrite (12 g, 0.17 mole) was added portionwise, with stirring, to a solution of 10 g (0.14 mole) of 2-α- or 2-β-naphthylethylamine-1-C^{14} in 50 ml of glacial acetic acid. After complete addition, stirring was continued for $\frac{1}{2}$ hour and the mixture was then poured into ice water. The resulting material was extracted with ether, and the combined extracts were washed with saturated sodium bicarbonate solution and with water and then dried over magnesium sulphate before the ether was removed. A solution of 8 g of sodium in 250 ml of 95% ethanol was added and the mixture refluxed for 8 hours and then poured into cold hydrochloric acid. The resulting mixture was extracted with ether, and the extracts were washed and dried as described above. The products were collected at 136–142° C at 0.12 mm and 159–166° C at 4 mm for the α- and β-isomers, respectively. Both alcohols solidified on being cooled and were recrystallized twice from petroleum ether. Average yields of twice-recrystallized 2-α- and 2-β-naphthylethyl alcohols for the various runs were 20%. The α-isomer melted at 61–62° C (lit. (6) m.p. 60.5–61.5° C), the β-isomer melted at 67–68° C (lit. (13) m.p. 67.5–68° C).

In another experiment with 2-α-naphthylethylamine-1-C^{14}, 2-α-naphthylethyl acetate was isolated in 57% yield and then reduced to the alcohol with lithium aluminum hydride by the method of Lee and Spinks (2).

Reaction of Amines with Nitrous Acid in Aqueous Medium

2-α-Naphthylethylamine-1-C^{14} (10g, 0.14 mole) was placed in a 1-liter flask and 800 ml of water added. Sufficient concentrated hydrochloric acid was introduced to bring the pH of the solution to 5. The solution

was then frozen to a slush, and stirred while 8.0 g of sodium nitrite in 20 ml of water was added portionwise. With continued stirring during the next hour, small amounts of sodium nitrite were added, together with sufficient hydrochloric acid to maintain a pH of 5. The mixture was stirred for an additional 2 hours, heated to boiling, removed from the heat, and then stirred overnight. It was then extracted with ether and the combined extracts were washed with dilute hydrochloric acid, sodium bicarbonate solution, and distilled water. After drying and removal of the ether, the residue was distilled under reduced pressure.

The reaction with the β-isomer was carried through in the same manner, except that about 1600 ml of water was used for 10 g of amine. Even at this dilution, the amine hydrochloride was almost insoluble and the reaction was carried out with the hydrochloride in suspension.

Although crude yields of the 2-α- and 2-β-naphthylethyl alcohols were comparable to those obtained in acetic acid medium, there was greater contamination by a yellow impurity, necessitating four to five recrystallizations to give the pure products in overall yields of about 5–10%.

Oxidation of 2-α- or 2-β-Naphthylethyl Alcohol or Amine

One gram of the alcohol or amine was placed in 50 ml of distilled water containing 2.5 g of potassium permanganate and 1.0 g of sodium hydroxide. The mixture was heated on the steam bath until complete discoloration of the permanganate occurred (15–20 minutes). The manganese dioxide was removed by filtration and the filtrate washed twice with ether before it was acidified with sulphuric acid. The crude α- or β-naphthoic acid was collected by suction in yields of 30–40%. The use of larger amounts of permanganate and sodium hydroxide and a longer reaction time resulted in decreased yields.

The crude α-naphthoic acid was recrystallized three times from cyclohexane, the β-naphthoic acid recrystallized once from cyclohexane and twice from ligroin, giving pure acids, m.p. 161.5–162° C and 184.5–185° C, respectively (lit. (14) m.p. 162° C and 185° C).

ACKNOWLEDGMENTS

The financial support given by the National Research Council of Canada is gratefully acknowledged.

REFERENCES

1. J. D. ROBERTS and C. M. REGAN. J. Am. Chem. Soc. **75**, 2069 (1953).
2. C. C. LEE and J. W. T. SPINKS. Can. J. Chem. **31**, 761 (1953).
3. J. D. ROBERTS and J. A. YANCEY. J. Am. Chem. Soc. **74**, 5943 (1952).
4. M. J. S. DEWAR. J. Am. Chem. Soc. **74**, 3357 (1952).
5. R. F. NYSTROM and W. G. BROWN. J. Am. Chem. Soc. **69**, 1197 (1947).
6. H. ADKINS and E. E. BURGOYNE. J. Am. Chem. Soc. **71**, 3528 (1949).
7. M. J. S. DEWAR and R. J. SAMPSON. J. Chem. Soc. 2789 (1956).
8. H. GILMAN and J. E. KIRBY. J. Am. Chem. Soc. **51**, 3475 (1929).
9. W. WISLICENUS and H. ELVERT. Ber. **49**, 2820 (1916).
10. J. VON BRAUN and K. MOLDAENKE. Ber. **56**, 2169 (1923).
11. L. H. AMUNDSEN and L. S. NELSON. J. Am. Chem. Soc. **73**, 242 (1951).
12. I. HEILBRON and H. J. BUNBURY. Dictionary of organic compounds. Vol. 3. Eyre and Spottiswoode, London. 1953. p. 587.
13. D. SONTAG. Compt rend. **197**, 1130 (1933).
14. R. L. SHRINER and R. C. FUSON. Identification of organic compounds. 3rd ed. John Wiley and Sons, New York. 1948. p. 224–225.

THE REACTION OF ISOPROPANOL VAPOR WITH Hg 6($^3P_1$) ATOMS

PART I. PURE SUBSTRATE

ARTHUR R. KNIGHT AND HARRY E. GUNNING
Department of Chemistry, University of Alberta, Edmonton, Alberta

Received February 8, 1962

ABSTRACT

The reaction of isopropanol vapor with Hg 6($^3P_1$) atoms has been investigated under static conditions at 25° C under continuous and intermittent illumination. The effect of added inert gas and isolation of the 2537 Å Hg resonance line were also studied.

The products of the reaction are H_2 (0.72), CH_3COCH_3 (0.25), CO, CH_4, C_2H_6, CH_3CHO, and H_2O, with the numbers in parentheses representing the quantum yields at zero exposure time. The non-volatile product remaining in the cell was a mixture of C_6-glycols, containing 98.6% pinacol, 1.2% 2-methyl-2,4-pentanediol, and ca. 0.2% or less of 2,5-hexanediol.

Under intermittent illumination, the quantum yield of hydrogen production, measured as a function of light period, t_L, rose linearly with log t_L, and had a constant value of unity for $t_L < 0.45$ msec. A mechanism is proposed involving the primary formation with perfect efficiency of isopropoxy radicals and H atoms.

INTRODUCTION

Recent investigations of the reactions of alcohol vapors with Hg 6($^3P_1$) atoms have shown that for methanol (1, 2, 3) and ethanol (4) the primary process is an almost exclusive split into an alkoxy radical and hydrogen atom. Utilizing intermittent-illumination techniques, values for the primary quantum yield, Φ^0, of hydrogen atom production of at least 0.89 for methanol (3) and 0.96 for ethanol (4) have been found. The corresponding values, as determined by extrapolation to zero extent of reaction, under steady illumination, were 0.45 and 0.53 respectively. The lower values for $\Phi(H_2)$ under continuous illumination were ascribed to a rapid back reaction between hydroxyalkyl radicals and hydrogen atoms competing with H_2 formation by abstraction from the substrate. As the light period was made progressively shorter the mean radical concentration decreased, favoring the abstraction reaction, with a resulting increase in the hydrogen yield. Thus for ethanol, where the α C—H bond energy is presumed to be lower than for methanol, the abstraction step competes more effectively with the back reaction, and higher values of $\Phi(H_2)$ are observed under both steady and intermittent illumination. In isopropanol, which has a tertiary C—H bond, still higher yields of H_2 would be expected under comparable conditions. Furthermore, since the tertiary C—H bond energy in isopropanol would be considerably lower than that of the O—H, demonstration of an exclusive O—H bond scission would give strong evidence in support of the generality of preferential quenching of Hg 6($^3P_1$) atoms at the oxygen site, in the alcohol series.

In the present investigation, the studies carried out in this laboratory on the alcohols (2, 3, 4) have been extended to isopropanol. The reactions of this alcohol with Hg 6($^3P_1$) atoms, under continuous and intermittent illumination, have been examined.

The details of the investigation follow.

EXPERIMENTAL

The apparatus used for the continuous-illumination experiments was essentially identical with that employed for the methanol reaction (2). The techniques and equipment used for the intermittent-illumination studies have also been described previously (4).

The isopropanol was Nichols reagent grade. After degassing and trap-to-trap distillation, rejecting large head and tail fractions, the reagent was stored in a quartz trap connected to the reaction system. Gas chromatographic analysis showed no detectable impurities other than ca. 0.05% water. Mass spectrometric analysis proved the absence of any triisopropylborate in a sample of the alcohol which had been stored in a pyrex vessel for 48 hours. The neon (Airco assayed reagent) was used without further purification.

The analysis of the reaction products was carried out by gas chromatography and mass spectrometry. Products condensable in liquid nitrogen were separated by a 2.5-m 8% didecylphthalate-on-Fluoropak column, operating at 35°, with a hydrogen flow of 80 cc/min. Carbon monoxide and methane were determined on a molecular-sieves column, and by mass spectrometric analysis of the total non-condensable yield. Hydrogen was obtained from the difference between the total non-condensable gas and the yield of CO + CH_4. Mass spectrometry was also employed for hydrogen analyses in the runs with added neon.

For the analysis of the involatile products, which formed as a deposit on the cell walls, two 10-hour runs were performed, and the cell deposit was dissolved in acetone and analyzed for glycols by the same procedure as used in the ethanol investigation (4). The presence of pinacol was confirmed by the sodium metaperiodate titration of Dal Nogare and Oemler (5). Here the cell deposit formed in a 3-hour run was analyzed by carrying out the titration on an aqueous solution of three washings of the reaction vessel.

The condensable products of the reaction were identified by their column retention times and the identification was confirmed by mass spectrometric analysis of each peak trapped from the chromatographic effluent.

In the experiments with filtered light, one reaction was performed with the light beam filtered by a solution of *trans,trans*-1,4-diphenyl-1,3-butadiene in a 1-cm path length cell (6). The solution had a narrow transmission band centered at ca. 2600 Å, with 39% transmission at 2537 Å. In the comparison run, using the same geometry, the light beam was attenuated by several quartz plates arranged to give 40% transmission of the 2537 Å line.

Light intensities were determined with propane as actinometer (7), using the differential method of Back (8) to determine the steady-state value of dH_2/dt. Four light intensities were employed in the experiments and the values, in μeinsteins/min, were (*a*) 1.25 (double sector); (*b*) 1.43 (single sector); (*c*) 1.78 and 1.35 (continuous illumination).

RESULTS

All experiments were carried out at a pressure of 40.0 mm isopropanol at room temperature, 25±1° C. The products of the reaction were found to be H_2, CO, CH_4, C_2H_6, MeCHO, $Me_2(CO)$, H_2O, pinacol, 2,5-hexanediol, and 2-methyl-2,4-pentanediol.

The results of the investigation of the reaction as a function of exposure time are presented in Figs. 1 and 2 as follows: Fig. 1 $\Phi(H_2)$, $\Phi(Me_2CO)$; Fig. 2 $\Phi(CO)$, $\Phi(CH_4)$, $\Phi(C_2H_6)$, and $\Phi(MeCHO)$. In these and subsequent figures for continuous-illumination work, the points given usually represent the mean value for two runs. Water was not determined, but a semiquantitative estimate showed it to be a minor product of the reaction. Glycol formation was not studied as a function of exposure time, but gas chromatographic analysis of the cell deposit gave a distribution among the three glycols of 98.6% pinacol, 1.2% 2-methyl-2,3-pentanediol, and ca. 0.2% or less of 2,5-hexanediol.

The effect of intermittent illumination on the reaction was also investigated, and the yields of hydrogen and acetone, as a function of light period t_L, for dark periods, t_D, of 0.102 and 0.160 sec and a net exposure time of 1 minute, are presented in Fig. 3. No separate study was made on the effect of varying t_D, but as for methanol and ethanol, the quantum yield appeared to be independent of t_D at values greater than 100 msec (cf. Fig. 3). It must be pointed out here that, although the actual value of $\Phi(H_2)$ on the plateau of the curve is 0.98, this should be considered to be unity within experimental error on an absolute scale.

Two runs were carried out at a reaction time of 10 minutes with added neon, with substrate pressure of 40.0 mm. The yields of Me_2CO, H_2, C_2H_6, and MeCHO, uncorrected for competitive quenching by neon, are presented in Table I, along with the same results for a neon-free run at the same exposure time.

To assess the importance of light of wavelength other than 2537 Å on the secondary decomposition of acetone, two reactions at approximately the same absorbed intensity

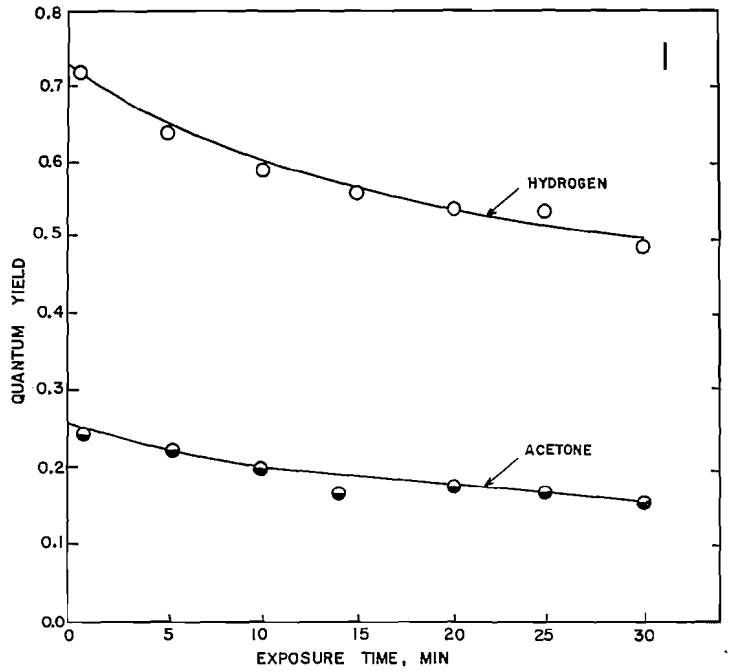

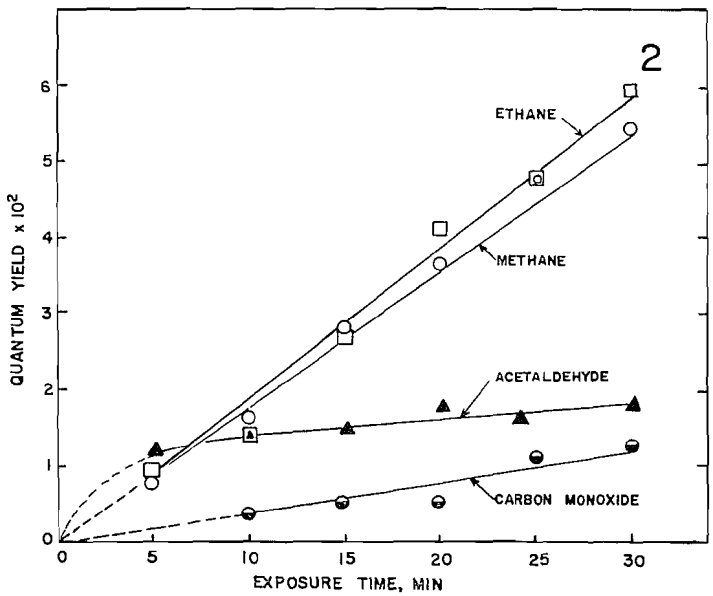

FIG. 1. Quantum yield of hydrogen, ○; and acetone, ◒, as a function of exposure time for pure isopropanol, at a pressure of 40 mm.

FIG. 2. Quantum yield of ethane, □; methane, ○; acetaldehyde, ▲; and carbon monoxide, ◒, as a function of exposure time for pure isopropanol, at a pressure of 40 mm.

at 2537 Å were carried out, with I_a calculated to be 0.6 μeinstein/min. In one of these experiments only the 2537 Å line was admitted using the filter described above. The results of the two experiments at exposure times of 30 minutes are given in terms of ratios of moles of products formed, in Table II.

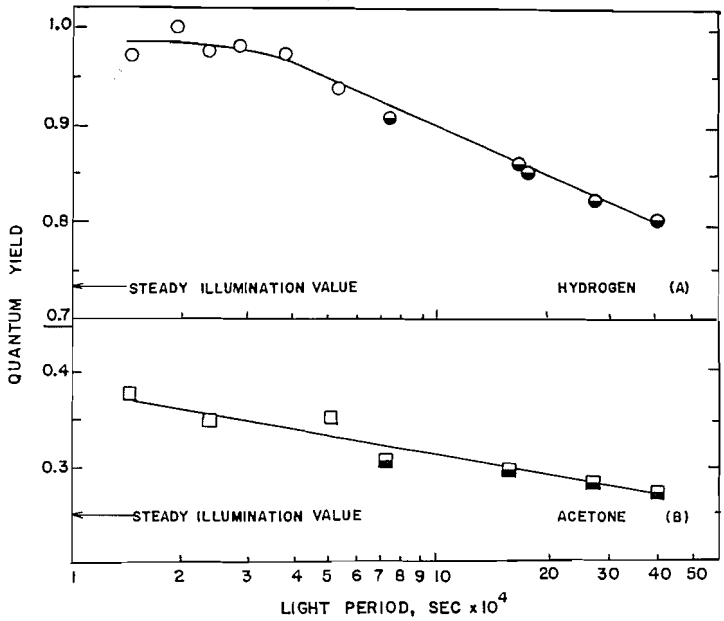

FIG. 3. Quantum yield of hydrogen, curve A, and acetone, curve B, as a function of light period, for dark periods of 160 msec, open symbols, and 103 msec, half-closed symbols, for pure isopropanol at a pressure of 40 mm. The Φ values obtained by extrapolation of the steady illumination data are indicated on the ordinate.

TABLE I

Effect of added inert gas on the reaction of isopropanol with Hg $6(^3P_1)$ atoms at a substrate pressure of 40 mm

P (neon), mm	$\Phi(H_2)$	$\Phi(Me_2CO)$	$\Phi(MeCHO) \times 10^2$	$\Phi(C_2H_6) \times 10^2$
0	0.583	0.197	1.48	1.4
100	0.551	0.195	1.56	1.4
300	*	0.178	1.55	*

*No analysis made.

TABLE II

Effect of filtered light on the secondary decomposition of acetone

	Ratio of moles formed in 30 minutes	
Product	Filtered light	Unfiltered light
Me_2CO	100	100
C_2H_6	14	14
MeCHO	7.8	6.7

DISCUSSION

In Part II of this series it will be demonstrated that the primary process is a scission of the O—H bond, leading to the production of an isopropoxy radical and a hydrogen atom. Including this reaction as the initial step, the following mechanism is proposed to account for the salient features of the isopropanol reaction:

$$Me_2CHOH + Hg\ 6(^3P_1) \rightarrow Me_2C\dot{H}O + H + Hg\ 6(^1S_0) \quad [1]$$

$$Me_2CHOH + H \rightarrow Me_2\dot{C}OH + H_2 \quad [2]$$

$$Me_2CHOH + Me_2C\dot{H}O \rightarrow Me_2\dot{C}OH + Me_2CHOH \quad [3]$$

$$2Me_2\dot{C}OH \rightarrow Me_2CO + Me_2CHOH \quad [4]$$

$$2Me_2\dot{C}OH \rightarrow Me_2C(OH)(HO)CMe_2 \quad [5]$$

$$H + Me_2\dot{C}OH \rightarrow Me_2CHOH. \quad [6]$$

Abstraction from the α-carbon atom in reactions [2] and [3] is indicated by the formation of pinacol as the predominant non-volatile product, and is in agreement with several investigations of radical abstraction reactions from alcohols (9, 10, 11, 12). Trotman-Dickenson and Steacie (13) estimate the activation energy for methyl abstraction from isopropanol to be 7.3 kcal/mole. It appears unlikely that E_{act} for reaction [3] would exceed this value. From the observed yield of the two glycols other than pinacol, reactions [2] and [3] must also result in a small but finite yield of the $\dot{C}H_2CH(OH)Me$ radical.

Reaction [4], as the mode of acetone production, is proposed in preference to the alternative routes:

$$Me_2CHOH + Hg\ 6(^3P_1) \rightarrow Me_2CHOH^* + Hg\ 6(^1S_0) \quad [1']$$

or

$$Me_2COH + H \rightarrow Me_2CHOH^*, \quad [6']$$

both being followed by

$$Me_2CHOH^* \rightarrow Me_2CO + H_2. \quad [4']$$

If an excited molecule were the precursor for acetone, then at high pressures of added inert gas, where collisional deactivation would be the predominant fate of Me_2CHOH^*, a decreased yield of both acetone and hydrogen would be observed. The data in Table I indicate, however, that apart from a slight decrease due to competitive quenching of the resonance radiation by the neon, the yields of these products are independent of pressure of added neon. Furthermore, in Part II of this series it will be shown that at short exposure times in the presence of nitric oxide, there is not the equivalence of $\Phi(H_2)$ and $\Phi(Me_2CO)$ which would be expected if reaction [4'] were an important step in the reaction sequence.

The other possible route to acetone formation would be from the disproportionation of isopropoxy radicals. However, the low stationary-state concentration of this species, as indicated by the absence of hydroxy ethers among the products, would suggest that this reaction is unimportant in the present system.

The increase in $\Phi(Me_2CO)$ at progressively shorter light periods under intermittent illumination, shown in Fig. 3, also favors reaction [4]. Certainly it appears reasonable to assume that the lifetime of H atoms in the system is considerably shorter than that of $Me_2\dot{C}OH$, and hence there should be a major segment of the dark period during which the H-atom concentration is essentially zero, and consequently the sole fate of $Me_2\dot{C}OH$ would be reactions [4] and [5], resulting in the observed increase in acetone production.

Figure 2 indicates that ethane, methane, and carbon monoxide have primary quantum yields of zero, indicating that these products are not of primary origin. It is likely that these products arise from the secondary decomposition of acetone. The experiments with filtered light, given in Table II, in which the secondary decomposition of acetone is shown to be unaffected by isolation of the 2537 Å resonance line, suggest that the acetone is reacting with Hg $6(^3P_1)$ atoms or with the resonance line itself. Steacie and Darwent

(14) have given evidence of the close similarity between the sensitized reaction and the photolysis at 2537 Å. The overall result of the secondary decomposition of acetone can be represented as:

$$Me_2CO + Hg\ 6(^3P_1) \rightarrow 2CH_3 + CO + Hg\ 6(^1S_0) \quad [7]$$

and accounts for the appearance of methane, ethane, and carbon monoxide as reaction products.

Whether the yield of the minor product, acetaldehyde, does in fact extrapolate to zero at zero extent of reaction remains uncertain, but it appears likely that at least some of this minor product may be arising from the decomposition of isopropoxy radicals by the reaction

$$Me_2CHO \rightarrow MeCHO + CH_3, \quad [8]$$

as observed by Wijnen (15) in the photolysis of isopropyl propionate.

Finally, our data for the reaction under intermittent illumination require comment. The observed increase in the yield of hydrogen, as the light period is made progressively shorter, indicates that as the mean radical concentration is reduced, the importance of reaction [6] as a fate of hydrogen atoms produced in the primary process is diminishing, and, in the plateau region of the curve of Fig. 3, the exclusive fate of hydrogen atoms is step [2], resulting in the observed quantum yield of unity.

CONCLUSIONS

The overall features of the reaction are similar to those of the *n*-chain alcohols previously investigated. The presence of a particularly weak C—H bond in isopropanol, however, leads to some important differences. In particular, $\Phi^0(H_2)$ is 0.72 for isopropanol, compared to 0.46 for methanol (2) and 0.53 for ethanol (4). In the intermittent illumination studies, a similar effect is observed. Here at $t_L = 0.15$ msec, the shortest light period studied, values for $\Phi(H_2)$ are 0.89 for methanol (3); 0.96 for ethanol (4), and 1.0 for isopropanol. It may be concluded that for ethanol and isopropanol and likely for methanol, H atoms are produced with perfect efficiency in the primary process.

ACKNOWLEDGMENTS

The authors take pleasure in expressing their thanks to Mr. R. K. Taylor of this laboratory for performing the mass spectrometric analyses.

This research was supported in part by the National Research Council under Block Term Grant No. T 162 (Gunning), which support is gratefully acknowledged.

REFERENCES

1. R. F. Pottie, A. G. Harrison, and F. P. Lossing. Can. J. Chem. **39**, 102 (1961).
2. A. R. Knight and H. E. Gunning. Can. J. Chem. **39**, 1231 (1961).
3. A. R. Knight and H. E. Gunning. Can. J. Chem. **39**, 2251 (1961).
4. A. R. Knight and H. E. Gunning. Can. J. Chem. **39**, 2466 (1961).
5. S. Dal Nogare and A. N. Oemler. Anal. Chem. **24**, 902 (1952).
6. N. Slagg and R. A. Marcus. J. Chem. Phys. **34**, 1013 (1961).
7. S. Bywater and E. W. R. Steacie. J. Chem. Phys. **19**, 319 (1951).
8. R. A. Back. Can. J. Chem. **37**, 1834 (1959).
9. M. S. Karasch, J. L. Rowe, and W. H. Ury. J. Org. Chem. **16**, 905 (1951).
10. W. R. McDonnell and A. S. Newton. J. Am. Chem. Soc. **76**, 4651 (1954).
11. W. H. Ury, W. H. Stacey, E. S. Huyser, and O. O. Juveland. J. Am. Chem. Soc. **76**, 450 (1954).
12. S. R. Symons and M. Townsend. J. Chem. Phys. **25**, 1299 (1956).
13. A. F. Trotman-Dickenson and E. W. R. Steacie. J. Chem. Phys. **19**, 329 (1951).
14. E. W. R. Steacie and B. DeB. Darwent. Can. J. Chem. **16**, 230 (1948).
15. M. H. J. Wijnen. Can. J. Chem. **36**, 691 (1958).

SYNTHESIS IN THE PYRIDINE SERIES

II. THE SYNTHESIS OF NEW 3,4,5-TRIALKYLATED PYRIDINES

JAMES P. KUTNEY AND T. TABATA
Department of Chemistry, University of British Columbia, Vancouver, British Columbia
Received February 12, 1962

ABSTRACT

A synthetic sequence leading to new and inaccessible 3,4,5-trialkylated pyridines has been developed. The nature of the synthesis allows the preparation of virtually any type of 3,4,5-trialkylated pyridine by simple, straightforward variations at the appropriate stage.

Recently, in connection with the structural elucidation of a new alkaloid, we became involved in the developing of a synthetic sequence to new 3,4,5-trialkylated pyridines. In Part I of this series (1) we described a general approach to this goal and, in particular, indicated that the substance 3,4-dimethyl-5-cyanopyridine (I) was a valuable intermediate for the synthesis of various new trialkylated pyridines of this type. We now wish to describe some of our results which support this view.

There are numerous possible modifications of the cyano group and we have already indicated (1) the conversion of this group to an ester function to provide an intermediate for the preparation of pyridines of the type A. In order to provide entry into another series of branched-chain pyridines (type B) we reacted 3,4-dimethyl-5-cyanopyridine with methylmagnesium iodide to obtain 3,4-dimethyl-5-acetylpyridine (II). The success of this reaction was readily evident from the infrared spectrum of the product, which indicated a virtual disappearance of the absorption due to the cyano function (4.48 μ) and the appearance of the characteristic carbonyl band (5.94 μ). This ketonic substance was subsequently treated with ethylmagnesium iodide, and the expected alcohol, III, was obtained as a light yellow viscous liquid. This substance resisted all attempts to crystallize —a rather surprising behavior since the analogous substance, 3,4-dimethyl-5-(2-hydroxy-2-propyl)-pyridine, reported previously (1), was a crystalline material. Nevertheless, characterization of the substance established, beyond doubt, that it possessed the expected structure. The infrared spectrum possessed a typical hydroxyl absorption and the nuclear magnetic resonance (n.m.r.) spectrum was particularly instructive. The presence of a triplet at high magnetic field (9.22 τ) indicated a methyl group flanked by a methylene carbon which in turn was indicated by a quartet centered at 8.16 τ. Another signal at 8.5 τ was assigned to a methyl group attached to an oxygen-bearing carbon and a weak signal at 4.6 τ was attributed to a proton on oxygen. This evidence established the presence of the 2-hydroxy-2-butyl group attached to the pyridine nucleus. The remaining signals—two sharp spikes at 7.85 and 7.58 τ characteristic of methyl protons attached to the pyridine ring (1), and a doublet at low field (2.08 τ) attributable to α protons on the pyridine ring (1, 2)—served to establish, beyond doubt, the structure III.

The removal of the hydroxyl function had been successfully accomplished in our previous work by means of red phosphorus and hydriodic acid and we attempted to utilize this reaction in this series. In contrast to the successful conversion of 3,4-dimethyl-5-(2-hydroxy-2-propyl)-pyridine to 3,4-dimethyl-5-isopropylpyridine by conducting the reaction at the reflux temperature for 24 hours, the corresponding conversion of III to the desired 3,4-dimethyl-5-*s*-butylpyridine (V) did not proceed to completion. Even

under more drastic conditions (48 hours' reflux), the reaction product always consisted of a mixture, the olefinic substance IV and the desired V. The greater resistance of the olefinic bond to reduction was further indicated by catalytic hydrogenation studies. When the hydrogenation of IV was performed under conditions previously used for 3,4-dimethyl-5-isopropenylpyridine (Adams catalyst, atmospheric pressure, and room temperature), incomplete reduction was observed, as evidenced by an olefinic signal in the n.m.r. spectrum. However, the desired pyridine, V, was obtained when the reduction was allowed to proceed at more stringent conditions (Adams catalyst, 32 p.s.i.). The ultraviolet spectrum of this product was characteristic of an alkylated pyridine and the n.m.r. spectrum provided strong support for this structure.

For the preparation of 3,4-dimethyl-5-ethylpyridine, which was necessary for further studies in this area, we considered the direct reduction of the acetyl function in II to an ethyl group. The most convenient method appeared to be the Wolff–Kishner reduction, a reaction frequently employed in the pyridine series (3). Indeed, reaction of 3,4-dimethyl-5-acetylpyridine under the Huang-Minlon modification of the Wolff–Kishner reduction (4) provided the expected 3,4-dimethyl-5-ethylpyridine. The n.m.r. spectrum was in complete agreement with the assigned structure. It indicated a triplet at high field (8.84 τ) and a quartet at lower field (7.42 τ), to provide strong evidence for the ethyl group. The intense signal at 7.86 τ, characteristic of methyl protons attached to the pyridine ring, and a weak signal at low field, typical of α protons, accounted for the remaining hydrogen atoms.

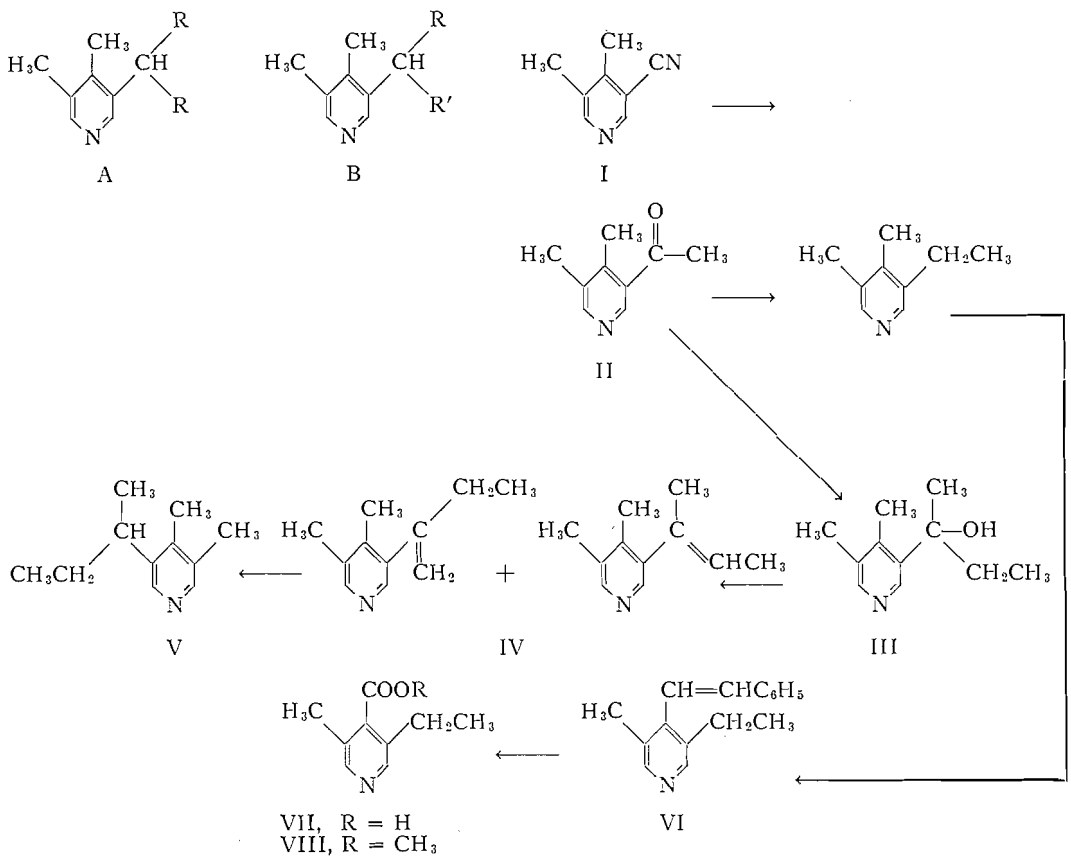

The successful synthesis of 3,4-dimethyl-5-ethylpyridine allowed us to consider the steric effects of the substituents attached to carbon atoms 3 and 5 on the reactivity of the methyl group at the 4 position. We became interested in this aspect of the problem, since some of our previous work has already indicated that this steric effect could be substantially important in certain reactions. For example, we had indicated previously (1) that 3,5-dimethyl-4-acetylpyridine possesses a very unreactive carbonyl group to organometallic reagents, a factor which must be attributed, at least in part, to the steric influence of the neighboring methyl groups. It appeared to us that some more information regarding this point could be deduced from the aldol-type condensation reactions of 3,4-dimethyl-5-ethylpyridine with such aldehydes as benzaldeyde. This reaction has been utilized in pyridine chemistry on numerous occasions and has proved to be of considerable synthetic value (5, p. 200). When 3,4-dimethyl-5-ethylpyridine was reacted with benzaldehyde under rather drastic conditions, the corresponding 3-methyl-5-ethyl-4-styrylpyridine, VI, was formed in moderate yield. The success of the reaction was easily recognized from consideration of the spectral data. The infrared spectrum, with a weak band at 6.12 μ, was consistent with the presence of a new olefinic bond and the n.m.r. spectrum was particularly informative. The characteristic signals for the ethyl group were still present and, in particular, the intense signal due to the C_3- and C_4-methyl groups in the starting material was considerably reduced and consistent with the presence of only *one* methyl group. The olefinic proton region exhibited a characteristic *AB* splitting pattern with a separation of 17 c.p.s., suggesting a trans orientation of the olefinic bond, and the appearance of the usual aromatic signals served to further confirm the 4-styrylpyridine structure. The ultraviolet spectrum was very interesting in that it was considerably different from the spectra reported previously for compounds of this type (6, 7). The main absorption band at 278 mμ represented a small bathochromic shift from the usual alkyl pyridine absorption (263–268 mμ) but this absorption is nevertheless significantly lower than that of such compounds as 4-styrylpyridine (307 mμ), and the intensity of the absorption of VI is lower. We believe that this rather anomalous spectrum is due to the fact that the neighboring alkyl substituents at the 3- and 5-positions cause the styryl moiety to lie out of the plane of the pyridine ring, thereby reducing the effect of the additional conjugation. From the above results it can be concluded that although the 4-methyl function is somewhat hindered it is still capable of entering into condensation reactions with carbonyl compounds. The yield in this reaction is, however, somewhat lower than reported in other series (8).

The isolation of 3-methyl-5-ethyl-4-styrylpyridine from the condensation reaction was useful in providing a synthetic intermediate for the synthesis of pyridine derivatives possessing different functions at the 4-position. We therefore considered several methods to convert the olefinic linkage to a carboxyl function. This type of reaction has been used in pyridine chemistry for the synthesis of pyridine carboxylic acids or aldehydes (5, p. 207). The reaction of choice involved ozonolysis, and we subjected 3-methyl-5-ethyl-4-styrylpyridine to this reaction. The product of this reaction was the expected carboxylic acid, VII, obtained as a high-melting, crystalline substance. Recently the ozonolysis of vinylpyridines has been shown to yield, under similar conditions, the corresponding pyridinecarboxylic acids (9). This material was readily converted to the methyl ester VIII by treatment with an ethereal solution of diazomethane. The structure of the ester was established, beyond doubt, by the n.m.r. spectrum of this substance. Apart from the characteristic signals for the presence of the ethyl and methyl groups attached directly to the pyridine nucleus, a sharp signal at 6.21 τ confirmed the presence of the ester methyl.

In conclusion, we would like to point out that these studies have provided intermediates which can be used to prepare virtually any type of 3,4,5-trialkylated pyridine. Firstly, it is obvious that any Grignard reaction on 3,4-dimethyl-5-cyanopyridine, followed by the appropriate steps, provides numerous variations to the type of group attached at C_5. Secondly, the appropriate ester analogous to VIII provides entry into various possibilities at C_4 and finally the nature of the alkyl group at C_3 can be likewise varied. It is pertinent to note that in the original Guareschi cyclization, which provides the starting material for the above work, the nature of the alkyl group at C_3 is determined by the nature of the acetoacetic ester molecule used in the cyclization. Consequently appropriate variations in the synthetic sequence will yield numerous new and otherwise difficultly accessible 3,4,5-trialkyl pyridines.

EXPERIMENTAL

All melting points were determined on a Fischer–Johns apparatus and are uncorrected. The ultraviolet spectra were recorded in 95% ethanol on a Cary 14 recording spectrophotometer. Infrared spectra were recorded on a Perkin–Elmer model 21 spectrophotometer. The n.m.r. spectra were taken at 60 Mc on a Varian A60 instrument. In all cases integration of areas under the signals was carried out and the number of protons corresponding to each signal is indicated in parentheses. Values are given in the Tiers τ scale with tetramethylsilane used as the external standard, set at 10.0 τ units. The solvent used was carbon tetrachloride. The analyses were performed by Dr. A. Bernhardt and his associates, Mulheim (Ruhr), Germany, and by Mrs. A. Aldridge, University of British Columbia.

3,4-Dimethyl-5-acetylpyridine (II)

A solution of 3,4-dimethyl-5-cyanopyridine (I, 22.2 g) in anhydrous ether (350 ml) was added slowly to a stirred solution of methylmagnesium iodide, prepared in the usual manner (48.5 g Mg, 385 g methyl iodide) in dry ether (630 ml). After the addition was complete, the reaction mixture was refluxed for 4 hours and then allowed to stand overnight at room temperature. The excess Grignard and the complex were destroyed by the addition of dilute ammonia until there was no further reaction. The resulting mixture was saturated with sodium chloride and extracted exhaustively with ether. The ether extract was dried over anhydrous magnesium sulphate and the solvent evaporated to yield a liquid product. Distillation of this material at a bath temperature of 120–130° at 2.5 mm provided a clear liquid product (10.9 g). This material was suitable for subsequent reactions although it contained traces of the starting cyano compound, which was very difficult to remove by distillation.

Chromatography of a small portion (3.8 g) of this liquid on alumina (250 g) provided a good separation. Elution with petroleum ether – ethyl ether (4:1) yielded a mixture of the acetylpyridine and the cyanopyridine in the initial fractions, and then the pure 3,4-dimethyl-5-acetylpyridine (1.2 g) was obtained in the later fractions. Elution with pure ether removed the remaining material.

An analytical sample of the acetylpyridine distilled at 144° at 22 mm; n_D^{20} 1.4166; infrared: 5.94 μ; ultraviolet: λ_{max} 231 mμ (log ϵ 3.73), λ_{max} 271 mμ (log ϵ 3.40), λ_{min} 254 mμ (log ϵ 3.24). Found: C, 72.43; H, 7.38; O, 10.74; N, 9.39. Calc. for $C_9H_{11}ON$: C, 72.45; H, 7.43; O, 10.72; N, 9.39.

A picrate, m.p. 162–163°, was prepared in ethanol and recrystallized several times from ethanol. Found: C, 47.82; H, 3.81; O, 33.52; N, 14.90. Calc. for $C_{15}H_{14}O_8N_4$: C, 47.62; H, 3.73; O, 33.84; N, 14.81.

3,4-Dimethyl-5-(2-hydroxy-2-butyl)-pyridine (III)

A solution of 3,4-dimethyl-5-acetylpyridine (0.81 g) in anhydrous ether (14 ml) was added slowly to a stirred solution of ethylmagnesium iodide (1.8 ml ethyl iodide, 0.52 g Mg turnings) in ether (20 ml). After the addition was complete, the reaction mixture was refluxed for 12 hours and then allowed to stand overnight at room temperature. The mixture was cautiously treated with dilute ammonia and the resulting basic mixture was saturated with sodium chloride. The reaction mixture was then extracted several times with ether and the ethereal layer dried over anhydrous magnesium sulphate. Removal of the solvent yielded a viscous liquid (1.07 g). This material was taken up in a small amount of chloroform and placed on a column of alumina (100 g). Elution with petroleum ether – ethyl ether (9:1) yielded traces of the starting material. Further elution with ethyl ether and chloroform provided the desired alcohol (III, 0.54 g). A small portion of this material was distilled to yield the analytical sample of the alcohol, as a light yellow viscous liquid (b.p. 144° at .01 mm); infrared: 2.95–3.2 μ, very broad; ultraviolet: λ_{max} 263 mμ (log ϵ 3.36), λ_{max} 271 mμ (log ϵ 3.30), λ_{min} 236 mμ (log ϵ 2.83); n.m.r. signals: triplet centered at 9.22 τ (methyl of ethyl group, area = 3H), 8.5 τ (CH_3—C—OH, area = 3H), quartet centered at 8.16 τ (methylene of CH_3CH_2—C—OH), 7.85, 7.58 τ (methyls attached to ring, area = 6H), 4.6 τ (OH, area = 1H), doublet centered at 2.08 τ (—αH, area = 2H). Found: C, 73.37; H, 9.40; O, 9.11; N, 8.27. Calc. for $C_{11}H_{17}ON$: C, 73.70; H, 9.56; O, 8.93; N, 7.81.

The picrate, prepared in the usual manner, was recrystallized several times from ethanol to yield an analytical sample which melted at 136–137.5°. Found: C, 50.32; H, 4.40; O, 31.22; N, 13.73. Calc. for $C_{17}H_{20}O_8N_4$: C, 50.00; H, 4.84; O, 31.34; N, 13.72.

Subsequent preparations of this alcohol were carried out very conveniently from the acetylpyridine without careful purification of the intermediates. That is, the crude product from the reaction of 3,4-dimethyl-5-acetylpyridine and methylmagnesium iodide was treated directly with ethylmagnesium iodide and this product chromatographed as above. An overall yield of 27% of the pure alcohol was obtained.

3,4-Dimethyl-5-s-butylpyridine (V)

A mixture of 5-(2-hydroxy-2-butyl)-3,4-dimethylpyridine (0.85 g), concentrated hydriodic acid (9.3 ml, 47%), and red phosphorus (1.1 g) was refluxed for 24 hours. After the mixture had been cooled, the phosphorus was removed by filtration and the filtrate concentrated by distillation *in vacuo*. The dark residual oil was taken up in water (6 ml) and decolorized by the addition of sodium bisulphite. The mixture was made alkaline by the addition of potassium hydroxide pellets and the alkaline mixture was then extracted thoroughly with ether. After the ethereal extract had been dried over anhydrous sodium sulphate, the solvent was removed and the residual liquid was distilled using a bath temperature of 60–100° at 0.07 mm. The yield of the colorless liquid product was 478 mg. This product was a mixture of the desired material and some olefin resulting from incomplete reduction (n.m.r. signal at 4.5 τ). This olefinic material was present in small quantities even if the reflux period was increased to 48 hours. Consequently, it was found most convenient to carry out the reduction under catalytic hydrogenation conditions. A portion of the distilled liquid product (102 mg) was dissolved in glacial acetic acid (14 ml) and catalytically hydrogenated over Adam's catalyst (100 mg) at room temperature with a hydrogen pressure of 32 p.s.i. After 5 hours, the catalyst was filtered and the solvent removed on a steam bath *in vacuo*. The residue was treated with water (3 ml), and made alkaline by the addition of sodium bicarbonate and the resulting mixture was extracted exhaustively with ether. After the ethereal extract had been dried over anhydrous magnesium sulphate, the solvent was removed and the residual liquid distilled at 60–70° (bath temp.) at 0.05 mm to provide 73 mg of a pure liquid. A small portion was redistilled for an analytical sample (b.p. 135° at 22 mm); n_D^{20} 1.5078; ultraviolet: λ_{max} 264 mμ (log ϵ 3.41), λ_{max} 272 mμ (log ϵ 3.33), λ_{min} 231 mμ (log ϵ 2.39); n.m.r. signals: triplet centered at 9.18 τ (methyl of ethyl group, area = 3H), doublet centered at 8.80 τ (CH_3—C—H, area = 3H), multiplet centered at 8.38 τ (methylene of ethyl group, area = 2H), 7.83 τ (intense, methyls attached to ring, area = 6H), multiplet centered at 7.2 τ (H—C—CH_3, area = 1H), doublet centered at 1.98 τ (αH, area = 2H). Found: C, 80.95; H, 10.52; N, 8.40. Calc. for $C_{11}H_{17}N$: C, 80.92; H, 10.50; N, 8.58.

A picrate was readily prepared in the usual manner, and this upon several recrystallizations from alcohol provided a pure sample, m.p. 131–132°. Found: C, 52.07; H, 5.03; N, 14.43; Calc. for $C_{17}H_{20}N_4O_7$: C, 52.04; H, 5.14; N, 14.28.

3,4-Dimethyl-5-ethylpyridine

The reaction product (11.1 g) resulting from the reaction of 3,4-dimethyl-5-cyanopyridine (20 g) with a fourfold excess of methylmagnesium iodide was treated with hydrazine (6.5 ml), potassium hydroxide pellets (90 g), and diethylene glycol (13 ml) and heated in an oil bath at 150–170° for 2 hours. The bath temperature was then raised to 200° and the reaction mixture was kept at this temperature for a further 2 hours. The cooled reaction mixture was treated cautiously with a small portion of water and the resulting mixture was distilled. The fraction which came over at 109–116° was treated with more water (250 ml) and this aqueous mixture was thoroughly extracted with ether. After the ether extract had been dried over anhydrous magnesium sulphate, the solvent was removed and the residual liquid was distilled from potassium hydroxide pellets. A fraction (7.6 g) distilling over at 50–70° (bath temp.) at 0.14 mm was completely free from any carbonyl or cyanide impurities and proved to be the desired material. A small portion of this liquid was redistilled (b.p. 115–116° at 22 mm) and provided an analytical sample. n_D^{20} 1.5151; ultraviolet: λ_{max} 263 mμ (log ϵ 3.39), λ_{max} 266 mμ (log ϵ 3.38), λ_{max} 271 mμ (log ϵ 3.31), λ_{min} 238 mμ (log ϵ 2.91); n.m.r. signals: triplet centered at 8.84 τ (methyl of ethyl group, area = 3H), 7.86 τ (intense, area = 6H, methyls attached to ring), quartet centered at 7.42 τ (methylene of ethyl group, area = 2H), 1.98 τ (αH, area = 2H). Literature values (10): n_D^{20} 1.5136; b.p. 217° at 744 mm. Found: C, 79.82; H, 9.69; N, 10.25. Calc. for $C_9H_{13}N$: C, 79.95; H, 9.69; N, 10.36.

A picrate of the substance was prepared in ethyl alcohol and after several recrystallizations from this solvent an analytical sample, m.p. 130–131°, was obtained. Literature (10): m.p. 133°. Found: C, 49.54; H, 4.34; O, 30.88; N, 15.23. Calc. for $C_{15}H_{16}N_4O_7$: C, 49.45; H, 4.43; O, 30.74; N, 15.38.

3-Methyl-4-styryl-5-ethylpyridine (VI)

A mixture of 3,4-dimethyl-5-ethylpyridine (2.82 g), benzaldehyde (6.3 ml), potassium acetate (1.95 g), acetic anhydride (5.9 ml), and a small crystal of iodine was refluxed for 40 hours. The resultant dark brown reaction mixture was cooled and treated with aqueous hydrochloric acid until acidic, and the excess benzaldehyde was removed by steam distillation. The residue from the steam distillation was extracted with ether to remove acidic or neutral materials and the resulting aqueous layer was then made basic by the addition of sodium hydroxide pellets. This basic layer was extracted several times with ether, the ether extract dried over anhydrous magnesium sulphate, and the solvent removed. The residual liquid product was fractionally distilled and a fraction distilling up to 140° (bath temp.) at 0.4 mm, which contained a considerable amount of starting material, was separated. The subsequent fraction (2.59 g) came over as a

yellow slightly viscous liquid at a bath temperature up to 240° at 0.45 mm. A small portion was distilled again to provide an analytical sample (b.p. 153° at 0.02 mm). Infrared: 6.12 μ; n_D^{20} 1.6144; ultraviolet: λ_{max} 276 mμ (broad, log ϵ 4.20), λ_{min} 239 mμ (log ϵ 3.73); n.m.r. signals: triplet centered at 8.84 τ (methyl of ethyl group, area = 3H), 7.78 τ (methyl attached to ring at C_3, area = 3H), quartet centered at 7.37 τ (methylene of ethyl group, area = 2H), four signals centered at 3.2 τ (olefinic H, area = 2H), multiplet centered at 2.72 τ (aromatic H, area = 5H), 1.82 τ (αH, area = 2H). Found: C, 85.42; H, 7.52; N, 6.44. Calc. for $C_{16}H_{17}N$: C, 86.05; H, 7.67; N, 6.27.

A picrate of this substance was prepared in ethyl alcohol and after several recrystallizations from this solvent, an analytical sample, m.p. 182–183°, was obtained. Found: C, 58.23; H, 4.50; O, 24.50; N, 12.52. Calc. for $C_{22}H_{20}N_4O_7$: C, 58.40; H, 4.46; O, 24.76; N, 12.39.

3-Methyl-5-ethyl isonicotinic Acid (VII)

A solution of 3-methyl-4-styryl-5-ethylpyridine (2.32 g, 0.01 mole) in glacial acetic acid (70 ml) was treated with ozone (0.015 mole) at room temperature. The reaction mixture was treated with 3% aqueous hydrogen peroxide (10 ml) and the mixture was refluxed for 10 minutes. The solvent was removed *in vacuo* and the residue washed with ether to remove the benzoic acid. To the ether-insoluble residue water (4 ml) was added, and the mixture was warmed in a steam bath until all the material had dissolved. As the solution gradually cooled, small, needle-like crystals separated (304 mg). Recrystallization of this substance from absolute ethanol provided the pure acid, m.p. 268–269°, infrared: 5.88 μ.

An additional 1.51 g of material was recovered from the mother liquors. Although this latter crop was not as crystalline as the initial crop, it was shown to be the desired acid since on esterification with diazomethane, in a subsequent experiment, it provided the identical methyl ester. Found: C, 65.29; H, 7.00; O, 19.69. Calc. for $C_9H_{11}O_2N$: C, 65.44; H, 6.71; O, 19.37.

Methyl 3-Methyl-5-ethyl-4-pyridinecarboxylate (VIII)

To a stirred solution of 3-methyl-5-ethyl isonicotinic acid (1.5 g) in absolute ethyl alcohol (300 ml) an ethereal solution of diazomethane (containing 2 g CH_2N_2) was added. The reaction mixture was cooled in ice and stirred at ice-bath temperature for 3 hours. The reaction mixture was then treated with 2 *N* hydrochloric acid (35 ml) and extracted with ether to remove any neutral contaminants. The aqueous layer was made basic by the addition of sodium bicarbonate and then extracted continuously with ether for 20 hours. The ether extract was dried over anhydrous magnesium sulphate and the solvent removed to yield a liquid product. Distillation of this material at 70–100° (bath temp.) at 0.2 mm yielded 0.50 g of a clear liquid. A small portion of this substance was distilled again to provide an analytical sample (b.p. 135° at 22 mm); n_D^{20} 1.5025; infrared: 5.78 μ; ultraviolet: λ_{max} 274 mμ (log ϵ 3.48), λ_{min} 238 mμ (log ϵ 2.85); n.m.r. signals: triplet centered at 8.9 τ (methyl of ethyl group, area = 3H), 7.85 τ (methyl attached to ring, area = 3H), quartet centered at 7.5 τ (methylene of ethyl group, area = 2H), 6.21 τ (—$COOCH_3$, area = 3H), 1.83 τ (αH, area = 2H). Found: C, 67.16; H, 7.26; N, 7.90. Calc. for $C_{10}H_{13}O_2N$: C, 67.02; H, 7.31; N, 7.82.

The ester formed a picrate readily and this derivative, after recrystallizing from alcohol, melted at 151–153°. Found: C, 47.21; H, 4.09; O, 35.15; N, 13.43. Calc. for $C_{16}H_{16}O_9N_4$: C, 47.06; H, 3.95; O, 35.27; N, 13.72.

It should be pointed out that we found it very convenient to convert the entire reaction product into the picrate, purify the picrate by several crystallizations from alcohol, and finally regenerate the ester by decomposition of the picrate with lithium hydroxide (11). The recovery in this reaction is good and this provided an excellent method for purifying small quantities.

ACKNOWLEDGMENTS

Financial aid from the National Research Council of Canada and Eli Lilly and Company is very gratefully acknowledged.

REFERENCES

1. J. P. KUTNEY and R. C. SELBY. J. Org. Chem. **26**, 2733 (1961).
2. W. G. SCHNEIDER, H. J. BERNSTEIN, and J. A. POPLE. Can. J. Chem. **35**, 1487 (1957).
3. C. T. KYTE, G. H. JEFFERY, and A. I. VOGEL. J. Chem. Soc. 4454 (1960).
4. HUANG-MINLON. J. Am. Chem. Soc. **68**, 2487 (1946).
5. E. KLINGSBERG. Heterocyclic compounds, pyridine and its derivatives. Part 2. Interscience Publishers Inc., New York. 1961.
6. E. R. BLOUT and V. W. EAGER. J. Am. Chem. Soc. **67**, 1315 (1945).
7. J. L. R. WILLIAMS, S. K. WEBSTER, and J. A. VAN ALLAN. J. Org. Chem. **26**, 4893 (1961).
8. A. P. PHILLIPS. J. Am. Chem. Soc. **76**, 3986 (1954).
9. R. H. CALLIGHAN and M. H. WILT. J. Org. Chem. **26**, 4912 (1961).
10. A. S. BAILEY and J. S. A. BRUNSKILL. J. Chem. Soc. 2554 (1959).
11. A. BURGER. J. Am. Chem. Soc. **67**, 1615 (1945).

METHYLATION OF SUGAR DITHIOACETALS

III. D-GALACTOSE DIETHYL DITHIOACETAL[1]

G. G. S. DUTTON AND Y. TANAKA[2]

Department of Chemistry, University of British Columbia, Vancouver, British Columbia

Received March 7, 1962

ABSTRACT

Partial methylation of D-galactose diethyl dithioacetal in tetrahydrofuran with Purdie's reagents yielded 2-, 3-, and 6-*O*-methyl-D-galactoses in approximately equal amounts. Poly-*O*-methyl-D-galactoses were not investigated. These three mono-*O*-methyl ethers were identified as crystalline 2-*O*-methyl-D-galactose, 3-*O*-methyl-D-galactose phenylosazone, and 6-*O*-methyl-D-galactose phenylhydrazone. Paper chromatographic separation of all monomethyl-D-galactopyranoses was achieved by addition of borax to the irrigating solvent.

As a continuation of our study on the relative reactivity of hydroxyl groups in dithioacetals (1, 2) this paper reports the results obtained from the partial methylation of D-galactose diethyl dithioacetal. The dithioacetal was shaken at room temperature with amounts of silver oxide and methyl iodide adjusted to give a reasonable amount of the mono-*O*-methyl ethers. The methylated dithioacetal was hydrolyzed with acid and the deionized hydrolyzate was examined by paper chromatography in butanone–water azeotrope. When the chromatogram was irrigated for a long period the original compact spot of mono-*O*-methyl ethers (R_f 0.08) was found to streak, indicating considerable differences in the mobilities of the mono-*O*-methyl-D-galactoses.

It has been shown that the addition of boric acid to a butanol–water system greatly enhances the resolution obtainable in paper chromatography (3) and the use of borate with charcoal columns has also been recommended (4). The latter method has been used for the separation of 3- and 4-*O*-methyl-D-galactoses (5). In the original paper (3) no ethers of galactose were mentioned and it is now shown that all the mono-*O*-methyl-D-galactopyranoses may be readily separated on paper when the irrigating solvent is butanone–water azeotrope saturated with borax. The $R_{\text{galactose}}$ values of these compounds were 3.60 (2-*O*-methyl-), 2.67 (3-*O*-methyl-), 2.28 (4-*O*-methyl-), and 3.02 (6-*O*-methyl-D-galactose) (60 hours). The methylation product was then shown to contain 2-, 3-, and 6-*O*-methyl-D-galactoses. Neither authentic samples nor the methylation product gave clear separation of these isomers when they were chromatographed for 60 hours in butanone–water azeotrope in the absence of borax. Paper electrophoresis confirmed the presence of 2-, 3-, and 6-*O*-methyl-D-galactoses in the methylation product; M_g values of these isomers were 0.43, 0.76, and 0.90, respectively (cf. ref. 5). Absence of 5-*O*-methyl-D-galactose in the methylation product was shown by electrophoresis of the components in the di-*O*-methyl area of the chromatograms which gave very slowly migrating spots only. In general, monomethylglycofuranose sugars travel on chromatograms about as fast as the corresponding dimethylglycopyranoses (6). The two groups may be readily differentiated by the high electrophoretic mobility of the former (7).

Colorimetric analysis, by the phenol – sulphuric acid method (8), of the mixture of mono-*O*-methyl ethers isolated from the methylation product gave an approximately

[1]*Previous papers in this series have used the term mercaptal. This has been altered to dithioacetal to accord with current carbohydrate nomenclature (rule 32).*

[2]*Present address: Department of Chemistry, Queen's University, Kingston, Ontario.*

equal ratio for these three isomers which was consistent with the weights of these components isolated by paper chromatography.

The 2-*O*-methyl ether isolated from the methylation mixture crystallized as the free sugar. The 3-*O*-methyl ether was identified as 3-*O*-methyl-D-galactose phenylosazone, and the 6-*O*-methyl ether as 6-*O*-methyl-D-galactose phenylhydrazone.

The results reported here thus differ from the case of L-arabinose dithioacetal (2) in that there appears to be no selective reactivity of any one hydroxyl group in D-galactose diethyl dithioacetal.

EXPERIMENTAL

Methylation of D-*Galactose Diethyl Dithioacetal*

D-Galactose diethyl dithioacetal (0.50 g) was dissolved in tetrahydrofuran (150 ml), and silver oxide (2.00 g), drierite (3 g), and methyl iodide (20 ml) were added to the solution. The mixture was shaken for 7 hours at room temperature. The inorganic substances were filtered and then washed with tetrahydrofuran (20 ml). The filtrate and washing were evaporated to a sirup, which was redissolved in chloroform (20 ml) in order to remove a small amount of inorganic impurities by filtration. The chloroform solution gave on evaporation a yellow sirup (470 mg).

The methylation product (470 mg) was dissolved in ethanol (10 ml), and 18% hydrochloric acid (2 ml) was added to the solution, which was refluxed for 5 hours. A yellow sirup (255 mg) was obtained by evaporation of the neutralized hydrolyzate (Duolite A-4 resin) and treatment with charcoal.

Paper chromatography in butanone–water azeotrope showed that the sirup was a mixture of mono-*O*-methyl-D-galactoses (R_f 0.05 (strong)) and unchanged D-galactose (R_f 0.01 (strong)), plus several fast-running components with very weak intensities.

Chromatographic Separation of the Mixture of Methylated D-*Galactoses*

To butanone–water azeotrope (100 ml) sodium borate decahydrate (1 g) was added; the mixture was shaken and left to stand for several hours. The solution was decanted and used as the developing solvent.

The mixture of methylated D-galactoses was chromatographed in this solvent for 40 hours together with standard samples and the mixture was shown to contain 2-, 3-, and 6-*O*-methyl-D-galactoses. The mixture was resolved into its three components by streaking on four 15 cm wide Whatman 3 MM sheets and was developed for 60 hours in the same solvent. Each component was extracted with water (50 ml×3) and was obtained as a sirup on evaporation. These sirups were shown to be electrophoretically homogeneous.

The separation was repeated on a second mixture of methylated galactoses (529 mg) and the results shown in Table I were obtained. The 2-, 3-, and 6-*O*-methyl-D-galactoses were obtained in yields of 13.2, 14.7, and 8.1 mg respectively.

TABLE I

Chromatography* and electrophoresis† of mono-*O*-methyl-D-galactoses

Ether	Movement in mm	$R_{galactose}$	M_g
2-*O*-Methyl	205	3.46	0.45
3-*O*-Methyl	143	2.34	0.81
4-*O*-Methyl	127	2.16	
6-*O*-Methyl	176	2.89	0.90
Mixture	205, 176, 143	3.46, 2.89, 2.34	0.45, 0.81, 0.90
D-Galactose	59	1.00	1.00

*In butanone–water saturated with borax for 40 hours.
†In 0.05 *M* sodium borate, 950–1050 v, 25–30 ma, 45 minutes.

Colorimetric Analysis of the Mono-O-methyl Ethers and Examination of Fast-running Components

A methylation under the same conditions using 2.0 g of the dithioacetal gave a sirup (1.0 g) of methylated D-galactoses, and paper chromatography in butanone–water azeotrope showed the following R_f values: R_f 0.34 (weak), 0.17 (weak), 0.12 (medium), 0.05 (strong), and 0.01 (strong).

The sirup (1.0 g) was chromatographed on a cellulose–hydrocellulose column in butanone–water azeotrope (rate of flow: 10 ml/10 minutes). In tubes No. 80–200 (10-minute intervals) the component of R_f 0.05 was found and this fraction gave on evaporation a sirup (48.2 mg) which showed three spots ($R_{galactose}$ 3.37, 2.88, and 2.38) by paper chromatography in butanone–water azeotrope saturated with borax.

A part of this sirup was chromatographed for 60 hours in the same solvent and the ratio of these three components was estimated by the phenol – sulphuric acid method (8), which gave approximately 1:1:1 for 2-, 3-, and 6-*O*-methyl-D-galactoses.

In tubes No. 40–70 the components of R_f 0.17 and 0.12 were detected without clear separation. Evaporation of these fractions gave a sirup (21.2 mg) which showed two strong spots (M_g 0.23 and 0.28) by electrophoresis (950–1050 v, 25–30 ma, 50 minutes in 0.05 *M* sodium borate solution).

Identification of the Component $R_{galactose}$ 3.46 as 2-O-Methyl-D-galactose

The components which were isolated from the methylation mixtures and corresponded to 2-*O*-methyl-D-galactose were combined. An aqueous solution was deionized with Amberlite IR-120 and traces of borate were removed as follows (9). To the sirup (18.2 mg) was added methanol (5 ml), and the solution was evaporated *in vacuo* without heating. After this procedure was repeated about 20 times, the residue was dissolved in a small amount of warm absolute ethanol, and ether was added to turbidity. After seeding with an authentic sample of 2-*O*-methyl-D-galactose, colorless crystals were precipitated. The solvent was decanted, the crystals were washed with ether and had m.p. 152–154° C. Admixture with authentic 2-*O*-methyl-D-galactose (m.p. 153–156° C (5)) gave no depression of the melting point.

Identification of the Component $R_{galactose}$ 2.34 as 3-O-Methyl-D-galactose

Since the sirup (23.4 mg) corresponding to 3-*O*-methyl-D-galactose failed to crystallize after treatment with methanol, it was dissolved in 20% acetic acid (3 ml) and heated for 5 hours in boiling water with phenylhydrazine (39.1 mg) in absolute ethanol (0.22 ml) and a little sodium metabisulphite. The yellow crystals which precipitated on cooling of the reaction mixture were recrystallized from water and had m.p. 177–179° C, lit. (10) m.p. 176–179° C, and the melting point was not depressed when mixed with 3-*O*-methyl-D-galactose phenylosazone derived from 2,3-di-*O*-methyl-D-galactose.

Identification of the Component $R_{galactose}$ 2.89 as 6-O-Methyl-D-galactose

The sirup (16.5 mg) which corresponded to 6-*O*-methyl-D-galactose did not crystallize after treatment with methanol. It was dissolved in absolute ethanol (1 ml), and phenylhydrazine (9.2 mg) in absolute ethanol (0.06 ml) was added to the solution. The mixture was warmed for about 20 minutes and addition of petroleum ether precipitated white crystals, which were recrystallized from ethanol – petroleum ether and had m.p. 161–162° C. When the product was recrystallized from aqueous methanol the melting point was raised to 171–173° C and the mixed melting point with authentic 6-*O*-methyl-D-galactose phenylhydrazone, m.p. 172–173° C (11), was 171–172° C.

Synthesis of 2,3-Di-O-methyl-D-galactose

The published procedure (10) provided this compound, $[\alpha]_D^{25}$ 51.8° (*c*, 2.15 in water), R_f 0.29 and $R_{galactose}$ 5.00 (20 hours) in ethyl acetate – pyridine – water (2:1:2). This sirupy product gave 3-*O*-methyl-D-galactose phenylosazone, m.p. 178° C, lit. (10) m.p. 176–179° C.

ACKNOWLEDGMENTS

The financial support of the Research Corporation is gratefully acknowledged. We wish to thank Dr. B. Lindberg, Stockholm, Sweden, for a gift of mono-*O*-methyl-D-galactoses. One of us (Y. T.) thanks the National Research Council for the award of a studentship.

REFERENCES

1. G. G. S. Dutton and K. Yates. Can. J. Chem. **36**, 550 (1958).
2. G. G. S. Dutton and Y. Tanaka. Can. J. Chem. **39**, 1797 (1961).
3. G. R. Barker and D. C. C. Smith. Chem. & Ind. (London), 19 (1954).
4. S. A. Barker, E. J. Bourne, and O. Theander. J. Chem. Soc. 4276 (1955).
5. H. Bouveng and B. Lindberg. Acta Chem. Scand. **10**, 1283 (1956).
6. G. G. S. Dutton, Y. Tanaka, and K. Yates. Can. J. Chem. **37**, 1955 (1959).
7. A. B. Foster. *In* Advances in carbohydrate chemistry. Vol. 12. Academic Press, New York. 1957. p. 81.
8. M. Dubois, K. A. Gilles, J. K. Hamilton, P. A. Rebers, and F. Smith. Anal. Chem. **28**, 350 (1956).
9. C. T. Bishop. Can. J. Chem. **38**, 1636 (1960).
10. G. T. Robertson and R. A. Lamb. J. Chem. Soc. 1321 (1934).
11. K. Freundenberg and K. Smeykal. Ber. **59**, 100 (1926).

5-METHYL-1,2,3-CYCLOHEXANETRIONETRIOXIME: A COMPARATIVE STUDY WITH SOME *vic*-DIOXIMES[1]

R. A. HAINES, D. E. RYAN, AND G. E. CHENEY
Department of Chemistry, Dalhousie University, Halifax, Nova Scotia

Received September 11, 1961

ABSTRACT

A comparative study has been made of 5-methyl-1,2,3-cyclohexanetrionetrioxime with nioxime and dimethylglyoxime; complexes with nickel, copper, and cobalt have been investigated. Dissociation constants of the three reagents, in aqueous solution, have been determined and formation constants of their copper complexes evaluated. Spectrophotometric and potentiometric studies were used to obtain the results.

INTRODUCTION

Numerous investigations of the reactions between *vic*-dioximes and metal ions have been reported (1–5) since the initial report on dimethylglyoxime by Tschugaeff (6). These dioximes can exist in three isomeric forms, as the hydroxy groups can be anti, syn, or amphi to one another; only the anti configuration gives the familiar red precipitate with nickel; the amphi form gives a yellow or green-yellow compound in which one molecule of dioxime is attached to one nickel while the syn form is incapable of reacting with metallic salts (1).

A trioxime, 5-methyl-1,2,3-cyclohexanetrionetrioxime, has been prepared recently (7) and, in preliminary studies, appeared to possess many of the selective properties of similar *vic*-dioximes. However, the presence of the third oxime group makes possible the existence of four isomers: the three hydroxy groups can be oriented so that they are all amphi, two are syn, and the third either anti or amphi to the common central group, and two are anti and the third group amphi. It was thought worthwhile, in view of possible reaction of this third hydroxy group, to evaluate the chelating properties of this trioxime through a comparison with dimethylglyoxime and nioxime employing absorption spectrophotometry and potentiometric titration techniques.

SPECTROPHOTOMETRIC STUDIES

In these studies, absorption spectra of 5-methyl-1,2,3-cyclohexanetrionetrioxime and its complexes with copper and cobalt were determined at various pH values; spectrophotometric studies for dimethylglyoxime and nioxime have been carried out previously by Banks (5). Measurements were made in matched 1-cm silica cells using a Beckman "DU" spectrophotometer equipped with an electronic power supply and photomultiplier attachment; a Beckman Model "G" pH meter, with saturated calomel and glass electrode couple, was used for pH measurements.

Reagent

Aqueous solutions of "White Label" Eastman Kodak 5-methyl-1,2,3-cyclohexanetrionetrioxime were prepared and diluted quantitatively to 0.0001 *M*. The absorption spectra of these solutions were determined at various pH values, adjustments to the

[1]*This work received financial assistance from the National Research Council, and is taken, in part, from the M.Sc. thesis of R. A. Haines.*

desired pH being made with dilute sodium hydroxide and perchloric acid. The difference in the nature of the spectral transmission curves at low and high pH is shown in Fig. 1.

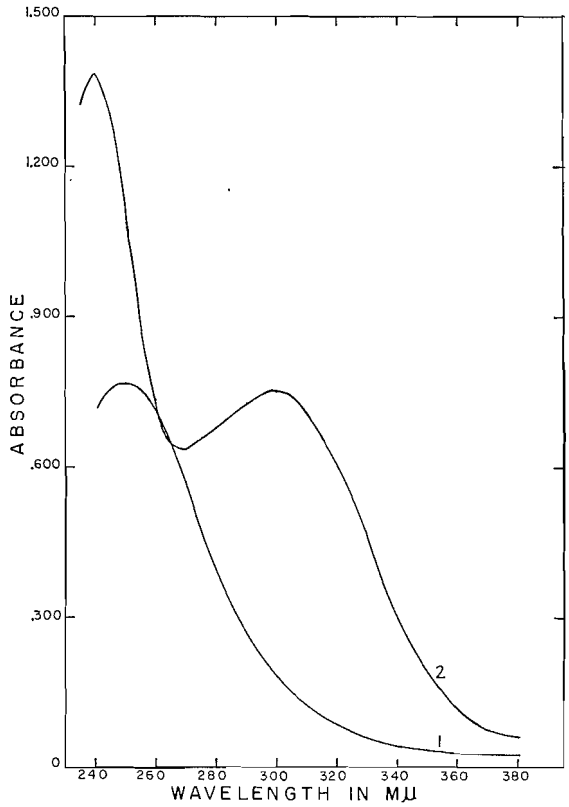

FIG. 1. Absorption spectra of trioxime. 1.16×10^{-4} aqueous solution at pH 2 (1) and pH 11 (2).

The absorption spectra of the reagent shows a maximum at approximately 245 mμ at pH 1, which undergoes a hypsochromic shift and an increase in absorptivity with an increase in pH. In solutions of pH greater than 7, a second maximum is present at approximately 300 mμ and the solution develops a yellow color. Spectrophotometric studies by Banks (5) on nioxime and dimethylglyoxime have shown that maxima occur, for these two oximes, at approximately 230 and 270 mμ. The introduction of the third oxime group into the ring system has resulted in a bathochromic shift of these maxima, which is consistent with an increase in the conjugation of the trioxime system relative to the nioxime system. Molecular extinction coefficients for the trioxime at 240 mμ and 300 mμ are recorded in Table I.

TABLE I

Molecular extinction coefficients of 5-methyl-1,2,3-cyclohexanetrionetrioxime

pH	240 mμ	300 mμ
2	4,770	1,520
4	6,250	1,580
6	6,490	1,620
8	9,010	2,850
10	12,100	5,310
11	12,000	6,500

Metal Chelates

Metal perchlorates, obtained from the G. Frederick Smith Chemical Co., were used to prepare the stock 0.01 *M* standard solutions, volumes of reagent and metal ions were mixed in the desired proportions, pH adjustments made with dilute sodium hydroxide and perchloric acid, and the spectral transmission curves of each mixture determined. Figure 2 shows curves for the complexes of the trioxime with copper and cobalt. Neither the cobalt nor copper complexes shows a resolvable maximum in the visible region; for both chelates a "shoulder" is present at approximately 300 mμ. Cobalt shows a maximum at about 260 mμ but this is unsuitable for most direct analytical measurements due to the strong absorbance of trioxime itself at this wavelength.

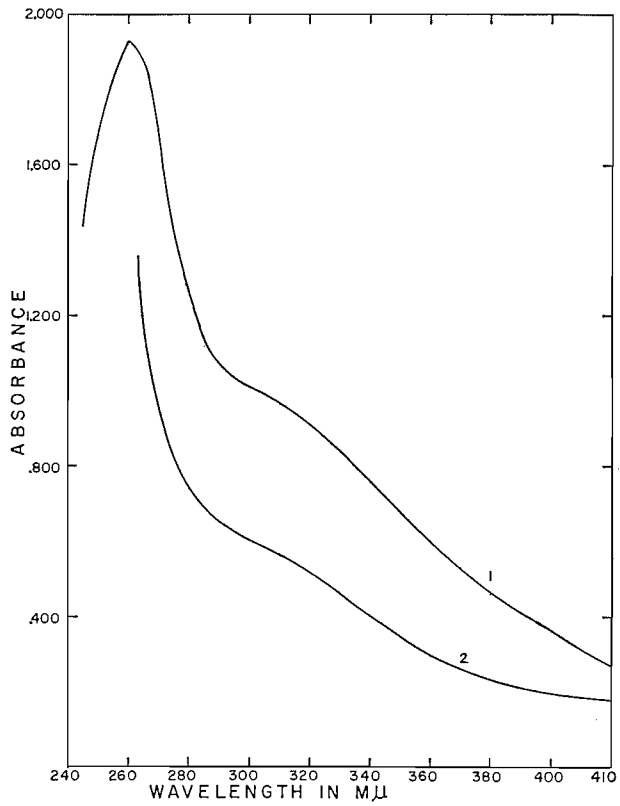

FIG. 2. Absorption spectra of metal complexes: 1, solution 2.33×10^{-4} *M* in cobaltous perchlorate and 6.99×10^{-4} *M* in trioxime at pH 6; 2, solution containing similar concentrations of copper perchlorate and trioxime at pH 4.

Job's method of continuous variations (8) and the molar ratio method of Yoe and Jones (9) were used to determine the stoichiometry of the trioxime copper and cobalt chelates. The continuous variations study yielded results in agreement with those obtained potentiometrically (*vide infra*); as shown in Fig. 3, a 2:1 complex with copper and a 3:1 complex with cobalt are indicated.

The mole ratio method, Fig. 4, showed different results. At 360 mμ the existence of both 1:1 and 2:1 copper complexes are indicated but only a 1:1 copper complex is apparent from measurements made at 410 mμ. With cobalt, at both wavelengths, complexes containing 1, 2, and 2.5 moles of reagent for each mole of cobalt are evident.

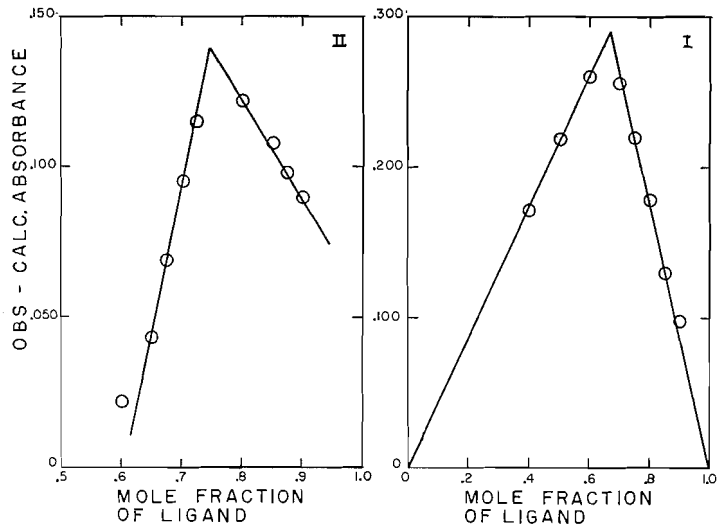

FIG. 3. Continuous variations plot: I, trioxime and copper perchlorate at pH 4 and wavelength 450 mμ (total concentration of copper plus reagent, 3.81×10^{-4} M); II, trioxime and cobaltous perchlorate at pH 6 and wavelength 330 mμ (total concentration of cobalt plus reagent, 3.68×10^{-4} M).

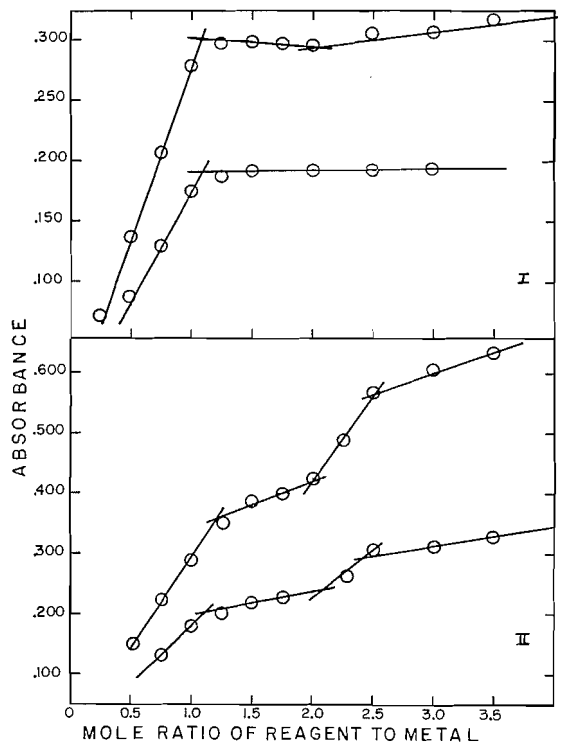

FIG. 4. Mole ratio plot: I, trioxime and copper perchlorate at pH 4; II, trioxime and cobaltous perchlorate at pH 6. Total metal concentration 2.41×10^{-5} M; curves are given for 360 and 410 mμ.

The results obtained by Job's method agree with those previously recorded for other oximes; a 2:1 complex of dimethylglyoxime with copper has been known for some time, and it has recently been shown that 1,2,3-cyclohexanetrionetrioxime forms a 3:1 complex with cobalt II (10).

POTENTIOMETRIC STUDIES

Potentiometric titrations, using carbonate-free 0.1 *N* potassium hydroxide as titrant, were carried out on 5-methyl-1,2,3-cyclohexanetrionetrioxime and its complexes with nickel II, cobalt II, and copper II. Potentiometric methods have been used sparingly for the dioximes and the data reported give formation constants only for dimethylglyoxime in 50% dioxane–water solution (4); it was necessary, therefore, for comparison purposes, to also investigate dimethylglyoxime and nioxime by this technique. These titrations permitted the calculation of the dissociation constants of the three oximes in water and gave information regarding the stoichiometry of the chelates and the relative stability of the copper II complexes based on the magnitude of the respective overall formation constants as evaluated by the Bjerrum technique (11).

Apparatus

The course of the titrations was followed with a Radiometer 4 pH meter equipped with a Beckman saturated calomel and an E-2 glass electrode couple. Titrations were carried out in a pyrex vessel equipped with an outer jacket through which water from a constant-temperature bath was circulated. A temperature of 25±0.1° C was maintained with a Wilkens–Anderson "lo-temp" constant-temperature bath. The vessel was fitted with a loose plastic cover, through which holes were drilled to accommodate a 10-ml microburet, the two electrodes, two nitrogen inlet tubes, a thermometer, and a glass rod for removing drops of liquid from the buret tip. During the titration, nitrogen gas was bubbled both through the solution and passed over it; in order to minimize evaporation losses, the nitrogen was previously saturated with water vapor at 25° C. The buret and reservoir of potassium hydroxide were connected by a continuous system of glass tubing and the atmosphere above each was protected by glass towers containing "caroxite" and indicating "drierite". Magnetic stirring was used throughout the titrations.

Reagents

Nioxime, obtained from the G. Frederick Smith Chemical Co., was recrystallized from water and dried at 50° C in a vacuum oven; the dried material melted at 189° C (reported, 188–190° C (12)).

5-Methyl-1,2,3-cyclohexanetrionetrioxime was a "White Label" grade product of Eastman Kodak. It was recrystallized from water and dried at 50° C in a vacuum oven; this material decomposed at 171–172° C on melting (reported, 170° C (7)) and a titration showed the reagent to be 99.1% pure on the basis of acid assay.

Dimethylglyoxime was "White Label" grade Eastman Kodak reagent. It was recrystallized from an alcohol–water mixture, dried in a vacuum oven at 50° C, and had a melting point of 239° C.

Each of these reagents was dissolved in redistilled water and titrated with 0.1 *N* potassium hydroxide, both in water alone and in solutions containing a known amount of perchloric acid. Titration curves in the presence of perchloric acid are shown in Fig. 5.

The titration curves show that the trioxime is a much stronger acid than the other two oximes; two end points are obtained corresponding to the neutralization of the perchloric acid and of one of the oxime groups. Dimethylglyoxime and nioxime are both extremely

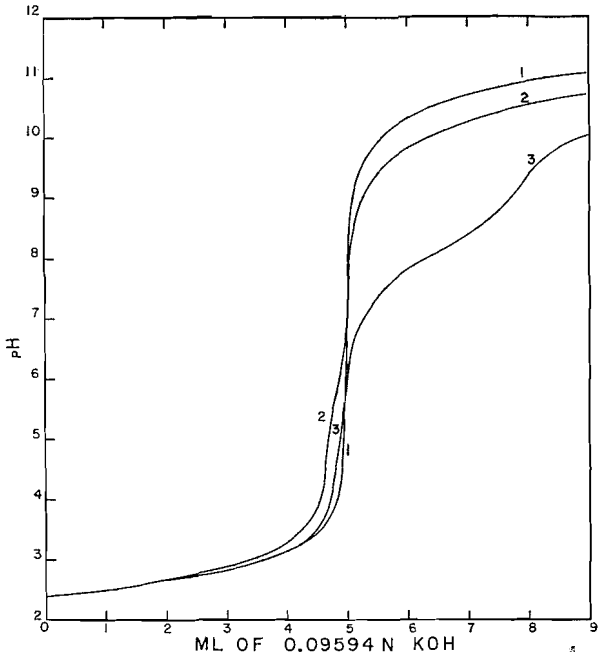

FIG. 5. Titration curves of 2.86×10^{-4} mole of reagent in presence of 50.0 ml of 9.81×10^{-3} N perchloric acid: 1, dimethylglyoxime; 2, nioxime; 3, trioxime.

weak acids and no break occurs in their titration curves after the perchloric acid end point. The titration curve of nioxime (Fig. 5, curve 2) shows one major difference from those of the other oximes—a break occurs before all the perchloric acid has been titrated. The end point cannot be correlated with any common multiple of the quantity of reagent used and it is followed by a second break corresponding to the complete neutralization of perchloric acid. Such an end point must be due to the nature of the reagent itself and not to any basic impurity; repeated recrystallization of reagent had no effect on the end points and the sharp melting point (in agreement with that reported in the literature) also suggests that the reagent is of high purity. The first end point might be due to a protonated species but there is little supporting evidence for this.

Dissociation constants of the three oximes were determined from equations derived for "non-overlapping" and "overlapping" dissociation constants. Data used for the calculations were taken from the half-neutralization portion of the titration curves. For dimethylglyoxime and nioxime, because of the close proximity of their values, graphical determinations of the dissociation constants were necessary. The equilibria involved are:

$$H_2R \rightleftarrows H^+ + HR^-, K_1 = \frac{(H^+)(HR^-)}{(H_2R)}$$

$$HR^- \rightleftarrows H^+ + R^=, K_2 = \frac{(H^+)(R^=)}{(HR^-)},$$

where H_2R represents the oxime under consideration, and parentheses denote molar concentrations. From these equilibria, together with equations for material and charge balance, it can be shown that:

$$\frac{(H^+)+(K^+)-(OH^-)}{T_{H_2R}} = \frac{K_1[(H^+)+2K_2]}{(H^+)^2+(H^+)K_1+K_1K_2},$$

where T_{H_2R} is the total concentration of the oxime.

If

$$\frac{(H^+)+(K^+)-(OH^-)}{T_{H_2R}} = S,$$

then

$$\frac{(H^+)^2S}{(S-2)}+(H^+)K_1\frac{(S-1)}{(S-2)}+K_1K_2 = 0$$

and a plot of $[(H^+)^2S]/(S-2)$ against $(H^+).[(S-1)/(S-2)]$ gives a straight line with a slope equal to K_1 and intercept equal to K_1K_2. Results are shown in Fig. 6.

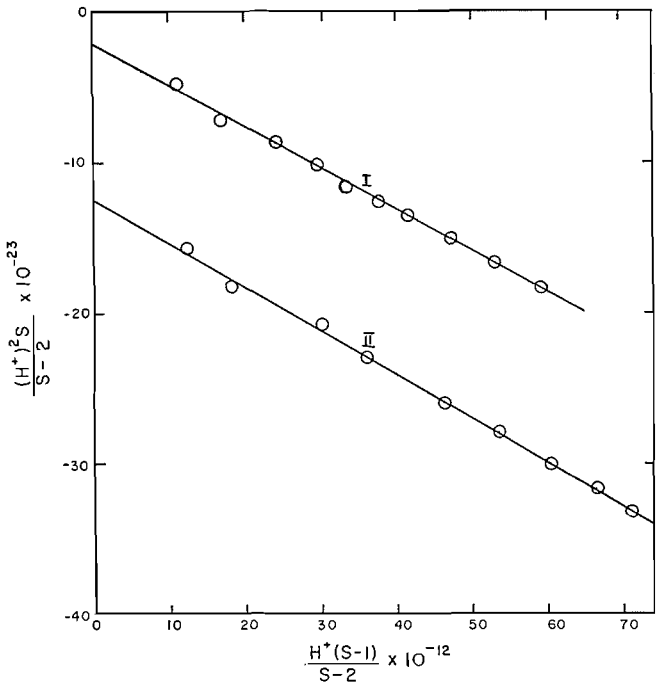

FIG. 6. Graphical determination of dissociation constants: I, dimethylglyoxime; II, nioxime.

The trioxime is a sufficiently strong acid to enable the direct calculation of pK_1 and pK_2, assuming no overlapping of these constants but, in its third ionization, it is too weak an acid in water to permit satisfactory calculations of pK_3 from the potentiometric curves. The results are given in Table II; these are not corrected with respect to activity coefficients of the various species and are from titrations on solutions containing reagent alone.

TABLE II

Acid dissociation constants of oximes, in water, at 25° C

Oxime	pK_1	pK_2
Dimethylglyoxime	10.60	11.85
Nioxime	10.68	11.92
5-Methyl-1,2,3,-cyclohexanetrionetrioxime	8.16	11.30

Metal Complexes

In these titrations different mole ratios of reagent and metal perchlorate solutions were mixed (varying from 4:1 to 1:1) and the liberated hydrogen ion titrated with 0.1 *N* potassium hydroxide; in each instance a known amount of perchloric acid was also present. A plot of the number of moles of hydrogen ion released for each mole of metal ion present should be indicative of the stoichiometry of the chelates; titration curves for each oxime in the presence of metal ions are shown in Figs. 7 and 8.

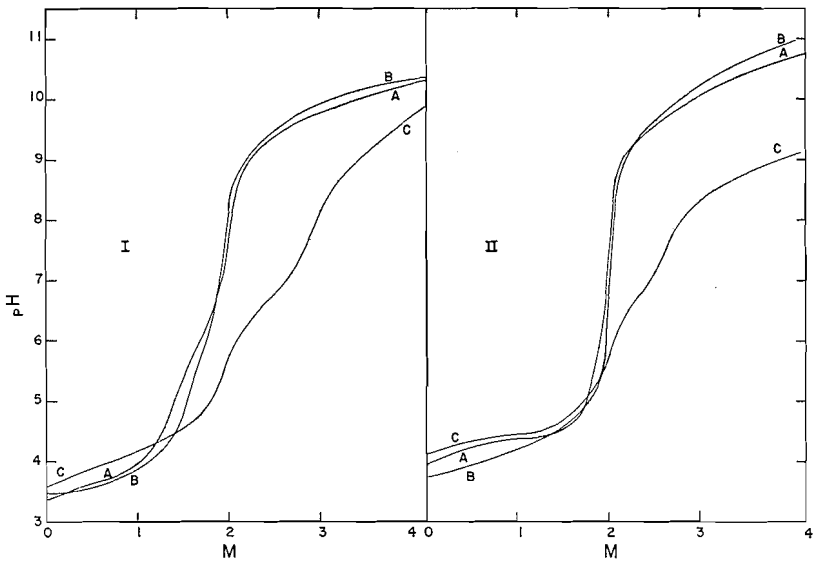

FIG. 7. Plot of moles of base used per mole of metal ion: I, nioxime; II, dimethylglyoxime. Curves A, B, and C are for nickel (3.28×10^{-5} mole), copper (4.06×10^{-5} mole), and cobalt (3.68×10^{-5} mole) respectively at a reagent-to-metal mole ratio of 3:1.

With nickel II, the titration curves for the three oximes were similar, and trioxime formed the familiar red precipitate; the break in the titration curves occurs at a proton-to-metal mole ratio of 2:1. With copper II, all oximes formed yellowish-brown complexes; the titration curves again are similar and show the formation of a 2:1 copper complex. These results suggest that the trioxime is similar, in its behavior with nickel and copper, to the other dioximes.

The reactions with cobalt II, however, appeared to be quite complex and differed with the reagent used. For the trioxime, at a mole ratio of reagent to cobalt of 3:1 or higher, 3 moles of proton were liberated; the solution was colored yellow initially and this color intensified to an orange as the titration progressed. In order to give a more complete

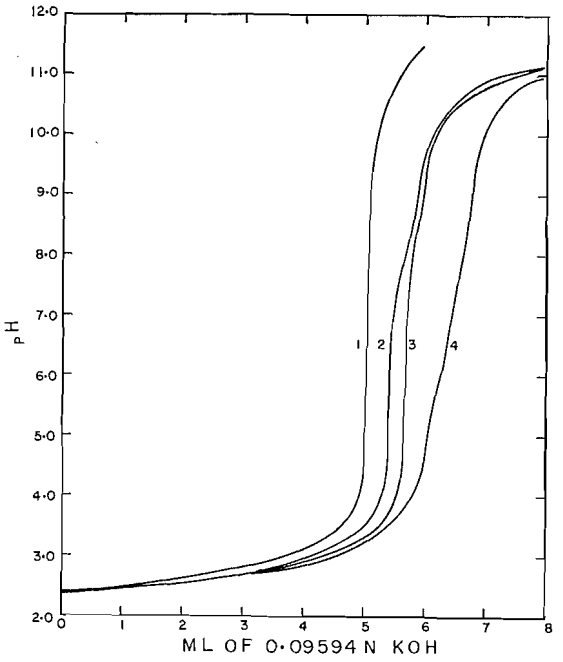

FIG. 8. Titration curves of metal chelates: 1, 50.0 ml of 9.811×10^{-4} *N* perchloric acid; 2, perchloric acid, 2.032×10^{-5} mole copper perchlorate, and 6.096×10^{-5} mole trioxime; 3, perchloric acid, 3.279×10^{-5} mole nickel perchlorate, and 9.837×10^{-5} mole trioxime; 4, perchloric acid, 3.359×10^{-5} mole cobaltous perchlorate, and 10.08×10^{-5} mole trioxime.

representation of the reactions of this reagent, Fig. 8 reproduces the titration curves obtained; two end points are evident corresponding to the liberation of 3 moles of hydrogen ion and a further 2 moles of proton. At a reagent-to-cobalt ratio of 2:1, using the same amount of cobalt, a precipitate occurred at pH 3; it subsequently dissolved between pH 6 and 7, causing a distinct drop in pH, and the number of moles of hydrogen ion ultimately released for each mole of cobalt was 2.70 ± 0.05.

Nioxime also shows the release of 3 moles of proton at ratios of reagent to cobalt of 3:1 or higher (Fig. 7A); no color was present in solution until after the addition of the first few drops of potassium hydroxide, when the solution developed a brownish-yellow color. Nioxime formed no precipitate when it was present in a 2:1 ratio with cobalt II but, as with trioxime, the number of moles in hydrogen ion released was 2.70 ± 0.05.

Dimethylglyoxime differed in its reactions with cobalt (Fig. 7B). A yellow color was formed at all ratios and the titration curve shows two end points corresponding to the liberation of 2 and 2.70 ± 0.05 moles of hydrogen ion.

Formation constants of the copper II complexes of the three oximes were calculated by the Bjerrum method (11). A plot of the formation function $\bar{n}$ (the concentration of bound ligand divided by the total concentration of metal present) against pHR^- (the negative logarithm of the equilibrium concentration of the ligand HR^-) enables the values of the logarithm of the formation constants, $\log K_1$ and $\log K_2$, to be read directly from the curve at $\bar{n}$ values of 0.5 and 1.5 respectively; the $\log K_{av}$ is read at $\bar{n}$ equal to 1.0. These values were read directly from the curves shown in Fig. 9; for nioxime, however, the $\log K_2$ value had to be calculated from the relationship $\log K_1+\log K_2 = 2\log K_{av}$.

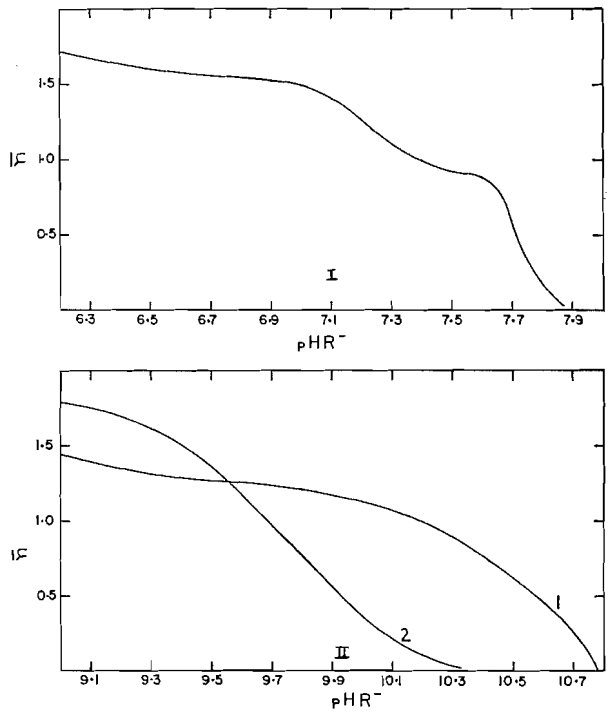

FIG. 9. Formation curves with copper at reagent-to-metal mole ratio of 3:1: I, trioxime; II, nioxime (1) and dimethylglyoxime (2).

Table III shows values calculated from titrations on solutions containing 50 ml or 0.009811 N perchloric acid, 4 ml of 0.01016 M cupric perchlorate, and 1.167×10^{-4} mole

TABLE III

Formation constants of copper II complexes at 25° C

Oxime	2 log K_{av}	log K_1	log K_2
Dimethylglyoxime	19.3_4	9.9_2	9.4_0
Nioxime	20.3_8	10.5_6	9.8_2
5-Methyl-1,2,3-cyclohexanetrionetrioxime	14.7_2	7.7_6	6.9_8

of reagent in a total initial volume of 110 ml (i.e. a reagent-to-copper mole ratio of approximately 3:1). Similar constants for the complexes with nickel were not evaluated because of their low solubility; the value of the solubility product would have been necessary for these calculations. The formation constants of the cobalt complexes were not calculated because of the uncertainty as to the actual species present.

DISCUSSION

The reactions of 5-methyl-1,2,3-cyclohexanetrionetrioxime with copper (II) and nickel (II), as contrasted with similar reactions between nioxime and dimethylglyoxime, indicate that the trioxime reacts in an analogous manner with these two metal ions. It is thus suggested that in the trioxime two oxime functional groups are anti, and thus reactive

toward these metal ions, and the third such group is syn to these two anti-oxime functionalities.

A comparison of the overall formation constants (2 log K_{av}) of the copper II reactions with these three oximes clearly reveals that the copper II – trioxime complex is much weaker than the corresponding complexes formed with nioxime and dimethylglyoxime. This comparatively low value for 2 log K_{av} may be partially attributed to the fact that the trioxime is the strongest acid of the three oximes; however, there is no linear correlation between either the acid dissociation constants of the ligands or the sum of these constants versus 2 log K_{av} for the copper II complexes. This is suggestive that some other factor in addition to ligand basicity is involved in the comparison of the stability of these copper II complexes.

In contrasting the reactions of the three oximes with cobalt II, two significant differences are apparent in the case of the trioxime. First, evidence for a 3:1 trioxime – cobalt II complex has been presented (Fig. 3), and a precipitate is formed on the addition of lead II, nickel II, or more cobalt II to solutions containing molar ratio of trioxime to cobalt II of 3:1 or greater. The corresponding complex with nioxime does not show these reactions; consequently, it is probable that the formation of precipitates by the 3:1 trioxime – cobalt II complex with these dipositive metal ions involves coordination of the additional metal ions with the third oxime group of the reagent.

Second, the presence of a second end point corresponding to the liberation of 5 moles of hydrogen ion per mole of cobalt II added initially (Fig. 8), is characteristic of the trioxime only, and is suggested to be due to an increase in the acidity of the third oxime group.

5-Methyl-1,2,3-cyclohexanetrionetrioxime does not appear, from studies to date, to be a satisfactory reagent for direct gravimetric determinations. Nickel, copper, and cobalt complexes that were precipitated from solution, washed with cold water, dried at 100° C, and then analyzed gave a metal content considerably *higher* than that anticipated from theoretical values and were inconsistent; no decomposition of the complexes was evident and preparation under nitrogen, followed by drying in a vacuum oven, failed to yield more coherent results. These results may be due to the formation of mixtures or to the third oxime group undergoing some reaction in solution that is preventing isolation of pure chelates by this method; this, and a more thorough study of the cobalt complexes of these oximes, are presently under investigation.

ACKNOWLEDGMENT

R. A. H. gratefully acknowledges the award of a bursary from the National Research Council.

REFERENCES

1. H. DIEHL. The applications of the dioximes to analytical chemistry. G. Frederick Smith Chemical Co., Columbus, Ohio. 1940.
2. R. C. VOTER, C. V. BANKS, and H. DIEHL. Anal. Chem. **20**, 458 (1948).
3. D. T. HOOKER and C. V. BANKS. Preparation, properties, and analytical applications of some substituted vic-dioximes. Ames Laboratory, Iowa State College. ISC-597.
4. R. G. CHARLES and H. FREISER. Anal. Chim. Acta, **11**, 101 (1954).
5. C. V. BANKS and A. B. CARLSON. Anal. Chim. Acta, **7**, 291 (1952).
6. L. TSCHUGAEFF. Z. anorg. Chem. **46**, 144 (1905).
7. D. C. BATESKY and N. S. MOON. J. Org. Chem. **24**, 1694 (1959).
8. P. JOB. Ann. chim. Ser. 10, **9**, 113 (1928).
9. J. H. YOE and A. L. JONES. Ind. Eng. Chem., Anal. Ed. **16**, 111 (1944).
10. J. FRIERSON, N. PATTERSON, H. HARRILL, and N. MARABLE. Anal. Chem. **33**, 1096 (1961).
11. J. BJERRUM. Metal ammine formation in aqueous solution. P. Haase and Son, Copenhagen. 1957.
12. E. G. BANK, G. F. SMITH, C. V. BANKS, and H. DIEHL. J. Org. Chem. **10**, 199 (1945).

INFLUENCE OF STERIC AND POLAR EFFECTS ON BASE STRENGTHS OF BICYCLIC GUANIDINES[1]

A. F. McKay and M.-E. Kreling
L. G. Ryan Research Laboratories of Monsanto Canada Limited, Lasalle, Que.

Received March 1, 1962

ABSTRACT

The pK_a and $E_{1/2}$ values of a number of bicyclic guanidines and their keto derivatives were determined. The influence of steric and polar effects on their base strengths is discussed.

INTRODUCTION

Recently it was observed (1) that the guanidine nucleus in 5-keto-2,3,6,7-tetrahydro-1(H),5(H)-imidazo(1,2-*a*)pyrimidine could not be converted into a nitroguanidine by the strong nitration medium of absolute nitric acid – acetic anhydride – ammonium chloride, whereas 2,3,6,7-tetrahydro-1(H),5(H)-imidazo(1,2-*a*)pyrimidine is readily nitrated to 1-nitro-2,3,6,7-tetrahydro-1(H),5(H)-imidazo(1,2-*a*) pyrimidine (2) by this medium. The failure of the guanidine structure in 5-keto-2,3,6,7-tetrahydro-1(H),5(H)-imidazo(1,2-*a*) pyrimidine salt (I) to nitrate was explained (1) by the electron displacements within structure I. There are two opposing electron-attractive forces operating on N_4; one force

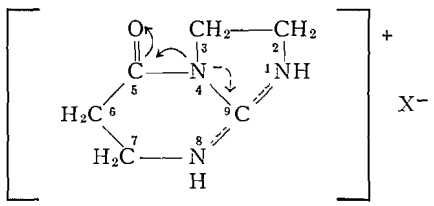

I

tends to displace the electrons towards participation in the guanidinium ion while the other force tends to displace electrons in the direction of the curved solid arrows. These opposing forces were considered to give the resonance ion structure more of an amidinium ion character than a guanidinium ion character. This would then explain the failure of 5-keto-2,3,6,7-tetrahydro-1(H),5(H)-imidazo(1,2-*a*)pyrimidine to nitrate.

Since the high base strength of guanidine is dependent upon the resonance stabilization of the guanidinium ion (3), it should be possible to measure the quantitative importance of the polar effect indicated by the solid curved arrow in I on the resonance stabilization of the guanidium ion by comparing the pK_a values of bicyclic guanidines with the pK_a values of their keto derivatives. The present study shows that an electronegative substituent adjacent to the guanidine nucleus in bicyclic guanidines has a very pronounced effect on their base strengths.

DISCUSSION

The pK_a values given in Table I show that the base strengths of the 5–6 (II), 6–6 (III), and 5–7 (IV) membered bicyclic guanidines are equivalent. In the 2,3,5,6-tetrahydro-1(H)-imidazo(1,2-*a*)imidazolium ion (V) containing two 5-membered fused rings considerable strain already exists in the bonding of the ring structure. This strain would be

[1]*Contribution No. 35.*

TABLE I

pK_a values and millivoltage half-neutralization values for bicyclic guanidines

Compound	pK_a, H_2O	$E_{1/2}$, acetic acid	ΔpK_a	$\Delta E_{1/2}$
3-Keto-1,2,5,6-tetrahydro-3(H)-imidazo(1,2-*a*)imidazole	6.82	367	—	—
2,3,5,6-Tetrahydro-1(H)-imidazo(1,2-*a*)imidazole	10.60	340	3.78	−27
3-Keto-1,2,6,7-tetrahydro-3(H),5(H)-imidazo(1,2-*a*) pyrimidine	8.15	369	—	—
5-Keto-2,3,6,7-tetrahydro-1(H),5(H)-imidazo(1,2-*a*) pyrimidine	8.25	373	—	—
2,3,6,7-Tetrahydro-1(H),5(H)-imidazo(1,2-*a*)pyrimidine	11.22	342	2.97; 3.07	−27; −31
4-Keto-2,3,6,7,8,9-hexahydro-4(H)-pyrimido(1,2-*a*) pyrimidine	—	370	—	—
2,3,6,7,8,9-Hexahydro-4(H)-pyrimido(1,2-*a*)pyrimidine	11.22	344	3.02	−26
1,2,5,6,7,8-Hexahydro-3(H)-imidazo(1,2-*a*)-1,3-diazepine	11.26	—	—	—

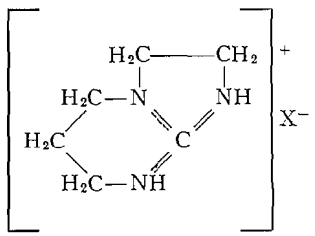

II

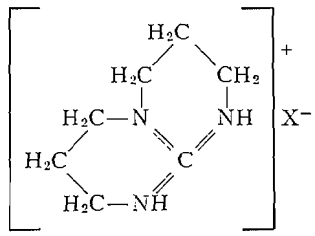

III

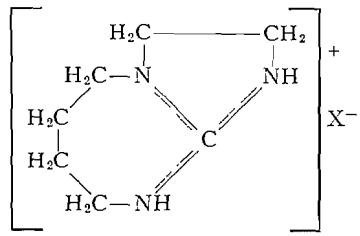

IV

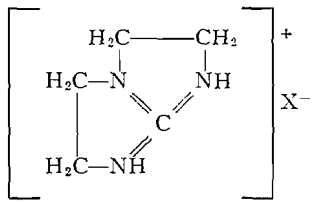

V

increased further by the shortening effect of resonance on the three C- N bonds. Thus the full resonance stabilization of the guanidinium ion cannot be realized in structure V and the base strength is lowered to a pK_a value of 10.60. In the 5–6-fused ring structure II, this strain is relieved by the puckering of the 6-membered ring.

A comparison of the pK_a values of the bicyclic guanidines II, IV, and V with their corresponding keto derivatives I, VI, and VII shows that the effects of the electron displacements indicated by the solid arrows on the resonance stabilization of the guanidinium ion are considerable. The base strengths of the keto derivatives I and VI are 3 pK_a

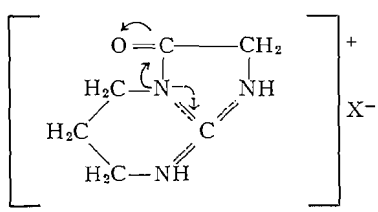

VI

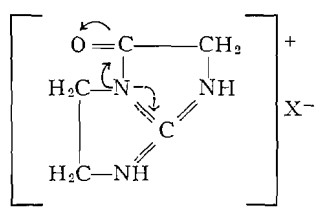

VII

units less than the corresponding parent bicyclic system II. As anticipated, the ΔpK_a value (3.78) is much greater between the 2,3,5,6-tetrahydro-1(H)-imidazo(1,2-*a*)imidazolium ion (V) and its keto derivative (VII). As seen above, the conformation of this almost planar bicyclic system offers some steric inhibition to the resonance stabilization of the guanidinium ion and thus it favors the electron displacement depicted by the solid arrows.

Since it was not possible to determine the pK_a value for 4-keto-2,3,6,7,8,9-hexahydro-4(H)-pyrimido(1,2-*a*)pyrimidine (4) (VIII) in aqueous solutions, all of the compounds,

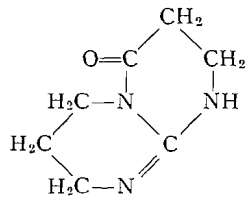

VIII

with the exception of 1,2,5,6,7,8-hexahydro-3(H)-imidazo(1,2-*a*)-1,3-diazepine,[2] were titrated with standard perchloric acid in glacial acetic acid solutions. The $E_{1/2}$ values for these determinations are given in Table I. No differences were observed in the base strengths of 2,3,5,6-tetrahydro-1(H)-imidazo(1,2-*a*)imidazoline and the other bicyclic guanidines II and III due to the levelling effect of the solvent medium. However, the pronounced effect of the adjacent keto groups in lowering the base strengths of the bicyclic guanidines is still apparent.

The rates of hydrolyses of the keto derivatives of the bicyclic guanidines were investigated in order to estimate the effect of their hydrolyses on the accuracy of the pK_a determinations. These studies are reported in the experimental section. It was found that 4-keto-2,3,6,7,8,9-hexahydro-4(H)-pyrimido(1,2-*a*)pyrimidine would be almost completely hydrolyzed in aqueous solution within the 3 minutes required to run the potentiometric titration. The errors in the pK_a values due to hydrolysis of 3-keto-1,2,6,7-tetrahydro-3(H),5(H)-imidazo(1,2-*a*)pyrimidine and 5-keto-2,3,6,7-tetrahydro-1(H),5(H)-imidazo(1,2-*a*)pyrimidine are less than 5% while the error due to the hydrolysis of 3-keto-1,2,5,6-tetrahydro-3(H)-imidazo(1,2-*a*)imidazole is less than 2%.

EXPERIMENTAL

Bicyclic Guanidines

2,3,5,6-Tetrahydro-1(H)-imidazo(1,2-*a*)imidazole (5), 3-keto-1,2,5,6-tetrahydro-3(H)-imidazo(1,2-*a*)imidazole (4), 2,3,6,7-tetrahydro-1(H),5(H)-imidazo(1,2-*a*)pyrimidine (2), 3-keto-1,2,6,7-tetrahydro-3(H),5(H)-imidazo(1,2-*a*)pyrimidine (4), 5-keto-2,3,6,7-tetrahydro-1(H),5(H)-imidazo(1,2-*a*)pyrimidine (1), 2,3,6,7,8,9-hexahydro-4(H)-pyrimido(1,2-*a*)pyrimidine (2), 4-keto-2,3,6,7,8,9-hexahydro-4(H)-pyrimido(1,2-*a*)pyrimidine (4), and 1,2,5,6,7,8-hexahydro-3(H)-imidazo(1,2-*a*)-1,3-diazepine (2) were prepared as previously described. Only highly purified, freshly sublimed samples were used for rate studies and pK_a determinations.

Kinetic Measurements

Weighed samples (0.005 mole) of the keto derivatives of the bicyclic guanidines were placed in volumetric flasks (10 ml) and water at 30.5° was added to the graduation mark to give 10 ml of 0.5 *M* solutions. The flask containing the solution was placed in a constant-temperature (30.5°) bath and samples (1 ml) were withdrawn at timed intervals. Aqueous picric acid solution (11 ml representing approximately 30% excess picric acid) was added to the withdrawn aliquots and after 2 minutes the precipitated picrate was removed by filtration using weighed micro sintered-glass funnels. The picrate was washed twice with 1 ml of water,

[2]*This compound was named incorrectly as* Δ^9*-1,4,9-triazabicyclo(5.3.0)decene in reference 2.*

dried, and weighed. Each lot of picrate was checked for purity by a melting-point determination. The rate of formation of 2-carboxymethylamino-Δ^2-tetrahydropyrimidine from 3-keto-1,2,6,7-tetrahydro-3(H),5(H)-imidazo(1,2-*a*)pyrimidine under the above conditions is kinetically first order with mean deviations within 10%. These deviations were due to the variations in efficiency of precipitation of bicyclic picrate and in some cases to coprecipitation of the picrate of the hydrolyses product.

Time, sec $\times 10^{-2}$	11.6	17.6	29.6	44.5	53.7
Reaction %	42.2	53.9	72.4	89.7	99.2
10^4K, sec^{-1}	4.72	4.39	4.31	3.95	4.22

Under the above conditions the half-life for 3-keto-1,2,6,7-tetrahydro-3(H),5(H)-imidazo(1,2-*a*)pyrimidine was calculated to be approximately 27.6 minutes while the half-life for 3-keto-1,2,5,6-tetrahydro-3(H)-imidazo(1,2-*a*)imidazole was calculated to be approximately 2 hours and 23 minutes.

It was not possible to calculate the rates of hydrolysis of 5-keto-2,3,6,7-tetrahydro-1(H),5(H)-imidazo-(1,2-*a*)pyrimidine and 4-keto-2,3,6,7,8,9-hexahydro-4(H)-pyrimido(1,2-*a*)pyrimidine even with this small degree of accuracy because of the coprecipitation of the hydrolysis product with the bicyclic guanidine in the first case and the very rapid hydrolysis of the latter bicyclic guanidine. The hydrolysis of 4-keto-2,3,6,7,8,9-hexahydro-4(H)-pyrimidino(1,2-*a*)pyrimidine was practically complete within 5 minutes. These studies showed that the relative susceptibility of the keto substituted bicyclic guanidines to hydrolysis falls in the following order: 4-keto-2,3,6,7,8,9-hexahydro-4(H)-pyrimido(1,2-*a*)pyrimidine (VIII) $\gg$ 5-keto-2,3,6,7-tetrahydro-1(H),5(H)-imidazo(1,2-*a*)pyrimidine (I) > 3-keto-1,2,6,7-tetrahydro-3(H),5(H)-imidazo-(1,2-*a*)pyrimidine (VI) $\gg$ 3-keto-1,2,5,6-tetrahydro-3(H)-imidazo(1,2-*a*)imidazole (VII).

Potentiometric Titrations

Aqueous solutions (0.01 moles) of the freshly sublimed bicyclic guanidines were prepared with carbon dioxide free water. These magnetically stirred solutions at a constant temperature of 30.5° were titrated with 0.1 *N* hydrochloric acid using a Beckman Model G pH meter equipped with glass electrode (Beckman No. 1190-80) and sealed calomel electrode (Fisher No. 11-505-80).

The pK_a values for 2,3,5,6-tetrahydro-1(H)-imidazo(1,2-*a*)imidazole and 2,3,6,7-tetrahydro-1(H),5(H)-imidazo(1,2-*a*)pyrimidine also were determined by potentiometric titration of their purified hydrochloride salts with 0.1 *N* sodium hydroxide solution. The pK_a values obtained in this manner were identical (within experimental error) with those determined from potentiometric titration of the corresponding free bases.

The potentiometric titrations of the aqueous bicyclic guanidines with 0.1 *N* hydrochloric acid were also conducted with an automatic potentiometer (Potentiograph E 336, Metrohm Ltd., Herisau, Switzerland, with combined glass/calomel electrode). The rate of titration was approximately 1 ml/min. The results with the automatic potentiometer were in agreement with the Beckman Model G pH meter.

The automatic potentiometer was used to titrate solutions of the bicyclic guanidines in glacial acetic acid with 0.1009 *N* perchloric acid in glacial acetic acid. The standard perchloric acid solution was prepared by the method of Fritz (6). The pK_a values determined in aqueous solution and the $E_{1/2}$ mv values determined in glacial acetic acid are given in Table I. The apparent pK_a values were determined from the readings at the half-neutralization points of the aqueous solutions of the bicyclic guanidines.

REFERENCES

1. A. F. McKay and M.-E. Kreling. Can. J. Chem. **38**, 1819 (1960).
2. A. F. McKay and M.-E. Kreling. Can. J. Chem. **35**, 1438 (1957).
3. L. Pauling. The nature of the chemical bond. 3rd ed. Cornell University Press, Ithaca, New York. 1959. p. 286.
4. A. F. McKay and M.-E. Kreling. Can. J. Chem. **40**, 205 (1962).
5. A. F. McKay, W. G. Hatton, and R. O. Braun. J. Am. Chem. Soc. **78**, 6144 (1956).
6. J. S. Fritz. Acid–base titrations in nonaqueous solvents. Twin City Printing Co., Champaign, Illinois. 1952. p. 13.

VIBRATIONALLY INDUCED PERTURBATIONS IN MOLECULAR ELECTRON DISTRIBUTIONS

RICHARD F. W. BADER
Department of Chemistry, University of Ottawa, Ottawa, Canada
Received January 17, 1962

ABSTRACT

It is demonstrated that second-order perturbation theory is useful in determining the manner in which the electron density present in a molecule is changed during a nuclear vibration. Furthermore, it is shown that one nuclear motion will lead to a particularly favorable electronic distortion such that this motion is energetically favored over the other possible motions of the molecule. This allows one to employ the theory to predict the symmetry of the reaction coordinate in both unimolecular and bimolecular reactions. The chemical implications of the electron density changes are discussed.

A reaction has associated with it a reaction coordinate, and any detailed analysis of a reaction mechanism requires a knowledge of how the electron distribution changes for various modes of motion of the system. For example, in a unimolecular decomposition there are a number of conceivable (and actual) ways in which a molecule may dissociate, depending on which vibrational mode corresponds to the most energetically favorable reaction coordinate. In the present approach we consider what effects the possible molecular motions have on the electron distribution. When the nuclei are displaced from their equilibrium positions the electron distribution relaxes in such a fashion as to follow the motion of the nuclei and thus leads to a smaller increase in energy than would be obtained if the electron distribution was static. By determining which nuclear motion allows for the most favorable relaxation of the electron density, we in effect determine the reaction coordinate.

We may treat the nuclear displacements as perturbations and in this way determine what effect these perturbations have on the electronic energy and wave function of the molecule in question. Making use of second-order perturbation theory we find that the energy of the distorted molecular configuration for extension in the i'th normal coordinate, Q_i, is

$$E(Q_i) = E_0 + \frac{1}{2}V_{00}^{ii} \cdot Q_i^2 + \sum_k{}' \frac{V_{0k}^{i} \cdot V_{k0}^{i}}{E_0 - E_k} Q_i^2. \qquad [1]$$

We employed this equation previously and applied it to an interpretation of potential interaction constants (1). We limit our present discussion to an interpretation of the terms appearing in the expression. E_0 is the energy of the undistorted configuration. The perturbations are given by the expressions

$$V_{00}^{ii} = \int \rho_{00} \frac{\partial^2 \phi(\mathbf{r},\mathbf{R})}{\partial Q_i^2} d\mathbf{r}$$

$$V_{0k}^{i} = \int \rho_{0k} \frac{\partial \phi(\mathbf{r})}{\partial Q_i} d\mathbf{r}$$

in which $\phi(\mathbf{r},\mathbf{R})$ is the total potential of the nuclei and $\phi(\mathbf{r})$ is the potential interaction of the nuclei with the i'th electron. We may employ the electron density functions ρ_{00} and ρ_{0k} in the above integrals, as neither $\phi(\mathbf{r},\mathbf{R})$ nor $\phi(\mathbf{r})$ contains terms which involve the

coordinates of more than a single electron. This fact makes it possible to give simple interpretations to $V_{00}{}^{ii}$ and $V_{0k}{}^{i}$. The quantity ρ_{00} is the electron density for the undistorted molecule. Thus the term $\frac{1}{2}V_{00}{}^{ii}\cdot Q_i{}^2$ determines the increase in the energy of the molecule when the nuclei are displaced from their equilibrium positions and the electron distribution is held fixed.

It is the term $V_{0k}{}^{i}$ which allows for a relaxation of the electron distribution and it is this term with which we shall be mainly concerned. The relaxation is brought about by mixing in with the ground state $|0\rangle$ the wave function for an excited state $|k\rangle$. The density expression ρ_{0k} appearing in $V_{0k}{}^{i}$ is thus termed the transition density.[1] *It is a measure of the amount of charge which is transferred within the molecule when the nuclei are displaced from their equilibrium positions.* The expressions ρ_{0k} are the corrections to the electron density of the undistorted molecule. The first-order correction to the wave function due to the mixing effect is

$$|0\rangle' = |0\rangle + Q_i \sum_k{}' [V_{0k}{}^{i}/(E_0 - E_k)]|k\rangle, \qquad [2]$$

and thus the transition density will make a contribution to the electron density found in the distorted molecule,

$$\rho_{0'0'} = \rho_{00} + 2Q_i \sum_k{}' [V_{0k}{}^{i}/(E_0 - E_k)]\rho_{0k} \ldots . \qquad [3]$$

By this mechanism we may explain how distortions of the nuclear framework introduce symmetric or antisymmetric components into the original charge distribution of the molecule.

The transition density does not represent any absolute amount of charge (its integral over all space is equal to zero) but instead gives a three-dimensional representation of the movements of charge density within the molecule. In the molecular orbital terminalogy, ρ_{0k} will be given simply as

$$\rho_{0k} = c\phi_i{}^{*}\phi_j,$$

where $\phi_i{}^{*}$ is the orbital which was occupied in the state $|0\rangle$, ϕ_j is the orbital occupied in its stead in the state $|k\rangle$, and c is a numerical constant. The forms of the ρ_{0k} are thus simple to determine and thus so is the magnitude and direction of the charge shift.

With the above interpretation of ρ_{0k} we may now interpret the integral $V_{0k}{}^{i}$ as the *force* exerted on the nuclei (those which are displaced in the mode Q_i) by the displaced charge density. Differentiation of $\phi(\mathbf{r})$ with respect to Q_i is mathematically equivalent to placing a point dipole, orientated in the direction of the nuclear displacement, on each nucleus which moves in the mode Q_i. Thus, alternatively, $V_{0k}{}^{i}$ may be interpreted as the interaction of the point dipoles centered on the nuclei with the displaced charge distribution.

The manner in which equation [1] may be applied is as follows. It is evident from the denominator in the expression for E that the lowering in energy due to the relaxation effect will be greatest for that mode of vibration which allows for an interaction with the lowest of the excited states. Furthermore, the transition force $V_{0k}{}^{i}$ will be different from zero only if the transition density ρ_{0k} and Q_i have identical symmetries. We then assume that

[1] $\rho_{0k} = \langle 0|-e\{\sum_i \delta(\mathbf{r}-\mathbf{r}_i)\}|k\rangle$ *(see reference 1 or 4).*

the most favored motion, i.e., the one which leads to the smallest increase in potential energy, will be that one whose symmetry allows for an interaction with the lowest of the excited states.[2] The principal change brought about in the electron distribution for any of the nuclear motions is assumed to be determined by the admixture of the lowest excited state of the proper symmetry, an assumption founded on the presence of the term $E_0 - E_k$ in the denominator of the coefficient in equation [3]. Thus we are now in a position to predict the major changes in the electron density accompanying any nuclear displacement, and, in addition, pick out that mode which allows for the greatest relaxation of the electron distribution. Using this method with the same assumptions, we have previously been able to correctly predict the signs of potential interaction constants for a large number of molecules (1). Since the successful prediction of the sign of an interaction constant by this method is determined by the proper selection of the mode which gives the greatest relaxation in the electron distribution, we base our confidence in the present approach on these previous results.

We now show how the information available from an application of equation [1] is of use in the understanding of the chemical properties of molecules, by providing us with information regarding the possible reaction coordinate and the accompanying changes in the electron density during the reaction.

Unimolecular Decompositions

The most obvious application of equation [1] is to the unimolecular decomposition of a molecule. We are interested in determining which relative motion of the nuclei corresponds to the reaction coordinate. We shall consider some triatomic systems first.

We have previously shown (1) that the transition density arising from the admixture of the lowest excited state of the triatomic molecules which possess 16 valence electrons (e.g., CO_2, CS_2, $HgCl_2$) is of Σ_u^+ symmetry,

$$\ldots (\pi_u)^4(\pi_g)^4;\ {}^1\Sigma_g^+ \rightarrow \ldots (\pi_u)^4(\pi_g)^3(\bar{\pi}_u);\ {}^1\Sigma_u^+$$

(the other states resulting from this excited configuration are of irrelevant symmetries ${}^1\Delta_u$ and ${}^1\Sigma_u^-$). The vibration which brings about the mixing in of this lowest excited state is the antisymmetric stretching vibration which is, therefore, predicted to be the energetically favored vibration and the reaction coordinate. The present method then correctly predicts that the unimolecular decomposition of these molecules will proceed so as to produce an atom and a diatomic molecule. The transition density is given as

$$\rho_{gu} = \pi_g^* \bar{\pi}_u.$$

We can employ this information to obtain a qualitative picture of how the electron density is changed during a Σ_u^+ vibration. From the form of the transition density (shown in Fig. 1) we see that charge is displaced from one end atom to the other and removed (in the opposite sense) from one binding region and concentrated in the other. Such a charge migration clearly weakens one bond and strengthens the other. The magnitude of this asymmetric contribution to the charge density increases as the extension in the asymmetric coordinate is increased.

It is possible, of course, that the symmetry of the transition density will change as the molecular dimensions are appreciably altered due to a crossing of orbital energies and

[2]*See the Appendix for further justification of this procedure.*

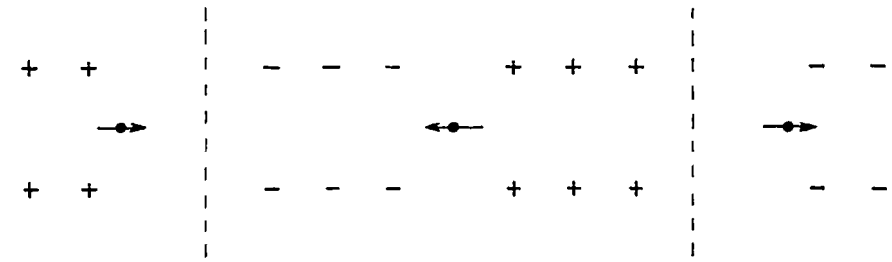

FIG. 1. Schematic representation of ρ_{gu} and its interaction with the antisymmetric stretching vibration. (The negative signs indicate an increase in the electron density, the positive signs a decrease.)

hence to the appearance of a new low-lying excited state. For molecules which contain relatively few atoms, the order of the orbital energies can be predicted with some certainty even for distorted configurations and thus this possibility may be allowed for. For example, in the above-mentioned triatomic molecules, the symmetry of the transition density remains unchanged even for appreciable extensions of the asymmetric coordinate. In more complicated molecules, the order of the orbitals, especially for distorted configurations, is not always predictable with great certainty and the method then loses its usefulness.

As another simple example of the application of the present method to unimolecular reactions we consider the decomposition of the ozone molecule. The method should in this case correctly predict the favored asymmetrical dissociation into an oxygen molecule and an oxygen atom. The ozone molecule contains 18 valence electrons and is therefore bent and of C_{2v} symmetry. Mulliken has given the molecular orbital description of this molecule (3), and we have previously discussed the symmetries of the relevant transition densities (1). The ground state is $^1A_1$ and the lowest excited state which gives a relevant transition density is of B_1 symmetry. Such a transition density favors the unsymmetrical extension of the molecule, which induces an asymmetry in the electronic charge distribution corresponding to a weakening of one of the bonds and a strengthening of the other.

Consider next the unimolecular decomposition of the dialkyl mercury compounds by taking dimethyl mercury as a typical case. The electronic configuration of this molecule, in terms of molecular orbitals is

$$(a_{1g})^2(a_{2u})^2(e_g)^4(e_u)^4(a_{1g})^2(a_{2u})^2;\ ^1A_{1g}.$$

The first four of these orbitals represent the bonding between the hydrogen and carbon atoms, the last two, the bonding between the mercury atom and the carbon atoms. The lowest excited orbital of dimethyl mercury is the antibonding orbital between the carbon and mercury atoms of $\bar{a}_{1g}$ symmetry. The carbon–hydrogen antibonding orbitals are certainly of much greater energy than the $\bar{a}_{1g}$ antibonding orbital, as is the $7s$ orbital of the Hg atom. (Transitions to the $6p_\pi$ orbitals of the mercury atom give an irrelevant transition density of E_g symmetry.) The lowest excited electronic state is, therefore,

$$\ldots (a_{1g})^2(a_{2u})(\bar{a}_{1g});\ ^1A_{2u}.$$

The transition density is of A_{2u} symmetry and the reaction coordinate will be of the same symmetry, i.e., an unsymmetrical vibration of the C—Hg bonds. Since it is the mercury–carbon orbitals which are involved in determining this transition density, it will be the

electron density in the region of the mercury carbon bonds which will be most strongly affected. The transition density is given by

$$\rho_{a\bar{a}} = a_{2u}\bar{a}_{1g}$$

and will be similar in appearance to that for ρ_{gu} in Fig. 1. The theory predicts that the molecule will decompose by the rupture of one of the carbon–mercury bonds to form a methyl radical and $Hg—CH_3$.

Laidler and Steel (2) have pointed out that the high-frequency factors which are found for certain unimolecular reactions may be explained by the simultaneous rupture of more than one bond in the molecule. The azo compounds are examples of molecules which exhibit high-frequency factors in their unimolecular decompositions. Laidler and Steel (2) postulate that their decomposition is via a symmetrical stretching of both $N—CH_3$ bonds. It is of interest, therefore, to apply the present approach to these molecules and determine whether it does indeed predict a symmetrical, as opposed to an unsymmetrical, reaction coordinate.

The order of the molecular orbitals for the C—N—N—C framework is most easily determined by the construction of a correlation diagram which shows the variation in the relative energies of the orbitals as the C—N—N angle is varied. Such diagrams, together with a simple set of rules regarding the degree of hybridization have been shown by Walsh (5) to be of great value in such assignments. The order of the molecular orbitals in the linear case are easily determined. These are listed on the right of Fig. 2. The correlated orbitals for a C—N—N—C framework of C_{2h} symmetry are given on the left of

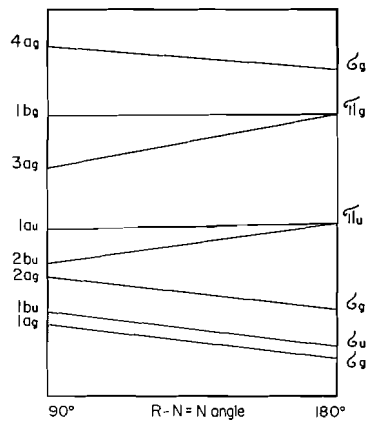

FIG. 2. A schematic representation of the correlation of molecular orbitals in the bent and linear C—N=N—C framework.

Fig. 2. The decrease of the C—N—N angle results in a splitting of the π degeneracies found in the linear case. Notice that if only 10 electrons are involved the molecule will remain linear, as a decrease in the C—N—N angle results in an overall raising of the orbital energies for reasons given by Walsh. In general, however, tetratomic molecules which possess more than 10 electrons (there are 12 in the azo compounds) will be bent due to the occupation of the $3a_{1g}$ orbital, which undergoes a drop in energy as the C—N—N angle is decreased.[3] The reason for this increased stabilization of the $3a_g$ orbital is

[3]*There are similarities and some understandable differences between our Fig. 2 and Walsh's figure for* HAAH *molecules.*

to be found in the fact that in the bent molecule this component of the π orbital takes on an increasing amount of s character. The ground-state electronic configuration of the azo compounds may be represented by

$$(1a_g)^2(1b_u)^2(2a_g)^2(2b_u)^2(1a_u)^2(3a_g)^2;\ ^1A_g.$$

The lowest excited state arises from a transition to the $1b_g$ orbital

$$\ldots (1a_u)^2(3a_g)(1b_g);\ ^1B_g,$$

which gives an irrelevant transition density of symmetry B_g, irrelevant since the C—N —N—C framework possesses no vibrational motions of B_g symmetry. The transition of next lowest energy is due to a transition to the $4\bar{a}_g$ orbital, which is strongly antibonding between the N and C atoms and bonding between the two nitrogen atoms, which gives a transition density of A_g symmetry,

$$\ldots (1a_u)^2(3a_g)(4\bar{a}_g);\ ^1A_g.$$

Therefore, the most favored motions are those of the same symmetry, and the molecule should decompose in a symmetrical fashion, giving two methyl radicals and a nitrogen molecule in one step. This mechanism is thus supported in preference to an unsymmetrical stepwise decomposition corresponding to a B_u motion and a B_u transition density. It is worth noting that as the C—N distance is increased the $3a_g$ orbital will rise in energy (ultimately becoming the same as the $1b_g$ orbital) and the $4a_g$ orbital will decrease in energy. The vibrationally induced A_g component of the electron density thus becomes more prominent as the decomposition proceeds.

Bimolecular Reactions

The transition state of a bimolecular reaction represents the configuration of maximum potential energy along the reaction coordinate, and therefore, as for a stable molecule, the energy is independent of the nuclear displacements to the first order. We may apply second-order perturbation theory to the transition-state molecule to again determine the most favored mode of decomposition. An insight into the electronic changes underlying the reaction may be obtained from a knowledge of the relevant transition density. Or, we may employ the method to test a proposed transition-state configuration. If a transition state is put forward for a reaction which possesses a favored mode of motion which does not lead to the observed products, then it must be discarded.

It is worthwhile noting that the "mixing in" of the excited state in the case of a transition-state molecule must be very pronounced, for the potential energy actually must decrease as the configuration of the transition state is distorted in such a manner as to correspond to a motion along the reaction coordinate. For this to be possible within the framework of the present theory, the following inequality must hold:

$$\frac{(V_{0k}{}^t)^2}{E_0-E_k} > \frac{1}{2}V_{00}{}^{tt}.$$

Thus, in general, we should expect to find that at least one excited state is relatively low lying for transition-state molecules in order that the above requirement may be met. This is in general true, and it is the nature of this first excited state which determines the course of the reaction.

As a simple first example of the application of the present method to a bimolecular reaction consider the complex H—H—H obtained in the hydrogen atom–molecule reaction. The electronic configuration of the complex is $(\sigma_g)^2(\sigma_u)$; $^2\Sigma_u^+$. The first excited state is obtained from the configuration $(\sigma_g)^2(\bar{\sigma}_g)$; $^2\Sigma_g^+$. The transition density is of Σ_u^+ symmetry and it follows that such a complex should decompose in an unsymmetrical fashion to give a hydrogen molecule and atom. Thus, due to the fact that the first excited state is of Σ_g^+ symmetry, an asymmetrical distortion of the charge density is the one most easily accomplished, and thus the asymmetric motion of the nuclei is favored. Such a motion leads to a concentration of charge in one bond and to its depletion in the other and to the observed formation of a hydrogen molecule and a hydrogen atom.

The transition state proposed for an S_N2 displacement on a substituted carbon atom is one in which the attacking nucleophile, the carbon atom, and the leaving group lie on a line. We shall use this case as a simple example of how, in general, a low-lying excited state arises in the formation of a transition-state molecule. In Fig. 3 we show the orbitals

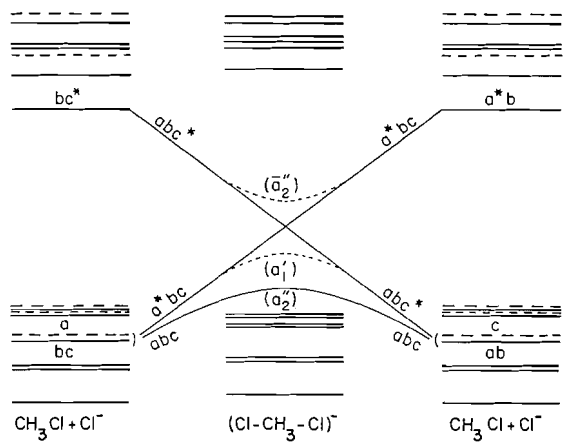

FIG. 3. An orbital correlation diagram between reactants, transition state, and products for $CH_3Cl + Cl^-$. The dashed lines in the right and left columns represent the Cl^- ion orbitals, the solid lines the CH_3Cl orbitals. The $\bar{a}_2''$ orbital and the ones lying above it are unoccupied.

of the reactants, of the transition state, and of the products. The p_z orbital on the entering chloride ion we label *a*, the original C—Cl bonding and antibonding orbitals in the reactant we label *bc* and *bc**, the asterisk denoting antibonding. The approach of the chloride ion to CH_3Cl will result in the formation of three new orbitals, *abc*, *a***bc*, and *abc**; the remaining orbitals in CH_3Cl and on the chloride ion are affected to a much smaller extent. The orbital *abc* will be the most stable of the three. The orbital *a***bc* will start out low in energy (degenerate with *abc* at large separations) and rise in energy as the reaction proceeds. The orbital *abc** will be high in energy at the start of the reaction (corresponding to an excited orbital of C—Cl for large separations) and will fall in energy, as the reaction progresses, to a value below that of *a***bc*. In effect, *a***bc* and *abc** interchange their roles during the reaction. In a first, very crude approximation, we might expect *a***bc* and *abc** to be degenerate in the transition-state molecule. This of course does not occur and the two orbital energies are instead "pushed apart" in the region where the crude approximation would have them intersect. The effect of the formation of the transition state is thus to lower the energy of what was initially an antibonding orbital

between carbon and chlorine and form a new occupied orbital which, as we have seen, will lie relatively close in energy to the vacant, lowered antibonding orbital. The new occupied orbital is high in energy because the bonds it describes are long and weak and the antibonding character of the vacant orbital is lessened for the same reason. The remaining excited orbitals of the complex (e.g., the carbon–hydrogen antibonding orbitals) are, to a first approximation, not affected by these changes in bonding and thus do not undergo any significant lowering in energy. The result is, therefore, the formation of a new low-lying excited state involving the occupation of an antibonding orbital which has been stabilized to a point well below the other excited orbitals of the system.

In the transition state (D_{3h} symmetry) the orbitals will be of symmetries a_2'' ($p_{z\mathrm{Cl}} + p_{z\mathrm{C}} + p_{z\mathrm{Cl}}'$, bonding), a_1' ($p_{z\mathrm{Cl}} - p_{z\mathrm{Cl}}'$, bonding), and $\bar{a}_2''$ ($p_{z\mathrm{Cl}} - p_{z\mathrm{C}} + p_{z\mathrm{Cl}}'$), the bar over the last symbol signifying its antibonding character. The electronic configuration of the transition state molecule will be

$$\ldots (a_2'')^2 (a_1')^2; {}^1A_1'.$$

It follows that since the C—Cl bonds are the weakest (and longest) in the molecule, the lowest lying of the antibonding orbitals found in the transition state will be that associated with the antibonding between the carbon atom and the halogens, $\bar{a}_2''$. The lowest excited state is

$$\ldots (a_2'')^2 (a_1')(\bar{a}_2''); {}^1A_2''$$

and the transition density is of symmetry A_2''. Therefore, the most easily imposed electronic distortion for the transition state is an unsymmetrical one and the vibration which will induce such a distortion is the asymmetrical motion of A_2'' symmetry,

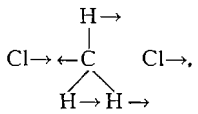

It is of interest to note that the motion of the hydrogen atoms, which is of A_2'' symmetry, corresponds to an inversion of the molecule as is observed in S_N2 reactions. While one cannot say to what extent the hydrogens participate in this particular coordinate, the motion required to bring about the inversion of the molecule is of the proper symmetry to be both allowed and favored.

As further examples of how the present method may be of use in determining possible reaction coordinates we shall consider the "branched" transition states recently proposed by Thrush and Clyne (6) for the reactions of oxygen atoms with NO_2, O_3, and ClO_2 and of nitrogen atoms with NO_2. The transition states proposed for these reactions are all of the form shown below for $O + NO_2$. Again, applying Walsh's molecular orbital

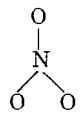

methods, we find that the transition-state molecules N_2O_2, NO_3, and O_4 (with 22, 23, and 24 valence electrons respectively) should be planar, while ClO_3 (with 25 valence

electrons) should be pyramidal. Thrush has pointed out that the formation of such a transition state is likely in each case, as the highest electron density in the top-filled orbital is found on the central atoms in NO_2, O_3, and ClO_2.

Consider first the complex NO_3 of D_{3h} symmetry. Does this molecule possess a transition density of the symmetry required to favor that nuclear motion which leads to the observed products (NO + O_2)? The structure of the vibrational representation for such a molecule is

$$\Gamma_{vib} = A_1' + A_2'' + 2E'.$$

The electronic configuration of the ground state of NO_3 will be (1, 5) (omitting the 2*s* electrons on the oxygen atoms)

$$(a_1')^2(1e')^4(a_2'')^2(2e')^4(2e'')^4(a_2')^1;\ ^2A_2'.$$

The two lowest unoccupied molecular orbitals are of symmetries $\bar{a}_1'$ and $\bar{a}_2''$ (the bar denoting their antibonding character). Of the excited states arising from occupation of a_2', $\bar{a}_1'$, or $\bar{a}_2''$, only two give states of relevant symmetries, they are

$$\ldots (2e')^3(2e'')^4(a_2')^2;\ ^2E'$$
$$\ldots (2e')^4(2e'')^3(a_2')(\bar{a}_2'');\ ^2E'.$$

The transition density is, therefore, of symmetry E', and the E' vibration is favored as the reaction coordinate over the A_1' or A_2'' motions. Of the possible vibrational motions of this molecule, only those of E' symmetry could give the observed products; both A_1' and A_2'' lead to the formation of N + 3O or perhaps (for A_2'') N + O_3. One component of each of the E' transition densities is illustrated in Fig. 4 together with the

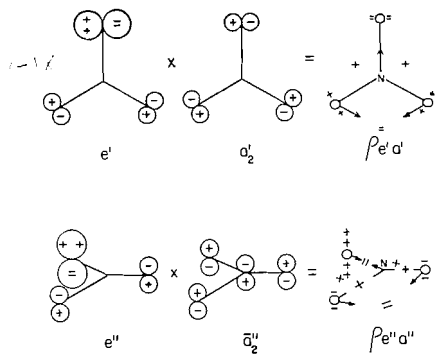

FIG. 4. Schematic representations of $\rho_{a'e'}$ and $\rho_{a''e''}$ for the NO_3 molecule and their interaction with an E' vibration.

contributing molecular orbitals. In each case charge is shifted so as to facilitate an E' vibration. The vibration may, of course, lead to any one of the three oxygen atoms combining with the nitrogen atom, since it is a degenerate motion. This proposed transition state is thus an acceptable one according to the tenets of the present theory, for it possesses a favored mode of motion which leads to the observed products.

The reaction of O with O_3 would, by this mechanism, give a planar D_{3h} transition-state molecule with the electronic configuration

$$\ldots (2e')^4(2e'')^4(a_2')^1(\bar{a}_2'')^1;\ ^3A_1''.$$

The transition state must be a triplet in order to preserve the spin correlation rules. This will force the occupation of the $\bar{a}_2''$ orbital in the case of a planar transition state. The lowest transition of a relevant symmetry is to the state

$$\ldots (2e')^4(2e'')^3(a_2')^1(\bar{a}_2'')^2;\ ^3E'',$$

which again gives a transition density of E' symmetry. Even though NO_3 and O_4 possess different numbers of electrons, both possess the same type of favored motion for their decomposition.

We can most rapidly predict the behavior of the $N + NO_2$ reaction via the proposed branched transition state by considering first the transition complex of greater symmetry obtained from $O + NO_2$ with 22 rather than 23 electrons. The electronic structure for such a complex would be (again it must be in a triplet state to preserve the spin correlation rules)

$$\ldots (2e')^4(2e'')^3(a_2')^1;\ ^3E''.$$

Now consider how the orbitals and states of such a symmetrical complex are perturbed as the nuclear charge of one of the oxygen atoms is decreased by one unit. The symmetry is now lowered to C_{2v} and all the degeneracies are lifted. The $2e''$ orbital now gives orbitals of symmetries $2a_2$ and $2b_2$, a_2' becomes b_1, and the orbital $\bar{a}_2''$ is transformed into one of b_2 symmetry. Before the perturbation, $2a_2$ and $2b_2$ were degenerate and it is reasonable to assume that their splitting is not too great. Therefore, the two states resulting from the splitting of the ground state $^3E''$ may be expected to differ little in energy.

$$\ldots (2a_2)^2(2b_2)^1(b_1)^1;\ ^3A_2$$

$$\ldots (2a_2)^1(2b_2)^2(b_1)^1;\ ^3B_2$$

The relative order of the two states is irrelevant (reversing the order of $2a_2$ and $2b_2$ reverses their order) as the symmetry of the transition density remains unchanged. This symmetry is B_1 and thus a B_1 vibration is favored. There are two possible B_1 motions, one would lead to the formation of 2NO and the other to $N_2O + O$. Thrush has actually postulated that the reactions of $N + NO_2$ to give 2NO and $N_2O + O$ do proceed through the same transition state, from considerations of the relative entropies and energies of activation. The present theory agrees with this postulate, as the removal of the degeneracy of the orbitals should lead to the appearance of two states close together in energy and giving a transition density of B_1 symmetry. Each of the E' vibrations is of course split into an A_1 and a B_1 component by the same perturbation. The transition density will favor the two B_1 components. Thrush also feels that the other products observed for this reaction, $N_2 + O_2$, might arise from the same transition state. This would require a transition density of A_1 symmetry. While an excited state of the proper symmetry to give an A_1 transition density is certainly present, it is, of course, beyond the capabilities of the present method to predict whether or not it is low enough in energy to compete with the B_1 transition density.

The molecule ClO_3 with 25 valence electrons will be pyramidal in shape of C_{3v} symmetry. Its ground state (1) will be (again ignoring the oxygen 2*s* electrons)

$$(1a_1)^2(1e)^4(2a_1)^2(1\bar{a}_1)^2(2e)^4(3e)^4(1\bar{a}_2)^1;\ ^2A_2.$$

The first excited state of proper symmetry is

$$\ldots (3e)^3(1\bar{a}_2)^2;\ ^2E.$$

The molecule ClO_3 should thus decompose to give ClO and O_2, as observed for this reaction, as an E vibration is the favored mode. Neither of the A_1 vibrations, which are the other possible modes of vibration, could lead to such products.

In all of the above applications to transition-state molecules we are describing their instability as due to the presence of a low-lying excited state. The bonds in a transition-state molecule are longer and weaker than usual, and hence the top-most orbitals will be higher in energy and the antibonding combinations will be correspondingly lower in energy, i.e., the separation between the bonding and antibonding combinations in general decreases as the bonding decreases. In such molecules we can thus expect to find a low-lying excited state. In the $O + NO_2$ and $O + O_3$ reactions, both are unstable due to a mixing in of a low-lying E' state arising from the occupation of the $\bar{a}_2''$ orbital. This orbital is antibonding between the outer atoms and the central atom and is formed from the *p* orbitals which are perpendicular to the plane of the molecule. Since all the bonds are long, we expect this to be a low-lying state in these cases, i.e., the $\bar{a}_2''$ orbital is only weakly antibonding. Thus, close to the ground state there is actually an orbitally degenerate state which must be inherently unstable with respect to an E' vibration. In these cases we thus have a situation in which the most easily attained charge distortion is one which is inherently unstable to a motion which does lead to the formation of the observed products.

APPENDIX

This appendix is to provide further discussion of the assumption basic to the present approach that the lowest of the excited states will determine the symmetry of the favored vibration. As a simple numerical example, we may consider the following two nuclear motions of H_2^+ (ground state $^2\Sigma_g^+$):

The lowest excited states of H_2^+ are $^2\Sigma_u^+$ and $^2\Sigma_g'^+$ (which is made orthogonal to $^2\Sigma_g^+$), $^2\Sigma_u^+$ being the lower of the two. We wish to compare

$$(\langle {}^2\Sigma_g^+|\partial\phi(\mathbf{r})/\partial Q_u|{}^2\Sigma_u^+\rangle)^2/(E_0-E_u),\quad T_u$$

with

$$(\langle {}^2\Sigma_g^+|\partial\phi(\mathbf{r})/\partial Q_g|{}^2\Sigma_g'^+\rangle)^2/(E_0-E_g),\ T_g.$$

These quantities are easily evaluated using simple molecular orbitals, and it is found that $T_u = 730$ and $T_g = 70$ (in a.u. $\times 10^4$). Since the terms contribute to a sum it is the difference in their magnitudes which is important. The difference ($T_u - T_g = 660$) is in

fact approximately 10 times greater than the whole contribution from the second lowest of the excited states. This difference is due mainly to the rapid fall in the integral, rather than to the increased energy difference on going from T_u to T_g. We can expect this to be a general result from the following considerations. From Schrödingers equation for the electronic wave function at the equilibrium position,

$$H\psi_k = E_k\psi_k,$$

we may obtain (7)

$$\langle k|\partial H/\partial Q_i|0\rangle = \langle k|\partial\phi(\mathbf{r})/\partial Q_i|0\rangle = (E_0-E_k)\langle k|\partial/\partial Q_i|0\rangle.$$

The term $\langle k|\partial/\partial Q_i|0\rangle$ will in turn reduce to

$$\int \phi_p(\partial\phi_j/\partial Q_i)d\tau,$$

where ϕ_p and ϕ_j are the same molecular orbitals which contribute to ρ_{0k}. The value of this latter integral decreases rapidly as the difference in the orbital energies of ϕ_p and ϕ_j increases (as may be easily demonstrated for simple systems). It represents simply an overlap integral between the derivative of one molecular orbital with another. The more the energies of the two orbitals differ, the smaller is the value of this overlap integral. Furthermore, the value of this overlap decreases much more rapidly than the energy difference (E_0-E_k) increases. Thus the low-lying states will make the major contribution to this particular kind of second-order sum and the lowest of these states will make the largest single contribution.

Terms of the form $\langle k|\partial/\partial Q_i|0\rangle$ occur in the off-diagonal matrix elements of the Born–Oppenheimer approximation (7). It is well known that when an excited state $|k\rangle$ lies very close to the ground state $|0\rangle$ the Born–Oppenheimer approximation breaks down because the terms $\langle k|\partial/\partial Q|0\rangle$ become very large. In fact, when $|k\rangle$ and $|0\rangle$ are degenerate, we have a Jahn–Teller instability. The present approach may be thought of as a second-order Jahn–Teller effect. When $|k\rangle$ and $|0\rangle$ are degenerate, there is no question as to the instability of the system with respect to certain normal modes. When $|k\rangle$ and $|0\rangle$ differ slightly in energy we pass from a first-order effect to the presently described second-order effect where the lowest-lying state $|k\rangle$ will still determine the major effect.

REFERENCES

1. R. F. W. Bader. Mol. Phys. **3**, 137 (1960).
2. C. Steel and K. J. Laidler. J. Chem. Phys. **34**, 1827 (1961).
3. R. S. Mulliken. Revs. Modern Phys. **14**, 204 (1942).
4. H. C. Longuet-Higgins. Proc. Roy. Soc. (London), A, **235**, 537 (1956).
5. A. D. Walsh. J. Chem. Soc. 2260, 2266, 2301 (1953).
6. M. A. A. Clyne and B. A. Thrush. Trans. Faraday Soc. **57**, 69 (1961).
7. W. D. Hobey and A. D. McLachlan. J. Chem. Phys. **33**, 1695 (1960).

METAL OXIDE ALKOXIDE POLYMERS

PART V. THE HYDROLYSIS OF SOME ALKOXIDES OF TIN (IV), CERIUM (IV), AND URANIUM (V)[1]

D. C. BRADLEY[2] AND H. HOLLOWAY[3]
Department of Chemistry, Birkbeck College, London, W.C.1, England

Received February 23, 1962

ABSTRACT

The polymers formed by the hydrolysis of stannic isopropoxide, ceric isopropoxide, and uranium pentaethoxide have been studied by means of an ebulliometric method. The metal oxide alkoxide polymers formed from the tin (IV), cerium (IV), and uranium (V) alkoxides conform to the requirements of a structural theory. In view of the fundamental nature of the theory a formal mathematical presentation is now given.

INTRODUCTION

Previous work has shown that the remarkable variation of number-average degree of polymerization of the oxide alkoxides of titanium (1), zirconium (2), and tantalum (3) as a function of degree of hydrolysis may be satisfactorily explained on the basis of certain key structures in which the metal atom exhibits a higher coordination number. The success of the theory in explaining the behavior of compounds of both quadrivalent and quinquevalent elements on the same basic structural models suggested that it may be of fundamental importance in relation to metal oxide alkoxides in general and that it should have predictive ability. Accordingly we have set out in a formal manner the mathematical aspects of the theory, including a useful terminology for describing the various structural models. In an attempt to test the predictive possibilities of the theory we have extended the work to the hydrolysis of the isopropoxides of tin (IV), cerium (IV), and the pentaethoxide of uranium (V). The derivatives of tin and cerium both form dimeric solvates of the type $M_2(OPr^i)_8,(Pr^iOH)_2$ and should give polymeric oxide isopropoxides based on mixtures of the model II and model III or of the model II and model IV basic structures. Similarly, the uranium oxide ethoxides would be expected to conform to the same structural models as the tantalum oxide ethoxides, provided that the uranium exhibits a coordination number of six.

EXPERIMENTAL

Preparation of Metal Alkoxides

Stannic isopropoxide was prepared by alcoholysis of the ethoxide, which was obtained by the method of Bradley, Caldwell, and Wardlaw (4). The isopropoxide was purified by crystallization of the solvate $Sn_2(OPr^i)_8,(Pr^iOH)_2$, which lost the coordinated isopropanol when heated *in vacuo*. The resulting $Sn(OPr^i)_4$ was distilled *in vacuo*. Cerium isopropoxide was prepared from dipyridinium cerium hexachloride by the method of Bradley, Chatterjee, and Wardlaw (5). It was purified by recrystallization of the solvate $Ce_2(OPr^i)_8,(Pr^iOH)_2$. Uranium pentaethoxide was prepared by the three-stage synthesis from UCl_4 and sodium ethoxide using bromine as the oxidant, as developed by Jones *et al.* (6). The product was purified by distillation *in vacuo*. All of these compounds are extremely susceptible to hydrolysis and the usual precautions were adopted to control the hydrolysis in these experiments. The uranium compound is also susceptible to oxidation and the experiments were carried out under an atmosphere of oxygen-free nitrogen.

Ebulliometry

The previously described technique (3) was essentially followed throughout. Solutions of $Ce_2(OPr^i)_8,(Pr^iOH)_2$ and $Sn_2(OPr^i)_8,(Pr^iOH)_2$ in boiling isopropanol were prone to decomposition if the amount of

[1] *For Part IV, see reference 3.*
[2] *Present address: The University of Western Ontario, London, Ontario.*
[3] *Present address: Post Office Research Station, Dollis Hill, London, N.W.2, England.*

superheating was high or if the heating was localized. However, by using a silicone oil heating bath and lagging the ebulliometer satisfactory conditions were obtained and the results were reproducible. With the exception of $Ce_2(OPr^i)_8,(Pr^iOH)_2$, which has a low volatility and was recrystallized immediately prior to use, the alkoxides were freshly distilled *in vacuo* immediately before an ebulliometric hydrolysis.

Stannic Isopropoxide

Three separate determinations of the molecular weight were carried out, each involving several additions of solute. Although the concentrations covered almost a 30-fold range there was no evidence of concentration dependence of the molecular weight. The values of n_0 (the number-average degree of polymerization of the metal alkoxide, i.e. n at zero degree of hydrolysis) were: 1.84, 1.88, 1.84. The mean value of $n_0 = 1.85$ was adopted. The results of two ebulliometric hydrolyses are recorded in Table I.

TABLE I

A. Initial concentration of $Sn(OPr^i)_4 = 0.264$ g-mol./kg						
h	0.100	0.190	0.332	0.507	0.724	0.919
n	1.87	2.06	2.43	2.98	3.81	4.95
n_{calc}	1.95	2.09	2.35	2.78	3.59	4.86
B. Initial concentration of $Sn(OPr^i)_4 = 0.310$ g-mol./kg						
h	0.204	0.483	0.822	1.078	1.449	
n	1.98	2.73	4.02	6.14	17.0	
n_{calc}	2.11	2.71	4.13	6.84		

Ceric Isopropoxide

The two determinations of the molecular weight of the solvate $Ce_2(OPr^i)_8,(Pr^iOH)_2$ gave $n_0 = 1.86, 1.87$. The value of 1.86 was adopted. The results of four ebulliometric hydrolyses are recorded in Table II.

TABLE II

A. Initial concentration of $Ce_2(OPr^i)_8,(Pr^iOH)_2 = 0.109$ g-mol./kg					
h	0.111	0.271	0.506	0.704	1.026
n	2.02	2.26	2.79	3.51	6.34
n_{calc}	2.02	2.28	2.83	3.55	6.08
B. Initial concentration of $Ce_2(OPr^i)_8,(Pr^iOH)_2 = 0.127$ g-mol./kg					
h	0.109	0.265	0.471	0.688	1.042
n	2.02	2.26	2.71	3.46	5.90
n_{calc}	2.02	2.27	2.74	3.48	6.25
C. Initial concentration of $Ce_2(OPr^i)_8,(Pr^iOH)_2 = 0.205$ g-mol./kg					
h	0.088	0.217	0.413		
n	1.98	2.21	2.62		
n_{calc}	1.98	2.19	2.59		
D. Initial concentration of $Ce_2(OPr^i)_8,(Pr^iOH)_2 = 0.173$ g-mol./kg					
h	0.128	0.289	0.505		
n	2.04	2.37	2.91		
n_{calc}	2.04	2.32	2.83		

Uranium Pentaethoxide

The molecular weight of uranium pentaethoxide was determined in boiling ethanol in two separate experiments covering a 15-fold range in concentrations but no evidence of concentration dependence was found. The values of n_0 were 1.47 and 1.49. The average value, $n_0 = 1.48$, was adopted. The results for two ebulliometric hydrolyses of uranium pentaethoxide are given in Table III.

TABLE III

A. Initial concentration of $U(OEt)_5 = 0.217$ g-mol./kg									
h	0.093	0.219	0.349	0.478	0.630				
n	1.56	1.70	1.85	2.03	2.31				
n_{calc}	1.61	1.69	1.85	2.03	2.31				
h	0.804	0.969	1.163	1.339	1.500				
n	2.72	3.28	4.25	6.07	10.0				
n_{calc}	2.73	3.30	4.55	6.21	10.7				
B. Initial concentration of $U(OEt)_5 = 0.167$ g-mol./kg									
h	0.075	0.226	0.354	0.482	0.655	0.779	0.866	0.992	1.081
n	1.55	1.70	1.86	2.00	2.32	2.62	2.98	3.42	4.14
n_{calc}	1.55	1.70	1.85	2.04	2.36	2.66	2.92	3.40	3.84

DISCUSSION

A General Structural Theory for Metal Oxide Alkoxide Polymers

A formal presentation of the theoretical aspects of the metal oxide alkoxides will simplify the discussion of the latest experimental results.

First we define a regular polymer series as a set of metal oxide alkoxides having structures which fulfill the following requirements: (*a*) Each polymer in the series may be considered as derived from an integral number of unhydrolyzed metal alkoxide units linked together by metal–oxygen–metal bridges formed in the condensation $M(OR) + H_2O + (RO)M \rightarrow M\cdot O\cdot M + 2ROH$. (*b*) The metal alkoxide repeating units may themselves be polymers but they must have integral values of degree of polymerization which remain constant throughout the polymer series. (*c*) The number of $M\cdot O\cdot M$ links between adjacent units of the metal oxide alkoxide polymer must be constant. Secondly, we define the following variables: (i) the degree of polymerization of the metal oxide alkoxide (i.e. number of metal atoms per molecule) $= n$; (ii) the degree of polymerization of the metal alkoxide repeating unit $= p$; (iii) the degree of hydrolysis (i.e. ratio of water molecules added per metal atom) $= h$; (iv) the number of $M\cdot O\cdot M$ links between adjacent repeating units $= q$.

It follows from the definition of the regular polymer series that $n = p(x+1)$, where x is 0, 1, 2, 3, etc. Since one water molecule produces one $M\cdot O\cdot M$ link between adjacent repeating units, it also follows that $hn = xq$. By eliminating x we obtain the following general description of the members of the regular polymer series:

$$n^{-1} = p^{-1} - q^{-1}h. \qquad [1]$$

The regular polymer series will consist of a distribution of the members of the series so that the number-average degree of polymerization $\bar{n}$ and the average degree of hydrolysis $\bar{h}$ need not necessarily have integral values. Consider a regular polymer series comprising a mole fraction N_1 of the species with $n = n_1$ and $h = h_1$; N_2 of the species with $n = n_2$ and $h = h_2$; and N_i of the species with $n = n_i$ and $h = h_i$. The number-average degree of polymerization

$$\bar{n} = \sum N_i n_i / \sum N_i = \sum N_i n_i \qquad [2]$$

and the average degree of hydrolysis $\bar{h} = \sum h_i n_i N_i / \bar{n}$. Equation [1] will hold (p and q are constant) for each member of the series, i.e. $n_i^{-1} = p^{-1} - q^{-1}h_i$, which may be rearranged to $pq = qn_i - pn_ih_i$. Summation over the whole series gives the following expression:

$$\sum pqN_i = \sum qn_iN_i - \sum pn_ih_iN_i, \qquad [3]$$

i.e.

$$pq = q\bar{n} - p\bar{n}\bar{h}. \qquad [4]$$

Equation [4] may be rearranged to [5].

$$(\bar{n})^{-1} = p^{-1} - q^{-1}\bar{h} \qquad [5]$$

An important feature of equation [5] is the determination of the number-average degree of polymerization $\bar{n}$ by the average degree of hydrolysis $\bar{h}$, since p and q are constant for any given regular polymer series. This is important because it has the consequence

that once $\bar{h}$ is fixed then $\bar{n}$ is fixed irrespective of the distribution of polymer sizes in the system. Thus a redistribution of the polymer sizes for a given value of $\bar{h}$ will not affect $\bar{n}$. Another consequence of equation [5] is a simple classification of regular polymer series. Thus the system can be defined as (p_x,q_y), where x is the numerical value of p, and y the numerical value of q. For example, the regular polymer series based on trimeric titanium ethoxide and termed Model I by Bradley, Gaze, and Wardlaw (1) would simply be the system (p_3,q_4) with $(\bar{n})^{-1} = 0.333_4-0.25\bar{h}$. The regular polymer series called model II and based on either the solvated dimeric metal tetraalkoxide $M_2(OR)_8,(ROH)_2$ (1, 2) or the dimeric tantalum pentaalkoxide $M_2(OR)_{10}$ (3) would be (p_2,q_3) with $(\bar{n})^{-1} = 0.5-0.333_4\bar{h}$. Model III based on the solvated monomeric alkoxides $M(OR)_4,2ROH$ or $M(OR)_5,ROH$ would be (p_1,q_3) with $(\bar{n})^{-1} = 1.0-0.333_4\bar{h}$, whilst the alternative model IV is (p_1,q_2) with $(\bar{n})^{-1} = 1.0-0.5\bar{h}$. The fundamental aspect of the theory of regular polymers is the consequence that the classification (p_x,q_y) fixes the variation of $\bar{n}$ with $\bar{h}$, which will be the same for all systems with the same values of x and y irrespective of the valency of the metal or the geometrical structures involved. It follows that with a knowledge of the structure of the original metal alkoxide and hence the value of x the possible values of y may be deduced from geometrical considerations. Having fixed x and y the variation of number-average degree of polymerization with degree of hydrolysis for the metal oxide alkoxides may be predicted by means of equation [5]. The structures of polymeric metal alkoxides have been discussed by Bradley (7) in terms of the valency of the metal, its higher coordination number, and stereochemistry. The fact that some metal alkoxides have non-integral values of n suggests that more than one value of x may be adopted. However, it is readily shown that the metal oxide alkoxides may still conform to an equation of the same general form as [5]. For example, let us consider a metal alkoxide existing in two polymeric species with $n = a$ and $n = b$ together in a system and let them form metal oxide alkoxides which conform to the regular polymer series (p_a,q_r) and (p_b,q_s). The proportions of the a-mer and b-mer initially present are defined by α_a, where α_a = the ratio of the number of metal atoms present in a-mers divided by the total number of metal atoms in the system. Obviously $\alpha_b = 1-\alpha_a$. Then

$$(\bar{n})^{-1} = \alpha n_a^{-1}+(1-\alpha)n_b^{-1},$$

where

$$n_a^{-1} = p_a^{-1}-q_r^{-1}h,$$

and

$$n_b^{-1} = p_b^{-1}-q_s^{-1}h.$$

Therefore,

$$(\bar{n})^{-1} = \alpha_a p_a^{-1}-\alpha_a q_r^{-1}h+(1-\alpha_a)p_b^{-1}-(1-\alpha_a)q_s^{-1}h.$$

$$= [\alpha_a p_a^{-1}+(1-\alpha_a)p_b^{-1}]-[\alpha_a q_r^{-1}+(1-\alpha_a)q_s^{-1}]h. \quad [6]$$

Substitution of

$$(\bar{p})^{-1} = \alpha_a p_a^{-1}+(1-\alpha_a)p_b^{-1}$$

and

$$(\bar{q})^{-1} = \alpha_a q_r^{-1}+(1-\alpha_a)q_s^{-1}$$

in equation [6] results in [7], which is identical in form with [5]:

$$[7] \qquad (\bar{n})^{-1} = (\bar{p})^{-1} - (\bar{q})^{-1}h.$$

Since α_a may be evaluated from the number-average degree of polymerization of the original metal alkoxide the values of $\bar{p}$ and $\bar{q}$ may be calculated for the metal oxide alkoxides. By similar reasoning it may be shown that for a metal alkoxide existing as three different polymeric species giving rise to the regular polymer series' (p_a,q_r),(p_b,q_s), and (p_c,q_t), equation [8] may be derived:

$$[8] \qquad (\bar{n})^{-1} = [\alpha_a p_a^{-1} + \alpha_b p_b^{-1} + (1-\alpha_a-\alpha_b)p_c^{-1}] - [\alpha_a q_r^{-1} + \alpha_b q_s^{-1} + (1-\alpha_a-\alpha_b)q_t^{-1}]h,$$

where α_a, α_b, and $(1-\alpha_a-\alpha_b)$ are the proportions of metal atoms in species (p_a,q_r), (p_b,q_s), and (p_c,q_t) respectively. By determining the intercept $(\bar{p})^{-1}$ and the slope $(\bar{q})^{-1}$ of equation [7] from the experimental plot of $(\bar{n})^{-1}$ versus h, it is possible to solve equation [8] for α_a and α_b and hence calculate $1-\alpha_a-\alpha_b$. It is clear that we cannot solve a system containing a mixture of more than three regular polymer series.

Stannic Oxide Isopropoxides

Since stannic isopropoxide forms a solvate, $Sn_2(OPr^i)_8,(Pr^iOH)_2$, which is practically dimeric in boiling isopropanol we should expect the variation of $\bar{n}$ with $\bar{h}$ for the oxide isopropoxides to be close to the equation for the (p_2,q_3) regular polymer series. The results plotted in Fig. 1 show that this is indeed the case. A least-squares fit of $(\bar{n})^{-1}$

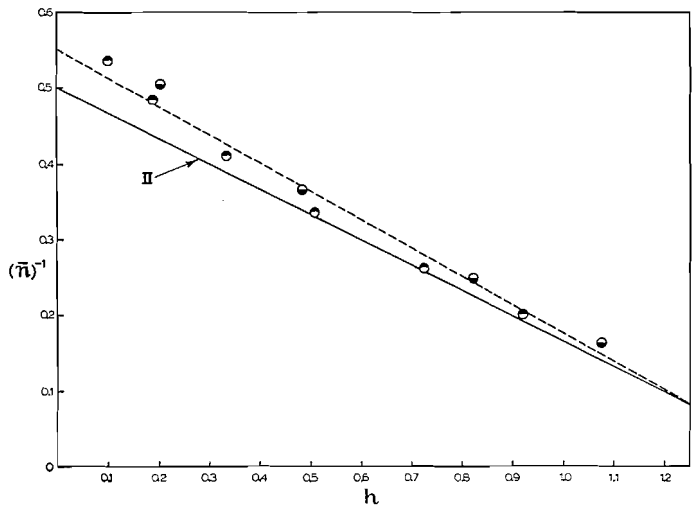

FIG. 1. The variation of $\bar{n}$ with $\bar{h}$ for the hydrolysis of stannic isopropoxide: ◓, data from Table 1A; ◒, data from Table IB. Curve II, $\bar{n} = 6/(3-2\bar{h})$.

versus $\bar{h}$ gave the equation $(\bar{n})^{-1} = 0.5505 - 0.3751\bar{h}$ with a coefficient of variation $\sigma_n = \pm 5.2\%$. There are five changes in sign in the error $\delta\bar{n} = \bar{n}_{calc} - \bar{n}$ ($\bar{n}_{calc}$ given in Table I) when the 11 points are arranged in ascending order of $\bar{h}$. From the intercept $(\bar{n})_0^{-1} = 0.5505$ at $\bar{h} = 0$, a value of $(\bar{n})_0 = 1.82$ was calculated, which compares favorably with the value of 1.85 determined from the molecular weight of stannic isopropoxide.

Assuming that the (p_2,q_3) regular polymer series is accompanied by either the (p_1,q_2) or (p_1,q_3) series we derive the value of $\alpha_{II} = 0.899$ for the proportion of tin atoms in the (p_2,q_3) series. If the (p_1,q_3) series is present then the slope $d(\bar{n})^{-1}/d\bar{h}$ should be -0.333_4. If the (p_1,q_2) series is present then $d(\bar{n})^{-1}/d\bar{h}$ is calculated from equation [6] to be -0.350. The "least-squares" value of -0.375 is obviously closest to that predicted for the mixture of (p_2,q_3) and (p_1,q_2) series.

Ceric Oxide Isopropoxides

Ceric isopropoxide also forms a solvate, $Ce_2(OPr^i)_8,(Pr^iOH)_2$, which is practically dimeric in boiling isopropanol and hence would be expected to produce oxide isopropoxides conforming nearly to series (p_2,q_3). The plot of $\bar{n}$ versus $\bar{h}$ in Fig. 2 shows that such is

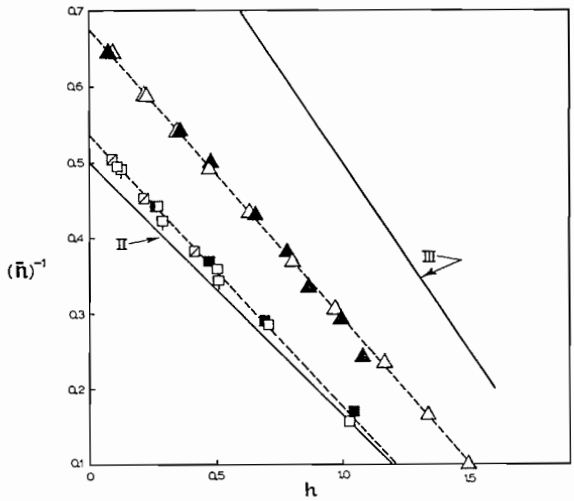

FIG. 2. The variation of $\bar{n}$ with $\bar{h}$ for the hydrolysis of ceric isopropoxide and uranium pentaethoxide: □, data from Table IIA; ■, data from Table IIB; ▨, data from Table IIC; ▫, data from Table IID; △, data from Table IIIA; ▲, data from Table IIIB. Curve II, $\bar{n} = 6/(3-2\bar{h})$; Curve III, $\bar{n} = 2/(2-\bar{h})$.

the case. The least-squares fit of $(\bar{n})^{-1}$ versus $\bar{h}$ gave the equation $(\bar{n})^{-1} = 0.5358-0.3608\,\bar{h}$, with a coefficient of variation $\sigma_n = \pm 2.1\%$. In fact a considerable part of the error resides in the two points of highest and next-highest value of $\bar{h}$, and the coefficient of variation for the first 14 points is only $\pm 1.2\%$, with 8 changes in sign of $\delta\bar{n}$. Values of $(\bar{n})_{calc}$ are listed in Table II. The intercept $(\bar{n})_0 = 0.5358$ at $\bar{h} = 0$ leads to a value of $(\bar{n})_0 = 1.87$, in good agreement with the value 1.86 calculated from the molecular weight of ceric isopropoxide. Accordingly the proportion of cerium in the (p_2,q_3) series is $\alpha_{II} = 0.928$. The slope $d(\bar{n})^{-1}/d\bar{h} = 0.3608$ is much closer to the figure of -0.3456 calculated (eq. [6]) for the (p_1,q_2) series than the -0.3334 calculated for the (p_1,q_3) series. It appears from these calculations that the ceric oxide isopropoxides resemble the stannic oxide isopropoxides in conforming to a mixture of the regular polymer series' (p_2,q_3) and (p_1,q_2).

Uranium (V) Oxide Ethoxides

Although uranium pentaethoxide is practically dimeric in boiling benzene its molecular weight in boiling ethanol ($\bar{n} = 1.48$) suggests that a considerable proportion of monomeric species is present in the alcohol, no doubt due to solvation to $U(OEt)_5,EtOH$. This is extremely interesting because the two previously discussed alkoxides were predominantly

dimeric and a quantitative distinction between the alternative series (p_1,q_2) and (p_1,q_3) was not favored. However, with the larger proportion of monomer species in the uranium pentaethoxide, discrimination between the alternative series should be facilitated. The plot of $\bar{n}$ versus $\bar{h}$ in Fig. 2 for the uranium oxide ethoxides appears to follow a path almost midway between curves II and III. The least-squares fit for the 20 points between $\bar{h} = 0$ to 1.500 was in accordance with the equation $(\bar{n})^{-1} = 0.6755 - 0.3841\bar{h}$, with a coefficient of variation $\sigma_n = \pm 3.2\%$ and 10 changes of sign in $\delta\bar{n}$ ($\bar{n}_{calc}$ values are listed in Table III). A major portion of the errors in $\bar{n}$ occurred for the highest four values of $\bar{h}$. Thus, $\sigma_n = \pm 1.4\%$ for the first 16 points ($h = 0$ to 0.992) and there are 9 changes of sign. From the intercept $(\bar{n})_0^{-1} = 0.6755$ ($\bar{h} = 0$), the value of $(\bar{n})_0 = 1.48$ was calculated in exact agreement with the value determined from the molecular weight of the pentaethoxide. The low value of $\alpha_{II} = 0.649$, calculated from $(\bar{n})_0$, predicts a slope $d(\bar{n})^{-1}/d\bar{h} = 0.3919$ if series (p_1,q_2) is present with (p_2,q_3) and this is close to the least-squares slope of -0.3841. The results thus point unambiguously to the presence of the (p_1,q_2) series and the absence of the alternative (p_1,q_3).

It should be noted that the theory is not confined to metal oxide alkoxide systems but is applicable to any system involving regular polymer series as defined in the text. For example, it is evident that the formation of linear polydialkylsiloxanes by hydrolysis and condensation of dialkyldialkoxysilanes should conform to the requirements of the theory since (p_1,q_1) series will be formed. In this particular system the "central" atom (silicon) of the monomer has a coordination number which is the same as its group valency.

CONCLUSIONS

A general theory to account for the number-average degree of polymerization of metal oxide alkoxides has been formulated mathematically. In addition to explaining the properties of some oxide alkoxides of titanium, zirconium, and tantalum reported earlier, the theory also provides a rational interpretation of some oxide alkoxides of tin, cerium, and uranium. A characteristic feature of the metal oxide alkoxide polymers, namely the formation of relatively low polymers, appears to be a logical consequence of the theory.

ACKNOWLEDGMENTS

We are grateful to the Department of Scientific and Industrial Research for a Maintenance Grant (to H. H.).

REFERENCES

1. D. C. BRADLEY, R. GAZE, and W. WARDLAW. J. Chem. Soc. 3977 (1955); 469 (1957).
2. D. C. BRADLEY and D. G. CARTER. Can. J. Chem. **39**, 1434 (1961); **40**, 15 (1962).
3. D. C. BRADLEY and H. H. HOLLOWAY. Can. J. Chem. **39**, 1818 (1961); **40**, 62 (1962).
4. D. C. BRADLEY, E. V. CALDWELL, and W. WARDLAW. J. Chem. Soc. 4775 (1957).
5. D. C. BRADLEY, A. K. CHATTERJEE, and W. WARDLAW. J. Chem. Soc. 3469 (1956).
6. R. G. JONES, E. BINDSCHADLER, G. KARNAS, F. A. YOEMAN, and H. GILMAN. J. Am. Chem. Soc. **78**, 4287 (1956).
7. D. C. BRADLEY. Nature, 182, 1211 (1958).

ALKOXIDES OF VANADIUM (IV)

D. C. BRADLEY[1] AND M. L. MEHTA[2]
Department of Chemistry, Birkbeck College, London, W.C.1, England

Received February 23, 1962

ABSTRACT

A number of tetraalkoxides of vanadium (IV) have been prepared by alcoholysis of tetrakis(diethylamino)vanadium (IV). Volatilities and molecular weights were determined on the new compounds and compared with the properties of the corresponding titanium compounds. Some of the primary alkoxides of vanadium are polymeric and this polymerization affects not only the volatility but also the color of the compound.

INTRODUCTION

In recent years the alkoxides of a number of quadrivalent metals have been prepared and their physicochemical properties have been studied (1). A notable feature of these metal alkoxides is their polymeric nature, which is believed to be caused by intermolecular bonds between metal and oxygen due to covalency expansion of the metal. An attempt has been made to rationalize the size of these polymers in terms of the stereochemistry of the metal (2). The metal alkoxides thus constitute an important class of coordination polymers. For theoretical purposes it is desirable to study various properties of a series of transition metal tetraalkoxides $M(OR)_4$ (e.g. Ti, V, Cr, etc.) and as part of a wider program we have investigated the preparation and properties of vanadium (IV) tetraalkoxides. The recent discovery of chromium (IV) tetra(tertiary-butoxide) (3) raises the possibility, now being investigated, of synthesizing chromium (IV) tetraalkoxides.

RESULTS AND DISCUSSION

The synthesis of vanadium tetraalkoxides proved to be a major problem due to the ease of hydrolysis and oxidation of these compounds. Thus it was shown by Bradley, Multani, and Wardlaw (4) that vanadium tetrachloride reacted vigorously with alcohols to form vanadium dichloride dialkoxide alcoholates $VCl_2(OR)_2,ROH$; but these authors were unable to prepare the tetraalkoxides by further substitution of chlorine in the presence of ammonia or sodium alkoxide. In attempting to prepare vanadium (III) triisopropoxide by the action of sodium in alcohol on vanadium trichloride we obtained some vanadium (IV) tetraisopropoxide (5) but the method did not seem very promising for synthesizing other vanadium tetraalkoxides. The synthesis of tetrakis(diethylamino)-vanadium (IV) from VCl_4 and lithium diethylamide by Thomas's method (6) offered a convenient route to the vanadium tetraalkoxides by alcoholysis and we have applied this method in the present research.

$$VCl_4 + 4LiNEt_2 \rightarrow V(NEt_2)_4 + 4LiCl$$

$$V(NEt_2)_4 + 4ROH \rightarrow V(OR)_4 + 4R_2NH$$

A large number of vanadium tetraalkoxides have now been prepared and this has established beyond doubt that these compounds do exist although they are rather unstable. Previous work on metal tetraalkoxides (1) has shown how markedly the physical properties of the alkoxide of a given metal depend on whether the alkoxide group contains

[1]*Present address: Department of Chemistry, University of Western Ontario, London, Ontario.*
[2]*Present address: Department of Chemistry, Munshi Singh College, Bihar University, India.*

primary, secondary, or tertiary alkyl groups. Therefore we shall discuss these new vanadium compounds under the three headings primary, secondary, and tertiary, and compare them with the corresponding alkoxides of other quadrivalent metals.

Primary Alkoxides

The primary alkoxides $V(OR)_4$, where R = Me, Et, Pr^n, Bu^n, Bu^i, Am^n, Am^{iso}, $Am,^{act}$ and neopentyl were prepared. Vanadium tetramethoxide and tetraethoxide were brown solids whereas the tetraneopentyloxide was a green solid. The other compounds were dark brown liquids at room temperature. All of the new alkoxides were soluble in benzene, ether, petrol, or the parent alcohol. The tetramethoxide was heated to 200° C at 0.05 mm but would not sublime, and above this temperature it decomposed. This behavior contrasts with that of $Ti(OMe)_4$, which sublimes at ca. 180° C at 0.1 mm, although the latter is practically insoluble in common organic solvents. All of the other vanadium primary alkoxides could be distilled under reduced pressure but some decomposition occurred, as shown by the yield (75–80%) and purity of the distillate. This thermal instability precluded the determination of true boiling points so that the figures quoted in the tables are generally the bath temperatures at which distillation occurred in conventional vacuum distillation apparatus. These temperatures will be 10–20° higher than the boiling points under the specified pressure. The solubility of the vanadium alkoxides enabled us to determine molecular weights ebullioscopically in benzene. In Table I are recorded the volatility and number-average degree of polymerization of the new compounds together with comparable data (7) on the corresponding titanium alkoxides.

TABLE I

	Volatility (°C/mm)		Degree of polymerization	
Alkoxide	Ti	V	Ti	V
$M(OMe)_4$	180/0.1	Non-volatile	Insol.	2.79
$M(OEt)_4$	102/0.1	100–110/0.05*	2.4	2.04
$M(OPr^n)_4$	124/0.1	140–150/0.5*	—	1.39
$M(OBu^n)_4$	142/0.1	150–160/0.5	—	1.31
$M(OBu^i)_4$	—	114/0.05	—	1.30
$M(OAm^n)_4$	158/0.1	160–180/0.5*	1.4	1.27
$M(OAm^{iso})_4$	148/0.1	112/0.01	1.2	1.30
$M(OAm^{act})_4$	140/0.1	142/0.5	1.1	1.10
$M(OCH_2Bu^t)_4$	111/0.1	100/0.1	1.3	1.03

*Bath temperature.

It is clear that with the exception of the methoxides the volatilities of the vanadium and titanium alkoxides are similar. Where comparative data are available it appears that the degree of polymerization is generally smaller for the vanadium alkoxide than for the titanium compound. This is strikingly so in the case of the methoxides, where the titanium compound is insoluble and presumably highly polymeric. The value of 2.79 for the degree of polymerization of $V(OMe)_4$ suggests that it is predominantly in the trimeric form, which is the limiting degree of polymerization for a metal tetraalkoxide in which the metal is octahedrally 6-coordinated (2). It was first shown by Caughlan *et al.* (8) by cryoscopic studies in benzene that in titanium alkoxides $Ti(OR)_4$, where R = Et, Pr^n, Bu^n, the degree of polymerization increased with increase in concentration to a limiting value of 3.0. More recently the very precise measurements of Martin and Winter (9) have not only confirmed that titanium tetrabutoxide attains a limiting trimeric state but also have demonstrated that the concentration dependence of the molecular weight fits a monomer–trimer equilibrium.

$$[Ti(OBu)_4]_3 \rightleftharpoons 3Ti(OBu)_4$$

Although there was no evidence for the variation of molecular weight with concentration in our ebullioscopic measurements with vanadium *n*-alkoxides we nevertheless suggest, on the basis of the non-integral values of the degrees of polymerization, that the vanadium alkoxides resemble the titanium alkoxides in having mixtures of monomers and trimers. It is relevant to observe that ebullioscopic measurements on the titanium alkoxides (7) also showed no evidence of concentration dependence of molecular weight, although non-integral values for the degrees of polymerization were obtained. At present we have no satisfactory explanation of this paradox. A rare example of the detection of concentration dependence of molecular weight for a metal alkoxide by ebulliometric measurements was found by Holloway (15) for niobium pentaethoxide, which exhibits a well-defined monomer–dimer equilibrium. In the straight-chain alkoxides there is a rapid decrease in degree of polymerization with lengthening of the alkyl chain from $V(OMe)_4$ to $V(OPr^n)_4$ but from $V(OPr^n)_4$ to $V(OAm^n)_4$ there is very little change. This is presumably the result of changes in steric effects, which will be most noticeable between the early members of the homologous series. Inspection of a trimer model shows that in the longer-chain derivatives lengthening of the alkyl chains does not cause much additional interference with the polymerization of the trimer.

The lower degree of polymerization exhibited by the vanadium alkoxides compared with the corresponding titanium alkoxides can also be interpreted as due to differences in steric effects. Thus in the case of a given alkoxide group, shielding of the central atom and consequent opposition to polymerization will depend on the size of the central atom, other factors being equal. Hence vanadium, which has a slightly smaller covalent radius (1.22 Å, ref. 11) than titanium (1.32 Å, ref. 11), will be better shielded and accordingly should achieve a smaller degree of polymerization in its tetraalkoxides. Moreover, chromium with a still smaller atomic radius (1.17 Å, ref. 11) would be expected to achieve a smaller degree of polymerization in tetraalkoxides than vanadium. Branching of the alkyl groups will have a pronounced tendency to oppose polymerization and this is shown to a marked degree in the neopentyloxide, which gives practically a monomeric vanadium compound. This is also reflected in the higher volatility of the neopentyloxide compared with *n*-amyloxide.

Secondary Alkoxides

The following secondary alkoxides were prepared: $V(OR)_4$, where R = Me_2CH, MeEtCH, $MePr^nCH$, $MePr^iCH$, and Et_2CH. The tetraisopropoxide was a dark green solid whilst the other compounds were green liquids. Molecular weight determination (ebullioscopically in benzene) showed that all except $V(OPr^i)_4$ were monomeric within experimental error. The degree of polymerization of 1.17 determined for $V(OPr^i)_4$ may be erroneously high due to the high volatility of the solute, and the compound is probably monomeric. The volatilities of these new vanadium compounds are compared in Table II with those of the corresponding titanium and zirconium alkoxides (10). Here it is noteworthy that the monomeric titanium and vanadium compounds are very similar in volatility whereas the polymeric zirconium compounds (degree of polymerization given in parentheses) are considerably less volatile. Another interesting feature is that the monomeric secondary alkoxides of vanadium (IV) are green in contrast to the brown primary alkoxides (except the neopentyloxide which is monomeric and green), which are polymeric. It seems feasible that the brown color of the primary alkoxides is due to the polymeric species. This problem is receiving further investigation. There is little doubt that the monomeric nature of the secondary alkoxides is a consequence of the steric hindrance of the branched alkoxide groups to polymerization.

TABLE II

Alkoxide	Volatility (°C/mm) Ti	V	Zr
$M(OPr^i)_4$	49/0.1	70–80/0.1*	160/0.1 (3.0)
$M(OBu^s)_4$	105/1.2	81/0.05	164/0.1 (2.5)
$M(OCHMePr^n)_4$	115/0.1	110/0.05	175/0.05 (2.0)
$M(OCHMePr^i)_4$	131/0.5	104/0.05	156/0.01 (2.0)
$M(OCHEt_2)_4$	112/0.05	108/0.05	178/0.05 (2.0)

*Bath temperature.

Tertiary Alkoxides

The following tertiary alkoxides were prepared: $V(OR)_4$, where R = Me_3C, Me_2EtC, Me_2Pr^nC, Me_2Pr^iC, Et_3C, and $MeEtPr^nC$. These new compounds are all liquids, the tertiary butoxide being blue and the others dark green. The compounds may be distilled under reduced pressure but some decomposition occurs. They are soluble in common organic solvents and are readily hydrolyzed. Molecular weight determinations in boiling benzene confirmed that the tertiary alkoxides were, without exception, monomeric. The data on the volatilities of the vanadium tertiary alkoxides are presented in Table III with the data on the corresponding titanium and zirconium compounds (12).

TABLE III

Alkoxide	Volatility (°C/mm) Ti	V	Zr
$M(OCMe_3)_4$	64.5/0.4	60–70/0.1*	55/0.2
$M(OCMe_2Et)_4$	109.5/0.3	83/0.05	93/0.1
$M(OCMe_2Pr^n)_4$	141/0.8	111/0.05	133/0.7
$M(OCEt_3)_4$	180/0.5	128/0.05	180/0.4

*Bath temperature.

It is clear that when allowance is made for the different pressures at which the boiling points are recorded, the volatilities of the monomeric tertiary alkoxides of titanium, vanadium, and zirconium are approximately the same. This is to be expected if the central metal atoms contribute little to the intermolecular forces, which are determined primarily by the peripheral atoms in these molecules. Thus the steric effect of the highly branched tertiary alkoxide groups by shielding the central metal atom not only prevents polymerization but also reduces the importance of the metal atom in determining intermolecular forces. Precise vapor pressure measurements on titanium, zirconium, and hafnium tetra(tertiary-alkoxides) revealed that a "heavier" molecular species of this type may produce a more volatile liquid than a lighter species (13). Unfortunately the low thermal stability of vanadium tetraalkoxides makes the determination of accurate vapor pressures a doubtful proposition. However, it is hoped that magnetic and spectral data will be determined on some of these interesting compounds in due course.

EXPERIMENTAL

General Techniques

Since the vanadium tetraalkoxides are very sensitive to moisture and oxygen, special precautions were taken in drying the all-glass apparatus and conducting reactions under an atmosphere of oxygen-free nitrogen. The analytical methods and the methods of drying the methanol, ethanol, isopropanol, and tertiary-butanol were the same as described in the work on vanadium trialkoxides (5). The other alcohols

(prepared as reported previously, refs. 12, 10, 7) were dried azeotropically using ethanol and benzene to remove water as the volatile ternary azeotrope of water–ethanol–benzene. Vanadium tetrachloride was prepared by chlorination of vanadium at 130–150° C and was vacuum distilled immediately prior to use.

Preparation of the Vanadium Alkoxides

The vanadium tetraalkoxides were prepared by alcoholysis of tetrakis(diethylamino)vanadium, which was obtained as a dark green liquid (b.p. 110° at 0.05 mm; found: V, 14.8; Et_2N, 83.8; valency, 4.02; $V(NEt_2)_4$ requires: V, 15.0; Et_2N, 85%) by the reaction of lithium diethylamide with vanadium tetrachloride (6). Since the alcoholysis experiments all involved the same technique, we record here the details of one preparation and summarize the remainder of the results in Table IV.

TABLE IV

Alkoxide	$V(NEt_2)_4$ taken (g)	Alcohol taken (g)	Benzene taken (g)	Weight of product (g)	Analysis: Found V	Found OR	Found Valency	Calc. V	Calc. OR
$V(OMe)_4$	6.6	9.0	14.5	3.6	28.3*	68.6	4.10	29.1	70.9
$V(OEt)_4$	10.5	20.5	14.2	7.4	20.8†	73.0	4.14	22.1	77.9
$V(OPr^n)_4$	3.6	7.9	7.3	3.2	18.1	—	4.08	17.8	—
$V(OBu^t)_4$	4.8	75 ml‡	—	4.6	15.0	—	4.05	14.9	—
$V(OBu^n)_4$	5.2	12.2	18.6	5.4	14.55	—	4.06	14.9	—
$V(OBu^i)_4$	4.8	20.4	25.2	4.6	15.0	—	4.04	14.9	—
$V(OBu^s)_4$	4.1	10.2	15.2	4.3	14.9	—	4.04	14.9	—
$V(OAm^n)_4$	2.5	4.2	22.3	2.9	13.0	—	4.10	12.8	—
$V(OAm^i)_4$	6.2	20.8	13.3	7.3	12.9	—	4.08	12.8	—
$V(OAm^{act})_4$	6.6	10.6	8.2	7.5	13.0	—	4.05	12.8	—
$V(OCH_2CMe_3)_4$	2.8	4.3	23.2	3.1	12.8	—	4.03	12.8	—
$V(OCHMePr^i)_4$	2.3	4.1	18.3	2.5	12.8	—	4.04	12.8	—
$V(OCHMePr^n)_4$	2.4	3.5	6.1	2.65	12.8	—	4.04	12.8	—
$V(OCHEt_2)_4$	4.7	11.8	19.3	5.5	12.7	—	4.10	12.8	—
$V(OAm^t)_4$	5.8	18.9	17.4	6.7	12.8	—	4.01	12.8	—
$V(OCMe_2Pr^i)_4$	3.1	4.9	11.4	4.3	11.1	—	4.04	11.2	—
$V(OCMe_2Pr^n)_4$	3.7	7.9	20.8	4.9	11.2	—	4.08	11.2	—
$V(OCEt_3)_4$	2.4	5.9	12.8	3.5	10.2	—	4.06	10.0	—
$V(OCMeEtPr^n)_4$	3.3	7.3	19.6	4.9	10.0	—	—	10.0	—

*MeO, found: 68.6; calc.: 70.9%.
†EtO, found: 73.0; calc.: 77.9%.
‡Benzene – *tert*-butanol azeotrope.

TABLE V

R in $V(OR)_4$	Alkoxide: Initial wt.	Alkoxide: Final wt.	Alkoxide: Slope (mm/g)	Fluorene: Initial wt.	Fluorene: Final wt.	Fluorene: Slope (mm/g)	Mol. wt.: Found	Mol. wt.: Calc.
Me	0.0240	0.2832	5.76	0.0132	0.1254	16.73	488	175
Et	0.0444	0.1442	5.03	0.0350	0.1418	14.10	466	231
Pr^n	0.0256	0.1356	5.84	0.0364	0.1230	14.07	400	287
Pr^i	0.0622	0.1518	7.23	0.0230	0.1055	14.60	336	287
Bu^n	0.0384	0.1101	5.51	0.0222	0.1111	14.85	448	343
Bu^i	0.1112	0.2825	4.73	0.0506	0.1660	12.65	445	343
Bu^s	0.0205	0.0792	7.92	0.0354	0.1312	15.85	334	343
Bu^t	0.0200	0.0752	7.40	0.0230	0.0994	14.93	335	343
Am^n	0.0426	0.1952	4.97	0.0262	0.1068	15.16	506	399
$Me_2CHCH_2CH_2$	0.0334	0.1296	5.13	0.0258	0.2184	16.06	520	399
$MeEtCHCH_2$	0.0486	0.1754	4.91	0.0136	0.1758	13.01	440	399
Me_3CCH_2	0.0484	0.1004	6.35	0.0272	0.0910	13.50	418	399
Pr^nMeCH	0.0334	0.2170	5.80	0.0240	0.1092	13.50	387	399
Pr^iMeCH	0.0291	0.1350	5.83	0.0280	0.1110	13.47	383	399
Et_2CH	0.0394	0.1602	6.20	0.0252	0.1176	14.73	394	399
$EtMe_2C$	0.0434	0.2242	6.36	0.0156	0.0980	14.86	388	399
Pr^nMe_2C	0.0214	0.2114	7.33	0.0244	0.0744	18.42	418	455
Pr^iMe_2C	0.0207	0.1401	5.60	0.0160	0.0778	15.12	449	455
Et_3C	0.0844	0.1606	5.37	0.0190	0.0896	16.10	499	511
Pr^nEtMeC	0.0266	0.1350	5.19	0.0152	0.0689	15.30	490	511

Vanadium Tetraisopropoxide

A solution of tetrakis(diethylamino)vanadium (5.4 g) in benzene (10.3 g) was frozen at ca. −78° C and to it was added, with vigorous stirring, isopropanol (10.1 g) in benzene (13.1 g). An exothermic reaction occurred and produced a green solution. Removal of the excess of benzene, isopropanol, and the liberated diethylamine, under reduced pressure, left a green solid (4.4 g). Found: V, 17.9; Pr^iO, 80.8; valency, 4.06. $V(OPr^i)_4$ requires: V, 17.8; Pr^iO, 82.2%. Distillation of a sample (3.1 g) under 0.1 mm with the bath temperature at 70° C gave a green solid distillate (2.4 g) which was less pure (found: V, 18.3; Pr^iO, 80.6%; valency, 4.22) than the starting material.

Molecular Weight Determinations

An all-glass ebulliometer incorporating a differential water thermometer was used. The internal calibration technique (14) with fluorene as the standard solute was employed for determining the molecular weights in boiling benzene. The data are recorded in Table V.

About 20–25 ml of benzene were used in each determination and five to six separate additions of each solute were made. We have recorded only the initial and final weights of solute to indicate the range in concentrations covered. The elevation of the boiling point was a linear function of the weight of solute for each compound. The slopes of elevation vs. weight of solute are recorded in terms of mm readings of the differential thermometer per g of solute.

ACKNOWLEDGMENT

M. L. Mehta thanks the authorities of Munshi Singh College, Bihar University, India, for granting him study leave.

REFERENCES

1. D. C. Bradley. Progress in inorganic chemistry. Vol. II. Interscience, New York. 1960. p. 303.
2. D. C. Bradley. Nature, **182**, 1211 (1958).
3. N. Hagihara and H. Yamazaki. J. Am. Chem. Soc. **81**, 3160 (1959).
4. D. C. Bradley, R. K. Multani, and W. Wardlaw. J. Chem. Soc. 4647 (1958).
5. D. C. Bradley and M. L. Mehta. Can. J. Chem. In Press.
6. I. M. Thomas. Can. J. Chem. **39**, 1386 (1961).
7. D. C. Bradley, R. C. Mehrotra, and W. Wardlaw. J. Chem. Soc. 2027 (1952). D. C. Bradley, R. C. Mehrotra, J. D. Swanwick, and W. Wardlaw. J. Chem. Soc. 2025 (1953).
8. C. N. Caughlan, H. S. Smith, W. Katz, W. Hodgson, and R. W. Crowe. J. Am. Chem. Soc. **73**, 5652 (1951).
9. R. L. Martin and G. Winter. J. Chem. Soc. 2947 (1961).
10. D. C. Bradley, R. C. Mehrotra, and W. Wardlaw. J. Chem. Soc. 5020 (1952).
11. T. Moeller. Inorganic chemistry. Wiley, New York. 1952. p. 135.
12. D. C. Bradley, R. C. Mehrotra, and W. Wardlaw. J. Chem. Soc. 4204 (1952).
13. D. C. Bradley and J. D. Swanwick. J. Chem. Soc. 3207 (1958); 748 (1959); 3773 (1959).
14. D. C. Bradley, W. Wardlaw, and A. Whitley. J. Chem. Soc. 5 (1956).
15. H. Holloway. Private communication.

REACTIONS OF OZONIDES

II. REDUCTIVE AMINATION OF OZONIZATION PRODUCTS WITH ETHANOLIC AMMONIA[1,2]

D. G. M. DIAPER AND D. L. MITCHELL[3]
Department of Chemistry, Royal Military College of Canada, Kingston, Ontario
Received October 19, 1961

ABSTRACT

Reductive amination of the ozonolysis products of the terminal olefins 10-undecen-1-ol, ethyl 10-undecenoate, 10-undecenoic acid, and 10-undecenamide produces 10-aminodecan-1-ol, ethyl 10-aminodecanoate, 10-aminodecanoic acid, and 10-aminodecanamide respectively. Esters are also formed, in a competitive reaction, by thermal decomposition of the ozonolysis product.

INTRODUCTION

The reaction of ozone with unsaturated compounds has been intensively studied for several decades and has been the subject of two major reviews (1, 2). Early investigations concentrated on the characterization of the fragments obtained by reductive or hydrolytic scission of the ozonization products, while more recent work has examined the structure of these products (3, 4), reaction conditions, choice of solvent (5–7), and selective ozonization (8–11). The study of ozonides as a functional class with particular reference to exploring fully the limits of their reactivity has received considerably less attention than other aspects of this subject. Ozonization as a preparative method has been used by few workers (12–16) and its industrial use is still in its infancy.

It is well known that mild catalytic reduction of ozonization products forms fragments with an introduced aldehyde or ketone function (1, 2). The vigorous reducing agent lithium aluminum hydride, reductively cleaves ozonization products, giving a pair of primary alcohols, but other groups in the molecule are also affected (17–19). Selective reduction of ozonization products, leaving acid, ester, and amide functions intact, may be achieved by sodium borohydride in ethanol or by nickel-catalyzed hydrogenation (15, 17).

The present investigation involves the conversion of the product from 10-undecenoic acid (undecylenic acid) directly to 10-aminodecanoic acid. Similar conversions of the olefin to the primary amine function were performed starting with the amide or the ethyl ester of 10-undecenoic acid or with 10-undecen-1-ol. Reductive amination of aldehydes and ketones is a standard reaction (20–24) but only one example of one-step reductive amination of ozonization products has as yet been reported (25). In the four examples studied, yields of the primary amine product were moderate, but its isolation was complicated by formation of nickel complexes and by the presence of the non-basic by-products, described below. It has been shown, however, that ozonization products may be exploited, on a preparative scale, as aldehyde precursors, and it is possible that, under reducing conditions, they may demonstrate other general aldehyde or ketone reactions.

From ethyl 10-undecenoate (I), the compound most extensively studied, ethyl 10-aminodecanoate (V) was obtained in 35–45% yield, this being identified by comparison

[1]*The financial support for this work was supplied by the Defense Research Board under D.R.B. Grant No. 9530-17.*
[2]*For Part I of this series see reference 15.*
[3]*Defense Research Board of Canada Postdoctorate Fellow, 1959–61. Present address: Department of Chemistry, Makerere College, The University College of East Africa, Kampala, Uganda.*

with an authentic sample. This was obtained by reduction of ethyl 10-oximinodecanoate and its identity was checked by analyses, infrared spectrum, and comparison of the derived crystalline hydrochloride and N′-phenylurea.

A non-basic fraction, in 30% yield, was shown to contain at least three major and four minor components. Only one was obtained pure and was conclusively identified as diethyl sebacate (IX). From gas chromatograms the yield was estimated to be about 20%. Ethyl undecanoate and ethyl 10-ethoxydecanoate were tentatively identified by vapor phase chromatography with authentic samples. Ethyl undecanoate doubtless resulted from incomplete ozonization. The ethoxy ester may be formed by nucleophilic ethoxide attack upon an amino group (a known reaction, but unusual) or by reduction of the peroxidic ozonization product.

Basic products (VI, VII, VIII) and the corresponding non-basic fractions (X, XI, XII) were obtained from 10-undecenoic acid (II) its amide (III) and 10-undecen-1-ol (IV). Authentic amino compounds were synthesized as above and the basic products were identified. The major non-basic product from 10-undecenoic acid was ethyl hydrogen sebacate (approx. 8% yield), that from the amide was 9-carbethoxynonanamide (20–30% yield of crude solid) and that from 10-undecen-1-ol was ethyl 10-hydroxydecanoate (approx. 12% yield). Under the conditions employed, reductive amination and ester formation, as indicated in the reaction scheme below, are competitive in a degree largely independent of the nature of the functional group at the far end of the chain:

$$Z(CH_2)_8CH{=}CH_2 \rightarrow \text{ozonization product} \begin{cases} \nearrow Z(CH_2)_9NH_2 \\ \quad \text{V–VIII} \\ \searrow Z(CH_2)_8COOEt \\ \quad \text{IX–XII} \end{cases}$$

I–IV

I, V, IX; Z = COOEt
II, VI, X; Z = COOH
III, VII, XI; Z = $CONH_2$
IV, VIII, XII; Z = CH_2OH

Ethanol is a good solvent for starting materials, ozonization products, and ammonia. It is shown that alcohols react with the zwitterionic ozonization products, giving alkyl hemiperacetals and the peroxidic products of further condensation reactions (1, 5, 26). It is suggested that the ester by-products of the present investigation come from the alkyl hemiperacetals or their derivatives and it may be seen that the esters (IX–XII) may be formed by loss of water from $Z(CH_2)_8CH(OEt)OOH$.

To investigate the above hypothesis of ester formation, ethyl 10-undecenoate was ozonized and heated in *n*-butanol in the absence of hydrogen, nickel, or ammonia. *n*-Butyl 10-undecenoate was treated similarly in ethanol. From both reactions ethyl *n*-butyl sebacate was obtained. Thermal decomposition of alkyl hemiperacetals or other peroxidic products may therefore be exploited as a preparative method for unsymmetrical esters.

These results led us to re-examine the hydroxy esters previously prepared (15) and thought to be impure on the grounds of wide boiling range and difficulty of reaction with phenyl isocyanate. These products were examined by gas chromatography, a technique not available at that time, and it was found that, depending on conditions, hydrogenolysis of the ethanolic ozonization product from ethyl 10-undecenoate may give a ratio of diethyl sebacate to ethyl 10-hydroxydecanoate as high as 2:1. Ester formation is, however, negligible under the conditions of borohydride reduction. Further experiments on the scope and conditions of this hitherto unreported formation of aliphatic esters from ozonization products are in progress.

EXPERIMENTAL

Melting points were uncorrected. Infrared spectra were determined using the potassium bromide pellet technique.

Ethyl 10-Aminodecanoate

A solution of ethyl 10-undecenoate (ethyl undecylenate) (50.0 g) in absolute ethanol (100 ml) was ozonized to completion at a temperature of 10–20° C. Tests for the absence of olefin (bromine in glacial acetic acid) were carried out on aliquot portions and verified by the infrared spectrum of a chloroform solution. The product was not isolated but was transferred to an autoclave hydrogenator* containing Raney nickel W-2 catalyst (6–9 ml settled volume) (27). After assembly of the hydrogenator, the alcoholic solution was saturated with ammonia gas delivered from a storage cylinder at 120–150 p.s.i. The ammonia supply was disconnected, hydrogen was introduced to a pressure of 1200–1400 p.s.i., and the reaction mixture was stirred for 3 hours at 100° C and for a further 3 hours while the hydrogenator was cooling to room temperature. The gases were vented outside the building. After dilution of the reaction product with ethanol (100 ml) and filtration of the solution free from the nickel catalyst, the product was concentrated to a thick syrup under reduced pressure at 40° C. The syrup was repeatedly dissolved in benzene (50–100 ml) and evaporated to dryness under reduced pressure to remove traces of ethanol. The benzene solution (100 ml) of the product was saturated with hydrogen chloride while maintaining external cooling (0–5° C). The solution was warmed to 60° C on the water bath and ethyl acetate or ether was added to incipient turbidity. The solution was stored at room temperature for a day and subsequently at refrigerator temperatures for several days. Additional ether (500 ml) was then added to complete the crystallization. The crude aminoester hydrochloride (18 g) was collected by filtration, washed with ether, and dried under reduced pressure. The mother liquors were concentrated at a small volume, diluted with ether, and extracted with 4 *N* hydrochloric acid (3×100 ml). Basification of these extracts liberated a further small amount of syrupy amino ester (2.5 g), which was collected by ether extraction. Total yield of crude ethyl 10-aminodecanoate hydrochloride was 38%.

In another experiment, under identical experimental conditions except that of increased hydrogenation pressure (2200 p.s.i.), the syrupy reaction product was isolated by ether extraction. The ethereal solution was extracted with cold 4 *N* hydrochloric acid (4×100 ml) and was retained for examination of non-basic products (see below). Basification of the aqueous acidic extracts at 0–5° C with solid sodium hydroxide liberated the amino ester as an oily layer, which was collected in ether or benzene and dried (magnesium sulphate). The product was isolated as the crude solid amino ester hydrochloride (19.0 g, 40%).

A solution of the above hydrochloride (11.2 g) in absolute ethanol was passed down a column of Amberlite IR-400 (OH form) ion exchange resin which had been previously washed with absolute ethanol. Concentration of the eluate gave syrupy ethyl 10-aminodecanoate (8.2 g, 82%), which was distilled to give a major fraction of b.p. 103–104° C at 0.2 mm (6 g) and m.p. 20.5–21.5° C (thermometer immersed). Anal. Calc. for $C_{12}H_{25}O_2N$: saponification equiv., 215; N, 6.5. Found: saponification equiv., 212; N, 6.6%.

The Reinecke salt had m.p. 120–122° C (decomposes on standing). Anal. Calc. for $C_{16}H_{34}CrN_7O_3S_4$: N, 17.7. Found: N, 16.3%. Attempts to distill the amino ester without prior purification via the hydrochloride gave significantly lower yields (9–10% overall) accompanied by large non-volatile pot residues. Attempts to reduce the proportion of non-basic products were unsuccessful. Employment of dilute solutions, low temperatures (−20° C), rapid stirring, "super dry" ethanol, and incomplete ozonization did not significantly alter the yields of the two fractions. Runs using N,N-dimethylformamide as a solvent gave poor yields of amino ester and an increased amount of non-basic product.

Examination of Non-Basic Components

Examination of the concentrated ethereal solution by gas chromatography (200° C, Apiezon M on firebrick, H_2) showed a recording revealing seven components, with 3 major peaks and 4 minor peaks. One of the major components (see fraction *c*) constituted about 70% of the sample. Distillation gave a broad boiling fraction (b.p. 90–130 at 0.1 mm) (14–19 g, 24–30% yield from ethyl undecylenate). Infrared examination revealed that no hydroxyl or amino groups were present but a strong ester carbonyl absorption was present and the spectrum was remarkably similar to that of an ester of a long-chain fatty acid. Fractional distillation through a short jacketted column gave two of the three components, (*a*) and (*c*), as pure fractions:

(*a*) B.p. 76–78° C at 0.1 mm, n_D^{23} 1.4365, chromatographed as a single peak upon admixture with ethyl undecanoate.

(*b*) Not isolated, but the major component chromatographed with ethyl 10-ethoxydecanoate.

(*c*) B.p. 108–112° C at 0.1 mm, n_D^{23} 1.4363, chromatographed with authentic diethyl sebacate. Saponification gave sebacic acid, m.p. 129–130° C, mixed m.p. 130–131° C, acid equiv., 103 (calc., 101.1). The infrared spectrum was identical with that of an authentic specimen of sebacic acid.

A synthetic specimen of fraction (*b*) was prepared by refluxing ethyl 10-hydroxydecanoate (12 g), ethyl iodide (40 ml), and freshly prepared silver oxide (6 g) (28), which was added in portions over a period of 6 hours. After warming for 24 hours, the silver salts were separated and washed with chloroform. The product was concentrated to a syrup under reduced pressure. The above reaction was repeated until a

**Superpressure Division of the American Instrument Company, Inc., Silver Springs, Maryland, U.S.A.*

negligible hydroxyl absorption was observed in the infrared. Fractional distillation through a short column gave a fraction of b.p. 98–100° at 0.4 mm and n_D^{24} 1.4330 which was observed as a single peak when analyzed by gas chromatography. Anal. Calc. for $C_{14}H_{28}O_3$: C, 68.8; H, 11.5. Found: C, 68.3; H, 11.1%.

10-Ethoxydecanoic Acid

The above ethoxy ester was saponified with alcoholic sodium hydroxide for 10 hours at 80° C. A solid formed when the reaction mixture was poured into a slurry of ice and 2 *N* hydrochloric acid and was collected while the solution was cold. After drying over silica gel at 10° C, the solid, after several crystallizations from light petroleum, had m.p. 32–33° C. Anal. Calc. for $C_{12}H_{24}O_3$: acid equiv., 216. Found: acid equiv., 207.

The derived methyl ester, obtained using diazomethene, analyzed as a single component in the gas chromatograph at 225° C.

Ethyl 10-Aminodecanoate Hydrochloride

From ethyl 10-aminodecanoate (1.5 g) in benzene – ethyl acetate the hydrochloride was obtained, m.p. 137–138° C. Anal. Calc. for $C_{12}H_{26}ClNO_2$: C, 57.2; H, 10.4; N, 5.6. Found: C, 56.5; H, 10.2; N, 5.8%.

N-Phenylurea of Ethyl 10-Aminodecanoate

Ethyl 10-aminodecanoate gave the corresponding N-phenylurea on treatment with phenyl isocyanate. It was crystallized from benzene–hexane and from methanol, m.p. 77–79° C. Anal. Calc. for $C_{19}H_{30}O_3N_2$: C, 68.2; H, 9.0; N, 8.4. Found: C, 68.1; H, 8.8; N, 8.5%.

10-Aminodecan-1-ol

The ozonization product prepared from 10-undecen-1-ol (37 g) in absolute ethanol was hydrogenated over nickel in the presence of ammonia as before. The crude product, after solvent removal, was diluted with ether and extracted with cold 4 *N* hydrochloric acid (3×200 ml). The ethereal layer was dried (magnesium sulphate) and concentrated to give a crude non-basic product (11.8 g). The ice-cold acid solution was basified with potassium hydroxide pellets and the separated oily layer was extracted with ether (3×300 ml). After drying and removal of the ether, the crude product solidified in the refrigerator. Wt. 21.3 g (66%). The product was dissolved in benzene, filtered through a pad of charcoal, and allowed to crystallize, first at room temperature and finally in the refrigerator (15° C). After several crystallizations in this manner a melting point of 72° C was obtained. Lit. m.p. 72° (29, 30). Anal. Calc. for $C_{10}H_{23}NO$: C, 68.9; H, 13.3; N, 7.8. Found: C, 68.9; H, 13.3; N, 7.8%. The derived Reinecke salt formed glistening flakes of m.p. 131–132° C (monohydrate). Anal. Calc. for $C_{14}H_{32}CrN_7O_2S_4$: N, 19.2. Found: N, 19.3%.

A portion of the crude non-basic fraction (8.5 g) was distilled to yield two major fractions, (*a*) and (*b*), and a pot residue of which the major portion was lubricating oil expelled from the hydrogenator:

(*a*) 0.95 g, 86–102° at 1 mm. The major component chromatographed with undecan-1-ol.

(*b*) 3.30 g, b.p. 142–145° at 3 mm, n_D^{24} 1.4452. Infrared spectrum identical with that of authentic ethyl 10-hydroxydecanoate. Upon admixture with ethyl 10-hydroxydecanoate, (*b*) chromatographed as a single peak (Apiezon T, on silver-coated glass beads, 290 μ, 170° C) (31, 32). (Lit. n_D^{24} 1.4460 (15).) Saponification gave 10-hydroxydecanoic acid, m.p. 72–73° C (15).

10-Aminodecan-1-ol Hydrochloride

Gaseous hydrogen chloride, passed into a benzene solution of the above aminoalcohol, gave the hydrochloride which, after crystallization from ethyl acetate – ethanol (20:1), was obtained as white flakes, m.p. 126–131° C. Anal. Calc. for $C_{10}H_{24}NOCl$: C, 57.0; H, 11.5; N, 6.7. Found: C, 57.2; H, 11.2; N, 6.5%. The derived Reinecke salt had m.p. 129–132° C.

10-(N-Phenylurea)-1-(N-phenylcarbamate) of 10-Aminodecan-1-ol

10-Aminodecan-1-ol (0.20 g) was warmed on the water bath with phenyl isocyanate (0.3 ml), giving the derivative, which was recrystallized twice from benzene, m.p. 172–175° C. Anal. Calc. for $C_{24}H_{33}N_3O_3$: C, 70.0; H, 8.1; N, 10.2. Found: C, 70.2; H, 8.5; N, 10.2%.

Reductive Amination of 10-Undecenoic Acid with Ammonia

10-Undecenoic acid (57 g) was ozonized as a neat liquid (or alcoholic solution) at room temperature. The product was diluted with ethanol (50 ml) and transferred to a precooled (ca. −60° C) hydrogenator containing Raney nickel catalyst. Liquid ammonia (400 ml) was added and hydrogen (100 p.s.i.) was introduced. After stirring at room temperature for 2 hours, and at 50° C for a further 2 hours, hydrogen was introduced to a pressure of 1500 p.s.i. and stirring was continued for 4 hours. Upon opening the hydrogenator, about 4 g of white product was collected from the walls of the vessel and the shaft of the stirrer. Several crystallizations from hot water gave a product of m.p. 182° C which was identified as 10-aminodecanoic acid, lit. m.p. 183–186° C (33). Anal. Calc. $C_{10}H_{21}NO_2$: N, 7.5. Found: N, 7.1%. The alcoholic solution was filtered and concentrated to a green viscous syrup. The syrup was poured into a slurry of 4 *N* hydrochloric acid and ice, and a yellow doughy solid separated. It was collected and dried over silica gel to give an amorphous resin (40 g, ca. 60%). Increased hydrogenation temperatures gave this solid in yields of ca. 40%. Infrared examination indicated peaks at 3570 (m), 3175 (s), 1710 (s), 1638 (w), and 1570 (w) $cm^{-1} \pm 10$ cm^{-1}.

A portion of the solid (6.7 g) was esterified with absolute ethanol (50 ml) and concentrated sulphuric acid (5 drops). Neutralization was effected by passage down Amberlite IR-400 (OH form) ion exchange resin which had been previously washed with ethanol. Distillation of the ester gave two fractions: (*a*) b.p. 60–105° C at 0.5 mm (1.7 g). This fraction, upon gas chromatographic examination, was found to contain two major components, the higher-boiling component chromatographing with ethyl undecanoate. (*b*) The second fraction, b.p. 120–130° at 0.5 mm (2.15 g), m.p. 23–25° C, had an infrared spectrum identical with that of ethyl 10-aminodecanoate. The derived ester hydrochloride had an infrared spectrum identical with the product described above. The remainder of the product formed a tarry pot residue.

A second portion of the resin was triturated several times with boiling 2,2,4-trimethylpentane. Concentration of the extracts gave a syrup which was esterified with ethereal diazomethane. The extract was examined in the gas chromatograph (225–230°, Apiezon M on firebrick, H_2, 9-ft column) and revealed three main components, (*a'*), (*b'*), (*c'*), and three very minor components which were not identified.

(*a'*) This fraction constituted approximately 80% of the extract. It chromatographed with authentic methyl undecanoate as a single component.

(*b'*) This fraction constituted less than 5% of the extract. It chromatographed with authentic dimethyl sebacate.

(*c'*) This fraction constituted 10–15% of the extract. It chromatographed with authentic methyl ethyl sebacate, which was prepared by treating ethyl hydrogen sebacate (m.p. 35.5–36.5° C) with ethereal diazomethane.

10-Aminodecanamide

A solution of the ozonolysis product prepared from 10-undecenamide (25 g) in absolute ethanol (300 ml) was hydrogenated similarly over nickel in the presence of an excess of dry ammonia. The product was obtained as a green semisolid mass after removal of the catalyst, ethanol, and ammonia. After crystallization from benzene – ethyl acetate, a crude green-colored product (14.65 g), A, giving a positive test for nickel with dimethylglyoxime solution was obtained. Product A was repeatedly triturated with hot 2,2,4-trimethylpentane and the extracts were combined with the mother liquors saved from the above crystallization. The combined extracts on concentration yielded a second product, B, which was crystallized from hot 2,2,4-trimethylpentane. Compound B did not form a Reinecke salt nor did it exhibit color reactions characteristic of amines. Repeated crystallization from 2,2,4-trimethylpentane raised the melting point to 63–65° C and its infrared spectrum was almost identical with that of the amide of ethyl hydrogen sebacate (m.p. 70–71° C). Anal. Calc. for $C_{10}H_{23}NO_3$: C, 62.9; H, 10.1; N, 6.1. Found: C, 63.4; H, 10.6; N, 7.5%.

A portion of the nickel-containing product (3.0 g), A, in ethanol (50 ml) was saturated with hydrogen sulphide and the precipitate was separated by filtration. The filtrate was concentrated to a yellow solid possessing a pungent odor. Several crystallizations from acetone at −20° C gave a pale yellow powder (2.15 g). This product (1.25 g) in absolute ethanol was deionized on a column of Amberlite IR-401 (OH form) resin and the eluate was concentrated to give a white solid (0.67 g). Crystallization from acetone–water gave the aminoamide, m.p. 133–143° C. Anal. Calc. for monohydrate $C_{10}H_{22}N_2O.H_2O$: C, 58.8; H, 11.8; N, 13.7. Found: C, 59.2; H, 11.8; N, 13.4%.

Another run at a higher hydrogenation pressure (1900 p.s.i.) and temperature (100° C) in the presence of liquid ammonia (200 ml) converted the ozonolysis product of 10-undecenamide (25 g) into 17.8 g of A (crude) and 8.4 g of B (found: N, 7.9%).

From the purified 10-aminodecanamide, the derived Reinecke salt (monohydrate) was prepared, m.p. 120–122° C. Anal. Calc. for $C_{14}H_{31}CrN_8O_2S$: N, 21.4. Found: N, 21.2%.

N'-Phenylurea of 10-Aminodecanamide

The phenylurea was prepared in the usual manner and was recrystallized from methanol, m.p. 139–140°. Anal. Calc. for $C_{17}H_{27}N_3O_2$: N, 13.8. Found: N, 14.1%.

10-Oximinodecan-1-ol, Ethyl 10-Oximinodecanoate, 10-Oximinodecanoic Acid, and 10-Oximinodecanamide

Ethanolic solutions of the ozonization products obtained from 10-undecen-1-ol, ethyl 10-undecenoate, 10-undecenoic acid, and 10-undecenamide were hydrogenated at room temperature and at 60–70 p.s.i. over palladium on calcium carbonate catalyst (34). The solution was filtered and warmed with a slight excess of hydroxylamine hydrochloride solution buffered with sodium acetate to yield the following oximes:

(*a*) 10-Oximinodecan-1-ol, from benzene, m.p. 83–84° C. Anal. Calc. for $C_{10}H_{21}NO_2$: C, 64.1; H, 11.3; N, 7.5. Found: C, 63.5; H, 11.2; N, 7.7%.

(*b*) Ethyl 10-oximinodecanoate, from aqueous ethanol, m.p. 56–59° C. Anal. Calc. for $C_{12}H_{23}NO_3$: C, 62.9; H, 10.1; N, 6.1. Found: C, 62.9; H, 9.9; N, 5.9%.

(*c*) 10-Oximinodecanoic acid, from ethanol, m.p. 108–110° C. Anal. Calc. for $C_{10}H_{19}NO_3$: N, 7.0. Found: N, 6.6%. Lit. m.p. 111° (35).

(*d*) 10-Oximinodecanamide, from ethanol, m.p. 138–140° C. Anal. Calc. for $C_{10}H_{20}N_2O_2.H_2O$: C, 55.0; H, 10.2; N, 12.8. Found: C, 54.75; H, 9.84; N, 12.7%.

Lithium aluminum hydride reduction of oximes (*a*), (*b*), and (*c*) in ether gave 10-aminodecan-1-ol (36), m.p. 71–72° C, in yields of 80%, 82%, and 16% respectively with infrared spectrum identical with that of the product prepared by reductive amination of the ozonization product from 10-undecenol (see above).

10-Aminodecanoic Acid

10-Oximinodecanoic acid (0.5 g) in absolute ethanol (60–80 ml) was hydrogenated at 65 p.s.i. and at room temperature over platinum oxide catalyst (37). The product (0.27 g, 57%) was recrystallized from hot water and had m.p. 181–182° C and mixed m.p. 180–182° C with the crystalline product obtained from 10-undecenoic acid. Comparison of their infrared spectra revealed that the two products were identical. Lit. m.p. 183–186° C (33). Anal. Calc. for $C_{10}H_{21}NO_2$: N, 7.5. Found: N, 7.0%.

Ethyl 10-Aminodecanoate

Under hydrogenation conditions identical with those described above, ethyl 10-oximinodecanoate gave syrupy ethyl 10-aminodecanoate. The N′-phenylurea was prepared and had m.p. 78–79° C with the N′-phenylurea described above. The infrared spectra of both specimens were identical in all respects. Anal. Calc. for $C_{19}H_{30}N_2O_3$: N, 8.4. Found: N, 8.6%.

The derived hydrochloride of the amine (m.p. 105–110° C) could not be separated from traces of the secondary amine hydrochloride but had an infrared spectrum identical with that of the ethyl 10-aminodecanoate hydrochloride described above. Anal. Calc. for $C_{12}H_{26}ClNO_2$: N, 5.6. Found: N, 5.5%.

Bis-(9-carbethoxy-n-nonyl)amine

Hydrogenation of a more concentrated solution of ethyl 10-oximinodecanoate (5 g) in ammoniacal ethanol (40 ml) over platinum on charcoal gave a mixture of the primary amine and the secondary amine (2.4 g). The latter amine was recrystallized from light petroleum at −20° C and had m.p. 49–50° C. Anal. Calc. for $C_{24}H_{47}NO_4$: C, 69.7; H, 11.4. Found: C, 69.5; H, 11.6%.

10-Aminodecanamide

A solution of 10-oximinodecanamide (0.5 g) in 85–95% ethanol (75 ml) was hydrogenated over Raney nickel W-2 catalyst for 10 hours at 60 p.s.i. and 22° C. Platinum oxide was then added and hydrogenation was continued a further 8 hours. The solution was filtered and concentrated to a crystalline mass. The product had an infrared spectrum identical with that of the 10-aminodecanamide described above. Anal. Calc. for $C_{10}H_{22}N_2O.H_2O$: N, 13.7. Found: N, 13.4%.

The derived Reinecke salt (monohydrate), m.p. 115–117° C, had an infrared spectrum identical with that of the above Reinecke derivative. Anal. Calc. for $C_{14}H_{31}CrN_8O_2S_4$: N, 21.4. Found: N, 21.9%.

The N-phenylurea derivative had a melting point (from methanol) and had an infrared spectrum identical with that of the N′-phenylurea of 10-aminodecanamide prepared above. Anal. Calc. for $C_{17}H_{27}N_3O_2$: N, 13.8. Found: N, 13.2%.

Thermal Decomposition of Ozonolysis Products in Alcohols

A solution of ethyl 10-undecenoate (20 g) in *n*-butanol (150 ml) was ozonized at 0° C until an aliquot portion gave a negative test for unsaturation (bromine in glacial acetic acid). The solution was autoclaved in a pressure vessel over Raney nickel (5 ml settled volume) at 150° C for 6 hours. The *n*-butanol was removed by evaporation under reduced pressure, at a bath temperature of 90–100° C, and the residual syrup was examined by gas chromatography (Apiezon T on silver-coated glass beads, 270 μ, 9-ft column, oven temperature 175°, H_2 at 40 ml/min). In addition to the volatile fractions, a large single peak and 2 minor less volatile peaks were observed. Fractional distillation at 125° at 0.1 mm gave *n*-butyl ethyl sebacate (9.6 g, 32%), n_D^{22} 1.4402. Saponification equiv.: calc., 143; found, 143.

n-Butyl 10-undecenoate in ethanol was ozonized and autoclaved by the procedure described above. Examination of the products by gas chromatography indicated that the major component had a retention time identical with that of *n*-butyl ethyl sebacate. The presence of other components in the same boiling range was considerably greater when ethanol was used as the solvent, and the above procedure (i.e. *n*-butanolysis) gave a product of higher purity.

REFERENCES

1. P. S. Bailey. Chem. Revs. **58**, 925 (1958).
2. L. Long, Jr. Chem. Revs. **27**, 437 (1940).
3. P. S. Bailey, S. B. Mainthia, and C. J. Abshire. J. Am. Chem. Soc. **82**, 6136 (1960).
4. R. Criegee. Record Chem. Progr. (Kresge-Hooker Sci. Lib.), **18**, 111 (1957).
5. P. S. Bailey. J. Org. Chem. **22**, 1548 (1957).
6. E. Bernatek and T. Ledaal. Tetrahedron Letters, No. 26, 30 (1960).
7. F. Dobinson and P. S. Bailey. Tetrahedron Letters, No. 13, 14 (1960).
8. E. J. Moriconi, W. F. O'Connor, and L. B. Taranko. Arch. Biochem. Biophys. **83**, 283 (1959).
9. E. J. Moriconi, W. F. O'Connor, and F. T. Wallenberger. J. Am. Chem. Soc. **81**, 6466 (1959).
10. G. Slomp and J. L. Johnson. J. Am. Chem. Soc. **80**, 915 (1958).
11. E. J. Moriconi, W. F. O'Connor, W. J. Schmitt, G. Cogswell, and B. P. Furer. J. Am. Chem. Soc. **82**, 3411 (1960).
12. W. H. Lycan and R. Adams. J. Am. Chem. Soc. **51**, 625 (1929).
13. C. R. Noller and R. Adams. J. Am. Chem. Soc. **48**, 1074 (1926).
14. D. G. M. Diaper. Can. J. Chem. **33**, 1720 (1955).
15. D. G. M. Diaper and D. L. Mitchell. Can. J. Chem. **38**, 1976 (1960).

16. A. S. CARPENTER and F. REEDER. Brit. Patent No. 743,491 (1956); Chem. Abstr. **50**, 16,838 (1956).
17. J. A. SOUSA and A. L. BLUHM. J. Org. Chem. **25**, 108 (1960).
18. F. L. GREENWOOD. J. Org. Chem. **20**, 803 (1955).
19. B. WITKOP and J. B. PATRICK. J. Am. Chem. Soc. **74**, 3855 (1952).
20. J. C. ROBINSON, JR. and H. R. SNYDER. Organic syntheses. Coll. Vol. III. John Wiley and Sons, Inc., New York. 1955. p. 717.
21. F. KAGEN, M. A. REBENSTORF, and R. V. HEINZELMAN. J. Am. Chem. Soc. **79**, 3541 (1957).
22. F. W. HOLLY, C. H. SHUNCK, and K. FOLKERS. U.S. Patent No. 2,621,175 (1952).
23. F. W. HOLLY, E. W. PEEL, R. MOZINGO, and K. FOLKERS. J. Am. Chem. Soc. **72**, 5416 (1950).
24. W. WAYNE and H. ADKINS. J. Am. Chem. Soc. **62**, 3314 (1940).
25. R. E. FOSTER and H. E. SCHROEDER. U.S. Patent No. 2,657,240 (October 27, 1953).
26. J. L. WARNELL and R. L. SHRINER. J. Am. Chem. Soc. **79**, 3165 (1957).
27. R. MOZINGO. Organic syntheses. Vol. 21. John Wiley and Sons, Inc., New York. 1941. p. 15.
28. B. HELFERICH and W. KLEIN. Ann. **450**, 219 (1926).
29. W. S. BISHOP. U.S. Patent No. 2,330,107; Chem. Abstr. **38**, 1248 (1944).
30. E. DYER and H. SCOTT. J. Am. Chem. Soc. **79**, 672 (1957).
31. S. W. GUNNER, J. K. N. JONES, and M. B. PERRY. Can. J. Chem. **39**, 1892 (1961).
32. H. G. JONES, J. K. N. JONES, and M. B. PERRY. Private communication.
33. D. E. AMES and R. E. BOWMAN. J. Chem. Soc. 2925 (1956).
34. A. I. VOGEL. Elementary practical organic chemistry. Longmans Green, New York. 1957. p. 820.
35. G. H. HARGREAVES and L. N. OWEN. J. Chem. Soc. 753 (1947).
36. D. R. SMITH, M. MAIENTHAL, and J. TIPTON. J. Org. Chem. **17**, 294 (1952).
37. A. H. SOMMERS and A. W. WESTON. J. Am. Chem. Soc. **73**, 5749 (1951).

THE STRUCTURE OF A SYNTHETIC GLUCAN[1]

I. GENERAL STRUCTURAL FEATURES

G. G. S. DUTTON AND A. M. UNRAU[2]

Department of Chemistry, University of British Columbia, Vancouver, British Columbia

Received December 4, 1961

ABSTRACT

Only D-glucose was obtained on acid hydrolysis of the glucan. Periodate oxidation released formaldehyde, which was believed to arise from C_6 of D-glucofuranose units. From the additional formaldehyde liberated from the borohydride-reduced glucan the degree of polymerization was estimated to be about 165. Complete hydrolysis of the derived polyalcohol gave glycerol, erythritol, D-glucose, and D-xylose. Partial hydrolysis gave glycerol, erythritol, and at least seven non-reducing oligosaccharides. Direct evidence for the existence of relatively large numbers of 1 → 6 and 1 → 4 linkages was found, together with smaller numbers of 1 → 2 linkages. The methylated glucan was freely soluble in chloroform – petroleum ether (5:95), and hydrolysis gave tetra, tri, di, and mono-*O*-methyl-D-glucoses in a 6:6:3:1 molar ratio.

There are many reports in the literature on the polymerization of D-glucose and a few papers on other monosaccharides (e.g. 1–10). Most of these polymerizations have been acid catalyzed at temperatures ranging from room temperature to about 200° C and the yields of polymeric material have varied greatly. There appears to have been no detailed study on the structures of these synthetic glucans, although there is general agreement that 1 → 6 linkages are commonly present and that there is a high proportion of α-glucosidic bonds. In a paper (6) on the glucan obtained by polymerization in the presence of metaboric acid it was inferred, on the grounds of hydrolytic behavior, that there were no glucofuranose units present. It was further stated that the polymer was highly branched, as shown by the large amount of 2,3,4,6-tetra-*O*-methyl-D-glucose obtained. Another recent paper on the glucan obtained by polymerization of 1,6-anhydro-D-glucose again demonstrated the branched nature of the polymer on the basis of periodate oxidation (11).

Since 1958 there has been a group of papers published by Mora and his associates at the National Institutes of Health on the preparation of several synthetic polysaccharides (2–4). Since some derivatives of these synthetic materials have been shown to be biologically active (12, 13) it was of interest to look more closely at the structures of these polymers. The present paper reports the general structural features of the glucan designated as polyglucose II in Table I of reference 3.

Complete hydrolysis of the glucan by boiling it with 1 *N* sulphuric acid followed by chromatography of the product showed only glucose, which was isolated in the crystalline state. Alkaline oxidation or bromine oxidation of the sugar to the corresponding aldonic acid followed by adsorption of the acid on an anion exchange resin left no residue which reacted with Tollens (23) or *p*-anisidine trichloroacetate (24) spray reagents when the effluent was evaporated, thus demonstrating the absence of any sugar alcohols. The low optical rotation of the glucan, $[\alpha]_D^{22}$ 65° (*c*, 1.0 in water), compared with the high positive rotation of alpha-linked glucans, such as amylose (195–210°), suggested that a number of beta-glycosidic linkages were likely present. Exclusively beta-linked glucans, such as laminarin, exhibit a negative rotation between −10 and −25°.

[1]*Presented at the 44th Chemical Institute of Canada Meeting in Montreal, August, 1961.*

[2]*Present address: Department of Plant Sciences, University of Manitoba, Winnipeg, Manitoba.*

Oxidation of the glucan with periodic acid (0.15 *M*) at 5° C resulted in the immediate liberation of formaldehyde (3.92 mg per hexose unit after 20 minutes) with no significant change observed after 3.5 hours, at which time 4.53 mg formaldehyde had been liberated per hexose residue. The glucan had consumed 1.218 moles of periodate per hexose unit when no further formaldehyde production could be detected after 12, 48, and 72 hours. Reduction ($NaBH_4$) of the glucan prior to periodate oxidation resulted in the liberation of more formaldehyde (a total of 4.88 mg per hexose unit), and about 1.235 moles of periodate had been consumed per hexose unit when no further formaldehyde was released. On the assumption that the additional formaldehyde produced in the periodate oxidation of the borohydride-reduced glucan stemmed from the glucitol end-residue (and that the glucitol was not substituted at C_2), the degree of polymerization (D.P.) was estimated (14) to be about 165. These results were in good agreement with those reported by Mora and his associates (2, 3).

Reduction ($NaBH_4$) of the polyaldehyde, $[\alpha]_D^{22}$ 39°, followed by complete hydrolysis of the polyalcohol gave glycerol and erythritol in major proportions and xylose and glucose in lesser quantities. The ratio of glycerol to erythritol was 7:1. The proportionately large quantity of glycerol indicated that numerous branch points and $1 \rightarrow 6$ linkages were present in the glucan. Glycerol and erythritol were converted to the corresponding *p*-nitrobenzoates with m.p. and mixed m.p. 189–193° C and 248–250° C, respectively (25).

D-Xylose, approximately 1% of the original sample, was identified as the crystalline sugar, m.p. and mixed m.p. 142–144° C, $[\alpha]_D^{23}$ 17.5° (*c*, 1.4 in water). This sugar would arise from internal glucofuranose units in which the C_5 and C_6 hydroxyls were not substituted. It was believed that the rapid liberation of formaldehyde upon periodate oxidation of the glucan stemmed from the presence of D-glucofuranose units. Those units occupying terminal positions would be degraded to glycerol whereas some of the internal D-glucofuranose units would appear as D-xylose. D-Glucose, approximately 6% of the original sample, was identified as the crystalline sugar, m.p. and mixed m.p. 142–144° C, $[\alpha]_D^{23}$ 51.8° (*c*, 1.5 in water) and as the phenylosazone, m.p. and mixed m.p. 205–207° C.

Mild acid hydrolysis (0.1 *N* H_2SO_4, room temperature, 8–12 hours) (15) of the polyalcohol resulted in the formation of glycerol, a small quantity of erythritol, and a number of non-reducing oligosaccharides, which will be described more fully in a future communication. The alcohols were transformed, as before, to the crystalline *p*-nitrobenzoates.

In an effort to determine the nature of the aldehydic residues liberated in the mild acid hydrolysis of the polyalcohol, a part of the hydrolyzate was treated with bromine and an excess of barium carbonate, and the mixture left for 24 hours. The bromine was removed by aeration and the barium carbonate by filtration of the solution, which was then passed through cation and anion exchange resins. Acidic material was eluted from the anion resin with alkali and the free acids were regenerated with fresh cation resin. Evaporation of the acidic solution, lactonization, and reduction ($NaBH_4$) of the lactones gave rise to some glycerol (4–5% of original polysaccharide), m.p. and mixed m.p. of tri-*p*-nitrobenzoate 189–192° C, and a number of non-reducing oligosaccharide components, the nature of which was not determined. The isolation of glycerol by this route indicated the presence of some $1 \rightarrow 2$ linkages in the glucan.

The glucan was difficult to methylate. Only after four separate and extended methylations (4–5 days) of the partially methylated product (Kuhn procedure) by Purdie's reagents was a product obtained which showed no OH absorption in the infrared spectrum and which contained 45.4% methyoxyl. This difficulty of methylation of these synthetic glucans has been noted by other workers (3, 6). The product was completely soluble in a

mixture of 5% chloroform in petroleum ether (30–60°). Hydrolysis of the alkylated glucan gave tetra-, tri-, di-, and mono-methyl glucoses in a 6:6:3:1 ratio (approx.). A small quantity (1–2%, approx.) of glucose was also present.

The results of these periodate oxidations indicated that this glucan was highly branched, a fact which was substantiated by the methylation data. The high yield of formaldehyde indicated that at least 15% of the D-glucose units were of the furanose type while the large amount of glycerol obtained shows that the 1 → 6 linkage is of major importance. The ratio of erythritol to glycerol indicated that about 20% of the glucose units were linked at positions 1,4 and/or 1,4,6. The isolation of glycerol from the acidic fraction was definite evidence for the 1 → 2 linkage while the isolation of unoxidized glucose may be due to 1 → 3 linkages. We believe that this is the first time that definite proof has been obtained for the existence of furanose residues in a synthetic glucan, although their presence has been indicated by the work of Mora (13).

EXPERIMENTAL

Paper chromatographic separations were carried out by the descending technique using solvent systems A, ethyl acetate:acetic acid:water (8:2:2); B, ethyl acetate:pyridine:water (9:2:2); and C, butanone:water azeotrope. Whatman No. 1 filter paper was used for qualitative and quantitative studies while Whatman 3 MM paper was generally used to resolve larger quantities of mixtures. The *p*-anisidine trichloroacetate spray reagent was used for detection of reducing compounds while non-reducing polyols were located using ammoniacal silver nitrate.

Unless otherwise stated, evaporations were carried out under reduced pressure with a bath temperature around 40° C. Melting points are uncorrected and specific rotations are equilibrium values at 22±2° C.

Hydrolysis of Glucan

Polyglucose, 1.50 g, $[\alpha]_D^{22}$ 65° (*c*, 1.0 in water) was dissolved in 0.3 *N* sulphuric acid (15 ml) and the solution was boiled for 16 hours. The solution was neutralized ($BaCO_3$) and the filtrate was deionized and evaporated to a sirup which crystallized overnight. A portion (55 mg) of the crystalline material was recrystallized from ethanol to give glucose, m.p. and mixed m.p. 143–144° C, $[\alpha]_D^{23}$ 52.1° (*c*, 0.8 in water).

Bromine Oxidation of Glucan Hydrolyzate

The remainder (approx. 1.10 g) was dissolved in water (15 ml), the flask was wrapped with aluminum foil, and a few drops of bromine were added periodically over the next 72 hours. The solution was kept neutral by addition of excess barium carbonate. The solution was finally filtered to remove excess barium carbonate, deionized, and evaporated. No *p*-anisidine or Tollens-positive residue was noted; hence no polyols were present in the original polysaccharide.

Periodate Oxidation and Determination of Formaldehyde Produced

Glucan (0.383 g) was dissolved in water (20 ml) containing acetic acid (6 *N*, 2 ml) and to this solution was added 0.5 *M* sodium periodate (5 ml). The mixture was left at 5° C and formaldehyde was determined periodically by a method described elsewhere (14). After 20 minutes, 9.27 mg formaldehyde had been liberated, 10.15 mg after 12 hours, and 10.70 mg after 48 and 72 hours. When no further formaldehyde was formed, the periodate uptake was determined by the arsenite method (16) and 1.218 moles of periodate had been consumed per hexose unit.

Reduction ($NaBH_4$) and Complete Hydrolysis of Polyalcohol

To the mixture from the previous experiment was added barium carbonate and barium chloride, the solution filtered, and to the clear filtrate was added sodium borohydride (150 mg). Excess reductant was decomposed with hydrochloric acid after 18 hours and the solution was evaporated to dryness. Methanol containing hydrogen chlorine (3%) was added and evaporated to remove borate (17). The residue, in water (10 ml), was deionized, and upon evaporation of the effluent, the sirup was chromatographed. Non-reducing compounds corresponding to glycerol and erythritol and reducing compounds corresponding to xylose and glucose were observed. The ratio of components was determined by developing a chromatogram in solvent A for 12 hours. The four components were located by spraying guide strips with Tollens reagent, and the components eluted with water from the respective areas. The alcohols were determined by a periodate–chromotropic acid procedure (14) and the sugars by the phenol–sulphuric acid method (18). The molar ratio of glycerol:erythritol:xylose:glucose thus found was approximately 105:15:1:5.

Periodate Oxidation of Reduced ($NaBH_4$) Glucan and Determination of D.P.

To a solution (20 ml) of glucan (0.291 g) was added sodium borohydride (60 mg) and the solution was left at room temperature for 24 hours. The solution was acidified with 10 *N* acetic acid (2 ml), 0.5 *M* sodium periodate (5 ml) was added, and the mixture was left at 5° C. The formaldehyde was determined as before

and 7.415 mg were found after 15 minutes, 8.76 mg after 3.5 hours, with no change after 12, 48, and 72 hours. Comparing the formaldehyde produced after 48 and 72 hours with that found before reduction of the glucan, then 0.383 g of glucan would produce 0.85 mg additional formaldehyde after reduction. Assuming that 2 molar proportions of formaldehyde were produced from the glycitol end-group, the D.P. of the polymer was 165 (approx.). The polyaldehyde was reduced ($NaBH_4$) and hydrolyzed as described in a previous section. The molar ratio of glycerol:erythritol:xylose:glucose was again determined as described above and found to be 110:16:1:5.

Identification of Compounds

The sirups from the above two experiments were combined and the mixture was resolved on Whatman 3 MM paper by development for 12–14 hours in solvent A. *Glycerol:* to the dry sirup was added a 10% molar excess of *p*-nitrobenzoyl chloride and pyridine (2–3 ml) and the mixture was heated at 60–70° C for 30 minutes. Excess aroyl halide was decomposed by the addition of a few drops of water followed by excess saturated sodium bicarbonate. The solid was collected by filtration, washed thoroughly with water, and after recrystallization from acetone, the tri-*p*-nitrobenzoate of glycerol had m.p. and mixed m.p. 188–190° C (25). *Erythritol:* This compound was converted to the tetra-*p*-nitrobenzoate as described for glycerol, m.p. and mixed m.p. 248–250° C. D-*Xylose:* the sirup had $[\alpha]_D^{23}$ 17.5° (*c*, 0.9 in water) and crystallized on seeding. The xylose was dried by washing with ether and had m.p. and mixed m.p. 143–145° C. D-*Glucose:* the sirup, $[\alpha]_D^{22}$ 49° (*c*, 1.2 in water), crystallized spontaneously. The glucose was washed with ethanol and ether and had m.p. and mixed m.p. 144–145° C. The derived D-glucosazone had m.p. and mixed m.p. 206–208° C.

Partial Hydrolysis of Polyalcohol (15)

Glucan (4.50 g) was dissolved in water (120 ml); the solution was cooled (5° C) and 0.5 *M* periodic acid (80 ml) was added. Periodate uptake became constant after 72 hours at which time 1.192 moles of periodate had been consumed per hexose unit. The polyaldehyde, $[\alpha]_D^{22}$ 39° (approx.), was reduced ($NaBH_4$, 2.5 g) after removal of periodate and iodate with barium carbonate. After standing for 24 hours at room temperature, the solution was evaporated to dryness. Borate was removed by repeated evaporations with methanol and finally with methanol containing 1% hydrogen chloride at a bath temperature not exceeding 25° C. The residue was dissolved in 0.2 *N* hydrochloric acid and the solution was left at room temperature for 10 hours. Excess barium carbonate was added, the flask was wrapped with metal foil, and periodically over the next 24 hours, a few drops of bromine were added. The solution was filtered and passed through cation and anion exchange resin columns and the effluent was evaporated to give a sirupy, neutral product. Chromatographic examination in solvents A and B demonstrated the presence of seven non-reducing components with a wide range of R_f values lower than glycerol. Glycerol and a small quantity of erythritol were also identified. The oligosaccharides and the two alcohols were resolved on Whatman 3 MM paper using solvents A and B to effect maximum purification. Glycerol was converted to the tri-*p*-nitrobenzoate, m.p. and mixed m.p. 188–190° C. The tetra-*p*-nitrobenzoate of erythritol had m.p. and mixed m.p. 248–250° C. The composition and characterization of the oligosaccharide fragments will be described in a future communication (19).

Isolation and Reduction of Acidic Fragments

The acidic material, from the bromine oxidation described above, was displaced with 1 *N* sodium hydroxide from the anion exchange resin and regenerated by passage through a cation resin. The solution of free acids together with hydrochloric and hydrobromic acid was neutralized with lead carbonate. After filtration and treatment of the filtrate with hydrogen sulphide gas, the acidic material was finally obtained free from inorganic ions. Chromatography of the acidic residue gave a series of Tollens-positive components and the one with the greatest R_f value was presumed to be glyceric acid. The residue was heated in a cold-finger apparatus at 90° C under vacuum for about 3 hours, after which the residue was dissolved in water (20 ml), and sodium borohydride added (200 mg). The solution was evaporated to dryness after 36 hours at room temperature and borate was removed by careful treatment with methanol containing hydrogen chloride (1%). An aqueous solution (about 15 ml) of the residue was deionized. Evaporation of the effluent left a sirupy product which upon chromatographic examination was found to contain glycerol and a series of non-reducing components with lesser R_f values. After resolution of the mixture using Whatman 3 MM paper and solvent A, glycerol was identified as the tri-*p*-nitrobenzoate in the usual manner, m.p. and mixed m.p. 188–190° C. The nature and composition of the other components have not yet been examined.

Methylation of the Glucan

To polyglucose (3.00 g) suspended in dimethylformamide (DMF) (opalescent solution resulted) was added strontium oxide (10 g), strontium hydrate (1 g), and methyl iodide (20). The consistency of the mixture became thick soon after addition of the methyl iodide and an apparently exothermic reaction took place. Upon stirring (magnetic stirrer) and at the reflux temperature of methyl iodide, the suspension became thin after 1 hour. After 8 hours, additional strontium oxide (8 g) and methyl iodide (25 ml) were added. After 48 hours, methyl iodide was recovered and the slurry was extracted with liberal quantities of chloroform. Evaporation of the chloroform and DMF gave a yellow-brown glass. The product was treated again as described above followed by one treatment with silver oxide, DMF, and methyl iodide (21) and four methylations with Purdie's reagents (26). The final product, a yellow glass, 3.06 g, had a methoxyl

content of 44.4%, a very small OH absorption band in the infrared spectrum, and $[\alpha]_D$ 71° (*c* 2.2 in chloroform). Practically no insoluble residue was noted when the product was dissolved in petroleum ether (30–60° C) containing 5% chloroform.

Hydrolysis of the Methylated Glucan

The methylated glucan (3.00 g) was hydrolyzed with sulphuric acid (22). Neutralization ($BaCO_3$) of the hydrolyzate followed by deionization of the filtrate and evaporation gave a sirup (2.89 g) which upon chromatographic examination using solvent C showed tetra-, tri-, di-, and mono-methyl glucoses as well as a small quantity of glucose. Resolution of these methyl glucoses into the above four classes was effected using sheets of Whatman 3 MM paper and solvent C. The weights of tetra- (985 mg), tri- (880 mg), di- (410 mg), and mono-methyl glucose (135 mg) correspond to an approximate molar ratio of 60:57:28:10. Approximately 1.3% glucose (35–36 mg) was present. The identity of the different methyl ethers of glucose will be the subject of a future paper.

ACKNOWLEDGMENTS

This investigation was supported by a P.H.S. research grant (RG7652) from the Division of General Medical Sciences, Public Health Service (U.S.A.), to whom we express our thanks. We are also indebted to Miss J. Hunter for skillful technical assistance.

REFERENCES

1. E. Pacsu and P. T. Mora. J. Am. Chem. Soc. **72**, 1045 (1950).
2. P. T. Mora and J. W. Wood. J. Am. Chem. Soc. **80**, 685 (1958).
3. P. T. Mora, J. W. Wood, P. Maury, and B. G. Young. J. Am. Chem. Soc. **80**, 693 (1958).
4. P. T. Mora, J. W. Wood, and V. W. McFarland. J. Am. Chem. Soc. **82**, 3418 (1960).
5. P. W. Kent. Biochem. J. **55**, 361 (1953).
6. H. W. Durand, M. F. Dull, and R. S. Tipson. J. Am. Chem. Soc. **80**, 3691 (1958).
7. C. R. Ricketts. J. Chem. Soc. 4031 (1954).
8. C. R. Ricketts and C. E. Rowe. J. Chem. Soc. 3809 (1955).
9. T. Nakamura. J. Chem. Soc. Japan, Ind. Chem. Sect. **63**, 1769 (1960).
10. C. T. Bishop. Can. J. Chem. **34**, 1255 (1956).
11. J. da S. Carvalho, W. Prins, and C. Schuerch. J. Am. Chem. Soc. **81**, 4054 (1959).
12. J. W. Wood and P. T. Mora. J. Am. Chem. Soc. **80**, 3700 (1958).
13. P. T. Mora, E. Merler, and P. Maury. J. Am. Chem. Soc. **81**, 5449 (1959).
14. A. M. Unrau and F. Smith. Chem. & Ind. (London), 330 (1957).
15. I. J. Goldstein, G. W. Hay, B. A. Lewis, and F. Smith. Abstracts of Papers, 135th American Chemical Society Meeting, Boston, Mass. April, 1959. p. 3D.
16. P. P. Fleury and J. Lange. J. pharm. chim. **17**, 107 (1933).
17. D. R. Briggs, E. F. Garner, R. Montgomery, and F. Smith. Anal. Chem. **28**, 1333 (1956).
18. N. Dubois, J. K. Hamilton, K. A. Gilles, P. A. Rebers, and F. Smith. Anal. Chem. **28**, 350 (1956).
19. G. G. S. Dutton and A. M. Unrau. Unpublished results.
20. R. Kuhn, J. Egge, R. Brossmer, A. Gauke, P. Klesse, W. Lochinger, E. Rohm, H. Trischmann, and D. Tschampel. Angew. Chem. **72**, 805 (1960).
21. R. Kuhn, I. Löw, and N. Trischmann. Ber. **90**, 203 (1957).
22. I. Croon, G. Herrström, G. Kull, and B. Lindberg. Acta Chem. Scand. **14**, 1338 (1960).
23. W. E. Trevelyan, D. P. Procter, and J. S. Harrison. Nature, **166**, 444 (1950).
24. L. Hough, J. K. N. Jones, and W. H. Wadman. J. Chem. Soc. 1702 (1950).
25. F. Wild. *In* Characterisation of organic compounds. C.U.P., London. 1958. p. 82.
26. T. Purdie and J. C. Irvine. J. Chem. Soc. **83**, 1021 (1903).

STUDIES ON THE CHEMICAL BASIS FOR CHOLINOMIMETIC AND CHOLINOLYTIC ACTIVITY

PART I. THE SYNTHESIS AND CONFIGURATION OF QUATERNARY SALTS IN THE 1,3-DIOXOLANE AND OXAZOLINE SERIES

D. J. TRIGGLE[1] AND B. BELLEAU
Department of Chemistry, University of Ottawa, Ottawa, Canada

Received February 19, 1962

ABSTRACT

Structure activity relationships in the muscarine and the quaternary 1,3-dioxolane (Fourneau series) series are briefly discussed. The most active member of the latter series (2-methyl-4-dimethylaminomethyl-1,3-dioxolane methiodide, (IX), F2268) was shown to consist of a mixture of 60% cis and 40% trans isomers. The same was found to apply to all synthetic intermediates in that series. Unequivocal assignments of configuration were made by relating various intermediates leading to (IX) and its analogs to D-*cis*-1,3-dimethyl-1,3-dioxolane itself, obtained by degradation of 1,6-anhydrogalactose. Attempted separation of cis–trans isomers in the 1,3-dioxolane series was not successful. However, a mixture of *cis*,*trans*-2-trichloromethyl-4-hydroxymethyl-1,3-dioxolane (XVI) could be fractionated by crystallization of the corresponding tosylates. Catalytic hydrogenolysis converted the pure *cis*- and *trans*-trichloromethyl derivatives (XVII) and (XVIII) to pure *cis*- and *trans*-2-methyl-4-hydroxymethyl-1,3-dioxolane tosylates (XIX) and (XX), which eventually afforded for the first time pure *cis*-F2268 and *trans*-F2268 (XXII) and (XXIII).

Optically active members in the 1,3-dioxolane series were prepared. Members of the D(−)-series were conveniently obtained from D-isopropylidene glycerol. Members of the L(+)-series could be obtained in optically impure forms by resolution of *dl*-tertiary bases such as (XXXVI) with D- and L-dibenzoyltartaric acid. The best preparations had an optical purity not exceeding 32%. The resolution of the cis base (X) was unsuccessful.

The synthesis of an oxazoline analog, (XLIV), of F2268 was accomplished. The reaction sequence involves solvolysis of N-acetyl-2,3-dibromo-*n*-propylamine (XLI) to give the 5-bromomethyl-2-methyloxazoline (XLII). This unstable intermediate was reacted with dimethylamine to give the tertiary base (XLIII), which was quaternized with methyl iodide whereupon the quaternary base (XLIV) was formed in good yield. The structure of the latter was established by an independent synthesis of the hydrolysis product (XLV).

Preliminary pharmacological data are reported for the various new quaternary salts. The compounds were assayed for cholinomimetic activity. It is concluded from these studies that quaternary 1,3-dioxolanes display structure-activity relationships analogous to the muscarones. The use of triethylammonium analogs has revealed a large degree of preference of cholinergic receptors for the presence of a cis configuration in 2,4-disubstituted-1,3-dioxolanes. It was also noted that the oxazoline derivative (XLIV) ranks amongst the most active cholinomimetics thus far reported. Relationships between configuration and activity are briefly discussed.

INTRODUCTION

The recent structure elucidation and synthesis of muscarine (1(*a*), 1(*b*)) has created renewed interest in the relationship between the structure and activity of drugs acting on the muscarinic cholinergic receptors. A variety of muscarine analogs have been synthesized and their cholinomimetic activity determined. This subject has been recently reviewed (2), and since then, Waser (3) has examined a number of additional structural analogs. Mention should also be made of the report of Friess, Witkop, and co-workers (4) on the inhibitory properties of a number of muscarine-related compounds towards acetylcholinesterase. It emerges from all these important studies that the optimal structural requirements for muscarinic activity are as follows: (1) The muscarinic receptor displays an almost absolute optical specificity, the non-natural enantiomorph (II)

[1]*Holder of a National Research Council of Canada Postdoctoral fellowship, 1959–1961.*

(Chart 1) being essentially inactive (5, 6). (2) The relative configuration of the substituents on the furan ring of natural muscarine represents also the optimum geometry

CHART 1

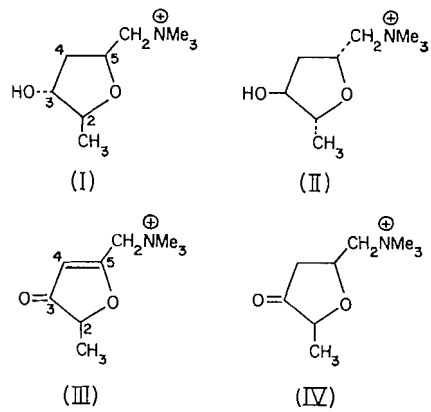

for activity. (3) The asymmetric center at position 5 can be destroyed as in 4,5-dehydromuscarone (III) without drastically changing the activity (7). However, inversion of configuration at the same position but in muscarine is detrimental to activity. The asymmetric center at position 2 is relatively unimportant in the muscarones (IV) (8) but of critical importance in muscarine. (4) The presence of a methyl group at C2 leads to maximum activity; its absence (9, 10), or its substitution for a larger group is detrimental to activity (10). (5) Replacing the furan oxygen by sulphur decreases potency (10). (6) The muscarinic receptor does not display absolute optical specificity towards the muscarones and 4,5-dehydromuscarone, in marked contrast to the specificity towards the muscarine enantiomorph (I) (3, 7, 8).

Some attempts at the interpretation of these unusual and puzzling structure-activity relationships have been made (11) and this problem will be dealt with in a future publication. There is little doubt that much knowledge about the nature of muscarinic receptors will be gained when the stereochemical interrelationships become understood. Some interesting generalizations concerning the optimum structural requirements for cholinomimetic activity have been put forward by Ing (11). The kinetics of drug interaction with cholinergic receptors has been examined in considerable detail, especially by Ariëns and van Rossum (12), who extended the original approach of Clark (13). The principles governing the ability of a drug receptor complex to produce an effect were defined in kinetic terms by Ariëns, Stephenson (14), and more recently by Paton (15). It is now recognized that the properties of drugs can best be quantitated in terms of their intrinsic activity, affinity for receptors, and rate of combination with the latter. In spite of these important contributions to the field of receptor theory, the biochemical nature of cholinergic receptors remains unsolved. We have initiated a program aimed at the elucidation of the stereochemical requirements for muscarinic activity with the hope that these studies might throw light on the nature of the receptors.

It has long been known that certain 1,3-dioxolanes exhibit a high degree of parasympathomimetic activity, a discovery due to Fourneau and his collaborators (16). The most active member of this series is 2-methyl-4-trimethylammoniummethyl-1,3-dioxolane

(IX) (Chart 2), which was reported to match muscarine in potency. All of the structural analogs of (IX) appear to be less active. The structural relationship of (IX) with muscarine

CHART 2

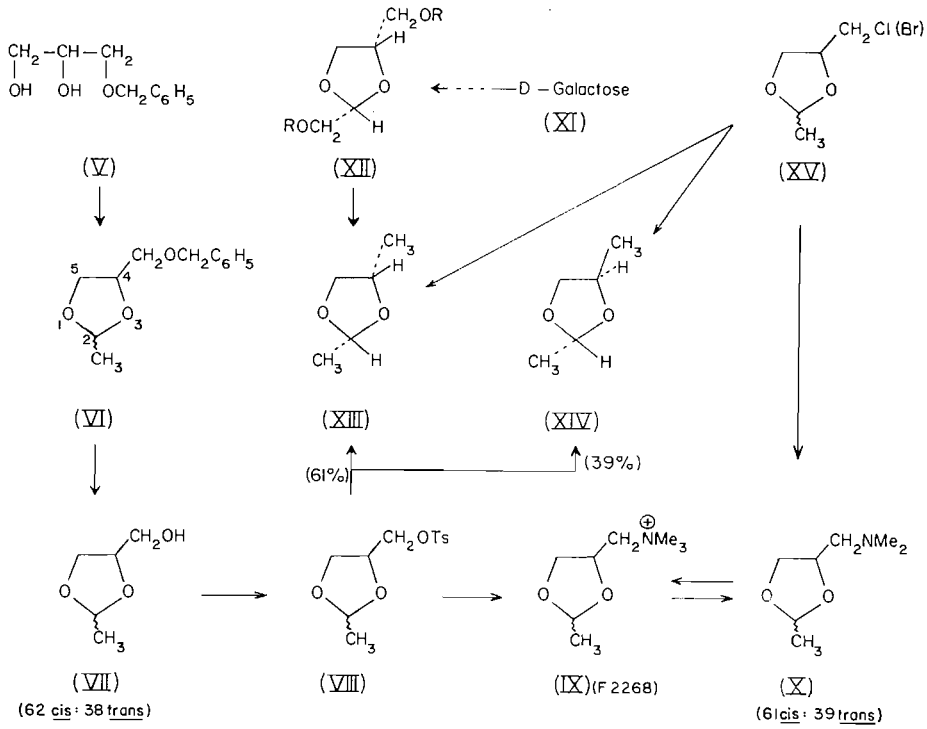

and its analogs is obvious and it was of interest to examine the relation between stereochemistry and activity in the Fourneau series. The effect of structural variations about the 2-position and the cationic head of (IX) has been studied by van Rossum and Ariëns (17), who confirmed the operation of the concept of affinity and intrinsic activity in this series. However, the stereochemistry of (IX) in relation to activity has not been investigated. Because activity in the muscarine series is highly dependent on configuration, relative and absolute, similar dependency would be expected in the Fourneau compound (IX). It is a rather curious phenomenon that the configuration of (IX) has never been established, and of the two possible stereoisomers, only one appears to have ever been obtained or prepared. It is not known as yet whether the high activity of (IX) is associated with a trans or cis configuration about the 2- and 4-positions, a situation which, however, has been clarified in the muscarine series. The optical forms of any quaternary-1,3-dioxolanes have also never been reported or tested. The possible inhibitory effect of these drugs on acetylcholinesterase has also not been investigated.

In this first paper of a series, the synthesis and the configuration of (IX) and a number of analogs will be described. Subsequent publications will deal with their effect on acetylcholinesterase and with generalizations regarding the probable nature of the muscarinic cholinergic receptors.

Relative Configuration of (IX)

The method most generally employed for the synthesis of 2-methyl-4-trimethylammoniummethyl-1,3-dioxolane iodide (IX) (F2268) involves the reaction of epichlorohydrin with acetaldehyde in the presence of stannic chloride whereupon the intermediate 2-methyl-4-chloromethyl-1,3-dioxolane (XV) is produced and thence reacted with dimethylamine to give (X), which is finally quaternized using methyl iodide (16). The quaternary salt (IX) so obtained has been repeatedly reported to melt sharply at 140–141° and we have confirmed this. van Rossum (17) has also showed it to be apparently homogeneous as judged from results of paper chromatography. A total of 38 homologous structures in this series were prepared by this author and all were reported to melt sharply and to give rise to single spots when chromatographed on paper.

Since the relative configuration of (IX) must be the same as that of the starting dioxolane (XV), we sought to establish the configuration of the latter by relating it to a 2,4-dimethyl-1,3-dioxolane of proven configuration. The reaction of propylene glycol with acetaldehyde has been reported to give a mixture of *cis*- and *trans*-2,4-dimethyl-1,3-dioxolane, (XIII) and (XIV), which has been claimed to be separable by fractional distillation (18). In our hands this separation proved to be far from complete (see Experimental); the fraction of lower boiling point has been assigned the cis configuration. Because of our need for a much more rigorous proof of configuration we sought to synthesize the cis isomer by unambiguous methods. Cleavage of 1,6-anhydrogalactose to D-*cis*-1,3-dioxolane-2,4-dicarboxaldehyde has been reported in the literature (19). Reduction of the latter with sodium borohydride gave the cis diol (XII) (Chart 2), which gave a crystalline di-*p*-nitrobenzoate and a crystalline ditosylate. Attempts to prepare a monotosylate were fruitless, a bicyclic ether being presumably the only product. Hydrogenolysis of the ditosylate with lithium aluminum hydride afforded D-*cis*-2,4-dimethyl-1,3-dioxolane (XIII), which gave rise to a single sharp peak in the vapor phase chromatography (v.p.c.) instrument.

The dioxolane (VI) resulting from the condensation of glycerol 1-monobenzyl ether and acetaldehyde was hydrogenolyzed and the resulting 2-methyl-4-hydroxymethyl-1,3-dioxolane (VII) converted to a crystalline tosylate, (VIII), which eventually afforded F2268 (IX) after reaction with dimethylamine followed by quaternization with methyl iodide. The identity of this material was ascertained by direct comparison (infrared and n.m.r.) with a sample obtained by the general literature method outlined earlier. Hydrogenolysis of the intermediate tosylate (VIII) with lithium aluminum hydride or catalytic hydrogenolysis of the 4-chloromethyl intermediate (XV) afforded 2,4-dimethyl-1,3-dioxolane, which was shown by v.p.c. to consist of a mixture of cis–trans isomers in a ratio of 60:40 (authentic D-*cis*-2,4-dimethyl-1,3-dioxolane (XIII) being used as a standard). In order to establish that crystallization of the quaternary base (IX) did not change the isomer ratio, it was submitted to N-dealkylation by treatment with lithium aluminum hydride (20) and the tertiary base (X) analyzed by v.p.c. The cis–trans isomer ratio proved to be 61:39, thus conclusively establishing that F2268 consists of a mixture of cis and trans isomers in a ratio closely approximating 60:40. This conclusion was confirmed by n.m.r. spectroscopy, which showed clearly the presence of two split methyl groups in a ratio of 60:40 (see Experimental). Moreover, identical v.p.c. patterns were obtained with the product resulting from the reaction of propylene glycol and acetaldehyde. Therefore the synthesis of (IX) proceeds non-stereospecifically and all the intermediates consist of a mixture of 60% of cis and 40% of trans isomers. We have subsequently found this to apply to virtually all solid derivatives in this series. It is clear that *cis*- and *trans*-2,4-disubstituted-1,3-dioxolanes crystallize as molecular compounds and display very

great similarities in their physical properties. Since the time F2268 (IX) was first synthesized *all the pharmacological properties reported for it are, therefore, those of a 60:40 mixture of the cis and trans isomers.* The same would appear to apply to all other homologs, as judged from additional observations recorded below. In view of the structural analogy of (IX) with muscarine, none of the previous pharmacological data can be relied upon for purposes of correlation between stereochemistry and activity.

Numerous attempts to achieve separation of the isomers of (IX) or its precursors on a practical scale by a combination of various techniques were fruitless. However, both the cis and the trans isomers of (IX) could eventually be obtained in pure form by an indirect synthetic route which is described below (Chart 3).

CHART 3

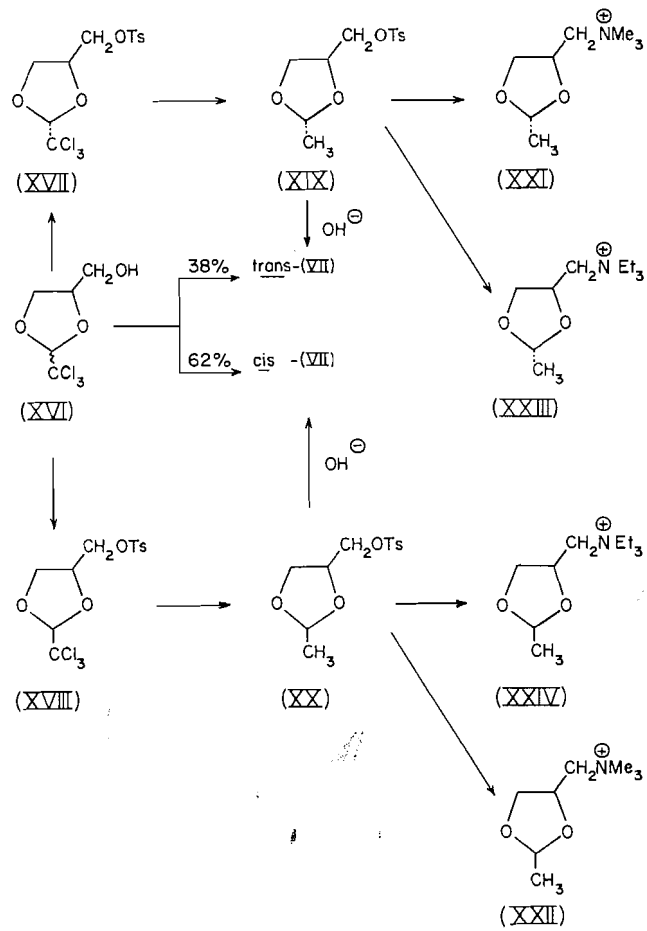

It was found that the reaction product of glycerol and chloral (XVI) (Chart 3) gave a crystalline tosylate melting over a wide range, thus indicating that molecular compound formation was apparently suppressed in this type of 1,3-dioxolane. This proved to be the case, since fractional crystallization of the tosylate led to the isolation of two sharp-melting isomers, isomer A (XVII), m.p. 133–134°, and isomer B (XVIII), m.p. 95–96°. The trichloromethyl group of each isomer was converted to methyl by catalytic hydrogenolysis. The resulting tosylate (XIX) from A had m.p. 66–68° and when submitted to

aqueous alkaline hydrolysis gave pure *trans*-2-methyl-4-hydroxymethyl-1,3-dioxolane (VII), as determined by v.p.c. Similarly, the tosylate (XX) from B had m.p. 64–66° and gave, after alkaline hydrolysis, pure *cis*-2-methyl-4-hydroxymethyl-1,3-dioxolane (VII), as established by v.p.c. Reaction of the pure trans tosylate (XIX) with dimethylamine followed by quaternization with methyl iodide afforded *trans*-2-methyl-4-trimethylammoniummethyl-1,3-dioxolane (XXI) (*trans*-F2268), m.p. 131–132°. The homogeneity of the product was confirmed by n.m.r. spectroscopy (single methyl doublet). Similar treatment of the pure cis tosylate (XX) gave *cis*-2-methyl-4-trimethylammoniummethyl-1,3-dioxolane (XXII) (*cis*-F2268), m.p. 143–144°. The n.m.r. spectrum of this compound also proved it to be homogeneous. *This is the first time that the powerful cholinomimetic F2268 becomes available in its pure stereoisomeric forms.*

In view of the fact that the experimental basis for the concept of affinity and intrinsic activity as elaborated by Ariëns and van Rossum lies principally on the inversion of agonistic activity when a trimethylammonium cationic head is changed for a triethylammonium one, it was of interest to prepare the pure *cis*- and *trans*-triethylammonium analogs (XXIV) and (XXIII) of *cis*- and *trans*-F2268. It should be emphasized that Ariëns and van Rossum used what we now recognize to be a 60:40 mixture of cis–trans isomers, thus preventing any definite conclusion regarding the effect of stereochemistry on the cholinolytic activity of triethylammonium analogs.

Synthesis in the Optically Active Series

Because of the dramatic difference in cholinomimetic activity between optical isomers in the muscarine series, it was of interest to make available a number of optical isomers in the 1,3-dioxolane series. Quaternary salts of the D-series could be prepared in optically pure forms from optically pure D-isopropylidene glycerol (XXV) (Chart 4). The latter could be converted by way of the D-tosylate (XXVI) to D(−)-2,2-dimethyl-4-trimethylammoniummethyl-1,3-dioxolane iodide (XXVII). The preparation of the 2,2-bisnor

CHART 4

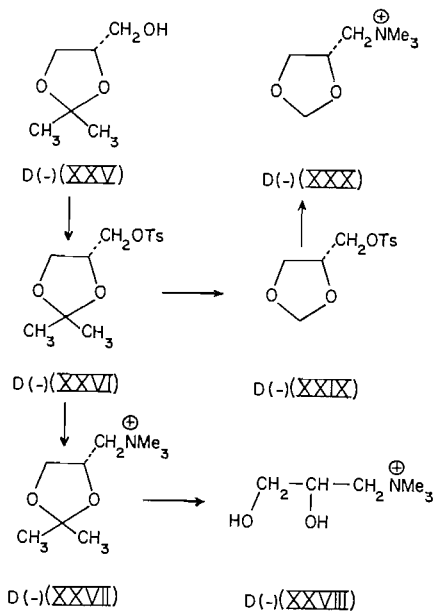

analog (XXX) in optically pure form was best accomplished by mild acid hydrolysis of D-isopropylidene glycerol tosylate (XXVI) followed by condensation with formaldehyde whereupon the tosylate (XXIX) was obtained. Conversion of the latter to D(−)-4-trimethylammoniummethyl-1,3-dioxolane iodide (XXX) was accomplished in the conventional manner described above. In order to gain access to the L-series, the resolution of the corresponding racemic tertiary bases was investigated (Chart 5). Racemic

CHART 5

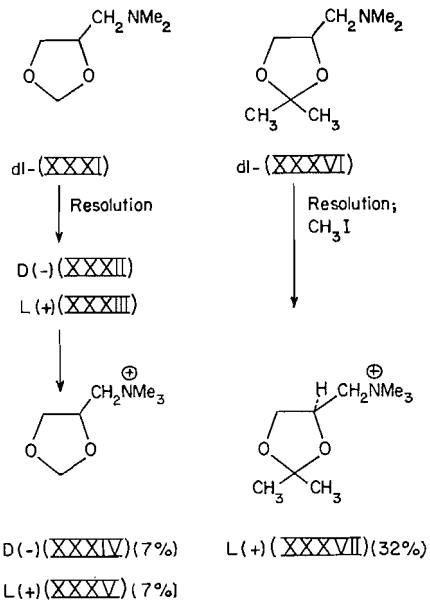

4-dimethylaminomethyl-1,3-dioxolane (XXXI) gave crystalline D- and L-dibenzoyltartrates (XXXII) and (XXXIII), which were recrystallized to constant rotation. The bases were regenerated and converted to the methiodides (XXXIV) and (XXXV). The levorotatory salt is therefore of the D-series. The rotations showed them to be only 7% optically pure. This difficulty in achieving resolution must again reflect the tendency for diastereoisomers of the 2,4-disubstituted-1,3-dioxolane series to crystallize as molecular compounds. Because L-dibenzoyltartaric acid gives rise to (+)-dioxolanes of the L-series, the 2,2-dimethyl tertiary base (XXXVI) (Chart 5) was converted to a crystalline L-dibenzoyltartrate which was recrystallized to constant rotation. Regeneration of the base followed by quaternization with methyl iodide gave L(+)-2,2-dimethyl-4-trimethylammoniummethyl-1,3-dioxolane iodide (XXXVII), which was 33% optically pure.

Application of these procedures to racemic *cis*- and *trans*- (X) was only partially successful. With *cis*-(X) it was not possible to obtain crystalline dibenzoyltartrate salts. However, *trans*-(XXXVIII) (Chart 6) gave a crystalline D-dibenzoyltartrate which was recrystallized to constant rotation. Regeneration of the base and quaternization in the usual way gave D(−)-*trans*-F2268 (XXXIX). The optical purity of the latter was established as follows: It was hydrolyzed with dilute hydrochloric acid and the rotation of the resulting quaternary diol (XXVIII) determined. Comparison of this rotation with that of an optically pure sample (Chart 4) derived from optically pure D(−)-(XXVII) by acid hydrolysis under identical conditions showed the D(−)-*trans*-(XXXIX) to be 32%

CHART 6

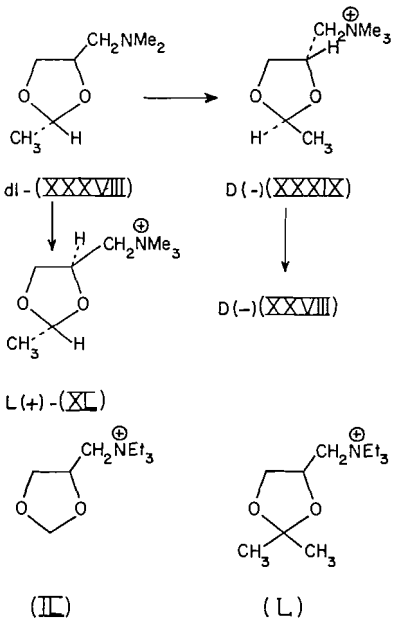

optically pure. Using again *trans*-(XXXVIII) but L-dibenzoyl tartaric acid as the resolving agent, L(+)-*trans*-F2268 (XL) was ultimately obtained with an optical purity of 32% (Chart 6).

With these isomers of variable optical purity it should be possible to establish whether activity will depend on absolute configuration, as is the case in the muscarine series. If the analogy between muscarine and the 2,4-disubstituted-1,3-dioxolane is real, it would be expected that the isomers of the L(+)-series should similarly be more active cholinomimetics. It will also be of interest to determine the anti-acetylcholinesterase inhibitory property of the various isomeric forms of the above quaternary dioxolanes. This aspect of our work will be reported separately.

Synthesis of 5-Trimethylammoniummethyl-2-methyl-oxazoline Bromide (XLIV)

Perhaps one of the most striking aspects of structure-activity relationships in the muscarine series is the observation that racemic 4,5-dehydromuscarone (III) surpasses L(+)-muscarine in potency (Chart 1). Because D(−)-muscarine displays a very low order of activity, it is surprising that the absence of an asymmetric center at position 5 of 4,5-dehydromuscarone should lead to such a highly active cholinomimetic. Moreover, and in sharp contrast to the muscarine series, the relative configuration of the methyl group in the muscarone series is relatively unimportant, racemic allomuscarone (*trans*-(IV)) being only slightly less active than racemic muscarone (*cis*-(IV)). This result also suggests that destruction of the asymmetric center at position 2 through the introduction of a double bond between carbons 2 and 3 (if this were feasible) might not alter activity in the muscarone series. While this problem is being investigated, it appeared of more immediate interest to transpose this reasoning to the 1,3-dioxolane series and it is obvious that in order to produce a trigonal carbon at position 2 of 1,3-dioxolanes, it is essential that the oxygen atom at position 1 be substituted by a trivalent heteroatom such as

nitrogen. It should be noted that no oxazoline analog in the Fourneau series of cholinomimetics has as yet been reported. Several of the most obvious methods for the synthesis of the desired analog (XLIV) (Chart 7) of (IX) proved unsuccessful. A convenient and

CHART 7

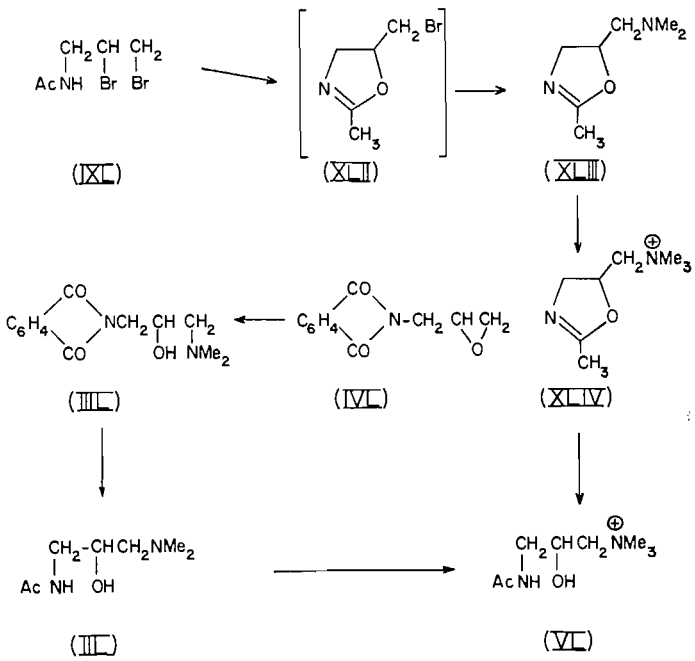

expedient method of synthesis was ultimately discovered which requires the readily available starting material N-allyl acetamide. This was converted to the dibromide (XLI) (Chart 7) as described elsewhere and then solvolyzed in acetonitrile in the presence of silver carbonate. The participation of neighboring amido groups in such solvolyses has previously been demonstrated (21) and allows the prediction that the dibromide (XLI) must be converted largely to 5-bromomethyl-2-methyl-oxazoline (XLII). Attempts to isolate this intermediate were unsuccessful, rapid polymerization of the compound taking place upon removal of the solvent. However, if excess anhydrous dimethylamine was added to the reaction mixture as soon as maximum precipitation of silver bromide had occurred, a good yield of 2-methyl-5-dimethylaminomethyloxazoline (XLIII) was obtained. Quaternization of the latter with methyl iodide finally gave the crystalline salt (XLIV) in high yield. It was desirable to establish the structure of the latter by unambiguous means, since the course of the solvolysis can only be inferred. The quaternary base (XLIV) was hydrolyzed with hot water to give a quantitative yield of 1-acetamido-3-trimethylammonium-2-propanol iodide (XLV). An authentic specimen of the latter was secured by reacting 1-phthalimido-2,3-epoxypropane (XLVI) with dimethylamine, whereupon (XLVII) was produced. Hydrolysis of the latter followed by acetylation and quaternization with methyl iodide afforded (XLV), which proved to be identical with the sample obtained by hydrolysis of the oxazoline (XLIV). It is clear that this method of synthesis of (XLIV) could be extended to the preparation of a variety of trialkylammonium analogs.

PRELIMINARY PHARMACOLOGICAL RESULTS*

The various quaternary dioxolanes and the oxazoline derivative (XLIV) were assayed for muscarinic activity using the guinea pig ileum as the test organ. The minimum concentration of drug necessary to elicit a response is recorded in Table I. Of immediate

TABLE I

Compound number	Concentration, mg/ml, guinea pig ileum ($c \times 10^{-7}$)	Compound number	Concentration, mg/ml, guinea pig ileum ($c \times 10^{-7}$)
Acetyl choline	2.5	L(+)-(XXXIX)†	12.5
(XXI)	12.5	L(+)-(XL)†	0.125
(XXII)	2.5	(XXIII)	500,000.
(XXX)	5,000.	(XXIV)	500.
D(−)-(XXVII)	250,000.	(XLIV)	2.5
L(+)-(XXXV)*	2,500.	(IL)	500,000.
L(+)-(XXXVII)†	2,500.	(L)	5,000,000.

*Optical purity of this isomer is 7%.
†Optical purity is 32%.

interest is the fact that quaternary compounds of the L(+)-series are uniformly much more active than their D(−) counterparts. Hence, the same absolute configurational requirement as in the muscarine series is operative. It is also interesting that *cis*-F2268 (XXII) surpasses *trans*-F2268 (XXI) in potency by a factor of 5. This also parallels the effect of epimerization about the C_2-methyl group of muscarine, racemic allomuscarine being very much less active. However, the magnitude of the differences in potency between *cis*-(XXII) and *trans*-(XXI) on the one hand and (±)-muscarine and (±)-allomuscarine on the other is such as to indicate that the asymmetric center at C_2 of (XXI) and (XXII) is not nearly as important as it is in the muscarine series. In this respect, the ratio of the potencies of *cis*- and *trans*-F2268 suggests that they resemble the muscarones much more than the muscarines. It should be mentioned that Barlow had speculated that *cis*- and *trans*-F2268 would not differ greatly in potency because of a loose structural analogy with the muscarones (IV) (22). It is striking, however, that the L(+)-*trans*-F2268 (XL), which is only 32% optically active, should surpass acetylcholine in potency by a factor of 20. Consideration of the fact that a 32% enrichment in the L(+) isomer increases the potency by a factor of 100 over the pure racemic mixture (XXI) and that the cis racemate (XXII) is five times more active than the latter, suggests that the pure L(+) cis isomer of (XXI) should possess extraordinary potency surpassing all known cholinomimetic drugs. The synthesis of this L(+) cis isomer is under way.

Confirmation that the configuration of the asymmetric center at C_2 of F2268 may not be a critical factor (although it has an influence) for activity is supplied by the high cholinomimetic activity of the quaternary oxazoline (XLIV) in which C_2 is now trigonal. We are fully aware, however, that in this latter case, the presence of a basic nitrogen in the ring introduces an additional factor which may alter the mechanism of interaction with the receptors. We are presently attempting to establish whether the oxazoline (XLIV) interacts with the receptors in the protonated form or as the free base.

Of great interest finally is the marked difference in the relative potencies of the triethylammonium analogs (XXIV) and (XXIII) of *cis*- and *trans*-(F2268). In contradiction with the conclusions regarding the significance of the asymmetric center at C_2 of F2268

Results of our work and that of Dr. M. Pindell and his staff, Bristol Laboratories, Syracuse, N.Y.

(IX), it appears that *in the triethylammonium series (XXIII) and (XXIV) the configuration of the C_2 methyl group is of critical importance.* An interpretation of these results will be given in a forthcoming publication.

EXPERIMENTAL*

cis,trans-2-Methyl-4-hydroxymethyl-1,3-dioxolane (VII)

This was prepared according to the method of Brimacombe, Foster, and Haines (23). The pure alcohol was analyzed by v.p.c. and shown to consist of a mixture of cis–trans isomers in a ratio of 64:36. (see Table II, entry 1). The *tosylate (VIII)* was prepared by treatment with *p*-toluenesulphonyl chloride and

TABLE II

Isomer composition of 2,4-disubstituted-1,3-dioxolanes

Entry	Compound No.	2-Subst.	4-Subst.	% *cis-*	% *trans-*	Column packing*
1	(VII)	Me	CH_2OH	64.0	36.0	A
2	(XIII)+(XIV)†	Me	Me	61.0	39.0	B
3	(X)	Me	CH_2NMe_2	60.5	39.5	A
4	(XV)	Me	CH_2Cl	62.0	38.0	B
5	(XV)	Me	CH_2Br	64.0	36.0	B
6	(XIII)+(XIV)‡	Me	Me	63.0	37.0	B
7	(XIII)+(XIV)§	Me	Me	62.0	38.0	B
8	(XIII)	Me	Me	100.0	—	B
9	(VII)‖	Me	CH_2OH	62.0	38.0	A
10	(XIII)+(XIV)¶	Me	Me	73.0	27.0	B
11	(XIII)+(XIV)**	Me	Me	46.0	54.0	B

*Obtained from Perkin–Elmer and used as such. The v.p.c. apparatus was a Perkin–Elmer instrument. Percentage compositions were determined by taking the ratio of peak areas in the usual way.
†Obtained from (VII) by way of (VIII).
‡Obtained from (XV), entry 4.
§Obtained from (XV), entry 5.
‖Obtained from *cis,trans*-(XVI) by hydrogenolysis.
¶Lower-boiling fraction.
**Higher-boiling fraction.

pyridine at 0°, whereupon an oily tosylate was obtained which crystallized from hexane as colorless needles, m.p. 49–53°. Yield: 74%. Calc. for $C_{12}H_{16}SO_5$: C, 52.9; H, 5.9. Found: C, 52.9; H, 5.9%.

cis,trans-2,4-Dimethyl-1,3-dioxolane (XIII) and (XIV)

A solution of the tosylate of *cis,trans*-2-methyl-4-hydroxymethyl-1,3-dioxolane (VIII) (13.5 g, 0.05 mole) in diglyme was added dropwise to a stirred solution of lithium aluminum hydride (1.9 g, 0.05 mole) in diglyme at 100°. The mixture was kept at this temperature for 2 hours, cooled, and treated with 10% sodium hydroxide and distilled (bath temperature 150°). The distillate was dried (Na_2SO_4) and redistilled to give *cis,trans*-2,4-dimethyl-1,3-dioxolane (4.4 g, 86%), b.p. 90–95°. The results of the vapor phase chromatographic analysis are given in Table II (entry 2).

Attempted Separation of cis and trans Isomers of 2,4-Dimethyl-1,3-dioxolane (XIII) and (XIV)

Two hundred grams of the cis–trans mixture was prepared according to the method of Lucas and Guthrie (18). Repeated fractional distillation and vapor phase chromatographic examination of the fractions revealed an increase in the cis content of the lower-boiling fraction and an increase in the trans content of the higher-boiling fraction, but as the results in Table II (entries 10 and 11 respectively) show, the separation was far from complete.

cis,trans-2-Methyl-4-dimethylaminomethyl-1,3-dioxolane Methiodide (IX)

cis,trans-2-Methyl-4-toluenesulphonyloxymethyl-1,3-dioxolane (VIII) (13.5 g, 0.05 mole) was dissolved in 100 ml of a 30% solution of anhydrous dimethylamine in benzene and kept at 100° for 12 hours; the mixture was cooled, filtered, and the excess dimethylamine removed by heating on the steam bath. Addition of an excess of methyl iodide gave a near quantitative yield of the quaternary iodide; crystallization from isopropanol gave colorless needles (82%), m.p. 141° (unchanged on further crystallization). The n.m.r. spectrum (in pyridine) showed two methyl doublets with an intensity ratio of 3:2.

**All melting points were determined microscopically on a Kofler hot stage and are uncorrected. The boiling points are also uncorrected. Infrared spectra were determined using a Perkin–Elmer Infracord instrument. The n.m.r. spectra were recorded with a Varian instrument operating at 60 Mc. Microanalyses by Miss E. Busk, Chemistry Department, University of Ottawa.*

cis,trans-2-Methyl-4-dimethylaminomethyl-1,3-dioxolane (X)

The finely powdered preceding methiodide (IX) (7.2 g, 0.025 mole) was suspended in diglyme (20 ml) with lithium aluminum hydride (0.025 mole) and the reaction mixture heated to 150° for 6 hours and then decomposed with 10% sodium hydroxide (10 ml), filtered, saturated with salt, and extracted several times with ether to give *cis,trans*-2-methyl-4-dimethylaminomethyl-1,3-dioxolane (2.6 g, 71.2%). The results of the vapor phase chromatographic analysis are given in Table II (entry 3).

cis,trans-2-Methyl-4-chloro- (or bromo-) methyl-1,3-dioxolane (XV)

These were prepared from glycerol α-monochlorhydrin or monobromhydrin and acetaldehyde by reaction in boiling benzene, the water being continuously removed with a Dean–Stark trap. The results of the vapor phase chromatography experiments are given in Table II (entries 4 and 5). The configurations were established by hydrogenolysis to the corresponding 2,4-dimethyl-1,3-dioxolanes as follows: *cis,trans*-2-methyl-4-halomethyl-1,3-dioxolane (0.1 mole) in absolute ethanol in which was suspended sodium bicarbonate (0.5 mole) and 10% Pd/C (0.5 g) was reduced at 3 atm pressure of hydrogen for 3 hours. The reaction mixture was filtered and a sample of the filtrate analyzed by vapor phase chromatography to give the results shown in Table II (entries 6 and 7). These results (Table II) confirm the configurations suggested by vapor phase chromatographic analysis of the halomethyl derivatives themselves (see above).

D-*cis-2,4-(Dihydroxymethyl)-1,3-dioxolane (XII)*

Crude 1,3-dioxolane-*cis*-2,4-dicarboxaldehyde (19) (0.1 mole) was dissolved in absolute methanol and cooled in ice. A solution of sodium borohydride (6.0 g, 0.15 mole) in water was added dropwise with stirring at 10–15°. Stirring at room temperature was continued for a further 3 hours, 25 ml of 10% sodium hydroxide was added, and carbon dioxide bubbled in until the solution was saturated. The solution was evaporated to dryness and the residue extracted with ethyl alcohol to give D-*cis*-2,4-bis(hydroxymethyl)-1,3-dioxolane (XII) as a viscous oil (12.1 g, 90.3%). Calc. for $C_5H_{10}O_4$: C, 44.8; H, 7.5. Found: C, 44.3; H, 7.1%. Without further purification, this D-*cis*-2,4-(dihydroxymethyl)-1,3-dioxolane (6.7 g, 0.05 mole) was dissolved in dry pyridine and the solution added dropwise to a stirred and cooled solution of *p*-nitrobenzoyl chloride (20.5 g, 0.11 mole) in dry pyridine; after 12 hours the reaction mixture was poured over ice, filtered, washed with ice-cold water, dried, and recrystallized from benzene to give the *cis*-bis(2,4-dinitrobenzoate) as very pale yellow needles (15.0 g, 71.2%), m.p. 94°. $[\alpha]_D^{22} = -18.5°$ (c = 1.2, acetone). Calc. for $C_{19}H_{16}N_2O_{10}$: C, 52.8; H, 3.7. Found: C, 52.6; H, 3.3%.

The *bis(dinitrobenzoate)* (10.8 g, 0.025 mole) was dissolved in aqueous ethanol (100 ml) containing sodium hydroxide (6 g) and heated under reflux for 5 hours. The solution was cooled, saturated with carbon dioxide, evaporated to dryness, and extracted with absolute ethanol to give D-*cis*-2,4-(dihydroxymethyl)-1,3-dioxolane (XII) (2.5 g, 74.6%) as a viscous oil. Calc. for $C_5H_{10}O_4$: C, 44.8; H, 7.5. Found: C, 44.3; H, 7.2%.

The pure D-*cis-(2,4-dihydroxymethyl)-1,3-dioxolane* (2.0 g, 0.015 mole) so obtained was dissolved in dry pyridine at 0°, and *p*-toluenesulphonyl chloride (6 g, 0.033 mole) was added. After 24 hours at room temperature a large excess of ether was added and the solution was extracted with 10% hydrochloric acid until free from pyridine. The ethereal solution was dried (Na_2SO_4), filtered, and evaporated to give the ditosylate as colorless needles (4.4 g, 66%), m.p. 84–86°. $[\alpha]_D = -25.5$ (c = 2, acetone). Calc. for $C_{19}H_{22}S_2O_8$: C, 51.6; H, 5.0. Found: C, 52.1; H, 5.1%.

D-*cis-2,4-Dimethyl-1,3-dioxolane (XIII)*

This was prepared by lithium aluminum hydride reduction of the preceding ditosylate by the procedure described above in the case of the preparation of *cis,trans*-2,4-dimethyl-1,3-dioxolane (XIII) + (XIV). The yield of crude D-*cis*-2,4-dimethyl-1,3-dioxolane was only 23% and the quantity was not sufficient for purification and empirical analysis. However, vapor phase chromatographic analysis was unambiguous as it showed that the compound could only be pure *cis*-2,4-dimethyl-1,3-dioxolane (XIII) (Table II, entry 8).

cis,trans-2-Trichloromethyl-4-hydroxymethyl-1,3-dioxolane (XVI)

This was prepared according to the method of Hibbert (24). It was found that by increasing the reaction temperature and time to 90° and 24 hours respectively the yield was increased to 65–70%.

The dioxolane so obtained (22.0 g, 0.1 mole) was dissolved in 80% aqueous methanol (100 ml) containing sodium bicarbonate (33.6 g, 0.4 mole) and 10% Pd/C (0.5 g). The mixture was reduced at 5 atm pressure of hydrogen for 5 hours. The solution was filtered and distilled to give *cis,trans*-2-methyl-4-hydroxymethyl-1,3-dioxolane (VII) (7.5 g, 63.5%), b.p. 70–75° at 8 mm. The isomer ratio was 62:38 (Table II, entry 9). Calc. for $C_5H_{10}O_3$: C, 50.9; H, 8.5. Found: C, 51.1; H, 8.6%.

Separation of cis,trans-2-Trichloromethyl-4-hydroxymethyl-1,3-dioxolane (XVI)

The above trichloromethyl dioxolane (892 g, 4.0 moles) was dissolved in dry pyridine (1.5 liters) and the solution cooled to 0° and treated with *p*-toluenesulphonyl chloride (840 g, 4.4 moles) over a period of 12 hours. The reaction mixture was then allowed to stand for 24 hours at room temperature and then poured into 5 liters of ice water. The precipitate was filtered, washed with water, and dried in air to give the *p*-toluenesulphonate (1495 g, 99%), white needles, m.p. 110–120°, which upon repeated recrystallization from methanol yielded the trans tosylate (XVII), m.p. 133–134° (250 g). Calc. for $C_{12}H_{13}SO_5Cl_3$: C, 38.3;

H, 3.5. Found: C, 38.1; H, 3.4%. The mother liquors from the first crystallization yielded, on repeated crystallization from methanol, the cis tosylate (XVIII), m.p. 95–96° (130 g). Found: C, 38.4; H, 3.4%.

cis- and trans-2-Methyl-4-hydroxymethyl-1,3-dioxolanes (cis-VII) and (trans-VII)

The preceding trans tosylate (XVII) (19.0 g, 0.05 mole) was added to 200 ml of aqueous methanol (1:1, v/v) together with sodium bicarbonate (14.8 g, 0.2 mole) and hydrogenated at 3–5 atm pressure with 10% Pd/C catalyst (0.5 g) for 24 hours to give the trans tosylate (XIX), m.p. 66–68°; yield 10.1 g. It was recrystallized from pentane. Calc. for $C_{16}H_{16}SO_5$: C, 52.9; H, 5.9. Found: C, 52.7; H, 5.9%. By the same procedure, the cis tosylate (XVIII) gave the cis tosylate (XX), m.p. 64–66°; yield 9.8 g. It was recrystallized from pentane. Calc. for $C_{12}H_{16}SO_5$: C, 52.9; H, 5.9. Found: C, 52.9; H, 5.6%.

The trans tosylate (XIX) (5.4 g, 0.02 mole) was heated under reflux for 4 hours with a 10% excess of sodium hydroxide in 70% aqueous ethanol. The solution was then saturated with carbon dioxide, evaporated to dryness, and the residue extracted with absolute ethyl alcohol to give chromatographically pure (v.p.c.) *trans*-2-methyl-4-hydroxymethyl-1,3-dioxolane (*trans*-VII), b.p. 76–80° at 9 mm (2.1 g, 70.0%). Similarly, the cis tosylate (XX) yielded chromatographically pure (v.p.c.) *cis*-2-methyl-4-hydroxymethyl-1,3-dioxolane (*cis*-VII), b.p. 78–80° at 10 mm (2.0 g, 67.0%).

Lithium aluminum hydride reduction of the trans tosylate (XIX) and the cis tosylate (XX) by the procedure described above in the case of (VIII) gave the corresponding pure *cis*- and *trans*-2,4-dimethyl-1,3-dioxolanes, as evidenced by v.p.c.

cis- and trans-2-Methyl-4-dimethylaminomethyl-1,3-dioxolane Methiodides (XXII) and (XXI)

cis- and *trans*-2-Methyl-4-*p*-toluenesulphonyloxymethyl-1,3-dioxolanes (XX) and (XIX) (5.4 g, 0.02 mole) were converted into the corresponding 4-dimethylaminomethyl derivatives by the method described above for the mixture of cis–trans isomers. Treatment with methyl iodide and crystallization from ethyl acetate – isopropanol gave pure *cis*-(XXII) and pure *trans*-2-methyl-4-dimethylaminomethyl-1,3-dioxolane methiodides (XXI), m.p. 143–144° and 131–132° respectively. Calc. for: $C_8H_{18}N_1O_2I$: (*trans*): C, 33.5; H, 6.3. Found: (*cis*): C, 33.8; H, 6.1; (*trans*): C, 33.6; H, 6.2%. The n.m.r. spectra (in pyridine) of both isomers showed a single methyl doublet.

cis- and trans-2-Methyl-4-diethylaminomethyl-1,3-dioxolane Ethiodides (XXIV) and (XXIII)

These were prepared in a way similar to that used for the corresponding 4-dimethylaminomethyl compounds. Pure *trans*-2-methyl-4-diethylaminomethyl-1,3-dioxolane ethiodide (XXIII) had m.p. 129–131° (from isopropanol – ethyl acetate) but the cis isomer (XXIV) failed to crystallize. Calc. for $C_{11}H_{24}NO_2I$: C, 40.2; H, 7.3. Found: (*trans*): C, 40.4; H, 7.0; (*cis*): C, 40.5; H, 7.1%.

Other Quaternary Salts of 1,3-Dioxolanes

These were the previously known 4-dimethylaminomethyl- and 2,2-dimethyl-4-dimethylaminomethyl-1,3-dioxolane methiodides (*dl*-XXX) and (*dl*-XXVII), and the 4-diethylaminomethyl- and 2,2-dimethyl-4-diethylaminomethyl-1,3-dioxolane ethiodides (IL) and (L). Their physical constants agreed with the literature values (16).

Resolution of 4-Dimethylaminomethyl-1,3-dioxolane (XXXI)

The amine (XXXI) (0.15 mole) was dissolved in dry ether, and a solution of D-dibenzoyltartaric acid (0.15 mole) in dry ether added and the mixture allowed to stand overnight. The ether was decanted and the viscous precipitate recrystallized to constant rotation from ethanol to give 13.0 g of colorless crystals, m.p. 131–132°, $[\alpha]_D^{20} = -90°$ ($c = 2$, methanol). Calc. for $C_{24}H_{25}NO_{10}$: C, 59.1; H, 5.2. Found: C, 59.0; H, 5.7%.

It was not possible to obtain the (+)-salt from the mother liquors. The above procedure was therefore repeated using L-dibenzoyltartaric acid, whereupon the (+)-salt was obtained in the same state of purity as the (−)-salt.

The free bases were regenerated from the (+)- and (−)-salts by treatment in dry ethanol with an equimolar amount of sodium ethoxide. The precipitated disodium dibenzoyltartrates were removed by filtration after dilution with ether. The filtrate was treated with excess methyl iodide and the pure methiodides collected after 24 hours. Both had m.p. 157–158°. The *D(−)-quaternary salt* (XXXIV) had $[\alpha]_D^{20} = -2.2$ ($c = 2$, H_2O). The optical purity was 7% (see below). Calc. for $C_7H_{16}O_2NI$: C, 30.8; H, 5.9. Found: C, 30.9; H, 5.6%. The *L(+)-quaternary salt* (XXXV) had $[\alpha]_D^{20} = 2.2°$ ($c = 2$, H_2O). The optical purity was 7%. Calc. for $C_7H_{16}O_2NI$: C, 30.8; H, 5.9. Found: C, 30.9; H, 5.8%.

Optically Pure D(−)-4-Dimethylamino-1,3-dioxolane Methiodide (XXX)

D-Isopropylidene glycerol (25) was converted to the *tosylate* (XXVI) by the general procedure outlined above. It crystallized from hexane as colorless needles, m.p. 24–27°. Calc. for $C_{13}H_{18}O_5S$: C, 54.5; H, 6.3. Found: C, 54.7; H, 6.2%.

The *tosylate* was hydrolyzed by heating to 50° in excess 2 *N* hydrochloric acid for 4 hours. The solution was taken to dryness *in vacuo* and the residue reacted in benzene with paraformaldehyde in the presence of some *p*-toluenesulphonic acid. The water was continuously removed with a Dean–Stark trap and the product

isolated in the usual manner. It crystallized from benzene–pentane, m.p. 35.7°. This optically pure D(−)-4-tosyloxymethyl-1,3-dioxolane (XXIX) had $[\alpha]_D^{20} = -10.0°$ (c = 2, isopropanol). Calc. for $C_{11}H_{14}O_5S$: C, 50.5; H, 5.5. Found: C, 50.8; H, 5.4%.

This *tosylate* (*XXIX*) was converted to D(−)-4-dimethylaminomethyl-1,3-dioxolane methiodide (XXX) by the general procedure outlined above. The *methiodide* had m.p. 147–148° (isopropanol); $[\alpha]_D^{20} = -32.5°$ (c = 2, H_2O). Calc. for $C_7H_{16}O_2NI$: C, 30.8; H, 5.9. Found: C, 31.3; H, 5.8%.

D(−)-2,2-Dimethyl-4-dimethylaminomethyl-1,3-dioxolane Methiodide (XXVII)

The preceding tosylate of D-isopropylidene glycerol (XXVI) was reacted with dimethylamine and the resulting base quaternized with methyl iodide by the procedures described above. The quaternary iodide (XXVII) had m.p. 215–216° (ethanol); $[\alpha]_D^{20} = -12.0°$ (c = 2, H_2O). Calc. for $C_9H_{20}O_2NI$: C, 35.9; H, 6.7. Found: C, 36.1; H, 6.4%.

Of this quaternary salt, 200 mg was heated at 90° in excess 2 *N* hydrochloric acid for 5 hours. The solution was taken to dryness *in vacuo* and the residue (XXVIII) made up to 5 ml with water. The solution had $\alpha_D^{20} = -1.38°$. This solution was used as a standard for the determination of the optical purity of other dioxolanes described below.

L(+)-2,2-Dimethyl-4-dimethylaminomethyl-1,3-dioxolane Methiodide (XXXVII)

The corresponding tertiary base *dl*-2,2-dimethyl-4-dimethylaminomethyl-1,3-dioxolane (XXXVI) was resolved with L-dibenzoyltartaric acid in the same manner as described above in the case of (XXXI). The salt was recrystallized to constant rotation. It had m.p. 133–136°; $[\alpha]_D^{20} = 70°$ (c = 2, methanol). Calc. for $C_{26}H_{31}O_{10}N$: C, 60.35; H, 6.05. Found: C, 60.5; H, 6.2%.

This L-dibenzoyltartrate salt was decomposed as described above in the case of (XXXI) and the regenerated base reacted with methyl iodide whereupon the methiodide (XXXVII) was obtained, m.p. 204–208° (isopropanol). It had $[\alpha]_D^{20} = 4.0°$ (c = 2, H_2O). Since the rotation of the optically pure enantiomorph (XXVII) is −12.0°, the optical purity of this L(+)-isomer (XXXVII) is 33%. Calc. for $C_9H_{20}O_2NI$: C, 35.9; H, 6.7. Found: C, 36.1; H, 6.9%.

D(−)-trans-2-Methyl-4-dimethylaminomethyl-1,3-dioxolane Methiodide (XXXIX)

The tertiary base (XXXVIII) was resolved with D-dibenzoyltartaric acid by the same procedure outlined above in the case of (XXXI). The salt, obtained in 25% yield, was recrystallized to constant rotation, m.p. 131–132°, $[\alpha]_D^{20} = -84°$ (c = 2, methanol). Calc. for $C_{25}H_{27}O_{10}N$: C, 60.0; H, 5.4. Found: C, 60.3; H, 5.5%.

Regeneration of the base followed by quaternization with methyl iodide in the usual manner afforded the D(−)-methiodide (XXXIX), m.p. 100–110° (isopropanol), $[\alpha]_D^{20} = -8.25$ (c = 2, H_2O). Calc. for $C_8H_{18}ONI$: C, 33.5; H, 6.3. Found: C, 33.8; H, 6.1%.

A 200-mg portion of the methiodide was hydrolyzed in 2 *N* hydrochloric acid as described above in the case of (XXVII). The resulting quaternary diol (XXVIII) had $[\alpha]_D^{20} = -0.44°$. Since the pure D(−) quaternary diol had $[\alpha]_D^{20} = -1.38°$ under the same conditions, the optical purity of the D(−)-*trans*-methiodide (XXXIX) obtained by resolution is 32%.

L(+)-trans-2-Methyl-4-dimethylaminomethyl-1,3-dioxolane Methiodide (XL)

The same procedure just described above in the case of (XXXIX) was applied throughout except that L-dibenzoyltartaric acid was used. The L-dibenzoyltartrate salt of (XXXVIII) had m.p. 131–132°, $[\alpha]_D^{20} = 85°$ (c = 2, methanol). Calc. for $C_{25}H_{27}O_{10}N$: C, 60.0; H, 5.4. Found: C, 60.1; H, 5.8%.

The L(+)-methiodide (XL) had m.p. 100–110°, $[\alpha]_D^{20} = 8.3°$ (c = 2, H_2O).

The quaternary diol (XXVIII) obtained by hydrolysis had $[\alpha]_D^{20} = 0.44°$. The optical purity of the L(+)-*trans*-methiodide (XL) obtained by resolution is therefore 32%.

With *cis*-2-methyl-4-dimethylaminomethyl-1,3-dioxolane (*cis*-X) no crystalline salts with D- or L-dibenzoyltartaric acid could be obtained.

2-Methyl-5-dimethylaminomethyl-oxazoline (XLIII) and Its Methiodide (XLIV)

After several trial runs, the following procedure proved to be the most convenient: to a solution of 30 g of N-acetyl-2,3-dibromo-1-propylamine (IXL) (prepared by bromination of N-allyl acetamide according to the literature) (26) in 130 ml of dry acetonitrile was added, with stirring, 16 g of dry and freshly precipitated silver carbonate. When all the silver carbonate appeared to have been converted to silver bromide (about 1/2 to 1 hour), it was quickly filtered and 100 ml of a 20% solution of dry dimethylamine in benzene was added. The mixture was stirred and allowed to stand overnight. Another portion of 16 g of dry silver carbonate was added and the precipitated silver bromide filtered off. The filtrate was evaporated *in vacuo* at 40° and the residue distilled *in vacuo*; at 57–58° at 5 mm, 8.5 g of colorless liquid (XLIII) was obtained. It gave a strong band at 1675 cm^{-1} in the infrared. Calc. for $C_7H_{14}ON_2$: C, 59.15; H, 9.85. Found: C, 59.30; H, 10.0%.

The *methiodide* (XLIV) was obtained in high yield by reacting the base with 20% less than the theoretical amount of methyl iodide in acetone (a purer product is obtained in this manner). The yield of colorless crystals, m.p. 134.5–135°, was quantitative (based on methyl iodide). The product can be recrystallized from methanol–acetone. Calc. for $C_8H_{17}ON_2I$: C, 33.8; H, 5.98. Found: C, 33.7; H, 5.88%.

N-Acetyl-N'-dimethyl-1,3-diamino-2-propanol Methiodide (VL) by Hydrolysis of (XLIV)

A solution of 100 mg of the quaternary iodide (XLIV) was heated to 100° in distilled water for 60 hours. The water was evaporated *in vacuo* and the residue crystallized from methanol–acetone, m.p. 119–120°, unchanged by recrystallization. It proved identical with an authentic sample of (VL) synthesized as described below.

1-Phthalimido-3-dimethylamino-2-propanol (IIIL)

A solution of 1-phthalimido-2,3-epoxypropane (40 g) in 250 ml of 20% dimethylamine in benzene was heated to 100° for 4 hours. Evaporation of the solvent gave (IIIL) as a viscous oil. Calc. for $C_{13}H_{16}O_3N_2$: C, 62.8; H, 6.5; N, 11.29. Found: C, 62.3; H, 6.9; N, 11.01%.

N-Acetyl-N'-dimethyl-1,3-diamino-2-propanol Methiodide (VL)

The preceding phthalimido derivative (IIIL) was hydrolyzed by heating under reflux with concentrated hydrochloric acid for 10 hours. The phthalic acid was filtered from the cooled solution and the filtrate concentrated *in vacuo* to give the dihydrochloride salt as an uncrystallizable oil. A crystalline dipicrate, m.p. 207–209° (isopropanol), was prepared. Calc. for $C_{17}H_{20}O_{15}N_8$: C, 35.4; H, 3.5. Found: C, 35.4; H, 3.5%.

The N,N-dimethyl-1,3-diamino-2-propanol dihydrochloride (0.04 mole) was converted to the N'-acetyl derivative by reaction with an equimolar amount of acetic anhydride in some water containing 4 g of sodium acetate. The reaction mixture stood for 2 hours, was neutralized with sodium hydroxide, and evaporated to dryness. The residue was extracted with alcohol–ether and the extract distilled; at 130° at 0.01 mm the acetyl derivative (IIL) was obtained as a vicous oil which could not be induced to crystallize. Calc. for $C_7H_{16}O_2N_2$: C, 52.5; H, 10.1. Found: C, 52.65; H, 10.1%.

The *methiodide* was obtained in the usual manner and crystallized from methanol–acetone, m.p. 119–120°. No depression of the melting point was observed when it was admixed with a sample secured by hydrolysis of (XLIV) as described above. The infrared spectra of the two compounds (Nujol mull) were superimposable. Calc. for $C_8H_{19}O_2N_2I$: C, 31.8; H, 6.3. Found: C, 31.9; H, 6.0%.

ACKNOWLEDGMENTS

The authors are grateful to the National Research Council of Canada for the financial support of this work.

REFERENCES

1. (*a*) F. Kögl, C. A. Salemink, H. Schouten, and F. Jellinek. Rec. trav. chim. **76**, 109 (1957). H. C. Cox, E. Hardegger, F. Kögl, P. Liechti, F. Lohse, and C. A. Salemink. Helv. Chim. Acta, **41** (1958).
(*b*) C. H. Eugster and P. G. Waser. Helv. Chim. Acta, **40**, 888 (1957). C. H. Eugster. Helv. Chim. Acta, **40**, 2462 (1957). C. H. Eugster, F. Höfliger, R. Denss, and E. Girod. Helv. Chim. Acta, **41**, 205, 583, 705, 886 (1958).
2. S. Wilkinson. Quart. Revs. (London), **15**, 153 (1961).
3. P. G. Waser. Experientia, **17**, 300 (1961).
4. B. Witkop, R. C. Durant, and S. L. Friess. Experientia, **15**, 300 (1959).
5. P. G. Waser. Experientia, **14**, 356 (1958).
6. S. L. Gyermeck and K. R. Unna. Proc. Soc. Exptl. Biol. Med. **98**, 882 (1958).
7. L. Gyermeck and K. R. Unna. J. Pharmacol. Exptl. Therap. **128**, 37 (1960).
8. L. Gyermeck and K. R. Unna. J. Pharmacol. Exptl. Therap. **128**, 30 (1960).
9. G. Zuricky, P. G. Waser, and C. H. Eugster. Helv. Chim. Acta, **42**, 1177 (1959).
10. P. G. Waser. Experientia, **16**, 347 (1960).
11. H. R. Ing, P. Kordik, and D. P. H. T. Williams. Brit. J. Pharmacol. **7**, 103 (1952).
12. E. J. Ariëns. Arzneimittel-Forsch. **6**, 282 (1956). E. J. Ariëns and J. M. van Rossum. Arch. Intern. Pharmacodynamie, **110**, 275 (1957). J. M. van Rossum. Arch. Intern. Pharmacodynamie, **118**, 418 (1959).
13. A. J. Clark. The mode of action of drugs on cells. Williams and Wilkins, Publ., Baltimore. 1937.
14. R. P. Stephenson. Brit. J. Pharmacol. **11**, 379 (1956).
15. W. D. M. Paton. Proc. Roy. Soc. (London), Ser. B, **154**, 21 (1961).
16. J. P. Fourneau, D. Bovet, F. Bovet, and G. Montézin. Bull. soc. chim. biol. **26**, 134, 516 (1944).
17. J. M. van Rossum. Ph.D. Thesis, R.C. University, Nijmegen. 1958. J. M. van Rossum and E. J. Ariëns. Experientia, **13**, 161 (1957).
18. H. J. Lucas and M. S. Guthrie. J. Am. Chem. Soc. **72**, 5490 (1950).
19. R. M. Hann and C. S. Hudson. J. Am. Chem. Soc. **64**, 2435 (1942).
20. A. C. Cope, E. Ciganek, L. J. Fleckenstein, and M. A. P. Meisinger. J. Am. Chem. Soc. **82**, 4651 (1960).
21. L. Goodman, S. Winstein, and R. Boschan. J. Am. Chem. Soc. **80**, 4312 (1958).
22. R. B. Barlow. Steric aspects of the chemistry and biochemistry of natural products. University Press, Cambridge. 1960. p. 46.
23. J. S. Brimacombe, A. B. Foster, and A. H. Haines. J. Chem. Soc. 2582 (1960).
24. H. Hibbert, J. G. Morazain, and A. Paquet. Can. J. Research, **2**, 131 (1930).
25. E. C. Baer. Biochem. Preparations, **2**, 31 (1952).
26. M. Bergmann, F. Dreyer, and F. Radt. Ber. B, **54**, 2139 (1921).

NOTES

PHOTOCONDUCTION OF CRYSTALLINE 9,10-DIBROMOANTHRACENE AND 9,10-DICHLOROANTHRACENE

I. C. Smith and E. Bock

It is well known that the absorption and fluorescence emission characteristics in organic crystals can be derived on a molecular basis; i.e. by postulating that crystal interactions exert only a small perturbing influence on the molecules of the crystal, and that the molecules retain their individuality to a large extent in the crystalline lattice. Recently several authors have applied a similar treatment to the process of photoconduction in organic crystals (1–4). According to these theories the major contribution to the photocurrent comes from molecules which have undergone radiationless transitions from the first excited singlet states to the first triplet states (4).

Craig and Hobbins (5) have shown that electronic transitions in the crystalline lattice depend to a large extent on vibrational interactions and multipole electrostatic interactions. This fact would lead one to expect that many strong transitions in the free molecule would be weakened in favor of the low-probability transitions; e.g. singlet–triplet transitions. Consequently, by the triplet-state theory, one would expect a higher order of photoconductivity in halogenated hydrocarbons than in the parent compounds (4). Indeed, as the work of Schneider *et al.* (6) on 9,10-dichloroanthracene has shown, the photocurrent in this compound is several orders of magnitude larger than in the parent hydrocarbon, anthracene. However, in a recent paper Kleinerman and McGlynn (7), on the basis of their results on the photoconductivity of acridine and phenazine—molecules in which the molecular energy levels are more suitably disposed for the population of the triplet state—suggest that the population of the triplet state may be detrimental to the photoconduction process.

In order to facilitate the elucidation of the role played by the triplet state in the photoconduction process we decided to investigate the photoconductivity of 9,10-dibromoanthracene, and also the temperature dependence of the photocurrent in 9,10-dichloroanthracene—a dependence not hitherto determined.

In what follows we give a brief account of our results. Further work is in progress, and we hope in the near future to expand upon this note.

All measurements were made on optically clear crystals grown from solution by cooling or by recirculating supersaturated solvent over seed crystals. The chemicals were purified by primary recrystallization, chromatography on columns of silica and alumina, and final recrystallization. These purifications, and the subsequent growth of crystals, were performed in subdued light under nitrogen. Some of the crystals were stored under nitrogen, but others were stored under air to see if this had any effect upon the surface photocurrent.

Only direct-current conductances were measured. The electrodes were always mounted on the same face of the prismatic crystals—a "surface cell" arrangement. Contact was made by thin platinum wires attached to the crystals by means of an alcoholic suspension of graphite. Except in special cases, all measurements were made *in vacuo* or under dry

nitrogen. The dependence of the surface photocurrents on applied field was found to be linear up to 3000 volt cm^{-1} for all crystals studied of each compound. The variation of the photocurrent in 9,10-dibromoanthracene with light intensity was also linear for the wavelengths 3650 Å, 4050 Å, and 4360 Å. The temperature dependence of the photocurrent fitted an expression of the form $i = i_0 \exp(-\Delta E/KT)$. For crystals stored under nitrogen, $\Delta E = 0.14 \pm .01$ ev. Crystals stored in air showed a discontinuity in a plot of $\log i$ versus $1/T$, yielding two straight lines of different slope. The high-temperature portions of these curves yielded $\Delta E = 0.11 \pm .01$ ev. The low-temperature portions gave $\Delta E = 0.20 \pm .01$ ev. This behavior is similar to that observed by Northrop and Simpson for the dark conductivity of solid solutions of aromatic hydrocarbons (8).

Crystals grown from solutions containing 0.001 mole of anthraquinone per mole of 9,10-dibromoanthracene also showed discontinuous temperature dependences. They yielded values for ΔE of $0.13 \pm .005$ and $0.17 \pm .01$ ev for the high- and low-temperature curves respectively. Crystals of 9,10-dichloroanthracene stored in air showed very little dependence upon temperature in the range 273–373° K. In fact some crystals showed a decrease in photocurrent for $T > 330°$. This is in agreement with work done by Bock, Ferguson, and Schneider (6). Low-temperature studies on these crystals gave exponential temperature dependences with $\Delta E = 0.16 \pm .01$ ev. A discontinuity occurred at approximately 200° K, and the low-temperature straight line gave $\Delta E = 0.23 \pm .01$ ev. Replacement of the nitrogen atmosphere above the crystals by oxygen resulted in an increase in the photocurrent in both 9,10-dichloro- and 9,10-dibromo-anthracene. The dependence of the photocurrent upon the partial pressure of ambient oxygen was found to concur with a Langmuir isotherm for a monomolecular adsorbed layer, as found by Bree and Lyons for anthracene (9). The effect of oxygen was reversible and could be removed by pumping. Ammonia gas was found to decrease the photocurrent in both compounds. Evidence for space charges in both compounds was found, indicating the presence of trapping centers in the crystals. The level of photoconductivity in the chloro compound was several orders of magnitude higher than that in the bromo compound under similar conditions.

These results show that 9,10-dichloroanthracene and 9,10-dibromoanthracene are easily oxidized on exposure to air, and that the oxidation products affect their surface photoconductivities. The reversibility with respect to adsorbed gases shows that the gases also affect the photocurrent through electrical double-layer formation. By analogy with the results of Northrop and Simpson (8) we quote photoconductivity activation energies of $0.14 \pm .01$ and $0.16 \pm .01$ ev for 9,10-dibromoanthracene and 9,10-dichloroanthracene respectively, and impurity activation energies of $0.19 \pm .015$ ev and $0.23 \pm .01$ ev. We quote $0.14 \pm .01$ ev for the activation energy of 9,10-dibromoanthracene, since this value was obtained from measurements on pure crystals which were stored in an atmosphere of dry nitrogen and showed no discontinuity in the temperature dependence over a range of 180 centigrade degrees. The earlier-mentioned value of 0.11 ev for the activation energy, obtained from measurements on crystals which were stored in air and hence were subject to surface oxidation of unknown extent, is significantly different from 0.14 ev, a difference of 0.03 ev, which is three times the estimated experimental precision of 0.01 ev. We are tempted to attribute this discrepancy to the unknown extent of surface oxidation and also to the unknown nature of the impurity resulting from oxidation. We are especially tempted to do so since the activation energies of crystals grown from pure compound, but doped with anthraquinone, the most likely oxidation product of 9,10-dibromoanthracene, yielded values of $0.13 \pm .01$ ev, which are

in agreement, within the experimental error, with the activation energy of pure 9,10-dibromoanthracene. Moreover, since the low-temperature straight-line plot of log i vs. $1/T$ for anthraquinone-doped crystals of 9,10-dibromoanthracene yielded an activation energy of 0.17 ev, and since the corresponding low-temperature lines for air-stored crystals of 9,10-dibromoanthracene and of 9,10-dichloroanthracene gave values of 0.19 ev and 0.23 ev respectively, we suggest that the impurity activation (8) is probably chiefly due to the presence of anthraquinone—the main impurity in these crystals. This suggestion, as to the nature of the main impurity, is in general agreement with the observation of other authors (10, 11). The relative orders of magnitude of the photocurrents are not what one would expect on the basis of the triplet-state theory. Further measurements on the dark conductivities are being made to confirm this statement. The effect of gases on the surface photocurrent shows the majority charge carriers to be positive holes.

ACKNOWLEDGMENTS

The authors are most grateful for the financial support given to this project by the National Research Council of Canada and the F. G. Cottrell Research Corporation grant.

1. L. E. Lyons and G. C. Morris. Proc. Phys. Soc. (London), **69**, 1162 (1956).
2. D. J. Carswell and L. E. Lyons. J. Chem. Soc. 1734 (1955).
3. A. N. Terenin. Radiotekh. i Elektron. **1**, 1127 (1956).
4. B. Rosenberg. J. Chem. Phys. **29**, 1108 (1958).
5. D. P. Craig and R. C. Hobbins. J. Chem. Soc. 539, 2309 (1955).
6. E. Bock, J. Ferguson, and W. G. Schneider. Can. J. Chem. **36**, 507 (1958).
7. M. Y. Kleinerman and S. P. McGlynn. Conference on Organic Semiconductors, Chicago. April, 1961.
8. D. C. Northrop and O. Simpson. Proc. Roy. Soc. (London), A, **234**, 124 (1956).
9. A. Bree and L. E. Lyons. J. Chem. Soc. 5179 (1960).
10. C. Dufraisse and J. Mathieu. Bull. soc. chim. France, 307 (1947).
11. S. P. McGlynn, M. Kasha, and M. R. Padhye. J. Chem. Phys. **24**, 588 (1956).

Received January 29, 1962.
Parker Chemistry Laboratory,
University of Manitoba,
Winnipeg, Manitoba.

CRYSTALLOGRAPHIC DATA FOR DI(PHENYLETHYNYL) MERCURY, POTASSIUM 2,4,6,2′,4′,6′-HEXANITRODIPHENYLAMIDE, AND *dl*-α-ALANINE HYDROCHLORIDE

J. Trotter

Preliminary X-ray examinations of three (unrelated) compounds have been carried out, but, for various reasons, detailed structural analyses are not proposed. The crystallographic data, which might be useful, are outlined in this note.

DI(PHENYLETHYNYL) MERCURY

Crystals of $(Ph.C{\equiv}C)_2Hg$ are small, colorless, diamond-shaped plates, with (100) developed and smaller {011} forms and occasionally (001) faces. The density was measured by flotation in aqueous silver nitrate, but as the crystals appeared to decompose fairly rapidly in this solution the value is only approximate. The unit cell dimensions and space group were determined from various rotation, oscillation, Weissenberg (Cu K_α), and precession (Mo K_α) photographs.

in agreement, within the experimental error, with the activation energy of pure 9,10-dibromoanthracene. Moreover, since the low-temperature straight-line plot of log i vs. $1/T$ for anthraquinone-doped crystals of 9,10-dibromoanthracene yielded an activation energy of 0.17 ev, and since the corresponding low-temperature lines for air-stored crystals of 9,10-dibromoanthracene and of 9,10-dichloroanthracene gave values of 0.19 ev and 0.23 ev respectively, we suggest that the impurity activation (8) is probably chiefly due to the presence of anthraquinone—the main impurity in these crystals. This suggestion, as to the nature of the main impurity, is in general agreement with the observation of other authors (10, 11). The relative orders of magnitude of the photocurrents are not what one would expect on the basis of the triplet-state theory. Further measurements on the dark conductivities are being made to confirm this statement. The effect of gases on the surface photocurrent shows the majority charge carriers to be positive holes.

ACKNOWLEDGMENTS

The authors are most grateful for the financial support given to this project by the National Research Council of Canada and the F. G. Cottrell Research Corporation grant.

1. L. E. Lyons and G. C. Morris. Proc. Phys. Soc. (London), **69**, 1162 (1956).
2. D. J. Carswell and L. E. Lyons. J. Chem. Soc. 1734 (1955).
3. A. N. Terenin. Radiotekh. i Elektron. **1**, 1127 (1956).
4. B. Rosenberg. J. Chem. Phys. **29**, 1108 (1958).
5. D. P. Craig and R. C. Hobbins. J. Chem. Soc. 539, 2309 (1955).
6. E. Bock, J. Ferguson, and W. G. Schneider. Can. J. Chem. **36**, 507 (1958).
7. M. Y. Kleinerman and S. P. McGlynn. Conference on Organic Semiconductors, Chicago. April, 1961.
8. D. C. Northrop and O. Simpson. Proc. Roy. Soc. (London), A, **234**, 124 (1956).
9. A. Bree and L. E. Lyons. J. Chem. Soc. 5179 (1960).
10. C. Dufraisse and J. Mathieu. Bull. soc. chim. France, 307 (1947).
11. S. P. McGlynn, M. Kasha, and M. R. Padhye. J. Chem. Phys. **24**, 588 (1956).

Received January 29, 1962.
Parker Chemistry Laboratory,
University of Manitoba,
Winnipeg, Manitoba.

CRYSTALLOGRAPHIC DATA FOR DI(PHENYLETHYNYL) MERCURY, POTASSIUM 2,4,6,2′,4′,6′-HEXANITRODIPHENYLAMIDE, AND *dl*-α-ALANINE HYDROCHLORIDE

J. Trotter

Preliminary X-ray examinations of three (unrelated) compounds have been carried out, but, for various reasons, detailed structural analyses are not proposed. The crystallographic data, which might be useful, are outlined in this note.

DI(PHENYLETHYNYL) MERCURY

Crystals of $(Ph.C{\equiv}C)_2Hg$ are small, colorless, diamond-shaped plates, with (100) developed and smaller {011} forms and occasionally (001) faces. The density was measured by flotation in aqueous silver nitrate, but as the crystals appeared to decompose fairly rapidly in this solution the value is only approximate. The unit cell dimensions and space group were determined from various rotation, oscillation, Weissenberg (Cu K_α), and precession (Mo K_α) photographs.

Crystal Data

Di(phenylethynyl) mercury, $C_{16}H_{10}Hg$: molecular weight = 402.9; melting point = 125°.

Monoclinic; $a = 32.3 \pm 0.1$, $b = 17.90 \pm 0.05$, $c = 19.63 \pm 0.05$ Å; $\beta = 110.8 \pm 0.5°$.

Volume of the unit cell = 10612 Å^3.

Density: calculated (with $Z = 32$), 2.0, measured, ~2 g cm^{-3}.

Absorption coefficients for X rays: $\lambda = 1.542$ Å, $\mu = 114$ cm^{-1}; $\lambda = 0.7107$ Å, $\mu = 66$ cm^{-1}.

Total number of electrons per unit cell = $F(000) = 5952$.

Absent spectra: $h0l$ when l is odd, $0k0$ when k is odd; space group is $P2_1/c$.

In addition to the systematically absent reflections, all reflections with $(h+k)$ odd are either absent or very weak, indicating a C-centered arrangement of Hg atoms. However, the long crystal axes and large number of molecules in the cell make the structure too complex for detailed analysis. The presence of 32 molecules in a cell requiring only four asymmetric crystal units suggested that the molecule might be an octamer, but measurement of the molecular weight in camphor by the Rast method gave a value of 373, corresponding to a monomer. The forces holding the eight units together in the crystal are probably then only of the van der Waals type.

POTASSIUM HEXANITRODIPHENYLAMIDE

The structure of the potassium salt of 2,4,6,2′,4′,6′-hexanitrodiphenylamine was investigated because of an interest in the structure of the anion. It was hoped that some useful information about its symmetry might be obtained from the space group and the number of molecules in the cell. The density was measured by displacement of carbon tetrachloride, and the cell dimensions and space group were determined from precession films (Mo K_α).

Crystal Data

Potassium 2,4,6,2′,4′,6′-hexanitrodiphenylamide, $C_{12}H_4N_7O_{12}K$: mol. wt. = 477.3.

Monoclinic; $a = 12.20 \pm 0.03$, $b = 13.01 \pm 0.03$, $c = 10.97 \pm 0.03$ Å; $\beta = 94.4 \pm 0.2°$.

Volume of the unit cell = 1736 Å^3.

D_{calc} ($Z = 4$) = 1.815, D_{meas} = 1.81 g cm^{-3}.

Absorption coefficient for X rays: $\lambda = 0.7107$ Å, $\mu = 4.4$ cm^{-1}.

Total number of electrons per unit cell = $F(000) = 960$.

Absent spectra: $(h0l)$ when $(h+l)$ is odd, $0k0$ when k is odd; space group is $P2_1/n$.

No information regarding the symmetry of the anion can be deduced from the crystal data, three-dimensional methods would be required to determine the structure, and the potassium ion is not heavy enough to apply the heavy-atom method (for the light atoms $\sum f_j^2 = 1562$; for K^+, $f^2 = 324$). Detailed analysis is therefore not being carried out.

dl-α-ALANINE HYDROCHLORIDE

Crystals of *dl*-α-alanine ethyl ester hydrochloride were examined to assist in the interpretation of the e.s.r. spectra of irradiated crystals. Specimens suitable for recording e.s.r. (and X-ray) data were obtained from Eastman Kodak CP grade by slow recrystallization from water. These crystals were thick plates elongated along the c-axis with (100) developed and smaller (001) faces. The density was measured by flotation in a benzene–CCl_4 mixture, and the crystal data determined from precession films (Mo K_α).

It was immediately apparent that an integral number of molecules of *dl*-alanine ethyl ester hydrochloride (molecular weight = 154) could not be accommodated in the unit

cell, so that the crystals under examination must be some other compound. Assumption of four molecules in the cell corresponded to a molecular weight of 125 (*dl*-alanine ethyl ester has molecular weight 117, and *dl*-alanine hydrochloride 126). Analysis of the original specimen indicated that it was the ethyl ester hydrochloride. (Found: C, 39.04; H, 7.84; N, 9.20%. Calc. for $C_5H_{12}O_2NCl$: C, 39.09; H, 7.87; N, 9.12%.) The recrystallized material, however, gave a different result (together with a positive test for chloride), which indicated that it must be *dl*-alanine hydrochloride. (Found: C, 29.78; H, 6.82; N, 11.03%. Calc. for $C_3H_8O_2NCl$: C, 28.70; H, 6.42; N, 11.16%.) Either, then, the ester has been hydrolyzed during crystallization (an unlikely occurrence) or, more probably, the original material contains a small quantity of *dl*-alanine hydrochloride as an impurity, which has crystallized preferentially. The C and H analyses suggest that the crystals contain a small amount of the ethyl ester hydrochloride. (Calc. for $0.93C_3H_8O_2NCl$: $0.07C_5H_{12}O_2NCl$: C, 29.57; H, 6.54; N, 10.98%.)

Crystal Data

dl-α-Alanine hydrochloride, $C_3H_8NO_2Cl$ (slightly impure—probably contains about 7% ethyl ester): mol. wt. = 125.6.

Monoclinic; $a = 9.20 \pm 0.02$, $b = 9.04 \pm 0.02$, $c = 7.31 \pm 0.02$ Å; $\beta = 95° 21' \pm 5'$.

Volume of the unit cell = 605.3 Å^3.

D_{calc} ($Z = 4$) = 1.37, D_{meas} = 1.36 g cm^{-3}.

Absorption coefficient for X rays: $\lambda = 0.7107$ Å, $\mu = 5.4$ cm^{-1}.

$F(000) = 264$.

Absent spectra: $h0l$ when l is odd, $0k0$ when k is odd; space group is $P2_1/c$.

No further work on these crystals is proposed.

The author thanks the National Research Council for financial support, and Dr. W. McCrae, Dr. R. Stewart, Professor C. A. McDowell, and Dr. W. C. Lin for crystal samples.

Received February 20, 1962.
Department of Chemistry,
University of British Columbia,
Vancouver 8, British Columbia.

THE EFFECT OF PRESSURE ON THE SPONTANEOUS HYDROLYSIS OF ACETYL PHOSPHATE MONO-ANION AND DI-ANION AND OF ACETYL PHENYL PHOSPHATE MONO-ANION[1]

G. Di Sabato,[2] W. P. Jencks,[2] and E. Whalley[3]

The spontaneous hydrolysis of acetyl phosphate mono-anion and di-anion and of acetyl phenyl phosphate has been studied in a number of ways in order to determine the mechanisms (1). The effect of pressure on the rates of reactions in solution has been used

[1]*Issued as contribution No. 146 from the Graduate Department of Biochemistry, Brandeis University, Waltham 54, Massachusetts, and as N.R.C. No. 6804 from the National Research Council, Ottawa, Canada. Supported in part by the National Cancer Institute of the National Institutes of Health (Grant C-3975, Training Grant CRT-5033) and the National Science Foundation.*
[2]*Graduate Department of Biochemistry, Brandeis University, Waltham 54, Massachusetts.*
[3]*Division of Applied Chemistry, National Research Council, Ottawa, Canada.*

cell, so that the crystals under examination must be some other compound. Assumption of four molecules in the cell corresponded to a molecular weight of 125 (*dl*-alanine ethyl ester has molecular weight 117, and *dl*-alanine hydrochloride 126). Analysis of the original specimen indicated that it was the ethyl ester hydrochloride. (Found: C, 39.04; H, 7.84; N, 9.20%. Calc. for $C_5H_{12}O_2NCl$: C, 39.09; H, 7.87; N, 9.12%.) The recrystallized material, however, gave a different result (together with a positive test for chloride), which indicated that it must be *dl*-alanine hydrochloride. (Found: C, 29.78; H, 6.82; N, 11.03%. Calc. for $C_3H_8O_2NCl$: C, 28.70; H, 6.42; N, 11.16%.) Either, then, the ester has been hydrolyzed during crystallization (an unlikely occurrence) or, more probably, the original material contains a small quantity of *dl*-alanine hydrochloride as an impurity, which has crystallized preferentially. The C and H analyses suggest that the crystals contain a small amount of the ethyl ester hydrochloride. (Calc. for $0.93C_3H_8O_2NCl$: $0.07C_5H_{12}O_2NCl$: C, 29.57; H, 6.54; N, 10.98%.)

Crystal Data

dl-α-Alanine hydrochloride, $C_3H_8NO_2Cl$ (slightly impure—probably contains about 7% ethyl ester): mol. wt. = 125.6.

Monoclinic; $a = 9.20 \pm 0.02$, $b = 9.04 \pm 0.02$, $c = 7.31 \pm 0.02$ Å; $\beta = 95° 21' \pm 5'$.

Volume of the unit cell = 605.3 Å^3.

D_{calc} ($Z = 4$) = 1.37, D_{meas} = 1.36 g cm^{-3}.

Absorption coefficient for X rays: $\lambda = 0.7107$ Å, $\mu = 5.4$ cm^{-1}.

$F(000) = 264$.

Absent spectra: $h0l$ when l is odd, $0k0$ when k is odd; space group is $P2_1/c$.

No further work on these crystals is proposed.

The author thanks the National Research Council for financial support, and Dr. W. McCrae, Dr. R. Stewart, Professor C. A. McDowell, and Dr. W. C. Lin for crystal samples.

Received February 20, 1962.
Department of Chemistry,
University of British Columbia,
Vancouver 8, British Columbia.

THE EFFECT OF PRESSURE ON THE SPONTANEOUS HYDROLYSIS OF ACETYL PHOSPHATE MONO-ANION AND DI-ANION AND OF ACETYL PHENYL PHOSPHATE MONO-ANION[1]

G. Di Sabato,[2] W. P. Jencks,[2] and E. Whalley[3]

The spontaneous hydrolysis of acetyl phosphate mono-anion and di-anion and of acetyl phenyl phosphate has been studied in a number of ways in order to determine the mechanisms (1). The effect of pressure on the rates of reactions in solution has been used

[1]*Issued as contribution No. 146 from the Graduate Department of Biochemistry, Brandeis University, Waltham 54, Massachusetts, and as N.R.C. No. 6804 from the National Research Council, Ottawa, Canada. Supported in part by the National Cancer Institute of the National Institutes of Health (Grant C-3975, Training Grant CRT-5033) and the National Science Foundation.*
[2]*Graduate Department of Biochemistry, Brandeis University, Waltham 54, Massachusetts.*
[3]*Division of Applied Chemistry, National Research Council, Ottawa, Canada.*

to help determine mechanisms (2). In this note the effect of pressure up to about 2.5 kilobars on the rates of hydrolysis of acetyl phosphate mono-anion and di-anion and of acetyl phenyl phosphate is described and the results are discussed in relation to the mechanisms.

EXPERIMENTAL METHODS AND RESULTS

The analytical and high-pressure techniques have been described in previous papers (1, 3). The buffer solutions were as described by Di Sabato and Jencks (1); the effect of pressures up to 2.5 kilobars on the pH of the buffers is not enough to change significantly the relative concentrations of the ions of the substituted phosphates. The first-order rate constants are listed in Table I, and shown graphically in Fig. 1. The accuracy is about 5%.

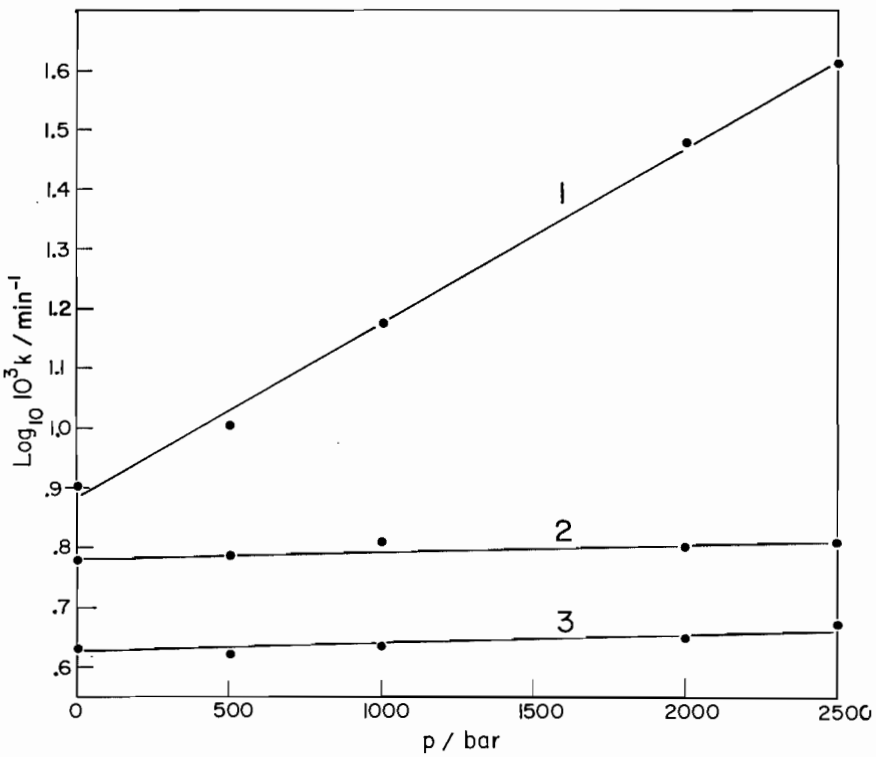

FIG. 1. Effect of pressure on the spontaneous hydrolysis of: curve 1, acetyl phenyl phosphate mono-anion at 60° C, ordinate increased 0.9 units; curve 2, acetyl phosphate mono-anion at 39° C, ordinate decreased 0.4 units; curve 3, acetyl phosphate di-anion at 39° C.

The volumes of activation $\Delta V‡$ at zero pressure calculated from the usual relation $\partial \ln k/\partial p = -\Delta V‡/RT$ are as follows:

acetyl phosphate mono-anion	$-0.6\pm\sim1.0$ cm^3 mole^{-1} at 39° C
acetyl phosphate di-anion	$-1.0\pm\sim1.0$ cm^3 mole^{-1} at 39° C
acetyl phenyl phosphate mono-anion	$-19\pm\sim2$ cm^3 mole^{-1} at 60° C

DISCUSSION

The main mechanisms of hydrolysis to be considered appear to be a unimolecular decomposition of the anion, a bimolecular reaction of water with the anion, and a bimolecular reaction of hydroxide ion with the conjugate acid of the anion.

TABLE I

Spontaneous hydrolysis of acetyl phosphate mono-anion and di-anion and of acetyl phenyl phosphate

Substrate	Temperature/°C	p/kilobar	10^3k/min^{-1}
Acetyl phosphate di-anion*†	39.0	0	4.20, 4.39
		0.5	4.19, 4.15
		1.0	4.32, 4.26
		2.0	4.41, 4.47
		2.5	4.59, 4.35
Acetyl phosphate mono-anion†‡	39.0	0	15.3, 15.0
		0.5	15.5, 15.0
		1.0	15.9, 16.5
		2.0	15.6, 16.0
		2.5	15.9, 15.6
Acetyl phenyl phosphate mono-anion†§	60.0	0	1.00, 1.01
		0.5	1.33, 1.19
		1.0	1.87
		2.0	3.82, 3.71
		2.5	5.43, 5.30

*Potassium phosphate buffer, 0.1 M, pH 6.7 at 1 atm.
†Ionic strength brought to 0.6 with KCl.
‡Potassium formate buffer, 0.2 M, pH 2.9 at 1 atm.
§Potassium phenyl phosphate buffer, 0.1 M, pH 4.8 at 1 atm. Control experiments showed no hydrolysis of the buffer under the experimental conditions employed.

The spontaneous hydrolyses of acetyl phosphate mono-anion and di-anion occur with P—O bond cleavage (4, 5). The volumes of activation are $-0.6\pm\sim1.0$ cm^3 mole^{-1} for the mono-anion and $-1.0\pm\sim1.0$ cm^3 mole^{-1} for the di-anion. If the mechanisms involved the attack of water on the phosphorus atom, then the volumes of activation should be considerably more negative because volume would be lost due to the formation of a partial valence bond and to a possible increased polarity. If the mechanism involved a reaction of hydroxide ion with the conjugate acid of the phosphate ion then, from arguments similar to those developed below for acetyl phenyl phosphate mono-anion, a large negative volume of activation would also be expected. For the di-anion, therefore, the mechanism is probably a unimolecular decomposition to give metaphosphate ion (1):

$$CH_3CO_2PO_3^{2-} \xrightarrow{\text{slow}} CH_3CO_2^- + PO_3^- \xrightarrow[\text{fast}]{H_2O} H_2PO_4^-, \qquad [1]$$

as is suggested (6–8) for the hydrolysis of phosphate monoester mono-anions. For the mono-anion, both a similar mechanism,

$$CH_3CO_2PO_3H^- \xrightarrow{\text{slow}} CH_3CO_2^- + HPO_3 \xrightarrow[\text{fast}]{H_2O} H_2PO_4^- + H^+, \qquad [2]$$

and one in which a proton has been transferred to the leaving acetate group and the transition state is close to acetic acid and metaphosphate ion are consistent with the volume of activation.

The hydrolysis of acetyl phenyl phosphate mono-anion in 90% aqueous methanol occurs with C—O bond cleavage (1) and we shall assume that this also occurs in aqueous solution. The rate is decreased 2.5-fold in deuterium oxide solution (1) and the entropy and volume of activation are, respectively, -28.8 cal deg^{-1} mole^{-1} (1) and -19 cm^3 mole^{-1}. The volume of activation does not allow us to distinguish between the possible

mechanisms, as the following considerations show. A unimolecular decomposition to give acylium ion:

$$CH_3COOPO_3C_6H_5^- \rightarrow CH_3CO^+ + C_6H_5OPO_3^{2-}, \quad [3]$$

is consistent with the volume and entropy of activation, because the polarity is greatly increased in the transition state. However, the relatively large effect of solvent deuterium oxide, which seems to require that at least one O—H (O—D in deuterium oxide) bond be strongly modified in the transition state, and the great stability of benzoyl phenyl phosphate (9) are difficult to explain by this mechanism. A bimolecular reaction involving solvent could proceed through transition states I, II, III, or IV, which differ in the position

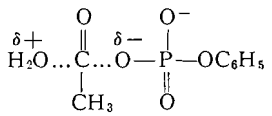

I

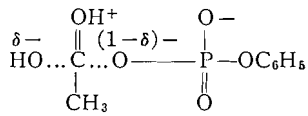

II

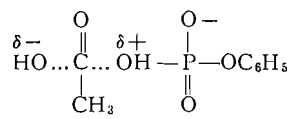

III

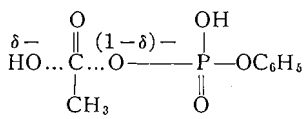

IV

of a proton. Each has, of course, resonating forms. The structures might be further modified if the incoming group adds rather than substitutes, as has been suggested (10) for some carboxyl reactions, and if several water molecules are incorporated into the transition state to aid in proton transfer (1, 11). All of these mechanisms appear to be consistent with the volume of activation and other (1) data. It is interesting to compare the experimental data with calculated values for a special case of mechanism IV, according to reactions [4] and [5]:

$$CH_3COOPO_3C_6H_5^- + H_2O \overset{\text{fast}}{\rightleftharpoons} CH_3COOPO_3HC_6H_5 + OH^- \quad [4]$$

$$CH_3COOPO_3HC_6H_5 + OH^- \xrightarrow{\text{slow}} CH_3COOH + C_6H_5PO_4H^-. \quad [5]$$

It seems likely that the volume and entropy change and the deuterium isotope effect of reaction [4] will be similar to those for the reaction

$$H_2PO_4^- + H_2O \rightleftharpoons H_3PO_4 + OH^-, \quad [6]$$

and those for reaction [5] will be similar to those for the alkaline hydrolysis of esters, in which a hydroxide ion also attacks an acetate group:

$$CH_3COOR + OH^- \rightarrow CH_3COOH + OR^-. \quad [7]$$

The thermodynamic parameters for reaction [6] can be obtained from those for the reactions

$$H_3PO_4 \rightleftharpoons H_2PO_4^- + H^+ \quad [8]$$

and

$$H_2O \rightleftharpoons H^+ + OH^-. \quad [9]$$

The data are given in Table II. They are mostly for temperatures near 25° C but this should not affect the conclusions in any important way. It is clear that the volume and entropy of activation and the deuterium isotope effect are quantitatively consistent with the mechanism given in reactions [4] and [5].

TABLE II

Reaction No.	ΔV/cm³ mole^{-1}	ΔS/cal deg^{-1} mole^{-1}	K_H/K_D or k_H/k_D
8 equil.	−15.1 (12)	−15.6 (15, p. 758)	1.61 (17)
9 equil.	−23.4 (13)	−18.7 (15, p. 667)	5.43 (17–19)
6 equil.	−7.9	−3.0	3.37
7 rate	−9 (14)	−27 (16)	0.75 (20)
4 and 5 rate, expected value	−17	−30	2.53
Exptl. value	−19±~2 (this work)	−28.8 (1)	2.5 (1)

NOTE: K_H/K_D and k_H/k_D are the ratio of equilibrium and rate constants in H_2O and D_2O.

1. G. DI SABATO and W. P. JENCKS. J. Am. Chem. Soc. **83**, 4393, 4400 (1961).
2. E. WHALLEY. Trans. Faraday Soc. **55**, 798 (1959), and later papers.
3. J. KOSKIKALLIO and E. WHALLEY. Trans. Faraday Soc. **55**, 809 (1959). A. R. OSBORN and E. WHALLEY. Can. J. Chem. **39**, 1094 (1961).
4. R. BENTLEY. J. Am. Chem. Soc. **71**, 2765 (1949).
5. J. H. PARK and D. E. KOSHLAND. J. Biol. Chem. **233**, 986 (1958).
6. W. W. BUTCHER and F. H. WESTHEIMER. J. Am. Chem. Soc. **77**, 2420 (1955).
7. J. KUMAMOTO and F. H. WESTHEIMER. J. Am. Chem. Soc. **77**, 2515 (1955).
8. C. A. BUNTON, D. R. LLEWELLYN, K. G. OLDHAM, and C. A. VERNON. J. Chem. Soc. 3574 (1958).
9. H. CHANTRENNE. Biochim. et Biophys. Acta, **2**, 286 (1948).
10. M. L. BENDER. J. Am. Chem. Soc. **73**, 1626 (1951).
11. W. P. JENCKS and J. CARRIUOLO. J. Am. Chem. Soc. **83**, 1743 (1961).
12. S. D. HAMANN and S. D. LIM. Australian J. Chem. **7**, 329 (1954). A. J. ELLIS and D. W. ANDERSON. J. Chem. Soc. 1765 (1961).
13. B. B. OWEN and S. R. BRINKLEY. Chem. Revs. **29**, 461 (1941).
14. K. J. LAIDLER and D. CHEN. Trans. Faraday Soc. **54**, 1026 (1958).
15. H. S. HARNED and B. B. OWEN. Physical chemistry of electrolytic solutions. 3rd ed. Reinhold Publishing Corp. 1958.
16. F. TOMMILA, A. KOIVISTO, J. P. LYYRA, K. ANTELL, and S. HEIMO. Ann. Acad. Sci. Fennicae. A, II, No. 47 (1952).
17. G. SCHWARZENBACH, A. EPPRECHT, and H. ERLENMEYER. Helv. Chim. Acta, **19**, 1292 (1936).
18. W. F. K. WYNNE-JONES. Trans. Faraday Soc. **32**, 1397 (1936).
19. E. ABEL, E. BRATU, and O. REDLICH. Z. physik. Chem. (Leipzig), A, **173**, 353 (1935).
20. W. F. K. WYNNE-JONES. Chem. Revs. **17**, 115 (1935).

RECEIVED JANUARY 29, 1962.
GRADUATE DEPARTMENT OF BIOCHEMISTRY,
BRANDEIS UNIVERSITY,
WALTHAM, MASS., U.S.A.,
AND
DIVISION OF APPLIED CHEMISTRY,
NATIONAL RESEARCH COUNCIL,
OTTAWA, CANADA.

ULTRAVIOLET SPECTRA OF SOME SUBSTITUTED STYRENES[1]

OWEN H. WHEELER AND CELIA B. COVARRUBIAS

Styrene has its main ultraviolet absorption band at 250 mμ (1–4). Methyl groups in the ortho positions have been found (1) to force the ethylenic group out of resonance

[1]*Contribution No. 125 from the Instituto de Quimica de la Universidad Nacional Autonoma de Mexico, Mexico, D.F.*

The data are given in Table II. They are mostly for temperatures near 25° C but this should not affect the conclusions in any important way. It is clear that the volume and entropy of activation and the deuterium isotope effect are quantitatively consistent with the mechanism given in reactions [4] and [5].

TABLE II

Reaction No.	ΔV/cm³ mole^{-1}	ΔS/cal deg^{-1} mole^{-1}	K_H/K_D or k_H/k_D
8 equil.	−15.1 (12)	−15.6 (15, p. 758)	1.61 (17)
9 equil.	−23.4 (13)	−18.7 (15, p. 667)	5.43 (17–19)
6 equil.	−7.9	−3.0	3.37
7 rate	−9 (14)	−27 (16)	0.75 (20)
4 and 5 rate, expected value	−17	−30	2.53
Exptl. value	−19±~2 (this work)	−28.8 (1)	2.5 (1)

NOTE: K_H/K_D and k_H/k_D are the ratio of equilibrium and rate constants in H_2O and D_2O.

1. G. DI SABATO and W. P. JENCKS. J. Am. Chem. Soc. **83**, 4393, 4400 (1961).
2. E. WHALLEY. Trans. Faraday Soc. **55**, 798 (1959), and later papers.
3. J. KOSKIKALLIO and E. WHALLEY. Trans. Faraday Soc. **55**, 809 (1959). A. R. OSBORN and E. WHALLEY. Can. J. Chem. **39**, 1094 (1961).
4. R. BENTLEY. J. Am. Chem. Soc. **71**, 2765 (1949).
5. J. H. PARK and D. E. KOSHLAND. J. Biol. Chem. **233**, 986 (1958).
6. W. W. BUTCHER and F. H. WESTHEIMER. J. Am. Chem. Soc. **77**, 2420 (1955).
7. J. KUMAMOTO and F. H. WESTHEIMER. J. Am. Chem. Soc. **77**, 2515 (1955).
8. C. A. BUNTON, D. R. LLEWELLYN, K. G. OLDHAM, and C. A. VERNON. J. Chem. Soc. 3574 (1958).
9. H. CHANTRENNE. Biochim. et Biophys. Acta, **2**, 286 (1948).
10. M. L. BENDER. J. Am. Chem. Soc. **73**, 1626 (1951).
11. W. P. JENCKS and J. CARRIUOLO. J. Am. Chem. Soc. **83**, 1743 (1961).
12. S. D. HAMANN and S. D. LIM. Australian J. Chem. **7**, 329 (1954). A. J. ELLIS and D. W. ANDERSON. J. Chem. Soc. 1765 (1961).
13. B. B. OWEN and S. R. BRINKLEY. Chem. Revs. **29**, 461 (1941).
14. K. J. LAIDLER and D. CHEN. Trans. Faraday Soc. **54**, 1026 (1958).
15. H. S. HARNED and B. B. OWEN. Physical chemistry of electrolytic solutions. 3rd ed. Reinhold Publishing Corp. 1958.
16. F. TOMMILA, A. KOIVISTO, J. P. LYYRA, K. ANTELL, and S. HEIMO. Ann. Acad. Sci. Fennicae. A, II, No. 47 (1952).
17. G. SCHWARZENBACH, A. EPPRECHT, and H. ERLENMEYER. Helv. Chim. Acta, **19**, 1292 (1936).
18. W. F. K. WYNNE-JONES. Trans. Faraday Soc. **32**, 1397 (1936).
19. E. ABEL, E. BRATU, and O. REDLICH. Z. physik. Chem. (Leipzig), A, **173**, 353 (1935).
20. W. F. K. WYNNE-JONES. Chem. Revs. **17**, 115 (1935).

RECEIVED JANUARY 29, 1962.
GRADUATE DEPARTMENT OF BIOCHEMISTRY,
BRANDEIS UNIVERSITY,
WALTHAM, MASS., U.S.A.,
AND
DIVISION OF APPLIED CHEMISTRY,
NATIONAL RESEARCH COUNCIL,
OTTAWA, CANADA.

ULTRAVIOLET SPECTRA OF SOME SUBSTITUTED STYRENES[1]

OWEN H. WHEELER AND CELIA B. COVARRUBIAS

Styrene has its main ultraviolet absorption band at 250 mμ (1–4). Methyl groups in the ortho positions have been found (1) to force the ethylenic group out of resonance

[1]*Contribution No. 125 from the Instituto de Quimica de la Universidad Nacional Autonoma de Mexico, Mexico, D.F.*

conjugation with the benzene ring and reduce the intensity of absorption without significantly changing the wavelength. Very few data exist in the literature concerning the absorption of substituted styrenes (2, 6–8) and accordingly a number of ortho and para methoxy- and halogeno-substituted styrenes have been prepared and their ultraviolet spectra recorded.

Apart from the main maximum at 250–275 mμ, other weaker bands were also found in some cases at higher wavelength (styrene 282 (60), 290 (30); *o*-methoxystyrene 320 (1440); *o*-chlorostyrene 295 (840)) and such bands, although often of higher intensity, have been previously reported (2–4, 6–8). It seems unlikely that a simple chromophore like styrene would have other maxima above 280 mμ of high intensity, although weak *B* bands can be expected, and part of this extra absorption may be due to polymerized material in solution.

A *p*-methoxy group produced a large displacement (+26 mμ) in the 250 mμ maximum and the para halogeno atoms caused smaller displacements of about the same order (10 mμ). These shifts are consistent with the electronic effects of these substituents (5). The corresponding ortho isomers all showed smaller displacements than the para compounds and the intensities were considerably reduced. Such effects are typically steric in origin (1, 5). Since the styrenes polymerize in solution, the recorded intensity values cannot be considered reliable. However, the ratios of intensities of the para to ortho isomers were MeO ~ Cl > Br, the order expected on the basis of the steric interference of these groups.

EXPERIMENTAL

Styrenes

The substituted styrenes were prepared from the corresponding substituted benzaldehydes by reaction with methyl magnesium iodide in ether and dehydration of the so-formed phenylcarbinol by distillation with potassium bisulphate (9). The styrenes formed by the decarboxylation of the cinnamic acids (10) were less pure and readily polymerized. The styrenes were all redistilled by short-path distillation at 5 mm with a bath temperature of 100–120°. Their refractive indices are given in Table I.

TABLE I*

	λ_{max}		n_D^{25}
Styrene	249	(15,500)	1.5458
p-Methyl	251.5	(9,000)†	—
o-Methyl	245	(12,600)‡	—
	246	(2,300)§	—
p-Methoxy	275	(19,900)	1.5600
o-Methoxy	253	(6,800)	1.5650
p-Chloro	259	(15,600)	1.5575
	254	(20,000)‖	—
o-Chloro	250	(6,900)	1.5595
p-Bromo	258	(16,700)	1.5720
o-Bromo	254	(4,600)	1.5785
p-Iodo	260	(18,650)	(m.p. 44°)¶

*λ in mμ; molar extinction coefficients in parenthesis; data determined in 95% ethanol.
†Ref. 6 in water.
‡Ref. 2.
§Ref. 7.
‖Ref. 8.
¶From ethanol.

o-Methoxybenzaldehyde was prepared by methylation of salicylaldehyde (11) and many of the halogenobenzaldehydes by Etard oxidation of the corresponding toluenes (12).

Spectra

The ultraviolet spectra were determined on freshly distilled or recrystallized samples using 95% ethanol. A Beckman D.K.2 spectrophotometer was employed under normal operating conditions.

1. E. A. BRAUDE and F. SONDHEIMER. J. Chem. Soc. 3773 (1955).
2. P. RAMART-LUCAS and J. HOCH. Bull. soc. chim. France, 327 (1935); 848 (1938).
3. E. A. BRAUDE. J. Chem. Soc. 1902 (1949).
4. C. G. OVERBURGER and D. TANNER. J. Am. Chem. Soc. **77**, 369 (1955).
5. O. H. WHEELER and P. H. GORE. J. Org. Chem. **26**, 3298 (1961).
6. R. ANDRISANO and A. TUNDO. Atti accad. naz. Lincei. Rend. Classe sci. fis. mat. e nat. **13**, [8], 158 (1952).
7. Y. HIRSHBERG. J. Am. Chem. Soc. **71**, 3241 (1949).
8. D. W. ADAMSON, P. A. BARRETT, J. W. BILLINGHURST, and T. S. G. JONES. J. Chem. Soc. 2315 (1957).
9. C. G. OVERBERGER, J. H. SAUNDERS, R. E. ALLEN, and R. GANDER. Org. Syntheses, Coll. Vol. III, 200 (1955). C. G. OVERBERGER and J. H. SAUNDERS. Org. Syntheses, Coll. Vol. III, 204 (1955).
10. G. WALLING and K. B. WOLFSTIRN. J. Am. Chem. Soc. **69**, 852 (1947).
11. A. I. VOGEL. Practical organic chemistry. Longmans, Green and Co., New York, N.Y. 1948. p. 640.
12. O. H. WHEELER. Can. J. Chem. **36**, 667 (1958).

RECEIVED AUGUST 3, 1961.
DEPARTMENT OF CHEMISTRY,
UNIVERSITY OF PUERTO RICO,
MAYAGUEZ, PUERTO RICO,
AND
INSTITUTO DE QUIMICA,
UNIVERSIDAD NACIONAL AUTONOMA DE MEXICO,
MEXICO 20, D.F.

SPECTROPHOTOMETRIC OBSERVATIONS ON THE CLEAVAGE OF *vic*-DIOLS BY LEAD TETRAACETATE[1]

A. S. PERLIN AND S. SUZUKI[2]

Oxidative cleavage of *vic*-diols and related groups by lead tetraacetate (1) is generally detected and estimated by iodometric titration. An alternative, and in some ways advantageous, means for examining such reactions is offered by the fact that tetravalent lead may be estimated spectrophotometrically (2). Measurements are made at 280–300 mμ, a region in which absorption by Pb (IV) is not maximal (2) (see also Fig. 1, curve A) but in which there is no interference from acetic acid (a reaction product and also the most common solvent) nor from divalent lead.

With the spectrophotometric method lead tetraacetate oxidations can be carried out at higher dilution (ca. 10^{-4} M) than formerly. One advantage gained in this way is that reaction rates for very fast glycols (such as those in which the dihedral angle of the carbon–oxygen bonds approximates 0 degree (3, 4)) are slowed sufficiently[3] for satisfactory measurement, particularly with a recording spectrophotometer. To illustrate, the rate of cleavage of the 2,3-*cis* diol of methyl α- or β-D-erythrofuranoside was found earlier (5) to be virtually instantaneous even at 0° C, so that comparative data were not available. However, the rate for each compound at high dilution has now been estimated readily, and a substantial anomeric difference detected. As with the very much slower methyl D-threofuranosides (5), the 1,2-*cis*-alkoxy-hydroxy anomer (α-D-erythroside) was found to be more reactive than the 1,2-*trans* anomer, the ratio of their second-order rate constants being 3.5 to 1.

[1]*Issued as N.R.C. No. 6821.*
[2]*National Research Council of Canada Postdoctorate Fellow, 1960–61.*
[3]*The retarding effect of high dilution on the oxidation rate of relatively slow glycols (e.g., those of 6-membered ring or acyclic compounds) is very marked. Hence, in using the spectrophotometric method as a microprocedure for examining compounds of this type it may be desirable to accelerate the oxidation with potassium acetate (6, 7; see experimental section).*

1. E. A. BRAUDE and F. SONDHEIMER. J. Chem. Soc. 3773 (1955).
2. P. RAMART-LUCAS and J. HOCH. Bull. soc. chim. France, 327 (1935); 848 (1938).
3. E. A. BRAUDE. J. Chem. Soc. 1902 (1949).
4. C. G. OVERBURGER and D. TANNER. J. Am. Chem. Soc. **77**, 369 (1955).
5. O. H. WHEELER and P. H. GORE. J. Org. Chem. **26**, 3298 (1961).
6. R. ANDRISANO and A. TUNDO. Atti accad. naz. Lincei. Rend. Classe sci. fis. mat. e nat. **13**, [8], 158 (1952).
7. Y. HIRSHBERG. J. Am. Chem. Soc. **71**, 3241 (1949).
8. D. W. ADAMSON, P. A. BARRETT, J. W. BILLINGHURST, and T. S. G. JONES. J. Chem. Soc. 2315 (1957).
9. C. G. OVERBERGER, J. H. SAUNDERS, R. E. ALLEN, and R. GANDER. Org. Syntheses, Coll. Vol. III, 200 (1955). C. G. OVERBERGER and J. H. SAUNDERS. Org. Syntheses, Coll. Vol. III, 204 (1955).
10. G. WALLING and K. B. WOLFSTIRN. J. Am. Chem. Soc. **69**, 852 (1947).
11. A. I. VOGEL. Practical organic chemistry. Longmans, Green and Co., New York, N.Y. 1948. p. 640.
12. O. H. WHEELER. Can. J. Chem. **36**, 667 (1958).

RECEIVED AUGUST 3, 1961.
DEPARTMENT OF CHEMISTRY,
UNIVERSITY OF PUERTO RICO,
MAYAGUEZ, PUERTO RICO,
AND
INSTITUTO DE QUIMICA,
UNIVERSIDAD NACIONAL AUTONOMA DE MEXICO,
MEXICO 20, D.F.

SPECTROPHOTOMETRIC OBSERVATIONS ON THE CLEAVAGE OF *vic*-DIOLS BY LEAD TETRAACETATE[1]

A. S. PERLIN AND S. SUZUKI[2]

Oxidative cleavage of *vic*-diols and related groups by lead tetraacetate (1) is generally detected and estimated by iodometric titration. An alternative, and in some ways advantageous, means for examining such reactions is offered by the fact that tetravalent lead may be estimated spectrophotometrically (2). Measurements are made at 280–300 mμ, a region in which absorption by Pb (IV) is not maximal (2) (see also Fig. 1, curve A) but in which there is no interference from acetic acid (a reaction product and also the most common solvent) nor from divalent lead.

With the spectrophotometric method lead tetraacetate oxidations can be carried out at higher dilution (ca. 10^{-4} *M*) than formerly. One advantage gained in this way is that reaction rates for very fast glycols (such as those in which the dihedral angle of the carbon–oxygen bonds approximates 0 degree (3, 4)) are slowed sufficiently[3] for satisfactory measurement, particularly with a recording spectrophotometer. To illustrate, the rate of cleavage of the 2,3-*cis* diol of methyl α- or β-D-erythrofuranoside was found earlier (5) to be virtually instantaneous even at 0° C, so that comparative data were not available. However, the rate for each compound at high dilution has now been estimated readily, and a substantial anomeric difference detected. As with the very much slower methyl D-threofuranosides (5), the 1,2-*cis*-alkoxy-hydroxy anomer (α-D-erythroside) was found to be more reactive than the 1,2-*trans* anomer, the ratio of their second-order rate constants being 3.5 to 1.

[1]*Issued as N.R.C. No. 6821.*
[2]*National Research Council of Canada Postdoctorate Fellow, 1960–61.*
[3]*The retarding effect of high dilution on the oxidation rate of relatively slow glycols (e.g., those of 6-membered ring or acyclic compounds) is very marked. Hence, in using the spectrophotometric method as a microprocedure for examining compounds of this type it may be desirable to accelerate the oxidation with potassium acetate (6, 7; see experimental section).*

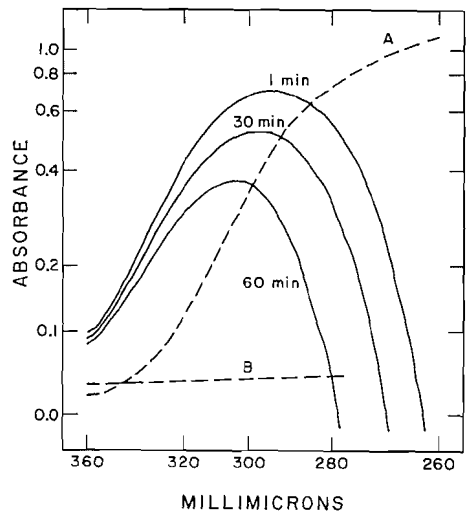

FIG. 1. Absorption spectrum at 1, 30, and 60 minutes' reaction time for a reaction mixture containing lead tetraacetate (84 μg/ml) and D-glucosamine hydrochloride (11 μg/ml) in acetic acid, using a solution of lead tetraacetate (84 μg/ml) in acetic acid as the reference liquid. The broken-line plots represent the absorption curve for (A) lead tetraacetate (84 μg/ml) and (B) D-glucosamine hydrochloride (11 μg/ml) in acetic acid, using acetic acid as the reference liquid.

Another possibility offered by the use of highly dilute solutions is that of examining the oxidation of compounds that are insufficiently soluble under the usual conditions. The behavior of amino sugars, for example, could not be compared directly with that of the 2-hydroxy analogues in earlier studies (8) because of poor solubility (of the crystalline amine hydrochlorides) in acetic acid. Some 2-amino-2-deoxy-D-aldohexoses (the D-gluco, D-galacto, and D-manno isomers), which have now been examined at high dilution, show the unusual property of promoting a marked *increase* in optical density at the outset of the reactions[4] (Fig. 1). This effect was not found with *N*-acetyl D-glucosamine nor with a wide variety of 1,2-dihydroxy compounds, and hence undoubtedly involves complexing between Pb (IV) and the amino group. Although all three aminohexoses show this effect, it appears to be steric dependent since it has not been observed with an acyclic α-amino alcohol (serine), nor with methyl 3-amino-3-deoxy-β-D-xylopyranoside, the 1,2,3-hydroxy-amino-hydroxy grouping of which should be fixed more rigidly than that of the aminohexoses. The present data do not show clearly that the complex is of the 5-membered cyclic type postulated by Criegee (3, 9), but an initial increase in optical density (at 220 mμ) detected during periodate oxidation of some 1,2-diols is consistent with the formation of such an intermediate (10).[5]

The aminohexoses, like the 2-hydroxy analogues (11), are only partially oxidized by lead tetraacetate and show pronounced isomeric differences, but the 1,2-amino hemiacetal group is cleaved much less readily than is the 1,2-hydroxy hemiacetal group.[4]

The spectrophotometric procedure should also facilitate the structural examination of oligosaccharides and partially substituted sugars, particularly when only small quantities

[4]*Thus, at 1, 30, 120, and 360 minutes, respectively, the apparent lead tetraacetate uptake (moles/mole) was:* D-*glucosamine, −0.46, −0.17, 1.02, 2.37;* D-*galactosamine, −0.23, 0.78, 1.10, 1.30;* D-*mannosamine, −0.22, 1.25, 2.19, 2.72. The* actual *uptake of oxidant by* D-*glucosamine in 30 minutes was about 0.3 mole/mole, as estimated by iodometric microtitration of large volumes of the reaction mixture, whereas in half this reaction period* D-*glucose reduced 2.0 moles of lead tetraacetate/mole.*

[5]*B. Coxon and L. Hough (private communication) have recently detected complex-formation between periodate and methyl 3-amino-4,6-O-benzylidene-3-deoxy-α-*D-*altropyranoside.*

of such compounds are available. This possibility has been checked for several oxidations carried out earlier under both potassium-acetate-catalyzed and uncatalyzed conditions (12, 13). The characteristics of the uncatalyzed oxidation, i.e., those dealing primarily with the degradation of reducing end-units (13), remain essentially the same at high dilution. However, the rate of reaction is retarded much more by the concentration change when the linkage is at position 4 than when at 6 or 3, which is of particular value in differentiating between the first two types. (Since 2-substituted aldoses are very unreactive, (1 → 2)- and (1 → 4)-linked oligosaccharides may be differentiated by oxidation at higher concentrations (13).) Also, these differences indicate some possibilities for effecting selective oxidation in mixtures of oligosaccharides, perhaps facilitating chromatographic separations; e.g., with three admixed oligosaccharides, the reducing end-units of which are substituted at positions 4, 3, and 6, respectively, the latter two should be oxidized preferentially at high dilution (yielding a 2-substituted pentose and a 3-substituted tetrose derivative, respectively (13)).

EXPERIMENTAL

Spectrophotometric measurements were made with a Beckman Model DU type instrument or with a Spectracord recording spectrophotometer.

All chemicals used were of reagent grade.

Estimation of Lead Tetraacetate

A stock solution (about 10%) of lead tetraacetate in acetic acid was prepared, the concentration of oxidant measured iodometrically (1), and appropriate dilutions were then made for the spectrophotometric studies.

The absorption curve for lead tetraacetate in acetic acid over the range 250–320 mμ (using acetic acid as the reference liquid) exhibits a shoulder in the region of 280 mμ (Fig. 1, curve A). At this wavelength the relation between optical density and lead tetraacetate concentration was linear and was plotted to serve as a standard curve. There was no indication during the present study that prolonged irradiation exerts an adverse effect on the reaction mixtures, such as is found with periodate oxidation (10, 14). However, in using potassium acetate for catalyzed oxidations, solutions containing more than 5 mg of the salt per milliliter were found to be too unstable for reactions requiring more than 30 minutes.

Lead Tetraacetate Oxidations

The following experiments illustrate the various oxidation conditions used:

(1) A solution of methyl α- or β-D-erythrofuranoside (64 μg) in acetic acid (2 ml) was syringed[6] into a solution of lead tetraacetate (240 μg) in acetic acid (2 ml), and the content of oxidant was measured continuously. Duplicate experiments showed only small variations. The calculated second-order rate constants (min^{-1} $mole^{-1}$ liter) were as follows:

Time (min)	0.35	0.40	0.50	0.60	0.70
k_{27} ($\times 10^{-3}$) α-D-isomer	41.6	38.8	36.3	36.4	37.6
k_{27} ($\times 10^{-3}$) β-D-isomer	10.8	11.9	11.0	11.3	11.3

(2) To a solution of lead tetraacetate (392 μg) in acetic acid (2 ml) was added a solution of 1,2:5,6-di-*O*-isopropylidene-D-mannitol (153 μg) in acetic acid (2 ml). The uptake of oxidant (moles/mole hr) was: 0.49 (1); 0.77 (2); 0.91 (3); 0.97 (4).

When the reaction was repeated in the presence of potassium acetate (5 mg/ml) the uptake of lead tetraacetate (moles/mole min) was: 0.59 (5); 0.79 (10); 0.96 (20); 0.98 (30); 1.03 (90).

(3) A solution of lactose (1.0 mg) in 90% acetic acid (0.2 ml) was added to a solution of lead tetraacetate (20 mg) and potassium acetate (10 mg) in 90% acetic acid (1.0 ml) (12). Portions (0.15 ml) of the reaction mixture were diluted, each to 25 ml, with acetic acid, and the lead tetraacetate content measured. The uptake of oxidant (moles/mole min) was: 4.07 (10); 4.74 (30); 4.91 (60); 5.08 (120).

(4) A solution of a given oligosaccharide (75–100 μg) in water (0.05 ml) was diluted with acetic acid (2 ml) and added to a solution of lead tetraacetate (400 μg) in acetic acid (2 ml). The uptake of oxidant (moles/mole) observed for the representative compounds listed below was:

[6]*An* all-glass *syringe is recommended; spurious absorption, possibly by metal ions, was observed when a stainless steel tip was used repeatedly.*

Time (min)	5	10	30	60
6-*O*-α-D-mannopyranosyl-D-glucose	1.27	1.62	1.91	1.93
4-*O*-β-D-glucopyranosyl-D-glucose	—	—	0	0.10
3-*O*-β-D-cellobiosyl-D-glucose	0.84	0.98	1.04	—

ACKNOWLEDGMENTS

The authors express their gratitude to Dr. L. C. Vining and Dr. W. A. Waters for helpful discussion and to Mrs. J. Nuttall for valuable technical assistance. Dr. J. C. Sowden kindly supplied a sample of D-mannosamine hydrochloride.

1. R. CRIEGEE. Ber. **64**, 260 (1931).
2. D. BENSON, L. H. SUTCLIFFE, and J. WALKLEY. J. Am. Chem. Soc. **81**, 4488 (1959).
3. R. CRIEGEE, L. KRAFT, and B. RANK. Ann. **507**, 159 (1933).
4. R. E. REEVES. Advances in Carbohydrate Chem. **6**, 107 (1951).
5. J. N. BAXTER and A. S. PERLIN. Can. J. Chem. **38**, 2217 (1960).
6. R. CRIEGEE and E. BÜCHNER. Ber. **73**, 563 (1940).
7. A. S. PERLIN. J. Am. Chem. Soc. **76**, 5505 (1954).
8. A. S. PERLIN. Advances in Carbohydrate Chem. **14**, 9 (1959).
9. G. E. MCCASLAND and D. A. SMITH. J. Am. Chem. Soc. **73**, 5164 (1951).
10. G. J. BUIST, C. A. BUNTON, and J. H. MILES. J. Chem. Soc. 4575 (1957).
11. A. S. PERLIN and C. BRICE. Can. J. Chem. **34**, 541 (1956).
12. A. S. PERLIN. Anal. Chem. **27**, 396 (1955).
13. A. J. CHARLSON and A. S. PERLIN. Can. J. Chem. **34**, 1200 (1956).
14. G. O. ASPINALL and R. J. FERRIER. Chem. & Ind. (London), 1216 (1957).

RECEIVED FEBRUARY 8, 1962.
NATIONAL RESEARCH COUNCIL OF CANADA,
PRAIRIE REGIONAL LABORATORY,
SASKATOON, SASKATCHEWAN.

EFFECT OF NUCLEAR SPIN ON THE EMISSION OF THE FORBIDDEN LINE Hg 6^3P_0–6^1S_0

G. H. KIMBELL[1] AND D. J. LE ROY

In a previous paper (1) we described a study of the formation and consumption of Hg 6^3P_0 atoms in mixtures of mercury vapor and nitrogen illuminated with 2537 Å. For a mercury pressure of 7.7×10^{-4} mm and nitrogen pressures in the range 0–140 mm we proposed the following mechanism:

$$\mathrm{Hg} + h\nu^* = \mathrm{Hg}^* \quad [1]$$

$$\mathrm{Hg}^* = \mathrm{Hg} + h\nu^* \quad [2]$$

$$\mathrm{Hg}^* + \mathrm{N_2} = \mathrm{Hg} + \mathrm{N_2} \quad [3]$$

$$\mathrm{Hg}^* + \mathrm{N_2} = \mathrm{Hg}^0 + \mathrm{N_2} \quad [4]$$

$$\mathrm{Hg}^0 = \mathrm{Hg}\ (\text{on wall}) \quad [5]$$

$$\mathrm{Hg}^0 = \mathrm{Hg} + h\nu^0 \quad [6]$$

$$\mathrm{Hg}^0 + \mathrm{N_2} = \mathrm{Hg} + \mathrm{N_2} \quad [7]$$

$$\mathrm{Hg}^0 + \mathrm{N_2} = \mathrm{Hg}^* + \mathrm{N_2} \quad [8]$$

$$\mathrm{Hg}^0 + \mathrm{N_2} = \mathrm{Hg} + \mathrm{N_2} + h\nu^0, \quad [9]$$

[1]*Present address: Department of Chemical Engineering, Imperial College, University of London, London, England.*

Time (min)	5	10	30	60
6-*O*-α-D-mannopyranosyl-D-glucose	1.27	1.62	1.91	1.93
4-*O*-β-D-glucopyranosyl-D-glucose	—	—	0	0.10
3-*O*-β-D-cellobiosyl-D-glucose	0.84	0.98	1.04	—

ACKNOWLEDGMENTS

The authors express their gratitude to Dr. L. C. Vining and Dr. W. A. Waters for helpful discussion and to Mrs. J. Nuttall for valuable technical assistance. Dr. J. C. Sowden kindly supplied a sample of D-mannosamine hydrochloride.

1. R. CRIEGEE. Ber. **64**, 260 (1931).
2. D. BENSON, L. H. SUTCLIFFE, and J. WALKLEY. J. Am. Chem. Soc. **81**, 4488 (1959).
3. R. CRIEGEE, L. KRAFT, and B. RANK. Ann. **507**, 159 (1933).
4. R. E. REEVES. Advances in Carbohydrate Chem. **6**, 107 (1951).
5. J. N. BAXTER and A. S. PERLIN. Can. J. Chem. **38**, 2217 (1960).
6. R. CRIEGEE and E. BÜCHNER. Ber. **73**, 563 (1940).
7. A. S. PERLIN. J. Am. Chem. Soc. **76**, 5505 (1954).
8. A. S. PERLIN. Advances in Carbohydrate Chem. **14**, 9 (1959).
9. G. E. MCCASLAND and D. A. SMITH. J. Am. Chem. Soc. **73**, 5164 (1951).
10. G. J. BUIST, C. A. BUNTON, and J. H. MILES. J. Chem. Soc. 4575 (1957).
11. A. S. PERLIN and C. BRICE. Can. J. Chem. **34**, 541 (1956).
12. A. S. PERLIN. Anal. Chem. **27**, 396 (1955).
13. A. J. CHARLSON and A. S. PERLIN. Can. J. Chem. **34**, 1200 (1956).
14. G. O. ASPINALL and R. J. FERRIER. Chem. & Ind. (London), 1216 (1957).

RECEIVED FEBRUARY 8, 1962.
NATIONAL RESEARCH COUNCIL OF CANADA,
PRAIRIE REGIONAL LABORATORY,
SASKATOON, SASKATCHEWAN.

EFFECT OF NUCLEAR SPIN ON THE EMISSION OF THE FORBIDDEN LINE Hg 6^3P_0–6^1S_0

G. H. KIMBELL[1] AND D. J. LE ROY

In a previous paper (1) we described a study of the formation and consumption of Hg 6^3P_0 atoms in mixtures of mercury vapor and nitrogen illuminated with 2537 Å. For a mercury pressure of 7.7×10^{-4} mm and nitrogen pressures in the range 0–140 mm we proposed the following mechanism:

$$\mathrm{Hg} + h\nu^* = \mathrm{Hg}^* \quad [1]$$

$$\mathrm{Hg}^* = \mathrm{Hg} + h\nu^* \quad [2]$$

$$\mathrm{Hg}^* + \mathrm{N_2} = \mathrm{Hg} + \mathrm{N_2} \quad [3]$$

$$\mathrm{Hg}^* + \mathrm{N_2} = \mathrm{Hg}^0 + \mathrm{N_2} \quad [4]$$

$$\mathrm{Hg}^0 = \mathrm{Hg\ (on\ wall)} \quad [5]$$

$$\mathrm{Hg}^0 = \mathrm{Hg} + h\nu^0 \quad [6]$$

$$\mathrm{Hg}^0 + \mathrm{N_2} = \mathrm{Hg} + \mathrm{N_2} \quad [7]$$

$$\mathrm{Hg}^0 + \mathrm{N_2} = \mathrm{Hg}^* + \mathrm{N_2} \quad [8]$$

$$\mathrm{Hg}^0 + \mathrm{N_2} = \mathrm{Hg} + \mathrm{N_2} + h\nu^0, \quad [9]$$

[1]*Present address: Department of Chemical Engineering, Imperial College, University of London, London, England.*

in which Hg represents 6^1S_0, Hg* represents 6^3P_1, and Hg^0 represents 6^3P_0 atoms. This mechanism was based on a kinetic analysis of the effect of nitrogen pressure on the absorption of 4047 Å (7^3S_1–6^3P_0) and on the intensity of the emission of the forbidden line 2656 Å (6^3P_0–6^1S_0). The lifetime, τ, of the 6^3P_0 atom with respect to radiation (the reciprocal of k_6) was found to be 4.2×10^{-4} sec.

The question naturally arose as to whether or not the spontaneous emission of the forbidden line was confined to the mercury isotopes having nuclear spin (odd atomic weight), as has been suggested by Mrozowski (2, 3, 4) and Bowen (5). There are a number of experimental methods of verifying this. In the present communication we report the results of one of these methods.

Assuming that $\tau_{even} \gg \tau_{odd}$, the steady-state concentration of Hg^0_{even} should be greater than that calculated from the natural isotope ratio when a mixture of nitrogen and natural mercury is illuminated by 2537 Å originating from a "natural" low-pressure mercury arc. Thus, the apparent value of τ should be greater than we found previously (1) if the analysis beam of 4047 Å contained only the hyperfine component from an isotope of even atomic weight.

The experimental method was similar to that used previously except that the 4047-Å beam was not derived from one of the primary lamps, but from a separate lamp containing only the isotope of atomic weight 198. The lamp consisted of a quartz tube 20 cm long and 7 mm in O.D. containing Hg^{198} and approximately 5 mm pressure of a 95% argon – 5% xenon mixture. It was operated by 2450-Mc microwave radiation from a 125-watt generator.

The temperature of the lamp was maintained within ±0.1° C by a water-cooled quartz jacket. Under fixed conditions in the reaction cell, the absorption of 4047 Å from this lamp was studied as a function of its temperature. The absorption remained constant at approximately 30% over the range 17 to 21° C, but rose to about 40% when the temperature of the lamp was raised to 27° C. For the measurements described below the lamp was operated at 20° C, at which temperature there was apparently insufficient pressure broadening in the lamp to cause any absorption by Hg^0 atoms of odd atomic weight in the reaction cell. The hyperfine structure of the 4047-Å line has been discussed by Schuler and Keyston (6) and by Burns and Adams (7).

To minimize pressure broadening of the absorption line in the reaction cell, nitrogen pressures were confined to the range 0.18 to 8.7 mm. For pressures less than 1 mm the results fitted the equation (1)

$$1/K^0L(Hg^0) = A/(N_2)^2+B/(N_2)+C,$$

with $A = 0.237$, $B = 3.16$, $C = 4.25$. These results are shown in Fig. 1 in the form of a plot of $(N_2)^2/K^0L(Hg^0)$ vs. (N_2).

In our previous work a plot of $(N_2)/K^0L(Hg^0)-A/(N_2)$ was linear up to approximately 6 mm. In the present measurements, shown in Fig. 2, the results are quite similar, an upward curvature setting in at about 5.5 mm. From the linear portion of this curve we derived the values $B = 3.06$, $C = 4.66$, in good agreement with the values obtained in the lower-pressure range. Taking $B/A = 3.06/0.237 = 12.9$ mm^{-1}, and $k_5 = 206$ mm sec^{-1}, it follows (1) that $k_6 = 12.9\times206 = 2.66\times10^3$ sec^{-1}, or $\tau = 3.8\times10^{-4}$ sec. Following the method used previously, the value of $k_7+k_8+k_9$ obtained from C/A was 0.75×10^{11} cm^3 mole^{-1} sec^{-1}, compared to the previous value of 1.09×10^{11}; nuclear spin would not be expected to influence these reactions. Individual values of the three rate constants could not, of course, be obtained from the present data.

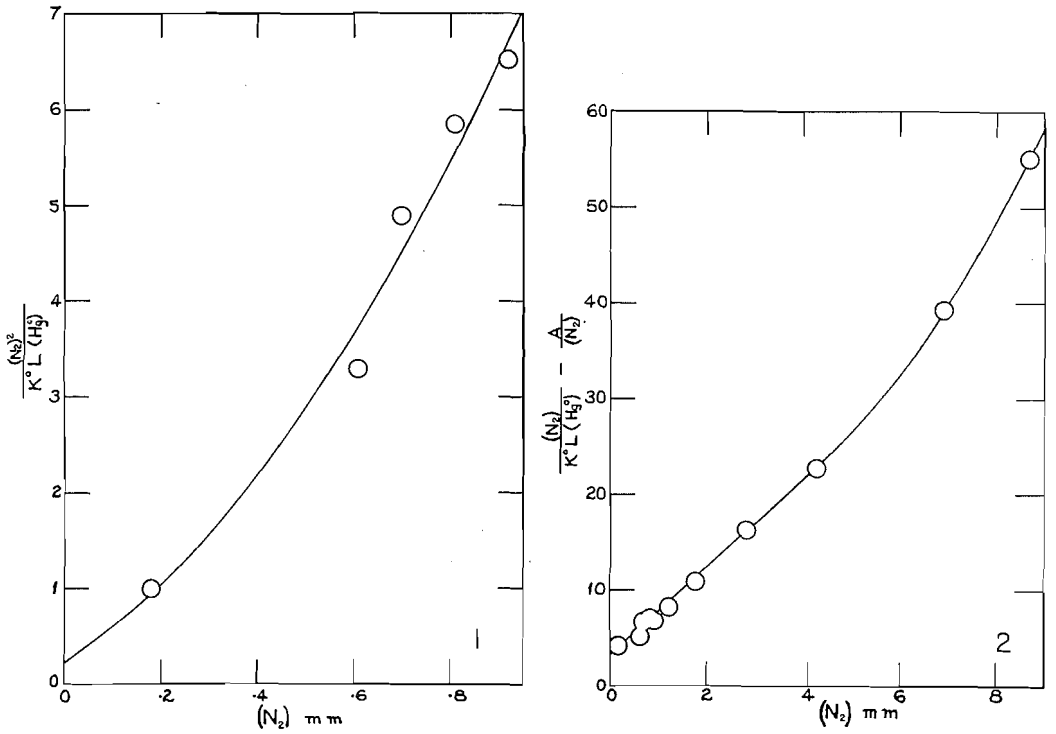

FIG. 1. $(N_2)^2/K^0L(Hg^0)$ vs. (N_2) in the low-pressure range, in which $K^0L(Hg^0)$ is the optical density for the absorption of the Hg^{198} hyperfine component of 4047 Å.

FIG. 2. $(N_2)/K^0L(Hg^0) - A/(N_2)$ vs. (N_2) in the medium-pressure range, in which $K^0L(Hg^0)$ is the optical density for the absorption of the Hg^{198} hyperfine component of 4047 Å and A is the intercept of Fig. 1.

The close agreement of the present value of τ with the value 4.2×10^{-4} sec obtained previously indicates that there is no significant difference between the lifetime of the Hg^0 isotope of mass 198, with no nuclear spin, and the "average" lifetime of all Hg^0 isotopes. It should also be recalled that our earlier work showed good agreement between the results obtained from the absorption of 4047 Å and those obtained from the emission of the forbidden line. One can only conclude that *either* the transition probability for emission of the forbidden line is essentially independent of nuclear spin *or* the exchange reaction $Hg^0_{even} + Hg_{odd} = Hg_{even} + Hg^0_{odd}$ is extremely fast.

ACKNOWLEDGMENTS

The continued financial support of the National Research Council of Canada is gratefully acknowledged, as is the award of a Studentship to one of us (G. H. K.).

1. G. H. KIMBELL and D. J. LE ROY. Can. J. Chem. **38**, 1714 (1960).
2. S. MROZOWSKI. Z. Physik, **108**, 204 (1938).
3. S. MROZOWSKI. Phys. Rev. **67**, 161 (1945).
4. S. MROZOWSKI. Revs. Modern Phys. **16**, 153 (1944).
5. I. S. BOWEN. Revs. Modern Phys. **8**, 55 (1936).
6. H. S. SCHULER and J. KEYSTON. Z. Physik, **72**, 423 (1931).
7. K. BURNS and K. B. ADAMS. J. Opt. Soc. Am. **42**, 56 (1952).

RECEIVED FEBRUARY 23, 1962.
THE DEPARTMENT OF CHEMISTRY,
UNIVERSITY OF TORONTO,
TORONTO 5, ONTARIO.

TRITIUM RELEASE FROM THE NEUTRON-IRRADIATED LITHIUM-DOPED NICKEL OXIDE

CONSTANȚA MĂNTESCU AND T. COSTEA

Nickel oxide is well known as a catalyst, often used in a series of chemical reactions. Recently one has tried to improve the properties of some semiconductor oxide catalysts by irradiation with high dosages or by doping them with other oxides and irradiating the mixture. To this purpose we have studied the behavior of neutron-irradiated lithium-doped nickel oxide during a post-irradiation thermal treatment. The $Li^6(n,\alpha)H^3$ nuclear reaction takes place by irradiation of the lithium-doped nickel oxide. We thought it would be interesting to pursue the fate of the recoil tritium atoms produced in the crystalline lattice of the doped oxide, as well as the possible chemical reactions of this hydrogen during the thermal spike and/or after reaching thermal equilibrium with the medium.

The lithium-doped nickel oxide was obtained by sintering reagent grade nickel oxide and lithium carbonate at 800° C to obtain $5Li_2O$:100NiO. The powder obtained was then heated under high vacuum for 3 hours at 200° C, after which it was sealed in quartz tubes. The samples were irradiated in these tubes in the IFA reactor, being exposed to an integral thermal neutron flux of 7×10^{15} n/cm^2. Irradiated samples of the same weight underwent isothermal treatment in the temperature range 100–800° C. The activity of the released tritium was measured in a G.M. gas counter using a known technique (1). A trap at liquid nitrogen temperature was placed between the quartz furnace, where the samples were heated, and the counter, so as to trap the condensable tritiated compounds and thus separate them from the free tritium.

It was observed that the bulk of the activity was trapped in the crystalline lattice of the lithium-doped nickel oxide, the released activity during the irradiation being under 1% of the total activity. This activity was divided approximately equally between the condensable fraction at the liquid nitrogen temperature and the uncondensable fraction at the same temperature. This fact shows that the release process requires an activation energy, the tritium or the tritiated compounds being trapped in the crystalline lattice. A second observation indicates that only tritium oxide has been produced—the only volatile compound of tritium at room temperature under vacuo conditions, but condensable at the liquid nitrogen temperature. The results of the isothermal treatment are shown in Fig. 1. It may be observed that for the temperature of 100° C, the samples release free tritium but, at higher temperatures, only tritium oxide is being released. The release process is characterized by a great rate in the first minutes of heating, after which the slope of the curves decreases gradually, reaching at last a pseudo plateau characteristic for a certain temperature. The released activity increases up to a temperature of 400–500° C, after which it decreases substantially at 600° C. For temperatures higher than 600° C, an increase of the activity may be observed.

The investigations are continuing, but some conclusions may already be drawn. There is no doubt that the results obtained may be interpreted if we admit that, in the crystal, the reaction of the formation of the tritium oxide takes place as follows:

$$T + O \rightarrow T_2O. \qquad [I]$$

The oxygen required by the first reaction may arise from the excess of oxygen atoms in the crystal (the nickel oxide corresponds to a formula NiO_{1+x}), or from the oxygen atoms distributed at random as a consequence of the thermal spikes. One puts the question as to whether this reaction takes place in the irradiation period or in the thermal period.

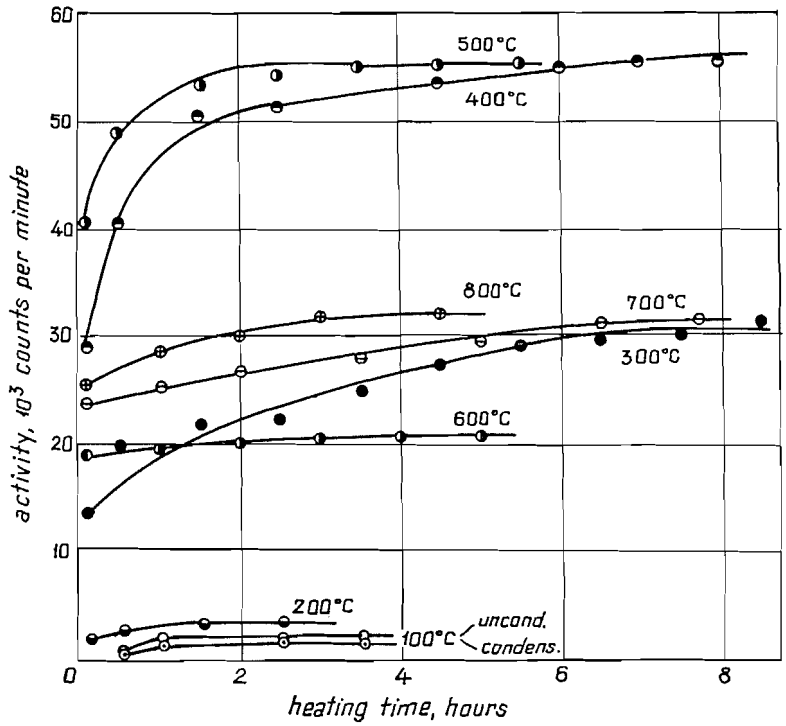

FIG. 1. The release of the tritium activity from the neutron-irradiated lithium-doped nickel oxide at different temperatures.

The fact that the released activity at 600° C is smaller than that released at 400–500° C may be due to any concurrent reaction

$$T + Li \rightarrow LiT \qquad [IIa]$$

or

$$T_2O + Li \rightarrow LiOT + T. \qquad [IIb]$$

The reaction [II*a*], which takes place just at 600–630° C, favors the appearance of the tritium oxide the moment the reactants reach thermal equilibrium with the medium. On the other hand, while reaction [II*b*] supposes that the tritium oxide is formed in the irradiation period, it is not experimentally confirmed because the release of the free tritium concomitant to the decrease of the combined tritium activity is not observed. In favor of reaction [II*a*] is the observation of faint sparks, which shows the presence of oxygen at higher temperature during the thermal treatment.

$$LiT + O \rightarrow Li_2O + T_2O \qquad [III]$$

For the released activity increase at temperatures higher than 600° C, reaction [III] may be used. In this way reaction [I] should be considered as a scavenger of the tritium by the oxygen, especially since, in the respective range of temperature, nickel oxide is a catalyst for the formation of water from oxygen and hydrogen.

It is intended to publish full details of this work elsewhere at a later date.

1. C. MĂNTESCU and M. FITI. Studii Cercetări Fizică, **11**, 788 (1960).

RECEIVED DECEMBER 27, 1961.
LABORATORY OF RADIOCHEMISTRY,
INSTITUTE OF ATOMIC PHYSICS,
BUCHAREST, ROUMANIA.

Canadian Journal of Chemistry

Issued by THE NATIONAL RESEARCH COUNCIL OF CANADA

VOLUME 40 JULY 1962 NUMBER 7

REACTIONS OF 2,3,5,6-TETRAKIS(β-HYDROXYETHYLMERCAPTO)-1,4-HYDROQUINONE AND RELATED COMPOUNDS

MARSHALL KULKA

Research Laboratories, Dominion Rubber Company Limited, Guelph, Ontario

Received February 19, 1962

ABSTRACT

The treatment of chloranil (I) with alkali and 2-mercaptoethanol resulted not only in replacement of the chlorine atoms but also in reduction to form 2,3,5,6-tetrakis(β-hydroxyethylmercapto)-1,4-hydroquinone (II). The conditions for the preparation of 2,3,5,6-tetrakis(β-chloroethylmercapto)-1,4-hydroquinone (III) from II differed from those required for the preparation of a lower-melting compound (IV) from II by such a narrow margin that exact control of temperature and concentration were necessary in order to avoid erratic behavior in the preparation. The structure of the lower-melting compound has been established as 2,3-dihydro-5,7,8-tris(β-chloroethylmercapto)-6-hydroxy-1,4-benzoxathiin (IV) by analyses and cyclization reactions. The treatment of 2,3-dichloro-1,4-naphthoquinone (VIII) with 2-mercaptoethanol yielded 2,3-bis(β-hydroxyethylmercapto)-1,4-naphthoquinone (IX) and not the quinol as was the case with chloranil. The quinone (IX) could not be converted to 2,3-bis(β-chloroethylmercapto)-1,4-naphthoquinone by treatment with hydrogen chloride because under these conditions only 1,4-oxathio-5,10-anthraquinone (X) was formed. A mechanism for the formation of X which involves intramolecular addition, elimination, and cyclization is described.

A few years ago 2,3,5,6-tetrakis(β-chloroethylmercapto)-1,4-hydroquinone (III) was synthesized in this laboratory in connection with another project. This "four-pronged" sulphur mustard was then submitted to the National Institutes of Health, Bethesda, Maryland, U.S.A., for evaluation in cancer chemotherapy. Preliminary screening results showed it to be active and curative to some extent. This provided a stimulus for further study and a second attempt to prepare III was made. Surprisingly enough the original preparation could not be duplicated and instead of III a lower-melting compound was isolated in high yield. The identification of this lower-melting compound and the explanation for the erratic behavior experienced in the preparation of III constitute the subject of this paper.

The synthesis of 2,3,5,6-tetrakis(β-chloroethylmercapto)-1,4-hydroquinone (III) consisted of two steps—the preparation of 2,3,5,6-tetrakis(β-hydroxyethylmercapto)-1,4-hydroquinone (II) from chloranil (I) followed by the conversion of II to III. It was the second step of the synthesis (II → III) which proved troublesome.

In the first step, the treatment of chloranil (I) with 2-mercaptoethanol in the presence of potassium hydroxide resulted in two simultaneous reactions—the displacement of the chlorine atoms by β-hydroxyethylmercapto groups and the reduction of the quinone to form 2,3,5,6-tetrakis(β-hydroxyethylmercapto)-1,4-hydroquinone (II). 2-Mercaptoethanol proved to be such a powerful nucleophile (as well as a reducing agent) that it attacked

other substituted benzoquinones besides I. Thus when 2,5-dichloro-3,6-bis(dimethylamino)-1,4-benzoquinone or 2,5-dichloro-3,6-di-N-morpholino-1,4-benzoquinone (1) was heated with 2-mercaptoethanol and pyridine, II was formed in high yield. The reduction of chloranil (I) to the quinol by mercaptides with the accompanying nucleophilic attack has been observed before when I was treated with ω-mercapto fatty acids (2, 3).

The second step in the synthesis of III, which required the conversion of the hydroxy compound II to 2,3,5,6-tetrakis(β-chloroethylmercapto)-1,4-hydroquinone (III), presented difficulties. Thionyl chloride could not be used for this purpose because II was completely insoluble in cold thionyl chloride and the hot reagent caused decomposition. However, 2,3,5,6-tetrakis(β-hydroxyethylmercapto)-1,4-hydroquinone (II) dissolved readily in cold concentrated hydrochloric acid and when the solution was allowed to stand at room temperature a white precipitate deposited. Analyses and melting point of this product indicated that it was incompletely chlorinated. However, the crude precipitate was now quite soluble in chloroform and the completion of the chlorination could be accomplished with thionyl chloride in chloroform solution. The conversion of II to III was therefore satisfactorily accomplished by the consecutive treatment with concentrated hydrochloric acid and thionyl chloride at room temperature.

Some time after this method of conversion (II $\rightarrow$ III) was developed, an attempt was made to repeat it. It was found that the treatment of II with concentrated hydrochloric acid at room temperature followed by the reaction with thionyl chloride gave a low-melting compound in high yield and no III. After considerable experimentation it became evident that the conditions required for the preparation of III and those for the preparation of the lower-melting compound differed by a small margin only and that "room temperature" had to be defined more precisely. Precise conditions for the preparation of III and those for the preparation of the lower-melting compound are described in the experimental section.

The lower-melting compound, which formed at lower temperatures (20–25°) in strong hydrochloric acid, was shown to be a product of cyclization. Analyses showed the presence of one phenolic group and three β-chloroethylmercapto groups and that its empirical formula was one hydrogen chloride molecule less than that of III. On this basis the structural formula IV was proposed. A study of the properties of this compound gave support to the postulated structure IV.

Pyrolysis of IV yielded ethylene dichloride. The liberation of ethylene dichloride on heating is characteristic of compounds bearing reactive β-chloroethylmercapto substituents (4). Infrared spectra showed the presence of a phenolic hydroxyl and this was confirmed by acetylation. The treatment of IV with 1 mole of alcoholic potassium hydroxide caused dehydrochlorination and cyclization to form 2,3,8,9-tetrahydro-5,6-bis(β-chloroethylmercapto)benzo(1,2-*b*:4,3-*b'*)bis(1,4-oxathiin) (V). The structure V was chosen in preference to the other possible isomer VI because V yielded on pyrolysis a tetracyclic compound VII which sublimed *in vacuo*. The isomer VI would be expected to yield on pyrolysis a polymer which would not sublime. Further support for the assignment of the structure IV lies in the fact that when 2,3,5,6-tetrakis(β-chloroethylmercapto)-1,4-hydroquinone (III) was treated with 2 moles of potassium hydroxide a double ring closure occurred to form the same tricyclic compound V as was obtained from IV by a similar treatment.

The properties of chloroquinones and their derivatives in the naphthalene series differed from those of the benzene series. Unlike chloranil, 2,3-dichloro-1,4-naphthoquinone (VIII) reacted with 2-mercaptoethanol and potassium hydroxide to give mostly tar and

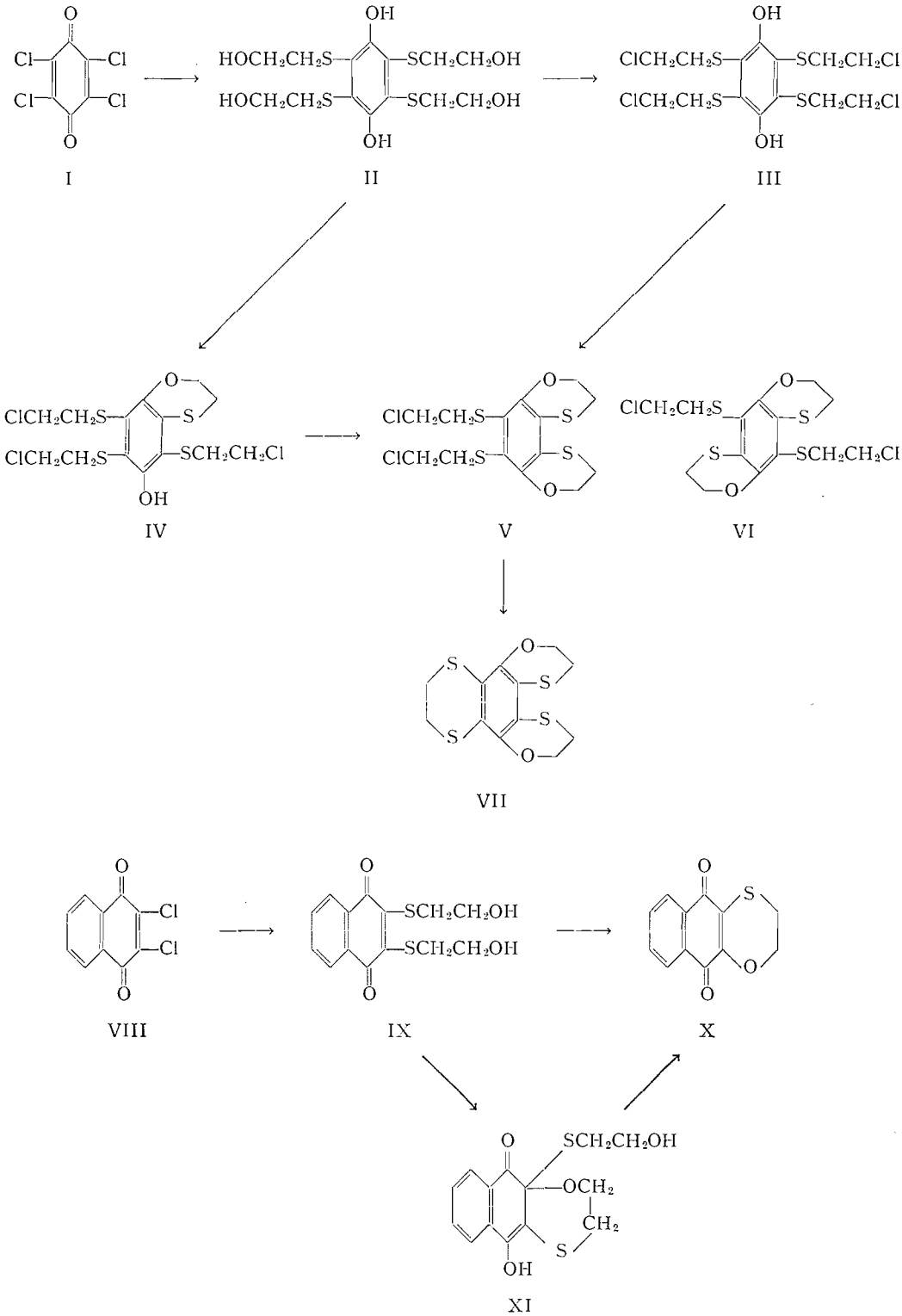

a small yield of an orange-colored compound. When pyridine was substituted for the potassium hydroxide and the temperature strictly controlled a high yield of the orange-colored compound was obtained. This proved to be 2,3-bis(β-hydroxyethylmercapto)-1,4-naphthoquinone (IX) and not the quinol as was the case in the benzoquinone series. All attempts to convert IX to the sulphur mustard 2,3-bis(β-chloroethylmercapto)-1,4-naphthoquinone were unsuccessful. The treatment of IX with thionyl chloride, or with alcoholic hydrogen chloride, or with acetic acid – hydrogen chloride yielded in each case a chlorine-free black compound which sublimed readily *in vacuo* and crystallized as sparkling black crystals. Infrared spectra showed the presence of carbonyl group(s), the absence of hydroxyl groups, and analyses indicated the structure to be 1,4-oxathia-5,10-anthraquinone (X). Apparently this was formed by displacement of one of the β-hydroxyethylmercapto groups and cyclization.

There is one example in the literature (5) of displacement of a β-hydroxyethylmercapto group from 2,3,5,6-tetrachloro-1,4-bis(β-hydroxyethylmercapto)benzene but in this case it occurred in alkaline solution. However, the displacement of methoxy groups in the benzoquinone series by other alkoxy groups (6), by amines (1, 7, 10), and by other groups (1, 7, 8) is not uncommon.

The mechanism of the conversion of IX to X is probably similar to that proposed by Fieser (9) for the methylation of 2-hydroxy-1,4-naphthoquinone by methanolic hydrogen chloride. Intramolecular addition of one hydroxyl group to the conjugated system of the quinone IX occurs to form the intermediate XI. From this, mercaptoethanol is eliminated to form the oxathianthraquinone X.

EXPERIMENTAL

2,3,5,6-Tetrakis(β-hydroxyethylmercapto)1,4-hydroquinone (II)

(a) From Chloranil (I)

To a stirred solution of 2,3,5,6-tetrachloro-1,4-benzoquinone (chloranil) (100 g) in benzene (3.5 l.) warmed up to 45° was added dropwise a solution of 2-mercaptoethanol (200 ml) and potassium hydroxide (96 g) over 2 hours. The temperature of the reaction mixture dropped to 41° during the first few minutes and then rose gradually to 48°. The stirring was continued for another 2 hours. The dark, sticky material which precipitated changed gradually to a light-colored solid which floated in the stirred benzene. The reaction mixture was allowed to stand overnight and then the benzene was decanted from the sticky solid. The solid was stirred with cold water for ½ hour, filtered, washed, and dried, m.p. 141–143°; yield 138 g. Crystallization from aqueous methanol yielded (120 g; 72%) yellowish sparkling crystals melting at 144–145°. Anal. Calc. for $C_{14}H_{22}O_6S_4$: C, 40.58; H, 5.31. Found: C, 40.55; H, 5.18.

Infrared spectra of this compound indicated that it was the quinol and not the quinone. Furthermore, on treatment with zinc and acetic acid, II remained unchanged.

(b) From 2,5-Dichloro-3,6-dimorpholino-1,4-benzoquinone

To a solution of 2,5-dichloro-3,6-dimorpholino-1,4-benzoquinone (3 g) (1) in benzene (250 ml) was added 2-mercaptoethanol (10 ml) and pyridine (10 ml), and the dark reaction mixture heated under reflux for 15 hours. The benzene was removed from the light-colored mixture, the residue was treated with water, and the solid was filtered and crystallized from aqueous methanol. The sparkling crystals (2 g) melted at 144–145° alone or in admixture with those obtained in (*a*).

(c) From 2,5-Dichloro-3,6-di(N,N-dimethylamino)-1,4-benzoquinone

2,5-Dichloro-3,6-di(N,N-dimethylamino)-1,4-benzoquinone (1) was treated with 2-mercaptoethanol as above. The chloro as well as the dimethylamino groups were replaced and reduction occurred to form 2,3,5,6-tetrakis(β-hydroxyethylmercapto)-1,4-hydroquinone (IV) in 70% yield.

2,3,5,6-Tetrakis(β-acetoxyethylmercapto)1,4-hydroquinone

(a) Using Acetic Anhydride

To a solution of 2,3,5,6-tetrakis(β-hydroxyethylmercapto)-1,4-hydroquinone (II) (5 g) in pyridine (15 ml) was added acetic anhydride (10 ml) and the solution was heated under reflux for 2 hours. The pyridine and excess anhydride were removed *in vacuo*. The residue was pulverized, washed with water, and the white solid (6.5 g) was crystallized three times from methanol. This yielded white prisms melting at 90–91°. Anal. Calc. for $C_{22}H_{30}O_{10}S_4$: S, 21.99. Found: S, 22.42, 22.52.

(b) Using Acetic Acid and Hydrogen Chloride

Into a solution of 2,3,5,6-tetrakis(β-hydroxyethylmercapto)-1,4-hydroquinone (II) (35 g) in acetic acid (750 ml) at 60°, hydrogen chloride gas was passed until saturation, and the solution was allowed to stand overnight. The acetic acid was removed *in vacuo* from the amber solution and the residue was crystallized from benzene. The white needles (32 g) melted at 85–87°. Two further crystallizations from methanol yielded a product melting at 90–91° alone or in admixture with that obtained in (*a*).

2,3-Dihydro-5,7,8-tris(β-chloroethylmercapto)-6-hydroxy-1,4-benzoxathiin (IV)

(a) Using Hydrochloric Acid Saturated with Hydrogen Chloride

A solution of 2,3,5,6-tetrakis(β-hydroxyethylmercapto)-1,4-hydroquinone (II) (25 g) in concentrated hydrochloric acid (250 ml) was saturated with hydrogen chloride at room temperature (20°) and the resulting solution was allowed to stand overnight. The hard cake which precipitated was separated from the hydrochloric acid, pulverized, washed with water, and dried. This crude product (27 g), which melted at 98–105°, was dissolved in chloroform (100 ml) and treated with thionyl chloride (15 ml) at 30° in order to complete the chlorination. The solution was allowed to stand overnight and then the solvent was removed *in vacuo* and the residue crystallized from benzene. White needles (20 g) arranged in rosettes and melting at 129–130° were obtained. Repeated recrystallizations did not raise the melting point. Anal. Calc. for $C_{14}H_{17}Cl_3O_2S_4$: C, 37.21; H, 3.76; Cl, 23.6; S, 28.3. Found: C, 37.55, 37.27; H, 3.90, 3.67; Cl, 23.64, 23.19; S, 29.01, 28.84.

(b) Using Concentrated Hydrochloric Acid

In several other experiments the saturation of the concentrated hydrochloric acid solution with hydrogen chloride was omitted. The results obtained were the same as in (*a*). However, in a few runs the 2,3-dihydro-5,7,8-tris(β-chloroethylmercapto)-6-hydroxy-1,4-benzoxathiin (IV) was not obtained but instead the higher-melting 2,3,5,6-tetrakis(β-chloroethylmercapto)-1,4-hydroquinone (III) (see below) was formed. It is believed that the runs which yielded III were performed on hot and humid days.

(c) Using a Higher Temperature

A solution of 2,3,5,6-tetrakis(β-hydroxyethylmercapto)-1,4-hydroquinone (10 g) in concentrated hydrochloric acid (100 ml) was heated at 35–37° for 6 hours. The white, sticky precipitate was extracted with chloroform and the chloroform solution dried and treated with thionyl chloride (5 ml) as in (*a*). The yellow crystals (4.5 g) which precipitated melted at 175–176° and proved to be 2,3,5,6-tetrakis(β-chloroethylmercapto)-1,4-hydroquinone (III) (see below). The mother liquors were taken to dryness *in vacuo* and the residue on crystallization from benzene yielded 3.5 g of 2,3-dihydro-5,7,8-tris(β-chloroethylmercapto)-6-hydroxy-1,4-benzoxathiin (IV) melting at 129–130° alone or in admixture with that obtained in (*a*).

2,3-Dihydro-5,7,8-tris(β-chloroethylmercapto)-6-acetoxy-1,4-benzoxathiin

A mixture of 2,3-dihydro-5,7,8-tris(β-chloroethylmercapto)-6-hydroxy-1,4-benzoxathiin (10 g), acetic anhydride (50 ml), and two drops of concentrated sulphuric acid was heated on the steam bath for 4 hours. The excess anhydride was removed *in vacuo* and the residue washed with ether and with methanol and crystallized from benzene–methanol. The white prisms (5.5 g) melted at 120–122°. Anal. Calc. for $C_{16}H_{19}O_3Cl_3S_4$: C, 38.94; H, 3.85; Cl, 21.58. Found: C, 38.56, 39.32; H, 3.84, 3.99; Cl, 21.37, 21.05.

2,3,5,6-Tetrakis(β-chloroethylmercapto)-1,4-hydroquinone (III)

(a) Using 30% Hydrochloric Acid and Thionyl Chloride

To a solution of concentrated hydrochloric acid (d = 1.19, 200 ml) and water (55 ml) was added 2,3,5,6-tetrakis(β-hydroxyethylmercapto)-1,4-hydroquinone (II) (25 g), and the mixture shaken until dissolved. Then chloroform (250 ml) was added and the mixture was heated under reflux for 3 hours. The chloroform layer was separated, concentrated to 75 ml *in vacuo* at 40°, cooled to 30°, and treated with thionyl chloride (15 ml) at 30–35°. Precipitation began immediately. The reaction mixture was allowed to stand at room temperature for 3 hours and then cooled to 0° and filtered. The lemon-yellow prisms (20.5 g or 70%) melted at 179–181°. Anal. Calc. for $C_{14}H_{18}O_2Cl_4S_4$: C, 34.42; H, 3.69; Cl, 29.10. Found: C, 34.05; H, 3.59; Cl, 28.35, 28.94.

In another experiment, to a solution of II (35 g) in methanol (200 ml) and water (40 ml) was added concentrated hydrochloric acid (500 ml), and the solution was heated under reflux on the steam bath for ½ hour. The precipitate was extracted with chloroform and then treated with thionyl chloride as in the first experiment above. There was obtained 27 g of III melting at 174–176° and at 178–179° after crystallization from benzene.

(b) Using Alcoholic Hydrogen Chloride

Methanol (450 ml) (or ethanol) was saturated with hydrogen chloride at 10°. To this was added 2,3,5,6-tetrakis(β-hydroxyethylmercapto)-1,4-hydroquinone (II) (25 g). After about half an hour of shaking it dissolved. The solution was allowed to stand at room temperature for 2 days and then cooled to 0°. The white precipitate on filtration and drying melted at 159–161°. Repeated recrystallizations raised the melting point by a few degrees only. However, when the crude product was treated with thionyl chloride in chloroform pure III melting at 180° was obtained.

2,3,8,9-Tetrahydro-5,6-bis(β-chloroethylmercapto)benzo(1,2-b:4,3-b')bis(1,4-oxathiin) (V)

(a) From 2,3,5,6-Tetrakis(β-chloroethylmercapto)-1,4-hydroquinone (III)

To a boiling solution of 2,3,5,6-tetrakis(β-chloroethylmercapto)-1,4-hydroquinone (III) (1.0 g) in acetone (150 ml) and methanol (50 ml) was added a solution of potassium hydroxide (0.25 g) in methanol (25 ml). The resulting solution was boiled for a few minutes. The white precipitate which formed quickly was filtered, washed, and dried. It weighed 0.45 g and melted at 226–227° with decomposition. Recrystallization from ethylene dichloride raise the melting point to 228–229° with decomposition. Anal. Calc. for $C_{14}H_{16}O_2Cl_2S_4$: C, 40.48; H, 3.86. Found: C, 40.28, 40.11; H, 3.84, 3.91.

(b) From 2,3-Dihydro-5,7,8-tris(β-chloroethylmercapto)-6-hydroxy-1,4-benzoxathiin (IV)

To a hot solution of IV (35 g) in acetone (700 ml) was added methanol (700 ml) followed by a solution of potassium hydroxide (4.5 g) in methanol (200 ml). After standing for 1 hour the reaction mixture was filtered and the white solid (22 g) melting at 218–220° with decomposition was crystallized from ethylene dichloride. The white prisms melted at 228–229° with decomposition, alone or in admixture with that obtained in (*a*).

2,3,8,9-Tetrahydro-5,6-ethylenedithio-benzo(1,2-b:4,3-b')bis(1,4-oxathiin) (VII) and Ethylene Dichloride from V

2,3,8,9-Tetrahydro-5,6-bis(β-chloroethylmercapto)benzo(1,2-*b*:4,3-*b'*)bis(1,4-oxathiin) (V) (1.0 g) was heated in a Späth bulb at 250° for a few minutes, the distillate being collected in a dry-ice trap. The distillate was treated with a solution of excess potassium *p*-chlorothiophenate in methanol, yielding a white compound (0.32 g) which melted at 92–94° and which did not depress the melting point of 1,2-bis(*p*-chlorophenylmercapto)ethane. This showed that the distillate was mainly ethylene dichloride.

The residue in the Späth bulb was then sublimed at 250° at 0.5 mm pressure. The chlorine-free sublimate was crystallized from benzene, yielding 0.25 g of almost white needles, m.p. 239–240°. Anal. Calc. for $C_{12}H_{12}O_2S_4$: C, 45.57; H, 3.79; S, 40.50. Found: C, 45.61, 45.48; H, 4.04, 3.98; S, 40.68, 41.14.

Pyrolysis of 2,3-Dihydro-5,7,8-tris(β-chloroethylmercapto)-6-hydroxy-1,4-benzoxathiin (IV)

2,3-Dihydro-5,7,8-tris(β-chloroethylmercapto)-6-hydroxy-1,4-benzoxathiin (IV) (25 g) was heated in a distilling flask equipped with a condenser at 200° until no more liquid distilled. The distillate (5 g) had all the physical properties of *ethylene dichloride*. A derivative was prepared by heating the distillate (2 g) with a methanolic solution of excess potassium *p*-chlorothiophenate. The product (4 g) melted at 93–94° and did not depress the melting point of 1,2-bis(*p*-chlorophenylmercapto)ethane.

Pyrolysis of 2,3,5,6-Tetrakis(β-chloroethylmercapto)-1,4-hydroquinone (III)

2,3,5,6-Tetrakis(β-chloroethylmercapto)-1,4-hydroquinone (III) was pyrolyzed in the same manner as was IV above. Ethylene dichloride (0.5 g) was obtained from 2 g of III.

2,3-Bis(β-hydroxyethylmercapto)-1,4-naphthoquinone (IX)

(a) Using Potassium Hydroxide and 2-Mercaptoethanol

To a stirred solution of 2,3-dichloro-1,4-naphthoquinone (VIII) (60 g) in benzene (2 l.) was added dropwise a solution of 2-mercaptoethanol (45 ml) and potassium hydroxide (30 g) over $1\frac{1}{4}$ hours. The temperature was kept at 40° by cooling. The dark reaction mixture was stirred for 2 hours and then let stand overnight. The warmed benzene solution was decanted from the salt and tar, concentrated to about 700 ml, and allowed to cool. The precipitate was filtered and crystallized from methanol, yielding orange needles (12 g) melting at 117–118°. Anal. Calc. for $C_{14}H_{14}O_4S_2$: C, 54.19; H, 4.51. Found: C, 54.53, 54.12; H, 4.51, 4.63.

(b) Using Pyridine and 2-Mercaptoethanol

A solution of 2,3-dichloro-1,4-naphthoquinone (VIII) (100 g) in benzene (1600 ml) and 2-mercaptoethanol (72 ml) was stirred and the temperature adjusted to exactly 54°. Then pyridine (80 ml) was added all at once. When the temperature reached 66° (in a few minutes) the reaction mixture was cooled occasionally on a water bath in order to keep the temperature at 65–67°. In about 15 minutes precipitation was complete and the temperature began to fall. The reaction mixture was cooled, treated with water, the precipitate filtered, washed with water, and crystallized from methanol. The yield of orange needles from two crops melting at 115–116° was 94 g. This compound turned dark and decomposed on standing in air after a few weeks.

2,3-Bis(β-hydroxyethylmercapto)-1,4-naphthoquinol

To a suspension of 2,3-bis(β-hydroxyethylmercapto)-1,4-naphthoquinone (IX) (62 g) in glacial acetic acid (620 ml) was added portionwise, with cooling on a water bath, zinc dust (25 g). The temperature was kept at 25–30°. After being stirred for 1 hour the reaction mixture was filtered and the filtrate taken to dryness *in vacuo*. The residue on crystallization from methanol yielded 39 g of white prisms melting at 124–126°. Anal. Calc. for $C_{14}H_{16}O_4S_2$: S, 20.51. Found: S, 20.52, 20.54. This quinol turned red on exposure to the air.

1,4-Oxathia-5,10-anthraquinone (X)

To a solution of 2,3-bis(β-hydroxyethylmercapto)-1,4-naphthoquinone (IX) (25 g) in methanol (300 ml) at 50° was added a solution of dry hydrogen chloride (120 g) in methanol (200 ml). The temperature rose to

60° and cooling was necessary in order to keep it below 60°. The dark purple solution was allowed to stand overnight and then the precipitated black sparkling crystals (10.5 g) were filtered, washed with methanol and benzene, and dried. This halogen-free compound melted at 230–232° and at 231–233° after sublimation at a temperature of 200° and a pressure of 1 mm. Anal. Calc. for $C_{16}H_8O_3S$: C, 62.07; H, 3.45; S, 13.8. Found: C, 61.52, 62.51; H, 3.49, 3.07; S, 14.16.

The same results were obtained when IX was treated with hydrogen chloride in acetic acid instead of in methanol.

REFERENCES

1. D. Buckley, H. B. Henbest, and P. Slade. J. Chem. Soc. 4891 (1957).
2. A. Blackhall and R. H. Thomson. J. Chem. Soc. 1138 (1953).
3. M. Schubert. J. Am. Chem. Soc. **69**, 712 (1947).
4. M. Kulka. Can. J. Chem. **37**, 325 (1959).
5. M. Kulka. J. Org. Chem. **24**, 235 (1959).
6. C. H. Shunk, D. E. Wolf, J. F. McPherson, B. O. Linn, and K. Folkers. J. Am. Chem. Soc. **82**, 5914 (1960).
7. D. Buckley, S. Dunstan, and H. B. Henbest. J. Chem. Soc. 4901 (1957).
8. J. A. D. Jeffreys. J. Chem. Soc. 2153 (1959).
9. L. F. Fieser. J. Am. Chem. Soc. **48**, 2922 (1926).
10. W. K. Anslow and H. Raistrick. J. Chem. Soc. 1446 (1939).

THE ACID-CATALYZED CLEAVAGE OF PHENYLSULPHINYLACETIC ACID

DEREK WALKER[1] AND JOSEPH LEIB
Research Laboratory, Dominion Tar and Chemical Company, Ltd., Ville LaSalle, Que.

Received January 22, 1962

ABSTRACT

A study of the hydrogen peroxide oxidation of phenylmercaptoacetic acid led to a new interpretation of the mechanism of the acid-catalyzed cleavage of phenylsulphinylacetic acid.

Phenylsulphinylacetic acid is known to undergo a facile cleavage to benzenethiol and glyoxylic acid in the presence of mineral acids (1) (equation [1]).

$$C_6H_5\overset{\uparrow}{S}(O)CH_2CO_2H \xrightarrow{H^{\oplus}} C_6H_5SH + OHCCO_2H \qquad [1]$$

This reaction has not been studied in detail although Pummerer (1) and, more recently, Kenney, Walsh, and Davenport (2) have suggested possible mechanisms based on the evidence available to them. The mechanism advanced by Pummerer is summarized in equation [2].

$$C_6H_5\overset{\uparrow}{S}(O)CH_2CO_2H \xrightarrow{H^{\oplus}} \underset{\text{I}}{C_6H_5S(OH)=CHCO_2H} \longrightarrow \underset{\text{II}}{C_6H_5S(OH)CHCO_2H} \downarrow \; C_6H_5SH + OHCCO_2H \qquad [2]$$

Kenney, Walsh, and Davenport put forward the scheme illustrated by equation [3].

$$C_6H_5\overset{\uparrow}{S}(O)CH_2CO_2H \xrightarrow{H^{\oplus}} \left[C_6H_5\overset{\uparrow}{\underset{H}{S}}(O)CH_2CO_2H\right]^{+} \longrightarrow \left[C_6H_5\underset{H}{S}\!-\!O\!-\!\underset{H}{CHCO_2H}\right]^{+} \downarrow \; \underset{\text{II}}{C_6H_5S(OH)CHCO_2H} \rightleftharpoons C_6H_5SH + OHCCO_2H \qquad [3]$$

Thus, according to Kenney, Walsh, and Davenport, phenylmercaptohydroxyacetic acid (II) results from a recombination of benzenethiol and glyoxylic acid. Pummerer, on the other hand, suggested that II was formed prior to benzenethiol and glyoxylic acid.

In this paper evidence is presented to support the view suggested by Pummerer. A new interpretation of the mechanism of the acid-catalyzed cleavage of phenylsulphinylacetic acid is also proposed.

In contrast with previous workers, our study of the cleavage of phenylsulphinylacetic acid was carried out without adding acid to catalyze the reaction. In other words phenylsulphinylacetic acid was the sole source of the protons necessary for catalysis. The

[1]*Present address: Arapahoe Chemicals, Inc., Boulder, Colorado, U.S.A.*

cleavage of phenylsulphinylacetic acid was accomplished in supersaturated aqueous solution, in methyl ethyl ketone, and in benzene. The supersaturated aqueous solution used in the present work was prepared by mixing equimolecular quantities of 30% hydrogen peroxide and phenylmercaptoacetic acid, and controlling the temperature below 40° until the hydrogen peroxide had been consumed. The clear solution thus obtained is supersaturated with respect to phenylsulphinylacetic acid since the solubility of this acid in water at 25° is only about 5%.

Phenylsulphinylacetic acid, in supersaturated aqueous solution at room temperature, is first converted into a water- and benzene-soluble acidic syrup which, in turn, breaks down into benzenethiol and glyoxylic acid. Further interactions between benzenethiol, glyoxylic acid, and the above-mentioned syrup occur over a period of time. The major products of these interactions are bis(phenylmercapto)acetic acid, diphenyl disulphide, and an unidentified oil. The unidentified oil was isolated from a supersaturated solution of phenylsulphinylacetic acid which had stood for 3 months.

All of these changes are accelerated by heat; higher temperatures favor the formation of bis(phenylmercapto)acetic acid.

The water- and benzene-soluble acidic syrup described above was also obtained by boiling phenylsulphinylacetic acid in dry methyl ethyl ketone or in dry benzene. If a pure sample of phenylsulphinylacetic acid is used no odor of benzenethiol is detectable during the course of this reaction. The properties of the water- and benzene-soluble acidic syrup obtained from the above preparations are compatible with those expected of phenylmercaptohydroxyacetic acid (II). Thus, the water- and benzene-soluble acidic syrup gave benzenethiol in high yield when it was warmed with aqueous mineral acid, and gave a high yield of bis(phenylmercapto)acetic acid when it was allowed to stand with benzenethiol in the presence of an acid catalyst. Further, the water- and benzene-soluble acidic syrup gave tests for an α-hydroxy acid with lead tetraacetate (3) and N-bromosuccinimide (4). Throughout the rest of this paper the water- and benzene-soluble acidic syrup will be referred to as II even though absolute proof of the correctness of this assignment is lacking.

The methods of preparing II suggested that this material was formed by an intramolecular rearrangement of phenylsulphinylacetic acid, and, hence, not by the recombination of benzenethiol and glyoxylic acid, as proposed by Kenney, Walsh, and Davenport (equation [3]).

Further proof for an intramolecular rearrangement of phenylsulphinylacetic acid to II was obtained by studying the reactions illustrated by equation [4].

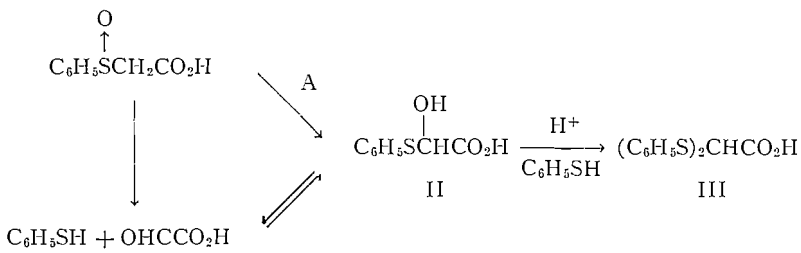

[4]

According to equation [4], if II is formed intramolecularly (route A), glyoxylic acid will not intervene in the formation of bis(phenylmercapto)acetic acid (III). Thus, formation of III in the presence of a scavenger for glyoxylic acid should provide clear evidence for route A.

When equimolecular amounts of phenylsulphinylacetic acid and benzenethiol were allowed to react in the presence of hydrazine sulphate, III was obtained in 32% yield. This experiment was repeated using equivalent amounts of glyoxylic acid and benzenethiol in place of the phenylsulphinylacetic acid; no III was isolated. These experiments were also carried out without adding hydrazine sulphate. Phenylsulphinylacetic acid and benzenethiol gave a 40% yield of III and glyoxylic acid and benzenethiol gave a 15% yield of III.

The above experiments, while clearly supporting an intramolecular rearrangement of phenylsulphinylacetic acid to II, do not prove that such a rearrangement is the exclusive reaction. It is our impression, however, that the rearrangement of phenylsulphinylacetic acid to II is the predominant reaction.

The above study led us to perfect a novel method for cleaving phenylmercaptoacetic acid to benzenethiol. The cleavage was accomplished by adding 30% hydrogen peroxide to a suspension of phenylmercaptoacetic acid in boiling aqueous mineral acid. Benzenethiol was removed as it was formed, by passing steam into the reaction mixture.

EXPERIMENTAL[2]

Formation and Cleavage of Phenylsulphinylacetic Acid

(1) Uncontrolled Reaction

Phenylmercaptoacetic acid (16.8 g) was treated with 30% hydrogen peroxide (11.4 ml). The resultant mixture soon turned liquid and erupted into vigorous boiling, which continued for about 5 minutes. When the reaction was over the mixture was allowed to cool to room temperature and water was removed under vacuum, in a rotary evaporator heated to about 60° C. A clear syrup was obtained. Digestion of this syrup with hot benzene (2×100 ml) for a few minutes left essentially pure phenylsulphinylacetic acid (9.2 g, 50%), m.p. 108–111° C. The benzene solution was extracted first with aqueous sodium bicarbonate and then with aqueous sodium hydroxide. Repeated extraction of the acidified sodium bicarbonate extract with chloroform removed phenylmercaptohydroxyacetic acid (2.6 g, 14%), which was recovered as a clear syrup by evaporation of the dried chloroform solution. Benzenethiol (0.8 g, 7.3%) was obtained by acidification of the sodium hydroxide extract. Evaporation of the neutral benzene layer gave diphenyl disulphide (1.0 g, 9.2%).

(2) Controlled Reaction

Phenylmercaptoacetic acid (16.8 g) was treated with 30% hydrogen peroxide (11.4 ml). The reaction mixture was stirred and held at about 40° C, by a cold-water bath, until all the hydrogen peroxide had been consumed (starch–iodide paper). At the end of the reaction a clear, colorless supersaturated solution of phenylsulphinylacetic acid was obtained. Evaporation of the water was carried out by the method described for the uncontrolled reaction above. Digestion of the product with hot benzene (2×100 ml) for a few minutes left phenylsulphinylacetic acid (17.5 g, 95%), m.p. 108–111° C. Vacuum evaporation of the benzene gave phenylmercaptohydroxyacetic acid (0.9 g, 5%), which was obtained as a syrup.

Supersaturated solutions of phenylsulphinylacetic acid obtained in the above-described manner were allowed to stand at room temperature in stoppered flasks for longer times:

(a) 6 days.—Faint signs of phase separation appeared in 3–4 days. After 6 days the water was removed by the method described for the uncontrolled reaction above. The following products and yields were obtained: phenylsulphinylacetic acid (11.7 g, 64%, m.p. 107–110° C), phenylmercaptohydroxyacetic acid (3–4 g of a syrup containing some bis(phenylmercapto)acetic acid), benzenethiol (0.8 g, 7.3%), diphenyl disulphide (0.4 g, 3.7%, m.p. 58–60° C).

(b) 3 months.—At the end of this period a heavy yellow oil and voluminous white crystals had separated from the original clear solution. The white crystals were filtered and shown to be diphenyl disulphide (1 g, 9.2%, m.p. 59–60° C). The filtrate when diluted with three times its volume of water still comprised two layers. These were separated and worked up individually. The aqueous layer was repeatedly extracted with benzene, evaporation of which yielded bis(phenylmercapto)acetic acid (0.5 g, 3.6%, m.p. 101–103° C) and benzenethiol (0.5 g, 4.5%). The water layer was evaporated, in a rotary evaporator at about 60°, and yielded phenylmercaptohydroxyacetic acid (1.5 g, 8%). The oil layer (15.5 g) gave an emulsion when treated with benzene (50 ml). The benzene–oil emulsion reacted vigorously with an excess of aqueous sodium bicarbonate; carbon dioxide was evolved and two clear phases resulted. Acidification of the aqueous layer gave bis(phenylmercapto)acetic acid (2.5 g, 18%, m.p. 100–103° C). The aqueous acid solution, after filtration of bis(phenylmercapto)acetic acid, was kept for further work-up. Extraction of the benzene layer with aqueous sodium hydroxide and acidification of the latter gave benzenethiol (2 g, 18%). The aqueous acid solution,

[2]*Melting points and boiling points are uncorrected.*

after removal of benzenethiol, was kept for further work-up. The benzene on evaporation gave diphenyl disulphide (0.5 g, 4.6%). The two aqueous acid solutions obtained above were combined and steam-distilled for several hours. Benzenethiol (2.8 g, 25%) was collected.

(3) Bis(phenylmercapto)acetic Acid Formation

A supersaturated solution of phenylsulphinylacetic acid, prepared from phenylmercaptoacetic acid (33.6 g) in the manner described above, was heated at about 100° C for 4 hours. A heavy oil separated during the reaction and on cooling this solidified. Some water was added, and the solid was broken up, filtered, and washed with water. The aqueous filtrate and water washings were combined and extracted with chloroform. The water on evaporation (rotary evaporator at about 60°) gave phenylmercaptohydroxyacetic acid (9.1 g, 25%).

The chloroform extract was combined with the solid on the filter, and a homogeneous solution was prepared by the addition of benzene. Extraction of this solution with aqueous sodium bicarbonate and acidification of the extract gave bis(phenylmercapto)acetic acid (18.2 g, 66%, m.p. 102–103° C). A trace of benzenethiol was extracted from the benzene–chloroform solution with aqueous sodium hydroxide. Evaporation of the neutral solvent gave diphenyl disulphide (1.8 g, 8.3%).

Cleavage of Phenylsulphinylacetic Acid in Organic Media

(1) Methyl Ethyl Ketone

Phenylsulphinylacetic acid (10 g) was refluxed in methyl ethyl ketone (50 ml) for 4 hours. At the end of this period the methyl ethyl ketone was removed under vacuum (rotary evaporator) and the product was digested with hot benzene. The benzene-insoluble portion was unchanged phenylsulphinylacetic acid (6.5 g, 65%, m.p. 107–110° C). Evaporation of the benzene extract gave phenylmercaptohydroxyacetic acid (3.3 g, 33%).

(2) Benzene

This reaction was conducted in the same manner as was the previous experiment. The benzene suspension was cooled, and unchanged phenylsulphinylacetic acid (8.6 g, 86%, m.p. 108–111° C) was filtered. Evaporation of the benzene gave phenylmercaptohydroxyacetic acid (1.5 g, 15%).

Evidence for the Structure of Phenylmercaptohydroxyacetic Acid (II)

This acid was always obtained as a clear, water- and benzene-soluble acidic syrup. The syrup was miscible with water in all proportions; however, its solubility in benzene was only moderate. The syrup has been described as benzene-soluble throughout this paper because benzene proved a convenient solvent for extracting syrup away from phenylsulphinylacetic acid.

Steam distillation of an acidified aqueous solution of phenylmercaptohydroxyacetic acid led to an almost quantitative recover of benzenethiol.

Phenylmercaptohydroxyacetic acid (3.2 g) and benzenethiol (10 g), when allowed to stand with concentrated sulphuric acid (1 drop) for 4 days, gave bis(phenylmercapto)acetic acid (3.0 g, 62%, m.p. 99–102° C).

Phenylmercaptohydroxyacetic acid gave the tests for an α-hydroxy acid with lead tetraacetate (3) and N-bromosuccinimide (4).

Bis(phenylmercapto)acetic Acid from Phenylsulphinylacetic Acid and Benzenethiol

(1) In the Presence of Hydrazine Sulphate

Benzenethiol (1.1 g) was added to a freshly prepared solution of phenylsulphinylacetic acid (1.84 g) in a mixture of acetic acid (7 ml) and water (3.7 ml). Hydrazine sulphate (1.43 g) was added followed by concentrated sulphuric acid (4 drops). After the mixture had been refluxed for 2 hours it was poured into water (50 ml). The water suspension was extracted with ether, the ether was washed with water, and was then extracted with aqueous sodium bicarbonate. The sodium bicarbonate extract was acidified to give bis-(phenylmercapto)acetic acid (0.88 g, 32%, m.p. 102–104° C).

(2) Without Hydrazine Sulphate

The experiment just described was repeated without the hydrazine sulphate. Bis(phenylmercapto)acetic acid, m.p. 102–104°, was obtained in 40% yield.

Bis(phenylmercapto)acetic Acid from Glyoxylic Acid and Benzenethiol

(1) In the Presence of Hydrazine Sulphate

Benzenethiol (2.2 g) was added to a freshly prepared solution of glyoxylic acid hydrate (0.92 g) in a mixture of acetic acid (7 ml) and water (3.5 ml). Hydrazine sulphate (1.43 g) was added followed by concentrated sulphuric acid (4 drops), and the mixture was refluxed for 2 hours. The resulting yellow suspension was poured into water (50 ml), and the mixture thus obtained was extracted with ether. The ether solution was washed with water and extracted with aqueous sodium bicarbonate. Acidification of the sodium bicarbonate gave no bis(phenylmercapto)acetic acid.

(2) Without Hydrazine Sulphate

The experiment just described was repeated without the hydrazine sulphate. Bis(phenylmercapto)acetic acid, m.p. 102–103° C, was obtained in 14.5% yield.

Oxidative Cleavage of Phenylmercaptoacetic Acid to Benzenethiol

Phenylmercaptoacetic acid (8.4 g) and 10% aqueous sulphuric acid (75 ml) were charged to a 250-ml 3-necked flask equipped as for a steam distillation. The third neck was fitted with a dropping funnel. Steam was passed into the mixture in the flask until a steady distillation was in progress. Hydrogen peroxide (10 ml of 30% aqueous solution) was added dropwise over 60 minutes. Benzenethiol started to distill in the steam shortly after addition of the hydrogen peroxide was commenced. Steam distillation was continued until benzenethiol ceased to pass over. Zinc dust (1 g) was then added to the flask and the steam distillation continued until no further benzenethiol distilled. The steam distillate was extracted with ether and the ether dried with anhydrous sodium sulphate. Benzenethiol (4.4 g, b.p. 166–169° C, 80%) was recovered from the ether by distillation.

This process was applied to *p*-tolylmercaptoacetic acid; *p*-toluenethiol (m.p. 42–44° C) was obtained in 75% yield.

DISCUSSION

Conjugate acids of sulphoxides with proton have been described by Connor (5) as possessing either structure IV or structure V.

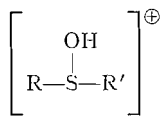

IV

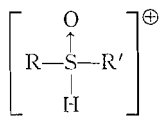

V

The oxygen atom of sulphoxides is, however, generally regarded as being more basic than the sulphur atom (2, 6, 7). Thus, in the case of the rearrangement of the conjugate acid of phenylsulphinylacetic acid a structure of type IV (R = $C_6H_5\cdot$, R′ = $\cdot CH_2CO_2H$) would appear to be more important than a structure of type V (R = $C_6H_5\cdot$, R′ = $\cdot CH_2CO_2H$).

Our observations provide strong support for an intramolecular rearrangement of IV (R = $C_6H_5\cdot$, R′ = $\cdot CH_2CO_2H$) to II. The following scheme (equation [5]) would seem to fit the experimental facts best:

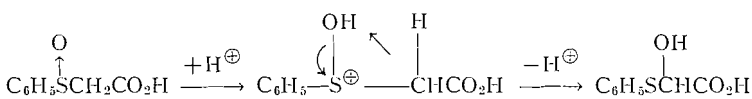

[5]

The reaction may be concerted in that loss of proton from the methylene carbon atom could coincide with the rearrangement as indicated. On the other hand, such associations as illustrated by the dotted lines in structure VI may lead to a collapse of the molecule in the manner illustrated by equation [6].

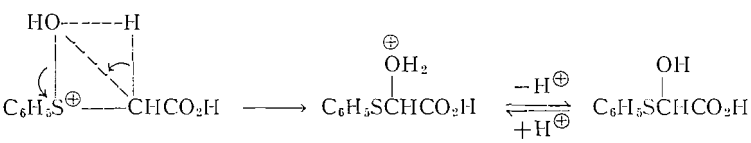

[6]

VI

In regard to equation [5] it is interesting to note that anions in solution do not appear to assist, to a significant extent, in the removal of proton from the methylene carbon atom. Thus, when sodium chloride was added to a standard preparation of II no noticeable increase in the yield of II was observed.

The carboxylic acid group probably plays an important part in the above mechanism by weakening the carbon–hydrogen bonds of the methylene group.

The mechanism proposed in equation [5] shows similarities to that suggested, on intuitive grounds, by Pummerer (equation [1]). The intermediate (I), suggested by Pummerer, might well arise from the conjugate acid of phenylsulphinylacetic acid thus:

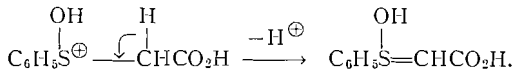

I

A close relationship exists between the mechanism proposed in equation [5] and the rearrangement of the chlorosulphonium chloride of thioanisole described by Bordwell and Pitt (8). The work described by Bordwell and Pitt led us to establish a parallel between equation [5] and the intramolecular rearrangement of halosulphonium halides of arylmercaptoacetic acids (9).

The mechanism by which bis(phenylmercapto)acetic acid (III) is formed from benzenethiol and phenylmercaptohydroxyacetic acid (II) undoubtedly follows the general scheme suggested by Campaigne and Leal (10). Resonance stabilization of the carbonium ion intermediate was not suggested by these workers but seems very likely in view of the work of Bordwell, Cooper, and Morita (11). The mechanism may thus be written:

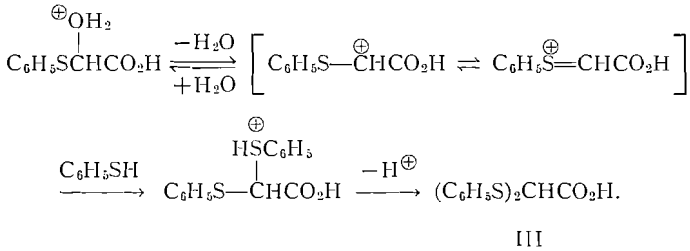

III

The foregoing mechanisms appear to account, in reasonable manner, for the formation of glyoxylic acid, benzenethiol, and bis(phenylmercapto)acetic acid by the acid-catalyzed cleavage of phenylsulphinylacetic acid. Some observations, however, still remain unexplained. Thus, on occasion, supersaturated aqueous solutions of phenylsulphinylacetic acid have given more diphenyl disulphide than can be accounted for by the oxygen of the air in the system. Perhaps the sulphoxide acts as an oxidizing agent (8).

The present paper raises questions concerning the generality of the intramolecular rearrangement of sulphoxides. The influence of ring substituents on the rearrangement of arylsulphinylacetic acids will be mentioned in future papers by us (9). However, since our work was restricted to arylsulphinylacetic acids and related compounds it is pertinent to draw attention to the acid-catalyzed rearrangement of diamyl sulphoxide for which Szmant (12) has tentatively suggested an intermolecular mechanism.

ACKNOWLEDGMENT

We thank the directors of Dominion Tar and Chemical Company for permission to publish this work.

REFERENCES

1. R. PUMMERER. Ber. **42**, 2282 (1909); Ber. **43**, 1401 (1910).
2. W. J. KENNEY, J. A. WALSH, and D. A. DAVENPORT. J. Am. Chem. Soc. **83**, 4019 (1961).
3. E. BAER. J. Am. Chem. Soc. **62**, 1597 (1940).
4. M. Z. BARAKAT and M. F. A. EL-WAHAB. J. Am. Chem. Soc. **75**, 5731 (1953).
5. R. CONNOR. *In* Organic chemistry, an advanced treatise. John Wiley and Sons, Inc., New York, N.Y. 1945. p. 872.
6. R. G. LAUGHLIN. J. Org. Chem. **25**, 864 (1960).
7. S. G. SMITH and S. WINSTEIN. Tetrahedron, **3**, 317 (1958).
8. F. G. BORDWELL and B. M. PITT. J. Am. Chem. Soc. **77**, 572 (1955).
9. D. WALKER and J. LEIB. To be published.
10. E. CAMPAIGNE and J. R. LEAL. J. Am. Chem. Soc. **76**, 1273 (1954).
11. F. G. BORDWELL, G. D. COOPER, and H. MORITA. J. Am. Chem. Soc. **79**, 376 (1957).
12. H. H. SZMANT. *In* Organic sulfur compounds. N. Kharasch. Pergamon Press, New York, N.Y. 1961.

THE PHOTODIMERS OF COUMARIN AND RELATED COMPOUNDS[1]

RAGINI ANET
Department of Chemistry, University of Ottawa, Ottawa, Canada
Received February 28, 1962

ABSTRACT

The photodimer of coumarin is shown to have the head-to-head cis cyclobutane structure I. An isomer, obtained by the lactonization of *o*-hydroxy-*trans*-cinnamic acid, is shown to have the head-to-tail trans structure II. The photodimers of *o*-methoxy- and *o*-hydroxy-*trans*-cinnamic acids have been interrelated.

The photodimer of coumarin has been known for nearly 60 years (1). In the last 20 years, the photodimers of several substituted coumarins have also been prepared (2). These have been of interest, as the substituted coumarins, e.g., the furanocoumarins, are known to react with the skin in presence of light (3). Some of these furanocoumarins, e.g. xanthotoxin, have in fact been used for the treatment of skin depigmentation as occurs in leucoderma, in both the Middle East and in India (2, 4). The photodimers of these compounds are known (5) but the structure of the dimers have not been determined. The present work describes the elucidation of the structure and stereochemistry of the photodimer of coumarin, the parent compound in this series.

A cyclobutane-type structure was assigned to these dimers (2) by analogy with the dimerization of the cinnamic acids to 1α,3β-diphenylcyclobutane-2α,4β-dicarboxylic (α-truxillic)[2] and 1α,2α-diphenylcyclobutane-3β,4β-dicarboxylic (β-truxinic) acid (6). The similarity in ultraviolet absorption spectra of 3,4-dihydro-7-methoxycoumarin and of the photodimer of 7-methoxycoumarin (III) lent support to a cyclobutane structure in which the 3,4-double bonds of the two pyrone rings were involved (8). An incomplete X-ray diffraction study on III published in 1958 (9) confirmed the presence of a cyclobutane ring; no conclusions regarding the disposition of the rest of the molecule were drawn.[3]

On the basis of a cis fusion[4] of the cyclobutane ring to the 6-membered pyrone rings, four structures can be considered for coumarin dimers, and are represented in Fig. 1. There are two sets of structural isomers, head-to-head and head-to-tail, each of which can exist in a cis or trans form. The problems of isomerism are simpler than in the case of dimeric cinnamic acids, where 11 possible isomers can exist.

The elucidation of the structures of the cinnamic acid dimers is largely due to the extensive work of Störmer and his collaborators (for a summary see ref. 6). The German workers distinguished among the various isomers by carrying out optical resolutions on suitable derivatives. With the physical methods now available, these time-consuming procedures are no longer necessary. For example, infrared spectroscopy can be useful in distinguishing between 5- and 6-membered anhydrides, thus allowing a distinction to be

[1]*A preliminary account of this work was published in Chem. & Ind. (London), 897 (1960). Presented in part at the Annual Conference of the Chemical Institute of Canada, Ottawa, June 13–15, 1960.*

[2]*The relative stereochemistry of substituents on the cyclobutane ring is designated α and β following Fieser's convention for carbohydrate derivatives (7).*

[3]*This work is erroneously reported in the Annual Reports of the Chemical Society (London), 1958, as showing a head-to-head structure for III.*

[4]*Recently, Corse, Finkle, and Lundin (10) have postulated a transfusion of cyclobutane rings to a cyclohexane-1,4-dione ring to explain the n.m.r. spectrum of the photodimer of 1,5-dicarbomethoxy-3-ketopenta-1,4-diene.*

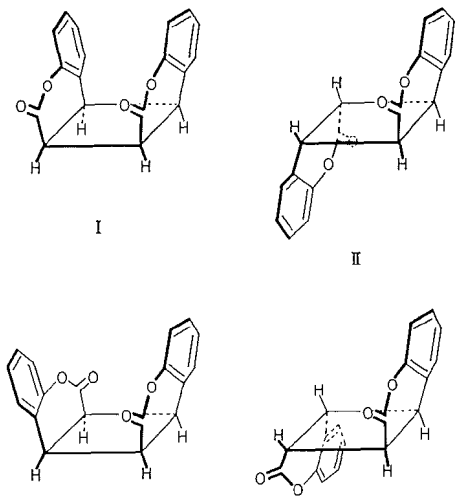

FIG. 1. Four isomeric structures for coumarin dimers. I represents the photodimer of coumarin, and II, the dilactone derived from the photodimer of *o*-hydroxy-*trans*-cinnamic acid.

made between the head-to-head (truxinic) and head-to-tail (truxillic) type dimers. Furthermore, n.m.r. spectroscopy can be a powerful tool in determining the relative stereochemistry of substituents on a cyclobutane ring, by taking advantage of the symmetry properties of these derivatives. Both these methods proved very valuable in the present work.

The photodimer of coumarin was prepared according to the method of Ciamician and Silber (1), viz., irradiation of an ethanolic solution of coumarin with sunlight. The same compound was also obtained by Schönberg's method (11), irradiation of a suspension of coumarin in water.

The only meaningful work reported on the photodimer of coumarin was Schönberg's observation (11) that it dissociated to coumarin on heating. This has been confirmed in the present study. de Jong's experiments (12) on I were of little value, as the products obtained were poorly characterized; no elemental analyses were recorded. For example, alkali fusion of I was reported to give an acid, m.p. 157°, which was claimed to be a cyclobutane dicarboxylic acid. Attempted repetition gives only salicylic acid, m.p. 158°.

In the present work, I was found to give a di-*o*-hydroxyphenylcyclobutane-dicarboxylic acid (IV), $C_{18}H_{16}O_6$, by dissolution of I in hot alkali, followed by careful acidification below 0°. The acid cyclized very readily to I in presence of a trace of acid at room temperature. The cyclization also took place on heating, so that the melting point of IV was not its true melting point, but that of I. The stereochemistry of IV and I was therefore identical.

In order to obtain a dimethyl ether dimethyl ester of the same stereochemistry as I, methylation of IV was tried with diazomethane. However, even after prolonged treatment, the material was largely phenolic. Methylation with dimethyl sulphate and alkali took place slowly, but after 36 hours at room temperature, 65–75% of phenolic compound had reacted, as estimated by the change in ultraviolet absorption spectrum in going from an alkaline to an acid solution (13). As this was expected to be a mixture of epimeric, as well as partially and fully methylated, products, the crude material was treated with diazomethane. A crystalline dimethyl ether dimethyl ester, V, $C_{22}H_{24}O_6$, m.p. 110°, was obtained in 70% overall yield. It was found to be homogenous by chromatography.

The n.m.r. spectrum of V (Fig. 2) was very informative. The spectrum revealed the presence of four different[5] methoxyl groups (τ, 6.26, 6.32, 6.59, and 6.82 (15)). Thus V can

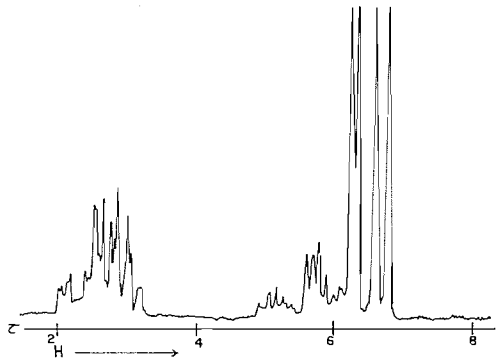

FIG. 2. The n.m.r. spectrum of V in carbon tetrachloride solution. τ values refer to tetramethylsilane as internal standard.

contain no elements of symmetry (axis, plane, or center), based on a time-average structure. This was in agreement with the unsymmetrical nature of the spectrum of the cyclobutane protons (τ, 5.0–6.3). The aromatic protons occurred at lowest field (τ, 1.98–3.6), and intensity measurements showed that the ratio of aromatic protons to methoxyl protons was 8.12.

The absence of symmetry deduced from the n.m.r. spectrum eliminated 9 of the 11 possible structures for a dimethyl ether dimethyl ester derived from the four possible structures for I (Fig. 1), taking into account the possibilities of epimerization. The 11 structures (*dl*-structures being counted as one) are shown in Fig. 3.

The esters can be divided into two groups, five, *a* to *e*, derived from a head-to-tail (truxillic type) and six, *f* to *k*, from a head-to-head (truxinic type) acid. Structures *a* to *e* can be eliminated for V, as all of them have an element of symmetry; *a* has a center, *b* and *e* have a plane, and *c* and *d* have both a plane and an axis of symmetry. None of these compounds can give rise to four methyl bands in the n.m.r. spectrum. Whereas *a*, *c*, and *d* should give rise to only two bands corresponding to six protons each, *b* and *e* would be expected to give rise to three bands in the ratio of 3:3:6. The ester V, and therefore I, can not be derived from a head-to-tail type structure. Of the six truxinic or head-to-head types, four structures, *f*, *g*, *h*, and *i*, can be eliminated. All these will give rise to only two methyl bands, as *f* and *g* have a plane of symmetry and *h* and *i* have an axis of symmetry in the plane of the cyclobutane ring. The two remaining structures, *j* and *k*, are the only possible structures for V, as they contain no element of symmetry. Each of them is formed from a head-to-head type structure for I.

In order to distinguish between the two possible structures *j* and *k* for V, the ester was treated with sodium methoxide in methanol. An epimeric ester, VI, $C_{22}H_{24}O_6$, m.p. 138°, was obtained. The n.m.r. spectrum of VI showed only two methyl bands (τ, 6.32 and 6.46), each corresponding to six protons; an element of symmetry had been restored during this epimerization. The ester VI was shown to be a cis diester as follows. Hydrolysis of VI with alkali gave a dicarboxylic acid, VII, $C_{20}H_{20}O_6$, m.p. 202°. With acetic anhydride, VII gave an anhydride, VIII, $C_{20}H_{18}O_5$, m.p. 121°. No epimerization took

[5]*The bands at τ 6.26 and 6.32 are tentatively assigned to the methoxyl groups on the phenyl rings by comparison with the n.m.r. spectrum of the fully methylated product obtained from the photodimer of 7-methoxycoumarin (14).*

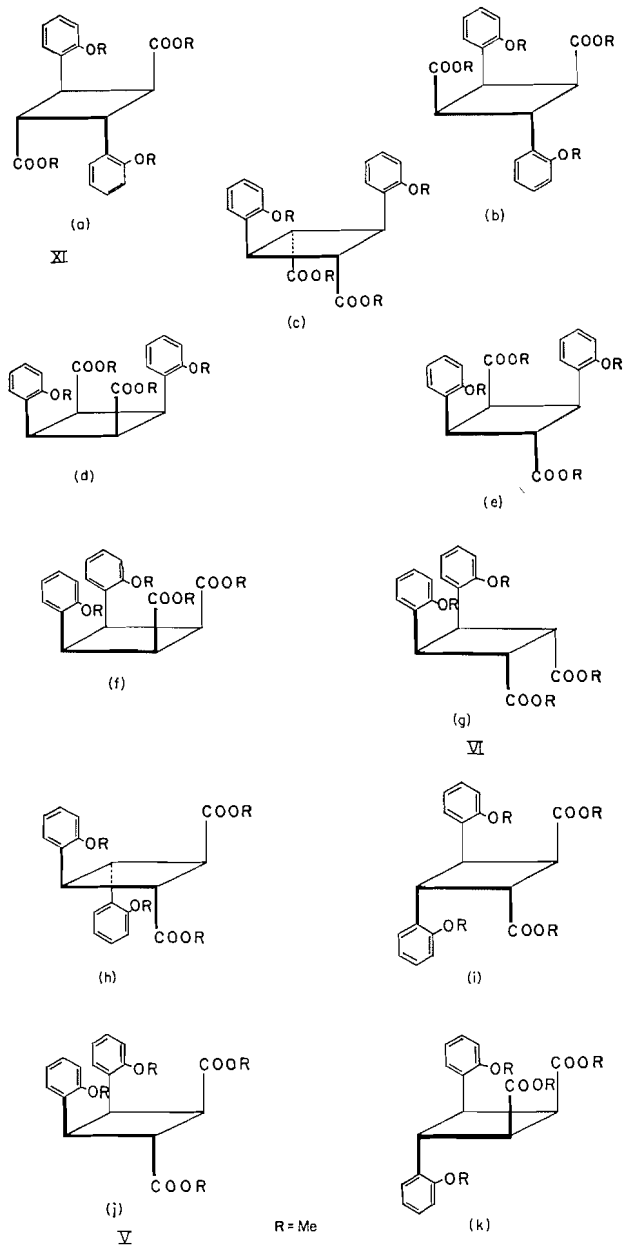

FIG. 3. The 11 isomeric structures for a dimethyl ether dimethyl ester derived from the four structures depicted in Fig. 1. V, VI, and XI are referred to in the text. Only one enantiomer of a *dl*-structure is shown.

place in this sequence of reactions, as VIII could be converted to VII with alkali at room temperature and further to VI with diazomethane. The carbonyl frequencies of the anhydride (1854 and 1768 cm^{-1}) were characteristic of a 5-membered anhydride (16) and were identical with those of the model compound 1α,2α-diphenylcyclobutane-3β,4β-dicarboxylic (β-truxinic) anhydride (6). The formation of a 5-membered anhydride from VI, via the reaction sequence described above, confirmed the head-to-head type

structure for VI, and therefore for V. The application of symmetry principles to the interpretation of the n.m.r. spectrum of V was correct.

Of the two structures for V, viz., *j* and *k*, only the former can give rise to an epimeric cis diester. The latter, *k*, which is itself a cis diester, can not epimerize to a new cis ester, but can only give rise to a trans ester. The structure *k* is therefore excluded for V, which must be 1α,2α-di-*o*-methoxyphenylcyclobutane-3α,4β-dicarboxylate *j*. Epimerization of this ester can lead to two possible cis esters, the all-cis 1α,2α-di-*o*-methoxyphenylcyclobutane-3α,4α-dicarboxylate (*f*) or 1α,2α-di-*o*-methoxyphenylcyclobutane-3β,4β-dicarboxylate (*g*). Of these, the former can be ruled out as it is unlikely that V, with three eclipsed interactions, would epimerize to an ester with four eclipsed interactions, and the ester VI must be 1α,2α-di-*o*-methoxyphenylcyclobutane-3β,4β-dicarboxylate (*g*).

The structure for V establishes the stereochemistry of the two aryl groups. These are 1:2-cis in V and VI, and must also be cis in their precursors, IV and I, as no epimerization of aryl groups is likely under the reaction conditions employed. Since the dicarboxylic acid IV cyclizes so readily to the dilactone I, the two carboxyl groups must be cis to the *o*-hydroxyphenyl groups. The complete structure and stereochemistry of IV and I is therefore 1α,2α-di-*o*-hydroxyphenylcyclobutane-3α,4α-dicarboxylic acid for IV, and the corresponding dilactone for I. These compounds therefore represent the hitherto unknown ω-truxinic acid type.[6]

Having established the structure for the photodimer of coumarin, the structures of the photodimers of two related compounds, viz., *o*-hydroxy-*trans*-cinnamic acid and *o*-methoxy-*trans*-cinnamic acid, can be considered. These are of interest, as the photodimer of *o*-hydroxy-*trans*-cinnamic acid has been reported to cyclize to a dilactone, II, m.p. 320° (19, 20), which is isomeric with the photodimer of coumarin.

The photodimers of the substituted cinnamic acids were prepared by irradiation of the crystalline acids with sunlight (19, 21), or with ultraviolet light (20). The photodimer of the *o*-hydroxy acid IX was reported to melt at 320°, which is undoubtedly not its true melting point, but the melting point of the cyclized dilactone II. The photodimer of the *o*-methoxy acid was reported to melt at 264°. These dimers were assigned a head-to-tail trans cyclobutane structure by Stobbe and Bremer (22) by analogy with the dimerization of *trans*-cinnamic acid to 1α,3β-diphenylcyclobutane-2α,4β-dicarboxylic acid (α-truxillic acid). However, this analogy is not strictly valid, as Bernstein and Quimby (23) demonstrated that different crystalline forms of *trans*-cinnamic acid give structurally different acids, i.e. head-to-tail (α-truxillic) or head-to-head (β-truxinic acid). The structures of IX and X could not be considered as established.

In the present work, IX and X were prepared by irradiation of the crystalline acids with ultraviolet light. In the case of the *o*-methoxy acid, the dimer obtained by this method had the same melting point (264°) as that reported in the literature (21). The structures of these compounds were investigated, by essentially the same approach as followed for I. However, as both the *o*-hydroxy and *o*-methoxy compounds were available in this series, the stereochemistry was established by making use of the interrelationships shown in the scheme below.

The dimers IX and X were shown to have the same stereochemistry at all the centers, by preparing the same dimethyl ether dimethyl ester XI, m.p. 132°, from each acid with diazomethane in ether. No epimerization seemed likely under the conditions employed.

[6]*Although all 11 dimeric cinnamic acids have been reported (6), the preparation of 1α,2α-diphenylcyclobutane-3α,4α-dicarboxylic (ω-truxinic) and 1α,2β-diphenylcyclobutane-3β,4α-dicarboxylic (μ-truxinic) acids by Shemyakin (17) is doubtful. Ettlinger (18) has suggested that these are lactonic acids, but the evidence has not been published.*

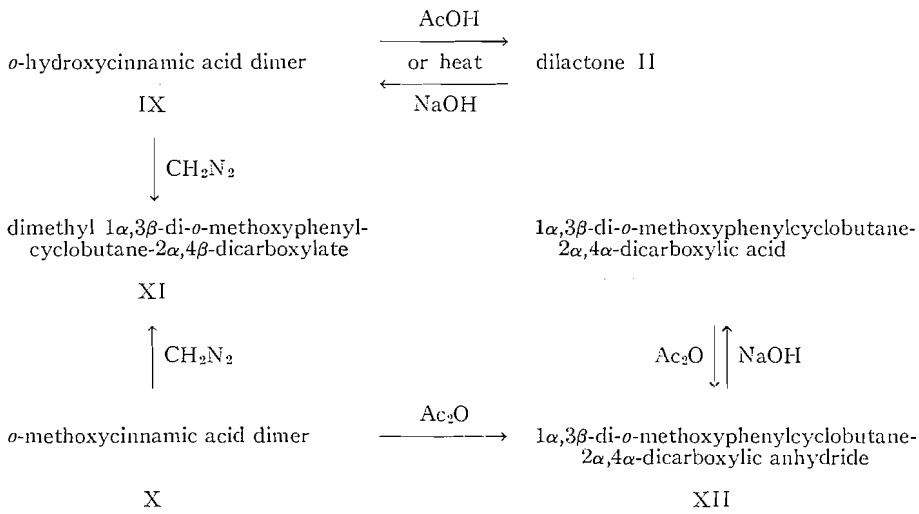

Treatment of X with boiling acetic anhydride containing a trace of *p*-toluenesulphonic acid gave an anhydride, $C_{20}H_{18}O_5$, m.p. 188° (XII), in good yield. The same anhydride could be obtained if the toluene sulphonic acid was omitted, but the yield of XII was very poor. The anhydride was shown to be intramolecular from its molecular weight (323) and 6-membered from its infrared spectrum (carbonyl bands at 1814 and 1762 cm^{-1}) (16). The model compound 1α,3β-diphenylcyclobutane-2α,4α-dicarboxylic anhydride (γ-truxillic anhydride) (6) showed the same frequencies, and these were slightly higher than those of glutaric anhydride (1802 and 1761 cm^{-1}) (16). This may reflect the strain involved in fusing a 6-membered anhydride 1:3 on a cyclobutane ring. The n.m.r. spectrum of XII, measured in pyridine (24), showed two methoxyl bands (τ, 6.87, 6.93); the two aryl groups were in different stereochemical environment, i.e., one group was cis and the other trans to the anhydride ring. Thus the aryl groups were situated 1:3-trans on the cyclobutane ring.

The stereochemistry of the two carboxyl groups relative to the aryl groups was shown as follows. The dilactone II was easily hydrolyzed to IX and the latter relactonized to give II. The stereochemistry of II and IX was identical. The easy interconversions of II and IX implied a cis relationship of the carboxyl and *o*-hydroxyphenyl substituents. The carboxyl groups were therefore 1:3-trans, and each of them was cis to one of the aryl substituents. That the lactonization of IX to give II involved the formation of 6-membered dihydropyrones was shown by the thermal decomposition of II to give coumarin. The compounds IX and X were indeed derivatives of 1α,3β-diphenylcyclobutane-2α,4β-dicarboxylic (α-truxillic) acid, and the isomer II was the head-to-tail trans compound.

The formation of the anhydride XII had involved the epimerization of one of the carboxyl groups. This was confirmed by treating XII with alkali at room temperature, which gave a new acid, $C_{20}H_{20}O_6$, m.p. 225–226° (XIII), mixed m.p. with X, 199–220°. The acid XIII was readily converted into its anhydride, and was therefore 1α,3β-di-*o*-methoxyphenylcyclobutane-2α,4α-dicarboxylic acid. Treatment of XIII with diazomethane gave a low-melting ester which readily epimerized to XI. The ester was not obtained crystalline, but its n.m.r. spectrum did show three methyl bands in the ratio of 1:1:2. The pattern changed rapidly to that given by dimethyl 1α,3β-di-*o*-methoxyphenyl-2α,4β-dicarboxylate (XI), if traces of acid or alkali were added.

The assignment of the cis structure for the photodimer of coumarin (I) has now received full confirmation by Professor Griffin, Yale University (private communication). Ozonolysis of I gives 1α,2α,3α,4α-tetracarboxycyclobutane identical with the one prepared by Griffin and Veber (25).

It is of interest that Schenck has recently reported (26) that irradiation of coumarin in presence of benzophenone gives a new dimer. A head-to-head trans structure has been suggested for it.

EXPERIMENTAL

All melting points are uncorrected. Infrared spectra were determined on a Perkin–Elmer 'Infracord' instrument except those of anhydrides, which were measured on a Perkin–Elmer single-beam double pass instrument. The n.m.r. spectra were recorded on a Varian V-4302 60 Mc/s instrument.

1α,2α-Di-o-hydroxyphenyl-3α,4α-dicarboxylic Acid Dilactone: the Photodimer of Coumarin (I)

Coumarin (300 g) was dissolved in 3 l. ethanol and exposed to sunlight in eight stoppered pyrex flasks (500 ml) for 4 weeks (May–June). After 1 week, the solution turned pale yellow and started depositing crystals. These were removed periodically, and a total of 4.5 g was collected in 4 weeks. Two crystallizations from glacial acetic acid gave 4 g of I, m.p. 260–262° (decomp.) (lit. m.p. 260° (1)). The ethanolic mother liquors were once again irradiated; after a further 6 weeks, 1 g of I was collected. No crystalline material apart from coumarin was isolated from the deep red solution.

The same compound was also obtained when a suspension of 20 g coumarin in 300 ml water was irradiated with sunlight. The yield of I was 185 mg, which was isolated by extraction of unchanged coumarin with ether.

Alkali Fusion of I: Formation of Salicyclic Acid

One hundred milligrams of I was heated with 0.5 g solid potassium hydroxide at 275° for 10 minutes. The melt was cooled, 5 ml water added, and the mixture acidified with hydrochloric acid. Extraction with ethyl acetate gave a gum from which 22 mg salicylic acid was isolated by extraction with hot petroleum ether (b.p. 80–100°). Recrystallization from the same solvent gave a sample, m.p. 158°, undepressed with an authentic sample. The infrared spectra (nujol mull) of the two samples were superposable.

Hydrolysis of I: 1α,2α-Di-o-hydroxyphenylcyclobutane-3α,4α-dicarboxylic Acid (IV)

Three hundred milligrams of I were dissolved in 5 ml of hot 10% potassium hydroxide. The solution was filtered and cooled to 0°. An ice-cold solution of 2% hydrochloric acid was added gradually with strong cooling, taking care to keep the temperature at 0–5°. The addition of acid was stopped when the solution turned milky. This was then allowed to stand at 0° for 15 minutes. The precipitated acid was filtered off and washed with 10 ml of a citrate–phosphate buffer of pH 7, and then with 5 ml water, followed by 20 ml pentane. The solid was taken up in acetone and filtered. The acetone solution gave 127 mg of the cyclobutane acid IV on evaporation of the solvent below 10°. (Found: C, 66.0; H, 4.7. Calc. for $C_{18}H_{16}O_6$: C, 65.8; H, 4.9%.)

Methylation of I: Dimethyl 1α,2α-Di-o-methoxyphenylcyclobutane-3α,4β-dicarboxylate (V)

A solution of 1 g of I in 10% potassium hydroxide was stirred with dimethyl sulphate (1 ml added at intervals) for 36 hours. The solution was kept strongly alkaline, more potassium hydroxide was added as necessary. After acidification with hydrochloric acid, the product was extracted with ethyl acetate when a gum (0.98 g) was obtained. Attempts to obtain a crystalline material did not succeed. The gum was therefore treated with excess ethereal diazomethane at room temperature. After 2 hours, the excess diazomethane was destroyed by cautious addition of acetic acid and the ether extracted with 1% alkali (twice) and then with water till neutral. The ether extract was dried over anhydrous sodium sulphate and the ether removed under reduced pressure. The residue (0.78 g) crystallized on treatment with a little ethyl acetate followed by petroleum ether (b.p. 30–60°). The crystals, m.p. 104–108°, were chromatographed over alumina, and benzene–ether (9:1) eluted 0.75 g of the dimethyl ether dimethyl ester V, m.p. 110°. (Found: C, 68.7; H, 6.2. Calc. for $C_{22}H_{24}O_6$: C, 68.7; H, 6.3%.)

Epimerization of V: Dimethyl 1α,2α-Di-o-methoxyphenylcyclobutane-3β,4β-dicarboxylate (VI)

The dimethyl ester V (200 mg) was refluxed under nitrogen with a solution of 100 mg of sodium in 25 ml methanol. After 6 hours the methanol was removed, and the residue treated with dilute hydrochloric acid and extracted with ethyl acetate (3×20 ml). The organic layer was washed with dilute alkali and dried (sodium sulphate). Removal of ethyl acetate gave 171 mg of VI, crystallizing from ethyl acetate – petrol ether in colorless plates, m.p. 138°. (Found: C, 68.5; H, 6.2. Calc. for $C_{22}H_{24}O_6$: C, 68.7; H, 6.3%.)

Hydrolysis of VI: 1α,2α-Di-o-methoxyphenylcyclobutane-3β,4β-dicarboxylic Acid (VII)

The ester VI (100 mg) was refluxed with 10% potassium hydroxide (8 ml) containing a few drops of dioxane for 8 hours. The alkaline solution was extracted with ethyl acetate to remove unchanged ester VI,

and the aqueous layer acidified with hydrochloric acid. Extraction with ethyl acetate gave 60 mg of VII, which after crystallization from the same solvent melted at 202° with decomposition. (Found: C, 67.2; H, 5.5. Calc. for $C_{20}H_{20}O_6$: C, 67.4; H, 5.9%.)

Methylation of VII

The acid VII (20 mg) was treated with diazomethane in ether. After 1 hour at room temperature, the ether was evaporated to give 20 mg of VI, m.p. 137–138°, mixed m.p. with VI 138°. The infrared spectra of the two samples (nujol mull) were superposable.

Anhydride from VII: 1α,2α-Di-o-methoxyphenylcyclobutane-3β,4β-dicarboxylic Anhydride (VIII)

The acid VII (40 mg) was refluxed with acetic anhydride (3 ml) for 1 hour. The acetic anhydride was removed under reduced pressure, and the residue dissolved in chloroform. The chloroform solution was washed with aqueous sodium carbonate, and the chloroform layer dried over anhydrous sodium sulphate. Evaporation of the solvent followed by crystallization from acetone – petrol ether gave 28 mg of the anhydride VIII, m.p. 121° after three crystallizations. (Found: C, 70.8; H, 5.5. Calc. for $C_{20}H_{18}O_5$: C, 71.0; H, 5.6%.)

Hydrolysis of VIII

The anhydride VIII (20 mg) was stirred with 5% aqueous sodium hydroxide at room temperature for 10 hours. The aqueous layer was extracted with chloroform to remove unchanged anhydride (2 mg). Acidification of the aqueous layer followed by extraction with ethyl acetate gave 15 mg of an acid, m.p. 202° (decomp.). Mixed melting point with a sample of VII was undepressed, and the infrared spectra (nujol mull) were superposable.

Photodimer of o-Hydroxy-trans-cinnamic Acid: 1α,3β-Di-o-hydroxyphenylcyclobutane-2α,4β-dicarboxylic Acid (IX)

Two grams of *o*-hydroxy-*trans*-cinnamic acid prepared from coumarin (27) was irradiated with ultraviolet light (Hanovia, Type 306). From time to time, the solid was stirred. After 48 hours the solid was extracted with hot chloroform, in which the monomer is insoluble. Evaporation of VIII gave 0.4 g of VIII. The melting point of VIII reported in the literature (320°) was the same as that of the dilactone II, into which it is converted on heating.

Dilactone of IX: 1α,3β-Di-o-hydroxyphenylcyclobutane-2α,4β-dicarboxylic Acid Dilactone (II)

The acid IX (200 mg) was heated with acetic anhydride for 5 minutes. The anhydride was removed under reduced pressure and the residue treated with aqueous sodium carbonate. The insoluble dilactone (163 mg) was collected and crystallized from glacial acetic acid, m.p. 324° (decomp.).

Hydrolysis of II

The dilactone II (100 mg) was dissolved in 5% aqueous potassium hydroxide on heating. The solution was filtered, cooled to 0°, and acidified cautiously with hydrochloric acid till neutral. After standing for 15 minutes, the precipitated acid was collected (40 mg) and found to be identical with IX (infrared spectra).

Decomposition of II: Formation of Coumarin

The dilactone II (50 mg) was heated at 300° for 10 minutes in a test tube. An oily distillate collected at the top of the tube and was treated with a little ether when it crystallized. The crystals, m.p. 68°, were found to be identical with coumarin (mixed m.p.).

Methylation of IX: Dimethyl 1α,3β-Di-o-methoxyphenylcyclobutane-2α,4β-dicarboxylate (XI)

The acid IX (100 mg) was suspended in 30 ml ether containing a few drops of methanol. An excess of diazomethane in ether was added and the mixture allowed to stand at room temperature for 3 hours. It was worked up in the usual manner to give 25 mg of the dimethyl ether dimethyl ester XI, m.p. 132° after crystallization from ether. (Found: C, 68.4; H, 6.4. Calc. for $C_{22}H_{24}O_6$: C, 68.7; H, 6.3%.)

Photodimer of o-Methoxycinnamic Acid: 1α,3β-Di-o-methoxyphenylcyclobutane-2α,4β-dicarboxylic Acid (X)

An acetone solution of *o*-methoxy-*trans*-cinnamic acid prepared by the methylation of coumarin (28) was evaporated on two watchglasses (7-cm diameter) by a fast stream of air. The small crystals thus deposited were irradiated by a Hanovia lamp for 36 hours. From time to time the solid was taken up in cold acetone to remove the sparingly soluble dimer X, and the acetone solution recycled. X (1.8 g) as collected from 4 g of the monomer, and crystallized from chloroform–methanol, m.p. 264° (lit. (21) m.p. 264°).

Methylation of X: Dimethyl 1α,3β-Di-o-methoxyphenylcyclobutane-2α,4β-dicarboxylate (XI)

The acid (120 mg) was esterified with diazomethane as described above to give the same diester (130 mg), XI, m.p. 132°. Mixed melting point with a sample prepared from IX was undepressed and the infrared spectra (nujol mull) were superposable.

Anhydride from X: 1α,3β-Di-o-methoxyphenylcyclobutane-2α,4α-dicarboxylic Acid Anhydride (XII)

The acid X (200 mg) was refluxed with 7 ml acetic anhydride containing 5 mg *p*-toluenesulphonic acid for 6 hours. The acetic anhydride was removed under reduced pressure and the residue taken up in chloroform. The chloroform extract was washed with alkali and dried over anhydrous sodium sulphate. Concentration of the chloroform solution followed by addition of petrol ether (b.p. 30–60°) gave a crystalline anhydride

(154 mg) which, after three crystallizations from chloroform – petrol ether, melted at 188°. (Found: C, 70.9; H, 5.6; mol. wt. (Rast), 323. Calc. for $C_{20}H_{18}O_5$: C, 71.0; H, 5.6; mol. wt., 338.) The infrared spectrum (CCl_4) showed carbonyl bands at 1814 and 1762 cm^{-1}.

Hydrolysis of XII: 1α,3β-Di-o-methoxyphenylcyclobutane-2α,4α-dicarboxylic Acid (XIII)

The anhydride XII (170 mg) was treated with 10% aqueous sodium hydroxide at room temperature for 18 hours. The aqueous layer was extracted once with chloroform to remove unchanged anhydride, and the aqueous layer acidified. Ethyl acetate extraction gave the acid XII (104 mg), which after crystallization from acetone – petrol ether melted at 225–226°. Mixed melting point with X was 199–220°. (Found: C, 67.2; H, 5.9. Calc. for $C_{20}H_{20}O_6$: C, 67.4; H, 5.9%.)

ACKNOWLEDGMENT

I thank Professor A. T. Blomquist, Cornell University, for a gift of β-truxinic acid.

REFERENCES

1. P. CIAMICIAN and G. SILBER. Ber. **35**, 4229 (1902).
2. A. SCHÖNBERG. Präparativ organische Photochemie. Springer-Verlag, Berlin. 1958.
3. L. MUSAJO, G. RODIGHIERO, and G. CAPAROLE. Bull. soc. chim. biol. **36**, 1213 (1954).
4. PSORALENS and Radiant Energy Proceedings of a Symposium. J. Invest. Dermatol. **32**, 131 (1959).
5. G. RODIGHIERO and V. CAPELLINA. Gazz. chim. ital. **91**, 103 (1961).
6. R. A. RAPHAEL. *In* Chemistry of carbon compounds. Vol. IIA. *Edited by* E. H. RODD. Elsevier Publishing Co., Amsterdam. 1953.
7. L. F. FIESER. J. Am. Chem. Soc. **72**, 623 (1950).
8. R. FISCHER. Arch. Pharm. 279 (1941).
9. E. FRASSON, G. RODIGHIERO, and C. PANATTONI. Ricerca sci. **28**, 517 (1958).
10. J. CORSE, B. J. FINKLE, and R. E. LUNDIN. Tetrahedron Letters, No. 1, 1 (1961).
11. A. SCHÖNBERG, N. LATIF, R. MOUBASHER, and W. I. AWAD. J. Chem. Soc. 374 (1950).
12. A. W. K. DE JONG. Rec. trav. chim. **43**, 316 (1924).
13. A. E. GILLAM and E. S. STERN. An introduction to electronic absorption spectroscopy in organic chemistry. Edward Arnold, London. 1954.
14. R. ANET. Unpublished work.
15. G. V. D. TIERS. J. Phys. Chem. **62**, 1151 (1958).
16. L. J. BELLAMY. The infrared spectra of complex molecules. 2nd ed. John Wiley and Sons Inc., New York. 1958.
17. M. M. SHEMYAKIN. Compt. rend. acad. sci. U.R.S.S. **24**, 768 (1939); Brit. Chem. and Physiol. Abstr. AII, 169 (1941). Zhur. Obshchei. Khim. **11**, 219 (1941); Chem. Abstr. **35**, 7944 (1941).
18. M. G. ETTLINGER. J. Am. Chem. Soc. **77**, 6646 (1955).
19. K. T. STRÖM. Ber. **37**, 1383 (1904).
20. F. WESSELY and I. PLAICHINGER. Ber. **75**, 971 (1942).
21. J. BERTRAM and R. KÜRSTEN. J. prakt. Chem. **51**, 322 (1895).
22. H. STOBBE and R. BREMER. J. prakt. Chem. **123**, 1 (1929).
23. H. I. BERNSTEIN and W. J. QUIMBY. J. Am. Chem. Soc. **65**, 1845 (1943).
24. G. SLOMP and F. MACKELLAR. J. Am. Chem. Soc. **82**, 999 (1960).
25. G. W. GRIFFIN and D. F. VEBER. J. Am. Chem. Soc. **82**, 6417 (1960).
26. G. O. SCHENCK, W. HARTMANN, S. P. MANNSFELD, W. METZNER, R. STEINMETZ, I. V. WILLUCKI, R. WOLGAST, and C. H. KRAUCH. Angew. Chem. **73**, 764 (1961).
27. W. VON MILLER and F. KINKELIN. Ber. **22**, 1714 (1889).
28. S. RANGASWAMI and T. R. SESHADRI. Proc. Indian Acad. Sci. A, **5**, 249 (1936).

THE BINARY (ANHYDROUS) SYSTEMS $NaNO_3$–$LiNO_3$, $LiClO_3$–$NaClO_3$, $LiClO_3$–$LiNO_3$, $NaNO_3$–$NaClO_3$ AND THE QUATERNARY SYSTEM $NaNO_3$–$LiNO_3$–$LiClO_3$–$NaClO_3$

A. N. Campbell, E. M. Kartzmark, and M. K. Nagarajan
Chemistry Department, University of Manitoba, Winnipeg, Manitoba

Received January 29, 1962

ABSTRACT

The equilibrium diagrams of the systems $NaNO_3$–$LiNO_3$, $LiClO_3$–$NaClO_3$, $LiClO_3$–$LiNO_3$, $NaNO_3$–$NaClO_3$, and $NaNO_3$–$LiNO_3$–$LiClO_3$–$NaClO_3$ have been investigated by thermal analysis and, to some extent, by X-ray powder photography. All the binary systems are of the simple eutectic type, accompanied, in one instance, by considerable solid solubility. The allotropic transformation of sodium nitrate complicates the equilibria involving sodium nitrate somewhat, especially when there is solid solution.

The quaternary diagram shows that in the (fused) reaction

$$NaNO_3 + LiClO_3 \rightleftarrows LiNO_3 + NaClO_3$$

lithium nitrate and sodium chlorate constitute the stable solid pair. The two invariant points of this system are both congruent.

As a preliminary to an investigation of the thermodynamic and electrical properties of molten salt mixtures, we found it advisable to investigate the equilibrium diagrams of mixtures of the salts named in the title. Because of the low melting point of lithium chlorate we were able to obtain a quaternary eutectic lying at 92.6° C. Such a relatively low temperature greatly facilitates the ease and accuracy of fused salt investigations. In addition, the quaternary system is of interest in itself, since very few investigations of quaternary salt systems have been made in the absence of water. In other words, most of the previous investigations have been isothermal studies of two anions, two cations, and water.

Of the component binary systems, only $NaNO_3$–$LiNO_3$ had been previously investigated, by Benrath and Tesche (1) and by Favorskii (2). Both investigators reported a simple eutectic-type diagram but made no mention of solid solubility.

EXPERIMENTAL

All the salts, except lithium chlorate, were purchased and were of the highest purity. The original method for the preparation of lithium chlorate, viz., double decomposition between barium chlorate and lithium sulphate, is due to Potilitzin (3) and to Kraus (4). We used the technique devised by Griffiths (5). Lithium chlorate is extremely hygroscopic and must be handled in a nitrogen-filled dry-box. We used barium oxide to dehydrate the dry-box atmosphere. The final product was heated at 100° C, under high vacuum, for 6–8 weeks. The melting point was 127.8° C.

For the melts which did not contain lithium chlorate, and which were therefore not markedly hygroscopic, it was not necessary to evacuate the space above the melt and the simple apparatus of Fig. 1 was used: it held about 100 g of salt mixture. The figure shows the thermocouple well and inlet and outlet tubes for the introduction of nitrogen. The stirrer passed through a water-jacketted mercury-seal.

Another type of cell (Fig. 2) was used for systems containing lithium chlorate. In this cell the melt was not stirred, but that does not appear to have affected the reproducibility of the results. The cell was loaded with lithium chlorate in the dry-box. After connecting up, it was immediately placed under high vacuum, which was only broken for the introduction of weighed amounts of the second component, an operation requiring only a few seconds.

In order to increase the sensitivity of thermal analysis the furnace in which the salt mixtures were melted was not allowed to cool freely. The current to the furnace was progressively reduced, by using a geared-down motor to operate a "Variac". The motor itself had a low speed. With this apparatus it was possible to continuously reduce the current over about 20 hours. Since only the input voltage was regulated, there was

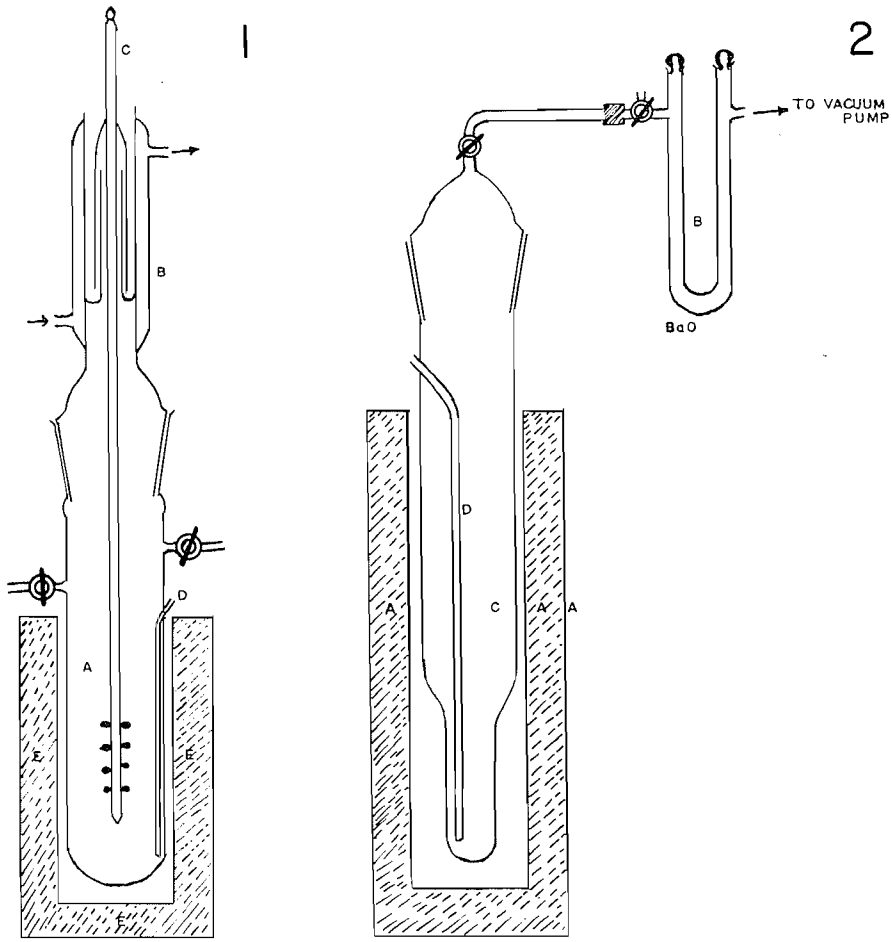

FIGS. 1 and 2.

a faster lowering of power input at the start than later on and a consequent more rapid decrease of temperature at the beginning of cooling, but this was an advantage since, when a system is partially solid, slower rates of cooling are necessary to establish equilibrium by solid diffusion.

The copper–constantan thermocouple was calibrated using the freezing points of tin (231.9° C) and cadmium (320.9° C) and the steam point corrected for barometric pressure. For thermal analysis the thermocouple was connected through a six-point switch to a Brown Electronik single-point recorder (range 20 mv). The other two points of the switch were connected to a precision potentiometer for the accurate determination of temperature whenever the cooling current indicated a point of interest.

Systems containing large amounts of lithium chlorate supercool considerably, as much as 18°, before solid lithium chlorate separates. Because of the very hygroscopic nature of lithium chlorate direct seeding was impossible, so the following procedure was used. After the approximate location of a point of interest by a preliminary thermal analysis, the experiment was repeated and when a temperature some three or four degrees above the expected temperature was reached, the cell was removed from the furnace, placed on a block of ice, till the liquid became fogged, and then reinserted in the furnace, an operation occupying barely 45 seconds.

It is notorious that the transitions

$$\alpha\text{-}NaNO_3 \rightleftarrows \beta\text{-}NaNO_3 \text{ and } \alpha\text{-}LiClO_3 \rightleftarrows \beta\text{-}LiClO_3$$

are very slow. In order to obtain a satisfactory "break" on the cooling curve the material was kept for 24 hours at a temperature above that of transition. After this treatment, a very sharp "break" was obtained on cooling. In most of these cases, however, heating curves gave equally reliable results and hence were

extensively employed. The equilibrium curves within the solid region, showing the effect of successive addition of sodium chlorate to sodium nitrate on the transition temperature of the latter, were obtained entirely by this procedure.

Use was occasionally made of differential thermal analysis. Copper was found to be a suitable inert body but, when investigating the effect of sodium chlorate on the transition temperature of sodium nitrate and of lithium chlorate, it was found more convenient to use an equal weight of the appropriate pure salt itself. A five-junction copper–constantan thermocouple was used in this work. Since the transition temperature is lowered by the addition of the second salt, due to solid solubility, the transition occurring in the pure material does not prevent its use as the "inert" material.

When investigating the quaternary system, we always commenced from one of the binary eutectics and added a known mixture of the other two salts. After some preliminary attempts, the approximate direction of the eutectic trough became apparent, and it was possible to add salts in the correct proportion to remain in the trough. When a given mixture was off the trough this was of course indicated on the cooling curve by a preliminary point of inflection.

X-Ray powder photographs were taken by the usual technique.

EXPERIMENTAL RESULTS

The experimental results are given in Tables I–VII.

TABLE I

System $LiClO_3$–$NaClO_3$

	Weight% $LiClO_3$	Temperature (°C)		
		Liquidus	Solidus	Transition (in $LiClO_3$)
1	100.00	—	127.9	99.1
2	94.27	126.5	107.1	99.9
3	90.63	125.4	107.1	—
4	81.38	120.1	107.0	98.6
5	73.38	114.2	107.2	89.0
6	67.04	108.7	107.2	—
7	63.52	110.8	107.1	—
8	59.54	119.6	107.2	—
9	55.48	129.9	107.1	100.0
10	49.61	143.9	107.1	97.1
11	38.92	170.3	107.0	99.1
12	26.82	197.9	107.0	99.8
13	15.51	226.4	106.9	99.2
14	5.10	248.5	107.1	—
15	0.00	—	259.9	—

The data of Tables II and III are represented graphically in Fig. 3.

The data of Table VI are plotted by the method of Jänecke in Fig. 4. Table VII contains the eutectic temperatures and compositions of the four binary systems, together with the two eutectics of the quaternary system.

DISCUSSION

The general accuracy of the results is about ±0.5° C, but that of the transition temperatures, freezing points of pure salts, and the eutectic temperatures is higher, about ±0.05° C, since these temperatures were read directly on a precision potentiometer.

$LiClO_3$–$NaClO_3$

When the data of Table I are plotted as the usual T–x diagram, the system appears to be of the simple eutectic type, unaccompanied by appreciable solid solubility. The eutectic temperature is 107.1°±0.05°, and the eutectic composition 34.55 weight% sodium chlorate. The approximate constancy of the figures in the last column of Table I shows that the temperature of the transition α-$LiClO_3 \rightleftarrows \beta$-$LiClO_3$ is unaltered by the addition of sodium chlorate.

TABLE II
System $NaClO_3$–$NaNO_3$

	Weight% $NaClO_3$	Temperature (°C)		
		Liquidus	Solidus	Others
1	0.00	—	306.6	—
2	9.92	291.4	265.6	89.7†
3	14.85	283.3	270.4	—
4	18.44	277.2	262.1	—
5	20.02	273.7	257.8	131.6†
6	23.32	269.2	247.0	251.4
7	28.06	260.9	236.9	251.5†
8	32.13	255.6	230.2	251.8
9	35.21	251.8	224.9	187.8†
10	38.74	245.6	218.7	199.1†
11	44.34	237.2	210.9	—
12	49.99	227.9	211.1	—
13	53.70	219.2	211.2	—
14	57.09	—	211.0	—
15	50.02	213.9	211.2	—
16	62.78	217.3	211.4	—
17	66.47	222.0	211.9	—
18	71.22	226.7	211.3	—
19	76.91	231.4	210.8*	—
20	79.79	234.5	214.0	—
21	81.07	235.6	215.3	192.8‡
22	83.34	237.4	219.0	—
23	86.40	239.8	222.3	—
24	88.69	241.6	226.0	133.9‡
25	90.99	244.3	230.4	—
26	93.29	248.1	238.2	—
27	96.48	253.5	248.6	94.1‡
28	100.00	—	259.9	—

*Eutectic.
†Reaction I.
‡Reaction II.

TABLE III
Effect of $NaClO_3$ on the transition α-$NaNO_3 \rightleftarrows \beta$-$NaNO_3$

	Weight% $NaClO_3$	Transition point (°C)	
		First inflection	Second inflection
1	0.00	274.6	
2	9.92	269.8	267.3
3	14.85	265.1	261.7
4	18.44	260.4	257.1
5	23.32	—	251.4
6	28.06	—	251.5
7	32.13	—	251.8
8	35.21	—	251.8

$NaClO_3$–$NaNO_3$

The column entitled "others" in Table II gives the temperatures corresponding to solid transformations below the eutectic temperature. Both components exhibit solid solubility and at the eutectic temperature this is considerable. The extents of solid solubility at the eutectic temperature are 21.7% sodium nitrate and 57.2% sodium nitrate respectively. As the temperature falls the solid solubility decreases and the following solid-state reactions occur: (1) α-solid solution of sodium nitrate in sodium chlorate $\rightarrow$ β-solid solution of sodium chlorate in sodium nitrate and (2) β-solid solution

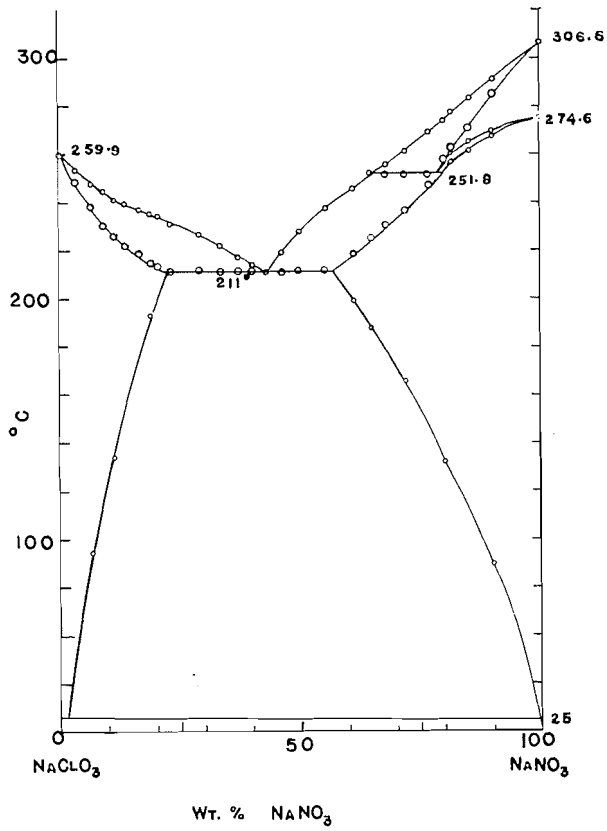

FIG. 3.

TABLE IV
System $LiNO_3$–$NaNO_3$

	Weight% $NaNO_3$	Temperature (°C)	
		Liquidus	Solidus
1	0.00	—	255.07
2	8.87	241.2	183.0
3	13.36	233.4	183.0
4	17.98	227.5	183.1
5	26.08	215.5	183.2
6	32.10	207.1	183.3
7	37.47	198.1	182.9
8	46.31	183.04 (eutectic)	
9	49.91	192.3	183.1
10	61.33	219.9	183.0
11	70.92	241.9	182.9
12	79.11	260.8	183.0
13	85.03	274.7	183.1
14	91.47	288.8	183.0
15	100.00	—	306.6

of sodium chlorate in sodium nitrate → α-solid solution of sodium nitrate in sodium chlorate. The crossing of the solid solubility curve, when a mixture of given composition

TABLE V

System $LiClO_3$–$LiNO_3$

	Weight% $LiNO_3$	Temperature (°C)	
		Liquidus	Solidus
1	0.00	—	127.9
2	3.84	126.4	101.0
3	11.51	123.3	100.8
4	22.48	117.1	100.4
5	30.01	111.0	100.7
6	35.09	106.4	100.7
7	39.78	100.8 (eutectic)	
8	44.49	111.1	100.6
9	48.93	123.9	101.0
10	53.47	134.8	100.9
11	63.32	159.9	100.9
12	72.91	184.0	100.8
13	74.78	189.5	100.9
14	84.00	213.7	100.8
15	89.44	227.4	100.6
16	100.00	—	255.07

TABLE VI

Quaternary system Li–Na–ClO_3–NO_3

	$\frac{ClO_3}{ClO_3+NO_3}\times 100$	$\frac{Na}{Na+Li}\times 100$	Trough temperature (°C)
X	0.00	41.28	183.04 (binary eutectic I)
	5.85	43.82	180.7
	11.18	46.39	178.4
	43.99	51.14	158.1
	49.92	64.01	153.1
	55.51	66.72	147.2 (quaternary eutectic) A
	51.46	100.00	211.0 (binary eutectic III)
	51.55	97.71	209.1
	52.28	92.85	203.9
	54.32	75.03	172.5
Y	100.00	30.96	107.1 (binary eutectic IV)
	93.50	32.42	105.2
	78.93	35.61	98.5
	71.40	37.32	92.6 (quaternary eutectic) B
	53.60	0.00	100.8 (binary eutectic II)
	55.61	4.58	100.1
	57.45	8.37	99.4
	61.13	15.99	98.0
Z	58.0	62.0	156.3
	58.6	58.8	158.9
	60.2	56.8	149.0

NOTE: Mixtures X solidify completely at 147.2° C. Mixtures Y solidify completely at 92.6° C. Mixtures Z lie on the line AB (see Fig. 4).

is cooled, was observed in thermal analysis and is given in Table II. The limits of solid solubility at room temperature were determined by X-ray analysis.

Table III shows the effect of additions of sodium chlorate on the transition temperature of sodium nitrate, α-sodium nitrate $\rightleftarrows$ β-sodium nitrate. This transition from a high-temperature cubic form to a low-temperature rhombohedral form was first observed by Kracek (6). He reported the transition temperature as 275° C. This transition proceeds so slowly and is accompanied by so small a heat effect that it is difficult to detect by direct thermal analysis, but it can be detected by differential thermal analysis as 274.6° C.

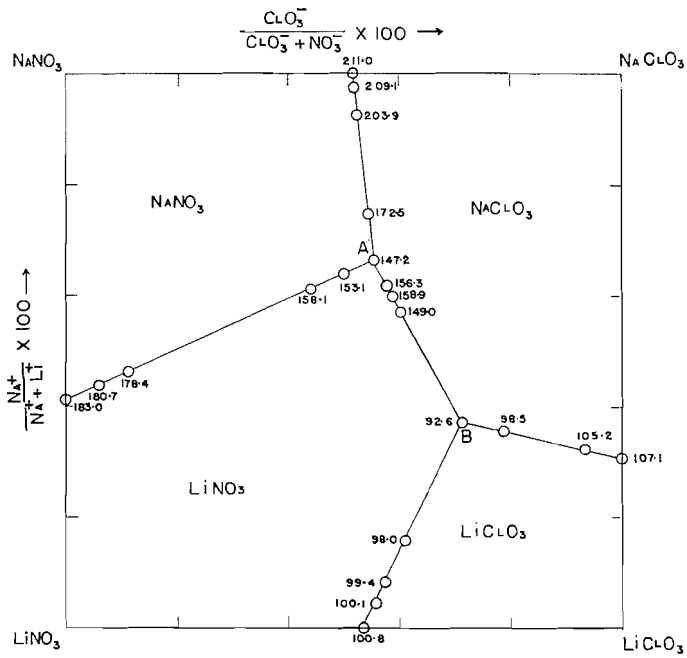

FIG. 4.

TABLE VII

Eutectic composition (mole%) and eutectic temperatures

	Binary eutectics		
I	$LiNO_3$	58.72	183.04° C
	$NaNO_3$	41.28	
II	$LiClO_3$	53.60	100.8° C
	$LiNO_3$	46.40	
III	$NaClO_3$	51.46	211.0° C
	$NaNO_3$	48.54	
IV	$LiClO_3$	69.04	107.1 °C
	$NaClO_3$	30.96	
	Quaternary eutectics		
A	Solid phases: $NaNO_3$, $NaClO_3$, $LiNO_3$		147.2° C
	Mole% ClO_3 = 55.51		
	Mole% Na = 66.72		
B	Solid phases: $NaClO_3$, $LiClO_3$, $LiNO_3$		92.6° C
	Mole% ClO_3 = 71.40		
	Mole% Na = 37.32		

The occurrence of two transition temperatures in mixtures containing sodium chlorate shows that sodium chlorate dissolves in both α- and β-sodium nitrate. The equilibrium diagram Fig. 3 is self-explanatory.

The results of the X-ray powder photographs were unequivocal. The line spacings and visual intensities were measured for the pure salts and found to agree with the ASTM index. The lines in the mixtures were all found to be identifiable with those belonging

either to pure sodium chlorate or pure sodium nitrate. It therefore appears that solid solubility at room temperature does not exceed, say, 5%.

$LiNO_3$–$NaNO_3$

The data for the system $LiNO_3$–$NaNO_3$ (Table IV) when plotted give a simple eutectic diagram, unaccompanied by solid solution. In the absence of solid solution, the temperature of the transition α-$NaNO_3 \rightleftarrows \beta$-$NaNO_3$ will not be affected by the presence of lithium nitrate. The α–β change does not appear on an ordinary cooling diagram.

$LiClO_3$–$LiNO_3$

The data for this system (Table V) when plotted also give a simple eutectic diagram, unaccompanied by detectable solid solution.

The data for the quaternary system (Table VI) when plotted by the method of Jänecke yield Fig. 4. Unlike the usual Jänecke diagram, this is not an isothermal diagram but a projection on the base of a composition–temperature model. The diagram shows that in the (fused) reaction

$$NaNO_3 + LiClO_3 \rightleftarrows LiNO_3 + NaClO_3$$

$LiNO_3$ and $NaClO_3$ constitute the stable solid pair. There are two invariant points in this quaternary system, both congruent. The crystallization paths on this diagram are obvious and might well serve as exercise for undergraduate students.

REFERENCES

1. A. Benrath and H. Tesche. Z. physik. Chem. (Leipzig), **96**, 474 (1920).
2. L. I. Favorskii. Ann. secteur anal. physico-chim., Inst. chim. Gén. (U.S.S.R.), **13**, 281 (1940).
3. A. Potilitzin. J. Russ. Phys.-Chem. Soc. **16**, 840 (1883).
4. C. A. Kraus and W. M. Burgess. J. Am. Chem. Soc. **49**, 1226 (1927).
5. A. N. Campbell and J. E. Griffiths. Can. J. Chem. **34**, 1647 (1958).
6. F. C. Kracek. J. Am. Chem. Soc. **53**, 2609 (1931).

THE STRUCTURE OF LINSEED MUCILAGE

PART II

K. HUNT[1] AND J. K. N. JONES

Department of Chemistry, Queen's University, Kingston, Ontario

Manuscript received January 25, 1962

ABSTRACT

Linseed mucilage has been separated into an acidic and a neutral fraction. The acidic fraction was further separated, by the use of cupric acetate solution, into two fractions, CuI and CuII. *Fraction CuI* contained L-rhamnose, L-galactose, and D-galacturonic acid. The methylated reduced polysaccharide gave on hydrolysis 2,3,4-tri-*O*-methyl-L-rhamnose, 3,4-di-*O*-methyl-L-rhamnose, 4-*O*-methyl-L-rhamnose, 2,3,4,6-tetra-*O*-methyl-D-galactose, 2,3,6-tri-*O*-methyl-D-galactose, and 2,3-di-*O*-methyl-D-galactose (?); L-galactose was lost during the methylation process. Periodate oxidation studies on the material indicated that the polymer was composed of a main chain of L-rhamnose units with most of the L-galactose units attached as non-reducing end groups. *Fraction CuII* contained L-rhamnose, L-fucose, L-galactose, and D-galacturonic acid. The methylated reduced polysaccharide gave on hydrolysis 2,3,4-tri-*O*-methyl-L-fucose, 2,3,4,6-tetra-*O*-methyl-L-galactose, 2,3,6-tri-*O*-methyl-D-galactose, 4-*O*-methyl-L-rhamnose, L-rhamnose, and possibly 2,3-di-*O*-methyl-D-galactose and 3-*O*-methyl-D-galactose. Periodate oxidation studies and a degradation by the Smith procedure indicated the presence of a L-rhamnose backbone with L-fucose and L-galactose units attached as non-reducing end groups.

The neutral fraction yielded a periodate-oxidizable material after one Smith-type degradation. Periodate oxidation studies indicated that the degraded material was branched. Methylation of the degraded polysaccharide followed by hydrolysis yielded 2,3,4-tri-*O*-methyl-D-xylose, 2,3-di-*O*-methyl-D-xylose, 2,4-di-*O*-methyl-D-xylose, 4-*O*-methyl-D-xylose, D-xylose, and traces of 2,3,4-tri-*O*-methyl- or 2,5-di-*O*-methyl-L-arabinose, 2,4-di-*O*-methyl-D-xylose, and 3-*O*-methyl-D-xylose. The main backbone of the degraded polysaccharide appeared to consist of (1 → 4)-linked D-xylose units. Linkages of the (1 → 3) type were also present. The smaller fragments from the Smith-type degradation, L-arabinose, 2-*O*-α-L-arabinosyl glycerol, and glycerol were characterized. A partial acid hydrolysis of the neutral fraction yielded a number of oligosaccharides.

DISCUSSION

The work described here is a continuation of that described in Part I by Erskine and Jones (1). Further work was performed on the neutral fraction which was isolated by these authors and new work on the two acidic fractions is presented.

Recently, mucilages have been separated into acidic and neutral fractions by 'cetavlon' (cetyltrimethylammonium bromide) precipitation (2). Using a combination of borate solution and 'cetavlon' a fractionation of neutral mixtures has been achieved (3–5). This 'cetavlon' method was shown to be very successful in the separation of the components of linseed mucilage. Repeated precipitation of a 'cetavlon' complex yielded an insoluble fraction which contained no pentose sugars, L-rhamnose, L-fucose, L-galactose, and D-galacturonic acid being the only sugars detected. The 'cetavlon' supernatant, after dialysis and subsequent concentration, yielded a neutral fraction which contained only a trace of acidic material. This could usually be removed by a second 'cetavlon' precipitation. Cupric acetate solution (7%) was used to fractionate the acidic mixture into a copper-insoluble fraction (fraction CuI) and a copper-soluble fraction (fraction CuII) (1).

Fraction CuI

Fraction CuI had physical properties which did not differ greatly from samples previously isolated by similar means (6, 7). Whereas other workers reported xylose in this

[1]*Present address: Chemistry Department, The University, West Mains Road, Edinburgh 9, Scotland.*

fraction, only L-rhamnose, L-galactose, and D-galacturonic acid were found, in the approximate molar ratio 2:1:2. Examination of fraction CuI by the Tiselius electrophoresis procedure indicated the presence of two components. The trace component had a mobility identical with that of fraction CuII.

Oxidation of fraction CuI with sodium metaperiodate resulted in the uptake of 1.34 moles of periodate and the liberation of 0.33 mole of formic acid per anhydrohexose unit. The figures indicate that about one third of the residues in the polysaccharide possessed sugar residues with hydroxyl groups on each of three contiguous carbon atoms. Assuming that no significant overoxidation had occurred, the figures above indicate that all the monosaccharide residues had been oxidized. Methylation results indicated that this conclusion was incorrect and hence some overoxidation had probably occurred. The periodate-oxidized polysaccharide was reduced with sodium borohydride and the product after hydrolysis showed, on chromatograms, small amounts of L-rhamnose, L-galactose, and D-galacturonic acid. The high uronic acid content (43%) of fraction I made it labile to alkalies. The uronic acids in the polysaccharide were therefore reduced to hexoses in an effort to keep alkaline degradation to a minimum (8). The reduced polymer was methylated five times using the Haworth procedure, the solution being kept at 0° C and close to pH 7. By using these conditions it was hoped to reduce still further the amount of alkaline degradation. A further reduction with lithium aluminum hydride followed by four Purdie-type and one Kuhn-type methylations produced a fully methylated polysaccharide (OMe, 43.6%) which showed a negligible hydroxyl peak in the infrared. At least half of the material was soluble in light petroleum. This strongly suggests that a large amount of the material was of low molecular weight. No doubt a certain amount of degradation took place during the reduction and methylation and this could account for the low yield. The presence of a large amount of methyl pentose (rhamnose) in the methylated polymer might also have some effect on the solubility of the methylated polymer in light petroleum. The sugars fully characterized were 2,3,4-tri-*O*-methyl-L-rhamnose, 2,3,4,6-tetra-*O*-methyl-D-galactose, 3,4-di-*O*-methyl-L-rhamnose, 2,3,6-tri-*O*-methyl-D-galactose, and 4-*O*-methyl-L-rhamnose. A sugar which might be 2,3-di-*O*-methyl-D-galactose was also obtained but not definitely characterized. Only L-galactose had been detected in the original polysaccharide. It is reasonable to suggest that all the methylated D-galactose derivatives arose from what were originally D-galacturonic acid residues. No L-galactose derivatives were found; it is possible that the majority of L-galactose units were near the periphery of the molecule and were lost during the methylation. From the methylation data the backbone of the polysaccharide appears to consist of L-rhamnose residues linked by a (1 → 2)-type glycosidic bond with some branching at position 3. The D-galacturonic acid was present as (1 → 4)-linked residues either in the main chain or as part of a side chain.

Autohydrolysis of the original polymer supports the above results because L-galactose was the first sugar to appear, followed later by D-galacturonic acid and L-rhamnose residues, the last appearing only after a long time of hydrolysis. This would indicate either that the methyl pentose is attached to the polymer by acid-resistant linkages or that hydrolysis of the L-rhamnose is hindered by the structure of the polymer.

Fraction CuII

Fraction CuII contained L-rhamnose, L-fucose, L-galactose, and D-galacturonic acid in the approximate molar ratio 4:1:2:2 in contrast to the ratio 1:1:3:2 reported by Erskine (6). Examination of this fraction by the Tiselius electrophoresis procedure showed only one peak. This mobility corresponded with that of the trace component in fraction CuI.

Oxidation of fraction CuII with sodium metaperiodate resulted in the uptake of 0.76 mole of periodate and the liberation of 0.13 mole of formic acid per hexose unit. The figures indicate that about one third of the residues was not oxidized. This was confirmed by hydrolysis of the periodate-oxidized reduced material, which gave crystalline L-rhamnose and L-galactose. The high yield of L-rhamnose suggested that the residues were well protected from oxidation. Glycerol, which most probably arose from the oxidation of L-galactose end groups, was also obtained and characterized as the tri-*O*-*p*-nitrobenzoate (9). Fraction CuII was reduced and methylated by the Haworth- and Kuhn-type procedures to yield a methylated material (OMe, 44.9%) containing a negligible hydroxyl peak (infrared). Methylated fraction CuII also contained a large percentage of light petroleum soluble material. After hydrolysis and separation, the methylated fragments definitely characterized were 2,3,4-tri-*O*-methyl-L-fucose, 2,3,4,6-tetra-*O*-methyl-L-galactose, 2,3,6-tri-*O*-methyl-D-galactose, 4-*O*-methyl-L-rhamnose, and L-rhamnose. Easterby (10) had previously methylated a similar fraction and obtained an uncharacterized monomethyl rhamnose which he suggested was the 4-*O*-methyl derivative. In addition, two other sugars which were not characterized were obtained. One was the suspected 2,3-di-*O*-methyl-D-galactose previously obtained from the methylated fraction CuI. The other sugar has the properties of a mono-*O*-methyl-D(?)-galactose, and chromatographic evidence points to its identity as the 3-*O*-methyl derivative. The results indicated that all the L-fucose and most of the L-galactose were present as end groups. From the periodate results one would have expected to find some L-galactose present along the chain length of the polymer. Methylated derivatives corresponding to this were not found, but since only small amounts would be present, they could have escaped detection. The D-galacturonic acid units appear to be combined by $(1 \rightarrow 4)$-type linkages either in the main or side chains.

Neutral Fraction

The neutral fraction was subjected to a Tiselius electrophoresis fractionation and the indications were that it consisted of three components. One component was present in very small amounts and had a high mobility. The other two were present in about equal amounts and possessed low mobilities. A Smith-type degradation (11) performed on the neutral fraction yielded a periodate-resistant polysaccharide as well as a large number of other compounds. The degraded polysaccharide had an optical rotation little changed from the original material. Most of the L-arabinose and all of the D-galactose residue were oxidized by the metaperiodate. The degraded polysaccharide consumed 0.57 mole of periodate and produced 0.10 mole of formic acid per pentose unit. There was still unoxidized D-xylose remaining after this second oxidation. The ratio of xylose to arabinose in the once degraded polysaccharide was 6:1 (estimated).

The degraded material was methylated once with Haworth reagents at pH 6–7 and then once with Purdies reagents. The resulting methylated material (OMe, 37.6%) showed a negligible hydroxyl peak (infrared). The methylated fragments fully characterized were 2,3,4-tri-*O*-methyl-D-xylose, 2,3-di-*O*-methyl-D-xylose, 4-*O*-methyl-D-xylose, and D-xylose. A fragment isolated in small amounts gave L-arabinose on demethylation, and judging by its mobility on paper it was either 2,3,4-tri-*O*-methyl-L-arabinose or 2,5-di-*O*-methyl-L-arabinose. A material with the same rate of movement as 2,4-di-*O*-methyl-D-xylose was also obtained, although no crystalline derivative could be prepared. During the isolation of the 4-*O*-methyl-D-xylose a substance with a rate of movement identical with that of 3-*O*-methyl-D-xylose was obtained. No derivative, however, could

be obtained. The evidence indicates that the main backbone consists of D-xylose units many of which are linked (1 → 4). It is reasonable to assume that considerable branching exists, as indicated by the amount of mono-*O*-methyl and unsubstituted xylose obtained. Erskine (1) did not isolate any 4-*O*-methyl-D-xylose from his methylated pentosan. The original neutral polysaccharide after methylation contained a much higher percentage of unsubstituted D-xylose than did the methylated degraded material. It seems possible that sugar residues originally attached to the 4-position of such D-xylose units in the undegraded polymer were removed during the Smith degradation procedure and left the 4-position available for methylation in the degraded material. These D-xylose units were therefore also linked through C_1, C_2, and C_3 in the undegraded polysaccharide. The isolation by Erskine (1) of 2,4-di-*O*-methyl-D-xylose from the original material suggests the presence of some (1 → 3)-linked D-xylose units. Xylans from the hemicellulose A of wattle wood (12) and the red alga *Rhodymenia palmata* (13) have been postulated to contain some (1 → 3)-linked D-xylose residues.

The alcohol-soluble material from the Smith degradation (11) was separated by acetone into a higher molecular weight insoluble fraction and a lower molecular weight soluble fraction. Very little information was obtained from this higher molecular weight fraction. The acetone-soluble fraction yielded some glycerol after repeated fractionation. The glycerol probably arose as a result of oxidation of hexose end groups or pentofuranose end groups. Free L-arabinose was also identified and could have arisen as a consequence of mild acid hydrolysis of the L-arabofuranoside units left unoxidized by periodate. A third substance obtained pure was probably 2-*O*-α-L-arabopyranosyl-glycerol. The α-configuration was assigned because of the low positive rotation. The (1 → 2)-type linkage seems probable since the glycerol was not oxidized by periodate. Jones (14) has isolated a material of closely similar properties. In neither instance has the material been obtained crystalline.

A controlled partial hydrolysis was performed on the neutral fraction using conditions which differed slightly from those of Erskine (6). At least 12 oligosaccharides were obtained in an approximately 10% total yield. The large number of disaccharides made the task of separating them very difficult and quite often the separated disaccharide was only represented by a very small amount of material. The 4-*O*-β-D-xylopyranosyl-D-xylose previously characterized by Erskine (6) was obtained again and identified. This fact would point to the presence of some (1 → 4)-linked xylose units in the polymer. A second xylobiose, which had $[\alpha]_D$ +94°, and is therefore probably α-linked, was also separated. A crystalline osazone, m.p. 146–148°, was obtained, indicating that the linkage was not of the (1 → 2) type. The R_f value on paper differed from that of both 3-*O*-α-D-xylopyranosyl-D-xylopyranose (15) and the xylobiose already characterized. A D-xylose → L-arabinose disaccharide which Erskine had obtained but not characterized was isolated in good yield. The material had $[\alpha]_D^{22}$ +84°, and arabinose was shown to be the reducing residue by bromine oxidation. The disaccharide had a higher R_f value than galactose in all solvents, and was distinct from 3-*O*-α-D-xylopyranosyl-L-arabinose (16, 17), 5-*O*-β-D-xylopyranosyl-L-arabinose (18, 19), 2-*O*-β-D-xylopyranosyl-L-arabinose (20); it yielded small amounts of a crystalline osazone, m.p. 121–123°. The periodate oxidation results for both the original disaccharide and reduced disaccharide were slightly low for a (1 → 5)-linked pentose disaccharide. This could be the result of the presence of a small amount of contaminant. Until definite proof is available it is suggested that the material could be 5-*O*-α-D-xylopyranosyl-L-arabofuranose (1). Two other disaccharides, which contained (?) D-galactose and L-arabinose, were isolated in small yields. In both materials, L-arabinose was the reducing residue. A second D-xylosyl-L-arabinose disaccharide was isolated

which had an R_f value different from any of the others described earlier. The material yielded an osazone with m.p. 185–187°. Periodate oxidation results were inconclusive. Separation of the higher oligosaccharide by an ion-exchange resin (21) gave various impure fractions. One yielded crystalline material, m.p. 238–240°, which gave only xylose upon hydrolysis. R_f values indicate that the material may consist of three to four D-xylose units. Conclusive identification was hampered by the lack of sufficient material. This work is continuing.

EXPERIMENTAL

Methods

Paper chromatography was carried out on Whatman No. 1 filter paper using the following solvent systems (v/v):

(A) ethyl acetate:acetic acid:formic acid:water (18:3:1:4),
(B) butan-1-ol-ethanol:water (3:1:1),
(C) butan-1-ol:pyridine:water (10:3:3),
(D) butan-1-ol:pyridine:water (5:3:2),
(E) ethyl acetate:pyridine:water (10:4:3).

Whatman 3 MM paper was used in all quantitative separations. Columns for separations of large quantities of sugar mixtures were packed with Whatman 'Cellulose Powder' by the dry method. Borate buffer (pH 9.6) was used in all electrophoretic separations. Optical rotations were observed in water unless otherwise stated. All solutions were concentrated under reduced pressure at 40–45° C. Demethylation of methylated sugars were carried out by the procedure of Allen *et al.* (22). All infrared spectra were made using either chloroform solution (6%) or potassium bromide pellets (0.8%) using a Perkin–Elmer model 21 infrared spectrophotometer. All moving-boundary electrophoresis determinations were performed on a Perkin–Elmer model 38-A apparatus with a standard 2-ml cell. The initial power input was adjusted to 2 watts.

Preparation of Linseed Mucilage

Samples of the crude linseed mucilage were prepared as described in Part I (1). The de-ashed mucilage had $[\alpha]_D^{21}$ −3° (*c*, 0.62 in 0.3 *N* NaOH) and a neutralization equivalent of 683. Hydrolysis of a sample followed by quantitative chromatographic separation of the hydrolyzate on paper using solvents (A), (B), and (C) confirmed the presence of L-fucose, D-xylose, L-galactose, D-galacturonic acid, and L-rhamnose and indicated the presence of arabinose and an aldobiouronic acid.

Fractionation of the Mucilage with 'Cetavlon' (Cetyltrimethylammonium Bromide)

The crude mucilage (10 g) was dissolved in distilled water (1500 ml) and the solution was deionized with Amberlite IR-120(H) resin. An aqueous solution of 'cetavlon', supplied by Eastman Chemicals (10%, 100 ml), was added to the deionized solution, and the precipitate which formed was allowed to settle (2). The precipitate was removed by centrifugation and washed with water. The 'cetavlon' complex was decomposed in sodium chloride solution (10%, 100 ml) and the resulting solution was poured into ethanol. The precipitate was collected by centrifugation, washed with ethanol, acetone, ether, and finally it was dried to a white powder (5.1 g). The 'cetavlon' supernatant was dialyzed against running water for several days. The dialyzate was concentrated and poured into ethanol. The precipitate (2.6 g) was collected by filtration and was then isolated as described above. The acidic and neutral fractions were treated a second time with 'cetavlon'. Each fraction was hydrolyzed and then examined chromatographically in solvents (A) and (B). The 'cetavlon' precipitate contained rhamnose, fucose, galactose, and galacturonic acid and the 'cetavlon' supernatant contained galactose, xylose, and arabinose.

Fractionation of the Acidic Material with Cupric Acetate

The de-ashed acidic material (3.5 g) was dissolved in water (350 ml), and cupric acetate solution (7%, 20 ml) was added. The green gelatinous precipitate which formed was allowed to settle for 5 hours and was then removed by centrifugation. The precipitate was decomposed with ethanol containing hydrochloric acid (1%). The insoluble material was further washed with ethanol until a negative test with silver nitrate was obtained. The precipitate was dried to yield fraction CuI as a brown powder (540 mg). The supernatant was poured into ethanol and the precipitate was removed by centrifugation. This complex was decomposed as before to yield fraction CuII as a white powder (2.47 g). The alcohol supernatant from the last precipitation was concentrated and dialyzed against running water. The dialyzate after concentration yielded only a very small amount of polysaccharide.

Properties of Fraction CuI Polysaccharides

The material was de-ashed by passage through IR-120(H) resin and then isolated as a white powder. Hydrolysis of the material followed by chromatography in solvents (A), (B), and (C) indicated the presence

of rhamnose, galactose, and galacturonic acid in the ratio 2:1:2 as determined by the weights of the fractions. The material had an ash content (23) of 0.7%; it had $[\alpha]_D^{22}$ +121° (*c*, 0.15) and a neutralization equivalent of 400 (pH meter), indicating a 43.4% anhydrouronic acid content.

Tiselius Investigation of the Fraction

Fraction CuI (25 mg) was dissolved in veronal buffer (0.1 *M*, 10 ml). Photographs were taken of the ascending arm in a Tiselius apparatus after 17 minutes (A) and 55 minutes (B). Two peaks were observed, a large one with a mobility (μ) of 14.3×10^{-5} $cm^2v^{-1}sec^{-1}$ and the other small peak with a mobility (μ) of 12.0×10^{-5} $cm^2v^{-1}sec^{-1}$.

Oxidation of Fraction CuI by Periodate

Samples of de-ashed polysaccharide ((1) 0.0549 g and (2) 0.0518 g) were dissolved in distilled water in volumetric flasks (100 ml) and the solutions were adjusted to pH 7 with sodium hydroxide solution (0.01 *N*). Sodium metaperiodate solution (0.3 *M*, 3 ml) was added and the solution was made up to volume (100 ml) and kept in the dark. The periodate uptake was determined by the thiosulphate method (24), and the formic acid by titration with sodium hydroxide solution (screened methyl red as indicator) after addition of ethylene glycol. The following results were obtained as mean values of the two series of analyses and are quoted as moles per mole of hexose unit (calculated as $C_6H_{10}O_5$). Extrapolation of the 'overoxidation' part of the periodate uptake and formic acid yield curve gave a periodate uptake of 1.34 moles and a formic acid yield of 0.33 mole.

Time (hours)	5	19	45.5	69	93
Periodate uptake	0.66	1.22	1.41	1.50	1.54
Formic produced	0.08	0.35	0.44	0.45	0.50

Large-scale Oxidation of Fraction CuI by Periodate

The freeze-dried polysaccharide (203 mg) in water (400 ml) was oxidized with sodium metaperiodate solution (0.3 *M*, 12 ml) for 20 hours. Ethylene glycol was added to destroy excess periodate. After dialysis to remove formaldehyde, ethylene glycol, and salts the polyaldehyde was reduced with sodium borohydride solution (0.6 g in 10 ml) for 9 hours. The excess borohydride was destroyed with dilute acetic acid and the solution was dialyzed against running water for 3 days. The dialyzate was concentrated and poured into alcohol. The precipitate was removed by centrifugation and dried to yield a white powder (192 mg) having $[\alpha]_D^{22}$ +19° (*c*, 0.16). The polyol (170 mg) was hydrolyzed (1 *N* H_2SO_4) for 16 hours on a boiling-water bath. After neutralization ($BaCO_3$) the concentrated solution was fractionated chromatographically using solvent (A). Spraying of the chromatogram with *p*-anisidine indicated the presence of rhamnose and galacturonic acid, with a trace of a material which gave a pink color, R_{rham} 1.53. Chromatograms developed in solvents (B) and (C) and sprayed with silver nitrate showed the presence of several other fast-moving components.

Smith-type Degradation of Fraction CuI

A further portion (500 mg) of this fraction was oxidized with metaperiodate as before and then reduced with sodium borohydride. The polyol was dissolved in sulphuric acid (1 *N*, 36 ml) and left at room temperature overnight (11). The solution was neutralized ($BaCO_3$) and the precipitate was removed by centrifugation. The centrifugate was passed through IR-120(H) resin and the eluate concentrated to a syrup. The syrup was poured into ethanol and the precipitate (5 mg) was removed by filtration. The alcohol supernatant was concentrated to a syrup (350 mg). A portion of each material was hydrolyzed. Chromatography in solvents (A) and (C) indicated the presence of rhamnose, galacturonic acid, and a trace of galactose in the precipitated material. Glycerol, a trace of galactose, and many unidentified materials were indicated in the alcohol supernatant.

Reduction of Fraction CuI

Fraction CuI (5.0 g) was deionized by IR-120(H) resin and then freeze-dried. The freeze-dried material was powdered and suspended in ether (25 ml). Diazomethane (3 g) (25) in ether was added dropwise until a faint yellow color persisted. The ether was removed by filtration and the material was dissolved in water 250 ml). Lithium borohydride solution (1 g in 100 ml) was added dropwise to the solution, which was allowed to stand overnight. The excess borohydride was destroyed with dilute acetic acid and the solution was dialyzed against running water for 3 days. The dialyzate was concentrated and then freeze-dried. The reduction procedure was repeated twice in a boric acid buffer (0.4 *M*) (18). The resulting material (2.1 g) showed a very much reduced carbonyl peak in the infrared spectrum.

Methylation of the Partially Reduced Fraction CuI

The freeze-dried material (2.1 g) was dissolved in water (45 ml). The solution was kept at 0° C (ice) and then adjusted to pH 6 by addition of dimethyl sulphate. Sodium hydroxide solution (30%, 15 ml) was

added dropwise, with vigorous stirring, to the slightly acid solution. After each addition of base the pH was carefully adjusted to pH 6 by further addition of dimethyl sulphate over an 8-hour period until dimethyl sulphate (10 ml) had been added to the solution. This procedure was repeated over 2 days. The alkaline solution was heated for 1 hour at 60° C. After cooling, the solution was brought to pH 6 and extracted several times with chloroform. The aqueous layer was dialyzed for 3 days against running water. The dialyzate was concentrated and the solution remethylated. This procedure was repeated five times. The chloroform extracts were united and then concentrated to a syrup (1.6 g). The syrup was dissolved in water and passed through IR-120(H) resin. The eluate was concentrated and dried to constant weight. This syrup was dissolved in redistilled tetrahydrofuran (20 ml), and diazomethane was added to the solution until nitrogen ceased to be evolved. The solvent was removed and the syrup dried once again. The syrup was redissolved in tetrahydrofuran (35 ml) and the solution added dropwise to a refluxing solution of lithium aluminum hydride (1 g) in tetrahydrofuran (35 ml). After addition of the partially methylated polysaccharide, the mixture was allowed to reflux for a further hour. The excess hydride was destroyed with moist ethyl acetate and the resulting mixture was acidified. The aqueous solution was extracted several times with chloroform. The chloroform extracts were concentrated, and yielded a syrup (1.5 g). The syrup was subjected to four Purdie-type methylations but the syrup (1.14 g) obtained still exhibited a slight hydroxyl peak in the infrared spectrum. The syrup was then methylated by the Kuhn (26) procedure to give a product with a negligible hydroxyl peak in the infrared. The methylated polysaccharide had a methoxyl content of 43.6%. No fractionation of the material could be obtained using chloroform – light petroleum (60–80° C).

Hydrolysis of Methylated Fraction CuI

The polysaccharide was hydrolyzed with formic acid (90%, 50 ml) in the cold for 13 hours. Water (50 ml) was added and the solution was heated on a boiling-water bath for a further 9 hours. The formic acid was removed by vacuum distillation and the formyl esters present were hydrolyzed by several codistillations with water. The resultant syrup was dissolved in a small volume of water and the solution was passed through IR-120(H) resin and A-4(OH) resin. The eluate was concentrated to a syrup (66 mg).

Separation of the Methylated Fragments

The syrup was separated on cellulose with light petroleum (b.p. 100–120°) – butan-1-ol (7:3 changed later to 6:4) and butan-1-ol – methanol (6:4) as eluants to give 11 fractions.

Fraction 1 (21 mg).—This sugar had $[\alpha]_D^{25}$ +26° (*c*, 0.7) and gave rhamnose when demethylated with boron trichloride (22). The syrup yielded a crystalline aniline derivative, which after recrystallization from light petroleum (40–60° C), had m.p. 108–110°, undepressed on admixture with authentic *N*-phenyl-2,3,4-tri-*O*-methyl-L-rhamnosylamine (27).

Fraction 2 (99 mg).—This fraction had $[\alpha]_D^{22}$ +94° (*c*, 1.98) and R_G value identical with that of 2,3,4,6-tetra-*O*-methyl-D-galactose in all solvents. The derived *N*-phenyl-galactosylamine, after recrystallization from ethanol, had m.p. and mixed m.p. 192–193° C (28).

Fraction 3 (76 mg).—This mixture was separated electrophoretically. The faster-moving component was eluted from the paper and yielded a syrup (18 mg) which was added to fraction 4. The slower-moving component was 2,3,4,6-tetra-*O*-methyl-D-galactose.

Fraction 4 (90 mg).—The sugar gave a positive reaction with triphenyltetrazolium chloride (29) and crystallized from ether – light petroleum. The crystals had $[\alpha]_D^{24}$ +22° (*c*, 1.8) and m.p. 97–98° C undepressed on admixture with authentic 3,4-di-*O*-methyl-L-rhamnose.

Fraction 5 (40 mg).—This mixture of sugars was also separated electrophoretically. The slower-moving component was identified as 3,4-*O*-methyl-L-rhamnose.

Fraction 6 (62 mg).—This syrup had an R_G value identical with that of 2,3,6-tri-*O*-methyl-D-galactose in all solvents. It had $[\alpha]_D^{24}$ +70° (*c*, 1.2), which changed to −14° (*c*, 0.2) when dissolved in methanolic hydrogen chloride (1%). A sample of the sugar was oxidized for 3 days with bromine in water. The crude crystalline lactone (30) was isolated and recrystallized from ether to yield 2,3,6-tri-*O*-methyl-D-galactonolactone, m.p. 98° C (31).

Fraction 7 (26 mg).—This fraction was separated electrophoretically into two components. The slower component was added to fraction 8.

Fraction 8 (35 mg).—This syrup, which had $[\alpha]_D^{22}$ +11° (*c*, 0.7), gave rhamnose on demethylation. Paper electrophoresis indicated that the material had the same R_G value as 4-*O*-methyl-L-rhamnose. However, the syrup did not crystallize even when seeded. A portion of the syrup was oxidized with bromine water (3 drops in 1 ml) for 5 days. The crude lactone was isolated in the usual manner. Recrystallization of the material from acetone – light petroleum gave crystalline 4-*O*-methyl-L-rhamnono-δ-lactone, m.p. and mixed m.p. 81–82° C (32).

Fraction 9 (15 mg).—This fraction was not investigated.

Fraction 10 (24 mg).—This syrup had $[\alpha]_D^{27}$ +52° (*c*, 1.2), which became negative in methanolic hydrogen chloride (1%). Demethylation of the syrup afforded galactose. The material failed to give a 'tetrazolium red' test, and it was chromatographically indistinguishable from sugar 5 obtained after methylation of fraction CuII. This was believed to be 2,3-di-*O*-methyl-D-galactose. A crystalline aniline derivative could not be obtained (33).

Acetolysis of Fraction CuI

Fraction CuI (200 mg) was mixed with acetic anhydride (4 ml) and concentrated sulphuric acid (0.1 ml) at 0° C for 28 hours. The solution was then heated at 80–90° C for 15 minutes and poured into ice water (34). The white precipitate was removed by filtration and washed several times with water. The material was dried to a white powder (170 mg).

The acetylated material (59 mg) was deacetylated with sodium hydroxide in acetone. The solution was deionized by passage through IR-120(H) resin and the eluate was concentrated to a syrup. Chromatography in solvent (A) indicated the presence of galacturonic acid and an orange spot, R_{gal} 0.43, and a pink spot, R_{gal} 0.13. A large streak, which probably represented higher oligosaccharides, was noted near the base line. A small portion (50 mg) of the original acetylated product was subjected to acetolysis and the product isolated and deacetylated as before. Chromatography in solvent (A) indicated the presence of three sugars, all of which gave a pink color when detected with the *p*-anisidine spray and had R_{gal} values of 1.00, 0.42, and 0.12.

Autohydrolysis of Fraction CuI

Fraction CuI (100 mg) was dissolved in water (20 ml) and the solution was passed through IR-120(H) resin. The acidic eluate (pH 2) was concentrated to a small volume (10 ml). This solution was refluxed and samples were removed at intervals and examined chromatographically in solvent (A). Galactose was the first to appear after 3 hours. Galacturonic acid appeared only after 5 hours. A disaccharide (R_{gal} 0.7) appeared after 10 hours; the disaccharide had disappeared when the next sample was examined. Rhamnose appeared between 10 and 21 hours and increased until, at 53 hours, the concentration was almost equal to that of the galacturonic acid.

Tiselius Investigation of Fraction CuII

Fraction CuII (25 mg) was treated in the same manner as fraction CuI. Photographs were taken of the 'buffer arm' after 10 minutes (*a*) and 75 minutes (*b*). A single peak was observed which had a mobility (μ) of 12.3×10^{-5} $cm^2v^{-1}sec^{-1}$. Fraction CuII had $[\alpha]_D^{22}$ −5° (*c*, 0.35 in water) and neutralization equivalent of 607.

Oxidation of Fraction CuII by Periodate

The polysaccharide samples (*a*) 0.0488 g and (*b*) 0.0470 g were placed in volumetric flasks (100 ml) and oxidized with sodium metaperiodate as described for fraction CuI. The periodate uptake and formic acid released per mole of hexose unit (calculated as $C_6H_{10}O_5$) were determined as before. The following results were obtained as mean values of the two series of analysis:

Time (hours)	5	11.5	24	35	48	59	72
Periodate uptake	0.54	0.72	0.78	0.80	0.81	0.82	0.84
Formic produced	0.09	0.11	0.15	0.20	0.23	0.24	0.25

Extrapolation of the 'overoxidation' part of the periodate uptake and formic acid yield curve gave, for the periodate uptake, 0.76 mole and for the formic acid yield, 0.13 mole per mole of hexose.

Large-scale Oxidation of Fraction CuII by Periodate

The polysaccharide (1.21 g, $[\alpha]_D^{22}$ −5°) was oxidized with sodium metaperiodate for 30 hours as described before. The resulting polyaldehyde was reduced with sodium borohydride (2 g in 100 ml) overnight. The excess borohydride was destroyed with dilute acetic acid and the solution was dialyzed against running water for 3 days. The dialyzate was concentrated to a syrup and poured into a large excess of ethanol. The resulting white material was collected and dried to yield a powder (1.15 g) which had $[\alpha]_D^{22}$ −95° (*c*, 0.13). The polyol was hydrolyzed with sulphuric acid (1 *N*, 100 ml) for 16 hours on a boiling-water bath. The hydrolyzate was neutralized ($BaCO_3$), filtered, and the filtrate passed through columns of IR-120(H) resin and A-4(OH) resin. The neutral eluate was concentrated to a syrup (381 mg). The A-4 resin was eluted with sodium hydroxide solution (1 *N*, 10 ml) and the eluate passed directly through IR-120(H) resin. The acidic eluate was concentrated to a syrup (139 mg). Separation of the acidic eluate was not attempted.

Separation of the Neutral Fraction

The syrup (381 mg) was separated on a cellulose column with butan-1-ol half saturated with water as eluant, to give 11 fractions.

Fraction A and B.—This material had the same R_f value as glycolic aldehyde in solvents (A) and (C); however, glyoxal phenylosazone could not be prepared from it.

Fraction C.—This syrup was not investigated.

Fraction D (70 mg).—This syrup was identified as glycerol. The derived tri-*O*-*p*-nitrobenzoate of glycerol had m.p. and mixed m.p. 191–193° (9).

Fraction E (138 mg).—This syrup crystallized after a short time. The crystals were recrystallized twice

from moist acetone to yield L-rhamnose hydrate, m.p. and mixed m.p. 91–92° C and $[\alpha]_D^{22}$ +9° (*c*, 0.18).

Fraction F (70 mg).—This material was not investigated.

Fraction J and K (50 mg).—This material crystallized, and after recrystallization from methanol the crystals had m.p. 160–162° C and $[\alpha]_D^{22}$ −87° (*c*, 0.56) (35). Admixture with authentic L-galactose produced no depression in the melting point.

Smith-type Degradation of Fraction CuII

Fraction CuII (500 mg) was oxidized with sodium metaperiodate and this material was worked up as described previously. After cold acid hydrolysis (N H_2SO_4) an alcohol-insoluble material (5 mg) and an alcohol-soluble syrup (310 mg) were obtained. Both materials were hydrolyzed and then chromatographed in solvents (A) and (C). The precipitate contained a large amount of rhamnose, with traces of galactose and galacturonic acid, whereas the syrup contained glycerol, a tetritol, and many unidentified components.

Reduction and Methylation of Fraction CuII

Fraction CuII (10.5 g) was deionized by passage through IR-120(H) resin and the eluate was freeze-dried. The freeze-dried material was powdered and treated with diazomethane in ether (25 ml) until the yellow color persisted. The ethereal solution was removed by decantation and the powder was dissolved in water (500 ml). Sodium borohydride (3.0 g) in water (100 ml) was added dropwise over a 3-hour period. The excess borohydride was destroyed with dilute acetic acid and the solution was dialyzed for 4 days. The reduction procedure was repeated until the infrared spectrum showed that the carbonyl peak had been greatly reduced. The partially reduced polysaccharide was then methylated by the Haworth procedure (four times). The chloroform extracts (of the acidified solution) from each methylation were combined and concentrated to a syrup (4.1 g). This partially methylated polysaccharide was reduced with lithium aluminum hydride in tetrahydrofuran as described before. A Kuhn-type methylation followed by a Purdie methylation yielded a syrup (2.45 g) which had $[\alpha]_D^{22}$ −15° (*c*, 1.42 in $CHCl_3$) and a methoxyl content of 44.9%. The material was not fractionated by light petroleum – chloroform and was soluble in a high percentage of light petroleum. The methylated material was hydrolyzed with formic acid as described before.

Separation of the Methylated Sugars

The syrup was separated on cellulose with light petroleum (100–120°) – butan-1-ol (7:3 later 6:4) and butan-1-ol containing some methanol as eluants, to give seven fractions.

Sugar 1 (39 mg).—The syrup from fractions 1 and 2 had an R_f value identical, in all solvents, with that of 2,3,4-tri-*O*-methyl-L-fucose, $[\alpha]_D^{22}$ −104° (*c*, 0.15). The syrup gave a crystalline aniline derivative which, after recrystallization from ether, yielded *N*-phenyl-2,3,4-tri-*O*-methyl-L-fucosylamine, m.p. and mixed m.p. 133–134° C.

Sugar 2 (280 mg).—This material, from fraction 3, had $[\alpha]_D^{22}$ −94° and was identified as 2,3,4,6-tetra-*O*-methyl-L-galactose. The negative rotation suggested that the L-form had been obtained. The aniline derivative, after recrystallization from ethanol, had $[\alpha]_D^{21}$ −48° (*c*, 0.17 in acetone) and m.p. 194–195°, depressed 15° on admixture with authentic *N*-phenyl-2,3,4,6-tetra-*O*-methyl-D-galactosylamine.

Sugar 3 (122 mg).—This material was obtained as the slower zone from fraction 4, using solvent (B). Further amounts were obtained from the slower zone of fraction 5 after paper electrophoresis. The syrup had $[\alpha]_D^{23}$ +84° (*c*, 1.22). The syrup (6 mg) in methanolic hydrogen chloride (1.5%, 5 ml) had $[\alpha]_D^{23}$ −56° (*c*, 0.12) after 24 hours. The material was chromatographically indistinguishable from 2,3,6-tri-*O*-methyl-D-galactose. The sugar solution was oxidized for 3 days with bromine (3 drops) in water (1 ml) and the lactone was isolated in the usual manner. Crystallization from ether yielded 2,3,6-tri-*O*-methyl-D-galactonolactone, m.p. and mixed m.p. 97–98° C, and possessed $[\alpha]_D^{22}$ −37° (*c*, 0.98) (30, 31).

Sugar 4 (181 mg).—This material was obtained from the electrophoretic separation of fractions 5 and 6. A portion of the syrup on demethylation afforded rhamnose. The sugar moved at a different rate to authentic 2-*O*-methyl and 3-*O*-methyl-L-rhamnose. The syrup consumed 1.9 moles of periodate, suggesting it to be 4-*O*-methyl-L-rhamnose. The syrup crystallized after 4 months. Recrystallization from acetone yielded white crystals, m.p. 110–111° C and $[\alpha]_D^{21}$ +26° (*c*, 1.2). A portion of the syrup was oxidized with bromine. The resulting 4-*O*-methyl-L-rhamnonolactone after recrystallization from chloroform – light petroleum had m.p. and mixed m.p. 81–82° C (32). A further portion of the sugar was refluxed with aniline in ethanol to give *N*-phenyl-4-*O*-methyl-L-rhamnosylamine, which after recrystallization from ethanol had m.p. 157–158° C and $[\alpha]_D^{22}$ +142° (*c*, 0.33 in pyridine) (36).

Sugar 5 (58 mg).—This sugar was isolated from fraction 7 by multiple development with solvent (B) on Whatman 3MM paper. The syrup showed galactose on demethylation and had $[\alpha]_D^{23}$ +71° (*c*, 1.11) (37). The material was electrophoretically identical with 2,3-di-*O*-methyl-D-galactose. A portion of the syrup in water (2 ml) was oxidized with bromine (3 drops) for 3 days. The resultant lactone was treated with methanolic ammonia (3%, 2 ml) for 2 days. Removal of the solvent yielded a white material which had $[\alpha]_D^{21}$ +24° (*c*, 0.08). This amide, spotted on paper, was sprayed with sodium periodate followed by a solution of inositol, then with a mixture of ammonia and acetyl acetone (37), when a yellow spot resulted, indicating release of formaldehyde. Oxidation of the amide with sodium periodate resulted in a periodate uptake of 1.85 moles and a formic acid production of 0.90 mole per sugar molecule. The original syrup after treatment for 5 days with methanolic hydrogen chloride (1.5%) had $[\alpha]_D^{22}$ −16° (*c*, 1.0) (38). A crystalline aniline derivative could not be obtained.

Sugar 6 (95 mg).—This material was obtained from fraction 7 after multiple development in solvent (B). The syrup had zero rotation and showed galactose after demethylation. The sugar was chromatographically different from 2-*O*-methyl and 6-*O*-methyl-D-galactose but was identical chromatographically with 3-*O*-methyl-D-galactose. Neither a crystalline aniline derivative nor an osazone could be obtained from the syrup.

Sugar 7 (55 mg).—This sugar was also obtained from fraction 7 by multiple development. The sugar was chromatographically indistinguishable from L-rhamnose in all solvents and had $[\alpha]_D^{22}$ +2° (*c*, 0.7). The material formed a phenylhydrazone which, after recrystallization from water, had m.p. 157–158° C and $[\alpha]_D^{22}$ +42° (*c*, 0.1) (39). Admixture with authentic L-rhamnose phenylhydrazone failed to depress the melting point.

Tiselius Investigation of the Neutral Fraction

The neutral fraction (50 mg) was dissolved in borate buffer (0.05 *M*, 5 ml) and dialyzed against borate buffer for 24 hours. The electrophoresis was performed with the aid of the compensator. Pictures were taken of the 'buffer arm' after 20 minutes (*a*), 80 minutes (*b*), and 390 minutes (*c*). A small fast peak was observed followed by two slow peaks of about the same size.

When the fast-moving peak was no longer visible on the observation screen, the cell was closed and the current switched off. The solutions contained in the 'buffer arm' and 'solution arm' were removed and hydrolyzed separately. Chromatography indicated that there was little difference in the sugar composition of each fraction, although the solution obtained from the 'solution arm' was apparently richer in arabinose.

Large-scale Smith-type Degradation of the Neutral Fraction

The neutral fraction (5.9 g) was dissolved in distilled water (1.2 l.), and sodium metaperiodate solution (0.3 *M*, 162 ml) was added. The reaction mixture was kept in the dark for 96 hours. The excess periodate was destroyed with ethylene glycol (20 ml), and after dialysis to remove formaldehyde, ethylene glycol, and salts, the polyaldehyde was reduced with a solution of potassium borohydride (5 g in 100 ml). The excess borohydride was destroyed with dilute acetic acid. The solution was dialyzed for several days and then concentrated to a thick gel. The volume was adjusted to 150 ml with sulphuric acid (1 *N*) and the solution kept at room temperature for 12 hours. After neutralization ($BaCO_3$), the precipitate was removed by centrifugation. The centrifugate was passed through IR-120(H) resin. The eluate was concentrated and poured into ethanol. The precipitate was collected by centrifugation and dried to a white powder (850 mg). The alcohol supernatant was concentrated to a syrup (2.1 g).

Properties of the Smith-type Degraded Polysaccharide

Hydrolysis of a portion (10 mg) of the polysaccharide followed by chromatography in solvents (A) and (C) showed the presence of xylose and a trace of arabinose. The polysaccharide had $[\alpha]_D^{22}$ −54° (*c*, 0.2).

The degraded material (4 mg) and Enzyme AP19 (supplied by Rohm and Haas Co.) (4 mg) were dissolved in water (5 ml) and incubated at 37° C. Aliquots were removed at intervals and chromatographed in solvent (A). Xylose, xylobiose, xylotetraose, and oligosaccharides were produced.

The degraded material (45.5 mg) was dissolved in water and sodium metaperiodate solution (0.3 *M*, 3 ml) added. The solution was made up to volume (100 ml) and kept in the dark while the oxidation proceeded. Periodate uptake and formic acid production were determined as previously described. Extrapolation of the 'overoxidation' part of the curves to zero time indicated that 0.57 mole of periodate was consumed and 0.10 mole of formic acid was produced per pentose unit (calculated as $C_6H_8O_4$). Hydrolysis of the mixture after oxidation followed by chromatography in solvents (A), (B), and (C) showed the presence of xylose only.

Methylation of the Degraded Polysaccharide

The polysaccharide (800 mg) was dissolved in water (10 ml), and dimethyl sulphate (30 ml) and sodium hydroxide solution (30%, 10 ml) were added, while the solution was vigorously stirred. The solution was kept at 0° C and at pH 6–7. After 24 hours the basic solution was heated at 60° C. The solution was neutralized with acetic acid and concentrated to a small volume (20 ml). This solution was extracted several times with chloroform and the combined chloroform extracts were concentrated to a syrup (770 mg). The syrup was dissolved in methyl iodide and methylated by Purdie's method. The syrupy methylated material (450 mg) was extracted with boiling light petroleum (40–60°). The solution was decanted from the insoluble material and concentrated to a syrup (113 mg). The light petroleum insoluble material (537 mg) was dissolved in chloroform and concentrated to a glass. The glass (found: OMe, 37.6%) displayed a negligible hydroxyl peak in the infrared spectrum.

The methylated material (525 mg) was hydrolyzed with formic acid as previously described to yield a syrup (481 mg) of methylated fragments. The syrup was separated on a cellulose column using light petroleum (100–120°) – butan-1-ol (7:3) and later butan-1-ol – methanol (10:1) as eluants, to give six fractions which were again separated chromatographically to give the following sugars.

Identification of the Methylated Fragments

Sugar 1.—This syrup (46 mg) had an R_f value identical with that of 2,3,4-tri-*O*-methyl-D-xylose and crystallized completely on nucleation. Recrystallization from ether yielded crystals, m.p. and mixed m.p. 88–89° C, which had $[\alpha]_D^{21}$ +19° (*c*, 0.7) (40). The mother liquors were separated on paper using solvent (A) and a further crop of crystals (16 mg) was obtained.

Sugar 2.—This syrup (128 mg) was crystallized from acetone – light petroleum and yielded 2,3-di-*O*-methyl-D-xylose, m.p. and mixed m.p. 80–81° C, and had $[\alpha]_D^{22}$ +25° (*c*, 0.34) (41). The derived *N*-phenyl glycosylamine was recrystallized from ethanol and yielded *N*-phenyl-2,3-di-*O*-methyl-D-xylosylamine, m.p. and mixed m.p. 124–125° C, which had $[\alpha]_D^{22}$ +88° (*c*, 0.14 in ethyl acetate, 5% acetic acid) (40).

Sugars 3 and 4.—The syrup (145 mg) was separated into two components by paper electrophoresis. The faster-moving material (9 mg) corresponded to authentic 3-*O*-methyl-D-xylose and had $[\alpha]_D^{22}$ +6° (*c*, 0.9); demethylation of the derivative afforded xylose. A crystalline aniline derivative could not be obtained. The slower-moving fraction (101 mg) yielded xylose after demethylation; it moved slower than 2- or 3-*O*-methyl-D-xylose on paper chromatograms. The material gave a positive tetrazolium red test and had $[\alpha]_D^{22}$ +6° (*c*, 1.01), in good agreement with the value reported by Hough and Jones (42) for syrupy 4-*O*-methyl-D-xylose. When oxidized with sodium periodate the syrup (4.5 mg) liberated 2 moles of formic acid per mole of mono-*O*-methyl pentose. The syrup failed to yield a crystalline aniline derivative. The derived phenylosazone had m.p. 160–161° C (43). Admixture with the authentic 4-*O*-methyl-D-xylosazone prepared by the method of Hough and Jones (42) failed to depress the melting point.

Sugar 5.—This material (10 mg) was obtained from the same separation as sugars 3 and 4. The syrup was chromatographically indistinguishable from xylose in solvents (A), (B), and (C); it could not be induced to crystallize. The syrup was treated with benzaldehyde and methanolic hydrogen chloride (44) for several days. The derived dibenzylidene dimethyl acetal of D-xylose after recrystallization from chloroform – light petroleum had m.p. and mixed m.p. 207–208° C.

Sugar 6.—This material (15 mg) was obtained from the paper chromatographic separation of sugars 5 and 6. The syrup had an R_f value identical with that of 2,4-di-*O*-methyl-D-xylose in solvents (A), (B), and (C). The syrup failed to crystallize or yield a crystalline aniline derivative.

Sugar 7.—This material (10 mg) was obtained from the separation of sugar 2. The syrup yielded arabinose after demethylation and had an R_f value in solvents (A) and (B) of 0.91 and 0.85 respectively. The data suggest that it is either 2,3,4-tri-*O*-methyl-L-arabinose or 2,5-di-*O*-methyl-L-arabinose (45); crystalline derivatives could not be obtained.

Investigation of the Alcohol-soluble Smith-type Degradation Products

1. Acetone Separation

The syrup (2.1 g) was extracted three times with boiling acetone. The acetone solutions were decanted, combined, and concentrated to a syrup (1.1 g).

2. Separation of the Acetone-insoluble Material

The syrup (1.0 g) in water (3 ml) was absorbed on a column of Dowex 50W resin 2% crosslinked (lithium salt) (46). Water was used as the developing solvent and six fractions were collected. Chromatography of the first three fractions indicated the presence of higher molecular weight material. Hydrolysis of portions of each fraction indicated a mixture of glycerol and one or two sugars.

3. Separation of the Acetone-soluble Material

This material (1.1 g) was separated in the same manner as the acetone-insoluble material and the following fractions were obtained.

Fraction	Tube No.	Component (R_{rham}, solvent (B))	Weight (mg)
A	0–81	0.22, 0.16	110
B	82–100	1.52, 1.14, 0.93 0.75, 0.60, 0.30, 0.14	230
C	101–146	1.50, 1.11, 0.90 0.75, 0.60	317
		Total	657

Fraction A.—This fraction was not investigated.

Fraction B (230 mg).—This fraction was separated on cellulose using butan-1-ol half saturated with water as eluant to give seven fractions.

Fraction B_3 (30 mg).—This fraction had an R_f value corresponding to glycerol in all solvents. The syrup was characterized as the tri-*O*-*p*-nitrobenzoate, m.p. 190–191° C undepressed on admixture with authentic glycerol-tri-*O*-*p*-nitrobenzoate (9). All the other fractions were hydrolyzed and appeared to be glycerol glycosides of arabinose and galactose.

Fraction C (317 mg).—This fraction was fractionated in a manner similar to that used for fraction B to yield five fractions.

Fraction C_1.—This syrup was separated into two components (R_{rham} 1.64 and R_{rham} 1.24) using solvent (A). The fast-moving component (R_{rham} 1.64) yielded glycerol and a trace of arabinose after hydrolysis. The slow-moving component (R_{rham} 1.24) yielded glycerol and traces of arabinose and galactose after hydrolysis.

Fraction C_2.—This syrup had $[\alpha]_D^{22}$ +13° (*c*, 1.3) and yielded equal amounts of glycerol and arabinose after hydrolysis. The material had an R_{glyc} value of 0.87 in solvent (A) and 0.92 in solvent (B). When oxidized with metaperiodate, the syrup consumed 1.80 moles of periodate and released 0.81 mole of formic acid per sugar molecule. Hydrolysis of the periodate-oxidized material followed by chromatography in solvent (A) indicated that no monosaccharide was present but confirmed the presence of glycerol. The material did not crystallize but possessed optical rotation and R_f values similar to those of 2-*O*-α-L-arabinosyl glycerol glycoside obtained by Jones (14).

Fraction C_3.—This material was not further investigated.

Fraction C_4.—This fraction was separated into three components by paper electrophoresis. The zones (α, β, and γ) were eluted with water and concentrated to syrups.

Fraction α.—This syrup (48 mg) had $[\alpha]_D^{22}$ +29° (*c*, 0.94) and R_{rham} value 0.61 in solvent (A) which was identical with that of arabinose. The syrup was treated with saturated benzoyl hydrazine solution for 48 hours. The derived L-arabinose benzoyl hydrazone had m.p. and mixed m.p. 189–191° C (47).

Fraction β.—This material (27 mg) had $[\alpha]_D^{22}$ +18° (*c*, 1.38) and R_{rham} value 0.68 in solvent (A). The syrup yielded arabinose and glycerol after hydrolysis.

Fraction γ.—This syrup (27 mg) was a mixture and consisted of two components (R_{rham} 0.68 and 0.77) in solvent (A). Hydrolysis of the mixture followed by chromatography indicated the presence of arabinose, galactose, and glycerol.

Fraction C_5.—This syrup (5 mg) had $[\alpha]_D^{27}$ +23° (*c*, 0.38) and R_{gal} values of 1.10 in solvent (A) and 1.2 in solvent (B). The material gave a dark brown color with *p*-anisidine and yielded about equal amounts of arabinose and galactose after hydrolysis. Sufficient material was not available for further study.

Partial Hydrolysis of the Neutral Fraction

The neutral material (1 g) in sulphuric acid solution (0.5 *N*, 10 ml) was heated on a boiling-water bath. Samples were removed at hourly intervals for a period of 9 hours and examined chromatographically in solvents (A) and (B). The maximum yield of oligosaccharides was obtained at about 5 hours. These conditions were therefore chosen for a large-scale partial hydrolysis.

The neutral fraction (29 g) was swollen in sulphuric acid solution (0.5 *N*, 290 ml) and heated on a boiling-water bath for 5 hours. The hydrolyzate was neutralized ($BaCO_3$) and the precipitate removed by centrifugation. The centrifugate was passed through IR-120(H) resin and A-4(OH) resin. The neutral eluate was concentrated to a small volume (75 ml) and dialyzed against distilled water for several days. The water used in the dialysis was concentrated to a syrup (23 g). The dialyzate was concentrated and then poured into alcohol to yield the degraded polysaccharide (1.79 g) which had $[\alpha]_D^{21}$ −15° (*c*, 0.23). Hydrolysis of this material (30 mg) followed by chromatography in solvents (B) and (C) indicated the presence of xylose and galactose but the absence of arabinose; trace amounts of rhamnose and galacturonic acid were also detected. The disaccharides were separated from the monosaccharides in the syrup (23 g) on a charcoal–celite (1:1, w/w) column (48) using water as eluant. The disaccharides were removed with ethanol in water and yielded a syrup (2.1 g) upon concentration.

Column Separation of the Oligosaccharides

The syrup (2.1 g) was adsorbed on a cellulose column previously equilibrated with the developing solvent (*n*-propanol:ethyl acetate:water) (7:1:1, v/v). Thirteen fractions were collected, all of which were mixtures. All but fractions 12 and 13 were further separated on paper, using solvent (A).

Identification of the Disaccharide Fragments

Disaccharide 1

This material (352 mg) had $[\alpha]_D^{22}$ +84° (*c*, 1.75) and showed R_{gal} values of 1.18, 1.29, and 1.33 in solvents (A), (B), and (D) respectively. Hydrolysis of the syrup followed by chromatography indicated equal amounts of arabinose and xylose. Bromine oxidation showed that arabinose was the reducing end-group.

A small portion (20 mg) of the disaccharide was dissolved in water (3 ml). Redistilled phenylhydrazine (0.18 ml) and glacial acetic acid (0.20 ml) were added and the mixture heated for several hours at 40–45° C. Upon cooling of the solution, yellow crystals appeared, which were collected and recrystallized from water. The crystals rapidly turned a dark brown color and had m.p. 121–125° C.

A further portion of the syrup (25 mg) was dissolved in borate buffer (0.1 *M*, pH 7) and reduced with potassium borohydride solution (3 mg in 1 ml) for 1 day (49). The excess borohydride was destroyed with dilute acetic acid and the solution was then passed through IR-120(H) resin and A-4(OH) resin. The eluate was concentrated and codistilled several times with methanol. The dried syrup was treated twice with acetic anhydride (3 ml) and pyridine (5 ml) at room temperature for 40 hours. The acetate was isolated in the usual manner but failed to crystallize. The syrup had $[\alpha]_D^{22}$ +6° (*c*, 1.27 in chloroform). The disaccharide acetate was dissolved in acetone (20 ml) and the solution refluxed with sodium hydroxide solution (0.1 *N*, 5 ml) for 5 hours. The solution was cooled and passed through IR-120(H) resin. The eluate was then concentrated to a syrup. Paper chromatography indicated a trace of unreduced disaccharide (R_{gal} 1.2) and the syrupy sugar alcohol derivative which was separated using solvent (A). The zone (R_{gal} 0.70) was eluted with water and finally yielded a syrup (14.5 mg) which had $[\alpha]_D^{23}$ +46° (*c*, 1.45). When the material was oxidized with lead tetraacetate in a Warburg apparatus, 1.5 moles of formic acid were released. The reduced

disaccharide consumed 3.47 moles of periodate and liberated 1.60 moles of formic acid and 0.70 mole of formaldehyde (50) per mole of sugar when oxidized with sodium metaperiodate. Disaccharide 1 when chromatographed in solvents (A) and (B) had R_{gal} 1.16 and in solvent (C) had R_{gal} 1.31. This material had R_{gal} values which differed from those of 5-*O*-β-D-xylopyranosyl-L-arabofuranose, 3-*O*-α-D-xylopyranosyl-L-arabinose, and 2-*O*-β-D-xylopyranosyl-L-arabinose.

Disaccharide 2

This material (125 mg) had $[\alpha]_D^{17}$ +94° (*c*, 1.23). The R_{gal} values in solvents (A), (B), and (D) were respectively 1.00, 0.88, and 1.02. The syrup was not identical with 3-*O*-α-D-xylopyranosyl-D-xylose and the xylobiose already identified. Hydrolysis of a small portion indicated only xylose. The syrup (7 mg) was treated with phenylhydrazine to yield yellow crystals which darkened in color very rapidly. After recrystallization from hot water the crystals had m.p. 154–156° C. When oxidized with sodium metaperiodate, the disaccharide consumed 3.10 moles of periodate and released 1.60 moles of formic acid per sugar molecule.

Disaccharide 3

This syrup (41 mg) had $[\alpha]_D^{17}$ −16° (*c*, 2.04). The R_f value in all solvents was identical with that of 4-*O*-β-D-xylopyranosyl-D-xylose. Hydrolysis of a portion of the syrup showed only xylose. When seeded the material crystallized. It was recrystallized from methanol and had m.p. 194–196° C, undepressed on admixture with authentic 4-*O*-β-D-xylopyranosyl-D-xylose (40). The derived phenylosazone had m.p. and mixed m.p. 210–212° C (decomp.).

Disaccharide 4

A small amount of this material (3 mg) was available. The syrup had $[\alpha]_D^{17}$ +34° (*c*, 0.29). Hydrolysis followed by chromatography indicated arabinose and galactose. Bromine oxidation left the galactose unit untouched. The R_{gal} values on chromatograms in solvents (A) and (B) were 0.92 and 0.65 respectively.

Disaccharide 5

This material (5 mg) possessed R_{gal} 0.42 in solvent (A) and R_{gal} 0.65 in solvent (B). The syrup had $[\alpha]_D^{17}$ +25° (*c*, 0.48) and was shown to be a galactosyl-arabinose from the results of hydrolysis and bromine oxidation.

Disaccharide 6

This syrup (164 mg) had $[\alpha]_D^{18}$ +14° (*c*, 8.2). Hydrolysis followed by chromatography indicated the presence of xylose and arabinose. Bromine oxidation indicated arabinose to be the reducing end-group. The derived phenylosazone had m.p. 185–187° C. The disaccharide consumed 4.34 moles of periodate and produced 1.95 moles of formic acid. The material had R_{gal} values of 0.90 in solvents (A) and (C) and 0.80 in solvent (B).

Resin Separation of Fractions 12 and 13

The combined fractions 12 and 13 (155 mg) were placed on a column of Dowex 50W resin, 2% cross-linked (46). Aqueous ethanol (50%) was used as the developing solvent, to give four fractions. All fractions proved to be mixtures. Fraction 4 crystallized and was recrystallized from ethanol containing a trace of water. The crystals had m.p. 238–240° C. Hydrolysis followed by chromatography indicated only xylose. The sugar had R_{glu} values in solvent (E) of 0.13 and R_{malt} value of 0.20.

ACKNOWLEDGMENTS

One of the authors (K. H.) is indebted to Queen's University and the National Research Council for the award of scholarships. The authors thank the National Research Council for a grant (NRCT-39).

REFERENCES

1. A. J. ERSKINE and J. K. N. JONES. Can. J. Chem. **35**, 1174 (1957).
2. B. C. BERA, A. B. FOSTER, and M. STACEY. J. Chem. Soc. 3788 (1955).
3. S. A. BARKER, M. STACEY, and G. ZWEIFEL. Chem. & Ind. (London), 330 (1957).
4. H. O. BOUVENG. Acta Chem. Scand. **13**, 1869 (1959).
5. H. O. BOUVENG. Acta Chem. Scand. **13**, 1877 (1959).
6. A. J. ERSKINE. Ph.D. Thesis, Queen's University, Kingston, Ontario. 1957.
7. J. K. N. JONES. Unpublished results.
8. J. K. N. JONES and M. B. PERRY. J. Am. Chem. Soc. **79**, 2787 (1957).
9. J. E. CADOTTE, G. G. S. DUTTON, J. J. GOLDSTEIN, B. A. LEWIS, F. SMITH, and J. W. VAN CLEVEN. J. Am. Chem. Soc. **79**, 691 (1957).
10. D. G. EASTERBY. Ph.D. Thesis, University of Bristol, Bristol, England. 1951.
11. F. SMITH and A. M. UNRAU. Chem. & Ind. (London), 636 (1959).
12. H. H. SEPHTON. Private communication.
13. B. H. HOWARD. Biochem. J. **67**, 643 (1957).
14. J. K. N. JONES. Unpublished results.
15. D. H. BALL and J. K. N. JONES. J. Chem. Soc. 33 (1958).
16. P. ANDREWS and J. K. N. JONES. J. Chem. Soc. 4134 (1954).

17. R. L. WHISTLER and W. M. CORBETT. J. Am. Chem. Soc. **77**, 6328 (1955).
18. P. ANDREWS, D. H. BALL, and J. K. N. JONES. J. Chem. Soc. 4090 (1953).
19. D. H. BALL and J. K. N. JONES. J. Chem. Soc. 4871 (1957).
20. R. L. WHISTLER and D. I. J. MCGILVRAY. J. Am. Chem. Soc. **77**, 2212 (1955).
21. J. K. N. JONES, R. A. WALL, and (in part) A. O. PITTET. Chem. & Ind. (London), 1196 (1959).
22. S. ALLEN, T. G. BONNER, E. J. BOURNE, and M. M. SAVILLE. Chem. & Ind. (London), 630 (1958).
23. R. F. MILTON and W. A. WATERS. Methods of quantitative micro-analysis. Edward Arnold Ltd. 1955. p. 102.
24. G. NEUMÜLLER and E. VASSEUR. Arkiv. Kemi, **2**, 235 (1953).
25. T. J. DE BOER. Rec. trav. chim. **73**, 229 (1954).
26. R. KUHN, H. TRISCHMANN, and I. LOW. Angew. Chem. **67**, 32 (1955). Chem. Abstr. 16,812 (1956).
27. F. SMITH. J. Chem. Soc. 1035 (1940).
28. F. SMITH. J. Am. Chem. Soc. **70**, 3249 (1948).
29. R. H. COTE. J. Chem. Soc. 2248 (1959).
30. E. L. HIRST and S. DUNSTAN. J. Chem. Soc. 2332 (1953).
31. R. L. WHISTLER and H. E. CONRAD. J. Am. Chem. Soc. **76**, 1673 (1954).
32. P. ANDREWS, L. HOUGH, and J. K. N. JONES. J. Am. Chem. Soc. **77**, 125 (1955).
33. D. J. BELL and G. D. GREVILLE. J. Chem. Soc. 1136 (1955).
34. F. SMITH and H. C. SRIVASTAVA. J. Am. Chem. Soc. **78**, 1404 (1956).
35. R. J. BLOCK. Anal. Chem. **22**, 1327 (1950).
36. G. W. HUFFMAN and F. SMITH. J. Am. Chem. Soc. **77**, 3141 (1955).
37. M. B. PERRY. Unpublished results.
38. G. J. ROBERTSON and R. A. LAMB. J. Chem. Soc. 1321 (1934).
39. C. L. BUTLER and L. H. CRETCHER. J. Am. Chem. Soc. **53**, 4358 (1931).
40. I. EHRENTHAL, M. C. RAFIQUE, and F. SMITH. J. Am. Chem. Soc. **74**, 1341 (1952).
41. H. A. HAMPTON, W. N. HAWORTH, and E. L. HIRST. J. Chem. Soc. 1739 (1929).
42. L. HOUGH and J. K. N. JONES. J. Chem. Soc. 4349 (1952).
43. O. WINTERSTEINER and A. KLINGSBERG. J. Am. Chem. Soc. **71**, 939 (1949).
44. L. J. BREDDY and J. K. N. JONES. J. Chem. Soc. 738 (1945).
45. R. W. HUMPHREYS, J. PRYDE, and E. T. WATERS. J. Chem. Soc. 1298 (1937).
46. J. K. N. JONES, R. A. WALL, and (in part) A. O. PITTET. Can. J. Chem. **38**, 2285 (1960). J. K. N. JONES and R. A. WALL. Can. J. Chem. **38**, 2290 (1960).
47. E. L. HIRST, J. K. N. JONES, and E. A. WOODS. J. Chem. Soc. 1048 (1947).
48. R. L. WHISTLER and D. F. DURSO. J. Am. Chem. Soc. **72**, 677 (1950).
49. P. D. BRAGG and L. HOUGH. J. Chem. Soc. 4347 (1957).
50. H. NEUKOM and H. DEUCH. Chem. & Ind. (London), **23**, 683 (1958).

ISOTOPE RATE EFFECTS IN THE ENOLIZATION OF OXALACETIC ACID

GEORGE W. KOSICKI
Department of Chemistry, Essex College, Assumption University of Windsor, Windsor, Ontario
Received February 16, 1962

ABSTRACT

Acid-catalyzed enolization of oxalacetic acid in H_2O and D_2O gives rise to a constant isotope rate effect k_{H_2O}/k_{D_2O} of 2.4 over the pH (pD) range of 5.5 to 7.5. Base-catalyzed enolization of oxalacetic acid in H_2O and D_2O gives rise to a constant isotope rate effect k_{H_2O}/k_{D_2O} of 4.5 over the pH (pD) range of 7.0 to 8.0. The percentage of enol form of oxalacetic acid was calculated to be 15.3% at pH 8.0, using the absorption of the enol form in ether at 255 mμ and the absorption of the keto form at pH 0.5 in an aqueous system. The spectrophotometric measurement of the isotope rate effect involved in the enolization of oxalacetic acid gives direct evidence for the rate-determining step in both the acid- and the base-catalyzed reactions without subsequent reactions.

INTRODUCTION

During the study of the isotope rate effects of the citrate-condensing enzyme we observed certain spectral changes in the assay involving the enolization of oxalacetic acid (1). Oxalacetic acid has been found to exist in the enol form to the extent of 15.2 to 15.8% in aqueous systems from pH 5 to 10 (2). Enolizations of this type are general acid- and base-catalyzed reactions (3, 4):

Acid-catalyzed:

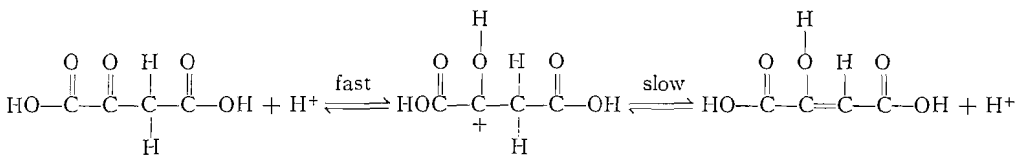

Base-catalyzed:

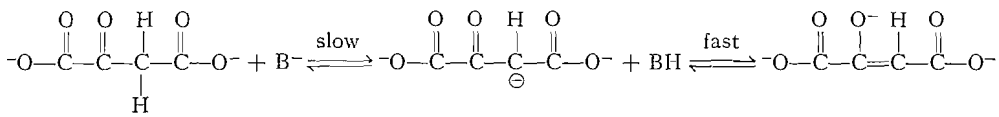

The step involving the C—H bond cleavage has been shown to be rate limiting by following the rate of enolization by subsequent bromination (5, 6), racemization, and deuteration (7) of the resulting enol. The rate of the base-catalyzed bromination is proportional to the concentrations of the ketone and base but is independent of the concentration of bromine. The acid-catalyzed halogenation has properties similar to those of the base-catalyzed reaction, i.e. the rate is proportional to the concentration of the ketone and acid but independent of the concentration of the halogen. This means that although halogen is consumed in the overall reaction of both acid- and base-catalyzed enolizations, it becomes involved after completion of the rate-determining step.

The rate of enolization of oxalacetic acid can also be followed spectrophotometrically because the enol form has a markedly increased absorption at 255 mμ. This increased absorption is due to the conjugated bond system of the enol form. In this paper the rate

of enolization of oxalacetic acid is measured spectrophotometrically as a function of pH and pD. The results show an isotope rate effect in both the acid- and base-catalyzed enolizations, indicating directly that C—H bond cleavage is involved in the rate-determining step.

EXPERIMENTAL

The following materials were commercial preparations: reduced diphosphopyridine nucleotide (DPNH), oxalacetic acid, and malate dehydrogenase (C. F. Boehringer and Son, Mannheim, Germany). The D_2O (99.78 atom% excess D) was purchased from Atomic Energy of Canada Limited, Ottawa. Tris(hydroxymethyl)aminomethane (THAM) was primary standard grade.

Oxalacetic acid concentrations were measured enzymatically using malate dehydrogenase and DPNH in 0.1 *M* potassium phosphate buffer, pH 7.2 (8). In these cases, however, the malate dehydrogenase reaction was followed to completion in the presence of an excess of enzyme (200 units) and a limiting concentration of oxalacetic acid. In a 1.0-ml volume and 1.0-cm light-path reaction cell, 1.0 μmole of DPNH consumed, which is equivalent to 1.0 μmole of oxalacetic acid, gives a change of 6.22 absorbancy units at 340 mμ. Freshly dissolved oxalacetic acid samples were stored in ice during the time of running a given series of readings in order to minimize decarboxylation.

The pH of each reaction cell was measured at the end of the assay by a Beckman Model G pH meter. For the D_2O systems the numerical reading of pH was converted to pD by adding 0.4 units as described by Lumry *et al.* (9, 10). This calculation received experimental confirmation by Glascoe and Long (11). For the assays in D_2O the same reagents used in the H_2O systems were made up in D_2O. The D_2O concentrations were routinely above 98% in the reaction cell.

The rates of reaction were measured with a Beckman Model D.U. spectrophotometer. The temperature of the reaction cell was kept at 25±0.2° C by a water-circulating bath.

RESULTS

Figure 1 shows the absorbancy of the equilibrium mixture of enol and keto forms of oxalacetic acid measured in the direction of enol formation. The equilibrium mixture at pH 8.0 contains 15.3% enol as calculated from the 255-mμ absorption of oxalacetic acid in ether; the ketoacid in ether is known to be in the enol form (12). The molar absorbancy index at 255 mμ is 5.60×10^3. The aqueous absorption at pH 8.0 was corrected for the

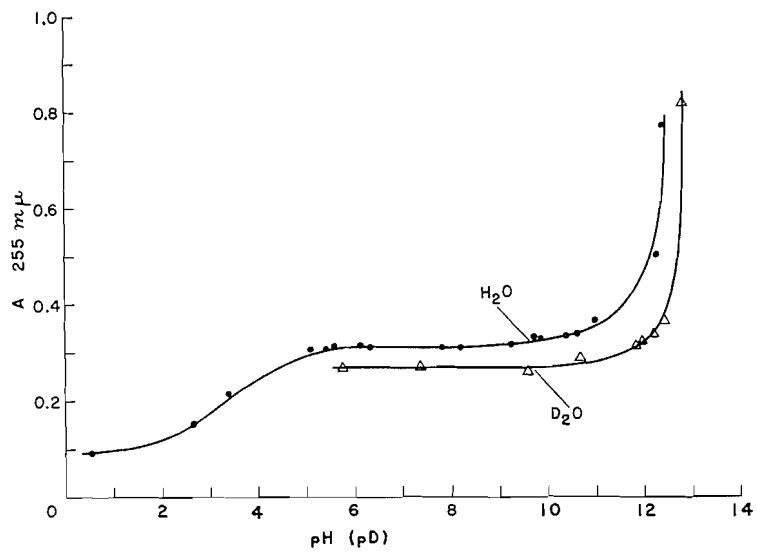

FIG. 1. Equilibrium absorbancy of oxalacetate. Each cell (0.5-cm light-path) contained 0.795 μmole of oxalacetic acid and sufficient NaOH (or HCl) to give the resulting pH (pD) values, and water to make the final volume 1.5 ml. For D_2O systems the reagents were made up in D_2O. The absorbancy values are the highest readings reached for each reaction.

absorption of the keto form by using the absorption of oxalacetic acid at pH 0.5, where the molar absorbancy index is 0.41×10^3. At pH 2.5 oxalacetic acid in H_2O is 2.8% in the enol form and at pH 12.4, 49%. The equilibrium absorption is approximately constant from pH 5 to 10.

The equilibrium absorption in D_2O is decreased, corresponding to 12.7% enol form from pD 5 to 11. Above pD 11 the absorption in D_2O is shifted about 0.5 pD units.

The same equilibrium values are reached by ketonization. Oxalacetic acid in NaOH (pH 12.5) or in ethanol, where the enol form predominates, was neutralized with varying amounts of HCl or NaOH to give a range of resulting pH and equilibrium values. At 25° C the rate of ketonization is too fast to be followed by our method.

Figure 2 shows the rate of absorbancy change as a function of pH in the range of acid-catalyzed enolization. The solid acid (enol form) equilibrated in H_2O (pH 2.5) corresponds

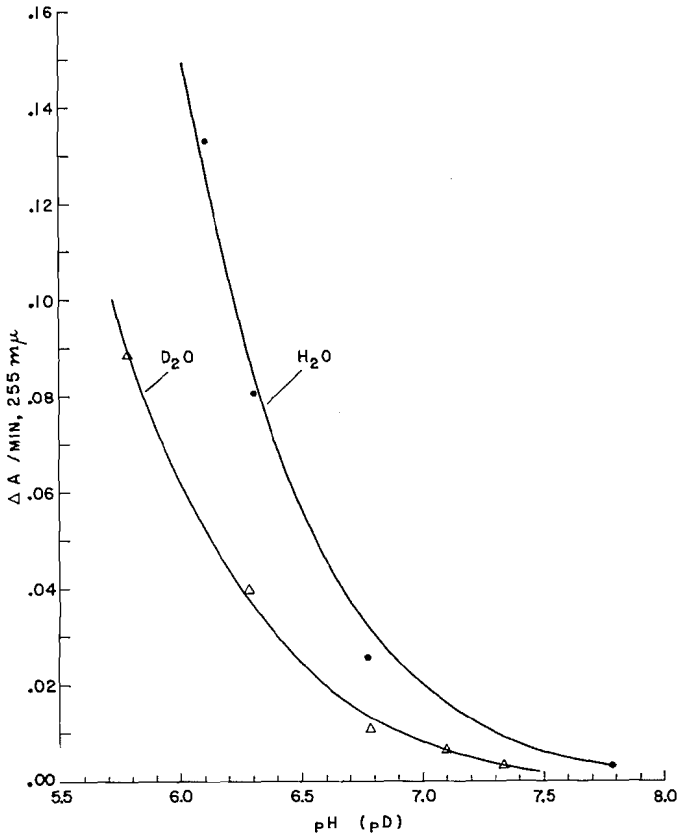

FIG. 2. Acid-catalyzed enolization. Each reaction cell (0.5-cm light-path) contained 0.765 μmole of oxalacetic acid, sufficient NaOH to give the resulting pH (pD) values, and water to make the final volume 1.5 ml. The reactions were started by additions of 0.10 ml of a solution of oxalacetic acid in H_2O (pH 3) or in D_2O (pD 2.5). The curve for the H_2O system is drawn with a constant isotope rate effect of k_{H_2O}/k_{D_2O} of 2.4.

to 2.8% enol form. This solution of the keto form of oxalacetic acid was added to a solution of NaOH of varying concentrations so that the resulting pH values would be within the range of pH 5.5 to 7.5. The initial rates of absorbancy increase were measured at 255 mμ and expressed as absorbancy change per minute.

The rate of absorbancy change as a function of pD (Fig. 2) shows a similar acid-catalyzed enolization. The D_2O system was measured under identically corresponding conditions, replacing H_2O with D_2O. The rate of enolization in D_2O depends on a higher concentration of acid, giving rise to a constant isotope rate effect k_{H_2O}/k_{D_2O} of 2.4.

In Fig. 3 the base-catalyzed enolization is shown for both H_2O and D_2O systems. A solution of the keto form (pH 3.0) was added to 0.67 *M* THAM–HCl, with the HCl

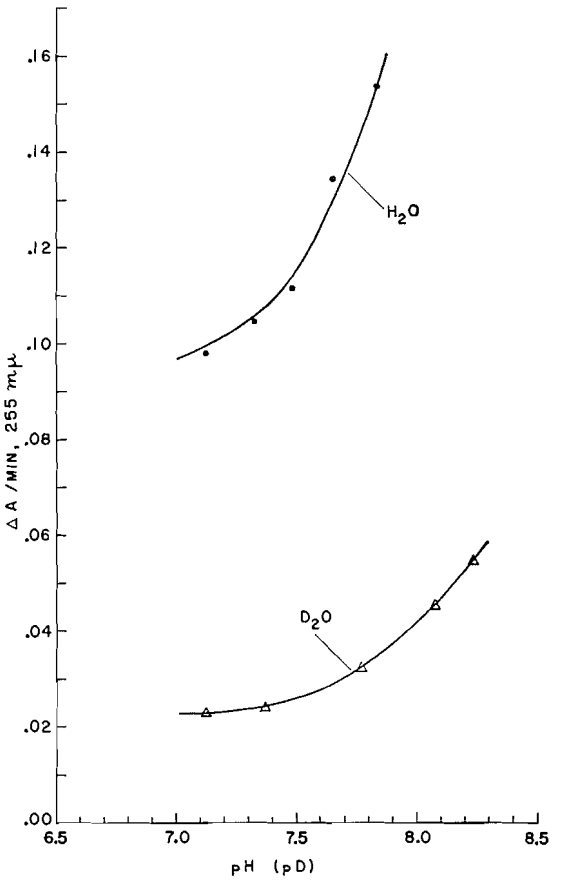

FIG. 3. Base-catalyzed enolization. Each reaction cell (0.5-cm light-path) contained 0.680 μmole of oxalacetic acid, 100 μmoles of basic THAM, sufficient HCl to give the resulting pH or pD values, and water or D_2O to make the final volume 1.5 ml. The curve for H_2O is drawn with a constant isotope rate effect k_{H_2O}/k_{D_2O} of 4.5.

concentrations varying so as to adjust the resulting pH or pD values. The rate of base-catalyzed enolization was similarly followed by the absorption increase at 255 mμ. The isotope rate effect of k_{H_2O}/k_{D_2O} is a constant value of 4.5. Additions of salts of weak acids such as $KHCO_3$ or THAM–acetate increased the rate of enolization, thus shifting the rate curve of the base-catalyzed reaction to lower pH values.

DISCUSSION

Approximately the same equilibrium value of 15.3% enol for the pH range of 5 to 10 is reached by acid or base catalysis whether approached from the enol or keto side of

the equilibrium. In the pH (pD) ranges where the rate of reaching the equilibrium is comparatively slow the equilibrium absorption is slightly variable and decreases because of decarboxylation of oxalacetic acid to pyruvic acid (13, 14). In the strongly basic region the equilibrium absorption increases because of the formation of the enolate. The magnitude of the shift of the absorption curve for D_2O to a higher pD value corresponds well to shift of pK values of weak acids in D_2O as compiled by Glascoe and Long (11).

In the strongly acid range the absorption of equilibrated oxalacetic acid decreases because full protonation of the carboxyl groups decreases any tendency to a conjugated double-bond system which is responsible for the 255-mμ absorption. This is borne out by the fact that the 255-mμ absorption of oxalacetic acid at pH 0.5 can be used as the absorption of the keto form.

The isotope rate effects in both acid- and base-catalyzed enolizations of oxalacetic acid indicate that proton cleavage is involved in the rate-limiting step of both reactions. When the oxalacetic acid is equilibrated in D_2O prior to the experiment it quickly exchanges to form the fully deuterated substrate (15). The C—D bond is then cleaved in the slow step.

These data give further and direct evidence that the proton–carbon bond cleavage is the rate-limiting step in acid- and base-catalyzed enolizations.

ACKNOWLEDGMENTS

The author wishes to thank the National Research Council of Canada for financial assistance and Doctors P. A. Srere, R. J. Thibert, and K. G. Rutherford for their many valuable discussions.

REFERENCES

1. G. W. Kosicki and P. A. Srere. J. Biol. Chem. **236**, 2566 (1961).
2. B. E. C. Banks. J. Chem. Soc. 5043 (1961).
3. E. S. Gould. Mechanism and structure in organic chemistry. Henry Holt and Co., New York. 1959. p. 372.
4. B. E. C. Banks. J. Chem. Soc. 63 (1962).
5. R. P. Bell and H. C. Longuet-Higgins. J. Chem. Soc. 636 (1946).
6. F. A. Long and D. Watson. J. Chem. Soc. 2019 (1958).
7. K. S. Hsu, C. K. Ingold and C. L. Wilson. J. Chem. Soc. 78 (1938).
8. S. Ochoa. *In* Methods in enzymology. Vol. I. S. P. Colowick and N. O. Kaplan (*Editors*). Academic Press Inc., New York. 1955. p. 735.
9. R. Lumry, E. L. Smith, and R. R. Glantz. J. Am. Chem. Soc. **73**, 4330 (1951).
10. P. A. Srere, G. W. Kosicki, and R. Lumry. Biochem. Biophys. Acta, **50**, 184 (1961).
11. P. K. Glascoe and F. A. Long. J. Phys. Chem. **64**, 188 (1960).
12. A. Hantzsch. Ber. **48**, 1407 (1915).
13. H. Krebs. Biochem. J. **36**, 303 (1942).
14. T. T. Tchen and B. Vennesland. J. Biol. Chem. **213**, 533 (1955).
15. R. P. Bell. The proton in chemistry. Cornell University Press, Ithaca, New York. 1959. p. 138.

A NUCLEAR MAGNETIC RESONANCE INVESTIGATION OF MOLECULAR COMPLEXES OF POLAR MOLECULES IN AROMATIC SOLVENTS*

J. V. HATTON† AND W. G. SCHNEIDER
Division of Pure Chemistry, National Research Council, Ottawa, Canada

Received February 14, 1962

ABSTRACT

In order to confirm the existence of specific molecular complexes in solutions of polar solutes in *aromatic* solvents previously proposed, the temperature variation of the proton resonance shifts of the solutes acetonitrile, *p*-benzoquinone, and N,N-dimethylformamide in 5 mole% concentration in toluene were measured. The large temperature coefficients of the solute shifts observed strongly support molecular complex formation. For the same solutes dissolved in methylcyclohexane the temperature coefficients were negligibly small. The temperature at which onset of free rotation of the N-dimethyl group of N,N-dimethylformamide occurs is solvent and concentration dependent. These observations are consistent with the proposed geometry of the molecular complex in the aromatic solvents.

INTRODUCTION

The proton chemical shifts of solute molecules in solution may be affected by a number of factors (1). The observed shift, δ, can be written

$$\delta = \delta_G + \delta_B + \delta_A + \delta_W + \delta_E + \delta_C,$$

where δ_G is the shift of an isolated gaseous molecule, δ_B is the shift due to the bulk diamagnetic susceptibility of the solvent, δ_A is the shift arising from the solvent magnetic anisotropy, and the term δ_W is the shift due to the van der Waals interaction between solute and solvent molecules. These contributions are important in the interpretation of the shifts of non-polar solute molecules, but, for polar molecules, an additional term, δ_E, must be taken into account. This is the shift arising from the reaction field of the solvent. Finally, δ_C is the shift due to specific molecular interaction or complex formation in solution. Theoretical calculations of the magnitude of δ_A have been made for the disk-shaped aromatic molecules, and the observed high-field dilution shifts of non-polar solutes in aromatic solvents agree reasonably well with theory (2–4).

Of particular interest is the exceptional behavior shown by polar solutes in aromatic solvents. Very large "high-field" dilution shifts have been observed (5–8). These have been tentatively interpreted in terms of complex formation between the polar solute and aromatic solvent molecules. Further supporting evidence for this interpretation would be highly desirable. The present paper describes an investigation of the temperature coefficient of the chemical shift of solute protons for three selected systems, each comprising a polar solute in an aromatic solvent. The large temperature variations observed provide strong evidence for molecular complex formation in these systems.

EXPERIMENTAL

The proton chemical shifts of dilute solutions of N,N-dimethylformamide, acetonitrile, and *p*-benzoquinone in toluene and methylcyclohexane have been measured at different temperatures on a Varian spectrometer operating at 60 Mc/sec. The variable temperature probe previously described (9) was used throughout the work and this gives temperatures which are accurate to $\pm 1/2°$ C.

*Issued as N.R.C. No. 6893.
†*National Research Council Postdoctorate Fellow, 1961–63.*

The solutions were made up by weight and contained 5 mole% solute. At this dilution, solute-solute interactions may be ignored. The strongest solution of *p*-benzoquinone in methylcyclohexane that could be obtained was 1 mole%.

All the liquids used were of White label or Research grade purity; the *p*-benzoquinone was purified by repeated sublimation.

Chemical shifts were measured by the side-band technique using T.M.S. (tetramethylsilane) as internal reference. These are accurate to ±0.1 cycle/sec. Tetramethylsilane was chosen because of its sharp resonance over the entire temperature range studied, −100° C to +140° C.

RESULTS AND DISCUSSION

The variation of chemical shift with temperature of dilute solutions of acetonitrile, *p*-benzoquinone, and N,N-dimethylformamide in methylcyclohexane and toluene are shown in Figs. 1 to 3 respectively. It is observed that in all three systems the proton

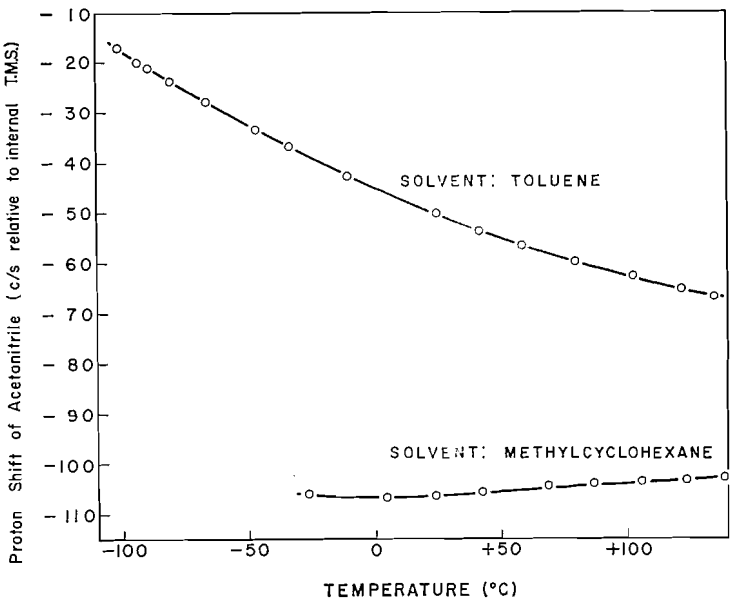

FIG. 1. The temperature dependence of the proton chemical shift of acetonitrile in toluene and methylcyclohexane. The negative sign indicates a displacement of the signal to the low-field side of the reference, T.M.S.

shifts are almost completely independent of temperature when methylcyclohexane is used as solvent, confirming the absence of solute–solvent complex species in these solutions. On the other hand, there is a progressive high-field shift of the solute protons in toluene solutions as the temperature is reduced.

Large shifts to high field occur in the *p*-benzoquinone–toluene system below +10° C. This is the result of the solution becoming more dilute as the solubility of the solid decreases. For this reason, the temperature coefficients of the shifts have been calculated using +10° C as the lower limit. The upper limit, +90° C, is fixed by the internal rotational behavior of N,N-dimethylformamide just above this temperature. The temperature coefficients are shown in Table I.

The methyl derivatives, toluene and methylcyclohexane, rather than the parent hydrocarbons, were chosen as solvents since their much lower freezing points enable a wide temperature range to be investigated. In addition, certain physical properties, i.e.

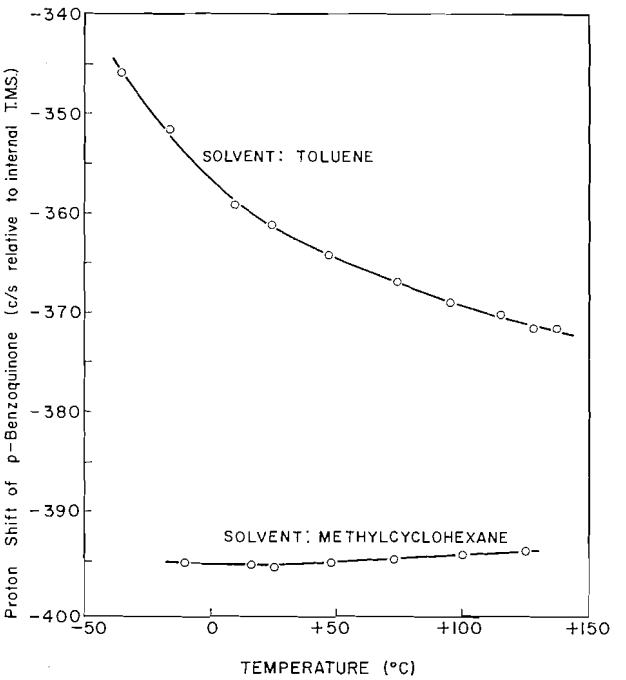

FIG. 2. The temperature dependence of the proton chemical shift of *p*-benzoquinone in toluene and methylcyclohexane.

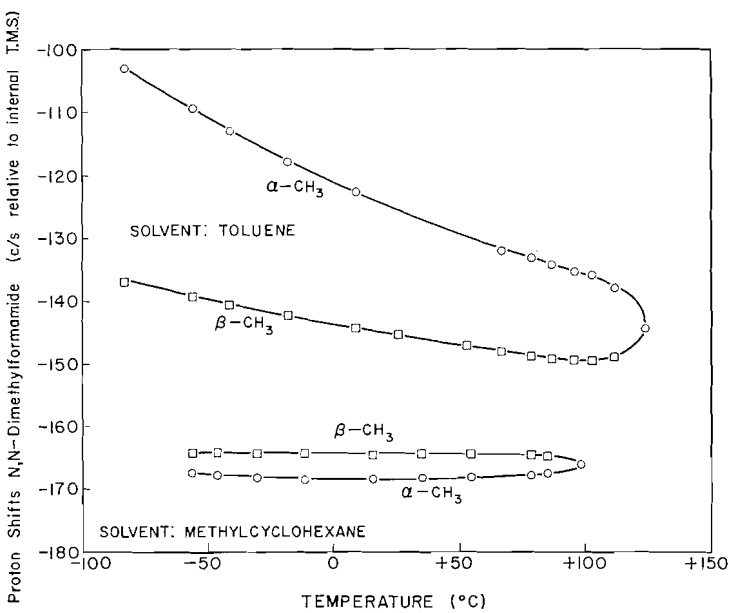

FIG. 3. The temperature dependence of the proton chemical shifts of the N-dimethyl group of N,N-dimethylformamide in toluene and methylcyclohexane.

TABLE I

Temperature coefficients* of the proton shifts in toluene, $d\delta/dT$

Solute	Concentration of solute (mole%)	$d\delta/dT$ ((cycle/sec)/°C) (between +10° C and +90° C)	$d\delta^{\alpha}/dT$	$d\delta^{\beta}/dT$
Acetonitrile	5	−0.180		
	10	−0.147		
p-Benzoquinone	5	−0.120		
N,N-Dimethylformamide	5		−0.146	−0.062
	10		−0.100	−0.040
	25		−0.057	−0.0194

*The negative sign indicates a shift to low field on raising the temperature.

shape, molar volume, and dielectric constant, of these two molecules are so similar that we are justified in making the following two assumptions:

(*a*) The van der Waals interactions between solute and solvent molecules will be comparable for both solvents.

(*b*) The electric "reaction field" experienced by polar solute molecules will also be small and comparable in toluene and methylcyclohexane.

Furthermore, the use of an internal reference eliminates the effect of the bulk susceptibility of the solvent. Thus, we can neglect the terms δ_B, δ_W, and δ_E, and the observed difference between the solute shifts in toluene and methylcyclohexane, $\Delta\delta$, will be a direct measure of the effect of $(\delta_A+\delta_C)$ on the solute molecule.*

The formation of the complexes can be represented by the equilibrium

$$\text{solute} + \text{toluene} \rightleftharpoons \text{toluene:solute}. \qquad [1]$$

At sufficiently high temperatures complex formation is very unfavorable and the distribution of molecules is completely random. Here, $\Delta\delta$ is small and, in the limit, tends to zero. At lower temperatures the distribution of solvent molecules around each solute molecule becomes increasingly more ordered as a result of complex formation, causing an increase in $\Delta\delta$.

Under the present experimental conditions the complexes are short-lived and it is not possible to isolate a pure species† and to measure the chemical shift. Thus, the actual value of $\Delta\delta$ at any temperature will depend, not only upon the geometry of the complex, but also upon the averaged configuration determined by the equilibrium constant of equation [1].

We have previously proposed, independently, that the complexes are planar and that the molecular interaction is dipolar‡ in nature (5, 6). The values of the temperature coefficients of the proton shifts (Table I) are consistent with the structure of these complexes, shown schematically in Fig. 4. The temperature coefficients decrease in the order $CH_3CN > \alpha\text{-}CH_3$ (N,N-dimethylformamide) > *p*-benzoquinone > $\beta\text{-}CH_3$ (N,N-dimethylformamide). This is also the order of the magnitudes of the anisotropic high-field shifts at each of these proton sites.

Since $\Delta\delta$ is observed to be positive, and δ_C may be expected to make a negative contribution, δ_A, the contribution due to the magnetic anisotropy, is responsible for the large "high-field" shifts of the solute protons in aromatic solvents.

†*A solid phase compound with an incongruent melting point in the acetonitrile–benzene system has recently been reported (10) and observed independently in this laboratory.*

‡*The complexes formed by p-benzoquinone with aromatic solvents may be regarded as arising from quadrupole-induced quadrupole interaction.*

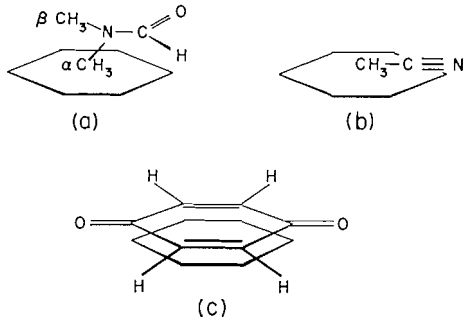

FIG. 4. Schematic representation of the complexes formed between toluene and (*a*) N,N-dimethylformamide, (*b*) acetonitrile, and (*c*) *p*-benzoquinone.

According to Gutowsky and Holm the potential barrier to free rotation of the NMe_2 group of N,N-dimethylformamide about the C—N bond is 7 kcal/mole (11). In Fig. 3 it is observed that onset of "free" rotation of the NMe_2 group (sufficient to cause averaging of the methyl chemical shifts) in the dilute solution in methylcyclohexane occurs at a temperature of 99° C. However, in the toluene solution, free rotation (in the above sense) does not begin until a temperature of 125° C is reached. The temperatures at which onset of free rotation occurs in toluene solutions of different N,N-dimethylformamide concentrations are shown in Table II. At first sight it would appear that, since

TABLE II

The temperatures at which free rotation of the N-dimethyl group of N,N-dimethylformamide occurs

Solvent	Concentration of solute (mole%)	Temperature (°C)
Methylcyclohexane	5	99
Toluene	5	125
	10	121
	25	112
Nitrobenzene	10	103

molecular interaction of the type considered here may be expected to hinder internal rotation in the solute, these values are consistent with the existence of complexes in the aromatic solvent. However, since the separations of the N-dimethyl resonances in the toluene solutions are larger than those in the methylcyclohexane, the faster exchange rates required in the former may well account for the higher temperatures at which free rotation sets in.* From the broadening of the resonance lines of N,N-dimethylformamide (below the coalescence temperature) in toluene and in methylcyclohexane, values of τ, the average time spent by each methyl group in a given environment, have been calculated. For the toluene solution these are $\tau = 0.078$ second (99° C) and 0.014 second (125° C). In methylcyclohexane, the value of τ at coalescence is 0.06 second (99° C). The larger value of τ at 99° C in toluene compared to that in methylcyclohexane could arise from the association postulated to occur between amide and aromatic molecules. However, this conclusion cannot be definitely confirmed since the present data were not sufficiently extensive to make an adequate assessment of errors and to establish the level of significance of the observed difference in τ values.

**We are indebted to the referee for drawing our attention to this point.*

The calculation of thermodynamic quantities governing the formation of these complexes is possible from the shape of the curves but their usefulness is questionable. The method involves a number of assumptions, which can introduce large errors.

The very weak molecular interaction proposed suggests a small heat of formation. This has been confirmed by calculations of ΔH for these systems, which imposes lower and upper limits of -1 and -2 kcal/mole respectively. Recently, Abraham has proposed that methyl iodide forms a complex with toluene in which the C—I bond lies along the sixfold symmetry axis of the ring, with the methyl protons nearest the ring center (12). We venture to suggest that the interaction could equally be one in which the C—I bond lies parallel to the plane of the ring. It may be that halogenated methanes do associate with a T-shape geometry, but numerous polar unsaturated solutes almost certainly associate with the aromatic ring, so that the planes of both molecules are parallel (5–8). Moreover, there is no doubt that in complexes between polar solutes and non-polar aromatic hydrocarbons the solute protons tend to be located above the plane of the ring and adjacent to the axis of symmetry.

The situation existing in solutions of polar aromatic molecules is more complicated. The shift of the methyl protons of N,N-dimethylformamide in a dilute solution of nitrobenzene is to low field from their position in a dilute solution of cyclohexane. Furthermore, the temperature at which onset of free rotation of the NMe_2 group occurs in a 10 mole% solution of N,N-dimethylformamide in nitrobenzene is 103° C. This is very much lower than the value of 121° C observed for the corresponding solution in toluene.

REFERENCES

1. A. D. Buckingham, T. P. Schaefer, and W. G. Schneider. J. Chem. Phys. **32**, 1227 (1960).
2. A. A. Bothner-By and R. E. Glick. J. Chem. Phys. **26**, 1651 (1957).
3. C. E. Johnson and F. A. Bovey. J. Chem. Phys. **29**, 1012 (1958).
4. J. S. Waugh and R. W. Fessenden. J. Am. Chem. Soc. **79**, 846 (1957).
5. J. V. Hatton and R. E. Richards. Mol. Phys. **3**, 253 (1960).
6. W. G. Schneider. J. Phys. Chem. In press.
7. J. V. Hatton and R. E. Richards. Mol. Phys. **5**, 139 (1962).
8. J. V. Hatton and R. E. Richards. Mol. Phys. **5**, 153 (1962).
9. W. G. Schneider, H. J. Bernstein, and J. A. Pople. J. Chem. Phys. **28**, 601 (1958).
10. J. R. Goates, J. B. Ott, and A. H. Budge. J. Phys. Chem. **65**, 2162 (1961).
11. H. S. Gutowsky and C. H. Holm. J. Chem. Phys. **25**, 1228 (1956).
12. R. J. Abraham. Mol. Phys. **4**, 369 (1961).

EFFECT OF ADDED AMMONIA ON THE REACTIONS OF ACTIVE NITROGEN WITH CH_4, C_2H_6, AND C_2H_4[1]

A. N. WRIGHT[2] AND C. A. WINKLER

Upper Atmosphere Chemistry Research Group, Physical Chemistry Laboratory, McGill University, Montreal, Que.

Received March 7, 1962

ABSTRACT

The small HCN yield from the CH_4 and C_2H_6 reactions in an unheated, cylindrical reaction vessel is greatly reduced in the presence of added NH_3. The addition of NH_3 completely quenches the flame emission from the CH_4 reaction, and greatly reduces that from the C_2H_6 and C_2H_4 reactions. Both flame emission and HCN production from the CH_4 and C_2H_6 reactions appear to be initiated, at reaction temperatures of about 83° C, by an excited nitrogen molecule similar to that responsible for NH_3 decomposition.

INTRODUCTION

The quenching effect of added NH_3 on the flame emission from the reactions of active nitrogen with compounds of the type XCN, where X represents a halogen atom, and also with CCl_4, recently led Bayes (1) to conclude that the CN light emission from these reactions is initiated by $N_2(A^3\Sigma_u^+)$ molecules. Since it is known (2) that NH_3 is quite efficient in removing from active nitrogen the excited molecule responsible for its decomposition, a brief study has been made of the effect of NH_3, not only on the flame emission, but also on the HCN production, from the reactions of active nitrogen with CH_4 and C_2H_6, which, according to earlier suggestions (3, 4), might be initiated by excited N_2 molecules. At the same time, a brief examination has been made of the effect of NH_3 on the flame from the C_2H_4 reaction, where it has been established (5) that addition of NH_3 does not reduce the production of HCN.

EXPERIMENTAL

The experiments were made in apparatus (II) of a previous paper (5). The apparatus was poisoned against surface recombination of N atoms by the introduction of a minute amount of water vapor. This treatment avoided ambiguity due to the poisoning effect of NH_3 itself (5, 6). The operating pressure was 3 mm and the products from a reaction of 100 seconds duration were trapped at liquid air temperature. The amount of NH_3 in the products was estimated by titration with standard sulphuric acid while HCN was analyzed by titration with silver nitrate in the presence of added NH_3, with potassium iodide as indicator.

To study the effect of added NH_3 on HCN production from the hydrocarbons, various flow rates of hydrocarbon were introduced through a mobile jet at levels 15 and 30 cm below a fixed NH_3 jet at the "0-cm" or reference level. A glass-encased thermocouple on the mobile jet column permitted a measure of the reaction temperature at a point 3.0 cm below the position at which the hydrocarbon was introduced.

Changes in the intensity of light emission in the active-nitrogen stream upon introduction of hydrocarbon, or hydrocarbon plus added NH_3, were measured with a 1P21 photomultiplier tube (hereafter referred to as PM) coupled to an Eldorado photometer. The PM was positioned so as to view the active nitrogen stream at a level corresponding to the maximum light intensity for medium flow rates of hydrocarbon, i.e., at a point 2 cm below a fixed jet at the 0-cm level through which, in these experiments, the hydrocarbon was introduced. Another fixed reactant inlet, 0.5 cm above the jet at the 0-cm level, permitted the simultaneous introduction of NH_3, when its effect on the light emission was to be studied. Although the PM readings are only proportional to the light intensity in the active-nitrogen stream, and no resolution of the emission into the red and violet systems (7, 8) of CN was attempted, the quenching effect of added NH_3 on the hydrocarbon reaction flames was readily observed.

[1]*This work supported by the Geophysics Research Directorate, Air Force Cambridge Research Division, and by the Defence Research Board of Canada.*

[2]*Postdoctoral Fellow.*

RESULTS

Although HCN and H_2 were previously reported (9) to be the only significant products of the CH_4 and C_2H_6 reactions in a spherical reaction vessel, NH_3 was found to be a product from both reactions in an unheated cylindrical vessel. The very small NH_3 yield increased with flow rate of reactant, as illustrated in Table I for the CH_4 reaction at the 15-cm level.

TABLE I

Effect of added NH_3 on HCN production from CH_4

CH_4 flow rate, mole sec^{-1} ($\times 10^6$)	Flow rate of added NH_3, mole sec^{-1} ($\times 10^6$)	HCN produced, mole sec^{-1} ($\times 10^6$)	NH_3 produced from CH_4, mole sec^{-1} ($\times 10^6$)
	15-cm level		
8.3	0	0.4_3	0.1_8
8.3	12.7	0.1_4	—
18.7	0	0.7_1	0.2_3
18.7	12.7	0.1_9	—
34.8	0	0.7_6	0.2_7
34.8	12.7	0.2_4	—
51.6	0	0.8_1	0.4_2
51.6	0	0.8_6	0.4_6
51.6	12.7	0.2_8	—
	30-cm level		
8.3	0	0.2_6	
8.3	12.7	0.1_4	
18.7	0	0.4_7	
18.7	12.7	0.1_9	
34.8	0	0.6_7	
34.8	6.3	0.2_9	
34.8	12.7	0.1_9	
51.6	0	0.6_7	
51.6	12.7	0.3_8	

The Effect of NH_3 on HCN Production from CH_4 and C_2H_6

The extent of HCN production from the CH_4 reaction was very small* (Table I) but increased as the flow rate of reactant was increased. Even with the highest flow rates of CH_4 alone, there was no significant change in the temperature of the active nitrogen (87° and 78° C at the 15- and 30-cm levels respectively), no visible reaction flame, and no visible diminution of the nitrogen afterglow downstream. In the presence of NH_3 added upstream, there was a slight (1° to 2° C) decrease in the temperature of the active nitrogen, and a marked decrease in HCN production, as shown in Table I.

Although the HCN yield from the C_2H_6 reaction (Table II) was also small, it was considerably larger than that obtained from CH_4† and approached the extent to which NH_3 was decomposed (5) by the active nitrogen at the same levels. The HCN yield remained dependent upon C_2H_6 flow rate, up to the highest flow rate of the hydrocarbon used. Even at the highest flow rates of C_2H_6, there was a negligible temperature change in the active-nitrogen stream and, although the eye could distinguish a weak reaction flame that extended about 8 cm downstream, the afterglow did not appear to be diminished to any large extent further downstream. When NH_3 was added, at various flow rates

The N-atom flow rate, inferred from maximum HCN production from C_2H_4 (5), was 22.6×10^{-6} and 20.2×10^{-6} mole sec^{-1} at the 15- and 30-cm levels respectively.

†*The small production of HCN from CH_4 was apparently not due to a trace of C_2H_6 as an impurity in the CH_4 (9), since mass spectrometric analysis, kindly performed by Dr. Leon Phillips of this department, showed that, in the CH_4 used for the present experiments, C_2H_6 could not have been present to an extent greater than 1 part in 250.*

TABLE II

Effect of added NH_3 on HCN production from C_2H_6

C_2H_6 flow rate, mole sec^{-1} ($\times 10^6$)	Flow rate of added NH_3, mole sec^{-1} ($\times 10^6$)	HCN produced, mole sec^{-1} ($\times 10^6$)
	15-cm level	
14.1	0	2.5
14.1	0	2.4
14.1	6.3	1.7
14.1	12.7	1.5
26.7	0	3.0
26.7	0	3.2
26.7	12.7	2.0
38.2	0	4.1
38.2	12.7	3.2
51.0	0	4.6
51.0	0	4.4
51.0	12.7	3.8
	30-cm level	
14.1	0	2.3
14.1	12.5	1.3
26.7	0	3.1
26.7	12.5	1.6
26.7	12.7	1.7
31.0	12.5	2.4
38.2	0	3.2
38.2	12.5	2.7
51.0	0	3.5
51.0	6.1	3.5
51.0	12.7	2.5

through the fixed jet, the temperature of the active-nitrogen stream, 3 cm below the C_2H_6 inlet, was decreased by about 1° C, and the HCN production was significantly reduced, as shown in Table II.

The Effect of NH_3 on the Reaction Flames from CH_4, C_2H_6, and C_2H_4

When NH_3, at flow rates of 6.3×10^{-6} and 12.7×10^{-6} mole sec^{-1}, was introduced above CH_4, the PM reading was decreased (Table III) to the same value as that* observed when NH_3 alone was added to the active nitrogen. With C_2H_6 as reactant, however, addition of NH_3 did not completely reduce the PM reading to that obtained in the absence of hydrocarbon. As shown in Table III, the overall increase in the PM reading became greater, for either flow rate of added NH_3, as the flow rate of C_2H_6 was increased. Finally, although NH_3 reduced the light emission from the C_2H_4 reaction, the results in Table III indicate that its effectiveness was considerably less than with either CH_4 or C_2H_6. It may be noted that, for the highest flow rate of C_2H_4 (7.0×10^{-6} mole sec^{-1}), the PM reading could be reduced to values of 380, 330, and even 200 (i.e. lower than with 12.7×10^{-6} mole sec^{-1} of NH_3 alone) by adding NH_3 at flow rates of about 26×10^{-6}, 31×10^{-6}, and 40×10^{-6} mole sec^{-1} respectively.

DISCUSSION

Although the extent of NH_3 production from the CH_4 and C_2H_6 reactions was quite small, it amounted to about one-third of the small HCN yield. It appears that some NH_3 formation may be a fairly general characteristic (10) of active nitrogen reactions

**A decrease in intensity of the active-nitrogen afterglow has been observed (6) down to the 45-cm level for introduction of various flow rates of NH_3 at the 0-cm level in the poisoned system.*

TABLE III

Effect of added NH_3 on the flame emission during the reactions of hydrocarbons

Hydrocarbon flow rate, mole sec^{-1} ($\times 10^6$)	Flow rate of added NH_3, mole sec^{-1} ($\times 10^6$): 0	6.3	12.7
	PM readings 2 cm below the hydrocarbon inlet (% trans.)		
CH_4			
0	480	420	340
1.4	870	420	340
3.4	940	420	350
6.4	970	420	350
C_2H_6			
0	470	410	360
1.1	>1000*	420	360
3.0	>1000	450	365
5.0	>1000	470	370
7.0	>1000	495	380
9.0	>1000	510	390
11.0	>1000	535	390
13.0	990†	540	390
16.0	940†	540	400
18.0	930†	530	405
C_2H_4			
0	440	380	330
0.5	>1000	470	375
0.7	>1000	545	430
1.1	>1000	920	585
3.0	>1000	>1000	830
5.0	>1000	>1000	990
7.0	>1000	>1000	>1000

*The upper limit of the PM was reached at a reading of 1000.
†The smaller PM readings for these higher flow rates of C_2H_6 are probably due simply to a shift in position of the flame to a position closer to the inlet jet.

(5) and that its extent may depend on the structure of the reactant, as found by Dewhurst and Cooper (11) for the methyl-substituted silanes.

The low HCN yields from the CH_4 and C_2H_6 reactions, in the unheated cylindrical reaction vessel, indicate that these hydrocarbons react directly with N atoms only to a very limited extent, if at all, at the low temperatures involved. This is perhaps not surprising, since a change of spin must occur before HCN can be produced from N-atom attack on these saturated hydrocarbons. Moreover, the persistence of the nitrogen afterglow downstream, in the presence of large amounts of CH_4 and C_2H_6, suggests that, as with the C_2H_4, *n*-butane, and but-2-ene reactions in an unheated cylindrical reaction vessel (5), there is little or no loss of N atoms through rapid recombination catalyzed by reactant, such as appears to occur at low reaction temperatures in a spherical reaction vessel (4). These results offer evidence, then, that the CH_4 and C_2H_6 reactions may be induced, at low reaction temperatures, by a second reactive species present in active nitrogen. It is not possible to calculate, as for the NH_3 reaction (5), the lifetime of the reactive species responsible for initiating the CH_4 and C_2H_6 reactions since, although the extent of HCN formation was less for reaction at the 30-cm than at the 15-cm level, it showed some dependence on the flow rate of reactant, even at high flow rates.

Although addition of NH_3 reduces the amount of HCN produced during the CH_4 and C_2H_6 reactions, no similar reduction is observed (5) when NH_3 is added to the C_2H_4 reaction. It would appear that, in an unheated cylindrical reaction vessel, destruction of the added NH_3, and formation of HCN from CH_4 and C_2H_6, are competitive reactions. The competitive nature of these reactions is also indicated by the further observation

that when NH_3 was added at the 0-cm level its extent of destruction was progressively reduced when CH_4 or C_2H_6 was added at the 30- or 15-cm level. It seems reasonable to conclude, therefore, that the reactions of these hydrocarbons, like the destruction of NH_3, involve an excited nitrogen molecule, presumably $N_2(A^3\Sigma_u^+)$. It is suggested that a collision of the Second Kind between CH_4 or C_2H_6 and the excited nitrogen molecule leads to some fragmentation of the hydrocarbon, followed by rapid reaction (3) of these fragments with N atoms to produce HCN. Since CH_4 produces considerably less HCN than C_2H_6, it is apparently less effective in competition with NH_3 for the excited nitrogen molecule involved. The small increase in HCN production at higher flow rates of the hydrocarbons might be due partly to reaction initiated by small amounts of $N_2(A)$ molecules formed by the recombination of N atoms in the presence of reactant (2), and partly to a slow direct reaction of N atoms with the hydrocarbon. The much higher maximum HCN yield at higher reaction temperatures (approximately equal to that from C_2H_4 at about 400° C in either a spherical or cylindrical vessel (9, 4, 5)) is almost certainly due to a much faster rate of the direct N-atom attack under such conditions.

The PM measurements indicate that the reaction flames from all three of the CH_4, C_2H_6, and C_2H_4 reactions are also initiated by $N_2(A)$ molecules. In this respect their behavior is similar to the reactants investigated by Bayes (1). However, the actual mechanism leading to the emission of the CN flame remains unresolved.

Since there is no effect of increased temperature (5, 12), or of NH_3 added upstream (5), on HCN production from C_2H_4 in a cylindrical reaction vessel, HCN formation from this reactant need not be initiated by excited nitrogen molecules. Nevertheless, the results indicate that the C_2H_4 reaction flame is reduced in intensity in the presence of NH_3, although the quenching efficiency of NH_3 is less than with CH_4 or C_2H_6. This reduced efficiency of NH_3 might be due to a greater ability of C_2H_4 to compete with NH_3 for $N_2(A)$ molecules. On the other hand, part of the flame emission from the C_2H_4 reaction might result from a direct reaction, at a considerable rate even at the low temperature involved, between N atoms and the unsaturated hydrocarbon molecule. This is indicated by the similar rate constants obtained for the active nitrogen – C_2H_4 reaction by measuring the extent of HCN production (2), or by application of flame diffusion techniques (13, 12).

REFERENCES

1. K. D. Bayes. Can. J. Chem. **39**, 1074 (1961).
2. A. N. Wright and C. A. Winkler. Can. J. Chem. **40**, 5 (1962).
3. H. G. V. Evans and C. A. Winkler. Can. J. Chem. **34**, 1217 (1956).
4. R. Kelly and C. A. Winkler. Can. J. Chem. **38**, 2514 (1960).
5. A. N. Wright, R. L. Nelson, and C. A. Winkler. Can. J. Chem. **40**, 1082 (1962).
6. A. N. Wright and C. A. Winkler. Unpublished results.
7. K. R. Jennings and J. W. Linnet. Trans. Faraday Soc. **56**, 1737 (1960).
8. N. H. Kiess and H. P. Broida. J. Mol. Spectroscopy, **7**, 194 (1961).
9. P. Gartaganis and C. A. Winkler. Can. J. Chem. **34**, 1457 (1956).
10. H. A. Dewhurst. J. Phys. Chem. **63**, 1976 (1959).
11. H. A. Dewhurst and G. D. Cooper. J. Am. Chem. Soc. **82**, 4220 (1960).
12. E. R. V. Milton and H. B. Dunford. J. Chem. Phys. **34**, 51 (1961).
13. J. H. Greenblatt and C. A. Winkler. Can. J. Research, B, **27**, 732 (1949).

THE REACTIONS OF ACTIVE NITROGEN WITH BORON TRICHLORIDE AND GERMANE[1]

ROSEMARY STORR,[2] A. N. WRIGHT,[3] AND C. A. WINKLER
Upper Atmosphere Chemistry Research Group, Physical Chemistry Laboratory, McGill University, Montreal, Que.

Received March 7, 1962

ABSTRACT

Chlorine and tetrachlordiborine were the main products from the reaction of active nitrogen with boron trichloride. The maximum flow rate of chlorine recovered, about 4% of the available N-atom flow rate, was essentially independent of temperature in the range 100° to 395° C. It is suggested that the reaction is initiated by $N_2(A^3\Sigma_u^+)$, and that this is followed by N-atom attack on the resulting BCl_2 radical. A similar mechanism is suggested for a slight extent of reaction observed with germanium tetrachloride.

Hydrogen and germanous nitride (Ge_3N_2) were the products of the reaction of active nitrogen with germane. The amount of germane decomposed increased with an increase of temperature from 100° to 200° C; at the higher temperature it corresponded to not more than two-thirds of the N-atom flow rate used. It is suggested that the reaction involves the direct and complete displacement of hydrogen by atomic nitrogen.

INTRODUCTION

Of the many reactions of active nitrogen that have been studied, those with inorganic reactants have revealed several points that appear to be of interest in any consideration of the nature of active nitrogen. For example, the experimental data available at present indicate that the maximum extent to which NH_3 is decomposed by active nitrogen is only about one-sixth of the maximum extent to which HCN may be produced from hydrocarbons or hydrocarbon derivatives (1–3). This, in turn, is comparable with the maximum extents to which active nitrogen reacts with O_2 (4) and NO_2 (5), but is considerably less than the maximum extent to which it reacts with NO (5, 6). Again, at least some of the reactions with inorganic molecules, e.g. PH_3 (7), HBr (8), SiH_4 (9), apparently involve hydrogen abstraction by atomic nitrogen, whereas this does not seem to occur with any of the organic molecules yet studied.

In the continuing program of investigations into the behavior of active nitrogen that has been in progress in this laboratory for several years, part of the effort is devoted to the study of reactions for which little or no information is yet available, but which might conceivably reveal interesting aspects of the nature of active nitrogen. Of these, the reactions with BCl_3 and GeH_4 have now been examined, the first as a convenient inorganic halide, the second for comparison with the data available for SiH_4 and CH_4.

Jevons (10) believed that he observed three intense bands due to BN in the spectrum of BCl_3, excited with active nitrogen, while BN was deposited on the wall of the vessel. Mulliken (11) later showed that Jevons had really observed the spectrum of BO, due to oxygen impurity in the nitrogen used. However, evidence for a band system around 3600 Å, due to BN, has been obtained by Douglas and Herzberg (12), by passing a trace of BCl_3 into a discharge through helium containing a small amount of nitrogen.

[1]*This work supported by the National Research Council and the Defence Research Board.*
[2]*Present address: Ayerst, McKenna and Harrison, Ltd., Rouses Point, N.Y.*
[3]*Postdoctoral Fellow.*

The reaction of active nitrogen with SiH_4 (9) yields no condensable product. Presumably the silane is decomposed to yield H_2 and, possibly, SiN. It was suggested that the reaction proceeded by a hydrogen-abstraction mechanism,

$$SiH_4 + N \rightarrow SiH_3 + NH,$$

followed by

$$2NH \rightarrow N_2 + H_2 \text{ or } NH + N \rightarrow N_2 + H.$$

On the other hand, the products from the reaction of active nitrogen with CH_4, in an unheated cylindrical vessel, are about two-thirds HCN and one-third NH_3, and the reaction appears to be initiated by excited nitrogen molecules (6).

EXPERIMENTAL

The apparatus and procedures of the present study were similar in all essentials to those outlined in the earlier papers from this laboratory. The reactions occurred at 1.45 mm pressure, in a spherical reaction vessel.

The products of the reaction with BCl_3 were separated with the Le Roy still (13). Chlorine distilled at $-110°$ C, at 3 mm pressure; BCl_3 at $-80°$ C, at 4 mm pressure; and tetrachlordiborine at room temperature. Chlorine was analyzed by absorption in distilled water and titration with sodium thiosulphate, with thyodene as indicator (14). Unreacted BCl_3, and the tetrachlordiborine, were both estimated by hydrolysis and titration with standard NaOH in the presence of mannitol to increase the extent of ionization of the boric acid formed (14). This method was used in preference to the less simple $AgNO_3$ titration of the chloride, but concordant results were obtained by the two methods.

The amount of unreacted GeH_4, following an experiment, was determined from its pressure in a known volume at room temperature. Germanium nitride, formed as a solid on the wall of the vessel, was treated in a manner that will be described later.

RESULTS

Reaction with BCl_3

With this reactant, the yellow afterglow of active nitrogen was completely replaced by a pale green reaction flame, and a small amount of white solid was deposited on the wall of the reaction vessel.

In Fig. 1 are plotted the yields of Cl_2 at 100, 353, and 395° C, and of B_2Cl_4 at 395° C. These yields are obviously very low in comparison with the active-nitrogen flow rate of 9.5×10^{-6} mole/sec, estimated from the maximum amount of HCN produced from C_2H_4

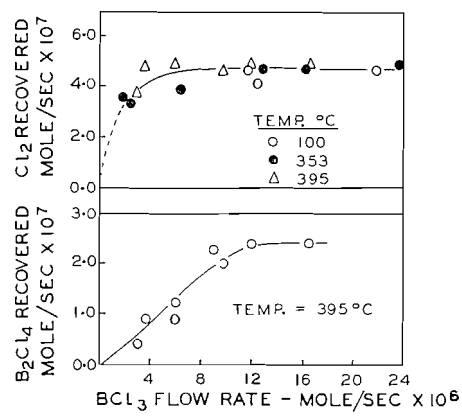

FIG. 1.

at 350° C. It might be noted that the ratio of the B_2Cl_4 yield to that of Cl_2 increased from about 1:10 at low flow rates of BCl_3 to 1:2 at the highest flow rates of reactant used.

The amount of solid deposited on the wall of the reaction vessel was insufficient for analysis. It was assumed to be BN. If it is assumed that the only chlorine-containing compounds in the products were BCl_3 and B_2Cl_4, it may be estimated that, since the Cl_2 plateau (0.5×10^{-6} mole/sec) corresponds to 1×10^{-6} mole/sec of Cl, and the B_2Cl_4 plateau (0.25×10^{-6} mole/sec) also corresponds to 1×10^{-6} mole/sec of Cl, the total rate of Cl recovery is 2×10^{-6} mole/sec, equivalent to BCl_3 destruction of 0.66×10^{-6} mole/sec. Hence, the amount of boron not accounted for in the trap is 0.66×10^{-6} mole/sec minus 0.5×10^{-6} mole/sec appearing as B_2Cl_4, or 0.16×10^{-6} mole/sec. This would, presumably, correspond to the amount of BN formed on the wall.

Reaction with $GeCl_4$

A few experiments were made with $GeCl_4$, instead of BCl_3, but even less reaction occurred. The nitrogen afterglow was completely quenched, and a reaction flame was observed. This was pale blue at low flow rates of $GeCl_4$ and a beautiful royal blue at higher flow rates. No noticeable amount of solid material was deposited on the wall of the vessel, and the maximum yield of Cl_2 at 65° C was only about 0.13×10^{-6} mole/sec, even at relatively high flow rates of $GeCl_4$ (of the order of 20×10^{-6} mole/sec). Accordingly, study of this reaction was not pursued further.

Reaction with GeH_4

This reaction produced a yellowish-orange flame and destroyed the nitrogen afterglow completely. No NH_3 or other condensable product was obtained in the cold trap, but a dark brown solid was deposited on the wall of the reaction vessel and of the tube connecting the reaction vessel to the cold trap. Reproducible results were obtained only after several experiments had been made and a uniform layer of the solid deposited on the wall. Data were then obtained for the amount of GeH_4 that reacted with active nitrogen at 100° and 200° C, as illustrated in Fig. 2. Higher temperatures were avoided, since

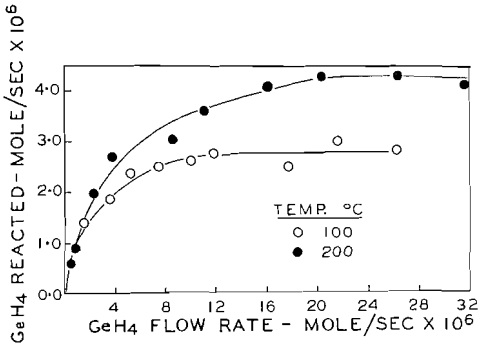

FIG. 2.

GeH_4 decomposes thermally at about 280° C (15). The flow rate of active nitrogen was obtained by titration with NO (16–18), in the presence of the brown solid, and found to be about 10×10^{-6} mole/sec (corresponding to about 6×10^{-6} mole/sec if based on HCN production from C_2H_4 (6)).

The solid product was insoluble in H_2SO_4 or HCl, but dissolved in H_2O or dilute NaOH to give a colorless solution from which the brown solid could be reprecipitated on acidification. Ammonia was evolved when the alkaline solution was heated. The color of the solid slowly became lighter when it was left exposed to air. These observations agree with the behavior of Ge_3N_2 (19), but not with that of Ge_3N_4, which is insoluble in H_2O and common organic solvents, and is not affected by air at ordinary temperatures (20). Hence, the product from the GeH_4 – active nitrogen reaction appeared to be mainly Ge_3N_2. Analysis of the solid by the micro-kjeldahl method gave a value of 5.3% N (theoretical for Ge_3N_2, 11.4%). The discrepancy was almost certainly due to air oxidation of the nitride. Accordingly, a known weight of the material was treated with $HClO_4$ to convert it completely to oxide, and from the change in weight it was found that 37% of the germanium in the original sample was converted from the nitride to oxide. This may be compared with a calculated value of 41% for a material containing 5.3% N and assumed to be Ge_3N_2. Again, the data indicate that the solid product from the GeH_4 – active nitrogen reaction was mainly Ge_3N_2. Examination of the solid by X-ray methods showed only that it was amorphous.[4]

DISCUSSION

Reactions with BCl_3 and $GeCl_4$

Of three possible modes of attack of N atoms on BCl_3, two may be ruled out from energy considerations. These are

$$BCl_3 + N \rightarrow BCl_2 + NCl, \Delta H = +63 \text{ kcal};$$

and

$$BCl_3 + N \rightarrow BN + Cl_2 + Cl, \Delta H = +175 \text{ kcal}.$$

The third possibility is a "catalyzed" atom recombination (21), which may be represented by

$$BCl_3 + N \rightarrow BCl_3.N \xrightarrow{N} N_2 + BCl_2 + Cl. \quad [1]$$

Such a sequence would probably have a negative temperature coefficient, since, without any other energetically favorable path available to it, the complex can only suffer reversion to the original reactants, and its lifetime (hence the rate of the overall reaction) should decrease with increase of temperature. Moreover, an initial reaction such as [1], followed by similar reactions with BCl_2 and BCl, or by direct attack of N on BCl to form BN + Cl, would be expected to cause much more destruction of BCl_3 than that observed, unless back reactions, probably involving a third body, occurred to a considerable extend, e.g.

$$Cl + BCl_2 + W \rightarrow BCl_3$$
$$Cl_2 + BCl + W \rightarrow BCl_3.$$

However, Holliday and Massey (22) and Frazer and Holzmann (23) have shown recently that B_2Cl_4 may be efficiently produced, at pressures less than 4 mm, from the decomposition of BCl_3 in a microwave discharge, which suggests that such back reactions should be quite unimportant at the pressures used in the present experiments. Catalyzed recombination of N atoms on the reactant therefore does not seem to provide an adequate mechanism for the reaction.

[4]*We are indebted to Dr. A. J. Frueh for the X-ray study of the solid product.*

The small extent of BCl_3 decomposition, relative to the concentration of N atoms available, and the negligible temperature coefficient of the reaction would both be consistent with an assumption that BCl_3 is decomposed by energy transfer from an excited nitrogen molecule, e.g. $N_2(A^3\Sigma_u^+)$:

$$BCl_3 + N_2(A^3\Sigma_u^+) \rightarrow BCl_2 + Cl + N_2. \quad [2]$$

The increase in the ratio of Cl_2:B_2Cl_4 in the products is then readily explained if the BCl_2 formed in [2] suffered extensive reaction with N atoms at low flow rates of BCl_3, but dimerized to a progressively larger extent as the flow rate of BCl_3 was increased. It is interesting to note that, since the ground state of BN appears to be a triplet (24), the reaction

$$BCl_2 + N \rightarrow BN + Cl_2, \Delta H = -18 \text{ kcal}$$

may be both energetically and spin favorable.

The reaction of active nitrogen with $GeCl_4$ is probably also initiated by excited molecules, but to a lesser extent than BCl_3, owing to the greater number of degrees of freedom into which the energy might pass.

Reaction with GeH_4

Since an increase of temperature from 100 to 200° C increased the plateau value for the amount of GeH_4 decomposed by only about 25%, it seems reasonable to assume that the plateau value at 200° (4.2×10^{-6} mole/sec) represents roughly the maximum extent of reaction possible with the flow rate of active nitrogen used (ca. 6×10^{-6} mole/sec on the basis of HCN production from C_2H_4). If this be true, there would seem to be far too few N atoms available for the reaction to proceed by stepwise hydrogen abstraction, followed by disproportionation of NH radicals, since this would require 4 N atoms per GeH_4 decomposed (i.e. 16.8×10^{-6} mole/sec of N atoms) plus 2.8 N atoms to convert 4.2 Ge atoms to Ge_3N_2, or a total flow rate of 19.6×10^{-6} mole/sec of N atoms.[5]

Decomposition of GeH_4 by excited N_2 molecules alone also seems to be an unsatisfactory explanation, since this would require at least 4.2×10^{-6} mole/sec of such a species, which would probably require a flow rate of active nitrogen much greater than that measured even by NO titration (6). To achieve the observed extent of reaction, following initiation by excited molecules, a sequence of reactions involving H- and N-atom reactions might be suggested, e.g.

$$GeH_4 + N_2^* \rightarrow GeH_3 + H$$
$$GeH_4 + H \rightarrow GeH_3 + H_2$$
$$GeH_3 + N \rightarrow GeN + H + H, \text{ etc.}$$

However, the last reaction would be less favorable energetically than the direct and complete displacement of H_2,

$$GeH_4^* + N \rightarrow GeN + 2H_2,$$

which is almost certainly exothermic.[6] It is suggested, therefore, that this represents the most acceptable mechanism for the reaction of GeH_4 with active nitrogen. It is interesting,

[5]*The data given in ref. 9 are inadequate for detailed analysis, but this argument does not seem to apply with nearly the same force to the silane reaction. Approximately 1.65×10^{-7} mole/sec of SiH_4 seems to have been decomposed, apparently with little SiN formation, and this would require some 6.5×10^{-7} mole/sec of N atoms. Actually, the HCN production from C_2H_4 indicated about 5×10^{-7} mole/sec of N atoms available (about 8.5×10^{-7} mole/sec on the basis of a NO titration).*

[6]*No value for the bond strength of GeN is available in the literature. A rough, and probably exaggerated, estimate of 80 kcal may be made by considering nitrides of other elements in neighboring groups in the periodic table. An average of 70 kcal may be similarly estimated for the GeH bond in GeH_4.*

perhaps, though obviously no argument in its favor, that such a mechanism would not seem to be applicable to any other active nitrogen reaction previously studied.

Regardless of the mechanism assumed for its formation, it does seem reasonable that GeN is a precursor to Ge_3N_2, the main solid product of the reaction. Transformation of the simpler to the more complex nitride is probably accomplished in wall reactions, which might be relatively simple, e.g.

$$3GeN \rightarrow Ge_3N_2 + \tfrac{1}{2}N_2,$$

or might be considerably complicated by the attack of N atoms on the nitride film.

REFERENCES

1. G. R. Freeman and C. A. Winkler. J. Phys. Chem. **59**, 371 (1957).
2. R. Kelly and C. A. Winkler. Can. J. Chem. **38**, 2514 (1960).
3. A. N. Wright and C. A. Winkler. Can. J. Chem. **40**, 5 (1962).
4. C. Mavroyannis and C. A. Winkler. International Symposium on the Chemistry of the Lower and Upper Atmosphere. San Francisco, Calif. April, 1961.
5. G. J. Verbeke and C. A. Winkler. J. Phys. Chem. **64**, 319 (1960).
6. A. N. Wright, R. L. Nelson, and C. A. Winkler. Can. J. Chem. **40**, 1082 (1962).
7. D. M. Wiles and C. A. Winkler. J. Phys. Chem. **61**, 902 (1957).
8. H. B. Dunford and B. E. Melanson. Can. J. Chem. **37**, 641 (1959).
9. H. A. Dewhurst and C. D. Cooper. J. Am. Chem. Soc. **82**, 4220 (1960).
10. W. Jevons. Proc. Roy. Soc. (London), A, **91**, 120 (1914).
11. R. S. Mulliken. Phys. Rev. **25**, 259 (1925).
12. A. E. Douglas and G. Herzberg. Phys. Rev. **57**, 752 (1940).
13. D. J. Le Roy. Can. J. Research, B, **28**, 492 (1950).
14. I. M. Kolthoff and E. B. Sandell. Textbook of quantitative inorganic analysis. Macmillan Co., New York. 1943.
15. T. R. Hogness and W. C. Johnson. J. Am. Chem. Soc. **54**, 3583 (1932).
16. M. L. Spealman and W. H. Rodebush. J. Am. Chem. Soc. **57**, 1474 (1935).
17. F. Kaufmann and J. R. Kelso. J. Chem. Phys. **28**, 510 (1958).
18. G. B. Kistiakowsky and G. G. Volpi. J. Chem. Phys. **27**, 1141 (1957).
19. W. C. Johnson and G. H. Ridgely. J. Am. Chem. Soc. **56**, 2395 (1934).
20. W. C. Johnson. J. Am. Chem. Soc. **52**, 5160 (1930).
21. W. Forst, H. G. V. Evans, and C. A. Winkler. J. Phys. Chem. **61**, 320 (1957).
22. A. K. Holliday and A. G. Massey. J. Am. Chem. Soc. **80**, 4744 (1958).
23. S. W. Frazer and R. I. Holzmann. J. Am. Chem. Soc. **80**, 2907 (1958).
24. E. R. Lippincott, D. Steele, and P. Caldwell. J. Chem. Phys. **35**, 123 (1961).

CONSTITUENTS OF THE OLEORESIN OF THE MALE FERN (DRYOPTERIS FILIX MAS L.)

PART I. ALCOHOL AND STEROL FRACTIONS[1]

TELFER LAWSON THOMAS[2] AND ALFRED TAURINS
Department of Chemistry, McGill University, Montreal, Que.

Received in original form December 23, 1960; as revised March 27, 1962

ABSTRACT

The solid alcohol fraction of the oleoresin of the male fern was shown to contain two higher primary alcohols, 1-tricosanol and 1-docosanol. The sterol fraction was found by means of chemical and spectrographic evidence to be 5,11(?)-stigmastadien-3β-ol.

1-Tricosanol was synthesized from behenic (docosanoic) acid via tricosanoic acid, the latter being the product of Arndt–Eistert synthesis. 1-Docosanol was synthesized by $LiAlH_4$ reduction of behenic acid.

DISCUSSION

The oleoresin of the rhizome of the male fern, *Dryopteris filix mas* L. (or *Aspidium filix mas* L.), has been used as an anthelmintic since the time of Ancient Greece, although its composition was not investigated until the end of the nineteenth century. The anthelmintic activity of the oleoresin was ascribed to a group of related compounds commonly known as "phenol fraction of the oleoresin" which were derivatives of 2-acylcyclohexane-1,3-dione. Recently a review on these compounds has been published by Hassal (1), who gives a number of references to the previous work.

In addition to the phenolic fraction, the oleoresin of the fern rhizome contains a large amount of glycerides of fatty acids. Maizite (2–4) has investigated oleoresins of several fern species, including *D. filix mas* L. Upon saponification of the fat fraction, *n*-butyric and linoleic acids as well as glycerol were isolated from all the fern oleoresins. From *Nephrodium filix mas* L. Maizite isolated, in addition, palmitic and stearic acids. He also obtained an unsaponifiable fraction which he thought was phytosterol, but did not investigate further.

The present paper describes the study of the solid alcohol and sterol fractions obtained from the male fern (*D. filix mas* L.) oleoresin. When the phenol fraction had been separated by the method described in the experimental part, the phenol-free residue was hydrolyzed and petroleum ether soluble and insoluble fractions were obtained. The former was found to consist of higher aliphatic alcohols, and the latter of a sterol.

Alcohol Fraction

The crude solid alcohol fraction was recrystallized from petroleum ether and esterified with *p*-phenylazobenzoyl chloride in order to facilitate the separation of substances by chromatography. Two main products were isolated from the chromatogram, and these esters were hydrolyzed to the original substances.

The major product melted at 73.4–73.7°, showed no ultraviolet absorption, and had a molecular weight of 343. Analysis indicated that the compound had the empirical formula $C_{23}H_{48}O$. The infrared spectra of the alcohol, its acetate, and azoate indicated that the substance was a straight-chain primary alcohol with little, if any, branching. A monolayer of the alcohol was tested on a film balance of the vertical pull type, similar to that used

[1]*This work received financial assistance from the National Research Council of Canada, Ottawa, Canada.*
[2]*Holder of Quebec Provincial Bursary 1955–1956, and of a National Research Council Studentship 1956–1957.*

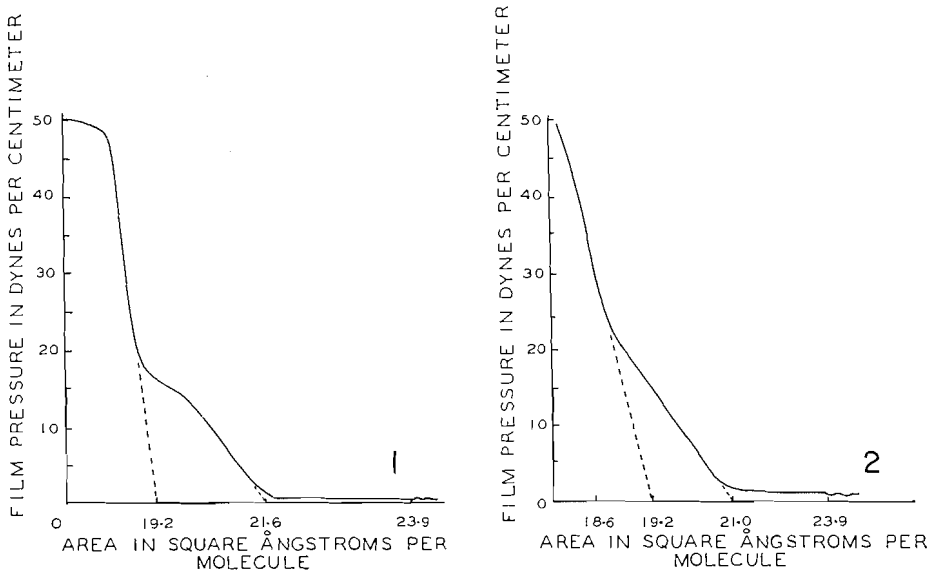

Fig. 1. Pressure–area isotherm of major product extracted from alcohol fraction of oleoresin.
FIG. 2. Pressure–area isotherm of 1-tricosanol.

by Harkins and Anderson (5). The change in pull on the immersed plate was recorded electrically. The shape of the pressure–area isotherm (Fig. 1), the area of the methylene chain, and the area of zero compression (area of the polar group in this case) all indicated that the substance was a high molecular weight, saturated, straight-chain, primary alcohol.

On the basis of the foregoing evidence, the substance was believed to be 1-tricosanol (6). In order to obtain further proof, an authentic sample of 1-tricosanol was prepared from erucic acid. Erucic acid was hydrogenated, using Adams catalyst, to behenic or docosanoic acid, $CH_3(CH_2)_{20}COOH$, and the latter was converted via an Arndt–Eistert synthesis to tricosanoic acid, $CH_3(CH_2)_{21}COOH$. The methyl ester of tricosanoic acid was reduced with lithium aluminum hydride to 1-tricosanol, $C_{23}H_{47}OH$. Comparison of the infrared spectra, pressure–area isotherms (Figs. 1 and 2), and determination of the mixed melting point showed that 1-tricosanol and the naturally occurring product were indeed identical. The spectra and melting points of 1-tricosanyl acetate and 1-tricosanyl azoate and the corresponding esters prepared from the natural product also were in complete agreement.

The second product isolated from the chromatogram melted at 72–73.3° and gave no precipitate with digitonin. The infrared spectrum of this material and that of an authentic sample of 1-docosanol (6) were found to be identical. A mixed melting point determination of the two substances showed no depression.

1-Tricosanol and 1-docosanol were found to be present in the original fern rhizome oleoresin to the extent of approximately 0.16–0.25% and 0.02–0.03% respectively.

Sterol Fraction

The petroleum ether insoluble portion of the unsaponifiable fraction of the oleoresin was recrystallized from ethanol. It was further purified via the digitonide, followed by recrystallization. Infrared absorption spectra of the crude and purified material, taken in Nujol, were identical, and it was concluded that only one sterol was present in the fraction.

The pure product melted at 136.1–137°, and had the empirical formula $C_{29}H_{50}O_2$. The sterol was tested for unsaturation with tetranitromethane, and the presence of at least two double bonds was indicated. The absence of absorption in the ultraviolet region of the spectrum led to the conclusion that the double bonds were not in conjugation. The material was found to contain 1 molecular equivalent of water of crystallization. Two derivatives, the azoate and the benzoate, were synthesized and characterized (Table I).

TABLE I

Comparison of analytical data for sterol isolated from male fern oleoresin and 5,11(?)-stigmastadien-3β-ol (10)

Physical constants	Sterol isolated from male fern oleoresin	5,11(?)-Stigmastadien-3β-ol from oats
M.p.	136.1–137° (corr.)	137°
$[\alpha]_D$	−36.7±2° at 18° C	−37.6±3° at 26° C
Benzoate derivative m.p.	148.8–149°	157°
Benzoate derivative $[\alpha]_D$	−11.0±2° at 20° C	−11.8±2° at 26° C
p-Phenylazobenzoate derivative m.p.	189–191°	191°

The presence of the hydroxyl group in the molecule was further verified by the existence of bands in the infrared at 3610 and 1050 cm^{-1} (in CS_2 solution). Since the sterol formed a digitonide, the hydroxyl group was considered to be in the 3β-position. When the spectrum was taken in chloroform solution, two distinct bands appeared in the C=C stretching region at 1665 and 1600 cm^{-1}. The higher-frequency band could be due to a double bond in either the 5- or 7-position of the steroid nucleus (7, 8). It was believed that the absorption at 1600 cm^{-1} was due to the existence of a double bond at either position 11 or 16, although bands due to double bonds in these two positions generally absorb at somewhat higher frequencies (9). Since the steric strain of a double bond in the five-membered D ring of the steroid nucleus usually results in an intense absorption in the olefinic C—H stretching region (3100–3000 cm^{-1}), and this phenomenon was absent in the present case, it was felt that the double bond was likely located at position 11. In the region 790–850 cm^{-1}, in which the characteristic bands due to the out-of-plane bending vibrations of an olefinic C—H occur, there was absorption at 837 and 782 cm^{-1} (in CS_2 solution).

The infrared spectrum of the fern sterol (Table II and Fig. 3) was found to be identical

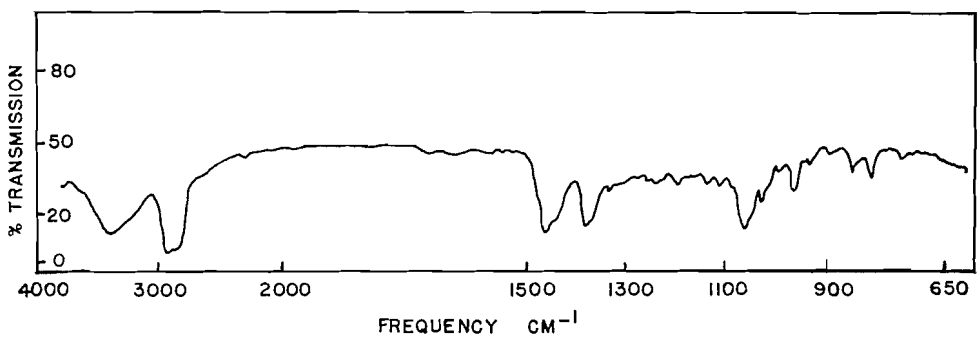

FIG. 3. The infrared spectrum of the sterol from fern (in KBr pellet).

TABLE II

Positions of the maxima (in cm^{-1}) of the absorption bands in the infrared spectra of the sterol isolated from the fern and its derivatives (in KBr pellets)

5,11(?)-Stigmastadien-3β-ol	5,11(?)-Stigmastadien-3β-yl azoate	5,11(?)-Stigmastadien-3β-yl benzoate
3630, 3610, 3460		
2960	2940	2950
2880	2870	2870
	1707	1711
1664	1670	1668
1636	1602	1600
1473	1486	1490
1450	1445	1452
	1410	
1387	1384	1384
1374		1356
1336	1319	1335
1259	1280	1274
1245	1220	
1198	1198	1200
1160		
1135	1144	1130
1110	1118	1110
	1095	
1082	1085	1080
1065	1070	1066
1058		
1026	1025	1025
1010	1010	1008
990	998	995
	977	977
961	962	955
938	945	945
928	925	924
885	882	884
	864	852
840	838	845
		837
		825
803	800	800
	776	768
	770	
741	736	736
	695	708
	685	680

with the spectrum obtained by Idler and his co-workers (10) for the sterol from oats. The analytical data and physical constants of the fern sterol and its derivatives were found to correspond quite closely with those of 5,11(?)-stigmastadien-3β-ol (Table I) which had been isolated from oats.

A quantitative Liebermann–Burchard reaction was run on the male fern oleoresin sterol. The graph of the reaction taken at 420 mμ was identical with that published by Idler and co-workers (10) (Fig. 4). Unfortunately it was not possible to obtain a sample of 5,11(?)-stigmastadien-3β-ol from oats for further comparison purposes. The sterol comprised approximately 0.17–0.25% of the oleoresin.

EXPERIMENTAL

The melting points below 200° were determined in an electrically heated Scientific Glass Apparatus Company No. 1855 interjoint melting point apparatus containing dibutyl phthalate. Melting points above 200° were carried out in a melting point block constructed according to the specifications given by Fieser (11). All melting points are corrected. Carbon, hydrogen, nitrogen, and oxygen analyses for all compounds except the benzoate of the sterol were carried out in the Schwarzkopf microanalytical laboratory, Woodside,

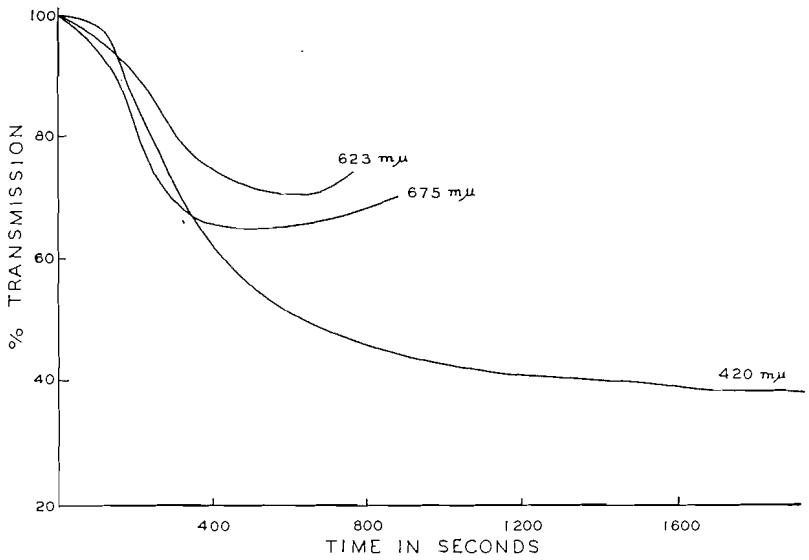

FIG. 4. Liebermann–Burchard reaction of sterol isolated from oleoresin of male fern.

N.Y., U.S.A. The analysis of the benzoate derivative was performed in the laboratory of W. Manser in Zurich, Switzerland. The infrared absorption spectra were determined by means of a Perkin–Elmer Model 21 double-beam spectrophotometer equipped with a sodium chloride prism, and the ultraviolet absorption spectra were determined using a Beckman DK-1 spectrophotometer.

Isolation of the Phenolic Fraction

Previous methods (12, 13) used for the separation of the phenol fraction of the oleoresin were excessively laborious and the method following was devised. Male fern oleoresin (453 g) was dissolved in diethyl ether and the solution was added to magnesium oxide (900 g), enough ether being present to form a thick paste with the oxide. More magnesium oxide was then added to this paste until "solidification" occurred. The ether was then allowed to spontaneously evaporate from the mixture. The magnesium phenolates were removed from the ether-free mixture by leaching with water (5×5 liters). The aqueous solution (about 25 liters) was acidified with dilute sulphuric acid, filtered, and a red-brown amorphous product separated. This material, consisting of the phenolic substances, was washed with water until the washings were neutral. The anhydrous phenolic material was obtained in a yield of 26.4 g, i.e. 5.9% based on the original oleoresin.

Isolation and Separation of Alcohols and Sterols

The oil (200 g) remaining after removal of the phenol fraction was hydrolyzed with 4% ethanolic potassium hydroxide (1500 ml) in a nitrogen atmosphere. The mixture was refluxed for 5 hours, then the ethanol was removed under reduced pressure. The residual material was diluted with water (1000 ml). The slightly turbid solution which formed was extracted continuously with diethyl ether for 12 hours. The aqueous solution was discarded and the ether extract was dried over anhydrous magnesium sulphate. The ether was removed, leaving a semisolid residue (1.9 g). This residue was triturated with petroleum ether (30–60°) and the insoluble fraction (0.75 g) was recrystallized from ethanol. The soluble fraction (1.15 g), after recrystallization from a minimum volume of petroleum ether, weighed 0.9 g. Ethanolic digitonin had no effect on the petroleum ether soluble portion but produced a flocculent precipitate with the insoluble fraction.

Esterification and Identification of the Components of the Alcohol Fraction

The recrystallized petroleum ether soluble material (0.9 g) was mixed with pyridine (10 ml) and azoyl chloride (0.9 g). The orange-colored solution was refluxed gently for 2 hours. It was then cooled, poured into cold 2% sodium bicarbonate solution, filtered, washed with water, and dried *in vacuo* over phosphorus pentoxide.

The ester mixture was chromatographed using a Pyrex glass column 5 cm in diameter, the sides of which had been treated with a solution of silicone oil in chloroform. The adsorbent employed was 3:1 silicic acid: Celite 503. The chromatograms were carried out in a nitrogen atmosphere, using as eluent a mixture of petroleum ether (b.p. 90–120°) and benzene, which was gradually changed from 3:1 to 5:1 petroleum ether: benzene. The change was completed when the lowest band had reached the middle of the column. Three bands were obtained in this way. The column was extruded and the colored sections were separated. Each band was extracted with hot benzene. The top band was found to contain mainly pyridinium compounds

and unesterified alcohols. About 2 cm below the top of the column was a very narrow band of azoyl ester and at the bottom of the column there was a large band of ester. The chromatographed esters were recrystallized from benzene and dried *in vacuo* over phosphorus pentoxide.

1-Tricosanyl Azoate

The azoyl ester from the lower band (0.45 g) melted at 82.0–82.2° after three recrystallizations from benzene. The infrared spectrum of the ester was determined in potassium bromide pellets (Table III). Molecular weight (Rast), 548. A mixed melting point determination with an authentic sample of 1-tricosanyl azoate showed no depression. Anal. Calc. for $C_{36}H_{56}N_2O_2$: C, 78.83; H, 10.30; N, 5.11. Found: C, 79.30; H, 10.03; N, 4.81%.

TABLE III

Positions of the maxima (in cm^{-1}) of the absorption bands in the infrared spectra of 1-tricosanol, 1-tricosanyl azoate, 1-tricosanyl acetate, and 1-docosanol (in KBr pellets)

1-Tricosanol	1-Tricosanyl azoate	1-Tricosanyl acetate	1-Docosanol
3340			3400
2930 vs	2925	2925	2930 vs
2860 vs	2850	2850	2860 vs
	1715	1737	
1645 vw			1645 vw
1630 vw			1630 vw
1487			1487
1465	1470	1470	1466
1380 w	1385 w	1368	1380 w
	1273	1245	
	1216		
1123	1145		1085
	1110		1075
	1100		1066
1070	1070	1050	1050
1060		1040	1035 vw
1030			1025 vw
1012 vw	1008		1007 vw
965 vw		963	970 vw
940 vw	936		
915	925		
885 vw	865	890	
	777		
728			729
718	720	718	718
	695		
	685		

Isolation of 1-Tricosanol

The azoyl ester (150 mg) from the lower band was dissolved in benzene (5 ml) and treated with 8% potassium hydroxide in 70% aqueous ethanol (3 ml). The mixture was refluxed for 1 hour, and then was cooled and extracted with benzene. The benzene extract was dried, and the solvent removed *in vacuo*. The solid residue was recrystallized from methanol and melted at 73.4–73.7°. Both bromine and potassium permanganate tests for unsaturation in the molecule were negative. The substance showed no absorption in the ultraviolet region of the spectrum. A monomolecular film of the alcohol was tested on a film balance similar to that used by Harkness and Anderson (5). The balance was of the vertical pull type, and the pull on the immersed plate was electrically recorded on a Minneapolis-Honeywell Brown continuous recorder. The film was spread on 0.1 *N* hydrochloric acid from dilute benzene solution. The pressure–area isotherm is shown in Fig. 1. The area of zero compression was 21.6 $Å^2$, and the area per molecule at the liquid–solid film phase transition was 19.2 $Å^2$. Molecular weight determinations by the Rast and gravimetric methods indicated that the compound had a molecular weight of 343. A mixed melting point determination with the authentic sample of 1-tricosanol remained undepressed. The infrared spectrum of 1-tricosanol was taken in KBr (Table III). Anal. Calc. for $C_{23}H_{48}O$: C, 81.07; H, 14.22. Found: C, 81.09; H, 13.78%.

1-Tricosanyl Acetate

1-Tricosanol (0.5 g) was refluxed with acetyl chloride (4 ml) and pyridine (3 drops) for 30 minutes. The solution was cooled and poured into ice water and allowed to stand for 1 hour. The precipitate which formed

was filtered, recrystallized from ethanol, and dried. The substance melted at 52.0–52.5°, and a mixed melting point determination with the authentic sample of 1-tricosanyl acetate showed no depression. The infrared spectrum of 1-tricosanyl acetate is recorded in Table III.

Isolation of 1-Docosanol

The material from the middle band of the chromatogram (0.16 g), after recrystallization from benzene, melted at 79–82°. The azoate (185 mg) was refluxed with 8% potassium hydroxide in 70% ethanol (3.8 ml), ethanol (8.7 ml), water (2.6 ml), and benzene (9.0 ml) for 1 hour. The product was isolated, and after recrystallization from ethanol it melted at 71–72°. A mixed melting point with the authentic sample of 1-docosanol was not depressed. The infrared spectrum of the alcohol (Table III) was identical with that of the authentic 1-docosanol.

Synthesis of 1-Tricosanol

Behenic or docosanoic acid, $CH_3(CH_2)_{20}COOH$ (10 g) (m.p. 79.5–80°) was converted by means of thionyl chloride to the acid chloride. The latter was added to an excess of ethereal diazomethane, and the solvent and excess diazomethane were removed *in vacuo* at 10°. The crude diazoketone was dissolved in 1,4-dioxane (100 ml), and the solution was added dropwise to a stirred mixture of sodium thiosulphate (11 g) and freshly precipitated silver oxide (7 g) in water (200 ml). The mixture was heated at 75° for 90 minutes, then the solid residue was filtered and washed with water. The precipitate was treated with dilute nitric acid, refiltered, washed with water, and dried. The material was then extracted with four 500-ml portions of boiling ether, each extraction lasting 1 hour. The ethereal solution was decolorized with Norite, concentrated to 250 ml, dried over anhydrous magnesium sulphate, and concentrated further until crystals precipitated. The crystalline material, after five recrystallizations from ligroin and finally from benzene, yielded tricosanoic acid, m.p. 79.5–80.5°. The tricosanoic acid was converted with diazomethane to methyl 1-tricosanoate (3 g). The ester was reduced with ethereal lithium aluminum hydride, yielding 1-tricosanol, which after recrystallization from isopropyl alcohol – ethanol (1:1) melted at 73.4–73.5° (reported m.p. 73.5–74.5 (6)).

Synthesis of 1-Docosanol

Methyl behenate was prepared by esterification of behenic acid with diazomethane. The ester was reduced with lithium aluminum hydride to 1-docosanol, which after recrystallization from isopropyl alcohol – ethanol (1:1) melted at 71.0–72.0° (reported m.p. 70.5–71.5° (6)).

Sterol Fraction

The unsaponifiable, petroleum ether insoluble fraction (410 mg) was recrystallized from ethanol.

The filtrate from the recrystallization was treated with digitonin, and the precipitate which formed was filtered and washed with cold 1,4-dioxane. The digitonide was decomposed in pyridine solution, and ether was added to precipitate the free digitonin, which was then removed by filtration and washed with diethyl ether. The pyridine–ether solution was evaporated *in vacuo* at 30°, leaving the sterol residue (140 mg). After three recrystallizations from ethanol, the melting point of the material remained unchanged at 135–136°.

The recrystallized sterol (m.p. 127–130°; 200 mg) which had been obtained from the petroleum ether insoluble fraction was also purified via the digitonide as above. The sterol (124 mg) obtained in this case, after three recrystallizations from ethanol, melted at 136.1–137°, and remained unchanged on further recrystallization.

A mixed melting point determination of the two sterols showed no depression and their infrared spectra (Nujol) were identical.

The sterol was tested for unsaturation with tetranitromethane (12). Cetyl alcohol was used as a blank. The color produced by the sterol was compared to, and found to be considerably deeper than, that produced by cholesterol. The cetyl alcohol – tetranitromethane mixture remained colorless. It was concluded that the sterol contained at least two double bonds. The ultraviolet absorption spectrum was taken, and there was no absorption in this region.

Attempts to determine the molecular weights by the Rast method gave unsatisfactory results due to the fact that the sterol underwent a considerable amount of decomposition above its melting point.

A sample of the sterol (25.16 mg) was heated at 110° under 0.005 mm pressure until a constant weight was achieved. The loss of weight was 1.03 mg, indicating the presence of 1 molecular equivalent of water of crystallization for a compound of molecular weight 439. There was no change in melting point after dehydration.

A quantitative Liebermann–Burchard reaction was run on the sterol using the Beckman ultraviolet and visible spectrophotometer. The sterol concentration was 0.097 mg/ml in chloroform. One-centimeter cells were used. There was absorption at 420 mμ (Fig. 4), and at 623 mμ and 675 mμ as well. At 623 and 675 mμ the rate of decrease of light transmission was slightly faster at first, but on standing for a short time the transmission began to increase again. The initial rate of decrease of transmission was greatest at 675 mμ, next at 623 mμ, and slowed at 420 mμ. $[\alpha]_D^{18}$ $-36.7\pm2°$ (*c*, 6.4, $CHCl_3$). Infrared spectrum (Table II). Anal. Calc. for $C_{29}H_{48}O.H_2O$: C, 80.87; H, 11.70; O, 7.43. Found: C, 80.91; H, 11.75; O, 7.99%.

5,11(?)-Stigmastadien-3β-yl Benzoate

5,11(?)-Stimastadien-3β-ol (25 mg), freshly distilled benzoyl chloride (7 ml), and pyridine (3 drops) were heated together for 4 hours on a steam bath. Then the reaction mixture was poured into cold water. When the excess benzoyl chloride had decomposed, the solid product was filtered, and the benzoic acid was removed by extraction with ethanol. The insoluble benzoate was separated by filtration, washed with ethanol, and recrystallized from acetone. The 5,11(?)-stigmastadien-3β-yl benzoate obtained in this way melted at 148.8–149°. $[\alpha]_D^{18}$ $-11.0\pm2°$ (*c*, 1.6, $CHCl_3$). Infrared spectrum was taken in KBr (Table II). Anal. Calc. for $C_{35}H_{52}O_2$: C, 83.68; H, 10.15. Found: C, 83.30; H, 10.54%.

5,11(?)-Stigmastadien-3β-yl Azoate

5,11(?)-Stigmastadien-3β-ol (40 mg), *p*-phenylazobenzoyl chloride (36 mg), and pyridine (0.4 ml) were refluxed together in an oil bath for 2 hours. The orange-colored solution was cooled and added to ice water. The material which precipitated was filtered and dried. Then the product was dissolved in benzene and the insoluble pyridinium salts were filtered and discarded. The filtrate was evaporated under reduced pressure, and the solid residue was recrystallized from benzene–ethanol. The recrystallized material softened at 180° and melted at 190–200°. The crude ester was chromatographed on a 20-mm column using 3:1 silicic acid: Celite 503 as the adsorbent. The eluent was a petroleum ether (90–120°) – benzene mixture, the ratio of which was changed rapidly from 4:1 to 6:1. The column was extruded when the main band reached about 2 cm from the bottom of the column. The center section of this band was cut out, extracted with benzene, and recrystallized from benzene–ethanol. After two recrystallizations, the ester softened at 181° and melted at 191–193°. Infrared spectrum (Table II).

ACKNOWLEDGMENTS

The authors wish to thank Dr. W. A. Rabinovitch for his aid in the film balance work, and Dr. Barbara G. Ketcheson for the editing of the manuscript.

REFERENCES

1. C. H. HASSAL. *In* Progress in organic chemistry. *Edited by* J. W. Cook. Butterworths Scientific Publications, London. 1958. pp. 115–123.
2. J. Maizite. Acta Univ. Latviensis, Kim. Fak. Ser. **4**, No. 1–5 (1938); Chem. Abstr. **32**, 7213 (1938).
3. J. MAIZITE. Acta Univ. Latviensis, Kim. Fak. Ser. **4**, No. 14 (1939); Chem. Abstr. **34**, 1812 (1940).
4. J. MAIZITE. Arch. Pharm. **280**, 132 (1942).
5. W. D. HARKNESS and T. F. ANDERSON. J. Am. Chem. Soc. **59**, 2189 (1937).
6. A. LEVENE and F. A. TAYLOR. J. Biol. Chem. **59**, 905 (1924); Chem. Abstr. **18**, 2126 (1924).
7. R. N. JONES, P. HUMPHRIES, E. PACKARD, and K. DOBRINER. J. Am. Chem. Soc. **72**, 86 (1950).
8. P. BLADON, J. M. FABIAN, H. B. HENBEST, H. P. KOCH, and G. W. WOOD. J. Chem. Soc. 2402 (1951).
9. R. N. JONES and F. HERLING. J. Org. Chem. **19**, 1252 (1954).
10. D. K. IDLER, S. W. NICKSIC, D. R. JOHNSON, V. W. MELOCHE, H. A. SCHUETTE, and C. A. BAUMANN. J. Am. Chem. Soc. **75**, 1712 (1953).
11. L. F. FIESER. Experiments in organic chemistry. 2nd ed. D. C. Heath and Co., New York. 1941. p. 329.
12. R. BÖHM. Arch. exptl. Pharm. **38**, 33 (1897).
13. A. MCGOOKIN, A. ROBERTSON, and T. H. SIMPSON. J. Chem. Soc. 1828 (1953).

THE PYROLYSIS OF TOLUENE

S. J. PRICE
Department of Chemistry, Essex College, Assumption University of Windsor, Windsor, Ontario
Received September 28, 1961

ABSTRACT

The pyrolysis of toluene has been studied in a flow system from 913 to 1143° K. First-order rate constants are independent of the toluene concentration but decrease approximately 9% when the contact time is reduced from 1.0 to 0.41 second. Increasing the contact time from 1.0 second to 2.07 seconds does not affect the rate constant. The overall rate has been resolved into homogeneous and heterogeneous components. It is suggested that the activation energy of the homogeneous process, 85 kcal/mole, may be associated with $D(C_6H_5CH_2—H)$.

INTRODUCTION

Attempts to determine $D(C_6H_5CH_2—H)$ by pyrolysis, photobromination, and mass spectrometric methods have led to values differing by 15 kcal/mole. The mechanisms proposed for all three types of studies have been questioned and it seemed possible that none of these methods could be used to obtain this bond dissociation energy.

The initial research on the pyrolysis of toluene was carried out by Szwarc (1). He reported a first-order homogeneous process represented by $\log k = 13.3 - 77{,}500/2.3RT$ and associated the activation energy with $D(C_6H_5CH_2—H)$. The mechanism proposed by Szwarc has been extensively reviewed (2–5) and seems to be substantially correct, although it does not explain the formation of solid products other than dibenzyl.

A second pyrolytic study was carried out by Blades, Blades, and Steacie (2). Their work disagreed with that of Szwarc in several important details. First, the rate constant was found to double when the contact time was increased from 0.068 to 0.568 second. Second, the rate was slightly increased by an increase in toluene pressure. Thirdly, the solid and involatile liquid products reported by Szwarc to be dibenzyl were shown to be only 50 to 75% dibenzyl, the bulk of the remainder being a mixture of dimethyl diphenyls. Fourthly, they found that the decomposition was partly heterogeneous. Blades *et al.* did confirm the constancy of the $CH_4:H_2$ ratio, but their ratio of 30:70 is considerably lower than the 40:60 ratio reported by Szwarc. Blades *et al.* preferred not to associate their activation energy of 90 kcal/mole with any single bond rupture process.

Anderson *et al.* (6) have tried to establish $D(C_6H_5CH_2—H)$ by studying the photobromination of toluene. They obtained a value of 89.5 kcal/mole, but this has been criticized by Sehon and Szwarc (3), who point out that the reaction of the benzyl radical with bromine, which was assigned zero activation energy by Anderson *et al.* in their calculations, may have an activation energy of 5–8 kcal/mole, giving $D(C_6H_5CH_2—H)$ a value of 81.5 to 84.5 kcal/mole.

Sehon and Szwarc (3) have also reviewed the mass spectrometric studies on toluene. It must be concluded that these studies cannot be used to obtain $D(C_6H_5CH_2—H)$.

Recently Takahasi (4) has studied the pyrolysis of toluene prepared from *o*-toluidine. Following Takahasi's suggestion (private communication), his results using a reaction zone of only 6.4 cc have been disregarded. It therefore appears that, qualitatively at least, his rate constants do seem to decrease with decreasing contact time. Although his results are somewhat scattered, it would also appear that his rate constants are independent of toluene concentration. Identification of the main solid products seems to agree

with the results of Blades *et al.* Takahasi reports, however, that the Arrhenius plot of the rate constants is curved and he assigns activation energies from 74 to 105 kcal/mole to different portions of the curve. His results do not seem sufficiently accurate to warrant such detailed analysis and for the present work his results will be represented by a best straight line giving an activation energy of approximately 86 kcal/mole.

EXPERIMENTAL

Materials

(*a*) Unprepyrolyzed toluene: Fischer reagent grade toluene dryed over sodium, fractionally distilled twice, degassed by bulb-to-bulb distillation, and stored over sodium.

(*b*) 1.5% prepyrolyzed toluene: reagent grade toluene passed through a quartz tube at 828° C with a contact time of approximately 1 second and then treated as in (*a*).

(*c*) 30% prepyrolyzed toluene: reagent grade toluene passed through a quartz tube at 900° C with a contact time of 3 to 4 seconds and then treated as in (*a*).

(*d*) Toluene from *o*-toluidine: toluene prepared by the diazotization of *o*-toluidine followed by deamination with sodium hypophosphite. The organic layer was fractionally distilled. The fraction boiling between 109–110° C (uncorrected) was dried over sodium and then treated as in (*a*).

Apparatus and Procedure

The apparatus used was a modified Szwarc toluene carrier system. Toluene pressures were measured using a mercury – dioctyl phthalate differential manometer. The volume of the reaction zone in the unpacked quartz vessel was 179 cc except as noted in the tables of results. The reaction vessel used to test for heterogeneity was packed with thin-walled vitrosil tubing approximately 2-mm O.D. It had a volume of 150 cc and a surface area approximately 10 times that of the unpacked vessel. Care was taken to completely fill the cross section of the reaction zone so that flow would occur evenly through the tubes and not above them. The contact time was varied by changing the flow controlling the capillary sealed into the line on the outlet side of the reaction vessel. A dry ice – acetone trap removed toluene, dibenzyl, and similar products. The remaining products were transferred by a diffusion pump to a Le Roy still kept at −160° C to remove traces of toluene and then to a pump-down trap (−200° C) to remove C_2H_6 and C_2H_4. The remaining H_2 and CH_4 were transferred with the aid of a Toepler pump, at intervals, past a non-return valve into a gas burette. After the $CH_4 + H_2$ mixture had been measured samples were taken for combustion over CuO and/or chromatographic analysis. The burette was then cleared, the pump-down trap was brought to room temperature, and the C_2 hydrocarbons were similarly measured and then collected for chromatographic analysis. The products which can be condensed by a dry ice – acetone trap have been well characterized and were not analyzed in the present work.

The chromatographic analyses were carried out using a 1-m silica gel column at 40° C with a flow rate of helium of approximately 20 cc/min. Internal standards were run with each set of analyses, so that peak heights could be used. In the $CH_4 + H_2$ mixtures the CH_4 was determined and the H_2 calculated by difference. Experiments with known CH_4–H_2 mixtures showed that this method yielded satisfactory results.

RESULTS

Tables I, II, and III give the results of the three major divisions of this investigation. In addition, two experiments were carried out at 845° K using unprepyrolyzed toluene. Rate constants calculated from the usual first-order rate expression assuming

$$\text{fraction decomposed} = \frac{\text{moles } CH_4 + \text{moles } H_2}{\text{moles toluene}}$$

were approximately eight times as large as those subsequently found at this temperature using toluene from *o*-toluidine.

Quantities of C_2 hydrocarbons were observed in all experiments. These ranged from 1 to 40 mole% of the $CH_4 + H_2$. In runs with 30% prepyrolyzed toluene this ratio was never above 10%, while in runs with toluene from *o*-toluidine it was rarely more than 2–3%. Analysis showed that the C_2 products were 0 to 5% C_2H_6, the remainder being C_2H_4. When prepyrolyzed toluene is used, C_2H_6 and C_2H_4 are undoubtedly produced by the decomposition of impurities. In experiments using toluene from *o*-toluidine, C_2H_4

TABLE I

Pyrolysis of 1.5% prepyrolyzed toluene

Temp. (°K)	Pressure (mm)	CH_4 (10^{-5} mole)	H_2 (10^{-5} mole)	Toluene (10^{-2} mole)	Contact time (sec)	k (sec^{-1})
1110	11.8	17.3	23.0	3.58	1.02	1.11×10^{-2}
1108	11.8	37.0	49.0	4.01	1.01	2.12 "
1108	26.5	17.9	20.3	3.71	0.75	1.38 "
1107	2.0	6.7	10.1	0.246	3.55	1.99 "
1106	17.0	23.8	31.5	3.74	0.85	1.74 "
1106	27.8	18.5	24.6	5.91	0.73	1.00 "
1105	12.9	39.8	52.6	3.74	1.07	2.31 "
1105	15.0	18.2	25.3	3.06	0.92	1.58 "
1104	11.9	21.7	28.8	4.10	0.90	1.37 "
1103	12.0	40.6	63.4	3.58	1.31	2.22 "
1100	12.0	19.1	31.2	3.85	0.98	1.33 "
1098	7.1	11.8	16.4	1.70	1.64	1.01 "
1098	3.25	9.8	16.7	0.87	2.33	1.33 "
1095	12.8	15.8	28.2	3.66	1.10	1.09 "
1092	12.5	19.8	23.3	3.53	1.12	1.09 "
1091	11.6	10.2	15.3	2.80	1.01	9.00×10^{-3}
1033	34.0	2.24	2.34	7.50	0.83	7.35×10^{-4}
1031	13.4	2.05	2.85	5.30	1.05	8.80 "
1026	12.0	3.62	3.48	4.25	1.19	1.40×10^{-3}
1025	11.6	1.92	2.66	3.60	1.08	1.19 "
1025	11.5	1.97	2.14	3.58	1.08	1.07 "
1018	11.6	1.38	1.75	3.48	1.12	8.05×10^{-4}
991	12.9	0.37	0.63	6.13	1.10	1.47 "
970	12.2	0.97	1.29	7.58	1.14	2.56 "
970	11.1	0.88	0.99	6.90	1.14	2.37 "
970	12.3	0.76	0.86	7.72	1.13	1.85 "

TABLE II

Pyrolysis of 30% prepyrolyzed toluene

Temp. (°K)	Pressure (mm)	CH_4 (10^{-5} mole)	H_2 (10^{-5} mole)	Toluene (10^{-2} mole)	Contact time (sec)	k (sec^{-1})
1143	12.3	41.0	64.0	1.85	0.97	5.97×10^{-2}
1143	12.1	37.8	59.2	1.76	0.98	5.85 "
1125	11.4	16.5	29.2	1.80	0.97	2.62 "
1125	12.0	17.2	32.0	1.96	0.97	2.59 "
1106	13.8	14.2	26.3	3.12	0.98	1.33 "
1106	9.5	10.1	20.5	2.07	1.06	1.40 "
1106	6.4	9.2	17.8	1.47	1.31	1.40 "
1077	11.7	8.0	12.1	3.82	0.98	5.38×10^{-3}
1018	12.5	1.30	1.94	4.08	0.99	8.03×10^{-4}
993	10.8	0.248	0.527	3.32	1.13	2.06 "
993	11.4	0.252	0.489	3.66	1.11	1.82 "
940	13.6	0.133	0.311	9.00	1.11	4.45×10^{-5}
940	10.9	0.077	0.189	5.00	1.20	4.44 "

probably arises from secondary reactions of the benzyl radical and possibly from rupture of the aromatic ring, while C_2H_6 is assumed to be formed by the recombination of two CH_3 radicals. The fraction of decomposition in experiments using toluene from *o*-toluidine should therefore be calculated from the moles of $H_2 + CH_4 + 2C_2H_6$. However, the quantities of C_2H_6 were often so small that they could not be detected chromatographically and even the largest quantities of C_2H_6 found would increase the calculated rate by less than 0.5%. The fraction of decomposition has therefore been calculated from moles $CH_4 + H_2$.

TABLE III

Pyrolysis of toluene prepared from *o*-toluidine

Temp. (°K)	Pressure (mm)	CH_4 (10^{-5} mole)	H_2 (10^{-5} mole)	Toluene (10^{-2} mole)	Contact time (sec)	k (sec^{-1})
1120	11.8	11.9	24.1	1.90	0.96	1.97×10^{-2}
1118	11.5	11.7	24.8	1.79	0.99	1.95 "
1089*	10.5	3.76	7.64	0.85	2.07	6.40×10^{-3}
1089*	10.5	3.23	6.87	3.86	0.45	5.80 "
1087	12.0	5.95	11.05	2.86	1.00	5.95 "
1085	11.9	2.68	5.96	4.36	.41	4.80 "
1069	12.3	3.91	7.59	3.86	1.03	2.90 "
1053	6.3	1.06	2.24	1.43	1.43	1.60 "
1053	22.1	1.89	3.66	4.30	0.84	1.55 "
1050	11.8	1.59	3.54	3.66	1.05	1.33 "
1022	12.7	0.70	1.36	4.01	1.07	4.80×10^{-4}
1022	11.2	1.01	2.16	5.13	1.11	5.57 "
997	11.9	0.409	0.911	5.63	1.09	2.20 "
997†	10.8	0.540	1.54	2.40	0.98	8.85 "
988	11.7	0.197	0.400	3.64	1.12	1.46 "
972	12.0	0.254	0.591	7.50	1.14	1.00 "
964	12.0	0.065	0.159	2.58	1.11	7.93×10^{-5}
964	11.9	0.090	0.230	3.64	1.17	7.51 "
939†	10.4	0.204	0.610	2.45	1.05	3.16×10^{-4}
929	12.2	0.040	0.115	3.92	1.15	3.44×10^{-5}
913†	10.8	0.119	0.356	1.95	1.09	2.24×10^{-4}

*Volume of reaction zone 195 cc.
†Packed vessel, volume 150 cc, surface approx. 2500 cm^2.

The results in Table I show that the rate constants obtained with 1.5% prepyrolyzed toluene are badly scattered. All attempts to reduce this scatter were unsuccessful. Furthermore, the percentage of CH_4 in the CH_4:H_2 mixture was generally higher than expected and very erratic (43±8%), although excellent agreement between chromatographic analysis and CuO combustion was always obtained on any one mixture.

Table II shows the results using toluene that had been approximately 30% decomposed in prepyrolysis. The rate constants from these experiments are included in Fig. 1. Reproducibility was satisfactory and the CH_4 percentage was lower and less scattered (36±4%). However, the quantities of C_2 hydrocarbons were still larger than expected.

Following the work of Takahasi (4) toluene prepared from *o*-toluidine was used for the experiments recorded in Table III. The percentage of CH_4 in the $CH_4 + H_2$ mixtures was slightly lower and more consistent (33±2%) than in runs with 30% prepyrolyzed toluene. Closer consideration of the results is therefore restricted to the results in Tables II and III, with major emphasis on those in Table III.

Runs at 1106° K (Table II) and 1053° K (Table III) show that over the range studied the first-order rate constants are unaffected by changes in the toluene concentration. Table IV shows that the rate constant apparently decreases approximately 9% when the contact time is reduced from 1.0 to 0.41 second, although increasing the contact time from 1.0 second to 2.07 seconds does not affect the rate constant. The effect of contact time

TABLE IV

The effect of contact time on the first-order rate constant at 1089° K for the pyrolysis of toluene prepared from *o*-toluidine

Contact time (sec)	0.41	0.45	1.00	2.07
k (sec^{-1})	5.83	5.80	6.43	6.40

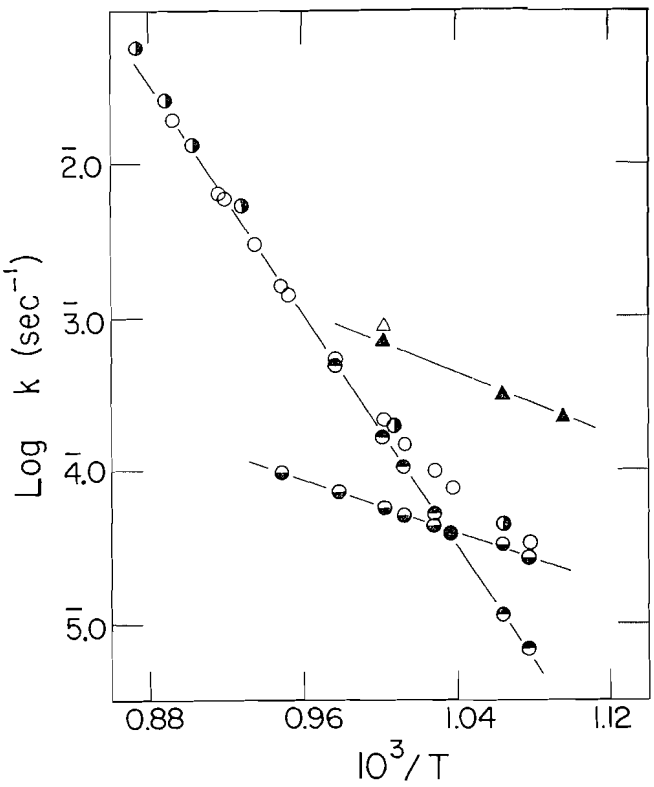

FIG. 1. Arrhenius plot for the pyrolysis of toluene. All points calculated assuming fraction decomposed given by moles H_2 plus moles CH_4 divided by moles toluene. ○ overall reaction (*o*-toluidine toluene); ◑ overall reaction (30% prepyrolysis toluene); ◓ homogeneous component; ◒ heterogeneous component; △ overall reaction in packed vessel; ▲ heterogeneous component in packed vessel.

will be discussed in detail later in this paper. Rate constants calculated on the basis of the Szwarc mechanism are shown as open circles in Fig. 1. The curvature in the lower portion of the plot was attributed to a competing surface reaction. The slope of this lower portion indicated that above approximately 1050° K the rate constants should be effectively those of the homogeneous reaction. Therefore the upper portion of the Arrhenius curve was linearly extrapolated and used as a basis for several approximations. The results of these calculations are shown by the resolved Arrhenius plots in Fig. 1. To confirm the heterogeneous nature of the competing process, the surface-to-volume ratio was increased by a factor of approximately 12. As may be seen from Table III and Fig. 1, the rate constants in the packed vessel increased by roughly the same ratio as the increase in surface to volume. The Arrhenius equation for the homogeneous process is given by $\log k = 14.8 - 85{,}000/2.3RT$.

DISCUSSION

Before any simple mechanism for the thermal decomposition of toluene can be considered, the effect of contact time on the rate constant observed both in this and previous work (2, 4) must be explained. Surface effects would appear to be unimportant under the experimental conditions used to check the effect of contact time, and it is unlikely that

any homogeneous process could cause the observed effect unless benzyl radicals are undergoing extensive side reactions. The decomposition of dibenzyl has been studied by Blades *et al.* (2). They report that no CH_4 was formed, although considerable quantities of hydrogen were produced. The invariance of the CH_4:H_2 ratio with contact time would therefore indicate that under the conditions used to study the thermal decomposition of toluene little breakdown of benzyl or dibenzyl is occurring. This is further substantiated by an experiment at 788° C carried out in the study of the pyrolysis of dimethyl zinc in a toluene carrier system (7). The quantity of hydrogen found in the products was essentially that expected from the decomposition of toluene, even though methane, and therefore benzyl radicals, were being produced at approximately 12 times the rate at which they would be produced in the decomposition of toluene under the same experimental conditions.

One further possibility is that as the contact time is decreased thermal equilibrium is not achieved in the initial part of the reaction zone, thus effectively reducing the reaction volume. It is tentatively suggested that this is the case and that the rate constants obtained in the present work using contact times of approximately 1 second are within 3 to 5% of the true first-order rate constants. Accepting this postulate, the thermal decomposition of toluene may be represented by the following mechanism:

$$C_6H_5CH_3 \rightarrow C_6H_5CH_2 + H \quad [1]$$

$$H + C_6H_5CH_3 \rightarrow C_6H_5CH_2 + H_2 \quad [2]$$

$$H + C_6H_5CH_3 \rightarrow C_6H_6 + CH_3 \quad [3]$$

$$CH_3 + C_6H_5CH_3 \rightarrow C_6H_5CH_2 + CH_4 \quad [4]$$

$$H + C_6H_5CH_3 \rightarrow C_6H_4CH_3 + H_2 \quad [5]$$

$$CH_3 + C_6H_5CH_3 \rightarrow C_6H_4CH_3 + CH_4 \quad [6]$$

$$2CH_3 \rightarrow C_2H_6 \quad [7]$$

plus the dimerization of benzyl and the various methyl phenyl radicals to give dibenzyl, dimethyl diphenyl, etc. and the breakdown of small quantities of these products to form the other solid and liquid products observed by Blades, Blades, and Steacie (2).

Whether reactions [5] and [6] occur at a sufficient rate to explain all the dimethyl diphenyl formation is uncertain. Blades and Steacie (5) indicate that at 1000° K approximately 10% of the radicals may be abstracting from the ring. Takahasi's work with deuterated toluene (8) would indicate considerable reactivity for the meta and para positions at least. Berezin *et al.* (9), using tritium labeling, find reaction [6] insignificant compared to reaction [4]. However, Berezin's work was carried out at much lower temperatures and may not be particularly relevant to the present study.

The possibility that reactions [8] and/or [9] occur to any appreciable extent seems

$$C_6H_5CH_3 \rightarrow C_6H_5 + CH_3 \quad [8]$$

$$H + C_6H_5CH_3 \rightarrow C_6H_5 + CH_4 \quad [9]$$

unlikely in view of the results of Leigh and Szwarc on the decomposition of *n*-propylbenzene in the presence of normal toluene (10) and of Blades and Steacie (5) on the decomposition of *n*-propylbenzene in the presence of "toluene-d_3".

The activation energy of the homogeneous process, 85 kcal/mole, may therefore be associated with $D(C_6H_5CH_2—H)$ within the limits of the kinetic method. This would

give a resonance energy of 17.5 kcal/mole to the benzyl radical. It should perhaps be pointed out that the observed frequency factor is within the limits expected in unimolecular processes (11).

Finally it is of interest to compare the results of the four kinetic studies of the pyrolysis of toluene. This has been done in Fig. 2. The results of Szwarc are of the same order as

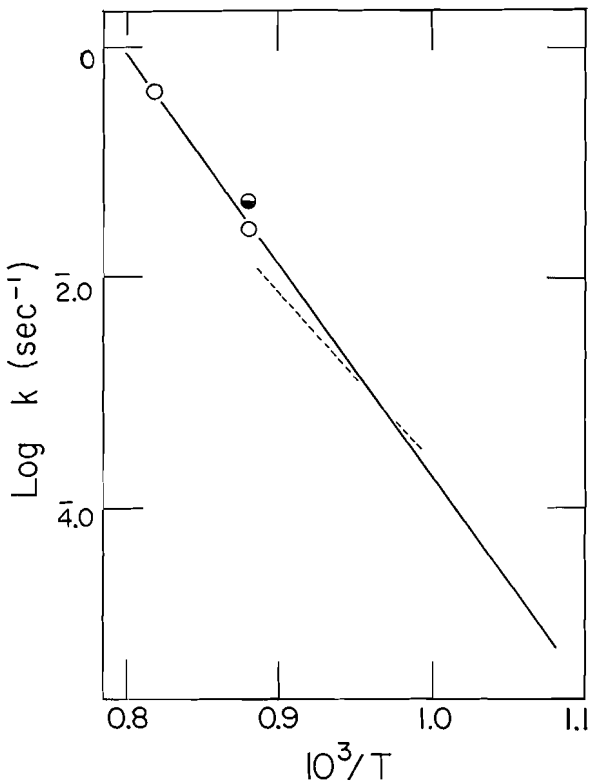

FIG. 2. Comparison of the present results with those of previous investigations. Broken curve, Szwarc; open circle, Blades, Blades, and Steacie using contact time of 0.068 second (half-fitted circle, correction of open circle to 1 second contact time); solid curve from $10^3/T = 0.875$ to $10^3/T = 1.08$, present work; solid curve from $10^3/T = 0.800$ to $10^3/T = 0.990$, Takahasi.

those of the other three investigations but detailed agreement is lacking. The agreement between the present results and the present author's interpretation of Takahasi's work is good. The agreement with the results of Blades *et al.* is somewhat unexpected. Both Blades *et al.* and the present work report decreasing rate constants as the contact time is decreased. Yet, agreement has apparently been obtained using contact times differing by a factor of 15. The effect of contact time in any one investigation seems real and it must be presumed that the agreement observed is due to systematic errors in either Blades' work or in both Takahasi's work and the present results.

ACKNOWLEDGMENTS

The author wishes to thank Mr. M. Jacko and Mr. M. Krech for carrying out preliminary experiments. This work has been supported by a grant from the National Research Council of Canada.

REFERENCES

1. M. SZWARC. J. Chem. Phys. **16**, 128 (1948).
2. H. BLADES, A. T. BLADES, and E. W. R. STEACIE. Can. J. Chem. **32**, 298 (1954).
3. A. H. SEHON and M. SZWARC. Ann. Rev. Phys. Chem. **8**, 445 (1957).
4. M. TAKAHASI. Bull. Chem. Soc. Japan, **33**, 801 (1960).
5. A. T. BLADES and E. W. R. STEACIE. Can. J. Chem. **32**, 1142 (1954).
6. H. R. ANDERSON, H. A. SCHERAGA, and E. R. VAN ARTSDALEN. J. Chem. Phys. **21**, 1258 (1953).
7. S. J. W. PRICE and A. F. TROTMAN-DICKENSON. Trans. Faraday Soc. **53**, 1208 (1957).
8. M. TAKAHASI. Bull. Chem. Soc. Japan, **33**, 808 (1960).
9. I. V. BEREZIN, N. F. KAZANSKAYA, and K. MARTINEK. Zhur. Obshcheĭ Khim. **30**, 4092 (1960).
10. C. H. LEIGH and M. SZWARC. J. Chem. Phys. **20**, 403 (1952).
11. C. STEEL and K. J. LAIDLER. J. Chem. Phys. **34**, 1827 (1961).

PERIODATE-OXIDIZED PHOSPHOMANNAN Y-2448: STRUCTURAL SIGNIFICANCE OF ITS REACTION WITH ALKALI[1]

ALLENE JEANES AND P. R. WATSON

Northern Regional Research Laboratory, Northern Utilization Research and Development Division, Agricultural Research Service, U.S. Department of Agriculture, Peoria, Ill., U.S.A.

Received January 29, 1962

ABSTRACT

The diesterphosphomannan produced by *Hansenula holstii* NRRL Y-2448 was shown by periodate-oxidation analysis to have 20% of its D-mannose units linked through carbon-1 only (or carbons-1 and -6), 33% through carbons-1 and -2, and 47% through carbons-1 and -3. Information regarding branching in this macromolecular polysaccharide derivative was not established. The periodate-oxidation product neutralized dilute alkali rapidly at pH 8.5–10.0, with elimination of about 30% of the phosphorus as inorganic orthophosphate. About 80% inorganic orthophosphate was obtained by longer treatment at pH 10.1–10.5. These observations are shown to support the hypothesis that diesterorthophosphate groups (0.20 mole/mole mannose unit) are held between carbon-6 of units otherwise linked only through carbon-1, and carbon-1 of 60% of the carbon-2-linked units. After periodate oxidation, both phosphoester bonds may undergo β-aldehydo elimination by alkali; the unit having phosphate in hemiacetal linkage and a mannosidic attachment at carbon-2 is presented as the more reactive site. Periodate oxidation also produces sites for β-dealkoxylation by alkali.

The exocellular polysaccharide derivative synthesized by the yeast *Hansenula holstii* NRRL Y-2448 and isolated as the neutral potassium salt has the constituents D-mannose, phosphorus, and potassium in the ratio of 5:1:1 (1). This phosphomannan is sensitive to overoxidation by sodium metaperiodate unless the reaction is conducted in the cold; after neutralization of the formic acid liberated, the oxidized product shows activity with mild alkali unusual for a polysaccharide. We have sought an explanation for these behaviors in relation to the structure of phosphomannan Y-2448.

It is reasonable to consider overoxidation of this substance possible since it seems characteristic of yeast mannans to have a significant proportion of their mannose units (MU) linked glycosidically at carbon-2 and/or carbon-3 (2–5). If in a reducing end position, such units are known to be susceptible to overoxidation (3–5). Phosphate groups in sugar phosphates (6) and in a polyribose phosphate (7) do not cause overoxidation unless the position of the phosphate results in formation of an active methylene group (6).

There are indications in the literature, however, that the presence of phosphate groups might be involved in the high activity of periodate-oxidized phosphomannan with alkali. Phosphates of β-aldehydo alcohols readily undergo phosphate elimination by mild alkali (8). Possibly closer parallels are provided by the smooth β-elimination, under mild alkaline conditions, of the phosphate moiety from dialdehydes produced by periodate oxidation of substances such as ribonucleoside-5′-phosphate (9) and by the adaptation of this procedure to oligo- and poly-nucleotides (9, 10).

Previously a fading end point during alkaline titration for formic acid in periodate-oxidation solutions of carbohydrates usually has been associated with the presence of *O*-formyl esters derived from reducing end groups (11–13), although other interpretations have been made (14, 15). *O*-Formyl groups appear to be excluded as the source of "ester" acidity in phosphomannan Y-2448 by the high proportion of ester-type acidity in relation

[1]*Presented before the Division of Carbohydrate Chemistry at the 139th Meeting of the American Chemical Society, St. Louis, Missouri, March 1961.*

to the reducing power of the polymer (1), and also by the relatively slow rate of reaction we have observed at pH 8.5–10.0. Since *O*-formyl esters saponify in the pH range 5.7–7.6 (11) or 5.0–9.5 (12) they should react almost instantaneously under our conditions for titrating ester-type acidity.

EXPERIMENTAL

Materials

The phosphomannan Y-2448 used, and the procedure for assuring samples of known dry weight, have been described previously (1). Visking tubing,[2] from which soluble matter had been removed by soaking in water, was used for dialysis.

Phosphorus Analysis

Carbohydrate-bound phosphate and inorganic phosphate were determined by adapting the method of Dryer, Tammes, and Routh (16). In the digesting of samples to determine carbohydrate-bound phosphorus, nitric acid was used instead of hydrogen peroxide (17). Since this method does not detect pyrophosphate under the conditions for inorganic phosphate (18, 19), any inorganic phosphate reported here is the ortho form.

Paper Chromatography

Solvent systems used for separating the inorganic components of dialyzates obtained from periodate-oxidation products after treatment with alkali or glycine buffer and neutralization were: *n*-propyl alcohol – water – aqua ammonia (6:1:3, v/v) (20); and the upper phase of *n*-butyl alcohol – pyridine – 1.5 *N* ammonium hydroxide (2:1:2, v/v) (21).

Phosphate was detected by dipping chromatograms in an ammonium molybdate – perchloric acid reagent (22) and using ultraviolet light (2537 Å) to bring out the spots (23).

Periodate Oxidation

For convenience in calculation and expression of periodate-oxidation results, sample weights of the phosphomannan (which is considered to have a repeating unit, $(C_6H_{10}O_5)_{10}(PO_3K)_2$) were calculated on the basis of $(C_6H_{10}O_5)_{10}$.

Oxidations were carried out in the dark; after a preliminary run of unbuffered solution at 25° C all subsequent oxidations were made at 4° C. Solutions for periodate oxidation contained phosphomannan Y-2448 and sodium metaperiodate at concentrations of 0.1% and 0.0074 *M* respectively, giving a ratio of 1.2 mole periodate ion per mole MU.

Analytical data for structural analysis were from unbuffered oxidation mixtures in which initial and final pH values were 5.0 and 4.0, respectively. For studies on quantitative elimination of phosphate groups from periodate-oxidized phosphomannan, periodate oxidations were conducted without buffer, in 0.065 *M* acetate buffer (pH 5.0), and in 0.025 *M* phthalate buffer (pH 6.0).

Periodate was measured by the method of Fleury and Lange as described by Jackson (24). Solutions were cooled to 4° C before and during titration with iodine (25).

Free Acidity

Ethylene glycol (1 ml) was added to aliquots (10 ml) of unbuffered oxidation mixtures and then the free acidity was titrated rapidly to the first phenolphthalein end point with 0.01 *N* barium hydroxide under an atmosphere of nitrogen. Comparable results were obtained by potentiometric titration. Acid titration values were corrected for a reagent blank. Evidence that this free acid was formic was obtained by subjecting 25-ml aliquots from a 400-hour oxidation mixture to distillation and finding 91% of the titratable free acidity in the distillate.

"Ester"-type Acidity

Measurement for ester-type acidity was made after titrating free acid in the oxidation reaction solution. When titrating for free acid, the first phenolphthalein end point faded within a few minutes and the pH decreased steadily. A more permanent end point was achieved by adding 0.2- to 1.0-ml portions of barium hydroxide solution at about 5-minute intervals during about 1.5 hours to maintain pH within the lower and upper limits of 8.5 and 10.0. Throughout this time, air was excluded by use of nitrogen gas.

Measurements on periodate-oxidation solutions showed inorganic phosphate present after titrating ester acidity but not before, and thus indicated that alkali was breaking some phosphate bonds. Conditions then were sought for more complete elimination of phosphate.

Elimination of Phosphate from Periodate-oxidized Phosphomannan

Except as stated otherwise, this procedure was applied to periodate-oxidation-reaction solutions after 240 hours' oxidation, when further change had become very slow. The pH of unbuffered oxidation solutions

[2]*Mention of trade names should not be construed as a recommendation or endorsement by the Department of Agriculture over those not mentioned.*

was made to about 5 before adding, to both buffered and unbuffered oxidation reaction mixtures, 1.01 times the calculated amount of ethylene glycol to reduce excess periodate. The solutions then were dialyzed (4° C) against distilled water until free of iodate and buffer salts. All phosphate remained in the residue.

Dialysis residues were treated (25° C) with dilute potassium hydroxide solution under an atmosphere of nitrogen, or with glycine buffer at pH 10.3–10.5 to eliminate the phosphate combined in the periodate-oxidized phosphomannan. Conditions for treatment with 0.1 *N* potassium hydroxide were (A) adding alkali to pH 11.90 and allowing to stand 1.5 hours, (B) adding alkali during 0.5 hour to pH 11.35 and allowing to stand 18 hours, and (C) adding alkali during 36 hours to maintain pH 10.45 and then allowing to stand 14 hours. Treatment with 0.02 *M* glycine buffer consisted of combining dialysis residue and 0.08 *M* glycine buffer in ratio of 10:3 by volume and allowing to stand 18 hours. The solutions then were neutralized with hydrochloric acid and analyzed for phosphate. At times the neutralized solutions were dialyzed and dialyzates and residues were analyzed separately for phosphate.

RESULTS

Oxidation in Unbuffered Solution

Oxidation of phosphomannan Y-2448 with sodium metaperiodate (1.2 mole/mole MU) in unbuffered solution at 25° C resulted in extensive overoxidation. Eventually all periodate was reduced and iodine was liberated. Unbuffered oxidation at 4° C apparently followed a normal course of reaction which, however, did not reach a sharp end point but continued to progress very slowly. Oxidation for 400 hours at 4° C resulted in essentially the same measured values as 24 hours' oxidation at 25° C.

As seen in Table I, reduction of periodate at 4° C was rapid during the first 24 hours,

TABLE I

Sodium metaperiodate oxidation of phosphomannan Y-2448 in unbuffered solution at 4° C

	Time, hours:			
	24	72	240	400
	Mole/mole MU			
IO_4^- reduced	0.47	0.57	0.64	0.73
Free acid	0.072	0.096	0.154	0.201
Single cleavage (A)*	0.326	0.378	0.332	0.328
"Ester"-type acidity (B)	0.293	0.293	0.329	0.337
(A)−(B)	0.033	0.085	0.003	−0.009

*Calculated from: IO_4^- reduced minus two times the free acid produced.

but proceeded more slowly thereafter. Liberation of formic acid occurred slowly; only 35% of the final amount was found at 24-hour reaction time. In contrast, when the neutral polysaccharide dextran B-512 is oxidized under the same conditions, it liberates 63% of the final amount of formic acid (0.60 mole/mole glucose unit) within the first 24 hours. In contrast to the slow liberation of free acid from the phosphomannan, 87% of the total ester-type acidity was obtained in 24 hours, and the value remained relatively constant the rest of the time. Cleavage of individual bonds (in 1,2-linked units) also was very rapid, and for each mole MU oxidized in this way there appears to be approximately one mole of ester acidity. The difference in these values, shown in Table I as (A)−(B), might represent the first, relatively rapid cleavage of MU from which formic acid would be liberated after the second, apparently much slower, cleavage was accomplished. The value, −0.009, suggests that by 400-hour reaction time some formic acid was being liberated by oxidation of only one bond. This reaction would result if reducing end groups became available by acid hydrolysis.

Oxidation in Buffered Solutions at 4° C

Curves for oxidation of phosphomannan in solutions buffered at pH 5.0 and pH 6.0 paralleled that for unbuffered solution after the rapid, initial stages, but the rate increased with pH. Thus, mole periodate reduced per mole MU was 0.59 for unbuffered solution at 122 hours, but at 85 hours it was 0.62 for pH 5.0 and 0.68 for pH 6.0. These values at pH 5.0 and 6.0 seemed to be approaching the 0.73 mole periodate reduced per mole MU observed for unbuffered solutions at 400 hours (Table I).

Elimination of Inorganic Phosphate from Periodate-oxidized Phosphomannan

Analysis for inorganic phosphate in solutions of phosphomannan Y-2448 oxidized 400 hours in unbuffered solution at 4° C (Table I) showed none before or after titrating free formic acid, but 0.06 mole per mole MU after titrating ester-type acidity.

Investigation of conditions for maximum elimination of phosphate in inorganic form showed the influence of rate of addition of alkali, maximum pH reached, and duration of reaction with alkali. Complete conversion to inorganic phosphate was accomplished only by adding the periodate-oxidation product to 1 *N* alkali. Milder treatment under conditions (A) and (B) resulted in 64% inorganic phosphate. Application of condition (C) to products of unbuffered and buffered periodate oxidation (Table II) shows that the

TABLE II

Elimination of phosphate from periodate-oxidized phosphomannan Y-2448 by treatment at pH 10.10–10.45

	Oxidation with $NaIO_4$		
Buffer	None	Acetate	Phthalate
pH during oxidation	5.0–4.0	5.0	6.0
Oxidation time, hours, at 4°	122	85	85
Mole IO_4^- reduced/mole MU	0.59	0.62	0.68
	Oxidation product + 0.1 *N* KOH, pH 10.45		
Inorganic P, % of total	57	63*	78
	Oxidation product + glycine buffer, pH 10.10		
Inorganic P, % of total	58	64	81

*If it be assumed that the amount of free acid was the same as for the unbuffered reaction, the mole OH^-/mole free PO_4^{3-} would be 5.1 for the acetate-buffered and 4.4 for the phthalate-buffered reaction. Since from these buffered reactions the free acid may be expected to be greater than from the unbuffered, their ratios actually would be lower than those shown.

amount of phosphate eliminated increased directly in relation to the pH at which periodate oxidation was conducted, that is, directly in relation to the extent of oxidation. Essentially no change in results were observed when glycine buffer was used to maintain mild pH conditions for phosphate elimination. Our use of glycine buffer was an application of the procedure previously reported for elimination of phosphate from periodate-oxidized nucleotides (9).

DISCUSSION

Previous work on phosphomannan Y-2448 has established that the molar ratio of phosphorus to mannose is 1:5 (1), that phosphate occurs in diester linkage between the carbon-6 position of one mannose unit (26) and the carbon-1 hemiacetal position of another (1, 26), and that the phosphate appears to cross-link chains (1, 26). We now have strong evidence that phosphate is present in the ortho rather than in the pyro form.

Our analytical measurements and paper chromatography of dialyzates of the dephosphorylated periodate-oxidized phosphomannan (19) demonstrated that orthophosphate was the only inorganic form present. The experimental conditions for these reactions appear to preclude hydrolysis of pyrophosphate if it had been present in the phosphomannan.

The nature and proportion of the mannosidic linkages, as determined by periodate oxidation, are shown in Table III. On the basis of all these experimental findings, the

TABLE III

Linkages of mannopyranose units as indicated by periodate oxidation

%	Out of 10	Carbon atoms bearing linkages
20	2	1 or 1 and 6
33 (20+13)	3	1 and 2 (or 4)*
47	5	1 and 3*

*Linkage at carbon-6 is indeterminate.

types and proportions of groups constituting the average hypothetical repeat unit are depicted in Fig. 1. A total of 10 MU are present, distributed on an average of 5 between

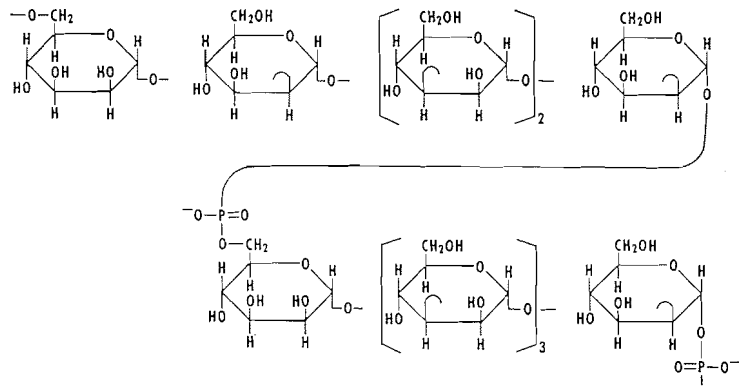

FIG. 1. Structural types and relative proportions of constituent mannose units in phosphomannan Y-2448. Absence of branching and some details of sequence have not been established.

a diesterorthophosphate group linked between carbon-6 of one MU and carbon-1 of another which appears to be mannosidically linked at carbon-2. As an average, phosphate is linked to 20% MU at carbon-6 and to 20% at carbon-1. The presence of sequences of 1,3-linked mannose units has been established by isolation of neutral di- and tri-saccharides containing this linkage from partial hydrolyzates of the periodate-oxidized phosphomannan (27). Evidence indicating 1,2-linkages rather than 1,4- will be discussed later in this article. The relative positions of 13% of the units linked through carbons-1 and -2 and of the sequences of 1,3-linked units are not established, nor is it known whether branching occurs. Therefore, linkages are not shown between the types of groups comprising the hypothetical repeating unit (Fig. 1).

These structural relationships (Fig. 1) appear to be compatible with all our observations relating to periodate oxidation and subsequent elimination of phosphate by alkali. Formic acid is believed to come from the unit linked through carbon-6 to phosphate.

Cleavage of the ring between cis hydroxyls would be rapid; subsequent cleavage between carbons-3 and -4 might be retarded by the electron-shielding effect of the phosphate ion, especially in unbuffered solution. Neutralization of this charge in buffered solution should permit an increased rate of oxidation, as was observed. In unbuffered solution, formic acid would be released slowly. Single ring cleavages presumably occur in units linked through carbons-1 and -2, and the rate of completion of this oxidation is striking (Table I). If the acid-sensitive hemiacetal-phosphate linkage should be hydrolyzed from one of these units, as might occur during unbuffered oxidation, overoxidation would occur and continue down the chain until a linkage through C_6 was encountered.

The structural representation is compatible with our observations that the native phosphomannan yields no inorganic phosphate under the conditions used for measuring ester acidity, nor even when heated at 60° C for 12 hours in 1 *N* sodium hydroxide solution. After this heating in 1 *N* alkali, the product showed no secondary phosphoryl hydrogen ions and no change in the primary ones. However, in the presence of weak acid, the native phosphomannan readily yields a secondary phosphoryl hydrogen ion, but no inorganic phosphorous is produced (1, 26). Direct correlation between the extent of periodate oxidation and the subsequent susceptibility of the phosphate to elimination by dilute alkali (Table II), as well as the high percentage of phosphate which can be eliminated, shows that both ester linkages of the phosphate become activated.

After periodate oxidation both phosphoester bonds are in β-aldehydo positions (Fig. 2, units I and II). The phosphoester attachment in I is directly analogous to that in

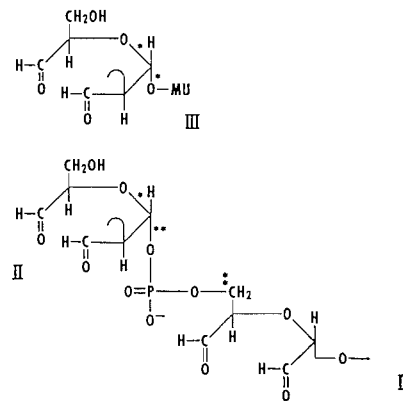

FIG. 2. Types of units from periodate-oxidized phosphomannan Y-2448 susceptible to β-alkoxy carbonyl (*) and β-phospho carbonyl (**) reaction with alkali.

periodate-oxidized adenosine-5′-phosphate. From this dialdehyde nucleotide, phosphate is eliminated in 85–90% yield by consumption of 2 equivalents of alkali per mole of phosphate liberated (9); we have employed the same manner of treatment with alkali.[3] There is analogy also btween the phosphoester attachment in I and that of the carbon-3 alkoxy group in 2:3-di-*O*-methyl D-glucose, which is eliminated readily by dilute alkali (28). There appears to be no previous report of a phosphoester attachment entirely comparable with that in II. However, the 3-carbon aldehyde to which the phosphate is attached is similar to the systems which react with alkali in 2:3-di-*O*-methyl D-glucose

[3]*An improved method for eliminating phosphate from dialdehyde nucleotides, reported recently by J. X. Khym and W. E. Cohn, J. Biol. Chem.* **236**, *PC9 (1961), also should be applicable to a system such as ours.*

and in periodate-oxidized methyl cellobioside (29) in having substituents at carbons-2 and -3 and in the absence of an α-hydroxyl. High activity might be expected at the carbon-3 position of this aldehyde fragment (originally the carbon-1 position of MU) since it is the site from which either (or both) the phosphoryl or α-glyceraldehyde group might undergo β-elimination.

Periodate-oxidized phosphomannan Y-2448 has still other alkali-sensitive bonds. In units glycosidically linked through carbons-1 and -2 (III), β-dealkoxylation might split out either of the two alkoxy groups attached at the original carbon-1 position. An additional postulated source for β-dealkoxylation would be a unit linked at carbon-3 if it were to become a reducing end group (30, 31).

The moles alkali consumed per mole inorganic phosphate eliminated from periodate-oxidized phosphomannan Y-2448 is 5.5 under the conditions of Table I (400 hour) and 4–5, or less, as estimated in Table II. These ratios are high in relation to the value 1 expected for normal dealkoxylation from a reducing sugar (32), 2 as observed for phosphate from periodate-oxidized adenosine-5′-phosphate (9), and 0 expected from a β-alkoxy aldehyde having no α-hydroxyl (28). Conditions contributing to our apparently high values might be conversion of some phosphate merely to the monoester state (81% being the maximum inorganic obtained), and the presence of alkali-sensitive groups other than phosphate.

The ester-type acidity observed stems from bonds which become labile to alkali during periodate oxidation and which, at least in part, are phosphate bonds. However, this lability is not all of equal degree. The main liberation of inorganic phosphate occurred relatively slowly or required strong alkali. Much more active was the ester acidity which apparently reached its full value within 24 hours' oxidation time, which showed a strikingly constant ratio of near unity to single bond cleavages by periodate, and which reacted relatively rapidly with alkali under mild conditions but resulted in elimination of only about 30% of the phosphate (Table I). These observations support our belief that this more active ester acidity arises from unit II rather than I.

These observations and the fact that both phosphoester attachments become activated support our hypothesis of a mannosidic bond at carbon-2 rather than at carbon-4 of unit II. Cleavage of a carbon-4-linked unit would result in a substituted α-phosphoglycol aldehyde, which would be expected to be much less reactive with alkali than the β-phosphoglyceraldehyde postulated (8, 29, 32, 33).

Additional evidence of a mannosidic bond at carbon-2 of the unit carrying phosphate in hemiacetal linkage (II) is the low reducing activity with alkaline copper reagents observed after mild acid hydrolysis of the native phosphomannan (26).

ACKNOWLEDGMENT

We are indebted to Jay E. Pittsley for paper chromatographic separation and identification of orthophosphate and of the mannose oligosaccharides.

REFERENCES

1. A. Jeanes, J. E. Pittsley, P. R. Watson, and R. J. Dimler. Arch. Biochem. Biophys. **92**, 343 (1961).
2. J. A. Cifonelli and F. Smith. J. Am. Chem. Soc. **77**, 5682 (1955).
3. L. Hough and M. B. Perry. Chem. & Ind. (London), 768 (1956).
4. P. A. J. Gorin and A. S. Perlin. Can. J. Chem. **34**, 1796 (1956).
5. D. H. Ball and G. A. Adams. Can. J. Chem. **37**, 1012 (1959).
8. J. R. Dyer. *In* Methods of biochemical analysis. Vol. 3. Interscience Publishers, Inc., New York. 1956. p. 143.
7. S. Zamenhof, G. Leidy, P. L. Fitzgerald, H. E. Alexander, and E. Chargaff. J. Biol. Chem. **203**, 695 (1953).

8. D. BROWN, F. HAYES, and A. TODD. Ber. **90**, 936 (1957).
9. D. M. BROWN, M. FRIED, and A. R. TODD. J. Chem. Soc. 2206 (1955).
10. P. R. WHITFELD. Biochem. J. **58**, 390 (1954).
11. K. H. MEYER and P. RATHGEB. Helv. Chim. Acta, **32**, 1102 (1949).
12. M. MORRISON, A. C. KUPYER, and J. M. ORTEN. J. Am. Chem. Soc. **75**, 1502 (1953).
13. I. A. WOLFF, B. T. HOFREITER, P. R. WATSON, W. L. DEATHERAGE, and M. M. MACMASTERS. J. Am. Chem. Soc. **77**, 1654 (1955).
14. D. M. W. ANDERSON, C. T. GREENWOOD, and E. L. HIRST. J. Chem. Soc. 225 (1955).
15. D. O'MEARA and G. N. RICHARDS. J. Chem. Soc. 1204 (1958).
16. R. L. DRYER, A. R. TAMMES, and J. I. ROUTH. J. Biol. Chem. **225**, 177 (1957).
17. C. H. FISKE and Y. SUBBAROW. J. Biol. Chem. **66**, 375 (1925).
18. J. M. R. BEVERIDGE and S. E. JOHNSON. Can. J. Research, E, **27**, 159 (1949).
19. P. R. WATSON, J. E. PITTSLEY, and A. JEANES. Unpublished.
20. C. S. HANES and F. A. ISHERWOOD. Nature, **164**, 1107 (1949).
21. R. J. BLOCK, E. L. DURRUM, and G. ZWEIG. Paper chromatography and paper electrophoresis. Academic Press, New York. 1958. p. 415.
22. S. BURROWS, F. S. M. GRYLLS, and J. S. HARRISON. Nature, **170**, 800 (1952).
23. E. S. ROREM. J. Chromatog. **4**, 162 (1960).
24. E. L. JACKSON. *In* Organic reactions. Vol. II. John Wiley and Sons, Inc., New York. 1944. p. 361.
25. J. C. RANKIN and A. JEANES. J. Am. Chem. Soc. **76**, 4435 (1954).
26. M. E. SLODKI. Biochim. et Biophys. Acta, **57**, 525 (1962).
27. A. JEANES, J. E. PITTSLEY, P. R. WATSON, and J. H. SLONEKER. Unpublished.
28. J. KENNER and G. N. RICHARDS. J. Chem. Soc. 2921 (1956).
29. F. S. H. HEAD. J. Textile Inst. **38**, T389 (1947).
30. J. KENNER and G. N. RICHARDS. J. Chem. Soc. 278 (1954).
31. W. M. CORBETT and J. KENNER. J. Chem. Soc. 3274 (1954).
32. W. M. CORBETT and J. KENNER. J. Chem. Soc. 2245 (1953).
33. C. E. BALLOU. Arch. Biochem. Biophys. **78**, 328 (1958).

THE FERMENTATION OF LONG-CHAIN COMPOUNDS BY TORULOPSIS MAGNOLIAE

I. STRUCTURES OF THE HYDROXY FATTY ACIDS OBTAINED BY THE FERMENTATION OF FATTY ACIDS AND HYDROCARBONS[1]

A. P. TULLOCH, J. F. T. SPENCER, AND P. A. J. GORIN
National Research Council of Canada, Prairie Regional Laboratory, Saskatoon, Saskatchewan

Received February 22, 1962

ABSTRACT

The yield of extracellular glycolipid produced by *Torulopsis magnoliae* is increased three- to five-fold by the addition of suitable compounds to the growing culture. The supplement, which can be a long-chain acid, ester, hydrocarbon, or glyceride, is hydroxylated and converted to hydroxy fatty acid sophorosides. Fatty esters of all chain lengths from C_{16} to C_{22}, including several unsaturated esters, and even-numbered hydrocarbons from C_{16} to C_{24} are readily fermented. Shorter-chain compounds are used poorly or not at all. With compounds of 16 to 18 carbon atoms, hydroxylation occurs at the terminal or penultimate carbon atom, depending on degree of unsaturation and chain length. Substrates of more than 18 carbon atoms are mainly reduced in chain length by one or more two-carbon units and hydroxylated, giving C_{17} or C_{18} acids with the hydroxyl group on the penultimate carbon atom. The various enzymic reactions which occur during the fermentation are discussed.

The extracellular oil produced by a particular strain of *Torulopsis magnoliae* in submerged culture has been the subject of an earlier investigation (1). It is heavier than water and consists of a mixture of hydroxy fatty acid glycosides of partially acetylated sophorose. The major components of the fatty acid portion of this "normal product" were 17-L-hydroxyoctadecanoic acid and 17-L-hydroxy-9-octadecenoic acid. Several minor components have since been identified as described below.

It has now been found that many long-chain compounds can be fermented by *Torulopsis magnoliae* with a substantial increase in the yield of glycolipid. The products are partially acetylated glycosides of hydroxy fatty acids as before, but the composition of the fatty acid portion varies with the substance added. To study this variation the glycolipids were subjected to acid methanolysis and the hydroxy fatty acid esters produced were analyzed by gas–liquid chromatography (GLC).

The compositions found when various fatty acid esters are incorporated into the medium are compared in Table I with that of the "normal product". Two hydroxy palmitic acids are the major components of the hydroxy acids obtained from the fermentation of methyl palmitate and also occur as minor components of the "normal product". One was shown to be 16-hydroxypalmitic acid by oxidation to hexadecanedioic acid. The other was thought to be 15-hydroxypalmitic acid by analogy with the 17-hydroxy C_{18} acid previously found (1). Bromination–dehydrobromination followed by oxidation with permanganate–periodate gave tetradecanedioic acid (2), and the derived oxo acid was shown to be identical with synthetic 15-oxopalmitic acid. The starting material for preparation of the latter was erucic acid; cis hydroxylation gave *threo*-13,14-dihydroxybehenic acid, which, after lead tetraacetate oxidation and hydrogenation, gave 13-hydroxytridecanoic acid. The ω-hydroxy acid was brominated to yield 13-bromotridecanoic acid,

[1]*Issued as N.R.C. No. 6856.*
Presented at the 44th Canadian Chemical Conference of the Chemical Institute of Canada, Montreal, August 1961.

TABLE I

Hydroxy acids obtained by fermentation of esters of fatty acids with an even number of carbon atoms

Added compound	Percentage of hydroxy acid						Yield of hydroxy ester from 1 g of ester (g)
	15-Hydroxy C_{16}	16-Hydroxy C_{16}	17-Hydroxy C_{18}	Unsaturated 17-hydroxy C_{18}	Unsaturated 18-hydroxy C_{18}	Others	
Palmitate	40	40	5	14	1	—	0.73
Stearate	2	2	80	9	—	8	0.68
Oleate	2	2	6	77	13	—	0.85
Linoleate	1	2	4	37	56	—	0.60
11-Eicosenoate	2	3	9	56	11	19	0.52
Erucate	2	4	5	65	12	12	0.51
None	9	10	21	50	6	4	0.16

which was converted to 15-oxopalmitic acid by the method of Bergström *et al.* (3). 15-Hydroxypalmitic acid is dextrorotatory and is assumed to have the L-configuration (1). The other minor component of the normal product examined was an unsaturated 18-hydroxy C_{18} acid, hydrogenation and oxidation of which yielded octadecanedioic acid.

On addition of ethyl stearate and methyl oleate to the culture the principal fatty acid components of the glycosides are 17-hydroxystearic and 17-hydroxyoleic acids respectively. The acids obtained from the fermentation of methyl linoleate were shown to be mainly a mixture of 17- and 18-hydroxy C_{18} diunsaturated acids, since on hydrogenation followed by oxidation with chromium trioxide they yielded a mixture of 17-oxooctadecanoic and octadecanedioic acids. Also, the known 18-hydroxyoctadecanoic acid was isolated from the mixture of hydrogenated acids. The double bonds in all the unsaturated hydroxy acids derived from the various fermentation products start at the ninth carbon atom since azelaic acid is the only dicarboxylic acid isolated on permanganate–periodate oxidation (4, 5).

It appears from these results that the substrate largely determines the structure of the hydroxy acid portion of the product; thus when stearate is added the fatty acids are more saturated and when oleate is added they are more unsaturated than in the "normal product". The hydroxy acids are probably produced by direct hydroxylation of the substrate and not by breakdown to acetate and resynthesis. Convincing evidence for this view was obtained by fermenting selectively hydrogenated soya bean oil methyl esters. Since this material contains isomeric mono- and di-enoic esters produced during hydrogenation, permanganate–periodate oxidation yields a number of other dicarboxylic acids besides azelaic acid. Oxidation of the hydroxy fatty acids obtained after fermentation gave the same mixture of dicarboxylic acids as did oxidation of the soya esters, showing that direct hydroxylation had occurred.

When methyl 11-eicosenoate and methyl erucate were fermented another aspect of the reaction appeared. The major acid produced from both is 17-L-hydroxyoleic acid as shown by hydrogenation to 17-L-hydroxystearic acid and oxidation to azelaic and 8-hydroxypelargonic acids. Since the double bond in the added esters is in the 11,12- or 13,14-positions respectively and is in the 9,10-position in the product, two or four carbon atoms must have been removed from the carboxyl end of the molecule. A hydroxy C_{20} acid is a minor component of eicosenoate fermentation, and is probably 19-hydroxy-11-eicosenoic acid, since undecanedioic acid was found in the oxidation products of the fatty acid mixture in an amount corresponding to the amount of C_{20} acid present. A small percentage of a hydroxy C_{20} acid appears to be produced from erucate, but no hydroxy C_{22} acid was found. The methyl esters of linolenic, pentadecanoic, and myristic acids were poorly utilized by the organism, and the products were complicated mixtures. Lower fatty acids were even less readily fermented.

Table II shows the composition of the fatty acid portion of the product obtained when some esters of odd-numbered fatty acids are fermented. Heptadecanoate gives 16-L-hydroxyheptadecanoic acid and some 17-hydroxy acid. The former acid is also obtained from nonadecanoate by loss of two carbon atoms, through 18-L-hydroxynonadecanoic acid is the major component of the hydroxy acids. With heneicosanoate, reduction in chain length by four carbon atoms is the principal reaction leading to 16-L-hydroxy- and 17-hydroxy-heptadecanoic acids but some 18-L-hydroxynonadecanoic acid is also produced by loss of two carbon atoms. Only a very small amount of hydroxyheneicosanoic acid is obtained. The location of the hydroxyl group was established for 16-hydroxyheptadecanoic and 18-hydroxynonadecanoic acids by hypoiodite oxidation to yield iodoform and hexadecanedioic and octadecanedioic acids respectively.

It appears likely that the production of "normal product" usually proceeds slowly at the same time as the supplement is fermented, which would account for the presence of C_{18} acids in the palmitate, nonadecanoate, and heneicosanoate fermentations and the presence of unsaturated acids in the stearate fermentation.

The hydroxy acids derived from the products of fermentation of some hydrocarbons are listed in Table III. The results are similar to those obtained with esters of the same chain length; chain shortening occurs with eicosane, docosane, and tetracosane, and the principal acid produced is 17-L-hydroxystearic acid. 19-L-Hydroxyeicosanoic acid was isolated as a minor component of eicosane fermentation. The hydroxyl group was shown to be at C_{19} by the formation of nonadecanedioic acid on oxidation with hypoiodite and the formation of a mixture of nonadecanedioic and octadecanedioic acids on oxidation with permanganate in acetic acid (6). However, no hydroxy C_{22} acid could be detected in the products of the docosane fermentation.

Finally the fermentation of substituted fatty acid esters was examined. Methyl 12-hydroxyoctadecanoate is much less readily utilized than the other supplements but a small amount of dihydroxy acid, which is probably 12,17-L-dihydroxyoctadecanoic acid, is obtained. Methyl 10-methyloctadecanoate is readily fermented to products assumed to be 17-L-hydroxy-10-methyloctadecanoic acid and minor amounts of 15-L-hydroxy-methylpalmitic acid and the corresponding ω-hydroxy acids.

Methyl 8-hydroxyoctadecanoate, which was isolated from hydrogenated isano oil, is also easily fermented, giving a good yield of 8,17-L-dihydroxyoctadecanoic acid. The positions of the hydroxyl groups in the starting material and in the product were confirmed by permanganate oxidation (6), the former yielding mainly pimelic and suberic acids, and the latter azelaic and sebacic acids, in addition to the other two acids. The configuration of the hydroxyl group in the hydroxy acid of isano oil does not appear to have been determined.

Glycerides such as olive oil and tallow, and free fatty acids such as tall oil acids, are also fermented easily and the products are very similar to those obtained before. The mixture of hydroxy acids produced is always that expected from the composition of the substrate. Thus, the product from tall oil acids contains ω-hydroxy C_{18} acids corresponding to the amount of linoleic acid in the tall oil.

The possibility that the "normal product" is produced by direct hydroxylation of glycerides in the yeast cells has been examined. If this occurs the composition of the acids of the "normal product" should be similar to that of the cell glycerides in chain length and degree of unsaturation. Cells grown on a low-nitrogen medium, when no extracellular oil is obtained but appreciable amounts of intracellular lipid are produced, and cells recovered after isolation of "normal product" were extracted and the fatty acid composition of the lipids determined. They were quite similar to each other, with a high percentage of oleic acid and more palmitoleic than palmitic acid. Oils with this composition would be expected to give a considerably higher percentage of unsaturated hydroxy acids than actually found in the "normal product". Therefore, the glycolipid is probably not produced in this way.

The fermentation reaction may have practical applications, as quite good yields of hydroxy acids can be obtained. With hydrocarbons and C_{20} and C_{22} esters 50–60% of the supplement is converted to hydroxy fatty acids and with palmitate and C_{18} esters 70–80%. No supplement is recovered unchanged. Except for ricinoleic, long-chain hydroxy acids are not readily available and not easily synthesized. Unsaturated hydroxy acids, which can be prepared by fermenting inexpensive materials such as inedible tallow or tall oil fatty acids, might be useful in resin or polymer preparation.

TABLE II

Hydroxy acids obtained by fermentation of esters of fatty acids with an odd number of carbon atoms

Added compound	Percentage of hydroxy acid							Yield of hydroxy esters from 1 g of ester (g)
	15-Hydroxy C_{16}	16-Hydroxy C_{16}	16-Hydroxy C_{17}	17-Hydroxy C_{17}	17-Hydroxy C_{18}	18-Hydroxy C_{19}	20-Hydroxy C_{21}	
Heptadecanoate	—	—	87	13	—	—	—	0.64
Nonadecanoate	3	5	24	9	6	53	—	0.63
Heneicosanoate	4	9	54	17	5	8	3	0.60

TABLE III

Hydroxy acids obtained by fermentation of normal hydrocarbons

Added compound	Percentage of hydroxy acids							Yield of hydroxy esters from 1 g of hydrocarbon (g)
	15-Hydroxy C_{16}	16-Hydroxy C_{16}	17-Hydroxy C_{18}	Unsaturated 17-hydroxy C_{18}	Unsaturated 18-hydroxy C_{18}	19-Hydroxy C_{20}	Others	
Hexadecane	36	43	5	13	2	—	1	0.56
Octadecane	2	4	85	4	—	—	5	0.55
Eicosane	8	7	57	8	2	14	4	0.54
Docosane	8	9	67	9	3	—	4	0.64
Tetracosane	8	8	63	16	5	—	—	0.51

From a practical point of view the most important result of the chain-shortening reaction is that compounds with an even number of carbon atoms greater than 18 are converted to 17-hydroxy C_{18} acids and compounds with an odd number of carbon atoms greater than 17 are converted to 16-hydroxy C_{17} acids. Therefore, the hydroxy fatty acid portion of the glycolipid obtained by fermenting a mixture of compounds of various chain lengths should consist largely of only one or two components. Preliminary experiments, using rapeseed oil and a crude petroleum fraction containing normal hydrocarbons with from 13 to 23 carbon atoms, have indicated that this is in fact the case.

Enzymic Reactions Involved

Since this type of fermentation has not been observed before, it is useful to consider the mechanism by which the added compounds are converted to hydroxy acids. As the carboxyl group is free in the end product and esters are readily utilized the first stage may be hydrolysis by an esterase to the free acid. The next stage would probably be oxidation of $-CH_3$ to $-CH_2OH$ or $\rangle CH_2$ to $\rangle CHOH$. This reaction is similar to that occurring in the well-known microbiological hydroxylation of steroids. The enzyme appears to be fairly specific in its action since the relative amounts of hydroxylation at the terminal and penultimate carbon atoms, which are shown in Tables I and II, can be correlated with the length of the substrate molecule. Figures derived from the work of Nicolaides and Laves (7), who measured the lengths of fatty acids and esters as urea complexes, were used. ω-Hydroxylation does not occur with stearic acid (25.05 Å), but with the shorter oleic (24.22 Å) and heptadecanoic acids (23.80 Å) it occurs to a small extent (13%). Elaidic acid (24.91 Å), very close to stearic acid in length, was also not terminally hydroxylated. With linoleic (23.31 Å) and palmitic (22.55 Å) acids, which are both shorter still, considerable ω-hydroxylation occurs but to a lesser extent with palmitic than with linoleic acid, suggesting that palmitic acid is shorter than the most favorable length for ω-hydroxylation. Pentadecanoic and myristic acids are apparently too short for appreciable hydroxylation of any type to occur. Since linolenic acid (calculated length 22.51 Å) is about the same length as palmitic acid it is probable that it is not hydroxylated readily because the 15,16-double bond is too close to the site of the reaction. Also, 12-hydroxyoctadecanoic acid probably does not react easily because the hydroxyl group is too near the reaction site. However, substituents in the 10- and 8-positions appear to be too far away to interfere. It may be that there are two active sites on the enzyme, one which can hold the carboxyl group and one which is involved in the oxidation, and only substrates of a certain critical length can fit onto these sites.

In the case of esters of more than 18 carbon atoms another enzyme system must be involved as the chain is reduced in length before hydroxylation. Since two carbon units are removed from the carboxyl end of the molecule, the reaction probably proceeds by β-oxidation similar to that occurring in fatty acid metabolism. The results of the fermentation of methyl erucate, for example, where about 50% is converted to hydroxyoleic acids, can be explained by assuming that the chain-shortening reaction and the hydroxylation reaction are proceeding independently. When the erucic acid has been reduced to 18 carbon atoms it can be hydroxylated by the other enzyme system, but part is broken down too far and metabolized in other ways, accounting for the lower percentage conversion.

In the utilization of hydrocarbons yet another type of oxidation probably occurs, that is the conversion of $-CH_3$ to $-COOH$. A number of examples are now known in which

Nocardia and other bacteria oxidize long-chain hydrocarbons to fatty acids of the same chain length (8, 9) and it is assumed that this type of terminal oxidation takes place. Hydrocarbon oxidation to acids of shorter chain length has also been observed (10) and apparently proceeds by β-oxidation. With *Torulopsis magnoliae* the probable course of reaction is oxidation to the fatty acid, and for longer-chain substances reduction to 18 carbon atoms and then hydroxylation as before.

Linday and Donald (11), who studied hydrocarbon oxidation by *Pseudomonas* and *Nocardia*, found the percentage conversion to long-chain fatty acids to be very low and suggested that this was due to further oxidation to short-chain acids. In the present work this degradation does not occur to any great extent probably because rapid hydroxylation followed by formation of the sophoroside effectively protects the fatty acid. Stewart and co-workers (8) found a gram-negative coccus which converted hexadecane to cetyl palmitate in moderately good yield. Also Raymond and Davis (9), working with *Nocardia*, obtained nearly 50% conversion of octadecane to cell lipids which were partly glycerides and partly ester waxes. Here the fatty acids may be protected by the formation of esters either with long-chain alcohols or with glycerol.

EXPERIMENTAL

Melting points were determined using a Leitz hot-stage microscope. Optical rotations were measured at 25° C in a 1-dm tube. Davison silica gel, 60–200 mesh, was used without activation for column chromatography. Petroleum of boiling range 60–80° C was used except where other boiling ranges are mentioned.

Preparation of the Substrates

Methyl palmitate, ethyl stearate, methyl oleate, methyl linoleate, methyl 11-eicosenoate, and methyl erucate were prepared from vegetable oils and purified by the usual methods. These esters were shown by gas–liquid chromatography to be more than 99% pure. Ethyl linoleate was prepared by fractional crystallization of the ethyl esters of safflower seed oil and contained 20% of ethyl oleate. Selectively hydrogenated soya bean oil esters were obtained from Dr. C. G. Youngs.

Methyl heptadecanoate was prepared as follows. 1-Octadecene was hydroxylated (12) and the diol crystallized four times from methanol. 1,2-Octadecanediol (10 g), m.p. 75–80° C, was dissolved in glacial acetic acid (150 ml), and lead tetraacetate (ca. 22 g) added. After 45 minutes benzene (150 ml) was added, the mixture was poured into water (600 ml) and shaken, the aqueous layer was further extracted with benzene (100 ml), the extract was washed twice with water, and the solvent was removed. The residual aldehyde was taken up in glacial acetic acid (80 ml) and a solution of chromium trioxide (3.17 g) in water (5 ml) and acetic acid (20 ml) added in portions. After 30 minutes the mixture was poured into water, sulphur dioxide passed in to reduce excess oxidant, and the precipitated acid filtered off. The acid, m.p. 60–61° C after crystallization from petroleum, was converted to methyl heptadecanoate by refluxing with 4% methanolic hydrogen chloride.

Methyl nonadecanoate was prepared by the method of Levene and Taylor (13).

Methyl heneicosanoate was prepared as follows. A mixture of tridecanoic acid (16 g) and methyl hydrogen sebacate (14) (8 g) was dissolved in methanol (130 ml) containing sodium (0.09 g) and electrolyzed, and the reaction mixture worked up as described by Greaves *et al.* (15). The neutral product (8.1 g) was extracted with petroleum and the acids (8.5 g) extracted with ether after acidification. Purification of the neutral fraction by distillation (b.p. 150° C at 0.1 mm) and crystallization from methanol (1500 ml) gave pure tetracosane (3.9 g), m.p. 50.5° C. The acid fraction after crystallization from methanol (100 ml) gave crude heneicosanoic acid (3.4 g), m.p. 67–72° C (lit. (16) gives 74.3° C). The acid (3 g) was esterified with methanolic hydrogen chloride and the ester, crystallized from methanol (75 ml), had m.p. 46–47° C (lit. (16) gives 47.2° C).

Hexadecane, octadecane, eicosane, and docosane were pure commercial products. Tetracosane was obtained as a by-product of the synthesis of methyl heneicosanoate.

Methyl 12-hydroxystearate was prepared from commercial 12-hydroxystearic acid.

Methyl 10-methyloctadecanoate was prepared as described by Linstead and co-workers (17).

Methyl 8-hydroxyoctadecanoic acid was prepared from isano oil (18) obtained from the Pacific Vegetable Oil Corporation. Isano oil (65 g) was hydrogenated at 40° C and 1800 p.s.i. over 5% palladium on charcoal (6 g) in ethanol (100 ml) for 5 hours. The product was saponified and the acids distributed between 85% methanol and petroleum in two separating funnels. The polar fraction, after two crystallizations from acetone, gave 8-hydroxyoctadecanoic acid (6.5 g), m.p. 77.5–79° C. The methyl ester was prepared as usual and distilled, $[\alpha]_D$ −0.4° (c, 12.7, MeOH).

Method of Fermentation

An oil-producing strain of *Torulopsis magnoliae* was used. The medium consisted of glucose (10%), yeast extract (0.8%), and urea (0.1%). The medium (50 ml) was put in a 500-ml conical flask and agitated on a shaker of 230 r.p.m. and a radius of 1 inch. The flask was shaken for 1 day after inoculation, then the supplement (1 g) added as a stable emulsion or suspension in water, and the shaking continued for 2–3 days. The oil was isolated by allowing it to separate from the medium in a 50-ml centrifuge tube. The product formed a layer at the bottom of the tube, from which the yeast cells and medium could be siphoned off. The mixture was not centrifuged because if this was done the yeast cells were mixed with the product. The fermentation conditions and the yields obtained from a number of fermentations which were carried out on a larger scale are described elsewhere (19).

Isolation of the Methyl Esters

The product was taken up in ethyl acetate, separated from the water, liberated, and dried over sodium sulphate. The dry oil was refluxed overnight with 4% methanolic hydrogen chloride (25 ml) poured into water, and the methyl esters of the hydroxy acids extracted with chloroform. The yield of methyl esters obtained from 50 ml of inoculated medium without supplement was the average of two separate fermentations. Exact figures for the percentage conversion cannot be obtained because the results varied slightly with different fermentations and the amount of "normal product" produced at the same time can not be measured accurately.

Gas–Liquid Chromatographic Analysis

The apparatus used was described previously (20, 21). For routine analysis of the hydroxy acid methyl esters a 2-ft×1/4-in. copper column packed with 1:6 silicone grease on 60–80 mesh acid-washed celite was used. The apparatus was operated at 200° C with injector at 250° and a flow rate of 60 ml of helium/min. A typical result of the analysis of esters from the "normal product" is shown in Fig. 1.

Not very much work has been done on the gas chromatography of hydroxy acids (22) and apparently none at all on the quantitative aspects of the results or on mixtures of hydroxy acids of the same chain length. As shown in Fig. 1 there is a good separation between ω-hydroxy esters and esters with the hydroxyl

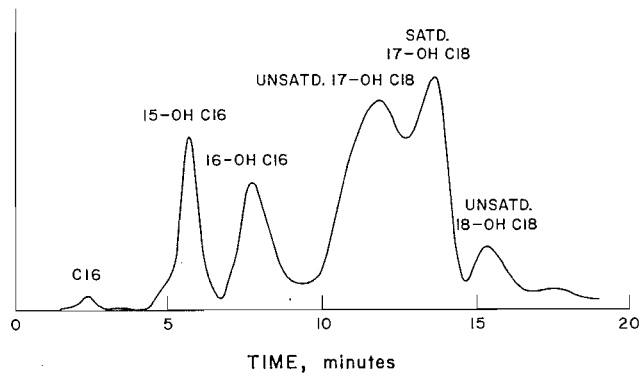

FIG. 1. Gas–liquid chromatographic analysis of hydroxy fatty acid esters using a silicone column.

group on the penultimate carbon atom. When the equivalent chain lengths (E.C.L.) (22) for the hydroxy esters are calculated the difference between the two types of ester amounts to almost 1 unit. The figures for the saturated hydroxy methyl esters obtained in the fermentations are as follows: 15-hydroxypalmitate 18.0, 16-hydroxypalmitate 18.8, 16-hydroxyheptadecanoate 19.0, 17-hydroxyoctadecanoate 20.0, 18-hydroxyoctadecanoate 20.8, and 19-hydroxyeicosanoate 22.0. The corresponding oxo esters had the same E.C.L.'s: 15-oxopalmitate 18.0, 17-oxooctadecanoate 20.0, 19-oxoeicosanoate 22.0. When the more polar fluorinated silicone QF-1 (23) is used the E.C.L.'s of the hydroxy esters are increased by 2 units compared to the results with the ordinary silicone: 15-hydroxypalmitate 20.0, 16-hydroxyheptadecanoate 21.0, 18-hydroxynonadecanoate 23.0. This difference in E.C.L. on the two types of silicone columns may be used as another way of distinguishing oxygenated esters from normal esters which have the same E.C.L. on one column. The column used was 18-in.×1/4-in. stainless steel, was packed with 1:6 silicone QF-1 on Gas-Chrom P (40–60 mesh), and was operated at 200° C.

Figure 1 also shows that the silicone column can give a partial separation of saturated and unsaturated hydroxy esters (20), sufficient to allow a rough estimation of the relative amounts present. It was not possible to use a polyester column to separate the saturated and unsaturated hydroxy esters, as can be done with ordinary esters (21, 24), because extensive decomposition or reaction with the liquid phase occurred.

Accordingly the following procedure was used in the analysis of the products. The ratio of the combined area of the saturated and unsaturated 17-hydroxy C_{18} peaks to the area of one of the hydroxy C_{16} peaks (the C_{16} esters are almost entirely saturated) is calculated. The spread between the saturated and unsaturated ester peaks can be much reduced by using a chart speed of one quarter of that used to give Fig. 1. A portion of the esters is oxidized with the permanganate–periodate reagent and separated into neutral and acidic fractions. From the analysis of the former by GLC the ratio of the area of the saturated 17-hydroxy C_{18} peak to the area of the hydroxy C_{16} peak is calculated. The complete composition of the ester mixture can then be worked out. The quantitative results obtained by gas chromatography agreed with the known values for a made-up mixture of saturated hydroxy esters and also with the percentages obtained by fractional crystallization, distillation, and chemical separations, within 5%. Some decomposition occurs on the column but since all the components are hydroxy compounds it is assumed that they all decompose to the same extent.

To separate azelaic acid and other products obtained by oxidation of the unsaturated esters or in permanganate – acetic acid oxidations a 10-ft×3/16-in. copper column packed with ethylene glycol – *o*-phthalate (24) 1: 4.5 on 40–60 mesh acid-washed firebrick was used. The oven temperature was 209° C and the flow rate 60 ml helium/min. To separate dicarboxylic esters of 16 or more carbon atoms obtained in hypoiodite oxidations the oven temperature was raised to 230° C.

Chemical Analysis of the Hydroxy Acids Produced by Fermentation

Palmitate Fermentation

The percentage of unsaturated esters was determined by two methods. (1) By oxidation: Esters (1.03 g) were dissolved in tertiary butanol (40 ml) and added to a mixture of permanganate–periodate solution (0.097 *M* in sodium metaperiodate and 0.0025 *M* in potassium permanganate) (40 ml), 0.25% potassium carbonate solution (40 ml), and tertiary butanol (80 ml), and the solution shaken for 6 hours. Ethylene was then passed in to destroy the excess oxidant, several milliliters of the carbonate solution added to raise the pH to 9, the butanol removed under vacuum at 50° C, and the saturated esters (0.89 g, 87%, measured by GLC 85%) extracted with ether. The amount of saturated C_{18} esters in this fraction was measured by GLC. After acidification the acidic products (0.16 g) were extracted with ether, converted to methyl esters with diazomethane, and found by GLC to be mainly azelaic and 8-hydroxypelargonic acids. (2) By hydrogenation: Esters (4.99 g) were hydrogenated in ethanol (65 ml) over 5% palladium on charcoal (0.5 g) and took up 59 ml hydrogen, corresponding to 14% monoene (theoretical volume required for monoene is 412 ml). The percentage of ω-hydroxy ester was determined by quantitative chromium trioxide oxidation (25). The hydrogenated and distilled ester consumed 1.46 atoms of oxygen, corresponding to 46% ω-hydroxy compound (calculated by GLC 44%).

Isolation of 16-Hydroxypalmitic Acid

A seven-stage fractional crystallization of the crude methyl esters (4.20 g) from acetone at −10° C gave pure methyl 16-hydroxypalmitate (0.57 g), m.p. 55.5–56° C (lit. (26) gives 55–55.5° C). Calculated for $C_{17}H_{34}O_3$: C, 71.3%; H, 12.0%. Found: C, 71.3%; H, 11.95%. Saponification gave 16-hydroxypalmitic acid, which, after crystallization from acetone, had m.p. 95–96.5° C (lit. (26) gives 95° C). Calculated for $C_{16}H_{32}O_3$: C, 70.5%; H, 11.8%. Found: C, 70.8%; H, 11.8%. On chromium trioxide oxidation the acid consumed 1.96 atoms of oxygen and gave hexadecanedioic acid, m.p. 119–122° C. The mixed melting point with the synthetic acid, m.p. 124–127° C, prepared by the method of Greaves *et al.* (15) was 121–125° C. 15-Hydroxypalmitate could not be obtained in pure form from the mother liquors of the fractional crystallization due to the presence of hydroxy C_{18} esters.

Isolation of 15-L-Hydroxypalmitic Acid

Partial acetylation of the crude esters, by refluxing with 85% acetic acid for 2 hours, and distribution of the product between petroleum and 80% ethanol in two separating funnels gave a polar fraction in which the concentration of the desired ester had been increased to 60%. This material was chromatographed on a silicic acid column and elution with petroleum containing 4% acetone gave an ester of 84% purity. The main impurity was 17-hydroxy C_{18} esters. The ester was acetylated by treatment with acetic anhydride at 100° C for 2 hours and finally purified by preparative gas chromatography. Batches of 42 mg were put through an 8-ft×5/16-in. copper column containing 1:6 silicone grease on acid-washed celite (60–80 mesh) operated at 240° C with injector at 290° and a flow rate of 60 ml helium/min. The recovery was about 88%. Deacetylation and crystallization from petroleum (b.p. 60–80° C) yielded pure methyl 15-L-hydroxypalmitate, m.p. 46–47° C. Calculated for $C_{17}H_{34}O_3$: C, 71.3%; H, 12.0%. Found: C, 71.1%; H, 12.1%; $[\alpha]_D$ +5.0° (*c*, 10.0, MeOH). 15-L-Hydroxypalmitic acid was obtained by hydrolysis and crystallization from acetone at 0°, m.p. 74–75° C. Calculated for $C_{16}H_{32}O_3$: C, 70.5%; H, 11.8%. Found: C, 70.45%; H, 11.7%; $[\alpha]_D$ +5.4° (*c*, 6.5, CH_3COOH). On oxidation with chromium trioxide the acid consumed 1.14 atoms of oxygen and gave 15-oxopalmitic acid, m.p. 81–82° C, after one crystallization from petroleum. The melting point was not depressed by the synthetic acid.

Synthesis of 15-Oxopalmitic Acid

Methyl erucate (25 g, prepared from rapeseed oil) was stirred with a mixture of 100% formic acid (60 ml) and 30% hydrogen peroxide (9 g) at 40° C, and propionic acid (20 ml) was added to give a homogeneous solution. After 3 hours' reaction the solvent was removed, the residue saponified with 10% potassium

hydroxide, and the acid isolated. Methyl *threo*-13,14-dihydroxybehenate was prepared by esterification with methanolic sulphuric acid (2%) and crystallized from petroleum, m.p. 77–79° C. The ester glycol was oxidized with lead tetraacetate, as described for the oxidation of octadecanediol above, and the aldehyde hydrogenated over Raney nickel at 100° C in ethanol. Saponification and crystallization from benzene gave 13-hydroxytridecanoic acid (7 g), m.p. 72–77° C (lit. (26) gives 79° C). The acid was brominated with 30% hydrogen bromide in acetic acid, esterified with diazomethane, and converted to the iodoester by refluxing with sodium iodide in dry acetone. After crystallization from ethanol the methyl 13-iodotridecanoate had m.p. 32–34° C. The iodoester (1.00 g), acetoacetic ester (0.36 g), potassium carbonate (1.15 g), and 2-pentanone (10 ml) were refluxed for 22 hours (3). Water was added and the product was extracted with ether and hydrolyzed with 10% methanolic potassium hydroxide (20 ml) at 50° C for 24 hours. After dilution with water and acidification crude 15-oxopalmitic acid (0.77 g) was extracted with ether. Two crystallizations from ethanol gave the pure acid, m.p. 81–82° C. Calculated for $C_{16}H_{30}O_3$: C, 71.1%; H, 11.2%. Found: C, 71.2%; H, 11.3%.

Isolation of Minor Components of the "Normal Product"

Crude hydrogenated hydroxy acids, prepared as before (1), were crystallized from acetone to remove most of the C_{18} acids (19.5 g). The residue (4.1 g) in the mother liquors was converted to methyl esters, acetylated, and separated in batches with a silicone column similar to that used above to give the two hydroxypalmitic acids. The 15-L-hydroxypalmitic acid had m.p. 75° C, $[\alpha]_D$ +4.6° (*c*, 4.6, CH_3COOH). Bromination of the acid (15 mg) with hydrogen bromide in acetic acid (1 ml) followed by dehydrobromination, by refluxing with S-collidine, and oxidation with aqueous permanganate–periodate reagent gave a dicarboxylic acid product. This material was found to be mainly tetradecanedioic acid when the methyl esters were analyzed on the polyester column and also on the silicone column at 200° C. Oxidation of the hydroxy acid with chromium trioxide gave 15-oxopalmitic acid, m.p. 80–81.5° C, undepressed on admixture with the synthetic acid, the X-ray powder photographs of the two acids were indistinguishable. Calculated for $C_{16}H_{30}O_3$: C, 71.1%; H, 11.2%. Found: C, 70.7%; H, 11.1%. The 16-hydroxypalmitic acid had m.p. 81–88° C, and oxidation yielded hexadecanedioic acid, m.p. 123–124° C, which did not depress the melting point of the synthetic acid, and the X-ray photographs of the two were indistinguishable. The hydrogenated crude acids were oxidized with chromic oxide and the oxo acids were removed by crystallization from ethanol. Hexadecanedioic and octadecanedioic acids were isolated from the mother liquors by crystallization from hexane and separated as methyl esters on the silicone column. Thus purified the octadecanedioic acid had m.p. 122–123° C and did not depress the melting point of a synthetic sample (15). The X-ray powder photographs were indistinguishable.

Stearate Fermentation

The crude ester was hydrolyzed and the acid crystallized once from acetone, m.p. 79–81° C, no depression with authentic 17-L-hydroxyoctadecanoic acid.

Oleate Fermentation

The crude esters were distilled, b.p. 168–170° C at 0.07 mm, $[\alpha]_D$ +3.2° (*c*, 8.0, MeOH). A portion was oxidized with the permanganate–periodate reagent and separated into saturated material (10%) and oxidation products as described for the palmitate product. The saturated material was analyzed by GLC to estimate the percentage of saturated C_{18} esters in the original product. GLC of the methyl esters of the oxidation products showed the presence of only azelaic and 8-hydroxypelargonic acids. Another portion of the esters was hydrogenated and 17-L-hydroxyoctadecanoic acid isolated, m.p. 77–80° C; the melting point of the authentic acid was not depressed.

Linoleate Fermentation

On permanganate–periodate oxidation in tertiary-butanol (5) the esters used 7.8 atoms of oxygen; the products were azelaic acid and short-chain hydroxy acids. The esters for this experiment were prepared by the fermentation of pure methyl linoleate but all the other reactions were carried out on esters derived from ethyl linoleate containing 20% ethyl oleate. The esters were distilled, b.p. 170–180° C at 0.08 mm, $[\alpha]_D$ +2.1° (*c*, 10.1, MeOH). During hydrogenation over 5% palladium on charcoal (0.36 g) the distilled esters (3.06 g) in ethanol (55 ml) took up 359 ml of hydrogen (calculated for 1.8 double bonds 398 ml). The hydrogenated esters (5 g) were oxidized with chromic oxide (3 g) in acetic acid (60 ml) as described before. The product (4.33 g) was crystallized from petroleum (b.p. 40–60° C) (150 ml) at 25° C and gave crude methyl hydrogen octadecanedioate (1.73 g, 40%). The pure half ester was obtained by crystallization from petroleum, m.p. 74–76° C (lit. (27) gives m.p. 72–74° C). Octadecanedioic acid was obtained by saponification and crystallized from ethyl acetate, m.p. 123–125.5° C, mixed melting point with the synthetic acid 124–127.5° C. The mother liquors, after separation of the half ester, yielded crude methyl 17-oxooctadecanoate (2.60 g), which gave the pure ester after crystallization from petroleum at 0° C, m.p. and mixed m.p. with the synthetic ester (1) 53–55° C. 17-Oxooctadecanoic acid was obtained by hydrolysis and crystallized from ethanol, m.p. and mixed m.p. with synthetic acid 85.5–87.5° C (1).

Isolation of 18-Hydroxyoctadecanoic Acid

Hydrogenated esters (20 g) were acetylated, by treatment with acetic anhydride (250 ml) at 100° C for 2 hours, and the reagent was removed under vacuum at 70° C. The acetate ester was taken up in methanol (200 ml), urea (34 g) added, and the mixture warmed to give a solution. The solid (33 g) was collected after 18 hours, decomposed with water, extracted with ether, and deacetylated with sodium methoxide in

methanol. The methyl esters (7.66 g) so obtained, contained about 75–80% ω-hydroxy ester. A portion (4.9 g) was chromatographed on a silicic acid column and eluted with petroleum containing 6% acetone. Methyl 17-hydroxyoctadecanoate came off first followed by pure methyl 18-hydroxyoctadecanoate (2.91 g), which was obtained as very long colorless needles after crystallization from petroleum, m.p. 61–62° C (lit. (3) gives 62.5° C). 18-Hydroxyoctadecanoic acid was prepared by saponification and crystallized from acetone, m.p. 97–99° C (lit. (3) gives 99° C). Calculated for $C_{18}H_{36}O_3$: C, 71.95%; H, 12.1%. Found: C, 71.8%; H, 12.0%.

Selectively Hydrogenated Soya Bean Oil Methyl Esters Fermentation

The composition of the original esters was palmitic 11.8, palmitoleic 0.2, stearic 5.6, oleic and isomers 62.7, linoleic and isomers 19.5%. Oxidation of these esters with the permanganate–periodate reagent (5) gave the following dicarboxylic acids expressed as molar percentages: C_6 1.2, C_7 1.6, C_8 5.1, C_9 58.7, C_{10} 10.3, C_{11} 10.7, C_{12} 9.6, C_{13} 2.8. Oxidation of the hydroxy methyl esters obtained after fermentation gave: C_6 2.3, C_7 2.0, C_8 3.8, C_9 57.6, C_{10} 11.8, C_{11} 9.6, C_{12} 10.6, C_{13} 2.2.

11-Eicosenoate Fermentation

Crude hydroxy esters (0.162 g) were oxidized as described for the palmitate fermentation and gave neutral product (0.018 g, 12.5% of original material). The oxidation products were 8-hydroxypelargonic acid and azelaic acid (85%, as a molar percentage of the total dicarboxylic acids) and undecanedioic acid (15%). Part of the esters was hydrogenated, purified by GLC as the acetate, and saponified, giving 17-L-hydroxyoctadecanoic acid, m.p. and mixed m.p. 79–81° C.

Erucate Fermentation

The acidic products obtained by the oxidation procedure used above were almost entirely azelaic and 8-hydroxypelargonic acids. A portion was hydrogenated and hydrolyzed to give 17-L-hydroxyoctadecanoic acid, m.p. and mixed m.p. 78–80° C.

Heptadecanoate Fermentation

Esters (0.63 g) were chromatographed on a silicic acid column and eluted with petroleum containing 4% of acetone, giving methyl 16-L-hydroxyheptadecanoate (0.44 g) free from the ω-hydroxy compound, m.p. 51.5–52.5° C, $[\alpha]_D$ +4.8° (*c*, 4.75, MeOH). Calculated for $C_{18}H_{36}O_3$: C, 71.95%; H, 12.1%. Found: C, 71.95%; H, 12.1%. The ester was saponified, giving 16-L-hydroxyheptadecanoic acid, which after crystallization from acetone had m.p. 86.5–87.5° C, $[\alpha]_D$ +5.2 (*c*, 4.0, CH_3COOH). Calculated for $C_{17}H_{34}O_3$: C, 71.3%; H, 12.0%. Found: C, 71.1%; H, 11.9%. Acid (10 mg) was dissolved in dioxane (2 ml), 5% aqueous potassium hydroxide (1 ml) added, followed by a solution (ca. 1 ml) of iodine in aqueous potassium iodide (10 g iodine in 50 ml of 30% potassium iodide solution) until the brown color persisted when heated to 60° C. The mixture was kept at 60° C for 2 minutes, potassium hydroxide added to dissolve excess iodine, and water (5 ml) added. Iodoform crystallized on standing. The solution was evaporated to a volume of 3–4 ml, acidified with 4 *N* sulphuric acid, sodium metabisulphite added, the acids extracted with ether, and treated with diazomethane. The principal dicarboxylic acid was shown by GLC to be hexadecanedioic acid together with a very small amount of the C_{15} acid.

Nonadecanoate Fermentation

Batchwise separation of the acetylated esters by GLC, as described under 15-hydroxypalmitate purification, and working up as usual yielded 18-L-hydroxynonadecanoic and 16-L-hydroxyheptadecanoic acids. Crystallization of the former from acetone gave pure 18-L-hydroxynonadecanoic acid, m.p. 91.5–92.5° C, $[\alpha]_D$ +4.4° (*c*, 2.8, CH_3COOH). Calculated for $C_{19}H_{38}O_3$: C, 72.6%; H, 12.2%. Found: C, 72.7%; H, 12.3%. Oxidation with hypoiodite as described above yielded mainly octadecanedioic acid and a small amount of the C_{17} acid. Treatment with diazomethane yielded methyl 18-L-hydroxynonadecanoate, m.p. 56–57° C, $[\alpha]_D$ +3.4° (*c*, 3.5, $CHCl_3$). Calculated for $C_{20}H_{40}O_3$: C, 73.1%; H, 12.3%. Found: C, 73.1%; H, 12.35%. The 16-L-hydroxyheptadecanoic acid was also crystallized from acetone and had m.p. 86–88° C. Calculated for $C_{17}H_{34}O_3$: C, 71.3%; H, 12.0%. Found: C, 71.5%; H, 12.2%. The X-ray powder photographs of this acid and of the 16-L-hydroxy C_{17} acid described earlier were indistinguishable.

Heneicosanoate Fermentation

Chromatography of the esters on silicic acid and elution with petroleum containing 4% of acetone yielded a fraction largely free from ω-hydroxy esters. This fraction was acetylated and separated into C_{17} and C_{19} ester acetates on the silicone column by GLC as above. After working up and crystallizing from acetone, 16-L-hydroxyheptadecanoic acid was isolated, m.p. and mixed m.p. 86.5–88° C. The 18-L-hydroxynonadecanoic acid had m.p. and mixed m.p. 90.5–92° C.

Hexadecane Fermentation

The products were identified by comparison of the GLC results with those obtained by palmitate fermentation.

Octadecane Fermentation

On hydrolysis the esters yielded 17-L-hydroxyoctadecanoic acid, m.p. and mixed m.p. 80–81° C. Oxidation of the esters as above gave 93% of neutral material.

Eicosane Fermentation

The crude hydroxy esters were first purified by rapid distillation, b.p. 160–180° C at 0.1 mm, then C_{16} and C_{18} compounds removed by fractional distillation through a spinning band column. Saponification of

a portion of the distillate and two crystallizations from acetone yielded 17-L-hydroxyoctadecanoic acid, m.p. and mixed m.p. 78–80° C. The distillation residue consisted of polymeric material, produced during the prolonged heating, and hydroxy C_{20} esters. The latter were largely separated from polymer by rapid distillation at 200° C and 0.04 mm. The ester so obtained was separated from a small amount of ω-hydroxy ester by chromatography on a silicic acid column and elution with petroleum containing 6% acetone. After hydrolysis 19-L-hydroxyeicosanoic acid was obtained and crystallized from acetone, m.p. 86.5–87.5° C, $[\alpha]_D$ +5.2° (*c*, 1.4, CH_3COOH). Calculated for $C_{20}H_{40}O_3$: C, 73.1%; H, 12.3%. Found: C, 73.3%; H, 12.4%. Esterification with 4% methanolic hydrogen chloride gave methyl 19-L-hydroxyeicosanoate, which was crystallized from petroleum, m.p. 58–60° C, $[\alpha]_D$ +3.6° (*c*, 2.4, MeOH). Calculated for $C_{21}H_{42}O_3$: C, 73.6%; H, 12.4%. Found: C, 73.75%; H, 12.3%. When the acid was oxidized with potassium permanganate in acetic acid (6) the principal acids produced were nonadecanedioic and octadecanedioic in about equal amounts; minor amounts of shorter-chain acids were also found. Chromium trioxide oxidation of the acid yielded 19-oxoeicosanoic acid, which crystallized from ethanol, m.p. 88.5–90.5° C. Calculated for $C_{20}H_{38}O_3$: C, 73.6%; H, 11.7%. Found: C, 73.4%; H, 11.5%. Oxidation of the oxo acid with hypoiodite gave mainly nonadecanedioic acid with small amounts of C_{18} and C_{17} dicarboxylic acids.

Docosane and Tetracosane Fermentations

17-L-Hydroxyoctadecanoic acid was isolated from both products by saponification and crystallization from acetone, m.p. and mixed m.p. 78–80° C.

12-Hydroxyoctadecanoate Fermentation

The ester product (0.49 g, derived from 2 g supplement) was saponified and chromatographed on silicic acid; elution with chloroform removed monohydroxy acids and elution with acetone gave a dihydroxy acid (0.19 g). Crystallization from ethyl acetate – hexane yielded 12,17-L-dihydroxyoctadecanoic acid, m.p. 71–72° C, $[\alpha]_D$ +8.2 (*c*, 4.9, CH_3COOH). Calculated for $C_{18}H_{36}O_4$: C, 68.3%; H, 11.5%. Found: C, 68.2%; H, 11.5%. Chromic acid oxidation gave 12,17-dioxooctadecanoic acid, which crystallized from ethyl acetate, m.p. 53–56° C. Calculated for $C_{18}H_{32}O_4$: C, 69.2%; H, 10.3%. Found: C, 68.9%; H, 10.3%.

10-Methyloctadecanoate Fermentation

ω-Hydroxy esters were removed from the product (0.53 g, from 1 g supplement) by silicic acid column chromatography as described for the heptadecanoate fermentations. Saponification yielded gummy 17-L-hydroxy-10-methyloctadecanoic acid (0.2 g), containing about 10% of a 17-hydroxymethyl C_{16} acid, $[\alpha]_D$ +3.2° (*c*, 7.5, CH_3COOH). Chromic acid oxidation gave 10-methyl-17-oxooctadecanoic acid, which was purified by GLC as the methyl ester. The acid, after crystallization from petroleum, had m.p. 35–36° C. Calculated for $C_{19}H_{36}O_3$: C, 73.0%; H, 11.6%. Found: C, 72.95%; H, 11.5%.

8-Hydroxyoctadecanoate Fermentation

The crude esters (1.01 g, from 1 g supplement) were extracted with boiling petroleum, and crystalline dihydroxy ester (0.49 g) was obtained on cooling. This ester was saponified and the product crystallized from acetone to give 8,17-L-dihydroxyoctadecanoic acid, m.p. 82–83° C. Calculated for $C_{18}H_{36}O_4$: C, 68.3%; H, 11.5%. Found: C, 68.05%; H, 11.45%, $[\alpha]_D$ +3.9° (*c*, 5.0, CH_3COOH). Methyl 8,17-L-dihydroxyoctadecanoate was prepared by treatment with methanolic hydrogen chloride and crystallized from acetone, m.p. 77–78° C, $[\alpha]_D$ +3.9° (*c*, 2.4, MeOH). Calculated for $C_{19}H_{38}O_4$: C, 69.0%; H, 11.6%. Found: C, 69.0%; H, 11.6%. Oxidation of the acid with permanganate in acetic acid yielded the following dicarboxylic acids: C_7 and C_8, lesser amounts of C_9 and C_{10}, and minor amounts of C_6, C_5, and C_4. Oxidation of 8-hydroxystearate in the same way gave mainly C_7 and C_8 dicarboxylic acids.

Composition of the Oil of Torulopsis magnoliae Cells

The yeast was grown on the following "low-nitrogen" medium: glucose 10%, yeast extract 0.2%, and urea 0.1%. The air flow was 1 liter per minute per fermentor, the agitator speed 400 r.p.m., and the temperature 30° C. No extracellular oil was produced. The yeast was also grown on the usual medium for oil production and the oil produced was separated. In both cases the cells were collected by centrifuging, washed twice with distilled water, and dried *in vacuo* at room temperature. The dry cells were ground and extracted with petroleum using the modification of Troéng's method (28) developed for use with fungus spores (29). The oil content of the cells grown on the "low-nitrogen" medium was 11%. Methyl esters were prepared in the usual way and analyzed by GLC (30). The fatty acid composition was: myristic 0.5, palmitic 12.9, palmitoleic 15.4, stearic 6.7, oleic 62.8, linoleic 0.7, and unidentified 0.9%. The extract from the oil-producing cells was 2.4% and only about 20% of this was fatty acid esters. The fatty acid composition was: palmitic 6.7, palmitoleic 16.5, stearic 2.7, and oleic 74.1%.

ACKNOWLEDGMENTS

The authors are indebted to Dr. C. G. Youngs for suggesting the fermentation of, and supplying, selectively hydrogenated soya bean oil esters. The authors wish to thank Mr. N. R. Gardner, Mr. L. L. Hoffman, and Miss S. F. Lubin for technical assistance, Miss I. M. Gaffney for the X-ray powder photographs, and Mr. M. Mazurek for the microanalyses.

REFERENCES

1. P. A. J. GORIN, J. F. T. SPENCER, and A. P. TULLOCH. Can. J. Chem. **39**, 846 (1961).
2. K. HOFMANN, G. J. MARCO, and G. A. JEFFREY. J. Am. Chem. Soc. **80**, 5717 (1958).
3. S. BERGSTRÖM, G. AULIN-ERDTMAN, B. ROLANDER, E. STENHAGEN, and S. ÖSTLING. Acta Chem. Scand. **6**, 1157 (1952).
4. R. U. LEMIEUX and E. VON RUDLOFF. Can. J. Chem. **33**, 1701 (1955).
5. E. VON RUDLOFF. Can. J. Chem. **34**, 1413 (1956).
6. A. T. JAMES, J. P. W. WEBB, and T. D. KELLOCK. Biochem. J. **78**, 333 (1961).
7. N. NICOLAIDES and F. LAVES. J. Am. Chem. Soc. **80**, 5752 (1958).
8. J. E. STEWART, R. E. KALLIO, D. P. STEVENSON, A. C. JONES, and D. O. SCHISSLER. J. Bacteriol. **78**, 441 (1959).
9. R. L. RAYMOND and J. B. DAVIS. Appl. Microbiol. **8**, 329 (1960).
10. D. M. WEBLEY, R. B. DUFF, and V. C. FARMER. Nature, **178**, 1467 (1956).
11. E. M. LINDAY and M. B. DONALD. J. Biochem. Microbiol. Technol. Eng. **3**, 219 (1961).
12. D. SWERN, G. N. BILLEN, and J. T. SCANLAN. J. Am. Chem. Soc. **68**, 1504 (1946).
13. P. A. LEVENE and F. A. TAYLOR. J. Biol. Chem. **59**, 905 (1924).
14. L. J. DURHAM, D. J. MCLEOD, and J. CASON. *In* Organic syntheses. Vol. 38. John Wiley & Sons, Inc., New York. 1958. p. 57.
15. W. S. GREAVES, R. P. LINSTEAD, B. R. SHEPHARD, S. L. S. THOMAS, and B. C. L. WEEDON. J. Chem. Soc. 3326 (1950).
16. F. FRANCIS and S. H. PIPER. J. Am. Chem. Soc. **61**, 577 (1939).
17. R. P. LINSTEAD, J. C. LUNT, and B. C. L. WEEDON. J. Chem. Soc. 3331 (1950).
18. J. P. RILEY. J. Chem. Soc. 1346 (1951).
19. J. F. T. SPENCER, A. P. TULLOCH, and P. A. J. GORIN. Paper presented at the 140th Meeting of the American Chemical Society, Chicago, Illinois. September, 1961.
20. B. M. CRAIG and N. L. MURTY. Can. J. Chem. **36**, 1297 (1958).
21. B. M. CRAIG and N. L. MURTY. J. Am. Oil Chemists' Soc. **36**, 549 (1959).
22. T. K. MIWA, K. L. MIKOLAJCZAK, F. R. EARLE, and I. A. WOLFF. Anal. Chem. **32**, 1739 (1960).
23. W. J. A. VANDENHEUVEL, E. O. A. HAAHTI, and E. C. HORNING. J. Am. Chem. Soc. **83**, 1513 (1961).
24. B. M. CRAIG. Chem. & Ind. (London), 1442 (1960).
25. R. U. LEMIEUX. Can. J. Chem. **31**, 396 (1953).
26. P. CHUIT and J. HAUSSER. Helv. Chim. Acta, **12**, 463 (1929).
27. G. MORGAN and E. WALTON. J. Chem. Soc. 442 (1938).
28. S. TROÉNG. J. Am. Oil Chemists' Soc. **32**, 124 (1955).
29. A. P. TULLOCH and G. A. LEDINGHAM. Can. J. Microbiol. **8**, 379 (1962).
30. A. P. TULLOCH and G. A. LEDINGHAM. Can. J. Microbiol. **6**, 425 (1960).

THE GAS–LIQUID PARTITION CHROMATOGRAPHY OF CARBOHYDRATE DERIVATIVES

PART II. THE SEPARATION OF METHYL GLYCOSIDES AND OF ACETYLATED DISACCHARIDES

H. G. JONES AND M. B. PERRY

Department of Organic Chemistry, Queen's University, Kingston, Ontario

Received March 15, 1962

ABSTRACT

Gas–liquid partition chromatography has been used to separate anomeric methyl glycosides and also fully acetylated disaccharides.

DISCUSSION

Earlier work in this laboratory (1, 2) showed that gas–liquid partition chromatography (G.L.P.C.) provided an excellent method for the separation of glycitol and glycose acetates. These results encouraged us to investigate the possibility of extending the method to the analysis of unsubstituted monosaccharides and of acetylated carbohydrates of higher molecular weight. This paper describes the separation of unsubstituted methyl glycosides and of acetylated disaccharides by G.L.P.C.

The recorded separations were obtained using samples (5–20 γ) of the methyl glycosides in dry methanol and of the acetylated disaccharides in dry chloroform solution developed on a Pye Argon Chromatograph fitted with an ionization detector (3), and in cases where larger amounts of material (50–150 mg) were separated and collected, the Burrell Kromo-Tog K-2 apparatus was used.

Bishop *et al.* (4, 5) and Kircher (6) have shown that G.L.P.C. can be applied to the separation of methyl *O*-methyl glycosides but that under the conditions used, methyl mono-*O*-methyl hexopyranosides and methyl hexopyranosides (5) have such large retention volumes that resolution of these compounds was not satisfactory. In our work it was found that the substitution of part of the usual Chromosorb W support material by glass beads coated with a suitable non-polar liquid phase greatly reduced the retention volumes of these compounds, thus making their separation by G.L.P.C. practical.

For the separation of methyl glycosides the two most suitable column packing materials found, from many trial experiments, were (*a*) a column made up of an intimate mixture of Apiezon M grease on Chromosorb W and butanediol succinate polyester on Chromosorb W packed on top of a column of methyl silicone rubber gum on glass beads (column packing I), and (*b*) an intimate mixture of Apiezon M grease on Chromosorb W, butanediol succinate polyester on Chromosorb W, and Apiezon M grease on glass beads (column packing II). Typical separations of glycosides on column packing I are shown in Fig. 1, and on column packing II in Fig. 2. The retention volumes of glycosides on these column packings are given relative to methyl β-L-arabinopyranoside (= 1.00) in Table I.

The most suitable operating temperature was found to be 200–210°, under which condition good separations were obtained on the Pye Argon Chromatograph without apparent decomposition of the compounds. However, although methyl pentosides were recovered unchanged from the effluent gas stream from preparative separations using the Burrell Kromo-Tog K-2 apparatus, methyl glucosides and methyl galactosides collected were found to be contaminated with β-glucosan (?) and β-galactosan respectively. It is

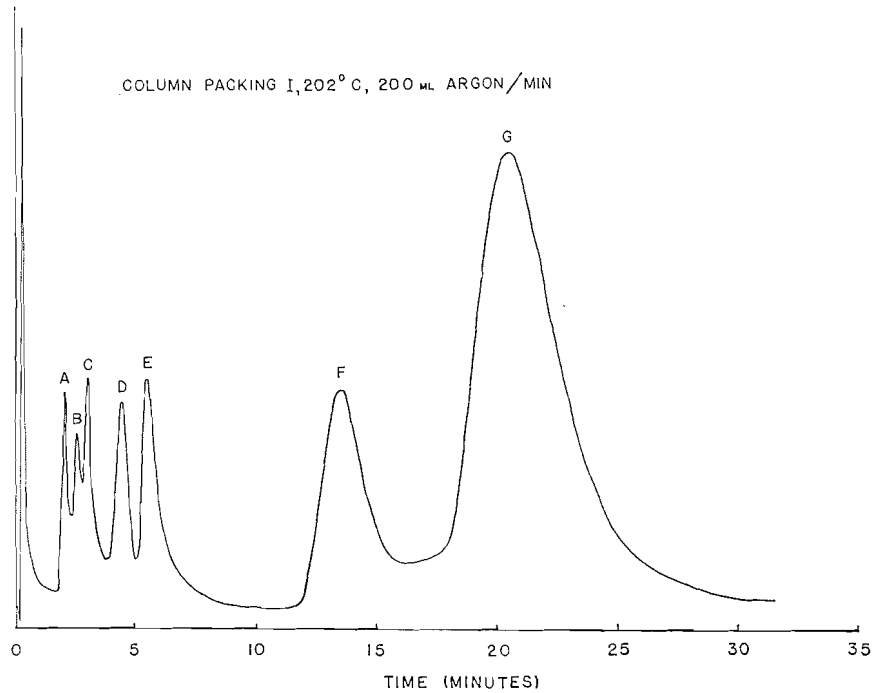

FIG. 1. Separation of glycosides: (A) methyl α-L-fucopyranoside, (B) methyl β-L-arabinopyranoside, (C) methyl β-D-xylopyranoside, (D) methyl α-L-arabinofuranoside, (E) β-galactosan, (F) methyl (methyl β-D-glucopyranosid) uronate, and (G) methyl β-D-galactopyranoside.

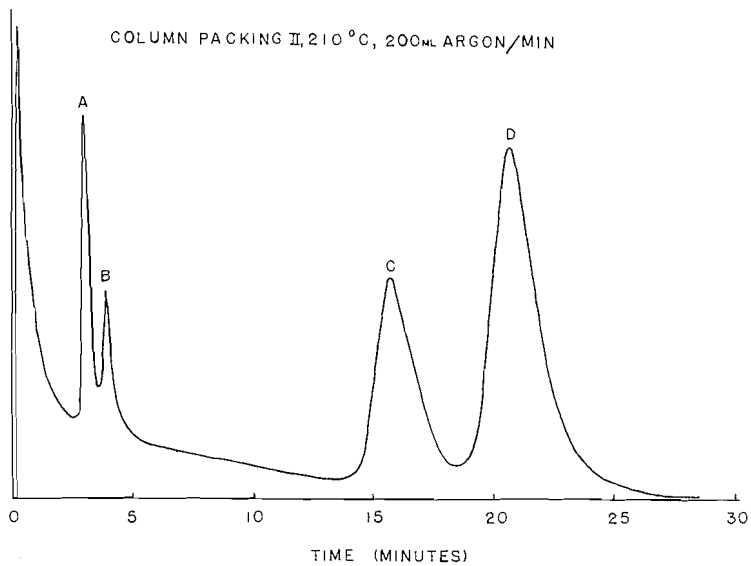

FIG. 2. Separation of methyl glycosides: (A) methyl β-L-arabinopyranoside, (B) methyl β-D-xylopyranoside, (C) methyl α-D-glucopyranoside, and (D) methyl β-D-glucopyranoside.

considered that the decomposition of the methyl hexosides takes place in the heated part of the collection device and not on the column packing material. A general relationship between the structures of the methyl glycosides and their relative retention volumes

TABLE I

Retention volumes of glycosides relative to methyl β-L-arabinopyranoside

Glycoside	Column packing	
	I (202°)	II (210°)
Methyl α-L-fucopyranoside	0.77	0.79
Methyl β-L-arabinopyranoside	1.00 (2.5 min)	1.00 (3 min)
Methyl α-L-rhamnopyranoside	1.06	1.00
Methyl β-D-xylopyranoside	1.20	1.25
Methyl β-D-ribofuranoside	1.70	1.75
Methyl α-L-arabinofuranoside	1.73	1.56
Methyl α-D-arabinopyranoside	2.20	—
β-Galactosan	2.30	1.00
Methyl α-D-glucopyranoside	5.50	5.40
Methyl (methyl β-D-glucopyranosid) uronate	5.60	2.53
Methyl α-D-galactopyranoside	5.70	5.34
Methyl α-D-altropyranoside	6.40	6.13
Methyl β-D-glucopyranoside	7.11	7.00
Methyl α-D-mannofuranoside	7.40	6.90
Methyl β-D-glucofuranoside	—	7.21
Methyl α-D-mannopyranoside	8.30	7.10
Methyl β-D-galactopyranoside	8.52	7.74
Methyl β-D-glycero-D-gulopyranoside	31.8	—
Phenyl β-D-glucopyranoside	39.0	—

could not be made since it was found that reversal of the order of elution occurred in some cases on changing the nature of the liquid phases. In the case of each glycoside investigated it was found that the anomers showed fairly wide separation and it is considered that the G.L.P.C. method will provide a convenient procedure for the detection, quantitative analysis, and preparative-scale separation of these compounds. In general, paper chromatography has not provided a successful method for the separation of anomeric methyl glycosides (6, 7), although some success has been achieved using cellulose column chromatography (8) separations on Florex XXX (9) and on Dowex-1 resin in the chloride and borate forms (10).

Attempts to separate oligosaccharide acetates by G.L.P.C. were successful only when glass beads were used as the inert support material for the liquid phases. Two of the most successful columns were prepared using (*a*) a mixture of polyphenylether on glass beads and D-C silicone oil 710 on glass beads (column packing III) and (*b*) methyl silicone rubber gum on glass beads (column packing IV) at 236–238°. Typical separations of disaccharide acetates are shown in Fig. 3 (column packing III) and in Fig. 4 (column packing IV), and the retention volumes of these derivatives, relative to octa-*O*-acetyl sucrose (= 1.00), are recorded in Table II.

The acetates of reducing disaccharides gave broad peaks under the conditions described above, and good separations of the anomers were not achieved. The best results were obtained with the acetates of non-reducing disaccharides and with glycosyl-glycitol derivatives prepared by acetylation with pyridine and acetic anhydride of reduced ($NaBH_4$) reducing disaccharides.

EXPERIMENTAL

Apparatus

Separations were carried out using the Pye Argon Chromatograph fitted with an ionization detector (80 μc radium D) and employing straight glass columns (117×0.5-cm I.D.) packed with the appropriate support, enclosed at each end by small glass-wool plugs. The samples (5–20 γ) in dry methanol or chloroform solution were placed on the top of the columns using a micropipette, and development was made using dry argon as the carrier gas.

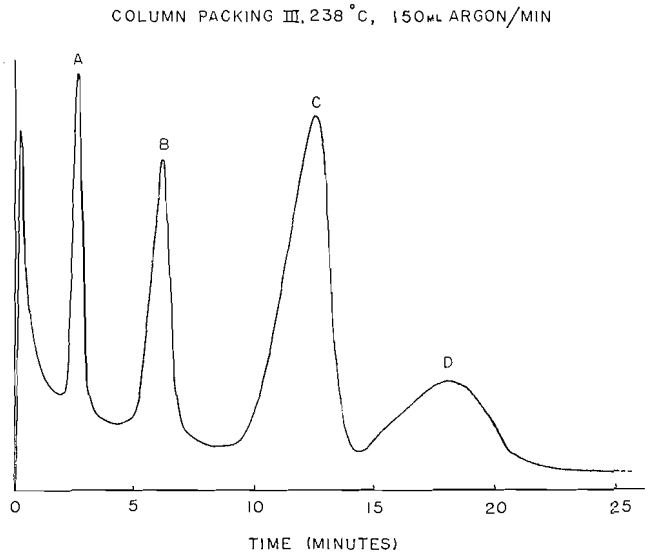

FIG. 3. Separation of disaccharide acetates: (A) α-D-xylopyranosyl α-D-xylopyranoside, (B) 5-*O*-β-D-xylopyranosyl-L-arabitol, (C) sucrose, and (D) cellobiitol.

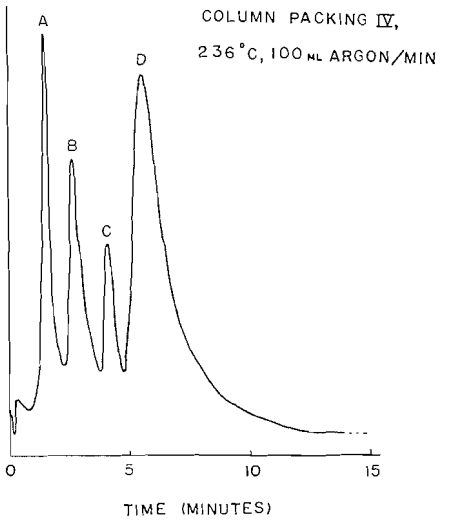

FIG. 4. Separation of disaccharide acetates: (A) α-D-xylopyranosyl α-D-xylopyranoside, (B) 5-*O*-β-D-xylopyranosyl-L-arabitol, (C) sucrose, and (D) maltitol.

Preparative-scale separations (50–150 mg) were made on U-shaped glass columns (250×1.3-cm I.D.) filled with the support material, using the Burrell Kromo-Tog K-2 apparatus fitted with a thermal detector and employing helium as the carrier gas.

Column Packings

Chromosorb W (Johns-Mansville), 60–80 mesh, was washed with 2 *N* hydrochloric acid and then with distilled water until the washings were neutral, was dried at 110°, and was then screened to remove fines. Glass beads, 60 plus mesh (MS-H; Microbeads Inc., Jackson, Mississippi), were washed with chloroform, acetone, water, hot dilute nitric acid, and then with distilled water and dried at 150°.

TABLE II

Retention volumes of fully acetylated disaccharides relative to octa-*O*-acetylsucrose

Disaccharide acetate	Column packing	
	III (238°)	IV (236°)
α-D-Xylopyranosyl α-D-xylopyranoside	0.21	0.34
5-*O*-β-D-Xylopyranosyl-L-arabitol	0.47	0.62
α,α-Trehalose	0.88	1.22
Sucrose	1.00 (12.5 min)	1.00 (4 min)
3-*O*-β-D-Mannopyranosyl-D-mannitol	1.09	1.00
Maltitol	1.30	1.38
Lactitol	—	1.35
Cellobiitol	1.46	1.72
Melibiitol	1.46	1.50
Gentiobiitol	1.74	1.60

The following liquid phases were used: (*a*) Apiezon M vacuum grease (Fisher Scientific Co.), (*b*) butanediol succinate polyester (m.p. 107–109°) prepared according to the directions of Bishop *et al.* (4), (*c*) polyphenylether (F & M Scientific Corp.), (*d*) D-C silicone oil 710 (F & M Scientific Corp.), and (*e*) methyl silicone rubber gum SE-30 (General Electric Co.). The packing materials were prepared by stirring a slurry of a weighed amount of the liquid phase dissolved in chloroform with a weighed amount of the inert support while the bulk of the solvent was removed by stirring the mixture, which was heated on a boiling-water bath. The last traces of the solvent were removed by heating the material *in vacuo* at 140°.

The packing materials were prepared as described below.

(1) Column packing I.—A column constructed of 40 cm of (*a*) a 1:1 v/v mixture of 20% w/w Apiezon M grease on Chromosorb W, 60–80 mesh, and 20% w/w butanediol succinate polyester on Chromosorb W, 60–80 mesh, placed on top of a 77-cm column of (*b*) column packing IV.

(2) Column packing II.—A 1:1:2 v/v intimate mixture of (*a*) 20% w/w Apiezon M grease on Chromosorb W, 60–80 mesh, (*b*) 20% w/w butanediol succinate polyester on Chromosorb W, 60–80 mesh, and (*c*) 0.1% w/w Apiezon M grease on 60 plus mesh glass beads.

(3) Column packing III.—A 1:2 w/w intimate mixture of (*a*) 1% w/w polyphenylether on 60 plus mesh glass beads and (*b*) 1% w/w D-C silicone oil 710 on 60 plus mesh glass beads.

(4) Column packing IV.—Methyl silicone rubber gum SE-30, 1% w/w, on 60 plus mesh glass beads.

The dried column packings were run into the glass columns under gravity, with gentle tapping to ensure even packing and the absence of any cavities. The packed columns were purged with argon gas for 3–4 hours at 20–30° above the operating temperatures before use. The columns could be used for at least 100 analyses before any noticeable deterioration in their resolving power became apparent.

ACKNOWLEDGMENTS

We wish to thank the National Research Council for financial assistance (Grant NRC 706) and Canadian Industries Ltd. for the award of a scholarship to one of us (H. G. J.). We also would like to thank Professor J. K. N. Jones, F.R.S., for his advice and encouragement.

REFERENCES

1. S. W. Gunner, J. K. N. Jones, and M. B. Perry. Chem. & Ind. (London), 255 (1961).
2. S. W. Gunner, J. K. N. Jones, and M. B. Perry. Can. J. Chem. **39**, 1892 (1961).
3. J. E. Lovelock. J. Chromatog. **1**, 35 (1958).
4. A. G. McInnes, D. H. Ball, F. P. Cooper, and C. T. Bishop. J. Chromatog. **1**, 556 (1958).
5. C. T. Bishop and F. P. Cooper. Can. J. Chem. **38**, 388 (1960).
6. H. W. Kircher. Anal. Chem. **32**, 1103 (1960).
7. E. Lederer and M. Lederer. Chromatography. Elsevier Publishing Co. 1957.
8. I. Augestad and E. Berner. Acta Chem. Scand. **8**, 251 (1954).
9. D. F. Mowery, Jr. and G. R. Ferrante. J. Am. Chem. Soc. **76**, 4103 (1954).
10. M. A. Chambers, L. P. Zill, and G. R. Noggle. J. Am. Pharm. Assoc., Sci. Ed. **41**, 461 (1952).

HALF-LIVES OF Cs^{141}, Cs^{142}, AND Cs^{143}

K. FRITZE
McMaster University, Hamilton, Ontario
Received March 27, 1962

ABSTRACT

The method of timed precipitations has been used to measure the half-lives of Cs^{141}, Cs^{142}, and Cs^{143}, which were found to be 24 ± 2 sec, 2.3 ± 0.2 sec, and 2.0 ± 0.4 sec respectively.

(A) INTRODUCTION

The occurrence of Cs^{141}, Cs^{142}, and Cs^{143} among the fission products of U^{235} was implied by the discovery of their respective xenon precursors (1–3). Recently Wahl *et al.* (4) reported a half-life of 25 ± 3 sec for Cs^{141} and also gave evidence that the half-life of Cs^{142} is less than 8 sec.

To measure the decay periods of the three cesium isotopes the method of timed precipitations (5) was used. Cesium is precipitated from a fission-product solution and the resulting compound is later analyzed for a suitable daughter isotope. For this purpose 32-day Ce^{141}, 92-min La^{142}, and 14-min La^{143} were selected. Their activity will be proportional to the number of cesium-parent atoms which were present at the time of the precipitation. By correlating the results of several runs with the time schedule of the precipitations, it is possible to obtain the half-life of each of the three cesium isotopes. Each half-life determination requires a separate set of experiments since it is necessary to optimize precipitation times and counting conditions. Employing perchloric acid as the precipitation agent, this method has been used earlier to measure the half-lives of Rb^{92}, Rb^{93}, and Rb^{94} (6, 7). Because of the very similar chemical behavior of rubidium and cesium, only minor changes had to be made to adopt the principal part of the procedure for the work on the cesium isotopes.

(B) Cs^{141}

Samples of 200 μg U^{235} were irradiated in the pneumatic-rabbit system of the McMaster Reactor in a flux of 3×10^{12} neutrons $cm^{-2}sec^{-1}$ for 20 seconds. The irradiated uranyl nitrate solution (2 ml) was mixed with 25 ml carrier solution containing 900 mg cesium and divided into two approximately equal portions. Cesium was then precipitated as the perchlorate by the addition of the first portion of the fission-product solution to 10 ml perchloric acid (20%) contained in a large membrane-filter assembly. Upon formation of the cesium perchlorate, which occurred immediately, the time was recorded and simultaneously the suction pump was started to draw off the liquid. The precipitate was washed once with dilute perchloric acid. This procedure was then repeated with the second portion of the fission-product solution. The two cesium perchlorate samples were dissolved in 3 *M* hydrochloric acid and small aliquots withdrawn for the later determination of the chemical yield of the cesium precipitation. After the addition of Ba, La, and Ce carriers the main portions were set aside for 2 days. During this time all the Cs^{141} and the intermediate members of its decay chain (18-min Ba^{141} and 3.9-hr La^{141}) decayed to 32-day Ce^{141}. The cerium was then isolated and purified using the method of Glendenin *et al.* (8). The resulting cerium oxalate was β-counted for several days in an automatic low-level unit to determine the relative quantities of Ce^{141} in the two samples.

The chemical yields were obtained by ashing the cerium oxalate and weighing the resulting cerium dioxide. The chemical yields of the cesium precipitations were usually measured by bringing the small aliquots of the perchlorate solutions to complete dryness, dissolving the cesium perchlorate in water, passing the solution over a cation-exchange column, and titrating the resulting acid with 0.05 *M* sodium hydroxide solution. In one case (run No. 4) the Cs^{141} was carried down on rubidium perchlorate and the relative cesium yields were determined by analyzing the small aliquots for their contents of Cs^{137}, which had been added to the rubidium-carrier solution.

Table I shows the results of four half-life measurements for Cs^{141}. The average value

TABLE I

Summary of Cs^{141} half-life data

Run	U^{235} (μg)	Flux (neutrons cm^{-2} sec^{-1} 10^{12})	Duration of irradiation (sec)	$CsClO_4$ precipitation times (sec)		Cs^{141} half-life (sec)
				1st ppt.	2nd ppt.	
1	200	3	20	23.8	47.2	23.7
2	200	3	20	31.4	41.8	21.2
3	200	3	20	24.0	69.6	26.4
4	300	3	20	24.0	48.0	25.6

of 24±2 sec is in very good agreement with the half-life of 25±3 sec obtained by Wahl *et al.* (4).

(C) Cs^{142}

A preliminary estimate had indicated that the half-life of Cs^{142} would be around 5 sec. This was based on an experiment completely analogous to the kind described for Cs^{141}. The two perchlorate precipitates were analyzed for La^{142} using γ-ray spectroscopy. Further work, however, indicated a considerably lower value. In fact, it was found impossible to perform two precipitations in a sufficiently short time interval. The quantity of Cs^{142} in the second precipitate was so small that the amount of the lanthanum daughter could just be detected and not properly measured. Therefore, it was decided to modify the method in the following manner: samples of a mixture of uranyl nitrate and cesium nitrate dissolved in 5 ml water were irradiated. The quantities of U^{235} (300 μg) and cesium (300 mg) were the same for all experiments and the irradiation time of 10 seconds was kept constant within 0.1 second. The recording of the precipitation time was achieved by connecting an electric stop watch to the rabbit-control system. This timer was started by the "reverse air-flow" signal which marks the end of the irradiation and was stopped when the cesium precipitate appeared. Filtration and washing were done as described in Section (B). Besides analysis of the cesium perchlorate for La^{142}, determination of the amount of Cs^{131} which resulted from the (n,γ) reaction on the cesium carriers was carried out. The latter analysis permits the calculation of a correction factor which takes into account both the cesium yields and the possible day-to-day variations in the neutron flux. In other words the method is based on the assumption that the number of Cs^{142} atoms produced is constant for each irradiation and that the quantity of Cs^{142} in the cesium precipitate is only a function of the precipitation time.

Each cesium perchlorate sample was dissolved in dilute hydrochloric acid, and barium and lanthanum carriers were added. Forty minutes after the end of the irradiation

lanthanum hydroxide was precipitated and reprecipitated in the presence of barium-hold-back carrier. The collected supernatants were set aside for the later determination of the correction for the cesium yield and flux variations. The lanthanum hydroxide was dissolved and further purified using tributyl phosphate (9). The lanthanum was finally counted as the oxalate.

The counting of the La^{142} is hampered by the presence of much larger quantities of La^{141}. A gross β-decay curve shows practically no deviation from the 3.9-hr half-life of La^{141}. Associated with the decay of La^{142} is a strong γ ray at 640 Kev (10). In contrast, the only γ line of La^{141} (1.37 Mev) is quite weak (10). The lanthanum samples were therefore γ-counted for 40 minutes through a 2 g cm^{-2} polyethylene absorber using a shielded 3×3 in. NaI (Tl) crystal in connection with a 256-channel analyzer. The area of the 640 Kev peak was determined by numerical integration. Finally, the lanthanum oxalate samples were ashed and the lanthanum oxide weighed to obtain the chemical yields.

From the collected supernatants of the first and second lanthanum hydroxide precipitations, barium was removed as the carbonate and the filtrates were γ-counted under identical geometrical conditions. The γ spectra were quantitatively analyzed for Cs^{134} and gave the correction factor for the chemical yield of the cesium precipitation and the neutron-flux variations.

A total of seven cesium perchlorate precipitations were carried out. The precipitation times ranged from 4.9 to 12.3 seconds, measured from the end of the respective irradiations. Figure 1 shows the resulting decay curve, indicating a half-life of 2.3±0.2 sec for Cs^{142}. The value is consistent with the upper limit of 8 sec given by Wahl *et al.* (4).

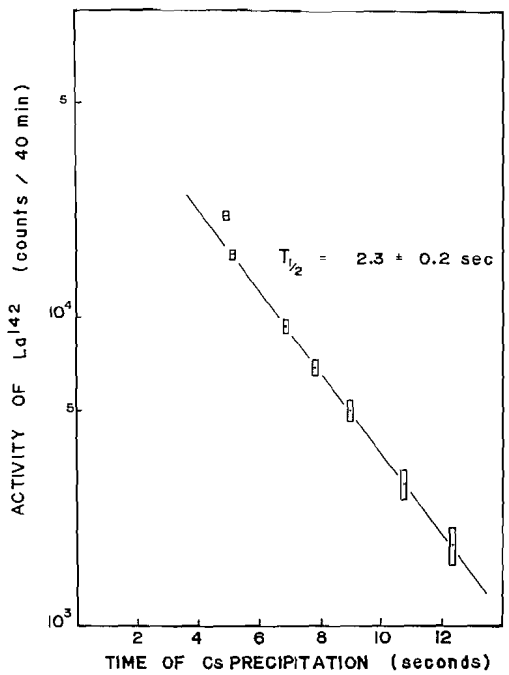

FIG. 1. Half-life of Cs^{142} from the timed precipitation of fission-product cesium. The normalized activity of La^{142} found during the later analysis of each cesium precipitate is plotted against the time of the cesium perchlorate precipitation as measured from the end of the respective irradiation.

(D) Cs^{143}

The half-life of Cs^{143} was determined using the same procedure as outlined for Cs^{142}. Since the fission yield of Cs^{143} is lower (4), the amount of U^{235} was increased to 500 μg. The cesium perchlorate samples were analyzed in the following manner. The precipitate was rinsed off the membrane filter into a 50-ml centrifuge tube containing barium and lanthanum carriers. Lanthanum hydroxide was precipitated and centrifuging was started at exactly 2 minutes after the end of the irradiation. At this time the intermediate member of the decay chain, 12-sec Ba^{143} (4), had decayed completely. On the other hand, only relatively small quantities of La^{142} and La^{141} had been formed, due to the holdup by the 11-min Ba^{142} and the 18-min Ba^{141}. From then on the purification of the lanthanum, as described in Section (C), was carried out as rapidly as possible and the counting was usually started at 21 minutes after the end of the irradiation.

The lanthanum oxalate samples were β-counted with a unit consisting of a 2×2 in. plastic scintillator coupled with an EMI 9536 photomultiplier tube, a DD2 amplifier, and a single-channel analyzer. Only β rays with energies in the interval 2.6 to 3.2 Mev were recorded, in 200-second intervals automatically for about 4 hours. In this way the conditions for the analysis of the La^{143} having a β energy of 3.3 Mev (9) were optimized. The β energies of La^{141} and La^{143} are 2.4 and 4.4 Mev respectively (10). The resulting decay curves were analyzed for their 14-min La^{143} and 92-min La^{142} components. The contribution of La^{142} to the initial counting rate ranged from approximately 10 to about 20%, depending on the time of the original cesium perchlorate precipitation. The initial counting rate itself was 450 c.p.m. for the strongest lanthanum sample (corresponding to the earliest cesium precipitation) and only about 70 c.p.m. for the weakest lanthanum sample. Consequently the statistics of the individual points which make up the decay curve of Cs^{143} were fairly poor. The preparation and analysis of five cesium perchlorate precipitates was done over a period of 3 days. A test of the counting unit over a similar time showed that there was a random drift of the window. No pattern in the shifting could be detected. For example, the unit would be perfectly stable for hours, then fairly slowly drift in one direction, remain constant, and after many hours return slowly to more or less the original position. The total spread of the shifting did not exceed 1%. However, the counting of a Ru–Rh^{106} standard, which has a spectrum similar to that of La^{143}, showed that this can cause fluctuations of approximately 10% in the counting rate. An effort was made to correct for this by storing the events which passed through the window in a 256-channel analyzer concurrently with the decay measurement. From the position of the window an estimate of the correction term was made and applied to the result of the decay-curve analysis. But since this is only an estimate the uncertainty in each point of the Cs^{143} decay curve is necessarily increased.

The corrections for the chemical yields were carried out using identical procedures as described above for Cs^{142}. The decay curve of Cs^{143} is shown in Fig. 2, giving a half-life of 2.0 ± 0.4 sec. It was pointed out above that in the lanthanum samples the amount of La^{142} increased relative to the quantity of La^{143} with increasing time of precipitation. Knowing the half-life of Cs^{142}, it is, in principle, possible to calculate the half-life of Cs^{143} from these data. In practice the errors of these ratios are too large to permit a meaningful calculation. However, the trend of the ratio values indicates that the half-life of Cs^{143} is shorter than that of Cs^{142}, even though the errors are such that the individual measurements overlap (Cs^{142} = 2.3 ± 0.2 sec and Cs^{143} = 2.0 ± 0.4 sec).

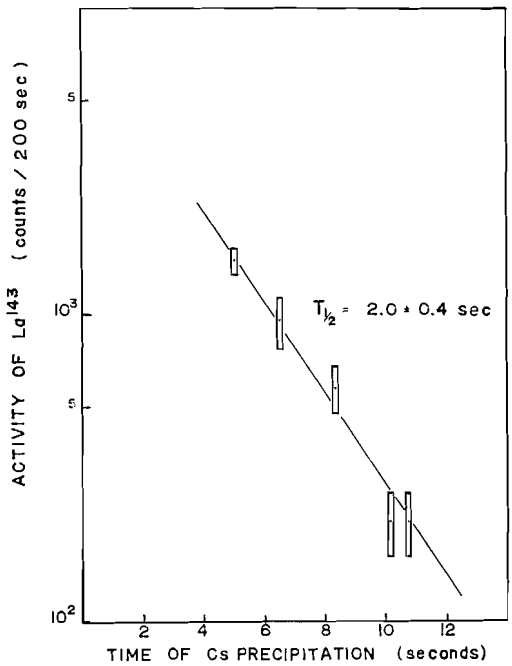

FIG. 2. Half-life of Cs^{143} from the timed precipitation of fission-product cesium. The normalized activity of La^{143} found during the later analysis of each cesium precipitate is plotted against the time of the cesium perchlorate precipitation as measured from the end of the respective irradiation.

(E) DISCUSSION

All features and possible limitations of the method of timed precipitations have been discussed previously (5–7). One would usually expect that the largest errors originate from the uncertainty of the timing and particularly from the assumption that the formation process of the precipitate is identical from sample to sample. Furthermore, it has been shown that daughter atoms (i.e. Sr and Ba) are easily extracted from the precipitate by the washing solution (6). This effect should have the most serious consequences in cases of short half-lives (<10 sec) since it is, in practice, impossible to exactly duplicate the precipitation and washing procedure on a time scale involving fractions of seconds. The very good agreement of the results of Wahl *et al.* (4) and those of this work for the half-life of Cs^{141} (25 ± 3 sec and 24 ± 2 sec) indicates that these effects are at least not too serious for somewhat longer half-lives. Although Wahl's method was similar, it was based on the timed removal of the Ba^{141} daughter (as the nitrate) rather than on the direct precipitation of the cesium.

Recently Stehney and Perlow (11) detected a delayed-neutron precursor among the decay products of fission-product krypton and found its half-life to be about 6 sec. This value agrees with the 5.3 ± 0.5-sec half-life of Rb^{92} and the 5.6 ± 0.5-sec half-life of Rb^{93} (6). Although certain other considerations favor Rb^{93} as a delayed-neutron precursor, the measurements of Stehney and Perlow indicate, in any case, that the method of timed precipitations is quite reliable for short half-lives.

For the case of very short half-lives (<3 sec), which require a new irradiation for each point of the decay curve, no independent check is available at present. Here an additional source of error is introduced by the possibility that the production of the nuclide in

question is not constant from sample to sample. Experimental evidence, however, indicates that the errors in the counting of the respective daughter isotopes are more serious. This is mainly due to the fact that these nuclides themselves are fairly short-lived and that their relative quantities must be determined in the presence of the large amounts of other isotopes of the same element.

ACKNOWLEDGMENTS

The author wishes to thank T. J. Kennett for many helpful discussions and W. V. Prestwich and T. Erme for assistance during the course of the experimental work. The financial assistance given by the National Research Council and the cooperation of the reactor staff are greatly appreciated.

REFERENCES

1. O. Hahn and F. Strassmann. Naturwiss. **30**, 324 (1942).
2. K. Wolfsberg, D. R. Nethaway, H. P. Malan, and A. C. Wahl. J. Inorg. & Nuclear Chem. **12**, 201 (1960).
3. E. L. Brady and N. Sugarman. National nuclear energy series—PPR. Vol. 9. McGraw-Hill Book Co., New York. 1951. p. 613.
4. A. C. Wahl, R. L. Ferguson, D. R. Nethaway, D. E. Troutner, and K. Wolfsberg. To be published.
5. N. Sugarman. J. Chem. Phys. **17**, 11 (1949).
6. K. Fritze and T. J. Kennett. Can. J. Phys. **38**, 1614 (1960).
7. K. Fritze, T. J. Kennett, and W. V. Prestwich. Can. J. Chem. **39**, 675 (1961).
8. L. E. Glendenin, K. F. Flynn, R. F. Buchanan, and E. P. Steinberg. Anal. Chem. **27**, 59 (1955).
9. K. Fritze, T. J. Kennett, and W. V. Prestwich. Can. J. Phys. **39**, 662 (1961).
10. Nuclear Data Sheets. Natl. Acad. Sci.—Natl. Research Council, Publ. Washington, D.C.
11. A. F. Stehney and G. J. Perlow. Bull. Am. Phys. Soc. Ser. II, **6**, 62 (1961).

COORDINATION COMPLEXES OF METAL ALKOXIDES

PART I. METAL ALKOXIDE – HYDRAZINE COMPLEXES

M. S. BAINS[1] AND D. C. BRADLEY[2]
Department of Chemistry, Birkbeck College, Malet Street, London, W.C.1, England

Received February 1, 1962

ABSTRACT

The field of metal alkoxide coordination compounds is surveyed briefly. The preparation of moderately stable complexes of hydrazine with aluminum isopropoxide, titanium ethoxide, titanium isopropoxide, and zirconium isopropoxide is described. Some reactions of these new complexes are reported.

INTRODUCTION

An interesting feature of the metal alkoxides is their preference for auto complex formation (i.e. polymerization) rather than the formation of addition complexes with typical donor molecules. A general rule stating that the metal alkoxide strives to achieve covalency expansion of the metal with the minimum degree of polymerization has been proposed to explain this behavior in terms of structural models (1). Another property of these compounds is the formation of double alkoxides (alkoxide salts), such as: $Li[Al(OEt)_4]$; $Ca[Al(OEt)_4]_2$; $K_2[Be(OEt)_4]$; $K[Li(OC_3H_7)_2]$. More than 50 such compounds were isolated by Meerwein and Bersin (2) and these formulations were supported by appropriate titrations of the reactants in non-aqueous solvents, using conventional indicators.

In spite of this great tendency on the part of the metal to attain its covalency maximum, no coordination complexes resulting from the simple union of an alkoxide and a neutral molecule were reported prior to 1951 (3), and among the large number of new alkoxides of transition metals prepared in recent years only the following complexes have been reported: $Ti(OBu^i)_4,Bu^iOH$; $Zr(OPr^i)_4,Pr^iOH$; $Zr(OPr^i)_4,C_5H_5N$; $Zr(OC_6H_5)_4,C_6H_5OH$; $Ce(OPr^i)_4,Pr^iOH$; $Ce(OPr^i)_4,C_5H_5N$; $Ce(OC_4H_6Cl_3)_4,C_5H_5N$; $Pu(OPr^i)_4,Pr^iOH$; $Pu(OPr^i)_4,C_5H_5N$; $Hf(OPr^i)_4,Pr^iOH$; $Th(OC_4H_6Cl_3)_4,2C_5H_5N$; $Sn(OPr^i)_4,Pr^iOH$.

The lack of complex formation in boron and aluminum alkoxides was discussed on the basis of X-ray crystallographic data, and the difference in the reducing power of boron and aluminum alkoxides in the Meerwein–Ponndorf–Verley reduction was attributed to their relative ability to coordinate with carbonyl compounds in solution (3).

It has been suggested (4) that oxygen in the alkoxide group attached to a metal atom has a greater electron density and hence can be a better donor than oxygen in the typical organic donor molecules (e.g. alcohols, ethers, esters, ketones, etc.). This may well explain why metal alkoxides polymerize instead of complex with donor molecules. The alkoxide salt formation is readily interpreted as due to the greater negative charge on the oxygen of the alkoxide group attached to the more electropositive metal. It also appears from experimental observation that even nitrogen bases rarely form complexes with metal alkoxides. Zirconium isopropoxide, which forms fairly stable addition compounds with isopropyl alcohol and pyridine, would not coordinate with donors such as diethyl ether, triethylamine, thiourea, dimethylamine, or α,α-dipyridyl (5). We have also found that aluminum alkoxides do not form stable complexes with bases such as ammonia, pyridine,

[1]*Present address: Department of Chemistry, Panjab University, Chandigarh 3, India.*
[2]*Present address: Department of Chemistry, The University of Western Ontario, London, Ontario.*

diethylamine, dimethylamine, triethylamine, quinoline, and picolines; ether; or acetone. However, the fact that the donor character of the solvent lowered the degree of polymerization of tantalum alkoxides (6) under ebullioscopic conditions coupled with Chelinzev's evidence (7) based on thermal data gives strong support to the view that addition complexes may be formed in solution. Moreover, coordination is proposed as the first step in the mechanism of certain organic reactions which are catalyzed by polymeric alkoxides. An interesting example of the formation of weak complexes was revealed by the existence of an insoluble ammoniate of ferric ethoxide, $Fe(OEt)_3,xNH_3$, where $x = 1$–3, which was coprecipitated with ammonium chloride in the synthesis of ferric ethoxide by the ammonia method (8).

A consideration of the addition complexes of metal chloride alkoxides (4) suggested that as chlorines are successively replaced by alkoxide groups, the acceptor ability of the central metal atom decreases. Polymerization due to metal–oxygen intermolecular bonding increases and the coordination of the nucleophilic reagent to the metal atom of the alkoxide steadily decreases. Thus in the case of zirconium, the compounds $ZrCl_4$,-CH_3COOEt; $ZrCl_3OEt,EtOH$; $ZrCl_2(OPr^i)_2,Pr^iOH$; $ZrCl(OEt)_3,EtOH$; and $Zr(OEt)_4$ were obtained. The compound $ZrCl_3(OEt),EtOH$ is so stable that the alcohol of addition cannot be removed from it but zirconium ethoxide does not form an addition complex.

If an electron-attracting group is substituted in the alkyl group of the alkoxide group, the electron density on the oxygen atom can be decreased and thus coordination of a ligand is enhanced. For example, when zirconium isopropoxide was treated with anhydrous chloral (5) the tetrakis-(trichloroethoxy)-zirconium produced retained 2 molecules of acetone in the complex $Zr(OCH_2CCl_3)_4,2(CH_3)_2CO$. This emphasizes the electronic arguments for the absence of coordination complexes of metal alkoxides. The chlorine atoms in the trichloroethoxide group have made the chloroalkyl group electron attracting instead of electron releasing. This has consequently drawn on the electron density of the oxygen atom on the one hand and to a diminished extent made the metal more electrophilic. Thus the oxygen in the trichloroethoxide group is a weaker donor than the oxygen in acetone. Gal *et al.* (11) have shown that certain insoluble carbonyl compounds would dissolve in the presence of aluminum monochloride diisopropoxide, but not in the presence of aluminum triisopropoxide. It appears that the carbonyl compound coordinates more readily with the monochloride and thus goes into solution.

Besides these electronic factors, the steric factors cannot be ignored in the formation of addition complexes, although it seems likely that in many cases steric factors would favor the addition of a ligand rather than polymerization. The monomeric nature of certain alkoxides was interpreted in terms of steric arguments (9).

In a recent publication (10) it was reported that the complex $Ti(OPr^i)_4,EtNH_2$ crystallized from a concentrated mixture of the alkoxide and excess ethylamine in *n*-decane. It was also established by the vapor pressure method that both $Ti(OPr^i)_4$,-$2EtNH_2$ and $Ti(OPr^i)_4,EtNH_2$ existed in solution as unstable complexes.

In attempts to find insoluble complexes of aluminum alkoxides we have found that hydrazine forms stable soluble complexes with metal alkoxides. The compounds isolated and the related reactions are described and discussed in this communication.

EXPERIMENTAL

Materials

The alkoxides used for this research were prepared by the methods described in the literature and were purified by distillation under reduced pressure: aluminum isopropoxide (12, 13); aluminum *tert*-butoxide (14); titanium ethoxide (15); titanium isopropoxide (16); zirconium isopropoxide isopropylate (17). The purity of the above compounds was checked by the standard analytical methods given in the cited literature.

Solvents

The solvents used were of "Analytical Reagent" grade. Benzene, diethyl ether, and petroleum ether (b.p. 40–60; 60–80°) were dried over freshly extruded sodium wire. Sodium-dried benzene was further dried by azeotropic distillation.

Bases

Pyridine, diethylamine, triethylamine, quinoline, α-picoline, and β-picoline were kept over potassium hydroxide pellets and then refluxed over a fresh batch of potassium hydroxide and fractionally distilled. A second distillation was performed if it was thought necessary. Dimethylamine was used as such from the ampoule.

Hydrazine (98%) was kept over potassium hydroxide for 2 days and then three successive distillations over potassium hydroxide through a small reflux column were performed. The liquid thus obtained was titrated against potassium iodate solution in strong hydrochloric acid, when 100±0.5% hydrazine was estimated. This purified hydrazine was kept in a desiccator and if left for more than a week was freshly distilled before use.

Analytical Methods

Zirconium and titanium were determined using the method described in the source describing the preparation of their alkoxides. Aluminum was determined by precipitating and weighing as the oxinate (18).

The alkoxide content of the pure metal alkoxides was determined by the method described by Bradley *et al.* (19) in the case of pure alkoxides.

The hydrazine content of the complexes was determined by the following iodate method. Hydrochloric acid (conc., 30 ml) and water (20 ml) were taken in an iodine flask (250 ml), and carbon tetrachloride (5 ml) was added as indicator. A sample containing about 0.05 g of hydrazine was added and the solution titrated with 0.15 *N* potassium iodate solution with shaking between the addition until the organic layer (CCl_4) was first decolorized. This method was reliable even in the presence of alkoxide groups, since under the conditions described, blank experiments with known amounts of hydrazine and excess alcohols showed no interference by the alcohol. However, the alkoxide content could not be estimated by the usual chromic acid method due to interference by the hydrazine.

1. Reaction between Aluminum Isopropoxide and Hydrazine

To a solution of aluminum isopropoxide (4.7 g) in anhydrous petroleum ether (40–60° C) in a flask (100 ml) an excess of hydrazine (8.5 g) was added and caused the precipitation of a white solid. The reaction mixture was mildly refluxed and allowed to cool, when a crystalline product separated. The excess of solvent and hydrazine was evaporated off at low pressure and the product was dried under 0.1 mm pressure. The crystalline product on analysis corresponded to aluminum isopropoxide hydrazinate, $Al(OPr^i)_3,N_2H_4$. Found: Al, 11.4, 11.5; N_2H_4, 13.50, 13.54%. $Al(OPr^i)_3,N_2H_4$ requires: Al, 11.47; N_2H_4, 13.56%.

In another experiment hydrazine (1.5 g) was added to a benzene solution (50 g) of aluminum isopropoxide (9.4 g). On shaking, a small precipitate appeared, and a sticky product was obtained on evaporation of the benzene under reduced pressure. An effort to crystallize it from benzene failed but when an excess of hydrazine was added to the petroleum ether solution heat was evolved and a precipitate appeared. The product gave the same results as before. Found: Al, 11.4, 11.4; N_2H_4, 13.52%. The above product on further evacuation at 0.1 mm pressure for 5–6 hours corresponded to $Al(OPr^i)_3,\frac{1}{2}N_2H_4$. Found: Al, 12.5, 12.7; N_2H_4, 7.51, 7.48%. $Al(OPr^i)_3,\frac{1}{2}N_2H_4$ requires: Al, 12.3; N_2H_4, 7.30%. The final product did not lose any further amount of hydrazine.

2. Reaction between Aluminum tert-Butoxide and Hydrazine

To a solution of aluminum *tert*-butoxide (1.82 g) in ether, hydrazine (0.5 g) was added. The clear supernatant solution was decanted off and the solvent removed under low vacuum. The analysis of the product corroborated with the empirical composition $Al(OBu^t)_3,2\frac{1}{2}N_2H_4$. Found: Al, 8.6, 8.5; N_2H_4, 25.50, 25.70%. $Al(OBu^t)_3,2\frac{1}{2}N_2H_4$ requires: Al, 8.30; N_2H_4, 24.54%.

The above product fumed strongly in the air. It was subjected to evacuation at 0.1 mm pressure for half an hour. On analysis the product was found to have no hydrazine. Found: Al, 11.8, 11.9%. $Al(OBu^t)_3$ requires: Al, 10.95%.

Attempts to isolate coordination complexes of quinoline, pyridine, diethylamine, triethylamine, dimethylamine, ether, or ammonia with aluminum isopropoxide failed. The product on removal of volatile contents always corresponded to aluminum isopropoxide.

3. Reaction between Titanium Ethoxide and Hydrazine

To a solution of titanium ethoxide (2.2 g) in ether (60 ml) hydrazine (0.75 g) was added. A colorless precipitate appeared, which turned light yellow after some time. Then the crystals redissolved until a very small amount remained. On evaporation of the solvent under water pump pressure a colorless crystalline product was obtained. It was then dried at 0.1 mm pressure for a while, and left a product whose analysis suggested that $Ti(OEt)_4,\frac{1}{2}N_2H_4$ was formed. Found: Ti, 21.0, 20.9, 21.1; N_2H_4, 6.3%. $Ti(OEt)_4,\frac{1}{2}N_2H_4$ requires: Ti, 19.65; N_2H_4, 6.56%.

4. Reactions of Titanium Isopropoxide and Hydrazine

Titanium isopropoxide (7.7 g) in diethyl ether (100 ml) was caused to react with an excess of hydrazine and the solution was shaken during mixing. After being allowed to stand for a few minutes the clear solution was decanted off from the excess of hydrazine, which remained as a lower layer. Ether was removed under water pump pressure and a colorless crystalline product obtained gave an analysis corresponding with the composition $Ti(OPr^i)_4,N_2H_4$. Found: Ti, 15.3, 15.0, 15.0; N_2H_4, 9.8, 9.7%. Calculated for $Ti(OPr^i)_4,N_2H_4$; Ti, 15.16; N_2H_4, 10.13%.

In another experiment titanium isopropoxide (2.39 g) and hydrazine (3.4 g) were heated by means of an oil bath for about 3 hours at about 130° C. An explosion took place when the temperature was raised a little further. The green material collected from the side of the condenser did not react even with hot chromic acid. In these experiments it was noted that the addition of hydrazine to the alkoxide was an exothermic process.

5. Reactions between Zirconium Isopropoxide Isopropylate and Hydrazine

Hydrazine (0.33 g) in diethyl ether (50 ml) was allowed to react with zirconium isopropoxide isopropylate, $Zr(OPr^i)_4,Pr^iOH$ (2.5 g). Removal of the solvent and excess hydrazine by evaporation under 0.1 mm pressure left zirconium isopropoxide hydrazinate. Found: Zr, 25.9; N_2H_4, 8.3%. $Zr(OPr^i)_4,N_2H_4$ requires: Zr, 25.4; N_2H_4, 8.9%.

DISCUSSION

The situation in the coordination complexes of metal alkoxides has been briefly surveyed in the introduction. This study has shown that hydrazine forms some interesting, moderately stable complexes with metal alkoxides. The following complexes appear to be established by analytical evidence: aluminum isopropoxide hydrazinate, $Al(OPr^i)_3,N_2H_4$; aluminum isopropoxide hemihydrazinate, $Al(OPr^i)_3,\frac{1}{2}N_2H_4$; titanium isopropoxide hydrazinate, $Ti(OPr^i)_4,N_2H_4$; titanium ethoxide hemihydrazinate, $Ti(OEt)_4,\frac{1}{2}N_2H_4$; zirconium isopropoxide hydrazinate, $Zr(OPr^i)_4,N_2H_4$.

Although it is clear that more work must be done in order to elucidate the structure of these complexes a few comments now are not out of place. For example, it is noteworthy that aluminum isopropoxide has a much greater affinity for hydrazine than has aluminum *tert*-butoxide. The failure of $Al(OBu^t)_3$ to coordinate hydrazine is presumably not due to steric factors, since the *tert*-butoxide is dimeric and there is less steric hindrance to the coordination of a molecule of hydrazine than to dimerization. We assume that bridging by *tert*-butoxide groups is favored by the high electron density on the oxygen which results from the large electron release of the Bu^t group.

The ability of hydrazine to form complexes with metal alkoxides is at first sight surprising in view of the fact that this ligand is a fairly weak base. It is tempting to suggest that the hydrazine behaves as a chelating ligand, thereby enhancing the stability of the complex. This would require the unusual arrangement (I) of a three-membered ring involving the metal and two nitrogens.

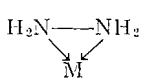

(I)

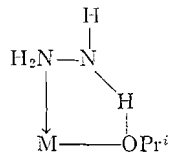

(II)

Alternatively the hydrazine might behave as a monodentate ligand but with additional stabilization due to ring formation in the hydrogen-bonded structure (II). We were unable to determine accurate molecular weights on any of the new complexes due to their instability in solution. Therefore it is not possible to assign structures to these complexes at present.

During this work it was observed that the hydrazine complexes with titanium and zirconium alkoxides underwent further chemical reaction on standing in solution and on being heated. The details of these reactions have not yet been elucidated but preliminary results suggest that alkoxide groups may be replaced by hydrazine, giving compounds of the type $M(OR)_{4-x}(N_2H_{4-x})$. This is remarkable because it has been found that amines do not as a rule displace alkoxide groups whereas alcohols displace amines very vigorously from dialkylamino derivatives (21). However, it was found that the "titanium hydrazinate" prepared by means of the following reaction:

$$x\mathrm{Ti(NEt_2)_4} + x\mathrm{N_2H_4} \rightarrow [\mathrm{Ti(N_2)}]_x + 4x\mathrm{Et_2NH},$$

exploded violently after the removal of volatile products at room temperature (20). Thus it seems reasonable to suggest that the explosion in experiment 4 was due to an unstable compound, $Ti(OPr^i)_{4-x}(N_2H_{4-x})$, where $x \rightarrow 4$.

ACKNOWLEDGMENT

One of the authors (M. S. Bains) wishes to thank S. Bhagar Singh Bains for the financial support which enabled him to carry out this research.

REFERENCES

1. D. C. Bradley. Nature, **182**, 1211 (1958).
2. H. Meerwein and T. Bersin. Ann. **476**, 113 (1929).
3. L. M. Jackman and A. K. Macbeth. J. Chem. Soc. 3252 (1952).
4. M. S. Bains. Ph.D. Thesis, University of London, London, England. 1959. D. C. Bradley. Progress in inorganic chemistry. Vol. 2. Interscience, New York. 1960. p. 334.
5. D. C. Bradley, R. N. P. Sinha, and W. Wardlaw. J. Chem. Soc. 4651 (1958).
6. D. C. Bradley, W. Wardlaw, and A. Whitley. J. Chem. Soc. 726 (1955).
7. V. Chelinzev. Bull. soc. chim. France, **35**, 741 (1924).
8. D. C. Bradley, R. K. Multani, and W. Wardlaw. J. Chem. Soc. 126 (1958).
9. D. C. Bradley. Alkoxides, Advances in Chem. Ser. No. 23. 10 (1959).
10. C. M. Cook, Jr. J. Am. Chem. Soc. **81**, 3828 (1959).
11. Gy. Gal, G. Tokar, and I. Simonyi. Acta Chim. Acad. Sci. Hung. **7**, 421 (1955).
12. R. C. Mehrotra. J. Indian Chem. Soc. **30**, 585 (1953).
13. W. G. Young, W. H. Hartung, and F. S. Crossley. J. Am. Chem. Soc. **58**, 100 (1936).
14. W. Wayne and H. Adkins. Org. Syntheses, **21**, 8 (1941).
15. D. C. Bradley, D. C. Hancock, and W. Wardlaw. J. Chem. Soc. 2773 (1952).
16. D. C. Bradley, R. C. Mehrotra, and W. Wardlaw. J. Chem. Soc. 2027 (1952).
17. D. C. Bradley and W. Wardlaw. J. Chem. Soc. 280 (1951).
18. A. I. Vogel. Quantitative inorganic analysis. 2nd ed. 1951. p. 365.
19. D. C. Bradley, F. M. A. Halim, and W. Wardlaw. J. Chem. Soc. 3450 (1950).
20. M. S. Bains. Unpublished results.
21. D. C. Bradley and I. M. Thomas. J. Chem. Soc. 3857 (1960). I. M. Thomas. Can. J. Chem. **39**, 1386 (1961).

METALLO-ORGANIC COMPOUNDS CONTAINING METAL–NITROGEN BONDS

PART III. DIALKYLAMINO COMPOUNDS OF TANTALUM[1]

D. C. BRADLEY AND I. M. THOMAS[2]
Department of Chemistry, University of Western Ontario, London, Ontario

Received March 6, 1962

ABSTRACT

Reactions involving $TaCl_5$ and LiX (where X = NMe_2, NEt_2, NPr^n_2, NBu^n_2, $NMeBu^n$, and NC_5H_{10}) were shown to produce substantially the pentaderivatives TaX_5. The thermal decomposition of TaX_5 (X = NMe_2, NEt_2, NPr^n_2, NBu^n_2, and $NMeBu^n$) was studied and only $Ta(NMe_2)_5$ could be sublimed unchanged. In other cases the main product of decomposition was a quinquevalent compound $RN{=}Ta(NR_2)_3$ and the secondary amine R_2NH. Some olefin and quadrivalent $Ta(NR_2)_4$ were also detected and it is believed that decomposition involves the following sequence:

$$Ta(NR_2)_5 \rightarrow Ta(NR_2)_4 + NR_2 \rightarrow RN{=}Ta(NR_2)_3 + HNR_2 + (R{-}H, \text{olefin}).$$

This is in contrast to the behavior of niobium compounds, which appears to be:

$$Nb(NR_2)_5 \rightarrow Nb(NR_2)_4 + NR_2 (\rightarrow HNR_2, \text{imine, etc.}).$$

INTRODUCTION

In a previous communication (1) we reported that lithium dialkylamides reacted with the tetrachlorides of titanium or zirconium and formed the corresponding tetrakis-(dialkylamino)-metal compounds:

$$MCl_4 + 4LiNR_2 \rightarrow M(NR_2)_4 + 4LiCl;\ M = Ti, Zr.$$

Aminolysis reactions (viz. $M(NR_2)_4 + HNR'_2 \rightarrow M(NR'_2)(NR_2)_3 + HNR_2$) revealed that the dialkylamino groups exerted considerable steric hindrance to nucleophilic attack on the central metal atom. In a recent communication (2) we reported on the reactions involving niobium pentachloride and several lithium dialkylamides. It appeared that the very powerful steric effects of the dialkylamino groups precluded the formation of stable pentakis-(dialkylamino)-niobium compounds except in the cases of the least bulky ligands, such as —NMe_2, —$NMeBu^n$, and —NC_5H_{10} (piperidide). With the more bulky ligands (—NR_2, where R = Et, Pr^n, Bu^n) the final products of distillation *in vacuo* were the tetrakis-(dialkylamino)-niobium(IV) derivatives. Preliminary results on the reactions of tantalum pentachloride with lithium dialkylamides (3) showed that tantalum resembled niobium in forming a stable pentakis-(dimethylamino) compound. However, with lithium diethylamide the final products obtained by distillation *in vacuo* contained mainly the surprising compound $EtN{=}Ta(NEt_2)_3$. In this paper we report the results from a detailed study of the reactions of tantalum pentachloride with various lithium dialkylamides, with special attention to the composition of the initial products of reaction.

RESULTS AND DISCUSSION

In these reactions the tantalum pentachloride was added to a suspension of the equivalent quantity of lithium dialkylamide in pentane at room temperature. After removal of the insoluble lithium chloride by filtration the tantalum product was isolated

[1]*For Part II see ref. 2.*
[2]*Present address: Stauffer Chemical Company, Anderson Division, Weston, Michigan, U.S.A.*

by evaporation of the solvent *in vacuo*, thus avoiding the heating involved in our earlier technique (3). By this means it was demonstrated that pentakis-(dialkylamino) derivatives $Ta(NR_2)_5$ (R = Me, Et, Pr^n, Bu^n) and also $Ta(NMeBu^n)_5$ and $Ta(NC_5H_{10})_5$ were initially formed in a substitution reaction:

$$TaCl_5 + 5LiNR_2 \rightarrow Ta(NR_2)_5 + 5LiCl.$$

This is in contrast to the behavior of niobium pentachloride, which under comparable conditions (2) gave products which contained increasing proportions of quadrivalent niobium as the size of the dialkylamino group was increased.

The thermal stability of $Ta(NMe_2)_5$ was demonstrated by the recovery of 73% of the compound as a pale yellow sublimate (100° C at 0.1 mm). After heating a sample at 180° C for an hour about 60% was recovered by sublimation *in vacuo*.

The impure $Ta(NEt_2)_5$ decomposed when heated and a volatile product distilled over at 120° C at 0.1 mm. From the tantalum and nitrogen analyses and a chemical determination of the valency it was deduced that the product consisted of $Ta(NEt_2)_4$ (55%), $Ta(NEt_2)_5$ (10%), and $EtN{=}Ta(NEt_2)_3$ (35%). In a repetition of the experiment the final distillate appeared to be $Ta(NEt_2)_4$ (38%), $Ta(NEt_2)_5$ (15%), and $EtN{=}Ta(NEt_2)_3$ (47%). These results are significantly different from those obtained when the reaction was conducted in diethyl ether (3) and the final distillate appeared to be substantially pure $EtN{=}Ta(NEt_2)_3$. Repetition of the reaction in ether has confirmed the earlier work, since the final distillate appeared to consist of $Ta(NEt_2)_4$ (20%) and $EtN{=}Ta(NEt_2)_3$ (80%). Further experiments showed that the product obtained by distillation from the reaction in petrol, when heated in diethylamine solution, was also converted to a mixture of $Ta(NEt_2)_4$ (20%) and $EtN{=}Ta(NEt_2)_3$ (80%). This suggests that the tetrakis-(diethylamino)-tantalum is slowly oxidized by loss of an ethyl group from one diethylamino group and converted to $EtN{=}Ta(NEt_2)_3$. This behavior underlines the lower stability of the quadrivalent tantalum compound relative to $Nb(NEt_2)_4$, which does not appear to be converted to $EtN{=}Nb(NEt_2)_3$.

The principal product from the reaction involving lithium di-*n*-propylamide and tantalum pentachloride was pentakis-(di-*n*-propylamino)-tantalum contaminated with about 10% of tetrakis-(di-*n*-propylamino)-tantalum. Heating the product *in vacuo* gave an orange liquid which distilled at 150° at 0.1 mm and contained 93% quinquevalent tantalum. Analysis showed that this product was substantially $Pr^nN{=}Ta(NPr_2^n)_3$. Treatment of this product with isopropanol liberated both primary-propylamine and di-*n*-propylamine and converted the tantalum to tantalum pentaisopropoxide. In addition to forming $Pr^nN{=}Ta(NPr_2^n)_3$ the thermal decomposition of $Ta(NPr_2^n)_5$ gave two more volatile fractions. One fraction, which condensed at ca. −78° C, was shown by gas chromatographic analysis (g.c.a.) to be 95% di-*n*-propylamine. The amount of di-*n*-propylamine was approximately 1 molecule per molecule of $Ta(NPr_2^n)_5$. The most volatile fraction, which condensed at ca. −180°, was shown by g.c.a. to contain propylene with some propane and butane or isobutylene.

A similar sequence of reactions occurred following the addition of $TaCl_5$ to lithium di-*n*-butylamide. The initial product was substantially $Ta(NBu_2^n)_5$ and this when heated at 180° *in vacuo* gave two volatile fractions. The most volatile was predominantly 1-butene (85%) with small proportions of isobutylene (or butane) and *cis*- and *trans*-2-butene. The other fraction was di-*n*-butylamine (95%) in an amount corresponding to 1 molecule per molecule of $Ta(NBu_2^n)_5$. Besides the two organic fractions a third, least volatile fraction (b.p. 180° at 0.1 mm) was predominantly $Bu^nN{=}Ta(NBu_2^n)_3$. The presence of both primary butylamino and di-*n*-butylamino groups in the latter was

confirmed by gas chromatographic analysis of the products of *n*-butanolysis, by means of which the tantalum was converted to tantalum pentabutoxide.

It appears that the overall products of thermal decomposition of tantalum pentadialkylamides conform to the following equation (for the di-*n*-propylamide):

$$Ta[N(CH_2CH_2CH_3)_2]_5 \rightarrow CH_3CH_2CH_2N{=}Ta[N(CH_2CH_2CH_3)_2]_3 + HN(CH_2CH_2CH_3)_2 + CH_2{=}CHCH_3.$$

This behavior is in striking contrast to that of the corresponding niobium compounds, which are converted to tetrakis-(dialkylamino) compounds. We are inclined to the view that the primary cause of decomposition of $M(NR_2)_5$ (M = Nb, Ta) is the same in both cases, namely intramolecular congestion due to the steric effect of dialkylamino groups. It is tempting to suggest that a dialkylamino radical is released from the pentakis compounds and that in the case of niobium a relatively stable tetrakis-(dialkylamino)-niobium(IV) is produced together with the products of reaction of the R_2N radical (amine, imine, etc.). However, in the case of tantalum the quadrivalent $Ta(NR_2)_4$ is unstable and interacts with the R_2N radical to produce $RN{=}Ta(NR_2)_3$, R_2NH, and olefin. It is noteworthy that the ligands (NMe_2, $NMeBu^n$, and NC_5H_{10}) which gave relatively stable pentacompounds with niobium also gave stable pentacompounds with tantalum. The thermal decomposition of $Ta(NMeBu^n)_5$ was considered likely to furnish further information on the mechanism of decomposition since there was the possibility that either $MeN{=}Ta(NMeBu^n)_3$ or $Bu^nN{=}Ta(NMeBu^n)_3$ would be formed. A sample heated *in vacuo* at 160–180° gave one volatile fraction which was predominantly N-methylbutylamine in the proportion of 1 molecule per molecule of $Ta(NMeBu^n)_5$. The volatile tantalum product was a mixture of $Bu^nN{=}Ta(NMeBu^n)_3$ (major fraction) and $Ta(NMeBu^n)_4$, which was separated by fractional distillation. It thus appears that in the cleavage of the BuMeN group it is the methyl group which is detached.

Work in this field is still in progress and further results on magnetic and spectroscopic properties of these and related compounds will be reported when complete.

EXPERIMENTAL

General Techniques

All reactions were conducted in carefully dried all-glass apparatus under an atmosphere of oxygen-free dry nitrogen.

Amines were stored over sodium wire and distilled from freshly cut sodium as required. The purity of the amines was checked by gas chromatographic analysis (g.c.a.).

Alcohols were dried azeotropically with benzene, and stored in contact with "molecular sieve" drying agent until required.

Commercially available tantalum pentachloride was used without further purification.

Analytical Techniques

Tantalum.—Samples of the dialkylamido compound were weighed directly into weighed platinum crucibles, allowed to hydrolyze, and finally ignited to tantalum pentoxide.

Nitrogen.—Weighed samples were hydrolyzed in caustic soda solution and the liberated amine steam-distilled into an excess of standard acid. The excess acid was back-titrated with standard alkali.

Valency.—The average valency of the tantalum in these compounds was deduced by determining the equivalent weight of the tantalum by oxidation of quadrivalent tantalum with ceric sulphate solution. To avoid premature oxidation of Ta(IV) whilst effecting solution of the sample prior to titration with ceric sulphate the following procedure was developed: Weighed samples were added to 10-ml aliquots of a solution containing anhydrous ferric chloride (15 g) in absolute ethanolic (150 ml) sulphuric acid (15 ml). When a clear solution was obtained (usually within 10 seconds), dilute sulphuric acid was added and the solution then titrated against standard ceric sulphate. A "blank" determination was made on the alcohol – ferric chloride – sulphuric acid reagent.

Preparation of Pentakis-(dimethylamino)-tantalum

Tantalum pentachloride (14.4 g) was added to a stirred suspension of lithium dimethylamide (0.202 g-equiv) in pentane. A rapid reaction occurred with the transient appearance of an orange solid and the formation of a pale yellow solution. After the mixture had been stirred for 18 hours it was filtered and the filtrate

evaporated *in vacuo*. A yellow solid (15.4 g, theory for $Ta(NMe_2)_5$, 16.1 g) remained. Found: Ta, 43.4; Me_2N, 50.1; Cl, trace; Li, zero; valency of Ta, 5.0. $Ta(NMe_2)_5$ requires: Ta, 45.1; Me_2N, 54.9%. A sample (14.2 g) was sublimed at 100° C at 0.1 mm, giving a pale yellow solid (10.8 g). Found: Ta, 44.8; Me_2N, 53.5%. Another sample (3.74 g) was heated at 180° for 1 hour under an atmosphere of nitrogen. The yellow solid melted to an orange liquid. A red sublimate (2.12 g) was recovered at 80–90° at 0.1 mm. Found: Ta, 45.4%. Gas chromatographic analysis of the amine liberated by isopropanolysis showed that only dimethylamino groups were present.

Reactions between $TaCl_5$ and Lithium Diethylamide

Tantalum pentachloride (13.8 g) was added over a period of 30 minutes to a stirred suspension of lithium diethylamide (0.215 g-equiv) in pentane. A slow reaction occurred and the system became light brown in color. After 20 hours' stirring it was filtered and an orange liquid (20.0 g) remained after the removal of volatile products and solvent *in vacuo*. Found: Ta, 33.9; Et_2N, 63.1; Li, trace; Cl, trace; valency of Ta, 4.92. $Ta(NEt_2)_5$ requires: Ta, 33.4; Et_2N, 66.6%. Gas chromatographic analysis of the product of *n*-butanolysis showed that only diethylamine was liberated.

A sample (17.2 g) of the foregoing product was heated *in vacuo* and gave a red distillate (12.7 g; b.p. 125° at 0.1 mm). Found: Ta, 38.8; N, 12.2; valency of Ta, 4.45. Calc. for a mixture of $Ta(NEt_2)_4$ (55%), $Ta(NEt_2)_5$ (10%), and $EtNTa(NEt_2)_3$ (35%): Ta, 38.8; N, 12.3%. Gas chromatographic analysis of the amines liberated by *n*-butanolysis showed that both primary ethylamine and diethylamine were present.

In another experiment under essentially the same conditions as before the $Ta(NEt_2)_5$ was decomposed to give a liquid (b.p. 120° at 0.1 mm) with the composition $Ta(NEt_2)_4$ (38%), $Ta(NEt_2)_5$ (15%), $EtNTa(NEt_2)_3$ (47%). Found: Ta, 39.0; N, 12.1%; valency of Ta, 4.63; ratio N:Ta, 4.01. The product was then heated under reflux at 120° at 0.1 mm for 3 hours and then distilled. Found: Ta, 39.6; N, 12.4%; valency of Ta, 4.75; ratio N:Ta, 4.04. The product was then refluxed in diethylamine for 24 hours and finally recovered by distillation *in vacuo*. Found: Ta, 40.2; N, 12.35%; valency of Ta, 4.77; ratio N:Ta, 3.99. Finally the product was refluxed in diethylamine for 4 days and the tantalum compound isolated as before. Found: Ta, 40.0; N, 12.5%; valency of Ta, 4.81; ratio N:Ta, 4.04. It is noteworthy that the five tantalum compounds analyzed in the foregoing sequence of experiments had a constant nitrogen-to-tantalum ratio (4.02 ± 0.02) but a steadily increasing valency. The constancy of the N:Ta suggests that very little $Ta(NEt_2)_5$ was present and that the change in analysis corresponds to the conversion of $Ta(NEt_2)_4$ to $EtN{=}Ta(NEt_2)_3$.

In a repetition of the previous experiment the product of the thermal decomposition of $Ta(NEt_2)_5$ (9.10 g; Ta, 39.2; N, 12.0%; valency of Ta, 4.66) was refluxed with diethylamine (20 ml) in pentane (20 ml) for 40 hours. Removal of solvent and diethylamine left a light brown liquid (9.00 g; found: Ta, 39.2%; valency of Ta, 4.72). Distillation of some of this liquid (7.22 g) gave a light brown distillate (7.10 g; b.p. 110° C at 0.1 mm; found: Ta, 39.7%; valency of Ta, 4.71).

In an earlier experiment in which $TaCl_5$ was added to lithium diethylamide in diethyl ether the solvent was removed and a tantalum compound (found: Ta, 40.0%) distilled out *in vacuo*. Gas chromatography of the amines liberated by *n*-butanolysis showed that the compound contained both primary-ethylamine and diethylamine. Redistillation of the product gave at 100–105° at 0.05 mm a compound with an analysis (Ta, 40.3; N, 12.2%; N:Ta, 3.91) similar to those of the final products of the previous two experiments. It thus appears that in the reaction carried out in ether the formation of $EtN{=}Ta(NEt_2)_3$ is facilitated. Following the development of the technique for determining the valency of the tantalum we repeated the experiment carried out in ether as follows: Tantalum pentachloride (17.7 g) was added to a stirred ethereal solution of lithium diethylamide (250 ml of 1.1 *N* solution). The ether was evaporated off and replaced by an equal amount of benzene and the system was then refluxed for 3 hours. After being allowed to cool overnight the mixture was filtered and the filtrate evaporated to dryness. Distillation of the residue gave a light brown liquid (11.6 g; b.p. 120° at 0.1 mm). Found: Ta, 40.6; N, 12.4%; valency of Ta, 4.80; ratio N:Ta, 3.94. Calc. for a mixture of $EtN{=}Ta(NEt_2)_3$ and $Ta(NEt_2)_4$: Ta, 40.5; N, 12.6%. It is evident that the $TaCl_5$–$LiNEt_2$ reaction gives reproducible products whether it is carried out in pentane or in ether.

Reactions between $TaCl_5$ and Lithium Di-n-propylamide

Tantalum pentachloride (13.7 g) was added to a stirred suspension of lithium di-*n*-propylamide (0.200 g-equiv) in pentane and the fast reaction was accompanied by the development of an orange color. After the system had been stirred at room temperature for 6 hours the crude $Ta(NPr_2^n)_5$ was isolated in the usual manner as a deep orange viscous liquid (25.9 g). Found: Ta, 25.6; Pr_2^nN, 67.7; Li, trace; Cl, trace; valency of Ta, 4.89. $Ta(NPr_2^n)_5$ requires: Ta, 26.5; Pr_2^nN, 73.5%. Distillation *in vacuo* of this product (19.4 g) gave an orange distillate (14.7 g, i.e. 93% recovery of Ta; b.p. 150° at 0.1 mm). Found: Ta, 31.7; N, 10.0; valency of Ta, 4.93; ratio N:Ta, 4.07. $Pr^nNTa(NPr_2^n)_3$ requires: Ta, 33.6; N, 10.4%. To a sample of the distillate (5.86 g) was added isopropanol (10 ml) cooled to 0° C. After refluxing, the volatile products were shown by g.c.a. to contain both primary-*n*-propylamine and di-*n*-propylamine. Removal of the volatile products and isopropanol followed by vacuum distillation afforded tantalum pentaisopropoxide (see also ref. 4) in quantitative yield (4.87 g, 98% of theory; m.p. 100° C, b.p. 110° at 0.1 mm). Found: Ta, 38.0; N, zero. $Ta(OPr^i)_5$ requires: Ta, 38.0%.

In a repetition of this experiment there was obtained from $TaCl_5$ (14.5 g) and $LiNPr_2^n$ (0.22 g-equiv) an orange liquid (26.3 g): Found: Ta, 27.4; N, 9.69%; valency of Ta, 4.92. A sample of this product (24.5 g) was heated *in vacuo* and volatile fractions were trapped at −78° and −180°. The most volatile fraction

(0.5 ml colorless liquid) was shown by g.c.a. to contain propylene, propane, and isobutylene or butane. The less volatile fraction (4.0 g) was shown by g.c.a. to be 95% Pr_2^nNH. Titration with acid gave the equivalent weight of the base as 121.6 (Pr_2^nNH requires 113). The ratio of molecules Pr_2^nNH produced per molecule of $Ta(NPr_2^n)_5$ was 1.0 based on the g.c.a. and 0.88 based on the volumetric analysis. The least volatile fraction was the tantalum compound, which was redistilled to give an orange liquid (16.6 g, 78% recovery of original Ta; b.p. 150° at 0.1 mm). Found: Ta, 32.1; N, 9.88%; valency of Ta, 4.90; ratio N:Ta, 3.98. Both primary-*n*-propylamine and di-*n*-propylamine were identified by g.c.a. as products of ethanolysis of the foregoing product.

Reactions of $TaCl_5$ with Lithium Di-n-butylamide

Tantalum pentachloride (12.0 g) was added to a stirred suspension of lithium di-*n*-butylamide (0.188 g-equiv) in pentane. During the fast reaction a yellow color developed. Afer refluxing for 6 hours and working up in the usual manner a red liquid tantalum compound (26.4 g) was obtained. Found: Ta, 21.7; Bu_2^nN, 74.4; valency of Ta, 4.89. $Ta(NBu_2^n)_5$ requires: Ta, 22.0; Bu_2^nN, 78.0%. Only di-*n*-butylamine was identified by g.c.a. as the product of *n*-butanolysis of this compound. When heated *in vacuo* a sample of $Ta(NBu_2^n)_5$ (22.8 g) gave a yellow liquid distillate (10.5 g, 57% recovery of Ta; b.p. 180° at 0.1 mm). Found: Ta, 27.6; N, 8.58; valency of Ta, 5.00; ratio N:Ta, 4.01. $Bu^nNTa(NBu_2^n)_3$ requires: Ta, 28.4; N, 8.80%. To this product (4.67 g) was added *n*-butanol (10 ml) and after refluxing the solution both primary-butylamine and di-*n*-butylamine were identified by g.c.a. as products of the reaction. Removal of the amines and excess *n*-butanol gave a near-quantitative yield of tantalum penta-*n*-butoxide as a pale yellow distillate (3.74 g; 83% recovery of Ta; b.p. 200° at 0.05 mm). Found: Ta, 33.2; N, zero. $Ta(OBu^n)_5$ requires: Ta, 33.1%.

From another reaction involving $TaCl_5$ (16.8 g) and $LiNBu_2^n$ (0.25 g-equiv) the red liquid product (40.3 g) was predominantly $Ta(NBu_2^n)_5$. Found: Ta, 20.9; N, 8.20%; valency of Ta, 4.92; ratio N:Ta, 5.07. A sample (38.8 g) was heated under reflux at 180° at 0.1 mm for 1 hour and the volatile products were condensed into two fractions at −78° and −180°. The most volatile fraction (0.5 ml) was shown by g.c.a. to be predominantly 1-butene (85%) with a small amount of isobutylene (or butane) (10%) and traces of *cis*- and *trans*-2-butene. The less volatile fraction (6.40 g) was shown by g.c.a. to be mainly di-*n*-butylamine (95%) and by titration to have an equivalent weight of 133.1±1.0 (di-*n*-butylamine requires 129). The molar proportion of Bu_2^nNH to $Ta(NBu_2^n)_5$ was calculated to be 1.05 (by g.c.a.) or 1.07 (by titration). The residual tantalum compound was then distilled and gave a yellow liquid (14.6 g; 50% recovery of Ta; b.p. 175° at 0.1 mm). Found: Ta, 27.7; N, 8.60; valency of Ta, 4.98; ratio N:Ta, 4.01. $Bu^nNTa(NBu_2^n)_3$ requires: Ta, 28.4; N, 8.80%. Ethanolysis of the product was shown by g.c.a. to liberate both Bu^nNH_2 and Bu_2^nNH.

Preparation of Pentakis-(piperidino)-tantalum

Tantalum pentachloride (10.9 g) was caused to react with lithium piperidide (0.155 g-equiv) in petrol (boiling range 35–60° C). After refluxing for 4 hours the system was allowed to cool and was then filtered. Evaporation of the filtrate to dryness gave impure pentakis-(piperidino)-tantalum as a light brown solid (19.4 g). Found: Ta, 27.1; $C_5H_{10}N$, 62.3; valency of Ta, 4.90; ratio N:Ta, 4.96; Li, trace; Cl, trace. $Ta(NC_5H_{10})_5$ requires: Ta, 30.1; $C_5H_{10}N$, 69.9%. Some of this product (16.5 g) was fractionally crystallized from petrol (boiling range 35–60°). The first crop of light brown crystals (4.75 g) were still contaminated by impurities (found: Ta, 26.7; $C_5H_{10}N$, 57.0; Li, trace; Cl, trace; valency of Ta, 4.99; ratio N:Ta, 4.58). The second crop appeared to be pure pentakis-(piperidino)-tantalum (6.90 g; found: Ta, 30.1; $C_5H_{10}N$, 69.2%; valency of Ta, 5.00). The third fraction was a red paste (4.31 g; Found: Ta, 27.7; $C_5H_{10}N$, 61.0%; valency of Ta, 4.75).

The pentakis-(piperidino)-tantalum was also prepared by aminolysis as follows: Piperidine (7.5 g) was added to $Ta(NMe_2)_5$ (4.32 g) in petrol (boiling range 35–60°), and dimethylamine was rapidly evolved. The system was refluxed for 3 days, the solvent then evaporated off, and the crude product recrystallized from petrol to give a pale yellow solid (1.62 g; 25% recovery of Ta). Found: Ta, 30.3; $C_5H_{10}N$, 70.2%.

Reaction of $TaCl_5$ with Lithium N-Methyl-n-butylamide

From the reaction involving $TaCl_5$ (19.0 g) and $LiNMeBu^n$ (0.27 g-equiv) in pentane at room temperature (4 hours), the pentakis-(N-methyl-*n*-butylamino)-tantalum was isolated after removal of lithium chloride as an orange liquid (32.2 g). Found: Ta, 29.7; N, 11.23; valency of Ta, 5.00; ratio N:Ta, 4.90; Li, zero; Cl, trace. $Ta(NMeBu^n)_5$ requires: Ta, 29.6; N, 11.45%. Butanolysis of a sample was shown by g.c.a. to liberate only N-methyl-*n*-butylamine.

Some $Ta(NMeBu^n)_5$ (29.7 g) was refluxed at 160–180° at 0.1 mm for 1 hour and the volatile products were condensed at −180°. The volatile fraction (4.50 g) was shown by g.c.a. and by titration (equiv. wt., 94.5±0.2; Bu^nMeNH requires: equiv. wt., 87) to be mainly a secondary amine and the molar ratio of amine to $Ta(NMeBu^n)_5$ was 0.98. The residual red liquid tantalum compound (25.0 g) was distilled to an orange liquid (22.5 g, b.p. 150° at 0.1 mm). Found: Ta, 34.8; N, 10.72; valency of Ta, 4.69; ratio N:Ta, 3.98. $Ta(NMeBu^n)_4$ requires: Ta, 34.4; N, 10.67%. $Bu^nNTa(NMeBu^n)_3$ requires: Ta, 35.4; N, 10.79%. These analytical data suggested that the orange liquid was a mixture of $Bu^nNTa(NMeBu^n)_3$ and $Ta(NMeBu^n)_4$. Fractional distillation of the substance (15.9 g) gave two fractions: An orange liquid (9.00; b.p. 150–155° at 0.1 mm) which appeared to be $Bu^nNTa(NMeBu^n)_3$; found: Ta, 35.3; N, 10.9; valency of Ta, 4.95; ratio N:Ta, 4.0. $BuNTa(NMeBu^n)_3$ requires: Ta, 35.4; N, 10.8%. The less volatile fraction was a red liquid (6.80 g; b.p. 155–180° at 0.1 mm) which according to its tantalum and nitrogen analysis was $Ta(NMeBu^n)_4$, but the valency determination indicated the presence of a considerable proportion of quinquevalent material.

Found: Ta, 34.4; N, 10.57; valency of Ta, 4.75; ratio N:Ta, 3.97. $Ta(NMeBu^n)_4$ requires: Ta, 34.4; N, 10.67%. A sample (5.31 g) of the $Bu^nNTa(NMeBu^n)_3$ was refluxed in *n*-butanol (9.0 g) and it was shown by g.c.a. that both primary-butylamine and N-methyl-*n*-butylamine were liberated, but no primary-methylamine was detected. After the removal of amines and butanol the residue was distilled *in vacuo*, giving a quantitative yield of tantalum penta-*n*-butoxide (5.40 g, 95% recovery of Ta; b.p. 200° at 0.1 mm). Found: Ta, 33.1; N, zero. $Ta(OBu^n)_5$ requires: Ta, 33.1%.

ACKNOWLEDGMENTS

We are indebted to the U.S. Air Force for supporting this research through the Wright Air Development Division, Air Research and Development Command. We also thank the National Research Council, whose support has greatly facilitated our research.

REFERENCES

1. D. C. Bradley and I. M. Thomas. J. Chem. Soc. 3857 (1960).
2. D. C. Bradley and I. M. Thomas. Can. J. Chem. **40**, 449 (1962).
3. D. C. Bradley and I. M. Thomas. Proc. Chem. Soc. 225 (1959).
4. I. M. Thomas. Can. J. Chem. **39**, 1386 (1961).

A SIMPLE THERMOBALANCE FOR STUDIES OVER A PRESSURE RANGE OF 0 TO 60 ATMOSPHERES

WENDELL J. BIERMANN AND MENNO HEINRICHS
Parker Chemical Laboratories, University of Manitoba, Winnipeg, Manitoba
Received January 15, 1962

ABSTRACT

A design is presented for a thermogravity balance usable to a pressure of 1000 p.s.i. The mass sensitive element is a tool steel cantilever rod, the displacement of which is measured by a linear variable differential transformer. Thermograms for the pyrolysis of calcium oxalate, chromium (VI) oxide, and Mohr's salt are included to show typical performances.

A search of the literature to find a thermogravity balance design which would enable us to study solid–gas reactions over an extended temperature and pressure range disclosed only one design, that reported by Rabatin and Card (1). This design employs a modified torsion balance as the mass sensitive element and an optical lever – photoelectric cell transducer system to develop a voltage proportional to mass, for automatic recording. While there is no question of the intrinsic excellence of their design, the construction of their balance would seem to offer a major challenge to the machine shop facilities available in most university laboratories.

In the present design, the mass sensitive element is a tool steel cantilever rod, rigidly fixed on one end and undergoing varying displacement on the free end as the sample, supported on the free end, changes mass. The amount of displacement is determined by a linear variable differential transformer (LVDT), whose output is demodulated and fed to a recording potentiometer. Easy zero adjusting of the transducer after closing and pressurizing the system is incorporated in the design, overcoming the major criticism of Rabatin and Card to the application of an LVDT as a displacement transducer.

The cross-sectional drawing of Fig. 1 shows the mechanical construction of the thermobalance. Since recent papers by Newkirk (2) and Garn (3) outline in detail various general considerations regarding the design of thermogravity balances, it would seem superfluous to repeat them here. Suffice it to say that the present design is in harmony with their various suggestions.

DESCRIPTION OF THE APPARATUS

The Pressure Vessel

The pressure vessel consists of three cylindrical chambers. An upper chamber M, with a removable top plate, houses the furnace and sample. Communicating with the upper chamber through a tube is the transducer chamber S, from the side of which projects the third cylindrical chamber, housing the cantilever rod and its associated adjustment mechanisms. A removable bottom plate and a removable end plate permit access to these latter chambers. The entire construction was from type 304 stainless steel, employing wall thickness of 0.25 inch for the chambers, 0.50 inch for the flanges welded onto the open ends of the chambers, and 0.75 inch for the access plates. These plates were secured by hardened steel cap screws, and gas-tight closure was effected with Teflon "O" rings.

Instead of using flat plates on the ends of the pressure chambers, they could alternately be machined to spherical segments which would permit the same pressures to be contained

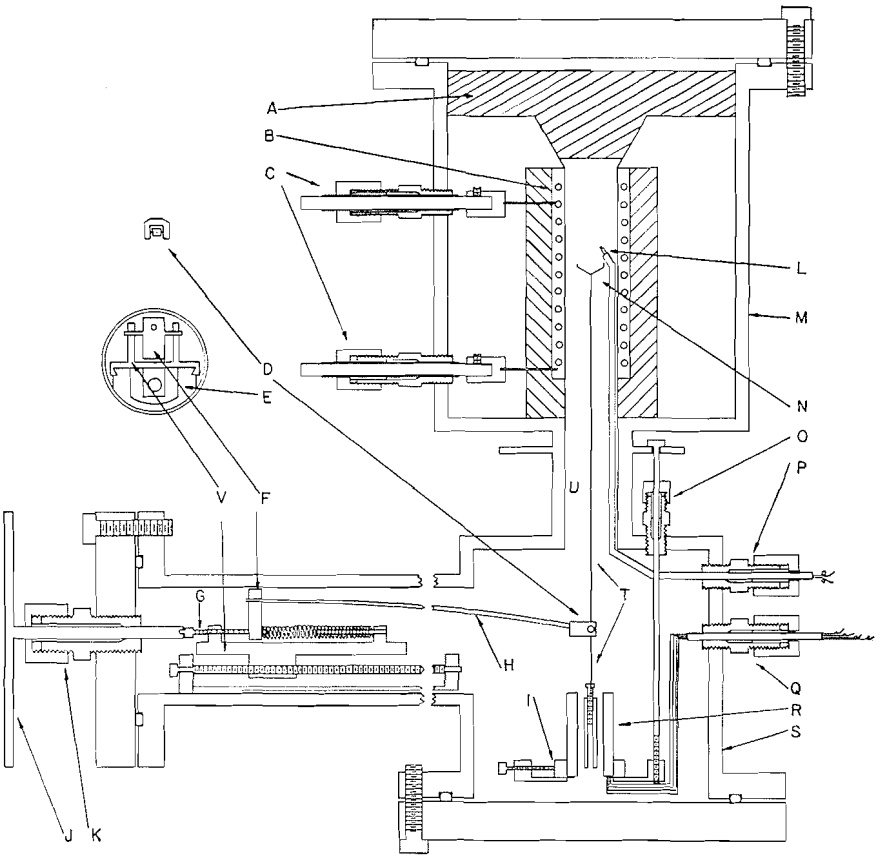

FIG. 1. Mechanical construction of the thermobalance.

with thinner walls. It would also be better practice to use radius cuts on the terminations and joinings of the chambers rather than the right-hand cuts which are shown on the drawing.

A tripod support, not shown on the drawing, holds the pressure vessel about 6 inches off the vibration pad on which it rests, permitting adjustments to be made through the lower access port, using a mirror for vision. The vibration pad consists of several layers of lead and cork, sandwiched between plywood, and mounted onto a concrete block wall by rigid brackets and was originally intended to support an analytical balance.

Calculations indicate that the pressure vessel should safely hold a pressure of about 1500 p.s.i., and it has been tested up to 1100 p.s.i. by applying oxygen from a cylinder.

A vertical quartz rod T supports the dish-shaped platinum foil sample pan on a tripod support N in the center of an electrically heated furnace. Fixed on the bottom of the quartz rod is the core of a Schaevitz Type 175 ES-L LVDT. This particular LVDT was chosen because we had anticipated more vibration background than was actually experienced; the amount of deflection needed is much less than the linear range of this unit. A much shorter range LVDT can therefore be substituted.

Immediately above the core, the quartz rod is supported by the cantilever rod H, a jewel-bearing supported pivot D allowing the quartz rod to remain vertical as the angle between it and the cantilever rod changes as a result of displacement. As displacements

of only a few thousandths of an inch are used, this assembly is essentially a strain gauge. Originally it had been planned to use a quartz rod for the cantilever, but experience showed that a rod thin enough to give adequate sensitivity was subject to frequent breakage. A 10-inch length of alloy steel drill rod (3/32-inch diameter) was then substituted and it has proved to be highly satisfactory both as regards mechanical strength and retention of calibration.

The furnace in the upper chamber was wound with Kanthal A-1 wire, backed with Alundum cement to give a rigid, cylindrical heating element B, which surrounds the sample. Asbestos fibers were packed in the space between the heating element and the wall of the pressure vessel. Closure of the top was effected with a lid A, fabricated from an insulating firebrick, which sits on the packed asbestos fibers. When the furnace is operated at 1000° C, very little heating of the outer vessel takes place. Two platinum foil radiation shields, in the vicinity of U in Fig. 1, minimize heat transfer to the lower sections of the pressure vessel.

Electrical connection to the heating element was made by slipping a cover of Teflon tubing over brass rods and then leading them through the wall of the pressure vessel with Conax sealants (Conax Corporation, Buffalo, N.Y.) with Teflon seals, as shown at C on Fig. 1.

Temperature in the vicinity of the sample is measured by means of a conventional high-temperature thermocouple L, led in through a Conax sealant P and having an exposed platinum, platinum–rhodium junction for low thermal lag. A similar thermocouple employing a chromel–alumel junction has also been employed. Placement of the thermocouple in different positions gives no change in the temperatures at which mass changes occur, indicating that no important thermal gradients exist in the vicinity of the sample pan.

The LVDT R in the lower compartment was mounted on a triangular brass plate, supported near each corner by an adjusting screw, one of which is shown at O, permitting leveling and approximate vertical positioning of the transducer body. Conax pressure sealants with neoprene seals were used to pass the adjusting screws through the wall of the pressure vessel. Three adjusting screws, one of which is shown at I, were used to center the transducer case about the core. Once the transducer case has been positioned, it requires no further adjustment between runs, vertical adjustment of the core for zeroing being done with the cantilever rod adjustment.

The fixed end of the cantilever rod H is anchored in a small brass plate, shown in both side and front view as F, which is in turn supported on a pivot which can rotate in ball bearing assemblies fixed to the carriage V. The angular position of this small plate is fixed by the end of the threaded rod G, against which it is pressed by a firm coil spring. This rod can be moved horizontally by rotation, being threaded through a block on the end of the carriage (40 threads/inch). A conax sealant, with a neoprene seal, passes this adjusting rod through the end plate with a gas-tight seal, and permits it to be turned with the 3-inch handwheel J after pressure buildup. This very simple system permits surprisingly precise adjustments of core position with no difficulty whatever.

The entire carriage assembly can be moved horizontally along the dovetail track E by means of a drive screw. This adjustment was intended to allow coarse adjustments of sensitivity by changing the length of the cantilever rod. Thus far it has been superfluous, the linear range of the LVDT being sufficiently long, and the stability and sensitivity of the other components sufficiently high that a change in range is more easily accomplished by taking greater or lesser fractions of the demodulator output.

Demodulator

Although the output of the LVDT is greater than would be required for full-scale deflection of a 10-mv recorder, the output signal is put through an amplifier stage before rectification to circumvent the difficulty of finding a rectifier with linear characteristics at low voltages. Following half-wave rectification of the amplified signal, a portion, usually 1/12, is selected by a variable potential divider network for feeding to a 10-mv recorder. The demodulator circuit is shown as Fig. 2. It will be noticed that the recorder

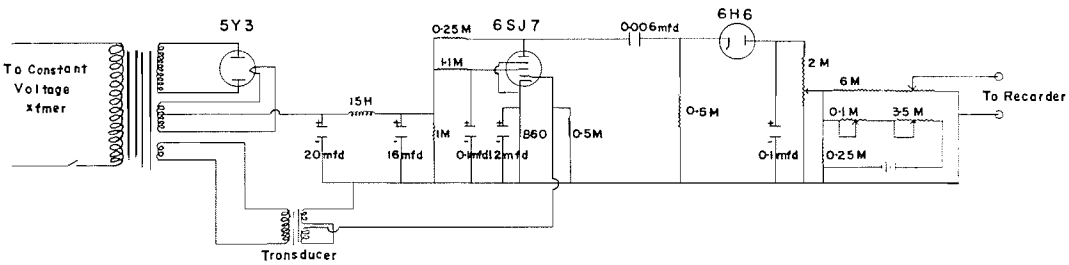

FIG. 2. Demodulator circuit.

output voltage fed to the recorder is opposed by a variable voltage taken from a mercury cell. This is a convenient way of setting the recorder to zero when beginning a run with the transducer slightly removed from its null point to get into a more linear region, and also to eliminate the effects of any constant inductive effects before the rectifier.

This demodulator is probably more complex than required. In principle, as there is adequate voltage from an LVDT in this situation to drive a recorder directly, it should only be necessary to follow the rectifier, even though non-linear, with an RC circuit having a time constant several times as long as the duration of a cycle in the LVDT output. We have not yet explained our failure to achieve satisfactory operation with the simpler circuit.

The recorder used was a two-pen, 10 mv/channel ServoRiter recording potentiometer (Texas Instrument Company, Houston, Texas) which permitted simultaneous recording of the LVDT and thermocouple outputs with 10-inch deflections on a common time axis.

Temperature Programmer

When the power supplied to the furnace was varied by linear variation of the voltage across the heater with time, the resulting time–temperature plots showed only moderate changes of slope. As this curvature was not great enough to be a handicap in any work we have in mind, a relatively simple motor and gear box drive was used to turn a variable autotransformer, with a limit switch at the end of its range. This was fed by a second variable autotransformer, much in the manner used by Reisman (4). By selecting suitable gear combinations a wide range of heating rates can be selected.

PERFORMANCE OF THE THERMOBALANCE

Operation

With the bottom plate removed, the transducer case is centered coaxially about the core in the vicinity of the null point by manipulation of the six adjusting screws which determine its position. As mentioned previously, this adjustment seldom needs to be repeated.

As the demodulator is not phase sensitive, deflections on either side of the null point are not distinguishable by the recorder. It is, therefore, easy to locate the null point by moving the cantilever rod with the handwheel until minimum deflection of the recorder is noted. Because an LVDT is generally non-linear in the immediate vicinity of its null point, it is most convenient to displace the core downward sufficiently to come into a linear region, the displacement with this apparatus being equivalent to about 40 mg in the sample pan. The region of linearity of the LVDT, in this apparatus, extends over a sample mass in excess of 1 g and the voltage developed across the 2-meg potential divider in the 6H6 plate circuit is about 1.0 mv/mg load in the sample pan. Since the recorder used gave full-scale deflection with 10-mv input, it was found convenient in most cases to use 1/12 of the demodulator output and to choose samples of such size that the mass change would be of the order of 0.1 g.

When set up as above, calibration was done directly by the addition of a succession of fractional weights, and the resultant sensitivity was 1.23 mg/chart division (0.1 inch), linear within the uncertainty of interpolating between chart markings. Greater or lesser sensitivity can be obtained, if experimentally convenient, by using a different fraction of the demodulator output. Zeroing of the recorder at different positions within the linear range is accomplished by applying a counter voltage in series with the demodulator output. The magnitude of the counter voltage, obtained from a mercury cell, is determined by the settings of the 3.5- and 0.1-meg potentiometers functioning as variable resistors and giving a coarse and fine control, respectively.

With the transducer core positioned at the beginning of the linear region, an appropriate-sized sample is then placed on the sample pan. If mass is to be lost, the recorder is set near full-scale deflection, and where mass is to be gained by reaction with the atmosphere within the pressure vessel, the recorder is set near zero deflection. While it would be possible to record the absolute mass of the sample, greater use is made of the sensitivity of the apparatus by weighing the sample on a balance and, using the above method of setting the recorder and an appropriate setting of the sensitivity selector, recording only the loss or gain in mass.

Results

Typical plots of mass and temperature as functions of time were traced from the recorder charts of the apparatus described above, and are reproduced as Figs. 3, 4, and 5. The temperature curve is easily distinguished from the loss of weight curve by the absence of inflection points. Calibration of the thermocouples by conventional calibration at invariant points served to fix the temperature axis.

Figure 3 shows the pyrolysis of a 0.2-g sample of calcium oxalate. The first plateau, representing completion of drying, begins at a temperature of 230° C, and the third plateau, completion of conversion to calcium oxide, occurs at 860° C, both temperatures being in substantial agreement with Newkirk (2). The center plateau, formation of calcium carbonate by the loss of carbon monoxide, is apparently reached at 435° C, substantially lower than Newkirk's value, but the irregularity in the temperature curve in this vicinity suggests that oxidation of the carbon monoxide is probably responsible for the rise in sample temperature, and served to underline the stress laid by Newkirk and by Garn and Kessler (5) on the effect of atmosphere and venting on the shape of the thermogram.

Figure 4 is a thermogram for the pyrolysis of chromium (VI) oxide under an oxygen atmosphere of 200 p.s.i. A precision potential divider allowed all, half, or one fifth of the

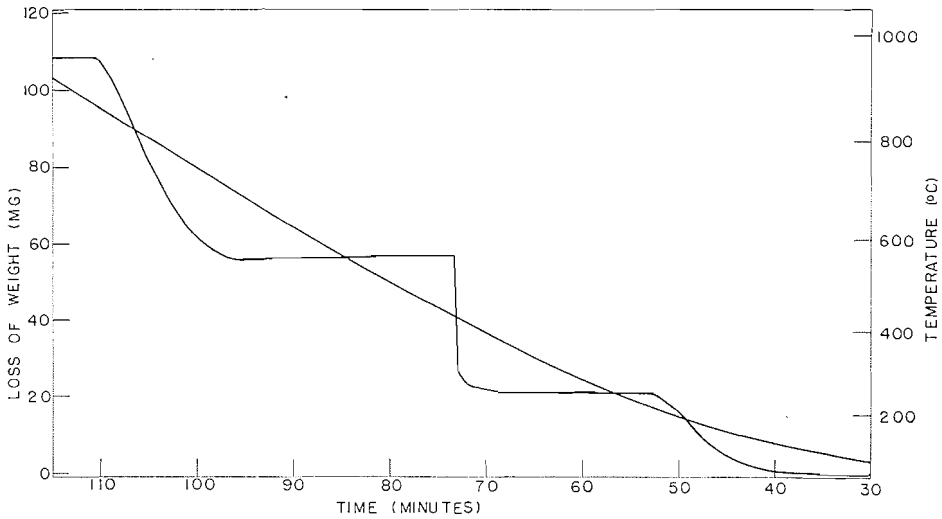

FIG. 3. Thermogram obtained by heating calcium oxalate.

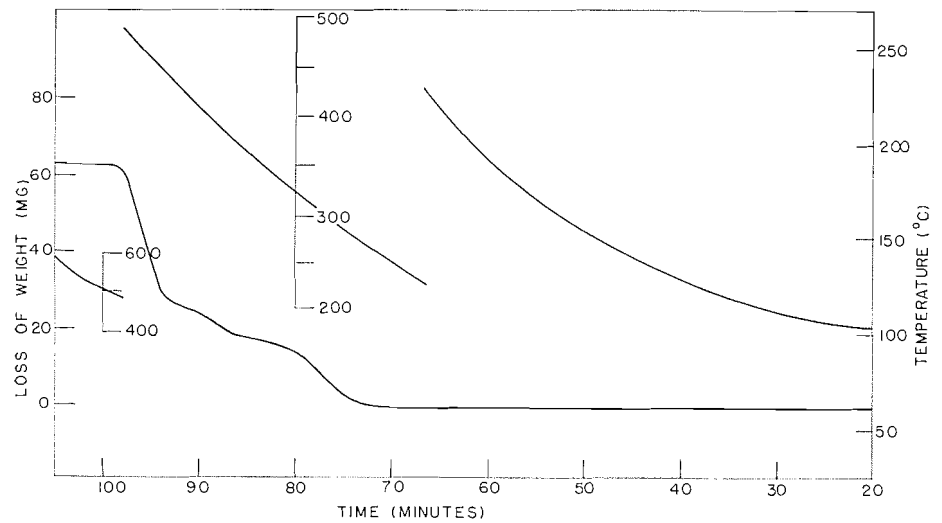

FIG. 4. Thermogram for heating chromium (VI) oxide under oxygen pressure of 200 p.s.i.

chromel–alumel thermocouple output to be fed into the recorder, thus leading to the three temperature axes shown on this thermogram. Oxygen is lost in three steps, the weight losses in these steps being in the ratio 4.10:1.97:9.00, which agrees with the successive formation of Cr_5O_{13}, Cr_5O_{12}, and Cr_2O_3, as reported by Mellor (6). The 258.2-mg sample gave a residue of 194.8 mg, compared to the theoretical value of 196.1 mg.

Figure 5 is a pyrolysis curve for Mohr's salt. This thermogram can be tentatively interpreted by postulating a decomposition in the following steps:

(1) a loss of 4, and subsequently 2 more, moles of water per mole of Mohr's salt, with the loss of mass being 34.68% of the sample weight (34.58% theoretical);

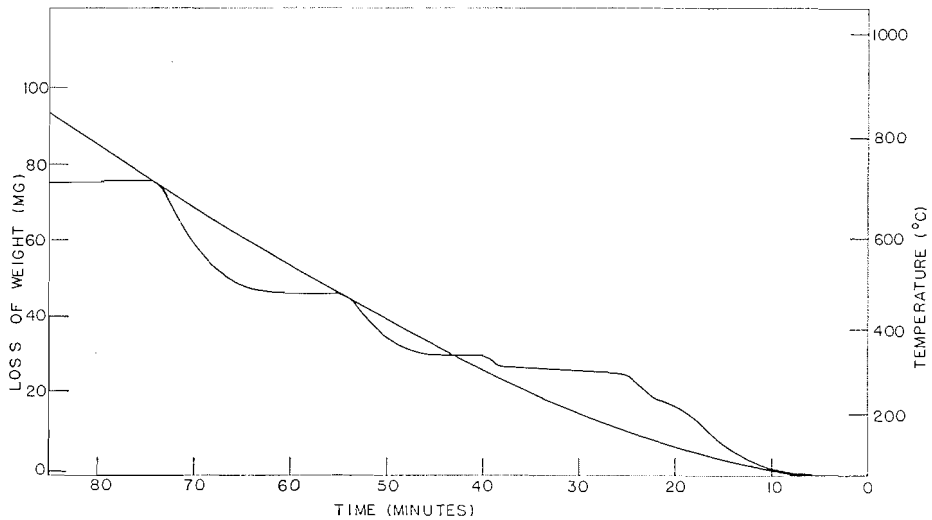

FIG. 5. Thermogram obtained on heating Mohr's salt.

(2) a loss of 1 mole of ammonia and $\frac{1}{2}$ mole of hydrogen simultaneously, the loss of mass being 5.64% (5.69% theoretical);

(3) the simultaneous loss of 1 mole of ammonia and $\frac{1}{2}$ mole of sulphuric acid, the mass loss being 21.29% (21.19% theoretical);

(4) the loss of $1\frac{1}{2}$ moles of sulphur trioxide, corresponding to a mass loss of 38.39% (38.42% theoretical).

ACKNOWLEDGMENTS

The authors are indebted to Mr. L. W. Wilkins for the construction of much of this apparatus and for his suggestions about its design. We also gratefully acknowledge the financial aid given by the National Research Council.

REFERENCES

1. J. G. REBATIN and C. S. CARD. J. Am. Chem. Soc. **31**, 1689 (1959).
2. A. E. NEWKIRK. Anal. Chem. **32**, 1558 (1960).
3. P. D. GARN. Anal. Chem. **33**, 1247 (1961).
4. A. REISMAN. Anal. Chem. **32**, 1566 (1960).
5. P. D. GARN and J. E. KESSLER. Anal. Chem. **32**, 1563 (1960).
6. J. W. MELLOR. Comprehensive treatise on inorganic chemistry. Vol. XI. Longmans, Green and Co., New York. 1931. p. 206.

LIQUID–LIQUID EXTRACTION OF BERYLLIUM

I. A STUDY OF FACTORS AFFECTING EXTRACTION

WENDELL J. BIERMANN AND ROBERT MCCORKELL
Department of Chemistry, University of Manitoba, Winnipeg, Manitoba

Received March 7, 1962

ABSTRACT

A consideration of factors known to govern the formation of coordination compounds with metal ions led to the conclusion that the best ligands to use in attempting to separate beryllium from other metal ions of inert gas configuration by liquid–liquid extraction would be easily polarizable, monofunctional ligands. It is suggested that the thiocyanate ion, as ammonium thiocyanate, is particularly promising for metallurgical application.

The organic solvent was shown to play an active role in the extraction, ketone or hydroxy groups on chains containing six to eight carbons giving good extraction with low solvent loss.

INTRODUCTION

Most of the existing literature concerning the chemical metallurgy of beryllium is directed towards the processing of beryl, until recently the only commercially important beryllium mineral, to produce beryllium oxide, destined for use mainly as a ceramic oxide or for production of beryllium–copper alloy (1–3). Recently there has been a resurgence of interest in the extractive chemistry of beryllium as a result of the discovery of new types of mineralization, extensive and rich enough to be more attractive than the traditional hand-cobbed beryl (4). The requirements of the nuclear energy field have also placed a far greater emphasis on purity than has heretofore existed.

A variety of studies has been in progress in this laboratory, designed to establish process information useful in meeting these new requirements. A series of communications, of which this is the first, will describe one aspect of this work—the separation of beryllium from other elements which might coexist in natural deposits by liquid–liquid extraction techniques.

In order to be useful on a commercial production scale, several criteria must be met. First, and most obvious, costly reagents and solvents must be avoided, otherwise there will be no practical advantage over existing practice. Recovery of reagents and solvents, by economical means, likewise is an advantageous situation. Second, some selectivity of the extraction system for beryllium is necessary if anything is to be accomplished. Third, after partition of the beryllium between the liquid phases, it must be easily possible to strip the beryllium-rich phase.

In principal, any reagent or group of reagents which can react with the aquated beryllium ion and, by displacement of water molecules in the primary hydration layer, produce an uncharged structure would enhance the solubility of the beryllium ion in "organic" solvents and could thus serve as the basis of a solvent extraction system. A brief consideration of some of the principals involved shows, however, that most of the potential systems will be of little practical value.

Various classifications of liquid–liquid extraction systems have been proposed (5, 6), a broad classification into ion association systems and coordination complexes being common.

Whether the ion association aggregate has any physically real distinction from the more common interaction involving coordination of ligands to the central atom is debatable. Generally, members of the ion association groups are those in which one would predict

weak coordination bonds between the central atom and the ligands. Since there seemed to be no possible advantage to maintaining these categories in planning a search for practical extraction systems, we considered that all extractions of beryllium would be of species containing coordinately bonded ligands with two associated negative charges, required to give an electrically neutral species.

A large amount of the modern solvent extraction literature is concerned with the coordination of polyfunctional bases to the central atom, giving the generally very stable chelate complexes. It has been shown by various investigators that the formation constants of chelates with a given ligand but various central ions can be, at least qualitatively, related to the charge of the central ion and its radius. Beryllium is often an exception to this generalization, the formation constants being too low, presumably because of steric hindrance effects arising from its very small radius. Advantage is frequently taken of this effect, as when beryllium is separated from ions with similar or smaller charge-to-radius ratios, notably aluminum, by chelating agents such as ethylenediaminetetraacetic acid or 8-quinolinol. Where a stable chelate is formed with beryllium ion, the 1,3-diketones being familiar examples, almost all other cations except those of groups I*a* and II*a* form equally, or more, stable complexes. We therefore rejected polyfunctional ligands as generally not meeting our criterion of specificity and, secondarily, as generally being on the expensive side.

This left us with only monofunctional ligands as potential extraction agents. Here we restricted most of our experimental work to those systems in which a priori considerations and reagent costs together established at least an hypothetical basis for an efficient and reasonably selective extraction system.

While the orbital theories of chemical bonding are useful in predicting formulae and geometry of coordination compounds, the electrostatic approach was far more useful in attempting to predict the usefulness of various ligands. In general the strength of the bonds, and hence the formation constant, will be determined by Coulomb's law (7). In the case of small, noble gas configuration cations and small anions one generally can get at least semiquantitative results by the simple use of conventional ionic charges and radii. When dealing with larger anions, particularly when the central cation shows a high effective charge-to-radius ratio, polarization effects can completely alter the expectations derived from the simple picture. The inversion of the order of stabilities of the halo complexes of the elements at the ends of the transitional series has been successfully explained on this basis, it being postulated that the effective charges on these ions are unduly high because of the ineffectual screening of the nucleus by the electrons in the *d* orbitals.

We now have two possible paths, regarding selectivity, for a solvent extraction system to follow. We might employ small ligands, such as fluoride ion, and use a basic solvent to supply the remaining two ligands to give an uncharged beryllium complex with the usual coordination number of four satisfied, or we might seek a large negatively charged anion and rely on the polarizing power of beryllium to distort the anion sufficiently to give a sufficiently stable bond to permit extraction.

The first would not be expected to give good separation from aluminum, lithium, or other elements of fairly high charge-to-radius ratio, but might be effective with some of the heavier elements, which are, however, seldom a difficulty in the metallurgy of beryllium. Because of the large energy of such coordinate bonds, for example between beryllium and fluoride ions, it is difficult to avoid a negatively charged, hence less extractable, ion.

Using large, hence deformable, anions seems to be the more promising approach. Since the polarizing power of an ion varies with the ratio of the charge to the square of the radius, such an easily polarizable ion should give good selectivity from elements with inert gas configurations, because the beryllium ratio is much larger than for other commonly coexisting ions like aluminum and lithium. Interference would be expected from those elements which occur about the ends of the transitional series, but since it seems to us that interference is inevitable, this would at least constitute the less objectionable type of interference. The fact that formation constants with ligands of this type would be lower than for small, or highly charged, ligands can also be advantageous in that it becomes easier to avoid anionic forms of beryllium and that stripping should be facilitated.

Because this picture includes the solvent as a coligand to the actual anionic reagent, the basic nature and water solubility of the solvent should be closely related to the extraction of beryllium. Solubility in water should, by a mass-law effect, increase extractability, and some strongly basic functional group should be necessary for appreciable extraction.

The systems studies were chosen in accordance with the above considerations, and the results were completely consistent with expectation.

EXPERIMENTAL

In essence, the experimental work consisted of taking water solutions of known beryllium concentration and any other reagents whose effects were to be studied and equilibrating with an appropriate organic solvent. The actual extractions were made in glass-stoppered separatory funnels, shaking until extraction was complete. It was assumed that when the beryllium concentration of the aqueous phase was reproducible after longer shaking intervals, equilibrium had been reached. In no cases studied were more than 1 or 2 minutes required to reach such equilibrium. For simplicity of comparison, equal volumes (40 ml) of aqueous and organic phases were used. Analysis of the aqueous phase after extraction then permitted calculation of the percent beryllium extracted, which is simply related to the distribution coefficient by D = (percent extraction)/(100-percent extraction) in the equal volume situation, provided the two solvents show little miscibility, as was generally the case.

Where extraction was sufficiently high to be promising, the experiments were repeated using an equivalent amount of aluminum ion in place of the beryllium, the distribution coefficients of aluminum and beryllium serving as a measure of the selectivity of the extraction for inert gas configuration ions.

A major part of the experimental work was analysis of aqueous and organic phases for beryllium and aluminum, and some complications were encountered here because of the coordination of beryllium and aluminum ions to thiocyanate and solvent. There seemed to be a tendency to prevent complete precipitation of the beryllium in some gravimetric methods, and in the determination of beryllium by optical absorption of beryllium–reagent complexes, results were similarly often low.

Ultimately two standard methods were adopted, a photometric method using *p*-nitrobenzeneazoorcinol (8) which proved applicable in some cases, and the precipitation of beryllium as NH_4BePO_4 (9), followed by ignition to $Be_2P_2O_7$ at 900° C. The latter method proved to be generally reliable, the uncertainty being no worse than $\pm 0.5\%$.

Aluminum was determined by EDTA titration using hematoxylin as an indicator (10). The reliability was shown to be within $\pm 0.5\%$ under the prevailing conditions.

The aqueous aluminum solutions were prepared from reagent grade aluminum sulphate, with no further purification. Beryllium solutions were prepared from beryllium sulphate tetrahydrate, supplied by A. D. MacKay, Inc., and whose purity was verified by chemical analysis. A range of grades of solvents, determined mostly by availability, was used and, when the results were thought to be significant, the solvents were purified by fractional distillation.

EXPERIMENTAL RESULTS

Our attempts to extract a solvated hydroxy complex of beryllium, using solvents with oxygen donor atoms in various functional groups, proved uniformly unpromising and were soon discontinued. The percentages of beryllium extracted were generally less than 0.1%.

Commercial di-*n*-butyl phosphate proved to be a fairly able extractant for beryllium when used in kerosene suspension, but as shown by representative results collected in Table I, it is not notably selective. Since, in addition, we encountered some difficulty in

TABLE I

The extraction of beryllium and other metals from 1.0 *M* aqueous nitric acid solution by kerosene suspensions of commercial di-*n*-butyl phosphate
(Initial metal concentration 0.050 *M*, extraction time 5 minutes, equal volumes of organic and aqueous phases)

Metal ion	Butyl phosphate concentration (moles/liter)	Percentage metal extracted
Be^{+2}	0.10	18.6
Be^{+2}	0.20	50.8
Be^{+2}	0.40	72.9
Be^{+2}	0.60	75.3
Be^{+2}	1.00	91.1
Ti^{+4}	0.10	48.6
Al^{+3}	1.00	45.5

getting clean separations of the liquid phases, due to emulsion formation, we discarded this as an impractical system.

In Table II are collected results of extractions using anions of various weak aliphatic acids as ligands. The aqueous layer was prepared by raising the pH until the beryllium

TABLE II

Extraction of 0.2 *M* beryllium solutions, in the presence of various carboxylic acids, with chloroform

Acid	Acid concentration (moles/liter)	Percentage extraction	Percentage Al^{+3} extraction
Acetic	5.0	3.3	
Propionic	5.0	21.9	95
Butyric	2.0	87.5	100
Butyric	3.0	92.3	100
Butyric	4.0	91.7	100
Butyric	5.0	94.7	
Hexanoic*		100	100
Octanoic		100	100

*Used instead of chloroform as organic phase.

precipitated as an hydroxide, after which it was redissolved by addition of an excess of the acid being tested. While the results showed good beryllium extraction, little differentiation from aluminum was noted, so no further attempts were made to develop this as a practical system.

As would be predicted from the introductory considerations the large, polarizable, halide-type anions proved to be particularly suitable for extraction. Table III shows the extractability of chloride, bromide, iodide, and thiocyanate complexes of beryllium and aluminum under similar experimental conditions. Of these ions, the low cost of ammonium thiocyanate made this reagent look particularly attractive, and seemed to justify a concentration of work on thiocyanate extraction systems.

TABLE III

Extraction of metal ions from solutions of halide-type ions with *n*-amyl alcohol (Initial metal concentration 0.100 *M*, pH = 3.00)

Metal	Salt	Percentage metal extracted
Be	4 *M* NH_4Cl	0.0
Be	4 *M* KBr	1.3
Be	4 *M* KI	66.6
Be	3 *M* NH_4CNS	81.0
Al	3 *M* NH_4CNS	41.2

Since we postulated that the solvent would play an active role in forming the co-ordination compound, which is the actual extracted species, distribution coefficients were determined with a variety of solvents.

The standard conditions of comparison were: an initial beryllium concentration of 0.100 *M*, as beryllium sulphate; an initial thiocyanate concentration of 3.00 *M*, as ammonium thiocyanate; and a pH of 3.00±0.01. It was noted that the distribution coefficient was pH sensitive, probably because a high proton concentration lowers the concentration of the somewhat basic thiocyanate ion, and a low proton concentration lowers extraction, presumably because of the formation of species like $BeOH^+$. The results of the solvent studies are tabulated in Table IV.

TABLE IV

The distribution ratios between the organic and aqueous phases of beryllium and aluminium ions in the presence of thiocyanate ion, for various organic phases (Initial concentration of metal in the aqueous phase 0.100 *M*, of thiocyanate ion as ammonium thiocyanate 3.0 *M*, pH = 3.00+0.01)

	Distribution ratio			Distribution ratio	
Organic solvent	Aluminum	Beryllium	Organic solvent	Aluminum	Beryllium
Alcohols			Ketones		
Cyclohexanol	3.0	6.70	Methyl isobutyl ketone	0.122	2.38
n-Amyl alcohol	0.701	3.27	Acetophenone	0.103	2.37
Isoamyl alcohol	0.673	4.55	Methyl isopropyl ketone		4.87
Methyl amyl alcohol	0.145	2.03	Methyl *n*-amyl ketone	0.110	1.63
1-Hexanol	0.770	2.59	2,4-Dimethylpentanone	0.005	0.138
2-Ethylhexanol	0.30	0.49	Aldehydes		
1-Octanol	0.513	1.66	Paraldehyde		0.235
2-Octanol	0.089	1.28	Paraldehyde (2 *M* kerosene solution)		0.11
Thioalcohols			Butyraldehyde	0.161	2.5
Lauryl mercaptan		0.004	Butyraldehyde (2 *M* in kerosene)	0.075	0.64
Octyl mercaptan		0.000	Acetaldehyde (4 *M* in kerosene)		0.51
Hexyl mercaptan		0.030	Ethers		
Esters			Butyl ether	0.000	0.000
Ethyl acetate	0.256	1.27	Isopropyl ether		0.000
Amyl acetate	0.012	0.115			
Isoamyl acetate	0.183	1.22			
2-Ethyl hexyl acetate	0.000	0.0039			
2-Ethyl butyl acetate	0.008	0.0395			

DISCUSSION

These results seem to be consistent with our analysis of the problem. The degree of differentiation that thiocyanate ion shows between the extraction of aluminum and beryllium is generally more than adequate to serve as the basis of a liquid–liquid extraction system for beryllium.

The best organic solvents to use seem to be six- to eight-carbon alcohols, or solvents containing double-bonded oxygens associated with five or six carbon atoms. Probably the lower efficiency of longer-chain compounds is merely a lowering of the concentration in the water phase as a result of the lower solubility.

It would seem that polarizability of the solvent is not an important contribution to the stability of the complex, as noted by the very poor extraction by the thioalcohols. This seems reasonable because the charge seen by the ligand should be quite low after the negative thiocyanate ions have been coordinated.

With cost considerations, as well as effectiveness of extraction and separation considered, methyl isobutyl ketone, 1-hexanol, isoamyl acetate, and 2-octanol seemed to be particularly promising solvents. A detailed investigation of beryllium–thiocyanate extraction systems using these solvents has therefore been undertaken, and a description of this work will constitute the second paper in this series.

The emphasis given to the thiocyanate ion in this work raises the question of the uniqueness of thiocyanate ion, implied by the failure to investigate the numerous other negatively charged ions which could coordinate to beryllium ions. If polarizability of the anion is an essential factor, then it seems evident that the negative ligand must be produced by dissociation of an acid in which the proton is associated with some element other than oxygen, since the nucleophilic atom would be more subject to polarization than atoms more remote from the coordinate bond. The cyanide ion, for example, would seem to meet our basic requirements of a ligand, but it does not exist as a free ion in the pH region where beryllium is free of hydroxylation. Other ions, such as selenocyanate, might work as well, or better than, the thiocyanate, but those which have occurred to us were rejected either on the basis of toxicity or economic consideration.

REFERENCES

1. D. W. BURKE, JR. and J. E. WHITE. The metal beryllium. American Society for Metals, Cleveland. 1955.
2. B. R. F. KJELLGREN. Beryllium. *In* Rare metals handbook. 2nd ed. *Edited by* C. A. Hampel. Reinhold, New York. 1961.
3. G. E. DARWIN and J. H. BUDDERY. Beryllium. Butterworth, London. 1960.
4. A. W. KNOERR. Eng. Mining J. 93 (1960).
5. G. H. MORRISON and H. FREISEN. Solvent extraction in analytical chemistry. John Wiley and Sons, Inc., New York. 1957. Chap. 3.
6. R. M. DIAMOND and D. G. TUCK. Extraction of inorganic compounds into organic solvents. *In* Progress in inorganic chemistry. Vol. II. *Edited by* F. A. Cotton. Interscience Publishers, New York. 1960.
7. F. BASOLO and R. G. PEARSON. Mechanisms of inorganic reactions. John Wiley and Sons, Inc., New York. 1958. p. 46.
8. J. C. WHITE, A. S. MEYER, and D. L. MANNING. Anal. Chem. **28**, 956 (1956).
9. E. S. MELICK. The analytical chemistry of beryllium in analytical chemistry in nuclear reactor technology. *Edited by* C. D. Susano, H. S. House, and M. A. Marler. AEC publication TID-7555. 1958.
10. F. J. WELCHER. The analytical uses of ethylenediaminetetraacetic acid. Van Nostrand, Princeton, N.J. 1958. p. 165.

A SYNTHESIS OF MIMOSINE

IAN D. SPENSER AND ALBERT D. NOTATION
Department of Chemistry, McMaster University, Hamilton, Ontario
Received March 9, 1962

ABSTRACT

DL-Mimosine has been synthesized by debenzylation and detosylation of the product obtained by condensation of 3-benzyloxy-4-pyrone with β-amino-α-tosylaminopropionic acid. A new method for the isolation of mimosine from *Leucaena glauca* Benth. is described.

The amino acid mimosine (VIII ↔ XV) was first isolated (1) from the sap of *Mimosa pudica* L. Investigation of its structure (1, 2) and of the structure of leucaenol (leucaenine) (3–9), isolated somewhat later (10) from *Leucaena glauca* Benth. (Kao Haole), made it likely that the two compounds were identical (1, 3–7). Direct comparison (11) confirmed this identity[1] and a synthesis of mimosine has been reported (12).

In connection with an investigation of the biosynthesis of mimosine, we required the compound in quantities which could not be conveniently obtained from *M. pudica*. Attempts to repeat the reported synthesis were disappointing. By reaction of 3-methoxy-4-pyridone (III) with α-acetamidoacrylic acid (IV), Adams and Johnson (12) had obtained an uncharacterized adduct, regarded as *O*-methyl-*N*-acetylmimosine (V), which gave mimosine (VIII) in 25% yield on vigorous hydrolysis with hydriodic acid. We were unable to obtain the amino acid by this method. The final product of the reaction was a mixture which, on the basis of paper chromatographic analysis, did not contain mimosine but appeared to consist mainly of 3-hydroxy-4-pyridone (VI) and alanine.

Another approach to synthesis, which had failed, was by the Strecker route. Although condensation of 3-methoxy-4-pyridone (III) with bromoacetaldehyde diethylacetal (13) and condensation of 3-methoxy-4-pyrone (I) with aminoacetaldehyde diethylacetal (14) gave derivatives of the requisite aldehyde (VII), further conversion of these to mimosine proved unsuccessful (13, 15).

The present synthesis was based on the condensation of suitably substituted derivatives of 3-hydroxy-4-pyrone and α,β-diaminopropionic acid. It had been reported earlier that 3-hydroxy-4-pyrone or 3-methoxy-4-pyrone did not react with glycine, α,β-diaminopropionic acid, β-amino-α-bromopropionic acid (15), or with β-amino-α-hydroxypropionic acid (12). Since the crucial step in the pyrone–pyridone conversion is generally regarded as analogous to carbinolamine formation (16), a nonprotonated amine is required as the nucleophilic reactant, and it was likely that the failure of these amino acids to condense was due to their zwitterion structure, in which the amino group is protonated. No attempt had been made to control the ionic state of the reactants (12, 15). Indeed, it was subsequently shown (17) that condensation of glycine with a number of 4-pyrone derivatives takes place only in the presence of an equimolar amount of base.

The desired condensation of a pyrone with α,β-diaminopropionic acid requires the species $NH_2—CH_2—CH(NH_3^+)COO^-$ of the latter. The assignment of pK values (pK_2, 6.69 (α-NH_2); pK_3, 9.50 (β-NH_2)) (18) indicates that in aqueous solutions this species in unobtainable in significant amounts. The species $NH_3^+—CH_2—CH(NH_2)COO^-$,

[1]*Since the name "mimosine" was the first to be coined (1), proof of identity makes the names "leucaenol" (10), "leucenol" (4), and "leucaenine" (5) redundant.*

which overwhelmingly predominates in the isoelectric range of the amino acid, would on condensation with 3-hydroxy-4-pyrone yield an isomer (IX) of mimosine. Condensation of the pyrone with the amino acid at pH > 11, i.e., with the species $NH_2—CH_2—CH(NH_2)COO^-$, would lead to a mixture of mimosine (VIII) and its isomer (IX). For an unequivocal synthesis of mimosine, protection of the α-amino group was therefore required.

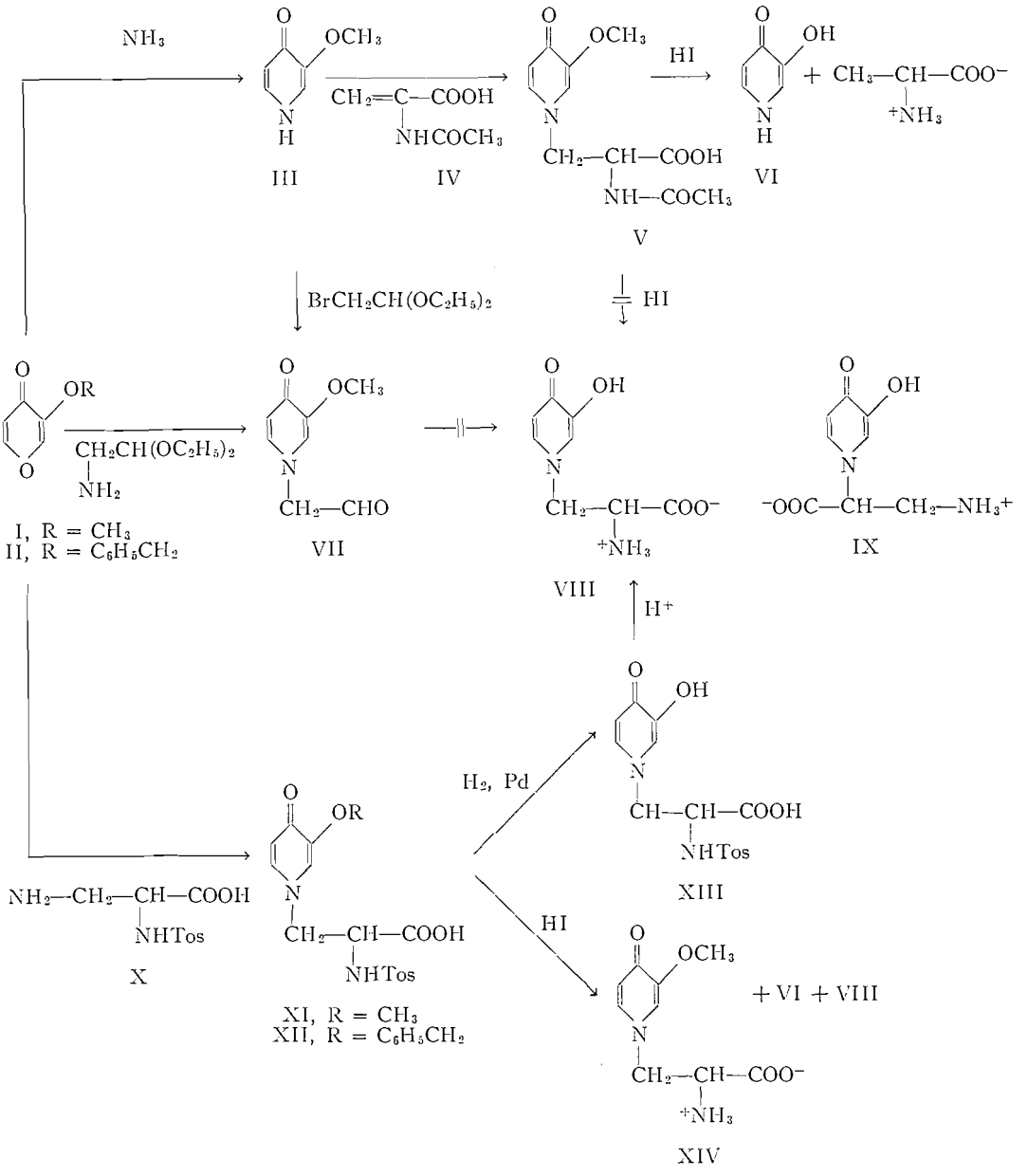

The chosen derivative was DL-β-amino-α-tosylaminopropionic acid (X), which was prepared, according to Rudinger (19), by Hofmann rearrangement of α-*N*-tosylasparagine.

Condensation of the tosylamino acid with 3-methoxy-4-pyrone in the presence of an equimolar quantity of sodium hydroxide gave β-(1,4-dihydro-3-methoxy-4-oxo-1-pyridyl)-*N*-tosylalanine (*O*-methyl-*N*-tosylmimosine) (XI) in 46% yield. Hydrolysis with hydrobromic or hydriodic acid under a variety of conditions gave mimosine (VIII), but was accompanied by considerable *N*-alkyl cleavage. It would appear that whereas mimosine itself is stable towards halogen acids (4, 5), derivatives of its *O*-methyl ether are not; this was presumably the reason why Adams and Johnson obtained a poor yield in their synthesis (12), and why we could not repeat their work. Under conditions where removal of the alanyl side chain from XI was minimal, detosylation did take place, but ether cleavage was incomplete. The product was a mixture of mimosine (VIII) and its *O*-methyl ether (XIV), fractionation of which proved to be tedious.

The difficulty was overcome by a minor variation in the route of synthesis. Condensation of DL-β-amino-α-tosylaminopropionic acid (X) with 3-benzyloxy-4-pyrone (II) gave β-(3-benzyloxy-1,4-dihydro-4-oxo-1-pyridyl)-*N*-tosylalanine (*O*-benzyl-*N*-tosylmimosine) (XII) in 70% yield, which on catalytic debenzylation yielded β-(1,4-dihydro-3-hydroxy-4-oxo-1-pyridyl)-*N*-tosylalanine (*N*-tosylmimosine) (XIII) in yields of 80%. Hydrolysis of the tosyl group by hydrogen bromide in glacial acetic acid gave DL-β-(1,4-dihydro-3-hydroxy-4-oxo-1-pyridyl)-alanine (VIII),[2] melting at 228–230° (decomp.). The melting point and infrared absorption of this synthetic material were very similar to the melting point (11, 12, 20) and infrared absorption[3] (9, 12, 20) of samples of natural mimosine, obtained from *M. pudica* L. and from *L. glauca* Benth. The ultraviolet absorption curves of the synthetic and the natural (4, 9) material were identical.

Synthetic and natural mimosine showed identical dissociation constants (pK_1, 2.1 (COOH); pK_2, 7.2 (NH_3^+); pK_3, 9.2 (OH)). The values for pK_2 and pK_3 are in good agreement with those calculated (7.28 and 9.19 respectively) from reported potentiometric data (5). The dissociation, pK_2, was the only one depressed in the presence of formaldehyde and must therefore be assigned to the α-amino group of mimosine. Its value, unusually low for the α-amino group of an amino acid, corresponds to reported values of the dissociation constants of similar NH_3^+ groups in 1,2-diammonium derivatives (e.g., $NH_3^+CH_2CH(NH_3^+)COO^-$, pK_2, 6.69 (α-NH_3^+) (18); $NH_3^+—CH_2—CH_2—NH_3^+$, pK_1, 6.98 (22)). The factor which lowers the basicity of the NH_2 group in these compounds is the polar effect of the proximal, charged NH_3^+ group. Since the pK_a of the α-amino group of mimosine is of similar magnitude, it is likely that the species XV is an important resonance contributor.

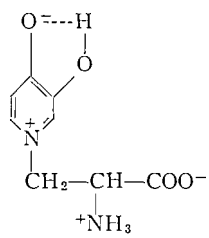

XV

[2]*An attempt to synthesize the* L-*isomer, starting from* L-α-*tosylamino-*β-*aminopropionic acid, failed, since condensation of this compound with 3-benzyloxy-4-pyrone under our conditions was accompanied by racemization.*

[3]*The observation that the infrared spectrum of a* DL-*amino acid in the solid state (*KBr*) differs from the spectra of the individual* D- *and* L-*isomers has been repeatedly confirmed (e.g., ref. 21).*

Unequivocal proof of identity, and incidentally, confirmation of structure, were obtained by comparison of the nuclear magnetic resonance spectra of synthetic and natural mimosine, recorded on samples dissolved in deuterium oxide containing sodium deuteroxide. A trace of water (H_2O) was present for internal reference. The two spectra were superimposable and showed four signals (chemical shift in parts per million from water): (*a*) a triplet +1.20, +1.12, +1.03 (—CH—); (*b*) a doublet +0.71, +0.63 ($—CH_2—$); (*c*) a doublet −1.57, −1.67 (C_5—H); (*d*) a singlet −2.49 (C_2—H) superimposed on a doublet −2.52, −2.62 (C_6—H). The areas of the signals were in the ratio 1:2:1:2. This spectrum fully accounts for the structure of the amino acid.

Extraction of mimosine from the seeds of *L. glauca* Benth. by reported methods (3–6) requires large volumes of solvent and the removal from the extracts of considerable quantities of protein and polysaccharides (23). Partial hydrolysis of the latter in the course of extraction leads to gummy intractable residues from which the desired product is obtainable only with great difficulty.

A simple but effective method for the separation of mimosine from the seeds of *L. glauca* has now been developed. Finely powdered seeds were dialyzed against distilled water. When the dialyzate was concentrated and allowed to stand overnight, almost pure mimosine crystallized in high yield.

Mimosine was also isolated from the exudate obtained on cutting the stems of *M. pudica*.

In biosynthetic experiments with *M. pudica*, radioactivity from carbon-14 dioxide and DL-3-C^{14}-aspartic acid was incorporated into mimosine. Degradation of the labelled mimosine from the latter experiment is in progress.

EXPERIMENTAL

3-Hydroxy-4-pyrone (Pyromeconic Acid)

3-Hydroxy-4-pyrone, melting at 116–118°, was prepared (24) in 66% yield by pyrolysis of anhydrous meconic acid and was purified by sublimation at 110° and 10^{-3} mm.

3-Methoxy-4-pyrone (I)

3-Methoxy-4-pyrone, melting at 93–95°, was obtained in 84% yield by methylation of pyromeconic acid with diazomethane in ether solution (24). It was purified by distillation at 5×10^{-3} mm and 100–110°.

3-Benzyloxy-4-pyrone (II)

A mixture of 3-hydroxy-4-pyrone (2.24 g, 0.02 mole), potassium iodide (0.30 g, 0.00019 mole), anhydrous potassium carbonate (2.67 g, 0.019 mole), and benzyl chloride (2.70 g, 2.45 ml, 0.022 mole) in dimethylformamide (100 ml) was heated for 8 hours on the steam bath with continuous stirring. The hot mixture was filtered, the residue washed repeatedly with ethanol, the combined filtrates evaporated to dryness, and the residual solid exhaustively extracted with ether. The extract was dried (Na_2SO_4) and concentrated to yield crystals of *3-benzyloxy-4-pyrone* (3.30 g, 81%), melting at 84–85° after recrystallization from ether. (Found: C, 71.0; H, 5.0. $C_{12}H_{10}O_3$ requires: C, 71.3; H, 5.0%.)

L- *and* DL-*β-Amino-α-tosylaminopropionic Acid (X)*

This was prepared according to Rudinger *et al.* (19) from L- and DL-*α-N*-tosylasparagine respectively.

β-(1,4-Dihydro-3-methoxy-4-oxo-1-pyridyl)-N-tosylalanine (O-Methyl-N-tosylmimosine) (XI)

3-Methoxy-4-pyrone (1.39 g, 0.011 mole) in water (10 ml) was added to a solution of DL-β-amino-α-tosylaminopropionic acid (2.58 g, 0.01 mole) in 0.1 *M* sodium hydroxide (100 ml, 0.01 mole). The mixture was heated for 3 hours on the steam bath and then concentrated to a volume of 50 ml, when the pH, originally above pH 11, had dropped to pH 9. The pH was adjusted to pH 7 by dropwise addition of concentrated hydrochloric acid and the solution was allowed to stand at 5° for several hours. Unreacted tosylamino acid (0.31 g, 0.0012 mole) was filtered off and the pH of the filtrate was adjusted to pH 2 with concentrated hydrochloric acid. Crystallization of the product started almost immediately and was complete after 12 hours at 5°, yielding DL-*β-(1,4-dihydro-3-methoxy-4-oxo-1-pyridyl)-N-tosylalanine* (1.51 g, 47%), melting at 200–201° (decomp.) after recrystallization from water. (Found: C, 52.7; H, 5.1; N, 7.6; S, 9.0. $C_{16}H_{18}N_2O_6S$ requires: C, 52.5; H, 5.0; N, 7.7; S, 8.7%.)

Condensation of 3-methoxy-4-pyrone with L-β-amino-α-tosylaminopropionic acid in place of the DL-compound was accompanied by racemization, also yielding optically inactive condensation product.

β-(3-Benzyloxy-1,4-dihydro-4-oxo-1-pyridyl)-N-tosylalanine (O-Benzyl-N-tosylmimosine) (XII)

3-Benzyloxy-4-pyrone (2.24 g, 0.011 mole) in ethanol (15 ml) was mixed with a solution of DL-β-amino-α-tosylaminopropionic acid (2.58 g, 0.01 mole) in 0.1 *M* sodium hydroxide (100 ml, 0.01 mole). The mixture was warmed and shaken until homogeneous, and the solution was heated on the steam bath under reflux for 8 hours. Concentrated hydrochloric acid (3 ml) was added with rapid stirring and the solution allowed to stand at 5° overnight, when *β-(3-benzyloxy-1,4-dihydro-4-oxo-1-pyridyl)-N-tosylalanine* (3.25 g, 74%), melting at 203–205° (decomp.) after recrystallization from ethanol, was obtained. (Found: C, 59.5; H, 5.3; N, 6.3; S, 7.4. $C_{22}H_{22}N_2O_6S$ requires: C, 59.7; H, 5.0; N, 6.3; S, 7.2%.)

β-(1,4-Dihydro-3-hydroxy-4-oxo-1-pyridyl)-N-tosylalanine (N-Tosylmimosine) (XIII)

O-Benzyl-*N*-tosylmimosine (1.00 g, 0.0023 mole) in dimethylformamide (100 ml) was shaken 45 hours at room temperature under hydrogen at 18 p.s.i. in the presence of 5% palladium on charcoal (1.00 g), the catalyst having been prehydrogenated at 25 p.s.i. in ethanol (50 ml) at room temperature for 3 hours. The reaction mixture was heated and filtered and the catalyst exhaustively washed with hot ethanol. The filtrate was evaporated to dryness and the residue crystallized from ethanol, yielding *β-(1,4-dihydro-3-hydroxy-4-oxo-1-pyridyl)-N-tosylalanine* (0.64 g, 80%), melting at 203–205° (decomp.). (Found: C, 51.0; H, 4.8; N, 7.8; S, 9.3. $C_{15}H_{16}N_2O_6S$ requires: C, 51.1; H, 4.6; N, 8.0; S, 9.1%.)

β-(1,4-Dihydro-3-hydroxy-4-oxo-1-pyridyl)-alanine (DL-Mimosine) (VIII)

The tosyl derivative (XIII) (0.40 g) was dissolved in sufficient glacial acetic acid (approximately 25 ml) to give a homogeneous solution. Phenol (0.40 g) was added and the solution was saturated at room temperature with dry hydrogen bromide and left at 60–65° in a stoppered flask. The reaction mixture was repeatedly monitored by ascending paper chromatography (phenol–ethanol–water, 3:1:1) and incubation was continued until the phenolic spot corresponding to *N*-tosylmimosine (R_f 0.78) failed to appear and only that corresponding to mimosine (R_f 0.27) was observed on development of the chromatogram with ferric chloride solution. This generally required 2–3 days but in some runs additional hydrogen bromide was passed into the solution after 3 or 4 days in order to complete hydrolysis. The cooled solution was diluted with dry ether (400 ml) and allowed to stand at 5° until the separation of mimosine hydrobromide was complete. The supernatant liquid was decanted and the residue repeatedly extracted with ether and then dissolved in water. The aqueous solution was basified with concentrated ammonium hydroxide and evaporated to dryness under reduced pressure. The remaining solid was repeatedly moistened with water and evaporated to dryness under reduced pressure to remove excess ammonia, and finally dissolved in hot water, decolorized with charcoal, and allowed to crystallize, yielding DL-mimosine (0.10 g, 45%) melting at 222–225° (decomp.). For analysis a sample was recrystallized from boiling water and the product filtered from the hot solution, to give anhydrous DL-mimosine, melting at 228–230° (decomp.). (Found: C, 48.7; H, 5.4; N, 14.1. Calculated for $C_8H_{10}N_2O_4$: C, 48.5; H, 5.1; N, 14.1%.) Dissociation constants (determined by half-titration of mimosine in 0.04 *M* aqueous solution with 0.10 *M* sodium hydroxide and 0.10 *M* hydrochloric acid, and application of water correction): pK_1, 2.1 (—COOH); pK_2, 7.2 (α-NH_3^+); pK_3, 9.2 (phenolic —OH). Only pK_2 was depressed in the presence of formaldehyde. Ultraviolet absorption (λ_{max}, mμ (log ε)): in water: 283 (410); in 0.07 *M* HCl: 277 (3.87); in 0.07 *M* NaOH: 309 (4.04). Infrared absorption (KBr) (cm^{-1}): 3400 (broad) (OH), 2900 (broad) (NH), 1640 (s) (C=O), 1588 (s) (COO^-), 1490 (s) (NH_3^+).

Mimosine from the Seeds of Leucaena glauca

Coarsely crushed dried seeds were pulverized to a fine powder in a ball mill. The powdered seeds (50 g) were placed into a dialysis bag (length 35 cm, cross section 3 cm) which was then filled with distilled water and completely immersed in distilled water (1 l.). After three changes of external solvent the dialyzate showed only a weak phenolic reaction. Each dialyzate was concentrated at reduced pressure to 25 ml, when almost pure product crystallized. Mimosine (0.61 g, 1.2%), melting at 227–228° (decomp.), after recrystallization from water, was obtained from 50 g of seeds. Dissociation constants: pK_1, 2.1; pK_2, 7.2 (α-NH_3^+); pK_3, 9.2 (OH). Ultraviolet absorption: (λ_{max}, mμ (log ε)): in water: 283 (4.11); in 0.07 *M* HCl: 277 (3.86); in 0.07 *M* NaOH: 309 (4.04). Infrared absorption (KBr) (cm^{-1}): 3400 (broad) (OH), 2850 (broad) (NH), 1640 (s) (C=O), 1590 (s) (COO^-), 1530 (s), 1490 (s) (NH_3^+).

Mimosine from Mimosa pudica (cf. Ref. 1)

The exudate from freshly cut green stems and petioles of *Mimosa* was aspirated into a lambda pipette. A sample (250 μl) was rubbed with ethanol (5 ml), when crude mimosine (12 mg) precipitated, which after treatment with charcoal and recrystallization from water melted at 224–226° (decomp.). A sample of exudate (250 μl) was evaporated to dryness in a vacuum desiccator to give a brown residue (39 mg) which was dissolved in water, decolorized with charcoal, and yielded mimosine, melting at 221–223° (decomp.).

A sample of exudate (250 μl) was dissolved in phthalate buffer (pH 4, 0.2 *M*) (3 ml), and applied to a cation exchange column (Dowex 50-X4) in the hydrogen form. Water eluted a fluorescent material which was not further investigated. Mimosine was displaced with ammonia (0.02 *M*). The eluate was concentrated *in vacuo* and dried in a vacuum desiccator over concentrated sulphuric acid, yielding mimosine (9 mg), melting at 225–226° (decomp.).

Paper Chromatography

Reaction mixtures and plant extracts were monitored by ascending paper chromatography on Whatman No. 1 paper, using phenol–ethanol–water, 3:1:1, as the solvent. Spots were developed with ferric chloride (1%) and/or ninhydrin (3% in acetone). Before development the papers were dried for 1 hour at 80° to ensure complete removal of phenol.

Under these conditions the following R_f values were found: 3-hydroxy-4-pyrone, R_f 0.83; 3-hydroxy-4-pyridone, R_f 0.70; *O*-methylmimosine, R_f 0.61; *N*-tosylmimosine, R_f 0.78; mimosine, R_f 0.27.

ACKNOWLEDGMENTS

We are greatly indebted to Professor R. Adams, University of Illinois, for a gift of *L. glauca* seeds; to Dr. H. Matsumoto, University of Hawaii, for a generous supply of ground seeds of Kao Haole; and to Dr. C. Lamoureux, University of Hawaii, for a gift of dried Kao Haole plants. We are also grateful to Mr. B. Lipinski, who, as a visiting fellow, took part in the early stages of this investigation.

Financial assistance by the National Research Council of Canada and by the Ontario Research Foundation is gratefully acknowledged.

REFERENCES

1. J. Renz. Z. physiol. Chem. Hoppe-Seyler's, **244**, 153 (1936).
2. H. Nienburg and K. Tauböck. Z. physiol. Chem. Hoppe-Seyler's, **250**, 80 (1937).
3. R. K. Yoshida. Ph.D. Thesis, University of Minnesota, Minneapolis, Minn. 1944.
4. R. Adams, S. J. Cristol, A. A. Anderson, and A. A. Albert. J. Am. Chem. Soc. **67**, 89 (1945).
5. A. F. Bickel and J. P. Wibaut. Rec. trav. chim. **65**, 65 (1946).
6. D. Kostermans. Rec. trav. chim. **65**, 319 (1946); **66**, 93 (1947).
7. J. P. Wibaut. Helv. Chim. Acta, **29**, 1669 (1946).
8. A. F. Bickel. J. Am. Chem. Soc. **69**, 1805 (1947); **70**, 326 (1948).
9. R. Adams, W. Jones, and J. L. Johnson. J. Am. Chem. Soc. **69**, 1810 (1947).
10. M. Mascré. Compt. rend. **204**, 890 (1937).
11. R. J. C. Kleipool and J. P. Wibaut. Rec. trav. chim. **69**, 37 (1950).
12. R. Adams and J. L. Johnson. J. Am. Chem. Soc. **71**, 705 (1949).
13. A. F. Bickel. J. Am. Chem. Soc. **70**, 328 (1948).
14. R. J. C. Kleipool and J. P. Wibaut. Rec. trav. chim. **66**, 459 (1947).
15. R. J. C. Kleipool and J. P. Wibaut. Rec. trav. chim. **69**, 1041 (1950).
16. E. Klingsberg (*Editor*). Pyridine and its derivatives. Part One. Interscience Publishers, New York. 1960. pp. 179, 185.
17. K. Heyns and G. Vogelsang. Chem. Ber. **87**, 1377 (1954).
18. A. A. Albert. Biochem. J. **50**, 690 (1951).
19. J. Rudinger, K. Poduška, and M. Zaoral. Collection Czechoslov. Chem. Commun. **25**, 2022 (1960).
20. J. P. Wibaut and J. P. Schuhmacher. Rec. trav. chim. **71**, 1017 (1952).
21. R. J. Koegel, J. P. Greenstein, M. Winitz, S. M. Birnbaum, and R. A. McCallum. J. Am. Chem. Soc. **77**, 5708 (1955).
22. G. Schwarzenbach. Helv. Chim. Acta, **16**, 522 (1933).
23. A. M. Unrau. J. Org. Chem. **26**, 3097 (1961).
24. A. F. Bickel. J. Am. Chem. Soc. **69**, 1801 (1947).

ABSOLUTE YIELDS IN THE γ-RADIOLYSIS OF GASES[1]

R. A. BACK, T. W. WOODWARD,[2] AND K. A. MCLAUCHLAN[3]
Division of Pure Chemistry, National Research Council of Canada, Ottawa, Canada

Received March 27, 1962

ABSTRACT

Absolute yields of hydrogen from the γ-radiolysis of hydrocarbon gases have been obtained by relating the hydrogen produced to saturation ion currents measured in the radiolysis vessel. Values for G_{H_2} of 1.28, 1.20, 6.25, 5.40, and 5.00 have been estimated for ethylene, propylene, propane, *n*-butane, and isobutane respectively. These values are consistently lower than those obtained previously with α-rays, and this is discussed as an effect of radiation quality. Arguments are advanced for the use of M/N, the yield per ion pair, rather than G, as a measure of yields in the radiolysis of gases.

Despite the very considerable amount of work done in recent years on the γ-radiolysis of gases, the dosimetry of these systems, especially the absolute dosimetry, is very far from satisfactory. Most workers have calculated G-values by a comparison with other gas-phase "dosimeters", such as ethylene, acetylene, or nitrous oxide, using a correction for differences in stopping power (usually simply an electron-density correction), although these "dosimeters" have never been well calibrated for gamma radiation. Others have simply estimated the energy absorbed from the measured γ-ray flux, with some assumption about an energy absorption coefficient for the gas, which can lead to large errors for gases at atmospheric pressure or lower. The basic difficulty in γ-ray dosimetry at these pressures is that in most cases the direct absorption of γ-radiation in the gas is quite negligible, and almost all the chemical effects are due to secondary electrons ejected from the walls of the irradiation vessel. The accurate estimation of absorbed energy becomes very difficult in this situation, especially in the absence of precise knowledge of the energy distribution of the electrons, and of their rate of energy loss in the gas.

Surprisingly little use has been made in the radiation chemistry of gases of the measurement of saturation ion currents in the gases themselves during irradiation. Essex and co-workers (1), using very weak sources of α-rays, have related chemical yields to saturation ion currents for a few gases, but the method has never been applied to γ-radiolysis systems. It appears to offer a very simple way to obtain absolute yields in the γ-radiolysis of gases, and the present paper describes the results of some measurements made with simple hydrocarbons.

EXPERIMENTAL

Unlike α-rays, γ-radiation cannot be restricted conveniently to a region between two parallel plates, so a cylindrical reaction vessel, shown in Fig. 1, was used in which the cylindrical wall itself was the collecting electrode. The vessel was made of 60-mm o.d. Pyrex tubing, while the cathode and guard ring consisted of graphite coatings, originally applied as colloidal graphite in aqueous suspension. The anode was a tungsten wire of 1.5-mm diameter, while tungsten leads through the glass walls made connections to the cathode and guard ring. The vessel was thoroughly baked under vacuum before its initial use, and before each experiment. In the initial baking at 400° C, a tarry material slowly distilled out, presumably formed from the decomposition of the suspension agent mixed with the graphite. After the first several hours of baking, no further material was ever evolved.

[1]*Issued as N.R.C. No. 6906.*
[2]*National Research Council of Canada Postdoctoral Fellow, 1960–62.*
[3]*National Research Council of Canada Postdoctoral Fellow, 1959–60. Present address: National Physical Laboratory, Teddington, Middlesex, England.*

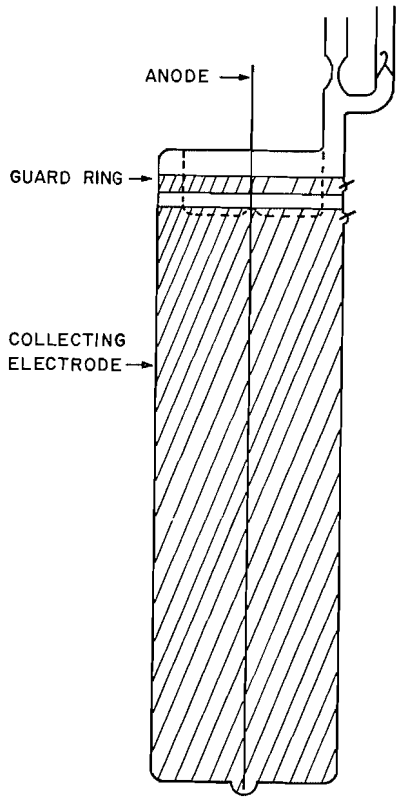

FIG. 1. Vessel used for γ-radiolysis of hydrocarbon gases, and for measurement of saturation ion currents

The preparation of the reaction vessel and the hydrocarbon gases, and the analytical techniques, were similar to those previously described (2). The hydrocarbons were all Phillips Research Grade, and showed no change in behavior upon careful treatment with sulphuric acid to remove any olefin present. Hydrogen was the only product accurately measured, and conversions were always low enough so that the yields were close to true initial values (2).

Ion currents were measured by passing the current from the collecting electrode to earth through a calibrated Rubicon spot galvanometer equipped with a suitable shunt. The guard ring was held at the same potential as the collecting electrode, while a variable high potential, up to 5 kv, could be applied to the central anode. Saturation ion currents were always measured at the beginning of the irradiation, and the time during which the field was applied was always negligible compared to the total time of irradiation, which was usually about 16 hours, and sometimes much longer. In a few experiments, ion currents were also measured at the end of the radiolysis period, and were found to be unchanged.

The source of γ-radiation was a Co^{60} unit, nominally of about 200 curies. The radiolysis vessel was mounted in an approximately reproducible position, end-on to the source, and about 8 inches away.*

RESULTS AND DISCUSSION

Figure 2 shows typical plots of ion current against applied voltage for ethylene and *n*-butane at 800 mm pressure. The slower approach to saturation in the latter is probably due partly to the higher electron density, with consequent higher rate of absorption of energy, higher ion concentrations, and hence faster gas-phase recombination, and partly to a slower diffusion of electrons and ions to the electrodes through the heavier gas. Similarly good saturation behavior was found with all the gases studied.

We are grateful to the Division of Applied Physics of these Laboratories for the use of the Co^{60} source.

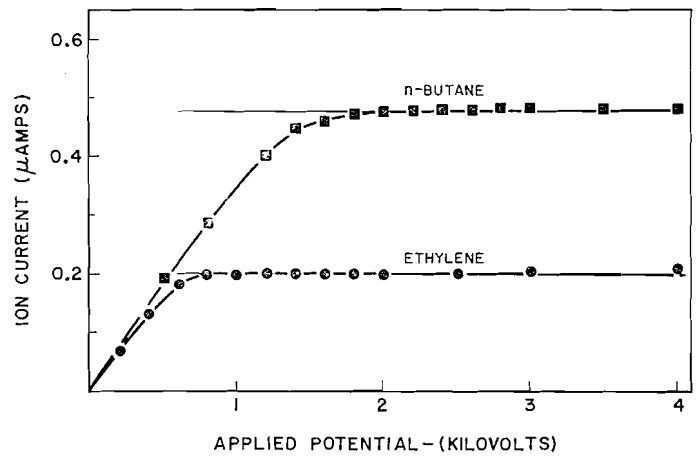

FIG. 2. Ion currents in the γ-radiolysis of ethylene and n-butane at 800 mm.

In Table I are shown values of the yield of hydrogen per ion pair, $(M/N)_{H_2}$ (following Lind's usage (3)), for several pure hydrocarbons, and several with added scavenger. Also

TABLE I

Hydrogen yields in the γ-radiolysis of hydrocarbon gases

Gas	Saturation ion current (μamp)	Hydrogen yield (μmoles/hr) $\times 10^2$	$(M/N)_{H_2}$ (molecules/ion pair)	W (ev/ion pair)	G_{H_2} This work	G_{H_2} Other values
C_2H_4	0.196	0.275	0.34	26.5*	1.28	2.0 (4) 1.14 (5) 1.3 (6) 1.2 (7)
C_3H_6	0.319	0.386	0.30	25†	1.20	1.1 (8)
C_3H_8	0.390	2.36	1.50	24‡	6.25	6.4 (9) 5.9 (10) 8.2 (α-rays (11))
C_3H_8 + scavenger	0.400	0.645	0.40	24	1.67	2.1 (6) 1.6 (9)
n-C_4H_{10}	0.520	2.72	1.29	24§	5.40	9.0 (α-rays (11))
n-C_4H_{10} + scavenger	0.488	0.864	0.42	24	1.75	
i-C_4H_{10}	0.471	2.29	1.20	24‖	5.0	7.4 (α-rays (11))
i-C_4H_{10} + scavenger	0.487	0.774	0.42	24	1.75	

*W. P. Jesse and U. Sadauskis. Phys. Rev. 97, 1668 (1955).
†Estimated from value for propane.
‡Ref. 6.
§Estimated from value of 25.9 for α-rays (G. J. Hine and G. L. Brownell. Radiation dosimetry. Academic Press, New York. 1956).
‖Taken to be the same as n-butane.

shown are values of W, the average energy absorbed per ion pair, taken from the literature, and values of G_{H_2} calculated from the relation $G = (M/N) \times 100/W$. All the pure hydrocarbons in Table I were studied at 800 mm pressure and room temperature, and each of the values of $(M/N)_{H_2}$ represents an average of at least two experiments agreeing to $\pm 2\%$ or better. To all the data in Table I, a correction of about 5% was applied to take

into account the "dead space" around the guard ring and in the side arm from which ions were not collected and measured.

The systems with added ethylene scavenger, ranging from 3 to 10 mole%, were maintained at constant electron density, equal to that of the pure paraffin at 800 mm and 25° C. The data were then extrapolated back to 0% scavenger in a way similar to that described previously (2). The W-values then used in computing G_{H_2} for unscavengable hydrogen were those for the pure paraffin. The similarity of the values of W for paraffins and olefins, and the almost unchanged ion currents observed with added scavenger, justify this procedure.

Several features of the results in Table I deserve comment. The ratio of G-values obtained with and without scavenger for propane, butane, and isobutane are almost identical with those found previously by simple measurements of relative hydrogen yields (2). This indicates that olefin impurities were not affecting the results, and shows that the saturation ion current method at least yields reasonable relative values in the presence and absence of olefin scavenger.

The values of W shown in Table I, and used in the calculation of G_{H_2}, were estimated by a variety of means, as indicated, and while probably not very reliable, they are unlikely to be grossly in error. There is no direct information available about W-values for γ-radiation, as their measurement is practically impossible. The values of W appropriate to the secondary electrons which are effective in the present systems are probably close to those measured for β-radiation.

In the last column of Table I are some values of G_{H_2} taken from the literature. The agreement between our measured values for ethylene and propane and the more recent literature values for γ-radiation is quite good. The values of G_{H_2} for α-radiolysis of propane, *n*-butane, and isobutane are consistently much higher than our present measured values for γ-radiation. This may be a true effect of radiation quality, and, if so, is one of the few examples of such an effect to be observed in gases. The larger hydrogen yield found in the α-radiolysis might be explained by the neutralization of a large fraction of the hydrocarbon ions in the α-ray tracks, with subsequent decomposition of the highly excited neutral species. With γ-rays, especially at the low intensities used in the present work, neutralization could be predominantly at the wall, with stabilization of the resultant fragment or molecule, and a decreased yield of products. In some recent experiments (12), it has been found that a saturation field applied during the course of the γ-irradiation of *n*-butane and isobutane causes a decrease in $(M/N)_{H_2}$ of about 30%, which supports the suggestion that neutralization at a surface could cause a reduction in hydrogen yield. This also suggests that at least 30% of the ions in the γ-radiolysis normally do *not* reach the wall, but this would still allow enough neutralization at the wall to account for the difference between α- and γ-radiolysis.

The absolute values of G_{H_2} for α-radiolysis found by Back and Miller (11) depend essentially upon a single measurement of the strength of their polonium source, and while this is reasonably certain, some confirmation of these values would be very desirable. Freeman and Ramaradhya (13), in the only comparable work,* have reported a similarly

*It should be noted that all the early work on the α-radiolysis of hydrocarbons (3), using radon, was done at such high conversions that the reported values of hydrogen yields are undoubtedly much lower than the initial ones, due to scavenging effects of products, and cannot be usefully compared with more recent measurements. Even in the work of Essex and Williams (14), using the saturation-current method in the α-radiolysis of ethane, and from which $G_{(H_2+CH_4)} = 5.7$ can be computed, the conversion of about 0.05% which was attained was high enough so that much of the original scavengeable hydrogen must have been lost, so that the higher value of $G_{H_2} = 8.8$ found recently by Yang and Gant (8) for the γ-radiolysis of ethane at much lower conversions probably does not represent a reversal of the dependence on radiaton quality discussed above.

"high" value of $G_{H_2} = 8.0$ for the α-radiolysis of cyclohexane vapor, which is again much higher than the values reported for β- and γ-radiation, although the latter data are very uncertain. Thus while there is some confirmation of a strong dependence on radiation quality in these systems, further measurements with both α- and γ-radiation, particularly the former, would be very useful.

Finally, some cogent arguments may be advanced for the general use of M/N rather than G as a measure of absolute yields in the radiolysis of gases. Both quantities are empirical, but G depends upon the measurement of total energy absorbed in the gas, which is almost impossible to determine directly for γ-radiation, and is usually estimated by some rather arbitrary, indirect, and uncertain method of dosimetry. M/N, on the other hand, when measured by the saturation-current method, is obtained directly from two well-defined and easily measured quantities. The saturation-current method is applicable to most gases, and to all types of radiation, and should be very useful in the comparison of results in different systems and from different laboratories. The use of M/N was, of course, common in the early days of radiation chemistry, when it was regarded as somewhat akin to a quantum yield. It fell into disrepute when it became evident that processes other than ionization could be important in radiolysis. However, M/N is still a more fundamental quantity than G, and a more directly useful one, especially for relating radiolysis products to mass spectra, as has become very popular recently. It is generally realized today that radiolysis mechanisms are undoubtedly very complex, and there seems to be little danger now that anyone would assume that the use of M/N implied a one-to-one relation between ion pairs and product molecules. Thus the reinstatement of M/N as a respectable quantity in the radiolysis of gases appears to offer few drawbacks and several distinct advantages. If W, the average energy dissipated per ion pair, could be more easily measured, then M/N and G would of course be readily interchangeable.

REFERENCES

1. H. ESSEX. J. Phys. Chem. **53**, 42 (1954).
2. R. A. BACK. J. Phys. Chem. **64**, 124 (1960).
3. S. C. LIND. Radiation chemistry of gases. Reinhold, New York. 1961.
4. K. YANG and P. J. MANNO. J. Phys. Chem. **63**, 752 (1959).
5. F. W. LAMPE. Radiation Research, **10**, 691 (1959).
6. L. M. DORFMAN and M. C. SAUER. J. Chem. Phys. **32**, 1886 (1960).
7. L. M. DORFMAN and M. C. SAUER. J. Phys. Chem. **66**, 322 (1962).
8. K. YANG and P. L. GANT. J. Phys. Chem. **65**, 1861 (1961).
9. K. YANG. J. Am. Chem. Soc. **84**, 719 (1962).
10. K. YANG and P. J. MANNO. J. Am. Chem. Soc. **81**, 3507 (1959).
11. R. A. BACK and N. MILLER. Trans. Faraday Soc. **55**, 911 (1959).
12. R. A. BACK and T. W. WOODWARD. To be published.
13. J. M. RAMARADHYA and G. R. FREEMAN. J. Chem. Phys. **34**, 1726 (1961).
14. N. T. WILLIAMS and H. ESSEX. J. Chem. Phys. **17**, 995 (1949).

HYDROGEN FORMATION IN γ-IRRADIATED HYDROGEN CHLORIDE

D. A. ARMSTRONG

Department of Chemistry, University of Alberta, Calgary, Calgary, Alberta

Received March 9, 1962

ABSTRACT

Hydrogen yields from pure liquid and solid hydrogen chloride irradiated with Co^{60} γ-rays were G_{H_2}(liquid) = $6.5_0 \pm 0.1_0$ and G_{H_2}(solid) = $3.3_0 \pm 0.1_0$ at −79° C and −196° C respectively. The yield from solid hydrogen chloride was only slightly reduced by the addition of chlorine; but the yield from liquid samples was reduced sharply by low concentrations of chlorine to a value of about 4.5, and then much more gradually by larger concentrations. A G_{H_2} value of 2.1 persisted at 10 mole% chlorine. The results were interpreted in terms of the formation of hydrogen in the reactions

$$H + HCl \rightarrow H_2 + Cl \quad [11]$$

and

$$H\ (hot) + HCl \rightarrow H_2 + Cl. \quad [11^*]$$

Reduction of the hydrogen yields by chlorine was attributed to the reactions

$$H + Cl_2 \rightarrow HCl + Cl \quad [15]$$

and

$$H\ (hot) + Cl_2 \rightarrow HCl + Cl. \quad [15^*]$$

Values of k_{11}/k_{15} and k_{11}^*/k_{15}^* were estimated to be 1.7×10^{-3} and 0.10 respectively, while those of G_H and $G_{H(hot)}$ were 2.4 ± 0.2 and 4.0 ± 0.2. Electron scavenging by chlorine was considered as a less likely mechanism for reduction of the hydrogen yield. Sources of the thermal and hot hydrogen atoms were examined and it was suggested that the decomposition of electronically excited molecules might be an important mode of decomposition.

INTRODUCTION

The decomposition of hydrogen halides by ionizing radiation has long been a subject of interest. Most of the earlier work was carried out with radon α-particles (see for example ref. 1), but more recently, Zubler, Hamill, and Williams (2) have irradiated gaseous hydrogen bromide with X rays. In this study the results were interpreted according to the mechanism of Eyring, Hirshfelder, and Taylor (3). Although it was suggested that the dissociation of electronically excited molecules might make a small contribution, most of the observed decomposition was considered to result from the ionization of hydrogen bromide molecules. Very few studies of the radiolysis of hydrogen halides in the liquid and solid states have been reported, and it seems that the effects of free-radical scavengers on the hydrogen and halogen yields have never been investigated. The present work was therefore initiated with the intention of extending our knowledge of the radiation chemistry of these compounds to condensed phases, and of determining the effect of scavengers on the product yields. This paper describes the results of an investigation of the radiolysis of liquid and solid hydrogen chloride (hereafter referred to as HCl). The effect of chlorine and ethylene on the hydrogen yields is also reported.

EXPERIMENTAL

Apparatus

A mercury-free vacuum line for purifying and storing HCl and chlorine was fitted with an oil diffusion pump and constructed so that samples of hydrogen and other volatile gases could be transferred from it via the oil diffusion pump to a conventional hydrogen analysis system. This feature permitted repeated irradiations of the same sample of hydrogen chloride without its being contaminated with mercury vapor from the analysis system. Pyrex bulbs and traps were provided for purifying the gases and storing them at liquid

nitrogen temperature, and a set of calibrated bulbs was used for measuring out samples of chlorine. These were connected to one side of a differential diaphragm manometer, the other side of which was attached to an auxiliary vacuum line with a conventional mercury manometer. Chlorine pressures were read on the mercury manometer, the differential manometer being used as a "null" instrument to equate the pressure in the auxiliary line to that of the chlorine in the calibrated bulb. The measured quantity of chlorine was distilled into the irradiation cell prior to the introduction of the HCl.

The 16-mm O.D. pyrex irradiation cells were cleaned by standard techniques and attached to the vacuum line via capillary "seal off" tubes. They were provided with "break seals" for re-entry into the vacuum line after radiolysis and were flamed to the sodium emission temperature under vacuum before the reagents were introduced. After they had cooled a small quantity of HCl was introduced and left in them for about 30 minutes to displace or react with possible contaminants adsorbed on the walls. The cells were then reflamed while the HCl was pumped out to an ultimate pressure of 5×10^{-6} mm of Hg.

A 200-curie Co^{60} source, housed in a concrete cave, was used for the radiolysis. Liquid HCl samples were irradiated at $-79°$ C in a dry ice – alcohol bath. Solid samples were irradiated at $-196°$ C in liquid nitrogen. The Fricke dosimeter was used and corrections were made for the different electron density of HCl. Chlorine molecules would undoubtedly have contributed a certain fraction of the total primary absorption of γ-rays in the system. However, they should also have absorbed a roughly equivalent fraction of the energy of the electrons set in motion in the medium. In solutions containing chlorine, the dose was therefore calculated for HCl alone, and energy absorption by chlorine was neglected.

Materials

Chlorine (99.5% minimum purity) from a Matheson lecture bottle was purified by bulb-to-bulb distillation and stored in a liquid nitrogen trap. Degassed hydrogen chloride of 99.0% minimum purity, also obtained from Matheson, was purified from hydrogen bromide and other impurities by preirradiation for a day or by treatment with chlorine. Both procedures oxidized the hydrogen bromide to bromine, which (together with excess chlorine) was subsequently removed by passage through copper foil. The hydrogen chloride was then stored in a liquid nitrogen trap. Samples for irradiation were further purified by sublimation from a trap at $-100°$ C through a second trap at the same temperature into a liquid nitrogen trap. A second sublimation from $-100°$ C to a calibrated bulb followed. The required quantity of this HCl was then roughly measured out as a liquid at its melting point and sublimed into the irradiation cell. Ethylene was purified in the same way as the chlorine.

Analytical Apparatus and Technique

The hydrogen analysis system, consisting essentially of a McLeod Gauge and Toepler pump, was similar to that described by Allen and co-workers (4) except that a palladium thimble was used, in place of the combustion technique, for identification of the hydrogen.

The liquefied HCl samples were shaken after irradiation to equilibrate the dissolved hydrogen with that in the vapor phase, and then frozen. All the non-condensable gas was introduced into the analytical apparatus by either connecting the irradiation cells directly to it or by connecting them to the purification system and transferring the gas with the diffusion pump. There was no difference between hydrogen yields measured by these two methods, and the hydrogen content of this first sample of gas was usually 95% or better. After melting and refreezing the hydrogen chloride a second portion of non-condensable gas was taken off. Its hydrogen content was usually about 10% of the first, and that of further degassings was negligible.

After the hydrogen had been extracted the HCl was either purified from halogen and transferred to another cell for a second irradiation or absorbed in water and titrated with standard sodium hydroxide to determine accurately the size of the sample. The latter was the eventual fate of all HCl samples except those with an appreciable concentration of chlorine. These were absorbed in standard sodium hydroxide and "back-titrated" to determine the total chloride. The original molecular chlorine content was then determined from the hypochlorite formed by iodimetry, and the HCl by difference. The chlorine content determined in this way agreed within a few percent with the gas phase measurement. The quantity of HCl used was usually in the range 2.4 to 2.7 g.

RESULTS

Hydrogen yields from pure liquid HCl and from solutions of ethylene and chlorine in liquid HCl have been plotted as a function of dose in Fig. 1. In all cases they were linear with dose over the range used, and for pure HCl repeated irradiation of the same sample to a total dose of 5×10^{19} ev/g produced no change in the hydrogen yield. The yields were reproducible to within $\pm1\%$ when reasonably large doses were used. The absolute accuracy is probably ±0.1 G units.

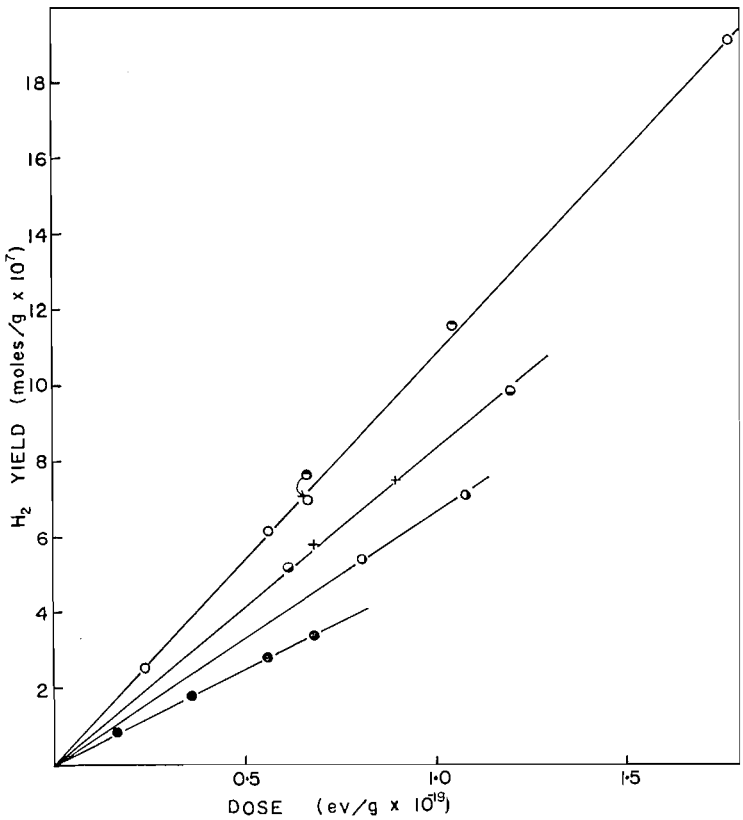

FIG. 1. Hydrogen yields from liquid HCl at −79° C plotted against absorbed dose: ○ pure HCl; ◓ HCl + NO (10^{-2} *M*); ◒ HCl + C_2H_4 (5.6×10^{-1} *M*); + HCl + Cl_2 ($7.1_7\times10^{-2}$ *M*); ◑ HCl + Cl_2 (4.65×10^{-1} *M*); ● HCl + Cl_2 (1.52 *M*).

It can be seen from Fig. 1 that ethylene was by far the less efficient of the two scavengers, and very high concentrations of it would have been required to reduce the hydrogen yield to the levels achieved with chlorine. In view of this and of the fact that there is a free-radical chain addition reaction between ethylene and HCl (5), which would have consumed the olefin, chlorine was chosen as the scavenger most suitable for detailed study. In the two experiments which were conducted with ethylene a small quantity of nitric oxide was added to inhibit the chain reaction. This quantity of nitric oxide was shown to be without effect on the hydrogen yield, but its efficiency as an inhibitor can only be presumed until a detailed study of the reaction is made.

The results for solutions of chlorine at several different concentrations in HCl have been summarized in Fig. 2. The hydrogen yields have been plotted as G_{H_2} values against the corresponding solute concentrations and it can be seen that an abrupt decrease in hydrogen yield from 6.5 to 4.5 resulted over the concentration range $0\text{-}2\times10^{-4}$ mole chlorine/g HCl. Further addition of chlorine caused a much more gradual decrease. A G_{H_2} value of 2.1 was finally reached at a chlorine concentration of 2.9×10^{-3} mole/g or about 10 mole%. Obviously, two hydrogen-forming species, which are scavenged with different efficiencies by chlorine, must be present.

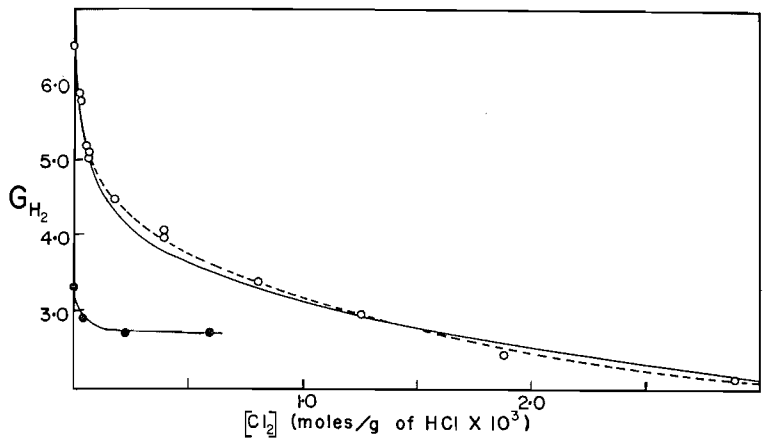

FIG. 2. Values of G_{H_2} plotted against chlorine concentration, which is expressed in moles/g HCl: ○ liquid HCl at −79° C; ● solid HCl at −196° C.

Note: The curves are theoretical and were calculated on the basis of equation [ii]: —— values of G_H, G_{H^*}, k_{15}/k_{11}, and k_{15}^*/k_{11}^* uncorrected; - - - values of G_H, G_{H^*}, k_{15}/k_{11}, and k_{15}^*/k_{11}^* corrected by successive approximation.

Hydrogen yields from pure HCl samples irradiated in the solid state were much lower than those from liquid HCl, and showed a tendency to decrease with dose. Yields were therefore measured at the minimum practical dose ($\sim 2\times10^{18}$ ev/g), and these have been presented in Fig. 2. The addition of chlorine to these samples had a much less pronounced effect than in the liquid samples. A concentration of 2×10^{-4} mole chlorine/g HCl caused a decrease in G_{H_2} from 3.3 to 2.7 and further addition of chlorine appeared to have little or no effect. It may be concluded from this that the more readily scavenged species does not produce much hydrogen in the solid state. Experiments with still larger amounts of chlorine (10 mole%) would have shown whether the second species was scavenged by chlorine with the same efficiency in the solid state as in the liquid state. This information is obviously highly desirable, but such experiments were not conducted because of the difficulty of obtaining homogeneous solid solutions of high concentration.

DISCUSSION

At this point it will be convenient to review briefly the ionic reactions which are likely to occur in irradiated HCl. Mass spectrometric studies (6, 7) have demonstrated the formation of the following positive ions on bombardment of HCl with electrons: HCl^+, HCl^{++}, Cl^+, Cl^{++}, and H^+. From the data of reference 7 the approximate relative abundances of the first four of these may be estimated to be 100:2:10:12 respectively at electron impact energies of 150 ev. The parent ion (HCl^+) is thus by far the most abundant ion in the mass spectrum, and it may be inferred that this will also be the predominant ionic species formed in irradiated HCl:

$$HCl \text{ —}\sim\sim\rightarrow HCl^+ + e. \qquad [6]$$

A consideration of the electron-stopping power and electron density (3.5×10^{23} electrons/ml) of HCl in the liquid state at −79° C leads to the conclusion that the L.E.T. (and hence the distribution of ions along the radiation tracks) should not be very different from that occurring in liquid water for the same type of radiation.

Secondary electrons ejected from the ionized molecules would lose energy to the liquid medium and might eventually become thermalized. Because of the comparatively small dielectric constant of HCl (approx. 10 at −79° C (8)), interionic forces would be large and thermalized electrons would be unlikely to escape recombination with positive ions. They would probably give rise to energetic radicals through dissociative combinations:

$$e + HCl^+ \rightarrow HCl^* \rightarrow H + Cl + \text{energy.} \qquad [7]$$

As usual, the time required for the thermalization and return to the positive ions cannot be determined with any degree of certainty. However, as a first approximation it may be assumed that this period will be similar to that estimated by Samuel and Magee for electrons in liquid water ($\sim 10^{-13}$ sec, see ref. 9). Obviously, other ionic processes which could occur within this time and lead to alternative decomposition mechanisms must also be considered.

The reaction

$$HCl^+ + HCl \rightarrow H_2Cl^+ + Cl \qquad [8]$$

has been shown to proceed with a rate constant of 4.4×10^{-10} ml/molecule sec in the gas phase (10). Assuming the same rate constant in liquid HCl, where the concentration of HCl molecules is $1.9_7 \times 10^{22}$/ml, it can readily be shown that the lifetime of HCl^+ ions with respect to this reaction should be of the order of 10^{-13} sec. Hence reaction [8] could conceivably precede ion recombination, and reactions [9*a*] and [9*b*]:

$$e + H_2Cl^+ \rightarrow H + HCl + \text{energy} \qquad [9a]$$

$$\rightarrow H + H + Cl + \text{energy,} \qquad [9b]$$

must be regarded as alternatives to reaction [7].

Several investigations of the electron resonance capture reaction:

$$e + HCl \rightarrow H + Cl^-, \qquad [10]$$

have recently been reported (11–13). The value of the energy threshold in the gas phase is virtually the same as the calculated endothermicity (0.65 ev), and most studies indicate that the capture cross section passes through a maximum at about 0.8 ev and then falls to a very low value at 1.5 ev. Obviously during the course of their thermalization in liquid HCl the secondary electrons must pass through this energy range. Their lifetime with respect to capture while in it can be estimated using the data of Buchelnikova (mean cross section for the above energy range $\simeq 2 \times 10^{-18}$ cm^2/molecule in the gas phase) and the concentration of molecules in liquid HCl. This lifetime again turns out to be of the order of 10^{-13} sec. Thus the possibility of capture cannot be excluded. Furthermore, there is strong evidence for hydrogen bonding (14) in the condensed phases of the hydrogen halides, and Cl^- ions are known to associate strongly with HCl molecules (15–17). Thus the reaction

$$e + H\text{—}Cl \cdots H\text{—}Cl \rightarrow H + Cl\text{—}H\text{—}Cl^- \qquad [10a]$$

should replace reaction [10] in liquid HCl. Because of the greater thermodynamic stability of the $ClHCl^-$ ion, the endothermicity of this reaction should be less than that of reaction [10]. Electron capture would therefore be extended to lower energies than in the gas phase, and could in fact be the exclusive fate of secondary electrons in liquid HCl. If formed in reaction [10*a*] the $ClHCl^-$ ions would diffuse relatively slowly. There would

then be no doubt that reaction [8] would occur prior to neutralization. The H_2Cl^+ and $ClHCl^-$ ions would react according to the equation

$$H_2Cl^+ + ClHCl^- \rightleftharpoons 3HCl. \qquad [10b]$$

This reaction is the reverse of the self-ionization process in HCl, for which there are now at least two independent sources of evidence (16, 17).

From the preceding discussion it can be seen that several reaction paths of the "Samuel–Magee" type are possible in liquid HCl: reactions [6]–[7]; reactions [6]–[8]–[9*a*]; and reactions [6]–[8]–[9*b*]. These are all likely to produce "hot" hydrogen atoms. As in the case of HBr the decomposition of electronically excited molecules must be included, and present knowledge (18) of the energy levels of the HCl molecule indicates that dissociation to H and Cl atoms in their ground states would occur, with the fragments gaining a considerable excess of kinetic energy (up to about 50 kcal). Most of this energy would again be acquired by the hydrogen atoms (cf. the photolysis of HBr and HI, ref. 20). The fraction of the hot hydrogen atoms from these sources which would be thermalized before reacting with HCl (see reaction [11*] below) should be comparatively small. "Hot-atom effects" similar to those observed in other irradiated systems are therefore to be expected. In contrast to the above processes the alternative "Lea" type decomposition path involving reactions [6], [8], [10*a*], and [10*b*] should produce hydrogen atoms of thermal or comparatively low energies.

Hydrogen and chlorine atoms may undergo the following reactions in HCl:

$$H + HCl \rightarrow H_2 + Cl \qquad [11]$$

$$H\ (hot) + HCl \rightarrow H_2 + Cl \qquad [11^*]$$

$$H + Cl + M \rightarrow HCl + M \qquad [12]$$

$$H + H + M \rightarrow H_2 + M \qquad [13]$$

$$Cl + Cl + M \rightarrow Cl_2 + M. \qquad [14]$$

The activation energy of reaction [11] is considered to be about 5 kcal (19). Assuming identical steric factors for all of the above reactions and activation energies of zero for the last three, simple calculation shows that the ratio of k_{11} to k_{12} or k_{15} at $-79°$ C should have a value of about 10^{-5}. The excessively large concentration of HCl in the pure liquid at $-79°$ C would be more than sufficient to compensate for this, and only a few hydrogen atoms would be expected to take part in reactions [12] and [13]. At $-196°$ C, however, the ratio of k_{11} to k_{12} or k_{15} would be of the order of 10^{-11} and hardly any thermal hydrogen atoms would react with HCl. Hot hydrogen atoms on the other hand should react almost exclusively with HCl at both temperatures. The large difference between the hydrogen yields in the solid and liquid samples of HCl can thus be attributed largely to loss of the hydrogen which is formed in reaction [11] at the higher temperature. The slight effect of chlorine in the solid phase may be due to the scavenging of thermal hydrogen atoms, which would otherwise have undergone reaction [13]. The remainder of the hydrogen yield, $G_{H_2} = 2.7$, at $-196°$ C must be formed in reaction [11*], and therefore gives a measure of the yield of hot hydrogen atoms, G_{H^*}. It seems that this is considerably less than in the liquid (see below).

As products accumulated in the system, reactions [15] and [16] would have been expected:

$$H + Cl_2 \rightarrow HCl + Cl \qquad [15]$$

$$Cl + H_2 \rightarrow HCl + H. \qquad [16]$$

In pure HCl their occurrence would have resulted in a decrease in the hydrogen yield at higher doses. Since the yields in liquid HCl were linear, we may consider that reactions [15] and [16] were negligible for the small chlorine and hydrogen concentrations which accumulated during the radiolysis. However, in the more concentrated synthetic solutions of chlorine in HCl reaction [15] must have been occurring, but it appears that reaction [16] was still insignificant since the yields remained linear. Hence in all cases the hydrogen yields from liquid HCl may be regarded as true "initial" yields unaffected by secondary radical reactions. The tendency for the yields from solid HCl to decrease with dose may be attributed in part to reaction [15], and also to reaction [12] since chlorine atoms would have been trapped in the solid matrix and their concentration should have built up to a fairly high level at the larger doses.

At the concentration employed ethylene could only have reacted with the thermal hydrogen atoms:

$$H + C_2H_4 + M \rightarrow C_2H_5 + M. \qquad [17]$$

Reduction of the hydrogen yield by it may be taken as further evidence for the formation of hydrogen in reaction [11]. Chlorine, on the other hand, may react with electrons:

$$e + Cl_2 \rightarrow Cl^- + Cl, \qquad [18]$$

as well as with thermal hydrogen atoms. Reduction of the hydrogen yield might then arise in three ways: (*a*) a competition between reaction [18] and reactions [7] or [9]; (*b*) a competition between reactions [18] and [10*a*]; and (*c*) a competition between reactions [15] and [11]. If it is assumed that the last competition (*c*) is responsible for the reduction in the hydrogen yield, then the usual steady-state approximation leads to the equation

$$\frac{1}{\Delta G_{H_2(S)}} = \frac{1}{G_H}\left\{1+\frac{k_{11}(HCl)}{k_{15}(Cl_2)_S}\right\}. \qquad [i]$$

$\Delta G_{H_2(S)}$ is the reduction of the total hydrogen yield at chlorine concentration $(Cl_2)_S$ and G_H is the yield of thermal hydrogen atoms, which in the absence of chlorine would have undergone reaction [11]. A similar treatment of alternative (*b*) above would have yielded an analogous expression except that G_e, k_{10}, and k_{18} would have replaced G_H, k_{11}, and k_{15} respectively. A plot of $1/\Delta G_{H_2}$ against $1/(Cl_2)$ for all but the two very dilute solutions of chlorine in HCl, which have very large possible errors in ΔG_{H_2} ($\pm 10\%$) and do not warrant inclusion, has been given in Fig. 3. This plot resolves into two parts: a linear portion corresponding to the low chlorine concentrations at which the abrupt decrease in hydrogen yield occurred and a second steeply curving portion which intercepts the Y axis at about 0.15. As would have been expected this intercept corresponds to a total ΔG_{H_2} of 6.5 at infinite chlorine concentration. The intercept for the linear portion, $1/G_H$, gives a value of 2.6 for the yield of thermal hydrogen atoms in the system and from the slope a value of $1.9\pm0.2\times10^{-3}$ was calculated for k_{11}/k_{15}. Klein and Wolfsberg (21) have recently shown that the ratio of k_{11} to k_{15} for thermal hydrogen atoms in the gas phase is given by the equation $k_{11}/k_{15} = (0.14_3\pm0.03)\exp -(1540/RT)$. Extrapolation of their data to the temperature used in this study predicts a value of 2.5×10^{-3}. The substantial agreement of this figure with the present result strongly supports the assumption made above, and the calculations in the following paragraph are based on it. However, as already indicated, electron scavenging could give rise to entirely analogous effects. It should not, therefore, be categorically excluded at this time.

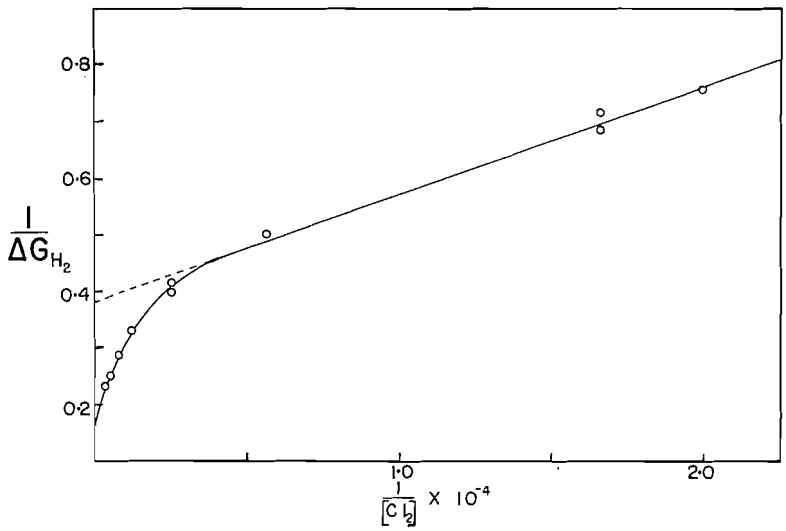

FIG. 3. The reciprocal of the reduction in the hydrogen yield ($1/\Delta G_{H_2}$) plotted against the reciprocal of the chlorine concentration ($1/(Cl_2)$).

Reaction [11*] appears to be the most reasonable process which can account for the relatively large hydrogen yield persisting in the presence of 10 mole% chlorine. On the assumptions that a competition between reaction [15*]:

$$H\ (hot) + Cl_2 \rightarrow HCl + Cl, \qquad [15^*]$$

and reaction [11*] is responsible for the reduction in the hydrogen yield at the higher chlorine concentrations, and that H and H (hot) are formed and react independently, equation [ii] may be derived:

$$G_{H_2(total)} = G_{H_2} + G_{H_2^*} = G_H \frac{1}{1+\frac{k_{15}(Cl_2)}{k_{11}(HCl)}} + G_{H^*} \frac{1}{1+\frac{k_{15}(Cl_2)}{k_{11}(HCl)}}. \qquad [ii]$$

Here G_H and G_{H^*} represent the yield of H and H (hot) in the system and are assumed to be independent of chlorine concentration. G_{H_2} and $G_{H_2^*}$ are their contributions to the total hydrogen yield, $G_{H_2(total)}$. Using this equation along with G_H and k_{15}/k_{11} determined above, G_{H_2} may be calculated and subtracted from $G_{H_2(total)}$ to give $G_{H_2^*}$. The values of $G_{H_2^*}$ determined in this way remained constant until a Cl_2 concentration of 2×10^{-4} mole/g Cl_2 was reached, and only then did they decrease in a regular manner. The initial constancy is no doubt due to the assumption which was implicit in the calculation of G_H and k_{15}/k_{11}, namely that the entire ΔG_{H_2} at the lower chlorine concentrations was due to thermal hydrogen atom scavenging. By substituting the values of $\Delta G_{H_2^*}$ for the higher chlorine concentrations into an equation analogous to [i] and using $G_{H^*} = 6.5_0 - 2.6_0 = 3.9_0$, the rate constant ratio k_{15}^*/k_{11}^* can be evaluated. The figure obtained, 0.13, was then used to correct ΔG_{H_2}, and thus to evaluate G_H, G_{H^*}, k_{11}/k_{15}, and, in turn, k_{15}^*/k_{11}^* more accurately. This method of successive approximation gave: $G_H = 2.3$; $G_{H^*} = 4.2$; $k_{15}/k_{11} = 1.7\times10^{-3}$; and $k_{15}^*/k_{11}^* = 0.1_0$. These values differ little from the original ones and k_{15}^*/k_{11}^* is still comparable to the pre-exponential factor of Klein and Wolfsberg, which would seem to be a reasonable ratio for the rate constants concerned.

The validity of equation [ii] was further tested by inserting the values of the four parameters and calculating the total hydrogen yield, $G_{H_2(total)}$. The "solid curve" in Fig. 2 was obtained with the uncorrected parameters and the "dashed curve" with those found by successive approximation. The agreement in the latter curve is a clear indication that the results can be explained on the basis of chlorine scavenging first thermal hydrogen atoms and then highly energetic ones.

Although an unequivocal choice of the origin of the hot hydrogen atoms is not at present possible, it should be pointed out that at high concentrations chlorine would be expected to react both with electrons and with positive ions in the exothermic charge-transfer reaction:

$$HCl^+ + Cl_2 \rightarrow HCl + Cl_2^+. \qquad [19]$$

If reactions [7] and [9] are responsible for the formation of the hot hydrogen atoms, chlorine should then behave as a dual scavenger, removing both the hot atoms and their precursors. A much more drastic reduction in the hot-hydrogen yield would therefore have been expected in the presence of 10 mole% chlorine. In view of this it may be suggested that electronically excited molecules and not ions are the precursors of the hot atoms. As indicated earlier in the discussion, reaction [10*a*] is a very likely source of the thermal hydrogen atoms.

Further work with other scavengers of different types is now in progress and the effects of these on the chlorine yield will also be investigated.

ACKNOWLEDGMENTS

The author wishes to express his appreciation to the Chemistry and Metallurgy Division of Atomic Energy of Canada Ltd. for a summer appointment in 1960. He also acknowledges many helpful discussions with Dr. F. C. Adam and other members of the University of Alberta, Calgary, Chemistry Department.

REFERENCES

1. S. C. Lind. The radiation chemistry of gases. Reinhold Publishing Corporation, N.Y. 1961.
2. E. G. Zubler, W. H. Hamill, and R. R. Williams. J. Chem. Phys. **23**, 1263 (1955).
3. H. Eyring, J. O. Hirschfelder, and H. S. Taylor. J. Chem. Phys. **4**, 570 (1936).
4. E. R. Johnson and A. O. Allen. J. Am. Chem. Soc. **74**, 4147 (1952).
5. J. H. Raley, F. F. Rust, and W. E. Vaughan. J. Am. Chem. Soc. **70**, 2767 (1948).
6. A. O. Nier and E. E. Hanson. Phys. Rev. **48**, 477 (1935).
7. W. H. Johnston and J. R. Arnold. J. Chem. Phys. **21**, 1499 (1953).
8. R. W. Swenson. Ph.D. Thesis, Brown University, Providence, R.I. 1953.
9. A. H. Samuel and J. L. Magee. J. Chem. Phys. **21**, 1080 (1953).
10. E. H. Field and F. W. Lampe. J. Am. Chem. Soc. **80**, 5583 (1958).
11. F. H. Field and J. L. Franklin. Electron impact phenomena. Acad. Press, N.Y. 1957.
12. (*a*) R. Fox. J. Chem. Phys. **26**, 1281 (1957).
    (*b*) D. C. Frost and C. A. McDowell. J. Chem. Phys. **29**, 503 (1958).
13. N. S. Buchelnickova. Soviet Phys.–Tech. Phys. **35**, 783 (1959).
14. D. F. Hornig and G. L. Hiebert. J. Chem. Phys. **27**, 752 (1957).
15. D. W. Sharp. J. Chem. Soc. 2558 (1958).
16. G. Glockler and R. E. Peck. J. Chem. Phys. 4, 658 (1936).
17. M. E. Peach and T. C. Waddington. J. Chem. Soc. 2329 (1960); 1238 (1961).
18. J. K. Jacques and R. F. Barrow. Proc. Phys. Soc. **73**, 538 (1959).
19. S. W. Benson. The foundations of chemical kinetics. McGraw Hill, Toronto. 1960.
20. (*a*) H. A. Schwarz, R. R. Williams, and W. H. Hamill. J. Am. Chem. Soc. **74**, 6008 (1952).
    (*b*) R. J. Carter, R. R. Williams, and W. H. Hamill. J. Am. Chem. Soc. **77**, 6457 (1955).
21. F. S. Klein and M. Wolfsberg. J. Chem. Phys. **34**, 1494 (1961).

SULPHONIUM SALT SOLVOLYSIS

PART III. NUCLEOPHILIC ROLE OF ANIONS IN SOLVOLYSIS OF DIMETHYL-*t*-BUTYL SULPHONIUM SALTS

J. B. HYNE AND J. H. JENSEN
Department of Chemistry, University of Alberta, Calgary, Alberta

Received March 22, 1962

ABSTRACT

The effect of variation of added anion type (I^-, Cl^-, NO_3^-, ClO_4^-, CH_3COO^-) on the kinetics of solvolysis of dimethyl-*t*-butyl sulphonium ions is interpreted as evidence supporting a nucleophilic role for the anion in low-polarity solvents. The specific case of acetate is discussed in terms of its relation to biochemical transmethylation reactions involving methionine.

INTRODUCTION

In the previous paper of this series (1) it was suggested that the anion plays an increasingly important role as a nucleophilic species in the solvolysis of sulphonium salts as the polarity of the solvent medium is reduced. In the particular case of solvolysis of dimethyl-*t*-butyl sulphonium salts in ethanol–water mixtures, it has been shown (1, 2) that in highly aqueous media the rate of solvolysis is independent of anion character, in keeping with the S_N1-type mechanism involving the production and subsequent fast solvolysis of the *t*-butyl carbonium ion. As the solvent polarity is decreased by increasing the ethanol content the observed rate of solvolysis becomes increasingly dependent on anion type. The form of this dependence has been analyzed in terms of a kinetic expression involving the onset of both ion pairing and a nucleophilic role of the anion (2) as solvent polarity diminishes. Previous experimental study of such solvolyses has been limited to a narrow range of anions of relatively similar nucleophilicities (e.g. the halides). In order to investigate further the possible nucleophilic role of the salt anions in solvolysis we report here a series of kinetic studies of the solvolysis of dimethyl-*t*-butyl sulphonium salts in highly ethanolic solvent media with variation of anion over the series I^-, Cl^-, NO_3^-, ClO_4^-, and CH_3COO^-.

EXPERIMENTAL

All kinetic studies were carried out by the radiochemical gas flow counting technique used in previous work (1, 2) and described by Hyne and Wolfgang (3). Labelled (C^{14}-methyl) dimethyl-*t*-butyl sulphonium iodide was prepared as described previously (3) and metathesized with the corresponding silver salts. In a few cases this metathesis was not carried out so that the kinetic system contained 10^{-3} *M* iodide in addition to the anion concentration of the added salt. It was found that the effect of this iodide ion was very small at the high concentrations of added salt used and was within the experimental uncertainty of the kinetic data. All working solutions were 10^{-3} *M* sulphonium salt in 0.945 mole fraction ethanol–water mixtures. Added anions were I^-, Cl^-, CH_3COO^-, NO_3^-, and ClO^-_4 in the form of their lithium salts. In a few selected runs potassium salts were used instead of lithium to check the independence of rate on cation type. This was found to be true in every case tested. All salts were vacuum-dried and assayed for water of crystallization. Since our primary interest in this work was in the dependence of k_{ip}' (see equation [1]) on anion nucleophilicity, rate investigations were limited to the linear portion of the k_{obs} vs. $[X^-]$ relationship, i.e. higher added salt concentration. In the acetate case, however, rate studies were carried out over the complete range of added salt concentrations. All rates were run at 69.46° C and rate analysis from the log (counts/min) versus time plots (see ref. 3) were made by least mean square analysis on an IBM-1620 computer. Rate data are presented in tabular form in Table I and plotted in Fig. 1.

TABLE I

Overall rate of solvolysis (rate of production of dimethyl sulphide) for dimethyl *t*-butyl sulphonium salts in 0.945 mole fraction ethanol in water at 69.46° C as a function of added anion (LiX) concentration

$[X^-]\times10^3$ (molar)	$k_{obs}\times10^4$ (sec^{-1})	$[X^-]\times10^3$ (molar)	$k_{obs}\times10^4$ (sec^{-1})	$[X^-]\times10^3$ (molar)	$k_{obs}\times10^4$ (sec^{-1})
CH_3COO^-		I^-		NO_3^-	
3.39	2.84	22.4	3.39	13.39	2.30
5.83	3.08	28.1	3.45	25.90	2.29
10.17	3.12	28.2	3.35	44.63	2.40
10.54	3.39	44.7	3.66	50.96	2.38
14.60	3.51	56.6	3.90	75.00	2.48
19.02	3.69	56.6	3.88		
24.92	3.73				
25.36	3.67	Cl^-		ClO_4^-	
36.07	3.96	13.01	2.91	13.88	2.31
46.98	4.12	26.55	3.05	25.20	2.35
58.10	4.28	39.57	3.20	44.94	2.32
58.85	4.12	53.72	3.22	66.91	2.37
69.77	4.42	71.47	3.31	74.21	2.36
70.70	4.50				
83.04	4.68				

NOTE: No added salt $k_{obs} = 2.34\pm0.02\times10^{-4}$ sec^{-1}.

DISCUSSION

A rate equation was previously derived (1) which described the observed solvolytic rate behavior (k_{obs}) as a function of anion concentration $[X^-]$. This equation has the form

$$[1] \qquad k_{obs} = \frac{k_+ + k_{ip}K_A[X^-] + k_{ip}'K_A[X^-]^2}{1+K_A[X^-]},$$

where k_+ is the rate of S_N1 solvolysis of the sulphonium ion predominating in high-polarity solvent media; k_{ip} is the rate of reaction of the sulphonium ion pair (association constant K_A) and is possibly associated with an S_Ni mechanism where the ion-pair anion acts internally as a nucleophile; and k_{ip}' is the rate of nucleophilic attack of an external anion on the ion pair and predominates at high added anion concentration, accounting for the observed linear dependence of k_{obs} on $[X^-]$ (see Fig. 1). As was shown in the previous paper (1), equation [1] reduces to the approximate form [2] at higher $[X^-]$, where $K_A[X^-]$ becomes large compared with unity and k_+:

$$[2] \qquad k_{obs} \doteq k_{ip} + k_{ip}'[X^-].$$

According to equation [2] approximate values for both k_{ip}' and k_{ip} can be obtained from the slope and intercept of the linear sections of the plots in Fig. 1. The rate values thus obtained are tabulated in Table II. If the postulated mechanism involving a nucleophilic role for the anion in both the k_{ip}' and k_{ip} rate steps is correct, we would expect the k_{ip}' and k_{ip} values to be related to the nucleophilicity of the anion.

In Table II nucleophilicity **n** values (4) are recorded for the anions used. Since the nucleophilicity constants are derived from a free-energy type of relationship ($\log k/k_0 = S\mathbf{n}$), $\log k_{ip}'$ rather than k_{ip}' is plotted against **n** in Fig. 2. The precise value of the nucleophilicity constant for ClO_4^- is not known but it is generally assumed to be less than zero on the arbitrary scale used here (4). A value of -1.2 would place the ClO_4^- point on the straight line established in the plot of Fig. 1 based on the three points for

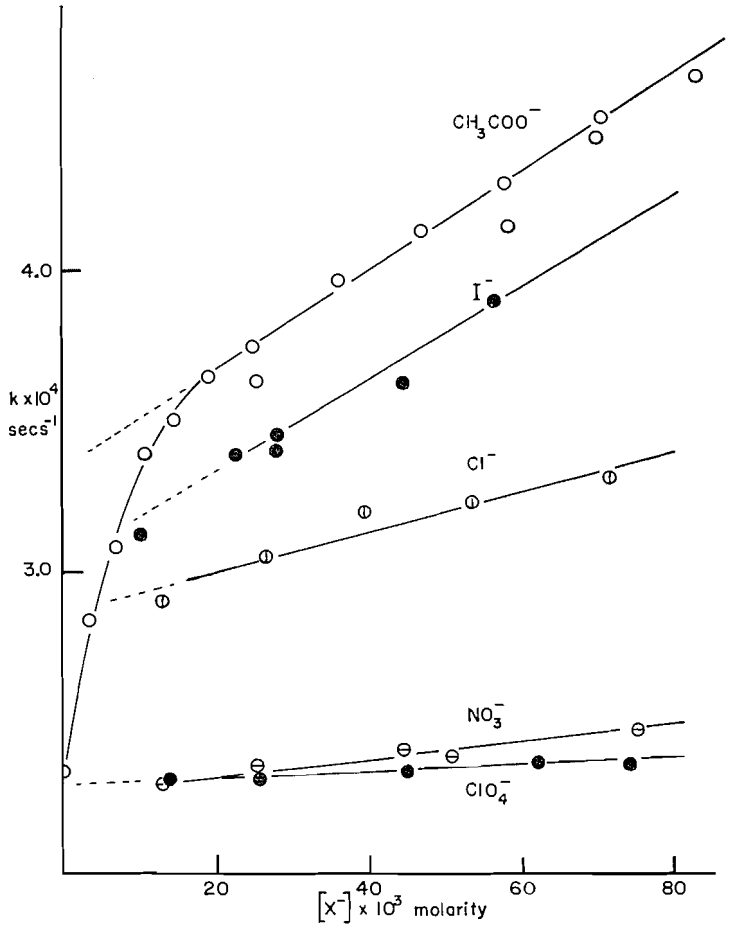

FIG. 1. Observed rate of solvolysis of dimethyl-*t*-butyl solphonium salts in 0.945 mole fraction ethanol in water at 69.46° C as a function of added anion concentration.

TABLE II

Apparent k_{ip} and k_{ip}' at 69.46° C for various anions from equation [2]

X^-	$k_{ip} \times 10^4$ (sec^{-1})	$k_{ip}' \times 10^3$ l./mole sec	**n** (nucleophilicity X^-)
CH_3COO^-	3.35	1.60	2.72*
I^-	3.03	1.52	5.04
Cl^-	2.85	0.66	3.04
NO_3^-	~2.30	0.32	1.03
ClO_4^-	~2.30	0.12	0.0 (−1.12)†

*Values of **n** from ref. 4.
†Bracketed value is that required for linearity in Fig. 2.

I^-, Cl^-, and NO_3^-. It is, however, not critical to the argument that this linear relationship should hold precisely. It appears justifiable to claim that the rate constant (k_{ip}') does in fact depend on the nucleophilicity of the added anion, X^-, thus constituting further support for the claim that this step involves the nucleophilic attack of the anion on the ion pair.

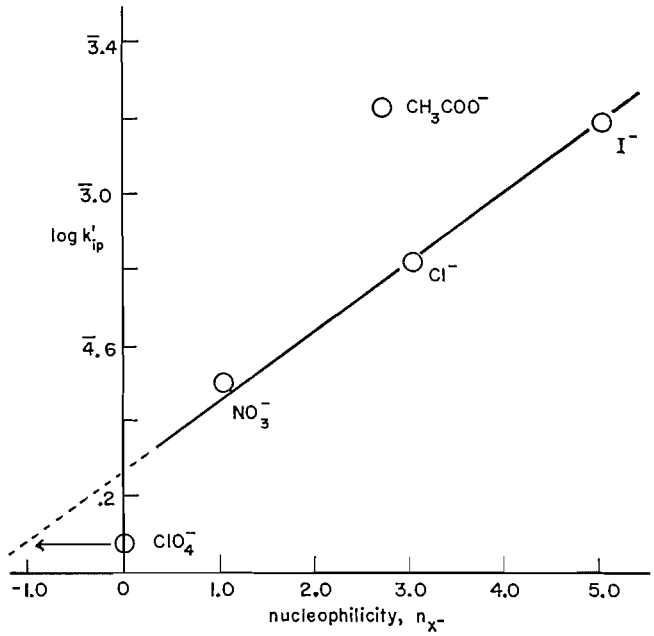

FIG. 2. Log k_{ip}' rate values (equation [2]) versus nucleophilicity constants (**n**) for various added anions.

The failure of the acetate anion to conform to the relationship apparently obeyed by the other anions is of particular interest on several counts. The apparent enhancement of nucleophilicity of the acetate anion in this particular mechanism over that expected from the **n** value may be related to the fact that in its nucleophilic role in sulphonium salt solvolysis the duality of the carboxylate group as a nucleophile, due to the two resonance forms possible, is of importance. This would suggest that the precise configuration of the ions with respect to one another in the transition state of the nucleophilic attack is of importance. It should also be noted that this enhanced nucleophilicity of acetate is also reflected in the higher k_{ip} value for acetate. Since this rate is presumably associated with the internal nucleophilic attack of the acetate anion of the ion pair on the *t*-butyl entity of the sulphonium ion, it is to be expected that the duality of the carboxylate anion as a nucleophile would enhance the number of favorable configurations possible for internal nucleophilic attack. It is also noteworthy that the carboxylate anion is probably involved in the analogous sulphonium salt reaction of methionine in biological transmethylations. The particular facility of acetate anion in enhancing the rate of cleavage of the sulphonium salt therefore raises the interesting question as to the possibility of a

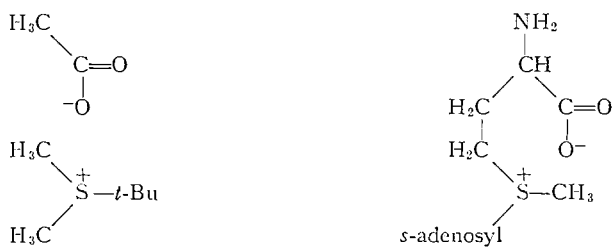

similar role of the methionine carboxylate anion in biological transmethylation. Further investigation of this aspect of anion involvement in transmethylation is now in progress.

In the NO_3^- and ClO_4^- cases it would appear from the values of k_{ip} obtained by back extrapolation that these ionic entities are such weak nucleophiles that cleavage of the sulphonium ion by internal nucleophilic attack within the ion pair is kinetically unimportant. The value of k_{ip} obtained by back extrapolation in these cases is virtually identical with the observed rate in the absence of added anion.

By virtue of the fact that the approximate form of the rate expression (equation [2]) has been used in the analysis of the rate data presented here, no reference has been made to the effect of variation of the ion-pair association constant K_A as the anion character is changed. It should be noted, however, that the major effect of changes in K_A on the observed rate of reaction is in determining how rapidly the linear relationship between k_{obs} and $[X^-]$ is attained as $[X^-]$ is increased. The larger the value of K_A the greater will be the effect of initial increases in $[X^-]$ in converting the sulphonium ion essentially completely to ion pairs. The effect of K_A variation on the k_{ip} and, particularly, the k_{ip}' values obtained by equation [2] will therefore be small.

CONCLUSIONS

The kinetic effect of variation of anion type in the solvolysis of dimethyl-*t*-butyl sulphonium salts in low-polarity media is clearly related to the nucleophilicity of the anion. This observation represents further evidence for the nucleophilic role of the salt anion under conditions where the S_N1-type mechanism is suppressed. The failure of the kinetic effect of the acetate anion to conform with the nucleophilicity of that species as observed in other reactions is suggestive of the fact that in sulphonium salt reactions the specific orientation of the anion nucleophile is important. This observation is in keeping with the involvement of ion pairs in the kinetic mechanism proposed and suggests possible interesting extensions to the case of biological transmethylation mechanisms involving methionine.

ACKNOWLEDGMENTS

The authors wish to acknowledge financial support from Research Corporation (scholarship to J. H. J.) and the National Research Council in this work.

REFERENCES

1. J. B. HYNE and J. W. ABRELL. Can. J. Chem. **39**, 1657 (1961).
2. J. B. HYNE. Can. J. Chem. **39**, 1207 (1961).
3. J. B. HYNE and R. WOLFGANG. J. Phys. Chem. **64**, 699 (1960).
4. J. HINE. Physical organic chemistry. McGraw-Hill. 1956. p.140.

5,6-DIMETHYLBENZ[*a*]ANTHRACENE AND 5,6-DIMETHYLBENZO[*c*]PHENANTHRENE

P. M. G. BAVIN[1]
Chemistry Department, the University, Hull, England

Received March 12, 1962

ABSTRACT

5,6-Dimethylbenz[*a*]anthracene and 5,6-dimethylbenzo[*c*]phenanthrene have been synthesized, the latter by a novel route.

The synthesis of benzo[*c*]phenanthrene and its derivatives has presented interesting problems, largely overcome by the use of partially hydrogenated intermediates (1, pp. 158–160; 2; 3). The successful ring expansion of benzo[*c*]fluorenone by the Schmidt reaction (4) and our earlier work with benzo[*b*]fluorene (5) prompted experiments with benzo[*c*]fluorene.

7-Acetylbenzo[*c*]fluorene (I*a*) was prepared by the Claisen condensation and was methylated in the usual way (cf. fluorene (6) and 9-acetylfluorene (7)). Reduction and subsequent dehydration–rearrangement by heating with phosphorus pentoxide under xylene (8) gave crude 5,6-dimethylbenzo[*c*]phenanthrene (II*a*) in 80% yield. Purification through the trinitrobenzene complex and by chromatography gave the pure hydrocarbon, m.p. 98–99°, characterized by comparison of its ultraviolet spectrum with those of benzo[*c*]phenanthrene and its methylated derivatives (9, 10). The availability of benzo[*c*]-fluorenones from arylpropiolic acids (11, 12 and references quoted therein) may make this novel route to benzo[*c*]phenanthrenes and other sterically hindered hydrocarbons an attractive one.

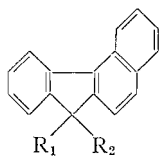

I

a, $R_1 = H$; $R_2 = CO.CH_3$
b, $R_1 = CH_3$; $R_2 = CO.CH_3$
c, $R_1 = H$; $R_2 = CO_2CH_3$
d, $R_1 = CH_3$; $R_2 = CO_2CH_3$
e, $R_1 = CH_3$; $R_2 = CH_2OH$
f, $R_1 = CH_3$; $R_2 = CH_2OTos$
g, $R_1 = CH_3$; $R_2 = CH_2OCO.CH_3$

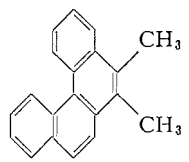

II

a, $R_1 = CH_3$; $R_2 = CH_3$
b, $R_1 = CH_3$; $R_2 = H$
c, $R_1 = H$; $R_2 = CH_3$

To extend the above synthesis methyl benzo[*c*]fluorene-7-carboxylate (I*c*) was prepared and methylated by a general method (5). Reduction gave the alcohol (I*e*) as an oil, the tosylate (I*f*) not being obtained pure. The acetate (I*g*) crystallized during 18 months and was recrystallized only with difficulty. Sufficient experiments were carried out to show spectroscopically that dehydration–rearrangement of I*e* gave a mixture of approximately equal amounts of 5- and 6-methylbenzo[*c*]phenanthrenes (II*b* and II*c*).

[1]*I.C.I. Fellow, 1958–60. Present address: Smith Kline and French Laboratories Ltd., Mundells, Welwyn Garden City, England.*

5,6-Dimethylbenz[*a*]anthracene (III), of interest because its carcinogenic index has been predicted from the results of quantum mechanical calculations (13), has been synthesized by a more conventional route (cf. 5-methoxybenz[*a*]anthracene (14)). The Friedel–Crafts reaction of 1,2-dimethylnaphthalene with phthalic anhydride gave a good yield of keto acid, assigned structure IV*a* by analogy with other substitution reactions of 1,2-dimethylnaphthalene (bromination, sulphonation (15); chloromethylation (16); acetylation (15, 17)). Cyclization of the reduced acid (IV*b*) using a variety of reagents has not been achieved in satisfactory yield. However, reduction of the crude cyclization product and careful purification gave pure 5,6-dimethylbenz[*a*]anthracene, m.p. 111–112°, in 5–10% yield. The hydrocarbon was characterized as its trinitrobenzene complex and by comparison of its ultraviolet spectrum with those of benz[*a*]anthracene and its methylated derivatives (18–20).

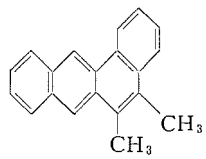

III

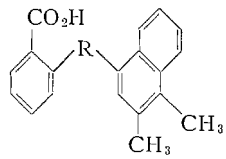

IV

a, R = C=O; *b*, R = CH_2

EXPERIMENTAL

Microanalyses marked SKF are by Miss Doreen Hardiman, Smith Kline and French Laboratories Ltd; others are by Weiler and Strauss, Oxford. Melting points are uncorrected.

7-Acetyl-7-methylbenzo[c]fluorene (Ib)

Benzo[*c*]fluorene (4 g) (21) was acetylated in the usual way (6).* The crude ketone was unstable (cf. 9-acetylfluorene (6)) and was immediately methylated (7). The *ketone* crystallized from acetone–methanol as lustrous plates (0.9 g), m.p. 170.0–170.5°. Found: C, 88.41; H, 5.97. Calc. for $C_{20}H_{16}O$: C, 88.20; H, 5.92%. Carbonyl stretching frequency: 1702 cm^{-1}.

5,6-Dimethylbenzo[c]phenanthrene (IIa)

The ketone (0.3 g) was reduced with lithium aluminum hydride to give the alcohol as an oil. Dehydration–rearrangement by boiling in xylene (10 ml) with phosphorus pentoxide (1 g) for 4 hours gave crude II*a*. Preliminary purification by passage of a solution in hexane through a column of activated alumina gave a colorless oil showing an intense blue fluorescence. The *1,3,5-trinitrobenzene complex* separated as bright orange needles (0.42 g, 82%) from ethanol, m.p. 145.0–145.5° after sintering at 144°. Found (SKF): C, 67.0; H, 4.26; N, 8.76. Calc. for $C_{26}H_{19}N_3O_6$: C, 66.52; H, 4.08; N, 8.95%. The hydrocarbon was regenerated by passage of a solution of the complex in hexane through a column of alumina, crystallization of the eluted material from methanol giving small, colorless, lustrous plates, m.p. 98–99°. Found (SKF): C, 93.6, 93.8; H, 6.30, 6.50. Calc. for $C_{20}H_{16}$: C, 93.71; H, 6.29%.

Benzo[c]fluorene-7-carboxylic Acid

Prepared in the usual way (5), the *acid* crystallized from benzene–hexane as colorless needles (81%), m.p. 212–214° with decomposition. Found: C, 83.21; H, 4.59. Calc. for $C_{18}H_{12}O_2$: C, 83.06; H, 4.65%. Equivalent wt. found: 262; calc.: 260.3.

The *methyl ester* (Ic), prepared by esterification in methanol–chloroform (1:1) saturated with hydrogen chloride, crystallized from acetone–methanol as colorless, glistening plates (86%), m.p. 129–130°. Found: C, 83.40; H, 5.11. Calc. for $C_{19}H_{14}O_2$: C, 83.20; H, 5.15%.

Methyl 7-Methylbenzo[c]fluorene-7-carboxylate (Id)

Methylation of the preceding ester by a general method (5) gave the *ester* (Id) as glistening plates (92%), m.p. 184–185°. Found: C, 83.46; H, 5.59. Calc. for $C_{20}H_{16}O_2$: C, 83.31; H, 5.59%.

**For alternative syntheses of 9-acetylfluorene from methyl 9-hydroxyfluorene-9-carboxylate and 9-ethinyl-9-fluorenol see refs. 22, 23; for the product of the reaction between acetyl chloride and fluorenyl lithium see refs. 24, 25.*

Hydrolysis and decarboxylation by boiling with potassium hydroxide in ethylene glycol (26) gave 7-methylbenzo[*c*]fluorene, which crystallized from acetone–methanol as white needles, m.p. 85–86°. (Lit. m.p. 80.2–82.0° cor. (21).) Found: C, 92.35; H, 7.86. Calc. for $C_{18}H_{14}$: C, 92.26; H, 7.74%.

7-Methyl-7-benzo[c]fluorenylmethyl Acetate (Ig)

Reduction of the ester (I*d*) with ethereal lithium aluminum hydride gave alcohol (I*e*) as an oil, not obtained crystalline during 2 years. The tosylate (I*f*), prepared in the usual way (26), was not obtained pure. It was obtained after several crystallizations from benzene–hexane as an amorphous powder which sintered between 80 and 120° and finally turned black at 180°. Found: C, 76.48, 76.49; H, 5.57, 5.60. Calc. for $C_{26}H_{22}O_3S$: C, 75.33; H, 5.35%.

Esterification of the alcohol with acetic anhydride containing a trace of concentrated sulphuric acid gave the *acetate* (I*g*) as a yellow gum. Material eluted from alumina with hexane–benzene (10:1) was colorless and crystallized during 18 months. Two recrystallizations from hexane, which required careful seeding, gave colorless needles, m.p. 79.5–81.0°. Found: C, 83.66; H, 5.85. Calc. for $C_{21}H_{18}O_2$: C, 83.42; H, 6.00%. Reduction with lithium aluminum hydride gave alcohol (I*e*) identical (infrared spectra) with that obtained from ester (I*d*).

5- and 6-Methylbenzo[c]phenanthrenes (IIb and IIc)

The alcohol (II*d*) (0.2 g) and xylene (10 ml) were boiled under reflux for 6 hours with phosphorus pentoxide (1 g). The product remaining after evaporation of the xylene was dissolved in hexane and passed through a column of activated alumina. The eluted oil (0.17 g) was colorless. Examination of the ultraviolet and infrared spectra suggested the presence of approximately equal amounts of 5- and 6-methylbenzo[*c*]phenanthrenes. The ultraviolet spectra have been reported elsewhere (9, 10); infrared spectra were obtained from small samples of authentic specimens (2) provided by Professor M. S. Newman. Attempts to separate the hydrocarbons through complexes with trinitrobenzene, picric acid, or trinitrofluorenone were not successful.

2-(1',2'-Dimethyl-4-naphthoyl)-benzoic Acid (IVa)

Finely powdered anhydrous aluminum chloride (14.8 g) was added to a solution of 1,2-dimethylnaphthalene (7.8 g) (15) and phthalic anhydride (7.4 g) in dry sulphur-free benzene (100 ml), maintained at 5°. After being kept at room temperature for 12 hours the mixture was poured onto ice, acidified, and steam-distilled. The residual solid acid was dissolved in aqueous sodium bicarbonate solution, clarified with charcoal, and poured into excess hydrochloric acid. One crystallization from benzene–hexane gave pale yellow prisms (10.5 g, 71%), m.p. 187–189°. Found: C, 78.71; H, 5.52. Calc. for $C_{20}H_{16}O_3$: C, 78.93; H, 5.30%. Equivalent wt. found: 310; calc.: 304.3.

2-(1',2'-Dimethyl-4-naphthylmethyl)-benzoic Acid (IVb)

The preceding acid (10 g) was reduced by stirring and boiling under reflux for 15 hours with aqueous sodium hydroxide (250 ml, 10%) and zinc dust (30 g) activated with copper. Aqueous ammonia solution (5 ml, *d* 0.88) was added every half hour for the first few hours. The *acid* separated from benzene–hexane as colorless prisms (7 g), m.p. 211–212°. Found: C, 82.46; H, 6.37. Calc. for $C_{20}H_{18}O_2$: C, 82.73; H, 6.25%. Equivalent wt. found: 285; calc.: 290.3.

5,6-Dimethylbenz[a]anthracene (III)

The reduced acid (1.45 g) was dissolved in concentrated sulphuric acid (10 g, 98%) containing boric acid (0.5 g) (27). The dark solution, protected from atmospheric moisture, was left at room temperature for 12 hours and then poured onto ice. The precipitated yellow gum was reduced by boiling and stirring for 15 hours with aqueous sodium hydroxide solution (250 ml, 10%), toluene (50 ml), and zinc dust (30 g) activated with copper, aqueous ammonia (5 ml, *d* 0.88) being added at half-hourly intervals for the first few hours. The crude hydrocarbon was dissolved in hexane and the solution passed through a column of activated alumina. Eluted material readily crystallized from methanol as colorless needles (0.15 g, 11%), m.p. 111–112°. Found: C, 93.40; H, 6.57. Calc. for $C_{20}H_{16}$: C, 93.71; H, 6.29%. The *1,3,5-trinitrobenzene complex* crystallized from methanol as deep orange needles, m.p. 179–180°. Found: C, 66.93; H, 4.13. Calc. for $C_{26}H_{19}N_3O_6$: C, 66.52; H, 4.08%.

Attempts were made to improve the cyclization, using hydrogen fluoride, aluminum chloride and the acid chloride, benzoyl chloride, zinc chloride, and acetic acid – acetic anhydride, but without marked success.

Ultraviolet Spectra

The ultraviolet spectra were obtained using a Beckmann DK-2 recording spectrophotometer, with ethanol as solvent. Shoulders are marked by an asterisk. Wavelengths are in mμ; intensities are recorded as log ϵ.

5,6-Dimethylbenzo[c]phenanthrene

379.5 (2.41); 361 (2.62); 330*; 317.2 (4.05); 305*; 298.9 (4.25); 285.8 (4.84); 276.2 (4.72); 266.5*; 255*; 245.8*; 221.0 (4.39); 225*.

5,6-Dimethylbenz[a]anthracene

389 (2.52); 367*; 358 (3.18); 352*; 341.5 (3.32); 301*; 292.8 (4.47); 282 (4.42); 272 (4.23); 260 (4.17); 237*; 229.5 (4.70); 224.5 (4.71).

ACKNOWLEDGMENTS

Some of the preliminary experiments with benzo[*c*]fluorene were carried out by D. F. Arnold and R. C. Wilson at Hull, where the author carried out most of the work.

REFERENCES

1. E. CLAR. Aromatische Kohlenwasserstoffe. Verlag von Julius Springer, Berlin. 1952.
2. M. S. NEWMAN, H. V. ANDERSON, and K. H. TAKEMURA. J. Am. Chem. Soc. **75**, 347 (1953).
3. M. S. NEWMAN and D. K. PHILLIPS. J. Am. Chem. Soc. **81**, 3667 (1959).
4. B. R. T. KEENE and K. SCHOFIELD. J. Chem. Soc. 2609 (1958).
5. F. A. L. ANET and P. M. G. BAVIN. Can. J. Chem. **38**, 240 (1960).
6. J. VON and E. C. WAGNER. J. Org. Chem. **9**, 155 (1944).
7. P. M. G. BAVIN. Can. J. Chem. **38**, 911 (1960).
8. W. G. BROWN and B. BLUESTEIN. J. Am. Chem. Soc. **62**, 3256 (1940).
9. G. M. BADGER and I. S. WALKER. J. Chem. Soc. 3238 (1954).
10. R. N. JONES and E. SPINNER. Spectrochim. Acta, **16**, 1060 (1960).
11. A. D. CAMPBELL. J. Chem. Soc. 3659 (1954).
12. F. G. BADDAR, L. S. EL-ASSAL, and N. A. DOSS. J. Chem. Soc. 1027 (1959).
13. N. BUU-HOI *et al.* Compt. rend. **225**, 238 (1947).
14. L. F. FIESER, E. B. HERSHBERG, L. LONG, and M. S. NEWMAN. J. Am. Chem. Soc. **59**, 475 (1937).
15. P. A. PLATTNER and A. RONCO. Helv. Chim. Acta, **27**, 400 (1944).
16. C. L. HEWETT. J. Chem. Soc. 293 (1940).
17. R. T. ARNOLD, J. S. BUCKLEY, and J. RICHTER. J. Am. Chem. Soc. **69**, 2322 (1947).
18. G. M. BADGER, R. S. PEARCE, and R. PETTIT. J. Chem. Soc. 1112 (1952).
19. C. SANDORFY and R. N. JONES. Can. J. Chem. **34**, 888 (1956).
20. R. N. JONES and C. SANDORFY. National Research Council of Canada. Bull. No. 4. 1956.
21. L. F. FIESER and L. M. JOSHEL. J. Am. Chem. Soc. **62**, 957 (1940).
22. G. F. HENNION and B. R. FLECK. J. Am. Chem. Soc. **77**, 3253 (1955).
23. F. D. MILLER and E. C. WAGNER. J. Org. Chem. **16**, 279 (1951).
24. H. F. MILLER and G. B. BACHMANN. J. Am. Chem. Soc. **57**, 766 (1935).
25. M. MASAKI and M. OHTA. Bull. chem. soc. Japan, **34**, 1257 (1961).
26. F. A. L. ANET and P. M. G. BAVIN. Can. J. Chem. **34**, 991 (1956).
27. H. BROCKMANN, F. KLUGE, and H. MUFELDT. Ber. **90**, 2302 (1957).

STRUCTURES OF CYCLOHEXANONE–UREA CONDENSATION PRODUCTS[1]

C. PODESVA, E. J. TARLTON, AND A. F. MCKAY
L. G. Ryan Research Laboratories of Monsanto Canada Limited, Lasalle, Que.

Received March 9, 1962

ABSTRACT

A new series of urea derivatives was prepared by condensing cyclohexanone with urea, thiourea, and their monosubstituted derivatives.

A new series of urea derivatives was prepared by condensing urea, thiourea, and their monosubstituted derivatives with cyclohexanone in the presence of acid. The derivatives formed by the condensation of 2 mole equivalents of cyclohexanone with the ureas and thioureas were formed also by condensing 2-cyclohexylidene-cyclohexanone with the same ureas and thioureas. The new compounds prepared in this study are described in Table I.

Two structures (I and II) were considered for the product from the condensation of

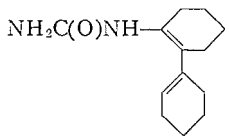

I

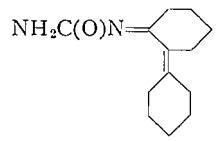

II

cyclohexanone with urea. If one assumes the substituted N atom to be equivalent to carbon for calculating the ultraviolet λ maxima of these unsaturated structures then the calculated values for structures I and II are 239 mμ and 326 mμ respectively (1). The observed λ_{max} of 238.5 mμ given in Table II is in good agreement with the calculated value for structure I. This structure was confirmed by an n.m.r. spectrum of the compound. The vinylic proton peak at 4.67 p.p.m. definitely excluded structure II from consideration. A peak at 7.99 p.p.m. is assigned to the four hydrogens of the methylene groups which are unshielded by the diene system. The rest of the hydrogen atoms of the remaining methylene groups gave a peak at 8.4 p.p.m.[2]

The infrared spectra listed in Table III show that all of the urea and thiourea derivatives possess this same general structure III. The bands between 3060 and 3080 cm^{-1} are

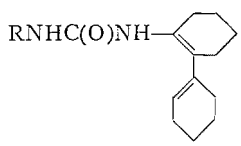

III

R = hydrogen, aryl, cyclohex-1-enyl, or alkyl

assigned to C—H stretching vibration of the —C=C—H group. The strong absorption band between 1673 and 1685 cm^{-1} is tentatively assigned to the stretching vibrations

[1]*Contribution No. 36.*
[2]*Sixty-megacycle n.m.r. spectrum was measured with Varian model HR-60 high-resolution spectrometer.*

TABLE I

Urea and thiourea derivatives

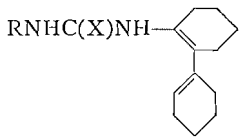

R	X	M.p. (°C)	Yield	Formulae	C		H		N	
					Calc.	Found	Calc.	Found	Calc.	Found
Hydrogen	O	234–235[a]	16.3[e]	$C_{13}H_{20}N_2O$	70.95	71.10	9.16	9.18	12.73	12.56
Hydrogen	S	274–276[a]	67.0[f]	$C_{13}H_{20}N_2S$	66.05	66.01	8.53	8.46	11.86	11.74[g]
Ethyl	O	164–166[b]	88.0[f]	$C_{15}H_{24}N_2O$	72.53	72.48	9.74	9.76	11.28	11.56
Allyl	O	154–155[b]	85.5[f]	$C_{16}H_{24}N_2O$	73.80	73.97	9.29	9.29	10.76	11.05
Phenyl	O	233[c]	31.2[f]	$C_{19}H_{24}N_2O$	76.99	76.78	8.16	8.24	9.45	9.49
Phenyl	S	195 (decomp.)[c]	37.5[f]	$C_{19}H_{24}N_2S$	73.03	73.32	7.74	7.93	8.97	9.13[h]
4-Chlorophenyl	O	241–243[c]	42.4[f]	$C_{19}H_{23}ClN_2O$	68.97	68.94	7.01	6.99	8.47	8.66[i]
4-Chlorophenyl	S	211 (decomp.)[a]	62.0[f] (18.4[e])	$C_{19}H_{23}ClN_2S$	65.78	65.76	6.68	6.66	8.08	8.35[j]
4-Hydroxyphenyl	O	268–269[a]	68.3[f]	$C_{19}H_{24}N_2O_2$	73.05	73.02	7.74	7.71	8.97	8.96
3,4-Dichlorobenzyl	O	243–244[d]	86.8[f] (73.3[e])	$C_{20}H_{24}Cl_2N_2O_2$	63.32	63.13	6.38	6.24	7.39	7.48[k]
3,4-Dichlorophenyl	O	228–229[a]	31.0[e]	$C_{19}H_{22}Cl_2N_2O_2$	62.47	62.75	6.07	6.25	7.67	7.92[l]
α-Naphthyl	O	257[a]	37.6[f]	$C_{23}H_{26}N_2O$	79.73	79.65	7.56	7.52	8.09	8.14

[a]Crystallized from ethanol.
[b]From aqueous ethanol.
[c]From benzene–ethanol (1:1).
[d]From butyl cellosolve.
[e]Method B.
[f]Method A.
[g]S calc. 13.56%, found 13.29%.
[h]S calc. 10.26%, found 9.96%.
[i]Cl calc. 10.72%, found 10.80%.
[j]Cl calc. 10.22%, found 10.00%; S calc. 9.24%, found 8.92%.
[k]Cl calc. 18.69%, found 19.01%.
[l]Cl calc. 19.41%, found 19.60%.

TABLE II

Ultraviolet absorption[a]

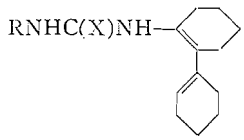

R	X	λ_{max} (mμ)	ϵ_{max}
Hydrogen	O	238.5	3,865
Cyclohex-1-enyl	O	233	6,670
Phenyl	O	247[b]	5,850
		220	End absorption
Hydrogen	S	275	9,020
		256	9,580
		220	End absorption
Phenyl	S	305[b]	10,280
		220	End absorption

[a]The ultraviolet spectra were determined on ethanolic solutions of the compounds with a Beckman DK-1 recording spectrophotometer.
[b]These absorption bands were broad and unsymmetrical. The phenyl groups contribute to the general absorption in the region covered by these broad bands.

of the —NH—C=C—C=CH or —NH—C=C— group. The CRR=CHR group gives an absorption band around 1670 cm^{-1} (2). This absorption is generally weak. Conjugation in a diene system shifts the absorption some 30 cm^{-1} to a lower frequency but the intensity of the band is generally increased considerably. In aliphatic conjugation of C=C bonds splitting of the two double-bond absorption bands usually occurs (2). In most of the compounds in Table III the band assigned to the —C=O group appears as a strong, separate band while in 2-cyclohex-1-enyl cyclohex-1-enyl-urea, 1-(cyclohex-1-enyl)-3-(2-cyclohex-1-enyl cyclohex-1-enyl)-urea, and 1-(4-hydroxyphenyl)-3-(2-cyclohex-1-enyl cyclohex-1-enyl)-urea the C=O absorption band has coalesced with the strong band tentatively assigned to the conjugated unsaturated group.

During this study 1,2-dicyclohexylisourea was prepared. This compound gave a strong, broad infrared absorption band at 1630 cm^{-1} which includes the C=N stretching and N—H bending modes.

EXPERIMENTAL[3]

2-Cyclohexylidene-cyclohexanone

2-Cyclohexylidene-cyclohexanone (b.p. 153–155° at 20 mm) was prepared in 69% yield by the method of Gault *et al.* (3).

3,4-Dichlorobenzylurea

3,4-Dichlorobenzylurea (m.p. 164–165°) was prepared in 82% yield from 3,4-dichlorobenzylamine hydrochloride and sodium cyanate by the general procedure described by Vogel (4). Anal. Calc. for $C_8H_8Cl_2N_2O$: C, 43.86; H, 3.68; Cl, 32.37; N, 12.79%. Found: C, 44.04; H, 3.77; Cl, 32.38; N, 12.55%.

Ethylenediurea

Ethylenediurea (m.p. 199° decomp.) was prepared in 73% yield by a modification of Volhard's (5) method. Sodium cyanate was used in place of silver cyanate.

Preparation of 2-Cyclohex-1-enyl cyclohex-1-enyl Derivatives of Ureas and Thioureas

The compounds described in Table I were prepared by either of the processes given in detail below for the preparation of 1-(3,4-dichlorobenzyl)-3-(2-cyclohex-1-enyl cyclohex-1-enyl)-urea.

[3]*All melting points were determined on samples sealed in evacuated capillary tubes. This technique was essential in obtaining reproducible melting points. Microanalyses were determined by Micro-Tech Laboratories, Skokie, Illinois.*

TABLE III

Infrared absorption band (cm^{-1}) assignments[a]

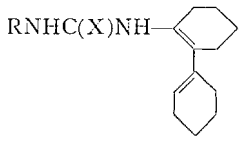

R	X	Stretching modes N—H		Other bands
Hydrogen	O	3350, 3250, 3200	1675	3080 (C=CH)
Allyl	O	3330, 3240	1683, 1672 (C=O)	3060 (C=CH), 1620 (C=C)
Cyclohex-1-enyl	O	3250	1673	3070 (C=CH), 1623 (C=C)
Phenyl	O	3350, 3215	1685, 1668 (C=O)	3075 (C=CH), 1623 (C=C), 1595 (aryl)
4-Chlorophenyl	O	3345, 3235, 3105	1688, 1670 (C=O)	1623 (C=C), 1593 (aryl)
3,4-Dichlorophenyl	O	3315, 3250	1683, 1651 (C=O)	3070 (C=CH), 1623 (C=C), 1586 (NH)
α-Naphthyl	O	3192	1681, 1661 (C=O)	3059 (C=CH), 1594 (aryl)
4-Hydroxyphenyl	O	3360, 3270, 3170	1677	3080 (C=CH), 1628 (C=C), 1592 (aryl)
3,4-Dichlorobenzyl	O	3310, 3250	1683, 1651 (C=O)	3060 (C=CH), 1610 (aryl)
1-(2-Cyclohex-1-enyl cyclohex-1-enyl)-ureidoethylene	O	3330, 3190	1678, 1650 (C=O)	3060 (C=CH)
Hydrogen	S	3370, 3225, 3175	1685	3060 (C=CH), 1553 (NH), 1366 (C=S)
4-Chlorophenyl	S	3345, 3200, 3115	1674	1610 (aryl), 1366 (C=S)

[a]Absorption spectra on Nujol mulls of the crystalline compounds.

Method A

A mixture of 3,4-dichlorobenzylurea (10.25 g, 0.047 mole), cyclohexanone (49 g, 0.5 mole), and concentrated hydrochloric acid (5 g, 0.05 mole) was refluxed for 30 minutes. Crystals separated from the solution during the refluxing period. These were separated and washed with ethanol, yield 15.4 g (86.8%). The melting point (243–244°) was not altered by further crystallization.

Method B

This procedure was the same as given in Method A with the exception that 2-cyclohexylidene-cyclohexanone (17.8 g, 0.1 mole) was used instead of cyclohexanone. The yield of product (m.p. 243–244°) was 13 g (73.3%).

1,2-Dicyclohexylisourea

A solution of bromocyanogen (5.3 g, 0.05 mole) in ether (50 ml) was added dropwise over a period of 35 minutes to a cold (−5 to 0°) solution of freshly distilled cyclohexylamine (9.9 g, 0.1 mole) in ether (50 ml). After the mixture was stirred for an additional 30 minutes, the precipitate of cyclohexylamine hydrobromide was removed by filtration and the filtrate at 0° was treated with cyclohexanol (50 g, 0.5 mole). The solution was stirred for 90 minutes, after which dry HCl gas (5.7 g) was added. This solution was allowed to stand at room temperature for 5 days and then the ether and excess cyclohexanol were removed *in vacuo*. The residue was suspended in water (20 ml) and the pH of the suspension was adjusted to 10 with sodium hydroxide solution. A crystalline suspension was obtained after the mixture had remained at room temperature for 4 days. The crystals (m.p. 78°) were recovered by filtration, yield 11.2 g (100%). Two crystallizations from petroleum ether (b.p. 65–110°) (5 ml/g) raised the melting point to 96°, yield 73.3%. Anal. Calc. for $C_{13}H_{24}N_2O$: C, 69.60; H, 10.78; N, 12.49%. Found: C, 69.80; H, 10.76; N, 12.51%.

1,1'-Bis-(2-cyclohex-1-enyl cyclohex-1-enyl)-ethylenediurea

Ethylenediurea (14.6 g, 0.1 mole), cyclohexanone (58.8 g, 0.6 mole), and concentrated hydrochloric acid (0.2 mole) were heated under reflux for 75 minutes. The crystals were removed from the cool solution by filtration, yield 35.1%. These crystals did not melt below 300° and they were very insoluble in the common organic solvents. Anal. Calc. for $C_{28}H_{42}N_4O_2$: C, 72.05; H, 9.07; N, 12.00%. Found: C, 72.18; H, 9.06; N, 12.32%.

1-(Cyclohex-1-enyl)-3-(2-cyclohex-1-enyl cyclohex-1-enyl)-urea

Urea (60 g, 1 mole), cyclohexanone (98 g, 1 mole), and concentrated hydrochloric acid (100 g, 1 mole) were heated under reflux for 90 minutes. After cooling of the mixture to room temperature the organic layer was separated and the unreacted cyclohexanone, together with some water, was removed *in vacuo*. The oily residue was diluted with ethanol (25 ml) and the solution poured into water (400 ml). This mixture was neutralized with aqueous sodium hydroxide, after which the oil solidified. The product (m.p. 180–200°) was separated by filtration and washed with water, yield 98 g (98%). Two crystallizations from ethanol–benzene (1:1) raised the melting point to a constant value of 221–223°. In some preparations a crystalline modification melting at 238° was obtained. The infrared spectra of these two crystalline modifications were identical. Anal. Calc. for $C_{19}H_{28}N_2O$: C, 75.96; H, 9.39; N, 9.33%. Found: C, 75.62; H, 9.40; N, 9.14%.

ACKNOWLEDGMENT

The infrared and ultraviolet spectra were determined by Dr. C. Sandorfy of the University of Montreal, Montreal, Quebec.

REFERENCES

1. L. F. Fieser and M. Fieser. Steroids. Reinhold Publishing Corp., New York. 1959. pp. 17, 19.
2. L. J. Bellamy. The infrared spectra of complex molecules. 2nd ed. Richard Clay and Co. Ltd., Bungay, Suffolk, Great Britain. 1958. pp. 36, 37.
3. H. Gault, L. Daltroff, and J. Eck-Tridon. Bull. soc. chim. France, **12**, 952 (1945).
4. A. I. Vogel. Textbook of practical organic chemistry. 2nd ed. Longmans, Green and Co., London. 1951. p. 616.
5. J. Volhard. Ann. **119**, 349 (1861).

THE REACTION OF SULPHURYL CHLORIDE WITH REDUCING SUGARS

PART I

H. J. JENNINGS AND J. K. N. JONES
Department of Chemistry, Queen's University, Kingston, Ontario

Received February 13, 1962

ABSTRACT

The reaction of sulphuryl chloride with D-glucose, with D-xylose, and with maltose is described. The products were fully substituted compounds containing both chlorodeoxy and chlorosulphate groups. Formation of the methyl glycosides and subsequent removal of the chlorosulphate groups enabled structural investigations to be carried out on the resultant chlorodeoxy methyl glycosides.

INTRODUCTION

Previous communications (1, 2) on the reaction of sulphuryl chloride with methyl glycosides have described the isolation of fully substituted glycosides containing chlorodeoxy and cyclic sulphate groups. In the case of methyl α-D-glucopyranoside the 2,3-cyclic sulphate derivative was desulphated to yield substances characterized as methyl 4,6-dichloro-4,6-dideoxy-α-D-galactoside and 4,6-dichloro-4,6-dideoxy-D-galactose (2). When conditions similar to those described by Bragg *et al.* (1) were employed the reaction of sulphuryl chloride with reducing sugars produced considerable degradation of the carbohydrate, and a crystalline product, tentatively identified as a dichloro pyridine derivative, was isolated. When the reaction was carried out at a much lower temperature degradation of the sugar was reduced and good yields of carbohydrate derivatives were obtained. Changes in reaction conditions also produced a new range of carbohydrate derivatives which contained the chlorosulphate group.

DISCUSSION

In view of the work of Bragg *et al.* (1, 2) it was considered likely that sulphuryl chloride would react with reducing sugars in pyridine solution to yield cyclic sulphate derivatives with the possible replacement of the hydroxyl group of C_1 by a chloro group. Analysis of the crystalline derivative from maltose indicated that such a reaction had in fact occurred but that the cyclic sulphate grouping was absent. Further examination of the crystalline derivative from maltose and of the syrupy products from D-glucose and D-xylose showed that chlorosulphate residues as well as chlorodeoxy groupings were present in the products. The infrared spectra of the compounds had two characteristic strong absorption frequencies, at 1431–1435 cm^{-1} and 1195–1200 cm^{-1}, the values of which compared well with the frequencies of absorption of the O—SO_2—Cl group reported by Robinson (3). The spectra also showed the absence of hydroxyl absorption. The presence of the chlorosulphate group was further substantiated by the reaction of the compounds with aniline and pyridine (4) to give a characteristic red dye. This dye was previously reported by König and Bayer (5) and was prepared by them from a wide range of inorganic acid chlorides.

The reactions of sulphuryl chloride with D-glucose (experiments i and ii) gave syrupy products which were probably mixtures of the α- and β-chlorodeoxy compounds (I). The formation of the methyl glycosides and the simultaneous dechlorosulphation with methanol alone produced, as the main product, methyl 4,6-dichloro-4,6-dideoxy-α-D-

galactopyranoside (II). The corresponding β-anomer (III) was obtained when methanol and silver oxide were employed. This was evident because both II and III gave on hydrolysis 4,6-dichloro-4,6-dideoxy-D-galactose (2) (IV). The reason for the isolation of both the α and β methyl glycosides is not clear and could be attributed to either a preponderance of the α- or β-1-chloro compound in the original product (I) due to different reaction conditions, or to the different methods used for the formation of the methyl glycosides from I. If it is assumed that in all these reactions the chlorosulphate group is substituted and removed without inversion, discounting the less likely process of double inversion; then compound I was 4,6-dichloro-4,6-dideoxy-D-galactopyranosyl chloride 2,3-dichlorosulphate.

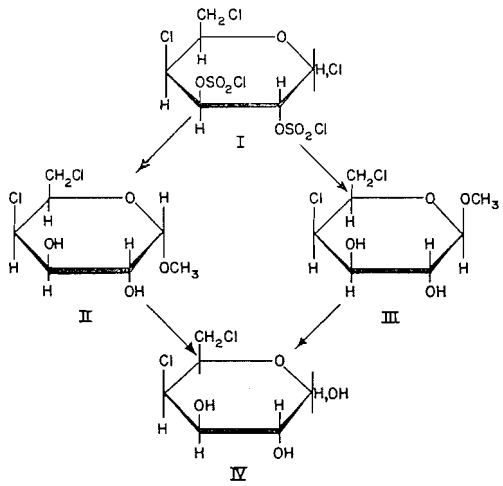

The reaction of sulphuryl chloride with D-xylose gave a syrup (V) which was dechlorosulphated with great difficulty using silver oxide and aqueous methanol. Analysis indicated the presence of one chlorodeoxy group in the dechlorosulphated methyl glycoside (VI) and periodate oxidation of VI gave results (1 mole/mole uptake) consistent with the presence of adjacent hydroxyl groups. Hydrolysis of VI yielded a monochloropentose (VII) which formed a phenylosazone which still contained chlorine. D-Xylose may have reacted in the pyranose or furanose form and the chlorodeoxy group could be assigned to positions C_4 or C_5 depending whether V was a pyranose or furanose derivation. Periodate oxidation of the monochloropentitol (VIII) (produced by reduction of VII) liberated 0.9 mole of formic acid and proved that the chlorodeoxy group was on position C_4 of the molecule, thus establishing that the original sugar had reacted in the pyranose form. The high positive rotation of VI (+237°) suggested that inversion of configuration had taken place at C_4, forming an L-arabinose derivative, and this was supported by the fact that VI remained unchanged when treated with sodium hydroxide solution. If inversion had not occurred the compound would have remained in the D-xylose configuration, and it is known that under alkaline conditions chlorine is eliminated from methyl 4-chloro-4-deoxy-α-L-xyloside to give the 3,4-anhydro compound (2). Compound VI was found to have a specific rotation similar to that of methyl β-L-arabinopyranoside (+245.5°) (6) and therefore it was characterized as methyl 4-chloro-4-deoxy-β-L-arabinopyranoside. On this evidence V was probably 4-chloro-4-deoxy-L-arabinopyranosyl chloride 2,3-dichlorosulphate.

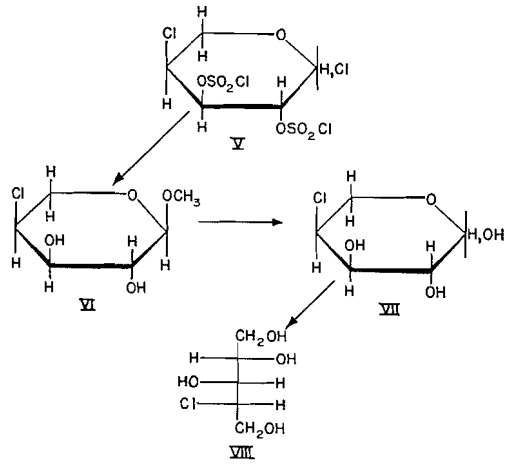

The reaction of sulphuryl chloride with maltose gave a crystalline product (IX) ($C_{12}H_{14}O_{15}Cl_8S_4$). Formation of the methyl glycoside and dechlorosulphation using sodium iodide gave two crystalline products, one of which was shown by analysis to be a trichlorotrideoxy methyl glycoside (X). Sodium iodide was employed because of the difficulty encountered in dechlorosulphating this product by the previous methods. Hydrolysis of X produced a syrup from which two main products were separated and identified as chlorodeoxy hexoses (III and XI). The crystalline dichlorodideoxy hexose (III) was characterized as 4,6-dichloro-4,6-dideoxy-D-galactopyranose (2). The other chlorohexose (XI), which could not be obtained crystalline, was identified as 6-chloro-6-deoxy-D-glucopyranose on the following evidence. It was found to have a specific rotation similar to that of the equilibrium value obtained for crystalline 6-chloro-6-deoxy-D-glucopyranose (7) and gave a phenylosazone (XII) identical with the phenylosazone of 6-chloro-6-deoxy-D-glucopyranose obtained by a synthetic route (8). The phenylosazone (XII) was oxidized with periodate by the method of Hough, Powell, and Woods (9) and initially consumed 1.93 moles of periodate, releasing 0.64 mole of formic acid and no formaldehyde, with an immediate precipitation of the 1,2-bisphenylhydrazone of mesoxaldehyde (XIII). The low yield of formic acid agreed with the findings of Hough, Powell, and Woods, who obtained similar results from the periodate oxidation of phenylosazones (9), but the gradual loss of formic acid with time cannot be satisfactorily explained. The initial results, however, are consistent with the presence of a chlorodeoxy group on position C_6 of the molecule. Accordingly compound X was characterized as methyl 4-*O*-α-4′,6′-dichloro-4′,6′-dideoxy-D-galactopyranosyl 6-chloro-6-deoxy-D-glucopyranoside, and the fully substituted compound (IX) from which it was obtained would be 4-*O*-α-4′,6′-dichloro-4′,6′-dideoxy-D-galactopyranosyl-6-chloro-6-deoxy-D-glucopyranosyl chloride 2,3,2′,3′-tetrachlorosulphate.

The other crystalline compound obtained from IX gave, on hydrolysis, products similar in properties to those observed when X was hydrolyzed. Failure to obtain a sharp melting point and a consistent analysis of the crystalline product from IX indicates that it is probably a mixture containing the α- and β-anomers of compound X.

EXPERIMENTAL

Melting points were determined on a Kofler hot stage and were uncorrected. Optical rotations were measured at 21±3° C. Solutions were concentrated under reduced pressure below 50° C. Paper chromatography was carried out by the descending method on Whatman No. 1 filter paper using the following

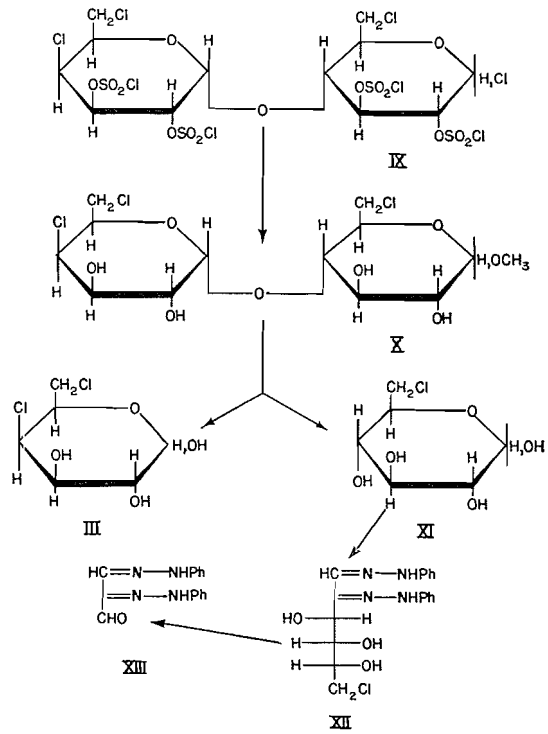

solvent systems (v/v): (*a*) ethyl acetate, acetic acid, formic acid, water (18:3:1:4) and (*b*) butan-1-ol, ethanol, water (3:1:1). Sugars were located on chromatograms by *p*-anisidine hydrochloride (10) or alkaline silver nitrate (11) sprays and the rates of movement are quoted relative to that of D-xylose (R_x). Sugars containing the chlorosulphate group were located specifically with a spray made of a butan-1-ol solution of aniline and pyridine (4). Infrared absorptions were measured as solutions in chloroform or as a powder suspended in a potassium bromide pellet on a Perkin–Elmer Model 21 spectrophotometer. All solutions were deionized by passage through Amberlite IR120 (H form) and Duolite A4 (OH form) unless otherwise stated.

General Method

The reducing sugar (10 g), previously dried over phosphoric oxide, was partially dissolved in dry pyridine (40 ml). Chloroform (100 ml), dried over anhydrous sodium sulphate, was added to the pyridine solution, and precipitation of some of the reducing sugar occurred. The heterogeneous reaction mixture was cooled in a solid carbon dioxide – acetone bath, and an excess of redistilled sulphuryl chloride was added drop by drop over a period of half an hour with vigorous stirring (21 ml of sulphuryl chloride for a pentose and 26 ml for a hexose or disaccharide). Cooling was continued for a further 2 hours and the reaction mixture was then allowed to come to room temperature. During this rise in temperature the viscosity of the solution decreased rapidly and a white precipitate, possibly of pyridine salts, was formed. The precipitate was filtered from the chloroform solution, and the chloroform solution was washed successively with 10% sulphuric acid, saturated sodium bicarbonate solution, and distilled water. The final chloroform solution was dried over anhydrous sodium sulphate, filtered, and the filtrate was concentrated to a syrup which crystallized on standing, in the case of maltose.

D-*Glucose (i)*

The general method was applied and the reaction mixture was allowed to stand for 24 hours at room temperature. D-Glucose gave a pale yellow syrup (8.8 g) which could not be obtained crystalline. It had $[\alpha]_D$ +66° (*c*, 2.8 in chloroform) and paper chromatography in solvent (*a*) gave one spot that moved with the solvent front (aniline/pyridine spray).

*Methyl 4,6-Dichloro-4,6-deoxy-α-*D*-galactopyranoside*

The above syrup (8.2 g) was refluxed in anhydrous methanol (200 ml) solution for 12 hours. The methanolic solution was passed through Duolite A4 (OH form) ion exchange resin and concentrated to a pale yellow syrup (4.5 g) which crystallized on standing. The crude crystals were dissolved in water, the solution was continuously extracted with chloroform, and the chloroform solution on concentration gave a crystalline

mass. Recrystallization from chloroform – light petroleum (b.p. 40–60° C) gave long colorless needles (2.5 g) of m.p. 157° C and $[\alpha]_D$ +179° (*c*, 2.1 in water). The mixed melting point with an authentic sample of methyl 4,6-dichloro-4,6-dideoxy-α-D-galactopyranoside (1, 2) was 157° C. The crystals gave an infrared spectrum identical with that of the authentic specimen of the galactoside derivative.

D-*Glucose (ii)*

The same method was applied as in the previous case (i) except that the reaction product was isolated immediately after the reaction mixture had attained room temperature. D-Glucose gave a pale yellow syrup (8 g) which could not be obtained crystalline and paper chromatography in solvent (*a*) gave one spot that moved with the solvent front (aniline/pyridine spray).

Methyl 4,6-Dichloro-4,6-dideoxy-β-D-galactopyranoside

The above syrup (6 g) was dissolved in anhydrous methanol (150 ml) and the solution was shaken in an aluminum foil covered flask with silver oxide (10 g), 'drierite' (5 g), and glass beads for 24 hours. Distilled water (10 ml) was then added to the reaction mixture, which was shaken for a further 24 hours. The heterogeneous mixture was filtered and the filtrate was deionized and concentrated to a syrup (2.5 g) which crystallized immediately. Two recrystallizations from chloroform – light petroleum (b.p. 40–60° C) gave colorless needles (0.5 g) of m.p. 154° C and $[\alpha]_D$ −8° (*c*, 0.8 in water). Analysis: Calc. $C_7H_{12}Cl_2O_3$: C, 36.4%; H, 5.2%; Cl, 30.7%. Found: C, 36.3%; H, 5.5%; Cl, 30.4%.

The crystals were hydrolyzed with *N* sulphuric acid and the solution was neutralized with barium carbonate, filtered, and the filtrate was deionized to give a syrup which crystallized on standing. Recrystallization from methanol gave colorless crystals of m.p. 184° C (decomp.), $[\alpha]_D$ +130° (30 minutes) → +97° (equilibrium, 24 hours) (*c*, 0.98 in methanol), and mixed melting point with authentic 4,6-dichloro-4,6-dideoxy-D-galactose (2) 184° C (decomp.).

D-*Xylose*

The reaction was carried out by the general method and the reaction product was isolated after the reaction mixture had been allowed to stand at room temperature for 4 hours. D-Xylose gave a yellow syrup (9.5 g) which had $[\alpha]_D$ −41° (*c*, 5.8 in chloroform) and did not crystallize. Paper chromatography in solvent (*a*) gave one spot that moved with the solvent front (aniline/pyridine spray).

Methyl 4-Chloro-4-deoxy-β-L-arabinopyranoside

The above syrup (5.5 g) was treated in the same way as the syrup from D-glucose (ii). Dechlorosulphation of the syrup using silver oxide, methanol, and distilled water was found to be incomplete even after 96 hours. Therefore, the sulphur-containing syrup (3.75 g) was dissolved in chloroform and the chloroform solution was extracted with distilled water. The distilled-water fraction was concentrated to a syrup (0.75 g) which partially crystallized and which was found to be free of sulphur. The semicrystalline mass was then dissolved in water and continuously extracted with ether. The ether extract on concentration produced a crystalline product (0.7 g). Recrystallization from ethyl acetate gave needle-shaped crystals of m.p. 152° C and $[\alpha]_D$ +237° (*c*, 0.96 in methanol). Analysis: Calc. $C_6H_{11}ClO_4$: C, 39.4%; H, 6.0%; Cl, 19.5%. Found: C, 39.4%; H, 6.3%; Cl, 19.1%.

4-Chloro-4-deoxy-L-arabinose

The above crystals (0.36 g) were refluxed in *N* sulphuric acid solution (50 ml) for 10 hours. The solution was neutralized with barium carbonate, filtered, and the filtrate was deionized and concentrated to a syrup (0.33 g) which crystallized on standing. Recrystallization from ethanol gave colorless crystals of m.p. 150° C and $[\alpha]_D$ +155° (10 minutes) → +119° (equilibrium, 36 hours) (*c*, 0.4 in water). Analysis: Calc. $C_5H_9ClO_4$: C, 35.6%; H, 5.4%; Cl, 21.0%. Found: C, 35.6%; H, 5.6%; Cl, 20.4%.

The phenylosazone of the above compound was made and purified by three successive precipitations from methanol solution using distilled water to give fine yellow crystals of m.p. 123° C (decomp.). Analysis: Calc. $C_{17}H_{19}ClN_4O_2$: Cl, 10.3%; N, 16.2%. Found: Cl, 10.0%; N, 15.8%.

4-Chloro-4-deoxy-L-arabitol

The crystalline monochloropentose (0.15 g) was dissolved in distilled water (50 ml) and an excess of sodium borohydride (0.15 g) was added. When the solution became non-reducing acetone was added to decompose the excess sodium borohydride. The solution was deionized and concentrated to a syrup which was codistilled (×10) with methanol. The resultant colorless syrup (0.14 g) did not crystallize and had $[\alpha]_D$ +10° (*c*, 0.9 in water). The syrup contained chlorine and gave one spot with alkaline silver nitrate (11) at R_x 1.0 on paper chromatograms when developed in solvents (*a*) and (*b*).

Periodate Oxidations

The oxidations were carried out in the dark at 25° C, using a small sample (20 mg) of the compounds in distilled water (25 ml) containing 0.3 *M* sodium metaperiodate (1 ml). Aliquots (1 ml) were removed at intervals and the consumption of periodate (12) and the production of formic acid (13) were measured.

Oxidation of Methyl 4-Chloro-4-deoxy-β-L-arabinopyranoside

The moles of periodate consumed were as follows: 0.37 (3.25 hours); 0.37 (5 hours); 1.01 (23 hours); 1.13 (68 hours). No formic acid was produced.

Oxidation of 4-Chloro-4-deoxy-L-arabitol

The moles of periodate consumed and moles of formic acid produced were respectively as follows: 2.04, 0.89 (0.5 hour); 2.08, 0.9 (9.5 hours).

Reaction of Methyl 4-Chloro-4-deoxy-β-L-arabinopyranoside with Sodium Hydroxide

The crystals (18 mg) were dissolved in 0.1 *N* sodium hydroxide solution (2 ml) and the solution was left to stand for 8 hours. Titration of the solution with 0.1 *N* sulphuric acid, using phenolphthalein as the indicator, indicated that only a negligible quantity of the sodium hydroxide solution had been spent in the reaction (0.02 ml). The solution was deionized and concentrated to a crystalline mass (18 mg) which was recrystallized from ethyl acetate to give a product with m.p. 151° C and mixed melting point with the starting material 150–151° C.

Maltose

The general method was applied except that the reaction product was isolated immediately after the reaction mixture had attained room temperature. Maltose gave a pale yellow syrup (11.6 g) which crystallized on standing. Recrystallization was carried out by cooling a saturated solution of the crude crystalline product in chloroform in an acetone – solid carbon dioxide bath. The crystals (6.8 g) were isolated by filtration and washed with chloroform – light petroleum (b.p. 40–60° C) (1:1, v/v). The crystals had m.p. 203° (decomp.) and $[\alpha]_D$ +143° (*c*, 1.28 in chloroform). Analysis: Calc. $C_{12}H_{14}Cl_8O_{15}S_4$: C, 18.2%; H, 1.8%; Cl, 35.8%; S, 16.1%. Found: C, 18.0%; H, 2.0%; Cl, 35.4%; S, 15.7%. Paper chromatography in solvent (*a*) gave one spot that moved with the solvent front (aniline/pyridine spray).

Methyl 4-O-α-4′,6′-dichloro-4′,6′-dideoxy-D-galactopyranosyl 6-chloro-6-deoxy-D-glucopyranoside

The above crystals (10 g) were dissolved in anhydrous methanol and refluxed for 8 hours to form the methyl glycoside. Sodium iodide (10 g) was added to the solution and an immediate evolution of iodine and sulphur dioxide was noticed. The reaction mixture was left to stand for 8 hours. Iodine was removed from the solution by passing hydrogen sulphide through it and the excess hydrogen sulphide was removed by aeration. The solution was neutralized with barium carbonate and filtered. Silver nitrate was added to remove the iodides from solution and after filtration of the silver iodide, potassium chloride was added to the solution to remove the excess silver nitrate. Finally the silver chloride was filtered from the solution and the solution was concentrated to a semicrystalline mass, which was extracted with cold acetone (×3). Evaporation of the acetone solution gave a colorless syrup (5 g). The syrup was dissolved in water and extracted continuously with chloroform for 4 hours and then for a further 4 hours, giving two fractions, A and B.

Fraction A

Concentration of the chloroform solution gave a colorless syrup (2 g) which did not crystallize. Crystallization occurred from ethyl acetate – chloroform and recrystallization from *n*-propanol gave colorless needles (0.25 g) of m.p. 184–186° C and $[\alpha]_D$ +174° (*c*, 0.58 in methanol). Analysis: Calc. for the monohydrate $C_{13}H_{24}O_9Cl_3$: C, 36.2%; H, 5.6%; Cl, 24.7%. Found: C, 36.0%; H, 5.0%; Cl, 24.6%. The sample above was dried to constant weight at 60° C *in vacuo* over phosphoric oxide. Analysis: Calc. for $C_{13}H_{22}O_8Cl_3$: C, 37.8%; H, 5.3%; Cl, 25.8%. Found: C, 37.8%; H, 5.1%; Cl, 26.1%.

6-Chloro-6-deoxy-D-glucose and 4,6-Dichloro-4,6-dideoxy-D-galactose

The crystals of the monohydrate above (0.25 g) were dissolved in *N* sulphuric acid (50 ml) and the solution was refluxed for 16 hours. The reaction mixture was neutralized and deionized as described for previous hydrolyzates. Concentration of the resultant solution gave a syrup (0.2 g) which was shown by paper chromatography in solvents (*a*) and (*b*) to contain two major reducing components at R_x 1.7 and R_x 2.5. A minor reducing component at R_x 0.63 cochromatographed with D-glucose in solvents (*a*) and (*b*). The syrup was fractionated on Whatman 3MM paper using solvent (*b*). End strips of the chromatogram were sprayed with alkaline silver nitrate and the areas of paper corresponding to the two components at R_x 1.7 and R_x 2.5 were eluted with water to give solutions of the two components.

Component at R_x 2.5

The solution was filtered and concentrated to give a crystalline mass (120 mg) which was recrystallized from ethanol. The crystals had m.p. 183–184° C (decomp.) and mixed melting point with an authentic sample of 4,6-dichloro-4,6-dideoxy-D-galactose (2) 184° C (decomp.). The crystals also cochromatographed with the authentic specimen in solvents (*a*) and (*b*).

Component at R_x 1.7

The solution was filtered and concentrated to give a syrup (100 mg) which could not be obtained crystalline. It had $[\alpha]_D$ +34° (*c*, 0.98 in water), and formed a phenylosazone which was recrystallized from methanol–

water to give yellow needles of m.p. 167–168° C (decomp.). Analysis: Calc. $C_{18}H_{21}ClN_2O_3$: C, 57.2%; H, 5.6%; Cl, 9.4%; N, 14.9%. Found: C, 57.6%; H, 5.7%; Cl, 9.1%; N, 15.0%.

Preparation of 6-Chloro-6-deoxy-D-glucose

This was carried out essentially by the method of Wiggins and Wood (8). 6-*O*-Tosyl methyl α-D-glucoside (0.5 g) was heated with anhydrous lithium chloride (0.25 g), absolute methanol (10 ml), and anhydrous acetone (10 ml) at 150° C in a sealed tube for 60 hours. The solution was concentrated to a syrup which was dissolved in water, deionized, and reconcentrated to a syrup (0.35 g) which did not crystallize and gave no spots on paper chromatograms developed in solvents (*a*) and (*b*). The syrup was refluxed with *N* sulphuric acid for 8 hours, and the solution was neutralized and deionized as in previous hydrolyses. The solution was concentrated to a syrup which was shown to consist of one major reducing component (R_x 1.9) and two minor reducing components (R_x 0.65 and R_x 1.35) by paper chromatography in solvents (*a*) and (*b*). The syrup was fractionated on Whatman 3MM paper in solvent (*b*) and the component at R_x 1.9 was isolated by the method used in the previous fractionation by chromatography on 3MM paper. Concentration of the aqueous solution gave a syrup (0.17 g) which could not be obtained crystalline. The syrup gave a phenylosazone of m.p. 165° C (decomp.) and had a mixed melting point with the phenylosazone from above of 166–167° C (decomp.). The two phenylosazones also gave identical infrared spectrums.

Periodate Oxidation of 6-Chloro-6-deoxy-D-glucose Phenylosazone

The crystalline phenylosazone (above) (14.7 mg) was oxidized with sodium metaperiodate in 50% aqueous ethanol by the method of Hough, Powell, and Woods (9). A yellow-orange precipitate was filtered from the solution after 30 minutes and the moles of periodate consumed and the formic acid produced were respectively as follows: 1.93, 0.64 (0.66 hour); 2.06, 0.62 (2.66 hours); 2.09, 0.17 (29.5 hours). No formaldehyde was produced.

1,2-Bisphenylhydrazone of Mesoxaldehyde (9)

The yellow-orange precipitate was recrystallized from 50% aqueous ethanol and gave crystals of m.p. 189° C. An authentic specimen had m.p. 193–194° C and the mixed melting point was 187–189° C. The infrared spectra of the authentic and derived specimens were identical over the range 4000–600 cm^{-1}.

Fraction B

The chloroform solution gave on concentration a syrup (2 g) which crystallized on the addition of hot chloroform. Recrystallization from chloroform – ethyl acetate gave non-reducing colorless crystals (1 g) of m.p. 98–102° C and $[\alpha]_D$ +76° (*c*, 1.0 in methanol). A consistent analysis could not be obtained for this compound even after repeated recrystallizations; therefore it was considered to be a mixture.

6-Chloro-6-deoxy-D-glucose and 4,6-Dichloro-4,6-dideoxy-D-galactose

The crystals from fraction B gave results similar to those observed when the crystalline product from fraction A was hydrolyzed under the same conditions. Paper chromatography produced reducing spots of the same intensities with similar R_x values at R_x 0.63, R_x 1.7, and R_x 2.5. The hydrolysis product was fractionated as described for the crystalline product from fraction A and both 6-chloro-6-deoxy-D-galactose and 4,6-dichloro-4,6-dideoxy-D-glucose were isolated and characterized.

ACKNOWLEDGMENTS

The authors wish to thank Mr. J. C. Turner for the sample of 6-*O*-tosyl methyl α-D-glucoside. They would also like to thank the National Research Council for financial assistance (grant N.R.C./T19).

REFERENCES

1. P. D. Bragg, J. K. N. Jones, and J. C. Turner. Can. J. Chem. **37**, 1412 (1959).
2. J. K. N. Jones, M. B. Perry, and J. C. Turner. Can. J. Chem. **38**, 1122 (1960).
3. E. A. Robinson. Can. J. Chem. **39**, 247 (1961).
4. G. Crank. M.Sc. Thesis, Queen's University, Kingston, Ontario. 1960.
5. W. König and R. Bayer. J. prakt. Chem. **83** (2), 325 (1911).
6. C. S. Hudson. J. Am. Chem. Soc. **47**, 265 (1925).
7. B. Helferich and H. Bredereck. Ber. **60**, 1995 (1927).
8. L. F. Wiggins and D. J. C. Wood. J. Chem. Soc. 1180 (1951).
9. L. Hough, D. B. Powell, and B. M. Woods. J. Chem. Soc. 4799 (1956).
10. L. Hough, J. K. N. Jones, and W. H. Wadman. J. Chem. Soc. 1702 (1950).
11. W. E. Trevelyan, D. P. Proctor, and J. S. Harrison. Nature, 166, 444 (1950).
12. G. Neumüller and E. Vasseur. Arkiv. Kemi, **5**, 235 (1953).
13. D. M. W. Anderson, C. T. Greenwood, and E. L. Hirst. J. Chem. Soc. 225 (1955).

CONSTITUTIONS OF POLYSACCHARIDES FROM SERRATIA MARCESCENS[1]

H. C. SRIVASTAVA[2] AND G. A. ADAMS
Division of Applied Biology, National Research Council, Ottawa, Canada

Received March 1, 1962

ABSTRACT

Constitutional studies of three polysaccharides prepared from *Serratia marcescens* cells by a sequence of phenol extraction, ultracentrifugation, and fractionation by Cetavlon are described. Methylation of the polysaccharides followed by acid hydrolysis yielded 2,3,4,6-tetra-*O*-methyl-D-glucose, 2,4,6-tri-*O*-methyl-D-glucose, 2,4,6-tri-*O*-methyl-D-mannose, 4,6-di-*O*-methyl-D-glucose, 2,6-di-*O*-methyl-D-glucose, and an unidentified di-*O*-methyl-glucose. The acidic components found were: 2,3,4-tri-*O*-methyl-D-mannuronic acid, 3-*O*-(2,3,4-tri-*O*-methyl-D-mannuronosyl)-2,4,6-tri-*O*-methyl-D-glucose, and *O*-2,3,4-tri-*O*-methyl-D-mannuronosyl-(1 → 3)-*O*-2,4,6-tri-*O*-methyl-D-glucosyl-(1 → 3)-2,4,6-tri-*O*-methyl-D-glucose. The polysaccharides are composed of a main chain of D-glucose and D-mannose residues joined by 1,3-glycosidic bonds. Some glucose residues carry branches at C_2 and C_4 which terminate in either D-glucose or D-mannuronic acid residues. The three polysaccharides studied had similar chemical structures but varied in the amounts of component sugars and degree of branching.

Because of the tumor-necrotizing properties of the polysaccharides of *Serratia marcescens* (*Bacillus prodigiosus*), much work has been carried out during the last two decades on isolation from their culture filtrates as well as from the cells, on analysis, and on biological properties (1–8). However, only one attempt has been made to investigate the chemical structure of the carbohydrate polymer. Thus, Rathgeb and Sylven (9) carried out structural studies on a glucan isolated by fractionation of Shear's polysaccharide (1) with trichloroacetic acid and ethanol followed by treatment with hot picric acid (7). On the basis of methylation and periodate oxidation, data suggested that the polysaccharide was composed of glucose residues combined mutually by alternating 1,4- and 1,6-glycosidic bonds. However, a weakness in this work is that identification of the methylated sugar fragments was based solely upon paper chromatographic analysis. It is now known that methyl ethers of different sugars having the same degree of methylation can have the same R_f value in a particular solvent. It is rather speculative to assign any structural significance to the periodate-oxidation data unless some reasonable idea about the inter-sugar linkages in the polysaccharide is available. The present communication describes constitutional studies on polysaccharides (or lipopolysaccharides) isolated from the cells of *S. marcescens* by phenol–water extraction followed by fractionation of the polysaccharide mixture by (i) high-speed centrifugation and (ii) by complex formation with cetyltrimethylammonium bromide (Cetavlon) (10). Figure 1 shows an abbreviated scheme of the preparative procedures for polysaccharides used in the present study (for details see ref. 10).

Graded hydrolysis of a main polysaccharide fraction (6NR) with *N* sulphuric acid produced three uronic acid components (A, B, and C), which were separated from neutral sugars by ion-exchange resins and from each other by chromatography on thick filter paper sheets. Component A was identified as D-mannuronolactone. Component B had an equivalent weight of 356 and proved to be an aldobiouronic acid. It turned dark rapidly, thus precluding optical rotation measurements. The aldobiouronic acid was converted to its methyl ester methylglycoside and the latter was reduced with lithium aluminum

[1]*Issued as N.R.C. No. 6863.*
[2]*National Research Council Postdoctorate Fellow 1957–1959. Present address: Ahmedabad Textile Industry's Research Association, Ahmedabad-9, India.*

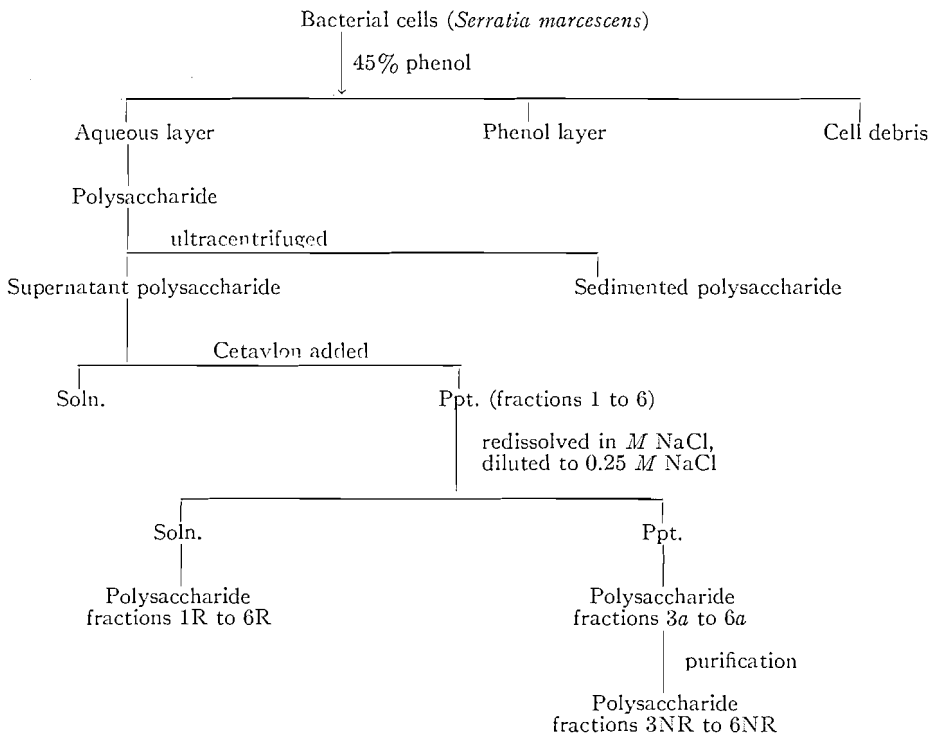

FIG. 1. Preparation of polysaccharides. Fractions 3R, 4R, and 5R were combined for methylation study; fraction 6NR was studied by methylation methods.

hydride to produce the methyl glycoside of a neutral disaccharide. Hydrolysis of the glycoside with acid produced D-glucose and D-mannose in equal proportions. The sugars were characterized as their *p*-nitroanilides. Similar experiments with component C revealed that it was an aldotriouronic acid in which a mannuronic acid residue was combined with two glucose units.

Fractions 6NR and combined fractions 3R, 4R, and 5R (see Fig. 1) were methylated separately with dimethyl sulphate and alkali and the methylation was completed by methyl iodide and silver oxide. The methylated polysaccharides were fractionated and the fractions having the highest methoxyl values were examined.

Methanolysis of 6NR methylated polysaccharide produced a mixture of methylated glycosides, a portion of which was separated by gas–liquid chromatography (11, 12) into three components. One of them crystallized and was shown to be methyl 2,4,6-tri-*O*-methyl-β-D-glucoside, m.p. 68–69° (13).

The methyl glycosides were hydrolyzed with acid to give a mixture of methylated sugars and methylated uronic acids. The uronic acids were converted to their barium salts and separated from the methyl glycosides by selective solvent extraction. The mixture of neutral methylated sugars was resolved by cellulose-column chromatography and the components were weighed and then identified as follows: (i) 2,3,4,6-tetra-*O*-methyl-D-glucose, characterized as *N*-phenyl 2,3,4,6-tetra-*O*-methyl-D-glucosylamine, m.p. 134–135°, $[\alpha]_D$ +240° in chloroform (14); (ii) 2,4,6-tri-*O*-methyl-D-glucose, m.p. and mixed m.p. 123–125° (15), identified as anilide, m.p. 162–165° (16); (iii) 2,4,6-tri-*O*-methyl-D-mannose, m.p. 63–65°, $[\alpha]_D$ +17.6° in water (17); the identity of the compound

was confirmed by ionophoresis and by its characteristic crystalline aniline derivative, m.p. and mixed m.p. 132°, $[\alpha]_D$ +7.8° in methanol (18), (iv) 4,6-di-*O*-methyl-D-glucose, m.p. and mixed m.p. 157–158°, $[\alpha]_D$ +62° in water (15); (v) 2,6-di-*O*-methyl-D-glucose, $[\alpha]_D$ +58° (19); and (vi) 2,3- or 2,4-di-*O*-methyl-D-glucose; the lack of sufficient material prevented complete identification of this component. The identification of 2,6-di-*O*-methyl-D-glucose, which was obtained as a sirup, is based upon the following evidence. Demethylation gave glucose and its mobility on paper chromatogram and paper electrophoretogram was the same as that of an authentic specimen of 2,6-di-*O*-methyl-D-glucose. It gave a negative color reaction with alkaline triphenyltetrazolium chloride (20, 21), indicating that C_2-hydroxyl of the sugar was substituted. The sugar was therefore 2,3-, 2,4-, or 2,6-di-*O*-methyl-D-glucose. Periodate oxidation of the sugar on paper followed by benzidine spray (22) showed that oxidation had taken place. Since, of the three possibilities, only 2,6-di-*O*-methyl-glucose is oxidizable, its identity is established.

Three methyl ether derivatives of acidic components were isolated from the hydrolyzate of the methylated polysaccharide. They were shown to be 2,3,4-tri-*O*-methyl-D-mannuronic acid (I), 3-*O*-(2,3,4-tri-*O*-methyl-D-mannuronosyl)-2,4,6-tri-*O*-methyl-D-glucose (II), and *O*-2,3,4-tri-*O*-methyl-D-mannuronosyl-(1 → 3)-*O*-2,4,6-tri-*O*-methyl-D-glucosyl-(1 → 3)-2,4,6-tri-*O*-methyl-D-glucose (III) on the basis of the following experimental evidence. The components I, II, and III were each transformed into their methyl ester methyl glycoside derivatives, which were reduced with lithium aluminum hydride and hydrolyzed. Component I gave only 2,3,4-tri-*O*-methyl-D-mannose, $[\alpha]_D$ +1° in water (23), which was identified by paper and gas chromatography and by preparation of the crystalline derivative 2,3,4-tri-*O*-methyl-D-mannonophenylhydrazide, m.p. 166° (24), via 2,3,4-tri-*O*-methyl-D-mannono-δ-lactone. Component II afforded a mixture of 2,3,4-tri-*O*-methyl-D-mannose and 2,4,6-tri-*O*-methyl-D-glucose (in approximately equal proportions), the methylated sugars being identified by the methods described earlier. Component III also yielded 2,3,4-tri-*O*-methyl-D-mannose and 2,4,6-tri-*O*-methyl-D-glucose but the proportion of the two sugars in this case was approximately 1:2.

Two methylated polysaccharides (S_0,S_I) which were isolated by fractionation of the methylated combined polysaccharides 3R, 4R, and 5R (Fig. 1) were also analyzed in the manner described for methylated 6NR polysaccharide. Both methylated fractions gave upon hydrolysis 2,3,4,6-tetra-*O*-methyl-D-glucose, 2,4,6-tri-*O*-methyl-D-glucose, 2,4,6-tri-*O*-methyl-D-mannose, and di-*O*-methyl sugars, besides the methylated aldobiouronic acid 3-*O*-(2,3,4-tri-*O*-methyl-D-mannuronosyl)-2,4,6-tri-*O*-methyl-D-glucose. There was also evidence for the presence of small amounts of methylated glucuronic acid, indicating thereby that some D-glucuronic acid residues were present in the polysaccharide in addition to the main acid component, D-mannuronic acid. The ratios of the methylated sugars produced upon hydrolysis of the methyl ethers of different polysaccharide fractions are given in Table I.

TABLE I

Mole ratios of methylated sugars

Methylated sugar	Fraction 6NR	Fraction S_0	Fraction S_I
2,3,4,6-Tetra-*O*-methyl-D-glucose	4.5	1.0	1.0
2,4,6-Tri-*O*-methyl-D-glucose	21.0	20.0	10.0
2,4,6-Tri-*O*-methyl-D-mannose	11.0	9.0	3.0
4,6-Di-*O*-methyl-D-glucose	2.5	1.0	1.0
2,6-Di-*O*-methyl-D-glucose	2.0		
Di-*O*-methyl-D-glucose (?)	1.0	—	—

6NR and 4R polysaccharides were oxidized with sodium metaperiodate, when 0.52 and 0.50 mole of periodate were consumed and 0.122 and 0.125 mole of formic acid were produced respectively per anhydrohexose unit.

DISCUSSION

Polysaccharide (6NR)

Isolation of D-mannuronolactone from the hydrolyzate of the polysaccharide and 2,3,4-tri-*O*-methyl-D-mannuronic acid from the products of hydrolysis of the methylated polysaccharide established beyond doubt that D-mannuronic acid was a component part of this polymer. As far as the authors are aware, this is the second polysaccharide in which D-mannuronic acid occurred as a building unit of the polymer, the other well-known example being that of alginic acid. D-Mannuronic acid has been suggested by Barker *et al.* to be a constituent of the capsular polysaccharide of *Aerobacter aerogenes*; however, definitive identification of the acid has not been made (25).

Although the methylation data were not sufficient for the formulation of a unique structure for the polysaccharide, the following points of constitutional significance emerged from these studies. The isolation of 2,4,6-tri-*O*-methyl-D-glucose and 2,4,6-tri-*O*-methyl-D-mannose showed that the polysaccharide had a backbone of D-glucose and D-mannose residues linked by 1,3-glycosidic bonds. Some of these glucose residues carried branches at C_2 or C_4 which terminated either in D-glucose or D-mannuronic acid residues, as indicated by the identification of 2,6-di-*O*-methyl, 4,6-di-*O*-methyl, 2,3,4,6-tetra-*O*-methyl ethers of D-glucose and 2,3,4-tri-*O*-methyl-D-mannuronic acid. Di-*O*-methyl sugars may arise from undermethylation and/or demethylation of the polysaccharide, but the isolation of tetra-*O*-methyl-glucose and the fact that no di-*O*-methyl ethers of mannose were obtained showed that the di-*O*-methyl-glucoses have definite structural significance.

Isolation of the aldobiouronic acid (B) from the polysaccharide and the identification of 3-*O*-(2,3,4-tri-*O*-methyl-D-mannuronosyl)-2,4,6-tri-*O*-methyl-D-glucose (II) as one of the methylated fragments from the methylated polysaccharide proved that the D-mannuronic acid was combined to the rest of the polymer through D-glucose residues and by 1,3-glycosidic bonds. It also proved that the D-mannuronic acid was in a terminal position. In the same way, the isolation of an aldotriouronic acid composed of mannuronic acid and two glucose residues and its corresponding methyl ether from the methylated polysaccharide provided evidence that the D-mannuronic acid is joined to one of two continuous D-glucose residues in the molecule.

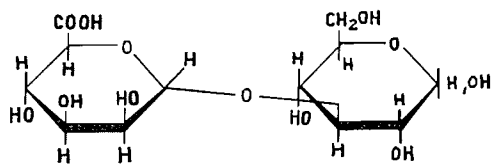

B

A high positive specific optical rotation of the polysaccharide as well as of its methyl ether indicated that the majority of the intersugar linkages had an α-configuration. The low consumption (0.5 mole) of periodate per anhydrohexose unit indicated that most of the sugar residues in the polysaccharide are immune to periodate oxidation and those which were oxidized were the non-reducing end groups of D-glucose and D-mannuronic

acid. The interpretation of the periodate-oxidation data was complicated by the presence of uronic acid residues, which tend to become oxidized, and also by the possibility that some of the sugar residues might be esterified by the phospholipid moiety of the lipopolysaccharide.

Polysaccharides (Combined 3R, 4R, 5R)

These polysaccharides were built up of similar sugar residues and the sugars were linked in the same manner as in the 6NR polysaccharide. However, they differed from the latter polysaccharide in the degree of branching and in their glucose:mannose ratio.

EXPERIMENTAL

All evaporations were carried out under diminished pressure below 40° unless otherwise stated.

Paper chromatograms were run by the descending method using the following solvent systems (v/v): (A) pyridine – ethyl acetate – water (2:1:2); (B) butanone–water azeotrope containing ammonia; (C) benzene–ethanol–water–ammonia (200:47:14:1); (D) 1-butanol–ethanol–water (40:11:19); and (E) ethyl acetate – acetic acid – formic acid – water (18:3:1:4). *p*-Anisidine hydrochloride was used to detect the sugars and their methyl ethers on paper chromatograms (26). R_g and M_G represent rates of movement of sugar paper chromatographically and electrophoretically in relation to 2,3,4,6-tetra-*O*-methyl-D-glucose and D-glucose respectively.

Hydrolysis of the Polysaccharide and Isolation of Uronic Acid Components

Polysaccharide (2.37 g) was heated in *N* sulphuric acid (50 ml) at 70° C for 23 hours and then at 100° C for 8 hours. The hydrolyzate was neutralized with barium hydroxide and barium carbonate, and the barium sulphate was removed by filtration. The barium ions were removed by Amberlite IR-120 and the acidic components were adsorbed on a column of Dowex 1 resin (acetate form). After the neutral sugars were washed off with water, the acids were eluted with *N* formic acid (yield of uronic acids 1.003 g). Chromatography on paper in solvent E showed three spots; one spot (component A) had the same mobility as mannuronolactone, the other two spots (components B and C) had $R_{\text{mannurone}}$ values of 0.22 and 0.36 respectively. The acids were separated on Whatman No. 3 MM paper using solvent E and gave the following yields: A, 82 mg; B, 334 mg; and C, 76 mg.

Attempts to crystallize A, $[\alpha]_D^{25}$ +91° (*c*, 1 in water), were unsuccessful. Reduction of its methyl ester methyl glycoside yielded a sugar which was identified chromatographically (solvent A) as mannose.

Component B, which appeared to be an aldobiouronic acid (acid equivalent: calculated 340, found 356), turned dark rapidly on standing and optical rotation measurements were impossible. Component B (134 mg) was heated for 10 hours at 75° C with 2% methanolic hydrogen chloride (3 ml). The methyl glycoside methyl ester was dissolved in tetrahydrofuran (25 ml) and reduced with lithium aluminum hydride (27). The recovered disaccharide glycoside (130 mg), $[\alpha]_D^{25}$ +34.8° (*c*, 2.3 in methanol), was hydrolyzed with *N* sulphuric acid. Chromatographic examination on paper using solvent A showed glucose and mannose in approximately equal amounts.

The sugars were separated on sheets of paper using solvent A, when mannose (53.6 mg) and glucose (57.9 mg) were obtained. The sugars were converted to their *p*-nitroanilides by heating with *p*-nitroaniline in methanol. The recovered *N*-*p*-nitrophenyl-D-mannopyranosylamine dihydrate had a melting point of 219° and the *N*-*p*-nitrophenyl-D-glucopyranosylamine dihydrate a melting point of 184° C, which are in good agreement with the reported values (13).

Similar examination of the derived neutral glycoside of component C showed that it was composed of mannose and glucose in the proportion of approximately 1:2.

Methylation of Fraction 6NR

The polysaccharide (4.01 g) was methylated three times by dimethyl sulphate and alkali (28) to yield chloroform-soluble (0.76 g) and chloroform-insoluble (5.03 g) fractions. These two fractions were then methylated five times by Purdies reagents (29); the chloroform-insoluble fraction yielded a product (0.85 g) with OCH_3 26.9%, and the chloroform-soluble material gave a product (4.73 g) with OCH_3 32.6%. Further methylation of this latter product did not increase its methoxyl content. The methylated polysaccharide (4.7 g) was dissolved in a mixture of chloroform – ethyl ether (60 ml, 1:5, v/v) and fractionated by addition of petroleum ether (b.p. 30–60°). A total of nine fractions were recovered and their specific rotations and methoxyl values are given in Table II. On the basis of similarity of these values, fractions 1, 2, and 3 were combined for methanolysis studies.

Methanolysis of Methylated Polysaccharides

The combined methylated polysaccharides (2.8 g) were refluxed on a water bath in 8% methanolic hydrogen chloride (80 ml). The course of methanolysis was followed by the changes in specific rotation: $[\alpha]_D$ initial (not observable); +75.5° (2 hours); +88° (6 hours); +90° (12 hours, constant value).

TABLE II

Fractionation of methylated polysaccharide from chloroform solution by petroleum ether

Fraction	Weight (g)	$[\alpha]_D^{27}$ in $CHCl_3$	OCH_3 value (%)
1	0.1535	+118°	36.1
2	1.5274	+100°	36.4
3	1.1200	+108°	38.4
4	0.6547	+ 64.5°	32.5
5	0.3929	+ 64°	35.3
6	0.1554	+ 4.56°	20.6
7	1.4791	+ 3.5°	23.0
8	0.1338	+ 55.5°	32.7
9	0.0430	+ 5.5°	—

A small portion of the mixture of methyl glycosides, after neutralization (Ag_2CO_3), was examined by gas–liquid chromatography (11, 12) using Apiezon M at 150° C and a flow rate of 75 ml of argon/min. Three distinct peaks were observed and the components of the mixture were collected separately. One of the components from the column crystallized as needles, which were recrystallized from ethyl – petroleum ether. The crystals had m.p. 67.5–69° and showed no depression when mixed with an authentic sample of methyl 2,4,6-tri-*O*-methyl-β-D-glucoside.

Acid Hydrolysis

A portion (65 mg) of the mixture of methyl glycosides was reserved and the remainder was hydrolyzed with hydrochloric acid (60 ml, 0.8 *N*) on a steam bath for 8 hours. The solution became dark upon hydrolysis and had a final $[\alpha]_D$ of +50° (*c*, 5). The hydrolyzate was neutralized (Ag_2CO_3), filtered, and silver ions were removed by H_2S. Evaporation of the solution afforded a light brown, clear syrup (2.67 g) which upon chromatography using solvent B gave spots with the following M_G values: 0.24; 0.59; 0.66; 1.00. From the chromatographic analysis the following sugars were tentatively identified: (i) 2,3,4,6-tetra-*O*-methyl-D-glucose; (ii) 2,4,6-tri-*O*-methyl-D-glucose; (iii) 2,4,6-tri-*O*-methyl-D-mannose; (iv and v) two di-*O*-methyl-hexoses; and (vi) uronic acid containing material which remained on the starting line.

The mixture of methylated sugars and uronic acids was passed over IR-120 and the acids were converted subsequently to their barium salts by heating with barium hydroxide at 65°. The neutral sugars were removed by continuous extraction with ethyl acetate for 4 days. The extract was evaporated to a sirup (1.734 g) which partly crystallized. The aqueous solution left after ethyl acetate extraction was acidified with *N* sulphuric acid and the extraction was continued with ethyl acetate for 48 hours. The extract was dried (Na_2SO_4) and evaporated to give a mixture of methylated uronic acid as a sirup (0.615 g). Examination of the acids by chromatography (solvent E) showed that there were three main components having R_g values 1.0, 0.8, and 0.55 respectively. They were separated from each other by sheet-filter-paper chromatography using solvent E and were designated fractions I, II, and III respectively.

Separation of the Mixture of Neutral Methylated Sugars on a Cellulose Column

The mixture (1.484 g) was put on a cellulose column and the column was developed with 1-butanone–water azeotrope. Ten-milliliter fractions were collected every 20 minutes. The appropriate fractions were combined and identified as described below.

Identification of Methylated Sugars

2,3,4,6-Tetra-O-methyl-D-glucose

The sirupy product (253 mg), $[\alpha]_D$ +83° in water (*c*, 1), was dissolved in 50% aqueous methanol and the insoluble material removed by filtration. Chromatographic examination in three different solvent systems (B, C, and D) showed that the sugar moved as a single spot and had the same mobility as 2,3,4,6-tetra-*O*-methyl-D-glucose. Examination of the methyl glycoside of the sugar by gas–liquid partition chromatography (11, 12) gave the same retention time as methyl 2,3,4,6-tetra-*O*-methyl-α,β-D-glucoside. Demethylation with boron trichloride (30) showed that glucose was the only parent sugar. The methylated sugar was identified as *N*-phenyl 2,3,4,6-tetra-*O*-methyl-D-glucosylamine, m.p. and mixed m.p. 134–135°; $[\alpha]_D$ +240° ±3° in chloroform (*c*, 0.3) (14).

The tri-*O*-methyl fraction, which was a mixture, was resolved into two components by chromatography on Whatman No. 3MM paper using solvent C. The two methylated sugars were identified as follows.

2,4,6-Tri-O-methyl-D-glucose

This sugar gave a bright red color with *p*-anisidine spray and yielded only glucose on demethylation. Its R_g (solvent C) was 0.47, which is the same as that of an authentic sample of 2,4,6-tri-*O*-methyl-D-glucose. The sirup crystallized and, after recrystallization from ethyl ether, had m.p. and mixed m.p. 123–125° (15).

Refluxing with aniline in ethanolic solution yielded *N*-phenyl 2,3,6-tri-*O*-methyl-D-glucosylamine, m.p. 162–165° (16). Examination of the methyl glycoside of the sugar by gas–liquid partition chromatography showed that it had the same retention time as that of authentic methyl 2,4,6-tri-*O*-methyl-α,β-D-glucoside.

2,4,6-Tri-O-methyl-D-mannose

This sugar had R_g 0.61 (solvent C) and M_G 0.0 in borate buffer, values which are in agreement with those of an authentic sample of 2,4,6-tri-*O*-methyl-D-mannose. On demethylation with boron trichloride it gave only mannose. Upon seeding with 2,4,6-tri-*O*-methyl-D-mannose, the sirup crystallized and, after recrystallization from ether–hexane, had m.p. and mixed m.p. 63–65° and showed $[\alpha]_D$ +17.6° in water (*c*, 1). These values are in good agreement with those reported for this sugar (17). The anilide, after recrystallization from ethyl ether, had m.p. and mixed m.p. 132° and $[\alpha]_D$ +7.8° in methanol (*c*, 0.35). The reported values for *N*-phenyl 2,4,6-tri-*O*-methyl-D-mannosylamine are m.p. 134° and $[\alpha]_D$ +8° (18).

The di-*O*-methyl sugar fraction did not give satisfactory separation of its components on paper using solvents B, C, and D. However, it was separable by electrophoresis on paper strips in 0.05 *M* borate buffer at 800 volts for 2 hours. Two main components (X, Y) and a minor one (Z) were separated. The methylated sugars were recovered from the paper by elution with water. Sodium ions were removed by Amberlite IR-120 and boric acid was removed by repeated distillation with methanol. The M_G values of the fractions were: X, 0.17; Y, 0.071; Z, 0.00 and the colors produced with the *p*-anisidine spray were: X, brown; Y, pink; and Z, bright red. Identifications of the sugars were made as follows.

4,6-Di-O-methyl-D-glucose

The rate of movement of the sugar on paper chromatogram (solvents B and C) was the same as that of 4,6-di-*O*-methyl-D-glucose and the brown color given by the *p*-anisidine spray was the same as that of an authentic specimen. Demethylation of this component produced only glucose. The sugar crystallized as fine needles from ethyl acetate solution, and after recrystallization from the same solvent, the crystals had m.p. 157–158° and showed $[\alpha]_D$ +62° in water (*c*, 1.9). The reported melting point and $[\alpha]_D$ for 4,6-di-*O*-methyl-D-glucose are 156–158° (19) and +62.4° (15) respectively.

2,6-Di-O-methyl-D-glucose

The sugar gave glucose on demethylation. Its mobility on paper in solvents B and C and by electrophoresis in borate buffer were the same as that of an authentic sample of 2,6-di-*O*-methyl-D-glucose. The specific rotation, +58° in water (*c*, 1), agreed closely with the reported value of +58.3° (19). The sugar gave a negative reaction with triphenyltetrazolium chloride (20, 21) but was detectable on the paper with periodate–benzidine spray (22).

Di-O-methyl Sugar (Component Z)

Its M_G value in borate buffer was 0.0, and upon demethylation, the sugar yielded glucose. It gave a negative triphenyltetrazolium test, showing thereby that C_2 was substituted. It was not oxidized by periodate. From these results the component appeared to be either 2,3- or 2,4-di-*O*-methyl-D-glucose. Scarcity of material precluded further investigation.

Identification of Methylated Uronic Acid Components

Fractions I, II, and III (10 mg each) were converted to their methyl ester methyl glycoside derivatives by heating with 2.5% methanolic hydrogen chloride (2 ml) at 100° in a sealed tube for 15 hours. Reduction with lithium aluminum hydride (50 mg) in tetrahydrofuran (40 ml) yielded sugars, which, after recovery by extraction with chloroform, were hydrolyzed with *N* sulphuric acid for 15 hours. The hydrolyzates were neutralized ($BaCO_3$) and chromatographed in solvent C. Fraction I yielded one main component, R_g 0.61; fractions II and III gave two components each, R_g 0.61 and 0.47 respectively. Chromatography of the sugars on paper using solvents B and C indicated that the sugar having R_g 0.61 (solvent C) and R_g 0.71 (solvent B) was 2,3,4-tri-*O*-methyl-D-mannose and the other sugar (R_g 0.47 (solvent C) and R_g 0.60 (solvent B)) was 2,4,6-tri-*O*-methyl-D-glucose.

Thus, fraction I yielded only 2,3,4-tri-*O*-methyl-D-mannose and fractions II and III yielded a mixture of this sugar and 2,4,6-tri-*O*-methyl-D-glucose. The mixtures were resolved by sheet-filter-paper chromatography and the sugars identified in the following manner.

2,4,6-Tri-O-methyl-D-glucose

The sugar crystallized and, after recrystallization from ethyl ether, had m.p. and mixed m.p. 123–125° (15). It gave an anilide, m.p. 162–165° (16). The identification was further confirmed by examination of its methyl glycosides by gas–liquid chromatography as described earlier.

2,3,4-Tri-O-methyl-D-mannose

The sirup, $[\alpha]_D$ +1° in water (*c*, 1), when examined on paper chromatograms in solvents B and C showed the same rate of movement as an authentic sample of 2,3,4-tri-*O*-methyl-D-mannose. Gas–liquid partition chromatography of the methyl glycoside of the sugar gave the same retention time as an authentic specimen of methyl 2,3,4-tri-*O*-methyl-α-D-mannoside.

The sugar (107 mg) was dissolved in water (2 ml), and barium carbonate (90 mg) and bromine (0.5 ml) were added. The oxidation was allowed to take place in the dark for 48 hours, after which time the excess of bromine was expelled by aeration. The reaction mixture was filtered, the filtrate acidified and extracted with chloroform. Evaporation of the chloroform extract gave 2,3,4-tri-*O*-methyl-D-mannonic acid, which

was distilled, b.p. (bath temp.) 110–120° (0.005 mm), to afford 2,3,4-tri-*O*-methyl-D-mannono-δ-lactone. Treatment of methanolic solution of the lactone (63 mg) with phenylhydrazine (33 mg) for 3 hours at 100° yielded crystalline 2,3,4-tri-*O*-methyl-D-mannonophenylhydrazide, which on recrystallization from ethyl acetate had m.p. 166° (reported value 166°) (26).

Methylation of Combined Fractions 3R, 4R, and 5R

The combined fractions (2.0 g) were methylated three times with dimethyl sulphate and alkali, using each time 50 ml of dimethyl sulphate and 150 ml of 45% potassium hydroxide. The first methylation was done in an atmosphere of nitrogen; acetone was added in subsequent methylations to keep the methylated product in solution. The rest of the procedure was the same as that described for 6NR. The chloroform-soluble material was methylated five times with methyl iodide and silver oxide, acetone being added in the first methylation to dissolve the partially methylated product. The methylated polysaccharide was recovered as a light brown friable glass (1.2 g; OMe 41.55%). The methylated polysaccharide was fractionated from chloroform – ethyl ether solution with petroleum ether and the analytical data on the fractions are given in Table III.

TABLE III

Analytical data of fractions of methylated polysaccharide

Fraction*	Weight (g)	$[\alpha]_D^{27}$ in $CHCl_3$	OCH_3 (%)
P I	0.1582	+106°	43.56
P II	Negligible	—	—
P III	0.0860	+109°	35.76
P IV	0.2536	+110°	38.8
S I	0.5704	+ 62°	41.34
S II	0.1000	+ 67°	25.95
S III	0.0396	+ 10°	2.4
S IV	0.0522	+ 11.5°	7.6

*P I, P II, P III, and P IV were combined to give S_0.

Examination of Methylated Fractions S_0 and S_I (See Table III)

Methanolysis and Hydrolysis

Fraction S_0.—This had $[\alpha]_D$ +114° (*c*, 1.18 in methanol) and was heated for 12 hours in 8% methanolic hydrogen chloride (20 ml). A portion of the methyl glycosides was hydrolyzed by heating with 0.5 *N* hydrochloric acid for 10 hours at 100° (final $[\alpha]_D$ +69°).

Fraction S_I.—This showed $[\alpha]_D$ +83° (*c*, 0.93 in methanol). It was treated the same way as described for S_0. After hydrolysis it had $[\alpha]_D$ +66°.

Chromatographic Examination of Methylated Sugars

The hydrolyzate of S_0 when examined by chromatography using solvents B and D showed the following components: 2,3,4,6-tetra-*O*-methyl-D-glucose; 2,4,6-tri-*O*-methyl-D-glucose; 2,4,6-tri-*O*-methyl-D-mannose; dimethyl sugar fraction; and uronic acid fraction.

Hydrolysis of fraction S_I gave the same components as S_0. The uronosides and glycosides from S_0 were separated by converting the former into their barium salts, from which the neutral glycosides were extracted with chloroform.

Examination of Neutral Sugar Fractions

The neutral glycosides of fraction S_0 were examined by gas–liquid partition chromatography and the retention times were compared with those of known sugar glycosides. By this means, the following sugars were found: 2,3,4,6-tetra-*O*-methyl-D-glucose; 2,4,6-tri-*O*-methyl-D-glucose; 2,4,6-tri-*O*-methyl-D-mannose; and an unresolved dimethyl fraction. Paper electrophoresis of the dimethyl fraction in borate buffer showed the presence of 4,6-di-*O*-methyl-D-glucose, 2,6-di-*O*-methyl-D-glucose, and an unidentified dimethyl spot.

Examination of fraction S_I by the same means as described for fraction S_0 showed that the same sugars were present, although the proportions were different. The ratios of the methylated fragments are given in Table I. Since it was clear from chromatographic evidence that the same sugars were present in all three fractions (6NR, S_0, and S_I) of the methylated polysaccharide and identification had been made of those in fraction 6NR, it was considered unnecessary to identify those in fractions S_0 and S_I further.

Methylated Uronic Acid Components of Fractions S_0 and S_I

The amounts of material were small and the whole quantity of each was treated as in the case of 6NR methylated polysaccharide. Reduction of the methyl ester methyl glycosides with lithium aluminum hydride yielded disaccharides which were subjected to acid hydrolysis. The sugars were separated by paper chromatography using solvent C and were found to be 2,3,4-tri-*O*-methyl-D-mannose and 2,4,6-tri-*O*-methyl-D-glucose. A portion of the sugars in the acid hydrolyzate was treated with methanolic hydrogen chloride

and the methyl glycosides thus formed were examined by gas–liquid chromatography. In addition to the above-mentioned sugars, there was present in the mixture a small amount of the glycosides of 2,3,4-tri-*O*-methyl-D-glucose.

Periodate Oxidation

Samples 4R (0.0854 g) and 6NR (0.0864 g) were each dissolved in water (50 ml), and 0.1 *M* sodium periodate (50 ml) was added. The samples and the blanks were put in brown, 250-ml glass-stoppered flasks and stored in the refrigerator (5° C). From time to time aliquots were taken out and periodate consumption and formic acid production were determined in the following manner.

Periodate Consumption

To 5 ml of aliquot, sodium bicarbonate (1.7 g), sodium arsenite solution (10 ml), and potassium iodide (1 ml) were added. The flasks were stored in the dark for 15–20 minutes and then titrated against 0.0203 *N* iodine using starch as indicator.

Formic Acid Production

To 10 ml of aliquot, seven drops of 2-methyl-1,2-propanediol were added. After 20 minutes, 1 ml of 20% potassium iodide was added and the liberated iodine was titrated against 0.01 *N* sodium thiosulphate.

Since the rate of oxidation was very slow during the first 24 hours, the samples were removed from the refrigerator and stored in a room maintained at 15° C. The results are given in Table IV.

TABLE IV

Periodate oxidation of fractions 4R and 6NR

Sample	Time (hours)	IO_4^- consumption (moles)	HCOOH produced (moles)
4R	5	0.27	0.076
	24	0.32	—
	48	0.29	0.080
	72	0.37	0.096
	196	0.50	0.125
6NR	5	0.17	0.071
	24	0.19	—
	48	0.38	0.086
	72	—	0.095
	196	0.52	0.122

ACKNOWLEDGMENTS

The authors wish to record their grateful thanks to Professor F. Smith for the specimens of 2,4,6-tri-*O*-methyl ethers of D-glucose and D-mannose, to Dr. C. T. Bishop and Mr. F. P. Cooper for gas-chromatographic analyses, and to Mr. W. R. Rowsome for valuable technical assistance.

REFERENCES

1. M. J. Shear and F. C. Turner. J. Natl. Cancer Inst. **4**, 81 (1943).
2. J. L. Hartwell, M. J. Shear, and J. R. Adams, Jr. J. Natl. Cancer Inst. **4**, 107 (1943).
3. H. Kahler, M. J. Shear, and J. L. Hartwell. J. Natl. Cancer Inst. **4**, 123 (1943).
4. A. Perrault and M. J. Shear. Cancer Research, **9**, 626 (1949).
5. H. J. Creech, L. H. Koehler, H. F. Havas, R. M. Peck, and J. Andre. Cancer Research, **14**, 817 (1954).
6. H. J. Creech and R. F. Hankwitz, Jr. Cancer Research, **14**, 824 (1954).
7. P. Rathgeb and B. Sylvén. J. Natl. Cancer Inst. **14**, 1099 (1954).
8. H. Malmgren. J. Natl. Cancer Inst. **14**, 1119 (1954).
9. P. Rathgeb and B. Sylvén. J. Natl. Cancer Inst. **14**, 1109 (1954).
10. H. C. Srivastava, E. Breuninger, H. J. Creech, and G. A. Adams. Can. J. Biochem. and Physiol. **40**, 905 (1962).
11. A. G. McInnis, D. H. Ball, F. P. Cooper, and C. T. Bishop. J. Chromatog. **1**, 556 (1953).
12. C. T. Bishop and F. P. Cooper. Can. J. Chem. **38**, 388 (1960).
13. J. W. A. Oldham. J. Am. Chem. Soc. **56**, 1360 (1934).
14. J. C. Irvine and A. M. Moodie. J. Chem. Soc. **93**, 95 (1908).
15. W. N. Haworth and W. G. Sedgwick. J. Chem. Soc. 2573 (1926).
16. H. Granichstädten and E. G. V. Percival. J. Chem. Soc. 54 (1943).
17. N. Prentice, W. S. Guendet, and F. Smith. J. Am. Chem. Soc. **78**, 4439 (1956).
18. W. N. Haworth, R. L. Heath, and S. Peat. J. Chem. Soc. 833 (1941).
19. D. J. Bell and R. L. M. Synge. J. Chem. Soc. 833 (1958).

20. D. S. FEINGOLD, L. AVIGAD, and S. HESTERIN. Biochem. J. **64**, 351 (1956).
21. S. HAQ and W. J. WHELAN. Nature, **178**, 1221 (1956).
22. J. A. CIFONELLI and F. SMITH. Anal. Chem. **26**, 1132 (1954).
23. W. H. HAWORTH, E. L. HIRST, F. A. ISHERWOOD, and J. K. N. JONES. J. Chem. Soc. 1878 (1939).
24. J. K. N. JONES. J. Chem. Soc. 3292 (1950).
25. S. A. BARKER, A. B. FOSTER, I. R. SIDDIQUI, and M. STACEY. J. Chem. Soc. 2358 (1958).
26. L. HOUGH, J. K. N. JONES, and W. H. WADMAN. J. Chem. Soc. 1702 (1950).
27. B. LYTHGOE and S. TRIPPETT. J. Chem. Soc. 1983 (1950).
28. W. N. HAWORTH. J. Chem. Soc. **107**, 8 (1915).
29. T. PURDIE and J. C. IRVINE. J. Chem. Soc. **83**, 1021 (1903).
30. S. ALLEN, T. G. BONNER, E. J. BOURNE, and N. M. SAVILLE. Chem. & Ind. (London), 630 (1958).

SINGLET METHYLENE FROM THERMAL DECOMPOSITION OF DIAZOMETHANE. UNIMOLECULAR REACTIONS OF CHEMICALLY ACTIVATED CYCLOPROPANE AND DIMETHYLCYCLOPROPANE MOLECULES[1,2]

D. W. SETSER[3]
Department of Chemistry, University of Washington, Seattle, Wash., U.S.A.

AND

B. S. RABINOVITCH[4]
Division of Applied Chemistry, National Research Council, Ottawa, Canada

Received February 2, 1962

ABSTRACT

The thermal decomposition of diazomethane (DM) into singlet methylene radicals and nitrogen has been studied from 225° to 450° in 10:1 olefin–diazomethane mixtures. At 2.5 cm pressure, $k = 1.2\times10^{12} \exp(-34{,}000/RT)$ sec^{-1}. The methylene radicals have similar reactivity to methylene generated from photolytic decomposition of DM, as judged by the follow-up reactions with ethylene and *cis*-butene-2. The structural isomerization reactions of energized cyclopropane and the structural and geometric isomerization of 1,2-dimethylcyclopropane (DMC), formed from the addition of the thermally generated methylene to the olefins, were measured from 250° to 450° over a wide range of pressures. For comparison, cyclopropane formed from photolysis at 4358 Å and 25° of DM and ethylene was studied. As judged from comparison of the experimental isomerization rate constants, the energy of the cyclopropanes formed at 350° in the thermal DM system is about the same as for cyclopropanes formed by photolysis at 4358 Å of DM at 25°. The experimental rate constants obtained on the assumption of strong collisions are compared with calculated rate constants which are based on quantum statistical models for k_E which fit literature data on conventional thermal isomerization of cyclopropane and DMC. From this comparison, the average energies of the formed molecules in the thermal systems are estimated to be between 107 and 115 kcal/mole, depending upon the temperature. Photolysis at 25° of the ketene–ethylene system (3200 Å) and of DM–ethylene system (4358 Å) give cyclopropane characterized as being at 103 and 111 kcal/mole respectively. These energies deduced from kinetic data are compared with available thermochemical quantities; the existing value of $\Delta H_f^0(CH_2N_2)$ is questioned. Further support for fast intramolecular relaxation of vibrational energy in DMC, relative to the relaxation process for reaction, is noted. Comparison of data in the literature on the ketene and DM photolytic systems strongly suggests that a larger fraction of the excess light energy resides with methylene from ketene (0.65–0.8) than with methylene from DM (0.3–0.5). Various approximations for the calculation of k_E are examined and are compared with accurate quantum statistical evaluation.

In a preliminary communication (1), we reported that thermal decomposition of diazomethane (DM) (2–4) proceeds with conservation of spin angular momentum to give singlet methylene radicals and nitrogen, in contradistinction to the thermal decomposition of the isoelectronic molecule nitrous oxide (5). The studies have now been extended to include more data on the thermal decomposition of DM; on the follow-up reactions of methylene with *cis*-butene at three temperatures, and with ethylene at two temperatures; and on the photolysis (6) of DM at 25° in the presence of ethylene, which was done for comparison.

[1]*Issued as N.R.C. No. 6873.*
This work was supported by the National Science Foundation and in part by the Office of Naval Research.
[2]*Abstracted in part from the Ph.D. Thesis, University of Washington, 1961, of D. W. S., which should be consulted for further details.*
[3]*National Science Foundation Predoctoral Fellow.*
[4]*Visiting Scientist, N.R.C.; John Simon Guggenheim Memorial Fellow, 1961–1962; and International Award Fellow, Petroleum Research Fund, American Chemical Society, 1961–1962.*

The predominant reactions of singlet methylene with olefins, insertion across C—H bonds (7) and addition to the double bond (8), give vibrationally excited molecules which may either decompose or be deactivated through collisions with bath molecules (8 (*c* and *e*), 9). (Reference 9 is most closely related to this work.) Recent explanation (10) of the pressure dependence of methylene radical in terms of singlet–triplet transitions of the methylene are not believed to apply in this work for reasons we have previously presented (1), and which are further supported here.

The use of singlet methylene radicals arising from photolysis of ketene and DM at various wavelengths with different substrates offers the possibility, beautifully exploited by Butler and Kistiakowsky (9(*c*)), of producing relatively monoenergetic molecules at variable, high vibrational energies. Unfortunately, due to the uncertainty in $\Delta H_f(CH_2)$ and in the fraction of excess light energy carried by the methylene, the energy of the hot cyclopropanes has not been well known. In the present work, utilizing a DM *thermal* decomposition source of CH_2 radicals, the energy of the formed cyclopropanes may, in principle, be changed in known manner by variation of temperature. The situation turns out not to be so simple; but by use of all these data, together with a relatively accurate quantum statistical formulation for the magnitude and energy dependence of the structural isomerization rate constants of the energized molecules, an attempt has been made to rationalize the various experimental rate constants and energies of cyclopropane and dimethylcyclopropane formed via these different sources of methylene radicals.

EXPERIMENTAL

Materials

DM prepared from N,N′-nitrosomethylurea was stored in butyl phthalate at −196° (9(*b*)). Ethylene and *cis*-butene-2 were Phillips research grade. The *cis*-butene-2 was distilled and corrections were applied for the remaining 0.4% *trans*-butene impurity.

Apparatus

A conventional vacuum system was used for gas handling. Pyrolyses were performed in seasoned pyrex bulbs of various sizes. Temperature gradients across the bulbs were less than 2°.

A G.E. AH-6 high-pressure (quartz-jacket) mercury lamp was used in the photolysis of DM. A combination of Dow Corning No. 5543 and No. 3389 filters isolated the 4358 Å line with the following distribution of absorbed radiation: 75% at 4450–4250 Å, 11% at 4450–5000 Å, and 14% at 4250–4000 Å.

All analyses were performed by gas–liquid phase chromotography.[2]

Procedure

Vessels were conditioned by treating with air at 375° for several hours, evacuating, and seasoning with *cis*-butene (5–10 cm Hg) for 8 hours at 300°; a run was done and discarded. The vessel was then, usually, properly seasoned. Data from unseasoned vessels were characterized by excess stabilization products (cyclopropanes).

Runs were performed by flash-distilling a liquid mixture of DM and olefin into the furnace as with butene, or by premixing the two gases and expanding in the gaseous mixture as with ethylene. Most runs were made with 1:10 mixture of DM to olefin; at the lowest pressure and highest pressure, the ratios approached 1:5 and 1:50, respectively. For photolysis, the ratios were at least 1:10.

RESULTS AND DISCUSSION

Thermal Decomposition of DM

Temperature Dependence of Products from DM Decomposition with Butene

Principal products from thermal decomposition of DM with *cis*-butene-2 above 220° are the expected C_5H_{10} compounds (9(*b*)). Figure 1 shows the variation of the C_2H_4/C_5H_{10}

$$CH_2N_2 \xrightarrow{k_1} CH_2 + N_2 \qquad [I]$$

$$CH_2 + C_4H_8 \longrightarrow C_5H_{10}$$

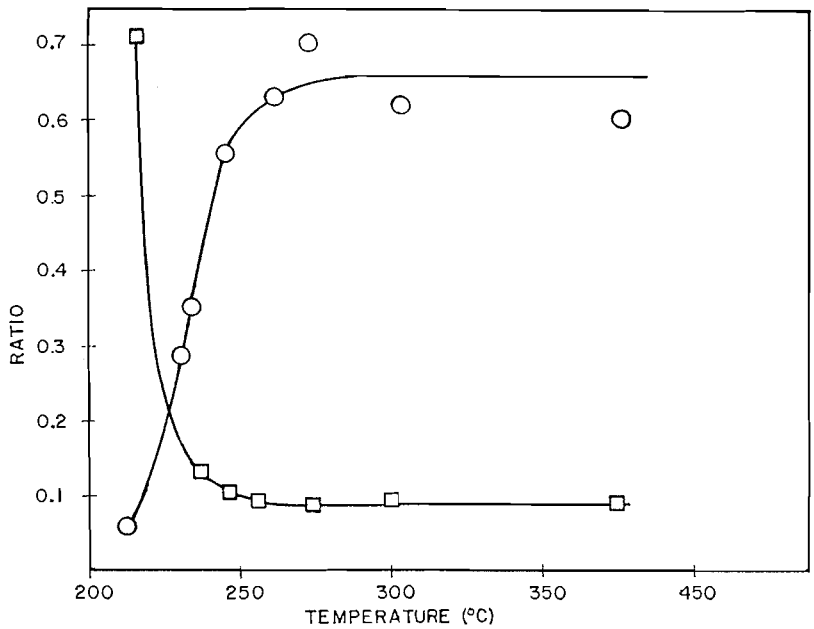

FIG. 1. Variation of the C_5H_{10}/DM ratio, ○, and of the C_2H_4/C_5H_{10} ratio, □, with temperature, for DM with *cis*-butene-2; total pressure = 2.5 cm.

product ratio and the C_5H_{10}/DM ratio with temperature. These runs were made with 1:20 mixtures of DM to *cis*-butene, at constant concentration of 7.4×10^{-7} mole/cc (~2.5 cm) of butene. In all cases complete decomposition of DM occurred. The deficit in material balance in Fig. 1 is due to deposition of polymethylene upon the reactor walls. Below 250°, ethylene product predominates; above 250°, only ~10% of the products are ethylene and propene and their production is directly dependent upon the DM/butene ratio. This suggests that ethylene arises at lower temperatures mainly by the molecular reaction [II*a*] reported by Steacie (3), and by attack mainly of methylene upon DM (reaction [II*b*]) (6(*a*)) at higher temperatures. Products formed in trace

$$2CH_2N_2 \longrightarrow C_2H_4 + 2N_2 \qquad [II a]$$

$$CH_2 + CH_2N_2 \longrightarrow C_2H_4 + N_2 \qquad [II b]$$

quantities were ethane, propane, butane, pentane, and isopentane, which may arise from reactions of CH_3 radicals resulting from H abstraction by methylene (7(*b*), 9(*b*)); these products were not followed quantitatively.

Kinetic Order and Activation Energy

C_5H_{10} production, i.e. the rate law for DM decomposition, followed first-order kinetics (Fig. 2). The data were obtained under the same conditions as those in Fig. 1. At low temperatures (below 225°) reproducible data could not be obtained in our system; it also appeared that at the lower temperatures the rate constants were high, suggesting heterogeneity. In view of the low C_5H_{10} yields and importance of C_2H_4 production below 250°, the activation energy determination here is based upon the three higher temperatures (Fig. 3). The rate constant $k_1 = 1.2\times10^{12}\exp(-34{,}000/RT)$ sec^{-1} for the thermal homogeneous decomposition of DM was obtained. Shantarovich (4) has reported $k_1 = 8\times10^{10}\exp(-31{,}400/RT)$ sec^{-1} in a nitrogen flow system; we prefer our value. E_a

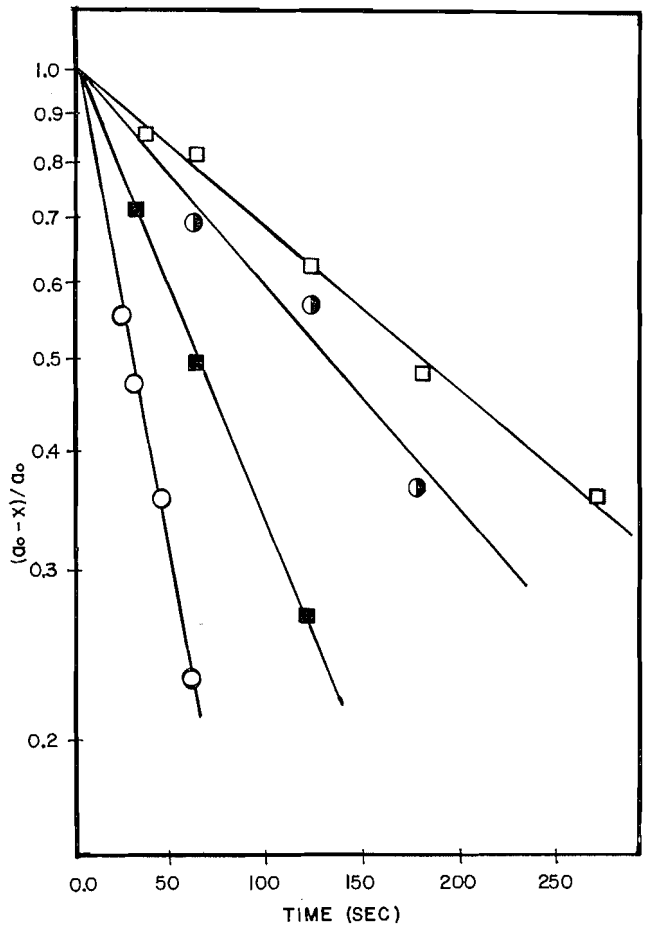

FIG. 2. Illustration of kinetic first-order behavior for formation of methylene-derived C_5H_{10} products: 212°, □; 232°, ◑; 245°, ■; 257°, ○.

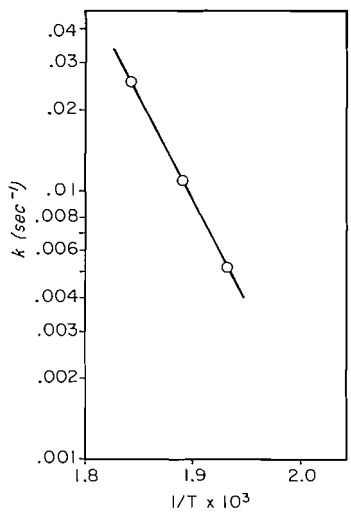

FIG. 3. Arrhenius plot for the three highest temperatures.

was measured here in a region of falloff which is estimated theoretically, and also by comparison with results for CH_3NC (11) (a molecule having somewhat similar complexity, structure, reaction temperature, and activation energy) to be ~1 kcal/mole below E_∞. A_∞ should also rise to the value of $\sim 10^{13}$ sec^{-1}, normal for many cases in which no change in electronic multiplicity is involved.

Homogeneity of Reactions of Methylene

The homogeneity of the methylene reactions that form cyclopropanes was tested in a 110-cc vessel packed with glass wool to give a tenfold increase in surface area. The results for *cis*-butene-2 at 1.3 cm pressure and 300° are as follows:

Product	Unpacked, seasoned (%)	Packed, seasoned (%)	Packed, unseasoned (%)
trans-DMC[a]	15.8	15.2	11.0
cis-DMC[a]	17.2	20.6	38.0
2-Methylbutene-2	18.2	17.4	13.7
trans-Pentene-2	8.9	8.5	7.1
cis-Pentene-2	36.8	35.1	27.9
2-Methylbutene-1 / 3-Methylbutene-1	3.1	3.2	2.3

[a]1,2-Dimethylcyclopropane.

Wall reactions are obviously important in unseasoned vessels and are characterized by formation of excess stabilized *cis*-DMC. However, in properly seasoned vessels above 250°, wall reactions[2] account for not more than 1–3% of the total C_5H_{10} products.

Temperature Variation Due to Self-Heating

The possibility of the true reaction temperature being significantly higher than the measured temperature of the furnace, due to the exothermicity of the reaction of methylene radicals with olefins, must be considered. The overall exothermicity for methylene-derived C_5H_{10} or C_3H_6 products is shown later to be ~80 kcal/mole. At 250°, the half-life, $t_{1/2}$, for DM decomposition is 90 sec; the theoretical equations (12) predict an insignificant temperature rise of <10°.

At 300° and 2.5 cm, it was shown by experiment with *cis*-butene that self-heating did not give rise to detectable effects: Runs made with DM/butene ratios of 1/40 and 1/8 resulted in no change of the observed rate constants for structural or geometric isomerization of DMC.

At an apparent temperature of 375°, DM decomposition is practically instantaneous. Experiments with various DM/butene ratios between 1/60 and 1/8 gave a variation in the measured values of the rate constants. Most experiments were done with DM/butene ratios of 1/10, and the average self-heating was estimated as ~25° for the butene system and ~50° for the ethylene system. Nominal temperatures of 375° and 400° thus correspond more closely to 400° and 450° for the *cis*-butene and ethylene systems, respectively, *and will be referred to as such, hereafter*. At these temperatures, conventional thermal isomerization reactions of the cyclopropane products are negligible for the short residence times employed (<3 min).

Reaction of Methylene with Ethylene

Products of Reaction and Variation with Pressure

Major products were cyclopropane and propene. Side products were ethane, propane, butane, butene-1, and unidentified compounds in trace quantities. The total quantities

of all side products increased from a few percent to 20% at lowest pressure. In general, the pyrolysis system gives less side reactions than the corresponding photolysis system.

The percent of cyclopropane product increases at higher pressures (Fig. 4). These data are characteristic of an energized cyclopropane molecule (8(*c*), 9), which can either

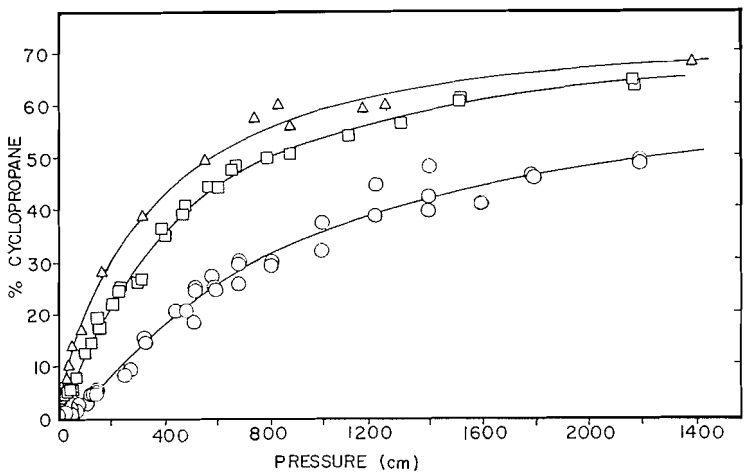

FIG. 4. Percent cyclopropane at different pressures; DM + C_2H_4 at 325°, □; DM + C_2H_4 at 450°, ○; photolysis (4358 Å) of DM with C_2H_4 at 25°, △. In the interest of clarity, a considerable amount of data was omitted from Figs. 4, 6, 7, 8, in the lower-pressure region especially.

isomerize to propene or be stabilized through collisions with bath molecules. Limiting high-pressure values of <100% cyclopropane reflect the direct insertion of methylene across C—H bonds to give propene:

$$\begin{array}{lcccl} & \xrightarrow{k_{11}} & \triangledown^* & \xrightarrow[M]{\omega} & \triangledown \\ CH_2+C_2H_4 & & \Big\downarrow k_a & & \\ & \xrightarrow{k_{12}} & CH_3CH{=}CH_2^* & \xrightarrow[M]{\omega} & CH_3CH{=}CH_2. \end{array} \qquad [III]$$

The asterisk represents a vibrationally excited molecule resulting from chemical reaction. At higher pressures no reaction of $CH_3CH{=}CH_2^*$ is expected; at low pressures it may decompose, and this may in part explain the increase in side reactions at low pressure.

Extrapolations (9(*c*)) of plots of propene/cyclopropane vs. ω^{-1} to infinite pressure gave the relative magnitudes of k_{12} and k_{11} in Table I. Such plots[2] of the 325° and photolysis data show little curvature and illustrate the relatively monoenergetic character of the energized cyclopropane molecules. The 450° data shows considerable scatter,[2] but no significant curvature either. Discussion of Table I is delayed until presentation of the butene data.

Experimental Average Rate Constants k_a

For the ethylene–cyclopropane systems, average experimental rate constants for structural isomerization of $\triangledown^*$ were computed according to the expression (13) $k_a = \omega \cdot D/S$

TABLE I

Summary of rate constants of cyclopropanes produced by chemical activation from methylene plus olefins

Olefin	CH_2 source	Relative CH_2 addition rates per C—H bond			Experimental rate constants ($10^8 sec^{-1}$)			E_{min} (kcal/mole)	E_{av} (kcal/mole)
		C=C	Allyl H	Vinyl H	k_a	k_{g1}	k_{g2}/k_{g1}		
cis-Butene-2[a]	DM 250°	1.00	0.14	0.15	0.43[g]	3.5	0.66	101[n]	109[n]
cis-Butene-2[a]	DM 300°	1.00	0.14	0.14	0.59[g]	4.4	0.66	102	112
cis-Butene-2[a]	DM 400°[f]	1.00	0.15	0.16	1.0[g]	11.5	0.72	102	116
trans-Butene-2[b]	DM 25° 4358 Å	1.00	0.15	0.11	1.1[j]	9.0			116[i]
Isobutene[b]	DM 25° unfiltered radiation	1.00	0.11	0.091	1.6[k]				119[i]
Isobutene[c]	CH_2CO 25° 3100 Å	1.00	0.053	0.063					
Ethylene[a]	DM 325°	1.00		0.068	380[g]			104	110
Ethylene[a]	DM 450°[f]	1.00		0.083	800[g]			107	116
Ethylene[a]	DM 25° 4358 Å	1.00		0.079	450[g]				111
Ethylene[d]	CH_2CO 25° 3200 Å	1.00		0.036	180				104[i]
Ethylene-d_2[e]	CH_2CO 25° 3200 Å	1.00		0.036	110	1580		98[m]	
Ethylene-d_2[e]	CH_2CO 25° 3320 Å	1.00		0.038	63	1180		95[m]	
Propene[c]	DM 25°	1.00	0.11	(0.091, 0.091)	16.5[h, l]				
Propene[c]	CH_2CO 25° 2600 Å	1.00	0.091	(0.067, 0.061)	5.5[h, l]				
	CH_2CO 25° 3130 Å	1.00	0.060	(0.025, 0.035)	8.2[h, l]				

[a]This work.
[b]Ref. 9(*b*). For photolysis in liquid phase (−70°) Frey (7(*b*)) found ratios of CH_2 addition to C=C:allylic C—H:vinylic C—H of 1.00:0.13:0.99 for *trans*-butene-2.
[c]Ref. 9(*c*).
[d]Ref. 14.
[e]Ref. 9(*a*) with corrected (14) estimate here of effective radiation involved.
[f]Corrected temperature as described in text earlier.
[g]Average values: DMC, Fig. 9, S/D between 0.2 and 1.5 for the 400° case, and between 0.2 and 3 for the lower temperatures; cyclopropane, average of all values shown in Fig. 5.
[h]For internal consistency, Butler and Kistiakowsky's (9(*c*)) data have been converted to the collision cross sections used here (Appendix I).
[i]In selecting E_{av}, the magnitude of k_E (Fig. 13) was set equal to k_a, since the distribution in wavelengths is small; for a similar system, DM photolysis with C_2H_4, where the distribution of absorbed radiation was used, this was shown to be a good approximation.
[j]Values of k_a (9(*b*)) range from 1.4×10^8 sec^{-1}, at $S/D = 3.8$, to 0.9×10^8 sec^{-1}, at $S/D = 0.5$; an intermediate value of 1.1×10^8 sec^{-1} was taken by the present authors.
[k]An average value of 1.6×10^8 sec^{-1} was taken by the present authors.
[l]In his higher-energy radiation studies with ketene and cyclobutene, Frey (9(*d*)) does not find the inversion of lifetimes, shown here for 3130 Å and 2600 Å as reported by Butler and Kistiakowsky.
[m]Given as sum of $\Delta E_0' + \bar{E}_{ex}$.
[n]True values for thermal DM systems may be lower by ~3 kcal/mole if allowance is made for inefficient collisional deactivation, particularly for C_2H_4 system.

and are presented in Fig. 5; S is the stabilized cyclopropane, D is the propene isomerization product, and ω is the specific collision rate (Appendix I).

Lifetimes of Cyclopropane from Different Sources

The similarity in magnitudes of k_a obtained from photolysis work at 4358 Å and from thermal DM decomposition at 325° indicates that the cyclopropane derived from these two sources have similar energy.

The average lifetimes of reacting molecules in conventional thermal structural isomerization of cyclopropane at 445° is $\sim10^{-7}$ sec (9(*a*)). This may be contrasted with the shorter lifetimes ($<10^{-10}$ sec) of the chemically activated molecules (Table I). The cyclopropanes obtained with ketene as the methylene precursor have longer lifetimes

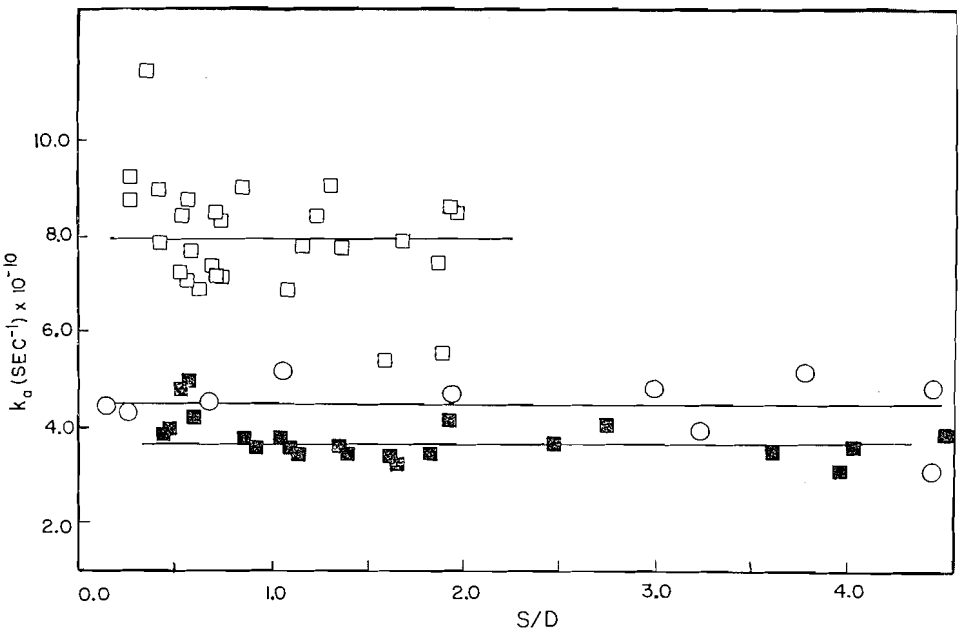

FIG. 5. Rate constants for isomerization of cyclopropane to propene: DM + C_2H_4 at 450°, □; DM + C_2H_4 at 325°, ■; photolysis (4358 Å) DM with C_2H_4 at 25°, ○.

than those derived from DM. Similar results have been found earlier for other systems (9(*c* and *d*)). Quantitative interpretation of these magnitudes is presented later. In this connection, it is desirable to mention now some different k_a data from the photolysis of ketene with ethylene. The data of Kistiakowsky and Frey (8(*e*)) give $k_a = 1.3\times10^{10}$ sec^{-1} for photolysis at 3130 Å. For a similar study with ethylene-d_2 (9(*a*)) $k_a = 1.1\times10^{10}$ was reported. For the photolysis at 3200 Å of ketene with ethylene (14), k_a[5] is 1.8×10^{10} sec^{-1}. The latter value will be used later for estimation of the energy of the formed cyclopropane molecules, while the variation of k_a with wavelength in the ketene–ethylene-d_2 system (Table I) will be used as a test of the energy dependence of the calculated rate constants.

Reaction of Methylene with *cis*-Butene-2

Variation of Products with Pressure and Methylene Source

Methylene adds to butene to give chemically energized DMC, or inserts across the allylic and vinylic C—H bonds to give *cis*-pentene-2 and 2-methylbutene-2, respectively. These energized molecules undergo characteristic isomerization reactions or are deactivated by collisions with bath molecules:

$$\begin{aligned} & \xrightarrow{k_{21}} \quad H_3C\bigtriangledown CH_3^* \\ CH_2 + CH_3CH{=}CHCH_3 \quad & \xrightarrow{k_{22}} \quad cis\text{-}CH_3CH_2CH{=}CHCH_3^* \\ & \xrightarrow{k_{23}} \quad CH_3CH{=}C(CH_3)_2^*. \end{aligned} \qquad [IV]$$

[5]*An isotope effect accounts in part for the difference between the cyclopropane-d_2 and cyclopropane values.*

Figures 6, 7, and 8 illustrate the product dependence upon pressure; the approach to constant limiting percentages at high pressure verifies reactions [IV]. The relative magnitudes of these processes (Table I) were again determined from ω^{-1} extrapolations of

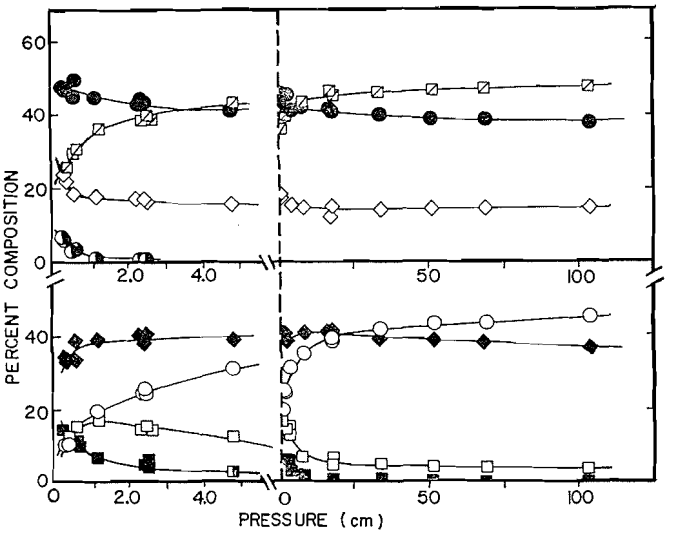

FIG. 6. Variation of the product composition with pressure, DM + *cis*-butene system, 250°: □, *trans*-DMC; ○, *cis*-DMC; ◆, *cis*-pentene-2; ■, *trans*-pentene-2; ◑, 2- and 3-methylbutene-1; ◇, 2-methylbutene-2; ⊠, total DMC; ●, total pentene-2. See Fig. 4.

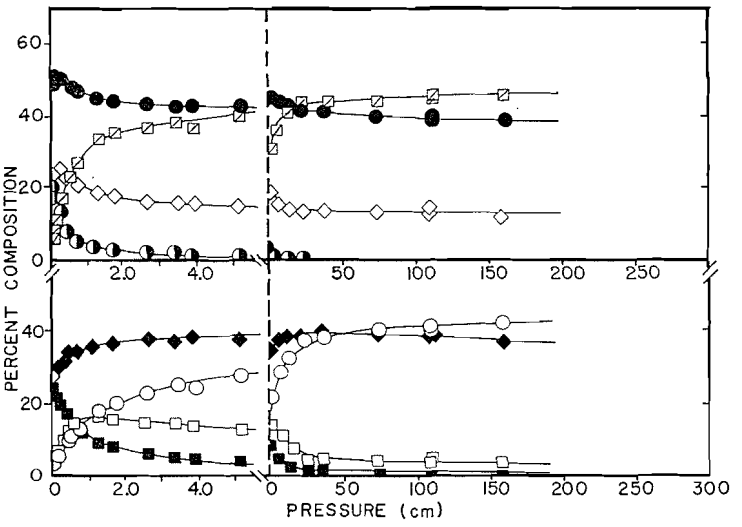

FIG. 7. Variation of the product composition with pressure, DM + *cis*-butene system, 300°: □, *trans*-DMC; ○, *cis*-DMC; ◆, *cis*-pentene-2; ■, *trans*-pentene-2; ◑, 2- and 3-methylbutene-1; ◇, 2-methylbutene-2; ⊠, total DMC; ●, total pentene-2. See Fig. 4.

product ratios: total pentene/DMC; (*cis* + *trans* + pentene-2)/DMC; and (2-methylbutene-2 + 2- and 3-methylbutene-1)/DMC. Due to the greater energy spread of the excited DMC relative to cyclopropane (*cf.* $f(E)$, Fig. 13), these plots[2] at 300° and

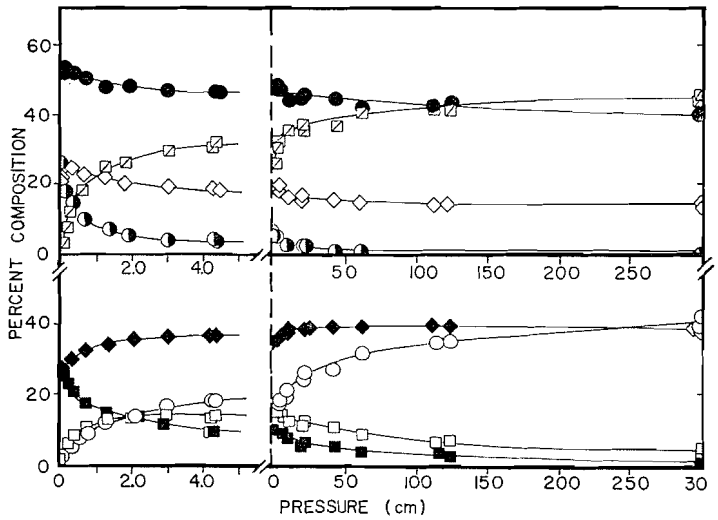

FIG. 8. Variation of product composition with pressure, DM + *cis*-butene system, 400°: □, *trans*-DMC; ○, *cis*-DMC; ◆, *cis*-pentene-2; ■, *trans*-pentene-2; ◑, 2- and 3-methylbutene-1; ◇, 2-methylbutene-2; ⊠, total DMC; ●, total pentene-2. See Fig. 4.

especially 400° show considerable curvature at higher pressures, in contrast with the cyclopropane plots.

For both ethylene and *cis*-butene the reactivity of methylene generated from thermal decomposition of DM is similar to that from photolytic (4358 Å) decomposition of DM (Table I). Both sources give nearly the same degree of discrimination between C=C and C—H bonds; any apparent trend is within experimental error. As was reported by other workers (9(*c*), 10), in the gas phase CH_2 from DM was found much less selective than CH_2 from ketene, both in regard to C—H insertion vs. double-bond addition and in regard to discrimination between different types of C—H bonds. Within experimental error (Table I), methylene derived from DM is indiscriminate in its attack on vinylic and allylic C—H bonds in the gas phase (note footnote *b*, Table I). The apparent difference (10, 7(*b*)) for alkanes, i.e. random insertion in the liquid phase and selective insertion (tert. > sec. > prim.) in the gas phase for methylene produced from photolysis of DM, does not hold for vinylic and allylic C—H bonds.

The constancy in this work of the relative magnitudes of k_{21}, k_{22}, and k_{23} from 250° to 400°, as shown in Table I, indicates that little difference in activation energy exists for addition of methylene to the double bond vs. C—H insertion; or, alternatively, the methylene carries excess translation energy, which negates small activation energy differences. Methylene from photolysis of DM is thought to carry excess translational energy (9(*b*)).

Reactions of Energized Product Molecules

A. Dimethylcyclopropane

The vibrationally excited *cis*-DMC, *cis*-pentene-2, and 2-methylbutene-2 species may undergo further reactions. *cis*-DMC may isomerize to the trans isomer, undergo intramolecular H migration in the ring to give *cis*- and *trans*-pentene-2, 2-methylbutene-2, and 2-methylbutene-1, or be de-energized by collisions with bath molecules. Still another possible reaction suggested by the data, and which involves the CH_3 substituent, will

be considered later. The *trans*-DMC also undergoes these reactions unless collisionally deactivated. These processes are defined in the manner of Frey (9(*b*)):

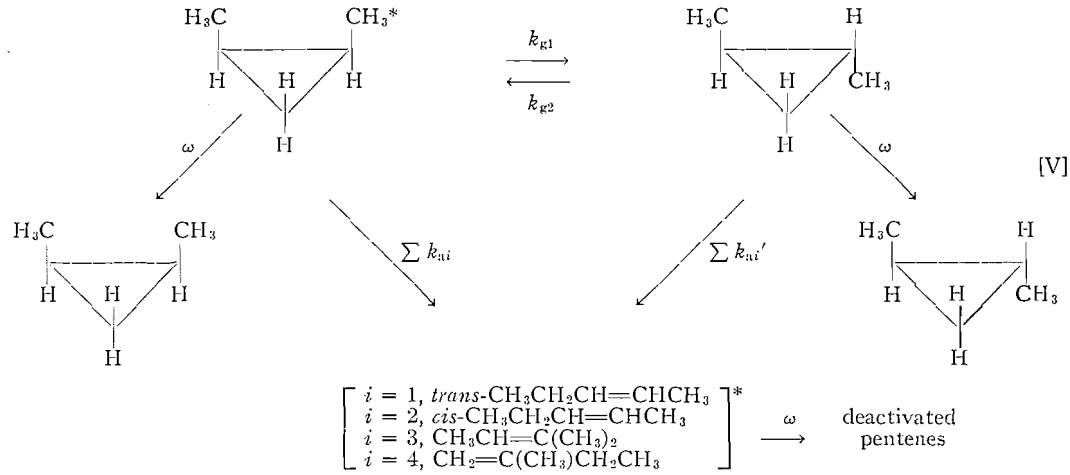

Consider the variation of the products with the total pressure under this scheme. The percent *trans*-DMC should go through a maximum when plotted as a function of pressure, since k_{g1} is approximately ninefold greater than $\sum_i k_{ai}$, as shown below (15).[6] Also, the percent of pentenes should increase from their high-pressure limits given by equations [IV], as total pressure is reduced. Figures 6, 7, and 8 exhibit these features.

The above mechanism also predicts that as the reaction temperature, and consequently the energy of the formed molecules, is increased, then k_{g1}, $\sum_i k_{ai}$, and $\sum_i k_{ai}'$ should increase. Indeed, at 400°, 300°, and 250° approximately one-half of the *cis*-DMS had isomerized to the *trans* isomer at 2.2 cm, 1.0 cm, and 0.6 cm, respectively; one-half of the total DMC had decomposed to pentenes at 1.2 cm, 0.5 cm, and 0.35 cm, respectively. This aspect of the data further supports an excited molecule mechanism.

B. Reactions of cis-Pentene-2

The energized *cis*-pentene-2 may isomerize to *trans*-pentene-2 unless de-energized by collisions with bath molecules. This is illustrated by the decline in *cis*-pentene-2 at lower pressures as reaction k_{g1}' of eq. [VI] overtakes reactions k_{a2} and k_{a2}' of eq. [V] (Figs. 6, 7, and 8).

$$cis\text{-}CH_3CH_2CH{=}CHCH_3^* \underset{k_{g2}'}{\overset{k_{g1}'}{\rightleftarrows}} trans\text{-}CH_3CH_2CH{=}CHCH_3^* \qquad [VI]$$

Pentene-1 was found only in trace quantities, indicating that rearrangement of pentene-2 to pentene-1 did not occur.

C. Reactions of 2-Methylbutene-2

Isomerization reactions [VII],

$$CH_3CH{=}C(CH_3)_2^* \longleftrightarrow CH_2{=}CHCH(CH_3)_2^* \qquad [VIIa]$$
$$CH_3CH{=}C(CH_3)_2^* \longleftrightarrow CH_2{=}C(CH_3)CH_2CH_3^*, \qquad [VIIb]$$

[6] *Flowers and Frey (15) find* $k_{g1} = 23 \sum_i k_{ai}$ *in thermal studies.*

between 3-methylbutene-1, 2-methylbutene-1, and 2-methylbutene-2 are known (16), and indeed the experimental data at the lowest pressures and highest temperature suggest that some 2-methylbutene-2 may be disappearing. For reactions [VII] at 1500°, roughly the "temperature" of these energized molecules, the equilibrium constants (17) for the formation of 3-methylbutene-1 and 2-methylbutene-1 from 2-methylbutene-2 are 0.25 and 3.7, respectively. This suggests that 2-methylbutene-1 could be formed from 2-methylbutene-2, and reaction [VII*b*] explains the decrease in percentage of 2-methylbutene-2 at the lowest pressures (Figs. 7 and 8).

D. Formation of 3-Methylbutene-1 and Possible Occurrence of Triplet Methylene

All products and their pressure dependence, except for 3-methylbutene-1, are reasonably explained by the above mechanism.

Within the pressure range 1 to 300 cm, the ratio of 3-methylbutene-1/2-methylbutene-1 was constant and slightly greater than unity. At the lowest pressure this ratio increased to nearly 3. In contrast to Frey (9(*b*), 19), we also find that photolysis of DM with *cis*-butene-2 gives 3-methylbutene-1 in similar amounts. Neither heterogeneity nor the intervention of triplet methylene (as discussed below) is thought to be primarily responsible for 3-methylbutene-1 formation. Also, thermodynamic considerations weigh against reaction [VII*a*] as a source. Indeed, Frey (9(*b*)) found evidence for the *reverse* of [VII*a*] in his studies of methylene with isobutene. Possible modes for its formation are the additional paths [VIII] and [IX]:

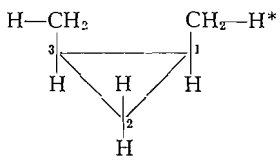

$$\xrightarrow{k_{a5}} \quad CH_2{=}CHCH(CH_3)_2 \qquad [VIII]$$

$$:CH_2 + CH_3CH{=}CHCH_3 \longrightarrow \cdot CH_3 + \cdot CH_2CH{=}CHCH_3 \qquad [IXa]$$

$$\cdot CH_2CH{=}CHCH_3 \longleftrightarrow CH_2{=}C\dot{H}CHCH_3 \qquad [IXb]$$

$$\cdot CH_3 + CH_2{=}C\dot{H}CHCH_3 \longrightarrow CH_2{=}CHCH(CH_3)_2$$

$$\cdot CH_3 + \cdot CHCH_2{=}CHCH_3 \longrightarrow CH_3CH_2CH{=}CHCH_3. \qquad [IXc]$$

Reaction [VIII] involves intramolecular hydrogen transfer from a methyl group to carbon atom 2 with rupture of C_1—C_2 or C_3—C_2. (Hydrogen transfer from a methyl to carbon atoms 1 or 3 with rupture of C_1—C_3 or C_2—C_3, respectively, would give pentene-1, or ethylcyclopropane; pentene-1 was not formed and unfortunately no search was made for ethylcyclopropane.) Alternatively, transfer of a methyl group between carbons 1 and 3 would also give this same result as well as some others to be mentioned next; isotopic studies could distinguish these possibilities. Other experimental evidence is cited now to support these transfer reactions.

Flowers and Frey (16) have earlier suggested methyl–hydrogen transfer, with an estimated activation energy as high as 68 kcal/mole, to explain small quantities of 2-methylbutene-2 in the thermal decomposition of 1,1-dimethylcyclopropane. In another study of energized 1,1-dimethylcyclopropane (9(*b*)) from CH_2 + isobutene, this methyl–hydrogen transfer reaction was not mentioned; however, a possible interpretation of this data at the lowest pressures could also include it. Again, Frey (9(*d*)) has found ethylacetylene to be one of the products of energized methylene cyclopropane from CH_2 + allene, and he has explained it by the migration of two hydrogen atoms; alternatively, it could also result from methylene hydrogen transfer.

Scheme [IX] remains to be considered. A minor reaction of singlet methylene radicals is abstraction of H from hydrocarbons (7(*b*), 9(*d*)) (reaction [IX*a*]). Equation [IX*b*] represents two resonance structures of the butenyl radical. Combination with methyl radical, reactions [IX*c*], gives 3-methylbutene-1 or pentene-2 in the ratio 1:2.5 at 25° (18), and 1:6 at 200° (19).

Since the proportions of DM and *cis*-butene are held constant, the relative amount of products arising through scheme [IX] would tend to be only weakly dependent on pressure. Figures 6, 7, and 8 show, instead, that the methylbutene-1 fraction goes to zero at high pressure, which suggests that an abstraction scheme, [IX], involving singlet methylene is not operative in an important way.

It is important, therefore, to consider again the proposal of Richardson *et al.* (10): Methylene radicals in the gas phase undergo singlet–triplet transitions before they react with the olefins; the lower the pressure the larger is the fraction converted to the triplet state; important reactions of triplet methylene radicals are non-stereospecific addition to the double bond (20) as well as postulated abstraction of H, followed by recombination of the methyl and hydrocarbon radical to give both *apparent* C—H insertion products and *apparent* cyclopropane isomerization products.

Now Frey (20) has found that *triplet* methylene reacts with *cis*-butene to give *cis*- and *trans*-DMC, 3-methylbutene-1, and *cis*- and *trans*-pentene-2, but not 2-methylbutene-2 or 2-methylbutene-1, as occur here. In addition, the following arguments pertaining to our reaction system, as well as previous evidence cited above and earlier (1), weigh further against involvement of triplet methylene in the main course of reaction: (*a*) The dependence of the methylbutene-1 fraction upon temperature at a given pressure (0.5 cm: 400°, 13%; 300°, 9%; and 250°, 4%) is clearly consistent with the reactions of energized molecules whose energy content varies somewhat with temperature. (*b*) Frey's studies of triplet methylene (20) at 25° show that at butene partial pressures of 2–10 mm, inert gas to butene ratios of 300:1 are necessary to convert 50% of the singlet methylenes to the triplet state and inert gas addition is necessary to produce characteristic "triplet" products. Therefore, at the same low butene pressures in our system, but with no intervening inert gas perturbing collisions, spontaneous singlet–triplet transitions cannot be important. (*c*) As noted above, the combination of methyl and butenyl radicals gives more pentene-2 than 3-methylbutene-1 (18). No such proportionate rise in the total pentene-2 fraction accompanies the rise in the 3-methylbutene-1 fraction (Figs. 6, 7, and 8) at lower pressures.

Thus reaction [VIII], whether methyl H or methyl group migration, fits best as the process giving 3-methylbutene-1. Reaction [IX] may conceivably explain the small (less than 1%), nearly constant amounts of *trans*-pentene-2 and methylbutene-1 fractions at high pressures, as well as the ethane, propane, and similar products.

Experimental Rate Constants k_a and k_g for Activated DMC

Individual values of the overall structural isomerization rate constant k_a are shown in Fig. 9. The previous definition of k_a is again used: $k_a = \omega(D/S)$, where S is stabilized *cis*- and *trans*-DMC and D is the total olefins, including 3-methylbutene-1, derived from excited cyclopropanes; ω is the specific collision rate (Appendix I). The above definition gives an *average* rate constant for both *cis*- and *trans*-DMC. The study of *trans*-DMC and of *cis*-DMC thermal isomerization reactions (15) indicates for our purposes a minor, although real, variation between $\sum_i k_{ai}$ and $\sum_i k_{ai}'$.

At 250° and 300°, the k_a values were quite reproducible. An upward trend with increasing S/D (i.e. increasing pressure) is evident, and is consistent (13) with a larger

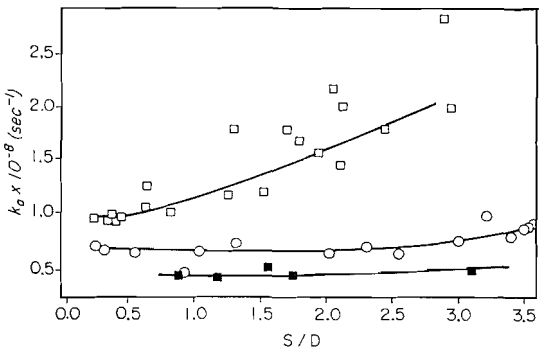

FIG. 9. Rate constant for isomerization of DMC to pentene: ■, DM and *cis*-butene-2 at 250°; ○, DM and *cis*-butene-2 at 300°; □, DM and *cis*-butene-2 at 400°.

energy spread in the formed DMC molecules. Values of k_a at very high pressure are more unreliable due to their sensitivity to the detailed choice of extrapolated high-pressure limits; thus a quantitative estimate of the energy spread is not available on this basis. At the highest temperature, 400°, there is more scatter in k_a at high S/D. This is possibly due to different degrees of self-heating in the various runs. The considerable rise in k_a at 400° with increase of S/D is also indicative of a greater energy spread of the formed molecules. However, the apparent increase is too large to be explained by this effect alone and may reflect, in part, the inaccuracy of the ω^{-1} extrapolation to $p = \infty$; such error becomes less important in the determination of k_a at the lower range of S/D.

Experimental values for k_{g1}^{-1} and k_{g2}/k_{g1} were calculated by least-squares analysis (Fig. 10) of the linear, low-pressure portion of the function

$$cis\text{-DMC}/trans\text{-DMC} = (k_{g2}/k_{g1}) + \omega \cdot (1 + D/S) \cdot k_{g1}^{-1}.$$

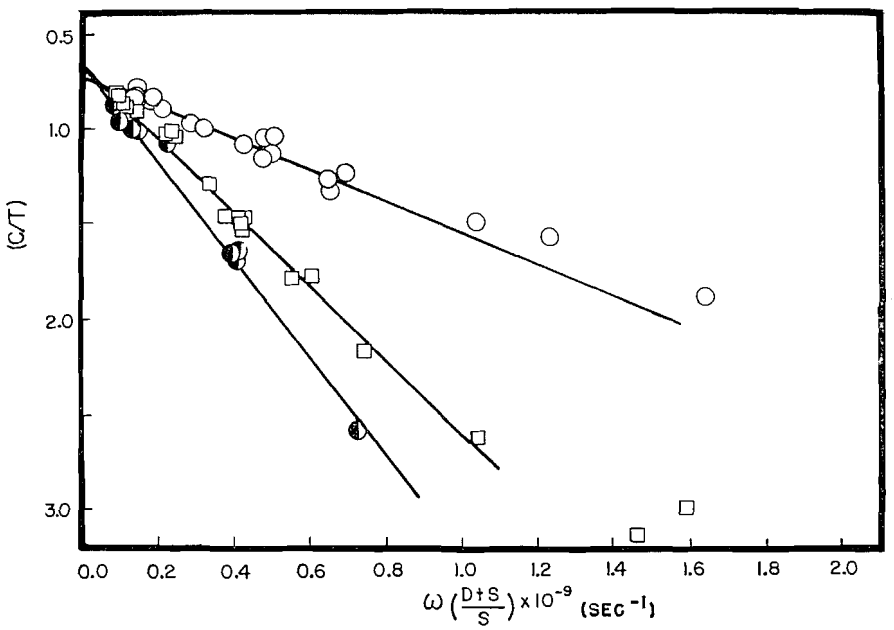

FIG. 10. Plot of *cis*-DMC/*trans*-DMC against $\omega \cdot (D+S)/S$: 400°, ○; 300°, □; 250°, ◐.

This relation follows (9(*b*))[2] from the steady-state expression for energized *trans*-DMC, on setting $k_a = \sum_i k_{ai} = \sum_i k_{ai}'$. The least-squares results for k_{g1} and k_{g2}/k_{g1} are 3.5×10^8 sec^{-1} and 0.66, 4.45×10^8 sec^{-1} and 0.66, 1.15×10^9 sec^{-1} and 0.72, at 250°, 300°, and 400°, respectively. Figure 11 illustrates the magnitude of k_{g1} for all S/D.

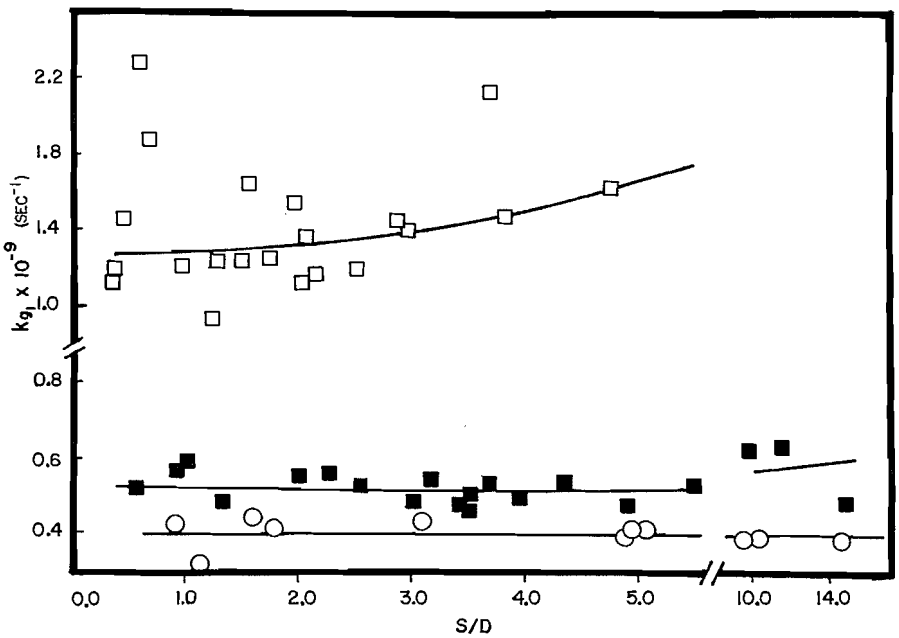

FIG. 11. Rate constants for *cis–trans* isomerization of *cis*-DMC: ○, DM and *cis*-butene at 250°; ■, DM and *cis*-butene at 300°; □, DM and *cis*-butene at 400°.

To obtain a ratio of k_{g1}/k_a, the least-squares value of k_{g1} was compared to k_a evaluated at $S/D = 1.0$. The ratio k_{g1}/k_a is 8 at 250°, 7.4 at 300°, and 11 at 400°; an average of 9 is taken; this is in agreement with related earlier findings that geometric isomerization of cyclopropanes proceeds faster than structural isomerization (9(*a*)).

k_g' for Pentene-2

The following expression obtained from the steady-state equation was used to calculate k_{g2}':

$$(k_{a1}/k_{g2}')(S/T_p) - (\omega/k_{g2}) + (k_{g1}'/k_{g2}') \cdot (C_p/T_p) = 1.0,$$

where S is the total DMC product, T_p is *trans*- and C_p is *cis*-pentene-2 product. The equilibrium constant for cis $\rightleftharpoons$ trans, i.e. k_{g1}'/k_{g2}', was calculated as 1.1 at these high vibrational "temperatures" from thermodynamic data (17). The values for k_{a1} and k_{g2}' were obtained by trial and error procedure with an IBM 709 computer for the data in Figs. 7 and 8, in conjunction with estimation of the contribution of k_{a1} to k_a. The best fit was given by $k_{a1}/k_{g2}' = 1\pm0.2$, and $k_{g2}' = 1.6\pm0.5\times10^7$ sec^{-1} and $3\pm1\times10^7$ sec^{-1} for 300° and 400° respectively.

The average ratio obtained for k_{g1}'/k_a was 0.27. Since the isomerization of *cis*-pentene-2 (i.e. k_{g1}') is expected to have an activation energy nearly equal to that for *cis*-butene-2 ($\geq$62.8 kcal/mole), which in turn is closely the same as that for the overall structural isomerization of *cis*-DMC (15), the ratio of 0.27 *may* largely reflect a difference in reaction path degeneracy—which is 8 for *cis*-DMC and only 2 for *cis*-butene-2 (21).

Some Remarks on Experimental Rate Constants

(a) Comparison of Energy of Chemically Activated DMC

Table I lists the average rate constants for geometric and structural isomerization in different DMC systems. The correspondence between the photolysis of a DM + *trans*-butene-2 mixture at 4358 Å and the thermal decomposition of a DM + *cis*-butene-2 mixture at 400° indicates that the energized DMC product molecules have nearly the same energy in both cases. A similar correspondence has been noted above for cyclopropane produced by DM pyrolysis at 325°. Sources of error in such comparisons include some uncertainty in the effective average wavelength for photolysis, and in the estimation of the change of the effective collision cross section with temperature by use, for example, of the Sutherland constant.

(b) Equilibrium Constant for cis–trans-DMC

For DM with *trans*-butene at 4358 Å Frey has found a low-pressure limit for k_{g2}/k_{g1} of 0.33 (9(*b*)). Within the validity of the approximation, $\sum k_{a\,i} = \sum k_{a\,i}'$, the low-pressure ratio of k_{g2}/k_{g1} corresponds to the apparent equilibrium constant of the *activated cis–trans*-DMC molecules (equation [V]). In view of the small differences in the heats of formation (1.02 kcal/mole) of *cis*- and *trans*-DMC (15), and in consideration of the high vibrational "temperatures" of these energized molecules, our present average of 0.68 for k_{g2}/k_{g1} seems more valid. In some work on DM photolysis, we obtain 0.80, again closer to unity.

(c) Evidence for Intramolecular Relaxation of Energy

The ratios of k_{g1}/k_a from the thermal isomerization of *cis*-DMC (15) and from this work are ~23 and ~9, respectively. This difference can be explained by the appreciable activation energy difference (15) (2 kcal/mole) between structural and geometric isomerization of *cis*-DMC. At the comparatively low energies of the conventional thermal system, this difference is important; at the higher energies here (Appendix IV) k_{g1}/k_a *tend* to approach the ratio of the pre-exponential factors. This reconciliation of the actual change in k_{g1}/k_a for these two different methods of activation provides additional support for fast intramolecular relaxation of vibrational energy relative to the relaxation process for decomposition (9(*c*), 22).

Calculation of k_a Values. Evaluation of Energy of Chemically Activated Cyclopropanes

In this section, a model for k_a is constructed which gives good fit of conventional thermal unimolecular data, i.e. systems of known energy. Values of k_g will not be computed here. The model is applied to the estimation of the cyclopropane energies involved in chemical activation work by treating the unknown energies as parameters which give fit of experimental and calculated values of k_a. This procedure is useful in view of the uncertainty in many of the thermochemical quantities involved and, together with all experimental data, also provides a test of various "thermochemical" assumptions and data.

Thermochemical Quantities. Distribution Function of the Formed Cyclopropanes

In order to calculate a value for k_a the energy distribution function of the formed cyclopropane molecules $f(E)$ must be obtained. Figure 12 illustrates and defines the thermochemical quantities.[7] The cyclopropane molecules are formed in an energy range

[7]*All quantities refer to 0° K. Although many quantities must be estimated, so that almost any reference should be sufficiently accurate, it seems best to adopt this base.*

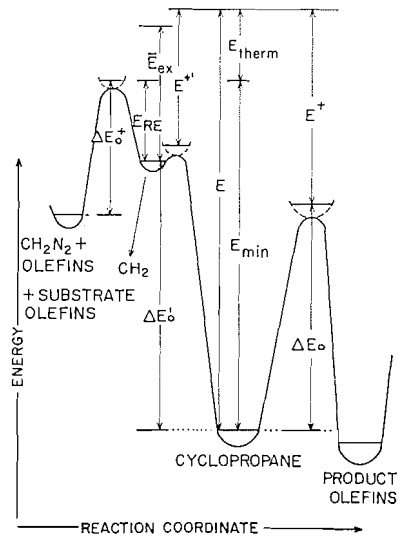

FIG. 12. Illustration and definition of thermochemical quantities for the addition of methylene to olefins. $\bar{E}_{ex}$ pertains only to photolysis systems and is that part of the excess light energy captured by the methylene and assumed to be retained up to reaction.

above E_{min} and isomerize to produce olefins unless their energy is reduced below ΔE_0 by collisions with heat bath molecules. E_{min} is the sum of $\Delta E_0'$, the heat of the addition reaction of CH_2 to the substrate olefin, and E_{RE}, the fraction of reorganization energy in the DM decomposition associated with methylene (Appendix III). E_{RE} is assumed to be largely retained by the methylene, which adds efficiently to olefins (8(*c*)). This is supported by the ability of CH_2 to carry from its genesis excess photolysis light energy (of varying amount) into the product cyclopropanes (9). The activation energy for addition of methylene to olefins is small (8(*c* and *d*), 23) (<2.0 kcal/mole) and, for simplicity, *relative translational* energy of the reacting methylene and olefin is simply lumped into E_{RE}.

The formed cyclopropanes are not in equilibrium with the heat bath. For the calculation of $f(E)$, the principle of detailed balancing is applied as before (13). As a reasonable approximation (and a desirable one, also, due to our ignorance of the spread in E_{RE}) we shall take E_{RE} to be a constant quantity, which can be added to the heat of reaction $\Delta E_0'$, but which does not affect the form of $f(E)$. $f(E)$ spans a large range of energies at the high temperatures used here in any case. Details are given in Appendix II and the form of $f(E)$ is illustrated for two cases in Fig. 13. Neither $\Delta E_0'$ or E_{RE} is well known, so that the procedure adopted here means that $f(E)$ is started at a value of E_{min} that gives agreement between experimental and calculated rate constants.

Formulation of k_E and k_a

The chemically activated cyclopropane molecules, $\triangledown$, with energy $E = E_{min} + E_{therm}$, may isomerize to olefin product with specific rate constant k_E, or may lose energy by collision with bath molecules with specific probability ω (equation [XI]). The asterisk denotes a cyclopropane molecule having energy above ΔE_0, and capable of undergoing

$$\triangledown (E') \xleftarrow{\omega} \triangledown (E)^* \xrightarrow{k_E} \text{olefin product} \qquad [XI]$$

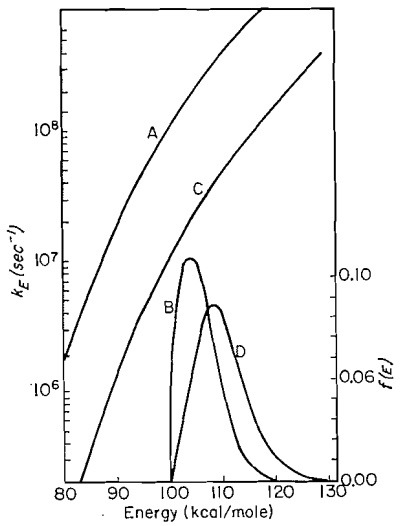

FIG. 13. Plots of k_E and $f(E)$ as a function of energy: (A) k_E for cyclopropane; all values have been multiplied by 10^{-2} to show them on the graph. (B) $f(E)$ for cyclopropane at 325° C. (C) k_E for DMC. (D) $f(E)$ for DMC at 300° C. Both distribution functions were started at 100 kcal/mole only for purposes of comparison.

isomerization. We consider only the case of strong collisions, i.e. $E' \leqslant E_0$. Detailed low-pressure experimental data and more refined collisional transition probabilities, including inefficient energy transfer, to be presented elsewhere, indicate that little error results here for this case.

The observed average rate constant is (13)

$$k_a = \omega \,.\, (D/S) = \omega \,.\, \frac{\int_{E_{min}}^{\infty} \{k_E/(k_E+\omega)\} f(E)dE}{\int_{E_{min}}^{\infty} \{\omega/(\omega+k_E)\} f(E)dE}, \qquad [a]$$

where the expression for k_E is (24)

$$k_E = P_1^+ N_E^+ / h P_1^* N_E^*. \qquad [b]$$

N_E^+ is the total sum over the active energy states of the activated complex up to its energy E_v^+; N_E^* is the total density of the active rotational and vibrational states at the energy E for the energized molecule; P_1^+/P_1^* is the residue of the partition function ratio for adiabatic degrees of freedom of overall rotation, including reaction path degeneracy. Reference 13 may be consulted for more detailed description of these equations and others of Appendix II.

The molecular and activated complex models used, as well as further calculational details, are summarized in Appendix II. Resulting k_E values for cyclopropane and DMC at various high energies are shown in Fig. 13. Combination of k_E with $f(E)$ gives k_a at different pressures (ω), according to equation [a]. With use of the strong collision model Table I lists the values of E_{min} and of the average energy of the formed cyclopropanes, $E_{av} = E_{min} + \bar{E}_{therm}$, necessary to give a magnitude of k_a that matched the observed rate

constant. $\bar{E}_{\text{therm}}$ was calculated from $f(E)$. On the basis of the agreement with conventional thermal data described in Appendix III, supported somewhat by the comparisons of the following section, the E_{av} values are considered known to within 5 kcal/mole. The remark may be added that inefficient collisional energy transfer indicates a lowering of the energies in Table I by 2–3 kcal/mole in some cases (thermal DM), which for cyclopropane, particularly, is opposed in effect by neglect of anharmonicity (11).

Energy Dependence of k_a

The calculational models predict that above 100 kcal/mole a change in excitation energy of 4–5 kcal/mole produces a twofold variation in k_E for both cyclopropane and DMC (Fig. 13). At lower energies, the energy dependence is somewhat stronger. The calculated change in k_E is compared to experimentally observed change in k_a for known energy change in Table II. Comparison of k_a with k_E is adequately valid since the energy dispersion (13) of the activated cyclopropanes is actually quite small in view of the large values of E_{min}.

TABLE II

Variation of rate constants with energy change, ΔE

System	ΔE (kcal/mole)	Observed change in k_a (factor)	Predicted change in k_E (factor)
DMC (DM, 250°)	1.7	1.4	1.3
DMC (DM, 300°)	1.7	1.4	1.3
DMC (DM, 400°)	5.4[a] 3.7[a]	2.3[a] 1.7[a]	2.1 1.6
Cyclopropane (DM, 325°)	2.7	2.0[b]	1.4[b]
Cyclopropane (DM, 450°)	2.7	2.0[b]	1.4[b]
Cyclopropane-d_2 (ketene, 3320 Å)	3	1.76	1.6
Cyclopropane-d_2 (ketene, 3200 Å)	3	1.76	1.6

[a]For 250–400° and 300–400°, respectively.
[b]Consideration of inefficient collisional deactivation reduces this discrepancy.

For the thermal DM–*cis*-butene systems the agreement between predicted and observed changes in the rate constants is well within experimental error. In these thermal DM systems, although E_{min} is treated as an unknown to be evaluated empirically, the increment in $\bar{E}_{\text{therm}}$ with temperature is reasonably well known.

The comparison of the cyclopropane results at 325° and 450° is less rewarding due to larger self-heating and to less efficient collisional deactivation for this smaller molecule.[2] Considerations of more inefficient stepwise deactivation from low-pressure studies bring the cyclopropane data within experimental error.

Since Fig. 13 shows closely similar *relative* energy dependence of k_E for both cyclopropane and DMC, it would be expected that k_E for methylcyclopropane should display similar energy dependence. Butler and Kistiakowsky (9(*c*)) have measured the rate constants for structural isomerization of energized methylcyclopropane formed from photolysis of ketene and of DM with propene and with cyclopropane, to make three pairs of systems: The exothermicity of the reaction of methylene with cyclopropane is known to be 7.9 kcal/mole greater than the reaction with propene. Using the present collision cross sections (Appendix I) the average ratio of rate constants for their three

pairs of systems is 3.8±0.4, and dependent a little upon the choices of collision cross sections. Around 100 kcal/mole, a change in energy of 7.9 kcal/mole changes k_E by a calculated factor of 3.5 and 3.3 for DMC and cyclopropane, respectively.

Pressure Dependence of k_a

As shown in Fig. 9, the values of k_a increase at higher pressures due to the rather large energy spread (Fig. 13) of the formed molecules. However, quantitative experimental measurement is difficult due to the sensitivity of the k_a values to the extrapolated high-pressure limits. It is sufficient to note that on the unit deactivation efficiency model the calculated $k_{a\infty}/k_{a0}$ ratio for the 300° DMC system is 1.45, and for the 325° cyclopropane system is 1.2. An inefficient collisional deactivation model would reduce these calculated ratios, but in any case these are sensible magnitudes of the energy dispersion (13).

Comparison of Calculated E Values with Those Based on Existing Thermochemical Quantities. $\Delta H_f^0(CH_2N_2)$

A comparison may now be made of the E_{min} values determined above with estimates of E_{min} from thermochemical data (17). A commonly used value of $\Delta H_f^0(CH_2)$ is 67 kcal/mole (25); $\geq$80 kcal/mole[8] may be a better estimate (8). The heat of reaction of CH_2 with ethylene to form cyclopropane ($\triangledown$) is $\Delta E_0' = [\Delta H_f^0(C_2H_4)+\Delta H_f^0(CH_2) - \Delta H_f^0(\triangledown)]$. Taking $\Delta H_f^0(C_2H_4)$ = 14.5 kcal/mole, $\Delta H_f^0(\triangledown)$ = 15.5 kcal/mole, and $\Delta H_f^0(CH_2)$ = 67–80 kcal/mole, limits of 66 and 79 kcal/mole for $\Delta E_0'$ are set. Since $E_{min} = \Delta E_0' + E_{RE}$ is ~101 kcal/mole (Table I, footnote *n*), E_{RE} is required to be between 35 and 22 kcal/mole. A significant part of the reorganization energy in DM decomposition should actually be in the nitrogen ($r(CH_2N{=}N)$ = 1.18 Å, $r(N{\equiv}N)$ = 1.094 Å) (27, 28), and E_{RE} would be expected to be less than the total reorganization energy.

The maximum possible value of E_{RE} is $\{\Delta H_f^0(CH_2N_2)+\Delta E_0^+ - \Delta H_f^0(CH_2)\}$. The activation energy ΔE_0^+ for DM decomposition seems here established at ~35 kcal/mole. Electron impact data (26) give $\Delta H_f^0(CH_2N_2)$ as 46 kcal/mole; this value of $\Delta H_f^0(CH_2N_2)$ leads to a range of E_{RE} of 1–14 kcal/mole, which is incompatible with the kinetic data and the above discussion on E_{RE}. This suggests that $\Delta H_f^0(CH_2N_2)$ must be >67 kcal/mole. Hence, high values for both $\Delta H_f^0(CH_2)$ and for $\Delta H_f^0(CH_2N_2)$ best fit the kinetic data; in terms of present evidence, $\Delta H_f^0(CH_2) \geq 80$ kcal/mole is favored and is used henceforth. Even if the models for k_E were in error by a factor of two and E_{min} were to be lowered by about 5 kcal/mole, this would not change the nature of the above arguments.

The Fraction of Excess Light Energy, $\bar{E}_{ex}$, Carried by the Methylene in Photolysis Systems

A. Ketene

The observed structural isomerization rate constant for cyclopropane formed from photolysis (3200 Å, 25°) corresponds to $E_{av} \simeq 100$ kcal/mole (Table I). At 25°, $\bar{E}_{therm}$ is 2 kcal/mole, so $\Delta E_0' + \bar{E}_{ex}$ = 98 kcal/mole.[9] Since $\Delta E_0'$ is 79 kcal/mole, $\bar{E}_{ex}$ = 19

[8]*We cite here three examples favoring a higher $\Delta H_f^0(CH_2)$: First, the existence of close-lying singlet and triplet states make interpretation of electron impact data difficult; Herzberg (Proc. Roy. Soc. (London), A,* ***262****, 291 (1961)) has reported an ionization potential of 10.4 ev for methylene ($^3\Sigma_g^-$), as opposed to the previous value of 11.9 ev (25), and a value for $\Delta H_f^0(CH_2)$ of $\leqslant$ 93 kcal/mole^{-1}. Second, Gesser and Steacie (Can. J. Chem.* ***34****, 113 (1956)) interpret the reaction of methylene with hydrogen to give $\Delta H_f^0(CH_2) \simeq$ 80 kcal/mole. Third, a recent value of 93 kcal/mole for the activation energy of the reaction $CH_4 \rightarrow CH_2 + H_2$ (where $CH_2(^1A_1)$ is presumably formed according to spin conservation) leads to $\Delta H_f^0(CH_2) \simeq$ 76 kcal/mole (V. Kevorkian, C. E. Heath, and M. Boudart. J. Phys. Chem.* ***64****, 964 (1960)).*

[9]*Due to the wavelength distribution of the incident radiation and some distribution in fraction of excess light energy retained by the methylene, we use only an average excess energy $\bar{E}_{ex}$, and do not define an E_{min} quantity for photolysis systems.*

kcal/mole. The *total* excess light energy is $\{\Delta H_f^0(CH_2CO)+h\nu-\Delta H_f^0(CH_2)-\Delta H_f^0(CO)\}$, and for $\Delta H_f^0(CH_2) = 80$ kcal/mole, this quantity is 23.8 kcal/mole. It follows that $\bar{E}_{ex}$, the fraction of the excess light energy in the methylene when it reacts, is $\simeq 0.80$ of the total excess light energy.

B. DM

We set $\Delta H_f^0(CH_2N_2) = 70$ kcal/mole for purposes of discussion. The kinetic data suggest $(\Delta E_0' + \bar{E}_{ex}) \simeq 107$ kcal/mole for the DM–ethylene system, and $\bar{E}_{ex}$ is here 28 kcal/mole. The total excess light energy is $\{\Delta H_f^0(CH_2N_2)+h\nu-\Delta H_f^0(CH_2)\}$ and equals 55 kcal/mole at 4358 Å ($h\nu$ = 65 kcal/mole). Hence $\bar{E}_{ex} \sim 0.50$ of the total excess light energy. A higher value for $\Delta H_f^0(CH_2N_2)$ would reduce this fraction.

Frey (9(*d*)) has studied energized methylcyclobutane and methylenecyclopropane formed from photolysis of DM + cyclobutane and DM + allene, respectively, at 4358 Å and 3660 Å. Assuming that the average wavelength absorbed was indeed the mentioned values, then the maximum energy difference of each pair would be 12 kcal/mole. The observed change in the structural isomerization rate constants was only a factor of 1.5 for both the methylenecyclopropane and the methylcyclobutane. This strongly suggests that the real energy change of the formed molecules was even less than $12\times0.50 = 6$ kcal/mole and that $\bar{E}_{ex} < 0.4$ of the total excess light energy.

In the same paper, Frey (9(*d*)) reported methylcyclobutane formed by photolysis of ketene and cyclobutane with 3130 Å, and with unfiltered, radiation in a quartz vessel (effective radiation was mainly 3000 Å and 2800 Å), and found an increase in the isomerization rate constant by a factor of 2. The maximum difference in absorbed wavelength was 3130 Å and 2800 Å, or a difference in total excess light energy of ~11 kcal/mole and probably somewhat smaller. Comparison of this data with that for Frey's DM system just described also supports the above finding that an appreciably greater fraction of the excess light energy remains with the reacting methylene from ketene photolysis than from DM photolysis.

If a high value for $\Delta H_f^0(CH_2)$ of 90 kcal was used, many of the quantities calculated above would change appropriately. The estimated fractions would decrease from 0.8 to 0.65 for ketene and from 0.5 to 0.4 for DM so that the relative relations and previous conclusions are unchanged. In addition, if the arbitrary estimate of $\Delta H_f^0(CH_2N_2) = 70$ kcal was raised to 80 kcal, this latter value when coupled with $\Delta H_f^0(CH_2) = 90$ kcal would reduce the fraction for DM further to 0.33.

Little information on the electronically excited DM and ketene states is available. However, it is of interest to compare r(C—O) in ground-state ketene and in the carbon monoxide product (1.15 Å (28) and 1.13 Å, respectively) with r(N—N) in ground-state DM and in the nitrogen product (1.18 Å (28) and 1.094 Å, respectively). The relative invariance of r(C—O) may help to explain the higher fraction of excess light energy that remains with the methylene in ketene photolysis.

ACKNOWLEDGMENTS

B. S. R. thanks Dr. I. E. Puddington, Director, for the splendid hospitality afforded him by the Applied Chemistry Division.

The present study has benefited greatly from the related work of Dr. H. M. Frey.

APPENDIX I

Calculation of the Specific Collision Frequency

A Sutherland correction was used to obtain the effective collision frequency at the different temperatures. Furthermore, it was necessary to apply molecular volume and

self-shielding corrections to the experimental ideal gas pressure at the high pressures used in the DM–ethylene systems (9(*a*)). For the cyclopropane system, DM and/or its products were counted fully in the calculation of the total ω. For the DMC system, DM and/or its products were counted in arbitrarily as one-half their value (to allow for decreased deactivation efficiency relative to *cis*-butene-2). The following tabulation lists the constants employed.

Molecule	Diameter (Å)	Sutherland constant
Ethylene	4.95	226[a]
Cyclopropane	4.92	
Diazomethane	6.4	
Propene	5.9	
cis-Butene-2	6.5	500[b]
Methylcyclopropane	5.9	
Dimethylcyclopropane	7.0	

[a]S. Chapman and T. G. Cowling. The mathematical theory of non-uniform gases. Cambridge University Press. 1952. p. 275.
[b]Estimated from molecules of similar complexity.

APPENDIX II

Computation of k_a

Formulation of f(E)

The process of interest for the calculation of $f(E)$ in the thermal DM system is the reverse dissociation of cyclopropane into methylene and substrate olefin (13). Then we may define

$$f'(E)dE = \frac{k_E'K(E)dE}{\int_{E_{\min}}^{\infty} k_E'K(E)dE}, \qquad [c]$$

where $K(E)$ is a Boltzmann distribution function for cyclopropane molecules at the reaction temperature, and k_E' is the specific rate at which energized molecules would decompose into methylene and substrate olefins. On substitution of equation [*b*] into [*c*], the distribution function $f'(E)$ takes the form

$$f'(E)dE = \frac{N_E^{+\prime}e^{-E/RT}dE}{\int_{E_{\min}}^{\infty} N_E^{+\prime}e^{-E/RT}dE} \qquad [d]$$

and $f'(E)$ becomes $f(E)$ upon superposition of E_{RE}.

For the photolysis system the energy distribution of the formed activated molecules corresponds to the combination of the thermal distribution at the reaction temperature, usually 25°, with the wavelength distribution of the absorbed light.

Numerical Calculations and Vibrational Models

Values of N_E^*, N_E^+, $N_E^{+\prime}$ were calculated directly with an IBM 709 (29). In order to do the sums of quantum states it is economical to group the molecular frequencies somewhat; in this case, five frequency groups (each group a degenerate oscillator with frequency equal to the geometric mean of the molecular frequencies of the group) give an accurate representation of the species concerned. Comparison of the zero-point energy

and partition function for the molecular cyclopropane frequencies (30) to that from the present model indicates that less than 10% error is introduced by this simplification.[2] *All vibrational and internal rotational degrees of freedom of molecules and complexes were taken as active.* The molecular frequencies for DMC were estimated. The grouped molecular frequencies are shown below.

For the activated complex for structural isomerization of cyclopropane, the previously described model (31, 32) (the representation of the activated complex in ref. 32 contains a slight typographic distortion) was used:

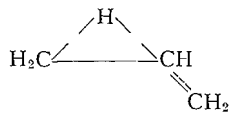

Relative to cyclopropane, the principal changes are the elimination of one C—H stretching frequency, and lowering of three frequencies corresponding to two new torsional modes of the methylene groups and a whole molecule bending frequency. These frequencies and bond lengths were chosen in accord with bond order rules. In formulation of the activated complex for structural isomerization of DMC, no distinction was made between either the two geometric isomers of DMC or between the formation of different structural isomers. The frequencies of this activated complex were obtained by changing the DMC frequencies in analogy with the above treatment of cyclopropane. As has been shown (32, 33), calculational results are fairly insensitive to variations in the assignment of frequencies for the activated complex. This is particularly true for large molecules whose frequency pattern is little affected by such variations. The assignment of vibrational frequencies for the methylene plus olefin *association* complex is, again, not a critical feature of these calculations. Methylene addition to olefins is stereospecific (8) and no internal rotation in the association activated complex is postulated.

Models for the cyclopropane (I) and DMC (II) systems

Energized molecule freq. (cm^{-1})	Activated complex freq. (cm^{-1})	Association complex freq. (cm^{-1})
I[a]		
3050 (6)	3020 (5)	3050 (6)
1460 (3)	1430 (3)	1410 (4)
1080 (7)	1100 (4)	1040 (5)
870 (3)	900 (5)	830 (3)
740 (2)	550 (3)	400 (2)
II		
3000 (10)	3000 (9)	3000 (10)
1450 (7)	1380 (8)	1430 (8)
1010 (13)	1000 (14)	1030 (7)
815 (5)	560 (3)	860 (7)
420 (2)	420 (2)	410 (4)
Int. rot. (2)	Int. rot. (2)	Int. rot. (2)

[a]Frequencies for cyclopropane molecule as given most recently by S. J. Cyvin, Spectrochim. Acta., **16**, 1022 (1960), would be slightly different, but the calculational results would be virtually unchanged.

The ratio $[(I_A{}^+I_B{}^+I_C{}^+)/(I_AI_BI_C)]^{1/2}$ was calculated to be 1.21 for cyclopropane and estimated as 1.1 for DMC. Combination of these models and the observed activation energies give 60.0 and 62.7 kcal as the values for ΔE_0 for DMC and cyclopropane respectively.

Fit of the Cyclopropane Models to Thermal Isomerization Data

The frequency assignments and calculational methods employed here do, in fact, provide an excellent fit of thermal unimolecular isomerization data, where $E_{\min} \equiv E_0$ is a known quantity: For k_∞ for cyclopropane, we have already found (32) with these models A_∞(calc.) = $10^{15.32}$; A_∞(exptl.) (34) = $10^{15.30}$. In addition, the model was shown to give the correct curvature for the experimental falloff curve of cyclopropane (35, 36). The absolute pressure fit is given to within a factor of $\sim$2, depending somewhat on the calculation of collision cross sections and on the particular experimental data. These models also satisfy (32) the observed (37) pressure dependence of the intermolecular isotope effect, (k_H/k_D), between cyclopropane and cyclopropane-d_6. This involved simultaneous fit of the observed activation energy difference, frequency factor ratio, and reasonable satisfaction of the Teller–Redlich product rule.

The models employed for DMC and its activated complex give $A_\infty = 7.0\times10^{14}$ sec^{-1} for the high-pressure frequency factor for thermal isomerization at 740° K. The theoretical rate is given by factors of 1.8 and 1.2 for *cis*-1,2-DMC and *trans*-1,2-DMC, respectively, relative to experimental values (15), and by a factor of 0.6 relative to 1,1-DMC (16).

The agreement described above supports the validity of the application here of these k_a calculational models to the chemical activation data for the evaluation of $E_{\min}$ and E_{av} by using these as parameters which bring k_a (calc.) into correspondence with k_a (exptl.).

APPENDIX III

Potential Surface for the Decomposition of DM

Herzberg[8] has shown from spectroscopic evidence that the triplet ($^3\Sigma_g^-$) rather than the singlet ($^1A_1$) is the ground state of methylene. Similar conclusions have been drawn from stereochemical evidence (20). The separation of these levels is not known but is believed to be small (Fig. 14).

The decomposition of DM is similar in principle to that of N_2O, for which (38) $k_\infty = 10^{11.9}\exp(-60{,}000/RT)$ and the decomposition proceeds (5) on surfaces I and III of Fig. 14 to give O(^3P). Gill and Laidler (39), using Stearn and Eyring's analysis (5(*a*)) together with an estimated normal frequency factor of 3×10^{13} sec^{-1}, find a separation of 500 cal/mole at the crossing of the $N_2O(^1\Sigma)$ surface with the $N_2(^1\Sigma)$–O(^3P) surface. This is of the magnitude given by McClure (40)[10] for N and O atom spin–orbit interactions and by Stearn and Eyring (5(*a*)) for O(^1D) and O(^3P) interaction.

The thermal decomposition of diphenyldiazomethane (ϕ_2DM) into diphenylmethylene radicals has recently been investigated (41) in an inert solvent; a rate constant of $10^{11.64}\exp(-26{,}000/RT)$ was reported at 100°. This low pre-exponential factor is similar to that for N_2O and is suggestive that the thermal decomposition gives triplet radicals. (Diphenylmethylene radicals from the photolysis of ϕ_2DM (42) may be produced in the triplet state.) Assuming this interpretation to be correct for the sake of this discussion, while subject to further investigation,[11] a "normal" frequency factor for the high-pressure decomposition would be $\gtrsim10^{13}$, and the transmission coefficient for the ϕ_2DM decomposition would be $\sim10^{-2}$. The Landau–Zener relation gives[12] in

[10]*McLure (40) estimates 28 cm^{-1} (80 cal/mole), 70 cm^{-1} (200 cal/mole), and 152 cm^{-1} (430 cal/mole) for the spin–orbit coupling parameters of atoms* C, N, *and* O, *respectively.*

[11]*The cautionary remarks of Fielding and Pritchard (J. Phys. Chem.* **74**, *278 (1960)) should be kept in mind.*

[12]*Based on tables from Stearn and Eyring (5(a)), with $|s_1-s_2|$, the difference in slopes of the two intersecting potentials, arbitrarily set the same as for* N_2O.

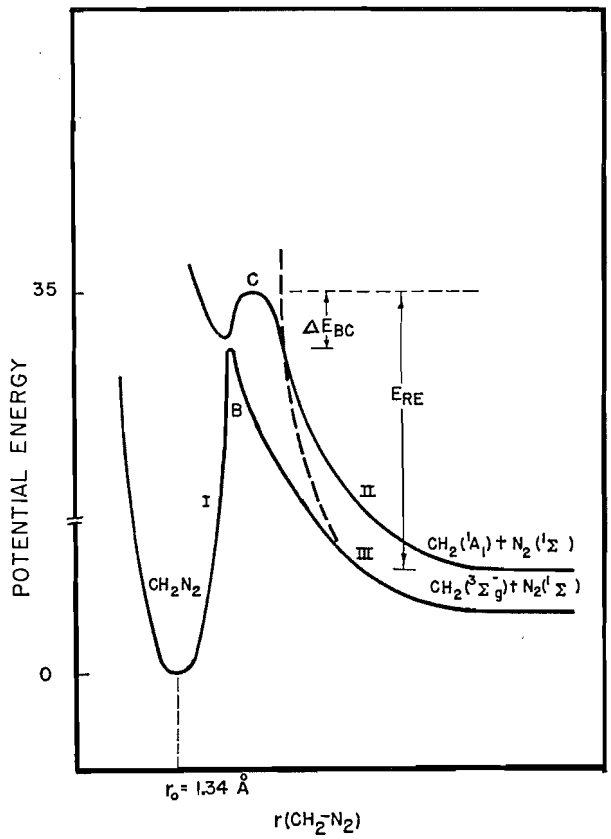

FIG. 14. Two-dimensional schematic representation of potential surfaces for diazomethane, singlet and triplet methylene. Zero-point energies have been omitted for simplicity. Variation of energy along the HCH angle coordinate may be inferred from the text, corresponding to the dotted curve for $CH_2(^3B_1)$.

this case a resonance separation of ~80 cal/mole. This would be a reasonable order of magnitude for the spin–orbit interaction.

For DM, it would not have been unexpected, therefore, had the reaction followed surface III rather than II. Without prejudice to factors that may alter the splitting at B as between ϕ_2DM and DM, we consider here only one other factor: The HCH bond angle in DM is around 120° while those in $CH_2(^1A_1)$ and $CH_2(^3\Sigma_g^-)$ are 103° and 180°, respectively.[8] As noted by Thrush (43), the energy of surface III with reduction of HCH angle from 180° toward 120° should follow the dotted line which lies in large part outside of the plane of Fig. 14. The latter represents, for surfaces I and II, a cut at a slightly varying HCH angle (120°–103°). After this paper was submitted, some calculations by Pedley (44) on the variation of CH_2 energy with HCH bond angle have appeared; these suggest that the dotted line could lie closer to the solid curve, and might cut surface I above B (Fig. 14) and within a few kcal of C, as would be required by our kinetic results and the Landau–Zener relation.

The explanation of the behavior of ϕ_2DM, if triplet product is indeed formed, would involve consideration both of a changed magnitude of separation of the singlet–triplet energies of the substituted methylene, and of the characteristic ϕ—C—ϕ angle in both states.

APPENDIX IV

Comparison of k_E Calculated from Quantum, Semiclassical, and Classical Models

Clarification of the relation of alternative expressions for the calculation of k_E may be worthwhile. Cyclopropane is used as a practical example. The well-known classical equation [*e*] of RRK has been widely used for estimation of k_E,

$$k_E = A\left\{\frac{E-E_0}{E}\right\}^{s-1}. \qquad [e]$$

A is a semiempirical constant; E_0 has its customary significance and is 62.7 kcal/mole for cyclopropane (32). The classical statistics give highly inaccurate results unless the index s is arbitrarily reduced to a fraction of the total number of vibrational modes (29, 33). For cyclopropane studied thermally at 500° C, $s \simeq 10.5$ (36).

By application of the Marcus–Rice semiclassical statistical approximation (24), Rabinovitch and Diesen (13) indicated an improved expression (equation [*f*]),

$$k_E = A'\left\{\frac{E-E_0+a^+E_z^+}{E+aE_z}\right\}^{s-1}. \qquad [f]$$

Here all vibrational modes are customarily to be taken (29, 33) as active ($s = 21$); E_z and E_z^+ are the zero-point energies of energized molecule (49.04 kcal/mole) and activated complex (42.8 kcal/mole), respectively. A' is evaluated from the properties of the species in question and is equal to $\sigma \cdot P_1^+ \cdot \Pi_{i=1}^{n} \nu_i^* / h \cdot P_1^* \cdot \Pi_{i=1}^{n-1} \nu_i^+$; for cyclopropane A' (Appendix II) is $10^{15.80}$. The quantities a^+ and a are empirical correction factors that bring the semiclassical expression for the sum of the vibrational states into agreement with exact count for the activated complex and energized molecule, respectively; values of a for cyclopropane have been given (29). Expression [*f*] has been applied previously (45).

Equation [*f*] has also been used in simplified form (9(*a*)) (denoted here as eq. [*f'*]) with $a = a^+ = 1$ and with A' simply set equal to A_∞ ($10^{15.30}$), as evaluated experimentally (34) from the high-pressure limit of thermal reaction as representing the correct order of magnitude. The approximation $a = 1$ is tolerable, but a^+ only approaches unity for E values much above E_0. The present experimental system represents a favorable case since $E-E_0 > 40$ kcal.

The results for cyclopropane given by eq. [*e*] and [*f'*] are compared to the results from the accurate direct quantum count for k_E (eq. [*b*]) in Table III. The Table shows that [*e*] is a gross underestimate of k_E at all energies and that [*f'*] becomes a good order of magnitude approximation to the direct count k_E at moderately high excess energies, but does not have the proper energy dependence. Use of tabulated values for a and a^+ shown in Table III provide a fit of eq. [*f*] to the accurate value of k_E given by eq. [*b*].

TABLE III

Values of k_E compared in various approximations (sec^{-1})

Energy (kcal/mole)	Eq. [*e*]	Eq. [*f'*]	Eq. [*f*]		Eq. [*b*] (Fig. 13)
			a	a^+	
85	4.6×10^3	1.05×10^9	0.922	0.834	6.0×10^8
100	5.4×10^6	7.98×10^9	0.929	0.878	1.07×10^{10}
115	6.6×10^8	1.49×10^{10}	0.942	0.901	6.4×10^{10}

REFERENCES

1. B. S. RABINOVITCH and D. W. SETSER. J. Am. Chem. Soc. **83**, 750 (1961).
2. (*a*) F. O. RICE and A. L. GLASEBROOK. J. Am. Chem. Soc. **56**, 2381 (1934). T. G. PEARSON, R. H. PURCELL, and G. S. SAIGH. J. Chem. Soc. 409 (1938).
   (*b*) A. LANGER and J. A. HIPPLE. Phys. Rev. **69**, 691 (1946).
3. E. W. R. STEACIE. J. Phys. Chem. **35**, 1493 (1931).
4. P. S. SHANTAROVICH. Doklady Akad. Nauk S.S.S.R. **116**, 255 (1957).
5. (*a*) A. E. STEARN and H. EYRING. J. Chem. Phys. **3**, 778 (1935).
   (*b*) B. G. REUBEN and J. W. LINNETT. Trans. Faraday Soc. **55**, 1543 (1959).
6. (*a*) F. W. KIRKBRIDE and R. G. W. NORRISH. J. Chem. Soc. 119 (1933). K. KNOX, R. G. W. NORRISH, and G. PORTER. J. Chem. Soc. 1447 (1952).
   (*b*) P. S. SKELL and R. C. WOODWORTH. J. Am. Chem. Soc. **78**, 4496 (1956).
   (*c*) W. VON E. DOERING and P. LA FLAMME. J. Am. Chem. Soc. **78**, 5447 (1956).
7. (*a*) W. VON E. DOERING, R. G. BUTTERY, R. G. LAUGHLIN, and N. Chaudhuri. J. Am. Chem. Soc. **78**, 3221 (1956). W. VON E. DOERING and H. PRINZBACH. Tetrahedron, **6**, 24 (1959).
   (*b*) H. M. FREY. Proc. Chem. Soc. 318 (1959); J. Am. Chem. Soc. **80**, 5005 (1958).
   (*c*) J. H. KNOX and A. F. TROTMAN-DICKENSON. Chem. & Ind. (London), 731 (1957).
8. (*a*) G. B. KISTIAKOWSKY and N. W. ROSENBERG. J. Am. Chem. Soc. **22**, 321 (1950). G. B. KISTIAKOWSKY and A. L. MARSHALL. J. Am. Chem. Soc. **74**, 88 (1952).
   (*b*) A. N. STRACHAN and W. A. NOYES, Jr. J. Am. Chem. Soc. **76**, 3258 (1954). R. A. HOLROYD and W. A. NOYES, Jr. J. Am. Chem. Soc. **78**, 4831 (1956).
   (*c*) G. B. KISTIAKOWSKY and K. SAUER. J. Am. Chem. Soc. **78**, 5699 (1956).
   (*d*) G. B. KISTIAKOWSKY and P. KYDD. J. Am. Chem. Soc. **79**, 4825 (1957).
   (*e*) H. M. FREY and G. B. KISTIAKOWSKY. J. Am. Chem. Soc. **79**, 6373 (1957).
9. (*a*) B. S. RABINOVITCH, E. TSCHUIKOW-ROUX, and E. W. SCHLAG. J. Am. Chem. Soc. **81**, 1981 (1959).
   (*b*) H. M. FREY. Proc. Roy. Soc. (London), A, **250**, 409 (1959); A, **251**, 575 (1959).
   (*c*) J. N. BUTLER and G. B. KISTIAKOWSKY. J. Am. Chem. Soc. **82**, 759 (1960); **83**, 1324 (1961).
   (*d*) H. M. FREY. Trans. Faraday Soc. **56**, 1201 (1960); **57**, 951 (1961).
10. D. B. RICHARDSON, M. C. SIMMONS, and I. DVORETSKY. J. Am. Chem. Soc. **82**, 5001 (1960); **83**, 1934 (1961).
11. F. W. SCHNEIDER and B. S. RABINOVITCH. Symposium on Elementary Reactions. American Chemical Society, St. Louis. March, 1961; Washington, March, 1962.
12. S. W. BENSON. Foundations of chemical kinetics. McGraw-Hill Book Co., New York. 1960.
13. B. S. RABINOVITCH and R. W. DIESEN. J. Chem. Phys. **30**, 735 (1959).
14. J. W. SIMONS and B. S. RABINOVITCH. Unpublished data.
15. M. C. FLOWERS and H. M. FREY. Proc. Roy. Soc. (London), A, **257**, 122 (1960); A, **260**, 424 (1961).
16. M. C. FLOWERS and H. M. FREY. J. Chem. Soc. 3953 (1959).
17. F. D. ROSSINI. Selected values of physical and thermodynamic properties of hydrocarbons and related compounds. American Petroleum Institute. 1953.
18. R. F. KUBIN. Ph.D. Thesis, University of Washington, Seattle, Wash. 1961.
19. S. A. RYCE and W. A. BRYCE. Trans. Faraday Soc. **57**, 943 (1961).
20. H. M. FREY. J. Am. Chem. Soc. **82**, 5947 (1960).
21. B. S. RABINOVITCH and K. W. MICHEL. J. Am. Chem. Soc. **81**, 5065 (1959).
22. R. E. HARRINGTON, B. S. RABINOVITCH, and H. M. FREY. J. Chem. Phys. **33**, 1271 (1960).
23. W. B. DEMORE, H. O. PRITCHARD, and N. DAVIDSON. J. Am. Chem. Soc. **81**, 5874 (1961).
24. R. A. MARCUS and O. K. RICE. J. Phys. & Colloid Chem. **55**, 894 (1951).
25. B. E. KNOX and H. B. PALMER. Chem. Revs. **61**, 247 (1961).
26. A. LANGER, J. A. HIPPLE, and D. P. STEVENSON. J. Chem. Phys. **20**, 1836 (1954).
27. J. C. POLANYI. J. Chem. Phys. **31**, 1338 (1959).
28. B. L. CRAWFORD and W. H. FLETCHER. J. Chem. Phys. **19**, 406 (1951).
29. B. S. RABINOVITCH and J. H. CURRENT. J. Chem. Phys. **35**, 2250 (1961).
30. H. GUNTHARD, R. C. LORD, and T. R. MCCUBBIN, Jr. J. Chem. Phys. **25**, 768 (1956).
31. B. S. RABINOVITCH, E. W. SCHLAG, and K. W. WIBERG. J. Chem. Phys. **28**, 504 (1958).
32. B. S. RABINOVITCH, D. W. SETSER, and F. W. SCHNEIDER. Can. J. Chem. **39**, 2609 (1961).
33. R. A. MARCUS and G. WIEDER. Ph.D. Dissertation (of G. W.), Polytechnic Institute of Brooklyn. 1961.
34. W. E. FALCONER, T. E. HUNTER, and A. F. TROTMAN-DICKENSON. J. Chem. Soc. 609 (1961).
35. H. O. PRITCHARD, R. G. SOWDEN, and A. F. TROTMAN-DICKENSON. Proc. Roy. Soc. (London), A, **217**, 563 (1953).
36. E. W. SCHLAG and B. S. RABINOVITCH. J. Am. Chem. Soc. **82**, 5996 (1960).
37. A. T. BLADES. Can. J. Chem. **39**, 1401 (1961).
38. H. S. JOHNSTON. J. Chem. Phys. **19**, 663 (1951).
39. E. K. GILL and K. J. LAIDLER. Can. J. Chem. **36**, 1570 (1958).
40. D. S. MCLURE. J. Chem. Phys. **17**, 905 (1949).
41. I. MURGULESCU and T. ONCESCU. J. chim. phys. **58**, 508 (1961).
42. R. M. ETTER, H. S. SKOVRONEK, and P. S. SKELL. J. Am. Chem. Soc. **81**, 1008 (1959).
43. B. A. THRUSH. Private communication.
44. J. B. PEDLEY. Trans. Faraday Soc. **58**, 23 (1962). *But see* P. C. H. Jordan and H. C. Longuet-Higgins. Mol. Phys. **5**, 121 (1962).
45. D. W. SETSER, B. S. RABINOVITCH, and E. G. SPITTLER. J. Chem. Phys. **35**, 1840 (1961).

INFLUENCE OF TEMPERATURE ON THE ELECTROLYTIC SEPARATION FACTOR OF HYDROGEN ISOTOPES[1]

L. P. Roy[2]

Research Chemistry Branch, Atomic Energy of Canada Limited, Chalk River, Ontario

Received August 12, 1960

ABSTRACT

An electrolysis cell and a tritium counting system are described for the study of the influence of temperature on the electrolytic separation of hydrogen isotopes on a mild steel cathode in alkaline solution. By careful control of the conditions for electrolysis, the separation factors could be determined with a probable error of ±4%. From the temperature coefficients of the three separation factors α, β, and γ, differences in activation energy of −1680, −2260, and −580 cal/mole have been calculated for electrolysis in the H–D, H–T, and D–T systems respectively. When conditions were less stringently controlled, the separation factor β was found to be a linear function of the separation factor α according to an equation of the form $\beta = D\alpha - E$. This relationship is of importance in the use of deuterium as a tracer in the electrolytic concentration of natural tritium. Some empirical equations showing the temperature influence on the variation of β as a function of α are also included.

INTRODUCTION

The study of the mechanisms of the cathodic evolution of hydrogen and the importance of obtaining an efficient separation of the hydrogen isotopes in the commercial production of heavy water by electrolysis have led investigators to determine the influence of factors which affect the separation of protium from deuterium. Among these factors may be cited: current density, overvoltage, nature of the electrode surface, presence of impurities in the electrolyte, time of electrolysis, and the influence of temperature on the separation of protium and deuterium. The efficiency of such a separation is usually expressed by its separation factor, which is defined by the ratio of the isotopic forms in the gaseous phase to that in the liquid phase. For the three hydrogen systems, protium–deuterium, protium–tritium, deuterium–tritium, the separation factors are:

$$\alpha = \frac{(h/d)_{\text{gas}}}{(h/d)_{\text{liquid}}}, \qquad [1]$$

$$\beta = \frac{(h/t)_{\text{gas}}}{(h/t)_{\text{liquid}}}, \qquad [2]$$

$$\gamma = \frac{(d/t)_{\text{gas}}}{(d/t)_{\text{liquid}}}, \qquad [3]$$

where h, d, and t represent the number of atoms of protium, deuterium, and tritium in the specified phase. The three separation factors are related to one another by the equation

$$\gamma = \beta/\alpha. \qquad [4]$$

Thus a knowledge of any two of these factors enables the third one to be calculated.

The results of previous workers have shown that the electrolytic separation factor of the hydrogen isotopes varies somewhat with temperature. Bell and Wolfenden (1) have reported a value of 4.3 at 10° C and 3.8 at 100° C for the separation factor α on a nickel cathode in alkaline solution. Walton and Wolfenden (2) have investigated the temperature

[1]*Issued as A.E.C.L. No. 1534.*

[2]*Present address: Laval Industrial Association (Incorporated), P.O. Box 124, Pointe-aux-Trembles, Montreal, Que.*

influence on five cathode materials. They have found a negative effect, i.e. a decrease of the separation factor α for an increase in temperature for Ni, Ag, Pt, and Hg, the temperature effect with the latter cathode being hardly detectable, while for Sn there seemed to be a slightly positive effect. They have reported a separation factor α of 7 at 15° C and 5.9 at 95° C on a nickel cathode in acid solution.

More recently, Brun and Varberg (3) have studied the temperature influence on the separation factor of protium and deuterium on a mild steel cathode in alkaline solution. They observed a decrease from 17.5 to 5.8 in the separation factor α for an increase of temperature from −19° C to +97° C. In such experiments carried out at various temperatures, it is possible to calculate the difference of activation energy for the rate-controlling step in the liberation of hydrogen isotopes by means of the Arrhenius equation applicable to the protium–deuterium system in the following way:

$$\frac{d \log \alpha}{dT} = \frac{\Delta H_\alpha}{2.3RT^2} \qquad [5]$$

where α is the separation factor at absolute temperature T, R is the molar gas constant, and

$$\Delta H_\alpha = E_H - E_D, \qquad [6]$$

where E_D is the free activation energy for the transfer of a deuteron to the cathode and E_H is the same activation energy for the transfer of a proton to the cathode.

Applying the above equation to the results of Brun and Varberg, an activation energy difference of −1800 cal/mole has been calculated for the H–D system on a mild steel cathode in alkaline solution.

On the other hand, the data available in the literature on the protium–tritium separation factor are very limited and do not involve any investigations of temperature dependence. Eidinoff (4) has observed a value of 14 on a smooth platinum cathode at 20° C in alkaline solution. Horiuti and Nakamura (5) have obtained, by theoretical calculations, values of 15.1 and 16.1 for nickel and platinum cathodes. Kaufman and Libby (6) have observed wide fluctuations for successive determinations of β and α but the ratio of β/α was found to be essentially constant at 2.1 ± 0.1. This ratio has been used by them and later workers to calculate, for purposes of low-level tritium measurements, the tritium recovery of an electrolytic enrichment from the observed deuterium recovery.

We observed a wide range of values in the electrolytic separation factors α and β during the first part of our investigation, and these results are discussed more fully below. Östlund and Werner observed the same behavior (7). We eventually improved our technique to the extent that reproducible results were obtained. This paper describes the electrolysis method finally adopted to study the influence of temperature on the electrolytic separation factors α and β on a mild steel cathode in alkaline solution. From our results and the relation given in equation [4] it was possible to calculate γ as a function of temperature. Linear Arrhenius relationships (equation [5]) allowed deduction of the activation energy differences of the three systems.

EXPERIMENTAL

(a) Electrolytic Cell and Oxidation Apparatus

The apparatus used is shown in Fig. 1. The electrolytic cell A, made of Pyrex glass, had a capacity of about 15 cc and was equipped with a ground-glass joint so that it could be opened readily. Two U traps, D, cooled with liquid nitrogen, kept the water of the electrolyte from contaminating the electrolytic gases. The simple manual Toepler pump E allowed quantitative transfer of the electrolytic gases from the cell

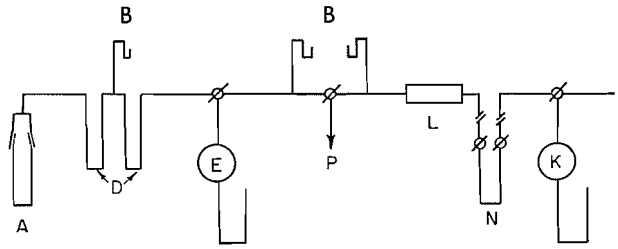

FIG. 1. Schematic representation of the electrolysis cell and oxidation apparatus.
A = electrolytic cell
D = condensate traps
B = differential manometers
E and K = Toepler pump
N = removable trap
P = vacuum pump
L = oxidation chamber

to the Vycor oxidation chamber L, which was filled with cupric oxide and kept at 750° C by means of an electric furnace. A second Toepler pump K was used to discard sweep gases while the water produced in the furnace was collected in the removable trap N, kept at liquid nitrogen temperature.

(b) Electrodes and Electrolyte

The 0.25 mm thick mild steel cathode containing 0.2±0.05% manganese and 0.1±0.05% carbon and the nickel anode were mounted as shown in Fig. 2. Two thin slots, cut in a small Teflon block located at

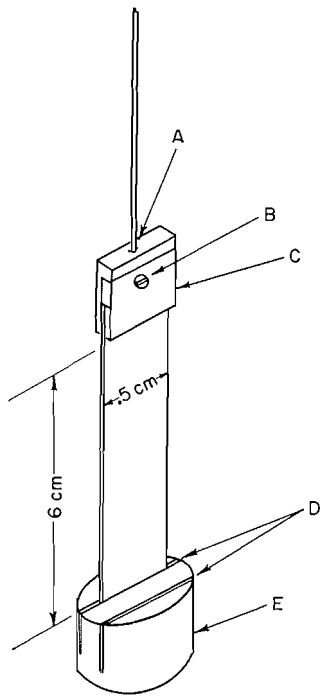

FIG. 2. Electrode arrangement.
A = electrical lead hard soldered to clamp
B = clamping screw
C = stainless steel clamp
D = slots for positioning electrodes
E = teflon block

the bottom of the cell, kept the electrodes in a fixed position. The electrical metal leads, extending about 3 cm from the top of the cell through small holes, were fastened to the glass with Armstrong cement. The direct current was supplied by a dry cell and was measured with a milliammeter. A variable resistance was inserted into the circuit to restore the small drop in current following the first one or two minutes of electrolysis.

The water used to make up the electrolyte was distilled three times from an alkaline permanganate solution. Some heavy water of known concentration was added to make the solution 2% in HDO and about 20 to 25 μc of tritium (as THO) was introduced into the water. The electrolyte was 4.4 weight% KOH.

(c) Reduction Apparatus and Tritium Counter

Figure 3 shows the reduction apparatus and the vacuum line associated with the operation of the tritium gas counter F. The water produced by the electrolysis and collected in the trap N (Fig. 1) was vacuum-distilled into E, with the Zn furnace at room temperature. Reduction was carried out by allowing the

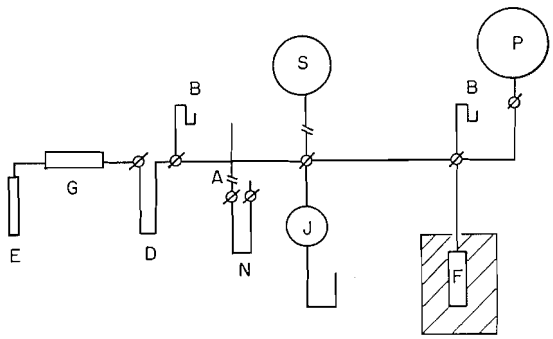

FIG. 3. Schematic representation of the reduction apparatus and of tritium gas counting system.

A = connection of trap N to vacuum system	F = tritium counter
E = water receiver	B = differential manometers
D = condensate trap	P = storage bulb
N = removable trap	G = reduction chamber
J = Toepler pump	S = removable sample bulb

sample to pass through a few grams of 20-mesh zinc metal at 375° C. Trap D served to recover any unreacted water. The hydrogen was transferred from the reduction system to the counter by the manual Toepler pump J.

Counter F, which was 8 cm in length and 1.8 cm in outside diameter, had a sensitive volume of 8.7 ml. The anode consisted of a 0.025-mm diameter tungsten wire, while the copper walls constituted the cathode. The use of an electronic quench unit (an A.E.C.L.-designed unit, number AEP 1702) with a self-quenching gas mixture of argon and ethylene provided a plateau with a slope of about 2%/100 v over a 400-v region. Six inches of lead were used for shielding, and this kept the background to about 12 counts/min. The counting gas mixture, consisting of 6 parts of argon to 5 parts of ethylene by volume, was stored in bulb P.

(d) Procedure

The electrodes were polished with 2/0 and 4/0 emery paper, cleaned with ethanol and benzene, inserted into the Teflon holder, and clamped to the connecting leads. The electrolyte was poured into the cell, the solution frozen with liquid nitrogen, and the air removed by pumping for a few minutes. Two or three freezing and pumping operations were sufficient to remove the last traces of dissolved air, which was then replaced by some 10 cm pressure of helium or argon. The electrolyte was purified by a pre-electrolysis at a current density of 15 ma/cm^2 for 1 hour, after which the solution was frozen by liquid nitrogen and the electrolytic gases along with the inert gas were removed by the series of operations outlined above. A fresh portion of inert gas was then added to the electrolytic cell and the pressure was maintained at 60 cm of Hg throughout the experiment by lowering of the mercury reservoir E. The solution, kept at constant temperature, was then electrolyzed for 30 to 60 minutes at a current density of 8 ma/cm^2. Current efficiencies of 95 to 98% were calculated from the hydrogen gas yield. At the end of the electrolysis, the solution was frozen with liquid nitrogen and the electrolytic gases, well mixed with the inert gas, were transferred, at a reduced pressure for safety purposes, to the evacuated cupric oxide furnace L by means of the mercury bulb E. (Fig. 1). The resulting water was collected in removable trap N, which was connected to the reduction apparatus at A (Fig. 3), and the water transferred into E. The reduction was carried out in the manner already described. Complete reduction of the water was very important in order to avoid a possible fractionation of the hydrogen isotopes at this stage. The presence of any unreacted water was detected by an increase of pressure when the evacuated, liquid nitrogen cooled trap D was heated gently to room temperature. In such a case, a second reduction was carried out. However, it was found that the incomplete reaction could be avoided by changing the zinc furnace frequently, e.g. after 5 or 6 runs. A portion of the hydrogen gas was put into a removable sample bulb, S (Fig. 3), for measurement of the protium–deuterium

ratio with a Model 21-610 Consolidated mass spectrometer. The remaining fraction of the hydrogen gas was transferred to the tritium counter F (Fig. 3) by the manual Toepler pump J and mixed four or five times with a constant amount of counting gas mixture supplied from P (Fig. 3). The hydrogen pressure varied between 10 and 15 cm of mercury while the argon–ethylene pressure was kept constant at 10.0 cm of mercury. A plateau was run for every tritium determination and the average activity over a 300-v interval was used as the true activity.

RESULTS AND DISCUSSION

The protium–deuterium separation factor α was calculated by means of equation [1], where the $(h/d)_{gas}$ and $(h/d)_{liquid}$ ratios were measured by a mass spectrometer after the water from the electrolyte (liquid phase) and the water from the electrolysis (gas phase) had been reduced to hydrogen gas. Two methods were used for the determination of the protium–deuterium separation factor. The first one consisted of calibration of the instrument with protium–deuterium mixtures of known composition so that the h/d ratios of the gaseous and liquid phases could be determined absolutely. The second method consisted of comparison of the HD peak height of the hydrogen derived from the electrolyte (liquid phase) to that derived from the electrolytic waters (gas phase) for the same hydrogen peak height in both phases. The ratio of the two peak heights under these conditions gave the separation factor of the protium–deuterium system. Both methods agreed within 2%.

A relative method was used to determine the protium–tritium separation factor β. The specific activity of the hydrogen derived from the electrolyte, relative to the specific activity of the hydrogen released during electrolysis, gave the separation factor directly. No absolute calibration of the counter was required. When the technique described in (*d*), Experimental, was followed carefully, the reproducibility was reasonable, as illustrated in Table I.

TABLE I

Reproducibility of the separation factors at 0.5° C

11.7	34.8
11.0	33.2
11.4	29.0
11.8	29.4
11.9	30.9
11.4	31.7
11.4	30.8
11.9	31.7
11.9	33.1
12.7	31.2
12.2	34.2
12.5	34.8
10.9	29.7
11.7	30.9
12.2	33.7
10.8	33.7
11.9	31.5
12.2	30.0
11.1	29.5
Average 11.7±0.4	31.8±1.3

The errors shown in Table I refer to the probable error obtained by a statistical treatment of the experimental data and lie well within the estimated combined errors of the individual measurements which were used to calculate the separation factors. Thus, uncertainties in the D content of the electrolyte and electrolytic water led to an error of ±2% in the separation factor, while a possible variation in temperature might produce an error of ±1%; finally, possible isotopic fractionation in the oxidation and reduction steps amounted to an error of ±3%. The latter value was obtained experimentally by

comparing the h/d ratio of the electrolytic hydrogen before and after it had undergone oxidation and reduction steps. The errors in the protium–tritium system were assessed as follows: statistical error due to tritium counting of the electrolyte and the electrolytic water amounted to ± 1 and $\pm 2\%$ in the final value of β, while measurement of hydrogen and of counting gas pressures introduced an error of $\pm 2\%$ in β. A possible variation in temperature might produce an error of $\pm 1\%$ while an error of $\pm 4\%$ in β was expected from the possible fractionation of hydrogen isotopes in the oxidation and reduction steps.

The results for the temperature effect on the electrolytic separation factors α, β, and γ are summarized in Table II. The separation factor γ has been calculated by the relation

TABLE II

Temperature effect on the electrolytic separation factors of hydrogen isotopes

	T (°C)	α	β	γ	log β/log α
	0.5	11.7±0.4	31.8±1.3	2.7_2±0.14	1.41
	22.5	9.6±0.2	24.9±1.0	2.6_0±0.12	1.42
	40	8.0±0.3	19.5±0.7	2.4_4±0.14	1.43
	60	6.7±0.3	15.0±0.7	2.2_4±0.14	1.42
ΔH (cal/mole)		$\Delta H_\alpha = -1680$	$\Delta H_\beta = -2260$	$\Delta H_\gamma = -580$	

given in [4]. The error quoted for over 15 determinations at each temperature refers to the most probable error. From Fig. 4, it can be seen that the Arrhenius relationship is obeyed in the temperature range studied. From the plots of Fig. 4, differences of activation energy of -1680, -2260, -580 cal/mole have been calculated for the H–D, H–T, and D–T systems, respectively. The value of -1680 cal/mole for the protium–deuterium system compares reasonably well with the value of -1800 cal/mole calculated from the results of Brun and Varberg (3). The ratio of log β/log α was found to be constant at 1.41±0.01, in agreement with the value of 1.40±0.01 reported by Bigeleisen (8) and of 1.40±0.09 reported by Kaufman and Libby (6).

When the technique described in (*d*), Experimental, was not followed, the agreement between successive runs was not very good, as shown in Fig. 5, in which the values of α varied from 6.7 to 12.7 at 0.5° C. This lack of reproducibility appears to arise from one or more of the following factors: nature of the electrode surface, impurities in the electrode or in the solution, omission of pre-electrolysis, presence of dissolved air in the electrolyte.

As a matter of practical interest in connection with measurement of tritium concentration in natural waters, it was desirable to determine whether or not β varies systematically with α. The practical usefulness of such a correlation will be evident when it is remembered that for determination of low levels of tritium in water, extensive preliminary electrolyses are necessary to concentrate the tritium (see for example ref. 6). In such electrolyses, β cannot be measured directly, i.e. only the H–D separation factor can be determined. Accordingly, all of the data obtained in the present work have been examined from this point of view. Table III summarizes the results. At all four temperatures, good empirical

TABLE III

Empirical equations at various temperatures

T (°C)	Limits		Number of determinations	Empirical equation
0.5	$6.7 < \alpha < 12.7$	$12.2 < \beta < 34.8$	45	$\beta = 3.80\alpha - 13.2$
22.5	$5.4 < \alpha < 10.5$	$9.2 < \beta < 29.8$	28	$\beta = 3.53\alpha - 9.7$
40.0	$3.5 < \alpha < 8.8$	$5.5 < \beta < 21.4$	26	$\beta = 3.16\alpha - 6.0$
60.0	$3.4 < \alpha < 7.4$	$5.8 < \beta < 18.6$	34	$\beta = 3.04\alpha - 5.4$

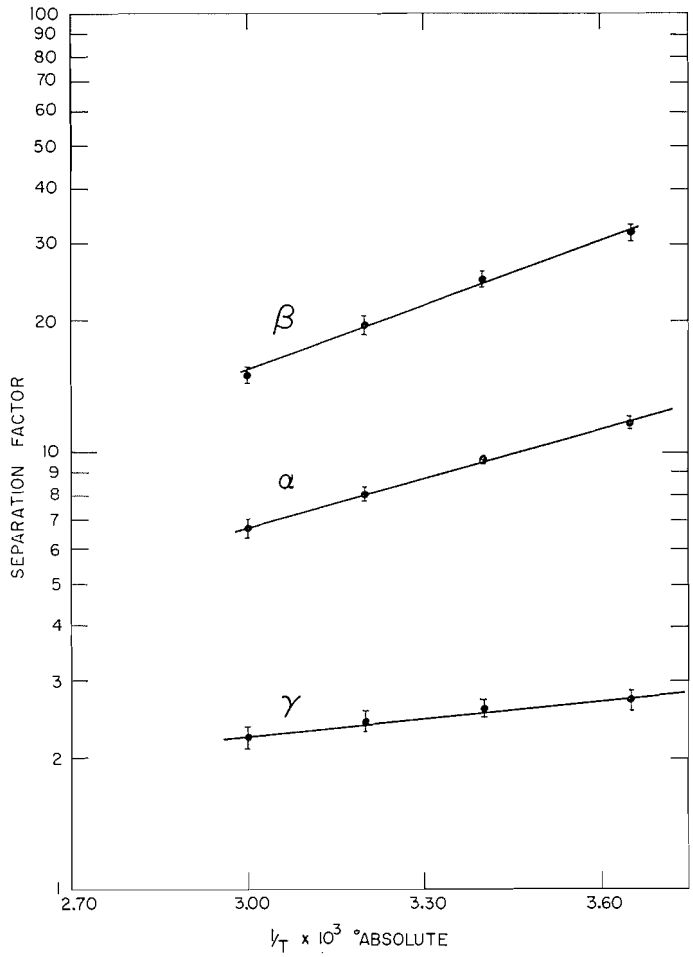

FIG. 4. Temperature variation of the separation factors α, β, and γ.

correlations of the form $\beta = D\alpha - E$ were observed between corresponding values of α and β. These are shown in the last column of Table III, and were derived from the data at each temperature by a least-squares analysis. The probable error in D and E was found to be 6% and 15% respectively.

The solid line in Fig. 5 represents the empirical correlation equation for 0.5° C. Correlations for other temperatures were fully as good as that shown in Fig. 5. Östlund and Werner (7) have also obtained a similar form of correlation between α and β for electrolysis at 10° C.

It is worthwhile emphasizing that γ, i.e. β/α, is not constant; for example, over the range of α observed at 0.5° C, γ was found to vary from 1.8 to 2.8, in contrast with the constant value of 2.1 ± 0.1 adopted by Libby and Kaufman (6) but in agreement with the values of 1.6 to 2.5 obtained by Östlund and Werner as reported by Bigeleisen (8).

CONCLUSION

When experimental conditions are carefully controlled, a good degree of reproducibility can be achieved in measurement of the isotopic separation which occurs during the electrolysis of alkaline water. For these conditions, a systematic increase of each separation

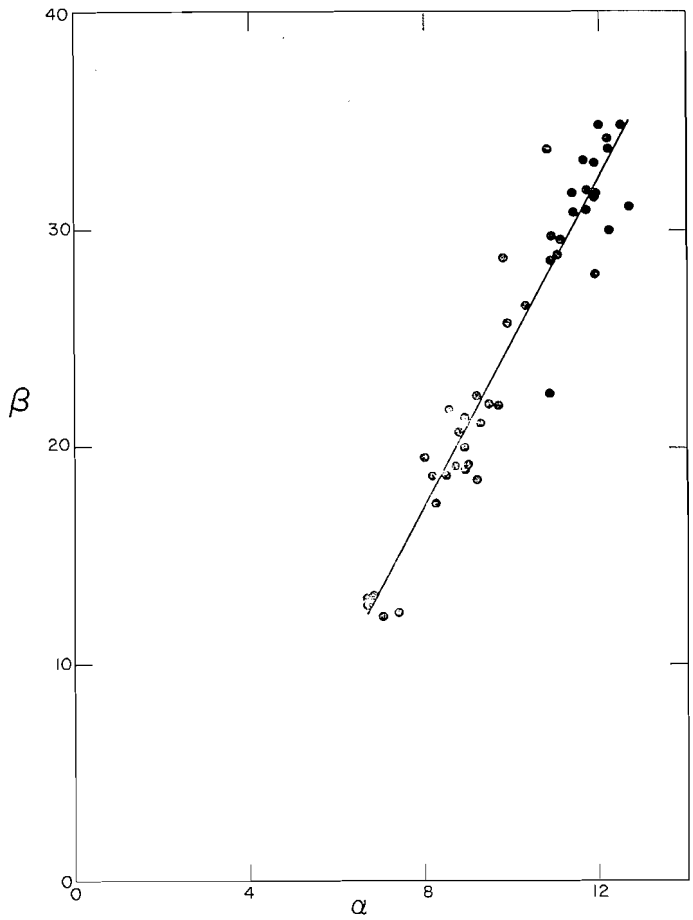

FIG. 5. Variation of separation factor β as a function of separation factor α, for $T = 0.5°$ C.

factor with decreasing temperature is observed; this effect can be expressed formally as an Arrhenius activation energy. The highest value observed for any separation factor was 34.8 for the H–T separation at 0.5° C.

When experimental conditions are less stringently controlled, variations up to a factor of 2 in the values of α occur, at a fixed temperature. For these less well defined conditions, it has been demonstrated that at each temperature a good empirical relationship of the form $\beta = D\alpha - E$ exists between corresponding values of α and β; D and E are temperature-dependent constants. As a consequence, γ is not a constant, as has been assumed previously, but varies with the value of α. These correlations have practical application in estimating the retention of tritium in the residual water after the extensive preliminary electrolyses frequently required as a concentration step in the determination of tritium in natural waters.

ACKNOWLEDGMENTS

The author is indebted to Drs. R. H. Betts, W. E. Grummitt, and R. M. Brown for numerous suggestions and helpful advice received in the course of this work.

REFERENCES

1. R. P. BELL and J. H. WOLFENDEN. Nature, **133**, 25 (1934).
2. H. F. WALTON and J. H. WOLFENDEN. Trans. Faraday Soc. **34**, 436 (1938).
3. J. BRUN and T. VARBERG. Kgl. Norske Videnskab. Selskabs Forh. **26**, 19 (1953).
4. M. L. EIDINOFF. J. Am. Chem. Soc. **69**, 2507 (1947).
5. J. HORIUTI and T. N. NAKAMURA. J. Chem. Phys. **18**, 395 (1950).
6. S. KAUFMAN and W. F. LIBBY. Phys. Rev. **93**, 1337 (1954).
7. H. G. ÖSTLUND and P. E. WERNER. Radioactive Dating Laboratory, Frescati, Stockholm 50. Private communication to R. M. Brown.
8. J. BIGELEISEN. Correlation of tritium and deuterium isotope effects. BNL 5314, April 1960.

FREE-RADICAL REACTIONS WITH AROMATIC ETHERS

PART I. BENZOYL PEROXIDE WITH ANISOLE[1]

BRIAN M. LYNCH[2] AND RALPH B. MOORE[3]

Chemistry Department, Memorial University of Newfoundland, St. John's, Newfoundland

Received January 22, 1962

ABSTRACT

A re-examination of the products of thermal decomposition of benzoyl peroxide in anisole has resolved anomalous findings by previous workers. The expected phenylation of the substrate is accompanied by appreciable benzoyloxylation, and the distribution of isomers in the phenylation and benzoyloxylation products has been examined; the theoretical implications of the results are discussed.

INTRODUCTION

Phenylation of aromatic substrates by benzoyl peroxide, discovered by Gelissen and Hermans (1) in 1925, was recognized as a free-radical process by Hey and Waters (2), and continues to receive much attention (for general reviews, see Augood and Williams (3), Dermer and Edmison (4), Walling (5), and Williams (6, 7)). In a series of some 20 papers, Hey and Williams and their co-workers (8, and previous papers cited therein) have applied Ingold's competitive method (Ingold and Shaw (9)) to evaluate the relative reactivities of many aromatic compounds towards the aryl radicals liberated by decomposing benzoyl peroxides.

Recently, it has been pointed out (5, 10–12) that there is considerable uncertainty attached to the application of the competitive method in such reactions, since many side reactions occur, and their importance varies markedly for different aromatic substrates. Further reservations have been expressed since the phenylation process does not occur by any one mechanism; differing processes may be dominant at different concentrations (Eliel *et al.* (13)). It is apparent that selection of the relative yields of substituted biphenyls as a measure of reactivity towards free-radical attack must be regarded with considerable reserve; a more acceptable procedure involves consideration of the distribution of products among the various possible reaction paths (cf. Lynch and Pausacker (11, 12)).

In the present paper, we have used this approach in a study of the various reaction products obtained when benzoyl peroxide decomposes in hot anisole, and we have resolved suggestions (14; 6, p. 65) that anisole is in some way anomalous in its behavior. A previously published study of this reaction system (15) neglects the occurrence of benzoyloxylation of the substrate.

EXPERIMENTAL

Analyses are by the Schwarzkopf Microanalytical Laboratory, Woodside, N.Y., and the Australian Microanalytical Service at the Chemistry Department, University of Melbourne. Infrared spectra were measured using a Unicam SP100 prism-grating spectrometer, and ultraviolet spectra were recorded with a Beckman DK2A spectrophotometer.

[1]*Presented in part at the 44th Annual Conference of the Chemical Institute of Canada, Montreal, Quebec, August 2–5, 1961.*

[2]*To whom requests for reprints should be addressed, at the Chemistry Department, St. Francis Xavier University, Antigonish, Nova Scotia.*

[3]*American Chemical Society – Petroleum Research Fund Undergraduate Scholar, 1961–1962.*

Materials

Anisole (Matheson, Coleman, and Bell) was redistilled before use, b.p. 154°, n_D^{25} 1.5151; the various samples contained from 0.02–0.08% phenol. Benzoyl peroxide was purified (minimum purity, 98%) by reprecipitation from ice-cold chloroform by methanol. Reference samples of the isomeric methoxybiphenyls, methoxyphenols, and methoxyphenyl benzoates, and of phenol and phenyl benzoate, were obtained by purification of commercially available samples or by established common syntheses; the physical constants of these samples agreed with those recorded in the literature.

General Procedure

Benzoyl peroxide and anisole were heated together under varying conditions (see Table I). After completion of reaction, the various products were separated and isolated as follows: the *carbon dioxide* evolved was estimated by passage through a gas-absorption train. *Free benzoic acid* was isolated by extraction with saturated sodium hydrogen carbonate solution, followed by acidification. Excess of substrate was removed under reduced pressure, and the residue was heated under reflux with 5% potassium hydroxide in ethanol (16 hours). The ethanol was removed under reduced pressure, and the residue was acidified to pH 2 and extracted with ether. The *phenolic fraction* and an additional quantity of benzoic acid (*benzoic acid from hydrolysis*) were obtained from the extract by standard methods, and the *methoxybiphenyls* were isolated, after evaporation of the ether, by careful distillation under reduced pressure, or by steam distillation. Any involatile residue was weighed and reserved. This procedure is based on that employed by Lynch and Pausacker (11).

The Phenolic Fractions: Distribution of Isomers in Benzoyloxylation

Element analysis, and infrared and ultraviolet spectra, indicate that the phenolic fractions isolated from the various experiments consist largely of methoxyphenols, with little phenol being present. The following infrared absorption bands were noted for the three methoxyphenols, and for a typical phenolic fraction (from expt. 2): guaiacol (capillary film) (cm^{-1}, intensity): 745 vs, 835 m, 920 w, 1005 w, 1022 s, 1040 m, 1112 s, 1220 m, 1265 s, 1380 m, 1440 m, 1480 m, 1510 vs, 1610 vs, 1620 m, 2840 m, 2960 m, 3010 m, 3430 s, 3500 s; *m*-methoxyphenol (capillary film): 690 s, 770 s, 840 m, 925 m, 996 w, 1045 s, 1080 w, 1160 vs, 1200 vs, 1290 s, 1445 m, 1470 m, 1500 s, 1600 vs, 1615 vs, 2835 m, 2950 m, 3000 m, 3400 s; *p*-methoxyphenol (KCl disk): 733 s, 825 vs, 1033 vs, 1105 s, 1151 w, 1170 w, 1182 m, 1240 s, 1280 s, 1302 m, 1379 s, 1455 s, 1510 vs, 1608 s, 2830 m, 2950 s, 3015 w, 3035 w, 3400 s; phenolic fraction from expt. 2 (capillary film): 690 vw, 735–760 s, 820 s, 840 s, 920 w, 1030 s, 1040 s, 1110 s, 1155 s, 1180 m, 1225 s, 1270 s, 1380 m, 1460 m, 1480 m, 1510 vs, 1600 vs, 1620 s, 2840 m, 2955 s, 3010 w, 3430 s, 3500 s. Virtually all of these bands can be assigned without difficulty, following the lines of previous work by Katritzky *et al.* (16, and previous papers cited therein). It is evident that guaiacol and *p*-methoxyphenol are major constituents of the phenolic fraction examined (the infrared spectra of the phenolic fractions were all closely similar), but the differences in the spectra of the three isomers are not sufficient for accurate analysis of the ratios of isomers.

Similarly, although the ultraviolet spectra of the mixtures of phenols from expts. 1–3 and 6–8 corresponded well to that of guaiacol, the differences between the spectra of the various isomers are small (in water containing 1% methanol by volume, guaiacol has λ_{max} 216 and 275 mμ, log ε 3.76 and 3.33; *m*-methoxyphenol has λ_{max} 217, 273, and 279 mμ, log ε 3.83, 3.28, and 3.23; *p*-methoxyphenol has λ_{max} 223 and 289 mμ, log ε 3.83 and 3.41; phenol has λ_{max} 211, 270, and 276 mμ, log ε 3.75, 3.18, and 3.08; and the various phenolic fractions showed λ_{max} 216 and 275 mμ, log ε 3.9 and 3.32). The infrared spectra of the three methoxyphenyl benzoates were recorded, and it was found that the meta and para isomers had characteristic absorption bands in the aromatic C—H deformation region. The following absorption bands were observed (bands characteristic of an isomer are italicized): guaiacyl benzoate (KCl disk) (cm^{-1}, intensity): 710 vs, 760 s, 810 w, 1025 s, 1040 m, 1065 vs, 1080 m, 1110 s, 1155 w, 1170 s, 1200 s, 1260 vs, 1310 w, 1450 s, 1585 w, 1600 s, 1735 vs, 2835 m, 2940 s, 2975 vs, 3000 s, 3065 s; *m*-methoxyphenyl benzoate (KCl disk): *690* s, 710 vs, *744* w, *782* s, 870 s, *930* s, *996* w, 1023 s, 1063 vs, 1081 vs, 1142 vs, 1160 m, 1175 m, 1190 s, 1270 vs, 1318 s, 1450 s, 1490 s, 1589 vs, 1605 vs, 1736 vs, 2825 m, 2930 s, 2950 s, 3000 s, 3065 m; *p*-methoxyphenyl benzoate (KCl disk): 710 vs, 765 m, *815* s, 870 m, 1030 m, 1040 m, 1070 s, 1075 s, 1115 w, 1185 m, 1205 s, 1255 s, 1280 s, 1320 w, 1440 m, 1520 vs, 1605 m, 1735 vs, 2835 s, 2935 s, 2960 s, 2995 vs, 3065 m. Samples of mixed methoxyphenyl benzoates, prepared by benzoylation of the phenolic fractions from expts. 1 and 2, showed the following bands (KCl disk): 710 vs, 760 m, 815 w, 870 w, 1024 s, 1040 m, 1065 vs, 1077 s, 1113 m, 1170 s, 1200 s, 1265 vs, 1315 w, 1450 s, 1520 s, 1600 s, 1735 vs, 2830 s, 2940 s, 2970 s, 2998 s, 3065 m. The absence of absorption at 690, 744, 782, 930, and 996 cm^{-1} in the samples of mixed benzoates indicated that very little *m*-methoxyphenyl benzoate was present; comparison with synthetic mixtures containing the other isomers showed that as little as 3% of the meta isomer could be detected readily by the above absorption bands. Comparison of the intensities of the 710 cm^{-1} and 815 cm^{-1} bands in the mixed benzoates with those in a series of synthetic mixtures (the 710 cm^{-1} band is common to all three isomers; the 815 cm^{-1} band is characteristic of the para isomer) indicated ortho:para ratios of from 20–25:1, suggesting that very little *p*-methoxyphenyl benzoate was present. However, a referee has drawn attention to bands in the infrared spectra of the phenolic mixtures (at 1155 cm^{-1}, and at 1180 and 820 cm^{-1}) indicating the presence of significant amounts of both *m*-and *p*-methoxyphenols; it thus appears possible that some fractionation of isomers occurred during esterification.

TABLE I

Products formed by reaction of benzoyl peroxide with anisole

Expt. No.:	1, 2, 3	4, 5	6, 7	8	9††	10‡‡	11§§
$(Ph.CO_2)_2$ (g)	20	40	20	6	3	3	20
$Ph.OCH_3$ (ml)	300	600	200	200	100	100	300
Temp. (°C)	154	96	80	80	80	80	96
Time of heating (hr)	4	15	30	50	50	50	15
Products* (g):							
Carbon dioxide	2.90, 2.90, —	4.51, 4.50	1.81, 1.75	0.53			
	(0.80, 0.80)	(0.62, 0.62)	(0.51, 0.48)	(0.49)			
Free benzoic acid†	8.40, 8.10, 8.99	22.6, 21.5	10.21, 9.70	3.20	1.91	2.41	9.95
	(0.83, 0.81, 0.90)	(1.13, 1.10)	(1.02, 0.97)	(1.06)	(1.26)	(1.60)	(0.99)
Phenolic fraction‡	1.2,§ 1.3, 1.2	—, —	1.9, 2.1	0.60			
	(0.12, 0.13, 0.12)		(0.19, 0.21)	(0.20)			
Benzoic acid from hydrolysis	1.2, 1.2, 1.2	5.0, 5.0	3.30, 3.80	—			
	(0.12, 0.12, 0.12)	(0.25, 0.25)	(0.33, 0.38)				
Methoxybiphenyls	7.3,‖ 7.3,¶ 7.0	16.0, 16.0	5.82, 6.00	—			
	(0.48, 0.48, 0.47)	(0.54, 0.54)	(0.39, 0.40)				
Involatile residue	0.8, 1.0, 1.0	0.8, 0.8	0.50, 0.50**	—			

*Yields in parentheses are in mole/mole benzoyl peroxide.
†Neutralization equivalents fell in the range 124–130.
‡Assumed to consist entirely of isomeric methoxyphenols.
§Anal. Calc. for $C_7H_8O_2$: C, 67.7; H, 6.5%. Found: C, 66.9; H, 5.6%.
‖Anal. Calc. for $C_{13}H_{12}O_2$: C, 84.8; H, 6.5%. Found: C, 84.7; H, 6.8%.
¶Anal. Found: C, 84.9; H, 6.5%.
**Anal. Found: methoxyl, 20.0%.
††Phenol (0.10 g) was added to the reaction mixture before heating was started.
‡‡Phenol (1.0 g) was added to the reaction mixture before heating was started.
§§Water (3.0 ml) was added to the reaction mixture before heating was started.

Consequently, further examination of the various phenolic mixtures was made by gas–liquid chromatography using a Beckman GC-2A gas chromatograph with a "Carbowax 4000 Dioleate"-on-firebrick column No. 70007, operated using helium at an inlet pressure of 30 p.s.i. (outlet pressure, atmospheric), at a column temperature of 160° C. Trial experiments established that the three methoxyphenols were satisfactorily resolved under these conditions, (the order of elution being ortho, para, meta), and that the ratio of peak areas was accurately proportional to the quantities of the isomers. The following isomer percentages were deduced: mixture from expt. 1: ortho, 65; para, 35%; from expt. 2: ortho, 70; para, 30%; from expt. 3: ortho, 82; para, 18%. No *m*-methoxyphenol was detected, confirming in part the results deduced from the infrared spectra of the mixed methoxyphenyl benzoates. The results of the trial experiments indicate that the individual experimental error is ±2%.

The Methoxybiphenyls: Isomer Ratios in Phenylation

The mixtures of methoxybiphenyls isolated from expts. 1 and 2 were analyzed by gas–liquid chromatography and by differential ultraviolet spectrophotometry.

In the gas–liquid chromatography, a Beckman GC-2A gas chromatograph was used, with the standard silicone-on-firebrick column No. 74346; helium at an inlet pressure of 30 p.s.i. (outlet pressure, atmospheric) was the carrier gas, and the column temperature was 190° C. Under these conditions, the three isomers were satisfactorily resolved (the order of elution being ortho, meta, para), and experiments with synthetic mixtures showed that the ratio of peak areas was proportional to the isomer ratios. The results obtained were: mixture from expt. 1: ortho, 76.2; meta, 10.5; para, 13.3%; mixture from expt. 2: ortho, 77.4; meta, 10.7; para, 11.9%. Results obtained with the synthetic mixtures indicate that the experimental error is ±2%.

The ultraviolet absorption spectra of the various methoxybiphenyls differed sufficiently for analysis of the mixtures by a standard method (cf. Lynch and Pausacker (17), Cadogan, Hey, and Williams (18)). Calibration spectra in 95% ethanol were recorded in the wavelength range 220–360 mμ, with the following results: *o*-methoxybiphenyl showed λ_{max} 246 and 285 mμ, log ε 4.09 and 3.70; *m*-methoxybiphenyl showed λ_{max} 250 and 280 (shoulder) mμ, log ε 4.18 and 3.62; *p*-methoxybiphenyl showed λ_{max} 261 mμ, log ε 4.28. The proportions of ortho, meta, and para isomers were found to be 80, 10, and 10% for the mixtures from expts. 1 and 2 (the two mixtures gave identical ultraviolet spectra). The experimental error is probably ±5%.

The infrared spectra of the various methoxybiphenyl mixtures were consistent with the isomer ratios as determined above, and no bands other than those due to the three isomers were present. The following absorption bands were noted for the methoxybiphenyls: (*a*) *o*-methoxybiphenyl (capillary film) (cm^{-1}, intensity): 700 vs, 732 s, 755 vs, 915 m, 937 w, 998 w, 1012 s, 1031 s, 1060 s, 1078 m, 1126 s, 1166 m, 1182 s, 1241 vs, 1264 vs, 1300 m, 1433 vs, 1465 m, 1485 vs, 1508 s, 1585 s, 1600 s, 2830 m, 2935 s, 2955 s, 3000 m, 3025 m, 3060 s; *m*-methoxybiphenyl (capillary film): 699 vs, 755 vs, 790 m, 860 m, 998 w, 1020 m, 1038 m, 1053 m, 1077 w, 1180 s, 1215 vs, 1270 sh, 1298 s, 1420 s, 1480 vs, 1570 s, 1600 vs, 2832 m, 2935 s, 2950 s, 3000 m, 3030 m, 3060 s; *p*-methoxybiphenyl (KCl disk): 688 m, 759 vs, 832 vs, 909 w, 1001 w, 1015 m, 1038 s, 1042 m, 1120 m, 1186 m, 1202 s, 1253 vs, 1271 m, 1290 s, 1441 m, 1450 m, 1466 m, 1490 vs, 1527 m, 1582 w, 1609 vs, 2835 m, 2935 s, 2960 s, 3000 m, 3030 m, 3070 m.

Infrared Spectra of Involatile Residues

These were recorded for the products from the various experiments, using the potassium chloride disk technique for sample preparation; all spectra were closely similar. A typical example (a sample prepared from the involatile residue from expt. 7) showed the following strong bands: 700, 755, 830, 1035, 1080, 1120, 1180, 1230, 1250, 1300, 1410, 1480, 1500, 1590, 1600, 2830, 2930–2960, 3000, 3030, 3060 cm^{-1}.

DISCUSSION

In most experiments, the sums of the yields of carbon dioxide, free benzoic acid, and benzoic acid from hydrolysis account almost quantitatively for the reacted benzoyl peroxide, and the yields of other products are quite reproducible. Although some losses are inevitable in the working-up processes, it appears that reasonably quantitative estimates of the various reaction products have been made.

In the following discussion, we interpret the anomalous behavior reported by previous workers, and attempt to show that anisole actually behaves in a typical manner in its reactions with the radicals from decomposing benzoyl peroxide.

The "Anomalous" Behavior of Anisole

The distribution of products in the present work differs from that reported previously (Suehiro (15)). Under conditions similar to those of expts. 4 and 5, Suehiro obtained the following yields of products (mole/mole peroxide): carbon dioxide, 0.51; free benzoic

acid, 1.22; methoxybiphenyls, 0.36. Thus, the contribution of the stoichiometric expression (A) to the total reaction is greater for our experiments.

$$Ph.OCH_3 + Ph.CO.O.O.CO.Ph \rightarrow Ph.C_6H_4.OCH_3 + CO_2 + Ph.CO_2H \quad (A)$$

Results similar to Suehiro's, in that yields of benzoic acid well in excess of 1 mole/mole peroxide were obtained, have also been reported by Augood (14) and Rondestvedt and Blanchard (19). Since the stoichiometric equations (A), summarizing phenylation, and (B), summarizing benzoyloxylation by benzoyl peroxide, predict a *maximum* yield of free benzoic acid of 1 mole/mole peroxide, processes other than (A) and (B) must account for the abnormally high yields of free benzoic acid.

$$Ph.OCH_3 + Ph.CO.O.O.CO.Ph \rightarrow Ph.CO.O.C_6H_4.OCH_3 + Ph.CO_2H \quad (B)$$

Augood and Williams (3) and Williams (6, p. 65) suggest that the high yields of benzoic acid noted in their reactions result from hydrogen abstraction from anisole by a benzoate radical, yielding the phenoxymethyl radical and benzoic acid (process (C)):

$$Ph.CO_2\cdot + Ph.OCH_3 \rightarrow Ph.CO_2H + Ph.OCH_2\cdot; \quad (C)$$

this radical is assumed to be incorporated in the high-boiling residues. If this suggestion is correct, it might be expected that 1,2-diphenoxyethane (formed by dimerization) and/or phenoxymethylanisoles (by nuclear substitution in anisole) would occur in the "methoxybiphenyl" fractions.* However, there were no indications of the presence of these substances in the methoxybiphenyls (see Experimental); furthermore, the infrared spectra of the involatile residues from the various experiments, and their methoxyl content (cf. Table I), indicate that these residues are probably of the quaterphenyl or tetrahydroquaterphenyl type to be expected from dimerization of the adduct between a phenyl radical and anisole (cf. Lynch and Pausacker (11), Pausacker (21), DeTar and Long (22)). Thus there is little supporting evidence for suggestions involving the extensive participation of process (C) in the total reaction scheme.

The key to an explanation of the anomalous yields of free benzoic acid obtained previously is simple; it is provided by the fact that although in the present work there is still an excess of free benzoic acid over the isolated nuclear substitution products, it is far less marked than reported previously. This implies that the anisole samples used in the various sets of experiments differ in some way. Since we noted in the course of the present work that our anisole samples contained traces of free phenol (which reacts extremely readily with benzoyl peroxide, yielding benzoic acid and other products (cf. refs. 23–25), it seems evident that the much higher yields of free benzoic acid obtained by previous workers are a result of the presence of higher proportions of free phenol as a contaminant in their anisole samples, and are not a consequence of any anomalous behavior of the anisole itself. Confirmation is afforded by the results of expts. 9 and 10, where deliberate addition of phenol to reaction mixtures markedly increased the yields of free benzoic acid.

It is also feasible that hydrolysis of the peroxide by small amounts of water present in the solvent might lead to increased yields of free benzoic acid (cf. the behavior of iodosobenzene dibenzoate and of lead tetrabenzoate (17, 26, 27); however, added water had no appreciable effect (expt. 11).

**Pfordte and Leuschner (20) have obtained 1,2-diphenoxyethane in low yield by irradiation of anisole with ultraviolet light, and Henbest, Reid, and Stirling (20(a)) have isolated phenoxymethylanisoles from the thermal decomposition of t-butyl peroxide in anisole.*

It is possible that another process may contribute to some of the excess of free benzoic acid noted in the present series of experiments, although there is no direct evidence in its favor: demethylation of anisole to phenol could occur by a route analogous to that commonly postulated for the dealkylation of tertiary amines (5, 28), i.e.

$$\mathrm{Ph.\ddot{O}{-}CH_3 + Ph.CO_2\cdot \rightarrow (Ph.\dot{O}{-}CH_3)^+ + Ph.CO_2^-}$$

$$\mathrm{(Ph.\dot{O}{-}CH_3)^+ + Ph.CO_2\cdot \rightarrow (Ph.\overset{+}{O}{=}CH_2) + Ph.CO_2H}$$

$$\mathrm{(Ph.\overset{+}{O}{=}CH_2) + H_2O \rightarrow Ph.OH + CH_2O + H^+.}$$

In unpublished experiments, we have shown that this reaction path is significant when substituted benzoyl peroxides react with anisole, since free phenol is generated from the substrate in sufficient amount for ready isolation from completed reaction mixtures. Cowley, Norman, and Waters (29) have found that methyl radicals effect dealkylation of anisole, and Kharasch and Huang (30) have shown that many phenol ethers can be dealkylated by free radicals, thus lending some support to this suggestion.

Nuclear Substitution Products

(a) Methoxyphenyl Benzoates

When benzenoid aromatic compounds react with benzoyl peroxide, benzoyloxylation (process (B) above) generally accompanies phenylation (process (A)) as a side reaction of varying importance.

Thus, benzoyloxylation has been observed when benzoyl peroxide decomposes in benzene (31), chlorobenzene (12, 31), nitrobenzene (12, 17), biphenyl (27, 31), *p*-dichlorobenzene (27), 1,2,3-trimethoxybenzene (32), pyridine (33), quinoline (33), and *p*-dimethoxybenzene (34). With the monosubstituted compounds, the extent of benzoyloxylation is small, and in some instances, the products (generally determined after hydrolysis to the corresponding substituted phenols) could have been formed by nucleophilic substitution of excess substrate during the hydrolysis step (e.g., nitrobenzene is converted into *o*- and *p*-nitrophenols by treatment with alkali in the presence of air (35, 36)).

However, in our present work we find that at 80° (expts. 6 and 7), the yields of methoxyphenyl benzoates are approximately one-half those of methoxybiphenyls; at higher temperatures, the extent of benzoyloxylation decreases, since the benzoyloxy radicals decarboxylate more rapidly.

These results imply that anisole is more reactive towards decomposing benzoyl peroxide than any monosubstituted benzene examined previously (since in a more reactive solvent, the benzoyloxy radical is more likely to react with the substrate before decarboxylating), conflicting with findings in previous studies employing the competitive method (3, 19, 37). Further discussion of this point is given below.

Acyloxylation of anisole under conditions favoring free-radical attack has been reported previously: with lead tetraacetate in acetic acid at 80°, *p*-methoxyphenyl acetate is a major product (38), while electrolysis of aqueous acetic acid in the presence of anisole gives mixed methoxyphenyl acetates (ortho:para ratio, 7:3) (39, 40).

In the present work, the most reliable values for the isomer distribution range from 65–82% *o*-methoxyphenol and from 18–35% *p*-methoxyphenol; no *m*-methoxyphenol could be detected. The large scatter in the isomer distributions for the various experiments (far beyond errors of analysis) probably reflects the occurrence of some preferential oxidation of the *p*-methoxyphenol during the hydrolysis of the methoxyphenyl benzoates

(which is effected under conditions known to oxidize phenols having electron-donating substituents (cf. ref. 40(*a*))). The apparent selectivity may thus result from the more rapid oxidation of *p*-methoxyphenol (for recent evidence indicating that *p*-methoxyphenol is oxidized more rapidly than *o*-methoxyphenol, see McClure and Williams (40(*b*))).

The occurrence of extensive ortho benzoyloxylation is in contrast to the results noted for thermal acetoxylation by Cavill and Solomon (38); it is suggested that the mechanism of ortho benzoyloxylation of anisole is analogous to that proposed for the benzoyloxylation of phenols by benzoyl peroxide (Walling and Hodgdon (41)). Thus, the second stage of the suggested dealkylation reaction (p. 1466) is replaced by coupling between the anisole ion–radical and a benzoate radical, followed by a cyclic rearrangement, i.e.

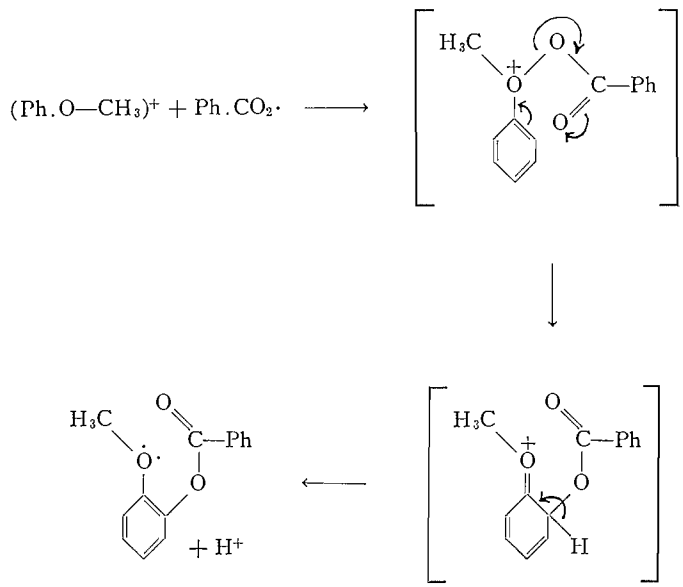

Walling and Hodgdon found that the reaction rates of phenols were increased by electron-donating substituents, and we find (34) that *p*-dimethoxybenzene is benzoyloxylated rapidly and almost quantitatively by benzoyl peroxide at 80° (apparent first-order rate constants for 0.125 *M* peroxide are (10^5k, sec^{-1}): *p*-dimethoxybenzene, 58.8; anisole, 8.3; benzene, 3.8), thus lending some slender support to the suggested mechanism.

A re-examination of the acetoxylation of anisole by lead tetraacetate in acetic acid, using infrared spectroscopy in the examination of products (42), further confirmed Cavill and Solomon's finding (38) of preferred para substitution (we could detect no *o*-methoxyphenyl acetate). It is possible that the differences in orientation between benzoyloxylation and acetoxylation reflect the occurrence of *polar* acetoxylation by lead tetraacetate (cf. Mosher and Kehr (43)).

Free phenol, present in our anisole samples, could lead to the occurrence of catechol in the phenolic fractions (arising from the above ortho benzoyloxylation, followed by hydrolysis), thus lessening the significance of the isomer ratios deduced above. This possibility was checked by extracting any phenolic material from completed reaction mixtures with aqueous sodium hydroxide, and brominating the extracted material; only

very small quantities (0.02 g from a reaction under conditions similar to expt. 6) were isolated. Therefore, this potential source of error is not significant (see also Experimental, p. 1462.

(b) Methoxybiphenyls

The isomer ratios for the free-radical phenylation of anisole at 154° (present work) and 100° (Suehiro (15)) and for methylation at 140° (Cowley *et al.* (29)) are assembled in Table II.

TABLE II

Percentages of isomers in the phenylation and the methylation of anisole

	Ortho	Meta	Para
Phenylation			
At 154°: analysis by gas–liquid chromatography	76.8	10.6	12.6
analysis by ultraviolet spectrophotometry	80	10	10
At 100°: analysis by infrared spectroscopy	67	18	15
Methylation			
At 140°: analysis by gas–liquid chromatography and infrared spectroscopy	74	15	11

Changes in orientation with temperature probably do not account for the differences between our results and Suehiro's, since isomer ratios in free-radical substitutions are not greatly temperature dependent. In our experience, infrared spectroscopy did not prove very suitable for the analysis of the isomer ratio in the phenylation of anisole, since considerable overlapping occurred among the various characteristic bands in the C—H out-of-plane deformation region (see Experimental); we believe that the figures based on gas–liquid chromatography are more reliable. However, the general pattern of the results is similar, and the agreement is reasonable on an absolute basis, although any revision of isomer distributions will have a large effect on partial rate factors.

Comparison of our results for phenylation of anisole with those for methylation reveals little difference in the behavior of the two radicals; in particular, no significant differences in the proportions of ortho isomer are noted, although it has been suggested (6, 29) that there may be slightly less steric hindrance to methylation than to phenylation. Since recent work (Weingarten (44)) indicates that the phenyl radical approaches almost perpendicularly to the plane of the aromatic ring in the substrate, steric effects will normally be insignificant. The appreciably lower meta:para ratio noted for phenylation probably reflects the greater electrophilicity of the phenyl radical.

High ortho:para ratios are typical of free-radical phenylations (for a summary, see Williams (7)), yet still await satisfactory explanation. Although preferred ortho–para orientation is to be expected from resonance theory if a σ-complex (the "Wheland intermediate" I*a*–I*b*–I*c*) is regarded as the transition state (since a σ-complex will be stabilized by conjugation or hyperconjugation by all substituents ortho or para to the site of attack), it is doubtful whether the formation of a σ-complex can be regarded as rate controlling in phenylations.

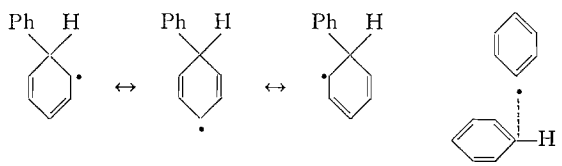

(Ia) (Ib) (Ic) (II)

The lack of selectivity noted in the phenylation and the methylation of naphthalene (12, 45–47) indicates that in the transition states for these reactions, the aromatic carbon being attacked is still partly conjugated with the rest of the system and the attacking radical is weakly bonded. Since the free-radical phenylations of all aromatic substrates are certainly very fast reactions with very low activation energies, showing low selectivity between the various possible positions of attack, and very little contrast in relative reaction rates (which, although derived using the somewhat suspect "competitive" method, possess empirical significance), a transition state involving a long "π-like" bond between radical and substrate (i.e., (II)) is probably appropriate for all phenylations (Walling (5, pp. 312, 434) has suggested that analogous "π-complexes" may be involved in other reactions involving the interaction of radicals with aromatic molecules). If so, however, the explanation of preferred ortho–para orientation noted above loses much of its force, although the relative stabilities of the various "π-complexes" may parallel those of the Wheland intermediates.

General Comments on the Significance of Partial Rate Factors and Relative Reactivities towards Phenyl-Radical Attack

Recent downward revisions of the scale of relative reactivities of aromatic compounds towards phenyl-radical attack (8), as evaluated by application of the "competitive" method, indicate that calculations of partial rate factors may not be meaningful for these reactions. Partial rate factors which are appreciably less than unity are noted for the meta positions of nitrobenzene (0.86), toluene (0.71), ethylbenzene (0.76), and isopropylbenzene (0.81). Further, if a relative reactivity of ca. 1.6 is assigned to anisole (cf. refs. 3, 6, 8, 14), then the calculated partial rate factor for a meta position is ca. 0.5. It is difficult to suggest a mechanism for *deactivation* of the *meta* positions relative to a benzene position.

Olah and his co-workers, in a study of another reaction (48) presenting a similar problem of low selectivity between different substrates, together with non-statistical isomer distribution (i.e., nitration of alkylbenzenes by nitronium tetrafluoroborate), suggest that partial rate factors are meaningless under such conditions, since the primary competition between substrates involves their molecular π-electron systems as entities, and not the individual positions of these molecules.

Unfortunately, such an interpretation accentuates the difficulty in suggesting a satisfactory explanation of the marked preference for ortho substitution found with phenylations. Waters' naive but remarkably fruitful suggestion that free radicals are essentially electrophilic (49–51) may be relevant, together with Rondestvedt and Blanchard's suggestion (19) that ortho substitution in nitrobenzene and benzonitrile results from preliminary radical complexing at the substituent (the region of highest electron density), followed by ready rearrangement to ortho product.

Further comment on the occurrence of concurrent benzoyloxylation and phenylation of anisole is pertinent. It has been noted previously (12, 19, 52) that application of the competitive method can lead to meaningful results only where side reactions are unimportant. This criterion is not satisfied for anisole, so that previously quoted relative reactivities (14, 19) can have little significance.

ACKNOWLEDGMENTS

Grateful acknowledgment is made to the donors of the Petroleum Research Fund, administered by the American Chemical Society, for support of this research, and also to the National Research Council of Canada, for an equipment grant.

REFERENCES

1. H. GELISSEN and P. H. HERMANS. Ber. **58**, 285 (1925).
2. D. H. HEY and W. A. WATERS. Chem. Revs. **21**, 169 (1937).
3. D. R. AUGOOD and G. H. WILLIAMS. Chem. Revs. **57**, 123 (1957).
4. O. C. DERMER and M. T. EDMISON. Chem. Revs. **57**, 77 (1957).
5. C. WALLING. Free radicals in solution. John Wiley and Sons, Inc., New York. 1957.
6. G. H. WILLIAMS. Homolytic aromatic substitution. Pergamon Press, London. 1960.
7. G. H. WILLIAMS. Chem. & Ind. (London), 1286 (1961).
8. S. ORMAN, D. H. HEY, and G. H. WILLIAMS. J. Chem. Soc. 565 (1961).
9. C. K. INGOLD and F. R. SHAW. J. Chem. Soc. 2918 (1927).
10. K. H. PAUSACKER. Current trends in heterocyclic chemistry. Butterworths Scientific Publications, London. 1958.
11. B. M. LYNCH and K. H. PAUSACKER. Australian J. Chem. **10**, 40 (1957).
12. B. M. LYNCH and K. H. PAUSACKER. Australian J. Chem. **10**, 165 (1957).
13. E. L. ELIEL, S. MEYERSON, Z. WELVART, and S. H. WILEN. J. Am. Chem. Soc. **82**, 2936 (1960).
14. D. R. AUGOOD. Ph.D. Thesis, University of London, London, England. 1952.
15. T. SUEHIRO. J. Chem. Soc. Japan, Pure Chem. Sect. **72**, 301 (1951).
16. A. R. KATRITZKY and P. SIMMONS. J. Chem. Soc. 2051 (1959).
17. B. M. LYNCH and K. H. PAUSACKER. Australian J. Chem. **10**, 329 (1957).
18. J. I. G. CADOGAN, D. H. HEY, and G. H. WILLIAMS. J. Chem. Soc. 794 (1954).
19. C. S. RONDESTVEDT and H. S. BLANCHARD. J. Org. Chem. **21**, 229 (1956).
20. K. PFORDTE and G. LEUSCHNER. Ann. **643**, 1 (1961).
20. (*a*) H. B. HENBEST, J. A. W. REID, and C. J. M. STIRLING. J. Chem. Soc. 5239 (1961).
21. K. H. PAUSACKER. Australian J. Chem. **10**, 49 (1957).
22. D. F. DETAR and R. A. J. LONG. J. Am. Chem. Soc. **80**, 4742 (1958).
23. S. L. COSGROVE and W. A. WATERS. J. Chem. Soc. 3189 (1949); 388 (1951).
24. J. J. BATTEN and M. F. R. MULCAHY. J. Chem. Soc. 2948 (1956).
25. J. J. BATTEN. J. Chem. Soc. 2959 (1956).
26. D. H. HEY, C. J. M. STIRLING, and G. H. WILLIAMS. J. Chem. Soc. 1475 (1956).
27. M. KARELSKY and K. H. PAUSACKER. Australian J. Chem. **11**, 39 (1958).
28. L. HORNER. J. Polymer Sci. **18**, 438 (1955).
29. B. R. COWLEY, R. O. C. NORMAN, and W. A. WATERS. J. Chem. Soc. 1799 (1959).
30. M. S. KHARASCH and R. L. HUANG. J. Org. Chem. **17**, 669 (1952).
31. D. I. DAVIES, D. H. HEY, and G. H. WILLIAMS. J. Chem. Soc. 562 (1961).
32. P. L. PAUSON and B. C. SMITH. J. Org. Chem. **18**, 1403 (1953).
33. K. H. PAUSACKER. Australian J. Chem. **11**, 200 (1958).
34. B. M. LYNCH. To be published. (For a preliminary account, see 6th Report of Research under the Sponsorship of the Petroleum Research Fund. American Chemical Society, Washington. 1962.)
35. A. WOHL. Ber. **32**, 3486 (1899).
36. M. J. S. DEWAR. The electronic theory of organic chemistry. Oxford University Press, Oxford. 1949. p. 168.
37. R. HUISGEN and G. SORGE. Ann. **566**, 162 (1950).
38. G. W. K. CAVILL and D. H. SOLOMON. J. Chem. Soc. 1404 (1955).
39. T. HAYASHI and C. L. WILSON. Abstracts of Papers, 126th Meeting of the American Chemical Society. 1954. p. 78.
40. C. L. WILSON and W. T. LIPPINCOTT. J. Am. Chem. Soc. **78**, 4290 (1956).
40. (*a*) H. ERDTMAN. Proc. Roy. Soc. (London), A, **143**, 191 (1933).
40. (*b*) J. D. MCCLURE and P. H. WILLIAMS. J. Org. Chem. **27**, 627 (1962).
41. C. WALLING and R. B. HODGDON. J. Am. Chem. Soc. **80**, 228 (1958).
42. B. M. LYNCH and R. B. MOORE. Unpublished experiments.
43. W. A. MOSHER and C. L. KEHR. J. Am. Chem. Soc. **75**, 3172 (1953).
44. H. WEINGARTEN. J. Org. Chem. **26**, 730 (1961).
45. D. I. DAVIES, D. H. HEY, and G. H. WILLIAMS. J. Chem. Soc. 1878 (1958).
46. J. A. KENT and R. O. C. NORMAN. J. Chem. Soc. 1724 (1959).
47. D. I. DAVIES, D. H. HEY, and G. H. WILLIAMS. J. Chem. Soc. 3112 (1961).
48. G. A. OLAH, S. J. KUHN, and S. H. FLOOD. J. Am. Chem. Soc. **83**, 4571 (1961).
49. W. A. WATERS. Trans. Faraday Soc. **37**, 770 (1941).
50. W. A. WATERS. The chemistry of free radicals. Oxford University Press, Oxford. 1946. p. 183.
51. J. F. TILNEY-BASSETT and W. A. WATERS. J. Chem. Soc. 3123 (1959).
52. D. F. DETAR. J. Am. Chem. Soc. **83**, 1014 (1961).

NOTES

DÉCOMPOSITION PYROLYTIQUE DE BORATES D'HEPTYLE

J. M. LALANCETTE

Brandenberg et Galat (1) rapportent que la déshydratation d'alcools peu volatils en présence d'acide orthoborique conduit aux alcènes correspondants avec de bons rendements. Ces auteurs expliquent cette réaction par formation initiale d'un orthoborate qui se décomposerait par la suite pour donner l'hydrocarbure non saturé. Cependant, O'Connor et Nace (2) postulent plutôt l'existence d'un métaborate comme intermédiaire à la formation de l'hydrocarbure. Leur argument s'appuie sur le fait qu'un orthoborate est relativement stable au traitement thermique et se transforme en métaborate en présence d'acide orthoborique. Récemment, Young et Anderson (3) ont pu montrer que l'on pouvait éliminer la possibilité de formation d'un métaborate comme intermédiaire à la déshydratation et apportent des évidences en faveur d'un intermédiaire orthoborique. Le mécanisme que proposent ces derniers auteurs, consiste en une décomposition de l'ester orthoborique en alcène et acide orthoborique suivie d'une déshydratation graduelle de l'acide orthoborique en anhydride borique. Cependant, j'ai constaté que la pyrolyse de l'orthoborate d'heptyle, en phase liquide et sous des conditions expérimentales permettant un dégagement rapide des produits volatils de la masse réactionnelle, a donné un mélange de deux moles d'hydrocarbure et d'une mole d'alcool par mole d'ester orthoborique décomposé. Le pourcentage relativement élevé d'alcool dans le distillat peut être expliqué en postulant un mécanisme d'élimination interne, la forme cyclique intermédiaire II constituant l'étape initiale de la réaction.

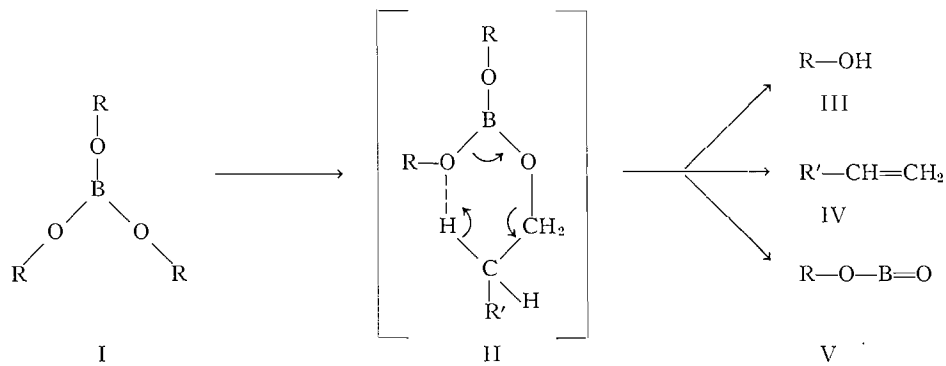

L'existence de II est d'ailleurs facilité par le caractère de lien double partiel que présente la liaison B—O (4). Un déplacement électronique concerté, du type postulé par Hurd et Blunck (5) pour expliquer la pyrolyse des acétates, conduit alors à la production d'une mole d'alcool III, d'hydrocarbure IV et de métaborate V. Ce métaborate, instable à la température de la réaction (6), se décompose par la suite pour donner une mole supplémentaire d'hydrocarbure.

Le mécanisme proposé justifie donc la proportion relative d'alcool et d'alcène dans le distillat donné par la pyrolyse. On conçoit cependant que si l'alcool est peu volatil ou si le temps de contact entre l'alcool généré *in situ* et le milieu réactionnel est trop long, une déshydratation subséquente de cet alcool viendra augmenter la proportion d'hydrocarbure jusqu'aux valeurs rapportées par Brandenberg et Galat (1). C'est probablement pour ces raisons que Young et Anderson ne retrouvent que peu d'alcool (0.040 mole par mole de borate) à la pyrolyse de l'orthoborate d'octyle.

Le mécanisme postulé incluant un métaborate, il a semblé indiqué d'effectuer une pyrolyse de cet ester afin d'étudier la composition du mélange d'hydrocarbure ainsi obtenu en regard de la composition trouvée à la pyrolyse de l'orthoborate correspondant. La grande divergence de composition (42% d'alcène monosubstitué pour l'orthoborate et 62% avec le métaborate, sous les mêmes conditions expérimentales) montre bien que la décomposition de l'ester orthoborique ne s'est pas accomplie par simple transformation de l'orthoborate en métaborate, ce qui vient s'ajouter aux arguments de Young et Anderson (3). Cependant, une contribution partielle d'une forme métaborique à l'élimination demeure possible en regard du mécanisme proposé.

PARTIE EXPÉRIMENTALE

1. Préparation de l'orthoborate d'heptyle

L'ester du titre a été préparé à partir d'heptanol "Reagent" et d'acide orthoborique "U.S.P." en quantités stoïchiométriques (distillation azéotropique de l'eau formée avec du benzène) et redistillé sous vide. P.é.: 175° sous 0.5 mm; n_D^{23}: 1.4300. Décrit (7): p.é.: 185° sous 2 mm; n_D^{20}: 1.4280. Spectre infrarouge (CCl_4): pas de bandes dans la région de 3400 cm^{-1}; bandes à 1415 cm^{-1} (forte), à 1330 cm^{-1} (très forte), 1050 cm^{-1} (moyenne), 1030 cm^{-1} (moyenne).

2. Pyrolyse

La pyrolyse de l'orthoborate d'heptyle a été effectuée dans un ballon Claisen d'une capacité de 50 ml muni d'une colonne haute de 10 cm, permettant de maintenir un reflux de l'ester sans en provoquer la distillation. Le système, préalablement purgé par de l'azote sec, a été gardé sous atmosphère inerte, à la pression atmosphérique au cours de la réaction qui dure de trois à quatre heures. La température de la masse réactionnelle demeure à 315–325° tout au cours de la réaction qui est arrêtée lorsqu'on voit apparaître un début de solidification. Le distillat brut est fractionné par distillation, en hydrocarbure et alcool. La nature de l'alcool est établie par ses constantes physiques et son spectre infrarouge. Le mélange d'hydrocarbure est analysé par chromatographie en phase gazeuse (colonne de 4 m, 15% éther benzylique sur Chromosorb No. 154-0262 Perkin–Elmer, élution par hélium, 50 cc/min, température: 100° C) et les pics identifiés par comparaison avec des chromatogrammes d'heptène synthétiques (8) de structure connue. Heptène-1: p.é.: 93° sous 750 mm; n_D^{23}: 1.4002. Décrit (9): p.é.: 94.9° sous 760 mm; n_D^{20}: 1.3999. Heptène-2 (mélange cis et trans): p.é.: 95° sous 750 mm; n_D^{23}: 1.4043. Décrit (9): p.é.: 98.1–98.4° sous 760 mm; n_D^{20}: 1.4041. Le distillat présente un indice de réfraction constant tout au cours de la pyrolyse et renferme des traces d'eau qu'on n'a pu évaluer avec précision. Une expérience de ce type effectuée à partir de 0.0241 mole d'orthoborate donne 0.0195 mole d'alcool et 0.0400 mole d'hydrocarbure. À la chromatographie en phase gazeuse, la fraction hydrocarbure indique 42% de monosubstitution, 25% d'alcène disubstitué cis et 33% d'alcène disubstitué trans. On assume ici que conformément aux mentions de la littérature (10), l'isomère trans sort le premier. Spectre infrarouge de la fraction hydrocarbure (CCl_4): bandes 990 cm^{-1} (faible), 965 cm^{-1} (moyenne), 905 cm^{-1} (moyenne).

3. Préparation du métaborate de n-heptyle

Le métaborate a été préparé à partir d'heptanol "Reagent" (0.240 mole) et d'acide orthoborique "U.S.P." (0.240 mole), l'eau formée étant éliminée par distillation azéotropique avec du toluène. Le toluène est distillé sous pression réduite et l'ester est maintenue à 100° C sous 0.7 mm, pendant 2 heures, sous bonne agitation pour enlever les dernières traces de solvant. Ce mode de purification a été adopté du fait que les métaborates sont rapportés instables à la distillation (6). On obtient ainsi une huile incolore, visqueuse; n_D^{23}: 1.4415. Spectre infrarouge (CCl_4): pas de bandes dans la région de 3400 cm^{-1}; bandes à 1470 cm^{-1} (moyenne), 1410 cm^{-1} (forte), 1335 cm^{-1} (très forte), 1080 cm^{-1} (moyenne). Calculé pour $BO_2C_7H_{15}$: C, 59.20; H, 10.64; B, 7.62. Trouvé: C, 59.22; H, 10.88; B, 7.72.

4. Pyrolyse

La pyrolyse du métaborate est faite suivant la méthode décrite précédemment, sauf que la température de la masse réactionelle demeure à 300° C et que l'opération dure 2 heures. Le distillat (15.9 g à partir de

35.0 g de métaborate) est fractionné en hydrocarbure (n_D^{23}: 1.4015; p.é.: 85–130° sous 750 mm; 10.3 g) et alcool (n_D^{23}: 1.4252; p.é.: 175–185° sous 750 mm; 3.6 g). Analyse chromatographique en phase gazeuse de la fraction hydrocarbure (méthode décrite plus haut): alcène monosubstitué: 62%; alcène interne: 19% cis; 19% trans.

Je désire remercier le Conseil National de Recherches du Canada de l'aide financière qu'il m'a accordée dans la poursuite de ce travail.

1. W. Brandenberg et A. Galat. J. Am. Chem. Soc. **72**, 3275 (1950).
2. G. L. O'Connor et H. R. Nace. J. Am. Chem. Soc. **77**, 1578 (1955).
3. D. M. Young et C. D. Anderson. J. Org. Chem. **26**, 2158 (1961).
4. R. L. Werner et K. G. O'Brien. Australian J. Chem. **8**, 355 (1955).
5. C. D. Hurd et F. H. Blunck. J. Am. Chem. Soc. **60**, 2421 (1938).
6. H. Schiff et E. Bechi. Compt. rend. **61**, 697 (1865).
7. M. F. Lappert. Chem. Revs. **56**, 959 (1956).
8. H. J. Lucas et R. T. Dillon. J. Am. Chem. Soc. **50**, 1460 (1928).
9. F. J. Soday et C. E. Boord. J. Am. Chem. Soc. **55**, 3293 (1933).
10. H. S. Knight. Anal. Chem. **30**, 9 (1958).

Reçu le 22 décembre 1961.
Département de Chimie,
Université de Sherbrooke,
Sherbrooke, Qué.

THE UNIT CELL, SPACE GROUP, INDEXED X-RAY POWDER PATTERN, AND MAGNETIC SUSCEPTIBILITY OF $VCl_3.2N(CH_3)_3$*

L. D. Calvert and C. M. Pleass†

This note records magnetic susceptibility measurements and X-ray data for the solid complex $VCl_3.2N(CH_3)_3$. The study was undertaken with the hope of showing that the vanadium atom was five-coordinated in solid $VCl_3.2N(CH_3)_3$. A trigonal bipyramidal coordination is not yet established for a solid vanadium complex and there is considerable interest in the structures of vanadium complexes (1). Recent measurements (2, 3) of magnetic susceptibility and molecular weight of $VCl_3.2N(CH_3)_3$ in nitrobenzene and chlorobenzene solutions have shown the vanadium to be five-coordinated. Since solid $VCl_3.2N(CH_3)_3$ sublimes readily at $\approx$100° C a non-ionic, molecular, five-coordinated structure seemed possible. Fivefold coordination in solution has been established for similar compounds such as $TiCl_3.2NMe_3$ (4), $NiBr_3.2PEt_3$ (5), $CoCl_3.2PEt_3$ (6), $VCl_3(OPr_3)_2$, etc. (7) but in no case is the solid structure known.

Magnetic Susceptibility Measurements

The magnetic susceptibility of a powdered sample of $VCl_3.2N(CH_3)_3$ sealed into a thin-walled glass ampoule was measured between 100 and 300° K using the Curie method with Henry pole-pieces (8). No decomposition was detected on an X-ray powder photograph of the sample after the measurements were completed. The results are plotted in Fig. 1. The effective magneton number, assuming no orbital contribution, is $\mu_{eff} = 2.49$ B.M. This is somewhat less than that calculated for two unpaired spins (2.83 B.M.) or that observed for $VCl_3.2N(CH_3)_3$ in chlorobenzene, 2.72 B.M. (2). This value does not establish a trigonal bipyramidal coordination for the vanadium since an ionic arrangement, as in solid PCl_5 (9), or shared octahedra would also have two unpaired spins.

*Issued as N.R.C. No. 6868.
†National Research Laboratories Postdoctoral Fellow. Present address: Bell Telephone Laboratories, Murray Hill, New Jersey, U.S.A.

35.0 g de métaborate) est fractionné en hydrocarbure (n_D^{23}: 1.4015; p.é.: 85–130° sous 750 mm; 10.3 g) et alcool (n_D^{23}: 1.4252; p.é.: 175–185° sous 750 mm; 3.6 g). Analyse chromatographique en phase gazeuse de la fraction hydrocarbure (méthode décrite plus haut): alcène monosubstitué: 62%; alcène interne: 19% cis; 19% trans.

Je désire remercier le Conseil National de Recherches du Canada de l'aide financière qu'il m'a accordée dans la poursuite de ce travail.

1. W. Brandenberg et A. Galat. J. Am. Chem. Soc. **72**, 3275 (1950).
2. G. L. O'Connor et H. R. Nace. J. Am. Chem. Soc. **77**, 1578 (1955).
3. D. M. Young et C. D. Anderson. J. Org. Chem. **26**, 2158 (1961).
4. R. L. Werner et K. G. O'Brien. Australian J. Chem. **8**, 355 (1955).
5. C. D. Hurd et F. H. Blunck. J. Am. Chem. Soc. **60**, 2421 (1938).
6. H. Schiff et E. Bechi. Compt. rend. **61**, 697 (1865).
7. M. F. Lappert. Chem. Revs. **56**, 959 (1956).
8. H. J. Lucas et R. T. Dillon. J. Am. Chem. Soc. **50**, 1460 (1928).
9. F. J. Soday et C. E. Boord. J. Am. Chem. Soc. **55**, 3293 (1933).
10. H. S. Knight. Anal. Chem. **30**, 9 (1958).

Reçu le 22 décembre 1961.
Département de Chimie,
Université de Sherbrooke,
Sherbrooke, Qué.

THE UNIT CELL, SPACE GROUP, INDEXED X-RAY POWDER PATTERN, AND MAGNETIC SUSCEPTIBILITY OF $VCl_3.2N(CH_3)_3$*

L. D. Calvert and C. M. Pleass†

This note records magnetic susceptibility measurements and X-ray data for the solid complex $VCl_3.2N(CH_3)_3$. The study was undertaken with the hope of showing that the vanadium atom was five-coordinated in solid $VCl_3.2N(CH_3)_3$. A trigonal bipyramidal coordination is not yet established for a solid vanadium complex and there is considerable interest in the structures of vanadium complexes (1). Recent measurements (2, 3) of magnetic susceptibility and molecular weight of $VCl_3.2N(CH_3)_3$ in nitrobenzene and chlorobenzene solutions have shown the vanadium to be five-coordinated. Since solid $VCl_3.2N(CH_3)_3$ sublimes readily at $\approx$100° C a non-ionic, molecular, five-coordinated structure seemed possible. Fivefold coordination in solution has been established for similar compounds such as $TiCl_3.2NMe_3$ (4), $NiBr_3.2PEt_3$ (5), $CoCl_3.2PEt_3$ (6), $VCl_3(OPr_3)_2$, etc. (7) but in no case is the solid structure known.

Magnetic Susceptibility Measurements

The magnetic susceptibility of a powdered sample of $VCl_3.2N(CH_3)_3$ sealed into a thin-walled glass ampoule was measured between 100 and 300° K using the Curie method with Henry pole-pieces (8). No decomposition was detected on an X-ray powder photograph of the sample after the measurements were completed. The results are plotted in Fig. 1. The effective magneton number, assuming no orbital contribution, is $\mu_{eff} = 2.49$ B.M. This is somewhat less than that calculated for two unpaired spins (2.83 B.M.) or that observed for $VCl_3.2N(CH_3)_3$ in chlorobenzene, 2.72 B.M. (2). This value does not establish a trigonal bipyramidal coordination for the vanadium since an ionic arrangement, as in solid PCl_5 (9), or shared octahedra would also have two unpaired spins.

Issued as N.R.C. No. 6868.

†*National Research Laboratories Postdoctoral Fellow. Present address: Bell Telephone Laboratories, Murray Hill, New Jersey, U.S.A.*

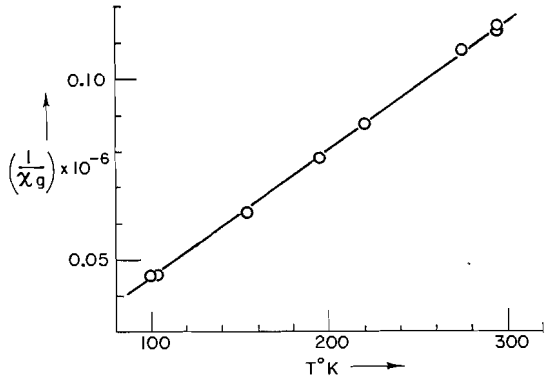

FIG. 1. Reciprocal mass susceptibility values plotted against absolute temperature.

A reversible reproducible color change from a "permanganate pink" to a pale green, without change of crystal form, was observed at about 170° K. Since there is no corresponding change in the χ/T curve the electron distribution must remain substantially unaffected.

Crystallographic Observations

$VCl_3.2N(CH_3)_3$ is strongly deliquescent, so the crystals used were slowly sublimed under reduced pressure into thin-walled glass capillaries which were then sealed off. Rosette-shaped aggregates were the most common form but a few, apparently hexagonal, tablets and one or two pyramidally terminated needles were found. Most crystals proved to be imperfect or multiple on X-ray examination. One selected crystal (0.15×0.15×0.10 mm) proved to be perfect and was used to record the bulk of the X-ray data; a second, less perfect, was used to confirm the data. Optical goniometry of the enclosed crystals was not possible but comparison of the X-ray precession photographs with the hexagonal tablet selected showed that the tablet face was (100) and that {010}, {110}, and {111} were the other forms present. The hexagonal outline is only superficial and arises from the angles $111 \wedge 010 \wedge \bar{1}1\bar{1} \wedge \bar{1}\bar{1}\bar{1}$ being 52°, 52°, and 76°.

The crystals were orthorhombic, *mmmPn—a*, a = 9.838 Å, b = 10.14 Å, c = 13.14 Å (all ±0.3%), vol. = 1311 Å^3, Z = 8, D_c = 2.79 g/cm^3, D_m 2.9 ±0.2 g/cm^3 (pycnometrically in dry varsol), F.W. = 275.55. The possible space groups are $Pnma(D_{2h}^{16})$ and $Pn2_1a(C_{2v}^{9})$ but no choice was made, although *Pnma* was the more probable.

X-Ray powder photographs were obtained from separate samples crushed, loaded, and sealed into thin-walled glass capillaries in an argon-filled dry box. Photographs of coarsely and finely powdered specimens were compared and no evidence of decomposition detected. Although Cu K radiation gave acceptable results, Cr K radiation gave a pattern more suitable for indexing. The powder pattern, indexed to d = 2.30 Å is given in Table I. The pattern, as observed, is given down to d = 1.439 Å; beyond this, the lines present are too weak to be of value in identification. The powder pattern of $TiCl_3.2N(CH_3)_3$ (4), which is almost identical, is given in columns 5 and 10 of Table I. It can also be indexed on a similar orthorhombic unit cell with a = 9.8 Å, b = 10.2 Å, and c = 13.1 Å. (The original data (4) do not allow greater precision in the axes.) $TiCl_3.2N(CH_3)_3$ is thus isomorphous with $VCl_3.2N(CH_3)_3$ and also has the diffraction symbol *mmmPn—a*.

TABLE I

X-Ray powder data for $VCl_3.2N(CH_3)_3$ and $TiCl_3.2N(CH_3)_3$*
($VCl_3.2N(CH_3)_3$: orthorhombic, $Pn—a$, a = 9.838 Å, b = 10.14 Å, c = 13.14 Å
$TiCl_3.2N(CH_3)_3$: orthorhombic, $Pn—a$, a = 9.8 Å, b = 10.2 Å, c = 13.1 Å)

d, Å	I/I_1	hkl	d, calc.	d, Å†	d, Å	I/I_1	hkl	d, calc.	d, Å†
7.8	13	101	7.88	—	2.67	11	321	2.69	2.66
6.5	26	002	6.57	6.73			033	2.67	
6.2	100 b‡	111	6.22	6.15	2.62	3	303	2.62	—
5.45	4	102	5.46	5.47	2.58	3	133	2.58	—
5.05	17	020	5.07	5.09			322	2.54	
4.79	9	112	4.81	4.87	2.53	7	105	2.54	2.55
4.61	6	201	4.61	—			040	2.53	
4.25	9	121	4.26	4.22	2.40	7			2.41
		013	4.02		2.36	2			—
4.01	3	022	4.01	3.99	2.31	9 b			2.33
		103	4.00		2.25	1§			—
3.92	3	202	3.94	—	—				2.06
3.70	17	113	3.72	3.70	1.96	11 b			1.97
		122	3.72		1.91	1 b			—
3.51	21	220	3.53	3.55	1.861	4 b			1.86
3.39	4	221	3.41	—	1.809	2			1.82
		004	3.28		1.750	4			1.76
3.27	13	031	3.27	3.27	1.722	1			1.72
		203	3.27		1.690	2			—
		104	3.11		1.644	3			—
3.10	17	213	3.11	3.14	1.616	1			—
		222	3.11		1.543	1§			1.55
		131	3.11		1.524	1			—
3.00	1§	311	3.04	—	1.471	1 b			1.47
2.92	21	302	2.93	2.95	1.439	1			1.41
2.85	3	132	2.87	—	‖				
2.77	9	230	2.78	2.79					

*Vanadium-filtered Cr radiation; camera diameter, 114.6 mm; cutoff, 20 Å; Intensities obtained by visual comparison with a logarithmic interval density scale; columns 1 to 4 refer to $VCl_3.2N(CH_3)_3$; column 5 refers to $TiCl_3.2N(CH_3)_3$.
†Data of Antler and Laubengayer (ref. 4).
‡b = broad line.
§Line barely visible, d-value not accurate.
‖Plus other, weak lines at lower d-values.

In the case of $SbCl_5$ (10) the space group and unit cell contents were sufficient to establish trigonal, bipyramidal coordination around the antimony atom. Unfortunately this is not the case for $VCl_3.2N(CH_3)_3$ and a full structural study was not possible in the limited time available. It is hoped that this study will be undertaken later.

The authors wish to acknowledge with gratitude the help of Dr. F. R. Ahmed, who calculated the d-values using an IBM650 program and Miss M. McLellan, who prepared the X-ray powder photographs.

1. A. E. Baker and H. M. Haendler. Inorg. Chem. **1**, 127 (1962).
2. G. W. A. Fowles and C. M. Pleass. Chem. & Ind. (London), **1743** (1955).
3. G. W. A. Fowles and C. M. Pleass. J. Chem. Soc. 2078 (1957).
4. M. Antler and A. W. Laubengayer. J. Am. Chem. Soc. **77**, 5250 (1955).
5. G. Giacometti, V. Scatturin, and A. Turco. Ricerca sci. **27**, 2449 (1957).
6. K. A. Jensen and B. Nygaard. Acta. Chem. Scand. **3**, 474 (1949).
7. K. Issleib and G. Bohn. Z. anorg. u. allgem. Chem. **301**, 188 (1959).
8. R. D. Heyding, J. B. Taylor, and M. L. Hair. Rev. Sci. Instr. **32**, 161 (1961).
9. D. Clark, H. M. Powell, and A. F. Wells. J. Chem. Soc. **642** (1942).
10. S. M. Ohlberg. J. Am. Chem. Soc. **81**, 811 (1959).

Received April 3, 1962.
Division of Applied Chemistry,
National Research Council,
Ottawa, Canada.

THE MEASUREMENT OF STREAMING POTENTIALS

G. H. E. SIMS AND R. G. GILSON

Many workers who have measured the streaming potentials of powders have used a layer of filter paper supported on a perforated platinum disk at each end of the cell to contain the powder. An exception has been Buchanan (1), who relied solely on perforated disks. This was possible with the materials he used since they were all available in large particle sizes, i.e. up to 500 μ; but with fine powders it is impracticable to drill sufficiently small holes in platinum. During some experiments in which the streaming potentials of phosphor particles of size 10–20 μ were being measured it was found that the pores of the filter paper were becoming clogged with powder as the experiments proceeded and thus the rate of flow of the streaming solution was being seriously reduced. This effect would give low values of E/P, where E is the streaming potential and P is the applied pressure, since the pressure drop in passing through the filter paper would be disproportionately high compared with the pressure drop through the powder. Also, the potential produced at the compacted interface between the powder and the cellulose fibers of the filter paper could produce unwanted results.

This difficulty was appreciated by Edelberg and Hazel (2), who measured the streaming potential of the filter paper used in their experiments. Then by assuming that the filter paper in an ordinary cell accounted for not more than 1% of the total hydrodynamic resistance they were able to calculate that the error introduced by it into the calculation of zeta potentials was well under 1%. It was felt that the arbitrary figure of 1% may not be justified even in the case of fairly large particles, e.g. −60 to +150 mesh, and certainly not in the case of very small particles. Accordingly a cell was constructed to determine the effect of filter paper on streaming potential measurements.

EXPERIMENTAL

The basic cell was that of Lauffer and Gortner (3) and consisted of two B14 ground-glass sockets joined end to end and fitted with two B14 cones. Perforated platinum disks (A and D) were placed over the ends of the cones and were connected by platinum leads to a valve voltmeter. The powder was contained in the cell formed by the two electrodes. Two platinum tubes (B and C) of 0.5-mm bore and 1.5-mm O.D. were sealed into the side of the cell at approximately equal spacing. The outer ends of the tubes were sealed into 1-mm-bore capillary tubing, which in turn was connected to mercury manometers. The bare platinum between the capillary tubing and the wall of the cell was connected to the potential measuring circuit. Thus we now have a cell in which the ratio E/P may be determined for three sections, A–B, B–C, and C–D, as well as the overall ratio A–D.

The material used in the cell was willemite phosphor which had been sintered at 1200° C for 4 hours in air and then ground to give a particle size fraction between 60 and 150 mesh. The material was elutriated several times in distilled water before use to remove 'fines' and was finally dried at 120° C.

The cell was filled by pouring into it a sludge of the material in distilled water, under a slightly reduced pressure and with the ends of the capillaries plugged to prevent loss of the powder through the side arms. The plugs were removed after filling and the capillary tubes were connected to two mercury manometers.

The streaming solution was distilled water and it was found that by increasing the streaming pressure slowly and continually adjusting the height of the mercury in the manometers, it was possible to obtain an air-free liquid/mercury interface in the manometer limbs close to the end of the capillary tubes. There was usually very little loss of material through the platinum tubes while these adjustments were being made. The streaming solution flows up through the cell from A to D.

When the streaming potential between the two perforated electrodes (A–D) had reached a steady value, potentials and pressures between points A–B, B–C, C–D, and A–D were measured. In order to allow for the polarization of the platinum electrodes the pressure was returned to zero and the potentials were measured again.

RESULTS

Several cells were prepared using filter paper (Whatman No. 54) and 200-mesh silk gauze to contain the powder, and several runs were made with each cell. Typical results for the ratio E/P are given in Table I for the two methods of containing the powder.

TABLE I

Ratios of E/P for two different methods of containing the powder

Containing material					
Filter paper (Whatman No. 54)			Silk gauze (200 mesh)		
Expt. No.	Measurement points	E/P (mv/cm Hg)	Expt. No.	Measurement points	E/P (mv/cm Hg)
1	A–B	26.3	3	A–B	63.2
1	B–C	64.0	3	B–C	61.2
1	C–D	11.1	3	C–D	43.8
1	A–D	34.4	3	A–D	56.8
2	A–B	25.3	4	A–B	63.1
2	B–C	61.3	4	B–C	62.4
2	C–D	10.0	4	C–D	43.7
2	A–D	32.8	4	A–D	55.0

It is to be expected that if the filter paper or gauze are contributing to the hydrodynamic resistance to any extent, then the effect will be most apparent at the upper end (C–D), where the powder is being forced against the containing material. It will be less evident at A–D, and at B–C a true value of E/P will be obtained. This is shown to be so by the experimental results.

Perhaps the most notable feature is the extent of the pressure drop at D when filter paper is used. It is also appreciable when 200-mesh gauze is used.

These results indicate that great care must be taken when comparing results by different workers using different methods of containing the material of their plugs. None would appear to give absolute values unless no hydrodynamic constraint is used. The best condition for accuracy would be the use of a filter of the same mesh size as the particles.

Due to difficulties associated with setting up the apparatus (particularly the fragility of the platinum/glass seals) it has not been possible to make extensive measurements of streaming potentials using the apparatus described above, and in further experiments it was decided that the error involved in using 200-mesh silk gauze would be accepted. The good agreement which has been subsequently found in measurements on different cells of the same material has shown that this error is constant.

Two interesting consequences arise from these experiments. The first is that a comparison of electrokinetic potentials derived from streaming or electroosmotic measurements with those obtained from electrophoretic measurements will show a poor correspondence if the potentials of the former are measured in a cell in which there is an extraneous hydrodynamic constraint. Bull (4) has found that the zeta potentials of quartz and cellulose derived from a streaming method were much lower than those derived from electrophoretic measurements.

The second consequence is that it is difficult to measure true zeta potentials of particles in the size range between say 5 μ and 50 μ. Below 5 μ an electrophoretic method can be used but for larger particles the effect of gravity becomes increasingly troublesome.

Above 50 μ it is possible to use an electroosmotic or streaming method by containing the particles in a cell by means of a fine-mesh gauze, as has been done in these experiments. The results, however, will become increasingly affected by the containing material as the particle size of the powder decreases, so that in the intermediate range 5–50 μ there is no easy method of electrokinetic measurement which will provide a true zeta potential.

ACKNOWLEDGMENT

This work was carried out at the Research and Development Laboratories of Electronic Tubes Ltd., High Wycombe, Bucks, England, and permission of the Directors to publish this note is gratefully acknowledged.

1. A. S. Buchanan and E. Heymann. Proc. Roy. Soc. (London), A, **195**, 150 (1948).
2. R. Edelberg and J. F. Hazel. Trans. Electrochem. Soc. **96**, 13 (1949).
3. M. A. Lauffer and R. A. Gortner. J. Phys. Chem. **42**, 641 (1938).
4. H. B. Bull. J. Phys. Chem. **39**, 577 (1935).

Received February 28, 1962.
Research and Development Laboratories,
Electronic Tubes Ltd.,
High Wycombe, Bucks, England.

Canadian Journal of Chemistry

Issued by THE NATIONAL RESEARCH COUNCIL OF CANADA

VOLUME 40 AUGUST 1962 NUMBER 8

THE CONSTITUTION OF A SYNTHETIC XYLAN

I. GENERAL STRUCTURAL FEATURES

G. G. S. DUTTON AND A. M. UNRAU[1]

Department of Chemistry, University of British Columbia, Vancouver, British Columbia

Received March 19, 1962

ABSTRACT

The polysaccharide was obtained by polymerization of D-xylose at 140° C in the presence of phosphorous acid. Complete hydrolysis of the xylan followed by bromine oxidation showed that the synthetic polymer contained only xylose. Periodate oxidation resulted in formation of a considerable quantity of formaldehyde, the origin of which is not known. Periodate oxidation of borohydride-reduced xylan gave additional formaldehyde and, from this, the average D.P. of the polymer was estimated to be about 55. Complete hydrolysis of the polyalcohol gave ethylene glycol, glycerol, and xylose in a ratio of 2:9:1. Partial hydrolysis gave ethylene glycol, glycerol, and at least seven non-reducing components. Hydrolysis of the fully methylated xylan gave tri-, di-, mono-methyl xyloses and xylose in a 32:32:18:5 ratio, and a carbonyl band was evident in the infrared spectrum of the hydrolyzate. No such band was evident in the hydrolyzate of the unsubstituted xylan. The xylan is highly branched and contains some D-xylofuranose units.

In contrast to the relatively ordered structures of naturally occurring enzymatically synthesized polysaccharides, it has usually been found that synthetic polysaccharides have highly random and branched structures (1–5). Recent investigations (6) on a synthetic glucan (7) have shown that almost all possible linkages were present and that glucofuranose residues occurred in the polymer. In contrast to the apparently simpler structure of a synthetic xylan investigated by Bishop (8), the results reported in this paper from experiments on a synthetic xylan prepared by Mora and associates (9) indicate that its structure is complex.

Complete hydrolysis of the xylan gave only D-xylose, which was obtained in crystalline form. Bromine oxidation of the hydrolyzate followed by adsorption of the xylonic acid on anion exchange resin left no residue that reacted with *p*-anisidine trichloroacetate or ammoniacal silver nitrate spray reagents, thus indicating the absence of any polyols. The facile partial hydrolysis of the xylan suggested the presence of some xylofuranose units (Table I). The oligosaccharides surviving the mild acid hydrolysis were presumed to consist primarily of xylopyranose units. The specific rotation of the xylan, $[\alpha]_D^{22}$ 45°, suggested that both alpha and beta glycosidic linkages were probably present, but if some of the D-xylose residues were present as open-chain acetals this point is less certain.

The rapid production of formaldehyde (1.52 mg per xylose unit after 20 minutes and 2.35 mg after 210 minutes, with no significant change thereafter) upon periodate oxidation of the xylan under controlled conditions (pH 4.0–4.5, 5° C) indicated the oxidation of some primary hydroxyl groups. A structural feature to accommodate this observation cannot

[1]*Present address: Department of Plant Science, University of Manitoba, Winnipeg, Manitoba.*

TABLE I

Partial hydrolysis of xylan: percent composition of hydrolyzate

Time (hr)	$[\alpha]_D$	Xylose	Disacch.	Tri- + tetra-sacch.	Oligosacch.
0	45°	—	—	—	100
0.5	46.5	9.0	2.6	4.4	84
1	50.3	9.8	2.8	4.4	83
1.5	50.8	10.0	3.0	4.6	83
2	50.8	10.1	3.0	4.7	83
4	50.8	10.5	3.1	4.6	82
6	51.4	11.1	3.1	4.9	81
27	52.4	11.7	3.2	5.2	80
48	53.0	12.5	3.3	5.9	78

be suggested with certainty at this point. Under the conditions of the oxidation, it does not seem probable that any appreciable overoxidation would have occurred. A possible explanation may be that there are present some open-chain xylose residues in which the C_4 and C_5 hydroxyls are not substituted. Periodate oxidation would result in the formation of formaldehyde from C_5 and the acetal system would be readily hydrolyzed by dilute acid. Periodate oxidation of the reduced ($NaBH_4$) xylan resulted in the liberation of additional formaldehyde, and by application of a reported procedure (10), the average degree of polymerization was estimated to be a minimum of 55. The assumption is made that the reducing end-group is not substituted at C_2 and hence gives 1 mole of formaldehyde on reduction and treatment with periodate.

The periodate uptake (0.91 mole per sugar residue, constant after 18 hours) indicated the presence of periodate-resistant xylose units in the xylan. Reduction ($NaBH_4$) of the xylan polyaldehyde followed by complete hydrolysis of the polyalcohol gave ethylene glycol (from non-reducing xylopyranose end-units and $1 \rightarrow 2$ linked pyranose units), glycerol (from internal xylopyranose and xylofuranose units, also from external xylofuranose units), and xylose in an approximate ratio of 2:9:1. About 7–8% xylose was not degraded. Since non-reducing xylofuranose end-units are present, the quantity of ethylene glycol formed in the periodate degradation compared to the estimated D.P. of the xylan cannot be used to calculate the approximate number of branch points in the molecule.

The controlled hydrolysis (11) of the polyalcohol gave ethylene glycol, glycerol, xylose, and at least seven oligosaccharide fragments with varying R_{xylose} values in several solvent systems. Free xylose is believed to have originated from relatively labile furanoside linkages. The oligosaccharides were composed of xylose and glycerol in varying ratios and further details concerning these will be reported later.

Methylation of the xylan was accomplished by employing successively the Haworth, Kuhn, and Purdie procedures. Only after extended and vigorous treatment with Purdie's reagents was the xylan fully methylated; methoxyl content 39.2%, no hydroxyl band in the infrared spectrum. The methylated xylan, $[\alpha]_D^{22}$ 42° (*c*, 8.2 in $CHCl_3$), was soluble in petroleum ether containing 4.5–5% chloroform. Hydrolysis of the methylated xylan gave tri-, di-, and mono-methyl xyloses and free xylose in a molar ratio of 32:32:18:5, respectively. The identity of the methylated sugars will be reported in a separate communication but it may be noted that the rotation, $[\alpha]_D^{22}$ 22.3° in water, of the trimethyl fraction indicated the presence of 37.5% 2,3,5-tri-*O*-methyl-D-xylofuranose; hence non-reducing xylofuranose end-units were present in the xylan. Since the methylated xylan was hydrolyzed with sulphuric acid under conditions known to minimize demethylation (12), the presence of xylose in the hydrolyzate indicates the occurrence of fully substituted residues in the xylan.

The infrared spectrum of the hydrolyzate of the methylated xylan showed absorption bands at 3400, 2930, 2825, 1725, 1650, 1460 cm^{-1}. The definite absorption at 1725 cm^{-1} suggested that aldehydic carbonyl groups might be present. It seemed unlikely that this absorption was due to furfural degradation products, since when a sample of the original xylan was hydrolyzed under similar conditions the band at 1725 cm^{-1} was absent. Xylose residues methylated at C_4 and C_5 would exist in the aldehyde form and could conceivably be responsible for absorption in the carbonyl region. As suggested previously, xylose residues occurring in the xylan in the open-chain form and not substituted at C_4 and C_5 would explain the rapid formation of formaldehyde upon periodate oxidation. The above spectroscopic observation lends support to this proposal.

EXPERIMENTAL

Chromatographic separations were carried out using the descending technique and Whatman No. 1 and 3MM paper. Solvent systems employed were A, ethyl acetate:acetic acid:water (8:2:2); B, ethyl acetate:pyridine:water (9:2:2); and C, butanone:water azeotrope. Spray reagents were D, *p*-anisidine trichloroacetate and E, ammoniacal silver nitrate solutions. Unless otherwise stated, evaporations were carried out under reduced pressure at a bath temperature of 40° C. Melting points are uncorrected and specific rotations were taken at 22±2° C.

Hydrolysis of Xylan

A quantity (750 mg) of xylan, $[\alpha]_D$ 45° (*c*, 2.0 in water), was dissolved in 0.2 *N* sulphuric acid (30 ml), and the solution boiled for 10 hours. The solution was neutralized ($BaCO_3$), deionized, and evaporated to a thick sirup which crystallized upon standing. After recrystallization from ethanol, D-xylose had m.p. and mixed m.p. 143–145°, $[\alpha]_D$ 18° (*c*, 1.8 in water).

Bromine Oxidation of Xylan Hydrolyzate

A portion (about 500 mg) of the hydrolyzate was oxidized with bromine in the usual manner until an aliquot of the solution no longer reduced Fehlings solution. After removal of excess bromine from the solution by aeration, the solution was passed through anion exchange resin. Evaporation of the neutral effluent left no residue which would react with either spray reagent D or E.

Partial Hydrolysis of Xylan

An aliquot (80 mg) of the polymer in 0.1 *N* hydrochloric acid (3 ml) was left at room temperature. The appearance of hydrolysis products was followed by paper chromatographic analysis in solvent A using the phenol – sulphuric acid method (13) to determine xylose and xylose oligosaccharides. The course of the hydrolysis was also followed polarimetrically. The change in the optical rotation and the extent of hydrolysis are summarized in Table I.

Periodate Oxidation, Reduction ($NaBH_4$), Complete Hydrolysis

Xylan (176 mg, 1.325 mmoles) was dissolved in water (20 ml) and the solution acidified with 6 *N* acetic acid (2 ml). After the solution was cooled, 0.5 *M* sodium periodate (5 ml) was added and the oxidation allowed to proceed at 5° C. Formaldehyde was determined (10) after $\frac{1}{3}$, $3\frac{1}{2}$, 12, 48, and 72 hours. After $\frac{1}{3}$ hour, 1.52 mg formaldehyde was produced per xylose unit and 2.43 mg after $3\frac{1}{2}$ hours, with no significant increase thereafter. After 72 hours, periodate consumption was determined and the xylan had consumed 0.905 mole of periodate per xylose unit. To the solution was added barium chloride and barium carbonate, and after filtration, sodium borohydride (200 mg) was added. The reduction was allowed to proceed overnight at room temperature, after which time the solution was acidified with hydrochloric acid and evaporated to dryness. Borate was removed by several evaporations with methanol and the residue hydrolyzed with sulphuric acid. The solution was deionized, concentrated, and the sirupy product chromatographed. Compounds corresponding to glycerol, ethylene glycol, and xylose were detected. The ratio of these was determined chromatographically using the periodate – chromotropic acid procedure (10) for the alcohols and the phenol – sulphuric acid method (13) for the determination of xylose. The ratio of ethylene glycol:glycerol:xylose thus found was about 2:9:1. A further quantity (650 mg) of xylan was treated as described above and the combined hydrolyzates resolved by paper chromatography (Whatman 3MM paper) using solvent A. The three compounds were located by spraying guide strips, and subsequently eluted. *Ethylene glycol*, 47 mg, was reacted with *p*-nitrobenzoyl chloride in pyridine solution to give the corresponding di-*p*-nitrobenzoate, m.p. and mixed m.p. 139–141° C. *Glycerol*, 435 mg, was similarly converted to the corresponding tri-*p*-nitrobenzoate, m.p. and mixed m.p. 188–190° C. D-*Xylose*, 70 mg, crystallized spontaneously and after recrystallization from ethanol had m.p. and mixed m.p. 143–144° C, $[\alpha]_D$ 17.7° (*c*, 1.4 in water).

Periodate Oxidation of Reduced ($NaBH_4$) Xylan and Determination of D.P. (10)

Xylan (230 mg) was dissolved in water (20 ml) and to the solution was added sodium borohydride (100 mg). The reduction was allowed to proceed at room temperature for 24 hours. The solution was acidified with acetic acid (2 ml), cooled to 5° C, and 0.5 *M* sodium periodate (5 ml) was added. Formaldehyde was determined (10) after $\frac{1}{3}$, $3\frac{1}{2}$, 12, 48, and 72 hours. After $3\frac{1}{2}$ hours, 4.20 mg formaldehyde had been formed per xylose unit, with no significant change thereafter. On the assumption that the extra formaldehyde formed in the periodate oxidation of the reduced xylan arose from the xylitol end-groups and that each such group produced 1 molecular proportion of formaldehyde, the approximate D.P. of the xylan was 55. The periodate consumption was determined after 72 hours and 0.92 mole of periodate had been consumed per pentose unit. The oxidation mixture was subsequently treated in the same manner as described in the previous section. Chromatography of the final product showed the presence of ethylene glycol, glycerol, and xylose. The ratio of these was determined and found to be about 2:10:1.

Partial Hydrolysis of Polyalcohol (11)

A quantity (100 mg) of xylan was dissolved in water (20 ml), cooled to 5° C, and 0.5 *M* periodic acid (5 ml) was added. After 72 hours, when 0.91 mole of periodate had been consumed per xylose unit, the solution was neutralized ($BaCO_3$), filtered, and sodium borohydride (75 mg) was added. The solution stood at room temperature overnight and was evaporated to dryness. Borate was removed by treatment with methanol containing 1% hydrogen chloride (14) and the residue was finally dissolved in 0.1 *N* sulphuric acid (30 ml) and left for 8 hours. The solution was neutralized ($PbCO_3$) and evaporated. Chromatographic examination of the sirupy residue indicated the presence of ethylene glycol, glycerol, xylose, and at least seven non-reducing components with a considerable range of R_{xylose} values. Further details of these periodate degradations will be reported separately.

Methylation of the Xylan

A quantity (4.0 g) of xylan was treated in the usual way with the Haworth methylating reagents, followed by two successive methylations using methyl iodide, silver oxide, and dimethylformamide (15). The product (4.59 g), a brittle, yellow glass, showed an OH band in the infrared spectrum and was therefore methylated three times with Purdie's reagents over extended periods (3–4 days). The final product (4.35 g) was dissolved in petroleum ether (30–60°) containing 5% chloroform, and a small quantity of insoluble material was removed by filtration. Evaporation of the solvent left a yellow, resinous solid which showed no OH character in its infrared spectrum and contained 39.2% methoxyl. Hydrolysis of a portion (80 mg) was effected using sulphuric acid (12). After neutralization ($BaCO_3$) and deionization, the solution was evaporated. Chromatographic examination using solvent C indicated the presence of tri-, di-, and mono-methyl xyloses and a small amount of free xylose. The ratio of the above-mentioned xylose methyl ethers was estimated chromatographically using the phenol – sulphuric acid reagent (13). The approximate molar ratio of tri-, di-, mono-methyl xyloses and xylose thus found was 32:32:18:5. The components of the hydrolyzate were subsequently separated by passage through a cellulose–hydrocellulose column using solvent C as the irrigant. The trimethyl fraction had a specific rotation of 22.3° in water, indicating that it was composed of 2,3,4- and 2,3,5-tri-*O*-methyl-D-xyloses in the ratio of 62.5:37.5. The identification of the other components will be reported later.

ACKNOWLEDGMENTS

This investigation was supported by a research grant (RE 7652) from the Division of General Medical Science, U.S. Public Health Service, to whom we express our thanks. We are also indebted to Miss J. Hunter for skillful technical assistance.

REFERENCES

1. P. T. Mora, J. W. Wood, P. Maury, and B. G. Young. J. Am. Chem. Soc. **80**, 693 (1958).
2. P. W. Kent. Biochem. J. **55**, 361 (1954).
3. C. R. Ricketts and C. E. Rowe. J. Chem. Soc. 3809 (1955).
4. H. W. Durand, M. F. Dull, and R. S. Tipson. J. Am. Chem. Soc. **80**, 3691 (1958).
5. J. da S. Carvalho, W. Prins, and C. Schuerch. J. Am. Chem. Soc. **81**, 4054 (1954).
6. G. G. S. Dutton and A. M. Unrau. Can. J. Chem. **40**, 1196 (1962).
7. P. T. Mora and J. W. Wood. J. Am. Chem. Soc. **80**, 685 (1958).
8. C. T. Bishop. Can. J. Chem. **34**, 1255 (1956).
9. P. T. Mora, J. W. Wood, and V. W. McFarland. J. Am. Chem. Soc. **82**, 3418 (1960).
10. A. M. Unrau and F. Smith. Chem. & Ind. (London), 330 (1957).
11. I. J. Goldstein, G. W. Hay, B. A. Lewis, and F. Smith. Abstracts of Papers, 135th Meeting of the American Chemical Society, Boston, Mass. April, 1959. p. 3D.
12. I. Croon, G. Herrström, G. Küll, and B. Lindberg. Acta Chem. Scand. **14**, 1338 (1960).
13. N. Dubois, J. K. Hamilton, K. A. Gilles, P. A. Rebers, and F. Smith. Anal. Chem. **28**, 350 (1956).
14. D. R. Briggs, E. F. Garner, R. Montgomery, and F. Smith. Anal. Chem. **28**, 1333 (1956).
15. R. Kuhn, I. Löw, and N. Trischmann. Ber. **90**, 203 (1957).

RELATIVE SIGNS OF GEMINAL AND VICINAL PROTON–PROTON COUPLING CONSTANTS IN α,β-DIPHENYLPROPIONIC ACID AND ITS METHYL ESTER

ROBERT R. FRASER
Department of Chemistry, University of Ottawa, Ottawa, Ontario
Received March 13, 1962

ABSTRACT

It has been shown that the geminal and vicinal coupling constants are of opposite sign in α,β-diphenylpropionic acid and its methyl ester. The significance of the results is discussed.

We recently reported the findings that from analysis of the n.m.r. spectra of a series of dioxolane derivatives (see Fig. 1) the sign of the geminal coupling constant J_{BC} was

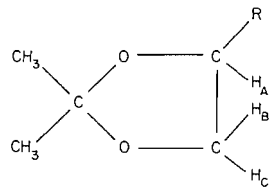

FIG. 1. The structures of the dioxolane derivatives from which the signs of the coupling constants between protons A, B, and C were determined.

opposite to that of the vicinal coupling constants J_{AB} and J_{AC} (1). Since the theoretical calculations of vicinal coupling constants by Karplus (2) and of geminal coupling constants by Karplus, Gutowsky, and Grant (3, 4) predicted the geminal and vicinal coupling constants to have the same sign as long as the bond angle between the geminal hydrogens is less than 125°, our results were surprising. Previously, in styrene oxide (3, 5), β-*p*-nitrophenyl-β-propiolactone (3), and several monosubstituted ethylene oxides (5, 6) the relative signs had been in accord with theory. Now, further examples of compounds in which the geminal and vicinal coupling constants have opposite signs have been reported, namely diethyl sulphite (7), epichlorohydrin (8), and hexadeuteriocyclohexanol (17), and prompts us to report our analysis of the spectra of α,β-diphenylpropionic acid and methyl α,β-diphenylpropionate.

In order to determine with any degree of certainty the relative signs of coupling constants between protons in a three-spin system from a complete analysis of the spectrum it is necessary that each of the three protons be slightly shifted in resonance position from one another. This is by definition an ABC system. Then the correctness of the parameters obtained by analysis is judged from a comparison of the theoretical and experimentally measured intensities. Final proof of the results is provided by comparing the spectrum measured at a lower frequency with that predicted from analysis of the original spectrum. It should be mentioned that a second, very useful method of determination of relative sign exists. This is the method of spin-decoupling, which has been described in detail by Freeman (9). We wished to examine the relative signs of coupling constants in open-chain aliphatic compounds and so examined a number of ethane derivatives of the general

structure XCH_2CHXY, where X and Y are substituents possessing appreciable magnetic anisotropy. Styrene dibromide, styrene glycol dibenzoate, α-bromobibenzyl, and α,β-diphenylpropionitrile produced spectra in which the aliphatic protons appeared as an ABX or AX_2 pattern and so were not studied in detail. On the other hand both α,β-diphenylpropionic acid and its methyl ester gave good ABC spectra.

A detailed description of a rigorous method of analysis of this type of spectrum has been given by Waugh and Castellano (10, 11). We have followed this method in our analysis, using an IBM 650 to perform the calculations. Any terms used subsequently, such as *arrangements*, *groupings*, *sets* of eigenvalues, will appear in italics and have the exact meaning defined by Waugh and Castellano (10). The spectrum of α,β-diphenylpropionic acid measured at 60 Mc/sec is shown in Fig. 2. Eleven transitions in all are

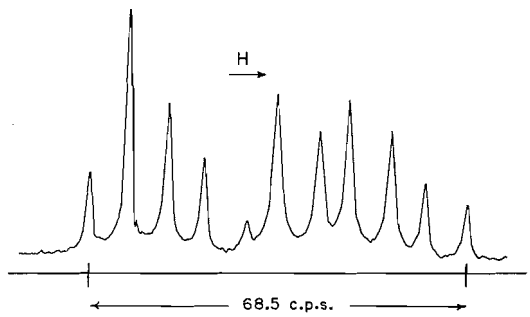

FIG. 2. Spectrum of a 25% solution (w/v) of α,β-diphenylpropionic acid in carbon tetrachloride at 60.0 Mc/sec.

visible and are assigned from the repeated spacings as being, in the first-order approximation, a triplet at low field (proton A) adjacent to two quartets (protons B and C), each at successively higher field. Since there are no visible combination bands,* there is no ambiguity in the assignment of this *grouping*. From the four possible *arrangements* four *sets* of eigenvalues are obtained. And from each *set* of eigenvalues two sets of chemical shifts, $\Delta\nu$'s, and coupling constants, J's, are calculated. In all, six sets of $\Delta\nu$'s and J's were obtained, two sets being discarded by failure to satisfy the condition of real roots. The theoretical intensities of all 15 transitions were then calculated for each of the six sets. From the obvious discrepancy between calculated and observed intensities three of the sets were immediately eliminated. The remaining three sets gave calculated intensities in fair agreement with the observed intensities, as is shown in Table I. To determine which set of parameters was correct the spectrum of the acid was also measured at 24.288 Mc/sec. This spectrum is compared in Fig. 3 with the spectra predicted from each of the three sets of chemical shifts and coupling constants given in Table I. Only for set I does the predicted spectrum agree with the observed spectrum to within 0.2 cycle/sec. It should be pointed out that although the chemical shifts and coupling constants are given to two decimal places they are estimated to be accurate only to ±0.08 cycle/sec.

The spectrum of methyl α,β-diphenylpropionate measured at 60 Mc/sec is shown in Fig. 4. Utilization of the same method of analysis provided three sets of chemical shifts and coupling constants compatible in theoretical intensities with the observed intensities. The comparison is shown in Table II. The spectrum of the ester was then measured at

A combination band arises from a transition which is forbidden in the first-order limit. It becomes increasingly intense when the chemical shifts between the nuclei become smaller.

TABLE I

A comparison of calculated and observed intensities in the 60 Mc/sec spectrum of α,β-diphenylpropionic acid

(The observed line positions have been adjusted to bring them into agreement with the rules of repeated spacings; $\Delta\nu_B = \nu_B - \nu_A$, the chemical shift in cycles/sec between protons A and B)

Line position			Calculated intensities			
Observed	Adjusted	Assignment	I	II	III	Observed intensities
—	−18.62	Comb.	<0.01	<0.01	<0.01	0.00
0.00	0.00	A	0.16	0.16	0.13	0.17
7.55	7.43	A	0.18	0.20	0.20	0.58
	7.47	A	0.26	0.26	0.27	
15.00	14.90	A	0.39	0.38	0.36	0.38
21.58	21.58	B	0.20	0.15	0.23	0.22
29.04	29.05	B	0.05	0.09	0.02	0.05
—	33.52	Comb.	0.01	<0.01	0.04	0.00
34.97	34.98	B	0.45	0.49	0.44	0.41
42.46	42.45	B	0.31	0.27	0.34	0.27
47.66	47.67	C	0.44	0.44	0.46	0.37
55.09	55.10	C	0.31	0.31	0.29	0.29
61.06	61.07	C	0.14	0.14	0.11	0.15
68.50	68.50	C	0.10	0.11	0.11	0.11
—	82.65	Comb.	<0.01	<0.01	<0.01	0.00
		Standard deviation	0.046	0.048	0.048	

Sets of parameters used to calculate the intensities

	$\Delta\nu_B$	$\Delta\nu_C$	J_{AB}	J_{AC}	J_{BC}
I	24.92	47.43	7.96	7.29	−13.75
II	25.05	47.69	7.09	7.97	13.25
III	24.72	46.96	−8.58	7.75	14.19

TABLE II

A comparison of calculated and observed intensities in the 60 Mc/sec spectrum of methyl α,β-diphenylpropionate

Line position			Calculated intensities			
Observed	Adjusted	Assignment	I	II	III	Observed intensities
—	−20.92	Comb.	<0.01	<0.01	<0.01	0.00
0.00	0.00	A	0.15	0.14	0.12	0.19
6.45	6.44	A	0.15	0.18	0.18	0.23
8.28	8.31	A	0.27	0.29	0.30	0.30
14.72	14.75	A	0.41	0.39	0.37	0.37
19.16	19.16	B	0.26	0.20	0.26	0.25 (assumed)
27.51	27.47	B	0.03	0.08	0.03	0.05
32.13	32.13	B	0.45	0.48	0.44	0.37
35.60	35.66	Comb.	0.02	<0.01	0.03	0.04
40.46	40.44	B	0.29	0.24	0.30	0.29
48.39	48.39	C	0.40	0.42	0.42	0.34
54.82	54.83	C	0.31	0.31	0.29	0.29
61.37	61.36	C	0.15	0.15	0.13	0.18
67.80	67.80	C	0.11	0.12	0.13	0.14
—	80.51	Comb.	<0.01	<0.01	<0.01	0.00
		Standard deviation	0.041	0.047	0.040	

Sets of parameters used to calculate intensities

	$\Delta\nu_B$	$\Delta\nu_C$	J_{AB}	J_{AC}	J_{BC}
I	22.01	47.57	8.85	6.50	−13.56
II	22.26	48.00	6.73	8.11	12.88
III	21.92	47.41	−9.10	6.39	13.80

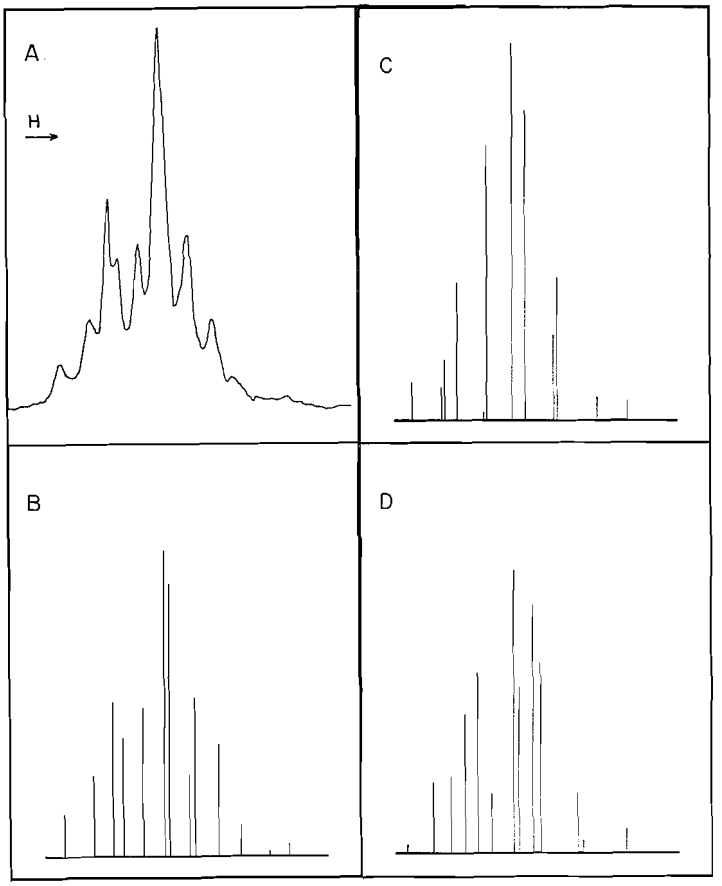

FIG. 3. Experimental and calculated spectra of α,β-diphenylpropionic acid. A. Spectrum of a 25% solution in carbon tetrachloride measured at 24.288 Mc/sec. Spectra B, C, and D were calculated using parameters I, II, and III in Table I, with the chemical shifts reduced in proportion to the change in frequency.

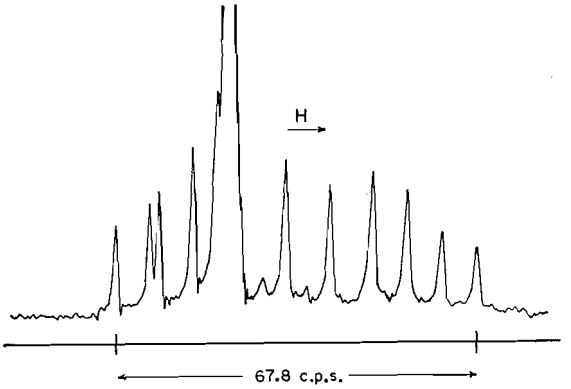

FIG. 4. Spectrum of a 14% (w/v) solution of methyl α,β-diphenylpropionate in carbon tetrachloride at 60.0 Mc/sec. The protons on the ester methyl group are responsible for the strong absorption in the center of the spectrum.

24.288 Mc/sec and compared with the spectra predicted from each of the three sets of parameters given in Table II. This comparison, as seen in Fig. 5, shows agreement in all

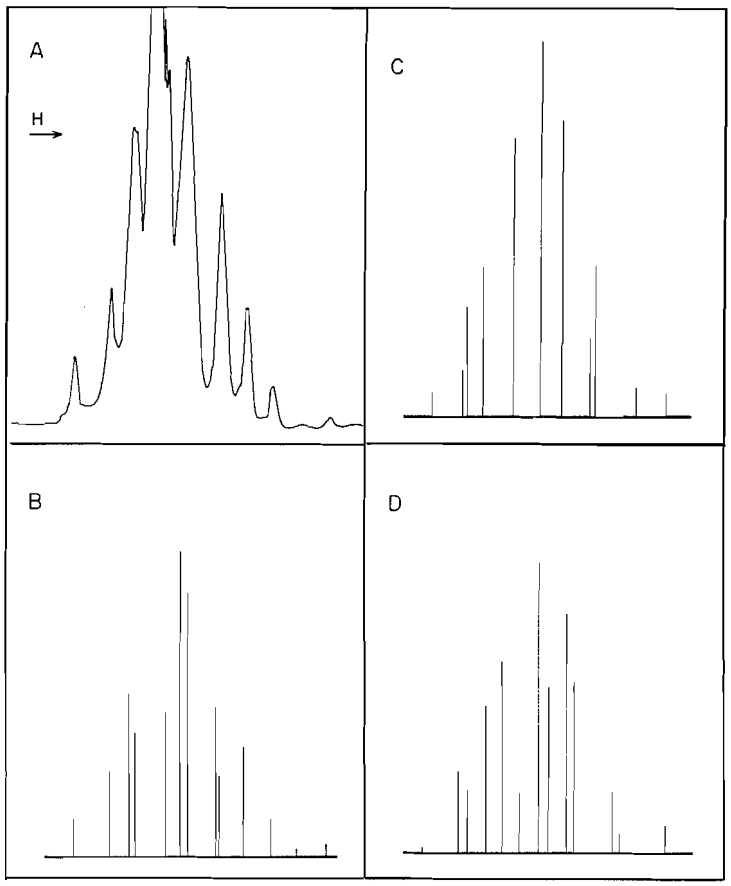

FIG. 5. Experimental and calculated spectra of methyl α,β-diphenylpropionate. A. Spectrum of a 14% (w/v) solution in carbon tetrachloride at 24.288 Mc/sec. Spectra B, C, and D were calculated using the parameters I, II, and III in Table II, with the chemical shifts reduced in proportion to the change in frequency.

line positions to within 0.4 cycle/sec for set I. Errors greater than 1 cycle/sec are found in the spectra predicted by the other sets. Thus in both compounds J_{BC} is opposite in sign to J_{AB} and J_{AC}.

Unambiguous assignment of the proton alpha to the carboxyl was made by measuring the spectra of the α-deuterated acid and ester. Exchange of the proton for deuterium was performed by heating the methyl ester with sodium in O-deuterated methanol. The spectrum of the aliphatic protons of the α-deuteroester was a pair of doublets of spacing 13.6 cycles/sec. Although the lower-field doublet was partially obscured by absorption of the ester methyl group, the spectrum was clearly devoid of absorption in the low-field region of the A proton. Hydrolysis of the deuterated ester in heavy water gave the α-deuterated acid, whose spectrum showed a pair of doublets of spacing 13.8 cycles/sec and no absorption in the region of the A proton. It is therefore concluded that in both compounds the proton attached to the alpha carbon atom appears at lowest field. The

magnitude of the spacing of the doublets agrees with the coupling constant obtained by the ABC analysis for each compound and serves to confirm its correctness.

To determine which of the remaining two protons represent signal B, deuterium gas was added to an aqueous solution of the sodium salt of *trans*-α-phenylcinnamic acid using 10% palladium on carbon as catalyst. The spectrum of the product showed only a single broadened peak whose chemical shift corresponded to that of proton C. If we assume that the deuterium added cis, the three protons can be assigned the positions shown in Fig. 6.

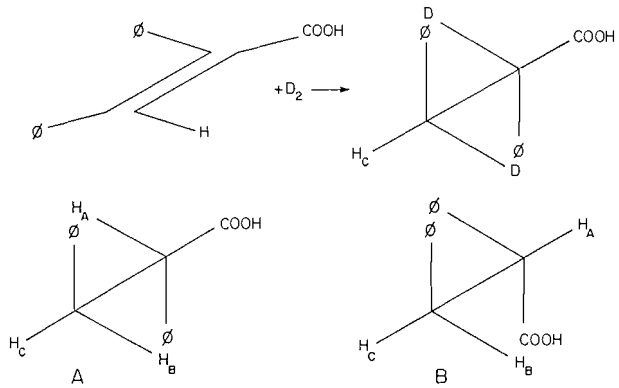

FIG. 6. Perspective formulae of the dideutero acid and the two most probable conformations of α,β-diphenylpropionic acid. The protons are labelled according to the conclusions of the deuteration experiments.

The two most probable conformations for the acid are shown. Since a phenyl group is larger than carboxyl,* conformation A would be more populated, as is indicated by J_{AB} being larger (7.96) than J_{AC} (7.29). This follows from the relation of the magnitude of J to the dihedral angle θ defined by two hydrogens on adjacent carbon atoms (2). When the two hydrogens are trans to each other ($\theta = 180°$) the coupling constant is three times as large as when the two hydrogens are gauche ($\theta = 60°$). Since carbomethoxyl is smaller than carboxyl, even less of conformation B should be present in the methyl ester. The larger difference between J_{AB} (8.85) and J_{AC} (6.50) in the methyl ester is attributed to this increase in the proportion of conformation A. Since proton A is in the alpha position, J_{BC} represents the geminal coupling constant. Thus in both α,β-diphenylpropionic acid and its methyl ester the geminal coupling constant is opposite in sign to the vicinal coupling constants.

It is now apparent that this opposition of sign is not simply peculiar to dioxolane derivatives. The question arises as to whether it is the theoretical calculations of the vicinal or of the geminal coupling constants which are at variance with the experimental evidence.

It would be most satisfying if all the experimental results could be accommodated by the present theory in a necessarily modified form. An indication of the point at which modification is required is most strikingly illustrated by Reilly's analysis of epichlorohydrin (8). For this compound the coupling constants were reported as shown in Fig. 7. Between protons 1, 2, and 3 all coupling constants are positive, as has been found in other epoxides. For protons 3, 4, and 5 the geminal and vicinal coupling constants are of opposite sign, as is the case in our substituted ethanes and diethyl sulphite. And further, it can be seen that this difference in relative sign is due to a change in sign of the *vicinal*,

**The A value, the difference in Gibbs free energy between axial and equatorial position of the substituent on a cyclohexane ring, has been found to be 2.6 for phenyl (12), 1.7 for carboxyl (13), and 1.1 for carbethoxyl (14). Presumably the carbomethoxyl group would have an A value slightly less than 1.1.*

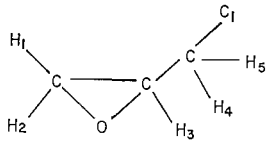

FIG. 7. Results of Reilly's analysis of epichlorohydrin.

$J_{1,2} = 5.0$	$J_{3,4} = -6.6$	$J_{1,4} = -0.2$
$J_{1,3} = 2.4$	$J_{3,5} = -4.0$	$J_{2,4} = 0.6$
$J_{2,3} = 4.0$	$J_{4,5} = 11.7$	$J_{2,5} = -0.1$
		$J_{1,5} = -0.1$

not the geminal, coupling constants $J_{1,2}$ and $J_{4,5}$, which both have the same sign. It must be realized that the possibility of other solutions of the spectrum of epichlorohydrin quite different in relative signs could exist, for this compound requires an exceedingly complex analysis. More results must be obtained before too much reliance can be placed on the above analysis.

EXPERIMENTAL

All 60.0 Mc/sec spectra were measured on a Varian V-4302 high-resolution n.m.r. spectrometer. The line positions in each spectrum were determined by the side-band technique and are reported as the average of 10 spectra. Intensities were obtained from peak heights and are also reported as the average of 10 spectra. They are generally considered to be accurate to within 10% of the reported value. The 24.288 Mc/sec spectra were recorded on a Varian V-4300B high-resolution n.m.r. spectrometer. The line positions reported are the average of four spectra.

α,β-Diphenylpropionic Acid

Condensation of benzyl chloride with phenylacetonitrile gave α,β-diphenylpropionitrile, m.p. 56–57.5° (lit. m.p. 58° (15)). Acid hydrolysis of the nitrile gave α,β-diphenylpropionic acid, which after two recrystallizations from heptane was seen to be a mixture of crystalline forms, m.p. 79–84° C (lit. m.p., plates 95–96°, prisms 88–89°, fused solid 82° (15)).

Methyl α,β-Diphenylpropionate

The above acid was converted to methyl α,β-diphenylpropionate, m.p. 31.5–32.5° (lit. m.p. 34° (15)), by treatment with diazomethane.

trans-α-Phenylcinnamic Acid

This acid was prepared by the procedure of Buckles and Hausman (16) in 45% yield. The product was a white solid, m.p. 169–170.5° (lit. m.p. 172° (16)).

ACKNOWLEDGMENTS

The author is grateful to the National Research Council of Canada for financial assistance. The technical assistance of Mrs. N. Stojanac is also appreciated.

REFERENCES

1. R. R. FRASER, R. U. LEMIEUX, and J. D. STEVENS. J. Am. Chem. Soc. **83**, 3901 (1961).
2. M. KARPLUS. J. Chem. Phys. **30**, 11 (1959).
3. H. S. GUTOWSKY, M. KARPLUS, and D. M. GRANT. J. Chem. Phys. **31**, 1278 (1959).
4. M. BARFIELD and D. M. GRANT. J. Am. Chem. Soc. **83**, 4726 (1961).
5. C. A. REILLY and J. D. SWALEN. J. Chem. Phys. **32**, 1378 (1960).
6. C. A. REILLY and J. D. SWALEN. J. Chem. Phys. **34**, 980 (1961).
7. F. KAPLAN and J. D. ROBERTS. J. Am. Chem. Soc. **83**, 4666 (1961).
8. C. A. REILLY and J. D. SWALEN. J. Chem. Phys. **35**, 1522 (1961).
9. R. FREEMAN. Mol. Phys. **4**, 321, 385 (1961).
10. S. CASTELLANO and J. S. WAUGH. J. Chem. Phys. **34**, 295 (1961).
11. J. S. WAUGH and S. CASTELLANO. J. Chem. Phys. **35**, 1900 (1961).
12. E. L. ELIEL and M. N. RERICK. J. Am. Chem. Soc. **82**, 1367 (1960).
13. R. D. STOLOW. J. Am. Chem. Soc. **81**, 5806 (1959).
14. E. L. ELIEL, H. HAUBENSTOCK and R. V. ACHARYA. J. Am. Chem. Soc. **83**, 2351 (1961).
15. H. HEILBRON and R. M. BUNBURY. Dictionary of organic compounds. Vol. II. Eyre and Spottiswoode, London. 1953. p. 425.
16. R. E. BUCKLES and E. A. HAUSMAN. J. Am. Chem. Soc. **70**, 415 (1948).
17. F. A. L. ANET. J. Am. Chem. Soc. **84**, 1053 (1962).

COMPLEX TELLURATES OF COBALT AND MANGANESE

M. W. LISTER AND Y. YOSHINO[1]
Department of Chemistry, University of Toronto, Toronto, Ontario
Received February 19, 1962

ABSTRACT

Complex tellurates of manganese and cobalt have been prepared by oxidizing mixtures of manganous or cobaltous sulphate with potassium (or sodium) tellurate by means of an alkaline hypochlorite solution. Cobalt gives $K_3H_6Co(TeO_6)_2.2H_2O$ as a dark green powder. The formula was confirmed by its oxidation equivalent with ferrous sulphate, by its displacement of chloride ions from an anion exchange resin, and by its magnetic susceptibility (-154×10^{-6} e.m.u./g-mol). The behavior of the compound on acidification is reported. Manganese gives $K_6H_8Mn(TeO_6)_3.5H_2O$ and $Na_7H_7Mn(TeO_6)_3.5H_2O$ as dark red crystals. The formula was confirmed as for the cobalt complex: its magnetic moment is 3.30 Bohr magnetons, which is reasonable for Mn(IV). The acid–base properties of the compound were examined. The ion is not very stable in solution, as shown by changes in its absorption spectrum; measurements of this gave evidence for the nature of the decomposition, and the equilibrium constant for this reaction. The main reaction is

$$H_7Mn(TeO_6)_3^{-7} + H_2O \rightleftharpoons H_4Mn(TeO_6)_2^{-4} + H_4TeO_6^{-2} + OH^-,$$

for which $K = 4\times10^{-5}$ (g-mol/l.)^2 at 25° C.

In recent papers (1), the present writers described the preparation and properties of complex periodates of cobalt and manganese. It seemed reasonable to expect that the same elements would give complex tellurates, especially in view of the behavior of trivalent copper, which has rather similar complex tellurates and periodates (2, 3). Issa, Khalafalla, and Issa (4) have deduced, from observations on the reduction of permanganate ions in the presence of sodium tellurate, that complex ions of manganese(IV) and tellurate must be formed, but they did not suggest any definite formula. The present paper reports the preparation of complex tellurates of cobalt and manganese, and gives an account of some of their properties. As will be seen, there is (as with copper) a general similarity between the complex periodates and tellurates, at least so far as the number of ligands attached to the metal is concerned; but the hydration of the salts, and the number of alkali metal ions present, are not the same. There can be no doubt that these are compounds of manganese(IV) and cobalt(III), as are the periodates.

Since it is perhaps rather more convenient to have all the information on the compounds of each central metal atom together, the cobalt compounds will be described first, followed by the manganese compounds.

Potassium Tellurato-cobaltate(III)

1. Preparation

Various rather similar methods were tried, but the most satisfactory proved to be as follows. A solution was prepared containing 2.0 g of cobalt chloride hexahydrate, 4.8 g of telluric acid, 1–2 ml of 6 *M* nitric acid, and 40 ml of water. A second solution contained 5 g of potassium hydroxide dissolved in 40 ml of 1.5 *M* potassium hypochlorite. These solutions were rapidly mixed, and allowed to stand while a dark green precipitate formed. Eighty milliliters of ethyl alcohol was added, and the solution allowed to stand. The supernatant liquid was poured off, and the precipitate was washed with 50% alcohol. The precipitate was then redissolved in 50 ml of 0.1 *M* potassium hydroxide, and an equal

[1]*Present address: College of General Education, University of Tokyo, Tokyo, Japan.*

volume of alcohol was added to the mixture. The new precipitate was then centrifuged off. This reprecipitation was repeated two or three times, and the final product was filtered off and dried over calcium chloride.

The yield was 3.7 g in a typical preparation. The compound is a dark green, microcrystalline powder. The precipitate was liable to be sticky; use of acetone instead of alcohol, or treatment of the solution with active charcoal, gave no improvement. It was necessary to add the alcohol very slowly, with stirring.

A similar preparation using sodium instead of potassium gave a somewhat similar precipitate, but analysis gave rather variable compositions and it appeared to contain sodium tellurate as an impurity.

Analysis of the potassium salt was carried out by dissolving a sample in concentrated hydrochloric acid, and adding first sulphur dioxide solution (to help it to dissolve) and then a solution of hydrazine chloride. The hydrochloric acid was now about 3 *M*. After 5 minutes' boiling, the precipitated tellurium was filtered off and weighed. The solution was evaporated to dryness, the hydrazine salts were destroyed by nitric acid, and after re-evaporation the residue was dissolved in very dilute hydrochloric acid. The metals were absorbed in a column of Dowex 50W-X8 in its hydrogen form; then the sodium was eluted by 0.4 *M* hydrochloric acid, and cobalt by 2 *M* hydrochloric acid. The potassium was weighed as K_2SO_4, and the cobalt was converted to $CoSO_4$. The cobalt content was also checked by EDTA titration. The water content of the compound was found from the loss in weight at 130° C.

The results of the analyses were: K 18.5, Co 8.94, Te 37.2, H_2O 5.97%; calculated for $K_3H_6Co(TeO_6)_2.2H_2O$: K 17.6, Co 8.86, Te 38.35, H_2O 5.42%. This formula assumes the presence of Co(III), which will be substantiated by other evidence below.

A check on this formula was obtained by dissolving a known weight of the compound, passing it through an anion exchange resin (Dowex 1-X4) in its chloride form, and titrating the potassium chloride liberated with silver nitrate. It was found that 1 g-mol of potassium chloride was liberated by 214 g of the compound; the calculated value is 221.8 g if the reaction is (R represents the resin)

$$K_3H_6Co(TeO_6)_2 + 3RCl \rightarrow R_3H_6Co(TeO_6)_2 + 3KCl.$$

2. Properties

Since telluric acid is not nearly as strong an oxidizing agent as periodic acid, it is not possible to check the formula of the complex tellurates by measuring the equivalent weight with a variety of reducing agents, as it is with complex periodates. However, an equivalent weight could be found by adding a known amount of ferrous ammonium sulphate in excess to a weighed sample of potassium tellurato-cobaltate, and the excess was titrated with decinormal potassium permanganate. The equivalent weight so found was 663; if $K_3H_6Co(TeO_6)_2.2H_2O$ is reduced by one oxidation step (i.e. Co(III) to Co(II)), the calculated equivalent weight is 665.4.

The most convincing evidence for the valency of the cobalt comes from the magnetic susceptibility of the compound. Measurements with a Goüy magnetic balance of the usual type gave a value for the susceptibility of -154×10^{-6} e.m.u./g-mol, at room temperature. Since the compound is diamagnetic, the cobalt is presumably trivalent. The susceptibility is a little lower than would be expected for this compound using, for instance, Angus' estimates (5) of the magnetic susceptibility of the atoms it contains: this gives a calculated value of -258×10^{-6} e.m.u./g-mol; but this is certainly not enough difference to cast any doubt on the trivalency of the cobalt.

3. Acid–Base Properties

A solution containing 2 g of potassium tellurato-cobaltate, on acidification with 5 ml of 3 *M* sulphuric acid, gave a dark green precipitate. The supernatant solution was pale pink, so some decomposition to Co(II) had occurred. The precipitate was washed, dried, and analyzed. It evidently contained a different Te/Co ratio, and in fact was approximately $KH_5Co_4(TeO_6)_3.10H_2O$. Addition of a weighed amount to a standardized ferrous ammonium sulphate solution and titration of the excess ferrous ion showed that the cobalt was still entirely trivalent. This substance has a sufficiently surprising formula that one might be inclined to dismiss it as a mixture. However, Malaprade (6, 7) has reported complex cobalt periodates with the same ratio of cobalt to ligand (e.g. $Na_3Co_4(IO_6)_3.10H_2O$).

If a solution of potassium tellurato-cobaltate was titrated with dilute perchloric acid (0.117 *N*) and the pH followed, the compound gave a normal pH curve. The pH curve makes pK_1 (the first stage of ionization) about 3.5, followed by considerably higher values of p*K* for the next two stages: roughly pK_2 is 7 and pK_3 is 9. This means that ionization to $Co(H_4TeO_6)_2^-$ is fairly easy, followed by two ionization steps to give $Co(H_3TeO_6)_2^{-3}$.

4. Absorption Spectrum

Like other complex tellurates or periodates, potassium tellurato-cobaltate gives an absorption spectrum with high absorption in the violet, falling to a minimum, followed by a single maximum as the wavelength is increased. The extinction coefficients at different wavelengths are: λ (mμ) 500, ϵ 139.1; 520, 95.6; 540, 74.7; 560 (min.), 68.0; 580, 71.0; 600, 75.4; 620, 80.0; 635 (max.), 81.6; 640, 81.1; 660, 75.9; 680, 63.7; 700, 49.9; 720, 34.5; 740, 23.7; 760, 14.7; 780, 9.9; 800, 6.9. These results were obtained from a 0.00435 *M* solution of the compound in 0.1 *M* potassium hydroxide. It was found that the addition of potassium tellurate caused no detectable change in the absorption curve, indicating that there is virtually no dissociation of the complex in a solution of this concentration.

Sodium and Potassium Tellurato-manganate(IV)

1. Preparation

After various preliminary trials, the most satisfactory methods devised were as follows. For the potassium salt, two solutions were made, one containing 2.0 g of manganous chloride tetrahydrate, 8.2 g of telluric acid, and a little nitric acid in 40 ml of water; the second contained 12 g of potassium hydroxide in 50 ml of 1.5 *M* potassium hypochlorite. The solutions were mixed, and, after standing, 100 ml of ethyl alcohol was added. The rather sticky red precipitate was separated by centrifuging and decantation. It was redissolved in 50 ml of 0.2 *M* potassium hydroxide, and reprecipitated by an equal volume of alcohol. This was repeated several times, and the final product was dried over calcium chloride or sulphuric acid. The yield on various occasions was 7.5 to 9.1 g of dark red crystals. In some preparations somewhat different ratios of manganese to tellurium were used.

The sodium salt was made similarly from sodium hydroxide and hypochlorite. It was less easy to purify, as sodium tellurate precipitated more easily than the potassium salt. However, the sodium tellurato-manganate is also less soluble.

The salts were analyzed by virtually the same methods as for the cobalt compound. The results for the potassium salt were: K 20.9, Mn 5.24, Te 36.5, H_2O 8.59%; calculated for $K_6H_8Mn(TeO_6)_3.5H_2O$: K 22.1, Mn 5.19, Te 36.2, H_2O 8.48%.

The results for the sodium salt were: Na 14.83, Mn 5.37, Te 39.2, H_2O 9.31%; calculated for $Na_7H_7Mn(TeO_6)_3.5H_2O$: Na 16.38, Mn 5.59, Te 38.9, H_2O 9.16%.

As with the cobalt compound, a check on the formula was made by passage of a weighed amount of the potassium salt in solution through an anion exchange resin in its chloride form; the liberated chloride ion was titrated. One gram-molecule of chloride ion was liberated by 185 g of the potassium salt. This is a little higher than the calculated value of 176 g for $K_6H_8Mn(TeO_6)_3.5H_2O$.

2. Valency of Manganese

This was obtained from equivalent weights in redox reactions, and from magnetic properties. The reducing agent that was found to give the best results was ferrous ammonium sulphate: excess of this was added, and the excess titrated with potassium permanganate. The equivalent weight so obtained was 518 for the potassium salt, and 534 for the sodium; if the ferrous ions reduced Mn(IV) to Mn(II), the calculated values are 529, and 492. Any other valency of manganese would give a very different equivalent weight, and, though the results are not very precise, there can be no doubt that the manganese is changing its valency by two.

The magnetic susceptibility of $K_6H_8Mn(TeO_6)_3.5H_2O$ was found to be 5230×10^{-6} e.m.u./g-mol at 25.1° C, and 4910×10^{-6} e.m.u./g-mol at 39.6° C. The correction for the diamagnetism of the various atoms is about 383×10^{-6} e.m.u./g-mol, making the corrected susceptibilities 5613×10^{-6} at 25.1° C, and 5293×10^{-6} at 39.6° C. If these susceptibilities obey the Curie–Weiss law, then the Weiss constant is −58°, and the Curie constant is 1.348. Hence the magnetic moment ($2.84C^{1/2}$) is 3.30 Bohr magnetons. This is somewhat lower than the calculated "spin only" value of 3.87 Bohr magnetons, but still near enough that it most probably indicates three unpaired electrons.

3. Acid–Base Properties

The potassium salt proved stable enough in solution to be titrated with dilute perchloric acid; or the solution on acidification could be back titrated with potassium hydroxide. The pH curve was the same in both directions. Starting at the acid end, the pH of 0.00204 *M* $H_{14}Mn(TeO_6)_3$ was 2.62. This corresponds to between one and two hydrogen ions/molecule, meaning that ionization is easy up to $Mn(H_4TeO_6)_3^{-2}$. When these acid hydrogens had been neutralized the pH rose steeply, and thereafter gave no marked rise until three more hydrogens had been neutralized. The third to fifth ionization steps, which cannot be clearly distinguished, have pK values about 7.5, corresponding to ionization as far as $Mn(H_3TeO_6)_3^{-5}$. The next ionization constant after this has pK about 11.5. These constants are consistent with the formula of the compound.

Stability of Tellurato-manganate Ion

Like other compounds of this type, sodium or potassium tellurato-manganate ions in solution gave an absorption spectrum which was high at the violet end, low at the red end, with a single minimum and maximum in between. The minimum was at about 420 mμ, and the maximum at 470 mμ. However, the absorption was considerably altered by addition of excess sodium tellurate, and it was evident that an equilibrium existed between ions differing in their content of tellurium. The absorption curves so obtained are shown in Fig. 1.

In the presence of excess sodium tellurate, the chief ion present contains three tellurate residues to each manganese atom. The evidence for this partly comes from the fact that the solid salts which were prepared contained this ratio of atoms, and partly from the following experiment. If a constant amount of manganese sulphate was mixed with varying

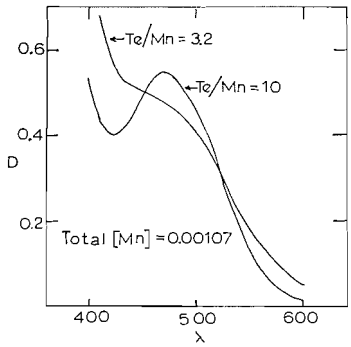

FIG. 1. Optical density of solutions with constant manganese and varying tellurium content.

amounts of sodium tellurate in solution, and the mixture oxidized by sodium hypochlorite, then some (or all) of the manganese was converted into a solution of sodium tellurato-manganate (the rest was precipitated as manganese dioxide). The amount in solution was determined by diluting the solution to a given volume, and measuring its optical density. The optical density increased steadily until the ratio of tellurium to manganese reached 3, and thereafter it levelled out.

Mixtures with various concentrations of manganese sulphate and sodium tellurate were oxidized by sodium hypochlorite, and the optical densities of the resulting solutions were measured at various wavelengths. The concentration of sodium hydroxide present was also varied. The temperature in all cases was 25° C. The results are summarized in Table I, which, however, only gives data for 470 mμ and 420mμ, which were the wavelengths where the greatest change in the optical density occurred. As indicated in Fig. 1, measurements were also made over most of the range 400–600 mμ.

In the interpretation of the results in Table I it was assumed that the equilibrium was of the type

$$\text{Mn(tellurate)}_3 \rightleftharpoons \text{Mn(tellurate)}_{3-n} + n.\text{tellurate}.$$

Let

Mn_0 = total manganese present,
R = tellurium/manganese ratio,
ϵ_1 = extinction coefficient of Mn(tellurate)_3,
ϵ_2 = extinction coefficient of $\text{Mn(tellurate)}_{3-n}$,
$A = \epsilon_1\text{Mn}_0$,
$B = \epsilon_2\text{Mn}_0$,
D = optical density.

Then it follows from the equations for the total manganese and tellurium present, and the Beer–Lambert law, that

$$K = \frac{D-A}{B-D}\,\text{Mn}_0\left[R-3+\frac{n(D-A)}{B-A}\right]^n.$$

K is the equilibrium constant of the reaction. If R is large, almost all the manganese will be converted to Mn(tellurate)_3, so $D = A$; hence a reasonably good value of A can be obtained by extrapolation of D at high values of R. Values of K were calculated

TABLE I

Run	[Mn]×10³ (*M*)	Ratio Te/Mn	Optical density 470 mμ	Optical density 420 mμ	[NaOH] (*M*)
1	1.07	3.2	0.468	0.574	0.180
		3.3	0.479	0.585	
		3.5	0.482	0.545	
		4.0	0.485	0.471	
		5.0	0.503	0.443	
		10.0	0.515	0.416	
2	0.535	3.5	0.233	0.298	0.19
		3.7	0.235	0.291	
		4.0	0.239	0.254	
		5.0	0.251	0.231	
		7.0	0.259	0.215	
		10.0	0.262	0.209	
3	1.07	3.5	0.508	0.506	0.460
		3.7	0.521	0.513	
		4.0	0.523	0.496	
		5.0	0.544	0.419	
		7.0	0.546	0.408	
		10.0	0.545	0.399	
4	0.713	3.5	0.341	0.375	0.505
		3.7	0.349	0.346	
		4.0	0.352	0.308	
		5.0	0.362	0.282	
		7.0	0.367	0.273	
		10.0	0.367	0.272	
5	0.713	3.7	0.338	0.321	0.295
		4.0	0.340	0.309	
		5.0	0.354	0.291	
		7.0	0.355	0.273	
		10.0	0.357	0.271	
		10.0	0.354	0.275	

from the data for different values of R, assuming various values of B and n. The value B was taken to be that for which the average deviation in K was least, and this deviation was compared for different values of n. Run 1, for instance, gave:

n	1	2	3
Average deviation in K (%)	3.8	13.2	22.2

Hence $n = 1$, and the equation for K reduces to

$$K = \mathrm{Mn}_0\left(\frac{D-A}{B-D}\right)\left(R-3+\frac{D-A}{B-A}\right).$$

The procedure adopted to find K was to select values of A and B for any one run, until the values of K obtained from that run showed a minimum average deviation (expressed as a percentage of K). This was done for both wavelengths studied, with the results given in Table II.

The values of K are fairly consistent, but tend to fall as the concentration of hydroxide ions rises. This drift is not quite as much as is required on the assumption that the equilibrium constant is inversely proportional to $[OH^-]$. Assuming that the ion in solution is the same as in the solid, and that tellurate is dissociated to $H_4TeO_6^{-2}$ in moderately alkaline solution, then the main reaction is

$$H_7Mn(TeO_6)_3^{-7} + H_2O \rightleftharpoons H_4Mn(TeO_6)_2^{-4} + H_4TeO_6^{-2} + OH^-.$$

TABLE II

Run	Wavelength (mμ)	A	B	$K\times10^4$	ϵ_1	ϵ_2
1	470	0.52	0.31	1.70	485	290
	420	0.40	1.10	1.71	375	1030
2	470	0.265	0.16	1.62	495	300
	420	0.194	0.55	1.55	365	1030
3	470	0.55	0.30	1.40	515	280
	420	0.39	1.10	1.42	365	1030
4	470	0.37	0.20	0.87	520	280
	420	0.26	0.75	0.98	365	1050
5	470	0.362	0.21	1.30	510	295
	420	0.255	0.75	1.16	360	1050

The equilibrium constant for this reaction will be the value of K given in Table II multiplied by the hydroxide ion concentration; this is about 4×10^{-5}. Hence this complex tellurato-manganate ion is of rather moderate stability. The extinction coefficients are also consistent, and average as follows:

$H_7Mn(TeO_6)_3^{-7}$: 470 mμ, $\epsilon_1 = 505$; 420 mμ, $\epsilon_1 = 290$;
$H_4Mn(TeO_6)_2^{-4}$: 470 mμ, $\epsilon_2 = 365$; 420 mμ, $\epsilon_2 = 1040$.

The absorption maximum found for $H_7Mn(TeO_6)_3^{-7}$ at 470 mμ seems to be absent for $H_4Mn(TeO_6)_2^{-4}$.

REFERENCES

1. M. W. LISTER and Y. YOSHINO. Can. J. Chem. **38**, 45, 1291 (1960).
2. L. MALATESTA. Gazz. chim. ital. **71**, 467, 580 (1941).
3. M. W. LISTER. Can. J. Chem. **31**, 638 (1953).
4. M. ISSA, S. E. KHALAFALLA, and R. M. ISSA. J. Am. Chem. Soc. **77**, 5503 (1955).
5. W. R. ANGUS. Proc. Roy. Soc. (London), A, **136**, 569 (1932).
6. L. MALAPRADE. Compt. rend. **210**, 504 (1940); **204**, 979 (1937).
7. L. MALAPRADE. Bull. soc. chim. France, **6**, 223 (1939).

INTERFACE KINETICS

HYDROGEN PEROXIDE OXIDATION OF CUPROUS ION

D. W. COLCLEUGH[1] AND W. F. GRAYDON[2]

Department of Chemical Engineering and Applied Chemistry, University of Toronto, Toronto, Ontario

Received March 9, 1962

ABSTRACT

It has been established (D. W. Colcleugh and W. F. Graydon. J. Phys. Chem. In press) that hydrogen peroxide is produced during the dissolution of polycrystalline copper in dilute aqueous solutions. The hydrogen peroxide formed during the dissolution further attacked the metal, producing additional cupric copper in solution. The kinetics of this heterogeneous reaction was investigated in aerated sulphuric acid solutions. Under these experimental conditions the ratio of the increase in concentration of cupric ion to the decrease in concentration of hydrogen peroxide was constant at the value of 2. In deaerated sulphuric acid this stoichiometric ratio was constant at the value of 1 under similar experimental conditions.

Rate equations for the formation of cupric ion in solution and for the decomposition of hydrogen peroxide in the solution were determined as a function of sample area, corroding solution volume, temperature, hydronium ion concentration, cupric ion concentration, and hydrogen peroxide concentration.

A reaction mechanism was suggested to describe the empirical rate equations and the stoichiometry obtained experimentally.

EXPERIMENTAL

Apparatus

The apparatus consisted of a cylindrical sample of polycrystalline copper rotating in a solution of sulphuric acid. The solution was kept saturated with either pure nitrogen or an oxygen–nitrogen mixture by continually bubbling the gas into the acid solution during an experimental run. The apparatus was described in full previously (1) and no modifications were made.

Analysis

A polarographic method of analysis was used for cupric ion, hydrogen peroxide, and, occasionally, dissolved oxygen determinations. Dissolved oxygen determinations were carried out prior to the start of a run to ensure that deaeration was complete.

The supporting electrolyte used was 1 M sodium acetate and the maximum suppressor was a 0.01% gelatin solution. The capillary had "m" and "t" values of 3.24 mg/sec and 3.19 sec respectively at 0.0 volts versus the saturated calomel electrode.

Procedure

The corroding solution consisted of a sulphuric acid solution containing cupric ion (dissolved cupric sulphate pentahydrate) and hydrogen peroxide. The gas stream was bubbled through the solution for several hours before the metal sample was immersed into the solution and the run was begun. The copper sample, before immersion in the solution, was polished mechanically with various grades of emery paper, progressing from rough to fine, and then cleaned thoroughly with distilled water and absolute alcohol.

Periodically, during the course of a run, samples of corroding solution were removed and analyzed for cupric ion and hydrogen peroxide content polarographically.

Unless otherwise stated in the discussion of the results the operating conditions were: a sulphuric acid concentration of 0.2 mole/liter, an ambient temperature of 25.8° C, a sample surface area of 11.4 cm^2, a corroding solution volume of 500 ml, partial pressure of oxygen in the gas stream of 0.21 atm, and a sample rotation speed of 880 r.p.m. In Section B of Discussion of Results, the oxygen concentration in the gas stream was zero.

DISCUSSION OF RESULTS

Introduction

Hydrogen peroxide was produced during the dissolution of polycrystalline copper in dilute aerated sulphuric acid solutions (2). At hydrogen peroxide concentrations less

[1]*N.R.C. Bursary 1959–60; N.R.C. Studentship 1960–61.*
[2]*Professor of Chemical Engineering, University of Toronto.*

than about 5×10^{-4} mole/liter the ratio of cupric ion concentration in solution to hydrogen peroxide concentration in solution was constant at the value of 2 under all experimental conditions. The plots of cupric ion concentration and hydrogen peroxide concentration to the one-half power versus time gave straight lines below this limit in hydrogen peroxide concentration.

It seemed logical to assume that the hydrogen peroxide, an active oxidizing agent, would be involved in the dissolution process. If the dissolution was allowed to continue beyond a hydrogen peroxide concentration of about 5×10^{-4} mole/liter, a marked increase in the ratio of cupric ion concentration to hydrogen peroxide concentration was observed. The slopes of the plots of cupric ion concentration and hydrogen peroxide concentration to the one-half power versus time began to increase and decrease respectively with increasing hydrogen peroxide concentration, as seen by Table I.

TABLE I

Time	$[H_2O_2]\times10^4$	$\frac{d[Cu^{++}]^{1/2}}{dt}\times10^4$	$\frac{d[H_2O_2]^{1/2}}{dt}\times10^4$	$\frac{[Cu^{++}]}{[H_2O_2]}$
7.5	0.97	11.4	7.80	2.0
15.0	2.54	11.3	7.67	2.1
25.0	5.29	12.2	6.82	2.3
35.0	8.39	13.0	5.35	2.6
45.0	11.35	14.2	3.85	3.3
58.5	12.73	16.4	0.60	5.1

These observations indicated that the copper dissolution process in aerated sulphuric acid solutions consisted of two oxidation steps, the oxidation of copper by dissolved oxygen (2) and the oxidation of copper by dissolved hydrogen peroxide formed in the first reaction.

The following empirical equations were postulated to explain the aforementioned phenomenon in a solution of constant sulphuric acid concentration and at a constant reaction temperature:

$$\frac{d[Cu^{++}]}{dt} = k_1[O_2]^{1/2}[Cu^{++}]^{1/2}+k_2[Cu^{++}]^{1/2}[H_2O_2] \quad [1]$$

$$2\times\frac{d[H_2O_2]}{dt} = k_1[O_2]^{1/2}[Cu^{++}]^{1/2}-k_2[Cu^{++}]^{1/2}[H_2O_2] \quad [2]$$

$$2\times\frac{d[Cu^{++}]^{1/2}}{dt} = k_1[O_2]^{1/2}+k_2[H_2O_2]. \quad [3]$$

At very low concentrations of hydrogen peroxide the equations above would reduce to the form of the rate equations reported previously (2):

$$2\times\frac{d[H_2O_2]}{dt} = \frac{d[Cu^{++}]}{dt} = k_1[O_2]^{1/2}[Cu^{++}]^{1/2}. \quad [4]$$

To test the validity of the above proposed equations [1], [2], and [3], several runs with initially added cupric ion and hydrogen peroxide were completed in aerated sulphuric acid solutions. Experiments of this sort were also carried out in deaerated sulphuric acid solutions. The exclusion of dissolved oxygen from the solution in contact with the metal

would serve to isolate part of the reaction for closer and more detailed examination. The data from these experiments were compared with the simplified forms of the equations [1] and [2] at zero oxygen concentration.

The dependence of the rate constants on dissolved oxygen concentration, sample area, corroding solution volume, rotation speed of the sample, temperature, and acid concentration was determined.

A. Experiments in Aerated Sulphuric Acid

Rate Dependence on Cupric Ion and Hydrogen Peroxide Concentrations

The basis of the proposed one-half-order dependence of rate with respect to cupric ion concentration and the first-order dependence of the rate with respect to hydrogen peroxide concentration was a series of experiments carried out under normal operating conditions with varying amounts of initially added cupric ion and hydrogen peroxide. These so-called normal operating conditions were specified in the Experimental Procedure.

The data obtained from these experiments when fitted to equations [1] and [2] gave constant values of k_1 and k_2 over the wide range of cupric ion and hydrogen peroxide concentrations used. The rates obtained, the average cupric ion and hydrogen peroxide concentrations over a run, and the calculated rate constants k_1 and k_2 are tabulated in Table II.

TABLE II

No.	$\frac{d[Cu^{++}]}{dt}\times10^4$	$\frac{d[H_2O_2]}{dt}\times10^4$	$[Cu^{++}]\times10^4$	$[H_2O_2]\times10^4$	k_1	k_2
1	1.75	0.38	52.9	15.8	0.107	0.43
2	1.95	0.35	48.0	15.0	0.117	0.60
3	1.21	0.31	20.6	8.62	0.126	0.75
4	1.76	0.62	54.8	8.56	0.125	0.41
5	1.51	0.49	35.5	6.82	0.130	0.65
6	1.38	0.20	27.1	16.3	0.105	0.58
7	2.18	−0.10	26.7	29.5	0.118	0.78
8	1.66	0.00	21.6	28.0	0.110	0.64
9	1.62	0.18	21.9	24.4	0.130	0.55
10	1.92	0.10	28.3	24.0	0.123	0.67
11	2.09	0.08	28.5	30.1	0.130	0.60
12	1.88	−0.20	15.1	50.2	0.119	0.58
13	1.81	−0.13	12.8	50.6	0.135	0.57
14	1.44	0.49	39.7	7.79	0.119	0.47
15	1.51	0.38	38.4	8.22	0.113	0.74
16	1.31	0.39	37.6	8.31	0.105	0.52
17	1.77	0.43	38.1	7.94	0.132	0.93
18	1.21	0.34	12.2	11.7	0.164	0.65
19	1.38	0.27	31.9	16.7	0.129	0.60
20	1.34	−0.04	15.1	28.6	0.099	0.64
21	1.67	0.08	23.4	28.8	0.115	0.54
22	1.84	−0.05	25.5	30.4	0.105	0.63
23	1.98	−0.25	19.7	37.9	0.101	0.73
24	2.18	0.08	46.1	32.7	0.104	0.46
25	1.81	−0.05	15.3	33.2	0.133	0.73
26	2.17	−0.07	20.3	37.4	0.138	0.69
27	1.44	−0.08	12.9	36.8	0.109	0.60
28	1.62	0.15	31.6	28.4	0.104	0.41
29	1.44	0.48	28.1	8.44	0.138	0.53
30	2.11	0.30	61.3	14.5	0.109	0.67

From Table II it can be seen that a wide selection of cupric ion concentrations and hydrogen peroxide concentrations were used in this part of the work. Average cupric ion concentrations in solution ranged from a low of 12.2×10^{-4} mole/liter to a high of

61.3×10^{-4} mole/liter, and the average hydrogen peroxide concentrations ranged from a low of 6.82×10^{-4} mole/liter to a high of 50.6×10^{-4} mole/liter. The ratio of average cupric ion concentration in solution to average hydrogen peroxide concentration in solution ranged from about 6.4 to 0.3. With these quite wide ranges in conditions the rate constants calculated from the proposed rate equations remained essentially constant with no observable trends.

Perhaps the most convincing part of the argument for acceptance of the proposed rate equations was the fact that at high enough concentrations of hydrogen peroxide, that is, concentrations above about 28×10^{-4} mole/liter, it was observed that the rate of formation of hydrogen peroxide was negative. At these high concentrations of hydrogen peroxide more hydrogen peroxide was being used up in reaction with the copper than was being produced in the reaction of the copper with dissolved oxygen. Again the rate constant remained at the same value without any significant trends.

It should also be noted that in run No. 8 a rate of hydrogen peroxide formation of zero was observed at a constant hydrogen peroxide concentration of 28.0×10^{-4} mole/liter. The cupric ion concentration increased throughout the run with no apparent change in the hydrogen peroxide concentration. The amount of hydrogen peroxide produced by the reaction of dissolved oxygen with copper discussed previously (2) was exactly balanced by the amount of hydrogen peroxide used up in reaction with the copper.

Rate Dependence on Dissolved Oxygen Concentration

A set of runs with initially added cupric ion and hydrogen peroxide was carried out in aerated 0.2 *M* sulphuric acid solutions with varying partial pressures of oxygen in the saturating gas phase.

The partial pressure of oxygen in the gas phase was found to be directly proportional to the concentration of dissolved oxygen in the condensed phase. The Henry's law constant for this concentration of solution at 25.8° C was found experimentally to be 8.00×10^{2} atm-liter/mole.

The values of the rate constants k_1 and k_2 calculated from the rate data and equations [1] and [2] and the corresponding partial pressures of oxygen in the gas phase are given in Table III. From this data it was observed that the rate constants k_1 and k_2 were independent of the oxygen concentration in the corroding solution.

TABLE III

Experimental variable	k_1	k_2
Oxygen partial pressure in gas:		
0.098	0.126	0.53
0.21	0.120	0.60
0.50	0.114	0.67
1.00	0.121	0.59
Rotation speed of sample:		
8	0.113	0.52
78	0.124	0.53
880	0.120	0.60
Sulphuric acid concentration:		
0.05	0.103	1.09
0.20	0.120	0.60
0.50	0.122	0.31

Rate Dependence on Sample Area and Corroding Solution Volume

A linear relationship between the rate constant k_2 and the ratio of sample area to

corroding solution volume was found as seen by Fig. 1. A similar dependence was previously found for the rate constant k_1 (1, 2), and was substantiated by this work.

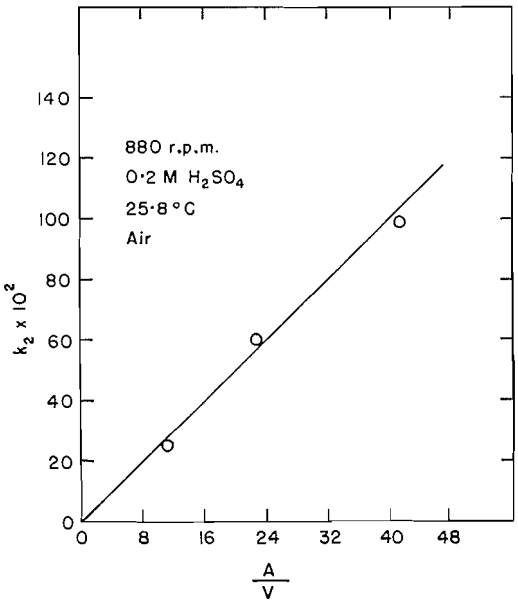

FIG. 1. Effect of sample area and corroding solution volume. Variation of rate constant from equations [1] and [2] with the ratio of sample area to dissolving solution volume.

Rate Dependence on Sample Rotation Speed

The cylindrical copper sample was rotated at three widely different speeds and the rate constants measured. Any dependence of rate on the rotation speed of the sample would indicate that the rate of diffusion of a reacting species to the copper surface played an important part in the control of the dissolution process.

The results shown in Table III clearly indicated that the rate constant k_2 was independent of sample r.p.m. and the reaction of hydrogen peroxide with copper was chemically controlled under these experimental conditions.

Rate Dependence on Sulphuric Acid Concentration

The variable in this series of experiments was sulphuric acid concentration. All other operating conditions were kept constant.

The variation in the values of k_1, as seen by Table III, was as expected from the previous work (2). The values of k_2 also showed a dependence on sulphuric acid concentration. The values of k_2 measured showed an inverse dependence on acid concentration, decreasing as the sulphuric acid concentration increased.

B. Experiments in Deaerated Sulphuric Acid

If the dissolved oxygen concentration in the solution is zero, equations [1] and [2] become

$$\frac{d[Cu^{++}]}{dt} = k_2[Cu^{++}]^{1/2}[H_2O_2], \qquad [5]$$

$$2\times\frac{d[H_2O_2]}{dt} = -k_2[Cu^{++}]^{1/2}[H_2O_2]. \qquad [6]$$

Thus one would expect, from the results in Section A, that the ratio of the increase in concentration of cupric ion in solution to the decrease in concentration of hydrogen peroxide in solution for the condition of no dissolved oxygen in solution would be constant at the value 2. However, it became increasingly evident as the path of the reaction between hydrogen peroxide and polycrystalline copper in deaerated sulphuric acid was followed that this stoichiometric ratio was in fact 1 and not 2.

Also, it was found that both the rate of formation of cupric ion and the rate of decomposition of the dissolved hydrogen peroxide were dependent upon the concentration of cupric ion in solution and upon the hydrogen peroxide concentration in solution to the one-half power and the first power respectively.

The results given in Table IV illustrate the above statements concerning the stoichiometry and the independence of the rate constant on cupric ion concentration and hydrogen

TABLE IV

No.	$[Cu^{++}]_{av}\times10^4$	$[H_2O_2]_{av}\times10^4$	K	$-\frac{\Delta[Cu^{++}]}{\Delta[H_2O_2]}$
1	45.1	7.15	0.47	1.08
2	55.4	14.5	0.48	1.60
3	51.2	11.3	0.59	0.59
4	128.0	35.4	0.59	1.04
5	23.0	15.5	0.59	1.00
6	75.5	41.5	0.55	0.48
7	65.1	19.2	0.65	0.51
8	49.0	122.4	0.57	0.93
9	22.7	38.5	0.55	0.70
10	45.5	6.98	0.69	1.00
11	47.1	6.20	0.73	0.80
12	40.0	23.4	0.66	1.70
13	47.5	18.7	0.60	1.10
14	14.2	9.07	0.57	1.80
15	24.8	12.6	0.55	0.93

peroxide concentration. The sample surface area was 11.4 cm², the corroding solution volume was 500 ml, the sample rotation speed was 880 r.p.m., and the ambient temperature was 25.8° C for all the runs given in Table IV.

The rate constant K given in Table IV was an average value over the length of the run and was defined by the following equations:

$$\frac{d[Cu^{++}]}{dt} = K[Cu^{++}]^{1/2}[H_2O_2] \qquad [7]$$

$$-\frac{d[H_2O_2]}{dt} = K[Cu^{++}]^{1/2}[H_2O_2]. \qquad [8]$$

The results from a typical run were illustrated graphically in Fig. 2, which corresponds to run No. 5 in Table IV.

It can be seen from the values of K that they are identical with the values of k_2 obtained in aerated solutions (Table II).

Rate Dependence on Sulphuric Acid Concentration

Figure 3 illustrates the effect of changing the acid concentration on the rate constant K. As was the case in Section A a decrease in the acid concentration increased the value of the rate constant k_2. The values of k_2 obtained from the experiments in aerated solutions

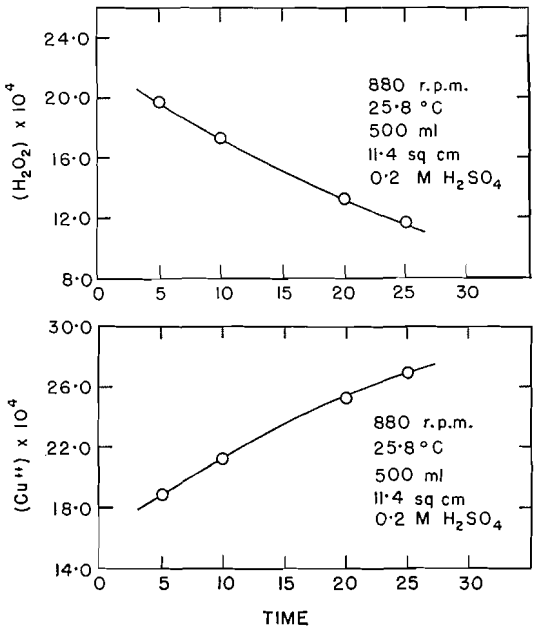

FIG. 2. Variation of concentration (mole/liter) with time (hours) in deaerated solution.

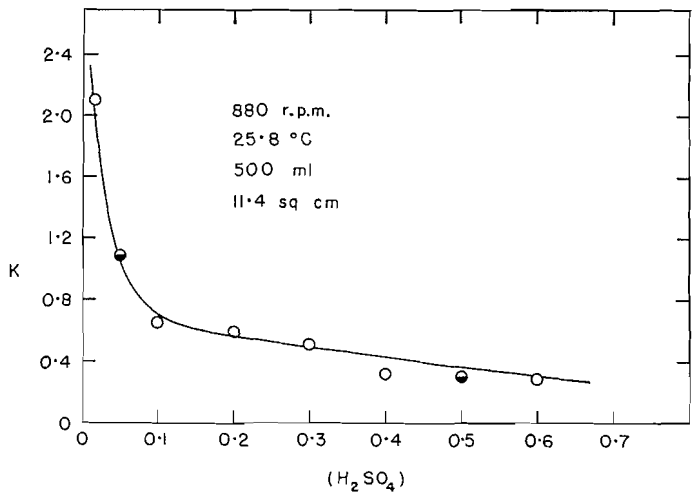

FIG. 3. Effect of sulphuric acid concentration. Variation of rate constant K from equations [7] and [8] with acid concentration (mole/liter) in deaerated solutions; ◒ shows variation of k_2 from equations [1] and [2] with acid concentration in aerated solutions.

and calculated from equations [1] and [2] were superimposed on Fig. 3, and found to agree well with the values of K obtained in deaerated solutions and calculated from equations [7] and [8].

The dependence of the rate constant K on sulphuric acid concentration did not appreciably affect the stoichiometry of the reaction, which remained at the value 1, as seen by Table V.

TABLE V

$[H_2SO_4]$	Temp.	A	V	r.p.m.	$-\frac{\Delta[Cu^{++}]}{\Delta[H_2O_2]}$
0.016	25.8	11.4	0.500	880	0.66
0.10	"	"	"	"	0.84
0.20	"	"	"	"	1.03
0.30	"	"	"	"	0.40
0.40	"	"	"	"	0.97
0.60	"	"	"	"	1.53
0.016	15.0	"	"	"	0.87
0.20	"	"	"	"	1.10
0.40	"	"	"	"	1.00
0.60	"	"	"	"	1.02
0.016	36.0	"	"	"	0.58
0.20	"	"	"	"	0.88
0.40	"	"	"	"	1.00
0.60	"	"	"	"	0.51
0.016	45.0	"	"	"	1.02
0.20	"	"	"	"	1.60
0.40	"	"	"	"	0.95
0.60	"	"	"	"	0.99
0.20	25.8	5.7	"	"	1.18
"	"	11.4	0.800	"	0.96
"	"	"	0.300	"	0.99
"	"	14.3	0.500	"	0.93
"	"	11.4	"	0	1.01
"	"	"	"	78	1.00
"	"	"	"	2300	1.05

The data in Fig. 3 when replotted as the reciprocal of the rate constant versus hydronium ion concentration (Fig. 4(*a*)) resulted in a good linear correlation. Similar data to that described above were obtained at ambient temperatures of 15.0° C (Fig. 4(*b*)), 36.0° C (Fig. 4(*c*)), and 45.0° C (Fig. 4(*d*)).

This data substantiated the linear relationship between hydronium ion concentration and the reciprocal of the rate constant.

Thus

$$K = \frac{K_1}{K_2 + [H_3O^+]}. \qquad [9]$$

Rate Dependence on Temperature

This series of experiments carried out with temperature as the variable was designed to determine the temperature dependence of the rate constants as well as to test the linear correlation of the reciprocal of the rate constant versus acid concentration as discussed above.

At the temperatures used, the stoichiometric ratio of the increase in concentration of cupric ion to the decrease in concentration of hydrogen peroxide remained at the value unity.

From the slopes and intercepts of Fig. 4(*a–d*) values of the rate constants K_1 and K_2 were determined and plotted as in Fig. 5. Arrhenius activation energies calculated from the slopes of Fig. 5 were 20.6 kcal/g-mole and 11.8 kcal/g-mole for the rate constants K_1 and K_2 respectively.

Rate Dependence on Sample Area and Corroding Solution Volume

As was the case in the experiments in aerated sulphuric acid solutions, a linear relationship between the rate constant K and the ratio of sample area to corroding solution volume was found as seen by Fig. 6.

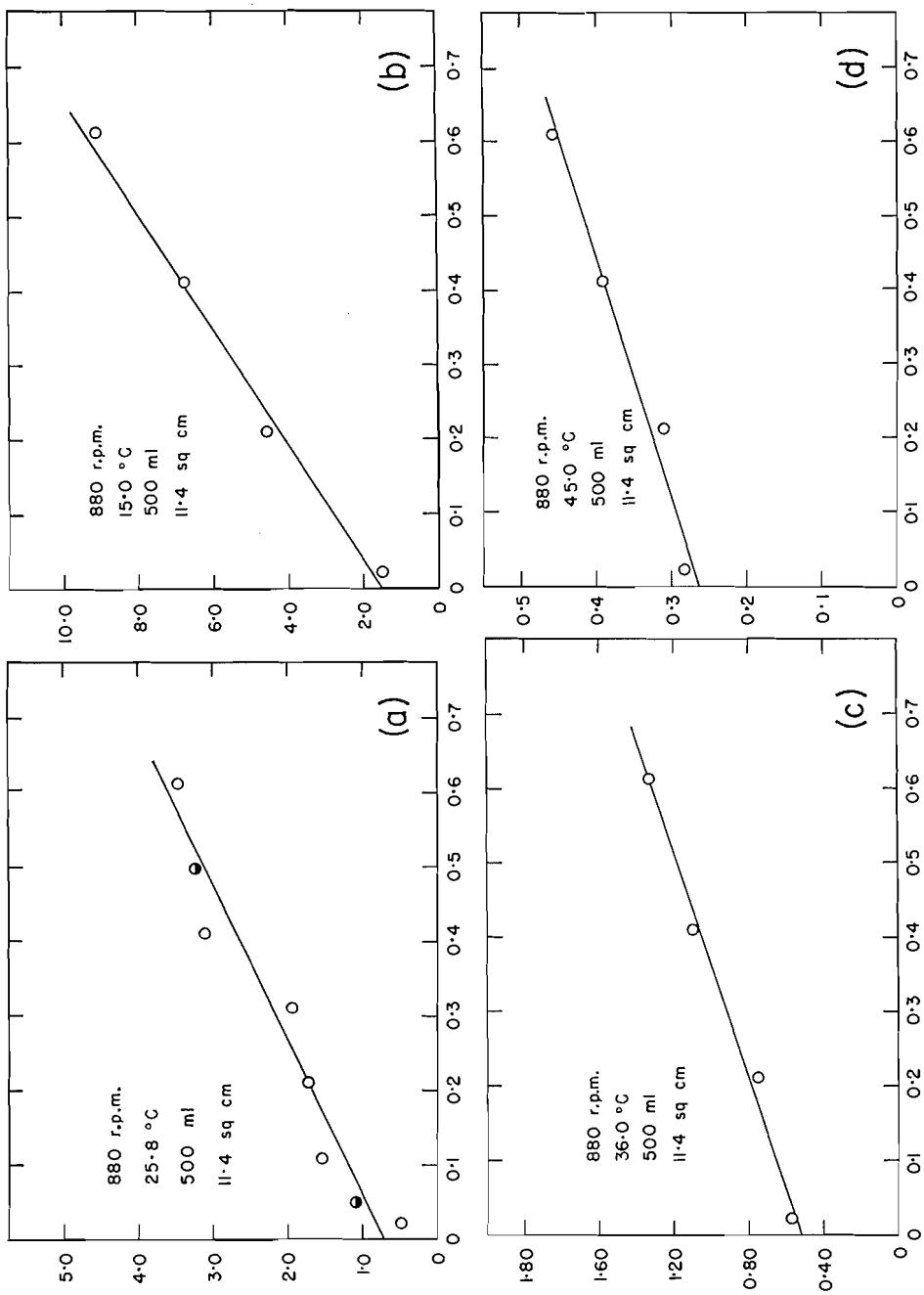

FIG. 4. Effect of hydronium ion concentration. Reciprocal of rate constant K from equations [7] and [8] versus hydronium ion concentration (mole/liter) in deaerated solutions at (*a*) 25.8, (*b*) 15.0, (*c*) 36.0, (*d*) 45.0° C. In Fig. 4(*a*) ◑ shows variation of reciprocal rate constant k_2 from equations [1] and [2] versus hydronium ion concentration in aerated solutions.

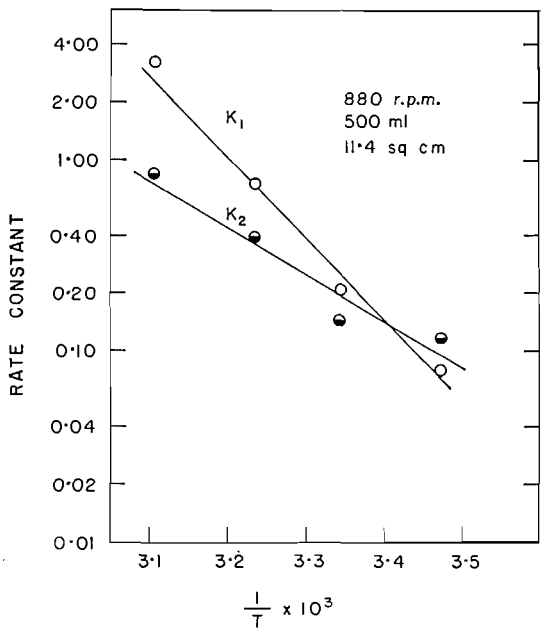

FIG. 5. Effect of temperature. Logarithms of rate constants K_1 and K_2 as defined by equation [9] versus the reciprocal of the corresponding absolute temperature in deaerated solutions.

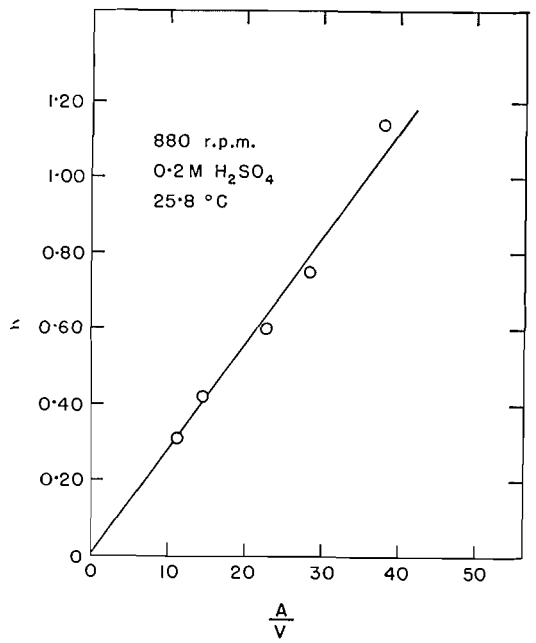

FIG. 6. Effect of sample area and corroding solution volume. Variation of rate constant K as defined by equations [7] and [8] with ratio of sample area to dissolving solution volume in deaerated solutions.

The stoichiometric ratio was unaffected by the variation in sample area and corroding solution volume, as illustrated in Table V.

Rate Dependence on Sample Rotation Speed

Variation in the rotation speed of the sample did not affect the value of the rate constant or the stoichiometric ratio and therefore the reaction must be chemically controlled under the existing experimental conditions.

Summary

From the discussion of the results obtained in this work and the results of previous work (1, 2), the overall rates of formation of cupric ion and hydrogen peroxide during the dissolution of polycrystalline copper in dilute sulphuric acid solutions could each be represented by the sum and difference, respectively, of two component rates:

$$\frac{d[Cu^{++}]}{dt} = R_1 + \frac{9.08\times10^{-3}(A/V)[Cu^{++}]^{1/2}[H_2O_2]}{0.145+[H_3O^+]}$$

$$\frac{d[H_2O_2]}{dt} = \frac{1}{2}R_1 - \frac{1}{\beta}\frac{9.08\times10^{-3}(A/V)[Cu^{++}]^{1/2}[H_2O_2]}{0.145+[H_3O^+]}.$$

The contribution to the overall rates of formation through the attack of the copper by dissolved oxygen, represented above by R_1, was discussed previously (1, 2). The rate constant obtained previously (2) for R_1, at 25.8° C in a sulphuric acid solution of 0.2 M, was $5.44\pm0.48\times10^{-3}$. The hydrogen peroxide concentrations were low enough so that the second term in each overall rate equation was negligible with respect to R_1.

In this investigation, in aerated solutions, the hydrogen peroxide concentration and the second term in each overall rate equation were not negligible with respect to R_1. The value of the rate constant for R_1 at 25.8° C in 0.2 M sulphuric acid, under these conditions of high hydrogen peroxide concentrations was $5.32\pm0.56\times10^{-3}$.

The value of β, the stoichiometric ratio, was 2 in aerated sulphuric acid solutions and 1 in deaerated sulphuric acid solutions.

At 25.8° C and a sulphuric acid concentration of 0.2 M the rate constant for the hydrogen peroxide oxidation of cuprous ion in aerated solutions was $26.3\pm3.71\times10^{-3}$ and in deaerated solutions was $26.3\pm2.11\times10^{-3}$.

Proposed Mechanism

The following reaction scheme was suggested as a possible reaction mechanism for the oxidation of polycrystalline copper by dissolved hydrogen peroxide in dilute acid solution under aerated or deaerated conditions.

In formulating the reaction mechanism the experimentally established facts were adhered to.

1. Both the rate of formation of cupric ion and the rate of decomposition of hydrogen peroxide were one-half order with respect to cupric ion and first order with respect to hydrogen peroxide.

2. One mole of cupric ion was formed for every mole of hydrogen peroxide reacted in deaerated solutions and 2 moles of cupric ion were formed for every mole of hydrogen peroxide reacted in aerated solutions.

3. The reaction was inhibited by increasing concentration of acid.

The following reactions were assumed to take place at the solid–liquid interface:

$$Cu + Cu_i^{++} \overset{K_a}{\rightleftharpoons} 2Cu_i^{+} \text{ (equilibrium)} \qquad [i]$$

$$Cu_i^{+} + H_2O_{2i} \underset{k_{-1}}{\overset{k_1}{\rightleftharpoons}} Cu^{+}.H_2O_2 \qquad [ii]$$

$$Cu^{+}.H_2O_2 \xrightarrow{k_3} Cu_i^{++} + OH + OH^{-} \qquad [iii]$$

$$Cu^{+}.H_2O_2 + H_3O^{+} \underset{k_{-4}}{\overset{k_4}{\rightleftharpoons}} Cu_i^{+} + H_3O_2^{+} + H_2O \qquad [iv]$$

$$H_3O_2^{+} + H_2O \underset{k_{-2}}{\overset{k_2}{\rightleftharpoons}} H_2O_2 + H_3O^{+}. \qquad [v]$$

Reaction [iv] represents the inhibition step. The hydronium ion enters into competition for and returns the cuprous ion, hydrogen peroxide transitory species to its original uncombined form of free cuprous ion and molecular hydrogen peroxide.

It is suggested that the hydroxyl free radical formed in reaction [iii] reacted predominantly in one of two ways depending upon the condition with respect to dissolved oxygen concentration.

In aerated solutions:

$$OH + O_s \xrightarrow{k_5} O_s.OH$$

$$O_s.OH + OH \xrightarrow{k_6} H_2O_{2i} + O_s.$$

In deaerated solutions:

$$OH + OH \xrightarrow{k_7} H_2O + \tfrac{1}{2}O_2.$$

The direct recombination of hydroxyl free radicals to form H_2O_2 was discounted by Weiss (3) because of dipolar repulsion, but he felt recombination in solution to form H_2O_2 was possible under the catalytic influence of various molecules or ions, such as dissolved oxygen (4). Stein (5) has suggested that many free radicals show a great tendency to combine with oxygen. Hydroxyl free radical, in this system, is thought to combine with surface oxygen in aerated sulphuric acid solutions; the product is subsequently rapidly reacted upon by more hydroxyl free radicals to form molecular hydrogen peroxide and regenerate the surface oxygen.

In the absence of surface oxygen, dismutation of hydroxyl radicals takes place by reaction at the solid–liquid interface, forming water and oxygen. The oxygen is removed from the solid–liquid interface by diffusion into the oxygen-free corroding solution and is swept out of the solution by the nitrogen stream bubbling through the solution.

The concentration of each of the four transitory species postulated was assumed to be small and in a stationary state with respect to time.

$$\frac{d[Cu^{+}.H_2O_2]}{dt} = 0 \qquad [10]$$

$$\frac{d[OH]}{dt} = 0 \qquad [11]$$

$$\frac{d[O_s.OH]}{dt} = 0 \qquad [12]$$

$$\frac{d[H_3O_2^{+}]}{dt} = 0 \qquad [13]$$

Therefore from equation [10] and assuming $k_{-4}[H_3O_2^+][H_2O]$ is much smaller than $k_1[H_2O_2]$

$$[Cu^+.\,H_2O_2] = \frac{k_1[Cu^+]_i[H_2O_2]_i}{k_{-1}+k_3+k_4[H_3O^+]}.$$

From the cuprous, cupric, copper equilibrium existing at the solution–solid interface,

$$[Cu^+]_i = K_a'[Cu^{++}]_i^{1/2}. \qquad [14]$$

There was no rate dependence on sample rotation speed so the diffusion gradient existing from bulk solution to interface is negligible.

$$[Cu^{++}]_i = [Cu^{++}] \qquad [15]$$

$$[H_2O_2]_i = [H_2O_2] \qquad [16]$$

In aerated solutions (from equations [11]–[16]):

$$\frac{d[Cu^{++}]}{dt} = \frac{k_3K_a'k_1[Cu^{++}]^{1/2}[H_2O_2]}{k_{-1}+k_3+k_4[H_3O^+]} \qquad [17]$$

$$\frac{d[H_2O_2]}{dt} = -\frac{1/2k_3K_a'k_1[Cu^{++}]^{1/2}[H_2O_2]}{k_{-1}+k_3+k_4[H_3O^+]}. \qquad [18]$$

In deaerated solutions (from equations [11]–[16]):

$$\frac{d[Cu^{++}]}{dt} = \frac{k_3K_a'k_1[Cu^{++}]^{1/2}[H_2O_2]}{k_{-1}+k_3+k_4[H_3O^+]} \qquad [19]$$

$$\frac{d[H_2O_2]}{dt} = -\frac{k_3K_a'k_1[Cu^{++}]^{1/2}[H_2O_2]}{k_{-1}+k_3+k_4[H_3O^+]}. \qquad [20]$$

Equations [17]–[20] are of the same form as those found experimentally for the rate of formation of cupric ion and the rate of decomposition of hydrogen peroxide due to the attack of the copper by dissolved hydrogen peroxide.

The rate constants in equations [17], [19], [20] are identical in form with those found empirically and the rate constant in equation [18] differs from the other three only by the factor 1/2, which was found experimentally.

Notation

[ ] —concentration in mole/liter;
A —exposed surface area of copper sample in cm²;
V —volume of corroding solution in liters;
i —denotes solid–liquid interface;
O_s —oxygen at surface of metal;
Time, t —reaction time in hours.

REFERENCES

1. B. C.-Y. Lu and W. F. Graydon. Can. J. Chem. **32**, 153 (1954).
2. D. W. Colcleugh and W. F. Graydon. J. Phys. Chem. In press.
3. J. Weiss. Trans. Faraday Soc. **36**, 856 (1940).
4. G. G. Jayson, G. Scholes, and J. Weiss. J. Chem. Soc. 1358 (1957).
5. G. Stein. J. chim. phys. **52**, 634 (1955).

THE POLYMERIZATION OF 1-BUTENE BY $TiCl_3$–$Al(i\text{-}Bu)_3$ CATALYSTS

M. H. JONES AND M. P. THORNE
Department of Chemistry, Ontario Research Foundation, Toronto, Ontario

Received March 14, 1962

ABSTRACT

An investigation has been made of the polymerization of 1-butene by $TiCl_3$–$Al(i\text{-}Bu)_3$ catalysts in heptane solution at 40° C. The polymerization curve has two segments covering initial and steady-state periods at which the rate increases several fold. The change in rate, which occurs after the formation of a constant amount of polymer for a given concentration of $TiCl_3$, is interpreted as an increase in surface area due to breakdown of the catalyst particles. For the steady-state period, it has been shown that the rate of polymerization is proportional to the monomer and titanium trichloride concentrations and approaches a constant value as the aluminum triisobutyl concentration increases.

The intrinsic viscosity of the bulk polymer and the crystallinity, as determined by infrared analysis, were found to be essentially independent of the concentrations of the catalyst components and the extent of polymerization.

The results are considered in terms of current theories on the mechanism of heterogeneous polymerization.

INTRODUCTION

Since the development of Ziegler–Natta type catalysts for the polymerization of α-olefins and dienes, many instances have been reported of the polymerization of 1-butene using, for the most part, catalysts prepared from aluminum alkyls and titanium tetrachloride or trichloride. However, kinetic studies (1, 2) have been confined to titanium tetrachloride systems, where problems have been encountered in making reproducible rate measurements. In part, this is understandable from the fact that the activity of these catalysts is believed to be associated with the formation of metal–organic complexes, involving titanium in a lower valency state, which are ill-defined and result from a series of complex reduction reactions between the tetrachloride and the metal alkyl (3–5). With propylene as the monomer, it has been found (6) that the use of titanium trichloride in place of the tetrachloride gives catalysts which are more reproducible and which yield polymers of greater stereoregularity. Similar observations have been reported (7) in a kinetic investigation of the polymerization of styrene by titanium trichloride – aluminum alkyl catalysts.

The present work is concerned with a kinetic study of the polymerization of 1-butene with aluminum triisobutyl – titanium trichloride catalysts and an examination of the effect of catalyst concentration and component ratio on the molecular weights and crystallinities of the polymers obtained.

EXPERIMENTAL

Polymerizations

The polymerization reactions were carried out in heptane solution at 40±0.2° C using Boston round bottles which were rotated end over end in a thermostatically controlled water bath. The methods employed for the purification of the solvent, catalyst components, etc., and the technique of catalyst preparation have been described previously (5).

For each series of reactions using the same ratio of catalyst components but different total concentrations, a single catalyst preparation was made and suitable samples withdrawn by a hypodermic syringe for injection into the monomer–solvent mixture. With bottle polymerizations it was not possible to follow the complete course of any single polymerization experiment because of the heterogeneous nature of the reaction mixture, and the fact that the polymer forms a gel around the catalyst particles, preventing effective sampling. Consequently, rates were determined from the amount of polymer formed during a

standard polymerization time. For each catalyst condition, duplicate reaction mixtures were prepared and the reactions stopped by the addition of ethanol at 24 and 48 hours respectively.

In several cases, the whole polymerization reaction for a given catalyst condition was followed by preparing a number of identical reaction mixtures and terminating them at suitable time intervals.

The polymers were recovered by precipitation in a 20-fold excess of ethanol while stirring in a Waring Blendor. After filtration and drying under vacuum, the crude products had ash contents of 1–2%. Further removal of the catalyst residue to an ash content of less than 0.5% was effected by reprecipitation and subsequent digestion in acidified 90% aqueous ethanol from a hot tetralin solution containing dibutyl *p*-phenylenediamine as antioxidant.

Viscosity Measurements

The intrinsic viscosities of the various polymer samples were determined in tetralin solution at 135° C using an Ubbelhode viscometer having a large bulb to permit dilution of the sample *in situ*. Polymer solutions (0.2 g/100 cc) were prepared at the bath temperature with a solvent containing 0.2% by weight of the antioxidant to prevent degradation. Under these conditions, solution flow times remained constant over a period of 3–4 hours and agreement between consecutive readings was found to be within 0.2 sec. It was established that the antioxidant had no detectable effect on the flow time of the pure solvent.

Polymer Fractionation

The polymer samples were separated into three fractions by extraction in a Soxhlet apparatus with ether and heptane. The ether extraction was continued until the solution failed to produce cloudiness when added to ethanol. The ether-soluble fraction was then obtained by evaporation of the solvent.

The extraction with heptane was continued for a standard time (4 hours) and the dissolved polymer recovered by precipitation in ethanol. Prolonged extraction with heptane resulted in complete removal of the polymer from the Soxhlet thimble in the form of a well-dispersed gel. The infrared absorption spectra of the separate fractions showed that the 4-hour extraction period was sufficient to increase the crystallinity of the residue to a constant level, which was assumed to be 100%.

The residue from the heptane extraction was dissolved in tetralin at 135° C, and reprecipitated from ethanol.

Crystallinity Measurements

The crystalline contents of the polymers were determined by infrared analysis on KCl pellets using the absorption peak due to crystallinity at 923 cm^{-1}. The samples were prepared by mixing a hot tetralin solution of the polymer with freeze-dried KCl at 120° C, the temperature of the mixture being maintained above 70° C while the solvent was removed by pumping under vacuum. The pellets, having an average thickness of 0.13 cm and containing a known concentration of polymer in the range 2.5–3.0%, were obtained by pressing the dried mixture under vacuum at a pressure of 100,000 p.s.i.

RESULTS

The results of a series of polymerization experiments covering a range of catalyst concentrations and component ratios are given in Table I. These were obtained using a single sample of titanium trichloride which, after pumping in vacuum, showed a residual tetravalent titanium content of 3%. Other samples from the same production lot were found to give lower rates of polymerization and also to contain lower amounts of tetravalent titanium. However, it was established that the addition of titanium tetrachloride to various samples of the trichloride to bring the Ti^{4+} content to a constant level resulted in comparable rates of polymerization. This method was employed to prepare reaction mixtures to study the course of the polymerization reaction under conditions in which the overall rates were similar to those reported in Table I.

Plots of the amount of polymer formed as a logarithmic function with respect to time for various catalyst concentrations are shown in Fig. 1. It is apparent that there are two segments to the rate curves. Both of these are essentially linear, indicating that the polymerization reaction is first order with respect to monomer concentration up to conversions of at least 85–90%. Values of the rate constants for the initial and final periods (k_1 and k_f) for different catalyst conditions are given in Table II. These data provide preliminary evidence that both rates increase progressively with the titanium trichloride concentrations and are independent of the ratio of catalyst components. More detailed information on these points has been obtained by calculating the values of k_f

TABLE I
Data on polymerization experiments

Expt. No.	[M] (mole l^{-1})	$[TiCl_3].10^2$ (mole l^{-1})	$[Al(i\text{-}Bu)_3].10^2$ (mole l^{-1})	Al:Ti	Time (hr)	% Polymn.	$k_f.10^2$ (hr^{-1})	Fractionation, % soluble in: Ether	Heptane	Residue	Crystallinity (%)	$[\eta]$ dl g^{-1}	$\bar{M}.10^{-3}$*
136	1.7	0.92	0.46	0.5	48	0	—						
135	1.7	1.8	0.90	0.5	48	0	—						
134	1.7	3.6	1.8	0.5	24	1.4	(0.35)						
133	1.7	3.6	1.8	0.5	48	4.8	(0.60)						
132	1.7	5.2	2.6	0.5	24	5.4	(1.45)						
131	1.7	5.2	2.6	0.5	48	17.8	(2.45)						
130	1.7	0.92	0.92	1.0	24	0.3	—						
129	1.7	0.92	0.92	1.0	48	3.6	(0.45)						
128	1.7	1.8	1.8	1.0	24	0.4	—						
127	1.7	1.8	1.8	1.0	48	5.0	(2.05)						
126	1.7	3.6	3.6	1.0	24	41.4	4.60	12	40	39	57.5	4.58	815
125	1.7	3.6	3.6	1.0	48	46.8	2.50						
124	1.7	5.2	5.2	1.0	24	52.2	6.55	25	36	29	49.0	3.92	665
123	1.7	5.2	5.2	1.0	48	80.6	5.15	24	37	24			
160	1.7	0.92	1.8	2.0	24	11.2	0.80				56.0	4.57	815
161	1.7	0.92	1.8	2.0	48	25.5	0.90						
162	1.7	1.8	3.6	2.0	24	36.3	3.00	21	25	38	57.0	4.10	705
165	1.7	1.8	3.6	2.0	48	56.0	2.30	17	27	29			
164	1.7	2.7	5.4	2.0	24	54.9	5.00						
163	1.7	2.7	5.4	2.0	48	85.5	5.05						
154	1.7	3.5	7.0	2.0	24	71.4	7.50	10	71	12	50.0	4.15	710
155	1.7	3.5	7.0	2.0	48	91.0	6.25						
152	1.7	4.3	8.6	2.0	24	75.0	8.55						
150	1.7	5.1	10.2	2.0	24	91.0	13.30	17	46	27	62.5	4.12	710
157	3.4	5.1	10.2	2.0	24	85.5	8.90						
151	1.7	5.1	10.2	2.0	48	~100	—	18	36	55			
122	1.7	0.92	2.8	3.0	24	7.2	0.65				45.0	4.33	760
121	1.7	0.92	2.8	3.0	48	30.0	1.00						
120	1.7	1.8	5.4	3.0	24	45.6	4.10				46.6	4.47	790
119	1.7	1.8	5.4	3.0	48	39.2	3.05						
118	1.7	3.4	10.2	3.0	24	70.8	7.30	14	48	37	53.5	4.77	865
117	1.7	3.4	10.2	3.0	48	88.0	5.40						
116	1.7	4.9	14.7	3.0	24	93.0	14.30	17	41	26	65.5	4.18	765
115	1.7	4.9	14.7	3.0	48	88.0	—						
144	1.7	0.92	4.6	5.0	24	15.6	1.05					4.53	805
143	1.7	0.92	4.6	5.0	48	25.5	0.80				54.5		
142	1.7	1.8	9.0	5.0	24	30.8	2.70	17	49	19	54.5	4.69	825
141	1.7	1.8	9.0	5.0	48	91.0	5.60						
140	1.7	3.4	17.0	5.0	24	84.5	9.85	17	43	31	64.5	4.51	805
139	1.7	3.4	17.0	5.0	48	~100	—	19	39	27			
138	1.7	4.9	24.5	5.0	24	~100	—	14	41	27	60.1	4.71	845
137	1.7	4.9	24.5	5.0	48	96.0	—	20	57	17			

*Derived from relationship for polypropylene, ref. 8.

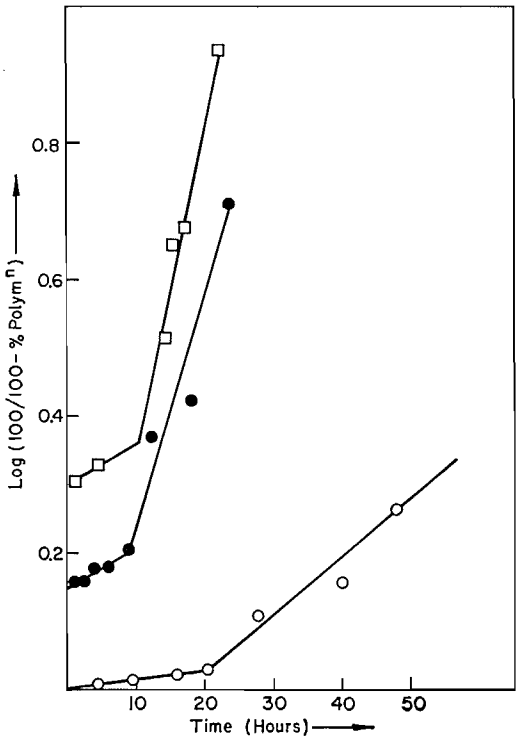

FIG. 1. First-order reaction plots for different catalyst concentrations with the same ratio of components (Al:Ti = 2.0); [$TiCl_3$]: ○ $1.8.10^{-2}$, ● $3.6.10^{-2}$, □ $5.1.10^{-2}$ mole l^{-1}. For clarity, two curves are displaced vertically from the origin.

TABLE II

Effect of catalyst conditions on k_i and k_f

Expt. No.	[$TiCl_3$].10^2	Al:Ti	$x_i.10^{2*}$	t_i* (hr)	x_i/[$TiCl_3$]	$k_i.10^3$ (hr^{-1})	$k_f.10^2$ (hr^{-1})	k_i/k_f
290	1.8	2.0	0.49	21	2.7	2.86	17.0	0.165
240	3.6	2.0	0.90	8.6	2.5	12.4	74.2	0.170
280	5.2	2.0	1.21	10.7	2.3	15.7	90.3	0.170
250	3.6	5.0	0.98	9.5	2.7	12.4	79.0	0.160
230†	3.6	2.0	0.89	48.0	2.5	1.57	8.87	0.175

*x_i = moles monomer consumed during initial period; t_i = time of initial period.
†Catalyst not activated with $TiCl_4$.

for the experiments listed in Table I, using the fact that the ratio of the initial and final rates, k_1/k_f, is constant for all polymerization conditions.

The dependence of the rate constant k_f on the concentration of titanium trichloride is shown in Fig. 2. Although there is some scatter in the data the rate is essentially independent of the Al:Ti ratio at values of 2 and above, and approaches a linear relationship with respect to titanium trichloride concentration in the high concentration range. Essentially the same result is obtained if the overall reaction rate is used, as determined from the amount of polymer formed after the standard polymerization times of 24 and 48 hours, although the curvature of the plot is greater.

A plot of the rate constant per unit concentration of titanium trichloride, k_f/[$TiCl_3$], as a function of the aluminum triisobutyl concentration is given in Fig. 3. It follows

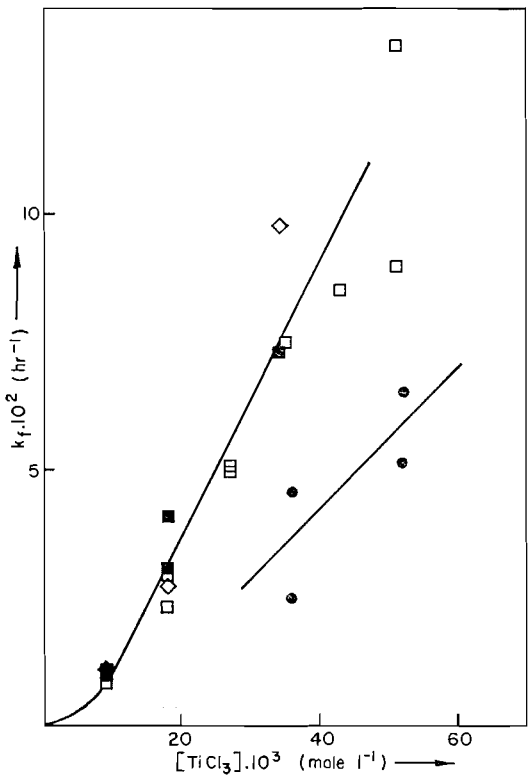

FIG. 2. Plot of k_f versus $[TiCl_3]$; Al:Ti: ● 1.0, □ 2.0, ■ 3.0, ◇ 5.0.

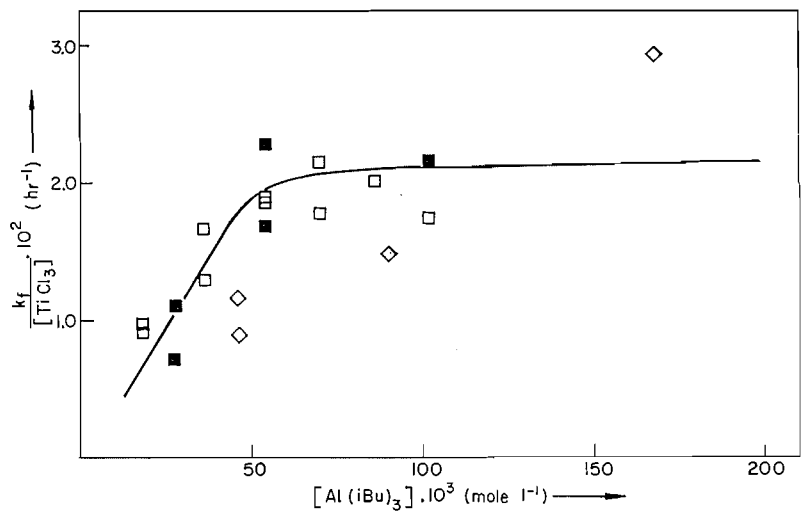

FIG. 3. Plot of $k_f/[TiCl_3]$ versus $[Al(i\text{-}Bu)_3]$; Al:Ti: □ 2.0, ■ 3.0, ◇ 5.0.

that the rate is dependent on $[Al(i\text{-}Bu)_3]$, approaching a constant value in the high range. This provides an explanation for the curvature of the plot of k_f versus $[TiCl_3]$,

since experiments in which the [Al(*i*-Bu)$_3$] is in the low range are also generally those in which the [TiCl$_3$] is in the low range. It may be assumed, therefore, that the rate of polymerization is essentially a linear function of the titanium trichloride concentration.

The apparent dependence of rate on the Al:Ti ratio below values of 2 may also be attributed, at least in part, to the effect of rate dependence on the [Al(*i*-Bu)$_3$] in the low concentration range.

Molecular Weights

The intrinsic viscosities of a number of unfractionated polymer samples are recorded in Table I. In the absence of data on a molecular weight – intrinsic viscosity relationship for poly-1-butene, approximate values of molecular weight for these samples have been calculated from that obtained by Moraglio (8) for polypropylene under identical conditions of solvent and temperature, viz.

$$[\eta] = 1.93.10^{-4}\bar{M}^{0.74}.$$

The effect of polymerization conditions on the molecular weight of the bulk polymer, expressed as a logarithmic function of the intrinsic viscosity ($\log [\eta] \propto \log \bar{M}$), is illustrated in Fig. 4. It is apparent that the molecular weight is essentially independent of

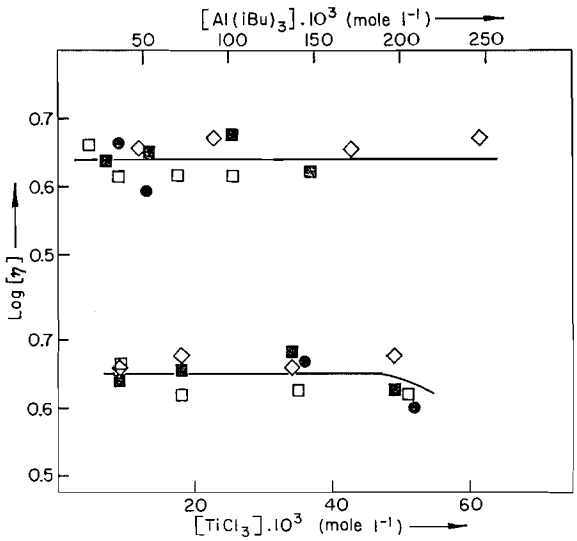

FIG. 4. Plots of log [η] versus [TiCl$_3$] and [Al(*i*-Bu)$_3$]; Al:Ti: ● 1.0, □ 2.0, ■ 3.0, ◇ 5.0.

both the concentration of titanium trichloride and aluminum alkyl. Similarly, it has also been found that the molecular weight is independent of the extent of polymerization, as shown in Fig. 5. In this case the individual points are for reactions carried out under widely different catalyst concentrations and ratios, and the constancy of molecular weight is dependent on the prior condition of no effect of catalyst variables as established above.

An example of the change in molecular weight with the fractions obtained by solvent extraction of a bulk polymer is given in Table III.

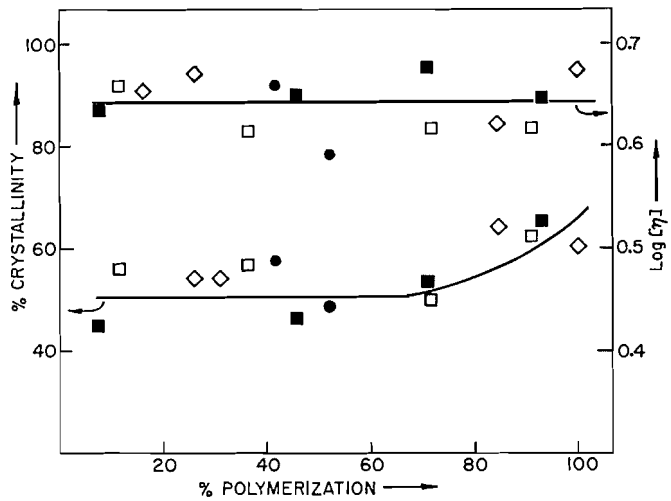

FIG. 5. Plots of log [η] (upper curve) and % crystallinity (lower curve) as a function of % polymerization; Al:Ti: ● 1.0, □ 2.0, ■ 3.0, ◇ 5.0.

TABLE III

Crystallinity and viscosity data for fractionated polymers

Expt. No.	Solvent	Crystallinity (%)	[η] (dl g^{-1})	$\bar{M}.10^{-3}$
162	Ether	0	1.18	130
118	Heptane	60.0	—	—
124	Heptane	67.0	—	—
150	Heptane	65.5	—	—
162	Heptane	—	4.65	835
118	Tetralin	94	—	—
124	Tetralin	108	—	—
140	Tetralin	94	—	—
162	Tetralin	100	5.28	990

Crystallinities

The infrared absorption spectra in the solid and molten states of the tetralin-soluble fractions of poly-1-butene, which should contain the greatest degree of isotacticity, were essentially identical with those reported by Natta (9). Two modifications exist in the solid state, the stable form having absorption bands at 1328, 1060, 1028, 1014, 976, 923, 848, 817, and 799 cm^{-1} which may be attributed to crystallinity. It was confirmed that the unstable modification is obtained on rapid cooling from the melt and it was found that conversion to the stable modification is not complete even after a period of several weeks. Some difficulty was experienced initially in the preparation of samples for optical density measurements in that as much as 40% of the unstable modification could be present if the polymer solution – KCl mixture was allowed to cool too rapidly during removal of the solvent. This is somewhat surprising in view of the pressure used in preparing the pellets, which was well in excess of that reported (9) to give rapid transformation to the stable modification.

The spectra of the ether-soluble fractions showed a complete absence of the crystalline peaks and the samples were assumed, therefore, to consist entirely of amorphous or atactic poly-1-butene. However, it was noted that the spectra were not identical with

those of the molten tetralin-soluble fractions, small differences being observed in the 900–1300 cm^{-1} region. In particular, a broad absorption band occurs at 937 cm^{-1}. This could not be attributed to solvent or catalyst residues and is unlikely to represent an end-group effect, in view of the comparatively high molecular weight of these fractions.

The crystalline contents of a series of unfractionated polymers are given in Table I. These were determined from optical density measurements using the strongest crystalline absorption band at 923 cm^{-1}. The calibration curve was prepared from synthetic mixtures of the ether-soluble or atactic polymer and the tetralin-soluble polymer. The latter was assumed to be 100% isotactic and, hence, to exhibit the maximum degree of crystallinity under the conditions of measurement. The optical densities of these fractions from different polymerization experiments were constant within the experimental accuracy (Table III).

The effect of polymerization conditions on crystallinity is shown in Fig. 6. Essentially, it is independent of both the titanium trichloride and aluminum triisobutyl concentration. There is some evidence of a trend to higher values with increasing concentration

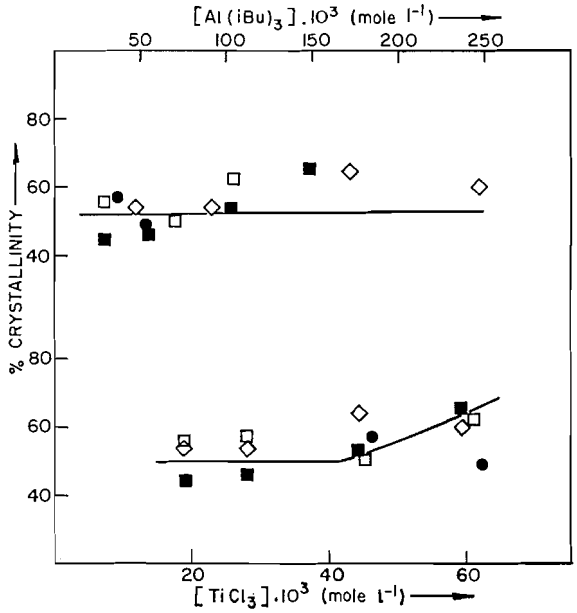

FIG. 6. Plots of % crystallinity versus $[TiCl_3]$ and $[Al(i\text{-}Bu)_3]$; Al:Ti: ● 1.0, □ 2.0, ■ 3.0, ◇ 5.0.

of the catalyst components but this probably represents a reflection of the small increase in crystallinity with the extent of polymerization as illustrated in Fig. 5. Higher yields of polymer were obtained with increasing titanium trichloride concentration.

Infrared analysis of some of the heptane-soluble fractions, Table III, gave crystallinity values of 60–70%, and the presence of the absorption band at 937 cm^{-1} indicated that the samples contained atactic polymer or atactic segments in the polymer chains. On the assumption that the crystalline content of these fractions is 65% and that of the tetralin-soluble fractions is 100%, crystallinity values have also been determined from the fractionation data listed in Table I. These fall in the range 58–72% and, as with the results for unfractionated polymer samples, are essentially independent of the polymerization conditions.

DISCUSSION

For the present catalyst system it has been shown that there are two segments to the overall polymerization curve, which may be termed the initial and steady-state periods, the rate during the latter being several fold greater. Also, the length of the initial period is determined by the amount of polymer formed for a given titanium trichloride concentration and is independent of the concentration of aluminum alkyl (Table II).

With heterogeneous catalysts of this type it is generally considered that polymerization occurs at active sites on the surface of the trichloride crystals (3, 10, 11). Thus, the increase in rate constant on the change to the steady-state period can be attributed to a breakup of the titanium trichloride crystals, revealing fresh surfaces at which additional polymerization centers can form by adsorption and complex formation with the excess aluminum alkyl present in the solution. The fact that the change in rate occurs at a fixed ratio of polymer to titanium trichloride suggests that cleavage of the crystals results from forces exerted by the polymer as it builds up on the catalyst surface, once a critical level is exceeded. This process of particle breakdown appears to take place in a uniform manner to provide a constant increase in surface area (more specifically of active sites) since the ratio of the rate constants for the initial and steady-state periods is independent of both the absolute rate and the titanium trichloride concentration. The occurrence of an initial adjusting period after which the rate of polymerization reaches a steady value has been noted with comparable catalyst systems (7, 12) and has been attributed to a similar cause (12).

For the steady-state period, it has been established that the rate is proportional to both the concentration of monomer and that of the titanium trichloride. In the case of the latter it is obvious that the relationship is not one of concentration but of surface area, since the system is heterogeneous, and the linear dependence of rate can be interpreted as the formation of a constant number of catalytic sites for each unit of available surface. Similarly, the trend in the values of $k_t/[TiCl_3]$ towards a constant level with increasing $[Al(i\text{-}Bu)_3]$ may be attributed to an approach to the condition of saturation of all potential polymerization sites on the surface. A similar kinetic pattern has been reported for the polymerization of propylene and styrene with $TiCl_3$–$AlEt_3$ catalysts (6, 7, 13), although the limiting condition of independence of rate on the metal alkyl concentration extends to much lower levels.

The higher rates observed with titanium trichloride samples containing residual amounts of tetravalent titanium appear to be related to the formation of a greater number of active sites on the trichloride base, as catalysts prepared from titanium tetrachloride at the impurity levels encountered are inactive.

Polymerization by Ziegler–Natta type catalysts is generally considered to proceed by an anionic mechanism and several possible steps have been suggested for the termination of growing polymer chains (13), viz.,

(i) direct intramolecular termination at the catalyst site by hydride ion transfer:

$$\overset{\delta+\ \delta-}{\text{cat. } CH_2CH(C_2H_5)\cdots} \rightarrow \overset{\delta+\ \delta-}{\text{cat. H}} + CH_2{=}C(C_2H_5)\cdots;$$

(ii) hydride ion transfer involving monomer:

$$\overset{\delta+\ \delta-}{\text{cat. } CH_2CH(C_2H_5)\cdots} + CH_2{=}CH(C_2H_5) \rightarrow \overset{\delta+\ \delta-}{\text{cat. } CH_2CH_2C_2H_5} + CH_2{=}C(C_2H_5)\cdots;$$

(iii) chain transfer involving metal alkyl:

$$\overset{\delta+\ \delta-}{\text{cat. CH}_2\text{CH}(\text{C}_2\text{H}_5)\cdots} + \text{AlR}_3 \rightarrow \overset{\delta+\ \delta-}{\text{cat. R}} + \text{R}_2\text{AlCH}_2\text{CH}(\text{C}_2\text{H}_5)\cdots;$$

(iv) a chain transfer process that is kinetically dependent on $[TiCl_3]$.

Process (iv) may be neglected, as the intrinsic viscosities of the polymers and, consequently, the molecular weights were found to be independent of the concentration of titanium trichloride. Hence the average polymeric chain length can be expressed in the form

$$\bar{P} = k_p[M]/(k_{t_1}+k_{t_2}[M]+k_{t_3}[A]),$$

where k_p, k_{t_1}, k_{t_2}, and k_{t_3} are the rate constants for propagation and termination by steps (i) to (iii), and [M] and [A] are the concentrations of monomer and aluminum alkyl. It follows that the reciprocal of the chain length is

$$1/\bar{P} = k_{t_1}/k_p[M]+k_{t_2}/k_p+k_{t_3}[A]/k_p[M].$$

This expression applies strictly to instantaneous rates or, in practice, to low polymer yields. However, the effects of the different termination steps will be apparent in the molecular weight of the polymer, at least qualitatively, over the range of yields encountered. As no significant influence on the intrinsic viscosity was noted with changes in the aluminum alkyl concentration, it may be assumed that the predominant termination reactions are processes (ii) and (iii) and that

$$k_{t_2}+k_{t_1}/[M] \gg k_{t_3}[A]/[M]$$

for the conditions employed. The range of average monomer concentrations encompassed, as reflected in the extent of polymerization, is small, but the constancy of molecular weight with polymer yield suggests that termination by monomer transfer (process (ii)) is favored.

In this simple analysis it has been assumed that the concentrations of the species involved in termination processes are those of the solution phase. The same conditions will be met for adsorbed species provided the concentrations in solution are linearly related to those in the adsorbed phase. This situation will apply for the limiting condition of low surface coverage in a Langmuir-type adsorption isotherm. The fact that the rate of polymerization is proportional to the monomer concentration supports this contention.

The influence of polymerization conditions on the crystallinity of the poly-1-butene is small. In this particular case, crystallinity is considered to represent the degree of stereoregularity in the polymer chains, although there may be no simple relationship between the two factors. Thus, the isotactic content of the polymer is also largely unaffected by polymerization variables. Similar observations have been reported for the polymerization of propylene (6). Chemical and X-ray analyses of the solid phase of the present catalyst system have shown (5) that it consists essentially of unchanged titanium trichloride with a small residual content of aluminum and alkyl groups, and it has been proposed (3, 10, 11) that the active sites for polymerization with such catalysts are locations on the crystal surface where the metal alkyl is adsorbed or enters into complex

formation with a particular configuration which provides steric control during the propagation step. In terms of this model, the relative constancy of the crystalline content of the polymer with the extent of polymerization implies that the configuration of the active centers formed on the new surfaces, revealed by breakdown of the titanium trichloride crystals during polymerization, is essentially the same as that present initially. Similarly, the nature of the sites is not affected by the aluminum alkyl concentration. The slight increase in crystallinity at high conversions may reflect a change in the nature of the complexes due to transfer.

ACKNOWLEDGMENTS

The authors are indebted to Miss E. Kirby for assistance with the infrared analyses.

This work was made possible by a research grant to the Ontario Research Foundation from the Province of Ontario.

REFERENCES

1. A. MEDALIA, A. ORZECHOWSKI, J. TRINCHERA, and J. MORLEY. J. Polymer Sci. **41**, 241 (1959).
2. A. TOPCHIEV, B. KRENTZAL, H. POKOTILO, and E. ERASOVA. Doklady Acad. Nauk S.S.S.R. **124**, 1255 (1959).
3. G. NATTA. J. Inorg. & Nuclear Chem. **8**, 589 (1958).
4. M. L. COOPER and J. B. ROSE. J. Chem. Soc. 795 (1959).
5. M. H. JONES, U. MARTIUS, and M. P. THORNE. Can. J. Chem. **38**, 2303 (1960).
6. G. NATTA, I. PASQUON, and E. GIACHETTI. Angew. Chem. **69**, 213 (1957).
7. G. M. BURNETT and P. J. TAIT. Polymer, **1**, 151 (1960).
8. G. MORAGLIO. Chim., e ind. (Milan), **41**, 879 (1959).
9. G. NATTA. Makromol. Chem. **31**, 94 (1960).
10. F. EIRICH and H. MARK. J. Colloid Sci. **11**, 748 (1956).
11. H. UELZMANN. J. Polymer Sci. **32**, 457 (1958).
12. G. NATTA, I. PASQUON, and E. GIACHETTI. Chim., e ind. (Milan), **39**, 1002 (1957).
13. G. NATTA. J. Polymer Sci. **34**, 21 (1959).

IONIZATION OF ORGANIC COMPOUNDS

IV. STUDIES OF ETHANOL AND ETHYL ETHER IN SULPHURIC ACID BY NUCLEAR MAGNETIC RESONANCE

J. T. EDWARD, J. B. LEANE,[1] AND I. C. WANG
Department of Chemistry, McGill University, Montreal, Que.

Received March 20, 1962

ABSTRACT

The chemical shift of the methyl protons relative to the methylenic protons of an ethyl group attached to a basic center increases with the acidity of the medium. This increase may be attributed to two effects: over a relatively narrow range of acidity function (H_0) values, to protonation of the basic center; over the complete H_0 range investigated, to a general solvent effect, which may be due to changing strengths of hydrogen bonds between the basic center or its conjugate acid and solvent water molecules. Protonation constants (pK_{BH^+}) of -1.1 for propionamide and -6.9 for propionic acid have been calculated, in good agreement with values obtained by the ultraviolet spectrophotometric method; the constants calculated for diethyl ether (-6.2) and ethanol (-4.8) are much less certain, because of the greater magnitude of the solvent effect with these compounds.

INTRODUCTION

The basicities of many aromatic compounds in aqueous acids have been determined since 1935 by Hammett's spectrophotometric method (1). However, the application of this method to aliphatic compounds has been restricted by their feeble absorption in the conveniently accessible range of ultraviolet frequencies (2–4), and new methods for following the ionization of such compounds are needed. Arnett and Wu (5) have made use of solubility changes attendant on the protonation of ethers for determining their basicities, and in the present work we have attempted to use nuclear magnetic resonance to follow the ionization of compounds having an ethyl group attached to the ionizing center. It is known that the difference in chemical shift of the methyl and methylenic protons of ethyl compounds CH_3CH_2X (which, following Stone (6), we shall term the "internal chemical shift" and symbolize by δ_1) is an approximately linear function of the electronegativity of the atom of X directly bonded to the ethyl group (7). Consequently, it can be expected that protonation of X will lead to a large increase in this difference. This expectation has been realized,* although it has become apparent that δ_1 is not only a sensitive index of protonation but also of other forms of interaction with the solvent.

EXPERIMENTAL

Materials

The purification of propionamide and propionic acid have already been described (4). Reagent grade ethanol, ethyl ether, and ethylamine were used without further treatment.

Procedure

Nuclear magnetic resonance spectra of approximately 3% solutions of the organic compounds in acid were measured at room temperature (ca. 23°) as soon as possible (10–15 minutes) after mixing of the solutions, using a Varian V4300-B high-resolution spectrometer operating at 60 Mc/sec. The chemical shift (δ_1) between the centers of the methyl triplet and the methylene quadruplet was measured to ± 0.5 c.p.s., the recorder trace being calibrated by the side-band technique using a Hewlett–Packard frequency counter. In most cases four to six measurements of δ_1 were made, alternately with increasing and decreasing

[1]*Present address: Perkin–Elmer Ltd., Beaconsfield, Bucks, England.*

**Stone and his collaborators (6) have recently observed a similar effect when X is coordinated with a Lewis acid.*

field. The concentration of acid in the solutions was determined by titration, and the H_0 values read from large-scale plots of H_0 against acid concentration constructed from the data of Paul and Long (8).*

RESULTS AND DISCUSSION

The internal chemical shifts of ethanol, ethylamine, and propionic acid in dilute aqueous solution (Table I) are close to the values found by Dailey and Shoolery (7) for the compounds in 50% benzene solution. As expected, δ_i of these and the other compounds

TABLE I

Internal chemical shifts (δ_i) and protonation constants (pK_{BH^+}) of compounds CH_3CH_2X

	δ_i (in p.p.m.)				
X	EtX*†	EtX‡	$EtXH^+$ *	$-pK_{BH^+}$*	$-pK_{BH^+}$§
—OH	2.49	2.55	2.80	4.8	—
—OEt	2.39	—	2.83	6.2	3.61 (5)
$—NH_2$	1.75‖	1.84	1.97¶	—	—
$—CO_2H$	1.32	1.23	1.59	6.9	6.8 (4)
$—CONH_2$	1.19	—	1.40	1.1	0.9 (4)

*Present study.
†In dilute aqueous acid.
‡Reported by Dailey and Shoolery (7) for compounds diluted with an equal volume of benzene.
§Reported values (lit. reference).
‖In 0.01 *N* NaOH.
¶In 0.01 *N* HCl.

increases with increasing acidity of the medium, and, furthermore, plots of δ_i against the acidity function H_0 (8) of the solvent give sigmoid curves, characteristic of the protonation of neutral Brønsted bases, as shown in Figs. 1 and 2. The pK_{BH^+} values in Table I have

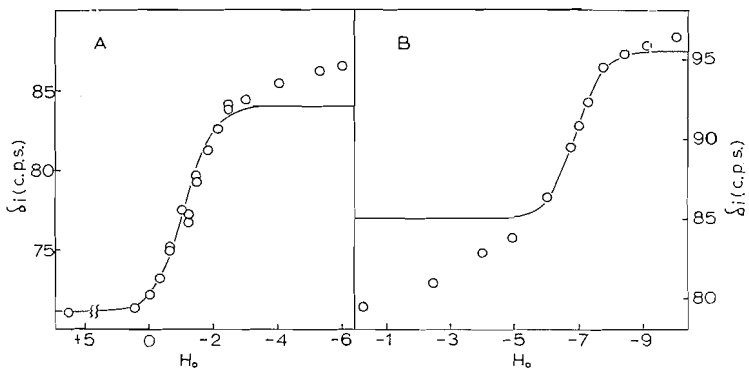

FIG. 1. Change in internal chemical shift (δ_i) with acidity. Points: experimental; curves: theoretical for equation [1], with parameters shown. A. Propionamide: $pK_{BH^+} = -1.1$, $\delta_i^{EtX} = 71.2$ c.p.s., $\delta_i^{EtXH^+} = 84.0$ c.p.s. B. Propionic acid: $pK_{BH^+} = -6.9$, $\delta_i^{EtX} = 85.0$ c.p.s., $\delta_i^{EtXH^+} = 95.5$ c.p.s.

been obtained from the H_0 values of the inflection points of these curves, this method having been shown previously to give the most reliable values (4). The protonation

**Such H_0 values strictly refer to aqueous solutions of acid containing extremely small concentrations of Brønsted base, comparable to the concentrations of indicators used in determining them (8). In the present studies the sulphuric acid is diluted by water plus organic compound, rather than water alone; when the organic compound is a stronger base than water (e.g. propionamide), this should cause the acidity of the solution to be less than that indicated by the data of Paul and Long. The low concentration of organic compound should make this effect a small one.*

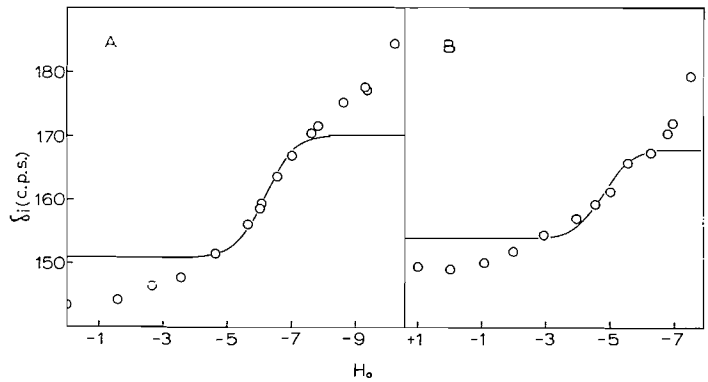

FIG. 2. Change in internal chemical shift (δ_i) with acidity. Points: experimental; curves: theoretical for equation [1], with parameters shown. A. Ethyl ether: $pK_{BH^+} = -6.2$, $\delta_i^{EtX} = 151.0$ c.p.s., $\delta_i^{EtXH^+} = 170$ c.p.s. B. Ethanol: $pK_{BH^+} = -4.8$, $\delta_i^{EtX} = 154.0$ c.p.s., $\delta_i^{EtXH^+} = 168$ c.p.s.

constants thus obtained for propionamide and propionic acid (Fig. 1) are close to the values previously obtained by the spectrophotometric method (4); the slightly weaker basicities found in the present study may be due in part to slight errors in the H_0 values caused by the fact, mentioned above, that the organic compound is present in higher concentrations than usual.

While these results with propionamide and propionic acid show the sigmoid shape of the δ_1–H_0 curves to be due to protonation of the compounds, the curves are very far from the ideal sigmoid shape (Fig. 1) required by the equation

$$[1] \qquad \log (\delta_1-\delta_1^{EtX})/(\delta_1^{EtXH^+}-\delta_1) = pK_{BH^+}-H_0,$$

which should describe (with fair precision (4)) the increase in δ_1 with H_0 if it were due to protonation alone. It is evident that, in addition, δ_1 of both neutral and protonated molecules increases continuously with increasing acidity of the medium. A possible explanation of this "solvent effect" is given later. Unfortunately the effect appears even more strongly in the curves for ethyl ether (Fig. 2A) and ethanol (Fig. 2B), and makes the estimation of precise pK_{BH^+} values for these compounds very uncertain; furthermore, the experimental points for ethanol in solutions more acidic than $H_0 = -6$ become progressively less reliable because esterification of the alcohol starts to become appreciable even in the short time required for making n.m.r. measurements after the mixing of the solutions (9). (Ethyl ether, however, is stable under the conditions of these experiments in the most strongly acidic solutions employed (5, 10).) Consequently the pK_{BH^+} value reported in Table I for diethyl ether and, even more, for ethanol can be considered only as highly tentative.

The divergence of our value for the basicity of ethyl ether from that of Arnett and Wu (5) is very large. It is possible that the changes in solubility observed by Arnett and Wu and attributed by them to formation of the protonated species Et_2OH^+ are in fact due to formation of a relatively stable hydrogen-bonded complex $Et_2O \ldots H_3O^+$. Dramatic increases in the solubility of nitrobenzene in sulphuric acid with increasing acidity were noted long ago by Hammett and Chapman (11), and shown not to be due to protonation; they are also probably due to the formation of hydrogen-bonded complexes. Arnett and Wu give reasons for rejecting this possibility, but for the moment it is reasonable to

consider the pK_{BH^+} values of aliphatic ethers unsettled, in the absence of further independent evidence. A pK_{BH^+} of -4.8 for ethanol is of about the magnitude expected from values reported for isopropyl alcohol (-3.2, -4.1) (12) and for *t*-butyl alcohol (-3.8) (13) from kinetic evidence.

The values in Table I of δ_1 of the protonated bases (except ethylammonium) are the values used in the calculation of the theoretical curves of Figs. 1 and 2, and hence, in view of the solvent effect, do not represent the maximum values of δ_1 for $EtXH^+$. However, accepting the values of the table, the increase in δ_1 accompanying protonation of the oxygen atom of ethyl ether (0.44 p.p.m.) is close to the increase accompanying its coordination with boron trifluoride (0.38 p.p.m.) (6). Further, the increase accompanying protonation of the nitrogen atom of ethylamine (0.22 p.p.m.) is almost identical with the increase accompanying the coordination of the nitrogen atom of triethylamine with boron trifluoride (0.23 p.p.m.) (6). It seems likely that about the same positive charge is developed by complexing with boron trifluoride and by protonation. The larger change in δ_1 accompanying the appearance of a positive charge on oxygen, as compared with nitrogen, is perhaps explained by the shorter carbon–oxygen bond length (14).

It is evident from the present work that the protonation of organic compounds may be followed by measurements of the internal chemical shift, but that the usefulness of the method is impaired by the magnitude of the solvent effect. Some understanding of this effect is, in consequence, desirable. At the moment only a tentative explanation for it can be advanced. It has been observed in spectrophotometric studies that donor molecules such as aliphatic ketones (3), propionic acid (4), and propionamide (4) form progressively stronger hydrogen bonds with the solvent as the acid concentration is increased, possibly with water molecules occupying the first (e.g. II) or second hydration layer of the oxonium ion. The increased strength of the hydrogen bond in going from I to II would be expected

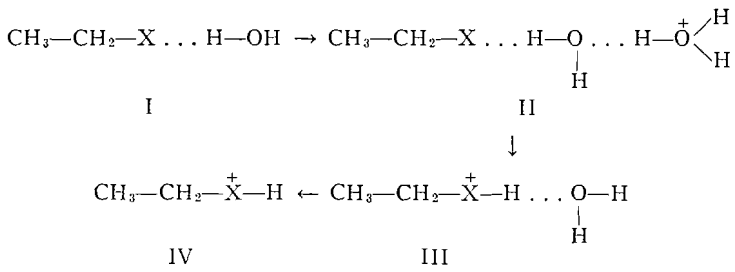

to increase the inductive effect of X, and hence to increase δ_1 of the unprotonated molecules. On the other hand, after protonation, the group XH^+ becomes the acceptor, and the oxygen of the free water molecules, the donor, as in III. With continued increase in acid strength the activity of the water decreases (15) and the hydration of protonated bases decreases (4, 16), shown schematically in III $\rightarrow$ IV. The hydration of XH^+ in III represents a slight neutralization of the partial positive charge on the hydrogen, and hence a diminution of the electron pull of the XH^+ group, so that progressive decrease in hydration (III $\rightarrow$ IV) should lead to an increase in δ_1 of the protonated molecule. The smaller solvent effects noted with the conjugate acids of propionic acid and propionamide may be due to the greater degree of charge dispersal in these compounds, with the result that hydration is less important.

Very recently Taft and Levins (17) have determined the pK_{BH^+} of *p*-fluorobenzamide and *p*-fluoroacetophenone from the change with increasing acidity in the position of the

F^{19} nuclear magnetic resonance lines, measured relative to an external standard. It was evident that the unshielding of the fluorine nuclei with increasing acidity was due to a solvent effect in addition to protonation of the carbonyl groups.

ACKNOWLEDGMENTS

We are grateful to Professors E. M. Arnett and N. C. Deno for information of unpublished results, and to the National Research Council for financial support.

REFERENCES

1. L. A. Flexser, L. P. Hammett, and A. Dingwall. J. Am. Chem. Soc. **57**, 2103 (1935).
2. A. R. Goldfarb, A. Mele, and N. Gutstein. J. Am. Chem. Soc. **77**, 6194 (1955).
3. H. J. Campbell and J. T. Edward. Can. J. Chem. **38**, 2109 (1960).
4. J. T. Edward and I. C. Wang. Can. J. Chem. **40**, 966 (1962).
5. E. M. Arnett and C.-Y. Wu. J. Am. Chem. Soc. **82**, 4999 (1960). C.-Y. Wu. Ph.D. Thesis, University of Pittsburgh, Pittsburgh, Pa. 1961.
6. T. D. Coyle and F. G. A. Stone. J. Am. Chem. Soc. **83**, 4139 (1961).
7. B. P. Dailey and J. N. Shoolery. J. Am. Chem. Soc. **77**, 3977 (1955).
8. L. P. Hammett. Physical organic chemistry. McGraw-Hill, New York. 1940. p. 262. M. A. Paul and F. A. Long. Chem. Revs. **57**, 1 (1957).
9. D. J. Clark and G. Williams. J. Chem. Soc. 4218 (1957).
10. R. L. Burwell. Chem. Revs. **54**, 615 (1954). D. Jaques and J. A. Leisten. J. Chem. Soc. 4963 (1961).
11. L. P. Hammett and R. P. Chapman. J. Am. Chem. Soc. **56**, 1282 (1934).
12. P. D. Bartlett and J. D. McCollum. J. Am. Chem. Soc. **78**, 1441 (1956). J. Rocek and J. Krupicka. Collection Czechoslov. Chem. Commun. **23**, 2068 (1958).
13. N. C. Deno, T. Edwards, and C. Perizzolo. J. Am. Chem. Soc. **79**, 2108 (1957).
14. A. Maccoll. *In* Progress in stereochemistry. Vol. I. *Edited by* W. Klyne. Butterworths, London. 1954. p. 361.
15. K. N. Bascombe and R. P. Bell. Discussions Faraday Soc. **24**, 158 (1957).
16. R. W. Taft. J. Am. Chem. Soc. **82**, 2965 (1960).
17. R. W. Taft and P. L. Levins. Anal. Chem. **34**, 436 (1962).

THE HYDROGEN ISOTOPE EFFECT IN THE PYROLYSIS OF ETHYL-1,1,2,2-d_4 CHLORIDE[1]

ARTHUR T. BLADES, P. W. GILDERSON, AND M. G. H. WALLBRIDGE
Research Council of Alberta, Edmonton, Alberta

Received February 16, 1962

ABSTRACT

The hydrogen isotope effect in the pyrolysis of ethyl-1,1,2,2-d_4 chloride has been investigated in the temperature range 758–989° C, yielding the relative rate constant expression

$$k_H/k_D = 1.16e^{985\pm50/RT},$$

where k_H and k_D are the rate constants for the production of C_2D_4 (and HCl) and of C_2D_3H (and DCl) per β-deuterium atom respectively.

The isotope effect is pressure dependent, its value increasing with decreasing pressure. The pressure effect in ethyl chloride has also been studied, and a qualitative explanation is given for the pressure dependence of intermolecular and intramolecular isotope effects.

The data are compared with the isotope effects in ethyl-d_4 bromide and ethyl-d_4 acetate, and the conclusion is reached that the evidence supports a four-centered transition-state complex in the case of the halides.

INTRODUCTION

The thermal decomposition of ethyl chloride is believed to be an example of a unimolecular reaction. Barton and Howlett (1) have shown that it decomposes into ethylene and hydrogen chloride in the stoichiometric ratio, and that increases in surface area and addition of propylene have no influence upon the kinetics. They concluded, therefore, that the mechanism does not involve a radical chain, but rather is a simple, homogeneous, unimolecular process. Further investigation by Howlett (2) has revealed that the rate constants are pressure dependent in the pressure region below 1 cm Hg.

The deuterium isotope effect in the pyrolysis of ethyl chloride is of interest because a carbon–hydrogen bond is being broken in the course of the reaction, and because the reaction is pressure dependent. In recent years, a number of isotope effects have been shown to be pressure dependent. R. E. Weston, Jr. (3), investigating the decomposition of cyclopropane-*t*, has observed a decrease in the isotope effect with lowering of pressure, and Langrish and Pritchard (4) have found a similar pressure effect in the pyrolysis of cyclobutane and octadeuterocyclobutane. Further, Blades (5) has demonstrated that the isotope effect in the cyclopropane–cyclopropane-d_6 decomposition is pressure dependent, the isotope effect at 482° C decreasing from 1.96 at 75 cm Hg to 1.35 at 0.0178 cm Hg.

The present work involves a re-examination of the pressure effect in the decomposition of ethyl chloride, and a study of the isotope effect in ethyl-1,1,2,2-d_4 chloride from the standpoint of its variation with pressure and temperature coefficient. If the generally accepted mechanism involving a four-centered transition state is correct, elimination from the ethyl-1,1,2,2-d_4 chloride molecule can yield two product ethylenes—C_2D_4 and C_2D_3H—from whose ratio the intramolecular isotope effect may be derived. The pressure dependency of this isotope effect is especially interesting because all the previously reported variations of isotope effects with pressure have involved intermolecular comparisons.

[1]*Contribution No. 175.*

EXPERIMENTAL

A conventional toluene carrier gas flow system, as has been described previously (6), was used for the investigation of the pressure effect in the pyrolysis of ethyl chloride. The hydrogen chloride produced was trapped at −196° C and titrated with standard 0.1 *N* sodium hydroxide, and the pressures, ranging from 1 to 6 cm Hg, were measured on a mercury – dibutyl phthalate magnifying manometer.

In the pyrolysis of ethyl-1,1,2,2-d_4 chloride, the same apparatus was used, with a large reaction cell being substituted at low temperatures to increase the contact time, as was done in the ethyl acetate study (7). In this flow system, the pressure was varied from 0.68 to 2.88 cm Hg. To extend the pressure range, a number of uninhibited static runs were performed in a seasoned vessel between the average pressures of 0.067 and 16.61 cm Hg.

The reaction products for all the flow runs were passed successively through traps at −80° C and −196° C. The contents of the latter trap, and all the contents of the reaction cell in the case of the static runs, were chromatographed on a silica gel column, using hydrogen as the carrier gas. It was shown by a separate experiment that the ratio of product ethylenes (C_2D_3H/C_2D_4) was unchanged by this treatment.

The ethylenes produced were analyzed on a mass spectrometer using the parent peaks 31 and 32 in the spectrum and correcting for the carbon-13 content of the ethylenes. A further small correction was introduced, as in the ethyl-1,1,2,2-d_4 acetate investigation (7), for production of C_2D_3H from impurities in the "99% deuterated as indicated" reactant.

RESULTS

(a) Ethyl Chloride

The effect of pressure on the first-order rate constant of ethyl chloride at 922.5° K is shown in Fig. 1.

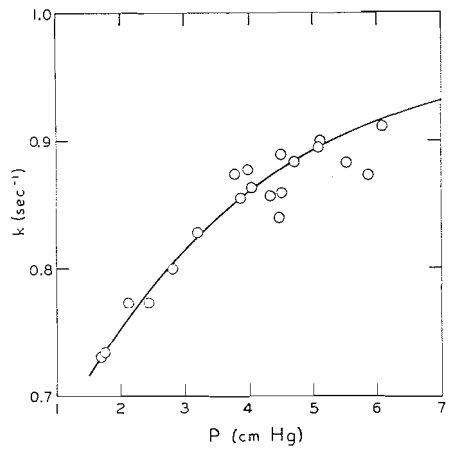

FIG. 1. The effect of pressure on the first-order rate constant (sec^{-1}) of ethyl chloride at 922.5° K.

(b) Ethyl-1,1,2,2-d_4 Chloride

The data for the effect of pressure on the isotope effect in ethyl-1,1,2,2-d_4 chloride are plotted in Fig. 2, indicating an increase in the isotope effect as the pressure is lowered. In this graph, the isotope effect, equivalent to twice the ratio of C_2D_4/C_2D_3H due to the multiplicity of β-deuterium atoms, is shown for both static and flow experiments. The flow experiments, being carried out at 857.6° K, have been corrected to the same temperature as the static experiments (831.9° K) by the use of the temperature coefficient of the isotope effect,

$$k_H/k_D = 1.22e^{985\pm50/RT},$$

derived from the data shown in Fig. 3. These data were obtained over the temperature range 758–989° K and has been normalized to a pressure of 1.80 cm Hg. Indications from

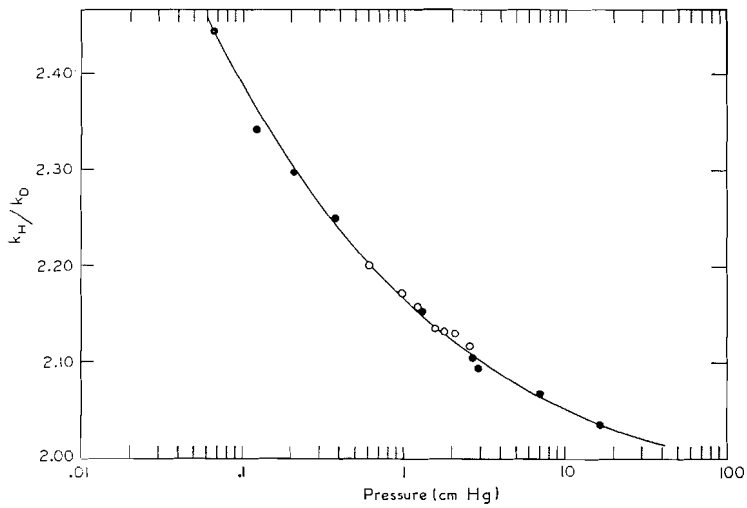

FIG. 2. The effect of pressure on the intramolecular isotope effect in ethyl-1,1,2,2-d_4 chloride at 831.9° K. ○, flow runs; ●, static runs.

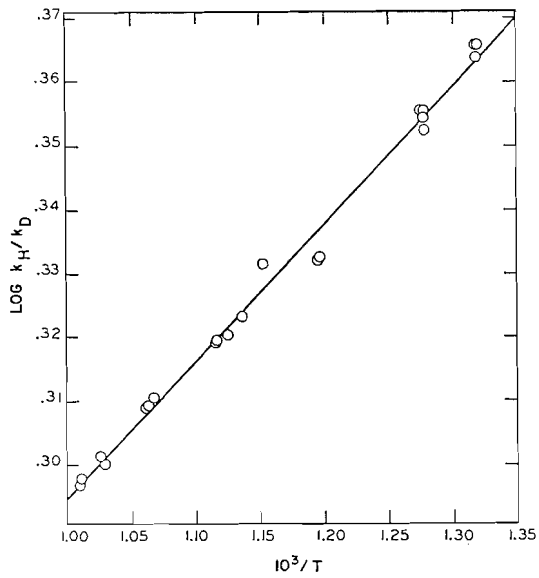

FIG. 3. The temperature dependence of the isotope effect in ethyl-1,1,2,2-d_4 chloride at 1.80 cm Hg pressure.

the pressure effect curve suggest that this effect is about 5% above that at infinite pressure, and the effect at infinite pressure would be given by

$$k_H/k_D = 1.16e^{985\pm50/RT}.$$

DISCUSSION

The Pressure Effects

Throughout our pressure range, the first-order rate constant for ethyl chloride is affected by pressure. However, the results from above 4 cm Hg are erratic, suggesting that the high-pressure limit of our technique has been reached at this pressure. This is

rather unfortunate, for the so-called critical pressure falls outside the range of not only our technique, but also that of Howlett, for he says (2) "that with (his) apparatus, the critical pressure was too low to allow a more quantitative study of the low pressure region". The critical pressure of 8 mm Hg that he does tentatively put forward is considerably lower than what might be expected from our data, which indicates that there is still curvature in the k vs. p plot at 6 cm Hg. Indeed, the fact that the isotope effect is still changing in the pressure region between 7 and 17 cm Hg suggests a "critical" pressure in excess of the former value and possibly greater than the latter. It is also significant that the falloff of the rate constant in ethyl chloride with decreasing pressure is essentially parallel to that observed for ethyl bromide (8).

At this stage it is relevant to give a qualitative explanation that will progressively explain, first the ordinary pressure effect as in ethyl chloride, then the pressure dependence of intermolecular isotope effects, and finally the pressure dependence of intramolecular isotope effects as in ethyl-d_4 chloride.

It has long been known that, if a sufficiently low pressure is attained, any unimolecular reaction will show an apparent increase in order, or, in other words, the value of the first-order rate constant will fall with decreasing pressure. This has been explained by indicating that below a certain pressure, molecular collisions are unable to maintain the equilibrium concentration of highly energized molecules in the energy region above the minimum energy required for reaction. According to the Rice, Ramsberger, and Kassel (R.R.K.) Theory and using Benson's (9) notation:

$P(E)$ = the energy distribution of the reactant molecules,
$k(E)$ = the reaction rate function,
$k(E)P(E)$ = the energy distribution of the chemical product,
E^* = the minimum energy required for the molecule to react,

when the pressure is drastically reduced, $P(E)$ is diminished in the energy region above E^* since the energetic molecules lost by reaction are not maintained at their equilibrium concentration by the decreased rate of collisional processes. Hence, the product distribution $k(E)P(E)$ is reduced below the high-pressure value, and thus the first-order rate constant decreases with decreasing pressure below the so-called critical pressure, as was found in the case of the ethyl chloride decomposition.

This simple model can be extended to account for the pressure effect in an intermolecular isotope effect (see Fig. 4). The areas under the product curves $(k(E)_HP(E)_H$

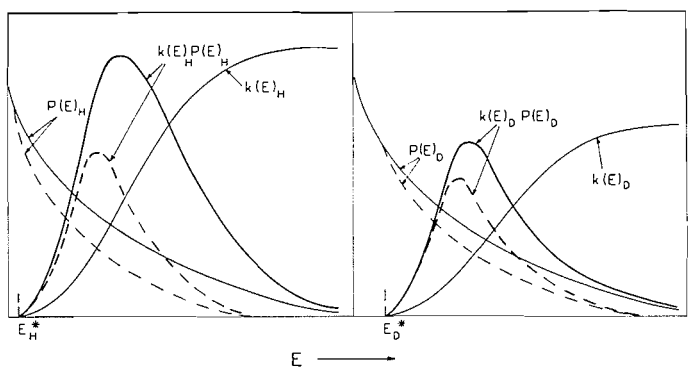

FIG. 4. The effect of pressure on an intermolecular isotope effect—graphical representation of the reaction rate functions for a hydrogen compound, $k(E)_H$, and for a deuterium compound, $k(E)_D$, the classical energy-distribution functions for the hydrogen and deuterium reactants, $P(E)_H$ and $P(E)_D$, in the region of E^*, and their products: $k(E)_HP(E)_H$ and $k(E)_DP(E)_D$.

and $k(E)_D P(E)_D$, solid lines) represent the rates for the hydrogen and deuterium compounds respectively at high pressure; their ratio is the isotope effect. At lower pressures (broken lines), the energy distribution curves, $P(E)_H$ and $P(E)_D$, deviate from the equilibrium high-pressure curves, this deviation becoming increasingly important with increasing energy due to the increase in the $k(E)$ curves with increasing energy. This results in product curves of similar shape, but with the maxima shifted to lower energies, the change in relative areas determining the direction of the trend of the isotope effect with pressure. Since the distortion of the $P(E)$ curves is due to reaction, the relative change in $P(E)_H$ and $P(E)_D$ depends on the relative shapes of the $k(E)_H$ and $k(E)_D$ curves. In the region of these curves of importance here, the value of $k(E)$ is influenced by the value of "s", the number of classical oscillators contributing to activation. As suggested by Rabinovitch, Setser, and Schneider (10), the "s" value for the deuterium compound (s_D) would be higher than that for the hydrogen compound (s_H) due to its more classical behavior and hence the $P(E)_H$ curve is more strongly influenced than the $P(E)_D$ curve by the pressure decrease, and the isotope effect would consequently decrease. This explanation is confirmed by all the available data on the subject.

In the intramolecular isotope effect, the situation is slightly different. The single energy distribution curve (Fig. 5), coupled with the two rate constant curves $k(E)_H$ and $k(E)_D$,

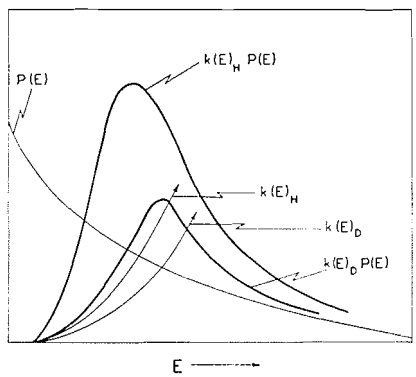

FIG. 5. The effect of pressure on an intramolecular isotope effect—graphical representation of the reaction rate functions $k(E)_H$ and $k(E)_D$ for the rupture of a carbon–hydrogen or a carbon–deuterium bond, the classical energy-distribution function $P(E)$, and their respective products: $k(E)_H P(E)$ and $k(E)_D P(E)$.

combine to give two product curves $k(E)_H P(E)$ and $k(E)_D P(E)$, the deuterium product curve being displaced to higher energies due to the higher activation energy required for this reaction. As the pressure is reduced, the energy distribution curve is more severely affected towards higher energies; the deuterium product, being more dependent on this part of the distribution curve, is thereby proportionately more reduced than the hydrogen product and an increase in the isotope effect results.

While this explanation, based on the R.R.K. Theory, adequately explains the behavior of intramolecular isotope effects, it should also be pointed out that a rate constant independent of the energy in excess of the minimum required for reaction also allows a rise in isotope effect with decreasing pressure, and indeed the arguments are not unrelated. It is also noteworthy that, although the isotope effect increases with decreasing pressure, the overall, and individual, rate constants decrease; in contradistinction to the intermolecular effect, however, s_H is now greater than s_D. This may be qualitatively explained in that when hydrogen is involved in reaction, vibrations involving four deuterium atoms

provide a more classical sink for energy than the three deuteriums and one hydrogen when deuterium is involved in reaction.

The Temperature Coefficient

The magnitude of the isotope effect at 500° C may be compared with the values obtained for similar reactions at the same temperature (see Table I). These values are approximately

TABLE I

High-pressure isotope effects at 500° C

Compound	Isotope effect	Ref.
Ethyl-d_4 chloride	2.20	—
Ethyl-d_4 bromide	2.17	11
Ethyl-d_4 acetate	2.00	7

equal to the "maximum" value to be expected for a reaction in which a carbon–hydrogen bond is essentially broken in the activated complex. From the extreme similarity between the effects in the bromide and chloride, and from the fact that an intermolecular isotope effect is observed in ethyl bromide (8), it may be assumed that this effect occurs in the rate-determining step in the decomposition. This serves as direct support for the generally accepted four-center mechanism for this reaction, in which the carbon–hydrogen and carbon–chlorine bonds are breaking simultaneously with bond formation between hydrogen and chlorine.

To assess the reasons for the differences in the magnitudes of the isotope effects for the ethyl-d_4 chloride, bromide, and acetate, it would be most instructive to consider the individual relative rate expressions:

$$\text{ethyl-}d_4\text{ chloride},\ k_H/k_D = 1.16 \exp(985/RT);$$
$$\text{ethyl-}d_4\text{ bromide},\ k_H/k_D = 1.18 \exp(925/RT);$$
$$\text{ethyl-}d_4\text{ acetate},\ k_H/k_D = 0.99 \exp(1145/RT).$$

Unfortunately, the experimental errors are such that only the differences in isotope effects can be stated with certainty, whereas the differences in the relative rate expression parameters between the halides and the acetate can merely be stated to be probable. It is tempting to associate this latter difference with the fact that the activated complex for the halides is four centered, while the complex for acetate is six centered. The lower temperature coefficient would then imply greater residual and (or) incipient bonding in the activated complex for the halides; this also has the effect of increasing the frequency factor ratio in accordance with observation. However, this would also require a reduced isotope effect, which is not consistent with the facts. Further discussion on this point is fruitless due to the wide variety of sometimes conflicting effects which may come into play.

ACKNOWLEDGMENTS

The authors wish to express their appreciation to Mr. J. Stauffer and Mr. F. Vaneldik for their valuable assistance in the mass spectrometric analyses, and to Dr. H. Habgood for his many helpful comments.

REFERENCES

1. D. H. R. Barton and K. E. Howlett. J. Chem. Soc. 165 (1949).
2. K. E. Howlett. J. Chem. Soc. 3695 (1952).
3. R. E. Weston, Jr. J. Chem. Phy. **26**, 975 (1957).

4. J. LANGRISH and H. O. PRITCHARD. J. Phys. Chem. **62**, 761 (1958).
5. A. T. BLADES. Can. J. Chem. **39**, 1401 (1961).
6. A. T. BLADES and G. W. MURPHY. J. Am. Chem. Soc. **74**, 6219 (1952).
7. A. T. BLADES and P. W. GILDERSON. Can. J. Chem. **38**, 1401 (1960).
8. A. T. BLADES. Can. J. Chem. **36**, 1043 (1958).
9. S. W. BENSON. The foundations of chemical kinetics. McGraw-Hill Book Company, Inc. 1960. p. 230.
10. B. S. RABINOVITCH, D. W. SETSER, and F. W. SCHNEIDER. Can. J. Chem. **39**, 2609 (1961).
11. A. T. BLADES, P. W. GILDERSON, and M. G. H. WALLBRIDGE. Can. J. Chem. This issue.

THE HYDROGEN ISOTOPE EFFECTS IN THE PYROLYSIS OF ETHYL-1,1,2,2-d_4 BROMIDE AND OF ETHYL-d_5 BROMIDE[1]

ARTHUR T. BLADES, P. W. GILDERSON, AND M. G. H. WALLBRIDGE
Research Council of Alberta, Edmonton, Alberta

Received February 16, 1962

ABSTRACT

The relative rate constant expression has been obtained for the decomposition of ethyl-1,1,2,2-d_4 bromide under inhibiting conditions in the temperature range 697.6 to 999.1° K,

$$k_H/k_D = 1.18e^{925\pm50/RT}.$$

The pressure dependence of the isotope effect has been investigated both with and without inhibitor, and in each case it has been shown that the isotope effect increases with decreasing pressure.

The relative rate constant expression for the ethyl-h_5, ethyl-d_5 bromide comparison was also obtained in the temperature range 730.9 to 964.8° K,

$$k_H/k_D = 0.502e^{2300\pm200/RT}.$$

The isotope effect is again pressure dependent, falling to lower values as the pressure is decreased.

The data are used to demonstrate that the inhibited decomposition of ethyl bromide is primarily a molecular process, and that the rate-controlling step involves a carbon–hydrogen bond break.

A side reaction that produces small amounts of ethane has been observed.

INTRODUCTION

Recent investigations (1–3) of the thermal decomposition of ethyl bromide have suggested that the reaction consists of two components, the first of which is a unimolecular splitting into ethylene and hydrogen bromide, the second being a faster chain reaction initiated by bromine from the interaction of hydrogen bromide and ethyl bromide. The rate of reaction may be reduced to a limiting value by the use of various inhibitors such as cyclohexene, propylene (2), and toluene (4), the conclusion being drawn that by this procedure the second component is eliminated. Further, the fact that no bibenzyl is found in the toluene-inhibited decomposition products has been interpreted (4) as evidence for the absence of radical reactions in the inhibited decomposition.

The results of these investigations have led to the belief that the reaction in the observed induction period in the uninhibited decomposition is identical with the reaction under the influence of inhibitors. Goldberg and Daniels (1) have pointed out that the initial rate during the induction period in their uninhibited experiments is in good agreement with the rate, under inhibited conditions, found by Blades and Murphy (4). Again, Blades (3) has shown that the rate constant of Goldberg and Daniels, when extrapolated to zero pressure, is comparable to the inhibited rate.

Although the relationship of the initial process to the inhibited decomposition may have been established, nevertheless the molecular nature of these reactions has not been unequivocally proved, and has in fact been cast in doubt recently by Wojciechowski and Laidler (6). These authors have suggested that inhibition limits such a reaction, not to a molecular component, but rather to a special type of radical process in which the inhibitor is involved in both the initial and final steps. Thus the absence of bibenzyl in the toluene-inhibited reaction products does not necessarily rule out such a limited chain in this

[1]*Contribution No. 176.*

reaction; neither does the finding of an isotope effect in ethyl-d_5 bromide by Blades (5), for an effect would in all probability be observed in the radical step

$$Br + C_2H_5Br \rightarrow HBr + C_2H_4Br.$$

If it can be shown that the initial step is indeed molecular, there is still a problem to be solved from the current literature on the nature of the transition state. Maccoll and his co-workers (7) have drawn an analogy between the gaseous decomposition of alkyl halides and S_N1 and E1 reactions in solution, concluding that the process is essentially heterolytic. Furthermore, Ingold (8) has gone as far as to suggest that the activated complex is a carbonium ion – halide ion pair, and that in its formation there is "no hydrogen loosening of any kind". However, the finding, by Blades (5), of an intermolecular hydrogen isotope effect on ethyl bromide (2.26 at 500° C) would appear to invalidate Ingold's argument. On the other hand, Maccoll and Thomas (9) have suggested that the β-hydrogen atom acts in a stabilizing capacity similar to the solvent in solution phase S_N1 and E1 mechanisms, allowing the transition state to be represented in essentially the same form as the often-proposed, four-centered complex.

The work reported in this paper is an investigation of the isotope effect in two deuterium-substituted ethyl bromides. In ethyl-1,1,2,2-d_4 bromide the isotope effect has been studied in an inhibited system from the standpoint of its pressure dependency and its temperature coefficient. Further, the isotope effect was examined over a wide range of pressures in an uninhibited system. In the second compound, ethyl-d_5 bromide, the influence of temperature and pressure variations on the isotope effect has again been studied in an inhibited system, using a technique different from that used previously (5) in order to check the unexpected Arrhenius parameters that have been reported.

EXPERIMENTAL

(a) Ethyl-1,1,2,2-d_4 Bromide

The apparatus and experimental procedure were essentially the same as for the ethyl-1,1,2,2-d_4 chloride as reported in the preceding paper.

In the inhibited pressure effect investigation the flow runs were conducted in the range 0.71 to 2.89 cm Hg, while one static run was performed at 20.4 cm Hg using *cis*-butene-2 as the inhibitor. Without an inhibitor, a further six runs were carried out between the average pressures of 0.0424 and 23.4 cm Hg. Data for the temperature coefficient were obtained over the range 697.6 to 999.1° K using the toluene flow system.

The hydrocarbon products were separated on a 24-inch silica gel column by vapor phase chromatography at room temperature, and the product ethylenes (C_2D_4 and C_2D_3H) were collected and analyzed on a mass spectrograph using the parent peaks (32 and 31) in the spectrum. Corrections to the ratios of the peak heights were made for the contributions of carbon-13 to the ethylenes, and for impurities in the reactants, as before (10).

(b) Ethyl-h_5 Bromide/Ethyl-d_5 Bromide Comparison

A gaseous mixture of ethyl-h_5 bromide and ethyl-d_5 bromide was prepared in the approximate ratio 5:1, and introduced from a graduated gas burette through a capillary into the toluene stream. The remainder of the apparatus and technique was essentially the same as for the 'd_4' pyrolyses, one static run (utilizing *cis*-butene-2 as inhibitor) being conducted at 11.4 cm Hg to extend the pressure range in the case of the pressure effect studies. For the temperature coefficient determination, two flow cells were used to enable the decomposition to be studied over the range 730.9 to 964.8° K.

The parent peaks 28 and 32 were used in the mass spectrum to measure the C_2H_4/C_2D_4 ratio. Successive corrections were made for the carbon-13 content of the ethylenes, for the contribution of C_2D_4 to the mass 28 peak, and for the reactant conversions, which were controlled to below 10%. In order to determine the contribution at 28 made by C_2D_4, a sample of C_2D_4 was prepared by pyrolyzing the 99% deuterated ethyl-d_5 bromide (Merck and Co.) in a large excess of toluene and separating as before. The contribution in question was then found on the mass spectrometer for the ionization potential that was used in the analysis of the C_2H_4, C_2D_4 mixtures.

RESULTS

(a) Ethyl-1,1,2,2-d_4 Bromide

The effect of pressure on the intramolecular isotope effect for ethyl-1,1,2,2-d_4 bromide is shown in Fig. 1, where the curves A and B show, respectively, the results of the inhibited

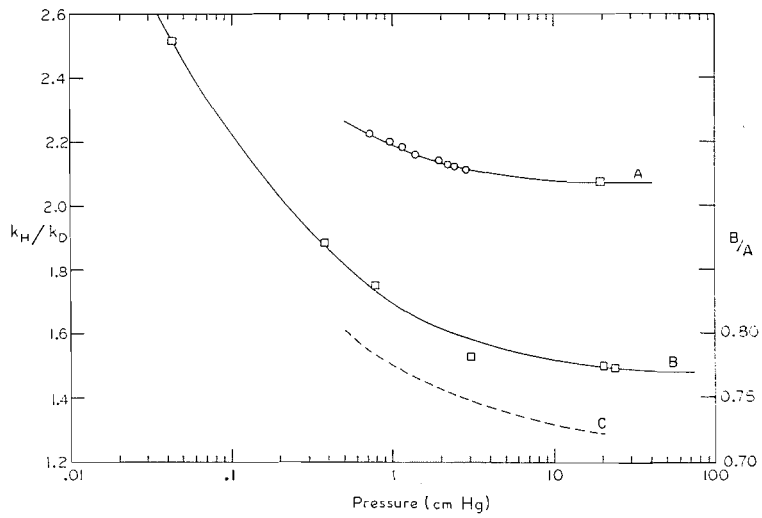

FIG. 1. The effect of pressure on the intramolecular isotope effect in ethyl-1,1,2,2-d_4 bromide at 826.4° K. Curve A shows the effect under inhibiting conditions; curve B, without inhibitor; and curve C is the ratio B/A.

and uninhibited decompositions. Curve C represents the variation in the ratio B/A with pressure, and demonstrates that the isotope effects under inhibiting and uninhibiting conditions converge at low pressures.

Figure 2 is a plot of the temperature coefficient of the isotope effect at 1.80 cm Hg, which may be expressed as

$$k_H/k_D = 1.22e^{925\pm50/RT}.$$

To obtain this expression, the data above 900° K were omitted from the least-squares process, for it is evident that these runs are consistently displaced above the linear plot.

At infinite pressure, the pre-exponential term in the above expression would be lower by about 3%, as indicated by curve A in Fig. 1. Thus the true relative rate expression is

$$k_H/k_D = 1.18e^{925\pm50/RT}.$$

(b) Ethyl-h_5/Ethyl-d_5 Bromide Comparison

The effect of pressure on the isotope effect in this comparison is shown in Fig. 3, which includes data from the previously published pressure effect curves for ethyl bromide and ethyl-d_5 bromide (5). The latter data, obtained at 889° K, were reduced to the temperature of the present investigations (826.4° K) by utilizing the coefficient reported below.

The relative rate constant expression for this comparison at 2.00 cm Hg is

$$k_H/k_D = 0.494e^{2300\pm200/RT},$$

from the data plotted in Fig. 4. The expression at infinite pressure is

$$k_H/k_D = 0.50e^{2300\pm200/RT}.$$

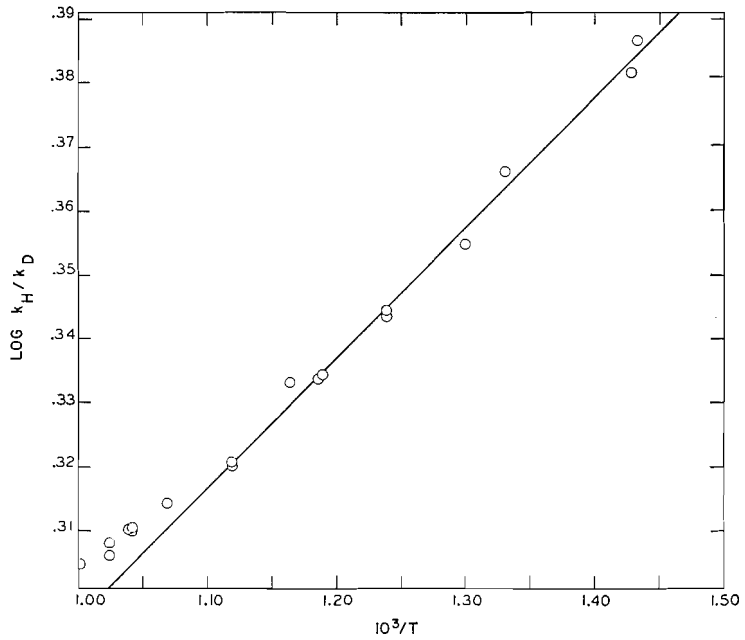

FIG. 2. The temperature dependence of the isotope effect in ethyl-1,1,2,2-d_4 bromide at 1.80 cm Hg pressure.

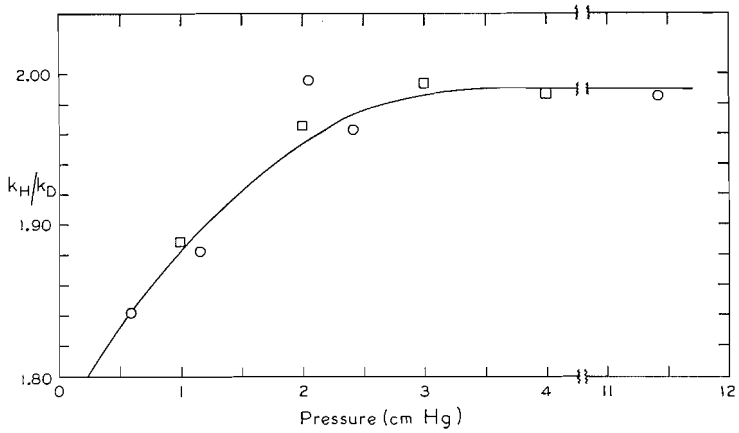

FIG. 3. The effect of pressure on the intermolecular isotope effect in the ethyl-h_5 bromide/ethyl-d_5 bromide comparison at 826.4° K. □, data from ref. 5; ○, results of present investigations.

(c) Ethane

Besides the ethylene, another product appeared in the chromatography of the hydrocarbon products. It was identified as ethane and was found to occur only to the extent of 1 or 2% of the total hydrocarbon products. Samples taken from the pyrolysis products of ethyl-d_5 bromide in toluene vapor were found to be approximately equimolecular mixtures of C_2D_5H and C_2D_6. In the few cases that were examined, no consistent trend could be established between the ratio of ethanes on the one hand, and either the temperature or the partial pressure of the bromide on the other.

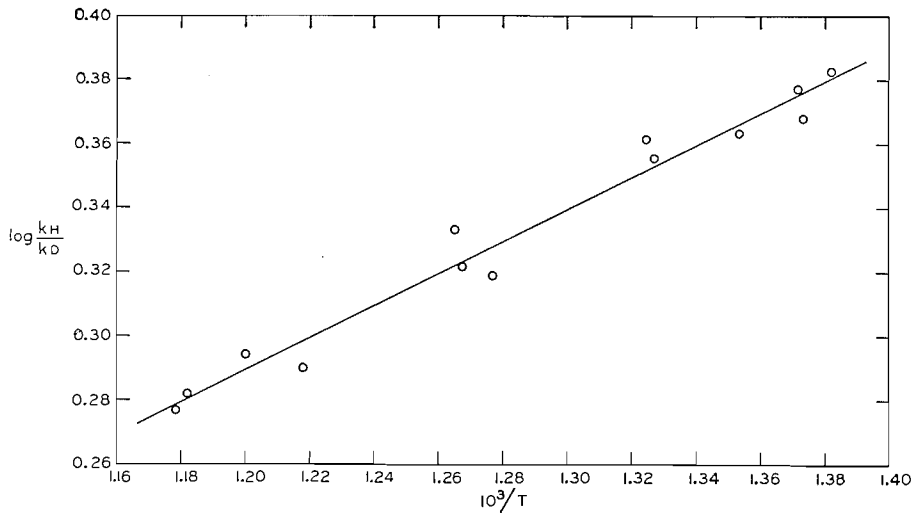

FIG. 4. The temperature dependence of the isotope effect in the ethyl-h_5 bromide/ethyl-d_5 bromide comparison at 2.00 cm Hg pressure.

DISCUSSION

Ethyl-1,1,2,2-d_4 Bromide

There is a great similarity between the isotope effects in the inhibited decomposition of ethyl-1,1,2,2-d_4 bromide and in the uninhibited decomposition of ethyl-1,1,2,2-d_4 chloride. The effects themselves at 500° C are 2.17 for the bromide and 2.20 for the chloride, while the relative rate expressions are:

$$\text{ethyl-}d_4 \text{ bromide, } k_H/k_D = 1.18e^{925/RT};$$
$$\text{ethyl-}d_4 \text{ chloride, } k_H/k_D = 1.16e^{985/RT}.$$

Further, it was demonstrated in the preceding paper that the pressure effects in ethyl bromide and ethyl chloride are almost identical, and this similarity is reflected in the pressure dependences of the isotope effects in the ethyl-d_4 bromide and in the ethyl-d_4 chloride. Not only do the isotope effects rise with falling pressure in both cases (in agreement with the theory postulated for intramolecular isotope effects in the preceding paper), but they do so in an essentially parallel fashion. Furthermore, the combination of these similarities sheds appreciable light on the mechanism of the ethyl bromide reaction.

If the ideas of Wojciechowski and Laidler (6) are applicable to the decomposition of ethyl bromide, then under the influence of inhibitors the reaction is limited to a special type of free-radical process. On this basis, and in addition, assuming the ethyl chloride decomposition to be a truly unimolecular reaction, it would be expected that there would be an appreciable difference in the isotope effects in the inhibited decomposition of ethyl-d_4 bromide and in ethyl-d_4 chloride. It has been shown here that this is not the case. Nevertheless, before rejecting the applicability of Wojciechowski and Laidler's ideas to this system, it is well to question the molecular nature of the ethyl chloride decomposition.

The pyrolysis of ethyl chloride has been considered to be a unimolecular process on the grounds that inhibitors do not affect the rate. It might be argued, however, that in this decomposition a special kind of radical chain is operating which is uninfluenced by inhibitors. Such a process must at the same time explain not only the intramolecular

isotope effect in ethyl-d_4 chloride but also its pressure dependence. Thus, although the chain-propagation reaction

$$Cl + C_2H_5Cl \rightarrow HCl + C_2H_4Cl$$

could produce the former, it would not be expected to account for the latter. It now seems inconceivable that any reasonable reaction scheme can be contrived which will explain the rise in k_H/k_D with decreasing pressure without the major reaction being intramolecular.

Thus far we have shown that the ethyl chloride decomposition is at least a predominantly unimolecular reaction, and it may now be inferred that the great similarities between the ethyl chloride and the maximally inhibited ethyl bromide decompositions indicate that in the latter a molecular reaction at all events has the preeminence. Hence, the only difference between the modes of decomposition of ethyl bromide and ethyl chloride is that in the bromide a radical chain reaction is known to exist in uninhibiting conditions. It now remains to be shown how the results of the uninhibited decomposition of ethyl-d_4 bromide fit into this scheme.

The isotope effect in the decomposition of ethyl-d_4 bromide increases with decreasing pressure over the pressure range studied, and curve C in Fig. 1 indicates that as the pressure is decreased, the isotope effects for the inhibited and uninhibited reactions approach one another. These observations are entirely in agreement with the previously noted (3) tendency for the uninhibited rate in ethyl bromide to approach the inhibited rate at low pressures due to the diminishing importance of the chain reaction. Again, the fact that the isotope effects at high pressure in the inhibited and uninhibited decompositions of ethyl-d_4 bromide are appreciably different adds further weight to the argument that distinct types of mechanism are predominant in each case, for if the source of both isotope effects was the radical-abstraction reaction

$$Br + C_2H_5Br \rightarrow HBr + C_2H_4Br,$$

and if the only difference between the inhibited and uninhibited decompositions was to be found in the length of the chain, then no estimable difference in the isotope effects should be seen.

If the above reaction does represent the chain-carrying step, it is apparent from Fig. 1 that the isotope effect in this reaction is less than 1.5 at 831.9° K. This would suggest that the curvature noted in the temperature coefficient (Fig. 2) cannot arise from a change to a free-radical mechanism in the temperature range above 900° K since this would result in the opposite curvature. If real, this effect may be due to the predicted curvature of such plots at high temperatures (10).

Ethyl-h_5/Ethyl-d_5 Bromide Comparison

The effect of pressure upon this intermolecular isotope effect (Fig. 4) is in accordance with the theory postulated in the preceding paper. It is satisfying that the results of our present investigations are in agreement with data obtained directly from previous work (5), which employed a different technique.

In the temperature coefficient studies there is also good agreement with the earlier results, and it would appear that there is indeed a large secondary isotope effect in this comparison, and that the carbon–hydrogen bond is being broken in the activation process in accordance with a four-centered activation complex.

Ethane

The production of C_2D_6 and C_2D_5H in approximately equal proportions in the inhibited decomposition of ethyl-d_5 bromide suggests that a small side reaction is occurring. The

two ethanes may be formed by a mechanism that involves an exchange reaction between DBr and toluene, occurring via a benzyl radical intermediate:

$$C_2D_5Br \rightarrow C_2D_4 + DBr$$
$$DBr + C_6H_5CH_3 \rightleftharpoons HBr + C_6H_5CH_2D$$
$$DBr + C_2D_5Br \rightarrow C_2D_6 + Br_2$$
$$HBr + C_2D_5Br \rightarrow C_2D_5H + Br_2.$$

The alternate mechanism of ethane production from ethyl radicals arising from the split of ethyl bromide cannot be definitely ruled out. It seems unlikely, however, since the amount of ethane is considerably higher than would be predicted from this reaction, and in any case ethyl radicals are known to decompose under these experimental conditions (11).

In conclusion, it has been shown that the ethyl bromide decomposition involves a radical and a molecular component, the former being largely eliminated under inhibiting conditions. The isotope effects reported are pressure dependent, following the general pattern laid down for such pressure effects in the preceding paper. The isotope effects are also consistent with the four-centered activated complex in which a hydrogen atom is transferring from a carbon atom to a bromine atom in the transition state. A side reaction producing small quantities of ethane has also been observed, and an explanation for the isotopic distribution of the ethane is suggested.

ACKNOWLEDGMENTS

The authors wish to thank Mr. J. Stauffer and Mr. F. Vaneldik for carrying out the mass spectrometric analysis.

REFERENCES

1. A. E. GOLDBERG and F. DANIELS. J. Am. Chem. Soc. **79**, 1314 (1957).
2. P. J. THOMAS. J. Chem. Soc. 1192 (1959).
3. A. T. BLADES. Can. J. Chem. **36**, 1129 (1958).
4. A. T. BLADES and G. W. MURPHY. J. Am. Chem. Soc. **74**, 6219 (1952).
5. A. T. BLADES. Can. J. Chem. **36**, 1043 (1958).
6. B. W. WOJCIECHOWSKI and K. J. LAIDLER. Can. J. Chem. **38**, 1027 (1960).
7. A. MACCOLL. Kekule Symposium, London. 1958. Butterworth's Scientific Publications.
8. C. K. INGOLD. Proc. Chem. Soc. 279 (1957).
9. A. MACCOLL and P. J. THOMAS. Nature, **176**, 392 (1955).
10. A. T. BLADES and P. W. GILDERSON. Can. J. Chem. **38**, 1401 (1960).
11. C. H. LEIGH and M. SZWARC. J. Chem. Phys. **20**, 403 (1952).

DITERPENOID QUINONES OF INULA ROYLEANA D.C.[1, 2]

O. E. EDWARDS, G. FENIAK,[3] AND M. LOS[3]
Division of Pure Chemistry, National Research Council, Ottawa, Canada
Received March 16, 1962

ABSTRACT

Three related diterpenoid quinones, royleanone, 9-acetoxyroyleanone, and 9-dehydroroyleanone, have been isolated from the roots of *Inula royleana* D.C. These have been assigned structures on the basis of degradation studies and the synthesis of royleanone from ferruginol.

The plant *Inula royleana* D.C. is a perennial shrub that grows in the western Himalayas at altitudes of 7,000 to 11,000 ft above sea level. It is considered to be poisonous and has been used as an insecticide and a disinfectant (1). Its roots have been shown to be rich in derivatives of the diterpenoid alkaloid lycoctonine (2–4). In addition, the presence of a yellow pigment has been reported (5). This pigment we now show to consist mainly of a mixture of diterpenoid quinones which we call 'royleanones'. The major component was an acetoxyroyleanone (I) ($C_{22}H_{30}O_5$). Small quantities of royleanone (IV) ($C_{20}H_{28}O_3$) and a dehydroroyleanone (III) ($C_{20}H_{26}O_3$) were also present. That these compounds were structurally closely related will become apparent in the sequel.

We first concerned ourselves with establishing the nature of the chromophoric system in royleanone. The compound was acidic (pK_a 8.5 in 50% aqueous methanol) and its alkaline solution was magenta in color. It reacted with diazomethane to give a monomethyl derivative. Royleanone took up 1 mole of hydrogen on catalytic hydrogenation and the colorless product was converted back to royleanone on standing in the presence of air. These properties, and the ultraviolet spectrum of royleanone, which was very similar to those of hydroxybenzoquinones (6), suggested that royleanone contained this unit. The hydrogen-bonded hydroxyl band ($\nu_{max}^{CHCl_3}$ 3350 cm^{-1}) and the two low-frequency carbonyl bands ($\nu_{max}^{CHCl_3}$ 1672 and 1632 cm^{-1}) in the infrared spectrum fitted this assignment. Finally, the reductive methylation of royleanone methyl ether (IX) to a trimethoxybenzene (VII) (λ_{max}^{EtOH} 208 mμ, ϵ 49,000, 281 mμ, ϵ 740) furnished conclusive evidence that royleanone was a hydroxybenzoquinone.

The structural relationship between royleanone, the dehydroroyleanone, and the acetoxyroyleanone was established as follows. Catalytic hydrogenation of the dehydroroyleanone (2 moles of hydrogen were taken up) followed by oxidation of the product by air gave royleanone. This indicated that dehydroroyleanone differed from royleanone only in having an additional double bond. A comparison of the ultraviolet spectra of royleanone (λ_{max}^{EtOH} 277, 283 (shoulder), and 403 mμ) and the dehydroroyleanone (λ_{max}^{EtOH} 212, 247 (shoulder), 330, and 459 mμ) showed that this double bond was conjugated with the quinone ring.

The similarity between the ultraviolet absorption spectra and many features of the infrared absorption spectra of acetoxyroyleanone and royleanone led us to believe that these compounds were related. The presence of an ester grouping in the acetoxyroyleanone was indicated by the carbonyl band at 1748 cm^{-1} in its infrared spectrum. In addition

[1]*Issued as N.R.C. No. 6930.*
[2]*Presented in part at the Annual Meeting of the Chemical Institute of Canada in Montreal, August, 1961.*
[3]*National Research Council of Canada Postdoctorate Fellow.*

the n.m.r. spectrum of acetoxyroyleanone methyl ether had an unsplit methyl signal[4] at τ 8.05 and a signal from a strongly deshielded single hydrogen at τ 4.25. These are consistent with the presence of a secondary acetoxyl group. The presence of the acetoxyl was confirmed by hydrolysis of the acetoxyroyleanone to acetic acid and an alcohol (II). Dehydration of II with *p*-toluenesulphonic acid in boiling xylene gave a compound identical with the natural dehydroroyleanone described above. Hence the acetoxyl was probably α or β to the quinone ring. Catalytic hydrogenation of acetoxyroyleanone (2 moles of hydrogen were taken up) followed by oxidation of the product with air gave royleanone. Such facile hydrogenolysis of the acetoxyl is compatible only with its being allylic or benzylic. Since there was no evidence for any unsaturation other than that in the quinone system, the acetoxyl was assigned to a carbon directly attached to this ring.

We were surprised to find that the acetoxy group of acetoxyroyleanone could be removed not only by catalytic hydrogenation but also by the action of sodium borohydride in methanol at room temperature. To our knowledge such a cleavage has not been previously reported.

There were no signals at lower field that τ 5.95 in the n.m.r. spectrum of royleanone methyl ether, showing that there were no hydrogens attached to the quinone ring. This evidence combined with the correlations described above allowed us to assign the following partial structures to the royleanones. As has been shown above, the differences in the partial structures are the only differences between these compounds.

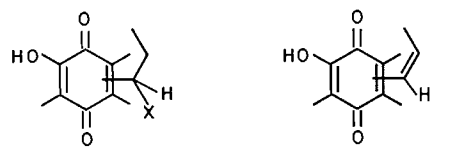

ROYLEANONE X = H
ACETOXYROYLEANONE X = OAc

DEHYDROROYLEANONE

Evidence for the remaining structural features was obtained by oxidation of dehydroroyleanone and royleanone. Alkaline hydrogen peroxide oxidation of either of these compounds gave rise to isobutyric acid. Since the oxidation conditions were relatively mild, this proved that an isopropyl group was attached to the quinone ring. Since isobutyric acid was obtained in both cases, the double bond in the dehydroroyleanone and consequently the acetoxyl group in the acetoxyroyleanone were not associated with the isopropyl group.

Oxidation of the dehydroroyleanone with alkaline potassium permanganate resulted in low yields of 1,3,3 trimethylcyclohexane-1,2-dicarboxylic acid (V). The assignment of structure to the latter compound was based on the n.m.r. spectrum of its methyl ester. The significant features of the latter were three unsplit C—CH_3 signals (τ 9.2, 9.15, 8.95), an unsplit signal (τ 7.1) which corresponded to a single hydrogen, and two unsplit O—CH_3 signals (τ 6.4, 6.35).

Only two structures for royleanone are compatible with the degradation products described above and the presence of signals due to an allylic hydrogen (τ 7.8) and two vinyl hydrogens (τ 3.4, 3.2) in the n.m.r. spectrum of the methyl ether of the dehydroroyleanone. The two possibilities are shown below.

[4]*The chemical shifts are given in τ values, following G. D. Tiers, J. Phys. Chem.* **62**, *1151 (1958). The n.m.r. spectra were of ca. 10% carbon tetrachloride or chloroform solutions with tetramethylsilane as an internal reference.*

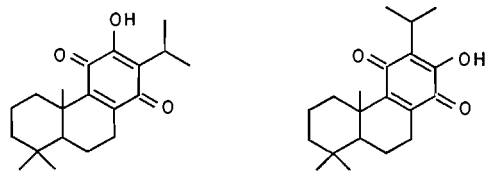

An attempt to distinguish between these two by dehydrogenation of royleanone was unsuccessful. Under the conditions required to complete the dehydrogenation the isopropyl group was lost. The isolation of small amounts of 1-methylphenanthrene (VI), however, supplied confirmation that one of these two structures was correct.

The structure of royleanone was finally proved to be IV by synthesis from ferruginol (VIII), a substance whose structure and absolute configuration have been firmly established (for leading references, see ref. 7). Oxidation of ferruginol with 98% hydrogen peroxide in acetic acid with sulphuric acid as catalyst gave a 7% yield of royleanone with optical rotation and other physical properties identical with those of the natural substance. The low conversion is probably due to the presence of two benzylic positions

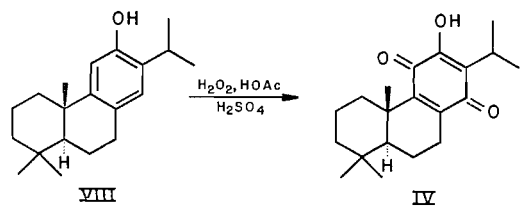

VIII IV

in ferruginol, which are known to be susceptible to oxidation (8). It follows that the companion quinones are 9-acetoxy- and 9-dehydro-royleanone, and that the reactions of these are as shown on the flowsheet.

The royleanones, thus, have the same trans A/B ring fusion and absolute configuration as all natural steroids and most diterpenes. The absolute configuration at the A/B junction bears a mirror image relationship to that found in lycoctonine (9), which, as was mentioned earlier, is found in the same plant. This indicates that although lycoctonine and the royleanones are both diterpenoid they are probably not closely linked biogenetically. Their syntheses in the plant must enter different pathways before the formation of the A/B junction.

After the structures of the royleanones had been established and their relationship to ferruginol recognized we considered the possibility that ferruginol is a direct royleanone precursor in the plant. Further examination of *Inula royleana* extracts indeed led to the isolation of small amounts of ferruginol from them. This leads us to suggest that the plant produces a 6-hydroxy diterpene by the route discussed by ApSimon and Edwards (10) and that this is isomerized and aromatized to ferruginol, which in turn is converted in stages to royleanone, 9-acetoxyroyleanone, and 9-dehydroroyleanone.

Examination of molecular models has convinced us that it is at present not possible to assign the configuration to the acetoxyl group in 9-acetoxyroyleanone on the basis of infrared (11) or n.m.r. (12) data because of the quasi-axial and quasi-equatorial configuration of the C_9 substituents and because of the proximity of the quinone carbonyl. This point, therefore, is still unsettled.

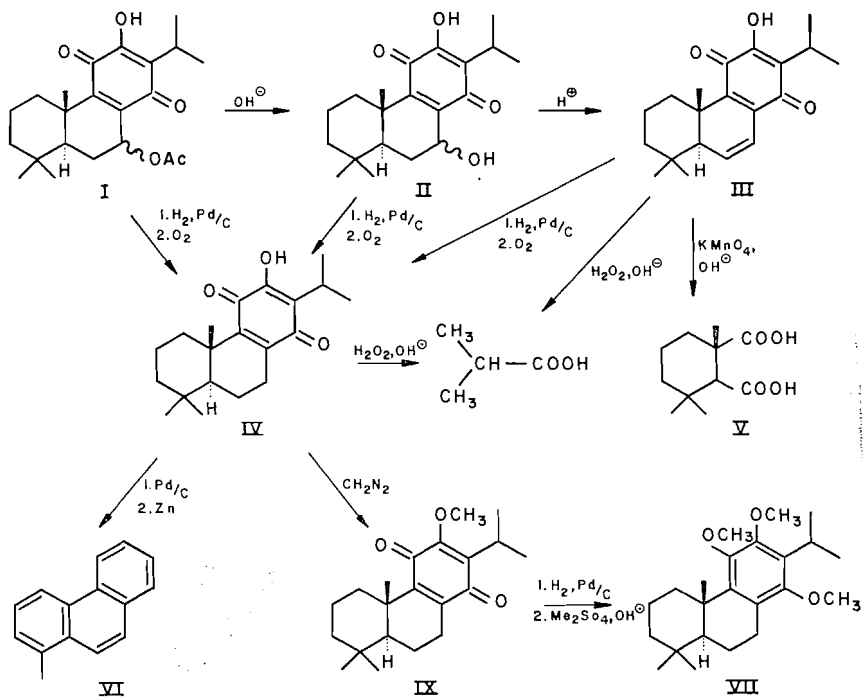

EXPERIMENTAL

Rotations were of chloroform solutions and melting points were taken in capillaries and are corrected.

Isolation of Royleanones

The dried ground roots of *Inula royleana* D.C., obtained from the S. B. Penick Company, N.Y., were extracted with methanol. During concentration of the extracts a dull yellow solid crystallized. This solid was predominantly 9-acetoxyroyleanone containing small quantities of royleanone. The mother liquors contained royleanone, 9-dehydroroyleanone, and ferruginol.

9-Acetoxyroyleanone (I)

The crude solid obtained above was purified by four recrystallizations from 2-butanone, a sublimation at 140° and 10^{-4} mm, and a final recrystallization from ethanol. It had m.p. 212–214.5°; $[\alpha]_D$ −14° (*c*, 1.07); $\nu_{max}^{CS_2}$ 3360, 1748, 1675, and 1645 cm^{-1}; λ_{max}^{EtOH} 272 mμ, ε 13,300, 407 mμ, ε 840. Neut. equiv. 378, 383. Found: C, 70.48; H, 7.86; OAc, 11.34. Calc. for $C_{22}H_{30}O_5$ (374.5): C, 70.56; H, 8.08; OAc, 11.49.

For most purposes material that had been recrystallized from ethanol three times (m.p. 208.5–212°) was used. The yield was approximately 1% of the weight of the dried roots.

The acetyl derivative of 9-acetoxyroyleanone, which was prepared by the treatment of 9-acetoxyroyleanone with acetic anhydride in the presence of sulphuric acid, melted at 122–122.5° (recrystallized from methanol–water); $[\alpha]_D$ +32° (*c*, 0.67); λ_{max}^{EtOH} 262 mμ, ε 14,900, 327 mμ, ε 320; $\nu_{max}^{CS_2}$ 1773, 1741, 1665, 1655 (shoulder), and 1607 cm^{-1}. Found: C, 69.06; H, 7.39; OAc, 20.38. Calc. for $C_{24}H_{32}O_6$: C, 69.21; H, 7.74; OAc, 20.66.

Treatment of a methanolic solution of 9-acetoxyroyleanone with excess ethereal diazomethane resulted in the formation of a monomethyl ether; m.p. 182.5–184.5° (recrystallized from methanol); $[\alpha]_D$ −121° (*c*, 1.32), λ_{max}^{EtOH} 270 mμ, ε 12,500, 375 mμ, ε 590; $\nu_{max}^{CS_2}$ 1740, 1660, 1645, and 1602 cm^{-1}. Found: C, 70.98; H, 8.21; OCH_3, 8.06. Calc. for $C_{23}H_{32}O_5$: C, 71.10; H, 8.30; OCH_3, 7.99.

Royleanone (IV)

A benzene solution of the solid that crystallized from the concentrated *Inula royleana* extract (see above) was chromatographed on silica gel. The first colored fractions that were eluted from the column with benzene were concentrated under reduced pressure and the residue was crystallized from hexane. Two different types of crystals separated, one yellow and the other orange in color. They were separated manually. The orange-colored crystals were recrystallized from glacial acetic acid until their melting point had risen to 181.5–183°. The yield was 0.008% of the weight of dried root extracted. $[\alpha]_D$ +134° (*c*, 1.03); $\lambda_{max}^{CCl_4}$ 277 mμ, ε 15,900, 283 mμ (shoulder), ε 15,200, 403 mμ, ε 510; $\nu_{max}^{CHCl_3}$ 3350, 1672, 1632, and 1602 cm^{-1}. Neut. equiv. 287, 306. Found: 75.93; H, 8.65. Calc. for $C_{20}H_{28}O_3$ (316.4): 75.91; H, 8.92.

The methyl ether of royleanone was prepared by treatment of a methanolic solution of royleanone with excess ethereal diazomethane. It melted at 119–120.5° (recrystallized from methanol); $[\alpha]_D$ −82° (*c*, 1.18), λ_{max}^{EtOH} 275 mμ, ε 12,300, 372 mμ, ε 460; $\nu_{max}^{CHCl_3}$ 1657 (shoulder), 1642, and 1602 cm^{-1}. Found: C, 76.03; H, 9.01; OCH_3, 9.75. Calc. for $C_{21}H_{30}O_3$: C, 76.32; H, 9.15; OCH_3, 9.39.

9-Dehydroroyleanone (III)

This material was obtained in pure form from 9-acetoxyroyleanone (*vide infra*). Evidence for its presence in the plant was obtained in the following manner. The mother liquors obtained after removal of the 9-acetoxyroyleanone from the plant extracts described above were concentrated until most of the methanol had been removed. The dark viscous mass was extracted with benzene. The benzene extracts were concentrated under reduced pressure, the residue was taken up in 1:1 benzene–hexane, and this solution was chromatographed on a silica gel column. The second colored band eluted with 1:1 benzene–hexane was collected, the eluate was concentrated, and the residue was recrystallized twice from ethanol. The yield of bright-orange-colored plates (m.p. 168–171°) was 0.07% of the weight of dried root. The infrared and ultraviolet spectra, the melting point, and the optical rotation of this material were identical with those of a ca. 45:55 mixture of royleanone and 9-dehydroroyleanone. We were unable to separate this mixture into its components.

This material, on hydrogenation over palladium on charcoal in glacial acetic acid, took up 1.6 equivalents of hydrogen. The product was oxidized by air to royleanone (mixed melting point and infrared spectrum).

Ferruginol (VIII)

The mother liquors obtained after the removal of the 9-acetoxyroyleanone from the plant extracts were concentrated until most of the methanol had been removed. The residue was extracted with hexane. The hexane extracts were concentrated, the residue was taken up in benzene, and the solution was washed well with 0.5 *N* aq. sodium hydroxide. The benzene layer was concentrated and the residue was chromatographed on silica gel. The fractions eluted with 1:1 hexane–benzene were combined, concentrated, and distilled. Material distilling below 140° at 10^{-3} mm was collected. The purification steps described above, i.e. the washing of a benzene solution of this material with 0.5 *N* aq. sodium hydroxide, the chromatography, and the distillation, were repeated. This time the material distilling below 125° at 10^{-3} mm was collected. The crude ferruginol, which was obtained as a viscous bright orange oil was characterized as the benzoate. After a crystallization from methanol and three recrystallizations from hexane, the benzoate was obtained as white needles that melted at 154–155.5°. It was identical with authentic ferruginyl benzoate (mixed melting point and infrared spectrum). The yield corresponded to 0.04% of the weight of the dried root.

Conversion of 9-Acetoxyroyleanone (I) to Royleanone (IV)

A suspension of 0.198 g of 9-acetoxyroyleanone in 30 ml of glacial acetic acid was hydrogenated over Adams' catalyst at atmospheric pressure. The reduction was complete within 2 hours. The uptake of hydrogen was 26.7 ml. The catalyst was removed by filtration, the filtrate was warmed to 90° and swirled for 20 minutes to promote aerial oxidation of the hydroquinone. The solution was concentrated under reduced pressure and the residue was recrystallized from glacial acetic acid, giving 0.123 g, m.p. 179–182.5°. The product was identical with natural royleanone (mixed melting point and infrared spectrum).

The catalytic reduction described above could be replaced by reduction with sodium borohydride in methanol at room temperature without any change in the course of the reaction.

9-Hydroxyroyleanone (II)

To a boiling solution of 0.513 g of 9-acetoxyroyleanone in 25 ml of ethanol was added 63 ml of 0.10 *N* aq. sodium hydroxide. The resulting magenta-colored solution was refluxed gently for 2 hours, cooled in an ice bath, and acidified with 15% phosphoric acid. The solid that separated was collected by filtration and air dried. It was purified by chromatography on silica gel followed by recrystallization from methanol–water, giving 0.23 g, m.p. 171–174°. After two additional recrystallizations from methanol–water the gold-colored plates melted at 172.5–174.5°, $[\alpha]_D$ −132° (*c*, 1.24). λ_{max}^{EtOH} 273 mμ, ε 11,900, 408 mμ, ε 800; $\nu_{max}^{CHCl_3}$ 3540, 3360, 1670, 1648, 1627, and 1604 cm^{-1}. Neut. equiv. 309, 325. Found: C, 72.46; H, 8.32. Calc. for $C_{20}H_{28}O_4$ (332.4): C, 72.26; H, 8.49.

In one run the acid liberated during the above hydrolysis was separated from the reaction mixture by codistillation with water. It was converted to the *p*-bromophenacyl ester, which was identical with authentic *p*-bromophenacyl acetate (mixed melting point and infrared spectrum).

9-Hydroxyroyleanone was converted to royleanone by catalytic reduction followed by air oxidation as is described above for the conversion of 9-acetoxyroyleanone to royleanone.

Treatment of a methanolic solution of 9-hydroxyroyleanone with excess ethereal diazomethane resulted in the formation of a monomethyl ether; m.p. 138.5–139.5° (recrystallized from methanol–water); $[\alpha]_D$ −310° (*c*, 1.05); λ_{max}^{EtOH} 270.5 mμ, ε 10,000, 372 mμ, ε 500; $\nu_{max}^{CHCl_3}$ 3550, 1661, 1640, and 1600 cm^{-1}. Found: C, 72.67; H, 8.54; OCH_3, 8.89. Calc. for $C_{21}H_{30}O_4$: C, 72.76; H, 8.73; OCH_3, 8.95.

Dehydration of 9-Hydroxyroyleanone (II) to 9-Dehydroroyleanone (III)

A mixture of 0.20 g of 9-hydroxyroyleanone, 10 ml of *p*-xylene, and 0.002 g of *p*-toluenesulphonic acid (monohydrate) was heated under reflux for 3½ hours. It was concentrated to a volume of ca. 0.5 ml under

reduced pressure, the residue was taken up in 1:1 hexane–benzene and the solution was poured onto a silica gel column. The column was eluted with 1:1 hexane–benzene and then with benzene. The benzene eluate was concentrated under reduced pressure and the residue was recrystallized from ethanol–water, giving 0.158 g; m.p. 166–168.5°; $[\alpha]_D$ −620° (*c*, 0.21); λ_{max}^{EtOH} 212 mμ, ε 16,700, 247 mμ (shoulder), ε 8,400, 330 mμ, ε 7,700, 459 mμ, ε 770; $\nu_{max}^{CHCl_3}$ 3340, 1666, 1635, 1615 (shoulder), 1595 (shoulder) cm^{-1}. Neut. equiv. 316. Found: C, 76.18; H, 8.30. Calc. for $C_{20}H_{26}O_3$ (314.4): C, 76.40; H, 8.34.

9-Dehydroroyleanone was converted to royleanone by catalytic reduction followed by air oxidation as is described above for the conversion of 9-acetoxyroyleanone to royleanone.

The methyl ether was prepared by the treatment of a methanolic solution of 9-dehydroroyleanone with excess diazomethane. It melted at 106.5–107.5° (recrystallized from methanol–water); $[\alpha]_D$ −615° (*c*, 0.21); λ_{max}^{EtOH} 212 mμ, ε 14,300, 246 mμ (shoulder), ε 8,400, 320 mμ, ε 5,600, 429 mμ, ε 770; $\nu_{max}^{CHCl_3}$ 1642, 1615 (shoulder) cm^{-1}. Found: C, 76.81; H, 8.49; OCH_3, 9.48. Calc. for $C_{21}H_{28}O_3$: C, 76.79; H, 8.59; OCH_3, 9.45.

Reductive Methylation of the Methyl Ether of Royleanone (IV) to VII (cf. ref. 13)

A solution of 0.185 g of royleanone methyl ether in 50 ml of methanol was hydrogenated over Adams' catalyst until the solution was colorless. The reaction mixture was left in the hydrogen atmosphere at room temperature, and during a period of 40 hours a total of 15 ml of 30% aq. sodium hydroxide and 13 ml of dimethyl sulphate was added to it. These were added in 1-ml portions; shaking was continued for 24 hours after the completion of the addition. The catalyst was removed by filtration, 50 ml of water was added, and the mixture was concentrated under reduced pressure to remove most of the methanol. The residue was extracted with benzene (75 ml). The benzene extract was washed with water (2×50 ml), dried over anhyd. magnesium sulphate, and passed through a column of alumina (activity I, 4 g). The colorless eluate was concentrated and the residue was crystallized from ethanol (0.11 g, m.p. 89–90.5°). After two additional recrystallizations from ethanol the product melted at 95–96.5°; $[\alpha]_D$ +99° (*c*, 0.91); λ_{max}^{EtOH} 208 mμ, ε 49,000, 281 mμ, ε 740. Found: C, 76.78; H, 10.09; OCH_3, 25.70. Calc. for $C_{23}H_{36}O_3$: C, 76.61; H, 10.07; OCH_3, 25.82.

Oxidation of 9-Dehydroroyleanone (III) with Alkaline Hydrogen Peroxide

To a solution of 0.200 g of 9-dehydroroyleanone in 81 ml of 0.10 *N* aq. sodium hydroxide at 70° was added 1.0 ml of 30% aq. hydrogen peroxide. The temperature was held at 70° for 3 hours. During this period three additional 1.0-ml portions of 30% aq. hydrogen peroxide were added. (The purple color of the sodium salt of the hydroxyquinone was completely discharged after the reaction had been in progress for 1½ hours.) The resulting pale yellow solution was made acid to Congo red with phosphoric acid and distilled. The volume of the pot residue was maintained at 30–90 ml by the addition of portions of water. Approximately 100 ml of distillate was collected. A small amount of oily material present in the distillate was removed and the residue was titrated with 0.100 *N* aq. sodium hydroxide (4.1 ml required). The resulting solution was concentrated to a volume of ca. 2 ml, made acid to Congo red with phosphoric acid, and extracted with ether (5×2 ml). The ether extracts were dried over anhydrous sodium sulphate, concentrated, and distilled. A colorless liquid, b.p. ca. 150°, 0.031 g, whose infrared spectrum was identical with that of isobutyric acid was obtained.

The oxidation of royleanone with alkaline hydrogen peroxide was carried out in the same fashion as was used with 9-dehydroroyleanone. The yield of isobutyric acid was comparable in the two cases.

Oxidation of 9-Dehydroroyleanone (III) with Alkaline Potassium Permanganate

Four percent aq. potassium permanganate was added to a solution of 1.22 g of 9-dehydroroyleanone in 100 ml of 2% aq. sodium hydroxide at such a rate that an excess of potassium permanganate was maintained in the reaction mixture. The temperature was held at 40–45° for 2 hours and at 65–70° for 1 hour. The solution was cooled to 30°, made acid to Congo red with conc. sulphuric acid, and the manganese dioxide was decomposed with sodium bisulphite. The volume of the solution was reduced to ca. 40 ml. The insoluble oil was separated and the residual aqueous layer was extracted continuously with ether. A yellow oil (0.44 g) was obtained when the ether extracts were concentrated. This oil was taken up in ether and treated with a slight excess of ethereal diazomethane at 5°. After 15 minutes at 5° the mixture was filtered through anhydrous sodium sulphate and the filtrate was concentrated under reduced pressure. The residue was taken up in 1:1 benzene–hexane and the solution was passed through a column of alumina (activity III, 10 g). The eluate was concentrated and distilled; the fraction distilling at 60–65° at 0.1 mm was collected; 0.130 g, $[\alpha]_D$ +26.5° (*c*, 1.83), $\nu_{max}^{CS_2}$ 1732 cm^{-1}. Found: C, 64.66; H, 9.06. Calc. for $C_{13}H_{22}O_4$: C, 64.44; H, 9.15.

Dehydrogenation of Royleanone (IV)

Royleanone (0.33 g) was passed through a heated column (100×8 mm) of 0.50 g of 30% palladium on charcoal supported on finely cut glass wool. The column was supported in a horizontal position in a furnace which was 20 cm in length and heated to 350°. The royleanone was distilled into the heated column with a small, movable furnace. A slow stream of hydrogen was used to sweep it through the catalyst bed. The product was passed through the catalyst bed in this manner five more times. It was then passed twice through a heated column (50×8 mm) of a mixture of zinc dust (Mallinckrodt Analytical Reagent) and pumice powder (B and A No. 2157) (2:1 by weight). The column was heated in the furnace described above.

Again a slow stream of hydrogen was used to carry the material through the column. Each of the passes described above required approximately 1 hour.

The material obtained from three such runs (0.54 g) was combined, dissolved in hexane, and chromatographed on 17 g of alumina (activity I). The column was eluted with hexane, hexane–benzene, and finally with benzene. The fractions eluted with hexane (0.14 g) were liquid and probably consisted of a mixture of naphthalenes (λ_{max} 228 mμ (strong), 280 mμ (medium), and ca. 320 mμ (weak doublet)). These fractions were not investigated further. The fractions eluted with hexane–benzene and with benzene were solid or semisolid (0.135 g). Their ultraviolet spectra were similar to those of phenanthrenes. These fractions were combined and fractionally recrystallized from ethanol. A total of 0.021 g of material with m.p. 118–120° was obtained. A mixed melting point with 1-methylphenanthrene (m.p. 119.5–121.5°) was not depressed (mixed m.p. 118–120.5°). Contamination of the 1-methylphenanthrene obtained by dehydrogenation of royleanone was indicated by a weak absorption band at 762 cm^{-1} in its infrared spectrum and a weak absorption band (ϵ 56) at 376 mμ in its ultraviolet spectrum. The spectra of the two samples were identical in all other respects.

Conversion of Ferruginol to Royleanone (IV)

To a solution of 0.360 g of ferruginol (liberated from the benzoate which melted at 156.5–157.5°) in 4 ml of glacial acetic acid at room temperature was added a drop of conc. sulphuric acid followed by 0.50 ml of 98% hydrogen peroxide. The reaction mixture quickly turned yellow and after an hour a solid began to separate. It was allowed to stand at room temperature for 12 hours. Water was added until the supernatant liquid was almost colorless. The gummy yellow precipitate was taken up in benzene, the solution was filtered through anhydrous sodium sulphate and concentrated under reduced pressure. The residue was chromatographed twice on silica gel. In each case the yellow band that was eluted with benzene–hexane was collected. The eluate was concentrated and recrystallized from acetic acid, giving 0.031 g, m.p. 176–180°. After an additional recrystallization from glacial acetic acid the product melted at 179–182°, 0.028 g, $[\alpha]_D$ +134° (*c*, 1.34). The melting point was not depressed by the admixture of authentic royleanone (mixed m.p. 179–182°). The infrared spectra of the two samples were identical (in chloroform).

ACKNOWLEDGMENTS

We wish to thank Mr. A. Knoll for the extractions and preliminary separations, Mr. H. Seguin for the analyses, Mr. J. Nicholson for the n.m.r. spectra, and Mr. R. Lauzon for the infrared spectra. We are grateful to Dr. P. K. Grant for a generous sample of ferruginol.

REFERENCES

1. I. C. Chopra, J. D. Kohli, and K. L. Handa. Indian J. Med. Research, **33**, 139 (1945).
2. O. E. Edwards and M. N. Rodger. Can. J. Chem. **37**, 1187 (1959).
3. A. Khaleque, S. Papadopoulos, I. Wright, and Z. Valenta. Chem. & Ind. (London), 513 (1959).
4. S. K. Talapatra and A. Chatterjee. J. Indian Chem. Soc. **36**, 437 (1959).
5. K. L. Handa, S. S. Chaudhary, and K. S. Jamwal. Indian J. Pharm. **20**, 211 (1958).
6. W. Flaig and J.-Ch. Salfeld. Ann. **618**, 117 (1958).
7. D. H. R. Barton. *In* Chemistry of carbon compounds. Vol. II B. *Edited by* E. H. Rodd. Elsevier Publishing Co. 1953. p. 718. G. Stork and J. W. Schulenberg. J. Am. Chem. Soc. **84**, 284 (1962).
8. J. B. Bredenberg. Acta Chem. Scand. **11**, 932 (1957).
9. M. Przybylska. Acta Cryst. **14**, 424 (1961).
10. J. W. ApSimon and O. E. Edwards. Can. J. Chem. **39**, 2543 (1961).
11. R. N. Jones, P. Humphries, F. Herling, and K. Dobriner. J. Am. Chem. Soc. **73**, 3215 (1951).
12. M. Karplus. J. Chem. Phys. **30**, 11 (1959).
13. P. K. Grant, A. W. Johnson, P. F. Juby, and T. J. King. J. Chem. Soc. 549 (1960).

OXIMES

I. THE SYNTHESIS OF SOME SUBSTITUTED 2-OXIMINOACETOPHENONES[1]

J. J. NORMAN,[2] R. M. HEGGIE, AND J. B. LAROSE
Defence Research Chemical Laboratories, Ottawa, Canada

Received March 16, 1962

ABSTRACT

The preparation of some *p*-(ω′-dimethylaminoalkyl)- and *p*-(ω′-dimethylaminoalkoxy)-2-oximinoacetophenones and their methiodides is described.

No general method was found for synthesis of short-chain (C_0, C_1, C_2) *p*-(ω′-dimethylaminoalkyl)-2-oximinoacetophenones. The longer-chain compounds (C_3, C_4) were prepared by a method which would appear to be general. ω-Phenyl-1-haloalkanes undergo Friedel–Crafts acylation to yield *p*-(ω′-haloalkyl)-acetophenones. These were converted to the dimethylamino compounds, which, subsequently, yielded 2-oximinoacetophenones. No method of preparation of *p*-(2′-dimethylaminoethyl)-2-oximinoacetophenone was found.

Synthesis of *p*-(ω′-dimethylaminoalkoxy)-2-oximinoacetophenones was accomplished using mixed α,ω-dihaloalkanes and *p*-hydroxyacetophenone. The *p*-(ω′-haloalkoxy)-acetophenones from these reactants were first converted to oximes and then to the dimethylamino compounds. Syntheses of *p*-(ω′-dimethylamino-ethoxy, -propoxy, -butoxy, and -pentoxy)-2-oximinoacetophenones were achieved. That of *p*-(dimethylaminomethoxy)-2-oximinoacetophenone was unsuccessful.

In the last few years, it has been shown that oximes are particularly effective reactivators of cholinesterases which have been inhibited by organophosphorus compounds (1–5). These inhibitors phosphorylate a group in the enzymatically active portion of the molecule, thus blocking hydrolysis of the normal substrate molecule (6–8). Kinetic and other studies with both inhibitors and substrates have revealed considerable detail regarding the structure of the active center of the enzyme (9, 10*). In this manner, it has been shown that both acetylcholinesterase (true cholinesterase) and pseudocholinesterase have a very similar "esteratic" site responsible for the actual hydrolysis of the substrate and that phosphorylation occurs at some point in this site (11, 12). The two enzymes, however, differ in the position and number of "anionic" sites which assist hydrolysis by aligning substrate molecules into positions favorable for interaction with the esteratic site (13, 14). For reactivation then, the enzyme must be dephosphorylated. With oximes, this results from nucleophilic attack of the oximate ion upon the phosphorus atom, with a resulting cleavage of the enzyme–phosphorus bond (15).

Incorporation into the reactivator molecule of a group capable of interaction with the anionic sites should assist dephosphorylation by aligning the oximate ion into a favorable position for attack on phosphorus. This would be entirely analogous to the substrate–enzyme interaction. Reasoning in this way, Wilson (16) and Davies and Green (17) tested pyridinium-2-aldoxime methiodide and found that it was both an effective reactivator of inhibited cholinesterase and, in conjunction with atropine sulphate, an excellent antidote for organophosphorus poisoning. By varying the distance of this interacting group from the oximino portion of the molecule, it should be possible to produce reactivators showing considerable specificity towards one or the other of the two types of cholinesterase and to map the enzyme surfaces by correlating the specificity patterns

[1]*Received as D.R.C.L. Report No. 372.*
Presented in part before the 5th Western Regional Conference of the CIC, Regina, 1960.
[2]*To whom inquiries should be addressed.*
**See also earlier papers by Friess.*

with the geometry of the oximes. Such an approach had been tried previously by Wilson (18, 19) in a much more limited way, using pyridinium-2-, -3-, and -4-aldoxime methiodides.

It has been shown previously (20) that the protonated dimethylamino group interacts with the anionic site nearly as well as the trimethylammonium group present in the choline portion of substrates. These two groups, therefore, were chosen for incorporation into the oxime molecule. The oxime portion chosen was based upon work by Childs, Davies, and Green (4, 5), who had shown that potent reactivators are obtained when a 1-oximino-2-oxo grouping is present in a wide variety of compounds. This grouping is present in 2-oximinoacetophenone, which itself is not an outstanding reactivator. It would be expected then that compounds related to 2-oximinoacetophenone carrying a trimethylammonium group or a dimethylamino group of suitable basicity would be better reactivators than the parent compound if they were specifically aligned for attack on the phosphorus atom, and any enhanced reactivity would reflect the fit of the oxime to the enzyme.

In this paper, the synthesis of the various oximes used in this study will be presented. Infrared spectra of the oximes and the results of reactivation studies will be reported in subsequent papers.

The first series of oximes synthesized had the general formula I, where n = 0, 1, 3,

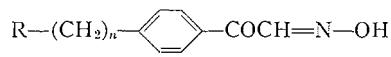

I

and 4, and R = $(CH_3)_2N$— and $I^-.(CH_3)_3\overset{+}{N}$—.

I (n = 0, R = $(CH_3)_2N$—) was synthesized from aniline. This was accomplished by a Friedel–Crafts acylation of acetanilide, followed by hydrolysis of the resulting *p*-acetaminoacetophenone to the free base.

Dimethyl sulphate converted this to the dimethylamino compound, which was treated with alkaline butyl nitrite to yield the required oxime. *p*-Aminoacetophenone was obtained in 40% yield from the starting materials but dimethylation and oximation resulted in low yields, about 20% in each case.

The following reaction scheme was utilized for synthesis of I (n = 1; R = $(CH_3)_2N$—). *p*-Toluidine was diazotized and treated with cuprous cyanide to form *p*-toluonitrile. This, on treatment with N-bromosuccinimide, yielded α-bromotoluonitrile, which in turn was converted to the dimethylamino compound. The cyano group was allowed to react with methylmagnesium iodide to form a methyl ketimine and, after hydrolysis, *p*-dimethylaminomethylacetophenone was obtained. This was treated with butyl nitrite to form *p*-(dimethylaminomethyl)-2-oximinoacetophenone.

The method of preparation of the *p*-alkyl compounds I (n = 3, 4; R = $(CH_3)_2N$—) was as follows. The ω-phenylalkanol-1 was converted to the bromide, which was acetylated with acetyl chloride in the presence of aluminum chloride. The resulting *p*-(ω'-bromoalkyl)-acetophenone was treated with dimethylamine to form the *p*-(ω'-dimethylaminoalkyl)-acetophenone, which, upon reaction with butyl nitrite in the presence of alkali, formed the oxime. Yields of bromoketones generally were good, about 80%, while those of the dimethylamino compounds were variable and poor, between 5 and 30%. The oximes were formed in about 25% yield.

It was found impossible to synthesize the compounds where n = 2, all attempts yielding only styrene derivatives.

As the length of the side chain increased, suitable starting materials became increasingly more difficult to obtain. A second series of compounds, therefore, was prepared from the readily available mixed α,ω-dihalides and *p*-hydroxyacetophenone. The resulting *p*-alkoxy compounds, II, where R = $(CH_3)_2N$— and $I^-.(CH_3)_3\overset{+}{N}$—, contain an ether link in the

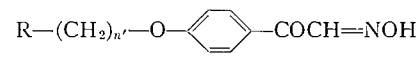

II

side chain, but such a substitution should have little effect upon the geometry of the system.

The synthesis of these compounds was accomplished in the following way. The mixed dihalide was treated with *p*-hydroxyacetophenone in the presence of potassium carbonate to yield a *p*-(ω'-haloalkoxy)-acetophenone. This, on reaction with butyl nitrite in the presence of sodium methoxide, formed the halooxime, which, subsequently, was treated with dimethylamine to yield the desired compound. Yields of the ω'-halo ketones were fair, 64–76%, while those of ω'-halooximes were variable, 30–70%. Yields of the ω'-dimethylaminooximes were poor, about 25%. In this manner, the compounds II (n' = 2, 3, 4, and 5; R = $(CH_3)_2N$—) were prepared. An attempt to prepare the compound II (n' = 1; R = Cl) was unsuccessful.

The dimethylamino compounds of both series I and II were quaternized with methyl iodide in absolute methanol, except for I, n = 0, where excess methyl iodide was used as solvent. Yields were approximately 50%.

Infrared spectra were run routinely to identify the products of reaction but are not reported here.

EXPERIMENTAL

Since methods were identical for many of the compounds prepared, only representative examples of the preparations will be given in detail. Starting materials for these preparations were commercially available C.P. grade chemicals.

Preparation of p-(ω'-Substituted alkyl)-2-oximinoacetophenones

p-Dimethylaminoacetophenone

p-Aminoacetophenone.—Acetanilide (0.2 mole) and aluminum chloride (0.3 mole) were suspended in carbon disulphide (250 ml), then acetyl chloride (0.2 mole) was added dropwise, with vigorous stirring. The reaction mixture was refluxed for 2 hours and then stirred overnight. Carbon disulphide and excess acetyl chloride were removed by distillation and the syrupy residue was poured onto ice. The solid material so obtained was suspended in 10% sodium hydroxide (200 ml) and the mixture was refluxed for 2 hours. After cooling, the solution was extracted with chloroform, the extracts were combined, and solvent was removed *in vacuo*. The residue was recrystallized from 50% aqueous ethanol. Yield: 0.082 mole, 41%, m.p. 103–105° C, lit. m.p. 105.8° C (28).

p-Dimethylaminoacetophenone.—*p*-Aminoacetophenone (0.74 mole) was added to warm water (500 ml, 70–80° C) and the stirred solution was treated dropwise with dimethyl sulphate (2.54 mole). A solution of 50% sodium hydroxide (135 ml) was placed in a dropping funnel and added at such a rate that the reaction mixture was kept mildly alkaline. When all the dimethyl sulphate had been added, the remainder of the alkali solution was run into the mixture and the whole was stirred for 10 minutes. The solid product was filtered, recrystallized from 70% methanol, and dried *in vacuo*. The dried material was shaken with warm (50° C) 10% sodium hydroxide (700 ml) and twice its weight of *p*-toluenesulphonyl chloride until the odor of the sulphonyl chloride had disappeared. The residual solid was separated and washed with 5% hydrochloric acid (5×50 ml). The acid extract was made alkaline (pH 9) with 10% sodium hydroxide and the precipitate was removed by filtration. This material was recrystallized from 65–110° C petroleum ether. Yield: 0.092 mole, 20.6%, m.p. 105–106° C, lit. m.p. 105° C (29).

p-(Dimethylaminomethyl)-acetophenone

α-Bromo-p-toluonitrile.—Toluonitrile (0.50 mole) (21) in carbon tetrachloride (200 ml) was added slowly, with stirring, to a mixture of N-bromosuccinimide (0.5 mole) and benzoyl peroxide (1 g) in a flask fitted with

a condenser. After refluxing for 45 minutes, half the solvent was removed by distillation and the mixture was allowed to cool. The precipitate was removed, washed three times with water, and dried. Yield: 0.30 mole, 60%, m.p. 114–116° C, lit. m.p. 114–115° (30).

p-(Dimethylaminomethyl)-benzonitrile.—α-Bromo-*p*-toluonitrile (0.30 mole) was dissolved in a mixture of ether (400 ml) and benzene (100 ml), the solution was chilled to −70° C, dimethylamine (0.3 mole) was added, and the flask was sealed and allowed to warm to room temperature. After 48 hours, the flask was cooled in an ice–salt bath to −10° C and opened. The solvent was removed *in vacuo* and the residue was dissolved in the minimum quantity of water. This solution was ether extracted, the extracts were combined and dried with anhydrous sodium sulphate, then distilled. Yield: 0.25 mole, 83.5%, b.p. 90–91° C at 0.6 mm, n_D^{25} 1.5234.

p-(Dimethylaminomethyl)-acetophenone.—*p*-(Dimethylaminomethyl)-benzonitrile (0.25 mole) was added dropwise to methylmagnesium iodide (0.50 mole) in toluene (400 ml) and the mixture was refluxed 48 hours. The reaction mixture was poured onto crushed ice, and 6 *N* hydrochloric acid was added until the precipitate just dissolved. This solution was heated on a steam cone for 2 hours, cooled, and extracted with ether. The aqueous layer was made basic with sodium carbonate and ether-extracted. The combined ether extracts were dried and distilled. Yield: 0.188 mole, 75%, b.p. 90° C at 0.05 mm, n_D^{25} 1.5248.

p-(4′-Dimethylaminobutyl)-acetophenone and p-(3′-Dimethylaminopropyl)-acetophenone

3-Bromopropylbenzene and 4-bromobutylbenzene.—3-Hydroxypropylbenzene and 4-hydroxybutylbenzene, prepared by lithium aluminum hydride reduction of ethyl 3-phenylpropionate and ethyl 4-phenylbutyrate (22), were converted to the corresponding bromides according to the procedure of Marvel (23).

p-(4′-Bromobutyl)-acetophenone.—Aluminum chloride (0.7 mole) was suspended in carbon disulphide (350 ml) in a 1-liter round-bottomed flask fitted with a stirrer, dropping funnel, and condenser with drying tube, then acetyl chloride (0.7 mole) was added over 10–15 minutes to the vigorously stirred mixture. This was cooled in an ice–salt bath, and a solution of 4-bromobutylbenzene (0.8 mole) and acetyl chloride (1.5 mole) was added as fast as possible. Stirring was continued until hydrogen chloride was no longer evolved. The complex was decomposed by pouring the reaction mixture onto crushed ice, the organic layer was separated, and the aqueous layer was extracted with benzene. The combined organic phases were dried and then distilled under reduced pressure. Yield: 0.16 mole, 20.3%, b.p. 125–127° C at 0.01 mm.

p-(3′-Bromopropyl)-acetophenone.—This compound was prepared in an analogous manner from 3-bromopropylbenzene in 70% yield.

p-(4′-Dimethylaminobutyl)-acetophenone.—*p*-(4′-Bromobutyl)-acetophenone (0.15 mole) was dissolved in anhydrous methanol (150 ml) in a pressure flask. The solution was chilled to −70° C, dimethylamine (0.35 mole) was added, and the flask was sealed. The solution was allowed to warm to room temperature and to stand for 24 hours. The flask was opened, the solvent was removed *in vacuo*, and the residue was dissolved in water. The dimethylamino compound was ether-extracted, the extracts were dried and distilled. Yield: 0.077 mole, 53%, b.p. 100° C at 0.005 mm, n_D^{25} 1.5195.

p-(3′-Dimethylaminopropyl)-acetophenone.—This compound was prepared similarly in 78% yield.

Preparation of Oximes

All the above acetophenones were converted to oximes in the same manner and one representative procedure only is given.

p-(4′-Dimethylaminobutyl)-2-oximinoacetophenone.—Butyl nitrite (0.08 mole) was added to a stirred, ice-cold solution of sodium ethoxide (from 0.088 mole of sodium) in absolute ethanol (100 ml). *p*-(4′-Dimethylaminobutyl)-acetophenone (0.077 mole) was added dropwise over 25–30 minutes, the solution was allowed to warm to room temperature and then to stand until the following day. The precipitate was filtered, washed with ether, and then dissolved in the minimum quantity of water. The solution was acidified with glacial acetic acid and the resulting yellow solid was filtered, recrystallized from ethanol, from isopropanol, and finally, from ether–acetone. Yield: 0.027 mole, 35%, m.p. 125° C. Other oximes were recrystallized twice from ethanol.

Preparation of p-(ω′-Substituted alkoxy)-2-oximinoacetophenones

Mixed α,ω-dihalides.—1-Chloro-3-bromopropane was prepared from 3-chloropropanol-1 and phosphorus tribromide (24), 1-chloro-4-idobutane from 1,4-dichlorobutane and sodium iodide (25), and 1-chloro-5-bromopentane from 5-chloro-*n*-amyl acetate and phosphorus tribromide (26). 1-Chloro-2-bromoethane was obtained from Fisher Scientific Co. Ltd.

p-(4′-Chlorobutoxy)-acetophenone.—*p*-Hydroxyacetophenone (1.5 mole) and potassium carbonate (2.0 mole) were suspended in 2-butanone (700 ml). To this vigorously stirred suspension, 1-chloro-4-bromobutane (1.5 mole) was added dropwise over 1 hour, then the mixture was refluxed for 5 hours. Inorganic solids were removed and the solution was taken to dryness *in vacuo*. The residue was taken up in ether, washed with 10% sodium carbonate, with water, then dried and distilled at reduced pressure. Yield: 0.98 mole, 64%, b.p. 131–132° C at 0.07 mm.

Other p-(ω′-chloroalkoxy)-acetophenones.—These compounds were prepared in a similar manner from 1-chloro-2-bromoethane, 1-chloro-3-bromopropane, and 1-chloro-5-bromopentane.

TABLE I

Preparation of *p*-ω'-substituted alkylacetophenones and 2-oximinoacetophenones

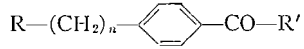

						Analysis					
						Calculated (%)			Found (%)		
n	R	R′	Yield (%)	B.p. or m.p. (°C)		C	H	N	C	H	N
0	$(CH_3)_2N$—	—CH_3*	20	m	105–105.5	73.56	8.07	8.39	73.70	7.98	8.88
	$(CH_3)_2N$—	—CH=NOH	23	m	175–177	62.51	6.19	14.25	62.61	6.25	.1457
	$I^-.(CH_3)_3\overset{+}{N}$—	—CH=NOH	18	m	189–190	39.53	4.53	8.38	39.94	4.57	8.14
1	$(CH_3)_2N$—	—CH_3†	75	b	90 at 0.05 mm	74.54	8.53	7.90	74.34	8.06	7.83
	$(CH_3)_2N$—	—CH=NOH	98	m	248–249	64.85	6.84	13.59	64.42	6.72	12.98
	$I^-.(CH_3)_3\overset{+}{N}$—	—CH=NOH	92	m	215	41.38	4.92	8.05	41.31	4.88	8.09
2	Br—	—CH_3	53	b	97–98 at 0.001 mm	Not analyzed					
	$(CH_3)_2N$—	—CH_3	69	m	34.5	75.35	8.96	7.32	75.58	8.47	7.50
3	Br—	—CH_3	70	b	112 at 0.04 mm	Not analyzed					
	$(CH_3)_2N$—	—CH_3‡	78	b	91 at 0.04 mm	Unstable					
	$(CH_3)_2N$—	—CH=NOH	15	m	113–114	66.62	7.74	11.69	66.35	7.41	11.55
	$I^-.(CH_3)_3\overset{+}{N}$—	—CH=NOH	97	m	214 decomp.	44.68	5.63	7.45	45.01	5.50	7.51
4	Br—	—CH_3§	20	b	125 at 0.01 mm	Not analyzed					
	$(CH_3)_2N$—	—CH_3‖	53	b	100 at 0.005 mm	Unstable					
	$(CH_3)_2N$—	—CH=NOH	35	m	125	67.71	8.09	11.26	67.78	7.79	10.99
	$I^-.(CH_3)_3\overset{+}{N}$—	—CH=NOH	48	m	171–172	46.19	5.91	7.17	46.13	5.80	7.02

NOTE: m = melting point; b = boiling point.
*Semicarbazone, m.p. 210° C. Calculated for $C_{11}H_{16}N_4O$: C 59.98%, H 7.27%, N 25.45%. Found: C 60.11%, H 7.35%, N 25.35%.
†2,4-Dinitrophenylhydrazone, m.p. 161.5° C. Calculated for $C_{17}H_{18}N_8O_4$: C 57.13%, H 5.36%, N 19.60%. Found: C 57.02%, H 5.17%, N 19.35%.
‡2,4-Dinitrophenylhydrazone, m.p. 139° C. Calculated for $C_{18}H_{20}N_8O_4$: C 58.12%, H 6.18%, N 18.66%. Found: C 58.19%, H 5.90%, N 18.50%.
§2,4-Dinitrophenylhydrazone, m.p. 142.5° C. Calculated for $C_{18}H_{19}BrN_8O_4$: C 49.66%, H 4.40%, N 12.88%. Found: C 50.68%, H 4.48%, N 12.60%.
‖2,4-Dinitrophenylhydrazone formed but was accidentally contaminated. Insufficient material remained to repeat the derivative preparation.

TABLE II

Preparation of *p*-ω'-substituted alkoxyacetophenones and 2-oximinoacetophenones

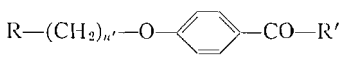

n'	R	R′	Yield (%)	B.p. or m.p. (°C)	Analysis					
					Calculated (%)			Found (%)		
					C	H	N	C	H	N
2	Cl—	—CH_3*	27	m 51	60.47	5.60	—	60.57	5.48	—
	Cl—	—CH=NOH	30	m 130–131	52.74	4.43	6.16	53.03	4.14	6.51
	$(CH_3)_2N$—	—CH=NOH	25	m 160–161	61.09	6.82	11.87	61.08	6.73	11.81
	$I^-.(CH_3)_3\overset{+}{N}$—	—CH=NOH	57	m 241	41.28	5.16	7.41	41.76	4.93	7.29
3	Cl—	—CH_3†	76	b 136 at 2 mm	62.12	6.16	—	61.52	5.70	—
	Cl—	—CH=NOH	57	m 95–96	54.67	5.00	5.79	54.70	4.94	5.48
	$(CH_3)_2N$—	—CH=NOH	12	m 122–123	62.36	7.24	11.19	62.42	7.02	10.91
	$I^-.(CH_3)_3\overset{+}{N}$—	—CH=NOH	52	m 190	42.87	5.40	7.14	43.08	5.16	7.07
4	Cl—	—CH_3‡	64	b 131–132 at 0.07 mm	63.58	6.67	—	63.42	6.31	—
	Cl—	—CH=NOH	70	m 110–112	56.36	5.51	5.49	56.45	5.66	5.25
	$(CH_3)_2N$—	—CH=NOH	41	m 122–123	63.60	7.58	10.59	63.36	7.38	10.36
	$I^-.(CH_3)_3\overset{+}{N}$—	—CH=NOH	43	m 135–136	44.28	5.71	6.89	44.16	5.67	6.85
5	Cl—	—CH_3§	77	m 40	64.86	7.12	—	64.64	6.85	—
	Cl—	—CH=NOH	16	m 68–69	57.88	5.98	5.19	60.02	5.99	5.62
	$(CH_3)_2N$—	—CH=NOH	27	m 122	64.72	7.97	10.06	64.81	7.65	10.03
	$I^-.(CH_3)_3\overset{+}{N}$—	—CH=NOH	76	m 235	45.72	5.99	6.67	45.56	5.90	6.57

NOTE: m = melting point; b = boiling point.
*2,4-Dinitrophenylhydrazone, m.p. 184.5° C. Calculated for $C_{16}H_{15}ClN_4O_5$: C 50.49%, H 3.99%, N 14.80%. Found: C 50.12%, H 3.59%, N 14.68%.
†2,4-Dinitrophenylhydrazone, m.p. 163° C. Calculated for $C_{17}H_{17}ClN_4O_5$: C 51.96%, H 4.36%, N 14.27%. Found: C, 52.43%, H 4.41%, N 14.62%.
‡2,4-Dinitrophenylhydrazone, m.p. 144° C. Calculated for $C_{18}H_{19}ClN_4O_5$: C 53.15%, H 4.17%, N 13.78%. Found: C 53.23%, H 4.68%, N 13.87%.
§2,4-Dinitrophenylhydrazone, m.p. 132.5° C. Calculated for $C_{19}H_{21}ClN_4O_5$: C 54.22%, H 5.03%, N 13.31%. Found: C 54.48%, H 5.08%, N 13.47%.

p-(ω'-Chloroalkoxy)-2-oximinoacetophenones.—These were prepared from the corresponding *p*-(ω'-chloroalkoxy)-acetophenones and butyl nitrite following the procedure outlined above for *p*-(4'-dimethylaminobutyl)-2-oximinoacetophenone.

p-(ω'-Dimethylaminoalkoxy)-2-oximinoacetophenones.—All the above chloroalkoxyacetophenones were converted to dimethylamino compounds in a fashion analogous to that described for *p*-(4'-dimethylaminobutyl)-acetophenone.

Quaternizations

The dimethylaminooxime (1.0 g) was dissolved in absolute methanol (10 ml), and then methyl iodide (15 ml) was added. The mixture was kept in a sealed tube at room temperature for 48 hours. The solvent was removed *in vacuo* and the residue was recrystallized from ethanol or acetonitrile. Yields varied from 18 to 97% but, in general, were 40% or better.

Derivatives

2,4-Dinitrophenylhydrazones were prepared for most acetophenone compounds, following the general procedure given in Shriner and Fuson (27, p. 171). When the acetophenone contained a dimethylamino group, this procedure had to be modified slightly, since the precipitate obtained was the hydrosulphate. This was treated with 15% sodium carbonate solution to regenerate the free base, which was recrystallized in the normal manner.

In one instance, the hydrazone did not form. The semicarbazone, however, was obtained readily (27, p. 170).

Analyses

Yields and anlyses for the various compounds prepared are listed in Tables I and II. Unfortunately, these compounds were all quite unstable and the analyses reported are the best obtained. It is realized that deviations between calculated and experimental values, in some instances, are somewhat larger than the generally accepted limits but further attempts at purification led to loss of nitrogen. The materials, however, are believed to be the oximes claimed because of their behavior in biological tests, which will be reported at a later date.

ACKNOWLEDGMENTS

The authors would like to thank Mr. I. G. Wright and Mr. R. Miller for their assistance in the preparation of some of these compounds, and Mr. J. Helie for performing the microanalyses.

REFERENCES

1. I. B. Wilson. Discussions Faraday Soc. **20**, 119 (1955).
2. I. B. Wilson and S. Ginsberg. Arch. Biochem. Biophys. **54**, 569 (1955).
3. I. B. Wilson, S. Ginsberg, and E. K. Meisich. J. Am. Chem. Soc. **77**, 4286 (1955).
4. A. F. Childs, D. R. Davies, and A. L. Green. Brit. J. Pharmacol. **10**, 462 (1955).
5. A. L. Green and H. J. Smith. Biochem. J. **68**, 28, 32 (1958).
6. J. C. Boursnell and E. C. Webb. Nature, **164**, 875 (1949).
7. W. N. Aldridge. Chem. & Ind. (London), 473 (1954).
8. A. L. Green and B. Saville. J. Chem. Soc. 3887 (1956).
9. W. N. Aldridge. Biochem. J. **53**, 62 (1953).
10. S. L. Friess. J. Am. Chem. Soc. **79**, 3269 (1957).
11. J. A. Cohen *et al.* J. Cellular Comp. Physiol. **54**, 231 (1959).
12. B. J. Jandorf *et al.* Discussions Faraday Soc. **20**, 134 (1955).
13. F. Bergmann. Discussions Faraday Soc. **20**, 126 (1955).
14. F. Bergmann and R. Segal. Biochem. J. **58**, 692 (1954).
15. D. R. Davies and A. L. Green. Biochem. J. **63**, 529 (1956).
16. I. B. Wilson and S. Ginsberg. Biochim. et Biophys. Acta, **18**, 168 (1955).
17. D. R. Davies and A. L. Green. Discussions Faraday Soc. **20**, 269 (1955).
18. I. B. Wilson. Federation Proc. **18**, 752 (1959).
19. I. B. Wilson, S. Ginsberg, and C. Quan. Arch. Biochem. Biophys. **77**, 286 (1958).
20. I. B. Wilson and F. Bergmann. J. Biol. Chem. **185**, 479 (1950).
21. H. T. Clarke and R. R. Read. Org. Syntheses, Coll. Vol. I, 514 (1941).
22. R. F. Nystrom and W. G. Brown. J. Am. Chem. Soc. **69**, 1197 (1947).
23. C. S. Marvel. Org. Syntheses, Coll. Vol. I, 25 (1941).
24. J. B. Cloke, R. J. Anderson, J. Lachmann, and G. E. Smith. J. Am. Chem. Soc. **53**, 2794 (1931).
25. K. Ahmed and F. M. Strong. J. Am. Chem. Soc. **70**, 1699 (1948).
26. M. S. Newman and J. Wotiz. J. Am. Chem. Soc. **71**, 1294 (1949).
27. R. L. Shriner and R. C. Fuson. The systematic identification of organic compounds. 3rd ed. John Wiley and Sons Inc., New York. 1948.
28. D. Kursanov. J. Gen. Chem. (U.S.S.R.), **13**, 286 (1943).
29. M. Suzuki and M. Nagawa. J. Pharm. Soc. Japan, **75**, 54 (1955).
30. J. Dzulynska. Roczniki Chem. **24**, 135 (1950).

INVESTIGATIONS IN THE BICYCLOHEPTANE SERIES

PART I. THE ELECTRONIC EFFECT OF METHYL GROUPS ON C_6 OF THE NORBORNYL CATION

DONALD E. MCGREER
Department of Chemistry, University of British Columbia, Vancouver, British Columbia
Received March 21, 1962

ABSTRACT

The addition of acetic acid to camphenilene has been carried out. The major products are the two expected from normal addition without rearrangement. From the product ratio it is possible to conclude that the difference between the electronic effect of a methyl and a hydrogen at C_6 of the norbornyl cation is small.

Winstein (1–3) and Roberts (4, 5) have proposed that a non-classical carbonium ion (I) is obtained in the norbornyl system by solvolysis of derivatives of *exo*-norborneol. This is analogous to the type of intermediate (II) proposed in a number of migration reactions (6). For many such reactions, i.e. the Baeyer–Villiger and pinacol rearrangement reactions,

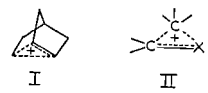

I II

a definite order of migrational aptitude of *t*-butyl > ethyl > methyl has been observed (7, 8) and this order has been partly attributed to electronic influence of the methyl groups on the migrating carbon. It is of interest to see if such pronounced effects are also present in the norbornyl system.

In our laboratories, we are studying the electronic and steric effects of substitution at C_6 of the norbornyl system and in this paper will report evidence concerning the electronic influence of two methyl groups at C_6.

Addition of acetic acid to camphenilene (apoisofenchene (III)) can potentially yield a simple norbornyl cation (IV) and/or a 6,6-dimethylnorbornyl cation (V) (the non-classical ion is used here for convenience since we do not have definitive evidence for or against its formation). Neglecting any steric differences (which are shown below to be small)

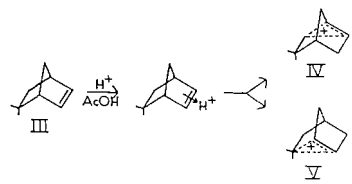

III IV V

and provided the product is not equilibrated, the product ratio should be a measure of the electronic influence of the methyl groups on the intermediate ion.

Beckmann and Bamberger (9) in 1953 reported the addition of acetic acid to camphenilene. They observed as the major product the acetate from IV (5-*exo*-camphenilanyl acetate (*β*-isofenchocamphoryl acetate) (VI)). Two other minor products resulting from

rearrangement were also found but there was no evidence for the acetate from V (6-*exo*-camphenilanyl acetate) (VII). We now have repeated this work and find that 5-*exo*-camphenilanyl acetate (VI) and 6-*exo*-camphenilanyl acetate (VII) are the major products and are formed in the ratio of 2:1 respectively.

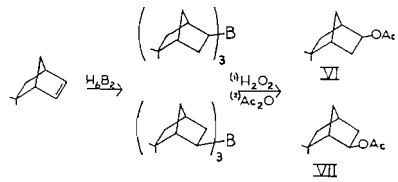

The acetate mixture from the addition of acetic acid to camphenilene was chromatographed by vapor chromatography and two major peaks were found to be present. These components were isolated and found to be identical with the pair of acetates prepared from camphenilene by the hydroboration method of Brown and Subba Rao (10). Hydroboration of camphenilene followed by oxidation and then acetylation gave two acetates, b.p. 211° and 214°, in a ratio of 45:55 respectively. From studies by Brown *et al.* on bicyclic systems and related structures (11, 12) it is unlikely that rearrangement of the carbon skeleton has occurred and it is probable that the two acetates are *exo*. It is important to note that for a reaction which has been shown to be sensitive to steric effects the ratio of acetates formed is close to 1. It is based on this observation that we feel that steric effects are minor in the addition reaction with acetic acid.

Further identification of the products has been based on the transformation of the acetates to the alcohols and derivatives and then to the ketones and derivatives. The

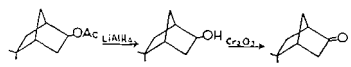

pertinent melting points of these and related compounds are given in Table I. From these data it can be concluded that the acetate, b.p. 214°, is 5-*exo*-camphenilanyl acetate (VI) and the acetate, b.p. 211°, is 6-*exo*-camphenilanyl acetate (VII).

TABLE I

Source	Melting point (°C)			
	Alcohol	Hydrogen phthalate	Ketone	Semicarbazone
5-*exo*-Camphenilanyl	60–61 (13)	130–131 (13)	64–65.5 (14)	193 (14)
3-Camphenilanyl "1"	103–104 (15)	178–179 (15)	38 (16)	223 (16)
3-Camphenilanyl "2"	75–76 (15)	154–155 (15)	38 (16)	223 (16)
α-Isofenchocamphoryl	132–133 (15)	174–175 (15)	109 (17)	220 (17)
6-*exo*-Camphenilanyl	—	—	b.p. 197 (18)	—
Acetate, b.p. 211°	30	138.5–140	55–56, b.p. 195	183–184
Acetate, b.p. 214°	55–56	130–131	—	189–190

Beckmann and Bamberger (9) missed the derivatives of the 6-*exo*-camphenilanyl system for the following reasons. In the attempted separation by crystallization of the hydrogen phthalates of the alcohol mixture the hydrogen phthalate of 6-*exo*-camphenilanol was

not obtained since it is more soluble than the 5-isomer in the solvents used. The ketone mixture of 6-camphenilanone and 5-camphenilanone under standard conditions yields the pure semicarbazone of the 5-isomer since the 6-isomer forms a semicarbazone at a much slower rate. The slow reactivity of the 6-ketone is presumably due to the large steric effort of an *endo*-methyl group at the 2-position.

There are two possible explanations for the observed product ratio from the addition of acetic acid to camphenilene. The first is that the presence of methyl substitution at C_6 of I (V) provides no additional stabilization over structure IV and thus the product ratio is close to 1. The ability of methyl attached to the carbon of a migrating group to give stabilization by electronic induction or hyperconjugation has been questioned in the case of the Wagner–Meerwein rearrangement reaction (19). Cram and Knight based their arguments on an observed migrational aptitude for methyl and ethyl of 35:1 respectively in the solvolysis of 3,4-dimethyl-4-phenyl-3-hexyl *p*-bromobenzoate. Unfortunately, there have been no other migrational aptitudes measured for the Wagner–Meerwein rearrangement reaction.

The second possible explanation is that C_6 does not participate during the addition and thus the effect of methyl substitution on C_6 is long range. It is hoped that further studies on the effect of substituents at C_6 of the norbornyl system will provide additional information from which our understanding of the factors involved will be increased.

EXPERIMENTAL

Melting points and boiling points are uncorrected. Boiling points of analytical samples were determined by the micro inverted capillary method.

Camphenilene

The camphenilene, m.p. 33–34°, b.p. 131°, and n_D^{35} 1.4525, used in this study was prepared by methods similar to those reported by Berson (20).

Addition of Acetic Acid to Camphenilene

A solution of 18 g (0.15 mole) of camphenilene in 70 ml of acetic acid containing 1 ml of 50% sulphuric acid was heated at 100° for 1 hour. The solution was poured into 500 ml of cold water and the two layers which formed were separated. The water layer was washed with ether and the ether washing combined with the organic layer. The resulting ether solution was washed with water, 10% sodium carbonate solution, and water and then dried over anhydrous magnesium sulphate. The ether solution was filtered and distilled to give 21 g of acetate product, b.p. 106–122° at 30 mm. Chromatographic separation of the two major components which comprised 90% of the product was carried out, first with a Megachrom instrument fitted with six 8-ft apiezon J columns fitted in parallel to give two acetate products which were shown by chromatography to be 95% pure. Further purification of the acetates with an Aerograph unit fitted with a 10-ft dinonyl phthalate column gave the two components pure.

Acetate, b.p. 211° and n_D^{21} 1.4597. Calc. for $C_{11}H_{18}O_2$: C, 72.53; H, 9.89. Found: C, 72.45; H, 9.66.

Acetate, b.p. 214° and n_D^{21} 1.4611. Calc. for $C_{11}H_{18}O_2$: C, 72.53; H, 9.89. Found: C, 72.41; H, 9.77.

The lower-boiling acetate was eluted first, on both columns.

The addition of acetic acid was carried out under a variety of conditions to determine the effect of time and temperature on the product ratio. For these experiments 1 g of camphenilene and 5 ml of acetic acid containing 1% of sulphuric acid were used. The results are given in Table II. A pure sample of the acetate,

TABLE II

Time (min)	Temp. (°C)	% acetate of b.p. 211°	% acetate of b.p. 214°	Comment
20	60	36	64	Reaction incomplete
60	60	39	61	5% camphenilene remaining
5	100	35	65	Reaction complete
30	100	39	61	
240	100	43	57	

b.p. 214°, was heated 5 minutes at 100° in acetic acid with sulphuric acid added. Work-up of the solution showed that there had been no isomerization of this acetate into the acetate, b.p. 211°. The product ratio is therefore kinetically controlled.

Hydroboration of Camphenilene

In a 200-ml 3-necked flask fitted with two gas adapters and a pressure-equalized dropping funnel was placed a solution of 10.73 g (0.088 mole) of camphenilene in 20 ml of purified diglyme. The flask was flushed with nitrogen, and 25 ml (0.025 mole) of 1 *M* sodium borohydride solution in diglyme was added. To the magnetically stirred solution was added dropwise a solution of 4.73 g (0.033 mole) of boron trifluoride etherate in 20 ml of diglyme over a 1-hour period. The solution was allowed to stand an additional hour and there was then added 7 ml of water and 14 ml of 3 *N* sodium hydroxide. The addition funnel was replaced by a condenser and 14 ml of 30% hydrogen peroxide was added in portions to maintain a steady reflux. The solution was cooled and added to 100 g of ice and extracted four times with water, and the ether extract was washed with ice water and dried over magnesium sulphate.

The ether solution was filtered and the ether removed by distillation. To the residual alcohol was added 40 ml of pyridine and 20 ml of acetic anhydride. The mixture was heated 3 hours on a steam bath and then poured into ice containing 15 ml of concentrated sulphuric acid. The resulting solution was extracted with ether and the ether solution washed with dilute sulphuric acid and water and then dried over magnesium sulphate. Distillation gave 9 g of acetate, b.p. 95–100° at 17 mm.

Vapor chromatographic separation of the product using a dinonyl phthalate column showed only 2 peaks. The first peak, n_D^{24} 1.4583, representing 45% of the total, was identical by infrared with the acetate, b.p. 211°, isolated from the addition reaction of acetic acid to camphenilene. The second peak, n_D^{24} 1.4600, representing 55% of the total, was identical with the acetate, b.p. 214°.

5-exo-Camphenilanol (β-Isofenchocamphorol)

A 15.1-g (0.0825 mole) sample of the acetate, b.p. 214°, which contained 5% of the acetate, b.p. 211°, was reduced in ether with 2.0 g of lithium aluminum hydride. After work-up in the usual way the dry ether solution of the alcohol product was reduced in volume to 20 ml, and 75 ml of pyridine was added. The resulting mixture was heated until all of the ethanol had distilled. Phthalic anhydride (11.3 g, 0.0825 mole) was added to the solution, which was then refluxed for 4 hours. The reaction mixture was poured into 1 liter of 10% sulphuric acid and extracted five times with 50-ml portions of benzene. The benzene solution was washed with water and dried. Evaporation of the benzene gave 23.3 g of product, m.p. 124–128°. Recrystallization from ethyl acetate and petroleum gave 10 g of the pure hydrogen phthalate of 5-*exo*-camphenilanol, m.p. 130–131° (lit. (13) m.p. 130–131°).

A solution of 9.4 g of the hydrogen phthalate of 5-*exo*-camphenilanol and 12.5 g of sodium hydroxide in 50 ml of water was steam-distilled to give 3.9 g of 5-*exo*-camphenilanol, m.p. 53–54° (lit. (13) m.p. 60–61°). Sublimation raised the melting point to 55–56°.

Semicarbazone of 5-Camphenilanone

To a solution of 0.5 g of 5-*exo*-camphenilanol in 1.5 ml of acetone at 5° was added dropwise 1.3 ml of chromic acid solution containing 10.3 g of chromium trioxide and 8.7 ml of concentrated sulphuric acid in 30 ml of water. After 1 hour at 5°, addition was complete, and the reaction was diluted with 13 ml of water and extracted with ether. The ether extract was washed and dried and then concentrated to give 0.5 g of an oil. The oil was treated with 0.5 g of sodium acetate, 0.5 g of semicarbazide hydrochloride, 5 ml of water, and 5 ml of methanol and heated at 65° for 20 minutes. After addition of 10 ml of water and cooling, the semicarbazone separated. Recrystallization from methanol gave 0.25 g, m.p. 189–190°, of the semicarbazone of 5-camphenilanone.

6-exo-Camphenilanol

A pure sample of 4 g of the acetate, b.p. 211°, was reduced with 1 g of lithium aluminum hydride in ether. After work-up in the usual way the product was distilled to give 2.8 g of 6-*exo*-camphenilanol, m.p. 30°, n_D^{31} 1.4187, and b.p. 200°. Calc. for $C_9H_{16}O$: C, 77.09; H, 11.50. Found: C, 77.13; H, 11.79.

The acid phthalate was prepared from a sample of the acetate, b.p. 211°, which contained 5% of the acetate, b.p. 214°, by the procedure used for the preparation of the hydrogen phthalate of 5-*exo*-camphenilanol. After three crystallizations from ethyl acetate and petroleum ether a constant melting point of 138.5–140° was obtained. Calc. for $C_{17}H_{20}O_4$: C, 70.81; H, 6.99. Found: C, 71.02; H, 7.13.

6-Camphenilanone

A solution of 2.6 g of 6-*exo*-camphenilanol in 20 ml of ether was treated at 20° with 8.8 ml of a solution made up from 5.00 g of sodium dichromate dihydrate and 3.75 ml of concentrated sulphuric acid diluted to 25 ml by the procedure of Brown and Garg (21). Chromatography of the product showed two peaks. The major peak, representing 82% of the total, was collected to give 1.0 g of 6-camphenilanone, m.p. 55–56° and b.p. 194° (lit. (18) b.p. 197°). Calc. for $C_9H_{14}O$: C, 78.21; H, 10.21. Found: C, 78.22; H, 9.95.

Semicarbazone, m.p. 183–184°, mixed m.p. with the semicarbazone of 5-camphenilanone 159–172°. Calc. for $C_{10}H_{17}N_3O$: C, 61.51; H, 8.78; N, 21.52. Found: C, 61.46; H, 8.66; N, 21.50. The semicarbazone, which

was prepared in methanol–water with semicarbazide hydrochloride and sodium acetate at room temperature, precipitated over a period of 4 weeks.

2,4-Dinitrophenylhydrazone, m.p. 164–165°. Calc. for $C_{15}H_{18}N_4O_4$: C, 56.59; H, 5.70; N, 17.60. Found: C, 56.65; H, 5.53; N, 17.61. The 2,4-dinitrophenylhydrazone took 3 weeks to form by the procedure of Shine (22). Camphor under the same conditions yields the derivative in 3 days.

The minor peak was collected but not identified. Analysis gave C, 72.09; H, 8.08.

ACKNOWLEDGMENTS

The author gratefully appreciates the support received for this work from the Research Corporation in the form of a Frederick Gardner Cottrell grant and from the National Research Council of Canada.

Thanks are also extended to Mr. K. Wong for his contribution to the synthetic work and to Mrs. A. Aldridge for the microanalysis.

REFERENCES

1. S. WINSTEIN and D. TRIFAN. J. Am. Chem. Soc. **71**, 2953 (1949).
2. S. WINSTEIN, B. K. MORSE, E. GRUNWALD, H. W. JONES, J. CORSE, D. TRIFAN, and H. MARSHAL. J. Am. Chem. Soc. **74**, 1127 (1952).
3. S. WINSTEIN and D. TRIFIN. J. Am. Chem. Soc. **74**, 1154 (1952).
4. J. D. ROBERTS and C. C. LEE. J. Am. Chem. Soc. **73**, 5009 (1951).
5. J. D. ROBERTS, C. C. LEE, and W. H. SAUNDERS, JR. J. Am. Chem. Soc. **76**, 4501 (1954).
6. J. A. BERSON and S. SUZUKI. J. Am. Chem. Soc. **81**, 4088 (1959).
7. M. F. HAWTHORNE, W. D. EMMONS, and K. S. MCCALLUM. J. Am. Chem. Soc. **80**, 6393 (1958).
8. M. STILES and R. P. MAYER. J. Am. Chem. Soc. **81**, 1497 (1959).
9. S. BECKMANN and R. BAMBERGER. Ann. **580**, 198 (1953).
10. H. C. BROWN and B. C. SUBBA RAO. J. Am. Chem. Soc. **81**, 6428 (1959).
11. H. C. BROWN and G. ZWEIFEL. J. Am. Chem. Soc. **81**, 247 (1959).
12. H. C. BROWN. Tetrahedron, **12**, 117 (1961).
13. G. KOMPPA and S. BECKMANN. Ann. **537**, 140 (1939).
14. D. MUKHERJI and J. C. BARDHAN. J. Chem. Soc. 195 (1949).
15. S. BECKMANN and R. BAMBERGER. Ann. **574**, 65 (1951).
16. W. HUCKEL. Ann. **549**, 186 (1941).
17. G. KOMPPA and R. H. ROSCHIER. Ann. Sci. Fennicae. A, **10**, 3 (1916); Chem. Abstr. **11**, 3276 (1917).
18. D. MUKHERJI. Science and Culture (Calcutta), **13**, 388 (1948).
19. D. J. CRAM and J. D. KNIGHT. J. Am. Chem. Soc. **74**, 5839 (1952).
20. J. A. BERSON, J. S. WALIA, A. REMANICK, S. SUZUKI, P. REYNOLDS-WARNHOFF, and D. WILLNER. J. Am. Chem. Soc. **83**, 3986 (1961).
21. H. C. BROWN and C. P. GARG. J. Am. Chem. Soc. **83**, 2952 (1961).
22. H. J. SHINE. J. Org. Chem. **24**, 252 (1959).

THE GAS–LIQUID PARTITION CHROMATOGRAPHY OF CARBOHYDRATE DERIVATIVES

PART III. THE SEPARATION OF AMINO GLYCOSE DERIVATIVES AND OF CARBOHYDRATE ACETAL AND KETAL DERIVATIVES

H. G. JONES, J. K. N. JONES, AND M. B. PERRY
Department of Organic Chemistry, Queen's University, Kingston, Ontario

Received April 24, 1962

ABSTRACT

Gas–liquid partition chromatography has been used to separate the anomeric acetates of 2-amino-2-deoxy-D-glucopyranose (D-glucosamine) and of 2-amino-2-deoxy-D-galactopyranose (D-galactosamine) and also their fully acetylated reduction products, 2-acetamido-2-deoxy-1,3,4,5,6-penta-*O*-acetyl-D-glucitol and 2-acetamido-2-deoxy-1,3,4,5,6-penta-*O*-acetyl-D-galactitol. The gas–liquid partition chromatographic method has also been successfully applied to the separation of unsubstituted carbohydrate acetal and ketal derivatives and to those derivatives in which the free hydroxyl groups have been substituted by *O*-acetyl, *O*-benzoyl, O-benzyl, carbonate, *O*-methanesulphonyl, *O*-methyl, and *O*-toluene-*p*-sulphonyl groups.

The Separation of Amino Glycose Derivatives

The present methods available for the analysis of amino glycoses mainly involve paper chromatographic procedures (1, 2) in which the compositions of the solvent systems have to be carefully chosen in order to prevent the decomposition of the free glycoses, which results in tailing, and the production of double spots. The *N*-(2,4-dinitrophenyl) (3) and *N*-acetyl derivatives of amino glycoses, however, behave like non-nitrogenous glycoses in the usual paper chromatographic solvent systems and their separations present no difficulties. Quantitative paper chromatographic procedures for the analysis of amino glycoses have been developed which use 2,3,5-triphenyl-2-*H*-tetrazolium hydroxide or ninhydrin as the detecting reagents (4). Methods involving ion-exchange chromatography have also been used in the separation of amino glycoses (5).

A variety of amino glycoses are now known to occur in nature (6), particularly in bacteria, lower fungi, and their soluble metabolites, and as components of mucopolysaccharides and glycoproteins. It was considered that a successful gas–liquid partition chromatographic procedure for their separation which would have the advantages of greater selectivity, speed, and simplicity and which could be used in the investigation of microamounts of material would provide a valuable supplement to the existing analytical methods.

The present investigations were confined to the two common naturally occurring amino glycoses 2-amino-2-deoxy-D-glucose (D-glucosamine) and 2-amino-2-deoxy-D-galactose (D-galactosamine). It was found that the acetates of these glycoses had such large retention volumes on the columns previously used for the analysis of non-nitrogenous glycose and glycitol acetates (7) that their successful resolution was not achieved. However, when a column packing made up of 5% w/w neopentylglycol sebacate polyester on Chromosorb W placed on top of a column approximately twice its length of 1% w/w SE-30 methyl silicone polymer on glass beads (column packing 3) at 214° C was used, good resolution of the anomers of 2-acetamido-2-deoxy-1,3,4,6-tetra-*O*-acetyl-D-glucose and of 2-acetamido-2-deoxy-1,3,4,6-tetra-*O*-acetyl-D-galactose and also of their acetylated reduction products 2-acetamido-2-deoxy-1,3,4,5,6-penta-*O*-acetyl-D-glucitol and 2-aceta-

mido-2-deoxy-1,3,4,5,6-penta-*O*-acetyl-D-galactitol were obtained. Table I records the retention volumes of these derivatives relative to penta-*O*-acetyl-L-arabitol (= 1.00) and a typical separation of the derivatives of 2-amino-2-deoxy-D-glucose is shown in Fig. 1.

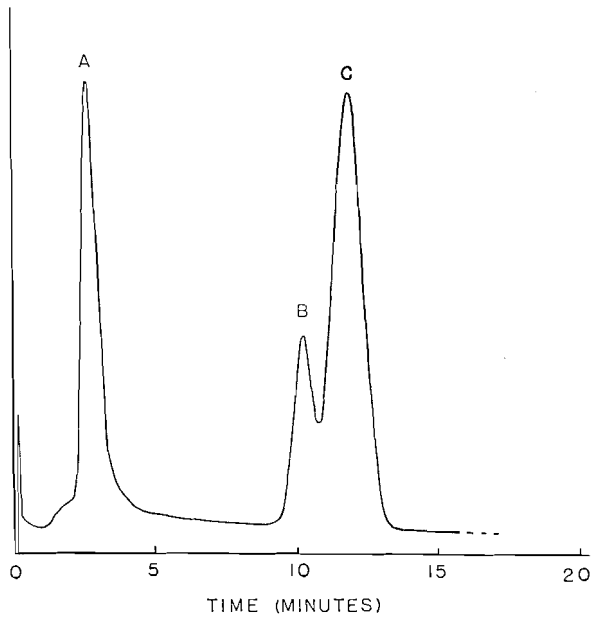

FIG. 1. Separation of 2-amino-2-deoxy-D-glucose derivatives: (A) 2-acetamido-2-deoxy-1,3,4,6-tetra-*O*-acetyl-β-D-glucopyranose, (B) 2-acetamido-2-deoxy-1,3,4,5,6-penta-*O*-acetyl-D-glucitol, and (C) 2-acetamido-2-deoxy-1,3,4,6-tetra-*O*-acetyl-α-D-glucopyranose. (Column packing 3, 214° C, 150 ml argon/min.)

TABLE I
Retention volumes of amino glycose derivatives relative to penta-*O*-acetyl-L-arabitol (= 1.00)

Amino glycose derivative	Retention volume column packing 3 214° C
2-Acetamido-2-deoxy-1,3,4,6-tetra-*O*-acetyl-β-D-glucopyranose	1.82
2-Acetamido-2-deoxy-1,3,4,5,6-penta-*O*-acetyl-D-glucitol	6.92
2-Acetamido-2-deoxy-1,3,4,6-tetra-*O*-acetyl-α-D-galactopyranose	7.93
2-Acetamido-2-deoxy-1,3,4,6-tetra-*O*-acetyl-α-D-glucopyranose	7.95
2-Acetamido-2-deoxy-1,3,4,6-tetra-*O*-acetyl-β-D-galactopyranose	8.12
2-Acetamido-2-deoxy-1,3,4,5,6-penta-*O*-acetyl-D-galactitol	8.14

Preliminary studies on the quantitative analysis of mixtures of 2-amino-2-deoxy-D-glucose and 2-amino-2-deoxy-D-galactose have been obtained by the G.L.P.C. separation of their fully acetylated glycitol derivatives (prepared by the sodium borohydride reduction of the 2-acetamido-2-deoxyglycoses followed by acetylation using pyridine and acetic anhydride) and measurement of the areas under the peaks obtained on the separation curves. Column packing 3 also resolved the acetates of non-nitrogenous pentitols and hexitols, and since the 2-acetamido-2-deoxy-penta-*O*-acetylhexitol derivatives investigated have much larger retention volumes than the former derivatives, it has been possible to analyze mixtures of neutral and basic glycoses on a single separation curve in a way analogous to that previously described for the analysis of neutral sugars alone

(8). The method has proved useful in this laboratory for the analysis of the hydrolyzates of glycoproteins and their lower molecular weight fragmentation products.

The Separation of Carbohydrate Acetal and Ketal Derivatives

The acetal and ketal derivatives of carbohydrates have proved to be important derivatives (9) which can be used for the characterization of glycitols, and as intermediates of known constitution from which substituted derivatives can be made and from which the protective alkylidene or arylidene groups may be subsequently removed under mild conditions. Hitherto, for acetal and ketal carbohydrate derivatives, there have been no generally satisfactory chromatographic methods of separation with the exception of a method developed by Barnett and Kent (10) using ascending chromatography on cellulose acetate strips. Our present results show that the G.L.P.C. method provides a sensitive micromethod for the detection and separation of carbohydrates containing one or more alkylidene or arylidene groups and also for such derivatives in which free hydroxyl groups have been substituted by *O*-acetyl, *O*-benzoyl, *O*-benzyl, carbonate, *O*-methanesulphonyl, *O*-methyl, and *O*-toluene-*p*-sulphonyl groups.

The most generally useful column packing was made up of an intimate mixture of Apiezon M grease on Chromosorb W and butanediol succinate polyester on Chromosorb W packed on top of a column of SE-30 methyl silicone polymer on glass beads (column packing 1), which at 206° C gave good separations of carbohydrate acetal and ketal derivatives. A representative group of derivatives separated on column packing 1, with their retention volumes quoted with reference to 1,2:5,6-di-*O*-isopropylidene-D-glucose (= 1.00), is recorded in Table II. Typical separations of D-fructose derivatives are shown in Fig. 2 and separations of 1,2:5,6-di-*O*-isopropylidene-D-glucose, 4,6-*O*-ethylidene-2,3-*O*-isopropylidene-D-mannose, and 1,2-*O*-isopropylidene-D-glucofuranose are shown in Fig. 3.

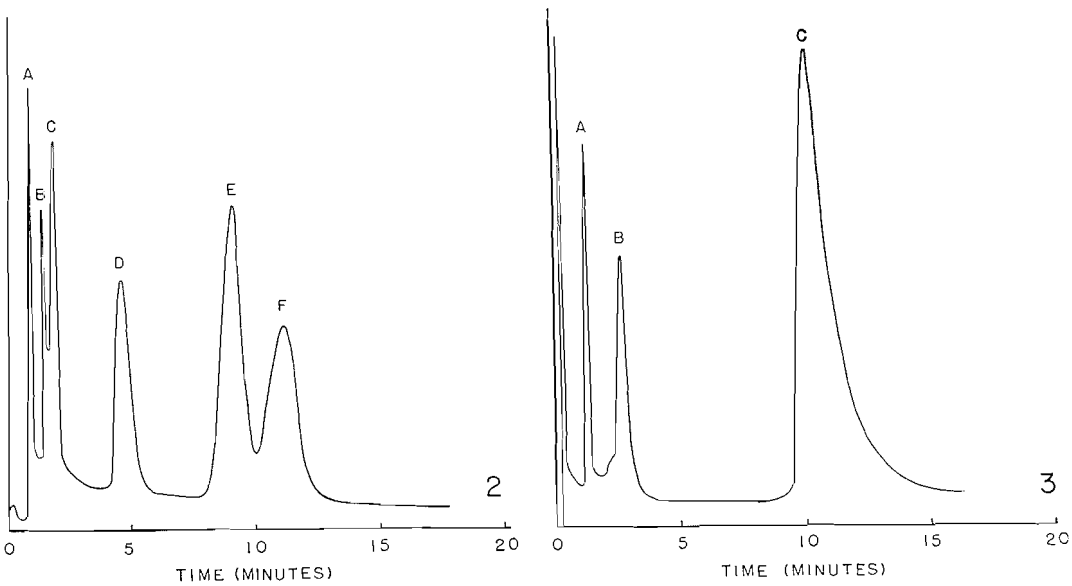

FIG. 2. Separation of D-fructose derivatives: (A) 1,2:4,5-di-*O*-isopropylidene-3-*O*-methyl-D-fructose, (B) 1,2:4,5-di-*O*-isopropylidene-D-fructose, (C) 2,3:4,5-di-*O*-isopropylidene-D-fructose, (D) 1,2-*O*-isopropylidene-D-fructose, (E) 3-*O*-benzyl-1,2:4,5-di-*O*-isopropylidene-D-fructose, and (F) 1,2:4,5-di-*O*-isopropylidene-3-*O*-methanesulphonyl-D-fructose. (Column packing 1, 206° C, 150 ml argon/min.)

Fig. 3. Separation of (A) 1,2:5,6-di-*O*-isopropylidene-D-glucose, (B) 4,6-*O*-ethylidene-2,3-*O*-isopropylidene-D-mannose, and (C) 1,2-*O*-isopropylidene-D-glucofuranose. (Column packing 1, 206° C, 150 ml argon/min.)

TABLE II

Retention volumes of carbohydrate acetal and ketal derivatives relative to 1,2:5,6-di-*O*-isopropylidene-D-glucose (= 1.00)

Carbohydrate acetal and ketal derivatives	Retention volumes column packing 1 206° C
1,2:4,5-Di-*O*-isopropylideneribitol	0.32
5-Deoxy-1,2-*O*-isopropylidene-L-arabinose	0.42
3-*O*-Methyl-1,2-*O*-isopropylidene-D-fructose	0.47
Methyl 2,3-di-*O*-methyl-4,6-*O*-isopropylidene-α-D-glucopyranoside	0.51
1,3:2,4-Di-*O*-methyleneribitol	0.58
1,2-*O*-Isopropylidene-α-D-glucofuranose 5,6-carbonate	0.58
Methyl 2,3-di-*O*-methyl-4,6-*O*-ethylidene-β-D-mannopyranoside	0.65
Methyl 2,3:4,6-di-*O*-isopropylidene-α-D-mannopyranoside	0.66
3-*O*-Acetyl-1,2:4,5-di-*O*-isopropylidene-D-fructose	0.72
2,3-*O*-Isopropylidene-L-rhamnose	0.79
1,2:4,5-Di-*O*-isopropylidene-D-fructose	0.82
Methyl 4,6-*O*-ethylidene-2,3-di-*O*-methyl-β-D-galactopyranoside	0.84
1,2-*O*-Isopropylidene-D-xylulose	0.97
1,2:5,6-Di-*O*-isopropylidene-D-glucose	1.00
2,3:4,5-Di-*O*-isopropylidene-D-fructose	1.04
3,4-*O*-Isopropylidene-β-D-galactosan	1.12
2,3:4,5-Di-*O*-isopropylidenegalactitol	1.13
1,2:4,5-Di-*O*-isopropylidenegalactitol	1.16
1,2:3,4:5,6-Tri-*O*-isopropylidene-D-mannitol	1.20
2,3:5,6-Di-*O*-isopropylidene-D-mannose	1.20
1,2:5,6-Di-*O*-isopropylidene-D-mannitol	1.40
1,2:4,5-Di-*O*-isopropylidene-D-mannitol	1.40
5-Deoxy-5-*S*-ethyl-1,2-*O*-isopropylidene-D-xylose	1.63
4,6-*O*-Ethylidene-1,2-*O*-isopropylidene-D-galactose	1.67
2,3:5,6-Di-*O*-isopropylidene-D-mannono-1 → 4-lactone	1.81
4,6-*O*-Ethylidene-2,3-*O*-isopropylidene-D-mannose	1.86
3,6-Di-*O*-acetyl-5-*O*-methyl-1,2-*O*-isopropylidene-D-glucose	1.91
5-Deoxy-5-*S*-ethyl-1,2-*O*-isopropylidene-L-arabinose	2.00
Methyl 3,4-*O*-isopropylidene-2-*O*-methanesulphonyl-β-D-arabinoside	2.24
2,3:4,5-Di-*O*-isopropylidene-1,6-di-*O*-methanesulphonylgalactitol	2.27
1,2-*O*-Isopropylidene-D-fructose	2.70
3,4:5,6-Di-*O*-isopropylidene-D-glucose dimethylacetal	3.13
2,3-*O*-Isopropylidene-D-ribono-1 → 4-lactone	4.05
3-*O*-Benzyl-1,2:4,5-di-*O*-isopropylidene-D-fructose	5.40
Methyl 4,6-*O*-benzylidene-2,3-di-*O*-methyl-α-D-glucoside	5.82
1,2:4,5-Di-*O*-isopropylidene-3-*O*-methanesulphonyl-D-fructose	6.54
1,2-*O*-Isopropylidene-D-glucofuranose	6.60
1,2:3,4-Di-*O*-isopropylidene-6-*O*-methanesulphonyl-D-galactose	6.64
2-*O*-Benzyl-3,4:5,6-di-*O*-isopropylidene-D-mannose dimethylacetal	7.46
1,3:2,4-Di-*O*-methylene-D-glucitol	8.88
2,3:5,6-Di-*O*-isopropylidene-4-*O*-toluene-*p*-sulphonyl-D-glucose dimethylacetal	8.92
3,5-Di-*O*-acetyl-2,4-*O*-benzylidene-D-xylose dimethylacetal	12.8
2,3:4,5-Di-*O*-isopropylidene-1-*O*-toluene-*p*-sulphonyl-D-fructose	16.7
1,3,5-Tri-*O*-acetyl-2,4-*O*-benzylidenexylitol	17.8
Methyl 3,4-*O*-isopropylidene-2-*O*-toluene-*p*-sulphonyl-β-D-arabinoside	18.0
1,2:5,6-Di-*O*-isopropylidene-3-*O*-toluene-*p*-sulphonyl-D-glucose	25.6
Methyl 4,6-*O*-isopropylidene-2,3-di-*O*-methanesulphonyl-α-D-glucoside	40.1
Methyl 4,6-*O*-isopropylidene-2,3-di-*O*-benzoyl-α-D-glucoside	42.7
4,6-*O*-Ethylidene-1,2-*O*-isopropylidene-3-*O*-toluene-*p*-sulphonyl-D-galactose	54.0
3,4-*O*-Ethylidene-1,2-*O*-isopropylidene-6-*O*-toluene-*p*-sulphonyl-D-galactose	56.8
Penta-*O*-acetyl-L-arabitol	2.46

In general it is found that substitution of free hydroxyl groups in carbohydrate acetal and ketal derivatives by *O*-methyl or *O*-acetyl groups reduces the retention volume below that of the parent compound whereas replacement by *O*-benzyl, *O*-methanesulphonyl, *O*-benzoyl, and *O*-toluene-*p*-sulphonyl groups causes increase in the retention volumes above that of the parent derivative, in the order listed.

Carbohydrates substituted by only one arylidene group, such as methyl 4,6-*O*-benzylidene-α-D-glucoside (retention time 2 min, column packing 2), and those derivatives containing two or more *O*-toluene-*p*-sulphonyl groups had such large retention volumes on column packing 1 that their separation proved impractical. However, a column made up of a very short length of a 1:1 v/v intimate mixture of (*a*) 20% w/w Apiezon M grease on Chromosorb W and (*b*) 20% w/w butanediol succinate polyester on Chromosorb W placed on top of a column of 1% w/w SE-30 methyl silicone polymer of glass beads at 206° C gave good separations of those compounds which had impractically high retention volumes on column packing 1.

EXPERIMENTAL

Apparatus

Separations were carried out using a Pye Argon Chromatograph fitted with an ionization detector (80 μc radium D) and employing straight glass columns (117×0.5-cm I.D.) packed with the support material and enclosed at each end by small glass wool plugs. The samples (3–5 γ) in dry methanol or chloroform solution were placed on the top of the columns with the aid of a micropipette and development was made using dry argon as the carrier gas.

Column Packings

Chromosorb W (60–80 mesh) and glass beads (60 plus mesh) were prepared and coated with the liquid phases under the previously described conditions (7). The columns were prepared as described below.

(1) Column packing 1.—A column was constructed of 40 cm of (*a*) a 1:1 v/v intimate mixture of 20% w/w Apiezon M grease on 60–80 mesh Chromosorb W and 20% w/w butanediol succinate polyester on 60–80 mesh Chromosorb W placed on top of a 77-cm column of (*b*) 1% w/w SE-30 methyl silicone polymer on 60 plus mesh glass beads.

(2) Column packing 2.—A column was constructed of 1.8 cm of (*a*) a 1:1 v/v intimate mixture of 20% w/w Apiezon M grease on 60–80 mesh Chromosorb W and 20% w/w butanediol succinate polyester on 60–80 mesh Chromosorb W placed on top of a 113-cm column of (*b*) 1% SE-30 methyl silicone polymer on 60 plus mesh glass beads.

(3) Column packing 3.—A column was constructed of 40 cm of (*a*) 5% w/w neopentylglycol sebacate (Applied Science Laboratories Inc., State College, Penna.) on 60–80 mesh Chromosorb W placed on top of a 74-cm column of (*b*) 1% w/w SE-30 methyl silicone polymer on 60 plus mesh glass beads.

The fresh columns were purged with argon gas for 6 hours at 15° above their operating temperatures before use. The columns could be used for several hundred analyses before any noticeable deterioration in their resolving power became apparent.

ACKNOWLEDGMENTS

We wish to thank the National Research Council of Canada (NRC 706) and the National Institutes of Health, Bethesda, Maryland, U.S.A., for financial assistance and Canadian Industries Ltd. for the award of a scholarship to one of us (H. G. J.).

REFERENCES

1. P. W. KENT AND M. W. WHITEHOUSE. Biochemistry of the aminosugars. Butterworths Scientific Publications, London. 1955. p. 163.
2. D. AMINOFF and W. T. J. MORGAN. Nature, **162**, 579 (1948).
3. P. W. KENT, G. LAWSON, and A. SENIOR. Science, **113**, 354 (1951).
4. F. G. FISCHER and H. J. NEBEL. Z. physiol. Chem., Hoppe-Seyler's, **302**, 10 (1955).
5. S. GARDELL, F. HEIJKENSKJOLD, and A. ROCHNORLAND. Acta Chem. Scand. **7**, 207 (1953).
6. A. B. FOSTER and D. HORTON. Advances in Carbohydrate Chem. **14**, 213 (1959).
7. S. W. GUNNER, J. K. N. JONES, and M. B. PERRY. Can. J. Chem. **39**, 1892 (1961).
8. S. W. GUNNER, J. K. N. JONES, and M. B. PERRY. Chem. & Ind. (London), 255 (1961).
9. S. A. BARKER and E. J. BOURNE. Advances in Carbohydrate Chem. **7**, 138 (1952).
10. J. E. G. BARNETT and P. W. KENT. Nature, **192**, 556 (1961).

ANIONIC POLYMERIZATION OF STYRENE

EFFECT OF TETRAHYDROFURAN[1]

S. BYWATER AND D. J. WORSFOLD
Division of Applied Chemistry, National Research Council, Ottawa, Canada
Received March 16, 1962

ABSTRACT

The propagation step in the butyllithium-initiated polymerization of styrene in benzene solution is thought to be due to a small concentration of highly active free ion-pairs in equilibrium with unreactive dimeric ion-pairs. This work shows that these dimers may be broken down by the addition of tetrahydrofuran. Small quantities of tetrahydrofuran form, first, a low concentration of a monoetherate of the ion-pair with a high reactivity, and this augments the propagation reaction without changing the kinetic order with respect to the initiator. This, at higher tetrahydrofuran concentrations, is followed by the complete breakdown of the dimers to give a dietherate in much higher concentration and lower reactivity compared with the initial ion-pair and monoetherate. The kinetic order with respect to the initial initiator species changes from one half to one during this process, and a maximum appears in the rate as the ether concentration increases.

Small amounts of ethers and amines have been found to cause a great increase in the rate of polymerization of styrene initiated by lithium alkyls in hydrocarbon solution (1, 2). Welch, and Tobolsky and O'Driscoll, have postulated the formation of a stable complex of the lithium alkyl or active chain end with two molecules of ether, when the ether is tetrahydrofuran (THF), and Welch made an estimate of the equilibrium constant for the association from the variation of rate with ether concentration.

Later data (3, 4), however, have indicated that the kinetic scheme used has to be modified. It is now thought that the lithium polystyryl salts formed in the polymerization in benzene solution are dimerized, because the rate of propagation is proportional to the half power of polystyryl anions present. Confirmation of this hypothesis could be sought by looking for the breakdown of the dimers by preferential coordination with THF, with a resultant change in the kinetic behavior. The more detailed study that is necessary has now been made, and although the formation of etherates is confirmed, the whole behavior is more complex than was previously thought.

EXPERIMENTAL

The experimental procedures were those used before (4). The THF was added via further fragile bulbs into which either a known volume of vapor was condensed or, for the highest concentrations, a known volume of liquid. Benzene was used as solvent throughout. All concentrations are in moles/liter, the time is in minutes, and except for the temperature dependence measurements the experiments were done at 20°.

RESULTS AND DISCUSSION

The first series of kinetic runs was designed to study the behavior of the reaction in the presence of a large excess of THF over *n*-butyllithium, the initiator used throughout. The first major effect of the THF is apparent in the initiation reaction. In the presence of 0.15 *M* THF the initiation step is completed virtually instantaneously on mixing of the reagents, in sharp contrast to the behavior in the absence of THF, where it is possible to follow the initiation reaction by the increase in optical density at 335 mμ over a period

[1]*Issued as N.R.C. No. 6889.*

of an hour or more. The optical density at 335 mμ attained a maximum before any measurements could be taken, and then declined at such a slow rate compared with that of the propagation reaction that the decline was negligible.

The shape of the ultraviolet absorption peak of the polystyryl anion in this benzene–THF mixture differs somewhat from that in pure benzene (4). Although the position of the maximum is still at 335 mμ the peak is broader and more akin to the spectrum in pure THF. There also appears to be a small increase in the integral extinction coefficient as found from the relative areas under the curves, and the area is closer to that of the absorption of the sodium polystyryl salt in THF solution. The extinction coefficient at 335 mμ changed from 1.30×10^4 in benzene to 1.20×10^4, and compares with 1.18 found in THF at 343 mμ. In subsequent series of experiments it was found that on the addition of smaller amounts of THF the spectrum was closer to that in pure benzene. When the [THF]/[butyllithium] ratio is about 2, at a butyllithium concentration of 10^{-3} M, the spectrum is almost identical with that in pure benzene solution. On addition of further THF the spectrum changes up to a ratio of 30/1 and then remains constant.

Even at the lowest concentration of THF used initiation was complete in a few seconds and no attempt was made to measure its kinetics. It is possibly this greatly increased rate of initiation that has caused other workers to comment on the greater overall rate of polymerization in the presence of THF. The propagation rate is generally increased as well, but far less markedly. Because of the fast initiation step, the concentration of polymerizing chain ends could always be taken to be the same as the initial butyllithium concentration.

The propagation reaction gives a normal first-order disappearance of styrene over several half-lifetimes, and good logarithmic plots of the decrease in optical density at 291 mμ were obtained as far as the limitations of the analysis would allow. The order with respect to the initial butyllithium concentration is changed from one half in the absence of THF to one in the presence of 0.15 M THF (Fig. 1). This is consistent with the breakdown by THF molecules of the dimerized active chain ends postulated to explain the half-order dependence in benzene. The actual increase in the rate of polymerization,

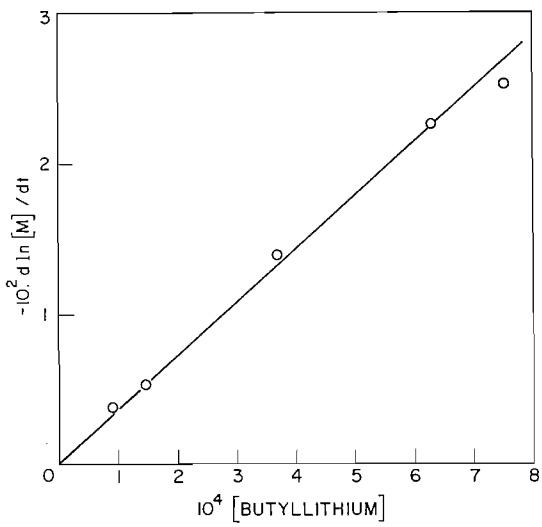

FIG. 1. The dependence of the propagation rate on the initial concentration of butyllithium in the presence of 0.15 M THF.

however, is only a few fold, and not at all proportional to the great increase in the number of monomeric active chain ends that must occur as all the chain ends separate. This can be explained by a sharp decrease in the intrinsic reactivity of the chain ends when complexed with THF. Alternatively, the reaction could be directly with the dimer instead of the single lithium polystyryl ion-pairs in equilibrium, but this view is not consistent with the rest of the data.

The next series of experiments was designed to find how the rate of propagation varied with the THF concentration. Propagation rates were measured over a wide range of THF concentrations, keeping the butyllithium nearly constant, at each of two median butyllithium concentrations (Fig. 2). It is seen that, although for small ratios of [THF]/

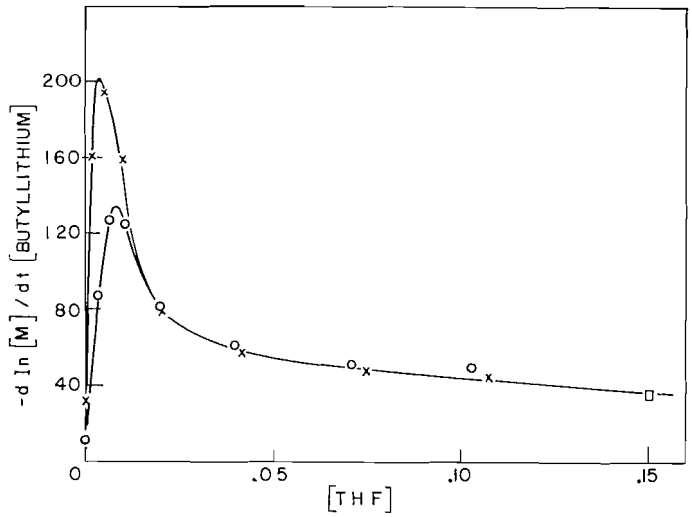

FIG. 2. The effect of wide variations in the tetrahydrofuran concentration on the propagation rate at two median butyllithium concentrations: O, [BuLi] = 0.96–1.2×10^{-3} M; ×, [BuLi] = 1.2–1.8×10^{-4} M.

[butyllithium] there is a sharp increase in rate, at ratios above about 10:1 the rates begin to decline.

The variation of the rate with the butyllithium and THF concentrations at the initial rising portion of these curves was next determined. Figure 3 is a plot of rate against the square root of half the initial butyllithium concentration at constant [THF] of 10^{-3} M, demonstrating that at this low THF concentration the order is still very close to a half in initiator. The difficulty of accurately reproducing this low THF concentration under these conditions is responsible for the rather undesirable scatter of the points.

Figure 4 shows a plot of rate/([butyllithium]/2)$^{1/2}$ vs. [THF] for low values of the latter, over a narrow range of initial butyllithium concentration. It is seen that the increase in rate approaches a linear dependence on the THF concentration as this decreases.

Hence at low [THF]/[butyllithium] ratios the propagation rate seems to be governed by the rate expression

$$-d \ln [\text{styrene}]/dt = ([\text{butyllithium}]/2)^{1/2}[\text{styrene}](k^{\text{I}}+k^{\text{II}}[\text{THF}]). \qquad [1]$$

At high ratios of [THF]/[butyllithium] it is possible to obtain a linear plot of rate against 1/[THF] with an intercept on the ordinate (Fig. 5). Hence as it has already been

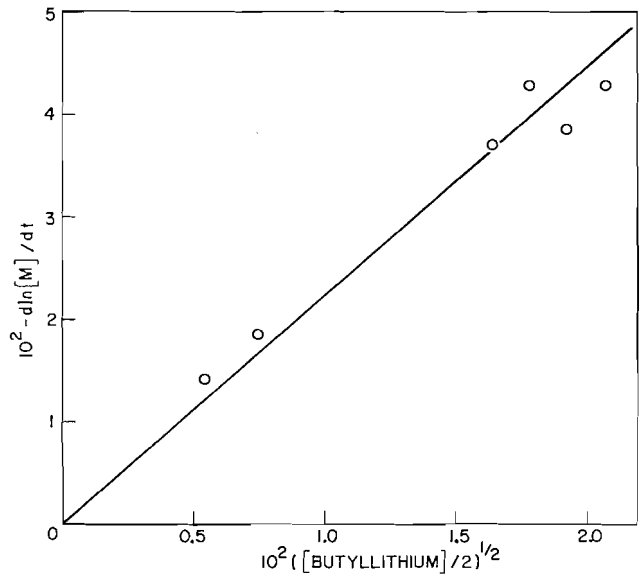

FIG. 3. The dependence of the propagation rate on the initial concentration of butyllithium in the presence of 1×10^{-3} M THF.

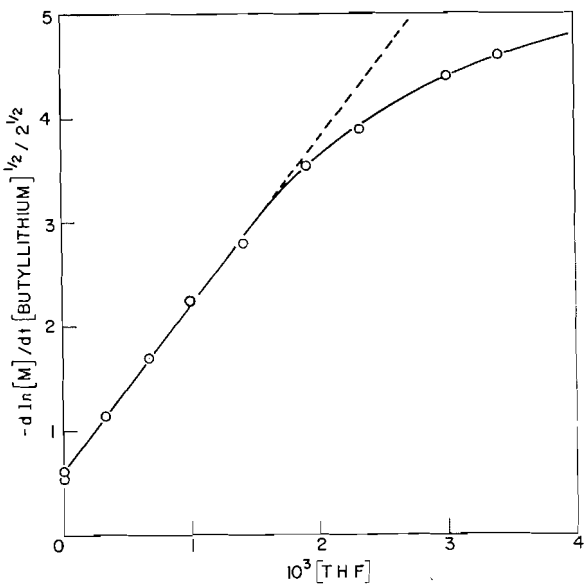

FIG. 4. The dependence of the propagation rate on low concentrations of THF. [BuLi] = $4.2\text{–}6.4\times10^{-4}$ M.

shown that the rate is of first order in initial [butyllithium], the propagation rate is governed by the equation

$$-d\ln[\text{styrene}]/dt = [\text{butyllithium}](k^{\text{III}}+k^{\text{IV}}/[\text{THF}]). \qquad [2]$$

These kinetics are consistent with a reaction scheme whereby the initial unreactive dimer ion-pair is in equilibrium with the free chain end ion-pair, which in turn is in equilibrium with a complex of this ion-pair with one molecule of THF, and this in turn can

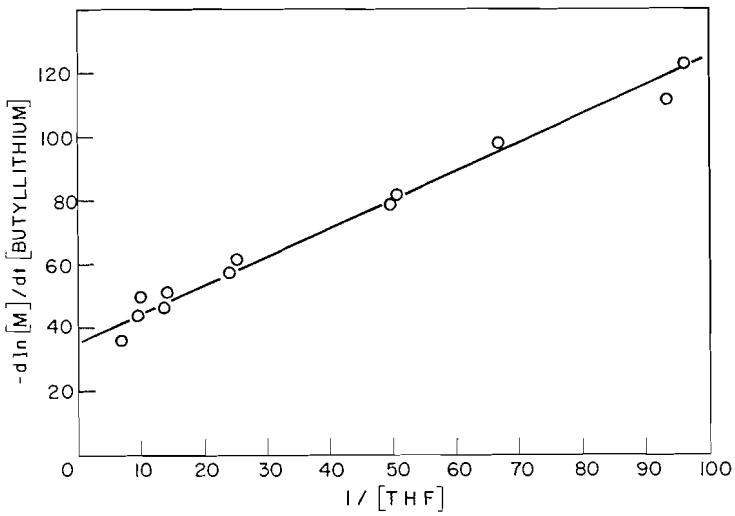

FIG. 5. The dependence of the propagation rate on higher concentrations of THF.

complex with one more molecule of THF to form a dietherate of comparatively low reactivity compared with the monoetherate or the bare ion-pair.

Hence,

$$(P_i)_2 \overset{K_1}{\rightleftarrows} 2P_i, \qquad P_i + M \overset{k_1}{\rightarrow} P_{i+1} \qquad [3]$$

$$P_i + THF \overset{K_2}{\rightleftarrows} P_i.THF, \qquad P_i.THF + M \overset{k_2}{\rightarrow} P_{i+1}.THF \qquad [4]$$

$$P_i.THF + THF \overset{K_3}{\rightleftarrows} P_i.2THF, \qquad P_i.2THF + M \overset{k_3}{\rightarrow} P_{i+1}.2THF \qquad [5]$$

At low THF concentrations only [3] and [4] will be of importance; hence,

$$-d \ln [M]/dt = k_1[P_i]+k_2[P_i.THF]$$
$$-d \ln [M]/dt = k_1K_1^{1/2}[(P_i)_2]^{1/2}+k_2K_1^{1/2}K_2[(P_i)_2]^{1/2}[THF].$$

Under these conditions both $[P_i]$ and $[P_i.THF]$ are small and $[(P_i)_2]$ is given by [butyllithium]/2. This is identical with [1] if $k^{I} = k_1K_1^{1/2}$ and $k^{II} = k_2K_1^{1/2}K_2$.

At high THF concentration, only [4] and [5] are of importance; hence,

$$-d \ln [M]/dt = k_2[P_i.THF]+k_3[P_i.2THF]$$
$$-d \ln [M]/dt = k_2[P_i.2THF]/K_3[THF]+k_3[P_i.2THF].$$

Under these conditions $[P_i.THF]$ is small, and in the limit $[P_i.2THF]$ is the total concentration of chain ends and hence equal to the initial butyllithium concentration. This is equivalent to [2] when $k^{III} = k_3$ and $k^{IV} = k_2/K_3$.

The overall reaction is governed by the equation

$$-d \ln [M]/dt = k_1[P_i]+k_2[P_i.THF]+k_3[P_i.2THF],$$

and if $[P_i]$ and $[P_i.THF]$ are assumed always small, then $2[(P_i)_2]+[P_i.2THF] = [c]$, where $[c]$ is the initial butyllithium concentration, and

$$-d \ln [M]/dt = k_1K_1^{1/2}\{(c-B)/2\}^{1/2}+k_2B/K_3[THF]+k_3[B], \qquad [6]$$

where

$$B = \{(A^2+4Ac)^{1/2}-A\}/2,$$
$$A = K_1K_2^2K_3^2[\mathrm{THF}]^4/2,$$
$$c = [\text{butyllithium}],$$

for all concentrations of THF.

The values $k_1K_1^{1/2} = 0.548$, $k_2K_1^{1/2}K_2 = 1.59\times10^3$, $k_2/K_3 = 0.89$, and $k_3 = 35.5$ can be derived from the slopes and intercepts in Figs. 1, 4, and 5, and from them it is possible to evaluate equation [6]. The calculated contributions of the three simultaneous propagation rates are given in Table I, together with their sum and the experimental value for all runs. Reasonable agreement is found, considering the range covered, which suggests that the approximations made were valid.

TABLE I

Calculated and observed propagation rates

10^3[BuLi] (moles/l.)	10^3[THF] (moles/l.)	10^2k_3[P_i.2THF]	10^2k_2[P_i.THF]	10^2k_1[P_i]	$-10^2d\ln[M]/dt$ (min^{-1}) Calc.	Obs.
1.20	3.24	1.35	10.4	1.1	12.9	10.4
1.14	6.66	3.15	11.9	0.6	15.7	14.4
1.09	10.4	3.67	8.84	0.27	12.8	13.6
1.22	19.8	4.31	5.46	0.11	9.88	9.9
1.18	39.7	4.19	2.65	0	6.84	7.18
0.98	70.7	3.48	1.23	0	4.71	4.95
0.96	102.0	3.41	0.84	0	4.25	4.79
0.603	0.333	0.012	.915	0.948	1.88	1.99
0.590	0.666	0.048	1.79	0.932	2.77	2.90
0.538	1.00	0.101	2.53	0.877	3.51	3.71
0.528	1.41	0.194	3.44	0.844	4.48	4.52
0.510	1.91	0.321	4.21	0.795	5.33	5.65
0.445	2.33	0.436	4.69	0.696	5.82	5.67
0.483	3.00	0.686	5.73	0.658	7.07	6.87
0.418	3.41	0.749	5.50	0.559	6.81	6.65
0.163	1.50	.115	1.92	0.44	2.48	2.60
0.145	4.99	.455	2.29	0.16	2.91	2.81
0.119	9.56	.415	1.09	0.05	1.56	1.89
0.185	20.1	.657	0.82	0	1.48	1.45
0.161	41.8	.572	0.343	0	0.915	0.92
0.140	74.2	.497	0.168	0	0.665	0.65
0.132	107.1	.469	0.110	0	0.579	0.58
0.739	1.00	.119	2.98	1.03	4.13	3.86
0.857	1.00	.128	3.22	1.11	4.46	4.28
0.057	1.00	.030	0.779	0.27	1.08	1.4
0.110	1.00	.044	1.11	0.38	1.53	1.42
0.635	1.00	.110	2.76	0.95	3.82	4.28
0.367	5.16	1.04	5.03	0.34	6.41	6.15
0.730	5.49	1.89	8.64	0.54	11.1	9.5
0.906	5.65	2.30	10.2	0.62	13.1	11.9
1.005	15.0	3.53	5.89	0.13	9.55	9.76
0.651	10.7	2.24	5.26	0.18	7.68	7.23

Because of the different rates of propagation of the three reactive species, if the establishment of the equilibria is not rapid, the polymer produced would not have the Poisson distribution expected from the fast initiation and slow propagation rates. To check this, two polymers were made under different conditions and their viscosity-average molecular weights found (5). The agreement shown in Table II with the number-average molecular weight calculated from the expression D.P. = [M]/[c] is sufficiently good to conclude that the equilibria must be very labile.

TABLE II

Measured and calculated molecular weights

			Molecular weight	
10^3[BuLi]	[Styrene]	10^3[THF]	Calc.	Visc.
1.24	0.452	3.95	37,900	39,600
1.38	1.050	6.05	79,100	82,800

The temperature coefficient of the reaction of the dietherate with styrene at a THF concentration of 0.15 M was found over the range 10° to 30°, and was equivalent to an activation energy of 10.4 kcal. This compares with the value of 9.2 kcal found by Gee, Allen, and Stretch (6) for the propagation reaction in the polymerization of styrene by sodium naphthalene in dioxane solution. The dielectric constants of the two solvents are similar, and both reactions have the same kinetics. No doubt the reactive species in dioxane is again an etherate.

It is not possible to determine the absolute concentration of the monoetherate from the data, but the assumption that it is small seems valid. The concentration of the dietherate can be calculated and shows that the tendency to complex is not very strong, since for an initiator concentration of 10^{-3} M nearly a 10-fold excess of THF is necessary before over 90% of the chains are in this form. Even then the rate is still largely governed by the small equilibrium concentration of monoetherate. The weakness of the complex is also illustrated by the slow change in appearance of the absorption peak in the ultraviolet with increasing THF concentration. It would seem that the ion-pair would prefer to associate with itself than with the THF. The interaction between two ion-pairs would be expected to be greater than that between one ion-pair and a polar molecule.

It should be noted that this analysis does not preclude the possibility of higher etherates forming at even higher THF concentration. Even in the range covered small amounts of such complexes would be overlooked unless they had again a markedly different reactivity.

REFERENCES

1. F. J. Welch. J. Am. Chem. Soc. **82**, 6000 (1960).
2. K. F. O'Driscoll and A. V. Tobolsky. J. Polymer Sci. **35**, 259 (1959).
3. M. Morton, E. E. Bostick, and R. Livigni. Rubber & Plastics Age, **42**, 397 (1961).
4. D. J. Worsfold and S. Bywater. Can. J. Chem. **38**, 1891 (1960).
5. J. M. G. Cowie, D. J. Worsfold, and S. Bywater. Trans. Faraday Soc. **57**, 705 (1961).
6. G. Allen, G. Gee, and C. Stretch. J. Polymer Sci. **48**, 189 (1960).

γ-FLUOROGLUTAMIC ACID

R. L. BUCHANAN, F. H. DEAN, AND F. L. M. PATTISON
Department of Chemistry, University of Western Ontario, London, Ontario
Received March 27, 1962

ABSTRACT

The synthesis of γ-fluoroglutamic acid, $HOOCCHFCH_2CH(NH_2)COOH$, was achieved by two independent methods, both of which involved the Michael reaction: (1) methyl α-fluoroacrylate and diethyl acetamidomalonate gave the transesterified intermediate, which on hydrolysis produced γ-fluoroglutamic acid (31% yield); (2) ethyl α-acetamidoacrylate and diethyl fluoromalonate reacted under mild conditions to give, after hydrolysis, the required amino acid in 56% overall yield. Of the two procedures, the second is preferable, since it is based on more readily available starting materials and gives a higher yield.

Virulent *Mycobacterium tuberculosis* var. *hominis* has a glutamic acid content averaging 50% higher than that of non-infective strains. The infective strain's virulence might thus conceivably be related in some way to its content of glutamic acid. From this it follows that antimetabolites of glutamic acid might have some chance of being effective against the tubercle bacillus. Because of the spatial similarity of fluorine and hydrogen atoms in organic compounds (1), γ-fluoroglutamic acid (I) was considered to be a promising candidate agent, and its synthesis was therefore undertaken.

The two routes which were examined initially proved to be unsuccessful. These are summarized below:

$$EtOOC\overline{C}HF + BrCH_2COCOOEt \rightarrow EtOOCCHFCH_2COCOOEt$$
$$\rightarrow EtOOCCHFCH_2CH(NH_2)COOEt \rightarrow \underset{\text{I}}{HOOCCHFCH_2CH(NH_2)COOH}, \quad [1]$$

$$\underset{\text{II}}{(EtOOC)_2CHF} + \underset{\text{III}}{BrCH_2C(NHAc)(COOEt)_2} \rightarrow (EtOOC)_2CFCH_2C(NHAc)(COOEt)_2$$
$$\rightarrow \underset{\text{I}}{HOOCCHFCH_2CH(NH_2)COOH}. \quad [2]$$

The first of these failed because the enolate of ethyl fluoroacetate (2) was found to attack the keto group of the ethyl bromopyruvate rather than effect nucleophilic substitution; attempts at blocking the keto group were no more successful.

For the second route, the preparation of diethyl bromomethylacetamidomalonate (III) proved to be unexpectedly difficult. Direct alkylation of diethyl acetamidomalonate using excess dibromomethane gave none of the desired product. Alkylation of diethyl acetamidomalonate with chloromethyl methyl ether gave the expected diethyl methoxymethylacetamidomalonate, but attempted cleavage of the ether with hydrobromic acid resulted either in no reaction or in extensive hydrolysis of the ester and amide groupings; this is in contrast to the behavior of diethyl methoxymethylmalonate, which readily forms diethyl bromomethylmalonate under similar treatment (3). The required diethyl bromomethylacetamidomalonate (III) was finally synthesized in satisfactory yield from diethyl acetamidomalonate by hydroxymethylation using formaldehyde and Amberlite IR-4B anion exchange resin at 30–35° (4), followed by treatment with excess phosphorus tribromide. However, on attempted reaction with diethyl fluoromalonate (II) (5), the

basic medium promoted ring closure of the bromo compound rather than the desired alkylation shown above; thus 4,4-dicarboethoxy-2-methyl-2-oxazoline (IV) was formed.

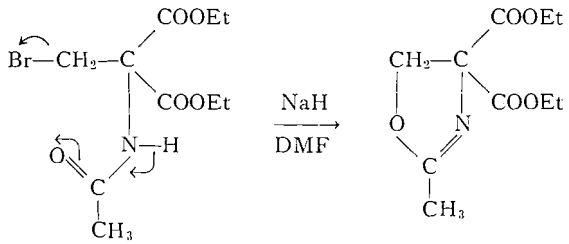

III IV

While oxazolines are susceptible to attack by some nucleophiles, trial runs indicated that 4,4-dicarboethoxy-2-methyl-2-oxazoline was resistant to ring opening by malonic ester anion.

Attention was next directed to schemes involving the Michael reaction:

$$\underset{\text{V}}{\text{ROOCCF=CH}_2} + \text{CH(NHAc)(COOEt)}_2 \rightarrow \underset{\text{VI}}{\text{EtOOCCHFCH}_2\text{C(NHAc)(COOEt)}_2}$$

$$\rightarrow \underset{\text{I}}{\text{HOOCCHFCH}_2\text{CH(NH}_2\text{)COOH}}, \quad [3]$$

$$\underset{\text{II}}{\text{(EtOOC)}_2\text{CHF}} + \underset{\text{VII}}{\text{CH}_2\text{=C(NHAc)COOEt}} \rightarrow \underset{\text{VIII}}{\text{(EtOOC)}_2\text{CFCH}_2\text{CH(NHAc)COOEt}}$$

$$\rightarrow \underset{\text{I}}{\text{HOOCCHFCH}_2\text{CH(NH}_2\text{)COOH}}. \quad [4]$$

While the first of these (scheme [3]) (6) was being studied, Hudlický (7, 8) described the identical procedure starting from ethyl α-fluoroacrylate (V, R = Et) (8, 9). Our work differed only in the use of methyl α-fluoroacrylate (V, R = Me) (10). Details of the synthesis may be obtained from Hudlický's reports. The only additional point of interest is that, during the Michael reaction, treatment with sodium ethoxide in ethanol caused the methyl ester grouping associated with the α-fluoroacrylate to be transesterified to the ethyl ester; thus both methyl and ethyl α-fluoroacrylate gave diethyl α-acetamido-α-carboethoxy-α′-fluoroglutarate (VI) as the Michael intermediate.

The above synthesis (scheme [3]) was based on α-fluoroacrylic esters, which are not readily available, and gave a rather low overall yield of γ-fluoroglutamic acid (31%, crude). Hence the second Michael reaction (scheme [4]) was next examined. Both starting materials are fairly easy to prepare. Diethyl fluoromalonate (II) (5) was obtained from ethyl fluoroacetate and ethyl chloroformate. Ethyl α-acetamidoacrylate (VII) (11) was synthesized from the half ethyl ester of acetamidomalonic acid by reaction with formaldehyde and dimethylamine; the resultant Mannich base gave the desired product at pH 8. The Michael reaction proceeded smoothly at room temperature to yield diethyl α-acetamido-α′-carboethoxy-α′-fluoroglutarate (VIII) and a small amount of 3,5-dicarboethoxy-3-fluoro-2-pyrrolidone by ring closure of VIII (12); the formation of the latter was inferred from the presence of traces of ethyl acetate in the reaction mixture. That the main product was VIII was indicated by a comparison of its amide carbonyl stretching frequency (1681 cm^{-1}) with that of diethyl α-acetamido-α-carboethoxy-α′-fluoroglutarate

(VI) (1686 cm^{-1}) and of 5,5-dicarboethoxy-2-pyrrolidone (1718 cm^{-1}). A separation was not attempted, because hydrolysis of the pyrrolidone and of VIII would give the desired γ-fluoroglutamic acid in both instances. The crude intermediate was heated under reflux with 6 *N* hydrochloric acid. Isolation and purification gave the pure material (I) in 56% overall yield, based on diethyl fluoromalonate. This procedure is the method of choice, in terms of yield, convenience, and availability of starting materials.

γ-Fluoroglutamic acid was non-toxic to mice ($LD_{50} > 80$ mg/kg by intraperitoneal injection). It was inactive in vitro at 20 γ/ml against the following bacteria: *Lactobacillus arabinosus*, *Lactobacillus casei*, *Streptococcus faecalis*, *Streptococcus pyogenes*, *Staphylococcus aureus*, *Proteus mirabilis*, *Pseudomonas aeruginosa*, *Salmonella typhimurium*, and *Mycobacterium tuberculosis* (H37Rv). It was inactive against the following important human pathogenic strains of virus (tissue culture test): polio, measles, herpes, and a virus isolated from respiratory infections (hemagglutinating virus No. 1). It showed weak activity against malignant cells (Eagle–Foley tests) in tissue culture (ED_{50}, 30 γ/ml). In short, no significant biological activity of any sort has been observed so far. The lack of positive results has led us to interrupt the synthesis of the isomeric β-fluoroglutamic acid, $HOOCCH_2CHFCH(NH_2)COOH$.

EXPERIMENTAL

Ethyl Fluoroacetate

This compound was prepared from technical sodium fluoroacetate (compound 1080) (13).

Diethyl Fluoromalonate (II)

This compound was prepared by the method of Bergmann, Cohen, and Shahak (5), but modified as follows: (*a*) The reaction was carried out on four times the scale (i.e. 2 *M*). (*b*) Sodium hydride dispersion (56.5%) in mineral oil was used in place of pure sodium hydride. (*c*) Ethyl fluoroacetate was added over 19 hours instead of 4 hours. (*d*) At the completion of the reaction, the ether extracts were washed with 1% sodium bicarbonate. Crude diethyl fluoromalonate (72.1 g, 27.7%) was obtained, b.p. 86–94° at 9 mm, and n_D^{25} 1.4063, which on fractionation through a platinum-plated spinning-band column yielded the pure fluoro ester (61.5 g, 23.6%), b.p. 97–97.5° at 12 mm, n_D^{25} 1.4056. Calc. for $C_7H_{11}FO_4$: C, 47.19; H, 6.22. Found: C, 46.82; H, 6.46.

Diethyl Methoxymethylacetamidomalonate

Sodium (4.6 g, 0.20 g-atom) was cut into small pieces under dry xylene, was washed with dry ether, and was added to 100 ml of anhydrous ethanol in a 1-liter, three-necked flask fitted with a stirrer, reflux condenser, and addition funnel. When all the sodium had reacted, diethyl acetamidomalonate (43.5 g, 0.20 mole) was added together with a further quantity of anhydrous ethanol (25 ml). The mixture was stirred at room temperature for 14 hours. Dry benzene (100 ml) was added to complete the precipitation of the enolate. The solid was filtered, was washed with dry benzene and dry ether, and was dried in a vacuum desiccator over P_2O_5; yield 37.6 g, 78.5%, m.p. 188–192° (decomp.). The dry enolate was transferred to a 1-liter, three-necked flask, fitted with a stirrer, reflux condenser, and addition funnel. Dry ether (150 ml) was added, and chloromethyl methyl ether (24.2 g, 0.3 mole) in dry ether (30 ml) was added over 15 minutes with vigorous stirring. The mixture was stirred at room temperature for an additional 4 hours, was heated under reflux for 2 hours, and was allowed to stand for 12 hours at room temperature. The precipitated sodium chloride was removed by filtration, and the filtrate was concentrated by evaporation on a steam bath. A small quantity (4.2 g) of diethyl acetamidomalonate crystallized, and the residual viscous liquid was distilled *in vacuo* through a short Vigreux column to yield the required product (10.4 g, 22.0%), b.p. 106–111° at 0.20 mm, n_D^{25} 1.4507. Infrared spectrum in $CHCl_3$, cm^{-1}: 3448 (NH) s, 3012 (CH) s, 2950 (CH) s, 2833 (OCH_3) m, 1745 (ester C=O) vs, 1681 (amide C=O) vs, 1497 s, 1479 s, 1449 m, 1393 m, 1374 s, 1304 s, 1222 s, 1110 s, 1078 m, 1022 s, 858 m. Calc. for $C_{11}H_{19}NO_6$: C, 50.65; H, 7.33. Found: C, 50.37; H, 7.20.

Diethyl Hydroxymethylacetamidomalonate (4)

A slurry of 12 ml of Amberlite IR-4B anion exchange resin in 95% ethanol was placed in a chromatographic column (0.9-cm internal diameter) which was maintained at 30–35° by means of heating tape. Diethyl acetamidomalonate (4.4 g, 22 mmoles) was dissolved in 95% ethanol (100 ml), and 37% formalin solution (2.6 g, 32 mmoles) was added. This solution was added dropwise to the column over 2 hours. The eluate was collected, and about 70 ml of 95% ethanol was passed through the column at the same rate to elute the remainder of the product. The ethanol was removed on a steam bath using a rotatory evaporator; the

resultant viscous syrup was dissolved in benzene, and petroleum ether (b.p. 60–80°) was added. On scratching and cooling, colorless crystals of the hydroxymethyl compound (3.4 g, 62.5%) separated, m.p. 61–65°. Yamada *et al.* (4) quote m.p. 64–65°. Calc. for $C_{10}H_{17}NO_6$: C, 48.57; H, 6.93. Found: C, 48.83; H, 7.13.

Diethyl Bromomethylacetamidomalonate (III)

To diethyl hydroxymethylacetamidomalonate (23.92 g, 96.8 mmoles) in the minimum quantity of benzene was added pyridine (two drops) and then, dropwise and with stirring, phosphorus tribromide (26.2 g, 97 mmoles). The mixture was stirred at 70° for 3½ hours. An equal volume of cold water was added and the resultant layers were separated. The aqueous layer was extracted four times with benzene, and the extracts were added to the original organic layer. The benzene solution was washed with 5% sodium bicarbonate and then with water, and was dried over anhydrous sodium sulphate. The solution was concentrated to a small volume, which on cooling deposited colorless crystals (17.5 g, 58.2%), m.p. 68.5–71.5°. Infrared spectrum in $CHCl_3$, cm^{-1}: 3448 (NH) s, 3021 (CH) s, 1751 (ester C=O) vs, 1681 (amide C=O) vs, 1497 vs, 1449 m, 1427 m, 1395 m, 1376 s, 1304 vs, 1247 s, 1196 s, 1163 m, 1100 m, 1063 m, 1014 s, 946 m, 881 m, 860 s, 630 (C—Br) s. Calc. for $C_{10}H_{16}BrNO_5$: C, 38.72; H, 5.20; Br, 25.77. Found: C, 38.92; H, 5.36; Br, 25.64.

4,4-Dicarboethoxy-2-methyl-2-oxazoline (IV)

Sodium hydride dispersion (56.5%) in mineral oil (137 mg, 3.23 mmoles) was suspended in dry dimethylformamide (25 ml). The bromoester III (1.0 g, 3.23 mmoles) was added, and the mixture was stirred at 65–70° for 7 hours. By this time evolution of hydrogen had ceased and the solution was clear. After standing at room temperature for a further 12 hours, the mixture was poured into water. Extraction with ether, washing the extracts with water, drying (Na_2SO_4), and distillation gave the oxazoline (0.40 g, 54.2%), b.p. 85–87.5° at 0.01 mm, n_D^{25} 1.4489. Infrared spectrum in CCl_4, cm^{-1}: 2985 (CH) s, 1745 (ester C=O) vs, 1667 (C=N) s, 1471 m, 1447 m, 1389 s, 1370 s, 1351 m, 1299 vs, 1247 vs, 1200 vs, 1103 vs, 1029 s, 1001 s, 917 s, 861 m. Calc. for $C_{10}H_{15}NO_5$: C, 52.39; H, 6.60; N, 6.11. Found: C, 52.21; H, 6.74; N, 6.25.

Methyl α-Fluoroacrylate

This compound (V, R = Me) (10) was kindly provided by Dr. J. J. Baron, Jr., General Aniline and Film Corporation, Easton, Pa.

γ-Fluoroglutamic Acid (I) (Scheme [3])

The method was essentially the same as that described by Hudlický (8), but with minor modifications. Methyl α-fluoroacrylate was used in place of the ethyl ester. However, this gave the transesterified Michael intermediate VI, m.p. 99–100.5°. Calc. for $C_{14}H_{22}FNO_7$: C, 50.14; H, 6.61; N, 4.18; F, 5.67; M.W., 335. Found: C, 50.42; H, 6.52; N, 4.22; F, 5.38; M.W. (Rast), 326. It is essential that vigorous and complete hydrolysis of the Michael intermediate be carried out; mild hydrolysis leaves the amide grouping intact, which in turn causes difficulty in the subsequent purification. The free amino acid had m.p. 188–192°. Calc. for $C_5H_8FNO_4$: C, 36.37; H, 4.88; N, 8.48. Found: C, 36.50; H, 5.17; N, 8.70.

Ethyl Hydrogen Acetamidomalonate

This compound was prepared by the method of Hellmann *et al.* (11).

Ethyl α-Acetamidoacrylate (VII)

This compound was prepared by the method of Hellmann *et al.* (11). To ensure the required decarboxylation, it is important to acidify the formalin–dimethylamine solution to a pH of ca. 8 by the addition of dilute hydrochloric acid before adding the acetamidomalonate half ester.

γ-Fluoroglutamic Acid (I) (Scheme [4])

Sodium (41.2 mg, 1.79 mg-atom) was dissolved in absolute ethanol (10 ml) contained in a 50-ml three-necked flask fitted with a stirrer, reflux condenser, and addition funnel. Diethyl fluoromalonate (3.78 g, 21.2 mmoles) was added, and the resultant mixture was stirred for 10 minutes. Ethyl α-acetamidoacrylate (3.2 g, 22.3 mmoles) in absolute ethanol (5 ml) was added dropwise and with stirring, causing a rise in temperature. The mixture was stirred for a further 30 minutes, and then was allowed to stand for 11 hours. The mixture, which had a distinct odor of ethyl acetate, was acidified with dilute hydrochloric acid, and the solvent was removed on a steam bath. The residue (5.65 g), a viscous oil, afforded a satisfactory infrared spectrum for VIII, cm^{-1}: 3413 (NH) s, 2985 (CH) s, 1742 (ester C=O) vs, 1681 (amide C=O) s, 1502 m, 1468 m, 1445 m, 1372 s, 1302 s, 1263 vs, 1159 s, 1096 (C—F) s, 1068 s, 1024 s, 942 m, 858 m.

The viscous oil (5.65 g) was heated under reflux with concentrated hydrochloric acid (14 ml) for 5¾ hours. The resultant solution was evaporated *in vacuo* on a steam bath, and was diluted with water and evaporated twice more. The syrup was dissolved again in water and treated with an excess of freshly prepared silver oxide to remove chloride ions, and filtered through "Supercel" to remove residual traces of silver chloride. The filtrate was evaporated at 70° in a water bath to a volume of about 50 ml. Further evaporation at 35° caused the amino acid to crystallize. After the solid had been collected by filtration, the remainder of the product was precipitated by the addition of 95% ethanol. The fluoroglutamic acid was obtained as a light brown solid (1.96 g, 56%). Two recrystallizations from water and drying *in vacuo* over P_2O_5 gave the pure

acid, m.p. 189–191°. The samples obtained by the two methods (schemes [3] and [4]) gave, on mixing, a melting point of 188–191°. Calc. for $C_5H_8FNO_4$: C, 36.37; H, 4.88; N, 8.48. Found: C, 36.10; H, 5.13; N, 8.28.

The nuclear magnetic resonance spectrum (Table I) of the γ-fluoroglutamic acid (10% w/v in redistilled trifluoroacetic acid) was obtained with a Varian 60 Mc/sec V-4302B spectrometer, using tetramethylsilane as internal standard. The data for DL-glutamic acid, obtained under the same conditions, agree with those already published (14).

TABLE I

N.M.R. spectrum of $HOOCCHFCH_2CH(\overset{+}{N}H_3)COOH$

Group	Chemical shift (τ)		Coupling constants (cycles/sec)
—COOH	−1.60	(under solvent signal)	—
$-\overset{+}{N}H_3$	2.36	(broad)	—
—CHF—	4.47	(doublet of triplets)	J_{HF} 47.3; J_{HH} 5.6
$-CH(\overset{+}{N}H_3)-$	5.25	(multiplet)	—
$-CH_2-$	6.99	(doublet of triplets)	J_{HF} 23.5; J_{HH} 5.6

ACKNOWLEDGMENTS

We wish to express our indebtedness to the National Research Council for financial support and for a studentship (R. L. B.), and to Canadian Industries Limited for the award of a fellowship (F. H. D.). We wish also to acknowledge with thanks the gift of a sample of methyl α-fluoroacrylate from Dr. J. J. Baron, Jr., Central Research Laboratory, General Aniline and Film Corporation, Easton, Pa. We are grateful to Dr. J. B. Stothers of this department for help with the nuclear magnetic resonance spectra, to Dr. M. K. McPhail, Suffield Experimental Station, Ralston, Alberta, for determining the toxicity, and to Parke, Davis and Co., Research Laboratories, 2800 Plymouth Road, Ann Arbor, Michigan, for carrying out or arranging for the bacterial, viral, and anticancer screening of γ-fluoroglutamic acid.

REFERENCES

1. F. L. M. PATTISON. Toxic aliphatic fluorine compounds. Elsevier Publishing Co., Amsterdam, 1959. pp. 24–26.
2. E. D. BERGMANN and S. SZINAI. J. Chem. Soc. 1521 (1956).
3. J. L. SIMONSEN. J. Chem. Soc. **93**, 1777 (1908).
4. S. YAMADA, I. CHIBATA, T. TSURUI, and H. MATSUMAE. Japanese Patent No. 5368 (1956); Chem. Abstr. **52**, 11905h (1958).
5. E. D. BERGMANN, S. COHEN, and I. SHAHAK. J. Chem. Soc. 3286 (1959).
6. H. R. SNYDER, J. F. SHEKLETON, and C. D. LEWIS. J. Am. Chem. Soc. **67**, 310 (1945).
7. M. HUDLICKÝ. Tetrahedron Letters, No. 14, 21 (1960).
8. M. HUDLICKÝ. Collection Czechoslov. Chem. Commun. **26**, 1414 (1961).
9. A. L. HENNE and C. J. FOX. J. Am. Chem. Soc. **76**, 479 (1954).
10. H. D. ANSPON and J. J. BARON, Jr. Wright Air Development Center, Tech. Rept. 57–24, Parts I and II. 1957–58.
11. H. HELLMANN, K. TEICHMANN, and F. LINGENS. Chem. Ber. **91**, 2427 (1958).
12. G. TALBOT, R. GAUDRY, and L. BERLINGUET. Can. J. Chem. **34**, 1440 (1956).
13. F. L. M. PATTISON, S. B. D. HUNT, and J. B. STOTHERS. J. Org. Chem. **21**, 883 (1956).
14. F. A. BOVEY and G. V. D. TIERS. J. Am. Chem. Soc. **81**, 2870 (1959).

INFRARED ABSORPTION STUDIES ON PEROXY TITANIUM SULPHATE

G. V. JERE AND C. C. PATEL
Department of Inorganic and Physical Chemistry, Indian Institute of Science, Bangalore 12, India

Received February 23, 1962

ABSTRACT

The infrared absorption spectrum of peroxy titanium sulphate has been studied in the region from 2 to 23 μ and the various bands are characterized. The sulphate group in the compound is shown to have C_{2v} symmetry, indicating its bidentate nature.

Orange-red peroxy titanium sulphate, $TiO_2SO_4.3H_2O$, was prepared in the solid state by Mohan and Patel (1). The compound was subjected to various physicochemical studies and assigned the structure (A). No infrared absorption studies were, however, carried out on the complex.

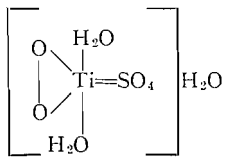

(A)

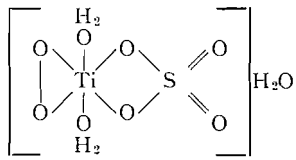

(B)

The infrared spectrum was taken with a single-beam Perkin–Elmer IR spectrometer, model 112, with a KBr prism, employing the mull technique. The absorption curve in the region from 2 to 23 μ is given in Fig. 1. The observed bands with group assignments are listed in Table I. The assignments of the frequencies are based on the available data in the literature. Wherever the bands are broad, the frequency at the center of gravity of the band is given.

The sulphate ion has a regular tetrahedral structure belonging to the point group T_d (2). In its ionic state, SO_4 has nine vibrational degrees of freedom, distributed in four normal modes of vibration. Out of these, only two are infrared active (2). When SO_4 functions as a unidentate ligand, the oxygen coordinating to a metal atom is no longer symmetrically equivalent to the other three oxygens and the effective symmetry of SO_4 is lowered to C_{3v} (3). In C_{3v} symmetry, six infrared absorption bands are observed. When SO_4 functions as a bidentate group, its effective symmetry is further lowered to C_{2v}. In C_{2v} symmetry, eight modes of vibration, out of the total of nine, are infrared active (3). It is thus possible to arrive at the symmetry of the SO_4 group in peroxy titanium sulphate from the observed bands. The observed infrared absorption bands of the SO_4 group for different point group symmetries are listed in Table II, along with the observed bands of the sulphate group of peroxy titanium sulphate. The results of Table II show that the sulphate group in peroxy titanium sulphate has a point group symmetry C_{2v} and the bands agree fairly well with those reported by Nakamoto and co-workers (3) for SO_4 having C_{2v} symmetry. This shows that the SO_4 group functions as a bidentate ligand in peroxy titanium sulphate, confirming the earlier observation of Mohan and Patel (1, 4). In peroxy titanium sulphate, two of the oxygens of the sulphate group are coordinated to the central titanium atom, as given in formula (B).

The band at 3030 cm^{-1} is attributed to the O—H stretching vibration and the one at 1681 cm^{-1} to O—H bending of H_2O groups in the complex. The lowering of the stretching frequency and the raising of the bending frequency from the corresponding frequencies

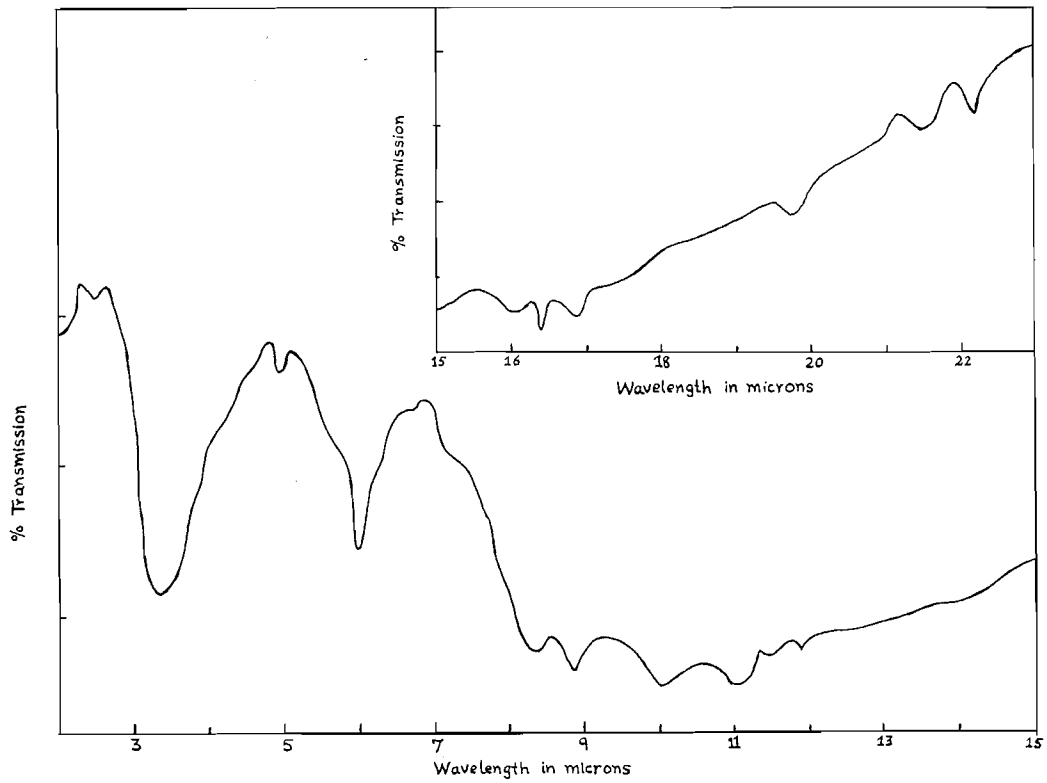

FIG. 1. Infrared spectrum of peroxy titanium sulphate.

TABLE I
Assignments of observed frequencies in the infrared spectrum of peroxy titanium sulphate

Frequency (cm^{-1})		Assignment
3030	(vs)	$\nu(H_2O)$
1681	(vs)	δ (H_2O)
1199	(vs)	(SO_4)
1142	(s)	(SO_4)
1005	(s, b)	(SO_4) overlapping with Ti—O of the triangular peroxy titanyl group,
917	(s)	(SO_4)
877	(w)	Ti—O of
848	(vw)	H_2O rock
621	(s)	(SO_4)
609	(s)	(SO_4)
592	(s)	(SO_4)
506	(s)	ν(Ti—O)
466	(s, b)	(SO_4)
448	(s)	δ(Ti—O)

NOTE: vs = very strong; s = strong; s, b = strong and broad; m = medium; w = weak; vw = very weak; ν = stretching; δ = bending.

of free water (2) are due to the combined effect of coordination and hydrogen bonding in water molecules (5). The weak band at 848 cm^{-1} is due to the rocking mode of vibration of the coordinated water (5). The bands at 1005 and 877 cm^{-1} are assigned to the triangular

TABLE II

Infrared absorption bands of the sulphate group of different point group symmetries (3), and of peroxy titanium sulphate, in cm^{-1}

T_d free ion		C_{3v} unidentate		C_{2v} bidentate		In peroxy titanium sulphate	
ν_1	—	970	(m)	995	(m)	917	(s)
ν_2	—	438	(m)	462	(m)	466	(s, b)
ν_3	1104 (s)	1130	(s)	1170	(s)	1199	(vs)
				1105	(s)	1142	(s)
		1038	(s)				
				1055	(s)	1005	(s, b)
ν_4	613 (s)	645	(s)	641	(s)	621	(s)
				610	(s)	609	(s)
		604	(s)				
				571	(m)	592	(s)

peroxy titanyl group, Ti$\begin{smallmatrix} O \\ | \\ O \end{smallmatrix}$. This assignment is based on the observation of similar bands in titanium peroxide (6), $TiO_2(OH)_2$, and the absence of the same bands in meta-titanyl hydroxide, $TiO(OH)_2$. The peroxy titanyl group bands are also found in the same region in peroxy titanium oxalate, maleate, and malonate complexes (our unpublished data). Unlike the peroxy bands in other peroxy titanium compounds, the band at 1005 cm^{-1} in peroxy titanium sulphate overlaps with one of the SO_4 bands in the same region, resulting in the broadening of the band. The bands at 506 and 448 cm^{-1} are due to the fundamental modes of vibration of Ti—O, as assigned earlier by Narayanan (7) and by Last (8) in rutile and several titanates respectively.

It has been observed, in the infrared spectra of a number of peroxy and deperoxygenated compounds including titanyl peroxide and hydroxide, investigated by the present authors, that there is a broad shallow absorption band extending from about 1000 to 700 cm^{-1}. Nyholm and co-workers (9) have also observed very broad absorption between 800 and 900 cm^{-1} in $TiOSO_4$ and $K_2TiO(C_2O_4)_2$. Kendall (10) has also found continuous absorption in the region 700–1200 cm^{-1} in the spectra of TiO_2 in its three polymeric forms. Narayanan (7) has also observed a broad absorption band extending from 1000 to 1200 cm^{-1} in the Raman spectrum of the rutile. The average region of absorption thus extends from 700 to 1200 cm^{-1} in various compounds having the Ti—O group. This broad absorption seems to be a characteristic feature of the Ti—O system of various titanium compounds. In the infrared spectrum of peroxy titanium sulphate, some of the bands due to the sulphate and the peroxy groups are superimposed on this broad absorption band.

ACKNOWLEDGMENTS

The authors are thankful to Professor M. R. A. Rao for his interest and to the authorities of the Physics Department of this Institute for taking the spectrum.

REFERENCES

1. M. S. Mohan and C. C. Patel. Proceedings of the Symposium on Coordination Compounds, Agra (India). 1959; Natl. Acad. Sci. India, Part II, 105 (1960).
2. G. Herzberg. Infrared and Raman spectra of polyatomic molecules. D. Van Nostrand Co., New York. 1956.
3. K. Nakamoto, J. Fujita, S. Tanaka, and M. Kobayashi. J. Am. Chem. Soc. **79**, 4904 (1957).
4. M. S. Mohan and C. C. Patel. Nature, **186**, 803 (1960).
5. G. V. Jere and C. C. Patel. Nature, **194**, 470 (1962).
6. G. V. Jere and C. C. Patel. Z. anorg. u. allgem. Chem. In press.
7. P. S. Narayanan. Proc. Indian Acad. Sci. A, **32**, 279 (1950).
8. J. T. Last. Phys. Rev. **105**, 1742 (1957).
9. C. G. Barraclough, J. Lewis, and R. S. Nyholm. J. Chem. Soc. 3552 (1959).
10. D. N. Kendall. Anal. Chem. **25**, 382 (1953).

ISARIIN, A NEW DEPSIPEPTIDE FROM ISARIA CRETACEA[1]

L. C. VINING AND W. A. TABER
National Research Council of Canada, Prairie Regional Laboratory, Saskatoon, Saskatchewan

Received April 2, 1962

ABSTRACT

One of the metabolic products of the fungus *Isaria cretacea* has been found to yield four different amino acids and a hydroxyacid on acid hydrolysis. The amino acids were identified as glycine, L-alanine, L-valine, and D-leucine, and a quantitative analysis showed them to be present in the molar ratio of 1:1:2:1, respectively. The hydroxyacid was identified as D-β-hydroxydodecanoic acid. These units appear to be combined in a simple cyclic structure by means of peptide bonds and an ester linkage between the hydroxyl of hydroxydecanoic acid and the carboxyl of the C-terminal amino acid. The sequence valine $\rightarrow$ β-hydroxydodecanoic acid $\rightarrow$ glycine has been established.

In an earlier study (1) it was reported that two strains of *Isaria cretacea* van Beyma had been isolated from the heterokaryotic parent organism. The most noteworthy difference between them was the ability of strain A to produce phototropic synnemata under suitable conditions of growth, whereas strain B formed only a highly branched aerial mycelium. Nutritional differences were also discovered, and the ability to develop synnemata was correlated with a low rate of growth.

During an examination of the metabolic products of the two strains a new depsipeptide, which has been named isariin, was isolated. It was found to be present in both strains A and B as well as the parent heterokaryon.

Isariin was obtained as colorless needles, m.p. 249.5–250.5° C, after repeated recrystallization from aqueous ethanol. Analyses and molecular weight estimations indicated the molecular formula $C_{33}H_{59}O_7N_5$. The infrared absorption spectrum provided evidence for ester and secondary amide groups. Isariin possessed neither acidic nor basic functions, but could be hydrolyzed in mild alkaline conditions to the monobasic isariic acid $C_{33}H_{61}O_8N_5$. That the infrared absorption maximum at 1727 cm^{-1} in this product was that of a carboxyl and not the unchanged ester carbonyl was shown by converting it to the sodium salt, when the maximum was shifted to 1603 cm^{-1}.

Vigorous acid hydrolysis of isariin yielded an ether-soluble product which was separated into neutral and acidic fractions. The acid, m.p. 62.8–63.2° C, gave analyses and a neutralization equivalent indicating the molecular formula $C_{12}H_{24}O_3$. The infrared spectrum showed maxima attributable to an aliphatic hydroxyacid, and upon distillation *in vacuo* a product was obtained which had infrared maxima consistent with those of an unsaturated aliphatic acid. This was converted with the uptake of approximately 1 mole of hydrogen, over palladium catalyst, to lauric acid. From the ease with which the hydroxyacid was dehydrated and from the properties of the unsaturated acid the hydroxyl group was thought to be in the β-position. This was confirmed by synthesis and resolution of DL-β-hydroxydodecanoic acid. Fractional crystallization of the D-amphetamine salt of the racemate afforded a levorotatory acid which was indistinguishable from the hydroxyacid of isariin. The dextrorotatory isomer was also separated and on admixture with an equal part of the natural acid or synthetic levorotatory isomer gave a product which was identical with the synthetic DL-racemate. The dextrorotatory isomer was also

[1]*Issued as N.R.C. No. 6898.*
Presented, in part, before the 41st Annual Conference of the Chemical Institute of Canada in Toronto, Ontario, May 26-28, 1958.

indistinguishable from a sample of authentic L-β-hydroxydodecanoic acid kindly furnished by Dr. K. Serck-Hanssen, who synthesized the compound by anodic chain extension (2) of methyl L-β-acetoxy-γ-carboxybutanoate. Admixture of the authentic L-isomer with the natural acid or the levorotatory isomer obtained by resolution of the racemate gave a product indistinguishable from the racemate. It is therefore concluded that the compound present in isariin is D-β-hydroxydodecanoic acid.

The neutral fraction from acid hydrolysis of isariin was an oil with an infrared maximum at 1765 cm^{-1}, suggestive of a lactone group. Upon alkaline hydrolysis β-hydroxydodecanoic acid was obtained as the only product, indicating that the material was a lactide formed by interesterification of the hydroxyacid.

Paper chromatographic examination of the aqueous solution from the acid hydrolyzate detected glycine, alanine, valine, and leucine. These were separated on a cellulose column; alanine and valine were found to be of the L- and leucine of the D-configuration. Quantitative analysis of the hydrolyzate showed that glycine, alanine, valine, leucine, and β-hydroxydodecanoic acid were present in the ratio 1:1:2:1:1, respectively.

Hydrazinolysis of isariic acid indicated that one of the two molecules of valine possessed a free carboxyl group and must, therefore, have been esterified with the hydroxyacid in isariin. This result was confirmed by subjecting isariic acid to the Dakin–West reaction (3). Vigorous acid hydrolysis of the product showed all four amino acids to be present in equimolecular amounts. Carboxypeptidase also released valine, but no other amino acid. Absence of enzymatic hydrolysis after the removal of valine suggests that the D-leucine may then have been in the penultimate position. It is unlikely that D-leucine was the newly formed C-terminal unit since its initial presence in the penultimate position should have prevented any action by carboxypeptidase on isariic acid. Less probably the lack of further action on the peptide by carboxypeptidase might have been due to the appearance of alanine in the terminal position, thus providing a relatively poor substrate for continued hydrolytic cleavage (4).

Partial hydrolysis of isariin gave an ether-extractable fraction which, on complete hydrolysis, yielded mainly glycine and β-hydroxydodecanoic acid. It was concluded that these two components were directly linked in the original compound. Five ninhydrin-reacting products, in addition to the constituent amino acids, were separated paper chromatographically from the partial hydrolyzate. In each instance they were found to contain all five amino acids and probably also the hydroxyacid. They are presumed to have been formed by ring opening of isariin at the various peptide bonds. For the depsipeptide a partial structure which is supported by the evidence at present available is shown in Fig. 1.

During the early part of this investigation it was noted that analysis of the components in various preparations of isariin did not yield whole numbers of amino acids. In particular, the content of alanine was frequently higher, and of valine lower, than found in samples which had been repeatedly recrystallized from aqueous ethanol. The presence of traces of an amino acid with an R_f corresponding to that of α-aminobutyric acid was also noted. Attempts to separate the crude material into components by paper chromatography were unsuccessful, but these observations suggested that *I. cretacea* produced a mixture of depsipeptides related to isariin, and that the latter was not the major constituent under all conditions of culture.

Depsipeptides containing a β-hydroxyacid are relatively uncommon. To the authors' knowledge, they have been reported only in esperin (5), an antibiotic containing β-hydroxytridecanoic acid obtained from *Bacillus mesentericus*, and in serratamolide,

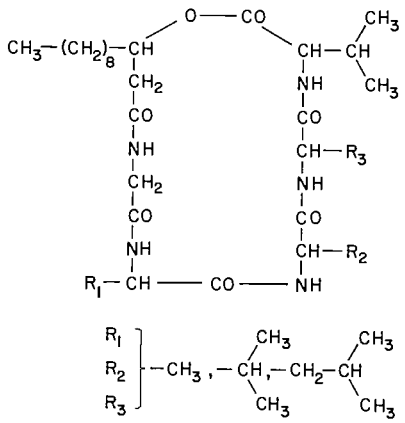

FIG. 1.

recently isolated (6) from *Serratia* strains and shown (7) to possess D-β-hydroxydecanoic acid. β-Hydroxydodecanoic acid appears not to have been previously isolated and unequivocally identified from a natural source, although Bergström and co-workers (8) appear to have obtained some evidence for its presence in the fatty acid components of crude pyolipic acid from *Pseudomonas pyocyanea*.

EXPERIMENTAL

Production of Isariin

In a typical experiment a covered glass tray (9×15 inches) containing 400 ml W.G.A. medium (9) supplemented with neomycin (5 mg) was seeded with the parent strain of *I. cretacea* van Beyma by flooding the surface of the agar with a suspension (27 ml) of a standard spore inoculum (1) and incubated at 28–30° C for 16 days. The mycelium (wet weight 1.1 g) was then scraped from the agar surface, suspended in ethanol (100 ml), and macerated in a Waring blender. The slurry was filtered and the residue re-extracted twice in the same manner. The extracts were combined and evaporated to dryness. The residual solid thus obtained was twice extracted with ethyl acetate (250 ml) under reflux for 30 minutes. The solution was concentrated to dryness and the gummy residue triturated with several portions of petroleum ether, b.p. 30–60° C. The insoluble white solid was crystallized from ethyl acetate as fine needles and constituted crude isariin (18 mg), m.p. 250–252° C. Found: C, 60.84%; H, 8.88%; N, 11.85%.

Strains A and B grown in the same manner yielded 1.6 and 1.0 g of wet mycelium from which 44 and 21 mg, respectively, of crude isariin were isolated.

In an alternative procedure 250-ml Erlenmeyer flasks containing W.G.B. medium (50 ml) were inoculated with 0.5 ml of a standardized spore suspension (1) of strain A incubated at 28–30° C on a rotary shaker for 8 days. The mycelium was then separated and extracted with ethanol as above. The filtrate was extracted with three portions of one-half volume each of *n*-butanol. The ethanolic and butanolic extracts were combined, evaporated to dryness, and the residue worked up, as described above. The yield of crude isariin in a typical experiment was 250 mg/liter of culture medium used.

Purification and Properties

Crude isariin was recrystallized twice from ethyl acetate, and then six times from aqueous ethanol to give fine, colorless needles, m.p. 249.5–250.5° C. Found: C, 62.12%; H, 9.11%; N, 11.14%; molecular weight (Rast in D-borneol) 551, (isothermal distillation in ethanol) 609; saponification equivalent, 638. Calculated for $C_{33}H_{59}O_7N_5$: C, 62.11%; H, 9.32%; N, 10.98%; molecular weight, 637.8. The ultraviolet spectrum in ethanol showed end absorption. Principal infrared maxima (KBr disk) were at 3300, 3060 (w), 2950 (shoulder), 2920, 2855, 1735, 1650 (broad), 1533 (broad), 1470, 1450 (shoulder), 1380 (broad), and 1190 cm^{-1}. Isariin is easily soluble in ethanol, methanol, or chloroform, less readily in acetone, poorly in ether or ethyl acetate, and insoluble in benzene, petroleum ether, water, 2 *N* sodium hydroxide, or hydrochloric acid solution.

Alkaline Hydrolysis of Isariin

Isariin (31.6 mg) was dissolved in methanol (4 ml), and 0.1 *N* KOH solution (1 ml) added. After 48 hours at 40° C the solution was acidified with 0.1 *N* HCl (2 ml) and cooled to 0° C. The gelatinous precipitate was separated, washed with water, and dried. The residue (24 mg) was crystallized twice from aqueous ethanol

as fine needles, melting indefinitely from 194 to 200° C. Found: C, 60.35%; H, 9.37%; N, 10.49%; molecular weight (Rast in D-borneol) 570; neutralization equivalent, 651. Calculated for $C_{33}H_{61}O_8N_5$: C, 60.43%; H, 9.38%; N, 10.68%; molecular weight, 655.9. Infrared maxima (KBr disk) for the free acid were at 2600 (broad, w), 1727, 1635 (broad), and 1543 (broad) cm^{-1}; for the sodium salt at 1655 (broad), 1603, and 1542 (broad) cm^{-1}.

Acid Hydrolysis

Isariin (98.5 mg) was heated for 48 hours at 100° C in a sealed tube with 20% (w/v) HCl (5 ml). The reaction mixture, which contained a brownish oil at the surface, was diluted with water to 20 ml and extracted thoroughly with ether. The ethereal extracts, on evaporation, left a partially crystalline oil (25.8 mg). Calculated for formation of 1 mole of $C_{12}H_{24}O_3$: 33.2 mg. This was separated into acidic (18.7 mg) and neutral (6.8 mg) fractions by distribution between ether and 0.5 *N* Na_2CO_3 solution.

The acidic fraction was crystallized twice from petroleum ether as colorless needles, m.p. 62.8–63.2° C, $[\alpha]_D^{25} - 15.2°$ ($c = 3.4$ in $CHCl_3$). Found: C, 66.42%; H, 11.06%; neutralization equivalent, 218. Calculated for $C_{12}H_{24}O_3$: C, 66.63%; H, 11.18%; molecular weight, 216.3. Principal infrared maxima (KBr disk) were at 3525, 3425, 3090, 2920, 2850, 2660 (broad), 1735, 1706, 1675, 1472, 1436, 1416, 1395, 1365, and 1295 cm^{-1}.

The neutral fraction was hydrolyzed by being heated for 3 hours under reflux in a mixture of ethanol (4 ml) and 4 *N* NaOH (1 ml). The acidic product (7 mg) was crystallized from petroleum ether to give fine needles, m.p. 62.5–63.0° C, undepressed on admixture with the acid obtained directly from hydrolysis of isariin.

The aqueous solution from the acid hydrolysis was evaporated to dryness over solid NaOH. It gave a strongly positive ninhydrin test and paper chromatography in several common solvent systems showed four ninhydrin-reacting substances to be present. These were identified by direct comparison with standards as glycine, alanine, valine, and leucine.

The residue dissolved in a mixture of *sec*-butanol (12 ml) and 3% aqueous ammonia (4 ml) was chromatographed on a column (2.5×60 cm) of powdered cellulose developed with the same solvent system. Fractions (10 ml) were collected and tested for the presence of amino acids by paper chromatography. Appropriate fractions were combined and evaporated to dryness. The residue from each was crystallized from aqueous ethanol and then sublimed under high vacuum for analysis.

The first yielded glistening, colorless plates from aqueous ethanol, $[\alpha]_D^{27} -13.0°$ ($c = 0.67$ in 6 *N* HCl). Found: C, 54.96%; H, 9.84%; N, 10.58%. Calculated for $C_6H_{13}O_2N$: C, 54.94%; H, 9.99%; N, 10.68%. The infrared spectrum (KBr disk) was indistinguishable from that of authentic D-leucine.

The second compound crystallized as colorless plates, $[\alpha]_D^{28} +30.0°$ ($c = 0.61$ in 6 *N* HCl). Found: C, 51.34%; H, 9.50%; N, 11.96%. Calculated for $C_5H_{11}O_2N$: C, 51.26%; H, 9.47%; N, 11.96%. The infrared spectrum (KBr disk) was indistinguishable from that of authentic L-valine.

The third compound crystallized as colorless prisms, $[\alpha]_D^{27} +17.0°$ ($c = 0.56$ in *N* HCl). Found: C, 40.44%; H, 7.60%; N, 15.49%. Calculated for $C_3H_7O_2N$: C, 40.44%; H, 7.92%; N, 15.72%. The infrared spectrum (KBr disk) was indistinguishable from that of authentic L-alanine.

The fourth compound crystallized as colorless needles, m.p. 232° C (decomp.). Found: C, 32.10%; H, 6.54%; N, 18.43%. Calculated for $C_2H_5O_2N$: C, 32.00%; H, 6.71%; N, 18.66%. A mixed melting point with authentic glycine showed no depression, and the infrared spectra (KBr disk) of the two substances were indistinguishable.

Lauric Acid

When the ether-soluble acid from the acid hydrolysis of isariin was distilled *in vacuo* (10^{-2} mm Hg) in a sublimation block at a block temperature of 100° C a discrete fraction was collected which, on cooling in an ice bath, formed a white crystalline solid, m.p. 25–26° C, with infrared maxima (film) at 2920, 2850, 2680 (broad), 1695, 1650, 1470, 1423, 1380, and 983 cm^{-1}. The substance took up hydrogen equivalent to 0.91 mole/mole, calculated on the basis that it was dodecenoic acid, and yielded an acid, m.p. 40–41° C, which gave a single peak on gas–liquid partition chromatography, using a column containing diethylene glycol succinate as liquid phase, with the same retention time as lauric acid. A mixture with authentic lauric acid, m.p. 42.5–43° C, gave m.p. 41.5–43° C. The infrared spectra of the two substances were indistinguishable.

Synthesis and Resolution of β-Hydroxydodecanoic Acid

Ethyl β-ketododecanoate was prepared in a yield of 70% by condensing caproyl chloride with the sodio derivative of ethyl acetoacetate and hydrolyzing the intermediate with sodium methylate in methanol, according to the procedure of Hunsdiecker (10). The keto ester was hydrogenated for 2½ hours at 1600 p.s.i. and 300° F over Raney nickel, as described by Skogh (11), hydrolyzed with alcoholic KOH under reflux, and the product crystallized from petroleum ether (b.p. 60–80° C) to yield DL-α-hydroxydodecanoic acid, m.p. 68.3–69.2° C, in an overall yield of 47% based on caproic acid.

To the racemic acid (1.22 g) in ether (120 ml) was added a solution of D-amphetamine prepared by treating D-amphetamine sulphate (2 g) with *N* NaOH (20 ml) and extracting the base into ether (25 ml). The precipitated salt was redissolved by adding just sufficient ethanol to the refluxing mixture, and allowed

to cool slowly to 10° C. The mass of fine needles (776 mg, m.p. 125–129° C) which separated was removed by filtration and recrystallized twice from ether–ethanol to give 360 mg of material of m.p. 119–121° C. The free acid was regenerated by shaking the product with dilute HCl and ether; the ethereal solution was dried over anhydrous sodium sulphate and evaporated to dryness. The residue, after crystallization from petroleum ether (b.p. 60–80° C), gave needles (172 mg), m.p. 62.5–63.25° C, $[\alpha]_D^{25}$ $-15.2(\pm 1)°$ (c = 1.6 in $CHCl_3$). Found: C, 66.38%; H, 10.94%. A mixture of equal parts of this substance and the hydroxyacid from isariin melted at 62.5–63.25° C. The infrared spectra (KBr disks) of the two compounds were indistinguishable.

The mother liquor from the initial crystallization of the D-amphetamine salt was cooled to −40° C to yield a crop of feathery needles (581 mg) melting mainly at 78–79° C. After two recrystallizations from ether at low temperature the material (495 mg) gave a sharp m.p. of 78–79° C. The free acid, regenerated as before, yielded 249 mg of small needles, m.p. 61–63.25° C, $[\alpha]_D^{25}$ $+14.4(\pm 1)°$ (c = 2.8 in $CHCl_3$). Found: C, 66.70%; H, 11.28%. The infrared spectrum of a sample in a KBr disk, prepared by evaporating an ethereal solution to dryness on KBr powder, was identical with that of the levorotatory isomer examined similarly.

No depression of melting point was observed when a sample was mixed with authentic L-β-hydroxydodecanoic acid, m.p. 62.2–63.2° C, $[\alpha]_D^{25}$ $+15.6(\pm 1)°$ (c = 2.1 in $CHCl_3$), and the two samples had virtually identical infrared spectra (KBr disk). When admixed with an equal amount of the hydroxyacid from isariin and recrystallized from petroleum ether (b.p. 60–80° C), the compound melted at 69–69.75° C. A similar mixture of authentic L-β-hydroxydodecanoic acid with the natural acid melted at 68–69.5° C. Mixtures of this compound or the authentic L-isomer with the levorotatory product from resolution of the racemate melted at 68.7–69.7° C and 69–69.75° C, respectively. All such mixtures of compounds with opposite optical rotations gave no depression when admixed with the unresolved racemate, and had infrared spectra (KBr disks from ether) which were indistinguishable from each other and from the racemate, but different from that of the optically active substances.

A comparison of authentic L-β-hydroxydodecanoic acid with the acids from isariin and from resolution of the racemate carried out by Dr. Serck-Hanssen yielded results similar to those obtained in this laboratory.

Quantitative Amino Acid Analysis

A sample of isariin (6.00 mg), hydrolyzed in a sealed tube with 25% w/v HCl at 110° for 2½ days, was extracted with ether, the aqueous phase freed of excess hydrochloric acid and made to 2 ml with water. Measured amounts of this solution were applied in triplicate to paper strips and chromatographed in *n*-butanol – acetic acid – water (4:1:1) at the same time as mixtures containing known amounts of leucine, valine, alanine, and glycine. The developed chromatograms were dried, treated with ninhydrin, the density of the spots measured with a densitometer, and the amount of each amino acid estimated by comparison with the standards, according to the procedure of Redfield and Guzman Barron (12).

The values obtained for a sample of crude isariin showed the content of glycine, alanine, valine, and leucine to be (to the nearest 0.05 mole/mole) 0.95, 1.30, 1.75, and 0.90, respectively. In addition, there was a trace of an amino acid with R_f values in several solvent systems corresponding to those of α-aminobutyric acid. For preparations of isariin purified by repeated crystallization from aqueous ethanol the content of amino acids was 1.0, 0.95, 2.05, and 1.0 mole/mole, respectively.

Hydrazinolysis of Isariic Acid

Isariic acid (1.5 mg), hydrazine sulphate (30 mg), and hydrazine (1 ml) were heated in a sealed tube at 60° C for 16 hours. Excess hydrazine and hydrazides were removed by the method of Bradbury (13). Paper chromatography of an aliquot of the aqueous solution showed only a single ninhydrin-reacting substance with R_f values in several solvent systems corresponding to valine. When the remainder of the solution was treated with 1-fluoro-2,4-dinitrobenzene and the dinitrophenylamino acids were separated and paper chromatographed in *n*-butanol – 3% aqueous ammonia (9:1), a spot corresponding in R_f value with 2,4-dinitrophenylvaline was obtained.

Dakin–West Reaction

The procedure described by Turner and Schmerzler (14) was used. Isariic acid (2.5 mg) was heated in a sealed tube at 135° C with pyridine (0.25 ml) and acetic anhydride (0.625 ml). The contents of the tube were then evaporated to dryness and hydrolyzed by heating under reflux with 6 *N* HCl for 24 hours. Excess acid was removed in a desiccator containing solid NaOH, and the amino acid composition of the product estimated quantitatively by paper chromatography as described above. Glycine, alanine, valine, and leucine were present in the ratio 1.0:1.0:1.05:1.0.

Action of Carboxypeptidase on Isariic Acid

Isariic acid (4.75 mg) was dissolved in water (4.5 ml) by adding 0.1 *N* NH_4OH to pH 9.0. A suspension of carboxypeptidase (2 mg) in water (0.1 ml) was added, the pH adjusted with dilute acetic acid to 7.8, and the final volume made up accurately to 5 ml with water. The suspension was agitated gently at room temperature and aliquots removed for quantitative paper chromatographic amino acid analysis at 0.5, 1, 2, 4, 8, and 24 hours. The only amino acid detected was valine in amounts of 0.58, 0.62, 0.73, 0.75, 0.86, and 0.88 mole/mole of isariic acid.

Partial Acid Hydrolysis of Isariin

Isariin (10 mg) was dissolved in glacial acetic acid (1.5 ml), and concentrated HCl (1.5 ml) added. The solution was kept at 40° C in a stoppered flask. At intervals, 0.5-ml aliquots were removed, evaporated to dryness, and the residue distributed between equal volumes of ether and water. At 4 days the ether-soluble fraction contained no products reacting with ninhydrin, but gave a strong positive test after further hydrolysis of the material with 6 *N* HCl under reflux for 18 hours. Paper chromatographic examination showed this to be due mainly to glycine, although small amounts of alanine, valine, and leucine were also present. After 6 days, only glycine could be detected in the hydrolyzate of this fraction. Paper chromatography of the aqueous fraction showed small amounts of all four amino acids present after 4 days with traces of ninhydrin-reacting material having R_f values higher than leucine in all solvent systems examined. The proportion of the latter substances appeared highest after 6 days. No compounds with R_f values lower than leucine, other than single amino acids, were detected during the 10-day period in which the hydrolyzate was examined.

The remaining water-soluble products from all sampling times were combined and separated by paper chromatography on a preparative scale. The mixture was applied as a line along the origin of a sheet of Whatman 3 MM paper and the chromatogram developed ascendingly with *n*-butanol – pyridine – 3% w/v aqueous ammonia (2:1:1). Marker strips cut from each edge of the paper and treated with ninhydrin showed, in addition to the expected single amino acids of R_f values 0.09 (gly), 0.16 (ala), 0.27 (val), and 0.37 (leu), five distinct purple zones at R_f values of 0.50, 0.58, 0.65, 0.78, and 0.87. Segments corresponding to these were cut from the untreated paper and eluted with 50% aqueous methanol. Each was evaporated to dryness and the residue hydrolyzed with 20% w/v HCl in sealed tubes for 24 hours at 110° C. The hydrolyzates all gave the characteristic odor associated with the presence of β-hydroxydodecanoic acid and, upon paper chromatographic examination, were found to contain all of the four amino acids present in isariin.

ACKNOWLEDGMENTS

The authors are indebted to Dr. B. M. Craig of this laboratory for the identification of lauric acid by means of gas–liquid partition chromatography, and to Dr. K. Serck-Hanssen of the Medicinsk–Kemiska Institutionen, Göteborgs Universitet, Sweden, for the gift of a sample of L-β-hydroxydodecanoic acid expressly synthesized for comparison with the acid from isariin. We also wish to express our thanks to Dr. Serck-Hanssen for communicating the results of comparisons carried out in his laboratory. Expert technical assistance was provided by Misses M. J. A. Gates and C. Marshall. Miss I. M. Gaffney and Mr. M. Mazurek of this laboratory performed microanalyses and prepared infrared spectra, respectively.

REFERENCES

1. W. A. Taber and L. C. Vining. Can. J. Microbiol. **5**, 513 (1959).
2. K. Serck-Hanssen. Arkiv. Kemi, **10**, 135 (1956).
3. H. D. Dakin and R. West. J. Biol. Chem. **78**, 91 (1928).
4. S. Yanari and M. A. Mitz. J. Am. Chem. Soc. **79**, 1150 (1957).
5. T. Ito and H. Ogawa. Bull. Agr. Chem. Soc. Japan, **23**, 536 (1959).
6. H. H. Wasserman, J. J. Keggi, and J. E. McKeon. J. Am. Chem. Soc. **83**, 4107 (1961).
7. N. J. Cartwright. Biochem. J. **67**, 663 (1957).
8. S. Bergström, H. Theorell, and H. Davide. Arch. Biochem. **10**, 165 (1946).
9. W. A. Taber. Can. J. Microbiol. **6**, 503 (1960).
10. H. Hunsdiecker. Ber. **75**, 450 (1942).
11. M. Skogh. Acta Chem. Scand. **6**, 809 (1952).
12. R. R. Redfield and E. S. Guzman Barron. Arch. Biochem. Biophys. **35**, 443 (1952).
13. J. H. Bradbury. Biochem. J. **68**, 475, 482 (1958).
14. R. A. Turner and G. Schmerzler. J. Am. Chem. Soc. **76**, 949 (1954).

SOME 5,5′-FREE PYRROKETONES[1]

J. M. OSGERBY[2] AND S. F. MACDONALD
Division of Pure Chemistry, National Research Council, Ottawa, Canada

Received February 23, 1962

ABSTRACT

5,5′-Dicarbethoxypyrromethanes are oxidized to the pyrroketones by lead tetraacetate – lead dioxide in acetic acid. The 5,5′-free pyrroketones obtained by decarboxylating the latter have not yet proved synthetically useful.

INTRODUCTION

Redistribution reactions may complicate the synthesis and further reactions of pyrromethenes and pyrromethanes. In this respect pyrroketones (2,2′-dipyrrylketones) should be more reliable intermediates in the synthesis of polypyrranes and porphyrins (1), although the behavior of some benzophenones (2) suggests that the difference might be relative rather than absolute. To explore their synthetic possibilities, we prepared some 5,5′-free pyrroketones corresponding to pyrromethanes which had proved synthetically useful (1).

Fischer's only general route to 5,5′-free pyrroketones lay in converting the 5,5′-dimethyl derivatives to dicarboxylic acids with sulphuryl chloride and decarboxylating these (3). 5,5′-Dimethylpyrroketones have been prepared by ring synthesis (4). More generally, they have been obtained by combining 5-methyl-2-free pyrroles with phosgene or with derivatives of 5-methyl-2-carboxypyrroles by the Grignard (5, pp. 361 ff.), Friedel–Crafts (5, pp. 361 ff.), or Vilsmeier (6) methods. It is uncertain whether this general approach could be usefully modified, avoiding both methyl groups for blocking. Both a 5-carbethoxy- (3) and a 5-free pyrrole-carboxylic acid chloride (7) had been used as the acylating component, though there is no general route to the latter. However, the use of a 2,5-free pyrrole as the other component was ambiguous (3), and the less reactive 5-carbethoxy-2-free pyrroles have not been used.

We found that the pyrroketones I*b*, II*b*, III*b*, and IV*b* (5, pp. 361 ff.) are easily obtained from the corresponding pyrromethanes I*a* (1), II*a* (1), III*a* (8), and IV*a* (5, p. 343) by oxidizing with lead tetraacetate in the presence of lead dioxide. Under similar conditions porphyrins have been oxidized to xanthoporphinogens (5, Vol. II/2, pp. 423 ff.). Selenium

I,	A	P	P	A
II,	P	A	A	P
III,	A	P	A	P
IV,	Me	Et	Et	Me
V,	Et	Me	Me	Et

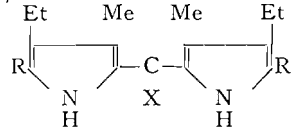

A = $CH_2.COOEt$
P = $CH_2CH_2.COOEt$

a,	X = H_2,	R = COOEt
b,	X = O,	R = COOEt
c,	X = O,	R = H
d,	X = H_2,	R = Me
e,	X = O,	R = Me
f,	X = H_2,	R = CHO

[1]*Issued as N.R.C. No. 6904.*
[2]*National Research Council Postdoctorate Fellow, 1960–62.*

dioxide, manganese dioxide, and permanganate left the pyrromethanes unchanged. The 5,5′-carbethoxy groups may be essential for this oxidation for, although pyrromethenes may reasonably be assumed to be intermediates, our attempts to oxidize 3,3′,5,5′-tetramethyl-4,4′-diethylpyrromethene to its ketone (5, pp. 361 ff.) were unsuccessful. Further, other reagents had oxidized both the 3,3′- and the 4,4′-dicarbethoxytetramethylpyrromethanes to pyrromethenes rather than to pyrroketones (9, 10). Also, 5-positions in pyrromethenes which bear hydrogen or carboxy and other labile groups there (like the methyl group in 2-methylpyrroles (11)) may be hydroxylated by lead tetraacetate (12, 13).

Four 5,5′-free pyrroketones have been previously prepared, the parent dipyrrylketone directly from pyrryl magnesium bromide and phosgene (5, pp. 361 ff.). Representing Fischer's general route, sulphuryl chloride converted the 5,5′-dimethyl pyrroketone V*e* into the 5,5′-dicarboxylic acid corresponding to V*b*, which at 180° *in vacuo* decarboxylated to V*c*; analogous transformations giving IV*b* and IV*c* from IV*e* were carried out but not described (3). Finally, a compound formulated as 3,4-dichlor-3′-methyl-4′-ethyl-5-carbethoxypyrroketone has been decarboxylated in 10% sodium hydroxide at 190° (3), essentially the conditions under which the pyrromethanes I*a*, II*a*, and III*a* lose their 5,5′-carboxyls (1). The free acetic acid groups of pyrrole-acetic acids, unlike their salts, are relatively easily decarboxylated by heat. Consequently we heated the free acids corresponding to I*b*, II*b*, III*b*, and IV*b* with 10% sodium hydroxide at about 160° to obtain acids corresponding to the 5,5′-free pyrroketones I*c*, II*c*, III*c*, and IV*c*.

In general, Fischer's general route and ours will lead to isomeric 5,5′-carboxy- and 5,5′-free pyrroketones from given pyrroles, e.g. to V*b*, V*c* and IV*b*, IV*c* respectively from 2,4-dimethyl-3-ethylpyrrole or its 5-carbethoxy derivative. Although our sequence gives symmetrical ketones more directly, unsymmetrical ones are reached through pyrromethane intermediates whose purity must be scrutinized (8).

The reduction of the ketones was studied both to confirm their structures and as a model for the conversion of derived intermediates into natural products. Xanthoporphinogens had been reduced to porphyrins (5, Vol. II/2, pp. 423 ff.) and the parent dipyrrylketone had been reduced to dipyrrylmethane (5, p. 335). The statements that V*e* was reduced to the pyrromethane are hard to reconcile with the experimental work (14). We reduced the ketone I*b* by Clemmensen's method to the dipyrrylmethane I*a* after catalytic methods had failed.

The carbonyl groups of dipyrrylketones were known to be unusual (5, pp. 361 ff.). In the absence of absorption at normal carbonyl frequencies in the infrared, it is reasonable to assume that exceptionally low frequencies are associated with the carbonyl groups of the ketones: 1627 cm^{-1} in I*b*, 1582 cm^{-1} in I*c*, 1543 cm^{-1} in IV*c*, 1522 cm^{-1} in V*e*.* This last, V*e*, was prepared for comparison from 2,4-dimethyl-3-ethylpyrryl magnesium bromide and phosgene (5, pp. 361 ff.).

The ketone V*e* gives a dibromo derivative (3) and our 5,5′-free pyrroketones all gave Ehrlich's reaction strongly in the cold. However, under conditions which had been successfully applied to the corresponding pyrromethanes (1), they were unreactive or gave no pure products. Attempts to introduce formyl groups into II*c* by the Gattermann–Hoesch method led to recovered starting material, by the Vilsmeier method to intractable tars. Nothing was isolated following attempts to condense II*c* with the methyl ester corresponding to II*f*, with 5,5′-di(bromomethyl)-3,3′-dimethylpyrromethene-4,4′-dipropionic

*NOTE ADDED IN PROOF: *The carbonyl groups in dipyrrylketone and its 4-methoxy derivative absorb at 1597 and 1595 cm^{-1} respectively (H. Rapoport and C. D. Willson. J. Am. Chem. Soc. **84**, 630 (1962)). That of 4,4′-bis(dimethylamino)-benzophenone absorbs, we find, at 1598 cm^{-1}.*

acid, or with formic and hydrobromic acids. Also, heating with formaldehyde in acid solution, which converts rather unreactive pyrroles into pyrromethanes (15), left II*c* unchanged.

There is no pronounced general deactivation peculiar to pyrroketones, for 3,3′,5,5′-tetramethylpyrroketone can be acylated in the 4,4′-positions (5, pp. 361 ff.). Also, we found that the pyrroketones were insoluble in hydrochloric acid and showed no evidence of forming presumably unreactive meso-chloropyrromethenes (5) therein. However, the expected interaction (16) between the 2- and 5- (or 2′- and 5′-) positions may be greater in pyrroketones than in monopyrroles. Thus, in contrast to the 5,5′-free pyrroketones, 2-carbethoxy- and 2-cyano-pyrroles have given 5-aldehydes by the Gatterman–Hoesch (5, pp. 162 ff.) and Vilsmeier (17) methods respectively, and 2,5-diacylpyrroles have been obtained otherwise (5, p. 206). Conversely, nucleophilic attack on 5-bromo-2-carbethoxy-pyrroles is apparently not facilitated (18).

In pyrromethenes there is definitely interaction between the 2- and 5- (or 2′- and 5′-) positions which is incidental to strong interaction between the 5- and 5′-positions. Fischer thus explained the extremely easy acid-catalyzed exchange of halogen for hydroxyl in 5-carbethoxy-5′-bromo- as opposed to 5,5′-dibromo-pyrromethenes (19). Other reactions can be rationalized in the same way. Thus under alkaline conditions the halogen of 5-methyl-5′-bromo- but not of 5-methoxy-5′-bromo-pyrromethenes is exchanged for methoxy (19). Conversely, 5-methoxy-5′-free pyrromethenes condense rapidly with formaldehyde in the presence of acid at room temperature (19) whereas a 5,5′-free pyrromethene condensed slowly at 125° (20).

EXPERIMENTAL

The infrared spectra and their interpretation are by Dr. R. N. Jones and Mr. R. Lauzon, the microanalysis by Mr. H. Séguin. Melting points (block) are corrected.

5,5′-Dicarboxypyrroketone-3,3′-dipropionic acid-4,4′diacetic acid Hexaethyl Ester (Ib)

A solution of 5,5′-dicarboxypyrromethane-3,3′-dipropionic acid-4,4′-diacetic acid hexaethyl ester (1) (2 g) in glacial acetic acid (75 ml) was treated with lead tetraacetate (2.9 g) and stirred at room temperature for 4 days. Lead dioxide (90%, 2.3 g) was then added and stirring continued for 2 days. The mixture was then centrifuged and the supernatant poured into ice water (500 ml). The colorless precipitate was separated, washed with water, and dissolved in ether. The ethereal solution was washed successively with water, 5% aqueous sodium bicarbonate, and water, then dried (sodium sulphate) and concentrated. The crystals which separated (1.27 g, 62%) were recrystallized from ether, affording colorless prisms, m.p. 152.5–153.5°, λ_{max} (log ϵ) in 95% ethanol: 251 mμ (4.35), 303 mμ (4.17), 336 mμ (4.29). Found: C, 58.34; H, 6.34; N, 4.40. Calc. for $C_{33}H_{44}O_{13}N_2$: C, 58.57; H, 6.55; N, 4.14.

Attempted Oxidation of a Pyrromethene

When 1.54 g of 3,5,3′,5′-tetramethyl-4,4′-diethylpyrromethene hydrobromide in 70 ml of acetic acid and 0.45 g of anhydrous sodium acetate was oxidized exactly as above, the product was a black precipitate insoluble in organic solvents.

Reduction of Ib to the Pyrromethane Ia

The ketone I*b* (0.668 g) in 5 ml of ethanol was added to water (1 ml), concentrated hydrochloric acid (1 ml), and amalgamated zinc (0.78 g). The mixture was refluxed for 3 hours, cooled, and filtered. When the filtrate was concentrated and then refrigerated, the pyrromethane I*a* (146 mg, 20%) crystallized; m.p. and mixed m.p. 94° after recrystallization.

5,5′-Dicarboxypyrroketone-3,3′-diacetic acid-4,4′-dipropionic acid Hexaethyl Ester (IIb)

This was prepared from 5,5′-dicarboxypyrromethane-3,3′-diacetic acid-4,4′-dipropionic acid hexaethyl ester (1) (7.91 g), acetic acid (200 ml), lead tetraacetate (11.7 g), and lead dioxide (9.2 g) as described for the isomer I*b* above. The ketone formed colorless prisms (5 g, 62%) after recrystallization from ether (thimble), m.p. 156°, λ_{max} (log ϵ) in 95% ethanol: 250 mμ (4.34), 304 mμ (4.17), 336 mμ (4.29). Found: C, 58.13; H, 6.60; N, 4.39.

5,5′-Dicarboxypyrroketone-3,4′-diacetic acid-4,3′-dipropionic acid Hexaethyl Ester (IIIb)

This was prepared from 5,5′-dicarboxypyrromethane-3,4′-diacetic acid-4,3′-dipropionic acid hexaethyl

ester (8) (1.56 g), lead tetraacetate (2.3 g), and lead dioxide (1.5 g) as described for I*b* above. The crude product (0.694 g, 43.5%) was recrystallized from ether (thimble), affording colorless microneedles, m.p. 149–150°. Found: C, 58.45; H, 6.37; N, 4.12.

4,4′-Dimethyl-3,3′-diethyl-5,5′-dicarbethoxypyrroketone (IVb)

This was prepared from 4,4′-dimethyl-3,3′-diethyl-5,5′-dicarbethoxypyrromethane (5, p. 343) (1.065 g), glacial acetic acid (35 ml), lead tetraacetate (1.45 g), and lead dioxide (1.2 g) as described for I*b*. The product formed colorless rods (300 mg, 27%) from ethanol, m.p. 190–191°. Found: C, 65.04; H, 7.08; N, 7.34. Calc. for $C_{21}H_{28}N_2O_5$: C, 64.92; H, 7.27; N, 7.21.

5,5′-Dicarboxypyrroketone-3,3′-dipropionic acid-4,4′-diacetic acid

Aqueous sodium hydroxide (10%, 3 ml) was added to a solution of the corresponding ester I*b* (400 mg) in ethanol (4 ml) and the mixture heated to dryness on the steam bath in an open flask (about 4 hours). Water (5 ml) was added to the residue. The resulting clear solution was brought to pH 1 with dilute hydrochloric acid, heated to dissolve the colorless precipitate, and allowed to cool. The crystals which separated were washed with water, with ether, then recrystallized from 5 ml of hot water. The product formed colorless needles (170 mg, 56%), m.p. (softening from 159°) 164–168°, Ehrlich's reaction negative in the cold. Found: C, 49.61; H, 4.24; N, 5.41. Calc. for $C_{21}H_{20}N_2O_{13}$: C, 49.61; H, 3.96; N, 5.51.

Pyrroketone-3,3′-dipropionic acid-4,4′-diacetic acid (Compare Ic)

A solution of the ketone I*b* (1.186 g) in ethanol (10 ml) and sodium hydroxide (10%, 5 ml) was hydrolyzed by heating to dryness in an open flask on the steam bath. The residue in water (4 ml) and sodium hydroxide (10%, 4 ml) was heated for 10½ hours at 155–158° in a Teflon-lined closed metal tube. The crude product (0.654 g, 89%) precipitated when the cooled solution was acidified to Congo red with sulphur dioxide. When recrystallized from acetone (thimble) it formed colorless needles, m.p. 203–205°, Ehrlich's reaction positive cold. Found: C, 54.11; H, 5.43; N, 6.51. Calc. for $C_{19}H_{20}N_2O_9$: C, 54.28; H, 4.80; N, 6.66.

Pyrroketone-3,3′-diacetic acid-4,4′-dipropionic acid (Compare IIc)

The ester II*b* (1.14 g) was hydrolyzed and then decarboxylated like the isomer above, giving the crude product (0.583 g, 82%). From aqueous acetone it formed colorless cubes, m.p. 272° (decomp.), Ehrlich's reaction positive cold. Found: C, 54.18; H, 4.94; N, 6.58.

The Tetraethyl Ester (IIc)

The above acid (145 mg) was left at room temperature overnight in 10 ml of 5% ethanolic hydrogen chloride. The solvent was removed *in vacuo* (<50°), leaving a red oil. This was extracted with hot *n*-hexane, from which the product separated as fine colorless plates (60 mg, 33%), m.p. 94–95°, λ_{max} (log ϵ) in 95% ethanol: 297.3 mμ (4.01), 334.5 mμ (4.23). Found: C, 60.64; H, 6.70; N, 5.21. Calc. for $C_{27}H_{36}N_2O_9$: C, 60.89; H, 6.82; N, 5.27.

The same ester (72%) was obtained by treating an ethereal suspension of the acid with freshly distilled ethereal diazoethane.

Pyrroketone-3,4′-diacetic acid-4,3′-dipropionic acid (Compare IIIc)

The ester III*b* (0.873 g) was hydrolyzed and decarboxylated like its isomers. The crude product (255 mg, 47%) was recrystallized from acetone (thimble) as colorless cubes, m.p. 260–262° (decomp.), Ehrlich's reaction positive cold. Found: C, 54.24; H, 4.88; N, 6.51.

4,4′-Dimethyl-3,3′-diethylpyrroketone (IVc)

The ester IV*b* (0.2 g) was heated to dryness with ethanol (25 ml) and sodium hydroxide (10%, 3 ml). The residue was heated in a closed tube for 10 hours at 155–160° with water (4 ml) and sodium hydroxide (10%, 3 ml). The cooled solution was extracted with chloroform. The chloroform extract was washed with dilute hydrochloric acid and then with water, dried (sodium sulphate), and evaporated. The residue was dissolved in ether, and *n*-hexane added, precipitating the products as colorless fluffy rods (108 mg, 86%), m.p. 180–180.5° (lit. 166° (3)), Ehrlich's reaction strongly positive cold, λ_{max} (log ϵ) in 95% ethanol: 344 mμ (4.26), 295 mμ (3.96), 207 mμ (3.95). Found: C, 74.02; H, 8.04; N, 11.36. Calc. for $C_{15}H_{20}N_2O$: C, 73.73; H, 8.25; N, 11.47.

3,5,3′,5′-Tetramethyl-4,4′-diethylpyrroketone (Ve)

This was prepared by the method of Fischer and Orth (5, pp. 361 ff.). The crude product (68%) was recrystallized from ethanol, giving slightly yellow needles, m.p. 208.5–210° (lit 207°), λ_{max} (log ϵ): 301 mμ (3.92), 364 mμ (4.44).

Attempted Reactions with IIc

(*a*) It was added to a mixture of phosphorus oxychloride and dimethylformamide, then left at 20° for 18 hours or at 100° for 10 minutes. In both cases working up gave a black tar from which nothing was isolated.

(*b*) It was dissolved in hydrogen cyanide – ether – chloroform, and dry hydrogen chloride passed in at 0°. Evaporation left ether-soluble material, from which the starting ketone (25%) was recovered, but no water-soluble aldimine hydrochloride.

(*c*) It was refluxed for 1 hour in 5% ethanolic hydrogen chloride containing formaldehyde (2 moles). Only the starting ketone (57%) was recovered.

(*d*) Like II*b* it was recovered quantitatively after attempted reduction by hydrogen over palladium black in ethanol or acetic acid.

(*e*) It was recovered (85%) after refluxing with hydroxylamine hydrochloride and sodium acetate in 90% ethanol.

REFERENCES

1. G. P. ARSENAULT, E. BULLOCK, and S. F. MACDONALD. J. Am. Chem. Soc. **82**, 4384 (1960).
2. R. C. FUSON, G. R. BAKKER, and B. VITTIMBERGA. Abstracts of Papers, 135th Meeting of the American Chemical Society. April, 1959. p. 13. M. Wenzing. Ber. **47**, 2152 (1914).
3. H. FISCHER and KLARA GANGL. Hoppe-Seyler's, Z. physiol. Chem. **267**, 188 (1941).
4. A. TREIBS and K. H. MICHL. Ann. **577**, 129 (1952).
5. H. FISCHER and H. ORTH. Chemie des Pyrrols. Vol. I. Leipzig. 1934.
6. A. H. JACKSON. Proc. Chem. Soc. 198 (1961).
7. H. FISCHER and H. ORTH. Ann. **502**, 239 (1933).
8. E. J. TARLTON, S. F. MACDONALD, and E. BALTAZZI. J. Am. Chem. Soc. **82**, 4389 (1960).
9. A. H. CORWIN and K. J. BRUNINGS. J. Am. Chem. Soc. **64**, 2106 (1942).
10. H. FISCHER and H. BELLER. Ann. **444**, 238 (1925).
11. W. SIEDEL and F. WINKLER. Ann. **554**, 162 (1943).
12. W. SIEDEL and H. MÖLLER. Hoppe-Seyler's, Z. physiol. Chem. **259**, 113 (1939).
13. H. v. DOBENECK. Hoppe-Seyler's, Z. physiol. Chem. **269**, 268 (1941).
14. H. FISCHER and H. ORTH. Ann. **489**, 62 (1931).
15. S. F. MACDONALD. J. Chem. Soc. 4176 (1952).
16. A. TREIBS and G. FRITZ. Ann. **611**, 162 (1958).
17. G. P. ARSENAULT and S. F. MACDONALD. Can. J. Chem. **39**, 2043 (1962).
18. W. SIEDEL. Ann. **554**, 144 (1943).
19. H. FISCHER and J. ASCHENBRENNER. Hoppe-Seyler's, Z. Physiol. Chem. **229**, 71 (1934).
20. H. FISCHER and W. LAMATSCH. Ann. **462**, 249 (1928).

STEREOCHEMISTRY OF ARSENIC

PART IV. CHLORODIPHENYLARSINE

J. TROTTER

Department of Chemistry, University of British Columbia, Vancouver, British Columbia

Received March 28, 1962

ABSTRACT

Crystals of chlorodiphenylarsine, $(C_6H_5)_2AsCl$, are monoclinic with four molecules in a unit cell of dimensions $a = 11.09$, $b = 8.55$, $c = 11.93$ Å, $\beta = 95.0°$. The crystals are isomorphous with crystals of the corresponding bromo derivative, and the structure has been determined by the isomorphous replacement method. The mean values of the bond lengths and valency angles (with standard deviations) are: As—Cl = 2.26±0.02 Å, As—C = 1.97±0.04 Å, C—C = 1.39±0.02 Å, ∠ Cl—As—C = 96±1°, ∠ C—As—C = 105±2°, ∠ As—C—C = 120±2°, ∠ C—C—C = 120±2°. The general molecular configuration and the intermolecular separations are very similar to those in bromodiphenylarsine.

INTRODUCTION

Crystals of chlorodiphenylarsine are isomorphous with crystals of bromodiphenylarsine, whose structure has been determined (1), but it has been considered useful to carry out a complete analysis of the chloro derivative to provide further details of the stereochemistry of arsenic, and to measure the As—Cl bond distance. The investigation has followed similar lines to that of Ph_2AsBr, and details of the molecular dimensions and of the intermolecular contacts have been obtained.

EXPERIMENTAL

The colorless crystals of chlorodiphenylarsine used in this investigation were removed from the walls of a bottle, where they had been deposited by very slow sublimation. The unit cell dimensions, space group, and density were determined as for the bromo derivative (1).

The crystal data were: Chlorodiphenylarsine, $C_{12}H_{10}AsCl$; M, 264.6; m.p. 38–40°. Monoclinic, $a = 11.09 \pm 0.04$, $b = 8.55 \pm 0.03$, c = 11.93±0.04 Å, $\beta = 95.0 \pm 0.5°$. Volume of the unit cell = 1127 Å^3. d_c (with $Z = 4$) = 1.550, $d_m \sim 1.5$ g cm^{-3}. Absorption coefficient for X rays: $\lambda = 1.542$ Å, $\mu = 69$ cm^{-1}. Total number of electrons per unit cell = $F(000) = 528$. Absent spectra: $h0l$ when h is odd, $0k0$ when k is odd. Space group is C_{2h}^5—$P2_1/a$.

Intensity data for the $0kl$ and $h0l$ zones were recorded as for bromodiphenylarsine, but a small crystal was used and no absorption corrections were applied.

Structure Analysis

The signs of most of the $h0l$ and $0kl$ structure factors were determined by comparison with the bromo derivative, using the isomorphous replacement method; refinement then proceeded by Fourier methods. After two cycles of F_o syntheses no further sign changes were indicated, and the discrepancy factors were $R_{h0l} = 14.8\%$ and $R_{0kl} = 15.8\%$; the scattering factors for As and C and an overall isotropic temperature factor were similar to those for Ph_2AsBr, and the scattering factor used for Cl was that of Tomiie and Stam (2). Measured and calculated structure factors are listed in Table I, and final electron-density maps are shown in Fig. 1.

Coordinates and Molecular Dimensions

The final positional parameters are listed in Table II, x, y, and z being fractions of the monoclinic cell axes, and X', Y, and Z' coordinates in Å units referred to orthogonal axes a', b, and c.

The bond distances and valency angles are shown in Fig. 2. The closest intramolecular C . . . C contacts between phenyl groups are: C_1—C_{12} = 3.29 Å; C_6—C_{12} = 3.43 Å; C_6—C_7 = 3.59 Å. The distance between the hydrogen atoms attached to C_6 and C_{12} (assuming C—H = 1.08 Å) is 2.87 Å.

The equations of the planes of the aromatic rings are:

$$C_1—C_6: \quad 0.2597X' - 0.5498Y + 0.7939Z' - 1.7213 = 0$$
$$C_7—C_{12}: \quad 0.6965X' + 0.6410Y - 0.3226Z' + 0.1296 = 0$$

TABLE I

Measured and calculated structure factors

h	k	l	F_o	F_c	h	k	l	F_o	F_c	h	k	l	F_o	F_c	h	k	l	F_o	F_c
0	0	1	Not obs.	−21	4	0	2	79	−78	10	0	$\frac{2}{1}$	12	−9	0	4	1	7	−12
		2	94	−91			3	<6	−9			0	25	−16			2	53	+56
		3	77	−78			4	84	+84			1	10	−9			3	<7	− 5
		4	38	+38			5	10	−18			$\frac{3}{2}$	15	+9			4	27	− 5
		5	13	− 6			6	40	−45			$\frac{1}{2}$	10	+16			5	<8	− 5
		6	52	− 53			7	<8	+14				<8	− 6			6	15	+16
		7	17	+ 23			8	45	+44				12	− 2			1	41	+33
		8	<5	0			9	<9	− 6					8			2	11	−12
		9	20	− 22			10	14	− 9								3	31	−29
		10	5	+ 2			$\frac{11}{10}$	9	+ 8								4	9	+13
		11	14	+ 17	6	0	$\frac{9}{8}$	9	− 7								5	31	+25
		12	<6	− 1			$\frac{8}{7}$	14	−19								6	10	−19
		13	8	0			$\frac{7}{6}$	28	+13								7	24	−20
		14	<4	+			$\frac{6}{5}$	<8	+34								8	7	+1
		15	4	5			$\frac{5}{4}$	50	+ 1								9	23	+23
2	0	0	32	− 39			$\frac{4}{3}$	22	−51								10	<8	− 8
		1	17	+ 5			$\frac{3}{2}$	54	+16								11	25	−16
		2	45	+ 50			$\frac{2}{1}$	8	+47								12	21	+21
		3	10	− 11			$\frac{1}{0}$	32	− 4								13	17	+15
		4	<6	− 16			0	18	− 35								14	7	−13
		5	44	+ 42			1	<7	+ 8								15	14	−19
		6	45	− 44			2	41	− 15								16	8	+10
		7	31	+ 32			3	<7	− 41								17	6	+ 9
		8	115	+126			4	48	+14								18	6	−10
		9	82	− 77			5	<8	+50								19	10	− 5
		10	194	− 198			6	13	− 12								20	6	+ 4
		11	6	− 7			7	<9	− 29								21	4	+ 3
		12	118	+121			8	12	+ 5								22	4	+ 3
		13	6	− 12			9	<9	+24								23	4	− 6
		14	46	− 49			10	14	− 4								24	2	+ 1
		15	7	− 4			$\frac{10}{9}$	14	− 12								25	2	0
4	0	0	30	+ 31			$\frac{9}{8}$	12	+13								26	2	− 2
		1	<9	+ 17			$\frac{8}{7}$	40	− 18										
		2	21	− 4			$\frac{7}{6}$	10	− 32										
		3	<8	− 24			$\frac{6}{5}$	45	+ 8										
		4	37	+ 7			$\frac{5}{4}$	28	+40										
		5	7	+ 38			$\frac{4}{3}$	32	− 17										
		6	67	− 71			$\frac{3}{2}$	<8	− 25										
		7	28	+ 10			$\frac{2}{1}$	31	+ 24										
		8	16	+ 39			$\frac{1}{0}$	10	− 3										
		9	37	− 27			0	9	− 9										
		10	25	+ 24			1	14	+ 26										
		11	88	+ 80			2	17	− 11										
		12	25	− 32			3	11	+ 10										
							4	21	+17										

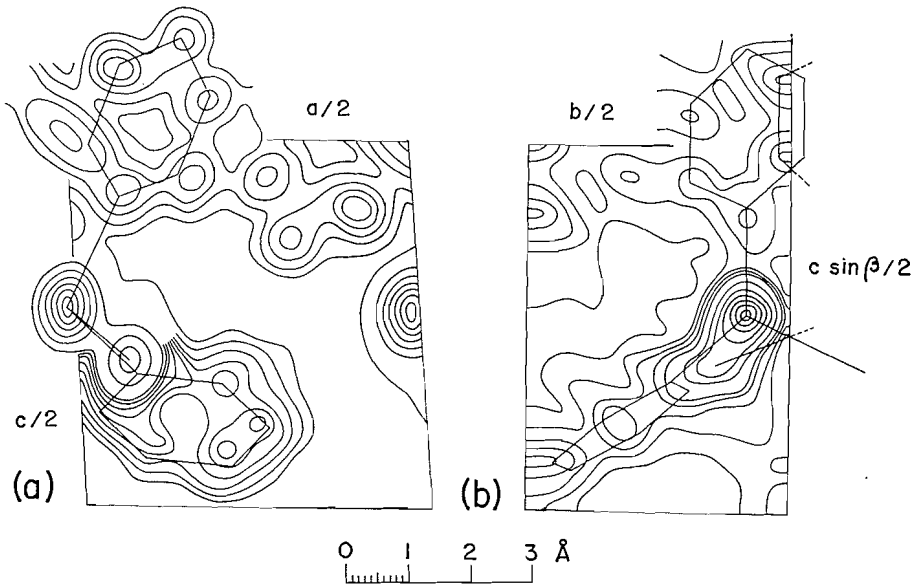

FIG. 1. (*a*) Electron-density projection along the *b*-axis. Contours at intervals of 1 e Å^{-2}, starting at 2 e Å^{-2}, but with contours above 10 e Å^{-2} at intervals of 5 e Å^{-2}.
(*b*) Electron-density projection along the *c*-axis. Contours at intervals of 2 e Å^{-2}, except at the As and Cl atoms, where contours above 10 e Å^{-2} are at intervals of 5 e Å^{-2}.

TABLE II

Final positional parameters, and deviations (Δ) from the mean aromatic planes

Atom	*x*	*y*	*z*	*X'*	*Y*	*Z'*	Δ_1 (Å)	Δ_2 (Å)
As	−0.0130	0.1673	0.2659	−0.144	1.430	3.185	−0.02	−0.08
Cl	0.0715	0.3857	0.2000	0.790	3.298	2.317	—	—
C 1	0.083	0.026	0.178	0.915	0.220	2.040	+0.02	—
2	0.025	−0.102	0.125	0.277	−0.870	1.462	−0.01	—
3	0.089	−0.200	0.063	0.988	−1.708	0.668	+0.01	—
4	0.213	−0.163	0.053	2.357	−1.392	0.427	−0.01	—
5	0.271	−0.033	0.106	2.991	−0.284	1.006	+0.01	—
6	0.206	0.062	0.165	2.271	0.526	1.771	−0.02	—
7	0.071	0.167	0.418	0.781	1.430	4.914	—	+0.01
8	0.031	0.275	0.489	0.347	2.350	5.806	—	+0.01
9	0.083	0.275	0.599	0.913	2.350	7.070	—	−0.01
10	0.176	0.167	0.638	1.944	1.430	7.438	—	0
11	0.213	0.059	0.559	2.351	0.500	6.464	—	0
12	0.159	0.059	0.450	1.761	0.500	5.208	—	0

and the deviations of the atoms from these planes are listed in the final columns of Table II. The angle between the planes is 65°.

The standard deviations of the atomic positions (3) are $\sigma(x) = \sigma(y) = \sigma(z) = 0.007$ Å for As, 0.014 Å for Cl, and 0.05 Å for C.

The intermolecular separations correspond to van der Waals interactions, and are very similar to those in bromodiphenylarsine.

DISCUSSION

Differences between chemically equivalent bond lengths and valency angles are not significant, the mean values being (with standard deviations):

$$\text{As—Cl} = 2.26 \pm 0.02 \text{ Å}$$
$$\text{As—C} = 1.97 \pm 0.04 \text{ Å}$$

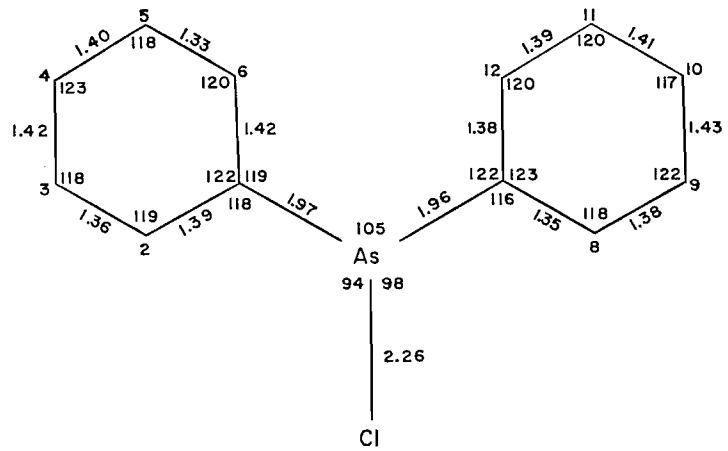

FIG. 2. Measured bond lengths (Å) and valency angles (degrees).

$$\text{C—C} = 1.39 \pm 0.02 \text{ Å}$$
$$\angle \text{ Cl—As—C} = 96 \pm 1°$$
$$\angle \text{ C—As—C} = 105 \pm 2°$$
$$\angle \text{ As—C—C} = 120 \pm 2°$$
$$\angle \text{ C—C—C} = 120 \pm 2°.$$

Apart from the shorter As—Cl distance in comparison with As—Br, these dimensions are very similar to those of bromodiphenylarsine (1). The molecular configuration of chlorodiphenylarsine is also almost identical with that of the bromo derivative; in comparison with an ideal model similar to that described for Ph_2AsBr, ring I (C_1—C_6) is rotated 76°, and is therefore in a position where interaction with the arsenic lone pair is almost at a minimum, while ring II (C_7—C_{12}) is twisted by 35°, so that interaction is still appreciable.

The author thanks the National Research Council of Canada for financial support, and Dr. W. R. Cullen for the crystal samples and for helpful discussion.

REFERENCES

1. J. TROTTER. J. Chem. Soc. In press.
2. Y. TOMIIE and C. H. STAM. Acta Cryst. **11**, 126 (1958).
3. D. W. J. CRUICKSHANK. Acta Cryst. **2**, 65 (1949).

AN APPARATUS FOR THE STUDY OF SHORT-LIVED FISSION PRODUCT RARE GASES

D. W. Ockenden[1] and R. H. Tomlinson
Department of Chemistry, McMaster University, Hamilton, Ontario
Received April 4, 1962

ABSTRACT

A procedure is described for the isolation, separation, and study of short-lived krypton and xenon isotopes formed by thermal fission of uranium. The gases are swept out from a thin film of uranium-235 stearate, rapidly separated by gas chromatography, and examined by gamma-spectrometric techniques. Krypton isotopes have been studied within 10 seconds of their formation in the reactor and xenon isotopes within 25 seconds. Spectra are reported for krypton-89 and -90, xenon-137, -138, and -139.

INTRODUCTION

Although the first uranium chain reaction took place 20 years ago, the amount of information available on the short-lived fission products ($T_{1/2}$ < a few minutes) is still relatively small. The main difficulty has been the development of extremely rapid and complete separation procedures. The fission product rare gases krypton and xenon have been examined more than most elements since, although they are difficult to separate from each other, they may easily be isolated from other fission products. Dillard and co-workers (1) measured the half-lives of several krypton and xenon nuclides without separation, by passing an active rare gas mixture at a known flow rate through a tube containing a coaxial charged wire. By measuring the distribution of the decay products along the wire, these workers were able to calculate half-lives.

In 1951, Kofoed-Hansen and Kristensen (2, 3) used an isotope separator for the isolation of particular species, and reported β-ray-energy end-point values and half-lives for the krypton and rubidium isotopes of mass numbers 89–91.

Wahl (4), in 1958, determined the cumulative yields of short-lived krypton and xenon isotopes from the thermal neutron fission of uranium-235, using the emanating properties of certain inorganic stearates for the isolation of the gases. Rubidium and cesium isotopes formed from the decay of some of the fission product gases were reported by O'Kelley *et al.* (5) and by Bunker *et al.* (6).

In 1960, Prakash (7) reported a study of krypton-89 and xenon-137, which were obtained by gas sweeping an irradiated uranyl nitrate solution. These were separated from each other by an adsorption–desorption technique which took 4 minutes. From an examination of the gamma-ray spectra and the relative intensities of the gamma rays in each, provisional decay schemes for the two isotopes were presented.

In 1961, Koch and Grandy (8) described an apparatus for the determination of radioactive fission gases, the radioisotopes being separated by gas chromatography, using charcoal as the fixed phase and helium as the carrier gas. The quickest separation obtained by these authors took 20 minutes, the xenon elution being accelerated by column heating. The shortest-lived isotopes studied, 3.2-min Kr-89 and 17-min Xe-138, were determined indirectly by study of their immediate decay products. Little gamma-spectrometric data was given.

[1]*Present address: Chemical Services Department, Windscale Works, U.K.A.E.A., Sellafield, Seascale, Cumberland, England.*

Wahlgren (9) has described the first extended study of the short-lived fission product rare gases. He has studied the gases evolved from solid uranium nitrate using a hypodermic needle sampling system which drew the gas mixture slowly through a thin charcoal bed. This produced pure radiokrypton in the gas phase and left radioxenon on the charcoal. Each phase was then examined separately, the minimum time from reactor to detector being 24 seconds for krypton and 30 seconds for xenon. Gamma-ray spectra of several short-lived nuclides were reported, together with some beta-ray spectra and a few beta–gamma and gamma–gamma coincidence measurements.

EXPERIMENTAL

Apparatus

The apparatus used in this work, for the preparation, isolation, and study of the rare gas fission products, may be discussed under the following headings: (*a*) beam port irradiation facility; (*b*) irradiation cell, with its neutron shutter; (*c*) gas chromatography; and (*d*) gas handling system.

(a) Beam Port Irradiation Facility

A beam port of the McMaster University reactor was used as a source of neutrons. The arrangement, including shielding, is shown in Fig. 1 along with the capped tube for containing the apparatus in the beam

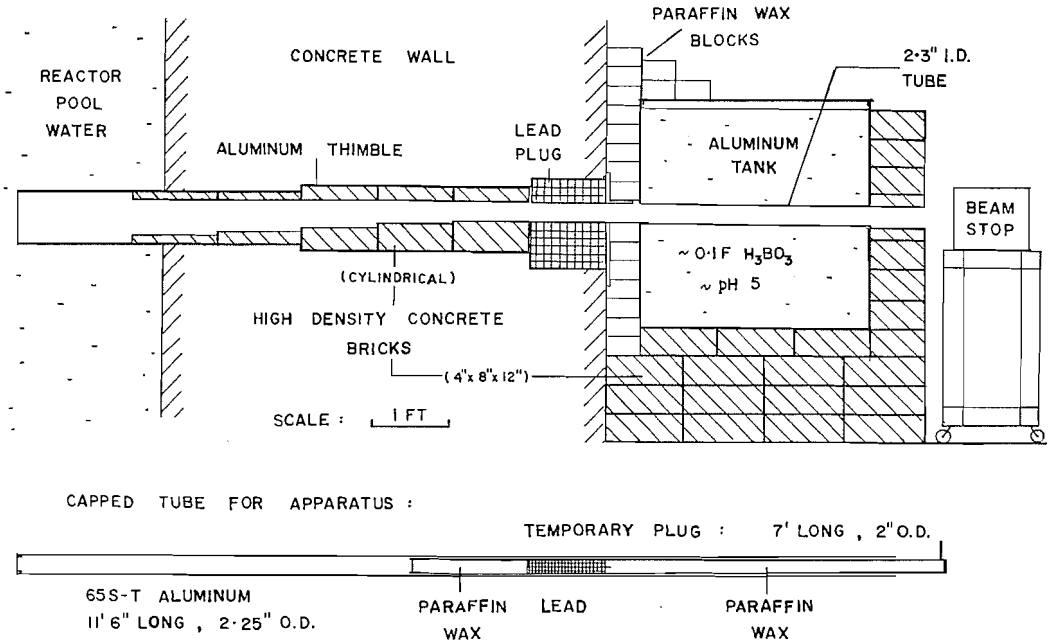

FIG. 1. Section through beam port No. 2, McMaster University swimming pool reactor. Main tube for the apparatus, and its associated plug also shown.

port, and the beam plug. The short space between the reactor core and the end of the beam port thimble contained, besides water, a 1 ft thick plug of graphite, a 6-in. can of air, and a 6-in. canned plug of bismuth. With the reactor operating at 1 MW, the thermal neutron flux at the reactor end of the beam port was found to be 2×10^{10} neutrons $cm^{-2}sec^{-1}$.

(b) Irradiation Cell and Neutron Shutter

The irradiation cell with its thermal neutron shutter is shown in Fig. 2. This apparatus fits inside the capped tube and beam port shown in Fig. 1. It is made in three interlocking aluminum sections and allows a fast stream of helium to flush out the emanated fission product rare gases. The gas leads are coiled throughout the length of the apparatus and also pass through sections of paraffin wax and lead. The hemispherical inside surfaces of the irradiation cell are coated with a uranium-235 stearate film approximately 2 mg cm^{-2} thick, and containing about 70 mg of uranium-235. The production of radioactivity from a short-lived isotope, rather than that from a long-lived one, is favored by a short irradiation. Hence, the

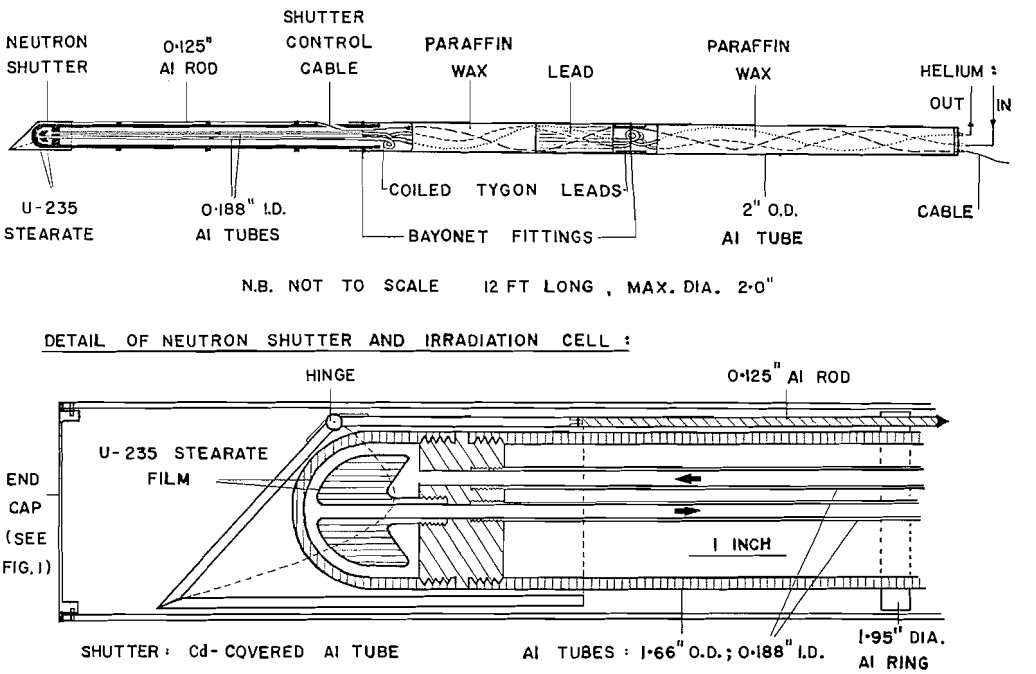

FIG. 2. Apparatus for the production and sweeping out of short-lived fission product rare gases.

irradiation cell is surrounded by a moveable thermal neutron shutter, which can be pulled back to expose the cell to the neutron beam for any predetermined length of time. The shutter is made from the aluminum tube covered with 1/32-in. cadmium sheet, and has a hinged, curved flap on the front, so that when the whole unit is drawn backwards by means of the rod and control cable, the flap fits snugly between the irradiation cell tube and the outer capped tube. The observed fission rate is reduced by a factor of about 80 when the shutter is in the closed position. The shutter is operated by a pneumatic barrel and plunger system, which is shown in Fig. 3. By means of the solenoid-operated valves, the compressed air system opens or closes the thermal neutron shutter in a fraction of a second.

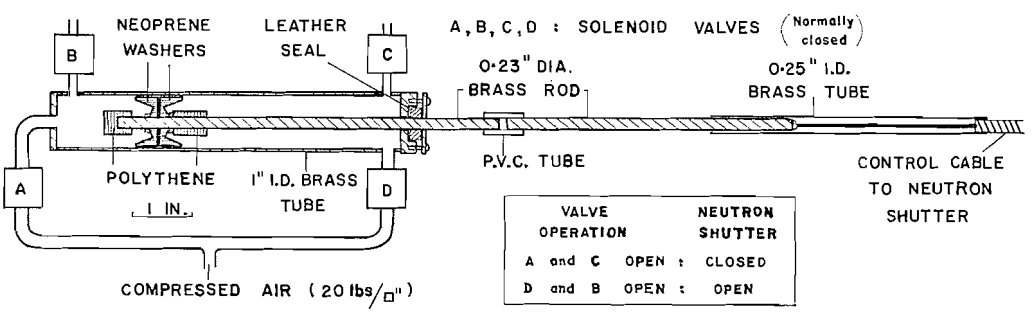

FIG. 3. Pneumatic system for the consistent and quick operation of the neutron shutter.

(c) Gas Chromatography

Separation of the active krypton and xenon isotopes outside the beam port was achieved by gas chromatographic means. Considering the relatively small number of radioactive atoms involved, it seemed likely that previous workers had used too much solid adsorbent in their separations. Accordingly, a gas chromatographic column was prepared which had the advantages of providing a high flow rate of carrier gas through a column containing only a small amount of activated charcoal.

The column packing was made by shaking up short pieces of glass wool, 2–3 cm long, with a small amount of very fine (200–400 mesh) activated charcoal, until the glass wool became a dark grey color without

retaining any obviously free charcoal. This packing was then tamped gently into several 4-mm bore glass tubes, varying in length from 5–30 cm at 5-cm intervals. The performance of these columns was tested at room temperature (70° F) using helium as carrier gas, and krypton–xenon mixtures from the irradiation cell. A shielded geiger tube, operating a rate meter and pen recorder, was used at the end of the column as the detector.

Excellent separations were obtained from all but the shortest columns, the best performance being from a 15-cm column which, at a helium flow rate of 310 cc/min, showed a krypton peak after 4 seconds and a xenon peak after 27 seconds. A typical trace is shown in Fig. 4, and the effect of helium flow rate on the performance of the 15-cm column is indicated in Table I.

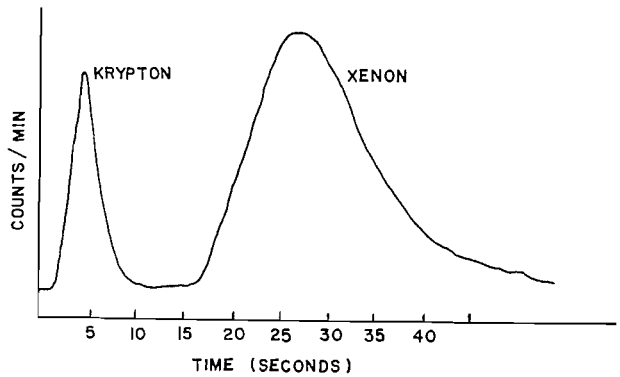

FIG. 4. High-speed gas chromatographic separation of radio-krypton and -xenon.

TABLE I

Effect of helium flow rate on krypton–xenon separation

Flow rate (cc/min)	Time to emergence of peak (seconds)	
	Krypton	Xenon
130	7	48
175	6	40
220	5	34
270	4.5	30
310	4	27
360	3.5	23
400	3.5	22
450	3.5	21

The fastest flow rates gave elution peaks which were even closer together, but in which tailing started to occur. For most of the work described subsequently, the 310 cc/min flow rate was used. Some improvements could, no doubt, be made on this separation by further adjustment of charcoal particle size, column length, flow rate, and temperature.

(d) Gas Handling Apparatus

The apparatus used for sweeping out the rare gas fission products from the irradiation cell is shown diagrammatically in Fig. 5. This enables either krypton or xenon isotopes to be studied by the gamma-ray spectrometer. The system is controlled by several solenoid-operated valves, which are normally closed. Commercial helium, at 15 lb/in^2 pressure, is used to flush out the irradiation cell and is used also as carrier gas for the chromatographic separation.

When valves E, G, and H are opened together, the mixture of rare gas isotopes from the irradiation cell is swept out through the sampling tube and on towards the trap, which contains activated charcoal granules cooled in liquid air. The flow is adjusted so that after 2 seconds the maximum amount of radioactivity is passing through the sampling tube. The flow is then stopped, trapping the sample between valves G and H. After any predetermined time the valves F and J are opened together and allow the sample to be swept into the gas chromatographic column, the separation being shown by the geiger-operated pen recorder. Depending on which gas is to be studied, valves K and L are operated so that one is swept into the trap, and the other into a replaceable 50-cc bulb, supported at the center of a 2×2×2-ft cave made from high-density concrete bricks. The outlet leads from the bulb return to the trap. The bulb, which is flattened on

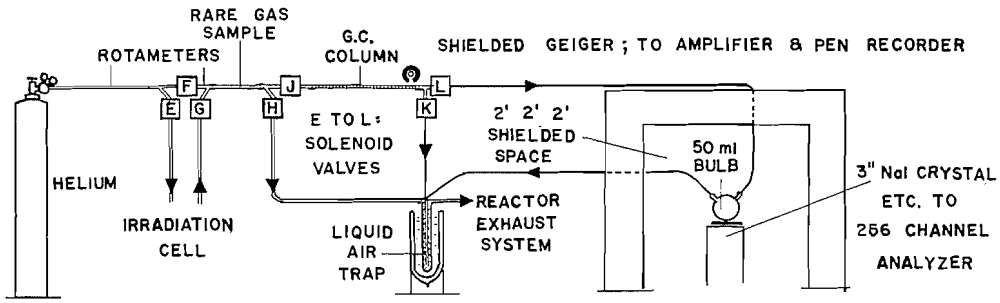

FIG. 5. Diagram of apparatus outside beam port.

one side, is fixed with the flat side facing a 3-in. sodium iodide (T1) γ-scintillation crystal connected via a photomultiplier to an R.C.L. 256-channel pulse height analyzer.

The bulb system was chosen to contain the gas sample rather than a cooled trap, since it allows the rapid removal of the gas and rapid study of the solid decay products deposited on the walls. It is housed in a small concrete cave in order to reduce reactor background and back-scattered radiation. While not as large or as effectively shielded as that suggested by Heath (10), it was found to be adequate for the relatively active samples counted in this work. The gas sweeping and gas chromatographic operations of any experiment were worked either manually or automatically by means of an electronic timing mechanism. This unit was designed to provide (i) a variable sweeping-out time (T_1), although this was always set at 2 seconds; (ii) a hold-up time (T_2) outside the beam port, varying from 2–81 seconds; and (iii) a chromatographic time (T_3) which could be set from 1–10 seconds, or to continuous running. By this means, reproducible samples could be obtained. The manual and automatic controls were usually used in conjunction with each other as outlined below.

Procedure

The procedure used in all experiments was as follows:

1. The irradiation cell was swept free of all gases for 10 seconds, using manual control.
2. The stearate sample was irradiated for a given period by opening and finally closing the thermal neutron shutter.
3. The emanated gases were allowed to "cool" for a predetermined time inside the cell. This time could, of course, be zero.
4. Automatic operation: the gases were swept out for 2 seconds ($T_1 = 2$), the maximum amount of activity being trapped in the sampling section.
5. The gases were held up in the sampling section (T_2 from 2–81 seconds).
6. Chromatographic separation: for krypton samples, T_3 was set at 10 seconds, or less if very fast flow rates were used. For xenon samples, T_3 was set for continuous running and the krypton was diverted to the trap by manual switching.
7. Gamma-spectrometric examination of the gas sample in the bulb.
8. If necessary, the bulb was flushed out with helium and the solid decay products examined.

Using this procedure, several fission product rare gas isotopes were studied and also a few of their decay products.

RESULTS

Krypton-89

After a 1-minute irradiation, the emanated gases were allowed to decay for 5 minutes inside the cell in order to allow krypton-90 to decay completely, and then treated by the above procedure. The time settings were $T_1 = 2$, $T_2 = 30$, $T_3 = 10$ seconds. The krypton sample was then counted by the 256-channel analyzer through a 1.5 g cm^{-2} aluminum absorber for a predetermined time. In the first experiments, the instrument was set for 0–1.0 Mev operation, and half-life determinations were made on the major photopeaks in this region. The results showed that these all decayed with a half-life of 3.2±0.2 min in agreement with previous work (1–3).

In order to obtain a gamma spectrum relatively free from the contributions of other longer-lived krypton isotopes or decay products, an accumulation technique was used.

Several identical samples were produced and counted for 1 minute only, the spectra being allowed to accumulate, and the sample bulb being changed for each count. The accumulated spectrum from five such samples of krypton-89 is shown in Fig. 6. The

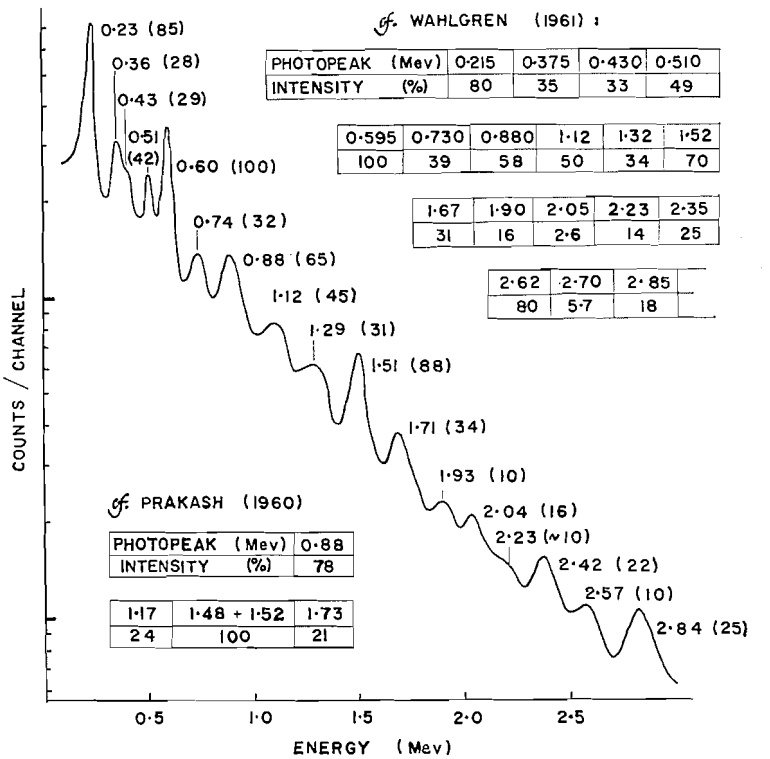

FIG. 6. Gamma spectrum of krypton-89.

energies of the photopeaks are shown, together with their relative intensities, which were calculated from the respective peak areas and an empirical efficiency curve. This was produced by study of isotopes with known decay schemes. The agreement with Wahlgren's data is seen to be reasonably good. On close examination, the photopeak at 1.51 Mev did appear to be composed of two very closely spaced peaks, as suggested by Prakash, but since they are normally unresolved, the photopeak was treated as a single one, with a single intensity. The incompleteness of Prakash's data make it unlikely that his proposed decay scheme for krypton-89 is valid.

It is probable that some of the low-intensity photopeaks may be sum or escape peaks. Coincidence measurements, which are currently being conducted, should elucidate this decay scheme.

A sample of short-lived krypton was produced as in the above experiments, allowed to decay for 5 minutes in the sample bulb, and then blown out by a stream of helium. The solid decay products were then studied from 0–1.5 Mev. The only photopeaks were at 0.66, 1.06, and 1.25 Mev, and, since all decayed with a half-life of 15.0 min, were due to the well-studied rubidium-89 (5, 9). It was not, therefore, examined any further.

Krypton-90

In order to minimize the effects of krypton-89, irradiations of 5 seconds were used.

The emanated gases were allowed to cool in the cell for 30 seconds and then treated according to the timing periods $T_1 = 2$, $T_2 = 30$, $T_3 = 10$ seconds. The major photopeaks were found to be at 0.125, 0.55, and 1.12 Mev and all decayed with a half-life of 35 ± 3 sec. A lower-intensity photopeak at 0.24 Mev was obscured by the 0.23 Mev peak of krypton-89.

To obtain a gamma spectrum relatively free from this effect, the accumulation technique was used. The krypton-90 samples were isolated as above and each was counted by the analyzer for 10 seconds only. The spectrum accumulated from 20 such samples is shown in Fig. 7. Under these conditions the effect of krypton-89 was negligible and the intensity

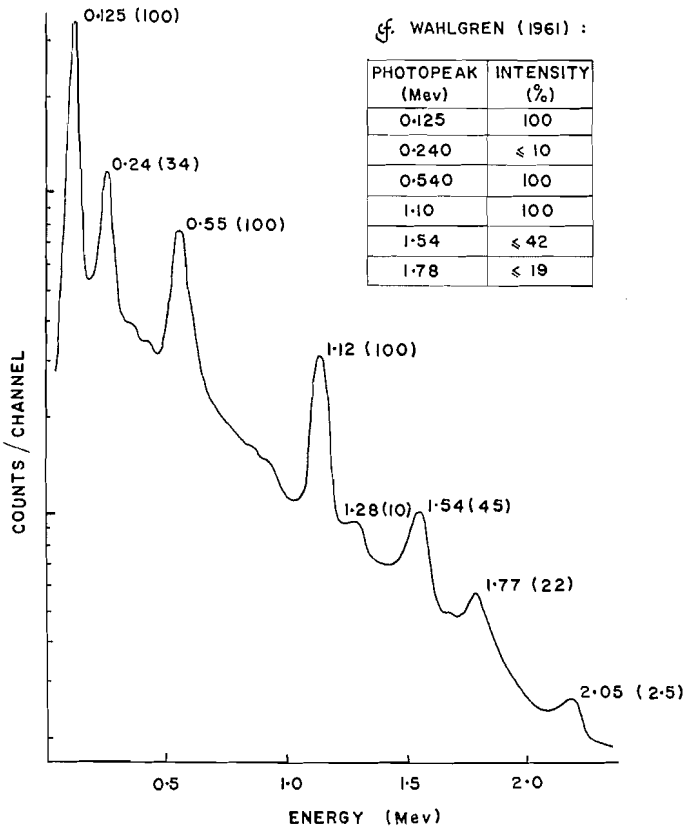

FIG. 7. Gamma spectrum of krypton-90.

of the 0.24 Mev photopeak was calculated to be 34%, much higher than the $\leq 10\%$ estimated by Wahlgren in allowing for krypton-89 interference. Otherwise the agreement is excellent.

In exactly the same way as described for the study of rubidium-89, a sample of krypton-90 was produced and allowed to decay for 90 seconds to rubidium-89. The krypton was then blown out of the cell and the decay products examined. The only photopeak which it was possible to study was the 0.84 Mev peak of rubidium-90, which decayed with a half-life of 2.8 ± 0.2 min, in agreement with O'Kelley (5) and Wahlgren (9). Other photopeaks were noted at 0.51 and 0.61 Mev, as stated by O'Kelley, but these were too small for half-life determinations.

Krypton-91

Although the half-life of this isotope is reported to be 10 sec (1, 2), no gamma rays of this period could be detected. Using 2-second irradiations and the fastest possible processing, such that the krypton sample was being counted only 9 seconds after leaving the reactor, the spectra produced were identical with that of krypton-90. The accumulation technique also failed to show evidence of this isotope, the final spectrum from 20 samples, each counted for only 5 seconds, again being identical with that of krypton-90.

This result is unusual in view of the energy available for the decay of krypton-91.

Xenon-137

This isotope, for which a half-life of 3.8 min is quoted (11), was produced by a 1-minute irradiation followed by a 2-minute cooling period, and was obtained in the cell by the separation procedure outlined above.

The gamma spectrum of the sample was similar in shape to that noted by Prakash (7) and showed photopeaks at 0.16, 0.26, 0.44 (a complex of three: 0.42, 0.44, and 0.46), and 0.53 Mev. However, only the single photopeak at 0.44 Mev showed a half-life of 3–4 min, the others being due either to xenon-138 ($t_{1/2}$ = 17 min) or its daughter cesium-138 ($t_{1/2}$ = 32 min). Only an approximate value of the 0.44 Mev half-life could be obtained because of the proximity and similar decay rates of the neighboring photopeaks.

The accumulation technique was used to establish that the 0.44 Mev photopeak did originate from xenon-137. Short-lived xenon samples were produced after 1-minute irradiations and 5-minute cooling periods, and counted for 1 minute only. Eight such samples were accumulated and showed a major photopeak at 0.44 Mev superimposed on a xenon-138 spectrum (*q.v.*). No other photopeaks of xenon-137 were noted.

The decay scheme for xenon-137 suggested by Prakash (7) must therefore be regarded as incorrect.

Xenon-138

Manual operation of the apparatus was used to obtain samples of this isotope, which was examined after 5-minute irradiations and 45 minutes' cooling outside the reactor.

The gamma spectra of these samples showed photopeaks mainly at low energies, at 0.16, 0.26, 0.42, 0.44 (trace Xe-137), 0.46, and 0.53 Mev. Those at 0.16 and 0.26 Mev decayed with a half-life of 17.5±0.5 min while the 0.42 Mev peak decayed with a half-life of 18±1 min. These are therefore attributed to xenon-138. The photopeaks at 0.46 and 0.53 Mev showed half-lives of 32±3 min and belong to cesium-138. Further proof of the xenon photopeaks was shown when a typical xenon-138 sample was allowed to decay for 30 minutes, then swept out of the cell by a stream of helium. The residual activity showed only the gamma spectrum of cesium-138, which has been thoroughly studied by Bunker *et al.* (6).

Thulin (12) had noted the 0.42 Mev peak of xenon-138 together with others at 0.51, 1.78, and 2.01 Mev. In order to establish the existence of these photopeaks, the accumulation technique was used over the energy range 0–2.5 Mev. The gamma spectrum from five xenon-138 samples is shown in Fig. 8 together with a cesium-138 spectrum produced under similar conditions. A low-intensity photopeak was produced at 0.51 Mev which had a relative intensity ratio of 0.2 compared to the 0.42 Mev peak, as found by Thulin. Since cesium-138 consistently showed a photopeak at 0.53 Mev, 0.51 Mev was assigned to xenon-138.

The photopeaks at 1.78 and 2.02 Mev are shown to be prominent in the xenon-138 spectrum and are missing from that of cesium-138.

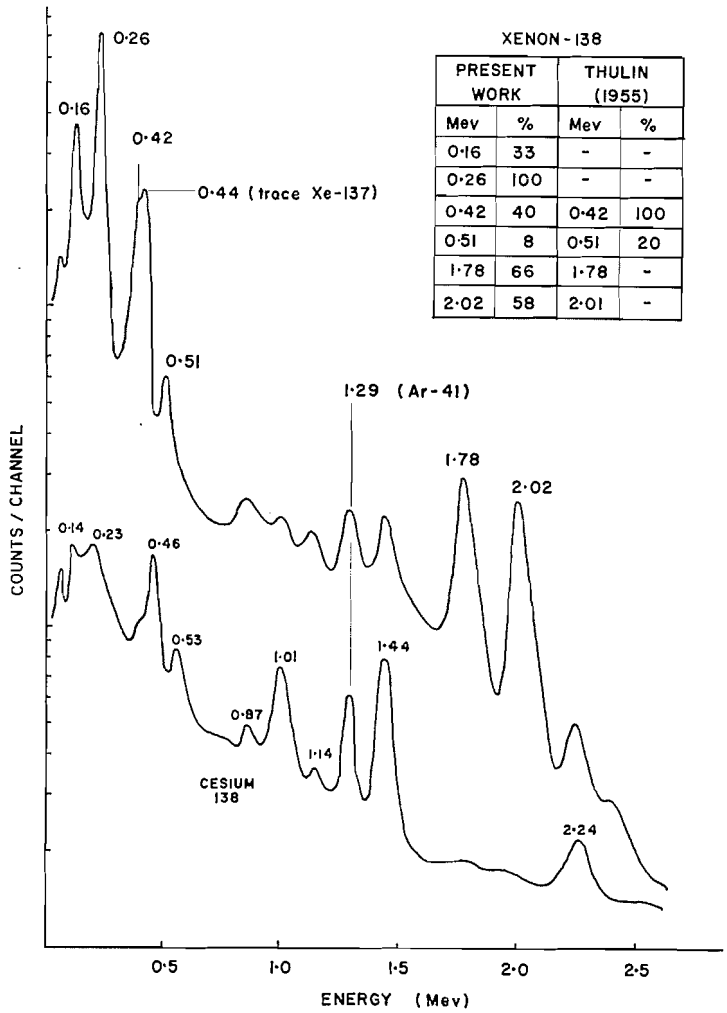

FIG. 8. Gamma spectra of xenon-138 and cesium-138.

Those attributed to xenon-138, therefore, are: 0.16, 0.26, 0.42, and 0.51±0.01 Mev; 1.78 and 2.02±0.02 Mev; their approximate relative intensities are shown in Fig. 8.

Xenon-139

In order to minimize the effect of xenon-138, a gamma spectrum of 41-sec xenon-139 was produced by the accumulation technique. Irradiations of 15 seconds were made, followed by the cycle $T_1 = 2$ seconds, $T_2 = 2$ seconds, $T_3 = \infty$ and with the xenon fraction being flushed into the cell. The spectrum, after 10×20 second counts, showed photopeaks at 0.18, 0.22, 0.30, 0.40, and 1.15 Mev as well as others due to other xenon and cesium isotopes. Subsequent half-life determinations on the 0.18, 0.22, 0.30, and 1.15 Mev peaks showed a decay period of 43±2 sec and these are all attributed to xenon-139, the first three being in agreement with Wahlgren (9). The photopeak at 0.40 Mev was too weak to study, although this also was attributed to xenon-139 by Wahlgren. The accumulated spectrum is shown in Fig. 9, with the calculated relative intensity values for the xenon-139 photopeaks. Agreement with Wahlgren's figures is good.

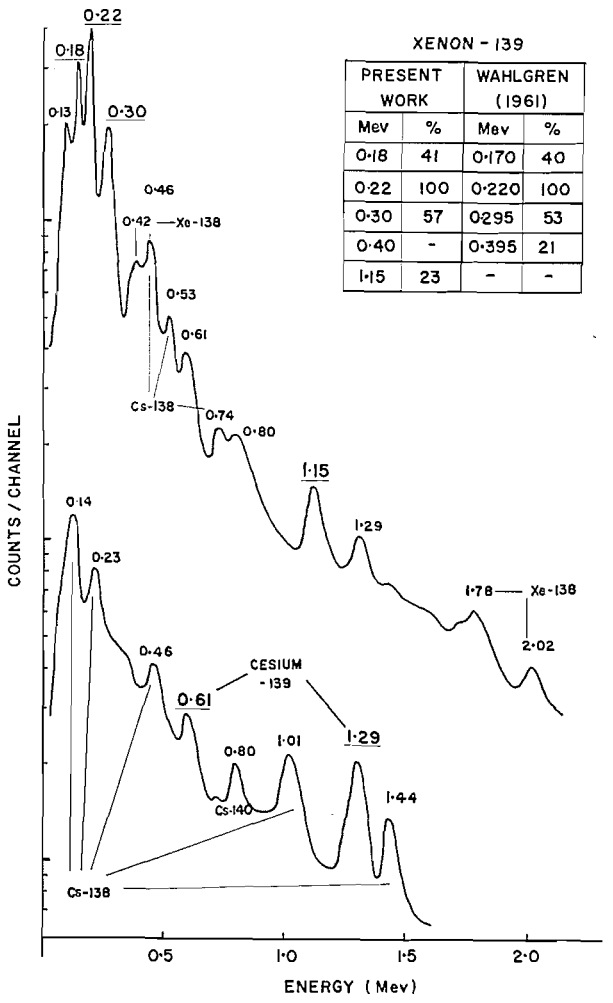

FIG. 9. Gamma spectra of xenon-139 and cesium-139.

The gamma-ray spectrum showing cesium-139 was also produced by accumulation. Xenon-139 samples were produced as described above and allowed to decay for 90 seconds, after which the xenon was blown out of the cell and the radiocesium counted for 5 minutes. Six samples were accumulated, and the resulting spectrum is shown on the lower part of Fig. 9.

Of all the photopeaks shown, only those at 0.61 and 1.29 Mev were attributed to cesium-139, the others being mainly due to cesium-138. Half-life studies confirmed this, values of 10 ± 1 min being obtained from both peaks. The 1.29 Mev peak contained a contribution from argon-41 ($t_{1/2}$ = 110 min) in the air, but a correction was made for this. Again these results are in agreement with those of Wahlgren (9).

Xenon-140

In all the gas samples containing xenon-139, a photopeak appeared at 0.13 Mev which decayed with a half-life of approximately 15 sec. This is due to xenon-140. No other gamma rays from this isotope could be detected, even when using the accumulation

technique in conjunction with 2-second irradiations and the quickest gas chromatographic separation.

CONCLUSION

The apparatus described has allowed the production of a large number of rare gas fission product samples, and the rapid gas chromatographic separation has enabled them to be studied within very short times. The results so far have confirmed recent studies (9) on krypton-89 and -90. No gamma rays from krypton-91 could be detected. New data have been obtained on xenon-137, -138, and -140, and previous work on xenon-139 has been corroborated. Some rubidium and cesium decay products have also been studied.

Coincidence measurements and decay scheme studies are being made on several of the above nuclides, and will be reported later.

ACKNOWLEDGMENTS

Thanks are offered to Dr. A. K. Das Gupta and Mr. M. D. Silbert for their assistance in building the beam port shielding, and to Mr. Edward Beaver for the design and construction of the electronic timer.

The authors acknowledge financial support from the National Research Council of Canada and from Atomic Energy of Canada Limited. One of us (D. W. O.) thanks the U.K. Atomic Energy Authority for leave of absence, and for supporting part of the work.

REFERENCES

1. C. R. Dillard, R. M. Adams, H. Finston, and A. Turkevitch. *In* Radiochemical studies: the fission products. *Edited by* C. D. Coryell and N. Sugarman. McGraw-Hill Book Co. Inc., New York. 1951. p. 624.
2. O. Kofoed-Hansen and P. Kristensen. Phys. Rev. **82**, 96 (1951); Dan. Mat. Fys. Medd. **26**, No. 6, (1951).
3. O. Kofoed-Hansen and K. O. Nielson. Phys. Rev. **82**, 96 (1951); Dan. Mat. Fys. Medd. **26**, No. 7, (1951).
4. A. C. Wahl. J. Inorg. & Nuclear Chem. **6**, 263 (1958).
5. G. D. O'Kelley, E. Eichler, and N. R. Johnson. Geneva Conference. 1958. Vol. 15. Paper 672.
6. M. E. Bunker, R. B. Duffield, J. P. Mize, and J. W. Starner. Phys. Rev. **103**, 1417 (1956).
7. S. Prakash. Z. Elektrochem. **64**, 1037 (1960).
8. R. C. Koch and G. L. Grandy. Anal. Chem. **33**, 43 (1961).
9. M. A. Wahlgren. U.S. Atomic Energy Comm. Rept. T1D–11807. 1961.
10. R. L. Heath. U.S. Atomic Energy Comm. Rept. 1DO–16408. 1957.
11. W. Seelmann-Eggebert and H. J. Born. Naturwiss. **31**, 59 (1943).
12. S. Thulin. Arkiv Fysik, **9**, 137 (1955).

THE RANGE OF Cs^{137} IONS OF KEV ENERGIES IN GERMANIUM[1]

J. A. DAVIES, J. D. MCINTYRE,[2] AND G. SIMS
Research Chemistry Branch, Atomic Energy of Canada Ltd., Chalk River, Ontario

Received April 25, 1962

ABSTRACT

The range of Cs^{137} ions in germanium has been measured at 4-, 20-, and 40-kev bombardment energy. Two independent methods of determining the depth of penetration were used. The results are in reasonable agreement with our previous range measurements in aluminum, and with the recently published theoretical treatment of Lindhard and Scharff. A possible explanation has been found for the abnormally large value reported by Bredov for the penetration depth of 4-kev Cs^{134} ions in germanium.

INTRODUCTION

Some years ago, Bredov and co-workers (1–3), reported an anomalously large penetration depth for alkali metal ions in germanium. They observed that a 4-kev Cs^{134} beam had a median penetration depth in germanium of approximately 35 $\mu g\ cm^{-2}$; in contrast with this, our recent experimental value (4) for 5-kev Cs^{137} ions in aluminum is only 0.9 $\mu g\ cm^{-2}$. The theoretically predicted increase in range in changing from an aluminum to a germanium target is somewhat less than a factor of 2; hence, Bredov's result is at least an order of magnitude higher than one would expect.

There are several completely different experimental techniques now available for measuring the range of atomic particles of kev energies in solid targets (5–7); the experimental results, except those of Bredov for germanium, are in reasonable accord with one another, and with the recent theoretical treatment of Lindhard and Scharff (8). However, most of this work has been confined to targets of low atomic number, particularly to aluminum. Hence, it was decided that a further investigation of germanium as a target material was necessary in order to determine whether an anomalously large range actually exists.

Bredov's experimental technique was to bombard a germanium target with a beam of Cs^{134} ions, and then to immerse the target for various periods of time in an aqueous H_2O_2 solution. From the observed decrease in the counting rate of the target after each immersion, and the known rate of etching of germanium in aqueous H_2O_2, he calculated the depth of penetration of the embedded radioactivity. Such a calculation involves two rather doubtful assumptions: (i) that the rate of etching is uniform over the target surface, and (ii) that it is unaffected by the Cs ion bombardment. The latter assumption is particularly questionable in view of the known effect of ionic bombardment on the electrical properties of semiconductors such as germanium and silicon (9–12).

EXPERIMENTAL

The present investigation may be divided into two parts:

(1) Duplication of Bredov's technique, using as small a beam intensity as possible in order to minimize any effect of radiation damage on the etching rate.

(2) Measurement of the transmission of Cs ions through thin germanium films in order to eliminate completely the above assumption about the rate of etching.

(1) Etching of Germanium Disks

Disks of pre-etched transistor-grade germanium were bombarded in a specially constructed electrostatic

[1]*Issued as A.E.C.L. No. 1538.*

[2]*Present address: Department of Chemistry, Princeton University, Princeton, N.J., U.S.A.*

ion accelerator (13) with a beam of 4-kev Cs^{137} ions. The beam was swept back and forth over the target in order to bombard as large an area as possible. The integrated flux in each case was about 3×10^{13} Cs ions per cm^2 of surface. After bombardment, the amount of radioactivity in each disk was measured with an end-window proportional β-counter of the methane flow type. The disks were then subjected to several successive immersions in aqueous H_2O_2. After each immersion, the disks were carefully weighed on a microbalance to determine the average thickness of the germanium layer removed, and then counted in order to obtain the residual Cs^{137} content. The results are illustrated in Fig.1. In one run, the $[H_2O_2]$, and hence

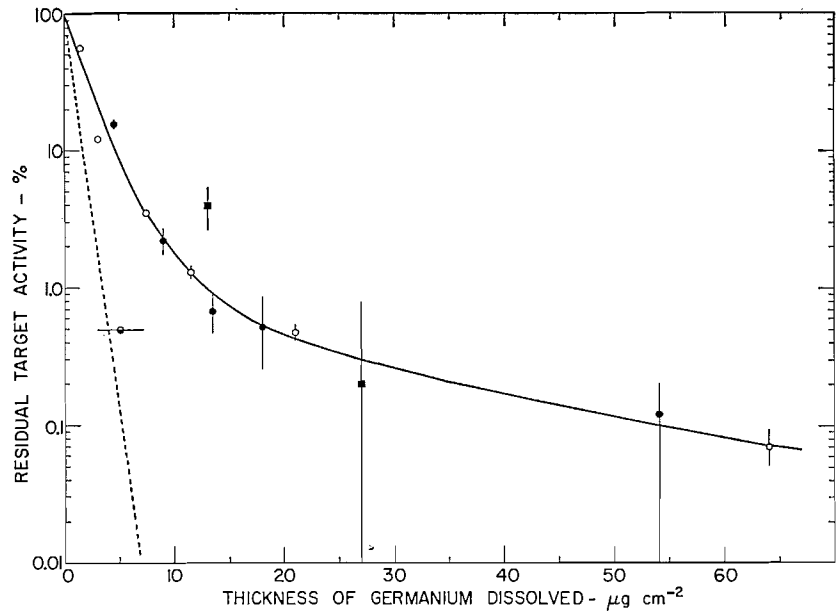

FIG. 1. Apparent depth of penetration of 4-kev Cs^{137} ions in germanium disks: ●, ○ using 0.3% aqueous H_2O_2 etch; ■ using 3% aqueous H_2O_2 etch; ◒ using the transmission method; – – – distribution curve for 5-kev Cs^{137} ions in aluminum.

the rate of etching, was increased 10-fold; this did not markedly affect the observed distribution curve. The broken line represents the observed distribution for 5-kev Cs^{137} ions in aluminum, using a previously established technique for removing *uniform* layers of accurately known thickness: viz. anodic oxidation at constant voltage, followed by dissolution of the oxide layer (5). The shape of the distribution curve in germanium approaches that observed in aluminum targets asymptotically. The observed shape of the curve might suggest the existence of an extremely penetrating component in the case of germanium. However, this penetrating "tail" was not found in the case of aluminum, and may be due merely to non-uniform etching of the germanium surface. It would require only a few percent of the incident beam to have become embedded in a corrosion-resistant region to account entirely for this "tail". The set of experiments described below provides considerable support for such an explanation.

(2) Transmission Through Thin Germanium Layers

Since the assumption of uniform etching of a germanium surface by aqueous H_2O_2 is subject to doubt, the range of Cs ions in germanium was also determined by a completely independent technique: viz. by measuring the transmission of Cs^{137} through thin films of germanium. The method consisted of three steps: (i) deposition of a thin film of germanium on an aluminum target by vacuum sublimation; (ii) bombardment of the target by a beam of Cs^{137} ions; and (iii) complete removal of the germanium layer by a 10-minute immersion in 3% aqueous H_2O_2 solution. By counting the target immediately before and after step (iii), the fraction of the Cs^{137} beam penetrating through the germanium film into the aluminum was obtained. Since the germanium film is completely dissolved in this experiment, no assumption about uniform etching rate is required. A similar technique has been used by Jech (14) to obtain approximate penetration depths for 4- to 6-kev Kr^{84} ions in nickel films.

Vacuum sublimation of the germanium was carried out slowly, with the collecting surface at least 20 cm from the heated filament, in order to obtain a fairly uniform layer. The rate of deposition was approximately 5 $\mu g\ cm^{-2}\ min^{-1}$.

The thickness of each germanium layer was determined radiochemically, using germanium containing a small amount of the 12-hr Ge^{77} isotope. This enabled extremely thin sublimed layers to be measured accurately by comparison of the counting rate of each target with that of a germanium standard of known weight. This radiochemical analysis was complicated by one factor: the Ge^{77} isotope decays to As^{77}, which in turn decays, with a 39-hr half-life, to the stable isotope Se^{77}. Since arsenic is much more volatile than germanium, it was found that the As^{77} content of the sublimed layer was considerably greater than that of the standard source. A suitable correction term for this effect was obtained by following the decay of each target for several days. With this procedure, it was possible to determine the average thickness of the germanium to ±15%. Some of the thicker layers were also measured by observing the increase in weight of the aluminum targets. There was no significant difference between the two methods (see Table I).

TABLE I

Transmission of Cs^{137} ions through germanium

	Film thickness ($\mu g\ cm^{-2}$)		
E_1 (kev)	Radiochemical analysis	Weight change	% transmission of Cs^{137}
4.0	—	5±2	0.5
20	1.8	—	95.5
	8.3	—	48
	18	14±2	4.0
40	11	—	47
	32	38±2	0.6
	58	—	0.1

After the film thickness was obtained, the (Ge^{77}+As^{77}) activity was allowed to decay to a negligible level before proceeding with the Cs^{137} bombardment.

Two additional tests were carried out in order to confirm that the aqueous H_2O_2 solution dissolves the germanium completely, without attacking the underlying aluminum.

To determine whether the aqueous H_2O_2 treatment dissolves the germanium film completely, a blank run was made with radioactive germanium of high specific activity and using the inactive Cs^{133} isotope in step (ii). After a 10-minute immersion in aqueous H_2O_2, it was found that less than 0.05% of the germanium activity remained on the aluminum foil. Hence, the dissolving of germanium was essentially quantitative.

To verify that the peroxide solution does not attack the underlying aluminum surface, another blank run was performed in which the Cs^{137} ions were injected directly into the aluminum target, i.e. before the germanium film was added. Any decrease in counting rate of the target after the germanium film was dissolved would indicate that the H_2O_2 solution was dissolving some of the underlying aluminum. The Cs^{137} ions were injected into the aluminum at 10-kev energy, and a thin, uniform layer of aluminum of known thickness (1.6 $\mu g\ cm^{-2}$) was then dissolved away by the standard anodizing and film stripping technique (5). This thickness corresponds roughly to the "most probable range" of 10-kev Cs^{137} ions in aluminum; hence, its removal effectively exposes a surface layer of aluminum with maximum Cs^{137} content. After measuring the target activity, a layer of inactive germanium approximately 30 $\mu g\ cm^{-2}$ in thickness was deposited on the surface, and subsequently dissolved by immersion in 3% aqueous H_2O_2. The decrease in Cs^{137} content was less than 1%. From this experiment, and the known distribution of the embedded Cs^{137} ions in the aluminum (13), it is estimated that the amount of aluminum dissolved by the aqueous H_2O_2 treatment was less than 0.05 $\mu g\ cm^{-2}$, i.e. less than one atom layer.

These preliminary experiments have shown that a thin layer of germanium of known thickness can be sublimed onto an aluminum surface, bombarded with Cs ions, and then removed completely without removing a significant amount of the underlying aluminum. Hence, the major sources of error for obtaining range data in germanium by chemical etching have been eliminated in the "transmission method".

Three different bombardment energies have been investigated—4, 20, and 40 kev; the results are summarized in Table I. The 4-kev result has been included in Fig. 1; the extremely small transmission through a 5 $\mu g\ cm^{-2}$ layer confirms our earlier suggestion that the "tail" observed above in Fig. 1 is not an abnormal penetration phenomenon but is due to a non-uniform rate of etching across the germanium surface.

A completely unexpected, direct observation of this non-uniformity in etching rate across a germanium surface occurred in several of these transmission experiments. During the dissolving of the sublimed layers, it was noticed that the bombarded area of the germanium dissolved somewhat more slowly than the unbombarded area; in fact, the last part to disappear resembled closely the shape of the bombarding beam. In subsequent runs, this effect was confirmed by obtaining an autoradiograph of the bombarded foil, and then comparing this autoradiograph visually with the appearance of the aluminum surface during the

dissolving of the germanium. In every case, immersion in the aqueous H_2O_2 produced on the aluminum surface a fleeting pattern of undissolved germanium which was identical in shape with the distribution of Cs^{137} atoms in the autoradiograph. Evidently, the ionic bombardment inhibits very markedly the rate of dissolution of the germanium layer—in the present case, the reduction in rate corresponded roughly to a factor of 3.

DISCUSSION

Depth-of-penetration curves for each of the energies studied are plotted in Fig. 2, together with the earlier results of Bredov *et al.* (2). No evidence of an abnormally large

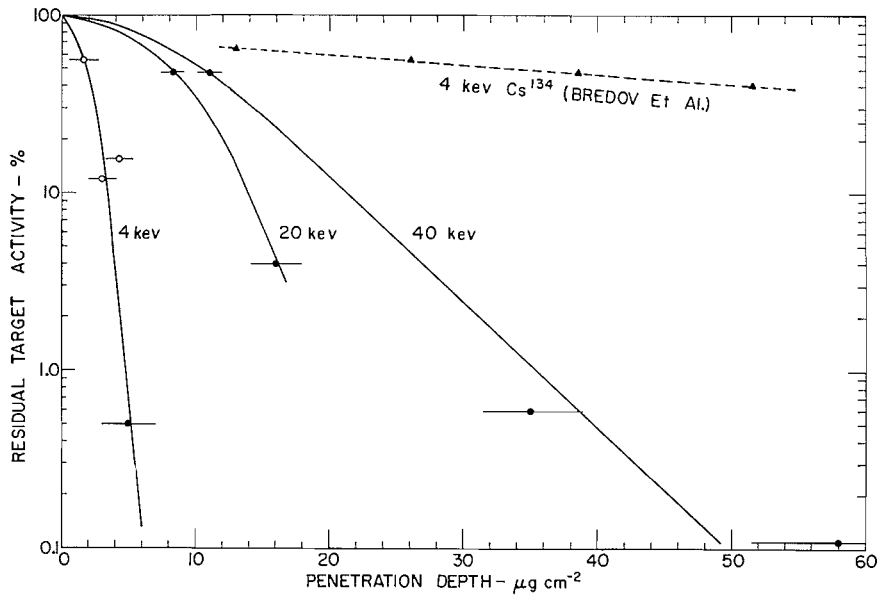

FIG. 2. Depth of penetration of Cs^{137} ions in germanium as a function of energy: ○ using method (1); ● using method (2); ▲ Bredov's data for 4-kev Cs^{134}.

penetration of germanium by Cs ions has been observed in the present investigation; in fact, even the 40-kev beam penetrated only a small fraction of the depth reported by Bredov for 4-kev ions.

A probable explanation for this discrepancy may be found in the marked reduction in etching rate that accompanies Cs ion bombardment. Bredov *et al.* determined their rate of etching, not on the bombarded specimen, but by weight loss of a control specimen which had not been subjected to the Cs ion bombardment. Consequently, the actual rate of etching of the bombarded surface (and hence, the penetration depth of the Cs ions) would be considerably less than the values calculated from the etching rate of an unbombarded specimen. It is, nevertheless, surprising that the discrepancy should have been so large, and suggests that chemical etching is not a reliable method of determining small depths of penetration.

Values of the median range obtained from the penetration curves of Fig. 2 are listed in Table II together with corresponding values for Cs^{137} ions of similar energy in aluminum targets.

In order to compare the aluminum and germanium results on a common basis, Lindhard and Scharff's recent theoretical treatment (8) has been used. They define a suitable

range parameter ρ and an energy parameter ϵ, such that all range–energy data expressed in terms of these parameters should fall on the same curve. The expressions for these two parameters may be written

$$\rho = R_m\left(1 + \frac{A_2}{3A_1}\right)\cdot\frac{166}{(Z_1^{2/3}+Z_2^{2/3})}\cdot\frac{A_1}{(A_1+A_2)^2}\ \mu g\ cm^{-2}$$

and

$$\epsilon = \frac{a}{b} = \frac{32{\cdot}5}{Z_1Z_2(Z_1^{2/3}+Z_2^{2/3})^{1/2}}\cdot\frac{A_2}{A_1+A_2}\cdot E_1,$$

where the subscripts 1 and 2 refer to the projectile and target atom respectively, a is the appropriate screening distance, b the collision diameter, and E_1 is the projectile energy in kev. By substituting the appropriate range–energy data from Table II into

TABLE II

Range of Cs^{137} ions in germanium and aluminum

E_1 (kev)	R_m, median range ($\mu g\ cm^{-2}$)	
	In aluminum	In germanium
2	0.6±0.3	—
4	—	1.8±0.5
5	0.9±0.3	—
20	4.8±0.3	8.1±1.2
30	7.4±0.4	—
40	—	10.5±1.6
50	9.0±0.5	—

the above equations, the ρ–ϵ plot shown in Fig. 3 is obtained. An earlier approximate treatment by Nielsen (15) is included for comparison. It will be noted that the germanium

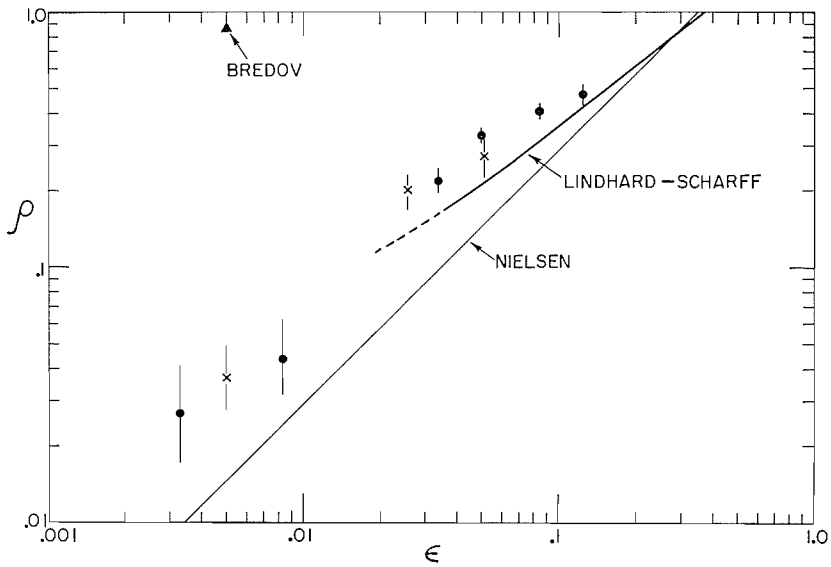

Fig. 3. ρ–ϵ plot for Cs^{137} ions: ● in aluminum; × in germanium; ▲ Bredov *et al.*

and aluminum results do in fact agree extremely well with one another, and that deviations from the theoretical $\rho-\epsilon$ curve predicted by Lindhard and Scharff, although significant, are not unreasonable and are within the limitation of the theory. In a future paper, the application of this $\rho-\epsilon$ plot to all our previous experimental measurements will be considered in detail.

REFERENCES

1. M. M. Bredov, R. F. Komareva, and A. R. Regel. Doklady Akad. Nauk S.S.S.R. **99**, 69 (1954).
2. M. M. Bredov and N. M. Okuneva. Doklady Akad. Nauk S.S.S.R. **113**, 795 (1957).
3. M. M. Bredov, I. G. Lang, and N. M. Okuneva. Zhur. Tekh. Fiz. **28**, 252 (1958).
4. J. A. Davies and G. A. Sims. Can. J. Chem. **39**, 601 (1961).
5. J. A. Davies, J. Friesen, and J. D. McIntyre. Can. J. Chem. **38**, 1526 (1960).
6. V. A. J. VanLint, R. A. Schmitt, and C. S. Suffredini. Phys. Rev. **121**, 1457 (1961).
7. R. D. Powers and W. Whaling. Bull. Am. Phys. Soc. **6**, 519 (1961).
8. J. Lindhard and M. Scharff. Phys. Rev. **124**, 128 (1961).
9. R. S. Ohl. Bell System Tech. J. **31**, 104 (1952).
10. E. F. Kingsbury and R. S. Ohl. Bell System Tech. J. **31**, 802 (1952).
11. R. Lawrance, A. F. Gibson, and J. W. Granville. Proc. Phys. Soc. (London), B, **67**, 625 (1954).
12. W. D. Cussins. Proc. Phys. Soc. (London), B, **68**, 213 (1955).
13. J. A. Davies, J. D. McIntyre, R. L. Cushing, and M. Lounsbury. Can. J. Chem. **38**, 1535 (1960).
14. C. Jech. *In* Chemical effects of nuclear transformations. International Atomic Energy Agency, Vienna. 1961. p. 243.
15. K. O. Nielsen. *In* Electromagnetically enriched isotopes and mass spectrometry. Academic Press, Inc., New York. 1956. pp. 68–81.

SOME REACTIONS INVOLVED IN THE PHOTOBROMINATION OF SIMPLE ALCOHOLS AND KETONES IN THE VAPOR PHASE

E. BUCKLEY* AND E. WHITTLE
Department of Chemistry, University College, Cathays Park, Cardiff, Wales
Received April 2, 1962

ABSTRACT

The vapor phase brominations of methanol, ethanol, formaldehyde, and acetaldehyde are all photosensitive. The products have been identified and mechanisms postulated to explain their formation. The vapor phase reactions between formaldehyde and HBr, acetaldehyde and HBr, acetaldehyde and acetyl bromide, and ethanol and acetyl bromide have also been studied.

The vapor phase reactions between bromine and simple organic compounds containing oxygen have received little attention. We are currently studying the kinetics of reactions of this type and have obtained considerable information about the chemistry involved, which will now be described. Unless otherwise stated, all reactions involve mixtures of the vapors of the reactants at room temperature.

We have shown previously (1) that the reaction between bromine and methanol is photosensitive and is given by

$$CH_3OH + 2Br_2 \rightarrow CO + 4HBr. \qquad [1]$$

A mechanism was proposed for this overall process involving successive stripping of hydrogen atoms from methanol by bromine atoms, thus giving formaldehyde as an intermediate. This was subsequently confirmed by kinetic studies (2). From separate experiments (1) it was found that the bromination of formaldehyde is also photosensitive and is given by

$$CH_2O + Br_2 \rightarrow CO + 2HBr. \qquad [2]$$

If more formaldehyde is used than is required by eq. [2] the yield of HBr falls considerably and separate experiments showed that formaldehyde and HBr react immediately with a 1:1 stoichiometry, producing drops of liquid on the walls of the container. If condensation is prevented the number of moles of products may be estimated from the pressure change. The results of two experiments are given in Table I. The products are water and *sym*-dibromodimethyl ether, and if the reaction is

$$2CH_2O + 2HBr \rightarrow BrCH_2OCH_2Br + H_2O, \qquad [3]$$

TABLE I
The reaction between formaldehyde and HBr

HBr	CH_2O	Total products
120	81	118
113	87	115

NOTE: all quantities are in μmoles.

**Present address: Department of Chemistry, University of British Columbia, Vancouver, British Columbia.*

then the number of moles of products should equal the number of moles of HBr reacted. If there is an excess of HBr, the final moles of products including unreacted HBr should still equal the initial moles of HBr, and this is confirmed by the data of Table I.

Tischtschenko (3) has shown that reaction [3] occurs when HBr reacts with solid polyoxymethylene and that similar reactions occur when HI or HCl is used. We have prepared the ethers $(XCH_2)_2O$, where X = Cl, Br, I, and have measured their infrared spectra, which are of interest, since Bellamy (4) has pointed out that the influence of α-halogenation on the C—O stretching vibration has not been studied. The following wave numbers of this vibration were found for solutions of the ethers in carbon disulphide: $(CH_3)_2O$, 1164; $(CH_2Cl)_2O$, 1099; $(CH_2Br)_2O$, 1080; $(CH_2I)_2O$, 1057 cm^{-1}.

The vapor pressure of the dibromoether was measured in the temperature range 284–307° K and is given by the equation

$$\log P_{mm} = 9.24 \pm 0.20 - 2420 \pm 60/T.$$

The unknown compound methyl hypobromite could be produced by

$$CH_3OH + Br_2 \rightarrow CH_3OBr + HBr, \qquad [4]$$

a reaction frequently postulated to occur in solutions of bromine in methanol. It could also be formed by

$$CH_2O + HBr \rightarrow CH_3OBr. \qquad [5]$$

However, we could detect no trace of it in the products of the vapor phase reactions. In 1894, Henry (5) isolated an unstable compound which he claimed to be $BrCH_2OH$. We have repeated his experiment, which consists of passing HBr into aqueous 40% formalin at room temperature. After about 90 minutes, an oily liquid separated but its infrared spectrum was the same as that of *sym*-dibromodimethyl ether and indeed this is a convenient way of making the compound.

Bromine and Acetaldehyde

The reaction between bromine and acetaldehyde is almost instantaneous in daylight but there is no dark reaction. A series of experiments was done using progressively increasing amounts of bromine measured photometrically. The following result is typical: initial acetaldehyde 29.1 mm, initial bromine 34.9 mm, residual bromine 6.7 mm. Clearly the stoichiometry is close to 1:1 when using excess bromine. Infrared analysis indicated that acetyl bromide and HBr are the only major products, with traces of acetic acid, CO, and CH_4. Hence the overall reaction is

$$CH_3CHO + Br_2 \rightarrow CH_3COBr + HBr. \qquad [6]$$

This was confirmed by dissolving the products in water and titrating the H^+ liberated. In one experiment 40.6 μmole of bromine reacted with 46.0 μmole of acetaldehyde, and 118.6 μmole of H^+ was found, compared to the expected value of $3 \times 40.6 = 121.8$ μmole.

In view of these facts the probable mechanism of reaction [6] is

$$Br_2 + h\nu \rightarrow 2Br \qquad [7]$$

$$Br + CH_3CHO \rightarrow HBr + CH_3CO \qquad [8]$$

$$CH_3CO + Br_2 \rightarrow CH_3COBr + Br \qquad [9]$$

plus a suitable termination step, e.g.

$$Br + Br + M \rightarrow Br_2 + M. \qquad [10]$$

The traces of CO and CH_4 amounted to less than 0.4% of the acetaldehyde reacted and could be owing to the breakdown of the acetyl radical:

$$CH_3CO \rightarrow CH_3 + CO \quad [11]$$

$$CH_3 + CH_3CHO \rightarrow CH_4 + CH_3CO. \quad [12]$$

The formation of acetic acid is discussed later.

If more acetaldehyde is used than is required by reaction [6], additional products are obtained, the main one being an ester, and it seems likely that the excess acetaldehyde reacts with the products of reaction [6]. This was confirmed by reacting 42.3 μmole of bromine with 79.7 μmole of acetaldehyde. The products were dissolved in water and on rapid titration (to avoid appreciable hydrolysis of the ester by reaction [14]) the measured H^+ was 56.1 μmole compared with the expected 3×42.3 μmole. We have therefore studied the reactions of acetaldehyde with acetyl bromide and with HBr.

Reaction between Acetaldehyde and Acetyl Bromide

On mixing equimolar amounts of the vapors of these compounds, both react completely and no HBr is liberated. The product has a fruity smell and an infrared spectrum rather like that of ethyl acetate. The carbonyl absorption is at 1773 cm^{-1} compared to 1745 cm^{-1} for ethyl acetate.

The product of the reaction was shown to be α-bromoethyl acetate, produced by the reaction

$$CH_3COBr + CH_3CHO \rightarrow CH_3COOCH(Br)CH_3. \quad [13]$$

The bromoester is unstable and is difficult to free from acetic acid as it is fairly readily hydrolyzed by water according to the equation

$$CH_3COOCH(Br)CH_3 + H_2O \rightarrow CH_3COOH + HBr + CH_3CHO, \quad [14]$$

and the fact that this reaction was found to be quantitative plus the information given above are strong proof of the identity of the compound.

The bromoester has been little studied since Tawildarow (6) made it by heating a mixture of acetaldehyde and acetyl bromide to 130° and distilling the product. We find that, on mixing the liquids at 20°, heat is liberated and good yields of the ester are obtained. Its infrared spectrum is identical with that of the ester formed when bromine reacts with excess acetaldehyde; clearly the acetyl bromide formed reacts with excess acetaldehyde.

The Reaction between Acetaldehyde and HBr

On mixing gaseous acetaldehyde and HBr, the changes seen are the same as when formaldehyde is used. The lower layer of the two liquids produced has an infrared spectrum characteristic of an ether, with two intense absorptions at 1076 and 1128 cm^{-1} compared with a single band at 1120 cm^{-1} in diethyl ether. By analogy with reaction [3], the ether could be *di-α-bromoethyl ether*, produced by

$$2CH_3CHO + 2HBr \rightarrow CH_3CH(Br)OCH(Br)CH_3 + H_2O. \quad [15]$$

This compound is unstable and is rapidly hydrolyzed by water, which reverses reaction [15]; this has been used to check the assigned formula. It does not seem to have been reported previously, although the corresponding dichloroether was made by Moffett (7) from acetaldehyde and HCl in the liquid phase.

If reaction [15] occurs to some extent when bromine reacts with acetaldehyde, then the water formed could react with the acetyl bromide present to give the traces of acetic acid mentioned earlier.

The Bromination of Ethanol

The reaction between bromine and aqueous ethanol has been studied in detail (8, 9) and it was found that in concentrated aqueous ethanol the only products are ethyl acetate and hydrobromic acid, whereas in dilute solution acetic acid is formed rather than ethyl acetate. The mechanism has not been definitely established.

In the vapor phase, we find that ethanol and bromine react only in light. The results of two experiments are shown in Table II and it is clear that the stoichiometry is close to 1:1. The main products are ethyl acetate and HBr, so the overall reaction is

$$2C_2H_5OH + 2Br_2 \rightarrow CH_3COOC_2H_5 + 4HBr. \qquad [16]$$

TABLE II

The reaction between bromine and ethanol

Initial pressure (mm)		Final pressure (mm)	Br_2 reacted (mm)
C_2H_5OH	Br_2	Br_2	
26.6	35.0	7.4	27.6
29.1	44.6	14.4	30.2

When methanol is brominated, formaldehyde is formed as an intermediate so it is likely that ethanol will give acetaldehyde on bromination. But acetaldehyde is rapidly brominated to acetyl bromide, which could react with residual ethanol. If the vapors of ethanol and acetyl bromide are mixed there is an immediate reaction which gives only ethyl acetate and HBr, presumably by

$$C_2H_5OH + CH_3COBr \rightarrow CH_3COOC_2H_5 + HBr. \qquad [17]$$

In view of the above facts the following mechanism is postulated to explain reaction [16]:

$$Br_2 + h\nu \rightarrow 2Br \qquad [7]$$

$$Br + CH_3CH_2OH \rightarrow HBr + CH_3CHOH \qquad [18]$$

$$CH_3CHOH + Br_2 \begin{cases} \nearrow \; CH_3CHO + HBr + Br & [19a] \\ \text{or} & \\ \searrow \; CH_3CH(Br)OH + Br & [19b] \end{cases}$$

$$CH_3CH(Br)OH \rightarrow CH_3CHO + HBr \qquad [19c]$$

followed by reactions [8], [9], and [17]. The termination step of this chain sequence has not been identified. Reaction [19*a*], and the alternatives [19*b*] and [19*c*] are analogous to those discussed by Buckley and Whittle (1) in connection with the bromination of methanol. If each molecule of acetyl bromide produced is converted to ethyl acetate, the above mechanism gives reaction [16] as the overall result.

A minor product of the bromination of ethanol is acetic acid, probably because of hydrolysis of some of the intermediate acetyl bromide. The necessary water could be produced by reaction [15] or by

$$C_2H_5OH + HBr \rightarrow C_2H_5Br + H_2O. \qquad [20]$$

There would also be traces of water in the original ethanol. Any ethyl bromide formed by this reaction would be very difficult to detect.

EXPERIMENTAL

Materials

Br_2 and CH_2O were treated as described previously (1). HBr was made from Br_2 and tetralin. B.D.H. spectroscopic ethanol was dried with anhydrous Na_2SO_4, distilled, and finally subjected to bulb-to-bulb distillations on a vacuum line. A middle cut was stored at −80°. May and Baker acetaldehyde was subjected to several bulb-to-bulb distillations on the vacuum line and a small middle cut stored at −80°.

Procedure

The reactions took place in a conventional high vacuum apparatus and all materials were thoroughly degassed before mixing.

sym-Dibromodimethyl Ether

This was made by (*a*) mixing the vapors of CH_2O and HBr or (*b*) treatment of paraformaldehyde with HBr. In each case the products were two immiscible liquids, the lower one being the ether and the upper layer aqueous HBr. The ether was dried with anhydrous Na_2SO_4. It fumes and decomposes in air and reacts very rapidly with aqueous NaOH. Because of this instability the ether cannot be obtained completely pure. A Carius estimation gave 74% Br (theor. 78.4%). A sample was hydrolyzed with dilute NaOH, and the H^+ and Br^- ions liberated were estimated independently and were found to be equivalent. Two samples of the ether, weighing 0.046 and 0.042 g respectively, gave 0.034 and 0.031 g of HBr (theor. HBr from reverse of eq. [3], 0.0365 and 0.0335 g). This is satisfactory in view of the instability of the compound.

Procedure (*b*) above was also used to make $(CH_2Cl)_2O$ and $(CH_2I)_2O$ starting with HCl and HI respectively. There is no apparent reaction between HCl and CH_2O vapors, and HCl gas must be left in contact with paraformaldehyde for several days at 100° C before liquid products are formed.

α-Bromoethyl Acetate

This was made (*a*) by mixing the vapors of CH_3CHO and CH_3COBr or (*b*) more conveniently by mixing the corresponding liquids, using a slight excess of CH_3CHO. When reaction was complete, the mixture was cooled to 20° and any excess CH_3CHO pumped away. The residue was distilled and a fraction with boiling point range of 108–132° was collected. This was rapidly washed with dilute aqueous $NaHCO_3$ followed by water and it was dried with anhydrous Na_2SO_4. The final product could not be freed of traces of acetic acid, probably because of the ready hydrolysis of the ester; this was studied with the following results.

Ester (0.329 g, 1.97 mmole) was dissolved in water and left until hydrolysis was complete. On the basis of eq. [14] we expect 1.97 mmole Br^-, 1.97 mmole CH_3CHO, and 3.94 mmole H^+. The Br^- and H^+ were determined volumetrically as 1.74 and 3.66 mmole respectively. The CH_3CHO should equal the Br^- and was found to be 1.73 mmole using a gravimetric determination based on the 2,4-dinitrophenylhydrazone. The results are satisfactory since the ester could not be completely freed of acetic acid.

Di-α-bromoethyl Ether

This was made by mixing the vapors of CH_3CHO and HBr. The subsequent results and procedure were similar to those given above under *sym*-dibromodimethyl ether. A sample of 0.088 g of di-α-bromoethyl ether was hydrolyzed with excess aqueous NaOH, and 0.056 g of HBr was liberated (theor. on the basis of the reverse of reaction [15], 0.061 g).

One of us (E. B.) wishes to thank the D.S.I.R. for a maintenance grant.

REFERENCES

1. E. Buckley and E. Whittle. Trans. Faraday Soc. **55**, 1536 (1959).
2. E. Buckley and E. Whittle. Trans. Faraday Soc. **58**, 529, 536 (1962).
3. W. Tischtschenko. Ber. ref. 20, 701 (1887).
4. L. J. Bellamy. The infrared spectra of complex molecules. Methuen, London. 1958.
5. L. Henry. Ber. ref. 20, 336 (1894).
6. N. Tawildarow. Ann. **176**, 21 (1875).
7. E. Moffett. J. Am. Chem. Soc. **56**, 2009 (1934).
8. L. Kaplan. J. Am. Chem. Soc. **80**, 2639 (1958).
9. L. Farkas, B. Perlmutter, and O. Schachter. J. Am. Chem. Soc. **71**, 2829 (1949).

NOVEL DEVIATIONS FROM THE 'MIXTURE LAW' IN THE RADIOLYSIS OF HYDROCARBON MIXTURES[1]

P. J. DYNE AND J. DENHARTOG
Research Chemistry Branch, Atomic Energy of Canada Limited, Chalk River, Ontario

Received April 10, 1962

ABSTRACT

The 'mixture law' states that, if the radiolysis of material A gives a product M with yield G_M, then, in a mixture where the mole fraction of A is X_A, the yield of M is $G_M X_A$.

In the radiolysis of dilute mixtures of cyclohexane-d_{12} or of methylcyclohexane-d_{14} with other aliphatic hydrocarbons D_2 is formed in a process which is first order with respect to the deutero compound. As a consequence these mixtures provide a sensitive method of detecting deviations from the mixture law.

Experimentally the yield of D_2 and the yield of HD vary widely from one solvent to another amongst the C_5 to C_{10} hydrocarbons selected. The yields of D_2 and HD are, approximately, linearly related. The solvents have similar quantitative effects on the yields for both deuterated hydrocarbons.

These deviations from the mixture law cannot be explained in terms of kinetic effects (variations in rate constants caused by differing bond strengths), because the D_2 yield measures a process without free radical intermediates. Mechanisms involving excitation transfer, ion–molecule reactions, and subexcitation electrons are discussed.

INTRODUCTION

An effective method of exploring mechanisms of radiolysis is to examine the radiation chemistry of mixtures. Here effects and interactions unsuspected from the radiolysis of a pure compound may be clearly revealed.

The first expectation about the radiolysis of a binary mixture is that the product yields will follow a simple mixture law. Suppose G^0_M is the yield of M derived from a material A, and suppose that X_A is the fraction of energy absorbed by A in a binary mixture of A and B. The yield of M in the mixture is then expected to be $G^0_M X_A$. Put another way, the yield G_M *per 100 ev absorbed in component A* is expected to be independent of composition.

In practice, mixtures obeying this simple law are the exception. Many physical and chemical interactions are possible between the compounds in the mixture and the intermediates in the decomposition, and, as a consequence, the yields depart widely from the simple mixture law. This is hardly surprising considering the diversity of compounds studied in a single mixture, e.g. cyclohexane–benzene (1–3), carbon tetrachloride and diphenyl-picryl-hydrazyl (4), hexane and methyl methacrylate (5). Mechanisms of energy transfer, charge transfer, and radical scavenging have been proposed for these interactions and have been demonstrated with varying degrees of rigor.

If the components of the mixture are similar, interactions are expected to be small or non-existent, as shown, for instance, by the hydrogen yield from mixtures of benzene (10) and toluene (6). The present paper describes experiments on mixtures of aliphatic and alicyclic hydrocarbons where large deviations from the simple mixture law are observed.

In these experiments we measure the yield of D_2 and HD from mixtures of cyclohexane-d_{12} (or methylcyclohexane-d_{14}) with other hydrocarbons (called "solvents"). Kinetic analysis (7, 8) shows that, at low concentrations of the deuterated hydrocarbon, the D_2 comes exclusively from the first-order decomposition

$$c\text{-}C_6D_{12} \longrightarrow D_2 + \text{products},$$

[1]*Issued as A.E.C.L. No. 1543.*

in which both deuterium atoms come from the same hydrocarbon molecule. The yield of D_2 is equivalent to the yield of M referred to in an earlier paragraph. We calculate the yield of this first-order decomposition, $G_1(D)$, from the relation

$$G_1(D) = G(D_2)/100 \text{ ev absorbed in cyclohexane-}d_{12}.$$

We assume that the fraction of energy absorbed by the cyclohexane-d_{12} is equal to its mole fraction.* We find that $G_1(D)$ is not a constant, as expected from the mixture law, but varies widely from solvent to solvent.

The use of a deuterated hydrocarbon as one component of a mixture gives, via the analysis of D_2 and HD, a sensitive method of detecting the reactions of one component in a mixture. Consequently we call the deuterated hydrocarbon molecule 'the detector molecule' and the other, non-deuterated hydrocarbon 'the solvent' since it is always present in large excess.

EXPERIMENTAL

The techniques of irradiation (Co-60 γ-rays), dosimetry, and isotopic analysis of the hydrogen have been described previously (7, 8). In cases where the methane yield is appreciable the total amount of gas, not condensed in liquid N_2, was measured and analyzed mass spectrometrically for methane and the hydrogen isotopes.

Cyclohexane-d_{12}, methylcyclohexane-d_{14}, and benzene-d_6 of >99% isotopic purity were obtained from Merck & Co. The isotopic purity was confirmed by mass spectrometric analysis.

The hydrocarbon solvents were: Fisher Spectrograde: *n*-hexane and cyclohexane; Phillips Pure Grade: methylcyclopentane, *n*-decane, methylcyclohexane, cyclopentane, *n*-pentane, and *n*-octane; Phillips Research Grade: *n*-hexane, cyclohexane, cyclopentane, neohexane, isopentane, isohexane, and *n*-pentane; Anachemia: (purified with H_2SO_4) methylcyclohexane, ethylcyclohexane, *n*-nonane, and *n*-decane; Matheson, Coleman and Bell: (purified with H_2SO_4) isooctane and decalin. The Phillips chemicals were used as received after we had found that refluxing with sulphuric acid to remove olefins, according to the method of Hardwick (5), did not increase $G(H_2)$. With the exception of *n*-hexane, which will be discussed later, no significant difference was found in the behavior of solvents from different manufacturers.

In general, measurements were made at two concentrations of the deuterated hydrocarbon, one at about 3 mole% and one at about 6 mole%. These gave yields of HD and D_2 which lay on a line passing through the origin. The estimated uncertainty in the percentage of D_2 and hence in $G_1(D)$ amounts to about ±5%; the uncertainty in the percentage of HD is less than this and amounts to ±3%. The values of $G(H_2)$ in Table I were obtained from 20-ml samples at a dose of 5×10^{22} ev/l. Values of G(total hydrogen) for the

TABLE I

Summary of D_2 and HD yields in hydrocarbon solvents

Hydrocarbon solvent	$G(H_2)$ (pure solvent)	Solutions of cyclohexane-d_{12}		Solutions of methylcyclohexane-d_{14}	
		$G_1(D)$	g(HD)	$G_1(D)$	g(HD)
1. *n*-Pentane	4.5	2.6	11.5	2.1	14.5
2. Isopentane	4.0	1.3	6.5	1.0	7.9
3. Cyclopentane	4.9	1.6	10.0	1.10	11.0
4. *n*-Hexane	5.1	2.6	10.5	2.2	14.4
5. Isohexane	3.9	0.69	4.4	0.48	4.9
6. Neohexane	3.7	0.51	3.1	—	—
7. Methylcyclopentane	4.2	0.35	3.4	0.54	5.5
8. Cyclohexane	5.3	0.33	4.1	1.38	9.0
9. Dimethylpentane	3.8	0.44	3.3	—	—
10. Methylcyclohexane	4.7	0.21	2.9	0.22	3.2
11. *n*-Octane	5.0	0.57	3.5	0.95	7.5
12. Isooctane	3.3	0.30	2.3	0.25	2.8
13. Ethylcyclohexane	4.6	0.25	2.2	—	—
14. *n*-Nonane	4.9	0.34	2.9	—	—
15. *n*-Decane	4.8	0.28	2.5	0.43	3.9
16. Decalin	3.9	0.08	1.6	0.075	1.72

**In the mixtures studied the mole fraction is approximately equal to the electron fraction, the parameter chosen by many workers. The effects reported in this paper are much larger than the differences between mole fraction and electron fraction.*

smaller isotopic samples containing the heavy hydrocarbon gave results of somewhat lower precision, deviating by as much as 5% from the results obtained with the larger samples. The values of $G_1(D)$ and $g(HD)$ are based on the amounts actually measured on the small samples. These, again, will be somewhat lower than the limiting values at zero dose.

This study is essentially a survey; observations were made at fewer concentrations of the deuterated hydrocarbon than in the earlier studies (7, 8). The reliability and reproducibility of all these experiments is good and so the smaller number of experimental points does not materially reduce the significance of the data.

Experiments with *n*-hexane showed that while Fisher Spectrograde material and Phillips Research Grade gave essentially the same $G(H_2)$, the values of $G_1(D)$ and $g(HD)$ from the isotopic mixtures with the Fisher material were about half those found in the Phillips material. We naturally looked for this type of variation with other hydrocarbons. However, cyclohexane from several manufacturers, viz. Phillips Pure and Research grades, Fisher Spectrograde, all gave essentially identical results. This impurity effect is, so far as we know, restricted to *n*-hexane: it is noteworthy that this 'impurity' does not markedly affect $G(H_2)$ although it affects both $g(HD)$ and $G_1(D)$ proportionately.

THE KINETIC ANALYSIS

The kinetic scheme used has been given previously (7, 8) and is summarized below for the reader's convenience. In essence it separates hydrogen-forming processes into two classes: those which are first order with respect to the hydrocarbon and those which are second order.

The scheme is:

$$\left.\begin{aligned} C_H &\xrightarrow{\sim\sim} H_2 + P \\ C_D &\xrightarrow{\sim\sim} D_2 + P \end{aligned}\right\} \text{first-order yields} \quad \begin{matrix} G_1(H) \\ G_1(D) \end{matrix}$$

$$\left.\begin{aligned} C_H &\xrightarrow{\sim\sim} X_H + P \\ C_D &\xrightarrow{\sim\sim} X_D + P \end{aligned}\right\} \text{second-order yields} \quad \begin{matrix} G_2(H) \\ G_2(D) \end{matrix}$$

$$\begin{aligned} X_H + C_H &\rightarrow H_2 + P \quad \text{rate constant } k_1 \\ X_D + C_H &\rightarrow HD + P \quad \text{" " } k_2 \\ X_H + C_D &\rightarrow HD + P \quad \text{" " } k_3 \\ X_D + C_D &\rightarrow D_2 + P \quad \text{" " } k_4 \end{aligned}$$

where C_H is the light hydrocarbon, C_D the deuterated hydrocarbon, P is any residue, and X_H and X_D the reactive intermediates in the bimolecular, second-order processes. We have shown that in mixtures containing C_D moles of the heavy hydrocarbon and C_H moles of the light hydrocarbon the yield of D_2 is given by:

$$G(D_2) = G_2(D) \times k_4/k_2 \times (C_D/C_H)^2 + G_1(D) \times C_D/C_H \qquad [1]$$

when $C_H > C_D$, and that in the limit $C_H \gg C_D$,

$$G_1(D) = G(D_2) \times (C_H/C_D). \qquad [2]$$

The yield of HD is given by

$$G(HD) = C_D/C_H[(k_3/k_1) \times G_2(H) + G_2(D)] \qquad [3]$$

when $C_H \gg C_D$.

We define

$$g(HD) = G(HD) \times (C_H/C_D) = (k_3/k_1) \times G_2(H) + G_2(D). \qquad [4]$$

This analysis assumes that the excitation is partitioned between the components according to their mole fraction, and the simple expectation is that $G_1(D)$ is independent

of the nature of C_H, the solvent. As will be seen, $G_1(D)$ varies with the solvent and we interpret this in terms of interaction of the detector molecule with the solvent.

RESULTS AND CORRELATIONS

(a) Aliphatic Solvents

The results are tabulated in Table I and are plotted in Figs. 1–3. The range of values of $G_1(D)$ and $g(HD)$ is large: values of $G_1(D)$ for C_6D_{12} in decalin and in *n*-pentane differ

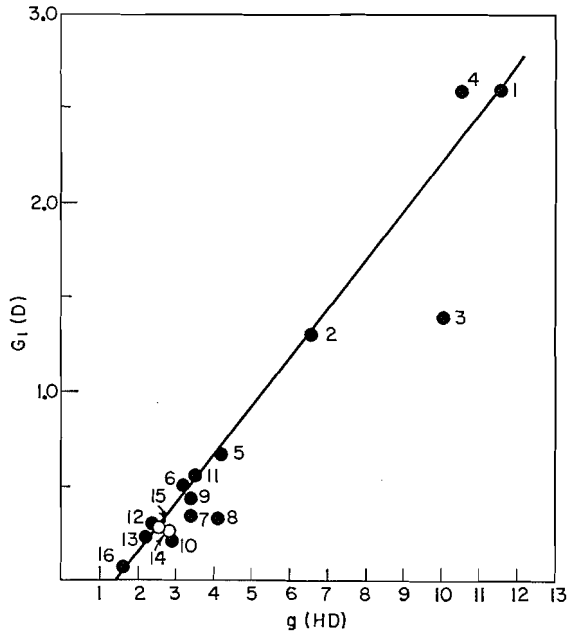

FIG. 1. Variation of $G_1(D)$ with $g(HD)$ for solutions of cyclohexane-d_{12} in various solvents. The key to the numbers identifying the solvents is in Table I.

by a factor of 30, values of $g(HD)$ for the same mixture differ by a factor of 7. In its simplest experimental terms the percentages of D_2 and HD differ by these amounts, since the yield of total hydrogen is relatively constant. The range in G(total hydrogen) for these same mixtures amounts to 15%. The effect we are studying is consequently of much greater magnitude than the variations in hydrogen yield between one hydrocarbon and another. It is also much greater than any corrections which might be made to the calculation of mole fraction due to non-ideality of the solution and other corrections which might alter the initial estimate of the energy partitioning.

There is a correlation between $G_1(D)$ and $g(HD)$. Solvents in which $G_1(D)$ is large are also solvents in which $g(HD)$ is large. This is shown in Figs. 1 and 2, where values of $g(HD)$ are plotted against $G_1(D)$. To a first approximation this correlation is linear, i.e. it can be expressed by

$$g(HD) \simeq AG_1(D)+B, \qquad [5]$$

where B is a constant.

There is also a correlation between $G_1(D)$ for cyclohexane-d_{12} solutions and $G_1(D)$ for methylcyclohexane-d_{14} solutions. Solvents in which $G_1(D)$ is large for one detector molecule also give large values for the other detector molecule. This is shown in Fig. 3.

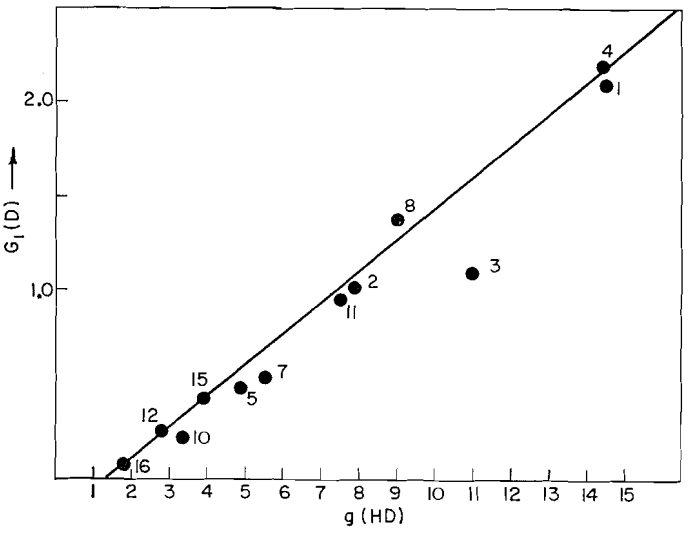

FIG. 2. Variation of $G_1(D)$ with $g(HD)$ for solutions of methylcyclohexane-d_{14} in various solvents. The key to the numbers identifying the solvents is in Table I.

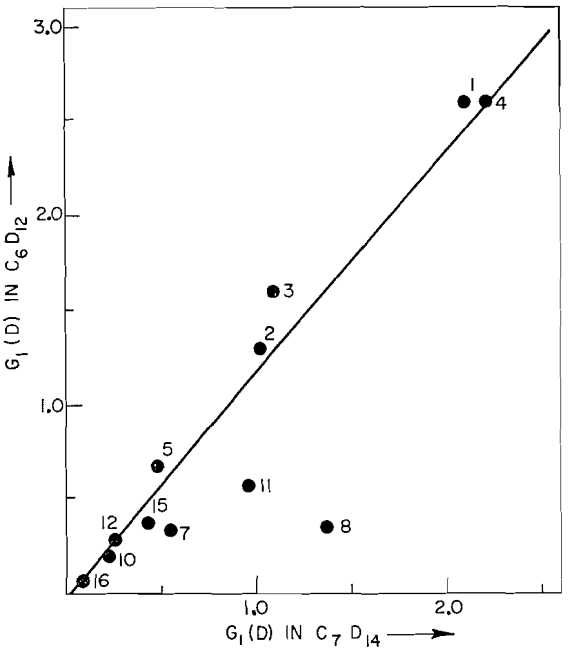

FIG. 3. The effect of solvent on $G_1(D)$ from C_6D_{12} (abscissa) against $G_1(D)$ from C_7D_{14} (ordinate). The key to the numbers identifying the solvents is in Table I.

These results show that the effective reactivity of the detector molecule, as measured by HD and D_2 yields, varies widely from solvent to solvent. This variation in reactivity must appear in the yields of all the other products derived from the detector molecule. To take an example, the yields of cyclohexene and high molecular weight hydrocarbons with a C_6 ring must differ between mixtures in pentane or in heptane. Muccini and Schuler (9)

have studied mixtures of cyclohexane and cyclopentane, analyzing the $(C_6)_2$, (C_6,C_5), and $(C_5)_2$ hydrocarbons. They conclude that the solutions are regular and show no evidence of energy transfer. These product yields are not symmetric with concentrations; they attribute this to reactions changing the identity of free radicals:

$$C_6H_{11} + C_5H_{10} \rightarrow C_6H_{12} + C_5H_9. \quad [6]$$

No measurements were made of the yields of olefins. If this change of identity reaction occurred it could mask the effects of the interaction we observe through the yields HD and D_2. While Muccini and Schuler's experiment gives no inkling of the interaction we observe we do not consider that it is in conflict with our data.

A further conclusion from the experimental results is that, since $G_1(D)$ varies with solvent, no unique significance can be placed on the value obtained from solutions of C_6D_{12} in C_6H_{12} (7). There is no reason to suppose that it gives the first-order yield in 'pure' C_6D_{12}, since we cannot assume that there is no interaction between molecules which differ only in isotopic substitution.

(b) Solutions of Aromatic Hydrocarbons

Experiments were carried out with benzene-d_6 as the detector molecule in both aromatic and aliphatic solvents.

From a complete analysis of mixtures of benzene and benzene-d_6 we have shown (10) that, within experimental error, the mixtures are regular. The isotopic composition of hydrogen evolved from a 50:50 benzene–benzene-d_6 mixture can be accurately predicted from the kinetic analysis which is confined to the two ends of the concentration range, $C_H \gg C_D$ and $C_D \gg C_H$.

Values of $G_1(D)$ and $g(HD)$ for benzene-d_6 in four aromatic solvents are shown in Table II.

TABLE II

Solutions of benzene-d_6 in aromatic hydrocarbons

Solvent	$10^3 G_1(D)$	$10^2 g(HD)$
Benzene	3.2	2.7
Toluene	3.2	5.2
Cumene	3.2	5.7
p-Xylene	2.6	6.2

The extreme errors in $G_1(D)$ amount to $\pm 5 \times 10^{-4}$ G(unit), in $g(HD)$ to $\pm 2 \times 10^{-3}$ G(unit). Values of $G_1(D)$ show little variation with solvent. In view of the wide variations observed with aliphatic mixtures it is reassuring to find some mixtures in which the simple expectation, the invariance of $G_1(D)$, is realized. Variations in $g(HD)$ due to kinetic effects are to be expected in these systems because of the aliphatic side chains in the solvents other than benzene.

Data on solutions of benzene-d_6 in aliphatic hydrocarbons are more difficult to interpret. The percentage of D_2 in the radiolytic gas is very small so that $G_1(D)$ can only be determined with low precision. $G(HD)$ is a markedly non-linear function of the concentration of the deutero compound, so $g(HD)$ can only be estimated from the limiting slope of the yield curve. Solutions of benzene-d_6 in cyclohexane, *n*-hexane, cyclopentane, isopentane, and *n*-octane have these points in common: firstly, the limiting value of $g(HD)$ is about 3

in all cases, showing a reactivity of benzene which is fully comparable to that of cyclohexane-d_{12}, and, secondly, $G_1(D) \geqslant G(D_2)$ for pure benzene-d_6. This last observation was first made by Patrick and Burton (11), who commented that it was apparently inconsistent with the amount of HD obtained from mixtures of benzene and benzene-d_6. It is likely that a solvent interaction is affecting the value of $G_1(D)$ (10).

THE MECHANISM OF THE INTERACTION

Any proposed mechanism must predict:

(1) changes in that yield of D_2 which is first order with respect to the deuterated hydrocarbon;

(2) the empirical relation $g(HD) = AG_1(D)+B$.

Let C_H and C_D represent the concentrations of these hydrocarbons and I_H and I_D the concentration of intermediates derived from them. I_H and I_D symbolize any ion, excited state, or molecular fragment derived from C_H and C_D.

The dominant terms in the rate equation describing the first-order D_2 yield cannot be of the form kC_D^2, kC_DI_D, or kI_D^2, since these will give a second-order dependence of $G(D_2)$ on C_D. A first-order dependence will be given by algebraic terms of the form kC_D, kC_DC_H, kI_DC_H, kC_DI_H, and kI_DI_H. The first term does not contain any explicit interaction with the solvent, and the second describes a reaction which would take place in the absence of radiation. The first two terms can therefore be discarded. Speculating on the reactions which would generate the last three rate expressions, we see that these would arise from

$$I_D + C_H \rightarrow D_2 + \ldots \quad [7]$$

$$C_D + I_H \rightarrow D_2 + \ldots \quad [8]$$

$$I_D + I_H \rightarrow D_2 + \ldots \quad . \quad [9]$$

Conventional free radical reactions, in particular H atom reactions, of the form of [7] and [8] provide paths for the formation of HD but not of D_2. Reaction [9] is implausible.

We have therefore to speculate on novel reactions of the forms of [7] and [8]. We present two possibilities: in the first the intermediates are unspecified excited states, in the second the intermediate is specifically identified as an ion.

An Excitation Transfer Mechanism

Writing the intermediates as excited states C_D^* and C_H^*, reaction [8] becomes

$$C_D + C_H^* \rightarrow C_D^* + \ldots \quad . \quad [10]$$

We follow an earlier suggestion (8) that C_D^* decomposes by two parallel routes:

$$C_D^* \xrightarrow{\alpha} D_2 + P \qquad C_D^* \xrightarrow{\beta} X_D + P \quad [11]$$

i.e., the first-order process giving D_2 and the second-order process giving HD have a common precursor. Algebraic treatment of steps [10] and [11] combined with the kinetic scheme of the section "The Kinetic Analysis" yields a relation of the form of equation [5]. This can be seen directly as follows:

The rates of the first- and second-order decompositions will be given by $\alpha k_{11}C_D^*$ and $\beta k_{11}C_D^*$. If α and β are constant and independent of the solvent, then $G(D_2)$ and $G(HD)$ will vary proportionately. We can write

$$g(HD) = k_3/k_1G_2(H)+G_2(D) = k_3/k_1G_2(H)+\beta/\alpha G_1(D).$$

Comparing with equation [5] we see $A = \beta/\alpha$, $B = k_3/k_1G_2(H)$. The solvent effect appears in the variation of $G_1(D)$, which is given by

$$G_1(D) = \alpha\left[G_D + \frac{k_{10}G_H C_H}{k_{12}+k_{10}C_D}\right], \qquad (C_H \gg C_D)$$

where G_D and G_H are the primary yields of C_D^* and C_H^*, and k_{12} is the sum of the rate constants of the concurrent processes:

$$C_H^* \begin{cases} \nearrow H_2 + P \\ \searrow X_H + P \end{cases} . \qquad [12]$$

At low concentrations of C_D the effective variable is k_{10}/k_{12}.

If this mechanism is correct and our identification of equation [5] is valid, this implies that the constant term is $k_3/k_1G_2(H)$. This does seem possible.

If an excitation transfer mechanism is operating then the magnitude of the interaction must be, in part, determined by the relative energies of the excited species involved. Now the order of the solvents in decreasing values of $G_1(D)$ (approximately the order of Table I) is roughly the order of increasing carbon number. Since the ionization potential of hydrocarbons decrease with increasing carbon number this correlation is qualitatively in agreement with the supposition of excitation transfer. However, the ionization potential is also a measure of the energy levels of excited states so this argument alone does not favor charged excited species over uncharged excited species. It would appear from these results that the net probability of excitation transfer increases as the difference between the energy levels of the solvent and detector molecule increases.

Taking this excitation transfer picture we note that $G_1(D)$ for C_6D_{12} in cyclohexane is greater than it is in methylcyclohexane. Methylcyclohexane is therefore an energy acceptor relative to cyclohexane. It follows that $G_1(D)$ for methylcyclohexane-d_{14} should be higher in cyclohexane than it is in methylcyclohexane and also higher than $G_1(D)$ for cyclohexane in methylcyclohexane. Both these differences are observed.

It is also possible that this effect is produced by subexcitation electrons. This is briefly discussed in the last section.

An Ion–Molecule Mechanism

Williams (12) has argued that ion–molecule reactions play a significant role in the radiolysis of liquid alkanes. The major point of Williams' paper is that ion–molecule reactions are allowed thermochemically.

The mechanism proposed by Williams for the formation of the dimer is

$$C_nH_{2n+2} + C_nH_{2n+2}^+ \rightarrow C_nH_{2n+3} + C_nH_{2n+1}^+ \qquad [13]$$

by either H atom or hydride ion transfer, followed by

$$C_nH_{2n+3} \rightarrow C_nH_{2n+1} + H_2$$

$$2C_nH_{2n+1} \rightarrow C_{2n}H_{4n+2}.$$

If this reaction is written for two hydrocarbons, one of them deuterated, the reaction path for H atom transfer is

$$C_nH_{2n+2}^+ + C_eD_{2e+2} \rightarrow C_nH_{2n+1}^+ + C_eD_{2e+2}H \text{ (H atom transfer).} \qquad [14]$$

Elimination of hydrogen from the $C_eD_{2e+2}H$ radical may take two paths:

$$C_eD_{2e+2}H \rightarrow HD + C_eD_{2e+1} \qquad [15a]$$

$$C_eD_{2e+2}H \rightarrow D_2 + C_eD_{2e}H \qquad [15b]$$

In reaction [15*b*] we have a process giving D_2 which will be first order with respect to the concentration of the deuterated hydrocarbon. The possibility of D_2 elimination rather than HD elimination depends on the extent to which the transferred H atom keeps its identity in the radical. This reaction also says that HD is formed by molecular elimination. Since $G(HD) \sim 10G(D_2)$ we have simply to assume that only 1 in 10 of the eliminations gives D_2. This is a relatively small amount of randomization compared with the statistical reaction in which D_2 would be greatly in excess since $(2e+2) \gg 1$.

The effect of solvent appears through the relative probabilities of reactions [14] and [15]. It can be shown that a scheme based on reactions [13], [14], and [15] can give relations of the form of our correlation equation [5].

This argument neglects contributions to the first-order hydrogen yield by the ionic molecular elimination

$$C_nH_{2n+2}^+ \rightarrow C_nH_{2n}^+ + H_2.$$

The yield of this reaction, in an isotopic experiment, could change with solvent due to preferential charge exchange. This is a mechanism which is formally equivalent to the first mechanism discussed in the first part of this section.

Possible Mechanisms of Excitation Transfer or Preferential Excitation

The formation of excited states by ionizing radiation has always raised the intriguing possibilities of energy transfer playing a dominant role in radiation-induced reactions. For energy transfer to be efficient the time-constant characteristic of the transfer process must be at most as long as the lifetime of the excited state. This often requires the energy transfer cross section to be appreciably greater than the gas-kinetic cross section.

One mechanism which permits the energy transfer cross sections to be large has been outlined by Lipsky and Burton (13) and Nosworthy, Magee, and Burton (14). In simple terms the idea is this: molecules in liquids are geometrically ordered over small distances and electronic excitation of one molecule may, to some extent, be delocalized and be more accurately described as a state of the ordered group of molecules. This delocalization will give the excitation a mobility and range greater than that expected for molecules with interaction and collision cross sections comparable to their gas-kinetic cross sections.

Again, while the chemical nature of the molecules has little effect on their initial probability of excitation it may affect the process in which the delocalized energy is focused onto one particular molecule prior to the molecular dissociation.

This hypothesis could be tested by examining the radiolysis of isotopic mixtures in the vapor phase: we are planning to do this.

It is also possible that these experiments reveal the effects of subexcitation electrons whose properties have been outlined by Platzman (15). Secondary electrons with energies greater than the minimum electronic excitation energy of the irradiated substance lose their energy rapidly: below this energy they lose their energy by relatively slow thermal processes. Another substance, with a lower electronic excitation energy will, however, act as an efficient sink for the energy of these 'subexcitation' electrons. Chemical effects resulting from this excitation of the second substance would be apparent at low concentrations ($\sim$1%) and would appear as a greater sensitivity to radiation than expected. It is clear that, in a qualitative sense, our observations follow this pattern: this model permits us to accept the observation that very small differences in excitation energy, as measured by the ionization potential, can have a large effect on the reactivity.

REFERENCES

1. J. P. Manion and M. Burton. J. Phys. Chem. **56**, 560 (1952).
2. G. R. Freeman. J. Chem. Phys. **33**, 71 (1960).
3. J. A. Stone and P. J. Dyne. Radiation Research. In Press.
4. S. Ciborowski, N. Colebourne, E. Collinson, and F. S. Dainton. Trans. Faraday Soc. **57**, 1123 (1961).
5. T. J. Hardwick. J. Phys. Chem. **65**, 101 (1961).
6. R. B. Ingalls. J. Phys. Chem. **65**, 1605 (1961).
7. P. J. Dyne and W. M. Jenkinson. Can. J. Chem. **38**, 539 (1960).
8. P. J. Dyne and W. M. Jenkinson. Can. J. Chem. **39**, 2163 (1961).
9. G. A. Muccini and R. H. Schuler. J. Phys. Chem. **64**, 1436 (1960).
10. P. J. Dyne, W. M. Jenkinson, and J. Denhartog. A.E.C.L. Rept. CRC-1066. December, 1961.
11. M. Burton and W. N. Patrick. J. Phys. Chem. **58**, 421 (1954).
12. T. F. Williams. Trans. Faraday Soc. **57**, 755 (1961).
13. S. Lipsky and M. Burton. J. Chem. Phys. **31**, 1221 (1959).
14. J. M. Nosworthy, J. L. Magee, and M. Burton. J. Chem. Phys. **34**, 83 (1961).
15. R. L. Platzman. Radiation Research, **2**, 1 (1955).

SYNTHÈSES DE DÉRIVÉS DE LA LYSINE[1]

LOUIS-MARIE BABINEAU ET LOUIS BERLINGUET
Département de Biochimie, Faculté de Médecine, Université Laval, Québec, Qué.

Reçu le 26 mars 1962

ABSTRACT

New N-ε-substituted lysines have been synthetized as follows: by condensing 5-δ-bromobutylhydantoin with different primary amines, 5-δ-alkylaminobutylhydantoins were obtained, the alkaline hydrolysis of which gave the corresponding N-ε-substituted lysines. N-α-Substituted hexahomoserines have also been prepared by acid hydrolysis of the reaction product between α,ε-dihydroxycaproic nitrile and primary amines. 5-Amino-5-carboxypentane sulphonamide has been prepared in the following way: 5-δ-bromobutylhydantoin was reacted with thiourea, and the resulting isothiouronium salt was oxidized with chlorine. Gaseous ammonia was then bubbled through an ethereal suspension of the 5-δ-chlorosulphonyl butylhydantoin and the resulting sulphonamide was hydrolyzed under pressure with barium hydroxide. 5-Amino-5-carboxypentane sulphonamide was then isolated and crystallized.

À l'heure actuelle, le métabolisme de la lysine est passablement bien connu même si l'on n'a pu encore démontrer de façon certaine la présence de quelques intermédiaires dont on a postulé l'existence (1). Cependant, on est loin d'avoir précisé tous les aspects de ce métabolisme. Ainsi, on rencontre encore peu d'études biochimiques des dérivés de cet acide aminé: on n'a en effet synthétisé jusqu'à présent qu'un petit nombre d'analogues de la lysine. Au cours de ce travail, nous avons synthétisé plusieurs nouveaux dérivés de la lysine. Nous en avons fait une étude biologique préliminaire et nous publierons ailleurs les résultats de cette étude.

On peut classifier en deux groupes les analogues de la lysine déjà existants: les uns sont porteurs de radicaux alkylés situés sur l'un ou l'autre atome d'azote ou sur les deux à la fois; les autres sont des dérivés de la lysine où l'on a greffé des chaînes latérales ou encore des composés où on a remplacé l'un ou l'autre des groupements aminés de la lysine par un radical quelconque. Nous avons synthétisé quelques représentants de ces deux groupes: les acides N-ε-méthyl-, N-ε-éthyl-, N-ε-cyclohexyl- et N-ε-pipéridyl-lysine et les acides éthylamino-2 hydroxy-6 et cyclohexylamino-2 hydroxy-6 caproïques. Enfin, au cours de ce travail, nous avons préparé un nouvel acide aminé porteur d'un groupement sulfonamide en ε: l'acide amino-5 carboxy-5 pentanesulfonamide.

Voici maintenant les modalités de notre synthèse de dérivés de la lysine porteurs de groupements alkylés sur l'azote en ε. La condensation de la δ-bromobutylhydantoïne-5 (I) avec différentes amines primaires donne une δ-alkylaminobutylhydantoïne-5 (II). L'hydrolyse de cette hydantoïne soit en milieu alcalin et sous pression, soit en milieu acide donne un acide alkylamino-6 amino-2 caproïque (III). Les rendements de la condensation sont de l'ordre de 45%; par contre, les rendements de l'hydrolyse de l'hydantoïne en acide aminé sont meilleurs (75%). À l'exception de la N-ε-méthyl-lysine et de la N-ε-pipéridyl-lysine, les produits obtenus sont relativement faciles à purifier. Le schéma suivant résume le processus suivi:

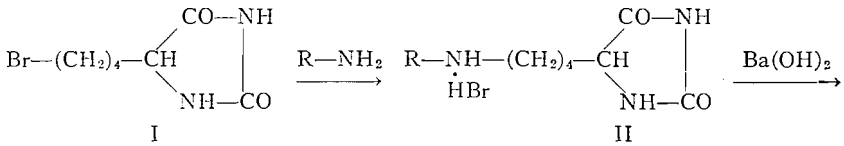

I II

[1]*Présenté en partie au congrès de l'ACFAS à Montréal en novembre 1959.*

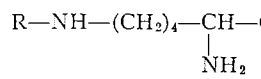

III

Enger et Steib (2), Neuberger et Sanger (3) et Poduska (4) ont déjà synthétisé la N-ε-méthyl-lysine mais en utilisant comme produit de départ l'acide ε-aminocaproïque qu'ils ont méthylé en ε. Pour la synthèse de dérivés N-α-alkylés de la lysine, d'autres auteurs (5) utilisent comme produit de départ la lysine ou l'acide ε-aminocaproïque. Dans ce dernier cas, ils procèdent de la façon suivante: la fonction ε-aminée étant protégée, ils greffent sur le carbone alpha de la molécule une fonction aminée puis remplacent cette dernière fonction aminée par un halogène et enfin, l'halogène par l'amine choisie.

Nous avons voulu obtenir ces dérivés par synthèse totale à partir de produits facilement accessibles comme le dihydropyranne. Gaudry a déjà publié (6) une synthèse de la lysine à partir de cette substance. L'hydrolyse acide du dihydropyranne donne la δ-hydroxy-valéraldéhyde dont le traitement par la méthode classique de Bucherer et Lieb (7) conduit à la formation de la δ-hydroxybutyl-5 hydantoïne et finalement à l'acide amino-2 hydroxy-6 caproïque. En remplaçant dans cette synthèse l'ammoniac par des amines primaires, nous espérions obtenir des dérivés de l'hexahomosérine à azote substitué en position alpha. Il était toutefois à prévoir que le traitement au carbonate d'ammonium des aminonitriles substitués entraînerait un remplacement du groupe alkylé par l'ammoniac. En effet, on avait déjà observé (8) que le traitement au carbonate d'ammonium de l'aminonitrile du cyclopentane donnait la spirohydantoïne non substituée sur l'azote. De plus, on avait noté que l'hydrolyse acide à chaud dissociait l'aminonitrile pour redonner la cyclopentanone de départ et non l'acide aminé attendu.

Dans notre cas, nous avons réussi à obtenir, à partir de la δ-hydroxyvaléraldéhyde et de l'éthylamine ou de la cyclohexylamine, deux alkylaminonitriles que nous avons isolés et dont l'hydrolyse par l'acide sulfurique concentré à froid a finalement donné deux acides alkylamino-2 hydroxy-6 caproïques.

Pour transformer ces deux acides hydroxylés en dérivés de la lysine, il ne restait plus qu'à protéger le groupement alpha aminé soit par acylation, soit par la formation d'une hydantoïne substituée et qu'à remplacer l'hydroxyle terminal par le brome. Une amination de l'hydantoïne ou du dérivé acylé ainsi préparé, suivie d'une hydrolyse, aurait alors donné l'acide particulier recherché. Nous n'avons pu, cependant, obtenir de cette façon des dérivés alkylamino-2 de la lysine. Il a été impossible, en effet, d'isoler une hydantoïne cristalline par traitement à l'isocyanate de phényle ou au cyanate de potassium du nitrile cyclohexylamino-2 hydroxy-6 caproïque.

Au cours de ces recherches, nous avons préparé un nouvel acide α-aminé contenant un groupement sulfonamide en position 6. Reisner (9) a déjà synthétisé plusieurs acides γ-sulfonamide α-aminés qui sont des analogues de l'acide glutamique. L'un de ces acides, l'amino-3 carboxy-3 propane sulfonamide, est un bon inhibiteur in vitro de la croissance de *Escherichia coli* T_2 et supprime la multiplication du coliphage T_2. Comme il n'existe aucun analogue de la lysine à groupement ε-sulfonamide, nous avons pensé en préparer un. Nous avons réussi de la façon suivante la synthèse de l'acide ε-sulfonamide α-amino-caproïque ou amino-5 carboxy-5 pentane sulfonamide.

On transforme d'abord la δ-bromobutylhydantoïne-5 (I) en un sel d'isothio-uronium (IV) au cours d'une réaction presque quantitative et d'exécution facile. On peut préparer ensuite le chlorure de sulfonyle de la butylhydantoïne-5 (VI) de deux manières différentes:

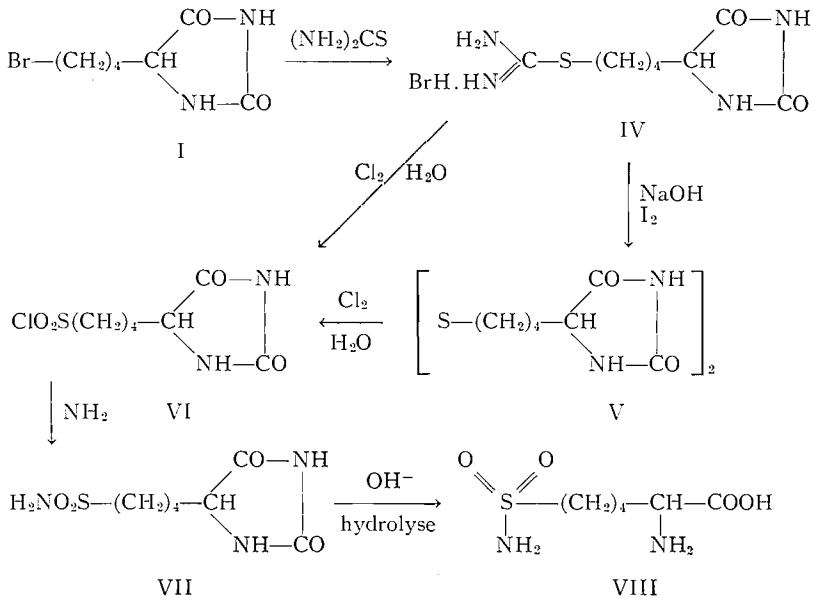

(*a*) On soumet le sel d'isothio-uronium (IV) à une hydrolyse alcaline modérée que l'on fait suivre d'une oxydation à l'iode. On obtient ainsi le dérivé dithio (V) que l'on traite au chlore après l'avoir suspendu dans l'eau.

(*b*) On dissout le sel d'isothio-uronium (IV) dans l'eau et l'on traite immédiatement la solution aqueuse par le chlore. On obtient aussitôt le chlorure de sulfonyle de la butylhydantoïne-5 (VI) avec un rendement beaucoup plus élevé dans ce cas que dans le premier. Après avoir préparé la sulfonamide (VII) par traitement à l'ammoniac gazeux d'une suspension éthérée du chlorure de sulfonyle (VI), on obtient facilement l'acide aminé recherché (VIII) par une hydrolyse alcaline et sous pression de la sulfonamidebutylhydantoïne-5 (VII). Le rendement final en acide ϵ-sulfonamide α-aminocaproïque est de 22.5% ou de 35.8% selon que l'on utilise ou non la bis(thio-δ-butylhydantoïne-5) (V), le rendement étant calculé à partir de la δ-bromobutylhydantoïne-5.

PARTIE EXPÉRIMENTALE

δ-Bromobutylhydantoïne-5 (I)

On prépare ce produit selon la méthode décrite par Gaudry (6). À partir de 0.2 mole (34.4 g) de δ-hydroxybutylhydantoïne-5, on obtient finalement, après recristallisation, 47 g de δ-bromobutylhydantoïne-5. Rendement: 70%; p.f. 126–127° (lit. 129–131°) (6). Anal. Calc. pour $C_7H_{11}O_2N_2Br$: N, 11.97%. Obtenu: N, 11.81%.

Bromhydrates de δ-alkylaminobutylhydantoïnes-5 (II)

Premier cas: On dissout 0.1 mole (23.5 g) de δ-bromobutylhydantoïne-5 dans un excès de méthylamine à 30% ou d'éthylamine à 70%.

Deuxième cas: On dissout la même quantité de δ-bromobutylhydantoïne-5 dans 55 ml d'éthanol chaud et on ajoute, lentement, 0.2 mole de cyclohexylamine ou 0.3 mole de pipéridine. La réaction est passablement exothermique avec la méthyl- ou l'éthyl-amine, légèrement exothermique avec la cyclohexylamine et la pipéridine. On laisse reposer le mélange réactionnel à la température ambiante pendant 2 jours. Des cristaux n'apparaissent qu'avec la cyclohexylamine. On se débarrasse du solvant et de l'excès d'amine par une évaporation à sec du mélange, sous vide et à basse température. Dans le cas de la réaction avec la pipéridine, il faut dissoudre le résidu dans l'eau et l'extraire plusieurs fois à l'éther pour le débarrasser de toute trace d'amine.

On dissout l'hydantoïne substituée dans l'éthanol absolu à l'exception du bromhydrate de la δ-méthylaminobutylhydantoïne-5 que l'on dissout dans le méthanol. On laisse la solution alcoolique plusieurs jours

à la glacière. On filtre des cristaux blancs que l'on recristallise de l'éthanol absolu ou du méthanol (cas de la δ-méthylaminobutylhydantoïne-5).

On trouvera au Tableau I la liste des δ-alkylaminobutylhydantoïnes-5 préparées.

TABLEAU I

δ-Alkylaminobutylhydantoïnes-5

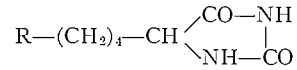

R	Rendement, %	P.f., °C	N, % Trouvé	N, % Théorie	Br, % Trouvé	Br, % Théorie
HBr.CH_3—NH—	45	141–142	15.82	15.79	—	30.03
HBr.C_2H_5—NH—	63	179–181	14.85	15.00	29.32	28.52
HBr.C_6H_{11}—NH—	47	190–192	12.36	12.53	24.10	23.84
HBr.  N—	44	185–187	11.96	13.12	25.00	24.95

Bromhydrates d'acides amino-2 alkylamino-6 caproïques

On hydrolyse ces hydantoïnes au moyen de $Ba(OH)_2.8H_2O$ en solution aqueuse, sous pression, à 170° pendant une demi-heure (6), ou encore, au moyen de HBr à 48%, à reflux pendant 15 heures. Les rendements de l'hydrolyse acide sont toutefois très inférieurs à ceux de l'hydrolyse alcaline. On recristallise de l'eau et de l'alcool les divers bromhydrates de la lysine à l'exception du bromhydrate de la N-ε-cyclohexyl-lysine qui recristallise de l'alcool absolu. On trouvera au Tableau II la liste des dérivés de la lysine ainsi préparés.

TABLEAU II

Acides amino-2 alkylamino-6 caproïques

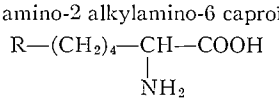

R	Rendement, %	P.f., °C	N, % Trouvé	N, % Théorie	Br, % Trouvé	Br, % Théorie
HBr.CH_3—NH—	74	234–235	10.71	11.61	33.14	32.00
HBr.C_2H_5—NH—	82	215–217	10.93	10.97	31.05	31.32
	40*					
HBr.C_6H_{11}—NH—	65	249–251	8.96	9.03	25.15	25.76
HBr.  N—	77	223–225	9.30	9.49	26.83	27.06

*Obtenu par hydrolyse acide.

Ces acides amino-2 alkylamino-6 caproïques migrent vers la cathode à l'électrophorèse sur papier à pH 8.6 et donnent une coloration violette à la ninhydrine.

Phénylcarbamates des acides amino-2 alkylamino-6 caproïques

On a caractérisé les divers acides amino-2 alkylamino-6 caproïques en en préparant les phénylcarbamates par la méthode habituelle (Tableau III).

Alkylamino-2 hydroxy-5 capronitriles

(a) Ethylamino-2 hydroxy-5 capronitrile

On dissout 0.77 mole (100 g) de dihydroxy-2,5 capronitrile dans 2 moles d'éthylamine à 70%. On abandonne le mélange pendant 3 jours à la température ambiante. On évapore l'excès d'amine sous vide et à basse température. On dissout le résidu dans l'éther anhydre et l'on extrait la solution éthérée au moyen de l'éther de pétrole bouillant. On refroidit cette dernière solution et l'on filtre des cristaux de nitrile éthylamino-2 hydroxy-5 caproïque. P.f. 44–45°. Rendement: 36.5 g (30%). Anal. Calc. pour $C_8H_{16}ON_2$: N, 17.93%. Obtenu: N, 17.58%. L'acétylation de ce produit a donné une huile que nous n'avons pas caractérisée.

(b) Cyclohexylamino-2 hydroxy-5 capronitrile

On laisse tomber lentement 1.6 moles de cyclohexylamine dans 0.8 mole (104 g) de dihydroxy-2,5 capronitrile. On note un fort dégagement de chaleur et le produit de la réaction ne tarde pas à cristalliser. On le

TABLEAU III

Phénylcarbamates des acides amino-2 alkylamino-6 caproïques

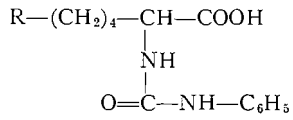

R	P.f., °C	N, % Trouvé	N, % Théorie
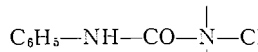	115–125	13.63	14.06
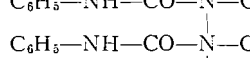	163–165	13.47	13.58
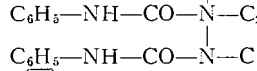	127–128	11.96	12.01
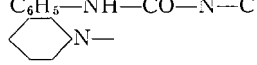	237–240	12.71	12.60

filtre et on le recristallise de l'alcool. P.f. 103–105°. Rendement: 122.5 g (73%). Anal. Calc. pour $C_{12}H_{22}ON_2$: N, 13.32%. Obtenu: N, 13.32%. L'acétylation de ce produit n'a pas donné de dérivé cristallin.

Acides alkylamino-2 hydroxy-6 caproïques

On hydrolyse pendant 15 heures 0.1 mole de l'un ou de l'autre nitrile au moyen d'un excès d'acide chlorhydrique concentré. On évapore à sec et l'on chasse toute trace d'eau. On dissout le résidu dans l'alcool anhydre, l'on filtre le NH_4Cl formé et l'on ajoute un excès de pyridine. On porte à la glacière et l'on obtient dans les deux cas un précipité amorphe. On recristallise de l'acétone l'acide éthylamino-2 hydroxy-6 caproïque. P.f. 184–185°. Rendement: 7 g (40%). Anal. Calc. pour $C_8H_{17}O_3N$: N, 7.99%. Obtenu: N, 7.30%. Quant à l'acide cyclohexylamino-2 hydroxy-6 caproïque, on peut le purifier en en préparant le chlorhydrate que l'on traite à nouveau par la pyridine. P.f. 210–211°. Rendement: 16.8 g (73%). Anal. Calc. pour $C_{12}H_{23}O_3N$: N, 6.11%. Obtenu: N, 5.87%.

Le traitement de ces deux acides aminés à l'isocyanate de phényle ne donne que des huilles non cristallisables.

Bromhydrate de la δ-isothio-uronium butylhydantoïne-5 (IV)

On prépare ce dérivé en modifiant comme suit la technique de Snyder et Cannon (10). On dissout dans un minimum d'alcool absolu et bouillant 23.5 g (0.1 mole) de δ-bromobutylhydantoïne-5 et 7.6 g (0.1 mole) de thiourée. On fait bouillir le tout à reflux au bain-marie pendant 21 heures. Le dérivé cristallise dans le ballon. On porte à la glacière pour quelques heures. On filtre des cristaux blancs qu'on lave à l'acétone. Les cristaux, très solubles dans l'eau et le méthanol, fondent à 176–177°. Rendement: 28.6 g (92%). Anal. Calc. pour $C_8H_{15}O_2N_4BrS$: N, 18.00%. Obtenu: N, 18.03%.

Bis(thio-δ-butylhydantoïne-5) (V)

On dissout 73 g (0.23 mole) d'isothio-uronium de la butylhydantoïne-5 dans un minimum d'eau bouillante et on y ajoute, lentement, 100 ml d'une solution de soude à 18.8%. On agite le tout pendant une heure. On oxyde (11) ensuite le produit par addition d'une solution d'iode ioduré (0.23 mole) jusqu'à apparition d'une coloration brune permanente. On filtre le précipité et on le dissout dans 250 ml de cellosolve bouillant. On purifie la solution par addition de noir animal et on lui ajoute 300 ml d'eau. On porte à la glacière. On obtient 28.0 g (63.0%) de cristaux blancs fondant à 178–180°. Anal. Calc. pour $C_{14}H_{27}O_4N_4S_2$: N, 14.96%. Obtenu: N, 14.64%.

δ-Chlorosulfonylbutylhydantoïne-5 (VI)

(*a*) On réduit 26.8 g (0.07 mole) de bis(thio-δ-butylhydantoïne-5) en une poudre fine que l'on suspend ensuite dans 100 ml d'eau. On place le ballon dans un bain de glace et l'on agite la suspension. On fait passer un courant de chlore pendant 80 minutes. Une masse solide se forme. On décante, on dissout la masse dans l'acétate d'éthyle et l'on traite l'eau cinq fois avec ce même solvant. On sèche l'acétate d'éthyle avec du sulfate de sodium anhydre, on le filtre et on le distille sous vide. On dissout le résidu dans l'acétate d'éthyle, on ajoute de l'éther de pétrole et on place le tout dans la glacière. On filtre 25.0 g (69%) de cristaux blancs fondant à 128–130°. Anal. Calc. pour $C_7H_{11}O_4SCl$: N, 11.00%. Obtenu: N, 10.82%.

(*b*) On prépare la δ-chlorosulfonylbutylhydantoïne-5 en traitant directement par le chlore, après une élimination préliminaire du brome sous forme de bromure d'argent, le bromhydrate de la δ-isothio-uronium butylhydantoïne-5 (12). En partant de 31.0 g (0.1 mole) du sel d'isothio-uronium de la butylhydantoïne-5,

on obtient 18.0 g (72%) de cristaux blancs fondant à 123–125°. Anal. Calc. pour $C_7H_{11}O_4SCl$: N, 11.00%. Obtenu: N, 11.30%.

δ-Sulfonamidebutylhydantoïne-5 (VII)

On prépare ce dérivé selon la méthode décrite par Reisner (9). On utilise 24.0 g (0.094 mole) de δ-chlorosulfonylbutylhydantoïne-5 et l'on obtient finalement, après recristallisation, 14.0 g (63%) de δ-sulfonamidebutylhydantoïne-5 sous forme de cristaux blancs fondant à 159–160°. Anal. Calc. pour $C_7H_{13}O_4N_3S$: N, 17.88%. Obtenu: N, 17.93%.

Acide DL-*amino-5 carboxy-5 pentane sulfonamide (VIII)*

L'hydrolyse alcaline, suivant la méthode de Gaudry (6), de 8.2 g (0.035 mole) de δ-sulfonamidebutylhydantoïne-5 a donné 6.5 g (89%) de cristaux blancs d'acide DL-amino-5 carboxy-5 pentane sulfonamide fondant à 243–245°. Anal. Calc. pour $C_6H_{14}O_4N_2S$: N, 13.33%. Obtenu: N, 13.45%.

Le traitement de ce nouvel acide aminé par l'isocyanate de phényle a donné un dérivé non cristallin qui se transforme par une hydrolyse acide avec HCl 6 *N* en une δ-sulfonamidebutyl-[(phényl-3)hydantoïne-5] recristallisable de l'alcool. P.f. 146–148°. Anal. Calc. pour $C_{13}H_{17}N_3O_4S$: N, 13.46%. Obtenu: N, 13.26%.

REMERCIEMENTS

Les auteurs remercient Monsieur Benoit Mercier de sa précieuse collaboration technique à ce travail. Ils remercient également le Conseil National de Recherches Médicales du Canada d'y avoir participé par l'octroi de subventions (octroi MA-831).

BIBLIOGRAPHIE

1. E. WORK. *Dans* A symposium on amino acid metabolism. W. D. McElroy et B. Glass (*Éditeurs*). The Johns Hopkins Press, Baltimore. 1955. pp. 464–465.
2. R. ENGER et H. STEIB. Hoppe-Seyler's Z. physiol. Chem. **191**, 97 (1930).
3. A. NEUBERGER et F. SANGER. Biochem. J. **38**, 125 (1944).
4. K. PODUSKA. Chem. listy, **52**, 153 (1958); Chem. Abstr. **52**, 16235*i* (1958).
5. A. NEUBERGER et F. SANGER. Biochem. J. **37**, 515 (1943).
6. R. GAUDRY. Can. J. Research, B, **26**, 387 (1948).
7. H. T. BUCHERER et V. A. LIEB. J. Prakt. Chem. **141**, 5 (1934).
8. L. NICOLE et L. BERLINGUET. Résultats non publiés.
9. D. B. REISNER. J. Am. Chem. Soc. **78**, 5102 (1956).
10. H. R. SNYDER et G. W. CANNON. J. Am. Chem. Soc. **66**, 511 (1944).
11. R. GAUDRY, L. BERLINGUET, R. GINGRAS et F. MARTEL. Rev. can. biol. **11**, 132 (1952).
12. T. B. JOHNSON et J. W. SPRAGUE. J. Am. Chem. Soc. **58**, 1348 (1936).

TERPENOIDS

II. CEANOTHENIC ACID: A C_{29} A-NORLUPANE DERIVATIVE

P. DE MAYO AND A. N. STARRATT
Department of Chemistry, University of Western Ontario, London, Ontario

Received April 9, 1962

ABSTRACT

Extraction of *Ceanothus americanus* (Jersey Tea) has afforded a new pentacyclic triterpenoid of the empirical formula $C_{29}H_{42}O_4$. It is a dicarboxylic acid containing two ethylenic linkages. The environment of one carboxyl group and one ethylenic linkage has been shown by diagnostic transformations characteristic of ring E of the lupeol–betulin series. The other ethylenic linkage has been shown to be present in a contracted ring A from which one carbon atom has been lost. The position of the second carboxyl group has been established by introduction of the 11-oxo-12-ene system, when monodecarboxylation occurred under mild conditions. This and other evidence establishes ceanothenic acid to be A-norlupa-1,22-diene-14,17-dicarboxylic acid.

Investigations of the triterpenoid constituents of *Ceanothus americanus* (Jersey Tea) were first initiated by Julian, Pikl, and Dawson (1), who reported the presence of ceanothic acid, a hydroxy dicarboxylic acid. Subsequent investigations (2) established the structure and stereochemistry of ceanothic acid to be as in (I) and have also established its identity with emmolic acid (3–5).

During the isolation of ceanothic acid a number of simple aromatic acids were isolated (see Experimental) together with the triterpenoids lupeol, betulin, and betulinic acid (II, R = CH_3, R = CH_2OH, and R = COOH respectively). In addition there was obtained a new acid, ceanothenic acid.[1]

Ceanothenic acid analyzed for $C_{29}H_{42}O_4$ or $C_{30}H_{44}O_4$, and was a dicarboxylic acid. It gave a non-crystalline dimethyl ester, reconverted to the acid on lithium iodide halolysis (6), and gave a tetrahydro acid on hydrogenation over platinum oxide. This, in turn, gave a crystalline dimethyl ester. Both the tetrahydro acid and its ester were optically transparent in the ultraviolet in the region 195–220 mμ and gave no color with tetranitromethane. No points of unsaturation other than the carboxyl functions therefore remained in the molecule: ceanothenic acid thus contained two ethylenic linkages and was pentacarbocyclic. The tetrahydro acid was converted into the acid chloride and thence, with lithium aluminum hydride, to the saturated diol characterized as the diacetate and, by oxidation, as the dialdehyde. The dicarboxylic acid recovered by oxidation of the diol had properties identical with those of the starting material, thus confirming its homogeneity.

In the infrared, ceanothenic acid exhibited two bands, at 893 and 753 cm^{-1} (nujol mull). The former band was in the position expected for the methylene out-of-plane deformation in an isopropenyl group. This assignment was confirmed by the obtention of formaldehyde on ozonolysis of ceanothenic acid and by the presence, in the n.m.r. spectrum of dimethyl ceanothenate (Fig. 1(*b*)), of bands at τ 5.29 and 5.41 (two multiplets, 2 H, $\diagdown$C=CH_2[2]) and 8.34 (singlet, 3 H) (7, p. 57) for the methylene and methyl moieties of the isopropenyl group.

[1]*The isolation of this acid was reported in the experimental section of Part I of this series. An improved isolation procedure is here presented.*

[2]*In an earlier paper (2) this was inadvertently referred to as a doublet. We wish to thank Dr. J. B. Stothers and a Referee for drawing this to our attention.*

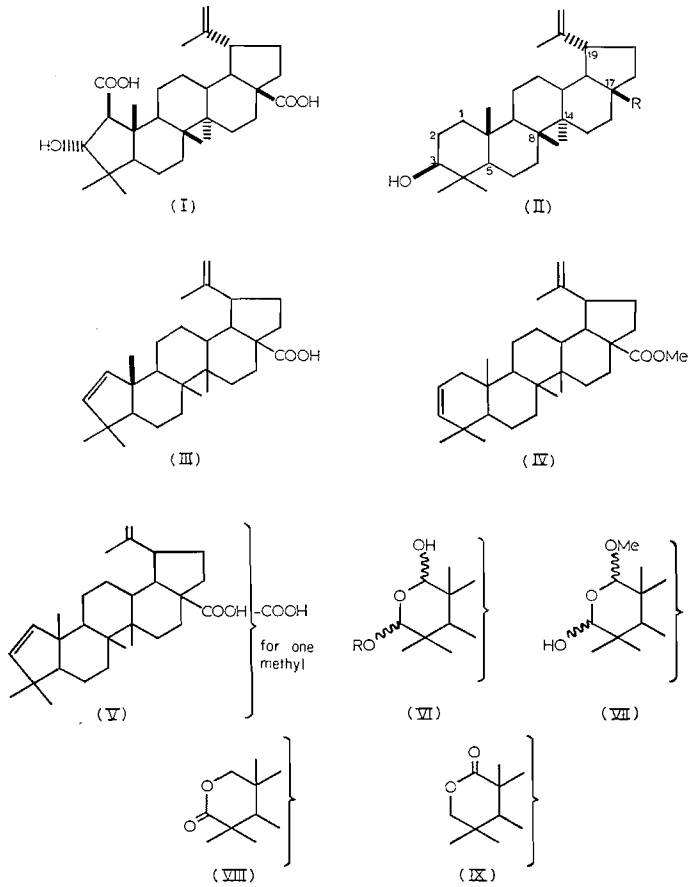

The band at 753 cm^{-1} was suggestive of a cis disubstituted ethylenic linkage. In the n.m.r. spectrum there were two doublets, at τ 4.66 and 4.11 ($J \sim 5.7$) (2 H), in accord with the presence of vicinal vinyl hydrogen atoms. Further, the similarity of this pattern to that obtained from the substance (III)—derived from ceanothenic acid (see Fig. 1(*a*)) by dehydration–decarboxylation—was indicative of a like environment for the double bond in ceanothenic acid. Methyl anhydrobetulinate (IV), in contrast, showed no such pattern (Fig. 1(*c*)).

If such were the case it seemed plausible that the extruded ring A carbon in ceanothic acid (I) had been eliminated in ceanothenic acid. This should, therefore, contain only 29 carbon atoms. The molecular weight, determined mass spectroscopically on dimethyl tetrahydroceanothenate, confirmed the hypothesis.[3] At this point it was possible to consider the part structure (V) for ceanothenic acid. Chemical evidence, in confirmation, was then sought.

Methyl ceanothenate, on treatment with osmium tetroxide gave the expected tetrol. Cleavage with periodic acid in methanolic solution, with the appropriate oxygen uptake, gave, however, a crystalline product differing from the expected analysis by the elements of methanol. Methanol of crystallization could be discounted since the process of purification involved chromatography and subsequent crystallization from ether and light

[3]*We are much indebted to Dr. K. Biemann (M.I.T.) for this determination.*

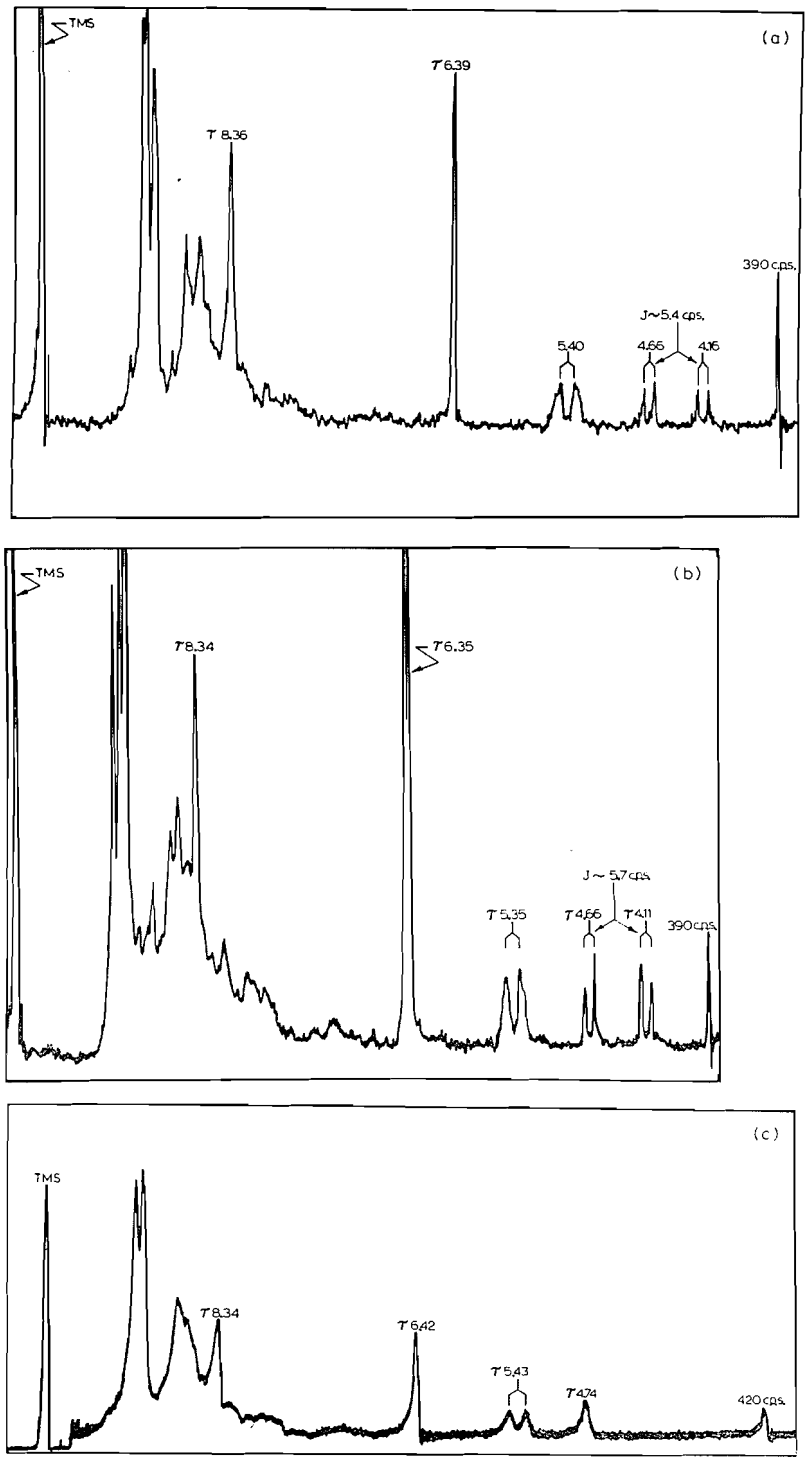

FIG. 1. N.M.R. spectra of (*a*) methyl decarboxyanhydroceanothate, (*b*) dimethyl ceanothenate, and (*c*) m ethyl anhydrobetulinate.

petroleum. Finally, any aldehydic structures could be rejected, since no low-field bands attributable to such hydrogen (7, p. 62) could be discerned in the n.m.r. spectrum.

The presence of the expected acetyl group was indicated by a singlet (3 H) at τ 7.84. A singlet (3 H) at τ 6.57 confirmed the presence of a methoxyl function. In addition there was, clearly discernible, bands (1 H each) at τ 5.84 and 5.43 in addition to the two methyl esters, which, at such low field, were required to be attributed to the environment of the moiety of the molecule under discussion. This pattern was compatible with expectation for the acetal and hemiacetal hydrogens of structures (VI; R = Me) or (VII) and this interpretation was confirmed, as follows.

Under the acidic conditions of 2,4-dinitrophenylhydrazone formation, the hemiacetal, being in equilibrium with the aldehyde, would be expected to react, and, in the event, the cleavage product gave the predicted tris-2,4-dinitrophenylhydrazone. Cleavage of the tetrol was then carried out in aqueous dioxane. The product, which was, however, not crystalline, showed bands at τ 0.85 and 0.73 compatible with aldehydes bearing no α hydrogen atoms. Since the infrared spectrum exhibited hydroxyl absorption at 3360 cm^{-1} it appeared possible that the product might be a mixture of aldehyde and hemiacetal (VI, R = H). Treatment with 2,4-dinitrophenylhydrazine in acid gave the same tris-2,4-dinitrophenylhydrazone obtained previously.

When the aqueous dioxane cleavage product was heated in aqueous methanol containing 2% of sodium hydroxide for 30 minutes the resultant product was almost entirely acidic. Acidification of the alkaline solution, however, gave material which was neutral. Such behavior and spectral properties (ν_{max} 1708 cm^{-1}) are compatible with those of a δ-lactone such as (VIII) or (IX). In agreement there was present, in the n.m.r. spectrum ($\tau \sim 5.85$, $J \sim 11$ c.p.s.), one half of the non-equivalence quartet expected for the lactonic methylene group, the other half being obscured by the ester methoxyl groups. The same substance was obtained by allowing the cleavage product to stand at room temperature with methanolic sodium methoxide. The formation of the lactone, an internal Cannizzaro reaction, has analogy in the chemistry of the monoterpenoid iridodial (8).

The above transformations establish the nature of ring A and, further, exclude from consideration positions 23, 24, and 25 for the unplaced carboxyl group. Had it been present at any one of these points a very facile deformylation would have been expected in the cleavage product, in view of its nature as an α-formyl ester, under the conditions of the Cannizzaro reaction: none was observed. Two positions, C_8 and C_{14}, remained.

A characteristic and diagnostic test for the terminal ring E in the lupeol–betulin series is the acid-catalyzed expansion of this ring with, in the case of substances having a carboxyl at C_{17}, subsequent lactonization (9). When a solution of ceanothenic acid was refluxed in 98% formic acid or in hydrochloric–acetic acids the product recovered was neutral, both carboxyl groups evidently having been involved in lactonization. The band at 893 cm^{-1}, indicative of the isopropenyl methylene, was no longer present in the infrared spectrum as was the allylic methyl in the n.m.r. spectrum, observations expected for the ring E expansions. In an attempt to achieve this transformation whilst leaving ring A untouched, dimethyl ceanothenate was dissolved in benzene, and a solution of sulphuric acid in acetic acid added (9). After 5 days at room temperature the same dilactone was obtained.

The part structure (V) now having been substantiated, it was required to place the remaining carboxyl group. Since the formation of the dilactone involved a rearrangement both in ring E and ring A no information could be forthcoming from it. The simplest approach appeared to be the introduction into ring C of a functional group so as to

effect a selective decarboxylation. A route to the introduction of such a group lay in the well-known conversion of substances of the lupeol–betulin class into that of β-amyrin (9), but a prerequisite for such an approach was the removal of the unsaturation from ring A.

Attempted selective hydrogenation, bromination, and peracid oxidation were unavailing in attempts to discriminate between the two ethylenic linkages. Recourse to diimide (11) as the reducing agent was successful and, in fact, under the conditions of the reaction the isopropenyl group was entirely resistant. A brief survey of other ethylenic systems showed that, whilst norbornylene was reduced to norbornane, lupeol, α-amyrin benzoate, cholesterol, and cholest-2-ene were largely unaffected.

With dihydroceanothenic acid (X) available, the β-amyrin conversion now appeared feasible. Treatment with formic acid gave the expected acid lactone (XI), characterized as the methyl ester, which was reduced to the diol (XII) with lithium aluminum hydride. It was intended to dehydrate the secondary alcohol (10) and oxidize further with selenium dioxide (12), but preliminary tests indicated that these later steps proceeded in too poor yield for the quantity of material available.

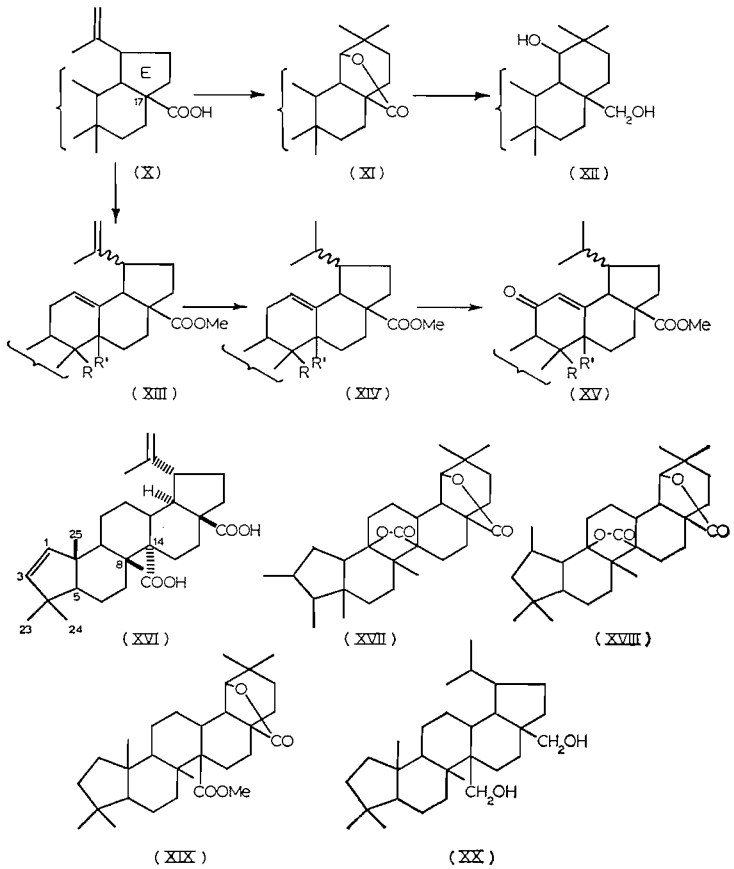

At this point the recently reported oxidation of compounds of the lupeol–betulin class with mercuric acetate became available (13). With this reagent the direct introduction of a Δ^{12} ethylenic linkage has been shown to be possible. Oxidation of methyl

dihydroceanothate with mercuric acetate, in the manner described (13), gave the dehydro compound (XIII; R or R′ = COOMe, R′ or R = Me). Hydrogenation over platinum oxide saturated the isopropenyl group, giving (XIV; R or R′ = COOMe, R′ or R = Me) characterized as the acid by lithium iodide halolysis (6). Although evolving gas at the melting point, as to be expected of a β,γ-unsaturated acid, the product of this decarboxylation could not be obtained crystalline. Oxidation of (XIV) with chromic acid in acetic acid gave the desired 11-ketone (XV; R or R′ = COOMe, R′ or R = Me).

The keto diester, unlike its precursor (XIV) and in keeping with its nature as a vinylogous β-ketoester, was readily hydrolyzed by 5% potassium hydroxide to a non-crystalline dicarboxylic acid monoester (14). This decarboxylated at 145° to give the crystalline monoester (XV; R = Me, R′ = H). The carboxyl unallocated in (V) must therefore be placed at C_{14}. Any possibility that the ethylenic linkage might have moved β,γ into the C_{13}—C_{18} position and that the C_{17} carboxyl had been lost could be discounted since the monoester retained its α,β-unsaturated ketone. Ceanothenic acid is, therefore, to be represented as (XVI), a disposition of carboxyl groups paralleled in the α-amyrin series by quinovic acid (15).

Although no direct evidence is available, it seems possible that the configuration of the isopropenyl group in (XIII)–(XV) may be opposite that (α) in lupeol, ceanothic acid, or ceanothenic acid. The n.m.r. spectrum shows a significant change, the original two multiplets now appearing as a single broad band at τ 5.24. In addition, on mechanistic grounds, since it has been shown (13) that the isopropenyl group is required for oxidation, inversion would seem necessary to allow approach of the reagent to C_{12}.

Since the direct lactonization from C_{27} to C_1 or C_3[4] is not possible, rearrangement must occur on dilactonization. Two more probable structures may be considered, (XVII) and (XVIII), the formation of both of which involves only the generation of tertiary carbonium ions after the initial migration. These are derived by protonation at either end of the cyclopentene ethylenic linkage. These two formulations differ in the number of potential acetic acid molecules obtainable by Kuhn–Roth oxidation. The monolactone (XI), now to be represented as (XIX), has two methyl groups and two geminal dimethyl groups. The same obtains in formulation (XVIII) for the dilactone. The alternative (XVII) has, in contrast, four methyl groups and one geminal dimethyl group. Since geminal dimethyl functions are known to give only a small fraction of a molecule of acetic acid, (XVII) would be expected to have a greatly increased Kuhn–Roth yield of acetic acid over (XIX). In fact, (XIX) gave 2.3 C—Me and the dilactone 2.2,[5] and, on this basis, (XVII) may be excluded. The position of the lactone is that found in the acid-catalyzed lactone from quinovic acid, novic acid (16).

EXPERIMENTAL

For general experimental details see Part I (2). Nuclear magnetic resonance spectra were determined in carbon tetrachloride solution. Silica gel was B.D.H. grade except where specified differently.

Extraction of Ceanothus americanus

(*a*) The ground root bark (10 kg) was extracted by standing with alcohol for approximately 24 hours, after which time the solvent was drained off. This was repeated seven times. The combined alcohol extract (30 l.) was concentrated to about 2 l., diluted with water, and extracted with ether. The ethereal solution was extracted exhaustively with potassium hydroxide solution, the insoluble potassium salts removed by filtration, and the defatted acids derived from the soluble salts isolated as previously described (2).

The larger benzene-soluble portion of the acid mixture was chromatographed on silica gel (730 g; Davison). Elution with benzene–ether (19:1) yielded a material which, after recrystallization of a portion from ether–benzene followed by ether–methanol, gave ceanothenic acid, m.p. 350–354° (decomposition) undepressed

[4]*In numbering ceanothenic acid it has been assumed that* C_2 *is extruded.*

[5]*We are greatly indebted to Mr. J. M. L. Cameron (Glasgow) for these determinations.*

on admixture with the acid from the earlier isolation (2), $[\alpha]_D$ +39° (*c*, 1.25; pyridine). Calc. for $C_{29}H_{42}O_4$: C, 76.61; H, 9.31; O, 14.08%. Found: C, 76.45; H, 9.23; O, 14.43%. Further elution produced the previously reported triterpenoids, betulinic acid, and ceanothic acid (I).

Additional amounts of ceanothenic acid were obtained upon addition of alcohol to the benzene-insoluble portion of the acid mixture. This then crystallized (m.p. 340–346°) and combination of this with the ceanothenic acid obtained upon chromatography yielded 8 g of crude acid.

The ether solution remaining after removal of the acidic material was washed with aqueous hydrochloric acid (2 *N*; 5×300 ml) and the neutral fraction isolated by evaporation.

The neutral material (17.6 g) from 19 kg root bark was refluxed for 3 hours under nitrogen with aqueous alcoholic (1:8) potassium hydroxide solution (5%; 300 ml).[6] The neutral fraction (30 g) from this, separated by ether extraction, was chromatographed on silica gel (650 g). Elution with light petroleum – benzene (3:7) afforded lupeol, identified by melting point (207–208°), mixed melting point, rotation ($[\alpha]_D$ +27°), and infrared spectrum. Elution with benzene–ether (9:1) produced a fraction which was recrystallized to give β-sitosterol, m.p. 136–137°, identical in every respect with authentic material. Further elution with benzene–ether (3:1) gave betulin, identified by melting point and mixed melting point. Acetylation gave the acetate identical in every respect with authentic betulin diacetate.

Acidification of the aqueous phase of the hydrolysis mixture followed by ether extraction of the acidic material afforded a fraction (9.9 g) which was chromatographed on silica gel. Elution with benzene–ether (1:3) gave a substance shown by melting point, mixed melting point, ultraviolet and infrared spectra to be phthalic acid.

(*b*) After alcoholic extraction of the root bark (10 kg) with alcohol, a further extraction was carried out using chloroform (3×4 l.).[6] After evaporation of the chloroform the residue was extracted exhaustively with refluxing light petroleum, dissolved in ether, the acidic fraction isolated by extraction with potassium hydroxide solution (2%), acidification, and ether extraction. The residue (7.2 g) was chromatographed on silica gel (210 g). Elution with benzene–ether (9:1) gave crystalline material, m.p. 201–202°. Calc. for $C_8H_8O_4$: C, 57.14; H, 4.80%. Found: C, 57.52; H, 4.79%. Methylation with diazomethane gave a crystalline compound, m.p. 58–59°. The substances were identified as vanillic acid and its methyl ether, and their melting points were undepressed on admixture with authentic specimens.

Elution with benzene–ether (4:1) gave material, m.p. 184–185°, raised to 207–208° after further purification. Calc. for $C_9H_{10}O_5$: C, 54.54; H, 5.09; O, 40.37%. Found: C, 54.22; H, 5.20; O, 40.78%. Methylation with diazomethane produced a compound, m.p. 80–81°. The original compound was identified as syringic acid by melting point, mixed melting point, and infrared spectrum.[7]

Dimethyl Ceanothenate

Ceanothenic acid was methylated with diazomethane to yield a non-crystalline ester, $[\alpha]_D$ +32° (*c*, 0.81), ν_{max} 1720, 1642, 890 cm^{-1} (CCl_4). Calc. for $C_{31}H_{46}O_4$: C, 77.13; H, 9.61%. Found: C, 77.17; H, 9.20%.

Tetrahydroceanothenic Acid

Ceanothenic acid (33 mg) absorbed 2.0 mole of hydrogen when hydrogenated in glacial acetic acid over platinum oxide catalyst. Recrystallization from ether gave tetrahydroceanothenic acid, m.p. 340° (decomposition), $[\alpha]_D$ −34° (*c*, 0.51; pyridine), ν_{max} 1686 cm^{-1} (nujol mull). Calc. for $C_{29}H_{46}O_4$: C, 75.94; H, 10.11%. Found: C, 75.88; H, 9.90%.

Dimethyl Tetrahydroceanothenate

Tetrahydroceanothenic acid (20 mg) was methylated with diazomethane to give the dimethyl ester, m.p. 159–163°, $[\alpha]_D$ −21° (*c*, 1.2). Calc. for $C_{31}H_{50}O_4$: C, 76.50; H, 10.36; OCH_3, 12.72%. Found: C, 76.58; H, 10.17; OCH_3, 11.52%. The molecular weight (mass. spec.) was 486 (calc. 486.7).

Ozonolysis of Ceanothenic Acid

Ozonolysis of ceanothenic acid (56 mg) in acetic acid solution at room temperature for 30 minutes followed by distillation into aqueous dimedone gave formaldehyde, characterized as the dimedone derivative, in 12% yield. A similar ozonolysis of undecylenic acid (21 mg) produced a 21% yield of formaldehyde as the dimedone derivative. Addition of alkali (10% potassium hydroxide solution) to the non-crystalline acidic product from ozonolysis followed by I_2–KI solution produced a precipitate of iodoform.

Ceanothenic Acid Dilactone

(*a*) Ceanothenic acid (68 mg) was refluxed 5 hours with formic acid (10 ml; 98%). The residue, obtained upon evaporation of the formic acid *in vacuo*, was chromatographed on alumina (Grade 1; 3 g). Elution with light petroleum – benzene (1:1) afforded crystalline material which gave, after recrystallization from chloroform–methanol, ceanothenic acid dilactone (19 mg), $[\alpha]_D$ −17° (*c*, 1.04). Calc. for $C_{29}H_{42}O_4.0.5MeOH$: C, 75.32; H, 9.36%. Found: C, 75.33; H, 9.20%. The dilactone possessed a complex melting point, undergoing transition in the range 250–285°, before finally completely melting, at 285°.

[6]*We wish to express our thanks to Mr. M. P. Li for this experiment.*

[7]*We are grateful to Dr. Irwin A. Pearl (The Institute of Paper Chemistry, Wisconsin) for a specimen of syringic acid.*

(*b*) Ceanothenic acid (110 mg) was refluxed with a mixture of acetic acid (36 ml) and concentrated hydrochloric acid (4 ml) for 2 hours. Additional hydrochloric acid (2 ml) was added and the refluxing continued for 3 hours. Dilution with water and ether extraction yielded a neutral product which gave, after recrystallization from ether, ceanothenic acid dilactone (42 mg).

(*c*) Methyl ceanothenate (22 mg) was dissolved in benzene (1 ml), and acetic acid (5 ml) and sulphuric acid (1 ml) added. After 5 days' standing at room temperature, ether extraction followed by chromatography on alumina yielded ceanothenic acid dilactone identical in every way with the material described above.

Conversion of Tetrahydroceanothenic Acid to the Diol (XX)

Tetrahydroceanothenic acid (32 mg) was refluxed 1 hour with thionyl chloride (3 ml). The thionyl chloride was removed under reduced pressure, then dry benzene (5 ml) added and likewise removed. The residue was dissolved in dioxane, an excess of lithium aluminum hydride added, and the mixture refluxed for 12 hours. After working up in the usual manner and filtering through alumina (Grade 4; 1 g), crystalline material (25 mg) was obtained which, after recrystallization from ether–methanol, afforded the diol (XX), m.p. 253–254°, $[\alpha]_D$ −41° (*c*, 0.99; pyridine), ν_{max} 3330 cm^{-1} (nujol mull). Calc. for $C_{29}H_{50}O_2$: C, 80.87; H, 11.70%. Found: C, 80.51; H, 11.56%.

Oxidation of the diol with an acetic acid solution of chromic anhydride at room temperature regenerated tetrahydroceanothenic acid identical in every respect with that obtained directly.

The crude diol (400 mg) was acetylated (30 minutes at 100° with acetic anhydride – pyridine (1:2)), and the isolated product chromatographed on alumina (8 g; Grade 1). Light petroleum – benzene (19:1) eluted crystalline material which, after recrystallization from ether–methanol, gave the diacetate, m.p. 121–122°, $[\alpha]_D$ −31° (*c*, 0.99), ν_{max} 1730 cm^{-1}. Calc. for $C_{33}H_{54}O_4$: C, 76.99; H, 10.57%. Found: C, 76.98; H, 10.51%.

Methyl Anhydrobetulinate

Methyl betulinate benzoate (134 mg) was heated under nitrogen for 30 minutes on a metal bath at 320–330°. The crude product was refluxed under nitrogen with alcoholic potassium hydroxide (10%) followed by isolation of the neutral material with ether and chromatography on alumina (2 g; Grade 1). Elution with light petroleum and crystallization from chloroform–methanol gave methyl anhydrobetulinate, m.p. 154–157°, $[\alpha]_D$ +25° (*c*, 2.44), ν_{max} 1720, 1642, 889 cm^{-1}. Calc. for $C_{31}H_{48}O_2.0.5MeOH$: C, 80.76; H, 10.62%. Found: C, 80.33; H, 10.62%.

Osmic Acid Oxidation

Methyl ceanothenate (195 mg) was dissolved in dioxane (2.5 ml), and pyridine (3.5 ml) and osmic acid (350 mg) added. This mixture was kept in the dark at room temperature for 9 days, when the osmic ester was decomposed with sodium bisulphite (17). The crude product was isolated by ether extraction and filtered through alumina with methanol–benzene (1:5). Recrystallization from methanol afforded the tetrol (112 mg), m.p. 254–260°, $[\alpha]_D$ −25° (*c*, 0.62; alcohol), ν_{max} 3440, 1712 cm^{-1}. Calc. for $C_{31}H_{50}O_8$: C, 67.61; H, 9.15%. Found: C, 67.75; H, 9.16%.

Periodic Acid Titration of the Tetrol in Methanol

The tetrol (114 mg), dissolved in methanol (24 ml) and water (3 ml), was titrated with periodic acid (3 ml; approx. 0.4 *N*). After 4 hours the uptake of oxidant had ceased, with consumption of 2.3 moles. The product was isolated by ether extraction and chromatographed on alumina (6 g; Grade 1). Elution with benzene–ether (19:1) gave a compound, m.p. 185–190° after recrystallization from ether – light petroleum. The substance showed ν_{max} 1708 cm^{-1}, and n.m.r. bands at τ = 7.87, 6.60, 6.37, 6.21, and 5.88. Further elution gave a second compound ((VI; R = Me) or (VII)), m.p. 184–186° after recrystallization from ether – light petroleum, $[\alpha]_D$ −10° (*c*, 0.54), ν_{max} 3400, 1720 cm^{-1}, n.m.r. bands at τ = 7.84, 6.57, 6.35, 6.22, 5.84, and 5.43. Calc. for $C_{31}H_{48}O_8$: C, 67.85; H, 8.82; OMe, 16.95%. Found: C, 67.91; H, 8.92; OMe, 16.61%.

To the cleavage product ((VI; R = Me) or (VII)) (16 mg) in alcohol (35 ml) was added a solution of 2,4-dinitrophenylhydrazine (45 mg) in alcohol (4 ml) containing hydrochloric acid (6 drops). After refluxing for 4.5 hours, the product was isolated and chromatographed on alumina. Benzene removed some non-crystalline material and on further elution with chloroform a substance was obtained which was recrystallized from chloroform–methanol to give the tris-2,4-dinitrophenylhydrazone, m.p. 281–282°. Calc. for $C_{48}H_{56}O_{16}N_{12}$: C, 54.56; H, 5.30; N, 15.90%. Found: C, 55.03; H, 5.88; N, 15.68%.

Periodic Acid Titration of the Tetrol (XXI) in Dioxane

The tetrol (35 ml) was titrated with periodic acid in the same manner as above, using dioxane (8 ml) and water (1 ml) as solvent. At the end of 4 hours, reaction was complete, with the consumption of 2.1 moles of oxidant.

Chromatography of the product did not afford any crystalline material. The n.m.r. spectrum of the oil showed bands at τ = 7.94, 6.34, 6.18, 0.85, and 0.73 and the compound possessed ν_{max} 3360 and 1708 cm^{-1}. Reaction of this product with 2,4-dinitrophenylhydrazone afforded the same derivative, m.p. 281–282°, as was obtained from the methanolic titration.

Cannizzaro Reaction

Sodium hydroxide solution (2 ml; 10%) was added to the periodic acid – dioxane cleavage product (20 mg), dissolved in methanol (8 ml). The solution was refluxed under nitrogen for 0.5 hours. Ether extraction yielded a trace of neutral material (3 mg). Acidification of the alkaline solution followed by re-extraction with ether gave crystalline material (16 mg). This material could not now be extracted from the ethereal solution with aqueous potassium hydroxide (2%). Recrystallization from ether–petrol gave the δ-lactone, m.p. 212–215°, $[\alpha]_D$ −18° (*c*, 1.04), ν_{max} 1708 cm^{-1}, τ = 7.80, 6.28, 6.21. Calc. for $C_{30}H_{44}O_7$: C, 69.74; H, 8.58%. Found: C, 70.28; H, 8.30%. The periodic acid – dioxane cleavage product (24 mg) in a sodium methoxide solution (2%) maintained overnight at room temperature afforded the same lactone.

Dihydroceanothenic Acid

Potassium azodicarboxylate (200 mg; 1.1 mmoles) prepared from azodicarbonamide was added to a solution of ceanothenic acid (20 mg) in methyl cellosolve (2 ml). Acetic acid (155 mg; 2.2 mmoles) was added and the mixture stirred under nitrogen until the disappearance of color (approx. 10 minutes). Recrystallization from ether–methanol gave dihydroceanothenic acid, m.p. 340° (decomposition), $[\alpha]_D$ +15° (*c*, 0.99; pyridine), ν_{max} 1692, 1646, 888 cm^{-1} (nujol mull). Calc. for $C_{29}H_{44}O_4.0.5MeOH$: C, 75.00; H, 9.76%. Found: C, 75.01; H, 9.72%. In the same manner norbornylene (220 mg) was reduced with potassium azodiformate (4 g) and acetic acid (3.6 g). The product was identified as norbornane by melting point and infrared spectrum.

Dihydroceanothenic Acid Lactone

Dihydroceanothenic acid (84 mg) was refluxed 3 hours with formic acid (25 ml; 97%). The product, after removal of the formic acid *in vacuo*, was chromatographed on silica gel (4.5 g). Elution with benzene–ether (19:1) yielded material which was recrystallized from ether – light petroleum to give dihydroceanothenic acid lactone, m.p. 289–291°, $[\alpha]_D$ +47° (*c*, 1.21), ν_{max} 1764, 1695 cm^{-1}. Calc. for $C_{29}H_{44}O_4$: C, 76.27; H, 9.71%. Found: C, 76.11; H, 9.47%.

Methyl Dihydroceanothenate Lactone (XIX)

Methylation of the acid with diazomethane gave methyl dihydroceanothenate lactone, recrystallized from ether – light petroleum, m.p. 179–180°, $[\alpha]_D$ +43° (*c*, 1.05), ν_{max} 1760, 1712 cm^{-1}. Calc. for $C_{30}H_{46}O_4$: C, 76.55; H, 9.85%. Found: C, 76.44; H, 9.79%.

Methyl Dehydrodihydroceanothenate

Methyl dihydroceanothenate (106 mg) in chloroform (4 ml) was refluxed with mercuric acetate (2 g) in acetic acid (20 ml) for 5 hours. The residue obtained after chloroform extraction was dissolved in pyridine and hydrogen sulphide passed through it for 1 hour. The precipitated sulphide was removed by filtration and the pyridine removed *in vacuo*. The residue, in ether, was washed with ammonium sulphide solution and the remaining material was chromatographed on alumina (2 g; Grade 1). Elution with benzene–ether (19:1) afforded material (47 mg) which recrystallized from ether–methanol to give methyl dehydrodihydroceanothenate, m.p. 160–161°, $[\alpha]_D$ +54°, (*c*, 1.09), ν_{max} 1723, 1669, 1625, 902 (shoulder), 894 cm^{-1} (CCl_4). Calc. for $C_{31}H_{46}O_4$: C, 77.13; H, 9.61%. Found: C, 76.70; H, 9.49%.

Methyl Dehydrotetrahydroceanothenate

Methyl dehydrodihydroceanothenate (332 mg) in acetic acid (18 ml) was hydrogenated over platinum oxide catalyst (82 mg). Recrystallization of the product from ether – light petroleum gave methyl dehydrotetrahydroceanothenate, m.p. 190–192°, $[\alpha]_D$ +8° (*c*, 0.93), ν_{max} 1716 cm^{-1}. Calc. for $C_{31}H_{48}O_4$: C, 76.81; H, 9.98%. Found: C, 77.33; H, 10.03%.

Lithium Iodide Halolyses

(*a*) Methyl ceanothenate (31 mg), in 2,4,6-collidine (2.8 ml), was refluxed for 8 hours with anhydrous lithium iodide (114 mg). The cooled solution was poured into a mixture of 2 *N* HCl (15 ml) and ether – methylene chloride (15 ml; 2:1). The aqueous portion was twice washed with ether – methylene chloride (2:1). The combined organic extract was then washed with dilute hydrochloric acid and water before evaporation of the solvent. Recrystallization of the product gave ceanothenic acid (22 mg), m.p. 347–351°.

(*b*) Methyl dehydrotetrahydroceanothenate (XIV; R = Me, R′ = COOMe) (57 mg) with lithium iodide (200 mg) in 2,4,6-collidine (4 ml) was refluxed for 8 hours. The reaction mixture was worked up as above. The product was recrystallized from ether–methanol to give the corresponding acid (28 mg), m.p. 320–330° (gas evolution), $[\alpha]_D$ −4° (*c*, 0.75; pyridine), ν_{max} 1692 cm^{-1} (nujol mull). Calc. for $C_{29}H_{44}O_4$: C, 76.27; H, 9.71%. Found: C, 76.09; H, 9.56%. Methylation of the acid gave back methyl dehydrotetrahydroceanothenate, identified by melting point, mixed melting point, and infrared spectrum.

Methyl 11-Oxodehydrotetrahydroceanothenate

An acetic acid solution of methyl dehydrotetrahydroceanothenate (50 mg) was allowed to stand overnight at room temperature with an excess of chromic acid solution (10 ml; 0.16 *N* in acetic acid). Isolation of the product and recrystallization from ether – light petroleum gave methyl 11-oxodehydrotetrahydroceanothenate, m.p. 217–219°, $[\alpha]_D$ −34° (*c*, 1.04), λ_{max} 239 mμ (ϵ = 12,200), ν_{max} 1718, 1699, 1615 cm^{-1}. Calc. for $C_{31}H_{46}O_5$: C, 74.66%; H, 9.30%. Found: C, 74.74; H, 9.43%.

Hydrolysis and Decarboxylation of the Ketone (XV; R = Me, R′ = COOMe)

Methyl 11-oxotetrahydrodehydroceanothenate (52 mg) was refluxed under nitrogen for 4 hours with methanolic potassium hydroxide (20 ml; 5%). The mixture was worked up as usual and the crude acidic fraction (22 mg) in methanol (10 ml) titrated with *N*/100 sodium hydroxide to a phenolphthalein end point. A titration value of 82% of the calculated was obtained.

This acid material was decarboxylated by heating 10 minutes at 145° under nitrogen. Filtration through alumina with benzene and recrystallization from ether–methanol afforded the neutral ketoester (XV; R = Me, R′ = H), m.p. 182–185°, $[\alpha]_D$ −95°, (*c*, 1.11), λ_{max} 241 mμ (ϵ = 13,200), ν_{max} 1717, 1690, 1614 cm^{-1}. Calc. for $C_{29}H_{44}O_3$: C, 79.04; H, 10.07%. Found: C, 79.07; H, 9.78%.

Oxidation of the Diol (XX) with Chromic Acid

The diol (62 mg) in Analar acetic acid (3 ml) was oxidized by standing overnight at room temperature with 0.17 *N* chromic acid in acetic acid (5.8 ml). Following isolation, the product was separated into acidic and neutral fractions. The neutral fraction was chromatographed on alumina (2 g), elution with light petroleum – benzene (19:1) affording crystalline material in poor yield. Recrystallization from ether–methanol gave the dialdehyde, m.p. 138–142°, $[\alpha]_D$ −22° (*c*, 0.75), ν_{max} 2740, 1715 cm^{-1}. Calc. for $C_{29}H_{46}O_2$: C, 81.63; H, 10.87%. Found: C, 81.52; H, 10.16%.

Reduction of Dihydroceanothenic Acid Lactone (XI)

Dihydroceanothenic acid lactone (97 mg) in tetrahydrofuran (9 ml) was refluxed with an excess of lithium aluminum hydride (300 mg) for 0.5 hour. The product was isolated in the usual manner and methylated with diazomethane. The crude product was filtered through alumina (2 g; Grade 1) in benzene and recrystallized from ether – light petroleum to yield the diol (XII), m.p. 236–238°, $[\alpha]_D$ +23°, (*c*, 0.90), ν_{max} 3350, 1709 cm^{-1}. Calc. for $C_{30}H_{50}O_4$: C, 75.90; H, 10.62%. Found: C, 76.05; H, 10.50%.

ACKNOWLEDGMENTS

The authors wish to thank Mr. R. E. Klinck for the determination of the n.m.r. spectra. Grateful acknowledgment is made to the National Research Council of Canada and to Abbott Laboratories for financial support.

REFERENCES

1. P. L. JULIAN, J. PIKL, and R. DAWSON. J. Am. Chem. Soc. **60**, 77 (1938).
2. P. DE MAYO and A. N. STARRATT. Can. J. Chem. **40**, 788 (1962).
3. J. P. BOYER, R. A. EADE, H. LOCKSLEY, and J. J. H. SIMES. Australian J. Chem. **11**, 236 (1958).
4. R. MECHOULAM. Chem. & Ind. (London), 1835 (1961).
5. T. G. HALSALL. Private communication.
6. F. ELSINGER, J. SCHREIBER, and A. ESCHENMOSER. Helv. Chim. Acta, **43**, 113 (1960).
7. L. M. JACKMAN. Applications of nuclear magnetic resonance spectroscopy in organic chemistry. Pergamon Press Inc., New York. 1959.
8. G. W. K. CAVILL, D. L. FORD, and H. D. LOCKSLEY. Australian J. Chem. **9**, 288 (1956).
9. G. S. DAVY, T. G. HALSALL, and E. R. H. JONES. J. Chem. Soc. 2696 (1951).
10. D. H. R. BARTON, C. J. W. BROOKS, and N. J. HOLNESS. J. Chem. Soc. 278 (1951).
11. E. J. COREY, W. L. MOCK, and D. J. PASTO. Tetrahedron Letters, No. 11, 347 (1961). S. HÜNIG, H. MÜLLER, and W. THIER. Tetrahedron Letters, No. 11, 353 (1961). E. E. VAN TAMELEN, R. S. DEWEY, and R. J. TIMMONS. J. Am. Chem. Soc. **83**, 3725 (1961).
12. S. DAVID. Bull. soc. chim. France, 159 (1949).
13. J. M. ALLISON, W. LAWRIE, J. MCLEAN, and G. R. TAYLOR. J. Chem. Soc. 3353 (1961). J. M. ALLISON, W. LAWRIE, J. MCLEAN, and J. M. BEATON. J. Chem. Soc. 5224 (1961).
14. L. RUZICKA, O. JEGER, and M. WINTER. Helv. Chim. Acta, **26**, 265 (1943).
15. A. BROSSI, B. BISCHOF, O. JEGER, and L. RUZICKA. Helv. Chim. Acta, **34**, 244 (1951).
16. D. H. R. BARTON and P. DE MAYO. J. Chem. Soc. 3111 (1953).
17. J. S. BARAN. J. Org. Chem. **25**, 257 (1960).

INFLUENCE OF THE DEFECT CENTERS ON THE SZILARD–CHALMERS ANNEALING

IRINA NEGOESCU AND T. COSTEA
Laboratory of Radiochemistry, Institute of Atomic Physics, Bucharest, Roumania

Received December 19, 1961

ABSTRACT

Reactor-irradiated copper and cobalt oxinates were studied for the behavior of Cu^{64} and Co^{60} atoms produced by radiative thermal neutron capture. The annealing processes associated with the Szilard–Chalmers effect were followed by means of retention. Both substances exhibit annealing at room temperature, formally following first-order kinetics. The retention was found to increase with reactor exposure time, following kinetics similar to that for post-irradiation thermal annealing. The interpretation of experimental data relies on the assumption that fractions annealed at room temperature decrease with increasing density of defect centers containing an annealable Szilard–Chalmers atom.

INTRODUCTION

The mechanism of the processes occurring in radiation-damaged solids is still considered to be in question in spite of the number of works published hitherto on this topic. In this connection the usefulness and importance of the Szilard–Chalmers method, which by its very simple radiochemical procedures obtains many results hardly available by the use of other methods, are well known.

The complexity of these processes is shown by the lack of reproducibility of experimental data. Attempts were made to follow the influence of various factors such as crystal fragment size, irradiation conditions (dose, dose rate, temperature), sample type (treated or untreated), etc. As a matter of fact most of these factors determine in a straightforward manner the crystal damage range along with the retention value, as shown by Maddock and Vargas (1), although variations were found not only in a unique direction. Certainly, definite conclusions may not be drawn until new experimental data can lead to a more precise knowledge of the way crystal defects act on recombination of recoil species.

The discussion of experimental results will rely on Harbottle and Sutin's hot-zone model (2); the processes arising after hot-zone cooling will be examined according to Vand–Primak's hypothesis on processes group distributed in activation energy (3).

Oxinates were chosen for the investigation of processes associated with the Szilard–Chalmers effect because, on the one hand, for chelate compounds, the exchange reaction between the recoil and complexed atom does, properly, not occur; on the other hand, owing to the solubility of oxinates in organic solvents there appears the possibility of carrying out the separation of recoil atoms through water extraction, without using more intricate analytical methods which may eventually change the original distribution of recoil fragments. Moreover, oxinates exhibit radiation and thermal stability against irradiation decomposition as well as radiation and thermal sensitivity against annealing. In the present work copper and cobalt oxinates were chosen. Cobalt (4), tungsten, calcium (5), copper, manganese, and nickel oxinates (6) were also studied but only in order to obtain high specific activity radioisotopes.

EXPERIMENTAL

Irradiation

Samples contained in quartz tubes were irradiated in the thermal column of the I.F.A. reactor. The irradiations were carried out in air at hole temperature (30–35° C); irradiation times ranged from 15 minutes

to 10 hours for copper oxinate and from 1 hour to 8 hours for cobalt oxinate. Irradiation conditions were as follows: thermal neutron flux 1.2×10^{11} $cm^{-2}sec^{-1}$, fast neutron flux 6.3×10^{9} $cm^{-2}sec^{-1}$, gamma dose rate 3.5×10^{6} r hr^{-1}.

Extraction

Irradiated 1-mg samples were dissolved in freshly distilled chloroform. Cobalt oxinate dissolution was carried out at a temperature of 45–50° C, *m*-toluidine traces being present. The recoil atoms were water-extracted at pH = 6 with Cu^{2+} and Co^{2+} respectively as carriers.

To test the separation method the following operations were performed: (*a*) Extraction of Cu^{64} synthetized copper oxinate from chloroformic phase to aqueous phase at pH 6; no active copper ions were found in the aqueous phase. (*b*) Extraction of active copper ions from aqueous solution at pH 6 to chloroformic phase; no activity was found in the chloroformic phase. (*c*) No exchange reaction was found between complexed active copper in the chloroformic phase and inactive Cu^{2+} used as carrier in the aqueous phase. Similar procedures were used for cobalt oxinate.

Counting

Both phases activity was measured using an immersion G.M. counter. Measurements were made after Cu^{66} (5.18 minutes) and Co^{60m} (10 minutes) activities had decreased to a negligible value. Retention was computed from the ratio between chloroformic and total activity of both phases. Each result consists of the average value obtained for two or three irradiation sets, with similar irradiation conditions. The uncertainty affecting the average value is ±1.5%.

RESULTS AND DISCUSSIONS

Copper Oxinate

The retention of samples reactor-irradiated for 15 minutes–9.5 hours was determined at room temperature and found to increase with time. In a few hours it reached a value of 94%, which remained constant even 24 hours after irradiation. An exception was found for the 9.5-hours irradiated sample, which exhibited from the very beginning a retention of 94%. Therefore, the conclusion may be drawn that in neutron-irradiated copper oxinate a fast annealing characterized by the decrease in annealing rate with time and by the appearance of a pseudo plateau occurs at room temperature. The following step, the slow annealing process taking place with constant annealing rate, was not yet tested owing to the short life of recoil radioactive atoms (7).

It must also be pointed out that for samples treated immediately after irradiation, the shorter the irradiation time the smaller the retention value, the existence of various original retention values hence depending on reactor exposure time. The ordinary plot of $R(t)$ could not account for this assumption because retention values in the range of greatest annealing rates were unknown, as determinations could only be made during the first few minutes after irradiation. The uncertainty affecting the retention value did not even allow the plot of a curve representing exactly the annealing kinetics, by extrapolation of which the retention at the end of irradiation might be obtained. The question was solved in another way.

As Harbottle and Sutin (8) pointed out, annealing of radiative neutron capture damages may be treated according to Vand–Primak's concept of group of processes distributed in activation energy (3). On the other hand it was demonstrated (9) that in first approximation, fast annealing may be formally considered as a first-order process characterized by apparent rate constants. The approximation is allowed for owing to the existence of a Primak spectrum consisting of a narrow band of activation energy.

In the present work a plot of log (ΔR) versus t is given, where $\Delta R = R_\infty - R$, R_∞ being the retention value at the pseudo plateau and R the retention value at time t. Straight lines exhibiting equal slopes were obtained, as was expected. Figure 1*a* shows the variation of annealing fraction with time at room temperature, for two samples irradiated with various integral neutron fluxes. The plot gives, by extrapolation, the original retention

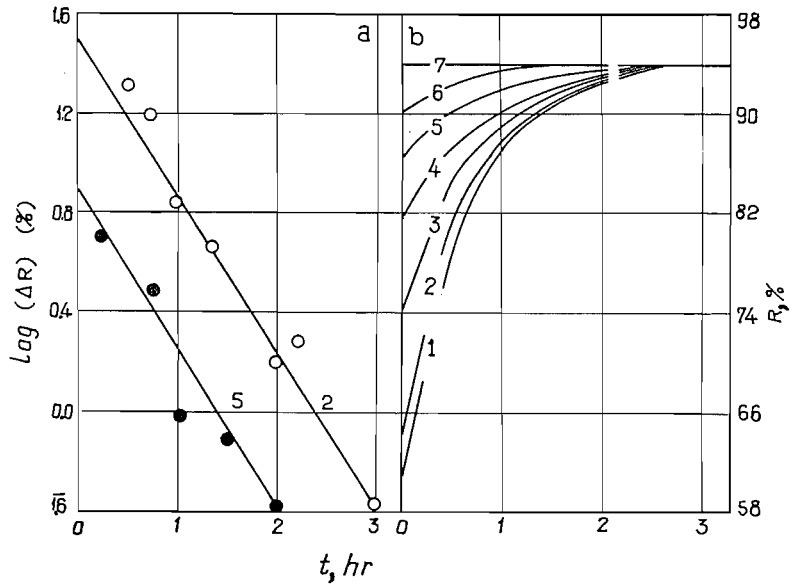

FIG. 1. The annealing at room temperture of copper oxinate irradiated as follows: 1, 15 minutes; 2, 30 minutes; 3, 1 hour; 4, 2 hours; 5, 3 hours; 6, 4 hours; 7, 9.5 hours.

R_0, i.e., the retention at the end of irradiation. R_0 increases with irradiation time; its values are given in Table I. The log (ΔR) versus t plot allowed also for the computation

TABLE I

Variation of the retention R_0 with the time of irradiation t' for copper oxinate

t', min	15	30	60	120	180	240	570
R_0, %	60.9	63.8	74.1	81.4	86.1	90.4	94.0

of a set of thermal annealing kinetic curves for various samples (Fig. 1*b*). The formal kinetic equation characterizing the process is:

$$[1] \qquad \Delta R = (\Delta R)_\infty \exp(-kt),$$

where $(\Delta R)_\infty = R_\infty - R_0$. The apparent rate constant has the value $k = 4.03 \times 10^{-4}$ sec^{-1}.

Similar considerations led to the description of the annealing during the irradiation. Reactor annealing is marked by prime superscripts; therefore $R_\infty' \equiv R_0$ and $(\Delta R)' = R_\infty' - R'$. A plot of log $(\Delta R)'$ versus irradiation time t' is a straight line, as shown in Fig. 2*a*. Hence, the annealing during irradiation may be formally considered as a first-order process. The kinetic curve of the annealing during irradiation corresponds to an equation of the same type as the former:

$$[2] \qquad (\Delta R)' = (\Delta R)_\infty' \exp(-kt'),$$

where $(\Delta R)_\infty' = R_\infty' - R_0'$. The numerical values obtained by graphical means from the plot in Fig. 2*a* are $k' = 1.73 \times 10^{-4}$ sec^{-1} and $R_0' = 54.6\%$. The condition $k \neq k'$ does not agree with the assumption that annealing could occur only under the influence of the temperature, although in this circumstance the temperature plays an important part.

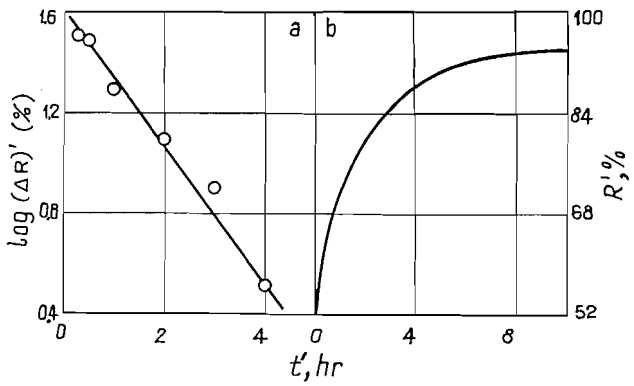

FIG. 2. The annealing concomitant with the irradiation of copper oxinate.

Moreover, curves similar to those plotted in Fig. 2*b* were reported for potassium chromate (10) and for hexammino-cobaltic nitrate (11); an equation of the type of eq. [2] was also found. It is worthwhile to point out the great original retention value R_0', which may be accounted for by applying only the hot-zone model because both the lack of nuclear inefficiency of gamma-ray emission and the lack of a Suess effect do not succeed in explaining the fact that about a half of the whole activity is retained by the original chemical compound or by compounds exhibiting a similar structure. However, it may be assumed that original retention results from recombination processes occurring in 10^{-11} second in the melt, which behaves as a cage for the recoil atom (12). Thus, the original retention arising from spontaneous recrystallization may quite possibly remain constant during the whole irradiation time. To this may be added the secondary retention, which also varies with time and which is due to radiation and thermal annealing of recoil atoms not yet rearranged and trapped in the hot zone during recrystallization. These processes require, also, activation energies as pointed out for thermal annealing, though radiation annealing might be accounted for by the appearance of hot spots behaving like hot zones.

Cobalt Oxinate

Cobalt oxinate behaves like copper oxinate. Annealing process at room temperature may be observed and the retention increases with time until reaching a saturation value, which is found to be constant even after 50 hours. However, the pseudo plateau is not the same for all samples, smaller values being found for samples irradiated with stronger integral neutron fluxes. The saturation retention values R_∞ for samples reactor-irradiated for 2–8 hours are given in Table II.

TABLE II

Variation of the retentions R_0 and R_∞ with the time of irradiation t' for cobalt oxinate

t', min	120	240	300	480
R_0, %	32.9	35.5	41.4	48.8
R_∞, %	83.0	71.0	67.0	64.0

According to reasons similar to those for copper oxinate, annealing curves are studied on a log (ΔR) versus time plot. Figure 3*a* shows that thermal annealing follows eq. [1]

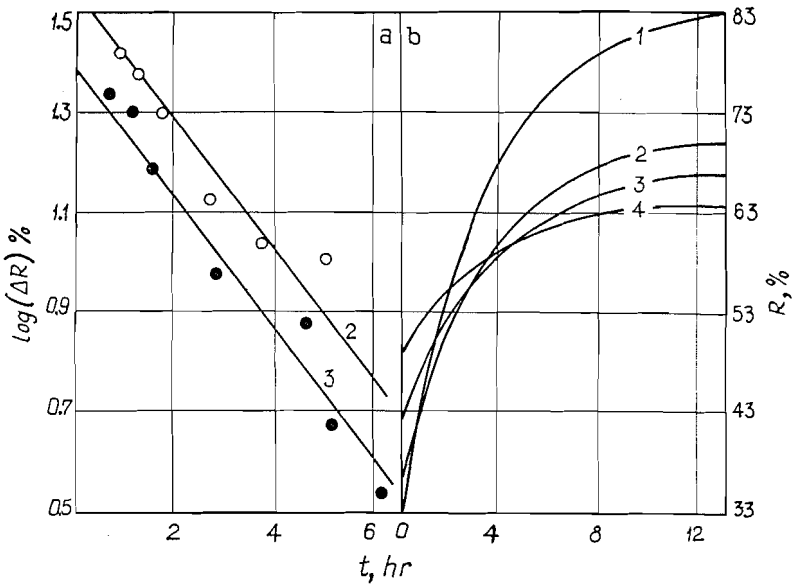

FIG. 3. The annealing at room temperature of cobalt oxinate irradiated as follows: 1, 2 hours; 2, 4 hours; 3, 5 hours; 4, 8 hours.

with $k = 0.80 \times 10^{-4}$ sec^{-1}. Figure 3*a* also allows computation of the original retention values R_0 (Table II), and thus a plot for thermal annealing kinetic curves is obtained. As shown in Fig. 3*b*, the curves cross one another according to their radiation history. As for copper oxinate, R_0 increases with reactor exposure time, attesting annealing during irradiation.

Influence of Defect Centers

Now two questions arise: saturation retention value depends on the one hand on heating temperature (room temperature) and on the other hand on irradiation time. An answer may be found by studying the variation of the annealable fraction at room temperature $(\Delta R)_\infty = R_\infty - R_0$ for the samples irradiated with various integral neutron fluxes. Moreover, the differences in crystal damages are also accounted for by various integral neutron fluxes. It may be shown that $(\Delta R)_\infty \propto 1/N$, where N is the density of defect centers.

Such a dependence was also found for hexammino-cobaltic nitrate (9). In a study of thermal annealing at various temperatures for various irradiation conditions it was found that, for a given heating temperature T, the annealable fraction $(\Delta R)_\infty$ may be written:

$$[3] \qquad (\Delta R)_\infty = \alpha_0 N^{1-\beta}(T - T_0),$$

where α_0 and β are constants characterizing the compound and T_0 is also a constant representing the characteristic annealing temperature, i.e., the temperature from which annealing begins and which is related to the minimum activation energy of Primak's spectrum (3) by the equation $E_0 = kT \ln (Bt)$. In eq. [3] N is the number of annealable defects, i.e., the number of cooled hot zones containing an annealable recoil atom.

For the present case, in which annealing occurs at room temperature, $T - T_0 = \Delta T$ is a constant; therefore,

[4] $$\alpha_0 \Delta T = c_1$$

[5] $$\beta - 1 = c_2,$$

so that eq. [3] may be written

[6] $$(\Delta R)_\infty = c_1 N^{-c_2}.$$

In Table III values of $(\Delta R)_\infty$ and N are given for copper and cobalt oxinates. It is noteworthy that an approximately linear relation is found between the logarithm of the change

TABLE III

The values of the fraction destined to be annealed and of the number of defect centers, for different irradiation times

	Copper oxinate		Cobalt oxinate	
t', min	$(\Delta R)_\infty$, %	N	$(\Delta R)_\infty$, %	N
15	33.1	1.35×10^{12}	—	—
30	30.2	3.47×10^{12}	—	—
60	19.9	6.84×10^{12}	—	—
120	12.6	1.33×10^{13}	50.1	2.95×10^{13}
180	7.9	1.94×10^{13}	—	—
240	3.6	2.53×10^{13}	35.5	5.68×10^{13}
300	—	—	25.6	6.45×10^{13}
480	—	—	15.2	9.02×10^{13}

in retention from the zero-time value to pseudo-equilibrium value and the logarithm of the density of the defect centers, although the slope between two successive points increases by degrees with the growth of the number of defect centers (Fig. 4). This proves

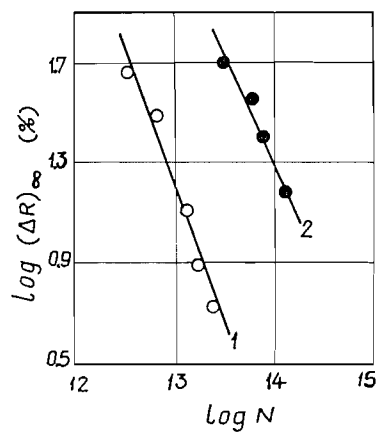

FIG. 4. The fraction destined to anneal at room temperature, as a function of the density of the defect centers: 1, copper oxinate; 2, cobalt oxinate.

the validity of eq. [6] for copper and cobalt oxinates. However, the imperfect linearity denotes that the phenomenon is more complex and we are under no illusions that the results are sufficient to generalize our equation, but hope that further studies will be suggested by them and that a theoretical consideration of this experimental evidence

will resolve the problem of the dependence between the annealing and the density of defect centers.

REFERENCES

1. A. G. MADDOCK and J. I. VARGAS. Nature, **184**, 1931 (1959).
2. G. HARBOTTLE and N. SUTIN. J. Phys. Chem. **62**, 1344 (1958).
3. W. PRIMAK. Phys. Rev. **100**, 1677 (1955).
4. A. NATH, J. SHANKAR, and S. B. SRIVASTAVA. Proceedings of the Second International Conference on the Peaceful Uses of Atomic Energy, Geneva. 1958. United Nations. 1958. 15/P/1650.
5. H. EBIHARA and K. YOSHIHARA. Bull. Chem. Soc. Japan, **33**, 116 (1960).
6. K. YOSHIHARA and H. EBIHARA. Japan Analyst, **9**, 815 (1960).
7. M. M. DE MAINE, A. G. MADDOCK, and K. TAUGBOL. Discussions Faraday Soc. **23**, 211 (1957).
8. G. HARBOTTLE and N. SUTIN. Advances in inorganic chemistry and radiochemistry. *Edited by* H. J. EMELEUS and A. G. SHARPE. Vol. 1. Academic Press, New York, London. 1959. p. 305.
9. T. COSTEA. J. Inorg. & Nuclear Chem. **19**, 27 (1961).
10. J. H. GREEN, G. HARBOTTLE, and A. G. MADDOCK. Trans. Faraday Soc. **49**, 1413 (1953).
11. T. COSTEA. J. Inorg. & Nuclear Chem. **17**, 20 (1961).
12. T. COSTEA and I. DEMA. Studii Cercetări Chimie, **9**, 109 (1961).

CLAM POISON

III. PAPER ELECTROPHORESIS OF CLAM POISON[1]

R. A. B. Bannard and A. A. Casselman
Defence Research Chemical Laboratories, Ottawa, Ontario

Received April 19, 1962

ABSTRACT

In paper strip electrophoretograms on Whatman 3MM paper, clam poison migrated toward the cathode when formic acid (1 *N* and 0.1 *N*), acetic acid (1 *N*), sodium acetate – acetic acid (0.1 *M*), monosodium dihydrogen phosphate – disodium monohydrogen phosphate (0.1 *M*), and sodium tetraborate (0.1 *M*) were used as electrolytes. Formic acid (1 *N*) proved the most suitable of these for examination of the quantitative electrophoretic behavior of clam poison. A method of pretreatment for the paper was developed to minimize introduction of extractable impurities into material recovered after electrophoresis by aqueous elution. Pure clam poison, on electrophoresis for 1.75 hours at 900 v on an 8×18-in. sheet of pretreated paper, migrated as a single, positively charged, Weber-positive band with apparent mobility 18.1 cm, which exhibited no fluorescence. Recovery was quantitative on both a weight and toxicity basis, and the toxicity, specific rotation, and infrared spectrum of the recovered toxin were identical with those of the starting material, thus providing an additional check on the homogeneity of the sample. Quantitative electrophoresis of toxin from clam poison tailings which had been purified by paper chromatography removed impurities which the latter method was incapable of eliminating, with resultant improvement in both the specific rotation and toxicity. Two such treatments provided toxin possessing a toxicity and specific rotation within the accepted limits for pure clam poison.

INTRODUCTION

The purification of clam poison by ion exchange followed by chromatography on acid-washed alumina, by chromatography on Norit A followed by crystallization as the helianthate, by countercurrent distribution (1), or by paper chromatography (2), provided material concluded to be chemically homogeneous because of the close correspondence in chemical, physical, and biological properties of the resultant specimens. Nevertheless, the fact that this exceedingly toxic substance of low molecular weight has not been obtained in a crystalline form possessing a definite melting point (2) makes it desirable to examine its purity by methods other than those mentioned above. Recently, we described a heavy-paper technique by means of which the toxin in clam poison tailings was enriched approximately fourfold in toxicity to 5000–5800 mouse units (MU)/mg in 67% yield. The recovered toxin exhibited physical, chemical, and biological characteristics which agreed in all respects with those reported previously for pure clam poison (1, 2), except that the specific rotation ($+98\pm4°$) was approximately 25% below normal. Since paper chromatography proved incapable of producing further improvement in the toxicity and rotation it was uncertain whether the low rotation referred to above was caused by the presence of impurities or whether the toxin recovered from the tailings differed from clam poison in some subtle manner. It therefore seemed worthwhile to examine the homogeneity of pure clam poison and tailings toxin by a method different from those previously employed, and the behavior of these materials during quantitative paper strip electrophoresis is reported herein.

RESULTS AND DISCUSSION

The paper strip electrophoresis of pure clam poison was examined in a series of electrolytes ranging in pH from 1.8 to 9.25 using Whatman 3MM paper and results are given

[1]*Issued as D.R.C.L. Report No. 367.*

in Table I. In all these electrolytes, the toxin migrated toward the cathode as a single, Weber-positive spot. In the first four electrolytes there was no ultraviolet fluorescence

TABLE I

Paper electrophoresis of clam poison

Electrolyte	pH	Time (hr)	True distance* (cm) migrated by: Toxin	UV-fluorescent material
HCOOH, 1 *N*	1.80	1.75	15.7	
HCOOH, 0.1 *N*	2.38	1.75	12.8	
HOAc, 1 *N*	2.30	1.75	10.4	
NaOAc/HOAc, 0.1 *M*	4.38	2.0	13.1	
NaH_2PO_4/Na_2HPO_4, 0.1 *M*	6.5	1.25	4.3	−1.0, 0.0, 4.6
$Na_2B_4O_7$, 0.1 *M*	9.25	1.0	3.0	−3.5, 0.2, 3.0

*Migration toward cathode designated as positive.

coincident with the toxin spot and none was anticipated since paper chromatograms performed on the same sample in the usual manner (2) revealed it to be free of fluorescence.* In the phosphate and borate buffers, however, there was ultraviolet fluorescence coincident with or overlapping the Weber-positive spot, together with two additional ultraviolet-fluorescent spots. The explanation for this phenomenon cannot be stated with certainty but could well be related to the frequent observation that the toxicity of clam poison decreases with increasing pH of its aqueous solutions (4–6), thus implying some destruction of the poison under these conditions. In this connection we have found that clam poison kept at 25° in aqueous solution at pH 6 for 11 days decomposed to the extent of 40%, with formation of a second Weber-positive substance of low toxicity and two additional ultraviolet-fluorescent substances, one of which is highly toxic (7). The appearance of multiple fluorescent spots in the phosphate and borate buffers makes these electrolytes less suitable for quantitative examination of the electrophoresis of clam poison than those electrolytes which do not cause such abnormalities. The sodium acetate – acetic acid buffer, although satisfactory for qualitative experiments, was not considered suitable for quantitative work because of the difficulty of removing salt from the recovered toxin. The 1 *N* formic acid proved the most satisfactory of the remaining acidic electrolytes, since it gave the most compact spots and the mobility of the poison was high. Whatman No. 1 and Reeve Angel No. 934-AH glass fiber papers gave more diffuse spots than No. 3MM paper and could not be loaded as heavily as the latter. Experiments with Whatman No. 17 and seed-test papers revealed them to be unsuitable for strip electrophoretic work, at least in this application, since 1-mg spots of toxin streaked very badly.

Earlier work on the purification of clam poison by quantitative paper chromatography in the acidic solvent system *t*-butanol:acetic acid:water (2:1:1) on Whatman No. 1, No. 17, and seed-test papers established the importance of extensive pretreatment of the papers to minimize introduction of impurities into the recovered toxin (2, 3). It was therefore necessary to ascertain the quantities of impurities introduced into toxin recovered by aqueous elution after electrophoresis on Whatman 3MM paper in 1 *N* formic

**Previously, samples of partially purified clam poison obtained from both the U.S. Army Chemical Corps Biological Laboratories and the U.S. Army Chemical Research and Development Laboratories exhibited fluorescence coincident with the Weber-positive toxin in paper chromatograms in t-butanol:acetic acid:water (2:1:1). This fluorescence proved separable from the toxin on electrophoresis in the first four electrolytes listed in Table I and was concluded to be a minor impurity present in partially purified samples, since pure specimens from both of the above-mentioned sources did not contain it.*

acid and, if possible, to develop a method of pretreatment for the paper capable of minimizing such impurities. To this end, 8×18-in. sheets of untreated 3MM paper were subjected to electrophoresis in blank runs under conditions identical with those described in the experimental section for electrophoresis of clam poison. Strips were removed from the dried sheet at preselected mobilities corresponding to the components in clam poison tailings, eluted with water, treated with Amberlite IRA-400 (Cl) resin, and filtered (2, 3). The filtrates were lyophilized and residues weighed. The experiments were repeated using Whatman 3MM papers which had been chromatographically pretreated by the procedure previously found to be most effective for removal of impurities from Whatman No. 1, No. 17, and seed-test papers (2, 3). Finally, 8×18-in. sheets of 3MM paper which had been chromatographically pretreated were conditioned further, by elution with 1 *N* formic acid and prolonged electrophoretic treatment as described in the experimental section, before the quantities of extractable impurities were determined. Results of these experiments are given in Table II, from which it is clear that untreated paper yields

TABLE II

Impurity recovered from Whatman 3MM paper

Mobility of band (cm)	Weight recovered (mg/in²) from:		
	Untreated	Pretreated	Pretreated and electrophoretically conditioned
5.1	0.074	0.046	0.024
6.7	0.076	0.060	0.024
8.2	0.075	0.068	0.036
18.0	0.057	0.044	0.025
18.8	0.103	0.079	0.031
22.5	0.106	0.069	0.034

substantial amounts of impurities which can be reduced appreciably by chromatographic pretreatment (2, 3). A further reduction can be effected by prolonged washing of the pretreated papers with 1 *N* formic acid, followed by electrophoretic conditioning. Preliminary experiments revealed the apparent mobility of clam poison under the experimental conditions used to be 18–19 cm and that the maximum loading attainable to confine the toxin to a 1×8-in. band after electrophoresis is 8–10 mg. It was concluded from the data in Table II that use of electrophoretically conditioned pretreated paper would introduce 2–3% of impurity into the recovered toxin, and although this level was somewhat greater than that realized by use of heavy-paper chromatography (3) it was still acceptable for the purpose of the present study.

A sample of pure clam poison dihydrochloride (5.02 mg, toxicity 6000 MU/mg, $[\alpha]_D^{25}$ +127°) was applied to an 8×18-in. sheet of electrophoretically conditioned pretreated paper and subjected to electrophoresis in 1 *N* formic acid at 900 v for 1.75 hours. Examination of a reference strip from the electrophoretogram under ultraviolet irradiation revealed no ultraviolet-fluorescent material. Spraying with Weber reagent revealed only one pink spot with apparent mobility 18.1 cm and ninhydrin produced a single yellow spot characteristic of the toxin (2) with the same mobility as the Weber-positive material. The substance was recovered by aqueous elution and the toxicity (5700 MU/mg) and specific rotation (+126°) were identical, within experimental error, with those of the starting material. The infrared spectrum was also identical with that reported previously for clam poison (2, 8). Since recovery was quantitative on both a weight (102%) and

toxicity (97.5%) basis it is evident that paper electrophoresis provides further support for the view that clam poison which possesses the physical constants delineated by Schantz and co-workers (1) is homogeneous.

Electrophoretograms on samples of tailings toxin (toxicity 5400±400 MU/mg, $[\alpha]_D^{25}$ +98±4°) on Whatman 3MM paper in 1 *N* formic acid at 900 v for 1.75 hours revealed the presence of Weber-positive toxin at an apparent mobility of 18–19 cm, ninhydrin-positive spots at 21 and 30 cm, and ultraviolet-fluorescent spots at 6.5 and 8 cm. These results indicated that electrophoresis is capable of separating components in the tailings toxin which are not separable by paper chromatography.

A sample of tailings toxin (8.40 mg, toxicity 5100 MU/mg, $[\alpha]_D^{25}$ +102°) was applied to an 8×18-in. sheet of electrophoretically conditioned pretreated Whatman 3MM paper and subjected to electrophoresis at 900 v for 1.75 hours in 1 *N* formic acid. A reference strip was examined under ultraviolet irradiation, then sprayed with Weber-reagent and ninhydrin for location of the components, which were recovered by aqueous elution. The eluates were lyophilized, weighed, and bioassayed as described in the experimental section. The results given in Table III clearly show that recovery on a weight basis is quantitative

TABLE III

Quantitative electrophoresis of tailings toxin*

Fraction No.	Chromogenic agent	Apparent mobility (cm)	Corrected weight (mg)	Toxicity (MU/mg)	Total MU
1	Ultraviolet	6.6	0.168	200	34
2	Ultraviolet	8.0	0.148	250	37
3	Weber	18.5	6.662	5,500	36,600
4	Ninhydrin	21.8	0.580	550	320
5	Ninhydrin	30.0	0.641	Nil	
			8.199 (101%)		37,000 (89.6%)

*Theoretical recovery 8.10 mg (41,300 MU).

whereas recovery on a toxicity basis is 90% of theoretical. Approximately 99% of the toxicity accounted for is contained in fraction 3, the specific rotation of which rose by 14% to +116° and the toxicity of which increased 8%. The infrared spectrum of the fraction was indistinguishable from that of clam poison (3). Because of the marked increase in rotation on electrophoretic treatment it appeared that the anomalous rotations of enriched tailings toxin (3) owe their origin to the presence of impurities (fractions 1, 2, 3, and 5) which possess low-order toxicities and little or no optical activity. (Fractions 1, 2, and 5 had no optical activity and fraction 4 had specific rotation +8.2°.) This point of view was confirmed by a second experiment in which fraction 3 was repurified by the same method. The recovered toxin had specific rotation +127° and toxicity 5800 MU/mg, which is within the range of values reported by Schantz and co-workers for pure clam poison (1), and the infrared spectrum of the sample remained unchanged. Recovery in the toxin fraction was 97% on a weight basis and 96% on a toxicity basis. The discrepancy between the recovery on a weight and toxicity basis in the experimental results given in Table III is ascribed to the difficulty of obtaining accurate bioassays on fractions possessing low-order toxicity, particularly when the latter contain rather large amounts of impurities from the paper. It is possible that such impurities may suppress the toxicity since it has been shown by Wiberg and Stephenson (6) that the presence of sodium chloride produces such an effect.

It is evident, therefore, that the toxin obtained by paper chromatographic purification of clam poison tailings (3) is clam poison containing toxic impurities with little or no optical activity and which are removable by paper electrophoresis. Clearly, the method described herein for electrophoretic purification of clam poison, although useful as a research tool, is quite impractical for purification of large quantities of tailings. However, it seems quite likely to us that a continuous electrophoretic apparatus would circumvent this drawback.

Schantz and co-workers (8) have reported clam poison to contain periodate-cleavable groups, the precise nature of which is unknown. The periodate-labile moiety could contain one or more of several well-known functional groups (9) and it is conceivable that one of these might be a 1,2-diol. It occurred to us that it might be possible to demonstrate the presence of the latter if it was present in a cis configuration in a five- or six-membered ring by the behavior of clam poison on paper electrophoresis in borate buffer, since under such circumstances a negatively charged borate–diol complex would be formed which would migrate toward the anode (10, 11). The observation (Table I) that clam poison migrates toward the cathode on electrophoresis in borate buffer could, therefore, be construed as evidence against the presence of the type of 1,2-diol group referred to above. However, it was also considered possible that the effect of borate in producing a negatively charged complex might have been masked by concomitant formation of ammonium-type ions on the basic centers known to be present (8). A brief examination of two model compounds demonstrated that masking of the borate-complexing effect with diols can indeed occur in the presence of a basic nitrogen atom. It was previously shown (12) that the N-*p*-nitrobenzoyl derivatives of *dl*-3α-amino-1α,2β-cyclohexanediol and *dl*-3β-amino-1α,2α-cyclohexanediol had M_G values of 0 and 0.34 respectively on electrophoresis in 0.1 M sodium tetraborate at 435 v; i.e., as anticipated, the *cis*-diol formed a borate complex which migrated toward the anode, whereas the *trans*-diol did not. Under identical conditions, the corresponding aminediols *dl*-3α-amino-1α,2β-cyclohexanediol and *dl*-3β-amino-1α,2α-cyclohexanediol behaved quite differently. Both migrated toward the cathode and the M_G values for the *cis*- and *trans*-diols were -0.24 and -0.49 respectively. These results suggest that the *trans*-diol formed only an onium-type ion and thus migrated toward the cathode more rapidly than the *cis*-diol, which in addition contained a negatively charged center due to borate complex formation. Thus, conclusions reached on the basis of paper electrophoresis in borate buffer regarding the stereochemical configuration of 1,2-diols in five- or six-membered ring compounds which also contain a basic nitrogen atom may be erroneous unless the basic center is protected from salt formation. It is therefore not possible to conclude from the present experiments whether or not clam poison contains a 1,2-diol function.

EXPERIMENTAL

All experiments were performed in a water-cooled closed strip-type apparatus (E.C. Apparatus Co., Model 401) containing the appropriate electrolyte. For qualitative experiments 10 λ (200 γ) of a 2% aqueous solution of clam poison was applied to strips of Whatman 3MM paper (6.3×46 cm) and placed in the apparatus, which was equipped with wicks of Whatman 3MM paper extending the strips to which the toxin was applied into the electrolyte (total path length of current = 60 cm). A voltage of 900 was applied (i.e. 15 v/cm) for the length of time given in Table I. The paper strips were dried for 7 minutes on a glass plate at 100°,* cut in half longitudinally, and the portion containing the clam poison sprayed with Weber reagent,

**Excessive heating of the paper strips must be avoided since it was found that heating at 100° for periods exceeding 10 minutes causes the appearance of ultraviolet-fluorescent material coincident with the toxin. Unlike other ultraviolet-fluorescent material which is observed to be coincident with the toxin in paper chromatograms of partially purified toxin, the fluorescent substance produced by action of heat on pure clam poison is not separable electrophoretically.*

after examination under ultraviolet irradiation to locate fluorescent material. The remainder of the electrophoretogram was sprayed with a chromogenic agent to reveal the particular reference compound used to define the electroendosmotic migration. *i*-Inositol was used as reference compound for the first four electrolytes shown in Table I and was revealed by spraying with ammoniacal silver nitrate, followed by heating. L-Proline (isoelectric point pH 6.3) was used as reference compound in the phosphate buffer and revealed by spraying with ninhydrin. The glucose and tetramethylglucose used with borate buffer were revealed by ammoniacal silver nitrate and by iodine in petroleum ether (0.2% w/v) respectively. Acid electrolytes were prepared from reagent grade acids, the strengths of which were determined by titration. The other buffers were prepared from appropriate reagent grade salts.

For the experiments with *dl*-3α-amino-1α,2β-cyclohexanediol and *dl*-3β-amino-1α,2α-cyclohexanediol in 0.1 *M* sodium tetraborate, 1% aqueous solutions were spotted on strips of Reeve Angel No. 934-AH glass fiber paper (6.3×46 cm) together with glucose and tetramethylglucose and subjected to electrophoresis under conditions identical with those previously described for the N-*p*-nitrobenzoyl derivatives (12). The strips were dried at 100° on a glass plate and sprayed with alkaline permanganate (13).

Pretreatment of Papers

Whatman 3MM papers were pretreated by chromatographic washing according to the method described previously (2) for Whatman No. 1 paper. For preparation of electrophoretically conditioned paper, the pretreated paper was eluted with 1 *N* formic acid for 2 days, with water for 2 days, air-dried, and cut into 8×18-in. sheets. The latter were subjected to electrophoresis in 1 *N* formic acid at 900 v for 5 hours, dried for 1.5 minutes at 100° then in air at room temperature, washed for 2 days with water, and air-dried.

Blank Runs on Pretreated Paper

Wicks used in all quantitative experiments were pretreated Whatman No. 1 paper. Whatman 3MM papers (8×18-in.), untreated, pretreated, and electrophoretically conditioned, were subjected to electrophoresis in 1 *N* formic acid at 900 v for 1.75 hours. The sheet was dried for 1.5 minutes at 100° and suspended horizontally at room temperature until completely dry. Bands (1/2 to 1 in. wide) were cut from the "electrophoretogram" in locations corresponding to the mobilities displayed by components in tailings toxin in qualitative experiments under equivalent conditions and eluted with water (3–5 ml). The eluates were passed through Amberlite IRA-400 (Cl) resin (1.5–2 ml), filtered through a fine-porosity sintered-glass funnel, lyophilized, and weighed. From the areas of the strips, the weights of residues recoverable per sq. in. of paper at the mobilities indicated in Table II were determined.

Paper Electrophoretic Purification of Tailings Toxin

Clam poison tailings toxin (8.40 mg, toxicity 5100 MU/mg, $[\alpha]_D^{25}+102°$) was applied as 28 spots from a 1% solution along a start line 4 in. from one end of an 8×18-in. sheet of electrophoretically conditioned Whatman 3MM paper. The sheet was subjected to electrophoresis under conditions identical with those for the blank runs. After drying as described above, a reference strip was examined under ultraviolet irradiation, sprayed with Weber reagent and ninhydrin for location of the components, and the bands removed. The latter were extracted as described in the blank runs and the weights of residues determined. From the weights thus obtained, the weights of impurities known to be introduced as a result of blank runs on the same batch of paper were subtracted to give the corrected weight of each fraction, as shown in Table III. Bioassays were performed on all the fractions as described previously (3, 5). The infrared spectrum of fraction 3 was recorded (KBr pellet) and the specific rotation (1% aqueous solution) was found to be $[\alpha]_D^{25}$ +116°. Fraction 3 was repurified in the same manner, yielding toxin with specific rotation +127° and toxicity 5800 MU/mg (recovery, 96% on a toxicity basis and 97% on a weight basis).

Paper Electrophoresis of Pure Clam Poison Dihydrochloride

Pure clam poison dihydrochloride (5.02 mg, toxicity 6000 MU/mg, $[\alpha]_D^{25}$ +127°) was subjected to quantitative electrophoresis as described for the tailings toxin. Only one Weber-positive band of apparent mobility 18.1 cm was obtained. Elution gave 4.78 mg (102% on a weight basis, 97.5% on a toxicity basis) of pale yellow glass with toxicity 5700 MU/mg and $[\alpha]_D^{25}$ +126°. The infrared spectrum was identical with that of the starting material.

ACKNOWLEDGMENTS

We are indebted to Dr. E. J. Schantz of the U.S. Army Chemical Corps Biological Laboratories for providing the sample of pure clam poison dihydrochloride used in this work. Thanks are also due Dr. A. D. Tennant and Mr. R. Tuszynski of the Laboratory of Hygiene, Department of National Health and Welfare, Ottawa, for performing the bioassays and to Dr. R. N. Jones and Mr. R. Lauzon, Division of Pure Chemistry, National Research Council, Ottawa, for measurement of infrared spectra.

REFERENCES

1. J. D. MOLD, J. P. BOWDEN, D. W. STANGER, J. E. MAURER, J. M. LYNCH, R. S. WYLER, E. J. SCHANTZ, and B. RIEGEL. J. Am. Chem. Soc. **79**, 5235 (1957).
2. A. A. CASSELMAN, R. GREENHALGH, H. H. BROWNELL, and R. A. B. BANNARD. Can. J. Chem. **38**, 1277 (1960).
3. R. A. B. BANNARD and A. A. CASSELMAN. Can. J. Chem. **39**, 1879 (1961).
4. H. SOMMER and K. F. MEYER. Arch. Pathol. **24**, 560 (1937).
5. E. J. SCHANTZ, E. F. MCFARREN, M. L. SCHAFER, and K. H. LEWIS. J. Assoc. Offic. Agr. Chemists, **41**, 160 (1958).
6. G. S. WIBERG and N. R. STEPHENSON. Toxicol. Appl. Pharmacol. **2**, 607 (1960).
7. R. A. B. BANNARD, R. GREENHALGH, and A. A. CASSELMAN. Unpublished results.
8. E. J. SCHANTZ, J. D. MOLD, W. L. HOWARD, J. P. BOWDEN, D. W. STANGER, J. M. LYNCH, O. P. WINTERSTEINER, J. D. DUTCHER, D. R. WALTERS, and B. RIEGEL. Can. J. Chem. **39**, 2117 (1961).
9. E. L. JACKSON. *In* Organic reactions. Vol. II. John Wiley and Sons Inc., New York. 1944. Chap. 8.
10. A. B. FOSTER. *In* Advances in carbohydrate chemistry. Vol. 12. Academic Press Inc., New York. 1957. pp. 81–115.
11. S. J. ANGYAL and D. J. MCHUGH. J. Chem. Soc. 1423 (1957).
12. R. A. B. BANNARD and L. R. HAWKINS. Can. J. Chem. **36**, 1241 (1958).
13. D. R. BRIGGS, E. F. GARNER, and F. SMITH. Nature, **178**, 154 (1956).

KINETIC SOLVENT EFFECT IN ETARD'S REACTION

R. A. STAIRS
Department of Chemistry, Queen's University, Kingston, Ontario
Received July 28, 1961

ABSTRACT

The rate of the reaction of chromyl chloride with toluene has been measured in a number of halogenated solvents. The data were correlated with the solubility parameters of the solvents and also with their dielectric constants. The results were taken as evidence against an ionic mechanism for the reaction.

INTRODUCTION

The initial stage of Etard's reaction may involve ionic or molecular attack upon the hydrocarbon by a species containing chromium VI. However, the kinetic study reported previously (1) was unable to discriminate between these two possibilities. In an attempt to subject this point to experimental scrutiny, we have now examined the effect of solvent on the rate of reaction of chromyl chloride with toluene. The influence of solvent on the rate of a chemical reaction has been discussed by Frost and Pearson from two points of view (2, pp. 132, 140). Following Hildebrand (3) they derive a relation between the rate constant and the molar volumes and solubility parameters of the various species (2, p. 132), which can be rearranged:

$$RT \ln (k/k_0) = (V_A\delta_A^2 + V_B\delta_B^2 - V_{\neq}\delta_{\neq}^2) - 2(V_A\delta_A + V_B\delta_B - V_{\neq}\delta_{\neq})\delta_l + (V_A + V_B - V_{\neq})\delta_l^2. \quad [1]$$

Here V represents a molar volume and δ a solubility parameter (related to internal pressure). The subscripts refer to the two reactants (A, B), the activated complex ($\neq$), and the solvent (l), and k_0 and k are the rate constants in a hypothetical ideal solution and in the real solution. For a given reaction at constant temperature, in different solvents having a range of values of the solubility parameter δ_l, by fitting an equation of the form $\log k = a + b\delta_l + c\delta_l^2$ to the data, it should be possible to evaluate $V_{\neq}$ from the coefficient of δ_l^2, and then $\delta_{\neq}$ from the coefficient of δ_l, if V_A, V_B, δ_A, δ_B are known or can be estimated. With imprecise data it should still be possible, by making an assumption about the volume of activation ($\Delta V_{\neq} = V_{\neq} - V_A - V_B$), to arrive at an estimate of $\delta_{\neq}$, and hence obtain some idea of the molecular character of the activated complex.

The other approach (2, p. 140), following Kirkwood (4), considers all the species A, B, and $\neq$ as more or less polar, ignores all but electrostatic forces, and yields

$$RT \ln (k/k_0) = \frac{N(\epsilon-1)}{2\epsilon+1}\left(\frac{\mu_A^2}{r_A^3} + \frac{\mu_B^2}{r_B^3} - \frac{\mu_{\neq}^2}{r_{\neq}^3}\right). \quad [2]$$

Here k is the rate constant in the real solvent of dielectric constant ϵ, and k_0 is that in a hypothetical solvent of dielectric constant unity, but otherwise identical with the first. N is Avogadro's number, and μ represents the electric dipole moment and r the molecular radius of the species indicated by the subscript. Thus, if estimates can be made of the dipole moments and the radii of the reactant species and of the radius of the activated complex, an estimate of the dipole moment of the complex can be obtained from the slope of a graph of $\log k$ against $(\epsilon-1)/(2\epsilon+1)$.

METHOD AND RESULTS

Kinetic measurements were made on the reaction between chromyl chloride and toluene (Etard's reaction), using the method already described (1), in a number of solvents. The solvents are listed in Table I, together with values of their dielectric constants and

TABLE I

Solvent properties

Solvent	ϵ_{298}*	δ_{298}
1,2-Dichloroethane	10.13	9.8‡
1,1,2,2-Tetrachloroethane	7.83	9.8§
Chloroform	4.96	9.3‡
1,1,2-Trichloro-*f*-ethane	2.48†	7.2§
Carbon tetrachloride	2.23	8.6‡
Pentachloroethane	3.60	9.4‡

*Values from International Critical Tables, unless otherwise indicated.
†Value from "Freon" Technical Bulletin B-2, E.I. du Pont de Nemours and Co. (Inc.), Wilmington 98, Delaware (adjusted to 25° C).
‡Value from ref. 2, p. 436.
§Value estimated by methods from ref. 2, chap. XXIII.

solubility parameters at 25° C. All the solvents were purified by treatment first with concentrated H_2SO_4 and then with water, followed by drying over $CaCl_2$, and distillation through a short column. The most satisfactory test of purity was found to be the clarity of the CrO_2Cl_2 solutions. Slow reaction of CrO_2Cl_2 with the solvent was observed, and roughly corrected for, in the case of dichloroethane.

Table II contains the results, in the form of second-order rate constants, each being the average of three to six determinations in each solvent at each temperature. Estimates of

TABLE II

Kinetic data

Solvent	t (°C)	k (liter mole^{-1}sec^{-1})	E^a (kcal/mole)	Steric factor
CCl_4	25.0	$1.55\pm0.04\times10^{-4}$	14.9*	2×10^{-5}
$C_2H_4Cl_2$	25.0	$7.8\pm0.6\times10^{-4}$	11.6	1×10^{-6}
"	0.4	$1.60\pm0.05\times10^{-4}$		
"	40.0	$2.33\pm0.20\times10^{-3}$		
$CHCl_3$	25.0	$2.59\pm0.14\times10^{-4}$	14.0	1.5×10^{-5}
"	35.0	$5.84\pm0.11\times10^{-4}$		
"	1.0	$3.28\pm0.07\times10^{-5}$		
$C_2H_2Cl_4$	27.5	$6.28\pm1.02\times10^{-4}$	13.6	2×10^{-5}
"	35.0	$1.16\pm0.11\times10^{-3}$		
"	1.0	$7.4\pm2.1\times10^{-5}$		
$C_2Cl_3F_3$	1.0	$1.83\pm0.09\times10^{-5}$	14.9	5×10^{-5}
"	13.0	$5.63\pm0.08\times10^{-5}$		
"	21.3	$1.38\pm0.25\times10^{-4}$		
C_2HCl_5	0.5	$2.5\pm0.5\times10^{-5}$	14.2	2×10^{-5}
"	25.0	$2.54\pm0.15\times10^{-4}$		
"	40.0	$7.7\pm0.7\times10^{-4}$		

*Stairs and Burns (1).

the Arrhenius activation energies and steric factors are also listed. The steric factors appear to be normal (2, p. 94) for a bimolecular reaction between two fairly complex molecules, except for the reaction in 1,2-dichloroethane, which may be anomalously slow, or in error owing to reaction with the solvent. The constants were based on initial rates

only, and are assumed to refer to the first stage of the complex overall reaction, i.e. to the reaction

$$PhCH_3 + CrO_2Cl_2 = PhCH_2OCrCl_2OH. \qquad [i]$$

DISCUSSION

Equation [i] may represent a molecular reaction, going essentially as written, or it may involve attack by a cation derived from CrO_2Cl_2. In the latter case it is necessary to assume a bimolecular ionization step, e.g.

$$2CrO_2Cl_2 = CrO_2Cl^+ + CrO_2Cl_3^-,$$

in order to explain the observed (1) partial order of unity with respect to CrO_2Cl_2. The activated complex would be cationic, but associated with an anion, and the dipole moment of this ion pair would be large, possibly as large as 10 debyes. If a meaningful solubility parameter could be assigned to such a polar entity, it would be large number. On the other hand, the molecular reaction would be expected to have an activated complex resembling a moderately polar molecule. It should be pointed out that the kinetic ambiguity between ionic and molecular mechanisms demonstrated by Weil and Morris (5) in the urea reaction does not apply here, owing to the distinctly different character of the activated complex postulated for the two mechanisms.

Figure 1(*a*) shows the results of plotting the logarithms of the observed rate constants versus the solubility parameters (δ_l) of the various solvents, all at 25° C. The data did not

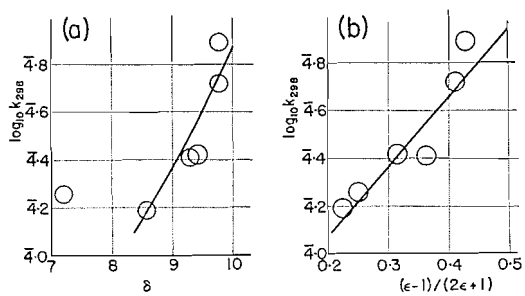

FIG. 1. Rate constants at 25° C in various solvents (as common logarithms) plotted (*a*) against the solubility parameters of the solvents, δ_l, and (*b*) against the function $(\epsilon-1)/(2\epsilon+1)$ of the dielectric constant.

appear to fit equation [1] well enough to justify calculation of the volume of activation, so the curve in the figure was drawn with an assumed value of $\Delta V_{\neq} = -10$ ml/mole. The point for the solvent $CF_2ClCFCl_2$ is the only one seriously off the curve.

The positive slope means that the activated complex has a higher solubility parameter than the reactants. Using molar volumes and solubility parameters of 107 ml and 8.9 for toluene (3, p. 437) and 81.0 ml and 10.4 for CrO_2Cl_2 (estimated by methods of ref. 3, chap. XXIII), the value of $\delta_{\neq}$ estimated from the slope is 11.5 ± 0.5, which represents only a moderate increase in intermolecular forces, and presumably in polarity.

In Fig. 1(*b*) the logarithms of the observed rate constants are plotted against $(\epsilon-1)/(2\epsilon+1)$ at 25° C. The positive slope of the line means that the activated complex is more polar than the reactants. Using radii estimated from the molar volumes used above, and the dipole moments 0.47 for CrO_2Cl_2 (6) and 0.4 (7) for toluene, one may calculate from the slope, using equation [2], $\mu_{\neq} = 2.0$. This value is typical of moderately polar molecules.

Analysis of the data by the two methods has shown that, in this case at least, the data are more compatible with the electrostatic than with the solubility parameter theories. However, within their limitations both approaches lead to the same conclusion, namely that the activated complex in Etard's reaction is somewhat more polar than the starting materials, but probably not polar enough to be described as ionic, even though in these relatively non-polar media an ionic activated complex would probably exist as an associated ion pair.

ACKNOWLEDGMENTS

The author wishes to acknowledge the assistance of Messrs. D. R. Morton and E. G. Dewar and Miss M. G. Gillies in making the measurements, a gift of 1,1,2-trichloro-*f*-ethane (Freon 113) from the Dupont Company of Canada, and a grant from the National Research Council.

REFERENCES

1. R. A. STAIRS and J. W. BURNS. Can. J. Chem. **39**, 960 (1961).
2. A. A. FROST and R. G. PEARSON. Kinetics and mechanism. John Wiley and Sons, Inc., New York. 1961.
3. J. H. HILDEBRAND and R. L. SCOTT. Solubility of non-electrolytes. 3rd ed. Reinhold Publishing Corp., New York. 1950.
4. J. G. KIRKWOOD. J. Chem. Phys. **2**, 351 (1934).
5. I. WEIL and J. C. MORRIS. J. Am. Chem. Soc. **71**, 1664 (1949).
6. C. P. SMYTH, A. J. GROSSMAN, and S. R. GINSBURG. J. Am. Chem. Soc. **62**, 192 (1940).
7. P. DEBYE. Polar molecules. Chem. Cat. Co., New York. 1929.

NITRONIUM SALTS

I. NEW METHODS FOR THE PREPARATION OF $NO_2^+BF_4^-$, $NO_2^+PF_6^-$, $NO_2^+AsF_6^-$ [1]

S. J. KUHN
Exploratory Research Laboratory, Dow Chemical of Canada, Limited, Sarnia, Ontario

Received April 13, 1962

ABSTRACT

Two new methods are presented for the preparation of complex salts of NO_2F using easily available starting materials such as nitric acid, HF, BF_3, etc. These methods produce very pure materials in a one-step reaction.

There is an increasing interest in the chemistry of nitronium salts since it has been proved that the attacking species in the nitration of aromatic compounds in many cases is the NO_2^+ ion which forms before or during the nitration. In the nitronium salts, the NO_2^+ ion is already present before the interaction with the aromatics. The nitronium salts are excellent nitrating agents (1–4) for aromatics, sometimes showing nitrating ability superior to that of the mixed acids or other nitrating agents. N- and O-nitrations have also been carried out with nitronium salts (5). The most frequently used nitronium salts for nitrations are $NO_2^+BF_4^-$ and $NO_2^+PF_6^-$ because of the ease of handling; generally, no side reaction occurs during nitrations by these compounds.

Most of the known nitronium salts other than the complex salts of NO_2F were prepared in pure state and studied by Goddard, Hughes, and Ingold (6).

The first nitronium salts of NO_2F were prepared by Woolf and Emeléus (7) in 1950 by the interaction of NO_2 together with BrF_3 on suitable non-metallic compounds like B_2O_3, As_2O_5, etc. With this method, they obtained $NO_2^+BF_4^-$, $NO_2^+PF_6^-$, $NO_2^+AsF_6^-$, and $NO_2^+SbF_6^-$. Since that time, other new methods have become known for the preparation of nitronium salts of NO_2F and a number of new salts have been prepared. Schmeisser and Elisher (8) prepared $NO_2^+BF_4^-$ and $(NO_2^+)_2SiF_6^{--}$ by adding the appropriate fluoride to a mixture of N_2O_5 and anhydrous HF in nitromethane. A number of nitronium salts have been prepared by reacting NO_2F (9, 10) with non-metallic elements or with their fluorides. Nitronium tetrafluoroborate has also been prepared by the ozone oxidation of the nitrozonium salt (11).

All of the above-mentioned methods present some difficulties. Some of them do not produce pure materials, others require separate preparation of sensitive starting materials.

In this work, two new possibilities were investigated for the preparation of nitronium salts of NO_2F. The aim of this investigation was to find methods which can produce large quantities of pure nitronium salt in a simple, one-step reaction using available starting materials.

The first reaction investigated was the interaction between nitric acid, anhydrous HF, and Lewis acid fluorides.

According to Gillespie and Millen (12), the following equilibrium exists if anhydrous HF is added to nitric acid:

$$2HF + HNO_3 \rightleftharpoons NO_2^+ + 2F^- + H_3O^+.$$

[1]*Contribution No. 46.*

In the infrared and Raman spectra of solutions of HNO_3 in liquid HF spectral features attributed to nitronium ion have also been observed by Del Gseco and Gryder (13). It was found in this investigation that if a sufficient amount of Lewis acid fluoride is added to an equimolar mixture of nitric acid and anhydrous HF, solid nitronium salt can be separated. The reaction proceeds without solvent but is easier to handle in nitromethane solution:

$$HNO_3 + HF + nBF_3 \rightarrow NO_2^+BF_4^- + H_2O.(n-1)BF_3.$$

The yields depend on the amount of Lewis acid used in the reaction, as it is shown in Tables I and II.

TABLE I

BF_3 (mole)	HNO_3 (mole)	HF (mole)	CH_3NO_2 (g)	Yield of NO_2BF_4 (g)	(%)
0.75	0.5	0.5	60.0	51.4	77.4
0.85	0.5	0.5	60.0	55.4	83.4
1.00	0.5	0.5	60.0	61.0	91.8
1.25	0.5	0.5	60.0	55.6	83.7

TABLE II

PF_5 (mole)	HNO_3 (mole)	HF (mole)	CH_3NO_2 (g)	Yield of NO_2PF_6 (g)	(%)
0.75	0.5	0.5	60	75.6	72.2
0.75	0.5	0.25	60	75.1	71.7
1.00	0.5	0.25	60	91.0	95.9
1.10	0.5	0.25	60	91.0	95.9
1.25	0.5	0.25	60	91.0	95.9

It was found that optimum yield was obtained if enough ($n = 2$) BF_3 is added to form the complex salt and HBF_3OH with the by-product water:

$$HNO_3 + HF + 2BF_3 \rightarrow NO_2^+BF_4^- + HBF_3OH.$$

The reaction is more complex if PF_5 or AsF_5 are used in the place of BF_3 because these compounds undergo hydrolysis with the water formed in the reaction.

It can be seen from Table II that maximum yield can be obtained if enough PF_5 is added to give the nitronium salt and POF_3 with the water formed in the reaction. It can also be seen that only a small amount of HF is necessary to start the reaction because the hydrolysis of PF_5 supplies more than a sufficient amount of HF for the reaction:

$$HNO_3 + 2PF_5 \xrightarrow{HF} NO_2^+PF_6^- + POF_3 + HF.$$

If the reaction is carried out under pressure a better utilization of the PF_5 can be achieved according to the following equation:

$$4HNO_3 + 5PF_5 \rightarrow 4NO_2PF_6^- + HF + H_3PO_4.$$

By using the described methods, $NO_2^+BF_4^-$, $NO_2^+PF_6^-$, $NO_2^+AsF_6^-$ were prepared with good purity and $NO_2^+SbF_6^-$, $(NO_2^+)_2SiF_6^{--}$ contaminated with hydrolysis by-products.

Later it was found that nitric acid can be replaced by esters of nitric acid in these reactions. Kuhn (14) investigated the solutions of ethyl nitrate in sulphuric acid and concluded that esters undergo ionization, yielding NO_2^+. He also found that the ultraviolet spectrum of this solution is almost identical with that of a solution of nitric acid in the sulphuric acid. Probably the same situation exists in the presence of anhydrous HF. This method is limited to the preparation of $NO_2^+BF_4^-$, $NO_2^+PF_6^-$, and $(NO_2^+)_2SiF_6^{--}$ because SiF_5 and AsF_5, being strong oxidizing agents, gave explosions when brought together with nitrate esters. It was found again (Table III) that optimum yield can be obtained if sufficient amount of BF_3 is added to produce the nitronium salt and remove the alcohol by-product in a form of $ROH.BF_3$:

$$R—O—NO_2 + HF + 2BF_3 \rightarrow NO_2^+BF_4^- + R—OH.BF_3.$$

TABLE III

BF_3 (mole)	$CH_3CH_2—ONO_2$ (mole)	HF (mole)	CH_3NO_2 (g)	Yield of NO_2BF_4 (g)	(%)
0.75	0.5	0.5	60.0	49.5	74.9
0.875	0.5	0.5	60.0	55.8	84.2
1.0	0.5	0.5	60.0	62.0	93.4
1.25	0.5	0.5	60.0	60.5	91.0

Methyl, ethyl, *n*-propyl, and butyl esters of nitric acid were used in these reactions and all of them gave similar results. The advantage of this second process is that the salts prepared in this way are extremely pure, ideal for kinetic investigations.

All of the described reactions can be carried out without the use of solvent or in excess HF. In these cases the ionization of nitric acid or the esters may occur before the addition of the Lewis acid fluoride. The situation is probably different in nitromethane solution, although the cryoscopic and spectroscopic properties of the solutions of HF and HNO_3 or HF and $R—ONO_2$ in nitromethane have not been investigated yet. An equilibrium probably exists between the unreacted acid and the protonated nitric acid or esters, and the formation of nitronium ion is promoted by the addition of the fluorides. The complex nitronium salts precipitate from the nitromethane solution, although $NO_2^+PF_6^-$ and $NO_2^+AsF_6^-$ are soluble in nitromethane, and for this reason it is advisable to use only a small amount of solvent. The optimum temperature for all these reactions is between -20 and $0°$. The HNO_3 content of the acid used is important because, in the case of dilute acid, large amounts of fluorides are needed to remove water and the yields are smaller due to the solubility of the salt in the by-product formed. Best results were obtained using 95–100% nitric acid. All these nitronium salts were prepared earlier by other methods. They are stable, white crystalline compounds if kept dry but hydrolyze in the presence of moisture. Only a few solvents can be found to dissolve these compounds because they interact with most of the usual solvents or they are not soluble at all. In previous work (12), it was found that tetramethylene sulphone is a good solvent for all of the salts. Solutions up to 10% can be made of this solvent. Nitromethane is an excellent solvent for $NO_2^+PF_6^-$ and $NO_2^+AsF_6^-$, especially for the latter ($\approx$50%). All of nitronium salts are soluble in anhydrous HF.

The infrared spectra of the nitronium salts (15) prepared by these methods were compared to the infrared spectra of nitronium salts prepared by other methods and were found to be identical.

EXPERIMENTAL

Reagents

The nitric acid used was either fuming nitric acid (HNO_3 assay 90%) or red fuming nitric acid (HNO_3 assay 100%). The HF used in the process was (HF assay 96–100%) supplied by the Matheson Co. The BF_3 and SiF_4 were also supplied by the Matheson Co. (BF_3 assay 99%, SiF_4 assay 99.5%). PF_5 and AsF_5 were supplied by Ozark and Mahoning Co. SbF_5 was supplied by Stauffer Chemicals Co. The alkyl nitrates and nitromethane used were Eastman white label chemicals or supplied by K and K Laboratories, Inc.

The HNO_3 Method

A solution of 40 g of anhydrous HF (2 moles) and 126 g of red fuming nitric acid (2 moles) in 250 g of nitromethane was placed in a 1-liter silica or polyethylene flask, and 271.3 g of BF_3 (4 moles) was introduced into this solution. The temperature was kept between −15 and 0° and the flask was shaken during the reaction. After the BF_3 addition, the precipitated white solid was filtered, washed twice with 40 g of nitromethane, then twice with 50 ml of Freon 113, chloroform, methylene chloride, or carbon tetrachloride. The complex was dried by pumping off the volatile washing solvents. Yield 91.8%, based on HNO_3 used. N% found, 10.55, calculated, 10.5.

NO_2PF_6, NO_2AsF_6 were made essentially in the same way using PF_5 or AsF_5 instead of BF_3 but the mole ratio of reagent used is different: $HF:HNO_3:PF_5(AsF_5) = 0.5:1:2$. In the preparation of NO_2BF_4, the $HF:HNO_3:BF_3$ mole ratio was 1:1:2. $(NO_2)_2SiF_6$ and NO_2SbF_6 can also be prepared by this method but the products are contaminated with SiO_2 and antimony oxide impurities.

The R—O—NO_2 Method

A solution of 20 g of anhydrous HF (1 mole) and 1 mole of alkyl nitrate in 120 g of nitromethane were placed in a 500-ml silica flask, and 2 moles of BF_3 were introduced into the reaction mixture. The temperature was kept between −20 and 0° C during the reaction. The product was filtered, washed twice with 25 g of nitromethane, then twice with 25 ml of low-boiling halogenated aliphatic hydrocarbon (Freon 113, chloroform, etc.).

Yield 93.4%, based on alkyl nitrate used. The product is very pure. N% calculated, 10.5, found, 10.5.

NO_2PF_6 and $(NO_2)_2SiF_6$ can also be made by this process.

The author is very grateful to Mrs. S. H. Flood for carrying out some of the experimental work and to Dr. Denys Cook and Miss C. D. Anderson for taking the infrared spectra of the compounds.

REFERENCES

1. G. A. Olah and S. J. Kuhn. Chem. & Ind. (London), 98 (1956).
2. G. A. Olah, S. J. Kuhn, and A. Mlinko. J. Chem. Soc. 4257 (1956).
3. S. J. Kuhn and G. A. Olah. J. Am. Chem. Soc. **83**, 4564 (1961).
4. G. A. Olah, S. J. Kuhn, and S. H. Flood. J. Am. Chem. Soc. **83**, 4571 (1961).
5. G. A. Olah, L. Noszko, S. J. Kuhn, and M. Szelke. Ber. **89**, 2374 (1956).
6. D. R. Goddard, E. D. Hughes, and C. K. Ingold. J. Chem. Soc. 2559 (1950).
7. A. A. Woolf and H. J. Emeleus. J. Chem. Soc. 1050 (1950).
8. M. Schmeisser and S. Elisher. Z. Naturforsch. Pt. b, **7b**, 583 (1957).
9. E. E. Aynsley, G. Hetherington, and P. L. Robinson. J. Chem. Soc. 1119 (1954).
10. H. C. Clark and H. J. Emeleus. J. Chem. Soc. 190 (1958).
11. R. W. Sprague, A. B. Garrett, and H. H. Sisler. J. Am. Chem. Soc. **82**, 1059 (1960).
12. R. J. Gillespie and D. J. Millen. Quart. Revs. (London), **2**, 277 (1948).
13. F. P. Del Gseco and J. W. Gryder. Abstract of Papers, 138th Meeting of the American Chemical Society, New York. 1960. p. 475.
14. L. P. Kuhn. J. Am. Chem. Soc. **69**, 1974 (1947).
15. D. Cook, S. J. Kuhn, and G. A. Olah. J. Chem. Phys. **33**, 1609 (1960).

ortho-DIQUATERNARY AROMATIC COMPOUNDS

I. THE SYNTHESIS OF *ortho*-DITERTIARYBUTYLBENZENE. SOME REACTIONS OF SIDE CHAIN SUBSTITUTED DERIVATIVES

L. R. C. BARCLAY, C. E. MILLIGAN, AND N. D. HALL
Department of Chemistry, Mount Allison University, Sackville, New Brunswick

Received April 24, 1962

ABSTRACT

1,1,4,4-Tetramethyltetralone (I) was converted by oxidative procedures into *o*-phenylene-diisobutyric acid (III). Hydride reduction of the dimethyl ester of III yielded β,β'-dihydroxy-*o*-di-*t*-butylbenzene (IV). The ditosylate of IV was converted by hydride reduction into *o*-di-*t*-butylbenzene (VI) (44%) together with rearrangement products. Ultraviolet spectral evidence indicated a slight distortion of the benzene ring in VI and its various side chain derivatives. Side reactions were encountered in the synthesis of III, which involved the conversion of this acid by periodate or lead tetraacetate oxidation into a lactone (X) and the anhydride (XI). A mechanism is postulated to account for the formation of X. The structures postulated for the various compounds were confirmed by n.m.r. spectral studies.

INTRODUCTION

The considerable interest in strained aromatic compounds bearing *o*-*t*-butyl groups has culminated in several recent syntheses of this system through the cyclization of *t*-butylacetylenic compounds with organometallic catalysts. Hubel and co-workers have successfully applied this method to the synthesis of 1,2,4-tri-*t*-butylbenzene (1), 1,2-di-*t*-butylbenzene (2), and 1,2,4,5-tetra-*t*-butylbenzene (3). Similarly Arnett and co-workers synthesized tetra-*t*-butylbenzene (4) and an impure version of *o*-di-*t*-butylbenzene (5). Earlier unsuccessful attempts to synthesize this system have been discussed (4–6).

In 1958 Bruson and co-workers (7) reported the syntheses of *o*-phenylene-diisobutyric acid, the first derivative of *o*-di-*t*-butylbenzene reported in the literature. In a preliminary communication (8) we reported the conversion of this acid into β,β'-dihydroxy-*o*-di-*t*-butylbenzene. We now wish to report on the details of this synthesis as well as the conversion of this diol to *o*-di-*t*-butylbenzene and some interesting reactions of side chain derivatives of *o*-di-*t*-butylbenzene. This strained system represents the initial research undertaken in our laboratory into the chemistry of various *o*-diquaternary aromatic systems.

DISCUSSION OF RESULTS

Bruson's procedure for the cyclialkylation of benzene with 2,2,5,5-tetramethyltetrahydrofuranone to produce 1,1,4,4-tetramethyltetralone* (I) was the starting point in our synthesis. The structure assigned to I was confirmed by its n.m.r. spectrum. A peak at 8.69 p.p.m. was attributed to the two methyl groups on carbon 4, while a peak at 8.56 of equal intensity was attributed to the two methyls on carbon 1, adjacent to the carbonyl function. The two methylene hydrogens appeared at 7.36 and a peak at 2.74 corresponded in relative intensity to the four aromatic protons. The conversion of I to *o*-phenylene-diisobutyric acid (III) by permanganate oxidation according to Bruson's procedure (7) was not very successful. A low yield of the acid (III) was obtained with a melting point of 218–219°. On the other hand Bruson reported a melting point of

**This synthesis actually yields a mixture of I and rearrangement products such as 1-acetyl-1,3,3-trimethylindan and 2,2,4,4-tetramethyl-1-indanone. These rearrangements will be the subject of a later publication.*

181–183° for this acid. In order to establish the identity of our acid, an alternate synthesis was carried out. In this synthesis I was oxidized with selenium dioxide to produce the yellow diketone (II) in high yield. Periodic acid oxidation of II at 70° readily yielded the acid (III). Treatment of III with diazomethane yielded the corresponding diester, dimethyl-*o*-phenylene-diisobutyrate. The structure of this ester (and therefore of the acid III) was confirmed by its n.m.r. spectrum. This spectrum showed a single band for C-methyl at 8.40 p.p.m. of relative intensity corresponding to the four C-methyls. The absorption for the two O-methyls appeared at 6.39 p.p.m. and the four aromatic protons absorbed at 2.73 p.p.m. On expansion of the spectrum, this band was resolved into the two groups of bands of the A_2B_2 type of pattern. The above diester was reduced with lithium aluminum hydride to yield β,β'-dihydroxy-*o*-di-*t*-butylbenzene (IV). The diol (IV) showed the expected n.m.r. spectrum. This spectrum showed a single peak attributable to C-methyl at 8.51 p.p.m. and of relative intensity corresponding to four such groups. A peak at 8.21 p.p.m. was assigned to the two hydroxyl hydrogens and one at 6.22 p.p.m. to the four methylene hydrogens. The aromatic protons showed the usual two groups of bands of the A_2B_2 pattern near 2.55 and 2.78 p.p.m. The infrared spectrum of a KBr pellet of this compound showed hydroxyl absorption at 3350 cm^{-1}, a strong band at 1037 cm^{-1} due to the $—CH_2OH$ groups, and a strong band at 750 cm^{-1} due to *o*-disubstitution. The relationships between these compounds are illustrated below.

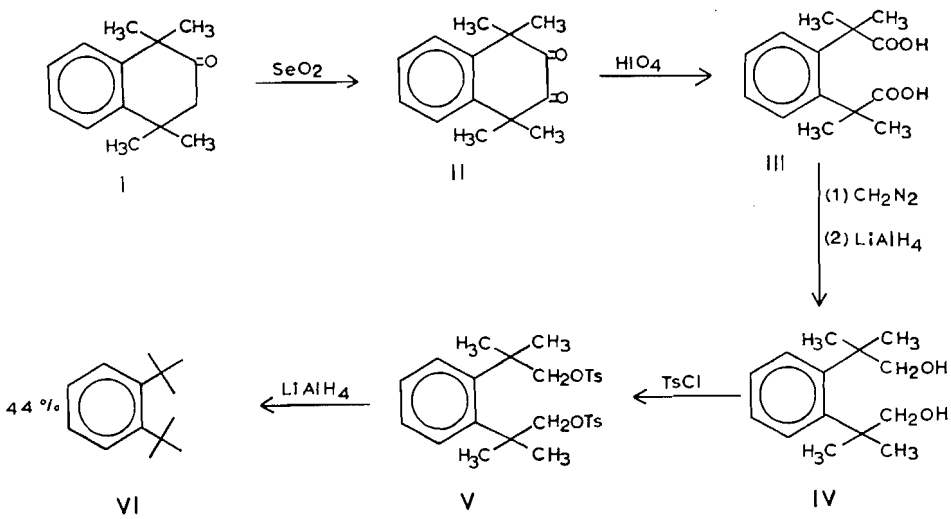

Treatment of the diol (IV) with *p*-toluenesulphonyl chloride in pyridine gave the corresponding ditosylate (V). Reduction of an ethereal solution of V with lithium aluminum hydride yielded a mixture of hydrocarbons showing parent masses of 190 and 188 in a high-temperature inlet mass spectrometer. Vapor phase chromatography indicated three major components in this mixture and, using this technique, *o*-di-*t*-butylbenzene (VI) (m.p. 24–27°) was separated in 44% yield. The structure of this hydrocarbon was confirmed by its n.m.r. spectrum, which showed one strong band for the C-methyls at 8.49 p.p.m. corresponding to the six such groups and the two groups of bands for the four aromatic protons near 2.63 and 3.09 p.p.m. The infrared spectrum of VI showed bands at 1390, 1360, 1230, and 1195 cm^{-1} attributed to the *t*-butyl groups, and a strong band for *o*-disubstitution was present at 755 cm^{-1}.

The two other major components formed by hydride reduction of V were found to consist of an unsaturated hydrocarbon (VII) and a hydrocarbon (VIII) of the same skeletal structure, since VII was converted to VIII by catalytic reduction. The structure of VII was established by its n.m.r. spectrum. This spectrum showed a band at 8.63 p.p.m. corresponding to the nine protons of a *t*-butyl group. There was a series of partially resolved symmetrical bands at 7.98, 8.10, 8.44, and 8.59 p.p.m. of relative intensity corresponding to six protons. The observed splitting can be explained by examination of a molecular model of *o*-*t*-butyl-β,β-dimethylstyrene, the structure postulated for VII. The bulky *t*-butyl group forces the ortho-situated unsaturated side chain out of the plane of the benzene ring. As a result one of the methyl groups on the olefinic carbon lies directly over the plane of the benzene ring, thereby causing a shielding effect on the protons in this group which is absent in the other methyl group on the olefinic carbon. An A_3B_3-type pattern is therefore observed for these two methyl groups. Absorption at 3.43 p.p.m. was attributed to the olefinic proton and a series of bands between 2.58 and 3.00 p.p.m. to the four aromatic protons.

Hydrocarbon VII showed the expected infrared spectrum with a band at 837 cm^{-1} attributed to the out-of-plane deformation of the olefinic proton and a band at 765 cm^{-1} due to *o*-disubstitution. On the other hand VII did not show the typical ultraviolet spectrum expected of an alkyl styrene. There was only comparatively weak general absorption, with no maxima observed. This can be attributed to steric inhibition of resonance whereby the olefinic double bond has been twisted out of the plane of the benzene ring.

Hydrocarbons VII and VIII undoubtedly formed by rearrangement accompanying the hydride reduction of V. In this case the nucleophilic displacement of the tosyl group may take place by an ionizing mechanism. The benzene ring can participate in this displacement (anchimeric assistance) through formation of a phenonium ion intermediate (IX). The relief of strain in the rearranged compounds VII and VIII would be a contributing driving force for this rearrangement. This is an interesting case of rearrangement accompanying hydride reduction; Winstein and co-workers (9) demonstrated that ethyl ether becomes a good ionizing medium in the presence of an added salt. It is possible that lithium aluminum hydride similarly promotes the ionization of V in ethyl ether.

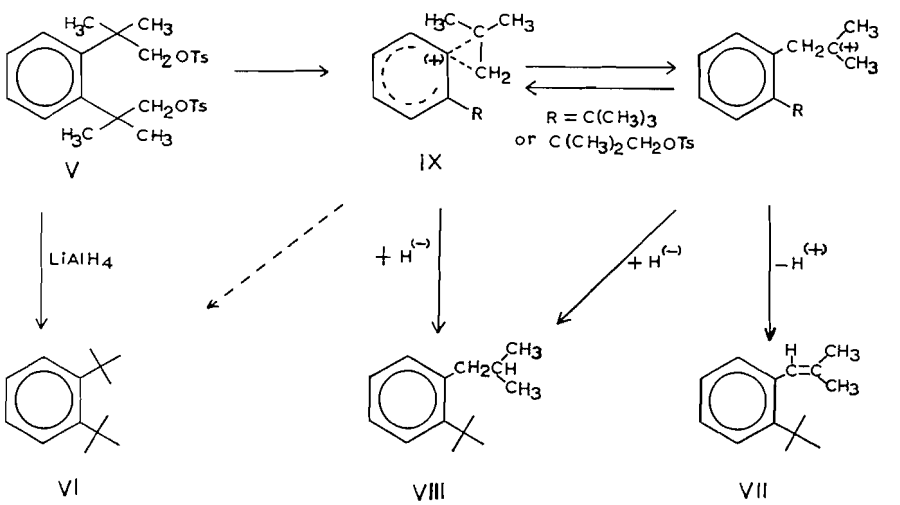

The ultraviolet absorption spectra of *o*-di-*t*-butylbenzene and derivatives are summarized in Table I. *o*-Di-*t*-butylbenzene and its derivatives all show a broad general

TABLE I

Ultraviolet absorption spectra

Compound	λ_{max} (mμ)	ϵ
1,1,4,4-Tetramethyltetralin	271, 264, 257	398, 457, 324
o-Phenylene-diisobutyric acid (III)	262	233
Dimethyl-*o*-phenylene-diisobutyrate	264	252
β,β'-Dihydroxy-*o*-di-*t*-butylbenzene (IV)	265	225
o-Di-*t*-butylbenzene	262.5	214

band in the region 262–265 mμ. The characteristic aspect of this absorption is the loss of aromatic vibrational fine structure typical of *o*-disubstituted benzenes such as 1,1,4,4-tetramethyltetralin. This effect has been the subject of some discussion (3–5, 8) including a detailed discussion of the infrared and ultraviolet spectrum of 1,2,4-tri-*t*-butylbenzene by Dale (10). The absence of vibrational fine structure has been attributed to a slight twisting of the benzene ring. This would result in a small decrease in overlap of the associated aromatic π-orbitals, which could account for the washing out of the aromatic fine structure in the ultraviolet spectrum. On the other hand the effect is a very subtle one compared to a seriously distorted benzene ring. Rapoport and Smolinsky (11) synthesized a highly strained 6,5,5,5-tetracyclic hydrocarbon which showed a much more dramatic change in ultraviolet absorption. In this case the spectrum was not only completely devoid of fine structure but showed a bathochromic shift of at least 8 mμ and approximately one-half the intensity of the corresponding unstrained analogue. A strikingly different behavior was shown by benzo[1,2:4,5]dicyclobutene examined by Cava and co-workers (12). The ultraviolet spectrum of this strained hydrocarbon showed a bathochromic displacement of 8–10 mμ from durene but the vibrational fine structure was preserved and furthermore the extinction coefficient of the strained hydrocarbon was 10 times *greater* than that of durene. Perhaps the strain in benzo[1,2:4,5]dicyclobutene manifests itself in an opening of the angles of the benzene ring which remains essentially planar, while the ring is actually slightly distorted in *o*-di-*t*-butylbenzene and derivatives.

If the *o*-*t*-butyl groups are seriously distorted from the plane of the ring, it is conceivable that derivatives of *o*-di-*t*-butylbenzene could exist in optically active forms (assuming the more likely "trans" distortion). Attempts to resolve *o*-phenylene-diisobutyric acid (III) through its brucine salt were completely unsuccessful. The salt was entirely homogeneous rather than consisting of diastereoisomeric forms. An attempt is being made to obtain detailed quantitative information on the "structure" of β,β'-dihydroxy-*o*-di-*t*-butylbenzene (IV) by X-ray analysis.* Unfortunately the crystal structure is a complex one with a large unit cell (approximately a cube of 17 Å) containing 16 molecules. The space group was found to be *Iba*2 with no center of symmetry and with two molecules in the asymmetric unit.

Periodic acid oxidation of 2,3-dioxo-1,1,4,4-tetramethyltetralin proceeded normally in aqueous dioxane at 70° to yield (64%) the acid (III). However a new neutral compound accompanied the formation of this acid and when the oxidation was carried out at the

*The authors are indebted to Dr. A. W. Hanson, Division of Pure Physics, National Research Council, for the X-ray measurements.

boiling point of the solvent this neutral product was formed in 90% yield. This neutral compound analyzed for $C_{13}H_{16}O_2$ and was shown to have the lactone structure (X) on the following evidence. Carbonyl absorption was shown in the ester region of the infrared at 1729 cm^{-1} and a strong band for *o*-disubstitution was present at 760 cm^{-1}. The ultraviolet spectrum of X showed characteristic aromatic absorption at 262.5 mμ, ϵ = 271 and 270 mμ, ϵ = 236 which was almost identical with that of 1,1,4,4-tetramethyltetralone (I). Mass spectral analysis of X showed the theoretical parent mass of 204, and fragment masses corresponding to loss of CH_3, CO_2, and $CO(CH_3)_2$ were observed. The n.m.r. spectrum of X showed two bands for C-methyl absorption. One appeared at 8.40 p.p.m. corresponding in intensity to six protons. The other band of equal intensity was shifted downfield to 8.30 p.p.m. due to the adjacent oxygen function. The four aromatic protons absorbed at 2.74 p.p.m.

Experiments on the mechanisms of formation of X showed that it formed from the acid (III). This acid was oxidized with periodic acid in aqueous dioxane to yield X. Treatment of III with lead tetraacetate in anhydrous dioxane or with periodic acid in glacial acetic acid yielded a mixture of approximately equal amounts of lactone (X) and the acid anhydride (XI) (m.p. 98–99°). The same anhydride resulted from dehydration of III with acetic anhydride. Colonge and Lagier earlier reported (13) the preparation of this anhydride with a melting point of 116°. Their compound probably has a different structure than XI since we have independent evidence that their starting material for oxidative degradation was not the proposed 1,1,5,5-tetramethyl-6,7-benzosuberane but rather was 1-isopropyl-4,4-dimethyltetralin. The acid (III) was recovered unchanged from heating with mineral acids or with hydrogen peroxide or benzoyl peroxide in various solvents. It appears that this reaction is specific for periodic acid and lead tetraacetate.

McCoy and Zagalo (14) reported a decarboxylation and lactonization of 2,3-diphenylglutaric acid with lead tetraacetate. Because the more stable (trans) lactone formed,

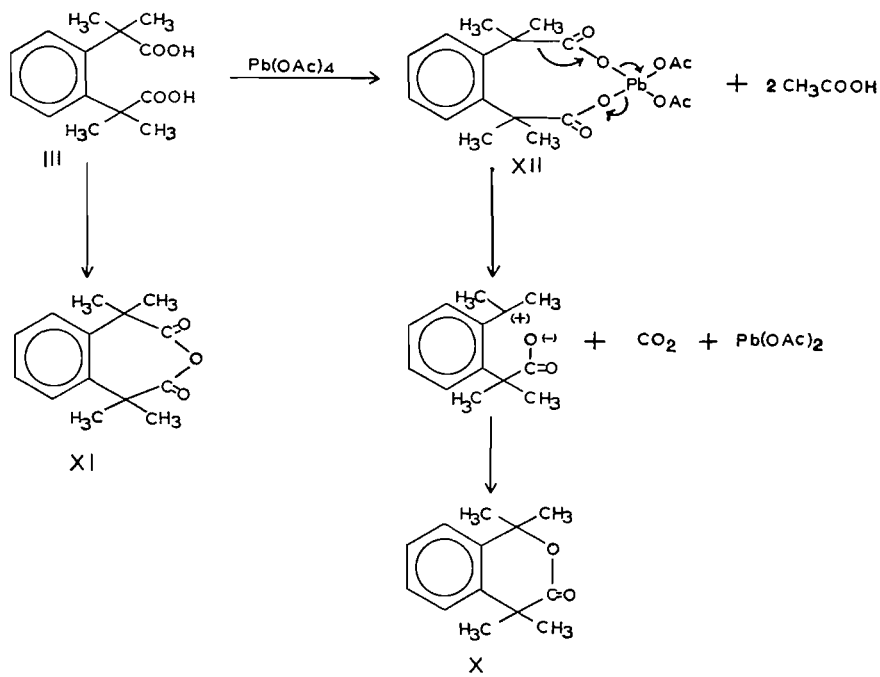

they favored a non-concerted mechanism, either radical or carbonium ion. Other workers (15) favor ionic mechanisms for the decarboxylation of organic acids by lead tetraacetate. It is possible that formation of the lactone (X) from the acid (III) involves intermediate formation of a cyclic compound such as XII. The latter could decompose by an ionic mechanism to the lactone. Anhydride formation which occurred in anhydrous solvents may take place prior to formation of the cyclic intermediate. A free radical mechanism can also be written for these reactions but the expectation that a free radical reaction could be catalyzed by peroxides was not realized.

EXPERIMENTAL

The melting points were obtained on a hot stage equipped with a microscope and are uncorrected. Ultraviolet spectra were recorded on a Beckman DK-2 spectrophotometer and infrared spectra on a Perkin–Elmer Model 136 Infracord. Reaction products were analyzed on a Perkin–Elmer Model 154-D vapor fractometer. The mass spectroscopic and nuclear magnetic resonance spectra were obtained in independent laboratories. The 1,1,4,4-tetramethyltetralone used was prepared by a procedure similar to that reported (7). The purified compound had m.p. 76.5–77.5°; λ_{max} 263.5 mμ, ϵ = 259 and 271 mμ, ϵ = 223. The infrared spectrum showed carbonyl absorption at 1700 cm^{-1} and a band for *o*-disubstitution at 755 cm^{-1}.

2,3-Dioxo-1,1,4,4-tetramethyltetralin (II)

1,1,4,4-Tetramethyl-2-tetralone (25.0 g, 0.12 mole) was dissolved in 200 ml of freshly purified dioxane, and selenium dioxide (14.0 g, 0.125 mole) was added. The reaction mixture was stirred and refluxed for 44 hours. After cooling and filtering, the solvent was removed under reduced pressure on the steam cone to yield a crude crystalline product. Recrystallization from petroleum ether yielded 22.3 g (86% yield) of yellow crystals (m.p. 61.5–63°). The ultraviolet spectrum of this compound had bands at 267 mμ, ϵ = 429 and 273 mμ, ϵ = 369. The infrared spectrum had a strong carbonyl band at 1700 cm^{-1} and a band for *o*-disubstitution at 755 cm^{-1}. Anal. Calc. for $C_{14}H_{16}O_2$: C, 77.74; H, 7.46; O, 14.80. Found: C, 77.85, 77.85; H, 7.57, 7.62; O, 14.89, 14.80.

The Action of Periodic Acid on II

(A) Preparation of o-Phenylene-diisobutyric Acid (III) and Methyl Ester

2,3-Dioxo-1,1,4,4-tetramethyltetralin (41.0 g, 0.19 mole) was dissolved in 435 ml of dioxane–water, and 50.1 g (0.22 mole) of paraperiodic acid was added. The reaction mixture was stirred and heated at 70° for a total of 40 hours. The solvent was removed under reduced pressure on the steam cone to leave a solid residue. This solid was taken up in ether and extracted with 10% sodium hydroxide. On acidification of the alkaline extract, a flocculent white precipitate was obtained. Recrystallization from ethyl acetate yielded 30.2 g (64% yield) of *o*-phenylene-diisobutyric acid (III) (m.p. 218–219°). The ultraviolet spectrum of this acid had a broad band at 262 mμ, ϵ = 233 (methanol). The infrared spectrum showed carbonyl absorption at 1680 cm^{-1} and *o*-disubstitution at 755 cm^{-1}. Anal. Calc. for $C_{14}H_{18}O_4$: C, 67.16; H, 7.25; neut. equiv., 125. Found: C, 67.03, 67.15; H, 7.32, 7.32; neut. equiv., 123.9, 124.4.

The neutral material from the preparation of the acid (III) was a viscous liquid (6.7 g). Vapor phase, infrared, and ultraviolet analyses of this material showed it to be identical with the neutral lactone (X) described below (B).

o-Phenylene-diisobutyric acid (25.0 g, 0.10 mole) was dissolved in ethyl ether and an ethereal solution of excess diazomethane was added slowly with stirring. The reaction mixture was allowed to stand in the refrigerator overnight. The solvent was then distilled, leaving a crude crystalline product. Recrystallization from petroleum ether yielded colorless crystals (27.3 g, 98%), m.p. 102–103°. Anal. Calc. for $C_{16}H_{22}O_4$: C, 69.03; H, 7.97; O, 23.00. Found: C, 69.33; H, 8.01; O, 23.39.

The ultraviolet spectrum of this ester showed a strong band at 264 mμ, ϵ = 252 (methanol). The infrared spectrum showed carbonyl absorption at 1720 cm^{-1} and a strong band at 752 cm^{-1} attributed to *o*-disubstitution (carbon disulphide).

(B) Formation of Lactone (X)

The diketone (II) (25.0 g, 0.12 mole) was oxidized with paraperiodic (31.0 g, 0.14 mole) in 250 ml of aqueous dioxane under similar conditions as above (A) except that the reaction mixture was refluxed (100°). On working up the reaction mixture as before, only 2.03 g (7%) of acidic material (III) was isolated. The major part of the reaction was a neutral product (22 g, 77%). This neutral compound was purified by chromatography of a petroleum ether solution on alumina. The compound crystallized on vacuum distillation from a Späth tube. Recrystallization from petroleum ether yielded colorless crystals, m.p. 50–51°. Anal. Calc. for $C_{13}H_{16}O_2$: C, 76.44; H, 7.89; O, 15.67. Found: C, 76.63, 76.49; H, 7.75, 7.85; O, 15.67,15.76.

The ultraviolet spectrum of this compound showed bands at 262.5 mμ, ϵ = 271 and 270 mμ, ϵ = 236 (cyclohexane). The infrared spectrum showed carbonyl absorption at 1729 cm^{-1} and a strong band attributed

to *o*-disubstitution at 765 cm^{-1} (carbon disulphide). High-temperature mass spectroscopic analysis showed a parent mass of 204. Large peaks for fragment masses were present at 189, 161, and 145.

β,β′-Dihydroxy-o-di-t-butylbenzene (IV)

Lithium aluminum hydride (14.8 g, 0.39 mole) was dissolved in 750 ml of dry ethyl ether in a three-necked flask equipped with a dropping funnel and a reflux condenser protected by a calcium chloride drying tube. Dimethyl-*o*-phenylene-diisobutyrate (27.1 g, 0.097 mole) was dissolved in 750 ml of dry ethyl ether and added dropwise to the reaction mixture over a period of 1.5 hours. The reaction mixture was refluxed for 27 hours. It was decomposed in ice water and made just acid with hydrochloric acid. The ether layer was separated, washed free from acid with water, and dried over sodium sulphate. Evaporation of the solvent left a white crystalline compound which, on recrystallization from petroleum ether – acetone, yielded 18.5 g (86% yield) of colorless crystals, m.p. 115–116°. Anal. Calc. for $C_{14}H_{22}O_2$: C, 75.63; H, 9.98; O, 14.39; active hydrogen, 0.90. Found: C, 75.34, 75.92; H, 9.98, 9.94; O, 15.12; active hydrogen, 0.90.

The infrared spectrum of this diol in a KBr pellet showed broad hydroxyl absorption at 3350 cm^{-1}. A strong band at 1037 cm^{-1} was attributed to the $—CH_2OH$ groupings and a strong band at 750 cm^{-1} to *o*-disubstitution. In chloroform solution the hydroxyl absorption appeared as two bands, at 3400 and 3570 cm^{-1}. The ultraviolet spectrum showed a broad band at 265 mμ, $\epsilon = 225$ (methanol).

Ditosylate (V) of IV

β,β′-Dihydroxy-*o*-di-*t*-butylbenzene (18.5 g, 0.083 mole) was dissolved in 100 ml of pyridine and cooled to 0°. Tosyl chloride (47.4 g, 0.249 mole) was similarly dissolved in 100 ml of pyridine and cooled to 0°. The tosyl chloride solution was then added to the diol solution and the resulting mixture left at room temperature for 24 hours. About 200 ml of water was then added and a white solid came out of solution. This was extracted with chloroform, washed with ice-cold 15% sulphuric acid, saturated sodium bicarbonate solution, and finally with water. After drying over sodium sulphate, the solvent was removed under reduced pressure at 38° to yield a white crystalline solid. Two recrystallizations from petroleum ether – chloroform yielded 36.7 g (83% yield) of ditosylate (V) (m.p. 110–111°). Anal. Calc. for $C_{28}H_{34}S_2O_6$: C, 63.37; H, 6.46; O, 18.09; S, 12.08. Found: C, 63.36, 63.32; H, 6.57, 6.67; O, 17.80, 17.79; S, 12.38, 12.49.

The ultraviolet spectrum of this compound showed bands at 262 mμ, $\epsilon = 1293$ and 273 mμ, $\epsilon = 1082$.

Lithium Aluminum Hydride Reduction of V, o-Di-t-butylbenzene

The ditosylate (V) (18.0 g, 0.034 mole) was dissolved in 1800 ml of anhydrous ethyl ether, and lithium aluminum hydride (14.2 g, 0.37 mole) was added all at once. The reaction mixture was stirred at room temperature for 2 days. It was then decomposed in ice water, made slightly acidic with hydrochloric acid and the resulting mixture extracted continuously with ethyl ether for 2 days. The extract was dried over anhydrous sodium sulphate and the solvent distilled to leave 6.3 g of a liquid residue. Vapor phase analysis at 198° of this product on a column of apiezon L grease (column "Q") indicated that there were three major components present (A, B, and C). These components were cleanly separated on this column with retention times of A = 95.5, B = 112.5, and C = 147 respectively. Quantitative vapor phase analysis indicated that the relative amounts of the components present were 19% A, 21% B, and 44% C. The original reaction product was reduced in methanol solution with hydrogen over a palladium – calcium carbonate catalyst at 50 p.s.i. Vapor phase analysis of the reduced material showed that component A had disappeared and component B was correspondingly increased. The proportion of component C was unchanged.

Larger quantities of the three components produced in the hydride reduction of V were obtained by vapor chromatography. This was accomplished by repetitive runs on an apiezon L grease column at 198° and by superheating the outlet from the vapor fractometer to 240° with electric heating tape. In this way the components were distilled into the collector as they eluted from the column rather than condensing and remixing.

The major component (C; *o*-di-*t*-butylbenzene) was a crystalline compound, m.p. 24–27°. Anal. Calc. for $C_{14}H_{22}$: C, 88.35; H, 11.65. Found: C, 88.13, 88.22; H, 11.60, 11.64.

The infrared spectrum of this compound showed a strong band at 755 cm^{-1} attributed to *o*-disubstitution. Bands at 1390, 1360, 1230, and 1195 cm^{-1} were assigned to *t*-butyl groups. The ultraviolet spectrum showed one band without fine structure at 262.5 mμ, $\epsilon = 214$.

Component A (unsaturated hydrocarbon) was similarly isolated by vapor phase analysis. This compound was obtained as a colorless oil. Anal. Calc. for $C_{14}H_{20}$: C, 89.29; H, 10.71. Found: C, 89.28, 89.15; H, 10.78, 10.72.

The infrared spectrum of this compound showed a strong band at 760 cm^{-1} attributed to *o*-disubstitution and a strong band at 837 cm^{-1} assigned to the out-of-plane deformation of an olefinic proton. The ultraviolet spectrum showed only general absorption (260 mμ, $\epsilon = 1055$).

Component B from the vapor phase analysis (also the reduction product of A) was not isolated for detailed analyses. However, the ultraviolet spectrum of B showed absorption typical of *o*-disubstituted aromatic hydrocarbons with vibrational fine structure.

The Action of Periodic Acid on o-Phenlyene-diisobutyric Acid (III)

(A) In Aqueous Dioxane

The acid (III) (1.0 g, 0.004 mole) and paraperiodic acid (0.91 g, 0.004 mole) were dissolved in a mixture of 15 ml of dioxane and 9 ml of water. The reaction mixture was stirred and refluxed for 45 hours. The solvent was removed under reduced pressure on the steam cone and the residue treated with ether. The ether extract was washed with 10% sodium hydroxide but no acid was recovered from the alkali extract. Distillation of the solvent from the ether extract left a semisolid residue (0.80 g). Ultraviolet, infrared, and vapor phase analyses of this material indicated it to be the lactone (X).

(B) In Glacial Acetic Acid

The acid (III) (0.50 g, 0.002 mole) and paraperiodic acid (0.46 g, 0.002 mole) were dissolved in glacial acetic acid and the solution heated at 100° for 2 days. The solvent was distilled under reduced pressure on the steam cone and the residue treated with ethyl ether. Some unreacted acid (III) (0.07 g) was recovered from this ether extract by extraction with 10% sodium hydroxide. The ether extract yielded 0.33 g of solid material. This material was analyzed on the vapor fractometer and found to contain 41% of the lactone (X) and 59% of the anhydride of *o*-phenylene-diisobutyric acid. The same anhydride was prepared for comparison purposes as described below.

o-Phenylene-diisobutyric acid (0.35 g, 0.0014 mole) was dissolved in 6.0 ml of acetic anhydride and the solution refluxed for 3 hours. The solvent was distilled under reduced pressure to yield 0.30 g (92%) of colorless crystals. Recrystallization from petroleum ether produced colorless crystals of m.p. 98–99°. Anal. Calc. for $C_{14}H_{16}O_3$: C, 72.39; H, 6.94; O, 20.67. Found: C, 72.28; H, 6.87; O, 20.41.

The infrared spectrum of this anhydride showed a doublet at 1770 and 1725 cm^{-1} for carbonyl absorption. A band at 765 cm^{-1} was attributed to *o*-disubstitution. The ultraviolet spectrum did not show definite maxima but exhibited shoulders at 260 mμ, ϵ = 339 and 267 mμ, ϵ = 212.

The Action of Lead Tetraacetate on III

o-Phenylene-diisobutyric acid (8.00 g, 0.032 mole) was dissolved in 300 ml of purified anhydrous dioxane, and lead tetraacetate (14.24 g, 0.032 mole) added. The mixture was stirred and heated at 75° for 21 hours. The solvent was distilled under reduced pressure on the steam cone and the organic residue dissolved in ethyl ether. The product from the ether extract was found to contain a mixture of approximately equal amounts of the lactone (X) and the anhydride (m.p. 98–99°) by vapor phase analysis.

ACKNOWLEDGMENTS

The authors express their appreciation to the National Research Council for financial support of this research. One of us (C. E. M.) was a recipient of a N.R.C. Studentship.

REFERENCES

1. U. KRÜERKE, C. HOOGZAND, and W. HÜBEL. Chem. Ber. **94**, 2817 (1961).
2. C. HOOGZAND and W. HÜBEL. Angew. Chem. **73**, 680 (1961).
3. C. HOOGZAND and W. HÜBEL. Tetrahedron Letters, No. 18, 637 (1961).
4. E. M. ARNETT, M. E. STREM, and R. A. FRIEDEL. Tetrahedron Letters, No. 19, 658 (1961).
5. E. M. ARNETT and M. E. STREM. Chem. & Ind. (London), 2008 (1961).
6. E. M. ARNETT. J. Org. Chem. **25**, 324 (1960).
7. H. A. BRUSON, F. W. GRANT, and E. BOBKO. J. Am. Chem. Soc. **80**, 3633 (1958).
8. L. R. C. BARCLAY, N. D. HALL, and J. W. MACLEAN. Tetrahedron Letters, No. 7, 243 (1961).
9. S. WINSTEIN, S. SMITH, and D. DARWISH. J. Am. Chem. Soc. **81**, 5510 (1959). S. WINSTEIN, P. E. KLINEDINST, and G. C. ROBINSON. J. Am. Chem. Soc. **83**, 885 (1961).
10. J. DALE. Chem. Ber. **94**, 2821 (1961).
11. H. RAPOPORT and G. SMOLINSKY. J. Am. Chem. Soc. **82**, 1171 (1960).
12. M. P. CAVA, A. A. DEANA, and K. MUTH. J. Am. Chem. Soc. **82**, 2524 (1960).
13. J. COLONGE and A. LAGIER. Compt. rend. **225**, 1160 (1947).
14. L. L. MCCOY and A. ZAGALO. J. Org. Chem. **25**, 824 (1960).
15. W. A. MOSHER and C. L. KIEHR. J. Am. Chem. Soc. **75**, 3172 (1953). D. BENSON, L. H. SUTCLIFFE, and J. WALKLEY. J. Am. Chem. Soc. **81**, 4488 (1959).

LIGNIN MODEL COMPOUNDS

II. PREPARATION AND PROPERTIES OF 1-HYDROXY-1-(4-HYDROXY-3-METHOXYPHENYL)-2-PROPANONE*

J. A. F. Gardner, D. W. Henderson, and Harold MacLean

Vancouver Laboratory, Forest Products Research Branch, Department of Forestry of Canada, Vancouver, British Columbia

Received April 3, 1962

ABSTRACT

Modern concepts of lignin structure suggest that the ketol 1-hydroxy-1-(4-hydroxy-3-methoxyphenyl)-2-propanone, VI, should be detectable in the hydrolysis products of lignin and wood. A reference sample of VI, previously unavailable, has now been prepared by catalytic hydrogenation of the diketone 1-(4-hydroxy-3-methoxyphenyl)-1,2-propanedione, II. Both fermentative and catalytic hydrogenation of II gave mixtures of, according to paper chromatography, mainly 2-hydroxy-1-(4-hydroxy-3-methoxyphenyl)-1-propanone, V; the desired ketol, VI; small amounts of vanillic acid; and traces of guaiacyl acetone and an unknown phenolic compound. The ketol VI was isolated from the catalytic hydrogenation products by solvent fractionation and was identified by absorption spectra, derivatives, and comparison with the other two possible isomeric ketols. Dilute alkali converted VI to the isomeric ketol V. Both ethanolysis and acidolysis of VI gave the same monomeric products as lignin.

Since the discovery by Hibbert and co-workers (1) that the four guaiacylpropane derivatives I–IV were produced by refluxing extractive-free coniferous wood with ethanol containing a small percentage of hydrogen chloride, extensive studies have been conducted on related monomers and dimers as model compounds for lignin reactions. In this way significant new knowledge of lignin structure and behavior has been acquired.

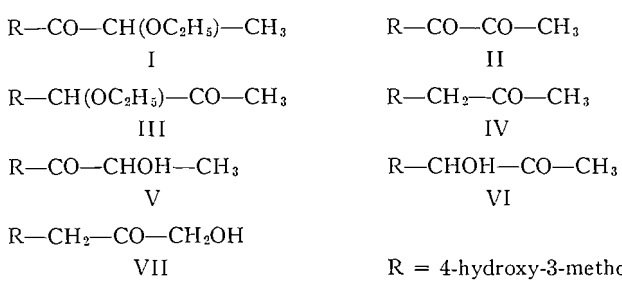

In seeking an explanation for the formation from lignin of the "ethanolysis" products, the synthesis and study of the three isomeric α-ketols V, VI, and VII were undertaken by the Hibbert group. The synthesis of V, 2-hydroxy-1-(4-hydroxy-3-methoxyphenyl)-1-propanone, and VII, 3-hydroxy-1-(4-hydroxy-3-methoxyphenyl)-2-propanone, was accomplished (2, 3) but repeated attempts failed to provide VI, 1-hydroxy-1-(4-hydroxy-3-methoxyphenyl)-2-propanone, and therefore it was necessary to perform ethanolysis and other reactions on its diacetate (4). Wacek and Horak (5) also attempted to prepare VI but found, as had Mitchell (6), that even very mild deacetylation techniques applied to the diacetate of VI invariably resulted in rearrangement to the more stable V. These findings were in accord with the results obtained with related alkylaryl α-ketols by Auwers and Noll (7) and Temnikova (8). Thus methylbenzoyl carbinol (V, R = phenyl) rearranged with a variety of reagents to phenylacetyl carbinol (VI, R = phenyl) whereas

*Paper presented at the 44th Annual Conference, Chemical Institute of Canada, Montreal, Quebec, August 3–5, 1961.

substitution of a methoxyl or hydroxyl group into the para position of the benzene ring stabilized the methylbenzoyl carbinol and completely reversed the order of stability. In the guaiacylpropane series, therefore, the para hydroxyl group stabilizes the 2-hydroxy derivative V and accounts for the difficulties experienced in attempts to prepare the 1-hydroxy derivative VI.

In a previous paper (9) strong experimental support was provided for Hibbert's proposal that the ethanolysis products, I–IV, are derived from lignin via a more reactive β-hydroxyconiferyl alcohol unit, VIII, by a series of rearrangements:

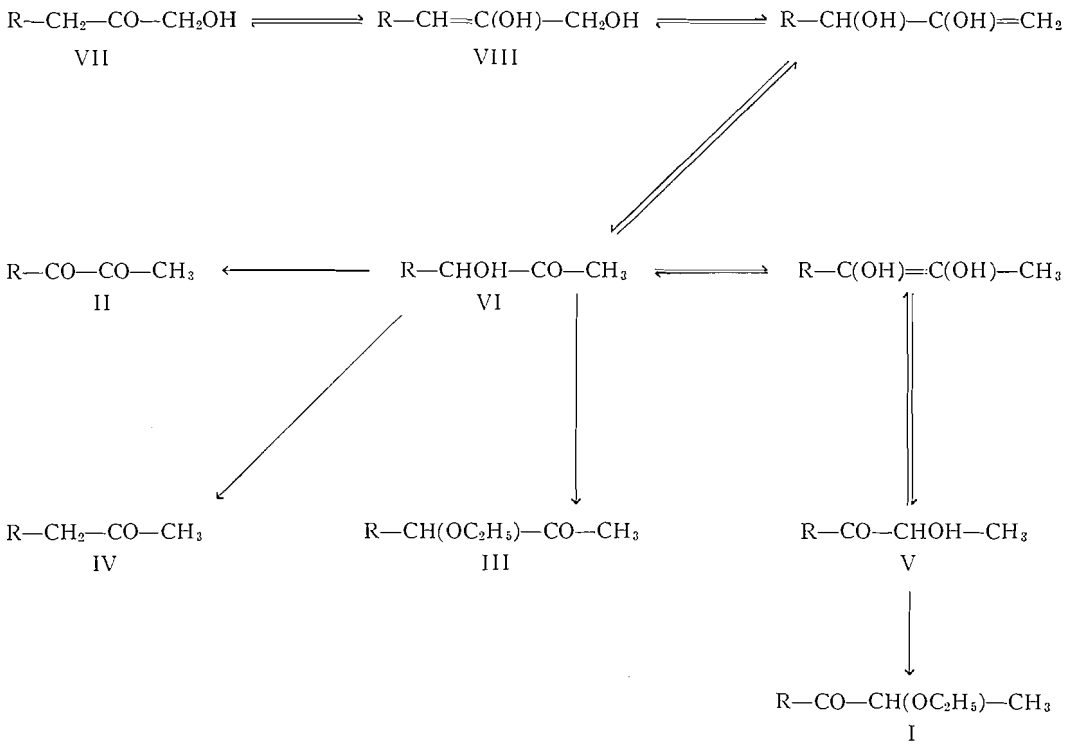

R = 4-hydroxy-3-methoxyphenyl

The relatively small amount of the ethyl ether, III, of the ketol VI compared to that of I of the ketol V obtained in lignin ethanolysis is consistent with the above scheme and the apparent relative stability of the ketols.

The same explanation applies to the formation of the lignin ethanolysis products by ethanolysis of guaiacylglycerol and its β-guaiacyl and β-coniferyl ethers, substances which have been found to be excellent model compounds for the study of characteristic lignin reactions (10). A primary α–β dehydration would yield an enol ether which would hydrolyze to β-hydroxyconiferyl alcohol, VIII. According to this scheme small amounts of the intermediate 1-hydroxy ketone VI should occur in the hydrolysis and acidolysis products of lignin and lignin model compounds. Goldschmid (11) suspected that an unknown substance detected among the products of aqueous hydrolysis of extractive-free western hemlock woodmeal was the 1-hydroxy derivative VI but this awaits confirmation. Adler *et al.* (12) showed that refluxing guaiacylglycerol-β-guaiacyl ether and two isolated lignins with dioxane–water containing 0.2 *N* hydrogen chloride ("acidolysis") gave a mixture

of products containing the 2-hydroxy ketone V, the diketone II, and guaiacyl acetone, IV. Other guaiacylpropane derivatives, if present, were not identified. The purpose of the present work was to prepare a sample of the 1-hydroxy compound VI for reference purposes in lignin hydrolytic studies and to permit a study of its properties in relation to lignin and related propylphenols.

In seeking methods that would avoid the chance of acid- and base-catalyzed rearrangements in the final stages, the possibility of preparing VI by treating vanillin with fermenting sugar solutions was investigated. Neuberg and Hirsh (13) had found that addition of benzaldehyde to sugar solutions yielded some phenylacetyl carbinol as well as benzyl alcohol. Application of this technique to vanillin showed that as well as the main product, vanillyl alcohol, minor amounts of vanillic acid, and two unknown compounds were produced. Paper chromatographic examination showed that neither of these was the known 2-hydroxy derivative V. While it was considered possible that some of the desired 1-hydroxy compound VI was present, this technique as a method of preparation was abandoned because of the obvious difficulties in purification. Subsequently, reports of the similar work of Higuchi *et al.* (14) came to hand. These workers also found that vanillyl alcohol, vanillic acid, and small amounts of the diketone II were formed from vanillin in fermenting sugar solution. Another minor product detected by paper chromatography (15) was believed to be the 1-hydroxy derivative VI but no confirmation has been published.

The hydrogenation of the diketone II as a means of preparing a sample of VI was investigated. This approach would eliminate contamination of the products with reduction products of vanillin. Both phytochemical and catalytic reduction methods were examined.

Addition of the yellow diketone to fermenting sucrose solution resulted in rapid decolorization. Descending paper chromatography in two solvent systems showed the presence of six phenolic substances: the ketol V (the main component), vanillic acid, unchanged diketone (trace), guaiacyl acetone, IV (trace), and two unknown compounds. One of these ($R_f = 0.89$ in butanol–ethanol–ammonia–water, 40:10:1:49 v/v) gave a pink color with diazotized sulphanilic acid (DSA) and was present in traces. The other ($R_f = 0.76$), present in substantial quantities, gave an orange color with DSA.

When the diketone II was treated in ethanol with 1 mole of hydrogen at room temperature and pressure over a palladium–barium sulphate catalyst prepared according to Kuhn (16), a very similar mixture of phenolic products was obtained according to paper chromatography. In this case the mixture was not contaminated with yeast and sugar fermentation products and it crystallized on standing. Recrystallization from benzene gave the pure 2-hydroxy derivative V. Attempts to isolate the other products by chromatography on celite and cellulose columns were unsuccessful. However, extraction of an ether solution of the mixture with aqueous bisulphite solution gave a bisulphite-soluble fraction containing the substance $R_f = 0.76$, believed to be the desired 1-hydroxy derivative, VI, contaminated with unreacted diketone, II. Distribution of this fraction between benzene and water gave a good separation, the diketone being retained in the benzene layer.

The product isolated from the aqueous layer as a colorless oil gave a strongly positive test for *p*-hydroxybenzyl alcohols with quinone monochloroimide (17) and exhibited only one spot on paper chromatograms using several solvent systems. It slowly crystallized and after recrystallization from ether–petroleum ether had a melting point of 53–54° C. The ultraviolet and infrared absorption spectra were consistent with a 1-aryl-2-propanone structure. Proof that it was the expected 1-hydroxy derivative, VI, was

provided by preparing the diacetate, which, obtained in high yield, was identical with an authentic sample of the diacetate of VI synthesized by the method of Mitchell and Hibbert (4).

It was of interest to determine the relative proportion of the two α-ketols V and VI produced by catalytic hydrogenation of the diketone. By quantitative paper chromatography (18), the mixture was found to consist of 73% 2-hydroxy derivative, V; 13% 1-hydroxy derivative, VI; 14% unchanged diketone; 2.6% vanillic acid; and a trace of guaiacyl acetone, IV, and an unknown ($R_f = 0.89$).

No systematic investigation of the effect different solvents or catalysts might have on the hydrogenation of the diketone was undertaken. However, after this paper was presented, the results of Adler and Marton (19) on the hydrogenation of a series of lignin model compounds became available. Using 93% acetic acid as solvent and a palladium chloride – barium sulphate catalyst, unwashed after prehydrogenation, they found that carbonyl groups conjugated to the guaiacyl ring, as in the ketol V and the diketone II, were reduced rapidly, whereas those in the position β to the ring, as in IV, were practically unaffected. Thus rapid addition of 2 moles of hydrogen to the diketone was reported to yield guaiacyl acetone, IV, via hydrogenation and then hydrogenolysis, the β-carbonyl not being reduced. This report prompted us to hydrogenate the diketone with Kuhn's catalyst (16) in 95% acetic acid instead of ethanol. After addition of 1 mole of hydrogen, the products were approximately the same as when ethanol was used as solvent, the main product being, as before, the 2-hydroxy derivative V. The indicated marked effect of the catalyst on the course of the reaction is now being investigated.

Ethanolysis of 1-hydroxy-1-(4-hydroxy-3-methoxyphenyl)-2-propanone, VI, gave the same propylphenol products, I–IV, as lignin, in accord with the prior work on the diacetate (4).

Treatment of VI with dilute alkali at 95° C rapidly brought about complete conversion to the 2-hydroxy derivative V, a result predictable from the findings of Mitchell (6) and of Wacek and Horak (5).

Acidolysis of VI in dioxane–water according to the method of Adler *et al.* (12) gave a mixture consisting of mainly the 2-hydroxy derivative V and the diketone II with traces of vanillic acid, vanillin, and an unknown phenol. Both V and II were obtained by Adler *et al.* by the acidolysis products of wood and isolated lignin. After 4 hours of acidolysis, roughly 10% of the ketol VI was unchanged. This measure of stability indicates that there is a good possibility of detecting the occurrence of the ketol VI in the acidolysis and hydrolysis products of lignins and wood.

The preparation of 1-hydroxy-1-(4-hydroxy-3-methoxyphenyl)-2-propanone, VI, completes the syntheses of the three possible α-ketols in the guaiacylpropane series and provides reference samples for use in lignin degradation studies. Its behavior in ethanolysis and acidolysis reactions confirms conclusions based on prior studies with derivatives and isomers.

EXPERIMENTAL

Solvent systems for paper chromatographic examinations were butanol–ethanol–ammonia–water (40:10:1:49 v/v) (BEAW) and tetrahydrofuran – petroleum ether (65–110°) – water (3:7:5 v/v) (THF). In the case of the latter system R_f's depended to a marked extent on the care exercised in equilibrating the paper with the solvent and therefore are not quoted.

Preparation of Diketone 1-(4-Hydroxy-3-methoxyphenyl)-1,2-propanedione, II

Two methods were used: 2-hydroxy-1(4-hydroxy-3-methoxyphenyl)-1-propanone was prepared from guaiacol and oxidized with copper sulphate by the method of Brickman *et al.* (20), or propiovanillone (22)

was converted with isobutyl nitrite by the method of Fodor *et al.* (21) to the α-oximino ketone, which was hydrolyzed to the diketone with 2% HCl at reflux or with 12 *N* H_2SO_4 at room temperature. The yellow diketone was extracted with benzene and recrystallized from petroleum ether, m.p. 62–63° C.

Preparation of 1-Hydroxy-1(4-hydroxy-3-methoxyphenyl)-2-propanone, VI

Kuhn's catalyst (16) (0.5 g) was added to 95% ethanol (50 ml), the flask evacuated, and the contents equilibrated with H_2 (13.7 ml) by mechanical shaking at slight pressure. The diketone (3 g = 0.0155 mole) was added, the flask again evacuated, and H_2 (348 ml = 0.0155 mole) added with mechanical shaking over 21 minutes. The catalyst was filtered and washed with ethanol, the filtrate and washings being evaporated under reduced pressure to yield a yellow oil (3 g). This oil gave a positive color test for *p*-hydroxybenzyl alcohols with quinone monochloroimide (17), and descending paper chromatographic examination showed the presence of six substances giving positive color reactions with DSA. The use of reference samples established the presence of vanillic acid (orange, R_f 0.22 BEAW); 2-hydroxy-1-(4-hydroxy-3-methoxyphenyl)-1-propanone, V (tan, R_f 0.54); diketone II (tan, R_f 0.60); guaiacyl acetone, IV (red, R_f 0.89); and two unknowns (strong orange, R_f 0.76; and weak red, R_f 0.89). The unknown with the same R_f on paper as guaiacyl acetone using BEAW was readily separated from it with the other solvent (THF).

The unknown with the orange color reaction, which also gave a positive 2,4-dinitrophenylhydrazone test, was isolated by the following fractionation, each step being monitored by paper chromatography. A diethyl ether solution (100 ml) was extracted with 15% sodium bisulphite solution (4×20 ml), then was back-extracted with diethyl ether (4×25 ml) to ensure removal of the 2-hydroxy derivative V and vanillic acid from the bisulphite-soluble compounds. The bisulphite solution was acidified to pH 3 with 6 *N* H_2SO_4, stripped of SO_2 using partial vacuum and a nitrogen bubbler, and then extracted with chloroform (5×25 ml). After drying, the chloroform was evaporated to leave a yellow oil which in benzene solution (50 ml) was extracted with water (5×25 ml). The water after back extraction with benzene (2×25 ml) was extracted with chloroform (7×25 ml). Drying and removal of the chloroform left a colorless oil (280 mg; 9% yield) which slowly crystallized. This material showed only one spot (orange, R_f 0.76 BEAW) on a papergram. Recrystallization from ether – petroleum ether gave colorless crystals, melting point 53–54° C. The infrared absorption spectrum, ν_{KBr}^{max} in cm^{-1} 3450, 3325, 2950, 2860, 1700 (unconjugated carbonyl), 1610, 1516, 1470, 1433, 1355, 1270, 1150, 1125, 1080, 1030, 866, 814, 735, was consistent with structure VI being very similar to that of the isomeric α-ketol VII (9). The ultraviolet absorption spectrum in ethanol (max. 282 mμ; min. 261 mμ; shoulder 234 mμ) was also consistent with this formulation. The semicarbazone, m.p. 170.5–172° C from hot water, differed from those of authentic specimens of the two α-ketols V and VII, m.p. 147–148 and 194–196° C respectively, prepared by identical procedures. The diacetate prepared in high yield (80%) by a 5-minute reflux in acetic anhydride – pyridine was identical by mixed melting point, 95.5–96° C, and infrared spectra with an authentic sample of 1-acetoxy-1-(4-acetoxy-3-methoxyphenyl)-2-propanone synthesized by the method of Mitchell and Hibbert (4).

If the oily hydrogenation product from the diketone was seeded with the 2-hydroxy-1-(4-hydroxy-3-methoxyphenyl)-1-propanone, V, partial crystallization occurred. Trituration with cold benzene followed by recrystallization from benzene gave colorless crystals, m.p. 110–111° C, identical with authentic V.

The presence of vanillic acid in the diketone hydrogenation product was proved by extraction of the ether solutions with cold 5% sodium bicarbonate solution. Acidification gave crystalline material identical with an authentic sample of vanillic acid.

Quantitative Estimation of Diketone Hydrogenation Products

A quantitative paper chromatographic method (18) with BEAW as developing solvent and Folin–Ciocalteu reagent for phenols was used, the spots being detected with ultraviolet light. Optical densities were measured at 750 mμ on a Beckman DK-2.

Ethanolysis of 1-Hydroxy-1-(4-hydroxy-3-methoxyphenyl)-2-propanone

A sample (20 mg) was refluxed with ethanol – 3% HCl (1.5 ml) for 24 hours in a carbon dioxide atmosphere. After cooling, the mixture was added to water (10 ml) and filtered. The filtrate was extracted with ether, the extract dried, and solvent removed. Paper chromatographic examination of the residue in comparison with synthetic mixtures of authentic specimens using BEAW, 20% aqueous KCl, and isopropanol–ammonia–water (8:1:1 v/v) as solvents showed the presence of the ethanolysis products I–IV.

Alkaline Rearrangement of 1-Hydroxy-1-(4-hydroxy-3-methoxyphenyl)-2-propanone

A sample (36 mg) was dissolved in 1% NaOH (15 ml), forming a yellow-colored solution which turned orange on warming under a nitrogen atmosphere on a steam bath (95° C) for ½ hour. Acidification and extraction with chloroform yielded, after removal of the solvent, a yellowish oil (30 mg) which slowly crystallized. It was shown to be the isomeric 2-hydroxy-1-(4-hydroxy-3-methoxyphenyl)-1-propanone by infrared absorption spectrum and chromatographic comparison with an authentic sample in BEAW and 20% aqueous KCl.

Acidolysis of 1-Hydroxy-1-(4-hydroxy-3-methoxyphenyl)-2-propanone

The ketol VI (10 mg) was refluxed in dioxane–water (9:1) (15 ml) containing 0.2 *N* hydrogen chloride by weight for 4 hours (12). The mixture was neutralized with sodium bicarbonate, evaporated to remove

most of the dioxane, diluted with water (10 ml), and extracted with chloroform (3×20 ml). Removal of the chloroform yielded a yellow oil (9 mg). Paper chromatography with BEAW solvent, THF solvent, and 20% aqueous KCl using DSA and ultraviolet light for detection showed, besides unchanged starting material (roughly 10%), the 2-hydroxy isomer V and the diketone II with traces of vanillin, vanillic acid, and an unknown phenol.

REFERENCES

1. H. HIBBERT. Ann. Rev. Biochem. **11**, 183 (1942).
2. A. B. CRAMER and H. HIBBERT. J. Am. Chem. Soc. **61**, 2204 (1939).
3. H. E. FISHER and H. HIBBERT. J. Am. Chem. Soc. **69**, 1208 (1947).
4. L. MITCHELL and H. HIBBERT. J. Am. Chem. Soc. **66**, 602 (1944).
5. A. WACEK and I. HORAK. Monatsh. **77**, 18 (1947).
6. L. MITCHELL, T. H. EVANS, and H. HIBBERT. J. Am. Chem. Soc. **66**, 604 (1944).
7. K. V. AUWERS and W. NOLL. Ann. **535**, 245 (1938).
8. T. I. TEMNIKOVA. Vestnick, Leningrad Univ. 138 (1947); Chem. Abstr. **42**, 4155 (1948).
9. J. A. F. GARDNER. Can. J. Chem. **32**, 532 (1954).
10. K. KRATZL and G. BILLEK. Tappi, **40**, 269 (1957).
11. O. GOLDSCHMID. Tappi, **38**, 728 (1955).
12. E. ADLER, J. M. PEPPER, and E. ERIKSOO. Ind. Eng. Chem. **49**, 1391 (1957).
13. C. NEUBERG and J. HIRSH. Biochem. Z. **115**, 282 (1921).
14. T. HIGUCHI, Y. ITO, and I. KAWAMURA. J. Japan. Forestry Soc. **37**, 239 (1955).
15. T. HIGUCHI. Physiol. Plantarum, **10**, 633 (1957).
16. R. KUHN and H. J. HAAS. Angew. Chem. **67**, 785 (1955).
17. J. GIERER. Acta Chem. Scand. **8**, 1319 (1954).
18. R. W. KEITH, D. LETOURNEAU, and D. MAHLUM. J. Chromatog. **1**, 534 (1958).
19. E. ADLER and J. MARTON. Acta Chem. Scand. **15** (2), 357 (1961).
20. L. BRICKMAN, W. L. HAWKINS, and H. HIBBERT. J. Am. Chem. Soc. **62**, 2149 (1940).
21. G. FODOR, J. KISS, and M. SZEKERKE. J. Org. Chem. **15**, 227 (1950).
22. S. B. BAKER, T. H. EVANS, and H. HIBBERT. J. Am. Chem. Soc. **70**, 60 (1948).

THE PROTON RESONANCE SPECTRUM OF 2-FURANACROLEIN

T. SCHAEFER
Department of Chemistry, University of Manitoba, Winnipeg, Manitoba
Received April 30, 1962

ABSTRACT

The proton resonance spectrum of 2-furanacrolein consists of two effectively independent ABX spectra, that due to the ring protons and that due to the side-chain protons. The solvent effects are such that the latter reduces to an AA^1X case. The ABX and AA^1X cases are discussed as deviations from the A_2X case. The difference is simply that forbidden singlet–triplet transitions in the A_2X case become allowed in the ABX case because the singlet and triplet states are uncoupled as the A_2 nuclei become nonequivalent. Energy level diagrams are given to illustrate this situation.

INTRODUCTION

Abraham and Bernstein give a detailed discussion of the analysis of deceptively simple high-resolution n.m.r. spectra (1). These arise, in the simplest instance, when a given nucleus, X, is coupled differently to two other nuclei, A and B, which themselves are strongly coupled. The observed splittings in the spectra of the three nuclei are then equal to the average of the coupling constants J_{AX} and J_{BX}. J_{AB} is unobservable in this case.

Musher (2) has recently remarked on this phenomenon in connection with an anomalous interpretation of certain fluorine–fluorine coupling constants (3) and calls it "virtual coupling". In the course of a study of solvent effects on proton resonance spectra we have noticed a good example of this. It appears profitable to discuss this example in terms of a general theorem on high-resolution n.m.r. spectra. It supplements the treatment of Abraham and Bernstein in an interesting way and should perhaps be read together with it.

The ABX, AA^1X, A_2X Systems

A pair of spins can be said to be isochronous if they have the same chemical shift. If, in addition, the spins have the same coupling constant with every other spin of the molecule they are said to be equivalent. A pair of spins can be equivalent only if they are isochronous. There is a well-known theorem stating that scalar couplings between equivalent spins are unobservable in a nuclear resonance experiment (4, 5). The proof of this theorem does not depend on symmetry in any way.

By definition the A protons of the A_2X system satisfy the theorem. The positions of the two A protons can usually be made to coincide through an operation of the symmetry group of the molecule. In that case their spin functions combine to form singlet and triplet states. Since singlet–triplet transitions are forbidden none of the observed transitions depend on the coupling constant between the A protons.

If the A protons are isochronous but unequally coupled to proton X they are nonequivalent and the theorem no longer applies. This situation is usually designated as AA^1X. The effect is to uncouple partially the singlet and $F_z(A) = 0$ triplet states of the A protons. This is also so if the A protons are not isochronous, but are equally coupled to proton X. When the nonequivalence arising in either of these two ways is large enough the coupling between the A protons becomes observable.

The two situations are intermediate stages in the conversion of an A_2X system, which gives rise to 5 lines, to the general ABX system, which has 14 lines in its spectrum. This is illustrated in Fig. 1, where the energy levels are given for six different cases as follows:

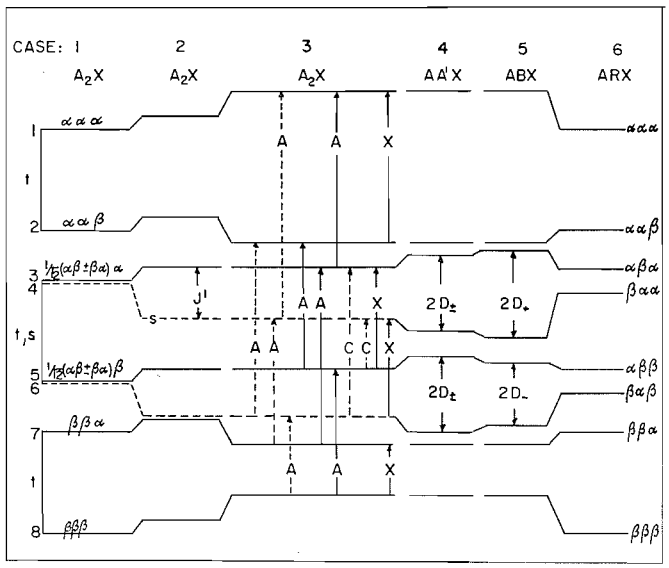

FIG. 1. The energy level diagram for a system of three-spin $\frac{1}{2}$ nuclei with one nucleus having a large relative chemical shift from the other two. The letters s and t indicate singlet and triplet states for the latter nuclei. Transitions are given by vertical arrows and those marked A are for the coupled nuclei. The various cases are described in the text.

(1) $\delta = 0 = J_1 = J_2 = J^1$;
(2) $\delta = 0 = J_1 = J_2, J^1 > 0$;
(3) $\delta = 0, J_1 = J_2 = J^1 > 0$;
(4) $\delta = 0, J_1 - J_2 > 0, J_1 + J_2 = 2J^1$ or $\delta > 0, J_1 = J_2 = J^1 > 0$;
(5) $\delta > 0, J_1 - J_2 > 0, J_1 - J_2 < \delta, J_1 + J_2 = 2J^1$;
(6) $\delta > 0, J_1 = J_2 = J^1 = 0$.

Here δ is the shift between the two A protons, J_1 and J_2 are the coupling constants between the A and X protons, and J^1 is the coupling constant between the A protons. We assume, of course, that the shift between A and X protons is so large that it does not affect the shape of the spectra. We take $J_1 + J_2 = 2J_1$, all positive, without too great a loss of generality.

In Fig. 1 the antisymmetric singlet levels are indicated by horizontal broken lines. The maximum number of 14 transitions in systems of this kind is indicated. There are eight transitions which are always allowed and six of these become pairwise isoenergetic in the A_2X limit. The other 6 of the 14 are singlet–triplet transitions in the A_2X limit and are forbidden. They are indicated by broken vertical arrows. In the AA^1X or ABX limit they no longer have singlet–triplet character and become allowed. But two of them involve a spin flip of all three nuclei and are usually very weak. Their occurrence, however, allows one to determine the relative signs of J_1 and J_2. They are marked C in Fig. 1. As can be seen from the figure we cannot observe J^1 when $2D_\pm - J^1$ is less than the resolution of a good spectrometer, presently about 0.3 cycle/sec. D_+ and D_- are defined by

$$2D_\pm = \{[\delta \pm 1/2(J_1 - J_2)]^2 + (J^1)^2\}^{1/2}.$$

Abraham and Bernstein derive the condition $[\delta \pm 1/2(J_1 - J_2)]^2/2J^1 < 0.3$. Physically

this condition describes the point at which singlet–triplet states are sufficiently strongly uncoupled to be detectable experimentally.

The various spectra for such three-spin systems are very easily deduced from Fig. 1 and three of them are reproduced in Fig. 2. Here broken lines indicate forbidden transitions. Otherwise the figure is self-explanatory. For the ABX case the two quartets in the

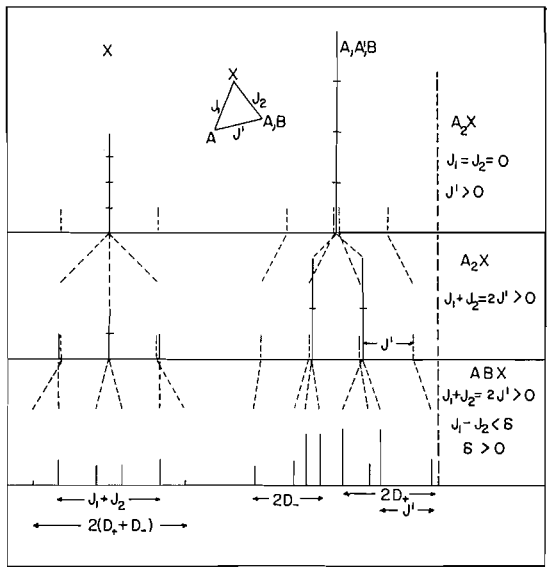

FIG. 2. The spectral shapes expected for three of the cases whose energy levels are illustrated in Fig. 1 and described in the text. Broken vertical peaks indicate forbidden transitions, allowed in the ABX case.

AB region corresponding to the two X spin states are easily picked out. It is, of course, the two outside lines of each quartet which disappear in the A_2X limit, and by comparison with the AB case it becomes perfectly obvious why J' should no longer be observable. In the more general ABR_pX_q . . . cases we would have $(p+1)(q+1)$ . . . such quartets, as discussed by Pople and Schaefer (6). Energy level diagrams for such cases could be constructed by simple extensions of Fig. 1.

EXPERIMENTAL

Proton spectra were taken of 2-furanacrolein at 60 Mc/sec at various concentrations in acetone and benzene. Peak separations were obtained by the side-band technique, taking averages of up to 10 spectra. Internal and external references were not used and concentrations were adjusted to obtain the desired spectral effects. The concentrations are therefore not known accurately but this is of no consequence for our purpose. τ values in chloroform have been given by Bhacca *et al.* (7). Figures 3 and 4 give the observed and calculated spectra in acetone and benzene solutions.

DISCUSSION

The spectrum is a superposition of two effectively independent ABX spectra, one due to the ring protons and one due to the side-chain protons. In Fig. 3 the calculated spectra are given as arrived at by the standard analysis (4). The peaks of the ring protons are indicated by broken lines. Table I presents the spectral parameters obtained from spectra run more slowly than that shown in Fig. 3.

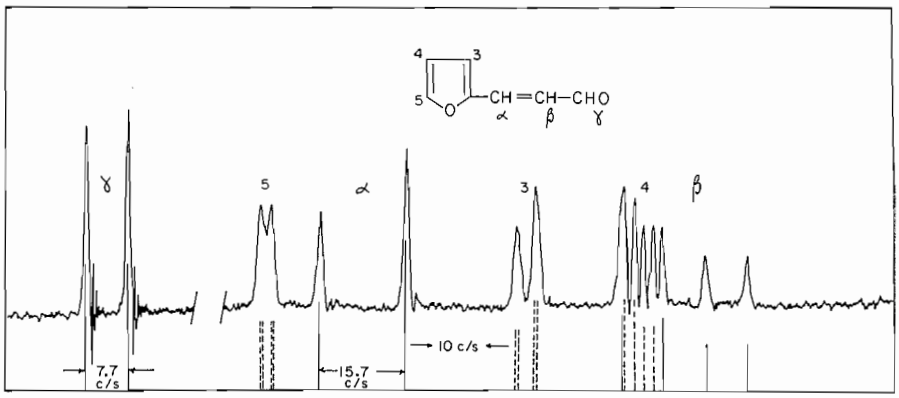

FIG. 3. The proton magnetic resonance spectrum of 2-furanacrolein as a saturated solution in acetone at 60 Mc/sec.

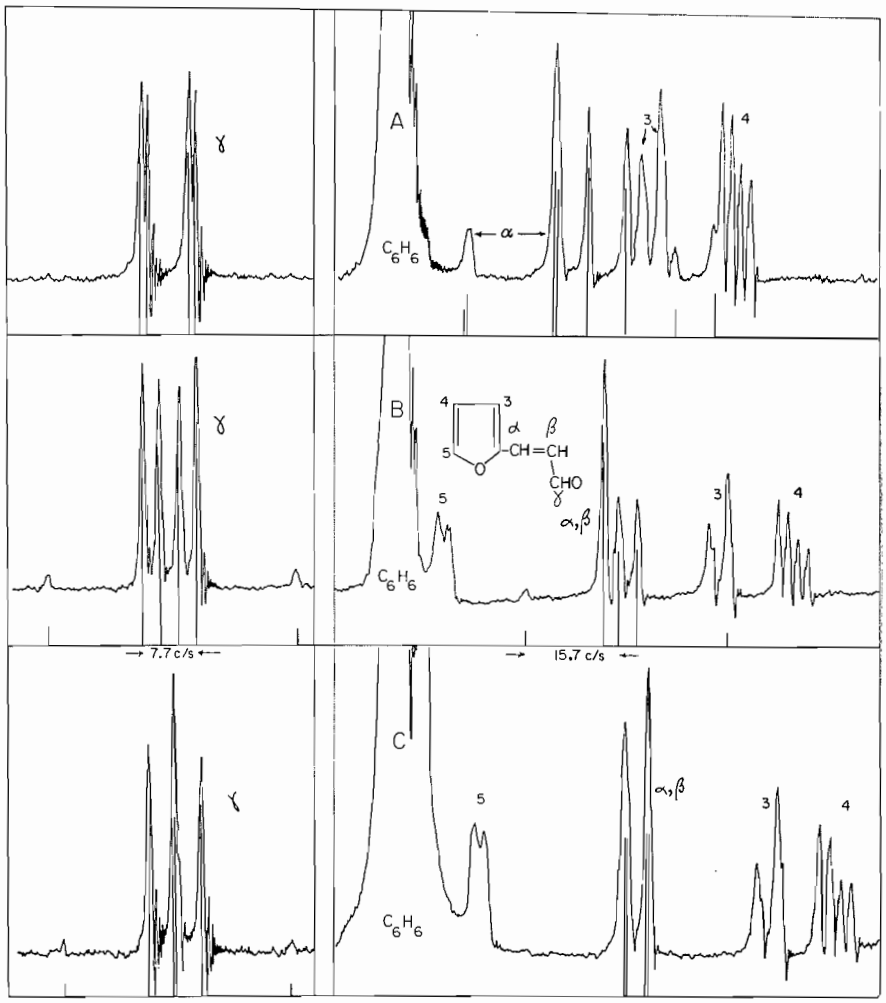

FIG. 4. The proton magnetic resonance spectrum of 2-furanacrolein at 60 Mc/sec at three concentrations in benzene, varying from a saturated solution in A to the most dilute solution in C.

TABLE I

Spectral parameters for 2-furanacrolein in acetone and benzene solutions in cycle/sec at 60 Mc/sec

	Relative chemical shifts*				
		Benzene			Coupling constants* †
	Acetone	A	B	C	
$H_0\ (\sigma_4-\sigma_3)$	20.0±0.5	15.3±0.3	12.5±0.3	10.9±0.3	J_{34} = 3.41±0.11
$H_0\ (\sigma_4-\sigma_5)$	68.5±1	54.7±1	59.5±1	66.1±1	J_{35} = 0.75±0.1
$H_0\ (\sigma_\beta-\sigma_\alpha)$	56.7±1	18.7±0.3	5.0±0.1	−0.6±0.1	J_{45} = 1.81±0.05
$H_0\ (\sigma_\beta-\sigma_\gamma)$	188.9±1	176.3±1	172.1±1	169.0±1	$J_{\alpha\beta}$ = 15.7±0.1
$H_0\ (\sigma_4-\sigma_\beta)$	−7.1±0.5	17.7±0.5	27.7±1	40.7±1	$J_{\alpha\gamma}$ = 0.0±0.1
					$J_{\beta\gamma}$ = 7.7±0.1
					$J_{\alpha 5}$ = 0.38±0.1

*See Fig. 3 or 4 for labelling of protons.
†All coupling constants are assumed to be positive.

(a) Ring Protons

There is no startling change in the shape of this ABX spectrum because the chemical shifts never become small compared to the coupling constants. The values of the latter agree well with the average values found for a large number of substituted furans (8) and also with those of furan itself, obtained by means of $C^{13}H$ patterns (9). Preferential shifts are discussed below.

(b) Side-chain Protons

As can be seen from Table I and Fig. 4, increasing dilution in benzene results in a preferential shift to high field of the α-ethylenic proton such that $\eta H_0(\sigma_\beta-\sigma_\alpha) = \delta$ decreases to about zero. The energy levels in Fig. 1 lead us to expect a transition from a 14-line ABX pattern to a 5-line AA^1X pattern if $D_\pm$ becomes indistinguishable from $J_{\alpha\beta}$. This will be so if $(\delta+1/2J_{\beta\gamma})^2/2J_{\alpha\beta} < 0.3$.

In the most concentrated benzene solution, A, there are 10 ABX lines. The two combination lines in the X region are too weak to be observed and since $J_{\alpha\gamma}$ is effectively zero there are only two α lines instead of four. These two lines are broadened by a weak coupling to proton 5 on the ring.

In benzene solution B the ABX situation still holds but δ is small enough that all six possible X lines are observable, including the two combination lines. In the AB region two of the weak transitions which become singlet–triplet transitions in the A_2X limit are already too weak to be observed.

Finally, in benzene solution C we are just on the borderline between AA^1X and ABX. δ is just a little less than zero and all AB transitions which become singlet–triplet transitions in the A_2X limit are too weak to be observed, but the two combination lines are detectable. Even if δ were zero we would still have a 0.4 cycle/sec splitting of the lines in the AB region. The combination lines would not be observable, however. Presumably because of the small coupling of proton α to proton 5 this is not observable in Fig. 4C. It is clear, of course, that the size of $J_{\alpha\beta}$ determines the rate at which one approaches a 5-line spectrum. Physically this means that the size of $J_{\alpha\beta}$ relative to δ and $J_{\alpha\gamma}-J_{\beta\gamma}$ determines the tightness of the coupling of the AB protons. We have the curious situation that the larger the relative magnitude of $J_{\alpha\beta}$ the sooner it becomes unobservable.

(c) Preferential Solvent Shifts

In going from acetone solution to the most dilute benzene solution the α-ethylenic proton shows a preferential shift to high field relative to the β-ethylenic proton of almost

1 p.p.m. Crotonaldehyde shows a similar behavior (6). In the ring it is proton 3 which shows the largest solvent shift and it is almost as large as that of the α-ethylenic proton. Some conformations of the molecule will have the α and 3 protons quite near. The implication is that the benzene molecules pack around the solute molecule in such a way as to avoid the oxygen atoms as far as possible. The shifts in Table I lend some support to this idea. Why this should be so is a problem.

ACKNOWLEDGMENTS

This work was supported by the National Research Council and the Research Corporation.

REFERENCES

1. R. J. ABRAHAM and H. J. BERNSTEIN. Can. J. Chem. **39**, 216 (1961).
2. J. I. MUSHER. J. Chem. Phys. **36**, 1086 (1962).
3. L. PETRAKIS and C. H. SEDERHOLM. J. Chem. Phys. **35**, 1174 (1961).
4. J. A. POPLE, W. G. SCHNEIDER, and H. J. BERNSTEIN. High resolution nuclear magnetic resonance. McGraw-Hill Book Co., New York. 1959.
5. A. ABRAGAM. The principles of nuclear magnetism. Oxford. 1961.
6. J. A. POPLE and T. P. SCHAEFER. Mol. Phys. **3**, 547 (1960).
7. N. S. BHACCA, L. F. JOHNSON, and J. N. SHOOLERY. NMR spectra catalog. Varian Associates. 1962.
8. R. J. ABRAHAM and H. J. BERNSTEIN. Can. J. Chem. **39**, 905 (1961).
9. G. S. REDDY and J. H. GOLDSTEIN. J. Am. Chem. Soc. **84**, 583 (1962).

THE EXTRACTION OF THORIUM AND SOME LOWER LANTHANIDE NITRATES BY DIBUTYL BUTYL PHOSPHONATE

P. G. MANNING*

Mineral Sciences Division, Mines Branch, Department of Mines and Technical Surveys, Ottawa, Canada

Received April 3, 1962

ABSTRACT

The distribution of thorium and a number of lanthanides between nitric acid and solutions of dibutyl butyl phosphonate in odorless kerosene has been examined as a function of the aqueous nitric acid concentration. Experiments were conducted at trace metal concentration using radioisotopes. Separation factors (denoted by S and defined as the ratio of the distribution coefficients, K, for two metal species) have been measured for some lanthanide–lanthanide couples and also for some thorium–lanthanide couples. Results indicate that separation factors between successive lanthanides (given by $S = K_{Z+1}/K_Z$) at the lower end of the rare-earth series are superior to those obtained with either tributyl phosphate (TBP) (D. Scargill *et al.* J. Inorg. & Nuclear Chem. **4**, 304 (1957)) or trioctyl phosphine oxide (TOPO) (J. M. Schmitt. Oak Ridge National Laboratory. Unpublished data), but as Z increases, $S_{DBBP} \sim S_{TBP} > S_{TOPO}$. For thorium–lanthanide couples, $S'_{DBBP} > S'_{TBP}$. Measurements over a range of extractant concentrations indicate that the lanthanides are extracted as trisolvates.

INTRODUCTION

Much work is being pursued at the present time in elucidating the metal-extractive properties of organophosphorus reagents. Of the neutral esters, tributyl phosphate (TBP) has found widespread application in the large-scale separation of metals, while a number of analytical procedures for the determination of metals with trioctyl phosphine oxide have also been devised (3). Siddall (4) and Madigan and Cattrall (5) have shown that dibutyl butyl phosphonate (DBBP) is a more efficient extractant for uranium and thorium than TBP. Other workers in these laboratories have produced uranium of nuclear-grade purity by a process, employing DBBP, which competes successfully with TBP in giving a product of high purity and in economy of operation (6, 7). Since DBBP can also compete with TBP in availability and initial cost, it possesses great potential in the large-scale separation of these metals. Some measurements have also been reported for the extraction of thorium and lanthanides with diphosphonates, these compounds being β-diketones (8). Radioisotopes of the rare-earth elements were used as tracers to obtain accurate values for the distribution coefficients achieved.

EXPERIMENTAL

DBBP was obtained from the Virginia–Carolina Chemical Corporation. Infrared spectra and titration against standard alkali indicated the presence of about 1% hydrogen-bonded acidic impurities. All organic solutions were, therefore, scrubbed with sodium hydroxide and then washed several times with distilled water prior to use. A 58% (v/v) solution of DBBP in kerosene was used in all distribution experiments. Trioctyl phosphine oxide (TOPO) was an Eastman Kodak White Label product and was used without further purification. The nitric acid used was Mallinckrodt analytical reagent grade and the kerosene was supplied by Anachemia.

La^{140} and Pr^{142} were obtained as carrier-free isotopes from Oak Ridge National Laboratory, $Eu^{152/154}$ from Atomic Energy of Canada Ltd., Chalk River, Ontario, and Tb^{160} from the Radiochemical Centre, Amersham, England. For the thorium measurements, carrier-free Th^{234} was prepared according to the method described by Berman *et al.* (9). The γ-emitting lanthanides were assayed using a NaI (Tl) scintillation assembly, and the β-active Th^{234} using a Geiger–Müller counter.

The distribution coefficient is defined as

$$K = \frac{\text{concentration of nuclide in organic phase}}{\text{concentration of nuclide in aqueous phase}}.$$

**National Research Council Postdoctorate Fellow.*

Ten milliliters of both phases were shaken together in Erlenmeyer flasks for a period of 1 hour, preliminary runs having shown that equilibration was attained in less than 30 minutes. All organic phases were pre-equilibrated. The temperature was 27±3° C; under these conditions the variation in K with temperature is well within experimental error (±3%).

RESULTS AND DISCUSSION

The Nature of the Species Extracted

To determine the nature of the species extracted, K was measured as a function of the neutral ester concentration in the organic phase. The application of dilute solutions of DBBP (desirable to maintain ideality in the organic phase) would involve the measurement of very low distribution coefficients. It was decided, therefore, to carry out this investigation, using another neutral organophosphorus reagent, trioctyl phosphine oxide (TOPO), since, according to Weaver (10), readily measurable distribution coefficients may be obtained at low extractant concentration. $Eu^{152/154}$ was employed as a tracer, and the aqueous phase was 0.316 M HNO_3. The results are listed in Table I, and are presented graphically in Fig. 1. The limiting slope is 2.9, which indicates the formation of the species

TABLE I

Distribution coefficients for $Eu^{152/154}$ at ranging TOPO concentrations

TOPO concn., M	0.232	0.0464	0.0232	0.0116	0.0058
K	20.6	1.006	0.178	0.0244	0.004

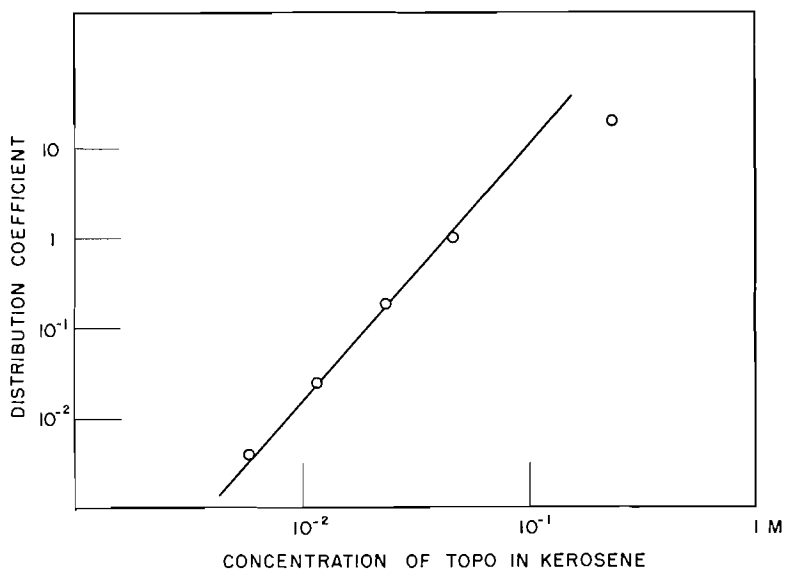

FIG. 1. Variation in K_{Eu} with TOPO, M.

$Eu(NO_3)_3(TOPO)_3$. Since it has been established previously that lanthanides are extracted by TBP as trisolvates (1), and since DBBP is intermediate between TBP and TOPO in both structure and electron-donor properties, it is reasonable to assume that the species extracted is $Eu(NO_3)_3(DBBP)_3$.

Extraction of Metal Nitrates with 58% DBBP in Kerosene

The measured distribution coefficients and equilibrium aqueous nitric acid concentrations are listed in Table II, and are plotted against each other in Fig. 2.

TABLE II

Distribution coefficients and equilibrium aqueous acidities

Nitric acid, M	K_{La}	K_{Pr}	K_{Eu}	K_{Tb}	K_{Th}	K_{HNO_3}
0.149	0.070			0.052		0.35
0.278	0.201			0.202		0.50
0.532	0.45		0.66			0.64
1.35	0.56	0.82	2.02	1.12	>300	0.59
2.89	0.30	0.60	1.41	1.47	>300	0.51
4.48	0.109	0.303	1.07	1.17	>300	0.41
6.14	0.0415	0.167	0.60	0.89	>300	0.33
7.80	0.0283	0.0905	0.61, 0.57	0.905	>300	0.28
9.30	0.025	0.115	0.70	1.28	>300	0.26
10.85	0.0253, 0.021		1.12	2.17		0.25
11.35		0.204				
12.36	0.0312, 0.032		1.84	4.15		0.25

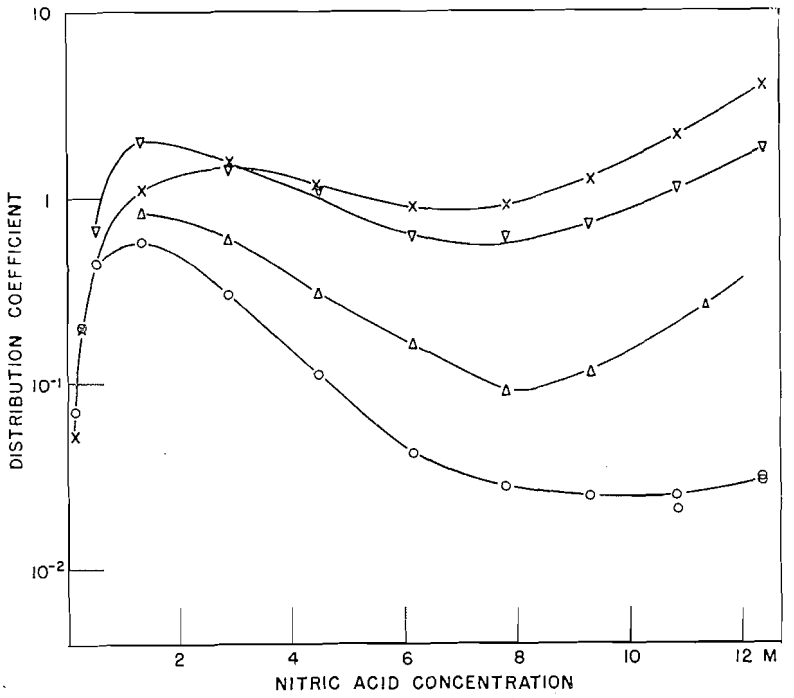

FIG. 2. Lanthanide nitrate distribution coefficients at varying nitric acid concentrations: ○ La^{140}; △ Pr^{142}; ▽ $Eu^{152/154}$; × Tb^{160}.

Although the plots follow the general pattern exhibited by the analogous lanthanide – HNO_3–48% TBP–kerosene system (1), the "valleys" are seen to be much deeper. Scargill *et al.* (1) and Hesford *et al.* (11) have discussed the shapes of the TBP curves, and stated that the important factors in operation are:

(*a*) The salting-out effect of the nitrate ion. This effect produces the initial increase in K with increasing nitric acid concentration.

(*b*) Lanthanide–nitrate complexing and HNO_3 competition for TBP molecules. These reactions would operate over the second portion of the curves and offer an explanation for the decreasing partition coefficients.

(*c*) Activity coefficients. According to Scargill *et al.*, this effect is responsible for the rising partition coefficients at the higher acidities.

That these factors are primary in determining the shapes of the rare earth – DBBP extraction curves is apparent from a qualitative comparison of the plots of Fig. 2 with the corresponding plots of Scargill *et al.* (1). As metal–nitrate complexing in both systems is identical under given aqueous conditions, the deeper "valleys" observed in the DBBP system may be attributed to greater DBBP–HNO_3 interaction, with the formation of the species DBBP.$(HNO_3)_n$. That the extraction of europium by TOPO also passes through a maximum has been demonstrated by Weaver (10).

Some K_{HNO_3} values between aqueous and DBBP phases are listed in Table II.

The non-parallel nature of the lanthanide–DBBP curves at very high acidities (Fig. 2) would suggest that another mechanism is operative in this region. Marcus and Abrahamer (12) have shown that the lanthanides are extracted by long-chain amines from nitrate solutions as anionic complexes, and, therefore, at the higher acidities employed in the present investigation, considerable lanthanide–nitrate complexing can be expected, the degree of which depends upon the hydration number of the ion. Since the ionic radii of the lanthanides decrease with increasing atomic number (the "lanthanide contraction"), the rare earths become progressively more hydrated, and, therefore, less prone to nitrate interaction.

This latter effect may account for the fact that the slope of the lanthanum distribution curve (Fig. 2) is much smaller, at higher nitrate concentration, than for Eu and Tb.

Allowing for the small difference in extractant concentration, DBBP is seen to be a better extractant for lanthanides than TBP.

At nitric acid concentrations greater than 4 *M*, distribution coefficients increase with *Z*, as is to be expected from the gradation in the ionic radii of the rare earths, but under no experimental conditions are the curves regularly spaced. At lower acidities, however, distribution coefficients increase with atomic number from La to Eu, but at this point in the lanthanide series a discontinuity occurs, and $K_{Tb} < K_{Eu}$. These points are illustrated in Fig. 3, which is a plot of *K* against *Z* at a number of nitric acid concentrations. Some TBP data have been included (1), and it is apparent in this system also that partition

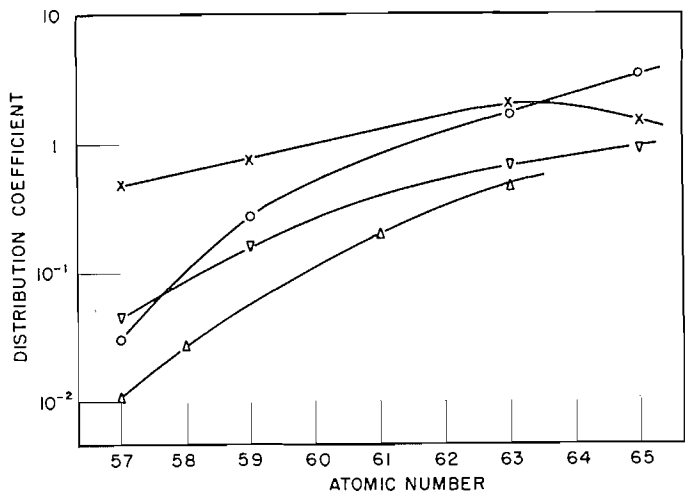

FIG. 3. Distribution coefficients for lanthanides as a function of atomic number: ○ 12 *M* HNO_3, DBBP; ▽ 6 *M* HNO_3, DBBP; × 2 *M* HNO_3, DBBP; △ 12 *M* HNO_3, 48% TBP.

coefficients are not proportional to the atomic number, although the authors state otherwise.

Separation Factors

In Table III are listed values for the separation factors for some lanthanide–lanthanide

TABLE III

S' and S values for metal–metal couples, 12 M HNO_3

	58% DBBP		48% TBP		TOPO	
Couple	S'	S	S'	S	S'	S
Ce–La			2.5	2.5		
Pr–La	8.5	2.9			2.3	1.5†
Pm–Ce			6.9	1.9		
Nd–Pr					1.2	1.2†
Sm–Nd						1.2†
Gd–Sm					0.8	
Eu–Pm			2.3	1.5		
Eu–Pr	6.6	1.6				
Tb–Eu	2.0	1.4				
Eu–La	56		42		<6 (est.)†	
Th–La	$>10^4$*		2.8×10^3*		$>5\times10^4$‡	
Th–Eu	>500*		180*			

*8 M HNO_3.
†0.1 M TOPO in kerosene, pH 1, ref. 2.
‡1 M HNO_3, 1 M $NaNO_3$, 0.6 M H_3PO_4, 0.1 M H_2SO_4, 0.1 M TOPO in cyclohexane, ref. 13.

couples and also for some thorium–lanthanide couples determined in the present investigation. S' and S are separation factors defined as follows.

$$S' = K_{M_1}/K_{M_2}, \text{ where } M_1 \text{ and } M_2 \text{ represent any two nuclides,}$$

and

$$S = \text{separation factor between successive lanthanides}$$

$$= \frac{K_{Z+1}}{K_Z} = \left(\frac{K_{Z_2}}{K_{Z_1}}\right)\frac{1}{Z_2 - Z_1}.$$

The TBP figures have been computed from the data of Scargill *et al.* (1), while the TOPO figures are those of Schmitt (2) and Ross *et al.* (13). As Table III indicates, DBBP is superior to TBP and TOPO in the separation of lanthanum from other lanthanides, but for all three extractants S decreases as Z increases, and for the Gd–Sm pair $S_{TOPO} < 1$. At the middle reaches of the rare-earth series, S_{DBBP} and S_{TBP} are comparable, $S_{DBBP} \sim S_{TBP} \sim 1.4$. For thorium–lanthanide mixtures, DBBP affords a higher degree of specificity of extraction than TBP, but it is difficult to compare directly the separation factors obtained with DBBP and TOPO as quantitative data are not available.

Lewis and Ingles (14), in these laboratories, from investigations involving the preferential adsorption of lanthanides on cation-exchange resins from sulphate solutions, obtained maximum separation factors of 6 between thorium and lanthanum.

CONCLUSIONS

Although the separation factors between successive lanthanides determined in this investigation are inferior to those obtained with acidic organophosphorus reagents (15, 16), the high S' values measured for the thorium–lanthanide system, coupled with the ready availability and relative cheapness of DBBP, would suggest that DBBP might

find ready application in the separation of thorium from rare earths on the industrial scale.

TOPO is among the best extractants of metals of all organophosphorus reagents, but it suffers from the disadvantage that it is expensive, and although TOPO has found application in the analytical separation of metals, its cost would preclude its use in large-scale processes.

Further investigations are being pursued to assess the influence on the magnitude of S' and S, by introducing acidic extractants into the organic phase in conjunction with DBBP. As thorium is known to complex more strongly than the lanthanides with such cation-exchangers as thenoyltrifluoroacetone, it is possible that any synergic effects which might occur would produce an enhancement of the separation factors.

ACKNOWLEDGMENT

This work was done while holding a National Research Council Postdoctorate Fellowship, the award of which is gratefully acknowledged.

REFERENCES

1. D. SCARGILL, K. ALCOCK, J. M. FLETCHER, E. HESFORD, and H. A. C. MCKAY. J. Inorg. & Nuclear Chem. **4**, 304 (1957).
2. J. M. SCHMITT. Oak Ridge National Laboratory. Unpublished data.
3. J. C. WHITE and W. J. ROSS. Separations by solvent extraction with tri-*n*-octyl phosphine oxide. Natl. Acad. Sci. Nuclear Science Series NAS-NS 3102. 1961.
4. T. H. SIDDALL. Ind. Eng. Chem. **51**, 41 (1959).
5. D. C. MADIGAN and R. W. CATTRALL. J. Inorg. & Nuclear Chem. **21**, 334 (1961).
6. V. M. MCNAMARA, H. W. PARSONS, and R. SIMARD. Mines Branch Investigation Report IR 60–120. Nov. 1960. Unpublished.
7. R. SIMARD, A. J. GILMORE, V. M. MCNAMARA, H. W. PARSONS, and H. W. SMITH. Can. J. Chem. **39**, 229 (1961).
8. H. SAISHO. Bull. Chem. Soc. Japan, **34**, 859 (1961).
9. S. S. BERMAN, L. E. MCKINNEY, and M. E. BEDNAS. Talanta, 4, 153 (1960).
10. B. WEAVER. Unpublished data.
11. E. HESFORD and H. A. C. MCKAY. Trans. Faraday Soc. 573 (1958).
12. Y. MARCUS and I. ABRAHAMER. J. Inorg. & Nuclear Chem. **22**, 141 (1961).
13. W. J. ROSS and J. C. WHITE. Anal. Chem. **31**, 1847 (1959).
14. D. C. LEWIS and J. C. INGLES. Mines Branch Research Report R 31. 1958.
15. D. F. PEPPARD, G. W. MASON, J. L. MEIER, and W. J. DRISCOLL. J. Inorg. & Nuclear Chem. 4, 334 (1957).
16. D. F. PEPPARD, G. W. MASON, and I. HUCHER. J. Inorg. & Nuclear Chem. **18**, 245 (1961).

ELECTROCHEMISTRY OF THE NICKEL OXIDE ELECTRODE

PART III. ANODIC POLARIZATION AND SELF-DISCHARGE BEHAVIOR

B. E. CONWAY AND P. L. BOURGAULT*

Department of Chemistry, University of Ottawa, Ottawa, Ontario

Received March 26, 1962

ABSTRACT

Further evidence that the rate-controlling process in self-discharge of the nickel oxide electrode is the anodic partial reaction of oxygen evolution is reported and is based on: (*a*) comparison of the heats of activation for open-circuit oxygen evolution and for d-c. anodic polarization with oxygen evolution; (*b*) comparison of the current potential behavior for d-c. anodic polarization and for rates of oxygen evolution on open circuit as a function of potential; and (*c*) comparison of H/D isotope effects for open-circuit and d-c. polarization behavior. In the latter cases, an unusual and characteristic inverse isotope effect is observed.

True Tafel slopes are deduced and interpreted in terms of possible mechanisms of oxygen evolution, taking account of the dependence of activation energy upon surface coverage by adsorbed intermediates.

INTRODUCTION

In previous papers (1, 2) we have discussed the mechanism of the self-discharge behavior of electrodes in a state of oxidation approaching and exceeding "Ni III" and have given some evidence that the rate-controlling process in self-discharge is a step in the anodic partial reaction of oxygen evolution. Since the converse view, that the cathodic step is rate limiting (but without a full appreciation of the electrochemical factors involved), has been presented elsewhere (3), we give, in the present paper, further unequivocal evidence for the identity of the rate-controlling process on open-circuit self-discharge, and hence of mechanism, by comparing the kinetics of the oxygen evolution process on open circuit and on driven anodic polarization of the charged (i.e. in a state of oxidation approximating to "$NiO_{1.5}$") nickel oxide electrode. Related data for the adsorption pseudocapacity associated with the surface layer at the nickel oxide electrode are also presented.

EXPERIMENTAL

Techniques used in the preparation of electrodes and solutions, in the e.m.f. measurements, and in the determination of oxygen evolution rates on open circuit (4) have been described in detail in our previous publications (1, 2). Evidence has also been given elsewhere (5) that ordinarily prepared aqueous solutions (made up from recrystallized analytical grade KOH and twice-distilled "conductance" water) give results identical, within experimental error, with those obtained using ultrapurified solutions prepared from potassium amalgam and pre-electrolyzed anodically before carrying out the kinetic runs at the nickel electrode. The ordinarily prepared solutions were hence used in the present work.

The following matters of experimental procedure require further mention:

(a) Steady-state Current-potential Behavior

A number of experiments were carried out in order to compare the kinetic parameters (viz. the apparent heats of activation and the exchange currents) for steady-state d-c. anodic oxygen evolution and open-circuit oxygen evolution. Since the nickel oxide electrode behaves electrically as a large capacitance (2, 5) due to discharge or desorption of O-containing radicals at its surface, normal procedures for examining steady-state polarization behavior at various current densities must be modified to allow for pseudo-Faradaic effects in charging the adsorption capacity (5, 6) which lead to time variation of the electrode potential when the current density is varied.

The impregnated plaques (7) were given three cycles of charging and discharging at 25° C before being used in the kinetic polarization measurements. The initial charging rate was at 38.5 ma g^{-1} of $Ni(OH)_2$

**Present address*: *Johnson Matthey and Mallory Co., Toronto, Ontario.*

for 30 hours and subsequent discharge and charge cycles were at about 55 ma g^{-1} for 5 hours. This conditioning of electrodes was necessary to obtain the best reproducibility (± 5 mv in polarization measurements; it is of interest that this figure is three or four times better than is normally attainable with pure solid metal electrodes). The electrodes were then transferred to the experimental cell containing two Hg/HgO reference electrodes and the KOH solution prepared from the recrystallized monohydrate. Final charging was then carried out at 38.5 ma g^{-1} $Ni(OH)_2$ for 30 hours and then at various higher and lower current densities until steady values of oxygen overpotential were attained.

The criterion of what constitutes a "steady state" is dependent upon the current density used. At high current densities (300 ma g^{-1}), e.m.f. was considered to be "constant" when it changed at a rate not exceeding 0.01 mv sec^{-1}. However, at a current density of 3 ma g^{-1} a rate of change of e.m.f. of 10^{-4} mv sec^{-1} is quite significant. This arises as follows: following a change of current density and polarization, the total current i_T passing into the electrode will be made up of a Faradaic contribution i_F (due to oxygen evolution) and a component i_C due to the change of charge held by the surface capacitance. Thus

$$i_T = i_F + i_C = i_F + C dV/dt.$$

The measured current i_T will thus only be equal to i_F, which is of significance in the kinetics of oxygen evolution, when the charging current has fallen to a negligible value. At low current densities, it is hence necessary to wait for a relatively greater constancy of e.m.f. with time (i.e., a low value of dV/dt) than would be the case at high current density, in order to obtain the same degree of accuracy in i_F. Estimates of the capacity were obtained from the slopes of electrode potential vs. volume of oxygen evolved on open circuit (1, 5) and from the θ values (1, 8) obtained in e.m.f. decay studies.

At the lowest current densities, several days* would be required for CdV/dt to become less that 1% of i_T. In order to overcome this difficulty, the value CdV/dt was obtained at various times and when it reached a value i_C' less that 10% of i_T, the current i_C' was subtracted from i_T, giving the required i_F for oxygen evolution. Allowing for a possible error of 10% in the estimate of CdV/dt, the error introduced into the corresponding estimate of i_F when $i_C = i_C' = i_T/10$ was only 1%. At higher current densities, the value of CdV/dt becomes negligible compared with i_T in a few minutes.

(b) Apparent Heats of Activation

The apparent (9, 10) heats of activation for the driven anodic oxygen evolution process and for the evolution of oxygen on self-discharge were evaluated by conducting the above steady-state measurements over a range of temperatures and also following the oxygen evolution rates on open circuit at various temperatures. In calculating the heat of activation, allowance was made for the e.m.f. of the Hg/HgO electrode and its temperature coefficient, so that the heats of activation would refer, in the usual way, to the oxygen evolution process at the *reversible* oxygen potential.

(c) Deuterium Isotope Effects

The effect of complete deuterium substitution in the "hydrated" oxide, the solvent and the electrolyte, on the kinetics of open-circuit decay of e.m.f. and on the rate of anodic oxygen evolution was investigated by examining the behavior of electrodes prepared from anhydrous nickel sulphate by precipitation of $Ni(OD)_2$ by means of KOD in D_2O. Control experiments were carried out using ordinary H-containing reagents but retaining the $NiSO_4$ instead of the normally used $Ni(NO_3)_2$ hydrate, which cannot be prepared anhydrous without decomposition. The purpose of this experiment was to obtain further confirmation of our previous evidence (1) that the open-circuit self-discharge process is controlled by the anodic oxygen evolution partial process rather than by the cathodic partial process of reduction of the higher oxide to $Ni(OH)_2$, as claimed by Pitman and Work (3).

(d) E.M.F. Decay and Surface Capacitance

Electromotive force decay studies were made as described previously (1), and from the evaluation of the term θ in the logarithmic decay of potential with time, the capacitance of the electrode was evaluated (1, 8, 5). Tests were performed (see Results) to check the validity of the estimates of θ and of the assignment of slopes of e.m.f. decay lines in log [time]. Surface capacitance values were also obtained from the slopes of the lines relating e.m.f. of the electrode to volumes of oxygen evolved, as described previously (1); new data were obtained at various temperatures and KOH concentrations which extend the range and applicability of our previous considerations (1).

RESULTS

(a) Steady-state d-c. Polarization Behavior

The steady-state Tafel lines obtained by the procedure described above are shown in Fig. 1 for 7 M (molal) aqueous KOH at five temperatures. Current densities are expressed

**It should be noted that the adsorption or pseudocapacitance of the nickel oxide electrodes is very large, e.g. of the order of 100 F g^{-1} (1, 5). It is for this reason that the charging currents, which are negligible at most other kinds of electrodes, except at the very lowest current densities, are important in the present work.*

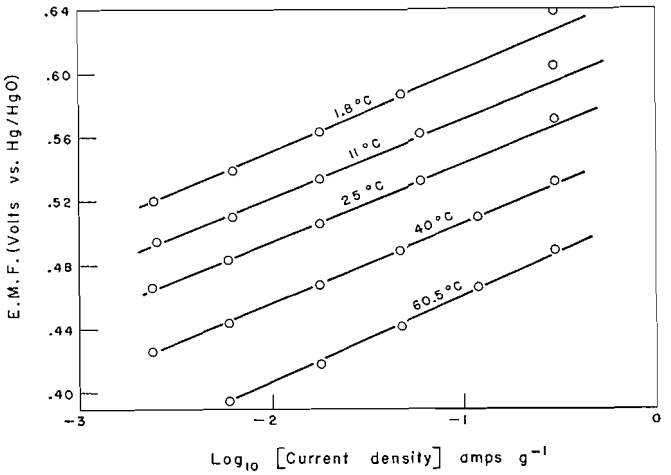

FIG. 1. Steady-state Tafel lines for d-c. anodic polarization of the nickel oxide electrode in 7 *M* KOH at various temperatures.

in amp g^{-1} as discussed previously (1, 2) since the real areas of the wet electrodes cannot be precisely determined (B.E.T. areas of the charged nickel oxide electrodes in the dry condition are about 40 m^2g^{-1} and of the uncharged electrodes 30 m^2g^{-1}; these values cannot be safely identified with the electrochemically accessible real areas of wet electrodes, although it is likely that areas of similar orders of magnitude are involved). The points shown are the mean values obtained from a series of measurements at increasing and decreasing current densities and are also averaged for runs with several electrodes. Reproducibilities of points are about ± 5 mv at a given current density. The slopes of the lines (calculated for 25° C) are 0.049 ± 0.002.

(b) Rates of Oxygen Evolution on Open Circuit

Typical plots of oxygen evolution rate as a function of electrode potential on open circuit are shown in Fig. 2 for various KOH solutions at 1°, 25°, and 60.5° C. Depending on concentration and temperature, these lines exhibit either one or two linear regions, as previously discussed, corresponding to the inflections in the e.m.f. decay lines (1, 5). The changes of slope in the latter plots of e.m.f. vs. log [time] are hence not due to incidental changes of capacitance with potential but must reflect a true change of mechanism (or rate-controlling step) in the oxygen evolution reaction. When a change of slope in the plot of e.m.f. vs. log [oxygen evolution rate] occurs, the two corresponding exchange currents can be evaluated and are shown, for 25° C, in Fig. 3 as a function of the log of the molal activity of KOH. It is seen that while the slopes of the e.m.f. – log [rate] plots vary significantly with KOH concentration, the exchange currents i_0 for oxygen evolution are not dependent, within the reproducibility* of the data, upon KOH activity (Fig. 3); however, the *difference* between the mean i_0 values for the processes in the upper and lower potential regions is certainly quite significant (Fig. 3). The datum for the steady-state anodic polarization in 7 *M* KOH at 25° C, indicated by the square point in Fig. 3, is also consistent with the other data obtained from the open-circuit measurements. The exchange currents for various temperatures are summarized in Table I.

**The reproducibility of the i_0 values appears to be less satisfactory than the claimed reproducibility (± 5 mv) for the overpotential values. This arises, however, since a relatively long extrapolation of the log [rate] plot is necessary down to the reversible oxygen potential, and the Tafel slopes are small.*

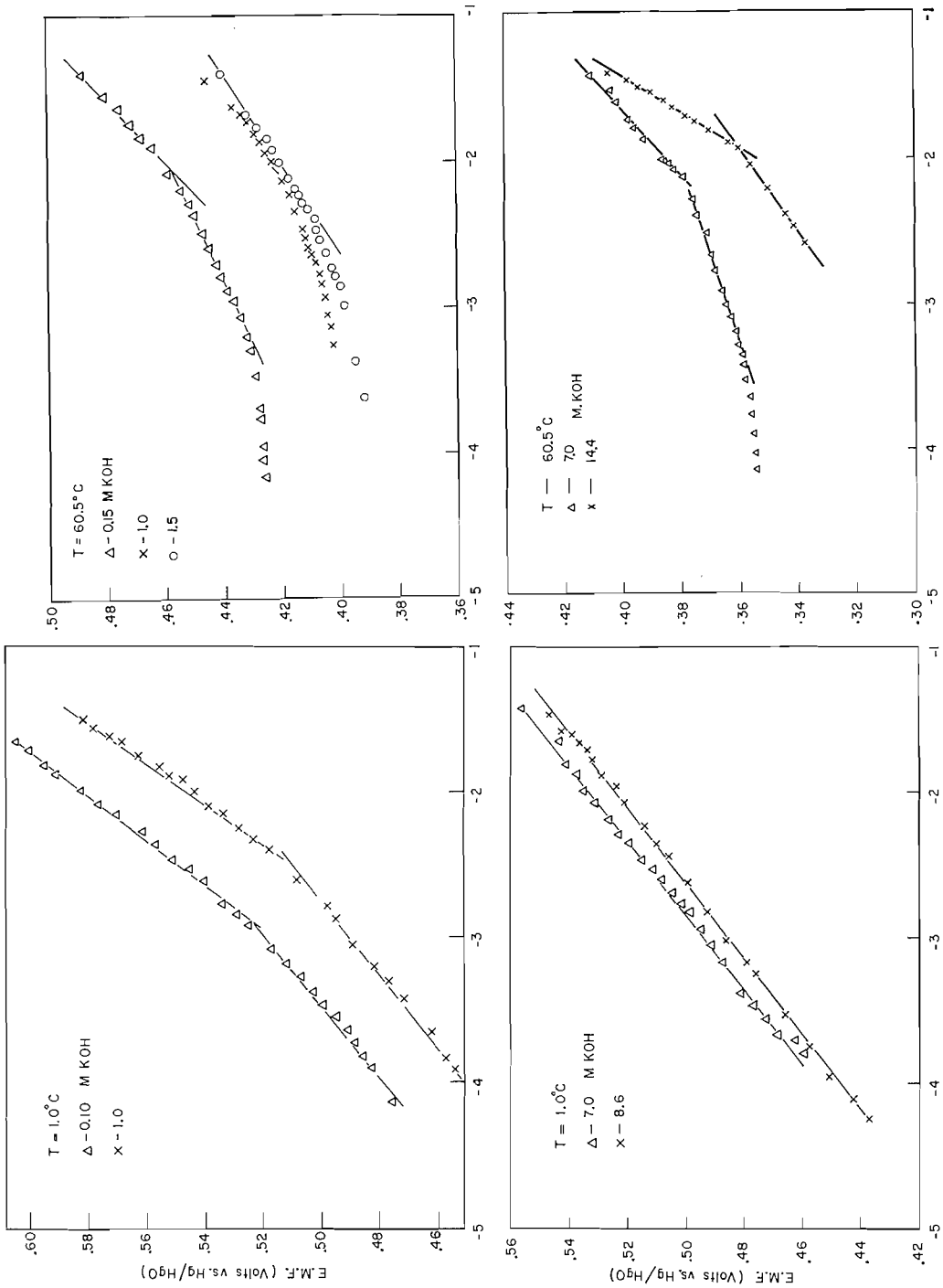

FIG. 2. Rates of oxygen evolution on open-circuit in KOH solutions at various concentrations and at 1° C, 25° C, and 60.5° C.

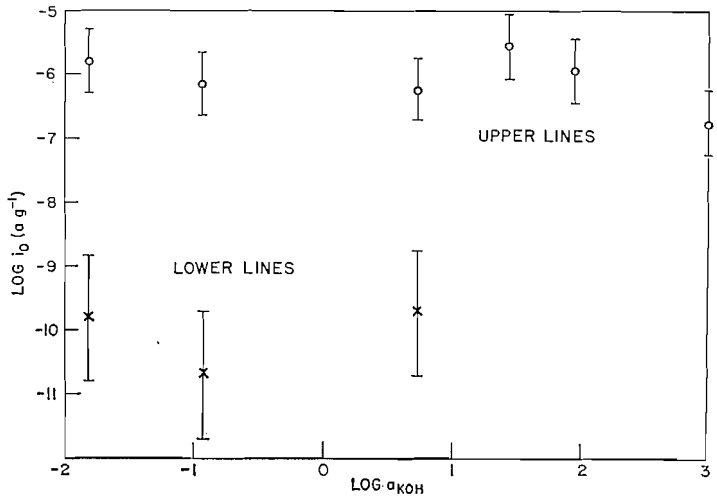

FIG. 3. Exchange currents for the two processes in oxygen evolution at high and low anodic overpotentials for various KOH activities at 25° C.

TABLE I

Exchange currents in amp g^{-1} from extrapolation of e.m.f. – log [rate of oxygen evolution] lines

Temp. (°C)	Concn.	Region I	Region II	Region III
−25	4.5		5×10^{-10}	
	8.2		6×10^{-10}	
	11.8		3×10^{-10}	
1.0	0.10	$[8\times10^{-7}]$*	1.4×10^{-8}	
	1.0	$[5\times10^{-6}]$	4.5×10^{-8}	
	7.0		2.7×10^{-8}	
	8.6		1.7×10^{-8}	
25	0.015		1.6×10^{-6}	1.5×10^{-10}
	0.15		7×10^{-7}	2.0×10^{-11}
	2.9		5.6×10^{-7}	2.2×10^{-10}
	7.0		2.7×10^{-6}	†
	9.4		1.2×10^{-6}	†
	14.6		2×10^{-7}	†
60.5	0.15		1.4×10^{-6}	
	1.5		5×10^{-6}	
	7.0		4×10^{-5}	
	14.4		8×10^{-5}	
	15.4		4×10^{-5}	

*These i_0 values correspond to the two values of b obtained for these conditions in the plots of oxygen evolution rate against potential.
†Values for i_0 for these concentrations cannot be obtained since no second region of the oxygen evolution rate line appears.

(c) Identity of Open-circuit and Steady-state Kinetic Behavior

(i) Current-potential Behavior

Direct comparison between the current-potential relationships obtained for steady-state d-c. and open-circuit oxygen evolution in 7 *M* aqueous KOH at 25° C is made in Fig. 4 and it is evident that, provided the electrode is conditioned by several cycles of charging and discharging, the kinetic behavior on open circuit is identical with that for steady d-c. polarization provided due allowance is made, as described above, for pseudo-Faradaic effects in charging the surface capacitance (2). In the plot for the open-circuit behavior in Fig. 4, the current density is identified with the self-discharge current

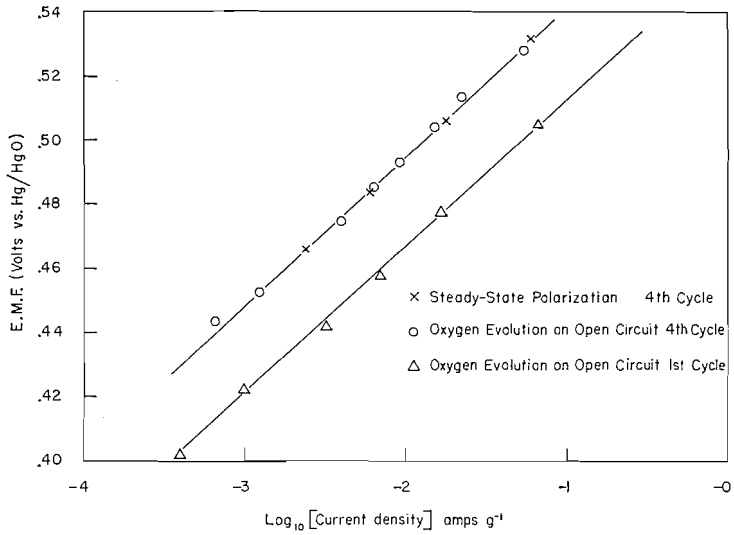

FIG. 4. Comparison of steady-state d-c. polarization behavior with that deduced from rates of oxygen evolution on open circuit (7 *M* KOH, 25° C).

expressed as $4F.dV_{O_2}/dt$, where V_{O_2} is the volume of oxygen evolved at N.T.P. (corrected for partial pressure of water vapor over the KOH solution (18)) as a function of time t.

From Fig. 4, it is evident that previous cycling history is of importance in determining the position of the Tafel line (i.e. the i_0 value) but not the slope and hence the rate-controlling mechanism. A number of experiments made at various times have indicated that the electrodes give reproducible behavior after the second or third cycle of charging and discharging. It is seen that fourth-cycle data for both open-circuit and steady-state kinetic behavior are identical within the experimental reproducibility (5 mv).

(ii) Apparent Heats of Activation

The apparent heat of activation (in the sense of Temkin (9, 10)) for steady-state d-c. polarization in 7 *M* KOH is derived from the Arrhenius plot shown in Fig. 5 by calculating $(\partial(\ln i)/\partial(1/T))_E$ at an oxygen overpotential of $E_{O_2} = 0.18$ v and is found to be 15.2 (± 1) kcal mole^{-1}. This corresponds, with the observed Tafel slope of 0.049 ± 0.002, to a heat of activation at the reversible oxygen potential of 20.2 (± 1.6) kcal mole^{-1}. In this calculation, allowance is made for the fact that the e.m.f. measurements were made with respect to the Hg/HgO electrode, which has a temperature coefficient of standard e.m.f. of -0.55×10^{-3} v (°C)$^{-1}$ (11).

The corresponding heat of activation for the evolution of oxygen on *open circuit* is identical with this value (see Fig. 5), although the Arrhenius plot is slightly shifted towards higher rates at a given temperature compared with that for the d-c. polarization. This may be due to slightly different electrode preparations used in these two experiments; in the oxygen evolution work, electrodes having maximum degree of impregnation (achieved by three successive vacuum impregnations (1, 2)) were used in order to achieve the highest possible extent of oxygen evolution with a given electrode.

(iii) Direction of H–D Isotope Effects

Open-circuit decay measurements were made in H_2O/KOH and D_2O/KOD solutions using electrodes prepared from anhydrous Ni_2SO_4 as described. Related experiments on oxygen evolution under d-c. polarization at nickel wires were also carried out in D_2O and H_2O. In both cases, the mercuric oxide reference electrode was used so that the

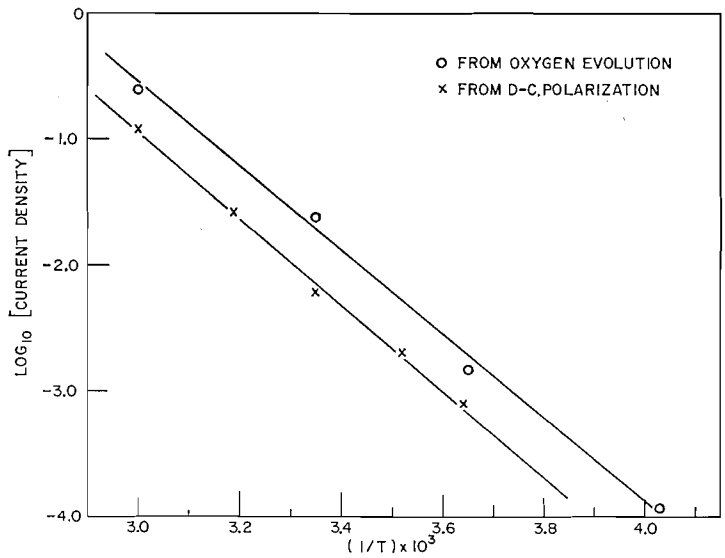

FIG. 5. Arrhenius plots for the apparent electrochemical heat of activation for the oxygen evolution reaction at nickel oxide electrodes (7 *M* KOH; overpotential for O_2 evolution = 0.18 v).

oxygen overpotential at a given current density or after a given time of decay could be compared directly in H_2O and D_2O, since the standard free energy and hence e.m.f. associated with the reaction

$$Hg + 1/2\,O_2 \rightleftharpoons HgO$$

is independent of the nature or activity of the water species.

Both for the open-circuit decay process and the d-c. polarization behavior, the H/D isotope effect on the rate of oxygen evolution is an *inverse* one having a magnitude of about 1/5, the reaction in the D-solvent being the faster at a given oxygen overpotential. This direction of the isotope effect has also been found at the partially charged electrodes in a formal state of oxidation "$NiO_{1.25}$" and has been referred to previously (2). The identity of the direction of the isotope effects for open-circuit and d-c. polarization behavior is further evidence that the rate-controlling process is the same in the two cases and is hence associated with oxygen evolution. The direction of the isotope effect observed is also important negative evidence that the cathodic reduction step* involving proton transfer, viz.

$$NiO.OH \xrightarrow{H^+, e} Ni(OH)_2,$$

which must occur in self-discharge, is *not*, as has been suggested by Pitman and Work (3), the rate-controlling partial process. The inverse isotope effect probably arises from preferential discharge of O from OD^- in D_2O than from OH^- in H_2O on account of different solvation energies of the isotopically analogous ions (12, 13).

(d) Open-circuit Decay of E.M.F., and Electrode Capacitance

Further (see ref. 1) e.m.f. decay studies have been made at various temperatures and the capacitance involved in the associated self-discharge process has been evaluated from

**The cathodic reduction step during relatively short times (less than about 1 day) and at room temperature mainly involves reduction of the surface phase (5) rather than the bulk phase, although self-discharge of the latter can be significant at elevated temperatures (e.g. 60° C) or over longer times (2).*

the θ constant defined (8) and discussed (1, 5) previously. The self-consistency of the e.m.f. decay data obtained was checked by establishing that:

(i) the θ term was inversely proportional to the current density prior to interruption of the current (see Fig. 6(*a*));

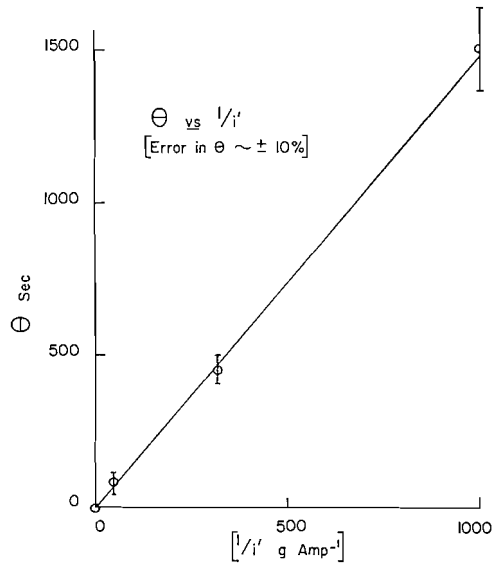

FIG. 6(*a*). θ values plotted against initial polarizing current density (0.72 *M* KOH, 25° C).

(ii) the e.m.f. decay lines taken from a series of different initial polarizing current densities were (almost) coincident (see Fig. 6(*b*));

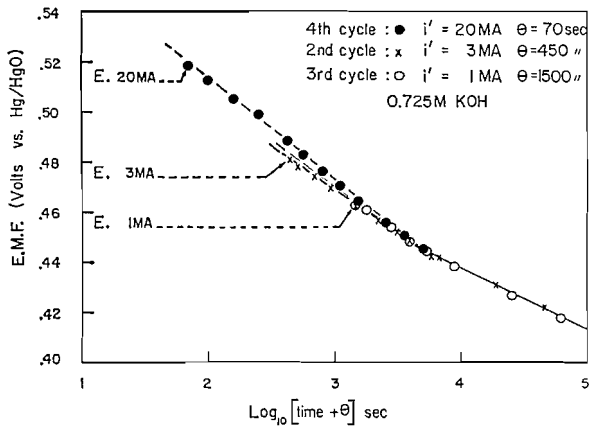

FIG. 6(*b*). Coincidence of e.m.f. decay lines taken from different initial polarizing current densities (0.72 *M* KOH, 25° C).

(iii) the same slope of the e.m.f. decay line was obtained by making an e.m.f. decay plot by the "difference" procedure (see Fig. 6(*c*)); this type of plot merely eliminates any arbitrariness in the estimation of θ. It is particularly useful in cases where it is suspected that a change of mechanism may occur with falling electrode potential at a potential near the starting value, i.e. after a time on open circuit comparable with θ.

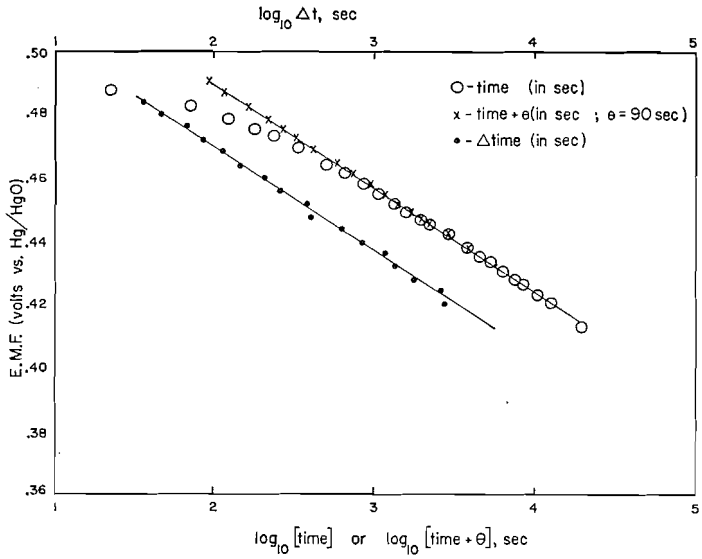

FIG. 6(*c*). Application of the difference method for evaluation of e.m.f. decay slopes without evaluation of θ (9.1 *M* KOH, 25° C); Δt values are the times required for successive falls of potentials of 4 mv, as a function of mean potential during these times. Log t and log $[t+\theta]$ plots for comparison.

The e.m.f. decay lines plotted in terms of E vs. log $[t+\theta]$ are shown in Fig. 7 for various concentrations at −25°, 1°, and 60.5° C. The behavior at 25° C, previously published (1), is included for comparison. The associated θ values lead (8, 1) to the capacities listed in Table II, where they are compared with the (initial) capacities deduced (cf. ref. 1) from

TABLE II

Surface capacitance and active oxygen content of electrodes as a function of temperature and KOH concentration

Temperature (°C)	Concn. (*M*/liter)	Surface capacitance ($F\,g^{-1}$)		Active O atom per Ni atom	
		From θ (±15%*)	From $dE/d\mathrm{O}_2$† (±15%*)	Initial (±0.03*)	Lost in first 24 hours (±0.005*)
−25	4.5	170	210	0.42	0.015
	8.2	170	130	0.42	0.010
	11.8	130	130	0.41	0.010
1.0	0.10	300	210	0.43	0.030
	1.0	300	230	0.49	0.035
	7.0	230	400	0.46	0.022
	8.6	180	210	0.43	0.020
25	0.015	320	230	0.41	0.035
	0.15	250	300	0.44	0.032
	0.93	400	600	0.43	0.035
	2.9	330	380	0.48	0.036
	7.0	330	480	0.52	0.028
	9.4	280	300	0.51	0.025
	14.6	180	240	0.57	0.020
60.5	0.15	150	130	0.28	0.050
	1.5	160	160	0.39	0.035
	7.0	200	260	0.57	0.028
	14.4	220	240	0.67	0.035
	15.4	280	320	0.66	0.035

*The margins of error indicated are the maximum deviations from the mean values observed between replicate runs done under the same conditions of temperature and concentration.

†The values recorded here are of "initial" capacitance at the highest anodic potential at the beginning of the e.m.f. decay. Substantially higher values arise at lower e.m.f.'s after the decay has proceeded for some time, particularly in the more dilute solutions at higher temperatures.

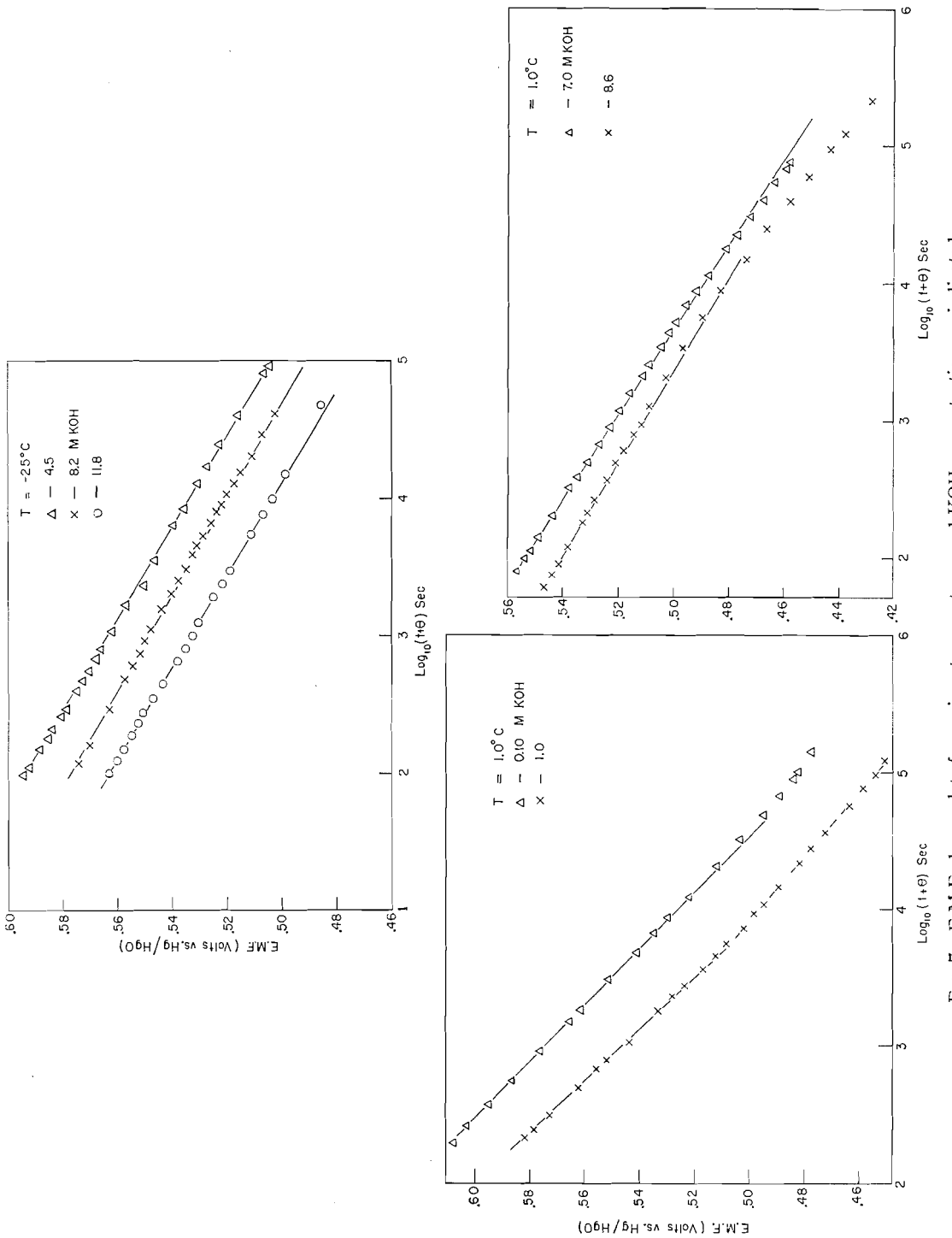

FIG. 7. E.M.F. decay plots for various temperatures and KOH concentrations as indicated.

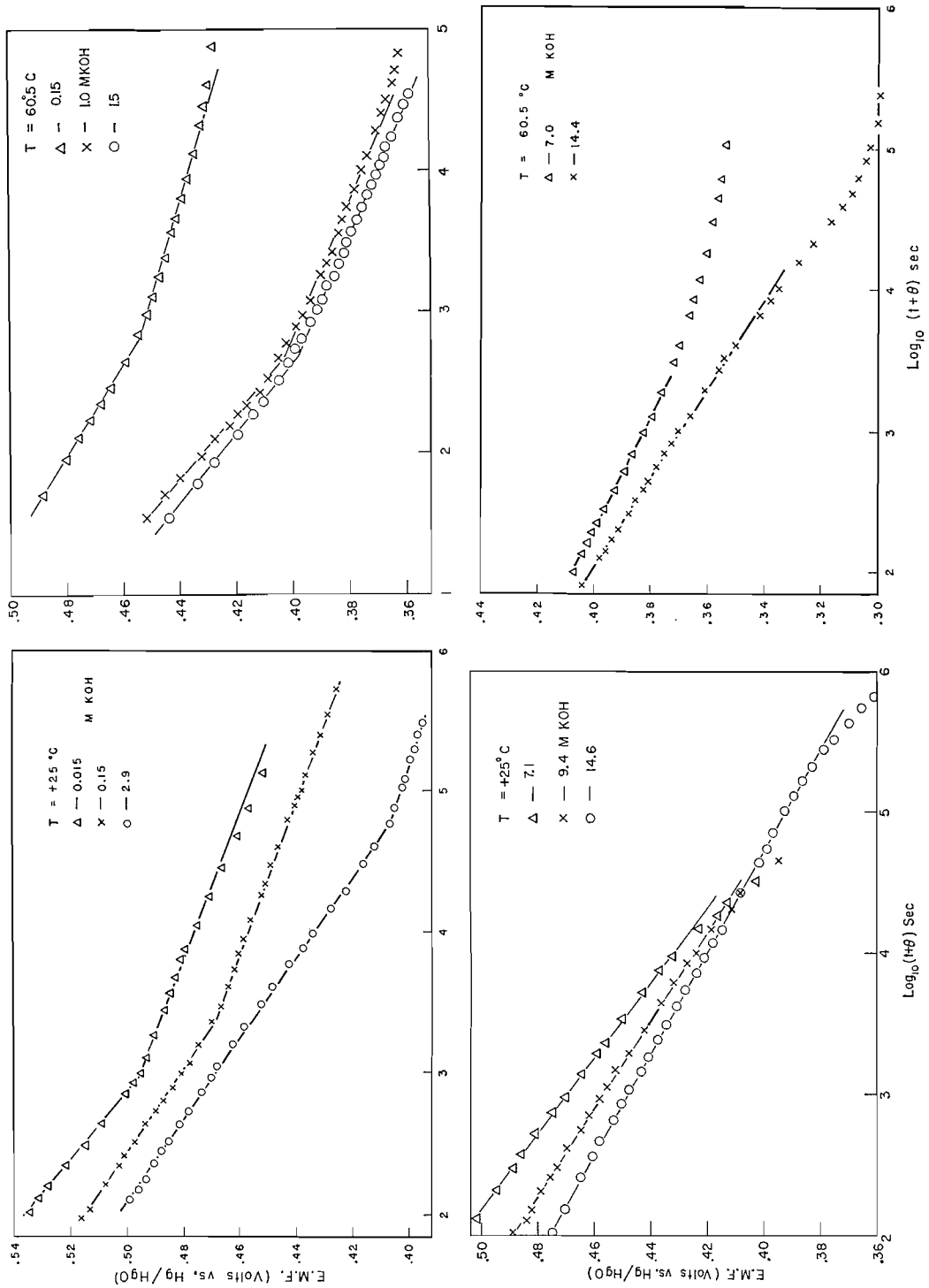

FIG. 7.

the volumes of oxygen evolved on open circuit as a function of electrode potential (as shown in Fig. 8). The corresponding total active oxygen to nickel ratios have been calculated from coulombic discharging and charging curves and are given in the last column of Table II.

DISCUSSION

(a) Rate-determining Mechanism in Self-discharge

From the above results, it is clear that three distinct lines of evidence strongly indicate that the self-discharge process is controlled by the *anodic* partial reaction of oxygen evolution rather than the cathodic one of reduction of nickel oxide in the bulk (or the surface) phase as suggested by Pitman and Work (3). Their differing conclusion evidently arises from the fact that *average* rates of oxygen evolution were estimated over a long time and hence over an appreciable range of falling potentials without making a proper allowance for the relation of the rate to the electrode potential. It may also be noted that the marked increase of the self-discharge rate at various given electrode potentials with increasing KOH activity cannot be related in a simple way to the nature of the self-discharge mechanism, since it is now evident that the effect arises mainly from the dependence of Tafel slopes of the rate-determining oxygen evolution reaction on the KOH activity; the corresponding i_0 values (see Fig. 3) are, in fact, almost independent of KOH activity within the reproducibility indicated.

The possibility that the self-discharge process in the overcharge region is simply a non-electrochemical decomposition or desorption from the surface phase at the interface of the nickel oxide particles (i.e. a process analogous to the decomposition reactions of the chemically prepared higher nickel oxide discussed by Howell (23)) can be eliminated on the basis of the identity of oxygen evolution rate and d-c. polarization Tafel slopes. Such a dependence of rates upon potential could only arise in a non-electrochemical decomposition if there was a remarkable and coincidental dependence of free energy of the surface phase (and hence associated electrode potential) upon coverage by adsorbed species leading to an apparent dependence of rate of decomposition on electrode potential. All the characteristics of the self-discharge process are consistent with an electrochemically controlled reaction, as also occurs for the partially charged material where an electrochemically controlled self-discharge process can quantitatively account for the steady-state mixed potential (2).

(b) E.M.F. Decay Slopes and Current-potential Behavior

Elsewhere (5) we have shown how the e.m.f. decay slopes ($dE/d \ln t$) may be related in a formal way to the mechanistically significant Tafel slopes when the surface capacitance (2, 5) involved in the self-discharge process is potential dependent. This case arises with the nickel oxide electrode only at room and higher temperatures but not at all at low temperatures in quite strong KOH solutions. When the e.m.f. decay slopes b_1 are obtained, the true Tafel slope b_3 follows (5, 14) from

$$b_1 = \frac{b_2 b_3}{b_3 - b_2},$$

where b_2 is the Nernst factor relating surface charge q_s or corresponding capacity dq_s/dE to potential E in the equation

$$q_s = ke^{E/b_2}$$

as we have shown previously (5).

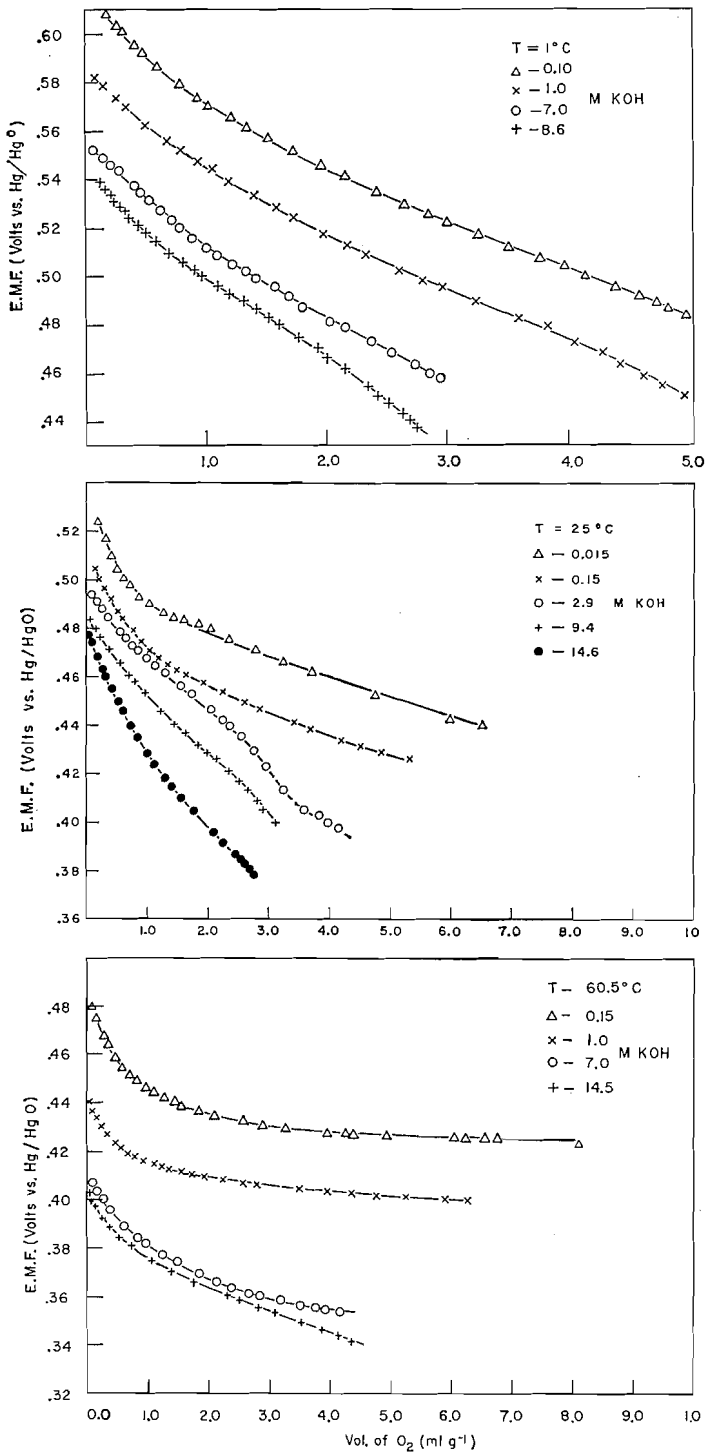

FIG. 8. Volumes of oxygen evolved on open circuit as a function of potential in various KOH solutions and at three temperatures.

In the dilute solutions (<1 M KOH) at 25° C, the *true* Tafel slopes may be calculated from the slopes of the e.m.f. decay lines (Fig. 7) using the observed dependence (1, 5) of surface charge upon potential (deduced from oxygen volume measurements (Fig. 8) as a function of potential (1)). The following values are obtained:

0.15 M KOH (25° C) upper potential region	$b_3 = 0.045$
0.15 M KOH (25° C) lower potential region	$b_3 = 0.022$
7 M KOH (25° C) upper potential region	$b_3 = 0.045$
7 M KOH (25° C) d-c. polarization (upper region)	$b_3 = 0.049$
0.15 M KOH (60.5° C) upper potential region	$b_3 = 0.051$
0.15 M KOH (60.5° C) lower potential region	$b_3 = 0.027$
1.5 M KOH (60.5° C) upper potential region	$b_3 = 0.044$
1.5 M KOH (60.5° C) lower potential region	$b_3 = 0.021$

We now consider the mechanistic significance of these true Tafel slopes in relation to our previous discussion (1) of rate-controlling mechanisms. By comparison with the steady-state Tafel lines for d-c. polarization (in 7 M KOH), it is seen that the Tafel slopes derived from the e.m.f. decay slopes in the upper potential region are now fairly consistent with the d-c. polarization values (viz. 0.049±0.002). In all cases, the Tafel slope in the lower potential region (corresponding to the lower i_0 values in Fig. 3) is approximately one half that for the mechanism occurring at higher potentials in cases where both the e.m.f. decay and oxygen evolution rate lines show a clear inflection.

Elsewhere (1) we have suggested consecutive mechanisms of oxygen evolution at the nickel oxide electrode that are consistent with limiting Tafel slopes of $\frac{2}{3}.2.3RT/F$ (0.038 v at 25° C), followed by either $\frac{2}{3}.2.3RT/F$ (0.023 v) or $2.3RT/3F$ (0.020 v). The true Tafel slopes (for the upper potential region) discussed above are seen to be between $2.3RT/F$ (0.059 v) and $\frac{2}{3}.2.3RT/F$. Thomas (15) has shown, by taking into account the variation of activation energy with surface coverage of intermediates, that the former value can arise in a simple radical recombination step, e.g. $H + H \rightarrow H_2$, in cathodic hydrogen evolution, when the activation energy for desorption in a molecule-producing step is greater than the net desorption energy, i.e., in the present case when the reverse process of chemisorption of O_2 as M—O is "activated". Inspection of the following possible oxygen-producing mechanisms involving recombination steps:

$$\text{I}\begin{cases} OH^- + M \rightarrow MOH + e & \text{(i)} \\ 2MOH \rightarrow MO + H_2O & \text{(ii)} \\ 2MO \rightarrow M + O_2 & \text{(iii)} \end{cases}$$

or

$$\text{II}\begin{cases} OH^- + M \rightarrow MOH + e & \text{(i)} \\ OH^- + MOH \rightarrow MO + H_2O + e & \text{(ii)} \\ 2MO \rightarrow M + O_2 & \text{(iii)} \end{cases}$$

where M refers to the surface of the nickel oxide, indicates (1, 19) that the final step in either case must be associated with a Tafel slope of $2.3RT/4F$ for low coverage by MO or MOH, with the Langmuir isotherm applying (15, 20). At appreciable coverages, different results can arise as discussed below. Since we have also to account for a lower slope of either $\frac{2}{3}.2.3RT/F$ or $2.3RT/3F$, which appears at lower potentials in dilute solutions, the scheme previously suggested (1), viz:

$$\text{III}\begin{cases} M + OH^- \rightarrow MOH + e & \text{(i)} \\ MOH + OH^- \rightarrow MO + H_2O & \text{(ii)} \\ MO + MOH \rightarrow MHO_2 & \text{(iii)} \\ MHO_2 + MOH \rightarrow M + H_2O + O_2 & \text{(iv)} \end{cases}$$

must still be considered under certain conditions.

Case 1: General Equations for the Recombination Mechanisms I(ii), I(iii), or II(iii)

Elsewhere (21) we have developed the treatment of Thomas (15) and applied it to steps similar to the recombination reactions I(ii), I(iii), or II(iii), allowing for variation of the free energy of activation of the various steps with coverage; analogous calculations of surface coverage effects have previously been carried out with regard to electrochemical H/D isotope effects (16). In another paper (5), we have shown from the direction of potential dependence of the adsorption pseudocapacity that the nickel oxide surface is appreciably covered with O-containing radical intermediates except at low anodic potentials.

The coverage by the adsorbed OH species at the surface must hence be considered sufficient to cause variation of the heat of adsorption ΔH of OH with coverage θ, according to the equation

$$\Delta H = \Delta H^0 - r_1\theta, \qquad [1]$$

per g radical of OH; then with I(i) or II(i) in quasi-equilibrium and with $\theta_{MOH} \doteqdot \frac{1}{2}$ (cf. ref. 15) and $\theta_{MOH} \gg \theta_{MO}$* so that the main effect of variations of θ is in the exponentials, we obtain (15, 24)

$$\Delta G_{-1} - \Delta G_1^{\neq} + VF = r_1\theta + K, \qquad [2]$$

where K is a constant at constant concentration and temperature, and the $\Delta G^{\neq}$ values are the standard free energies of activation for the indicated forward and backward reactions I(i) or II(i) proceeding at an interfacial p.d. of V.

The rate equation for rate-controlling I(ii) is

$$v_2 = k_2(\theta_{MOH})^2 \exp -[\Delta G_2^{\neq} - 2\gamma r_1\theta + (1-\gamma)r_2\theta]/RT, \qquad [3]$$

where γ is a symmetry factor similar to the usual β and r_2 refers to MO species in an equation similar to [1]. For intermediate coverage ($\theta \doteqdot 0.5$) the variation of v_2 with θ_{MOH} will be mainly due to variation of the exponentials with θ in the terms involving $r_1\theta$ and $r_2\theta$. For most examples of chemisorption, the heat of adsorption varies by at least 10 kcal (g-atom)$^{-1}$ over the range of fractional coverage 0 to say 0.9, so that r is of the order 10 kcal. A variation of θ from $\theta = 0.1$ to say 0.9 as potential is varied would change the velocity of a recombination step by a factor of 81 due to variation of the pre-exponential term in θ_{MOH}^2; however, the corresponding effect in the exponential, through the r term taken as 10 kcal, would give a rate factor of

$$\exp\left[\frac{2\,0.9r}{RT}\right] \Big/ \exp\left[\frac{2\,0.1r}{RT}\right].$$

This ratio is approximately exp [26.6] or $10^{11.6}$ so that the exponential θ term, even when θ varies over as large a range as 0.1–0.9, can be by far the principal factor determining the dependence of rate upon coverage. In practice, this means that the variation of θ

**In the original treatment (15) for hydrogen evolution the only intermediate is adsorbed* H. *When several consecutive steps are involved, as in the present case, limiting assumptions must be made about the* total *coverage by intermediates and about the relative values of coverage, e.g. by* O *and* OH *etc. Such assumptions are also the basis of the previous general analysis of oxygen evolution slopes (19) but neglecting coverage effects in exponential terms. In the present case, with I(ii) or II(ii) rate determining, θ_{MOH} will be much greater than θ_{MO}.*

with potential occurs over a much wider range of potential than is possible if only the pre-exponential terms in θ are involved in the rate expression (21).

Substitution of θr_1 from [2] into [3] leads to the Tafel slope of

$$dV/d \ln i = 2RT/F$$

when $r_1 = r_2$, as is likely for the similar chemical species OH and O at the water-covered surface (21). No activated adsorption case (cf. ref. 15) can arise with I(ii) since molecular oxygen is not a product (to be desorbed) of this step. The Tafel slope can hence never be $RT/2F$ for this step and the lowest Tafel slope obtainable is RT/F when $r_1 \gg r_2$.

If I(iii) or II(iii) were rate determining, the low coverage Tafel slope is obviously $RT/4F$ and the intermediate coverage slope is now $RT/2F$ (15) for non-activated adsorption conditions. However, since in I(iii) or II(iii), the molecular oxygen produced is the final product and must be desorbed, the activated adsorption case (cf. ref. 15) must be considered here and corresponds to the substitution of a term $2\gamma r\theta$ instead of $2r\theta$ in the rate equation similar to [3] for reactions I(iii) or II(iii), leading to a Tafel slope of RT/F when $\gamma = 0.5$, and r now refers to coverage effects due to MO + MOH if I(iii) or II(iii) is rate controlling. For I(iii) or II(iii) the Tafel slope could hence change in the sequence

$$RT/4F \text{ (low coverage)} \rightarrow RT/2F \text{ (intermediate coverage)} \rightarrow RT/F \text{ (intermediate coverage, "activated" adsorption).}$$

We may note that when surface coverage terms are introduced into the exponentials in the rate expressions the lowest Tafel slope that can arise is $RT/2F$ when the exponential terms in θ are more important that the pre-exponential θ terms. Steps such as I(iii) or II(iii), which give a slope less than $RT/2F$ at low coverage (1, 19), cannot hence be distinguished, under conditions of intermediate coverage, from steps I(ii) or II(ii) at low coverage. The same arises for ion–radical recombination steps which, independent of their position in the consecutive sequence of steps, will not give slopes less than RT/F when coverage by intermediates is appreciable (21, see below) except when they are terminal desorption steps for which the minimum slope will normally be $2.3(2RT/3F)$.

Case 2: Ion–Radical Rearrangement—Mechanism II(ii) or III(ii)

Here, following the same methods as above, the theoretically possible Tafel slopes are:

Langmuir adsorption	(low coverage)	$2.3(2RT/3F)$;
Temkin adsorption	(intermediate coverage)	$2.3(2RT/F)$ $(r_1 = r_2)$,
		$2.3(RT/F)$ $(r_1 \gg r_2)$.

Since molecular O_2 is not a product in these reactions, neither of the terminal desorption cases considered above are relevant to this case.

(c) Conclusions on Reaction Mechanism

If the observed slope of 0.049 in the upper potential region is to be identified with that considered above for recombination in reactions I(iii) or II(iii) with "activated" desorption, γ will be 0.6 while if the slope were to be identified with that for the desorption reactions II(ii) or III(ii) at low coverage, the symmetry factor β in

$$dV/d \ln i = RT/(1+\beta)F$$

would vary from 0.22 to about 0.33 depending on the value of the slope considered, which varies to some extent with concentration (e.g. see refs. 1, 5). At the present time, we cannot make a final distinction between the several above possibilities but we note that the low values of β which would now be required to account for the observed slopes with the radical–ion desorption mechanism (Langmuir case) are unusual, while the value of γ (which has a similar significance to that of β) required to account for the observed slopes in the upper potential region on the basis of a recombination reaction has the more reasonable value of 0.6, nearer to the normal expected value of about 0.5.

Under conditions corresponding to activated adsorption of oxygen, it is seen that the observed slope for the upper potential region must preferably be explained in terms of the radical recombination mechanism II(iii) or III(iii), with $\gamma \doteqdot 0.6$ since II(ii) or III(ii) at appreciable coverage can never give slopes less than $2.3RT/F$ ($r_1 \gg r_2$) (21). The lower slope of $2.3(2RT/5F)$ or $2.3(RT/3F)$ observed at lower potentials in dilute solutions still follows in terms of the same consecutive mechanisms previously suggested (1), although it must be noted that for these slopes to arise, the coverage must be low, since at intermediate coverage III(iii) cannot give a slope less than $2.3RT/F$ for the same reasons as those which determine the slope of I(ii) or II(ii). Similarly, if III(iv) were rate determining, only slopes of $2.3RT/2F$ or $2.3RT/2\gamma F$ could arise as in the case of I(iii) or II(iii).

Since the lower slopes are observed only after an appreciable volume of oxygen has been desorbed in the self-discharge, this requirement of low coverage is not inconsistent with the experimental situation; we have in fact shown (5) that the total amount of oxygen desorbed over about a day corresponds to about a monolayer, based on the B.E.T. area of the dry oxidized electrode. Also with decreasing potential, the pseudocapacitance increases, indicating a trend (5) from high to lower coverage.

For the oxygen-producing reactions at the nickel oxide electrode, the low coverage Langmuir case is almost certainly only applicable after appreciable desorption of oxygen on self-discharge, since we have shown (5) from the direction of the potential dependence of the adsorption pseudocapacitance (viz. decreasing capacitance with increasing anodic oxygen overpotential) that the adsorbed layer of O-containing radicals at the surface is approaching full coverage at high anodic potentials. Under these conditions, where the heat of adsorption of O-containing radicals will be far removed from the "initial" or zero-coverage value, it is likely that the condition of "activated" adsorption (15) will hold, corresponding to a slope of $2.3RT/F$ for the final desorption step.

We hence conclude that the observed slope in the upper potential region could correspond to the final recombination step at appreciable coverages under "activated adsorption" conditions and the change of slope with decreasing potentials (and coverage) could correspond to a real change of mechanism to process III(iii) or to the alternative process $MO + OH^- \rightarrow MHO_2 + e$, as previously suggested (1), corresponding to a slope of $2.3(2RT/5F)$ under conditions of low coverage.

(d) Electrode Surface Capacity and Active O:Ni ratio

Elsewhere (2, 5) we have discussed the significance of the surface capacitance in relation to the e.m.f. decay behavior and to the mechanism of charging of the electrode. The results in Table II extend the previous observations (1) to higher and lower temperatures. The capacitance values given are "initial" values corresponding to the highest anodic potential involved at the moment of commencement of e.m.f. decay on open-circuit oxygen evolution; the variation of capacitance with temperature at a given concentration is not significant but the active O:Ni ratio generally increases with increasing KOH

concentration at 25° C and 60.5° C and the extent of self-discharge measured by the oxygen evolved is larger at the higher temperature on account of the greater rate of the process at elevated temperatures, as indicated by the kinetic data given above. The actual surface capacitance values vary appreciably probably on account of the difficulty of reproducing surfaces of the same real area from one run to another. The trend of the active O:Ni ratios with increasing KOH concentration may reflect stabilization of the surface layer of higher degree of oxidation by adsorbed KOH. The trend of true reversible potentials for the "$NiO_{1.25}$" electrode with KOH concentration requires participation of adsorbed KOH (2); elsewhere (25) it will be shown that the reversible potentials for the nickel oxide electrode, even in a low state of charge, are determined by the surface phase at the nickel oxide – solution interface.

We may conclude by noting that from equation [2] we can write

$$d\theta/dV = F/r.$$

Since the pseudocapacity associated with the coverage θ by radicals is

$$C = dq/dV,$$

where q is the adsorbed charge corresponding to θ and given by

$$q = k\theta,$$

it is clear that a constant pseudocapacity contribution C arises, associated with the linear dependence of θ on V, given by

$$C = kF/r$$

and is determined by the rate of change of adsorption energy with coverage (cf. ref. 22). When the heat of adsorption varies with θ by some power other than unity, potential-dependent capacitance can be shown (21) to result, as is also the case (24) for Langmuir conditions when the pre-exponential θ terms are taken into account. When pre-exponential and exponential terms in θ are combined, a more complex expression for C can be shown to result (21).

REFERENCES

1. B. E. Conway and P. L. Bourgault. Can. J. Chem. **37**, 292 (1958).
2. P. L. Bourgault and B. E. Conway. Can. J. Chem. **38**, 1557 (1960).
3. A. L. Pitman and G. W. Work. U.S. Naval Res. Lab. Rept. 4845 (1956); 5031 (1957).
4. P. L. Bourgault and B. E. Conway. J. Electroanalytical Chem. **1**, 8 (1959).
5. B. E. Conway and P. L. Bourgault. Trans. Faraday Soc. In press.
6. A. N. Frumkin and M. Slygin. Acta Physicochim. U.R.S.S. **3**, 791 (1935); 819 (1936); **11**, 45 (1939).
7. E. J. Casey, P. L. Bourgault, and P. Lake. Can. J. Technol. **34**, 95 (1956).
8. H. B. Morley and F. E. W. Wetmore. Can. J. Chem. **34**, 359 (1956).
9. M. Temkin. Zhur. Fiz. Khim. **22**, 1081 (1948).
10. B. E. Conway. Phil. Trans. Roy. Soc. (Canada), **54** (III), 19 (1960).
11. W. Latimer. Oxidation potentials. 2nd ed. Prentice-Hall. 1952.
12. O. Reitz and E. F. Forster. Z. Elektrochem. **44**, 45 (1938).
13. B. E. Conway. Proceedings of the Symposium on Electrode Processes. Philadelphia. 1959. The Electrochemical Society. John Wiley and Son, New York. 1961.
14. P. D. Lukovtsev and S. A. Temerin. Trudy Akad. Nauk S.S.S.R., Otdel Khim. Nauk, 494 (1953).
15. J. G. N. Thomas. Trans. Farday Soc. **57**, 1603 (1961).
16. B. E. Conway. Proc. Roy. Soc. (London), A, **256**, 128 (1960).
17. A. M. Azzam and J. O'M. Bockris. Trans. Faraday Soc. **48**, 145 (1952).
18. G. C. Akerlof and P. Bender. J. Am. Chem. Soc. **70**, 2366 (1948).
19. J. O'M. Bockris. J. Chem. Phys. **24**, 817 (1956).
20. R. Parsons. Trans. Faraday Soc. **54**, 1053 (1958).
21. B. E. Conway and E. Gileadi. In press.
22. B. E. Conway and R. G. Barradas. Electrochim. Acta, **5**, 319, 349 (1961).
23. O. H. Howell. J. Chem. Soc. **123** (II), 1772 (1923).
24. J. O'M. Bockris and H. Kita. J. Electrochem. Soc. **108**, 676 (1960).
25. B. E. Conway and E. Gileadi. Part IV of this series. Can. J. Chem. In press.

NOTES

THE X-RAY POWDER DIFFRACTION PATTERNS OF AMMONIA – NICKEL CYANIDE COMPLEXES

V. M. BHATNAGAR[1] AND J. A. R. CLOUTIER[2]

Clathrate compounds of ammonia – nickel cyanide complexes can be prepared from a small group of organic molecules. The composition of this series of clathrates is represented by $[Ni(CN)_2.NH_3.M]$, where M is aniline, benzene, furan, phenol, pyridine, pyrrole, or thiophene. An X-ray structural investigation of benzene clathrate has been made by Rayner and Powell (1).

The three clathrates were prepared by the method described by Palmer (2). The hydrated ammonia – nickel cyanide complex was obtained as stated by Bhatnagar (3). The following code has been used for these compounds in this note:

JA = $[Ni(CN)_2.NH_3.C_4H_5N]$, pyrrole clathrate;
VM = $[Ni(CN)_2.NH_3.\frac{1}{4}H_2O]$, hydrated ammonia – nickel cyanide complex;
QR = $[Ni(CN)_2.NH_3.C_6H_5NH_2]$, aniline clathrate;
AB = $[Ni(CN)_2.C_5H_5N]$, pyridine clathrate.

The unground powder, except when indicated, was introduced into a 0.2-mm glass capillary tube of 0.01-mm wall thickness. Diffraction patterns were obtained using Philips Debye–Scherrer powder cameras, diameter 114.83 mm, and Cu K_α radiation. Exposures from 5 to 10 hours at 30 kv and 10 ma were used. Line positions were corrected for film shrinkage and converted into d-values using tables (4). Relative intensities were estimated visually on a scale of 100. The I/I_1 values, as recorded, take into account the widths of the lines.

The X-ray powder diffraction patterns of the four complexes studied are presented in Figs. 1(*a*), 1(*b*), 1(*c*), and 1(*e*). The corresponding diffraction data are given in Table I. Letters are used to report on the condition of some of the observed lines. A diffuse line is indicated by the letter "d". An unresolved doublet which appeared as an unusually wide line is marked "w".

The four patterns of Figs. 1(*a*), 1(*b*), 1(*c*), and 1(*e*) are different from one another and could be used to characterize the corresponding compounds. However, under close inspection, a number of lines repeat with about the same relative intensities in each of these powder diagrams. These lines are, limiting the discussion to the ones of larger d-values: 3.60, 3.21, 2.54, 2.27, and 2.19 Å. Qualitatively, it would therefore appear that these four complexes have some common structural feature.

The effect of mechanical grinding on the powder diagrams was studied. The patterns from complexes AB and JA remained unaffected. Many lines disappeared on the pattern from complex QR, as illustrated in Fig. 1(*d*). Complex VM showed the presence of some additional doublets in its pattern, Fig. 1(*f*). However, these changes attributed to the

[1]*Department of Chemistry, The University of Western Australia, Nedlands, Perth, Australia.*
[2]*Food and Drug Laboratories, Department of National Health and Welfare, Ottawa, Ontario.*

FIG. 1. X-Ray powder diffraction patterns: (*a*) complex AB, not ground; (*b*) complex JA, not ground; (*c*) complex QR, not ground; (*d*) complex QR, ground; (*e*) complex VM, not ground; (*f*) complex VM, ground; (*g*) the four complexes heated at 200±10° C for 30 minutes; (*h*) the four complexes heated at 300±10° C for 30 minutes.

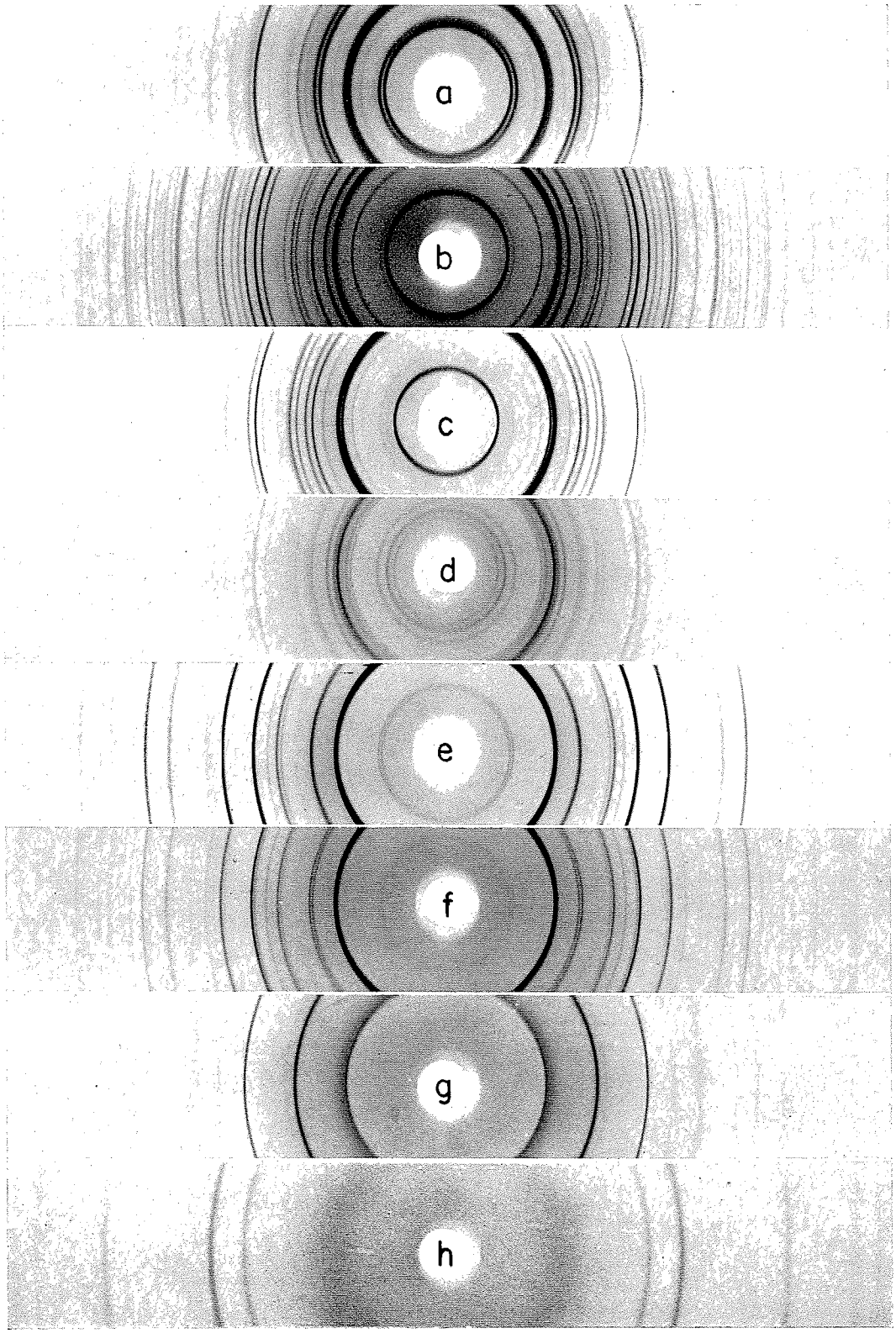

TABLE I
X-Ray diffraction data

d, Å	I/I_1	d, Å	I/I_1	d, Å	I/I_1	d, Å	I/I_1
			Complex AB (not ground)				
8.29	2	3.28	3	2.32	5	1.59	2
7.57	95	3.21	20	2.26	10 w	1.57	2
7.02	70	3.13	1	2.19	2	1.53	1
6.58	4	3.03	8	2.12	3	1.51	1
5.96	2 w	2.89	1	2.06	10	1.473	2
5.49	8	2.87	1	2.00	2	1.438	1
4.86	100	2.78	1	1.89	3	1.415	3
4.63	50	2.71	7	1.81	10	1.395	1
4.15	5	2.60	2 w	1.75	2	1.380	1
3.79	80	2.52	70	1.68	10	1.358	2
3.62	70	2.46	10	1.64	5	1.312	1
3.39	8	2.40	8	1.61	3	1.259	2
			Complex JA (not ground)				
7.91	50	2.97	10	1.78	1	1.371	3
7.18	7	2.63	25	1.75	5	1.342	1
6.20	1	2.54	45	1.72	2 w	1.327	7
5.07	25	2.49	2 w	1.69	5	1.296	1
4.71	2 d	2.42	40	1.65	10	1.285	2
4.28	100	2.34	14	1.63	2 w	1.272	1
4.11	1	2.27	12	1.60	5	1.253	1
3.95	45	2.18	20	1.57	4	1.242	2
3.60	40	2.14	16	1.56	10	1.213	1
3.46	5	2.05	1	1.51	1	1.196	1
3.40	1	1.97	15	1.486	8	1.181	2
3.21	15	1.94	1	1.423	3	1.146	2
3.12	20	1.84	20 w	1.408	3		
3.04	1	1.80	4	1.386	7		
			Complex QR (not ground)				
9.28	45	3.32	1	2.05	10	1.52	1
8.51	1 *	3.23	25	2.00	1	1.51	1
8.08	2 *	3.09	25 *	1.96	15	1.493	2
7.53	1 *	3.05	8 *	1.85	2	1.475	1
7.19	4 *	2.94	1	1.83	2	1.461	1
5.70	3	2.85	4	1.80	4	1.440	1
5.36	1	2.73	1	1.77	6	1.425	1
5.10	8	2.64	8	1.74	1	1.412	2
4.88	1	2.55	40	1.72	3	1.397	3
4.63	40	2.46	30	1.70	3	1.371	1
4.44	100	2.32	5	1.67	8 *	1.352	3
4.05	2	2.28	10	1.66	3 *	1.323	1
3.89	8	2.23	15 *	1.61	4	1.288	2
3.73	1	2.20	15 *	1.59	5	1.275	2
3.60	30	2.15	1	1.56	1		
3.43	25	2.11	10	1.55	1		
			Complex VM (not ground)				
7.52	10	2.24	1	1.74	4 w	1.359	1
7.13	10	2.19	70	1.70	2	1.348	1
4.81	2	2.15	1	1.69	2	1.330	1
4.40	100	2.11	3	1.66	50	1.317	1
3.59	45	2.08	3	1.60	15	1.295	1
3.50	1	2.05	7	1.54	1	1.266	15
3.21	2 w	2.01	1	1.52	1	1.250	1
2.94	10	1.98	1	1.50	15	1.226	1
2.87	40	1.92	5	1.462	15	1.215	5
2.72	15	1.87	4	1.429	1	1.197	1
2.53	80	1.81	1	1.407	1	1.188	1
2.27	2	1.79	35	1.385	25		

*Two lines which are closely spaced.

grinding of the powder were not predictable, since several patterns were obtained which were similar to Figs. 1(*c*) and 1(*e*), the diagrams from the unground QR and VM powders respectively.

The heat stability of the complexes was investigated. It was not possible to correlate the changes observed in the patterns with the expected ones associated with either the loss of the enclathrated organic molecules or the removal of NH_3 from the solid matrix. Therefore, it is not known how the initial dissociation of these complexes with heat takes place. However, it was observed that at 200±10° C the four complexes turned to a light brown color and yielded an X-ray diffraction pattern, Fig. 1(*g*), which was identified as that from anhydrous nickel cyanide (5). When the temperature was raised to 300±10° C, the four complexes gave the cubic pattern characteristic of nickel oxide, Fig. 1(*h*).

ACKNOWLEDGMENTS

This work was supported by research grants from the University of Western Australia, and one of us (V. M. B.) wishes to thank that body for its generosity. Grateful acknowledgment is made of the valuable technical assistance by J. C. Meranger for the X-ray diffraction work.

1. J. H. Rayner and H. M. Powell. J. Chem. Soc. 319 (1952).
2. W. G. Palmer. Experimental inorganic chemistry. Cambridge University Press, London. 1954.
3. V. M. Bhatnagar. J. Indian Chem. Soc. **39**, 143 (1962).
4. H. E. Swanson. Table for conversion of X-ray diffraction angles to interplanar spacings. App. Math. Ser. 10. Natl. Bur. Standards, Washington. 1950.
5. J. A. R. Cloutier. To be published.

Received April 9, 1962.
Department of Chemistry,
University of Western Australia,
Nedlands, Perth, Australia.

VANADIUM TRIALKOXIDES AND SOME ALCOHOLATES OF VANADIUM TRICHLORIDE

D. C. Bradley* and M. L. Mehta†

In attempting to prepare vanadium trialkoxides with vanadium trichloride as a starting material we have found that the lower aliphatic alcohols coordinate with vanadium trichloride, forming green solid alcoholates which are sparingly soluble in benzene, ether, toluene, carbon tetrachloride, or petrol, but more soluble in dimethylcellosolve. Methanol formed a 1:4 complex, VCl_3,4MeOH, whilst ethanol gave VCl_3,3EtOH, but neither complex could be crystallized from the alcohol. Isopropanol also gave a 1:4 complex, VCl_3,4Pr^{i}OH, which was recrystallized from boiling isopropanol. These alcoholates were readily oxidized on exposure to the air. It is noteworthy that chromium and iron trichlorides also form alcoholates (viz. $CrCl_3$,3ROH (1); $FeCl_3$,2ROH (2)).

The preparation of vanadium trialkoxides proved to be very difficult due to their ease of oxidation. Only the trimethoxide and triethoxide could be obtained in a reasonably pure state as green non-volatile solids. They were both prepared by the reaction involving vanadium trichloride and the appropriate lithium alkoxide:

$$VCl_3 + 3LiOR \rightarrow V(OR)_3 + 3LiCl.$$

**Present address: Chemistry Department, The University of Western Ontario, London, Ontario.*
†*Present address: Chemistry Department, Munshi Singh College, Bihar University, India.*

grinding of the powder were not predictable, since several patterns were obtained which were similar to Figs. 1(*c*) and 1(*e*), the diagrams from the unground QR and VM powders respectively.

The heat stability of the complexes was investigated. It was not possible to correlate the changes observed in the patterns with the expected ones associated with either the loss of the enclathrated organic molecules or the removal of NH_3 from the solid matrix. Therefore, it is not known how the initial dissociation of these complexes with heat takes place. However, it was observed that at 200±10° C the four complexes turned to a light brown color and yielded an X-ray diffraction pattern, Fig. 1(*g*), which was identified as that from anhydrous nickel cyanide (5). When the temperature was raised to 300±10° C, the four complexes gave the cubic pattern characteristic of nickel oxide, Fig. 1(*h*).

ACKNOWLEDGMENTS

This work was supported by research grants from the University of Western Australia, and one of us (V. M. B.) wishes to thank that body for its generosity. Grateful acknowledgment is made of the valuable technical assistance by J. C. Meranger for the X-ray diffraction work.

1. J. H. Rayner and H. M. Powell. J. Chem. Soc. 319 (1952).
2. W. G. Palmer. Experimental inorganic chemistry. Cambridge University Press, London. 1954.
3. V. M. Bhatnagar. J. Indian Chem. Soc. **39**, 143 (1962).
4. H. E. Swanson. Table for conversion of X-ray diffraction angles to interplanar spacings. App. Math. Ser. 10. Natl. Bur. Standards, Washington. 1950.
5. J. A. R. Cloutier. To be published.

Received April 9, 1962.
Department of Chemistry,
University of Western Australia,
Nedlands, Perth, Australia.

VANADIUM TRIALKOXIDES AND SOME ALCOHOLATES OF VANADIUM TRICHLORIDE

D. C. Bradley* and M. L. Mehta†

In attempting to prepare vanadium trialkoxides with vanadium trichloride as a starting material we have found that the lower aliphatic alcohols coordinate with vanadium trichloride, forming green solid alcoholates which are sparingly soluble in benzene, ether, toluene, carbon tetrachloride, or petrol, but more soluble in dimethylcellosolve. Methanol formed a 1:4 complex, VCl_3,4MeOH, whilst ethanol gave VCl_3,3EtOH, but neither complex could be crystallized from the alcohol. Isopropanol also gave a 1:4 complex, VCl_3,4Pr^{i}OH, which was recrystallized from boiling isopropanol. These alcoholates were readily oxidized on exposure to the air. It is noteworthy that chromium and iron trichlorides also form alcoholates (viz. $CrCl_3$,3ROH (1); $FeCl_3$,2ROH (2)).

The preparation of vanadium trialkoxides proved to be very difficult due to their ease of oxidation. Only the trimethoxide and triethoxide could be obtained in a reasonably pure state as green non-volatile solids. They were both prepared by the reaction involving vanadium trichloride and the appropriate lithium alkoxide:

$$VCl_3 + 3LiOR \rightarrow V(OR)_3 + 3LiCl.$$

**Present address: Chemistry Department, The University of Western Ontario, London, Ontario.*
†*Present address: Chemistry Department, Munshi Singh College, Bihar University, India.*

Several methods for preparing vanadium triisopropoxide were tried but the product always contained vanadium in a higher valence state than three. In one experiment the quinquevalent vanadyl compound $VO(OPr^i)_3$ was obtained whilst in another the quadrivalent vanadium tetraisopropoxide $V(OPr^i)_4$ was isolated. Similarly, attempts to prepare vanadium tri-*tert*-butoxide were unsuccessful because of oxidation. In view of the precautions taken to avoid atmospheric oxidation it seems probable that the vanadium trialkoxides are sufficiently powerfully reducing to liberate hydrogen from the alcohols (cf. action of alkali metals). Moreover, it seems likely that we succeeded in isolating $V(OMe)_3$ and $V(OEt)_3$ only because they are sparingly soluble and hence less prone to oxidation. It is noteworthy that a similar facile oxidation has been observed with cerium (III) (3), uranium(IV) (4), and niobium(IV) (5) alkoxides. The insolubility and nonvolatility of vanadium trimethoxide and vanadium triethoxide strongly suggest that these compounds are polymeric. Vanadium triethoxide thus differs from ferric ethoxide and aluminum ethoxide, which can both be volatilized under reduced pressure.

EXPERIMENTAL

Apparatus

All-glass apparatus specially adapted to exclude atmospheric moisture and oxygen was used. The apparatus was rinsed with ethanol, dried at 120° C, and allowed to cool *in vacuo*. All operations were conducted under an atmosphere of pure dry nitrogen. The gas was finally deoxygenated by scrubbing with a solution of the sodium ketyl of benzophenone in diphenyl ether. The gas was conducted to the apparatus through polyethylene tubing since the latter is less permeable to oxygen than P.V.C. tubing.

Chemicals

Vanadium trichloride was prepared as follows: vanadium metal was chlorinated at 130–150° C to form the tetrachloride, which was dissociated at 160–170° C to give the trichloride. Methanol was dried by refluxing for 24 hours over magnesium methoxide and then distilled. Ethanol was first dried azeotropically with benzene and then chemically with sodium ethoxide and diethylphthalate followed by distillation. Isopropanol was dried azeotropically with benzene. *tert*-Butanol was dried first over freshly ignited calcium oxide, then distilled over sodium, and finally subjected to azeotropic distillation with benzene. In the preparation of the vanadium(III) alkoxides the alcohols were passed through a column of dry chromatographic alumina to remove traces of peroxides.

Benzene, toluene, petrol, and diethyl ether were dried over sodium and distilled. Carbon tetrachloride was dried by distillation over phosphoric oxide.

Analytical Methods

Vanadium was determined volumetrically, after reduction to V(II) in a Jones Reductor, by titration with ceric ammonium sulphate using ferroin indicator. This gave the titer for "total" vanadium; the average valency of the vanadium in a compound was deduced by comparing the equivalent weight of vanadium given by the titration of total vanadium with the equivalent weight determined by direct titration of the sample with ceric ammonium sulphate. In the vanadium alkoxides the "total" vanadium was checked gravimetrically as follows: The sample (ca. 0.2 g) was weighed directly into a crucible and hydrolyzed with dilute nitric acid. After careful evaporation to dryness (infrared lamp) the residue was treated with a few drops of concentrated nitric acid, dried, then ignited to V_2O_5. Chlorine was determined gravimetrically by precipitation of silver chloride in acid solution. Methoxide, ethoxide, and isopropoxide were determined volumetrically using the chromic acid method (6) with corrections for the concomitant oxidation of V(III) to V(IV).

Preparation of VCl_3,4MeOH

Vanadium trichloride (4.4 g; V, 32.8; Cl, 67.5%; valency, 3.01) appeared not to react with methanol (30 g) even on shaking. Heating under reflux for 3 hours gave a green solution but the cooled solution did not crystallize. Evaporation of the excess methanol under reduced pressure at room temperature left a green solid (8.0 g). Found: V, 18.72, 18.57; Cl, 36.8, 36.8; MeOH, 45.9, 46.8; valency, 3.04. VCl_3,4MeOH requires: V, 17.89; Cl, 37.3; MeOH, 44.8%. Attempts to recrystallize the product from methanol were unsuccessful.

Preparation of VCl_3,3EtOH

Vanadium trichloride (5.2 g) appeared not to react with ethanol (38.5 g) at room temperature. After refluxing the mixture for 4 hours the excess alcohol was removed, leaving a green solid (9.4 g). Found: V, 17.6, 17.6; Cl, 33.66, 33.60; EtOH, 45.9, 46.1; valency, 3.24. VCl_3,3EtOH requires: V, 17.3; Cl, 36.01; EtOH, 46.7%.

Preparation of VCl_3,4Pr^{i}OH

Vanadium trichloride (11.5 g) was refluxed with isopropanol (105 g), and on cooling deposited green crystals which were separated by decantation and recrystallized from isopropanol. The green crystalline product (26.6 g) was dried *in vacuo* at room temperature. Found: V, 13.12, 13.15; Cl, 26.50, 26.50; Pr^{i}OH, 60.01, 59.96; valency, 3.05. VCl_3,4Pr^{i}OH requires: V, 12.83; Cl, 26.80; Pr^{i}OH, 60.4%.

Preparation of Vanadium Trimethoxide

Vanadium trichloride (10.2 g) was dissolved in methanol (150 ml) and to this solution was added a solution of lithium methoxide (from 1.36 g Li) in methanol (100 ml). Vanadium trimethoxide was precipitated as a green solid, which was filtered off and washed with methanol (800–1000 ml) until the washing was free from chloride. The final residue (6.8 g) was analyzed. Found: V, 34.8 (volumetrically), 34.7 (gravimetrically); MeO, 64.2, 64.6; valency, 3.08; ratio MeO:V, 3.04; Cl, 0; Li, 0. $V(OMe)_3$ requires; V, 35.4; MeO, 64.6%. The trimethoxide was heated to 150° at ca. 10^{-4} mm in a molecular still and a trace of greenish-yellow sublimate was obtained, but the green solid was non-volatile. Found: V, 35.4; MeO, 64.4; valency, 3.05; MeO:V, 2.96. The trace of sublimate was probably the quinquevalent vanadyl trimethoxide.

Preparation of Vanadium Triethoxide

From the reaction involving VCl_3 (12.8 g) and lithium ethoxide (from 1.7 g Li) in ethanol (500 ml) a green solid (9.1 g) was finally obtained after filtration and exhaustive washing with ethanol. Found: V, 27.1, 27.2; EtO, 70.0; Cl, 0; Li, 0; valency, 3.1; EtO:V, 2.93. $V(OEt)_3$ requires: V, 27.4; EtO, 72.6%. A sample of the triethoxide was heated to 250° at ca. 10^{-4} mm in a molecular still but gave only a trace of yellow sublimate (probably $VO(OEt)_3$). The non-volatile residue (found: V, 40.2%; valency, 4.8) was not the triethoxide.

Attempts to Prepare Vanadium Triisopropoxide

(a) From VCl_3 and Sodium Isopropoxide

The trichloride (8.2 g) suspended in isopropanol (175 ml) was refluxed in the boiler of a Soxhlet apparatus, which also contained sodium (3.59 g) in the extraction compartment. The sodium isopropoxide was thus extracted into the vanadium trichloride solution in an atmosphere of hydrogen. After filtration the green solution was evaporated under reduced pressure but gave a brown solid residue (12.1 g). Found: V, 24.4, 23.3; Pr^{i}O, 44.1, 43.7; valency, 4.58, 4.60; Pr^{i}O:V, 1.56. $V(OPr^i)_3$ requires: V, 22.4; Pr^{i}O, 77.6%.

(b) From $V(OMe)_3$ and Isopropanol

The trimethoxide (8.4 g) was suspended in isopropanol (200 ml) and benzene (20 ml) and then refluxed under a fractionating column. During 5 days of reaction the trimethoxide went into solution and the liberated methanol was removed as the methanol–benzene azeotrope. Removal of excess isopropanol from the green solution left a green solid (6.8 g). Found: V, 23.9 (volumetrically), 23.7 (gravimetrically); Pr^{i}O, 71.0; valency, 4.54, 4.52; Pr^{i}O:V, 2.57. When the foregoing product was heated to 100–120° at 0.5 mm a green liquid distilled over. Found: V, 20.1; Pr^{i}O, 66.0, 70.0; valency, 4.98; Pr^{i}O:V, 2.93. $VO(OPr^i)_3$ requires: V, 20.9; Pr^{i}O, 72.5%.

(c) From VBr_3 and Lithium Isopropoxide

The tribromide (15.8 g) was dissolved in isopropanol (200 ml) and mixed with lithium isopropoxide (from 0.587 g Li) in isopropanol (200 ml). Nothing precipitated, so the green solution was evaporated to dryness and the residue heated *in vacuo*. At 140° and 0.2 mm a green distillate was obtained. Found: V, 20.7; 20.4; Pr^{i}O, 72.2; valency, 4.95, 4.75. $VO(OPr^i)_3$ requires: V, 20.9; Pr^{i}O, 72.5%.

(d) From VCl_3 and Sodium in Isopropanol

The trichloride (11.8 g) was suspended in isopropanol (52.5 g) and benzene (74.7 g), and sodium (4.91 g) was added. The mixture was refluxed for 12 hours, giving a green solution which was evaporated to dryness, and the residue distilled at 100–110° at 0.1 mm. The green distillate solidified. Found: V, 17.3; Pr^{i}O, 79.8; valency, 4.17; Pr^{i}O:V, 3.89. $V(OPr^i)_4$ requires: V, 17.7; Pr^{i}O, 82.3%.

Attempts to Prepare Vanadium Tritertiary Butoxide

(a) From Vanadium Trimethoxide and Lanthanum tert-Butoxide

Vanadium trimethoxide (1.6 g) was mixed with lanthanum tri-*tert*-butoxide (4.49 g) in benzene (50.2 g). During 12 hours of refluxing a faint green color developed in the solvent. After filtration the filtrate was taken to dryness, giving a light green solid (0.2 g). Found: V, 17.9. $V(OBu^t)_3$ requires: V, 18.9%. The product was heated at 0.01 mm but nothing volatilized up to 340°.

(b) From Vanadium Trimethoxide and Aluminum tert-Butoxide

Vanadium trimethoxide (4.2 g) and aluminum tri-*tert*-butoxide (7.2 g) were mixed with petrol (20 ml, boiling range 40–60°) and well shaken. After evaporating off the solvent the residue was heated *in vacuo*. A green liquid distilled over (1.3 g; b.p. 140° at 0.3 mm). Found: V, 17.4; valency, 4.98. $VO(OBu^t)_3$ requires: V, 17.8%.

(c) From the Action of tert-Butanol on Vanadium Amide

Potassium amide was prepared in liquid ammonia (1000 ml) from potassium (8.27 g). Vanadium trichloride (10.6 g) was added, causing an exothermic reaction. After the mixture had stood overnight, *tert-*

butanol–benzene azeotrope (80 ml) was slowly added and the solvents were then evaporated off. The residue was extracted with petrol (200 ml, 40–60° boiling range) and gave a green solution which, upon evaporation and drying, left a violet solid (1.32 g). Found: V, 16.1, 16.3; valency, 5.0.

ACKNOWLEDGMENT

M. L. Mehta is indebted to Munshi Singh College, Bihar University, for the grant of study leave which allowed him to engage in this research.

1. KOPPEL. Z. anorg. Chem. **28**, 461 (1901).
2. R. K. MULTANI. Ph.D. Thesis, London University, London, England. 1956.
3. A. K. CHATTERJEE. Private communication.
4. D. C. BRADLEY, R. N. KAPOOR, and B. C. SMITH. J. Inorg. & Nuclear Chem. In press.
5. I. M. THOMAS. Can. J. Chem. **39**, 1386 (1961).
6. D. C. BRADLEY. Ph.D. Thesis, London University, London, England. 1950.

RECEIVED APRIL 24, 1962.
DEPARTMENT OF CHEMISTRY,
BIRKBECK COLLEGE,
MALET STREET,
LONDON, W.C.1, ENGLAND.

TRANSFORMATION OF ACONITINE TO AN ISOMER OF HYPACONITINE*

ROBERT E. GILMAN† AND LÉO MARION

Hypaconitine, $C_{33}H_{45}O_{10}N$, $[\alpha]_D = +23°$ ($CHCl_3$), m.p. 198°, has long been considered to be closely related to aconitine in structure. Majima and Tamura have reported that hypaconitine contains an N-methyl group rather than the N-ethyl group that is present in aconitine (1). They also found that hypaconitine is very resistant to chromic acid oxidation. It is known that aconitine (I) is oxidized with ease by chromic acid to a ketone, aconitinone, which readily loses the elements of methanol to form the α,β-unsaturated ketone aconitoline, and that it is a secondary hydroxyl in ring A that is oxidized in this reaction (2). Hence, if hypaconitine possesses the same ring structure as aconitine, it cannot contain a similarly placed hydroxyl in ring A.

It was then assumed as a working hypothesis that hypaconitine had the same structure as aconitine except that it contained an N-methyl instead of an N-ethyl group, and that it lacked the hydroxyl of ring A. An attempt to convert aconitine into the assumed structure II of hypaconitine was started in this laboratory by Dr. N. V. Riggs. By treatment of aconitine with thionyl chloride, anhydroaconitine ($C_{34}H_{45}O_{10}N$) was obtained, which, on catalytic hydrogenation, absorbed 1 mole of hydrogen and produced deoxyaconitine ($C_{34}H_{47}O_{10}N$). It has now been demonstrated that the ring A hydroxyl was the one that was removed in these reactions. Pyrolysis of deoxyaconitine gave pyrodeoxyaconitine, $C_{32}H_{43}O_8N$ (III). Transesterification of the pyro compound gave pyrodeoxyaconine (IV), which was isolated as the perchlorate. The infrared spectrum of pyrodeoxyaconine contained carbonyl absorption at 1705 cm^{-1}, like pyraconine, and it can thus be concluded that a secondary hydroxyl group must be present in ring D of deoxyaconitine (cf. ref. 3). If this ring D hydroxyl had been the one removed in the formation of deoxyaconitine, the pyrolysis product would have been an olefin like pyrodelphinine (4) instead of being a ketone.

Issued as N.R.C. No. 6896.
†*National Research Council of Canada Postdoctorate Fellow.*

butanol–benzene azeotrope (80 ml) was slowly added and the solvents were then evaporated off. The residue was extracted with petrol (200 ml, 40–60° boiling range) and gave a green solution which, upon evaporation and drying, left a violet solid (1.32 g). Found: V, 16.1, 16.3; valency, 5.0.

ACKNOWLEDGMENT

M. L. Mehta is indebted to Munshi Singh College, Bihar University, for the grant of study leave which allowed him to engage in this research.

1. KOPPEL. Z. anorg. Chem. **28**, 461 (1901).
2. R. K. MULTANI. Ph.D. Thesis, London University, London, England. 1956.
3. A. K. CHATTERJEE. Private communication.
4. D. C. BRADLEY, R. N. KAPOOR, and B. C. SMITH. J. Inorg. & Nuclear Chem. In press.
5. I. M. THOMAS. Can. J. Chem. **39**, 1386 (1961).
6. D. C. BRADLEY. Ph.D. Thesis, London University, London, England. 1950.

RECEIVED APRIL 24, 1962.
DEPARTMENT OF CHEMISTRY,
BIRKBECK COLLEGE,
MALET STREET,
LONDON, W.C.1, ENGLAND.

TRANSFORMATION OF ACONITINE TO AN ISOMER OF HYPACONITINE*

ROBERT E. GILMAN† AND LÉO MARION

Hypaconitine, $C_{33}H_{45}O_{10}N$, $[\alpha]_D = +23°$ ($CHCl_3$), m.p. 198°, has long been considered to be closely related to aconitine in structure. Majima and Tamura have reported that hypaconitine contains an N-methyl group rather than the N-ethyl group that is present in aconitine (1). They also found that hypaconitine is very resistant to chromic acid oxidation. It is known that aconitine (I) is oxidized with ease by chromic acid to a ketone, aconitinone, which readily loses the elements of methanol to form the α,β-unsaturated ketone aconitoline, and that it is a secondary hydroxyl in ring A that is oxidized in this reaction (2). Hence, if hypaconitine possesses the same ring structure as aconitine, it cannot contain a similarly placed hydroxyl in ring A.

It was then assumed as a working hypothesis that hypaconitine had the same structure as aconitine except that it contained an N-methyl instead of an N-ethyl group, and that it lacked the hydroxyl of ring A. An attempt to convert aconitine into the assumed structure II of hypaconitine was started in this laboratory by Dr. N. V. Riggs. By treatment of aconitine with thionyl chloride, anhydroaconitine ($C_{34}H_{45}O_{10}N$) was obtained, which, on catalytic hydrogenation, absorbed 1 mole of hydrogen and produced deoxyaconitine ($C_{34}H_{47}O_{10}N$). It has now been demonstrated that the ring A hydroxyl was the one that was removed in these reactions. Pyrolysis of deoxyaconitine gave pyrodeoxyaconitine, $C_{32}H_{43}O_8N$ (III). Transesterification of the pyro compound gave pyrodeoxyaconine (IV), which was isolated as the perchlorate. The infrared spectrum of pyrodeoxyaconine contained carbonyl absorption at 1705 cm^{-1}, like pyraconine, and it can thus be concluded that a secondary hydroxyl group must be present in ring D of deoxyaconitine (cf. ref. 3). If this ring D hydroxyl had been the one removed in the formation of deoxyaconitine, the pyrolysis product would have been an olefin like pyrodelphinine (4) instead of being a ketone.

Issued as N.R.C. No. 6896.
†*National Research Council of Canada Postdoctorate Fellow.*

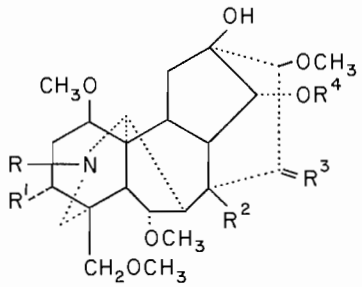

I: $R = Et; R^1 = OH; R^2 = OAc; R^3 = OH,H; R^4 = COC_6H_5$
II: $R = Me; R^1 = H; R^2 = OAc; R^3 = OH,H; R^4 = COC_6H_5$
III: $R = Et; R^1 = R^2 = H; R^3 = O; R^4 = COC_6H_5$
IV: $R = Et; R^1 = R^2 = R^4 = H; R^3 = O$

The N-ethyl group of deoxyaconitine was then removed by oxidation with mercuric acetate in 3% acetic acid solution. This method has been used previously in this laboratory to remove the N-ethyl group of delcosine (5). The oxidation of deoxyaconitine proceeded smoothly and yielded two products. The desired secondary amine was extracted into chloroform from the reaction mixture as its acetate salt. Conversion of the acetate to the free base gave an amorphous compound which could not be crystallized even after careful chromatography over Grade III alumina. The n.m.r. spectrum did not contain the triplet characteristic of an ethyl group at τ 8.9. The second product was obtained by chloroform extraction of the residual reaction mixture after it had been made basic. The base was crystallized from acetone–hexane to a melting point of 168–175°, but was not examined further, since its n.m.r. spectrum indicated that the N-ethyl group was still present.

A small quantity of the amorphous secondary amine was converted back to deoxyaconitine by treatment with ethyl iodide. Hence only the ethyl group attached to the nitrogen had been removed by the oxidation.

The secondary amine was then converted to the desired N-methyl compound by treatment with methyl iodide. The product was recrystallized from methanol until it had a constant melting point of 172–178° decomp.

This compound, which has structure II, has an infrared spectrum which is nearly superimposable on that of hypaconitine, but there are slight differences in the region between 950 and 1050 cm^{-1}. The X-ray powder patterns of the two compounds are also nearly identical, although definite differences are observable. Hence, although the compound derived from aconitine is very similar to hypaconitine, it is definitely different.

In the compound derived from aconitine there are 14 asymmetric centers, many of which have a fixed configuration because of the rigidity of part of the structure. A difference of configuration at any one of the remaining centers, however, could account for the slight differences observable in the infrared spectra and the X-ray patterns. It is probable that the ring structure of hypaconitine is the same as that of aconitine, but that the configuration of either a ring, or one or more of the substituents, is different. To determine what the difference is will necessitate degradative work with hypaconitine, which cannot be undertaken until a supply of the alkaloid becomes available.

EXPERIMENTAL

All melting points were measured on a hot-stage under the microscope. The infrared spectra were obtained in nujol mulls on a Perkin–Elmer model 21 double-beam instrument.

*Anhydroaconitine Perchlorate**

Aconitine (3 g) and redistilled thionyl chloride (10 ml) were refluxed for 3 hours, initial gas evolution apparently ceasing after 40 minutes. The mixture was evaporated at the water pump on a water bath at 60° to a dry froth which was evaporated twice similarly with methanol (5 ml). The residue dissolved in methanol (5 ml) was neutralized by the dropwise addition of 70–72% perchloric acid, the solid mass obtained diluted with methanol (5 ml), and the mixture set aside. The crystal crop (2.5 g) was recrystallized several times from methanol–ether, from which it separated as clumps of prisms, m.p. 200–204°, $[\alpha]_D^{25} = +12.9°$ (*c*, 1.90 in acetone). The material was dried at 100° and 0.4 mm for 16 hours for analysis. Found: C, 55.40; H, 6.38; Cl, 4.53; OCH_3, 17.66%. Calc. for $C_{34}H_{45}O_{10}N.HClO_4.0.5H_2O$: C, 55.39; H, 6.43; Cl, 4.81; $4\times OCH_3$, 16.84%. The water of crystallization was not removed by drying at 100° and 0.01 mm. Found: C, 55.51; H, 6.46%.

*Deoxyaconitine**

A solution of anhydroaconitine perchlorate (151 mg) in purified ethanol (20 ml) absorbed hydrogen (4.89 ml at 25° and 760 mm; calc. for 1 mole, 5.01 ml) in the presence of 5% palladium–95% barium sulphate catalyst during 5 hours, uptake then ceasing. Evaporation of the filtrate and crystallization of the residue from methanol with addition of ether gave prisms, m.p. 180° after softening at 165°, $[\alpha]_D^{25} = -11.7°$ (*c*, 2.33 in acetone). The material was dried at 100° and 0.5 mm for 16 hours. Found: C, 55.87; H, 7.16; Cl, 4.80. Calc. for $C_{34}H_{47}O_{10}N.HClO_4$: C, 55.92; H, 6.63; Cl, 4.86%.

The perchlorate was shaken with cold saturated sodium carbonate solution and the mixture extracted three times with chloroform. The combined extract was dried over sodium carbonate and evaporated to a froth which rapidly crystallized in contact with a little methanol. Recrystallization from acetone–water gave colorless leaves, m.p. 173–176°. The material was dried at 100° and 0.4 mm for 4 hours. Found: C, 64.84; H, 7.52; OCH_3, 19.43. Calc. for $C_{34}H_{47}O_{10}N$: C, 64.84; H, 7.52; $4\times OCH_3$, 19.71%.

Pyrodeoxyaconitine

Deoxyaconitine (85 mg) was placed in a sublimation tube and the tube evacuated to 5×10^{-4} mm. The tube was then placed in a block heater at 200–205° C and held at that temperature for 30 minutes while the pyrolysis product distilled slowly. Yield of faintly colored distillate, 70 mg. All attempts to crystallize the distillate were unsuccessful and it was redistilled for analysis. $[\alpha]_D^{20} = -82°$ (*c* = 1.0 in ethanol). Calc. for $C_{32}H_{43}O_8N$: C, 67.46; H, 7.61; N, 2.46. Found: C, 67.40; H, 7.49; N, 2.44%.

Pyrodeoxyaconine Perchlorate

Distilled pyrodeoxyaconitine (150 mg) was dissolved in dry methanol (10 cc). Sodium (1–2 mg) was added and the solution was kept at 0° for 1 hour. The methanol was then removed by distillation at 30° under reduced pressure. Chromatography of the residue over Grade IV alumina gave 66 mg of product that crystallized from a concentrated ether solution, m.p. 85–90°. Since the crystals could not be obtained in pure form, the base was converted to the perchlorate salt. Recrystallized from methanol–ether, m.p. 250–260° decomp., $[\alpha]_D^{20} = -86°$ (*c* = 0.6 in water). The infrared spectrum has a strong band at 1705 cm^{-1}. Calc. for $C_{25}H_{39}O_7N.HClO_4$: C, 53.05; H, 7.12; N, 2.47. Found: C, 53.11; H, 7.24; N, 2.45%.

N-Desethyl-deoxyaconitine

Deoxyaconitine (750 mg) was dissolved in 3% acetic acid (25 cc), and mercuric acetate (1.25 g) was added. The solution was heated on the steam bath for 1 hour. The crystalline mercurous acetate that formed was then removed from the cooled reaction mixture by filtration. The filtrate was extracted with three portions of chloroform and the combined chloroform extracts were washed with 5% potassium carbonate solution and then with water. Concentration of the dried chloroform solution to dryness left a white foam. Yield: 350 mg. All attempts to crystallize this material failed.

Chromatography over Grade III alumina gave a main fraction of 210 mg when the column was eluted with 50% benzene–chloroform. The lack of a triplet in the n.m.r. spectrum at a τ value of 8.9 indicated that the ethyl group attached to the nitrogen was absent.

Attempts to prepare crystalline salts of the secondary amine were also unsuccessful.

The original aqueous reaction mixture, which had been extracted with chloroform, was then made basic and extracted again with chloroform. Concentration of the washed and dried chloroform extract left a residue that was crystallized from ether – *n*-hexane, m.p. 168–175°. The n.m.r. spectrum indicated that the N-ethyl group was still present, so this product was not investigated further.

Ethylation of N-Desethyl-deoxyaconitine

The chromatographed secondary amine (50 mg) was dissolved in ether and treated with excess ethyl

**Experiments performed by Dr. N. V. Riggs.*

iodide. The solution was refluxed for 30 minutes. Excess ethyl iodide and ether were distilled off and the residue was dissolved in water. The aqueous solution was made basic with potassium carbonate and the precipitate was extracted with chloroform. Concentration of the washed and dried chloroform extracts left a white foam which was crystallized from ether – *n*-hexane to a constant melting point of 167–174° decomp. The melting point was not depressed when the product was mixed with deoxyaconitine. The infrared spectrum was identical with that of deoxyaconitine.

Methylation of N-Desethyl-deoxyaconitine

The chromatographed secondary amine (300 mg) was dissolved in ether and treated with excess methyl iodide. The solution was refluxed for 30 minutes and then concentrated to dryness *in vacuo*. The residue (370 mg) was worked up exactly as above and yielded a white foam (240 mg) that crystallized on contact with ether. This was recrystallized from methanol to a constant melting point of 172–178° decomp., $[\alpha]_D^{20} = +18°$ (*c*, 1.2 in $CHCl_3$). Calc. for $C_{33}H_{45}O_{10}N$: C, 64.37; H, 7.37; N, 2.27. Found: C, 64.57; H, 7.29; N, 2.33%.

ACKNOWLEDGMENTS

We acknowledge with thanks the kindness of Professor H. Suginome, who supplied us with a small sample of hypaconitine. We thank Dr. M. Przybylska for the X-ray patterns, Mr. R. Lauzon for the infrared spectra, and Mr. H. Seguin for the analyses.

1. R. MAJIMA and K. TAMURA. Ann. **526**, 116 (1936).
2. H. MAYER and L. MARION. Can. J. Chem. **37**, 856 (1959).
3. D. J. MCCALDIN and L. MARION. Can. J. Chem. **37**, 1071 (1959).
4. K. WIESNER, F. BICKELHAUPT, D. R. BABIN, and M. GÖTZ. Tetrahedron, **9**, 254 (1960).
5. R. ANET, D. W. CLAYTON, and L. MARION. Can. J. Chem. **35**, 397 (1957).

RECEIVED APRIL 19, 1962.
DIVISION OF PURE CHEMISTRY,
NATIONAL RESEARCH COUNCIL,
OTTAWA, CANADA.

A NEW SPRAY FOR THE DETECTION OF HIGHLY SUBSTITUTED ACETALS AND KETALS OF CARBOHYDRATES

J. W. BIRD

The detection of highly substituted acetals and ketals of carbohydrates on paper chromatograms is often difficult or impossible with the commonly used spray reagents (i.e. alkaline silver nitrate (1), *p*-anisidine hydrochloride (2)) unless vicinal hydroxyl or reducing groups are present. Pacak and Cerny (3) report the use of ceric ammonium nitrate for the detection of isopropylidene compounds. However, the author has found this reagent (2–3% aqueous solution heated at 120° C for 2–3 minutes) to give difficultly reproducible results and now reports a modification giving a more sensitive, reliable, and permanent method of detection.

The chromatograms developed in basic, acidic, or neutral solvent systems were dried (chromatograms from acidic solvents were air dried for 1 hour) and sprayed, first with a freshly prepared aqueous solution of ceric ammonium nitrate (2–3%) then immediately with a 2% solution of silver nitrate in acetone (1). The chromatograms, after drying at 120° C for 2–3 minutes, were sprayed with a 2% ethanolic solution of sodium hydroxide, and after 2–3 minutes the background color was bleached by immersion of the chromatogram in sodium thiosulphate solution. After application of the sodium hydroxide spray reagent, a further overspraying with the ceric ammonium nitrate solution was found to give improved definition.

iodide. The solution was refluxed for 30 minutes. Excess ethyl iodide and ether were distilled off and the residue was dissolved in water. The aqueous solution was made basic with potassium carbonate and the precipitate was extracted with chloroform. Concentration of the washed and dried chloroform extracts left a white foam which was crystallized from ether – *n*-hexane to a constant melting point of 167–174° decomp. The melting point was not depressed when the product was mixed with deoxyaconitine. The infrared spectrum was identical with that of deoxyaconitine.

Methylation of N-Desethyl-deoxyaconitine

The chromatographed secondary amine (300 mg) was dissolved in ether and treated with excess methyl iodide. The solution was refluxed for 30 minutes and then concentrated to dryness *in vacuo*. The residue (370 mg) was worked up exactly as above and yielded a white foam (240 mg) that crystallized on contact with ether. This was recrystallized from methanol to a constant melting point of 172–178° decomp., $[\alpha]_D^{20} = +18°$ (*c*, 1.2 in $CHCl_3$). Calc. for $C_{33}H_{45}O_{10}N$: C, 64.37; H, 7.37; N, 2.27. Found: C, 64.57; H, 7.29; N, 2.33%.

ACKNOWLEDGMENTS

We acknowledge with thanks the kindness of Professor H. Suginome, who supplied us with a small sample of hypaconitine. We thank Dr. M. Przybylska for the X-ray patterns, Mr. R. Lauzon for the infrared spectra, and Mr. H. Seguin for the analyses.

1. R. MAJIMA and K. TAMURA. Ann. **526**, 116 (1936).
2. H. MAYER and L. MARION. Can. J. Chem. **37**, 856 (1959).
3. D. J. MCCALDIN and L. MARION. Can. J. Chem. **37**, 1071 (1959).
4. K. WIESNER, F. BICKELHAUPT, D. R. BABIN, and M. GÖTZ. Tetrahedron, **9**, 254 (1960).
5. R. ANET, D. W. CLAYTON, and L. MARION. Can. J. Chem. **35**, 397 (1957).

RECEIVED APRIL 19, 1962.
DIVISION OF PURE CHEMISTRY,
NATIONAL RESEARCH COUNCIL,
OTTAWA, CANADA.

A NEW SPRAY FOR THE DETECTION OF HIGHLY SUBSTITUTED ACETALS AND KETALS OF CARBOHYDRATES

J. W. BIRD

The detection of highly substituted acetals and ketals of carbohydrates on paper chromatograms is often difficult or impossible with the commonly used spray reagents (i.e. alkaline silver nitrate (1), *p*-anisidine hydrochloride (2)) unless vicinal hydroxyl or reducing groups are present. Pacak and Cerny (3) report the use of ceric ammonium nitrate for the detection of isopropylidene compounds. However, the author has found this reagent (2–3% aqueous solution heated at 120° C for 2–3 minutes) to give difficultly reproducible results and now reports a modification giving a more sensitive, reliable, and permanent method of detection.

The chromatograms developed in basic, acidic, or neutral solvent systems were dried (chromatograms from acidic solvents were air dried for 1 hour) and sprayed, first with a freshly prepared aqueous solution of ceric ammonium nitrate (2–3%) then immediately with a 2% solution of silver nitrate in acetone (1). The chromatograms, after drying at 120° C for 2–3 minutes, were sprayed with a 2% ethanolic solution of sodium hydroxide, and after 2–3 minutes the background color was bleached by immersion of the chromatogram in sodium thiosulphate solution. After application of the sodium hydroxide spray reagent, a further overspraying with the ceric ammonium nitrate solution was found to give improved definition.

The compounds listed in Table I were detected as light brown to black spots on a light background after following the procedure above.

TABLE I

Compound	Reagent	
	$AgNO_3$, NaOH	Ceric $AgNO_3$
1,2:5,6-Di-*O*-isopropylidene-D-glucofuranose*	—	VS
Di-*O*-isopropylidene-ribitol	—	VS
1,2:4,5-Di-*O*-isopropylidene-3-*O*-methyl-D-fructose	—	M
5,6-Carbonate-1,2-*O*-isopropylidene-D-glucofuranose	—	M
2,3:5,6-Di-*O*-isopropylidene-D-mannose	—	S
2,3:5,6-Di-*O*-isopropylidene-D-mannitol	—	S
1,2:3,4:5,6-Tri-*O*-isopropylidene-D-mannitol*	—	VS
2,4-*O*-Benzylidene-5,6-*O*-isopropylidene-D-glucitol	—	S
Methyl-α-D-glucopyranoside	VW	S
Methyl-4,6-*O*-benzylidene-α-D-glucoside†	—	S
6-Chloro-6-deoxy-D-mannose	VW	M
3,6-Anhydro-D-mannoside	VW	M
Methyl 2,3,4,6-tetra-*O*-methyl-α-D-mannoside‡	VW	M
Methyl 2,3,4,6-tetra-*O*-methyl-α-D-galactoside	—	—
1,2,3,4,5-Penta-*O*-acetyl-L-arabinitol	M	M
Methyl 2,3,4-tri-*O*-acetyl-α-D-ribopyranoside	M	M
Sucrose octacetate	M	S
Maltose octacetate	S	S
Ethyleneglycol	W	S
Glycerol	M	VS

NOTE: S = strong positive; M = medium positive; W = weak positive; V = very.
*Detected in quantities of 8–12 μg.
†Detected in quantities of 15 μg.
‡Detected in quantities of 30–40 μg.

1. W. E. TREVELYAN, D. P. PROCTOR, and J. S. HARRISON. Nature, **166**, 444 (1950).
2. L. HOUGH, J. K. N. JONES, and W. H. WADMAN. J. Chem. Soc. 1702 (1950).
3. J. PACAK and M. CERNY. Collection Czechoslov. Chem. Communs. **24**, 3804 (1959); Chem. Abstr. **54**, 8643*i* (1960).

RECEIVED APRIL 25, 1962.
GORDON HALL,
QUEEN'S UNIVERSITY,
KINGSTON, ONTARIO.

THE STRUCTURE OF CARBOLINES AND RELATED COMPOUNDS

LEONELLO PAOLONI

In a recent paper Abramovitch and Adams (1) have made some remarks concerning the work of this author (2) on the concept of valence state and the electronic structure of carbolines and their anhydronium bases. They state in the footnote on p. 2518 of reference 1: ". . . his conclusion that it is unnecessary to represent the carboline anhydrobases as hybrids of dipolar and quinonoïd structures in view of the fact that his results '*illustrate eloquently the compromise between the tendency to form the (aromatic) sextet and that to neutralize the charges*' seems a contradiction in ideas".

The wording in italics, written by the Authors (1) between quotation marks, does not represent a *verbatim* translation of any sentence in the original paper (2), but it is, on the best, the abstract of their interpretation of the last paragraph of p. 1532 of reference 2.

The compounds listed in Table I were detected as light brown to black spots on a light background after following the procedure above.

TABLE I

Compound	Reagent	
	$AgNO_3$, NaOH	Ceric $AgNO_3$
1,2:5,6-Di-*O*-isopropylidene-D-glucofuranose*	—	VS
Di-*O*-isopropylidene-ribitol	—	VS
1,2:4,5-Di-*O*-isopropylidene-3-*O*-methyl-D-fructose	—	M
5,6-Carbonate-1,2-*O*-isopropylidene-D-glucofuranose	—	M
2,3:5,6-Di-*O*-isopropylidene-D-mannose	—	S
2,3:5,6-Di-*O*-isopropylidene-D-mannitol	—	S
1,2:3,4:5,6-Tri-*O*-isopropylidene-D-mannitol*	—	VS
2,4-*O*-Benzylidene-5,6-*O*-isopropylidene-D-glucitol	—	S
Methyl-α-D-glucopyranoside	VW	S
Methyl-4,6-*O*-benzylidene-α-D-glucoside†	—	S
6-Chloro-6-deoxy-D-mannose	VW	M
3,6-Anhydro-D-mannoside	VW	M
Methyl 2,3,4,6-tetra-*O*-methyl-α-D-mannoside‡	VW	M
Methyl 2,3,4,6-tetra-*O*-methyl-α-D-galactoside	—	—
1,2,3,4,5-Penta-*O*-acetyl-L-arabinitol	M	M
Methyl 2,3,4-tri-*O*-acetyl-α-D-ribopyranoside	M	M
Sucrose octacetate	M	S
Maltose octacetate	S	S
Ethyleneglycol	W	S
Glycerol	M	VS

NOTE: S = strong positive; M = medium positive; W = weak positive; V = very.
*Detected in quantities of 8–12 μg.
†Detected in quantities of 15 μg.
‡Detected in quantities of 30–40 μg.

1. W. E. TREVELYAN, D. P. PROCTOR, and J. S. HARRISON. Nature, **166**, 444 (1950).
2. L. HOUGH, J. K. N. JONES, and W. H. WADMAN. J. Chem. Soc. 1702 (1950).
3. J. PACAK and M. CERNY. Collection Czechoslov. Chem. Communs. **24**, 3804 (1959); Chem. Abstr. **54**, 8643*i* (1960).

RECEIVED APRIL 25, 1962.
GORDON HALL,
QUEEN'S UNIVERSITY,
KINGSTON, ONTARIO.

THE STRUCTURE OF CARBOLINES AND RELATED COMPOUNDS

LEONELLO PAOLONI

In a recent paper Abramovitch and Adams (1) have made some remarks concerning the work of this author (2) on the concept of valence state and the electronic structure of carbolines and their anhydronium bases. They state in the footnote on p. 2518 of reference 1: ". . . his conclusion that it is unnecessary to represent the carboline anhydrobases as hybrids of dipolar and quinonoïd structures in view of the fact that his results '*illustrate eloquently the compromise between the tendency to form the (aromatic) sextet and that to neutralize the charges*' seems a contradiction in ideas".

The wording in italics, written by the Authors (1) between quotation marks, does not represent a *verbatim* translation of any sentence in the original paper (2), but it is, on the best, the abstract of their interpretation of the last paragraph of p. 1532 of reference 2.

Because the quotation is in fact wrong and misleading, we give here its correct English version: "One consequence of this (valence state) interpretation is that it is no longer necessary to use two formulas (one with charge separation) in exchange equilibrium with one another to denote, for example, anhydronium bases. The balance between the *tendency to sextet formation* and the *tendency to charge neutralization*, used by Robinson (3) to justify the double formula, is indeed the consequence of the change which has taken place in the potential field where the electrons move. Since such a changed situation is clearly reflected in the classical formula, this is in itself completely adequate to describe the properties of anhydronium bases."

We would like also to remark that the emphasis of our paper (2) was not on the exact calculation of the pK_a or of the spectrum of the carboline anhydronium bases (whose general trend is correctly predicted), but rather on the relationship between the valence state of atoms in molecules and the chemical symbolism.

It may be convenient to point out, for those who do not read Italian, that an English translation of the paper (2) has been published recently (4).

1. R. A. ABRAMOVITCH and K. A. H. ADAMS. Can. J. Chem. **39**, 2516 (1961).
2. L. PAOLONI. Gazz. chim. ital. **90**, 1530 (1960).
3. J. W. ARMIT and R. ROBINSON. J. Chem. Soc. **127**, 1604 (1925).
4. L. PAOLONI. Sci. Repts. Ist. Super. Sanità, **1**, 86 (1961).

RECEIVED MAY 14, 1962.
LABORATORIES OF CHEMISTRY,
ISTITUTO SUPERIORE DI SANITÀ,
ROME, ITALY.

REACTIONS OF ALIPHATIC ARYLHYDRAZONES AND OF ANILINE WITH CARBON MONOXIDE TO YIELD UREAS

ALEX ROSENTHAL

It has been recently reported (1–3) that the cyclization of Schiff bases and of aromatic ketone phenylhydrazones with carbon monoxide yields N-phenylphthalimidines and phthalimidine-N-carboxyanilides, respectively. In this paper we wish to report the extension of the carbonylation reaction to aliphatic arylhydrazones and to aniline. Slightly modified conditions to those reported by Murahashi and Horiie (1, 2) were used.

When a solution of acetone phenylhydrazone in benzene was reacted with about 4000 p.s.i. of carbon monoxide at about 250° in the presence of preformed dicobalt octacarbonyl, the main products isolated were *sym*-diphenylurea, monophenylurea, and diphenyl. In addition, a crystalline organocobalt complex which, on degradation with molten sodium hydroxide, yielded aniline and ammonia was obtained. An unstable substance (B), having an empirical formula of $C_{10}H_{10}N$ (approximate), was separated from the mixture of products by chromatography on alumina. As the latter substance was present in low yield, and rapidly changed in the presence of air, further work on it was abandoned.

Similarly, acetaldehyde phenylhydrazone also reacted with carbon monoxide to yield *sym*-diphenylurea and monophenylurea.

Because the quotation is in fact wrong and misleading, we give here its correct English version: "One consequence of this (valence state) interpretation is that it is no longer necessary to use two formulas (one with charge separation) in exchange equilibrium with one another to denote, for example, anhydronium bases. The balance between the *tendency to sextet formation* and the *tendency to charge neutralization*, used by Robinson (3) to justify the double formula, is indeed the consequence of the change which has taken place in the potential field where the electrons move. Since such a changed situation is clearly reflected in the classical formula, this is in itself completely adequate to describe the properties of anhydronium bases."

We would like also to remark that the emphasis of our paper (2) was not on the exact calculation of the pK_a or of the spectrum of the carboline anhydronium bases (whose general trend is correctly predicted), but rather on the relationship between the valence state of atoms in molecules and the chemical symbolism.

It may be convenient to point out, for those who do not read Italian, that an English translation of the paper (2) has been published recently (4).

1. R. A. ABRAMOVITCH and K. A. H. ADAMS. Can. J. Chem. **39**, 2516 (1961).
2. L. PAOLONI. Gazz. chim. ital. **90**, 1530 (1960).
3. J. W. ARMIT and R. ROBINSON. J. Chem. Soc. **127**, 1604 (1925).
4. L. PAOLONI. Sci. Repts. Ist. Super. Sanità, **1**, 86 (1961).

RECEIVED MAY 14, 1962.
LABORATORIES OF CHEMISTRY,
ISTITUTO SUPERIORE DI SANITÀ,
ROME, ITALY.

REACTIONS OF ALIPHATIC ARYLHYDRAZONES AND OF ANILINE WITH CARBON MONOXIDE TO YIELD UREAS

ALEX ROSENTHAL

It has been recently reported (1–3) that the cyclization of Schiff bases and of aromatic ketone phenylhydrazones with carbon monoxide yields N-phenylphthalimidines and phthalimidine-N-carboxyanilides, respectively. In this paper we wish to report the extension of the carbonylation reaction to aliphatic arylhydrazones and to aniline. Slightly modified conditions to those reported by Murahashi and Horiie (1, 2) were used.

When a solution of acetone phenylhydrazone in benzene was reacted with about 4000 p.s.i. of carbon monoxide at about 250° in the presence of preformed dicobalt octacarbonyl, the main products isolated were *sym*-diphenylurea, monophenylurea, and diphenyl. In addition, a crystalline organocobalt complex which, on degradation with molten sodium hydroxide, yielded aniline and ammonia was obtained. An unstable substance (B), having an empirical formula of $C_{10}H_{10}N$ (approximate), was separated from the mixture of products by chromatography on alumina. As the latter substance was present in low yield, and rapidly changed in the presence of air, further work on it was abandoned.

Similarly, acetaldehyde phenylhydrazone also reacted with carbon monoxide to yield *sym*-diphenylurea and monophenylurea.

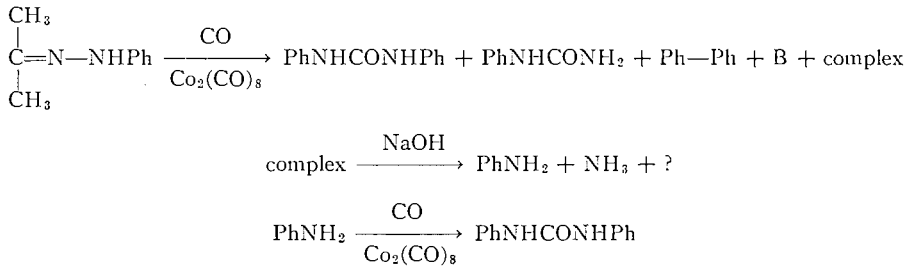

The fact that diphenyl was present in the reaction product suggests strongly that during the reaction phenyl free radicals were produced and these subsequently combined. It is possible that the phenyl free radicals were produced by thermal decomposition of the azo tautomer of acetone phenylhydrazone. Support for this hypothesis is provided by the recent work of Connor (6), who found that the phenylhydrazones of aldehydes and ketones rapidly tautomerize to benzene azoalkanes. The homolytic cleavage of the latter compound to yield nitrogen and free radicals is well known (7, 8).

Since *sym*-diphenylurea was produced by the reaction of aliphatic arylhydrazones with carbon monoxide, it was decided to determine if under similar conditions aniline would also yield the same product. The expected result was realized, although in much lower yield. Presumably the dicobalt octacarbonyl dehydrogenated the aniline, yielding *sym*-diphenylurea and possibly cobalt hydrocarbonyl. A similar dehydrogenation of aniline was recently reported by Franz and co-workers (4, 5), who found that aniline reacted with carbon monoxide in the presence of sulphur to yield *sym*-diphenylurea and hydrogen sulphide.

The explanation of the mechanism of the reaction is complicated by the fact that acetone phenylhydrazone is known to be thermally decomposed into aniline and ammonia (9). As the rate of formation of *sym*-diphenylurea from aniline was much slower than that from acetone phenylhydrazone, it would appear that the reaction must proceed by at least two independent mechanisms.

EXPERIMENTAL

General Considerations

The equipment was described previously (10).

Reaction of Acetone Phenylhydrazone with Carbon Monoxide

A mixture of 10 g (0.065 mole) of acetone phenylhydrazone (11) and 2 g of preformed dicobalt octacarbonyl in 40 ml of thiophene-free anhydrous benzene and carbon monoxide (1980 p.s.i. at 20°) was placed in the high-pressure bomb. The reactants were heated with rocking at 250–265° for 2 hours. An observed pressure drop of 50 p.s.i. at 20° was obtained. After the residual gases were vented, a blue crystalline residue (1.65 g) was removed by filtration. The residue was insoluble in ether, benzene, or acetone and very slightly soluble in N,N-dimethylformamide. Infrared (KBr): 3150–3450 (broad, m), 1715 (s), 1480 (m), 1330–1410 (broad, w), 1150 (w), 1065 (w), 1010 (w), 825 (m). Anal. Found: C, 44.22; H, 4.16; N, 16.44.

Combustion of 14.190 mg of blue crystals yielded 3.486 mg of cobalt residue. Reaction of the organocobalt complex with molten sodium hydroxide pellets produced basic gaseous and liquid nitrogen containing substances. The gaseous component was shown by means of infrared analysis to contain ammonia. The liquid component was converted to a bromo derivative, and shown to be identical with an authentic sample of 2,4,6-tribromoaniline. Reaction of the liquid component with gaseous hydrogen chloride produced aniline hydrochloride. Another compound in trace amount was shown, by nuclear magnetic resonance studies, to be present in the liquid.

After removal of the organocobalt complex, an aliquot of the filtrate containing 1.5 g of the product was subjected to exhaustive chromatographic fractionation on alumina (110×30-mm diam.). Petroleum ether (b.p. 65–80°) eluted traces of residual catalyst. A 1:1 mixture of benzene–petroleum ether (35–60°) yielded

0.32 g (20%) of substance A, which on recrystallization from petroleum ether at −50° yielded diphenyl, m.p. 68–70°; mixed m.p. with an authentic sample of diphenyl was 68–70°. The infrared spectra of both compounds were identical.

Substance B (0.16 g) was then eluted from the column with benzene. Fraction B (oil) turned red on addition of an acid (or after standing in the air for a few hours) and yellow on addition of a base. Infrared (KBr): 3400 (m), 3080 (w), 2950 (m), 1700 (w), 1620 (w), 1600 (w), 1550 (m), 1460 (s). The n.m.r. spectrum of fraction B in chloroform showed two main peaks at 2.15 and 7.32 τ having approximate areas of 22:18. Anal. Found: C, 81.45; H, 6.95; N, 9.70.

Substance C (*sym*-diphenylurea) was then eluted with a 1:1 mixture of benzene–chloroform. Recrystallization of compound C from chloroform gave pure material; m.p. 251–252°; mixed m.p. with an authentic sample (12) of *sym*-diphenylurea was 251–252°. The infrared spectra of both compounds were identical.

Compound E (monophenylurea) was eluted with a 9:1 mixture of benzene–ethanol; yield, 0.33 g. Recrystallization from chloroform gave pure monophenylurea, m.p. 146–148°; mixed m.p. with an authentic sample of monophenylurea (13) was 146–148°. The infrared spectra of both compounds were identical.

Reaction of Acetaldehyde Phenylhydrazone with Carbon Monoxide

A mixture of 8.3 g of acetaldehyde phenylhydrazone (14), m.p. 98–101°, was carbonylated at 250–260° for 70 minutes. The reaction products consisted of a highly intractable gum in addition to a blue-black solid (0.5 g). After removal of the solid and gum, the benzene filtrate was freed of catalyst and then subjected to chromatographic fractionation on alumina according to the procedure described previously in the experimental section. *sym*-Diphenylurea (55%) and monophenylurea 17% (based on the chromatographed material) were the chief products of the reaction.

Reaction of Aniline with Carbon Monoxide

A mixture of 1.5 g of aniline and 0.4 g dicobalt octacarbonyl in 15 ml of benzene was reacted with 3900 p.s.i. of carbon monoxide at 250–260° for 1.5 hours. The product was chromatographed on Florisil, as described previously in the experimental. *sym*-Diphenylurea was obtained; 0.04 g, m.p. 250–252°; mixed m.p. with an authentic sample of *sym*-diphenylurea 250–252°.

ACKNOWLEDGMENTS

This research was supported by a grant from the Petroleum Research Fund administered by the American Chemical Society. Grateful acknowledgment is hereby made to the donors of said fund.

The author wishes to thank Dr. D. McGreer of this department for carrying out the nuclear magnetic resonance studies. The phenylhydrazones were prepared by Mr. J. Matson.

Thanks are also due Dr. W. R. Cullen for determining the ammonia in the organocobalt complex.

1. S. Murahashi, S. Horiie, and T. Jō. Bull. Chem. Soc. Japan, **33**, 81 (1960).
2. S. Horiie and S. Murahashi. Bull. Chem. Soc. Japan, **33**, 247 (1960).
3. A. Rosenthal and M. M. S. Weir. Can. J. Chem. **40**, 610 (1962).
4. R. A. Franz, J. Applegath, F. V. Morriss, F. Baiocchi, and C. Bolze. J. Org. Chem. **26**, 3309 (1961).
5. R. A. Franz and F. Appligath. J. Org. Chem. **26**, 3304 (1961).
6. Rod O'Connor. J. Org. Chem. **26**, 4375 (1961).
7. H. C. Ramsperger. J. Am. Chem. Soc. **51**, 2134 (1929).
8. S. G. Cohen and Chi-Hua Wang. J. Am. Chem. Soc. **77**, 3628 (1955).
9. A. E. Arbuzov and Yu P. Kitaev. Trudy Kazan. Khim. Tekhnol. Inst. im. S. M. Kirova, **23**, 54 (1957); Chem. Abstr. **52**, 10080 (1958).
10. A. Rosenthal, R. F. Astbury, and A. Hubscher. J. Org. Chem. **23**, 1037 (1958).
11. H. Reisenegger. Ber. **16**, 662 (1883).
12. A. W. Hofmann. Ann. **74**, 15 (1850).
13. A. Fleischer. Ber. **9**, 995 (1876).
14. E. Fischer. Ber. **29**, 796 (1896).

Received January 22, 1962.
Department of Chemistry,
University of British Columbia,
Vancouver, British Columbia.

SOME DIELECTRIC PROPERTIES OF CARBONYL CHLORIDE[1]

D. W. DAVIDSON

Recent spectroscopic (1), crystal structure (2), and calorimetric (3) studies of carbonyl chloride (phosgene) seem to rule out the possibility of the existence of residual entropy in the stable solid form (1) of carbonyl chloride, in contrast with earlier suggestions (4). However, the identification by Giauque and Ott (3) of two additional, relatively unstable, solid forms (II and III) prompted a dielectric study with the aim of determining whether the residual disorder in these forms was accompanied by dipolar relaxation processes of appreciable rate. In addition, the static dielectric constant of the liquid between −132 and +20° and the dipole moment of the gas were measured.

Gas Measurements

These were undertaken primarily to check the performance of a recently constructed apparatus for measurements of dipole moments of substances in the vapor state. The apparatus is of the classical LC oscillator type in which the cell capacitance is connected in parallel with a series arrangement of a small fixed capacitor (C_s = ~23 pf) and a General Radio Type 722 variable air capacitor. Deviations of the oscillator frequency from 1 Mc/sec, shown directly on a General Radio Frequency Deviation Meter, are adjusted to zero (to within a fraction of a cycle/sec) with the variable capacitor. Readings of this capacitor (corrected by calibration) are taken with the cell evacuated (C_0'), filled with sample at a known pressure (C_g), and evacuated again (C_0'').

The gas cell consists of three coaxial cylindrical electrodes of gold-plated nickel, suspended in a stainless steel vessel. The intermediate (high-potential) electrode is slightly shorter than the other two and is held in circular grooves in Teflon rings which fit tightly between the ends of the inner- and outer-most (grounded) electrodes. The rings are backed with perforated nickel disks, grooved to receive the ends of the grounded electrodes. The electrode assembly is held rigid by bolts which bear on the backing disks and are threaded on a nickel shaft attached to the top of the cell vessel. A vacuum-tight seal between the top and body of the vessel, which are bolted together, is provided by a thin 2S0 aluminum gasket, placed between a 1/16-in. circular bead machined on the lower edge of the top and the highly polished upper edge of the body wall. The lead from the high-potential electrode is brought out through a double Kovar-glass seal and connected to the oscillator via a rigid Teflon-insulated coaxial cable. The cell is connected to the sample line via a Kovar-glass seal. The cell constant (C_{cell}) is ~170 pf.

Dielectric constants ϵ were determined from

$$\frac{(\epsilon-1)C_{cell}}{C_s^2} = \frac{C_0-C_g}{(C_0+C_s+C_p)(C_g+C_s+C_p)}$$

in which $C_0 = (C_0'+C_0'')/2$ and C_p = small effective capacitance in parallel with the variable capacitor. Values of the two constants, viz. C_s^2/C_{cell} and C_s+C_p, were determined from measurements with standard non-polar gases at different pressures and with the cell in parallel with a small variable condenser in which capacitance variations were known to 0.001 pf.

[1]*Issued as N.R.C. No. 6877.*

The cell is mounted in a thermostated oil bath. Temperatures are measured with a calibrated thermocouple located in a blind hole in the wall of the cell.

Gaseous phosgene from a cylinder (Matheson of Canada, Limited) was condensed into a cooled, evacuated flask. Vapor pressures of the original samples considerably exceeded the vapor pressure of carbonyl chloride itself, but after about one quarter of the samples had been distilled off at dry-ice temperatures the vapor pressures at 0° had fallen to within a few tenths of a millimeter of the value (564.3 mm) obtained from the equation of Giauque and Jones (4) for carbonyl chloride at 0°. The samples studied were obtained from the middle one third of the distillate.

Values of dielectric constant of the vapor were determined at 7 to 10 pressures between 40 and 600 mm at each of five temperatures between 20 and 180°. We obtain a dipole moment ($1.17_9 \pm 0.015$ debyes) almost identical with that of Smyth and McAlpine (5) (1.19 ± 0.01) as re-evaluated (6, 7) with modern constants. Our value of the polarizability contribution (A) to the molar polarization is 18.3 ± 0.5 cm^3 (vs. 18.4 ± 0.4 cm^3).

Liquid Measurements

Carbonyl chloride was distilled under vacuum into the dielectric cell. The electrical measurements and temperature control and measurement were essentially as previously described (8). Values of the static dielectric constant for two samples were obtained at 28 temperatures between +20° and −132°. At the latter temperature the sample is undercooled by some 4° below the melting point of the stable solid form I. Measurements were made at each temperature at 10 and 100 kc/sec. Direct-current conductivities ranged from $\sim 7 \times 10^{-10}$ at the melting point to $\sim 4 \times 10^{-8}$ ohm^{-1}cm^{-1} at 20°.

The results can be expressed as a function of T (°K) by

$$\epsilon_0 = -1.01_3 + \frac{1678.2}{T}$$

to within a standard deviation of ±0.36%. The temperature dependence of the dielectric constant is shown graphically in Fig. 1.

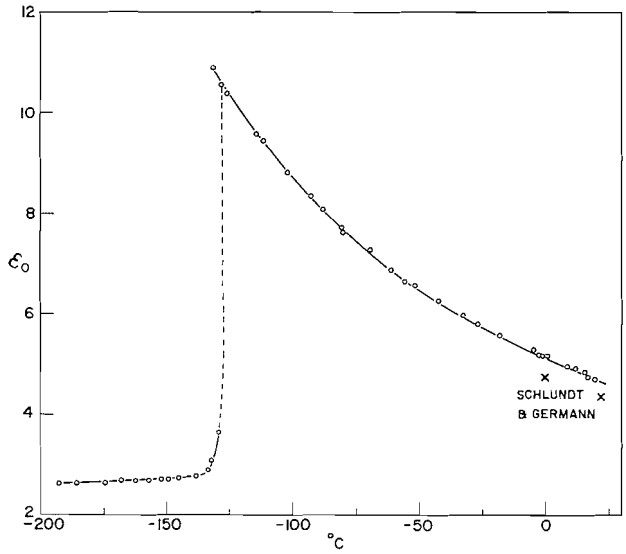

FIG. 1. Dielectric constant of carbonyl chloride. Solid data at 10 kc/sec, temperature increasing.

The only previous dielectric measurements on liquid carbonyl chloride are those reported in 1925 by Schlundt and Germann (9) at temperatures of 0 and 22°. Their dielectric constants, viz. 4.72 at 0° and 4.34 at 22°, are smaller by 7 to 8% than those found for corresponding temperatures in the present study. It appears that most of this difference may be attributed to the use by Schlundt and Germann of Drude's values (10) of the dielectric constants of acetone–benzene solutions for calibration of their apparatus. Comparison of Drude's values with those of more recent workers (e.g., those of Syrkin and Shedlovskaya (11)) in the range of concentration corresponding to dielectric constants between 3.5 and 5 shows the former values to be too low by almost 6%.

Dipole moments of carbonyl chloride have been calculated at different temperatures from the above values of the static dielectric constant of the liquid by use of the Onsager equation. For this we have taken values of ϵ_∞ derived from $A = 18.4$ cm^3 (6) and density values from the formula of Davies (12). The dipole moments obtained are effectively independent of temperature: at 0°, for example, the Onsager moment is 1.175 ± 0.014 debyes, at −100° 1.165 ± 0.038 debyes. The indicated uncertainty at 0° is primarily due to a standard deviation of 0.4 cm^3 in the value of A (6). That at −100° includes as well the possibility that the density given by the formula of Davies is in error by as much as 2%; this temperature is well below the range of the data on which the formula was based.

It is worth noting that, although the Onsager moment of carbonyl chloride is, within experimental error, the same as the moment of the gas, values obtained from measurements of the dielectric constants of dilute solutions in non-polar solvents are considerably smaller. Measurements of Le Fèvre *et al.* (13, 7) gave 1.11 debyes for carbonyl chloride in CCl_4 at 0° and 1.13 debyes in benzene at 25°.

Solid Measurements

Numerous dielectric constant and loss measurements were made on solid phosgene of different thermal histories in an attempt to determine whether solids II and III are characterized by rotational disorder of the type contributing to the dielectric constant. No disorder of this type was found within the considerable uncertainties of the quantities measured.

Dielectric constants were 2.7 ± 0.1 below the freezing point, and decreased by about 0.1 unit on cooling to liquid nitrogen temperature, probably because of some contraction of the sample away from the electrodes at very low temperatures. In general the dielectric losses in the solid were considerably less than those due to d-c. conductivity in the liquid at the same frequencies. No consistent differences were observed in the dielectric behavior of samples frozen slowly and rapidly (with, for example, the thermal histories specified by Giauque and Ott (3) for formation of solids II and III), except that samples frozen rapidly tended to show pronounced loss maxima at 10 kc/sec and lower frequencies at the onset of freezing.

Of seven cooling curves run on four samples of phosgene at cooling rates between 0.1°/min and 2°/min, five froze sharply into III, one into II, and one directly into I. Form III had a waxy appearance and, with further cooling or heating, frequently was observed to change into white crystals which grew from nucleation centers. It could only be melted without being converted into another form if it were immediately heated just after freezing was completed. Otherwise all samples melted as I. One or two showed signs of starting to melt as II, conversion to I, and melting as I. These observations are in general agreement with those of Giauque and Ott (3).

In view of the instability of III, it is possible that none of the dielectric measurements

was made on this form. However, since the freezing process was followed a number of times dielectrically with the invariable observation of only a monotonic fall in dielectric constant and loss, even when freezing started in the range of 130 to 135° K, it is probable that form III, like the other two forms, exhibits no appreciable dipolar polarization. Another possibility, that III has dielectric properties very similar to those of the supercooled liquid, may be excluded. All dielectric samples melted at the melting point of I.

Mention should be made of the occurrence in one sample (which had a d-c. conductivity in the liquid some 2.5 times as great as the best samples) of a broad loss maximum at temperatures near 118° K. This maximum developed some hours after the sample had frozen, and was subsequently observed on passing through this temperature range in either direction, on heating to the melting point of I and recooling, and on melting the sample completely and refreezing. The maximum must be attributed to solid I, but its origin is not clear. The magnitude of the maximum increases with decreasing frequency (change of the frequency from 10 kc/sec to 100 cycles/sec increased it by a factor of 20) and at low frequencies a maximum in the dielectric constant is also apparent. There appeared to be no dependence of the temperature of the maximum on frequency. It is possible that these effects were due to the presence of some HCl or water in the sample, and that the maximum corresponded to a eutectic temperature.

ACKNOWLEDGMENTS

The author is indebted to L. Kuhi and G. Young for assistance in construction of the vapor dipole moment apparatus.

1. E. CATALANO and K. S. PITZER. J. Am. Chem. Soc. **80**, 1054 (1958).
2. B. ZASLOW, M. ATOJI, and W. N. LIPSCOMB. Acta Cryst. **5**, 833 (1952).
3. W. F. GIAUQUE and J. B. OTT. J. Am. Chem. Soc. **82**, 2689 (1960).
4. W. F. GIAUQUE and W. M. JONES. J. Am. Chem. Soc. **70**, 120 (1948).
5. C. P. SMYTH and K. B. MCALPINE. J. Am. Chem. Soc. **56**, 1697 (1934).
6. TABLES of dielectric constants and electric dipole moments of substances in the gaseous state. Natl. Bur. Standards Circ. No. 537. 1953.
7. C. L. ANGYAL, G. A. BARCLAY, and R. J. W. LE FÈVRE. J. Chem. Soc. 3370 (1950).
8. D. W. DAVIDSON. Can. J. Chem. **35**, 458 (1957).
9. H. SCHLUNDT and A. F. O. GERMANN. J. Phys. Chem. **29**, 353 (1925).
10. P. DRUDE. Z. physik. Chem. **23**, 267 (1897).
11. A. N. SHEDLOVSKAYA and YA. K. SYRKIN. Zhur. Fiz. Khim. **22**, 913 (1948).
12. C. N. DAVIES. J. Chem. Phys. **14**, 48 (1946).
13. C. G. LE FÈVRE and R. J. W. LE FÈVRE. J. Chem. Soc. 1696 (1935).

RECEIVED MARCH 16, 1962.
DIVISION OF APPLIED CHEMISTRY,
NATIONAL RESEARCH COUNCIL,
OTTAWA, CANADA.

Canadian Journal of Chemistry

Issued by THE NATIONAL RESEARCH COUNCIL OF CANADA

VOLUME 40 SEPTEMBER 1962 NUMBER 9

THE PREPARATION AND RAMAN SPECTRUM OF DIPHOSPHORYL TETRAFLUORIDE: COMPARISON WITH THE SPECTRUM OF DIPHOSPHORYL TETRACHLORIDE

E. A. ROBINSON

Department of Chemistry, University of Toronto, Toronto, Ontario

Received May 10, 1962

ABSTRACT

Diphosphoryl tetrafluoride has been prepared by the dehydration of difluorophosphoric acid with phosphoric anhydride. The Raman and F^{19} n.m.r. spectra have been determined and are consistent with a symmetric structure $F_2P(O)—O—P(O)F_2$. The Raman spectrum is compared with that of diphosphoryl tetrachloride and partial assignments of the frequencies to normal modes of vibration are made by comparison with the spectra of POF_3 and $POCl_3$.

The compound $P_2O_3F_4$ has been reported previously (1) as a decomposition product of a white solid of approximate composition $P_7O_{10}F_{15}$ which was obtained at −75° C by the action of an electrical discharge on an equimolar mixture of oxygen and phosphorus trifluoride. In the present work, $P_2O_3F_4$ was prepared by the dehydration of difluorophosphoric acid with phosphoric oxide:

$$2HPO_2F_2 = P_2O_3F_4 + H_2O.$$

The F^{19} n.m.r. spectrum consisted of two peaks of equal intensity, indicating that all four fluorine atoms in the molecule are equivalent, the two peaks being due to spin–spin coupling between F^{19} and P^{31}. The method of preparation of the compound and its n.m.r. spectrum are consistent with its formulation as difluorophosphoric acid anhydride, I.

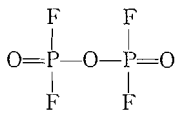

I

The spectrum is shown in Fig. 1. Table I gives the frequencies of the 22 observed lines and a comparison is made with the spectrum of $P_2O_3Cl_4$ (2, 3). The infrared spectrum of $P_2O_3Cl_4$ was checked and the measurements are also shown in Table I. The formulation of $P_2O_3Cl_4$ as dichlorophosphoric anhydride is reasonable since this acid is reported (4) as the product of hydrolysis of $P_2O_3Cl_4$ at −60°.

Gerding and co-workers (3) and Baudler and co-workers (2) attempted only a partial assignment of frequencies. Their conclusions are summarized in Table II. Gerding (3) made his assignment mainly by comparison with his previous assignment of the spectrum of $S_2O_5Cl_2$ (5), which has since been criticized (6).

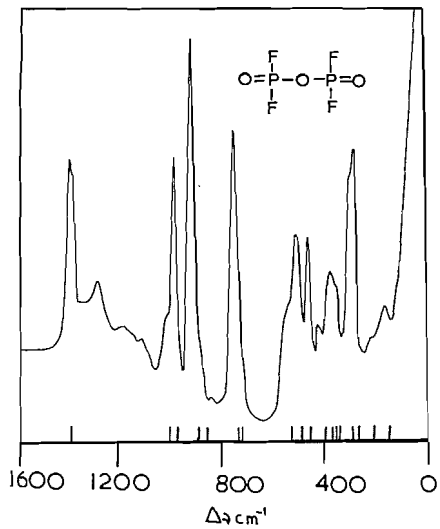

FIG. 1. The Raman spectrum of diphosphoryl tetrafluoride.

TABLE I

Vibrational spectra of $P_2O_3Cl_4$ and $P_2O_3F_4$
(Frequencies in cm^{-1})

$P_2O_3Cl_4$				$P_2O_3F_4$
Infrared		Raman		Raman
(*a*)	(*b*)	(*b*)	(*c*)	(*a*)
1310	1320	1314(9)	1312(15) p	1390(6) p
1248	1250			1370(4) ?
1135	—			1270(3) dp
962	966			1170(1) dp
—	950			1083(1) dp
885	897			987(3) dp
790	—		806(2)	951(7) p
706	714	713(3)	713(5) p	890(10) p
628	628	626(3)	649(1–2)	855(½)
		605(4)	611(2–3) dp	721(9) p
		559(7)	560(8) p	700(½)
		531(2)	531(1–2)	518(4) sh
		506(9)	507(15) p	480(6) p
		487(3)	454?(1)	440(3) p
		426(10)	425(20) p	395(1) dp
		407(3)	408(2)	362(3)
		355(3)	364(4)	352(3)
		341(8)	343(10) dp	340(3)
		320(3)	316(1)	295(4)
		296(3)	290(2–3) p	273(6) dp
		267(1)	—	205(1)
		246(5)	249(6) p	160(2) p
		237(3)	—	
		210(3)	213(1–2)	
		192(7)	192(5) dp	
		169(8)	166(10) dp	
		159(7)		
		96(3)		

NOTE: (*a*) present results; (*b*) Baudler and co-workers (2); (*c*) Gerding and co-workers (3); p, polarized; dp, depolarized; sh, shoulder.

TABLE II

Previous assignments of characteristic vibrations of $P_2O_3Cl_4$

Frequency (cm^{-1})		
(*a*)	(*b*)	Assignment
1312	1320	P—O stretch
806	966	P—O—P asym. stretch
713	714	P—O—P sym. stretch
611	—	PCl_2 asym. stretch
343	—	PCl_2 rocking or twisting

NOTE: (*a*) Gerding and co-workers (3); (*b*) Baudler and co-workers (2).

The normal modes of $P_2O_3X_4$ can be related to those of POX_3, as is shown in Table III, in a manner similar to that which was used previously to relate the spectra of disulphuryl

TABLE III

Correlation of the vibrational modes of $P_2O_3X_4$ with those of POX_3

POX_3			$X_2P(=O)—O—P(=O)X_2$	
	$POCl_3$*	POF_3†		Number of vibrations
P—O stretch	1290	1415	P—O stretch	2‡
PX_3 sym. stretch	486	873	PX_2 sym. stretch	2‡
PX_3 sym. bend	268	473	PX_2 sym. bend	2‡
PX_3 asym. stretch	581	990	PX_2 asym. stretch	2‡
PX_3 asym. bend	193	485	PX_2 rocking modes, ⊥ & ∥§	4‡
PX_3 rocking mode (or P—O wag)	337	386	P—O wags, ⊥ & ∥§	4‡
			Torsions	2
			P—O—P sym. stretch	1
			P—O—P asym. stretch	1
			P—O—P bend	1
			Total number of vibrations	21

*Delwaulle and Francois (10).
†Gutowsky and Liehr (11).
‡In phase and out of phase.
§⊥, perpendicular to P—O—P plane; ∥, parallel to P—O—P plane.

halides $S_2O_5X_2$ to those of the sulphuryl halides SO_2X_2 (6). Partial assignments for the molecules $P_2O_3Cl_4$ and $P_2O_3F_4$ which are shown in Table IV were made in this way and it is necessary therefore to comment on only a few of them.

For a molecule $P_2O_3X_4$ the maximum number of fundamental vibrational frequencies is 21. Baudler and co-workers report a total of 26 lines in the Raman and infrared spectra of $P_2O_3Cl_4$ and we have found 22 lines in the Raman spectrum of $P_2O_3F_4$. Some of the observed frequencies must therefore be combination or overtone bands. Since we expect only two frequencies greater than 1000 cm^{-1} (the in-phase and out-of-phase P—O stretches), we assign 1270, 1170, and 1083 cm^{-1} in the spectrum of $P_2O_3F_4$, and 1248 and 1135 cm^{-1} in the spectra of $P_2O_3Cl_4$, as combination or overtone bands.

Theoretically three vibrations are expected to be associated with the P—O—P bridging group and these are conveniently described as symmetric and asymmetric stretches, and a bend. The bend is assigned at 159 and 160 cm^{-1} (polarized), respectively, for $P_2O_3Cl_4$ and $P_2O_3F_4$, by comparison with the S—O—S bends near 150–160 cm^{-1} in disulphuryl

TABLE IV

Assignment of the vibrational spectra of $P_2O_3Cl_4$ and $P_2O_3F_4$

$P_2O_3Cl_4$		$P_2O_3F_4$	
Frequency (cm^{-1})	Assignment	Frequency (cm^{-1})	Assignment
1312 p	P—O stretch, i and o	1390 p	P—O stretch, i
1248	Overtone ?	1370	P—O stretch, o
1135	Overtone ?	1270 dp	overtone ?
962	P—O—P asymmetric stretch	1083 dp	overtone ?
885	?	987 dp	P—O—P asymmetric stretch
806	?	951 dp	
713 p	P—O wagging mode, ∥, o	890 p	PF_2 stretches
649	P—O wagging mode, ⊥, o	855	
611 dp		721 p	P—O wagging mode, ∥, o
560 p	PCl_2 stretching modes	700	P—O wagging mode, ⊥, o
531		518	PF_2 bend, o
507 p		480 p	P—O—P symmetric stretch
454?	?	440 p	PF_2 bend, i
425 p	P—O—P symmetric stretch	395	
408		362	
364	P—O wagging or torsional modes	352	PF_2 rocking modes,
343 dp		340	P—O wagging modes,
290 p	PCl_2 bend, ?, o	295	and torsional modes
249 p	PCl_2 bend, i	273 dp	
213		205	
192 dp	PCl_2 rocking modes	160 p	P—O—P bend
166 dp			
159	P—O—P bend		
96	?		

NOTE: i = in phase; o = out of phase.

halides (6) and the Si—O—Si bend in, e.g., $[(CH_3)_3Si]_2O$ at 180 cm^{-1} (7). The P—O—P asymmetric stretches are assigned at 962 cm^{-1} ($P_2O_3Cl_4$) and 987 cm^{-1} ($P_2O_3F_4$), and the symmetric stretches at 425 cm^{-1} ($P_2O_3Cl_4$) and 480 cm^{-1} ($P_2O_3F_4$). Bands near 950 cm^{-1} have been assigned to the P—O—P asymmetric stretches in the infrared spectra of pyrophosphates and pyrophosphate esters (8). The P—O—P stretches are to be compared with the assignment of Si—O—Si stretches at 500–600 cm^{-1} (symmetric) and approximately 1050 cm^{-1} (asymmetric) in several disiloxanes (7), and with our recent assignment of S—O—S stretches at approximately 300 cm^{-1} (symmetric) and approximately 800 cm^{-1} (asymmetric) in the spectra of disulphuryl halides (6).

The only other assignment which requires special comment is that of the lines at 713 cm^{-1} (polarized) and 649 cm^{-1} in the spectrum of $P_2O_3Cl_4$, and 721 cm^{-1} (polarized) and 700 cm^{-1} in the spectrum of $P_2O_3F_4$, to P—O wagging modes. These are to be compared with our recent assignment of 716 cm^{-1} (polarized) and 621 cm^{-1} in the spectrum of $S_2O_5Cl_2$, and 733 cm^{-1} (polarized) and 630 cm^{-1} in the spectrum of $S_2O_5F_2$, to SO_2 rocking modes (6). The relatively high values of these frequencies may be attributed to the close proximity of the $POCl_2$ groups.

Recently Stolzer and Simon (9) have reported the preparation of diphosphoryl difluoride dichloride, $P_2O_3F_2Cl_2$, by the reaction between P_4O_{10} and $POFCl_2$. They claim that the compound has the symmetrical structure II and have found bands at 1360 cm^{-1} (P—O stretch), 1020 cm^{-1} (P—O—P asymmetric stretch), 930 cm^{-1} (PF stretch), and 600 cm^{-1} (PCl stretch) in the infrared spectrum. It is of interest to note that the P—O stretching frequency is close to the mean of the frequencies of the similar vibrations in $P_2O_3Cl_4$ (1320 cm^{-1}) and $P_2O_3F_4$ (1390 cm^{-1}), which provides additional support for the symmetric formulation II.

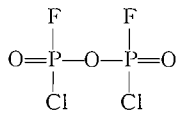

II

EXPERIMENTAL

Diphosphoryl tetrafluoride was prepared by the reaction between difluorophosphoric acid (Ozark-Mahoning Co.) and phosphoric anhydride. Difluorophosphoric acid (1.0 mole) and P_4O_{10} (0.25 mole) were heated under gentle reflux for 1 hour and the mixture was then distilled. The fraction boiling below 75° was collected and purified by fractional distillation using an efficient column. The product had b.p. 71°.

The Raman spectrum was measured with the apparatus previously described (6) and polarization measurements were carried out using polaroid cylinders to polarize the incident light perpendicular to and parallel to the axis of the Raman tube.

The n.m.r. measurements were carried out using a Varian Associates high-resolution n.m.r. spectrometer operating at 56.4 Mc.

ACKNOWLEDGMENTS

Professor R. J. Gillespie of the Chemistry Department, McMaster University, is thanked for discussion of the manuscript, and Dr. W. E. White of the Ozark-Mahoning Company, Tulsa, Oklahoma, for a gift of difluorophosphoric acid. The National Research Council of Canada is thanked for financial support.

REFERENCES

1. U. Wannagat and J. Rademachers. Z. anorg. u. allgem. Chem. **289**, 66 (1957).
2. M. Baudler, R. Klement, and E. Rother. Ber. **93**, 149 (1960).
3. H. Gerding, H. Gijben, B. Nieuwenhuijse, and J. G. van Raaphorst. Rec. trav. chim. **79**, 41 (1960).
4. H. Grunze and E. Thilo. Angew. Chem. **70**, 73 (1958).
5. H. Gerding and A. C. Linden. Rec. trav. chim. **61**, 735 (1942).
6. R. J. Gillespie and E. A. Robinson. Can. J. Chem. **39**, 2179 (1961).
7. H. Kriegsmann. Z. Elektrochem. **61**, 1088 (1957); Z. anorg. u. allgem. Chem. **299**, 78, 134 (1959).
8. L. J. Bellamy. The infra-red spectra of complex molecules. Wiley, New York. 1958. p. 318.
9. C. Stolzer and A. Simon. Ber. **94**, 1976 (1961).
10. M. Delwaulle and F. Francois. Compt. rend. **220**, 817 (1945).
11. H. S. Gutowsky and A. D. Liehr. J. Chem. Phys. **20**, 1653 (1952).

AN ELECTRON IMPACT STUDY OF CHLOROMETHYL AND DICHLOROMETHYL DERIVATIVES

A. G. Harrison and T. W. Shannon
Department of Chemistry, University of Toronto, Toronto, Ontario
Received May 3, 1962

ABSTRACT

The appearance potential of the CH_2Cl^+ ion has been measured from methyl chloride, dichloromethane, bromochloromethane, and ethyl chloride. The results lead to $\Delta H_f(CH_2Cl^+) = 230\pm3$ kcal/mole. The heat of formation of $CHCl_2^+$ is estimated to be 215 ± 3 kcal/mole from the appearance potential of this ion in the mass spectrum of chloroform and of bromodichloromethane. By the indirect mass spectrometric method $\Delta H_f(CH_2Cl) = 29\pm3$ kcal/mole and $\Delta H_f(CHCl_2) = 15\pm3$ kcal/mole are obtained. The ionization potentials of a number of chlorine-containing compounds have been measured.

INTRODUCTION

The literature contains little consistent information on the heats of formation of chloromethyl and dichloromethyl radicals and ions, and hence on bond dissociation energies involving these radicals. Reed and Sneddon (1) have reported the electron-impact ionization potential of CH_2Cl radical to be 9.70 ev and have combined this with $A(CH_2Cl^+) = 12.89$ ev from dichloromethane to give $D(CH_2Cl—Cl) = 74$ kcal/mole. However, their appearance potential is considerably higher than the value 12.3 ev reported by Gutbier (2), and, further, the radical ionization potential is in disagreement with the value 9.32 ev measured by Lossing, Kebarle, and deSousa (3).

The results for dichloromethyl derivatives are equally contradictory. Reed and Sneddon have reported $I(CHCl_2) = 9.54$ ev and have combined this with $A(CHCl_2^+) = 13.00$ ev from dichloromethane and 12.43 ev from chloroform to give respectively $D(CHCl_2—H) = 80$ kcal/mole and $D(CHCl_2—Cl) = 67$ kcal/mole. It should be noted that their ionization potential is again in disagreement with that reported by Lossing *et al.* (3), and also that the appearance potentials lead to mutually inconsistent values for $\Delta H_f(CHCl_2^+)$ when combined with standard thermochemical data.

Recently, Goldfinger and Martens (4) have estimated $D(CH_2Cl—H) = 98$ kcal/mole and $D(CHCl_2—H) = 95$ kcal/mole on the assumption of a monotonic decrease in bond dissociation energies from methane to chloroform. As justification for this assumption they refer to estimates of $D(C—Br)$ by Sehon and Szwarc (5) for the various chlorobromomethanes. Sehon and Szwarc obtained $D(CH_2Cl—Br) = 61.0$ kcal/mole and $D(CHCl_2—Br) = 53.5$ kcal/mole from the pyrolysis of the bromides by the toluene-carrier technique. However, the activation energies and hence the bond dissociation energies were estimated from rate measurements at one temperature on the basis of a pre-exponential factor of 2×10^{13} and, furthermore, the rates were found to be dependent on the toluene pressure. Hence the results obtained must be accepted with reservation.

The present work reports the measurement by electron-impact methods of the appearance potentials of CH_2Cl^+ and $CHCl_2^+$ from suitable derivatives to obtain further information concerning the heats of formation of these ions. In view of the lack of consistent information on bond dissociation energies we have also applied the indirect mass spectrometric method (6) to the determination of the heat of formation of the chloromethyl and dichloromethyl radicals.

The principles of the indirect method of obtaining radical heats of formation can be outlined briefly. The appearance potential for the process

$$RR_1 + e \rightarrow R^+ + R_1 + 2e,$$

where R_1 is the radical of interest, can be equated to standard heats of formation as follows.

$$A(R^+) = \Delta H_f(R^+) + \Delta H_f(R_1) - \Delta H_f(RR_1) + E,$$

where E is any excess energy which may be associated with either the charged or uncharged fragments. If E can be measured or can be assumed to be zero then the heat of formation of the radical can be evaluated provided $\Delta H_f(R^+)$ and $\Delta H_f(RR_1)$ are known independently. The main experimental difficulty lies in the estimation of the excess energy and consequently it is usually assumed to be zero. The large body of consistent results thus obtained (7) affords some justification for this assumption. It is apparent, however, that the presence of excess energy in any ionization process, if undetected, would lead to erroneous conclusions. Somewhat more reliable results can be obtained by measuring the appearance potentials of ions of known heat of formation from a number of derivatives where R_1 is the common neutral fragment. If consistent results for $\Delta H_f(R_1)$ are obtained then either the excess energy is the same in all cases or it is zero. Economy of hypothesis would suggest the latter. However, the method can only lead to upper estimates for radical heats of formation in the absence of accurate excess energy measurements.

EXPERIMENTAL

The ionization and appearance potentials were measured using an Associated Electrical Industries MS-2 mass spectrometer, which has been described previously (8). Tungsten filaments were used throughout this work since rhenium filaments were found to deteriorate rapidly in the presence of chlorinated compounds. The ionization efficiency curves for the unknown and standard were plotted in the semilogarithmic manner (9). For molecular ions these curves were parallel and the voltage difference could be determined directly. For the fragment ions these curves were frequently non-parallel and in these cases the threshold voltage was evaluated by extrapolation of the voltage difference curve to zero ion current.

In the dissociative ionizations studied in this work the postulated neutral fragment frequently contained a halogen atom. Since the formation of negative halide ions is frequent in electron impact the possibility of ion-pair processes cannot be neglected. The mass spectra of the compounds studied were therefore examined for negative ions. In many cases small negative ion currents were found. To check that this low abundance was not completely due to instrumental factors the O^- formation in oxygen was studied. The ratio $O^-/O^+ = 0.016_9$ was obtained at 35 volts electron energy, compared to the value of 0.04 obtained by Lozier (10) in a system presumably devoid of discrimination effects. We therefore conclude that the mass spectrometer is approximately 42% efficient in collecting negative ions, although this is undoubtedly a rather rough estimate.

The samples used were commercially available samples of high purity.

RESULTS AND DISCUSSION

Ionic Heats of Formation

The results obtained for the appearance potential of the CH_2Cl^+ ion from a number of derivatives are recorded in Table I and compared with previous results. The appearance potential of CH_2Cl^+ from methyl chloride obtained in the present work is in good agreement with the earlier result by Irsa (11). Both results are somewhat lower than the value obtained by Gutbier (2), although the discrepancy is not serious. The present result for $A(CH_2Cl^+)$ from dichloromethane is in essential agreement with Gutbier's result and in disagreement with the higher result obtained by Reed and Sneddon (1). There does not appear to have been any previous study of bromochloromethane. The appearance potential curve for CH_2Cl^+ from ethyl chloride showed a large curvature and led to a somewhat

TABLE I

Heat of formation of CH_2Cl^+ ion

$CH_2ClX + e \rightarrow CH_2Cl^+ + X + 2e$

X	$A(CH_2Cl^+)$, ev		$\Delta H_f(CH_2ClX)$, kcal/mole	$\Delta H_f(CH_2Cl^+)$, kcal/mole		
	This work	Literature		This work	Literature	Average
H	12.88±0.1	13.0±0.2*	−20.6§	224	227	228
		13.3±0.1†			234	
Cl	12.12±0.1	12.3±0.1†	−21‖	231	235	233
		12.89±0.03‡				
Br	11.56±0.1		−12¶	229		229
CH_3	13.20±0.2	13.6±0.2*	−26.2§	248	257	
						230±3

*Ref. 11. †Ref. 2. ‡Ref. 1. §Ref. 17. ‖Ref. 12. ¶Ref. 18.

lower result than that reported by Irsa. The error, however, is large due to the extrapolation involved.

The last three columns of Table I record values for $\Delta H_f(CH_2Cl^+)$ calculated from the present data and the literature data using the heats of formation recorded in column 4 for the neutral molecules and the following heats of formation (12): $H = 52.1$, $Cl = 29$, $Br = 27$, and $CH_3 = 32$, all in kcal/mole. With the exception of the results for ethyl chloride and the one high value for dichloromethane the calculated ionic heats of formation are in reasonable agreement and lead to $\Delta H_f(CH_2Cl^+) = 230\pm3$ kcal/mole. It would appear that the formation of CH_2Cl^+ from ethyl chloride involves considerable excess energy.

The alternative ion-pair process

$$CH_2ClX + e \rightarrow CH_2Cl^+ + X^- + e$$

would lead to much lower values for the ionic heats of formation. For methyl chloride the negative ion would be H^-, which could not be detected. Ion-pair processes involving H^- formation appear to be quite rare. For dichloromethane and bromochloromethane small ion currents for Cl^- and Br^-, respectively, were found. Using the collection efficiency of 42% discussed above, these negative ion currents were estimated to be less than 1% of the CH_2Cl^+ ion current in each case. This abundance, if arising from an ion-pair process involving CH_2Cl^+ as the positive fragment, would lead to considerable tailing of the appearance potential curves. For the chloro and bromo derivatives this tailing was relatively small, suggesting that negative ion formation was not interfering seriously with the measurements. For methyl chloride the appearance potential curve for CH_2Cl^+ was parallel to the standard krypton curve, lending further support to the conclusion that H^- was not formed. The agreement of the ionic heats of formation calculated from the three results suggests that ion-pair formation in the chloro and bromo compounds also is not interfering.

The appearance potential of the $CHCl_2^+$ ion was measured from chloroform and bromodichloromethane. The results are summarized in Table II. The appearance potential of the ion from dichloromethane could not be determined accurately because of the low abundance of the ion. The appearance potential of $CHCl_2^+$ from chloroform obtained in the present work is 0.73 ev lower than the value reported by Reed and Sneddon (1). Assuming the ionization process

$$CHCl_2X + e \rightarrow CHCl_2 + X + 2e$$

TABLE II

Heat of formation of $CHCl_2^+$ ion

$CHCl_2X + e \rightarrow CHCl_2^+ + X + 2e$

X	$A(CHCl_2^+)$, ev: This work	$A(CHCl_2^+)$, ev: Literature	$\Delta H_f(CHCl_2X)$, kcal/mole	$\Delta H_f(CHCl_2^+)$, kcal/mole
Cl	11.70±0.1	12.43±0.02*	−24.4†	216.4
Br	11.02±0.1		−14‡	213.4
			Average	215±3

*Ref. 1. †Ref. 12. ‡Ref. 18.

and, further, assuming that no excess energy is involved, the present results lead to consistent values for $\Delta H_f(CHCl_2^+)$, as shown in Table II, suggesting that the earlier appearance potential is in error. The alternative ionization process leading to ion-pair formation would result in ionic heats of formation 80–90 kcal/mole lower than the value 215 kcal/mole obtained. This does not appear possible by comparison with the well-established $\Delta H_f(CCl_3^+)$ = 216 kcal/mole (13, 14) and the low (about 1%) abundance of the corresponding negative ions.

Radical Heats of Formation

The ionic heats of formation reported above lead to $D(CH_2Cl—H)$ = 79 kcal/mole and $D(CHCl_2—H)$ = 68 kcal/mole when combined with $I(CH_2Cl)$ = 9.70 ev and $I(CHCl_2)$ = 9.54 ev as reported by Reed and Sneddon (1). When combined with the ionization potential of 9.3 ev reported for both radicals by Lossing *et al.* (3), they lead to $D(CH_2Cl—H)$ = 89 kcal/mole and $D(CHCl_2—H)$ = 74 kcal/mole. These results appear quite unlikely when compared with $D(CH_3—H)$ = 102 kcal/mole and $D(CCl_3—H)$ = 89 kcal/mole (15) and suggest that the radical ionization potentials reported by both groups may be in error. To obtain further information the indirect mass spectrometric method was used to obtain estimates for the radical heats of formation.

Table III records the results obtained by the indirect method for the chloromethyl

TABLE III

Heat of formation of CH_2Cl radical

$RCH_2Cl + e \rightarrow R^+ + CH_2Cl + 2e$

R	$A(R^+)$, ev (±0.1 ev)	$\Delta H_f(R^+)$, kcal/mole	$\Delta H_f(RCH_2Cl)$, kcal/mole	$\Delta H_f(CH_2Cl)+E$, kcal/mole
C_2H_5	12.48	224*	−31‖	33
i-C_3H_7	11.26	193†	−38¶	29
n-C_3H_7	11.92	193†	−35¶	46
CH_2Cl	12.52	230‡	−31**	28
CH_2OH	11.51	179§	−59††	27

*Ref. 7.
†Ref. 7 gives a value of 190 kcal/mole. However, the simpler processes involving loss of a single atom give an average of 193 kcal/mole.
‡This work.
§Calculated from data of Friedman *et al.* (J. Chem. Phys. **27**, 613 (1957)), and supported by unpublished work in this laboratory.
‖The heat of combustion reported by Smith (Acta Chem. Scand. **7**, 65 (1953)) leads to −36 kcal/mole and is out of line with other members of the series. Mortimer *et al.* (Trans. Faraday Soc. **48**, 220 (1952)) give −31 kcal/mole, in agreement with calculations by group methods.
¶Ref. 17.
Sinke (J. Phys. Chem. **62, 397 (1958)) and Kirkbride (J. Appl. Chem. (London), **6**, 11 (1956)) give values in excellent agreement.
††Calculated from ΔH_f of liquid and ΔH_v of liquid given in ref. 12, after correction of ΔH_v to 25° C.

radical. These appearance potentials do not appear to have been measured previously. Column 5 gives the values calculated for $\Delta H_f(CH_2Cl)+E$, assuming the following ionization process:

$$RCH_2Cl + e \rightarrow R^+ + CH_2Cl + 2e.$$

The alternative ionization process involving $CH_2 + Cl$ as the neutral fragments is of considerably higher energy. For example, using $\Delta H_f(CH_2) = 93$ kcal/mole, calculated from $D(CH_2—H) = 113$ kcal/mole (16), the appearance potential for the ionization process

$$CH_2ClCH_2Cl + e \rightarrow CH_2Cl^+ + CH_2 + Cl + 2e$$

is calculated to be 16.6 ev compared to the experimental value of 12.52 ev. On the other hand, the ion-pair process

$$RCH_2Cl + e \rightarrow R^+ + CH_2 + Cl^- + 2e$$

would lead to appearance potentials only slightly higher than the experimental values. To check this possibility the ratio Cl^-/R^+ was measured for each of the compounds studied. Over the range 20–50 volts electron energy this ratio was about 0.01 for dichloroethane and less than 0.0008 for all other compounds listed in Table III. The ionization efficiency curves for the negative ion were complex and could not be used to obtain information on the mechanism of formation of the ion. It would appear that ion-pair formation by the process indicated above is occurring to only a slight extent, if at all. The assumption of the simple ionization process leading to CH_2Cl as the neutral fragment is therefore justified.

With exception of the result for the $C_3H_7^+$ ion from *n*-butyl chloride the calculated values for $\Delta H_f(CH_2Cl)+E$ are in essential agreement. Neglecting this value, which must involve considerable excess energy, the results lead to an upper limit $\Delta H_f(CH_2Cl) = 29\pm3$ kcal/mole on the assumption that $E = 0$ for the other ionization processes.

The application of the indirect method to the estimation of the heat of formation of the dichloromethyl radical is hindered by the lack of accurate heat of formation data. The study was necessarily limited to two derivatives, 1,1,2,2,-tetrachloroethane and pentachloroethane, with the results shown in Table IV. The appearance potentials obtained,

TABLE IV

Heat of formation of $CHCl_2$ radical

$RCHCl_2 + e \rightarrow R^+ + CHCl_2 + 2e$

R	$A(R^+)$, ev (±0.1 ev)	$\Delta H_f(R^+)$, kcal/mole	$\Delta H_f(RCHCl_2)$, kcal/mole	$\Delta H_f(CHCl_2)+E$, kcal/mole
$CHCl_2$	11.55	215*	−37.3‡	14.1
CCl_3	11.54	216†	−34.7‡	15.4
			Average	15±3

*This work.
†Refs. 13 and 14.
‡Kirkbride. J. Appl. Chem. (London), **6**, 11 (1956).

when combined with the thermochemical data given in the table, yield consistent results leading to $\Delta H_f(CHCl_2) = 15\pm3$ kcal/mole on the assumption that no excess energy is involved in the ionization processes. Again small amounts of Cl^-, amounting to about 1% of the R^+ peak, were formed; however, the possible mechanisms of formation in the

polychlorinated derivatives are abundant. The low abundance of the negative ion would suggest that the ion-pair process

$$RCHCl_2 + e \rightarrow R + CHCl + Cl^- + e$$

is not occurring to a significant extent, and that calculations on the basis of the dissociation process

$$RCHCl_2 + e \rightarrow R + CHCl_2 + 2e$$

are justified.

Bond Dissociation Energies and Radical Ionization Potentials

The radical heats of formation reported above may be combined with standard thermochemical data to yield bond dissociation energies. Table V gives the results of these

TABLE V

Effect of chlorine substitution on bond dissociation energies

R	D(R—H), kcal/mole	D(R—Cl), kcal/mole	D(R—Br), kcal/mole
CH_3*	102	80	67
CH_2Cl	102±3	79±3	68±3
$CHCl_2$	88±3	68±3	56±3
CCl_3*	89	68	50–55

*Values for methyl and trichloromethyl derivatives from ref. 15.

calculations and compares the results with bond dissociation energies for methyl and trichloromethyl derivatives (15). The following heats of formation, all in kcal/mole, were used in the calculations: CH_3Cl = −20.6 (17), CH_2Cl_2 = −21 (12), $CHCl_3$ = −24.4 (12), CH_2ClBr = −12 (18), $CHCl_2Br$ = −14 (18), H = 52.1 (12), Cl = 29 (12), and Br = 27 (12).

Within experimental error the calculated bond dissociation energies for the chloromethyl derivatives are identical with the well-established values for the methyl derivatives. The value $D(CH_2Cl—H)$ = 102±3 kcal/mole is indistinguishable from the estimated value, 98 kcal/mole (4), within the combined limits of error, although $D(CH_2Cl—Br)$ = 68±3 kcal/mole is considerably higher than the value of 61 kcal/mole reported by Sehon and Szwarc (5). The present value for $D(CH_2Cl—H)$ is in reasonable agreement with $D(CH_2Br—H)$ = 99 kcal/mole at 0° K, obtained from photobromination experiments (19). This agreement suggests that the present results are not greatly in error, although the lower limit of error is more likely to apply than the upper limit.

The bond dissociation energies obtained for dichloromethyl derivatives do not fit a picture involving an even gradation of bond energies in the series from methyl to trichloromethyl. The present results indicate that the bond dissociation energies of dichloromethyl derivatives are identical with the bond dissociation energies of trichloromethyl derivatives. If the value $D(CCl_3—H)$ = 93 kcal/mole (4) is used the present results for dichloromethyl derivatives are lower than for trichloromethyl derivatives. It is interesting to note that recent measurements (4) of the activation energy of the reaction $Cl + RH \rightarrow HCl + R$ indicate that the activation energy for chlorine atom reaction with dichloromethane is somewhat less than that for reaction with chloroform. The present value $D(CHCl_2—Cl)$ = 68±3 kcal/mole is in agreement with an earlier result $\geqslant$ 72 kcal/mole obtained from the kinetics of the thermal decomposition of chloroform (20), although this result has been questioned (15). The result $D(CHCl_2—Br)$ = 56±3 kcal/mole is also in agreement with

$D(CHCl_2—Br)$ = 53.5 kcal/mole (5), although this value too must be accepted with reservations. The present results should represent an upper limit to the bond dissociation energies of dichloromethyl derivatives. The available experimental results are therefore in reasonable agreement and indicate that the bond dissociation energies of dichloromethyl derivatives are identical with or less than the bond dissociation energies of trichloromethyl derivatives.

From the radical and ionic heats of formation obtained in this work $I(CH_2Cl)$ and $I(CHCl_2)$ are calculated to be 8.72±0.26 and 8.67±0.26 ev respectively. The large error in these calculated values makes detailed comparison with $I(CH_3)$ = 9.95 ev (21) and $I(CCl_3)$ = 8.78 ev (13) of little value; however, it would appear that the ionization potentials of the three chloromethyl radicals do not differ greatly. The calculated ionization potentials are considerably lower than the experimental values reported by either Reed (1) or Lossing (3), suggesting that the vertical ionization potential reported by these workers is considerably above the adiabatic ionization potential.

Ionization Potentials of Parent Molecules

During the course of this investigation the appearance potentials of the molecular ions were determined wherever the parent ion was of sufficient intensity. The results are presented in Table VI and compared, where possible, with previous electron-impact

TABLE VI

Ionization potentials of chloro compounds

Molecule	Electron impact		Photoionization (reference 24)
	This work	Literature	
CH_3Cl	11.45±0.05	11.46,* 11.35†	11.28
C_2H_5Cl	11.16±0.05	11.18,* 11.2‡	10.98
n-C_3H_7Cl	11.05±0.05	10.96,* 10.7§	10.82
CH_2Cl_2	11.49±0.05	11.4‖	11.35
$ClCH_2CH_2Cl$	11.25±0.05		11.12
$Cl_2CHCHCl_2$	11.10±0.05		
CH_2ClBr	10.75±0.05		
$CHCl_2Br$	10.88±0.05		

*Ref. 22. †Ref. 7. ‡Ref. 11. §Ref. 23. ‖Ref. 2.

results (2, 7, 22, 23) and with photoionization results (24). In general the agreement with previous electron-impact results is within experimental error. The electron-impact results are consistently 0.15 to 0.20 ev higher than the photoionization results, as is frequently found.

ACKNOWLEDGMENTS

The authors are indebted to the Advisory Committee on Research, University of Toronto, and the National Research Council of Canada for financial support.

REFERENCES

1. R. I. Reed and W. Sneddon. Trans. Faraday Soc. **55**, 876 (1959).
2. H. Gutbier. Z. Naturforsch. A, **9**, 348 (1954).
3. F. P. Lossing, P. Kebarle, and J. B. deSousa. *In* Advances in mass spectrometry. Pergamon Press, London. 1959. p. 431.
4. P. Goldfinger and G. Martens. Trans. Faraday Soc. **57**, 2220 (1961).
5. A. Sehon and M. Szwarc. Proc. Roy. Soc. (London), A, **209**, 110 (1951).
6. D. P. Stevenson. J. Chem. Phys. **10**, 291 (1942).
7. F. H. Field and J. L. Franklin. Electron impact phenomena and the properties of gaseous ions. Academic Press, New York. 1957.

8. J. M. S. TAIT, T. W. SHANNON, and A. G. HARRISON. J. Am. Chem. Soc. **84**, 4 (1962).
9. F. P. LOSSING, A. W. TICKNER, and W. A. BRYCE. J. Chem. Phys. **19**, 1254 (1951).
10. W. W. LOZIER. Phys. Rev. **46**, 268 (1934).
11. A. P. IRSA. J. Chem. Phys. **26**, 18 (1957).
12. F. D. ROSSINI *et al.* Natl. Bur. Standards Circ. 500. 1952.
13. J. B. FARMER, I. H. S. HENDERSON, F. P. LOSSING, and D. G. H. MARSDEN. J. Chem. Phys. **24**, 348 (1956).
14. R. E. FOX and R. L. CURRAN. J. Chem. Phys. **34**, 1595 (1961).
15. T. L. COTTRELL. The strengths of chemical bonds. 2nd ed. Butterworths, London. 1958.
16. G. HERZBERG. Can. J. Phys. **39**, 1511 (1961).
17. H. A. SKINNER. Modern aspects of thermochemistry. Royal Institute of Chemistry, London. 1959.
18. P. G. MASLOV and YU. P. MASLOV. Khim. i Teckhnol. Topliv i Masel, **3** (10), 50 (1958); Chem. Abstr. **53**, 1910h (1959).
19. G. B. KISTIAKOWSKY and E. R. VANARTSDALEN. J. Chem. Phys. **12**, 469 (1944).
20. G. P. SEMELUK and R. B. BERNSTEIN. J. Am. Chem. Soc. **79**, 46 (1957).
21. F. P. LOSSING, K. U. INGOLD, and I. H. S. HENDERSON. J. Chem. Phys. **22**, 621 (1954).
22. J. D. MORRISON and A. J. C. NICHOLSON. J. Chem. Phys. **20**, 1021 (1952).
23. D. P. STEVENSON and J. A. HIPPLE. J. Am. Chem. Soc. **64**, 2766 (1942).
24. K. WATANABE, T. NAKAYAMA, and J. MOTTL. Final report on ionization potentials of molecules by a photoionization method. University of Hawaii. December 1959.

THE DISULPHONATION OF 2,6- AND 2,7-DI-*t*-BUTYLNAPHTHALENE

MARCEL MENARD, DENNIS AWANG, AND FRANCIS L. CHUBB
Research Laboratories, Frank W. Horner Limited, Montreal, Que.

Received March 21, 1962

ABSTRACT

It has been found that both 2,6- and 2,7-di-*t*-butylnaphthalene form the same disulphonic acid when treated with 2 molar equivalents of chlorosulphonic acid. It is suggested that this acid is 2,6-di-*t*-butylnaphthalene-4,8-disulphonic acid. The evidence, including the n.m.r. spectrum, on which the proposed structure is based is presented.

In a previous paper (1) it was shown that sulphonation of 2,6- and 2,7-di-*t*-butylnaphthalene (I and II) with 1 molar equivalent of chlorosulphonic acid gave high yields of the corresponding 4-sulphonic acids. It has now been found that I and II behave differently when treated with 2 molar equivalents of chlorosulphonic acid. From I a disulphonic acid, III, was obtained in high yield, whereas from II two products were obtained—a neutral product, 2,7-di-*t*-butylnaphthalene-4-sulphonyl chloride, and the disulphonic acid III. Thus in one of the above reactions a rearrangement must have occurred.

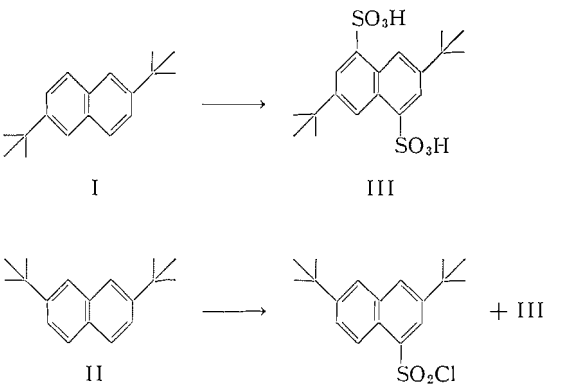

The structure of the disulphonic acid III, shown as 2,6-di-*t*-butylnaphthalene-4,8-disulphonic acid, was assigned from the following considerations. The ease of formation of III from I, as well as the fact that the ultraviolet absorption spectrum of the dimethyl ester of III was similar to that of ethyl 2,6-di-*t*-butylnaphthalene-4-sulphonate and different from that of ethyl 2,7-di-*t*-butylnaphthalene-4-sulphonate (Fig. 1), indicated that III was a 2,6-di-*t*-butylnaphthalene derivative. Since the low-temperature disulphonation of naphthalene yields the 1,5- (or 4,8-) disulphonic acid (2, 3) and since the 4 and 8 positions in I are the only available positions free of steric hindrance, it was believed that the sulphonic acid group entered these positions. Finally, the n.m.r. spectrum of the dimethyl ester of III (Fig. 2) was in excellent agreement with the proposed structure. The spectrum showed peaks at 510 and 534 c.p.s., due to the aromatic protons. These protons, occupying meta positions, revealed characteristic two-cycle coupling. The protons in the α position of the naphthalene nucleus, being less shielded, showed resonance lines at 534 c.p.s., while those located between the methyl sulphonate and *t*-butyl groups, being

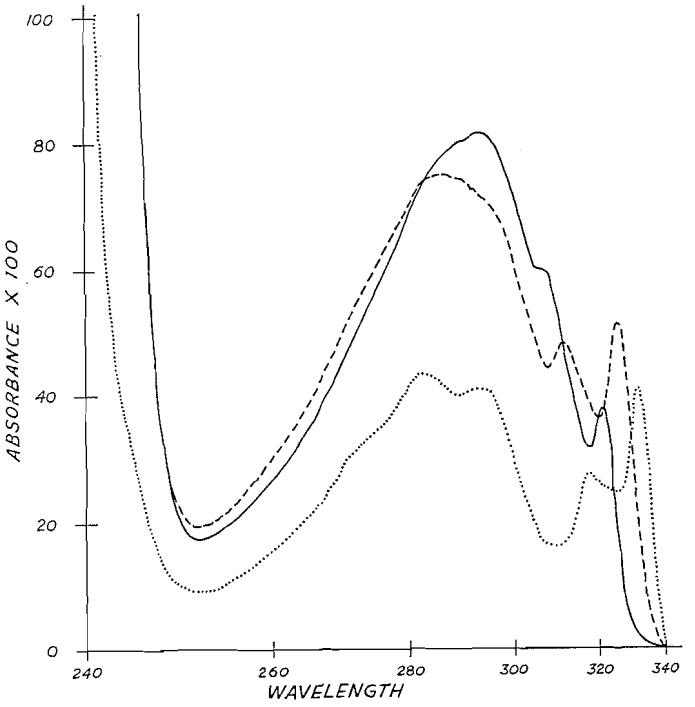

FIG. 1. The ultraviolet absorption spectra of: ethyl 2,7-di-*t*-butylnaphthalene-4-sulphonate (——) in methanol solution; ethyl 2,6-di-*t*-butylnaphthalene-4-sulphonate (- - -) in methanol solution; and dimethyl 2,6-di-*t*-butylnaphthalene-4,8-disulphonate (· · ·) in chloroform solution.

more shielded, showed resonance lines at 510 c.p.s. The spectrum would fit the isomeric dimethyl 1,5-di-*t*-butylnaphthalene-3,7-disulphonate (IV) equally well but this structure seems very unlikely. Apart from the evidence of the ultraviolet spectra it would require the shift of both *t*-butyl groups in both sulphonation reactions to relatively more hindered positions.

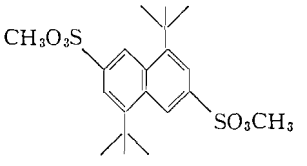

IV

Thus the disulphonation of 2,7-di-*t*-butylnaphthalene is accompanied by the rearrangement of one of the *t*-butyl groups. This may be a new example of the well-known Jacobsen rearrangement, although no evidence in favor of any particular mechanism has been obtained.

EXPERIMENTAL

Melting points are uncorrected. Ultraviolet absorption spectra were measured on a Beckman Model DK 2 recording spectrophotometer. Microanalyses were performed by E. Thommen, Thannerstrasse 45, Switzerland, and Dr. Claude Daesslé, 5757 Decelles, Montreal, Que.

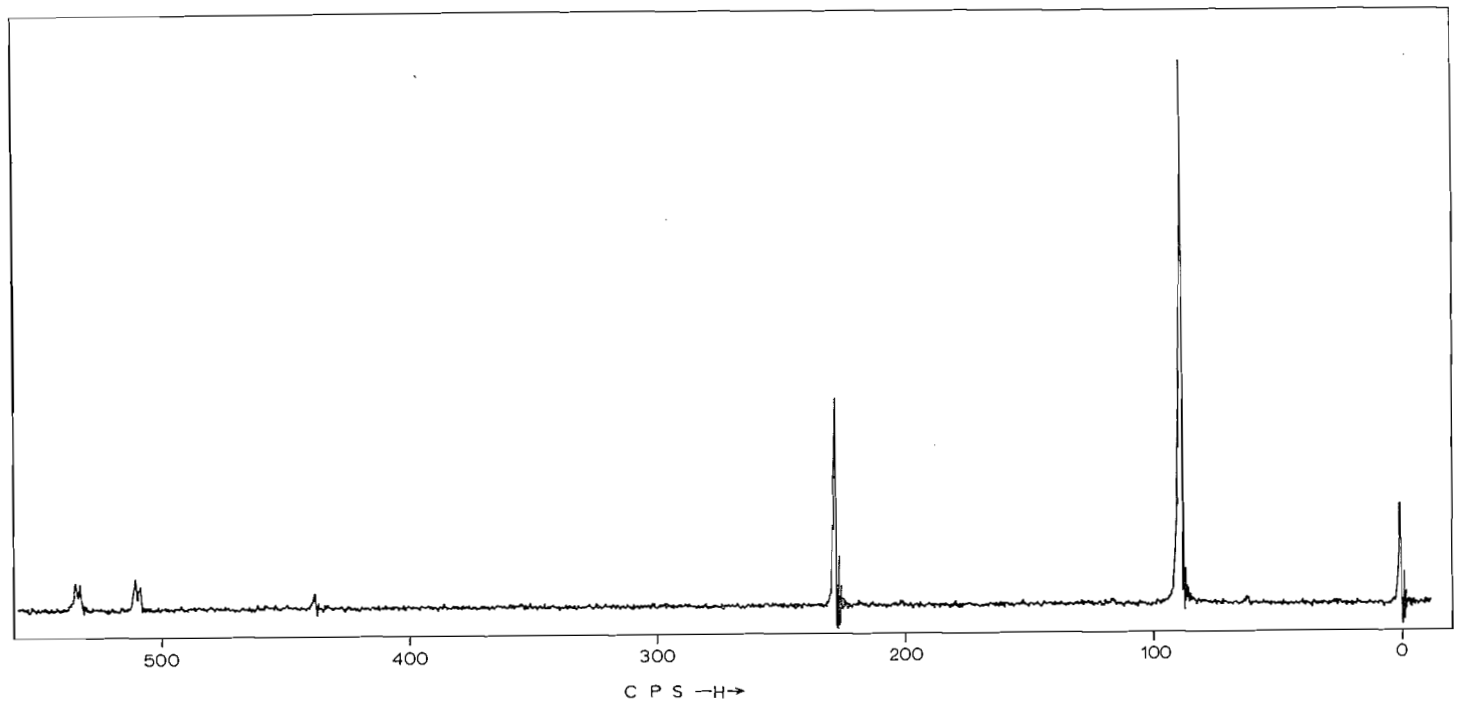

FIG. 2. The n.m.r. spectrum of dimethyl 2,6-di-*t*-butylnaphthalene-4,7-disulphonate in $CDCl_3$ solution with tetramethylsilane as the internal reference.

2,7-Di-t-butylnaphthalene (II)

A mixture of sodium 2,7-di-*t*-butylnaphthalene-4-sulphonate monohydrate (256 g) (1), water (100 ml), and concentrated sulphuric acid (750 g) was heated in an oil bath at 200–210° C and steam-distilled. Filtration of the distillate and recrystallization of the solid from ethanol gave 133 g (80%) of the hydrocarbon, m.p. 102–103° C (4).

2,6-Di-t-butylnaphthalene-4,8-disulphonic Acid (III)

To a stirred and cooled slurry of 2,6-di-*t*-butylnaphthalene (10 g, 0.042 mole) (4) in carbon tetrachloride (25 ml), chlorosulphonic acid (10.8 g, 0.094 mole) was added dropwise so that the temperature was maintained below 5°. The mixture was then stirred at room temperature for 2 hours and the white precipitate filtered and washed with petroleum ether. Recrystallization from acetic acid gave 14.4 g (86%) of the crude disulphonic acid III, m.p. 204° decomp. (5). Further recrystallization from acetic acid raised the melting point to 264–266°. No sulphonyl chloride could be isolated from the combined filtrates, the only contaminant being the corresponding monosulphonic acid (1). Analysis: Calc. for $C_{18}H_{24}O_6S_2.H_2O$ (418.52): C, 51.65; H, 6.26; S, 15.32%. Found: C, 52.03; H, 6.12; S, 15.42%. Neut. equiv.: Calc.: 209.3. Found: 209.9.

Dimethyl ester (from diazomethane).—M.p. 248–250°. Analysis: Calc. for $C_{20}H_{28}O_6S_2$ (428.56): C, 56.05; H, 6.59; S, 14.96%. Found: C, 56.30; H, 6.70; S, 15.00%. Ultraviolet spectrum ($CHCl_3$): maxima at 283, 317, and 331 mμ (ϵ = 635, 405, and 595). N.M.R. spectrum: peaks at 535, 533, 511, 509, 238, and 88 c.p.s.

Disulphonyl chloride.—Prepared by the method of Bosshard *et al.* (6), m.p. 260–263°. Analysis: Calc. for $C_{18}H_{22}O_4S_2Cl_2$ (437.40): C, 49.42; H, 5.07; S, 14.66%. Found: C, 49.98; H, 5.33; S, 14.34%.

Sulphonation of 2,7-Di-t-butylnaphthalene

Pure 2,7-di-*t*-butylnaphthalene (10 g) was treated, as described for the 2,6-isomer, with 2.2 molar equivalents of chlorosulphonic acid. Recrystallization of the solid gave pure 2,6-di-*t*-butylnaphthalene-4,8-disulphonic acid (8.5 g, 30%). The identity of this material with the dibasic acid described above was ascertained by a comparison of melting points and ultraviolet spectra.

Concentration of the combined filtrates and extraction of the solid residue with boiling ligroin (2×100 ml) gave 7.5 g (31%) of 2,7-di-*t*-butylnaphthalene-4-sulphonyl chloride, m.p. 167–169°, undepressed on admixture with an authentic sample (1).

ACKNOWLEDGMENT

The authors wish to thank Dr. N. S. Bhacca of Varian Associates, who obtained and analyzed the n.m.r. spectrum for us.

REFERENCES

1. M. MENARD, L. MITCHELL, J. KOMLOSSY, A. WRIGLEY, and F. L. CHUBB. Can. J. Chem. **39**, 729 (1961).
2. A. CORBELLINI. Giorn. chim. ind. ed appl. **9**, 118 (1927).
3. H. E. FIERZ-DAVID and A. W. HASLER. Helv. Chim. Acta, **6**, 1133 (1923).
4. C. C. PRICE, H. M. SHAFER, M. F. HUBERT, and C. BERNSTEIN. J. Org. Chem. **7**, 517 (1942).
5. H. KASPAREK and K. PFROEPFER. Ger. Patent No. 1,057,105 (May 14, 1959).
6. H. H. BOSSHARD, R. MORY, M. SCHMID, and HCH. ZOLLINGER. Helv. Chim. Acta, **42**, 1653 (1959).

SYNTHESIS OF CARBON-14 LABELED DEOXYRIBONUCLEOSIDES[1]

D. L. WILLIAMS
Los Alamos Scientific Laboratory, University of California, Los Alamos, New Mexico
Received May 10, 1962

ABSTRACT

The enzymatic transfer of deoxyribose from a purine or a pyrimidine deoxyriboside to a carbon-14 labeled purine or pyrimidine base affords an efficient means of preparing labeled deoxyribonucleosides. Deoxyadenosine-8-C^{14}, deoxyguanosine-8-C^{14}, deoxycytidine-2-C^{14}, and thymidine-2-C^{14}, with the natural β-configuration, were prepared in good yields and isolated in radiochemically pure form by large-scale paper chromatography.

INTRODUCTION

Carbon-14 labeled deoxyribonucleosides are not, as yet, commercially available. Strictly chemical syntheses of 2′-deoxyribosides (*a*) by the reduction at C2′ of ribofuranosylpurines (1) and -pyrimidines (2, 3); (*b*) through condensation of acylated 2-deoxyribosyl halides with suitably substituted purines (4–6) and pyrimidines (7); or (*c*) by the direct condensation of 2-deoxyribose with purines and pyrimidines catalyzed by polyphosphoric acid ester (8) are, in general, attended by requirements for difficultly obtainable intermediates, low yields, or the formation of both the α- and β-anomers. The β-anomer is the desired natural product.

In terms of high yields of solely the desired β-anomer and probable time consumption, enzymatic methods of synthesis appear much more of interest than the above chemical methods. The phosphorylase enzymes (9–13) give excellent yields of deoxyribosides from deoxyribose-1-phosphate and certain purines and pyrimidines, but the enzyme from a given tissue and species of organism is too specific and a number of enzyme preparations would be required to obtain the desired products. The *trans-N*-glycosidase first described by MacNutt (14), which was more specifically named *trans-N*-deoxyribosylase and further characterized by Roush and Betz (15), appeared to be the enzyme of choice, since it is nonspecific and transfers 2-deoxyribose from any deoxyriboside to a new purine or pyrimidine base, according to the following equilibrium:

$$\text{base}_1 + \text{base}_2 \text{ deoxyriboside} \rightleftarrows \text{base}_2 + \text{base}_1 \text{ deoxyriboside}.$$

This communication describes the enzymatic synthesis and isolation of 2′-deoxyadenosine-8-C^{14} (I), 2′-deoxyguanosine-8-C^{14} (II), 2′-deoxycytosine-2-C^{14} (III), and thymidine-2-C^{14} (IV).

EXPERIMENTAL

Carbon-14 Assays

Radiochemical yields were determined, with a Tri-Carb spectrometer,* by liquid scintillation counting of suitable aliquots in 15 ml of a dioxane system (naphthalene, 125 g/l.; 2,5-diphenyloxazole (PPO), 7.5 g/l.; and 2,2′-*p*-phenylenebis-(5-phenyloxazole) (POPOP), 0.375 g/l.) (16).

Paper Chromatography

Reaction mixtures were separated by chromatography on 18×44-in. sheets of Whatman No. 3 paper, and the chromatograms were developed with Hems' (17) solvent (85% saturated ammonium bicarbonate) in a combined descending and ascending manner. The paper was attached at both ends to supports in a

[1]*Work performed under the auspices of the U.S. Atomic Energy Commission.*
**Model 314EX, Packard Instrument Company, Inc., LaGrange, Illinois.*

Chromatocab. This procedure gave good separation of all components, including the pairs thymine–thymidine and cytosine–deoxycytidine. Upon rechromatography of aliquots of the isolated products on $1\frac{1}{2}\times44$-in. strips of Whatman No. 3 MM paper, only one ultraviolet-absorbing spot was observed, in each case. The only radioactivity which was observed with a windowless gas-flow strip scanning device* was concentrated in these spots.

R_f values for the compounds encountered in this work are shown in Table I.

TABLE I

Paper chromatography of purine and pyrimidine bases and their deoxyribosides

Compound	R_f value	Compound	R_f value
Adenine	0.36	Deoxyadenosine	0.51
Guanine	0.39	Deoxyguanosine	0.62
Cytosine	0.72	Deoxycytidine	0.77
Thymine	0.72	Thymidine	0.81

NOTE: Paper, Whatman No. 3. Solvent, 85% saturated ammonium bicarbonate.

Enzymes

trans-N-Deoxyribosylase enzyme was extracted from sonically disrupted *Lactobacillus helveticus* (ATCC 12046) bacteria with 0.1 *M* phosphate buffer (pH 6) and was partially purified, through the first ammonium sulphate precipitation step, as described by Roush and Betz (15). The protein which precipitated between 35% and 70% of saturation was redissolved in distilled water and dialyzed against distilled water at 4° C until free of sulphate ion. The final solution contained 6 mg of protein per ml, as determined by the method of Lowry *et al.* (18).

An auxiliary enzyme, xanthine oxidase, was prepared from fresh, whole cream according to the procedure of Horecker and Heppel (19). Oxidase activity was determined spectrophotometrically with hypoxanthine as substrate. The uric acid produced absorbs strongly at 293 mμ, and there is no interference from purines or pyrimidines or their deoxyribosides at this wavelength.

The specific activity of the transferase enzyme was also determined spectrophotometrically by a modification of the auxiliary enzyme procedure of Kalckar (20). In the transfer reaction between deoxyadenosine and hypoxanthine to form deoxyinosine, the rate of disappearance of hypoxanthine was measured with xanthine oxidase. At a hypoxanthine concentration of 101.3 μg/ml and a molar ratio of deoxyriboside to free purine base of 5 to 1 in pH 6.1 phosphate buffer at 37° C, the initial rate of disappearance of hypoxanthine was 13.13 μmoles per mg of protein per hour. These conditions were similar to those anticipated in subsequent synthesis experiments.

Transfer Reactions

(a) Deoxyadenosine-8-C^{14} (I)

A solution of adenine-8-C^{14} (300 μc, sp. act. 8.5 mc/mmole) and thymidine (42.8 mg, 0.1765 mmole) in 25 ml of 0.1 *M* phosphate buffer (pH 6.1) was incubated with 1 ml of enzyme solution at 37° C for 2 hours. The solution was overlaid with 5 drops of toluene to prevent bacterial growth. At the end of the incubation period, the solution was heated in boiling water for 5 minutes to denature the enzyme, cooled in ice, filtered, and chromatographed. The buffer salts, which moved with the solvent front, did not interfere with the complete separation of adenine-8-C^{14} and deoxyadenosine-8-C^{14}. The radioactive, ultraviolet-absorbing bands of residual adenine-8-C^{14} and the deoxyadenosine-8-C^{14} were cut from the large sheets and eluted with dilute ammonium hydroxide. The radiochemical yield of pure product was 91.4%; 2.7% of the initial adenine-8-C^{14} was also recovered. The results are shown in Table II.

Both the thymine and thymidine bands on the chromatogram were radioactive. The total activity in the two bands was 5.62 μc. This finding suggests that the commercial adenine-8-C^{14}, which is obtained from biologically labeled DNA, contained a small amount of C^{14}-thymine.

(b) Deoxyguanosine-8-C^{14} (II)

Guanine-8-C^{14} (300 μc, sp. act. 9.8 mc/mmole) was suspended in 100 ml of deionized water and heated in a boiling-water bath to dissolve as much of the guanine as possible. To the resulting suspension at 37° C was added 25 ml of 0.1 *M* phosphate buffer (pH 6.1), thymidine (37.1 mg, 0.153 mmole), and 1 ml of enzyme solution. A few drops of toluene were added, and the mixture was magnetically stirred in a stoppered flask for 24 hours at 37° C. After 24 hours, some guanine-8-C^{14} was still undissolved; 1 ml of enzyme solution was added, and incubation was continued an additional 24 hours with stirring. The reaction mixture was heated in boiling water for 7 minutes to coagulate protein and cooled to room temperature. The mixture was then desalted, prior to chromatography, by adsorption of the organic components on a mixture of 80-mesh

**Model D-47, Chicago-Nuclear Corporation, Chicago, Illinois.*

TABLE II

Enzymatic synthesis of carbon-14 labeled deoxyribonucleosides

Purine or pyrimidine						Deoxyriboside			
	C^{14} activity						C^{14} activity		
	Initial	Residual		Deoxy-ribose donor*	Time, hr	Product	Yield, μc	% of initial	% of recov-ered‖
Base	μc	μc	% of initial						
Adenine-8-C^{14}	300	8.1	2.7	t	2	I	274	91.4†	97.2
Guanine-8-C^{14}	300	21.6	7.2	t	48	II	240	80.0‡	91.8
Cytosine-2-C^{14}	300	146.0	49.4	a	6	III	132	44.0	47.5
	146.0	69.7	47.8	a	6		67.8	46.5	49.4
	69.7	35.1	50.4	a	6		33.0	47.3	48.3
	35.1	17.7	50.5	a	2		17.0	48.3	48.9
Thymine-2-C^{14}	300	166.8	55.6	a	2	IV	98.4	32.8‡	36.6
	166.8	109.0	65.4	a	6		46.2	27.7§	29.1
	109.0	68.8	63.2	a	6		38.0	34.9	35.6
	68.8	43.0	62.2	a	6		25.5	37.0	37.2
	43.0	26.9	62.5	a	6		15.7	36.4	36.8

*Abbreviations used are: thymidine, t; deoxyadenosine, a.
†Phosphate buffer salts not removed prior to chromatography.
‡Phosphate buffer salts removed prior to chromatography.
§Buffer was not used in this and subsequent thymidine runs.
‖This is percentage of activity recovered in the residual base and the deoxyriboside formed.

Fishers' activated charcoal (1 g) and Celite (1 g). The charcoal bed was washed free of phosphate ion with three 10-ml portions of distilled water.* The purines and deoxyribosides were eluted with 50% aqueous ethanol containing 5% pyridine (by volume). The eluate (ca. 1500 ml) was concentrated to ca. 30 ml on a rotary vacuum evaporator at 35° C. The components of the mixture were then separated by chromatography, as described above. The radiochemical yield of pure product was 80%; 7.2% of the initial guanine-8-C^{14} was also recovered. The results are given in Table II.

The thymine and thymidine bands, which were both radioactive, were eluted together and rechromatographed. When the two bands were eluted and assayed, the thymine contained 2.34 μc of activity and the thymidine contained 4.16 μc. As in the adenine-8-C^{14} case above, the guanine-8-C^{14} apparently contained C^{14}-thymine.

(c) Deoxycytidine-2-C^{14} (III)

A solution of cytosine-2-C^{14} (300 μc, sp. act. 5.07 mc/mmole) and deoxyadenosine (74.3 mg, 0.296 mmole) in 25 ml of distilled water was adjusted to pH 5.8 with carbon dioxide. One milliliter of enzyme solution and 5 drops of toluene were added, and the solution was incubated at 37° C for 6 hours. The reaction mixture was then heated in boiling water for 5 minutes, cooled in ice, filtered, and chromatographed as described above. As shown in Table II, it was necessary to treat the residual cytosine-2-C^{14} several times in this manner in order to approach quantitative conversion to the deoxyriboside. The total radiochemical yield of pure product was 83.3%; 11.7% of the initial cytosine-2-C^{14} was also recovered.

The pooled deoxyadenosine from all the deoxycytidine runs contained 5.16 μc of radioactivity, which was probably cytosine-2-C^{14}, since the adenine was not active.

(d) Thymidine-2-C^{14} (IV)

A solution of thymine-2-C^{14} (300 μc, sp. act. 5.0 mc/mmole) and deoxyadenosine (75.5 mg, 0.3 mmole) in 25 ml of 0.1 *M* phosphate buffer (pH 6.1) was incubated with 1 ml of enzyme solution for 2 hours. The reaction mixture was heated, cooled, and desalted, as described for II above, prior to chromatography. As illustrated in Table II, it was necessary to treat the residual thymine-2-C^{14} several times to effect a high degree of conversion to deoxyriboside. In the second thymidine run (Table II), the reaction was run in distilled water, but the pH was 6.7 due to a trace of residual ammonium bicarbonate. This is higher than the enzyme pH optimum of 5.8 (15), and apparently the 2-hour incubation was too short for equilibrium to be established. Subsequently, the reaction was run 6 hours in distilled water adjusted to pH 5.8–6 with carbon dioxide. The total radiochemical yield of pure product was 74.6%; 9% of the initial thymine-2-C was also recovered.

The pooled deoxyadenosine from all the thymidine runs contained 11.9 μc of radioactivity. This activity is probably all due to thymine-2-C^{14}, since the adenine was free of activity.

**The filtrate and washings contained 3.1 μc of C^{14} activity, which was not absorbed on an additional 1 g of charcoal.*

DISCUSSION

The *trans-N*-deoxyribosylase enzyme offers an efficient means of obtaining labeled deoxyribosides, with the natural configuration, providing the labeled bases or a deoxyriboside with the label in the deoxyribose moiety are available. Since the enzyme has no requirement for phosphate, the transfer reaction can be run in neutral aqueous medium or one adjusted with carbon dioxide to the optimum pH of 5.8, thus eliminating the need for a desalting step prior to chromatography.

Although guanine is only slightly soluble in a neutral or slightly acidic (pH 6) aqueous medium, high yields of deoxyguanosine are obtained by stirring a suspension of guanine in thymidine solution for an extended reaction period. Guanine dissolves as the reaction proceeds.

As indicated by the work of Roush and Betz (15), at equilibrium, in a reaction mixture containing the enzyme, a purine, a pyrimidine, and their deoxyribosides, the reaction rates greatly favor the formation of purine deoxyriboside. Therefore, thymidine is an excellent donor of deoxyribose in the preparation of labeled deoxyadenosine and deoxyguanosine. Comparison of the concentrations of deoxycytidine and thymidine in equilibrium with deoxyadenosine (Table II) and the equilibrium data of Roush and Betz (15) suggests that a pyrimidine deoxyriboside as deoxyribose donor would afford higher yields of labeled thymidine or deoxycytidine than does deoxyadenosine. However, separation of the resulting four-component mixture by paper chromatography or by cellulose column chromatography would be extremely difficult because of the narrow spread in R_f values for most solvents. In any case, it appears that several successive treatments of the pyrimidine bases are required in approaching quantitative conversion to their deoxyribosides.

ACKNOWLEDGMENT

The author is grateful to Dr. I. U. Boone of this laboratory for the *Lactobacillus helveticus* bacteria used in this work and for assistance and technical advice in the preparation of the *trans-N*-deoxyribosylase enzyme.

REFERENCES

1. C. D. Anderson, L. Goodman, and B. R. Baker. J. Am. Chem. Soc. **81**, 3967 (1959).
2. G. Shaw and R. N. Warrener. J. Chem. Soc. 50 (1959).
3. D. M. Brown, D. B. Parihar, C. B. Reese, and A. Todd. J. Chem. Soc. 3035 (1958).
4. H. Venner. Ber. **93**, 140 (1960).
5. R. K. Ness and H. G. Fletcher, Jr. J. Am. Chem. Soc. **82**, 3434 (1960).
6. C. Pedersen and H. G. Fletcher, Jr. J. Am. Chem. Soc. **82**, 5211 (1960).
7. M. Hoffer, R. Duschinsky, J. J. Fox, and N. Yung. J. Am. Chem. Soc. **81**, 4112 (1959).
8. G. Schramm, H. Grötsch, and W. Pollmann. Angew. Chem. **73**, 619 (1961).
9. H. M. Kalckar. J. Biol. Chem. **167**, 477 (1947).
10. M. Friedkin and H. M. Kalckar. J. Biol. Chem. **184**, 437 (1950).
11. M. Friedkin. Federation Proc. **11**, 216 (1952).
12. M. Friedkin and D. Roberts. J. Biol. Chem. **207**, 257 (1954).
13. L. A. Manson and J. O. Lampen. J. Biol. Chem. **193**, 539 (1951).
14. W. S. MacNutt. Biochem. J. **50**, 384 (1952).
15. A. H. Roush and R. F. Betz. J. Biol. Chem. **233**, 261 (1958).
16. D. G. Ott, F. N. Hayes, and T. T. Trujillo. Los Alamos Scientific Laboratory Report LAMS-2445. 1960. p. 213.
17. G. Hems. Arch. Biochem. Biophys. **82**, 484 (1959).
18. O. H. Lowry, N. J. Rosebrough, A. L. Farr, and R. J. Randall. J. Biol. Chem. **193**, 265 (1951).
19. B. L. Horecker and L. A. Heppel. *In* Methods in enzymology. Vol. II. Academic Press, Inc., New York. 1955.
20. H. M. Kalckar. J. Biol. Chem. **193**, 265 (1951).

ISOTOPIC COMPOSITION OF RADIOLYTIC HYDROGEN EVOLVED FROM MIXTURES OF BENZENE AND CYCLOHEXANE WITH THEIR DEUTERATED ANALOGUES[1]

P. J. DYNE AND W. M. JENKINSON
Research Chemistry Branch, Atomic Energy of Canada Limited, Chalk River, Ontario

Received May 16, 1962

ABSTRACT

We have measured the isotopic composition of radiolytic hydrogen evolved from mixtures of benzene and cyclohexane with their deuterated analogues. The data are interpreted in terms of first-order processes of the kinetic form (for C_6D_{12}) $C_6D_{12} \rightarrow C_6D_{10} + D_2$ and second-order processes $C_6D_{12} \rightarrow X_D + R$, $X_D + C_6H_{12} \rightarrow HD + R$.

A complete kinetic analysis for the system C_6D_6–C_6H_6 has been made from measurements at the two ends of the concentration range. This gives a satisfactory prediction of the isotopic composition of hydrogen evolved from an equimolar C_6H_6–C_6D_6 mixture. A first-order yield of D_2 is found in solutions of C_6D_{12} in benzene which persists to 'zero' C_6D_{12} concentration. The mechanisms of the first-order process studied in these experiments, and of the 'unscavengeable' or 'molecular' yields of radiolytic hydrogen, are discussed.

INTRODUCTION

Studies (1–3) of the isotopic composition of hydrogen formed in the radiolysis of light and heavy hydrocarbons have shown the existence of two radiolytic processes: a decomposition in which both hydrogen atoms in the H_2 molecule come from the same hydrocarbon molecule,

$$RH \text{—}\sim\sim\rightarrow H_2 + \text{residue}, \qquad [1]$$

and a decomposition which occurs via a reactive intermediate X_H,

$$RH \text{—}\sim\sim\rightarrow X_H + \text{residue} \qquad [2]$$

$$X_H + RH \longrightarrow H_2 + \text{residue}, \qquad [3]$$

where the hydrogen atoms in the H_2 molecule come from two hydrocarbon molecules. We call the first 'the first-order process' since its existence is shown, in our experiments, by a yield of D_2 which is first order with respect to the concentration of the deuterated hydrocarbon. The second we call 'the second-order process' since the yield of D_2 formed by it has a second-order dependence on the concentration of the deuterated hydrocarbon.

The yield of the first-order process is calculated with the assumption that the amount of energy absorbed by the deuterated hydrocarbon is proportional to its mole fraction in the mixture. We have previously called the first- and second-order yields the 'unimolecular' and 'bimolecular' yields. The new terminology emphasizes the operational definition and avoids confusion in discussion.

In reference 3 we have described experiments on hydrocarbon mixtures in which the variation of the first-order yield with solvent demonstrates that the energy absorbed by the deuterated hydrocarbon is not determined simply by its mole fraction. The major part of this paper is concerned with mixtures of heavy and light benzene in which the deviations from the mixture law as described in reference 3 appear to be absent. Experiments on other mixtures of benzene and cyclohexane, variously deuterated, are also described.

[1]*Issued as A.E.C.L. No. 1416.*

EXPERIMENTAL

The experimental techniques have been previously described (1, 2). Cyclohexane-d_{12} and benzene-d_6 of >99% isotopic purity were obtained from Merck and Co; the isotopic composition was confirmed by mass spectrometric analysis.

Cyclohexane and benzene were Fisher Spectrograde. Benzene samples (~2 ml) were irradiated for 40 hours at a dose rate of $\sim 3\times10^{22}$ ev/l. hr to give 1–2 μmoles of gas.

KINETIC ANALYSIS

It is convenient to use the kinetic analysis given previously (1, 2). The following steps are proposed:

$$\left.\begin{array}{ll} C_H \rightsquigarrow H_2 + P & \text{yield } G_1(H) \\ C_D \rightsquigarrow D_2 + P & \text{" } G_1(D) \end{array}\right\} \text{first-order yields}$$

$$\left.\begin{array}{ll} C_H \rightsquigarrow X_H + P & \text{" } G_2(H) \\ C_D \rightsquigarrow X_D + P & \text{" } G_2(D) \end{array}\right\} \text{second-order yields}$$

$$\begin{array}{ll} X_H + C_H \rightarrow H_2 + P & \text{rate constant } k_1 \\ X_D + C_H \rightarrow HD + P & \text{" " } k_2 \\ X_H + C_D \rightarrow HD + P & \text{" " } k_3 \\ X_D + C_D \rightarrow D_2 + P & \text{" " } k_4 \end{array}$$

where C_H refers to the 'light' hydrocarbon and C_D to the 'heavy', i.e. completely deuterated, hydrocarbon.

We have shown that when $C_H \gg C_D$ (1, 2) and putting $C_D/C_H = F$:

$$G(D_2) = G_1(D)\times F + (k_4/k_2)\times G_2(D)\times F^2 \quad \text{(i)}$$

$$G(HD) = F[G_2(D) + (k_3/k_1)\times G_2(H)]. \quad \text{(ii)}$$

It can readily be shown that when $C_D \gg C_H$ the analogous equations hold where $F' = C_H/C_D$:

$$G(H_2) = G_1(H)\times F' + (k_1/k_3)\times G_2(H)\times F'^2 \quad \text{(iii)}$$

$$G(HD) = F'[G_2(H) + (k_2/k_4)\times G_2(D)]. \quad \text{(iv)}$$

In equation (i) the second term is considerably smaller than the first and $G_1(D)$ can be obtained from the slope of the line obtained by plotting $G(D_2)$ vs. F. Alternatively, the function $G(D_2)/F$ can be plotted against F when $G_1(D)$ is obtained as the intercept of $G(D_2)/F$ when $F = 0$. This is the graphical method given in reference 1. The values of the bracketed terms in equations (ii) and (iv) are the slopes of the plot of $G(HD)$ vs. C_D/C_H and C_H/C_D respectively. We have defined (2) the slope of (ii) as

$$g(HD) = G_2(D) + (k_3/k_1)G_2(H). \quad \text{(v)}$$

We now define

$$g'(HD) = G_2(H) + (k_2/k_4)G_2(D). \quad \text{(vi)}$$

This analysis contains six independent quantities, $G_1(H)$, $G_2(H)$, $G_1(D)$, $G_2(D)$, k_3/k_1, and k_2/k_4. Noting that, for the pure compounds C_H and C_D, $G(H_2) = G_1(H) + G_2(H)$ and $G(D_2) = G_1(D) + G_2(D)$, measurements of $G_1(D)$ and $G_1(H)$ using equations (i) and (iii) and measurements of $g(HD)$ and $g'(HD)$ will determine all six quantities.

MIXTURES OF C_6H_6 AND C_6D_6

In this system all the constants in our kinetic analysis have been established using data obtained at both ends of the concentration range. Within our experimental precision no very large interactions occur in this mixture or in other mixtures of aromatic hydrocarbons (3). Small positive deviations in G(total hydrogen) are observed from that predicted on the basis of a simple mixture law: these differ in sign from deviations reported by Gordon and Burton (4), who made the first studies on this system.

(a) Mixtures where $C_6H_6 \gg C_6D_6$

Data on the isotopic composition of hydrogen evolved from benzene (C_6H_6) containing small amounts of C_6D_6 are given in Table I. The yields are shown in Fig. 1. A plot of $G(D_2)/F$ gives an intercept:

$$G_1(D) = (3.2 \pm 0.4) \times 10^{-3}, \qquad (C_6H_6 \gg C_6D_6)$$

TABLE I

Isotopic composition of hydrogen from C_6H_6–C_6D_6 mixtures
($C_H \gg C_D$)

Mole% C_6D_6	$F = C_6D_6/C_6H_6 \times 10^2$	G(hydrogen)	% HD	% D_2	$G(HD) \times 10^3$	$G(D_2) \times 10^3$	$\frac{G(D_2)}{F} \times 10^3$
2.43	2.45	0.037	1.97	0.23	0.73	0.08_5	3.46
4.74	4.97	0.037_5	3.80	0.45	1.42	0.16_8	3.38
6.99	7.20	0.036_5	5.83	0.75	2.12	0.27_3	3.83
9.09	10.0	0.037	7.65	1.05	2.83	0.38_8	3.88

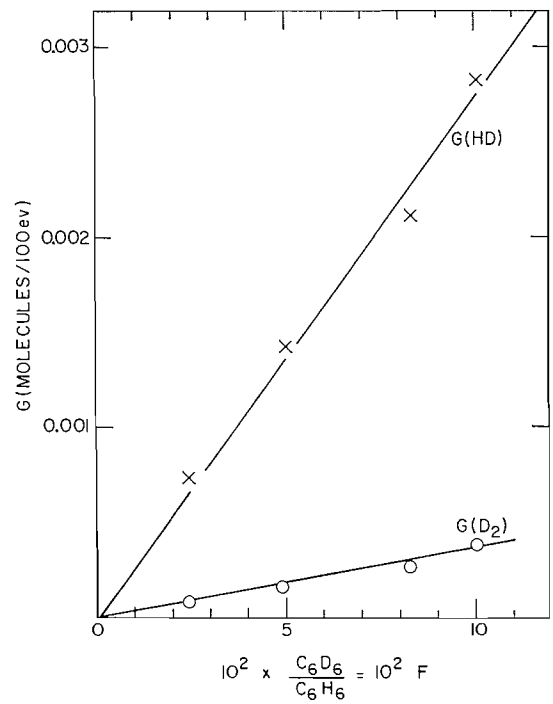

FIG. 1. Yields of HD and D_2 from dilute solutions of C_6D_6 in C_6H_6.

the uncertainty being derived from the intercepts of the extreme lines that could reasonably be drawn through the points.

Values of G(HD) are also shown in Fig. 1. The slope of G(HD) vs. C_6D_6/C_6H_6 gives

$$g(\mathrm{HD}) = k_3/k_1G_2(\mathrm{H})+G_2(\mathrm{D}) = 0.027.$$

(b) Mixtures where $C_6D_6 \gg C_6H_6$

Data on mixtures in which the heavy component is greatly in excess of the light component are given in Table II and are shown in Fig. 2. Since the major component is

TABLE II

Isotopic composition of gas from C_6H_6–C_6D_6 mixtures
($C_D \gg C_H$)

Mole% C_6H_6	$F' = C_6H_6/C_6D_6 \times 10^2$	G(hydrogen)	% HD	% H_2	G(HD) $\times 10^3$	$G(H_2)$ $\times 10^3$
0	0	0.0132	2.88	0	0.38	0
2.44	2.5	0.0143	10.02	3.28	1.43	0.47
2.44	2.5	0.0153	10.04	3.76	1.53	0.57
4.77	5.00	0.0164	14.57	6.18	2.38	1.01
4.77	5.00	0.0149	16.92	5.97	2.52	0.89
4.77	5.00	0.0160	15.65	6.49	2.50	1.04
4.77	5.00	0.0147	16.36	5.45	2.40	1.15
7.0	7.6	0.0183	20.80	9.06	3.80	1.65
9.1	10.0	0.0186	24.7	11.8	4.59	2.19

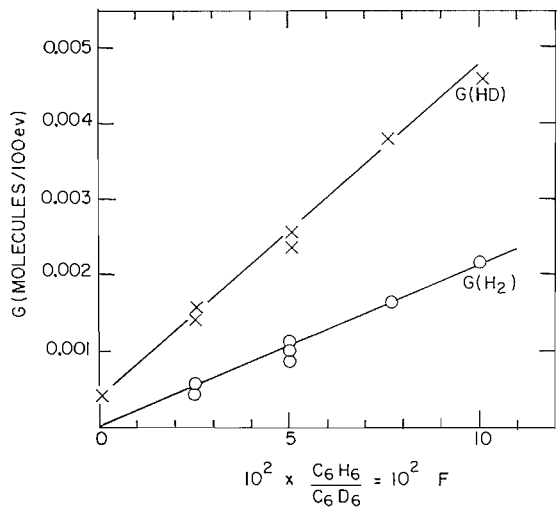

FIG. 2. Yields of HD and H_2 from dilute solutions of C_6H_6 in C_6D_6.

not isotopically pure this material gives gas containing 2.88% HD. The plot of G(HD) vs. mixture composition does not go through the origin: we have, however, taken g'(HD) to be the slope of this line. The mass spectrum of 'pure' D_2 contains about 1% of the D^+ ion, $m/e = 2$. The mass spectrometric results given in Table II have been corrected for this. In this connection we went to some trouble to avoid the accidental introduction of hydrogenous impurities into these samples. Rigorous exclusion of water vapor by handling materials and preparing samples in a 'dry' dry box and using 'Kel F' grease

(a perfluorinated hydrocarbon) in the vacuum lines made no noticeable difference to the amounts of H_2 or HD observed nor to the experimental scatter.

From these data we obtain

$$G_1(H) = 0.02 \pm 0.002 \qquad (C_6D_6 \gg C_6H_6)$$
$$g'(HD) = k_2/k_4G_2(D) + G_2(H) = 0.045.$$

(c) Mixtures where $C_6H_6 \sim C_6D_6$

Data on a few samples in the intermediate concentration region are given in Table III and plotted in Fig. 3. These data fit smoothly to the data given above for the two ends

TABLE III

Isotopic composition of hydrogen from C_6H_6–C_6D_6 mixtures ($C_H \sim C_D$)

Mole% C_6D_6	$G(H_2)$	G(HD)	$G(D_2)$	G(hydrogen)
20	0.0276	0.0052	0.00089	0.0337
50	0.0166	0.0102	0.00406	0.0308
80	0.00529	0.00777	0.00947	0.0225

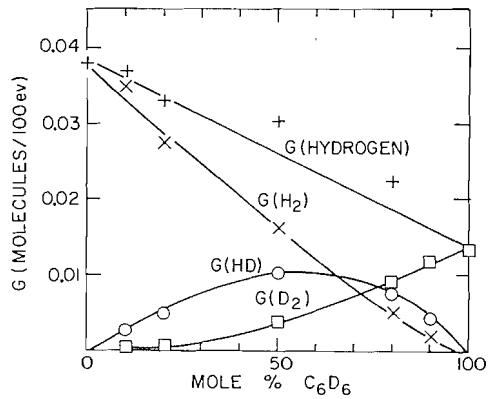

FIG. 3. Yields of H_2, HD, D_2, and total hydrogen from mixtures of C_6H_6 and C_6D_6.

of the concentration range. However, the values of G(hydrogen) = $G(H_2 + HD + D_2)$ differ significantly from the previously published data of Gordon and Burton (4), although there is good agreement in the percentage isotopic composition. At 50 mole% C_6D_6, for instance, we found G(hydrogen) = 0.03, whereas they report 0.02. The percentage composition we found was 53.8% H_2, 33.1% HD, and 13.1% D_2. They report 52.1% H_2, 33.1% HD, and 14.8% D_2. Our values of G(hydrogen) lie above the 'mixture line' for C_6H_6–C_6D_6 mixtures. Their results lie below the 'mixture line' and they concluded that C_6D_6 and C_6H_6 were in effect protecting one another. We have no explanation of this experimental discrepancy.

(d) Other Parameters of the System

Combining the values of G_1(H) and G_1(D) with the values of $G(H_2)$ and $G(D_2)$ we found for pure C_6H_6 and C_6D_6, viz.

$$G(H_2) = 0.038$$
$$G(D_2) = 0.0135,$$

and recalling that $G(H_2) = G_1(H)+G_2(H)$, $G(D_2) = G_1(D)+G_2(D)$, we find

$$G_2(H) = 0.018 \text{ and } G_2(D) = 0.01.$$

From the values of $g(HD)$ and $g'(HD)$ we find

$$k_3/k_1 = 0.95 \text{ and } k_2/k_4 = 2.7.$$

With the equations given above, these numbers can be used to calculate the isotopic composition of radiolytic hydrogen evolved from mixtures of any composition.

For a 50–50 mixture the calculated percentage composition is 56.5% H_2, 31.1% HD, and 12.1% D_2, which is in reasonable agreement with the observed compositions (see above). The calculated G(hydrogen) is 0.025, which is midway between the experimental results of Gordon and Burton and ourselves.

While this agreement in isotopic composition is satisfactory, it is probably not very significant since the kinetic analysis can be regarded as a curve-fitting procedure. As the parameters have been chosen to give a fit at the two ends of the composition range, it is not surprising that an interpolation at the midpoint of the composition is in good agreement with experiment.

MIXTURES OF C_6D_{12} AND C_6H_6

Data on mixtures of benzene with small amounts of cyclohexane-d_{12} are given in Table IV and plotted in Fig. 4. The dotted line, $G_0(H_2)\times$electron fraction, shows the

TABLE IV

Isotopic composition of hydrogen from C_6H_6–C_6D_{12} mixtures

Mole% C_6D_{12}	$F = C_6D_{12}/C_6H_6\times10^2$	G(hydrogen)	% HD	% D_2	$G(HD)\times10^3$	$G(D_2)\times10^3$	$G(D_2)/F$	$G(H_2)$
1.95	1.98	0.045_6	8.15	2.90	3.71	1.32	0.066	0.040_6
3.96	4.12	0.047_5	14.4	5.78	6.84	2.74	0.066	0.037_9
5.82	6.17	0.048_9	19.8	8.03	9.68	3.92	0.0635	0.035_3
7.60	8.22	0.052_7	23.7	10.61	12.48	5.58	0.072	0.034_6

decrease in $G(H_2)$ expected from simple dilution, neglecting any interactions such as the formation of HD. It can be seen that $G(D_2)$ is a linear function of the C_6D_{12} concentration and there is a finite first-order yield of D_2. For these mixtures

$$G_1(D) = 0.06\pm0.01 \qquad (C_6H_6 \gg C_6D_{12})$$
$$g(HD) = 0.17.$$

This first-order decomposition of C_6D_{12} in benzene is analogous to "$g_c(H_2)$", the unquenchable yield of H_2 from c-C_6H_{12}, which persists at "infinite benzene concentration", observed by Burton, Chang, Lipsky, and Reddy (5). This "unquenchable yield" was obtained by calculation from values of $G(H_2)$ in benzene–cyclohexane mixtures of the yield of H_2 from cyclohexane per 100 ev absorbed in the cyclohexane fraction. This yield, $g_c(H_2)$, extrapolated to 0.5 molecule/100 ev in pure benzene. While this yield is considerably greater than our value of $G_1(D)$ the experiments agree on the existence of this unquenched decomposition.

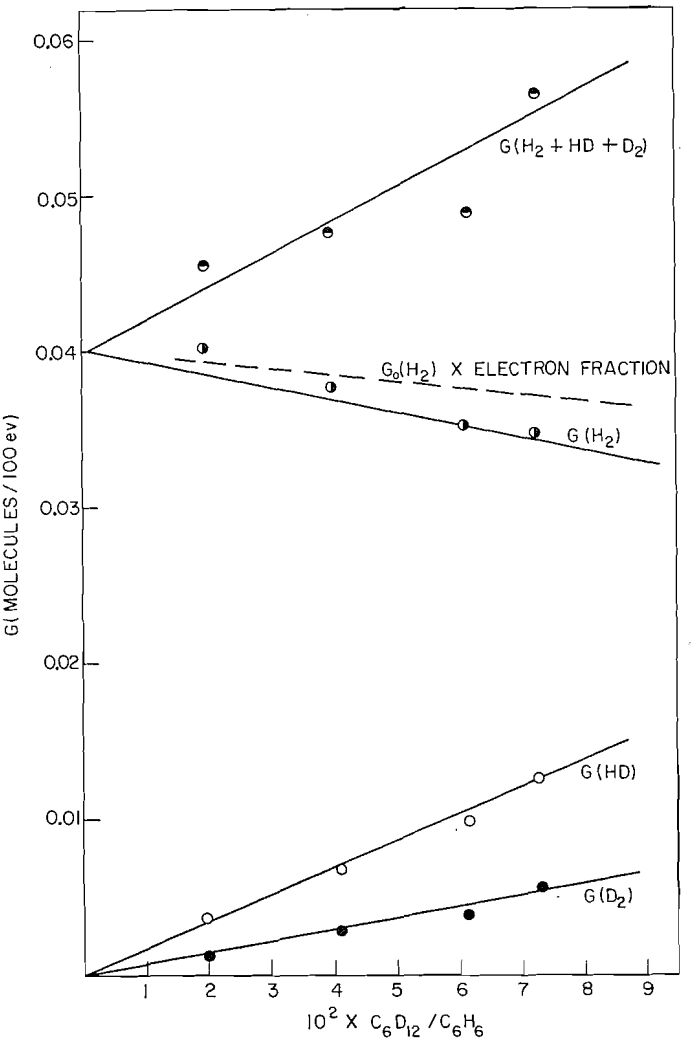

FIG. 4. Yields of HD, D_2, and total hydrogen from dilute solutions of C_6D_{12} in C_6H_6.

Burton and his co-workers suggest that this decomposition occurs via a precursor which cannot be quenched by benzene. It is not, however, necessary to make this assumption because the simple quenching scheme can lead to a finite yield. The sequence

$$C \sim\sim\sim\rightarrow C^x \text{ (yield } G) \qquad [4]$$

$$C^x \longrightarrow \text{products including hydrogen} \qquad [5]$$

$$C^x + B \longrightarrow \text{products excluding hydrogen,} \qquad [6]$$

where C ≡ cyclohexane, B ≡ benzene, leads to:

$$G(H_2) = \frac{GX_c}{1+k_6/k_5[B]},$$

where X_c is the mole fraction of cyclohexane. Burton's quantity $g_c(H_2)$ and our quantity $G_1(D)$ are both of the form $G(H_2)/X_c$. If $k_6/k_5 \sim 1$ and X_c is small (i.e. $[B] \rightarrow 10$ moles/liter) then $G/(1+k_6/k_5[B]) \sim G/10$, which is still a finite fraction of the yield in pure cyclohexane. From a more detailed analysis of the variation of $G(H_2)$ with composition Freeman (6) concluded that, at high benzene concentrations, the main interaction between benzene and the excited precursors C^x was a charge or energy-transfer step like [6] and that, in fact, $k_6/k_5 \sim 1$ ($k_6/k_5 \equiv k_3''/k_4''$ in Freeman's terminology). This correlation only shows, however, that similar kinetic treatments of the system lead to similar numerical values of the parameters.

At present it is only possible to make qualitative, comparative comments on the value of $g(HD)$. In solutions of c-C_6D_{12} in C_6H_6, $g(HD) = 0.17$, in solutions of C_6D_6 in C_6H_6 $g(HD) = 0.027$, so the deuterium atoms on a cyclohexane molecule are considerably more labile in benzene solutions than deuterium atoms on a benzene molecule.

MIXTURES OF C_6D_6 IN C_6H_{12}

The isotopic composition of hydrogen evolved from these mixtures has been previously studied by Burton and Patrick (7) and by Chang (8). In the present work more data were obtained in the low concentration range. These data are given in Table V and plotted in Fig. 5,

TABLE V

Mixtures of C_6D_6 with C_6H_{12}

Mole% C_6D_6	$F = C_6D_6/C_6H_{12} \times 10^2$	G(hydrogen)	% HD	% D_2	G(HD)	$G(D_2)$
0.51	0.512	4.14	0.36_6	—	0.015	—
1.17	1.18	4.04	0.63	—	0.0254	—
2.32	2.37	3.56	1.08	—	0.0384	—
4.63	4.85	3.07	1.86	—	0.057	—
23.4	—	1.204	7.54	0.29	0.091	0.003_4
54.8	—	0.390	18.78	1.84	0.074	0.007_7
82.92	—	0.106	33.56	10.93	0.034	0.109

together with some data for $G(HD)$ from C_6D_{12}–C_6H_{12} mixtures. The yield of HD from these solutions is not a linear function of C_6D_6 concentration, due mainly to the large reduction in G(hydrogen) on the addition of benzene. The initial slope of $G(HD)$, i.e. the limiting value of $g(HD)$ as $[C_6D_6] \rightarrow 0$, is 2.94 as measured from the lowest concentration point; conventional extrapolation techniques of the differential slope show that the limiting value may be as great as 3.5.

The experimental result is therefore

$$g(HD) \geqslant 2.9. \qquad (C_6H_{12} \gg C_6D_6)$$

The value of $g(HD)$ can only be subjected to a qualitative discussion. The main point of interest is that the value $g(HD) = 2.9$ where benzene-d_6 is the source of the D atoms in cyclohexane solutions is close to the value $g(HD) = 3.7$ (1, 2) where cyclohexane-d_{12} is the source of D atoms. The comparable reactivities of benzene and cyclohexane in this respect is somewhat surprising when one recalls the very low hydrogen yield from pure benzene. It must, however, be noted that in these solutions the absolute yield $G(HD)$ is a small fraction of the total hydrogen yield and is also a small fraction of the decrease in hydrogen yield from pure cyclohexane. At the lowest concentration of benzene-d_6,

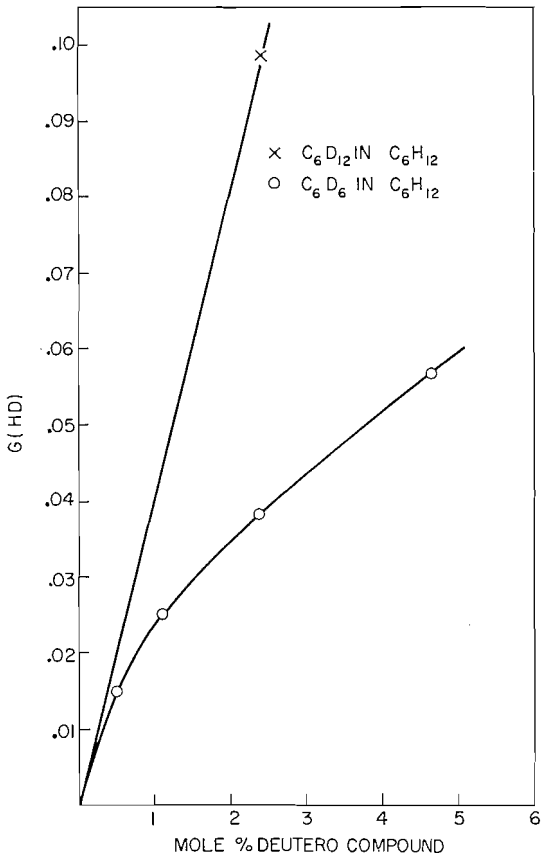

FIG. 5. Yields of HD from dilute solutions of C_6D_6 in C_6H_{12} and C_6D_{12} in C_6H_{12}.

$G(HD) \approx 0.015$, $\Delta G(\text{hydrogen}) \approx 1.4$, so there is a factor of the order of 100 between the efficiency (rate) of the abstraction reaction and that of the scavenging/quenching reactions which are responsible for the decrease in hydrogen yield.

A second point of interest is the variation of $G(D_2)$ at high benzene concentration: Burton and Patrick (7) reported that $G(D_2)$ is a linear function of mole% C_6D_6. Our results for D_2 yields plotted in Fig. 6 confirm this. We have also plotted values of $G(D_2)$ in C_6H_6–C_6D_6 mixtures, together with the extrapolated limiting slope measured at low C_6D_6 concentration which we have identified with $G_1(D)$. The measurements in cyclohexane solution show a linear slope such that $G_1(D)$ equals the yield of D_2 from pure benzene-d_6. This suggests that the deuterium from pure C_6D_6 (or hydrogen from C_6H_6) is produced wholly by the first-order mechanism. However, this cannot be since mixtures of C_6H_6 and C_6D_6 give appreciable amounts of HD.

This paradox is partially resolved if the results of reference 3 are recalled. It was noted that $G_1(D)$ varies with solvent; it could be greater or less than the first-order yield in the pure deuterated hydrocarbon and could very well be greater than the total yield of D_2 from the deuterated hydrocarbon. If it were greater, the curve of $G(D_2)$ vs. concentration would be concave to the concentration axis, a behavior which is shown in some of the data obtained by Chang (8) from C_6D_6–C_6H_{12} mixtures containing iodine. If the results

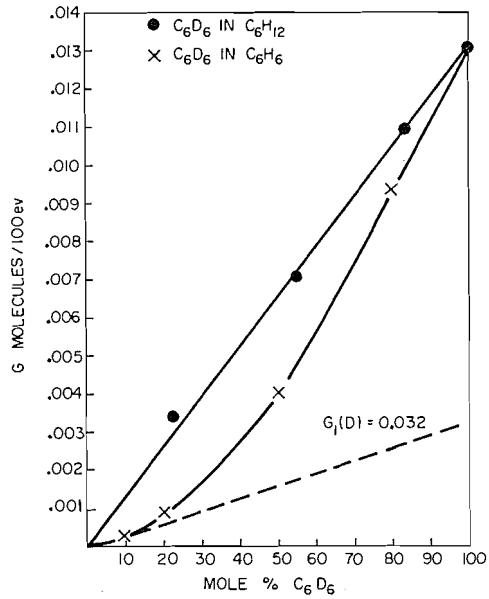

FIG. 6. Yields of D_2 from mixtures of C_6D_6 in C_6H_{12} and C_6D_6 in C_6H_6.

of reference 3 are taken to indicate energy transfer then this result apparently indicates energy transfer from cyclohexane to benzene-d_6.

MIXTURES OF C_6D_{12} AND C_6H_{12}

This section is a brief account of some experiments on 'pure' C_6D_{12}. This material has a 99.5% isotopic purity and consequently contains about 5–6% $C_6D_{11}H$. Radiolysis of this material gives hydrogen containing 6.4% HD. This result indicates an apparently 'infinite' isotope effect for the liberation of H atoms from $C_6D_{11}H$; if excitation is partitioned between components as their mole fraction, then this result implies that every $C_6D_{11}H$ molecule dissociates to give the X_H precursor with something approaching 100% efficiency. The gas obtained from the radiolysis of 'pure' $C_6D_{11}H$ contained 26% HD and 2.2% H_2. This compound contains 8% hydrogen atoms and the amounts of H_2 and HD found do not suggest any abnormal effects in the lability of H atoms. The amount of HD from 'pure' C_6D_{12} is equivalent to a material containing ~25% $C_6D_{11}H$.

This anomaly makes the interpretation of the data on mixtures of C_6D_{12} with small amounts of C_6H_{12} uncertain. Making a simple subtraction of the yield of H_2 from 'pure' C_6D_{12} our experiments show a wide experimental scatter but indicate $G_1(H) \sim 4.0 \pm 1.0$. This value is very close to the total hydrogen yield and apparently greater than the initial yield of cyclohexene, viz. 3.2 (9). Comparable experimental observations have been made by Burton and Chang (10).

THE MECHANISM OF THE 'FIRST-ORDER' PROCESS

Part of the hydrogen yield from alkanes is rapidly reduced by materials expected to have a high reactivity towards hydrogen atoms (11). As a consequence this part is often referred to as the 'scavengeable' hydrogen. The residue, which is "unscavengeable", is often called the 'molecular' hydrogen. Our first isotopic experiments (1) demonstrated the existence of the molecular detachment process formalized in eq. [1]. We have later

shown that benzene and iodine reduce the first-order yield with an efficiency closely comparable to the efficiency with which the total hydrogen yield is reduced. We have analogous results for solutions of benzoquinone and carbon tetrachloride in C_6D_{12}–C_6H_{12} mixtures and for benzene and iodine in mixtures of methylcyclohexane-d_{14} and methylcyclohexane (12). Since the 'molecular' process, observed in the isotopic experiments, is reduced concurrently with the bimolecular process (which would be reduced by a hydrogen atom scavenger) interpretations of the type given by Hardwick (11) and Freeman (20) need modification.

It is of interest to discuss possible mechanisms for the first-order yield.

For alkanes, these are:

(i) A true unimolecular decomposition mechanistically described by

$$C_H \text{—}\sim\sim\rightarrow C_H{}^X \rightarrow H_2 + \text{olefin.}$$

The excited precursor $C_H{}^X$ may be an ion or a neutral molecule. Williams (13) has argued that, for *n*-alkanes, this unimolecular decomposition of an ion is exothermic and may account for part of the olefin formation. Forrestall and Hamill (14) have suggested that the intermediate $C_H{}^X$ (our nomenclature) is formed following electron capture by the $C_6H_{12}{}^+$ ion. Sauer and Dorfman (15) have shown, for ethylene and *n*-butane, that a considerable amount of photolytic hydrogen is produced in a unimolecular decomposition via non-ionic precursors.

(ii) A bimolecular ion–molecule reaction, e.g.

$$CH_3{}^+ + CH_4 \rightarrow C_2H_5{}^+ + H_2$$

or, more generally (13),

$$C_nH_{2n+2}{}^+ + C_nH_{2n+2} \rightarrow C_{2n}\text{-hydrocarbon} + H_2. \qquad [7]$$

These reactions would not be affected by a radical scavenger and would consequently contribute to the unscavengeable hydrogen (or 'molecular' hydrogen) in contrast to the scavengeable hydrogen which, by definition, occurs via a radical reaction. If reaction [7] is rewritten for a mixture of isotopic hydrocarbons:

$$C_nH_{2n+2} + C_nD_{2n+2}{}^+ \rightarrow C_{2n}\text{-hydrocarbons} + \begin{cases} H_2 \\ HD \\ D_2 \end{cases} \qquad [8]$$

we see that there is no certainty as to the isotopic composition of the molecular hydrogen. Williams suggests that this reaction may proceed via hydride ion transfer—to give $C_nD_{2n+2}H$, which then eliminates 'hydrogen', which, in this case, could be D_2 or HD. The amount of D_2 formed by this process would be proportional to the concentration of the deutero compound and would contribute to the first-order yield.

(iii) A bimolecular radical–radical reaction

$$C_6D_{12} \text{—}\sim\sim\rightarrow C_6D_{11} + D \qquad [9]$$

$$D + C_6D_{11} \longrightarrow D_2 + C_6D_{10}, \qquad [10]$$

where the second step is a diffusion-controlled reaction between the species formed in the first step. We have discussed (15) the possibility of benzene acting as a radical scavenger in dilute benzene–cyclohexane solutions and competing with step [8], and conclude that the gas-phase values for the reactivity of H atoms with benzene are not large enough for effective competition at low benzene concentrations. We concluded that the mechanism

by which benzene reduces the 'molecular' yield must be a 'quenching' or energy-transfer type of mechanism.

Somewhat surprisingly, the gas-phase reactivity is not large enough to exclude this radical–radical reaction even in pure benzene solutions. In the equation given by Roy, Williams, and Hamill (16) the probability of a scavenger competing with a diffusion-controlled reaction is determined by the product P_2X (where, in this case, P_2 is the collision efficiency of the reaction of D atoms with benzene and X is mole fraction of benzene). Their data show that if $P_2 \sim 1$ a 50% efficiency of scavenger is observed when $X \sim 10^{-2}$. When the reaction occurs in pure scavenger ($X = 1$) P_2 must be $\sim 10^{-2}$ for effective competition. Since the collision efficiency P_2 for the reaction between hydrogen atoms and benzene in the gas phase is $1.3\text{–}7.9 \times 10^{-4}$ (17), it is still possible for the first-order yield to be occurring by a sequence like reactions [9] and [10] in pure benzene. This observation reinforces our conclusion (3, 15) that, at low benzene concentrations, benzene acts by 'quenching' precursors of the 'unimolecular' decomposition.

Smith (18), in this laboratory, has observed a first-order yield of D_2 in the radiolysis of C_6D_{12}–C_6H_{12} mixtures in the vapor phase which is somewhat greater than that in the liquid phase. The diffusion-controlled atom–radical reaction cannot occur in the vapor phase and consequently, one of the first two mechanisms must be occurring in the vapor. This again argues that they may be expected to occur in the liquid.

In benzene the situation is different. The total hydrogen yield is very small so while the first-order yield is a significant fraction of the total yield it corresponds, by comparison with cyclohexane, to a much less efficient process. It is, therefore, quite possible that the diffusion-controlled radical–radical reaction is significant in benzene whereas it is relatively insignificant in cyclohexane. Ingalls (19) has suggested that the radical–radical reaction is the mechanism for the first-order yield which he measured in toluene.

From the balance of this evidence it is our opinion that, in cyclohexane, the first-order yield measures a true molecular detachment. The ionic process discussed in (ii) is an interesting and provocative speculation. In benzene, the first-order yield could be a true molecular detachment or a diffusion-controlled radical–radical reaction.

REFERENCES

1. P. J. DYNE and W. M. JENKINSON. Can. J. Chem. **38**, 539 (1960).
2. P. J. DYNE and W. M. JENKINSON. Can. J. Chem. **39**, 2163 (1961).
3. P. J. DYNE AND J. DENHARTOG. Can. J. Chem. **40**, 1616 (1962).
4. S. GORDON and M. BURTON. Discussions Faraday Soc. **12**, 88 (1952).
5. M. BURTON, J. Y. CHANG, S. LIPSKY, and M. P. REDDY. Radiation Research, **8**, 203 (1958).
6. G. R. FREEMAN. J. Chem. Phys. **33**, 71 (1960).
7. M. BURTON and W. N. PATRICK. J. Phys. Chem. **58**, 421 (1954).
8. J. Y. CHANG. Ph.D. Thesis, Notre Dame University, Notre Dame, Ind. 1959.
9. P. J. DYNE and J. A. STONE. Can. J. Chem. **39**, 2381 (1961).
10. M. BURTON and J. Y. CHANG. Private communication.
11. T. J. HARDWICK. J. Phys. Chem. **65**, 101 (1961).
12. P. J. DYNE, J. DENHARTOG, and W. M. JENKINSON. Unpublished work.
13. T. F. WILLIAMS. Trans. Faraday Soc. **57**, 755 (1961).
14. L. J. FORRESTALL and W. H. HAMILL. J. Am. Chem. Soc. **83**, 1535 (1961).
15. P. J. DYNE. J. Phys. Chem. **66**, 767 (1962).
16. J. C. ROY, R. R. WILLIAMS, and W. H. HAMILL. J. Am. Chem. Soc. **76**, 3274 (1954); **77**, 2953 (1955).
17. P. E. M. ALLEN, H. W. MELVILLE, and J. C. ROBB. Proc. Roy. Soc. (London), A, **218**, 311 (1953).
18. D. R. SMITH. Unpublished work.
19. R. B. INGALLS. J. Phys. Chem. **65**, 1605 (1961).
20. G. R. FREEMAN. J. Chem. Phys. **33**, 71 (1960); **36**, 1542 (1962).

C^{13} SPLITTINGS IN SOME SUBSTITUTED BENZENES

H. M. HUTTON,* W. F. REYNOLDS,† AND T. SCHAEFER
Department of Chemistry, University of Manitoba, Winnipeg, Manitoba

Received May 4, 1962

ABSTRACT

C^{13} sidebands in the proton spectra of some symmetrically substituted benzenes have been used to obtain carbon–hydrogen coupling constants as well as proton coupling constants.

A long-range carbon–hydrogen coupling constant has also been found. Substituents which act as electron acceptors in an inductive manner are found to increase the $C^{13}H$ coupling constants by as much as 20 c.p.s. The patterns of the sidebands are discussed and possible errors in first-order analyses are indicated.

INTRODUCTION

The carbon–hydrogen spin–spin splittings in a wide variety of compounds have been measured, either by C^{13} resonances or from sidebands in proton resonances. They have been reviewed by Lauterbur (1). It has been proposed that they are mainly determined by the *s* character of the carbon-bonding orbital (2, 3). Long-range carbon–hydrogen coupling constants have been measured by Karabatsos *et al.* by means of C^{13} enrichment (4). A few carbon–hydrogen coupling constants for benzene rings have been reported from C^{13} measurements (1). We have measured these for a dozen substituted benzenes by means of proton spectra. All compounds were chosen so that the main proton resonance was a single line. In such cases the sidebands occurring due to splitting by C^{13} present in natural abundance are observable. The separations of the centers of gravity of the sidebands give the carbon–hydrogen coupling constants directly. The sidebands show interesting fine structure and these are discussed.

EXPERIMENTAL

The C^{13} sidebands of the proton resonance at 60 Mc/s were measured in natural abundance in the pure liquid or saturated solution. Peak separations were determined by the standard techniques using a frequency counter and sidebands obtained from the main proton resonance. Averages were taken of up to 10 spectra. The spectra were taken with a radio-frequency power of about 50 db below 0.5 watt. A compromise had to be reached between saturation effects and a rate of sweep of the field such that fine structure could be observed.

RESULTS AND DISCUSSION

In Table I the coupling constants are given for the various compounds run either as liquids or as saturated solutions in the solvents listed. The standard deviations are given. In Fig. 1 typical spectra are presented for symmetrically substituted benzenes as well as that of benzene itself. The different types of spectra will now be discussed in turn.

Pentasubstituted Benzene

The spectrum of molecules of 2,3,5,6-tetrachloronitrobenzene containing a C^{13} nucleus bonded to the hydrogen is of course a simple doublet, Fig. 1(*a*). The separation of the peaks is 175.0 ± 0.4 c.p.s. in carbon tetrachloride and 176.9 ± 0.6 c.p.s. in acetone. The difference is just larger than the standard deviations but it is not certain that this is significant.

The two peaks marked I in Fig. 1(*a*) are due to impurities. The unmarked peak next to the main proton resonance, however, is not caused by an impurity. It is one peak in

*Holder of a C.I.L. Fellowship.
†Holder of a N.R.C. Studentship.

TABLE I

Coupling constants in some symmetrically substituted benzenes in c.p.s.

Compound	State	$J_{C^{13}H}$*	Other coupling constants*
2,3,5,6-Tetrachloronitrobenzene	In CCl_4	175.0±0.4	$J_{C^{13}CH} = 4.9\pm0.3$
	In acetone	176.9±0.6	or $J_{C^{13}CCH} = 4.9\pm0.3$
2,4,6-Tribromophenol	In acetone	172.5±0.8	$J_m^{HH} = 2.3\pm0.2$
2,4,6-Trichlorophenol	In acetone	171.3±0.5	$J_m^{HH} = 2.5\pm0.2$
2,4,6-Trinitrophenol	In acetone	175.8±0.5	$J_m^{HH} = 2.8\pm0.2$
2,6-Dinitro-4-chlorophenol	In ether	174.1±0.4	$J_m^{HH} = 2.8\pm0.2$
2,6-Dibromo-4-nitrophenol	In acetone	172.8±1.3	$J_m^{HH} = 3.3\pm0.3$
1,3,5-Trichlorobenzene	In CCl_3Br	172.2±0.4	$J_m^{HH} = 2.1\pm0.2$
1,3,5-Tribromobenzene	In CCl_3Br	174.3±0.5	$J_m^{HH} = 1.7\pm0.3$
1,3,5-Trinitrobenzene	In acetone	179.5±1.5	$J_m^{HH} = 1.9\pm0.2$
p-Dichlorobenzene	In acetone	169.0±1.0	
p-Dimethoxybenzene	In acetone	161.1±1.0	
Benzene	Liquid	158.7±0.8	
2,4,6-Trimethylpyridine	Liquid	158.5±0.7	$J_{C^{13}H}(CH_3) = 126.4\pm0.5$

*Errors given are standard deviations.

the doublet due to long-range carbon–hydrogen coupling in those molecules where C^{13} is in the position ortho or meta to the proton. A spectrum run in reverse reveals the other peak of the doublet. Ringing of the large proton peak obscures the second peak of the doublet in each case. The coupling is 4.9±0.3 c.p.s. Since the intensity of the peaks in this doublet is greater than that of the peaks in the other doublet (the exact ratio is very hard to decide because of the proximity of the large ring resonance), we conclude that this coupling is either $J_{C^{13}CH}$ or $J_{C^{13}CCH}$. In less heavily substituted benzenes the peaks due to such coupling will be obscured by the more intense central hydrogen peak.

The only other value for a long-range coupling constant in benzenes is the one of 5 c.p.s. between the methyl protons and, presumably, the neighboring ring carbon in toluene (10). It is of the same order of magnitude as those found by Karabatsos *et al.* in molecules containing sp^2 hybridized carbon (4).

Tetrasubstituted Benzenes

All four of this type have the two protons in the meta position. A typical spectrum is shown in Fig. 1(*b*). Neglecting long-range coupling constants between carbon and hydrogen, we have, in first order, that the separation of the doublets is $J_{C^{13}H}$ and the doublet spacing is J_m^{HH}.

Consider now an exact approach to this three-spin system. The two ring protons and the C^{13} nucleus constitute an AA′X system (5). It follows that the separation of the outermost peaks of the doublets is $J_m^{HH}+1/2(J_{C^{13}H}+J_{C^{13}CCH})+2D$ and the separation of the innermost peaks is $-J_m^{HH}+1/2(J_{C^{13}H}+J_{C^{13}CCH})+2D$. Here $2D = \{[1/2(J_{C^{13}H}-J_{C^{13}CCH})]^2+(J_m^{HH})^2\}^{1/2}$. Only if both J_m^{HH} and $J_{C^{13}CCH}$ are much smaller than $J_{C^{13}H}$ do we make no error in a first-order analysis. Assuming a maximum long-range coupling constant of about 5 c.p.s. and a J_m^{HH} of 2 c.p.s. the error in $J_{C^{13}H}$ is only about 0.1 c.p.s. The error can reach significant proportions where J^{HH} is not small, as in cis and trans disubstituted ethylenes for instance.

Trisubstituted Benzenes

A typical spectrum is shown in Fig. 1(*c*). In first order we expect two triplets with spacings equal to J_m^{HH} and centers separated by $J_{C^{13}H}$. If J_m^{HH} and $J_{C^{13}CCH}$ cannot be neglected with respect to $J_{C^{13}H}$ we have the $AA_2'X$ case. The energy levels for this are written down rather easily. It is immediately clear that there are strong A transitions between antisymmetrical triplet states which are separated by $J_{C^{13}H}$. This constant can

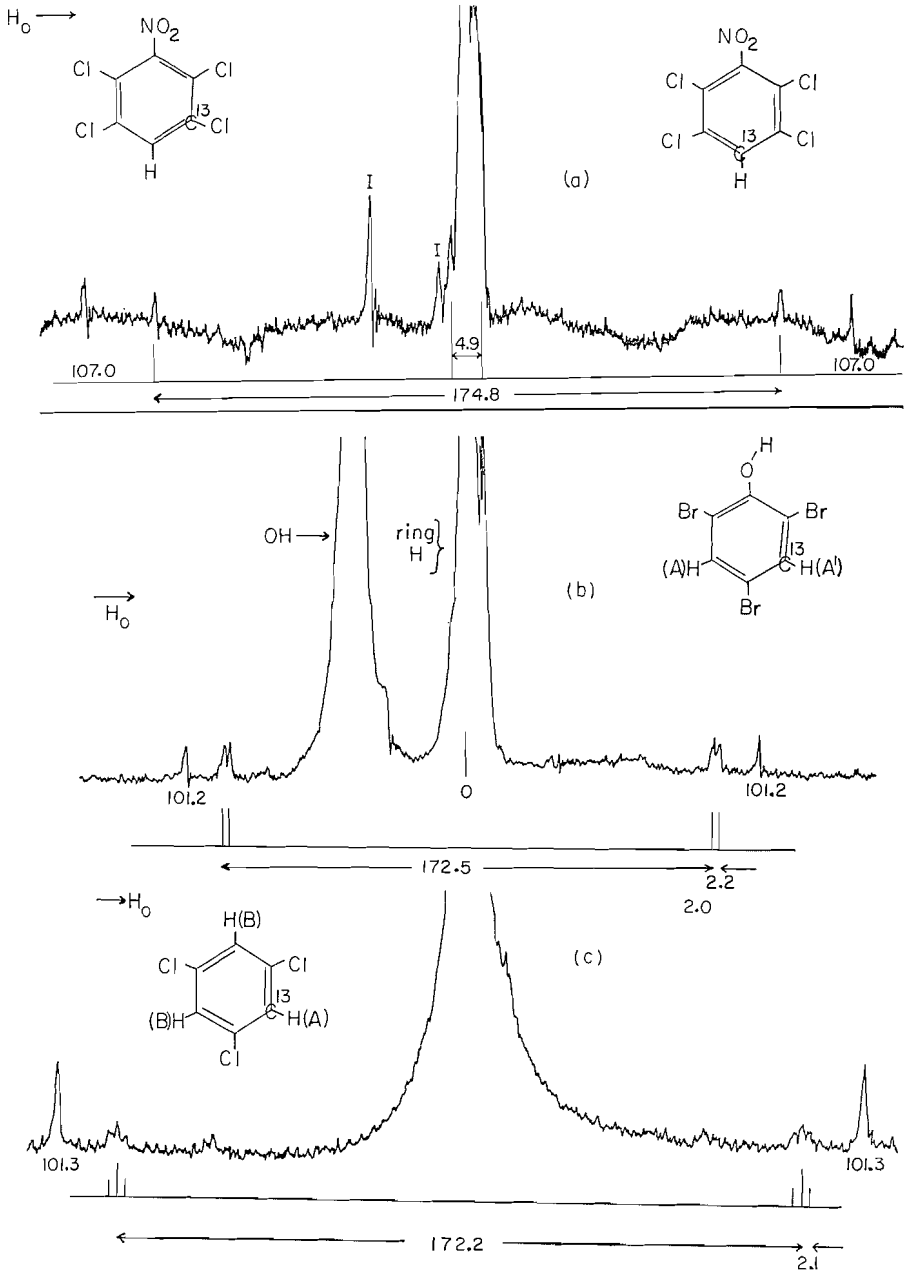

FIG. 1. The 60 Mc/s proton resonance spectrum at high radio-frequency power, showing the C^{13} sidebands in saturated solutions of (*a*) 2,3,5,6-tetrachloronitrobenzene in acetone, (*b*) 2,4,6-tribromophenol in acetone, (*c*) 1,3,5-trichlorobenzene in trichlorobromomethane. Peak separations in the observed and calculated spectra are given in c.p.s.

immediately be derived from the separation of the strong central lines of the triplets. In contrast to the tetrasubstituted benzenes the peak separations in the multiplets themselves deviate from J_m^{HH}, depending on the relative sizes of J_m^{HH}, $J_{C^{13}CCH}$, and $J_{C^{13}H}$. In our examples the error is less than the experimental one.

Disubstituted Benzenes

The spectrum obtained from a paradisubstituted benzene is typified by Fig. 2(*a*). It is

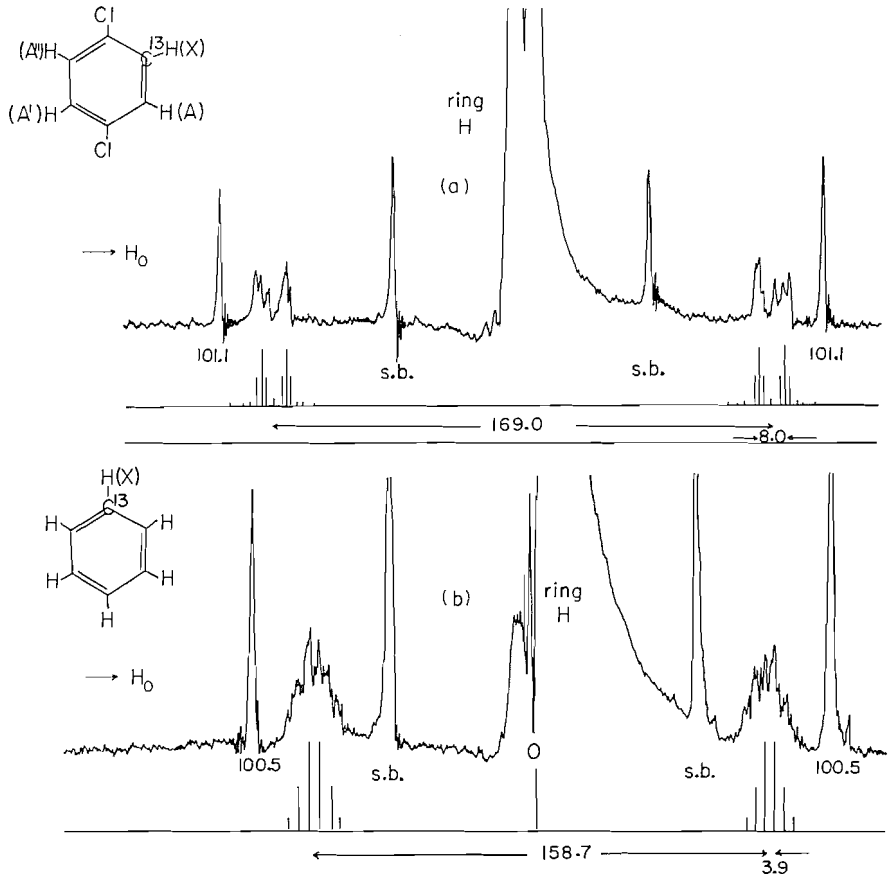

FIG. 2. The 60 Mc/s proton resonance spectrum at high radio-frequency power, showing the C^{13} sidebands of (*a*) paradichlorobenzene as a saturated solution in acetone, (*b*) liquid benzene. Peak separations in the observed and calculated spectra are given in c.p.s. The peaks marked s.b. are spinning sidebands.

immediately clear that it is not a first-order spectrum. The best approximation to the actual situation, for which explicit values for the transitions in terms of spectral parameters can be obtained, is AA'A''X, where long-range carbon–hydrogen coupling constants are neglected. The highest order of the submatrices is three and orthogonal matrices can be found which diagonalize them. This was done.

Taking $J_o^{HH} = J_{AX} = J_{A'A''} = 8$ c.p.s., $J_m^{HH} = J_{AA'} = J_{A''X} = 2$ c.p.s., and $J_p^{HH} = J_{AA''} = 0$ c.p.s., the calculated spectrum which results is shown in Fig. 2(*a*). This is exactly what one expects as soon as one realizes that proton X and proton A as well as protons A' and A'' are relatively tightly coupled.

The deviation from the calculated spectrum can result from the fact that $2J_o^{HH} \approx 0.1J_{C^{13}H}$. If the $J_{C^{13}H}$ values are large enough, they could aggravate the deviation from the case AA'A''X. We conclude that we are in fact dealing with the case AA'A''A'''X, where X is now a carbon nucleus. These systems show no symmetry and this is really where the difficulty lies. However, our analysis has accounted for the spread of the spectrum and we can extract a value of $J_{C^{13}H}$ which is accurate to about 1 c.p.s.

Benzene

The calculated spectrum in Fig. 2(*b*) is that resulting from the assumed case A_5X, where X is the proton bonded to C^{13}. This assumption is justified if (*a*) $J_{C^{13}H}$ is large compared to any J^{HH} and (*b*) J_o^{HH} is large compared to a fraction, about one quarter, of $J_o^{HH}-J_m^{HH}$. These conditions, hard to specify more closely in this complex situation, are roughly true here. In that case each half of the spectrum should be a sextet with separations between the multiplet peaks of $1/5(2J_o^{HH}+2J_m^{HH}+J_p^{HH})$. This is 3.9 c.p.s. on an average and it is seen that the calculated spectrum reproduces the shape of the observed spectrum. The situation is somewhat similar to that of fluorobenzene (6). A good general discussion of similar systems is given by Abraham and Bernstein (7). Further progress in the analysis of C^{13} sidebands in the proton spectra of substituted benzenes will no doubt involve enrichment of the carbon isotope in these molecules.

The Carbon–Hydrogen Coupling Constants

All the carbon–hydrogen coupling constants lie above that of benzene itself. If the relation $\rho_{CH} = 0.20J_{C^{13}H}$ is correct, as suggested by Muller and Pritchard (2), then the percentage of *s* character, ρ_{CH}, of the carbon atomic orbital of the CH bond varies from about 32% for benzene to about 36% for 1,3,5-trinitrobenzene. The carbon atomic orbital deviates only slightly from sp^2 hybridization. If, further, the linear relation between r(C—H) and percentage of *s* character of C—H is correct, the bond length shortens by 0.01 Å in going from benzene to 1,3,5-trinitrobenzene.

Lauterbur has obtained $J_{C^{13}H}$ coupling constants for a number of methyl-, hydroxy-, and methoxy-substituted benzenes from the C^{13} spectra (8). They are the same as that in benzene within experimental uncertainties. These substituents are all electron donors in an overall manner. Most of the substituents in the present set of compounds are electron acceptors in an inductive manner, including the halogens. The electron-withdrawing groups cause an increase in $J_{C^{13}H}$ and this is an indication of an increase in *s* character of the C—H bond if Muller's ideas are correct (2). The trinitrobenzene has the highest $C^{13}H$ coupling constant and it is one of the strongest meta-directing groups. No simple additivity relation is evident for the various substituents, such as the one found for substituted methanes (9), and this is probably due to resonance interactions among the substituents.

The $C^{13}H$ coupling constant in the pyridine is the same as in benzene and since the carbon is meta to the nitrogen this is perhaps not surprising.

ACKNOWLEDGMENTS

This work was supported by the National Research Council and by the Research Corporation.

REFERENCES

1. F. C. NACHOD and W. D. PHILLIPS (*Editors*). Determination of organic structures by physical methods. Academic Press. 1962. Chap. 7.
2. N. MULLER and D. E. PRITCHARD. J. Chem. Phys. **31**, 1471 (1959).
3. J. N. SHOOLERY. J. Chem. Phys. **31**, 1427 (1959).
4. G. J. KARABATSOS, J. D. GRAHAM, and F. M. VANE. J. Am. Chem. Soc. **84**, 37 (1962).
5. J. A. POPLE, W. G. SCHNEIDER, and H. J. BERNSTEIN. High resolution nuclear magnetic resonance. McGraw Hill. 1959.
6. A. ABRAGAM. Principles of nuclear magnetism. Oxford. 1961. p. 497.
7. R. J. ABRAHAM and H. J. BERNSTEIN. Can. J. Chem. **39**, 216 (1961).
8. P. C. LAUTERBUR. J. Am. Chem. Soc. **83**, 1846 (1961).
9. E. R. MALINOWSKI. J. Am. Chem. Soc. **83**, 4479 (1961).
10. D. R. MCADAMS. J. Chem. Phys. **36**, 1948 (1962).

DETERMINATION OF FREE FORMALDEHYDE BY VAPOR DIFFUSION TECHNIQUE: A STUDY OF THE GLYCINE–FORMALDEHYDE REACTION

JOHN L. MORRISON,[1] AUDREY S. LEE, AND PETER J. MOLONEY
Connaught Medical Research Laboratories, University of Toronto, Toronto, Ontario

Received May 8, 1962

ABSTRACT

A vapor diffusion technique has been modified to give absolute values of the free formaldehyde in glycine–formaldehyde mixtures. The equilibrium constant for the formation of the monomethylol addition compound of glycine and formaldehyde was found to be 40, which coincides with that calculated from Levy's measurements which were made with a hydrogen electrode. Values of the equilibrium constant for the formation of the dimethylol compound were variable and much higher than a single value reported by Levy. This uncertainty may be due to polymerization.

INTRODUCTION

The reaction of formaldehyde with glycine has been studied with the hydrogen (1) and glass (2) electrodes. Levy (1) has proposed addition reactions of one and two formaldehyde molecules on the amino group. Further support of Levy's assumptions would be given by a determination of the amount of free or unbound formaldehyde in the aqueous solution. Isolation procedures such as distillation or even precipitation of the formaldehyde as, for example, by dimedon reagent, do not avoid the rapid reversal of the reactions. It was found here that Nash reagent (3) gives a complete reversal of the reaction. Phloroglucinol reagent (4) probably gives a partial reversal.

In the present paper, a vapor diffusion technique (5, 6) has been modified to give an absolute measure of the free formaldehyde, and the equilibria proposed by Levy and others are applied to the measurements.

EXPERIMENTAL

Aqueous solutions of pure formaldehyde were obtained by fractional distillation from paraformaldehyde into water (7). The glycine was analytical grade. The aqueous mixtures were adjusted to various pH values by HCl and NaOH of 0.1 and 1.0 normalities; pH was measured on a Radiometer pH meter.

Formaldehyde was analyzed by means of the Nash test (3) at 420 mμ on a Coleman Universal spectrophotometer. Contrary to what Nash reports, it was found that his reagent retains its full strength for several months, provided that no pipette is dipped into the original reagent bottle. It was noted that standard formaldehyde solutions of over 0.03% concentration are stable for at least 1 month.

The vapor diffusion bottle, Fig. 1, was adapted from diffusion flasks described by Ward Smith (5). Exactly 0.1 ml of a known formaldehyde concentration is added to the small cup by a blowout T.D. type pipette and 5 to 10 ml of the glycine–formaldehyde mixture is measured into the bottle. Several concentrations of formaldehyde (5–8) are placed in the cups of a series of the vapor diffusion bottles above a fixed volume of glycine–formaldehyde mixture. The concentrations in the cups are chosen so as to bracket the free formaldehyde concentration in the mixture. The bottles are rotated on an *inclined* rotating machine (9) in a constant-temperature room. All solutions, bottles, and pipettes are allowed to come to thermal equilibrium in the room before the various additions are made. This precaution is necessary to prevent mass distillation of liquid to or from the small cups. After about 3 to 4 hours' rotation, the complete contents of each cup are carefully washed into separate volumetric flasks and made up to a volume suitable for formaldehyde analysis by the Nash test. Then for each cup the absolute change in formaldehyde concentration is plotted against the original concentration. Usually lines drawn through the increasing and decreasing concentration points are linear and meet at the point of zero change (Fig. 2). The concentration of formaldehyde represented by this point is a measure of the free formaldehyde in the glycine–formaldehyde mixture.

[1]*Present address: Ontario Research Foundation, Toronto, Ontario.*

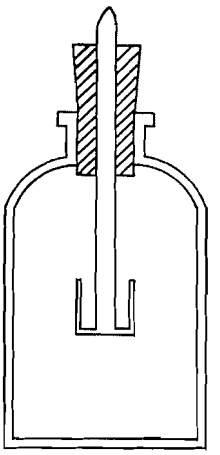

FIG. 1. Vapor diffusion bottle: 50 ml total capacity, No. 00 rubber stopper, borosilicate glass, small cup volume of 0.4 ml.

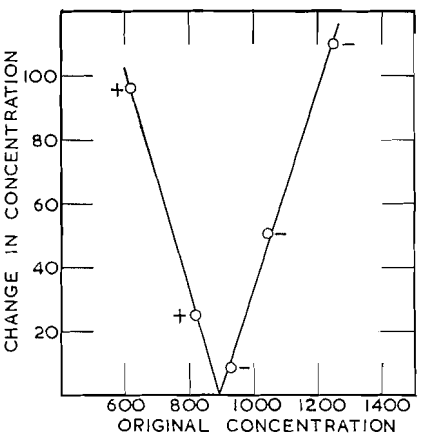

FIG. 2. Determination of free formaldehyde by vapor diffusion bottles; all concentrations and changes in concentration refer to solutions in the small cups; concentrations in parts per million.

It is the point of equal "escaping tendency" or activity (8) of the formaldehyde in the cup and in the mixture.

Blank experiments in which the concentrations in the cup and bottle were the same showed no change in the analysis of formaldehyde in the cup. This shows that during the course of an experiment thermal equilibrium is maintained between the formaldehyde solution and the glycine–formaldehyde mixture. All experiments were carried out in a room at 31.5±0.3° C.

Fixed amounts of 1% glycine and 0.1% formaldehyde were used in most of the experiments. The pH was varied from 2.8 to 9.7. In a few experiments, the ratio of glycine to formaldehyde was varied for both a fixed formaldehyde and a fixed glycine content at a pH of 8.30. This pH was chosen in a region where the free formaldehyde changes rapidly with pH change.

RESULTS AND DISCUSSION

The free formaldehyde values in 0.1% formaldehyde and 1% glycine mixtures at various pH values are given in Table I and plotted in Fig. 3. The only similar experiments in the literature were those of Hobohm (4). In general, except for the 90% free formaldehyde values below pH 7, his results were higher than ours. This is to be expected since he determined the free formaldehyde directly on the *bulk mixture* by the phloroglucinol

TABLE I

Free formaldehyde at various pH values

pH	Free formaldehyde, %	K_3	pH	Free formaldehyde, %	K_3
9.70	6.0		7.40	85	3,800
9.30	8.5		7.04	90	4,500
9.10	12	27,700	6.55	90	
8.55	23	19,700	5.63	90	
8.40	28	17,100	4.10	90	
7.99	52	7,750	2.8	90	
7.40	74	8,050			

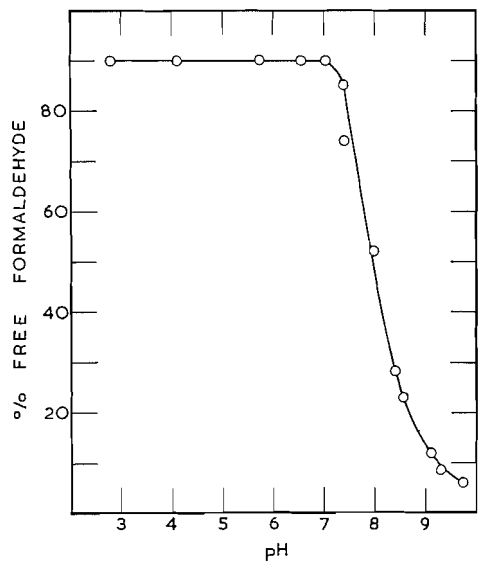

FIG. 3. The variation of free formaldehyde with pH for solutions of 1% glycine and 0.1% formaldehyde.

colorimetric method. Hobohm evidently assumed that phloroglucinol does not even partially reverse the reaction of glycine–formaldehyde compound formation. Our results suggest that this assumption is not valid. In fact, in the case of Nash reagent, there is a complete recovery of formaldehyde from glycine–formaldehyde mixtures at all pH values tested. Apparently phloroglucinol only partially reverses the reaction.

The effect of varying the formaldehyde concentration for a fixed glycine concentration, and the converse, are given in Table II. In order to treat the data theoretically it is necessary to consider the experimental measurements and theoretical calculations of Levy for the same system (1).

Levy considered that glycine reacted very rapidly with formaldehyde to form mono- and di-methylol addition compounds.

He postulated that the following equilibria determine the behavior of the system:

$$\underset{a}{\mathrm{CH_2(COOH)NH_2}} = \underset{b}{\mathrm{CH_2(COO^-)NH_2}} + \mathrm{H^+},\ K_1 = \frac{bh}{a} \qquad [1]$$

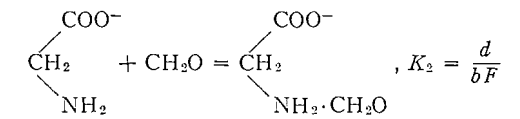

[2]

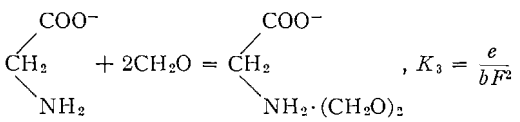

[3]

K_1 is the hydrogen ion dissociation constant of glycine.

TABLE II

Total formaldehyde, %	Total glycine, %	Free formaldehyde, %	Apparent K_2	K_3
A. Variation of free formaldehyde with formaldehyde concentration at pH 8.30 and 1% glycine				
0.0125		73	58.6	3,400
0.0250		64	90.5	4,650
0.0500		50	167.5	7,500
0.100		30*	444	18,250
0.150		27	585	17,000
B. Variation of free formaldehyde with glycine concentration at pH 8.30 and 0.1% formaldehyde				
	2.0	24		7,200
	1.0	30*		18,250
	0.5	55		14,300

*This value was obtained from an interpolation in Fig. 3.

Levy used the hydrogen electrode to measure the equilibrium relations. The pH values of half-neutralized amino acid at various formaldehyde concentrations were measured and designated pG_f. In order to obtain a simple relationship between the constants K_1, K_2, and K_3, he used the approximation that, when the amino acid concentration is small compared with the formaldehyde concentration, the amount of combined formaldehyde becomes negligible compared with the total formaldehyde. Then the total formaldehyde concentration can be substituted for F, the concentration of free formaldehyde. On the basis of this approximation, Levy obtained the equation

$$\left(\frac{G_f}{K_1}+1\right)\frac{1}{F} = K_2+K_3.F = M. \qquad [4]$$

An examination of Levy's results for some amino acids other than glycine indicates that his approximation is valid. However, in the case of glycine he extrapolated from results (in his Fig. 2) in which an appreciable amount of the total formaldehyde is combined with the glycine. For example, at $M = 100$, and on the assumption that the glycine is combined with 2 moles of formaldehyde, it is found that 13% of the formaldehyde has been combined. His extrapolation of the straight line for glycine to zero formaldehyde concentration gave a value of 60 for K_2. Our estimation of K_3 from the slope of his straight line gives a value of 520. He reported in his Table II a value of 290 for 0.01 M glycine only.

By using Levy's graphical data for glycine as given in his Fig. 1, we calculated the results given in our Fig. 4. These results are plotted over a range of pH values and formaldehyde concentrations similar to those of his other amino acids. From the graph, K_2 is

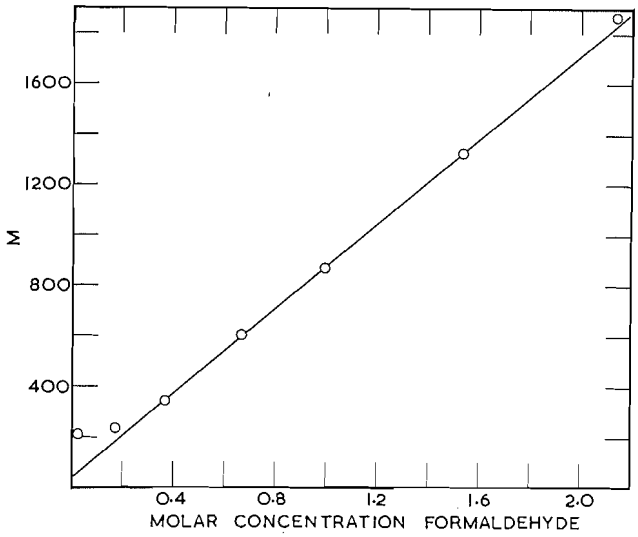

FIG. 4. A graph of calculations made from Levy's results (1) for glycine and formaldehyde. $M = K_2+K_3F$.

found to be 40 instead of 60. It is interesting to note that the points begin to depart from linearity at a formaldehyde concentration below which Levy's approximation is no longer valid. From the slope of the graph, the value of K_3 is found to be 830.

Most of Levy's measurements were made in a region of relatively high formaldehyde concentration; in contrast, the present measurements were made in a region of relatively low formaldehyde concentration. Levy's equilibrium equations can be applied directly to our measurements. In order to obtain K_2, equation [2], apparent values of K_2 were calculated on the assumption that no dimethylol compound was formed (reaction [3] not involved). Apparent K_2 values at various formaldehyde concentrations were calculated at pH 8.30 for a fixed glycine concentration (Table II, A). These were plotted against the total formaldehyde concentration (Fig. 5) and the curve was extrapolated to zero formaldehyde concentration, at which the assumption (no dimethylol compound formed) can be considered valid. The value of $K_2 = 40$ was obtained, which coincides with that obtained by the present calculations from Levy's results. In these calculations of K_2, the value of 9.6 for pK_1 was used.

K_3 was calculated in the following manner: The ratio of b to a is given by the ratio of pK_1 to pH from equation [1]. The total glycine equals $a+b+d+e$. The bound formaldehyde equals $d+2e$. With $K_2 = 40$, one obtains the ratio of b to d. Then one solves for b and e, thus obtaining K_3.

Values of K_3 are included in Tables I and II. K_3 varies from 3,400 to 27,700, in all cases much larger than the values calculated from Levy's data. An analysis of our data showed that when e, the molar concentration of dimethylol compound, was small, K_3 was small, and conversely, when e was large, K_3 was large. Separate calculations on the assumption that $K_2 = 60$ change the values of K_3 by less than 10%.

There are obviously anomalies in the reaction between glycine and formaldehyde. Not

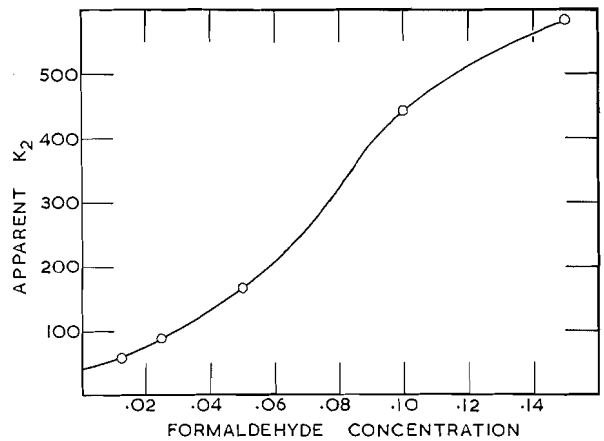

FIG. 5. Apparent K_2 values versus % total formaldehyde concentration for 1% glycine solutions.

only are the calculated values of K_3 variable both for the present results and for those of Levy, but our K_3 values are much larger than those of Levy. It is apparent that the three equations postulated by Levy do not completely describe the reactions between glycine and formaldehyde.

Also, some other experimental results are not accounted for by Levy's equations. For example, the fixed percentage of bound formaldehyde below pH 7.0 is not explained. Hobohm (4) also observed about the same magnitude of binding below pH 7.0.

Moreover, a slow, irreversible binding occurs between formaldehyde and glycine at pH values greater than 7.0. For example, at pH 8.7, 94% of the original formaldehyde remains after 5 days at 31.5° C, as shown by the results of the Nash test on the bulk mixture; after 6 weeks, only 65% can be accounted for by the Nash test. On the other hand at pH 5.65, 94% remains after 2 months.

Levy had reservations concerning the interpretation of his glycine results. He suggested by way of explanation that "there is evidence in this case that the formaldehyde compound is polymerized to a marked extent and the values of the constants are dependent to some extent on the actual glycine concentration" (1). Perhaps one or more of the many possible compounds suggested in the review by French and Edsall (10) is slowly being formed.

REFERENCES

1. M. LEVY. J. Biol. Chem. **99**, 767 (1932–33).
2. M. S. DUNN and A. LOSHAKOFF. J. Biol. Chem. **113**, 359 (1936).
3. T. NASH. Biochem. J. **55**, 416 (1953).
4. K. O. HOBOHM. Biochem. Z. **316**, 202 (1943–44).
5. H. J. WARD SMITH. J. Lab. Clin. Med. **38**, 762 (1951).
6. E. M. TAYLOR and P. J. MOLONEY. J. Am. Pharm. Assoc. Sci. Ed. **46**, 299 (1957).
7. J. F. WALKER. Formaldehyde. Reinhold Pub. Corp., New York. 1944.
8. G. N. LEWIS and M. RANDALL. Thermodynamics and the free energy of chemical substances. McGraw-Hill Book Co., Inc., New York. 1923.
9. D. SELIGSON and H. SELIGSON. J. Lab. Clin. Med. **38**, 324 (1951).
10. D. FRENCH and J. T. EDSALL. *In* Advances in protein chemistry. Vol. II. *Edited by* M. L. Anson and J. T. Edsall. Academic Press, Inc., New York. 1945. p. 277.

HIGH-TEMPERATURE STUDIES OF METALLURGICAL PROCESSES

PART II. THE THERMAL REDUCTION OF CALCINED DOLOMITE WITH SILICON

J. M. Toguri and L. M. Pidgeon
Department of Metallurgy, University of Toronto, Toronto, Ontario

Received May 18, 1962

ABSTRACT

The production of magnesium by the following reaction has been studied:

$$2CaO_{(s)} + 2MgO_{(s)} + Si_{(s)} = 2Mg_{(g)} + Ca_2SiO_{4\,(s)}. \qquad (a)$$

The rate of reaction (*a*) was followed by continuous weight loss measurements of the reactants. Keeping the particle size of the reactants and size and shape of the charge constant, the following factors which affect the yield of magnesium were investigated: (1) temperature, from 1050–1560° C; (2) pressure, from less than 1 μ to 261 mm of Hg; (3) catalysts, CaF_2, BaF_2, and MgF_2; and (4) ferrosilicon grade, from 18.7% to 96.7% Si.

It was found that the yield increased by a factor 1.55 for a 50° increase in temperature over the temperature range investigated. At temperatures below 1300° C the yield falls linearly with increase in pressure, while at temperatures above 1300° C the yield remains relatively constant until the pressure exceeds the equilibrium magnesium pressure. All fluoride additions were found to increase the yield, CaF_2 being the most effective. The rate of the reaction was also found to have a direct relationship with the silicon activity.

INTRODUCTION

The problem of extracting magnesium from its ores has resolved itself into two general methods: (1) electrolysis of fused magnesium chloride and (2) direct thermal reduction of magnesium oxide.

In the direct thermal reduction of magnesium oxide, various reducing agents are available. However, only three have been used commercially: carbon (1–4), calcium carbide (5), and silicon (6–11). Of these three, only the thermal reduction of calcined dolomite with silicon has survived. The overall reaction that occurs in this process can be expressed by the equation

$$2CaO_{(s)} + 2MgO_{(s)} + (Fe)Si_{(s)} = 2Mg_{(g)} + Ca_2SiO_{4(s)} + (Fe)_{(s)}. \qquad [1]$$

This reaction is endothermic, and CaO, the more basic of the two alkaline earth oxides, combines with the silica to form the dibasic silicate. Pidgeon and King (12) have measured the eqilibrium pressure of magnesium over this reaction by means of the entrainment method, obtaining a value of 10.1 mm of Hg at 1100° C, which has been confirmed recently by Rosenqvist and Ellingsaeter (13). This is to be compared with 1.9 mm Hg and 1200° C, obtained by Schneider and Hesse (14), for the reaction pressure of Mg over the system MgO and Si in the absence of CaO. In addition to the higher equilibrium pressure, the presence of CaO makes possible the use of dolomite as a raw material. This mineral is abundant and contains one molecule each of $CaCO_3$ and $MgCO_3$, frequently in a state of high purity.

To effect completion of this reaction, the ambient pressure must be below the equilibrium pressure and this can be accomplished by either a vacuum system or by sweeping out the magnesium by a stream of inert gas.

In one commercial application, this reaction takes place in vacuum (less than 0.1 mm of Hg) at a temperature of 1180° C in a horizontal tubular alloy steel retort (6, 7, 8, 15). Calcined dolomite is intimately mixed with silicon in the form of ferrosilicon. This mixture

is pressed into briquettes, which are then charged into the retort. Since magnesium is the only volatile component in the system, it is distilled from the reaction mixture and condensed as a dense, coherent deposit in the water-cooled end of the retort. The operation is essentially a vacuum distillation, and yields metal of high purity (99.97%). The magnesium crystals produced in this manner are melted and cast into ingots.

While this process has resulted in the production of substantial amounts of magnesium, relatively little has been published on the factors controlling reaction rates, and in fact little is known of the reaction mechanism. There are many variables in the reaction, and only by arbitrarily holding constant a few can the effect of others be examined. This paper describes experiments in which the effect of temperature (1050–1560° C), pressure, and composition of silicon alloys was examined and under conditions in which the reaction mixture was of uniform composition.

EXPERIMENTAL PROCEDURES

The experimental procedure adopted for the determination of the reaction rate has been previously described (16). Briefly, the method consisted of determining the weight loss with time of a briquetted reaction mixture due to the evolution of magnesium, by means of a calibrated helical steel wire spring suspended in a vacuum furnace. Since the particle size of the reactants and size and shape of the briquettes were held constant, the effect of factors such as temperature and pressure could be determined. These standardized experimental conditions permitted a direct comparison of the yields. However, because of the heterogeneous nature of the reaction concerned, the experimental results may not be interpreted in terms of exact kinetic laws.

The composition of the calcined dolomite used in these tests is shown in Table I. The dolomite was commercially calcined.

TABLE I

Analysis of calcined dolomite

Loss on ignition	1.38%
Insoluble	0.48
R_2O_3	0.40
CaO	57.5
MgO	38.8

The ferrosilicon used was 74.1% Si, −200 mesh, unless otherwise stated.

The charge was made up by mixing intimately the fine calcined dolomite with ferrosilicon. Fifteen percent excess of silicon was added to that required by the stoichiometry of equation [1]. All briquettes of the reaction mixture were made in a 1-inch-diameter mold at a pressure of 3000 p.s.i. without a binder. The weight of each briquette was approximately 17 g. Three briquettes were used for each experiment and these were arranged as previously described (16).

Blank runs using only calcined dolomite prepared in the same manner as the reaction mixture showed negligible weight loss when heated over the temperature range 1050–1356° C in the graphite retort. When briquetted calcined dolomite and ferrosilicon mixture were reacted in the graphite retort, weight losses of the retort were observed at temperatures exceeding 1300° C. At 1568° C, the highest temperature used in this investigation, the weight loss of the graphite accounted for 5.85% of the total loss in weight. Below 1300° C, however, the weight loss of the reactants and the weight of magnesium collected was found to be in good agreement within ±2.0%.

A. Effect of Temperature

Typical results are shown in Fig. 1, where percentage yield of Mg, based on the initial weight of MgO, is plotted against time in minutes. In Fig. 2, the results are summarized by plotting percentage yield after 10 minutes against temperature.

B. Effect of Pressure

The main function of vacuum in this process is to displace the equilibrium in such a way that the metal may be distilled or sublimed from the reaction mixture. A secondary function is to permit the formation of a dense solid condensate (17).

Figure 3 shows the result of the effect of pressure on the yield at various temperatures. At the lower temperatures, an increase of pressure has a marked effect on the yield, the yield appearing as a linear function

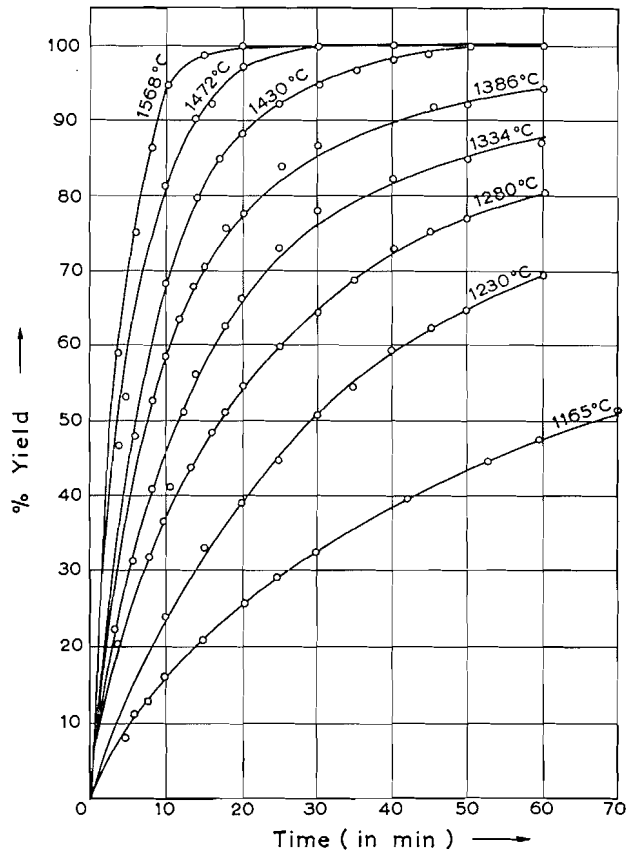

FIG. 1. Reaction rates for calcined dolomite and FeSi (74.1% Si).

of pressure. However, at the higher temperature, 1370° C, an increase in the pressure has much less effect on the yield until the equilibrium pressure (209 mm of Hg, calculated from an extrapolation of Pidgeon and King's measurement (12)) is reached, at which point the yield falls off rapidly.

The beneficial effect of high temperature is quite apparent from this curve. However, as expected, the physical nature of the condensate was found to be affected by the pressure. The results obtained were similar to those reported by Betcherman and Pidgeon (17). Under high-vacuum conditions, a very dense condensate is obtained regardless of the temperature of the reactor, but as soon as the pressure is increased, numerous loosely compacted dendrites are formed. Further increase in pressure caused a lacy network of innumerable fragile dendrites to appear. With a combination of high temperature (1370° C) and increased argon pressures, the condensate appeared to collect in a partly liquid state.

C. Effect of Ferrosilicon Grade

While theoretical considerations favor the use of 100% Si as a reducing agent, its cost is prohibitive in most cases and ferrosilicon is preferred. An examination of the iron–silicon phase diagram shows that in the region 60–100% silicon no solid solubility exists and solid alloys in this range consist of a mixture of free silicon and ferrosilicon alloy.

A range of alloys has been examined between 18.7% and 96.7% Si, as shown in Fig. 4, to ascertain the effect of ferrosilicon grade on the reaction rate at 1228° C. The weight percentages of free silicon, as calculated from the phase diagram, are shown in Table II. In Fig. 5, the initial rate constants are plotted against the mole fraction of silicon. The similarity of the plot with the activity curve of FeSi, as determined by Rosenqvist and Ellingsaeter (13), at 1200° C, is evident. It appears that the initial rate constant is a direct function of the activity of silicon. The decrease of the rate in the case of the 90% and 74.1% alloys after 15 minutes of reaction is to be attributed to the decrease in availability of silicon. While the decrease in the 46.7% and 18.7% alloys can be attributed to the activity of Si and to the formation of a liquid phase at 1128° C, which tends to agglomerate and decrease the effective reaction surface. Evidence that the liquid particles

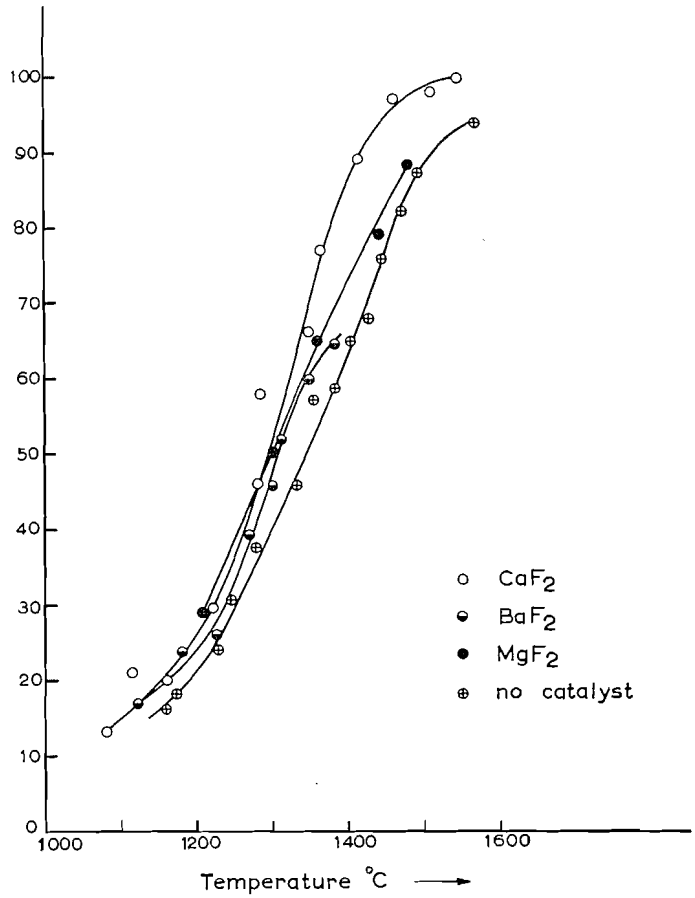

FIG. 2. Effect of Catalysts. Percentage yield after 10 minutes vs. temperature.

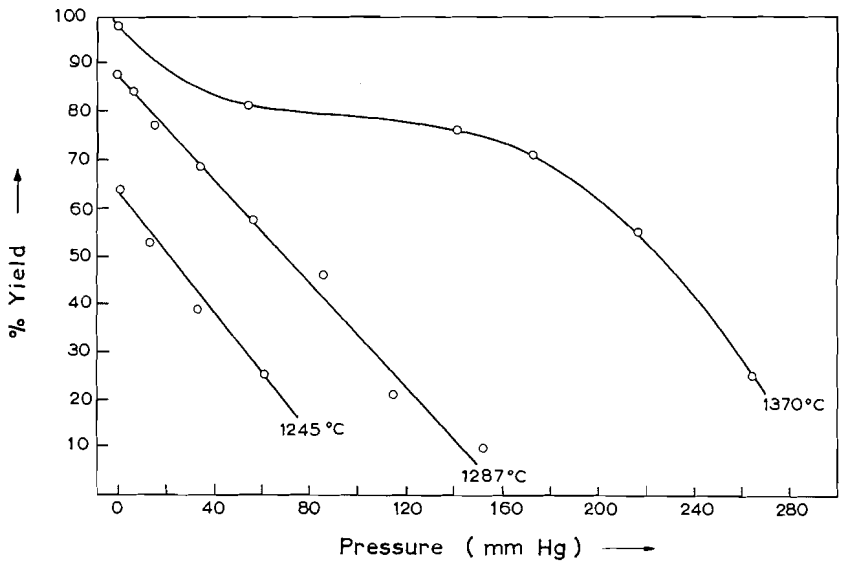

FIG. 3. Percentage yield after 20 minutes vs. pressure.

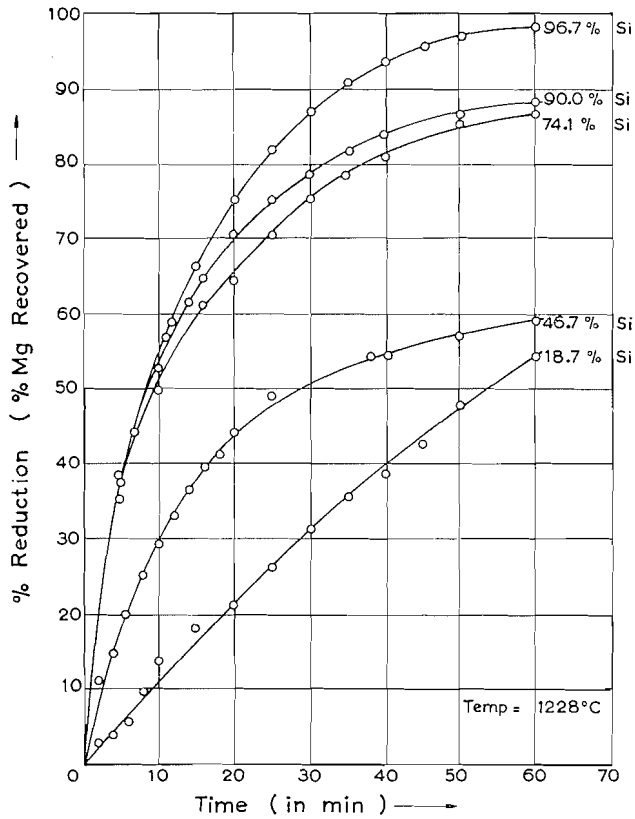

FIG. 4. Effect of ferrosilicon grade on the reduction of calcined dolomite.

TABLE II

Effect of FeSi grade

Grade of FeSi			Wt. of charge (g)			Si (g)			% excess based on	
% Si	% Free Si	N_{Si}	Calcine	MgO	FeSi	Total Si	Free Si	Theoretically required Si	Free Si	Total Si
96.7	93.1	0.98	42.572	16.518	6.791	6.567	6.322	5.748	+10.0	+14.2
90.0	77.6	0.95	42.542	16.506	7.432	6.689	5.767	5.744	+4.0	+16.4
74.1	41.4	0.85	42.445	16.081	8.655	6.413	3.583	5.596	−36.0	+14.6
46.7	0	0.64	36.978	14.347	12.682	5.922	0	4.922	−100.0	+18.6
18.7	0	0.31	22.679	8.799	35.817	6.698	0	3.062	−100.0	+118.7

coalesce was afforded by the existence in the residue of ferrosilicon balls of about 1.5-mm diameters. The initial size of the ferrosilicon was −200 mesh.

D. Effect of Catalyst

Alkali and alkaline earth fluorides are known to accelerate solid-state reactions in oxide systems. CaF_2 is commonly used as a catalyst in the calcined dolomite – ferrosilicon reaction (7, 18). In this investigation, the effects of CaF_2, BaF_2, and MgF_2 were studied. The amount of fluoride added in all cases was 2.5% of the charge. The results are summarized in Fig. 2, where the percentage yield after 10 minutes is plotted against temperature. CaF_2 is the most effective, while MgF_2 and BaF_2 appear to have approximately the same catalytic effect.

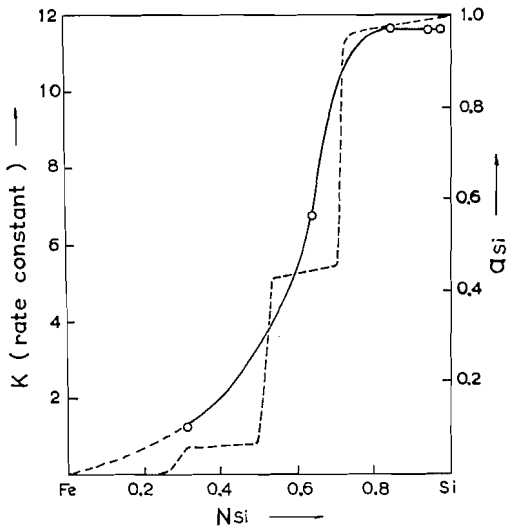

FIG. 5. Initial rate constant vs. N_{Si} at 1228° C. Solid line shows the initial rate constant while the broken line shows the activity of Si in FeSi as measured by Rosenqvist and Ellingsaeter (13).

E. Effect of Temperature on Purity of Magnesium Condensate

Magnesium was produced at temperatures between 1165° C and 1588° C. Magnesium crystals representative of the bulk of the condensate at any temperature were analyzed, with results shown in Table III.

TABLE III

Effect of temperature on purity

Temp.	Ca	Al	Ni	Cu	Mn	Zn	Pb	Sn	Si	Fe
1160	0.003	0.02	0.002	0.0002	0.004	0.03	0.06	0.002	0.07	
1165	0.0008	0.006	0.002	0.0002	0.004	0.03	0.06	0.002	0.009	
1222	0.003	0.035	0.002	0.0004	0.004	0.03	0.06	0.002	0.07	
1282	0.0025	0.009	0.002	0.0002	0.004	0.03	0.06	0.002	0.02	
1355	0.002	0.006	0.002	0.0002	0.004	0.03	0.06	0.002	0.009	
1350	0.003	0.035	0.002	0.0002	0.004	0.03	0.06	0.002	0.05	0.0014
1410	0.004	0.05	0.002	0.0002	0.004	0.03	0.24	0.002	0.08	
1422	0.0008	0.006	0.002	0.0001	0.004	0.06	0.06	0.002	0.009	
1460	0.003	0.05	0.002	0.0006	0.008	0.03	0.06	0.003	0.05	
1480	0.0025	0.015	0.002	0.0003	0.01	0.03	0.06	0.002	0.018	0.0019
1510	0.003	0.05	0.002	0.0002	0.008	0.03	0.06	0.004	0.07	
1545	0.003	0.05	0.002	0.0004	0.015	0.03	0.06	0.002	0.07	

NOTE: Analyses by spectrographic method—courtesy of Dominion Magnesium Ltd.

No effect of temperature is detectable. The metal produced from the dolomite used in these experiments is known to be of high purity (7) and the independence of temperature suggests that such impurities as appear are either absent in the original raw materials, completely distilled at all temperatures (impossible conclusions for Ca, Al, Si, and Fe), or are not a part of the distillation process as such (a few "high" values suggest salting).

DISCUSSION

It has been shown that small samples of calcined dolomite are reduced by silicon at extremely rapid rates at high temperatures. Between 1200 and 1500° C the increase in yield with temperature is approximately linear and involves a factor of 1.55 per 50° C. The presence of small amounts of certain catalysts (2.5% of the charge) was found to increase the rate. For example, at 1200° C, calcium fluoride increased the percentage

yield after 10 minutes from 21.5% to 27.0%. This effect was even more noticeable at 1400° C, where the corresponding values are 62.5% and 87.0%. In the presence of alkaline earth halides the residue showed a glassy appearance under the microscope, regardless of the temperature of the reaction. This suggests the formation of a liquid phase which may account for the catalytic effect (19). In finely divided reactants, the formation of a liquid phase may decrease the effective reaction surface and thus decreases the rate of reaction; however, it also creates a faster diffusion media and thereby increases the reaction rate. The phase diagram of the system CaF_2–$CaO.SiO_2$ shows a low-melting eutectic at 1125° C (20). It may be possible that, as small amounts of silicates appear, they form a eutectic with neighboring CaF_2, thus explaining the glassy appearance of the residue. Another possible explanation for the catalytic effect is that the fluorine anions tend to surround the highly charged silicon cations and thereby increase the silicon diffusion rate.

These factors seem insufficient to account for the rapid reaction rates which are observed, and it is natural to suggest that other gaseous or liquid intermediaries are present.

The vapor pressure of silicon seems too low to account for the rates measured. At 1370° C, the vapor pressure of silicon is approximately 3×10^{-3} mm Hg; yet the silicon was almost half reacted in 8 minutes at this temperature. A plausible gaseous intermediary is SiO. SiO gas is stable at these temperatures according to a number of investigators (23, 24). In a previous publication (16), it was shown that SiO is distilled from the reaction mixture of MgO + Si at temperatures above 1300° C. In the present work, where CaO was present, no SiO was distilled, even at 1565° C. Thus, if SiO is formed at all, it must be assumed that the presence of the basic CaO prevented loss of SiO from the system. (In the calculations shown, the thermodynamic values recommended by Kubaschewski and Evans (25) have been used.)

If the following reaction takes place:

$$MgO + Si = Mg_{(g)} + SiO_{(g)} \qquad [2]$$

$$P_{SiO} \text{ at } 1550° \text{ K} = 3.26\times10^{-1} \text{ mm Hg},$$

it may be followed by reaction [3]:

$$2SiO + 2CaO = Ca_2SiO_4 + Si \qquad [3]$$

$$\Delta G^0_{1550° \text{ K}} = -35.2 \text{ kcal/mole CaO}.$$

The calculated P_{SiO} over [3] at 1550° K is 8.24×10^{-3} mm Hg. This is too low to produce appreciable distillation, and reaction [3] should take place since P_{SiO} for reaction [2] is greater than P_{SiO} for reaction [3] (different from the case of MgO alone). Reaction [3] also offers a mechanism for depositing free silicon throughout the reaction system, acting as nuclei for further reaction.

Schneider *et al.* (21) have suggested that the primary reaction is the formation of calcium silicide by reaction between CaO and Si. At the temperature concerned, this silicide would be in the liquid state. Similarly, Kroll (22) has suggested the formation of calcium–magnesium silicides. X-Ray analysis of residues was carried out in this investigation at various stages of the reaction. No positive identification of either calcium or magnesium silicide was found in the diffractograms. It is possible that the large number of lines from the calcium orthosilicate had concealed those of the silicide; also, under the

condition of rapid reaction which existed the calcium silicide reacted as rapidly as it was formed. Current work indicates that calcium silicide is a likely intermediate in this reaction.

ACKNOWLEDGMENTS

Financial support in the form of a fellowship (to J. M. T.) from the Steel Company of Canada is gratefully acknowledged. The authors are also indebted to Dominion Magnesium Limited for supplying the dolomite and ferrosilicon used throughout this investigation.

REFERENCES

1. H. A. DOERNER. U.S. Bur. Mines. R.I.3635. May, 1942.
2. F. J. HANSGIRG. Iron Age, **152**, 56 (1943); U.S. Patent No. 2,025,740 (1936).
3. W. S. LANDIS. Trans. Electrochem. Soc. **72**, 1 (1937).
4. W. D. TREADWELL and J. HARTNAGEL. Helv. Chim. Acta, **17**, 1372 (1934).
5. C. MATIGNON. Comp. rend. **172**, 381 (1921); Fr. Patent No. 488,735 (1915).
6. A. MAYER. Trans. Am. Inst. Mining Met. Engrs. Iron Steel Div. **159**, 363 (1944).
7. L. M. PIDGEON and W. A. ALEXANDER. Trans. Am. Inst. Mining Met. Engrs. Iron Steel Div. **159**, 315 (1944).
8. L. M. PIDGEON. Trans. Can. Inst. Mining Met. **47**, 16 (1944); **49**, 621 (1946).
9. A. Z. SCHNEIDER. Z. Metallk. **41**, 210 (1950).
10. W. MOSCHEL. Angew Chem. **63**, 394 (1951).
11. W. J. KROLL. Rev. mét. **48**, 929 (1951).
12. L. M. PIDGEON and J. A. KING. Discussions Faraday Soc. **4**, 197 (1948).
13. T. ROSENQVIST and B. Ellingsaeter. J. Metals, **212**, 1111 (1956).
14. A. SCHNEIDER and E. HESSE. Z. Elektrochem. **46**, 279 (1940).
15. L. M. PIDGEON. U.S. Patent No. 2,373,812 (1945).
16. J. M. TOGURI and L. M. PIDGEON. Can. J. Chem. **39**, 540 (1961).
17. I. I. BETCHERMAN and L. M. PIDGEON. Trans. Can. Inst. Mining Met. **54**, 460 (1951).
18. I. G. FARBEN. Ger. Patent No. 666,353 (1939).
19. A. HEDVALL. Reaktionsfahigheit fester Stoffe. Leipzig. 1938. p. 72.
20. E. LEVIN, H. MCMURDIE, and F. HALL. Phase diagrams for ceramicists. Am. Ceram. Soc. 1956.
21. A. SCHNEIDER, J. F. CORDES, H. KRIBBE, and H. RUNGE. Erzberg. Metal, **12**, 103, 164, 224 (1959).
22. W. J. KROLL. Rev. mét. **48**, 929 (1951).
23. L. BREWER and R. K. EDWARDS. J. Phys. Chem. **58**, 35 (1954).
24. L. BREWER and F. T. GREENE. J. Phys. Chem., Solids, **2**, 286 (1957).
25. O. KUBASCHEWSKI and E. LL. EVANS. Metallurgical thermochemistry. Pergamon Press Ltd., London. 1958.

THE PROTON RESONANCE SPECTRA AND STRUCTURES OF SUBSTITUTED AZULENES IN TRIFLUOROACETIC ACID[1]

S. S. DANYLUK[2] AND W. G. SCHNEIDER
Division of Pure Chemistry, National Research Council, Ottawa, Canada

Received March 28, 1962

ABSTRACT

The proton resonance spectra for a number of substituted azulenes and their conjugate acids are reported at 22° C. From the spectra for the conjugate acids it is confirmed that monoprotonation occurs in the five-membered ring in each case. The unit electron deficiency is shown to be mainly localized in the seven-membered ring of the ion.

Chemical shift changes on protonation are interpreted qualitatively in terms of changes in local π electron charge densities on the carbon atoms.

Unusually large values are noted for the coupling constants between protons on the five-membered ring of the cations and are attributed in part to hyperconjugative effects.

INTRODUCTION

Aromatic hydrocarbons, both alternant and non-alternant, dissolve readily in strong protonic acids with formation of their conjugate acids. Proton addition is generally favored at the carbon atom with the greatest excess electron charge density. For example, molecular orbital calculations (1, 2) indicate the highest π electron density in positions 1 and 3 for the non-alternant hydrocarbon azulene, I. Protonation would therefore be favored as follows:

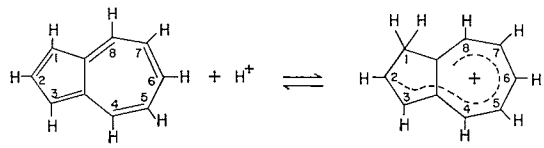

(I) (II)

with the formation of a methylenic carbon at position 1 and a delocalization of the unit charge deficiency in the five- and seven-membered rings. The proton resonance spectrum for the azulenium cation in trifluoroacetic acid, reported previously (3), strongly supports structure II for the conjugate acid.

In an earlier work Mclean *et al.* (4) confirmed from proton resonance spectra that proton addition occurs almost entirely in the 9 position when 9,10-dimethyl-1,2-benzanthracene is dissolved in CF_3COOH–$H_2O \cdot BF_3$ mixtures. Proton resonance spectra are therefore capable of providing useful information about the structures and charge distribution in the conjugate acids of aromatic hydrocarbons. In this paper proton resonance spectra are reported for several substituted azulenes in strongly acid media and the structures of the conjugate acids are confirmed. The possibility of monopositive ion–radical formation in oxygenated solutions has also been investigated and some preliminary observations on the effects of dissolved oxygen are also included.

[1]*Issued as N.R.C. No. 6958.*
[2]*National Research Council Postdoctorate Fellow 1958–1960. Present address: Department of Chemistry, University of Toronto, Toronto, Ontario.*

EXPERIMENTAL

The proton resonance spectra were measured at 22±0.5° C with a Varian 4300 high-resolution spectrometer equipped with a superstabilizer and operating at 60 Mc/s. Signal separations from the reference, CH_2Cl_2, were measured by the side-band technique and are accurate to ±0.2 c.p.s. Closely spaced multiplets were bracketed with side bands as the spectrum was recorded.

Reagent grade trifluoroacetic acid was redistilled through a fractionating column and the middle portion retained for use. Commercial, high-purity azulene, 4,6,8-trimethylazulene, and guaiazulene were used without further purification.

Solutions, approximately 7 mole% in the hydrocarbon, were prepared under a nitrogen atmosphere and were sealed in 5-mm spinning tubes. Spectra were recorded immediately after preparation of the solutions. A slow, irreversible reaction was noted recently by Lauterbur (5) for solutions of azulene in trifluoroacetic acid. In the present investigation the spectra of oxygen-free acid solutions of the cations did not alter appreciably over a period of several days.

All measurements were referred to methylene chloride as internal standard. The methylene chloride signal, measured relative to internal tetramethylsilane, was shifted only very slightly (less than 5 c.p.s.) on dilution from pure methylene chloride to a 10 mole% solution in trifluoroacetic acid.

The electron spin resonance spectra were recorded with a Varian 4500 spectrometer equipped with a 100 kc field modulation unit. Solutions were prepared as described previously and oxygen was bubbled directly into the samples prior to measurements. The "g" value was measured relative to diphenyl picryl hydrazyl (D.P.P.H.) radical as reference.

RESULTS

Azulene and Azulenium Cation

The proton resonance spectra for azulene and the azulenium cation are shown in Fig. 1. The five-membered-ring protons of azulene show a characteristic AB_2 spectrum

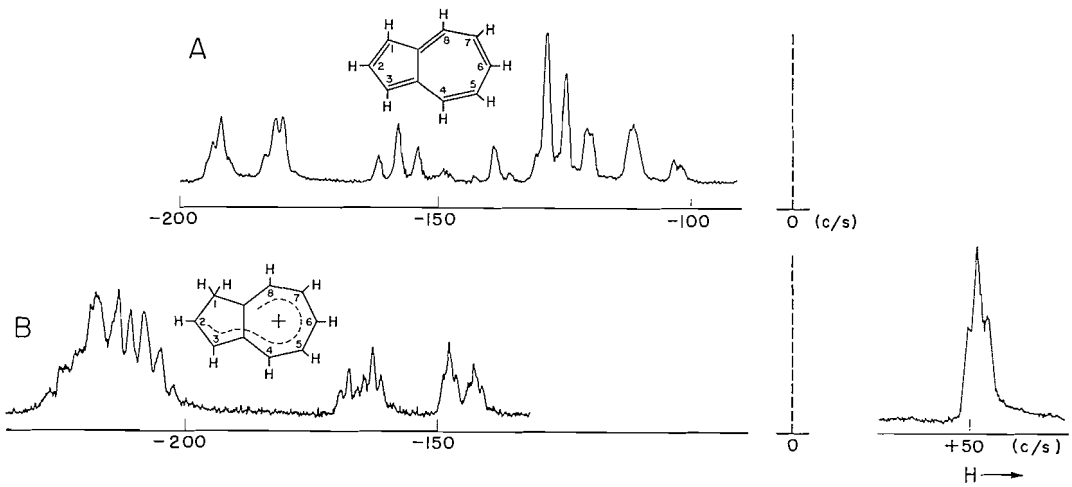

FIG. 1. Proton magnetic resonance spectra. A. 7 mole% solution of azulene in CH_2Cl_2. B. 7 mole% solution of azulene in CF_3COOH. CH_2Cl_2, internal reference.

and analysis gives a value of 3.9±0.2 c.p.s. for the coupling constant J_{12} (J_{23}) and 0.486±0.005 p.p.m. for the relative chemical shifts. A detailed analysis of the seven-membered-ring proton signals was not attempted, although it is of interest to note the displacement of proton 2 from the center of the signal for proton 4 (8), i.e.,

$$\delta_2 - \delta_4 = 0.448 \pm 0.005 \text{ p.p.m.}$$

Figure 1B reproduces the azulenium ion spectrum under somewhat higher resolution than previously reported (3). A typical ABX_2 type of spectrum is observed for the five-membered-ring protons and a first-order analysis of the splitting for the methylene signal

at 51.8 c.p.s. gives coupling constants of 1.8±0.2 c.p.s. and 1.3±0.2 c.p.s. for $J_{11',2}$ and $J_{11',3}$ respectively.[3] Analysis of the AB portion of the spectrum centered at −155.7 c.p.s. gives a value of 0.372 p.p.m. for the relative chemical shift between protons 2 and 3 and 5.5±0.2 c.p.s. for J_{23}. A further splitting of the AB spectrum into triplets (relative intensity, 1:2:1) is due to spin coupling with the methylene protons. The slightly larger splitting, 1.8±0.2 c.p.s., is attributed to interactions with proton 2, while the smaller splitting, 1.3±0.2 c.p.s., involves coupling with proton 3.

The broad unresolved bands at low field, −208 c.p.s. to −240 c.p.s., are assigned to the five non-equivalent protons on the seven-membered ring.

4,6,8-Trimethylazulene and Trimethylazulenium Cation

Figure 2 shows the proton resonance spectra for 4,6,8-trimethylazulene and its conjugate acid. Analysis of the AB_2 spectrum for the five-membered-ring protons in trimethylazulene gives a relative chemical shift of 0.300±0.005 p.p.m. and spin–spin coupling constant of 3.9±0.1 c.p.s. The resonance band at −110.3±0.3 c.p.s. is assigned to the protons in the 5 and 7 positions while the bands at 141.0±0.2 c.p.s. and 156.8±0.2 c.p.s. are assigned to the methyl groups in the 4 and 8 positions and the 6 position respectively.

The spectrum for the trimethylazulenium ion shows a band at 66.5 c.p.s. corresponding to the methylene protons in position 1 (or 3). A quadruplet, Fig. 2C, centered at −145.0 c.p.s. is due to non-equivalent protons in the 2 and 3 positions with a relative chemical shift of 0.181±0.005 p.p.m. and coupling constant, J_{23}, of 5.7±0.2 c.p.s. Spin coupling with the methylene protons further splits the components of the quadruplet into triplets with $J_{11',2} = 1.6\pm0.1$ c.p.s. and $J_{11',3} = 1.1\pm0.1$ c.p.s.

The broad bands at −192.5 c.p.s. and −199.8 c.p.s. are due to the two non-equivalent protons (5, 7) in the seven-membered ring while the three non-equivalent methyl groups account for the bands at 130.0, 132.1, and 134.8 c.p.s.

Guaiazulene and Guaiazulenium Ion

Proton resonance spectra for guaiazulene and its conjugate acid are shown in Fig. 3. An assignment and analysis of the proton spectrum for pure guaiazulene has been reported previously (7). Analysis of the spectrum for a 7 mole% solution in methylene chloride gives the following values:

$$(\delta_1-\delta_2) = 0.433\pm0.005 \text{ p.p.m.}$$
$$J_{12} = 3.8\pm0.2 \text{ c.p.s.}$$
$$(\delta_7-\delta_6) = 0.406\pm0.005 \text{ p.p.m.}$$
$$J_{76} = 11.0\pm0.2 \text{ c.p.s.} \qquad J_{46} = 2.0\pm0.2 \text{ c.p.s.}$$

An appreciable increase in magnitude of the relative chemical shifts is noted for both sets of protons (1,2 and 6,7) in the dilute solution as compared with pure guaiazulene. Furthermore the separation between the five-membered-ring and seven-membered-ring protons increases with dilution. Thus the separation between the midpoints of protons 1 and 2, and 4, increases from 0.753 p.p.m. for pure guaiazulene to 0.847 p.p.m. in a 7 mole% solution in methylene chloride.

Assignment of the remaining bands is straightforward with the septet (129 c.p.s.) and doublet (227, 236 c.p.s.) due to the isopropyl group and the two bands at 146.2 and 150 c.p.s. arising from the two non-equivalent methyl groups. The displacement of proton 2 relative to proton 4, 0.61 p.p.m., is significantly greater in guaiazulene as compared

[3]*The methylene protons on the protonated azulene have been labelled as 1,1'.*

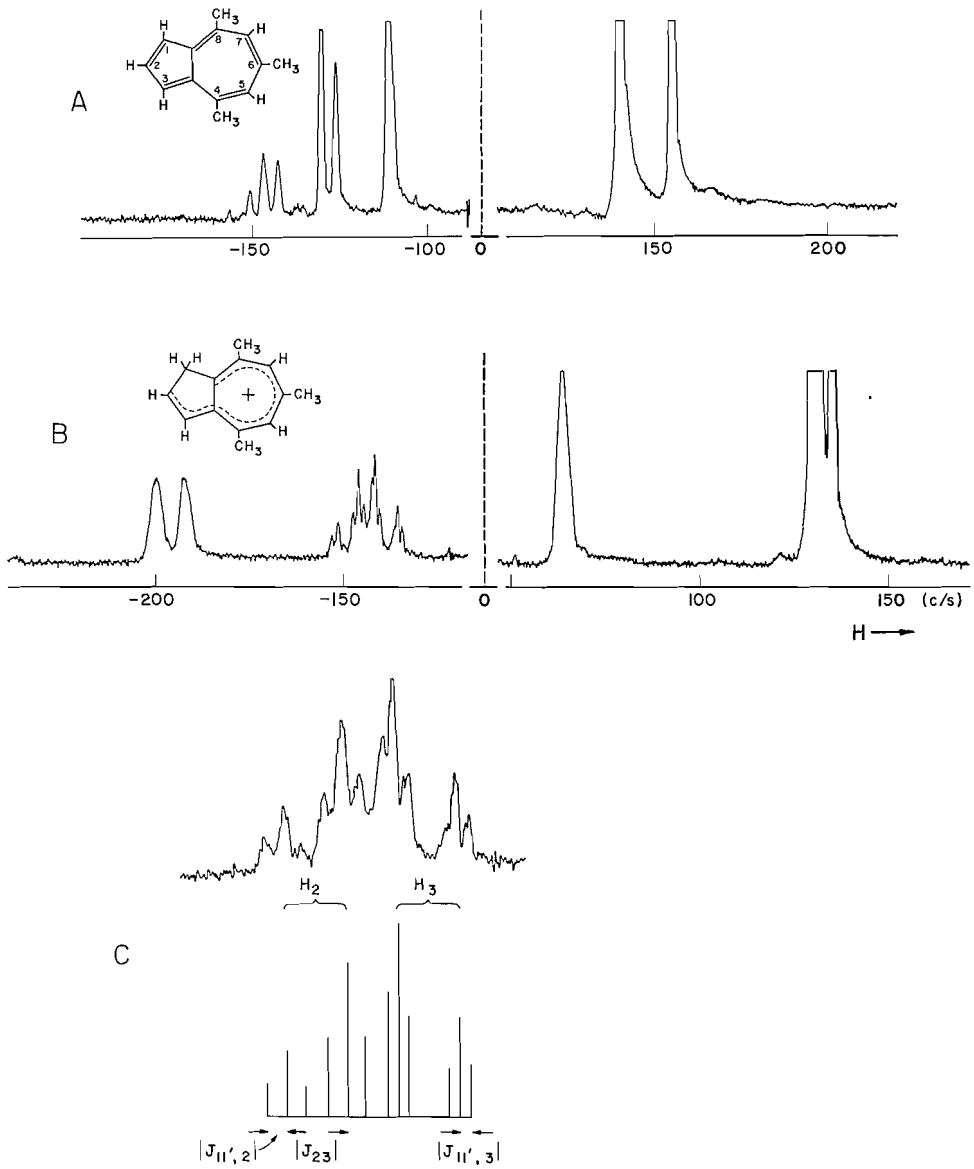

FIG. 2. Proton magnetic resonance spectra. A. 7 mole% solution of 4,6,8-trimethylazulene in CH_2Cl_2. B. 7 mole% solution of 4,6,8-trimethylazulene in CF_3COOH. C. Quartet centered at −118.7 c.p.s. CH_2Cl_2, internal reference.

with azulene. Since the azulene and guaiazulene solutions were relatively dilute (7 mole%) the larger $(\delta_2-\delta_4)$ value in the latter cannot be attributed to solvent effects solely but may reflect small changes in electron distribution brought about by the substituent alkyl groups.

Several distinct features are apparent in the spectrum of the guaiazulenium ion shown in Fig. 3B. The methylene protons in position 1 appear as a symmetric quintet, Fig. 3C (relative intensity 1:4:6:4:1), at 75.5 c.p.s. In order to account for the latter the spins of the methylene protons must interact equivalently with the proton in the 2 position and

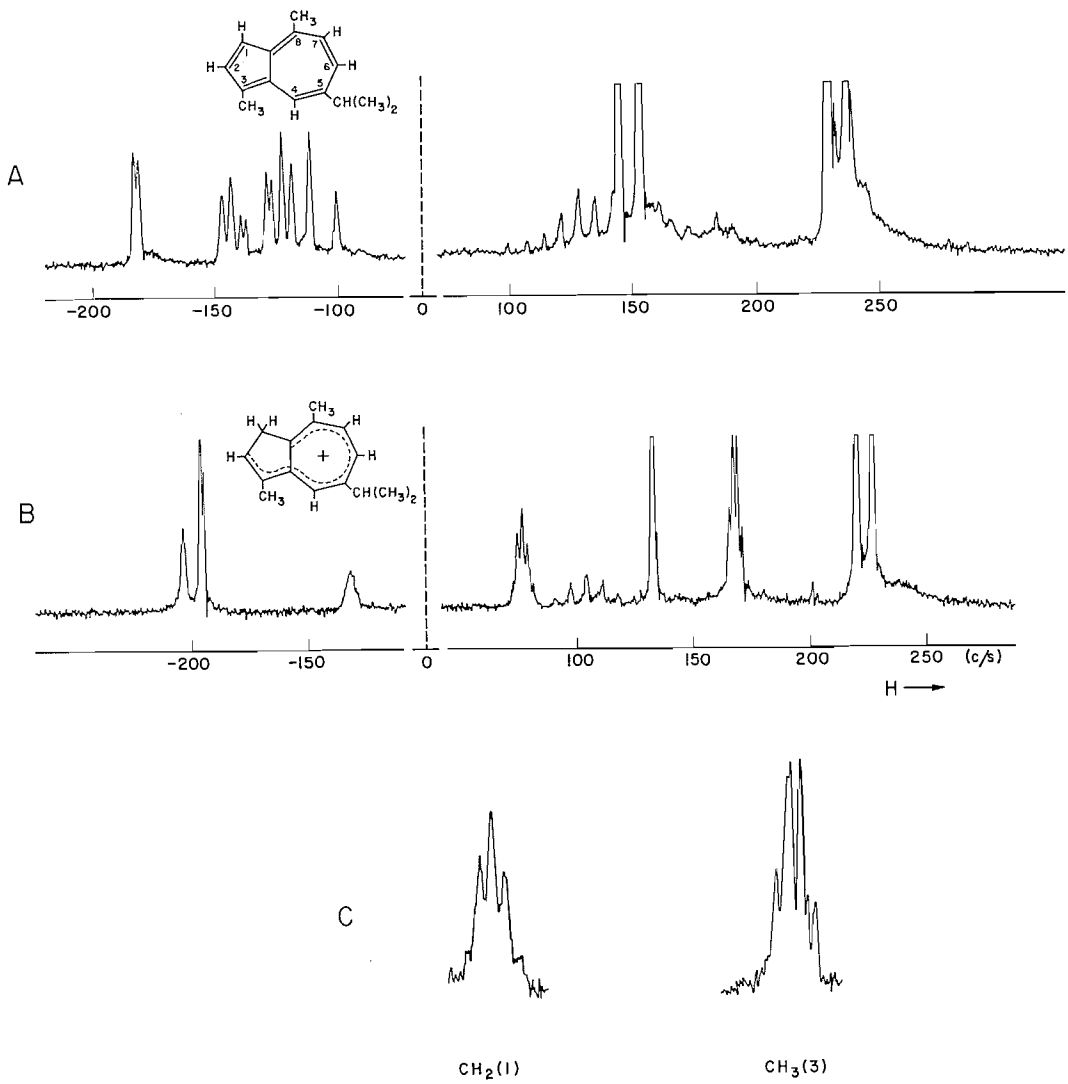

FIG. 3. Proton magnetic resonance spectra. A. 7 mole% solution of guaiazulene in CH_2Cl_2. B. 7 mole% solution of guaiazulene in CF_3COOH. C. Methylene protons in position 1 and methyl group in position 3 of guaiazulenium. CH_2Cl_2, internal reference.

the methyl protons attached to the 3 position, the coupling constant having a value of 2.0 ± 0.2 c.p.s. On this basis the quadruplet at 166.0 c.p.s. is assigned to the methyl group at position 3. Although long-range spin–spin coupling has been noted previously (8, 9), the magnitude of the spin interaction extending over five bonds in the guaiazulenium ion is unusually large.

An assignment of the bands at low field can be made from a comparison of relative intensities. Thus the broad unresolved multiplet at -133.5 c.p.s. is attributed to proton 2 while the bands at -197.6 and -204.0 c.p.s. arise from protons in positions 6 and 7 and 4 respectively. Both the methyl and isopropyl group on the seven-membered ring in the ion are shifted downfield slightly.

The addition of oxygen to 7 mole% solutions of azulene and guaiazulene in trifluoroacetic acid produced in both cases significant changes in the proton resonance spectra and led to the appearance of an electron spin resonance band. A noticeable broadening of the proton resonance lines associated with the cations occurred in the oxygenated solutions. In addition the electron spin resonance spectra show a single band with a half-band width of 5 ± 0.5 gauss and a "g" value of 2.0031. No evidence of hyperfine splitting is apparent under the present conditions.[4] The intensity of the e.s.r. band increases rapidly with time for freshly prepared solutions until equilibrium is attained, generally within 24 hours. An increase in the concentration of oxygen also increases the intensity of the e.s.r. signal, while a degassing of equilibrated solutions leads to a disappearance of the signal.

DISCUSSION

The values of the coupling constants J_{12} are identical for the three azulenes and in agreement with previous results (7, 10). No change in the coupling constants is noted when alkyl groups are present on the five- or seven-membered rings.

Comparison of the relative chemical shifts for the dilute solutions shows that the values of $(\delta_1-\delta_2)$ for guaiazulene, 0.433 p.p.m., and trimethylazulene, 0.300 p.p.m., are appreciably lower than for azulene, 0.486 p.p.m. This decrease is attributable primarily to changes in the local π electron charge densities on the carbon atoms induced by alkyl substituents. It has been demonstrated previously (10) that ring currents alone do not account for the shifts satisfactorily in azulene.

Both the trimethylazulene and guaiazulene show anomalous dilution shifts, the former being of slightly smaller magnitude than the dilution shift observed for azulene. For guaiazulene the anomalous shift leads to an increase of 0.094 p.p.m. in the separation between the protons in the five- and seven-membered rings.

The proton resonance spectra for the three ions show that monoprotonation takes place in the five-membered ring with formation of a characteristic methylene group in each case. Further proton addition does not occur under the present experimental conditions. Recent conductivity measurements by Long and Schulze (11) on acid solutions of azulene confirm monoprotonation in this system.

Protonation of the azulenes brings about pronounced changes in the chemical shifts and coupling constants, as is apparent from the proton resonance spectra. From Table I it is evident that protons in the seven-membered ring are shifted as much as 1.50 p.p.m. to low field in the ions.

Two effects might be expected to contribute to the chemical shift changes.

(1) Any alteration in the aromatic ring currents would result in a shift of the proton signals. In the azulenium ions the formation of a CH_2 group will alter the ring currents in the five-membered ring considerably. Information about ring currents in analogous rings, such as cyclopentadiene, is lacking and the effect on chemical shifts is uncertain. If it is assumed, however, that the ring current is hindered completely in the protonated ring, then relatively large changes in chemical shifts, amounting to 1.66 p.p.m., would be expected for protons in the 2 and 3 positions. Protons in the seven-membered ring would be shifted much less due to ring current change since the introduction of an excess charge into a ring does not affect the ring currents appreciably. In the tropylium ion, for example, the shift due to ring current changes amounts to 0.41 p.p.m. per unit electron deficiency

[4]*No e.s.r. absorption was noted for the original oxygen-free solutions. Furthermore, addition of oxygen to solutions of azulenes in methylene chloride and to pure trifluoroacetic acid does not affect the proton resonance spectra nor do these solutions show any e.s.r. band.*

TABLE I

Chemical shifts for ring protons in protonated and unprotonated azulenes

Compound		$\delta_{CH_2Cl_2}$*	δ_{acid}†
Azulene	5-membered (1,3)	−2.13	(3) −2.40
	(2)	−2.62	(2) −2.77
	7-membered (4,8)	−3.06	(4) −3.78‡
	(5,7)	−1.93	(5) −3.69‡
	(6)	−2.31	(6) −3.60‡
4,6,8-Trimethylazulene	5-membered (1,3)	−2.12	(3) −2.32
	(2)	−2.43	(2) −2.50
	7-membered (5,7)	−1.84	(5) −3.33
			(7) −3.22
Guaiazulene	5-membered (1)	−1.97	
	(2)	−2.41	(2) −2.22
	7-membered (4)	−3.02	(4) −3.40
	(6)	−2.20	(6) −3.29
	(7)	−1.75	(7) −3.29

*Chemical shifts are given in p.p.m. relative to CH_2Cl_2 as internal standard, with CH_2Cl_2 as the solvent.
†Chemical shifts in trifluoroacetic acid in p.p.m. relative to CH_2Cl_2 as internal standard.
‡Estimated.

(12). Since the unit electron deficiency is distributed between the two rings in the azulenium ion its effect on the seven-membered-ring currents is difficult to estimate. The effect would be less than 0.41 p.p.m., however, and assuming that an electron deficiency of 0.60 electron is localized on the seven-membered ring the shift change would amount to 0.25 p.p.m. to low field. The contributions of neighbor-ring currents to the chemical shifts range from 0.12 to 0.65 p.p.m., with protons in the 3 and 4 positions affected more than protons in the other positions.

(2) A second effect contributing to chemical shifts results from differences in local π electron charge densities. In particular, introduction of a positive charge into a ring generally produces shifts of the ring protons to lower fields (12–14). Surprisingly large shifts were noted by Fraenkel *et al.* (12) when a unit electron deficiency was present in aromatic rings ($C_7H_7^+$). In the present case the large decrease in screening and the near equivalence of the seven-membered-ring protons in the ions indicate a significant localization of the electron deficiency in the seven-membered ring. This suggests a configuration analogous to the tropylium ion and it is of interest to note that signals of the seven-membered-ring protons are in the same region as proton signals of the tropylium ion, −3.10 p.p.m. (12) relative to methylene chloride.

An estimate of the effect of protonation on the chemical shifts of ring hydrogens has been made recently (15) for a number of alternant aromatic carbonium ions on the assumption that ring currents and excess charges are the only significant factors affecting the shift. In each case the unit electron deficiency was found to be distributed fairly uniformly in the ion.

A similar uniform distribution of positive charge is noted in the azulenium ion. The π electron densities, ρ, for azulene and the azulenium ion have been calculated using the calibration equation $\delta = 10.6\rho$ (16) and the results are summarized in Table II and Fig. 4. Corrections due to the neighbor-ring current have been applied to the protons in the five- and seven-membered rings of azulene. The charge densities for azulene agree with the values reported earlier (16). In the case of the azulenium ion an estimate has been made of charge densities in the seven-membered ring, assuming the absence of a neighbor-ring current in the five-membered ring. A deficiency of approximately 0.7 electron charge is localized in the seven-membered ring and is distributed uniformly around the ring. The

TABLE II

Chemical shift changes of azulene ring protons on protonation

Proton	δ* (p.p.m.)	Correction for neighbor ring (p.p.m.)	Net shift (p.p.m.)	$\Delta\rho$	ρ
		Azulene			
1,3†	−0.07	+0.65	+0.58	+0.055	1.055
2†	−0.56	+0.35	−0.21	−0.022	0.987
4,8‡	−0.96	+0.61	−0.35	−0.933	0.967
5,7§	+0.22	+0.20	+0.42	+0.040	1.040
6‡	−0.14	+0.14	0	0	1.000
		Azulenium ion			
3	−0.34	—	—	—	—
2	−0.71	—	—	—	—
4,8	−1.34	—	−1.34	−0.13	0.87
5,7	−1.27	—	−1.27	−0.12	0.88
6	−1.23	—	−1.23	−0.12	0.88

*Chemical shifts relative to benzene with CH_2Cl_2 as solvent. The chemical shifts have been recalculated from Table I using the value −2.06 p.p.m. as the difference in chemical shifts between CH_2Cl_2 and benzene. The benzene reference point is used in applying the calibration equation $\delta = 10.6\rho$.
†Protons in 2 and 3 positions of azulene.
‡Protons in 4 and 6 positions of guaiazulene.
§Protons in 5 and 7 positions of 4,6,8-trimethylazulene.

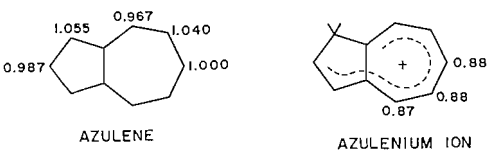

FIG. 4. Charge densities in azulene and the azulenium ion.

charge densities in the five-membered ring cannot be determined satisfactorily because of the uncertainty in the magnitude of the ring current and the change in hybridization at the carbon atom in the 1 position. However, a comparison of the chemical shifts for the five-membered-ring protons in the ion, Table II, with the chemical shift for the olefinic protons in cyclopentadiene, +0.84 p.p.m. relative to benzene, indicates a significant decrease in screening in the ion.

The magnitudes of the spin–spin coupling constants between protons in the five-membered rings are of considerable interest. Long-range proton spin–spin coupling extending over three and four bonds for both saturated and unsaturated hydrocarbons have been reported previously (9, 10, 18, 19). Values for these long-range coupling constants are generally less than 1 c.p.s. and decrease as the number of intervening bonds increases. Interactions between protons separated by five bonds have been reported recently (8). Fraser observed coupling constants of 1.46 c.p.s. and 1.17 c.p.s. between the protons of the methyl groups in angelic and tiglic acids respectively. In the present work, $J_{11',3}$ extending over four bonds has values of 1.3 and 1.1 c.p.s. for the azulenium and trimethylazulenium ions. A surprisingly large coupling constant, 2.0 c.p.s., extending over five bonds is noted between the methylene protons in the 1 position and the methyl group in the 3 position for the guaiazulenium ion. Long-range spin–spin interactions have been interpreted theoretically (17) in terms of a delocalization of electrons in the C—H bond and it is probable that this effect accounts at least qualitatively for the magnitude of the coupling constants observed in the five-membered ring of the ion. The magnitude

of J_{11',CH_3} in guaiazulenium suggests, in addition, the likelihood of a significant contribution to the delocalization of electrons due to hyperconjugation (1). Similar effects have been noted previously for substituted allenes (18), thiophenes (19), and mesitylene (20).

The electron paramagnetic resonance of oxygenated acid solutions of the azulenes can be accounted for by the additional formation of monopositive ions of the hydrocarbons along with the protonated ions. The formation of monopositive ions has been noted previously for solutions of perylene (21, 22), anthracene (22, 23), and other polycyclic aromatic compounds (23) in strongly acidic and oxidizing media. Although the mechanism is not clear it is likely that the paramagnetic monopositive ion $C_{10}H_8^+$ (as distinct from the protonated species $C_{10}H_9^+$) is formed by transfer of an electron from the azulene to the oxygen molecule, acting as an electron acceptor, to form the O_2^- ion. The width of the e.s.r. absorption band and the lack of hyperfine splitting indicate a rapid exchange reaction between the monopositive ion and the free hydrocarbon.

REFERENCES

1. E. Heilbronner. Non-benzenoid aromatic compounds. Interscience Publishers, Inc., New York. 1959. p. 196.
2. R. Pariser. J. Chem. Phys. **25**, 1112 (1956).
3. S. S. Danyluk and W. G. Schneider. J. Am. Chem. Soc. **82**, 997 (1960).
4. C. Mclean, J. H. van der Waals, and E. L. Mackor. Mol. Phys. **1**, 247 (1958).
5. P. C. Lauterbur. J. Am. Chem. Soc. **83**, 1841 (1961).
6. J. A. Pople, W. G. Schneider, and H. J. Bernstein. High-resolution nuclear magnetic resonance. McGraw-Hill Co., New York. 1959. p. 19.
7. H. J. Bernstein, J. A. Pople, and W. G. Schneider. Can. J. Chem. **35**, 65 (1957).
8. R. R. Fraser. Can. J. Chem. **38**, 549 (1960).
9. E. B. Whipple, J. H. Goldstein, and L. Mandell. J. Chem. Phys. **30**, 1109 (1959).
10. W. G. Schneider, H. J. Bernstein, and J. A. Pople. J. Am. Chem. Soc. **80**, 3497 (1958).
11. F. A. Long and J. Schulze. J. Am. Chem. Soc. **83**, 3340 (1961).
12. G. Fraenkel, R. E. Carter, A. McLachlan, and J. H. Richards. J. Am. Chem. Soc. **82**, 5846 (1960).
13. J. R. Leto, F. A. Cotton, and J. S. Waugh. Nature, **180**, 978 (1957).
14. E. Grunwald, H. Loewenstein, and S. Meiboom. J. Chem. Phys. **27**, 641 (1957).
15. C. Mclean and E. L. Mackor. Mol. Phys. **4**, 241 (1961).
16. W. G. Schneider and H. Speisecke. Tetrahedron Letters, No. 14, 468 (1961).
17. M. Karplus. J. Chem. Phys. **33**, 1842 (1960).
18. E. B. Whipple, J. H. Goldstein, and W. E. Stewart. J. Am. Chem. Soc. **81**, 4764 (1959).
19. S. Gronowitz and R. A. Hoffman. Acta Chem. Scand. **13**, 1687 (1959).
20. R. A. Hoffman. Mol. Phys. **1**, 326 (1958).
21. Y. Yokozawa and I. Miyashita. J. Chem. Phys. **25**, 796 (1956).
22. S. I. Weissman, E. de Boer, and J. J. Conradi. J. Chem. Phys. **26**, 963 (1957).
23. W. I. Aalbersberg, G. J. Hoijtink, E. L. Mackor, and W. P. Weijland. J. Chem. Soc. 3049 (1959).

KINETIC STUDIES OF PROTEIN–DYE AND ANTIBODY–HAPTEN INTERACTIONS WITH THE TEMPERATURE-JUMP METHOD[1,2]

A. FROESE[3] AND A. H. SEHON
Department of Chemistry, McGill University, Montreal, Que.

AND

M. EIGEN
Max-Planck-Institut für Physikalische Chemie, Göttingen, Germany

Received April 24, 1962

ABSTRACT

The kinetics of protein–dye and antibody–hapten reactions were studied with the temperature-jump method. The systems used consisted of (i) bovine serum albumin (BSA) and the dye 1-naphthol-4-[4-(4′-azobenzene azo)phenyl arsonic acid], referred to as N—R′, (ii) BSA and the dye 1-naphthol-2-sulphonic acid-4-[4-(4′-azobenzene azo)phenyl arsonic acid], referred to as NS—R′, and (iii) rabbit antibodies to phenyl arsonic acid [Ab] and the hapten N—R′.

Each of the systems exhibited a single relaxation time. From the analysis of the concentration dependence of the relaxation times, it was concluded that each system could be represented by the reactions

$$P + D \underset{k_{21}}{\overset{k_{12}}{\rightleftharpoons}} PD,$$

where P refers to BSA or Ab, and D to N—R′ or NS—R′. The following rate constants were calculated for the three systems at 25° C:

(i) BSA – N—R′ : $k_{12} = 2.1\times10^6\ M^{-1}\text{sec}^{-1}$; $k_{21} = 35\ \text{sec}^{-1}$
(ii) BSA – NS—R′ : $k_{12} = 3.6\times10^5\ M^{-1}\text{sec}^{-1}$; $k_{21} = 2.5\ \text{sec}^{-1}$
(iii) Ab – N—R′ : $k_{12} = 2\times10^7\ M^{-1}\text{sec}^{-1}$; $k_{21} = 50\ \text{sec}^{-1}$.

The effects of temperature and pH on the rate constants of the system BSA – N—R′ are discussed.

INTRODUCTION

In most biological reactions, such as in enzyme–substrate, antibody–antigen, or antibody–hapten reactions, at least one of the reactants is a macromolecule. Antibody–hapten systems are particularly suitable for the elucidation of the nature of the forces which are responsible for the specificity of these reactions, their main advantage being that antibodies to a variety of chemically well-defined substances can be produced. From equilibrium studies it has been shown that the free energy change for many antibody–hapten associations is of the order of -7 to -12 kcal/mole (1, 2). This means that even at high dilutions the extent of association is still appreciable.

Information about the mechanisms of chemical reactions can be obtained from kinetic studies. However, in the case of antibody–antigen and antibody–hapten associations only very few such studies have been performed so far. For some systems, containing polyvalent antigens and divalent antibodies (3–5), the rates were followed by measure-

[1]*This study was supported by grants from the National Institute of Allergy and Infectious Diseases, National Institutes of Health, Bethesda, Md., the National Research Council of Canada, Ottawa, and the Deutsche Forschungsgemeinschaft.*
[2]*This work was submitted in partial fulfillment for the degree of Ph.D. (A. F.) in the Department of Chemistry, McGill University; the kinetic experiments were performed at the Max-Planck-Institut für physikalische Chemie.*
[3]*Holder of Studentship from the National Research Council of Canada.*

ments of the light scattered as a function of time. Such systems involve complex, overall reactions leading to the formation of aggregates of different size. Therefore, it is conceivable that the initial reaction between the specific combining sites was obscured by re-equilibration steps resulting in some statistical redistribution of these aggregates with respect to their size. In other instances, such as the kinetic studies of the inhibition of luciferase (6) and the neutralization of bacteriophage (7) by the corresponding antibodies, rates of combination between antigen and antibody molecules were not measured directly. Only Berson and Yallow (8) have actually determined rate constants from the direct measurements of the rates of association between insulin and the corresponding antibodies; I^{131}-labelled insulin in concentrations as low as 10^{-9} M was used for this purpose and the values reported for the rate constants ranged from 10^4 to 10^6 $M^{-1}\text{sec}^{-1}$ (8).

Only two studies of the kinetics of antibody–hapten reactions have been reported so far. Schneider and Sehon (9) attempted to study the kinetics of the reaction between the reducible hapten 4-(4′-aminophenylazo)phenyl arsonic acid and its homologous antibody with the aid of cathode-ray polarography. They reported that the reaction had gone to completion within the time of mixing, which was estimated to be 1–2 seconds. Although rate measurements could not be made directly, lower limiting values of 10^6 $M^{-1}\text{sec}^{-1}$ and 1 sec^{-1} were calculated for the rate constants k_{12} and k_{21}, respectively, for the reaction

$$\text{Ab} + \text{H} \underset{k_{21}}{\overset{k_{12}}{\rightleftharpoons}} \text{AbH}. \qquad [1]$$

While the present investigation was in progress, Sturtevant *et al.* (10) studied the association between a dinitrobenzene derivative and its homologous antibodies using a stopped flow technique. These authors have shown that about two thirds of the reaction had gone to completion within the dead time of their instrument. Nevertheless, they were able to compute a rate constant of 10^6 $M^{-1}\text{sec}^{-1}$ for k_{12} for the slower region of the reaction, and suggested a value as high as 10^8 $M^{-1}\text{sec}^{-1}$ for the faster portion of the reaction.

In the present paper, studies of the kinetics of antibody–hapten interactions by means of the temperature-jump method are reported. This technique is generally applicable to rapid reactions involving a change in enthalpy and which occur within the range of 1 microsecond to 1 second. The reaction system is perturbed by a sudden jump in temperature (of about 10° C), which is achieved within 0.1–1 microsecond by discharging a condensor through a conducting solution containing the system to be studied. The rate of readjustment of the system to the new equilibrium conditions at the higher temperature is then determined by following the change in an appropriate physical parameter, which represents the concentration of one of the reactants. Provided the deviations from equilibrium are small, for a one-step reaction the linearized rate equation can be expressed as

$$\tau \frac{d(\Delta C)}{dt} + \Delta C = \Delta \bar{C}(t),$$

where $\Delta \bar{C}(t)$ is the change in equilibrium concentration of a given reactant, ΔC the concentration change from the original equilibrium value at any time t, and τ is the relaxation time (11). With the help of appropriate relations which are characteristic for a given reaction mechanism, τ yields the rate constants determining the new equilibrium. Thus, for a reaction of the type represented by equation [1] the relaxation time is expressed by

$$\frac{1}{\tau} = k_{21}+k_{12}[(\overline{\mathrm{Ab}})+(\overline{\mathrm{H}})],$$

where $(\overline{\mathrm{Ab}})$ and $(\overline{\mathrm{H}})$ represent equilibrium concentrations of the antibody and hapten, respectively.

In view of the scarcity of specific antibodies, the applicability of this relaxation technique to the present investigation was first established with a model system consisting of bovine serum albumin (BSA) and the two colored hapten molecules 1-naphthol-4-[4-(4′-azobenzene azo)phenyl arsonic acid] and 1-naphthol-2 sulphonic acid -4-[4-(4′azobenzene azo)phenyl arsonic acid. This system was chosen as a model since the results of equilibrium measurements for BSA–dye interactions are similar to those of antibody–hapten reactions (12, 13).

EXPERIMENTAL

Materials

Crystalline bovine serum albumin (BSA) was obtained from Armour Pharmaceutical Co., Kankakee, Ill. The molecular weight of BSA used for various calculations was taken as 69,000 (14).

Antibodies to the phenyl arsonate group were prepared by immunizing rabbits with the protein–hapten conjugates as described elsewhere (15). The antibody preparations used in this study were isolated by precipitation of the γ-globulin fraction according to the procedure of Marrack *et al.* (16).

The haptens used for the kinetic studies with both BSA and specific antibodies were the dyes 1-naphthol-4-[4-(4′-azobenzene azo)phenyl arsonic acid] and 1-naphthol-2 sulphonic acid-4-[4-(4′-azobenzene azo)phenyl arsonic acid], referred to hereafter as N—R′ and NS—R′, respectively. These compounds were prepared by coupling the diazonium salt of 4-(4′-aminobenzene azo)phenyl arsonic acid to 1-naphthol and 1-naphthol-2 sulphonic acid, respectively (17).

The buffers used were borate–KNO_3 (pH 8.0, 8.5, 9.0, $\Gamma/2 = 0.1$), borate–NaCl (pH 8.0, $\Gamma/2 = 0.1$), Tris[4]–KNO_3 (pH 7.5, $\Gamma/2 = 0.1$), and phosphate (pH 7.0, $\Gamma/2 = 0.1$).

Methods

The concentrations of the BSA solutions were determined spectrophotometrically at a wavelength of 280 mμ ($E^{1\%}_{1\,\mathrm{cm}} = 6.8$). Antibody concentrations were determined by the quantitative precipitin method of Heidelberger and Kendall (18), and the nitrogen contents of the precipitates were obtained by the micro-Kjeldahl procedure of McKenzie and Wallace (19).

The concentrations of bound and free dyes were determined spectrophotometrically (20, 21). If the molar extinction coefficients of the bound and free forms of the dye are known, the fraction of the free dye can be calculated from the equation

$$\alpha = \frac{\epsilon_{\mathrm{app}}-\epsilon_{\mathrm{b}}}{\epsilon_{\mathrm{f}}-\epsilon_{\mathrm{b}}},$$

where ϵ_{app} is the apparent molar extinction coefficient of the dye, and ϵ_{f} and ϵ_{b} are the molar extinction coefficients of the free and bound forms of the dye, respectively. The molar extinction coefficient of the free dye was calculated from the optical densities of solutions of known dye concentrations in appropriate buffers. To obtain ϵ_{b} the method of Westphal *et al.* (21) was used. Values for the apparent molar extinction coefficient were determined for a series of solutions containing a constant amount of dye and varying amounts of BSA or of the specific antibodies. For the calculation of ϵ_{b}, values of ϵ_{app} were plotted versus the ratios of dye/protein concentrations of the corresponding solutions, and ϵ_{b} was identified with the molar extinction coefficient of the solution for infinite protein concentration. All spectrophotometric measurements were made with a Zeiss spectrophotometer.

The number of binding sites on the BSA molecule was calculated with the help of the equation used previously by Nisonoff and Pressman (22) for antibody–hapten systems,

$$\frac{1}{b} = \frac{1}{K(\mathrm{P})c} + \frac{1}{(\mathrm{P})},$$

where b and c are the concentrations of bound and free dye, (P) is the total molar concentration of the protein binding sites, and K is the equilibrium constant. For this purpose varying amounts of dyes were added to a constant amount of BSA and the concentrations of bound and free dye were calculated from optical density measurements. The number of binding sites on the antibody molecules was taken as two (1, 23).

[4]*Tris refers to tris-(hydroxy methyl)-amino methane.*

Relaxation time measurements were made with the aid of the temperature-jump apparatus described elsewhere (11, 24), and the rate of re-equilibration at a higher temperature was followed spectrophotometrically at a wavelength of 590 mμ.

RESULTS AND DISCUSSION

(a) BSA–Dye Interactions

The rationale for synthesizing the particular dyes N—R′ and NS—R′ was that these compounds incorporated the antigenic determinant, the phenyl arsonate group, and had a structure similar to that of Orange I, which is a pH indicator. The pK values of these pH indicators as determined by spectrophotometric measurements in buffer solutions of various pH values were 8.7 and 7.2 for N—R′ and NS—R′, respectively. An increase in pH resulted in a shift of the absorption spectra of the dyes to longer wavelengths, which was considered to be due to the ionization of the naphtholic OH group. Similar shifts were observed when BSA or the specific antibody solutions were added to the dye solutions. To obtain maximum shifts in wavelength due to the binding of the dyes, experiments were performed in buffer solutions of pH values which were mainly below the pK values of the dyes. The effect of BSA on the absorption spectrum of N—R′ in borate–KNO_3 buffer (pH 8.0, $\Gamma/2 = 0.1$) is shown in Fig. 1, from which it is evident that the absorption maximum was shifted from 510 mμ (which corresponded to the free dye) to 610 mμ for the bound dye. Spectral shifts for the interaction of NS—R′ with BSA in phosphate buffer (pH 7.0, $\Gamma/2 = 0.1$) were not nearly as pronounced (Fig. 2).

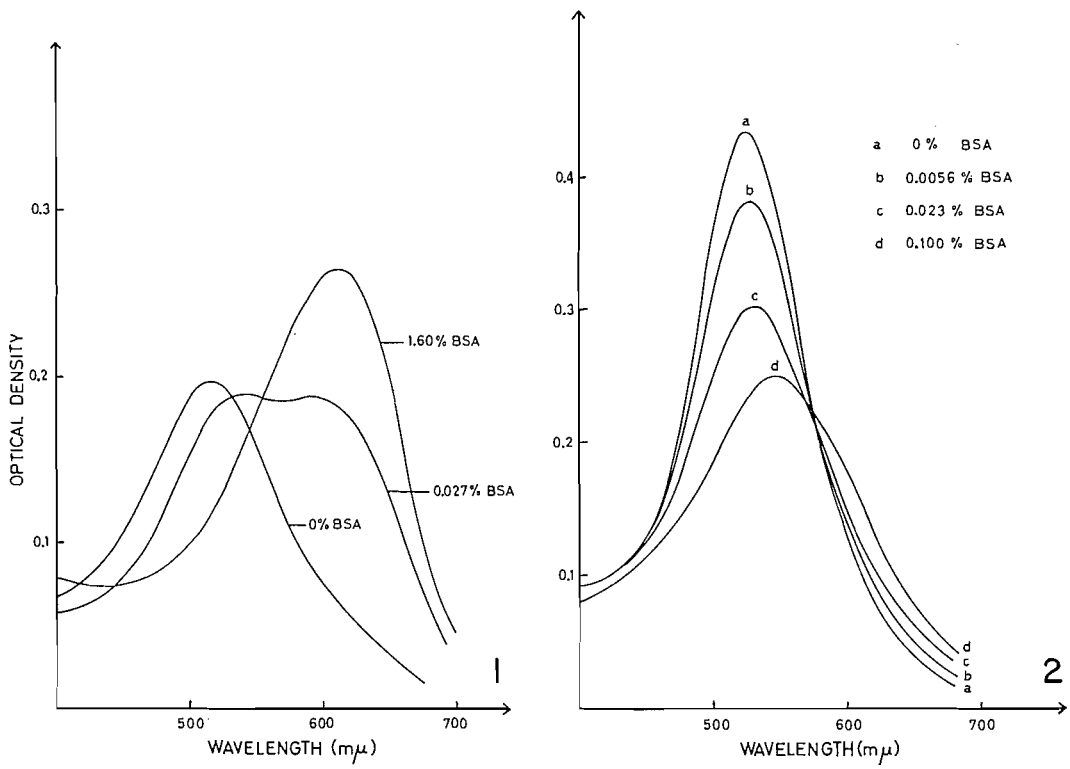

FIG. 1. The effect of BSA on the absorption spectrum of a 9.1×10^{-6} M solution of N—R′ in borate–KNO_3 buffer (pH 8.0, $\Gamma/2 = 0.1$).

FIG. 2. The effect of BSA on the absorption spectrum of a 9.1×10^{-6} M solution of NS—R′ in phosphate buffer (pH 7.0, $\Gamma/2 = 0.1$).

In the present study equilibrium dialysis could not be employed, since both dyes showed an extremely high affinity for the dialysis membranes. Therefore, only spectrophotometric methods were used for the determinations of free and bound reactants, as described under Methods. The molar extinction coefficient ϵ_f was determined as 0.58×10^4 M^{-1}cm^{-1} at 610 mμ and the value for ϵ_b was calculated (at pH 8.0, borate–KNO_3 buffer) from the plot shown in Fig. 3 as 2.80×10^4 M^{-1}cm^{-1}. The corresponding extinction

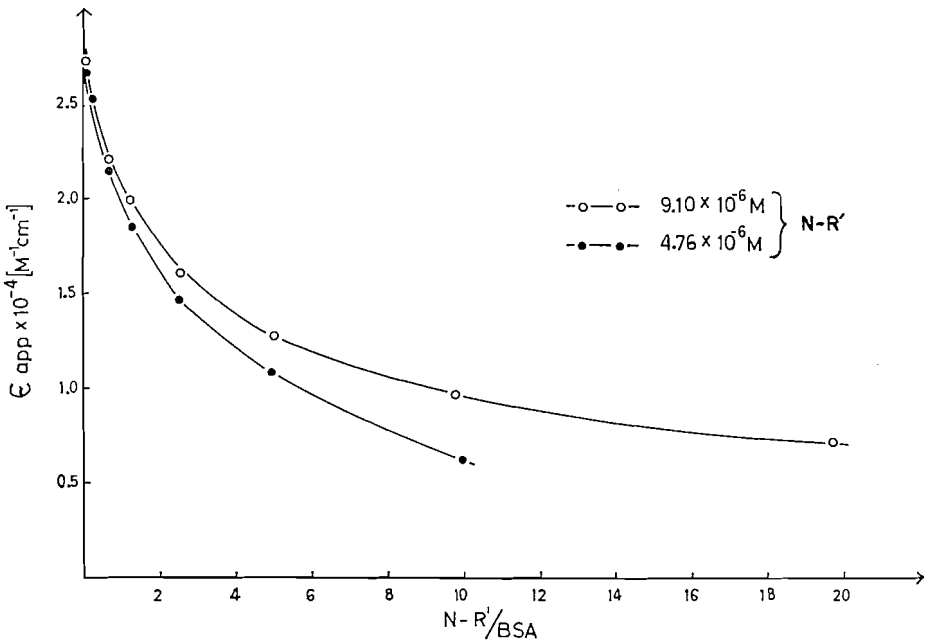

FIG. 3. Determination of ϵ_b of N—R′ bound by BSA for two different dye concentrations in borate–KNO_3 buffer (pH 8.0, $\Gamma/2 = 0.1$).

coefficients for NS—R′ in phosphate buffer (pH 7.0) were determined as 2.10×10^4 M^{-1}cm^{-1} and 1.04×10^4 M^{-1}cm^{-1} for ϵ_b and ϵ_f, respectively.

Binding curves for BSA with the dyes N—R′ and NS—R′ are shown in Figs. 4 and 5, respectively, and the corresponding number of binding sites per molecule of BSA for N—R′ and NS—R′ were calculated as five and one. The deviation of the curve from a straight line in Fig. 4 indicates that the binding sites on BSA have different affinities for N—R′ and a heterogeneity index (a) of 0.6 was calculated using the method of Nisonoff and Pressman (22). The average equilibrium constant K_0 for the association between N—R′ molecules and BSA was computed as 1×10^5 M^{-1}. On the other hand the plot in Fig. 5 suggests that the sites of BSA involved in the binding of NS—R′ were homogeneous. The equilibrium constant for this reaction was calculated as 5.5×10^4 M^{-1}.

To simplify the evaluation of the relaxation time measurements, it was assumed that all the binding sites on the BSA molecule were identical and independent of one another. Relaxation time measurements were performed on different solutions of varying dye/protein concentration ratios. A relaxation curve for the interaction between N—R′ and BSA is shown in Fig. 6. In all cases the curves were characterized by a single relaxation time. From the analysis of the concentration dependence of the relaxation time it was found that the relation

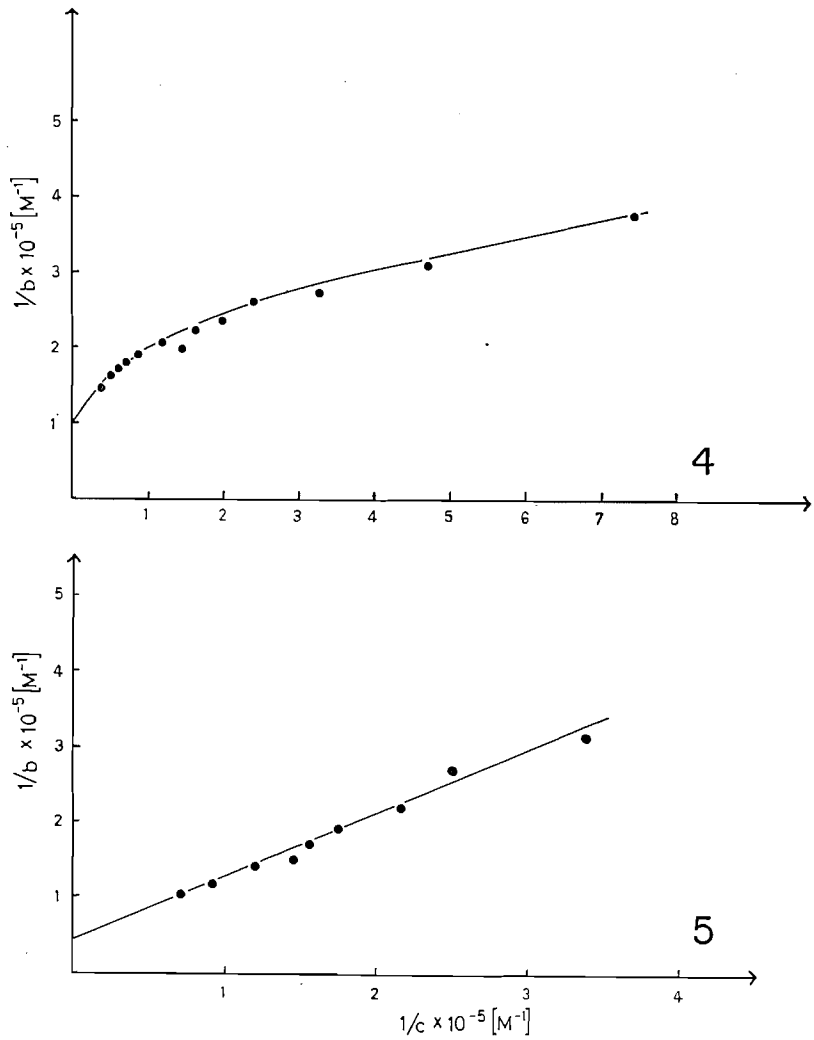

FIG. 4. The binding of N—R′ by BSA in borate-KNO_3 buffer (pH 8.0, $\Gamma/2 = 0.1$) at 25° C. Here c and b represent the free and bound dye concentrations, respectively.

FIG. 5. The binding of NS—R′ by BSA in phosphate buffer (pH 8.0, $\Gamma/2 = 0.1$) at 25° C. The symbols c and b represent the free and bound dye concentrations, respectively.

$$\frac{1}{\tau_{ii}} = k_{21}+k_{12}[(\overline{P})+(\overline{D})]$$

described the behavior of the system (11). In consequence it is suggested that the overall mechanism for the interaction of BSA with N—R′ is represented by the reactions

$$P + D \underset{k_{21}}{\overset{k_{12}}{\rightleftharpoons}} PD.$$

In Fig. 7 are given the plots of $1/\tau$ versus $[(\overline{P})+(\overline{D})]$ for 25, 30, and 35° C. The corresponding rate constants k_{12} and k_{21} at these temperatures are listed in Table I. It was shown also that the values for k_{12} and k_{21} were almost independent of the buffer ions used.

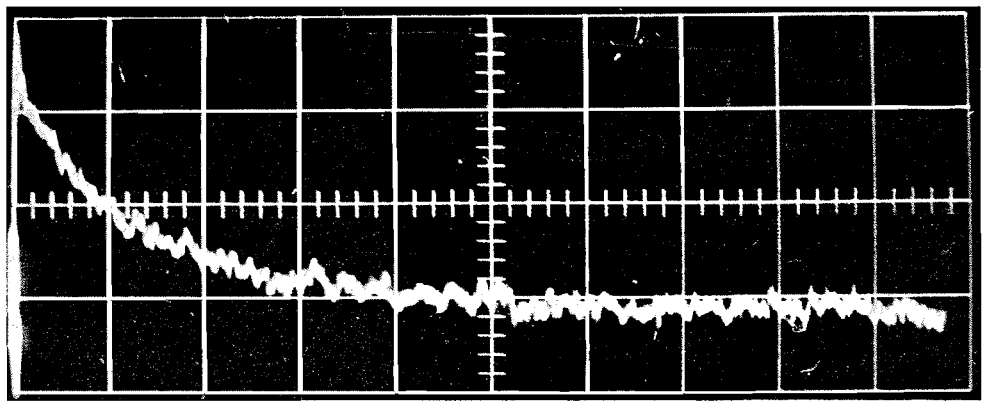

FIG. 6. Relaxation curve for the reaction between BSA and N—R′ (sweep rate 5 msec/cm).

TABLE I

Temperature (°C)	$k_{21}\times10^{-1}$ (sec^{-1})	$k_{12}\times10^{-6}$ ($M^{-1}sec^{-1}$)
25	3.5	2.1
30	7.0	3.2
35	13.6	3.7

The same relationship was found to be valid for the concentration dependence of the reaction between NS—R′ and BSA at 25° C (Fig. 8), and the appropriate rate constants were calculated as $k_{12} = 3.6\times10^5\ M^{-1}sec^{-1}$ and $k_{21} = 2.5\ sec^{-1}$. Thus, the equilibrium constants obtained from the ratio k_{12}/k_{21} for the systems consisting of BSA and N—R′ and NS—R′ are respectively $6\times10^4\ M^{-1}$ and $1.4\times10^5\ M^{-1}$ at 25° C. These values are of the same order of magnitude as the equilibrium constants calculated from static experiments, i.e. $1\times10^5\ M^{-1}$ and $5.5\times10^4\ M^{-1}$ for the N—R′ and NS—R′ systems, respectively (see also above).

In view of the different approaches used for obtaining these values, which represent only averages of the distribution of complex constants for the different binding sites, this agreement is considered satisfactory. Moreover, it ought to be stated that in the static experiments (Figs. 4 and 5) the concentration of the dyes had to be varied within wide limits, some of which were outside the range where the dye N—R′ obeyed Beer's law. This effect was probably caused by micelle formation and might introduce a serious error in the calculation of both the equilibrium constant and the number of binding sites. The latter error is carried over to the kinetic experiments in as much as the relaxation times are related to the total number of active sites.

In view of the heterogeneous population of the binding sites with respect to their affinity for the dye, which results in a distribution of equilibrium values (Fig. 4), it is reasonable to expect that there should be also a statistical distribution of the corresponding rate constants, k_{12} and k_{21}, rather than single values. From the equilibrium experiments with N—R′ an average value for the binding constant was determined. However, on the basis of the calculated heterogeneity coefficient of 0.6, the actual equilibrium constants for the different binding sites would vary over a wide range of values, differing by as much as two orders of magnitude (22). No account was taken of this complication in

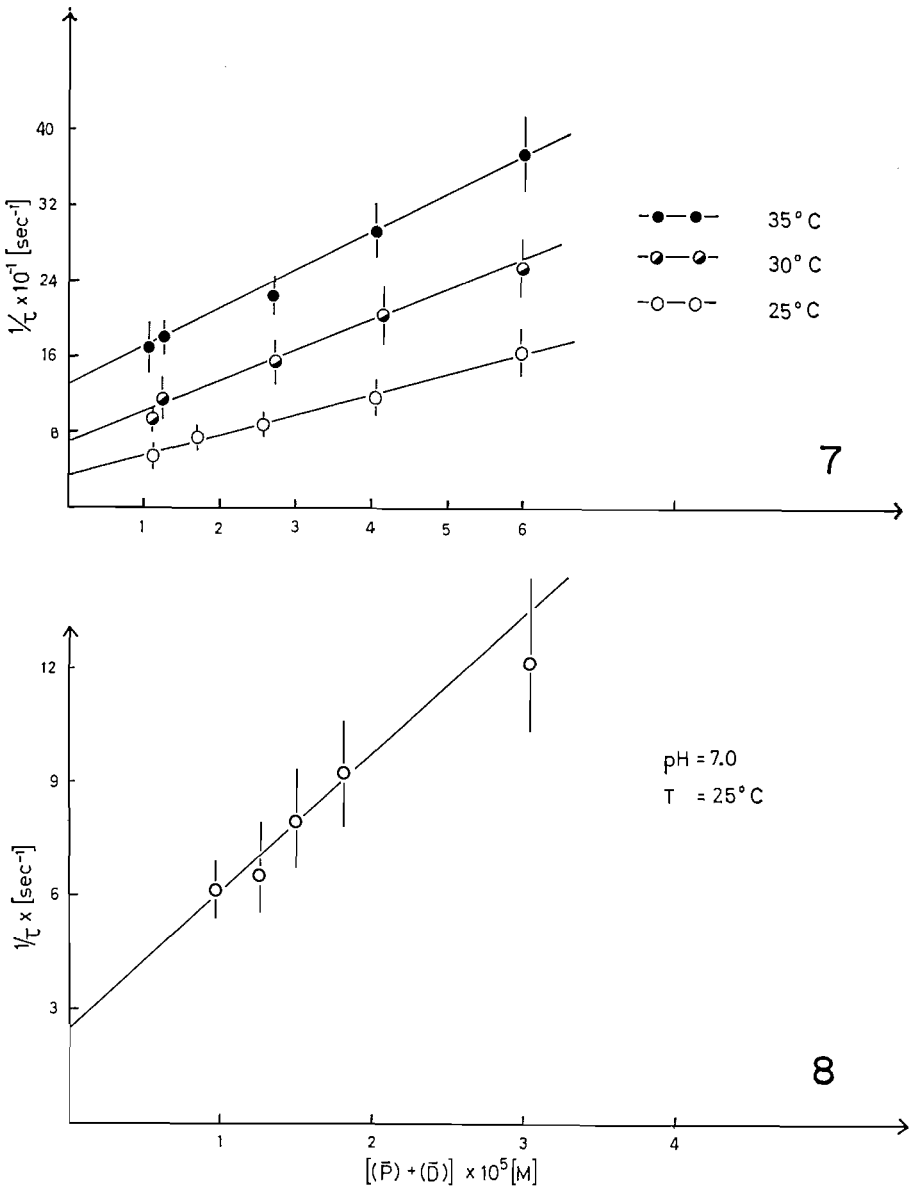

FIG. 7. Concentration dependence of $1/\tau$ for the reaction between BSA and N—R′ in borate–KNO_3 buffer (pH 8.0, $\Gamma/2$) at 25, 30, and 35° C.

FIG. 8. Concentration dependence of $1/\tau$ for the reaction between BSA and NS—R′ in phosphate buffer (pH 7.0, $\Gamma/2 = 0.1$) at 25° C; $k_{12} = 3.6 \times 10^5$ [M^{-1}sec^{-1}], $k_{21} = 2.5$ [sec^{-1}].

plotting the concentration dependence of τ from which the values of k_{12} and k_{21} were calculated. In consequence, at the lower concentrations of the dye, the contribution of the binding sites with the higher affinities will be more pronounced, and on increasing the concentration of the dye the binding sites having weaker affinities will come into play. Because of all these considerations it is obvious that the temperature dependence of the rate constants could not be obtained with the high degree of accuracy required for the

determination of an activation energy. Moreover, due to technical reasons, the present studies were restricted to a narrow temperature range of 10° C, so that relatively small errors in rate constants would have led to considerable uncertainties in activation energies, particularly in determining the activation energy of the dissociation step from the temperature dependence of k_{21}, which is obtained by extrapolation of $1/\tau$ to zero concentration of the free reactants. Therefore, the estimated activation energies, $E_{12}\simeq 10$ kcal/mole and $E_{21}\simeq 20$ kcal/mole, should be regarded as preliminary values and considered with some reservation. Studies over a wider temperature range are in progress and more definite values for these activation energies will be given later. From the difference in activation energies for the association and dissociation steps, it would appear that the reaction is exothermic to the extent of about 10 kcal/mole.

Because of the great number of protolytic equilibria involved, it is conceivable that the rate of dye–albumin interactions is affected greatly by pH. Relaxation time measurements at the three different pH values of 8.0, 8.5, and 9.0 at 25° C are shown in Fig. 9,

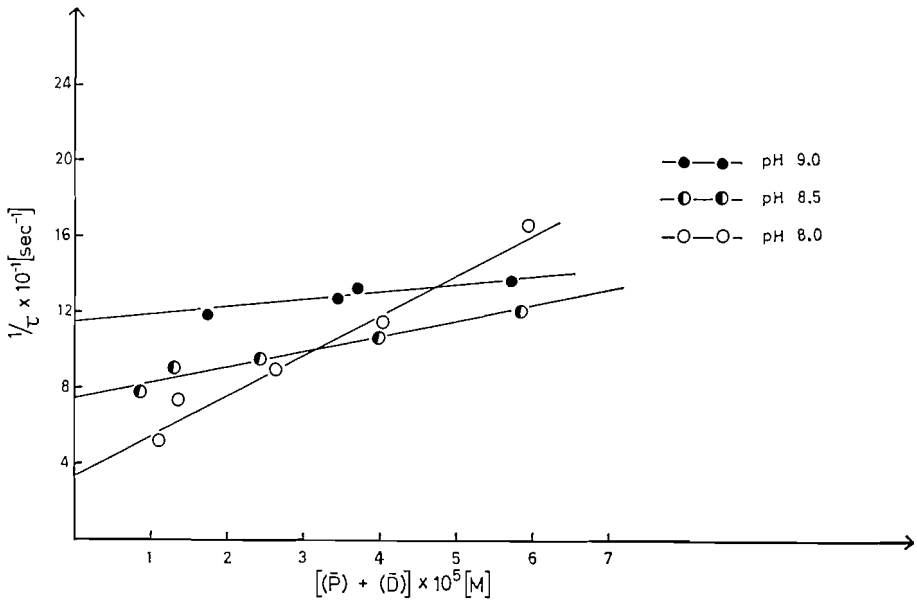

FIG. 9. Concentration dependence of $1/\tau$ for the reaction between BSA and N—R′ in borate–KNO_3 buffer at three different pH values.

from which it can be inferred that dissociation rates increase and association rates decrease with increasing pH. This could be explained partly by the increased repulsion between the negatively charged reactants, which becomes more pronounced at the higher pH values.

(b) Antibody–Hapten Interactions

Reactions between the haptens NS—R′ and N—R′ and the antibodies to the phenyl arsonate group resulted in a shift of the spectra of both dyes to longer wavelength. However, addition of normal rabbit gamma globulin to these dyes did not result in a detectable spectral shift. The change in the absorption spectrum of the NS—R′ dye due to the addition of antibody in Tris buffer at pH 7.5 is shown in Fig. 10.

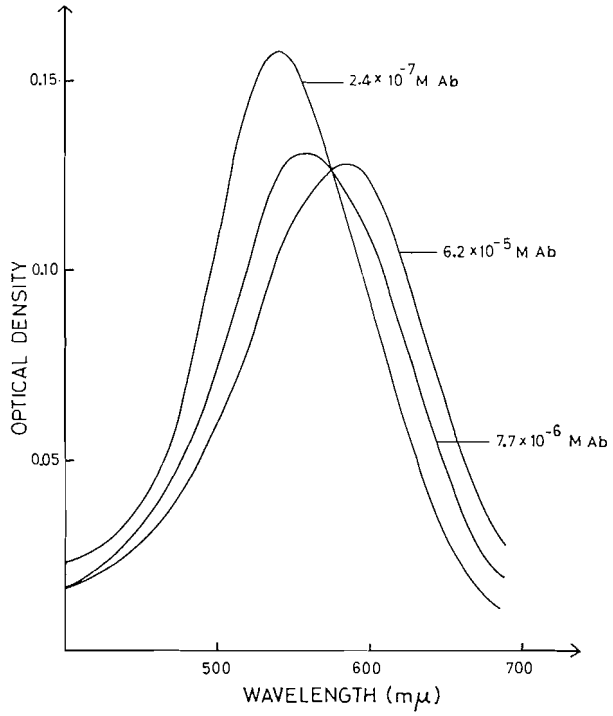

FIG. 10. The effect of anti-R antibodies on the absorption spectrum of a 4.8×10^{-6} M solution of NS—R′ in Tris–NaCl buffer (pH 7.5, $\Gamma/2 = 0.1$).

Unfortunately, it was not possible under the present experimental conditions to measure relaxation times for the reaction between NS—R′ and the antibodies in Tris buffer, because of the large temperature coefficient of the latter. This in turn led to a large change in the protolytic equilibrium of the dye, which masked any effect due to the dye–antibody interaction. Phosphate buffer could not be used either, since it was found to inhibit the reaction.

In spite of the fact that the N—R′ was univalent, precipitation was observed at some antibody-to-hapten ratios. This precipitation was most likely due to the aggregation of the hapten into micelles, an effect which was previously referred to. For this reason no binding studies were done with N—R′. Nevertheless, relaxation time measurements could be made with this system in borate buffer at pH 8.0 in a concentration range where no precipitation occurred. The value for ϵ_b for N—R′ was assumed to be 2.8×10^4 $M^{-1}cm^{-1}$, by analogy with the value determined for the BSA – N—R′ system.

From the concentration dependence of $1/\tau$ (Fig. 11) the rate constants k_{12} and k_{21} were calculated as $\sim2\times10^7$ $M^{-1}sec^{-1}$ and ~50 sec^{-1}, respectively. These values are higher by one order of magnitude than the lower limits estimated by Schneider and Sehon for the phenyl arsonate system (9). The value of k_{12} exceeds also the lower limit reported by Sturtevant *et al.* for the dinitrophenyl system (10) by one order of magnitude. Although rate constants as large as 10^9 $M^{-1}sec^{-1}$ could have been determined with the method used in the present investigation, no further second-order step representing the formation of specific complexes could be detected. The equilibrium constant calculated from the values of k_{12} and k_{21}, i.e. $\sim4\times10^5$ M^{-1}, agrees well with the equilibrium constants calculated for similar antibody–hapten reactions (9, 25).

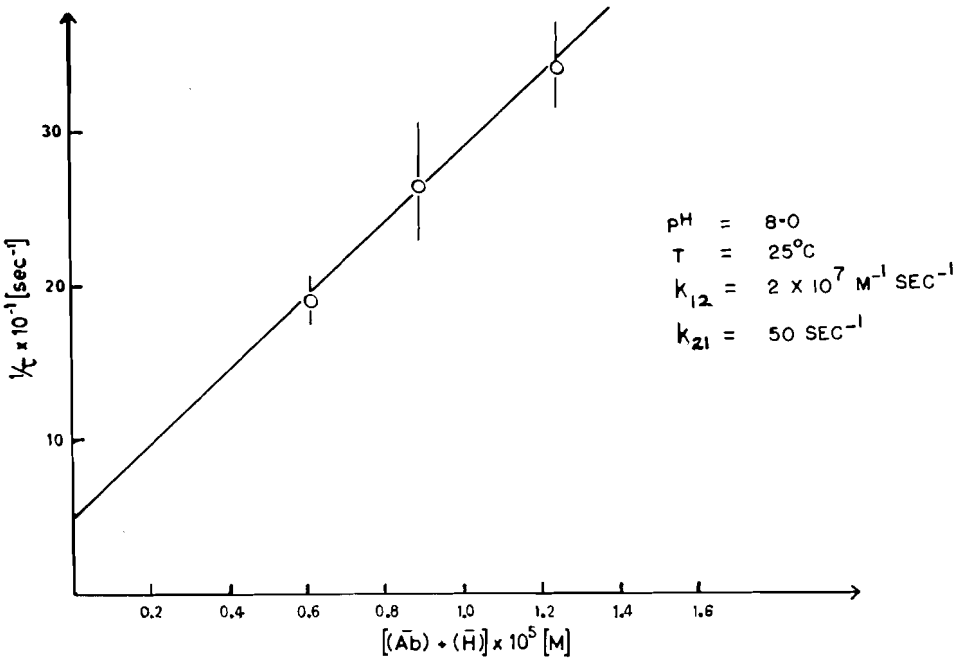

FIG. 11. Concentration dependence of $1/\tau$ for the reaction between anti-R antibodies and N—R′ in borate–NaCl buffer (pH 8.0, $\Gamma/2 = 0.1$) at 25° C.

GENERAL REMARKS

This study has demonstrated the applicability of the temperature-jump method to the investigation of the kinetics of protein–dye and antibody–hapten reactions. In view of the complicated mechanisms underlying these systems, the error limits of the rate constants obtained in these first studies might still be quite large. However, additional support for the kinetic values derived in this study is provided by the good agreement between the equilibrium constants calculated from the ratios of k_{12}/k_{21} and the equilibrium values computed from static experiments, both in this and other studies (1, 9, 25). The rate constant for the association between the hapten and the specific antibody at 25° C was found to be larger than that for the reaction between the hapten and BSA (by a factor of at least 10), but it is still more than one order of magnitude below the limit to be expected for a diffusion-controlled reaction. The fact that BSA reacts more slowly is not surprising since one might expect that repulsion between the negatively charged dye and albumin molecules is larger and that the extent of complementariness between the combining sites in the antibody–hapten system is more pronounced.

REFERENCES

1. D. TALMAGE and J. R. CANN. The chemistry of immunity in health and disease. C. C. Thomas, Springfield. 1961.
2. S. F. VELICK, C. W. PARKER, and H. N. EISEN. Proc. Natl. Acad. Sci. U.S. **46**, 1470 (1960).
3. B. GITLIN and H. EDELHOCH. J. Immunol. **66**, 67 (1951).
4. R. J. GOLDBERG and D. H. CAMPBELL. J. Immunol. **66**, 79 (1951).
5. P. JOHNSON and R. H. OTTEWILL. Discussions Faraday Soc. **18**, 327 (1954).
6. F. I. TSUJI, D. L. DAVIES, and R. SOWINSK. J. Immunol. **84**, 615 (1960).
7. J. R. CANN and E. W. CLARK. J. Am. Chem. Soc. **78**, 3627 (1956).
8. S. A. BERSON and R. S. YALOW. J. Clin. Invest. **38**, 1996 (1959).
9. H. SCHNEIDER and A. H. SEHON. Trans. N.Y. Acad. Sci. **24**, 15 (1961).
10. J. M. STURTEVANT, L. WOLFSY, and S. J. SINGER. Science, **134**, 1434 (1961).

11. M. EIGEN and L. DE MAEYER. *In* Technique of organic chemistry. Vol. 8. (Part 2), p. 793 ff 2nd ed. *Edited by* A. Weissberger.
12. F. KARUSH. J. Am. Chem. Soc. **72**, 2705 (1950).
13. W. KAUZMANN. *In* Advances in protein chemistry. Vol. 44. Academic Press, Inc., New York. 1959.
14. E. J. COHN, W. L. HUGHES, JR., and J. H. WEARE. J. Am. Chem. Soc. **69**, 1703 (1947).
15. A. FROESE and A. H. SEHON. Can. J. Biochem. and Physiol. **39**, 1067 (1961).
16. J. R. MARRACK, H. HOCH, and R. G. S. JOHNS. Brit. J. Exptl. Pathol. **32**, 212 (1951).
17. A. FROESE. Ph.D. Thesis, McGill University, Montreal, Canada. 1962.
18. M. HEIDELBERGER and F. E. KENDALL. J. Exptl. Med. **50**, 809 (1929).
19. H. A. MCKENZIE and H. S. WALLACE. Australian J. Chem. **7**, 55 (1954).
20. I. M. KLOTZ. *In* The proteins. *Edited by* H. N. Neurath and K. Bailey. Vol. I. Part B. Academic Press, Inc., New York. 1953.
21. U. WESTPHAL, B. B. ASHLEY, and G. L. SELDEN. J. Am. Chem. Soc. **80**, 5735 (1958).
22. A. NISONOFF and D. PRESSMAN. J. Immunol. **80**, 417 (1958).
23. F. KARUSH. J. Am. Chem. Soc. **78**, 5519 (1956).
24. G. CZERLINSKI and M. EIGEN. Z. Elektrochem. **63**, 652 (1959).
25. J. I. EPSTEIN, P. DOTY, and W. C. BOYD. J. Am. Chem. Soc. **78**, 3306 (1956).

BIOSYNTHESIS OF SUGARS FOUND IN BACTERIAL POLYSACCHARIDES

PART II. BIOSYNTHESIS OF D-*glycero*-D-*manno*-HEPTOSE

J. K. N. JONES, M. B. PERRY, AND R. J. STOODLEY
Department of Organic Chemistry, Queen's University, Kingston, Ontario

Received May 17, 1962

ABSTRACT

Azotobacter indicum was grown in media which contained D-glucose-1-C^{14}, D-glucose-2-C^{14}, D-glucose-6-C^{14}, D-mannose-1-C^{14}, or D-galactose-1-C^{14}. Each radioactive polysaccharide produced was hydrolyzed and the specific activity of the isolated D-*glycero*-D-*manno*-heptose was determined. The distribution of activity in the heptose molecule was determined by chemical degradation procedures.

The results suggest that the D-*glycero*-D-*manno*-heptose is formed from hexose precursors by pathways which involve the action of transaldolase, transketolase, and aldolase

INTRODUCTION

The role of D-*altro*-heptulose (sedoheptulose) 7-phosphate in cellular metabolism has been amply demonstrated. It has been detected as an early product of photosynthesis (1) and as an intermediate in the pentose phosphate cycle (2, 3). Aldoheptoses have been found in the polysaccharides of a number of Gram-negative bacteria (4), although there is little information about the structures of such polymers. The mode of biosynthesis of these 7-carbon sugars has not been reported, but it is logical to expect that they may be derived from D-*altro*-heptulose 7-phosphate.

Knight and his co-workers (5) have shown that *Azotobacter indicum* can produce a heptose-containing extracellular polysaccharide. Sowa (6) in this laboratory, has characterized the 7-carbon sugar as D-*glycero*-D-*manno*-heptose. The results of growing *A. indicum* in media containing a number of C^{14}-labelled sugar substrates were reported in Part I of this series (7). The polysaccharides produced were hydrolyzed and the distribution of activity in the isolated D-glucose and L-rhamnose was determined and possible origins of L-rhamnose were discussed. In this communication the results of the heptose degradations are reported and possible pathways for the biosynthesis of D-*glycero*-D-*manno*-heptose are presented.

EXPERIMENTAL

Azotobacter indicum was grown in media which contained D-glucose-1-C^{14}, D-glucose-2-C^{14}, D-glucose-6-C^{14}, D-mannose-1-C^{14}, or D-galactose-1-C^{14}. The methods for the production and hydrolysis of the polysaccharide, the isolation of the component monosaccharides, and the counting procedures were the same as those described earlier (7).

Paper chromatography was carried out by the descending method on Whatman No. 1 filter paper using the following solvent systems (v/v): (*a*) 1-butanol, ethanol, water (3:1:1), (*b*) ethyl acetate, acetic acid, formic acid, water (18:3:1:4), and (*c*) 1-butanol, pyridine, water (10:3:3). Sugars were located on the developed chromatograms by the *p*-anisidine hydrochloride spray (8).

The weights of D-*glycero*-D-*manno*-heptose isolated from the polysaccharide hydrolyzates were determined by the colorimetric phenol – sulphuric acid method (9); the estimated specific activities of the heptose are shown in Table I. The samples of radioactive D-*glycero*-D-*manno*-heptose were diluted with inactive heptose prior to their degradations.

Degradation of D-glycero-D-manno-*Heptose*

The heptose was degraded according to the reactions outlined in Fig. 1.

Determination of C^{14} in C1–6 and C7

D-*glycero*-D-*manno*-Heptose (20 mg) was dissolved in pH 8 phosphate buffer (10 ml), and 0.3 *M* sodium metaperiodate solution (2 ml) was added. Barium acetate solution was added after 2 hours and the precipitated barium salts were removed by filtration. The filtrate was acidified with acetic acid and dimedon was

TABLE I

Specific activities of D-*glycero*-D-*manno*-heptose

Sugar substrate	Specific activity of sugar substrate (μc/mmole C)	Specific activity of heptose (μc/mmole C)
D-Glucose-1-C^{14}	3.00	3.40
D-Glucose-2-C^{14}	3.00	3.22
D-Glucose-6-C^{14}	3.00	2.85

added. The precipitated formaldehyde dimedon (C7) was collected after 20 hours and was recrystallized from aqueous ethanol prior to the determination of its specific activity; m.p. 188° C. Mercuric acetate solution was added to the filtrate obtained after removal of the formaldehyde dimedon and the formic acid (C1–6) was oxidized to carbon dioxide (10), the specific activity of which was determined.

Determination of C^{14} in C1+7 and C2–6

The heptose (15 mg) was reduced with 1% sodium borohydride solution (2 ml). The excess borohydride was destroyed after 12 hours by the addition of 2 *N* sulphuric acid and the specific activity of C1+7 (formaldehyde) and of C2–6 (formic acid) were determined as described above.

Determination of C^{14} in C1–7, C1–2, C3–6, and C7

D-*glycero*-D-*manno*-Heptose *p*-nitrophenylhydrazone was prepared in the usual manner in 80% yield; m.p. 176–177° C. The hydrazone (40 mg) was dissolved in pH 8 phosphate buffer (10 ml) and was oxidized with excess sodium metaperiodate. Glyoxal *p*-nitrophenylhydrazone precipitated almost immediately and, after recrystallization from aqueous acetone, it was obtained in 65% yield; m.p. 199–200° C. The specific activity of C1–2 was then determined. The solution remaining after the removal of the glyoxal *p*-nitrophenylhydrazone was acidified with acetic acid, and dimedon was added. After 20 hours the formaldehyde dimedon was removed by filtration, and, after recrystallization from aqueous ethanol, it was obtained in 70% yield; m.p. 188° C. The material was plated and the specific activity of C7 was determined. The filtrate was acidified with sulphuric acid and distilled. The formic acid in the distillate was oxidized with mercuric acetate (10) and the specific activity of C3–6 was determined. The specific activity of C1–7 was determined by directly counting the heptose *p*-nitrophenylhydrazone.

Oxidation of D-glycero-D-manno-*Heptose p-Nitrophenylhydrazone with 1 Mole of Periodate*

D-*glycero*-D-*manno*-Heptose *p*-nitrophenylhydrazone (300 mg) was dissolved in hot water (20 ml). The solution was cooled in ice water, and periodic acid (198 mg) in water (10 ml) was added. Glyoxal *p*-nitrophenylhydrazone precipitated within a few seconds and was collected by filtration after 10 minutes. The material had m.p. 199–200° C and was obtained in 55% yield. Barium acetate solution was added to the filtrate and the precipitated barium salts were removed by filtration. The filtrate was evaporated to dryness under reduced pressure and the residue was examined by paper chromatography using solvents *a*, *b*, and *c*. A reducing component corresponding to ribose was detected with the *p*-anisidine hydrochloride spray (8). Minor amounts of other components were also detected.

The residue (170 mg) was fractionated on Whatman 3MM filter paper using solvent *a*. The area of paper containing ribose was eluted with water and the solution was evaporated to a pale yellow syrup (40.5 mg, 31%). The material was paper chromatographically homogeneous in solvents *a*, *b*, and *c*.

Determination of C^{14} in C3+7 and C4–6 of the Heptose

The ribose (15 mg) isolated above was reduced with sodium borohydride and then oxidized with sodium metaperiodate as described for D-*glycero*-D-*manno*-heptose. Formaldehyde dimedon (C3+7) was obtained in 65% yield after recrystallization from aqueous ethanol; m.p. 188° C. The formic acid (C4–6) was oxidized to carbon dioxide with mercuric acetate (10).

The specific activities of the fragments obtained during the degradation of D-*glycero*-D-*manno*-heptose are recorded in Table II.

The percentage distribution of activity in the carbon chain of D-*glycero*-D-*manno*-heptose is summarized in Table III.

The total activity of the heptose was determined by summing the individual activities of C1, C2, C3, C4–6, and C7. The isotope content of C1 was obtained by difference (activity of C7 subtracted from that of C1+7), while the activity of C2 was calculated by subtracting C1 from C1+2. When a negative value resulted, the activity of C2 was assumed to be zero. The activity of C3 was determined by subtracting C4–6 from C3–6 (in the cases when D-glucose-1-C^{14} or D-galactose-1-C^{14} were the substrates) or by subtracting C7 from C3+7 (when D-glucose-2-C^{14} and D-mannose-1-C^{14} were substrates). In the calculations the average isotope content of C7 (mean of determinations by two methods) was used.

TABLE II

Specific activities of heptose fragments (c.p.m./mmole C)

Heptose carbon	Sugar substrate				
	G-1-C^{14}	G-2-C^{14}	G-6-C^{14}	M-1-C^{14}	Gal-1-C^{14}
C1–6	—	15,750	4,040	29,540	16,560
C7*	—	10,080	112,350	6,720	16,590
C1+7	26,670	11,130	65,000	67,620	40,110
C2–6	—	17,720	630	10,330	5,540
C1+2	20,900	32,340	10,190	63,630	30,980
C3–6	3,360	10,970	630	13,810	7,510
C7†	5,250	4,640	105,420	6,720	10,920
C3+7	—	5,880	—	29,090	—
C4–6	1,190	8,400	—	1,540	2,680
C1–7	9,000	15,930	17,250	26,940	15,090

Abbreviations: G = D-glucose, M = D-mannose, Gal = D-galactose.
*Determined by periodate oxidation of heptose.
†Determined by periodate oxidation of heptose *p*-nitrophenylhydrazone.

TABLE III

Distribution of C^{14} in individual carbon atoms of D-*glycero*-D-*manno*-heptose

Sugar substrate	C^{14} as % total in the aldoheptose						
	C1	C2	C3	C4	C5	C6	C7
D-Glucose-1-C^{14}	72	0	15	←	5	→	8
D-Glucose-2-C^{14}	15	49	4	←	25	→	7
D-Glucose-6-C^{14}	16	←		2		→	82
D-Mannose-1-C^{14}	67	0	27	←	3	→	3
D-Galactose-1-C^{14}	59	0	25	←	7	→	9

DISCUSSION

There have been no reported degradations of C^{14}-labelled aldoheptoses. Preliminary studies were aimed at cleaving the heptose to a 6-carbon sugar, which could then be degraded by conventional methods. Antia and Perry (11) prepared methyl β-D-gulopyranoside by oxidizing methyl β-D-*glycero*-D-*gulo*-heptopyranoside with 1 mole of sodium metaperiodate followed by borohydride reduction of the resulting aldehyde. It was hoped to convert methyl α-D-*glycero*-D-*manno*-heptopyranoside to methyl α-D-mannopyranoside by this method; however, in practice only poor yields of mannose (ca. 15%) were obtained.

D-*glycero*-D-*manno*-Heptose *p*-nitrophenylhydrazone could be prepared in 80% yield and was used to determine the isotope content of C1+2, C3–6, and C7. Oxidation of the hydrazone with 1 mole of periodate under unbuffered conditions gave fair yields (ca. 30%) of a compound characterized chromatographically as ribose. The isolated ribose was reduced to ribitol and oxidation with sodium metaperiodate gave formaldehyde (C3+7) and formic acid (C4–6), from which the specific activities of C3+7 and C4–6 of the original heptose were determined.

The D-*glycero*-D-*manno*-heptose *p*-nitrophenylhydrazone would be expected to adopt the stable zig-zag conformation if it existed in the open-chain form, in which case the C2—C3 glycol system would be trans and unfavorable for attack by the periodate ion. The present results suggest that the heptose *p*-nitrophenylhydrazone exists mainly in a furanose ring form in which cleavage of the C2—C3 glycol system by the periodate ion is more favored than cleavage of the exocyclic C6—C7 glycol group.

The isotope contents of C1–6, C7, C1+7, and C2–6 were determined by periodate oxidation of the D-*glycero*-D-*manno*-heptose and its reduction product D-*glycero*-D-*manno*-heptitol according to the reactions outlined in Fig. 1.

Perry and Pietak (12) in an investigation of the periodate oxidation of aldoheptoses found that the production of an intermediary malondialdehyde derivative about C5 resulted in partial overoxidation, with the subsequent release of some carbon dioxide from C5. However, under the alkaline conditions used, the overoxidation is minimized and only a small proportion (0.08 mole) of carbon dioxide is released from C5 and the degradation proceeds essentially as illustrated in Fig. 1.

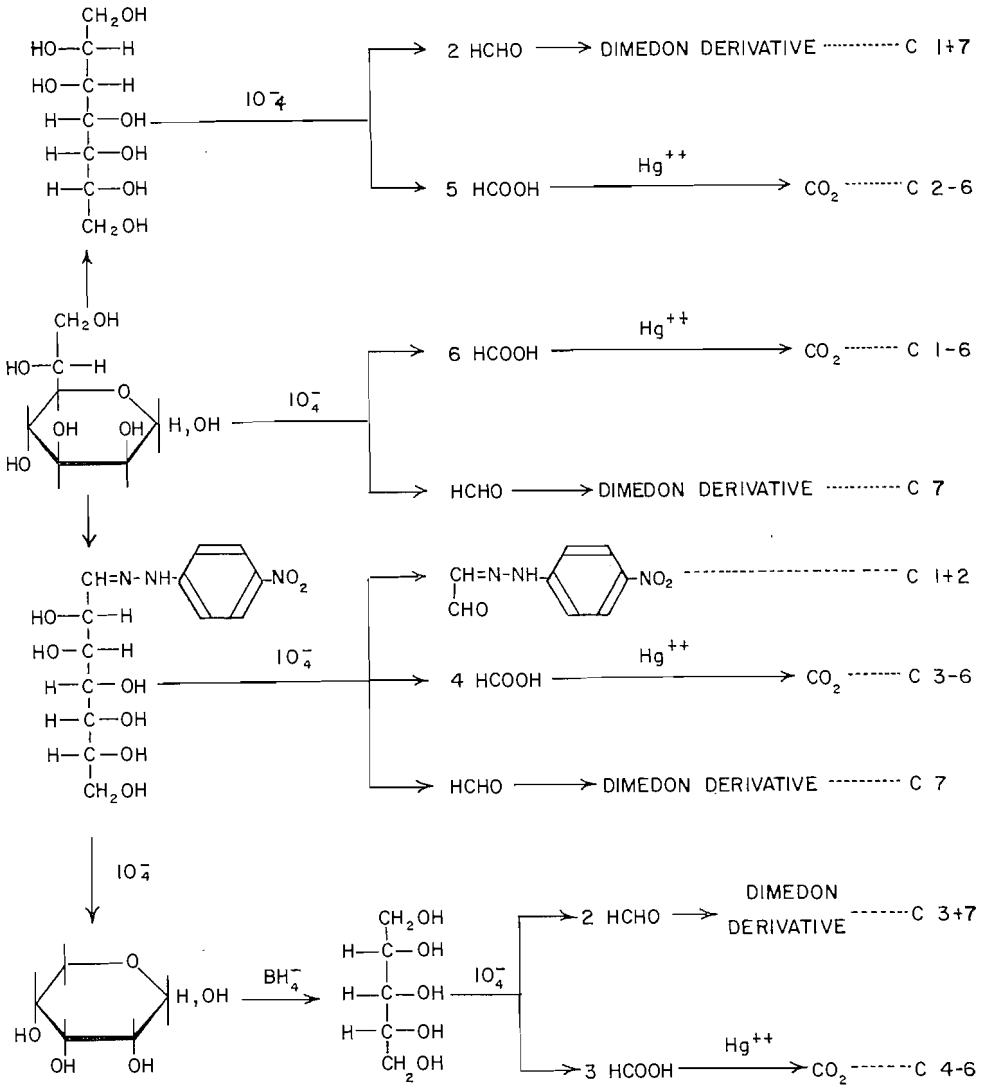

FIG. 1. Degradation of D-*glycero*-D-*manno*-heptose-C^{14}.

In this investigation the isotope contents of C4–6 and C7 were determined directly while those of C1, C2, and C3 were calculated by difference, using 2 mmoles of heptose.

It is generally unwise to determine activities of carbon atoms indirectly, since the errors are magnified. However, the objection is not so serious as it may first appear. When D-glucose-1-C^{14}, D-glucose-2-C^{14}, and D-mannose-1-C^{14} were substrates for extracellular polysaccharide synthesis by *A. indicum*, the isolated heptose samples contained very little activity in C7. The determination of C1+7 and C3+7 is, therefore, almost as satisfactory as a direct determination of C1 and C3.

When D-glucose-1-C^{14}, D-mannose-1-C^{14}, and D-galactose-1-C^{14} were substrates about $65\pm7\%$ of the activity was located in C1 of the isolated heptose. The majority of the remaining radioactivity was located in C3 ($21\pm6\%$). Most of the activity (82%) was found in C7 of the heptose when D-glucose-6-C^{14} was the substrate and the remaining activity was located in C1. When D-glucose-2-C^{14} served as the substrate about 50% of the activity was recovered in C2 of the heptose, 25% in C4–6, and 15% in C1. This latter result indicates that C1 decarboxylation is occurring and suggests that some of the pentose thus formed in the hexose monophosphate shunt is utilized for heptose synthesis.

The specific activities of the 7-carbon sugars isolated from the polysaccharide hydrolyzates were quite similar to each other ($\pm8\%$) and also to those of the corresponding hexose-1-C^{14}, -2-C^{14}, or -6-C^{14} substrates, indicating that C1, C2, and C6 of D-glucose make similar contributions to the heptose carbon skeleton.

The distribution of activity in the heptose samples may be largely interpreted in terms of the known reactions of the pentose phosphate cycle (13), which are summarized in Fig. 2. The routes which may be responsible for aldoheptose biosynthesis are shown in

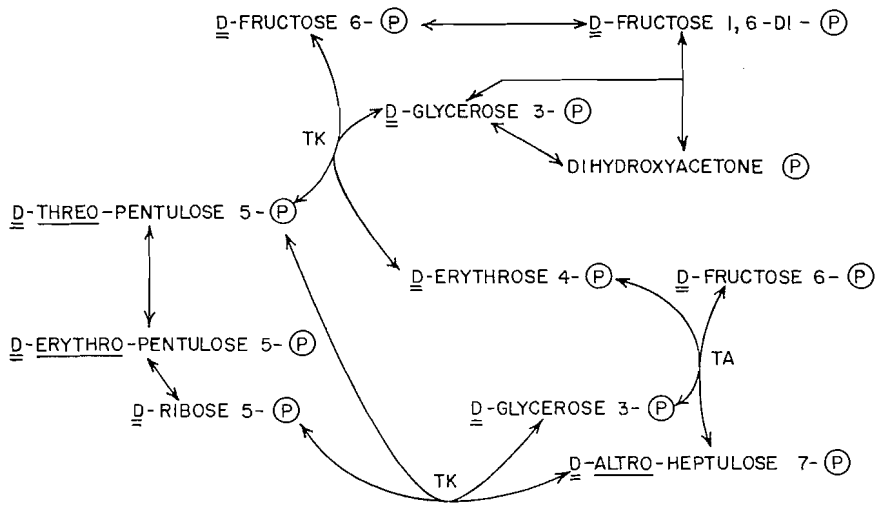

FIG. 2. Reactions of the pentose phosphate cycle.

Fig. 3. If reactions B and C (Fig. 3) are the sole pathways, the specific activity of the heptose isolated from the D-glucose-6-C^{14} substrate should be only 50–60% as much as the specific activities of the heptose samples isolated from the other substrates. In practice

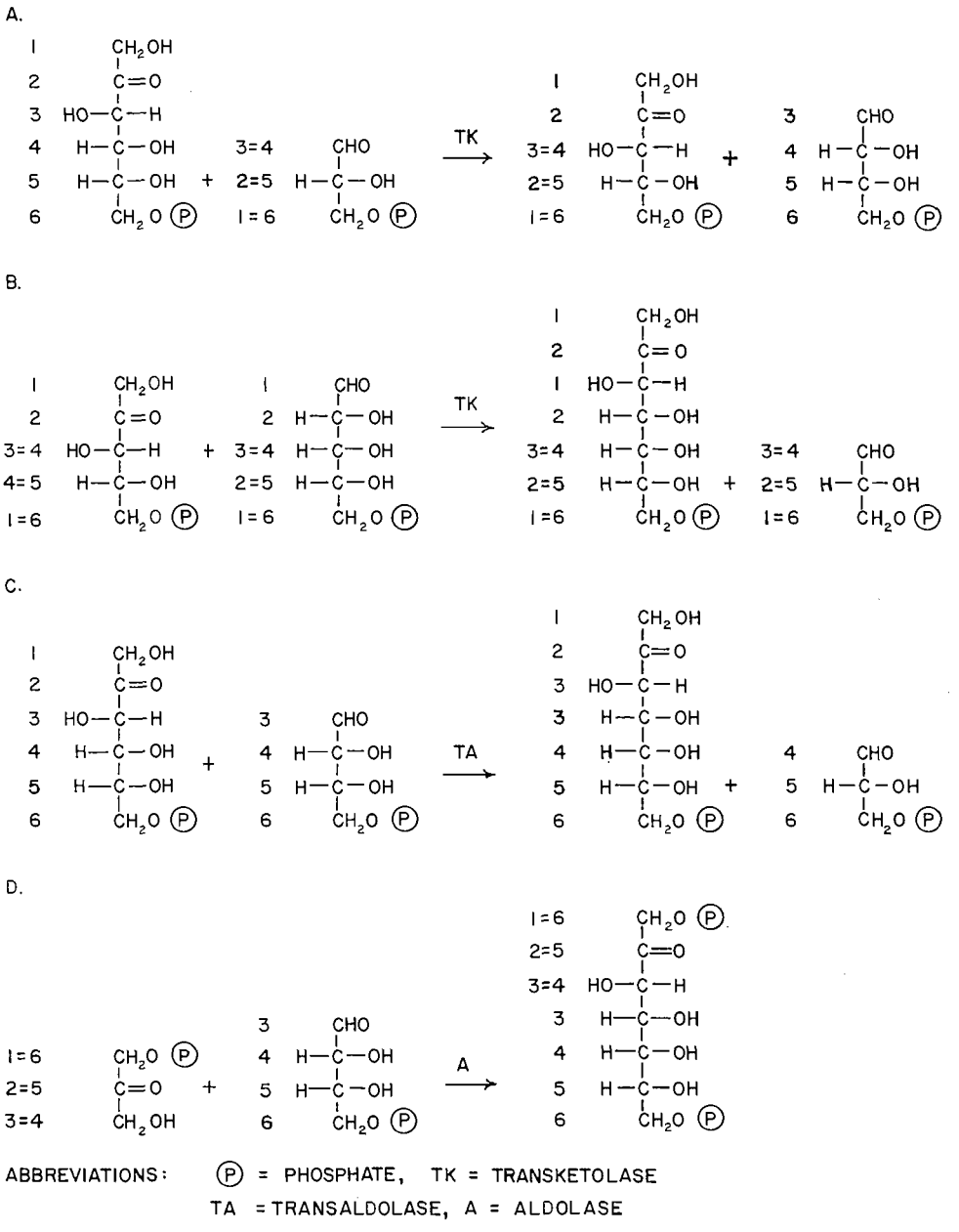

FIG. 3. Possible routes of heptose biosynthesis.

there was little difference between these specific activities, suggesting that there is an additional route for heptose synthesis in which C6 of D-glucose makes more of a contribution than C1 or C2.

Horecker *et al.* (14) and Ballou *et al.* (15) have shown that aldolase can catalyze the condensation of dihydroxyacetone phosphate with D-erythrose 4-phosphate to form D-*altro*-heptulose 1,7-diphosphate (route D, Fig. 3). If it is assumed that 25% of the heptose synthesized by *A. indicum* is formed by this route, 25% by route B, and 50%

by route C, the observed specific activities and the distributions of activity in the heptose can be explained.

There have been no previous investigations on the mechanism of formation of aldoheptoses found in polysaccharides. The present study suggests that D-*glycero*-D-*manno*-heptose may be synthesized by the action of transketolase on D-*threo*-pentulose 5-phosphate and D-ribose 5-phosphate. The pentoses may be derived from hexose and triose phosphates by the action of transketolase, or from hexonic acid phosphate via the hexose monophosphate shunt. The action of transaldolase on hexose and tetrose phosphates probably makes a significant contribution to the 7-carbon sugar biosynthesis. D-*altro*-Heptulose 7-phosphate is probably formed by these reactions while D-*altro*-heptulose 1,7-diphosphate may also be produced by the action of aldolase on dihydroxyacetone phosphate and D-erythrose 4-phosphate.

The heptulose phosphates are probably converted to aldoheptose phosphates, which are then transformed into the appropriate nucleotides, prior to incorporation into the polysaccharide. Palleroni and Doudoroff have shown that D-*altro*-heptulose and D-*glycero*-D-*manno*-heptose are interconvertible in the presence of a mannose isomerase from *Pseudomonas saccharophila* (16). Ginsburg (17) has recently isolated the guanosine diphosphate derivative of D-*glycero*-D-*manno*-heptose from bakers' yeast.

ACKNOWLEDGMENTS

The authors are greatly indebted to Dr. N. K. Richtmyer for a generous sample of D-*glycero*-D-*manno*-heptose hexaacetate. They thank Dr. G. B. Krotkov and Dr. C. D. Nelson of the Biology Department of Queen's University for making available the counting apparatus. They would also like to thank the National Research Council of Canada for financial assistance (Grants T-39 and NRC 706) and for the award of a Studentship to one of them (R. J. S.).

REFERENCES

1. A. A. BENSON, J. A. BASSHAM, and M. CALVIN. J. Am. Chem. Soc. **73**, 2970 (1951).
2. B. L. HORECKER and P. Z. SMYRNIOTIS. J. Am. Chem. Soc. **74**, 2123 (1952).
3. E. RACKER, G. DE LA HABA, and I. G. LEDER. Arch. Biochem. Biophys. **48**, 238 (1954).
4. D. A. L. DAVIES. Advances in Carbohydrate Chem. **15**, 271 (1960).
5. C. M. QUINNELL, S. G. KNIGHT, and P. W. WILSON. Can. J. Microbiol. **3**, 277 (1957).
6. W. SOWA. Ph.D. Thesis, Queen's University, Kingston, Ontario. 1962.
7. J. K. N. JONES, M. B. PERRY, and R. J. STOODLEY. Can. J. Chem. **40**, 856 (1962).
8. L. HOUGH, J. K. N. JONES, and W. H. WADMAN. J. Chem. Soc. 1702 (1950).
9. M. DUBOIS, K. A. GILLES, J. K. HAMILTON, P. A. REBERS, and F. SMITH. Anal. Chem. **28**, 350 (1956).
10. H. D. WEIHE and P. B. JACOBS. Ind. Eng. Chem., Anal. Ed. **8**, 44 (1936).
11. N. J. ANTIA and M. B. PERRY. Can. J. Chem. **38**, 1917 (1960).
12. M. B. PERRY and T. PIETAK. The periodate oxidation of aldoheptoses. Royal Society of Canada, June Meeting, Kingston, Ontario. 1960.
13. B. L. HORECKER and A. H. MEHLER. Ann. Rev. Biochem. **24**, 207 (1955).
14. B. L. HORECKER, P. Z. SMYRNIOTIS, H. H. HIATT, and P. A. MARKS. J. Biol. Chem. **212**, 827 (1955).
15. C. E. BALLOU, H. O. L. FISCHER, and D. L. MCDONALD. J. Am. Chem. Soc. **77**, 2658 (1955).
16. N. J. PALLERONI and M. DOUDOROFF. J. Biol. Chem. **218**, 535 (1956).
17. V. GINSBURG. J. Biol. Chem. **237**, 497 (1962).

TRIMETHYL ORTHOBORATE – AMINE INCLUSION COMPOUNDS[1]

D. M. YOUNG AND C. D. ANDERSON
Exploratory Research Laboratory, Dow Chemical of Canada, Limited, Sarnia, Ontario

Received May 17, 1962

ABSTRACT

A new class of non-stoichiometric crystalline inclusion compounds has been discovered, having the general formula

$$(CH_3O)_3B.(\text{amine})_n.(\text{solvent})_x,$$

where $0.5 < n < 1.0$ and $0 < x < 3$ depending on the method of preparation and on the nature of the amine and solvent. Such compounds have been prepared with ammonia and a variety of primary and secondary amines. Among the solvents which can be incorporated into the crystals are alcohols, ketones, ethers, esters, nitriles, nitroparaffins, and hydrocarbons. Such compounds are also formed by triphenyl orthoborate, with $1.7 < n < 2.4$ and $1.2 < x < 1.6$.

The incorporated solvent has been shown to exert a definite vapor pressure. Furthermore, many of the compounds sublime at room temperature to form large transparent crystals which also contain incorporated solvent. The mechanism probably involves dissociation, followed by reassociation on the walls of the vessel. Preliminary X-ray diffraction measurements suggest that the trimethyl orthoborate – ammonia inclusion compounds have essentially the same crystal lattice as pure trimethyl orthoborate – ammonia.

INTRODUCTION

In a discussion of various methods for preparing the compound $(CH_3O)_3B$, Schechter (1) reported that treatment of the trimethyl orthoborate – methanol azeotrope with ammonia afforded crystals with incorporated methanol. The present work was undertaken to determine whether this phenomenon is a general one and, if so, to make a preliminary study of the properties of these inclusion compounds.

The literature on adducts of orthoboric acid esters and amines is scant. As recently as 1950, these esters were thought (2) to be insufficiently acidic (in the Lewis sense) to form such compounds.

In a series of papers on the reaction of trimethyl orthoborate with ammonia and amines, Goubeau *et al.* (3–5) described the preparation of $(CH_3O)_3B.NH_3$ and its reactions with excess ammonia and with excess orthoborate. They also prepared and characterized the 1:1 addition compounds of trimethyl orthoborate with mono-, di-, and tri-methylamine (5). Urs and Gould (6) reported the formation of solid addition compounds on mixing trimethyl orthoborate with dimethyl-, diethyl-, di-*n*-propyl-, di-*n*-butyl-, di-*n*-amyl-, triethyl-, and tri-*n*-butyl-amine. The compounds formed with ethylenediamine, piperidine, methylamine, and *t*-butylamine were stable enough to be purified by sublimation *in vacuo*; melting points and analytical results were given for these 1:1 addition compounds. The addition reactions were strongly catalyzed by the lower aliphatic alcohols. No solids separated on mixing amines with triethyl, tri-*n*-butyl, and tri-*n*-amyl orthoborates, although considerable heat evolution was noted with the ethyl ester. Urs and Gould (6) found no evidence of interaction between trimethyl orthoborate and pyridine or quinoline, but a stable 1:1 adduct of tris(1,1,1-trifluoroethyl) orthoborate and pyridine has since been characterized by Gerrard *et al.* (7).

Horn and Gould (8) studied the interaction of trimethyl orthoborate with 19 aliphatic and 5 heterocyclic amines, by measuring partial vapor pressures of the borate over

[1]*Contribution No. 68.*

equimolar borate–amine mixtures. Departures from ideality, which were greatest for ethylenediamine, piperidine, and triethanolamine and least for trimethylamine, di-*i*-propylamine, and pyridine, afforded a measure of the degree of interaction. As found previously (6), methanol markedly increased the borate–amine interaction.

Addition compounds between triaryl orthoborates and amines have been prepared and characterized by Colclough, Gerrard, and Lappert (9, 10). Stable 1:1 adducts were obtained in most cases, but where steric hindrance was severe the adducts were found to be deficient in amine. Ammonia formed 3:1 and 2:1 adducts respectively with tris(2,4,6-trichlorophenyl) and triphenyl orthoborates.

EXPERIMENTAL

Materials

Trimethyl orthoborate – methanol azeotrope was prepared by fractionating orthoboric acid and methanol (1:4 mole ratio) at a 10:1 reflux ratio. Trimethyl orthoborate was separated by shaking the azeotrope with anhydrous lithium chloride (11) and purified by fractionation. The purity was checked by titrating a weighed sample with 0.1 *N* sodium hydroxide to the phenolphthalein end point in the presence of mannitol.

Triphenyl orthoborate was prepared by distilling orthoboric acid and phenol (1:5.3 mole ratio), the water formed being removed azeotropically with the excess phenol (9). The crude product was purified by vacuum distillation, the fraction boiling at 154–167° at 0.2 mm being used for subsequent experiments.

The ammonia was Dow refrigeration grade. The gaseous amines were supplied by the Matheson Company and the liquid amines and solvents were Eastman Kodak "White Label" quality.

Preparation of Inclusion Compounds

(i) Trimethyl Orthoborate plus Gaseous Amines

Trimethyl orthoborate (5 ml) and the solvent to be incorporated (10 ml) were mixed in a 50-ml Erlenmeyer flask and saturated with the amine under slight excess pressure. Cooling the mixture in an ice bath helped to initiate crystallization and was useful in controlling the subsequent temperature rise. The crystals were separated by filtration on a sintered-glass funnel, in a dry box, washed with the same solvent if sufficiently volatile, otherwise with methanol, acetone, or *n*-pentane. After drying by suction, samples of the solid were transferred to tared weighing bottles for analysis. A small quantity was crushed on a porous plate and placed in a melting point tube which was sealed immediately after removal from the dry box.

(ii) Trimethyl Orthoborate plus Liquid Amine

Trimethyl orthoborate, solvent, and amine (5 ml of each) were added in turn to a 50-ml Erlenmeyer flask cooled in an ice bath. The resultant crystals were filtered in the dry box as described above.

(iii) Trimethyl Orthoborate plus Liquid Ammonia

A few inclusion compounds were formed using liquid ammonia, in an attempt to obtain an exactly 1:1 ratio of B:N. A mixture of trimethyl orthoborate, solvent, and ammonia in the mole ratio 1:8:5 was found to provide a sufficient excess of ammonia and enough solvent to prevent the trimethyl orthoborate from freezing. One part of trimethyl orthoborate and four parts of solvent were cooled to −28° C (boiling CF_2Cl_2) and a mixture of five parts of liquid ammonia and four parts of solvent added cautiously with stirring. A soda lime trap was attached to the flask and the contents were allowed to warm to room temperature. Filtration was carried out in a dry box, as usual.

(iv) Triphenyl Orthoborate

Triphenyl orthoborate – ammonia compounds were made by dissolving the ester in the solvent to be incorporated (using a slight excess of solvent over that required to effect solution) and saturating the solution with ammonia.

Analysis of Inclusion Compounds

Weighed samples of the inclusion compounds were dissolved in water and titrated against 0.1 *N* hydrochloric acid to the methyl red end point. Mannitol was added and the solution then titrated against 0.1 *N* sodium hydroxide to the phenolphthalein end point. The first titration gives the amount of amine, the second gives the amount of boric acid liberated on hydrolysis.

The methanolysis procedure of Thomas (12) was used to determine the boron content of the triphenyl orthoborate inclusion compounds. Later experiments, however, showed that direct titration gives the correct answer despite the presence of free phenol.

All inclusion compounds were assumed to correspond to the formula

$$(RO)_3B.(amine)_n.(solvent)_x.$$

The values of n and x could be calculated from the above analytical results.

RESULTS

Trimethyl Orthoborate – Ammonia Compounds

Analytical and other data for inclusion compounds involving trimethyl orthoborate, ammonia, and a series of alcohols are given in Table I. The solvents used to wash the

TABLE I

$(CH_3O)_3B.(NH_3)_n.(alcohol)_x$

(Prepared by saturating an alcoholic solution of trimethyl orthoborate with ammonia gas)

Alcohol	% N	% B	n	x	Washed with	Appearance	Crystal growth
Methyl	8.95	5.98	1.16	1.79	MeOH	Wet	xxx
	8.04	5.73	1.09	2.09	*	Wet	xxx
Ethyl	4.55	4.23	0.83	2.99	MeOH	Wet	xxx
n-Propyl	6.92	5.15	1.04	1.47	MeOH	Wet	
i-Propyl	7.57	6.33	0.92	0.85	MeOH	Wet	xxx
n-Butyl	5.94	8.52	0.54	0.19	MeOH	Wet	
i-Butyl	7.76	6.53	0.92	0.62	*n*-Pentane		xx
s-Butyl	7.86	7.60	0.80	0.34	Col. 1	Slightly wet	xxx
t-Butyl	5.44	6.72	0.63	0.63	Col. 1		
n-Amyl	4.04	5.05	0.62	1.13	Col. 1	Wet	xx
i-Amyl	6.84	6.66	0.79	0.51	Col. 1	Wet	xxx
t-Amyl	7.57	7.58	0.77	0.29	Col. 1	Dry	xxx
n-Hexyl	4.50	6.50	0.54	0.52	Acetone	Wet	x
n-Heptyl	3.65	8.03	0.35	0.22	—	Wet	
n-Octyl	4.94	5.60	0.68	0.60	—	Wet	
n-Decyl	7.14	7.69	0.72	0.16	Acetone	Dry	xxx
n-Dodecyl	5.96	9.16	0.50	0.03	Acetone	Wet	xx

*Prepared using liquid ammonia.

crystals are listed in column 6 ("col. 1" means that the crystals were washed with the same alcohol). The appearance of the crystals is noted in column 7. These compounds were generally quite wet and sticky, so that it was not possible to measure melting points. Thus the compound containing ethanol became practically liquid on storage. Many of the compounds showed a marked tendency to sublime at room temperature. After a few weeks' storage in weighing bottles, large transparent crystals were deposited on the upper surfaces of the bottles. In some cases, such crystals were found buried in the original powder at the bottom of the bottles. The tendency for crystal growth by sublimation is indicated in column 8 (x = slight, xx = moderate, xxx = pronounced). The compounds with *t*-amyl and *n*-decyl alcohols formed large, dry crystals, which were removed with tweezers and analyzed (see Table IX).

In Table II are listed the results obtained for inclusion compounds containing trimethyl orthoborate, ammonia, and a series of saturated and unsaturated hydrocarbons. All these compounds were fine, dry powders. For all the alkanes except neopentane and cyclohexane, x is equal to zero within the experimental error. In contrast, significant values of x were found for all the unsaturated hydrocarbons except isoprene. Benzene and cyclohexane gave almost identical x values. Melting points (sealed tube) for some of these compounds are recorded in the last column.

Results for compounds containing trimethyl orthoborate, ammonia, and a variety of organic solvents are given in Table III. Some of these compounds were prepared using liquid ammonia and are designated "liq." in column 6. Crystals of the compound containing 1,1-dimethoxyethane, which had sublimed on storage, were removed and analyzed (Table IX). The compound containing CF_2Cl_2 (b.p. −28° C) was prepared as follows.

TABLE II

$(CH_3O)_3B.(NH_3)_n.(hydrocarbon)_x$

(Prepared by saturating a hydrocarbon solution of trimethyl orthoborate with ammonia gas)

Hydrocarbon	% N	% B	n	x	Washed with	Crystal growth	M.p. (°C)
			Alkanes				
n-Butane	10.38	9.26	0.87	−0.03	Col. 1		
n-Pentane	10.51	8.79	0.92	0.05	Col. 1		
2-Me-butane	10.37	9.48	0.85	−0.06	Col. 1	xxx	
Neopentane	9.46	8.31	0.87	0.16	Col. 1	x	
n-Hexane	11.17	9.35	0.92	−0.05	Col. 1		67.5–69
2-Me-pentane	11.11	9.08	0.95	−0.01	Col. 1		
3-Me-pentane	11.09	9.25	0.93	−0.03	Col. 1		60–63
2,3-DiMe-butane	11.28	9.00	0.97	0.00	Col. 1		
2,2-DiMe-butane	11.30	8.90	0.98	0.01	Col. 1		68–77
n-Heptane	10.05	8.72	0.89	0.04	Col. 1	xxx	
Cyclohexane	7.98	7.34	0.84	0.35	Col. 1	x	
			Alkenes				
2-Pentane	9.33	8.62	0.84	0.11	—		
Isoprene	10.67	9.22	0.89	−0.02	—		
2-Me-1-pentene	9.51	8.55	0.86	0.10	—		
1-Heptene	8.27	7.82	0.82	0.21	—		
3-Et-2-pentene	9.97	8.29	0.93	0.11	Col. 1	x	
			Aromatic hydrocarbons				
Benzene	7.89	7.65	0.81	0.31	Col. 1		

TABLE III

$(CH_3O)_3B.(NH_3)_n.(solvent)_x$

(Prepared with gaseous or liquid ammonia)

Solvent	% N	% B	n	x	Method	Washed with	Crystal growth	M.p. (°C)
CH_2Cl_2	5.92	6.65	0.69	0.55	Gas	Col. 1		
	7.53	8.20	0.71	0.19	Liq.	—		62–64
$CHCl_3$	7.94	7.79	0.79	0.18	Liq.	—		
CCl_4	5.36	5.65	0.73	0.49	Gas	Col. 1	x	
	5.15	5.80	0.69	0.46	Liq.	—		67–71
CF_2Cl_2					Gas	—	Loses CF_2Cl_2	
Et_2O	8.32	7.99	0.81	0.24	Liq.	—		
n-Pr_2O	7.15	6.46	0.86	0.48	Gas	Col. 1	xxx	
1,1-$(CH_3O)_2C_2H_4$	6.19	6.13	0.78	0.66	Gas	Col. 1	xxx	
MeCOEt	6.07	8.91	0.53	0.12	Liq.	—		
MeCOOEt	8.82	8.30	0.82	0.14	Gas	Col. 1		
$MeNO_2$	8.13	6.87	0.91	0.62	Gas	Col. 1	x	
$HCONH_2$	7.64	8.33	0.71	0.31	Gas	Acetone	x	
MeCN	8.72	7.80	0.86	0.49	Gas	—	x	
EtCN	7.55	7.48	0.78	0.50	Gas	—	xx	

A mixture of approximately equal volumes of trimethyl orthoborate and liquid CF_2Cl_2 (they are not completely miscible) was held at −28° C in a boiling-CF_2Cl_2 bath and saturated with ammonia gas. Extensive precipitation was observed in both gas and liquid phases. The mixture was warmed to room temperature, whereupon all the uncombined CF_2Cl_2 and ammonia evaporated. The weight of the residual solid was measured as a function of time; the sample lost weight continuously over a period of 24 hours. The same results were obtained in a subsequent experiment in which $(CH_3O)_3B.NH_3$ (1.785 g) was treated with excess liquid CF_2Cl_2 at its boiling point. After warming to room temperature and allowing the excess CF_2Cl_2 to boil off, the solid was reweighed and found to

have occluded 0.172 g of CF_2Cl_2 ($x = 0.096$). This sample also lost weight slowly at room temperature.

Trimethyl Orthoborate – Methylamine Compounds

Results for compounds of trimethyl orthoborate, monomethylamine, and alcohols are shown in Table IV. Under the conditions used, no crystals could be obtained in the

TABLE IV

$(CH_3O)_3B.(CH_3NH_2)_n.(alcohol)_x$

(Prepared by saturating an alcoholic solution of trimethyl orthoborate with methylamine gas)

Alcohol	% N	% B	n	x	Washed with	Appearance	Crystal growth	M.p. (°C)
Methyl	8.29	6.58	0.97	0.95	—		xx	
Ethyl	Could not be formed							
n-Propyl	Could not be formed							
i-Propyl	6.93	5.89	0.91	0.86	—	Dry	x	78–82
n-Butyl	Could not be formed							
i-Butyl	Could not be formed							
s-Butyl	7.24	6.24	0.90	0.56	—	Wet	xx	74
t-Butyl	7.22	5.95	0.94	0.66	—	Wet	x	73–74
n-Amyl	6.24	5.76	0.84	0.66	Col. 1	Wet	xx	
i-Amyl	Unstable							
t-Amyl	6.93	5.78	0.93	0.62	Col. 1	Dry	x	
n-Hexyl	5.85	5.45	0.83	0.67	Col. 1	Mod. dry	x	
n-Decyl	Unstable							
n-Dodecyl	Unstable							

presence of ethanol, *n*-propanol, *n*- and iso-butanol; with isoamyl alcohol, *n*-decanol, and *n*-dodecanol, the crystals were not stable enough to permit filtration. The remaining alcohols in Table IV formed stable compounds having substantial values of x, comparable (excepting methanol) to those found for the corresponding ammonia adducts (Table I). Values of n showed far less variation than those in Table I. In the case of methanol and *n*-hexanol, the crystals formed by sublimation during storage were hand-picked and analyzed (Table IX).

The results shown in Table V, for compounds involving trimethyl orthoborate, monomethylamine, and hydrocarbons, are remarkably similar to those for the corresponding

TABLE V

$(CH_3O)_3B.(CH_3NH_2)_n.(hydrocarbon)_x$

(Prepared by saturating a hydrocarbon solution of trimethyl orthoborate with methylamine gas. Crystals washed with the same hydrocarbon)

Hydrocarbon	% N	% B	n	x	Crystal growth	M.p. (°C)
n-Pentane	8.90	8.54	0.81	−0.03		73.5–76
Neopentane	7.36	7.88	0.72	0.15	x	
2-Me-butane	8.07	7.41	0.84	0.39	xxx	
n-Heptane	8.51	8.56	0.77	−0.01		
Cyclohexane	8.84	8.39	0.81	0.00		73.5–74
Benzene	7.90	6.88	0.89	0.33		71.5–72
CH_2Cl_2	7.75	8.26	0.73	0.05		
CCl_4	8.06	7.65	0.81	0.08		64–66

compounds made with ammonia (Table II). The values of x are almost identical except for 2-methylbutane, which is occluded with methylamine but not with ammonia, and

for cyclohexane, for which the reverse is true. With methylamine, the values of n are slightly lower than with ammonia. Results for CH_2Cl_2 and CCl_4 are also included in Table V. These solvents give very low x values, in contrast to their behavior with ammonia (cf. Table III).

Trimethyl Orthoborate – Higher Amine – Methanol Compounds

In Table VI are given the results for compounds involving trimethyl orthoborate and higher amines, methanol being the incorporated solvent in each case. The first five

TABLE VI

$(CH_3O)_3B.(amine)_n.(MeOH)_x$

(Prepared by treating a methanolic solution of trimethyl orthoborate with gaseous or liquid amine)

Amine	% N	% B	n	x	Appearance	Crystal growth	M.p. (°C)
Ammonia	8.95	5.98	1.16	1.79	Wet	xxx	
Monomethyl	8.29	6.58	0.97	0.95	Mod. wet	xx	
Dimethyl	Unstable at room temperature						
Trimethyl	Unstable at room temperature						
Monoethyl	7.50	5.52	1.05	1.40	Mod. dry	xxx	56–60
Diethyl	6.53	4.98	1.01	1.23	Wet	xxx	45–50
Triethyl	No crystals formed						
n-Butyl	5.99	4.66	0.99	1.74	Wet		
Tri-*n*-butyl	No crystals formed						
t-Butyl	Unstable at room temperature						
n-Amyl	6.21	4.86	0.99	1.02	Wet	xx	Decomp.
n-Heptyl	No crystals formed						
Piperidine	5.93	4.76	0.96	1.29	Mod. dry	xx	65–69

amines were added as gases. The data for ammonia and methylamine (from Tables I and IV) are listed for the sake of completeness. All the compounds analyzed contained substantial amounts of included methanol ($0.95 < x < 1.79$) and exhibited B:N ratios close to unity ($0.96 < n < 1.16$). The trimethyl orthoborate – diethylamine – methanol compound showed a pronounced tendency to sublime, producing spectacular clusters of large crystals on the walls of the weighing bottle in which it was stored. A photograph of the crystals is shown in Fig. 1; the black strip on the outside of the weighing bottle is 1 cm in length. These crystals were hand-picked and analyzed (Table IX).

In order to determine the effect of solvent concentration on the value of x, a number of preparations of the methyl borate – piperidine – methanol compound were made, by adding 5 ml of piperidine to 5 ml of methyl borate dissolved in 1–10 ml of methanol. The results, given in Table VIII, will be discussed later.

Sublimed Crystals

The n and x values for large sublimed crystals, which were hand-picked and analyzed, are compared in Table IX with the corresponding values for the fine crystals from which they were grown.

Triphenyl Orthoborate – Ammonia Compounds

Results for compounds involving triphenyl orthoborate, ammonia, and solvent are summarized in Table VII. The amounts of pentane, benzene, and methylene chloride incorporated are much larger than with the trimethyl orthoborate – amine compounds. Furthermore, n is nearer 2 than 1, in accord with the work of Colclough, Gerrard, and Lappert (10), who found $n = 2$ for the pure compound triphenyl orthoborate – ammonia.

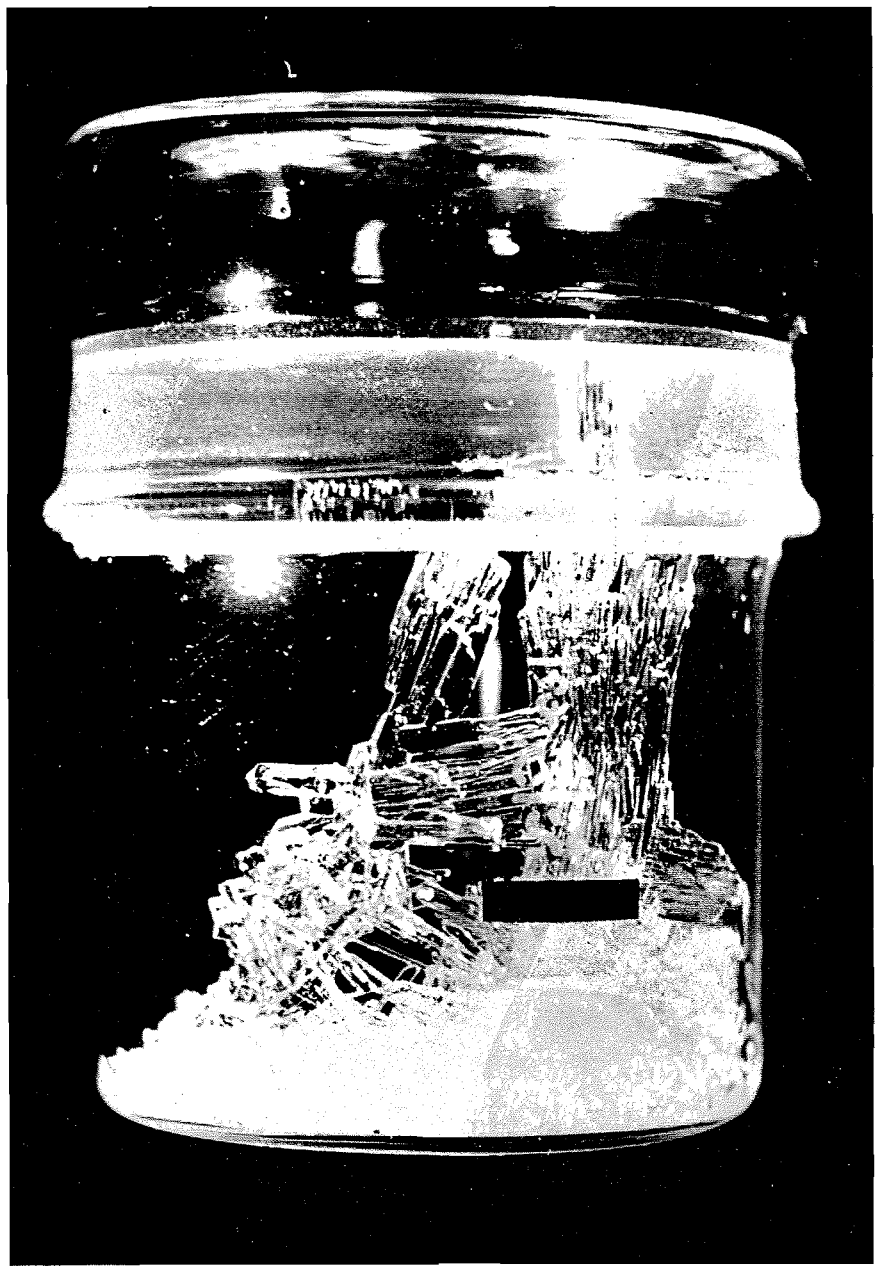

FIG. 1. Sublimed crystals of the trimethyl orthoborate – dimethylamine – methanol compound. The black strip is 1 cm long.

TABLE VII

$(C_6H_5O)_3B.(NH_3)_n.(solvent)_x$

(Prepared by saturating a solution of triphenyl orthoborate with ammonia gas. Crystals washed with same solvent)

Solvent	% N	% B	n	x	M.p. (°C)
n-Pentane	5.69	2.58	1.70	1.39	
Benzene	7.43	2.37	2.42	1.60	
CH_2Cl_2	5.90	2.54	1.80	1.24	84–88

DISCUSSION

In the absence of any detailed physicochemical or crystallographic information on the pure inclusion-free borate–amine compounds, there is little hope of being able to give a satisfactory interpretation of the mass of results obtained in this work. It may be worthwhile, however, to assemble the facts which theory must eventually explain.

The most striking feature of the compounds is that they are non-stoichiometric with respect to the B:N ratio. Thus with trimethyl orthoborate – ammonia – heptanol, n is as low as 0.35, while with the first member of the same series, trimethyl orthoborate – ammonia – methanol, $n = 1.16$. Triphenyl orthoborate – ammonia inclusion compounds also exhibit wide variations in n.

Considering now the values of x, it must be borne in mind that this parameter is sensitive to the method of preparation and time of drying with suction on the filter. In a number of instances, x and n have been determined as a function of time of drying. In all cases, long drying causes a decrease in x, but n remains constant. Care was therefore taken to prepare the compounds under similar conditions; indeed, duplicate preparations have shown x and n to be fairly reproducible.

The series trimethyl orthoborate – ammonia – alcohol (Table I) merits detailed examination, because it is the largest group and exhibits the widest range of x and n values. The results indicate a rough correlation between x and n, as shown in Fig. 2. Excluded from this graph are the data for ethanol, which exhibits an abnormally high affinity for trimethyl orthoborate – ammonia, the results for the methanol compound prepared using liquid ammonia, and those for the resublimed compounds. It should be emphasized that in all cases a constant volume of solvent was used. If the value of x is a function of the mole fraction of the solvent in the mixture during precipitation, more meaningful values of x might have obtained if in all preparations a constant initial mole fraction of solvent had been used.

In order to determine the dependence of x on the mole fraction of solvent in the mixture at the start of the reaction, a series of preparations of the compound $(CH_3O)_3B.(\text{piperidine})_n.(\text{methanol})_x$ was made, using varying amounts of methanol. This system was selected because liquid amines form adducts more rapidly than gaseous amines and because moderately dry crystals with high x values could be obtained. The variation of x with the amount of methanol used followed no regular pattern in this case (Table VIII). However, the results are of unusual interest in that they show very clearly the relation between x and n (see Fig. 3) and confirm the correlation inferred from Fig. 2.

If the incorporated solvent molecules occupy holes in the trimethyl orthoborate – amine crystal lattice, one would expect x to be high for small molecules and zero for large ones. This general behavior is found in the series trimethyl orthoborate – ammonia – alcohol. In Fig. 4, the value of x is plotted against the number of carbon atoms in the

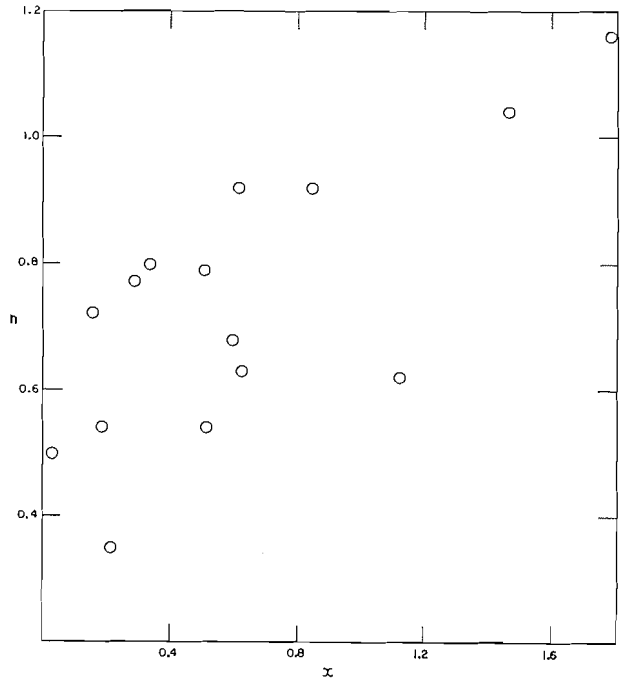

FIG. 2. Plot of n versus x for the series of compounds $(CH_3O)_3B.(NH_3)_n.(alcohol)_x$.

TABLE VIII

$(CH_3O)_3B.(piperidine)_n.(MeOH)_x$

(Prepared by adding 5 ml of piperidine to 5 ml of trimethyl orthoborate dissolved in methanol)

MeOH (ml)	% N	% B	n	x
1	6.33	5.34	0.92	0.65
1	6.53	6.17	0.82	0.05
2	6.42	5.55	0.89	0.47
3	6.39	5.40	0.92	0.57
4	6.32	5.38	0.91	0.62
5	6.31	5.19	0.94	0.77
7	6.54	5.76	0.88	0.29
7	6.34	5.16	0.95	0.78
10	6.45	5.54	0.90	0.47

alcohol, for primary straight-chain alcohols. Since it has been shown that x does not exhibit a systematic variation with the mole fraction of alcohol in the mixture (see above), the results in Fig. 4 may be cited as partial evidence for this "molecular sieve" effect.

The marked tendency of the trimethyl orthoborate – amine inclusion compounds to sublime is most probably due to dissociation, migration of the volatile components through the vapor space, and reassociation on the cooler parts of the vessel. The same behavior has been found with pure trimethyl orthoborate – ammonia. It is interesting to note (Table IX) that the sublimed crystals have substantially higher values of n and x than

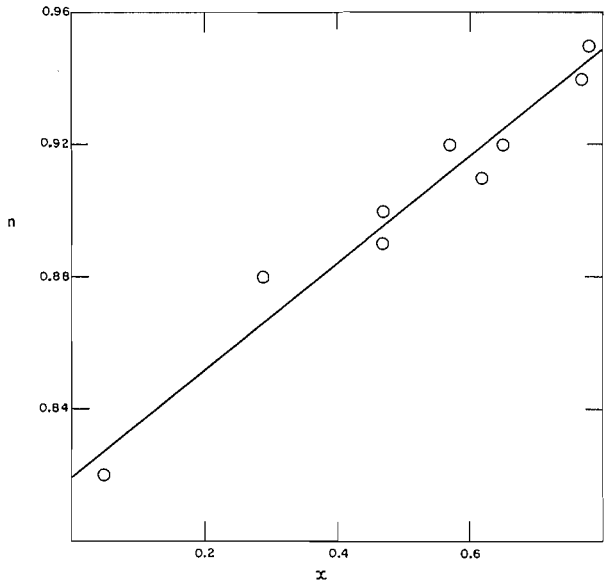

FIG. 3. Plot of n versus x for the series of compounds $(CH_3O)_3B.(piperidine)_n.(CH_3OH)_x$.

TABLE IX

Amine	Incorporated solvent	Original crystals		Large sublimed crystals	
		n	x	n	x
Ammonia	*t*-Amyl alcohol	0.77	0.29	1.03	0.89
	n-Decanol	0.72	0.16	0.93	0.24
	$1,1\text{-}(CH_3O)_2C_2H_4$	0.78	0.66	0.90	0.71
Monomethyl	Methanol	0.83	0.67	0.78	0.60
	n-Hexanol	0.97	0.95	0.97	0.95
Diethyl	Methanol	1.01	1.23	0.98	1.02

the original crystals, when ammonia is the amine, whereas with methylamine and diethylamine n and x are unchanged or lower than in the original crystals.

From the behavior of the CF_2Cl_2 inclusion compound it is clear that CF_2Cl_2 is incorporated into the crystal lattice of trimethyl orthoborate – ammonia in such a way that it is in equilibrium with a definite partial pressure of CF_2Cl_2, as if it were adsorbed on charcoal, for example. The same undoubtedly holds true for the other incorporated solvents. The problem of measuring this equilibrium partial pressure is complicated, however, by the fact that trimethyl orthoborate and the amine also exert appreciable equilibrium partial pressures. If a compound could be prepared from an involatile orthoborate ester and an involatile amine, this solid could be treated as the sorbent and the solvent to be incorporated as the sorbate, sorption isotherms could be measured, and the thermodynamic functions for the system calculated in the usual way.

The melting points of the inclusion compounds are thought to be dissociation temperatures rather than true melting points; therefore little significance is attached to the fact that those for the trimethyl orthoborate – ammonia compounds lie close to that (72° C) reported by Goubeau and Link (5) for the pure compound trimethyl orthoborate – ammonia. In contrast, the melting point of the methylene chloride inclusion compound

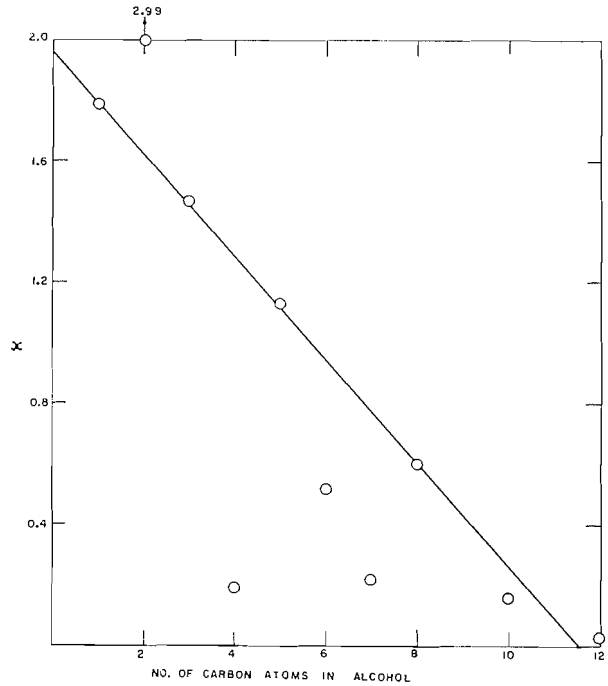

FIG. 4. Dependence of x on the number of carbon atoms in the alcohol, for the series of compounds $(CH_3O)_3B.(NH_3)_n.(\text{alcohol})_x$.

of triphenyl orthoborate – ammonia (84–88°) is much lower than the value (125°) reported for the pure adduct (10).

The finding that alkanes are not occluded by trimethyl orthoborate – ammonia and trimethyl orthoborate – methylamine forms the basis for a proposed method (13) for making these compounds, free from incorporated solvent, avoiding the disadvantages of the vapor phase method (1). It is interesting to note that, although the alkanes are not incorporated, the crystal growth of the pure amine compounds prepared from alkane solutions depends on the nature of the alkane. Thus (Table II), crystals of trimethyl orthoborate – ammonia prepared in 2-methylbutane or *n*-heptane show a pronounced tendency for crystal growth, whereas those prepared in other alkanes do not. In all these cases $x = 0$ within experimental error. The same general behavior is exhibited with trimethyl orthoborate – methylamine compounds prepared from alkane solutions (Table V).

Preliminary X-ray diffraction measurements on some trimethyl orthoborate – ammonia inclusion compounds have indicated that the crystal lattice is essentially the same as that of pure trimethyl orthoborate – ammonia, confirming the idea that the included solvent molecules occupy holes in the crystal lattice.

ACKNOWLEDGMENTS

Thanks are due Drs. D. R. Petersen and S. R. Curtis of the Dow Chemical Company for X-ray diffraction measurements.

REFERENCES

1. W. H. SCHECHTER. Can. Patent No. 538,655 (1957).
2. N. V. SIDGWICK. The chemical elements and their compounds. Vol. I. Oxford University Press. 1950. p. 403.
3. J. GOUBEAU and U. BOHM. Z. anorg. u. allgem. Chem. **266**, 161 (1951).
4. J. GOUBEAU and E. EKHOFF. Z. anorg. u. allgem. Chem. **268**, 145 (1952).
5. J. GOUBEAU and R. LINK. Z. anorg. u. allgem. Chem. **267**, 27 (1951).
6. S. V. URS and E. S. GOULD. J. Am. Chem. Soc. **74**, 2948 (1952).
7. E. W. ABEL, W. GERRARD, M. F. LAPPERT, and R. SHAFFERMAN. J. Chem. Soc. 2895 (1958).
8. H. HORN and E. S. GOULD. J. Am. Chem. Soc. **78**, 5772 (1956).
9. T. COLCLOUGH, W. GERRARD, and M. F. LAPPERT. J. Chem. Soc. 907 (1955).
10. T. COLCLOUGH, W. GERRARD, and M. F. LAPPERT. J. Chem. Soc. 3006 (1956).
11. H. I. SCHLESINGER, H. C. BROWN, D. L. MAYFIELD, and J. R. GILBREATH. J. Am. Chem. Soc. **75**, 213 (1953).
12. L. H. THOMAS. J. Chem. Soc. 820 (1946).
13. D. M. YOUNG and C. D. ANDERSON. Can. Patent No. 615,621 (1961).

THE WATER-SOLUBLE POLYSACCHARIDES OF DERMATOPHYTES

I. A GALACTOMANNAN FROM TRICHOPHYTON GRANULOSUM[1]

C. T. BISHOP
Division of Applied Biology, National Research Council, Ottawa, Canada

AND

F. BLANK[2]
Department of Bacteriology and Immunology, McGill University, Montreal, Que.

AND

M. HRANISAVLJEVIC-JAKOVLJEVIC[3]
Division of Applied Biology, National Research Council, Ottawa, Canada

Received May 2, 1962

ABSTRACT

A galactomannan containing D-galactose (16%) and D-mannose (84%) has been isolated from the water-soluble polysaccharides of *Trichophyton granulosum*. Methylation studies showed that the structure was highly branched, the predominant structural feature being a chain of α-D-mannopyranose units joined together by an equal number of $1 \rightarrow 2$ and $1 \rightarrow 6$ linkages. About 22% of the D-mannose units were doubly substituted at positions 2,6; 2,4; and 2,3 to form branch points. The branches were terminated by D-mannopyranose and D-galactofuranose residues, the latter accounting for all of the D-galactose present in the polysaccharide.

An earlier investigation (1) showed that the skeleton of the cell wall of dermatophytes is made up of chitin, a water-insoluble polysaccharide. However, the cells of these organisms also contain other polysaccharides which, when isolated, are soluble in water. These water-soluble polysaccharides are of considerable immunochemical importance because Bloch *et al.* (2) have shown them to be an essential part of "trichophytin". The latter is an antigenic material derived from cultures of dermatophytes and is used clinically in diagnostic skin tests.

Water-soluble polysaccharides from a number of dermatophytes have now been isolated as part of a program to determine if species differences occur and to test their antigenic properties. The present paper describes the isolation and constitution of the first of these to be studied, a water-soluble polysaccharide from *Trichophyton granulosum* Sabouraud, 1909.

A crude mixture of polysaccharides was isolated in 10% yield from powdered cells of *T. granulosum* by the procedure given in the experimental section. The product contained no nitrogen and hence was free from any proteinaceous material. On hydrolysis the mixture yielded large amounts of mannose with smaller amounts of glucose and galactose. Examination of the crude polysaccharides by moving-boundary electrophoresis in borate buffer (3) gave the separation pattern shown in Fig. 1A. In both separations shown in Fig. 1 the non-migrating peak was shown to be a false boundary. The peak of greatest mobility in Fig. 1A was sharp and symmetrical and obviously represented the major polysaccharide component of the mixture. The less mobile peak in Fig. 1A was low, broad,

[1]*Issued as N.R.C. No. 6910.*
Presented at the 141st Meeting of the American Chemical Society, Washington, D.C. 1962.
[2]*Present address: Department of Dermatology, Temple University Medical Center, Philadelphia, Pa., U.S.A.*
[3]*National Research Council Postdoctorate Fellow 1960–61.*

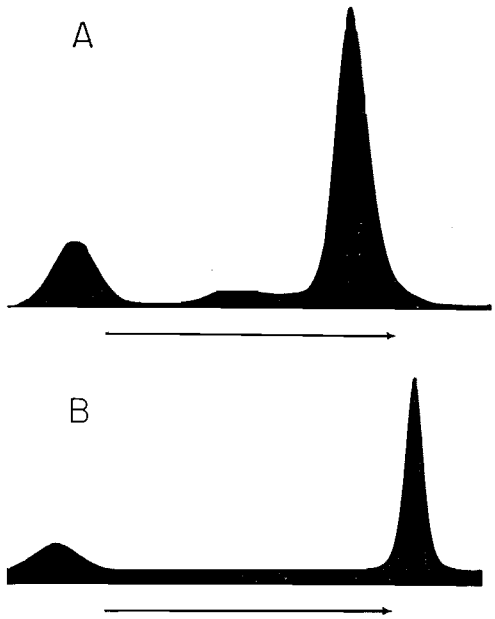

FIG. 1. Moving-boundary electrophoresis of polysaccharides from *T. granulosum*: A. Crude polysaccharides. B. Purified galactomannan (fractions 3+4, Fig. 2). Buffer: 0.05 *M* sodium tetraborate.

and diffuse, indicative of heterogeneity, and showed that the major polysaccharide was admixed with probably more than one minor component.

The mixture of polysaccharides was resolved by chromatography on diethylaminoethyl (DEAE) cellulose (4) into two fractions, as shown in Fig. 2; fractions 2 and 4 proved to be the same as fractions 1 and 3 respectively. On electrophoresis fractions 1+2 gave a broad, diffuse peak corresponding in mobility to the minor component in

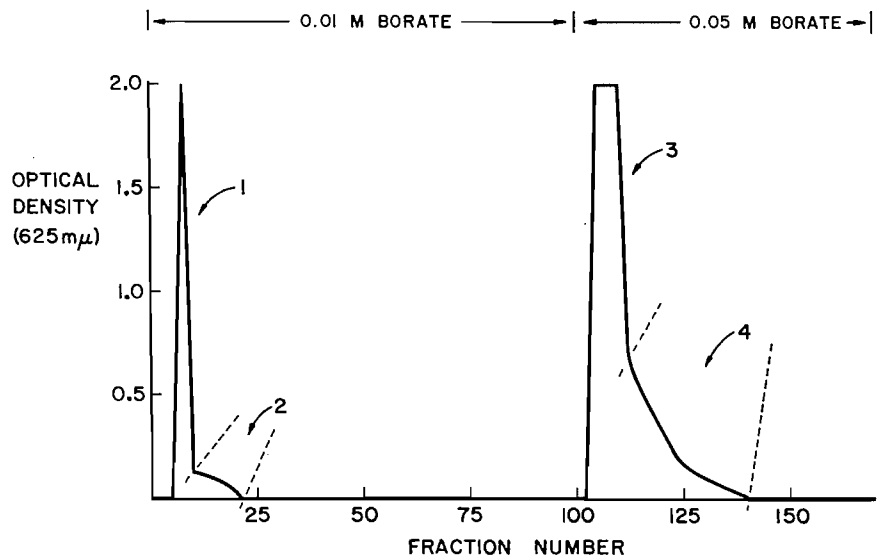

FIG. 2. Separation of *T. granulosum* polysaccharides on DEAE cellulose.

Fig. 1A and on hydrolysis yielded approximately equal amounts of glucose, galactose, and mannose. Fractionation of fractions 1+2 in ethanol–water mixtures yielded a small amount of material which gave only glucose on hydrolysis, and other fractions were enriched with respect to mannose and galactose. The material in fractions 1+2 was therefore a mixture of a glucan and a galactomannan or a glucogalactomannan. Fractions 3+4, Fig. 2, gave the electrophoresis pattern shown in Fig. 1B, and the single, sharp, symmetrical peak had the same mobility as the major component in Fig. 1A. Hydrolysis of fractions 3+4 yielded a large amount of mannose, a smaller amount of galactose, and a trace of glucose. Reprecipitation of this polysaccharide in 50% aqueous ethanol left the glucose-containing material in solution and yielded a pure galactomannan on which the balance of this work was done.

The galactomannan had a number-average degree of polymerization of 55 ± 1. On hydrolysis its specific rotation changed from $+71\pm1°$ to $+22\pm1.5°$, indicative of a predominance of α-glycosidic linkages. Three independent estimations of the monosaccharide composition gave the average values of 16% galactose and 84% mannose. Isolation of crystalline derivatives confirmed the identities of the two sugars and showed that both were present as the D-enantiomorphs.

The galactomannan was methylated and hydrolyzed; the *O*-methyl sugars in the hydrolyzate were isolated and estimated by a combination of gas–liquid chromatography (5, 6), liquid–liquid chromatography on cellulose (7), and paper electrophoresis (8). Thus, gas–liquid chromatography of the mixture of *O*-methyl sugars, as their methyl glycosides, gave the separation shown in Fig. 3. Although only one peak, the third,

FIG. 3. Gas–liquid chromatogram of methyl-*O*-methyl glycosides from methylated galactomannan of *T. granulosum*.

2 parts

1. Methyl 2,3,4,6-tetra-*O*-methyl-α-D-mannoside (1).
   Methyl 2,3,5,6-tetra-*O*-methyl(α,β)-D-galactoside (3).
   Small peaks are anomers of the same two sugars.

5 parts

2. Methyl 2,3,4-tri-*O*-methyl-α-D-mannoside (1).
   Methyl 3,4,6-tri-*O*-methyl-α-D-mannoside (1).
   Two of the small peaks are β-anomers of these.

1 part

3. Methyl 3,4-di-*O*-methyl-α-D-mannoside (1).

1 part

4. Methyl 3,6-di-*O*-methyl-α-D-mannopyranoside (1).
   Methyl 4,6-di-*O*-methyl-α-D-mannoside (1).

represented a single compound, this separation provided the overall quantitative ratio of di- to tri- to tetra-*O*-methyl hexosides as 2:5:2. The tetra-*O*-methyl hexoses were separated from the other components and from each other by liquid–liquid chromatography on cellulose, which gave 2,3,4,6-tetra-*O*-methyl-D-mannose (1 part) and 2,3,5,6-tetra-*O*-methyl-D-galactose (3 parts); both compounds were identified by formation of crystalline derivatives. The tri-*O*-methyl hexoses were separated from the other components but not from each other by liquid–liquid chromatography on cellulose. However,

paper electrophoresis of the tri-*O*-methyl fraction yielded 3,4,6-tri-*O*-methyl-D-mannose (1 part) and 2,3,4-tri-*O*-methyl-D-mannose (1 part), both of which were identified as crystalline derivatives. Individual components in the di-*O*-methyl fraction could not be resolved by paper chromatography or paper electrophoresis. They were separated by gas–liquid chromatography under the conditions given in Fig. 4. A portion of the 3,4-di-

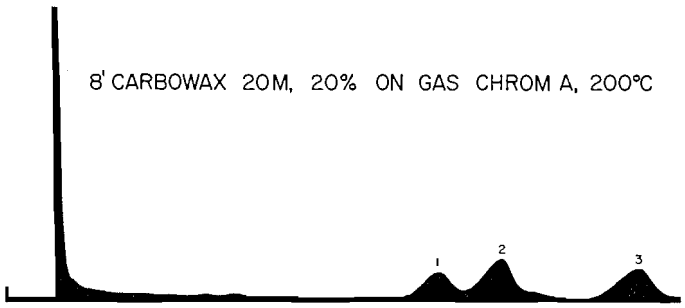

FIG. 4. Gas–liquid chromatogram of methyl-di-*O*-methyl-α-D-mannosides from methylated galactomannan of *T. granulosum*.

2 parts
1. Methyl 3,4-di-*O*-methyl-α-D-mannoside.

1 part
2. Methyl 3,6-di-*O*-methyl-α-D-mannopyranoside.

1 part
3. Methyl 4,6-di-*O*-methyl-α-D-mannoside.

O-methyl-D-mannose had crystallized from the di-*O*-methyl fraction and was removed for identification prior to this separation. This did not disturb the quantitative data because the ratio of 3,4-di-*O*-methyl-D-mannose to the other components was established by the separation shown in Fig. 3. Identifications of the three components shown in Fig. 4 were based on the following evidence. The di-*O*-methyl fraction obtained from chromatography on cellulose yielded 2,3,4,6-tetra-*O*-methyl-D-mannose exclusively on complete methylation, thus limiting the possibilities to di-*O*-methyl-D-mannopyranoses. The di-*O*-methyl fraction migrated as one component on paper electrophoresis and its mobility (M_G 0.38) showed that all components had a free hydroxyl at C_2. The three components shown in Fig. 4 were collected from the effluent gas stream and the first was identified as crystalline methyl 3,4-di-*O*-methyl-α-D-mannoside. The other two components then had to be the glycosides of 3,6- and 4,6-di-*O*-methyl mannose because these were the only possible remaining di-*O*-methyl mannopyranoses with a free hydroxyl at C_2. Distinction between the two possibilities was made by periodate oxidation of the glycosides collected from the gas–liquid chromatogram. The glycoside from peak 2 was resistant to periodate oxidation and was therefore the 3,6-di-*O*-methyl isomer; the compound from peak 3 was readily oxidized by periodate and was therefore the glycoside of 4,6-di-*O*-methyl-D-mannose. The separation shown in Fig. 4 gave a ratio of 3,6- to 4,6-di-*O*-methyl-D-mannoses of 1:1. Figure 3 showed that the amount of 3,4-di-*O*-methyl-D-mannose was equivalent to the sum of the other di-*O*-methyls. The ratio of 3,4- to 3,6- to 4,6-di-*O*-methyl-D-mannose was therefore 2:1:1.

Table I contains a summary of the methylation results which give some idea of the gross structure of the polysaccharide. The predominant feature was a chain of D-mannose units joined together by an equal number of $1 \rightarrow 2$ and $1 \rightarrow 6$ linkages. The polysaccharide was highly branched with about 22% of the D-mannose units being doubly substituted at positions 2,6; 2,4; and 2,3: the branches were terminated by D-manno-

TABLE I

Hydrolysis products from methylated galactomannan of *T. granulosum*

Compound	Molar proportion
2,3,5,6-Tetra-*O*-methyl-D-galactose	3
2,3,4,6-Tetra-*O*-methyl-D-mannose	1
2,3,4-Tri-*O*-methyl-D-mannose	5
3,4,6-Tri-*O*-methyl-D-mannose	5
3,4-Di-*O*-methyl-D-mannose	2
3,6-Di-*O*-methyl-D-mannose	1
4,6-Di-*O*-methyl-D-mannose	1

pyranose and D-galactofuranose residues. A polysaccharide such as that just described should consume 1.39 moles of periodate with production of 0.33 mole of formic acid per mole anhydrohexose unit. When the galactomannan was oxidized by periodate the results indicated extensive overoxidation and the data did not permit a valid extrapolation. The overoxidation was probably caused by α-hydrogen oxidation in the malondialdehyde-type structure (9) which would be formed by oxidation of the terminal D-galactofuranoside residues. The units giving rise to the methyl ethers in Table I could, of course, be joined together in many different ways. Fragmentation analysis is required to provide more detailed information, such as the sequence of $1 \rightarrow 2$ and $1 \rightarrow 6$ linkages along the mannan chain and the size of the branches.

The galactomannan from *T. granulosum* appears to be unique among the naturally occurring polysaccharides of this type. In the plant kingdom galactomannans occur most widely in the endosperms of the *Leguminosae* and have the general structure of a chain of $1 \rightarrow 4$ linked β-D-mannose units, some of which are substituted at the C_6 position by single α-D-galactopyranose residues (10). To the authors' knowledge, the polysaccharide from *T. granulosum* is the first galactomannan to be isolated from a microorganism but some of its structural features can be related to those occurring in other microbial polysaccharides. Thus, the mannan chain bears some resemblance to the mannan isolated from *Candida albicans* (11) in having both $1 \rightarrow 2$ and $1 \rightarrow 6$ but no $1 \rightarrow 3$ linkages. This absence of $1 \rightarrow 3$ linkages serves to distinguish both of these polysaccharides from the mannans isolated from *Saccharomyces cerevisiae* (12–14) and *Saccharomyces rouxii* (15).

The occurrence of all of the galactose units as terminal non-reducing furanoside residues was another distinguishing feature of the galactomannan from *T. granulosum*. D-Galactose appears to have been found in the furanose form in only three other polysaccharides, galactocaralose from *Penicillium charlesii* (16), an extracellular polysaccharide from *Gibberella fujikuroi* (= *Fusarium moniliforme*) (17), and the specific substance from type 34 *Pneumococcus* (18).

EXPERIMENTAL

Paper chromatograms were run by the descending method using the following solvent systems (v/v):

(A) pyridine:ethyl acetate:water—1:2.5:2.5 (upper phase);

(B) butanone saturated with water;

(C) *n*-butanol:ethanol:water—3:1:1;

(D) benzene:ethanol:water:concentrated ammonium hydroxide—200:47:14:1 (upper phase).

Paper electrophoreses (8) were done on Whatman 3 MM paper in 0.1 *M* sodium tetraborate at 750 v (potential gradient, 25 v/cm) and 25–40 ma for 2 1/2 hours. Unsubstituted sugars were detected on paper chromatograms by silver nitrate – sodium hydroxide sprays (19); methylated sugars were detected on the papers by the *p*-anisidine hydrochloride spray reagent (7). Gas–liquid chromatography (5, 6) was done on a Pye

Argon Chromatograph equipped with an ionization detector and on an F and M Model 500 Chromatograph which had a thermal-conductivity detector. All evaporations were at 35–40° C under diminished pressure; melting points are corrected; specific rotations are equilibrium values unless otherwise specified. R_g values represent movement relative to 2,3,4,6-tetra-*O*-methyl-D-glucose on paper chromatograms and M_G values refer to movement relative to glucose on paper electrophoresis.

Isolation of Crude Polysaccharides

Trichophyton granulosum was grown in 500-ml Erlenmeyer flasks containing 250–300 ml of a liquid medium consisting of the following nutrients: 4% maltose (technical grade), 1% neopeptone "Difco", 0.05% yeast extract "Difco", 0.001% thiamine, 0.005% inositol made up in tap water. The incubation period was 3–4 weeks at 25° C, after which the cultures were autocalved at 121° C for 20 minutes. The mycelium was collected and washed three times in boiling water to remove adhering medium. The washed mycelium was freeze-dried, ground in a ball mill, and extracted continuously with light petroleum (b.p. 30–60° C) in a Soxhlet apparatus for 8 days. The extracted mycelium (730 g) was suspended in 0.8% aqueous sodium carbonate (8500 ml) and the pH of the mixture was adjusted to 8.1 by addition of *N* hydrochloric acid. Trypsin (3.0 g, "Difco") was added to the mixture, which was then protected from contamination by a layer of toluene (10 ml per flask). The trypsin digests (four equal lots) were kept at 37° C and were shaken vigorously once every 24 hours during an incubation period of 14 days. The insoluble residue was centrifuged, washed three times with distilled water, and freeze-dried. Crude polysaccharides were removed from the freeze-dried material (510 g) by extraction with hot, 3% aqueous sodium hydroxide (10,200 ml) for 15–16 hours. The extract was clarified by centrifugation, neutralized with acetic acid, and dialyzed to remove salts and other low molecular weight impurities. The non-dialyzable polysaccharides were precipitated by ethanol, dissolved in water, reprecipitated, and dried by solvent exchange with ethanol, ether, and light petroleum (b.p. 30–60° C). The polysaccharide preparation thus obtained was a light tan powder (10% of the dried, powdered mycelium) which contained no nitrogen, as shown by microanalysis. A sample (5 mg) of this material was hydrolyzed by *N* sulphuric acid (0.5 ml) at 97° C in a sealed tube for 12 hours. Paper chromatography (solvent A) of the hydrolyzate showed the presence of a large amount of mannose with smaller amounts of glucose and galactose. Another sample (150 mg) of the polysaccharide preparation was dissolved in 0.05 *M* sodium tetraborate, equilibrated with the buffer by dialysis, and examined by moving-boundary electrophoresis (3). Figure 1A shows the separation obtained by this procedure. The first peak was a false boundary because the removal and hydrolysis of a sample yielded no sugars. The second peak was broad and diffuse, indicative of heterogeneity; it had an average mobility (μ) of 8.33×10^{-5} cm²/volt sec. The peak of greater mobility ($\mu = 11.28\times10^{-5}$ cm²/volt sec) was sharp and symmetrical and obviously represented the major component of the mixture.

Purification of Galactomannan

The mixture of crude polysaccharides (300 mg) was resolved on a column (32×3 cm) of diethylaminoethyl (DEAE) cellulose by stepwise elution with increasing concentrations of sodium tetraborate (4). Fractions (18 ml each) were collected automatically every 15 minutes; aliquots (1 ml) of each fraction were mixed with 2 ml of anthrone reagent (0.5% anthrone in 95% sulphuric acid) and the optical densities at 625 mμ were read on a colorimeter. Figure 2 shows the result of this separation, which gave four fractions. Each fraction was passed over Amberlite IR-120 exchange resin to remove sodium ions and was then evaporated until boric acid began to crystallize. Six volumes of methanol were then added and the precipitated polysaccharides were washed successively with methanol, ethanol, ether and were then dried. This procedure yielded fractions 1 (76.2 mg), 2 (16.3 mg), 3 (128.2 mg), and 4 (25.8 mg); recovery, 246.5 mg, 82%. The losses were accountable in part by the 5.5% of each fraction of eluate used for the anthrone test and in part by the irreversible absorption of highly pigmented impurities on the DEAE cellulose. The recovered polysaccharides were white, water-soluble powders and yielded the following sugars on hydrolysis, as shown by paper chromatography (solvent A): fractions 1 and 2—glucose, mannose, galactose; fractions 3 and 4—mannose, galactose, trace of glucose. On moving-boundary electrophoresis under the conditions described above, fractions 1+2 gave a broad, diffuse peak corresponding in mobility to the minor component shown in Fig. 1A. Fractions 3+4, under the same conditions, gave a sharp symmetrical peak (Fig. 1B) which had the same mobility as the major component in Fig. 1A. The above results showed that fractions 2 and 4 were the same as fractions 1 and 3 respectively and probably represented the normal elution pattern of these polysaccharides from DEAE cellulose.

The separation was repeated a sufficient number of times on a larger scale (2 g of crude polysaccharide on a column (7.6×50 cm) of DEAE cellulose, 230 g) to yield 5.0 g of fractions 3+4. Reprecipitation of this product from aqueous solution by addition of ethanol to a concentration of 50% yielded a pure galactomannan; the trace of glucose-containing material remained in solution. The number-average degree of polymerization of the galactomannan was 55±1 based on estimation of reducing end group by hypoiodite oxidation (20).

Estimation and Identification of Constituent Sugars

A sample (64.0 mg) of the galactomannan in *N* hydrochloric acid (5 ml) showed an initial specific rotation of +71±1°. When this solution was heated at 85° C the specific rotation changed to a constant value of

+22±1.5° after 11 hours. The calculated specific rotation for a mixture containing 13% galactose and 87% mannose is +22.7°. The sugars in the hydrolyzate were resolved by paper chromatography (solvent A) and estimated by the phenol–sulphuric acid method (21), which gave 18% galactose, 82% mannose. The amounts of *O*-methyl mannose and galactose derivatives (Table I) from hydrolysis of the methylated polysaccharide showed 16.5% galactose and 83.5% mannose. The average of these three estimations was 16% galactose, 84% mannose.

The two sugars in a hydrolyzate of 100 mg of the polysaccharide were isolated by preparative paper chromatography (solvent A), and identified as D-galactose and D-mannose by preparation of the phenylosazone (22), m.p. and mixed m.p. 194–196° C, and the *p*-nitroanilide (23), m.p. and mixed m.p. 217–218° C, respectively.

Methylation of Galactomannan

Galactomannan (3.0 g) was methylated five times by dimethyl sulphate and 30% sodium hydroxide (24). The partially methylated product (2.96 g), isolated by extraction into chloroform, was methylated three times by silver oxide and methyl iodide (25) to yield a product (2.6 g; OCH_3, 41.5%) showing weak hydroxyl absorption in its infrared spectrum. A portion of this material was insoluble in absolute ethanol and was removed by centrifugation. The ethanol solution was then evaporated to dryness and a small oily impurity was removed from the residue by extraction with hot light petroleum (b.p. 30–60° C). The residue from this extraction was the fully methylated galactomannan, a cream-colored powder; 2.23 g, $[\alpha]_D^{25}$ +42 ±1° (*c*, 2.3% in chloroform); OCH_3, 44.8%; calc. OCH_3, 45.6%.

Hydrolysis Products from Methylated Galactomannan

The methylated galactomannan (2.1 g) was dissolved in ice-cold 72% sulphuric acid (16 ml) and the solution was left at room temperature for 45 minutes. Water (112 ml) was added and the solution (now 12% sulphuric acid) was heated on a boiling-water bath for 4 hours (26). Acid was removed by Amberlite IR-45 exchange resin and the neutral solution was evaporated to dryness. A portion of the residue was refluxed with 2% methanolic hydrogen chloride for 6 hours and the solution was then neutralized with silver carbonate. The methyl glycosides in this solution were examined by gas–liquid chromatography to give the separation shown in Fig. 3. Subsequent identifications of the components showed that all but one of the peaks in Fig. 3 represented more than one compound. However, the areas of the peaks, determined by triangulation, gave the gross quantitative ratios of di- to tri- to tetra-*O*-methyl sugars as 2:5:2. Detailed quantitative ratios of individual components within each of these groups were obtained as described below.

The mixture of reducing *O*-methyl sugars was chromatographed in solvent B on a column of powdered cellulose to yield the following fractions:

Fraction 1

Fraction 1, 160 mg, gave R_g values (1.04, 0.99, and 1.07 in solvents B, C, and D respectively) identical with those given by an authentic sample of 2,3,5,6-tetra-*O*-methyl-D-galactose prepared by methylation and hydrolysis of methyl β-D-galactofuranoside (27), m.p. 66–67° C, $[\alpha]_D^{25}$ −113.5±1.0° (*c*, 2.94% in water). Oxidation by bromine yielded a lactone having an infrared spectrum identical in all respects with that of authentic 2,3,5,6-tetra-*O*-methyl-D-galactonolactone. Both spectra showed carbonyl absorption at 1775 cm^{-1} indicative of 5-membered (1765–1790 cm^{-1}), as opposed to 6-membered (1726–1760 cm^{-1}), lactone rings (28). The lactone yielded an amide which, after three recrystallizations from acetone, had $[\alpha]_D^{25}$ +7.7±1.0° (*c*, 4.92% in water) and a melting point of 157–158° C, unchanged on admixture with an authentic sample of 2,3,5,6-tetra-*O*-methyl-D-galactonamide (29).

Fraction 2

Fraction 2, 50.7 mg, contained two components with R_g values (1.04 and 0.98) in solvent B the same as those of 2,3,5,6-tetra-*O*-methyl-D-galactose and 2,3,4,6-tetra-*O*-methyl-D-mannose respectively. The two compounds were separated by preparative paper chromatography and the amounts obtained gave a ratio of 4 parts 2,3,5,6-tetra-*O*-methyl-D-galactose to 1 part 2,3,4,6-tetra-*O*-methyl-D-mannose.

Fraction 3

Fraction 3, 60.3 mg, contained one component with R_g values (0.98, 0.99, and 1.00 in solvents B, C, and D respectively) the same as those of 2,3,4,6-tetra-*O*-methyl-D-mannose and had $[\alpha]_D^{27}$ +44.7±0.6° (*c*, 3% in methanol). The derived anilide, recrystallized from ether:methanol (98:2), had $[\alpha]_D^{27}$ −11±2° (*c*, 0.88% in methanol) and a melting point of 146–147° C, unchanged on admixture with N-phenyl-2,3,4,6-tetra-*O*-methyl-D-mannosylamine (30).

Portions of fractions 1 and 3 were converted to their methyl glycosides by methanolic hydrogen chloride and examined by gas–liquid chromatography under conditions given in Fig. 3. The two sugars were not separated under these conditions and had the same retention time as peak 1, Fig. 3. The quantitative ratio of 3 parts 2,3,5,6-tetra-*O*-methyl-D-galactose to 1 part 2,3,4,6-tetra-*O*-methyl-D-mannose was obtained from the relative amounts of fractions 1, 2, and 3. Thus, 2,3,5,6-tetra-*O*-methyl-D-galactose = fraction 1 (160 mg) + 4/5 fraction 2 (4/5×50.7) = 200 mg and 2,3,4,6-tetra-*O*-methyl-D-mannose = fraction 3 (60.3 mg) + 1/5 fraction 2 (1/5×50.7) = 70.4 mg (ratio = 2.84:1).

Fraction 4

Fraction 4, 249 mg, showed only one spot on paper chromatograms in solvents B and C (R_g values 0.72 and 0.88 respectively) but gave two spots, not separated completely, of R_g 0.58 and 0.47 in solvent D.

Paper electrophoresis gave a separation of two components with M_G values of 0.00 and 0.31. Methylation (31) and hydrolysis of the mixture yielded only 2,3,4,6-tetra-*O*-methyl-D-mannose, as shown by chromatography in solvent B. R_g values in this solvent were 2,3,5,6-tetra-*O*-methyl-D-galactose (1.04), 2,3,4,6-tetra-*O*-methyl-D-mannose (0.98), and 2,3,4,6-tetra-*O*-methyl-D-galactose (0.81). Both components were therefore mannopyranose derivatives and the R_g values indicated that they were tri-*O*-methyl mannoses. Since the component with M_G 0.31 probably had a free hydroxyl at C_2 the mixture was seeded with crystalline 3,4,6-tri-*O*-methyl-D-mannose, which induced crystallization of that component. Crystallization from ether:hexane (2:1) yielded three crops of crystals which were combined and recrystallized from the same solvent to yield 3,4,6-tri-*O*-methyl-D-mannose (32), m.p. and mixed m.p. 102–104° C, $[\alpha]_D^{25}$ +36±1° (*c*, 1.15% in methanol).

The component with M_G 0.00 was separated from the 3,4,6-tri-*O*-methyl-D-mannose remaining in the mother liquors from the above crystallization by preparative paper electrophoresis (Whatman 3 MM paper 14×46 cm). The area of the paper containing the non-migrating component was eluted with water and the eluate was passed over Amberlite IR-120 exchange resin and evaporated. Boric acid was removed from the residue by repeated evaporation with methanol. The sirupy product was oxidized by bromine to yield a lactone which showed carbonyl absorption at 1715 cm^{-1} in its infrared spectrum, indicative of a 6-membered lactone ring (28). The lactone yielded an amide which was recrystallized from ethyl acetate and had m.p. 142–143° C, $[\alpha]_D^{25}$ = +4.5±1° (*c*, 1.3% in water), in good agreement with the reported values for 2,3,4-tri-*O*-methyl-D-mannonamide (33).

Small samples of 3,4,6- and 2,3,4-tri-*O*-methyl-D-mannose were refluxed with 2% methanolic hydrogen chloride for 6 hours and the products were examined by gas–liquid chromatography. The two components were not separated under conditions given in Fig. 3 and had the same retention time as peak 2. Small peaks from both of these samples had the same retention time as the small peaks following peak 2, Fig. 3. It is known that D-mannose yields predominantly the α-methyl glycoside on methanolysis and these small peaks were probably the β-anomers. The small amounts and the close similarity of their retention times precluded more positive identification.

The quantitative ratio (1:1) of the two tri-*O*-methyl-D-mannoses was established by the amounts recovered from a preparative paper electrophoresis carried out before crystallization of the 3,4,6-tri-*O*-methyl isomer. The two products were recovered as described above to yield 2,3,4-tri-*O*-methyl-D-mannose (14.9 mg) and 3,4,6-tri-*O*-methyl-D-mannose (14.1 mg) (ratio = 1.05:1.0).

Fraction 5

Fraction 5, 208 mg, showed one spot in solvents C and D (R_g 0.69 and 0.21 respectively) and a double spot (R_g 0.40 and 0.35) in solvent B. On paper electrophoresis the mixture migrated as an elongated spot with M_G 0.38 (center of spot). Methylation (31) and hydrolysis yielded only 2,3,4,6-tetra-*O*-methyl-D-mannose, as shown by chromatography in solvent B. The R_g values indicated di-*O*-methyl derivatives, the M_G value showed that there were free hydroxyls on C_2, and methylation proved that all components were derivatives of mannopyranose; this left only the 3,4-, 3,6-, and 4,6-di-*O*-methyl mannoses as possibilities. Peak 3, Fig. 3, had the same retention time as an authentic sample of methyl 3,4-di-*O*-methyl-α-D-mannoside so the mixture of reducing di-*O*-methyl mannoses was seeded with crystalline 3,4-di-*O*-methyl-D-mannose. The sirup crystallized partially and three crops of the product were obtained by crystallization from ethyl acetate. Recrystallization of this material from the same solvent yielded 3,4-di-*O*-methyl-D-mannose (15, 34), m.p. and mixed m.p. 71–73° C, $[\alpha]_D^{24}$ +32±1.5° (*c*, 1.55% in methanol).

The components in the mother liquors from crystallization of the 3,4-di-*O*-methyl-D-mannose were converted to their methyl glycosides and examined by gas–liquid chromatography. Under the conditions given for Fig. 4 a separation of three components was obtained and they were collected from the effluent gas stream. The material from peak 1, Fig. 4, crystallized when seeded with methyl 3,4-di-*O*-methyl-α-D-mannoside (13) and had m.p. and mixed m.p. 86–87° C. The material from peak 2, Fig. 4, was resistant to periodate oxidation when tested as follows. The compound was spotted on glass fiber paper, which was then sprayed with a saturated solution of sodium metaperiodate. The oxidation was allowed to proceed for 1 hour and the paper was then sprayed successively with acetonic silver nitrate and alcoholic sodium hydroxide (19), which showed up any oxidation products as dark brown spots. Because peak 1, Fig. 4, had been identified as the 3,4-di-*O*-methyl isomer, peak 2, Fig. 4, could only be the glycoside of 3,6- or 4,6-di-*O*-methyl-D-mannose. The negative periodate oxidation test showed that this component was the glycoside of 3,6-di-*O*-methyl-D-mannose. This compound does not appear to have been reported and attempts to prepare a crystalline derivative were unsuccessful. No crystalline osazone could be obtained from 2,3,6-tri-*O*-methyl-D-mannose and acetylation of the methyl 3,6-di-*O*-methyl-α-D-mannopyranoside yielded a sirupy product. Lack of sufficient material precluded attempts to prepare other derivatives.

The compound giving peak 3, Fig. 4, was readily oxidized by periodate under the test conditions described above, and by similar reasoning, was thereby proved to be the methyl glycoside of 4,6-di-*O*-methyl-D-mannose. An attempt to prepare 2,3-*O*-isopropylidine 4,6-di-*O*-methyl-D-mannose (35) from the reducing sugar did not yield sufficient material for characterization.

The glycosides of 3,6- and 4,6-di-*O*-methyl-D-mannose, as collected from peaks 2 and 3 respectively (Fig. 4) were not separable under the conditions cited in Fig. 3 and had the same retention time as peak 4, Fig. 3. No anomeric pairs were observed in these di-*O*-methyl mannosides and the α-configuration, proved for the 3,4-di-*O*-methyl isomer, was assumed for the other two.

Quantitative relationships between the three di-*O*-methyl mannoses were obtained from Figs. 3 and 4. Thus, the areas of peaks 3 and 4, Fig. 3, were in a 1:1 ratio (1 part of 3,4-di-*O*-methyl-D-mannose to 1 part 3,6- + 4,6-di-*O*-methyl-D-mannose). The separation in Fig. 4 showed that 3,6- and 4,6-di-*O*-methyl-D-mannose were present in a 1:1 ratio; some of the 3,4-di-*O*-methyl-D-mannose had been removed by crystallization from the mixture shown in Fig. 4. The overall ratio of 3,4- to 3,6- to 4,6-di-*O*-methyl-D-mannose was therefore 2:1:1.

The amounts of the five fractions recovered from the cellulose column gave a ratio of di- to tri- to tetra-*O*-methyl sugars of 1.00:1.25:1.3, which was different from that (2:5:2) obtained by gas–liquid chromatography. The recoveries from the cellulose column were regarded as unreliable, first because the above ratio, in disagreement with the results of gas–liquid chromatography, did not satisfy theoretical requirements and second because it would give a galactose content of 29% (4/5 of the tetra-*O*-methyl was galactose), quite different from the average value of 15.5% found by two other methods. There was no ready explanation for these anomalous recoveries from the cellulose column. However, it was apparent that compounds with hydroxyl groups (di-*O*- and tri-*O*-methyl isomers) were lost, possibly by irreversible adsorption on the particular batch of cellulose used. There was no evidence that a single isomer was lost preferentially and ratios of components within a single fraction were regarded as valid.

Periodate Oxidation

The galactomannan (118.9 mg, 0.734 mmole) was dissolved in water (125 ml), and 0.25 *M* sodium periodate (25 ml) was added. A reagent blank was also prepared and the oxidation was allowed to proceed at 25° C in the absence of light. At intervals samples were removed for estimation of formic acid by iodometric titration and of periodate by the excess arsenite procedure (36). The results, given below in moles per mole anhydrohexose unit, were indicative of extensive overoxidation.

Time (hr)	Formic	Periodate
72	0.57	1.05
96	0.63	1.58
144	0.68	1.85
168	0.72	2.05

ACKNOWLEDGMENT

The authors are grateful to Mr. F. P. Cooper for carrying out the gas–liquid chromatographic separations.

REFERENCES

1. F. BLANK. Biochim. et Biophys. Acta, **10**, 110 (1953).
2. B. BLOCH, A. LABOUCHÈRE, and F. SCHAAF. Arch. Dermatol. and Syphilol. **148**, 413 (1925).
3. D. H. NORTHCOTE. Biochem. J. **58**, 353 (1954).
4. H. NEUKOM, H. DEUEL, W. J. HERI, and W. KÜNDIG. Helv. Chim. Acta, **43**, 64 (1960).
5. A. G. MCINNES, D. H. BALL, F. P. COOPER, and C. T. BISHOP. J. Chromatog. **1**, 556 (1958).
6. C. T. BISHOP and F. P. COOPER. Can. J. Chem. **38**, 388 (1960).
7. L. HOUGH, J. K. N. JONES, and W. H. WADMAN. J. Chem. Soc. 1702 (1950).
8. A. B. FOSTER. Advances in Carbohydrate Chem. **12**, 81 (1957).
9. C. F. HUEBNER, S. R. AMES, and E. C. BUBL. J. Am. Chem. Soc. **68**, 1621 (1946).
10. R. L. WHISTLER and C. L. SMART. Polysaccharide chemistry. Academic Press Inc., New York. 1953.
11. C. T. BISHOP, F. BLANK, and P. E. GARDNER. Can. J. Chem. **38**, 869 (1960).
12. W. N. HAWORTH, E. L. HIRST, and F. A. ISHERWOOD. J. Chem. Soc. 784 (1937).
13. W. N. HAWORTH, R. L. HEATH, and S. PEAT. J. Chem. Soc. 833 (1941).
14. J. A. CIFONELLI and F. SMITH. J. Am. Chem. Soc. **77**, 5682 (1955).
15. P. A. J. GORIN and A. S. PERLIN. Can. J. Chem. **34**, 1796 (1956).
16. W. N. HAWORTH, H. RAISTRICK, and M. STACEY. Biochem. J. **31**, 640 (1937).
17. I. R. SIDDIQUI and G. A. ADAMS. Can. J. Chem. **39**, 1683 (1961).
18. W. K. ROBERTS, J. G. BUCHANAN, and J. BADDILEY. Biochem. J. **82**, 42p (1962).
19. W. E. TREVELYAN, D. P. PROCTER, and J. S. HARRISON. Nature, **166**, 444 (1950).
20. R. WILLSTÄTTER and G. SCHUDEL. Ber. **51**, 780 (1918).
21. M. DUBOIS, K. A. GILLES, J. K. HAMILTON, P. A. REBERS, and F. SMITH. Anal. Chem. **28**, 350 (1956).
22. E. FISCHER and J. TAFEL. Ber. **20**, 3390 (1887).
23. F. WEYGAND, W. PERKOW, and P. KUHNER. Chem. Ber. **84**, 594 (1951).
24. W. N. HAWORTH. J. Chem. Soc. **107**, 8 (1915).
25. T. PURDIE and J. C. IRVINE. J. Chem. Soc. **83**, 1021 (1903).
26. I. CROON, G. HERRSTRÖM, G. KULL, and B. LINDBERG. Acta Chem. Scand. **14**, 1338 (1960).
27. I. AUGESTAD and E. BERNER. Acta Chem. Scand. **8**, 251 (1954).

28. S. A. BARKER, E. J. BOURNE, R. M. PINHARD, and D. H. WHIFFEN. Chem. & Ind. (London), 658 (1958).
29. R. W. HUMPHREYS, J. PRYDE, and E. T. WATERS. J. Chem. Soc. 1298 (1931).
30. J. C. IRVINE and D. MCNICOLL. J. Chem. Soc. **97**, 1449 (1910).
31. R. KUHN, H. TRISCHMANN, and I. LÖW. Angew. Chem. **67**, 32 (1955).
32. H. G. BOTT, W. N. HAWORTH, and E. L. HIRST. J. Chem. Soc. 1395 (1930).
33. W. N. HAWORTH, E. L. HIRST, F. A. ISHERWOOD, and J. K. N. JONES. J. Chem. Soc. 1878 (1939).
34. D. H. BALL and G. A. ADAMS. Can. J. Chem. **37**, 1012 (1959).
35. R. G. AULT, W. N. HAWORTH, and E. L. HIRST. J. Chem. Soc. 1012 (1935).
36. P. FLEURY and J. LANGE. J. pharm. chim. **17**, 107 (1933).

THE KINETICS OF THE ALKALINE HYDROLYSES OF DIMETHYL TEREPHTHALATE AND THE TRANS ISOMER OF DIMETHYL 1,4-CYCLOHEXANEDICARBOXYLATE IN DIOXANE–WATER MIXTURES[1]

W. J. Svirbely and Patricia A. Cunniff
Department of Chemistry, University of Maryland, College Park, Md., U.S.A.
Received March 29, 1962

ABSTRACT

The kinetics of the alkaline hydrolyses of dimethyl terephthalate and *trans*-dimethyl 1,4-cyclohexanedicarboxylate was studied in dioxane–water mixtures varying in dielectric constant from 60 to 11. The effect of the medium on the mechanism and rate constants is, in general, similar to that previously observed in the study of the alkaline hydrolyses of aliphatic diesters.

INTRODUCTION

Recently (1) a study was made on the effect of the medium on the rate constant ratios of diester hydrolysis. Three diesters in the aliphatic series differing markedly in length, namely, diethyl malonate, diethyl succinate, and diethyl sebacate, were used. It was observed that as the dielectric constant decreased (or as the dioxane content in dioxane–water media increased), the two rate constants in each of the two-step competitive–consecutive second-order reactions approached each other, i.e. the rate constant ratio in each diester reaction approached unity. The observations can be explained on the basis that both steps of each reaction are proceeding by essentially the same mechanism in low-dielectric media. This situation would arise if one were dealing under such circumstances with solvated ion pairs or aggregates. One would expect the same general variation in the rate constants for the alkaline hydrolyses of cyclic diesters in low-dielectric media if structural features did not complicate the picture.

Consequently, in order to determine the effect of the medium on the alkaline hydrolyses of cyclic diesters, studies were made of the alkaline hydrolysis of *trans*-dimethyl 1,4-cyclohexanedicarboxylate and of dimethyl terephthalate in dioxane–water mixtures varying in dielectric constant from 60 to 11.

EXPERIMENTAL

Materials and Apparatus

Dioxane, water, sodium hydroxide solutions, and hydrochloric acid solutions were prepared or purified as before (2).

The dimethyl terephthalate was obtained from Eastman Kodak Co. Two recrystallizations from diethyl ether yielded a product which melted at 139.6–140.4° (corr.). Literature values are 140.5–141° and 140°. The saponification equivalent indicated 99.9±0.1% purity.

The trans isomer of dimethyl 1,4-cyclohexanedicarboxylate was obtained from a cis–trans mixture furnished by the Eastman Kodak Co.[2] which had an approximate isomer concentration of 60% cis and 40% trans. The solid material was filtered from the mixture and recrystallized five times from petroleum ether, m.p. 69.1–69.4° (corr.). Further recrystallization did not produce a change in the melting point. The saponification equivalent indicated 99.9±0.1% purity.

Procedure

The procedure has been described (1).

[1]*Abstracted in part from a thesis by Patricia A. Cunniff to the Graduate School of the University of Maryland in partial fulfillment of the requirements for the degree of Master of Science.*

[2]*Acknowledgment is hereby made to the Eastman Kodak Company for their grant of two pounds of the mixture.*

DATA AND CALCULATIONS

Evaluation of Rate Constants

The alkaline hydrolyses of the diesters used in this research may be represented by the equations

$$A + B \xrightarrow{k_1} C + E$$

$$A + C \xrightarrow{k_2} D + E,$$

where A, B, C, and D represent hydroxyl ion, diester, monovalent ion of the ester, and divalent ion of the ester respectively. The procedure for calculating the rate constants, based on the Frost and Schwemer method (3), has been described (1). Tables I and II summarize the calculations for two of our runs. In some of our calculations, the Burkhard (4) extension of the τ (defined $= B_0k_1t$) and time-ratio tables of Frost and Schwemer were used.[3]

TABLE I

Data for the dimethyl terephthalate reaction at 25.22°;
$D = 25.82$; $A_0 = 11.055\times10^{-3}$ mole/l.; $B_0 = 5.527\times10^{-3}$ mole/l.

Run A			Run B		
Time (min)	$A\times10^3$ (mole/l.)	$\alpha = A/A_0$	Time (min)	$A\times10^3$ (mole/l.)	$\alpha = A/A_0$
4.00	8.6559	0.7830	3.00	9.0403	0.8178
6.00	7.8348	0.7087	5.00	8.0619	0.7293
8.00	7.2931	0.6597	7.00	7.5028	0.6787
10.00	6.9087	0.6249	9.00	7.0310	0.6360
12.00	6.6292	0.5997	11.00	6.7689	0.6123
14.00	6.2972	0.5696	13.00	6.3846	0.5775
18.00	5.8080	0.5254	20.00	5.7381	0.5191
24.00	5.4236	0.4906	26.00	5.3537	0.4843
30.00	5.0742	0.4590	32.00	5.0392	0.4558
36.00	4.9518	0.4479	40.00	4.7422	0.4290
42.00	4.7247	0.4274	45.00	4.6548	0.4211
48.00	4.5500	0.4116	50.00	4.4976	0.4068
55.00	4.3928	0.3974	60.00	4.3403	0.3926
65.00	4.1831	0.3784	70.10	4.1481	0.3752
80.00	3.9909	0.3610	75.10	4.0433	0.3657
90.00	3.8511	0.3484	85.00	3.9559	0.3578
100.00	3.6589	0.3310	95.00	3.7638	0.3405

Table III summarizes the data at 25.22°. A_0 (starting hydroxide concentration) varied from 10.825×10^{-3} to 11.075×10^{-3} mole/l. in the various runs. Thus the data in Table III were obtained under essentially the same stoichiometric ionic strength conditions as far as the reactants were concerned. Solubility limitations prevented the study of the dimethyl terephthalate reaction over the same dielectric range as was used in the trans 1,4-cyclohexanedicarboxylate reaction.

Table III also summarizes the data obtained when KCl was added to the reaction mixtures.

[3]*In order to obtain the time-ratio derived data from the experimental data, values of α (defined as A/A_0) for duplicate runs were plotted against time on a large sheet of graph paper. From the resulting smooth curve, the times for fixed percentages of completion were determined. Time-ratios were then calculated from these times for the various percentages of reaction.*

TABLE II

Calculations of rate constants using data of Table I

% reaction	t (min)	Percentage compared	t ratio	$1/K$	τ	k_1 (l. mole^{-1}min^{-1})
20	3.38	60/20	15.775	15.81	0.2811	15.05
30	6.35	60/30	8.397	15.64	.5304	15.11
40	11.54	60/40	4.620	15.48	.9574	15.01
50	22.35	60/50	2.386	15.57	1.862	15.07
60	53.32	50/20	6.612	15.48	4.447	15.09
		50/30	3.520	15.76		
		50/40	1.937	15.44		
				Average 15.60		15.07

$$k_2 = \frac{15.07}{15.60} = 0.966 \text{ l. mole}^{-1}\text{min}^{-1}$$

TABLE III

Rate constants* for the hydrolyses of the cyclic diesters in dioxane–water media at 25.22° C

Ester	D	Wt% dioxane	Without salt			KCl added†		
			k_1	k_2	k_1/k_2	k_1	k_2	k_1/k_2
Dimethyl terephthalate	25.82	60	15.1	0.966	15.6			
	17.67	70	13.0	1.14	11.4	7.94	1.23	6.46
	10.70	80	11.8	1.74	6.78			
trans-Dimethyl 1,4-cyclohexane-dicarboxylate	60.72	20	9.47	1.92	4.93			
	42.90	40	6.81	1.19	5.72			
	25.82	60	5.05	0.974	5.18			
	17.67	70	3.85	1.05	3.67	2 60	1.24	2.09
	10.70	80	3.06	1.37	2.23			

*Duplicate runs were made in all cases. Average deviation from the mean of the $1/K$ values in each pair of runs was between 0.1% and 2.2%.
†Reading down the column, KCl added was = 0.1253 and 0.1398 mole/l. respectively.

DISCUSSION

Reference to Fig. 1 and to the literature (1) shows quite similar behavior in the effect of the medium on the rate constants obtained for the alkaline hydrolyses of cyclic diesters and aliphatic diesters in dioxane–water mixtures. These may be summed up as follows: (1) While there is a marked difference in the rate constants for the two steps of each reaction in high-dielectric media, this difference is markedly less in lower-dielectric media. (2) With the exception of the dimethyl terephthalate reaction, the curves of log k_2 vs. $1/D$ for the reactions go through a minimum in a narrow dielectric range, i.e. between 25 and 33. A minimum for the dimethyl terephthalate reaction could not be demonstrated because of solubility limitations. Our previous conclusion (1) "that this could be the point at which ion-pair formation becomes important and the second step of each reaction is changing from an ion–ion reaction to one involving ion-pairs" is thus also applicable to these cyclic diester reactions.

Since both of the diesters used in this research had, as substituents, the same electron-withdrawing groups, i.e. carbomethoxy groups, the larger values of k_1 obtained in the terephthalate reaction compared to the values of k_1 obtained in the cyclohexanedicarboxylate reaction can be accounted for by the assumption of greater electrophilicity of the carbonyl carbon atom in the terephthalate compound as the result of structural differences in the two ring structures. However, on examining the results for the second step

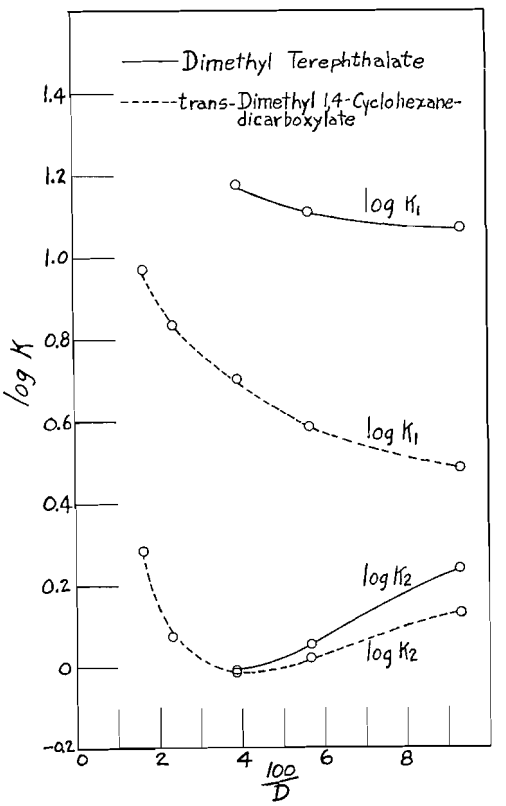

FIG. 1. Log K versus $100/D$ at 25.2°.

of each reaction, one observes that the k_2 values of the two esters are considerably closer to one another under similar environmental conditions. If structural differences can account for the differences in the k_1 values, they should also lead to differences in the k_2 values. Such is not the case. We can explain the above observations by the following argument. If one examines the k_2 values of aliphatic diesters (1) along with the k_2 values of the cyclic diesters, one observes that in low-dielectric media, i.e. $D \sim 11$, the magnitudes of the k_2 values are in the inverse order to the distances separating the substituents in the original compounds. If one assumes that an increase in electrophilicity of the carbonyl carbon atom in the second step of the reactions depends both on the distance between the residual charge on the so-called monovalent ion and its remaining carboxylate group and on the medium surrounding the ion rather than on any effect through the ion due to its structure, then one can rationalize the variation in the k_2 values. Since the residual charge on the so-called monovalent ion is affected by the extent of ion-pair or other aggregate formation, then a change in slope in the log k_2 vs. $1/D$ curve should occur as the composition of the medium is changed. This is in agreement with the observations.

REFERENCES

1. W. J. SVIRBELY and A. D. KUTCHA. J. Phys. Chem. **65**, 1333 (1961).
2. W. J. SVIRBELY and H. E. WEISBERG. J. Am. Chem. Soc. **81**, 257 (1959).
3. A. A. FROST and W. C. SCHWEMER. J. Am. Chem. Soc. **74**, 1268 (1952).
4. C. A. BURKHARD. Ind. Eng. Chem. **52**, 678 (1960).

THE HYDROGEN-ABSTRACTION REACTIONS IN THE PHOTOLYSIS OF PENTAFLUOROPROPANAL AND HEPTAFLUOROBUTANAL[1]

G. O. PRITCHARD, G. H. MILLER, AND J. K. FOOTE
Department of Chemistry, University of California, Santa Barbara, Goleta, Calif., U.S.A.

Received April 16, 1962

ABSTRACT

The main products of the photolysis of the aldehydes at 3130 Å were determined and the rates of H-atom abstraction relative to radical recombination were measured. They are $k_1/k_2^{\frac{1}{2}} = (3.09\pm0.12)10^3 \exp(-4500\pm200/RT)$ mole$^{-\frac{1}{2}}$cc$^{\frac{1}{2}}$sec$^{-\frac{1}{2}}$ for C_2F_5CHO, and $k_1/k_2^{\frac{1}{2}} = (1.86\pm0.14)10^3 \exp(-4000\pm300/RT)$ mole$^{-\frac{1}{2}}$cc$^{\frac{1}{2}}$sec$^{-\frac{1}{2}}$ for C_3F_7CHO. The derived Arrhenius parameters are compared with those determined in the photolysis of CF_3CHO, and also with the non-fluorinated aldehydes.

INTRODUCTION

The photolysis of the two aldehydes C_2F_5CHO and C_3F_7CHO was undertaken with a view to testing their suitability as convenient sources of $C_2F_5\cdot$ and $C_3F_7\cdot$ radicals for studying the rates of hydrogen abstraction from various hydrogen-containing compounds RH. It was first necessary to determine the rates of the self-abstraction reaction [1] in the systems, e.g.,

$$R_fCHO + h\nu \rightarrow R_f\cdot + CHO\cdot \qquad [I]$$

$$R_f\cdot + R_fCHO \rightarrow R_fH + R_fCO\cdot \qquad [1]$$

$$R_f\cdot + R_f\cdot \rightarrow R_{f_2}, \qquad [2]$$

where $R_f\cdot$ denotes $C_2F_5\cdot$ or $C_3F_7\cdot$, relative to the respective radical recombination reaction [2].

Our values of the Arrhenius parameters for reaction [1] showed a marked difference from those expected from the earlier work of Dodd and Smith (1) on the photolysis of trifluoroacetaldehyde ($R_f\cdot = CF_3\cdot$). A discussion of these differences constitutes the scope of this paper. Reactions of $R_f\cdot$ with other RH will be presented subsequently.

EXPERIMENTAL

A standard vacuum apparatus for this type of study was used. The light source was a British Thomson-Houston ME/D 250-watt high-pressure mercury arc. The beam was collimated by a quartz lens, and passed through a Corning 9863 blue-glass into the 10 cm long, cylindrical, quartz reaction vessel, volume 152.6 ml, fully illuminating it. It was connected to the remainder of the system with a mercury cutoff; the dead space was less than 10 ml. The temperature in the surrounding furnace was controlled to $\pm1°$ during the period of a run.

The aldehydes were obtained as the hydrates from K and K Laboratories and Columbia Organic, and dehydrated with P_2O_5 and H_2SO_4 (2). After low-temperature fractionation, their purity was established mass spectrometrically (3). They were stored in blackened bulbs at $-195°$, for decomposition and polymerization occurred at room temperature. The ultraviolet absorption spectra were taken on a Cary Model 14 recording spectrophotometer. They were identical in shape, with a maximum at 3190 Å. The C_3F_7CHO extinction coefficient ($\log_{10} I_0/I = \epsilon cl$), 22.8 l. mole^{-1}cm^{-1}, is about 50% higher than that for C_2F_5CHO, 15.5 l. mole^{-1}cm^{-1}.

After photolysis, product analysis was effected by low-temperature fractionation on Ward – Le Roy stills and mass spectrometry. The CO and H_2 were collected at $-195°$ and measured; after treatment in a CuO furnace at 300°, the CO was determined as CO_2, and the H_2 by difference. The remainder of the reaction products and the undecomposed aldehyde were condensed into a tube containing a solution of phenylhydrazine in carefully out-gassed, distilled water, made acid with HCl or H_2SO_4. The tube was allowed

[1]*Presented at the XVIIIth International Congress of Pure and Applied Chemistry, Montreal, August, 1961.*

to warm to room temperature, and left until the aldehyde had completely reacted. If pure water only is used, an equilibrium is established, and the aldehydes are volatile enough to interfere in the subsequent analysis. In our procedure they are removed, probably as hydrates, hydrazones, and polymer.

In the C_2F_5CHO experiments, C_2F_5H was collected at $-150°$, and C_4F_{10} at $-120°$. The separation of these two products by low-temperature distillation is tedious, and in many cases they were collected together and analyzed on the mass spectrometer, using the CF_2H^+ (51) ion peak for C_2F_5H, and the residual CF_3^+ (69) ion peak for C_4F_{10}. Pure standards were obtained by prolonged photolysis of the aldehyde, and careful fractionation. The mass spectra were identical with those previously recorded (4, 5). No disparity was found between the two methods.

In the C_3F_7CHO photolyses, C_3F_7H was collected at $-120°$, and C_6F_{14} at $-80°$. Their purity was checked from the mass spectra (5, 6).

RESULTS

The results are presented in Table I for C_2F_5CHO and in Table II for C_3F_7CHO.

TABLE I

Data on the photolysis of C_2F_5CHO

Run	Time (sec)	Temp. (°K)	$[C_2F_5CHO]_0$ (moles $cc^{-1}\times10^6$)	Products (moles$\times10^5$)			% decomp.	$k_1/k_2^{\frac{1}{2}}$ (mole$^{-\frac{1}{2}}$cc$^{\frac{1}{2}}$sec$^{-\frac{1}{2}}$)
				$CO+H_2$	C_2F_5H	C_4F_{10}		
10	2100	300	4.85	4.59	1.98	1.65	5.8	1.83
14	2820	301	3.48	5.66	2.52	1.46	10.3	3.05
17	1800	301	6.70	6.07	2.06	1.50	4.9	1.55
9	3600	300	3.01	7.94	2.96	2.46	17.3	2.93
1	3600	304	4.87	7.40	2.68	2.33	9.8	1.66
2	1800	305	3.33	3.34	1.68	1.29	8.4	2.80
12	1200	321	2.45	2.42	1.41	0.860	8.2	4.78
11	1200	322	4.34	2.67	1.36	1.01	5.1	2.36
18	1800	324	2.78	5.72	2.07	2.14	15.1	3.32
15	1800	326	3.07	4.13	2.08	1.54	10.7	3.49
16	1815	341	2.79	6.74	2.29	1.54	16.7	4.23
19	1800	343	2.81	6.79	2.67	2.37	17.4	4.09
5	1920	368	2.83	7.54	3.55	2.39	19.4	5.26
20	1800	384	2.67	10.7	5.09	3.20	42.9	7.46
4	1800	391	4.55	10.1	2.10	0.129	3.5	7.86
3	1800	393	2.16	8.06	4.50	2.35	27.8	9.52
13	900	393	4.02	4.70	3.24	1.17	9.2	6.67
21	1800	439	1.83	12.8	6.78	2.84	46.1	17.1
6	1930	457	1.93	11.4	7.07	1.91	36.8	18.9
22	90	508	1.64	2.46	1.56	0.613	11.0	34.7
7	1800	507	1.74	17.1	10.8	2.05	56.3	36.4
8	600	513	1.72	6.86	4.66	0.832	23.8	35.1
23	60	580	1.33	3.77	2.81	1.95	33.1	59.9

TABLE II

Data on the photolysis of C_3F_7CHO

Run	Time (sec)	Temp. (°K)	$[C_3F_7CHO]_0$ (moles $cc^{-1}\times10^6$)	Products (moles$\times10^5$)				% decomp.	$k_1/k_2^{\frac{1}{2}}$ (mole$^{-\frac{1}{2}}$cc$^{\frac{1}{2}}$sec$^{-\frac{1}{2}}$)
				CO	H_2	C_3F_7H	C_6F_{14}		
1	960	301	2.85	3.65	0.08	1.23	1.22	8.4	3.37
6	900	302	3.71	4.15	0.18	1.26	1.39	7.0	2.55
12	780	306	2.75	2.86		1.26	2.01	9.5	2.95
2	600	322	2.88	3.10	0.20	1.23	1.14	8.0	4.36
8	675	345	3.31	5.41	0.47	2.33	2.15	13.0	5.05
3	450	369	2.55	3.52	0.21	1.86	1.26	11.4	8.33
11	300	398	2.79	2.95	0.18	1.66	1.17	9.3	8.53
7	300	408	2.69	3.80	0.00	1.98	1.15	10.4	10.7
4	300	453	2.11	4.07	0.24	2.83	1.04	15.2	21.0
5	120	510	2.66	3.82	0.32	2.76	0.759	10.5	29.5
9	90	575	2.58	5.92	0.40	4.57	0.813	15.5	57.5
10	90	588	1.97	6.48		4.70	0.702	20.3	85.0

Hydrogen was a minor product, and it was not determined in all experiments. Differentiation between CO and H_2 is made only in Table II. The relative amounts of H_2 formed increased with temperature, as would be expected from the activation energy required for the decomposition of the formyl radical (7). No thermal decomposition

occurred up to 315° C, and no fluorocarbons resulting from F-atom abstraction reactions were detected. The absence of SiF_4 in the products shows that fluoroalkyl radicals do not react with silica at these temperatures.

The Arrhenius plots for $k_1/k_2^{\frac{1}{2}}$ mole$^{-\frac{1}{2}}$cc$^{\frac{1}{2}}$sec$^{-\frac{1}{2}}$ versus $10^3/T°$ K are given in Fig. 1.

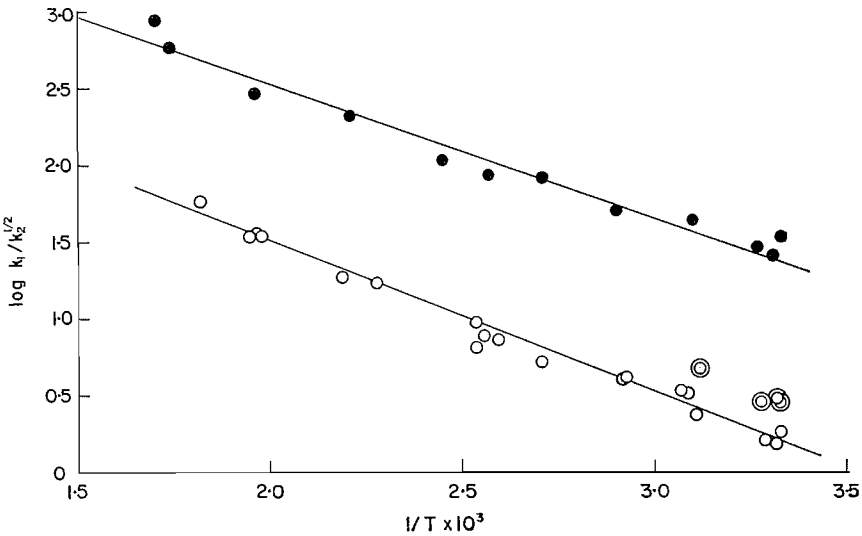

FIG. 1. Plot of log $k_1/k_2^{\frac{1}{2}}$ versus $1/T\times10^3$. ○ C_2F_5CHO photolysis; for double circles, see text. ● C_3F_7CHO photolysis; displaced upward by one log unit for clarity.

There was some scatter in the low-temperature end of the C_2F_5CHO plot (double circles), but as the run numbers indicate, it was random. However, there is a suggestion of curvature, and Dodd and Smith (1) found a distinct curvature of this kind in the CF_3CHO photolysis. As there is no other plausible source of R_{f_2}, other than reaction [2], they suggest the following possible reactions of low activation energy as competing sources of fluoroform, which are important at low temperatures:

$$CF_3\cdot + \cdot CHO \rightarrow CF_3H + CO \qquad [3]$$

and

$$CF_3\cdot + CF_3CHO \text{ (wall)} \rightarrow CF_3H + \text{products} \qquad [4]$$

and the intramolecular split:

$$CF_3CHO + h\nu \rightarrow CF_3H + CO, \qquad [II]$$

They discount [3], and contend that their results provide evidence for the occurrence of [4] and some mode [II] fission. It is certain that at higher temperatures, and at our intensities, the aldehyde decomposition is mainly due to the chain-propagating step, reaction [1], which is the only significant source of R_fH, and the absence of curvature in the plots in Fig. 1 indicates that reactions comparable to [3], [4], and [II] are relatively unimportant in this work. It may be noted, however, that due to the high value (see Discussion) found for the activation energy of reaction [1] for $CF_3\cdot$, competing sources of fluoroform formation of low activation energy will be more apparent.

A least-squares treatment of the results yields for C_2F_5CHO $k_1/k_2^{\frac{1}{2}} = (3.09\pm0.12)10^3\times \exp(-4500\pm200/RT)$ mole$^{-\frac{1}{2}}$cc$^{\frac{1}{2}}$sec$^{-\frac{1}{2}}$ exclusive of the double circles; including them,

$k_1/k_2^{\frac{1}{2}} = (1.64\pm0.25)10^3 \exp(-4000\pm600/RT)$ mole$^{-\frac{1}{2}}$cc$^{\frac{1}{2}}$sec$^{-\frac{1}{2}}$. For C_3F_7CHO we obtain $k_1/k_2^{\frac{1}{2}} = (1.86\pm0.14)10^3 \exp(-4000\pm300/RT)$ mole$^{-\frac{1}{2}}$cc$^{\frac{1}{2}}$sec$^{-\frac{1}{2}}$.

Values of $k_1/k_2^{\frac{1}{2}}$ were calculated from the steady-state approximation $(\bar{R}_{R_fH}/\bar{R}_{R_{f_2}}^{\frac{1}{2}} \times [\text{Ald.}]_{av})$, where $\bar{R}$ is the mean rate of formation, and the average aldehyde concentration is the arithmetic mean of the initial and final concentrations (assumed percentage decomposition = $(R_fH+2R_{f_2})/(\text{Ald.})_0$). Correction factors to the above approximation to allow for time fluctuations and cell gradients in the radical concentration have been discussed (8, 9). Some of the percentage decompositions in the C_2F_5CHO results are well beyond the normal limit of a steady-state condition, suggesting that we take cognizance of these factors in discussing these experiments. It is noticeable, however, that we have not observed any deviation from the Arrhenius plots for the high percentage decomposition runs; e.g., compare numbers 7 and 22 in Table I. Perhaps more important is the fact that the approximation is put to severe limitations if the two measured products can be consumed by secondary reactions, or produced from alternative sources, as the decomposition progresses. This is not the case in our system, for we have established that reactions other than [1] and [2] are unimportant, and the products, once formed, are not removed by subsequent reaction. Hydrogen transfer, e.g.,

$$C_3F_7\cdot + C_3F_7H \rightarrow C_3F_7H + C_3F_7\cdot,$$

does not disturb the product balance, and R_{f_2} is stable and not subject to radical attack. It is surprising that Henderson and Steacie (10) found no variation in the ratio $\bar{R}_{CH_4}/\bar{R}_{C_2H_6}^{\frac{1}{2}}[\text{Ac.}]_0$ from the photolysis of acetone above 10% decomposition, as this system must incorporate some of these limitations.

DISCUSSION

We may compare our results with the value of $k_1/k_2^{\frac{1}{2}} = (1.95\times10^4)T^{1/4} \exp(-8200/RT)$ mole$^{-\frac{1}{2}}$cc$^{\frac{1}{2}}$sec$^{-\frac{1}{2}}$ given by Dodd and Smith (1) from CF_3CHO photolysis, and it is seen that there is a large variation in the Arrhenius parameters. The values of $k_1/k_2^{\frac{1}{2}}$ differ much less markedly; at 182° C they are 10.6 (CF_3CHO), 21.1 (C_2F_5CHO), and 22.7 (C_3F_7CHO), all in mole$^{-\frac{1}{2}}$cc$^{\frac{1}{2}}$sec$^{-\frac{1}{2}}$. Variations between A and E can be accounted for by compensation between the two, but if rate data are to be interpreted in terms of the Arrhenius equation, reasons must be sought for significant differences in these parameters.

It has been demonstrated (11) that E_2 does not vary for simple perfluoroalkyl radicals, so that the variation in E_1 is real. The absolute magnitude of E_2 is uncertain; for $CF_3\cdot$ it has been suggested that it may be as high at 2 kcal/mole, due, in part, to the polarity of the radical (12). This result has been questioned (13), but recent studies by Szwarc and his co-workers (14, 15) on the "cage" recombination of $CF_3\cdot$ radicals from the photolysis of $(CF_3)_2N_2$ in isooctane solution at 65° C indicate a value of about 1.5 kcal/mole. The only direct determination of $CF_3\cdot$ radical recombination has been made by Ayscough (16), using a rotating sector, giving $k_2 = 2.34\times10^{13}$ mole^{-1}cc sec^{-1} at 400° K. From collision theory, we find at 400° K ($\sigma CF_3\cdot = 4.0$ Å) the collision number $Z_2 = 7.5\times10^{13}$ mole^{-1}cc sec^{-1} (not 1.5×10^{14} mole^{-1}cc sec^{-1}, as given by Ayscough, as Z_2 is one half of this value for combination between identical species). These values yield limits of E_2 and the steric factor P_2 of 0 kcal/mole and 0.31, and 0.93 kcal/mole and 1, respectively. The evidence favors the latter picture, especially if $CF_3\cdot$ is planar.

The recombination rates of $C_2F_5\cdot$ and $C_3F_7\cdot$ radicals have not been determined directly; the respective collision numbers are 1.1×10^{14} and 1.3×10^{11} mole^{-1}cc sec^{-1} at 400° K ($\sigma C_2F_5\cdot = 5.5$ Å, $\sigma C_3F_7\cdot = 6.5$ Å). If $P_2 = 1$ for all three radicals, we may equate

Z_2 with A_2. Using these values in conjunction with the experimental $A_1/A_2^{\frac{1}{2}}$ ratios, and assuming the following collision diameters: σCF_3CHO = 5.7 Å, σC_2F_5CHO = 7.2 Å, and σC_3F_7CHO = 8.2 Å, yields values of $P_1 = 3.8\times10^{-3}$ ($CF_3\cdot$), 1.2×10^{-4} ($C_2F_5\cdot$), and 6.8×10^{-5} ($C_3F_7\cdot$) at 400° K. If $P_2 < 1$, which may well be so for the larger radicals,[2] the values of P_1 will be further reduced.

The calculated steric factors for $C_2F_5\cdot$ and $C_3F_7\cdot$, which are maximum values, are lower than those generally expected in free-radical H-abstraction reactions, i.e., about 10^{-3}, but this might be expected, due to the smaller number of available hydrogen atoms in the molecule undergoing radical attack. As an example, we may consider the competing reactions

$$CD_3\cdot + CF_3H \rightarrow CD_3H + CF_3\cdot \quad [5]$$

and

$$CD_3\cdot + CD_3COCD_3 \rightarrow CD_4 + \cdot CD_2COCD_3 \quad [6]$$

where it was found (17) that $A_5/A_6 = 0.013$. Taking $A_6 = 6.3\times10^{11}$ $mole^{-1}cc\ sec^{-1}$ (18), this gives $P_5 = 1.3\times10^{-4}$ at 400° K (σCD_3 = 3.5 Å, σCF_3H = 4.0 Å).

A comparison of Dodd and Smith's value (1) with other known activation energies for H-abstraction reactions indicates that it is improbably high. A survey of these values (19) for $CH_3\cdot$ (E_m) and $CF_3\cdot$ (E_f) radicals shows a reasonably constant difference of $E_m - E_f = 3$ kcal/mole, suggesting that $E_7 = 8.2+3 = 11.2$ kcal/mole (for reaction

$$CH_3\cdot + CF_3CHO \rightarrow CH_4 + CF_3CO\cdot \quad [7]$$

[7]), which compares unfavorably with the established value of $E_8 = 7.5$ kcal/mole (18) (for reaction [8]).

$$CH_3\cdot + CH_3CHO \rightarrow CH_4 + CH_3CO\cdot \quad [8]$$

However, Dodd and Smith (1) do report $k_9/k_2^{\frac{1}{2}} = (2.5\times10^3)T^{\frac{1}{4}}\exp(-4000/RT)$ for the reaction

$$CF_3\cdot + CH_3CHO \rightarrow CF_3H + CH_3CO\cdot, \quad [9]$$

which is very compatible with our results, and $E_m - E_f = 3.5$ kcal/mole for reactions [8] and [9].

The main factors which determine the activation energies of simple metatheses of the type we are discussing are the strengths of the bonds broken and formed, and the repulsive forces between the attacking radical and molecule, and those between the new molecule and radical that are produced in the reaction (20). If the respective C—H bond strengths do not vary in the R_fCHO and R_fH series of molecules, we may anticipate a constant activation energy for reaction [1], provided that the repulsive forces do not vary with R_f. The constancy of E_2 with $R_f\cdot$ suggests that they do not, so that a value of $E_1 = \sim4$ kcal/mole may be expected for reaction [1]. The result of reaction [9] suggests that this may well hold true for aldehydes in general. A similar correspondence has been found for methane and ethane (4, 11) and cyclohexane (21, 22) subjected to $R_f\cdot$ radical attack.

[2]*In systems containing two radicals* A *and* B, *it is frequently found that the cross-combination ratio* $k_{AB}/k_{AA}^{\frac{1}{2}}k_{BB}^{\frac{1}{2}}$ *equals about 2, independent of temperature. As the collision number ratio* $Z_{AB}/Z_{AA}^{\frac{1}{2}}Z_{BB}^{\frac{1}{2}}$ *is also close to 2, it has been suggested that this is an indication that radical combination in the gas phase occurs on every collision (reference 13). We have found (reference 11) for* A = $CF_3\cdot$ *and* B = $C_3F_7\cdot$ *that* $k_{AB}/k_{AA}^{\frac{1}{2}}k_{BB}^{\frac{1}{2}} = 1.77\pm0.1$, *independent of temperature. This shows that* $E_{AB} = \frac{1}{2}(E_{AA}+E_{BB})$, *but the values are not necessarily zero, and that* $P_{AB} = (P_{AA}\cdot P_{BB})^{\frac{1}{2}}$, *but again not necessarily that* $P_{AB} = P_{AA} = P_{BB} = 1$. *We may cite an extreme case of* $P_{AB} = 0.1$, $P_{AA} = 1$, *and* $P_{BB} = 0.01$. *Further complexities can arise if disproportionation reactions occur; see A. R. Blake, J. F. Henderson, and K. O. Kutschke, Can. J. Chem.,* ***39****, 1920 (1961).*

For these compounds the rate constants at 182° C vary as $CF_3\cdot \gg C_2F_5\cdot > C_3F_7\cdot$, which indicates increasing steric effects with the larger radicals.

Trotman-Dickenson and his co-workers (13) have established the Arrhenius parameters of the reactions

$$R\cdot + RCHO \rightarrow RH + RCO\cdot \quad [10]$$

and

$$CH_3\cdot + RCHO \rightarrow CH_4 + RCO\cdot \quad [11]$$

compared to the relevant recombination reaction

$$R\cdot + R\cdot \rightarrow R_2, \quad [12]$$

where R· is Me·, Et·, *n*-Pr·, or *n*-Bu·. The rate constants for these reactions are remarkably constant. For reaction [11], $k_{11}/k_{12}^{\frac{1}{2}}$ ranges from 13 to 20 $mole^{-\frac{1}{2}}cc^{\frac{1}{2}}sec^{-\frac{1}{2}}$ (mean 17), which indicates that the alkyl group has little effect on the reactivity of the aldehydic hydrogen.

Our values of $k_1/k_2^{\frac{1}{2}} = 21.1$ ($C_2F_5\cdot$) and 22.7 ($C_3F_7\cdot$) compare favorably with those for $k_{10}/k_{12}^{\frac{1}{2}} = 16$, and appear to be quite constant, as in the case of the alkyl radicals.

The general pattern of the results suggests that the potential barrier to perfluoroalkyl radical H-abstraction reactions will be lower than that for the corresponding alkyl radical reaction. The reason for Dodd and Smith's result (1) is not clear.

ACKNOWLEDGMENTS

We thank Mr. A. K. Bakhtiar for performing the C_2F_5CHO photolyses, and the National Science Foundation for a grant-in-aid.

REFERENCES

1. R. E. Dodd and J. W. Smith. J. Chem. Soc. 1465 (1957).
2. M. Braid, H. Iserson, and F. E. Lawlor. J. Am. Chem. Soc. **76**, 4027 (1954).
3. G. H. Miller and G. O. Pritchard. Chem. & Ind. (London), 1314 (1961).
4. S. J. W. Price and K. O. Kutschke. Can. J. Chem. **38**, 2128 (1960).
5. F. L. Mohler, V. H. Dibeler, and R. M. Reese. J. Research Natl. Bur. Standards, **49**, 343 (1952).
6. G. H. Miller and E. W. R. Steacie. J. Am. Chem. Soc. **80**, 6486 (1958).
7. J. G. Calvert. J. Phys. Chem. **61**, 1206 (1957).
8. M. Szwarc. J. Chem. Phys. **19**, 256 (1951).
9. R. J. Cvetanović and E. Whittle. Can. J. Chem. **32**, 63 (1954).
10. J. F. Henderson and E. W. R. Steacie. Can. J. Chem. **38**, 2161 (1960).
11. G. O. Pritchard, G. H. Miller, and J. R. Dacey. Can. J. Chem. **39**, 1968 (1961).
12. G. O. Pritchard and J. R. Dacey. Can. J. Chem. **38**, 182 (1960).
13. J. A. Kerr and A. F. Trotman-Dickenson. *In* Progress in reaction kinetics. *Edited by* G. Porter. Pergamon Press. 1961.
14. L. Herk, M. Feld, and M. Szwarc. J. Am. Chem. Soc. **83**, 2998 (1961).
15. A. P. Stefani, L. Herk, and M. Szwarc. J. Am. Chem. Soc. **83**, 4732 (1961).
16. P. B. Ayscough. J. Chem. Phys. **24**, 944 (1956).
17. G. O. Pritchard, H. O. Pritchard, H. I. Schiff, and A. F. Trotman-Dickenson. Trans. Faraday Soc. **52**, 849 (1956).
18. A. F. Trotman-Dickenson. Gas kinetics. Butterworths, London. 1955.
19. G. O. Pritchard and G. H. Miller. J. Chem. Phys. **35**, 1135 (1961).
20. J. M. Tedder. Quart. Revs. (London), **14**, 336 (1960).
21. S. W. Charles and E. Whittle. Trans. Faraday Soc. **56**, 794 (1960).
22. G. O. Pritchard and G. H. Miller. J. Phys. Chem. **63**, 2074 (1959).

THE KINETICS OF THE FORMATION OF THE MONOSULPHATO COMPLEX OF IRON (III) IN AQUEOUS SOLUTION

G. G. DAVIS[1] AND W. MACF. SMITH
Department of Chemistry, Queen's University, Kingston, Ontario

Received May 31, 1962

ABSTRACT

The kinetics of formation of the monosulphato complex of iron (III) has been examined spectrophotometrically using a continuous-flow technique over the range of temperatures 15.6 to 34.5° C in an aqueous medium of ionic strength 0.5 and a range of concentrations of hydrogen ions 0.05 to 0.30 *M*. The experimental data may be interpreted on the assumption that the significant reactions are a bimolecular association opposed by a first-order dissociation ($Fe^{+++} + SO_4^{=} \rightleftharpoons FeSO_4^{+}$). For the forward reaction $\Delta H^{\mp}$ is 18.0 kcal mole^{-1} and $\Delta S^{\mp}$ is 19.4 cal mole^{-1}deg^{-1}.

INTRODUCTION

The kinetics of the association reactions of ferric ion with thiocyanate and chloride have been investigated by Connick and co-workers (1, 2), that of ferric ion with fluoride by Pouli and Smith (3). Although the equilibria involved in the reactions involving ferric and sulphate ions have been considerably studied, there has been no account of studies of the kinetics. This work was carried out to provide more information about the nature of the association reactions involving ferric ions.

EXPERIMENTAL

Reagents and Solutions

All solutions used in the spectrophotometric observations relating to solutions at equilibrium were prepared from triply distilled water, the second distillation being from alkaline permanganate. The solutions used for the kinetic studies were prepared mainly from singly distilled water. Checks of the absorption spectra of solutions of acidified ferric perchlorate in singly and triply distilled water were made and showed no indication of any difference. Sodium perchlorate (anhydrous), perchloric acid (70%), and ferric perchlorate (non-yellow) were reagent grade and obtained from G. Frederick Smith Chemical Company. The perchlorate was tested for chloride content by nephelometric methods and shown to contain less chloride than would correspond to a concentration of 10^{-5} *M* in any of the solutions used. The stock solutions of ferric perchlorate in perchloric acid were analyzed for acid and iron content by the method previously discussed (3). Sodium sulphate was Baker anhydrous reagent and was dried for 2 to 3 hours at 120° C before weighing. The *o*-cresol red was obtained as 0.02% solution from Fisher Scientific Company. In all solutions the acidity was adjusted with perchloric acid, the ionic strength to 0.5 with sodium perchlorate.

The Measurement of Equilibrium Constants

The spectrophotometric measurements on solutions at equilibrium were carried out with a Beckman DU spectrophotometer using Beckman quartz cells of 10-mm path length which were housed in a thermostating block permitting temperature control to ±0.10°.

The Kinetic Measurements

The kinetic measurements were carried out spectrophotometrically using a continuous-flow technique. Essentially this involves means of rapidly mixing two reactant solutions and of following the change in composition along the length of a reaction tube down which the mixed and reacting solution flows at a velocity which is constant and sufficiently high to prevent streamlining. The design of our apparatus is based on principles evaluated by Hartridge and Roughton (4), involves some features of a design by Dalziel (5), and is such as to permit its incorporation in a Beckman DU spectrophotometer. The reaction tube is quartz about 2 mm in inside diameter and 40 cm long. One end of this tube fits into a plexiglass mixing block containing the mixing chamber, which is continuous with the reaction tube and identical in diameter. The reactant solutions are forced from thermostated storage flasks by controlled gas pressure and enter the mixing chamber via two pairs of 0.5-mm jets whose axes are nearly tangential to the circumference of the chamber. The spectral character of the reacting mixture at various points along the reaction tube is determined by standard photometric techniques, and these measurements are then interpreted to yield the composition of the solution for reaction times equal to the times of flow between the regions of mixing and

[1]*Holder of an Ontario Research Council Scholarship 1960–61.*

observation. The reaction tube is held firmly in an aluminum housing which slides in a metal collar attached to the portion of the Beckman normally carrying the cell holder and the assembly is carefully constructed so that any part of the reaction tube may be slid reproducibly into the beam of radiation emerging from the monochromator. The beam is collimated by slits 1 mm wide and 4 mm long before and after passage through the reaction tube and, consequently, only the radiation passing through the central portion of the tube (an effective path length of just under 2 mm) reaches the photomultiplier unit. Flow rates of the solution were controlled to $\pm 2\%$ and tests involving the mixing of a solution of the acid form of *p*-nitrophenol with a solution of sodium hydroxide and examination of the resulting solution for optical homogeneity and completeness of transformation to the basic form indicated that mixing of the solutions was complete at the region of observation which is closest to the mixing chamber. This corresponded to a reaction time of about 5 milliseconds. No attempt was made to thermostat the reaction tube. A Sargent Thermistor Thermometer was used to measure the temperature of the solution leaving the exit of the reaction tube and also leaving the mixing chamber with no reaction tube attached. A temperature gradient of 0.4° occurred over the length of the tube under conditions of maximum difference in temperature between the solution and environment, and the average of the extremes was taken as the reaction temperature.

Details about Measurements Made with the Flow Apparatus

A kinetic run involved measurements of relative intensity of the beam of λ 305 mμ transmitted through the flow tube at various positions along its length while the mixed, reacting solution was flowing through it at uniform velocity. At λ 305 mμ, $FeSO_4^+$ has a maximum in its extinction coefficient (6). Uncomplexed iron has an effective coefficient which is constant at the constant acidity of a run but is dependent on the acidity (due to varying proportion of $FeOH^{++}$ to Fe^{+++}). The effective extinction coefficient is, however, substantially less than that of $FeSO_4^+$ over the range of our experimental conditions. Immediately before and after the kinetic run reference intensities were obtained at the same positions along the flow tube, which now contained a solution of the same ionic strength, acidity, and iron (III) content as that in the kinetic run but no sulphate. Since sulphate is transparent these intensities correspond to mixed but unreacted solution. If the predominant species involved in the reaction are Fe^{+++}, $SO_4^=$, and $FeSO_4^+$, and if the ratio $[Fe^{+++}]/[FeOH^{++}]$ remains constant, the difference (ΔD) in optical densities or absorbances of the two solutions at the same position along the flow tube is

$$\Delta D = x(\epsilon_{FeSO_4^+} - \epsilon_{Fe,\,eff})l,$$

where

$\epsilon_{FeSO_4^+}$ is the molar extinction coefficient of $FeSO_4^+$;

$\epsilon_{Fe,\,eff}$ is the effective molar extinction coefficient of the Fe (III) (in the forms Fe^{+++} and $FeOH^{++}$);

x is the concentration of $FeSO_4^+$ (moles liter^{-1});

l is the length of the optical path in centimeters;

and consequently

$$[1] \qquad \frac{\text{Concentration of } FeSO_4^+ \text{ at time } t}{\text{Concentration of } FeSO_4^+ \text{ at equilibrium}} = \frac{x}{c} = \frac{\Delta D_t}{\Delta D_\infty}$$

and

$$\frac{c-x}{c} = \frac{\Delta D_\infty - \Delta D_t}{\Delta D_\infty},$$

where c is the concentration of $FeSO_4^+$ at equilibrium; ΔD_t and ΔD_∞ the values of ΔD at times of observation and equilibrium.

For most runs reaction was nearly complete within the flow tube (i.e. within a time of 250 milliseconds) and the transmission (and absorbance) remained nearly constant over a range of positions near the exit. First approximations of the values of the rate constants for the reaction were made assuming that the values of ΔD_t obtained from readings close to the exit were those of ΔD_∞. The rate constant so obtained and the values of the time corresponding to positions near the exit when inserted into the integrated rate expression [7] given below indicated the fractional progress to equilibrium and also a correction to this first approximation for ΔD_∞. The corrected value for ΔD_∞ was used to estimate a corrected value for the rate constant.

The correlation between distance along the flow tube and time of reaction depends on cross section and volume rate of flow. The average cross section was determined by measuring the length of known weights of mercury in the tube and was found to be 0.0377 cm², and there was a maximum variation in average cross section for various 1-cm lengths of $\pm 1\%$. The rate of flow was determined by direct observation of the volume of liquid collected at the exit (checked by observation of the volumes leaving the storage flasks) over definite times. As indicated above, the two conditions which must apply before simple interpretation of the flow measurements may be made are (1) effective mixing at the point where the jets enter the mixing chamber and (2) flow along the flow tube at such a rate that it is turbulent and not significantly streamlined. The rate of flow in our kinetic runs was about 8.5 cc/sec, a value well in excess of the minimum value required to attain turbulence. To confirm that the conditions of flow and mixing were satisfactory, we have carried out runs using identical reacting solutions and different flow rates between 2.7 cc/sec and 9.1 cc/sec. The

temperature was 15° C, the total iron (III) concentration 1.0×10^{-2} M, the total sulphate concentration 2.0×10^{-3} M.

The results are given in Fig. 1 as plots of ΔD_t (called change of absorbance) against time and in Fig. 2

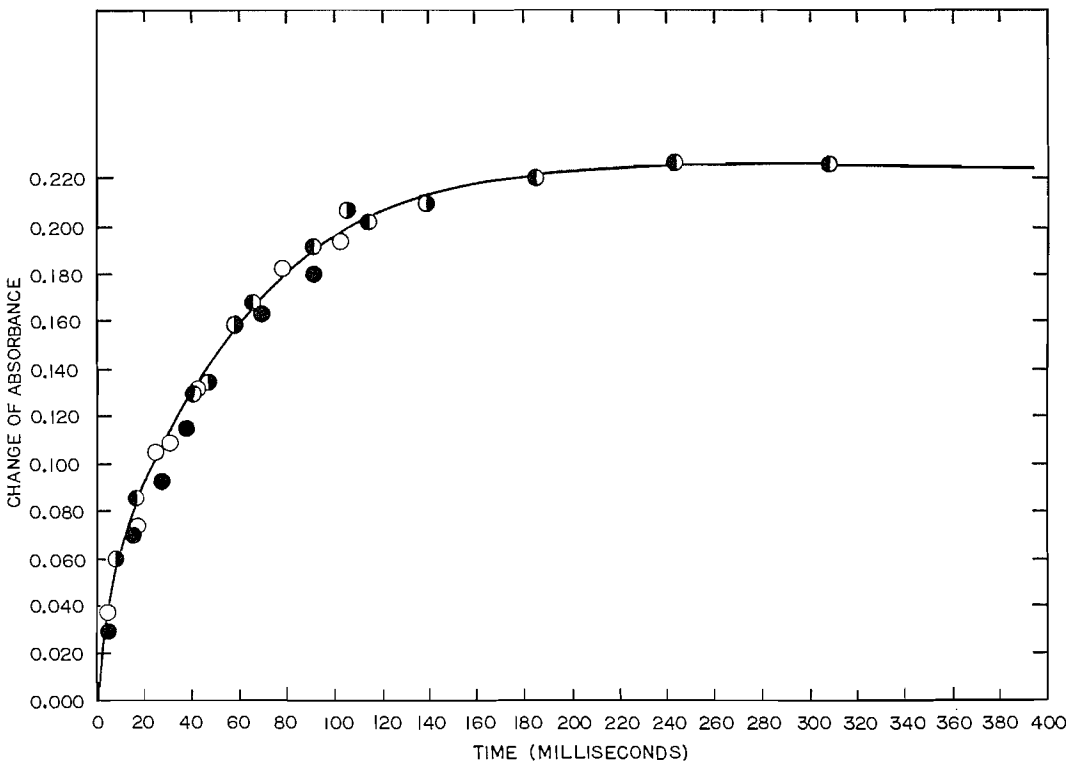

FIG. 1. Change of absorbance plotted against time for four different kinetic runs differing only in flow rate. Temperature 15.6° C, ionic strength 0.50, total iron (III) concentration 0.010 M, total sulphate concentration 0.0020 M, perchloric acid concentration 0.15 M. Flow rate: run 1 ● 9.09 cc/sec, run 2 ○ 8.69 cc/sec, run 3 ◑ 5.97 cc/sec, run 4 ◐ 2.68 cc/sec.

in partially reduced form as a plot of log $(c-x)$ against time, where c is the concentration of $FeSO_4^+$ at equilibrium and x its concentration at time t. This plot should be linear according to the integrated rate expression [7] developed below. Concentration c was determined using the relationship (5) given below and x was determined using the relationship $x = c\Delta D_t/\Delta D_\infty$. In Fig. 1 only one point of every three measured for runs 1, 2, and 3 and one of every two for run 4 are plotted. In Fig. 2 all data for run 2 for times up to 100 milliseconds are included. It will be noted that there is no significant dependence on the flow rate of the correlation between amount of reaction and time, and also that the data appear to extrapolate smoothly to $\Delta D = 0$ at $t = 0$. We had anticipated that there might be some immediate change in optical density on mixing, during which time ion pairs (with solvent between the positive and negative ions) but not complexes between ferric and sulphate ions might be formed. Experiments using higher concentrations of reactants and covering a wider range of wavelengths might indicate such an effect.

The Significance of the Species $FeHSO_4^{++}$ and $Fe(SO_4)_2^-$

The assumption implied above that ΔD is proportional to x would not be valid if the species $FeHSO_4^{++}$ or $Fe(SO_4)_2^-$ was in concentration comparable to that of $FeSO_4^+$ or in relatively small amounts if their contributions to optical density were appreciable.

Whiteker and Davidson's measurements (6) suggest that the extinction coefficient of the species $Fe(SO_4)_2^-$ is not greatly different from that of $FeSO_4^+$ at the wavelength used in our kinetic study. They indicate a value for the second association quotient $[Fe(SO_4)_2^-]/[FeSO_4^+][SO_4^=]$ of about 10 at ionic strength 1.0 and temperature 27°. We estimate that the maximum concentration of free sulphate ions existing under our experimental conditions is about 3×10^{-4}, and this implies a value for $[Fe(SO_4)_2^-]/[FeSO_4^+]$ of 0.003 if the value 10 is assumed to apply to ionic strength 0.5. The figure 0.003 must be considered as a very rough estimate, but as under most of our experimental conditions the formation of $Fe(SO_4)_2^-$ relative to $FeSO_4^+$ is much less favored than in this example, it seems justifiable to ignore its influence on free sulphate concentra-

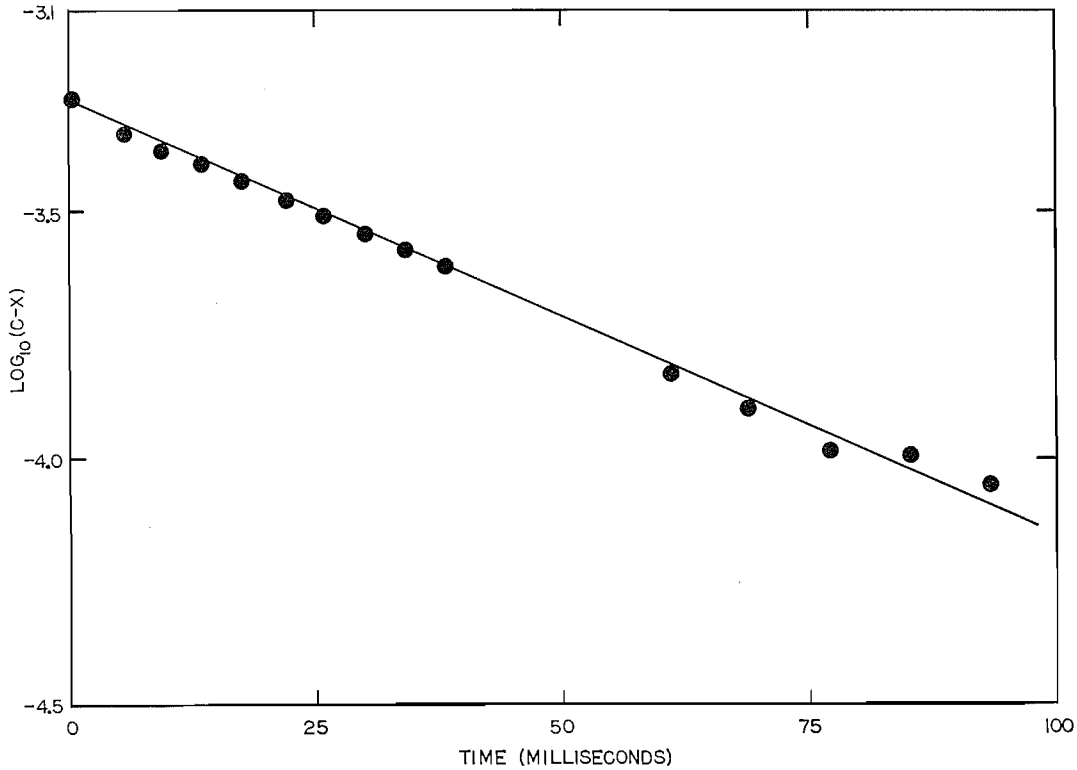

FIG. 2. Plot of log $(c-x)$ against time for data of run 2 of Fig. 1.

tion. Also, as the molar extinction coefficient of $Fe(SO_4)_2^-$ appears to be less than 50% greater than that for $FeSO_4^+$ (6), its contribution to optical density should be negligible.*

Whiteker and Davidson found no positive evidence for the formation of $FeHSO_4^{++}$ but Lister and Rivington (7) and Sykes (8) suggest values for the formation constant which, while applying to conditions different from ours, suggest that this species might be formed in significant amount under our experimental conditions. We have, therefore, attempted experimental evaluation of this constant along with those applying to the formation of $FeSO_4^+$ and the acid ionization of HSO_4^- at ionic strength 0.5.

The acid dissociation quotient of HSO_4^- at ionic strength 0.5 and temperatures between 1.4 and 35° C was determined spectrophotometrically using *o*-cresol red to indicate the hydrogen ion concentration in solutions containing sulphate and bisulphate. These solutions were prepared by adding perchloric acid to sodium sulphate and adjusting the ionic strength with sodium perchlorate. Values for the concentration of the hydrogen ion and of the total sulphate permitted estimation of the concentration of $SO_4^=$ and HSO_4^- and so of the ionization quotient. The ionic strength of these solutions depends on the extent to which H^+ and $SO_4^=$ associate, and to permit approximate adjustment to the ionic strength 0.5, we have calculated compositions on the basis of approximate values for the ionization constant for HSO_4^- determined from Monk's value at ionic strength zero (9) and the application of the Davies activity function. The relation between the absorbance of the *o*-cresol red solution and hydrogen ion concentration was determined at λ 520 mμ (where the indicator is the only significant absorber and its acidic and basic forms have marked differences in their extinction coefficients) with standards prepared from perchloric acid and sodium perchlorate. As the acid concentration was in the range 0.02 to 0.06 *M* it was legitimate to consider the concentration of hydrogen ions equal to that of perchloric acid. The *o*-cresol concentration in all solutions corresponded to 34.0 ml of 0.02% cresol red solution per liter. The values of acid ionization quotient

$$K_a \left(= \frac{[H^+][SO_4^=]}{[HSO_4^-]} \right),$$

which we have measured, are given in Table I.

**Lister and Rivington (7) suggest that the formation quotient* $([Fe(SO_4)_2^-]/[FeSO_4^+][SO_4^=])$ *at ionic strength 1.2 and temperature 25° C may be about 100. If this value is correct then the concentration of* $Fe(SO_4)_2^-$ *is higher at ionic strength 1.0 than we have estimated. Our data (discussed below) obtained from experiments designed to yield information about* $FeSO_4^+$ *and* $FeHSO_4^{++}$ *are generally more consistent with Whiteker and Davidson's with regards to the formation quotient of* $FeHSO_4^{++}$ *and the molar extinction coefficient of* $FeSO_4^+$*, although the difference in ionic strength makes strict comparison of the formation constants impossible.*

TABLE I

The acid ionization quotient (K_a) for bisulphate (ionic strength = 0.5)

Temperature (°C)	$K_a \times 10^2$ (mole liter^{-1})
35.0	3.36±0.09
25.0	4.33±0.05
15.0	5.40±0.10
1.4	7.40±0.10

The formation quotients of $FeSO_4^+$ (K_c) and of $FeHSO_4^{++}$ (K_m) at ionic strength 0.5 were measured using a method similar to that described by Lister and Rivington (7). The essential data involved the optical densities of solutions containing substantial excess of iron (III) over sulphate and adjusted for ionic strength and acidity, relative to a blank which differed in that it did not contain sulphate. Groups of solutions of different acidity were examined, with members of each group containing the same small concentrations of sulphate (1×10^{-3} M), the same relatively large concentration of perchloric acid, and varying concentrations of iron (III) (between 1×10^{-2} and 3×10^{-2} M). Our data for temperatures 1.4 and 15° C interpreted using the value of K_a given in Table I indicated the values for K_c given in Table II and were

TABLE II

The association quotients (K_c) for the monosulphato iron (III) complex (ionic strength = 0.5)

Temperature (°C)	K_c (mole^{-1} liter)
35.0	280±22
25.0	205±18
15.0	149±10
1.4	95±6

consistent with $K_m = 0\pm1$. The data for 25° and 35° were less consistent and suggested somewhat negative values for K_m. We have assumed that $K_m = 0$ in interpreting the data and obtain the values of K_c for 25.0 and 35.0° C given in the table. These values of K_c yield a fair linear plot of log K_c against $1/T$ and values of $\Delta H^0 = 5.5$ cal mole^{-1} and $\Delta S^0 = 29$ cal mole^{-1} deg^{-1}.

It appears then that the value for the formation quotient for $FeHSO_4^{++}$ is less than 0.01 that for $FeSO_4^+$ at ionic strength 0.5. The maximum value of $[HSO_4^-]/[SO_4^=]$ under our experimental conditions is about 8/1. Since

$$\frac{[FeHSO_4^{++}]}{[FeSO_4^+]} = \frac{K_m}{K_c}\frac{[HSO_4^-]}{[SO_4^=]}$$

the concentration of $FeHSO_4^{++}$ is probably less than 8% of that of $FeSO_4^+$ under the conditions most favoring its formation. Sykes estimates that the extinction coefficient at λ 305 mμ for $FeHSO_4^{++}$ is 850 mole^{-1}liter cm^{-1} and for $FeSO_4^+$ is 2160. Whiteker and Davidson find a value of 2200 for $FeSO_4^+$ (6). Our data do not cover the range of compositions or wavelengths which would permit an estimate of these quantities. However, our results, implying a small degree of formation of $FeHSO_4^{++}$, along with the reasonable assumption that $\epsilon_{FeHSO_4^{++}}$ is less than $\epsilon_{FeSO_4^+}$, suggest that the influence of $FeHSO_4^{++}$ on optical density is small under the conditions of our experiments.

We have, therefore, interpreted our kinetic data on the assumptions that the only species of importance are the absorbing species Fe^{+++}, $FeOH^{++}$, and $FeSO_4^+$ and the non-absorbing species HSO_4^- and $SO_4^=$. Additional support for this procedure is provided by the approximate proportionality between the overall change in absorbance during a kinetic run and the concentration of the species $FeSO_4^+$ calculated for the final equilibrium conditions, using the data from the equilibrium studies outlined above. In the kinetic runs the light path in the reacting solution had an effective length just under 2 mm and the change in absorbance ΔD_∞ due to reaction should be approximately

$$\Delta D_\infty = c(\epsilon_{FeSO_4^+} - \epsilon_{Fe,\,eff})l,$$

where c is the concentration of $FeSO_4^+$ at equilibrium, and l, the effective length of the optical path, is approximately 0.2 cm.

Consequently

$$\Delta D_\infty + c\epsilon_{Fe,\,eff}d = c\epsilon_{FeSO_4^+}l. \qquad [2]$$

Concentration c was calculated for the equilibrium conditions attained in the kinetic runs at 25° C using the value of the association quotient for $FeSO_4^+$ given in Table II and the value for the acid ionization quotient for HSO_4^- given in Table I and ignoring all effects due to $FeHSO_4^{++}$. The value for the left side of equation [2] was then evaluated and plotted against c. The plot was consistent with a straight line passing through the origin ($\Delta D = 0$ for $c = 0$) with a slope indicating $\epsilon_{FeSO_4} = 1940$ if the length of the light path be taken as 2 mm or $\epsilon = 2155$ if the path be taken as 1.8 mm. Richards and Sykes' value for this extinction coefficient (λ 305 mμ) is 2160, Whiteker and Davidson's 2210.

The Reduction of the Kinetic Measurements

We have found that our kinetic data may be satisfactorily interpreted on the assumption that the following rate equation applies:

$$[3] \qquad (d/dt)[FeSO_4^+] = k_1[Fe^{+++}][SO_4^{=}] - k_1/K_c[FeSO_4^+],$$

corresponding to a second-order association opposed by a first-order dissociation.

$$Fe^{+++} + SO_4^{=} \underset{k_{-1}}{\overset{k_1}{\rightleftharpoons}} FeSO_4^+$$

K_c is the association quotient of the complex ($=k_1/k_{-1}$).

If

a = total concentration of iron (III)
$= [Fe^{+++}]+[FeOH^{++}]+[FeSO_4^+]$;

b = total sulphate concentration
$= [SO_4^{=}]+[HSO_4^-]+[FeSO_4^+]$;

K_a = acid ionization quotient of HSO_4^-;

$$s = \frac{[SO_4^{=}]}{[SO_4^{=}]+[HSO_4^-]} = \frac{K_a}{K_a+[H^+]};$$

K_h = hydrolysis quotient of ferric ion;

$$r = \frac{[Fe^{+++}]}{[Fe^{+++}]+[FeOH^{++}]} = \frac{[H^+]}{K_h+[H^+]};$$

x = concentration of $FeSO_4^+$ at time t;

c = concentration of $FeSO_4^+$ at equilibrium;

then equation [3] becomes

$$[4] \qquad \frac{d}{dt}x = k_1rs(a-x)(b-x) - \frac{k_1}{K_c}x,$$

also

$$[5] \qquad K_c = \frac{c}{rs(a-c)(b-c)}.$$

Substituting [5] into [4] and solving yields

$$[6] \qquad \ln\frac{c-x}{ab-cx} = \frac{k_1sr}{c}(c^2-ab)t + \ln\frac{c}{ab}.$$

Under our experimental conditions, where a is present in considerable excess over b, cx is small relative to ab and equation [6] reduces to

$$[7] \qquad \log\frac{c-x}{c} = -k_1rs\frac{(ab-c^2)}{2.3c}t$$

but

$$\frac{c-x}{c} = \frac{\Delta D_\infty - \Delta D_t}{\Delta D_\infty}.$$

So

$$[8] \qquad \log(\Delta D_\infty - \Delta D_t) = \text{constant} - \frac{k_1rs(ab-c^2)}{2.3c}t$$

and a plot of log $(c-x)$ or log $(\Delta D_\infty - \Delta D_t)$ against time should yield a straight line with slope $[k_1 rs(ab-c^2)]/[2.3c]$, and knowledge of the values of a, b, c, r, and s permits evaluation of k_1. The value r has been estimated from values of K_h given by Connick and co-workers (10), s has been estimated from the values for K_a given in Table I, and c was estimated using the values of K_c given in Table II.

Results of the Kinetic Measurements

The values obtained for the rate constant k_1 under all conditions which we have examined in the kinetic measurements are given in Table III. Although the scatter in the values of k_1 is considerable, there seems

TABLE III

The forward rate constants (k_1) for the association reaction of iron (III) and sulphate (ionic strength = 0.5)

Hydrogen ion concentration (moles liter^{-1})	Total iron (III) concentration$\times 10^2$ (moles liter^{-1})	Total sulphate concentration$\times 10^3$ (moles liter^{-1})	$k_1 \times 10^{-3}$ (mole^{-1} liter sec^{-1})
Temperature = 15.6° C			
0.05	1.00	1.00	2.18
0.05	1.00	1.00	2.86
0.05	1.00	1.00	2.44
0.10	1.00	1.00	2.31
0.10	1.00	1.00	2.35
0.10	1.00	1.00	2.22
0.15	1.09	0.91	2.06
0.15	1.09	1.36	2.19
0.15	1.09	1.82	2.11
0.15	1.00	2.00	2.00
0.15	1.00	2.00	2.23
0.15	1.00	2.00	2.19
0.15	1.00	2.00	2.13
0.15	1.63	0.91	2.30
0.15	2.18	0.91	2.20
0.20	1.09	1.82	2.36
0.20	1.00	2.00	2.17
0.25	1.09	1.82	2.45
0.25	1.00	2.00	2.24
0.30	1.09	1.82	2.20
0.30	1.00	2.00	2.27
Temperature = 25° C			
0.15	1.09	0.91	6.50
0.15	1.09	1.36	6.90
0.15	1.09	1.82	6.05
0.15	1.63	0.91	5.90
0.15	2.18	0.91	6.65
0.20	1.09	0.91	6.30
0.25	1.09	0.91	6.65
0.30	1.09	0.91	6.00
Temperature = 34.5° C			
0.05	1.00	1.00	19.8
0.05	1.00	1.00	22.1
0.05	1.00	1.00	20.1
0.10	1.00	1.00	16.0
0.10	1.00	1.00	16.4
0.10	1.00	1.00	15.1
0.15	1.00	1.00	15.9
0.15	1.00	1.50	16.6
0.15	1.00	2.00	16.0
0.20	1.00	2.00	15.0
0.25	1.00	1.00	16.4
0.25	1.00	2.00	15.1
0.25	1.50	1.00	16.4
0.25	2.00	1.00	14.3
0.30	1.00	2.00	15.7

to be no significant dependence on the concentrations of the reactants or the acidity, with the possible exception of the values for the highest temperature and lowest acidity. This is in contrast with the result obtained by Connick and co-workers for the reactions of thiocyanate and chloride with ferric ion, where the species $FeOH^{++}$ was contributing appreciably to the overall rate and apparent rate constant at hydrogen

ion concentrations of 0.05, and is also in contrast with the findings of Smith and Pouli for the reaction between fluoride and iron (III) that there is a significant increase in apparent rate constant with hydrogen ion concentration over the range 0.1 to 0.4 *M*.

We have taken the arithmetic mean of all values at one temperature as the value of the bimolecular rate constant for the association reaction at that temperature. The values are given in Table IV, and are the basis of the log k_1/T against $1/T$ plot of Fig. 3.

TABLE IV

Average values of rate constant k_1 (ionic strength = 0.5)

Temperature (°C)	$k_1 \times 10^{-3}$ (mole^{-1} liter sec^{-1})
15.6	2.26±0.18
25.0	6.37±0.40
34.5	16.70±2.10

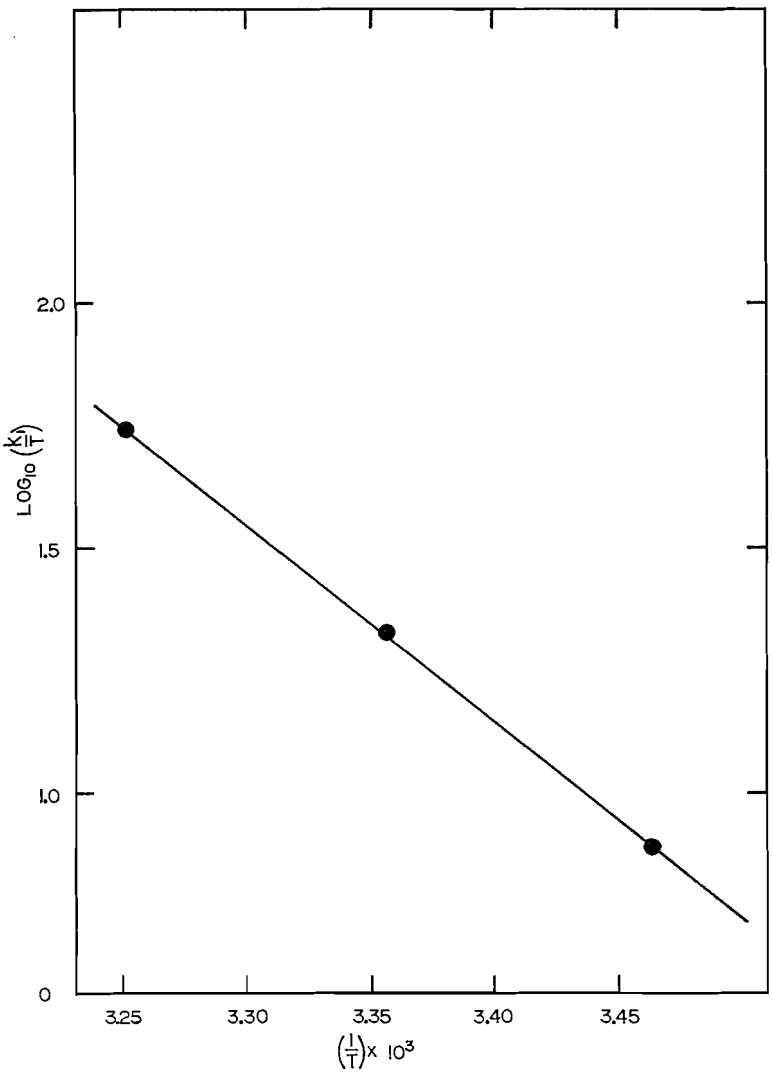

FIG. 3. Modified Arrhenius plot for the reaction $Fe^{+++} + SO_4^{=} \rightarrow FeSO_4^{+}$.

Values implied for the heat and entropy of activation are

$$\Delta H^{\ddagger} = 18.0 \pm 1.9 \text{ kcal mole}^{-1}$$

$$\Delta S^{\ddagger} = 19.4 \pm 6.7 \text{ cal mole}^{-1}\text{deg}^{-1}.$$

DISCUSSION

Pearson (11) has emphasized that for displacement reactions second-order kinetics (first order in both interacting species) may result from both an S_N2 mechanism

$$M(H_2O)_n + X \rightarrow X - - - - M(H_2O)_n \rightarrow M(H_2O)_{n-1}X + (H_2O)$$

or an "intermediate" S_N1 mechanism where the partially desolvated intermediate $M(H_2O)_{n-1}$ reacts to re-form $M(H_2O)_n$ much more rapidly than to form $M(H_2O)_{n-1}X$:

$$M(H_2O)_n \underset{k_b}{\overset{k_a}{\rightleftharpoons}} M(H_2O)_{n-1} + H_2O$$

$$M(H_2O)_{n-1} + X \xrightarrow{k_c} M(H_2O)_{n-1}X.$$

k_b is a first-order constant which involves the concentration of water.

Assuming that stationary-state conditions apply it may be shown that

$$\frac{d}{dt}[M(H_2O)_{n-1}X] = \frac{k_a k_c [M(H_2O)_n][X]}{k_b + k_c[X]}$$

and if $k_c[X] \ll k_b$,

$$\frac{d}{dt}[M(H_2O)_{n-1}X] = \frac{k_a k_c}{k_b}[M(H_2O)_n][X].$$

If $k_c[X] \gg k_b$ then the reaction becomes zero order in X with a first-order rate constant equal to k_a.

Our finding that the reaction is first order in sulphate implies that the mechanism is either S_N2 or intermediate S_N1 with $k_c[X] \ll k_b$ over the range of concentrations of sulphate (X) investigated. The rate constant is therefore identifiable with $k_a k_c/k_b$ if the mechanism is intermediate S_N1.

We find a value of 6.4×10^3 mole^{-1}liter sec^{-1} for the second-order constant for the ferric sulphate association at 25° C. Taube (12) has, from n.m.r. measurements, estimated that the first-order rate constant of water exchange from ferric ions is probably 1×10^4 sec^{-1} at 25° C, the assignment of this value being somewhat indefinite because of the possibility that the mean life of the magnetic spin state rather than the life of the freely solvated ferric ion is being measured.

If it is assumed that the value of k_a is that for water exchange and that the intermediate S_N1 mechanism operates, then

$$\frac{k_c k_a/k_b}{k_a} = \frac{6.4 \times 10^3}{1 \times 10^4} \quad \text{and} \quad \frac{k_c}{k_b} = 0.64.$$

Recalling that k_b involves the concentration of water, i.e. $k_b = k_b'[H_2O]$, then $k_c/k_b' = 0.64[H_2O] = 35$, where k_c and k_b' are both second-order rate constants. The implication that the rate constant for the association of sulphate with $Fe(H_2O)_5^{+++}$ is 35 times that for the association of water with this species seems reasonable. The concentration

of water is 2.7×10^4 times the maximum concentration of sulphate in our kinetic work. Consequently the rate of attack of water relative to that of sulphate on the five-coordinated intermediate would be $(2.7\times10^4)/35 = 770/1$, and the concentration of five-coordinated intermediate would remain close to its equilibrium value and a second-order rate law is implied. It would appear then that Taube's and our data are consistent with an intermediate S_N1 mechanism. They do not, however, rule out the S_N2 mechanism.

The absence of any considerable contribution to the rate by the species $FeOH^{++}$ does favor the assumption that the mechanism approaches S_N2. Decrease of positive charge associated with loss of a proton from the hydrated ferric ion should lead to enhancement of the rate constant if the mechanism were pure S_N1 and could lead to partially compensating effects if the mechanism were S_N2 (12). At a concentration of hydrogen ions of 0.05 *M* at 25° C, $FeOH^{++}$ is contributing appreciably to the rate of the reactions with chloride and thiocyanate but not to the reaction with sulphate. The facts concerning the first two associations do not alone rule out the possibility of predominately S_N2 mechanisms applying but the added fact of absence of significant reaction involving $FeOH^{++}$ and sulphate does suggest greater interaction of the entering ligand in the transition state involving sulphate than with those involving chloride or thiocyanate (i.e. that the reaction involving sulphate has more S_N2 character than do those involving thiocyanate and chloride).

The transition state should be a seven-coordinate configuration $(SO_4 \ldots Fe(H_2O)_6)^+$ if the S_N2 mechanism applies and a six-coordinate configuration $(SO_4 \ldots Fe(H_2O)_5)^+$ if the intermediate S_N1 applies. The decrease in charge accompanying the formation of the transition state should yield markedly positive entropies of activation for both mechanisms, with the value for the S_N1 mechanism being the larger and approaching the value for the overall association reaction. The observed value for $\Delta S^{\ddagger}$, i.e. 19.4, is less than the value ΔS^0, i.e. 29, and this fact is at least consistent with an S_N2 mechanism.

ACKNOWLEDGMENTS

We are particularly grateful to Mr. R. D. Bradfield, Instrument Maker of Queen's University, for his assistance with both the design and construction of the continuous-flow apparatus. We acknowledge helpful advice from Dr. Anthony C. Davies and one of us (G. G. D.) wishes to thank the Ontario Research Council for a scholarship.

This work was carried out with financial assistance from the National Research Council of Canada.

REFERENCES

1. R. E. Connick, C. P. Coppel, and J. F. Below, Jr. J. Am. Chem. Soc. **80**, 2961 (1958).
2. R. E. Connick and C. P. Coppel. J. Am. Chem. Soc. **81**, 6389 (1959).
3. D. Pouli and W. MacF. Smith. Can. J. Chem. **38**, 567 (1960).
4. H. Hartridge and F. J. W. Roughton. Proc. Roy. Soc. (London), A, **104**, 376 (1923).
5. K. Dalziel. Biochem. J. **55**, 79 (1953).
6. R. A. Whiteker and N. Davidson. J. Am. Chem. Soc. **75**, 3081 (1953).
7. M. W. Lister and D. E. Rivington. Can. J. Chem. **33**, 1591 (1955).
8. K. W. Sykes. The kinetics and mechanism of inorganic reactions in solution. Special Publication No. 1. The Chemical Society, London. 1954. p. 64.
9. C. W. Davies, H. W. Jones, and C. B. Monk. Trans. Faraday Soc. **48**, 921 (1952).
10. R. E. Connick, L. G. Hepler, ZZ. Hugus, Jr., J. W. Kury, W. M. Latimer, and Maak-Sang Tsao. J. Am. Chem. Soc. **78**, 1827 (1956).
11. F. Basolo and R. G. Pearson. Mechanisms of inorganic reactions. John Wiley and Sons Inc., New York. 1958. Chap. 3, p. 138.
12. H. Taube. Communication to R. G. Pearson. *Quoted in* J. Chem. Educ. **38**, 164 (1961).

THE ELECTROLYSIS OF ω-BROMOCARBOXYLIC ACIDS

R. G. WOOLFORD
Department of Chemistry, University of Waterloo, Waterloo, Ontario

Received May 29, 1962

ABSTRACT

The first successful preparation of ω,ω′-dibromides from the electrolyses of a series of ω-bromocarboxylic acids, $Br(CH_2)_nCOOH$ ($n = 5$ to $n = 11$), is reported. Under conditions of fairly low temperature and current density, yields from 54 to 71% of these dibromides were obtained.

The electrolysis of 11-bromoundecanoic acid is discussed as an example of how a small change in experimental conditions can produce a considerable change in the products of reaction. At 50°, the product was mainly 1,20-dibromoeicosane, whereas at 65° the products were mainly the esters methyl 11-bromoundecanoate and methyl 11-methoxyundecanoate.

It has been reported (1) that ω-bromocarboxylic acids with chain lengths of 10 carbons or less do not electrolyze normally to yield ω,ω′-dibromides, while those with greater chain lengths behave as expected (the acids used were of formula $Br(CH_2)_nCOOH$, where n = 1–5, 7, 9, 10, 15). No products were isolated and identified in these non-coupling reactions. Later, a successful mixed coupling reaction involving 3,5-dimethyl-6-bromohexanoic acid (I) was run (2), but no experimental details regarding conditions, yields,

$$\underset{\text{I}}{BrCH_2\underset{CH_3}{CH}CH_2\underset{CH_3}{CH}CH_2COOH} + HOOC(CH_2)_{16}CH_3 \rightarrow BrCH_2\underset{CH_3}{CH}CH_2\underset{CH_3}{CH}(CH_2)_{17}CH_3$$

etc. were given. Also, 11-bromoundecanoic acid, which has been electrolyzed normally on more than one occasion (1, 3), has been known (4) to split out bromine under a high temperature of reaction, to yield a neutral product not identified further.

In view of these unexpected and sometimes conflicting results, a thorough investigation of the electrolyses of ω-bromocarboxylic acids seemed necessary. This investigation has produced the first successful anodic couplings of 6-bromohexanoic acid, 7-bromoheptanoic acid, 8-bromooctanoic acid, 9-bromononanoic acid, 10-bromodecanoic acid, and 12-bromododecanoic acid, giving the corresponding ω,ω′-dibromides in yields of 54–71%. These dibromides, while known compounds, have not been made previously by the Kolbe reaction.

The work reported is part of a study being carried out on electrolyses of ω-bromocarboxylic acids which may or may not electrolyze normally, i.e. produce ω,ω′-dibromides in reasonable yield. The results show that ω-bromocarboxylic acids of chain lengths from 6 to 12 will electrolyze to give the expected symmetrical coupling products. The best experimental conditions seem to be a low temperature of reaction (at least below 50° and often below 40°) and not too high a current density. Normally such factors as concentration of acid, current density, temperature of reaction, etc. are not nearly so critical for electrolyses in absolute methanol as they are for electrolyses in aqueous media (5, 6). However, for the ω-bromocarboxylic acids, it appears that these factors may be much more critical than for various unhalogenated acids and half-esters. Certainly, temperature of reaction seems to be quite critical if a good yield of the dibromide is desired. So, while the results in the experimental section (Table I) reflect reasonably

good conditions for the production of ω,ω′-dibromides from the corresponding ω-bromocarboxylic acids, there are yet insufficient data to define more closely the best experimental conditions.

As an example of how the course of an electrolysis may change markedly with a relatively small change in experimental conditions, consider the electrolysis of 11-bromoundecanoic acid (II).

$$\underset{\text{II}}{Br(CH_2)_{10}COOH} \xrightarrow[CH_3OH\ \text{solvent}]{65^\circ} \underset{\text{III}}{Br(CH_2)_{10}COOCH_3} + \underset{\text{IV}}{CH_3O(CH_2)_{10}COOCH_3}$$

(71%) (2.4%)

$$\text{II} \xrightarrow[CH_3OH\ \text{solvent}]{50^\circ} \underset{\text{V}}{Br(CH_2)_{20}Br}$$

(64%)

At 50°, the major product in good yield is 1,20-dibromoeicosane (V). At 65°, no dibromide seems to be produced, but only the two esters, methyl 11-bromoundecanoate (III) and methyl 11-methoxyundecanoate (IV). These esters would be expected as possible side products in this electrolysis at any temperature but the almost complete production of esters under a slightly higher temperature of reaction is rather startling. A control reaction, in which an identical electrolytic solution was heated under reflux (65°) in the absence of an electric current, yielded a negligible conversion of 11-bromoundecanoic acid to any esters. Obviously, more details about the electrolysis of 11-bromoundecanoic acid and other ω-bromocarboxylic acids under varying experimental conditions are necessary before any conclusions can be drawn. It should be noted that the ω-bromocarboxylic acids behave rather sluggishly in the electrolyses (current efficiencies are low: reactions are often incomplete even after three times the theoretical time for the electrolysis). This sluggishness increases as the chain length of the acid increases. So it is not unreasonable that side reactions, such as ester formation, might play a greater role with the brominated acids than with their unsubstituted analogues, which do not possess the heavier bromine atoms, and which, therefore, are attracted faster to the electrodes.

The bromoacids necessary for the present work were either purchased commercially or synthesized by standard means. The preparation of 10-bromodecanoic acid by a Barbier–Wieland degradation of 11-bromoundecanoic acid is described in the experimental section; it is a modification of the work of Paulshock and Moser (7), who were not too explicit on details of the final oxidation step, which turned out to be the critical one. Not much is known of the stability of bromoacids under strong oxidizing conditions but in at least one instance (the conversion of 10-bromodecanol to 10-bromodecanoic acid in 31% yield (1)) the yields seem to be lower than those for their unsubstituted counterparts. More vigorous oxidizing conditions for the production of 10-bromodecanoic acid than those described always resulted in considerably lower yields and in greater difficulties in purification.

Recent speculations in print (2, 8) have suggested or implied that it is surprising that the ω-bromoacids with a chain length of 6 to 10 carbon atoms do not couple normally. The present work now shows that they do couple normally, provided the proper experimental conditions are used. These reactions represent a convenient synthetic route for some of the rarer long-chain ω,ω′-dibromoalkanes.

EXPERIMENTAL

General

All melting points were recorded on a Leitz hot-stage microscope. The melting points are corrected. The boiling points are uncorrected. The analyses were performed by Spang Microanalytical Laboratory, Ann Arbor, Michigan, and by Schwarzkopf Microanalytical Laboratory, Woodside, New York.

6-Bromohexanoic acid, 8-bromooctanoic acid, 9-bromononanoic acid, and 12-bromododecanoic acid were purchased from Sapon Laboratories, Lynbrook, New York. 11-Bromoundecanoic acid was purchased from Eastman Organic Chemicals, Rochester, New York. These bromoacids were all redistilled before use, and then recrystallized from low-boiling petroleum ether.

7-Bromoheptanoic Acid

7-Bromoheptanonitrile (150 g, 0.79 mole), 48% hydrobromic acid (300 ml), and glacial acetic acid (300 ml) were heated under reflux for 16 hours. The mixture was cooled, diluted with water (500 ml), and extracted with ether. The ether extract was washed with water and dried over anhydrous magnesium sulphate. The ether and acetic acid present were distilled at atmospheric pressure, and the residual liquid was fractionally distilled under reduced pressure. 7-Bromoheptanoic acid (126 g, 80%) of b.p. 112–116° (0.3 mm) and m.p. 28–29° was obtained. Ames *et al.* (9) report b.p. 140–142° (1.5 mm) and m.p. 29°.

Methyl 11-Bromoundecanoate

11-Bromoundecanoic acid (90.0 g, 0.34 mole) was dissolved in methanol (300 ml), and concentrated sulphuric acid (5 ml) was added. The solution was heated under reflux for 8 hours, cooled, and diluted with water (300 ml). The ester layer was separated, washed with 10% sodium carbonate solution, then water, and dried over anhydrous sodium carbonate. Distillation under reduced pressure yielded methyl 11-bromoundecanoate (76.0 g, 81%), b.p. 170–175° (12 mm), n_D^{25} 1.4630. Geiger-Berschandy (10) reports b.p. 175–176° (14 mm), n_D^{16} 1.4665.

1,1-Diphenyl-11-bromo-1-undecene

Methyl 11-bromoundecanoate (76.0 g, 0.27 mole) in anhydrous ether (150 ml) was added dropwise over a period of 2 hours to an ethereal solution of phenylmagnesium bromide (0.60 mole), made from 94.2 g of bromobenzene and 14.5 g of magnesium in 250 ml of ether. The reaction mixture was heated under reflux for 8 hours, and then poured into a mixture of 500 ml of 10% sulphuric acid and 300 g of ice. The ether layer was separated, washed with water, and dried over anhydrous magnesium sulphate. After removal of the ether, the residue was fractionated under reduced pressure to yield 1,1-diphenyl-11-bromo-1-undecene (80.0 g, 76%), b.p. 210–214° (1.2 mm), n_D^{25} 1.5596. Paulshock and Moser (6) report b.p. 190° (0.5 mm), n_D^{25} 1.557.

10-Bromodecanoic Acid

A solution of chromium trioxide (80.0 g, 0.80 mole) in 90% acetic acid (800 ml) was slowly added to a solution of 1,1-diphenyl-11-bromo-1-undecene (80.0 g, 0.21 mole) in glacial acetic acid (500 ml) at 90°, over a period of 3 hours. The solution was stirred for 5 hours at 90° and allowed to stand at room temperature overnight (10 hours). Ten-percent hydrochloric acid (2000 ml) was slowly added, and the reaction mixture was ether-extracted five times with 400 ml of ether each time. To separate the bromoacid from any benzophenone produced, the combined ether extract was washed with saturated sodium carbonate solution; the carbonate washings were separated, acidified with hydrochloric acid, and extracted with ether. After drying over anhydrous magnesium sulphate and removal of the ether, the residue was fractionated to yield 10-bromodecanoic acid (34.5 g, 65%), b.p. 134–138° (0.3 mm), m.p. 37–38°. Pattison *et al.* (1) report m.p. 37–38°.

Anodic Syntheses of ω,ω'-Dibromoalkanes

The cell used for all electrolyses was a water-jacketed, thick-walled test tube of dimensions 5×23 cm. A rubber stopper fitted with a reflux condenser held two platinum foil electrodes (2.5×5 cm) in place; these were spaced about 2 mm apart. A 50-volt d-c. supply produced the electrical current.

The ω-bromocarboxylic acid (10–15 g) was dissolved in absolute methanol (100 ml) along with sufficient sodium to neutralize 5% of the acid. A current of 1.0–1.5 amp was passed for about two to three times the theoretical time. Sometimes the end of the reaction was indicated when the electrolyte turned alkaline to litmus. In most cases, however, the solution remained slightly acid, either because the starting acid was too sluggish to react completely in the time allotted, or because traces of bromine were produced which seemed to keep the solution acidic even though electrolysis was complete. To isolate the products the current was stopped, sufficient glacial acetic acid was added to neutralize any sodium salt of unreacted starting material, and the bulk of the methanol was evaporated on a steam bath. The residue was diluted with water (100 ml) and extracted with ether several times. The combined extracts were washed with 10% sodium carbonate solution to remove any unreacted bromoacid, and then dried over anhydrous magnesium sulphate. Unreacted starting material was recovered by acidifying the carbonate washings, extracting with ether, and drying the extract over anhydrous magnesium sulphate. After removal of the

TABLE I

Symmetrical coupling reactions of ω-bromocarboxylic acids

Product*	Reactant	Wt. of reactant (g)	Temp. (°C)	Current (amp)	Time (hr)	Yield (%)	M.p. (°C)	Analytical results (%)					
								Carbon		Hydrogen		Bromine	
								Calc.	Found	Calc.	Found	Calc.	Found
1,10-Dibromodecane	6-Bromohexanoic acid	15	50	1.5	3.5	71	25.5–26.0‡	40.02	40.12	6.72	6.60	53.26	53.25
1,12-Dibromododecane	7-Bromoheptanoic acid	15	50	1.5	8.2	61	38.5–38.7	43.92	44.01	7.37	7.33	48.71	48.75
1,14-Dibromotetradecane†	8-Bromooctanoic acid	10	40	1.0	4.7	67	47.5–48.0	47.20	47.02	7.92	7.87	44.88	44.95
1,16-Dibromohexadecane†	9-Bromononanoic acid	10	50	1.0	5.0	68	53.5–55.0	50.00	50.12	8.40	8.45	41.60	41.45
1,18-Dibromooctadecane†	10-Bromodecanoic acid	10	35	1.5	3.7	70	58.0–59.0	52.43	52.26	8.80	8.68	38.77	38.54
1,20-Dibromoeicosane†	11-Bromoundecanoic acid	10	45	1.0	8.0	64	66.3–67.0	54.54	54.49	9.16	9.25	36.30	36.35
1,22-Dibromodocosane†	12-Bromododecanoic acid	10	40	1.0	15.0	54	69.2–70.5	56.39	56.18	9.47	9.57	34.15	34.16

*Recrystallized from petroleum ether (30–60°).

†In most cases, as the reactions proceeded the solid product settled on the electrodes, causing the current to drop; frequent changes of polarity were necessary to maintain the current. The current indicated and the temperature of the system (which varied with the current and depended on the heat of the electrodes) represent maximum values in these cases.

‡Boiling point 107–109° (0.45 mm), n_D^{28} 1.4914.

ether, the neutral and acidic products were purified by fractional distillation or by recrystallization. Table I lists the details of the electrolyses of the ω-bromocarboxylic acids containing from 6 to 12 carbon atoms.

Non-coupling Electrolysis of 11-Bromoundecanoic Acid

11-Bromoundecanoic acid was electrolyzed to yield 1,20-dibromoeicosane under conditions described above, the details being recorded in Table I. When the temperature of the reacting solution was increased from 50° to reflux (65°) the course of the reaction changed and different products were obtained. This non-coupling electrolysis is described here, along with the identification of the major products.

11-Bromoundecanoic acid (26.5 g, 0.10 mole) was dissolved in absloute methanol (200 ml) to which sodium (0.12 g, 0.005 mole) had been added. This solution was electrolyzed at 1.0 amp for 18 hours at reflux temperature (65°). Small amounts of bromine were liberated continuously during the electrolysis. The current was stopped and glacial acetic acid (1 ml) was added. Approximately 90% of the methanol was distilled off on a steam bath, and the residue was dissolved in 100 ml of ether. Any unreacted bromo-acid was removed from the ether solution by washings with 10% sodium carbonate. On acidification and ether extraction, only a trace of impure starting acid was recovered. The neutral ether extract was dried over anhydrous magnesium sulphate. On removal of the ether, a yellow-orange oil, which did not solidify, remained. Distillation under reduced pressure yielded two main fractions, both colorless liquids: (i) b.p. 100–102° (0.3 mm), n_D^{25} 1.4356, 0.54 g, and (ii) b.p. 112–116° (0.3 mm), n_D^{25} 1.4630, 20.0 g. These fractions were identified as follows.

Fraction (i).—This fraction proved to be methyl 11-methoxyundecanoate. Its physical constants and infrared spectrum were identical with those of authentic methyl 11-methoxyundecanoate prepared as described below. Its behavior in gas chromatography, using a column of diethylene glycol succinate on Chromosorb-W, was identical with that of the authentic ester. Hydrolysis (10% NaOH) of small samples of fraction (i) and the authentic ester yielded acids, both of which had m.p. 34–35° (recrystallized from low-boiling petroleum ether) and whose mixed melting point was undepressed. Bowman and Mason (11) report, for 11-methoxyundecanoic acid, m.p. 34.5–35°.

Fraction (ii).—This fraction proved to be methyl 11-bromoundecanoate. Its physical constants and infrared spectrum were identical with those of the authentic methyl 11-bromoundecanoate prepared previously. Its behavior in gas chromatography, as above, was identical with that of the authentic ester. Hydrolysis (10% NaOH) of a small sample yielded an acid of m.p. 49–50° (recrystallized from low-boiling petroleum ether), undepressed by admixture with authentic 11-bromoundecanoic acid. Analysis of fraction (ii): Calculated for $C_{12}H_{23}BrO_2$: C, 51.61; H, 8.30; Br, 28.62. Found: C, 52.07; H, 8.29; Br, 28.65.

The yields of these esters were: methyl 11-methoxyundecanoate, 2.4%; methyl 11-bromoundecanoate, 71%.

Methyl 11-Methoxyundecanoate

Methyl 11-bromoundecanoate (37.4 g, 0.13 mole) was added dropwise to a solution of sodium (3.0 g, 0.13 mole) in dry methanol (100 ml) over a period of 1 hour. The solution was heated under reflux for an additional 4 hours. Most of the methanol was evaporated on a steam bath and 50 ml of 10% hydrochloric acid was carefully added. The mixture was ether-extracted, and the ether extract washed with 10% sodium carbonate solution and dried over anhydrous magnesium sulphate. Removal of the ether and fractional distillation yielded methyl 11-methoxyundecanoate (25.0 g, 81%) of b.p. 109–112° (0.8 mm), n_D^{25} 1.4356. Bowan and Mason (11) report b.p. 104–105° (0.5 mm), n_D^{20} 1.4375.

ACKNOWLEDGMENTS

The author is indebted to the National Research Council of Canada for financial support. He is also grateful to Mr. David Roberts, Oxford University, for assistance during the summer 1961.

REFERENCES

1. F. L. M. Pattison, J. B. Stothers, and R. G. Woolford. J. Am. Chem. Soc. **78**, 2255 (1956).
2. C. Collin-Asselineau, J. Asselineau, S. Stallberg-Stenhagen, and E. Stenhagen. Acta Chem. Scand. **10**, 1035 (1956).
3. H. Korsching. Chem. Ber. **86**, 943 (1953).
4. W. E. Garrison. Private, unpublished communication on work done at the University of Illinois. 1958.
5. S. Glasstone and A. Hickling. Trans. Electrochem. Soc. **75**, 333 (1939).
6. W. S. Greaves, R. P. Linstead, B. R. Shephard, S. L. S. Thomas, and B. C. L. Weedon. J. Chem. Soc. 3326 (1950).
7. M. Paulshock and C. M. Moser. J. Am. Chem. Soc. **72**, 5073 (1950).
8. B. C. L. Weedon. Advances in Org. Chem. **1**, 1 (1960).
9. D. E. Ames, R. E. Bowman, and R. G. Mason. J. Chem. Soc. 174 (1950).
10. S. Geiger-Berschandy. Bull. soc. chim. France, 994 (1955).
11. R. E. Bowman and R. G. Mason. J. Chem. Soc. 4151 (1952).

THE INHIBITED AUTOXIDATION OF STYRENE

PART I. THE DEUTERIUM ISOTOPE EFFECT FOR INHIBITION BY 2,6-DI-*tert*-BUTYL-4-METHYLPHENOL*

J. A. HOWARD† AND K. U. INGOLD

Division of Applied Chemistry, National Research Council, Ottawa, Canada

Received May 29, 1962

ABSTRACT

Most previous work on the inhibition of autoxidation by phenols has indicated that the reaction involves abstraction of the phenolic hydrogen. However, the apparent absence of any appreciable deuterium isotope effect made it difficult to believe that abstraction could be rate controlling. The present work using styrene as the substrate, 2,6-di-*tert*-butyl-4-methylphenol as the inhibitor, and azo-bis-isobutyronitrile as the initiator has shown that this reaction has an unexpectedly large isotope effect, e.g. ~10.6 at 65° C. Previous failures to detect an isotope effect are attributed to the rapid exchange of deuterium which takes place between deuterated phenols and traces of moisture or other hydroxyl-containing compounds present in the substrate. Rate constants and activation energies for some of the elementary reactions in the inhibited and uninhibited oxidation of styrene have been measured. It is suggested that a compound which functions in the same way as a weak phenolic inhibitor is formed in the apparently uninhibited oxidation.

INTRODUCTION

Although the ability of phenolic compounds to inhibit the autoxidation of organic substances in the liquid phase has been known for many years, the exact mechanism by which this process occurs is still far from certain (1). Autoxidation is a free radical chain process which, for most organic substrates, can be described by the following simplified reaction scheme:

Initiation:	production of $R\cdot$ or $RO_2\cdot$	[1]
Propagation:	$R\cdot + O_2 \rightarrow RO_2\cdot$	[2]
	$RO_2\cdot + RH \rightarrow ROOH + R\cdot$	[3′]
	$RO_2\cdot + RH \rightarrow ROO\dot{R}H$	[3]
Branching:	$ROOH \rightarrow RO\cdot + \cdot OH$	[4]
Termination:	$RO_2\cdot + RO_2\cdot \rightarrow$ inactive products.	[5]

RH represents the organic substrate and $RO_2\cdot$ its peroxy radical. Hydroperoxides are produced by the majority of organic compounds (reaction [3′]) but certain polymerizable olefins yield, instead, polyperoxides (reaction [3]) (2).

The chain-breaking step by which phenolic inhibitors reduce oxidation rates has generally been considered to involve the hydrogen abstraction process

$$RO_2\cdot + AH \rightarrow ROOH + A\cdot, \qquad [6]$$

where AH is the inhibitor and $A\cdot$ is its resonance stabilized, comparatively unreactive, phenoxy radical. The radical $A\cdot$ will, in general, be destroyed by reaction with a second peroxy radical (1),

$$RO_2\cdot + A\cdot \rightarrow ROOA. \qquad [7]$$

If reaction [6] is truly a simple hydrogen abstraction process, replacement of the phenolic hydrogen by deuterium should reduce its rate, i.e., AD should be a less efficient inhibitor than AH. The magnitude of such an isotope effect would be expected to be larger than

Issued as N.R.C. No. 6922.

†*N.R.C. Postdoctorate Fellow 1961–62.*

that observed in reaction [3′] when RH is replaced by RD, since the transfer of a hydrogen atom between two identical atoms should, in general, proceed through a transition state in which the zero-point energy of the hydrogen is lost (3). Under these conditions the isotope effect will tend to be a maximum (3). The abstraction of a hydrogen atom from cumene (which is isoelectronic with a phenol) by peroxy radicals (E = 6.7 kcal/mole) has an isotope effect k_H/k_D = 5.5 (4). It might therefore be expected that deuteration of a phenol would decrease its efficiency by a factor of more than 5.5. However, several workers have either failed to detect any isotope effect with 2,6-di-*tert*-butyl-4-methylphenol (BMP)* (7) and similar hindered phenols (8), or else have found only comparatively small isotope effects, i.e. 1.3 with 3% BMP in butadiene – styrene rubber (9) and 1.6–1.7 in methacrylonitrile (10). The situation with other inhibitors—both of the phenolic and of the aromatic amine type—is similar. That is, either no isotope effect has been observed (11–13) or else only a very small one ~1.0–1.3 (9, 14–16). It should also be noted that abstraction of the phenolic hydrogen from BMP by diphenylpicrylhydrazyl radicals (E = 5.3±0.5 kcal/mole) has a reported kinetic isotope effect of 1.95 (7) whereas abstraction from 2,6-di-*tert*-butylphenol by the same radical (E = 6.0 kcal/mole) has a reported isotope effect of 8.1 (17).

Many of the above facts appear to be mutually contradictory unless it is assumed that the mechanism of reaction [6] (with phenols) is quite dissimilar to the mechanism of reaction [3′] (with hydrocarbons). That is, the very small, or even non-existent, isotope effect that has been reported for reaction [6] could only be a secondary isotope effect, which would imply that a straightforward hydrogen abstraction process is not rate determining. This is both unexpected and contrary to the fact—based on product analysis (1)—that the phenolic hydrogen is actually removed by peroxy radicals. Moreover, replacement of this hydrogen by an alkyl group completely destroys the antioxidant properties of the phenol.

We considered that the question of the existence of an isotope effect in reaction [6] was worth reinvestigating since the previous work is open to some criticism (1) owing to the fact that a phenolic hydrogen, even when sterically well protected, as in BMP, can exchange extremely rapidly if the phenol is dissolved in an organic liquid saturated with D_2O (15). It seems likely, therefore, that deuterated phenols can also exchange rapidly with the hydroperoxides that are the normal products of autoxidation. If this is the case, there is little hope of observing any appreciable isotope effect unless the deuterated phenol is used at such a high concentration that reaction [3′] is nearly completely suppressed. In this way, significant rate measurements might be made before appreciable exchange occurred but it would, of course, be very difficult to estimate how high the concentration should be under any given set of oxidative conditions. This difficulty can, however, be overcome by using as the substrate certain polymerizable olefins which form polyperoxides rather than hydroperoxides, i.e., reaction [3]. Styrene was chosen as the substrate in the present work since its products and also its kinetics for oxidation initiated by α,α'-azo-bis-isobutyronitrile (AIBN) have previously been examined in some detail (18). Moreover, among this type of olefin, styrene undergoes a minimum amount of side reactions leading to hydroxyl- or hydroperoxide-containing compounds. A further advantage that may be expected is that the peroxy radicals will probably be complexed with the aromatic π electron system of one or more adjacent styrene molecules (19) (cf. chlorine atoms in aromatic media (20)). Such complexing

**The activation energy for the reaction of* BMP *with various peroxy radicals has been reported to be 5.0±1.0 kcal/mole (5, 6).*

will reduce the reactivity of the peroxy radicals, which will tend to raise the activation energy for hydrogen abstraction from the added inhibitor, thereby increasing the magnitude of any isotope effect. That is, an isotope effect of this type is more likely to be observable in aromatic, than in aliphatic, media.

BMP was chosen as the inhibitor both because of the large amount of work already done with this phenol and also because the steric protection afforded to the OH group by the two adjacent *t*-butyl groups tends to suppress otherwise troublesome side reactions, e.g., the direct reaction of the phenol with peroxides, chain transfer processes, etc. A further advantage in using BMP is that these same steric factors may also directly increase the magnitude of the hydrogen isotope effect (21).

EXPERIMENTAL

The apparatus has been described previously (22). Styrene was degassed and distilled several times under vacuum before use. It was stored at −30° C under vacuum. α,α'-Azo-bis-isobutyronitrile (AIBN) was used as a thermal initiator of oxidation. It was stored in carbon tetrachloride solution at −15° C. The required volume of solution was added to the reaction vessel and the CCl_4 removed under vacuum. Following this, a BMP solution in CCl_4 was added and the solvent was again removed under vacuum. The styrene was then distilled into the reaction vessel.

Deuterated BMP (i.e., BMP-*d*) was very simply prepared by adding a small quantity of D_2O to a CCl_4 solution of BMP and shaking at room temperature for a few hours. The solution was stored under D_2O since it was found that back exchange with atmospheric moisture occurred extremely rapidly. Infrared analysis indicated that it contained >96% OD, and it might be noted that exchange was fairly rapid even in a dry, stoppered, infrared cell.

The oxidation was studied under 1-atm pressure of dry oxygen from 45–70° C at 5° temperature intervals with 5-ml samples of dry styrene. The AIBN and BMP concentrations were in the range 10^{-1} to 10^{-4} M and 2×10^{-2} to 2×10^{-5} M respectively.

RESULTS AND KINETICS

The Uninhibited Oxidation

At the temperatures used in this work initiation by peroxide decomposition (reaction [4]) can be neglected and therefore the only important initiation process is the unimolecular decomposition of AIBN. That is, reaction [1] can be represented by

$$I_2 \rightarrow 2I\cdot. \qquad [1]$$

Measurements of the rate of nitrogen evolution from AIBN dissolved in styrene under oxygen-free helium at six temperatures from 45° to 70° C give

$$k_1 = 1.99\times10^{15} \exp(-30{,}900/RT)$$

in excellent agreement with previous work in benzene and toluene (23).

The general shape of both the uninhibited and inhibited oxygen uptake curves are shown in Fig. 1. In the absence of BMP the rate of oxidation is constant for several hours. This rate was measured over quite a large range of AIBN concentrations at each temperature and was found to be proportional to $[AIBN]^{0.60\pm0.02}$. The results obtained at 50° and 65° demonstrating this relationship are shown in Fig. 2. Assuming a bimolecular chain termination step (i.e., reaction [5]) the rate should be proportional to the square root of the initiator concentration. That is, the rate of the uninhibited oxidation $(\rho)_0$ is given by:

$$(\rho)_0 = 2ek_1[I_2]+k_3[RH][RO_2\cdot]-k_1[I_2], \qquad [I]$$

where e is the efficiency of chain initiation by AIBN and the last term corrects for nitrogen evolution from the AIBN. The usual steady-state treatment yields the relation

$$(\rho)_0 = (2e-1)k_1[I_2]+k_3[RH]\left(\frac{ek_1[I_2]}{k_5}\right)^{1/2}. \qquad [II]$$

Since the first term is negligible compared with the second, this equation predicts that $(\rho)_0$ should be proportional to $[I_2]^{1/2}$. The observed rate law can be most easily explained by assuming that there is a concurrent first-order chain termination process even in the apparently uninhibited oxidation.* If this reaction is simply represented as

$$RO_2\cdot \rightarrow \text{inactive products}, \qquad [8]$$

then,

$$(\rho)_0 = k_3[RH]\left(\frac{(k_8^2+16ek_1k_5[I_2])^{1/2}-k_8}{4k_5}\right). \qquad [III]$$

Let

$$\frac{k_3k_8[RH]}{4k_5} = \alpha \qquad \text{and} \qquad \frac{ek_1k_3^2[RH]^2}{k_5} = \beta$$

then,

$$(\rho)_0 = (\alpha^2+\beta[I_2])^{1/2}-\alpha \qquad [IV]$$

and

$$\frac{[I_2]}{(\rho)_0^2} = \frac{1}{\beta}+\frac{2\alpha}{\beta}\cdot\frac{1}{(\rho)_0}. \qquad [V]$$

A plot of $[I_2]/(\rho)_0^2$ against $1/(\rho)_0$ should yield a straight line whose slope and intercept can be used to derive α and β. This procedure was followed at each temperature. Although the straight lines are not particularly good the oxidation rates calculated from α and β by equation [IV] represent the experimental results just about as well as the 0.60-order rate law over a wide range of AIBN concentration (see dotted curves in Fig. 2). The assumption that a unimolecular chain-terminating reaction occurs in the uninhibited oxidation of styrene is therefore not unreasonable. This assumption also receives some support from the experiments on the effects of light and heavy water on this oxidation (see below). However, the possibility that the non-integral rate law is due to some other cause cannot be ruled out.

The following activation energies were derived from the values of α and β obtained at each temperature and given in Table I:

$$E_\alpha = E_3+E_8-E_5 = 11.0\pm1.0 \text{ kcal/mole},$$

$$E_\beta = E_1+2E_3-E_5 = 46.0\pm1.0 \text{ kcal/mole}.$$

**Some other explanations which have been put forward in the past to account for non-integral kinetics in similar systems such as the mutual termination of geminate chains (24) or the radical-induced decomposition of* AIBN *can be ruled out since they would also apply to other substrates, whereas we have found that the rate of oxidation of cumene is accurately proportional to* $[AIBN]^{0.50}$ *under similar experimental conditions (25).*

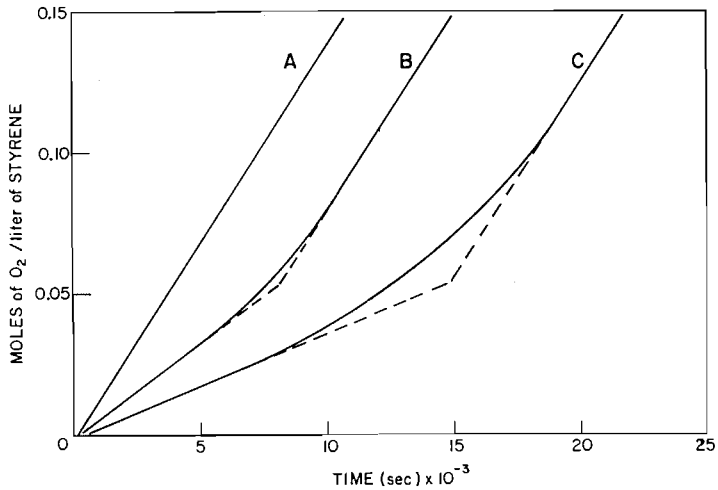

FIG. 1. Oxidation of styrene initiated by 0.01 mole/liter of AIBN, at 50° C. Key: A, no inhibitor; B, 1.38×10^{-4} mole/liter of BMP; C, 2.38×10^{-4} mole/liter of BMP.

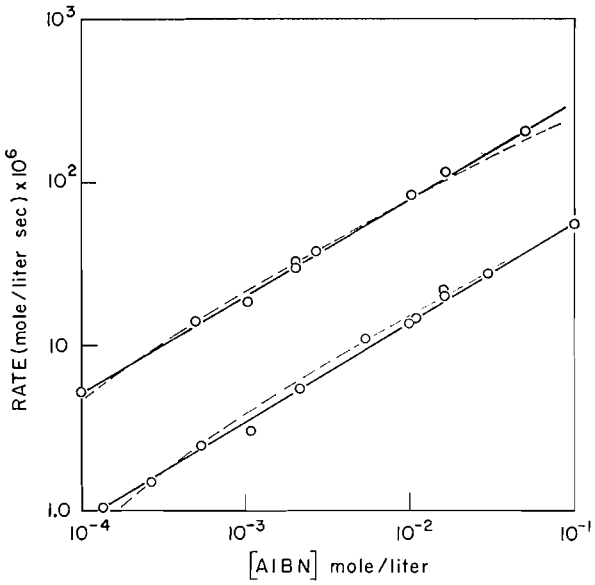

FIG. 2. Uninhibited oxidation of styrene at 50° C and 65° C.

Understandably, E_β compares very well with the activation energy derived directly from the measured oxidation rates at a given AIBN concentration. That is, from equation [II]:

$$E_{p_0} = \tfrac{1}{2}E_1 + E_3 - \tfrac{1}{2}E_5 = 23.3 \pm 0.5 \text{ kcal/mole.}$$

The Inhibited Oxidation

Figure 1 shows that the addition of BMP to the styrene–AIBN system reduces the initial rate to a smaller, but still constant, value. Thereafter, the rate increases slowly until it becomes the same as for the uninhibited oxidation, at which point all the BMP

TABLE I

AIBN-initiated oxidation of styrene

Temp. (°C)	Uninhibited oxidation: $\frac{\rho_0}{[AIBN]^{0.6}} \times 10^4$ ((mole/liter)$^{0.4}$ sec^{-1})	Uninhibited oxidation: $\alpha \times 10^6$ (mole/liter sec)	Uninhibited oxidation: $\beta \times 10^7$ (mole/liter sec^2)	Inhibited oxidation: $\frac{(\rho)_{[AH]\to 0}}{[BMP]}$ (sec^{-1})	Inhibited oxidation: $(\rho)_{[AH]\to max} \times \frac{[BMP]}{[AIBN]} \times 10^7$ (mole/liter sec) BMP	BMP-*d*
45.5	1.46	1.8	0.11	0.08_6	0.37_1	—
50	2.51	2.3	0.31	0.10	0.86_3	6.1_1
55	4.23	3.4	1.0	0.12	2.0_2	15.8
60	7.43	4.3	2.6	0.16	4.7_5	39.2
65	12.7	5.2	7.1	0.20	10.7	75.9
70.5	21.3	6.5	19.9	0.24	27.2	186

must have been consumed. The intersection of the extrapolated linear regions of the inhibited oxidation curves (see Fig. 1) gives an induction period which corresponds to the time at which the BMP would have been completely consumed had its rate of consumption remained constant. That is, this procedure makes allowance for the steady decrease in the concentration of BMP. The efficiency of chain initiation, e, can therefore be determined since the amount of AIBN decomposed during this induction period is known from k_1 and since each molecule of BMP is known to react with two peroxy radicals (26, 27). An average value of e at 50° equal to 0.67 ± 0.02 was obtained in this way. This value of e compares favorably with values obtained in benzene (0.61), chlorobenzene (0.57), and nitrobenzene (0.73) by the same technique (28) when it is remembered that in the present case the solvent is also the reactant. Rather similar values of e have been obtained in aromatic solvents by using iodine as the radical trap (28) and by using an isotopic dilution method (29). It is also interesting that e for the AIBN-initiated polymerization of styrene(0.66–0.82) is also in this range (30).

The kinetics applicable to the BMP-inhibited oxidation depend on the relative concentrations of BMP and AIBN. That is, at low concentrations of inhibitor,

$$(\rho)_{[AH]\to 0} = k_3[RH]\left(\frac{((k_8+2k_6[AH])^2+16ek_1k_5[I_2])^{1/2}-(k_8+2k_6[AH])}{4k_5}\right), \qquad [VI]$$

since reaction [7] will be very fast compared with reaction [6] for the inhibitor BMP (8). Therefore, the rate is approximately proportional to the square root of the initiator concentration. Subtracting equation [VI] from equation [III] we obtain

$$(\rho)_0 - (\rho)_{[AH]\to 0} \approx \frac{k_3k_6[RH][AH]}{2k_5}. \qquad [VII]$$

On the other hand, in the presence of sufficiently high concentrations of inhibitor, reactions [5] and [8] can be neglected. Therefore,

$$(\rho)_{[AH]\to max} = 2ek_1[I_2] + \frac{ek_1k_3[RH][I_2]}{k_6[AH]} - k_1[I_2] \qquad [VIII]$$

and the rate is proportional to the initiator concentration and inversely proportional to the inhibitor concentration.

Equation [VII] predicts that at a given temperature the decrease in rate produced

by the addition of a small concentration of inhibitor will be independent of the initiator concentration, i.e., independent of the uninhibited rate. This is confirmed by the results shown in Fig. 3 for the rates obtained at four AIBN concentrations at 65° C. Within the limits of experimental error the tangents to the curves at zero BMP concentrations are of equal slope. The activation energy derived from these slopes at each temperature is:

$$E_{VII} = E_3+E_6-E_5 = 9.4\pm1.0 \text{ kcal/mole.}$$

Owing to the difficulties which are always inherent in measuring tangents to experimental curves this activation energy is somewhat less accurate than the others obtained in this work.

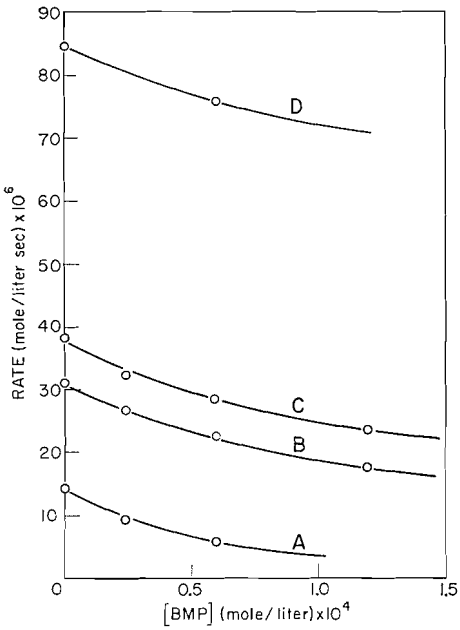

FIG. 3. Effect of low concentrations of BMP on the rate of oxidation of styrene at 65° C. Key: A, 5.0×10^{-4} mole/liter of AIBN; B, 2.0×10^{-3} mole/liter of AIBN; C, 2.63×10^{-3} mole/liter of AIBN; D, 1.0×10^{-2} mole/liter of AIBN.

Figure 4 shows that at high inhibitor concentrations a straight line is obtained by plotting $(\rho)_{[AH]\to max}/[I_2]$ against $1/[AH]$ as predicted by equation [VIII]. This line passes very close to the origin, but the expanded area of the graph shows that it actually has a finite intercept on the vertical axis. From equation [VIII], this intercept $= (2e-1)k_1 \approx 1.2\times10^{-5}$ sec^{-1} and therefore $e = 0.8$ at 65°, in fairly good agreement with the method based on induction periods. The slopes of these lines at different temperatures (see Fig. 5) give

$$E_{VIII} = E_1+E_3-E_6 = 36.9\pm0.5 \text{ kcal/mole.}$$

Both the low and the high concentrations of inhibitor can be treated together by using the same method as was used in deriving equation [V]. That is, neglecting reaction [8], the inhibited rate is given by

$$\rho_{AH} = (2e-1)k_1[I_2]+(\alpha^2[AH]^2+\beta[I_2])^{1/2}-\alpha[AH], \qquad [IX]$$

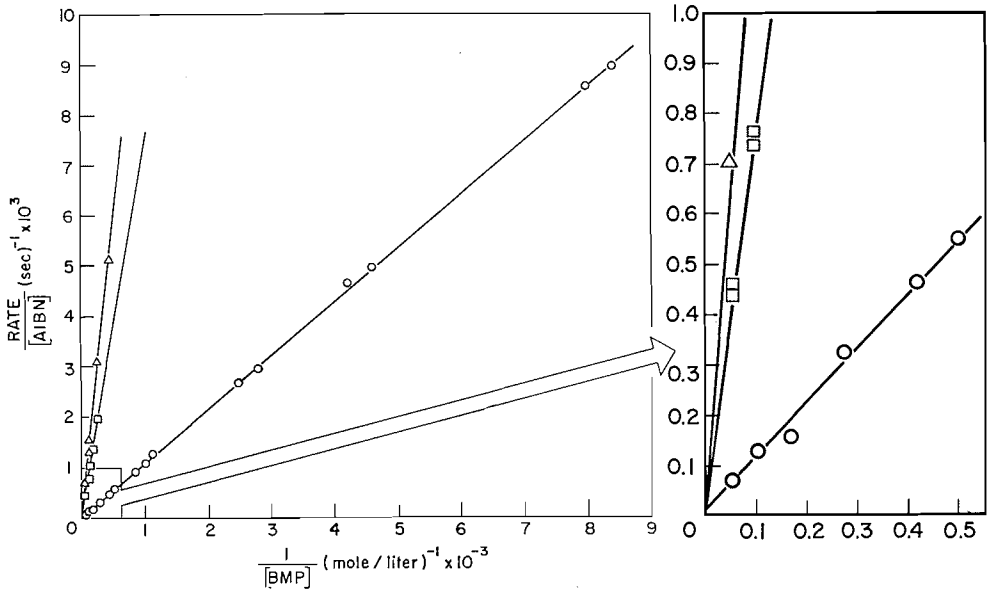

FIG. 4. Effect of high concentration of BMP on the rate of oxidation of styrene at 65° C. Key: ○ BMP; □ BMP-*d*; △ BMP-*d* + D_2O.

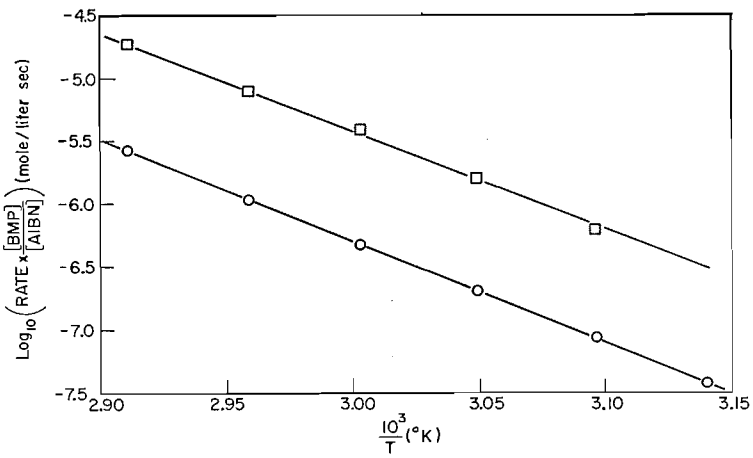

FIG. 5. Oxidation of styrene inhibited by high concentrations of BMP and BMP-*d* plotted against the reciprocal of the absolute temperature. Key: ○ BMP; □ BMP-*d* (92–95%, see text).

where $\alpha = k_3k_6[RH]/2k_5$ and $\beta = ek_1k_3^2[RH]^2/k_5$. Good straight lines yielding α and β are obtained by plotting $[I_2]/\rho_{AH}^2$ against $[AH]/\rho_{AH}$, and the activation energy derived from α is in good agreement with E_{VII}.

The Effect of BMP-d and Heavy Water on the Oxidation

Preliminary experiments showed that deuterated BMP was a much less efficient inhibitor than the undeuterated phenol, but that considerable precautions had to be taken to obtain reproducible results. For example, the temporary admission of air to the system just prior to a run or the use of low concentrations of BMP-*d* could result in rates little different from those obtained with an equivalent concentration of the

undeuterated phenol. Even with fairly high concentrations of BMP-*d* ($\sim 10^{-2}$ to 10^{-3} mole/liter) the rate of oxygen uptake decreases markedly with time (Fig. 6). That this is due to a fairly rapid loss of deuterium by the BMP was proved both by infrared analysis during the oxidation and by adding 1.0–2.0 ml of heavy water to the system.* The effect of this heavy water is to increase the rate by about two thirds based on the initial rate at the same BMP-*d* concentration (see Fig. 4). The rate remains unchanged at this high value throughout the reaction (see Fig. 6). The occurrence of a rapid exchange of the phenolic hydrogen during the oxidation was further confirmed by showing that, although H_2O has a small accelerating effect ($\sim 10\%$) on the rate of a normal BMP-inhibited reaction, D_2O causes the rate to rise towards that of the BMP-*d* + D_2O reaction a short time after oxidation commences. The addition of H_2O to the BMP-*d*-inhibited reaction rapidly reduces the rate to that of the normal BMP + H_2O reaction. The oxygen uptake curves obtained in all these experiments are shown in Fig. 6. It should be added that for both light and heavy water the effects on the rate were independent of the amount of water added and were the same whether the water was pipetted or vacuum distilled into the reaction vessel. The accelerating effects of H_2O and D_2O are therefore not due to traces of transition metal contaminants.

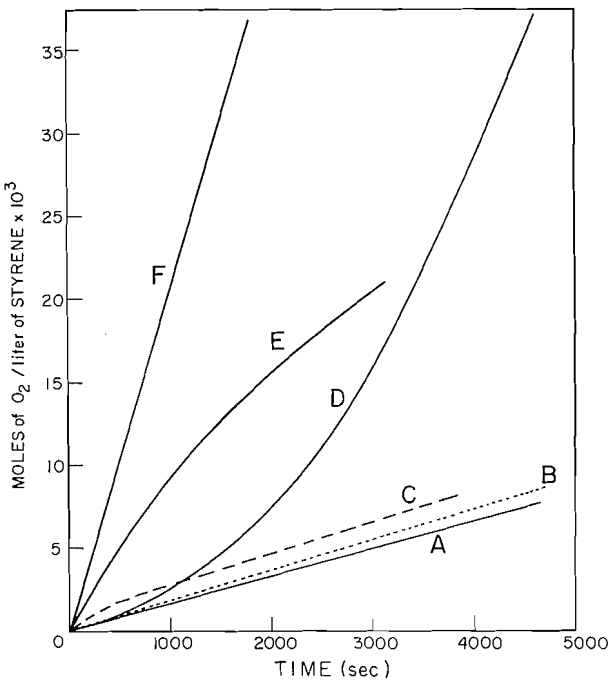

FIG. 6. Effect of H_2O and D_2O on the inhibited oxidation of styrene at an AIBN concentration of 1.32×10^{-2} mole/liter and a BMP concentration of 1.0×10^{-2} mole/liter. Key: A, BMP; B, BMP + H_2O; C, BMP-*d* + H_2O; D, BMP + D_2O; E, BMP-*d*; F, BMP-*d* + D_2O.

The initial rates of the BMP-*d*-inhibited oxidation in the absence of D_2O are compared with the rates of the normal BMP-inhibited reaction at 65° C in Fig. 4. The isotope effect, which is given by the relative slopes of the two lines (equation [VIII]), should probably be regarded as a lower limit, since some exchange occurs before sufficient

**Infrared spectra suggest that small quantities of water are produced in the uninhibited oxidation.*

measurements have been made to obtain an accurate rate. The infrared spectra of reaction samples inhibited by BMP-*d* at a number of stages from preparation to fairly extensive oxidation indicated that this exchange amounted to about 5–8% during the initial linear region of the oxidation curve. The approximately 67% increase in the rate produced by D_2O is, therefore, probably largely due to the maintenance of fully deuterated BMP in the oxidizing system. A lesser part of the increase is probably due to the same factors that cause H_2O to have a small accelerating effect, ~10%, on the inhibited reaction. That is, the measured isotope effect at 65° C in the absence of D_2O is 7.1. On the basis that 5–8% of the deuterium has already exchanged, the true isotope effect will be about 50% greater than this, i.e., $7.1 \times 1.5 = 10.6$. The measured isotope effect in the presence of D_2O is 11.7, which, after applying the 10% correction based on the effect of H_2O, gives an isotope effect of 10.5, in agreement with the value calculated for fully deuterated BMP. In view of the large effect of D_2O on the uninhibited oxidation (see below) it was considered to be safer to estimate the isotope effect from the experimental slopes of the lines obtained in the absence of D_2O rather than in its presence. These slopes are compared at each temperature in Fig. 5 with the slopes obtained with the undeuterated phenol, and they give the minimum isotope effect since they would probably be about 50% greater if allowance were made for deuterium loss. The activation energy with BMP-*d* is $(E_{VIII})_D = 35.8 \pm 0.5$ kcal/mole. Therefore, $(E_6)_D - (E_6)_H = 1.1 \pm 1.0$ kcal/mole.

In view of the catalytic effects of light and heavy water on the inhibited oxidation their effect on the uninhibited oxidation was also examined. H_2O increased the rate by about 12–15% and D_2O by nearly 50%. The increases appeared to be independent of temperature and AIBN concentration and were not due to metal catalysts.

DISCUSSION

From this study of the deuterium isotope effect of the autoxidation inhibition reaction it is apparent that styrene has certain advantages over many of the more usual oxidizable substrates. The most notable advantage is the very low concentration of hydroxyl-containing compounds in the products. On the other hand, the non-integral kinetics of uninhibited oxidation is very surprising, particularly in view of earlier reports about this reaction (18). As was discussed in the previous section, these kinetics can be most readily explained by assuming that a first-order termination process is competing with the usual bimolecular termination. The exact nature of this reaction is unknown but the effect of H_2O and D_2O on the "uninhibited" oxidation suggests that a free radical inhibitor containing a replaceable hydrogen is responsible. Since the rate of oxidation is constant for the "uninhibited" oxidation up to fairly high conversions the concentration of such an inhibitor must rapidly reach a steady state. That is, the inhibitor must be formed throughout the oxidation and must react with a small but constant percentage of the peroxy radicals produced by the decomposing AIBN. In view of the reaction conditions, it seems a reasonable assumption that such a compound contains a hydroxyl group and is therefore, quite probably, a phenol. If this is the case, the small catalytic effect of H_2O could be due to surface adsorption of some of the phenol on the water droplets. This would decrease its effective concentration, since the active centers would be oriented away from the peroxy radicals present in the organic phase. The larger catalytic effect of D_2O would be due to the decreased reactivity of the exchanged but unadsorbed deuterated phenol.

The suggestion that an inhibitor, which is probably a phenol, is produced in the AIBN-initiated oxidation of styrene receives further support from the observation (31)

that the AIBN-initiated oxidation of benzene gives a product which inhibits the thermal polymerization of styrene. Moreover, the fact that H_2O is a catalyst in the present system implies that some rather unusual reaction is occurring, since water generally has either no effect on a substrate (25) or else behaves as an inhibitor. Its usual inhibiting effect is most probably due both to the solvation of small initiating radicals and to the surface adsorption of the larger peroxy radicals.

Although the activation energies and rate constants of the uninhibited propagation and termination reactions cannot be separately evaluated from the present measurements, it is possible to determine $E_3-\frac{1}{2}E_5$ and $k_3/k_5^{1/2}$ from both ρ_0 and β. The two sets of data are in good agreement, as would be expected, and the average values can be represented by

$$E_3-\tfrac{1}{2}E_5 = 7.7\pm0.5 \text{ kcal/mole}$$

$$\frac{k_3}{k_5^{1/2}} = 2.6\times10^3 \exp(-7700/RT) \text{ (liter/mole sec)}^{1/2}.$$

Both these quantities compare very well with the values previously reported by other workers for a variety of fairly reactive substrates containing activated secondary hydrogen atoms, e.g., ethyl linoleate (32) and tetralin (33). It is interesting that a very similar relationship holds for the thermal polymerization of styrene (34), i.e.,

$$\frac{k_{\text{propagation}}}{(k_{\text{termination}})^{1/2}} = 4.17\times10^3 \exp(-6370/RT) \text{ (liter/mole sec)}^{1/2}.$$

Hydrocarbon structures appear to have little effect on the self-termination rate constant of secondary peroxy radicals, since all determinations of k_5 by non-stationary-state methods in substrates which yield these radicals lie fairly close to 10^7 liter/mole sec (5, 6, 32, 33, 35, 36). It therefore seems not unreasonable to assign this same value of k_5 to polystyryl peroxy radicals. Making the further assumption that $E_5 = 0$ within experimental error, we obtain

$$k_3 = 8.1\times10^6 \exp(-7700/RT) \text{ (liter/mole sec)}.$$

The corresponding values for thermal polymerization are (34)

$$k_{\text{propagation}} = 4.5\times10^6 \exp(-7300/RT) \text{ (liter/mole sec)}$$
$$k_{\text{termination}} = 5.8\times10^7 \exp(-1900/RT) \text{ (liter/mole sec)}.$$

An activation energy and an *apparent* first-order rate constant for the postulated first-order termination reaction in the uninhibited oxidation can be derived from α. That is,

$$E_8-\tfrac{1}{2}E_5 = 3.3\pm1.5 \text{ kcal/mole}$$

$$\frac{k_8}{k_5^{1/2}} = 4.4\times10^{-6} \exp(-3300/RT) \text{ (mole/liter)}^{1/2} \text{ sec}^{3/2}$$

or

$$k_8 = 1.4\times10^{-2} \exp(-3300/RT) \text{ sec}^{-1}.$$

The activation energy of this reaction is of the right order of magnitude for the reaction of a polystyryl peroxy radical with a phenolic inhibitor that is rather less reactive than BMP (see below).

At low concentrations of BMP we obtain from E_{VII} and the average value of $E_3-\frac{1}{2}E_5$:

$$E_6-\tfrac{1}{2}E_5 = 1.7\pm1.5 \text{ kcal/mole},$$

and hence,

$$\frac{k_6}{k_5^{1/2}} = 21.8 \exp(-1700/RT) \text{ (liter/mole sec)}^{1/2}$$

or

$$k_6 = 6.9\times10^4 \exp(-1700/RT) \text{ (liter/mole sec)}.$$

At high concentrations of BMP we obtain from E_{VIII} and equation [VIII]

$$E_6-\tfrac{1}{2}E_5 = 1.7\pm1.0 \text{ kcal/mole}$$

$$\frac{k_6}{k_5^{1/2}} = 33.8 \exp(-1700/RT) \text{ (liter/mole sec)}^{1/2}$$

or

$$k_6 = 1.0\times10^5 \exp(-1700/RT) \text{ (liter/mole sec)}.$$

The two sets of data derived by independent experiments are in excellent agreement, but it is probable that the results obtained at high concentrations are more accurate (Figs. 3 and 4). The absolute value of k_6 is in excellent agreement with the values reported for this reaction with cyclohexane and some methyl-substituted cyclohexanes as substrates (5). The activation energy is, however, less than half of the previous reported values but within the limits of accuracy of both methods, and considering the different substrates employed the agreement is satisfactory. Moreover, it is interesting to note that this activation energy is quite close to the value of 1.0 ± 0.5 kcal/mole recently found for the transfer of a hydrogen atom between 2,4,6-tri-*tert*-butylphenol and its phenoxy radical (37).

The present result is also in excellent agreement with the rate constant obtained for the reaction of 2,4,6-trimethylheptylperoxy radicals with the comparatively poor inhibitor diphenylamine (16), i.e.,

$$k = 6.0\times10^4 \exp(-3500/RT) \text{ (liter/mole sec)}.$$

This suggests that there is no fundamental difference in the mechanism of inhibition between phenols and secondary aromatic amines.

At high concentrations of BMP-*d* in the absence of D_2O, we obtain

$$(E_6)_D-\tfrac{1}{2}E_5 = 2.8\pm1.0 \text{ kcal/mole}.$$

Under these conditions maximum rate constants will be obtained, since no correction has been made for the fact that the BMP-*d* was no longer fully deuterated by the time

these measurements were made. On making this correction the pre-exponential factors will be decreased by one third to give minimum rate constants, since the correction factor (1.0/1.5) may have been somewhat overestimated. In the following expressions the first number represents the uncorrected pre-exponential and the second the corrected pre-exponential factor. The true values should lie between these limits.

$$\frac{(k_6)_D}{k_5^{1/2}} = 24.6\ (16.4)\ \exp\ (-2800/RT)\ (\text{liter/mole sec})^{1/2}$$

$$(k_6)_D = 7.8\ (5.2)\times 10^4\ \exp\ (-2800/RT)\ (\text{liter/mole sec})$$

Therefore,

$$\frac{(k_6)_H}{(k_6)_D} = 1.3\ (2.0)\ \exp\ (1100/RT).$$

The difference in activation energy for normal and deuterated BMP can be calculated on the basis of a simple zero-point energy effect from the O—H and O—D fundamental stretching frequencies (38). In styrene, $\nu_{O-H} = 3634\ cm^{-1}$ and $\nu_{O-D} = 2682\ cm^{-1}$ for BMP and hence,

$$(E_6)_D - (E_6)_H = 1.36\ \text{kcal/mole},$$

in excellent agreement with the measured value. The ratio of the pre-exponential factors should lie between 1.0 and $\sqrt{2.0}$ (38), giving a calculated isotope effect of 7.6 and 10.6 respectively at 65° C compared with an uncorrected measured value of 7.1 and a corrected measured value of 10.6. These values should also be compared with the rather smaller isotope effect, $(k_6)_H/(k_6)_D = 4.2\pm0.5$, which we have obtained very recently from the initial rates of the AIBN-initiated oxidation of cumene inhibited by BMP at 65° C (25).

The present results indicate that the rate-determining step for the inhibition of the autoxidation of aromatic substrates by BMP involves a straightforward abstraction of the phenolic hydrogen by peroxy radicals. There is therefore no need to postulate the formation of an intermediate complex as the rate-determining step with this particular inhibitor in an aromatic substrate. This result can probably be generalized to all strong phenolic inhibitors which show first-order kinetics but it is possible that complexing will be rate determining in non-aromatic media.

The determination of rate constants and activation energies would be greatly improved by using a photochemical method of initiation instead of the thermal method, since this would eliminate the large activation energy E_1 from the calculations. Moreover, a direct determination of k_5 could then be made by the rotating sector technique.

It might be added, in conclusion, that comparisons of deuterated and undeuterated inhibitors by measurements of the induction periods produced in a given substrate are extremely unlikely to detect appreciable isotope effects under either initiated or thermal conditions. In the first case, if the reaction is initiated by a compound such as AIBN it is obvious that the length of the induction period will not be affected by deuteration of the inhibitor. In the second case, where initiation is due to the thermal decomposition of hydroperoxide products, the hydroperoxide concentration which builds up during the induction period will generally be quite sufficient to ensure a virtually complete exchange of the deuterium before the end of the induction period. This will lead to nearly equal induction periods for the two inhibitors. That is, if deuteration reduces inhibitor efficiency

by a factor of 10 it will increase the chain length by an equal factor. Therefore, from the very beginning of the reaction, at least 10 molecules of inhibitor (and probably many more since this assumes a chain length of only one for the undeuterated compound) can lose deuterium by exchange with the product hydroperoxide for each molecule that reacts with a peroxy radical. That is, nearly all the deuterium can be lost by exchange in the early part of the induction period so that the measured induction periods will appear to be nearly identical for the deuterated and undeuterated inhibitor. This difficulty might be overcome either by extremely careful measurements at very low degrees of oxidation, although even these would not give the true isotope effect, or alternatively, by the addition of D_2O, provided the D_2O had no effect on the oxidation other than to maintain the inhibitor in its fully deuterated state.

ACKNOWLEDGMENT

The authors wish to thank Dr. I. E. Puddington for his continuing interest and advice throughout the course of this work.

REFERENCES

1. K. U. Ingold. Chem. Revs. **61**, 563 (1961).
2. F. R. Mayo, A. A. Miller, and G. A. Russell. J. Am. Chem. Soc. **80**, 2500 (1958).
3. C. A. Bunton and V. J. Shiner, Jr. J. Am. Chem. Soc. **83**, 3214 (1961).
4. G. A. Russell. J. Am. Chem. Soc. **79**, 3871 (1957).
5. J. C. Robb and M. Shahin. J. Inst. Petrol. **44**, 283 (1958); Trans. Faraday Soc. **55**, 1753 (1959).
6. J. A. Howard and J. C. Robb. Unpublished results.
7. A. F. Bickel and E. C. Kooyman. J. Chem. Soc. 2415 (1957).
8. K. U. Ingold. J. Phys. Chem. **64**, 1636 (1960).
9. J. R. Shelton and E. T. McDonel. J. Polymer Sci. **32**, 75 (1958).
10. C. E. Boozer and C. C. Snead. Private communication.
11. C. E. Boozer and G. S. Hammond. J. Am. Chem. Soc. **76**, 3861 (1954).
12. G. S. Hammond, C. E. Boozer, C. E. Hamilton, and J. N. Sen. J. Am. Chem. Soc. **77**, 3238 (1955).
13. C. J. Pedersen. Ind. Eng. Chem. **48**, 1881 (1956).
14. K. U. Ingold and I. E. Puddington. Ind. Eng. Chem. **51**, 1319 (1959).
15. J. R. Shelton, E. T. McDonel, and J. C. Crano. J. Polymer Sci. **42**, 289 (1960).
16. A. L. Buchachenko, K. Ya. Kaganskaya, and M. B. Neĭmen. Kinetika i Kataliz, **2**, 161 (1961); Trudy Khim. i Khim. Tekhnol. **4**, 31 (1961).
17. R. A. Bird, G. A. Harpell, and K. E. Russell. Can. J. Chem. **40**, 701 (1962).
18. A. A. Miller and F. R. Mayo. J. Am. Chem. Soc. **78**, 1017 (1956). F. R. Mayo and A. A. Miller. J. Am. Chem. Soc. **78**, 1023 (1956). F. R. Mayo. J. Am. Chem. Soc. **80**, 2465 (1958).
19. E. A. Blyumberg, A. D. Malievskii, and N. M. Emanuel. Doklady Akad. Nauk S.S.S.R. **136**, 1130 (1961).
20. G. A. Russell. J. Am. Chem. Soc. **79**, 2977 (1957); J. Am. Chem. Soc. **80**, 4987, 4997, 5002 (1958); J. Org. Chem. **24**, 300 (1959); Tetrahedron, **8**, 101 (1960).
21. E. Baciocchi, G. Illuminati, and G. Sleiter. Tetrahedron Letters, No. 23, 30 (1960).
22. K. U. Ingold. Can. J. Chem. **34**, 600 (1956).
23. J. P. Van Hook and A. V. Tobolsky. J. Am. Chem. Soc. **80**, 779 (1958).
24. P. E. M. Allen and C. R. Patrick. Nature, **191**, 1194 (1961).
25. K. U. Ingold and J. A. Howard. Nature. In press.
26. A. F. Bickel and E. C. Kooyman. J. Chem. Soc. 3211 (1953).
27. C. E. Boozer, G. S. Hammond, C. E. Hamilton, and J. N. Sen. J. Am. Chem. Soc. **77**, 3233 (1955).
28. G. S. Hammond, J. N. Sen, and C. E. Boozer. J. Am. Chem. Soc. **77**, 3244 (1955).
29. J. C. Bevington. Nature, **175**, 477 (1955).
30. L. M. Arnett and J. H. Peterson. J. Am. Chem. Soc. **74**, 2031 (1952).
31. J. C. Bevington and H. Troth. Trans. Faraday Soc. **58**, 186 (1962).
32. L. Bateman, G. Gee, A. L. Morris, and W. F. Watson. Discussions Faraday Soc. **10**, 250 (1951).
33. C. H. Bamford and M. J. S. Dewar. Proc. Roy. Soc. (London), A, **198**, 252 (1949).
34. C. Walling. Free radicals in solution. John Wiley and Sons, Inc., New York. 1957. Chap. 3.
35. T. A. Ingles and H. W. Melville. Proc. Roy. Soc. (London), A, **218**, 163 (1953).
36. V. F. Tsepalov and V. Ya. Shlyapintokh. Doklady Akad. Nauk S.S.S.R. **124**, 883 (1959).
37. R. W. Kreilick and S. I. Weissman. J. Am. Chem. Soc. **84**, 306 (1962).
38. L. Melander. Isotope effects on reaction rates. Ronald Press, New York. 1960. Chap. 2.

THE CHEMICAL SHIFT OF AROMATIC ALKOXY GROUPS

CLAYTON HEATHCOCK[1]
Research and Development, Humble Oil & Refining Co., Baytown, Texas, U.S.A.
Received May 31, 1962

ABSTRACT

The nuclear magnetic resonance (n.m.r.) spectra of 42 variously substituted anisoles and phenetoles have been obtained. The chemical shifts of the alkoxy hydrogens have been assembled in charts for ready use in interpreting the n.m.r. spectra of unknown compounds. For meta- and para-substituted anisoles, a reasonably good correlation has been shown to exist between the methyl resonance and the corresponding Hammett σ parameter. With anisole itself, a preferential solvent effect has been noticed which suggests a specific type of interaction between solute molecules.

In the interpretation of high-resolution nuclear magnetic resonance spectra, two features are of prime importance: the chemical shift and the spin–spin multiplicity pattern. Spin coupling shows the relative positions of various protons within a molecule, and the chemical shift derives its usefulness from its ability to "see" various functional groups which may be present. Chamberlain (1) has shown that the chemical shift can be a powerful tool in the identification of functional groups. Chamberlain's chemical shift charts contain the complete data on more than 400 organic compounds. By using these charts, the organic chemist is often able to identify an unknown resonance peak with a specific functional group.

In these data, however, only two compounds containing aromatic alkoxy groups are included. The only specific study of compounds of this type which has appeared in the literature is the work of Kun and Cassidy (2), who report the spectra of a number of methylated 1,4-dimethoxybenzenes.

In light of the fact that this functional group is very common in organic compounds, especially those of biological origin, we have obtained the n.m.r. spectra of 42 variously substituted anisoles and phenetoles and condensed the data into a chemical shift chart patterned after those of Chamberlain (1).

EXPERIMENTAL

Nuclear magnetic resonance spectra were produced with a modified Varian V-4300B spectrometer operating at a frequency of 60 Mc. The magnetic field was stabilized to a high degree by proton-resonance control in addition to the Varian Super Stabilizer. All spectra were run at room temperature (ca. 30° C) at an r.f. amplitude of 0.04 milligauss and a scan rate between 1.5 and 5.0 c.p.s./sec. All compounds studied were commercial samples and were used as delivered with no further purification. Spectra were referenced from internal tetramethylsilane (TMS) and chemical shifts are expressed on the "tau" scale (3). Concentrations were maintained at 10% or lower in carbon tetrachloride where solubility permitted. In duplicate measurements, an average difference of 0.012 p.p.m. was observed.

RESULTS AND DISCUSSION

The data are presented in Tables I and II. The range of values obtained is remarkably narrow, considering the number of compounds included and the range of ring substituents. This is fortunate, since it enables one to pinpoint rather precisely the shift expected for alkoxy hydrogens in almost any conceivable environment. It should be noted that the present data were obtained with concentrations no greater than 10% by weight in an inert solvent. The resonance positions are strongly solvent dependent,

[1]*Present address: Chemistry Department, University of Colorado, Boulder, Col., U.S.A.*

TABLE I

Chemical shifts of anisole and derivatives*

Compound	Ring	Methoxy	Methyl
Anisole	2.88–3.3	6.34	—
o-Methylanisole	3.08–3.36	6.35	7.86
m-Methylanisole	3.03–3.55	6.38	7.77
p-Methylanisole	3.03, 3.35	6.38	7.80
o-Aminoanisole	3.48	6.34	—
o-Nitroanisole	2.30–3.00	6.16	—
m-Nitroanisole	2.25–2.85	6.16	—
p-Nitroanisole	1.92, 2.82	6.16	—
p-Chloroanisole	2.88, 3.35	6.36	—
o-Bromoanisole	2.50–3.25	6.18	—
p-Bromoanisole	2.74, 3.35	6.36	—
o-Iodoanisole	2.28–3.36	6.22	—
o-Methoxybenzoic acid†	2.30–3.20	6.22	—
p-Methoxybenzoic acid†	2.58, 3.17	6.24	—
Methyl *o*-methoxy benzoate	2.30–3.15	6.20	6.20
Methyl-*p*-methoxy benzoate	2.13, 3.20	6.22	6.24
o-Acetamidoanisole‡	3.2	6.24	7.95
p-Acetamidoanisole‡	2.65, 3.20	6.30	7.95
p-Methoxybenzaldehyde	2.32, 3.12	6.21	—
o-Phenylanisole	2.55–3.23	6.37	—
m-Dimethoxybenzene	3.05–3.75	6.37	—
p-Dimethoxybenzene	3.32	6.43	—
p-Cyanoanisole	2.53, 3.12	6.18	—
p-Methoxybenzyl alcohol	2.95, 3.36	6.39	—
2,4-Dinitroanisole§		5.90	—
2,4-Dichloroanisole	2.75, 2.90, 3.30	6.23	—
2,5-Dimethoxytoluene	3.48	6.33, 6.37	7.87
2,3-Dimethoxybenzaldehyde	2.70–3.30	6.22	—
2-Amino-5-nitroanisole‖	2.25, 2.35, 3.40	6.13	—
2-Iodo-5-nitroanisole‖	2.12, 2.45, 2.50	6.11	—
2-Hydroxy-5-formylanisole	2.65, 3.00	6.13	—
2-Hydroxy-5-propenylanisole	3.35	6.26	—

*All spectra were run at a concentration of 10% in CCl_4 unless otherwise noted. The chemical shifts of the ring hydrogens are given as ranges where spin-coupling patterns were not readily interpretable. Resonance positions are expressed on the "tau" scale (3).
†10% hexamethylphosphoramide added as a solubilizer.
‡5% in $CDCl_3$.
§0.5% in CCl_4. Poor signal-to-noise ratio did not permit the location of the ring resonances.
‖2% in $CDCl_3$.

TABLE II

Chemical shifts of phenetole and derivatives*

Compound	Ring	Methylene	Methyl	Ring methyl
Phenetole	2.88–3.3	6.13	8.68	—
o-Methylphenetole	3.18–3.42	6.11	8.66	7.86
m-Methylphenetole	3.03–3.50	6.13	8.68	7.77
p-Methylphenetole	3.10, 3.36	6.15	8.69	7.80
o-Aminophenetole	3.48	6.10	8.68	—
m-Aminophenetole	3.15–4.02	6.20	8.73	—
p-Aminophenetole	3.50, 3.65	6.20	8.73	—
o-Diethoxybenzene	3.30	6.07	8.65	—
m-Diethoxybenzene	3.05–3.77	6.13	8.67	—
p-Diethoxybenzene	3.35	6.15	8.70	—
p-Nitrophenetole	1.85, 3.10	2.93	8.57	—

*All spectra were at a concentration of 10% in CCl_4. The chemical shifts of the ring hydrogens are given as ranges where spin-coupling patterns were not readily interpretable. Resonance positions are expressed on the "tau" scale (3).

and the use of concentrations greater than 10% leads to highly unreliable results. For example, the chemical shift of the methyl hydrogens in anisole varies from 3.34 τ for a 10% solution in CCl_4 to 3.63 τ for the neat liquid.

There seems to be a definite dependence of the resonance of the methoxy or ethoxy group on ring substitution. The data have been accumulated into a chemical shift chart (Fig. 1), although, with one exception, no effort has been made to show, on the chart,

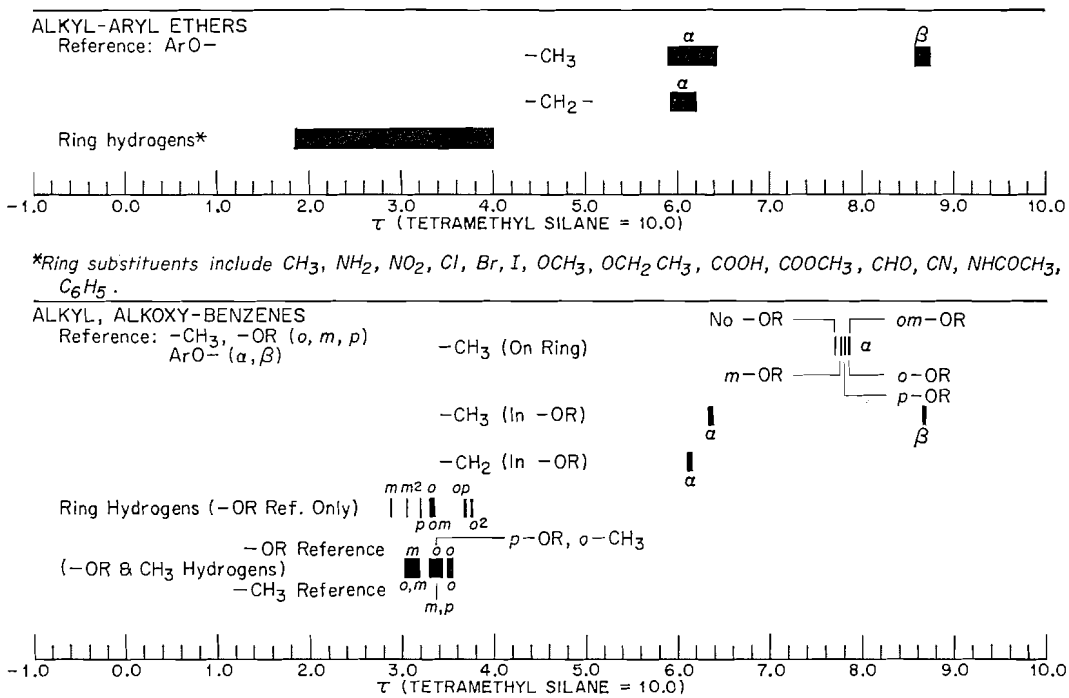

FIG. 1. Chemical shift chart for alkyl ethers of substituted phenols.

the fine distinctions caused by the ring substituents.[2] The one exception is in the alkyl, alkoxy benzenes. Because of the number of compounds studied in this category (14) and the regular trends observed, a separate part of the chart has been devoted to a summary of their chemical shifts.

The origin of the observed dependency of chemical shift on ring substituent is of interest. Figure 2 is a plot of the methyl resonances of meta- and para-substituted anisoles versus the corresponding Hammett σ functions. The Hammett functions are experimental parameters which provide a measure of the ability of a substituent to withdraw or donate charge through a combination of its inductive and resonance effects (4).

As is evident, the correlation is fairly good, although not perfect. The fact that a correlation exists is evidence that, at least to some extent, the dependence of the chemical shift of the alkoxy group on the nature of the ring substituent is due to the inductive and resonance effects of the substituent.

Several groups of workers have found analogous correlations in other systems. Taft (5) has found a precise correlation of the F^{19} resonance in meta- and para-substituted fluorobenzenes with the corresponding reactivity parameters. Bothner-By and Glick (6) noticed a relationship between the chemical shift of the para hydrogen in several mono-

[2]*See reference 1 for nomenclature of the chemical shift charts. The referencing nomenclature has been changed from the parts per 10 million from benzene scale originally proposed by Chamberlain to the "tau" scale in accordance with current usage.*

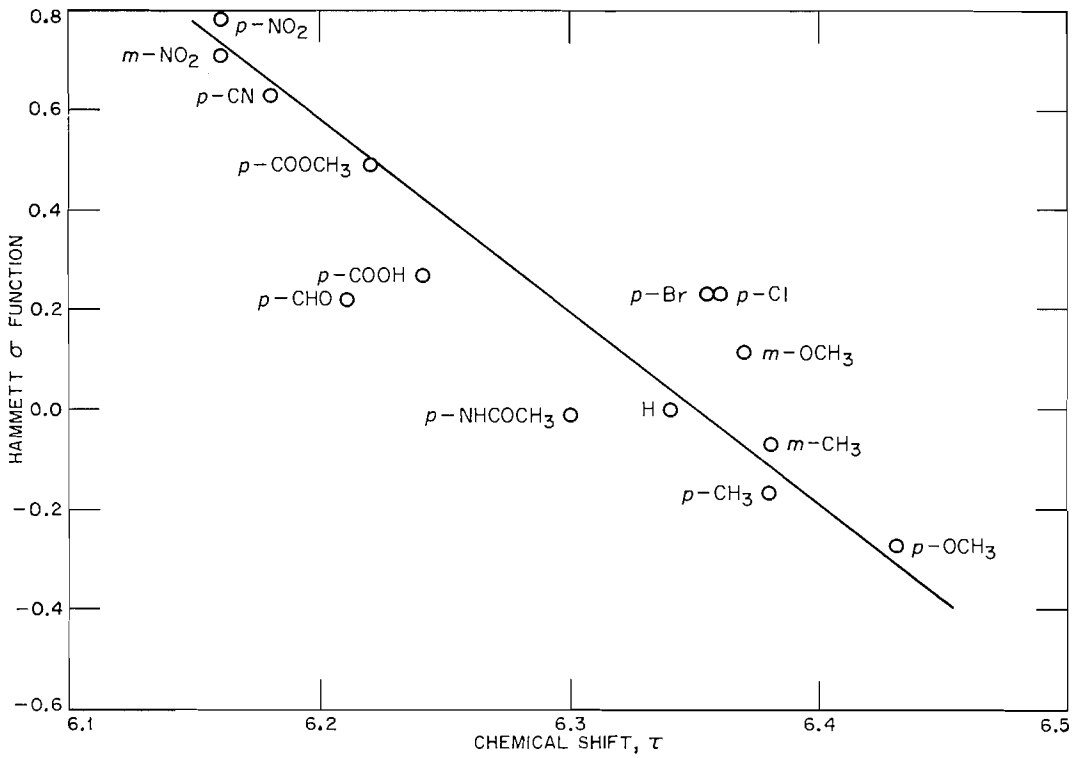

FIG. 2. Dependence of methoxy chemical shift on aromatic ring subtsituent.

substituted benzenes with the Hammett functions. More recently, Spiesecke and Schneider (7) were able to correlate the Hammett functions with the chemical shift of both C^{13} and H^1 in the para position of monosubstituted benzenes, although they failed to find a similar correlation in the meta position. Apparently, our work is the first example of a correlation between reactivity parameters and chemical shift of nuclei not a part of, or directly connected to, the ring. The fact that some of the points fall off the line of best fit simply indicates that these effects are not the only causes of the shifts observed. Also, the Hammett parameters are only accurate to $\pm 15\%$. In the case of substituents ortho to the alkoxy group, complexities are encountered. In this position, proximity effects must no doubt be taken into consideration.

As is mentioned above, the methyl resonance in anisole is highly solvent dependent. However, the ring hydrogen resonance is scarcely affected by dilution with CCl_4, as is shown in Fig. 3.

A similar behavior has been noticed by Hatton and Richards (8) with γ-picoline. These workers found that the resonances of the methyl and β-ring hydrogens shifted downfield upon dilution with CCl_4 while the α-ring hydrogens were not affected. They have proposed a structure for the neat liquid in which the molecules associate as dimers, with the methyl group of each molecule located roughly over the face of the ring of its partner molecule. Such an arrangement causes the methyl hydrogens and β-hydrogens to be shielded by the diamagnetic anisotropy of the adjacent aromatic ring, while the α-hydrogens are in approximately the right position for the net effect to be zero. Dilution with an inert solvent breaks up the association, with a resulting downfield shift for the hydrogens involved.

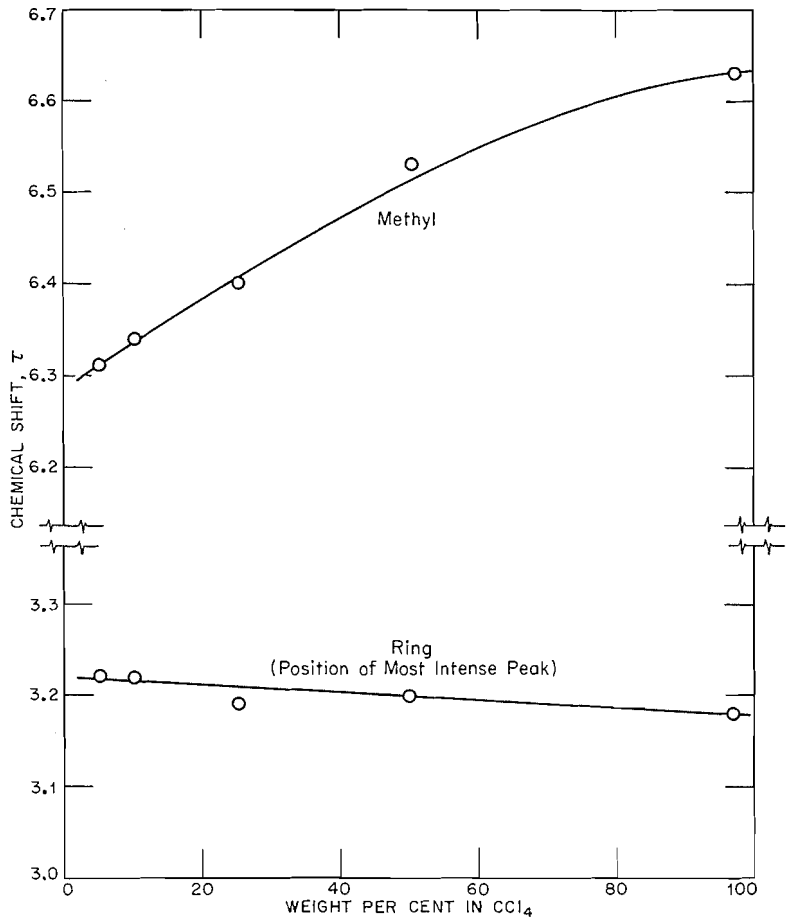

FIG. 3. Chemical shifts of anisole as a function of concentration.

An analogous arrangement seems to be indicated for anisole molecules. However, in the case of anisole, the inclusion of an oxygen between the aromatic ring and the methyl places all of the ring hydrogens in a region where the effect of the diamagnetic anisotropy of the partner molecule is negligible.

ACKNOWLEDGMENTS

The author wishes to thank N. F. Chamberlain and Dr. F. C. Stehling for many valuable discussions during the course of this work, and R. K. Saunders and T. J. Denson for obtaining some of the spectra used.

REFERENCES

1. N. F. CHAMBERLAIN. Anal. Chem. **31**, 56 (1959).
2. K. A. KUN and H. G. CASSIDY. J. Org. Chem. **26**, 3223 (1961).
3. G. V. D. TIERS. J. Phys. Chem. **62**, 1151 (1958).
4. (*a*) L. P. HAMMETT. Physical organic chemistry. McGraw-Hill, New York. 1940.
   (*b*) H. H. JAFFE. Chem. Revs. **53**, 191 (1953).
5. R. W. TAFT, JR. J. Am. Chem. Soc. **79**, 1045 (1957).
6. A. A. BOTHNER-BY and R. E. GLICK. J. Am. Chem. Soc. **78**, 1071 (1956).
7. H. SPIESECKE and W. G. SCHNEIDER. J. Chem. Phys. **35**, 731 (1961).
8. J. V. HATTON and R. E. RICHARDS. Mol. Phys. **5**, 153 (1962).

NUCLEAR MAGNETIC RESONANCE SPECTRA OF SIX-MEMBERED ALCYCLIC RING COMPOUNDS AT LOW TEMPERATURE

IV. PARTIALLY DEUTERATED 1,2-*trans*-CHLOROIODOCYCLOHEXANE

E. Premuzic and L. W. Reeves

Department of Chemistry, University of British Columbia, Vancouver, British Columbia

Received March 16, 1962

ABSTRACT

A 50/50 mole% mixture of 1-iodo-2-chloro-1,3,3-trideutero-, and 1-chloro-2-iodo-1,3,3-trideutero-cyclohexane has been synthesized. At −93° C in a CS_2 solution iodochlorocyclohexane shows resolution into diaxial and diequatorial halogen forms. Analysis of the adjacent proton resonance signal intensities shows that this compound exists 68±3 mole% in the diaxial halogan form. This is quite similar to 1,2-dibromocyclohexane, which has 70 mole% in the diaxial form, and is in contrast to 1,2-dichlorocyclohexane, which has a more stable diequatorial form.

INTRODUCTION

In six-membered alcyclic ring compounds, axial and equatorial protons have been distinguished by chemical shift measurements (1). The indirect spin–spin coupling constants between the various protons have energies decreasing in the order $Je_1a_1 > Ja_1a_2 > Je_1a_2 \simeq Je_1e_2$ (17). In this notation, e_1 corresponds to a proton equatorial on carbon 1, a_1 axial on carbon 1, e_2 equatorial on carbon 2, and a_2 axial on carbon 2.

Several other techniques have been used to determine the configurations in the six-membered ring compounds. In particular, electron diffraction methods (2) give the bond lengths and bond angles in some cases. The technique is limited to the gas phase and the method is not sensitive enough to give accurate populations of two chair forms in equilibrium. Infrared measurements have been made on these types of compounds, and the separation of the skeletal carbon vibrations from the vibrations of the $\rangle$CH bonds have been made (3–5). The $\rangle$CH stretching region of the infrared spectrum of these molecules is too complex to interpret in terms of the configurations of the rings. Selective deuteration of the rings and observation of the $\rangle$CD stretching region have been carried out (15, 14). Axial and equatorial deuterium atoms in the rings have been distinguished by this means, but the method has not been accurate enough to determine an analysis of a compound with an unsymmetrical inverting ring system, chair to chair. The infrared method has also been used to distinguish axial and equatorial $\rangle$CX groups from the region of the spectrum appropriate to the $\rangle$CX stretching frequency (16, 13). Analysis of cyclohexyl chloride and cyclohexane thiol for axial and equatorial sulphur or halogen groups has been achieved by this technique.

Six-membered ring compounds which are not locked by the substitution of large groups around the ring into one configuration undergo chair-to-chair inversion. The rate of chair-to-chair inversion can be studied by proton resonance measurements. At room temperature these inverting ring compounds have a spectrum which is the weighted average of the equilibrium forms (18, 6, 12). Between room temperature and −150° C the two distinct forms in equilibrium become distinguishable in the n.m.r. spectrum so

that it is possible to analyze the percentage of each chair form by either measuring the intensities under respective proton resonance peaks at low temperature or by the techniques suggested in the paper of Gutowsky and Saika (18). Measurements of chemical shifts and coupling constants of the two distinguishable chair forms at low temperature may be combined with average chemical shift and coupling constant measurements at room temperature to give an analysis of the rapidly interconverting mixture at room temperature. The proton resonance technique has already been used to study halogenated cyclohexane (6, 12), *trans*-disubstituted cyclohexanes (7), N,N-dimethylpiperazine (8), bicyclic systems such as decalins (9), cyclohexane (10), and perfluorocyclohexane (11).

The difficulties of the proton resonance method as applied to these molecules are the complexities of the proton resonance spectrum, which increase as the symmetry of the molecule is lowered by substitution. In most cases the energy barrier for chair-to-chair inversion has been estimated from the so-called "coalescence temperature", assuming a frequency factor of 10^{13}. It is apparent that substitution of the cyclohexane ring or the introduction of a hetero atom into the ring of carbons may result in the mechanism of chair-to-chair inversions being changed. The assumption of a frequency factor 10^{13} is then not justified, since in these different inversion mechanisms the entropy of activation will not be the same. In simple monosubstituted cyclohexanes the proton resonance adjacent to the substituted group is in general chemically shifted to low field from the rest of the ring protons, and indirect spin–spin interaction with the α protons renders the proton resonance spectrum of this adjacent proton quite complex and in many cases up to 12 cycles in apparent half-width. At low temperatures the resolution of the two chair forms into distinct n.m.r. spectra sometimes results in overlap between the axial and equatorial proton peaks. In order to overcome some of the difficulties of the n.m.r. technique in the study of these molecules, this paper will describe a selective deuteration around the cyclohexane ring so as to simplify the complex spectrum and obtain more accurate populations of chair forms.

EXPERIMENTAL

The variable-temperature n.m.r. apparatus is part of a 40 Mc/s Varian high-resolution spectrometer and is described in previous work (1). The verification of the structure of intermediates was greatly aided by the use of an A60 Varian spectrometer.

Preparation of Cyclohexanone-2,6-D_4

Cyclohexanone was treated with D_2O from Stuart Oxygen Co. (99.8% deuterium). Twenty milliliters of cyclohexanone and a solution of 1–2 g of sodium carbonate in 10 ml D_2O were refluxed overnight. The D_2O layer was then frozen and separated. The cyclohexanone layer was dried over sodium sulphate. The exchange was repeated four times until the A60 spectra showed, from integrated intensity measurements, that only 2% of the α protons remained.

Reduction of 2,6-Tetradeuterocyclohexanone

A typical reduction was carried out with lithium aluminum hydride in the following manner. A saturated solution of lithium aluminum hydride in dry ether was placed into a two-necked, round-bottomed flask. The flask was cooled with ice and the reaction mixture stirred magnetically. A reflux was set up and cyclohexanone-D_4 was added dropwise from a separatory funnel. When the reduction was complete, excess of lithium aluminum hydride was destroyed with slow addition of moist ether. Ice-cold 10% sulphuric acid was then added gradually, until all of the precipitated aluminum hydroxide dissolved. The ether layer was then separated out and dried over anhydrous sodium sulphate. The ether was removed by distillation and the fraction boiling at 155–157° C collected. On a 10-g preparation, yield of cyclohexanol-D_4 (2,6-tetradeuterocyclohexanol) was **7.2 g**.

Dehydration of Cyclohexanol-D_4 to 1,3,3-Trideuterocyclohexene

The conventional dehydration of cyclohexanol with phosphoric acid was used. Phosphoric acid (85%) was added dropwise to 6.33 g of cyclohexanol-D_4 until a homogeneous mixture resulted (2.5 ml of phosphoric acid). The reaction mixture was then subjected to distillation using a small glass-bead column and the

fraction distilling at 82–83° C collected. A good yield of 3.4 g or 65.6% of pure deuterated cyclohexene was thus obtained.

Addition of Iodine–Chloride across the Double Bond of Cyclohexene-D_3

Cyclohexene-D_3 (1.23 g) was dissolved in 3 cc of ice-cold glacial acetic acid. Iodine–chloride (2.3 g) dissolved in 6 ml of glacial acetic acid was then added dropwise to this solution. The reaction mixture was cooled throughout. At the end of the reaction, the product containing a slight excess of iodine–chloride was transferred into a separatory funnel, and then shaken well with 5 ml of saturated sodium thiosulphate. The oily chloroiodocyclohexane was allowed to separate out, treated further with sodium bicarbonate, and dried over anhydrous sodium sulphate. The almost quantitative yield of the mixture of 1-iodo-2-chloro-1,3,3-trideuterocyclohexane and 1-chloro-2-iodo-1,3,3-trideutero cyclohexane was then subjected to n.m.r. studies.

RESULTS

Figure 1 shows 60 Mc/s spectra of 1-chloro-2-iodo-cyclohexane and the 50/50 mole%

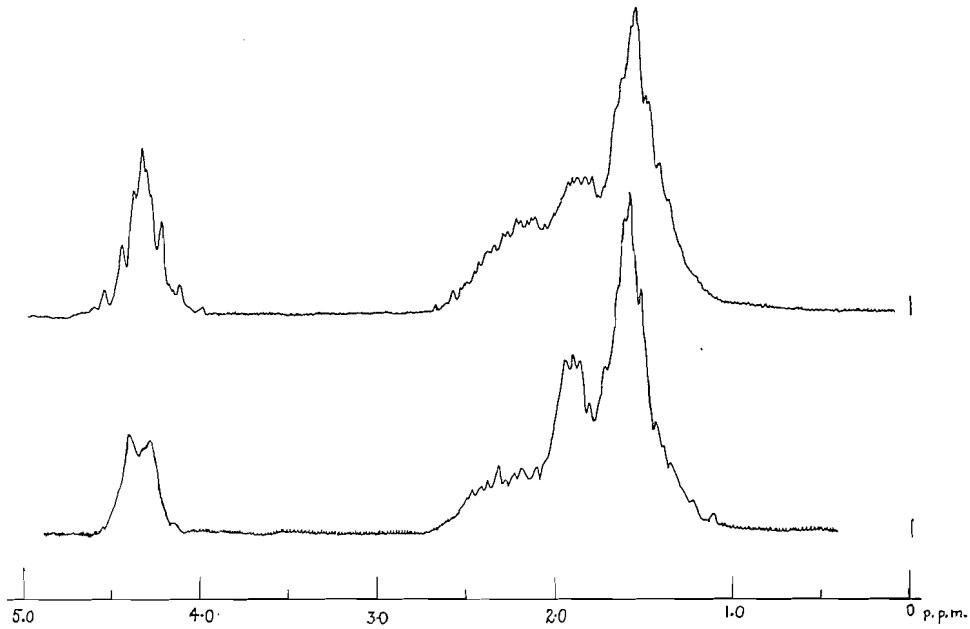

FIG. 1. Sixty-megacycle spectra of 1,2-*trans*-chloroiodocyclohexane (upper) and the 50/50 mixture of 1-iodo-2-chloro-1,3,3-trideuterocyclohexane and 1-chloro-2-iodo-1,3,3-trideuterocyclohexane. Both were diluted to 20 mole% in CS_2.

mixture of 1-iodo-2-chloro-1,3,3-trideutero cyclohexane and 1-chloro-2-iodo-1,3,3-trideuterocyclohexane. The chemical shift between the —CHI— proton and the —CHCl— is small and can be measured directly from the mixture of deuterated molecules (0.12 p.p.m. = 7.2 c.p.s.).

The peaks obtained for the —CHCl—CHI— group arise as follows. The two protons within this group comprise an AB spectrum requiring second-order theory in order to evaluate δ_{AB} and J_{AB}. The value for δ_{AB} is 7.2 c.p.s. (The —CH_2— groups adjacent to the —CHI—CHCl— group form a set of four inequivalent protons all of which are at least 120 c.p.s. removed to higher field.) There should be 16 lines in all, some of which may be coincident. Ten lines have been resolved in spectra taken under slower sweep conditions than those illustrated in Fig. 1. It has not been possible to satisfactorily assign these transitions to obtain coupling constant data.

Low-temperature Studies at 40 Mc/s

Figure 2 shows two spectra, at −44° C and −107° C, of the mixture of deuterated iodochlorocyclohexanes. There was no detectable change in the proton resonance spectra

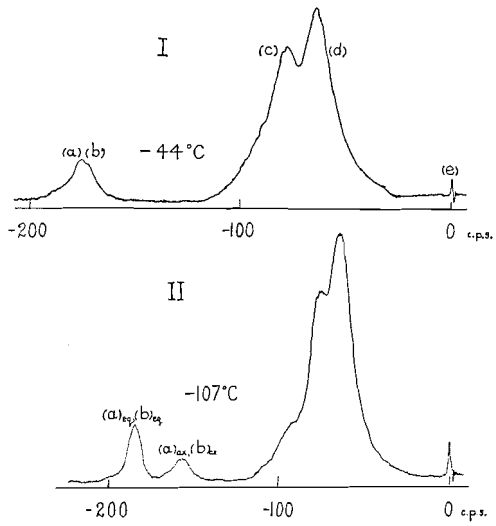

FIG. 2. Forty-megacycle spectra at −44° C and −107° C of the deuterated iodochlorocyclohexane at 40 mole% in CS_2.

between room temperature and −80° C so the spectrum at −44° C is typical of this temperature range. It can be related to the spectrum described in Fig. 1 at 60 Mc/s for the same sample. The low-field peak in spectrum I, Fig. 2, does not show complete resolution into the —CHI— and —CHCl— components. These are labelled (*a*) for the —CHI— proton resonance and (*b*) for the —CHCl— signal. Signals (*c*) and (*d*) marked in spectrum I, Fig. 2, correspond to the distinguishable peaks in the high-field spectra at 60 Mc/s in Fig. 1. The low-field tail of these peaks is barely distinguishable in the 40 Mc/s spectrum. The internal standard hexamethyldisiloxane appears in Fig. 2 marked as 0 c.p.s. The compound was dissolved in CS_2 at a concentration of 40 mole%.

The broadening of the low-field signals occurs below −80° C and they become clearly resolved into two peaks at −100° C. A single broad peak (the "coalescence temperature") is observed at −93° C. The two resolved low-field peaks are in fact composite so that at lowest field $(a)_{eq}(b)_{eq}$ are made up of equatorial proton signals geminal to chlorine in one half of the sample and to iodine in the rest. The corresponding axial proton resonances $(a)_{ax}(b)_{ax}$ are also designated in spectrum II of Fig. 2. The protons geminal to chlorine and iodine are not distinguishable at 40 Mc/s and so the spectra at low temperature can be analyzed into the percentage of the diaxial halogen chair form. Analysis of the spectra below −95° C shows that 68±3 mole% of this iodo–chloro compound exists in the diaxial halogen form. This result is based on the intensities obtained from 18 low-temperature spectra. The deviation from the mean is a maximum value. The mean chemical shift of $\rangle$CHI and $\rangle$CHCl protons at room temperature is −174.8 c.p.s. (−4.37 p.p.m.) from an internal hexamethyldisiloxane reference. At low temperature the mean of the two diaxial proton shifts adjacent to the halogens is −158.2 c.p.s. (−3.96 p.p.m.) and the

mean of the diequatorial protons is found at −185.2 c.p.s. (−4.66 p.p.m.). These values can be compared with earlier studies on dichloro- and dibromo-cyclohexane (7).

DISCUSSIONS

The difference in free energy, which is approximately the same as the energy content difference (6, 7) between diaxial and diequatorial halogen forms, is almost the same for iodochlorocyclohexane (+241 cal mole^{-1}) as for dibromocyclohexane (+305 cal mole^{-1}) (7). The repulsions of diequatorially substituted groups and the halogen with 3,5-diaxial hydrogens are almost exactly the same for iodochloro- as for dibromo-cyclohexane. The sum of the van der Waals radii of 1,2-*trans*-disubstituted groups appears to be the dominant effect in determining the stability of the configurations in the halogenated series of cyclohexanes.

This work has been generously supported by the Petroleum Research Fund of the American Chemical Society.

REFERENCES

1. R. U. Lemieux, R. K. Kullnig, H. J. Bernstein, and W. G. Schneider. J. Am. Chem. Soc. **80**, 6098 (1958).
2. O. Hassel. Quart. Revs. (London), **7**, 221 (1953).
3. D. Ramsey and G. B. B. M. Sutherland. Proc. Roy. Soc. (London), A, **190**, 245 (1947).
4. C. W. Beckett, K. S. Pitzer, and R. Spitzer. J. Am. Chem. Soc. **69**, 2488 (1947).
5. S. C. Burkett and R. M. Badger. J. Am. Chem. Soc. **72**, 4397 (1950).
6. L. W. Reeves and K. O. Strømme. Can. J. Chem. **38**, 1241 (1960).
7. L. W. Reeves and K. O. Strømme. Trans. Faraday Soc. **57**, 390 (1961).
8. L. W. Reeves and K. O. Strømme. J. Chem. Phys. **34**, 1711 (1961).
9. W. B. Moniz and J. A. Dixon. J. Am. Chem. Soc. **83**, 1671 (1961).
10. F. R. Jensen, D. S. Noyce, C. M. Sederholm, and A. J. Berlin. J. Am. Chem. Soc. **82**, 1256 (1960).
11. G. Van Dyke Tiers. Proc. Chem. Soc. 389 (1960).
12. A. J. Berlin and F. R. Jensen. Chem. & Ind. (London), 998 (1960).
13. G. Chinodoglu, J. Reisse, and M. Vander Stichelen Rogier. Chem. & Ind. (London), 1874 (1961).
14. F. R. Jensen and L. H. Gale. J. Am. Chem. Soc. **82**, 145 (1960).
15. E. J. Corey, M. G. Howell, A. Boston, R. L. Young, and R. A. Sueen. J. Am. Chem. Soc. **78**, 5036 (1956).
16. R. R. Rutledge, F. J. Corey, R. A. Sueen, M. G. Danaher, and R. L. Young. Chem. & Ind. (London), 1294 (1954).
17. J. A. Pople, M. J. Bernstein, and W. G. Schneider. High resolution nuclear magnetic resonance. McGraw Hill Co., New York. 1959.
18. H. S. Gutowsky and A. Saika. J. Chem. Phys. **21**. 1688 (1953).

NOTES

HIGH-FIELD KINETIC PROCESSES IN ANODIC OXIDE FILMS ON ALUMINUM

P. J. Ryan and M. J. Dignam

The electrode systems aluminum–alumina and tantalum–tantala afford a unique opportunity for the investigation of high-field ($\sim 10^6$ v/cm or higher) kinetic processes. A theory has been proposed by Bean, Fisher, and Vermilyea (1) to explain the complex transient behavior of these electrode systems. The qualitative predictions of this theory appear to be correct (2); however, critical analysis of data has indicated major discrepancies (3–5). This note presents some preliminary results which have bearing on the nature of these discrepancies and suggests a quantitative interpretation of them.

A full description of the model by Bean *et al.* can be found elsewhere (1–3, 5). Briefly, the ion current density, I, is assumed to depend on the electric field strength, E, and the concentration of interstitial cations, n, in accordance with Verwey's equation (6):

$$I = 2\,qa\nu n \exp\left[-(U-Eaq)/kT\right], \qquad [1]$$

where q is the charge on the ion, ν its vibrational frequency, U the activation energy for ion migration at zero field, and a the corresponding activation distance. Pairs of interstitial cations and cation vacancies (i.e. Frenkel defects) are assumed to be formed by the action of the field on lattice cations (N per unit volume), and to be destroyed by recombination, the collision cross-sectional area, πr^2, being assumed constant. The resulting equation is

$$dn/dt = N\nu \exp\left[-(W-E\lambda q)/kT\right] - I\pi r^2 n/q, \qquad [2]$$

where W is the zero-field activation energy and λ the activation distance for formation of a Frenkel defect. Equation [2] contains the assumption that the concentrations of interstitials and vacancies are essentially equal and are much smaller than N.

All measurements reported herein were performed by increasing the anodic overpotential, V, at a constant rate, $R = dV/dt$, the film thickness, δ, changing negligibly during a run. For these special conditions, elimination of n from equations [1] and [2] yields

$$\frac{d \ln I}{dV} = \frac{\pi r^2}{qR}\left[\frac{(\alpha \exp \beta E)^2}{I} - I\right] + \frac{qa}{kT\delta}, \qquad [3]$$

where α and β are constants occurring in the steady-state (i.e. $dn/dt = 0$) solution of equations [1] and [2]:

$$I = \alpha \exp \beta E, \qquad [4]$$

and are given by $\alpha = q\nu(2Na/\pi r^2)^{1/2} \exp\left[-(W+U)/2kT\right]$ and $\beta = q(\lambda+a)/2kT$. For R

sufficiently large, equation [3] predicts a linear relation between log I and V, the slope yielding the value of a. For smaller values of R, equation [3] can be rewritten as follows:

$$\ln Z = (2\beta/\delta)V + 2\ln\alpha, \qquad [5]$$

where

$$Z = I\left[\frac{qR}{\pi r^2}\left(\frac{d\ln I}{dV} - \frac{qa}{kT\delta}\right) + I\right].$$

Accordingly, for R sufficiently small, β (or $\lambda+a$) and α may be determined from a plot of log Z versus V, Z being calculated for various trial values for r, the value leading to the best linear plot being selected.

EXPERIMENTAL

Electropolished samples of superpurity aluminum were anodically oxidized at a constant current density, I_f, in a 30% solution of ammonium pentaborate in ethylene glycol (7) at room temperature. The instant the desired film thickness (100 → 500 Å) was achieved, the anodic overpotential was increased at a linear rate ranging from 10 to 2500 v/sec. The current during the rapid voltage sweep was recorded with an oscilloscope and camera. Details of the apparatus and procedure will be provided in a future publication.

RESULTS AND DISCUSSION

The results of our preliminary studies are summarized in Fig. 1 and Table I.

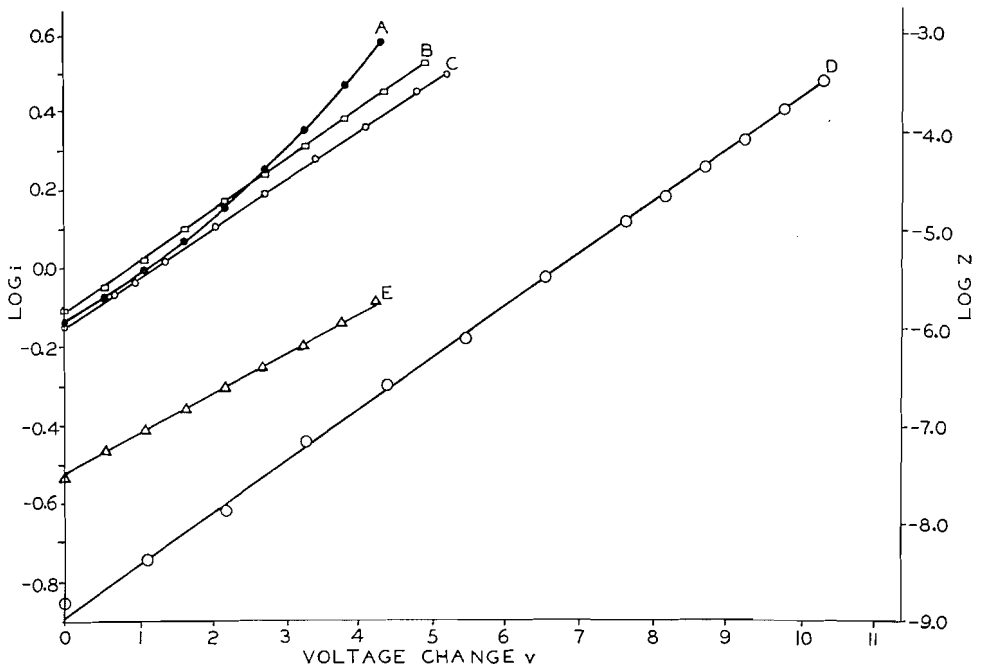

FIG. 1. Representation of transient conductivity measurements. Log i versus voltage change v: (A) $I_f \simeq 200$ μa/cm², $R = 107.6$ v/sec; (B) $I_f \simeq 200$ μa/cm², $R = 1076$ v/sec; (C) $I_f \simeq 200$ μa/cm², $R = 2703$ v/sec; (D) $I_f \simeq 20$ μa/cm², $R = 1076$ v/sec. Log Z versus voltage change v: (E) $I_f \simeq 200$ μa/cm², $R = 107.6$ v/sec. (Z in amp²/cm⁴, i in ma for an area $\simeq 3.4$ cm².)

TABLE I

Anodic oxidation parameters for the aluminum–alumina system

Reference	Method of measurement	$\lambda+a$ (Å)	a (Å)	r (Å)	α (amp/cm²)
Bernard and Cook (7)	Steady-state	8.2*			$\sim 10^{-22}$†
Present results	trans., $I_f = 2\times10^{-4}$	3.9	1.23	~4	$\sim 10^{-13}$
Present results	trans., $I_f = 2\times10^{-5}$	3.9	1.25	~4	$\sim 3\times10^{-1}$
Present results	trans., $I_f = 2\times10^{-6}$	4.0	~1.1	~4	$\sim 10^{-14}$

NOTE: trans. = transient; I_f in amp/cm².

*Steady-state values for $\lambda+a$ calculated from the literature from results obtained using aqueous electrolytes are: 7.1 to 8.1 Å (3), 7.3 Å (8), 7.2 Å (9), and 5.3 Å (10). All these results are ultimately interpreted as being $2(\lambda+a)$ rather than $\lambda+a$.

†Steady-state values for α for aqueous electrolytes are: 10^{-20} amp/cm² (8), 10^{-23} amp/cm² (9), and 10^{-18} amp/cm² (10). These results are ultimately interpreted as being α^2/I_f rather than α.

In accordance with the predictions, the logarithm of the current, i, is linear in the voltage change ($v = V(t) - V(t = 0)$) for $R \geqslant 1000$ v/sec. In addition, the resulting value of a (see equation [3]) is independent of R, within this limit, and also independent of the formation current density, I_f. Again, for runs in which $R \leqslant 100$ v/sec, log Z could be made linear in the voltage change, v, by a suitable choice for r, and $\lambda+a$ and α deduced from the slope and intercept. Within experimental error, r and $\lambda+a$ were also found to be independent of R and I_f. Neither r nor α could be determined with any degree of certainty. Values for the film thickness and sample area employed in the calculations were determined using the data of Bernard and Cook (7). Results of the calculations are presented in Table I.

The most interesting feature of these results is the disagreement, by a factor of 2, between $\lambda+a$ values calculated from steady-state and from transient data, and the corresponding discrepancy in the α values. The disagreement can be reconciled if it is assumed that N, the number of sites at which Frenkel defects may form, is not a constant equal to the number of lattice sites but is a function of the "amorphous" film structure, as proposed by Dignam (5). Quantitative agreement is obtained by setting N proportional to the rate of electrical energy dissipation per unit volume in the film for steady-state conditions, the rate of change of N with time being considered too slow to affect significantly the value of N during a transient measurement. Accordingly, setting $N = C'IE \simeq CI$ (since E varies by only a few percent for change of several powers of 10 in I) the steady-state solution of equations [1] and [2] becomes

$$I = \alpha' \exp 2\beta E, \qquad [6]$$

where $\alpha' = q^2\nu^2(2Ca/\pi r^2) \exp -(W+U)/kT$. Interpreting Bernard and Cook's steady-state data in terms of equation [6], $\lambda+a = 8.2/2 = 4.1$ Å, in agreement with the value of 3.9 Å obtained from the present transient measurements. Also, since $\alpha^2/\alpha' = I_f$, we have I_f equal to $(10^{-13})^2/10^{-22}$, $(3\times10^{-14})^2/10^{-22}$, and $(10^{-14})^2/10^{-22}$, which compare favorably with the measured values of 2×10^{-4}, 2×10^{-5}, and 2×10^{-6} amp/cm² respectively.

An extensive investigation of this system using techniques outlined herein is at present under way.

This work was supported by a grant from the National Research Council of Canada.

1. C. P. BEAN, J. C. FISHER, and D. A. VERMILYEA. Phys. Rev. **101**, 551 (1956).
2. J. F. DEWALD. Phys. and Chem. Solids, **2**, 55 (1957).
3. D. A. VERMILYEA. J. Electrochem. Soc. **104**, 427 (1957).
4. L. YOUNG. Proc. Roy. Soc. (London), A, **263**, 395 (1961).
5. M. J. DIGNAM. J. Electrochem. Soc. **109**, 184 (1962).

6. E. J. W. VERWEY. Physica, **2**, 1059 (1935).
7. W. J. BERNARD and J. W. COOK. J. Electrochem. Soc. **106**, 643 (1959).
8. K. NAGASE. Mem. Inst. Sci. and Ind. Research, Osaka Univ. **12**, 67 (1955).
9. A. GUNTHERSHULZE and H. BETZ. Z. Physik, **92**, 367 (1934).
10. A. CHARLESBY. Proc. Phys. Soc. (London), B, **66**, 317 (1953).

RECEIVED APRIL 3, 1962.
DEPARTMENT OF CHEMISTRY,
UNIVERSITY OF TORONTO,
TORONTO, ONTARIO.

STEREOCHEMISTRY OF ARSENIC
V. CRYSTAL DATA FOR TRIARYLARSINES

J. TROTTER

Crystal structure studies of the halogenodiphenylarsines (1) have shown that, as a result of steric interactions, the phenyl groups are rotated from the positions that they might be expected to occupy in an "ideal" structure with maximum interaction between the arsenic lone pair and the aromatic π-electrons. The deviations are not, however, symmetrical, one ring being rotated approximately 90° and the other only about 30° from the orientation with maximum interaction.

Similar steric effects are to be expected in triarylarsines, except that the deviations are probably symmetrical; the analyses of the crystal and molecular structures of a few molecules of this type have been undertaken to determine the molecular configurations. The unit cell dimensions and space groups of crystals of triphenylarsine, tri-*p*-tolylarsine, and tri-*p*-xylylarsine were determined from single crystal rotation, oscillation, Weissenberg (all with Cu K_α radiation, $\lambda = 1.542$ Å), and precession films (Mo K_α, $\lambda = 0.7107$ Å). These data and other relevant information are given in Table I.

TABLE I
Crystallographic data for triarylarsines, R_3As

	R:			
	Phenyl, C_6H_5—			
	Wetzel	Present	*p*-Tolyl, C_7H_7—	*p*-Xylyl, C_8H_9—
Molecular weight	306.2		348.3	390.4
Melting point (°C)	58		148–149	161
Crystal system	Triclinic		Rhombohedral	Monoclinic
a (Å)	15.23	15.20	9.84	10.81
b (Å)	17.72	17.81		33.4
c (Å)	11.14	11.16		5.72
α (deg)	99.8	98.9	80° 2′	
β (deg)	93.6	93.0		96° 28′
γ (deg)	85.0	84.6		
V (Å^3)	2947	2968	914	2052
Z	8	8	2	4
D_c (g cm^{-3})	1.37	1.36	1.258	1.256
D_m (g cm^{-3})	1.35		1.25	1.24
Space group	$P1$ or $P\bar{1}$		$R3$ or $R\bar{3}$	$P2_1/a$

6. E. J. W. VERWEY. Physica, **2**, 1059 (1935).
7. W. J. BERNARD and J. W. COOK. J. Electrochem. Soc. **106**, 643 (1959).
8. K. NAGASE. Mem. Inst. Sci. and Ind. Research, Osaka Univ. **12**, 67 (1955).
9. A. GUNTHERSHULZE and H. BETZ. Z. Physik, **92**, 367 (1934).
10. A. CHARLESBY. Proc. Phys. Soc. (London), B, **66**, 317 (1953).

RECEIVED APRIL 3, 1962.
DEPARTMENT OF CHEMISTRY,
UNIVERSITY OF TORONTO,
TORONTO, ONTARIO.

STEREOCHEMISTRY OF ARSENIC
V. CRYSTAL DATA FOR TRIARYLARSINES

J. TROTTER

Crystal structure studies of the halogenodiphenylarsines (1) have shown that, as a result of steric interactions, the phenyl groups are rotated from the positions that they might be expected to occupy in an "ideal" structure with maximum interaction between the arsenic lone pair and the aromatic π-electrons. The deviations are not, however, symmetrical, one ring being rotated approximately 90° and the other only about 30° from the orientation with maximum interaction.

Similar steric effects are to be expected in triarylarsines, except that the deviations are probably symmetrical; the analyses of the crystal and molecular structures of a few molecules of this type have been undertaken to determine the molecular configurations. The unit cell dimensions and space groups of crystals of triphenylarsine, tri-*p*-tolylarsine, and tri-*p*-xylylarsine were determined from single crystal rotation, oscillation, Weissenberg (all with Cu K_α radiation, $\lambda = 1.542$ Å), and precession films (Mo K_α, $\lambda = 0.7107$ Å). These data and other relevant information are given in Table I.

TABLE I
Crystallographic data for triarylarsines, R_3As

	R:			
	Phenyl, C_6H_5—			
	Wetzel	Present	*p*-Tolyl, C_7H_7—	*p*-Xylyl, C_8H_9—
Molecular weight	306.2		348.3	390.4
Melting point (°C)	58		148–149	161
Crystal system	Triclinic		Rhombohedral	Monoclinic
a (Å)	15.23	15.20	9.84	10.81
b (Å)	17.72	17.81		33.4
c (Å)	11.14	11.16		5.72
α (deg)	99.8	98.9	80° 2′	
β (deg)	93.6	93.0		96° 28′
γ (deg)	85.0	84.6		
V (Å^3)	2947	2968	914	2052
Z	8	8	2	4
D_c (g cm^{-3})	1.37	1.36	1.258	1.256
D_m (g cm^{-3})	1.35		1.25	1.24
Space group	$P1$ or $P\bar{1}$		$R3$ or $R\bar{3}$	$P2_1/a$

Crystal data for the triphenyl derivative have been reported previously by Wetzel (2), and these dimensions (with the cell reoriented by taking [101] as the new a axis) agree well with the present measurements (Table I). This compound has obviously a rather complex crystal structure, and no further work on it is proposed. We hope, however, to carry out detailed analysis of the *p*-tolyl and *p*-xylyl derivatives. A comparison of the configurations of these molecules will be of some interest, since tri-*p*-xylylarsine has a methyl group ortho to the arsenic, while the *p*-tolyl compound has no ortho substituent.

The author thanks Dr. W. R. Cullen for the crystal samples and helpful discussion, and the National Research Council for financial support.

1. J. Trotter. Can. J. Chem. **40**, 1590 (1962).
2. J. Wetzel. Z. Krist. **104**, 305 (1942).

Received May 17, 1962.
Department of Chemistry,
University of British Columbia,
Vancouver 8, British Columbia.

FORMATION OF KETENEIMINE LINKS IN ACRYLONITRILE POLYMERIZED UNDER FREE RADICAL CONDITIONS*

J. C. Crosthwaite, J. J. McLeskey, III,† and P. Smith‡

Recently it has been shown (1) that polyacrylonitrile prepared by X-ray irradiation of pure liquid acrylonitrile at −78° C contains keteneimine links. On the other hand, acrylonitrile polymerized in bulk at 50° C using benzoyl peroxide as initiator has been reported to give polymer not possessing keteneimine links (2). The object of the present work was to determine whether the formation of keteneimine structures was peculiar to X-ray-initiated polymer by testing whether polyacrylonitrile made using conventional free radical initiation at dry ice – ethanol temperatures could give rise to these structures. The results obtained gave positive evidence for keteneimine link production. Consequently, the tests were extended to higher temperatures, with similar success.

In the case of polymethacrylonitrile formed under free radical conditions, Grassie and McNeill (3) have shown that keteneimine links form mainly via the chain termination step. If this were the case for polyacrylonitrile, these structures would be more readily detected for short-chain polymer. Hence, the experimental conditions of this work were aimed at producing short-chain polymer. Also, because it was thought that the keteneimine link formed by coupling of polyacrylonitrile free radicals in this system

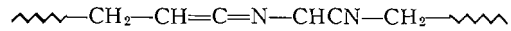

might be unstable towards water, special efforts were made to exclude water from reaction mixtures. As the investigation progressed, it was shown that this precaution was perhaps unimportant.

*Supported by grants from the Esso Research and Engineering Co. and the United States Public Health Service, Division of General Medical Sciences.
†National Defense Education Act Predoctoral Fellow.
‡To whom all correspondence should be addressed.

Crystal data for the triphenyl derivative have been reported previously by Wetzel (2), and these dimensions (with the cell reoriented by taking [101] as the new a axis) agree well with the present measurements (Table I). This compound has obviously a rather complex crystal structure, and no further work on it is proposed. We hope, however, to carry out detailed analysis of the *p*-tolyl and *p*-xylyl derivatives. A comparison of the configurations of these molecules will be of some interest, since tri-*p*-xylylarsine has a methyl group ortho to the arsenic, while the *p*-tolyl compound has no ortho substituent.

The author thanks Dr. W. R. Cullen for the crystal samples and helpful discussion, and the National Research Council for financial support.

1. J. Trotter. Can. J. Chem. **40**, 1590 (1962).
2. J. Wetzel. Z. Krist. **104**, 305 (1942).

Received May 17, 1962.
Department of Chemistry,
University of British Columbia,
Vancouver 8, British Columbia.

FORMATION OF KETENEIMINE LINKS IN ACRYLONITRILE POLYMERIZED UNDER FREE RADICAL CONDITIONS*

J. C. Crosthwaite, J. J. McLeskey, III,† and P. Smith‡

Recently it has been shown (1) that polyacrylonitrile prepared by X-ray irradiation of pure liquid acrylonitrile at −78° C contains keteneimine links. On the other hand, acrylonitrile polymerized in bulk at 50° C using benzoyl peroxide as initiator has been reported to give polymer not possessing keteneimine links (2). The object of the present work was to determine whether the formation of keteneimine structures was peculiar to X-ray-initiated polymer by testing whether polyacrylonitrile made using conventional free radical initiation at dry ice – ethanol temperatures could give rise to these structures. The results obtained gave positive evidence for keteneimine link production. Consequently, the tests were extended to higher temperatures, with similar success.

In the case of polymethacrylonitrile formed under free radical conditions, Grassie and McNeill (3) have shown that keteneimine links form mainly via the chain termination step. If this were the case for polyacrylonitrile, these structures would be more readily detected for short-chain polymer. Hence, the experimental conditions of this work were aimed at producing short-chain polymer. Also, because it was thought that the keteneimine link formed by coupling of polyacrylonitrile free radicals in this system

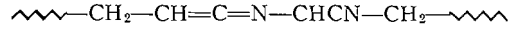

might be unstable towards water, special efforts were made to exclude water from reaction mixtures. As the investigation progressed, it was shown that this precaution was perhaps unimportant.

*Supported by grants from the Esso Research and Engineering Co. and the United States Public Health Service, Division of General Medical Sciences.
†National Defense Education Act Predoctoral Fellow.
‡To whom all correspondence should be addressed.

Initial attempts to polymerize acrylonitrile at dry ice – ethanol temperatures ($-72\pm 2°$ C) by ultraviolet irradiation of undiluted monomer were unsuccessful. The polymerization rate was too slow and insufficient polymer was obtained. With either benzoyl or *t*-butyl peroxide initiators added, the rate was increased sufficiently and the polymer was found in every case to possess the characteristic absorption of keteneimine structures at 4.93 μ (1–6).

In a like fashion, the bulk polymerization of acrylonitrile at $12\pm 2°$ C was carried out using ultraviolet irradiation both alone and with each of the two peroxide initiators mentioned above. No keteneimine links could be detected in the infrared absorption spectra of these polymers. This was attributed to their long chain length. Consequently, the polymerization was repeated with *t*-butyl peroxide as initiator under conditions similar to those above except that the monomer was made 1 *M* by dilution, in one case, with *n*-heptane and, in another, with methanol containing ca. 6–7% v/v water. In both experiments the polymer again showed an absorption at 4.93 μ.

Finally, to test the formation of keteneimine links at still higher temperatures, a 0.2 *M* solution of the monomer in absolute methanol with *t*-butyl peroxide as initiator was irradiated at $50\pm 2°$ C. Again, the polymer produced was found to possess the characteristic keteneimine absorption at 4.93 μ. A summary of all polymerizations may be found in Table I.

TABLE I

Summary of polymerization runs*

Run	[Monomer], *M*	Solvent	Initiator†	[Init.] $\times 10^2$, M	Temp., °C	Irrad. time,‡ hr
1	Bulk	None	None	—	−72	16
2	Bulk	None	A	0.5	−72	6
3	Bulk	None	A	3	−72	7
4	Bulk	None	B	9	−72	11
5§	Bulk	None	None	—‖	12	0.5
6	Bulk	None	A	0.6	12	0.4
7	Bulk	None	B	7	12	0.4
8	1.0	*n*-Heptane	B	7	12	0.3
9	1.0	Methanol¶	B	7	12	0.3
10	0.2	Methanol	B	14	50	1.0

*The polymers containing keteneimine links were tinted yellow when first formed and the color deepened on standing in air. All others appeared white.
†A and B refer to benzoyl peroxide and *t*-butyl peroxide, respectively.
‡The irradiation times correspond to ca. 1–2% conversion, except for run 1, where no polymer was isolated.
§Runs 5, 6, and 7 gave no infrared absorption at 4.93 μ; the others, except run 1 (see ‡), had an absorption peak at this wavelength.
‖The polymer from the prepolymerization runs at room temperature ($25\pm 2°$ C) showed no absorption peak at 4.93 μ.
¶Containing ca. 6–7% v/v water.

The usual tests (3) were run to confirm the presence of keteneimine structures. For details of these, see Experimental. As expected, the results of the tests further confirmed the presence of keteneimine structures in the polymers.

Recent work by Tsuda (7) indicates that a free radical mechanism predominates in the X-ray-induced bulk polymerization of pure liquid acrylonitrile at −78° C, while an anionic mechanism tends to be more important when the polymerization is carried out with dilute solutions of the monomer. The present results suggest that the keteneimine structures formed at −78° C with X-ray initiation may arise via a free radical mechanism, in harmony with the conclusions of Tsuda. Electrical discharges through acrylonitrile monomer also produce keteneimine structures (8). Details of this work are not complete

enough to allow much comment here. Nevertheless, it seems possible that some of the keteneimine structures formed by electrical discharge may also be free radical derived.

This investigation is being continued.

EXPERIMENTAL

The acrylonitrile was Monsanto 200 X grade,* purified by three fractionations from reagent grade P_2O_5, through a 20-plate column, under a nitrogen atmosphere, the middle 80% fraction being collected each time. (This method of collection applied to all fractionations and bulb-to-bulb distillations *in vacuo*.) The monomer from the last fractionation was collected over P_2O_5 and given two simple bulb-to-bulb distillations *in vacuo*. After each distillation, the monomer was prepolymerized to ca. 1% conversion by ultraviolet irradiation at room temperature, n_D^{25} 1.388_6. Benzoyl peroxide, Eastman White Label, was twice recrystallized from chloroform by precipitation with methanol (9). *t*-Butyl peroxide, Wallace and Tierman, Inc., Lucidol Div., 97% min., was given a simple bulb-to-bulb distillation *in vacuo*. *n*-Heptane, Eastman White Label, was washed with C.P. concentrated H_2SO_4, then water, dried over Drierite, fractionated, and finally dried with Linde Molecular Sieves, n_D^{25} 1.326_7. Deionized water (Amberlite MB-3) was used for the aqueous polymerization. Dimethylformamide, Eastman White Label, was given three fractionations from P_2O_5, n_D^{25} 1.427_0. Merck reagent grade chloroform was twice fractionated from P_2O_5. Merck reagent grade ethanol was used without further purification.

All reactions were carried out in cylindrical pyrex tubes, 25-cm length, 2.5-cm o.d., and 1-mm wall thickness, with ca. 30 ml of reaction mixture. For the irradiations at $-72\pm2°$ C the reaction vessel was immersed in a dry ice – ethanol mixture in an unsilvered pyrex dewar surrounded by a pyrex water jacket containing tap water. The ultraviolet radiation was provided by two B.T.H. Mazda Type ME/D 250-watt mercury vapor compact sources of the rectangular-box variety set side by side and aimed at the reaction mixture 10 ± 1 cm away. They were run with the supplied glass windows removed. However, there was still approximately 6 mm of pyrex in the light path. For the polymerizations at 12 and 50° C, the reaction vessel was placed in the water jacket alone and located 3.5 ± 0.5 cm from the lamps. Because the dewar was omitted, a total of only ca. 4 mm of pyrex remained in the light path. The prepolymerization runs described above were carried out following a procedure similar to that used for those at 12 and 50° C.

Since the effect of solvents on the anticipated keteneimine structures was not known, the first infrared spectra were obtained from polymers which had been freed of excess monomer by evacuation on a high-vacuum line. Later it was found that washing with methanol did not destroy keteneimine structures, but did dissolve some of the short-chain polymer. Consequently, all polymers were dried *in vacuo* and left unwashed. The infrared spectra were obtained in KBr disks on a Perkin–Elmer Model 21 double-beam spectrophotometer with sodium chloride optics.

The existence of keteneimine structures in the polymer was further investigated by the following tests. Heating *in vacuo* for 3 hours at $103\pm3°$ C caused a significant reduction in the infrared absorption at 4.93 μ. After 18 hours, the peak had completely disappeared. Treatment with methanol, water, or dilute aqueous HCl caused no detectable change in the 4.93-μ peak. This is not surprising since the polymer is insoluble in these reagents. However, when dissolved in dimethylformamide made 0.1 *M* in HCl by the addition of sufficient 6 *M* aqueous HCl, and heated *in vacuo* for 5 hours at $100\pm2°$ C, infrared absorption showed no indication of keteneimine structures. The action of chlorine on a dimethylformamide solution of the polymer again destroyed the absorption at 4.93 μ. The results of these tests are in agreement with those obtained for keteneimine structures in polymethacrylonitrile (3).

1. C. S. H. Chen, N. Colthup, W. Deichert, and R. L. Webb. J. Polymer Sci. **45**, 247 (1960).
2. M. Talât-Erben and S. Bywater. Ricerca sci. A, **25**, 11 (1955).
3. N. Grassie and I. C. McNeill. J. Polymer Sci. **33**, 171 (1958).
4. C. L. Stevens and J. C. French. J. Am. Chem. Soc. **76**, 4398 (1954).
5. R. Dijkstra and H. J. Backer. Rec. trav. chim. **73**, 575 (1954).
6. C. L. Stevens and J. C. French. J. Am. Chem. Soc. **75**, 657 (1953).
7. Y. Tsuda. J. Polymer Sci. **54**, 193 (1961).
8. W. G. Deichert and M. C. Tobin. J. Polymer Sci. **54**, S39 (1961).
9. K. Nozaki and P. D. Bartlett. J. Am. Chem. Soc. **68**, 1686 (1946).

Received May 7, 1962.
Department of Chemistry,
Duke University,
Durham, N.C., U.S.A.

Kindly provided by Dr. L. H. Peebles, The Chemstrand Corporation.

SYNTHESIS AND PHYSIOLOGICAL PROPERTIES OF 9-HYDROXY-2-DECENOIC ACID

Wm. H. Brown,[1] Ethel E. Felauer,[1] and M. V. Smith[2]

It has been recently reported by Brown and Felauer (1) that small amounts of 9-hydroxy-2-decenoic acid (VI) are present in the mixture of carboxylic acids isolated from royal jelly by the procedure described by Brown and Freure (2). It was of interest to synthesize the acid and determine its physiological properties since it is closely related to 9-keto-2-decenoic acid (VII). The latter acid is known as "queen substance" and has interesting effects on the behavior of worker bees (3). Several methods of synthesis for VII have been reported, the most recent by Kennedy *et al.* (4).

Our method of synthesis of (VI) is shown in the following scheme:

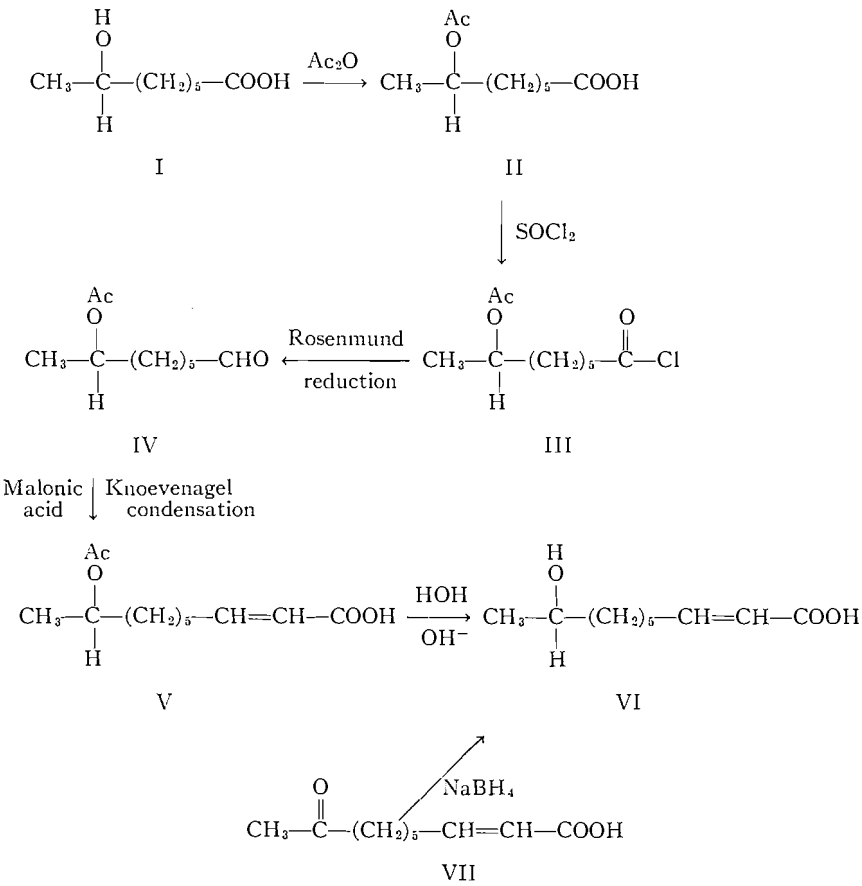

The 7-hydroxyoctanoic acid (I) was prepared by the method of Lease and McElvain (5). Since both 9-acetoxy-2-decenoic acid (V) and 9-hydroxy-2-decenoic acid (VI) are liquids which do not crystallize, a solid derivative, the *p*-bromophenacyl ester of VI, was

[1]*Department of Chemistry, Ontario Agricultural College.*
[2]*Department of Apiculture, Ontario Agricultural College.*

prepared. The latter was shown to be identical with the same derivative of authentic VI prepared by sodium borohydride reduction of 9-keto-2-decenoic acid (VII). The iodoform test is given readily by VI, which is contrary to the findings of Barbier and Hügel (6).

EXPERIMENTAL

Melting points are corrected. Infrared data were determined on a Beckman IR5 instrument and ultraviolet data on a Bausch and Lomb Spectronic 505.

9-Hydroxy-2-decenoic Acid (VI) and p-Bromophenacyl Ester

Saponification of 0.3 g of 9-acetoxy-2-decenoic acid (V) with 10% aqueous sodium hydroxide solution gave 0.2 g of crude VI, a liquid which did not crystallize. After chromatography on Whatman seed test paper using propanol-1 – ammonia (70:30) as the developing solvent (R_f 0.73 at 25°) the compound still failed to crystallize. The ultraviolet spectrum showed that the compound is unsaturated. The infrared spectrum showed bands for unsaturation and free hydroxyl group. The iodoform test was positive.

Treatment of VI with *p*-bromophenacyl bromide by the usual procedure gave the ester, white needles from hexane (150 ml/g), m.p. 73–74°. Anal. Calc. for $C_{18}H_{23}BrO_4$ (383.28): C, 56.4; H, 6.05; Br, 20.8. Found: C, 56.4; H, 6.08; Br, 21.0.

Physiological Activity

The bioassay method described by Butler and Gibbons (7) was used. The acid (VI) was supplied to 10 cages of test bees by dissolving 10 mg of the compound in 2 ml of acetone and dipping the dead bodies of worker bees in this solution. Two bee bodies, so treated, were placed in each cage. The 10 control cages all built queen cells but results with the acid were extremely variable, i.e., in some cages queen cells were constructed while in others they were not. Repeated tests and doubling of the amount of acid presented to the bees gave no clear-cut differences.

Presentation of the acid on filter paper to cages of young bees according to the method of Pain (8) gave no indication that it has any attractiveness to the bees.

Results of the evaluation of the antitumor activity of 9-hydroxy-2-decenoic acid (VI) will be reported in the series "Studies on the in vitro antitumor activity of fatty acids", of which the fourth paper appeared recently (9).

ACKNOWLEDGMENTS

The studies herein described were carried out in connection with projects supported by the National Cancer Institute of Canada, whose financial assistance is gratefully acknowledged.

We are indebted to Dr. R. K. Callow of the National Institute for Medical Research, London, England, for providing a sample of authentic 9-keto-2-decenoic acid. DuPont of Canada Limited supplied a generous amount of adipic acid.

1. W. H. Brown and E. E. Felauer. Nature, **190**, 88 (1961).
2. W. H. Brown and R. J. Freure. Can. J. Chem. **37**, 2042 (1959).
3. C. G. Butler. The world of the honeybee. Collins, London. 1954; Bee World, **40**, 269 (1959); Experientia, **16**, 424 (1960); Endeavour, **77**, 5 (1961).
4. J. Kennedy, N. J. McCorkindale, and R. A. Raphael. J. Chem. Soc. 3813 (1961).
5. E. J. Lease and S. M. McElvain. J. Am. Chem. Soc. **55**, 807 (1933).
6. M. Barbier and M.-F. Hügel. Bull. soc. chim. France, 951 (1961).
7. C. G. Butler and D. A. Gibbons. J. Insect Physiol. **2**, 61 (1958).
8. J. Pain. Institute National de la Recherche Agr. Serie A. No. 3674. 1961.
9. G. F. Townsend, W. H. Brown, E. E. Felauer, and B. Hazlett. Can. J. Biochem. Physiol. **39**, 1765 (1961).

Received January 19, 1962.
Departments of Chemistry and Apiculture,
Ontario Agricultural College,
Guelph, Ontario.

THE ELECTRON SPIN RESONANCE OF NON-ALTERNANT AROMATIC HYDROCARBON – IODINE COMPLEXES[1]

S. S. DANYLUK[2] AND W. G. SCHNEIDER

The electron spin resonance (e.s.r.) spectra have been reported recently for a number of molecular complexes of iodine with a variety of electron donors (1–3). Matsunaga (1) and Kommandeur and Singer (3) have observed e.s.r. in polycyclic alternant aromatic hydrocarbon – iodine complexes and Kommandeur and co-workers (3, 4) have shown a correlation between electron spin concentration and charge carrier concentration in electronic conduction for these complexes. Recently Kommandeur (5) reported hyperfine structure in the e.s.r. spectrum for a dilute solution of perylene in molten iodine. In this note we report the e.s.r. measurements for iodine complexes formed with the non-alternant aromatic hydrocarbons azulene, guaiazulene, and acepleiadylene.

The complexes were prepared by refluxing equimolar amounts of the hydrocarbon and iodine in oxygen-free benzene under an inert atmosphere for several hours. A deep blue-black precipitate was formed in each case, and after treatment with excess benzene to remove unreacted material the solids were analyzed for iodine composition. The analyses confirmed a 1:1 stoichiometry for each complex: azulene–iodine, calc. for $C_{10}H_8.I_2$: 66.3%, found: 66.1%; guaiazulene–iodine, calc. for $C_{15}H_{18}.I_2$: 56.1%, found: 54.8%; acepleiadylene–iodine, calc. for $C_{16}H_{10}.I_2$: 55.7%, found: 55.2%.

An X-ray examination[3] of the complexes showed the azulene.I_2 complex to be mainly amorphous while the acepleiadylene.I_2 complex was crystalline. All of the complexes decomposed when heated above 120° C in sealed tubes.

The e.s.r. spectra were measured with a Varian 4500 spectrometer equipped with 100 kc/s modulation. Polycrystalline samples of the complexes were examined in sealed quartz tubes. The line widths and g values were determined by calibration of the spectra with signals from diphenylpicrylhydrazyl and a single crystal of MgO doped with Cr^{+3} (6). Electron spin concentrations were measured by comparison of the integrated signals for the complex with the signal for a known standard D.P.P.H. sample. The results for these measurements are listed in Table I. Preliminary measurements of the spin concentration for the azulene.I_2 at low temperatures showed no appreciable change from the room temperature value.

TABLE I

E.S.R. spectra of non-alternant hydrocarbon–iodine molecular complexes

Complex	Number of spins per gram	g value	Line width (gauss)
Azulene.I_2 (1:1)	2.2×10^{19}	2.0039 ± 0.0002	13.9 ± 0.3
Acepleiadylene.I_2 (1:1)	1.3×10^{19}	2.0034 ± 0.0002	4.9 ± 0.2
Guaiazulene.I_2 (1:1)	2.5×10^{17}	2.0030 ± 0.0002	10.3 ± 0.3

A single relatively broad e.s.r. signal with a g value close to the free electron value was noted for each complex, confirming the presence of unpaired electron spins in these

[1]*Issued as N.R.C. No. 7008.*
[2]*National Research Council Postdoctorate Fellow 1958–60.*
[3]*We are indebted to Dr. A. Hansen for carrying out these examinations.*

systems. No hyperfine splitting was resolvable for the solids under the present conditions. The paramagnetic species present in these complexes are very probably aromatic radical ions, Ar^+, formed by electron transfer from the hydrocarbon to iodine in a charge-transfer reaction:

$$Ar + I_2 \rightarrow Ar^+I_2^-.$$

Evidence supporting the existence of aromatic radical ions in related systems has been reported recently (5). A marked similarity was noted between the e.s.r. spectra for perylene in molten iodine and sulphuric acid, indicating the presence of monopositive ions in the former solution.

Comparison of the line widths in Table I shows that the line width of the acepleiadylene. I_2 complex is considerably narrower than the line widths for the azulene complexes, and is close to the value observed for the isomeric pyrene–iodine complexes (3). No correlation between line widths and spin concentrations is apparent at room temperature and accordingly the line broadening is not primarily attributable to pure dipolar broadening. It is likely that an electron-exchange process between the radical ions and neutral molecules, similar to that proposed for the perylene–iodine complex (5), is the predominant cause of line broadening in the non-alternant complexes.

The spin concentrations for the azulene– and acepleiadylene–iodine complexes are of the same order of magnitude as observed in alternant hydrocarbon–iodine systems. However, a 100-fold decrease in spin concentration is noted for the guaiazulene complex. The lower spin concentration in this case could result from steric hindrance of the alkyl groups on the five- and seven-membered rings to complex formation with iodine.

1. Y. Matsunaga. J. Chem. Phys. **30**, 855 (1959).
2. H. M. Buck, J. H. Lupinski, and L. J. Oosterhoff. Mol. Phys. **1**, 196 (1958).
3. L. S. Singer and J. Kommandeur. J. Chem. Phys. **34**, 133 (1961).
4. J. Kommandeur and F. R. Hall. J. Chem. Phys. **34**, 129 (1961).
5. J. Kommandeur. Mol. Phys. **4**, 509 (1961).
6. W. Low. Phys. Rev. **105**, 801 (1957).

Received April 29, 1962.
Division of Pure Chemistry,
National Research Council,
Ottawa, Canada.

THE DE-*O*-ACETYLATION OF ACETYLATED AMINO SUGARS*

D. R. Whitaker, M. E. Tate,† and C. T. Bishop

In the course of attempts to prepare oligosaccharides of *N*-acetyl-D-glucosamine (2-deoxy-2-acetamido-D-glucose) by acetolysis of chitin, substantial amounts of products with R_f values greater than *N*-acetyl-D-glucosamine were found on chromatograms of the de-*O*-acetylated products. A similar experience has been reported by Barker *et al.* (1). As it seemed likely that these products would interfere with the isolation, in pure form, of the oligosaccharides of *N*-acetyl-D-glucosamine, the nature and source of these products was investigated to determine whether their occurrence could be prevented.

*Issued as N.R.C. No. 6921.
†*National Research Council Postdoctorate Fellow 1960–1962.*

systems. No hyperfine splitting was resolvable for the solids under the present conditions. The paramagnetic species present in these complexes are very probably aromatic radical ions, Ar^+, formed by electron transfer from the hydrocarbon to iodine in a charge-transfer reaction:

$$Ar + I_2 \rightarrow Ar^+I_2^-.$$

Evidence supporting the existence of aromatic radical ions in related systems has been reported recently (5). A marked similarity was noted between the e.s.r. spectra for perylene in molten iodine and sulphuric acid, indicating the presence of monopositive ions in the former solution.

Comparison of the line widths in Table I shows that the line width of the acepleiadylene. I_2 complex is considerably narrower than the line widths for the azulene complexes, and is close to the value observed for the isomeric pyrene–iodine complexes (3). No correlation between line widths and spin concentrations is apparent at room temperature and accordingly the line broadening is not primarily attributable to pure dipolar broadening. It is likely that an electron-exchange process between the radical ions and neutral molecules, similar to that proposed for the perylene–iodine complex (5), is the predominant cause of line broadening in the non-alternant complexes.

The spin concentrations for the azulene– and acepleiadylene–iodine complexes are of the same order of magnitude as observed in alternant hydrocarbon–iodine systems. However, a 100-fold decrease in spin concentration is noted for the guaiazulene complex. The lower spin concentration in this case could result from steric hindrance of the alkyl groups on the five- and seven-membered rings to complex formation with iodine.

1. Y. Matsunaga. J. Chem. Phys. **30**, 855 (1959).
2. H. M. Buck, J. H. Lupinski, and L. J. Oosterhoff. Mol. Phys. **1**, 196 (1958).
3. L. S. Singer and J. Kommandeur. J. Chem. Phys. **34**, 133 (1961).
4. J. Kommandeur and F. R. Hall. J. Chem. Phys. **34**, 129 (1961).
5. J. Kommandeur. Mol. Phys. **4**, 509 (1961).
6. W. Low. Phys. Rev. **105**, 801 (1957).

Received April 29, 1962.
Division of Pure Chemistry,
National Research Council,
Ottawa, Canada.

THE DE-*O*-ACETYLATION OF ACETYLATED AMINO SUGARS*

D. R. Whitaker, M. E. Tate,† and C. T. Bishop

In the course of attempts to prepare oligosaccharides of *N*-acetyl-D-glucosamine (2-deoxy-2-acetamido-D-glucose) by acetolysis of chitin, substantial amounts of products with R_f values greater than *N*-acetyl-D-glucosamine were found on chromatograms of the de-*O*-acetylated products. A similar experience has been reported by Barker *et al.* (1). As it seemed likely that these products would interfere with the isolation, in pure form, of the oligosaccharides of *N*-acetyl-D-glucosamine, the nature and source of these products was investigated to determine whether their occurrence could be prevented.

Issued as N.R.C. No. 6921.
†*National Research Council Postdoctorate Fellow 1960–1962.*

Reaction of *N*-acetyl-D-glucosamine or of α-D-glucosamine pentaacetate with 0.5 *N* sodium methoxide in methanol yielded substantial amounts of the unknown products. Hence these products were artifacts produced during the de-*O*-acetylation rather than during the acetolysis.

The major artifact had chromatographic mobility relative to *N*-acetyl-D-glucosamine (R_{NAG}) of 1.85; minor components of R_{NAG} 2.81 and 3.22 were found under some conditions of de-*O*-acetylation. Barker *et al.* (1) report R_{NAG} 1.87 for the major artifact found in their experiments. The component with R_{NAG} 1.85 gave a positive reaction with silver nitrate – alkali sprays (2) and negative reactions with *p*-anisidine hydrochloride

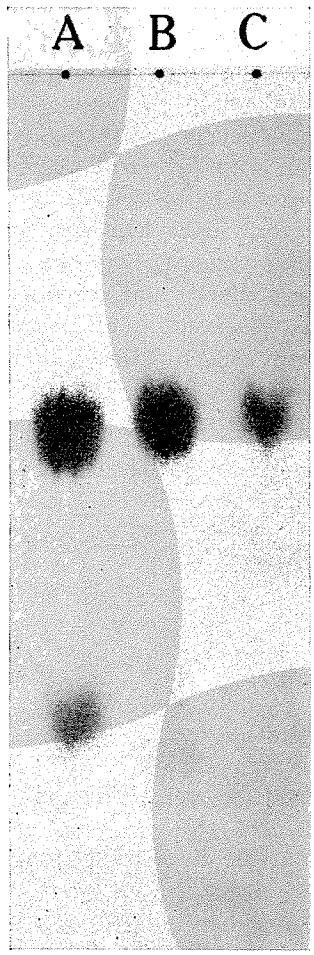

FIG. 1. Paper chromatogram of (A) de-*O*-acetylation of α-D-glucosamine pentaacetate by sodium methoxide; (B) de-*O*-acetylation of α-D-glucosamine pentaacetate by magnesium methoxide; (C) *N*-acetyl-D-glucosamine.

(3) and ferric hydroxamate (4) spray reagents. These results showed that the compound was polyhydroxylated, contained no aldehyde or hemiacetal groups, and was devoid of *O*-acetyl groups. The major artifact gave an immediate, intense, positive reaction when sprayed with an acidic solution of *p*-dimethylaminobenzaldehyde (Ehrlich reagent (5)) without prior spraying with alkali; under the same conditions *N*-acetyl-D-glucosamine gave no reaction. This result indicated that the artifact was the chromogenic

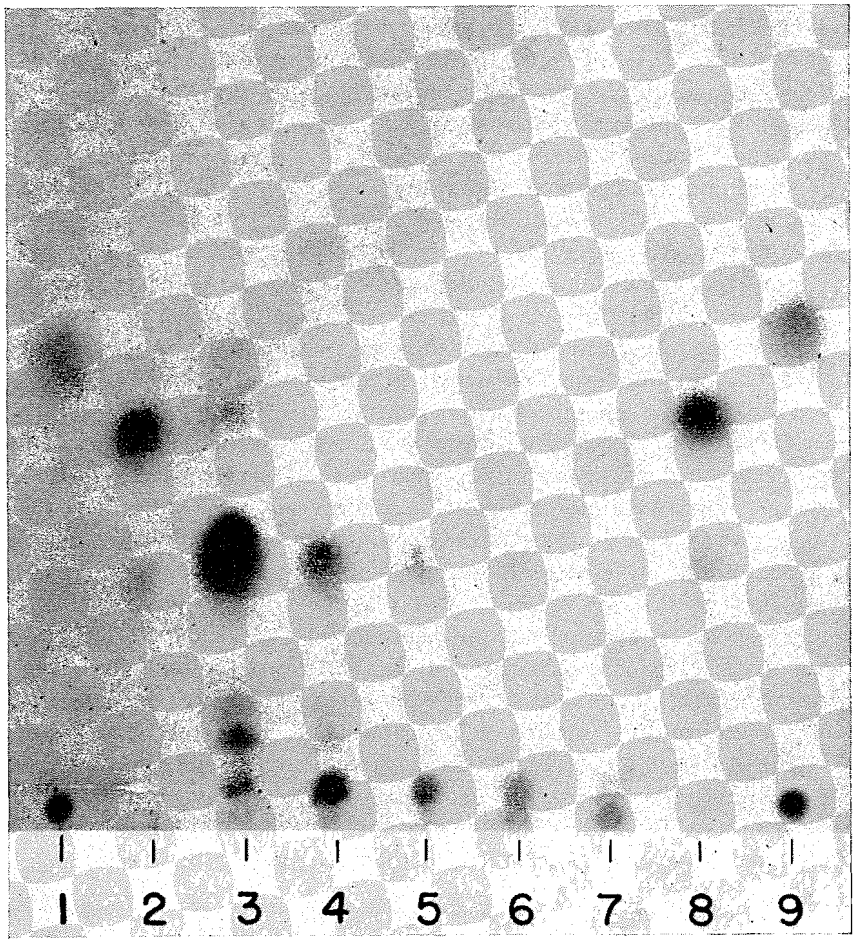

FIG. 2. Thin-layer chromatogram of de-*O*-acetylation of α-D-glucosamine pentaacetate by 1% magnesium methoxide at 0° C. (3) 1 minute; (4) 5 minutes; (5) 10 minutes; (6) 30 minutes; (7) 60 minutes; (1 and 9) marker dyes; (2 and 8) α-D-glucosamine pentaacetate.

material which is formed during the alkaline treatment of *N*-acetylhexosamines in the Morgan–Elson test (6). Three Ehrlich-positive chromogens can be obtained from *N*-acetyl-D-glucosamine depending on the conditions of alkaline treatment (7). The only one of these to be characterized, 3-acetamido-5-(1,2-dihydroxyethyl)furan, is formed at high temperatures (100° C) (8). The artifact in the present work was produced during de-*O*-acetylation of hexosamine acetates, which was carried out at room temperature (25° C) or lower, and therefore was probably one of the chromogens which has not yet been characterized. The minor artifacts of R_{NAG} 2.81 and 3.22 gave positive tests with both acidic *p*-dimethylaminobenzaldehyde and ferric hydroxamate sprays, indicating that they were probably *O*-acetyl derivatives of the major artifact.

Conditions were sought for de-*O*-acetylation which would minimize or prevent the formation of these artifacts. Reaction of α-D-glucosamine pentaacetate or of *N*-acetyl-D-glucosamine with the following reagents in methanol gave substantial yields of the major artifact under a variety of conditions of concentration, temperature, and time (see Experimental): sodium methoxide, barium methoxide, potassium hydroxide, and dry ammonia. A typical result is shown in Fig. 1,A.

The formation of artifact was least when magnesium methoxide in methanol was employed as a de-*O*-acetylating agent. Investigation of conditions showed that a high concentration of magnesium methoxide in methanol at low temperatures and for a short reaction time gave a smooth de-*O*-acetylation of α-D-glucosamine pentaacetate with practically no production of artifact; this is shown in Fig. 1,B. Apparently, the Ehrlich-positive chromogen is produced from acetylated hexosamines by only the slightest trace of hydroxyl ion. It is very difficult to keep the de-*O*-acetylation reactions absolutely anhydrous and any water in the system would yield hydroxyl ion with most de-*O*-acetylating agents. However, magnesium methoxide would tend to maintain anhydrous conditions and any hydroxyl ion formed would be removed from the reaction as insoluble magnesium hydroxide. Magnesium methoxide in methanol is therefore the preferred reagent for de-*O*-acetylation of alkali-sensitive compounds.

The de-*O*-acetylation of α-D-glucosamine pentaacetate by 1% magnesium methoxide in methanol at 0° C was followed by thin-layer chromatography (9). The results, Fig. 2, showed that the reaction was very rapid; most of the pentaacetate was converted into a tetraacetate in 1 minute and no pentaacetate was present after 5 minutes. The amounts of *O*-acetyl derivatives then decreased gradually until, at the end of 1 hour, only traces of ferric-hydroxamate-positive material were present. Figure 1,B shows the paper chromatogram of this de-*O*-acetylation reaction after 1 hour.

The reference spots of α-D-glucosamine pentaacetate, 2 and 8, Fig. 2, showed small amounts of a material which corresponded to the major product from the 1-minute de-*O*-acetylation (3, Fig. 2). These samples of α-D-glucosamine pentaacetate had been dissolved in magnesium-dried methanol for application to the chromatographic plates. The lability of the acetate groups together with the subsequent rearrangements of the glucosamine molecule emphasizes the need for care in the purification of hydroxylic solvents. Basic impurities such as magnesium methoxide or amines can be removed from alcohols by distillation from 2,4,6-trinitrobenzoic acid (10, p. 168).

EXPERIMENTAL

Materials

N-Acetyl-D-glucosamine (2-deoxy-2-acetamido-D-glucose) was a commercial product obtained from the California Corporation for Biochemical Research. α-D-Glucosamine pentaacetate, m.p. 133–134° C, $[\alpha]_D^{25}$ +84.3±2° (*c*, 1.21% in chloroform), was isolated from an acetylation of D-glucosamine hydrochloride with acetic anhydride and sodium acetate (11) by repeated recrystallization from ether. Methanol was refluxed with magnesium and distilled through a 2-ft column (10, p. 169). Paper chromatograms were run by the descending method using a solvent system of butan-1-ol:ethanol:concentrated ammonium hydroxide:water —40:10:1:49 (v/v, upper phase). Thin-layer chromatograms were run on silica gel G and were developed twice in an ascending direction with benzene:methanol (9:1, v/v).

De-O-acetylations

To solutions (2%) of *N*-acetyl-D-glucosamine and of α-D-glucosamine pentaacetate were added the de-*O*-acetylating reagents under conditions of temperature and reagent concentration given below. At the times indicated samples were removed for examination by paper chromatography (silver nitrate – alkali spray reagent). All samples showed varying but substantial amounts of the major artifact (R_{NAG} 1.85) and

Reagent	Concentration (*N*)	Temperature (°C)	Time (hr)
Sodium methoxide	0.24	0	1
	0.01	25	2, 5, 22
	0.0007	25	20
Barium methoxide	0.25	25	1, 5, 24
	0.01	5	20
Potassium hydroxide	0.25	25	20
Ammonia	2	25	2, 5, 16

the chromatogram shown in Fig. 1A was typical. The minor artifacts of R_{NAG} 2.81 and 3.22 were more pronounced in the samples taken at early times. No differences were found when the samples were acidified with acetic acid, diluted with water, and deionized by Amberlites IR-120 and IR-45 exchange resins before chromatography.

Magnesium methoxide was added to a 2% solution of α-D-glucosamine pentaacetate in dry methanol under the following conditions: (1) 1% at 0° C; (2) 0.01% at 0° C; (3) 1% at 28° C; (4) 0.01% at 28° C. At 1, 5, and 24 hours samples were removed from each of these solutions for examination by paper chromatography. The major artifact (R_{NAG} 1.85) was present under conditions 2, 3, and 4 but in smaller amounts than in the previous de-*O*-acetylations. Under the first condition (1% magnesium methoxide at 0° C) there was only a trace of the major artifact after 1 hour (Fig. 1B), the amount increasing in the samples taken at 5 and 24 hours. It was apparent that the optimum conditions for de-*O*-acetylation of acetylated hexosamines were a high concentration of magnesium methoxide at low temperatures for a short time.

De-*O*-acetylation of α-D-glucosamine pentaacetate under condition 1, given above, was followed by thin-layer chromatography (Fig. 2); the results showed the reaction to be complete in 1 hour.

ACKNOWLEDGMENT

The authors gratefully acknowledge the technical assistance of Mrs. Barbara Potvin.

1. S. A. BARKER, A. B. FOSTER, M. STACEY, and J. M. WEBBER. J. Chem. Soc. 2218 (1958).
2. W. E. TREVELYAN, D. P. PROCTER, and J. S. HARRISON. Nature, **166**, 444 (1950).
3. L. HOUGH, J. K. N. JONES, and W. H. WADMAN. J. Chem. Soc. 1702 (1950).
4. M. ABDEL-AKHER and F. SMITH. J. Am. Chem. Soc. **73**, 5859 (1951).
5. P. EHRLICH. Deut. med. Wochschr. **15**, 434 (1901).
6. W. T. J. MORGAN and L. A. ELSON. Biochem. J. **28**, 988 (1934).
7. R. KUHN and G. KRÜGER. Chem. Ber. **89**, 1473 (1956).
8. R. KUHN and G. KRÜGER. Chem. Ber. **90**, 264 (1957).
9. M. E. TATE and C. T. BISHOP. Can. J. Chem. **40**, 1043 (1962).
10. A. I. VOGEL. Practical organic chemistry. Longmans Green and Co., New York. 1956.
11. C. A. LOBRY DE BRUYN and W. ALBERDA VAN EKENSTEIN. Rec. trav. chim. **18**, 77 (1899).

RECEIVED MAY 11, 1962.
DIVISION OF APPLIED BIOLOGY,
NATIONAL RESEARCH COUNCIL OF CANADA,
OTTAWA, CANADA.

Canadian Journal of Chemistry

Issued by THE NATIONAL RESEARCH COUNCIL OF CANADA

VOLUME 40 OCTOBER 1962 NUMBER 10

THE STUDY OF HYDROGEN BONDING AND RELATED PHENOMENA BY SPECTROSCOPIC METHODS

PART VII. INTRAMOLECULAR HYDROGEN BONDING AND STERIC INTERACTIONS IN *o*-NITROBENZALDEHYDE AND RELATED COMPOUNDS[1]

W. F. FORBES[2]

Division of Protein Chemistry, Wool Research Laboratories, C.S.I.R.O., Parkville, N2, Victoria, Australia

Received January 22, 1962

ABSTRACT

Certain unusual features in the infrared spectra of *o*-nitrobenzaldehyde have been interpreted either in terms of an intramolecular hydrogen bond or in terms of steric interactions. As an extension of these studies we have investigated the ultraviolet, infrared, and n.m.r. spectra of *o*-nitrobenzaldehyde and of suitable reference compounds and have re-examined the available other evidence. It is concluded that the observed spectral changes can best be explained in terms of steric interactions rather than in terms of intramolecular hydrogen bonding.

INTRODUCTION

In 1955 Pinchas proposed that the increased infrared frequency of the aldehyde C—H stretching band in *o*-nitrobenzaldehyde (I) and related compounds may be explained by the formation of an intramolecular hydrogen bond as shown in I*a* (1, 2). West and

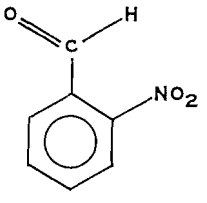

I

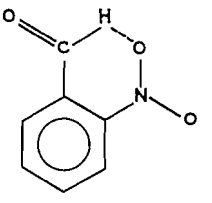

Ia

Whatley (3) criticized this interpretation because the infrared N—O stretching frequency is similar for the three isomeric nitrobenzaldehydes (i.e., the frequency is not appreciably lowered in the *o*-isomer), and they proposed instead that the effect results from steric interactions. That is, they supposed that the presence of bulky *o*-substituents forces the aldehyde group out of the preferred configuration coplanar with the aromatic ring. Pinchas (4) has criticized this steric interpretation because he maintains that the arguments against the formation of an intramolecular hydrogen bond are not convincing, and he, moreover, puts forward a number of arguments against the steric hypothesis.

[1]*Part VI: Can. J. Chem.* **38**, *1852 (1960).*
[2]*Present address: Chemistry Department, University of Waterloo, Waterloo, Ontario.*

Since ultraviolet and n.m.r. spectra can also provide information concerning intramolecular hydrogen bonding, we have determined the relevant spectra. We have also redetermined the infrared spectra of the nitrobenzaldehydes together with the infrared spectra of a number of reference compounds. The purpose of the present paper is to rediscuss the intramolecular interactions in *o*-nitrobenzaldehyde in the light of this additional information.*

EXPERIMENTAL

The infrared spectra were determined on a Beckman Model IR 7 spectrophotometer, calibrated against a polystyrene film, using a NaCl prism and a diffraction grating. The frequency accuracy in the 1700-cm^{-1} region is believed to be ± 2.0 cm^{-1} and the frequency reproducibility ± 0.5 cm^{-1}. Solutions were examined in 0.5- or 0.2-mm cells equipped with sodium chloride windows. The solute concentration was ca. 10^{-3} mole/l. Infrared data are shown in Tables I, II, and III and in Fig. 1.

The ultraviolet spectra were determined by standard methods in matched 1-cm silica quartz cells using both a Beckman DK 2 spectrophotometer and a Unicam SP 500 spectrophotometer calibrated against a didymium filter and solutions of potassium chromate and potassium nitrate. Wavelength readings obtained on the two instruments were found to be within 1 $m\mu$ of each other. The accuracy of λ_{max} values is estimated to be ± 1 $m\mu$, and the precision of molar absorptivities $\pm 5\%$ or better. Most molar absorptivity values were reproducible to $\pm 2\%$. Data are given in Table IV and Fig. 2.

Nuclear magnetic resonance data were determined by means of a 33-Mc spectrometer equipped with a Varian magnetic flux superstabilizer. Measurements were carried out in carbon tetrachloride solutions using tetramethylsilane as an internal indicator. Shift measurements were usually reproducible to within ± 1 cycle/sec.

The compounds examined were commercial samples purified by recrystallization until their melting points indicated that the samples were pure. Sample purity was also sometimes confirmed by vapor phase chromatography. The solvents used were commercially available spectroanalyzed solvents (Fisher).

THE SPECTRA OF *o*-NITROBENZALDEHYDE AND RELATED COMPOUNDS

A. Infrared Spectra

The infrared carbonyl band of *o*-nitrobenzaldehyde in carbon tetrachloride is structureless and does not show a doublet or shoulder such as might be expected if the molecule were to exist in two conformations with the NO_2 and C=O groups being either cis or trans with respect to each other (cf. ref. 5). The infrared carbonyl bands of *o*-nitrobenzaldehyde and reference compounds are listed in Fig. 1 and Table I. Although the carbonyl band doublet shown in Fig. 1 and Table I for *m*-nitrobenzaldehyde may be caused by factors other than *s*-cis, *s*-trans isomerism, the *absence* of fine structure in the carbonyl band of *o*-nitrobenzaldehyde indicates that *o*-nitrobenzaldehyde exists predominantly in only *one* form; this is probably a structure like I, in which the C=O and NO_2 groups are approximately trans with respect to each other, or more precisely a gauche form in which the substituent groups are twisted out of the plane of the benzene ring.

Next, the N—O stretching frequencies, as noted by West and Whatley (3), are not lowered in the *o*-isomer compared with the same band in the *p*-isomer. The relevant data are listed in Table II. West and Whatley deduce from the symmetrical stretching band data that no hydrogen bonding to the nitro group occurs in *o*-nitrobenzaldehyde. However, as Pinchas (4) correctly points out, the N—O stretching frequencies sometimes remain approximately constant, even if the nitro group is involved in an intramolecular hydrogen bond (cf. also ref. 6). Our more complete data for the nitrobenzaldehydes and the nitrophenols show that a displacement to lower frequency is observed in the

**Since this paper was submitted for publication, a referee has drawn our attention to the work of P. Coppens (to be published), who has shown, using X-ray crystallographic methods, that (1) the aldehyde group is forced out of the plane of the ring and (2) the oxygen atom of the nitro group is much too distant from the aldehyde hydrogen for hydrogen bonding to take place.*

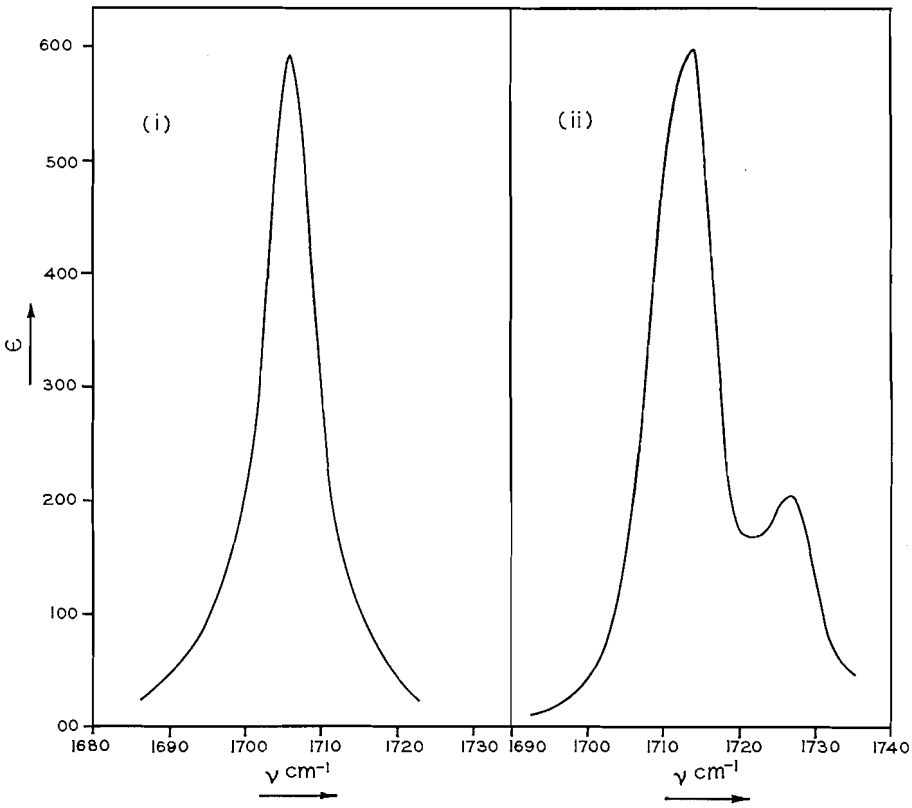

FIG. 1. The infrared C=O stretching bands of (i) *o*-nitrobenzaldehyde and of (ii) *m*-nitrobenzaldehyde in carbon tetrachloride solution.

TABLE I

Carbonyl stretching bands for *o*-nitrobenzaldehyde and reference compounds (carbon tetrachloride solution)

Compound	ν_{max} (cm^{-1})	Apparent molecular extinction coefficient ϵ^{a}_{max}
o-Nitrobenzaldehyde	1706	600
m-Nitrobenzaldehyde	1727	200
	1714	590
p-Nitrobenzaldehyde	1716	680
o-Nitroacetophenone*	1712	230
m-Nitroacetophenone†	1701	645

*No doublet could be detected for this compound (cf. ref. 5) and the compound was shown to be pure by vapor phase chromatography. The present data should therefore replace those previously reported.

†Jones, Forbes, and Mueller (5), using a Perkin Elmer Model 12 double-pass single-beam spectrometer.

symmetrical N—O stretching band for *o*-nitrophenol, a compound which is believed to contain an intramolecular hydrogen bond (7), but not for *o*-nitrobenzaldehyde. These data therefore indicate the absence of an intramolecular hydrogen bond in *o*-nitrobenzaldehyde.

TABLE II

N—O stretching bands for *o*-nitrobenzaldehyde and reference compounds (carbon tetrachloride solution)

Compound	Nitrobenzaldehydes* ν_{max} (cm^{-1})	Nitrophenols† ν_{max} (cm^{-1})
o-Isomer	1536 (s) 1347 (s) (1340)	1541 (s) (1530) 1332 (s)
m-Isomer	1546 (w) 1353 (vs) (1345)	1537 (vs) (1526) 1355 (vs)
p-Isomer	1538 (w) 1345 (vs) (1336)	1528 (s) (1500) 1346 (vs)

*Data in parentheses by West and Whatley (3).
†Values in parentheses in KBr; data by Franck, Hörmann, and Scheibe (6).

Pinchas in his later paper (4) also associates frequency displacements (to higher frequency) with quinonoid forms of type II and hence this may provide a third cause

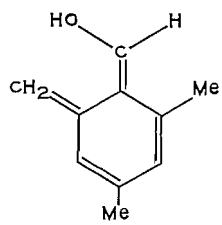

II

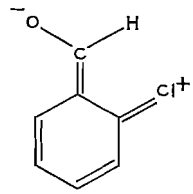

III

for the observed frequency displacement to higher frequency. However, a number of other *p*-substituted benzaldehydes, such as *p*-hydroxy- or *p*-nitro-benzaldehyde (1, 8), do not afford this displacement (although appropriate quinonoid forms can be written) and this points against the hypothesis that such displacements are caused by classical quinonoid forms.* On the other hand, it is possible that a displacement to higher frequency is caused by electrostatic interactions, which can be crudely represented by structures of type III and which are favored by a coplanar arrangement.

One argument against a steric explanation of the spectral displacements (4) is that one would anticipate, when comparing *o*-chloro- and *o*-bromo-benzaldehyde, that an *o*-bromo substituent should cause a greater frequency displacement relative to the C—H bands in benzaldehyde; in fact, *o*-chlorobenzaldehyde affords the greater displacement. However, compounds like *o*-substituted benzaldehydes may exist in *a number of conformations* in which the angle between the plane of the benzene ring and the plane of the formyl group assumes various values because of torsional vibrations across the C—C bond linking the two planar entities. Moreover, infrared data indicate that *o*-chloro- and *o*-bromo-acetophenone exist in both *s*-cis and *s*-trans forms (5) and the infrared carbonyl band of *o*-chlorobenzaldehyde affords a doublet which may indicate an equilibrium of *s*-cis and *s*-trans forms (unpublished information). It follows that other explanations may account for the relatively greater displacement to high frequency observed in *o*-chlorobenzaldehyde. For example, *o*-chlorobenzaldehyde may still be sufficiently coplanar for contributions of type III to be important, while for *o*-bromobenzaldehyde steric interactions

The author is grateful to a referee for drawing his attention to this result.

TABLE III

Principal aldehyde C—H absorption bands for benzaldehydes (carbon tetrachloride solution)

	ν_{max} (cm^{-1})	ν_{max} (cm^{-1})
(*a*) Compounds in which intramolecular hydrogen bonding may occur		
(Benzaldehyde)*	2729	2820
o-Nitrobenzaldehyde* ‡	2753	2888
o-Chlorobenzaldehyde	2754 (2752§)	2868 (2860§)
o-Bromobenzaldehyde†	2751 (2747§)	2868 (2860§)
2-Chloro-3-hydroxybenzaldehyde§	2750	2860
2-Chloro-5-hydroxybenzaldehyde§	2752	2866
2,4-Dichlorobenzaldehyde§	2765	2875
(*b*) Compounds in which steric interactions may displace the formyl group out of the plane of the benzene ring		
(Benzaldehyde)*	2729	2820
o-Chlorobenzaldehyde‡	2754 (2752§)	2868 (2860§)
o-Bromobenzaldehyde†	2751 (2747§)	2868 (2860§)
o-Methylbenzaldehyde	2730	2853‖
2,4,6-Trimethylbenzaldehyde* ¶	2761	2888±10
o-Nitrobenzaldehyde*	2753	2888

*West and Whatley (3).
†These runs were carried out not using high-resolution techniques and the frequency accuracy is therefore believed to be only ca. ±5.0 cm^{-1}.
‡The principal C—H absorption bands of the *m*- and *p*-isomers for most of the substances listed in the table are close to the value given for benzaldehyde.
§Pinchas (2).
‖This band shows some fine structure.
¶Structures of type III and related structures (see text) may also contribute to this displacement since 2,4-dihydroxybenzaldehyde also absorbs at higher frequency (2765 cm^{-1} (2)). An explanation for this latter displacement in terms of a dimeric hydrogen bond seems unlikely since no subsiduary maximal frequencies are evident in the relevant carbonyl band.

may inhibit these contributions and in this way a smaller frequency displacement may be observed for the principal C—H bands. Consequently a steric interpretation of the C—H band data cannot be rejected. Finally, in this discussion of the C—H bands near 2750 and 2850 cm^{-1}, it should be noted that the maximal frequency of infrared stretching bands is *normally lowered* if the relevant band is involved in a hydrogen bond, whereas the frequencies of the above C—H stretching bands are *raised* for the *o*-substituted benzaldehydes under discussion. Therefore such a displacement to higher frequency is inherently more readily interpreted in terms of steric interactions rather than in terms of intramolecular hydrogen bonding, since the latter explanation requires an additional hypothesis (cf. ref. 2).

B. Ultraviolet Spectra

Ultraviolet spectra, on the basis of previously noted generalizations, may contribute in two ways to the problem. First, intensity decreases are generally known to be indicative of steric interactions, and second, solvent changes, on determining ultraviolet spectra in different solvents, are sometimes decreased in the presence of intramolecular hydrogen bonding (see, for example, ref. 7).

Figure 2 shows the ultraviolet spectra of *o*- and *m*-nitrobenzaldehyde in constant-boiling ethanol. The spectral data in a number of solvents are also listed in Table IV. These data show that in both solvents the main absorption bands (indicative of conjugation) are considerably decreased in the *o*-isomer relative to the *m*-isomer, consistent with the explanation that the aldehyde and nitro groups are displaced from the plane of the benzene ring. Further, in intramolecularly hydrogen bonded nitrobenzenes—such as *o*-nitrophenol—the ultraviolet nitrobenzene band is displaced to *longer* wavelength relative to the similar absorption band in the *m*-isomer or other reference compound (7).

However, the ultraviolet absorption data for the nitrobenzaldehydes show (see Table IV) that the *o*-isomer absorbs at *shorter* wavelength than the *m*-isomer, which then again

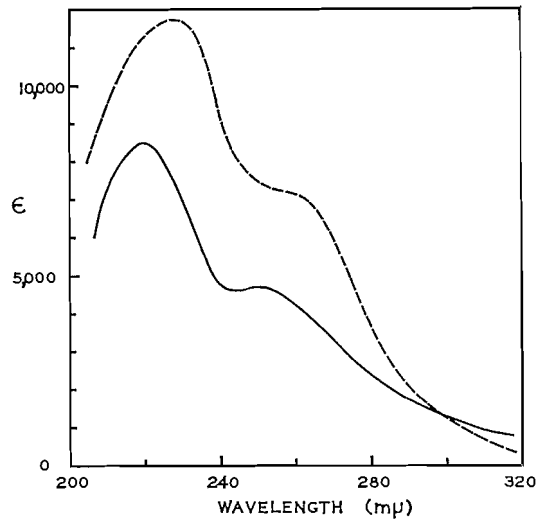

FIG. 2. The ultraviolet absorption spectra of *o*-nitrobenzaldehyde (——) and of *m*-nitrobenzaldehyde (– –) in constant-boiling ethanol (9).

TABLE IV

Main ultraviolet absorption bands of *o*- and *m*-nitrobenzaldehyde in various solvents

		Absorption band associated with benzaldehyde chromophore		Absorption band associated with nitrobenzene chromophore	
Compound	Solvent	λ_{max} (mμ)	ϵ_{max}	λ_{max} (mμ)	ϵ_{max}
o-Nitrobenzaldehyde	Cyclohexane	222	18,000	248	6,500
	Ether	222	18,000	*250*	*6,500*
	Chloroform			253	6,000
	Ethanol	219.5	9,500	252	5,000
	Water	225	12,000	259	5,000
m-Nitrobenzaldehyde	Cyclohexane	227	30,000	ca. *245* ca. *260*	*10,500* *6,000*
	Ether	226.5	26,000	ca. *260*	*6,000*
	Chloroform	242	13,500	ca. *262*	*6,500*
	Ethanol	227	11,000	258.5	7,500
	Water	233	22,000	ca. *266*	*7,000*

indicates steric interactions. Steric interactions between the *C—H* part of the aldehyde group and the ortho substituent are also suggested in compounds like *o*-chlorobenzaldehyde (λ_{max} 246 mμ, ϵ = 11,000; λ_{max} 252 mμ, ϵ = 8,500 (10)), *o*-bromobenzaldehyde (λ_{max} 245.5 mμ, ϵ = 12,500 (11)), *o*-tolualdehyde (λ_{max} 251 mμ, ϵ = 13,000), and 2,6-dimethylbenzaldehyde (λ_{max} 251 mμ, ϵ = 12,500 (12)), by the relatively low ϵ_{max} values of these compounds compared with the ϵ_{max} values of benzaldehyde (ϵ = 14,000 at 241 mμ and ϵ = 12,000 at 247 mμ (11)). (The ϵ_{max} of *o*-chlorobenzaldehyde is less than that of *o*-bromobenzaldehyde but, as previously noted in the discussion of the infrared spectra, a number of explanations can account for this.) Although these absorptivity decreases are

not directly related to steric interactions (since, for example, compounds like *m*-chlorobenzaldehyde in which steric interactions are small also show an absorptivity decrease relative to benzaldehyde), the general lowering of absorptivity observed in the above-mentioned *o*-substituted benzaldehydes, compared with the absorptivity of a number of reference compounds, strongly suggests the presence of some steric interactions. The absence of a direct, quantitative relationship between steric interactions and either ultraviolet absorptivities or infrared C—H frequency shifts is also indicated by the examples of *o*-tolualdehyde and mesitylaldehyde. Both compounds show similar ultraviolet spectra, indicative of steric interactions, but only mesitylaldehyde affords the C—H frequency increase which is also associated qualitatively with steric, though not necessarily with identical steric, interactions.

The data in Table IV also show that *o*-nitrobenzaldehyde does not afford a similar spectrum in various solvents in the same way as has been observed for intramolecularly hydrogen bonded nitrobenzenes such as nitrophenol (7). This then again tends to point against the existence of a strong intramolecular hydrogen bond except that the similarity of the spectra of the *o*-isomer in cyclohexane and ether solution may indicate some interactions between the formyl and nitro groups. Recent ultraviolet data obtained by Lutskii and Alekseeva for different solvents have similarly been interpreted to show the absence of intramolecular hydrogen bonding in *o*-nitrobenzaldehyde (13).

C. N.M.R. Spectra

The n.m.r. spectra of *o*- and *m*-nitrobenzaldehydes showed that in the *o*-isomer the proton signal of the formyl group is displaced by ca. 0.4 ± 0.1 p.p.m. to lower field with respect to this signal in the *m*-isomer. Since in intramolecularly hydrogen bonded compounds this displacement is usually much larger (14), the n.m.r. data also point against the existence of a strong intramolecular hydrogen bond in *o*-nitrobenzaldehyde in carbon tetrachloride solution.

CONCLUDING REMARKS

The spectral data discussed in the previous section favor the explanation that no intramolecular hydrogen bond exists in *o*-nitrobenzaldehyde and that the anomalous spectral effects are caused by steric interactions. It remains to discuss the evidence available from other physical data.

The most important of these is, as mentioned in the Introduction, that recent X-ray crystallographic evidence has in fact established the presence of appreciable steric interactions and the absence of intramolecular hydrogen bonding in *o*-nitrobenzaldehyde. Next, it may be noted that α-phthalimido-*o*-tolualdehyde (IV) is able to assume con-

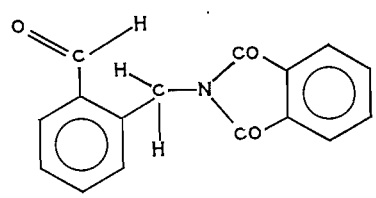

IV

formations which, as judged from molecular models, have a similar effect on the planarity of the benzaldehyde part of the molecule as has the *o*-methyl group in *o*-tolualdehyde.

Hence the similar *C—H* frequencies of α-phthalimido-*o*-tolualdehyde (IV) and *o*-tolualdehyde are not surprising on the basis of a steric interpretation of the spectral changes (cf. ref. 4). Further, the inhibited interaction of *o*-nitrobenzaldehyde with rhodamine B may be caused by the proximity of the nitro group preventing another molecule approaching the hydrogen atom of the aldehyde group. It does not necessarily imply the presence of an intramolecular hydrogen bond in *o*-nitrobenzaldehyde, as suggested by Lundgren and Binkley (15, cf. also 4).

It is concluded therefore that none of the data reported so far conclusively show the existence of an intramolecular hydrogen bond in *o*-nitrobenzaldehyde. On the other hand, many of the data can be explained satisfactorily in terms of a proximity effect between the formyl group and the nitro group, an effect to which a secondary steric interaction (that is, a steric effect involving a twisting of the formyl and nitro groups away from the plane of the benzene ring) makes a significant contribution. The spectral data therefore substantiate the X-ray data on *o*-nitrobenzaldehyde.

ACKNOWLEDGMENTS

Thanks are due to Mr. G. W. West for determining the n.m.r. spectra, to Mr. A. A. Sioumis for determining the infrared spectra, and to Miss V. R. Jellett for determining the ultraviolet spectra.

REFERENCES

1. S. PINCHAS. Anal. Chem. **27**, 2 (1955).
2. S. PINCHAS. Anal. Chem. **29**, 334 (1957).
3. R. WEST and L. S. WHATLEY. Chem. & Ind. (London), 333 (1959).
4. S. PINCHAS. Chem. & Ind. (London), 1451 (1959).
5. R. N. JONES, W. F. FORBES, and W. A. MUELLER. Can. J. Chem. **35**, 504 (1957).
6. B. FRANCK, H. HÖRMANN, and S. SCHEIBE. Ber. **90**, 330 (1957).
7. J. C. DEARDEN and W. F. FORBES. Can. J. Chem. **38**, 1837 (1960).
8. R. M. POWERS, J. L. HARPER, and H. TAI. Anal. Chem. **32**, 1287 (1960).
9. J. R. YOUNG. Unpublished information.
10. W. F. FORBES. Can. J. Chem. **38**, 1104 (1960).
11. J. C. DEARDEN and W. F. FORBES. Can. J. Chem. **36**, 1362 (1958).
12. E. A. BRAUDE and F. SONDHEIMER. J. Chem. Soc. 3754 (1955).
13. A. E. LUTSKII and V. T. ALEKSEEVA. Zhur. Obshcheĭ Khim. **29**, 3248 (1959).
14. L. M. JACKMAN. *In* Applications of nuclear magnetic resonance spectroscopy in organic chemistry Pergamon Press, London. 1959. p. 71.
15. H. P. LUNDGREN and C. H. BINKLEY. J. Polymer Sci. **14**, 139 (1954).

METHYLATION OF SUGAR DITHIOACETALS

IV. D-XYLOSE DIETHYL DITHIOACETAL

G. G. S. DUTTON AND Y. TANAKA[1]

Department of Chemistry, University of British Columbia, Vancouver, British Columbia

Received June 21, 1962

ABSTRACT

Partial methylation of D-xylose diethyl dithioacetal in tetrahydrofuran with methyl iodide and silver oxide yielded 2-, 3-, and 5-*O*-methyl-D-xyloses in the ratio of 20:10:1. The poly-*O*-methylated components were not examined. The 2-*O*-methyl-D-xylose was identified as the crystalline sugar and the 3-*O*-methyl ether as the phenylosazone and *p*-bromophenylosazone. An alternative preparation of the dithioacetal in tetrahydrofuran solution is described.

It has been reported in the preceding papers of this series (1, 2) that D-glucose and L-arabinose dithioacetals were predominantly methylated at their 2-hydroxyl groups with methyl iodide and silver oxide in tetrahydrofuran, and from the latter dithioacetal a small amount of 5-*O*-methyl-L-arabinose was also detected. The case of D-galactose diethyl dithioacetal was rather different in that positions 2, 3, and 6 were of approximately equal reactivity (3). The present paper is the fourth in a series on the relative reactivities of hydroxyl groups in sugar dithioacetals and describes the partial methylation of D-xylose diethyl dithioacetal.

D-Xylose diethyl dithioacetal was first prepared as a sirup by Fischer (4) in 1894 and was not crystallized until 1931 when it was obtained by the deacetylation of its crystalline tetraacetate (5). More recently the crystalline dithioacetal has been obtained directly by Zinner (6) using Fischer's method followed by neutralization of the reaction mixture with an ion-exchange resin. Repetition of Zinner's procedure failed to give us a crystalline product and we therefore carried out the preparation in tetrahydrofuran followed by neutralization with barium carbonate. This method also yielded a sirup but it was later found that dilution of the sirup with a small amount of 2-propanol caused rapid crystallization. Similar dilution of the sirups obtained by either Fischer's or Zinner's procedures gave crystalline material. The results discussed in this section are those obtained with the crystalline dithioacetal but essentially the same results were obtained starting from the sirupy compound as shown in the experimental part.

Since D-xylose diethyl dithioacetal was soluble in methyl iodide the methylation was first attempted in the absence of tetrahydrofuran. The methylation reaction was exothermic and the product gave, on hydrolysis, a mixture of poly-*O*-methylated D-xyloses. When the methylation was performed at 0° C in methyl iodide, no appreciable methylation was observed. Methylation to yield a reasonable amount of mono-*O*-methyl-D-xyloses was possible in a mixture of methyl iodide and tetrahydrofuran (1:1 by volume) at room temperature. The methylation product thus obtained was hydrolyzed with acid and a strong spot of mono-*O*-methyl ethers as well as spots of poly-*O*-methylated D-xyloses together with free D-xylose were detected by paper chromatography. The methylated mixture was chromatographed for 7 hours on Whatman No. 3MM filter papers using butanone–water azeotrope as a developing solvent, and the mono-*O*-methyl ethers were extracted from the appropriate area of the sheets. The area which corresponded to the di-*O*-methyl ethers was also extracted from the same chromatograms. It was necessary

[1]*Present address: Department of Chemistry, Queen's University, Kingston, Ontario.*

to examine this part of the chromatogram because in general monomethylfuranose sugars travel as fast as the corresponding dimethylpyranoses (7). The two groups may be readily differentiated by the high electrophoretic mobility of the former, e.g. 5-*O*-methyl-D-xylose, M_g 1.00. It was assumed that any di-*O*-methyl sugar would be substituted at C_2 and thus have a low mobility (8).

The mixture of mono-*O*-methyl-D-xyloses gave two spots, M_g 0.49 (strong) and 0.92 (weak), by paper electrophoresis, which corresponded to 2- and 3-*O*-methyl-D-xyloses, respectively. The mixture was also shown to contain 2- and 3-*O*-methyl-D-xyloses by paper chromatography (20 hours) in butanone–water azeotrope (R_{xylose} 3.16 (strong) and 3.65 (weak) respectively). Separation of these two spots was much clearer when one drop of concentrated ammonia was added to the developing solvent. The mixture of di-*O*-methyl-D-xyloses was examined by electrophoresis and showed three components, M_g 1.00 (weak), 0.37 (very weak), and 0.00 (strong). The component of M_g 1.00 was electrophoretically identical with a synthetic sample of 5-*O*-methyl-D-xylose but was obtained in too small an amount to be characterized.

The sirup of mono-*O*-methyl-D-xyloses was dissolved in absolute ethanol and 2-*O*-methyl-D-xylose crystallized on dilution with petroleum ether and seeding with an authentic sample. The mother liquor still showed a strong spot of the same compound as well as one of 3-*O*-methyl-D-xylose. The mother liquor was therefore rechromatographed and the 3-*O*-methyl-D-xylose converted into 3-*O*-methyl-D-xylose phenylosazone.

The phenol – sulphuric acid method (9) was used to estimate the ratio of 2- and 3-*O*-methyl-D-xyloses and of 5-*O*-methyl- and di-*O*-methyl-D-xyloses, and the combination of these results with the weights of the fast- and slow-running components isolated from the paper chromatograms gave approximately 20:10:1 for the ratio of 2-, 3-, and 5-*O*-methyl-D-xyloses. In experiments starting with sirupy dithioacetal the trace of the 5-*O*-methyl ether was not observed.

In the course of this work authentic samples of 3- and 5-*O*-methyl-D-xyloses were needed and these compounds were synthesized according to the procedure of Levene and Raymond (10). In this paper the melting points and rotations for the two *p*-bromophenylosazones have been transposed (11).

The results of this methylation study again demonstrate the superior reactivity at C_2 and differ from those for L-arabinose diethyl dithioacetal in that there is appreciable reactivity at C_3.

EXPERIMENTAL

Preparation of D-*Xylose Diethyl Dithioacetal*

Method I

D-Xylose (15.0 g) was suspended in dry tetrahydrofuran (100 ml) which had been saturated with hydrogen chloride at 0° C. The suspension was cooled in an ice-water bath, and ethanethiol (10 g) was added portionwise with vigorous shaking and occasional cooling in ice water. After all the thiol was added (ca. 10 minutes), the mixture was shaken for another 20 minutes, during which time all the D-xylose dissolved to give a homogeneous solution. The reaction mixture was diluted with dry tetrahydrofuran (100 ml), neutralized with excess barium carbonate, and filtered. The filtrate was dried with calcium chloride, the solvent was removed, and the residue was extracted with dry tetrahydrofuran (50 ml). Evaporation of the extract gave a product (20.3 g, 79%) which remained as a sirup for many weeks but which crystallized almost immediately on dilution with a small amount of 2-propanol. The crude product was recrystallized from 2-propanol – petroleum ether. Yield 15.8 g, m.p. 63–64° C, lit. (5) 63–65° C.

Method II

D-Xylose (4.5 g), ethanethiol (4.5 g), and concentrated hydrochloric acid (4.5 g) were shaken for 30 minutes with occasional cooling in an ice-water bath. To the clear reaction mixture was added ice water (50 ml), then sufficient Duolite A-4 resin to neutralize the acid. (An additional amount (50 ml) of water was needed to facilitate stirring.) The filtrate was evaporated to a sirup, which was diluted with isopropyl

alcohol (10 ml). Petroleum ether (3–4 ml) was added to the solution, and after several hours' storage of the solution at 5° C a crystalline mass was obtained. The crude crystals were recrystallized from isopropyl alcohol – petroleum ether. Yield 3.2 g (42%), m.p. 62–63° C. No depression of the melting point was observed when mixed with the sample prepared by the method I.

Methylation of Sirupy D-*Xylose Diethyl Dithioacetal*

Methylation I

D-Xylose diethyl dithioacetal (3.00 g, sirup) was dissolved in a mixture of methyl iodide (35.0 ml) and dry tetrahydrofuran (35.0 ml). Silver oxide (7.0 g) and drierite (7 g) were added to the solution, and the mixture was shaken at room temperature for 3 hours. The reaction mixture was filtered in order to remove the inorganic substances, which were washed with tetrahydrofuran (10 ml). The filtrate and washing were evaporated and the residue was redissolved in chloroform (10 ml). Evaporation of the filtered chloroform solution yielded a light brown sirup (2.49 g).

The sirup (2.49 g) was refluxed for 5 hours in a mixture of ethanol (20 ml), water (1.5 ml), and concentrated hydrochloric acid (1.5 ml). The hydrolyzate was neutralized with Duolite A-4 resin, and after treatment with charcoal, evaporation of the neutral solution gave a light yellow sirup (1.42 g). The sirup showed the following R_f values in butanone–water azeotrope: 0.94, 0.87, 0.79, 0.62, 0.54, 0.46, 0.18, and 0.05. The spot of R_f 0.18 was strong in intensity and the others were all weak.

Methylation II

Using the same quantities of reactants under the same conditions, a sirup (3.12 g) of the methylated mercaptals was obtained. Hydrolysis of this sirup under the same conditions provided a sirupy mixture (1.97 g) of the methylated D-xyloses which showed two strong spots (R_f 0.20 and 0.06) and a few very weak spots with higher R_f values in butanone–water azeotrope.

*Isolation and Examination of Mono-O-methyl-*D-*xylopyranoses*

The sirup (1.42 g) of the methylation I was chromatographed on twelve 15-cm-wide Whatman No. 3MM sheets for 7 hours, and the mono-*O*-methyl-D-xyloses, located by means of guide strips, were extracted with cold water (200 ml×3). Evaporation of the extracts gave a sirup, which was redissolved in methanol (ca. 5 ml), and a mixture (96.7 mg) of mono-*O*-methyl-D-xylopyranoses was obtained by evaporation of the filtered methanolic solution.

In a similar manner a sirup (118.6 mg) of mono-*O*-methyl-D-xylopyranoses was isolated from the hydrolyzate (1.97 g) of methylation II.

The mixtures were chromatographed for 20 hours and two spots (R_{xylose} 3.16 (strong) and 3.65 (weak)) were shown to be 2- and 3-*O*-methyl-D-xyloses, respectively. Separation of these spots was clearer when one drop of concentrated ammonia was added to the solvent.

Electrophoretic examination (900–1000 v, 20–90 ma, 90 minutes in 0.05 *M* sodium borate solution) of the mixtures also showed that they consisted of 2-*O*-methyl-D-xylose (M_g 0.49 (strong)) and 3-*O*-methyl-D-xylose (M_g 0.92 (weak)).

Isolation and Electrophoresis of the Fast-moving Components

From the same chromatograms used for the isolation of mono-*O*-methyl-D-xylopyranoses in methylation mixture I, the area which corresponded to the di-*O*-methyl ethers (R_f 0.54 and 0.46) was extracted with cold water (200 ml×3). A sirup (21.1 mg) was obtained by evaporation of the extracts, followed by the removal of methanol-insoluble impurities. The sirup gave only one spot of M_g 0.00.

Identification of the Component R_{xylose} *3.16 as 2-O-Methyl-*D-*xylose*

The mixture of mono-*O*-methyl-D-xylopyranoses isolated from methylation I was dissolved in warm absolute ethanol, and after cooling, petroleum ether was added to turbidity. Colorless crystals, m.p. 133° C, lit. (12) 132–133° C, precipitated from the solution on seeding. Admixture with an authentic sample gave no depression of the melting point.

Identification of the Component R_{xylose} *3.65 as 3-O-Methyl-*D-*xylose*

After 2-*O*-methyl-D-xylose crystallized, the mother liquor was decanted and evaporated to a sirup which still showed a strong spot for 2-*O*-methyl-D-xylose. The sirup (52.1 mg) was combined with that (118.6 mg) obtained from methylation II, and the combined sirup was chromatographed for 20 hours on three 15-cm-wide Whatman No. 3MM sheets using butanone–water azeotrope to which one drop of concentrated ammonia was added. The areas corresponding to 3-*O*-methyl-D-xylose were extracted with cold water (50 ml×3), and evaporation of the extracts gave a sirup (28.5 mg) which was electrophoretically homogeneous.

The sirup (28.5 mg) was dissolved in water (3 ml), and phenylhydrazine (56.2 mg) in ethanol (0.31 ml) and a small amount of sodium metabisulphite were added. The mixture was heated for 5 hours in boiling water and yellow crystals precipitated on cooling. The crystals (21.6 mg) were recrystallized from ethanol–water, m.p. 171–172° C, lit. (13) 172° C. No depression of the melting point was observed when mixed with synthetic 3-*O*-methyl-D-xylose phenylosazone.

Methylation Study on Crystalline D-*Xylose Diethyl Dithioacetal*

(1) Methylation

Crystalline D-xylose diethyl dithioacetal (1.00 g) was dissolved in a mixture of methyl iodide (12.0 ml) and tetrahydrofuran (12.0 ml). Silver oxide (2.40 g) and drierite (5 g) were added to the solution and the mixture was shaken for 3 hours at room temperature. The methylation product was treated as described above and the sirup (991 mg) thus obtained was hydrolyzed in a similar manner to yield a light yellow sirup (582 mg) which showed the following R_f values in butanone–water azeotrope: 0.91, 0.85, 0.73, 0.60, 0.51, 0.40, 0.20, and 0.07. Only the spot of R_f 0.20 was strong in its intensity; the others were weak.

*(2) Isolation and Electrophoresis of Mono-O-methyl-*D-*xyloses and Di-O-methyl-*D-*xyloses*

The sirup (583 mg) of the methylated D-xyloses was chromatographed for 7 hours on six 15-cm-wide Whatman No. 3MM sheets using butanone–water azeotrope as developing solvent, and the areas of R_f 0.20 and of 0.51 plus 0.40 were separately extracted with cold water (100 ml×3 each). A sirup (41.9 mg) was obtained from the extracts of the R_f 0.20 component, and a sirup (16.3 mg) from the components of R_f 0.51 and 0.40.

By electrophoresis in 0.05 *M* sodium borate solution, the component of R_f 0.20 showed two spots (M_g 0.45 (strong), 2-*O*-methyl-D-xylose; and 0.91 (weak), 3-*O*-methyl-D-xylose; 950–1100 v, 25 ma, 60 minutes), whereas the components of R_f 0.51 and 0.40 showed three spots (M_g 1.00 (weak) (5-*O*-methyl-D-xylose), 0.37 (very weak), and 0.00 (strong); 950–1100 v, 25–35 ma, 70 minutes).

The components of R_f 0.20 were separated by paper electrophoresis and analysis by the phenol – sulphuric acid method (9) gave a ratio of 2:1 for 2- and 3-*O*-methyl-D-xyloses. Similarly the components of R_f 0.51 and 0.40 gave a ratio of 1:10 for 5-*O*-methyl-D-xylose and poly-*O*-methyl-D-xyloses.

Combination of these results with the weights of these two sirups gives approximately 20:10:1 for the ratio of 2-*O*-methyl-D-xylose to 3- and 5-*O*-methyl isomers, respectively.

*Synthesis of 3-O-Methyl-*D-*xylose*

This compound was synthesized by the published method (10) from crude 1,2-*O*-isopylidene-D-xylofuranose (2.97 g) via the 5-*O*-trityl derivative. The yield of chromatographically and electrophoretically homogeneous product was 758 mg.

The sirup (238 mg) was treated in water (5 ml) with phenylhydrazine hydrochloride (650 mg) and anhydrous sodium acetate (400 mg), and 3-*O*-methyl-D-xylose phenylosazone, m.p. 179–181° C, lit (13) 172° C was obtained.

The sirup (351 mg) was heated for 3 hours in water (5 ml) with *p*-bromophenylhydrazine hydrochloride (1.5 g) and anhydrous sodium acetate (0.7 g). The osazone was recrystallized from ethanol–water, m.p. 168–170°, lit. (11) 174–175°.

*Synthesis of 5-O-Methyl-*D-*xylose*

Crystalline 1,2-*O*-isopropylidene-5-*O*-tosyl-D-xylose (6.25 g), m.p. 135–136° C, lit (10) 133–134° C, was obtained by the published procedure (10) from crude 1,2-*O*-isopropylidene-D-xylose (5.12 g). The tosylated compound (2.70 g) provided crystalline 1,2-*O*-isopropylidene-5-*O*-methyl-D-xylose (1.23 g), m.p. 85° C, lit. (10) 80.5–81.5° C, by treatment with sodium methoxide in a sealed tube. Chromatographically pure 5-*O*-methyl-D-xylose (593 mg) was obtained by chromatographic purification of the hydrolyzate of 1,2-*O*-isopropylidene-5-*O*-methyl-D-xylose.

The sirup (293 mg) of 5-*O*-methyl-D-xylose was treated for 3 hours in boiling water with *p*-bromophenylhydrazine hydrochloride (1.20 g) and anhydrous sodium acetate (0.5 g), and the precipitated *p*-bromophenylosazone was recrystallized from ethanol–water, m.p. 152–154° C with softening about 140–144° C, lit. (11) 153–155° C.

ACKNOWLEDGMENTS

We are grateful to the Research Corporation for financial support and one of us (Y. T.) thanks the National Research Council for the award of a studentship.

REFERENCES

1. G. G. S. Dutton and K. Yates. Can. J. Chem. **36**, 550 (1958).
2. G. G. S. Dutton and Y. Tanaka. Can. J. Chem. **39**, 1797 (1961).
3. G. G. S. Dutton and Y. Tanaka. Can. J. Chem. **40**, 1146 (1962).
4. E. Fischer. Ber. **27**, 673 (1894).
5. M. L. Wolfrom, M. R. Newlin, and E. E. Stakly. J. Am. Chem. Soc. **53**, 4379 (1931).
6. H. Zinner, G. Rembarz, H. W. Linke, and G. Ulbricht. Ber. **90**, 1761 (1957).
7. R. Montgomery and F. Smith. *In* Gums and mucilages. Reinhold, New York. 1959.
8. A. B. Foster. *In* Advances in carbohydrate chemistry. Vol. 12. Academic Press, New York. 1957.
9. M. Dubois, K. A. Gilles, J. K. Hamilton, P. A. Rebers, and F. Smith. Anal. Chem. **28**, 350 (1956).
10. P. A. Levene and A. L. Raymond. J. Biol. Chem. **102**, 331 (1933).
11. D. A. Applegarth, G. G. S. Dutton, and Y. Tanaka. To be published.
12. G. J. Robertson and T. H. Speedie. J. Chem. Soc. 824 (1934).
13. E. G. V. Percival and I. C. Wilcox. J. Chem. Soc. 1608 (1949).

ISOTOPE EFFECTS IN NEUTRAL H_2O–D_2O IRRADIATED SOLUTIONS AND THE NATURE OF THE REDUCING RADICAL

CHAVA LIFSHITZ[1]

Department of Physical Chemistry, The Hebrew University of Jerusalem, Israel

Received June 4, 1962

ABSTRACT

Neutral solutions of sodium formate in H_2O–D_2O mixtures were irradiated by 200-kv X rays. The atomic deuterium isotope effect (α_A) and its dependence on deuterium concentration were determined. In a 1×10^{-1} *M* HCOONa, 96% D_2O solution, G(hydrogen) = 1.14 and $\alpha_A = 4.3$. It is concluded that the hydrogen atom cannot be formed from a *single* water molecule. Possible mechanisms of hydrogen atom formation are discussed. The alternative possibilities for the atoms to react as H or H_2O^- are viewed in the light of the proposed mechanisms.

INTRODUCTION

The nature of the reducing radical produced in the radiolysis of aqueous solutions is the subject of several recent studies. It has been shown that two forms of hydrogen atoms are involved—basic and acidic (1–3)—and that these are the solvated electron H_2O^- and the hydrogen atom H, respectively (4). It has further been shown that the transition from H_2O^- to H is brought about in acid solution by H_3O^+.

The relative contribution of the two species to reactions with the solute at neutral pH's is still debated. Czapski and Allen (5), while studying H_2O_2–O_2 solutions, found that the total yield of the reducing species, $G = 2.85$ (where G is the number of radicals formed for 100 ev absorbed), is in the form of solvated electrons. Allan and Scholes (3) and Rabani (6), when studying aqueous solutions of organic solutes, found, on the other hand, that part of the yield of reducing species reacts in neutral solutions in the acid H form, with a yield of $G(H) \simeq 0.6$ (to be termed "residual" yield). This part of reducing species was attributed to hydrogen atoms having excited water molecules as their precursors (3).

All of these studies employed the use of competitive kinetics, the difference between them being the choice of solutes. The use of a different method to investigate the problem of the nature of the reducing radical and the mechanism by which it is formed in neutral solutions seems important. The present study employs the use of the deuterium isotope effect.

When a mixture of H_2O and D_2O is irradiated, the deuterium content of the reducing radicals is lower than that of the irradiated water (7–10). The isotope effect $\alpha_A = (H/D)_{atoms}/(H/D)_{water}$ was found experimentally to depend on the deuterium concentration of the solution, both in acid (8) and in neutral (10) solutions.

Statistical arguments show that if $\alpha_A > 2$ at $\sim$100% D, then more than one water molecule is involved in the reaction producing hydrogen atoms (9).

In the present study further attention is given to the determination of α_A in neutral solutions and its dependence on deuterium concentration, with special emphasis on the "residual" yield. The aim is to determine the value of α_A of these atoms, at high deuterium concentrations, specifically, whether α_A is smaller or bigger than 2. This will enable one to decide whether one or more water molecules are involved in the reaction producing these atoms.

[1]*Present address: Department of Chemistry, Cornell University, Ithaca, New York.*

α_A is determined by studying the isotopic composition of the hydrogen gas evolved from H_2O–D_2O solutions of sodium formate. Formate was chosen as solute, because only the "residual" hydrogen atoms react with it to form molecular hydrogen. It was found by Rabani (6) that, in fact, the relative rate constants of the reaction of formate and ferricyanide ions with hydrogen atoms are the same in acid and neutral solutions. This is explained if the formate reacts, at all the pH values studied, with the same hydrogen atom species (6).

The mechanism by which the "residual" atoms are formed will be discussed, as well as the alternative possibilities that these atoms react with the solute as H or H_2O^-.

EXPERIMENTAL

Mixtures of light and heavy water containing different solutes were irradiated. The yield and isotopic composition of the hydrogen gas were determined.

Irradiations were carried out with an X-ray machine operated at 200 kv and 15 ma. The vessels were cylindrical Pyrex tubes with about 200 cc free volume above the 10 cc liquid phase. Dose rates were approximately 6500 r/min, as measured by the Fricke dosimeter, taking $G(Fe^{+3}) = 15.5$ (11). Total doses given varied from 1×10^{22} to 3×10^{22} ev/l.

Solutions were prepared from triply distilled water. Heavy water (99.8% deuterium) was from Norsk Hydro-Elektrisk. The materials used were of "Analar" grade purity. α_A was determined from experiments on HCOONa solutions, with or without phosphate buffer. Auxiliary experiments were carried out on KBr, KNO_2, and $K_4Fe(CN)_6$ solutions.

The solutions were degassed to an ultimate air pressure of less than 10^{-4} mm Hg. After irradiation the evolved gas was pumped by a Toepler, through a liquid air trap, into a known volume and its pressure was measured by a McLeod gauge. In view of the possibility, that the gas contains oxygen, the hydrogen yields were determined in some auxiliary experiments, where the isotopic composition of the gas was not determined, by burning the gas on a Pt filament.

Mass spectrometric analysis of H_2, HD, and D_2 was carried out on a Consolidated 21-401 instrument.[2] The peak heights were determined in the order of m/e: 2, 3, 4, 3, 2, in order to take into account pressure changes in the mass spectrometer. From the mean peak height of each isotopic species and the total hydrogen yield, the individual HD, H_2, and D_2 yields could be calculated. Contribution to mass 2 by D^+ was taken into account, at high deuterium concentrations, while the isotopic concentrations at low deuterium content were checked by Zn-decomposed water mixtures.

RESULTS

Table I shows the results from experiments on HCOONa. The D_2O percentage is

TABLE I

Expt. No.	%D	$(D/H)_{water}$	Solute	G (hydrogen)	$G(H_2)$	$G(HD)$	$G(D_2)$	$(D/H)_{gas}$	α_A
1	2	1.98×10^{-2}	1.1×10^{-1} *M* HCOONa	1.4_4				6.8×10^{-3}	$3._1$
2	"	"	" "	1.4_9				6.7×10^{-3}	$3._1$
3	"	2.13×10^{-2}	1.1×10^{-1} *M* HCOONa + 1.0×10^{-1} *M* KH_2PO_4	3.3_0				$4._1\times10^{-3}$	$4._9$
4	50	1.00	1.0×10^{-1} *M* HCOONa	1.3_8				$2.5_5\times10^{-1}$	$3._6$
5	95	18.3	1.1×10^{-1} *M* "	1.1_2	0.1_1	0.6_5	0.3_6	1.5_8	$4._4$
6	96.5	28.2	1.0×10^{-1} *M* "	1.1_6	0.0_8	0.6_6	0.4_2	1.8_2	$4._3$
7	95.5	20.4	1.0×10^{-1} *M* HCOONa + 1.0×10^{-1} *M* KH_2PO_4	3.2_0	0.5_8	2.0_3	0.5_9	1.0_1	$6._7$
8	97	31.8	5×10^{-3} *M* HCOONa	1.0_0	0.0_5	0.5_7	0.3_8	1.9_8	$3._4$
9	100	499	1.1×10^{-1} *M* "	1.1_4	—	0.6_1	0.5_3	2.7_5	—
10	100	499	9×10^{-3} *M* "	1.0_3	—	0.5_6	0.4_7	2.6_8	—

rounded off to the nearest half percent, while the value $(D/H)_{water}$ is the exact value of free exchangeable D atoms to exchangeable H atoms in the irradiated solution. The

[2]*The author wishes to thank the Isotope Department of the Weizman Institute, Rehovoth, for performing these analyses.*

hydrogen atoms of sodium formate are not taken into account, in the calculation of $(D/H)_{water}$, because they do not exchange (12). G(hydrogen) means the total hydrogen yield, light and heavy, as measured by the McLeod and is expressed in molecules formed per 100 ev absorbed radiation. The yields of the different isotopic species were calculated as explained in the previous section. In some experiments the isotopic composition of the gas is expressed by the ratio $(D/H)_{gas}$ and not by the individual H_2, HD, and D_2 yields.

For α_A to be calculated from the isotopic composition of the gas, the composition of the "molecular" product formed by the primary radiation–chemical act has to be known (8). The auxiliary experiments, given in Table II, were carried out for this reason. The

TABLE II

%D	Solute	G(hydrogen)	α_M
1	10^{-2} M KBr	0.7_5	1.7_0
1	10^{-4} M KBr; 3×10^{-2} M KH_2PO_4	0.7_5	1.9_5
1	5×10^{-3} M $K_4Fe(CN)_6$	0.7_5	1.7_5
2	9×10^{-3} M $NaNO_3$; 6×10^{-2} M KH_2PO_4	0.6_9	1.8_0
1.5	8.6×10^{-3} M KNO_2	0.5_5	1.7_9
1.5	4.3×10^{-2} M "	0.4_7	1.7_5
52	5×10^{-3} M $K_4Fe(CN)_6$	0.7_0	2.1_0
96.5	10^{-2} M KBr	0.6_0	3.6_0
97	1.1×10^{-1} M KNO_2	0.3_6	4.3_0

hydrogen gas obtained in these experiments is the "molecular" product alone and α_M has its usual meaning (7, 8), namely: $\alpha_M = (H/D)_{gas}/(H/D)_{water}$. α_A is calculated from the formate results at high deuterium concentrations, by the procedure of Baxendale and Hughes (8). The experiments 9 and 10 in Table I show that this procedure is applicable, as part of the gas—$G(D_2)$—is the "molecular" yield, having the isotopic composition of the water (100% D), and the other part of the gas—G(HD)—is the atomic abstraction yield. This procedure is, however, inapplicable at low deuterium concentrations, since the solute contains light hydrogen atoms. The expression

$$G(\text{hydrogen})(D/H+D)_{gas} = \tfrac{1}{2}G(H)(D/H+D)_A+G_{H_2}(D/H+D)_M$$

is instead used, in order to calculate the isotopic composition of the atoms—$(D/H+D)_A$. In this expression G(H) and G_{H_2} are the "atomic" and "molecular" yields, respectively (light and heavy) and $(D/H+D)_M$ is the isotopic composition of the "molecular" product. $(D/H+D)_M$ and G_{H_2} are known from the independent experiments of Table II, while $G(H) = G(\text{hydrogen}) - G_{H_2}$. The experiments in Table II show that α_M is independent of the solute and, to a certain extent, of solute concentration, provided the gas yield and deuterium concentration remain the same.

In order to calculate α_A at low deuterium concentrations, the following values were taken: $G_{H_2} = 0.65$ and $\alpha_M = 1.75$.[3] α_M adopted at high concentrations was 3.9. These values are averages from experiments in Table II, where the scavenger concentrations and molecular yields are similar to the ones expected in the formate experiments. In experiments 9 and 10 of Table I, the $G(D_2)$ values are the "molecular" yields. A comparison of these yields with the yields of Table II at ~100% D shows that the "molecular" yield in formate is intermediate between the KBr and KNO_2 yields. The value of $G_{H_2} = 0.65$ was chosen at low deuterium concentrations, by analogy to the ~100% D experiments, as it is intermediate between the KBr and KNO_2 values.

[3] *For example, the isotopic composition of the atoms was calculated in experiment 1 from the following:* $1.44[6.8\times10^{-3}/(1+6.8\times10^{-3})] = \tfrac{1}{2}(1.44-0.65)(D/H+D)_A+0.65[(1.98\times10^{-2}/1.75)/(1+1.98\times10^{-2}/1.75)]$.

The results obtained for α_A are given in the last column of Table I. The values of α_A at low deuterium concentrations are less certain than those at high ones, because of some arbitrariness in the choice of G_{H_2}. The "molecular" yields, calculated for experiments 5, 6, and 8 from $\alpha_M = 3.9$ and from the experimental G_{D_2}'s (8), in these experiments, are close to the experimental G_{D_2} values for 100% D (experiments 9 and 10). This relates further confidence to the choice of α_M from the auxiliary experiments. Furthermore, even if a considerably different α_M is used, α_A is only slightly affected, in experiments 5, 6, and 8.

DISCUSSION

Fiquet-Fayard (9) has shown that if a single excited water molecule decomposes, independently of all other molecules, without prior energy transfer, then α_A should be lowered by high deuterium concentrations of the solution and α_A cannot be higher than 2 at $\%D \simeq 100$. At high deuterium concentrations the only isotopic water molecule species virtually present are HDO and D_2O. If the composition of the water is one HDO molecule for every n molecules of D_2O and if excitation is random, then there will also be one excited HDO for every n excited D_2O molecules. In the limit of an infinitely high isotope effect in favor of light hydrogen, HDO decomposes to give H only. But if every excited molecule decomposes independently of all others, there will be one H atom for every n D atoms formed. As the original *atom* concentration in the water is one H atom for every $2n$ D atoms, it is evident that the maximum isotope effect is 2. This statistical argument, developed by Fiquet-Fayard (9), holds for any process by which a *single* water molecule decomposes by itself; for instance, it holds also if

$$H_2O^- \rightarrow H + OH^- \qquad [1]$$

or if H_2O^- reacts with the solute, according to

$$H_2O^- + RH \rightarrow H_2 + R + OH^-. \qquad [2]$$

If the excitation energy or the electron is shared among several water molecules so that out of several D_2O and HDO molecules there is a bigger chance than the statistical one for HDO to decompose, although a D_2O molecule was originally excited, then α_A may be bigger than 2 at ~100% D (9).

The results in Table I show that α_A is higher at high deuterium concentrations than at low ones and that it is bigger than 2. A similar behavior was noted for acid solutions (8, 9) and was attributed to reaction (9)

$$H_3O^+ + e \rightarrow H + H_2O \qquad [3]$$

being the one responsible for hydrogen atom production, since H_3O^+ is formed by the interaction of more than one water molecule.

In the formate experiments, where low yields are obtained (Table I, except for experiments 3 and 7) one deals with the "residual" yield (3), after the majority of the electrons have been scavenged, without yielding hydrogen gas. It is apparent from α_A that this yield cannot be due to either [1], [2], or

$$H_2O^* \rightarrow H + OH. \qquad [4]$$

Reaction [4] has been proposed to account for this yield (3), because it could explain why, under certain conditions, electron scavengers do not affect this yield. If excited water molecules (as in [4]), and not solvated electrons, are the precursors of the hydrogen

atoms, electron scavengers would not be able to affect the "residual" yield (3). On the other hand, our isotopic results are incompatible with reaction [4].

If reaction [1] were fast enough, it could explain why, under some conditions, the "residual" yield is scavenged as H, while under others, it is scavenged as H_2O^-. But, as has already been said, this reaction would lead to a similar dependence of α_A on deuterium concentration, as reaction [4], if only one molecule is bound to the electron, in H_2O^-.

The *only* possible explanations for the "residual" yield which are compatible with the observed isotope effect are those reactions in which more than one water molecule is involved. Reaction [3] or sharing of excitation energy (or of the electron) among several water molecules belongs to that category.

Reaction [3] is very likely to occur, since H_3O^+ is formed in the track of the ionizing electron, by the sequence (9)

$$H_2O \rightarrow H_2O^+ + e \qquad [5]$$

and

$$H_2O^+ + H_2O \rightarrow H_3O^+ + OH. \qquad [6]$$

It is significant to note that the "residual" yield is suppressed by those solutes which are efficient electron scavengers, like H_2O_2, O_2 (5), and CO_2 (13). These could compete with reaction [3]. Reaction [3] thus accounts best for all the results.

It is seen that the addition of phosphate to the formate changes the yield, as well as the isotopic composition of the gas. The isotope effect, when full hydrogen yields are obtained in neutral solutions, was previously determined. It was shown by tracer exchange reactions that HDO decomposes independently of the medium (H_2O or D_2O) (10); moreover, a calculation of the numerical exchange results, according to our notation, gives $\alpha_A = 1.6$ at $\sim$100% D. These studies were done at low concentrations of the scavenger (hydrogen molecules) and at a complete absence of efficient electron scavengers. Under these conditions, reaction [1] followed by reaction of H with a hydrogen molecule, or reaction [2], where RH is H_2, can occur. α_A obtained by us in experiments 3 and 7 is not equal to that from the hydrogen experiments (10), either because of a different scavenger concentration—a factor which has not yet been studied—or because of the interaction of the $H_2PO_4^-$ ion with the electrons, to give hydrogen atoms.

The dependence of hydrogen yield on phosphate concentration will be given in a forthcoming publication (14), where the influence of buffers will be further discussed.

CONCLUSIONS

A mechanism for the production of the "residual" yield, compatible with the deuterium isotope effect, is one in which more than one water molecule is involved. A track reaction between H_3O^+ and an electron accounts best for isotopic, as well as scavenger, results.

ACKNOWLEDGMENTS

This research was sponsored by the Israel Atomic Energy Commission. The author wishes to thank Professors G. Stein and E. D. Bergmann for their continuous interest in this work. The author also thanks Professor M. Anbar for his help with the isotopic analyses.

REFERENCES

1. N. F. Barr and A. O. Allen. J. Phys. Chem. **63**, 928 (1959).
2. E. Hayon and J. Weiss. Proc. U.N. Intern. Conf. Peaceful Uses Atomic Energy, 2nd, Geneva. **29**, 80 (1958).
3. J. T. Allan and G. Scholes. Nature, **187**, 218 (1960).
4. G. Czapski and H. A. Schwarz. J. Phys. Chem. **66**, 471 (1962).

5. G. CZAPSKI and A. O. ALLEN. J. Phys. Chem. **66**, 262 (1962).
6. J. RABANI. J. Am. Chem. Soc. **84**, 868 (1962).
7. P. KELLY, T. RIGG, and J. WEISS. Nature, **173**, 1130 (1954).
8. J. H. BAXENDALE and G. HUGHES. Z. Phys. Chem. **14**, 323 (1958).
9. F. FIQUET-FAYARD. J. chim. phys. **57**, 467 (1960).
10. P. J. DYNE, J. W. FLETCHER, W. M. JENKINSON, and L. P. ROY. Can. J. Chem. **39**, 933 (1961).
11. F. T. FARMER, T. RIGG, and J. WEISS. J. Chem. Soc. 582 (1955).
12. P. A. SMALL and J. H. WOLFENDEN. J. Chem. Soc. 1811 (1936).
13. J. T. ALLAN, N. GETOFF, H. P. LEHMANN, K. E. NIXON, G. SCHOLES, and M. SIMIC. J. Inorg. Nucl. Chem. **19**, 204 (1961).
14. C. LIFSHITZ and G. STEIN. To be published.

PREPARATION OF ANTIDOTES FOR ANTICHOLINESTERASE POISONING

I. PARPANIT ANALOGUES[1]

R. A. B. BANNARD, J. H. PARKKARI, AND I. W. COLEMAN
Defence Research Chemical Laboratories, Ottawa, Ontario

Manuscript received June 13, 1962

ABSTRACT

Interaction of potassium 1-phenylcyclopentanecarboxylate and 2-diethylaminoethyl chloride in absolute ethanol proved the most satisfactory of four methods examined for the preparation of 2-diethylaminoethyl 1-phenylcyclopentanecarboxylate hydrochloride (Parpanit). This procedure was used to obtain 2-(ethyl-2′-fluoroethylamino)ethyl (I), 2-(ethylisopropylamino)-ethyl (II), 2-diisopropylaminoethyl (III), 2-pyrrolidinoethyl (IV), and 2-piperidinoethyl (V) 1-phenylcyclopentanecarboxylate hydrochlorides. 2-Diethylaminoethyl 1-(*p*-nitrophenyl)-cyclopentanecarboxylate hydrochloride (VI) was also prepared in this way but was obtained more conveniently by direct nitration of 2-diethylaminoethyl 1-phenylcyclopentanecarboxylate. The preparation of intermediates required in these syntheses is described.

Preliminary results are given on the potency of these compounds as substitutes for atropine sulphate in the usual oxime and atropine sulphate treatment of mice which have been poisoned with Sarin.

In connection with extension of our studies on the usefulness of substitutes for atropine in the treatment of Sarin poisoning (1, 2) it became necessary to prepare certain analogues of 2-diethylaminoethyl 1-phenylcyclopentanecarboxylate hydrochloride, which is known commercially as Parpanit, Panparnit, Caramiphen hydrochloride, or Pentaphen. Many compounds of this type have been synthesized previously and the method most frequently employed has been interaction of the acid chloride with the requisite aminoalcohol in an aromatic solvent (3–8) (method 1). Other procedures which have been utilized less frequently include transesterification of ethyl 1-phenylcyclopentanecarboxylate with an aminoalcohol and sodium in xylene (8–11) (method 2); interaction of an alkali metal salt of the acid and an aminoalkyl halide in a hydrocarbon solvent (5, 7, 12–14) (method 3); treatment of the acid chloride with an aminoalcohol hydrochloride in a hydrocarbon solvent (5) (method 4); and heating the acid with an aminoalkyl chloride hydrochloride in an alcohol (5) (method 5). Method 2 was considered unsuitable for preparation of the compounds required because it sometimes furnishes very poor yields (11). It was not clear, however, which of the other four procedures referred to above would be most satisfactory. Accordingly, the merits of methods 1, 3, 4, and 5 were briefly examined with respect to yield and manipulative convenience for preparation of 2-diethylaminoethyl 1-phenylcyclopentanecarboxylate hydrochloride (3).

Interaction of equimolar quantities of 1-phenylcyclopentanecarboxylic acid chloride and 2-diethylaminoethanol in anhydrous benzene under reflux for 2 hours furnished the ester hydrochloride in 65% yield. Prolonging the period of reflux did not improve the yield (method 1).

When potassium 1-phenylcyclopentanecarboxylate was heated under reflux in absolute ethanol for 18 hours with a 20 mole% excess of 2-diethylaminoethyl chloride, followed by treatment with hydrogen chloride, an 80% yield of 2-diethylaminoethyl 1-phenylcyclopentanecarboxylate hydrochloride was obtained. Lengthening the period of reflux did not improve the yield but the latter decreased to ca. 60% when heating periods shorter than 12 hours were employed (method 3).

[1]*Issued as D.R.C.L. Report No. 374.*

Interaction of equimolar quantities of 1-phenylcyclopentanecarboxylic acid chloride and 2-diethylaminoethanol hydrochloride in dry benzene at reflux temperature for 48 hours gave a 51% yield of the desired material. The yield decreased sharply when shorter reflux periods were used (method 4).

When equimolar quantities of 1-phenylcyclopentanecarboxylic acid and 2-diethylaminoethyl chloride hydrochloride were heated under reflux in absolute ethanol for 48 hours only a 29% yield of the desired ester hydrochloride was obtained (method 5).

From the foregoing results it is evident that method 3 is superior to the others examined on the basis of yield. It is also best from the standpoint of manipulative convenience, since the other methods either required much longer periods of heating under reflux and/or furnished products of inferior quality, which necessitated multiple recrystallizations to provide material equivalent to that obtained by method 3. This method was therefore adopted for preparation of the esters shown in Table II and was satisfactory in all cases.

1-Phenylcyclopentanecarbonitrile was prepared by interaction of phenylacetonitrile and tetramethylene dibromide with sodamide in liquid ammonia, following the general method of Case (15) as modified by Tilford and co-workers (9). The nitrile was hydrolyzed to the acid in 93% yield by the action of 48% hydrobromic acid, by modification of the method used by Weston (5) for preparation of 1-phenylcyclohexanecarboxylic acid. Interaction of the acid and thionyl chloride in dry benzene furnished the acid chloride in 79% yield. Potassium 1-phenylcyclopentanecarboxylate was obtained in 97% yield by neutralization of an alcoholic solution of the acid with 10% alcoholic potassium hydroxide. 1-(*p*-Nitrophenyl)cyclopentanecarboxylic acid was prepared in 80% yield by nitration of 1-phenylcyclopentanecarboxylic acid. The nitro group was concluded to be para to the phenylcyclopentanecarboxylic acid group on the basis of the infrared absorption pattern of the compound in the 1650- to 2000-cm^{-1} region (16). The potassium salt of this acid was readily obtained by the method employed for preparation of potassium 1-phenylcyclopentanecarboxylate.

2-(Ethyl-2′-fluoroethylamino)ethanol was prepared in 78% yield from 2-ethylaminoethanol and 2-fluoroethyl bromide (17), which were caused to react in dry benzene in the presence of anhydrous potassium carbonate. 2-(Ethylisopropylamino)ethanol was obtained similarly and in 41% yield from isopropylaminoethanol and ethyl bromide and was characterized as the halogen acid salts shown in Table I. Isopropylaminoethanol was prepared from isopropylamine and ethylene oxide following Biel's method (18) and characterized as the hydrochloride.

2-Diethylaminoethanol, N-(2-hydroxyethyl)pyrrolidine, N-(2-hydroxyethyl)piperidine, 2-(ethyl-2′-fluoroethylamino)ethanol, 2-(ethylisopropylamino)ethanol, and 2-diisopropylaminoethanol were converted to the corresponding chloride hydrochlorides in the yields given in Table I by treating them with thionyl chloride in dry chloroform (cf. Bartlett *et al.* (19)). These salts were treated with 20% aqueous sodium hydroxide and the free bases were recovered by ether extraction. The latter compounds were not analyzed but were kept at 4° until required in the esterifications.

Finally, 2-diethylaminoethyl 1-(*p*-nitrophenyl)cyclopentanecarboxylate hydrochloride (VI), which had been obtained by esterification of potassium 1-(*p*-nitrophenyl)cyclopentanecarboxylate with 2-diethylaminoethyl chloride, was prepared in 65% yield by direct nitration of 2-diethylaminoethyl 1-phenylcyclopentanecarboxylate. The identity of the two samples was established by comparison of melting points and infrared spectra.

The effectiveness of Parpanit analogues I–VI (Table II) as substitutes for atropine

TABLE I

2-Aminoethanol derivatives

Compound	M.p. (°C)	% yield	Solvent for recrystallization	Empirical formula	Analysis							
					Calculated %				Found %			
					C	H	N	X	C	H	N	X
2-Isopropylaminoethanol hydrochloride	69–70	75	Ethanol–ether	$C_5H_{14}NOCl$	43.01	10.11	10.03	25.40	43.13	9.99	10.09	25.46
2-(Ethylisopropylamino)ethanol hydrochloride	85–86	73	Ethanol–ether	$C_7H_{18}NOCl$	50.14	10.82	8.35	21.15	50.23	10.80	8.32	21.17
2-(Ethylisopropylamino)ethanol hydrobromide	71–72	72	Ethanol–ether	$C_7H_{18}NOBr$	39.63	8.55	6.60	37.67	39.90	8.68	6.65	37.59
2-(Ethylisopropylamino)ethanol hydriodide	76–77	38	Ethanol–ether	$C_7H_{18}NOI$	32.44	7.00	5.41	48.98	32.50	6.95	5.56	49.28
2-(Ethylisopropylamino)ethyl chloride hydrochloride	120–121	92	Acetone–ether	$C_7H_{17}NCl_2$	45.17	9.21	7.53	38.10	45.11	9.40	7.63	38.01
2-(Ethyl-2′-fluoroethylamino)-ethyl chloride hydrochloride	147–147.5	66	Methanol–ether	$C_6H_{14}NCl_2F$	37.91	7.42	7.37		37.73	7.30	7.30	
2-Diisopropylaminoethyl chloride hydrochloride	130–131*	84	Acetone–ether	$C_8H_{19}NCl_2$	48.00	9.57	7.00	35.43	48.27	9.44	6.96	35.44
2-Pyrrolidinoethyl chloride hydrochloride	169.5–170.5†	77	Ethanol–ether	$C_6H_{13}NCl_2$	42.37	7.70	8.24	41.69	42.60	7.61	7.97	41.56
2-Piperidinoethyl chloride hydrochloride	225–227‡	79	Ethanol	$C_7H_{15}NCl_2$	45.66	8.21	7.61	38.52	45.84	7.99	7.49	38.40

*J. B. Wright *et al.* (23) report m.p. 132°.
†J. B. Wright *et al.* (24) report m.p. 173.5–174°.
‡J. G. M. Dunlop (25) reports m.p. 231°.

TABLE II

1-Phenyl- and 1-(*p*-nitrophenyl)-cyclopentanecarboxylate hydrochlorides

Compound	M.p. (°C)	% yield	Empirical formula	Analysis							
				Calculated %				Found %			
				C	H	N	X	C	H	N	X
1-Phenylcyclopentanecarboxylate hydrochloride											
2-(Ethyl-2′-fluoroethylamino)ethyl (I)	131.5–132.5	77	$C_{18}H_{27}NO_2ClF$	62.87	7.92	4.07		62.74	8.11	4.07	
2-(Ethylisopropylamino)ethyl (II)	130–131	61	$C_{19}H_{30}NO_2Cl$	67.13	8.90	4.12	10.43	67.37	8.70	4.07	10.42
2-Diisopropylaminoethyl (III)	134–134.5	75	$C_{20}H_{32}NO_2Cl$	67.87	9.11	3.96	10.02	67.87	9.32	4.09	10.10
2-Pyrrolidinoethyl (IV)	142.5–143	83	$C_{18}H_{26}NO_2Cl$	66.75	8.09	4.33	10.95	66.64	8.17	4.34	10.93
2-Piperidinoethyl (V)	163.5–164.5	82	$C_{19}H_{28}NO_2Cl$	67.54	8.35	4.15	10.49	67.55	8.28	4.07	10.51
1-(*p*-Nitrophenyl)cyclopentanecarboxylate hydrochloride											
2-Diethylaminoethyl (VI)	182–182.5	51*	$C_{18}H_{27}N_2O_4Cl$	58.29	7.34	7.56	9.56	58.50	7.13	7.39	9.53

*Recrystallized from ethanol–ether, all others recrystallized from acetone–ether.

sulphate in the usual pyridine-2-aldoxime methanesulphonate (P-2-S) and atropine treatment of Sarin-poisoned mice is shown in Table III. The method of bioassay was

TABLE III

Atropine substitute activity of Parpanit analogues in protection of Sarin-poisoned mice

Compound	Atropine substitute activity PR-1*	Compound	Atropine substitute activity PR-1*
Atropine	2.03	III	4.5
Parpanit	3.2	IV	2.6
I	1.2	V	2.0
II	1.8	VI	1.3

*PR-1 = (LD_{50} Sarin in treated animals)/(LD_{50} Sarin in untreated controls).

identical with that described previously (1). Compounds III and IV are the only members of the group which exhibit greater protective ability than atropine sulphate. The marked improvement in protective effectiveness displayed by the diisopropyl analogue III relative to Parpanit suggests that further improvement in atropine substitute activity in the Parpanit molecule may result by placing suitable bulky electron-donating substituents on the nitrogen atom.

EXPERIMENTAL[2,3]

1-Phenylcyclopentanecarbonitrile

This compound was prepared in 64% yield (b.p. 144–148° at 12 mm pressure; n_D^{25} 1.5323) using the procedure of Tilford and co-workers (9), who report b.p. 148–153° at 20 mm pressure.

1-Phenylcyclopentanecarboxylic Acid

1-Phenylcyclopentanecarbonitrile (34.2 g, 0.020 mole) was heated under reflux with 48% hydrobromic acid (140 ml) for 3 days. The precipitated acid was collected by filtration, washed with water, and dissolved in ether (500 ml). The ether solution was extracted with 10% sodium hydroxide (2×150 ml) and the alkaline extract was acidified with 10% hydrochloric acid. The resultant precipitate was recrystallized from aqueous alcohol, yielding 35.5 g (93.4%) of light fawn plates, m.p. 159–160°. Case (15) reports m.p. 158–159°.

1-Phenylcyclopentanecarboxylic Acid Chloride

Thionyl chloride (11.9 g, 0.10 mole) was added dropwise to a mechanically stirred solution of 1-phenylcyclopentanecarboxylic acid (9.5 g, 0.05 mole) in anhydrous benzene (100 ml). Stirring was continued for 2 hours at room temperature, after which the solution was heated under reflux for 2 hours. Distillation *in vacuo* furnished 8.20 g (78.5%) of pale yellow oil, b.p. 114–115° at 4 mm pressure; n_D^{25} 1.5418. Levshina and Sergievskaya (13) report b.p. 149–150° at 20–23 mm pressure.

Potassium 1-Phenylcyclopentanecarboxylate

A solution of 1-phenylcyclopentanecarboxylic acid (3.80 g, 0.020 mole) in absolute ethanol (100 ml) was titrated with 10% ethanolic potassium hydroxide using phenolphthalein as external indicator. Removal of the solvent *in vacuo* followed by two recrystallizations from ethanol–ether gave 4.42 g (97.0%) of fine colorless needles which did not melt below 350°. Calc. for $C_{12}H_{13}O_2K$: C, 61.07; H, 5.74; K, 17.13%. Found: C, 61.18; H, 5.74; K, 17.08%.

1-(p-Nitrophenyl)cyclopentanecarboxylic Acid

1-Phenylcyclopentanecarboxylic acid (5.00 g, 0.0263 mole) was added portionwise with stirring to fuming nitric acid (75 ml) kept at −10°. Stirring was continued for a further hour at 0°, after which the reaction mixture was poured onto crushed ice (300 g). The resultant precipitate was collected by filtration and recrystallized from methanol, yielding 4.93 g (80.0%) of colorless to light tan platelets, m.p. 179–182°. Calc. for $C_{12}H_{13}NO_4$: C, 61.27; H, 5.57; N, 5.96%. Found: C, 60.94; H, 5.52; N, 5.98%. This procedure is based on that used by Rubin and Wishinsky (20) for preparation of 1-(*p*-nitrophenyl)cyclohexanecarboxylic acid.

[2]*All melting points and boiling points are uncorrected.*

[3]*Microanalyses were performed by J. G. Helie of these laboratories.*

Potassium 1-(p-Nitrophenyl)cyclopentanecarboxylate

This compound was prepared in 96% yield from the corresponding acid, using the method described for potassium 1-phenylcyclopentanecarboxylate and was obtained as fawn needles, m.p. 225°, after recrystallization from methanol–ether. Calc. for $C_{12}H_{12}NO_4K$: C, 50.56; H, 4.43; N, 5.12; K, 14.31%. Found: C, 50.81; H, 4.57; N, 4.93; K, 14.38%.

2-(Ethyl-2′-fluoroethylamino)ethanol

A mixture of 2-ethylaminoethanol (Eastman, 67.0 g, 0.750 mole), 2-fluoroethyl bromide (120 g, 0.940 mole) (17), anhydrous potassium carbonate (103 g, 0.750 mole), and dry benzene (475 ml) was heated under reflux with stirring for 40 hours. The solid which separated from the cooled solution was collected by filtration and washed with benzene. The benzene was removed by distillation and the residue fractionated *in vacuo*, yielding 79.0 g (78.0%) of 2-(ethyl-2′-fluoroethylamino)ethanol as a colorless liquid, b.p. 71–72° at 8 mm pressure; n_D^{25} 1.4330. Equivalent weight: Calc. for $C_6H_{14}NOF$: 135. Found: 134.

2-Isopropylaminoethanol

2-Isopropylaminoethanol, b.p. 169–170°, n_D^{25} 1.4388, was prepared in 78% yield by the method of Biel (18), who reported b.p. 169–171°. This compound was characterized as the hydrochoride, m.p. 69–70° (see Table I).

2-(Ethylisopropylamino)ethanol

A mixture of 2-isopropylaminoethanol (28.8 g, 0.280 mole), anhydrous potassium carbonate (38.7 g, 0.280 mole), ethyl bromide (30.5 g, 0.280 mole), and anhydrous benzene (50 ml) was heated under reflux with stirring for 5 hours. The solid was removed by filtration and discarded. The filtrate was dried over anhydrous magnesium sulphate, then distilled *in vacuo*, yielding 15.2 g (39.4%) of colorless oil, b.p. 95° at 57 mm; n_D^{25} 1.4380. Brill (21) reports b.p. 175°. This compound was further characterized as the hydrochloride, m.p. 85–86°, and hydrobromide, m.p. 71–72°, which were prepared by conventional methods (see Table I). The hydriodide was prepared directly as follows. A mixture of 2-isopropylaminoethanol (11.3 g, 0.11 mole), ethyl iodide (15.6 g, 0.10 mole), and 90% ethanol (50 ml) was heated under reflux for 24 hours, then kept at room temperature for 3 days. Volatiles were removed *in vacuo*; the oily residue was dissolved in water (100 ml) and extracted with ether (6×15 ml). The aqueous layer was concentrated and dried at 0.001 mm pressure, yielding an oil which crystallized on standing. Three recrystallizations from ethanol–ether gave 9.88 g (39.7%) of 2-(ethylisopropylamino)ethanol hydriodide as colorless needles, m.p. 76–77° (see Table I).

Dialkylaminoethyl Chloride Hydrochlorides

These compounds were all prepared in the same manner, by interaction of thionyl chloride with the dialkylaminoethanol in anhydrous chloroform. The preparation of 2-diisopropylaminoethyl chloride hydrochloride is typical.

A solution of thionyl chloride (5 ml, 8.3 g, 0.07 mole) in dry chloroform (5 ml) was added dropwise to a stirred solution of 2-diisopropylaminoethanol (7.26 g, 0.05 mole) in dry chloroform (50 ml) kept at −10°. The mixture was heated under reflux for 6 hours, and methanol (5 ml) was added. Removal of solvents, first at water pump pressure, then at 0.001 mm, followed by recrystallization of the solid residue from acetone–ether, gave 7.25 g (72.5%) of 2-diisopropylaminoethyl chloride hydrochloride as colorless needles, m.p. 130–131°. The dialkylaminoethyl chloride hydrochlorides prepared are shown in Table I.

Dialkylaminoethyl Chlorides

These compounds were prepared from the corresponding hydrochlorides according to the method used by Breslow and co-workers for the preparation of 2-diethylaminoethyl chloride (22). The preparation of 2-(ethylisopropylamino)ethyl chloride is typical.

A mixture of 2-(ethylisopropylamino)ethyl chloride hydrochloride (4.65 g, 0.025 mole), ice-cold 20% aqueous sodium hydroxide (5 ml), crushed ice (10 g), and ice-cold ether (25 ml) was stirred vigorously for 5 minutes. The ether layer was decanted and the aqueous layer extracted with ice-cold ether (2×15 ml). The combined extracts were dried for 3 hours at 4° over anhydrous magnesium sulphate. The drying agent was removed by filtration and the ether was removed *in vacuo*, yielding 2.85 g (76.0%) of colorless oil. No attempt was made to characterize the product and it was used immediately in the esterification conducted according to method 3. The dialkylaminoethyl chlorides are unstable on storage at room temperature but may be kept at 4° for periods up to 2 weeks without separation of solid, which is considered to be the cyclic dimer (cf. Breslow *et al.* (22) and Wright *et al.* (24)). The following dialkylaminoethyl chlorides were prepared by this method and yields are given in parentheses: 2-(ethylisopropylamino)ethyl (76), 2-(ethyl-2′-fluoroethylamino)ethyl (87), 2-diisopropylaminoethyl (89), 2-pyrrolidinoethyl (82), 2-piperidinoethyl (83).

Dialkylaminoethyl 1-Phenyl- and 1-(p-Nitrophenyl)-cyclopentanecarboxylate Hydrochlorides

(a) Method 1.—Freshly distilled diethylaminoethanol (Eastman, 5.85 g, 0.050 mole) dissolved in dry benzene (25 ml) was added dropwise with stirring to a solution of freshly prepared 1-phenylcyclopentanecarboxylic acid chloride (10.4 g, 0.050 mole) in dry benzene (100 ml) at 25°. The solution was heated under reflux with stirring for 2 hours, during which time a precipitate separated. The mixture was cooled to room

temperature and anhydrous ether (400 ml) was added to complete precipitation. The precipitate was recrystallized three times from acetone, yielding 10.9 g (69.0%) of 2-diethylaminoethyl 1-phenylcyclopentanecarboxylate hydrochloride as colorless needles, m.p. 142–143°. Swiss Patent 234,452 (3) reports m.p. 145–146° for this compound.

(b) Method 3.—Potassium 1-phenylcyclopentanecarboxylate (2.28 g, 0.01 mole) dissolved in absolute ethanol (25 ml) was added in one portion to freshly prepared 2-diethylaminoethyl chloride (1.62 g, 0.012 mole) dissolved in absolute ethanol (10 ml). The solution immediately became turbid and a precipitate began to separate. The mixture was heated under reflux for 18 hours and, after cooling to 0°, the precipitated inorganic salt was collected and discarded. The filtrate was evaporated to dryness *in vacuo* and the oily residue was extracted with anhydrous ether (4×25 ml). The ether solution on saturation with dry hydrogen chloride gave a precipitate which was recrystallized once from acetone, yielding 2.61 g (80.0%) of colorless needles, m.p. 145–147°.

(c) Method 4.—A mixture of 1-phenylcyclopentanecarboxylic acid chloride (4.18 g, 0.02 mole), 2-diethylaminoethanol hydrochloride (Eastman, 3.07 g, 0.02 mole), and dry benzene (50 ml) was heated under reflux for 2 days. The precipitate which separated on cooling was collected and the filtrate was evaporated to dryness *in vacuo*. The combined residue and precipitate were recrystallized from acetone, yielding 3.32 g (51.0%) of colorless needles, m.p. 140–141.5°.

(d) Method 5.—A mixture of 1-phenylcyclopentanecarboxylic acid (1.90 g, 0.01 mole) and 2-diethylaminoethyl chloride hydrochloride (1.72 g, 0.01 mole) in absolute ethanol (50 ml) was heated under reflux for 2 days. The dark precipitate was collected, discarded, and the filtrate was evaporated to dryness *in vacuo*. The residue was recrystallized three times from acetone, yielding 0.96 g (28.6%) of colorless needles, m.p. 144–146°.

The products from the four methods were shown to be identical with an authentic sample of Parpanit (2-diethylaminoethyl 1-phenylcyclopentanecarboxylate hydrochloride), kindly provided by Geigy Pharmaceuticals, Montreal, by comparison of melting points and infrared spectra.

The other esters of 1-phenylcyclopentanecarboxylic acid and 1-(*p*-nitrophenyl)cyclopentanecarboxylic acid shown in Table II were prepared by method 3.

2-Diethylaminoethyl 1-(p-Nitrophenyl)cyclopentanecarboxylate Hydrochloride (VI) by Nitration of 2-Diethylaminoethyl 1-Phenylcyclopentanecarboxylate

2-Diethylaminoethyl 1-phenylcyclopentanecarboxylate (5.00 g, 0.0153 mole) was added portionwise with stirring during a period of 1 hour to fuming nitric acid (75 ml) kept at −15°. The reaction mixture was stirred at 0° for an additional hour then poured onto crushed ice (200 g). The resultant mixture was neutralized with ice-cold 10% sodium hydroxide and extracted with ether (4×50 ml). The extract was dried over anhydrous magnesium sulphate, filtered to remove the desiccant, and saturated with hydrogen chloride. The precipitated solid was recrystallized twice from ethanol–ether, yielding 3.63 g (65.2%) of colorless crystals, m.p. 182–182.5° alone and in admixture with an authentic sample of 2-diethylaminoethyl 1-(*p*-nitrophenyl)cyclopentanecarboxylate hydrochloride (VI). The infrared spectra of the two samples were also identical.

ACKNOWLEDGMENT

We are indebted to Mr. J. R. Blanchfield for preparation of some of the 1-phenylcyclopentanecarboxylic acids used in this work and for providing the 2-diisopropylaminoethanol.

REFERENCES

1. I. W. Coleman, P. E. Little, and R. A. B. Bannard. Can. J. Biochem. and Physiol. **40**, 815 (1962).
2. I. W. Coleman, P. E. Little, and R. A. B. Bannard. Can. J. Biochem. and Physiol. **40**, 827 (1962).
3. J. R. Geigy A-G. Swiss Patent No. 234,452 (January 16, 1945); Chem. Abstr. **43**, 6229[b] (1949).
4. H. Martin and F. Häfliger. U.S. Patent No. 2,404,588 (July 23, 1946); Chem. Abstr. **40**, 6501[2] (1946).
5. A. W. Weston. J. Am. Chem. Soc. **68**, 2345 (1946).
6. J. R. Geigy A-G. Swiss Patent No. 240,160 (May 1, 1946); Chem. Abstr. **43**, 6655[h] (1949).
7. A. W. Weston. U.S. Patent No. 2,704,284 (March 15, 1955); Chem. Abstr. **50**, 1903[i] (1956).
8. H. G. Morren. Brit. Patent No. 753,779 (August 1, 1956); Chem. Abstr. **51**, 7443[c] (1957).
9. C. H. Tilford, M. G. Van Campen, and R. S. Shelton. J. Am. Chem. Soc. **69**, 2902 (1947).
10. M. G. Van Campen and C. H. Tilford. U.S. Patent No. 2,474,796 (June 28, 1949); Chem. Abstr. **44**, 3018[b] (1950).
11. J. H. Biel, H. L. Friedman, H. A. Leiser, and E. P. Sprenzler. J. Am. Chem. Soc. **74**, 1485 (1952).
12. T. Ito. Jap. Patent No. 5278 (December 12, 1952); Chem. Abstr. **48**, 8820[d] (1954).
13. K. V. Levshina and S. I. Sergievskaya. Zhur. Obshchei Khim. **22**, 2189 (1952).
14. W. A. Lott and J. Krapcho. U.S. Patent No. 2,688,025 (August 31, 1954); Chem. Abstr. **49**, 11697[i] (1955).
15. F. H. Case. J. Am. Chem. Soc. **56**, 715 (1934).

16. R. N. JONES and C. SANDORFY. *In* Technique of organic chemistry. Vol. IX. Chemical applications of spectroscopy. *Edited by* A. Weissberger. Interscience Publishers, Inc., New York. 1956. p. 397.
17. F. W. HOFFMANN. J. Org. Chem. **15**, 425 (1950).
18. J. H. BIEL. J. Am. Chem. Soc. **71**, 1306 (1949).
19. P. D. BARTLETT, S. D. ROSS, and C. G. SWAIN. J. Am. Chem. Soc. **71**, 1415 (1949).
20. M. RUBIN and H. WISHINSKY. J. Am. Chem. Soc. **68**, 828 (1946).
21. H. C. BRILL. J. Am. Chem. Soc. **54**, 2484 (1932).
22. D. S. BRESLOW, R. S. YOST, H. G. WALKER, and C. R. HAUSER. J. Am. Chem. Soc. **66**, 1921 (1944).
23. J. B. WRIGHT, E. H. LINCOLN, R. V. HEINZELMAN, and J. H. HUNTER. J. Am. Chem. Soc. **72**, 3536 (1950).
24. J. B. WRIGHT, H. G. KOLLOFF, and J. H. HUNTER. J. Am. Chem. Soc. **70**, 3098 (1948).
25. J. G. M. DUNLOP. J. Chem. Soc. **101**, 2002 (1912).

ORGANOPHOSPHORUS COMPOUNDS

IX. DIARYL PHOSPHOROFLUORIDATES AND DIARYL PHOSPHOROFLUORIDOTHIOATES[1, 2]

GEORGE A. OLAH AND ALEXIS A. OSWALD[3]
Exploratory Research Laboratory, Dow Chemical of Canada, Limited, Sarnia, Ontario
Received April 18, 1962

ABSTRACT

Diaryl phosphorofluoridates and diaryl phosphorofluoridothioates were prepared and their properties investigated.

INTRODUCTION

Of the diaryl phosphorofluoridates, diphenyl phosphorofluoridate was alone prepared by Saunders and co-workers (2) from phosphorus oxydichlorofluoride and phenol in the presence of dimethyl aniline, with 60% yield:

$$POCl_2F + 2C_6H_5OH + 2C_6H_5N(CH_3)_2 \rightarrow (C_6H_5O)_2POF + 2C_6H_5N(CH_3)_2HCl.$$

Gottlieb (3) claimed to have prepared this compound previously in 7% yield by the action of potassium fluoride on the corresponding diphenyl phosphorochloridate. The obtained compound was rapidly decomposed by water whereas diphenyl phosphorofluoridate is quite stable against water. As no fluorine analysis data were given by Gottlieb, it is doubtful that he had obtained the pure compound.

RESULTS AND DISCUSSION

No aryl phosphorofluoridothioates were reported in the literature although the preparation of diaryl phosphorochloridothioates from phosphorus thiotrichloride and anhydrous sodium phenolates is known (4–6):

$$PSCl_3 + 2ArONa \rightarrow (ArO)_2PSCl + 2NaCl.$$

In continuation of previous work on the biologically active phosphorofluoridates (7) it was of some interest to prepare diaryl phosphorofluoridates and diaryl phosphorofluoridothioates and investigate some of their properties.

O,O′-Phenyl,aryl phosphorofluoridates and O,O′-phenyl,aryl phosphorofluoridothioates were conveniently prepared from phenyl phosphorochlorido-fluoridate or -fluoridothioate and the corresponding phenol in the presence of pyridine or dimethylaniline as acid binding agent:

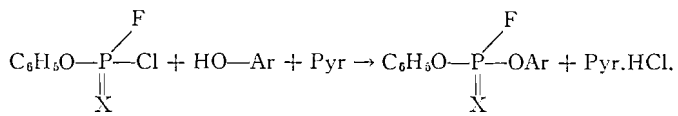

X = O, S

[1] *Contribution No. 67.*
[2] *For Part VIII, see reference 1.*
[3] *Present address: Esso Research and Engineering Company, Linden, New Jersey.*

Phenyl phosphorochlorido-fluoridate and -fluoridothioate were obtained from phosphorus oxydichloridefluoride or thiophosphoryl dichloridefluoride and phenol:

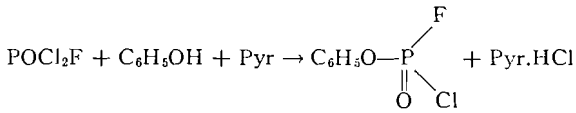

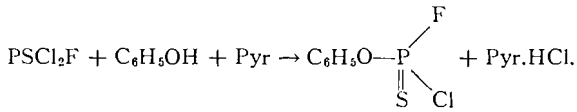

Diaryl phosphorofluoridates and fluoridothioates can also be obtained in one step from phosphorus oxydichloridefluoride or thiophosphoryl dichloridefluoride and 2 mole equiv of phenols:

$$POCl_2F + 2ArOH + 2Pyr \rightarrow (ArO)_2POF + 2Pyr.HCl$$
$$PSCl_2F + 2ArOH + 2Pyr \rightarrow (ArO)_2PSF + 2Pyr.HCl.$$

The one-step procedure, however, does not allow the preparation of "mixed" diaryl derivatives.

The prepared diaryl phosphorofluoridates and fluoridothioates, together with some of their properties and analytical data, are listed in Table I.

Both the diaryl phosphorofluoridates and fluoridothioates are quite stable against aqueous hydrolysis. They show practically no myotic effect. Although they show insecticide properties, they are considerably less toxic than their aliphatic analogues.

EXPERIMENTAL

Phenyl phosphorochloridofluoridothioate was prepared according to Olah and Oswald (J. Org. Chem. **25**, 603 (1960)).

Phenyl Phosphorochloridofluoridate

To a solution of 170 g (1.1 mole) phosphorus oxydichloridefluoride in 250 ml of toluene a solution of 1 mole of phenol in 300 ml toluene was added. To the resulting mixture 80 g (1 mole) of pyridine was added, diluted with 200 ml of toluene. (All operations were carried out with efficient stirring and external cooling, allowing the mixture to warm up from −50° slowly to room temperature.) The mixture was stirred for 2 hours at room temperature and another half hour at 40° to complete the reaction. The precipitated pyridine hydrochloride was filtered and the product fractionated in vacuum. Yield 87%, b.p. 66–70 at 5 mm. $C_6H_5OPOClF$: calc.: P 15.9, Cl 18.25, F 9.76; found: P 15.8, Cl 18.1, F 9.7%.

O-Phenyl,O'-Aryl Phosphorofluoridothioates

To a stirred solution of 0.1 mole of phenyl phosphorochloridofluoridothioate and 0.1 mole of the appropriate phenol in 150 ml of benzene, 7.9 g (0.1 mole) of anhydrous pyridine was added slowly, while the reaction mixture was cooled with ice water. After about half an hour the cooling was discontinued and the reaction mixture was heated for 15 minutes on a water bath and then was allowed to cool to room temperature. The pyridine hydrochloride crystals were removed by filtration and washed with benzene. The combined benzene filtrate was washed with water, 5% aqueous sodium carbonate solution, and again with water and dried over sodium sulphate.

Fractional distillation of the benzene solution *in vacuo* yielded the corresponding O,O'-phenyl,aryl phosphorofluoridothioate as a high-boiling colorless liquid fraction. Physical properties and analytical data of the products are shown in Table I.

O,O'-Diaryl phosphorofluoridothioates can also be prepared with a similar method in ether solvent. When using ether as solvent, a 3-day standing of the reaction mixture at room temperature was required to complete the reaction. Instead of pyridine, tertiary amines, e.g. triethylamine, are suitable to bind the hydrochloric acid formed during the reaction.

TABLE I

O,O′-Diaryl phosphorofluoridates and phosphorofluoridothioates

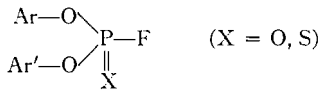

(X = O, S)

Ar′	Ar	X	Formula	% yield	B.p., °C/mm Hg	% calc. C	H	P	F	% found C	H	P	F
Phenyl	Phenyl	O	$C_{12}H_{10}FO_3P$	81	120–121/1	57.15	3.99	12.28	7.53	57.21	4.03	12.3	7.50
Phenyl	4-Tolyl	O	$C_{13}H_{12}FO_3P$	87	129–130/1.5	58.65	4.54	11.63	7.13	58.60	4.61	11.5	7.02
Phenyl	4-Chlorophenyl	O	$C_{12}H_9ClFO_3P$	83	133–134/1.5	50.28	3.16	10.80	6.62	49.97	3.20	10.6	6.55
Phenyl	Phenyl	S	$C_{12}H_{10}FO_2PS$	87	112–113/1	53.73	3.75	11.54	7.08	53.49	3.87	11.3	6.96
Phenyl	4-Tolyl	S	$C_{13}H_{12}FO_2PS$	92	123–124/1.5	53.31	4.28	10.97	6.73	53.29	4.24	10.2	6.81
Phenyl	2-Naphthyl	S	$C_{16}H_{12}FO_2PS$	85	155–157/1.5	60.37	3.80	9.73	5.96	60.39	3.92	9.6	5.87
Phenyl	4-Chlorophenyl	S	$C_{12}H_9ClFO_2PS$	87	130–131/1.5	47.61	2.99	10.23	6.27	47.56	3.03	10.2	6.25

O,O'-Diphenyl Phosphorofluoridothioate

To a stirred solution of 0.1 mole of thiophosphoryl dichloridefluoride and 0.2 mole of phenol in 150 ml of toluene 16 g (0.2 mole) of anhydrous pyridine was added slowly, while the reaction mixture was cooled with ice water. The reaction was thereafter carried out and the product isolated as previously described for the preparation of O-phenyl,O'-aryl phosphorofluoridothioates.

O-Phenyl,O'-Aryl Phosphorofluoridates

To a stirred solution of 0.1 mole phenyl phosphorochloridofluoridate and 0.1 mole of the appropriate phenol in 150 ml of benzene, 12 g (0.1 mole) of dimethylaniline was added, while the reaction mixture was cooled with ice water. The reactions were then further carried out and the products isolated similarly as described previously for the preparation of O-phenyl,O-aryl phosphorofluoridothioates using pyridine instead of dimethylaniline as acid binding agent.

REFERENCES

1. G. A. OLAH and A. A. OSWALD. Can. J. Chem. **38**, 2053 (1960).
2. N. B. CHAPMAN and B. C. SAUNDERS. J. Chem. Soc. 1010 (1948).
3. H. B. GOTTLIEB. J. Am. Chem. Soc. **58**, 532 (1936).
4. W. AUTENRIETH and O. HILDEBRAND. Ber. **31**, 1094 (1898).
5. W. AUTENRIETH and W. MEYER. Ber. B, **58**, 840 (1925).
6. J. LECOCQ and A. R. TODD. J. Chem. Soc. 2381 (1954).
7. G. A. OLAH and A. A. OSWALD. J. Org. Chem. **24**, 1443, 1568 (1959); **25**, 603 (1960).

NITRATION AND REDUCTION OF SUBSTITUTED AZOBENZENES AND AZOXYBENZENES[1]

JOGINDER SINGH,[2] PRITAM SINGH, JEAN L. BOIVIN, AND PAUL E. GAGNON
Department of Chemistry, Laval University, Quebec, Que.

Received May 4, 1962

ABSTRACT

The nitration of some symmetrically tetrasubstituted azo- and azoxy-benzenes in various nitrating media was found to yield the 4-nitro derivatives in some cases, while more drastic conditions gave the 4,4′-dinitro compounds. Some nitroazobenzenes were transformed to the 4-nitroazo and 4,4′-dinitroazoxy derivatives.

Reduction of the mononitroazo-, dinitroazo-, and azoxy-benzenes gave the monoaminoazo, diaminoazo, and azoxy derivatives under mild conditions while strong reducing agents converted the whole molecule to 1,4-diaminobenzene. One exception was found with 2,2′,5,5′-tetramethyl-4,4′-dinitroazobenzene, which was reduced to 2,2′,5,5′-tetramethyl-4,4′-dinitrohydrazobenzene.

INTRODUCTION

The nitration and bromination of the α- and β-isomers of *p*-nitroazoxybenzenes have been reported (1, 2) to take place at the para position with the β-isomers only, the α-isomer being unaffected due to the protective action of the oxygen atom on the adjacent ring:

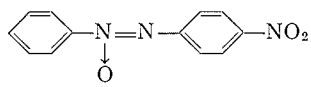

α-isomer

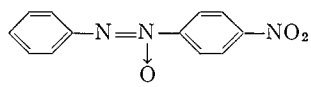

β-isomer

However, recently it has been reported (3) that, using a nitrating mixture of fuming nitric acid in phosphoric acid, nitration takes place in both rings. It was thought of interest to investigate the nitration and reduction of some symmetrically substituted azo- and azoxy-benzenes.

DISCUSSION OF RESULTS

Nitration

During the nitration of azo compounds, both mononitro and dinitro derivatives were obtained. 2,2′-Dimethyl-5,5′-dichloro- and 2,2′-dimethyl-3,3′-dichloro-azobenzenes, when treated with concentrated HNO_3 and glacial acetic acid produced mononitro derivatives, while 2,2′-dimethyl-5,5′-dichloro- and 2,2′,5,5′-tetramethyl-azobenzenes gave the dinitro compounds with fuming HNO_3. The ortho- and para-directing influence of azo groups was confirmed by the introduction of nitro groups in the para position. While in the above cases only nitration took place, 2,2′-dimethyl-3,3′-dichloroazobenzene treated with a mixture of fuming HNO_3 and glacial acetic acid gave both the oxidation and nitration derivative 2,2′-dimethyl-3,3′-dichloro-4,4′-dinitroazoxybenzene.

[1]*This paper constitutes part of a thesis submitted to the Graduate School, Laval University, by Joginder Singh, in partial fulfillment of the requirements for the degree of Doctor of Science.*

This work was supported in part by a grant from the Defence Research Board of Canada (1959).

[2]*Graduate Student, holder of scholarships from Canadian Industries Limited (1960) and Shell Oil Company of Canada (1961).*

The nitration of 2,2′-5,5′-tetrachloro-, 2,2′-dimethyl-5,5′-dichloro-3,3′,4,4′-tetrachloro-, and 2,2′-dimethoxy-5,5′-dichloro-azoxybenzenes gives rise to α-isomers only, in agreement with the work of Angeli (4).

Reduction

For the purpose of determining the constitution of substituted azo- and azoxy-benzenes, many reducing agents have been used, such as zinc in acetic acid, zinc in caustic soda (5), and tin in hydrochloric acid. When 2,2′-dimethyl-5,5′-dichloroazoxybenzene was treated with zinc and acetic acid, the corresponding hydrazo compound was obtained in good yield, but using alkaline reduction with zinc dust in caustic soda, the yield was low. The alkali decomposes the hydrazo derivative readily. 2,2′-Dimethyl-4,4′-dinitro-5,5′-dichloroazobenzene when reacted with sodium sulphide in methanol gave a diamino compound. The reduction of both nitro groups can easily be explained by considering the electromeric effect of adjacent chlorine atoms and the electron-donating nature of the azo group itself. These two effects increase electron density at the nitro groups and by doing so facilitate its reduction rather than that of the azo group (6).

Reduction of 2,2′-dimethyl-3,3′-dichloro-4,4′-dinitroazoxybenzene by excess hydrazine hydrate in ethanol gave the corresponding 4,4′-diaminoazoxy compound. In this case, the nitro groups rather than the azoxy groups are reduced; this is because the two electron-donating chlorine substituents are in positions ortho to the two electron-sink nitro groups. The reduction seems to stop after the nitro groups are reduced. When this compound was reduced with excess sodium sulphide in aqueous methanol, it gave the 4,4′-diaminoazobenzene.

Similar results were observed with the reduction of the 4,4′-dinitroazo derivatives. For instance, 2,2′,5,5′-tetramethyl-4,4′-dinitroazobenzene was reduced by sodium sulphide in ethanol to the 4,4′-diamino compound. The reduction of 2,2′,5,5′-tetramethyl-4,4′-dinitroazobenzene with ammonium sulphide in alcoholic solution gave a yellow crystalline compound which the analysis indicated to be the dinitrohydrazo compound. The attack in this case on the azo group rather than on the more vulnerable nitro groups is very surprising. A possible explanation for this is that methyl groups, due to their positive inductive effect, prevent the electromeric shift of electrons from the azo to nitro group, as shown below, thus keeping the electron density at the azo group sufficient to be attacked by ammonium sulphide.

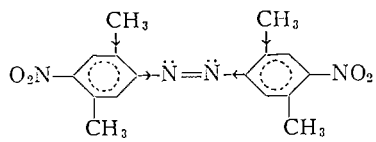

EXPERIMENTAL

General Procedure

(*a*) *Nitrations*

The azo- and azoxy-benzenes were nitrated in a mixture of nitric acid (*d*: 1.5) or fuming nitric acid in glacial acetic acid at temperatures of 60–90° C for a few hours. When the reaction was over the mixture was poured into crushed ice and the product which separated out was filtered and crystallized from suitable solvents. The conditions of nitration, yields, and physical properties of the nitro derivatives are recorded in Table I together with their analyses.

(*b*) *Reductions*

The reductions of substituted nitrobenzenes for the preparation of azoxy compounds were performed in 500-ml three-necked flasks fitted with a mercury-sealed stirrer, a condenser, and a thermometer. Magnesium turnings were added in small portions over a 30-minute period. The mixture was refluxed about 15

TABLE I

Nitration of substituted azo- and azoxy-benzenes

Compound	Nitro derivative	Nitrating mixture*	Reaction conditions	Cryst. solvent	M.p. (°C)	Yield (%)	Analysis for the nitration products	
							Calc. (%)	Found (%)
2,2′,5,5′-Tetrachloro-azoxybenzene	4′-Nitroazoxy†	B	65° C (4 hr)	Acetone	167.5	85	N, 11.0	10.7
2,2′-Dimethyl-5,5′-dichloroazobenzene	4-Nitroazo‡	A	90° C (1 hr)	Acetone, CH_3COOH	161–162	56	Cl, 21.9	21.9
	4,4′-Dinitroazo‡	B	90° C (1 hr)	Acetone, CH_3COOH	250 decomp.	57	Cl, 19.4	19.2
2′2′-Dimethyl-5,5′-dichloroazoxybenzene	4′-Nitroazoxy‡	B	65° C (30 min)	Ethanol	147–148	30	Cl, 20.8	20.8
2,2′-Dimethoxy-5,5′-dichloroazoxybenzene	4′-Nitroazoxy§	B	75° C (30 min)	Ethanol	170–172	36	Cl, 19.1	19.3
2,2′-Dimethyl-3,3′-dichloroazobenzene	4-Nitroazo‖	A	95° C (15 min)	CCl_4 or CH_3CN	164	75	Cl, 21.9	22.1
	4,4′-Dinitroazoxy‖	B	80° C (30 min)	Dioxane Acetone	261	70	N, 14.5	14.5
2,2′,5,5′-Tetramethyl-azobenzene	4,4′-Dinitroazo¶	B	45° C (10 min)	Ethanol	240	90	N, 17.0	17.1

*A: conc. HNO_3 (12 ml) and glacial CH_3COOH (5 ml); B: fuming HNO_3 (10 ml) and glacial CH_3COOH (5 ml).
†Reduced to 2,5-dichloro-1,4-diaminobenzene, m.p. 167.2° C.
‡Reduced to 2-methyl-5-chloro-1,4-diaminobenzene, m.p. 146° C.
§Reduced to 2-methoxy-5-chloro-1,4-diaminobenzene, m.p. 224–225° C.
‖Reduced to 2-methyl-3-chloro-1,4-diaminobenzene, m.p. 89° C.
¶Reduced to 2,5-dimethyl-1,4-diaminobenzene, m.p. 150° C.

TABLE II

Reduction of substituted azo- and azoxy-benzenes

Compound	Product derivative	Reducing agent	Reaction conditions	Cryst. solvent	M.p. (°C)	Yield (%)	Analysis	
							Calc. (%)	Found (%)
2,2′-Dimethyl-5,5′-dichloroazobenzene	Hydrazo	Zn in glac. CH_3COOH	80° C (1 hr)	$CHCl_3$	165–166	60	Cl, 25.3	25.5
2,2′-Dimethyl-4,4′-dinitro-5,5′-dichloro-azobenzene	4,4′-Diaminoazo	Na_2S in CH_3OH	50° C (30 min)	Ethanol*	332 decomp.*	75*	Cl, 18.0*	17.9*
2,2′-Dimethyl-3,3′-dichloro-4,4′-dinitro-azoxybenzene	4,4′-Diamino-azoxy	N_2H_4 in C_2H_5OH	100° C (90 min)	Ethanol	219–220	88	Cl, 21.8	21.9
	4,4′-Diaminoazo	Na_2S in CH_3OH (85%)	60° C (3 hr)	Methanol	230	90	Cl, 22.9	22.9
	,,	,,	,,	,,	310 decomp.*	93*	Cl, 18.0*	18.0*
2,2′,5,5′-Tetramethyl-4,4′-dinitroazobenzene	4,4′-Dinitro-hydrazo	CH_3OH, $(NH_4)_2S$	50° C (90 min)	Ethanol	146	45	N, 16.9	16.8
	4,4′-Diaminoazo	Na_2S in methanol	60° C (45 min)	,,	362 decomp.*		N, 15.9*	15.9*
2,2′,5,5′-Tetrachloro-4-nitroazobenzene	4-Nitroazo	$(NH_4)_2S$ in methanol	25° C (18 hr)	Ethanol	204		C, 39.4 H, 1.37	39.4 1.38
	,,	Na_2S in methanol	50° C (1 hr)	,,	204†	95		

*4,4′-Diacetylamino derivative.
†Mixed m.p. 204° was not depressed.

minutes to complete the reaction and the excess magnesium methylate was destroyed with dilute HCl. The precipitated compound was filtered and subjected to steam distillation, leaving a solid, which was crystallized from a suitable solvent.

The reductions for the structural determination of azo and azoxy compounds (1.0 g) were done in 50-ml round-bottomed flasks fitted with a microcondenser, using excess tin (1.0 g) and 50 ml of a solution containing equal volumes of concentrated HCl and alcohol. When alcohol was used as a solvent, the reaction mixture was always refluxed for another half hour after the disappearance of the initial color of the solution. When acetic acid was the solvent the reaction mixture was kept at about 90° C. After the reduction was over, the reaction mixture was filtered, made alkaline with an excess of 20% alkaline solution, and extracted with ether. In the case of hydroxyazo compounds, the aminophenols which remained in the alkaline solution were either obtained as the benzoyl derivatives by the addition of an excess of benzoyl chloride, or extracted with ether after the careful neutralization of the alkaline solution with dilute HCl.

The reduction products are recorded in Table II together with their analyses. The elemental analyses were performed by Micro-Tech Laboratories, Skokie, Illinois, U.S.A.

2,2'-Dimethyl-5,5'-dichloro-azo- and -azoxy-benzenes

2-Methyl-5-chloronitrobenzene (80 g, 0.47 mole) was dissolved in absolute methanol (700 ml) and, while the mixture was constantly stirred, magnesium turnings (32 g) were added in small portions. The mixture was thereafter refluxed for 5.5 hours. Methanol (200 ml) was added during the heating period to keep the reaction mixture in a semifluid state. When reaction was complete, excess magnesium methylate was destroyed by the addition of concentrated hydrochloric acid. The reaction products were precipitated by dilution with water, and unreacted 2-methyl-5-chloronitrobenzene was removed by steam distillation. The azo and azoxy compounds were separated by fractional crystallization from ethanol, the azo compound being less soluble. Both compounds were further purified by crystallization from ethanol. The azoxy compound melted at 124° C as compared with 123° C found in the literature (5); yield, 25 g (36%). The corresponding azo compound melted at 182–183° C; yield, 25 g (30%). Calc. for $C_{14}H_{12}N_2Cl_2$: Cl, 25.7%. Found: Cl, 25.6%.

2'-Nitro-4,4',5,5'-tetrachloroazoxybenzene, 3,3',4,4'-Tetrachloro-5'-nitroazoxybenzene, and 3,3',4,4'-Tetrachloro-5'-aminohydrazobenzene

3,3',4,4'-Tetrachloroazoxybenzene (1.0 g, 0.003 mole) was dissolved in glacial acetic acid (20 ml), and fuming nitric acid (30 ml) was added. The mixture was then heated at 70° C for 10 minutes. By subsequent dilution with water, a precipitate formed which crystallized from hot glacial acetic acid (50 ml) to give 0.15 g of yellow crystals, m.p. 168–169° C. Calc. for $C_{14}H_5N_3O_3Cl_4$: Cl, 37.3%. Found: Cl, 37.0%. The analysis corresponded to the 5'-nitro compound. When reduced by tin and HCl in glacial acetic acid, white crystals were obtained from ethanol, m.p. 191° C. Yield, 0.25 g (30%). Calc. for $C_{12}H_9N_3Cl_4$: Cl, 42.1%. Found: Cl, 42.4%. This analysis corresponded to the aminohydrazobenzene derivative, which was unusually stable in alkaline solution. When the mother liquor from the above crystallization was diluted with water, a precipitate was formed which, when dissolved in acetone or methanol–benzene, gave a non-crystalline yellow compound, m.p. 128.5° C. Yield, 0.5 g (45%). Calc. for $C_{12}H_5N_3O_3Cl_4$: Cl, 37.3%. Found: Cl, 36.9%. Reduction with tin and HCl gave 3,4-dichloro-1,6-diaminobenzene, m.p. 160° C (lit. 160° C) (7), confirming the position of the 2'-nitro group.

REFERENCES

1. A. Angeli and M. Marchetti. Atti accad. Lincei, **15**, 48 (1906).
2. A. Angeli. Atti accad. Lincei, **19**, 793 (1910).
3. T. Urbanski and J. Urbanski. Bull. acad. polon. sci. Classe (III), **6**, 305 (1958).
4. A. Angeli and B. Valori. Atti accad. Lincei, **21**, 155 (1912).
5. R. Gaudry and K. F. Keirstead. Can. J. Research, B, **27**, 897 (1949).
6. M. Khalifa. J. Chem. Soc. 1854 (1960).
7. D. W. Wooley. Proc. Soc. Exptl. Biol. Med. **75**, 745 (1950).

THE PRODUCTS OF THE PREVOST REACTION ON D-GLUCAL TRIACETATE

R. U. LEMIEUX[1] AND S. LEVINE[2]
Department of Chemistry, University of Ottawa, Ottawa, Ontario

Received May 7, 1962

ABSTRACT

The compound reported by Stanek and Schwarz (Collection Czechoslov. Chem. Communs. **20**, 42 (1955)) to be 1-*O*-benzoyl-2-iodo-2-deoxy-α-D-glucopyranose triacetate is actually an approximately equimolar mixture of 1-*O*-benzoyl-2-iodo-2-deoxy-β-D-glucopyranose triacetate and the stereoisomer with the α-D-manno configuration. Methanolysis of these compounds yielded methyl 2-iodo-2-deoxy-β-D-glucopyranoside and methyl 2-iodo-2-deoxy-α-D-mannopyranoside, respectively. Hydrogenolysis of the latter iodoglycosides using a palladium catalyst gave near-quantitative yields of the corresponding methyl 2-deoxy-D-glucopyranosides. Several other properties of the iodides are reported.

In 1955, Stanek and Schwarz (1) reacted D-glucal triacetate (I) with iodine and silver benzoate in dry benzene to form a substance termed 1-*O*-benzoyl-2-iodo-2-deoxy-α-D-glucopyranose triacetate, m.p. 129–130°, $[\alpha]_D^{31}$ +21.7° in chloroform. On repeating the experiment, we obtained a nicely crystalline product, $[\alpha]_D$ +25.9° in chloroform, in 96% yield. However, although the product possessed the expected iodine content, the melting point (microstage) was 123–148°.

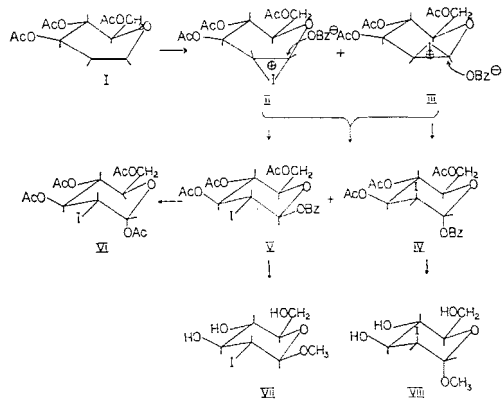

From a mechanistic point of view, it would be anticipated that, in the first stage of the reaction, both the 1,2-iodonium ions II and III would form. These would subsequently undergo nucleophilic attack by benzoate ion to form 1,2-*trans* adducts of the D-glucal triacetate (I). The positive charge of the iodonium ions should be localized mainly at the anomeric center in view of the ability of the ring oxygen to participate in the delocalization. Certainly, for this reason, nucleophilic attack by benzoate ion should occur largely at the 1-position. It may be noted in this regard that 1,2-anhydro-α-D-glucopyranose triacetate undergoes attack exclusively at the 1-position (2). Therefore, the Prevost reaction (3) would be expected to form, from D-glucal triacetate (I), a

[1]*Present address: Department of Chemistry, University of Alberta, Edmonton, Alberta.*
[2]*Present address: Department of Chemistry, University of Saskatchewan, Regina Campus, Regina, Saskatchewan.*

mixture of the two 1-*O*-benzoyl-2-iodo-2-deoxyhexose triacetates IV and V. The relative amounts of these two products presumably would depend either on the relative stabilities of the transition states leading to the two iodonium ions, if these are formed essentially irreversibly in the slow stage of the reaction, or the relative stabilities of the transition states for the nucleophilic attack on the iodonium ions, if the formation of the ions is relatively rapid and reversible. There appears to be no definitive information as to which of these two stages is rate controlling.

The large melting point range that we observed for the product suggested that the substance was a mixture of the isomers IV and V. This condition was clearly substantiated by the nuclear magnetic resonance spectrum of the product, which is reported in Fig. 1. The spectra of the pure compounds are also reproduced in Fig. 1 since this application

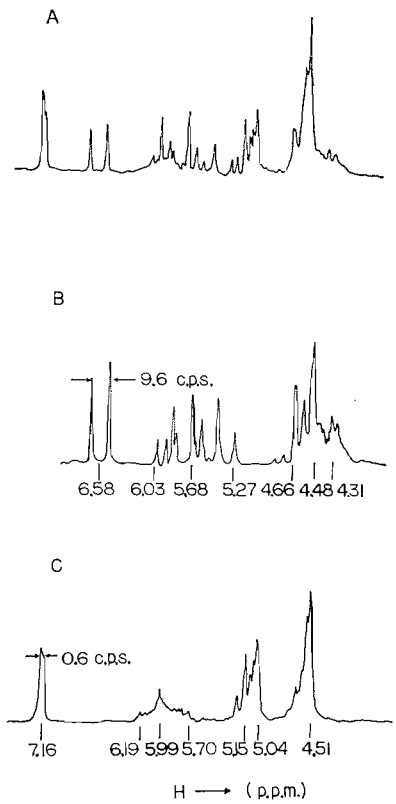

FIG. 1. The proton magnetic resonance spectra measured at 60 Mc/s in chloroform, with tetramethylsilane as an internal standard, of the products which are formed on reacting D-glucal triacetate with iodine and silver benzoate in benzene. Spectrum A is of the crude reaction product and shows that the material is an approximately equimolar mixture of the compounds whose spectra are reproduced in B and C. Spectrum B is of 1-*O*-benzoyl-2-iodo-2-deoxy-β-D-glucopyranose triacetate (V) and spectrum C is of the α-D-manno stereoisomer (IV).

clearly illustrates the power of this relatively new physical tool in the solution of problems related to purity in the field of carbohydrate chemistry. It was at once evident from the appearance of two doublets, at 7.16 and 6.58 p.p.m., in the general region characteristic of anomeric hydrogens for 1-*O*-acyl aldoses (4) that the substance was an approximately 1:1 mixture of two isomeric compounds. The doublet at 6.58 p.p.m. has a spacing of 9.6 c.p.s. and must therefore arise from the isomer (V) with the β-gluco configuration,

wherein the 1-hydrogen is in axial orientation and 1- and 2-hydrogens define a dihedral angle of about 180°. The doublet at lower field has a spacing of only about 0.6 c.p.s. and must arise from a compound with 1- and 2-hydrogens in gauche orientation. From the above-mentioned mechanistic considerations, the signal would be expected to arise from the compound (IV) which has the α-manno configuration. Definitive evidence for this assignment of structure is given below.

A scheme for the separation of IV and V by fractional crystallization was evolved. Compound IV melted at 159.5–160° with $[\alpha]_D$ +45.3° in chloroform whereas compound V melted at 150–151.5° with $[\alpha]_D$ +2.2° in chloroform.

Evidence that compounds IV and V were not anomeric was provided by the following acetolysis and methanolysis experiments. Treatment of V with 1:1 acetic acid – acetic anhydride containing sulphuric acid to constant rotation led to the formation of a substance, m.p. 109.5–111.5°, $[\alpha]_D$ +125° in chloroform, which, in view of its rotation and the fact that the signal for the anomeric hydrogen has a half-band width of only 3 c.p.s., must be 2-iodo-2-deoxy-α-D-glucopyranose tetraacetate (VI). On the other hand, a similar acetolysis of compound IV gave a viscous oil in 91% yield with $[\alpha]_D$ +41.5°. The nuclear magnetic resonance spectrum of this oily substance showed it to be a mixture of presumably anomeric compounds devoid of the benzoate group. The signals for the anomeric hydrogens were at 6.74 and 6.30 p.p.m., whereas the position of the signal for the anomeric hydrogen in compound VI was at 6.85 p.p.m. Therefore, it is highly improbable that compounds IV and V are anomeric since, if they were, they would be expected to yield common products on acetolysis. Treatment of compound V with methanolic hydrogen chloride produced methyl 2-iodo-2-deoxy-β-D-glucopyranoside (VII), m.p. 189–189.5° and $[\alpha]_D$ +6.9° in methanol. The identity of this substance was firmly established by ammonolysis followed by acetylation to methyl 3-amino-3-deoxy-β-D-altropyranoside tetraacetate (5–7). On the other hand, methanolic hydrogen chloride converted compound IV to a methyl 2-iodo-2-deoxyglycoside, VIII, m.p. 146–147° and $[\alpha]_D$ +49.2° in methanol, in 72% yield. Ammonolysis of this compound led to deep-seated degradation without the formation of an aminoglycoside. Further evidence for the configurations of compounds IV and VIII is available from a consideration of the optical rotations shown in Table I. It is seen that there is very good agreement between the molar rotations of compounds IV and VIII and those observed for the corresponding derivatives of α-D-mannose. Although the molar rotations for the configurationally related derivatives of D-glucose do not agree nearly as well, the general agreement is sufficiently good for the present purpose of assigning configurations to the various 2-iodo-2-deoxysugar derivatives. That compounds VII and VIII are in fact 2-iodo-2-deoxyglycosides was firmly established by their hydrogenolysis in near-quantitative yield to the methyl 2-deoxy-β- and -α-D-glucopyranosides, respectively.

Stanek and Schwarz (1) prepared 2-deoxy-D-glucose in low yield by reduction of the substance now known to be a mixture of IV and V using a zinc–copper couple in methanol. We observed this reaction to lead to the formation of water-soluble substances, starting either from IV or V and using the zinc–copper couple described by Shank and Schechter (8). These contained zinc and liberated D-glucal when hydrolyzed with base. Attempts to hydrogenolyze V using a palladium-on-charcoal catalyst in the presence of diethylamine in methanol led to the consumption of 2 moles of hydrogen per mole of V. The product of the reaction was not characterized.

Both the 2-iodo-2-deoxyglycosides VII and VIII rapidly consumed sodium hydroxide. The gluco compound (VII) consumed the base about three times more rapidly than the

TABLE I

Optical rotations of derivatives of D-glucose and D-mannose

Derivative	$[\alpha]_D$	Solvent	$[M]_D$
D-Glucose			
β-D-Glucopyranose pentaacetate	+ 3.8°	$CHCl_3$	+ 1,500°
1-*O*-Benzoyl-2-iodo-2-deoxy-β-D-glucopyranose triacetate (V)	+ 2.2	"	+ 1,100
Methyl β-D-glucopyranoside	− 34.2	H_2O	− 6,600
Methyl 2-iodo-2-deoxy-β-D-glucopyranoside (VII)	+ 6.9	CH_3OH	+ 2,100
Methyl β-D-glucopyranoside tetraacetate	− 18.2	$CHCl_3$	− 6,600
Methyl 2-iodo-2-deoxy-β-D-glucopyranoside triacetate (IX)	+ 6.2	"	+ 2,700
α-D-Glucopyranose pentaacetate	+101.6	"	+39,700
2-Iodo-2-deoxy-α-D-glucopyranose tetraacetate (VI)	+125	"	+57,200
D-Mannose			
α-D-Mannopyranose pentaacetate	+ 55	"	+21,500
1-*O*-Benzoyl-2-iodo-2-deoxy-α-D-mannopyranose triacetate (IV)	+ 45.3	"	+23,600
Methyl α-D-mannopyranoside	+ 79.2	H_2O	+15,400
Methyl 2-iodo-2-deoxy-α-D-mannopyranoside (VIII)	+ 49.2	CH_3OH	+15,000
Methyl α-D-mannopyranoside tetraacetate	+ 49.1	$CHCl_3$	+17,800
Methyl 2-iodo-2-deoxy-α-D-mannopyranoside triacetate (X)	+ 44.9	"	+19,300

manno epimer (VIII), presumably because of the trans configuration of the 2,3-iodohydrin group in VII. However, 1.9 equiv of base were consumed per mole of VII and 2.9 equiv per mole of VIII. These results undoubtedly are related to elimination of the iodine to form initially 2-deoxy-3-ketoglycosides, which under the influence of the base are degraded to acidic products. These reactions are under investigation.

Small amounts of methyl 2-iodo-2-deoxy-β-D-glucopyranoside (VII) were isolated from the methanolysis of pure 1-*O*-benzoyl-2-iodo-2-deoxy-α-D-mannopyranose triacetate (IV). The formation of this compound requires dissociation of the benzoyloxy group, with participation of the iodine atom, to lead initially to a 1,2-iodonium ion. This ion must then decompose to some extent to D-glucal and positive iodine (likely either as methyl hypoiodite or iodine chloride), which recombine to form a 2,3-*trans*-iodonium ion (such as II) which can lead to the formation of VII. It is of interest to note from the point of view of neighboring iodine participation (9) that the methanolysis of V afforded only a 20% yield of VII. Since VII proved highly resistant to change under the conditions of methanolysis, it could not be the main product of the reaction.

EXPERIMENTAL

Mixture of 1-O-Benzoyl-2-iodo-2-deoxy-triacetate Derivatives of β-D-Glucopyranose and α-D-Mannopyranose

D-Glucal triacetate (10), 37.5 g (0.133 mole), was added to 30 g (0.131 mole) of silver benzoate suspended in 400 ml of dry benzene. Iodine, 36 g (0.141 mole), was added to the stirred solution and the purple color which formed after the addition of each portion disappeared almost immediately. After all the iodine had been added the mixture had a faint brown coloration. The mixture was stirred for 30 minutes at room temperature, the silver iodide was collected by filtration, and the filter cake washed with benzene. The combined filtrates were washed with sodium thiosulphate and sodium bicarbonate and finally with water. The benzene was removed *in vacuo* to leave 65.4 g (96%) of a crystalline residue; m.p. 123–148°, $[\alpha]_D$ +25.9° (*c*, 2.0 in chloroform). A study of the solubility properties of the components of the mixture led to the following scheme for their separation by fractional crystallization.

1-O-Benzoyl-2-iodo-2-deoxy-β-D-glucopyranoside Triacetate (V)

The above-mentioned crystalline mixture, 50 g, was dissolved in 75 ml of acetone, and 150 ml of cyclohexane was added. There was obtained 6.13 g of crystals, $[\alpha]_D$ +7.1° (*c*, 2.1 in chloroform), and mother liquor A. After two recrystallizations from methanol there remained 4.70 g of white crystals, $[\alpha]_D$ +2.2 (*c*, 1.9 in chloroform), with a transition beginning at 145°. When the melting point was determined at a sufficiently slow rate to allow completion of the transition, the melting point was 150–151.5°. Further

recrystallization from either methanol or ethanol did not change the melting point or rotation. The n.m.r. spectrum (Fig. 1B) showed the presence of only one type of anomeric hydrogen.

In the presence of onefold excess of sodium hydroxide in 50% aqueous dioxane at 0°, compound V consumed within 60 minutes 5 equiv of base per mole with the liberation of 1 mole-equiv of iodide ion.

Anal. Calc. for $C_{19}H_{21}O_9I$: C, 43.86; H, 4.07; I, 24.40. Found: C, 43.61; H, 4.34; I, 24.71.

1-O-Benzoyl-2-iodo-2-deoxy-α-D-mannopyranose Triacetate (IV)

The crystalline residue obtained after evaporation of solvent from mother liquor A was dissolved in 350 ml of benzene, and 700 ml of 30–60° petroleum ether was added. Crystals, 9.84 g, were deposited, $[\alpha]_D$ +43.1° (*c*, 1.8 in chloroform), in mother liquor B. One recrystallization from methanol gave 7.43 g of large white crystals, $[\alpha]_D$ +45.3° (*c*, 2 in chloroform), m.p. 157–160° with a transition at about 150°. After the transition was complete, the melting point was 159.5–160°. The melting point and rotation were not changed by further recrystallization either from methanol or ethanol. The n.m.r. spectrum of the product (Fig. 1) showed the presence of only one type of anomeric hydrogen.

In the presence of a onefold excess of sodium hydroxide in 50% aqueous dioxane at 0° compound IV consumed within 40 minutes 6 equiv of base per mole with the liberation of 1 mole equiv of iodide ion. It is apparent that the elimination of the iodine atom led to the formation of acidic products.

Anal. Calc. for $C_{19}H_{21}O_9I$: C, 43.86; H, 4.07; I, 24.40. Found: C, 44.13; H, 3.96; I, 24.00.

Evaporation of mother liquor B left a crystalline residue with a composition approximately that of the original reaction product. The fractional crystallization was continued until 9.28 g of mixture remained. It was not possible to obtain a further yield from this residue. The total yields of 1-*O*-benzoyl-2-iodo-2-deoxy-β-D-glucopyranose triacetate and 1-*O*-benzoyl-2-iodo-2-deoxy-α-D-mannopyranose triacetate were 14.3 and 20.9 g, respectively.

Methyl-2-iodo-2-deoxy-β-D-glucopyranoside (VII)

A solution of 10 g (0.0192 mole) of 1-*O*-benzoyl-2-iodo-2-deoxy-β-D-glucopyranose triacetate in 400 ml of 2% methanolic hydrogen chloride was allowed to stand at room temperature until it had attained constant rotation (6 hours). The solution was then neutralized with silver carbonate and, after filtration, hydrogen sulphide was used to remove silver ion. After removal of the methanol, an aqueous solution of the residue was decolorized using charcoal and then evaporated to 5.61 g of viscous oil. Crystallization from ethyl acetate gave 1.19 g (20%) of a crystalline solid, m.p. 189–189.5°, $[\alpha]_D$ +6.9° (*c*, 2.1 in methanol).

Anal. Calc. for $C_7H_{13}O_6I$: C, 27.65; H, 4.31; I, 41.74. Found: C, 27.74; H, 4.53; I, 41.22.

All attempts to isolate crystalline methyl 2-iodo-2-deoxy-α-D-glucopyranoside from the mother liquors were unsuccessful.

Acetylation of VII in the usual manner using acetic anhydride and pyridine provided a near-quantitative yield of methyl 2-iodo-2-deoxy-β-D-glucopyranoside triacetate (IX), m.p. 85–86°, $[\alpha]_D$ +6.2° (*c*, 1.3 in chloroform).

Anal. Calc. for $C_{13}H_{19}O_8I$: C, 36.29; H, 4.45; I, 29.50. Found: C, 36.18; H, 4.69; I, 29.18.

In the presence of a 50% excess of aqueous sodium hydroxide at room temperature, compound VII consumed within 20 hours 1.88 milliequiv of base per mole with the liberation of 1 mole equiv of iodide ion.

Methyl 2-Iodo-2-deoxy-α-D-mannopyranoside (VIII)

Treatment of 1-*O*-benzoyl-2-iodo-2-deoxy-α-D-mannopyranose triacetate (IV) under the same conditions mentioned above for the gluco isomer led to the isolation of a compound, m.p. 145–146°, $[\alpha]_D$ +49.2° (*c*, 1 in methanol).

Calc. for $C_7H_{13}O_5I$: C, 43.86; H, 4.07; I, 24.40%. Found: C, 44.13; H, 3.96; I, 24.00%.

Acetylation of VIII in the usual manner using acetic anhydride and pyridine gave a product (X), $[\alpha]_D$ +44.9° in chloroform, which failed to crystallize. The nuclear magnetic spectrum left no doubt that the compound was essentially pure.

In the presence of a 50% excess of aqueous sodium hydroxide, compound VIII consumed within 40 hours at room temperature 3 equiv per mole with the liberation of 1 mole equiv of iodide ion.

2-Iodo-2-deoxy-α-D-glucopyranose Tetraacetate (VI)

A solution of 0.269 g (0.5 mmole) 1-*O*-benzoyl-2-iodo-2-deoxy-β-D-glucopyranose triacetate in 2 ml of 1:1 acetic anhydride – acetic acid was added to 0.256 g of 95.5% sulphuric acid in 2 ml of the acetic anhydride – acetic acid. After mixing, the volume was adjusted to 5 ml with the 1:1 acetic acid – acetic anhydride mixture to yield a solution 0.5 *M* in sulphuric acid and 0.1 *M* in the glucose derivative. The observed optical rotation in a 2-dm tube of the solution reached a constant value of 13.5° after 15 minutes at room temperature. After standing for 25 minutes, the product was isolated in the usual manner. An oil, 0.20 g (87%), was obtained which crystallized after trituration with 30–60° petroleum ether. Recrystallization from benzene – petroleum ether gave 0.12 g of material; m.p. 109.5–111.5° $[\alpha]_D$ +125° (*c*, 1.7 in chloroform).

Anal. Calc. for $C_{14}H_{19}O_9I$: C, 36.69; H, 4.18; I, 27.70. Found: C, 36.50; H, 3.99; I, 27.82.

Acetolysis of 1-O-Benzoyl-2-iodo-2-deoxy-α-D-mannopyranose Triacetate

The acetolysis was carried out in exactly the same manner as for 1-*O*-benzoyl-2-iodo-2-deoxy-β-D-glucopyranose triacetate. The specific rotation of the solution reached a minimum observed value of 1.47° (using a 2-dm tube) after standing the solution 9 minutes at room temperature and remained at this value for about 42 minutes. The observed rotation of the solution then rose to a constant value of 4.5°. The product, 0.21 g (91%) of a viscous oil, $[\alpha]_D$ +41.5° (*c*, 1.7 in chloroform), was isolated in the usual manner. The nuclear magnetic resonance spectrum showed two signals of about equal intensity in the region characteristic of anomeric hydrogens for this type of compound. One signal was in the form of a singlet at 6.74 p.p.m. and the other a doublet at 6.30 p.p.m. with a spacing of 8.5 c.p.s. The intensities of these signals were considerably lower than expected and it seems likely, therefore, that the reaction was not restricted to replacement of the benzoyloxy group by acetoxy group.

Methyl 3-Acetamido-3-deoxy-β-D-altropyranoside Triacetate

Methyl 2-iodo-2-deoxy-β-D-glucopyranoside, 0.20 g (0.66 mmole), was dissolved in 2.5 ml of dry methanol saturated with ammonia and the solution, in a sealed tube, was heated for 6 hours at 120°. The methanol and ammonia were removed and the residue was dissolved in water. After treatment with silver carbonate and then with hydrogen sulphide, the aqueous solution was decolorized with charcoal. Evaporation of the water *in vacuo* left 0.11 g of a deliquescent white powder, which was acetylated using 1 ml of pyridine and 0.7 ml of acetic anhydride for 22 hours. The product, 0.19 g of a light yellow oil, was isolated in the usual manner and dissolved in a small amount of absolute ethanol. After standing at 4° for 19 hours there was deposited 0.16 g (65%) of a crystalline material, m.p. 189.5–190°, $[\alpha]_D$ −123° (*c*, 1.1 in chloroform), −149° (*c*, 1.2 in methanol). The reported (5–7) physical constants for methyl 3-acetamido-3-deoxy-β-D-altropyranoside triacetate are: m.p. 188°, $[\alpha]_D$ −119° (chloroform).

Anal. Calc. for $C_{15}H_{23}O_9N$: C, 49.86; H, 6.42. Found: C, 50.04; H, 6.51.

Methyl 2-Deoxy-β-D-glucopyranoside

A solution of 0.303 g (1 mmole) of methyl 2-iodo-2-deoxy-β-D-glucopyranoside (VII) and 0.148 (2.04 mmoles) of diethylamine in 10 ml of water was hydrogenated at room temperature and pressure using 0.035 g of palladium on charcoal as catalyst. The theoretical amount of hydrogen was taken up in 16 minutes. After 30 minutes, the catalyst was removed by filtration and the filtrate was treated with silver carbonate to remove iodide ion and then with hydrogen sulphide to remove silver ion. After evaporation of the water and diethylamine *in vacuo* an aqueous solution of the residue was decolorized with charcoal. Evaporation of the water left 0.15 g (84%) of crystalline material which, after recrystallization from ethyl acetate, melted at 121.5–122°, $[\alpha]_D$ −46.9° (*c*, 1.0 water). The physical constants reported (11) for methyl 2-deoxy-β-D-glucopyranoside are: m.p. 122–123°, $[\alpha]_D$ −48.4° (water).

Methyl 2-Deoxy-β-D-glucopyranoside Triacetate

A solution of 0.10 g of methyl 2-deoxy-β-D-glucopyranoside in 0.7 ml of pyridine and 0.5 ml of acetic anhydride was allowed to stand for 18 hours at 4°. The product, 0.17 g of crystalline material, was isolated in the usual manner. After recrystallization from ether – 30–60° petroleum ether, the material melted at 97–99°, $[\alpha]_D$ −34.8° (*c*, 0.9 in chloroform). Methyl 2-deoxy-β-D-glucopyranoside triacetate is reported (5) to melt at 96–97°, $[\alpha]_D$ −30.2° (tetrachloroethane).

Methyl 2-Deoxy-α-D-glucopyranoside

Hydrogenation of 0.303 g (1 mmole) of methyl 2-iodo-2-deoxy-α-D-mannopyranoside (VIII) and purification of the product in the same manner as described above for the β-anomer gave 0.16 g (89%) of material which was recrystallized from ethyl acetate. The substance melted at 93.5–94.5°, $[\alpha]_D$ +143° (*c*, 0.9 in methanol). Methyl 2-deoxy-α-D-glucopyranoside is reported (11) to melt at 92–93°, $[\alpha]_D$ +145° (*c*, 0.8 in methanol). The tri-*O*-acetyl derivative failed to crystallize.

Reductions with Zinc–Copper Couple

1-*O*-Benzoyl-2-iodo-2-deoxy-β-D-glucose triacetate (0.15 g) was dissolved in 6.5 ml of absolute methanol, and 0.7 g of zinc–copper couple (8) was added. The mixture was stirred for 8 hours at room temperature. After filtration, the filtrate was evaporated to dryness *in vacuo* and the residue was taken up in chloroform. Evaporation of the clarified chloroform solution left 0.15 g of a white, semicrystalline, waxy solid which gave a strong positive test for zinc. The material, which was partially soluble in water and gave an immediate precipitate with silver nitrate, was suspended in water and titrated with aqueous sodium hydroxide. One equivalent of base per molecular weight of starting material was rapidly consumed. A further equivalent of base was consumed slightly less rapidly. A non-combustible precipitate was formed, which likely was zinc oxide. Filtration and evaporation *in vacuo* left a residue which was acetylated with pyridine and acetic anhydride. A 74% yield of a substance characterized as D-glucal triacetate (mixed melting point and infrared spectra) was obtained.

A similar reduction of 1-*O*-benzoyl-2-iodo-2-deoxy-α-D-mannopyranose triacetate gave a 79% yield of D-glucal triacetate.

ACKNOWLEDGMENTS

The authors wish to thank the Bristol Laboratories Incorporated and the National Research Council of Canada for the financial support of this research through grants to R. U. L. The nuclear magnetic resonance spectra were determined by Mrs. A. Westland and the microanalyses were conducted by Miss E. Busk of these laboratories.

REFERENCES

1. J. STANEK and V. SCHWARZ. Collection Czechoslov. Chem. Communs. **20**, 42 (1955).
2. R. U. LEMIEUX and G. HUBER. J. Am. Chem. Soc. **78**, 4117 (1956).
3. C. PREVOST. Compt. rend. **196**, 1129 (1933).
4. R. U. LEMIEUX, R. K. KULLNIG, H. J. BERNSTEIN, and W. G. SCHNEIDER. J. Am. Chem. Soc. **80**, 6098 (1958).
5. E. FISCHER, M. BERGMANN, and H. SCHOTTE. Ber. B, **53**, 509 (1920).
6. E. W. BODYCOTE, W. N. HAWORTH, and E. L. HIRST. J. Chem. Soc. 151 (1934).
7. W. N. HAWORTH, W. H. G. LAKE, and S. PEAT. J. Chem. Soc. 271 (1939).
8. R. S. SHANK and H. SCHECHTER. J. Org. Chem. **24**, 1825 (1959).
9. S. WINSTEIN, E. GRUNWALD, and L. L. INGRAHAM. J. Am. Chem. Soc. **70**, 821 (1948).
10. W. W. PIGMAN and H. S. ISBELL. J. Research Natl. Bur. Standards, **19**, 204 (1937).
11. F. SHAFIZADEH and M. STACEY. J. Chem. Soc. 3609 (1952).

ELECTROCHEMISTRY OF THE NICKEL OXIDE ELECTRODE

PART IV. ELECTROCHEMICAL KINETIC STUDIES OF REVERSIBLE POTENTIALS AS A FUNCTION OF DEGREE OF OXIDATION

B. E. CONWAY AND E. GILEADI

Department of Chemistry, University of Ottawa, Ottawa, Ontario

Received May 22, 1962

ABSTRACT

Electrochemical kinetic studies have been carried out at the nickel oxide electrode showing that the reversible potential for the Ni^{II}–Ni^{III} system is independent of the state of oxidation of the bulk oxide in the electrode over a wide range of degrees of oxidation. The properties of the electrode are shown to be determined by the state of a surface phase, which is completely charged when the bulk oxide material in the electrode has been charged to 10% of its total charge capacity. Experiments on sparingly charged electrodes have proved that charging of the bulk oxide does not commence significantly until the electrode is charged to about 1.5%. Consecutive electrochemical reactions possibly involved in the charging process are discussed.

INTRODUCTION

The real reversible potential of the nickel oxide (Ni^{II}–Ni^{III}) electrode has been the subject of controversy for some years and previously reported values are misleading since they have not been based on well-defined equilibrium conditions or a well-defined state of the system. Determination of the reversible potential is complicated by the self-discharge processes which occur at the electrode in the oxidized form and also by the fact that the electrode may exist in a range of chemical states corresponding to the extent of conversion of Ni^{2+} to Ni^{3+} (and possibly Ni^{4+} under certain conditions) in the hydrated oxide.

In an earlier paper (1), the true reversible potential of partially charged nickel oxide electrodes at a single controlled state of oxidation "$NiO_{1.25}$" was examined as a function of potassium hydroxide and water activities in aqueous alkali solutions, and distinguished from the mixed potential assumed in previous work (2, also 12, 13) to be the reversible potential. A polarization decay method was employed (1, 3, 4) in which the reversible potential was approached both from the anodic and the cathodic directions.

In the present phase of our work, the same method has now been applied to the study of the potential of partially charged nickel oxide electrodes as a function of the degree of charge, at constant electrolyte composition. This method was found to be applicable only over a limited range of degree of oxidation of the electrode ("$NiO_{1.10}$"–"$NiO_{1.30}$") owing to problems of extrapolation to the reversible potential to be discussed below. Stationary potentials, taken at very long times on open circuit, were therefore also measured as a function of the degree of charge over a much wider range of degree of oxidation ("$NiO_{1.025}$"–"$NiO_{1.50}$").

The role of the surface and bulk phases in determining the measured potential was deduced. It will be shown that three well-defined regions in the charging process can be distinguished experimentally. In the first, the surface phase alone is being charged; in the intermediate region, the Faradaic current is used to charge both phases, until the surface phase is fully charged, after which oxidation of the bulk is the main Faradaic process. (Most of the charging process occurs at a potential anodic to the reversible oxygen electrode, so that oxygen evolution must occur to a certain extent as a parallel process in all three regions described above. It does not, however, become appreciable until most of the bulk material has been charged.)

EXPERIMENTAL

(1) Electrodes

Nickel hydroxide electrodes were prepared in sintered-nickel plaques by methods described in detail previously (1, 3, 5). Each electrode was charged and discharged three times before use, at a 5-hour charging rate, in order to stabilize its electrochemical behavior (3, 4).

(2) Solutions

All solutions and reagents were prepared as described previously (1, 3), and most experiments were carried out in 1 *N* aqueous KOH at 25° C. Some comparative runs were carried out in 7.2 *N* KOH.

(3) Reversible Potentials

The reversible potential of the Ni^{II}–Ni^{III} system was obtained by extrapolating anodic and cathodic e.m.f. decay lines, plotted logarithmically in time, to the potential of their intersection, as described in a previous paper (1).

The "discharged" electrodes still contained a small amount of the higher oxide of nickel, which at the apparent end of discharging is evidently inaccessible, probably due to insulation by the less conducting $Ni(OH)_2$ (6). The electrodes were reduced completely by prolonged cathodic polarization until a total of 3 F/equivalent had been passed. The electrodes were then transferred to another cell containing freshly prepared electrolyte and reference electrodes, and left on open circuit overnight with purified oxygen bubbling through the cell.

The following sequence of operations was then performed at a current corresponding to a 2-hour charging rate, i.e. at 143 ma g^{-1} of active material calculated as $Ni(OH)_2$ (cf. ref. 1).

(*a*) The electrode was charged for 24 minutes to an extent of oxidation of 20% ($NiO_{1.10}$) based on the oxidation change $Ni^{II} \rightarrow Ni^{III}$ in the oxide. The current was then interrupted and open-circuit decay of potential followed for about an hour.

(*b*) Charging was then continued for 24 minutes, followed immediately by discharge for the same length of time. The current was then interrupted and buildup (i.e. recovery of potential on open circuit to more anodic values) was followed for an hour, the degree of charge again being 20%, as in (*a*).

Anodic and cathodic open-circuit decay and recovery of potential were followed in a similar manner at the 40%, 60%, and 80% charged electrodes, corresponding to formal degrees of oxidation of $NiO_{1.20}$, $NiO_{1.30}$, $NiO_{1.40}$ respectively. Charging and discharging curves for one of these experiments are shown in Fig. 1. Similar charging and discharging cycles were carried out to obtain data for electrodes in 25%, 50%, and 75% degrees of oxidation (see Table I).

TABLE I

Degree of charge (%)	KOH concn. (*N*)	Anodic decay slope		Cathodic buildup slope b_3 (mv)	E_{rev}† (mv)	Number of experiments
		Initial, b_1 (mv)	Lower, b_2 (mv)			
20	1	−12.7	−18.2	+11.0	423	1
25	1	− 9.5±0.6	−18.3±3.5	+13.1±2.1	424±4	5
40	1	−12.0	−15.2	+ 9.0	427	1
50	1	−10.8±1.5	−19.8±5.0	+10.9±1.6	423±5	9
60	1	−35.3	−17.8	+11.4	*	1
75	1	−32±13	−22±2.3	+ 9.4±1.2	*	5
80	1	−60	−21.0	+14.3	*	1
"Overcharge"	1	−45±2.6	—	—	*	6

*See comment in text with regard to these degrees of oxidation.
†The reversible potentials are given vs. that of a Hg/HgO reference electrode in the same solution.

(4) Stationary Potentials

In this series of experiments, the electrodes were charged to a given degree of oxidation, and decay of e.m.f. on open circuit was followed by means of a high-impedance recorder for about a week, at which time the e.m.f. varied at a rate of 1 mv/day or less.

(5) Sparingly Charged Electrodes

A series of experiments was conducted on electrodes charged to a very small extent (0.33% to 5% of total charge capacity).

RESULTS

Plots of decay of e.m.f. after anodic and cathodic polarization vs. log $(t+\theta)$ are shown in Fig. 2. The significance of this type of plot, of e.m.f. decay slopes, and of the parameter θ have been discussed previously (1, 3, 4, 7, 8).

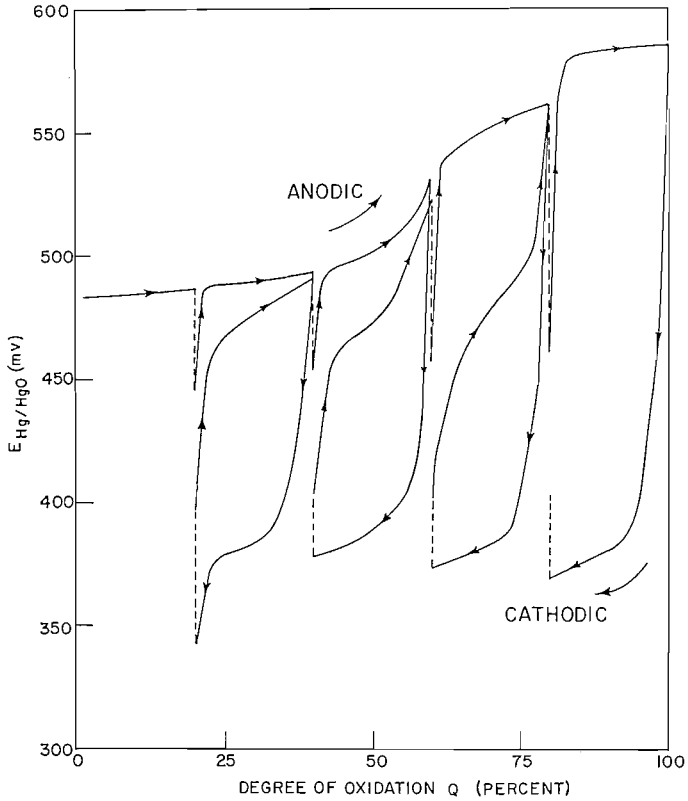

FIG. 1. Anodic and cathodic polarization curves for the nickel oxide electrode in 1 *N* KOH, 2-hour charging rate. Vertical broken lines correspond to open-circuit e.m.f. decay or recovery. Solid lines correspond to changes of potential associated with changes of degree of charge between successive open-circuit measurements.

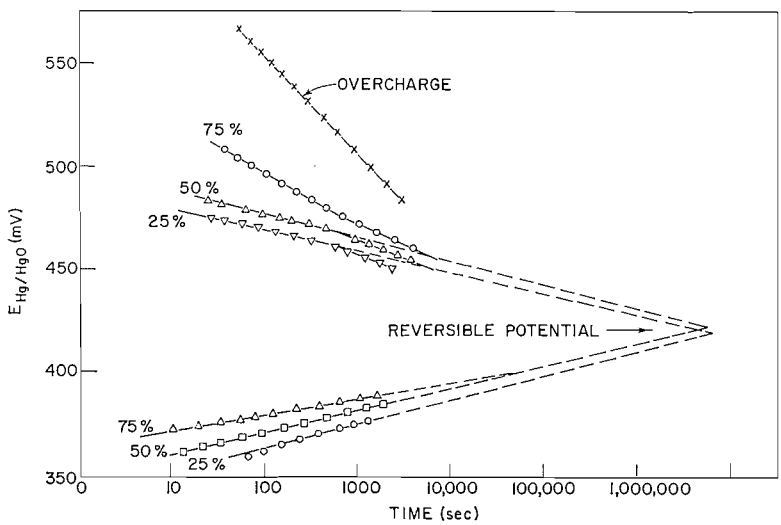

FIG. 2. Decay and recovery of e.m.f. of the nickel oxide electrode in log [time] at various degrees of charge after anodic and cathodic polarization, respectively (data for 1 *N* KOH); compare ref. 1.

All e.m.f. decay lines from anodic polarization are seen to have two distinct regions. For electrodes charged to 50% ("$NiO_{1.25}$") or less, an initial low slope (about −10 mv) is followed by a higher slope (about −20 mv). When the electrode is charged to 75%, a high initial slope (about −32 mv) is followed by the same slope (−20 mv) mentioned above, in the lower-potential region. Electromotive force recovery lines from cathodic polarization have a slope of about +11 mv, independent of degree of charge. Results for a typical individual experiment are given in Fig. 2 and some slight increase of recovery slope is apparent as the charge is reduced; however, this trend does not appear to be very significant statistically (e.g. see Table I).

In Table I, the reversible potentials for the Ni^{II}–Ni^{III} system, obtained by extrapolating cathodic and (initial) anodic e.m.f. decay lines (1), are given for different degrees of charge (between 20% and 50% formal degree of oxidation) of the electrode at 25° C, together with other kinetic parameters. An important result obtained here is that the reversible potential is seen to be *independent* of formal degree of charge over the above range of charge. Similar conclusions were arrived at from two comparative runs in 7.2 *N* KOH.

For reasons to be discussed, it is not possible to obtain the true reversible potentials by extrapolation of cathodic and anodic e.m.f. decay lines above degrees of oxidation of about 50%. In order, however, to study further the potentials of the nickel oxide electrode, the "stationary" or quasi-equilibrium potentials were examined at higher states of oxidation.

In Table II, the "stationary" potentials measured after 4×10^5 and 6×10^5 seconds on

TABLE II

Stationary potentials of the nickel oxide electrode in 1 *N* KOH, 25° C

Degree of charge (%)	Potential reached after 4×10^5 sec (mv, Hg/HgO)	Potential reached after 6×10^5 sec (mv, Hg/HgO)
"Overcharge"	426.5	422.6
50	426.5	424.0
20	420.4	417.2
10	422.6	419.9
7	406.0	404.8
5	401.5	399.3

open circuit are given for various degrees of charge of the electrode between 5% and 100% (overcharged electrode). These results were obtained by reducing the electrode completely, polarizing it anodically to the appropriate degree of charge, and then leaving it on open circuit for 6×10^5 seconds or longer. It is seen that the "stationary potential" measured after a long period of standing on open circuit is still independent of the degree of charge above 10% extent of oxidation ("$NiO_{1.05}$"), and in this respect exhibits a behavior similar to that of the true reversible potentials.

Results of experiments on sparingly charged electrodes (0.33% to 5% degree of oxidation) are shown in Fig. 3, where the e.m.f.–time relation is plotted for decay on open circuit after anodic charging for various degrees of charge. It is seen that the decay process changes qualitatively once quite low degrees of charge are reached. These results can, for the purpose of interpretation, be best represented graphically as plots of the degree of charge, Q, held by the electrode vs. the time required for the electrode potential to decay to a given value (Fig. 4) or in terms of the charge held vs. the potential reached after a given time (Fig. 5). These plots are equivalent to taking cuts at a given value

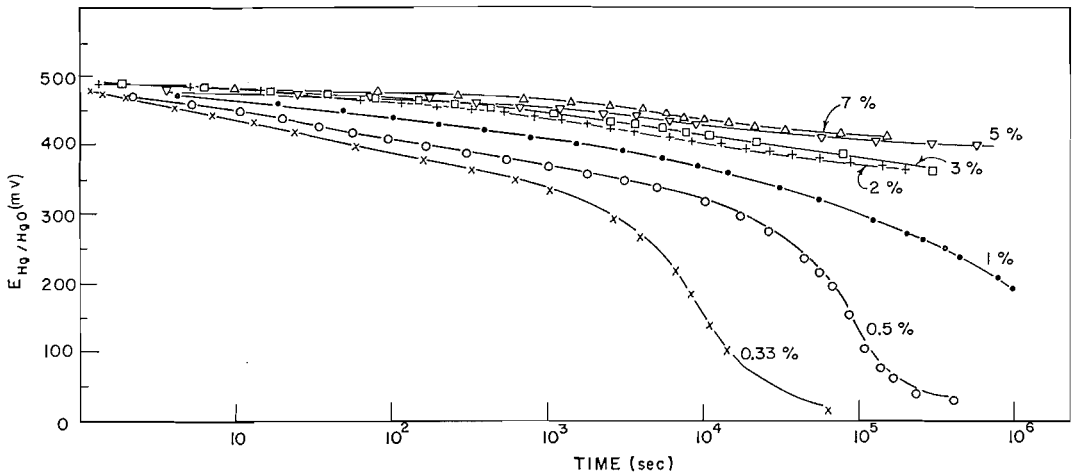

FIG. 3. Plots of e.m.f. decay at sparingly charged electrodes, for various degrees of charge.

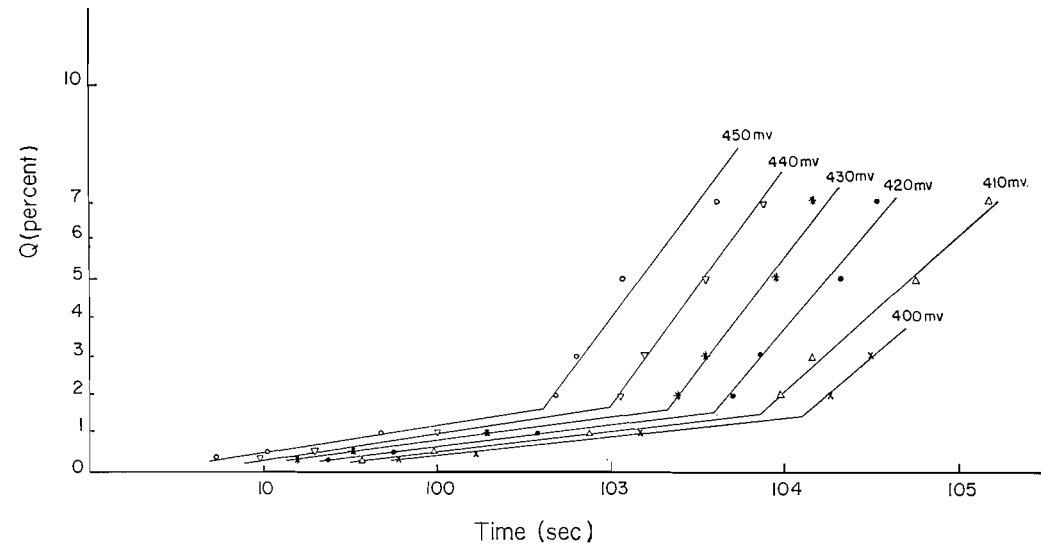

FIG. 4. The length of time necessary for the electrode to reach a certain potential on open circuit vs. the degree of charge of the electrode. (Lines show inflection at common degree of charge $Q = 1.6 \pm 0.1\%$.)

of the abscissa or ordinate in Fig. 3.

It is seen from both these derived plots that two linear regions are observed for each of the two families of lines, which intersect at a degree of charge of ca. $1.5 \pm 0.1\%$. This observation leads to the important conclusion that electrodes charged to 1.5% or less are in a fundamentally different state than electrodes charged to a greater extent of oxidation. This point is further demonstrated by examining the decay slopes listed in Table III below. It was shown previously (1) that the initial low slope (ca. -10 mv) is characteristic of the oxidation of the bulk nickel oxide. In the present work, this slope was only observed for electrodes charged to 2% or more. Below the latter extent of charge, no oxidation of the bulk material appears to occur, and the potential on open circuit drops much more rapidly.

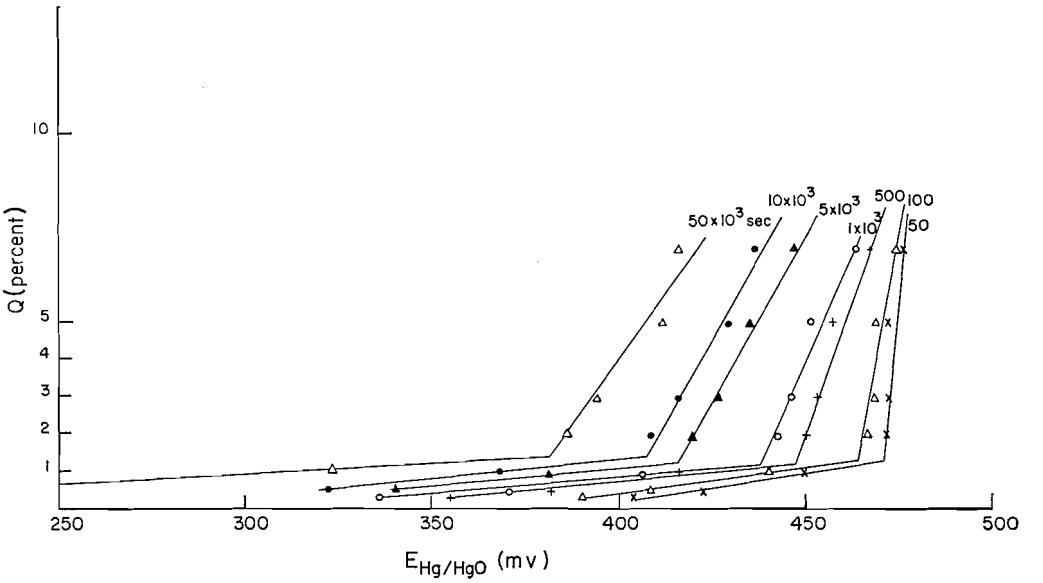

FIG. 5. The potential reached after a given length of time on open circuit vs. the degree of charge. (Lines show inflection at common degree of charge $Q = 1.35 \pm 0.1\%$.)

TABLE III

E.m.f. and e.m.f.–decay behavior at sparingly charged electrodes

Degree of charge (%)	Decay slopes (as in Table I)		E.m.f. V (mv) at time of last measurement	Time of last measurement (10^5 sec) after interruption of polarization	$\Delta V/\Delta t$ for the last day (mv/day)
	b_1 (mv)	b_2 (mv)			
7	—	—	404.8	6	0.2
5	−12.3	−23.2	398.3	7	0.8
3	−15.5	−34.1	366.5	2.8	5
2	−12.6	−34.2	356.1	6	2
1	−34.3	>100	188.6	9.5	8
½	−40	>100	41	4.1	1
⅓	−48	>300	18	0.7	1

DISCUSSION

The reversible potential for the Ni^{II}–Ni^{III} system in the electrochemically formed nickel oxide has been shown to be independent of the degree of charge of the electrode. Between 20% and 50% degree of charge, it was measured by extrapolating anodic and cathodic e.m.f. decay lines, plotted logarithmically in time, as described earlier (1). Values of the reversible potential could only be obtained over a limited range of degrees of oxidation (20–50% of total charge) since at a higher degree of charge the initial low anodic slope, characteristic of the oxidation of the bulk material (1), was not observed (see Fig. 2), and at a very low degree of charge, cathodic e.m.f. recovery lines were irregular and difficult to reproduce.

It is of interest to discuss why the reversible potential cannot be obtained by extrapolation of anodic and cathodic polarization decay lines above a degree of charge of about 50%. In Fig. 2 it is evident that the e.m.f. decay line, e.g. for 75% degree of charge, shows two linear regions in "concave" relationship to one another as also found for the

"overcharged" electrode (3), whereas (1) at lower degrees of charge, a "convex" relation is observed between two linear regions. We have previously shown (1, 3) how such relations arise, respectively, from two processes in an overall mechanism which are consecutive, so that one or the other becomes rate determining, depending on the potential range; or the two processes are parallel and the faster determines the kinetics. Above 50% degree of charge (for example, with the 75% charged electrode), it is clear that the former type of process is operative, as it is in oxygen evolution at overcharged nickel oxide electrodes (3); moreover, the Tafel slopes are similar to those obtained for the oxygen evolution process at the overcharged electrode. We cannot hence identify the initial process as involving the Ni^{II}–Ni^{III} oxidation reaction as we have done for the 50% charged electrode (1) and so cannot obtain the true reversible potential by the extrapolation procedure under these conditions. We can have, in effect, two pathways for the anodic reaction which could be written, for example, as

$$M + OH^- \rightarrow MOH + e \qquad (I)$$

$$MOH + OH^- \rightarrow MO + H_2O + e \qquad (II)$$

(A) oxide oxidation in bulk of material

(B) O_2 evolution by further steps (cf. refs. 1, 3, 15)

e.g.

$$MO + MOH \rightarrow MHO_2 \qquad (III)$$

$$MHO_2 + MOH \rightarrow O_2 + H_2O + M \qquad (IV)$$

or

$$MO + OH^- \rightarrow MHO_2 + e \qquad (V)$$

$$MHO_2 + MOH \rightarrow O_2 + H_2O + M \qquad (IV)$$

or

$$2MO \rightarrow O_2. \qquad (VI)$$

At the higher degrees of charge ($> \simeq 50\%$), the pathway is evidently one involving *consecutive* rate-determining steps and is therefore probably associated with the scheme (I), (II) with pathway (B) to oxygen evolution with, for example, (II) or (VI) (cf. ref. 16) rate determining.

At low degrees of charge, 50% or less, the course of the e.m.f. decay corresponds to alternative reactions, one or the other of which becomes predominant as the potential changes, as we have discussed previously (1). The pathway is thus probably (I), (II), and (A) at short times after decay (higher anodic potentials) and (I), (II), and (B) to oxygen evolution at longer times when the pathway which is faster at lower anodic potentials dominates the kinetics of the decay process.

The above discussion is intended only as a qualitative, plausible explanation of the effects associated with the e.m.f. decay behavior, as a function of charge and we have discussed in detail elsewhere (1, 3, 16) the evidence for assignment of some of the mechanisms involved in the oxygen evolution process in the scheme shown above.

In order to supplement the above data on true reversible potentials, steady or quasi-equilibrium potentials were measured over a wider range of degrees of oxidation (5–100%). The significance of these potentials as kinetically determined mixed potentials

has been discussed previously (1). They cannot be related directly to the reversible potential of the system at different degrees of charge, since the exchange current for the nickel II $\rightarrow$ III oxidation process may strictly depend on the degree of charge. Nevertheless, the constancy of these potentials over a large range of formal degree of oxidation of the electrode ("$NiO_{1.05}$" to "$NiO_{1.50}$"), combined with the fact that the true reversible potential has been shown above to be independent of degree of charge in the range where it is directly accessible, makes it most probable that the reversible potential is, in fact, constant over the whole range of degrees of oxidation where the steady potential is found to be constant. This is contrary to conclusions reported by Lukovtsev and Temerin (9) (using electrodes with a graphite matrix), who claimed that the apparent reversible potential of this system follows a Nernst-type equation with a slope of 0.050 v. The observed variation of actual potential during charging and discharging, on which the latter conclusion was based, may be due to a concentration polarization in the solid phase (6, 9), or a change in effective current density due to a change in available surface area, and not due to a variation of the true reversible potential of the system, as claimed by Lukovtsev and Temerin.

Our present findings are not in conflict with the equation

$$E = a + b_2' \log \left(\frac{q_{ox} - q_{red}}{q_{red}} \right),$$

discussed by Lukovtsev and Temerin and examined and evaluated by Conway and Bourgault (4), since that equation refers to the variation of electrode potential with degree of oxidation of the *surface* phase in the overcharge region, and in fact the potential of the electrode was shown (1) to involve a term corresponding to uptake of adsorbed KOH.

For electrodes charged to less than 10%, the open-circuit steady potential was found to depend on the degree of charge to a large extent. Electrodes charged to 1% or less behaved quite differently from those charged to a greater extent. The results suggest that up to a degree of charge $Q = 1.5 \pm 0.1\%$ (i.e., the average value of Q at the points of intersection of the lines in Figs. 4 and 5) only a surface phase is being charged. Above that, and up to a degree of oxidation of about 10%, both surface and bulk phases are being charged. When the electrode has been charged to 10% of its total charge capacity, it appears that the surface phase is completely charged, and any further charging can then only affect the bulk material.

The variation of the observed true reversible, and stationary or quasi-equilibrium potentials as a function of charge in 1 *M* KOH is shown in Fig. 6. The electrochemical behavior of the electrode is evidently determined by the *surface* phase, since the reversible (or steady) potential is independent of the degree of charge so long as the surface phase is apparently completely charged, i.e., above 10% formal degree of oxidation. The theoretical Nernst plot for a one-electron transfer process (in terms of formal degrees of charge) which would be observed for ideal solid-solution behavior, with the bulk material potential determining, is shown in Fig. 6 for comparison.

The independence of reversible (or steady) potential demonstrated, above a degree of oxidation of 10%, could formally arise for either of the following reasons: (*a*) If the electrode were a two-phase mixture of lower and higher oxide, the potential would be independent of apparent degree of oxidation so long as both oxides were present. (*b*) If the potential were determined by a surface phase of constant composition, superimposed on a bulk phase of varying degree of oxidation but not potential determining, the observed potential would be independent of composition of the bulk.

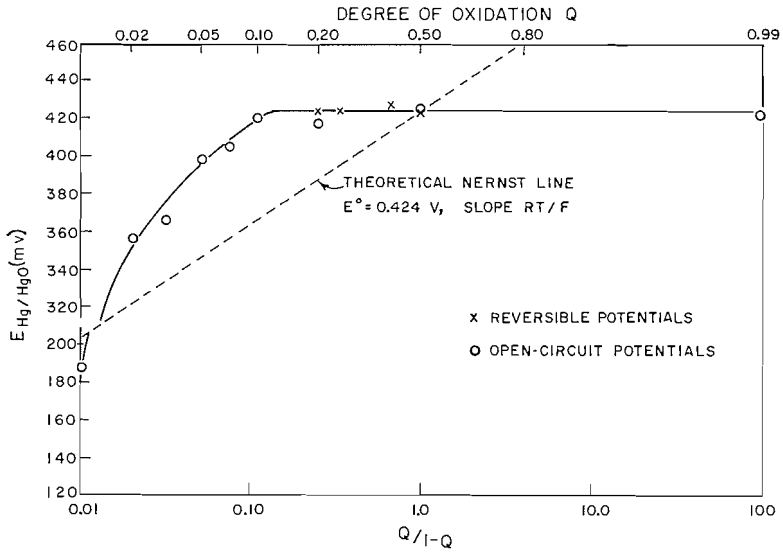

FIG. 6. True reversible potentials and quasi-equilibrium "stationary" potentials of the nickel oxide as a function of degree of oxidation. One-electron theoretical Nernst slope is shown for comparison.

The latter situation, (*b*), is consistent with our previous kinetic conclusions (1) on the mechanism of charging of the bulk material via a surface phase, and our observation of a large adsorption pseudocapacitance associated with the (overcharged) nickel oxide electrode. The former possibility, (*a*), is rendered unlikely by the X-ray diffraction pattern of nickel oxide at various degrees of charge (10, 11) where it was shown that there was a continuous variation of the pattern consistent with a complete range of solid solutions of Ni II and III oxide states. The observed variation of potential between 2% and 10% degree of oxidation confirms the view that a two-phase mixture cannot be present and potential determining, since such a mixture should give a constant potential except at a state of complete oxidation or complete reduction. We must hence conclude that the surface phase is potential determining, and that above a degree of oxidation of 10% of the whole material in the oxide electrode, a more or less constant potential is reached.

We may conclude by summarizing the reasons why previous assignments of reversible potentials (2, 12, 13) are of limited validity:

(*a*) In most cases, kinetically determined mixed potentials were involved which differ from the true reversible values by 0–30 mv depending on concentration of KOH.

(*b*) The species (14), e.g. "NiO_2", to which the potentials were assumed to refer have not been identified or characterized and their existence is doubtful (such species may correspond only to the surface phase at the overcharged electrode).

(*c*) The phase to which the potentials refer is evidently not the bulk phase oxide but the electrochemically active surface phase.

(*d*) Potentials attained during charging or discharging of the electrode differ substantially and neither can be identified with a thermodynamically significant reversible potential.

ACKNOWLEDGMENTS

We are indebted to the Defence Research Board, Department of National Defence, for support of this work on Grant No. 5480-12. One of us, E. G., is indebted to the National Research Council for the award of a scholarship for the year 1962–63.

REFERENCES

1. P. L. BOURGAULT and B. E. CONWAY. Can. J. Chem. **38**, 1557 (1960).
2. F. KORNFEIL. Proceedings of the 127th U.S. Army Battery Research and Development Conference. 1958.
3. B. E. CONWAY and P. L. BOURGAULT. Can. J. Chem. **37**, 292 (1959).
4. B. E. CONWAY and P. L. BOURGAULT. Trans. Faraday Soc. **58**, 593 (1962).
5. E. J. CASEY, P. L. BOURGAULT, and P. E. LAKE. Can. J. Technol. **34**, 95 (1956).
6. B. V. ERSHLER and E. M. KUCHINSKII. Zhur. Fiz. Khim. **20**, 539 (1946).
7. G. ARMSTRONG and J. A. V. BUTLER. Trans. Faraday Soc. **29**, 1261 (1933).
8. H. B. MORLEY and F. E. W. WETMORE. Can. J. Chem. **34**, 359 (1956).
9. P. D. LUKOVTSEV and V. I. TEMERIN. Akad. Nauk S.S.S.R., Otdel. Khim. Nauk, 494 (1953).
10. O. GLEMSER and J. EINERHAND. Z. anorg. Chem. **261**, 26 (1950); Z. Elektrochem. **54**, 302 (1950). G. W. D. BRIGGS and W. F. K. WYNNE-JONES. Trans. Faraday Soc. **52**, 1272 (1956).
11. W. FEITKNECHT, H. R. CHRISTEN, and H. STUDER. Z. anorg. u. allgem. Chem. **283**, 88 (1956).
12. F. FOERSTER. Z. Elektrochem. **13**, 414 (1907); **14**, 17, 285 (1908).
13. J. ZEDNER. Z. Elektrochem. **11**, 809 (1905); **12**, 463 (1906); **13**, 752 (1907).
14. W. M. LATIMER. Oxidation potentials. 2nd. ed. Prentice Hall. 1952.
15. J. O'M. BOCKRIS. J. Chem. Phys. **24**, 817 (1956).
16. B. E. CONWAY and P. L. BOURGAULT. Can. J. Chem. **40**, 1690 (1962).

A PROPOSED STRUCTURE FOR ANNEALED ANODIC OXIDE FILMS OF TANTALUM*

L. D. CALVERT AND P. H. G. DRAPER†
Division of Applied Chemistry, National Research Council, Ottawa, Canada
Received June 1, 1962

ABSTRACT

Anodic oxide films (~1500 Å thick) formed on tantalum in saturated H_3BO_3, saturated Na_2SO_4, 86% H_3PO_4, 1% H_2SO_4, and 100% H_2SO_4 have been examined by a simple but sensitive glancing angle X-ray technique. They are amorphous as formed but can be crystallized on annealing at various temperatures between 500 and 1000° C. The times and temperatures required for crystallization depend on the electrolyte used. The crystallization process is competitive with the dissolution of oxygen in the substrate metal. The observed powder diffraction patterns show considerable variation from sample to sample. Similar variations have been reported in the literature for different samples of Ta_2O_5. A structural model is proposed for β-Ta_2O_5 based on the isostructural relationship with U_2O_5, whose structure is related to that of α-UO_3. This proposed structure consists of linear chains of Ta—O—Ta—O— parallel to the *c* axis with varying disorder in the *ab* plane. This disorder accounts for the observed variations in the patterns. The proposed structure is a defect one and the ordering of these defects may account for some of the reports of irreversible transformations observed on heating Ta_2O_5.

INTRODUCTION

The present paper describes the results of an X-ray investigation of the structure of annealed anodic oxide films formed on tantalum sheet. A recent study of the kinetics of the growth of anodic films on tantalum and niobium by Draper (1) has shown that gross changes in electrolyte composition, for example from 0.1 *N* to 100% H_2SO_4, greatly affect the rate of growth and the voltage at which breakdown finally takes place. Radiotracer experiments showed that electrolyte ions were taken up into the films during growth and that these are associated with the anomalous electrical properties. Similar occlusion of foreign material had been observed previously with porous films formed, for example, on aluminum (2), but not with tantalum or niobium. Draper also obtained reflection and transmission electron diffraction patterns from films formed on tantalum single crystal planes of low index, and confirmed the findings of Vermilyea (3) that anodic films are amorphous. On heating, the films were found to crystallize to orthorhombic β-Ta_2O_5 or β-Nb_2O_5. For films stripped from tantalum crystallization occurred after 15 minutes at 715° C whereas films left on the metal crystallized after 15 minutes at 550° C. The transmission electron diffraction was carried out on thin films (~350 Å) stripped from the metal and on thinned foils (1). The reflection electron diffraction technique is open to the objection that only the surface is examined. Draper (1) and Vermilyea (4) have stated that the nature of the film at the metal/oxide interface is not necessarily the same as that at the surface during the anodization process. Furthermore, data taken from stripped films may not be representative for films on the metal. To overcome these difficulties an X-ray method was chosen for the present study and both stripped and attached films were examined. The simple glancing angle technique used yields good photographs from films as thin as 1000–1500 Å (5, 6) and reaches the metal below the oxide film.

The only other recent X-ray work on anodic films on tantalum is that of Vermilyea (3), who formed 5000 Å thick anodic films in 0.1% Na_2SO_4 and then stripped them from the

*N.R.C. No. 6931.
†National Research Laboratories. Present address: c/o Draper Bros., Dartford, Kent, England.

metal mechanically. Before heat treatment only amorphous X-ray halos were observed. Although no crystallization occurred after heating for 4 hours *in vacuo* at 500° C the three strongest lines of β-Ta_2O_5 appeared after 1 hour at 800° C. Subsequently Vermilyea (7) examined stacks of stripped films with a total thickness of about 2 μ. Increasing sharpness of the X-ray diffraction pattern was correlated with a decrease in the rate of solution in 48% hydrofluoric acid. Burgers *et al.* (8) in 1932, using qualitative X-ray techniques, reported that a thick oxide film on tantalum was crystalline Ta_2O_5.

It is convenient at this point to summarize some of the existing data in the literature concerning Ta_2O_5 and Nb_2O_5. Most workers agree that there are two forms, the β form stable below about 1300° C and the α form stable above that temperature. Others report several forms within this temperature range. There is general disagreement on the exact transition temperatures. King *et al.* (9) and Durbin *et al.* (10) while working at the Battelle Memorial Institute made a careful investigation using pure materials. They found two forms of Ta_2O_5, the β form below about 1300° C and the α form stable above about 1400° C. They proposed an orthorhombic unit cell with $a = 6.18$, $b = 3.66$, and $c = 3.88$ Å for the β form. They also pointed out that this was probably only a subcell because a few lines in the powder pattern could not be indexed on this basis. Lagergren and Magnéli (11) also found two forms, with the high-temperature form having an appreciable oxygen pressure. Schönberg (12) found only one form. Holser (13) reported diffraction patterns which could not be indexed on the simple orthorhombic cell proposed by King (9). Holser suggested that these extra lines may indicate a very large unit cell similar to that of $UO_{2.6}$. Zaslavskii (14), Simanov (15), and Harvey (16) have all reported forms of β-Ta_2O_5 requiring a multiple b axis for satisfactory indexing.

Brauer (17) found three forms of Nb_2O_5. Kramers and Smith (18) found that the presence of small amounts of various impurities in Ta_2O_5, both metallic and non-metallic, had a profound effect on the structures observed. Shafer and Roy (19) found three metastable and two stable forms of Nb_2O_5. Their results agree only in part with those of Brauer. Holtzberg *et al.* (20) also found two or possibly three metastable forms of Nb_2O_5. Frevel and Rinn (21) observed different patterns from different samples of Nb_2O_5 and Ta_2O_5 containing varying amounts of impurity. These three groups of observers report varying line widths in their X-ray patterns. Mohler and Hirst (22) have also reported a form of Ta_2O_5 with a modified electron diffraction pattern, but did not report the actual pattern. Lapitskii *et al.* (23) reported two forms of β-Ta_2O_5, one stable from 400° C to 600° C and the other stable above 600° C; both forms were orthorhombic. Wasilewski (24) examined the solubility of oxygen in tantalum and found a maximum solubility of 0.88 wt% at 1050° C. He also found two forms of Ta_2O_5.

EXPERIMENTAL

The tantalum used was in the form of rolled sheet (0.025 cm thick) obtained from A.E.R.E. Harwell, England, with a nominal analysis of 99.99% Ta, the remainder Nb except for 80 to 100 p.p.m. of N_2, O_2, and C. Sheet niobium was obtained from the same source with an analysis of Fe 420, Si 340, C 80, H_2 3, O_2 110, N_2 110 p.p.m. and the remainder Nb. The specimens were cut in the form of plates 2×0.5 cm with a thin, heavily oxidized tag at one corner to serve as a current lead. Each was first degreased, then chemically polished in a fresh solution of 40% HF, 70% HNO_3, 98% H_2SO_4 in the ratio 2:2:5 (3). X-ray examination of the surfaces prepared in this way showed a coarse-grained b.c.c. metal pattern ($a_0 = 3.3030$ Å) with the expected rolling texture. Initially, specimens were formed to a voltage just below breakdown in order to obtain the maximum amount of material. However, the X-ray technique used proved to be so sensitive that the greatest thickness was not needed and the more desirable procedure was adopted of forming all specimens to about 100 v at 1 ma/cm². For a dilute aqueous solution 1 volt ≈ 15 Å of anodic oxide on tantalum and hence these films were roughly 1500 Å thick. This thickness was also estimated from the interference color. The electrolytes used were 1% and 100% H_2SO_4, 86% H_3PO_4, and saturated solutions of Na_2SO_4 and H_3BO_3.

The films were examined in an 11.46 cm diameter powder camera using vanadium foil filtered Cr radiation, 0.25 mm aperture collimators, and an oscillation angle of 10° on either side of the mean glancing angle of 25°. Exposures for the films examined *in situ* ranged from 80 to 120 ma hr whilst stripped films required 650 ma hr. A modified single-crystal Unicam 3 cm diameter cylindrical camera was also used in checking for possible orientation of the oxide film. After examination in the "as-formed" state, specimens were annealed at 550, 700, and 1000° C, a few in open silica tubes and the rest in well degassed silica tubes sealed off at about 10^{-5} mm of air. The temperatures were selected to cover the range thought to be of potential significance. Attempts to extend the annealing range above 1000° C always resulted in the loss of the oxide film. No attempt was made to examine the known influence of electric fields on crystallization (25, 7).

RESULTS

Some 40 specimens were examined in all. The films as formed yielded X-ray patterns showing only the metal substrate plus considerable background scatter. Annealing first reduced this scatter and then produced a crystalline diffraction pattern. The time and temperature required to produce crystallization varied markedly with the forming electrolyte. For example a film formed in saturated boric acid required 15 minutes at 550° C whereas one anodized in 86% H_3PO_4 had not crystallized after heating for 100 hours at 550° C. These observations yield upper limits for the crystallization temperatures of films formed in the various electrolytes as follows: 550° C (25 hours) for 1% H_2SO_4, 700° C (4 minutes) for 100% H_2SO_4, 700° C (8 minutes) for 86% H_3PO_4, 750° C (15 minutes) for saturated Na_2SO_4, and 550° C (15 minutes) for saturated H_3BO_3. Table I gives representative observed patterns and also includes the Battelle Memorial Institute pattern (9) of Ta_2O_5 obtained from the Fansteel Metallurgical Corporation and fired at 1200° C. The observed d values are omitted for brevity, since they are equal to those in the standard pattern within the accuracy of the glancing angle technique used. Intensities were measured by visual comparison with a logarithmic interval scale; a dash signifies that the line in question was not observed; the breadth of the lines is indicated by letters s = sharp, b = broad, vb = very broad. The metal substrate pattern is omitted although present in all cases except the thick film formed by heating in air. The annealed oxide pattern never showed any preferred orientation. The air-formed film is very similar to the material examined by King *et al.* (9) but with the significant absence of the extra lines which they could not index on the basis of their unit cell. The patterns vary considerably, both in intensity and width of the observed lines. Despite this apparent variability it is possible to index all the patterns on the simple unit cell put forward by King *et al.* (9) in the setting $a = 6.18$, $b = 3.66$, $c = 3.88$ Å, provided one assumes varying degrees of disorder for the a or b axes or both. Thus the orders of $00l$ are sharp and the reflections hkl, $hk0$, $h00$, and $0k0$ are broadened to varying degrees, sometimes not being observed at all. The three lines (002) $d = 1.95$, (020) $d = 1.83$, and (310) $d = 1.80$ Å were observed to be particularly sensitive to the degree of ordering present. The pattern for the air-formed film is also similar to that reported by Frevel and Rinn (21).

It was also found that crystallization is a process competitive with the dissolution of oxygen in the substrate. The value of 3.3030 Å for the lattice parameter of the polished surface agrees well with the values of 3.3026 Å (24, 26) and 3.3029 Å (27) for oxygen-free metal. For certain intermediate times and temperatures of annealing much higher values for the metal lattice parameter were observed, e.g. after heating for 8 minutes at 700° C a specimen covered by a film formed in 86% H_3PO_4 gave a metal pattern with $a = 3.3140$ Å, equivalent to 0.75 wt% O_2. These values were associated with marked line broadening for the metal pattern, indicating the existence of a range of oxygen concentration near the surface. Prolonged heating *in vacuo* resulted, in many cases, in complete dissolution of all the available oxygen into the metal, as shown by the disappearance of the oxide

TABLE I

Representative data for annealed Ta_2O_5 films

	Ta_2O_5 pattern*									
	I_{obs}	d, Å	(hkl)	Air, 700° C	H_3BO_3,† 700° C	H_3BO_3, 700° C	1% H_2SO_4, 700° C	100% H_2SO_4, 700° C	86% H_3PO_4, 700° C	Na_2SO_4, 750° C
	90	3.87	001	80 s	100 s	100 vs	100 s	50 b	100 b	100 s
	10	3.36	—							
	100	3.15	110	100 b	15 b	20 s	5 b	100 b	35 vb	25 b
	50	3.09	200			40 s	16 s			
	20	2.55	—							
	100	2.46	111	17 b	15 b	45 s	3 b	50 b	45 vb	30 b
	60	2.43	201			45 s	16 s			
	20	2.36	210							
	10	2.11	300	2						
B	30	2.02	211	2		3 b				
	50	1.95	002	13 s	20 s	25 vs	15 s		15 b	40 s
	40	1.83	020	10 b	1					
	40	1.80	310		1	12 b	3 b		7 vb	
	20	1.76	120							
	10	1.71	012							
	10	1.68	—							
	100	1.661	021	10 b	13 b	1			1	20 b
	40	1.655	202							
	30	1.632	121		1	1				
	30	1.582	220	3 b	1				10 b	
	30	1.551	400							
	20	1.504	212							
	10	1.487	—							
	40	1.463	221	2 b	1					
	30	1.441	401							
	10	1.427	410							
B	30	1.405	302?							
	30	1.387	320?							
	70	1.338	022	2 vb	3 b					
	60	1.322	312							
	20	1.310	122							
	20	1.300	003	1 s	5 s	1				2 s
	10	1.272	103							
	20	1.252	—							
	10	1.237	500	2 vb	1 b					8 b
	40	1.227	222							
	20	1.215	402							
B	80	1.20	113+	3 vb	8 vb	8 b	5 b		3 vb	12 b
B	30	1.18	420							
	plus 5 lines to d = 1.097									

*From ref. 9.
†Stripped film.

diffraction pattern and the sharpening of the metal lines as the surface concentration fell to a constant value somewhat greater than that of the pure metal. However, at other times the oxide pattern remained, apparently because a diffusion barrier was set up between the oxide and metal before appreciable diffusion could take place. When annealed at 1000° C the oxide films coalesced into small particles and broke away completely from the metal. The loss of oxygen to the environment during annealing, while not ruled out, is apparently not a major process.

To examine the possible effect of the metal, some films formed in boric and 1% sulphuric acids were stripped from the substrate by cathodic polarization in 1% H_2SO_4, floated off onto water, and transferred to platinum grids for annealing in air and *in vacuo*. It was not found possible to strip films formed in 100% H_2SO_4. In all but one case these yielded Ta_2O_5 patterns similar to those listed in Table I, with the triplet (002),(020),(310) being present. This exception was a film formed in saturated boric acid and annealed *in vacuo*

for 10 hours at 700° C after stripping. This specimen yielded an hexagonal pattern with $a = 5.150$ and $c = 13.76$ Å which matches closely that reported for $LiNbO_3$ (28). The conditions for its formation, possibly a small loss of oxygen, were not investigated further. In another experiment a film formed by heating a sheet of tantalum in air for 10 minutes gave an hexagonal pattern with $a = 3.18$ and $c = 4.79$ Å. As this cell is closely related to that reported by Schönberg (29) for a Ta–N–O phase it is possible that a nitrogen-containing compound had been formed in this case.

Some preliminary experiments with anodically formed Nb_2O_5 films on niobium sheet indicated a disordered structure after annealing. The results were not extensive enough to establish the disordering scheme, which was not the same as that found for Ta_2O_5. The times and temperatures for crystallization are not the same as those required for similar Ta_2O_5 films.

DISCUSSION

A structure for orthorhombic Ta_2O_5 which accounts for the above results can be derived by noting that Ta_2O_5, Nb_2O_5, Pa_2O_5, and U_2O_5 (Table II) are isomorphous and

TABLE II

Selected data for compounds related to Ta_2O_5

Compound	a, Å	b, Å	c, Å	D_{calc}	Vol., Å^3	Ref.
Ta_2O_5	6.18	3.66	3.88	8.35	87.8	9
"	12.38	44.02	7.79	8.29	4245.0	38
"	6.2	69.6	3.9	8.28	1683.0	16
"	7.78	7.67	12.69	(7.75)	757.0	15
"	7.77	12.40	12.59	(7.99)	1213.0	15
"	7.75	6.48	7.48	(7.81)	376.0	23
"	6.19	44.02	3.90	8.28	1063.0	14
Nb_2O_5	6.19*	3.65*	3.94*	4.96	89.0*	32
U_2O_5	6.73	31.72	8.29	8.34	110.5*	33
U_3O_8	6.70	11.98	4.15	8.39	333.0	34
"	6.72	3.98	4.14	8.42	110.7	33
UO_3	6.88	3.97	4.17	8.35	113.8	31

*Subcell.

isostructural (30, 31, 13). Further, α-UO_3, U_3O_8, and U_2O_5 are special compositions existing within a range of continuous variation (32, 33). The structure derived for α-UO_3 by Zachariasen (31) is shown in Fig. 1. It consists of a somewhat distorted primitive cubic lattice of oxygen ions with uranium ions placed in the center of one out of every three

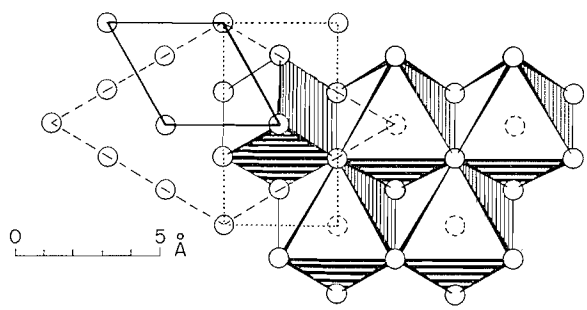

FIG. 1. Zachariasen's (31) structure for α-UO_3. The heavy lines show a single unit cell. Siegel's (34) cell for H.T. U_3O_8 is outlined in dashed lines. The cell proposed by Grønvold (35) for U_3O_8 is outlined in dotted lines. The octahedra of oxygens around the U sites are shown on the right of the diagram. The primitive cube of oxygens is also indicated in the center.

such cubes, giving the composition $U_3O_3-2U = UO_3$. The structure is referred to an hexagonal cell with $a = 3.971$, $c = 4.168$ Å where c is parallel to the body diagonal of the primitive cubic lattice of the oxygen ions. Using the space group $P\bar{3}m1$ (D_{3d}^3) there is one U in 1(a) at 000, one O_I in 1(b) at 0,0,1/2, and two O_{II} in 2(d) at 1/3,2/3,0.17 and 2/3,1/3,0.83. Grønvold (34) has proposed a structure for U_3O_8 that is essentially the same as that for α-UO_3 but the oxygen atoms are not located. The cell used (Fig. 1) is closely related to the orthohexagonal setting of α-UO_3. The densities observed for U_3O_8 (Table II) and U_2O_5 are compatible only with subtractive UO_3 structures. Siegel (33) has deduced a slight variation of the α-UO_3 structure for a high-temperature form of U_3O_8 which can be referred to hexagonal axes related to both the UO_3 axes and the low-temperature U_3O_8 axes (Fig. 1). He notes that the lattice is oxygen deficient to a variable extent depending on the heat treatment. More recently Andresen (36) has determined the U_3O_8 structure by neutron diffraction and found the same closely linked U—O—U—O chains. The U_2O_5 structure is closely related to the UO_3 and U_3O_8 structure (32, 36) and presumably contains the same metal lattice with the vacancies necessary to give the 2:5 formula. This structure will presumably have the same closely linked chains of U—O—U—O atoms (U—$O_I \approx 2.08$ Å) parallel to c with more loosely linked octahedra of six O_{II} atoms around each U (U—$O_{II} \approx 2.39$ Å). Since the O_I atoms are so closely bound to the U it seems reasonable to suppose that the O_{II} atoms will be the ones removed to provide the necessary vacancies in the U_2O_5 structure, as was shown to be the case for U_3O_8 (36). Assuming the same structure for β-Ta_2O_5, as suggested by Elson (30), the observations of disordered Ta_2O_5 diffraction patterns given above can be tentatively described in terms of a simple structural model.

In this model, the structure of Ta_2O_5 consists of linear chains of closely bonded Ta—O—Ta—O ions parallel to c with varying degrees of disorder in the ab plane perpendicular to c, i.e. a chain structure with the chains parallel but rotated randomly with respect to each other. This disorder arises from the possibility of choosing any one of six equivalent O_{II} atoms in each octahedron for the vacancies required by the 2:5 formula. This structure is a notably open one and has both cation and anion vacancies. The c axis, which has been assumed to be parallel to the chains of —Ta—O—Ta—O atoms, has a value close to that calculated on the basis of Zachariasen's equation for interionic distances (35); $D = R_c+R_a+\Delta N-K$. Here D is the interionic distance, R_c and R_a the cation and anion radii, ΔN a correction for coordination number, and K a constant equal to zero for an ionic compound. Taking 0.81 Å for Ta^{5+} and 1.46 Å for O^{2-} with $\Delta N = -0.31$ Å for 2-fold coordination, then $D = 0.81+1.46-0.31 = 1.96$ Å whilst c observed = 3.88 Å (9) $\approx (1.96\times2)$ Å.

From this structure three main types of diffraction pattern may be expected. Firstly, one with defects statistically disordered so that the mean unit cell is the orthorhombic pseudocell with $a = 6.18$, $b = 3.66$, and $c = 3.88$ Å. Secondly, another with the c axis well ordered but the defects so disordered in the plane perpendicular to c that the a or b axes or both are no longer well defined. Finally, in the exceptional cases where the ordering of the defects has been propagated over considerable distances single crystals result with axes which are multiple lengths of the basic mean orthorhombic cell (see Table II). Implicit in this model of the β-Ta_2O_5 structure is the possibility that the observed diffraction pattern for any Ta_2O_5 sample will be a function of its thermal history and that the presence of cationic or anionic impurities may markedly alter both the kinetics and the kind of ordering at any given temperature.

Examples of the diffraction pattern corresponding to a well-ordered structure with the

defects statistically distributed are those observed for the air-formed film or the stripped borate film (Table I). Both contain no lines which cannot be indexed on the orthorhombic Battelle Memorial Institute cell (9). It is interesting to note that the pattern of Frevel and Rinn (21), which is very similar to these two patterns, also contains the same sharp and broad lines.

The other type of diffraction pattern in which the *a* and *b* axes are defined in varying degrees can be represented by the remaining patterns in Table I. The many variations possible within this scheme encompass most of the published patterns for β-Ta_2O_5 and some of those for the isomorphous β-Nb_2O_5. Peterson *et al.* (37), in particular, give a table (their Table I, p. 1041) which shows all the features to be expected from a series of samples having varying degrees of order. Many of the reports of irreversible changes occurring on heating Ta_2O_5 and Nb_2O_5 can be interpreted as successive stages of ordering processes (17, 19, 20), since the difference observed between the various forms consists in the detection of additional lines upon continued annealing and the patterns contain both sharp and broad lines.

Finally in those cases where single crystals or very well crystallized powders have been studied (11, 13–16, 23) a very large unit cell related to the basic orthorhombic unit cell has been found or it has been necessary to use such a cell to index the observed powder pattern. The monoclinic cell reported for the stable β form has a β angle close to 120° and is geometrically related to the hexagonal subcell of the orthorhombic β-Ta_2O_5 cell. Plainly quite extensive variations of the basic orthorhombic cell are probable, as may be seen from the values given in Table II, and these are likely to be sensitively dependent on the presence of foreign material, e.g. water (14, 23) or traces of alkali (9, 10, 21) or common metallic contaminants (18).

It seems probable that the annealing of films in contact with a tantalum surface was responsible for the relative uniformity and simplicity of the X-ray-diffraction results in the present study. The purity of the tantalum and the thinness of the films may also have been determining factors.

CONCLUSIONS

(1) Anodically formed films of Ta_2O_5 are amorphous when formed at voltages below breakdown in the electrolytes used.

(2) Upon heating they crystallize to a disordered form of β-Ta_2O_5 with the *c* axis ordered while the *a* and *b* axes are disordered in varying degrees.

(3) A structural model composed of linear chains of Ta—O—Ta—O parallel to the *c* axis but randomly rotated around the *c* direction is consistent with the observed data.

ACKNOWLEDGMENTS

The authors wish to thank Miss M. McLellan, who prepared the X-ray photographs.

REFERENCES

1. P. H. G. Draper. Ph.D. Thesis, University of London, London, England. 1959.
2. J. E. Lewis and R. C. Plumb. J. Electrochem. Soc. **105**, 496 (1958).
3. D. A. Vermilyea. Acta Met. **1**, 282 (1953).
4. D. A. Vermilyea. Acta Met. **2**, 482 (1954).
5. J. D. Wilkinson and L. D. Calvert. J. Sci. Instr. **37**, 399 (1960).
6. J. D. Wilkinson and L. D. Calvert. J. Sci. Instr. **39**, 87 (1962).
7. D. A. Vermilyea. J. Electrochem. Soc. **104**, 485 (1957).
8. W. G. Burgers, A. Claasen, and J. Zernicke. Z. Physik. **74**, 593 (1932).
9. B. W. King, J. Schultz, E. A. Durbin, and W. H. Duckworth. Reports of the Battelle Memorial Institute. No. 1106. 1956. X-ray Powder Data File Card 8-255.

10. E. A. DURBIN, A. E. WAGNER, and C. G. HARMAN. Reports of the Battelle Memorial Institute. No. 792. 1952.
11. S. LAGERGREN and A. MAGNÉLI. Acta. Chem. Scand. **6**, 444 (1952).
12. N. SCHÖNBERG. Acta Chem. Scand. **8**, 240 (1954).
13. W. T. HOLSER. Acta Cryst. **9**, 196 (1956).
14. A. I. ZASLAVSKII, R. A. ZWINCHUK, and A. G. TUTOV. Doklady Akad. Nauk S.S.S.R. **104**, 409 (1955).
15. YU. P. SIMANOV, A. V. LAPITSKII, and E. P. ARTAMONOVA. Vestnik Moskov. Univ. Ser. Fiz.–Mat. i Estestven Nauk, **9**, 109 (1954).
16. J. HARVEY. Ph.D. Thesis, University of London, London, England. 1959. J. HARVEY and H. WILMAN. Acta Cryst. **14**, 1278 (1961).
17. G. BRAUER. Z. anorg. Chem. **248**, 1 (1941).
18. W. J. KRAMERS and J. R. SMITH. Trans. Brit. Ceram. Soc. **56**, 590 (1957).
19. M. W. SHAFER and R. ROY. Z. Krist. **110**, 241 (1958).
20. F. HOLTZBERG, A. REISMAN, M. BERRY, and M. BERKENBLIT. J. Am. Chem. Soc. **79**, 2039 (1957).
21. L. K. FREVEL and H. W. RINN. Anal. Chem. **27**, 1329 (1955).
22. D. MOHLER and R. G. HIRST. J. Electrochem. Soc. **108**, 347 (1961).
23. A. V. LAPITSKII, YU. P. SIMANOV, K. N. SEMENENKO, and E. I. YAREMBASH. Vestnik Moskov. Univ. Ser. Fiz.–Mat. i Estestven Nauk, **9**, 85 (1954).
24. R. J. WASILEWSKI. J. Am. Chem. Soc. **75**, 1001 (1953).
25. E. A. WOOD and R. C. MILLER. Abstr. Am. Cryst. Assoc. Meeting, Boulder, Colorado. 1961. No. D8.
26. M. C. NEUBERGER. Z. Krist. **93**, 312 (1936).
27. J. W. EDWARDS, R. SPEISER, and H. L. JOHNSTON. J. Appl. Phy. **22**, 424 (1951).
28. A. V. LAPITSKII and YU.P. SIMANOV. Zhur. Fiz. Khim. **29**, 1201 (1955).
29. N. SHÖNBERG. Acta Chem. Scand. **8**, 199, 620 (1954).
30. R. ELSON, S. FRIED, P. SELLERS, and W. H. ZACHARIASEN. J. Am. Chem. Soc. **72**, 5791 (1950).
31. W. H. ZACHARIASEN. Acta Cryst. **1**, 265 (1948).
32. R. E. RUNDLE, N. C. BAENZIGER, A. S. WILSON, and R. A. MCDONALD. J. Am. Chem. Soc. **70**, 99 (1948).
33. S. SIEGEL. Acta Cryst. **8**, 617 (1955).
34. F. GRØNVOLD. Nature, **162**, 70 (1948).
35. W. H. ZACHARIASEN. Z. Krist. **80**, 137 (1931); Phys. Rev. **73**, 1104 (1948); Abstr. Am. Cryst. Assoc. Meeting. 1950. p. 29.
36. A. F. ANDRESEN. Acta Cryst. **11**, 612 (1958).
37. R. C. PETERSON, W. M. FASSELL, and M. E. WADSWORTH. J. Metals, **6**, 1038 (1954).
38. A. I. ZASLAVSKII and R. A. ZWINCHUK. Zapiski Vsesoyuz. Mineral. Obshchestva, **81**, 323 (1952).

ORGANOPHOSPHORUS COMPOUNDS

X. PHOSPHORISOCYANATIDIC DIFLUORIDE AND CHLORIDE FLUORIDE. PREPARATION OF ALKYL CARBAMATOPHOSPHORODIFLUORIDATES AND UREIDOPHOSPHORODIFLUORIDATES[1,2]

STEPHEN J. KUHN AND GEORGE A. OLAH
Exploratory Research Laboratory, Dow Chemical of Canada, Limited, Sarnia, Ontario

Received April 18, 1962

ABSTRACT

Phosphorisocyanatidic difluoride and phosphorisocyanatidic chloride fluoride were prepared. Addition reactions with alcohols (phenol) and amines were investigated, leading to carbamatophosphorodifluoridates and ureidophosphorodifluoridates.

Phosphorus oxyhalides are used as starting materials for the preparation of many organophosphorus compounds. The reactive halogens can be easily replaced by alkoxy, amido, mercapto groups, etc. The replacement of one of the halogens with an isocyanate group in the phosphoryl halides increases the versatility of these compounds and enables the preparation of many new groups of organophosphorus compounds.

Phosphorisocyanatidic dichloride was prepared by Kirsanov (2) by the interaction of ethylcarbamate and phosphorus pentachloride:

$$CH_3—CH_2—O—\overset{\overset{O}{\|}}{C}—NH_2 + PCl_5 \rightarrow Cl—\overset{\overset{O}{\|}}{\underset{\underset{Cl}{|}}{P}}—NCO + C_2H_5Cl + 2HCl.$$

Phosphorisocyanatidic dichloride partially decomposes when distilled at atmospheric pressure or when stored at room temperature over long periods of time. It was hoped that by preparing the corresponding difluoridate or chlorofluoridate more stable compounds would be obtained. These could be useful new polyfunctional reagents for the preparation of derivatives of fluorophosphoric acid (3).

Phosphorisocyanatidic dichloride readily reacts with antimony trifluoride, in the absence of catalyst, to give a 90% yield of the corresponding difluoride, without interacting with the isocyanate group:

$$6Cl—\overset{\overset{O}{\|}}{\underset{\underset{Cl}{|}}{P}}—NCO + 4SbF_3 \rightarrow 6F—\overset{\overset{O}{\|}}{\underset{\underset{F}{|}}{P}}—NCO + 4SbCl_3.$$

The reaction is fast and exothermic; therefore the antimony trifluoride is added in small portions to the phosphorisocyanatidic dichloride. The lower-boiling difluoride distills out from the reaction vessel as it forms. Phosphorisocyanatidic difluoride is a colorless liquid which fumes if exposed to moist air. It boils at atmospheric pressure at 68–68.5°.

It is readily soluble in solvents like methylene chloride, chloroform, carbon tetrachloride, benzene.

[1]*Contribution No. 64.*
[2]*For Part IX, see reference 1.*

The infrared spectrum shows maxima at 2247, 1458, 1351, 952, 905, 752 cm^{-1}, indicating the presence of the isocyanate group and P—F bonds. (See Fig. 1.)

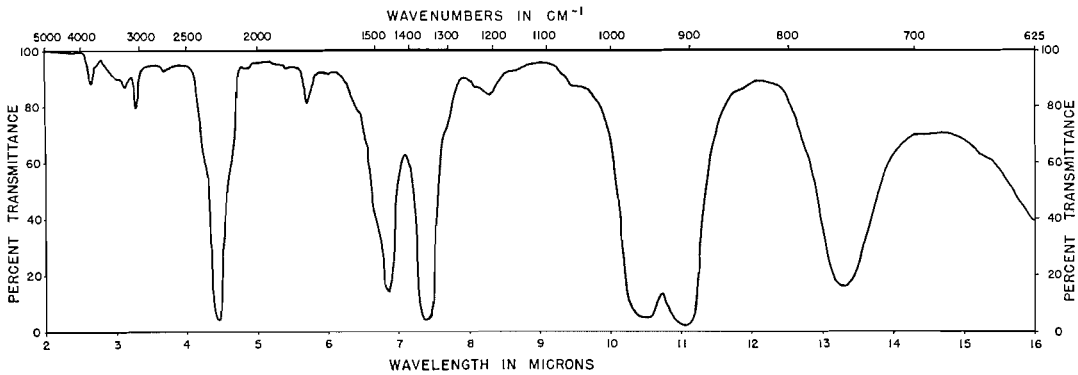

FIG. 1. Infrared spectrum of phosphorisocyanatidic difluoride.

Phosphorisocyanatidic difluoride can be distilled at atmospheric pressure and kept at room temperature for a long time without decomposition. It hydrolyzes, however, very rapidly with water. Therefore all operations must be carried out under dry conditions. In the halogen exchange reaction, in addition to the main product, about 10% phosphorisocyanatidic chloride fluoride, OCNPOFCl, b.p. 101–103°, is formed.

Phosphorisocyanatidic difluoride reacts easily with alcohols (phenol), yielding alkyl carbamatophosphorodifluoridates:

$$F{-}P(=O)(F){-}NCO + ROH \rightarrow F{-}P(=O)(F){-}NH{-}C(=O){-}OR.$$

The carbamate derivatives are stable solid compounds and can be distilled under reduced pressure without decomposition. Table I lists the new carbamates that have been prepared. With an excess of alcohol the fluorides can be replaced by alkoxy groups only with difficulty. The use of sodium alcoholates is more advantageous.

TABLE I

Carbamatophosphorodifluoridates, $RO{-}C(=O){-}NH{-}POF_2$

R	% yield	B.p., °C/mm Hg	M.p., °C	% N		% P	
				Calc.	Found	Calc.	Found
Methyl	90	95/5	51–52	8.80	8.74	19.44	19.31
Ethyl	94	91–92/3	35–36	8.09	7.97	17.91	17.80
Isopropyl	93	101–102/6	54–55	7.48	7.52	16.57	16.42
Phenyl	94	—	80–83	6.33	6.28	14.01	14.14

Primary and secondary amines react with phosphorocyanatidic difluoride to give substituted alkyl (aryl) ureidophosphorodifluoridates:

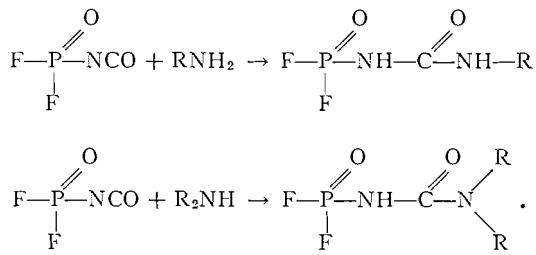

Table II summarizes data of the prepared ureidophosphorodifluoridates.

TABLE II

Ureidophosphorodifluoridates, R,R′—N—C(=O)—NH—POF_2

R	R′	% yield	M.p., °C	% N Calc.	% N Found	% P Calc.	% P Found
C_2H_5	H	91	66–67	16.28	16.16	18.00	17.85
C_2H_5	C_2H_5	90	Visc. oil	14.00	13.95	15.48	15.52
C_6H_5	H	94.4	111–112	12.73	12.64	14.08	14.15
$C_6H_5CH_3$	CH_3	92	87	11.96	11.87	13.23	13.30

EXPERIMENTAL

Preparation of Phosphorisocyanatidic Dichloride (2)

One mole of PCl_5 and 1 mole of ethylcarbamate were placed in a 1-liter round-bottomed flask equipped with a reflux condenser and drying tube, and kept at 10° by means of external cooling. In a few minutes HCl formation begins. The temperature of the bath was kept 10° for 45 minutes, then it was carefully raised at a rate of 1°/6 minutes up to 50°, then by 1°/2 minutes up to 80° (5.5 hours total reaction time). The by-product HCl and ethyl chloride escaped through the reflux condenser. Fractionation of the residual liquid product gave 140 g of pure $POCl_2NCO$ (87.5%), b.p. 64–60° at 50 mm. CCl_2NO_2P: found: P 19.5, Cl 44.3, N 8.6; Calc.: P 19.4, Cl 44.37, N 8.75%.

Preparation of Phosphorisocyanatidic Difluoride

Phosphorisocyanatidic dichloride (160 g, 1 mole) was placed into a two-necked flask equipped with powder feeder and condenser. SbF_3 (150 g) was added in 6–10 portions to the chloride. The reaction is exothermic and the product distills out as it forms. After the addition of the SbF_3 the flask was heated to remove all the remaining product. Liquid product (130 g) was obtained, which after fractionation through a 300-mm Widmer column gave two fractions: POF_2NCO: b.p. 68–68.5°; 115 g (90% yield); n_D^{25} 1.3381; d_{25} 1.5899 (CF_2NO_2P (127): calc.: N 11.0, P 24.4, F 29.9; found: N 10.80, P 23.9, F 29.7%) and POFClPNCO: b.p. 101–103°; 10 g; n_D^{25} 1.4024 (calc. N 9.76, P 21.0, Cl 24.7; found: N 9.78, P 21.4, Cl 24.6%).

Reaction of Phosphorisocyanatidic Difluoride with Alcohols

POF_2NCO (0.25 mole) was dissolved in 50 ml of CH_2Cl_2 and into the stirred solution 0.25 mole of alcohol in 20 ml of CH_2Cl_2 was added dropwise at 0°. The reaction is completed in a few minutes. Methylene chloride was pumped off and the residual liquid product fractionated under reduced pressure.

The reaction with phenol was carried out in essentially the same manner, but due to decomposition the product could not be distilled and was purified by recrystallization from chloroform or benzene.

Reaction of Phosphorisocyanatidic Difluoride with Amines

POF_2NCO (0.25 mole) was dissolved in 50 ml of CH_2Cl_2 and into the stirred solution 0.25 mole of amine in 20 ml of CH_2Cl_2 was added dropwise, while the temperature of the mixture was kept around 0°. The reaction is completed in a few minutes. The methylene chlorided was removed by distillation and finally

by pumping the product in vacuum. Attempted distillation of the products, even under pressure, resulted in decomposition. The products, which are essentially pure after removal of the solvent, and any possible volatile starting materials were recrystallized from chloroform or CCl_4.

ACKNOWLEDGMENTS

The authors thank D. G. Barnes for the infrared spectra and K. Sketris for the analyses.

REFERENCES

1. G. A. OLAH and A. A. OSWALD. Can. J. Chem. This issue.
2. A. V. KIRSANOV. J. Gen. Chem. (U.S.S.R.), **24**, 1033 (1954); Chem. Abstr. **49**, 8787 (1955).
3. G. A. OLAH and S. J. KUHN. Can. Patent No. 597,955 (1960).

OBSERVATIONS ON THE KARPLUS CURVE IN RELATION TO THE CONFORMATION OF THE 1,3-DIOXOLANE RING[1]

R. U. LEMIEUX,[2] J. D. STEVENS,[3] AND R. R. FRASER
Department of Chemistry, University of Ottawa, Ottawa, Ontario

Received March 19, 1962

ABSTRACT

The experimental evidence indicates that the Karplus curve, which relates the coupling constant between hydrogens on vicinal carbons and the dihedral angle defined by the hydrogens, is subject to displacement. An upward displacement of 2.2 c.p.s. is required to account for the coupling constants found for the neighboring hydrogens in both 1,3-dioxolane and its 2,2-dimethyl derivative. On this basis, the compounds exist in conformations wherein the cis neighboring hydrogens define dihedral angles of 35° and 41°, respectively.

The formation of cyclic ketals and acetals from glycol groups has found widespread application in isolation, structural, and synthetic studies. The formation of the *O*-isopropylidene derivatives of vicinal hydroxyl groups has been particularly useful. The ease for the preparation of these compounds has received considerable attention from the point of view of conformational analysis (1–6). For this purpose, it has generally been assumed that the 1,3-dioxolane ring is planar (4). Although this assumption has proved useful, it is clearly desirable to obtain more precise information on the conformation of the 1,3-dioxolane ring. Three types of conformations are possible, the planar conformation and the conformations wherein one or two of the atoms are out of the plane of the other atoms in the ring (7).

An examination of a precise conformational model (8) for the 1,3-dioxolane ring clearly indicates that the ring can be puckered substantially without the introduction of valence-angle strain. One of the carbon atoms of the ethylene group can readily move out of the plane of the other four atoms to the extent that the cis neighboring hydrogens define dihedral angles of about 35°. In view of the potential barrier to rotation which is present in ethane (9), the resulting increased staggering of the cis hydrogens must provide a conformation which is, energetically, substantially more favorable than is the planar conformation. In fact, the nuclear magnetic resonance spectrum of 1,3-dioxolane (10) is only readily understood if the compound possesses a puckered conformation. It was found (10) that the average coupling, J, of a hydrogen with one of the neighboring hydrogens plus the average coupling, J', of the same hydrogen with the other neighboring hydrogen was 13.3 c.p.s. The difference $J-J'$ was 1.3 c.p.s. (see Fig. 1). We have confirmed these experimental results. The so-called Karplus curve (11–14) relates coupling constant to the dihedral angle defined by neighboring hydrogens. Should the 1,3-dioxolane ring be planar, then, on the basis of the Karplus values, $J_{0°} = 8.2$ and $J_{120°} = 2.2$ c.p.s., one would expect $J-J'$ to equal 6.0 c.p.s. rather than the observed 1.3 c.p.s. Although, as will be seen below, the Karplus curve is subject to displacement, its general shape has received substantial experimental verification (11–13). Certainly, although values for $J_{0°}-J_{120°}$ somewhat greater than 6 c.p.s. may be anticipated, none of the substantial

[1]*Presented by R. U. L. at the XVIIIth International Congress of Pure and Applied Chemistry, Montreal, Que., August, 1961. Abstracts of Scientific Papers, p. 268.*
[2]*Present address: Department of Chemistry, University of Alberta, Edmonton, Alberta.*
[3]*Corn Industries Research Foundation postdoctorate fellow, 1960–62.*

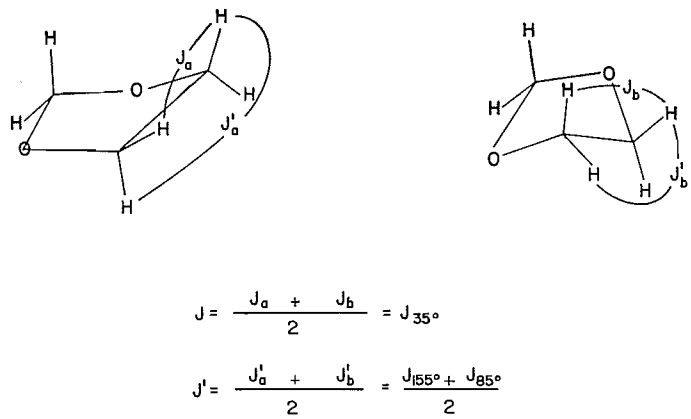

$$J = \frac{J_a + J_b}{2} = J_{35°}$$

$$J' = \frac{J'_a + J'_b}{2} = \frac{J_{155°} + J_{85°}}{2}$$

FIG. 1. The two energetically equivalent conformations for 1,3-dioxolane in which one of the C-methylene groups is puckered out of the plane of the other four atoms in the ring. The dihedral angles defined by the neighboring hydrogens are expected to be approximately those indicated. The experimentally determined coupling constants J and J' result from the averaging of the coupling constants in each of the conformations according to the relationships which are shown.

amount of information which has accumulated is in any way suggestive that the trough-shaped Karplus curve can be so very shallow as to provide a value for this difference in coupling constant as small as 1.3 c.p.s. Therefore, it can be concluded that the neighboring cis hydrogens in 1,3-dioxolane are not eclipsed.*

Although all the experimental evidence has substantiated the general shape of the Karplus curve, it is clearly apparent that the curve is subject to displacement depending on the chemical nature of the compound. This fact is demonstrated by the coupling constants reported in Table I for the hydrogens of a freely rotating methyl group and

TABLE I

Variation in the coupling constant between hydrogens on neighboring carbons which define the same dihedral angle but which differ in chemical nature

Compound	Coupling constant (c.p.s.)	Compound	Coupling constant (c.p.s.)
$(CH_3CH_2)_4Si$	7.9*	$CH_3CH(OCH_3)_2$	5.3
$(CH_3CH_2)_2S$	7.42*	$(CH_3CH_2)_3O^+BF_4^-$	4.7‡
CH_3CH_2Br	7.25†	$(CH_3)_2CHBr$	6.40†
CH_3CH_2Cl	7.07†	$(CH_3)_2CHCl$	6.31†
CH_3CH_2OH	6.97†	$(CH_3)_2CHOH$	6.05†
$(CH_3CH_2)_2O$	6.96†	$((CH_3)_2CH)_2O$	5.98†

*B. R. McGarvey and G. Slomp, Jr. J. Chem. Phys. **30**, 1586 (1959).
†A. A. Bothner-By and R. E. Glick. J. Chem. Phys. **25**, 362 (1956).
‡S. Brownstein, B. C. Smith, G. Ehrlich, and A. W. Laubengayer. J. Am. Chem. Soc. **81**, 3826 (1959).

the hydrogens on the neighboring carbon. The only important conformations for these compounds (CH_3CH_2X) are undoubtedly those wherein the hydrogens on the neighboring carbons are in the staggered arrangement. Therefore, on the basis of the Karplus curve, the average coupling of the neighboring hydrogens should be $(J_{180°}+2J_{60°})/3 = 4.2$ c.p.s. However, it is seen that the experimental values are in the range 4.7 to 7.9 c.p.s. For

Since this manuscript was first submitted, a publication appeared (R. J. Abraham, K. A. McLauchlan, L. D. Hall, and L. Hough. Chem. & Ind. (London), 213 (1962)) wherein it was concluded, on the basis of the nuclear magnetic resonance spectra of isopropylidene derivatives of sugars, that the currently held view that 2,2-dimethyldioxolane rings are planar is in need of modification.

compounds of structure $(CH_3)_2CHX$, the values range from 6.0 to 6.4 c.p.s. Karplus (11) has commented on this discrepancy, which renders it clearly apparent that the coupling constant between neighboring hydrogens is not only dependent on the dihedral angle which they define but also on the substituents other than the hydrogens on the vicinal carbons. The data in Table I indicate that a displacement of the Karplus curve can result from a change in the electronegativity of the substituent X in the compounds CH_3CH_2X. Experimental work on polyoxygenated six-membered ring compounds (15) and on substituted camphanes (12) are in good numerical agreement with the theoretical curve, which has also enabled consistent and reasonable conclusions to be drawn about ring conformations of other sugar derivatives (16, 17). However, Williamson and Johnson (18) have adjusted the Karplus curve to provide coupling constants of 16 and 10 c.p.s. for neighboring hydrogens which define dihedral angles of 180° and 0°, respectively, on the basis of the coupling constants found for neighboring hydrogens in the A-ring of 2- and 4-acetoxycholestane-3-ones. It was contended that perhaps the coupling constants for neighboring hydrogens in carbohydrate pyranose rings are smaller because the compounds do not possess conformational rigidity. Considerable evidence in fact exists that for many pyranose structures there must exist a very high degree of conformational purity. It has been ascertained, for example, that the coupling constants in 3-*O*-methyl-6,6-di-*C*-deutero-β-D-glucopyranose tetraacetate (I) are $J_{H_1,H_2} = 8.2$ c.p.s., $J_{H_2,H_3} = J_{H_3,H_4}$

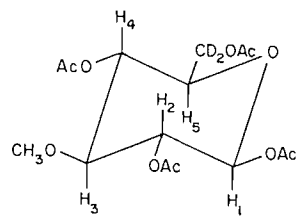

(I)

$= 9.3 \pm 0.1$ c.p.s., and $J_{H_4,H_5} = 9.7$ c.p.s. (19). The success encountered by Lemieux and Chü (20) in accounting for the anomeric equilibria of sugar acetates on the basis of conformational analysis with the pyranose ring in the chair conformation clearly requires conformational purity for many of the hexose pentaacetates. Clearly the indications are that the Karplus curve is subject to considerable displacement depending on the chemical nature of the compound being examined, and the use of the curve for the determination of fine points of conformation will require a knowledge of the position of the curve in the set of coordinates (coupling constant versus dihedral angle) for the type of structure under consideration. Thus, for example, in the above-mentioned glucose derivative, $J_{180°}$ appears to vary from 8.2 to 9.7 c.p.s. depending on the substituents on the various carbon atoms to which the hydrogens are bonded and in the manner expected from the data in Table I.

We have therefore interpreted the results of analysis of 1,3-dioxolane in the following manner. First of all we can calculate the values for $J-J'$ from the Karplus curve for varying amounts of puckering of the ring into a C_s conformation. A consideration of the C_2 conformation was omitted since examination of models showed that the differences in dihedral angles for the two conformations are relatively small. Let θ be the angle between the two hydrogens cis to each other on the two-carbon portion of the ring. Then for $\theta = 0°$, $J-J' = 6.0$; $\theta = 15°$, $J-J' = 5.1$; $\theta = 30°$, $J-J' = 2.65$; $\theta = 35°$, $J-J'$

$= 1.4$; $\theta = 40°$, $J-J' = 0.25$ c.p.s. Thus, it is seen that the value of $J-J'$ is in agreement with the experimental value when $\theta = 35°$, the angle which, on the basis of conformational models, appears near optimum for 1,3-dioxolane. However, the Karplus curve requires for $\theta = 35°$, $J+J'$ to be 11.1 c.p.s. In order to obtain agreement with the observed value of 13.3 c.p.s., it is necessary to displace the curve upwards by 2.2 c.p.s. Such a displacement of course leaves $J-J'$ unchanged.

We have now observed the carbon-13 side-band signal for the ethylenic group of 2,2-dimethyl-1,3-dioxolane. The signal is a triplet of spacing 12.6 c.p.s. Analysis of this signal as the A_2 part of an A_2X_2 spectrum yields $J = J' = 6.3$ c.p.s. (22). The Karplus curve allows $J = J'$ when $\theta = 41°$ and if the same upward displacement of 2.2 c.p.s. is assumed, then the curve yields values for $J_{41°} = 6.3$ c.p.s. and $J' = (J_{161°}+J_{79°})/2 = 6.3$ c.p.s., which are in agreement with the experimental values. It should be noted that only a rather limited variation in either θ ($\pm 2°$) or the upward displacement (± 0.2 c.p.s.) will still provide agreement within experimental error between the observed coupling constants and those predicted from the Karplus curve. On this basis the 1,3-dioxolane ring is puckered to a greater extent by the introduction of the two methyl groups at the 2-position. This conclusion would be in accordance with expectations based on the Thorpe–Ingold *gem*-dimethyl effect (23). That is, the introduction of the methyl groups should tend to decrease the O—C_2—O valence angle and thus requires a greater puckering of the ring.

It is interesting to compare the results of Anet (21) with ours. He found that in *trans*-4-*t*-butylcyclohexanol the coupling constants of the 1-hydrogen with the cis and trans 2-hydrogens were 4.31 and 11.07 c.p.s. respectively. Assuming that the cyclohexane ring exists in the ideal chair form in this compound then these values correspond to an upward displacement of the Karplus curve by 2.5 and 1.9 c.p.s. for $J_{60°}$ and $J_{180°}$, respectively.

The above conclusions regarding the conformations of 1,3-dioxolane rings are of direct importance to conformational analysis. Evidently, the formation of the *O*-isopropylidene derivative of an α-glycol does not require the two C—O bonds to achieve coplanarity. Angyal and MacDonald (2) have pointed out that a decrease of the 60° dihedral angle defined by the oxygen atoms in 1,2-*trans*-cyclohexanediol must introduce severely repulsive non-bonded interactions between opposing axial hydrogens. A distortion of about 19° would be required for the formation of *O*-isopropylidene-1,2-*trans*-cyclohexanediol without strain in the 1,3-dioxolane ring. It is therefore not surprising that the compound can be prepared only under strongly forcing conditions (24). A similar distortion for the cis isomer can be expected (1, 2) to introduce little strain in the cyclohexane ring. In fact, Kuhn has estimated, from the extent of hydrogen bonding, that the two oxygen atoms in 1,2-*cis*-cyclohexanediol define a dihedral angle of about 50°. The compound is well known to be readily transformed into the *O*-isopropylidene derivative. The oxygen atoms in 1,2-*cis*-cyclopentanediol can be expected to define a dihedral angle of about 46° (7), and the *O*-isopropylidene derivative forms readily (6). The dihedral angle defined by the oxygen atoms of the trans isomer is too large to allow formation of the *O*-isopropylidene derivative (6).

The above comments do not contradict the previous conclusions reached in conformational analyses involving the 1,3-dioxolane ring. However, the analyses were based on the erroneous assumption that the 1,3-dioxolane ring is planar. Clearly, the rings should be considered in their preferred puckered conformations unless evidence exists that the neighboring hydroxyl groups of the glycol are held rigidly in the eclipsed condition. Dihedral angles in the range 0–41° can be expected to be favorable for the for-

mation of the isopropylidene derivative, since there should not exist an appreciable barrier to rotation about the O—C_2—O bonds. The somewhat greater puckering of the ring in 2,2-dimethyl-1,3-dioxolane over that of the ring in 1,3-dioxolane can be expected to render it generally easier to prepare the former ring from neighboring hydroxyl groups in structures that resist conformations wherein the hydroxyl groups define angles as small as 40°. Certainly, the experience in carbohydrate chemistry (4) is in good general agreement with this expectation.

EXPERIMENTAL

The spectra were measured using a Varian V-4302 high-resolution spectrometer operating at a frequency of 60 Mc/s.

The 1,3-dioxolane and 2,2-dimethyl-1,3-dioxolane were prepared according to the directions provided by Dauben *et al.* (25) and were purified by fractional distillation using a Todd distillation apparatus. The carbon-13 triplet side bands occurred 74 c.p.s. to either side of the signal for the ethylenic hydrogens.

ACKNOWLEDGMENTS

This research was made possible through grants-in-aid for research by the National Research Council of Canada and the Corn Industries Research Foundation, Washington, D.C.

REFERENCES

1. O. Hassel and B. Ottar. Acta Chem. Scand. **1**, 929 (1947).
2. S. J. Angyal and C. G. MacDonald. J. Chem. Soc. 686 (1952).
3. H. C. Brown, J. H. Brewster, and H. Schechter. J. Am. Chem. Soc. **76**, 467 (1954).
4. J. A. Mills. Advances in Carbohydrate Chem. **10**, 1 (1955).
5. D. H. R. Barton and R. C. Cookson. Quart. Revs. (London), **10**, 44 (1956).
6. L. P. Kuhn. J. Am. Chem. Soc. **76**, 4323 (1954).
7. K. S. Pitzer and W. E. Donath. J. Am. Chem. Soc. **81**, 3213 (1959).
8. D. H. Barton. Chem. & Ind. (London), 1136 (1956).
9. G. B. Kistiakowsky, J. R. Lacher, and F. Stitt. J. Chem. Phys. **7**, 289 (1939).
10. N. Sheppard and J. J. Turner. Proc. Roy. Soc. A, **252**, 506 (1959).
11. M. Karplus. J. Chem. Phys. **30**, 11 (1959).
12. F. A. L. Anet. Can. J. Chem. **39**, 789 (1961).
13. H. Conroy. Advances in organic chemistry. Methods and results. Vol. II. R. A. Raphael, E. C. Taylor, and H. Wynberg (*Editors*). Interscience Publishers Inc., New York. 1960. p. 265.
14. C. D. Jardetzky. J. Am. Chem. Soc. **82**, 229 (1960).
15. R. U. Lemieux, R. K. Kullnig, H. G. Bernstein, and W. G. Schneider. J. Am. Chem. Soc. **80**, 6098 (1958).
16. R. U. Lemieux. Can. J. Chem. **39**, 116 (1961).
17. C. D. Jardetzky. J. Am. Chem. Soc. **83**, 2919 (1961).
18. K. L. Williamson and W. S. Johnson. J. Am. Chem. Soc. **83**, 4623 (1961).
19. R. U. Lemieux and J. D. Stevens. In preparation.
20. R. U. Lemieux and N. J. Chü. Abstracts of Papers, 133rd Meeting of the American Chemical Society, San Francisco, Calif. April 13–18, 1958. 31 N.
21. F. A. L. Anet. J. Am. Chem. Soc. **84**, 1053 (1962).
22. J. A. Pople, W. G. Schneider, and H. J. Bernstein. High-resolution nuclear magnetic resonance. McGraw-Hill Book Co., Inc., New York. 1959.
23. C. K. Ingold and J. F. Thorpe. J. Chem. Soc. 1318 (1928).
24. W. R. Christian, C. J. Gogek, and C. B. Purves. Can. J. Chem. **29**, 911 (1951).
25. H. J. Dauben, Jr., B. Löken, and H. J. Ringold. J. Am. Chem. Soc. **76**, 1359 (1954).

SYNTHÈSES D'ACIDES AMINOBUTYRIQUES

II. ACIDES ALKYLAMINO-2 HYDROXY-4 BUTYRIQUES

RÉAL LALIBERTÉ ET LOUIS BERLINGUET

Département de Biochimie, Faculté de Médecine, Université Laval, Québec, Qué.

Reçu le 27 septembre 1961

ABSTRACT

Starting from 2-bromo-4-butyrolactone which was treated with primary amines, five new 2-alkylamino-4-hydroxy-N-alkylbutyramides were obtained in good yields. Acid hydrolysis gave the corresponding lactones, which, when treated with $Ba(OH)_2$, gave the 2-alkylamino-4-hydroxybutyric acids. The new derivatives of homoserine thus prepared are: 2-methylamino-4-hydroxybutyric acid, 2-ethylamino-4-hydroxybutyric acid, 2-propylamino-4-hydroxybutyric acid, 2-butylamino-4-hydroxybutyric acid, and 2-cyclohexylamino-4-hydroxybutyric acid.

Some of these amides were easily lactonized in HCl–acetone medium. Two 2-alkylamino-4-chloro-N-alkylbutyramides were also prepared.

INTRODUCTION

Dans le cadre d'un travail portant sur la synthèse d'acides aminobutyriques N-alkylés (1), nous avons préparé cinq nouveaux dérivés de l'homosérine substitués sur l'azote.

Nous avons utilisé comme produit de départ la bromo-2 butyrolactone-4 (2). Knobler et Frankel (3) ont déjà montré que la bromo-2 butyrolactone-4 réagit avec l'ammoniaque pour donner l'amino-2 hydroxy-4 butyramide, qui après hydrolyse libère l'acide amino-2 hydroxy-4 butyrique (homosérine). En traitant de la même façon la bromo-2 butyrolactone-4 avec des amines primaires, nous avons isolé les amides suivants avec les rendements indiqués: méthylamino-2 hydroxy-4 N-méthylbutyramide (50%); éthylamino-2 hydroxy-4 N-éthylbutyramide (56%), propylamino-2 hydroxy-4 N-propylbutyramide (82%), butylamino-2 hydroxy-4 N-butylbutyramide (55%) et cyclohexylamino-2 hydroxy-4 N-cyclohexylbutyramide (82%).

Cette réaction se fait en deux étapes. Dans l'une, il y a substitution au brome de l'amine et dans l'autre, il y a ouverture du cycle par l'amine en excès pour donner le butyramide N-alkylé. Signalons que Sheradsky, Knobler et Frankel (4) viennent d'obtenir de la même façon le benzylamino-2 hydroxy-4 N-benzylbutyramide.

Ces amides hydroxylés en position 4 se cyclisent en milieu acide pour donner les butyrolactones correspondantes. Cette cyclisation s'effectue dans l'eau par l'acide sulfurique comme nous l'avons fait pour préparer les homosérines. On peut aussi l'effectuer dans un solvant organique saturé de HCl anhydre, ce qui permet l'isolement facile de la lactone. Il semble aussi que la transformation notée par Frankel, Knobler et Sheradsky (5) du benzamido-2 hydroxy-4 butyramide en benzamido-2 chloro-4 butyrate d'éthyle par le HCl anhydre dans l'éthanol se fasse par l'intermédiaire de la benzamido-2 butyrolactone-4.

Nous avons isolé facilement une lactone de ce type en saturant de HCl sec une suspension de cyclohexylamino-2 hydroxy-4 N-cyclohexylbutyramide (I, où $R = C_6H_{11}$) dans l'acétone ou le dioxanne. Dans les deux cas, on obtient après une semaine un rendement quantitatif en chlorhydrate de cyclohexylamino-2 butyrolactone-4 (III, où $R = C_6H_{11}$). Pour expliquer cette lactonisation de l'amide, on peut supposer la formation par l'action de HCl d'un chlorure d'imino-éther (II, où $R = C_6H_{11}$) instable en présence d'un acide fort (6, 7). En se réarrangeant, celui-ci donne la lactone qu'on peut isoler.

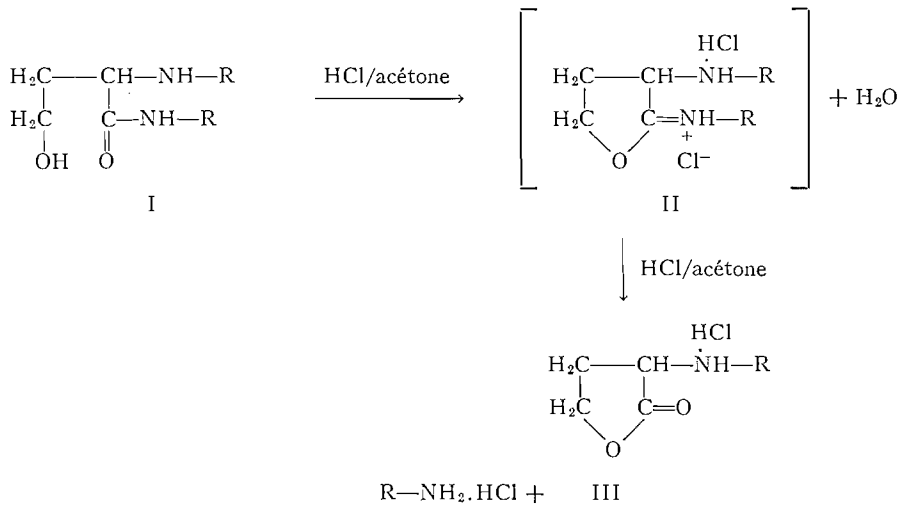

On peut répéter cette cyclisation dans des conditions semblables avec l'hydroxy-4 propylamino-2 N-propylbutyramide (I, où R = C_4H_9). Dans ce cas, on obtient le chlorhydrate de la propylamino-2 butyrolactone-4 avec un rendement de 82%.

Nous avons constaté que cette lactonisation des alkylamino-2 hydroxy-4 N-alkylbutyramides en alkylamino-2 butyrolactones sous l'action d'un acide fort, se fait plus rapidement dans l'eau que dans un solvant organique. Nous avons donc traité, sans les isoler, les amides résultant de l'action d'amines primaires sur la bromo-2 butyrolactone-4 par un excès d'acide sulfurique dilué à la température de la pièce pendant 24 heures. Nous avons ensuite éliminé l'acide sulfurique par un équivalent d'hydroxyde de baryum, ce qui a provoqué l'ouverture des lactones. Nous avons alors obtenu, avec les rendements indiqués, les acides butyriques suivants: acide méthylamino-2 hydroxy-4 butyrique (80%), acide éthylamino-2 hydroxy-4 butyrique (77%), acide propylamino-2 hydroxy-4 butyrique (70%), acide butylamino-2 hydroxy-4 butyrique (71%) et acide cyclohexylamino-2 hydroxy-4 butyrique (88%).

En traitant le cyclohexylamino-2 hydroxy-4 N-cyclohexylbutyramide et le propylamino-2 hydroxy-4 N-propylbutyramide par du chlorure de thionyle, on obtient les chlorhydrates du cyclohexylamino-2 chloro-4 N-cyclohexylbutyramide (rendement: 80%) et du butylamino-2 chloro-4 N-butylbutyramide (rendement: 50%).

En préparant le chlorhydrate du cyclohexylamino-2 chloro-4 N-cyclohexylbutyramide (IV), nous nous sommes demandé si la structure ouverte attribuée au produit était la bonne ou s'il ne s'agissait pas d'un produit cyclique (V) de type imino-éther comme en décrit Stirling (8). Ceci d'autant plus que l'action à chaud du chlorure de thionyle sur le cyclohexylamino-2 hydroxy-4 N-cyclohexylbutyramide (IV) dans le chloroforme donne un produit solide qui fond vers 130° (produit A). Mais en continuant à chauffer, ce produit redevient rapidement solide pour fondre à nouveau à 219° (produit B). De plus cette substance provenant du chloroforme (produit A) se dissout en quelques secondes dans l'acétone d'où elle cristallise quantitativement après quelques minutes pour donner le produit B.

Mais le produit obtenu de l'acétone (produit B) ne possède qu'un chlore inorganique et présente une bande à 1680 cm^{-1}, caractéristique d'un amide. Ceci n'est compatible qu'avec la structure ouverte (produit B, VI). Tant qu'à l'intermédiaire instable (produit

A), nous n'avons pu déterminer sa structure, mais on peut cependant supposer qu'il s'agit d'un chlorure de cyclohexylamino-2 N-cyclohexyltétrahydroiminofuranne (V).

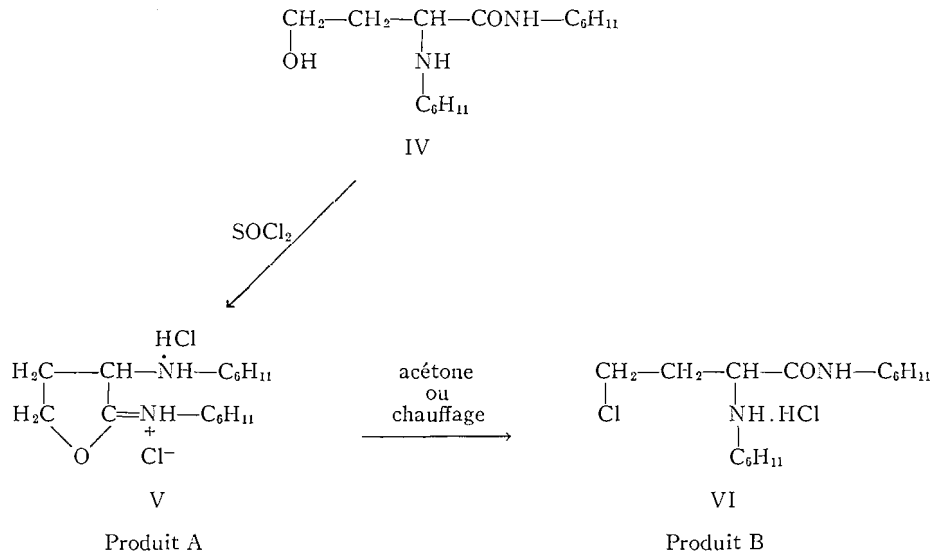

PARTIE EXPÉRIMENTALE

Alkylamino-2 hydroxy-4 N-alkylbutyramides

La synthèse des butyramides substitués se fait par addition de la bromo-2 butyrolactone-4 à l'amine choisie, suivant la technique décrite pour la méthylamino-2 hydroxy-4 N-méthylbutyramide.

Dans le cas de la butylamine et de la cyclohexylamine, il y a avantage à maintenir la température du mélange à 75–100° après l'addition, ce qui diminue le temps de réaction à 24 heures et à 2 heures respectivement.

On trouvera au tableau I les constantes physiques des produits obtenus.

TABLEAU I

Alkylamino-2 hydroxy-4 N-alkylbutyramides

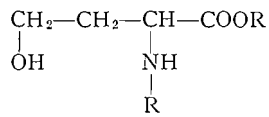

R	% rendement	P.f.*	Formule	% N Calculé	% N Trouvé	Solvants de recristallisation
CH_3—	50	95	$C_6H_{14}N_2O_2$	19.15	19.03	BuOH/éther/éther de pétrole
C_2H_5—	56	96	$C_8H_{18}N_2O_2$	16.07	15.80	Benzène/éther de pétrole
C_3H_7—	81	97	$C_{10}H_{22}N_2O_2$	13.84	13.82	Benzène ou eau
C_4H_9—	55	64	$C_{12}H_{26}N_2O_2$	12.15	12.05	Acétate d'éthyle/éther de pétrole
C_6H_{11}—	82	132	$C_{16}H_{30}N_2O_2$	9.91	9.94	EtOH/eau

*Les points de fusion ne sont pas corrigés.

Méthylamino-2 hydroxy-4 N-méthylbutyramide

A 200 ml (2.0 moles) de méthylamine en solution aqueuse à 30% placés dans une fiole conique refroidie, on ajoute en agitant 82.5 g (0.50 mole) de bromo-2 butyrolactone-4. La réaction est exothermique. Une fois l'addition terminée, on retire la fiole conique du bain de glace, puis on la laisse au repos pendant plusieurs jours à température de la pièce. On ajoute ensuite 50 ml de soude 10 *N* (0.50 mole), puis on évapore à sec l'excès d'amine. On recristallise l'amide obtenu d'un solvant organique dans lequel le bromure de sodium

demeure insoluble et qu'on filtre (voir tableau I). Le méthylamino-2 hydroxy-4 N-méthylbutyramide cristallise du butanol par addition lente d'un mélange d'éther et d'éther de pétrole. On obtient 36.5 g d'un solide blanc.

Chlorhydrate de cyclohexylamino-2 chloro-4 N-cyclohexylbutyramide

On dissout 10 g (0.035 mole) de cyclohexylamino-2 hydroxy-4 N-cyclohexylbutyramide dans 100 ml de chloroforme, puis on fait passer dans ce milieu du gaz chlorhydrique sec pendant 2 à 3 minutes. On ajoute ensuite 30 g (0.25 mole) de chlorure de thionyle et on chauffe à reflux pendant une heure. On refroidit puis on filtre (produit A). Le solide obtenu est versé en une fois dans 35 ml d'acétone où il se dissout rapidement, semble se réarranger et cristallise rapidement à température de la pièce. On refroidit la suspension dans l'acétone, on filtre et on lave le solide obtenu avec 30 ml d'acétone où il est maintenant insoluble (produit B). On obtient ainsi 10 g d'un solide blanc. Rendement: 84%. P.f. 219°. Anal. Calc. pour $C_{16}H_{29}ClN_2O.HCl$: N, 8.30; Cl, 21.0%. Trouvé: N, 8.28; Cl, 21.2%.

Le produit B ne contient qu'un chlore inorganique. Nous l'avons vérifié en faisant un dosage rapide par gravimétrie (AgCl) sans au préalable digérer la substance en milieu alcalin. Il donne à l'infra-rouge la bande de l'amide à 1680 cm^{-1} (KBr).

Le produit A obtenu du chloroforme est très soluble dans l'acétone. De plus, il fond vers 130° pour redevenir solide vers 150° et refondre à 219° comme le produit B. Mais il est très instable et se transforme très rapidement en produit B dès que nous le dissolvons dans un solvant quelconque. Il donne le même spectre que le produit ci-haut (KBr). Nous supposons cependant qu'il s'agit d'un chlorure d'imino-éther (V) très instable dans ce cas particulier.

Chlorhydrate de butylamino-2 chloro-4 N-butylbutyramide

On dissout 7.8 g (0.035 mole) de butylamino-2 hydroxy-4 N-butylbutyramide dans 100 ml de chloroforme en faisant barboter un peu d'acide chlorhydrique sec. On y ajoute 30 g (0.25 mole) de chlorure de thionyle, puis on fait refluer la solution pendant une heure. On évapore à sec et on dissout le résidu dans du méthanol que l'on traite avec du noir animal. Le produit cristallise en ajoutant de l'éther. On obtient ainsi 5 g de chlorhydrate de butylamino-2 chloro-4 N-butylbutyramide. Rendement: 50%. P.f. 193°. On peut le recristalliser de l'isopropanol. Anal. Calc. pour $C_{12}H_{25}ClN_2O.HCl$: N, 9.81; Cl, 24.86%. Trouvé: N, 9.76; Cl, 25.0%. Nous n'avons observé aucun réarrangement lors de la préparation de ce produit. Un dosage de chlore inorganique ne révèle qu'un halogène.

Chlorhydrate de cyclohexylamino-2 butyrolactone-4

On suspend dans 40 ml d'acétone ou de dioxanne 2 g (0.0071 mole) de cyclohexylamino-2 hydroxy-4 N-cyclohexylbutyramide. On fait passer dans cette suspension un courant d'acide chlorhydrique sec jusqu'à ce que la solution soit saturée à 40°. La lactone cristallise lentement à température de la pièce. Après 7 jours, on obtient avec un rendement quantitatif (1.5 g) le chlorhydrate de cyclohexylamino-2 butyrolactone-4, qu'on lave avec un peu d'acétone. P.f. 259°. Anal. Calc. pour $C_{10}H_{17}NO_2.HCl$: N, 6.37%. Trouvé: N, 6.42%.

Chlorhydrate de propylamino-2 butyrolactone-4

On dissout 3 g (0.014 mole) de propylamino-2 hydroxy-4 N-propylbutyramide dans de l'acétone saturé de HCl sec à 40°. On laisse au repos à température de la pièce pendant une semaine. On porte ensuite la fiole conique au froid où le produit cristallise après quelques jours. On filtre, puis on recristallise le chlorhydrate de propylamino-2 butyrolactone-4 du butanol ou du dioxanne. On obtient ainsi 2.1 g de solide. Rendement: 83%. P.f. 166°. Anal. Calc. pour $C_7H_{13}NO_2.HCl$: N, 7.79%. Trouvé: N, 7.97%.

Acides alkylamino-2 hydroxy-4 butyriques

Les acides substitués peuvent être obtenus par hydrolyse acide des amides. Toutefois on peut y passer directement à partir de la bromo-2 butyrolactone sans isoler les amides, suivant la synthèse décrite pour l'acide méthylamino-2 hydroxy-4 butyrique.

On trouvera au tableau II les constantes physiques des produits obtenus.

Les rendements indiqués sont calculés à partir de la bromo-2 butyrolactone-4.

Acide méthylamino-2 hydroxy-4 butyrique

On ajoute 10 g (0.060 mole) de bromo-2 butyrolactone-4 à 75 ml (0.75 mole) d'une solution à 30% de méthylamine dans l'eau contenue dans une fiole conique plongée dans un bain de glace. Lors de l'addition, on agite pour que les deux liquides se mélangent rapidement. On laisse au repos pendant plusieurs jours à la température de la pièce. On évapore ensuite l'amine en excès. On ajoute 100 ml d'acide sulfurique 6 *N* (0.30 mole). On chauffe la solution sur bain-marie pendant 30 minutes puis on la laisse au repos jusqu'au lendemain. Dans ces conditions, l'amide hydroxylé en position 4 se transforme en lactone. On verse celle-ci dans une solution chaude de 94 g (0.30 mole) de $Ba(OH)_2.8H_2O$. Après avoir laissé le mélange sur un bain-marie bouillant 30 minutes, on filtre le sulfate de baryum. Au filtrat on ajoute un peu de carbonate d'ammonium pour éliminer le léger excès de baryte, puis on filtre. On évapore ensuite le filtrat jusqu'à environ 25 ml. On y ajoute 400 ml d'acétone et on met la solution au froid. L'acide méthylamino-2 hydroxy-4 butyrique cristallise alors lentement à froid pour donner 6.5 g de solide.

TABLEAU II

Acides alkylamino-2 hydroxy-4 N-alkylbutyriques

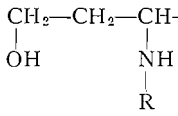

R	% rendement	P.f.*	Formule	% N Calculé	% N Trouvé	Solvants de recristallisation
CH_3—	80	225	$C_5H_{11}NO_3$	10.51	10.48	Eau/acétone
C_2H_5—	77	245	$C_6H_{13}NO_3$	9.51	9.43	Eau/EtOH
C_3H_7—	70	234	$C_7H_{15}NO_3$	8.68	8.65	Eau/EtOH ou acétone
C_4H_9—	71	228	$C_8H_{17}NO_3$	7.99	7.86	Eau/acétone
C_6H_{11}—	88	235	$C_{10}H_{19}NO_3$	6.96	7.12	Eau/acétone

*Les points de fusion ne sont pas corrigés.

REMERCIEMENTS

Les auteurs remercient le Conseil National de Recherches pour une bourse accordée à l'un d'eux (R. L.) ainsi que l'Institut National du Cancer pour aide financière.

BIBLIOGRAPHIE

1. R. Laliberté et L. Berlinguet. Can. J. Chem. **38**, 1933 (1960).
2. J. E. Livak, E. C. Britton, J. C. Van der Weele et M. F. Murray. J. Am. Chem. Soc. **67**, 2218 (1945).
3. Y. Knobler et M. Frankel. J. Chem. Soc. 1629 (1958).
4. T. Sheradsky, Y. Knobler et M. Frankel. J. Org. Chem. **26**, 1482 (1961).
5. M. Frankel, Y. Knobler et T. Sheradsky. Bull. Research Council Israel, Sect. A, **7**, 173 (1958).
6. I. H. Derby. Am. Chem. J. **39**, 437 (1908).
7. J. Stieglitz. Am. Chem. J. **39**, 402 (1908).
8. C. J. M. Stirling. J. Chem. Soc. 255 (1960).

THE MASS SPECTRA OF THREE DEUTERATED BROMOBUTANES[1]

W. H. McFADDEN[2] AND M. LOUNSBURY
Research Chemistry Branch, Atomic Energy of Canada Limited, Chalk River, Ontario

Received June 4, 1962

ABSTRACT

The mass spectra of 1,1-dideutero-1-bromobutane, 1,1,1,3,3-pentadeutero-2-bromobutane, and 1,1,1,2,3,3-hexadeutero-2-bromobutane have been obtained using 70-volt ionizing electrons. The cracking patterns of the deuterated molecules are compared with those of the undeuterated bromobutanes. It is shown that no hydrogen–deuterium exchange occurs in certain ions formed from the parent ion by simple bond break but that extensive exchange of hydrogen and deuterium occurs in ions formed by further decomposition of unsaturated daughter ions.

Formation of HBr^+ or loss of HBr to form $C_4H_8^+$ from 2-bromobutane is shown to favor sterically the hydrogen on carbon 4 and not to involve that on carbon 2. However, in the case of 1-bromobutane, formation of these ions does not appear to involve any particular hydrogen preferentially, because if one assumes that all hydrogens in the molecule are involved, then the hydrogen on carbon 1 appears to be involved to an almost statistical extent.

In two cases the isotopic substitution so modifies the rate of a metastable reaction that the metastable peak disappears from the spectra of the deuterated species.

INTRODUCTION

Some understanding of the reaction processes induced in alkyl halides by electron impact has been obtained in previous works (1–6). Methyl and ethyl halides have been studied at various electron energies (1, 2, 3). The energetics of several primary reactions were determined and important mechanistic differences were shown to exist between C_2H_5Cl and C_2H_5Br or C_2H_5I. McLafferty has studied series of organic halides and shown correlations between their spectra and that of similar hydrocarbons (4). Related studies have been performed by Momigny (5) and D'Or (6), and in the latter study considerable information was obtained on the fragmentation of bromopentanes from a study of the metastable ions observed. However, no fragmentation studies have been reported on deuterated alkyl halides of more than three carbons. Since this latter technique has often yielded important and sometimes unexpected information with other molecular systems, it seemed desirable to obtain the mass spectra of three deuterated bromobutanes which were available from a previous study (7).

EXPERIMENTAL

The three deuterated bromobutanes used in the present study are 1,1-dideutero-1-bromobutane, 1,1,1,3,3-pentadeutero-2-bromobutane, and 1,1,1,2,3,3-hexadeutero-2-bromobutane (hereafter referred to as *n*-bromobutane-D_2, *sec*-bromobutane-D_5, and *sec*-bromobutane-D_6 respectively). Their synthesis has been described previously (7). Before mass analysis, *n*-bromobutane-D_2 and *sec*-bromobutane-D_5 were purified by gas–liquid chromatography but because only an extremely small quantity of *sec*-bromobutane-D_6 was available it was used without further processing. The handling technique for *sec*-bromobutane-D_6 may have introduced an unknown amount of CO_2 and H_2O, and traces of other chemical impurities may be present due to the known slow decomposition of alkyl bromides.

All three compounds were concluded to be better than 97% isotopically pure from the mass spectra of the deuterated alcohols from which they were prepared (8). However, a good low-voltage analysis has not been obtained so doubt of isotopic purity may exist. This point is elaborated in detail where it is pertinent to the conclusions regarding the mechanics of fragmentation.

[1]*Issued as A.E.C.L. No. 1586.*
[2]*Present address: Western Utilization Research and Development Division, Agricultural Research Service, U.S. Department of Agriculture, Albany, Calif.*

The mass spectrometer (6-inch radius, 90° magnetic sector) and mass analysis techniques have been previously described (9, 8). The reported spectra were obtained with 70-volt electrons. The temperature of the ionization chamber was not measured.

EXPERIMENTAL DATA

The mass spectra of the undeuterated bromobutanes and deuterated bromobutanes are given in Table I. Ion abundances are reported in terms of the percentage of the

TABLE I

Mass spectra of the bromobutanes

	% ionization						% ionization				
	n-Bromobutane		*sec*-Bromobutane				*n*-Bromobutane		*sec*-Bromobutane		
m/e	D_0	D_2	D_0	D_5	D_6	*m/e*	D_0	D_2	D_0	D_5	D_6
14	0.14	0.10	0.13	0.10	0.10	61				3.46	1.33
15	0.51	0.35	0.60	0.28	0.26	62				29.1	3.56
16	0.12	0.25	0.13	0.25	0.22	63				1.34	27.9
17		0.12		0.19	(0.50)	64					1.25
18				0.26	(1.83)	79	0.94	0.95	0.81	0.99	1.01
26	1.94	1.13	1.50	0.28	0.24	80	1.67	1.48	1.37	1.15	1.22
27	8.42	4.57	6.71	1.19	0.81	81	1.00	1.19	0.84	1.59	1.62
28	4.47	4.35	2.56	2.38	2.46	82	1.65	1.47	1.35	1.15	1.23
29	11.7	7.00	14.3	3.84	2.18	83	0.08	0.27	0.05	0.62	0.64
30	0.36	6.94	0.36	3.43	4.23	92	0.04	0.01			
31		3.26		5.59	3.69	93	0.47	0.10	0.15	0.04	0.04
32				5.86	6.21	94	0.05	0.09	0.02	0.07	0.04
33				2.71	4.56	95	0.43	0.41	0.14	0.09	0.12
34				0.28	1.27	96	0.03	0.10	0.04	0.06	0.05
36	0.46	0.36	1.08	0.40	0.29	97		0.33		0.06	0.10
37	0.34	0.26	0.43	0.30	0.17	98					0.03
38	0.67	0.41	0.96	0.39	0.33	105	0.08	0.02	0.07	0.02	
39	3.66	1.67	4.63	0.65	0.40	106	0.16	0.04	0.10	0.03	
40	0.66	1.76	0.71	1.50	1.12	107	1.28	0.11	0.51	0.05	0.06
41	15.8	4.65	16.9	2.26	1.65	108	0.22	0.15	0.10	0.10	0.03
42	0.87	6.94	1.07	2.71	2.46	109	1.17	1.28	0.44	0.06	0.10
43	1.37	7.08	0.64	5.48	2.93	110	0.09	0.15	0.01	0.42	0.05
44	0.11	0.39		6.48	6.08	111		1.16		0.04	0.41
45		0.20		4.23	4.82	112		0.04		0.34	0.04
46				0.99	3.18	113					0.35
47				0.54	0.29	135	0.01		0.01		
50	0.42	0.17	0.58	0.11	0.18	136	1.73		0.12		
51	0.36	0.29	0.51	0.21	0.15	137	0.09	0.04	0.01		
52	0.12	0.23	0.17	0.24	0.23	138	1.69	1.36	0.12		
53	0.39	0.18	0.58	0.20	0.17	139	0.07	0.10	0.01		
54	0.21	0.22	0.24	0.15	0.16	140		1.34		0.01	0.01
55	1.81	0.31	1.83	0.25	0.26	141		0.06		0.18	0.02
56	4.16	0.51	2.33	0.27	0.35	142				0.02	0.51
57	25.5	1.55	31.3	0.36	0.35	143				0.17	0.05
58	1.15	4.70	1.41	0.42	0.18	144				0.01	0.49
59		25.4		0.88	0.55	145					0.02
60		1.19		1.52	0.81						

total ionization but the contribution due to metastable ions is not included. The usual methods of correcting for background contributions and memory effects have been applied. The corrections were insignificant for most of the important ions except for the CO_2 and H_2O contribution in the spectrum of *sec*-bromobutane-D_6. The H_2O could not be properly estimated and the values at m/e 18 and 17 for *sec*-bromobutane-D_6 are not reliable. The CO_2 contributions at $m/e = 44$ and 28 were obtained by assuming that the ionization observed at $m/e = 22$ was due to CO_2^{++}. The natural C^{13} abundance is reported as observed.

A number of broad non-integral peaks were observed corresponding to the so-called metastable ions. These metastable ions are particularly useful in determining reaction mechanisms because the mass at which they are observed is related to both the mass of the decomposing ion, m_o, and the actual mass of the daughter fragment, m_d. For the type of mass spectrometer used in this work, the relationship is $m^* = m_d^2/m_o$, where m^* is the observed mass of the metastable ion. The existence of a metastable peak definitely establishes the possibility of the corresponding reaction but it may not be used as a measure of its probability. Conversely, the absence of a metastable peak does not preclude the possibility of a particular reaction.

Table II presents the metastable peaks observed for *n*-bromobutane-D_0 and *sec*-bromobutane-D_0 and the corresponding kinetic processes. The metastable data for the

TABLE II

Metastable ions observed in the mass spectra of *n*-bromobutane and *sec*-bromobutane

Process	m^* calc.	*n*-Bromobutane m^* obs.	*n*-Bromobutane Intensity, % ionization	*sec*-Bromobutane m^* obs.	*sec*-Bromobutane Intensity, % ionization
$C_4H_9^+ \rightarrow C_2H_4^+ + \cdot C_2H_5$	13.75	13.75	0.004	13.75	0.004
$C_4H_9^+ \rightarrow C_2H_5^+ + C_2H_4$	14.75	14.75	0.01	14.75	0.008
$C_4H_7^+ \rightarrow C_2H_5^+ + C_2H_2$	15.28	15.3	0.009	15.3	0.008
$C_4H_9Br^+ \rightarrow C_4H_8^+ + HBr^{81}$	22.7	—		22.8	0.03
$C_4H_9Br^+ \rightarrow C_4H_8^+ + HBr^{79}$	23.0	—		23.1	0.04
$C_4H_9Br^+ \rightarrow C_4H_9^+ + \cdot Br^{81}$	23.6	23.6	0.02	—	
$C_4H_9Br^+ \rightarrow C_4H_9^+ + \cdot Br^{79}$	23.8	23.8	0.02	—	
$C_2H_4^+ \rightarrow C_2H_2^+ + H_2$	24.1	24.15	0.02	24.15	0.004
$C_2H_3^+ \rightarrow C_2H_2^+ + H_2$	25.1	25.15	0.02	25.15	0.02
$C_2H_4^+ \rightarrow C_2H_3^+ + \cdot H$	26.0	25.9	0.0004	—	
$C_2H_5^+ \rightarrow C_2H_4^+ + \cdot H$	27.0	26.9	0.01	—	
$C_4H_7^+ \rightarrow C_3H_3^+ + CH_4$	27.6	27.67	0.004	27.68	0.008
$C_4H_9^+ \rightarrow C_3H_5^+ + CH_4$	29.5	29.5	0.17	29.6	0.21
$C_4H_8^+ \rightarrow C_3H_5^+ + \cdot CH_3$	30.0	30.2	0.008	—	
$C_3H_5^+ \rightarrow C_3H_3^+ + H_2$	37.1	37.2	0.03	37.2	0.04
$C_3H_7^+ \rightarrow C_3H_5^+ + H_2$	39.1	39.1	0.03	—	
$C_4H_7^+ \rightarrow C_4H_5^+ + H_2$	51.0	51.2	0.004	51.2	0.008
$C_4H_8^+ \rightarrow C_4H_6^+ + H_2$	52.2	—		52.3	0.004

deuterated samples are given in Table III but the possible kinetic processes are not included. In many cases the metastable pattern is excessively smeared out as a result of contributions from various deuterated fragments, and the assignment of mass to the metastable peak is admittedly somewhat arbitrary. In addition the calculated masses for different reactions often have the same value, depending upon the particular deuterium content. An example of this is given by the data for *n*-bromobutane-D_2, from which one might expect the formation of $C_3H_5^+$ from $C_3H_7^+$ and $C_3HD_2^+$ from $C_3H_3D_2^+$. Both processes would give a metastable peak at mass 39.1 with a probable intensity of about 0.03% so that an unequivocal determination of the kinetic process is not possible. Nevertheless, many of the metastable processes occurring with the deuterated molecules can be correlated with those of the undeuterated compounds. Some of these reveal or confirm important features of the fragmentation pattern and are discussed in later sections.

DISCUSSION

(A) General

In the following discussion it is shown that ions from simple bond break occur without significant hydrogen–deuterium exchange, but, on the other hand, ion fragments that

TABLE III

Metastable ions observed in the mass spectra of *n*-bromobutane-D_2, *sec*-bromobutane-D_5, and *sec*-bromobutane-D_6

	Intensity, % ionization				Intensity, % ionization		
m^*	D_2	D_5	D_6	m^*	D_2	D_5	D_6
14.25	0.002			27.1		0.009	0.01
15.28	0.01		0.002	27.3		0.005	0.005
15.5		0.005		27.8			0.005
15.8	0.002			28.6	0.02		
16.3	0.004		0.007	28.9		0.005	
16.5		0.007		29.5			0.02
16.9	0.002			29.9	0.05	0.06	
17.3			0.006	30.8			0.05
17.5		0.004		31.25		0.10	
18.09			0.005	31.3	0.04		
24.1	0.003			32.1			0.03
24.3	0.003	0.003	0.002	32.65		0.03	
24.6		0.003	0.005	33.6			0.01
24.9	0.02			34.3		0.005	
25.18	0.01			36.3	0.001		0.002
25.2	0.02			37.2	0.01	0.007	0.005
25.3		0.007	0.006	38.2	0.005	0.007	0.01
26.1	0.01	0.02	0.005	39.2	0.006	0.006	0.005
26.3		0.02	0.005	40.1			0.005
27.0	0.004			40.9		0.006	0.006

do not contain bromine (C_1, C_2, and C_3 fragments) show extensive exchange. From these experimental facts it is concluded that in the parent ion the rate of H–D exchange is less than the rate of simple bond break (7), and, therefore, the formation of most of the hydrocarbon fragments must occur from the $C_4H_9^+$ ion. The observed metastable ions confirm this conclusion.

The slower rate of exchange observed in saturated parent ions as compared with the exchange rates observed in olefinic parents (10, 11) or radical daughter ions must be a consequence of the necessary intermediate structures of the saturated system, which would involve either pentavalent carbon or divalent hydrogen. The former would require extra energy in order to attain the probable bipyramidal dsp^3 hybridization, while the formation of an intermediate with a divalent hydrogen might impose a steric restriction on the system. On the other hand the exchange in an olefinic or unsaturated system can take place with very little change in the structure of the excited ion.

(B) Ions CH_2Br^+ and $C_2H_4Br^+$

(i) n-Bromobutane

From *n*-bromobutane an ion which contributes 2.4% to the total ionization, that is, the sum of the ionization due to $(C_2H_4Br^{79})^+$ and $(C_2H_4Br^{81})^+$ at $m/e = 107$ and 109, is formed by loss of $\cdot C_2H_5$. From *n*-bromobutane-D_2 this ion appears at 2 mass units higher, with the same percentage of ionization. The statistical probability of such an event is only 0.16 (assuming all hydrogens and deuteriums are equivalent) and the statistical probability for formation of $C_2H_3DBr^+$ from the ensemble $C_4D_2H_7Br^+$ is 0.56.

If a simple model is assumed in which a hydrogen from either carbon 3 or 4 is mixed with the deuterium on carbon 1 and then H or D statistically returned to carbon 3 or 4 (11), it is readily ascertained that with only one exchange of this type the probability of obtaining C_2H_3DBr is 0.66 (assuming no H–D isotope effect). This overly simplified model shows that a molecular system of this type requires very few exchanges in order

to bring about a considerable change in the H–D distribution. From such considerations one may conclude that the reaction $CH_2BrCH_2—CH_2CH_3^+ \rightarrow CH_2BrCH_2^+ + \cdot C_2H_5$ occurs at a rate much greater than the rate of H–D exchange. This conclusion assumes that exchanges occur at approximately the same rate between all carbon positions and that exchanges between carbons 1 and 2 do not occur exclusively (7).

The ion CH_2Br^+ formed by loss of $\cdot C_3H_7$ contributes 0.9% to the total ionization. Approximately 15% of these events appear to involve an exchange of hydrogen and deuterium. This is not likely to be due to the additional possibility of 1–2 exchanges and indicates a slightly slower rate for the reaction $CH_3CH_2CH_2—CH_2Br^+ \rightarrow CH_2Br^+ + \cdot C_3H_7$. It is again emphasized that the amount of exchange observed is considerably less than is expected for one hypothetical exchange of the type discussed.

(ii) sec-Bromobutane

From *sec*-bromobutane the ionization due to loss of $\cdot C_2H_5$ to form $C_2H_5Br^+$ contributes 0.95% to the total. As with loss of $\cdot C_2H_5$ from *n*-bromobutane, the deuterated molecules show no exchange so that one again concludes that the simple bond break occurs faster than the H–D exchange.

The ion CH_2Br^+ contributes only 0.3% to the total ionization and, as would be expected for an ion which requires rearrangement of the parent structure prior to dissociation, the deuterium and hydrogen show considerable exchange. Unfortunately, the amount of ionization is too small to permit speculation on possible mechanisms.

(C) Ions Br^+, HBr^+, and H_2Br^+

These ions contribute about 5% to the total ionization for both *n*-bromobutane and *sec*-bromobutane. From the data for *n*-bromobutane-D_2, it appears that the ion DBr^+ is formed in about 12% of this group of events (after making allowance for H_2Br^+). Statistically one would expect 22% but since the H–D isotope effect would decrease the possible transfer of deuterium to the bromine, the data suggest the possibility that HBr^+ may be formed from *n*-bromobutane by a random selection of hydrogen. This implies that the probable activated complex, $(C_4H_6D_2)—BrH^+$, is sufficiently stable to permit considerable exchange of H and D prior to its dissociation.

The data for the formation of HBr^+ from *sec*-bromobutane is more specific. The ion HBr^+ is formed in 65% of the events in the breakdown of both *sec*-bromobutane-D_5 and *sec*-bromobutane-D_6. The remarkable similarity of the spectra of these two molecules in the Br^+–HBr^+ region ($m/e = 79$ to $m/e = 83$) indicates that the hydrogen on carbon 2 is not involved in the formation of the HBr^+. The 65% of the rearrangement involving hydrogen for both of the deuterated molecules indicates that the hydrogen on carbon 4 is strongly favored, in accordance with accepted views that such rearrangements are often sterically dependent (8, 12). With the present data one cannot distinguish between contributions from carbon 1 and 3.

The ionization due to H_2Br^+ is relatively insignificant (about 0.1%) and nothing can be postulated regarding its formation. However, it must be considered in order to determine the contribution due to DBr^+ at $m/e = 81$ and 83.

(D) C_4 Ions Not Containing Bromine

(i) n-Bromobutane

The most abundant ion in the mass spectrum of *n*-bromobutane is $C_4H_9^+$ and it is formed by the reaction $C_4H_9Br^+ \rightarrow C_4H_9^+ + \cdot Br$. This is indicated by the metastable ions at masses 23.6 and 23.8. The possibility of the reaction $C_4H_9Br + e \rightarrow C_4H_9^+ + Br^- + e$ is however not excluded and such reactions have been shown to occur at

low electron energies (2, 3). The equivalent metastable peaks appear to be present in the spectrum of the deuterated molecule at masses 24.9 and 25.2, but because of the normal peak at 25 and a small metastable peak at 25.18 the unique pattern is partially obscured.

The butylene ion from *n*-bromobutane-D_2 is formed without any significant loss of D from position one. This indicates the expected reaction $C_4H_9Br^+ \rightarrow C_4H_8^+ + HBr$, but no corresponding metastable ions are observed. Because of the small amount of DBr^+ formed (11% of total hydrobromic ion) one might expect a corresponding amount of DBr to be lost in forming the butylene ion but doubts regarding the isotopic purity[3] of this compound make differences of this magnitude undiscernible.

(ii) sec-Bromobutane

The $C_4H_9^+$ ion is again the most abundant ion in the spectra, but contrary to the observations on *n*-bromobutane the metastable ions at masses 23.6 and 23.8 are not observed. This indicates an increase in the rate of the primary reaction $C_4H_9Br^+ \rightarrow C_4H_9^+ + \cdot Br$ so that decompositions do not occur in the metastable region of the mass spectrometer (13). A less likely possibility is that the pair formation reaction, $C_4H_9Br + e \rightarrow C_4H_9^+ + Br^- + e$, becomes predominant.

Metastable ions in the mass spectrum of *sec*-bromobutane-D_0 prove the occurrence of the expected reaction $C_4H_9Br^+ \rightarrow C_4H_8^+ + HBr$. However, before discussing the mechanics of this fragmentation it is necessary to appraise the data on the isotopic purity of the two deuterated samples.

Unfortunately, n.m.r. analysis was not available at the time the samples were mass analyzed (1958) and later n.m.r. analysis (1961) indicated chemical impurities due to the known instability of the alkyl bromides. These impurities were most likely absent during the mass analysis because of the prior purifying techniques but their presence during the n.m.r. analysis precluded any conclusion regarding isotopic purity and location of the deuterium.

The mass spectral data for the corresponding butanols (8) do furnish upper limits. An upper limit of 2.9% isotopic impurity on carbon 1 is obtained for *sec*-bromobutane-D_5 from the ratio of *m/e* 47 to *m/e* 48 from *sec*-butanol-D_5, (1.06% for *m/e* 47 and 36.5% for *m/e* 48). An upper limit of 4.4% isotopic impurity on carbons 1 and 2 is obtained for *sec*-bromobutane-D_6 from the ratio of *m/e* 48 to *m/e* 49 from *sec*-butanol-D_6 (1.68/37.6). If it is assumed from this that the deuteriums of carbons 1 and 3 would contain about 1% isotopic impurity *per deuterium* and carbon 2 about 1.4%, then, as an upper limit, one would have 5% $C_4H_5D_4Br$ in *sec*-$C_4H_4D_5Br$ and 6.4% $C_4H_4D_5Br$ in *sec*-$C_4H_3D_6Br$. These values could definitely be reduced by consideration of the fact that some of the ionization of the alcohols which was assumed due to the isotopic impurity would actually be due to the same species minus hydrogen. In previous work reduction by a factor of about 2 was considered a more reasonable estimate of the isotopic impurity. However, in order to be conservative in the present estimation of hydrogen versus deuterium in formation of the lost HBr group, the above figures were used for correcting the data.

Table IV presents corrected data for this small section of the mass spectra. For the rest of the spectra, in which considerable exchange of the hydrogen and deuterium occurs, such corrections have only modest influences on the nature of the spectra. The

[3]*The ionization at masses 58 and 57 in the mass spectrum of n-butanol-*D_2 *places an extreme upper limit of 11.8% on the isotopic impurity (8). However, the ionization at mass 57 must correspond primarily to loss of* H_3O *(rather than* H_2O *from* C_4H_8DOH*) in order to match the corresponding ionization from n-butanol-*D_0*. Taking this into account it was concluded that about 3.5% is a reasonable upper limit to the isotopic impurity.*

TABLE IV

Corrected partial mass spectra of deuterated *sec*-bromobutanes

D_0		D_5		D_6	
m/e	% ionization	*m/e*	% ionization	*m/e*	% ionization
54	0.24	59	0.9	60	0.8
55	1.83	60	1.5	61	1.3
56	2.33	61	2.0	62	1.7
57	31.3	62	30.6	63	29.8

corrections have been applied here only to the data for the ions due to loss of ·Br or HBr, because only negligible changes would be made in the other values. Because upper limit values of the possible corrections were used, the data at *m/e* 61 and 62 for *sec*-bromobutane-D_5 and *sec*-bromobutane-D_6 respectively may be taken as the minimum amount of ionization due to loss of HBr. The corrections impose uncertainties which make the difference between these values of no significance (D_6 is believed to be the more overcorrected) and because of observed differences in the total ionization of the C_4 group (as obtained from Table I, $\sum C_4$ ions is 38.9, 38.5, 37.4 for D_0, D_5, D_6) it is not certain how much ionization should be attributed to the combined loss of HBr and DBr. Nevertheless, a definite conclusion can be made that more than 86% (2.0/2.33) of the events forming the lost HBr involve either the hydrogen (deuterium) on carbons 2 or 4 and more than 73% (1.7/2.33) of the events involve only the hydrogen on carbon 4.

Because the two bromine isotopes Br^{79} and Br^{81} occur in about a 50–50 abundance the metastable ions corresponding to loss of HBr occur on an overlapping doublet with a characteristic shape. This shape was defined in these experiments from the spectrum of *sec*-bromobutane-D_0. It was observed in the spectrum of *sec*-bromobutane-D_5 with peaks at 26.0 and 26.4 corresponding to loss of HBr, but the metastable peaks corresponding to loss of DBr at *m/e* 25.5 and 25.2 were not observed. This would confirm the conclusions deduced from the corrected data of Table IV, namely, that loss of HBr to form $C_4H_8^+$ primarily involves the hydrogen on carbon 4 and may be considered as sterically dependent.

The spectrum of *sec*-bromobutane-D_6 showed no metastable ion doublet that could be attributed to the same molecular processes involving either loss of HBr or DBr. The absence of these very characteristic peaks must be due to an increase in the rate constant for the loss of HBr due to the additional isotopic substitution. It is interesting that this small isotopic change could so affect the rate of decomposition, but such an observation is in accordance with accepted views (13).

(E) C_3 Ions Not Containing Bromine

The metastable ions observed from the undeuterated bromobutanes indicate that many of the smaller ion fragments which do not contain bromine are secondary daughter fragments with $C_4H_9^+$ or $C_4H_8^+$ as their precursors. This results in an interesting comparison, namely, that many of the metastable peaks are also present in the mass spectra of the saturated and unsaturated hydrocarbons (14). A similar observation has been noted in the mass spectra of bromopentanes (6).

As a consequence of originating from unsaturated precursors, the hydrogens and deuteriums of most of the smaller daughter ions are significantly exchanged and in certain instances may be considered equilibrated. One notable exception is the propyl ion from *n*-bromobutane.

(i) n-Bromobutane

Because the total ionization of the C_3 group is the same for deuterated and undeuterated *n*-bromobutane (23.72% and 23.94%), one may confidently assume that the percentage of ionization for each type of ion is approximately the same. In order to establish the distribution of deuterium in the important ions ($C_3H_7^+$, $C_3H_5^+$, and $C_3H_3^+$) the less abundant ions at masses 42, 40, and 38 are assigned a statistical distribution of H and D. After a first-approximation calculation, minor corrections are made for the carbon 13 isotopes with the assumption of the same distribution of H and D as was found for the carbon 12 analogues. The $C_3H_8^+$ ion was assumed to have the same distribution as the propyl ion. Thus, one can approximate the amount of propyl ion containing zero, one, or two deuteriums. With this information the calculation of deuterium among the $C_3H_5^+$ ions can be determined and finally that for the $C_3H_3^+$ ions. The results are presented in Table V along with the values calculated on a statistical basis.

TABLE V

Distribution of H and D in the ions $C_3H_7^+$, $C_3H_5^+$, and $C_3H_3^+$ from $CD_2BrCH_2CH_2CH_3$

	% ionization					
	$C_3H_7^+$		$C_3H_5^+$		$C_3H_3^+$	
No. of deuteriums	Calc. data	Calc. stat.	Calc. data	Calc. stat.	Calc. data	Calc. stat.
0	1.17	0.04	3.7	4.4	1.5	1.5
1	—	0.53	6.6	8.7	1.6	1.8
2	0.20	0.82	5.5	2.5	0.6	0.3

The data of Table V show that most of the propyl ion is formed without involvement of the deuterium on carbon 1. A small amount (14% of total $C_3H_7^+$) appears to involve both of these deuteriums but apparently the ion $C_3H_6D^+$ is not formed to any appreciable extent. The assignment of the 0.39% of ionization observed at $m/e = 44$ to $C_3H_4D_2^+$, $C_3{}^{13}H_3D_2^+$, and $C_3H_8^+$ could not be in error enough to alter this conclusion. Thus, it appears that most of the propyl ion is formed by simple bond break without H–D exchange from the parent ion. A small amount appears to be formed by a path which involves the hydrogen on carbon 1 but which does not permit significant exchange. The statistically calculated values indicate the improbability of such data if many exchanges were occurring.

The data for the ions $C_3H_5^+$ and $C_3H_3^+$ show, on the other hand, a considerable exchange of hydrogen and deuterium. This is consistent with the observed metastable ion data indicating an unsaturated hydrocarbon ion as the precursor; for such ions, the rate of H–D exchange would be much greater than that obtained in saturated species. Comparison with the statistically calculated values indicates a close approximation to equilibrium with a slight preference for retention of the deuterium, but until a more refined understanding of the isotope effect and the intramolecular exchange reactions is obtained, these small differences cannot be interpreted.

In the spectrum of *n*-bromobutane-D_0 a metastable peak is observed at mass 29.5 corresponding to the reaction $C_4H_9^+ \rightarrow C_3H_5^+ + CH_4$. The equivalent metastable peaks are observed at masses 28.6, 29.9, and 31.3 (Table III) corresponding to the processes

$$\begin{aligned} C_4H_7D_2^+ &\rightarrow C_3H_5^+ + CH_2D_2 \\ &\rightarrow C_3H_4D^+ + CH_3D \\ &\rightarrow C_3H_3D_2^+ + CH_4. \end{aligned}$$

Metastable peak data indicate that $C_3H_3^+$ can be formed by the reactions $C_4H_7^+ \rightarrow C_3H_3^+ + CH_4$ and $C_3H_5^+ \rightarrow C_3H_3^+ + H_2$. The first of these paths gave only 0.004% of the ionization as a metastable ion so that, as is expected, none of the six possible paths leading to equivalent ions are observed in the spectrum of *n*-bromobutane-D_2. The second reaction gave a stronger metastable peak from the undeuterated molecule (0.03%). The six possible equivalent reaction paths for the deuterated molecule are:

$C_3H_5^+ \rightarrow$	$C_3H_3^+ + H_2$	$m^* = 37.1$
$C_3H_4D^+ \rightarrow$	$C_3H_3^+ + HD$	36.2
$\rightarrow$	$C_3H_2D^+ + H_2$	38.1
$C_3H_3D_2^+ \rightarrow$	$C_3H_3^+ + D_2$	35.4
$\rightarrow$	$C_3H_2D^+ + DH$	37.2
$\rightarrow$	$C_3HD_2^+ + H_2$	39.1

and all except $C_3H_3D_2^+ \rightarrow C_3H_3^+ + D_2$ are observed. That this reaction should be absent is a logical result of the low statistical probability for that process, and the small signal observed for the process $C_3H_4D^+ \rightarrow C_3H_3^+ + HD$ may also be attributed to that cause.

(ii) sec-Bromobutane

Determination of the distribution of deuterium among the more predominant C_3 ions from *sec*-bromobutane-D_5 and *sec*-bromobutane-D_6 was made in the same way as for *n*-bromobutane-D_2. Because the propyl ion contributes less to the total and because it makes an uncertain contribution to the mass 48 ionization it was arbitrarily assigned a statistical distribution. The results for the $C_3H_5^+$ and $C_3H_3^+$ ions are given in Table VI.

TABLE VI
Distribution of H and D in the ions $C_3H_5^+$ and $C_3H_3^+$ from $CD_3CHBrCD_2CH_3$ and $CD_3CDBrCD_2CH_3$

	% ionization							
	$CD_3CHBrCD_2CH_3$				$CD_3CDBrCD_2CH_3$			
	$C_3H_5^+$		$C_3H_3^+$		$C_3H_5^+$		$C_3H_3^+$	
No. of deuteriums	Calc. data	Calc. stat.	Calc. data	Calc. stat.	Calc. data	Calc. stat.	Calc. data	Calc. stat.
0	—	—	0.04	0.2	—	—	0.0	0.05
1	1.3	0.7	1.3	1.6	—	—	0.8	1.0
2	5.2	5.4	2.1	2.2	2.8	2.0	1.8	2.5
3	6.2	8.0	1.2	0.6	6.2	8.0	2.4	1.1
4	3.8	2.7			4.9	6.1		
5	0.4	0.1			3.0	0.8		

The data of Table VI again show considerable rearrangement of hydrogen and deuterium. In both cases, however, there is a tendency to retain deuterium, indicating that the lost CH_4 molecule may predominantly involve carbon 4.

The metastable ion at mass 29.5 from the undeuterated compound indicates the process $C_4H_9^+ \rightarrow C_3H_5^+ + CH_4$. From *sec*-bromobutane-D_5 this ion could be expected to occur at masses 28.4, 29.8, 31.2, 32.7, and 34.1, corresponding to formation of $C_3DH_4^+$, $C_3D_2H_3^+$, $C_3D_3H_2^+$, $C_3D_4H^+$, and $C_3D_5^+$. All are observed except that at 28.4 and the intensities are in reasonable agreement with the expected values, considering the difficulty in accurately measuring metastable peak heights.

Metastable ions due to the processes equivalent to $C_3H_5^+ \rightarrow C_3H_3^+ + H_2$ could occur by 11 processes from *sec*-bromobutane-D_5 and 9 from *sec*-bromobutane-D_6. All but two are observed and these two are low probability processes.

(F) C_2 and C_1 Ions Not Containing Bromine

The ethyl and ethylene ions from *n*-bromobutane and *sec*-bromobutane are shown by the metastable peaks to originate to a considerable extent from $C_4H_9^+$ or $C_4H_7^+$ and to be in turn the precursors of the vinyl and acetylene ions (Table II). From such origins one would expect that the hydrogen and deuterium of the deuterated molecules would be considerably exchanged prior to formation of these ions. In Table VII the observed

TABLE VII

Observed and statistically calculated ion intensities for the C_2 ions from *n*-bromobutane-D_2, *sec*-bromobutane-D_5, and *sec*-bromobutane-D_6

	$CD_2BrCH_2CH_2CH_3$		$CD_3CHBrCD_2CH_3$		$CD_3CDBrCD_2CH_3$	
m/e	Obs.	Stat.	Obs.	Stat.	Obs.	Stat.
26	1.1	1.2	0.3	0.2	0.2	0.1
27	4.6	4.3	1.2	1.2	0.8	0.8
28	4.4	5.6	2.4	2.9	2.5	2.1
29	7.0	5.1	3.8	3.7	2.2	3.7
30	6.9	7.4	3.4	2.0	4.2	2.4
31	3.3	3.5	5.6	5.4	3.7	2.9
32			5.9	7.0	6.2	7.1
33			2.7	2.5	4.6	5.3
34			0.3	0.2	1.3	0.9

ion ratio for the C_2 ions of the deuterated species is compared with that calculated assuming all ion types have complete equilibration of the original hydrogen and deuterium. It is seen that the experimental data are close to the statistical calculations and the small deviations may be considered due to isotope effects.

The three metastable processes leading to these ions in the undeuterated molecules (namely, $C_4H_9^+ \rightarrow C_2H_4^+ + \cdot C_2H_5$, $C_4H_9^+ \rightarrow C_2H_5^+ + C_2H_4$, and $C_4H_7^+ \rightarrow C_2H_5^+ + C_2H_2$, Table II) have 13, 19, and 16 equivalent processes from the molecules *n*-bromobutane-D_2, *sec*-bromobutane-D_5, and *sec*-bromobutane-D_6, respectively. This causes considerable overlap and since the position of metastable peaks cannot always be precisely determined, the 12 metastable ions reported in Table III between mass 14.25 and 18.09 cannot all be assigned to an unequivocal reaction. They are all accountable, however. Noteworthy is the fact that the metastable ions corresponding to the different possible isotopic reactions equivalent to $C_4H_9^+ \rightarrow C_2H_5^+ + C_2H_4$ are all absent in the spectra of the two deuterated *sec*-bromobutanes. This most likely indicates a change in the rate of that reaction due to the isotopic substitution.

The C_1 ions (primarily CH_3^+) do not constitute an important part of the total ionization. Considerable H–D exchange occurs, leading to values close to the statistical ones. This suggests that these small ions are formed from a number of the prior daughter fragments, consistent with recent conclusions based on data from large substituted hydrocarbons (15).

ACKNOWLEDGMENTS

We wish to thank Professor A. L. Wahrhaftig for making the deuterated samples available and Dr. R. E. Lundin and Mr. R. B. Block for attempting the belated isotopic analysis by n.m.r.

REFERENCES

1. H. BRANSON and C. SMITH. J. Am. Chem. Soc. **75**, 4133 (1953).
2. A. P. IRSA. J. Chem. Phys. **26**, 18 (1957).
3. J. COLLIN. Bull. soc. roy. sci. Liège, 426 (1956).
4. F. W. McLAFFERTY. Anal. Chem. **34**, 2 (1962).
5. J. MOMIGNY. Bull. soc. chim. Belges, **64**, 144 (1955).
6. L. D'OR, H. NEYNS, and J. MOMIGNY. Ann. soc. sci. Bruxelles, Sér. I, **71**, 61 (1957).
7. W. H. McFADDEN and A. L. WAHRHAFTIG. J. Am. Chem. Soc. **78**, 1572 (1956).
8. W. H. McFADDEN, M. LOUNSBURY, and A. L. WAHRHAFTIG. Can. J. Chem. **36**, 990 (1958).
9. R. L. GRAHAM, A. L. HARKNESS, and H. G. THODE. J. Sci. Instr. **24**, 119 (1947).
10. W. A. BRYCE and P. KEBARLE. Can. J. Chem. **34**, 1249 (1956).
11. W. H. McFADDEN. Paper presented at the 9th Annual Meeting of ASTM Committee E-14 on Mass Spectrometry, Chicago, 1961.
12. F. W. McLAFFERTY. Anal. Chem. **31**, 2072 (1959).
13. A. KROPF. Doctoral thesis, University of Utah, Salt Lake City, Utah. 1954. p. 54.
14. CATALOG OF MASS SPECTRAL DATA. Am. Pet. Inst., Research Project 44, A. and M. College of Texas, College Station, Texas. 1962.
15. J. H. BEYNON, R. A. SAUNDERS, A. TOPHAM, and A. E. WILLIAMS. J. Phys. Chem. **65**, 114 (1961).

GAS–LIQUID CHROMATOGRAPHIC ANALYSIS OF LIGNIN OXIDATION PRODUCTS

J. M. Pepper, M. Manolopoulo, and R. Burton
Department of Chemistry, University of Saskatchewan, Saskatoon, Saskatchewan

Received July 3, 1962

ABSTRACT

The gas–liquid chromatographic separation of vanillin, syringaldehyde, and *p*-hydroxybenzaldehyde has been effected using a 15% Apiezon N on Fluoropak column at 220° C. Using standard solutions of the reference compounds and measuring peak areas, the percentage composition of mixtures of milligram amounts of these aldehydes may be determined quantitatively to within 5%.

The method has been applied to the quantitative analysis of the phenolic aldehydes resulting from the alkaline nitrobenzene oxidation of aspen and spruce wood and wheat straw meals as well as the lignins isolated from these same plant materials. The results are reproducible and generally in good agreement with those reported earlier for similar lignified substances as determined using the spectrophotometer method of Stone and Blundell.

In a recent communication Pepper and Siddiqueullah (1) reviewed the chemical nature and the methods of separation and estimation of those lignin derivatives obtained by the oxidation and/or alkaline hydrolysis of woody plants and isolated lignins. Of these, the procedure developed in 1951 by Stone and Blundell (2) has been used most extensively for both the identification and quantitative estimation of the phenolic aldehydes vanillin, syringaldehyde, and *p*-hydroxybenzaldehyde. This method involves the paper chromatographic separation of the oxidation products, their extraction from strips cut from these papers, and their subsequent quantitative estimation spectrophotometrically. In our laboratory good reproducible results were obtained only after extensive experience with the procedure, especially with respect to the sampling of the whole oxidation reaction mixture. A modification has been suggested (3) to minimize these difficulties.

It has now been found that these lignin oxidation products may be separated readily and subsequently determined quantitatively using gas–liquid chromatography. The components of a mixture of vanillin, syringaldehyde, and *p*-hydroxybenzaldehyde were readily separated using a 1/4 in.×6 ft 15% Apiezon N on Fluoropak column at 220° C. Retention times of 8.2, 19.3, and 5.8 minutes respectively were observed using 30 p.s.i. helium carrier gas at a flow rate of 0.7 cc/sec. To determine if such an analysis could be used quantitatively, standard curves were prepared relating peak areas to weight of injected sample. The areas were determined by the triangulation method. A 1% solution of each pure aldehyde was prepared in absolute ethanol. For each compound five accurately measured sample volumes ranging from 10 to 60 μl were chromatographed using the column and conditions described above. The results so obtained and subsequently used to plot the standard calibration curves are given in Table I.

Subsequently a synthetic mixture of known composition of the three aldehydes was prepared in ethanol and analyzed using these calibration curves. Symmetrical, well-separated peaks were obtained, which permitted the ready calculation of areas and hence concentration. Agreement with the original composition was within 3%.

It was then necessary to show that a similar quantitative recovery of these aldehydes could be accomplished from the products of an alkaline nitrobenzene oxidation of lignin. To this end a study was made of the products of oxidation of each of a sample of aspen and spruce wood and wheat straw as well as a representative lignin fraction obtained

TABLE I

Relationship of peak area to sample weight for phenolic aldehydes

Sample (μl)	Aldehyde (mg)	Peak areas (cm²)		
		Vanillin	Syringaldehyde	*p*-Hydroxybenzaldehyde
10	0.10	8		7.8
15	0.15			12.0
20	0.20	16.7	15.4	15.8
25	0.25			19.5
30	0.30	24.2	22.8	23.2
35	0.35	28.2		
40	0.40	31.9	30.6	
50	0.50		39.3	
60	0.60		46.3	

from each of them. These six samples were independently oxidized at 180±2° C for 2 hours in small, rocking, stainless steel autoclaves. For each, the alkaline reaction product was extracted with ether to remove excess nitrobenzene and its reduction products, then acidified and re-extracted with ether to remove the lignin oxidation products. This ether extract was water-washed, dried, and concentrated to standard volume. Accurately measured aliquots were injected into the 6-ft Apiezon N on Fluoropak column under conditions as similar as possible to those used to prepare the standard calibration curves.

Well-separated, symmetrical peaks were obtained for each of the major components of each of the six oxidation products, as shown in Fig. 1. For those cases in which only trace

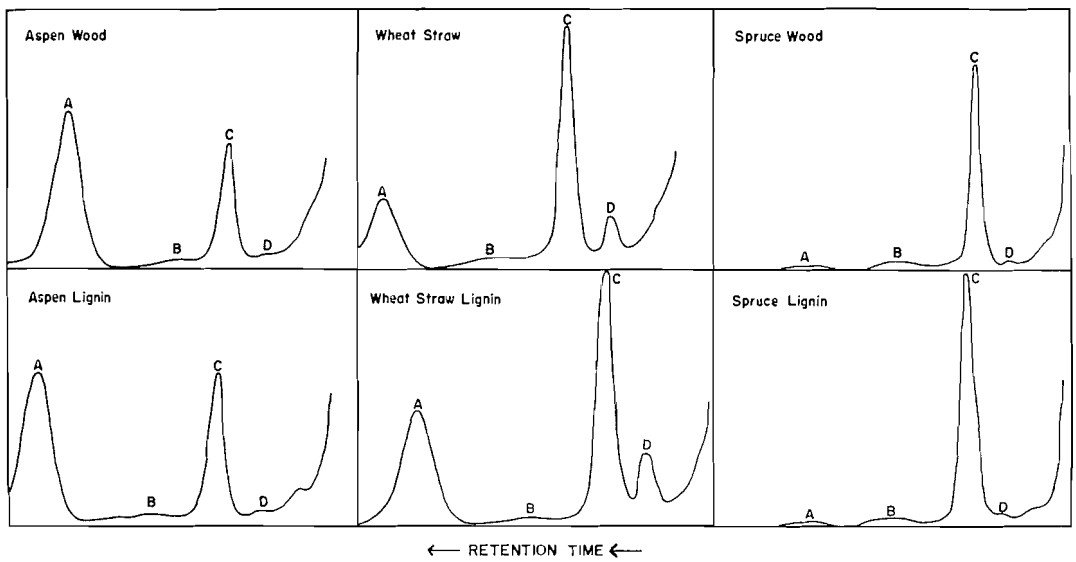

FIG. 1. Chromatographic separation of oxidation products of wood, straw, and isolated lignins. A, syringaldehyde; B, acetoguaiacone; C, vanillin; D, *p*-hydroxybenzaldehyde.

amounts of aldehydes or acetoguaiacone were indicated in these curves, larger, sharper peaks were obtained for these components by injection of a larger sample. From the peak areas both the relative abundance and the yield of each component were determined by reference to the standard calibration curves. From these yields the percentage yields based on either the Klason lignin content of the plant meals or on the isolated lignin

were calculated. These data, together with the yields obtained previously by the method of Stone and Blundell on similar or in some cases identical samples, are given in Table II.

For a simple, rapid analysis of both the chemical nature and the relative abundance of the simple products of lignin oxidation, this gas–liquid chromatographic method is superior to the paper chromatographic methods that have been used previously. For the more precise quantitative analysis of the oxidation products this method compares very favorably with that described by Stone and Blundell (2). It should be emphasized that it may be necessary to check the standardization curves more frequently due to the greater possibility of variation in the experimental conditions and especially in the characteristics of the particular column should it have been in use for any extended length of time. As may be seen from Table II, the percentage yields of the phenolic aldehydes as determined by the two methods are generally in good agreement. No doubt, part of the variation may be attributed to the problems of sampling and of small actual differences within the plant species themselves. Using the gas chromatographic method there is no need for correction for chromatographic losses, as Stone and Blundell suggest must be applied in the calculations using their method.

It is now quite evident that the lignin fraction of representative samples of deciduous and coniferous woods and of cereal straws gives rise to all three types of nuclei as seen in the compounds vanillin, syringaldehyde, and *p*-hydroxybenzaldehyde. However, the relative abundance of each such type still serves adequately as a form of taxonomic classification of such lignified tissues (7).

EXPERIMENTAL

The various samples of pre-extracted wood meals and wheat straw, as well as the lignins isolated from them, had been prepared by other workers, and their method of preparation described earlier (6).

The apparatus used for the oxidations consisted of small cylindrical (6 in.×1 in. O.D., 20-ml capacity) stainless steel reaction vessels with screw caps. Six such vessels could be inserted and held in an aluminum block which was heated electrically. A rocking device permitted a swing through approximately 120° at 50 cycles/min. One such vessel was designed to accommodate a thermometer and was filled with Stanolax oil as the heat exchange medium.

The chromatographic column was made from 6 ft×1/4 in. I.D. copper tubing and packed with Apiezon N grease on Fluoropak 80 (Wilkens Instrument and Research, Inc.) in the ratio of 3 to 17. A Beckman GC-2 chromatograph, with a thermal conductivity detector unit, was used, after some modification, to place the injection system as close as possible to one end of the column.

Oxidation and Analytical Procedure

For each oxidation 2 *N* sodium hydroxide (10 ml) was added to the reaction vessel. Subsequently the pre-extracted wood or straw meals or the isolated lignins were added. The dry weights of the lignified materials that were used to obtain the results given in Table II were 401, 579, 824 mg for the aspen, spruce, and straw meals respectively and 198, 210, and 210 mg for the corresponding isolated lignins. For each oxidation redistilled nitrobenzene (0.6 ml) was added. The vessels were sealed and the contents heated at 180±2° for 2 hours with rocking. After being cooled, the dark-colored reaction mixture was transferred, with careful rinsing with water and ether, to a continuous liquid–liquid extraction apparatus. Excess nitrobenzene and its reduction products were removed by the continuous ether extractions (24–30 hours).

The aqueous layer, after acidification to pH 3 by the slow addition of concentrated hydrochloric acid, was further continuously extracted with ether (24–30 hours) to remove the lignin oxidation products. The ether extract, after being washed with water, was dried over anhydrous magnesium sulphate and concentrated to a volume of 2–3 ml. Complete transfer of this extract to a 5-ml volumetric flask required two or three washings with dry ether, each of which was concentrated to 0.5–1 ml. Finally, by the addition of dry ether, the extract was diluted to exactly 5 ml. At least two samples of equal volume of about 60–100 μl were pipetted quickly from the 5-ml extract and injected immediately into the previously equilibrated column.

ACKNOWLEDGMENT

Grateful acknowledgment is made to the National Research Council of Canada for financial assistance.

TABLE II

Quantitative analyses of lignin oxidation products

	Lignin oxidized* (mg)	Total ether-soluble oxidation products (ml)	Injected sample (μl)	Lignin oxidation products†				
				Peak area‡ (cm^2)	Weight in injected sample (mg)	Weight in total sample (mg)	Percentage of original lignin	
							Found	Reported§
Aspen wood meal	72.2	5	90					
Vanillin				12.2	0.152	8.45	11.7	11.5
Syringaldehyde				30.9	0.40	22.2	30.8	29.1
p-Hydroxybenzaldehyde				0.4	0.007	0.38	0.2	
Aspen lignin	198	5	90					
Vanillin				15.6	0.195	10.8	5.5	6.7
Syringaldehyde				37.2	0.483	26.9	13.6	19.3
p-Hydroxybenzaldehyde				0.6	0.01	0.56	0.3	
Spruce wood meal	156	5	30					
Vanillin				24.6	0.305	50.9	32.6	27.5
Syringaldehyde				0.98	0.013	2.17	1.4	0.06
p-Hydroxybenzaldehyde				0.72	0.009	1.5	1.0	0.25
Spruce lignin	210	5	60					
Vanillin				34.4	0.428	35.7	17.0	15.8
Syringaldehyde				1.0	0.014	2.18	1.4	
p-Hydroxybenzaldehyde				1.2	0.015	1.25	0.6	
Wheat straw meal	173	5	90					
Vanillin				23.4	0.29	16.1	9.3	7.5
Syringaldehyde				17.3	0.225	13.9	8.0	8.2
p-Hydroxybenzaldehyde				3.05	0.039	2.17	1.3	1.2
Wheat straw lignin	210	3.85	100					
Vanillin				27.5	0.342	15.8	7.5	9.5
Syringaldehyde				26.8	0.351	16.1	7.7	8.3
p-Hydroxybenzaldehyde				4.7	0.062	2.8	1.35	

*Based on Klason lignin content of wood or straw meals.
†In each case traces of acetoguaiacone were noted but not determined quantitatively.
‡Average of two or three separate oxidations; maximum variation within 5%; in most cases variation did not exceed 2%.
§The values for aspen wood meal and aspen lignin were reported by Pepper and Siddiqueullah (4); for spruce wood by Leopold (5); for spruce and wheat straw lignin by Pepper and Wood (6); and for wheat straw meal by Stone and Blundell (2).

REFERENCES

1. J. M. PEPPER and M. SIDDIQUEULLAH. Can. J. Chem. **38**, 2324 (1960).
2. J. E. STONE and M. J. BLUNDELL. Anal. Chem. **23**, 771 (1951).
3. J. M. PEPPER and M. SIDDIQUEULLAH. Can. J. Chem. **39**, 390 (1961).
4. J. M. PEPPER and M. SIDDIQUEULLAH. Can. J. Chem. **39**, 1454 (1961).
5. B. LEOPOLD. Acta Chem. Scand. **6**, 38 (1952).
6. J. M. PEPPER and P. D. S. WOOD. Can. J. Chem. **40**, 1026 (1962).
7. R. H. J. CREIGHTON, R. D. GIBBS, and H. HIBBERT. J. Am. Chem. Soc. **66**, 32 (1944).

MECHANISM OF ALKALINE HYDROLYSIS OF HINDERED AROMATIC ESTERS, THE $B_{AL}2$ MECHANISM

L. R. C. BARCLAY, N. D. HALL, AND G. A. COOKE
Department of Chemistry, Mount Allison University, Sackville, New Brunswick

Received June 27, 1962

ABSTRACT

Kinetic and isotopic exchange data employing H_2O^{18} are presented to establish the bimolecular alkaline hydrolysis with alkyl–oxygen fission ($B_{AL}2$) for the highly hindered ester methyl 2,4,6-tri-*t*-butylbenzoate. Methyl 2-methyl-4,6-di-*t*-butylbenzoate also cleaved predominately by alkyl–oxygen fission. Other hindered esters, methyl 2,4,6-trimethylbenzoate and methyl 2,5-di-*t*-butylbenzoate, hydrolyzed by the usual acyl–oxygen fission.

INTRODUCTION

Attempts have been made to observe the relatively unknown bimolecular alkaline hydrolysis of carboxylic esters with alkyl–oxygen fission ($B_{AL}2$). Mechanistic studies on the saponification of di-ortho-substituted benzoic esters are of special interest. Bulky ortho substituents in the methylbenzoates might be expected to hinder nucleophilic attack at the carbonyl carbon and possibly permit observation of the unusual mechanisms of nucleophilic attack at the alkyl (methyl) carbon atom. In this connection Goering, Rubin, and Newman (1) provided kinetic evidence on the alkaline hydrolysis of 4-substituted-2,6-dimethyl benzoates (i.e. methyl mesitoate) which they suggested was indicative of the $B_{AL}2$ mechanism. The log PZ terms for hydrolysis of mono-ortho-substituted benzoic esters are about 10 times smaller than the value of approximately 8 observed for the meta and para isomers. Therefore the log PZ terms for hydrolysis of di-ortho-substituted benzoic esters were expected to be still smaller (1). However, these terms were at least as large as those observed for the unsubstituted ester and meta and para isomers. This anomalous result prompted Newman and co-workers to suggest a change in mechanisms from the usual acyl–oxygen fission to the unusual alkyl–oxygen fission. Bender and Dewey (2) later provided unequivocal tracer evidence with H_2O^{18} to show that the kinetic results (1) led to an incorrect conclusion. This tracer evidence established that this ester cleaved via acyl–oxygen fission. Bunton and co-workers (3) found that methyl 2,4,6-triphenylbenzoate underwent the usual bimolecular acyl–oxygen fission ($B_{AC}2$) in aqueous dioxane. In aqueous methanol this ester hydrolyzed to some extent by the $B_{AC}2$ mechanism and to some extent by the $B_{AL}2$ mechanism, but in the latter case the reaction apparently proceeded by attack of methoxide rather than hydroxide ion on the alkyl carbon.

Evidence was provided in a preliminary publication (4) for the $B_{AL}2$ mechanisms for hydrolysis of methyl 2,4,6-tri-*t*-butylbenzoate. We now wish to report the details of this research and also to report on the extension of this mechanism to methyl 2-methyl-4,6-di-*t*-butylbenzoate.

EXPERIMENTAL

Syntheses of Hindered Acids and Esters

(A) Methyl Mesitoate

Mesitoic acid (m.p. 154°), prepared as described in *Organic Syntheses* (5), was esterified with diazomethane in ethyl ether. The pure ester (n_D^{20} 1.5090) was obtained by chromatography in petroleum ether on alumina.

(B) Methyl 2,5-Di-t-butylbenzoate

2,5-Di-*t*-butylbenzoic acid was prepared as previously described (6) and converted into its methyl ester with diazomethane. The ester was purified by chromatography and distilled at 148–150° at 7 mm; n_D^{20} 1.5068.

(C) 2,4,6-Tri-t-butylbenzoic Acid and Methyl Ester

2,4,6-Tri-*t*-butylbenzoic acid was prepared from 2,4,6-tri-*t*-butylbromobenzene by a procedure similar to that previously described (6). The ester, methyl 2,4,6-tri-*t*-butylbenzoate, was prepared from the acid by the diazomethane method. The ester was purified by chromatography on alumina, m.p. 98–99°.

(D) Methyl 2-Methyl-4,6-di-t-butylbenzoic Acid and Related Compounds

(1) 3,5-Di-t-butyltoluene.—3,5-Di-*t*-butyltoluene was prepared by a procedure similar to that reported by Wepster and co-workers (7).

(2) 2-Methyl-4,6-di-t-butylbromobenzene.—3,5-Di-*t*-butyltoluene (20 g, 0.098 mole) was dissolved in 130 cc of glacial acetic acid. Aqueous nitric acid (80 cc of concentrated nitric acid in 80 cc of distilled water) was added to this mixture. Bromine (15 g, 0.094 mole) was added to the solution followed by a solution of 20 g of silver nitrate in 50 cc of water. The aqueous silver nitrate was added dropwise to the stirred reaction mixture over a period of 2 hours and the reaction was allowed to stand overnight. An oily organic layer was separated and traces of bromine were removed by washing with aqueous sodium bisulphite. The product was dried with anhydrous sodium sulphate and purified by distillation to yield 23 g of bromocompound (83%), b.p. 87–89° at 0.2 mm; n_D^{20} 1.5318.

(3) 2-Methyl-4,6-di-t-butylbenzoic acid and methyl ester.— 2-Methyl-4,6-di-*t*-butylbromobenzene (3.70 g, 0.013 mole) in 20 ml of anhydrous ethyl ether was added to 0.026 mole of *n*-butyl lithium in 65 ml of ethyl ether in an atmosphere of dry nitrogen. There was spontaneous refluxing for 15 minutes, which was continued for an additional 30 minutes by heating. Carbon dioxide was passed through the reaction mixture, with stirring, for 5 hours. The solvent was distilled to dryness and the residue treated with water. Acidification of this aqueous layer yielded 2.30 g, 72% of the crude acid, m.p. 147–152°. Crystallization from petroleum ether produced colorless crystals, m.p. 152–153°. The same acid was also prepared by chromic acid oxidation of 2-methyl-4,6-di-*t*-butylbenzyl alcohol, which was synthesized by the method of Beets and co-workers (8). They reported a melting point of 152.3–152.9°. The acid was esterified by the diazomethane method. On crystallization from methanol–water, the methyl ester melted at 46–48°. It was further purified by chromatography on alumina and gave a melting point of 47–48° (lit. (8) m.p. 53.5–54.0°).

(4) Oxidation of 2-methyl-4,6-di-t-butylbenzoic acid.—2-Methyl-4,6-di-*t*-butylbenzoic acid (1.0 g, 0.004 mole) was dissolved in aqueous sodium carbonate. Potassium permanganate (1.30 g) was added in portions and the reaction mixture was heated under reflux until the permanganate color had nearly disappeared (5 hours). Sulphur dioxide was passed into the reaction to destroy the precipitated manganese dioxide and the precipitated organic acid was filtered and dried (1.05 g, 95%). This crude acid was dissolved in aqueous sodium carbonate and reprecipitated, and the melting point found to be 175–183°. The infrared spectrum of this acid (KBr pellet) showed a doublet in the carbonyl region at 1690 and 1710 cm^{-1}. An attempt was made to purify this acid by sublimation *in vacuo*. The sublimed crystals had a melting point of 93–95° and double carbonyl absorption in the infrared (KBr pellet) at 1760 and 1820 cm^{-1}, typical of a cyclic anhydride. Calc. for $C_{16}H_{20}O_3$: C, 73.82; H, 7.74. Found: C, 73.40, 73.44; H, 7.97, 7.86.

Kinetics of Alkaline Hydrolysis of Methyl 2,4,6-Tri-t-butylbenzoate

The methanol which was used as the solvent was purified by the method of Morton and Mark (9). It was then distilled on a podbielniak column and the fraction which gave a negative test for carbonyl compounds used. The dioxane used was purified by the method of Fieser (10) and distilled from lithium aluminum hydride on a podbielniak column in an atmosphere of nitrogen. This solvent gave very large blanks with aqueous alkali in the kinetic apparatus even when the purification was repeated. Its use therefore had to be abandoned in the kinetic runs.

The kinetic runs were made in stainless steel tubes ($8\times\frac{1}{2}$ in.) which were fitted at each end with heavy stainless steel hexagonal caps. The caps contained an expansion chamber into which were fitted pure silver disks. The tubes were sealed by turning the caps on tightly so that the ends of the tubes were seated into the silver disks. The extent of hydrolysis was followed by removing aliquots and titrating the alkali remaining with standard hydrochloric acid from a microburette using phenolphthalein indicator.

The rate constants were determined from the integrated form of the second-order rate equation, $k = 1/t(a-b) \ln [b/a(a-x)/(b-x)]$, where a is the initial concentration of sodium hydroxide, b is the initial concentration of ester, x is the amount reacted at time t, and k is the second-order rate constant in liters/mole sec. The results of the measurements at six temperatures are summarized in Table I.

Isotopic Oxygen Tracer Studies

In the isotopic tracer studies, water enriched in H_2O^{18} was employed.*

The alkaline hydrolysis mixtures containing ester were made up to contain certain percentages of H_2O^{18} by dilution. The amount of oxygen exchange was determined from the isotopic abundance of oxygen in the acid

**Samples enriched to about 1.5% H_2O^{18} were supplied by Dr. R. E. Robertson of the N.R.C. Laboratory. Other samples were obtained from Dajac Laboratories, Philadelphia.*

TABLE I

Hydrolysis of methyl 2,4,6-tri-*t*-butylbenzoate in aqueous methanol (90%)

T (°C)	t (min)	$x\times10^4$ (moles)	$\ln \frac{b(a-x)}{a(b-x)}$	$k\times10^4$
95	6,830	0.2820	0.01732	1.225
	12,590	0.5234	0.03327	1.276
	18,390	0.6812	0.04431	1.164
($a = 9.56\times10^{-4}$ mole, $b = 6.109\times10^{-4}$ mole)				1.202*
110	1,197	0.3221	0.02368	4.587
	2,575	0.7118	0.05466	4.923
	5,480	1.5196	0.12870	5.447
	11,167	2.4684	0.23817	4.947
($a = 14.28\times10^{-4}$ mole, $b = 7.089\times10^{-4}$ mole)				5.035*
126	1,365	1.1544	0.09305	15.84
	2,790	2.1310	0.19505	16.25
	4,205	2.6648	0.26369	14.57
	8,505	4.0336	0.50705	13.85
($a = 14.275\times10^{-4}$ mole, $b = 7.1025\times10^{-4}$ mole)				14.21*
140	2,810	3.0568	0.27179	32.97
	3,975	3.9698	0.42234	36.21
	6,835	5.2030	0.76342	38.08
($a = 11.94\times10^{-4}$ mole, $b = 7.061\times10^{-4}$ mole)				37.09*
150	335	1.1018	0.10528	88.64
	1,075	2.6649	0.32957	86.47
	1,450	3.3580	0.48180	93.71
($a = 11.95\times10^{-4}$ mole, $b = 6.041\times10^{-4}$ mole)				91.06*
180	220	4.7624	0.70921	777.5
	290	5.4500	0.98966	823.1
	350	5.9184	1.28034	882.3
	390	6.0445	1.38309	855.4
($a = 13.96\times10^{-4}$ mole, $b = 7.046\times10^{-4}$ mole)				847.6*

*These values of k were determined by the method of least squares.

produced in the saponification by decarboxylation of the silver salts of the acids. The procedure was similar to that reported by Bunton and co-workers (3). The silver salts of the acids were prepared by dissolving the acids in ethanol, titrating with standard alcoholic potassium hydroxide, and then adding exactly an equivalent amount of silver nitrate. The silver salt of 2,4,6-tri-*t*-butylbenzoic acid precipitated best from an aqueous medium. These salts were dried by heating *in vacuo* over phosphorus pentoxide. Preliminary decarboxylations were carried out on the silver salts at 290° to establish the best technique to be used and to obtain carbon dioxide for mass spectroscopic analyses of "blanks". The reliability of the isotopic exchange technique was checked with methyl 2,4,6-trimethylbenzoate, known to cleave by acyl–oxygen fission (2). The mass spectroscopic analyses were determined in independent laboratories. The results obtained are summarized in Table II. Isotopic tracer experiments in aqueous dioxane were carried out in a pure silver apparatus manufactured by Johnson, Matthey and Mallory to a design described by Bunton (3).

TABLE II

Isotopic tracer analyses of the mechanism of fission of hindered esters

Methyl ester	Solvent	$CO^{16}O^{18}$ from acid (%)
2,4,6-Trimethylbenzoate	65% dioxane, 0.75% H_2O^{18}	0.7
2,5-Di-*t*-butylbenzoate	65% dioxane, 0.75% H_2O^{18}	0.8
2,4,6-Tri-*t*-butylbenzoate	90% methanol, 0.50% H_2O^{18}	0
2,4,6-Tri-*t*-butylbenzoate	65% dioxane, 0.90% H_2O^{18}	0
2-Methyl-4,6-di-*t*-butyl-benzoate	65% dioxane, 0.90% H_2O^{18}	0.02

RESULTS AND DISCUSSION

Structure and Properties of Hindered Aromatic Acids

2,4,6-Tri-*t*-butylbenzoic acid is a weaker acid than benzoic acid and this behavior was attributed to steric hindrance to solvation of the carboxylate ion (4). A similar explanation

can be offered to account for the unusual solubility of this acid. It extracts from aqueous alkali into ethyl ether as its sodium salt. This property was not exhibited by the other acids in this investigation.

The structure of 2-methyl-4,6-di-*t*-butylbenzoic acid was readily confirmed by oxidation to a dicarboxylic acid which spontaneously formed an anhydride.

Kinetics of Alkaline Hydrolysis of Methyl 2,4,6-Tri-t-butylbenzoate

A plot of the second-order rate constant against $1/T$ for the alkaline hydrolysis of methyl 2,4,6-tri-*t*-butylbenzoate is illustrated in Fig. 1.

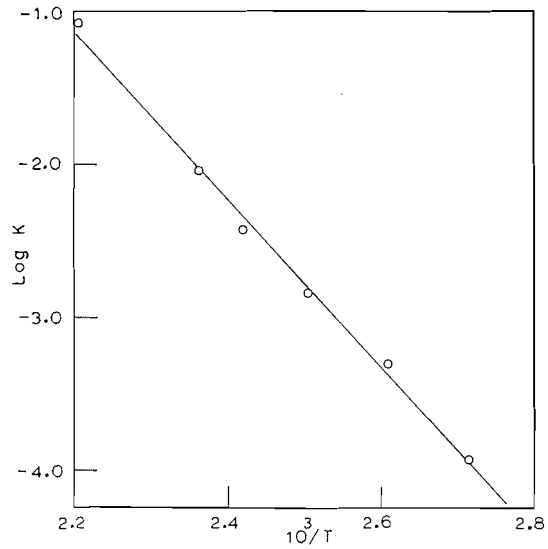

FIG. 1. Plot of log k against the reciprocal of the absolute temperature for the basic hydrolysis of methyl 2,4,6-tri-*t*-butylbenzoate.

The best straight line was estimated by the method of least squares. From this line the energy of activation was found to be 25.07 kcal/mole and the $\log_{10} PZ$ factor 10.93. This factor is much higher (by about at least 100 times) than that observed for alkaline hydrolysis of most benzoic esters which hydrolyze by the $B_{AC}2$ mechanism. The significance of this higher log PZ factor is not entirely obvious. It may be a result of a change in mechanism from the usual $B_{AC}2$, which would be highly hindered in this ester, to attack at the alkyl (methyl) carbon ($B_{AL}2$). The latter mechanism would be free of steric effects in this methyl ester and a resulting higher entropy of activation would be expected. This is reflected in the larger log PZ term. It is interesting that the steric effect in hydrolysis of methyl 2,4,6-trimethylbenzoate was not reflected in a lower log PZ term (1), especially since the cleavage has been found to be acyl–oxygen (2). It is conceivable that this ester undergoes hydrolysis mainly by acyl–oxygen fission but also partly by alkyl–oxygen fission. This could account for the somewhat high log PZ term and such a mixed mechanism might not be detected by the isotopic tracer evidence.

Tracer Evidence of the Position of Bond Fission of Hindered Esters. Evidence for a $B_{AL}2$ Mechanism

The isotopic tracer analysis on methyl 2,4,6-trimethylbenzoate (Table II) confirms the finding of Bender and Dewey that the cleavage is acyl–oxygen. The hindered ester

methyl 2,5-di-*t*-butylbenzoate also cleaved by this mechanism, since the carbon dioxide from the acid was similarly enriched in $CO^{16}O^{18}$ when the hydrolysis was carried out in the presence of H_2O^{18}. With the highly hindered ester methyl 2,4,6-tri-*t*-butylbenzoate, no exchange of O^{18} into the acid could be detected. This was the case not only in aqueous methanol but also in aqueous dioxane, where the reaction is not complicated by the possibility of methanolysis occurring along with hydrolysis (3). A small amount of enrichment in $CO^{16}O^{18}$ was found in the tracer hydrolysis of methyl 2-methyl-4,6-di-*t*-butylbenzoate. This can be interpreted as meaning that this ester cleaves mainly by alkyl–oxygen fission but some acyl–oxygen fission takes place. The $CO^{16}O^{18}$ isotopic tracer studies reported in Table II were determined on a mass spectrometer accurate to only one or at most two decimals. This was sufficient to give a positive or negative answer. In the crucial case of methyl 2,4,6-tri-*t*-butylbenzoate, the tracer analysis using 0.9% H_2O^{18} in aqueous dioxane was repeated for a mass spectroscopic analysis of higher precision. Compared to a standard sample of carbon dioxide, which showed an intensity of 0.04135 (arbitrary scale) for natural abundance of $CO^{16}O^{18}$, the carbon dioxide from the acid formed after 75% hydrolysis gave readings of 0.04137 and 0.04139,* that is, there has been no significant amount of enrichment of the carbon dioxide in $CO^{16}O^{18}$. The hydrolysis takes place practically completely by alkyl–oxygen fission. In view of the kinetic form of the hydrolysis this result establishes unequivocally the unusual $B_{AL}2$ mechanism.

An additional interesting observation on methyl 2,4,6-tri-*t*-butylbenzoate involved the reaction of this ester with the Grignard reagent methyl magnesium iodide. No reaction took place in boiling ethyl ether; however, in boiling butyl ether the ester was converted into an inorganic salt of the acid and ethane gas was evolved as detected by vapor phase chromatography. In other words, the Grignard reagent attacked the alkyl carbon instead of the usual carbonyl carbon.

ACKNOWLEDGMENTS

The mathematical calculations involving least-squares methods were made by Dr. D. Russell of the Mathematics Department. The stainless steel tubes for the kinetic runs were manufactured by Enamel and Heating Products Ltd., Sackville, N.B. We are indebted to the National Research Council for financial support of the research.

REFERENCES

1. H. L. GOERING, T. RUBIN, and M. S. NEWMAN. J. Am. Chem. Soc. **76**, 787 (1954).
2. M. L. BENDER and R. S. DEWEY. J. Am. Chem. Soc. **78**, 317 (1956).
3. C. A. BUNTON, A. E. COMYNS, J. GRAHAM, and J. R. QUAYLE. J. Chem. Soc. 3817 (1955).
4. L. R. C. BARCLAY, G. A. COOKE, and N. D. HALL. Chem. & Ind. (London), 346 (1961).
5. ORGANIC SYNTHESES. Coll. Vol. III. John Wiley & Sons, Inc., New York. 1955. p. 555.
6. L. R. C. BARCLAY and E. E. BETTS. Can. J. Chem. **33**, 1768 (1955).
7. J. GEUZE, C. RUINARD, J. SOETERBROCK, P. E. VERKADE, and B. M. WEPSTER. Rec. trav. chim. **75**, 301 (1956).
8. M. G. J. BEETS, W. MEERBURG, and H. VANESSEN. Rec. trav. chim. **78**, 570 (1959).
9. A. A. MORTON and J. G. MARK. Ind. Eng. Chem., Anal. Ed. **6**, 151 (1934).
10. L. F. FIESER. Experiments in organic chemistry. D. C. Heath and Co., New York, N.Y. 1941.

The authors are indebted to Dr. H. Taube of the University of Chicago for this analysis.

CONCURRENT ION–MOLECULE REACTIONS LEADING TO THE SAME PRODUCT ION

A. G. HARRISON AND J. M. S. TAIT
Department of Chemistry, University of Toronto, Toronto, Ontario
Received June 15, 1962

ABSTRACT

Seven of the major secondary ions in the high-pressure mass spectrum of cyclopropane have been studied. A method has been developed for studying concurrent ion–molecule reactions and it has been shown that four of the secondary ions are the products of more than one reaction. Cross sections for the separate reactions are reported. The appearance potentials of the major primary ions in the mass spectrum of cyclopropane have been measured.

INTRODUCTION

Theard and Hamill (1) have pointed out in a recent communication that many of the cross sections reported in the literature for ion–molecule reactions must be considered as suspect. This arises because the method of identification of the reactant ion by measurement of the secondary ion appearance potential only provides information on the reaction of lowest appearance potential. Frequently, other reactions involving ions of higher appearance potential are thermochemically possible, but are not detected due to the limited sensitivity of such determinations. The occurrence of undetected reactions will, of course, lead to erroneous values for reaction cross sections.

Recently, Hutchison and Pobo (2) have outlined a method for studying concurrent ion–molecule reactions leading to the same product ion in binary systems. They have shown that in nitrogen–deuterium systems the N_2D^+ ion is formed by the reaction

$$D_2^+ + N_2 \rightarrow N_2D^+ + D$$

in addition to the reaction detected previously (3, 4):

$$N_2^+ + D_2 \rightarrow N_2D^+ + D.$$

The present paper reports an extension of the method developed by these authors to the study of the major secondary ions in the high-pressure mass spectrum of cyclopropane.

Consider the two ion–molecule reactions

$$P_1^+ + M \rightarrow S^+ + N_1$$
$$P_2^+ + M \rightarrow S^+ + N_2$$

involving the reaction of two different primary ions with substrate molecules to produce the same product ion S^+. The secondary ion current I_s, arising from the two reactions, can be expressed as the sum of two independent contributions in the usual fashion (5):

$$I_s = f_1Q_1d[M]I_{P_1} + f_2Q_2d[M]I_{P_2}, \qquad [1]$$

where f_x is the collision efficiency, Q_x is the phenomenological cross section, d is the distance from the electron beam to the exit slit, [M] is the concentration of neutral molecules, and the I_x terms refer to measured ion currents. We have made the usual assumption that the collection efficiencies for all the ions are the same.

Equation [1] may be rearranged to give the following two equations:

$$\frac{I_s}{I_{P_1}} = f_1 Q_1 d[M] + f_2 Q_2 d[M]\frac{I_{P_2}}{I_{P_1}} \quad [2]$$

$$\frac{I_s}{I_{P_2}} = f_1 Q_1 d[M]\frac{I_{P_1}}{I_{P_2}} + f_2 Q_2 d[M]. \quad [3]$$

Equations [2] and [3] predict that for a secondary ion arising from two concurrent reactions a plot of I_s/I_{P_1} against I_{P_2}/I_{P_1} should lead to a straight line with slope proportional to f_2Q_2 and intercept proportional to f_1Q_1, while the similar plot of I_s/I_{P_2} against I_{P_1}/I_{P_2} should be a straight line with slope and intercept proportional to f_1Q_1 and f_2Q_2, respectively. With a knowledge of d and [M] the individual cross sections can be determined.

The ion current ratios in the above expressions are most easily varied by varying the electron energy at constant source pressure. The success of the method depends on two assumptions: first, that the relative collection efficiencies for the various ionic species do not vary with electron energy and, second, that the reaction cross sections are independent of electron energy. The evidence concerning these assumptions is very limited; however, the success of the method in the present investigation suggests that they are not a serious limitation.

EXPERIMENTAL

The experiments were performed using an Associated Electrical Industries MS-2 mass spectrometer. Rhenium filaments were used throughout the work and considerably more stable source characteristics were observed than have previously been obtained with this instrument using tungsten filaments (6). The ionizing current was 20 μa.

The electrical controls were altered to permit independent control of the repeller voltage from a potentiometer and battery. This voltage was read by a precision voltmeter. The distance from the repeller plate to the exit slit was calculated from the dimensions of the ion source, while the distance from the electron beam to the exit slit was estimated to be 0.12 cm from the variation of the appearance potential of argon with repeller voltage. This value is in agreement with estimates from source dimensions.

The sample inlet system supplied with the MS-2 was replaced by a system permitting measurement of the sample pressure with a Consolidated Electrodynamics micromanometer. For the sample pressures of 2–8 mm required for the ion–molecule reactions a series of expansions from known volumes was required to give pressures in the micromanometer range. For the latter part of the work an Atlas–Werke diaphragm-type micromanometer was added to the system. This manometer gives a direct pressure reading over the range 0.02 to 20 mm with an accuracy of ca. 1%. The molecular concentration in the ion source was related to the pressure in the inlet system by measuring the saturation ion current to the negatively biased repeller. Ion current – pressure measurements were carried out for argon, xenon, oxygen, ethylene, and cyclopropane at 70 v electron energy. Ionization cross sections in agreement with previous results (7, 8) were obtained. It was found that the source concentration was a linear function of the inlet pressure with the relation

$$[M]\ (\text{molecules/cc}) = 2.43\times10^{9}\times\text{pressure}\ (\mu).$$

In studying the ion–molecule reactions, the reactant ion of lowest appearance potential was determined by measurement of the appearance potential of the secondary ion using added krypton or xenon as standard. The reaction identification by this method was in essential agreement with the recent results of Pottie, Lorquet, and Hamill (9). The ratio of secondary ion current to primary ion current was then measured as a function of electron energy at constant source pressure. A decrease in this ratio with decrease in electron energy was taken to indicate the occurrence of a second reaction of higher appearance potential, while an increase in the ratio indicated a second ion of lower appearance potential was involved. The latter behavior was rarely encountered. It was necessary, of course, to select a range of electron energies such that the relative primary ion currents were changing markedly.

The choice of a second reactant ion was thus based on its appearance potential and the thermochemistry of the reaction involved. We have made the usual assumption that endothermic reactions will not occur. The electron energy was adjusted to give conditions, if possible, where only the two reactant ions of interest were of appreciable concentration in the ion source. The ion currents for the two primary ions and the secondary ion were then measured as a function of electron energy and the results treated in the manner indicated by equations [2] and [3]. The details will be discussed in the following section for each of the secondary ions studied.

The above procedure necessitated working at low electron energies and preliminary work at low repeller voltages did not lead to straight-line plots. This difficulty disappeared at high repeller voltages; consequently, no results were obtained at field strengths below 10 v/cm. For studies involving the $C_3H_6^+$ ion, where the lowest electron energies were used, field strengths of greater than 14 v/cm were necessary. This effect is not completely understood; however, it is probable that at low repeller voltages and low electron energies space charge effects in the electron beam are sufficient to change the ionic residence time and thus the apparent reaction cross sections. Similar space charge effects have been observed in the measurement of secondary ion appearance potentials at low repeller voltages (5, 10).

The cyclopropane was of 99.5% purity as supplied and was further purified by bulb-to-bulb distillation. Gas-chromatographic analysis showed no detectable impurities. The primary ion appearance potentials were determined by methods previously discussed (11).

RESULTS AND DISCUSSION

Primary Ion Appearance Potentials

During this work, we have measured the appearance potentials of the major primary ions in the mass spectrum of cyclopropane. The appearance potentials and the ionic heats of formation calculated therefrom are recorded in Table I. The limits of error

TABLE I

Primary ion appearance potentials

Ion	Neutrals	Appearance potential, v				ΔH_f (ion), kcal/mole	
		This work	Ref. 9	Ref. 12	Ref. 13	This work	Ref. 14
$C_3H_6^+$	—	10.39±0.05	10.2	10.23	10.53	252	249
$C_3H_5^+$	H	11.70±0.1	12.0	12.1	12.06	230	220 or 230
$C_3H_4^+$	H_2	11.57±0.1	12.4	12.26		279	279–284
$C_3H_3^+$	$H_2 + H$	13.73±0.1	14.4	14.09		286	274–283
$C_3H_2^+$	$2H_2$	—	16.4	13.8		—	ca. 360
C_3H^+	$2H_2 + H$	19.7±0.5	19.4	15.0		415	309 (?)
	$H_2 + 3H$					311	
$C_2H_3^+$	CH_3	13.3±0.2	13.6	13.37		288	280
$C_2H_2^+$	CH_4	13.28±0.2	14.6	13.62		344	317

represent the average deviation of three or more determinations. In general, the appearance potentials are somewhat lower than those obtained by previous workers (9, 12, 13); however, the calculated ionic heats of formation are in reasonable agreement with the "best values" quoted by Field and Franklin (14).

The major discrepancy in Table I is for the C_3H^+ ion, where the present result and that of Pottie *et al.* (9) differ from the result of Field (12) by over 4 v. From the appearance potential Field calculated $\Delta H_f(C_3H^+) = 306$ kcal/mole and this was supported by later measurements (15) of $A(C_3H^+)$ in 1-butyne and 1,3-butadiene which led to $\Delta H_f(C_3H^+) =$ 282 to 328 kcal/mole. As shown in Table I, the present result is in agreement with this heat of formation if $H_2 + 3H$ are assumed as the neutral fragments. However, we believe the higher value of ca. 415 kcal/mole is to be preferred. As will be shown below, the ion–molecule reaction

$$C_3H^+ + C_3H_6 \rightarrow C_4H_2^+ + C_2H_5$$

has been found to occur. Using $\Delta H_f(C_4H_2^+) = 332$ kcal/mole, the lowest value reported for this ion (16), $\Delta H_f(C_2H_5) = 25$ kcal/mole (17), and $\Delta H_f(C_3H_6) = 12.7$ kcal/mole (18) this reaction is 32 kcal/mole endothermic if $\Delta H_f(C_3H^+) = 311$ kcal/mole. Since the reaction does occur, a considerably higher heat of formation must be in order. To obtain further evidence, the appearance potentials of C_3H^+ in propene and in propyne were determined. The results are summarized in Table II and again the data can be interpreted to give $\Delta H_f(C_3H^+)$ equal to approximately 300 or 400 kcal/mole. We are inclined to

TABLE II
Appearance potentials of C_3H^+

Molecule	Neutrals	Appearance potential, v		ΔH_f (ion), kcal/mole	
		This work	Literature*	This work	Literature
Propylene	$2H_2 + H$	20.2±0.5	—	418	
	$H_2 + 3H$			314	
Propyne	$H_2 + H$	17.5±0.5	18.4±0.3	396	416
	$3H$			292	312

*F. H. Coats and R. C. Anderson. J. Am. Chem. Soc. 77, 895 (1955).

accept the higher value on the basis of the ion–molecule reaction, although we cannot explain the discrepancy with the results of Field (12, 15).

Ion–Molecule Reactions

As has been reported (9), the secondary ions in the high-pressure mass spectrum of cyclopropane consist of a series of ions from $C_4H_2^+$ to $C_4H_8^+$ inclusive with the further ions $C_5H_5^+$, $C_5H_6^+$, $C_5H_7^+$, $C_6H_5^+$, $C_6H_7^+$, and $C_6H_9^+$. The ions in the C_5–C_6 region are of low intensity and could not be treated in the manner described in this paper. The present results are therefore limited to a discussion of the ions in the C_4 region. In calculating the heats of reactions given in the following, the lowest reported heats of formation for the ions in the C_4 region were used to avoid rejection of possible reactions on the basis of a false endothermicity. The heats of formation of the reactant ions were taken from Table I and for neutral species, from standard sources.

m/e = 56 ($C_4H_8^+$)

The only exothermic reactions resulting in this ion are the following:

$$C_3H_6^+ + C_3H_6 \rightarrow C_4H_8^+ + C_2H_4 \qquad \Delta H = -43^* \qquad [4]$$

$$C_3H_4^+ + C_3H_6 \rightarrow C_4H_8^+ + C_2H_2 \qquad \Delta H = -29 \qquad [5]$$

The appearance potential of $C_4H_8^+$ coincided with $A(C_3H_6^+)$, indicating the occurrence of reaction [4]. Figure 1 shows the ion current for $C_4H_8^+$ as a function of I_{42} and I_{40} plotted in the manner of equations [2] and [3]. The zero slope of Fig. 1*a* and the zero intercept of Fig. 1*b* indicate that reaction [5] is not occurring. The results were obtained at a field strength of 14.2 v/cm and a source concentration of 9.80×10^{12} molecules/cc. From the intercept and slope of Fig. 1, *a* and *b* (7.10×10^{-3} and 7.14×10^{-4}, respectively), $fQ = 6.1\times10^{-16}$ cm²/molecule for reaction [4]. This value is in reasonable agreement with the result 10.1×10^{-16} (9) at 12 v/cm and 70 v electron energy.

m/e = 55 ($C_4H_7^+$)

On a thermochemical basis the following reactions can result in the formation of $C_4H_7^+$ by ion–molecule reactions, which involve reasonable neutral fragments. (We have eliminated from consideration, throughout the following, those reactions which would involve fragments such as C_2H, CH_2, and CH, even though these may be exothermic in some cases.)

$$C_3H_6^+ + C_3H_6 \rightarrow C_4H_7^+ + C_2H_5 \qquad \Delta H = -36 \qquad [6]$$

$$C_3H_5^+ + C_3H_6 \rightarrow C_4H_7^+ + C_2H_4 \qquad \Delta H = -27 \qquad [7]$$

$$C_3H_4^+ + C_3H_6 \rightarrow C_4H_7^+ + C_2H_3 \qquad \Delta H = -23 \qquad [8]$$

$$C_3H_3^+ + C_3H_6 \rightarrow C_4H_7^+ + C_2H_2 \qquad \Delta H = -32 \qquad [9]$$

**Throughout this section the heats of reaction given are in the units kcal/mole.*

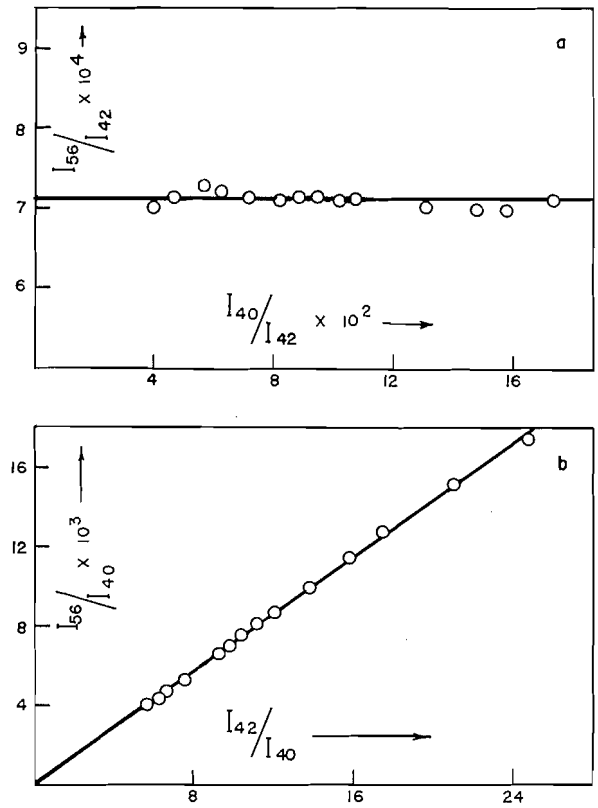

FIG. 1. Dependence of I_{56} ($C_4H_8^+$) on I_{42} ($C_3H_6^+$) and I_{40} ($C_3H_4^+$).

$A(C_4H_7^+)$ was intermediate between the appearance potential of $C_3H_6^+$ and $C_3H_5^+$ (or $C_3H_4^+$), suggesting that both reactions [6] and [7] might be occurring. Figure 2 shows the variation of I_{55} with I_{42} and I_{41} under conditions such that the source concentration of $C_3H_3^+$ was negligible. From the non-zero slopes and intercepts of both plots it is clear that two reactions are involved in the formation of $C_4H_7^+$. Since the ionization efficiency curves for $C_3H_5^+$ and $C_3H_4^+$ are essentially identical, it is impossible to separate the contribution from reactions [7] and [8]. In calculating cross sections, we have assumed that reaction [8] does not occur. Cross sections:

Reaction [6]: intercept (Fig. 2*a*) $= 3.00\times10^{-4}$; slope (Fig. 2*b*) $= 3.06\times10^{-4}$ $\Big\}$ $fQ = 2.5\times10^{-16}$ cm²/molecule

Reaction [7]: intercept (Fig. 2*b*) $= 1.02\times10^{-3}$; slope (Fig. 2*a*) $= 1.04\times10^{-3}$ $\Big\}$ $fQ = 9.0\times10^{-16}$ cm²/molecule

m/e = 54 ($C_4H_6^+$)

The exothermic reactions resulting in the ion $C_4H_6^+$ are the following:

$$C_3H_6^+ + C_3H_6 \rightarrow C_4H_6^+ + C_2H_6 \qquad \Delta H = -47 \qquad [10]$$
$$C_3H_4^+ + C_3H_6 \rightarrow C_4H_6^+ + C_2H_4 \qquad \Delta H = -42 \qquad [11]$$
$$C_3H_2^+ + C_3H_6 \rightarrow C_4H_6^+ + C_2H_2 \qquad \Delta H = -52 \qquad [12]$$
$$C_2H_3^+ + C_3H_6 \rightarrow C_4H_6^+ + CH_3 \qquad \Delta H = -30 \qquad [13]$$

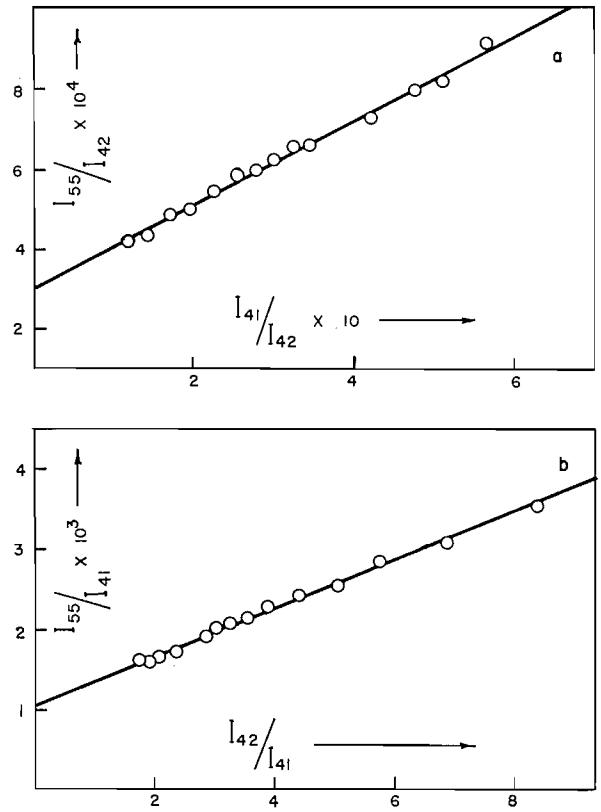

FIG. 2. Dependence of I_{55} ($C_4H_7^+$) on I_{42} ($C_3H_6^+$) and I_{41} ($C_3H_5^+$).

The appearance potential of $C_4H_6^+$ was in agreement with $A(C_3H_4^+)$, thus eliminating any significant contribution from reaction [10]. Figure 3 shows the variation of I_{54} with I_{40} and I_{27}. These results were obtained at 10 v/cm with a source concentration [M] = 11.45×10^{12} molecules/cc, under conditions where the ion $C_3H_2^+$ was of negligible concentration. The results clearly show that reaction [11] is occurring, but that reaction [13] is not. The intercept of Fig. 3*a* (1.10×10^{-3}) is in good agreement with the slope of Fig. 3*b* (1.12×10^{-3}) and leads to $fQ = 8.1\times10^{-16}$ cm^2/molecule for reaction [11]. It is possible that reaction [12] is occurring at higher electron energies. This could not be determined since it was not possible to obtain conditions such that I_{54}, I_{38}, and I_{40} could be measured simultaneously over a significant range.

m/e = 53 ($C_4H_5^+$)

The following reactions are energetically possible:

$$C_3H_5^+ + C_3H_6 \rightarrow C_4H_5^+ + C_2H_6 \qquad \Delta H = -8 \qquad [14]$$
$$C_3H_4^+ + C_3H_6 \rightarrow C_4H_5^+ + C_2H_5 \qquad \Delta H = -12 \qquad [15]$$
$$C_3H_3^+ + C_3H_6 \rightarrow C_4H_5^+ + C_2H_4 \qquad \Delta H = -23 \qquad [16]$$
$$C_3H_2^+ + C_3H_6 \rightarrow C_4H_5^+ + C_2H_3 \qquad \Delta H = -24 \qquad [17]$$
$$C_3H^+ + C_3H_6 \rightarrow C_4H_5^+ + C_2H_2 \qquad \Delta H = -119 \qquad [18]$$
$$C_2H_3^+ + C_3H_6 \rightarrow C_4H_5^+ + CH_4 \qquad \Delta H = -63 \qquad [19]$$
$$C_2H_2^+ + C_3H_6 \rightarrow C_4H_5^+ + CH_3 \qquad \Delta H = -63 \qquad [20]$$

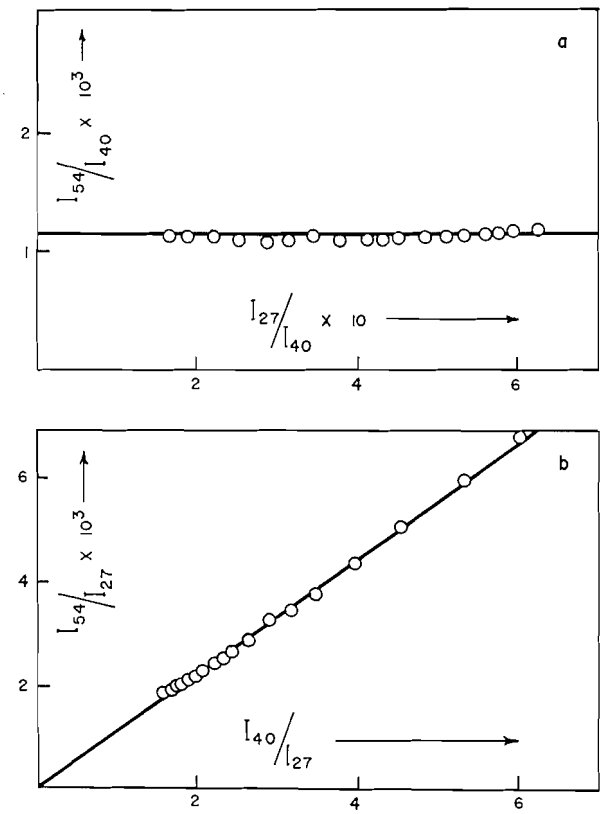

FIG. 3. Dependence of I_{54} ($C_4H_6^+$) on I_{40} ($C_3H_4^+$) and I_{27} ($C_2H_3^+$).

Within experimental error $A(C_4H_5^+)$ coincided with $A(C_3H_3^+)$, thus eliminating significant contributions from reactions [14], [15], [19], and [20]. However, the ratio I_{53}/I_{39} was found to decrease with decreasing electron energy near the appearance potential threshold, suggesting a second reaction of higher appearance potential. The only possible reactions are [17] and [18]; however, the source concentrations of $C_3H_2^+$ and C_3H^+ were negligible. A plot of I_{53} against I_{39} gave a result which was not found in other cases. Figure 4 shows the plot and, for comparison, a plot of I_{54} against I_{40} and a plot of I_{53} against I_{38}. The plot of I_{53} is a straight line, but does not pass through the origin as is found in other cases where a single reaction is occurring (I_{54}). On the other hand, no upward curvature is observed as in the plot of I_{51}, where a second reaction of higher appearance potential is involved (see below). The reasons for this are not clear. One possibility is that the reaction involves an excited $C_3H_3^+$ ion. From the slope of the line shown we estimate $fQ = 18.2 \times 10^{-16}$ cm^2/molecule at 10 v/cm; if an excited ion is involved this result may be in error, since the concentration of excited ions is not necessarily given by the measured ion current.

m/e = 52 ($C_4H_4^+$)

The following reactions are energetically possible:

$$C_3H_4^+ + C_3H_6 \rightarrow C_4H_4^+ + C_2H_6 \qquad \Delta H = -18 \qquad [21]$$
$$C_3H_2^+ + C_3H_6 \rightarrow C_4H_4^+ + C_2H_4 \qquad \Delta H = -38 \qquad [22]$$
$$C_3H^+ + C_3H_6 \rightarrow C_4H_4^+ + C_2H_3 \qquad \Delta H = -69 \qquad [23]$$
$$C_2H_2^+ + C_3H_6 \rightarrow C_4H_4^+ + CH_4 \qquad \Delta H = -74 \qquad [24]$$

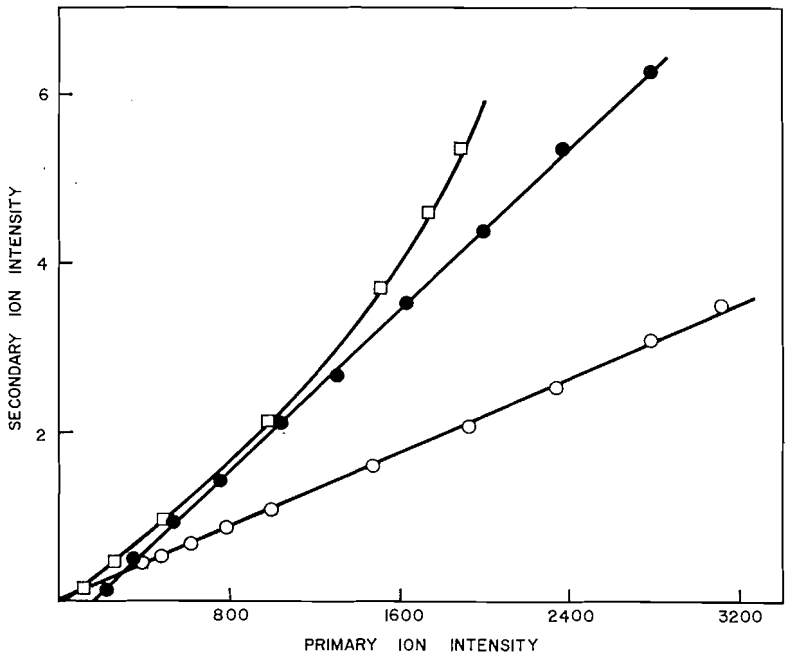

FIG. 4. Dependence of secondary ion intensity on primary ion intensity. □ $I_{51}/2$ as a function of I_{38}, ● I_{53} as a function of I_{39}, ○ I_{54} as a function of I_{40}.

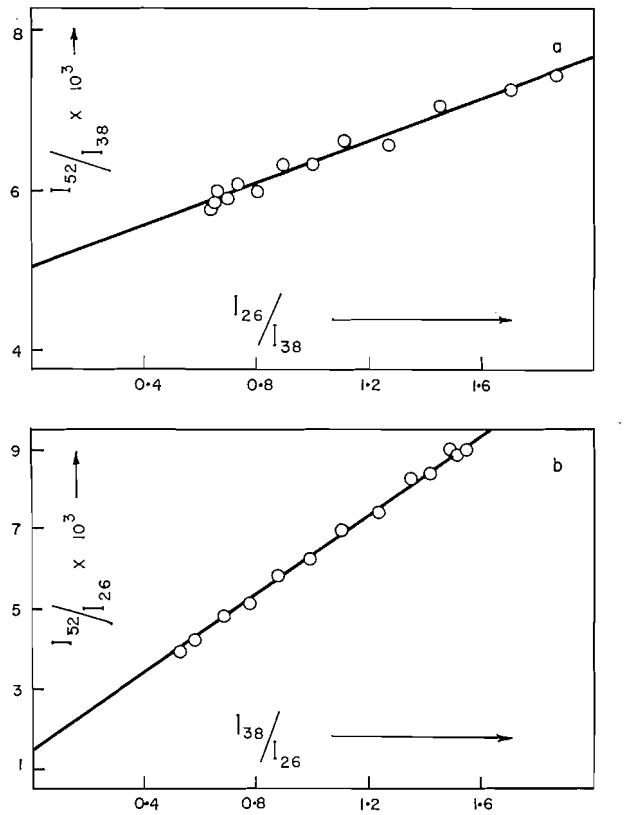

FIG. 5. Dependence of I_{52} ($C_4H_4^+$) on I_{38} ($C_3H_2^+$) and I_{26} ($C_2H_2^+$).

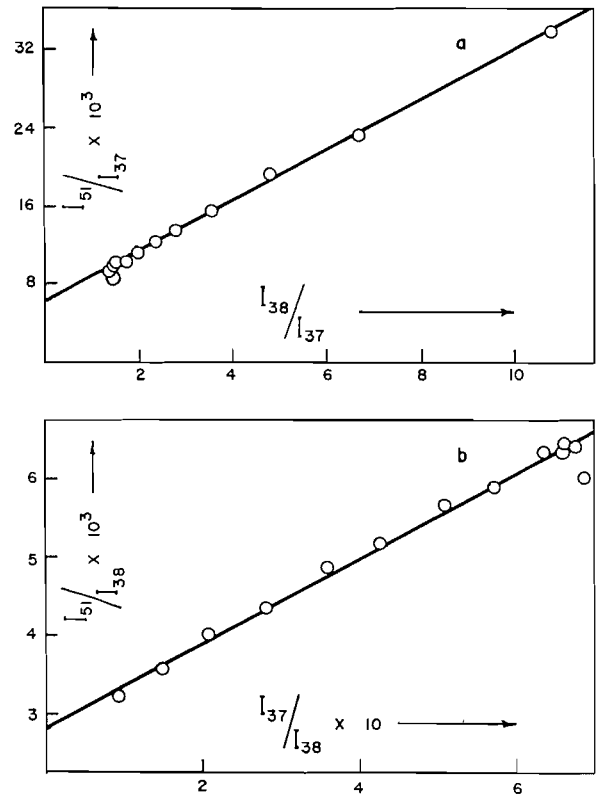

FIG. 6. Dependence of I_{51} ($C_4H_3^+$) on I_{38} ($C_3H_2^+$) and I_{37} (C_3H^+).

The appearance potential of $C_4H_4^+$ suggested the occurrence of reaction [22]; however, the ratio I_{52}/I_{38} increased with decreasing electron energy, suggesting the occurrence of a second reaction. Figure 5 shows the results obtained considering reactions [22] and [24]. The satisfactory straight lines obtained and the non-zero intercepts and slopes show that both reactions are occurring. Cross sections ([M] = 11.87×10^{12} molecules/cc, E = 10 v/cm):

Reaction [22]:	intercept (Fig. 5*a*) = 5.04×10^{-3} slope (Fig. 5*b*) = 4.93×10^{-3}	$fQ = 35.3\times10^{-16}$ cm²/molecule
Reaction [24]:	intercept (Fig. 5*b*) = 1.40×10^{-3} slope (Fig. 5*a*) = 1.30×10^{-3}	$fQ = 9.6\times10^{-16}$ cm²/molecule

m/e = 51 ($C_4H_3^+$)

The following reactions are thermochemically permitted:

$$C_3H_3^+ + C_3H_6 \rightarrow C_4H_3^+ + C_2H_6 \qquad \Delta H = -7 \qquad [25]$$

$$C_3H_2^+ + C_3H_6 \rightarrow C_4H_3^+ + C_2H_5 \qquad \Delta H = -16 \qquad [26]$$

$$C_3H^+ + C_3H_6 \rightarrow C_4H_3^+ + C_2H_4 \qquad \Delta H = -113 \qquad [27]$$

$$C_2H_3^+ + C_3H_6 \rightarrow C_4H_3^+ + CH_4 + H_2 \qquad \Delta H = -15 \qquad [28]$$

$$C_2H_2^+ + C_3H_6 \rightarrow C_4H_3^+ + \begin{Bmatrix} CH_3 + H_2 \\ CH_4 + H \end{Bmatrix} \qquad \Delta H = \begin{matrix} -15 \\ \text{or } -13 \end{matrix} \qquad [29]$$

The appearance potential of $C_4H_3^+$ and the shape of the ionization efficiency curve suggested reaction [26]; however, the variation of I_{51}/I_{38} with electron energy suggested reaction [27] was also occurring. Figure 6 shows the results obtained considering these two reactions. The straight lines obtained lead to the following cross sections at 10 v/cm and [M] = 10.82×10^{12} molecules/cc:

Reaction [26]:	slope (Fig. 6*a*) = 2.60×10^{-3} intercept (Fig. 6*b*) = 2.80×10^{-3}	$fQ = 21.0\times10^{-16}$ cm²/molecule
Reaction [27]:	slope (Fig. 6*b*) = 5.4×10^{-3} intercept (Fig. 6*a*) = 5.7×10^{-3}	$fQ = 43.1\times10^{-16}$ cm²/molecule

m/e = 50 ($C_4H_2^+$)

The exothermic reactions resulting in $C_4H_2^+$ are:

$$C_3H_2^+ + C_3H_6 \rightarrow C_4H_2^+ + C_2H_6 \qquad \Delta H = -32 \qquad [30]$$
$$C_3H^+ + C_3H_6 \rightarrow C_4H_2^+ + C_2H_5 \qquad \Delta H = -71 \qquad [31]$$
$$C_2H_2^+ + C_3H_6 \rightarrow C_4H_2^+ + CH_4 + H_2 \qquad \Delta H = -36 \qquad [32]$$

The appearance potential of $C_4H_2^+$ and the shape of the ionization efficiency curve indicated the occurrence of one or both of reactions [30] and [31]. Figure 7 shows the

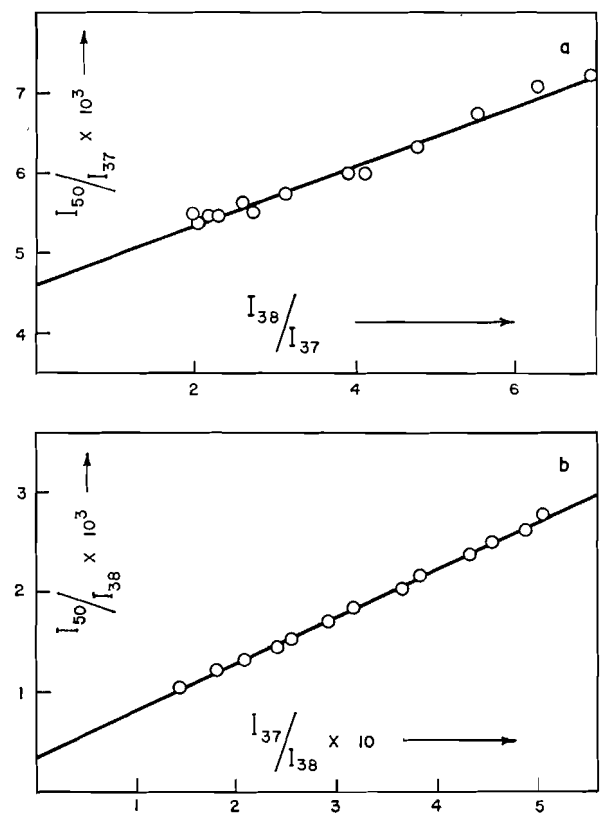

FIG. 7. Dependence of I_{50} ($C_4H_2^+$) on I_{38} ($C_3H_2^+$) and I_{37} (C_3H^+).

results obtained on the assumption that these two reactions are occurring. The straight lines obtained lead to the following cross sections at 10 v/cm and [M] = 15.35×10^{12} molecules/cc:

Reaction [30]:	slope (Fig. 7*a*) = 3.6×10^{-4} intercept (Fig. 7*b*) = 3.4×10^{-4}	$fQ = 2.0\times10^{-16}$ cm²/molecule
Reaction [31]:	slope (Fig. 7*b*) = 4.60×10^{-3} intercept (Fig. 7*a*) = 4.70×10^{-3}	$fQ = 25.4\times10^{-16}$ cm²/molecule

CONCLUSIONS

The present work has shown that four of the seven secondary ions studied in cyclopropane are formed by more than one ion–molecule reaction. A method of separating the contribution of the separate reactions has been developed. The ion–molecule reactions reported for other simple hydrocarbons may also be somewhat suspect due to the occurrence of concurrent ion–molecule reactions. These systems are presently being studied.

ACKNOWLEDGMENTS

The authors are indebted to the National Research Council of Canada and the Advisory Committee of the University of Toronto for financial support.

REFERENCES

1. L. P. Theard and W. H. Hamill. J. Am. Chem. Soc. **84**, 1134 (1962).
2. D. Hutchison and L. Pobo. Paper presented at ASTM E-14 meeting, Chicago. June, 1961.
3. D. O. Schissler and D. P. Stevenson. J. Chem. Phys. **24**, 926 (1956).
4. D. P. Stevenson. J. Phys. Chem. **61**, 1453 (1957).
5. D. P. Stevenson and D. O. Schissler. J. Chem. Phys. **29**, 282 (1958).
6. R. Taubert. Z. anal. Chem. **164**, 164 (1958).
7. J. W. Otvos and D. P. Stevenson. J. Am. Chem. Soc. **78**, 546 (1956).
8. F. W. Lampe, J. L. Franklin, and F. H. Field. J. Am. Chem. Soc. **79**, 6129 (1957).
9. R. F. Pottie, A. J. Lorquet, and W. H. Hamill. J. Am. Chem. Soc. **84**, 529 (1962).
10. J. H. Beynon, G. R. Lester, R. A. Saunders, and A. E. Williams. Trans. Faraday Soc. **57**, 1259 (1961).
11. A. G. Harrison and T. W. Shannon. Can. J. Chem. **40**, 1730 (1962).
12. F. H. Field. J. Chem. Phys. **20**, 1734 (1952).
13. R. F. Pottie, A. G. Harrison, and F. P. Lossing. J. Am. Chem. Soc. **83**, 3204 (1961).
14. F. H. Field and J. L. Franklin. Electron impact phenomena and the properties of gaseous ions. Academic Press, New York. 1957.
15. F. H. Field, J. L. Franklin, and F. W. Lampe. J. Am. Chem. Soc. **79**, 2665 (1957).
16. R. Barker, W. H. Hamill, and R. R. Williams. J. Phys. Chem. **63**, 825 (1959).
17. R. A. Bernecker and F. A. Long. J. Phys. Chem. **65**, 1565 (1961).
18. J. W. Knowlton and F. D. Rossini. J. Research Natl. Bur. Standards, **43**, 113 (1949).

INFRARED SPECTRA OF CARBON MONOXIDE AND CARBON DIOXIDE ADSORBED ON CHROMIA–ALUMINA AND ON ALUMINA[1]

L. H. LITTLE[2] AND C. H. AMBERG
Division of Applied Chemistry, National Research Council, Ottawa, Canada

Received May 24, 1962

ABSTRACT

Infrared spectra of CO and CO_2 adsorbed on chromia–alumina and on alumina surfaces have been determined. A band near 2200 cm^{-1} formed by CO on both surfaces at room temperature was due to a weak, non-activated sorption, but also contained a contribution from a more strongly sorbed, activated species on the chromia–alumina. The assignment of this band was discussed in some detail. Bands in the region 1200–1800 cm^{-1} were considered in terms of surface CO_2^- species, although in certain instances the appearance of bands at 1750 and 1430 cm^{-1} may have indicated carbonate ion formation.

Following an infrared study of carbon monoxide and carbon dioxide adsorbed on zinc oxide (1) investigations have now been extended to chromia–alumina and alumina catalysts. Previous studies of CO and CO_2 adsorption using the infrared method with both metals and metal oxides include the well-known work of Eischens and Pliskin (2, 3), correlations of vibration frequencies and number of valence electrons of CO surface species by Gardner and Petrucci (4, 5), and work on titania surfaces by Yates (6).

EXPERIMENTAL

The chromia–alumina catalyst was prepared by mixing chromium hydroxide and aluminum hydroxide gels which had been precipitated separately from solutions of the metal nitrates by ammonia. The mixed gel was then dried at 110° C for 24 hours and calcined at 500° C in oxygen, resulting in a composition of 41% by weight of Cr_2O_3. The powder was compressed at 40 tons/in^2 into a thin plate suitable for the infrared studies. The plate, which measured 1.3 cm × 2.8 cm × 0.1 mm, weighed about 100 mg and had a surface area of 108 m^2/g. It was mounted in a cell of 10-cm path length, similar to that described earlier (7). Cells of 5-mm path length were also used occasionally. Evacuation at 300–400° C and 10^{-4}–10^{-5} mm was carried out for 1–2 hours before gases were adsorbed. Spectra were then recorded on a Perkin–Elmer 21 spectrophotometer fitted with a sodium chloride prism. The percentage transmission through the sample was 10–15% at 1800 cm^{-1}. The alumina catalyst was prepared in a manner analogous to that described for the mixed gels.

RESULTS

Figure 1*a* shows the spectrum of the chromia–alumina sample, with a weak band appearing at 1370 cm^{-1} after heating for 1 hour in oxygen at 320° C and outgassing at 10^{-5} mm for 1 hour. Scattering by the sample of infrared radiation at higher frequencies precluded any study above 2500 cm^{-1}.

When the sample was allowed to stand in the cell at room temperature for 24 hours a weak band appeared at 1580 cm^{-1} (Fig. 1*b*). Then after further evacuation at 350° C a broad intense band appeared at 1530 cm^{-1} with shoulders at 1420 cm^{-1} and at about 1350 cm^{-1} (Fig. 1*c*). It was only after first heating the sample in oxygen at 300–350° C and then evacuating that the absorption in the 1300–1600 cm^{-1} region was decreased to the level shown in Fig. 1*a*. This oxygen treatment led to an intensification of the 1370 cm^{-1} band.

[1]*Issued as N.R.C. No. 6932.*
[2]*N.R.C. Postdoctorate Fellow 1958–1960. Present address: Department of Chemistry, University of Western Australia, Nedlands, Western Australia.*

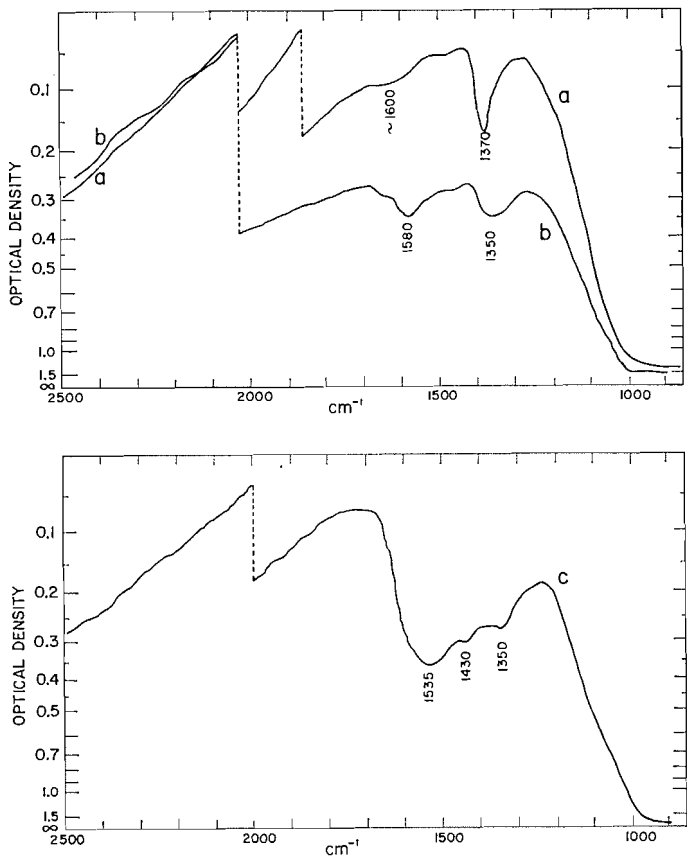

FIG. 1. (*a*) Chromia–alumina heated in 25 cm O_2 at 320° for 1 hour, outgassed to 10^{-5} mm at 320° for 1.5 hours.
(*b*) After 24 hours, standing *in vacuo* at 20°, following (*a*).
(*c*) Further outgassing at 320° for 3 hours, following (*b*).

After the sample had been standing in a cell for 1–2 days, the broad band reappeared at 1580 cm^{-1}. Depending on whether or not the sample had been heated with oxygen before evacuation, the spectrum resembled either that in Fig. 1*a* or Fig. 1*c*. This behavior was characteristic of the chromia–alumina sample.

A strong broad band which grew in intensity appeared at 1627 cm^{-1} upon exposure to the atmosphere of a sample which had been heated in oxygen and outgassed and which, as before, showed only the 1370 cm^{-1} band in its background spectrum. The 1627 cm^{-1} band was readily removed by evacuation at 300° C, without oxygen treatment, and was apparently due to adsorbed water.

When carbon monoxide at 3 cm pressure was admitted to the sample a sharp band immediately appeared at 2200 cm^{-1}. In addition to this, broad absorption occurred between 1500 and 1600 cm^{-1}. On standing for 8 hours the intensity of the 2200 cm^{-1} band remained unaltered while the 1500–1600 cm^{-1} absorption increased and a weak band appeared at 1230 cm^{-1} (Fig. 2*b*).

For the freshly prepared chromia–alumina sample the intensity of the 1370 cm^{-1} band was increased by adsorption of carbon monoxide. After several adsorption and desorption

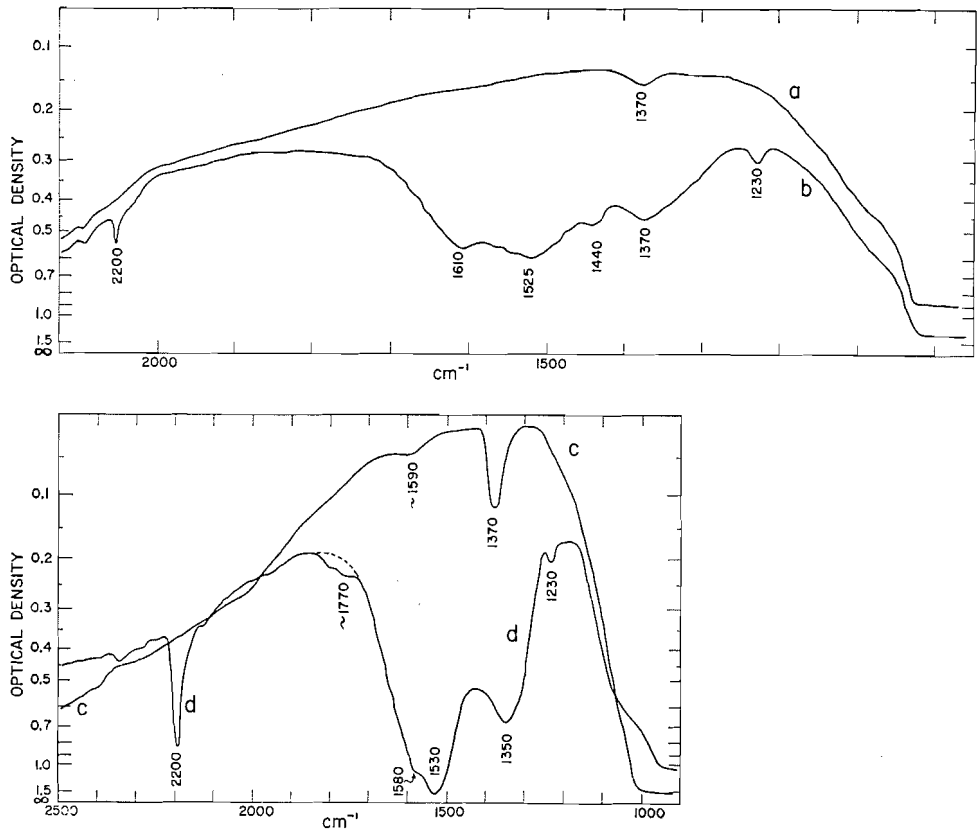

FIG. 2. (*a*) Chromia–alumina heated in 70 cm O_2 at 350° for 0.5 hour, outgassed at 350° for 1 hour.
(*b*) Two hours after admitting 3.8 cm CO at 20°, following (*a*).
(*c*) Sample heated in 30 cm O_2 at 320° for 3 hours, outgassed to 10^{-4} mm at 320° for 1 hour.
(*d*) Heated in 3.5 cm CO at 300° for 20 minutes, following (*c*).

experiments the band intensity eventually increased to the constant value shown in Fig. 3*c*. The intensity was then unaffected by further adsorption of carbon monoxide.

Evacuation at 20° C for 10 minutes entirely removed the species responsible for the 2200 cm^{-1} band, but the other bands were unaltered. The addition of dry oxygen did not change the spectrum. The absorption in the 1500 cm^{-1} region comprised bands at 1490–1500 and 1590–1610 cm^{-1}. The relative intensities of these bands varied slightly in different experiments on the same sample.

After heating the sample in oxygen at 320° C for 3 hours and outgassing at 320° C for 1 hour, the spectrum was the same as that before the addition of carbon monoxide. Further addition of CO to the sample in this condition at 20° C led to an identical sequence of spectra. However, when the chromia–alumina specimen was heated at 300° C for 20 minutes in the presence of 3.5 cm of carbon monoxide, a very great increase in the intensity of the 2200, 1500–1600, and 1230 cm^{-1} bands occurred (Fig. 2*d*). On further standing at 20° C the 2200 cm^{-1} band was unchanged while those at lower frequencies increased. Evacuation at 20° C for 10–15 minutes did not affect the low-frequency bands but greatly decreased the intensity of the 2200 cm^{-1} band, although it was not entirely removed by this treatment. Previously this band had been entirely removed by pumping at 20° C

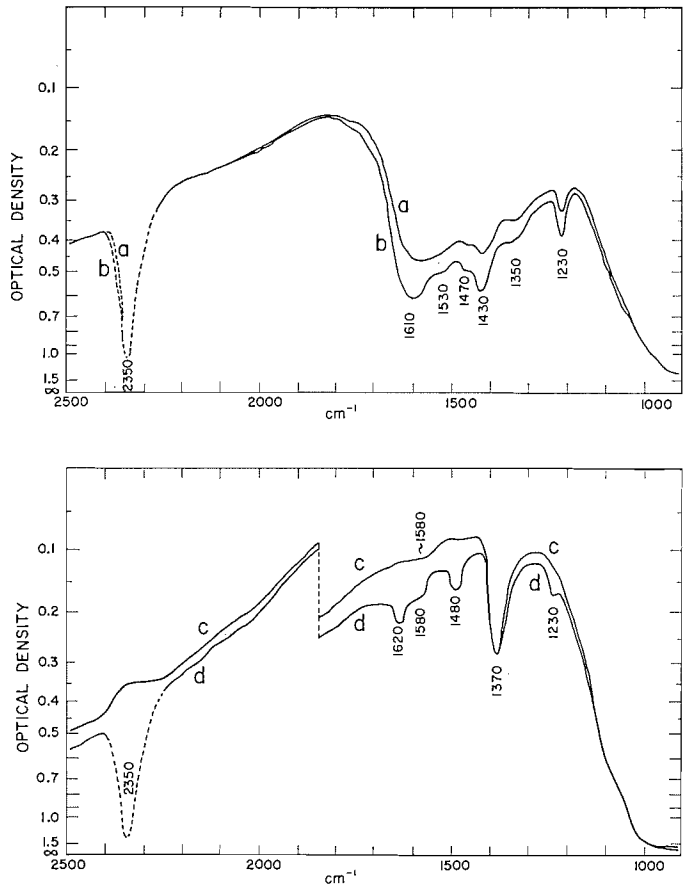

FIG. 3. (*a*) One-half hour after admitting 4.5 cm CO_2 at 20°, following Fig. 1*c*.
(*b*) After standing further 10 hours, following (*a*).
(*c*) After heating in 20 cm O_2 at 320° for 3.5 hours, then outgassing at 320° to 10^{-5} mm for 2 hours, following (*b*).
(*d*) One-half hour after admitting 5.0 cm CO_2 at 20°, following (*c*).

after adsorption had been carried out at the same temperature. The 2200 cm^{-1} band remained after the addition of 10 cm of oxygen at 20° C.

Carbon dioxide (4.5 cm) was admitted to the chromia–alumina sample and within 30 minutes produced absorption bands at 2350, 1620, 1580, 1480, and 1230 cm^{-1} (Fig. 3*d*). When carbon dioxide was adsorbed on a chromia–alumina sample which had been outgassed at 300° C but had not been heated with oxygen before this, a strong band appeared at 1430 cm^{-1} in addition to those above (Fig. 3*b*). This may have arisen from an intensification of an existing band at 1430 cm^{-1} in the background spectrum (Fig. 1*c*) of the sample prepared under these conditions or from the formation of a new surface species. In another experiment, when no band existed at 1430 cm^{-1} in the background spectrum, a weak band appeared at this frequency after CO_2 adsorption.

Bands appeared at 2200 cm^{-1} and weakly at 1750 and 1570 cm^{-1} when carbon monoxide was admitted to a pure alumina sample at 20° C. The latter bands were superimposed on broad bands in the alumina background at 1550 and 1470 cm^{-1}. There was a great intensity

decrease of the 2200 cm^{-1} band when the carbon monoxide was heated with the alumina, unlike the results observed for the chromia–alumina samples. New bands emerged at 1620, 1590, 1380, and 1230 cm^{-1} after the heating. The appearance of the 2200 cm^{-1} band on pure alumina is contrary to the experience of Yates (6), who was not able to observe it.

Carbon dioxide gave bands at 2350, 1750, 1635, 1500, and 1235 cm^{-1} on alumina. The band at 1750 cm^{-1} for carbon dioxide was stronger, judged on the basis of pressure and time of standing, than the band at that frequency for carbon monoxide.

DISCUSSION

Absorption Bands of Adsorbed CO in the Region 2100–2400 cm^{-1}

The adsorption of carbon monoxide on chromia–alumina to give the sharp band at 2200 cm^{-1} was extremely rapid at 20° C and the activation energy for the process must be very small. This band was unaltered in frequency and intensity on standing for 30 hours. The species was readily removed from the surface by evacuation at 20° C for 10–20 minutes; adsorption is thus very weak. Mass spectrometric analysis showed the gas removed from the surface to be entirely carbon monoxide, a result similar to that found for zinc oxide (1).

The proximity of this band to that of gaseous CO, as well as the available chemical evidence, would indicate a weak chemisorption process or adsorption by dipolar forces in which the essential carbon monoxide structure has been retained. Dipole attraction was suggested earlier in the analogous case for zinc oxide (1). However, the rather large displacement of 57 cm^{-1} to higher frequency remains to be rationalized. The shift is in a direction opposite to that normally produced by polar environments: in general it is found that the stretching frequencies of polar groups are displaced to lower values when material is transferred from vapor to liquid (8). This red shift usually increases with increasing polarity of the solvent.

In an endeavor to determine the influence of solvent environment on the carbon monoxide fundamental vibration frequency, the spectra of saturated solutions of the gas in carbon tetrachloride and in chloroform were recorded. The solubility of CO in these solvents is so low that only very weak bands were obtained, resulting in poor accuracy in the frequency values. Nevertheless the values obtained, 2137 ± 5 and 2144 ± 5 cm^{-1} respectively, showed quite clearly that large displacements to high frequency were not caused by solvent effects under homogeneous conditions. It should, however, be remembered that shifts in either direction may be produced by solute–solvent interaction. Buckingham (9) has analyzed the situation for diatomic molecules in an axially directed force field and has cited instances where a blue shift was observed for systems under high pressure. It is conceivable that similar conditions may hold for surface–adsorbate interactions.

Eischens and Pliskin (2) were the first to observe a high-frequency band for adsorbed CO (on nickel oxide, 2193 cm^{-1}), and ascribed it to the asymmetric C—O stretching vibration of a group such as M—O=C=O. The reasons for rejecting this explanation in favor of dipole attraction (1) were reinforced by the present findings in that again no band assignable to the corresponding symmetrical vibration could be detected. If this vibration had produced a band of extremely low intensity then one would have expected the M—O bond to be weak and the O=C=O group to behave essentially as carbon dioxide; in the latter compound this second band is forbidden in the infrared spectrum for symmetry reasons. However, the gas recovered was again CO rather than CO_2, which makes the covalent structure appear unlikely.

An alternative explanation for the spectra of CO adsorbed on metals and their salts in terms of a partially or completely ionized positive surface species has been advanced by Gardner and Petrucci (4). Terenin and Roev (10, 11) had earlier proposed both positive and negative ions as the surface species responsible for both increased and decreased frequencies in the adsorption of NO on transition metals and their salts. The electrons of highest energy in CO in the ground state occupy an antibonding orbital (12), so that ionization of one electron would strengthen the carbon–oxygen bonding, with an increase in the force constant and contraction of the internuclear distance. From the spectroscopic parameters for CO and CO^+ given by Herzberg (13), the vibrational frequencies are 2143 and 2184 cm^{-1}, the internuclear distances 1.128 and 1.115 Å respectively. While this would adequately account for bands at frequencies between the gaseous CO and CO^+ species (1, 4), shifts to frequencies higher than the latter need further explanation.

Apart from the generally possible blue shifts due to solute–solvent interaction mentioned earlier, two specific effects might contribute to a shift of this kind. A decrease in the anharmonicity of the vibration of the CO^+ ion in the adsorbed state could ideally cause shifts of up to 30 cm^{-1} ($\omega_e x_e$ = 15.2 cm^{-1} (13)). Bayliss and Rees some years ago proposed a theory to describe the interaction of a solvent cage with the solute which made use of the concepts of decreased anharmonicity (14). However, it was recently found by Ewing and Pimentel (15) that $\omega_e x_e$ decreases by only 2 cm^{-1} in the gas–solid transition of neutral CO, which makes this explanation unlikely, at least if one wishes to retain the solvent–solute analogy.

As another possibility it is suggested that a contribution from the second antibonding electron to the adsorbent–adsorbate bond could serve to shorten the C—O distance in the CO^+ ion and thus raise the frequency.* A difficulty that remains with all these explanations, and one that has also been noted by Terenin (11) for NO^+ adsorption, is the magnitude of the effect compared with the observed weakness of the adsorptive bond.

Further objections to postulating CO^+ as the surface species responsible for the high-frequency band may be raised, because this would necessitate the donation of an electron to the adsorbent. In the earlier work on zinc oxide (1) no intensity change in the broad electronic infrared absorption band was detectable, nor did Kubokawa (16) find an effect of preadsorbed oxygen on room temperature CO adsorption, oxygen being known in this case to act as an electron trap. Similarly Vilesov and Terenin (17) could not observe an appreciable change in the photoelectric work function for this system. The only way of invalidating this objection would be to assume that the electronic changes in the adsorbent lie below the limit of detectability. An indication that this might be so was given by Heiland *et al.* (18) for a reverse reaction—the trapping of conduction electrons by oxygen adsorption—in that the ratio of electrons trapped to oxygen atoms adsorbed was of the order of $1:10^5$. Unfortunately no infrared electronic absorption has as yet been assigned in chromia–alumina so that we are unable to use it as a criterion in the present case.

A considerable portion of the carbon monoxide responsible for the 2200 cm^{-1} band on chromia–alumina had a measurable activation energy of adsorption, since the intensity of this band increased 5-fold when the sample was heated for 20 minutes to 300° C in contact with 3.5 cm of carbon monoxide. This carbon monoxide was probably adsorbed on the chromia of the sample, since the 2200 cm^{-1} band did not increase when an alumina sample was heated in contact with the gas.

The formation of the 2198 cm^{-1} band for CO adsorbed on zinc oxide (1) also occurred through an activated process, since this frequency was approached only slowly on standing

**Dr. Gardner has calculated a CO^{++} vibration frequency of 2205 cm^{-1}; he has kindly put the data of ref. 5 at our disposal.*

at 25° C, whereas the 2174 cm^{-1} band appeared rapidly. Moreover the 2198 cm^{-1} band was produced occasionally when carbon monoxide adsorption was studied at 155° C on zinc oxide. The activated process by which the 2200 cm^{-1} band was formed may be surface diffusion of the CO molecule to other adsorption sites. It is unlikely to be diffusion into the metal oxide lattice: the band was readily eliminated by evacuation at 25° C and this would not be consistent with removal of carbon monoxide from the bulk.

Absorption Bands of Adsorbed CO and CO_2 in the Region 1200–1800 cm^{-1}

In both the present work and in the work on zinc oxide (1), carbon dioxide gave a band in the region 1610–1630 cm^{-1}, at higher frequency than did carbon monoxide on the corresponding oxide (1580–1610 cm^{-1}). Of the carbon–oxygen species considered by Gatehouse, Livingstone, and Nyholm (19) only the acid carbonates absorbed above 1600 cm^{-1}. This vibration was the asymmetric stretching mode of the $-C\begin{matrix}=O\\ \diagdown\\ \diagup\\ -O\end{matrix}$ group. The symmetric mode appeared at about 1300–1400 cm^{-1}. It is possible that the band above 1600 cm^{-1} for carbon dioxide and the band at 1580–1600 cm^{-1} for carbon monoxide may be due to a bicarbonate species formed by reaction with surface hydroxyl groups. The hydroxyl stretching region cannot be studied for the chromia–alumina samples because of scattering, but no change was observed for zinc oxide catalyst in this region (1).

The low-frequency band of the bicarbonate species may then be one of the bands at 1430 or 1370 cm^{-1}. However, a band persists at 1370 cm^{-1} even after evacuation at 300° C during which all other bands were removed. In view of this it is possible that the adsorption merely intensified the band already existing at 1370 cm^{-1} in the spectrum of the surface.

Eischens and Pliskin (2) have considered the spectrum of bicarbonate with absorption bands at 1630 and 1390 cm^{-1}, due respectively to the asymmetric and symmetric stretching modes of $-C\begin{matrix}=O\\ \diagdown\\ \diagup\\ -O\end{matrix}-$, and then assigned bands at these frequencies in the spectrum of carbon dioxide on nickel oxide to the following structure:

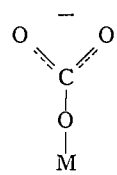

(i)

It would appear that the asymmetric $-C\begin{matrix}=O\\ \diagdown\\ \diagup\\ -O\end{matrix}-$ stretching mode of complex metal carbonates such as this would absorb at a rather lower frequency. Thus Gatehouse *et al.* (19) show the asymmetric stretching modes of

$$(\text{Co-en-}CO_3)Cl^* \text{ and } Na_2\left[Cu\begin{matrix}O-CO_2\\ \diagdown\\ \diagup\\ O-CO_2\end{matrix}\right]\cdot 3H_2O$$

to be 1577 and 1529 cm^{-1} respectively while the corresponding symmetric modes absorb at 1280 and 1326 cm^{-1}.

**en = ethylenediamine.*

Taylor and Amberg (1) considered the assignment of bands at 1560 and 1330 cm^{-1} to the asymmetric and symmetric modes of a surface carboxylate group, without specifying the surface atom to which it is bonded. The results of Gatehouse *et al.* (19) would at any rate make a distinction between structures (i) and (ii) uncertain.

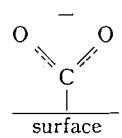

(ii)

In the work on chromia–alumina both carbon monoxide and carbon dioxide gave a band at 1230 cm^{-1} whereas for zinc oxide (1) only the latter gas gave a band at this frequency. The intensity of this band for carbon dioxide on chromia–alumina was greater than that for carbon monoxide for similar gas pressures and times of standing. Its assignment is uncertain but it may be the symmetric stretching mode of a structure such as (i) or (ii) displaced to a frequency below normal (19) or to the stretching of a carbon–oxygen single bond raised from the normal range (19) (1000–1100 cm^{-1}).

A weak band, which may be due to the structure 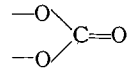 , similar to organic carbonates, appeared at 1750 cm^{-1} when carbon dioxide was heated over chromia–alumina and when carbon dioxide was adsorbed on thick alumina samples. The 1230 cm^{-1} band cannot be the carbon–oxygen single bond stretching mode of this structure since it occurs on samples when no 1750 cm^{-1} band appears.

The band which appears at 1430 cm^{-1} when carbon dioxide and in some cases carbon monoxide was adsorbed on the chromia–alumina may be due to the formation of carbonate ion, since this is the frequency of the asymmetric carbon–oxygen stretching mode of this species.

Absorption Bands of Chromia–Alumina and Alumina

The 1370 cm^{-1} band which appears in the spectrum of chromia–alumina seems independent of other bands in the spectrum. Thus it cannot be due to a complex carbonate species on the surface, since some other accompanying band would be expected, while this band is the only one remaining when the sample is heated with oxygen and outgassed. Carbonaceous impurities might have been introduced into the gel catalyst during its preparation by inclusion of atmospheric carbon dioxide.

The 1370 cm^{-1} band may be due to the carbonate ion vibration displaced to lower frequency from its normal value of 1430 cm^{-1}. It would be expected that carbon dioxide would form this band more readily than carbon monoxide since less oxygen is required, although when adsorption was carried out at 20° C carbon monoxide in certain cases appeared to give intensification of this band, whereas carbon dioxide did not. If the species responsible for the band is a carbonate ion the process may be an activated one. The band was intensified by heating carbon monoxide with both alumina and chromia–alumina samples.

Consideration must be given to the view that the band at 1370 cm^{-1} is due to nitrate impurity incorporated during the sample preparation. It seems unlikely, however, that this explanation is correct, since the intensity of the band fluctuated during the course

of the experiments on one sample and the final band intensity was larger than that for the freshly prepared sample.

The frequencies and intensities of bands in the 1300–1550 cm^{-1} region of the chromia–alumina spectrum have been shown to vary considerably during heating and evacuation, both with and without oxygen, and when no carbon monoxide or carbon dioxide was present. At least some of the bands in this region may be connected with the defect structure of the oxide rather than with the stretching vibrations of definite surface species. A chromia–alumina sample having initially only one band, at 1370 cm^{-1}, in its spectrum, after standing in an evacuated cell for 24 hours had a weak band at 1580 cm^{-1} in addition to the original band, which was decreased somewhat in intensity. Evacuation at 300° C gave a complex spectrum with broad intense bands at 1535, 1430, and 1350 cm^{-1}. When the sample was heated with oxygen and then evacuated only the 1370 cm^{-1} band remained. These changes seem incompatible with the presence of definite surface species. Nevertheless, in spite of some doubt expressed at the time of publication, a similar set of bands on zinc oxide (1) has now been quite definitely shown to arise from carbonaceous impurities (20). A number of differences remain however, in particular with respect to the band at 1370 cm^{-1}, which does not occur on zinc oxide, so that we do not feel justified in drawing the same conclusions by analogy. The 1580 cm^{-1} band cannot be due to the deformation mode of adsorbed water, since on exposing the sample completely to the atmosphere a very intense band appeared at 1627 cm^{-1}. There is no reason why evacuation at 320° C should not completely remove the 1580 cm^{-1} band if it were due to adsorbed water, especially since the band at 1627 cm^{-1} disappeared completely after this treatment.

Finally the possibility that certain bands produced during adsorption of gases such as carbon monoxide, carbon dioxide, or oxygen may be due to the introduction of valency or other defects by the adsorption process cannot be completely disregarded. This is most unlikely in the cases discussed in the previous sections, where the appearance or disappearance of well-characterized bands can be directly correlated with the adsorption or desorption of CO or CO_2. For example, our evidence leaves little doubt that the band at 2200 cm^{-1} arose from an adsorbed CO species; moreover the observed frequency was close enough to the fundamental vibrational frequency of the gaseous molecule to reinforce this view. Defects are equally unlikely to have been the source of spectra which are similar for chromia–alumina and zinc oxide, since these solids differ widely in structure. Thus only where assignments have so far been uncertain, as in some of the cases cited in this section, could defects be considered an alternative to impurities or adsorbates in trying to explain the observed bands.

ACKNOWLEDGMENTS

The authors express their gratitude to Dr. Y. Amenomiya for supplying the catalyst samples and to Dr. H. J. Bernstein for a helpful discussion. Experiments were completed in the Department of Mining and Metallurgy, University of Alberta, Edmonton, and L. H. Little is grateful for spectroscopic facilities provided there.

REFERENCES

1. J. H. Taylor and C. H. Amberg. Can. J. Chem. **39**, 535 (1961).
2. R. P. Eischens and W. A. Pliskin. Advances in Catalysis, **9**, 662 (1957).
3. R. P. Eischens and W. A. Pliskin. Advances in Catalysis, **10**, 1 (1958).
4. R. A. Gardner and R. H. Petrucci. J. Am. Chem. Soc. **82**, 5051 (1960).
5. R. A. Gardner and R. H. Petrucci. XVIIIth International Congress of Pure and Applied Chemistry, Montreal. 1961. Paper No. B1-30.
6. D. J. C. Yates. J. Phys. Chem. **65**, 746 (1961).

7. L. H. LITTLE, H. E. KLAUSER, and C. H. AMBERG. Can. J. Chem. **39**, 42 (1961).
8. L. J. BELLAMY. Spectrochim. Acta, **14**, 192 (1958).
9. A. D. BUCKINGHAM. Trans. Faraday Soc. **56**, 753 (1960).
10. L. M. ROEV and A. N. TERENIN. Optika i Spektroskopiya, **7**, 756 (1959).
11. A. TERENIN and L. ROEV. Actes du deuxième congrès international de catalyse, Paris. 1960. p. 2183. (Editions Technip, Paris, 1961.)
12. B. J. RANSIL. Revs. Modern Phys. **32**, 245 (1960).
13. G. HERZBERG. Spectra of diatomic molecules. 2nd ed. Van Nostrand, New York. 1950. p. 522.
14. N. S. BAYLISS and A. L. G. REES. J. Chem. Phys. **8**, 377 (1940).
15. G. E. EWING and G. C. PIMENTEL. J. Chem. Phys. **35**, 925 (1961).
16. Y. KUBOKAWA. Bull. Chem. Soc. Japan, **33**, 743 (1960).
17. F. I. VILESOV and A. N. TERENIN. Doklady Akad. Nauk S.S.S.R. **125**, 1053 (1959).
18. G. HEILAND, E. MOLLWO, and F. STÖCKMANN. Solid State Phys. **8**, 277 (1959).
19. B. M. GATEHOUSE, S. E. LIVINGSTONE, and R. S. NYHOLM. J. Chem. Soc. 3137 (1958).
20. J. H. TAYLOR and C. H. AMBERG. Unpublished work.

CARBON-13 KINETIC ISOTOPE EFFECTS IN BIMOLECULAR REACTIONS

J. B. STOTHERS[1] AND A. N. BOURNS
Department of Chemistry, McMaster University, Hamilton, Ontario

Received July 9, 1962

ABSTRACT

Carbon-13 kinetic isotope effects have been measured for the bimolecular reaction of 1-phenyl-1-bromoethane (I) and benzyl bromide (II) with alkoxide ion in alcohol solution. Compound I gave an effect, k^{12}/k^{13}, of 1.0032 ± 0.0005 for reaction with ethoxide ion in ethanol, while II gave $k^{12}/k^{13} = 1.0531 \pm 0.0004$ for reaction with methoxide ion in methanol. These surprisingly different effects are tentatively interpreted in terms of a model for the transition state having varying degrees of ionic character.

INTRODUCTION

Although nucleophilic substitution at a saturated carbon atom is one of the most commonly encountered organic reactions and as such has long been the subject of detailed study, many points concerning the nature of the reaction remain obscure. One of the newer tools available for the study of reaction mechanisms, that of kinetic isotope effects, would appear to provide an additional means of extending our understanding of this reaction, since isotopic fractionation in rate processes is extremely sensitive to bonding changes in the rate-determining stage. A priori, one might have expected that the isotope effect associated with the carbon atom at the seat of displacement could serve to distinguish between the two extremes of S_N1 and S_N2 behavior, since, intuitively, a larger effect might be predicted for a process involving simple bond rupture than for one in which bond rupture and formation are synchronous. This approach has been investigated by Bender and co-workers (1–3), who, contrary to this prediction, observed a much larger effect in the S_N2 reaction of various nucleophiles with methyl iodode-C^{14} ($k^{12}/k^{14} = 1.09$ to 1.14) than in the S_N1 hydrolysis of 2-chloro-2-methylpropane-2-C^{14} ($k^{12}/k^{14} = 1.03$). Melander (4) has recently shown that whereas the Bigeleisen method (5) for the theoretical evaluation of isotope effects leads to the conclusion that a change in mechanism should have very little influence on the magnitude of the effect, a treatment (4) based on an actual calculation of the moments of inertia leads to results which are consistent with Bender's experimental findings. It should be emphasized, however, that there is a danger in making a direct comparison of effects in S_N1 and S_N2 processes involving different substrates and one should not discount the possibility that other factors, such as the nature of the leaving group and the reaction medium, may have an important influence on the observed effect (2).

In a previous communication (6) from this laboratory a very small carbon-13 isotope effect, $k^{12}/k^{13} = 1.0065$, was reported for the S_N1 alcoholysis of 1-bromo-1-phenylethane and was interpreted in terms of a model for the transition state in which the bonding to the isotopic carbon is strengthened by conjugation of the electron-deficient center with the ring. Since this compound is known to undergo mainly bimolecular reaction when treated with an ethanolic solution of ethoxide ion in concentrations of 1.5 M or higher (7, 8), it appeared to be particularly well suited for an investigation of the relative magnitude of isotope effects in S_N1 and S_N2 reactions of the same substrate. Other practical considerations governing the choice of this halide for such a study and the reason for using a compound of natural isotopic abundance have been previously discussed (6).

[1]*Present address: Department of Chemistry, University of Western Ontario, London, Ontario.*

The isotope effect study of the S_N2 reaction of 1-bromo-1-phenylethane with ethoxide ion is described in the present paper and the results compared with those obtained previously (6) for the alcoholysis reaction. On the basis of these results, it appeared desirable to measure the isotope effect in a bimolecular reaction in which the bond-breaking and bond-formation processes are more nearly balanced than in the 1-phenylethyl system. Accordingly, a study has been made of the isotope effect in the reaction of benzyl bromide with methoxide ion in methanol. This work also is now reported.

EXPERIMENTAL

In general, the experimental procedures employed for these studies were similar to those described previously (6). Some minor modifications were introduced for the present system and these are indicated below.

Kinetic Studies

The reaction rates were determined by following the rate of formation of bromide ion in a series of sealed tubes containing aliquots of the reaction mixture. A modified Volhard method was used for this analysis (9) and the quenching mixture contained sufficient nitric acid to neutralize the unreacted base present. The rate constant, k_2, for a particular run was obtained by a least-squares analysis of a plot of time vs. $\log a(b-x)/b(a-x)$.

Isotope Effect Experiments

For each determination of the carbon-13 isotope effect a sample of alkyl bromide was allowed to react with alkoxide ion to a small known extent of reaction (ca. 5%), the reaction was stopped, and the ether product separated from unreacted starting material by fractional distillation. Samples of the product and original bromide were degraded by oxidation and decarboxylation to yield carbon dioxide derived exclusively from the carbon at which displacement occurred. The 1-phenylethyl derivatives were degraded by a two-step oxidation procedure, which has been previously described (6). In the first stage the compounds were treated with potassium permanganate in aqueous pyridine solution to give a mixture of benzoic and benzoylformic acids. This acid mixture, after isolation, was then further oxidized with hydrogen peroxide, whereby the benzoylformic acid was quantitatively converted to benzoic acid. With the benzyl derivatives, only the permanganate oxidation step is required. It was found that better yields (ca. 85%) are obtained for benzyl bromide if it is converted to the methyl ether before oxidation. The remaining steps in the isotope effect determinations were carried out as before.

RESULTS

The results of the kinetic studies are presented in Table I for the reactions of 1-bromo-1-phenylethane with ethoxide ion in ethanol and benzyl bromide with methoxide ion in

TABLE I

Kinetic results for the reaction $RBr + OR'^- \rightarrow ROR' + Br^-$

RBr	OR'^-	Solvent	Temp., °C	Concn. of RBr, *M*	Concn. of OR'^-, *M*	$k_2 \times 10^3$, l./mole min
1-Bromo-1-phenylethane	Ethoxide	Ethanol	25.0	0.470	2.175	3.16
				0.488	2.160	3.24
				0.498	1.848	3.28
						Average 3.23
Benzyl bromide	Methoxide	Methanol	0.0	0.537	1.108	5.33
				0.424	1.122	5.29
				0.519	0.911	5.31
						Average 5.31

methanol. The isotope effect values found for each of these reactions are shown in Tables II and III, respectively. Each determination refers to an individual partial reaction of alkyl bromide followed by degradation of the ether product and a sample of the original halide to carbon dioxide. The rate constant ratios, k^{12}/k^{13}, were calculated from the isotopic ratios and the extent of reaction (10).

TABLE II

C^{12}/C^{13} ratios and kinetic isotope effects in the reaction of 1-bromo-1-phenylethane with ethoxide ion in ethanol at 25° C

Expt. No.	Compound degraded	Reaction %	C^{12}/C^{13} ratios	k^{12}/k^{13}
1	RBr		91.16	1.0030
	ROC_2H_5	4.8	91.42	
2	RBr		90.74	1.0031
	ROC_2H_5	4.9	91.01	
3	RBr		91.52	1.0026
	ROC_2H_5	7.4	91.74	
4	RBr		93.15	1.0036
	ROC_2H_5	7.5	93.47	
5	RBr		91.07	1.0025
	ROC_2H_5	7.9	91.28	
6	RBr		91.16	1.0038
	ROC_2H_5	8.9	91.49	
7	RBr		91.16	1.0036
	ROC_2H_5	7.6	91.47	
			Mean value of isotope effect	1.0032*

NOTE: RBr concn. ca. 0.5 *M*; ethoxide ion concn. ca. 2 *M*.
*Standard deviation 0.0005; 95% confidence limit 0.0004.

TABLE III

C^{12}/C^{13} ratios and kinetic isotope effects in the reaction of benzyl bromide with methoxide ion in methanol at 0° C

Expt. No.	Compound degraded	Reaction %	C^{12}/C^{13} ratios	k^{12}/k^{13}
1	RBr		91.00	1.0530
	$ROCH_3$	7.1	95.65	
2	RBr		90.98	1.0530
	$ROCH_3$	6.2	95.65	
3	RBr		91.07	1.0528
	$ROCH_3$	8.6	95.67	
4	RBr		91.11	1.0536
	$ROCH_3$	7.0	95.82	
5	RBr		90.98	1.0533
	$ROCH_3$	8.3	95.63	
			Mean value of isotope effect	1.0531*

NOTE: RBr concn. ca. 0.5 *M*; methoxide concn. ca. 1 *M*.
*Standard deviation 0.0003; 95% confidence limit 0.0004.

DISCUSSION

The carbon-13 isotope effect of 0.3% found for the reaction of 1-bromo-1-phenylethane with ethoxide ion is slightly, but significantly, smaller than the 0.6% previously reported for the alcoholysis of this substrate. This result is the reverse of that reported by Bender (1, 2), who found a considerably higher effect for the S_N2 reaction of methyl iodide than for the hydrolysis of *t*-butyl chloride. As was pointed out in the Introduction, however, when quite different substrates are being compared, factors other than reaction molecularity may be important in determining the relative magnitude of the observed effects.

Since not only the difference in the isotope effects found for the S_N1 and S_N2 reactions of 1-bromo-1-phenylethane, but also the magnitude of the effects themselves, is small, it is rather fruitless to attempt any detailed theoretical interpretation. It is of interest to

note, however, that the temperature-independent factor of the Bigeleisen equation (5), evaluated by the method of Bigeleisen and Wolfsberg (11) using the mass-fragment model (12), has a value very slightly higher for the reaction with ethoxide ion than for the ethanolysis. Consequently, it would appear to be the temperature-dependent (free energy) factor which is mainly responsible for the lower effect in the S_N2 process.

In contrast to the very small isotope effect found for the reaction of alkoxide ion with 1-bromo-1-phenylethane, the reaction of benzyl bromide gives an effect of 5.3%, which is comparable to that reported by Bender (1) for the reaction of hydroxide ion with methyl iodide. Yet both the 1-bromo-1-phenylethane and the benzyl bromide reactions have been found to give good second-order kinetics under the conditions of the present study and they have always been considered to be typical bimolecular or S_N2 processes. This large difference in isotope effect cannot be attributed to the temperature-independent component, which is small and not significantly different in the two reactions. It, therefore, must have its origin in the free energy factor, which implies that there are important differences in the transition states of the two bimolecular reactions, differences which are not disclosed by conventional methods of investigating reaction mechanisms such as stereochemical or ordinary kinetic studies.

Now it is well known on the basis of kinetic studies that the 1-phenylethyl group tends to promote reaction by the unimolecular mechanism (13). For example, reaction with methanolic sodium methoxide has an important first-order component even at very high methoxide ion concentrations, and good second-order kinetics are found in the reaction with sodium ethoxide in ethanol only at an alkoxide ion concentration in excess of 1.5 *M*. It seems reasonable to conclude, then, that the transition state for the bimolecular reaction of this substrate has considerable carbonium ion character. On the other hand, there is strong evidence that in the benzyl system bond formation and bond rupture have occurred to about the same extent at the transition-state configuration (14–17). The present results indicate that this difference in the nature of the transition state is manifested in the observed kinetic isotope effects for the carbon undergoing substitution.

In the 1-phenylethyl system, the carbon atom at the seat of displacement is electron deficient in the transition state and there is conjugative interaction between its fairly well developed vacant p orbital and the π orbitals of the benzene ring. The result will be a contribution to the isotope effect by a free energy factor which is not greatly different from that associated with a unimolecular process. In the benzyl system, however, the charge on the carbon atom undergoing substitution would not be expected to change greatly in going from the initial to the transition state and there will be little conjugative interaction with the adjacent benzene ring. It is suggested that it is this difference in the extent of internal conjugation, and hence of carbon–carbon bond strengthening, in the transition state which is largely responsible for the marked difference in the isotope effect in the two reactions.

Although this interpretation is purely speculative and highly tentative, there is no doubt that kinetic isotope effect measurements provide a very sensitive means of obtaining information about the nature of the transition state. Clearly, more experimental work is required to adequately evaluate the significance of the results so far reported and studies to this end are now underway.

ACKNOWLEDGMENTS

This work was supported by the National Research Council and one of us (J. B. S.) wishes to acknowledge financial assistance in the form of N.R.C. Studentships.

REFERENCES

1. M. L. BENDER and D. F. HOEG. J. Am. Chem. Soc. **79**, 5649 (1957).
2. M. L. BENDER and G. J. BUIST. J. Am. Chem. Soc. **80**, 4304 (1958).
3. G. J. BUIST and M. L. BENDER. J. Am. Chem. Soc. **80**, 4308 (1958).
4. L. MELANDER. Isotope effects on reaction rates. Ronald Press, New York. 1960. pp. 143 f.
5. J. BIGELEISEN. J. Chem. Phys. **17**, 675 (1949).
6. J. B. STOTHERS and A. N. BOURNS. Can. J. Chem. **38**, 923 (1960).
7. E. D. HUGHES, C. K. INGOLD, and A. D. SCOTT. J. Chem. Soc. 1201 (1937).
8. E. D. HUGHES, C. K. INGOLD, S. MASTERMAN, and B. J. MCNULTY. J. Chem. Soc. 899 (1940).
9. H. DIEHL and G. F. SMITH. Quantitative analysis. J. Wiley and Sons, New York. 1952. p. 332.
10. W. H. STEVENS and R. W. ATTREE. Can. J. Research, B, **27**, 807 (1949).
11. J. BIGELEISEN and M. WOLFSBERG. J. Chem. Phys. **21**, 1972 (1953); **22**, 1264 (1954).
12. J. BIGELEISEN and M. WOLFSBERG. Advances in Chem. Phys. **1**, 15 (1958).
13. C. K. INGOLD. Structure and mechanism in organic chemistry. Cornell University Press, Ithaca, N.Y. 1953. pp. 324 ff.
14. C. W. L. BEVAN, E. D. HUGHES, and C. K. INGOLD. Nature, **171**, 301 (1953).
15. S. SUGDEN and J. B. WILLIS. J. Chem. Soc. 1360 (1951).
16. J. HINE. Physical organic chemistry. McGraw-Hill, New York. 1956. pp. 153 ff.
17. P. D. BARTLETT. *In* Organic chemistry. Vol. III. *Edited by* Henry Gilman. John Wiley and Sons, New York. 1953. pp. 33 ff.

REACTIONS OF METHYL RADICALS WITH NITRIC OXIDE

D. E. HOARE
Chemistry Department, Queen's College, University of St. Andrews, Dundee, Scotland

Received April 24, 1962

ABSTRACT

Methyl radicals have been produced by the photolysis of acetone at 200° C and their reaction with nitric oxide has been studied. The reaction $CH_3 + NO + M \rightarrow CH_3NO + M$ is shown to be third order with a rate constant of 8.8×10^{-31} $cm^6 molecule^{-2} sec^{-1}$, with acetone as M. It is further shown that the nitrosomethane formed reacts with either methyl radicals or nitric oxide. The probability of reactions such as $CH_3CO + NO \rightarrow CH_3CO.NO$ taking place is shown.

INTRODUCTION

The reaction of methyl radicals with nitric oxide has been studied by a number of investigators (3, 5, 6, 9, 10, 11, 17). Usually the reaction has been followed by estimating either the rate of disappearance of nitric oxide or the rate of removal of methyl radicals. The present investigation followed the reaction by both methods and it was therefore possible to discover the presence of other complicating reactions of both methyl radicals and nitric oxide.

EXPERIMENTAL

The apparatus was the same as that used in previous experiments (1). A beam of light, effectively limited to the wavelengths 3130 and 3020 Å, filled a silica reaction cell of 2.8-cm diameter and 20-cm length. The absorbed light intensities were 1.0×10^{13} quanta $cm^{-3} sec^{-1}$ and 1.0×10^{12} quanta $cm^{-3} sec^{-1}$ with 200 mm and 10 mm, respectively, of acetone present. Small amounts of nitric oxide were added to keep its pressure constant during the reaction. A magnetically operated stirrer kept the gases mixed during the reaction, but it was found necessary to allow time for each successive addition to mix, by cutting off the light with a screen immediately before each addition. Quantum yields were calculated by comparison with the yield of carbon monoxide from the photolysis of pure acetone, which is assumed to have a quantum yield of unity at 200° C.

The acetone and oxygen were prepared as described previously (1). Spectroscopically pure nitric oxide was prepared by Dr. P. Warsop from sodium nitrate, potassium iodide, and sulphuric acid. It was redistilled in the apparatus to give a blue liquid (with no traces of green color).

Carbon monoxide and methane were estimated in the usual manner (2) by the use of Le Roy – Ward stills and a mixture of copper and copper oxide heated to 200° C. Nitric oxide was estimated by condensation with ethane at −215° C followed by combustion at 350° C over copper and copper oxide. Small amounts of ethane which were present were thus converted to carbon dioxide and measured.

RESULTS

The photolysis of acetone at 200° C is said to occur by the following mechanism:

$$CH_3COCH_3 + h\nu \rightarrow CH_3CO + CH_3 \quad [1]$$

$$CH_3CO + M \rightarrow CH_3 + CO + M. \quad [2]$$

The methyl radicals may then react with acetone according to reaction [3]:

$$CH_3 + CH_3COCH_3 \rightarrow CH_4 + CH_3COCH_2, \quad [3]$$

or react with nitric oxide according to reaction [4]:

$$CH_3 + NO + M \rightarrow CH_3NO + M. \quad [4]$$

Only in the presence of low concentrations of nitric oxide will the reaction

$$2CH_3 \rightarrow C_2H_6 \quad [5]$$

be of importance.

Table I shows the quantum yields of methane and carbon monoxide in typical experiments and relates them to the nitric oxide which has been consumed. The yields of

TABLE I

Variation of pressure

Acetone (mm Hg)	CO_2 (mm Hg)	NO (μm Hg)	ϕ_{CH_4}	ϕ_{NO}	ϕ_{CO}	t (hr)
200	0	64	0.07	1.41	0.90	0.20
90	0	65	0.08	1.59	0.94	0.33
90	0	34	0.17	1.33	0.97	0.33
30	0	30	0.14	0.94	0.89	0.75
10	0	14	0.18	0.78	0.91	1.75
10	80	36	0.10	1.11	0.86	1.75
10	250	21	0.10	1.29	0.98	1.75

carbon monoxide were reduced by the addition of nitric oxide (Table I, experiments 2 and 3), and the most plausible explanation is that acetyl radicals may react with nitric oxide, e.g.,

$$CH_3CO + NO \rightarrow CH_3CO.NO, \quad [6]$$

rather than decompose according to reaction [2]. The increase in the yield of carbon monoxide when inert carbon dioxide was added (thus favoring reaction [2]) supports such a hypothesis (Table I, experiments 5 and 7). Below 200 mm pressure, acetone appears more effective than carbon dioxide as third body in reaction [2] (experiments 3, 4, and 6).

The amounts of ethane obtained were, as expected, very small. One would expect, therefore, that reactions [3] and [4] would account for the majority of the methyl radicals produced. Hence $\phi_{CH_4}+\phi_{NO}+2\phi_{C_2H_6}$ should be equal to 2. Table I shows clearly that this is not so and that methyl radicals must have another reaction, probably with the nitrosomethane which has been formed. Since the quantity of nitrosomethane formed would not have varied much from one experiment to another (the total absorbed intensity was kept approximately constant) this hypothesis was best tested by further experiments in which the nitric oxide was deliberately allowed to become very low (and not constant during an experiment). Under such extreme conditions the number of methyl radicals which did not form methane or ethane was very much greater than the number of nitric oxide molecules which were consumed. Even allowing for a possible reaction of methyl radicals with acetonyl (CH_3COCH_2) radicals an average of between 2 and 3 methyl radicals were consumed per nitric oxide molecule. This is illustrated in Table II(*a*).

At the other extreme of conditions, pressures of nitric oxide were used sufficiently high to cause reaction [4] to predominate so that no methane or ethane was experimentally detectable. Under such conditions the rate of consumption of nitric oxide exceeded the rate of formation of methyl radicals and the yield of carbon monoxide was much decreased by the favoring of a reaction such as reaction [6]. Under these conditions a gas which was not condensed at −215° C (presumably nitrogen) was formed in small yields. It was unchanged in volume by passage over heated copper and copper oxide at 350° C. The results are shown in Table II(*b*).

TABLE II

Extreme pressures of nitric oxide

Acetone (mm Hg)	NO (μm Hg)	ϕ_{CH_4}	ϕ_{NO}	ϕ_{CO}	$\phi_{C_2H_6}$	ϕ_{N_2}	t (hr)
		(*a*) Low pressures of nitric oxide					
10	0	0.53	0	1.00	0.56		2.00
10	low	0.46	0.13	0.97	0.48		1.75
10	low	0.38	0.33	0.93	0.34		1.75
10	14	0.18	0.78	0.91	0.06		1.75
		(*b*) High pressures of nitric oxide					
200	600		2.6	0.71		0.14	0.20
91	640		2.2	0.68		0.06	0.33
10	730		1.7	0.52		0.015	2.00

DISCUSSION

The possibility of the reaction between nitric oxide and methyl radicals being third order has been realized for some years. Experimental attempts to prove the kinetic dependence of the reaction upon a third body have often failed because experimentalists failed to realize the specificity of third bodies in their efficiency in performing the role of M. Thus Miller and Steacie (3) added up to 10 cm of nitrogen to 4.5 mm Hg of mercury dimethyl without causing any great increase in the rate of reaction [4]. Nitrogen would be expected to be ineffective compared with mercury dimethyl as M in such an energy transfer reaction. Preliminary results showed that nitric oxide reacted five times as rapidly with methyl radicals as does oxygen when acetone is the third body (4). Christie (5) found reaction [4] to be 100 times as fast as the corresponding reaction of methyl radicals with oxygen when methyl iodide was the third body. However, she neglected to allow for reactions between nitrosomethane and methyl radicals which could modify her conclusions.

The rate constant for reaction [4] in the present work may be derived by comparing it with reaction [3]. Using the experimental values presented in Table I (where the nitric oxide pressure was too low for it to react further with nitrosomethane) and correcting for reaction [6], one finds

$$k_4/k_3 = \frac{\phi_{NO}+\phi_{CO}-1}{\phi_{CH_4}} \times \frac{[\text{acetone}]}{[NO][M]}.$$

The plot of $\{(\phi_{NO}+\phi_{CO}-1)/\phi_{CH_4}\} \times \{[\text{acetone}]/[NO]\}$ $(=R)$ against [M] clearly shows the kinetic dependence of reaction [4] upon [M]. This is illustrated in Fig. 1. The small effect of adding carbon dioxide emphasizes the relative inefficiency of this gas in reaction [4]. Christie (5) found it to be similarly much less efficient than methyl iodide in this same reaction.

The evidence is strong that reaction [4] is third order and indeed it is difficult to account for a steric factor of 10^{-4}, which is obtained if a second-order mechanism is postulated (6). One would expect it to be third order by comparison with the corresponding reaction of methyl radicals with oxygen (7, 8). However, Christie (5) finds evidence of a transition from third to second order at total pressures approaching 100 mm Hg. No evidence of this was found in the present experiments and the discrepancy may be due to her neglect of other possible reactions of methyl radicals.

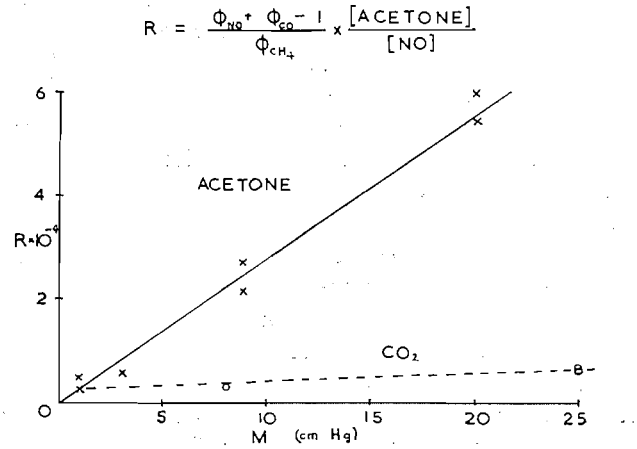

FIG. 1. Dependence of the reaction between CH_3 and NO upon a third body (M = acetone or CO_2).

The values obtained for the absolute rate constant of reaction [4] depend upon the accuracy with which the rate constant of the competing reaction is known. Reaction [3] has been much studied and is usually compared with reaction [5]. If a value of 3.2×10^{-12} $cm^{3/2}molecule^{-1/2}sec^{-1/2}$ is taken for $k_3/k_5^{1/2}$ at 200° C (2), the present work leads to a value for $k_4/k_5^{1/2}$ of 4.3×10^{-26} $cm^{9/2}molecule^{-3/2}sec^{-1/2}$ at 200° C. If reaction [5] is assumed to have a rate constant of 4.2×10^{-10} $cm^3molecule^{-1}sec^{-1}$ at 200° C then $k_4 = 8.8\times10^{-31}$ $cm^6molecule^{-2}sec^{-1}$ at 200° C.

Values calculated from the results of other workers are given in Table III in the same units.

TABLE III

Comparison of rate constants

Rate constants	Authors	Third body	Value	Temperature (°C)
$k_4/k_5^{1/2}$	Present work	Acetone	4.3×10^{-26}	200
"	Miller and Steacie (3)	$Hg(CH_3)_2$	3×10^{-25}	27
"	Birss, Danby, and Hinshelwood (9)	$[(CH_3)_3CO]_2$	1.7×10^{-27}	160
k_4	Present work	Acetone	8.8×10^{-31}	200
"	Christie (5)	CH_3I	3×10^{-30}–3×10^{-29}	Room
"	Durham and Steacie (6)	$[(CH_3)_3CO]_2$	8.5×10^{-30}	Room
"	Bryce and Ingold (10)	He	2.8×10^{-30}	900
"	Lossing, Ingold, and Tickner (11)	He	1×10^{-30}	950

Table III illustrates differing values for the rate constant of reaction [4], many of which depend upon mechanisms or uncertain values of rate constants. Some correlation may be made between the more recent determinations if a negative activation energy (ca. 4 kcal/g-mole) is assumed. This would correspond to a positive activation energy for the decomposition of the activated CH_3NO complex first formed by the combination of methyl radicals and nitric oxide. There is some evidence that at higher pressures of a suitable third body, reaction [4] becomes effectively second order (5, 17).

The nitrosomethane which is formed by reaction [4] has been investigated by Gowenlock and Trotman (12). They have shown that it may dimerize or rearrange to give formaldoxime. The latter reaction involves a high activation energy (ca. 40 kcal/mole) whereas the former is probably a wall reaction. In the present work it has been shown that up to 3 methyl radicals are removed by 1 molecule of nitric oxide without the formation of methane or ethane. The obvious solution is the formation of the molecule $N(CH_3)_2.OCH_3$ (trimethyl hydroxylamine) by addition of methyl radicals across the double bond of nitrosomethane. Such reactions are known to occur with more complex free radicals in solution (14). Similarly Batt and Gowenlock (13) have suggested that the reaction between nitric oxide and nitrosomethane, which they have detected (in agreement with the present work and that of Christie (5)), occurs by addition of 2 molecules of nitric oxide across the double bond of nitrosomethane. The compound formed decomposes with the evolution of some nitrogen, as has been observed in the present work.

It has been suggested earlier that nitric oxide reacts with acetyl radicals, thus reducing the yield of carbon monoxide formed by reaction [2]. Such a phenomena has been previously reported by Anderson and Rollefson (15). The ready reaction of nitric oxide with free radicals favors the plausibility of such a reaction. Reaction [6] appears to occur by a second-order mechanism and is appreciable at lower pressures of nitric oxide than the corresponding reaction of acetyl radicals with oxygen (16). This is to be expected by analogy of the reaction of methyl radicals with nitric oxide and with oxygen (4). It is interesting to note that the similar reaction of nitric oxide with *t*-butyl radicals also occurs readily (9).

Caldwell and Hoare (18) have shown that in the photolysis of acetone at 150 to 200° C oxygen has no effect on the rate of decomposition of acetone, i.e. reaction of oxygen with the triplet state of acetone is not important. This is probably due to the virtual absence of triplet state acetone at those temperatures and therefore one can assume that nitric oxide similarly has no effect on the rate of decomposition of acetone.

REFERENCES

1. D. E. Hoare. Trans. Faraday Soc. **49**, 1292 (1953).
2. D. E. Hoare. Trans. Faraday Soc. **53**, 791 (1957).
3. D. M. Miller and E. W. R. Steacie. J. Chem. Phys. **19**, 73 (1951).
4. D. E. Hoare and A. D. Walsh. Special Publ. Chem. Soc. **9**, 17 (1958).
5. M. I. Christie. Proc. Roy. Soc. (London), A, **249**, 248 (1959).
6. R. W. Durham and E. W. R. Steacie. J. Chem. Phys. **20**, 582 (1952).
7. D. E. Hoare and A. D. Walsh. Trans. Faraday Soc. **53**, 1102 (1957).
8. M. I. Christie. Proc. Roy. Soc. (London), A, **244**, 411 (1958).
9. F. W. Birss, C. J. Danby, and C. N. Hinshelwood. Proc. Roy. Soc. (London), A, **239**, 154 (1957).
10. W. A. Bryce and K. U. Ingold. J. Chem. Phys. **23**, 1968 (1955).
11. F. P. Lossing, K. U. Ingold, and A. W. Tickner. Discussions Faraday Soc. **14**, 34 (1953).
12. B. G. Gowenlock and J. Trotman. J. Chem. Soc. 4190 (1955).
13. B. G. Gowenlock and L. Batt. Trans. Faraday Soc. **56**, 682 (1960).
14. B. A. Gingras and W. A. Walters. J. Chem. Soc. 1920 (1954).
15. H. W. Anderson and G. K. Rollefson. J. Am. Chem. Soc. **63**, 816 (1941).
16. F. Marcotte and W. A. Noyes. J. Am. Chem. Soc. **74**, 783 (1952).
17. W. C. Sleppy and J. G. Calvert. J. Am. Chem. Soc. **81**, 769 (1959).
18. J. Caldwell and D. E. Hoare. J. Am. Chem. Soc. In press (1962).

EXTRACTIVES FROM POPULUS TREMULOÏDES HEARTWOOD

THE STRUCTURE AND SYNTHESIS OF TREMULONE[1]

R. A. ABRAMOVITCH AND R. G. MICETICH
Department of Chemistry, University of Saskatchewan, Saskatoon, Saskatchewan

Received May 28, 1962

ABSTRACT

Tremulone, a dienone isolated from *Populus tremuloïdes* heartwood, has been shown to be stigmasta-3,5-diene-7-one. This has been confirmed by a partial synthesis from β-sitosterol. The possibility that tremulone might be an artifact arising from the isolation procedure is discussed.

During a systematic analysis of the nature of the extractives from the heartwood of *Populus tremulöides* (aspen poplar or quaking aspen) (1) a ketone, m.p. 111°, $[\alpha]_D^{22}$ −273°, was isolated in very small yield (0.001% based on dry wood), and was named *tremulone*. Though this was a very minor component, its spectral properties were interesting enough that it was decided to determine its structure. The minor constituents of plant extractives have not, as a rule, been subjected to systematic investigation and it was thought possible that the determination of their structures in this case might, among other things, throw added light onto the biogenetic pathways available in such a plant.

Tremulone is a pleasant smelling compound (even when pure). Microanalytical values were not reproducible on samples obtained after repeated recrystallizations and chromatographic separations on alumina. An analytically pure specimen (melting point unchanged, $[\alpha]_D^{22}$ −288°) was finally obtained by 100-tube countercurrent distribution. Analytical values were consistent with either $C_{29}H_{46}O$ or $C_{30}H_{48}O$; the molecular weight determination (Rast) agreed better with the C_{30} formulation. The infrared spectrum indicated the presence of an α,β-unsaturated ketone grouping (1660 and 1600 cm^{-1}) and what at first was interpreted to be a $\rangle C{=}CH_2$ terminal methylene grouping (883 and 1630 cm^{-1}—the latter somewhat low for this assignment). Periodate–permanganate oxidation of a sample of tremulone before countercurrent purification gave a small amount of formaldehyde (detected by chromotropic acid). The presence of the keto group was confirmed by the ready formation of a 2,4-dinitrophenylhydrazone and an oxime. The ultraviolet absorption spectrum (λ_{max} 278 mμ; ε 20,000) indicated a conjugated dienone and the spectrum of the 2,4-dinitrophenylhydrazone (λ_{max} 375 mμ) was consistent with this formulation (2). Taking into account the suggested presence of a terminal methylene group and applying Woodward's rules (3) two chromophores are possible:

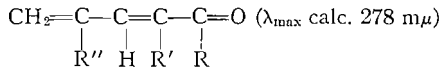

(λ_{max} calc. 278 mμ)

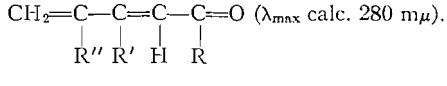

(λ_{max} calc. 280 mμ).

Catalytic hydrogenation of tremulone over palladium–charcoal led to the uptake of 2 molar equivalents of hydrogen and gave tetrahydrotremulone ($\nu_{C=O}$ 1705 cm^{-1}). The

[1]*Presented at the 45th Annual Conference of the Chemical Institute of Canada in Edmonton on May 29th, 1962.*

ketone group is, therefore, either in a side chain or in a six- or higher-membered ring, and the compound is tetracyclic. Again, analytical figures for the saturated ketone and its 2,4-dinitrophenylhydrazone did not lead to an unequivocal molecular formula, being consistent with either $C_{29}H_{50}O$ or $C_{30}H_{52}O$ for tetrahydrotremulone. Sodium borohydride reduction of tremulone did not yield a crystalline alcohol, but the mixture (of probably epimeric alcohols) had an ultraviolet absorption spectrum (λ_{max} 230, 237 mμ, λ_{infl} 245 mμ) indicating the presence of a conjugated diene (4). On the other hand, no band at 883 cm^{-1} was present in the infrared.

Tetrahydrotremulone was subjected to the Huang-Minlon modification of the Wolff–Kishner reduction and gave a hydrocarbon, $C_{29}H_{52}$ or $C_{30}H_{54}$, m.p. 85°, $[\alpha]_D^{22}$ +25.2°. These constants are in good agreement with those of stigmastane (5, p. 1442S), an authentic specimen of which was therefore prepared from β-sitosterol via β-stigmastanyl acetate and stigmastan-3-one. Both synthetic and natural samples exhibited the same infrared and n.m.r. spectra, their melting points were undepressed on admixture, and their retention times on vapor phase chromatography on two columns of different polarities were identical. On the other hand, the X-ray diffraction patterns of the two hydrocarbons were appreciably different. This, however, may be due to polymorphism; it has been shown (6) that in sterols that exhibit polymorphism the X-ray diffraction pattern depends on the crystal form. That the stigmastane ring system was indeed present was confirmed by a very accurate determination of the molecular weights of tremulone, tetrahydrotremulone, and the hydrocarbon by mass spectrometry (determination kindly performed by Mr. A. Burlingame of M.I.T.). The mass numbers found were 410, 414, and 400, respectively, supporting the molecular formulae $C_{29}H_{46}O$ and $C_{29}H_{50}O$ for the unsaturated ketone and its tetrahydro derivative.

The question of the location of the carbonyl group was considered next. If the presence of a terminal methylene group in tremulone is accepted then the keto group must be present in the side chain as in (A). This is biogenetically unlikely. Also, a study of the n.m.r. spectrum of tremulone indicated the absence of a terminal methylene group. Thus,

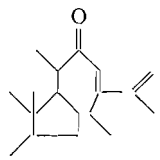

(A)

two signals at 3.9 τ and 4.46 τ in the intensity ratio of 2:1 were observed. These are characteristic of olefinic protons (7). On the other hand, the two-proton absorption was a singlet whereas a multiplet would have been expected for a terminal methylene group (8). The periodate–permanganate oxidation of tremulone was, therefore, reinvestigated but using this time a sample which had been purified by countercurrent distribution. No formaldehyde was detected. This explains the absence of a band at 883 cm^{-1} in the infrared spectrum of the sodium borohydride reduction product of tremulone. Tetrahydrotremulone underwent the Baeyer–Villiger oxidation to give a lactone, $C_{29}H_{50}O_2$, which could be hydrolyzed, but recyclized to the same lactone immediately on treatment with cold dilute mineral acid. The keto group is, therefore, present in a six-membered ring. To determine its position, use was made of the molecular rotations difference method (9). Here difficulties were initially encountered in that, using the values given in Klyne's article (9), the molecular rotation of tetrahydrotremulone was only consistent with its

being a 5-β-7-ketone, implying, therefore, an inversion of configuration at C_5 during the Wolff–Kishner reduction. A search of the literature and calculations made on known 7-ketosteroids reveal that the correct value of M_D for a 5-α-7-one is $-233°$ (10) and not $+223°$ (9). Using this value and $M_D = +102°$ for stigmastane gives $M_D = -131°$ for stigmastan-7-one, in good agreement with the value of $M_D = -126°$ found for tetrahydrotremulone.

The band at 883 cm^{-1} in the infrared spectrum of tremulone itself could be due to a C—H out-of-plane deformation in a system —CH$\overset{cis}{=}$CH—C=CH—C=O (which would also account for the observed ultraviolet and n.m.r. spectrum). Indeed, cholesta-3,5-diene-7-one exhibited a band at 883 cm^{-1} in the infrared and its spectrum was almost superimposable onto that of tremulone. Its n.m.r. spectrum also had two bands at 3.9 τ and 4.5 τ whose relative intensities were 2:1. The band at 3.9 τ is clearly due to the cyclic —CH=CH— protons (11) whereas that at 4.5 τ is due to the —C=CH—C=O proton. There is, therefore, no doubt that tremulone is actually stigmasta-3,5-diene-7-one (I). This compound had already been reported by Marker and Rohrmann (12), who prepared it from β-sitosterol via sitosteryl chloride and 7-ketositosteryl chloride. The only constant given for this compound was its melting point (106–107°). An authentic sample of stigmasta-3,5-diene-7-one has now been synthesized from β-sitosteryl acetate. Chromic acid oxidation gave 7-ketositosteryl acetate, which, on heating with p-toluenesulphonic acid in toluene, gave the required dienone in an overall yield of 10%. It was identical in all respects with tremulone. On selective catalytic reduction it gave stigmastan-7-one (II), identical with tetrahydrotremulone.

At an earlier stage of the investigation, tetrahydrotremulone was reduced with sodium borohydride in boiling ethanol. A single, crystalline alcohol was obtained in good yield and is formulated as stigmastan-7α-ol on the basis of its molecular rotation (+52.8°). Dauben, Blanz, Jiu, and Micheli (13) have studied the methanolic sodium borohydride reduction of cholestan-7-one and obtained a mixture containing the α- and β-epimeric alcohols in the ratio of 73:27. The predominant formation of the axial isomer was attributed to the steric bulk of the solvated borohydride ion, which would hinder its approach from the α-side. In the present case, no β-isomer was isolated; this is undoubtedly due to the even greater bulk of the solvated borohydride ion in ethanol. Catalytic hydrogenation of (II) over platinum oxide gave a mixture of alcohols as a wax; the epimers could not be separated by fractional crystallization or by column chromatography.

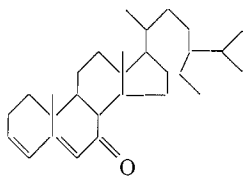

(I)

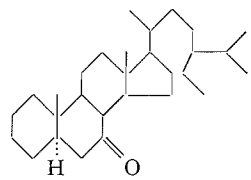

(II)

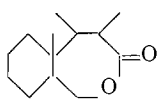

(III)

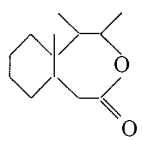

(IV)

Two structures (III or IV) are possible for the seven-membered-ring lactone obtained from the Baeyer–Villiger oxidation of (II). It was expected that (IV) was the more likely structure in view of the known greater ease of migration of tertiary than secondary carbon atoms in this reaction (14). Thus, 7-ketocholestan-3β-ol is oxidized to the lactone arising from migration of C_8 (15). The n.m.r. spectrum supported the assignment of structure (IV) to the lactone, a broad, not clearly resolved, single proton peak being observed at 5.93 τ corresponding to the —CO—O—CH— proton.

Finally, the question arises as to whether tremulone is actually present as such in the heartwood, or, in view of the small quantities in which it is found, whether it is an artifact arising during the isolation process. It is not possible to answer this at the moment. In the case of cholesta-3,5-diene-7-one, which has been isolated from the non-saponifiable fraction of swine spleen, sclerotic aortas, and wool fat, 7-ketocholesterol is considered to be the precursor, the dienone being an artifact (5, p. 2465S). It is known that passing oxygen through aqueous colloidal suspensions of sterols containing the 5-ene-3-ol system gives rise to the 3,7-diol and the 3-ol-7-one (16). Such an oxidation could have taken place in this case during the saponification step, for instance. On the other hand, Mitsui (17) isolated from sugar cane wax a compound in 0.1 to 0.2% yield which he called β-saccharostenone, and to which he assigned the molecular formula $C_{29}H_{48}O$. The melting points of β-saccharostenone (106°), its oxime (163–165°), and its 2,4-dinitrophenylhydrazone (211°) are very close to those found here for tremulone and its derivatives and it is felt that the two steroids are probably the same, though a direct comparison was not possible. It would seem somewhat less likely that up to 0.2% yield of an artifact should be formed under Mitsui's isolation conditions so that it is probable that β-saccharostenone occurs as such in sugar cane wax. It undoubtedly arises in the plant from β-sitosterol, which Mitsui was also able to isolate from the same source.

EXPERIMENTAL

Melting points are uncorrected. Infrared spectra were measured on potassium bromide disks of the compounds using a Perkin–Elmer model 21 instrument using sodium chloride optics. Only the main peaks are reported. Ultraviolet absorption spectra were measured on a Cary Model 14 recording spectrophotometer. The *Populus tremuloïdes* heartwood used in this study came from trees grown in the Prince Albert, Saskatchewan, area and was kindly supplied by Nisbet Plywood Co. Ltd., Prince Albert.

Isolation and Purification of Tremulone

The crude ketone mixture (5 g) obtained by column chromatography of the non-saponifiable fraction of the extractives from *Populus tremuloïdes* heartwood (1) was rechromatographed on a column of alumina (Type H; 200 g). Elution with light petroleum (b.p. 40–60°) gave a hydrocarbon (0.765 g). Elution with light petroleum (b.p. 63–65°) – ether (9:1) gave tremulone (1.483 g). Light petroleum (b.p. 63–65°) – ether (4:1) brought down a brown-red oil (1.280 g) whose infrared spectrum indicated it to be probably an unsaturated ketone. It was not investigated further.

Tremulone was recrystallized from acetone and then from methanol to give pleasant smelling, slightly yellow crystals, m.p. 111°, $[\alpha]_D^{22}$ −273° (chloroform). Repeated recrystallizations did not raise the melting point or alter the rotation. It was finally purified by countercurrent distribution in a 100-tube automatic machine (20 ml each phase), the solvents used being 85% methanol and light petroleum (b.p. 63–65°). After 100 transfers the contents of tubes 81–88 were combined and evaporated, and the ketone recrystallized from aqueous acetone to give pure tremulone, m.p. 111°, $[\alpha]_D^{22}$ −288° (chloroform), λ_{max} 278 mμ, ϵ 20,000 (in ethanol). (Found: C, 84.81, 84.83, 84.64; H, 11.30, 11.34, 11.91; mol. wt., 428 (Rast), 410 (mass spec.). Calc. for $C_{29}H_{46}O$: C, 84.81; H, 11.29; mol. wt., 411.) Infrared spectrum: 1660, 1630, 1603, 1390, 1375, 883 cm^{-1}. The *2,4-dinitrophenylhydrazone* separated from ethanol, and was purified by chromatography on a very short column of alumina (Woelm, neutral; Brockman activity III) and recrystallization from chloroform–ethanol. It had m.p. 211°, λ_{max} 395 mμ (in chloroform). (Found: C, 70.96, 71.45; H, 8.37, 8.31; N, 9.14. Calc. for $C_{35}H_{50}O_4N_4$: C, 71.15; H, 8.53; N, 9.48.) The *oxime* was recrystallized twice from aqueous ethanol and had m.p. 169° (decomp.).

Sodium Borohydride Reduction of Tremulone

Tremulone (147 mg), sodium borohydride (211 mg), and 95% ethanol (20 ml) containing a drop of 2 *N* sodium hydroxide were boiled under reflux for 5 hours. An excess of acetone was then added and the mixture was distilled on a steam bath. It was then extracted with chloroform and the extract washed with dilute mineral acid, dried, and evaporated to give a wax (140 mg). This did not crystallize even after chromatography on alumina. Its ultraviolet spectrum (in ethanol) had λ_{max} 230, 237 mμ, λ_{infl} 245 mμ.

Selective Catalytic Reduction of Tremulone—Stigmastan-7-one (Tetrahydrotremulone)

Tremulone (300 mg) in 95% ethanol (200 ml) was hydrogenated at atmospheric pressure and room temperature over 10% palladium-on-charcoal catalyst (50 mg) for 24 hours, when 2 molar equivalents of hydrogen were taken up. Filtration and evaporation gave *stigmastan-7-one*, which was recrystallized from aqueous ethanol and obtained as white needles (220 mg), m.p. 98–99°, $[\alpha]_D^{22}$ −30.3° (chloroform). (Found: C, 83.65, 83.53, 84.07; H, 11.90, 12.35, 11.96; mol. wt., 414 (mass spec.). Calc. for $C_{29}H_{50}O$: C, 83.99; H, 12.15; mol. wt., 414.7.) Infrared spectrum: 1705, 1385, 1375 cm^{-1}. The *2,4-dinitrophenylhydrazone*, purified as above, gave yellow needles, m.p. 188–189°. (Found: C, 70.63; H, 8.98. Calc. for $C_{35}H_{54}O_4N_4$: C, 70.67; H, 9.15.)

Wolff–Kishner Reduction of Tetrahydrotremulone—Stigmastane

Tetrahydrotremulone (126 mg), triethylene glycol (10 ml), hydrazine hydrate (3 ml, 99–100%), and potassium hydroxide (2 pellets) were boiled under reflux for 4 hours, and then distilled until the temperature of the vapors reached 195°. The solution was boiled under reflux for another 6 hours, diluted with water, and extracted with ether. The dried ($MgSO_4$) ether extract was evaporated and the residual oil was chromatographed on a column of Woelm neutral alumina (10 g) (Brockman activity III) and eluted with light petroleum (b.p. 63–65°). The product was sublimed under vacuum and then recrystallized from chloroform–ethanol to give stigmastane (80 mg), m.p. 85°, $[\alpha]_D^{22}$ +25.2° (chloroform), identical (m.p., mixed m.p., infrared and n.m.r. spectra) with the stigmastane prepared from β-sitosterol as described below. (Found: C, 86.54; H, 12.88. Calc. for $C_{29}H_{52}$: C, 86.92; H, 13.08.)

Stigmastane from β-Sitosterol

3-β-Stigmastanyl acetate (500 mg) (18) was hydrolyzed with 3% methanolic potassium hydroxide to give 3-β-stigmastanol, m.p. 136–137°,[$\alpha]_D^{22}$ +24° (chloroform). This was oxidized to stigmastan-3-one (m.p. 155°, $[\alpha]_D^{22}$ +38° (chloroform)) (Ives and O'Neill (18) give m.p. 156–157°, $[\alpha]_D$ +37°) with chromic acid in acetic acid, and the ketone reduced by the Wolff–Kishner method (Huang-Minlon modification) as described above for stigmastan-7-one. The stigmastane so obtained had m.p. 84–85°, $[\alpha]_D^{22}$ +25° (chloroform), in good agreement with the literature values (5, p. 1442S).

The synthetic and "natural" hydrocarbon were each subjected to vapor phase chromatography on two columns of differing polarities: (*a*) a 2½-ft SE-30 on glass beads (0.5% w/w) column operated at 220° and a helium inlet pressure of 30 p.s.i.; (*b*) a 12-ft ethylene glycol succinate polyester on glass beads (0.5% w/w) column operated at 220° and a helium inlet pressure of 25 p.s.i. Anthracene was used as an internal standard. The synthetic and the "natural" hydrocarbon were chromatographically indistinguishable on either column.

Baeyer–Villiger Oxidation of Tetrahydrotremulone

Tetrahydrotremulone (100 mg) in glacial acetic acid (1 ml) was treated with 10% peracetic acid in acetic acid (3 ml) and *p*-toluenesulphonic acid (15 mg), and the mixture kept in the dark at room temperature for 3 days. Water was added and the solid which precipitated was filtered and recrystallized from methanol to give the *lactone* (90 mg), m.p. 140°. (Found: C, 80.60; H, 11.75. Calc. for $C_{29}H_{50}O_2$: C, 80.87; H, 11.70.)

The lactone (50 mg) was boiled under reflux with an excess of 20% aqueous potassium hydroxide for 2 days, during which time an oil separated. On shaking the mixture with ether three layers formed. The ether layer contained very little starting material. The two bottom layers were extracted with chloroform (in which the oil dissolved), the chloroform was dried ($MgSO_4$) and evaporated, leaving behind a yellow solid whose infrared spectrum indicated the presence of an OH group and a —COO^- (characteristic broad band at ca. 1600 cm^{-1}). When this solid was treated with dilute acid the lactone was recovered.

Sodium Borohydride Reduction of Tetrahydrotremulone—Stigmastan-7α-ol

Tetrahydrotremulone (50 mg) in absolute ethanol (10 ml) containing a drop of 2 *N* sodium hydroxide was boiled under reflux and sodium borohydride (25 mg) in ethanol (5 ml) was added over a period of ½ hour. The mixture was boiled for a further 2 hours and then allowed to stand at room temperature overnight. Hydrochloric acid (5%; 2 ml) was added, the mixture was warmed for 5 minutes, and water (25 ml) was added. The ethanol was removed in a stream of air and the residual solution extracted with chloroform. The chloroform extract was washed with aqueous sodium carbonate and filtered through a short column of alumina. The product was recrystallized from acetone to give *stigmastan-7α-ol* (30 mg) as white flakes, m.p. 112°, $[\alpha]_D^{22}$ +12.7° (chloroform) (transparent in the ultraviolet). (Found: C, 83.48; H, 12.85. Calc. for $C_{29}H_{52}O$: C, 83.58; H, 12.58.)

7-Keto-β-sitosteryl Acetate

β-Sitosteryl acetate (500 mg), in glacial acetic acid (10 ml) containing sodium acetate (400 mg), was warmed to 60°, and chromic anhydride (400 mg) added over a period of ½ hour. The solution was warmed for another 4½ hours, diluted with water (10 ml), and the precipitated solid washed with water. The combined filtrates were treated with ethanol and extracted with chloroform. The chloroform extract was washed with aqueous sodium carbonate solution and then with water, dried ($MgSO_4$), and evaporated. The residue was combined with the solid that had precipitated before and was chromatographed on alumina (25 g). Elution with light petroleum (b.p. 40–60°) – ether (9:1) gave unchanged β-sitosteryl acetate (170 mg). Elution with light petroleum (b.p. 40–60°) – ether (1:1) gave 7-keto-β-sitosteryl acetate (183 mg), which was used as such in the next stage. Elution with ether–methanol (1:1) gave β-sitosterol (120 mg).

Stigmasta-3,5-diene-7-one

A mixture of 7-keto-β-sitosteryl acetate (183 mg), *p*-toluenesulphonic acid (150 mg), and toluene (5 ml) was boiled under reflux for 2 hours (solution turned dark brown). The mixture was dissolved in ether and the solution washed with aqueous sodium carbonate solution, then with water, and evaporated to dryness at 80°. The oil thus obtained was chromatographed on alumina to give stigmasta-3,5-diene-7-one (45 mg), m.p. 109°, identical in every respect with tremulone.

ACKNOWLEDGMENTS

This work was carried out during the tenure (by R. G. M.) of a National Research Council Studentship (1961–1962), and was supported financially by a generous grant from the Saskatchewan Research Council. The authors also wish to express their gratitude to Mr. A. L. Burlingame (M.I.T.) for the mass spectroscopic determinations, to Dr. O. E. Edwards (N.R.C.) for some of the n.m.r. spectra, and to Mr. W. Larson for the X-ray diffraction photographs, as well as to Dr. R. Altschul for a sample of 7-ketocholesterol.

REFERENCES

1. R. A. Abramovitch, R. G. Micetich, and S. J. Smith. In press.
2. E. Müller. Methoden der organischen chemie. Band III. Teil 2. Georg Thierne Verlag, Stuttgart. 1955. p. 675.
3. L. Dorfman. Chem. Revs. **53**, 47 (1953).
4. M. C. Dawson, T. G. Halsall, and R. E. H. Swayne. J. Chem. Soc. 590 (1953).
5. Elsevier's Encyclopaedia of organic chemistry. Vol. 14S. Part 3. Springer-Verlag. 1959.
6. J. Parsons, W. T. Beher, and G. D. Baker. Anal. Chem. **28**, 1514 (1956).
7. H. Conroy. Advances in organic chemistry. Vol. II. Interscience Publishers, Inc., New York. 1960. p. 289.
8. N. S. Bhacca, L. F. Johnson, and J. N. Shoolery. High resolution NMR spectra catalog. Varian Associates, Palo Alto. 1962. Nos. 62, 64, 65.
9. W. Klyne. *In* Determination of organic structures by physical methods. Academic Press, Inc., New York. 1955. p. 108.
10. D. H. R. Barton and W. Klyne. Chem. & Ind. (London), 755 (1948).
11. R. R. Fraser. Can. J. Chem. **40**, 78 (1962).
12. R. E. Marker and E. Rohrmann. J. Am. Chem. Soc. **62**, 516 (1940).
13. W. G. Dauben, E. J. Blanz, Jr., J. Jiu, and R. Micheli. J. Am. Chem. Soc. **78**, 3752 (1956).
14. W. Von E. Doering and L. Speers. J. Am. Chem. Soc. **72**, 5515 (1950).
15. H. Heusser, A. Segre, and Pl. A. Plattner. Helv. Chim. Acta, **31**, 1183 (1948).
16. S. Bergstrom. J. Biol. Chem. **145**, 327 (1942). S. Bergstrom and O. Wintersteiner. J. Biol. Chem. **141**, 597 (1941). W. Wunderlich. Z. physiol. Chem. Hoppe-Seyler's, **241**, 115 (1936). G. A. D. Haslewood. Biochem. J. **36**, 389 (1942).
17. T. Mitsui. J. Agr. Chem. Soc. Japan, **15**, 526 (1939).
18. D. A. J. Ives and A. N. O'Neill. Can. J. Chem. **36**, 434 (1958).

OXIMES

II. THE INFRARED SPECTRA OF SOME COMPLEX OXIMES[1]

J. J. NORMAN
Defence Research Chemical Laboratories, Ottawa, Canada

Received May 14, 1962

ABSTRACT

The infrared spectra of several ω'-substituted *p*-alkyl- and *p*-alkoxy-2-oximinoacetophenones were investigated. When the ω'-substituent was the dimethylamino group, the spectra were incompatible with a simple α-ketooxime structure. The spectra of these dimethylamino compounds showed a diffuse absorption with broad peaks at 2500 and 1850 cm^{-1}. The hydroxyl band at 3150 cm^{-1} and the dimethylamino doublet at 2820 and 2770 cm^{-1} had nearly disappeared while the carbonyl and N—O frequencies had undergone large shifts. The spectra are best interpreted in terms of a zwitterion carrying a novel anion. The structure of this anion is considered.

A series of oximes with the general structures I and II was prepared. During the syntheses, infrared spectra were obtained routinely to identify the various products

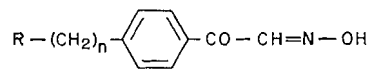

I

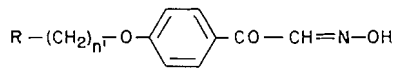

II

n = 1, 3, 4
a: R = $(CH_3)_2N$—
b: R = $I^-.(CH_3)_3\overset{+}{N}$—

n' = 2, 3, 4, 5
a: R = Cl—
b: R = $(CH_3)_2N$—
c: R = $I^-.(CH_3)_3\overset{+}{N}$—

obtained and, in some instances, it was found that spectra were incompatible with the structures shown above.

EXPERIMENTAL

The syntheses of the various compounds used in this study have been described elsewhere (1).

All spectra were obtained with 1–1.5% suspensions of the oxime in potassium bromide, pressed into disks. The spectra were obtained with a Baird Model AB-1 double-beam recording infrared spectrophotometer, which was calibrated daily to an accuracy of ± 5 cm^{-1} at 3060 cm^{-1} and ± 15 cm^{-1} at 700 cm^{-1}. No attempt was made to obtain quantitative intensity data, and band positions, quoted to the nearest 5 cm^{-1}, are listed in Table I.

DISCUSSION

Simple oxime spectra exhibit an OH band at 3115-3300 cm^{-1}, a C=N band at about 1640 cm^{-1}, and an N—O band at 950–990 cm^{-1} (2–4). Similarly, various acetophenones

[1]*Issued as D.R.C.L. Report No. 378.*
Presented in part before the 5th Western Regional Conference of the CIC, Regina, 1960.

TABLE I

Group frequencies of some substituted 2-oximinoacetophenones and related compounds

Compound type	Frequency range (cm^{-1})								
		—N(CH_3)		Zwitterion					
	—OH	ν_1	ν_2	ν_1	ν_2	—C=O	—C=N—	—N—O—	Other
2-Oximinoacetophenone	3290 s	—	—	—	—	1670 s	1650 i	985 s	—
p-(ω′-Dimethylaminoalkyl)-acetophenones	—	2900–2820 w	2810–2760 m	—	—	1675 vs	—	—	—
p-(ω′-Chloroalkoxy)-2-oximinoacetophenone	3350–3125 s	—	—	—	—	1675–1660 vs	—	985–975 s	—
p-(ω′-Dimethylaminoalkyl)-2-oximinoacetophenone	—	—	—	2525–2500 m	1925–1825 w	1630–1625 vs	—	1050–1030 s	—
p-(ω′-Dimethylaminoalkoxy)-2-oximinoacetophenone	—	—	—	2560–2480 m	1900–1845 w	1625–1620 vs	—	1030–1010 s	—
ω-Dimethylaminoalkan-3-oximino-2-ones	—	—	—	2520–2500 m	1890–1880 w	1655 s	—	1050–1040 m–s	—
p-(ω′-Trimethylammoniumalkyl)-2-oximinoacetophenone iodide	3160–3125 s	—	—	—	—	1670–1665 s	1640 i	995–975 m	
p-(ω′-Trimethylammoniumalkoxy)-2-oximinoacetophenone iodide	3195–3125 ms	—	—	—	—	1670–1660 m	1045 i	985–970 m	
p-(3′-Dimethylammoniumpropyl)-2-oximinoacetophenone chloride	3115 vs	—	—	—	—	1650 s	—	1010 vs	$\overset{+}{\text{N}}$—H 2685 vs
p-(3′-Dimethylaminopropyl)-2-oximino-acetophenone salt									
Sodium salt of keto form	—	2835 w	2780 m	—	—	1630 s	—	1040 vw	—
Sodium salt of enol form	—	2830 w	2770 m	—	—	1655 w	—	—	—N=O 1550 s
p-Dimethylamino-2-oximinoacetophenone	3200 m	2905 w	2860 m	—	—	1610 m	—	985 m	—
p-Trimethylammonium-2-oximinoaceto-phenone iodide	3160 s	—	—	—	—	1690 s	1645 m	975 s	—

NOTE: w = weak intensity, m = medium intensity, s = strong intensity, vs = very strong intensity, i = inflection.

show a C=O band in the region 1660–1685 cm^{-1} (5). These absorptions are exhibited by 2-oximinoacetophenone, whose spectrum has maxima at 3290 cm^{-1} (OH), 1670 cm^{-1}, (C=O), and 985 cm^{-1} (N—O). Absorption by C=N apparently is masked by that of C=O, although it was noted that an inflection is present on the low-frequency side of the carbonyl band. This shows the positions where one would expect absorption for compounds containing the structure III. On this basis, then, one would expect the spectra

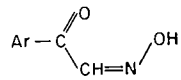

III

of the compounds of the two series I and II to show absorption bands in the above positions, perhaps with minor shifts of position, plus the bands characteristic of the para substituent.

The spectra of the *p*-(ω'-chloroalkoxy)-2-oximinoacetophenones (II*a*: $n' = 3, 4, 5$) exhibited O—H absorption at 3125–3350 cm^{-1}, N—O absorption at 975–985 cm^{-1}, and C=O absorption at 1660 cm^{-1}, while that of C=N appeared to be buried under the C=O peak. These spectral features then indicate that the structure III is present in these molecules.

When the substituent R was the dimethylamino group (I*a*, II*b*), the spectra were vastly different. Dimethylamino compounds normally exhibit a doublet at 2825 and 2775 cm^{-1} arising from the asymmetric and symmetric C—H stretching vibrations of the N—$(CH_3)_2$ group (6), analogous to those of the C—CH_3 and O—CH_3 groups (7, 8). In the present work, this doublet was observed at slightly varying frequencies, 2900–2820 cm^{-1} for the higher and 2810–2760 cm^{-1} for the lower band, with the parent compounds for the series I*a*, the *p*-(ω'-dimethylaminoalkyl)-acetophenones. For the oximes themselves (I*a*: $n = 1, 3, 4$; II*b*: $n' = 2, 3, 4, 5$), this doublet was missing and the O—H peak was greatly reduced in intensity. A diffuse absorption area in the region 3100–1700 cm^{-1}, with broad peaks at approximately 2500 and 1850 cm^{-1}, had appeared. Such a phenomenon had been noted in the spectra of amino acids and is attributed to zwitterion formation (9, 10). Bellamy (11, Ch. 13) ascribes these peaks to N^+—H groupings. Similar broad peaks have been noted (17, 18) in the spectra of isonicotinic, quinaldic, and cinchoninic acids and have been ascribed to *very strong* hydrogen bonding between carbonyl hydrogen and the ring hetero nitrogen atom.

Because the dimethylamino group is much more basic than the oximate ion, it is felt that the proton has been transferred to nitrogen and intact dimethylamino and oximino groups are not present in the molecule but are involved in the formation of a zwitterion such as IV. A very strongly hydrogen bonded structure is, however, also compatible with the spectral data but is thought to be much less likely than the zwitterion.

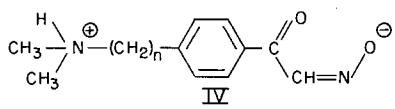

IV

A closer inspection of the spectra indicated the zwitterion to be more complex than this. The N—O band, normally at 950–990 cm^{-1}, has shifted to 1030–1050 cm^{-1}, an effect opposite to that expected for loss of the proton from the N—OH portion of the molecule.

At the same time, the carbonyl group frequency has shifted from the normal position of 1670 cm^{-1} in aromatic α-ketooximes to 1630 cm^{-1}. These are incompatible with a simple enolizing of the anion, where one would expect the disappearance of the C=O band and the appearance of an N=O band at 1570–1590 cm^{-1} (12). The observed effects, however, do agree with a resonance hybrid where carbonyl loses and N—O acquires double-bond character, as in V, although the C=O shift of about 40 cm^{-1} is quite large. It has been

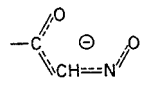

V

reported recently (without experimental details) that with α-oximino esters a very stable pseudoaromatic ring system is formed involving the ester carbonyl and the oximino group (16), which results in a lowering of the carbonyl frequency. It is possible to draw a tautomeric structure, VI, of the anion of IV in which a similar ring system is implicit.

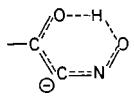

VI

This would be highly unstable as it requires carbon to become the site of negative charge. Formation of the ring system, however, would greatly assist stabilization and might, in large measure, overcome the inherent instability of such an anion. While such a structure could explain the lowering of the carbonyl frequency of these oximinoacetophenones, it is much less probable than the resonance hybrid V.

That the aromatic ring is not involved in these end group interactions is shown by the spectra of the aliphatic compounds 5-dimethylamino-3-oximino-2-oxopentane and 6-dimethylamino-3-oximino-2-oxohexane. The spectra of these compounds exhibited at 2500 and 1890 cm^{-1} the zwitterion doublet previously described. The hydroxyl and dimethylamino group absorptions were missing, and the carbonyl group frequency was at 1655 cm^{-1}, an abnormally low value for an aliphatic ketone (11, pp. 134–136). The N—O band was at 1050 cm^{-1}, a higher frequency than expected for an aliphatic oxime (3).

To show that the spectra observed for compounds of the series I*a* and II*b* arise from zwitterion formation, the basicity of the amine function was destroyed by quaternization. The amino group now carries a formal positive charge, resembling closely the dimethylammonium group postulated for the zwitterion. The inductive effects of the positively charged nitrogen, therefore, are unchanged but proton abstraction from the oximino group no longer can occur and no zwitterion can form. The spectra of these methiodide salts show a hydroxyl peak at 3150 cm^{-1}, carbonyl absorption at 1670 cm^{-1}, and the N—O bond is at 985 cm^{-1}, all conforming to the structure III for the ketooxime portion of the molecule. The absorptions at 2500 and 1850 cm^{-1} have disappeared. These peaks then must be characteristic of the zwitterion rather than of charged nitrogen since this latter is still present.

As a further test, *p*-(3′-dimethylaminopropyl)-2-oximinoacetophenone was converted to the sodium salt and to the hydrochloride salt. The spectra of these salts were quite different from that of the parent compound. The spectrum of the sodium salt exhibited

no hydroxyl absorption, the dimethylamino doublet was present at 2835 and 2780 cm^{-1}, while the carbonyl band was present at 1630 cm^{-1}, just resolved from the strong peak at 1610 cm^{-1} arising from aromatic ring vibrations. This low-frequency position of the carbonyl peak would indicate an increase in the amount of single-bond character of this bond. The N—O band, at 1030 cm^{-1} in the zwitterion, was greatly reduced in intensity. Two peaks of medium intensity, however, were observed at 1155 and 885 cm^{-1} and could arise from N—O^- bond vibrations but, because of lack of spectral data on other compounds containing such a bond, no assignments will be made. The spectrum of the hydrochloride salt featured a strong hydroxyl peak at 3115 cm^{-1}, a carbonyl peak at 1650 cm^{-1}, and N—O absorption at 1010 cm^{-1}. The dimethylamino doublet was obscured by the hydroxyl peak but a single intense peak was noted at 2685 cm^{-1}, and is ascribed to the N^+—H structure.

These spectra then indicate the structures VII and VIII for the sodium and hydrochloride salts.

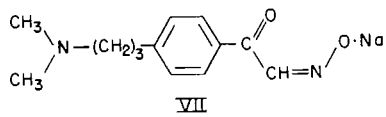

VII

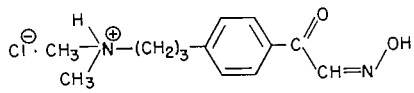

VIII

In connection with the work on the sodium salt, an interesting phenomenon was noted. After recording the spectrum of the salt, the KBr disk was heated, inadvertently, to 50° C. On re-examination, this disk yielded a spectrum which would indicate that the material had undergone an isomerization. The dimethylamino doublet was unaffected, but the carbonyl peak was greatly reduced in intensity and a new band had appeared at 1550 cm^{-1}. This spectral behavior is in accord with loss of a carbonyl group and formation of an N=O bond in the molecule and would suggest that the canonical form of V, IX*a*,

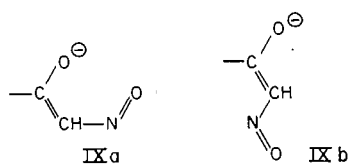

IXa IXb

makes a large contribution to the structure of the anion. This would be further stabilized by shifts in position of the skeletal atoms so that the nitroso oxygen is remote from the enol oxygen, as in IX*b*. This isomerization did not reverse on cooling. A repeat of this work in which the material was heated to 50° C before presssing into a pellet yielded a spectrum identical with that obtained when the KBr disk was heated. That this was an isomerization and did not arise from replacement of sodium ion by potassium ion from the pelleting material was shown by the fact that the potassium salt of the oxime underwent a similar isomerization when heated. On acidification, both carbonyl and nitroso forms of the sodium salt regenerated the original oxime.

It should be mentioned that the peaks at 1155 and 885 cm^{-1} in the spectrum of the keto form of the sodium salt became much less intense in that of the enol form. This would support their assignment to the N—O^- structure.

To test the conditions under which zwitterion formation occurs, an oxime was synthesized in which the basicity of the amine function was lowered but not destroyed. The pK_a of dimethylaminoalkanes is 10.0 (13) but that of dimethylaniline is 5.1 (14). This latter value is much lower than the pK_a of the oxime function in 2-oximinoacetophenones, 8.25 (15), and it would be expected that X would not undergo zwitterion formation. Its

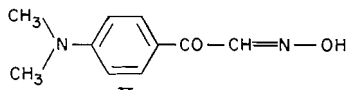

X

spectrum, then, in contrast to the spectra of the *p*-(ω'-dimethylaminoalkyl)-2-oximinoacetophenones, would not be expected to exhibit the zwitterion peaks and, indeed, such peaks were not observed experimentally. This spectrum, however, is different from that of other 2-oximinoacetophenones which are not in the zwitterion form, for the carbonyl and hydroxyl band intensities are very weak. In addition, the carbonyl band is at the abnormally low position of 1610 cm^{-1}. The dimethylamino doublet at 2905 and 2860 cm^{-1} (very poorly resolved) and the N—O band at 985 cm^{-1} are in their normal positions. These features are indicative of an interaction between the hydroxyl and carbonyl groups and of no particular change in the N—O portion of the molecule.

It can be seen that in compound X, the dimethylamino group is conjugated through the benzene ring with the carbonyl group. The mesomeric interaction of these two groups will lead to a partial negative charge on the keto oxygen, as in XI, which will greatly

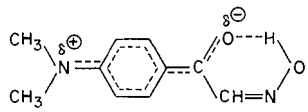

XI

facilitate hydrogen bonding of the OH and C=O groups, hence leading to the much reduced intensities observed for these two absorptions. The very large shift in position of the carbonyl band from its normal position of 1680–1670 cm^{-1} in oximinoacetophenones to 1610 cm^{-1} shows the combined effects of mesomerism with the dimethylamino group and the increased hydrogen bonding with the hydroxyl group. The weak hydroxyl peak is consistent with an intramolecular rather than an intermolecular hydrogen bond, since the latter increases the OH band intensity (11, p. 99).

The fact that the broad bands at 2500 and 1850 cm^{-1} are not observed with this compound cannot be taken as unequivocal proof that these bands in the spectra of other *p*-(ω'-dimethylamino-alkyl and -alkoxy)-2-oximinoacetophenones arise because of zwitterion formation and are not the result of a very tight hydrogen bond. One might not expect evidence for hydrogen bonding to nitrogen in the spectrum of X, since the oximino hydrogen is already involved in a very strong intramolecular hydrogen bond to carbonyl oxygen.

Upon quaternization of X, there can be no mesomeric interaction between the carbonyl and amino nitrogen functions because the free electron pair of the latter has been lost

The enhanced hydrogen bonding between the hydroxyl and carbonyl groups observed for X now should be suppressed and the spectrum of the resulting *p*-trimethylammonium-2-oximinoacetophenone iodide should show normal hydroxyl and carbonyl absorption. In actual fact, the major absorption bands, hydroxyl at 3160 cm^{-1}, carbonyl at 1690 cm^{-1}, and N—O at 975 cm^{-1}, all lie within the ranges normal for simple 2-oximinoacetophenones. The unusual feature of this spectrum is the presence of a small peak on the low-frequency side of the carbonyl peak. This band at 1640 cm^{-1} probably arises from the C=N linkage. Because of the strong inductive effect of the trimethylammonium portion of the molecule, the polarization of the carbonyl group has shifted the carbonyl frequency high enough for the C=N band to be resolved, rather than appearing as a shoulder.

SUMMARY

The incorporation of a highly basic dimethylamino group into an α-ketooxime molecule results in the formation of a zwitterion incorporating a novel anion. Quaternization results in loss of ability to form the zwitterion and the placement of a formal positive charge upon the amino nitrogen. The spectra of these quaternized compounds are quite different from those of the dimethylamino compounds, which also are considered to carry such a charge on the amino nitrogen. The basicity of the amino group was decreased so that no zwitterion formed, but in such a way that a charge was induced upon the carbonyl oxygen by a mesomeric effect. This resulted in formation of a hydrogen-bonded structure of the ketooxime which showed several of the spectral features associated with the zwitterion previously produced. Changes resulting in a suppression of the polarization of the carbonyl group resulted in the loss of these spectral features and the spectra resembled those of simple oximes. Sodium salts of these oximes were shown to undergo an interesting isomerization.

REFERENCES

1. J. J. Norman, R. M. Heggie, and J. B. Larose. Can. J. Chem. **40**, 1547 (1962).
2. A. Palm and H. Werbin. Can. J. Chem. **31**, 1004 (1953); **32**, 858 (1954).
3. S. Califano and W. Luttke. Z. physik Chem. (Frankfurt), **6**, 83 (1956).
4. G. Duyckaerts. Bull. soc. roy. sci. Liège, **21**, 196 (1952).
5. H. W. Thompson and P. Torkington. J. Chem. Soc. 640 (1945).
6. R. D. Hill and G. D. Meakins. J. Chem. Soc. 760 (1958).
7. J. J. Fox and A. E. Martin. Proc. Roy. Soc. (London), A, **175**, 208 (1940).
8. S. A. Francis. J. Chem. Phys. **19**, 942 (1951).
9. H. W. Thompson, D. Nicholson, and L. N. Short. Discussions Faraday Soc. **9**, 222 (1950).
10. J. T. Edsall and H. Scheinberg. J. Chem. Phys. **8**, 520 (1940).
11. L. J. Bellamy. The infra-red spectra of complex molecules. 2nd ed. Methuen and Co. Ltd., London. 1958.
12. W. Luttke. J. phys. radium, **15**, 633 (1954).
13. J. Hanson. Svensk Kem. Tidskr. **67**, 256 (1955).
14. N. F. Hall and M. R. Sprinkle. J. Am. Chem. Soc. **54**, 3469 (1932).
15. A. L. Green and B. Saville. J. Chem. Soc. 3887 (1955).
16. H. Reinheckel. Monatsber. deut. Akad. Wiss. Berlin, **1**, 42 (1959).
17. J. T. Braunholtz *et al.* J. Chem. Soc. 868 (1959).
18. J. T. Braunholtz and F. G. Mann. J. Chem. Soc. 3368 (1958).

NOTES

THE PREPARATION AND INFRARED AND N.M.R. SPECTRA OF MONODEUTERATED PYRIDINE AND 3-PICOLINE

R. A. Abramovitch, D. J. Kroeger, and B. Staskun

In connection with other studies it was of interest to get an estimate of the relative ground-state π-electron densities at the 2- and 6-positions of 3-picoline and its complex with a simple metallic salt. Smith and Schneider (1) recently estimated the charge distribution in pyridinium ion, assuming a simple proportionality between the proton resonance displacement and the electron charge deficiency on the carbon atom to which the proton is bonded. 3-Picoline-2*d*, 3-picoline-6*d*, and their zinc chloride complexes have been prepared and their n.m.r. and infrared spectra compared.

Bak, Hansen, and Rastrup-Andersen (2) obtained pyridine-2*d* by the action of zinc dust and sulphuric acid-d_2 on 2-bromopyridine. It was prepared more conveniently here from 2-pyridyllithium and deuterium oxide. Preliminary experiments indicated that there was no loss of deuterium when the pyridine-2*d* was extracted with mineral acid instead of being isolated as the mercuric chloride complex. This is in agreement with the recent finding by Katritzky and Ridgewell (3) that pyridine is very resistant to proton exchange. In the same way, 3-picoline-2*d*, 3-picoline-6*d*, and the corresponding tritiated compounds were obtained (the latter by using tritiated water).

The n.m.r. spectra were run in acetonitrile solutions of the compounds, due to the limited solubility of the zinc chloride complexes in carbon tetrachloride and to interference by chloroform when it was used. The results are summarized in Table I. The accuracy is ± 2 cycles/sec.

TABLE I

N.M.R. spectra (at 60 Mc/s) of deuterated picolines and their zinc chloride complexes (solutions in acetonitrile; band positions in cycles/sec from tetramethylsilane as internal standard; no solvent corrections applied)

	H_2, H_6	H_4	H_5	CH_3
3-Picoline	504	450	430	136.6
(3-Picoline)$_2$–$ZnCl_2$	515	475	452.5	143.5
3-Picoline-2*d*	502 (H_6)	450	429.5	135.5
(3-Picoline-2*d*)$_2$–$ZnCl_2$	509.5	475.5	451.2	143.5
3-Picoline-6*d*	504.5 (H_2)	451.5	431.5	136.0
(3-Picoline-6*d*)$_2$–$ZnCl_2$	508	472	449	140.5

In the case of 3-picoline (unlike that of myosmine (4)) and its zinc chloride complex the signals for the 2- and 6-protons overlap and no resolution is possible at 60 Mc/s. The shift between these two protons is seen to be +2.5 cycles/sec from the spectra of 3-picoline-6*d* and 3-picoline-2*d* respectively. From these values, the differences in π-electron densities are estimated to be very small. Complexing, as expected, gives rise to appreciable changes in chemical shift, particularly at the β- and γ-protons. The corresponding shift to lower field of the α-proton is appreciably smaller. This is probably due

to the change in the paramagnetic contribution of the nitrogen atom on complexing. Some "back-bonding" from the zinc chloride might also account for the smaller shift, though in this case one would have expected it to affect the γ- more than the α-protons (5). No clear indication of the relative ground-state π-electron densities at C_2 and C_6 may be obtained from these measurements.

The infrared spectrum of pyridine (6), its zinc chloride complex (7), and pyridine-2*d* (2) have been reported and analyzed. The spectra of (pyridine-2*d*)$_2$–$ZnCl_2$, 3-picoline, (3-picoline)$_2$–$ZnCl_2$, 3-picoline-2*d*, (3-picoline-2*d*)$_2$, 3-picoline-6*d*, and (3-picoline-6*d*)$_2$–$ZnCl_2$ were determined and exhibited no unexpected features. The main bands only are listed in Table II for the zinc chloride complexes.

TABLE II

Infrared spectra of zinc chloride complexes of some pyridine derivatives (as Nujol mulls)

(Pyridine)$_2$ –$ZnCl_2$	(Pyridine-2*d*)$_2$ –$ZnCl_2$	(3-Picoline)$_2$ –$ZnCl_2$	(3-Picoline-2*d*)$_2$ –$ZnCl_2$	(3-Picoline-6*d*)$_2$ –$ZnCl_2$
1609	1602	1612	1600	1604
			1590 (sh)	1575
1488		1480		
1452	1440		1410	1420 (sh)
	1304			1302
1218		1199	1206	1231
1067	1065	1130	1135	1137
1044	1042	1100		
1015	1010	1060		1060
				925 (w)
	901		915	910
	810 (sh)		815 (w)	850
	802		796	819
757	754	784	777 (w)	
			718 (w)	717 (w)
686		693		

An interesting difference was observed between the C—D stretching vibration frequencies of 3-picoline-2*d* and 3-picoline-6*d* (liquid films). Thus, whereas 3-picoline-2*d* exhibited a band at 2244 ± 2 cm^{-1}, the corresponding band for 3-picoline-6*d* was at 2259 ± 2 cm^{-1}. This difference reflects a slightly greater force constant for the C_6—D bond and probably indicates that C_2 is slightly less electronegative than C_6, in accord with simple predictions based on the generally accepted positive inductive effect of the methyl substituent.

EXPERIMENTAL

Deuterium analyses are by J. Nemeth, Urbana, Illinois.

Pyridine-2d

2-Bromopyridine (82 g, redistilled) in ether (10 ml) was added over a period of 10 minutes to a stirred solution of butyllithium (from 8.5 g lithium and 68 g butyl bromide in 250 ml of dry ether) at ca. −60° and stirring was continued for another 5 minutes. To the dark orange solution was added deuterium oxide (20 g, 99.7%) dropwise during 5 minutes and the temperature maintained at about −55° while the mixture was stirred. The stirred suspension was then allowed to reach room temperature. Water (100 ml) was added and then potassium hydroxide pellets to make the solution strongly alkaline, and the product was extracted repeatedly with ether. At this point the ether solution could be treated with a solution of mercuric chloride (200 g) in water (1 l.) to precipitate the mixture of complexes of pyridine-2*d* and 2-bromopyridine (containing some unreacted butyl bromide) according to the procedure of Bak *et al.* (2). Alternatively, and more conveniently, the reaction product which had been treated with water was added to a cooled solution of dilute hydrochloric acid (700 ml), extracted with ether to remove unchanged butyl bromide, the acid layer made strongly alkaline with potassium hydroxide and extracted repeatedly with ether. The dried (KOH)

ether extract was evaporated and the residue distilled to give crude pyridine-2*d*, b.p. 100–130°, followed by 2-bromopyridine (25 g), b.p. 192–194°. The crude pyridine-2*d* fraction was dried and distilled from potassium hydroxide pellets to give pure pyridine-2*d* (9.5 g), b.p. 113–114°. (Found: atom%×D, 18.80. Calc. for C_5H_4DN: 20.) No diminution in deuterium content occurred when the compound was boiled with dilute hydrochloric acid, or kept in hydrochloric acid solution at room temperature for 3 months.

3-Picoline-2d

Prepared similarly from 2-bromo-3-methylpyridine (4.4 g), it was obtained as a colorless liquid (1.1 g), b.p. 141–142°. (Found: atom%×D, 11.67. Calc. for C_6H_6DN: 14.2.)

3-Picoline-6d

It was obtained in 61% yield from 2-bromo-5-methylpyridine. (Found: atom%×D, 11.65. Calc. for C_6H_6DN: 14.2.)

Zinc Chloride Complexes

These were prepared by adding an aqueous solution of the pyridine to zinc chloride in water. A precipitate formed which was recrystallized from 95% ethanol repeatedly and then dried in a vacuum oven. The $(3\text{-picoline})_2$ – zinc chloride complexes had m.p. 143–144°.

ACKNOWLEDGMENTS

The authors are very grateful to Dr. W. G. Schneider for the first determinations of the n.m.r. spectra and for some very helpful comments. Thanks are due Dr. B. Gunn for the use of a Beckmann IR-4 spectrophotometer, and the National Research Council for financial assistance.

1. I. C. Smith and W. G. Schneider. Can. J. Chem. **39**, 1158 (1961).
2. B. Bak, L. Hansen, and J. Rastrup-Andersen. J. Chem. Phys. **22**, 2013 (1954).
3. A. R. Katritzky and B. J. Ridgewell. Proc. Chem. Soc. 114 (1962).
4. J. A. Pople, W. G. Schneider, and H. J. Bernstein. High-resolution nuclear magnetic resonance. McGraw-Hill Book Company, Inc., New York. 1959. p. 281.
5. R. K. Murmann and F. Basolo. J. Am. Chem. Soc. **77**, 3484 (1955).
6. J. K. Wilmshurst and H. J. Bernstein. Can. J. Chem. **35**, 1185 (1957).
7. N. S. Gill, R. H. Nuttall, D. E. Scaife, and D. W. A. Sharp. J. Inorg. Nuclear Chem. **18**, 79 (1961).

Received June 4, 1962.
Department of Chemistry,
University of Saskatchewan,
Saskatoon, Saskatchewan.

SYNTHESIS OF 19-NORTESTOLACTONE

Jehan F. Bagli

Modification of steroidal molecules resulting in dissociation of androgenic and myotropic activity is a problem of interest to steroid chemists. Testolactone is the only known steroid reported (1) to have anabolic activity without any androgenic side effect. It is well established (2) that, everything else being equal, the myotropic/androgenic ratio is increased in compounds devoid of C_{19}-methyl group. It was therefore of interest to synthesize 19-nortestolactone.

19-Nortestolactone[1] was first prepared from a product of the biological transformation of androst-4-ene-3,17-dione (3).

Estrolactone 3-acetate (I) was directly converted to its methyl ether (II) as described (4). A lithium aluminum hydride reduction of II yielded diol III.

[1]*Since completion of this work, an alternative route for the synthesis of 19-nortestolactone has appeared (M. Akhtar and D. H. R. Barton. J. Am. Chem. Soc. 84, 1496 (1962)).*

ether extract was evaporated and the residue distilled to give crude pyridine-2*d*, b.p. 100–130°, followed by 2-bromopyridine (25 g), b.p. 192–194°. The crude pyridine-2*d* fraction was dried and distilled from potassium hydroxide pellets to give pure pyridine-2*d* (9.5 g), b.p. 113–114°. (Found: atom%×D, 18.80. Calc. for C_5H_4DN: 20.) No diminution in deuterium content occurred when the compound was boiled with dilute hydrochloric acid, or kept in hydrochloric acid solution at room temperature for 3 months.

3-Picoline-2d

Prepared similarly from 2-bromo-3-methylpyridine (4.4 g), it was obtained as a colorless liquid (1.1 g), b.p. 141–142°. (Found: atom%×D, 11.67. Calc. for C_6H_6DN: 14.2.)

3-Picoline-6d

It was obtained in 61% yield from 2-bromo-5-methylpyridine. (Found: atom%×D, 11.65. Calc. for C_6H_6DN: 14.2.)

Zinc Chloride Complexes

These were prepared by adding an aqueous solution of the pyridine to zinc chloride in water. A precipitate formed which was recrystallized from 95% ethanol repeatedly and then dried in a vacuum oven. The (3-picoline)$_2$ – zinc chloride complexes had m.p. 143–144°.

ACKNOWLEDGMENTS

The authors are very grateful to Dr. W. G. Schneider for the first determinations of the n.m.r. spectra and for some very helpful comments. Thanks are due Dr. B. Gunn for the use of a Beckmann IR-4 spectrophotometer, and the National Research Council for financial assistance.

1. I. C. Smith and W. G. Schneider. Can. J. Chem. **39**, 1158 (1961).
2. B. Bak, L. Hansen, and J. Rastrup-Andersen. J. Chem. Phys. **22**, 2013 (1954).
3. A. R. Katritzky and B. J. Ridgewell. Proc. Chem. Soc. 114 (1962).
4. J. A. Pople, W. G. Schneider, and H. J. Bernstein. High-resolution nuclear magnetic resonance. McGraw-Hill Book Company, Inc., New York. 1959. p. 281.
5. R. K. Murmann and F. Basolo. J. Am. Chem. Soc. **77**, 3484 (1955).
6. J. K. Wilmshurst and H. J. Bernstein. Can. J. Chem. **35**, 1185 (1957).
7. N. S. Gill, R. H. Nuttall, D. E. Scaife, and D. W. A. Sharp. J. Inorg. Nuclear Chem. **18**, 79 (1961).

Received June 4, 1962.
Department of Chemistry,
University of Saskatchewan,
Saskatoon, Saskatchewan.

SYNTHESIS OF 19-NORTESTOLACTONE

Jehan F. Bagli

Modification of steroidal molecules resulting in dissociation of androgenic and myotropic activity is a problem of interest to steroid chemists. Testolactone is the only known steroid reported (1) to have anabolic activity without any androgenic side effect. It is well established (2) that, everything else being equal, the myotropic/androgenic ratio is increased in compounds devoid of C_{19}-methyl group. It was therefore of interest to synthesize 19-nortestolactone.

19-Nortestolactone[1] was first prepared from a product of the biological transformation of androst-4-ene-3,17-dione (3).

Estrolactone 3-acetate (I) was directly converted to its methyl ether (II) as described (4). A lithium aluminum hydride reduction of II yielded diol III.

[1]*Since completion of this work, an alternative route for the synthesis of 19-nortestolactone has appeared (M. Akhtar and D. H. R. Barton. J. Am. Chem. Soc. 84, 1496 (1962)).*

Reduction with lithium and liquid ammonia gave 1-(*n*-hydroxypropyl)-2-methyl-2-hydroxy-7-methoxy-1,2,3,4,4*a*,5,8,9,10,10*a*-decahydrophenanthrene (IV) in an overall yield of 42% from estrolactone acetate. Diol IV on treatment with dilute hydrochloric acid, followed by chromic acid oxidation, yielded 19-nortestolactone (V).

Dehydration of diol III with *p*-toluenesulphonyl chloride and pyridine gave the oxide VI (5).

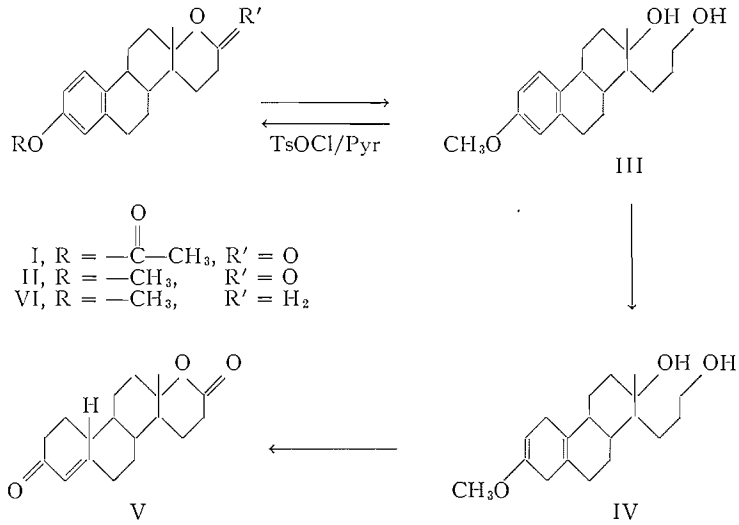

EXPERIMENTAL[2]

1-(n-Hydroxypropyl)-2-methyl-2-hydroxy-7-methoxy-1,2,3,4,4a,9,10,10a-octahydrophenanthrene

Estrolactone methyl ether (12 g) in dry tetrahydrofuran (220 ml) was added over 25 minutes, to a suspension of lithium aluminum hydride (11.8 g) in dry tetrahydrofuran (500 ml). The mixture was stirred for 30 minutes and worked up by adding hydrochloric acid (18%, 320 ml). The organic layer separated, and the aqueous layer was extracted with tetrahydrofuran. The organic liquor was washed with saturated sodium chloride, dried, and the solvent was removed to yield an oily semisolid (12.25 g). Elution from a column of florisil (440 g) with chloroform gave a solid (6.5 g, 54%), m.p. 128–129°. Recrystallization from chloroform–hexane gave an analytical sample, m.p. 130–132°, α_D +108°. Calc. for $C_{19}H_{28}O_3$ (304.41): C, 74.96; H, 9.27. Found: C, 75.04; H, 9.34.

1-(n-Hydroxypropyl)-2-methyl-2-hydroxy-7-methoxy-1,2,3,4,4a,5,8,9,10,10a-decahydrophenanthrene (IV)

Diol III (4.14 g) was dissolved in dry tetrahydrofuran (75 ml), and liquid ammonia (300 ml) was added to it. Lithium wire (4.2 g) was added in small pieces and the mixture was stirred for 25 minutes. Dry ethanol (50 ml) was added dropwise over 20 minutes. Ammonia was then removed and water carefully added. The organic layer was separated and the aqueous layer was extracted with ether. The organic extract was washed with water, dried, and the solvent removed to yield a solid (4 g). A crystallization from aqueous methanol gave colorless plates (3.21 g, 80%), m.p. 147–149°. An analytical sample melted at 148–149°. ν_{max} 1695, 1667 (unconjugated dihydroanisol system) cm^{-1} (6). Calc. for $C_{19}H_{30}O_3$ (306.41): C, 74.47; H, 9.87. Found: C, 74.37; H, 9.47.

19-Nortestolactone (V)

Diol IV (2.5 g) was dissolved in methanol (130 ml) and dilute hydrochloric acid (75 ml), and refluxed under nitrogen for 15 minutes. The mixture was neutralized with sodium carbonate, and the solvent removed under vacuum. The residue was taken up in chloroform, the solution was washed, dried, and the solvent was removed, leaving a colorless oil (2.7 g). λ_{max} 239 mμ (ϵ_{max} 19,350).

[2]*All melting points are uncorrected. Infrared spectra are recorded in chloroform using a Perkin–Elmer Model 21 spectrophotometer, and ultraviolet spectra in 95% ethanol. Rotations were determined in chloroform solution at a concentration of about 1% at room temperature. We wish to thank Dr. G. Papineau-Couture and his associates for microanalyses, rotations, and spectral data.*

Oxidation

The above oil was dissolved in acetone (150 ml, distilled over potassium permanganate), the solution was cooled to 0°, 8 *N* chromic acid (8 ml) was added, and the mixture was stirred for 10 minutes. Excess acid was destroyed with methanol, and the solvent was removed. The residue was taken up in chloroform, and worked up as usual to yield a colorless oil (2.4 g). Two crystallizations from acetone–hexane afforded crystals (0.82 g), m.p. 187–188°. An analytical sample furnished by further crystallizations had m.p. 198–199°, α_D −13°. ν_{max} 1720 (lactone carbonyl), 1667 (3-ketone), 1625 (Δ^4 double bond) cm^{-1}. λ_{max} 238 mμ (ϵ_{max} 19,700). Calc. for $C_{18}H_{24}O_3$ (288.37): C, 74.97; H, 8.39. Found: C, 74.67; H, 8.14.

*3-Methoxy-17a-oxa-*D*-homoestra-1,3,5(10)-triene (VI)*

Diol III (2 g) and *p*-toluenesulphonyl chloride (1.6 g) were dissolved in dry pyridine (26 ml), kept overnight at room temperature, and heated on a steam bath for 1 hour. A few milliliters of water was added and pyridine was removed. The residue was worked up in the usual manner. A crystallization from aqueous methanol afforded colorless plates (0.7 g), m.p. 150–151°. An analytical sample melted at 150–151°, α_D +91°. Calc. for $C_{19}H_{26}O_2$ (286.37): C, 79.68; H, 9.15. Found: C, 79.95; H, 8.86.

1. G. S. Gorden. A.M.A. Arch. Internal Med. **100**, 744 (1957).
2. H. P. Schedi, C. Delea, and F. C. Bartter. J. Clin. Endocrinol. and Metabolism, **19**, 921 (1959).
3. G. M. Richards. U.S. Patent No. 2,855,404 (October 7, 1958); Chem. Abstr. **53**, 8215*a* (1959).
4. R. P. Jacobson. J. Biol. Chem. **171**, 61 (1947).
5. G. R. Petit, U. R. Ghatak, B. Green, T. R. Kasturi, and D. M. Piatak. J. Org. Chem. **26**, 1685 (1961).
6. G. Stork. J. Am. Chem. Soc. **73**, 504 (1951).

Received June 4, 1962.
Ayerst Research Laboratories,
Montreal, Que.

Canadian Journal of Chemistry

Issued by THE NATIONAL RESEARCH COUNCIL OF CANADA

VOLUME 40 NOVEMBER 1962 NUMBER 11

THIOCARBONATES AS BLOCKING GROUPS FOR THE SYNTHESIS OF PARTIAL ESTERS OF CARBOHYDRATES

J. J. WILLARD[1]

Cellulose Research Institute, State University of New York College of Forestry, Syracuse, N.Y., U.S.A.

Received May 8, 1962

ABSTRACT

It has been found that the thiocarbonate, or (alkylthio)carbonyl derivative, serves as a versatile blocking group for the synthesis of partial ester derivatives of carbohydrates. The (alkylthio)carbonyl group is readily substituted in pyridine solution, is stable to mild acid conditions, but is decomposed by mild oxidation. Crystalline methyl 4,6-di-*O*-benzoyl-α-D-glucopyranoside has been synthesized and its structure proved by an independent synthesis of its 2,3-di-*O*-phenylcarbamate derivative. Methyl 4,6-di-*O*-benzoyl-β-D-glucopyranoside was also synthesized and its structure proved by acetylation to the known 2,3-di-*O*-acetyl derivative.

INTRODUCTION

During a study of the kinetics of acetylation of methyl glucosides in our laboratories, certain unknown di- and tri-acetate derivatives of the methyl glucosides became of interest. Many of the possible mono-, di-, and tri-acetates of the methyl glucosides are not known, as is true also for the benzoate derivatives (1), and the general methods for their synthesis have been limited. Apart from the few acetates and benzoates which can be synthesized by the specific substitution reactions or those which depend on the controlled migration of an ester group from one hydroxyl to another, the only derivatives known are those which have utilized acid-sensitive blocking groups such as 4,6-benzylidene (giving 2,3-diesters) or the triphenylmethyl ether (giving 2,3,4-triesters) for their preparation.

The (alkylthio)carbonyl[2] group, R—S—C(=O)—, has been utilized as a protective radical for amino groups in peptide synthesis (2). The (benzylthio)carbonyl derivative of methyl-α-D-glucopyranoside was encountered (3) as an intermediate during the two-step removal of the xanthate group from methyl 2,3,4-tri-*O*-benzoyl-6-*O*-(benzylthio)thiocarbonyl-α-D-glucopyranoside, and was shown to be readily decomposed by mild oxidation, the parent alcohol being liberated. Because it was proved that the benzoyl groups did not migrate during the reaction, the (benzylthio)carbonyl group was suggested as a promising blocking group for the synthesis of partial esters of carbohydrates. This paper describes the synthesis and proofs of structure of methyl 4,6-di-*O*-benzoyl-α-D-glucopyranoside and its β-anomer, demonstrating this principle.

[1]*Present address: Chemistry Department, University of Birmingham, Edgbaston, Birmingham 15, England.*

[2]*The nomenclature for thiocarbonates recommended by L. Hough, J. E. Priddle, and R. S. Theobald, Advances in Carbohydrate Chem., **15**, 91 (1960), is used in this communication.*

Methyl 4,6-di-*O*-benzoyl-β-D-glucopyranoside (VI) was synthesized in 21% overall yield, as seen from Fig. 1. Methyl 4,6-*O*-benzylidene-β-D-glucopyranoside (I) was treated

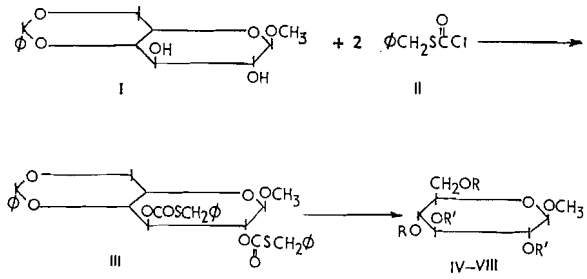

WHERE:

IV R = −H; R′ = $-\overset{O}{\overset{\|}{C}}SCH_2\phi$ VII R = $-\overset{O}{\overset{\|}{C}}\phi$; R′ = $-\overset{O}{\overset{\|}{C}}CH_3$

V R = $-\overset{O}{\overset{\|}{C}}\phi$; R′ = $-\overset{O}{\overset{\|}{C}}SCH_2\phi$ VIII R = $-\overset{O}{\overset{\|}{C}}CH_3$; R′ = $-\overset{O}{\overset{\|}{C}}SCH_2\phi$

VI R = $-\overset{O}{\overset{\|}{C}}\phi$; R′ = −H ϕ = $-C_6H_5$

FIG. 1.

in pyridine solution with a small excess of (benzylthio)carbonyl chloride (II), giving a crystalline 2,3-di-*O*-(benzylthio)carbonyl derivative (III). Removal of the benzylidene group by mild acid hydrolysis afforded methyl 2,3-di-*O*-(benzylthio)carbonyl-β-D-glucopyranoside (IV), which failed to crystallize. However, benzoylation gave a crystalline 4,6-di-*O*-benzoyl derivative (V) and acetylation, the crystalline diacetate (VIII). Oxidation of V with hydrogen peroxide in acetic acid – chloroform solution gave methyl 4,6-di-*O*-benzoyl-β-D-glucopyranoside (VI), the structure of which was proved by acetylation of VI to known (4) methyl 2,3-di-*O*-acetyl-4,6-di-*O*-benzoyl-β-D-glucopyranoside (VII).

Crystalline methyl 4,6-di-*O*-benzoyl-α-D-glucopyranoside (IX), Fig. 2, was synthe-

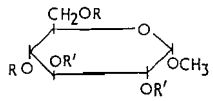

IX R = $-\overset{O}{\overset{\|}{C}}\phi$; R′ = −H

X R = $-\overset{O}{\overset{\|}{C}}\phi$; R′ = $-\overset{O}{\overset{\|}{C}}NH\phi$

XI R = −H; R′ = $-\overset{O}{\overset{\|}{C}}NH\phi$

FIG. 2.

sized in 36% yield in the same manner from methyl 4,6-*O*-benzylidene-α-D-glucopyranoside. It gave a crystalline 2,3-di-*O*-phenylcarbamate derivative (X). Its structure was proved by benzoylation of known (5) methyl 2,3-di-*O*-phenylcarbamyl-α-D-glucopyranoside (XI), giving a product identical with that prepared from the dibenzoate derivative (IX).

DISCUSSION

During the first attempts to synthesize methyl 4,6-di-*O*-benzoyl-α- and -β-D-glucopyranosides use was made of the known (6, 7) 2,3-di-*O*-benzyl ether derivatives (XII). Methyl 2,3-di-*O*-benzyl-α- and -β-D-glucopyranosides were benzoylated to the new crystalline 4,6-di-*O*-benzoyl derivatives (XIII) seen in Fig. 3. Repeated attempts to

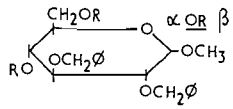

XII R = —H

XIII R = —C(=O)Ø

XIV R = —CH3

FIG. 3.

remove the benzyl ether groups by catalytic hydrogenolysis were not successful. This was surprising in view of the experience in this laboratory that methyl 4,6-di-*O*-methyl-β-D-glucopyranoside is readily obtained by catalytic reduction (Pd) of its 2,3-di-*O*-benzyl ether derivative (XIV), a reaction described by Freudenberg and Plankenhorn (8). No reports have been found, in the literature, in which benzyl ether groups were removed by catalytic reduction from a carbohydrate also carrying ester groups. Since no other method is available for removal of benzyl ethers without loss of ester groups, the benzyl ether does not appear to be a useful blocking group in the synthesis of partial esters of the methyl glucosides.

The use of (alkylthio)carbonyl derivatives can be combined with that of any acid-sensitive blocking groups, e.g., condensed aldehydes and ketones, or triphenylmethyl ethers. The action of (benzylthio)carbonyl chloride on 1,2-5,6-di-*O*-isopropylidene-D-glucofuranose (XV), Fig. 4, gave a crystalline (benzylthio)carbonyl derivative, 1,2-5,6-

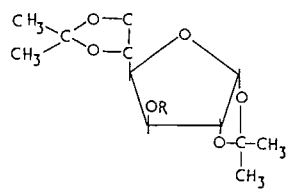

XV R = —H

XVI R = —C(=O)SCH2Ø

FIG. 4.

di-*O*-isopropylidene-3-*O*-(benzylthio)carbonyl-D-glucofuranose (XVI).

The properties of the thiocarbonate group which contribute to its value as a blocking agent are the following: (1) (benzylthio)carbonyl chloride, prepared by the action of 1 mole of phosgene on benzyl mercaptan in aqueous alkali (3, 9), can be purified by distillation and is stable during storage; (2) thiocarbonates are introduced conveniently

and in high yield in pyridine solution; (3) (benzylthio)carbonyl derivatives are generally crystalline; (4) they are stable under mild acid conditions; and (5) they can be removed by oxidative cleavage or by alkaline hydrolysis.

Although (alkylthio)carbonyl derivatives other than the benzyl analogue are prepared with equal ease, use has been confined chiefly to the (benzylthio)carbonyl ester in this laboratory.

It has been found that treatment of methyl 4,6-*O*-benzylidene-α-D-glucopyranoside with 1 mole of (benzylthio)carbonyl chloride gave a good yield of a crystalline monosubstituted (benzylthio)carbonyl derivative. This derivative increases even further the utility of the thiocarbonate as a precursor to partially esterified methyl glucosides. Investigations of this product will be reported in a later communication.

EXPERIMENTAL[3]

Methyl 2,3-Di-O-benzyl-4,6-di-O-benzoyl-α- and -β-D-glucopyranoside (XIII)

Methyl 4,6-*O*-benzylidene-β-D-glucopyranoside (I) was prepared according to the procedure of Freudenberg (10). It had m.p. 197–199°. This derivative was benzylated directly by the Zemplen procedure (11), the 2,3-di-*O*-benzyl derivative having m.p. 115–117°. The benzylidene group was removed by mild acid hydrolysis according to Bell and Lorber (12), furnishing methyl 2,3-di-*O*-benzyl-β-D-glucopyranoside (XII), m.p. 122–123°.

To 2.0 g XII in 10 ml anhydrous pyridine was added 2.5 ml benzoyl chloride, with cooling in ice bath. After standing overnight at room temperature, the product was isolated by pouring the solution into ice water, extracting the water with chloroform, and extracting the chloroform layer successively with excess 1 *N* hydrochloric acid, sodium bicarbonate solution, and finally with water. The chloroform layer was dried 0.5 hour over magnesium sulphate, filtered, and the chloroform evaporated *in vacuo*. As crystallized from ethanol, the product had m.p. 115–118°. After recrystallization it had m.p. 120–121° and $[\alpha]_D^{23}$ −7.5° (c = 1, $CHCl_3$). Anal. Calc. for $C_{35}H_{34}O_8$: C, 72.2; H, 5.84. Found: C, 70.8; H, 6.04.

The α-anomer was synthesized in the same manner and had m.p. 95–97° and $[\alpha]_D^{22}$ +20.5° (c = 1, $CHCl_3$). The product crystallized as long needles from methanol. Anal. Calc. for $C_{35}H_{34}O_8$: C, 72.4; H, 5.84. Found: C, 72.4; H, 6.04.

Repeated attempts to remove the benzyl ether groups from XIII by catalytic reduction using palladium, palladium on carbon, and platinum catalysts in various solvents resulted only in the recovery of starting materials.

1,2-5,6-Diisopropylidene-3-O-(benzylthio)carbonyl-D-glucofuranose (XVI)

To 2.0 g XV, m.p. 108–109°, in 5 ml anhydrous pyridine 1.2 ml II was added slowly with cooling in an ice bath. After standing several hours at room temperature, the product was worked up as usual. It crystallized from ligroin (unreacted diacetone glucose crystallizing out first from that solvent) after long standing in the refrigerator. The product had m.p. 66–67° and $[\alpha]_D^{22}$ −23.8° (c = 3, $CHCl_3$). Anal. Calc. for $C_{20}H_{26}O_7S$: C, 58.5; H, 6.34; S, 7.81. Found: C, 57.5; H, 6.46; S, 7.39.

(Benzylthio)carbonyl Chloride (II)

Compound II was prepared as described previously (3, 9), and had the following additional properties: $n_D^{22.5}$ 1.5748 and specific gravity 1.235.

Methyl 2,3-Di-O-(benzylthio)carbonyl-4,6-O-benzylidene-α-D-glucopyranoside (XVII)

To 6.0 g methyl 4,6-*O*-benzylidene-α-D-glucopyranoside in anhydrous pyridine was added 7.1 cc of II during 0.5 hour, with cooling in ice bath. It is essential that the pyridine be dry since II reacts preferentially with water in the presence of pyridine. The reaction can also be carried out entirely at room temperature with equivalent yields. The use of a larger excess of II resulted in increased yields.

The mixture was then allowed to come to room temperature during an additional 0.5 hour, after which it was poured into ice water. The product was extracted successively with dilute hydrochloric acid, twice with 0.5 *N* sodium hydroxide, and with water. The chloroform layer was dried over magnesium sulphate. Evaporation of the chloroform gave a sirup which crystallized as long needles from absolute ethanol, giving 10.0 g product with m.p. 130–133°. Two recrystallizations from ethanol gave 8.2 g (66%) having m.p. 133–134°. The product showed $[\alpha]_D^{22}$ +31.7° (c = 2, $CHCl_3$). Its melting point was not changed after recrystallization from methanol. Anal. Calc. for $C_{30}H_{30}O_8S_2$: C, 61.8; H, 5.16; S, 11.0. Found: C, 60.1; H, 5.44; S, 10.7.

[3]*All melting points are uncorrected. Solvents were removed in vacuo at 50°.*

Methyl 2,3-Di-O-(benzylthio)carbonyl-α-D-glucopyranoside (XVIII)

To 0.5 g of XVII in 20.0 cc of pure, dry acetone was added 6.0 cc of 0.20 *N* hydrochloric acid. The solution was refluxed and the optical rotation observed at 0.5-hour intervals. Although the material was not entirely soluble at room temperature initially, after 0.5 hour of refluxing it showed $[\alpha]_D$ +51°. A plot of the data log $(\alpha_{final}-\alpha)$ against time fits a final $[\alpha]_D$ of 87°. The solution was neutralized with barium carbonate after 3.5 hours' refluxing, the $[\alpha]_D$ being then +85.6°. The solution was filtered, evaporated to dryness, the sirup was taken up in anhydrous ether and filtered to remove additional insoluble salts. The product could not be obtained in crystalline form. It showed $[\alpha]_D^{22}$ +85.7° (c = 2, $CHCl_3$).

Methyl 2,3-Di-O-(benzylthio)carbonyl-4,6-di-O-benzoyl-α-D-glucopyranoside (XIX)

To 3.0 g of XVIII in 10 cc anhydrous pyridine was added 2.8 cc benzoyl chloride, with cooling in ice bath. The solution stood for 20 hours at room temperature. The reaction mixture was poured into ice water and isolated in the usual way. Evaporation of the chloroform solvent gave a sirup which failed to crystallize. It showed $[\alpha]_D^{22}$ +34.5° (c = 2, $CHCl_3$).

Methyl 4,6-Di-O-benzoyl-α-D-glucopyranoside (IX)

The product XIX from the previous experiment was dissolved in 15 cc glacial acetic acid. One gram of potassium acetate and 5.7 cc of 30% hydrogen peroxide solution were added. The reaction mixture stood at room temperature for 4 days, after which it was poured into water containing sufficient sodium bicarbonate to neutralize the acetic acid. The product was extracted into chloroform and the chloroform layer dried over magnesium sulphate. Evaporation of the chloroform gave a sirup which readily crystallized as fine needles from ether on the addition of petroleum ether. It showed m.p. 131–132°. Recrystallization from ethyl acetate – petroleum ether gave 1.35 g (55%) showing m.p. 133–133.5° and $[\alpha]_D^{22}$ +145.7° (c = 2, $CHCl_3$). Anal. Calc. for $C_{21}H_{22}O_8$: C, 62.8; H, 5.47. Found: C, 62.8; H, 5.44.

Methyl 2,3-Di-O-phenylcarbamyl-4,6-di-O-benzoyl-α-D-glucopyranoside (X)

To ½ g of IX dissolved in 10 cc anhydrous pyridine was added 1 cc of phenylisocyanate, and the mixture was warmed for 1 hour on the steam bath. After cooling, the reaction mixture was poured into ice water and isolated by the usual procedure. The product crystallized as needles from ethanol–water and had m.p. 154–155°. Recrystallization from ether – petroleum ether gave 0.71 g (90%) with m.p. 154–156°. The product showed $[\alpha]_D^{22}$ +56.5° (c = 2, $CHCl_3$). Anal. Calc. for $C_{35}H_{32}O_{10}N_2$: C, 65.7; H, 5.00; N, 4.38. Found: C, 66.6; H, 5.38; N, 4.10.

X from Methyl 2,3-Di-O-phenylcarbamyl-α-D-glucopyranoside

Methyl 2,3-di-*O*-phenylcarbamyl-4,6-*O*-benzylidene-α-D-glucopyranoside was prepared as described by Hearon, Hiatt, and Fordyce and had m.p. 216–217°. Reported (5) 216–217°. The benzylidene group was removed from 0.35 g by refluxing 5 hours in 20 cc acetone containing 6.0 cc 0.20 *N* hydrochloric acid. The product was recovered by the usual procedure, furnishing a sirup which was benzoylated directly, giving 0.13 g, crystallizing first from ethanol–water then from ether – petroleum ether. The product had m.p. 155–156° and $[\alpha]_D^{22}$ +56.7°. A mixed melting point with X from the previous experiment was not depressed.

Methyl 2,3-Di-O-(benzylthio)carbonyl-4,6-O-benzylidene-β-D-glucopyranoside (III)

This compound was prepared in 71% yield in the same manner as its alpha anomer, XVII, from methyl 4,6-*O*-benzylidene-β-D-glucopyranoside. The product was crystallized from a large quantity of ethanol and had m.p. 159–160° and $[\alpha]_D^{22}$ −54.75° (c = 2, $CHCl_3$). It was recrystallized from acetone – ether – petroleum ether and showed the same melting point. Anal. Calc. for $C_{30}H_{30}O_8S_2$: C, 61.8; H, 5.16; S, 11.0. Found: C, 61.8; H, 5.22; S, 10.87.

Methyl 2,3-Di-O-(benzylthio)carbonyl-β-D-glucopyranoside (IV)

One-half gram of III was treated with hydrochloric acid in acetone exactly as described for the alpha anomer while the reaction was observed polarimetrically. Five hours of reflux was required before the optical rotation was constant, its $[\alpha]_D$ then being +1.53°. The product, isolated as before, was obtained as a sirup with $[\alpha]_D^{22}$ +1.55° (c = 2, $CHCl_3$).

Methyl 2,3-Di-O-(benzylthio)carbonyl-4,6-di-O-benzoyl-β-D-glucopyranoside (V)

The product IV obtained from 4.0 g of III was benzoylated as described before for the alpha anomer. Evaporation of the chloroform gave a solid residue, which was triturated with a small amount of 95% ethanol and crystallized from 150 cc absolute ethanol, yielding 3.3 g (69%) of V, m.p. 115–116°. After recrystallization from methanol the product had m.p. 119–120° and $[\alpha]_D^{22}$ −10.7° (c = 2, $CHCl_3$). Anal. Calc. for $C_{37}H_{34}O_{10}S_2$: C, 63.3; H, 4.84; S, 9.13. Found: C, 63.1; H, 4.88; S, 9.23.

Methyl 4,6-Di-O-benzoyl-β-D-glucopyranoside (VI)

To 1.8 g of V dissolved in 20 cc glacial acetic acid containing 5 cc chloroform was added 4.2 cc 30% hydrogen peroxide and 0.6 g potassium acetate. After standing for 4 days at room temperature, the product was isolated as with the alpha anomer IX. The addition of water to an ethanol solution of the product gave 0.3 g of an unidentified product having m.p. 85° after recrystallization from ether – petroleum ether.

After the addition of more water to the filtrate and long standing, more crystalline material (needles) was obtained, giving 0.49 g (48%) with m.p. 135–137°. Recrystallization of the latter from ether – petroleum ether raised the melting point to 137–138°. The product had $[\alpha]_D^{22}$ +20.7° (c = 2, $CHCl_3$). Anal. Calc. for $C_{21}H_{22}O_8$: C, 62.8; H, 5.47. Found: C, 63.3; H, 5.50.

Methyl 2,3-Di-O-acetyl-4,6-di-O-benzoyl-β-D-glucopyranoside (VII)

To 0.30 g of VI in 5 cc anhydrous pyridine was added 1 cc of acetic anhydride. The solution was warmed 2 hours on the steam bath and cooled. On pouring the solution into ice water, a white solid was obtained which was recovered by filtration and washed with water. After crystallization twice from anhydrous ether there was obtained as prisms 0.26 g (72%) of VII, m.p. 165.5–166° and $[\alpha]_D^{22}$ −12.2° (c = 2, $CHCl_3$). Reported (4) for VII: m.p. 164–165° and $[\alpha]_D^{20}$ −5.8° (c = 2, $CHCl_3$).

Methyl 2,3-Di-O-(benzylthio)carbonyl-4,6-di-O-acetyl-β-D-glucopyranoside (VIII)

The benzylidene group was removed from 0.80 g of III as described before. The product was dissolved in 5 cc anhydrous pyridine and 2 cc acetic anhydride. After standing 24 hours at room temperature and warming 1 hour on the steam bath, the product was isolated in the usual manner. It crystallized as needles on standing in the presence of petroleum ether and was recrystallized twice from ether – petroleum ether, giving 0.60 g (75%) having m.p. 96–97° and $[\alpha]_D^{22}$ −3.0 (c = 2, $CHCl_3$). Anal. Calc. for $C_{27}H_{30}O_{10}S_2$: C, 56.0; H, 5.18; S, 11.1. Found: C, 55.6; H, 4.94; S, 11.3.

ACKNOWLEDGMENT

This investigation was carried out during the tenure of a Postdoctoral Fellowship supported by the National Science Foundation.

REFERENCES

1. G. N. Bollenback. Methyl glucosides. Academic Press, Inc., New York. 1958.
2. J. Kollonitsch, V. Gabor, and A. Hajos. Nature, **177**, 840 (1956).
3. J. J. Willard and E. Pacsu. J. Am. Chem. Soc. **82**, 4347 (1960).
4. P. A. Levene and A. L. Raymond. J. Biol. Chem. **97**, 763 (1932).
5. W. M. Hearon, G. D. Hiatt, and C. R. Fordyce. J. Am. Chem. Soc. **66**, 995 (1944).
6. O. Littman and K. Hess. Ber. **67**, 519 (1934).
7. J. C. Irvine and J. P. Scott. J. Chem. Soc. **103**, 575 (1913).
8. K. Freudenberg and E. Plankenhorn. Ber. **73**, 621 (1940).
9. H. Tilles. J. Am. Chem. Soc. **81**, 714 (1959).
10. K. Freudenberg, H. Toepffer, and C. Anderson. Ber. **61**, 1750 (1928).
11. G. Zemplen, Z. Csuros, and S. Angyal. Ber. **70**, 1848 (1937).
12. D. J. Bell and J. Lorber. J. Chem. Soc. (1941) 453.

3,4-DIHYDRO-β-CARBOLINES

I. THE ALKYLATION OF 1-SUBSTITUTED N_β-ALKYL-3,4-DIHYDRO-β-CARBOLINE ANHYDRO BASES

R. N. Gupta and Ian D. Spenser
Department of Chemistry, McMaster University, Hamilton, Ontario
Received June 13, 1962

ABSTRACT

Methylation of the anhydro base derived from 1-methyl-3,4-dihydro-β-carboline methiodide is accompanied by ring opening and yields 3-[2-acetylindolyl]-β-ethyltrimethylammonium iodide, and not a 2,2-dialkyl-1-methylene-1,2,3,4-tetrahydro-β-carbolinium salt, as reported.

Present knowledge of the reactions of the 3,4-dihydro-β-carboline (II) ring system is due almost entirely to the classical work of the schools of Fischer (1–5) and of Perkin and Robinson (6–11) on the structure of the alkaloid harmaline (III). The most recent relevant reference quoted in a current review (12) dates back more than 30 years.

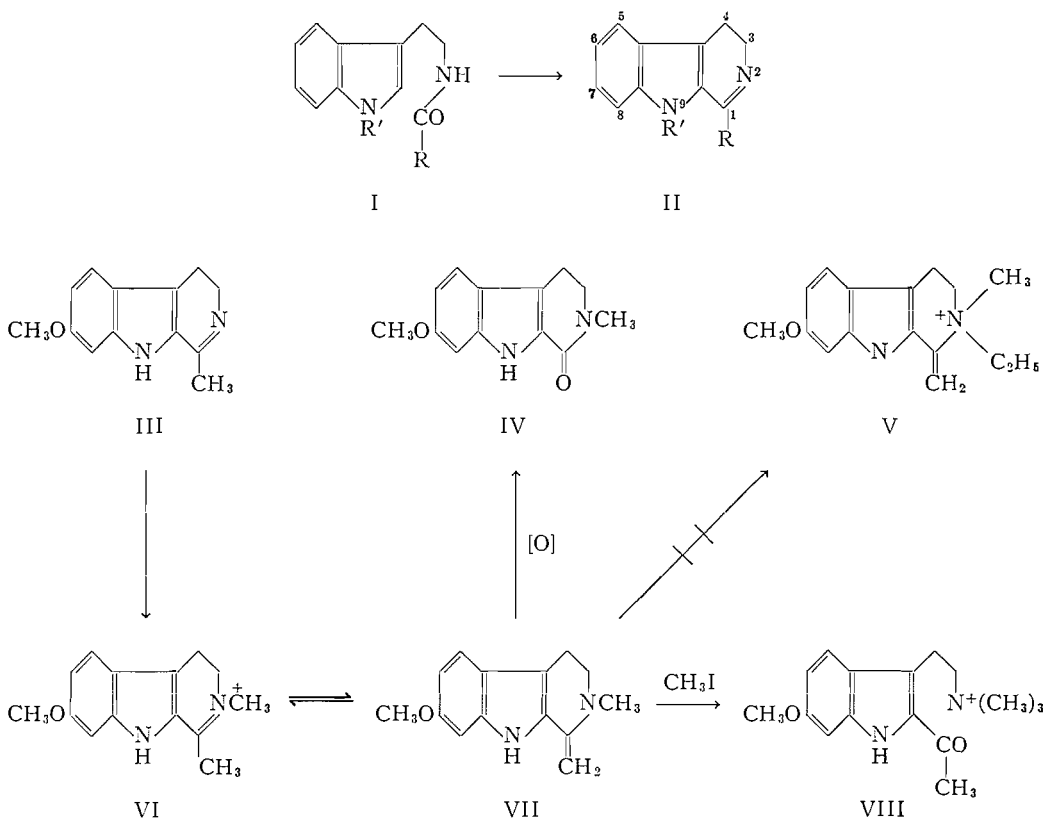

Harmaline (III) and a large number of other 1-substituted 3,4-dihydro-β-carbolines have been synthesized, almost invariably by Bischler–Napieralski ring closure of N-acyltryptamines (I) (13, 14). Three other methods of synthesis, based on cyclization of

2-acyltryptamines (10), and on controlled oxidation (7, 15) or dehydration (15) of suitably substituted 1,2,3,4-tetrahydro-β-carbolines, have so far found only limited application.

Alkylation studies in the 3,4-dihydro-β-carboline series have been carried out with harmaline (III) (1, 3, 5, 7, 9, 16). Quaternization of the base yielded the quaternary methiodide (VI), which on treatment with alkali gave an anhydro base, formulated as (VII) (9) because of its facile oxidation to the 1-oxoderivative (IV).

The structure of the anhydro base (VII) corresponds to that postulated for analogous 3,4-dihydroisoquinolines (cf. ref. 17) but differs markedly from that of the anhydro bases derived from 2-alkyl-β-carbolinium salts (18, and earlier references cited therein).

Reports on the course of further alkylation of 2-methylharmaline anhydro base (VII) are conflicting. On the one hand it was found by Fischer (5) that alkylation of harmaline (III) with methyl iodide in alcoholic solution yielded, in addition to the methiodide (VI), small amounts of another alkylation product of unknown structure, referred to as 'dimethylharmaline iodide', which on treatment with aqueous potassium hydroxide gave trimethylamine. On the other hand Konowalowa and Orechoff (16) claimed to have obtained alkali-stable salts of structure V by further alkylation of 2-alkylharmaline anhydro bases (e.g., VII).

We have reinvestigated the alkylation of 3,4-dihydro-β-carboline derivatives. Compounds used in this study were 1-methyl- (15), 1-ethyl- (14), and 1,9-dimethyl-3,4-dihydro-β-carboline. The latter was prepared by our new method (15) from 1-hydroxymethyl-9-methyl-1,2,3,4-tetrahydro-β-carboline. The 3,4-dihydro-β-carbolines were purified by high-vacuum distillation, when, contrary to a recent report (19), no decomposition was observed.

The ultraviolet spectra of 1-methyl-, 1-ethyl- and 1,9-dimethyl-3,4-dihydro-β-carboline (II) showed the expected bathochromic shift (20) accompanying the transformation $C{=}N \rightarrow C{=}\overset{+}{N}H$. In alcoholic solution, or in the presence of base, the compounds absorbed at 315 mμ. In acid solution a strong band at 350 mμ, due to the dihydro-β-carbolinium ion, was observed (cf. ref. 15, Fig. 1). In the infrared region the compounds showed bands of medium intensity at 1600–1620 cm^{-1} due to C=N stretching vibrations (21). Absorption due to NH was absent in the Nujol spectra. Similarly only weak NH absorption had been observed in the spectrum of harmaline (22).

Treatment of the bases with alkyl iodide in benzene solution gave the corresponding alkiodides (IX) in good yield. The infrared absorption curves of these 2-alkyl-3,4-dihydro-β-carbolinium salts showed strong bands due to $C{=}\overset{+}{N}$ at 1615–1650 cm^{-1} (20, 21). Their ultraviolet curves in water and in acid were identical, and similar to those of the parent bases in acid solution except for the expected bathochromic shift of 5–10 mμ due to N-alkylation (cf. ref. 18).

In alkaline solution, curves similar to those of the parent bases and that of 2-formylindole were obtained (cf. ref. 18, Fig. 4). Formation of anhydro bases of the accepted enamine (X) or of a ketoamine (XI) structure could account for this type of spectrum. Since the 9-methyl derivative also gave this absorption, an anhydro base structure (XII), of the type obtained in the β-carboline series, formation of which requires deprotonation at the indole nitrogen, is excluded.

The anhydro bases (X) were obtained as oily or amorphous yellow solids when an aqueous solution of the corresponding quaternary salt (IX) was treated with sodium hydroxide solution. The anhydro base derived from the methiodide of 1-methyl-3,4-dihydro-β-carboline was purified by distillation and obtained as a light yellow solid

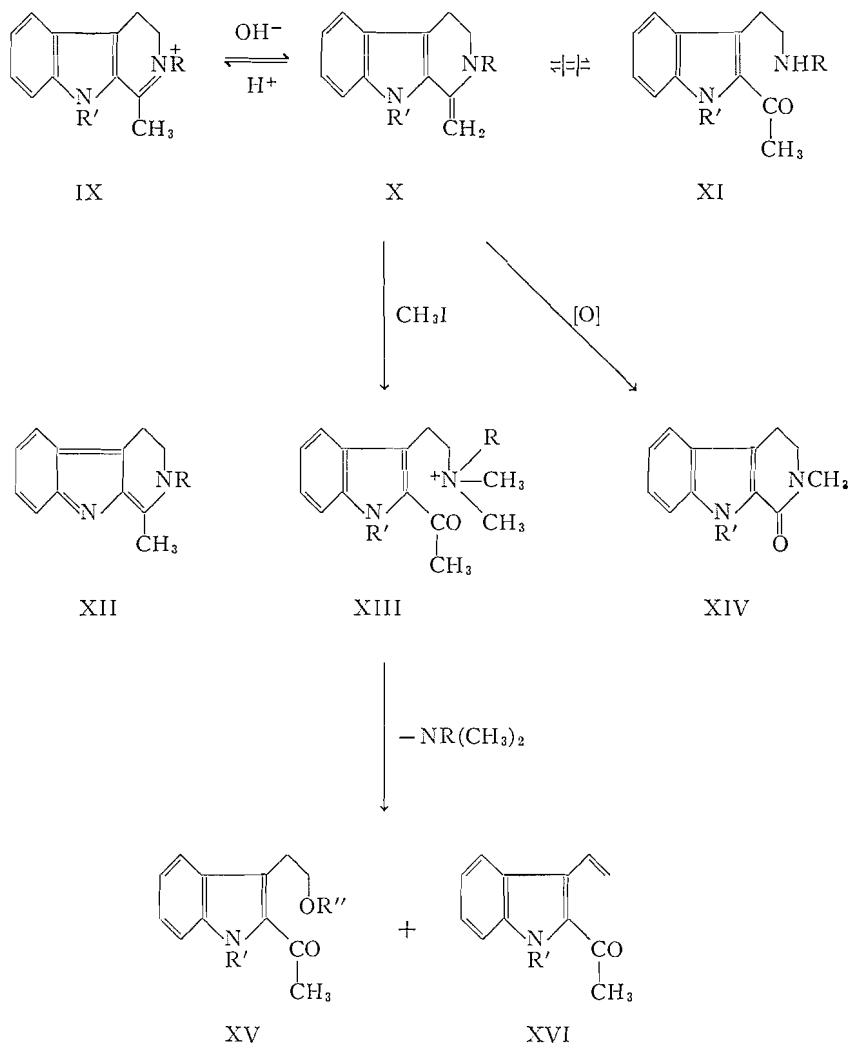

which darkened on keeping. Analysis showed the absence of oxygen and tends to eliminate a ketoamine structure (XI). The anhydro base from 1,9-dimethyl-3,4-dihydro-β-carboline methiodide oxidized on distillation. The small amount of distillate showed an ultraviolet spectrum with a band at 310 mμ, unaffected by change of pH, and an infrared spectrum identical with that of authentic 2,9-dimethyl-1-oxo-1,2,3,4-tetrahydro-β-carboline (XIV, R′ = CH_3) (23). An analogous compound, 2-methyl-1-oxo-1,2,3,4-tetrahydro-β-carboline (XIV, R′ = H), was obtained (23) by oxidation of the anhydro base derived from 1-methyl-3,4-dihydro-β-carboline methiodide.

The infrared spectra of the anhydro bases showed bands at 1625–1655 cm^{-1} which were not of high enough intensity to be attributable to carbonyl absorption; these bands are presumably due to C=C stretching vibrations. Infrared evidence thus also eliminates a ketoamine structure (XI). In accord with the known behavior of anhydro bases, all of which revert in ionizing solvents to the quaternary ion from which they are derived (cf. ref. 18 and earlier references cited therein), the ultraviolet absorption of the compounds

was that of the 3,4-dihydro-β-carbolinium ion, not only in acid solution, but also in ethanol. In non-ionizing solvents, such as ether and chloroform, and in alcoholic sodium hydroxide solution, absorption curves of the free anhydro bases, identical with those given by the parent salt in alkaline solution, were obtained.

Further alkylation of the anhydro bases is not as facile a reaction as reported by Konowalowa and Orechoff (16), who claimed to have obtained an almost theoretical yield of 2,2-dialkylated salts of structure V, when a 2-alkylharmaline anhydro base (VII) was refluxed with alkyl halide in alcoholic solution. We have found that alkylation does not take place readily under these conditions. The crystalline products which were obtained proved to be pure 3,4-dihydro-β-carbolinium alkiodides (IX) to which the anhydro bases had reverted. The hydriodic acid required for this reversal was presumably generated by solvolysis of the alkylating agent.

Alkylation of the enamine carbon atom, found in anhydro bases derived from fully aromatic systems in which N-alkylation would result in loss of ring resonance (e.g., ref. 24), and also known to compete with N-alkylation in some aliphatic enamine systems (e.g., ref. 25), was not observed. The ultraviolet spectra of the mother liquors from these alkylation experiments did show additional absorption at 310 mμ in acid solution. The compounds giving rise to this absorption were obtained as the major reaction products when alkylation was carried out under basic conditions.

Methylation of the anhydro bases in aqueous alcoholic potassium carbonate suspension gave a new quaternary salt in each case. These new compounds showed intense carbonyl absorption at 1645 cm^{-1}, and their ultraviolet spectra were unaffected by change of pH and were similar to that of 2-formylindole. Thus the anhydro base X (R = CH_3, R′ = H) gave a compound $C_{15}H_{21}IN_2O$ (XIII, R = CH_3, R′ = H) and the anhydro base X (R = n-C_3H_7, R′ = H) a compound $C_{17}H_{25}IN_2O$ (XIII, R = n-C_3H_7, R′ = H). On Hofmann degradation these yielded, respectively, trimethylamine and dimethyl-n-propylamine, characterized as picrates. Alkylation had thus taken place at N_β, and the methylation products must be formulated as 3-[2-acetylindolyl]-β-ethyltrialkylammonium iodides (XIII).

The neutral fragments from the Hofmann degradation of the two compounds were identical. They consisted of a mixture of the displacement product, 2-acetyl-3-[β-alkoxyethyl]-indole (XV, R′ = H), whose constitution, with respect to the ether group R″, depended on the alcohol used as a solvent in the experiment, and of the elimination product, 2-acetyl-3-vinylindole (XVI, R′ = H), which proved difficult to isolate. The ethers showed ultraviolet absorption curves, unaffected by change of pH, similar to that of 2-formylindole, and in the infrared had strong carbonyl absorption at 1660 cm^{-1} and ether absorption at 1000–1200 cm^{-1}. Methylation of the anhydro base derived from 1,9-dimethyl-3,4-dihydro-β-carboline methiodide (X, R = R′ = CH_3) yielded 3-[2-acetyl-1-methylindolyl]-β-ethyltrimethylammonium iodide, $C_{16}H_{23}IN_2O$ (XIII, R = R′ = CH_3), which on Hofmann degradation gave trimethylamine and 2-acetyl-1-methyl-3-vinylindole (XVI, R′ = CH_3). The infrared spectrum of this compound showed bands due to carbonyl (1650 cm^{-1}) and due to vinyl (912, 992 cm^{-1}) absorption, and in the ultraviolet region an intensification of absorption at 325 mμ was observed, consistent with the constitution of the compound.

No evidence for structures corresponding to V, of the type postulated by Konowalowa and Orechoff (16), was obtained. This structure was put forward on the basis of the supposed identity of two quaternary iodides obtained respectively by methylation of 2-ethylharmaline anhydro base and ethylation of 2-methylharmaline anhydro base. The

reported criteria of identity, mixed melting points and incomplete analysis (iodine only), were obviously inadequate. The fact that these products were obtained under conditions which have now been shown to lead to reconversion of the anhydro bases to their parent salts indicates that the compounds obtained by Konowalowa and Orechoff were in fact harmaline methiodide (VI) and ethiodide, and not dialkylated salts.

Fischer's 'dimethylharmaline iodide' (5), on the other hand, was presumably the quaternary salt (VIII), 3-[2-acetyl-6-methoxyindolyl]-β-ethyltrimethylammonium iodide.

EXPERIMENTAL

1-Alkyl-3,4-dihydro-β-carbolines

1-Methyl-3,4-dihydro-β-carboline (Harmalan)

Harmalan was obtained by dehydration of 1-hydroxymethyl-1,2,3,4-tetrahydro-β-carboline (15).

1-Ethyl-3,4-dihydro-β-carboline

This base was prepared by dehydration of N_β-propionyltryptamine, as described by Späth and Lederer (14).

1,9-Dimethyl-3,4-dihydro-β-carboline

The starting material for this preparation was ind-N-methyltryptamine, which was prepared by the gramine route from N-methylindole (26). The latter was obtained by lithium aluminum hydride reduction of N-methylindoxyl (27).

1-Hydroxymethyl-9-methyl-1,2,3,4-tetrahydro-β-carboline.—A solution of ind-N-methyltryptamine (3.4 g) and glycolaldehyde (1.27 g) in 200 ml water containing 20 ml 2 *N* hydrochloric acid was refluxed for 2 hours. The solution was decolorized, extracted with ether to remove non-basic impurities, and made alkaline with sodium hydroxide. A dark brown solid was obtained, which was dissolved in ethanol, decolorized, and crystallized from aqueous ethanol. It sublimed at 2.10^{-3} mm and 140–160° to give *1-hydroxymethyl-9-methyl-1,2,3,4-tetrahydro-β-carboline* (3 g, 70%) as a colorless crystalline solid melting at 144°. (Found: C, 72.4; H, 7.7; N, 13.1. $C_{13}H_{16}N_2O$ requires: C, 72.2; H, 7.5; N, 13.0%.)

1,9-Dimethyl-3,4-dihydro-β-carboline.—The above tetrahydro-β-carboline (2.5 g) was wetted with water, 85% phosphoric acid (30 ml) was added, and the mixture was kept on the steam bath until the absorption band at 280 mμ, characteristic of the indole chromophore of the starting material, had disappeared (4 hours). The dark brown solution was diluted with water, decolorized, and made alkaline with 20% sodium hydroxide, and the product was extracted into ether. The extract was dried, ether was removed, and the solid residue was dissolved in methanol. The solution was decolorized and evaporated and the residue was sublimed at 2.10^{-3} mm and 90° to yield 1,9-dimethyl-3,4-dihydro-β-carboline (1.2 g, 58%), melting at 80–84°, as a colorless solid. (Found: C, 78.8; H, 7.4; N, 14.2. Calc. for $C_{13}H_{14}N_2$: C, 78.8; H, 7.1; N, 14.1%.) (Reported melting point (14): 91–92°.) Infrared absorption (Nujol) (cm^{-1}): 1610 (m) (C=N). Ultraviolet absorption (λ_{max}, mμ (log ε)): in 0.1 *N* HCl: 352 (4.2), 250 (4.0); in 0.1 *N* NaOH: 318 (4.0).

1-Alkyl-3,4-dihydro-β-carboline Alkiodides and Anhydro Bases Derived from These Salts

1-Methyl-3,4-dihydro-β-carboline Methiodide (Harmalan Methiodide)

Harmalan (0.5 g) was suspended in nitrobenzene (5 ml), and benzene (100 ml) was added when a clear solution was obtained. Methyl iodide (2 ml) was added and the mixture was kept at 37° for 48 hours. A yellow precipitate was obtained which was crystallized from methanol after treatment with charcoal, yielding light yellow needles of the *methiodide* (0.8 g, 80%) melting at 288–290°. (Found: C, 47.8; H, 4.7; N, 8.7. $C_{13}H_{15}IN_2$ requires: C, 47.8; H, 4.6; N, 8.6%.) Infrared absorption (Nujol) (cm^{-1}): 3130 (m) (NH); 1618 (s) ($C{=}\overset{+}{N}$). Ultraviolet absorption (λ_{max}, mμ (log ε)): in 0.1 *N* HCl: 355 (4.3), 250 (4.1); in 0.1 *N* NaOH: 315 (4.2).

Anhydro base derived from 1-methyl-3,4-dihydro-β-carboline methiodide (i.e., 2-methyl-1-methylene-1,2,3,4-tetrahydro-β-carboline).—An aqueous solution of harmalan methiodide (0.5 g) was treated with 20% sodium hydroxide, when a yellow turbidity appeared. The solution was extracted with ether, the ether extract was dried and concentrated, and the residue distilled at 2.10^{-3} mm and 110–120° to give the *anhydro base*, melting at 115° after sintering at 105°, as a colorless solid which turned yellow on standing. (Found: C, 78.6; H, 7.2; N, 14.0. $C_{13}H_{14}N_2$ requires: C, 78.8; H, 7.1; N, 14.1%.) Infrared absorption (Nujol) (cm^{-1}): 3410 (m) (NH); 1625 (m) (C=C).

1-Methyl-3,4-dihydro-β-carboline n-Propiodide

Harmalan (0.5 g) was dissolved in a mixture of nitrobenzene (10 ml) and benzene (100 ml). 1-Iodopropane (3 ml) was added and the solution kept at 37° for 72 hours. An orange precipitate was obtained which crystallized from methanol after treatment with charcoal to yield *1-methyl-3,4-dihydro-β-carboline n-propiodide* (0.73 g, 70%) melting at 269–270°. (Found: C, 50.7; H, 5.5; N, 7.9. $C_{15}H_{19}IN_2$ requires: C, 50.8; H, 5.4;

N, 7.9%.) Infrared absorption (Nujol) (cm^{-1}): 3130 (m) (NH); 1615 (s) ($C{=}\overset{+}{N}$). Ultraviolet absorption (λ_{max}, $m\mu$ (log ϵ)): in 0.1 *N* HCl: 360 (4.4), 250 (4.1); in 0.1 *N* NaOH: 320 (4.2).

Anhydro base derived from 1-methyl-3,4-dihydro-β-carboline n-propiodide (i.e., 1-methylene-2-n-propyl-1,2,3,4-tetrahydro-β-carboline).—Treatment of an aqueous solution of harmalan propiodide with 20% sodium hydroxide gave a brown solid, melting at 104–106°, which darkened on drying in air. Sublimation under reduced pressure gave a glassy solid, which was not analyzed. Infrared absorption (Nujol) (cm^{-1}): 3410 (m) (NH); 1630 (m) (C=C).

1-Ethyl-3,4-dihydro-β-carboline Methiodide

1-Ethyl-3,4-dihydro-β-carboline (0.5 g), dissolved in a mixture of benzene (100 ml) and nitrobenzene (10 ml), was incubated at 40° with methyl iodide (2 ml). After 48 hours the yellow crystalline product was separated, washed with benzene and with ether, and recrystallized from ethanol, to yield the *methiodide* (0.64 g, 73%) as yellow needles, melting at 221–222°. (Found: C, 49.1; H, 5.2. $C_{14}H_{17}IN_2$ requires: C, 49.4; H, 5.0%.) Infrared absorption (Nujol) (cm^{-1}) 3100 (m) (NH); 1615 (s) ($C{=}\overset{+}{N}$). Ultraviolet absorption (λ_{max}, $m\mu$ (log ϵ)): in 0.1 *N* HCl: 355 (4.2); in 0.1 *N* NaOH: 315 (4.2).

1,9-Dimethyl-3,4-dihydro-β-carboline Methiodide

1,9-Dimethyl-3,4-dihydro-β-carboline (0.5 g) was treated with methyl iodide (2 ml) in 100 ml benzene and allowed to stand for 24 hours at 39°. A yellow solid was obtained, which was crystallized from water after treatment with charcoal, yielding the *methiodide* (0.8 g, 80%) in yellow needles melting at 216–218°. (Found: C, 49.6; H, 5.4; N, 7.9. $C_{14}H_{17}IN_2$ requires: C, 49.4; H, 5.0; N, 8.2%.) Infrared absorption (Nujol) (cm^{-1}): 1661 (m) ($C{=}\overset{+}{N}$). Ultraviolet absorption (λ_{max}, $m\mu$ (log ϵ)): in 0.1 *N* HCl: 355 (4.2), 250 (4.0); in 0.1 *N* NaOH: 310 (4.0).

Anhydro base derived from 1,9-dimethyl-3,4-dihydro-β-carboline methiodide (i.e., 2,9-dimethyl-1-methylene-1,2,3,4-tetrahydro-β-carboline).—The above methiodide (0.4 g) was dissolved in hot water and treated with 20% sodium hydroxide, when the anhydro base separated as a colorless solid which discolored rapidly on standing.

A sample of the product was distilled at 2.10^{-3} mm. The major portion decomposed but a small amount of distillate was obtained which showed ultraviolet and infrared absorption spectra identical with those of an authentic sample of 1-oxo-2,9-dimethyl-1,2,3,4-tetrahydro-β-carboline (23).

Exhaustive Methylation of 3,4-Dihydro-β-carboline Anhydro Bases

Further Methylation of 2-Methyl-1-methylene-1,2,3,4-tetrahydro-β-carboline

Attempted methylation in methanol solution.—Harmalan methiodide (0.20 g) was dissolved in hot water, 20% sodium hydroxide added, the solution was cooled and extracted with ether, and the dried ether extract concentrated. The residue was dissolved in methanol (10 ml), methyl iodide (2 ml) was added, and the mixture was refluxed 6 hours. Concentration of the reaction mixture and recrystallization of the residue from methanol gave harmalan methiodide (0.11 g, 55%), melting at 286°. (Found: C, 48.0; H, 4.7; N, 8.8. Calc. for $C_{13}H_{15}IN_2$: C, 47.8; H, 4.6; N, 8.6%.)

3-[2-Acetylindolyl]-β-ethyltrimethylammonium iodide.—Harmalan methiodide (1.0 g) was dissolved in hot water, 20% sodium hydroxide added, the solution cooled and extracted with ether. The ether extract was dried, solvent evaporated, and the residue dissolved in 50 ml moist methanol. Potassium carbonate (0.4 g) and methyl iodide (5 ml) were added. The mixture was kept for 24 hours at 40°. The solvent was evaporated and the residue washed with cold water and crystallized from 50% aqueous methanol after treatment with charcoal. Pale yellow plates (0.88 g, 70%) of the *quaternary salt*, melting at 278°, were obtained. (Found: C, 48.0; H, 5.4; N, 7.4. $C_{15}H_{21}IN_2O$ requires: C, 48.4; H, 5.7; N, 7.5%.) Infrared absorption (Nujol) (cm^{-1}): 3280 (m) (NH); 1660 (vs) (C=O). Ultraviolet absorption (λ_{max}, $m\mu$ (log ϵ)): in 0.1 *N* HCl and 0.1 *N* NaOH: 315 (4.1), 242 (4.1).

Hofmann degradation of 3-[2-acetylindolyl]-β-ethyltrimethylammonium iodide with methanolic potassium hydroxide.—The above quaternary salt (0.70 g) was treated with 2% methanolic potassium hydroxide (40 ml). The solution was kept at 50°, a current of nitrogen was passed for 4 hours, and the issuing gas passed through an alcoholic solution of picric acid. Concentration of the picric acid solution gave a picrate (0.45 g) melting at 216° (decomp.) after recrystallization from methanol, which was identified as trimethylamine picrate by comparison with an authentic sample and by analysis. (Found: C, 37.7; H, 4.1; N, 19.2. Calc. for $C_9H_{12}N_4O_7$: C, 37.5; H, 4.2; N, 19.4%.)

The reaction mixture was evaporated, water was added to the residue, the solution was extracted with ether, and the ether extract dried and evaporated. The residue was dissolved in benzene and applied to an alumina column. The column was eluted with benzene and the colorless eluate collected and evaporated, when *2-acetyl-3-[β-methoxyethyl]-indole* (0.10 g) was obtained as a colorless residue melting at 140°. (Found: OCH_3, 14.1; C, 71.7; H, 7.3; N, 6.2. $C_{13}H_{15}NO_2$ requires: OCH_3, 14.3; C, 71.9; H, 7.0; N, 6.5%.) Infrared absorption (Nujol) (cm^{-1}): 3250 (m) (NH); 1660 (vs) (C=O); 1028 (m), 1065 (m), 1090 (s) (OCH_3). Ultraviolet absorption (λ_{max}, $m\mu$ (log ϵ)): in 0.1 *N* HCl and in 0.1 *N* NaOH: 315 (4.1).

Hofmann degradation of 3-[2-acetylindolyl]-β-ethyltrimethylammonium iodide with ethanolic potassium hydroxide.—The quaternary salt was degraded as before with ethanolic potassium hydroxide. The basic

fragment was isolated as trimethylamine picrate and the neutral fragment was *2-acetyl-3-[β-ethoxyethyl]-indole*, isolated as a colorless solid, melting at 118°. (Found: OC_2H_5, 18.4; C, 72.4; H, 7.9; N, 6.1. $C_{14}H_{17}NO_2$ requires: OC_2H_5, 19.5; C, 72.7; H, 7.4; N, 6.1%.) Infrared absorption (Nujol) (cm^{-1}): 3230 (m) (NH); 1664 (vs) (C=O); 1032 (m), 1065 (m), 1090 (vs) (OC_2H_5). Ultraviolet absorption (λ_{max}, mμ (log ϵ)): in 0.1 *N* HCl and in 0.1 *N* NaOH: 315 (4.1).

Further Methylation of 1-Methylene-2-n-propyl-1,2,3,4-tetrahydro-β-carboline

3-[2-Acetylindolyl]-β-ethyldimethyl-n-propylammonium iodide.—Harmalan propiodide (1.0 g) was dissolved in hot water, treated with sodium hydroxide, the anhydro base extracted into ether and quaternized with methyl iodide as described earlier. The *quaternary salt* was isolated as pale yellow plates (0.87 g, 70%) melting at 197°. (Found: C, 51.1; H, 6.5; N, 6.6; I, 31.9. $C_{17}H_{25}IN_2O$ requires: C, 51.0; H, 6.3; N, 7.0; I, 31.8%.) Infrared absorption (Nujol) (cm^{-1}): 3390 (m, broad) (NH); 1640 (vs) (C=O). Ultraviolet absorption (λ_{max}, mμ (log ϵ)): in 0.1 *N* HCl and in 0.1 *N* NaOH: 315 (4.1).

Hofmann degradation of 3-[2-acetylindolyl]-β-ethyldimethyl-n-propylammonium iodide.—Treatment of the above quaternary salt with methanolic and ethanolic potassium hydroxide in the usual manner, and purification of the degradation products as before gave 2-acetyl-3-[β-methoxyethyl]-indole and 2-acetyl-3-[β-ethoxyethyl]-indole respectively, identical with those obtained by degradation of the corresponding trimethylammonium salt. The corresponding compounds had identical melting points and gave overlapping infrared spectra.

Isolation of dimethyl-n-propylamine picrate.—As before, the volatile degradation products were swept into an alcoholic solution of picric acid by means of a stream of nitrogen. After concentration of the solution dimethyl-*n*-propylamine picrate was obtained as lemon yellow plates melting at 108–109°, after recrystallization from ethyl acetate. (Found: C, 42.0; H, 5.3; N, 17.3. Calc. for $C_{11}H_{16}N_4O_7$: C, 41.8; H, 5.1; N, 17.7%.) There was no depression in the melting point on admixture of an authentic sample of dimethyl-*n*-propylamine picrate.

Further Methylation of 2,9-Dimethyl-1-methylene-1,2,3,4-tetrahydro-β-carboline

3-[2-Acetyl-1-methylindolyl]-β-ethyltrimethylammonium iodide.—Anhydro base, obtained from 0.5 g 1,9-dimethyl-3,4-dihydro-β-carboline methiodide, was dissolved in 25 ml methanol. Methyl iodide (2 ml) and potassium carbonate (0.4 g) were added and the reaction mixture was kept at 40° for 24 hours. The monohydrate of the *quaternary salt* (0.35 g, 62%), melting at 215–216°, crystallized from aqueous methanol. (Found: C, 48.0; H, 6.4; N, 7.2; I, 32.1. $C_{16}H_{23}IN_2O,H_2O$ requires: C, 47.5; H, 6.2; N, 6.9; I, 31.4%.) Infrared absorption (Nujol) (cm^{-1}): 1640 (vs) (C=O). Ultraviolet absorption (λ_{max}, mμ (log ϵ)): in 0.1 *N* HCl and in 0.1 *N* NaOH: 315 (4.1).

Hofmann degradation of the quaternary salt.—The above quaternary salt (0.2 g) was treated with 5% methanolic potassium hydroxide (20 ml) in the usual manner. The basic fragment was isolated and identified as trimethylamine picrate.

The reaction mixture was evaporated, water was added to the residue, the solution was extracted with ether, and the extract dried and evaporated. The residue was dissolved in methanol, the solution decolorized with charcoal and again evaporated. The residue was sublimed at 3.10^{-3} mm and 70°, when pale yellow crystals (0.02 g) of *2-acetyl-1-methyl-3-vinylindole* melting at 54° were obtained. (Found: C, 78.7; H, 6.9; N, 6.8. $C_{13}H_{13}NO$ requires: C, 78.4; H, 6.6; N, 7.0%.) Infrared absorption (Nujol) (cm^{-1}): 1650 (vs) (C=O); 1605 (s) (C=C); 912 (m), 992 (m) (vinyl).

ACKNOWLEDGMENTS

Financial assistance by the National Research Council of Canada and by the Ontario Research Foundation is gratefully acknowledged.

REFERENCES

1. O. Fischer and E. Täuber. Ber. **18**, 400 (1885).
2. O. Fischer. Ber. **22**, 637 (1889).
3. O. Fischer. Ber. **30**, 2481 (1897).
4. O. Fischer and W. Boesler. Ber. **45**, 1930 (1912).
5. O. Fischer. Ber. **47**, 99 (1914).
6. W. H. Perkin and R. Robinson. J. Chem. Soc. **101**, 1775 (1912).
7. W. H. Perkin and R. Robinson. J. Chem. Soc. **115**, 933 (1919).
8. W. O. Kermack, W. H. Perkin, and R. Robinson. J. Chem. Soc. **121**, 1872 (1922).
9. H. Nishikawa, W. H. Perkin, and R. Robinson. J. Chem. Soc. **125**, 657 (1924).
10. R. H. F. Manske, W. H. Perkin, and R. Robinson. J. Chem. Soc. 1 (1927).
11. H. S. B. Barret, W. H. Perkin, and R. Robinson. J. Chem. Soc. 2942 (1929).
12. W. O. Kermack and J. E. McKail. *In* Heterocyclic compounds. Vol. 7. *Edited by* R. C. Elderfield. John Wiley, New York. 1961. p. 237.
13. E. Späth and E. Lederer. Ber. **63**, 120 (1930); cf. W. M. Whaley and T. R. Govindachari. Org. Reactions, **6**, 142 (1951).

14. E. SPÄTH and E. LEDERER. Ber. **63**, 2102 (1930).
15. I. D. SPENSER. Can. J. Chem. **37**, 1851 (1959).
16. R. KONOWALOWA and A. ORECHOFF. Arch. Pharm. **272**, 748 (1934).
17. W. J. GENSLER, E. M. HEALY, I. ONSHUUS, and A. L. BLUHM. J. Am. Chem. Soc. **78**, 1713 (1956).
18. I. D. SPENSER. J. Chem. Soc. 3659 (1956).
19. R. TSCHESCHE and H. JENSSEN. Chem. Ber. **93**, 271 (1960).
20. B. WITKOP. Experientia, **10**, 420 (1954).
21. B. WITKOP and J. B. PATRICK. J. Am. Chem. Soc. **75**, 4474 (1953).
22. L. MARION, D. RAMSAY, and R. N. JONES. J. Am. Chem. Soc. **73**, 305 (1951).
23. R. N. GUPTA and I. D. SPENSER. Can. J. Chem. This issue.
24. J. W. ARMIT and R. ROBINSON. J. Chem. Soc. **121**, 827 (1922). W. H. MILLS and R. RAPER. J. Chem. Soc. **127**, 2466 (1925). R. ROBINSON and J. E. SAXTON. J. Chem. Soc. 976 (1952).
25. G. STORK, R. TERRELL, and J. SZMUSZKOVICZ. J. Am. Chem. Soc. **76**, 2029 (1954). E. ELKIN. Bull. Soc. Chim. France, 972 (1960).
26. H. R. SNYDER and E. L. ELIEL. J. Am. Chem. Soc. **70**, 1703 (1948).
27. P. L. JULIAN and H. C. PRINTY. J. Am. Chem. Soc. **71**, 3206 (1949).

3,4-DIHYDRO-β-CARBOLINES

II. THE EXHAUSTIVE METHYLATION OF 3,4-DIHYDRO-β-CARBOLINE

R. N. GUPTA AND IAN D. SPENSER
Department of Chemistry, McMaster University, Hamilton, Ontario

Received June 13, 1962

ABSTRACT

The methiodide of 3,4-dihydro-β-carboline yields a dimeric anhydro base which, on heating, disproportionates to a β-carboline and a tetrahydro-β-carboline derivative, and on methylation is converted to 3-[2-formylindolyl]-β-ethyltrimethylammonium iodide.

Although a large number of 1-substituted 3,4-dihydro-β-carbolines have been synthesized (1, 2), the parent base itself (II, R=H) has not been well characterized. 3,4-Dihydro-β-carboline was first obtained (3) by degradation of evodiamine. It was isolated as a tarry mass, which yielded a picrate, and was identified by oxidation to β-carboline (4). Attempted synthesis by conventional Bischler–Napieralski ring closure of N_β-formyltryptamine (I, R = H) gave an uncharacterized product in 2% yield (2). The base was later obtained by this method in 36% yield as an amorphous powder of indeterminate melting point, yielding a picrate and a perchlorate (5).

Crude 3,4-dihydro-β-carboline (II, R = H) has now been obtained in 50% yield from N_β-formyltryptamine (I, R = H), using polyphosphoric acid as the dehydrating agent. The compound resisted purification because of its sensitivity towards aqueous acid and its tendency to polymerization. Analysis of the free base was unsatisfactory. The methiodide, however, showed the expected composition. 9-Methyl-3,4-dihydro-β-carboline (II, R = CH_3), obtained from N_β-formyl-1-methyltryptamine (I, R = CH_3), behaved similarly. The ultraviolet absorption curves of both compounds (Fig. 1) were similar to those of 1-alkyl-3,4-dihydro-β-carbolines (6), and the infrared spectra were also consistent with the assigned structure.

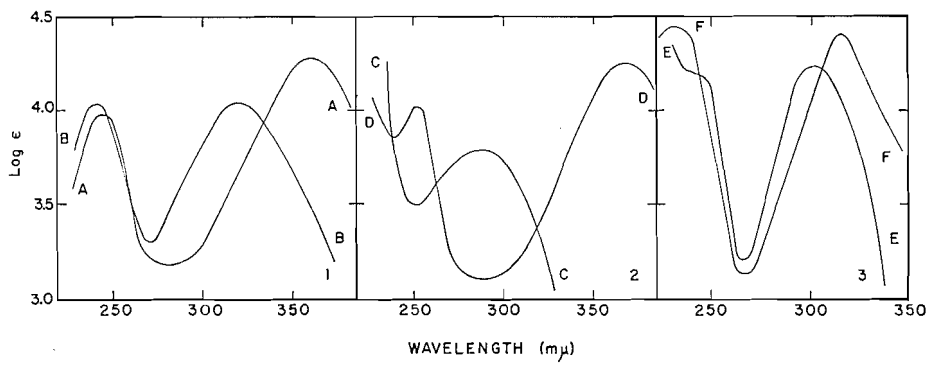

FIG. 1. 3,4-Dihydro-β-carboline (norharmalan). Curve A, in 0.1 *N* HCl in aqueous ethanol; curve B, in 0.1 *N* NaOH in aqueous ethanol.
FIG. 2. 3,4-Dihydro-β-carboline methiodide. Curve C, in 0.1 *N* NaOH in aqueous ethanol; curve D, in 0.1 *N* HCl in aqueous ethanol.
FIG. 3. Curve E: 2-methyl-1-oxo-1,2,3,4-tetrahydro-β-carboline in 0.1 *N* HCl in aqueous ethanol. Curve F: 2-formylindole in ethanol (20).

The difficulties encountered in the purification of the bases are in line with experience with analogous compounds of the dihydroisoquinoline series (7). A trimer, corresponding in structure to N,N′,N″-triphenylethylaminomalonamide (8), a substance obtained as a by-product in the cyclodehydration of N-formylphenylethylamine, was not detected in the intractable by-products of the present preparations.

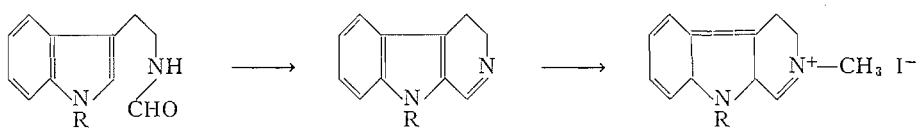

I II III

Treatment of the compounds with methyl iodide gave the corresponding methiodides (III) in good yield. The infrared curves of these 2-methyl-3,4-dihydro-β-carbolinium salts showed strong $C{=}\overset{+}{N}$ absorption at 1640 cm^{-1} (cf. ref. 9). Their ultraviolet absorption in alcohol and in 0.1 *M* acid was identical (Fig. 2, curve D), and similar to that of the parent bases in acid solution (Fig. 1, curve A). In alkaline solution absorption characteristic of indole was obtained (Fig. 2, curve C). This spectral change is consistent with the formation of pseudobases of structure IV, i.e., of 1-hydroxy-2-methyl-1,2,3,4-tetrahydro-β-carbolines, analogous in constitution to the pseudobases of the 3,4-dihydroisoquinoline series, such as hydrastinine (V, R = H) and cotarnine (V, R = OCH_3). This type of spectrum eliminates an aldehyde–amine formulation (VI), which would be expected to show absorption similar to that of 2-formylindole (Fig. 3, curve F). An anhydro base structure (VII) of the β-carboline type, formation of which would require deprotonation at the indole nitrogen, is also excluded, since the 9-methyl derivative also gave an indole spectrum in alkaline solution.

The compounds containing the indole chromophore were isolated when the parent salts were treated with aqueous alkali.

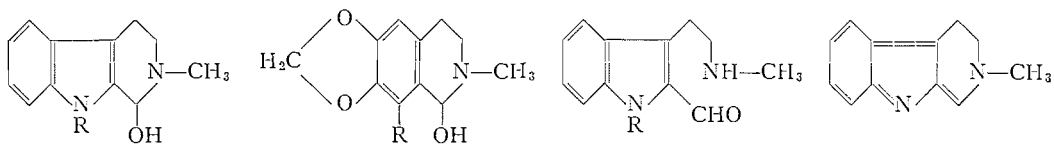

IV V VI VII

The 'pseudobase' derived from 3,4-dihydro-β-carboline methiodide was a colorless solid, melting at 185°. In non-aqueous solvents and in alkaline solution the compound gave an ultraviolet spectrum similar to that of indole. In aqueous acid the 3,4-dihydro-β-carbolinium spectrum of the parent salt was observed. Such behavior is characteristic of pseudobases and anhydro bases in general. The infrared spectrum of the compound did not show carbonyl absorption, confirming the absence of the aldehyde–amine structure VI, nor bands attributable to OH and NH. This lack of OH and NH absorption is not conclusive evidence against the carbinolamine structure IV (R = H). The absence of NH absorption in Nujol spectra of other 3,4-dihydro-β-carbolines has been noted (6), and a lack of OH absorption has been observed in other pseudobasic carbinolamines, such as hydrastinine (10) and cotarnine (11), while only very weak OH bands were observed in the infrared spectrum of vomalidine (12). Elementary analysis, although low in carbon,

indicated that carbon, hydrogen, and nitrogen fully accounted for the composition of the compound, which cannot therefore be represented either as the pseudobase (IV, R = H), or as an 'ether base' (cf. ref. 13).

Molecular weight determination showed the compound to be dimeric. The weight of evidence favors formulation of the product as a dimeric anhydro base (VIII). A similar dimeric structure has been proposed for a derivative obtained by dehydration of 1-hydroxy-1,2,3,4-tetrahydrocarbazole (14).

A chemical property of the compound, which is accounted for by this dimeric structure, is an unusual pyrolytic disproportionation reaction. On high-vacuum distillation the compound decomposes into 2-methyl-1,2,3,4-tetrahydro-β-carboline (IX) and 2-methyl-β-carboline anhydro base (X), whose identities were confirmed by comparison with authentic

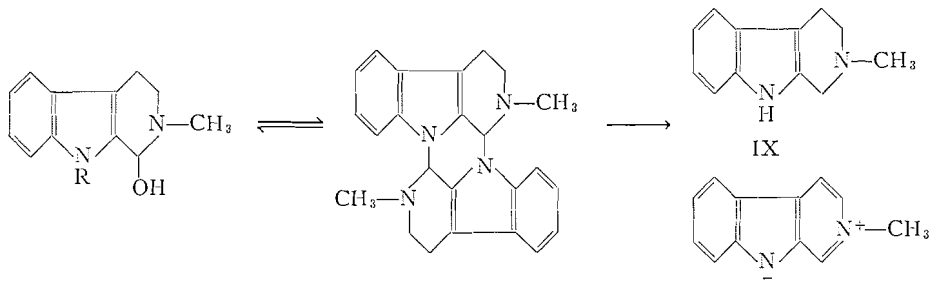

IV, R = H VIII X

samples (see refs. 15 and 16 respectively). 1-Phenyl-3,4-dihydroisoquinoline is known to undergo a similar pyrolytic disproportionation (17). Recently (18) such a disproportionation has been ascribed also to 1-methyl-3,4-dihydro-β-carboline to account for the chromatographic detection of 1-methyl-β-carboline, 1-methyl-3,4-dihydro-β-carboline, and 1-methyl-1,2,3,4-tetrahydro-β-carboline amongst the distillation products of 1-methyl-3,4-dihydro-β-carboline-3-carboxylic acid. 1-Methyl-3,4-dihydro-β-carboline has now been found (6) to distill without decomposition, however, and another explanation for the appearance of these decomposition products of the carbolinecarboxylic acid is therefore required.

9-Methyl-3,4-dihydro-β-carboline methiodide (III, R = CH_3), on treatment with alkali, gave the corresponding pseudobase (IV, R = CH_3) as a low-melting solid which decomposed on attempted distillation. The small amount of distillate consisted of an oxidation product, 2,9-dimethyl-1-oxo-1,2,3,4-tetrahydro-β-carboline (XI, R = CH_3), identical in infrared and ultraviolet absorption with an authentic specimen obtained by oxidation of 2,9-dimethyl-3,4-dihydro-β-carboline pseudobase (IV, R = CH_3) with alkaline ferricyanide. The same compound was also obtained as a minor product when the pseudobase was refluxed in alkaline solution, conditions which left the major portion of the starting material unchanged. Neither the dimeric anhydro base (VIII) nor the pseudobase (IV, R = CH_3) underwent base-catalyzed disproportionation to the 1,2,3,4-tetrahydro and the 1-oxo-1,2,3,4-tetrahydro derivatives,[1] analogous to the well-known conversion of hydrastinine to hydrohydrastinine and oxohydrastinine (19). This may be related to the fact that 2-formylindole does not appear to undergo the Cannizzaro reaction (20).

[1]*An authentic specimen of 2-methyl-1-oxo-1,2,3,4-tetrahydro-β-carboline (XI, R = H) was prepared by oxidation of harmalan methiodide.*

The dimeric anhydro base (VIII) and the pseudobase (IV, R = CH_3) reacted with hydroxylamine to yield products whose infrared spectra did not show oxime absorption and must therefore be formulated as 1-hydroxylamino-1,2,3,4-tetrahydro-β-carboline derivatives (XII), rather than as derivatives of the oxime of indole-2-aldehyde (XIII).

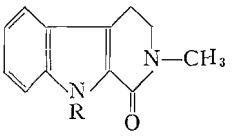

XI

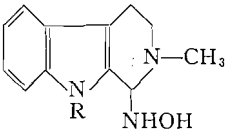

XII

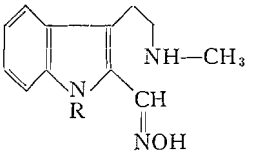

XIII

This accords with recent work (10, 11) on the structure of the hydroxylamine adducts of hydrastinine and cotarnine. The ultraviolet spectra of the hydroxylamine adducts, however, were similar to that of 2-formylindole rather than indole. This would appear to favor their existence in solution as XIII.

Methylation of the dimeric anhydro base and of the pseudobase in aqueous methanolic potassium carbonate suspension gave quaternary salts $C_{12}H_{19}IN_2O$ and $C_{15}H_{21}IN_2O$, respectively, which showed intense carbonyl absorption in the infrared, and whose ultraviolet absorption curves were similar to that of 2-formylindole. On Hofmann degradation both compounds yielded trimethylamine. From the neutral fraction of the Hofmann degradation, 2-formyl-3-vinylindole and 2-formyl-3-[β-methoxyethyl]-indole were isolated in the former case, 2-formyl-1-methyl-3-vinylindole in the latter. The methylation products are therefore 3-[2-formylindolyl]-β-ethyltrimethylammonium iodide (XIV, R = H) and its 1-methyl derivative (XIV, R = CH_3).

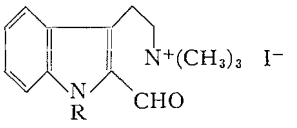

XIV

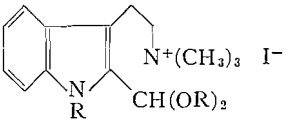

XV

When methylation was carried out under anhydrous conditions, acetals (XV) of the quaternary salts were obtained. These also yielded trimethylamine on Hofmann degradation.

The infrared absorption curves of these acetals showed ether bands in the region 1000–1200 cm^{-1} and lacked carbonyl absorption. Their ultraviolet absorption spectra in alkaline solution showed an indole chromophore. On acidification the absorption changed irreversibly to that of 2-formylindole. The acetals had been hydrolyzed to formyl derivatives on treatment with acid.

On exhaustive alkylation 3,4-dihydro-β-carboline and its 9-methyl derivative yield products which are analogous to those obtained similarly from 3,4-dihydroisoquinoline (21).

EXPERIMENTAL

3,4-Dihydro-β-carboline (Norharmalan)

$N_β$-Formyltryptamine (5) (1.5 g) and polyphosphoric acid (10 g) were heated at 100–110° for 40 minutes with constant stirring. The dark melt was poured into cold water, the solution was diluted to about 1 liter and decolorized. The clear filtrate was extracted with ether to remove non-basic impurities and was made

alkaline with 10% sodium hydroxide. The turbid solution was extracted with ether and the ether extract dried and evaporated, yielding crude 3,4-dihydro-β-carboline. Attempted purification by crystallization or chromatography gave an intractable brown polymeric material.

Sublimation at 2.10^{-3} mm and 130–140° gave 3,4-dihydro-β-carboline as a glassy solid (0.74 g, 52%) melting at 120–130° after sintering at 90°, pK_a 7.8. The product did not give a satisfactory analysis. Infrared absorption (Nujol) (cm^{-1}): 3380 (m) (NH); 1615 (m) (C=N). Ultraviolet absorption (λ_{max}, mμ (log ε)): in 0.1 *N* HCl: 355 (4.2), 245 (4.0); in 0.1 *N* NaOH: 318 (4.0), 242 (4.1).

A sample was converted to the picrate, melting at 233–234°. (Found: C, 51.1; H, 3.2. Calc. for $C_{17}H_{13}N_5O_7$: C, 51.1; H, 3.3%.) Reported melting point 241–242° (decomp.) (3), 233° (5).

9-Methyl-3,4-dihydro-β-carboline

Ind-N-methyl-N$_β$-formyltryptamine

Reduction of N-methylindoxyl with lithium aluminum hydride gave N-methylindole (22), which was converted to Ind-N-methyltryptamine by the gramine route (23).

Ind-N-methyltryptamine (3 g) was heated in a sealed tube with freshly distilled ethyl formate (25 ml) at 100° for 2 hours. The solution was diluted with ether, washed with dilute hydrochloric acid and with water, and dried. Ethyl formate and ether were evaporated and the residue was distilled at 5.10^{-3} mm and 165–170° to give *Ind-N-methyl-N$_β$-formyltryptamine* as a colorless viscous oil (2.8 g, 80%). (Found: N, 13.8. $C_{12}H_{14}N_2O$ requires: N, 13.9%.) Infrared absorption (Nujol) (cm^{-1}): 1640 (vs) (C=O).

9-Methyl-3,4-dihydro-β-carboline

Ind-N-methyl-N$_β$-formyltryptamine (1.5 g) was stirred for 1 hour with polyphosphoric acid (10 g) at 110–120°. The reaction mixture was worked up as in the preparation of 3,4-dihydro-β-carboline. The crude product was sublimed at 5.10^{-3} mm and 120°, when the product (0.75 g, 55%), melting at 120–130°, was obtained as a colorless solid. It did not give a satisfactory analysis. Infrared absorption (Nujol) (cm^{-1}): 1600 (m), 1620 (w) (C=N). Ultraviolet absorption (λ_{max}, mμ (log ε)): in 0.1 *N* HCl: 360 (4.1), 248 (4.1); in 0.1 *N* NaOH: 322 (4.0), 252 (3.9).

A sample was converted to the picrate, melting at 248–249° (decomp.). (Found: N, 16.6. $C_{18}H_{15}N_5O_7$ requires: N, 16.9%.)

3,4-Dihydro-β-carboline Methiodide

3,4-Dihydro-β-carboline (1 g) was dissolved in 50 ml dry benzene, the solution was filtered, and the residue rejected. The filtrate was diluted to 250 ml with dry benzene, methyl iodide (3 ml) was added and the mixture was allowed to stand at room temperature for 48 hours, when yellow needles, contaminated with a brown impurity, had deposited. The solid was dissolved in methanol, the solution treated with charcoal and concentrated, and the residue crystallized from aqueous methanol, when the *methiodide* (1.4 g, 70%) was obtained as long needles of the monohydrate, melting at 223° after sintering at 215°. (Found: H_2O, 4.9. $C_{12}H_{13}IN_2,H_2O$ requires: H_2O, 5.4%. After drying to constant weight, found: C, 46.2; H, 4.4; N. 8.9. $C_{12}H_{13}IN_2$ requires: C, 46.1; H, 4.2; N, 9.0%.) Infrared absorption (Nujol) (cm^{-1}): 3160 (m) (NH); 1640 (s) ($C=N^+$). Ultraviolet absorption (λ_{max}, mμ (log ε)): in 0.1 *N* HCl: 360 (4.3), 248 (4.0); in 0.1 *N* NaOH: 282 (3.7).

Dimeric Anhydro Base from 3,4-Dihydro-β-carboline Methiodide

3,4-Dihydro-β-carboline methiodide (0.25 g) was dissolved in 20 ml water, and 10% sodium hydroxide was added with constant stirring. The light yellow precipitate was washed with water, rubbed with methanol (5 ml), filtered, and again washed with a little methanol to yield a colorless amorphous powder (0.12 g, 85%), melting at 184–185°. The same product was obtained when more dilute sodium hydroxide or ammonia was used to liberate the anhydro base. Crystallization from dry chloroform did not raise the melting point. (Found: molecular weight,[2] 346±35; C,[3] 77.4; H, 6.8; N, 15.4. $(C_{12}H_{12}N_2)_2$ requires: molecular weight, 368; C, 78.2; H, 6.6; N, 15.2%.) Addition to a small quantity of the anhydro base of concentrated sulphuric acid containing a trace of ferric chloride gave an ultramarine color which on standing changed to crimson.

Treatment of the Dimeric Anhydro Base with Alkali

The anhydro base (0.02 g) was suspended in 30% potassium hydroxide in aqueous methanol (5 ml) and the solution refluxed on the steam bath for 4 hours. Alcohol was evaporated and the residue acidified with hydrochloric acid. The solution was extracted with ether, the ether extract dried and concentrated. The ether extract did not contain material absorbing in the ultraviolet region of the spectrum.

When the aqueous solution was made alkaline with excess 10% sodium hydroxide unchanged starting material was recovered.

Distillation of the Dimeric Anhydro Base

The anhydro base (0.1 g) was distilled at 1.10^{-2} mm and 140–150°. A mixture of a colorless and a yellow substance sublimed and a black residue remained. When the sublimate was redistilled at 1.10^{-2} mm below 100° the colorless substance sublimed and the yellow substance remained as residue.

[2]*Schwarzkopf Microanalytical Laboratory, Woodside, N.Y., U.S.A.*

[3]*Consistently low analytical values for carbon (eight determinations) were presumably due to contamination of the dimeric product by small amounts of pseudobase (IV, R = H).*

The colorless substance was 2-methyl-1,2,3,4-tetrahydro-β-carboline, melting at 216–217°, identical in melting point and infrared and ultraviolet spectra with an authentic sample (15).

The yellow substance, melting at 212–214°, proved to be identical by similar criteria with an authentic sample of 2-methyl-β-carboline anhydro base (16).

1-Hydroxylamino-2-methyl-1,2,3,4-tetrahydro-β-carboline

A solution of the dimeric anhydro base (0.1 g) and hydroxylamine hydrochloride (0.05 g) in methanol (25 ml) was refluxed for 15 minutes. The solvent was distilled off and the residue was dissolved in water. Addition of ammonia gave a precipitate, which was dissolved in ether. The ether solution was dried, the solvent evaporated, and the residue crystallized from methanol, yielding colorless crystals of *1-hydroxylamino-2-methyl-1,2,3,4-tetrahydro-β-carboline* (0.08 g, 75%) melting at 182°. (Found: C, 66.6; H, 7.5; N, 18.9. $C_{12}H_{15}N_3O$ requires: C, 66.3; H, 7.0; N, 19.3%.) Ultraviolet absorption (λ_{max}, mμ (log ε)): in 0.1 *N* HCl: 310 (4.3), 250 (4.2); in 0.1 *N* NaOH: 315 (4.3).

9-Methyl-3,4-dihydro-β-carboline Methiodide

9-Methyl-3,4-dihydro-β-carboline (0.5 g) was dissolved in 75 ml benzene, methyl iodide (2 ml) was added, and the solution was kept at 37° for 24 hours. A yellow solid separated which was recrystallized from water to give the *methiodide* as pale yellow needles (0.7 g, 70%) melting at 228°. (Found: C, 48.1; H, 4.9; N, 8.6; I, 38.9. $C_{13}H_{15}IN_2$ requires: C, 47.9; H, 4.6; N, 8.6; I, 39.0%.) Infrared absorption (Nujol) (cm^{-1}): 1648 (s) ($C{=}\overset{+}{N}$). Ultraviolet absorption (λ_{max}, mμ (log ε)): in 0.1 *N* HCl: 364 (4.4), 252 (4.1); in 0.1 *N* NaOH: 286 (3.8).

Attempted Characterization of 2,9-Dimethyl-1-hydroxy-1,2,3,4-tetrahydro-β-carboline

The above methiodide (0.5 g) was dissolved in a small amount of water. Addition of 20% sodium hydroxide gave an oil which, on cooling, solidified to an amorphous, light green solid melting at 55°. Ultraviolet absorption (λ_{max}, mμ): in 0.1 *N* HCl: 364, 252; in 0.1 *N* NaOH: 286; in ether: 287. The product was not analyzed.

High-vacuum distillation did not lead to a purer product and was accompanied by oxidation. At 3.10^{-3} mm and 110° a dark yellow oil was obtained. This was dissolved in ether, the solution was extracted with *N* hydrochloric acid, the acid extract made alkaline and extracted with ether, and the ether extract dried (Na_2SO_4) and evaporated. The amorphous residue showed an infrared spectrum identical with that of the crude pseudobase. The original ether solution, containing the non-basic fraction, was dried and evaporated. A small amount of colorless residue, melting at 68–70°, was obtained whose infrared absorption was identical with that of 2,9-dimethyl-1-oxo-1,2,3,4-tetrahydro-β-carboline.

Pseudobase obtained from 0.5 g methiodide was refluxed 2 hours with 35% potassium hydroxide solution (10 ml). The solution was extracted with ether, the ether extract was washed with *N* hydrochloric acid and with water, dried (Na_2SO_4), and evaporated. Sublimation of the residue at 3.10^{-3} mm and 90° gave 2,9-dimethyl-1-oxo-1,2,3,4-tetrahydro-β-carboline as a colorless solid melting at 68–70° identical in melting point and infrared and ultraviolet absorption with an authentic specimen (*vide infra*).

2,9-Dimethyl-1-hydroxylamino-1,2,3,4-tetrahydro-β-carboline

Pseudobase from 0.5 g methiodide was dissolved in methanol (30 ml), and hydroxylamine hydrochloride (0.13 g) and potassium carbonate (0.20 g) was added. The mixture was kept at 40° for 2 hours, the solvent was evaporated, the residue was washed with cold water (2×3 ml) and was crystallized from methanol after treatment with charcoal. The *product* (0.23 g, 65%) was obtained as a colorless solid melting at 156°. (Found: C, 67.2; H, 7.5; N, 18.1. $C_{13}H_{17}N_3O$ requires: C, 67.5; H, 7.4; N, 18.2%.) Ultraviolet absorption (λ_{max}, mμ (log ε)): in 0.1 *N* HCl: 310 (4.3), 243 (4.3); in 0.1 *N* NaOH: 315 (4.3).

2-Methyl-1-oxo-1,2,3,4-tetrahydro-β-carboline

1-Methyl-3,4-dihydro-β-carboline methiodide (6) (0.33 g) was dissolved in hot water. Acetone (50 ml) and *N* sodium hydroxide (2 ml) was added, the solution was cooled to −5°, and finely ground potassium permanganate (0.50 g) was added in small portions. The solution was acidified with *N* hydrochloric acid (2.5 ml), excess permanganate destroyed by addition of hydrogen peroxide, the mixture filtered, and the filtrate concentrated. Recrystallization of the residue from a large volume of boiling water gave fine needles of *2-methyl-1-oxo-1,2,3,4-tetrahydro-β-carboline* (0.09 g, 45%) melting at 237–238°. (Found: C, 72.1; H, 6.2. $C_{12}H_{12}N_2O$ requires: C, 72.0; H, 6.1%.) Infrared absorption (Nujol) (cm^{-1}): 3190 (m) (NH); 1620 (vs) (C=O). Ultraviolet absorption (λ_{max}, mμ (log ε)): in 0.1 *N* HCl and NaOH: 303 (4.2), 240 (4.2, shoulder) (Fig. 3, curve E).

2,9-Dimethyl-1-oxo-1,2,3,4-tetrahydro-β-carboline

Pseudobase from 0.32 g 9-methyl-3,4-dihydro-β-carboline methiodide was suspended in 10 ml 5% potassium hydroxide solution. Potassium ferricyanide (0.4 g), dissolved in 20 ml water, was added and the mixture heated on the steam bath for 4 hours. The solution was extracted with ether, the extract washed with *N* hydrochloric acid and with water, dried (Na_2SO_4), and the solvent evaporated. The residue sublimed at 3.10^{-3} and 80°, giving colorless crystals (0.07 g, 32%) of 2,9-dimethyl-1-oxo-1,2,3,4-tetrahydro-β-carboline melting at 69–71°. (Found: C, 72.8; H, 7.0; N, 13.1. Calc. for $C_{13}H_{14}N_2O$: C, 72.9; H, 6.6; N, 13.1%.)

Reported melting point: 65–66° (24). Infrared absorption (Nujol) (cm^{-1}): 1640 (vs) (C=O). Ultraviolet absorption (λ_{max}, $m\mu$ (log ϵ)): in 0.1 *N* HCl and 0.1 *N* NaOH: 305 (4.1).

Exhaustive Methylation of the Dimeric Anhydro Base

3-[2-Formylindolyl]-β-ethyltrimethylammonium Iodide

Dimeric anhydro base (0.4 g) was suspended in methanol (20 ml). Potassium carbonate (0.2 g) and methyl iodide (5 ml) were added and the mixture was kept at 40° for 24 hours. The solvent was evaporated, the residue was washed with cold water (3 ml) and crystallized from 50% aqueous methanol after treatment with charcoal, when colorless needles (0.42 g, 70%) of the *quaternary iodide*, melting at 270°, were obtained. (Found: C, 46.9; H, 5.3; N, 7.6; I, 35.8. $C_{14}H_{19}IN_2O$ requires: C, 46.9; H, 5.3; N, 7.8; I, 35.5%.) Infrared absorption (Nujol) (cm^{-1}): 3280 (m, broad) (NH); 1655 (vs) (C=O). Ultraviolet absorption (λ_{max}, $m\mu$ (log ϵ)): in 0.1 *N* HCl and in 0.1 *N* NaOH: 315 (4.1), 237 (4.1).

Hofmann Degradation of 3-[2-Formylindolyl]-β-ethyltrimethylammonium Iodide

A stream of nitrogen gas was passed for 2 hours through a solution of the above quaternary salt (0.35 g) in 5% methanolic potassium hydroxide (20 ml) at 50°. The issuing gas was passed through an alcoholic solution of picric acid. Concentration of the picric acid solution gave a picrate (0.28 g) which melted at 216° (decomp.) after recrystallization from methanol, and was identified as trimethylamine picrate by comparison with an authentic sample. (Found: C, 37.7; H, 4.3; N, 19.2. Calc. for $C_9H_{12}N_4O_7$: C, 37.5; H, 4.2; N, 19.4%.)

The reaction mixture was evaporated *in vacuo*, water (10 ml) was added to the residue, and the mixture was extracted with ether. The ether extract was washed with water, dried, and evaporated. The residue was dissolved in methanol, the solution decolorized with charcoal and evaporated. The residue was distilled at 3.10^{-3} mm and 70°, when two fractions were obtained.

The first fraction (0.035 g), a colorless solid melting at 110°, was *2-formyl-3-[β-methoxyethyl]-indole.* (Found: C, 70.9; H, 6.6. $C_{12}H_{13}NO_2$ requires: C, 70.9; H, 6.5%.) Infrared absorption (Nujol) (cm^{-1}): 3210 (m) (NH); 1650 (vs) (C=O); 1012 (m), 1070 (m), 1094 (s) (OCH_3). Ultraviolet absorption (λ_{max}, $m\mu$ (log ϵ)): in 0.1 *N* HCl and in 0.1 *N* NaOH: 317 (4.2), 238 (4.1).

The second fraction, a pale yellow solid (0.045 g) melting at 126° after sintering at 115°, was *2-formyl-3-vinylindole.* (Found: C, 77.0; H, 5.4; N, 8.0. $C_{11}H_9NO$ requires: C, 77.2; H, 5.3; N, 8.2%.) Infrared absorption (Nujol) (cm^{-1}): 3280 (m) (NH); 1640 (vs) (C=O); 1615 (s) (C=C); 918 (m), 972 (m) (vinyl). Ultraviolet absorption (λ_{max}, $m\mu$ (log ϵ)): in 0.1 *N* HCl and in 0.1 *N* NaOH: 322 (4.2), 252 (4.1).

Dimethylacetal of 3-[2-Formylindolyl]-β-ethyltrimethylammonium Iodide

Dimeric anhydro base (0.4 g) was suspended in 20 ml methanol. Anhydrous potassium carbonate (2.0 g) and methyl iodide (5 ml) were added and the reaction mixture was kept at 40° for 24 hours. The solvent was evaporated, the residue was washed with cold water (3 ml) and crystallized from aqueous methanol after treatment with charcoal to give colorless needles (0.58 g, 66%) of the *dimethylacetal* melting at 180°. (Found: C, 47.4; H, 6.2; N, 7.0. $C_{16}H_{25}IN_2O_2$ requires: C, 47.5; H, 6.2; N, 6.9%.) Infrared absorption (Nujol) (cm^{-1}): 3330 (m) (NH); 1030 (m), 1090 (s) (—OCH_3). Ultraviolet absorption (λ_{max}, $m\mu$ (log ϵ)): in 0.1 *N* HCl: 318 (3.9); in 0.1 *N* NaOH: 282 (3.7).

Hofmann Degradation of the Dimethylacetal

The acetal (0.20 g) was dissolved in 5% methanolic potassium hydroxide (20 ml). The solution was kept at 60° and swept out with a current of nitrogen for 4 hours and the issuing gas passed through an alcoholic solution of picric acid, from which trimethylamine picrate was isolated as described earlier. The reaction mixture was evaporated *in vacuo*, water was added to the residue, and the solution was extracted with ether. The ether extract was washed with water, dried, and evaporated. The residue was dissolved in methanol, treated with charcoal, and again evaporated.

The residue was distilled at 3.10^{-3} mm and 70°, when a small amount of a colorless solid, melting at 115°, was obtained, which may have been the dimethylacetal of 2-formyl-3-vinylindole. The quantity obtained was insufficient for analysis. Infrared absorption (Nujol) (cm^{-1}): 3215 (m) (NH); 1635 (s) (C=C); 970 (m), 910 (m) (vinyl); 1090 (m), 1045 (m) (OCH_3). Ultraviolet absorption (λ_{max}, $m\mu$ (log ϵ)): in 0.1 *N* HCl: 319 (4.1); in 0.1 *N* NaOH: 317 (3.9).

Diethylacetal of 3-[2-Formylindolyl]-β-Ethyltrimethylammonium Iodide

Dimeric 2-methyl-3,4-dihydro-β-carboline anhydro base was methylated in the presence of anhydrous potassium carbonate in ethanol suspension.

The *diethylacetal* was obtained in the form of colorless needles melting at 230°. (Found: C, 50.3; H, 6.8; N, 6.4. $C_{18}H_{29}IN_2O_2$ requires: C, 50.0; H, 6.7; N, 6.5%.) Infrared absorption (Nujol) (cm^{-1}): 3380 (m) (NH); 1030 (m), (1090) (s) (OC_2H_5). Ultraviolet absorption (λ_{max}, $m\mu$ (log ϵ)): in 0.1 *N* HCl: 318 (3.9); in 0.1 *N* NaOH: 282 (3.7).

Exhaustive Methylation of 2,9-Dimethyl-1-hydroxy-1,2,3,4-tetrahydro-β-carboline

3-[2-Formyl-1-methylindolyl]-β-ethyltrimethylammonium Iodide

Pseudobase from 0.5 g 9-methyl-3,4-dihydro-β-carboline methiodide was dissolved in methanol (20 ml). Potassium carbonate (0.2 g) and methyl iodide (5 ml) were added and the mixture kept at 40° for 24 hours.

The solvent was evaporated, the residue was washed with water and crystallized from 50% aqueous methanol after treatment with charcoal. Pale, shining plates (0.38 g, 60%) of the monohydrate of the *quaternary salt*, melting at 244°, were obtained. (Found: C, 46.3; H, 6.1; N, 6.8; I, 32.4. $C_{15}H_{21}IN_2O,H_2O$ requires: C, 46.2; H, 5.9; N, 7.2; I, 32.6%.) Infrared absorption (Nujol) (cm^{-1}): 1652 (vs) (C=O). Ultraviolet absorption (λ_{max}, mμ (log ϵ)): in 0.1 *N* HCl and 0.1 *N* NaOH: 318 (4.2), 240 (4.2).

Hofmann Degradation of 3-[2-Formyl-1-methylindolyl]-β-ethyltrimethylammonium Iodide

The above quaternary salt (0.25 g) was treated with 5% methanolic potassium hydroxide (15 ml) under nitrogen as described earlier and products isolated as before. The basic product was isolated as the picrate (0.17 g) melting at 216° (decomp.) and identified as trimethylamine picrate by comparison with an authentic sample.

The neutral product, *2-formyl-1-methyl-3-vinylindole*, was obtained as pale yellow crystals (0.020 g) melting at 82°. (Found: C, 77.9; H, 6.3; N, 7.6. $C_{12}H_{11}NO$ requires: 77.8; H, 6.0; N, 7.6%.) Infrared absorption (Nujol) (cm^{-1}): 1650 (vs) (C=O), 1605 (s) (C=C); 928 (m), 992 (m) (vinyl). Ultraviolet absorption (λ_{max}, mμ (log ϵ)): in 0.1 *N* HCl and in 0.1 *N* NaOH: 322 (4.2), 253 (4.2).

Oxime of 3-[2-Formyl-1-methylindolyl]-β-ethyltrimethylammonium Iodide

3-[2-Formyl-1-methylindolyl]-β-ethyltrimethylammonium iodide (0.20 g) was dissolved in 50% aqueous alcohol. Hydroxylamine hydrochloride (0.05 g) and potassium carbonate (0.05 g) were added. The reaction mixture was kept at 60° for ½ hour. Concentration yielded the *oxime* (0.15 g, 75%), melting at 256°, after recrystallization from aqueous alcohol. (Found: C, 46.6; H, 6.0; N, 11.1. $C_{15}H_{22}IN_3O$ requires: C, 46.3; H, 5.7; N, 10.9%.) Ultraviolet absorption (λ_{max}, mμ (log ϵ)): in 0.1 *N* HCl: 310 (4.1); in 0.1 *N* NaOH: 315 (4.1), 254 (4.1).

Dimethylacetal of 3-[2-Formyl-1-methylindolyl]-β-ethyltrimethylammonium Iodide

When the pseudobase was methylated in methanol solution in the presence of a large excess of anhydrous potassium carbonate, the *dimethylacetal* was obtained as colorless needles melting at 233°. (Found: C, 48.7; H, 6.6. $C_{17}H_{27}IN_2O_2$ requires: C, 48.8; H, 6.5%.) Infrared absorption (Nujol) (cm^{-1}): 1040 (m), 1095 (s) (OCH_3). Ultraviolet absorption (λ_{max}, mμ (log ϵ)): in 0.1 *N* HCl: 318 (4.3); in 0.1 *N* NaOH: 282 (4.0) (broad).

ACKNOWLEDGMENTS

Financial assistance by the National Research Council of Canada and by the Ontario Research Foundation is gratefully acknowledged.

REFERENCES

1. E. Späth and E. Lederer. Ber. **63**, 120 (1930); cf. W. M. Whaley and T. R. Govindachari. Org. Reactions, **6**, 142 (1951).
2. E. Späth and E. Lederer. Ber. **63**, 2102 (1930).
3. Y. Asahina and K. Kashiwaki. J. Pharm. Soc. Japan, No. 405, 1293 (1915).
4. Y. Asahina. J. Pharm. Soc. Japan, No. 503, 1 (1924).
5. C. Schöpf and H. Steuer. Ann. **558**, 124 (1947).
6. R. N. Gupta and I. D. Spenser. Can. J. Chem. This issue.
7. E. Späth, F. Berger, and W. Kuntara. Ber. **63**, 134 (1930).
8. H. Decker, W. Kropp, H. Hoyer, and P. Becker. Ann. **395**, 299 (1913).
9. B. Witkop. Experientia, **10**, 420 (1954).
10. W. Schneider and B. Müller. Ann. **615**, 34 (1958). W. Schneider. Private communication.
11. D. Beke, D. Korbonits, and R. Kornis-Markovits. Ann. **626**, 225 (1959).
12. A. Hofmann and A. J. Frey. Helv. Chim. Acta, **40**, 1866 (1957).
13. A. Hantzsch and M. Kalb. Ber. **32**, 3109 (1899). A. Kaufmann and P. Strübin. Ber. 44, 680 (1911).
14. A. C. Geale, J. M. G. Linnell, and M. L. Tomlinson. J. Chem. Soc. 1124 (1956).
15. V. Boekelheide and C. Ainsworth. J. Am. Chem. Soc. **72**, 2132 (1950).
16. I. D. Spenser. J. Chem. Soc. 3659 (1956).
17. C. I. Brodrick and W. F. Short. J. Chem. Soc. 2587 (1949).
18. R. Tschesche and H. Jenssen. Chem. Ber. **93**, 271 (1960).
19. M. Freund and W. Will. Ber. **20**, 2400 (1887).
20. W. I. Taylor. Helv. Chim. Acta, **33**, 164 (1950).
21. W. J. Gensler, E. M. Healy, I. Onshuus, and A. L. Bluhm. J. Am. Chem. Soc. **78**, 1713 (1956).
22. P. L. Julian and H. C. Printy. J. Am. Chem. Soc. **71**, 3206 (1949).
23. H. R. Snyder and E. L. Eliel. J. Am. Chem. Soc. **70**, 1703 (1948).
24. R. A. Abramovitch. J. Chem. Soc. 4593 (1956).

THE ULTRAVIOLET ABSORPTION SPECTRUM OF NITROUS ACID IN THE VAPOR STATE

G. W. KING AND D. MOULE[1]
Department of Chemistry, McMaster University, Hamilton, Ontario
Received July 3, 1962

ABSTRACT

The diffuse absorption bands of $HON^{14}O$, $HON^{15}O$, $DON^{14}O$, and $DON^{15}O$ in the near ultraviolet have been examined. Transitions from both rotational isomers of nitrous acid contribute to the vibrational structure, with the excited state $\sigma(N{=}O)$ stretching vibrations active in the most intense progressions. The cis–trans energy separation increases from 500 cal/mole in the ground state to 1200 cal/mole in the upper state. This is attributed to weakening of the internal hydrogen bond in the cis state upon an electronic promotion of primarily $n_O \rightarrow \pi^*$ type. The accompanying change in geometry is responsible for the appearance of the cis ground-state $\delta(ONO)$ bending mode in the spectrum.

INTRODUCTION

Gaseous mixtures of NO, NO_2, and water vapor exhibit a system of diffuse absorption bands in the 4000–3000 Å spectral region (1). The isotopic wavelength shift upon deuteration eliminates NO_2, N_2O_3, and N_2O_4, all of which absorb in the same region, as possible carrier species (2, 3). The intensity of absorption varies in proportion to the calculated equilibrium concentration of nitrous acid in gas mixtures of different composition and temperature and the spectrum is attributed to this molecule. Alkyl nitrites in general show, in the same spectral region, a similar diffuse absorption spectrum (4) which is typical of the —O—N=O group. Analysis of the nitrous acid spectrum is complicated by the diffuse nature of the bands, by the discrete background absorption of the NO_2 present in the gas mixture, and by perturbations between vibrational levels of the excited DONO molecule.

In addition to examining the spectra of HONO and DONO containing the naturally occurring N^{14} isotope under improved experimental conditions, we have also investigated the spectra of the additional isotopically substituted species $HON^{15}O$ and $DON^{15}O$. In this paper, the arguments of previous investigators are reconsidered in the light of our data, and a plausible interpretation of the spectrum of nitrous acid vapor is given. In a subsequent paper, the spectrum of nitrous acid in various solvents will be discussed on the basis of this interpretation.

EXPERIMENTAL

In order to minimize contamination of the nitrous acid spectrum by the intense discrete absorption bands of NO_2, the partial pressure of this oxide in the gas mixture was kept small. A typical mixture showing minimum background absorption was obtained by equilibrating NO, NO_2, and H_2O at initial partial pressures of 740, 2, and 15 mm respectively in a 50 cm path length absorption cell. The NO and NO_2 (Matheson Co. Inc.) were taken from cylinders without further purification. DONO was formed by substituting D_2O with deuterium content >99.7% for the H_2O in the mixture.

Five hundred cubic centimeters of $N^{15}O$ at S.T.P., with N^{15} content >98%, was supplied by the Isomet Corporation. Half of this was mixed at 260 mm pressure with O_2 at 1 mm and H_2O at 15 mm directly in the absorption cell to form $HON^{15}O$. The other half was used to form $DON^{15}O$ by a similar procedure.

Spectra of all four isotopic species were taken on a Bausch and Lomb 1.5-m grating spectrograph (Model 11), used in the first and second orders with resolving powers of 35,000 and 70,000 respectively. Wavelength measurements of the intensity maxima of the bands were made off microdensitometer traces, by interpolation between iron arc reference spectra that were also recorded on the spectrograms. The vacuum

[1]*Holder of a C.I.L. Fellowship, 1960–1962.*

wave numbers of the bands are given in Table I, together with an estimate of the uncertainty in measurement. (1) indicates a clearly resolved band with a sharp maximum, (2) indicates a band with a more rounded

TABLE I

Wave numbers of maxima of ultraviolet absorption bands of nitrous acid

Label	HONO	HON^{15}O	DONO	DON^{15}O	Assignment
A	26,034 (2)	26,043 (2)	26,050 (2)	26,060 (2)	0–0 (t)
B	27,150 (1)	27,145 (1)	27,197 (1)	27,185 (1)	$1\nu_2'$ (t)
C	28,225 (1)	28,209 (1)	28,308 (1)	28,283 (1)	$2\nu_2'$ (t)
D	29,253 (1)	29,223 (1)	29,384 (1)	29,344 (1)	$3\nu_2'$ (t)
E	30,231 (1)	30,195 (1)	30,460 (2)	30,403 (2)	$4\nu_2'$ (t)
F	31,175 (2)	31,121 (2)	(31,440)		$5\nu_2'$ (t)
G	(32,075)				$6\nu_2'$ (t)
A''	27,420 (3)	27,421 (3)	27,483 (2)	27,464 (2)	$1\nu_2'$ (c)
B''	28,495 (1)	28,477 (1)	28,551 (1)	28,526 (1)	$2\nu_2'$ (c)
C''	29,518 (1)	29,494 (1)	29,584 (1)	29,553 (1)	$3\nu_2'$ (c)
D''	30,505 (1)	30,472 (1)	30,612 (2)	30,570 (2)	$4\nu_2'$ (c)
E''	31,461 (2)	31,402 (2)	(31,426)		$5\nu_2'$ (c)
F''	(32,350)				$6\nu_2'$ (c)
A'	(26,910)				$1\nu_2'-\nu_5''$ (c)
B'	27,955 (3)	27,923 (3)	27,915 (3)*	27,914 (3)*	$2\nu_2'-\nu_5''$ (c)
C'	28,882 (2)	28,878 (2)	28,946 (3)†	28,928 (3)†	$3\nu_2'-\nu_5''$ (c)
D'	29,874 (2)	29,842 (2)	29,993 (2)‡	29,935 (2)‡	$4\nu_2'-\nu_5''$ (c)
E'	30,871 (2)	30,803 (2)	(30,830)§		$5\nu_2'-\nu_5''$ (c)
F'	31,808 (2)	31,758 (2)			$6\nu_2'-\nu_5''$ (c)
A'			27,036 (3)	27,031 (3)	$\nu_2'+\nu_4'$ (c) (?)
B'			28,146 (3)	28,099 (3)	$2\nu_2'+\nu_4'$ (c) (?)
C'			29,201 (2)	29,171 (2)	$3\nu_2'+\nu_4'$ (c) (?)
D'			30,239 (2)	30,201 (2)	$4\nu_2'+\nu_4'$ (c) (?)
E'			(31,280)		$5\nu_2'+\nu_4'$ (c) (?)
A''''			29,827 (2)	29,806 (2)	?

NOTE: (1) indicates an uncertainty of measurement <2 cm^{-1}, (2) indicates <10 cm^{-1}, and (3) indicates <50 cm^{-1}. Bracketed wave numbers are measured from spectrophotometer traces, with an uncertainty <30 cm^{-1}.

*A'''.
†B'''.
‡C'''.
§D'''.

peak, and (3) refers to weak bands overlapped by other bands. The bracketed wave numbers represent HONO and DONO bands which could not be clearly distinguished from the residual NO_2 absorption on the spectrograms, and which were measured off the spectrophotometer records described below.

In order to study the variation of absorption intensity of HONO and DONO with temperature, a Perkin–Elmer Spectracord Model 4000 was modified to accommodate an electrically heated absorption cell with a 1-m optical path length in the sample beam. The cell was sealed after filling with gas mixture and spectra were recorded over the temperature range 25–130° C. A 10-cm gas cell was inserted in the reference beam and heated to the same temperature as that of the sample cell. Before each spectrum was recorded, the reference cell was filled with sufficient NO_2 to balance out the interfering background, together with dry NO to bring the total pressure to 1 atm. This procedure also partly balanced out a weak continuous background absorption, probably due to N_2O_3 and N_2O_4, that was also present. Very clean nitrous acid spectra could be obtained in this manner; the residual continuous background absorption did not affect the temperature dependence studies, which involved comparison of the intensities of adjacent strong bands in the nitrous acid spectrum.

RESULTS

The ultraviolet absorption spectrum of HONO at 25° C is shown in Fig. 1. This is taken from a spectrophotometer record with compensated background. Comparison of microdensitometer traces of spectrograms of HONO and HON^{15}O shows that the two spectra have identical overall patterns apart from isotopic wavelength shifts. Three progressions of bands appear in both spectra. Each of these is labelled alphabetically in accordance with the nomenclature of previous workers (3) and identified below as the A, A', or A'' progression respectively.

The spectrum of DONO at 25° C is presented in Fig. 2. The prominent bands again can be grouped into three strong progressions, labelled A, A', and A'', and are displaced

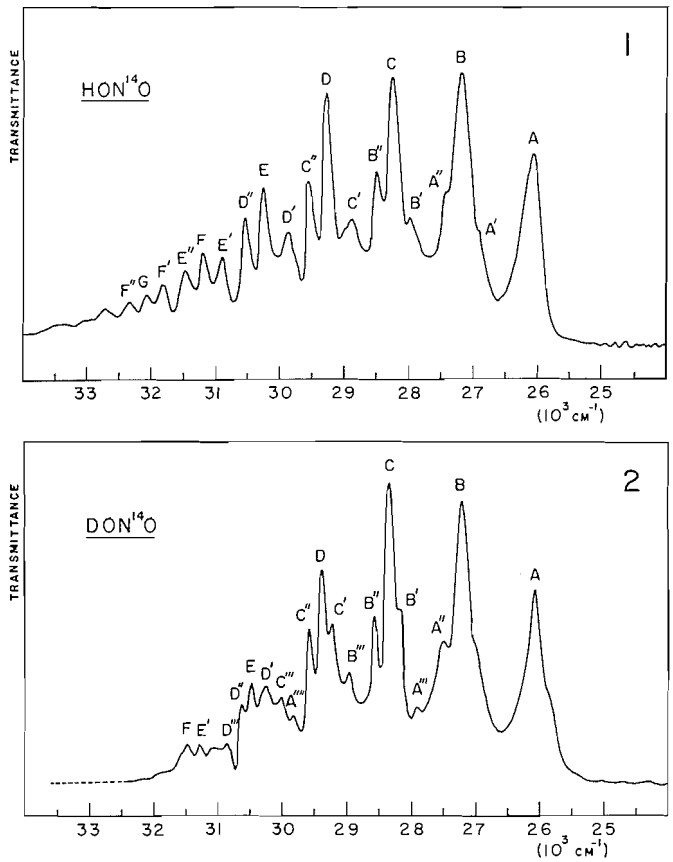

FIG. 1. The absorption spectrum of HONO at 25° C.
FIG. 2. The absorption spectrum of DONO at 25° C.

to slightly higher frequencies by comparison with their counterparts in the HONO spectrum. In addition, four weak bands labelled A''', B''', C''', and A'''' are also present in the DONO spectrum. The spectrum of DON^{15}O shows the same number of bands, with the same relative positions and intensities, as does the DONO spectrum.

The bands in all of the spectra show a peculiar diffuseness, having a symmetric form that is devoid of local undulations. No traces of fine structure were apparent even when the bands were photographed on a 20-ft grating spectrograph with a resolving power of 150,000; in these experiments, the lowest total pressure of the absorbing gas mixture that gave a detectable concentration of nitrous acid was 40 mm, so it is possible, but highly unlikely, that the diffuseness was due to residual pressure broadening. The band profiles did not alter as the pressure was decreased, an observation which indicates that intermolecular association is absent.

The A band in each spectrum is slightly broader, but apart from this, all the other strong bands are uniformly diffuse with a half width of $\sim$60 cm^{-1}. This diffuseness is different from the usual type that is observed in the spectra of light polyatomic molecules,

which is caused by vibrational predissociation in the excited electronic state and which increases markedly towards higher wave numbers.

At elevated temperatures, the increase of NO_2 and N_2O_4 and the decrease of nitrous acid concentration in the equilibrium gas mixture make band intensities difficult to measure accurately, owing to the greater background contamination appearing in the spectrum. Nevertheless, the intensities of the A', A'', and A''' progressions detectably increase relative to the A progression in each spectrum as the temperature is raised. This is illustrated by the portions of the HONO and DONO spectra shown in Fig. 3.

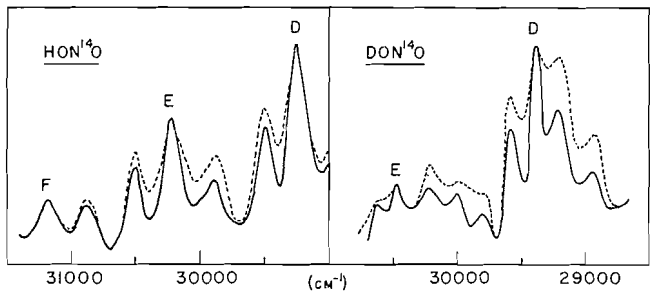

FIG. 3. Portions of the HONO and DONO spectra at 25° C (solid curves) and 135° C (broken curves).

ANALYSIS

Analysis of the infrared spectrum (5, 6) shows that nitrous acid consists of a mixture of two planar isomeric forms in the ground electronic state. These have the dimensions (5) shown in Fig. 4. The cis form is 506±250 cal/mole higher in energy than the trans form, with $p_{trans}/p_{cis} \sim 2.5$ at 25° C. The fundamental frequencies are listed in Table II.

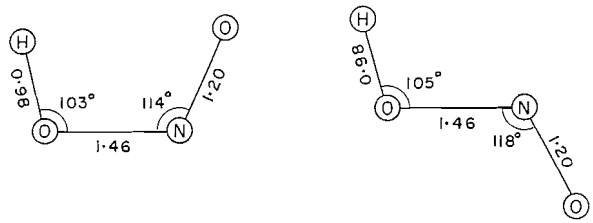

FIG. 4. Estimated dimensions (Å) of *cis*- and *trans*-nitrous acid in the ground state.

TABLE II

Fundamental vibration frequencies (cm^{-1}) of gaseous nitrous acid
(Ground-state values are averaged from Jones, Badger, and Moore (5) and D'Or and Tarte (6))

Cis				Trans					
HONO		DONO		HONO		DONO			
ν''	ν'	ν''	ν'	ν''	ν'	ν''	ν'		
3425		2533		3590		2659		ν_1 (a')	σ(O—H)
1639	1127	1618	~1100	1698	1139	1697	~1100	ν_2 (a')	σ(N=O)
1370 (?)		1086	~1000	1263		1016	~1000	ν_3 (a')	δ(NOH)
855		816	660 (?)	793		739		ν_4 (a')	σ(N—O)
620*		620*		598		591		ν_5 (a')	δ(ONO)
637		508		544		416		ν_6 (a'')	τ(O—H)

*Revised—see text.

Rotational isomerism is common in the ground states of alkyl nitrites (7–9) and the calculated barrier height of ~10 kcal/mole in nitrous acid (10) agrees with the value of ~9 kcal/mole for primary nitrites (9).

A singlet–singlet $n \rightarrow \pi^*$ type of electronic transition is undoubtedly responsible for the near-ultraviolet spectra of nitrites and nitrous acid. The low absorption intensity ($f = 0.002$ and $\epsilon_{max} = 110$ for nitrous acid in aqueous solution) is characteristic of such transitions and cannot be ascribed to an electronically forbidden $\pi \rightarrow \pi^*$ transition, since both the alkyl nitrites and nitrous acid are classified under the C_s point group for which all transitions are symmetry allowed.

The *A* progression is the most prominent feature in the spectrum of each isotopic species. The intensity distribution and wave number separations between successive bands in the progression are similar in the four spectra, and indicate an active excited-state vibration of ~1130 cm^{-1}. A similar interval is also prominent in the spectra of alkyl nitrites (7); hence the vibration must be localized primarily in the —O—N=O group: this interpretation is confirmed for nitrous acid by the observed small decrease in frequency upon N^{15} substitution and the absence of a large frequency decrease upon deuteration, both of which are apparent from the frequency differences listed in Table III. An electronic $n \rightarrow \pi^*$ excitation, in which a non-bonding electron is promoted into a

TABLE III

Band separations (cm^{-1}) in the *A* progression

Bands	HONO	$HON^{15}O$	DONO	$DON^{15}O$
B–A	1116	1102	1147	1125
C–B	1075	1064	1111	1098
D–C	1028	1014	1076	1061
E–D	978	972	1059	1059
F–E	944	926	(980)	
G–F	(900)			

relatively antibonding molecular orbital, is expected to cause a general decrease in the vibrational frequencies of groups affected by the promotion. This is true for such transitions in carbonyl compounds, where, for example, the C=O stretching frequency drops to ~1300 cm^{-1} from 1700 cm^{-1} in the ground state. At this stage in the analysis, therefore, we assign the intervals in the *A* progression to an excited-state N=O stretching vibration of nitrous acid. A similar frequency assignment has been made for nitroso and nitro compounds in their excited states (11).

Previous interpretations of the other bands in the spectrum (2, 4) were made before the cis–trans isomerism of the ground state was recognized, and it was assumed that only one absorbing species was present. An analysis would still be possible on this basis if the oscillator strength of the electronic transition differed greatly between the two isomers. The suggestion (2) that the intervals *A''–A*, *B''–B*, . . . represent an excited-state vibration of ~1350 cm^{-1} can be discounted, since the negligible change of frequency on deuteration shows that the motion would be localized in the ONO group; and it is unlikely that ν_4'' and ν_5'' would show a large frequency increase upon electronic excitation of the molecule. Another suggestion has been (4) that the intervals B–A'', C–B'', . . . represent a low-frequency torsional oscillation in the upper state, but these intervals are not constant in each of the spectra of the isotopic species. Neither of the suggested frequencies is active in the spectra of alkyl nitrites (7). Furthermore, these assignments would require

both the A and A'' progressions to show the same variation of intensity with temperature, whereas only the A'' progression is temperature dependent.

The most satisfactory explanation is that the A and A'' progressions are caused by excitation of the N=O stretching mode ν_2' in the excited trans and cis isomers respectively, with the temperature-dependent A'' progression bands originating in the isomer of higher ground-state energy. Both isomers must retain their approximate geometrical form upon electronic excitation, otherwise the Franck–Condon principle predicts the appearance of long and prominent progressions in those vibrations which would bring the nuclei into coincident positions in the combining electronic states, whereas maximum intensity occurs in the second or third members of all the observed progressions.

The A band is assigned to the 0–0 (trans) transition; but if the A'' band is assigned to the corresponding 0–0 (cis) transition, the separation between the cis and trans electronically excited states would be 4.5 kcal, an unexplicably large value. However, the broadness of the A band and also the slight displacement from its calculated position in the A progression leads to the suspicion that a second component is present here. If this is the 0–0 (cis) band and the A'' band is actually the second member of the progression, then the measured bands in the A'' progressions of HONO and $HON^{15}O$ can be fitted to an equation of type

$$[1] \qquad G(\nu_i) = G(0\text{–}0)+\omega_i^0\nu_i+x_{ii}^0\nu_i^2$$

to give

$$\text{HONO (cis)} \quad G(\nu_2') = 26{,}320+1126.9\nu_2'-19.75(\nu_2')^2$$

$$\text{HON}^{15}\text{O (cis)} \quad G(\nu_2') = 26{,}328+1113.0\nu_2'-19.25(\nu_2')^2.$$

In similar manner, the bands in the A progression, with $\nu_2' = 0$ for the A band itself, give

$$\text{HONO (trans)} \; G(\nu_2') = 26{,}034+1139.3\nu_2'-22.3(\nu_2')^2$$

$$\text{HON}^{15}\text{O (trans)} \; G(\nu_2') = 26{,}043+1127.2\nu_2'-22.3(\nu_2')^2.$$

This scheme of band numbering yields satisfactory isotope shifts of +8 and +9 cm^{-1} in the cis and trans isomers respectively for $G(0\text{–}0)$ upon N^{15} substitution. The substitution decreases the zero-point energy more in the ground than in the excited state, which is a reasonable expectation if the $n \rightarrow \pi^*$ excitation decreases the molecular binding. On the other hand, if the A'' band is assigned to the 0–0 (cis) transition, the isotope shift in the cis state only would be to lower frequencies, and this would imply large anomalous values for the cross-terms of type x_{ij}^0 that are necessarily ignored in equation [1].

The intensity distribution in the A and A'' progressions cannot be accurately determined because of the background of overlapping bands. However, a calculation after the method of Craig (12), with the simplifying assumption that the ν_2' motion is localized in the N=O bond, gives the extension of this in the excited state as 0.08 Å. This indicates $r_{NO}' \sim 1.28$ Å in both the cis and trans upper states. An extension of similar magnitude occurs in the $n \rightarrow \pi^*$ ($^1A_2 \leftarrow {}^1A_1$) transition in formaldehyde, for which $r''(CO) = 1.22$ Å and $r'(CO) = 1.32$ Å, although the bonding in this molecule is modified by the non-planar geometry of the excited state (13).

Porter (2) has attributed the enhanced separation between successive bands in the A progression of DONO to a perturbation between N=O stretching and D—O—N bending vibrations in the excited molecule. He assigned a frequency of "just under 1000 cm^{-1}"

to the latter motion. Our analysis confirms and extends this idea; Table III shows that anomalous frequency intervals also occur in the A progression bands of DON^{15}O but not of HON^{15}O. The E and F bands in the DONO and DON^{15}O spectra are strongly reduced in intensity and this is also attributable to the perturbation. The intervals between the A'', B'', and C'' bands for DONO and DON^{15}O also decrease irregularly by comparison with their undeuterated counterparts, and a similar kind of perturbation in the excited cis molecule may well be responsible. We conclude that ν_2' and ν_3' have similar values for both deuterated isomers, and that there is only a small drop in frequency of the ν_3'' vibration upon electronic excitation.

Although the bands in the A' and A''' progressions are weak and cannot be measured with precision, consideration of the frequency differences between bands in the spectra of all four isotopic species reveals that only one interpretation appears to be possible within the limits of experimental error. According to this, the A' progressions in the HONO and HON^{15}O spectra and the A''' progressions in the DONO and DON^{15}O spectra are produced by transitions from a cis ground-state level in which one quantum of a vibration of frequency $\sim$ 620 cm^{-1} is excited to upper-state levels in which successive quanta of ν_2' (cis) are excited. This assignment is consistent with the observed increase of intensity of the progressions with temperature.

In order to assign the 620 cm^{-1} interval to a lower-state vibrational mode, it is necessary to re-examine previous analyses of the infrared spectrum. D'Or and Tarte (6) have assigned values of 525 and 517 cm^{-1} to ν_5'' in *cis*-HONO and -DONO respectively, but these values are unexpectedly much smaller than the corresponding frequencies of 598 and 591 cm^{-1} in the trans species. In the alkyl nitrites, ν_5'' (cis) and ν_5'' (trans) are both at $\sim$600 cm^{-1} (7); indeed, this frequency is actually larger for *cis*-methyl nitrite than for *trans*-methyl nitrite, owing to internal non-bonded hydrogen–oxygen interactions in the former configuration. D'Or and Tarte's assignments for ν_5'' (cis) stem from two extremely weak bands in the KBr spectral region that were not observed by Jones, Badger, and Moore (5); the latter assume ν_5'' (cis) is buried under the strong ν_5'' (trans) band at 598 cm^{-1} in the HONO spectrum. This interpretation is preferable, since it enables us to assign the 620 cm^{-1} interval to ν_5'' (cis). Further support comes from the work of Balderschweiler and Pimentel (14), who produced enhanced concentrations of *cis*-nitrous acid in nitrogen matrices by irradiation, and yet reported no absorption bands in the 500–550 cm^{-1} region.

Finally, we note that the intervals B'–A'', C'–B'', . . . have the constant values of 660 and 645 cm^{-1} in the DONO and DON^{15}O spectra respectively, and tentatively assign these frequencies to ν_4' (cis) in the deuterated molecules.

DISCUSSION

According to the simple molecular orbital picture, the electronic transition may be either $n_O \rightarrow \pi^*$, $^1U \leftarrow {}^1A$ or $n_N \rightarrow \pi^*$, $^1W \leftarrow {}^1A$, in terms of Platt's notation (15). In either case, the overall symmetry change is $^1A'' \leftarrow {}^1A'$ with the transition moment perpendicular to the molecule plane. The lowest-energy transitions in nitroso and nitro compounds are often assigned as $n_N \rightarrow \pi^*$ on the grounds that nitrogen lone-pair electrons have a smaller ionization potential and are therefore more readily excited (16). This view may well be oversimplified, since more sophisticated molecular orbital calculations by McEwen (17) show that the promoted electron comes from an LCAO/MO in which the n_O orbital has the largest coefficient. In a review article by Sidman (18), differences in intensity are used as a criterion to distinguish between $^1W \leftarrow {}^1A$ ($f \sim 10^{-2}$, $\epsilon_{max} \sim 10^3$) and $^1U \leftarrow {}^1A$ ($f \sim 10^{-4}$, $\epsilon_{max} \sim 10^3$) transitions. Because of the low intensity, Sidman assigns the near-ultraviolet absorption of nitrites, and also of the nitrite ion which is

isoelectronic with nitrous acid, to an $n_O \rightarrow \pi^*$ transition, since $^1U \leftarrow {}^1A$ is forbidden by the local symmetry of the nitro group. The low intensity of the nitrous acid absorption ($f \sim 10^{-3}$, $\epsilon_{max} \sim 10^2$) indicates that the transition is *mainly* of $n_O \rightarrow \pi^*$ type, in the sense that n_O–n_N mixing occurs in LCAO/MO formation, but one-center ($2s$, $2p$) components localized on the hybridized nitrogen atom only make a small contribution to the transition moment.

In the ground state of *cis*-nitrous acid the separation between the terminal atoms is 2.17 Å, considerably less than 2.6 Å for the sum of the van der Waals radii of hydrogen and oxygen. Since the cis isomer is only 500 cal/mole less stable than the trans, hydrogen bonding to oppose the steric repulsion has been postulated in the ground state of the former species (5, 6, 10). The decrease of ν_1'', the increase of ν_3'' and ν_5'', and the decrease of $\angle$ NOH and $\angle$ ONO in the cis isomer relative to the trans isomer all indicate such bonding, which, from the molecular geometry, must be primarily an interaction between the hydrogen atom and the lone-pair n_O terminal oxygen electrons. The separation of the (0–0) band origins shows that the energy separation between the cis and trans isomers increases to 1300 cal/mole in the excited state, the intramolecular hydrogen bond being weakened by the electronic promotion. The ONO bond angle is expected to open slightly when the hydrogen bond is weakened, and since this motion of the nuclei is linked to the redistribution of charge that occurs in the electronic transition, we might predict that the ν_5 vibration would be active in the spectrum of *cis*-nitrous acid, as is actually the case. On the other hand, Goodman and Kasha's rule (19) that angular bending vibrations about the nitrogen atom are prominent in the spectrum of $n_N \rightarrow \pi^*$ transitions should apply to both *cis*- and *trans*-nitrous acid, whereas the angular deformation mode was not observed in the spectrum of the latter. It might be argued that transitions from the $1\nu_5''$ (trans) ground-state level are not observed because the bands are buried beneath other stronger bands. But if this were the case, the transition to the vibrationless excited state should appear $\sim$600 cm^{-1} to the red of the A band, and there is no trace of discrete absorption in this region. Owing to the displacement of the cis and trans band origins, the corresponding transition for the cis molecule is at the long wavelength edge of the A band; and this edge does indeed appear to broaden as the temperature is increased.

In a crude approximation, two mechanisms can contribute to the weakening of the hydrogen bond: (i) electrostatic interactions of the type normally associated with hydrogen bonding (20) are decreased by $n_O \rightarrow \pi^*$ excitation; (ii) orbital redistribution of electrons after excitation may produce changes in molecular geometry that increase the (O – – – H) separation and so indirectly weaken the bond. This could occur, for example, in an $n_N \rightarrow \pi^*$ transition where rehybridization occurs at the N atom. However, (i) is expected to predominate here, with a small contribution from (ii) due to the increased (N=O) distance in the excited state. The well-known "blue shifts" for $n \rightarrow \pi$ absorption bands that occur when ketonic compounds are dissolved in hydroxylic solvents have been ascribed to breaking of intramolecular hydrogen bonds upon electronic excitation (21). These shifts indicate bond energies of 0.5–4 kcal/mole, but this may only be the amount by which the bond is weakened (22); in any case, the magnitude of such blue shifts is of the same order as the increase in the cis–trans energy separation in nitrous acid upon excitation.

ACKNOWLEDGMENT

Financial assistance by the National Research Council of Canada is gratefully acknowledged.

REFERENCES

1. E. H. MELVIN and O. R. WULF. Phys. Rev. **38**, 2294 (1931); J. Chem. Phys. **3**, 755 (1935). D. M. NEWITT and L. E. OUTRIDGE. J. Chem. Phys. **6**, 752 (1938).
2. G. PORTER. J. Chem. Phys. **19**, 1278 (1951).
3. P. TARTE. Bull. Soc. Chim. Belges, **59**, 365 (1950). L. D'OR and P. TARTE. Bull. Soc. Roy. Sci. Liège, 685 (1951).
4. C. H. PURKIS and H. W. THOMPSON. Trans. Faraday Soc. **32**, 1466 (1936).
5. L. H. JONES, R. M. BADGER, and G. E. MOORE. J. Chem. Phys. **19**, 1599 (1951).
6. L. D'OR and P. TARTE. Bull. Soc. Roy. Sci. Liège, 478 (1951).
7. P. TARTE. J. Chem. Phys. **20**, 1570 (1952).
8. W. D. PHILIPS and C. E. LOONEY. J. Mol. Spectry. **1**, 35 (1957).
9. L. H. PIETTE and W. A. ANDERSON. J. Chem. Phys. **30**, 899 (1959).
10. A. PALM. J. Chem. Phys. **26**, 855 (1957).
11. J. MASON. J. Chem. Soc. 3904 (1957).
12. D. P. CRAIG. J. Chem. Soc. 2146 (1950).
13. J. C. D. BRAND. J. Chem. Soc. 858 (1956). G. W. ROBINSON and V. E. DIGIORGIO. Can. J. Chem. **36**, 31 (1958).
14. J. D. BALDESCHWIELER and G. C. PIMENTEL. J. Chem. Phys. **33**, 1008 (1960).
15. J. R. PLATT. J. Chem. Phys. **18**, 1168 (1950); J. Opt. Soc. Am. **43**, 252 (1953).
16. S. F. MASON. Quart. Rev. (London), **15**, 287 (1961).
17. K. L. MCEWEN. J. Chem. Phys. **34**, 547 (1961).
18. J. W. SIDMAN. Chem. Rev. **58**, 689 (1958).
19. L. GOODMAN and M. KASHA. J. Mol. Spectry. **2**, 58 (1958).
20. C. A. COULSON. Hydrogen bonding. *Edited by* D. Hadzi. Pergamon Press, London. 1959. p. 339.
21. G. J. BREALEY and M. KASHA. J. Am. Chem. Soc. **77**, 4462 (1955).
22. G. C. PIMENTEL. J. Am. Chem. Soc. **79**, 3323 (1957).

EXOCELLULAR BACTERIAL POLYSACCHARIDE FROM XANTHOMONAS CAMPESTRIS NRRL B-1459

PART I. CONSTITUTION[1]

J. H. Sloneker and Allene Jeanes

Northern Regional Research Laboratory, Northern Utilization Research and Development Division, Agricultural Research Service, U.S. Department of Agriculture, Peoria, Ill., U.S.A.

Received May 22, 1962

ABSTRACT

Polysaccharide B-1459 is the first bacterial polysaccharide reported to contain pyruvic acid as a constituent. The polysaccharide, isolated as the potassium salt, was shown to be composed of D-glucose, D-mannose, and D-glucuronic acid, acetic acid, and pyruvic acid in the ratio 2.8:3.0:2.0:1.7:0.51–0.63. One-third of the total mannose was released readily as free mannose by graded acid hydrolysis with only a slow loss of the high solution viscosity. The remainder of the mannose was isolated as the acid-stable aldobiouronic acid 2-*O*-(β-D-glucopyranosyluronic acid)-D-mannose. Partial acid hydrolysis and preparative paper chromatography afforded two higher oligosaccharides: an aldotriouronic acid composed of glucuronic acid β-linked 1,2 to mannose with glucose as the reducing end group, and what appears to be an aldotetraouronic acid composed of glucuronic acid, mannose, and glucose.

INTRODUCTION

Exocellular polysaccharides have been produced by several species of the bacterium *Xanthomonas* (1), but only that from a strain of *X. phaseoli* has been characterized (2). This highly viscous material is composed of D-glucose, D-mannose, and D-glucuronic acid in the ratio 1:1:1. At this laboratory a similar polysaccharide has been isolated from *X. campestris* NRRL B-1459 (3) and has been produced on a practical scale (4). Polysaccharide B-1459 has possibilities for utility based on its highly viscous, homogenous dispersions, its acid stability, and its unusual behavior with salts (3). Atypical of a polyelectrolyte, at low polysaccharide concentrations the viscosity is relatively insensitive to salts, and at higher polysaccharide concentrations salts increase the viscosity markedly. Furthermore, salts stabilize the viscosity to heat (3). In this investigation we have sought to correlate the unusual physical properties of this polysaccharide with its chemical constitution and structure. Succeeding papers will be concerned with the detailed structural aspects of this problem.

EXPERIMENTAL

Chromatography

The chromatographic solvents employed were as follows: for the free sugars (A) ethyl acetate – acetic acid – water (3:1:3) (5) and (B) *n*-butyl alcohol – pyridine – water (6:4:3) (6); for the hydroxamic acids (C) *n*-amyl alcohol – formic acid – water (4:1:5) and (D) *n*-butyl alcohol – acetic acid – water (4:1:5) (7); and for the polyalcohols (E) 2-butanone – acetic acid – water saturated with boric acid (9:1:1) (8) (all v/v). Spray reagents used for the detection of sugars and their derivatives were (A) *O*-aminobiphenyl (9) and (B) periodate–permanganate (10). Whatman paper No. 1[2] was used for quantitative and qualitative chromatography and No. 3MM was used to separate and isolate larger quantities of pure sugars.

Materials

Polysaccharide B-1459 is isolated as the potassium salt from cell-free media by a series of alcohol precipitations in the presence of 1% potassium chloride. The final precipitate is either dissolved in water and freeze-dried or dehydrated with alcohol and vacuum-dried. Products thus obtained contain only traces of

[1]*Presented before the Division of Carbohydrate Chemistry at the 137th Meeting of the American Chemical Society, Cleveland, Ohio, April 1961.*

[2]*Mention of trade names should not be construed as a recommendation or endorsement by the Department of Agriculture over those not mentioned.*

nitrogen, chloride, and phosphorus (3). Two different preparations were used in the composition studies and are designated T-42, a laboratory preparation (3), and MP-3, an experimental pilot-plant preparation (4).

Deacetylated MP-3 and T-42 were obtained by hydrolyzing a 1% solution of polysaccharide in 0.025 *N* potassium hydroxide and 1% potassium chloride (w/v) for 2 hours at 24–25° C under an atmosphere of nitrogen. The alkali was neutralized with 0.125 *N* hydrochloric acid and the polysaccharide was dialyzed until free of salt. The pH of the solution was adjusted to 6.5, and the polysaccharide was recovered by lyophilization.

Graded Acid Hydrolysis of Polysaccharide B-1459

To 36 mg of T-42 dissolved in 2 ml of water was added 2 ml of 8 *N* sulphuric acid, and the solution was heated at 100° C. At various time intervals 0.5-ml samples were removed, neutralized with saturated barium hydroxide, and centrifuged. The neutralized centrifugates were reduced in volume and qualitatively chromatographed in solvents A and B. In 20 minutes D-mannose appeared in the hydrolyzate in rather large amounts. After 45 minutes D-glucose appeared along with an aldobiouronic acid and several higher oligosaccharides. The hexuronic acid, D-glucuronic acid, appeared only weakly after 60 minutes.

Quantitative Determination of the Sugars in Polysaccharide B-1459

A sample of polysaccharide (100–120 mg) was dissolved in 30 ml of 2 *N* hydrochloric acid and heated for 2.5 hours at 100° C. After cooling in an ice bath, the hydrolyzate was neutralized with silver carbonate and filtered through Celite to remove silver chloride. Excess silver ions were precipitated with hydrogen sulphide, and the solution was reduced in volume and filtered through Celite into a 5-ml volumetric flask. The hydrolyzate, containing considerable quantities of aldobiouronic acid, D-glucose, and D-mannose along with smaller quantities of two higher oligosaccharides (approximately 5% total weight), was chromatographed in solvent (A) for 36 hours. The respective sugar fractions were eluted from the paper and determined quantitatively by the phenol – sulphuric acid method (11).

The D-glucuronic acid content was determined by the carbazole method on the intact polysaccharide (12). Reference materials for the determinations were as follows: U.S. National Bureau of Standards D-glucose; commercial mannose recrystallized from methanol; glucuronic acid dihydrate of established purity; and a chromatographically pure sample of the barium salt of the aldobiouronic acid 2-*O*-(β-D-glucopyranosyluronic acid)-D-mannose isolated from polysaccharide B-1459. For the small quantities of the two higher oligosaccharides, very pure polysaccharide was used as the standard. Between 90 and 95% of the polysaccharide sugars was recovered.

Table I summarizes the sugar analyses run on both native and deacetylated samples of polysaccharide

TABLE I

Composition of polysaccharide B-1459

Polysaccharide sample	Equivalents of: D-Glucose	D-Mannose	D-Glucuronic acid	Acetic acid	Pyruvic acid
Native					
T-42	2.8	3.0	2.0 (22.0%)*	1.73	0.627
MP-3			(22.0%)	1.74	0.509
Deacetylated					
T-42	2.6	2.8	2.0 (24.8%)	0.0	0.634
MP-3			(24.8%)	0.0	

*Determined on the intact polysaccharide by the carbazole method and expressed as $C_6H_8O_6$.

B-1459. Deacetylation produced no change (within experimental error) in the sugar composition, and the D-glucuronic acid content of all the samples is in good agreement.

Identification and Determination of the Acyl Group

Native polysaccharide B-1459 (3 g) was hydrolyzed for 1 hour in 300 ml of 4 *N* sulphuric acid at 100° C and extracted with 6 volumes of ethyl ether. The ether was reduced in volume under vacuum, titrated to pH 7 with 0.01 *N* potassium hydroxide, and then taken to dryness. Hydroxamic acid derivatives were prepared from a portion of the dry residue according to Block *et al.* (13) and chromatographed in solvents (C) and (D). Three spots appeared on the chromatogram when developed with acidic ferric chloride and were identified as to origin as follows: The major spot was from acetic acid; the second spot of medium intensity appeared to be from pyruvic acid; and the third, very weak spot was from formic acid, which probably originates as a breakdown product during hydrolysis.

The acyl content of polysaccharide B-1459 was determined by two methods. First, the polysaccharide (0.1% solution) was deacetylated in an oxygen-free system with 0.01 *N* potassium hydroxide in the presence

of potassium chloride (1% w/v) at room temperature. Aliquots were removed periodically and titrated with 0.01 *N* sulphuric acid with the aid of a pH meter. The acetyl content was 4.7% and the hydrolysis was complete in 5 hours (Table I). The second method was a colorimetric procedure based on the color complex formation of an acyl hydroxamic acid and ferric ions (14). The acetyl content was 4.6%.

Isolation and Determination of Pyruvic Acid

Pyruvic acid, which was identified tentatively as its hydroxamic acid during a routine identification of the acetyl groups in polysaccharide B-1459, was identified positively as its 2,4-dinitrophenylhydrazone derivative. A 2,4-dinitrophenylhydrazine reagent (15) was added to a water solution of a portion of the dry residue from the neutralized ether extract of acid-hydrolyzed polysaccharide used for the identification of the acyl groups. Small yellow crystals formed immediately. After three crystallizations from ethanol–water, 21.0 mg of a bright yellow crystalline material was obtained which had a melting point of 216° C. The melting point did not change when the sample was mixed with authentic pyruvic acid 2,4-dinitrophenylhydrazone. Calc. for $C_9H_8N_4O_6$: C, 40.3%; H, 3.01%; N, 20.9%. Found: C, 40.5%; H, 3.14%; N, 21.2%.

Quantitative analysis of the pyruvic acid as its 2,4-dinitrophenylhydrazone (16) revealed that the pyruvate content varied slightly between different polysaccharide preparations (Table I).

Neutral Equivalent Determination for Polysaccharide B-1459

A 0.1% solution of polysaccharide B-1459 as its potassium salt was passed slowly with the aid of pressure over a column containing a 30-fold excess of Dowex 50-X4, 20–50 mesh resin (H^+ form). The column was washed with at least six holdup volumes of water. The sample and washings were combined and concentrated in a rotary evaporator at 40° C. The sample was titrated with 0.01 *N* sodium hydroxide using a pH meter. The neutral equivalent values found by alkali titration of deionized native and deacetylated samples of polysaccharide and those obtained by calculation from the glucuronate and pyruvate contents are summarized in Table II.

TABLE II

Equivalent weight of polysaccharide B-1459

Polysaccharide sample	Equivalent weight	
	Theoretical*	By alkali titration
Native		
T-42	594	764
MP-3	594	675±21
Deacetylated		
MP-3	526	635±7

*Calculated from the glucuronic and pyruvic acid contents.

Isolation of the Acidic Oligosaccharides

Polysaccharide B-1459 (5.0 g) was hydrolyzed in 500 ml of 4 *N* sulphuric acid for 3 hours at 100° C. The solution was neutralized with barium carbonate, centrifuged, reduced in volume to 10 ml, and filtered to remove residual barium carbonate. A 300-ml aliquot of absolute ethanol was added, and the precipitate which formed was allowed to settle out at 4° C. The precipitate collected by centrifugation was redissolved in 10 ml of water, reprecipitated, and was finally washed with absolute ethanol. The yield as the barium salt after drying was 1.96 g.

The acidic oligosaccharides were separated by paper chromatography (200 mg per sheet) in solvent (A) for 6 days. The papers were dried overnight, and the fractions, four in all, were detected on guide strips with spray (A). The fractions were recovered by macerating the paper in distilled water, removing the pulp on a sintered-glass funnel, reducing the volume of the filtrate, and neutralizing to pH 7.0 with a saturated barium hydroxide solution. The fractions were then precipitated with ethanol, collected by centrifugation, and dried in vacuum over phosphorus pentoxide. The yield of each fraction was:

Fraction	Yield, mg
1	130
2	904
3	69
4	19

Identification of Fraction 1 as D-*Glucuronic Acid*

Fraction 1 was identified chromatographically in solvent (A) as D-glucuronic acid.

*Identification of Fraction 2 as 2-O-(β-*D-*Glucopyranosyluronic acid)-*D-*mannose*

Fraction 2 (4 mg) was hydrolyzed in 0.5 ml of 4 *N* sulphuric acid for 3 hours at 100° C. The hydrolyzate was neutralized with barium hydroxide, the precipitate was removed by centrifugation, and the supernatant solution was reduced in volume and chromatographed in solvent (A). The hydrolyzate contained D-glucuronic acid, D-mannose, and starting material.

Fraction 2 had an $[\alpha]_D^{25}$ value of −30.6 (*c*, 0.240, water). The specific rotation reported for the barium salt of 2-*O*-(β-D-glucopyranosyluronic acid)-D-mannose is $[\alpha]_D^{25}$ −30.0 (*c*, 0.96, water) (17). An authentic sample of 2-*O*-(β-D-glucopyranosyluronic acid)-D-mannose and fraction 2 both gave the same chromatographic results; neither reacted with triphenyltetrazolium chloride, a behavior characteristic of a 1,2-linked reducing disaccharide (18 and references cited therein). With spray reagent (A) both compounds gave an unexpected orange-brown spot in contrast to the characteristic greenish-brown color of hexoses (9) shown by 4-*O*-(glucopyranosyluronic acid)-D-galactose as well as by neutral disaccharides (maltose, isomaltose, and gentiobiose).

Both fraction 2 and the barium salt of 2-*O*-(β-D-glucopyranosyluronic acid)-D-mannose were oxidized with lead tetraacetate as described by Charlson and Perlin (19). In 9 hours fraction 2 reduced 13.6 moles of lead tetraacetate and produced 5.6 moles of carbon dioxide. In comparison, the known aldobiouronic acid reduced 13.4 moles of lead tetraacetate and produced 5.9 moles of carbon dioxide. Fraction 2, therefore, is 2-*O*-(β-D-glucopyranosyluronic acid)-D-mannose.

Identification of Fraction 3 as an Aldotriouronic Acid

Fraction 3 (4 mg) was hydrolyzed and chromatographed as described for fraction 2. The hydrolyzate showed D-glucose (strong), 2-*O*-(β-D-glucopyranosyluronic acid)-D-mannose (strong), D-mannose, and D-glucuronic acid (both weak). A second sample of fraction 3 (4 mg) was dissolved in 0.2 ml of water. Ten milligrams of sodium borohydride was added and was allowed to react at room temperature overnight. The solution was neutralized with solid carbon dioxide and was decationized by passing it through a Dowex 50 H^+ column. The eluate was taken to dryness, and the boric acid was removed with dilute methanolic hydrogen chloride. The residue was hydrolyzed in 4 *N* sulphuric acid for 2 hours and was neutralized as described. Chromatography of the hydrolyzed, reduced sample in solvent (E) revealed that the glucose was completely converted to sorbitol. The presence of sorbitol indicates that fraction 3 is a trisaccharide composed of D-glucuronic acid, D-mannose, and D-glucose, with D-glucose the reducing end group.

Identification of Fraction 4 as an Aldotetraouronic Acid

Fraction 4 (5 mg) was hydrolyzed in 4 *N* sulphuric acid for 1 hour at 100° C. The hydrolyzate was neutralized and chromatographed as described. The substances found and their relative concentrations were: D-glucose, high; 2-*O*-(β-D-glucopyranosyluronic acid)-D-mannose, medium; and the aldotriouronic acid, weak. This chromatographic evidence indicates that fraction 4 is an aldotetraouronic acid in which two glucose residues are adjacent.

RESULTS AND DISCUSSION

The polysaccharides produced in the laboratory (T-42) or on a pilot-plant scale (MP-3) appear to be the same in composition and structure except for a small variation in the pyruvic acid content (Table I). The polysaccharide from *X. phaseoli* contains the same sugar constituents but in a different ratio (1:1:1) (2). Acetic and pyruvic acids were not reported for this polysaccharide. The optical rotations, however, of the polysaccharides from both genera of *Xanthomonas* are zero, indicating some degree of structural similarity. The acetic acid (4.7% as acetyl) in polysaccharide B-1459 appears to be present as an ester because it can be removed readily with dilute alkali at room temperature. Removal of the acetyl groups produces a polysaccharide with improved physical properties, e.g., its viscosity in the presence of salts is significantly greater and it produces stronger and more flexible films than the native polysaccharide (20).

Pyruvic acid, a unique polysaccharide constituent, comprises 3.0 to 3.5% of the total weight of polysaccharide B-1459. Previously, only commercial preparations of a red seaweed agar have been reported to contain 1.0% pyruvic acid as a 4,6-*O*-(1-carboxyethylidene) unit attached to D-galactose (21). In the seaweed polysaccharide pyruvic acid is suspected of imparting gel properties to the polymer. In polysaccharide B-1459 there is evidence that the pyruvic acid is attached by the same linkage to a glucose unit (22). The effect that pyruvate has on the physical properties of the polysaccharide is

unknown. The small differences in the pyruvate content of the two preparations of polysaccharide B-1459 are possibly due to slight variations in fermentation conditions.

Neutral equivalent data determined on native and deacetylated polysaccharide B-1459 indicate that lactonization is occurring when the polysaccharide is decationized with ion exchange resin. Measurement of neutral equivalents of both native and deacetylated polysaccharide should, theoretically, reveal the extent of carboxyl esterification since the conditions of deacetylation are sufficient to saponify esters of either glucuronic acid or pyruvic acid if they exist. Any difference in the neutral equivalent between the two samples, beyond that caused by the weight loss of acetyl groups, would be a measure of the carboxyl ester content. However, when such measurements were made on decationized material, both native and deacetylated polysaccharide samples gave results that were inconsistent and also high as compared with theoretical values based on the sum of pyruvic and glucuronic acid contents (Table II). Like polysaccharide B-1459, the exocellular polysaccharide from *X. phaseoli* exhibited an inconsistency of neutral equivalent values (391 to 599) when determined by a similar method (2). These discrepancies probably result from formation of the 3,6-lactone of glucuronic acid in the polymer by the action of the acidic ion exchange resin. Extensive lactone formation has been reported previously in certain other polysaccharides containing 1,4-linked glucuronic or mannuronic acid when isolated from an acidic medium (23). On the other hand, free galacturonic acid lactonizes to a minor extent, if at all (24, 25). In a polysaccharide it should lactonize only negligibly and titration of a polymer containing galacturonic acid should give an accurate measure of carboxyl content. As expected, pectic substances yield identical results when the hexuronic acid content is measured either by alkali titration or by the carbazole assay (26).

In graded acid hydrolysis studies approximately one-third of the mannose is released rapidly into the hydrolysis medium and is presumed to be a single side-chain unit. The quantity of labile mannose liberated is equivalent to one mannose side chain for every eight sugar residues. Stability of the polysaccharide backbone, however, is indicated by the persistence of viscosity even after 1 hour's hydrolysis in 4 *N* sulphuric acid at 100° C. This acid stability coupled with an optical rotation of zero indicates that the majority of the glycosidic linkages are in the β-configuration.

The sugar sequence of the polysaccharide backbone is revealed in part through the oligosaccharides isolated by partial acid hydrolysis. The majority of the mannose that is stable to mild acid hydrolysis was recovered as an acid-stable aldobiouronic acid, 2-*O*-(β-D-glucopyranosyluronic acid)-D-mannose.

Isolated in lesser yield was an aldotriouronic acid composed of the above aldobiouronic acid and glucose, which occupies the reducing end position. A third acidic oligosaccharide isolated in quite small yield was also made up of the aldobiouronic acid and glucose. However, its rate of migration on paper chromatograms as compared with that of the aldotriouronic acid is somewhat slower and therefore it is believed to be an aldotetraouronic acid which contains two adjacent glucose residues. No other oligosaccharides were observed.

Polysaccharide B-1459 appears to be a relatively high molecular weight linear polymer which forms highly viscous gel-like solutions that produce strong, flexible films (3, 20, 27). From the chemical composition studies, the polysaccharide may be depicted as a linear polymer with an acid-stable β-linked backbone containing D-glucose, D-mannose, and D-glucuronic acid with 1 mannose side chain unit for every 8 sugar residues and possibly a 4,6-*O*-(1-carboxyethylidene)-D-glucose side-chain residue for every 16 sugar residues (22).

Additional structural details based on periodate oxidation procedures will be described in a subsequent paper.

ACKNOWLEDGMENTS

We wish to thank Dr. G. O. Aspinall and Dr. A. M. Stephens for their gifts of 2-*O*-(β-D-glucopyranosyluronic acid)-D-mannose and 4-*O*-(α-D-glucopyranosyluronic acid)-D-galactose. Our appreciation is also extended to Mr. S. P. Rogovin for supplying us with polysaccharide preparation MP-3 and to Mrs. Danute Orentas for portions of the analytical data presented.

REFERENCES

1. V. G. LILLY, H. A. WILSON, and J. G. LEACH. Appl. Microbiol. **6**, 105 (1958).
2. S. M. LESLEY and R. M. HOCHSTER. Can. J. Biochem. Physiol. **37**, 513 (1959).
3. A. JEANES, J. E. PITTSLEY, and F. R. SENTI. J. Appl. Polymer Sci. **5**, 519 (1961).
4. S. P. ROGOVIN, R. F. ANDERSON, and M. C. CADMUS. J. Biochem. Microbiol. Technol. Eng. **3**, 51 (1961).
5. M. A. JERMYN and F. A. ISHERWOOD. Biochem. J. **44**, 402 (1949).
6. E. CHARGAFF, C. LEVINE, and C. GREEN. J. Biol. Chem. **175**, 67 (1948).
7. A. R. THOMPSON. Australian J. Sci. Res. Ser. B, **4**, 180 (1951).
8. W. R. REES and T. REYNOLDS. Nature, **181**, 767 (1958).
9. T. E. TIMELL, C. P. J. GLAUDEMANS, and A. L. CURRIE. Anal. Chem. **28**, 1916 (1956).
10. R. U. LEMIEUX and H. F. BAUER. Anal. Chem. **26**, 920 (1954).
11. M. DUBOIS, K. A. GILLES, J. K. HAMILTON, P. A. REBERS, and F. SMITH. Anal. Chem. **28**, 350 (1956).
12. Z. DISCHE. *In* Methods in biochemical analysis. Vol. II. Interscience Publishers, New York. 1956. p. 342.
13. R. J. BLOCK, E. L. DURRUM, and G. ZWEIG. A manual of paper chromatography and paper electrophoresis. 2nd ed. Academic Press, New York. 1958. p. 220.
14. E. A. MCCOMB and R. M. MCCREADY. Anal. Chem. **29**, 819 (1957).
15. R. L. SCHRINER, R. C. FUSON, and D. Y. CURTIN. The systematic identification of organic compounds. 4th ed. John Wiley and Sons, New York. 1956. p. 219.
16. J. H. SLONEKER and D. G. ORENTAS. Nature, **194**, 478 (1962).
17. A. M. STEPHENS. J. Chem. Soc. 4487 (1956).
18. R. H. CÔTÉ. J. Chem. Soc. 2248 (1959).
19. A. J. CHARLSON and A. S. PERLIN. Can. J. Chem. **34**, 1200 (1956).
20. P. R. WATSON, A. JEANES, and C. E. RIST. J. Appl. Polymer Sci. **6**, S12 (1962).
21. S. HIRASE. Bull. Chem. Soc. Japan, **30**, 68, 70 (1957).
22. J. H. SLONEKER and D. G. ORENTAS. Can. J. Chem. This issue.
23. M. A. G. KAYE and P. W. KENT. J. Chem. Soc. 79 (1953).
24. M. GEE and R. M. MCCREADY. Anal. Chem. **29**, 257 (1957).
25. W. WLOSTOWSKA. Roczniki Chemji, **10**, 342 (1940); Chem. Abstr. **24**, 4508 (1930).
26. E. A. MCCOMB and R. M. MCCREADY. Anal. Chem. **24**, 1630 (1952).
27. R. L. WHISTLER and J. N. BEMILLER. Industrial gums. Academic Press, New York. 1959. p. 8.

STABILIZATION OF POLYMERIC CARBOHYDRATE NITRATES FROM STUDIES ON STARCH, AMYLOSE, AMYLOPECTIN, AND GLYCOGEN

AHMED MUSTAFA, ABDEL FATTAH DAWOUD, AND SALAH EL-SHOURBANI

Department of Chemistry, Faculty of Science, Cairo University, Cairo, U.A.R.

Received May 14, 1962

ABSTRACT

Whole starch, amylose, amylopectin, and glycogen (polymeric carbohydrates of the α-D-glycosidic linkage type) were nitrated by nitric acid in the presence of phosphoric anhydride and stability properties of the nitrated products were studied. Crude amylose nitrate is more stable than amylopectin nitrate and the latter is less stable than the whole-starch nitrate as judged by the Bergmann–Junk test. The stability of glycogen nitrate is closely similar to that of amylopectin nitrate.

Appreciable stabilization of the crude nitrates was brought about by boiling with slightly alkaline water for long periods (60–70 hours). All stabilized samples were found to possess closely similar stability properties. The Bergmann–Junk values of all examined nitrates ranged from 2.2 to 1.7 mg of nitrogen per gram sample; the latter value seems to represent the maximum stabilization which could be attained for the polymeric carbohydrate nitrates of the α-D-glycosidic linkage type. In the case of cellulose nitrate (β-D-glycosidic linkage type) Bergmann–Junk values of 1 to 1.25 mg of nitrogen were obtained.

Extensive work has been carried out on starch nitrate (from 1833 onwards) by different investigators (6, 7, 14), but most of this work has centered on the preparation and stabilization of whole-starch nitrate. Some trials, however, were made by Berl and Kunze (4), Centola (11), and Snelling (20) to separate the nitrated starch into two different fractions, namely, the amylose and amylopectin nitrates, and to study their properties; but the difficulty was that the authors did not have either a true amylose (unbranched fraction) or a true amylopectin (branched fraction), since, at that time, these two principal components of starch had not been thoroughly established (7).

In recent years improved techniques have been developed for fractionation of starch into its separate components (2, 17, 18). The availability of two starch fractions, namely, amylose and amylopectin, simplified the study of two considerably different polymeric carbohydrate nitrates (2, 8, 9, 24). Thus, recently the Will and Lenze method for the preparation of whole-starch nitrate (23) was revived once again by Ashford, Evans, and Hibbert (2) for nitrating the amylose and the amylopectin fractions of the starch granule. The nitrated products were fractionated by dissolution in ethanol. The authors have indicated that the unfractionated amylose nitrate possesses greater stability than the unfractionated amylopectin nitrate. A high stability was also found with both the alcohol-soluble and alcohol-insoluble amylose nitrate fractions, those of the corresponding amylopectin nitrate being less stable.

The method of Will and Lenze appeared to be experimentally tedious and gave products that required considerable effort to stabilize (24). On the other hand, it has been previously claimed that nitration of whole starch with nitric acid alone (12) or with nitric acid in the presence of phosphoric acid and/or phosphoric anhydride (3, 4, 7) gives nitrates of higher stabilities and higher viscosities (through less degradation). The investigation, herein described, was initiated in the belief that a study of the properties of the nitrates of starch, amylose (unbranched fraction), and amylopectin (branched fraction), prepared

by nitric acid in the presence of phosphoric anhydride, would provide valuable data on stability properties of those polymeric carbohydrate nitrates; an elusive problem in the chemistry of polymeric carbohydrate nitrates is that of stability. Moreover, the availability of glycogen, a polymeric carbohydrate possessing the branched-type structure of α-D-glycosidic linkages like that of amylopectin (branches of glycogen are shorter than those of amylopectin (13)), gives a new material for study of the nitration and stabilization of another polymeric carbohydrate nitrate of the α-D-glycosidic linkage type. No work has been done previously on the stabilization of glycogen nitrate.

DISCUSSION

Many tests have been devised to measure the stability of the nitrated polysaccharides (5, pp. 41–61; 15). The Abel heat test and the Bergmann–Junk test are the two most widely used tests for measuring the stability of starch nitrates.

There are some objections, however, to the application of the Abel test; the most essential ones are: (*a*) the test is extremely sensitive, the standard tint being produced by 0.000135 mg of nitrogen peroxide; (*b*) the test time is greatly affected by the moisture content of the sample (15); and (*c*) short test time is obtained for carefully stabilized explosives when the water used in the stabilization treatment has a high content of certain salts and impurities (5, pp. 41–61); on the contrary, the presence of minute amounts of certain adulterants, e.g., mercuric chloride, methanol, ethanol, etc., prolongs the test time (15).

In contrast to the Abel test, the Bergmann–Junk test is quantitative and gives a better idea of the actual stability or storage ability of explosives (5, pp. 41–61). This test was taken as the main measure of stability during the course of the present experiments. The ignition temperatures of the nitrates were recorded throughout all the work.

The crude nitrated products of whole starch, amylose, amylopectin, and glycogen were found to possess different stability properties as judged by the Bergmann–Junk test. Amylose nitrate is more stable than the amylopectin nitrate and the latter is less stable than the whole-starch nitrate. The stability of glycogen nitrate is closely similar to that of amylopectin nitrate. In the ignition temperature test, the examined nitrates had different ignition temperatures, as shown in Table I. The ignition temperature of glycogen nitrate is about 2.5° C lower than that for the amylopectin and for the whole-starch nitrates. Amylose nitrate has a higher ignition temperature (178° C).

Stabilization of the crude nitrates was brought about by boiling either with distilled water or with slightly alkaline water (0.025% sodium carbonate solution), for long periods, as followed in the industrial stabilization treatment of cellulose nitrates (16). The following results were obtained.

(1) Stability properties of the crude nitrates were improved by boiling with distilled water for 72 hours (cf. Table I). Although the Bergmann–Junk stability values of the so treated nitrates were still far away from the specifications of stable explosives (1.25 mg nitrogen for cellulose nitrate (5, pp. 41–61)), yet the most important observation was that the difference in stability properties of the examined esters was practically negligible. The ignition temperatures of the nitrates were also improved but still there is a slight difference, as shown in Table I; brown fumes appeared at about 169° C.

(2) Appreciable stabilization of the crude nitrates was brought about by boiling with slightly alkaline water. Thus, boiling with slightly alkaline water for 24 hours effected more stabilization than boiling with distilled water for 72 hours. A slight decrease in nitrogen content was observed in the first case. The stability of the esters was greatly

TABLE I

Nitrate sample	Nitrogen content, %	Ignition temp. test		Bergmann–Junk test, mg nitrogen	Abel heat test at 80° C (ref. 5, pp. 41–61), min
		Brown fumes, °C	Ignition temp., °C		
	(1) Crude untreated nitrates				
Starch	13.68	167	174.5	15.70	6
Amylopectin	13.78	167	174.4	18.10	4
Amylose	13.65	168	178.0	13.60	6
Glycogen	13.70	167	172.0	17.96	5
	(2) Boiling with distilled water under reflux for 72 hours				
Starch	13.50	169	177	8.36	—
Amylopectin	13.62	169	176	8.43	—
Amylose	13.60	169	178.6	8.39	—
Glycogen	13.43	169	175	8.35	20
	(3) Boiling with sodium carbonate solution (0.025%) for 24 hours				
Starch	13.35	170	176	6.57	—
Amylopectin	13.45	170	175	6.73	—
Amylose	—	—	—	—	—
Glycogen	13.30	169	173.1	6.60	22
	(4) Boiling with sodium carbonate solution (0.025%) for 48 hours				
Starch	13.22	170	176.5	4.75	—
Amylopectin	13.30	170	176.0	4.8	—
Amylose	13.12	170	178.2	4.75	—
Glycogen	13.16	169	173.6	4.75	37
	(5) Boiling with sodium carbonate solution (0.025%) for 60 hours				
Starch	12.81	171	177.5	2.22	—
Amylopectin	12.80	171	177.8	2.2	—
Amylose	12.82	171	178.6	2.18	—
Glycogen	12.78	170	174.2	2.17	50
	(6) Boiling with sodium carbonate solution (0.025%) for 72 hours				
Starch	12.53	171	177.5	1.70	—
Amylopectin	12.59	171	177.8	1.70	—
Amylose	12.62	172	179.0	1.73	—
Glycogen	12.58	170	174.5	1.72	60
	(7) Boiling with sodium carbonate solution (0.025%) for 84 hours				
Starch	12.19	171	178.5	1.65	—
Amylopectin	11.9	171	178.5	1.65	—
Amylose	12.10	—	—	1.65	—
Glycogen	11.85	170	175.5	1.65	—

improved by alkaline boiling for a period of 60 hours. It is to be noted that the so treated nitrates of starch, amylose, amylopectin, and glycogen possessed closely similar stability Bergmann–Junk values.

(3) Further improvement in stability of the discussed esters was obtained by boiling in slightly alkaline water for 72 hours, whereby an appreciable decrease in nitrogen content was also traced. This represents the most favorable conditions for attaining the best stabilization results, since boiling for 84 hours caused marked loss in nitrogen content and no appreciable improvement of the Bergmann–Junk stability values (cf. Table I).

Examinations of the explosive properties of the stabilized samples of glycogen, amylopectin, and whole-starch nitrates boiled for 60 hours (with carbonate solution) had shown that their nitrogen contents still provided them with good explosive properties; the Trauzl lead block test showed a net expansion of 325, 330, 340 ml respectively, as compared with a net expansion of 280 ml for standard T.N.T. The ignition temperature of glycogen nitrate was still lower (ca. 3° C) than that for the amylopectin and for the whole-starch nitrates. The amylose nitrate had a higher ignition temperature than all the examined nitrates.

In a nitrating medium composed of nitric acid and phosphoric anhydride the instability of the nitrated starch and its fractions is mainly attributed to the presence, in very small amounts, of either free mineral acid or certain nitrated oxidation products formed during the nitration reaction (10, 16). The fact that stabilization of the esters by boiling with slightly alkaline water is more effective than boiling with distilled water is not surprising, since (*a*) the dilute alkaline boiling is reported to effect decomposition of the unstable nitrated oxidation products (16) and (*b*) alkaline hydrolysis is more rapid and effects rapid fall in nitrogen content.

It remains, now, to interpret the solubility results of the above-discussed nitrates in absolute ethanol. The crude nitrated products were found to possess widely different solubilities. Amylopectin and glycogen nitrates are much more soluble, in absolute ethanol, than the amylose nitrate (59, 56, and 21% respectively). The whole-starch nitrate is less soluble than the amylose ester (16.5 and 21% respectively). The widely different solubilities of either amylopectin nitrate or glycogen nitrate, and of the amylose ester, may be related to the structural difference between amylose, amylopectin, and glycogen. It is evident that the amylose ester, which is composed of linear molecules capable of close packing, would be more insoluble than the somewhat loosely packed molecules of amylopectin ester (22). The glycogen nitrate is expected to behave like the amylopectin nitrate due to similarity in their branched-type structure (13). In the case of whole-starch nitrate the solvent is unable to break associative bonds necesssary for solution, while when the amylopectin is separated from the amylose, associative bonding is greatly lessened and solution of the former component can take place more readily; the amylose is responsible for association in whole-starch nitrate (cf. ref. 2).

On the basis of the above results, it could be concluded that stabilization of polymeric carbohydrate nitrates of amylose, amylopectin, whole starch, and glycogen, by boiling with slightly alkaline water, gives products of closely similar stability properties as judged by the Bergmann–Junk test. The stabilized samples had Bergmann–Junk values ranging from 2.2 mg of nitrogen (60 hours' boiling) to ca. 1.7 mg of nitrogen (72 hours' boiling) per gram sample, and these values are probably the maximum stability values attained for those polymeric carbohydrate nitrates of the α-D-glycosidic linkage type. When samples of commercial cellulose nitrates (β-D-glycosidic linkage type) were examined, during the course of the present experiments, Bergmann–Junk values ranging from 1 to 1.25 mg of nitrogen per gram sample were obtained. The present stability results throw light on stability of starch nitrate, and further investigations on the subject will follow.

EXPERIMENTAL

Amylopectin and glycogen (provided by the British Drug Houses) as well as potato starch (provided by Carlo Erba, Italy) were used during the course of the present experiments. Amylose was obtained from the potato starch by means of the selective adsorption method employing cotton cellulose as the adsorbent (2, 19, 21).

Preparation of the Nitrates

Nitration of starch, amylose, amylopectin, and glycogen was carried out under the following conditions: nitric acid/P_2O_5 (by weight), 19:1; starch/nitrating medium, 1:50; time of nitration, 3 hours; temperature of nitration, 10° C.

Nitration

Five hundred cubic centimeters of concentrated nitric acid (*d*, 1.52), in a 1-liter three-necked flask, fitted with a stirring motor, was placed in an ice bath at a temperature of about 10° C. Forty grams of phosphorus pentoxide (P_2O_5) were added to the nitric acid, in portions, so that the temperature of the nitrating mixture did not exceed 10° C. Well-dried starch, amylose, amylopectin, and glycogen (16 g) were added to the nitrating mixture over a period of 1 hour, during which time the mixture was stirred vigorously

and the temperature maintained at 10° C. Nitration was completed by continuing the stirring for a period of 2 hours at the same temperature.

The nitrated products were isolated by pouring the nitration mixture onto vigorously stirred, finely chopped ice, followed by filtration and then washing, on the filter, with large quantities of water. The crude ester was placed in a beaker with 250 ml of dilute sodium carbonate solution (0.025%) and boiled for ½ hour, cooled, filtered, and then washed with large quantities of cold water.

The nitrated products were dried cautiously at 45–55° C and weighed. Yields amounted to ca. 27.5 g, 172%.

Stabilization Treatment

Stabilization of the crude nitrates was carried out by boiling either with distilled water or with slightly alkaline water (0.025% sodium carbonate solution) for long periods, as followed in the industrial stabilization treatment of commercial cellulose nitrates (16). The nitrates were boiled under reflux for the periods illustrated in Table I; liquor ratio 15:1. After the boiling treatment the treated esters were washed thoroughly with water, followed by washing with 0.1% solution of ammonium hydroxide, and then finally with water.

Determination of Nitrogen Content

Nitrogen contents were obtained by the nitrometer method. The Lunge–Sederholm nitrometer (5, pp. 160–161) was used.

Solubility of the Nitrates in Absolute Ethanol

One-half gram of dry sample of nitrate was weighed out in a 250-ml glass cylinder. One hundred cubic centimeters of absolute ethanol (provided by E. Merck) was added and the stoppered cylinder was then shaken on a shaker for 2 hours. After centrifugation, 50 cc of ethanol was withdrawn by means of a pipette and evaporated in a tared glass dish on a water bath. It was then dried, cooled in a desiccator, and weighed to constant weight. The percentage of soluble matter was calculated.

Determination of Stabilities

The Bergmann–Junk Test

In the official Bergmann–Junk test, 2 g of the explosive of the cellulose nitrate type is heated at 132° C (±0.5° C) for a period of 2 hours, at the end of which the quantity of nitric oxide evolved per gram of sample is quantitatively determined as a measure of the stability of the explosive under examination. Results are usually given in milligram of nitrogen per gram of sample. The amount of nitric oxide present can be estimated by the Schultze–Tiemann method (15) or by titrimetric procedures (5, pp. 41–61).

The Bofor's titrimetric procedure, using 0.05 *N* sodium hydroxide solution and phenolphthalein as indicator (1 ml of 0.05 *N* sodium hydroxide is equivalent to 1 ml of nitric oxide (5, pp. 41–61), was employed. Results were checked by the Schultze–Tiemann method whereby reliable results were obtained. Triplicate samples were used.

During the course of the present investigation, the Bergmann-Junk test was modified in one respect only, namely, in the weight of the sample used. One-half-gram samples were used in the primary stabilization experiments and compared with 0.5-g samples of standard starch nitrate. When the best favorable conditions of stabilization were attained (e.g., by boiling with slightly alkaline water for 60 hours) the official Bergmann–Junk test with the 2-g sample was employed.

Determination of the Ignition Temperature

The ignition temperatures were obtained using Bofor's ignition temperature apparatus (5, pp. 41–61). The experiments were carried out by inserting four ignition test tubes, each containing 0.1 g of dry sample of the nitrate, into the corresponding holes of the ignition apparatus, as soon as its temperature attained 100° C. Heating was controlled to allow a rise of 5° C per minute.

REFERENCES

1. W. R. Ashford, L. M. Cooke, and H. Hibbert. Can. J. Res. B, **24**, 238 (1946).
2. W. R. Ashford, T. H. Evans, and H. Hibbert. Can. J. Res. B, **24**, 246 (1946).
3. E. Berl. U.S. Patent No. 2,384,415 (1945).
4. E. Berl and W. C. Kunze. Ann. **250**, 270 (1935).
5. AB. Bofors. Analytical methods for powders and explosives. Bofors Nobelkrüt, Sweden. 1960.
6. L. Brissaud and S. Ronssin. Mém. Poudres. **33**, 199 (1951).
7. G. V. Caesar. *In* Advances in carbohydrate chemistry. Vol. 13. Academic Press, Inc., New York. 1958. pp. 331–345.
8. G. V. Caesar and M. Goldfrank. J. Am. Chem. Soc. **68**, 372 (1946).
9. G. V. Caesar, N. S. Gruenhut, and M. L. Cushing. J. Am. Chem. Soc. **69**, 617 (1947).
10. W. A. Caldwell and J. Creasy. Paint Manuf. **24**, 435 (1954).
11. G. Centola. Gazz. Chim. Ital. **66**, 8 (1936).
12. J. Hackel and T. Urbanski. Z. Ges. Schiess- Sprengstoffw. **28**, 306, 350, 378 (1933); **29**, 14 (1934); **30**, 98 (1935).

13. W. Z. HASSID. *In* Organic chemistry, an advanced treatise. Vol. IV. *Edited by* H. Gilman. John Wiley and Sons, Inc., New York. 1953. pp. 901–950.
14. H. KESSELER and R. RÖHM. Z. Angew. Chem. **35**, 125 (1922).
15. A. MARSHALL. Explosives. J. and A. Churchill, Ltd., London. 1917. pp. 644–660.
16. E. D. MILES. Cellulose nitrate. Oliver and Boyd, London, 1955. pp. 101–102.
17. E. PACSU and J. W. MULLEN. J. Am. Chem. Soc. **63**, 1168 (1941).
18. J. A. RADLEY. Starch and its derivatives. Vol. I. 3rd ed. Chapman and Hall, Ltd., London. 1953. pp. 123–175.
19. T. J. SCHOCH. *In* Advances in carbohydrate chemistry. Vol. I. Academic Press, Inc., New York. 1945. pp. 247–277.
20. W. O. SNELLING and G. E. REES. U.S. Patent No. 2,271,877 (1942).
21. C. TANRET. Bull. Soc. Chim. France, **17**, 83 (1915).
22. R. L. WHISTLER. *In* Advances in carbohydrate chemistry. Vol. I. Academic Press, Inc., New York. 1945. pp. 279–307.
23. W. WILL and F. LENZE. Ber. **31**, 68 (1898).
24. M. L. WOLFROM, A. CHANEY, and K. S. ENNOR. J. Am. Chem. Soc. **81**, 3469 (1959).

IDENTIFICATION OF CONJUGATED TRIENE FATTY ACIDS IN CERTAIN SEED OILS[1, 2]

C. Y. Hopkins and Mary J. Chisholm
Division of Pure Chemistry, National Research Council, Ottawa, Canada

Received July 17, 1962

ABSTRACT

Seed oils were hydrolyzed under mild conditions and the major conjugated fatty acid of each oil was isolated and identified. In two families, species which were closely related botanically contained different but isomeric acids. Thus, in the Bignoniaceae, *Jacaranda chelonia* had *cis,trans,cis*-8,10,12-octadecatrienoic acid as a major acid while *Catalpa speciosa* had *trans,trans,cis*-9,11,13-octadecatrienoic acid. In the Cucurbitaceae, *Momordica charantia* had the ordinary *cis,trans,trans*-9,11,13-octadecatrienoic (α-eleostearic) acid while *M. balsamina* had *cis,trans,cis*-9,11,13-octadecatrienoic (punicic) acid. *M. balsamina* is a new and convenient source of punicic acid. α-Eleostearic acid was identified as a major acid in examples of Valerianaceae and Rosaceae. Further proof was obtained that the fatty acid of *Calendula officinalis* (Compositae) is *trans,trans,cis*-8,10,12-octadecatrienoic acid.

Until the year 1956 only two simple conjugated triene fatty acids were known to occur in seed oils, viz. α-eleostearic and punicic acids. Three additional acids of this type have been discovered since then (1, 2, 3, 4). All five of these simple conjugated acids have an 18-carbon straight chain; in two of them the unsaturated grouping occupies the 8,10,12 position but in the other three it is in the 9,11,13 position. The present work reveals the occurrence of four of these acids in plant species in which they were not known previously (Table I). Positive identification of each acid was made by orthodox chemical procedures.

TABLE I

Occurrence of conjugated octadecatrienoic acids

$CH_3(CH_2)_xCH{=}CH{-}CH{=}CH{-}CH{=}CH(CH_2)_yCOOH$

Species	Formula	Unsaturated grouping		Reference
		Position	Configuration	
Jacaranda chelonia (Bignoniaceae)	I	8,10,12	cis,trans,cis	*
Catalpa speciosa (Bignoniaceae)	II	9,11,13	trans,trans,cis	*
Momordica charantia (Cucurbitaceae)	III	9,11,13	cis,trans,trans (α-eleostearic)	5
Momordica balsamina (Cucurbitaceae)	IV	9,11,13	cis,trans,cis (punicic)	*
Calendula officinalis (Compositae)	V	8,10,12	trans,trans,cis	1, 2
Centranthus ruber (Valerianaceae)	III	9,11,13	cis,trans,trans	*
Cotia chestnut (Rosaceae, see text)	III	9,11,13	cis,trans,trans	*
Prunus mahaleb (Rosaceae)	III	9,11,13	cis,trans,trans	6

*Present work

Seed of *Jacaranda chelonia* Griseb. (Bignoniaceae) yielded an oil containing a substantial amount of conjugated triene acid, as shown by its ultraviolet spectrum. The acid was isolated and identified as *cis,trans,cis*-8,10,12-octadecatrienoic acid (I) by melting point, mixed melting point, and ultraviolet spectrum. The only previously known occurrence of this acid is in the oil of *Jacaranda mimosifolia* D. Don (4).

[1]*Presented in part at the VIth Congress of the International Society for Fat Research, London, April 9–13, 1962.*
[2]*Issued as N.R.C. No. 7006.*

The seed oil of *Catalpa speciosa* Warder, also a member of the Bignoniaceae family, yielded a different triene acid. It melted at 31–32° and gave an adduct with maleic anhydride which melted at 72–73°. Its ultraviolet spectrum indicated a triene grouping of two trans and one cis bond (cf. ref. 7). The acid was identified as *trans,trans,cis*-9,11,13-octadecatrienoic acid (II) by mixed melting point with an authentic sample. This was confirmed by mixed melting point of the maleic anhydride adducts. The acid is known to occur in the oil of *Catalpa ovata* Don (3) but has not been observed elsewhere. Occurrence of this trans,trans,cis acid nullifies an earlier suggestion that the 9:10 double bond in natural triene acids is always cis (8).

The existence of acid I in two species of *Jacaranda* and of acid II in two species of *Catalpa* provides rather striking confirmation of the botanical classification of these plants. It is notable that one genus produces the 8,10,12-triene while the other produces the 9,11,13-triene, also that the two acids differ in their geometric configuration. Although it cannot be taken for granted that a given species of plant will always produce the same isomer of a conjugated fatty acid, we are not aware of any evidence to the contrary.

The oil of *Momordica charantia* L. (Cucurbitaceae) has been studied in the past and the presence of α-eleostearic acid has been reported. Claims that the oil contained trichosanic (punicic) acid have apparently not been substantiated. Verma and Aggarwal (5) isolated the acid and identified it as α-eleostearic by melting point, ultraviolet absorption, and conversion to the all-trans form. However, they did not report any mixed melting points. Our sample of *Momordica charantia* seed yielded α-eleostearic acid (III) as the major acid and its identity was proved conclusively, thus confirming the work of Verma and Aggarwal.

Another species of the same genus, *M. balsamina* L., contained a different acid. Earle and co-workers (9) reported that the oil of this species contained 50% of a conjugated triene acid and listed it as trichosanic acid, although evidence of its identification was not given. Our sample of the oil was estimated to contain 58% of a conjugated triene acid which was identified unambiguously as punicic acid (synonymous with trichosanic), i.e. *cis,trans,cis*-9,11,13-octadecatrienoic acid (IV). Thus it appears that two species of the same genus produce different major fatty acids, indicating a marked specificity of fatty acid biosynthesis. The two acids from these species differ only in geometric configuration (cis,trans,trans and cis,trans,cis).

Punicic acid has been available hitherto only from *Punica granatum* (Punicaceae) and from *Trichosanthes* sp. (Cucurbitaceae). *Momordica balsamina* constitutes a useful new source of the acid since the seed is available commercially and the oil has a high content of punicic acid.

The oil of *Calendula officinalis* L. (Compositae) was shown by McLean and Clark to contain an 8,10,12-octadecatrienoic acid (1). Later, the configuration of this acid was found to be trans,trans,cis (V) by infrared studies and by degradation of its maleic anhydride adduct (2). The trans,trans,cis configuration was confirmed in the present work by hydrogenating the adduct (VI) and comparing the product with the compound (VIII) obtained by hydrogenating the adduct (VII) of *trans,trans*-8,10-octadecadienoic acid; both melted at 105.5–106.5° and a mixed melting point determination showed that they were identical. Hence, the two trans double bonds of the triene acid must be at positions 8 and 10.

Seed oil of *Centranthus ruber* DC. (Valerianaceae) was found to contain a conjugated triene acid which was isolated and identified as α-eleostearic acid. This appears to be the first identification of a conjugated triene acid in this family although Earle and co-

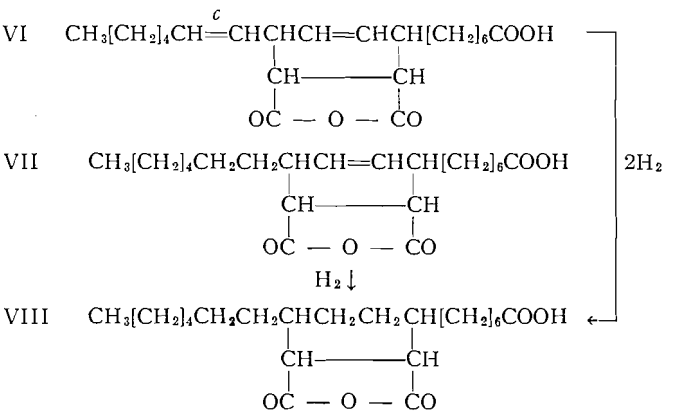

workers (9) reported infrared evidence for a triene acid in *Valeriana officinalis* that was listed as eleostearic acid. *Valerianella olitoria*, of the same family, was shown by Steger and van Loon to contain no conjugated acid (10) and we have confirmed this.

Two species of Rosaceae were examined. The kernel oil of the cotia chestnut was reported earlier to contain a conjugated acid on the basis of its diene value and drying properties (11). Our sample of this nut, obtained from the vicinity of Tefe, Amazonas, Brazil, yielded an oil containing about 23% of α-eleostearic acid, identified by means of its maleic anhydride adduct. There was no evidence of an hydroxy acid. The cotia chestnut is considered to be a species of *Parinarium* or *Licania* (family Rosaceae) but there is still some doubt concerning its classification.

The oil of *Prunus mahaleb* L. was re-examined. It was studied by Alpar and Esin (6), who isolated the triene acid and prepared derivatives which showed fairly conclusively that it was α-eleostearic acid. In the present work its identity has been confirmed by means of spectral analysis and mixed melting points of the acid and derivatives.

These results, taken in conjunction with previous data, indicate that α-eleostearic is the most commonly occurring conjugated triene acid; it is found in species of Rosaceae, Euphorbiaceae, Cucurbitaceae, and Valerianaceae. Punicic acid occurs in three species of Cucurbitaceae and one of Punicaceae. Other positional or geometric isomers of octadecatrienoic acid are found in four species of Bignoniaceae and one of Compositae.

EXPERIMENTAL

Cotia chestnuts were supplied through the kindness of Dr. K. S. Markley. Other seeds were obtained from commercial sources. Melting points were determined in capillary tubes and are corrected. Ultraviolet spectra were determined in cyclohexane solution, except where noted, with a Beckman DU spectrophotometer. Infrared spectra were determined in carbon disulphide in a Perkin–Elmer model 21 spectrophotometer with sodium chloride prism.

Jacaranda chelonia

Seed of *J. chelonia* Griseb. (10 g) was ground and extracted at room temperature by stirring with 30–60° petroleum ether. It yielded 19% of oil. The solvent was removed at 25–30° under nitrogen. The oil (1.9 g) had ultraviolet absorption λ_{max} 265, 275, 287 mμ and absorptivity $E^{1\%}_{1\ cm}$ 540 at 275 mμ, equivalent to about 31% of conjugated triene fatty acid. The oil was hydrolyzed, the unsaponifiable matter removed, and the acids recovered by methods described previously (3). The mixed acids were crystallized from acetone and then from pentane in the usual way (3), yielding 0.38 g of pure conjugated acid, m.p. 43.5–44°, λ_{max} 265, 275, 287 mμ. The melting point was unchanged in admixture with an authentic sample of *cis,trans,cis*-8,10,12-octadecatrienoic acid prepared from the oil of *J. mimosifolia* (4).

Catalpa speciosa

Seed of *C. speciosa* Warder, treated as described above, yielded 22% of oil having λ_{max} 262, 272, 283 mμ and absorptivity $E^{1\%}_{1\ cm}$ 604 at 272 mμ, equivalent to about 34% of conjugated triene fatty acid. The mixed

acids were crystallized at low temperature, giving a triene acid, m.p. 31–32°, λ_{max} 262, 272, 283 mμ. It reacted readily with maleic anhydride, giving an adduct, m.p. 72.5–73.5°. The melting point was unchanged in admixture with the corresponding adduct of *trans,trans,cis*-9,11,13-octadecatrienoic acid, prepared from the oil of *C. ovata* (3).

Momordica charantia

Seed of *M. charantia* L. was extracted and the fatty acids of the oil were crystallized in the usual way (3). A triene acid was obtained. It melted at 46–47°, alone and mixed with authentic α-eleostearic acid prepared from tung oil. Its maleic anhydride adduct melted at 63–64°, alone and mixed with the maleic anhydride adduct of α-eleostearic acid.

Momordica balsamina

Seed of *M. balsamina* L. yielded an oil having λ_{max} 266, 275, 286 mμ and absorptivity at 275 mμ equivalent to about 58% of conjugated triene fatty acid. Crystallization of the fatty acids yielded a triene acid, m.p. 44–45°, unchanged in admixture with punicic acid prepared from *Punica granatum*. The pure *Momordica* acid had λ_{max} 265, 275, 287 mμ; absorptivity $E^{1\%}_{1\,cm}$ 1694 at 275 mμ; infrared absorption, ν_{max} 933 (s), 983 (s) cm^{-1}. The absorption maxima were identical with those of punicic acid. The *Momordica* acid did not form an adduct with maleic anhydride under the normal conditions for this reaction. It formed a *p*-phenylphenacyl ester, m.p. 61.5–63.5°, alone and mixed with an authentic sample of the *p*-phenylphenacyl ester of punicic acid (4).

Calendula officinalis

trans,trans-8,10-Octadecadienoic acid was prepared from oleic acid by the method of Gupta and Kummerow (12). The diene acid (0.24 g), m.p. 55–56°, was refluxed with benzene (20 ml) containing maleic anhydride (0.21 g) for 6 hours. The product was crystallized from ether:petroleum ether (3:4) at 0°, giving 0.18 g of the pure adduct, 3-6′-carboxyhexyl-6-heptylcyclohexene-4,5-dicarboxylic anhydride (VII), m.p. 109–110°. Von Mikusch gives m.p. 110° (13). Calcd. for $C_{22}H_{34}O_5$: C, 69.8; H, 9.05. Found: C, 70.1; H, 9.06.

The adduct (VII) was hydrogenated in methanol with Adams catalyst and the product was crystallized from methanol at −30°, giving 3-6′-carboxyhexyl-6-heptylcyclohexane-1,2-dicarboxylic anhydride (VIII), m.p. 105.5–106.5°. Calcd. for $C_{22}H_{36}O_5$: C, 69.4; H, 9.5. Found: C, 69.5; H, 9.7.

The triene acid of *Calendula officinalis* L., 8,10,12-octadecatrienoic acid, and its adduct with maleic anhydride were prepared as described previously (2). The adduct, m.p. 73–74°, considered to be 3-6′-carboxyhexyl-6-*cis*-1′-heptenylcyclohexene-4,5-dicarboxylic anhydride (VI), was hydrogenated in methanol with Adams catalyst; it absorbed 2 moles of hydrogen. The product was crystallized from methanol at 0°. It melted at 105.5–106.5° and the melting point was not depressed in admixture with compound VIII, prepared from *trans,trans*-8,10-octadecadienoic acid. Hence the identity of VI is confirmed.

Centranthus ruber

Seed of *C. ruber* DC. yielded an oil having λ_{max} 262, 271, 282 mμ and absorptivity at 271 mμ equivalent to about 43% of conjugated triene fatty acid. The mixed fatty acids were crystallized, giving a triene acid that was somewhat difficult to purify. It melted at 42–43°. On treatment with iodine in pentane it gave β-eleostearic acid, m.p. and mixed m.p. 70–71°. The unisomerized acid reacted readily with maleic anhydride to give an adduct, m.p. 63.5–64.5° alone and mixed with the adduct of α-eleostearic acid (14).

Oil of *Valerianella olitoria* Poll. had negligible ultraviolet absorption in the conjugated triene region.

Cotia chestnut

Kernels of the cotia chestnut were extracted, yielding 61% of oil. The oil had λ_{max} 261, 270, 282 mμ in isooctane; absorptivity equivalent to about 24% of conjugated triene fatty acid; ν_{max} 957 (w), 986 (s) cm^{-1}. The triene acid was concentrated by crystallization but retained some saturated fatty acid. The concentrate was allowed to react with maleic anhydride, giving an adduct, m.p. 63–64° alone and mixed with the adduct of α-eleostearic acid.

Prunus mahaleb

Whole seeds of *P. mahaleb* L. yielded 15% of oil. The oil had λ_{max} 261, 270, 282 mμ in isooctane and absorptivity equivalent to about 29% of conjugated triene fatty acid. The mixed methyl esters of the fatty acids had infrared maxima at 960 (w) and 988 (vs) cm^{-1}. A concentrate of the triene acid was prepared and a portion was converted to its maleic anhydride adduct. The adduct melted at 63–64°, alone and mixed with the adduct of α-eleostearic acid. Another portion was isomerized by iodine in pentane solution to the all-trans form, m.p. and mixed m.p. with β-eleostearic acid, 70–71°.

ACKNOWLEDGMENTS

The authors are indebted to Mr. R. Lauzon for determination of infrared spectra and to Mr. H. Seguin for the microanalyses.

REFERENCES

1. J. McLEAN and A. H. CLARK. J. Chem. Soc. 777 (1956).
2. M. J. CHISHOLM and C. Y. HOPKINS. Can. J. Chem. **38**, 2500 (1960).
3. C. Y. HOPKINS and M. J. CHISHOLM. J. Chem. Soc. 573 (1962).
4. M. J. CHISHOLM and C. Y. HOPKINS. J. Org. Chem. In press.
5. J. P. VERMA and J. S. AGGARWAL. J. Indian Chem. Soc. **33**, 357 (1956).
6. S. R. ALPAR and S. ESIN. Rev. Fac. Sci. Univ. Istanbul, A, **13**, 199 (1948).
7. L. CROMBIE and A. G. JACKLIN. J. Chem. Soc. 1632 (1957).
8. F. D. GUNSTONE. *In* Progress in organic chemistry. *Edited by* J. W. Cook. Butterworth, London. 1958. p. 12.
9. F. R. EARLE, E. H. MELVIN, L. H. MASON, C. H. VAN ETTEN, and I. A. WOLFF. J. Am. Oil Chemists' Soc. **36**, 304 (1959).
10. A. STEGER and J. VAN LOON. J. Soc. Chem. Ind. (London), **56**, 298T (1937).
11. K. A. PELIKAN and J. F. GERKENS. Oil & Soap, **16**, 11 (1939).
12. S. C. GUPTA and F. A. KUMMEROW. J. Am. Oil Chemists' Soc. **37**, 32 (1960).
13. J. D. VON MIKUSCH. J. Am. Oil Chemists' Soc. **29**, 114 (1952).
14. K. ALDER and R. KUTH. Ann. **609**, 19 (1957).

GAS–LIQUID PARTITION CHROMATOGRAPHY OF SESQUITERPENE COMPOUNDS

ISHWAR C. NIGAM[1] AND LEO LEVI
Food and Drug Directorate, Department of National Health and Welfare, Ottawa, Canada

Received July 5, 1962

ABSTRACT

Sesquiterpene compounds were effectively separated by gas chromatography and identified by infrared spectrophotometry. Examples given include the recovery and characterization of β-caryophyllene and β-humulene from oil of balsam copaiba, of α- and β-vetivone from oil of vetiver, and of α- and β-santalol from oil of sandalwood.

INTRODUCTION

Gas–liquid partition chromatography has become a technique of choice for the investigation of volatile substances, particularly essential oils and related products. An increasing number of researches are being published dealing with its application to the characterization and estimation of major as well as minor constituents in natural and synthetic products used by the essential oils, flavor, cosmetic, and perfume industry. Recently, preparative columns have enabled investigators to collect effluent fractions in quantities sufficient for further physicochemical analysis by infrared and ultraviolet spectroscopy as well as the formation of characteristic derivatives.

Most efforts have, however, been directed toward the examination of monoterpene compounds (1, 2, 3, 4). Corresponding studies of sesquiterpenes are lacking, although some notable contributions have been made (5, 6, 7, 8, 9, 10, 11). Paucity of systematized data may, in part, be due to the low vapor pressure of these compounds—a property that restricts the choice of stationary phases permitting reasonable retention times—combined with a rather delicate nature, rendering them prone to degradation when kept at elevated temperature on potentially catalytic surfaces for some length of time.

Experiments carried out in the authors' laboratory showed that these compounds can be resolved effectively by gas chromatography within less than 30 minutes under relatively mild conditions. It is the purpose of this paper to report the separation of typical sesquiterpenoid mixtures occurring in balsam copaiba, vetiver, and sandalwood oil.

EXPERIMENTAL RESULTS AND DISCUSSION

Apparatus.—Gas chromatograph. Burrell Kromo-Tog K-2 equipped with thermal conductivity detector cell and separate heating baths for column and detector, respectively.

Column.—Glass tubing, 0.6 cm inside diameter, 215 cm long.

Packing.—Reoplex 400 (20 parts) deposited from ethanolic solution on 60- to 80-mesh, acid-washed Chromosorb W (80 parts). Length of packed column, 200 cm.

Carrier Gas.—Helium, inlet pressure 1.1 atm; outlet pressure 1.0 atm.

Recorder.—0 to 1 mv full scale deflection; 1 second.

Chart Speed.—0.5 inch per minute.

Analytical procedures were previously described (12, 13).

Infrared spectra of the eluates collected were charted by a Perkin–Elmer Model 221 spectrophotometer operated with fivefold ordinate scale expansion and their identity confirmed through reference to literature data (14).

Caryophyllene Fraction of Oil of Balsam Copaiba

Oil of balsam copaiba is known to contain a number of sesquiterpene hydrocarbons. α- and β-Caryophyllene were isolated in 1892 (15) and *l*-cadinene was detected in 1910 (16). α-Caryophyllene, later identified as

[1]*National Research Council of Canada Postdoctoral Fellow, 1961–62.*

humulene, is now itself considered to be composed of two isomers, α- and β-humulene. Separation of β-caryophyllene–humulene mixtures has been accomplished by careful distillation and repurification of the isolates via extensive column chromatography (17, 18).

Figure 1 shows the chromatogram of a fraction, b.p. 116–125° C/10 mm, obtained by vacuum distillation of a genuine Brasilian oil and the infrared spectra of the eluates, β-caryophyllene and β-humulene, collected

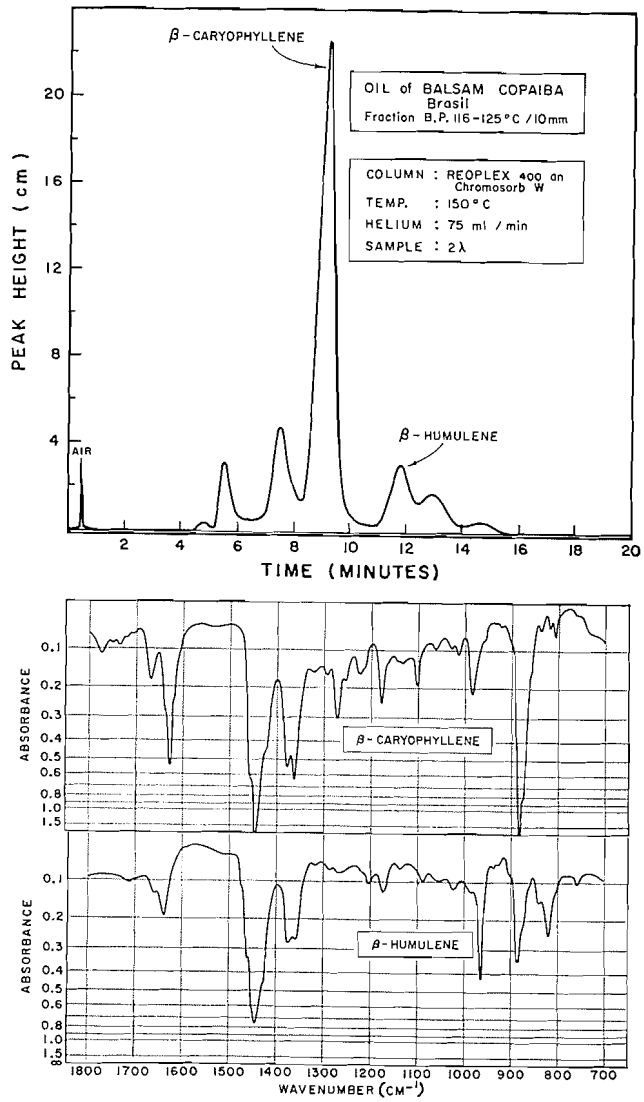

FIG. 1. Gas chromatographic separation and infrared spectra of sesquiterpenes. β-Caryophyllene: isolate from 10-λ sample injection examined with fivefold ordinate scale expansion; β-humulene: isolate from 3×8-λ sample injection examined with fivefold ordinate scale expansion.

for analysis. The identity of three other sesquiterpene compounds present and likewise well resolved is being established.

A column of SAIB (19) operated at 170° C was found to separate the hydrocarbons with equal efficiency.

Vetivone-enriched Fraction of Vetiver Oil

α- and β-Vetivone, two stereoisomeric sesquiterpene ketones differing only in the spatial configuration about their asymmetric $\rangle CH—CH_3$ group, are the major ketones present in oil of vetiver and considered

responsible for its characteristic odor. Their isolation has been achieved by treatment of the oil with Girard T reagent, conversion of the complexes formed to semicarbazones, and decomposition of the derivatives with phthalic anhydride following repeated fractional recrystallizations, or by careful distillation of the oil, reaction of the ketone fraction with semicarbazide, and analogous treatment of the isolated semicarbazones. Each method involves tedious and time-consuming operations and yields are poor (20, 21, 22, 23).

Figure 2 shows the chromatogram of a vetivone-enriched fraction obtained by column chromatography of a sample of Réunion Island vetiver oil and the infrared spectra of the well-separated isomers collected for examination. Characterization of other sesquiterpene ketones present and effectively resolved is underway.

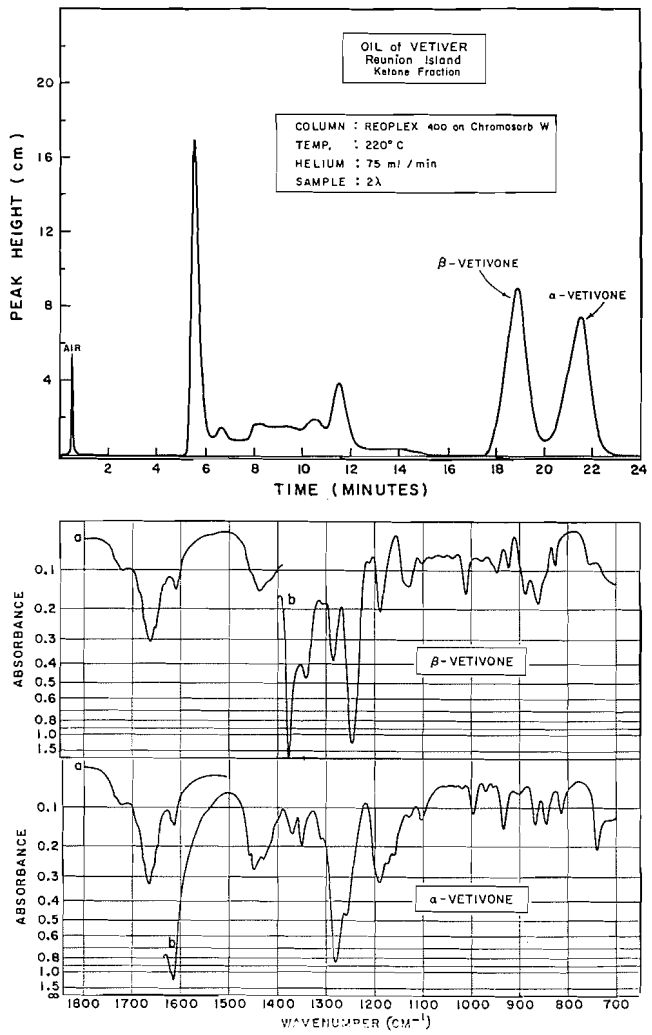

FIG. 2. Gas chromotographic separation and infrared spectra of sesquiterpene ketones. α- and β-Vetivone isolates from 8-λ sample injection examined (*a*) without and (*b*) with fivefold ordinate scale expansion.

East Indian Sandalwood Oil

East Indian sandalwood oil contains more than 90% of santalol, a high-boiling sesquiterpene alcohol occurring as an α- and β-isomer, respectively. Official methods of analysis based on acetylation and saponification reactions lack selectivity (24, 25, 26). An infrared procedure utilizing measurements of specific extinction coefficients observed throughout the 3.2–3.3 and 9.8–10.0 μ regions, respectively, has also been reported. Considered to be characteristic of cyclopropane ring compounds present, it provides an index of total cyclopropyl content including, in addition to α-santalol, such constituents as α-santalene, teresantalic acid, teresantalol, and nortricycloekasantalane, but leaving β-santalol unaccounted for (27).

Figure 3 shows the chromatogram of this oil and the infrared spectra of both isomers collected from a single 8-λ sample injection. Requiring only microamounts of products for analysis the method described should prove of general value to workers in the field.

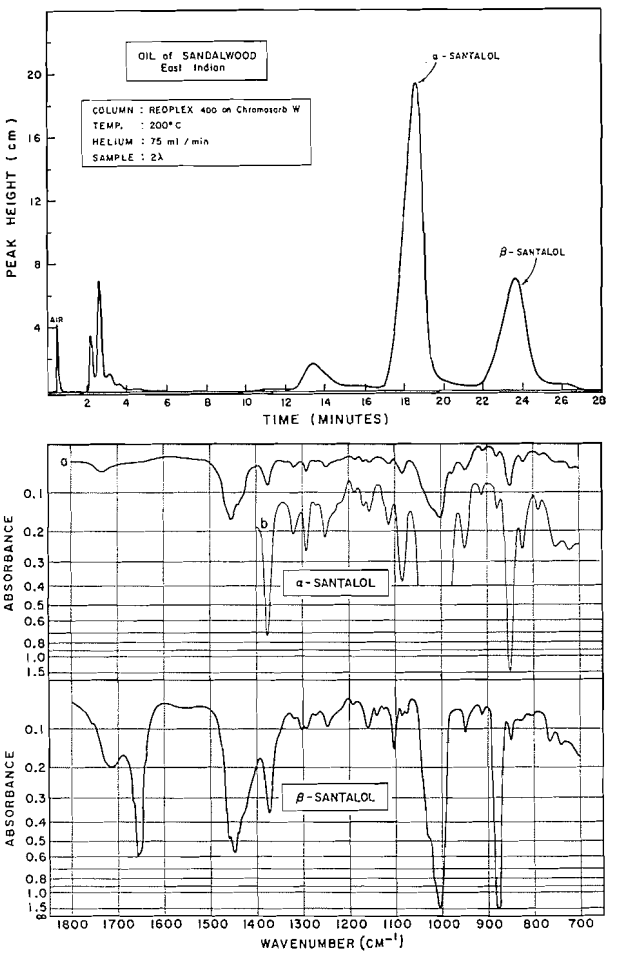

FIG. 3. Gas chromatographic separation and infrared spectra of sesquiterpene alcohols. α-Santalol: isolate from 8-λ sample injection examined (*a*) without and (*b*) with fivefold ordinate scale expansion; β-santalol: isolate from 8-λ sample injection examined with fivefold ordinate scale expansion.

Application of the technique to the examination and recognition of sandalwood oils of different geographical origins and further illustrations of sesquiterpene analyses by gas–liquid partition chromatography will be reported in forthcoming publications.

ACKNOWLEDGMENTS

The authors are indebted to Dr. E. Guenther, Fritzsche Brothers, Inc., New York, U.S.A., for the balsam copaiba oil fraction used in this study; to Dr. J. Gondran, Société Comores Bambao, Paris, France, for an authentic sample of Réunion Island vetiver oil; to Dr. Y. R. Naves, Givaudan and Co., Geneva, Switzerland, for a genuine specimen of β-vetivone; and to Dr. S. C. Bhattacharyya, National Chemical Laboratory, Poona, India, for an authentic sample of Mysore sandalwood oil.

REFERENCES

1. A. LIBERTI and G. P. CARTONI. Ric. Sci. **28**, 1192 (1958).
2. W. J. ZUBYK and A. Z. CONNER. Anal. Chem. **32**, 912 (1960).
3. E. VON RUDLOFF. Can. J. Chem. **38**, 631 (1960); **39**, 1, 1190, 1200 (1961).
4. M. H. KLOUWEN and R. TERHEIDE. J. Chromatog. **7**, 297 (1962).
5. E. VON RUDLOFF. Can. J. Chem. **39**, 1860 (1961).
6. E. VON RUDLOFF. Tappi, **45**, 181 (1962).
7. E. VON RUDLOFF. Chem. Ind. (London), 743 (1962).
8. J. RUNEBERG. Acta Chem. Scand. **14**, 803, 1985 (1960).
9. E. PETTERSSON and J. RUNEBERG. Acta Chem. Scand. **15**, 713 (1961).
10. A. OFNER, W. KIMEL, A. HOLMGREN, and F. FORRESTER. Helv. Chim. Acta, **42**, 2577 (1959).
11. N. NARASIMHACHARI and E. VON RUDLOFF. Can. J. Chem. **39**, 2572 (1961).
12. K. L. HANDA, D. M. SMITH, and L. LEVI. Perfumery Essent. Oil Record, **53**, 607 (1962).
13. I. C. NIGAM, M. SAHASRABUDHE, T. W. MCCONNELL DAVIS, J. C. BARTLET, and L. LEVI. Perfumery Essent. Oil Record, **53**, 614 (1962).
14. J. PLÍVA, M. HORÁK, V. HEROUT, and F. ŠORM. Die Terpene, Sammlung der Spektren und physikalischen Konstanten. Teil I: Sesquiterpene. Akademie-Verlag, Berlin. 1960.
15. O. WALLACH. Ann. **271**, 294 (1892).
16. SCHIMMEL & CO. Ber. 177 (1910).
17. V. HEROUT, M. STREIBL, J. MLEZIVA, and F. ŠORM. Collection Czech. Chem. Commun. **14**, 716 (1949).
18. V. BENEŠOVÁ, V. HEROUT, and F. ŠORM. Collection Czech. Chem. Commun. **26**, 1832 (1961).
19. D. M. SMITH, J. C. BARTLET, and L. LEVI. Anal. Chem. **32**, 568 (1960).
20. M. ROMAŇUK and V. HEROUT. Collection Czech. Chem. Commun. **25**, 2540 (1960).
21. A. S. PFAU and P. A. PLATTNER. Helv. Chim. Acta, **22**, 648 (1939).
22. S. SABETAY and L. TRABAUD. Bull. Soc. Chim. France, **6** (5), 740 (1939).
23. Y. R. NAVES and E. PERROTTET. Helv. Chim. Acta, **24**, 20 (1941).
24. BRITISH STANDARD SPECIFICATION. B.S.2999/30. British Standards Institution, London, England. 1959.
25. INDIAN STANDARD. IS: 329-1952. Indian Standards Institution, New Delhi, India.
26. BRITISH PHARMACOPOEIA. Pharmaceutical Press, London. 1932. p. 313.
27. V. K. BALAKRISHNAN, S. DASGUPTA, and S. C. BHATTACHARYYA. Perfumery Essent. Oil Record, **47**, 383 (1956).

LYCOPODIUM ALKALOIDS

IV. THE CONSTITUTION AND STEREOCHEMISTRY OF LYCOCLAVINE, AN ALKALOID OF LYCOPODIUM CLAVATUM VAR. MEGASTACHYON[1]

W. A. Ayer and D. A. Law
Department of Chemistry, University of Alberta, Edmonton, Alberta
Received May 22, 1962

ABSTRACT

The alkaloids of *Lycopodium clavatum* var. *megastachyon* have been examined and two hitherto unreported alkaloids, lycoclavine and acetyllycoclavine, were isolated and their structures determined. The nuclear magnetic resonance spectra of these and related compounds are discussed in terms of the conformation of ring B in these alkaloids.

The alkaloids of *Lycopodium clavatum* Linn. have been examined extensively (1–4) and a total of 16 different alkaloids isolated. We have now investigated the alkaloidal content of *L. clavatum* var. *megastachyon* Fern. and Bissel (5), and two closely related, but hitherto unreported, alkaloids have been isolated and their structures established. In addition, four other alkaloids of known constitution were isolated, along with a small amount of a base of undetermined constitution.

The total crude alkaloid of *L. clavatum* var. *megastachyon*, obtained by methanol extraction, amounted to approximately 0.12% of the dry weight of the plant. Separation of the alkaloids, achieved mainly by chromatographic techniques (see Experimental), yielded the following compounds: (i) lycopodine (30% of the total basic material); (ii) clavolonine (11%);[2] (iii) a compound, $C_{18}H_{29}O_3N$, m.p. 212–213° (7.5%), which appears to be new and which we have named lycoclavine; (iv) a compound, $C_{20}H_{31}O_4N$, m.p. 144–145° (11%), which proved to be the O-acetyl derivative of lycoclavine; (v) a substance, $C_{32}H_{52}O_3N_2$, m.p. 213–214° (1.5%), which was shown to be a 1:1 molecular complex of dihydrolycopodine ($C_{16}H_{27}ON$) and flabelliformine ($C_{16}H_{25}O_2N$).[3] In addition to the above-mentioned alkaloids, a small amount of an apparently new alkaloid, m.p. 261–263°, analyzing best for $C_{16}H_{25-27}O_2N$, was also isolated but has not yet been further characterized.

The structures of lycopodine (6), dihydrolycopodine (6), flabelliformine (7),[4] and clavolonine (8) are known. Furthermore, a comparison of the infrared spectrum of clavolonine with that of alkaloid L.34, first isolated by Manske in 1953 from *Lycopodium densum* Labill. (9), revealed their identity.[5] The composition of the molecular complex mentioned in (v) above was established in the following manner. Attempts to separate the complex by fractional crystallization and by chromatography were unsuccessful. However, treatment of the complex with chromium trioxide in pyridine oxidized the dihydrolycopodine to lycopodine and left the flabelliformine unchanged. The two components were then easily separable by chromatography. Finally, combination of equimolar quantities of dihydrolycopodine and flabelliformine gave a high yield of the C_{32} complex, identical in

[1]*Part III: W. A. Ayer and G. G. Iverach. Tetrahedron Letters, No. 3, 87 (1962).*
[2]*Identical in all respects with an authentic sample kindly furnished by Dr. R. H. Burnell, University of the West Indies, Jamaica.*
[3]*We wish to thank Dr. D. B. MacLean, McMaster University, for the comparison of our material with authentic flabelliformine.*
[4]*We wish to thank Dr. MacLean for a preprint of this paper.*
[5]*We wish to thank Dr. Manske for a sample of alkaloid L.34.*

all respects with that obtained from the plant. It is interesting to note that flabelliformine also forms stable 1:1 molecular complexes with both lycopodine and lycodoline, although these latter are readily separable by chromatography (10).

Turning now to the determination of the structure of lycoclavine, $C_{18}H_{29}O_3N$, the presence of a hydroxyl group and an acetoxyl group was established by the following observations. The infrared spectrum (in dilute CCl_4) showed a concentration-independent peak at 3600 cm^{-1}, with a shoulder at 3620 cm^{-1}, indicative (11) of an intramolecularly hydrogen-bonded hydroxyl group. Peaks at 1736 cm^{-1} and 1240 cm^{-1} in the infrared, and at 7.93 τ (3 H) in the n.m.r. suggested the presence of an O-acetyl group and this was confirmed by hydrolysis to acetic acid and a diol, $C_{16}H_{27}O_2N$, henceforth called desacetyllycoclavine. The secondary nature of these functional groups was indicated by the n.m.r. spectra of lycoclavine, which showed one-proton peaks at 5.11 τ (doublet, splitting 6.9 c.p.s., $\rangle$*C*HOAc) and 6.40 τ (singlet, $\rangle$*C*HOH). Acetyllycoclavine, prepared by acetylation of lycoclavine with acetic anhydride – pyridine, showed similar peaks at 4.92 τ (doublet, splitting 6.8 c.p.s.) and 5.32 τ (singlet), the latter peak being attributed to the proton on the carbon bearing the hydroxyl group in the unacetylated compound. The n.m.r. spectra also revealed the presence of a secondary C-methyl group (doublets at 9.09 τ and 9.08 τ, splitting ca. 6 c.p.s., in lycoclavine and acetyllycoclavine, respectively). Lack of NH absorption in the infrared spectra of lycoclavine and its acetyl derivative indicated the tertiary nature of the amino nitrogen. Since lycoclavine could not be reduced catalytically and showed no olefinic protons in the n.m.r., it appeared to be tetracyclic.

Oxidation of lycoclavine with chromic acid in acetic acid, followed by chromatography over alumina, yielded a basic compound, $C_{18}H_{27}O_2N$, m.p. 174–175°, which showed peaks in the infrared at 1751 cm^{-1} (O-acetyl) and 1724 cm^{-1} (cyclohexanone), and in the ultraviolet at 282 mμ (log ϵ, 2.56). Hydrolysis of this ketone, which we shall refer to as "lycoclavinone", with dilute sodium hydroxide yielded an amphoteric compound, $C_{16}H_{23}O_2N$, which had the properties of a diosphenol. In particular, the ultraviolet spectrum showed a maximum at 282 mμ (log ϵ, 3.99) in neutral solution, shifted to 327 mμ in dilute base, and to 248 mμ on acetylation. These values are indicative of the presence of the grouping 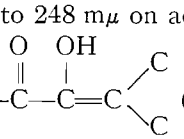 (12). The formation of the enolic α-diketone indicated that lycoclavinone was an α-acetoxy ketone, the α-diketone arising from aerial oxidation of the initially formed α-ketol. The susceptibility of α-ketols to aerial oxidation in alkaline solution is well authenticated (13) and it was found that the rate of formation of the diketone (as determined by the rate of increase of the ϵ value at 327 mμ) was substantially reduced when the reaction was carried out in a nitrogen atmosphere and accelerated when oxygen was bubbled through the hydrolysis solution. Hydrolysis of lycoclavinone with aqueous acid yielded the α-ketol, which underwent aerial oxidation to the diosphenol in alkaline solution. These results demonstrate the presence of the grouping —CHOH—CHOAc—, flanked on at least one side by a methine group, in lycoclavine.

The presence of the above-mentioned grouping, a $\rangle$$CHCH_3$ group, and a tertiary nitrogen, together with the fact that lycoclavine occurs along with lycopodine (I) and several other alkaloids having a lycopodine skeleton, and that all *Lycopodium* alkaloids

of known constitution bear an oxygen or its biogenetic equivalent (i.e. unsaturation or nitrogen) at C-5, suggested structure II (without stereochemical implications) as a possibility for lycoclavine, and hence III for the enolic α-diketone. Indeed, oxidation of lycopodine with 1 mole[6] of SeO_2 in refluxing dioxane gave, in addition to unchanged lycopodine, the enolic diketone III (25% yield), identical in all respects with that prepared from lycoclavine. Compound III has also been prepared by hydrolysis of bromolycopodine in the presence of air (14).

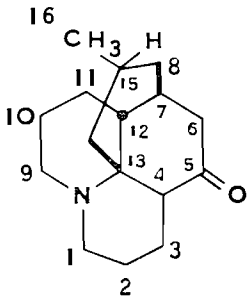

I

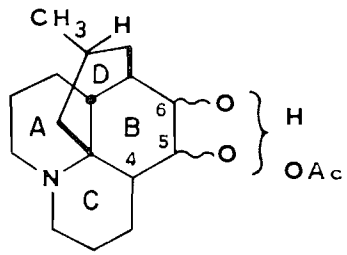

II

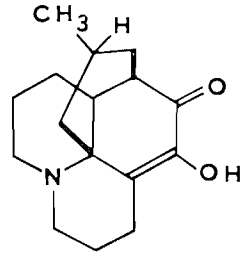

III

Since both the relative (15) and absolute (16) stereochemistry of lycopodine are known these results show that lycoclavine is represented by II, the only remaining points to be determined being the relative positions of the hydroxyl and acetoxyl groups and the stereochemistry at C-4, C-5, and C-6.[7] In order to simplify the discussion, the hydrogen at C-4 will now be placed trans to the C-7, C-13 bridge as in structures IV–VII. That this is indeed the correct orientation at C-4 will be demonstrated later.

On the basis of the n.m.r. data presented earlier, structure IV (R = Ac, R′ = H) was first favored for lycoclavine, since in this structure the axial proton on C-5 is flanked by an axial proton on C-4 which could lead to the observed splitting (ca. 7 c.p.s.), whereas the equatorial proton on C-6 is flanked by gauche protons on C-5 and C-7 and might be expected to be weakly coupled, resulting in the broadened singlet (half-height width about 3.5 c.p.s.) actually observed (17). Several facts, however, were not in agreement with this formulation. Thus, although lycoclavine showed weak intramolecular hydrogen bonding in the infrared, the corresponding diol, desacetyllycoclavine, obtained by alkaline hydrolysis or, better, by $LiAlH_4$ reduction of lycoclavine, showed a single OH stretching vibration at 3620 cm^{-1}. The diol was also resistant to oxidation with periodic acid. Both these facts speak against the cis relationship of the two groups. Furthermore, hydrolysis of acetyllycoclavine with refluxing 10% aqueous HCl for $1\frac{1}{2}$ hours gave lycoclavine in better than 90% yield. If IV (R = Ac, R′ = Ac) were indeed the correct formulation for the diacetate, the retention of the relatively unhindered equatorial acetoxyl at C-5 while the hindered axial acetoxyl group at C-6 was hydrolyzed would not be expected.

Structure V would also be expected to lead to a diol which would show intramolecular hydrogen bonding and react with periodic acid. Since it was felt that the oxygenated ring might be considerably distorted from the chair form (see below) structures VI and VII remained for consideration.

[6]*Use of excess* SeO_2 *led to the formation of compound(s) absorbing at 306, 340, and 380 mμ in the ultraviolet.*
[7]*The numbering system used (see structure I) is that suggested by K. Wiesner (16(b)).*

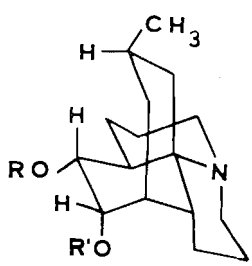

IV

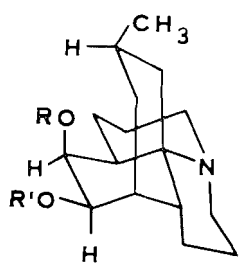

V

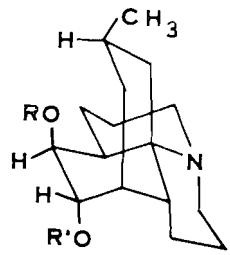

VI

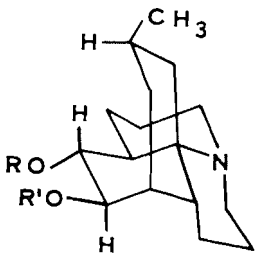

VII

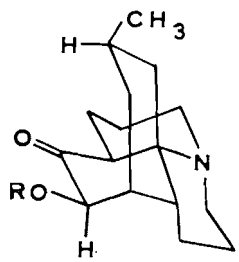

VIII

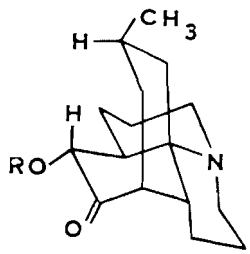

IX

The position of the acetoxyl group was determined in the following manner. Lycoclavinone, mentioned above, could be assigned structure VIII (R = Ac) on the following basis. The optical rotatory dispersion curve showed a positive Cotton effect with extrema at 308 mμ and 271 mμ and an amplitude of 23,000°. Lycopodine (VIII, RO replaced by H) under the same conditions also shows a positive Cotton effect with extrema at 306 mμ and 271 mμ, amplitude 17,000°. The octant rule (18) predicts a positive Cotton effect if the keto group is at C-5 (as in VIII) and a negative Cotton effect if it is at C-6 (as in IX). The equatorial nature of the acetoxyl group is indicated both by the position of the extrema in the optical rotatory dispersion spectrum (19) and by the position (282 mμ, lycopodine 285 mμ) of the ketonic maximum in the ultraviolet (20). The fact that the α-ketol obtained by acid hydrolysis of the acetoxy ketone was reconverted by acetic anhydride – pyridine to the same acetoxy ketone is also consistent with structure VIII, since under these equilibrating conditions ketol VIII (R = H), in which the serious non-bonded interaction between C-15 and C-5 is minimized, should be favored over ketol IX (R = H). The fact that the hydroxyl group in the ketol is intramolecularly hydrogen bonded (concentration-independent band at 3500 cm^{-1} in the infrared) is consistent with the assigned equatorial position.

Pyrolysis of VIII (R = Ac) at 240° for 8 minutes led to a good yield of the α,β-unsaturated ketone X, which had previously been prepared from bromolycopodine (14). Presumably this facile elimination of acetic acid proceeds via the enol form of the ketone, as formulated below, with the reacting material acting as its own base.

It was now important to determine whether lycoclavinone (VIII, R = Ac), which is

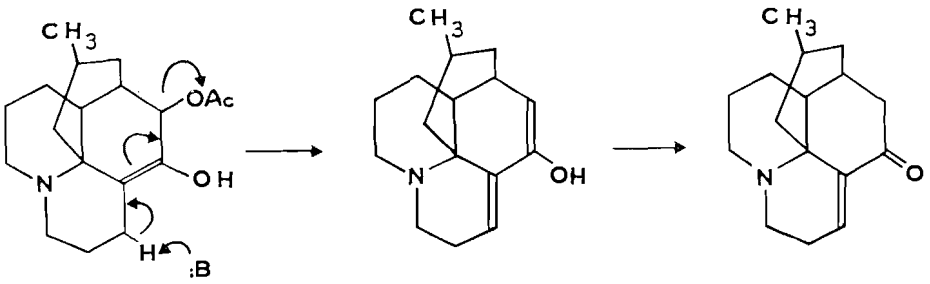

X

presumably the thermodynamically more stable of the four possible C-5, C-6 acetoxyketones, was actually the first product of the oxidation of lycoclavine. It was found that if the acetic acid oxidation solution was first diluted with $CHCl_3$ and then ice-cold ammonium hydroxide added, evaporation of the $CHCl_3$ extract and crystallization from *n*-hexane gave, instead of lycoclavinone, the α-acetoxyketone XI, m.p. 115–118°. If the oxidation solution was first made basic by addition of ammonium hydroxide, then extracted with $CHCl_3$ and filtered *rapidly* through alumina, the ketone IX (R = Ac), m.p. 143°, was obtained. Both IX (R = Ac) and XI were isomerized to VIII (R = Ac) when adsorbed on basic alumina for any extended length of time. Similar isomerizations of steroidal α-acetoxyketones have been reported (21). Acid hydrolysis of IX (R = Ac) gave the α-ketol VIII (R = H). The structural assignments are based mainly on optical rotatory dispersion and ultraviolet measurements. Both IX and XI showed *negative* Cotton effect curves, as predicted by the octant rule (see above). The extrema for IX (R = Ac) were at 312 mμ and 280 mμ (amplitude −2300°), for XI at 334 mμ and 297 mμ (amplitude −11,300°), indicative (19) of equatorial and axial α-acetoxy groups, respectively. The ultraviolet maxima were at 286 mμ for IX and 308 mμ for XI. The fact that XI shows a more negative Cotton effect than does IX no doubt reflects the distortion of the ketone-containing ring from an ideal chair (see below). Similar observations have been made with α-acetoxy 11- and 12-ketosteroids (22).

The formation of lycoclavinone I thus proceeds via the sequence

$$\text{lycoclavine} \xrightarrow{CrO_3\text{–HOAc}} \text{XI} \xrightarrow[Al_2O_3]{NH_4OH \text{ or}} \text{IX} \xrightarrow{Al_2O_3} \text{VIII}$$

and hence the acetoxyl group in lycoclavine is located on C-5 cis to the C-7, C-13 bridge, in agreement with structure VI (R = Ac, R′ = H) but not with structure VII.

Further evidence for the diaxial orientation of the substituents at C-5 and C-6 and for the configuration at C-4 was obtained by a study of the reduction products obtained from the various isomeric α-ketols and α-acetoxylketones now available to us. It has been shown (8) that lithium aluminum hydride reduction of lycopodine (I) leads to the axial alcohol dihydrolycopodine (XII, R = OH, R′ = H), whereas dissolving metal reduction gives the equatorial alcohol α-dihydrolycopodine (XII, R = H, R′ = OH). We have independently arrived at this same conclusion,[8] and, furthermore, have shown that

[8]*Since the previous workers (8) have not reported physical constants or experimental details for the preparation of α-dihydrolycopodine, this is included in the experimental section.*

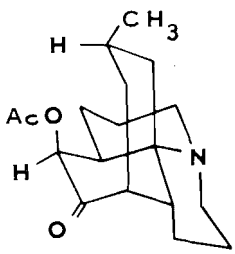

XI

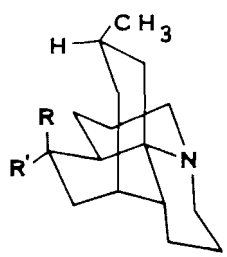

XII

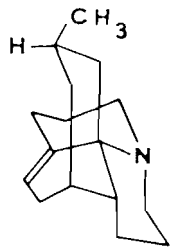

XIII

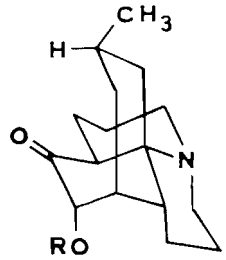

XIV

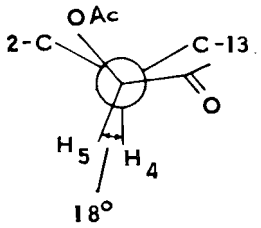

XV

the methiodide of the xanthate (XII, R = H, R′ = OCS_2CH_3), derived from α-dihydrolycopodine, yields anhydrodihydrolycopodine (XIII) on pyrolysis, confirming the cis arrangement of the hydroxyl and the C-4 hydrogen.

Reduction of alkaloid L.20 (XIV, R = H), in which the configuration at C-4 is known (14), with lithium aluminum hydride in ether yielded the diol VI (R = R′ = H) identical in all respects with desacetyllycoclavine. The structure VI (R = R′ = H) was assigned on the assumption that the approach of the reducing agent would be on the side opposite to the C-7, C-13 bridge, as is the case with lycopodine. This assumption is supported by the results obtained on reduction of ketones VIII and IX. Reduction of the ketol VIII (R = H) with $LiAlH_4$ gave a new diol, m.p. 230–231°, assigned structure V (R = R′ = H) on the basis of its mode of formation. Lithium–ammonia–methanol reduction of ketol VIII yielded a third diol, m.p. 209–210°, assigned the diequatorial structure VII (R = R′ = H), again on the basis of its mode of formation. Attempts to prepare the fourth diol (IV, R = R′ = H) by dissolving metal reduction of alkaloid L.20 were unsuccessful, leading only to reductive removal of the C-6 hydroxyl (14). However, reduction of IX (R = Ac) with $LiAlH_4$ led to a diol, m.p. 234–235°, differing from the other three, and therefore assigned structure IV (R = R′ = H). All four diols showed different infrared spectra, single spots on paper chromatography, and depression of mixed melting points, where appropriate. It is interesting to note that hydride reduction of IX (R = Ac) involves approach of the reducing species from the same side as the C-7, C-13 bridge. Presumably in this case approach to the opposite side is hindered by the C-12 methylene group. Since each of the latter three diols must have at least one equatorial

hydroxyl group, the hydride reduction product of alkaloid L.20, and hence desacetyllycoclavine, is the diaxial diol VI (R = R′ = H), and lycoclavine itself is VI (R = Ac, R′ = H).

As noted above, lycoclavine shows intramolecular hydrogen bonding but the corresponding diol does not. To account for this, it must be assumed that the oxygenated ring is severely distorted toward the half-chair, i.e., the dihedral angle between the two groups must approach 120°. It is known, for instance, that *trans*-1,2-pentanediol does not show intramolecular hydrogen bonding, but that the corresponding monoacetyl derivative does (23). Measurements on Drieding models indicate an internuclear distance of ca. 1 Å between the C-5 oxygen and the C-15 hydrogen in lycoclavine. The sum of the van der Waals radii is 2.6 Å, so that a distortion of ring B (and presumably also ring D) is to be expected.

A more quantitative estimate of this distortion can be obtained by a consideration of the n.m.r. spectra (Table I) of some of the compounds mentioned earlier. It is well

TABLE I

Nuclear magnetic resonance data for lycoclavine and related compounds

Compound	Chemical shifts* (splitting)†			
	C-5	C-6	—OCOCH$_3$	C-16
VI (R = Ac, R′ = H)	5.11 (6.9)	6.40 (3.3)‡	7.93	9.09 (6.0)
VI (R = R′ = Ac)	4.92 (6.8)	5.32 (3.2)‡	7.92, 7.93	9.08 (6.0)
VIII (R = Ac)		4.60 (5.5)	7.83	9.17 (5.5)
IX (R = Ac)	4.73 (11.5)		7.83	8.96 (5.8)
XI	4.61 (9.0)		7.89	9.03 (6.0)
XIV (R = Ac)		5.11 (3.5)	7.94	9.16 (4.5)
I				9.14 (5.0)
XII (R = R′ = H)				9.13 (6.0)
XII (R = OAc, R′ = H)	4.90§		7.96	9.08 (6.0)
XII (R = H, R′ = Ac)	4.98§		7.95	9.09 (5.7)

*τ-Values.
†In c.p.s. units.
‡Width at half height.
§Approximate center of multiplet.

known (17) that the coupling constant between vicinal hydrogens is related to their dihedral angle. In the particular case of α-acetoxycyclohexanones in fused-ring systems, the following relationships have been found (24) to apply:

$$J_{HH'} \begin{cases} 10\cos^2\phi & 0° \leqslant \phi \leqslant 90° \\ 16\cos^2\phi & 90° \leqslant \phi \leqslant 180°. \end{cases}$$

In compound XI the coupling constant between the protons on C-4 and C-5 (J_{45}) is 9 c.p.s. Using the Johnson expression given above this indicates a dihedral angle of about 18°, indicating a considerable distortion from the normal 60° angle. This is illustrated in the Newman projection XV. Compound IX (R = Ac) shows a similar distortion (J_{45} = 11.5 c.p.s., ϕ = 142° instead of 180°). In the C-5 ketone VIII (R = Ac), where the C-5, C-15 interaction is minimized because of the trigonal nature of C-5, the calculated angle is 42° ($J_{67} \simeq 5.5$ c.p.s.). The acetyl derivative of XIV gave a broadened singlet (width at half height about 3.5 c.p.s.), indicative of an angle of about 60°. Thus it appears that in the C-6 ketone series the non-bonded interaction between C-5 and C-15 is relieved, at least in part, by a distortion of ring B from an ideal chair towards the half-chair. This

strain could also be relieved if ring D assumed the boat conformation, but as has been pointed out previously (15), this introduces a serious bowsprit–flagpole interaction between C-12 and C-16. The n.m.r. results obtained with the C-5 ketones indicate a similar, but smaller, distortion of ring B in this series. Such a flattening of the B ring would increase the angle between C-4 and C-6 and account for the unusually low (1700 cm^{-1}) (6) carbonyl stretching frequency of lycopodine (27).

The n.m.r. spectra of lycoclavine and its acetyl derivative (Table I) are in good agreement with the proposed structure if we make the reasonable assumption that ring B is distorted to at least the same extent as in the C-6 ketones. Applying the Karplus–Conroy correlation (17) (the Johnson expression applies only to six-membered rings containing a trigonal carbon atom adjacent to the bonds under consideration (24)) a H_4—C—C—H_5 dihedral angle of 20° would lead to a coupling constant J_{45} of 7 c.p.s. (observed, 6.8 and 6.9 c.p.s.). J_{56} and J_{67} would be expected to be small (both angles approach 90–100° in the distorted chair), explaining the fact that C—H_5 is not further split and C—H_6 is a somewhat broadened singlet.

Inspection of Table I suggests a possible relationship between the chemical shift of the C-16 methyl group and the presence or absence of a carbonyl group at C-5. Thus those compounds with a C-5 keto group show the C-methyl resonance at 9.14–9.17 τ, while, with one exception, those without a carbonyl group in ring B show this peak at 9.08–9.09 τ. The exception is compound XII (R = R′ = H), not previously mentioned but readily available by Wolff–Kishner reduction of lycopodine, which has the C-methyl doublet centered at 9.13. The differences noted are possibly due to the long-range shielding effect of the carbonyl group (25). Inspection of models reveals that in the C-6 ketones the C-methyl group no longer lies in the shielding region of the carbonyl and may in fact be deshielded by it. In agreement with this view, the two C-6 ketones absorb at 8.96 τ and 9.03 τ.

In view of the fact that acetyllycoclavine is hydrolyzed by hot dilute mineral acid to lycoclavine, the possibility arose that the lycoclavine isolated was actually formed during the isolation process. Although this possibility cannot be completely excluded, it seems unlikely, since lycoclavine can also be isolated in good yield by percolation of the ground plant with cold dilute acetic acid and immediate extraction of the alkaloids into chloroform.

EXPERIMENTAL

Ultraviolet spectra were measured in 95% ethanol and, unless otherwise specified, infrared spectra in carbon tetrachloride. For hydrogen-bonding studies, spectra were determined on 0.1, 0.05, and 0.025 *M* solutions in CCl_4 using a Perkin–Elmer Model 221 spectrophotometer. Nuclear magnetic resonance spectra were measured on ca. 10% w/v solutions in chloroform using a Varian Associates Model A-60 spectrometer. Internal tetramethylsilane was used as a standard. Some of the optical rotatory dispersion curves were obtained by Dr. M. M. Marsh, Eli Lilly, Indianapolis, to whom we extend our best thanks; the others were determined by Mr. R. N. Swindlehurst of these laboratories using a Rudolph Automatic Recording Spectropolarimeter. Melting points were determined on a hot stage and are uncorrected. Alumina, unless otherwise specified, means basic alumina of activity III. Skellysolve B refers to Skelly Oil Company light petroleum, b.p. 62–70°. Microanalyses are by Pascher Mikroanalytisches Laboratorium, Bonn, West Germany, and C. Daesslé, Montreal, Quebec.

Isolation of the Alkaloids

Dried, powdered *L. Clavatum* var. *megastachyon* (15.5 kg) was Soxhlet-extracted for 24 hours with methanol. Most of the methanol was removed by distillation and the residue treated with ice-cold 1% hydrochloric acid (5 l.). The acid solution was filtered (celite) from insoluble material. The insoluble material was then vigorously stirred with cold 1% HCl (5 l.) for several hours, and the mixture again filtered. The combined acid solutions were basified (NH_4OH, ice) and extracted five times with chloroform. The chloroform was removed by distillation and the oily residue dissolved in ice-cold 1% HCl (5 l.) and washed three

times with ether to remove neutral material. The aqueous solution was then basified (ice-cold NH_4OH) and extracted four times with chloroform. Evaporation of the chloroform left 18.2 g of basic material as a dark brown gum.

Purification of the Alkaloids

The crude alkaloid was placed on a column of alumina (1 lb) in ether and eluted in four fractions: A, 9.01 g, 3 l. ether; B, 1.88 g, 6 l. ether; C, 8.50 g, 6 l. $CHCl_3$; D, 3.32 g, 1 l. MeOH.

Fraction B was crystallized from acetone to give the dihydrolycopodine–flabelliformine complex, m.p. 213–214° (0.3 g). Calc. for $C_{32}H_{52}O_3N_2$: C, 75.00; H, 10.16; O, 9.37; N, 5.47%. Found: C, 74.78; H, 10.16; O, 9.82; N, 5.44%. Infrared spectrum: ν_{max} (nujol) 3300–2600 (broad OH superimposed on C—H), 1710 cm^{-1} (C=O).

Fraction C crystallized from acetone to given clavolonine, m.p. 233–234° (1.53 g), identical with an authentic sample furnished by Dr. R. H. Burnell.

Fraction D was chromatographed over alumina and yielded further clavolonine (0.50 g) when eluted with $CHCl_3$. Elution with $CHCl_3$–MeOH (99:1) and crystallization from methanol–ether yielded 70 mg colorless needles, m.p. 261–263°. Found: C, 72.36, 72.49; H, 9.36, 9.58; N, 5.60%. The infrared spectrum (nujol) showed strong —OH absorption (3400 cm^{-1}) but no carbonyl absorption. This compound has not been further investigated.

Fraction A and the residues from fractions B and C were combined and carefully chromatographed over alumina (1 lb). Elution with benzene (5 l.) yielded lycopodine (5.36 g), identical with an authentic sample. Elution with ether (5 l.) and crystallization from Skellysolve B gave *acetyllycoclavine*, m.p. 144–145° (2.03 g). Calc. for $C_{20}H_{31}O_4N$: C, 68.74; H, 8.94; O, 18.31; N, 4.01%. Found: C, 68.74, 68.54; H, 8.69, 9.15; O, 19.03; N, 3.55%. Infrared spectrum: ν_{max} 1745, 1225 cm^{-1} ($OCOCH_3$).

Elution with chloroform and crystallization of the eluates from acetone yielded *lycoclavine* (1.32 g). The analytical sample, m.p. 212–213°, $[\alpha]_D$ −9° (95% ethanol), was prepared by several recrystallizations from acetone. Calc. for $C_{18}H_{29}O_3N$: C, 70.32; H, 9.51; N, 4.54; O, 15.57%. Found: C, 70.11, 70.19; H, 9.43, 9.48; N, 4.57; O, 15.71%. pK_a (50% MeOH) 9.6. Infrared spectrum: ν_{max} 3620 (sh), 3600, 1736, 1240 cm^{-1}. The methiodide melted at 314°, the perchlorate at 283–286°, and the hydrochloride at 281–285°.

Further small quantities of crystalline material could be obtained by chromatography of the mother liquors from the above operations.

Proof of Composition of Molecular Complex M.p. 213–214°

Dihydrolycopodine (10.6 mg) and flabelliformine (11.2 mg) were combined in hot acetone. The solution deposited colorless crystals (15.2 mg), m.p. 204–206°. The infrared spectrum (nujol) was identical with that of the material isolated from the plant, and the mixed melting point (206–210°) showed no depression.

Oxidation of the complex with CrO_3–pyridine and alumina chromatography of the resulting product yielded lycopodine (eluted with benzene) and flabelliformine (eluted with ether).

Desacetyllycoclavine (VI, R = R′ = H)

(a) By Alkaline Hydrolysis of Lycoclavine

Lycoclavine (0.109 g) was refluxed for 1 hour with 2% NaOH in 80% methanol. Removal of most of the methanol, dilution with water, and extraction with chloroform gave, after removal of solvents, a colorless foam (0.09 g). Crystallization from a small volume of acetone yielded elongated prisms (40 mg), m.p. 207–208°. The compound was difficult to crystallize in good yield and was sublimed for analysis. Calc. for $C_{16}H_{27}O_2N$: C, 72.41; H, 10.25; N, 5.28%. Found: C, 72.28, 72.48; H, 10.30, 10.34; N, 5.45%. The infrared spectrum showed a concentration-independent band at 3620 cm^{-1} and no carbonyl absorption.

The perchlorate, prepared by neutralization of an acetone solution of the base with 70% perchloric acid and crystallization from either acetone–ether or methanol–ether, exists in two crystalline forms, one melting at 230–238° and the other at 276–278°. The two forms have different infrared spectra (nujol mulls) but are readily interconverted by seeding.

(b) By $LiAlH_4$ Reduction of Acetyllycoclavine

Acetyllycoclavine (VI, R = R′ = Ac) (0.20 g) in ether (50 ml) was refluxed for 2½ hours with lithium aluminum hydride (0.25 g), then worked up using the method of Mićović and Mihailović (26). Sublimation of the crude product gave the diol (0.148 g), m.p. 203–206°, identical with that obtained above. Similar reduction of lycoclavine also gave the diol in good yield.

(c) By Acid Hydrolysis of Acetyllycoclavine

Acetyllycoclavine (60 mg) was refluxed for 16 hours in 20% aqueous HCl (30 ml), then the solution neutralized with sodium bicarbonate and continuously extracted with ether. Evaporation of the dried ether extract gave a colorless solid which on sublimation affords desacetyllycoclavine (32 mg), m.p. 201–206°.

(d) By $LiAlH_4$ Reduction of Alkaloid L.20

Alkaloid L.20 (XIV, R = H) (38 mg) was added to a slurry of $LiAlH_4$ (0.102 g) in ether (50 ml), and the mixture refluxed for 12 hours, then worked up as in part (*b*). Sublimation of the colorless semisolid remaining after removal of the solvents gave a colorless solid (32 mg), m.p. 191–196°, whose infrared

spectrum was virtually identical with that of authentic desacetyllycoclavine. The perchlorate, prepared from the sublimed material, was identical in all respects (melting point, mixed melting point, infrared spectrum) with the perchlorate of desacetyllycoclavine.

Acetylation of Lycoclavine

Lycoclavine (87 mg) was kept for 18 hours in acetic anhydride (4 ml) – pyridine (2 ml). The solution was then diluted with chloroform and shaken with ice-cold dilute ammonium hydroxide. The chloroform layer was separated, washed with water, dried, and evaporated. The off-white solid obtained was chromatographed on alumina (5 g). Elution with ether yielded a colorless solid (86 mg). Crystallization from Skellysolve B gave *actyllycoclavine*, m.p. 144–145°, identical in all respects with the naturally occurring compound described above.

Similar treatment of desacetyllycoclavine also gave acetyllycoclavine in high yield.

Lycoclavine from Acetyllycoclavine

Acetyllycoclavine (0.87 g) was refluxed for 1½ hours with 10% aqueous HCl, then the solution was neutralized with sodium bicarbonate and continuously extracted with ether. Evaporation of the ether and crystallization of the residue from acetone gave lycoclavine (0.71 g), m.p. 211–213°, identical with the natural material.

"Lycoclavinone" (VIII, R = Ac)

Lycoclavine (68 mg) was dissolved in 98% acetic acid (20 ml) containing chromium trioxide (70 mg) and the resulting solution kept at room temperature for 18 hours, then made basic with cold dilute ammonium hydroxide and extracted six times with chloroform. Evaporation of the chloroform gave a colorless semisolid (69 mg), which was chromatographed over alumina (5 g). Elution with ether gave "lycoclavinone" (40 mg). Elution with chloroform yielded unreacted lycoclavine (15 mg). Lycoclavinone, after recrystallization from Skellysolve B, melted at 174–175°. Calc. for $C_{18}H_{27}O_3N$: C, 70.79; H, 8.92; O, 15.72%. Found: C, 70.39, 70.64; H, 9.11, 9.06; O, 15.73%. Infrared spectrum: ν_{max} 1751, 1245 ($OCOCH_3$), 1724 cm^{-1} (C=O). Ultraviolet spectrum: λ_{max} 282 mμ (log ϵ 2.56). Rotatory dispersion in methanol (*c* 0.023): $[\phi]_{400}$ +290°, $[\phi]_{308}$ +8,300°, $[\phi]_{271}$ −15,400°, $[\phi]_{260}$ −7,500°.

Ketol VIII (R = H)

Lycoclavinone (VIII, R = Ac) (45 mg) was dissolved in 10% aqueous HCl and the solution refluxed for 2 hours, then cooled, basified with sodium bicarbonate, and extracted four times with chloroform. Evaporation of the chloroform and sublimation of the residue gave a colorless solid (23 mg), m.p. 127–132°. Four recrystallizations from Skellysolve-B gave analytically pure material, m.p. 135–136°. Occasionally, a second crystalline form, m.p. 122–123°, was obtained. The two forms had different infrared spectra in nujol mull, but identical solution spectra. Calc. for $C_{16}H_{25}O_2N$: C, 72.96; H, 9.57; N, 5.32%. Found: C, 72.88, 73.00; H, 9.62, 9.76; N, 5.26%. Infrared spectrum: ν_{max} 3510 (bonded OH), 1710 cm^{-1} (C=O). Ultraviolet spectrum: λ_{max} 280 mμ (log ϵ 1.95). Rotatory dispersion in methanol (*c* 0.11): $[\phi]_{400}$ 0∓20°, $[\phi]_{304}$ +6,400°, $[\phi]_{253}$ −19,100°, $[\phi]_{250}$ −19,000°.

Acetylation of the ketol VIII with pyridine – acetic anhydride at room temperature gave lycoclavinone in high yield.

Diosphenol III

(a) From Lycoclavinone

Lycoclavinone (VIII, R = Ac) (53 mg) was stirred at room temperature for 12 hours with 2% NaOH in 20% methanol (30 ml). The solution was then adjusted to pH 7.5 with dilute acetic acid and extracted with four 30-ml portions of chloroform. Evaporation of the chloroform gave a colorless solid which did not crystallize readily and was purified by sublimation. The analytical sample melted at 185–186°, $[\alpha]_D$ −45° (0.5 in ethanol). Calc. for $C_{16}H_{23}O_2N$: C, 73.53; H, 8.87; O, 12.24; N, 5.36%. Found: C, 73.41; H, 8.95; O, 12.12; N, 5.33%. Infrared spectrum: ν_{max} 3440 (bonded OH), 1672 (C=O), 1648 cm^{-1} (C=C). Ultraviolet spectrum: λ_{max} 282 mμ (log ϵ 3.99) shifted to 327 mμ in ethanolic NaOH.

When the reaction was carried out in an atmosphere of nitrogen the peak at 327 mμ developed at about one seventh the rate in air. When oxygen was bubbled through the reaction solution the rate of formation of diketone was about 1½ times that in air.

Acetylation of the diosphenol III with acetic anhydride – pyridine gave an oily product which showed a maximum at 248 mμ in the ultraviolet.

(b) From Lycopodine

A solution of lycopodine (I) (0.83 g) in dioxane (70 ml) was refluxed for 18 hours with selenium dioxide (0.37 g). The dark brown solution was then filtered from selenium and the dioxane removed at the pump. The resulting red-brown resin was dissolved in water, the pH adjusted to 7.5 with bicarbonate, and the solution extracted six times with chloroform. The reddish-brown oil (0.63 g) obtained by removal of the chloroform was chromatographed over alumina (12 g). Elution with ether gave a pale yellow solid (0.30 g) which proved to be mainly lycopodine. Elution with chloroform–methanol (49:1) yielded a dark brown

semisolid (0.22 g) which on sublimation furnished fairly pure diosphenol III, m.p. 183–185°, identical (infrared spectrum, ultraviolet spectrum, mixed melting point, rotation) with that prepared from lycoclavinone.

Pyrolysis of Lycoclavinone

Lycoclavinone (28 mg) was heated at 240° in a nitrogen atmosphere for 8 minutes, then cooled to 120° and distilled (0.1 mm). The distillate, a pale yellow oil, was chromatographed over alumina. Elution with ether gave a colorless oil (13 mg) which showed a maximum in the ultraviolet at 244 mμ (log ε, 3.9) and bands in the infrared at 1680 and 1610 cm^{-1}. Treatment of an acetone solution of the oil with methyl iodide yielded a solid methiodide which melted, after recrystallization from methanol–ether, at 273–274°. The methiodide was identical with an authentic sample (14) of the methiodide of X.

Acetoxyketone XI

A solution of lycoclavine (0.47 g) and chromium trioxide (0.47 g) in 98% acetic acid (20 ml) was kept at room temperature for 18 hours, then diluted with chloroform (50 ml), and the resulting solution washed with enough dilute ice-cold ammonium hydroxide to neutralize the acetic acid. The chloroform layer was separated, washed with water, and evaporated to leave a colorless oil (0.41 g). Crystallization from Skellysolve B gave compound XI (234 mg), m.p. 115–118°. Calc. for $C_{18}H_{27}O_3N$: C, 70.79; H, 8.92; N, 4.59%. Found: C, 71.03, 70.91; H, 8.88, 8.94; N, 4.63%. Infrared spectrum (nujol): ν_{max} 1747, 1260 ($OCOCH_3$), 1712 cm^{-1} (C=O). Ultraviolet spectrum: λ_{max} 308 mμ (log ε 1.85). Rotatory dispersion in methanol (*c* 0.11): $[\phi]_{589}$ −200°, $[\phi]_{500}$ −500°, $[\phi]_{333}$ −5060°, $[\phi]_{298}$ +6100°, $[\phi]_{280}$ +1100°.

Isomerization of XI to VIII (R = Ac)

The acetoxyketone XI (50 mg) was adsorbed on alumina (5 g) in ether and eluted (ether) after 2 hours. Crystallization of the product from Skellysolve-B gave lycoclavinone (32 mg), m.p. 172–174°, identical with an authentic sample. The infrared spectrum of the mother liquors from the crystallization indicated a mixture of acetoxyketones VIII and IX.

Acetoxyketone IX (R = Ac)

A solution of lycoclavine (0.39 g) and chromium trioxide (0.39 g) in 98% acetic acid (40 ml) was kept at room temperature for 20 hours, then made basic with cold dilute ammonium hydroxide and extracted four times with chloroform. Evaporation of the chloroform left a tan-colored oil (0.4 g), which was dissolved in ether and filtered rapidly through alumina (5 g) to give a colorless oil (0.30 g) which crystallized (0.22 g) from Skellysolve-B. The analytical sample, prepared by two recrystallizations from Skellysolve-B followed by sublimation, melted at 143°. Calc. for $C_{18}H_{27}O_3N$: C, 70.79; H, 8.93; N, 4.59%. Found: C, 70.96; H, 8.77; N, 4.36%. Infrared spectrum (nujol): 1752, 1238 (OAc), 1720 cm^{-1} (C=O). Ultraviolet spectrum: λ_{max} 286 mμ (log ε 1.79). Rotatory dispersion in methanol (*c* 0.1): $[\phi]_{589}$ −80°, $[\phi]_{400}$ −315°, $[\phi]_{312}$ −2135°, $[\phi]_{280}$ +190°, $[\phi]_{265}$ −1000°.

Isomerization to VIII (R = Ac) was carried out on an alumina column as described above for ketone XI. Hydrolysis of IX (R = Ac) with 10% HCl (as described above for VIII (R = Ac)) gave ketol VIII in 85% yield.

α-Dihydrolycopodine (XII, R = H, R′ = OH)

Lithium metal (0.9 g) was added in small portions over a period of 30 minutes to a solution of lycopodine (0.76 g) in methanol (40 ml) – liquid ammonia (200 ml). After most of the ammonia had evaporated, water (200 ml) was added and the mixture extracted four times with chloroform. Evaporation of the chloroform left a colorless glass (0.77 g) which crystallized from ether in colorless needles (0.63 g). The analytically pure material, obtained by recrystallization from ether, melted at 133–134°. Calc. for $C_{16}H_{27}ON$: C, 77.06; H, 10.91; N, 5.62%. Found: C, 76.93; H, 11.00; N, 4.69%. Infrared spectrum: ν_{max} 3620 cm^{-1}.

The perchlorate, after recrystallization from acetone–ether, melted at 245–246°. Calc. for $C_{16}H_{27}ON \cdot HClO_4$: C, 54.94; H, 8.01; N, 4.01%. Found: C, 55.31; H, 8.24; N, 4.44%.

Acetylation with pyridine – acetic anhydride at room temperature gave acetyl-α-dihydrolycopodine as a colorless oil (no OH in infrared) in almost quantitative yield. The perchlorate, after recrystallization from acetone–ether, melted at 276–278° (decomp.). Calc. for $C_{18}H_{29}O_2N \cdot HClO_4$: C, 55.24; H, 7.67; N, 3.58%. Found: C, 55.17; H, 7.68; N, 4.15%. Infrared spectrum (nujol): 3120 (+NH), 1730, and 1250 cm^{-1} (OAc). The free base, liberated from the perchlorate, solidified, and after distillation melted at 74–76°.

Anhydrodihydrolycopodine (XIII) from α-Dihydrolycopodine

Treatment of α-dihydrolycopodine with phosphorus oxychloride in pyridine gave the chloro compound XII (R or R′ = Cl), characterized as the perchlorate, m.p. 230–231°, in good yield. However, heating the xanthate (XII, R = H, R′ = OCS_2CH_3) methiodide (0.12 g) at 265° for 20 minutes followed by distillation (0.1 mm, 140°) gave anhydrodihydrolycopodine (XIII) (0.04 g), identified as the perchlorate, m.p. 238–239°. The xanthate was prepared by refluxing an ethereal solution of α-dihydrolycopodine (0.48 g) with sodium (0.06 g) for 60 hours, then adding carbon disulphide (1 ml) and refluxing for a further 24 hours. Addition of methyl iodide and further heating caused a white precipitate to separate. The precipitate

was filtered and recrystallized from ethanol to give the xanthate methiodide (0.54 g), m.p. 280–282° (decomp.). Calc. for $C_{18}H_{29}OS_2N \cdot CH_3I$: C, 47.39; H, 6.70; S, 13.32; N, 2.91; I, 26.36%. Found: C, 47.49, 47.69; H, 6.85, 6.66; S, 13.22; N, 3.07; I, 26.41%.

Diol V (R = R′ = H)

The ketol VIII (R = H) (86 mg) was refluxed for 3 hours with a slurry of $LiAlH_4$ (0.15 g) in ether (50 ml). Working up in the usual manner gave a colorless solid (84 mg), m.p. 217–222°. The analytical sample, m.p. 230–231°, was prepared by recrystallization from acetone followed by sublimation. Calc. for $C_{16}H_{27}O_2N$: C, 72.41; H, 10.25; N, 5.28%. Found: C, 71.78; H, 10.29; N, 5.44%. The infrared spectrum (nujol) showed a sharp band at 3500 cm^{-1} and broad —OH absorption at 2600–3300 cm^{-1}.

Diol VII (R = R′ = H)

A solution of the ketol VIII (R = H) (85 mg) in methanol (10 ml) was added to liquid ammonia (150 ml). The solution was stirred vigorously and lithium (0.2 g) added in small pieces over 10 minutes, then the ammonia was evaporated and water (100 ml) added. Continuous ether extraction yielded a yellow oil which, on distillation (0.1 mm, 150°), afforded a colorless oil that solidified on scratching. Four recrystallizations from acetone gave small, colorless needles of diol VII, m.p. 209–210°. Calc. for $C_{16}H_{27}O_2N$: C, 72.41; H, 10.25; N, 5.28%. Found (sublimed sample): C, 72.38, 72.21; 10.52, 10.55; N, 4.94%. Analysis of unsublimed material suggested that it was a monohydrate (found: C, 67.84; H, 9.31%). The infrared spectrum (nujol) showed OH stretching vibrations at 3580 (sharp) and 3080 (broad) cm^{-1}. The perchlorate melted at 243–245°. The mixed melting point with diol VI (m.p. 207–208°) was 176–184°.

Diol IV (R = R′ = H)

Acetoxyketone IX (27 mg) was refluxed with $LiAlH_4$ (0.1 g) in ether (30 ml) for 6 hours, then worked up in the usual manner to give a colorless solid (22 mg), m.p. 219–226°. Recrystallization from acetone raised the melting point to 234–235°. The compound, even after sublimation, analyzed as a hemihydrate. Calc. for $C_{16}H_{27}O_2N \cdot \frac{1}{2}H_2O$: C, 70.03; H, 10.28; N, 5.10%. Found: C, 70.38, 70.04; H, 10.49, 10.32; N, 5.79%. The mixed melting point with diol V (m.p. 230–231°) was 223–230°.

Wolff–Kishner Reduction of Lycopodine

Sodium (0.10 g) in diethylene glycol (40 ml) was heated to 180° and anhydrous hydrazine added until the solution refluxed freely at 180°. The solution was then cooled and lycopodine (0.63 g) added and refluxed for 17 hours. The temperature was then raised to 210° by distilling off excess hydrazine and refluxing was continued at this temperature for 24 hours. The cooled solution was diluted with water, acidified with hydrochloric acid, and continuously extracted with ether for 24 hours to remove diethylene glycol. Basification of the aqueous layer and further extraction with ether yield a colorless semisolid (0.5 g) which could not be recrystallized, but which was purified as the perchlorate, m.p. 224–225° (from ethanol–ether). Calc. for $C_{16}H_{27}N \cdot HClO_4$: C, 57.56; H, 8.45; N, 4.20%. Found: C, 57.38, 57.32; H, 8.73, 8.40; N, 4.71%. The free base, regenerated from the perchlorate, showed no absorption in the 3000–3600 cm^{-1} or 1500–1800 cm^{-1} regions in the infrared. The methiodide melted at 288–289° after recrystallization from ethanol–ether.

ACKNOWLEDGMENTS

We wish to thank Mr. M. A. Stillwell, Mouth of Keswick, New Brunswick, for the collection and identification of the plant material, Mr. R. N. Swindlehurst and Miss Gail Stayura for most of the infrared, nuclear magnetic resonance, and optical rotatory dispersion measurements, and the National Research Council of Canada for financial support.

REFERENCES

1. O. ACHMATOWICZ and W. UZIEBLO. Roczniki Chem. **18**, 88 (1938).
2. L. MARION and R. H. F. MANSKE. Can. J. Res. B, **22**, 137 (1944).
3. R. H. BURNELL and B. S. MOOTOO. Can. J. Chem. **39**, 1090 (1961).
4. W. A. AYER, D. A. LAW, and J. A. BEREZOWSKY. Unpublished.
5. H. A. GLEASON. New Britton and Brown illustrated flora of the northeastern United States and adjacent Canada. Vol. 1. Lancaster Press. 1952. p. 4.
6. W. A. HARRISON, M. CURCUMELLI-RODOSTAMO, D. F. CARSON, L. R. C. BARCLAY, and D. B. MACLEAN. Can. J. Chem. **39**, 2086 (1961).
7. M. CURCUMELLI-RODOSTAMO and D. B. MACLEAN. In press.
8. R. H. BURNELL and D. R. TAYLOR. Tetrahedron, **15**, 173 (1961).
9. R. H. F. MANSKE. Can. J. Chem. **31**, 894 (1953).
10. W. A. AYER and J. A. BEREZOWSKY. Unpublished.
11. A. R. H. COLE. Fortschr. Chem. Org. Naturstoffe, **13**, 30 (1956).
12. L. F. FIESER and M. FIESER. Natural products related to phenanthrene. 3rd ed. Reinhold Publishing

Corp. 1949. p. 195. D. H. R. BARTON, S. K. PRADHAN, S. STERNHELL, and J. F. TEMPLETON. J. Chem. Soc. 255 (1961).
13. S. J. ANGYAL and R. J. YOUNG. J. Am. Chem. Soc. **81**, 5251 (1959).
14. W. A. AYER, J. A. BEREZOWSKY, and D. A. LAW. In preparation.
15. F. A. L. ANET. Tetrahedron Letters, No. 20, 13 (1960).
16. (*a*) K. WIESNER, J. E. FRANCIS, J. A. FINDLAY, and Z. VALENTA. Tetrahedron Letters, No. 5, 187 (1961).
(*b*) K. WIESNER. Fortschr. Chem. Organ. Naturstoffe. In press.
17. H. CONROY. Advan. in Org. Chem. **2**, 308 (1960).
18. W. MOFFITT, R. B. WOODWARD, A. MOSCOWITZ, W. KLYNE, and C. DJERASSI. J. Am. Chem. Soc. **83**, 4013 (1961).
19. C. DJERASSI. Optical rotatory dispersion. McGraw-Hill. 1960. p. 113.
20. R. C. COOKSON and S. H. DANDEGAENKER. J. Chem. Soc. 352 (1955).
21. H. B. HENBEST, D. N. JONES, and G. P. SLATER. J. Chem. Soc. 4472 (1961).
22. W. KLYNE. Tetrahedron, **13**, 29 (1961).
23. T. C. BRUICE and T. H. FIFE. Tetrahedron Letters, No. 8, 263 (1961).
24. K. L. WILLIAMSON and W. S. JOHNSON. J. Am. Chem. Soc. **83**, 4623 (1961).
25. L. M. JACKMAN. Applications of nuclear magnetic resonance spectroscopy in organic chemistry. Pergamon Press. 1959. pp. 121–125.
26. V. M. MIĆOVIĆ and M. L. MIHAILOVIĆ. J. Org. Chem. **18**, 1198 (1953).
27. P. VON SCHLEYER and R. D. NICHOLAS. J. Am. Chem. Soc. **83**, 182 (1961).

THE CONSTITUTION OF A SYNTHETIC XYLAN

II. CONTROLLED PERIODATE DEGRADATION

G. G. S. DUTTON AND A. M. UNRAU[1]
Department of Chemistry, University of British Columbia, Vancouver, British Columbia
Received June 29, 1962

ABSTRACT

The controlled periodate degradation of the synthetic xylan resulted in the formation of ethylene glycol, glycerol, xylose, and at least eight non-reducing oligosaccharides. The composition, approximate D.P., periodate oxidation, and possible structure of these oligosaccharides are reported and discussed.

In a previous communication (1), some preliminary structural investigations of the xylan (2) used in this study were reported. These studies indicated that the xylan possessed a complex structure and evidence was obtained for the possible existence of some open-chain xylose residues. This communication is concerned with the application of the Smith periodate degradation (3) to the synthetic xylan. This structural analysis has been applied with considerable success and interesting consequences to a number of naturally occurring polysaccharides (3–6) and by the authors (7) to a synthetic glucan (8). Although it may be difficult to separate or resolve the various types of fragments that are formed when this degradation is applied to some polymers, it can be most useful in determining the fine structure of certain polysaccharides.

The controlled periodate degradation of the synthetic xylan gave ethylene glycol (from the non-reducing xylopyranose end units), glycerol (from internal xylose and non-reducing xylofuranose end units), xylose (from readily hydrolyzable xylofuranoside structural units), and at least eight different non-reducing oligosaccharides with R_{xylose} values ranging from 2.32 to 0.17, see Table I.

Component 2 was identified as 1′-*O*-glyceryl-D-xylofuranoside by the following reactions. Hydrolysis gave xylose and glycerol in a 1:1 ratio. Periodate oxidation gave 1 mole of formaldehyde and borohydride reduction of the trialdehyde followed by hydrolysis gave ethylene glycol and glycerol in a 1:1 ratio. Component 6 was treated similarly and gave xylose and glycerol in a 1:1 ratio but only ethylene glycol was obtained from the periodated and reduced material. Thus component 6 must be 1′-*O*-glyceryl-D-xylopyranoside. The isolation of these two components thus indicates the existence in the xylan of xylofuranosyl $1 \rightarrow 5$ xylose units and xylopyranosyl $1 \rightarrow 5$ xylose units.

The other oligosaccharides apparently possessed progressively more complex structures. Components 4 and 7 were primarily composed of 1′-*O*-glyceryl xylobioside units. In each molecule, apparently one xylose unit was substituted at either C_2 or C_3 to render it immune to periodate attack. Since the formaldehyde involved in the periodate oxidation suggested an approximate D.P. of 3, the ethylene glycol arose from the glyceryl residues linked through C_1 whereas glycerol then must have originated primarily from xylofuranose end units. Component 8 was apparently composed mainly of 1′-*O*-glyceryl xylotrioside residues, although, in this case, a proportionately lesser amount of formaldehyde was produced and indicated a D.P. of 4.7 or approximately 5. This observation suggested

[1]*Present address: Department of Plant Science, University of Manitoba, Winnipeg, Manitoba.*

that some of the molecules were terminated by 2′-*O*-glyceryl structures. Ethylene glycol primarily originated from 1′-*O*-glyceryl structures while glycerol probably arose mostly from xylofuranose end units. The 1:1.2:1.85 ethylene glycol:glycerol:xylose ratio suggested that a few internal 1,4-linked xylopyranose and 1,5-xylofuranose units would, however, also furnish glycerol; consequently the observed ratio of the three components cannot by itself be used to suggest branching or other glycerol-producing structures in the periodate degradation.

Although the structure of components 9 and 10 was generally comparable to that of component 8, even less-specific details could be deduced. In both cases formaldehyde undoubtedly arose from 1′-*O*-glyceryl structures and a comparable amount of ethylene glycol would be expected. Some ethylene glycol could also have arisen from xylopyranose end units. A comparison of the xylose:glycerol ratios of the undegraded oligosaccharides (approximately 4:1 and 6:1 for components 9 and 10, respectively) with the D.P. estimated from the formaldehyde produced upon periodate oxidation (6.2 and 9.9 for components 9 and 10, respectively) indicates that some molecules are terminated by 2′-*O*-glyceryl structures and hence some of the glycerol in the subsequent hydrolysis would originate from such a structural feature. Some of the glycerol probably arose from xylofuranose end units although internal $1 \rightarrow 4$ linked xylopyranose units would also furnish glycerol. Although it was suspected that some branched molecules were probably present, further investigations would be necessary to establish this possibility. In this connection methylation of the oligosaccharide fragments and the investigation of their hydrolytic products by vapor phase chromatography would be most useful.

The results presented here confirm the existence of xylofuranose units in the xylan and further demonstrate the utility of the Smith degradation.

EXPERIMENTAL

Chromatographic separations were carried out using the descending technique. Whatman No. 1 filter paper was used throughout unless otherwise stated. Solvent systems employed were (A) ethyl acetate:acetic acid:water (8:2:2), (B) ethyl acetate:pyridine:water (9:2:2), and (C) butanone:water azeotrope. Ammoniacal silver nitrate and *p*-anisidine trichloroacetate spray reagents were used for detection of compounds on paper chromatograms.

Evaporations were carried out under reduced pressure at bath temperatures of 40 to 45° C. Optical rotations are equilibrium values at 21±2° C. Melting points are uncorrected.

Periodate Oxidation of Xylan

Some details of the periodate oxidations of the synthetic xylan were reported in a previous communication (6). Xylan (2.50 g) dissolved in cold water (160 ml) was treated with periodic acid (40 ml 0.5 *M*) and the oxidation followed by the usual arsenite titration technique. After 18 hours' standing at 5° C, 0.905 mole of periodate had been consumed per xylose unit and 0.910 mole of periodate was consumed per monomer unit after 28 hours. The solution was neutralized ($BaCO_3$), a solution (40 ml) of sodium borohydride added (2.0 g), and the reduction allowed to proceed at room temperature for 24 hours. After neutralization with acetic acid, the solution was evaporated to dryness and borate removed by addition of methanol containing 2% hydrogen chloride followed by evaporation under vacuum at 25–28° C. The residue was dissolved in 0.1 *N* hydrochloric acid (90 ml) and left at room temperature for 4 hours. The solution was neutralized ($PbCO_3$), evaporated to a thick syrup, and chromatographed. The mixture was resolved using sheets of Whatman No. 1 paper and solvent A. The mobilities and quantities of the components are recorded in Table I.

Characterization of Components

Component 1.—37.5 mg, originating from xylopyranose end units, was treated with a 15% molar excess of *p*-nitrobenzoyl chloride in pyridine (3 ml) and the mixture heated at 70° for 45 minutes. After addition of saturated sodium bicarbonate solution, the insoluble di-*p*-nitrobenzoate of ethylene glycol was recrystallized from acetone–ethanol, m.p. and mixed m.p. 138–140° C.

Component 2.—98 mg, $[\alpha]_D^{22}$ 10.2° (*c*, 1.0 in water) was hydrolyzed in part (39 mg) in *N* sulphuric acid (steam bath, 14 hours). The solution was neutralized ($BaCO_3$), evaporated, and chromatographed. Glycerol and xylose were identified. The ratio of the two compounds was determined chromatographically using the

TABLE I

Smith degradation of synthetic xylan

Component No.	R_{xylose} Solvent A	R_{xylose} Solvent B	Yield (mg)
1 (ethylene glycol)	3.48	3.18	37.5
2	2.38	2.32	98.0
3 (glycerol)	2.43	1.92	93.3
4	1.46	1.29	120.1
5 (xylose)	1.00	1.00	113.0
6	0.86	0.79	75.8
7	0.74	0.68	88.2
8	0.64	0.51	105.7
9	0.36	0.30	143.8
10	0.21	0.17	291.7

periodate – chromatropic acid technique (9) for the polyols and the phenol – sulphuric acid method (10) for the sugar. In a typical analysis of the mixture, 128.3 mg or 1.395 μmoles glycerol and 232 mg or 1.545 μmoles xylose was found on a paper chromatogram. The ratio of xylose:glycerol was about 1:1. To an aliquot (49 mg) of the substance in water (5 ml) was added (2 ml) periodic acid solution (0.5 *M*) and the mixture left in the dark at 5° C. After 48 and 72 hours, formaldehyde was determined (9) and at these intervals 6.48 and 6.58 mg formaldehyde had been evolved. Using an average molecular weight of xylose and glycerol, and assuming that 1 mole of formaldehyde was formed from the glyceryl xyloside, the D.P. was calculated to be approximately 2. After 72 hours, the above mixture was neutralized ($BaCO_3$) and to the solution was added sodium borohydride (50 mg). The reduction was allowed to proceed at room temperature for approximately 20 hours after which time the solution was acidified, boiled for 3 hours, deionized, and evaporated to give a small quantity of syrupy material. Chromatographic examination using solvents A, B, and C revealed the presence of glycerol and ethylene glycol. In a typical analysis, 1.01 μmoles glycerol and 1.13 μmoles ethylene glycol were found on a chromatogram or the ratio of the two alcohols was about 1:1.

Component 3.—93.3 mg, was optically inactive and had a chromatographic mobility in solvents A, B, and C identical with that of glycerol. Treatment of the oily material with *p*-nitrobenzoyl chloride as described for ethylene glycol gave glycerol tri-*p*-nitrobenzoate, m.p. and mixed m.p. 189–191° C.

Component 4.—120 mg, $[\alpha]_D^{22}$ 26° (*c*, 1.2 in water), was analyzed as described for component 2. Hydrolysis of a portion (48 mg) gave two components identified by paper chromatography as xylose and glycerol. The ratio of xylose:glycerol was found to be about 2:1. Periodate oxidation of a sample (60 mg) gave 4.65 and 4.71 mg formaldehyde after 48 and 72 hours, which corresponded to an approximate D.P. of 3. Reduction ($NaBH_4$) and hydrolysis gave rise to ethylene glycol, glycerol, and xylose in a ratio of 1:1.3:1.2.

Component 5.—113 mg, $[\alpha]_D^{22}$ 17.5° (*c*, 1.1 in water), had a mobility identical with that of xylose in solvents A, B, and C. The substance reacted with *p*-anisidine trichloroacetate, hence was reducing. Upon standing, the sugar crystallized, m.p. and mixed m.p. 143–145°.

Component 6.—75.8 mg, $[\alpha]_D^{22}$ 29° (*c*, 0.8 in water), gave, upon hydrolysis of a sample (30 mg), xylose and glycerol in an approximate ratio of 1:1. Periodate degradation of a portion (40 mg) gave, after 48 and 72 hours, 4.45 and 4.58 mg formaldehyde. The estimated approximate D.P. was 2. Reduction ($NaBH_4$) and hydrolysis gave ethylene glycol and a trace of glycerol and xylose.

Component 7.—88 mg, $[\alpha]_D^{22}$ 32° (*c*, 0.9 in water), gave, upon hydrolysis of a portion (35 mg), xylose and glycerol in an approximate ratio of 2:1. Periodate oxidation of a sample (44 mg) gave, after 48 and 72 hours, 2.91 and 3.16 mg formaldehyde, which corresponded to a D.P. of 3.4. Reduction ($NaBH_4$) and hydrolysis gave ethylene glycol, glycerol, and xylose in approximately equimolar proportions.

Component 8.—106 mg, $[\alpha]_D^{22}$ 30° (*c*, 1.1 in water) gave, upon hydrolysis of a portion (42 mg), xylose and glycerol in a ratio of 3.3:1 or approximately 3:1. Periodate oxidation of a sample (53 mg) gave, after 48 and 72 hours, 2.07 and 2.16 mg formaldehyde, which corresponded to a D.P. of 4.7 or about 5. Reduction and hydrolysis gave ethylene glycol, glycerol, and xylose in a ratio of 1:1.2:1.85.

Component 9.—144 mg, $[\alpha]_D^{22}$ 33.5° (*c*, 1.4 in water), gave, upon hydrolysis of a sample (58 mg), xylose and glycerol in ratio of 4.5:1. Periodate oxidation (72 mg) gave, after 48 and 72 hours, 2.10 and 2.12 mg formaldehyde, which corresponded to a D.P. of 6.3. Reduction and hydrolysis gave ethylene glycol, glycerol, and xylose in a ratio of 1:3.2:2.2.

Component 10.—292 mg, $[\alpha]_D^{22}$ 24° (*c*, 1.45 in water), yielded, upon hydrolysis of a sample (58 mg), xylose and glycerol in a 6:1 ratio. Periodate oxidation (73 mg) gave, after 48 and 72 hours, 2.69 and 2.68 mg formaldehyde, which corresponded to a D.P. of 9.9. Reduction and hydrolysis gave ethylene glycol, glycerol, and xylose in a ratio of 1:2.8:5.1.

Identification of Components in Hydrolyzates

The hydrolyzates of the above oligosaccharides were combined and resolved by paper chromatography using solvent C. The xylose and glycerol areas were eluted and the solutions evaporated to a syrup. D-*Xylose*, the syrup, had $[\alpha]_D^{22}$ 17.7° (*c*, 1.3 in water) and crystallized upon standing, m.p. and mixed m.p. 144–145° C. *Glycerol* gave, upon treatment with *p*-nitrobenzoyl chloride in pyridine in the usual manner, the corresponding tri-*p*-nitrobenzoate, m.p. and mixed m.p. 188–191° C.

Identification of Periodate Degradation Products of the Oligosaccharides

The hydrolyzates from the different polyalcohols were combined and the components resolved by paper chromatography as described in the previous section. *Ethylene glycol*, treatment of the oily residue with *p*-nitrobenzoyl chloride in pyridine gave the di-*p*-nitrobenzoate, m.p. and mixed m.p. 139–142° C. *Glycerol*, similarly, converted to the tri-*p*-nitrobenzoate, m.p. and mixed m.p. 188–191° C. D-*Xylose*, the syrup, had $[\alpha]_D^{22}$ 17.3° (*c*, 1.2 in water) and upon standing crystallized. Recrystallization from acetronitrile gave D-xylose, m.p. 142–146° C.

ACKNOWLEDGMENTS

This investigation was supported by a research grant (RG 7652) from the Division of General Medical Sciences, Public Health Service (U.S.A.), to whom we express our thanks. We are also indebted to Miss J. Hunter for skillful technical assistance.

REFERENCES

1. G. G. S. Dutton and A. M. Unrau. Can. J. Chem. **40**, 1479 (1962).
2. P. T. Mora, J. W. Wood, and V. W. McFarland. J. Am. Chem. Soc. **82**, 3418 (1960).
3. I. J. Goldstein, G. W. Hay, B. A. Lewis, and F. Smith. Abstracts of Papers, 136th American Chemical Society Meeting, Boston, Mass. April, 1959. p. 3D.
4. D. V. Myhre and F. Smith. Abstracts of Papers, 139th American Chemical Society Meeting, St. Louis, Mo. March, 1961. p. 6D.
5. G. W. Hay and F. Smith. Abstracts of Papers, 139th American Chemical Society Meeting, St. Louis, Mo. March, 1961. p. 6D.
6. G. G. S. Dutton and A. M. Unrau. Can. J. Chem. **40**, 348 (1962).
7. G. G. S. Dutton and A. M. Unrau. Unpublished.
8. P. T. Mora and J. W. Wood. J. Am. Chem. Soc. **80**, 685 (1958).
9. A. M. Unrau and F. Smith. Chem. Ind. (London), 330 (1957).
10. N. Dubois, J. K. Hamilton, K. A. Gilles, P. A. Rebers, and F. Smith. Anal. Chem. **28**, 350 (1956).

THE CONSTITUTION OF A SYNTHETIC XYLAN

III. METHYLATION STUDIES[1]

G. G. S. DUTTON AND A. M. UNRAU[2]

Department of Chemistry, University of British Columbia, Vancouver, British Columbia

Received June 29, 1962

ABSTRACT

Hydrolysis of the fully methylated xylan gave a complex mixture of sugars indicating the highly branched nature of the polysaccharide. At least 27% of the internal xylose units were furanose and 38% of the terminal units were also furanose.

An earlier paper (1) has described the general properties of a synthetic xylan made by polymerizing D-xylose at 120° in the presence of phosphorous acid (2). The present paper is an attempt to investigate the structure of this synthetic xylan by the methylation technique. Previous workers (3, 4) have commented on the difficulty of completely methylating synthetic glucans and we have experienced similar trouble in the present study. Only after repeated treatments using the methods of Haworth (5), Kuhn (6), and Purdie (7) was a methylated xylan obtained which showed no hydroxyl absorption in the infrared and had a methoxyl content of 39.1%. The fully methylated polysaccharide showed unusual solubility properties in being soluble in petroleum ether (30–60°) containing as little as 5% chloroform. In this respect it resembled a methylated synthetic glucan (8).

Hydrolysis of the methylated xylan under conditions reported (9) to minimize demethylation gave tri-, di-, and mono-*O*-methyl-D-xyloses together with D-xylose in the ratio of 31:33:19:5 as determined by the phenol – sulphuric acid method (10). Many of the methyl ethers were positively identified as crystalline derivatives but because of the complexity of the hydrolysis products some were only identified by their chromatographic and electrophoretic mobilities. Separations were carried out on a cellulose–hydrocellulose column (11) using butanone–water azeotrope (12).

From the optical rotation of the tri-*O*-methyl-D-xylose fraction, it was calculated that 2,3,5-tri-*O*-methyl-D-xylose comprised 38% of the mixture, the remainder being the 2,3,4-tri-*O*-methyl isomer. The ease of methyl furanoside formation of the former was employed so that the water-insoluble 2,3,4-tri-*O*-methyl-D-xylose-1-*p*-nitrobenzoate could be obtained. The water-soluble trimethyl furanoside was subsequently hydrolyzed, reduced ($NaBH_4$) to the corresponding xylitol, and characterized as the crystalline di-*p*-nitrobenzoate. The above experimental result definitely showed that some of the terminal non-reducing xylose units were present in the polymer in the furanose form.

The different di-*O*-methyl xylose ethers were eventually separated by column chromatography and paper electrophoresis. By column chromatography, three fractions were obtained. The fastest-migrating fraction (R_f 0.63) was shown by electrophoresis to be composed of 3,5- and 2,5-di-*O*-methyl-D-xyloses. The next fraction (R_f 0.55) was shown by electrophoresis to be composed of 2,3- and 3,4-di-*O*-methyl-D-xyloses. The slowest-moving dimethyl xylose (R_f 0.45) was obtained crystalline and was 2,4-di-*O*-methyl-D-xylose. The ratio of 2,5- plus 3,5:2,3- plus 3,4-:2,4-di-*O*-methyl-D-xylose was approximately

[1]*Presented at the 45th Chemical Institute of Chemistry Conference, May 1962, Edmonton, Alberta.*
[2]*Present address: Department of Plant Science, University of Manitoba, Winnipeg, Manitoba.*

1.7:3.6:1. Approximately 27% of the internal xylose residues were thus shown to exist in the polymer in the furanose form. This value does not include the 2,3-di-*O*-methyl-D-xylose residues, which may also have existed in the furanose form in the original methylated xylan. Although 2,5- and 3,5-di-*O*-methyl-D-xylose have very different electrophoretic mobilities (borate buffer), the recovery of the sugars from the borate-impregnated paper was extremely poor. Similarly, a very low recovery was experienced when 2,3- and 3,4-di-*O*-methyl-D-xyloses were separated.

The various di-*O*-methyl sugars were identified as follows: 3,5-di-*O*-methyl-D-xylose as the *p*-bromophenylosazone; 2,5-di-*O*-methyl-D-xylose was oxidized to the acid and the derived amide shown to give a negative Weerman test (18) and the corresponding xylitol failed to give formaldehyde on periodate oxidation; 3,4-di-*O*-methyl-D-xylose on oxidation gave a positive Weerman test, the xylitol gave 1 mole of formaldehyde on periodate oxidation and the sugar gave the *p*-bromophenylosazone; 2,3-di-*O*-methyl-D-xylose on oxidation gave a negative Weerman test, the xylitol gave 1 mole of formaldehyde on periodate oxidation but the *N*-phenylglycosylamine was only obtained as a sirup.

The mono-*O*-methyl ethers of xylose were identified by electrophoresis. The apparent absence of 5-*O*-methyl-D-xylose indicated that the highly branched xylose residues existed in the pyranose form or, alternatively, those existing in the furanose form were also substituted at C_5.

The significant yield (5.2%) of D-xylose considering the hydrolysis conditions used (9) indicated that some xylose units were fully substituted.

These results confirm the earlier findings (1) based on periodate oxidation that this synthetic xylan contains an appreciable proportion of D-xylofuranose units. It is interesting to compare these findings with those of Bishop (13), who examined a xylan of low D.P. obtained by polymerizing D-xylose at room temperature in the presence of concentrated hydrochloric acid. In this case (13) there was no evidence for any D-xylofuranose units.

In our previous paper (1) we commented on the rapid liberation of formaldehyde when the xylan was oxidized with periodate and suggested the possible existence of D-*aldehydo*-xylose residues with the formaldehyde coming from a C_{4-5} glycol system. This would require that amongst the hydrolysis products of the methylated polysaccharide there should be at least 4,5-di-*O*-methyl-D-xylose. This was not detected but may have been missed in the rather complex di-*O*-methyl ether fraction.

EXPERIMENTAL

Paper chromatographic separations were carried out using the descending technique and butanone:water azeotrope as the developing solvent. Whatman No. 1 filter paper was employed and sugars were detected with the *p*-anisidine trichloroacetate spray reagent (14).

Evaporations were carried out under reduced pressure at a bath temperature of 40–45° C. Optical rotations recorded are equilibrium values at 21±2° C. Melting points quoted are uncorrected.

Methylation of the Xylan

Polyxylose (4.5 g) was methylated once by the Haworth procedure. The product, which was insoluble in water, was subsequently methylated by dissolving it in dimethylformamide and adding excess silver oxide and methyl iodide (3) and raising the temperature to the reflux temperature of methyl iodide. The mixture was continuously stirred by means of a magnetic stirrer. The product, a yellow, brittle glass, showed a small but definite OH absorption band in the infrared spectrum; consequently it was dissolved in methyl iodide, silver oxide was added, and the mixture boiled in a flask fitted with an efficient condenser on a steam bath for at least 96 hours before re-isolation. This treatment was repeated four times until finally no OH band was found in the infrared spectrum. The yellow, resinous product contained 39.1% methoxyl and was soluble in petroleum ether (30–60°) containing 4% chloroform. The final yield of methylated product was 4.24 g and had $[\alpha]_D^{22}$ 45.2° (*c*, 8.1 in $CHCl_3$).

Hydrolysis of Methylated Xylan

The bulk (4.05 g) of the methylated xylan was dissolved in 72% sulphuric acid (9); the sirupy and rather dark mixture was diluted with cold water until the acid was 2 *N*. The solution was boiled for 12 hours after which time the acid was neutralized ($BaCO_3$), decolorized with charcoal, and filtered. Evaporation of the filtrate gave a sirup which, upon chromatography, was apparently composed of xylose, and mono-, di-, and tri-methyl xyloses. The ratio of the four classes of sugars was determined paper chromatographically using the phenol – sulphuric acid method (10) and the standard curve for xylose. The result of the analysis is recorded below.

Components	μg on paper	Molar ratio
Xylose	5.0	5
Mono-*O*-methyl	18.8	19
Di-*O*-methyl	31.6	32
Tri-*O*-methyl	31.3	31

Resolution of Mixture by Cellulose Chromatography (11)

The mixture of sugars (4.05 g) was placed on a cellulose–hydrocellulose column in about four equal portions and the column irrigated with butanone:water azeotrope. The effluent was collected in tubes at 6-minute intervals for the tri- and di-methyl xyloses and at 30-minute intervals for the monomethyl xyloses and xylose. By chromatographic examination of the tubes containing the dimethyl xyloses, three quite distinct components were obtained after the column separation. The yield of the different components, their R_f values, and their probable identity are summarized in Table I.

TABLE I

Hydrolysis products of methylated xylan

Component	Description	Weight (g)	R_f
1	Trimethyl (2,3,4 and 2,3,5)	1.265	0.80
2	Tri- and di-methyl mixture	0.050	
3	Dimethyl (2,5 and 3,5)	0.344	0.63
4	Dimethyl mixture	0.070	
5	Dimethyl (2,3 and 3,4)	0.736	0.55
6	Dimethyl mixture	0.065	
7	Dimethyl (crystalline) (2,4)	0.205	0.45
8	Unknown	0.035	0.32
9	Monomethyl	0.615	0.22
10	Xylose	0.200	0.06
		3.585	

Identification of Components

Component 1 had $[\alpha]_D^{22}$ 22.2° in water. Reported rotation for 2,3,5-tri-*O*-methyl-D-xylose is 29.5° and that for 2,3,4-tri-*O*-methyl-D-xylose is 18.0° (15). The component is therefore a mixture containing 37.5% of 2,3,5-tri-*O*-methyl-D-xylose or approximately 470 mg. The two isomers were identified in the following manner. The sirup was dissolved in dry methanol containing 1% hydrogen chloride and the solution left at room temperature until no further change in the rotation could be observed. The solution was neutralized (Ag_2CO_3) and evaporated to a sirup. The product was dissolved in pyridine (6 ml) an excess quantity of *p*-nitrobenzoyl chloride was added (5% molar excess assuming all material was 2,3,4-tri-*O*-methyl-D-xylose) and the mixture was heated at 60° C for about 45 minutes, then left overnight at room temperature. Saturated sodium bicarbonate was added and the insoluble *p*-nitrobenzoate removed. The 2,3,4-tri-*O*-methyl-D-xylose-1-*p*-nitrobenzoate was recrystallized from a mixture of acetone and ether, m.p. 133–135° C, $[\alpha]_D^{22}$ −75.2° (*c*, 1.5 in $CHCl_3$), lit. m.p. 136°, $[\alpha]_D$ −76° in $CHCl_3$ (16). The filtrate, which presumably contained the methyl 2,3,5-tri-*O*-methyl-D-xyloside, was evaporated to remove pyridine and an aqueous solution of the residue extracted with chloroform. The product (375 mg) was boiled in 0.5 *N* sulphuric acid (15 ml) for 3 hours after which time the solution was neutralized ($BaCO_3$) and evaporated to a sirup, $[\alpha]_D^{22}$ 28.9° (*c*, 2.5 in water). The sugar in water (20 ml) was reduced with sodium borohydride (350 mg) at room temperature for 48 hours. The solution was neutralized (HCl) and evaporated and an aqueous solution of the residue extracted with chloroform. Evaporation of the solvent gave a sirupy product (335 mg) which did not react with Tollens reagent. The alcohol was treated with *p*-nitrobenzoyl chloride in the usual way to give 2,3,5-tri-*O*-methyl-1,4-di-*p*-nitrobenzoyl-D-xylitol, which, after recrystallization from acetone, had m.p. and mixed m.p. 147–150° C, $[\alpha]_D^{22}$ 7.1° (*c*, 1.8 in pyridine). An authentic sample was prepared from methyl αβ-D-xylofuranoside. Calculated for $C_{22}H_{24}N_2O_{10}$: N, 5.9; OCH_3, 19.5%. Found: N, 5.6; OCH_3, 19.2%.

Component 3 showed $[\alpha]_D^{22}$ 33° (*c*, 2.5 in water). Electrophoresis using 0.05 *M* borate buffer, Whatman No. 1 paper, 1000 volts, 35 milliamperes for 45 minutes revealed the presence of two components with M_g (migration relative to D-glucose) values 0.0 and 0.88. A trace of material had M_g 0.16. The substance with M_g 0.88 corresponded to 3,5-di-*O*-methyl-D-xylose whereas 2,5-di-*O*-methyl-D-xylose would not be expected to migrate and was presumed to be the substance with M_g 0.00. The ratio of the two sugars was determined by the phenol – sulphuric acid method and found to be about 1:1. The mixture was resolved using Whatman 3 MM paper and the above specified conditions. The recovery of the sugars was extremely low. *3,5-Di-O-methyl-D-xylose*, 12 mg, $[\alpha]_D^{22}$ 23.5° (*c*, 0.55 in water), 10.3° (*c*, 0.55 in $CHCl_3$), was dissolved in 80% aqueous ethanol (5 ml) and a 5% molar excess of *p*-bromophenylhydrazine in ethanol (20 ml) added. The mixture was heated on a steam bath for 45 minutes and, upon cooling, the *p*-bromophenylosazone of 3,5-di-*O*-methyl-D-xylose separated. The product was collected on a filter paper, dried with ether and petroleum ether, and had m.p. 103–105° C, lit. m.p. 107–108° (17). *2,5-Di-O-methyl-D-xylose*, 18.8 mg, $[\alpha]_D^{22}$ 43° (*c*, 0.38 in water), 15.5° (*c*, 0.94 in ethanol). A small portion (3 mg approx.) was oxidized with bromine and the Weerman test (18) applied. The test was negative, indicating that C_2 was blocked by methoxyl. The remainder was reduced with sodium borohydride in the usual manner and the 2,5-di-*O*-methyl-D-xylitol obtained as a sirup. Oxidation of a small portion (about 2.5 mg) gave no formaldehyde. The alcohol was treated with *p*-nitrobenzoyl chloride in the usual manner to give the insoluble *p*-nitrobenzoate, which was not obtained crystalline.

Compound 5, 836 mg, showed $[\alpha]_D^{22}$ 21° (*c*, 4.2 in water). Electrophoretic examination of the sirup as described for component 3 showed that two compounds were present, one with an M_g value of 0.26 and corresponding to that of 3,4-di-*O*-methyl xylose, the other with an M_g of 0.0 was 2,3-di-*O*-methyl xylose. The electrophoretic behavior in conjunction with the R_f of 0.55 for the mixture indicated that the two sugars were 3,4- and 2,3-di-*O*-methyl-D-xylose. The components were separated by electrophoresis using Whatman 3 MM paper and the conditions described previously except that the time was increased to 105 minutes. The recovery of material was extremely poor, approximately 15%. *3,4-Di-O-methyl-D-xylose*, 82 mg, showed $[\alpha]_D^{22}$ 19.8° (*c*, 1.64 in water), 39° (*c*, 1.64 in $CHCl_3$). About 5 mg was oxidized and the Weerman test (18) applied to the derived amide. The test gave positive results, hence the C_2-hydroxyl was not substituted. Similarly, 5 mg of the sugar was reduced ($NaBH_4$) to the corresponding xylitol and after removal of borate, the alcohol was oxidized with periodate and the amount of formaldehyde liberated was determined (19). Approximately 0.835 mg formaldehyde or almost 1 molar proportion of the aldehyde was formed. The remainder (about 70 mg) was dissolved in 75% aqueous ethanol (15 ml), a 5% molar excess of *p*-bromophenylhydrazine in ethanol (30 ml) added, and the solution refluxed. Upon cooling, the osazone separated and was collected by centrifugation. After drying in a vacuum desiccator, the compound had m.p. 130–134° C. *2,3-Di-O-methyl-D-xylose*, 28 mg, showed $[\alpha]_D^{22}$ 22° (*c*, 1.4 in water). The sirupy material did not crystallize. A small portion (3 mg) was oxidized with bromine and after conversion to the amide a negative Weerman test (18) was obtained, showing that the C_2-hydroxyl was substituted. Another small portion (3 mg) was reduced ($NaBH_4$) and the alcohol subsequently oxidized with periodate as described previously. Approximately 0.490 mg formaldehyde or 1 molar proportion of the aldehyde was liberated. The remaining material (about 20 mg) was dissolved in absolute ethanol (5 ml), freshly distilled aniline (2 drops) was added, and the mixture refluxed for 1 hour. Evaporation of the solvent under vacuum gave a sirupy product, $[\alpha]_D^{22}$ 170° in ethyl acetate having the characteristically high rotation of 2,3-di-*O*-methyl-*N*-phenylxylosylamine but which failed to crystallize. *2,4-Di-O-methyl-D-xylose*, 205 mg, showed $[\alpha]_D^{22}$ 21° (*c*, 1.5 in water), −24.5° (*c*, 1.5 in $CHCl_3$). The sirup crystallized upon standing. When it was washed with cold ether and petroleum ether and dried on a porous plate, the compound had melting point 109–112° C, lit. (20, 21) m.p. 111°, 114–116° C. Mixed m.p. 110–112° C. The crystalline compound mutarotated in water, $[\alpha]_D^{22}$ −28° → +22°. The physical constants obtained show that the sugar was 2,4-di-*O*-methyl-D-xylose.

Component 8, 35 mg, had an M_g value of 0.05 upon electrophoresis. The sirup was boiled in *N* sulphuric acid (10 ml) for 6 hours. The solution was neutralized ($BaCO_3$) and evaporated, and the residue chromatographed. Compounds were observed corresponding to tri-, di-, and mono-*O*-methylxyloses and xylose.

Component 9, 615 mg, was found to be composed of three different mono-*O*-methyl xyloses, with M_g values of 0.82 (3-*O*-methyl-D-xylose), 0.25 (2-*O*-methyl-D-xylose), and 0.16 (4-*O*-methyl-D-xylose). No 5-*O*-methyl-D-xylose was apparently present. The ratio of 3-, 2-, and 4-*O*-methyl-D-xylose, determined by the phenol – sulphuric acid method was about 3:4:1.

Component 10, D-xylose, 200 mg, showed $[\alpha]_D^{22}$ 17.8° in water. The sirup crystallized upon standing. Recrystallization from hot ethanol gave D-xylose, m.p. and mixed m.p. 143–145° C.

ACKNOWLEDGMENTS

This investigation was supported by a P.H.S. research grant (RG 7652) from the Division of General Medical Sciences, Public Health Service (U.S.A.), to whom we express our thanks. We are also indebted to Miss J. Hunter for skillful technical assistance, to Dr. Elizabeth Percival for a sample of 2,4-di-*O*-methyl-D-xylose, and to Mrs. A. Aldridge for analyses.

REFERENCES

1. G. G. S. DUTTON and A. M. UNRAU. Can. J. Chem. **40**, 1479 (1962).
2. P. T. MORA, J. W. WOOD, and V. W. MCFARLAND. J. Am. Chem. Soc. **82**, 3418 (1960).
3. P. T. MORA, J. W. WOOD, P. MAURY, and B. G. YOUNG. J. Am. Chem. Soc. **80**, 693 (1958).
4. J. DA S. CARVALHO, W. PRINS, and C. SCHUERCH. J. Am. Chem. Soc. **81**, 4054 (1959).
5. W. N. HAWORTH. J. Chem. Soc. **107**, 8 (1915).
6. R. KUHN, I. LOW, and N. TRISCHMAN. Ber. **90**, 203 (1957).
7. T. PURDIE and J. C. IRVINE. J. Chem. Soc. **83**, 1021 (1903).
8. G. G. S. DUTTON and A. M. UNRAU. Can. J. Chem. **40**, 1196 (1962).
9. I. CROON, G. HERRSTROM, G. KULL, and B. LINDBERG. Acta Chem. Scand. **14**, 1338 (1960).
10. N. DUBOIS, J. K. HAMILTON, K. A. GILLES, P. A. REBERS, and F. SMITH. Anal. Chem. **28**, 350 (1956).
11. J. D. GEERDES, B. A. LEWIS, R. MONTGOMERY, and F. SMITH. Anal. Chem. **26**, 264 (1954).
12. L. BOGGS, L. S. CUENDET, I. EHRENTHAL, R. KOCH, and F. SMITH. Nature, **166**, 520 (1950).
13. C. T. BISHOP. Can. J. Chem. **34**, 1255 (1956).
14. L. HOUGH, J. K. N. JONES, and W. H. WADMAN. J. Chem. Soc. 1702 (1950).
15. G. G. MAHER. *In* Advances in carbohydrate chemistry. Academic Press, New York. 1955. p. 260.
16. F. SMITH and R. MONTGOMERY. *In* Plant gums and mucilages. Reinhold, New York. 1959. p. 517.
17. P. A. LEVENE and A. L. RAYMOND. J. Biol. Chem. **102**, 331 (1933).
18. R. A. WEERMAN. Rec. Trav. Chim. **37**, 16 (1917).
19. A. M. UNRAU and F. SMITH. Chem. Ind. (London), 330 (1950).
20. R. A. LAIDLAW and E. G. V. PERCIVAL. J. Chem. Soc. 528 (1950).
21. O. WINTERSTEINER and A. KLINGSBERG. J. Am. Chem. Soc. **71**, 939 (1949).

STUDIES ON THE INFRARED SPECTRA OF A MERCAPTOTRIAZOLE AND MERCAPTOTHIAZOLINE AND THEIR ADSORPTION ON SILVER IODIDE[1]

L. H. LITTLE[2]
Division of Applied Chemistry, National Research Council, Ottawa, Canada

AND

R. H. OTTEWILL
Department of Colloid Science, Free School Lane, Cambridge, England

Received May 7, 1962

ABSTRACT

An investigation has been carried out on the infrared spectra of 3-mercapto-4-methyl-5-ethyl-1,2,4-triazole and 2-mercaptothiazoline, both in solution and in the crystalline form. The spectra of the deuterated compounds and the silver salts have also been examined. The results allow some assignment of bands to be made. The spectra of these compounds adsorbed on silver iodide were then examined. It would appear that in the concentration range examined physical adsorption occurs.

INTRODUCTION

Although many studies have been made of the adsorption of various types of organic molecules on silver halide particles, little direct evidence is available as to the actual state of the molecule on the surface. In many cases the material adsorbed was an organic ion and the adsorption was electrostatic in nature (1); in such cases little change in structure of the ion would be expected. However, there are a number of organic compounds which are of great importance in flotation processes and in the photographic industry which contain the —N(H)—C(=S)— grouping; these are often added to suspensions at a pH where they exist mainly as unionized molecules. Compounds such as 3-mercapto-4-methyl-5-ethyl-1,2,4-triazole flocculate silver halides at neutral pH and are also found to influence the crystal shapes of silver iodide when crystallization is carried out in their presence (2). The latter behavior appeared to be due to the preferential adsorption of this material onto certain crystal faces of silver iodide. The exact mode of adsorption was not easy to determine but it appeared highly probable that perturbation of the —N(H)—C(=S)— group would occur in the adsorbed state and that this would be detectable by infrared spectroscopy.

The infrared spectroscopic technique has proved invaluable in the elucidation of the structures of adsorbed molecules in many systems but there is considerable limitation to its application, owing to the loss of radiation, by absorption and scattering, in the solid substrate upon which the molecules are adsorbed. The difficulties inherent in the technique have been discussed by Eischens and Pliskin (3) for adsorption at the gas–solid interface.

[1]*Issued as N.R.C. No. 6965.*
[2]*Present address: Department of Chemistry, University of Western Australia, Nedlands, W. Australia.*

Two further problems may arise when adsorption is studied at the liquid–solid interface. Firstly, the molecules studied in these systems are invariably larger than those studied at the gas–solid interface and consequently at high concentrations of adsorbate, multilayer adsorption may occur. In such cases it may not be possible to distinguish the first layer, which interacts with the substrate, from subsequent overlaying deposits. Secondly, adsorption of solvent may compete with that of the adsorbate under investigation and wide spectral regions may be excluded from study if the solvent absorption is intense. In the present system investigation was confined to regions considerably below completion of a monolayer of adsorbate and no problems were encountered due to retention of water by the solid.

Silver halides, moreover, form suitable adsorbents since they do not have absorption bands of their own in the regions to be studied. By using finely divided sols a relatively large surface area can be obtained and thus sufficient adsorbed material can be included in the sample to yield a spectrum of moderate intensity. Further, with such finely divided materials, radiation losses by scattering are not large, especially at frequencies below ca. 2000 cm^{-1}.

EXPERIMENTAL

Materials

All inorganic chemicals used were of A.R. grade.

3-Mercapto-4-methyl-5-ethyl-1,2,4-triazole (I, II) was kindly supplied by Messrs. Ilford Ltd.,* and 2-mercaptothiazoline (III, IV) by Messrs. I.C.I. Ltd.* These compounds are referred to as MCT and MCTH respectively.

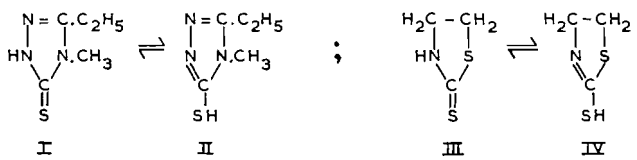

Preparation and Flocculation of Sols

Two methods may be employed to study the flocculation of sols by a specific reagent. Either the reagent may be added to a preformed sol (4) or alternatively the sol may be formed in the presence of the reagent (5). In the latter case the effect of the reagent on the nucleation and the crystal growth process may also be investigated. Both methods have been utilized in the present studies. All silver iodide sols and suspensions were employed at pI = 4 to ensure a negative charge on the particles (4).

Preparation of Silver Iodide Sols in the Presence of MCT

Silver nitrate (0.16 ml, 0.0155 *N*) was added with stirring to 5 ml of a solution composed of 0.5 ml 0.0207 *N* potassium iodide, 0.9 ml 0.1393 *M* MCT, and 3.6 ml distilled water. Flocculation of the sol occurred rapidly under these conditions and the whitish fluffy floccules settled out in a few hours. The suspension was then centrifuged, the supernatant decanted, and the floccules washed several times with distilled water followed by centrifugation; it appeared unlikely that a strongly adsorbed film would be removed by this washing procedure. After removal of as much supernatant as possible the remaining water was pumped off. The dried material was then ground up in a small volume of nujol and examined in this state in the spectrometer. Nujol and hexachlorobutadiene were used as mulling agents to provide complete coverage of the spectrum between 4000 and 650 cm^{-1}. Spectra were recorded on a Perkin–Elmer 21 spectrophotometer fitted with a calcium fluoride or a sodium chloride prism.

These conditions were employed since it has been shown that it is at this concentration of MCT that flocculation occurs; this point also corresponds with the zero point of charge as measured by microelectrophoresis (6). From experiments with other systems it has been found that this point usually corresponds to ca. 30% of a monolayer (4). The silver iodide particles formed under these conditions do not have the usual hexagonal or tetrahedral shapes but form long rods, suggesting the strong adsorption of the MCT onto certain crystal faces (2). Microelectron diffraction patterns indicated that the crystals were silver iodide; spots due to silver mercaptotriazole were not detected, suggesting that coprecipitation had not occurred.

**We wish to express our thanks to these organizations for gifts of material.*

Experiments with Preformed Silver Iodide Sols

Concentrated silver iodide sols with an average particle diameter of 500 Å were prepared in the manner described by Harmsen, van Schooten, and Overbeek (7). MCT solution (1.5 ml, 0.1038 *M*) was added to 1.5 ml of the concentrated sol (ca. 40% w/v). Instantaneous flocculation of the sol occurred and the particles were then spun down and treated as previously described. In this manner a sample of large specific surface was obtained.

Alternatively, powdered silver iodide having a specific surface of 0.7 m^2/g was employed (2). To 0.5 g of this powder 1.25 ml of 0.1038 *M* MCT solution was added. The suspension was agitated for 4 hours and then treated as described above.

Preparation of Deuterated MCT

To assist in the assignment of vibrational bands a study was also made of the spectrum of deuterated MCT.

MCT (70 mg) was sealed in a glass ampoule with 4 ml of heavy water. The ampoule was heated to 70° C until all the MCT had dissolved and was then allowed to stand for 24 hours at room temperature. The solvent was then pumped off and the sample stored *in vacuo*. This treatment gave about 50% deuteration, so a further sample was treated with successive amounts of D_2O. Complete deuteration was still not achieved, suggesting that very stringent precautions are necessary to prevent exchange with atmospheric water vapor. Preparation of samples for infrared purposes was carried out in a dry box.

Preparation of Silver MCT

The silver salt of MCT was prepared for spectral comparison with MCT adsorbed on silver iodide. The preparation was carried out by adding excess silver nitrate solution to an MCT solution, centrifuging off the precipitate, washing with water, and then drying.

Experiments with MCTH

Experiments and preparations parallel to those described above for MCT were carried out with MCTH. The infrared spectrum of MCTH, while similar in some respects to that of MCT, was generally much simpler and was of assistance in assigning bands in the MCT spectrum.

RESULTS AND DISCUSSION

Infrared Spectra of MCT and MCTH

Absorption in the Region 3500–2000 cm^{-1}

Cyclic secondary thioamides such as MCT have been studied previously (8, 9) but since certain difficulties are associated with their spectra some discussion is warranted before the spectra of films adsorbed on silver iodide are considered. It has been shown that such compounds exist in the thiolactam form (I, III) rather than in the mercapto form (II, IV). Figure 1 shows the spectrum of MCT in the solid state and in solution in chloroform. SH— absorption is apparently absent whilst bands due to the —N—H stretching vibration, at ca. 3100 cm^{-1} (solid) and 3410 cm^{-1} (solution), are intense. There are some very weak bands at 2550 and 2480 cm^{-1} in the spectrum of solid MCT, at 2450 cm^{-1} in the spectrum of the chloroform solution, and at 2450 cm^{-1} in the spectrum of MCTH in carbon tetrachloride solution. This is the region where S—H groups might be expected to absorb (10). However, any S—H group in the solid material would be hydrogen bonded and would probably absorb at frequencies below that found for the solutions in carbon tetrachloride and chloroform. It is possible that these weak bands are overtones of bands at lower frequencies. The N—H groups are all hydrogen bonded in the crystalline material, possibly as dimers.

The spectrum of MCT was examined in solution in carbon tetrachloride, carbon disulphide, and in chloroform. The molecules again exist largely, if not entirely, in the N—H form rather than in the S—H form. However, in solution there is a large proportion of N—H groups not involved in hydrogen bonding and hence a mixture exists of free molecules with dimers or higher combinations. Similarly MCTH exists in the thiolactam form rather than in the mercapto form.

Absorption in the Region 2000–650 cm^{-1}

One of the most prominent features of the spectra of MCT and MCTH is the intense band at 1500–1520 cm^{-1}. Since these compounds are secondary thioamides it is expected

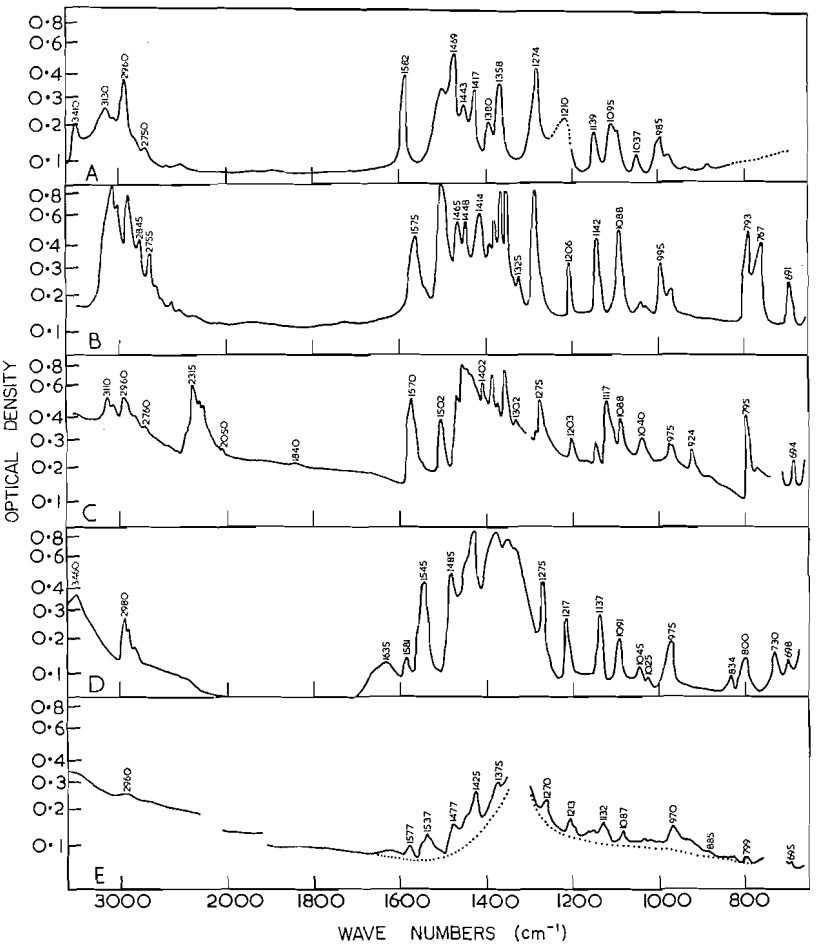

FIG. 1. Infrared spectra of (A) MCT solution in chloroform, (B) MCT mull, (C) MCT (partly deuterated) mull, (D and E) silver MCT mull.

that a band will appear in this region of the spectrum similar to that classified as the amide II band (10). Considerable controversy has surrounded the assignment of this band and it has been variously attributed to the N—H in-plane deformation vibration and to the C—N stretching vibration of the amide group. The frequency is higher than that normally associated with the C—N single bond, but this fact is attributed to the partial double-bond character of the band in the thioamide structure.

Previous deuteration studies (10) have favored the assignment of the 1500–1550 cm^{-1} band to the in-plane N—H deformation mode, since, on substitution of deuterium for hydrogen, the band disappears and a new band appears at about 1120 cm^{-1}. The frequency displacement is that expected for substitution of H by D (12). In the present study deuteration of MCT and MCTH was accompanied by a decrease in intensity of the 1500–1520 cm^{-1} band and the appearance of a new band at 1110–1120 cm^{-1} (Figs. 1 and 2). With more complete deuteration of the MCT than that shown in Fig. 1C, the band at 1502 cm^{-1} almost entirely disappeared.

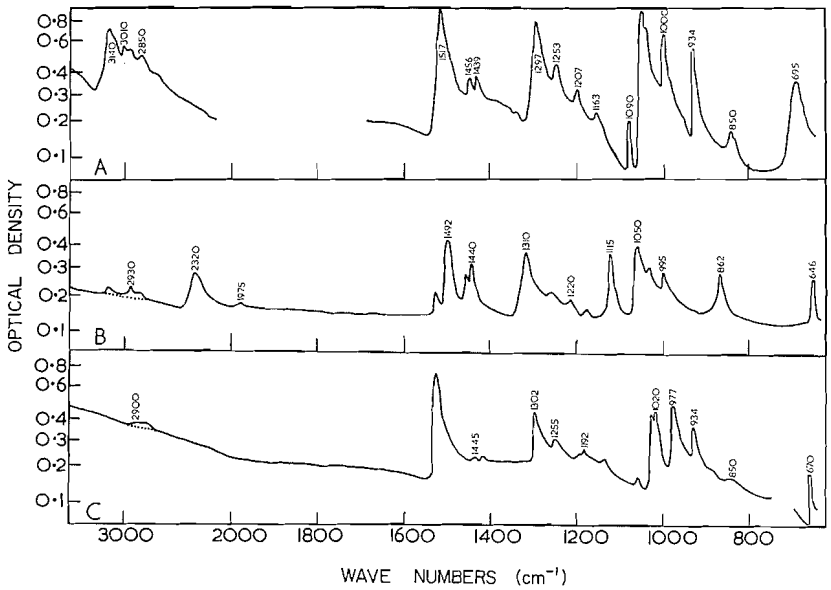

FIG. 2. Infrared spectra of (A) MCTH mull, (B) deuterated MCTH mull, (C) silver MCTH mull.

When MCT was dissolved in chloroform the 1502 cm^{-1} band was displaced to 1480 cm^{-1}. In carbon tetrachloride the frequency of the 1520 cm^{-1} band of MCTH was displaced to 1490 cm^{-1}. The direction of displacement is that expected if the band was due to a deformation mode, since hydrogen bonding in the crystal would stiffen the N—H group against deformation and increase the frequency of the vibration.

However, the spectra of silver MCT and silver MCTH do not support the latter conclusion. When the silver salts are formed the N—H stretching band disappears completely, as indicated by the spectra (Figs. 1 and 2), thus proving the complete replacement of hydrogen by silver. The frequency of the 1520 cm^{-1} band of MCTH, whose assignment is in question, was merely displaced upwards by 10 cm^{-1} and the intensity was unaffected on formation of the silver salt. The situation was not so well defined in the case of the silver salt of MCT, but the 1500 cm^{-1} band still remained, being either displaced upwards in frequency to 1540 cm^{-1} or downward to 1485 cm^{-1}, as discussed below. The displacement of this band from 1500 cm^{-1} in solid MCT to 1485 cm^{-1} in chloroform solution was mentioned earlier. The 1500–1520 cm^{-1} band cannot, therefore, be due to the N—H deformation mode and must largely be due to the C=N stretching of the thiolactam group.

The band which appeared at 3440 cm^{-1} in the spectrum of the silver salt of MCT (Fig. 1D) is not due to a N—H stretching vibration. The frequency and half width of this band show that it belongs to a hydrogen-bonded O—H stretching vibration. This must be due to adsorbed water on the silver salt and the assignment is confirmed by the presence of the O—H deformation band of water at 1630 cm^{-1}.

Chatt, Duncanson, and Vinanzi (11) found an intense band at 1480–1530 cm^{-1} in the spectrum of N,N-dialkyldithiocarbamates. No N—H group occurred in these compounds and this band was assigned to the stretching vibration of the C—N group, which has partial double-bond character. They found that the frequency of the 1500 cm^{-1} band of methyl N,N-dimethyldithiocarbamate and of several metal N,N-dialkyldithiocarbamates

was decreased when the solid material was dissolved in solvents. These results are in agreement with those mentioned above for MCT and again suggest that the 1500 cm^{-1} band cannot be assigned to the N—H deformation vibration.

It would appear that, in the spectra of deuterated MCT and MCTH, the band which appears at 1115 cm^{-1} is due to the N—D in-plane deformation vibration. Although the 1500 cm^{-1} band decreased on deuteration, a new intense band appeared at 1450 cm^{-1}, superimposed on existing bands of MCT. This suggests that the band did not disappear completely, but was displaced to a lower frequency. For MCTH the 1520 cm^{-1} is the strongest band in this region and it can readily be seen that the corresponding band in deuterated MCTH occurs at 1492 cm^{-1}. This band must be due to C—N stretching. The sensitivity of the C=N band to the replacement of hydrogen by deuterium must mean that the N—H in-plane deformation mode contributes to the C=N stretching mode. Hadži (12) has concluded that the two vibrations are strongly coupled in secondary thioamides. In the absence of a separate band, which may be assigned to the N—H in-plane deformation mode in the spectra of MCT and MCTH, it must be concluded that the deformation mode is strongly coupled with the C=N stretching mode, which absorbs at 1500–1520 cm^{-1} in the solid.

The intense band at 1570 cm^{-1} in the spectrum of MCT was due to the 3,4 C=N stretching vibration. The 3,4 bond is saturated in MCTH and consequently the band does not appear in the spectrum of this compound.

Two possible explanations may be advanced for the changes which occur in the region 1450–1600 cm^{-1} when silver MCT is formed. Firstly, the 1502 cm^{-1} band due to the C=N stretching mode is displaced downward in frequency to 1430–1480 cm^{-1} and the 3,4 C=N stretching mode is displaced from 1575 cm^{-1} to 1545 cm^{-1}. The small remaining band at 1575 cm^{-1} in the silver MCT spectrum must then belong to some unreacted MCT. Secondly, with the formation of the silver salt the frequency of the 1502 cm^{-1} band of solid MCT is raised to 1545 cm^{-1} and the 1575 cm^{-1} band suffers a very great intensity decrease. In favor of the second explanation is the observation that the C=N stretching frequency of MCTH is raised 10 cm^{-1} on forming the silver salt of this compound. There seems no reason to expect the intensity of the 3,4 C=N stretching vibration of MCT to be affected so greatly by silver salt formation, although it is possible that the C=N group is rendered less polar by the replacement of the thioamide hydrogen atom with silver, and as a result the intensity of the C=N stretching vibration is decreased.

In other instances, the C=N band frequency has shown variations over a range similar to that considered for MCT and silver MCT, i.e. 1502–1545 cm^{-1}. Thus the frequency of the C=N band of metal N,N-dialkyldithiocarbamates was found to range from 1480 to 1530 cm^{-1} as the metal was varied (11). However, the systems are not completely similar since in the latter compounds the metal is attached to the sulphur atom, whereas in silver MCTH, and probably in silver MCT, the silver atom replaces hydrogen from the nitrogen. This is shown by the appearance of the C=S stretching band with normal frequency and intensity in the silver MCTH spectrum (Fig. 2).

A band appearing at 1050 cm^{-1} in the MCTH spectrum has been assigned by Mecke *et al.* (13) to the C=S stretching mode of the thioamide group. The band is one of the most intense in the spectrum of MCTH (Fig. 2). With the formation of the silver salt the frequency of this band was displaced downward by about 20 cm^{-1}.

Although several moderately intense bands occur in this region in the spectrum of MCT, no band appears which may be assigned with certainty to the C=S stretching vibration of this compound. The two compounds MCT and MCTH differ in that the

former has a double bond in the 3,4 position. Should the interpretation of the 1500–1520 cm^{-1} band assignment be correct, in so far as the C—N bond in the 1,2 position has double-bond character, then conjugation may occur between the two double bonds in MCT and be responsible for the difference between its spectrum and that of MCTH. It is of interest to consider that in the case of MCT conjugation effects may cause the structure to lie somewhere between V and VI.

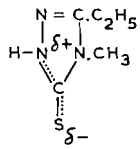

V

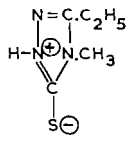

VI

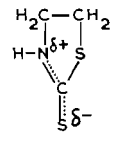

VII

According to the magnitude of the contribution of VI to the structure, the carbon–sulphur stretching vibration may not absorb as a normal C=S mode. MCTH, without the opportunity for conjugation, may exist more as a structure of type V, i.e. the carbon–sulphur bond preserves essentially double-bond character as in VII. Gingras *et al.* (14) consider from chemical evidence that, for thiosemicarbazones, the polar form

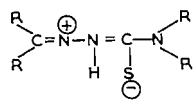

contributes to the overall structure because of stabilization by conjugation.

If the zwitterion form VI contributes more to the structure of MCT than to that of MCTH, it would be expected that this effect should be reflected in different frequencies for the N—H stretching modes for these compounds. However, this is not supported by the spectral evidence. The frequencies of the N—H stretching modes are identical in solution and the value for solid MCT is only slightly below that for solid MCTH.

Refn (15) considers that the N—H stretching mode of $=\overset{+}{N}H-$ in pyrazol-5-ones absorbs at about 1800–2400 cm^{-1} due to strong hydrogen bonding of the zwitterion form. This is well below the frequencies found in the present work but stronger bonding should be expected in the system $\overset{+}{N}—H\cdots\overset{-}{O}-$ than in $\overset{+}{N}—H\cdots\overset{-}{S}—$.

The study of solvent effects on the C=S stretching vibration led Bellamy and Rogasch (16) to develop a technique for the assignment of this vibration. However, they found that mercaptobenzothiazole, which exists in the C=S form, did not show the expected solvent-induced frequency displacements. This was attributed to the molecules existing as dimers in solution. None of the bands at 1350, 1275, 1140, 1090, 985, or 965 cm^{-1} in the spectrum of MCT follow the solvent frequency pattern expected for normal C=S stretching bands in carbon tetrachloride, carbon disulphide, and chloroform, although a considerable proportion of the molecules exists as single species in these solutions (see discussion above). A band in the 1200 cm^{-1} region was obscured by strong solvent absorption in chloroform and in carbon tetrachloride. However, this band occurred at 1206 cm^{-1} in the spectrum of solid MCT and at 1201 cm^{-1} in carbon disulphide solution, a result which is not expected for a C=S stretching mode. MCTH was too insoluble for a complete investigation.

Assignment of the 770 cm^{-1} band in the spectrum of MCT to the out-of-plane N—H deformation mode was confirmed by deuteration studies. The spectra were measured with a cesium bromide prism. The only change in the spectrum between 800 and 300 cm^{-1}, on deuteration, was the replacement of the 770 cm^{-1} band by one at 550 cm^{-1}. This band is normally referred to as the amide V band (10).

The band at 1275 cm^{-1} in the MCTH spectrum and at 1297 cm^{-1} in that of MCTH must be the one normally classified as the amide III band (10). When the amide II band is attributed to the N—H in-plane deformation this band is associated with the C—N stretching vibration (10). However, its origin is uncertain when the amide II band is largely due to C=N stretching. The band is little affected by the various environments shown in Figs. 1–5.

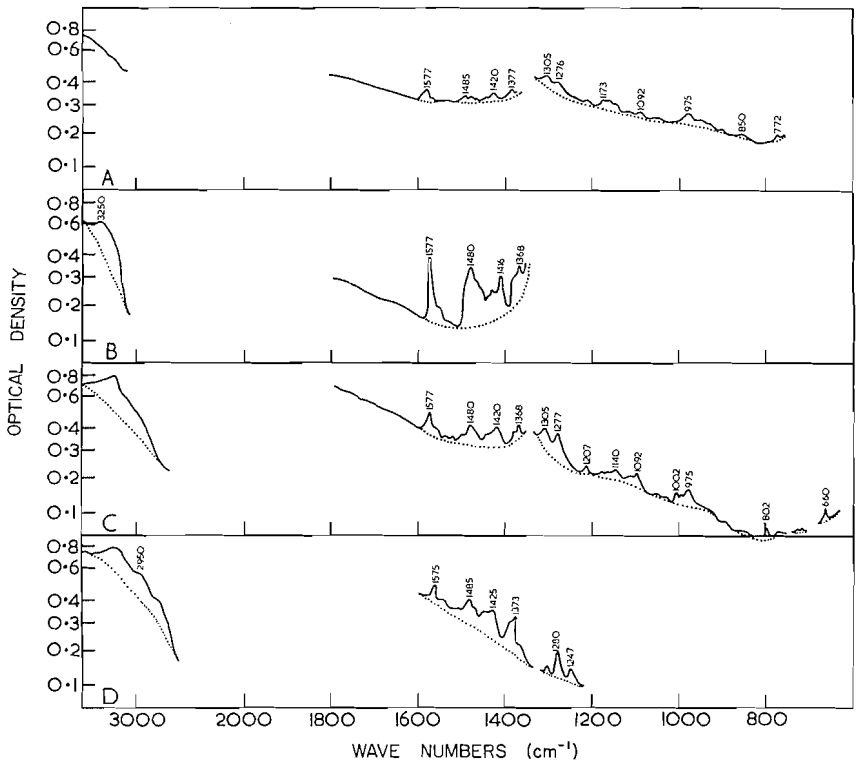

FIG. 3. Infrared spectra of (A, B, C) MCT adsorbed on preformed silver iodide sol, (D) MCT adsorbed on silver iodide powder.

Adsorption Studies

Adsorption of MCT on Silver Iodide

The spectra (Figs. 3 and 4) show that MCT adsorbed on silver iodide has a similar structure to that of the material in bulk or in solution. This appears to be independent of whether the MCT was used to coagulate a preformed sol or whether the sol was formed in its presence. Titration studies have shown that MCT behaves as a weak acid with a pK of ca. 8.5 (17). This means that at the pH of the coagulation, ca. 5.0, the MCT would be present in aqueous solution mainly in the non-ionized form. On this basis the spectra would be consistent with adsorption of the MCT molecule in the neutral form.

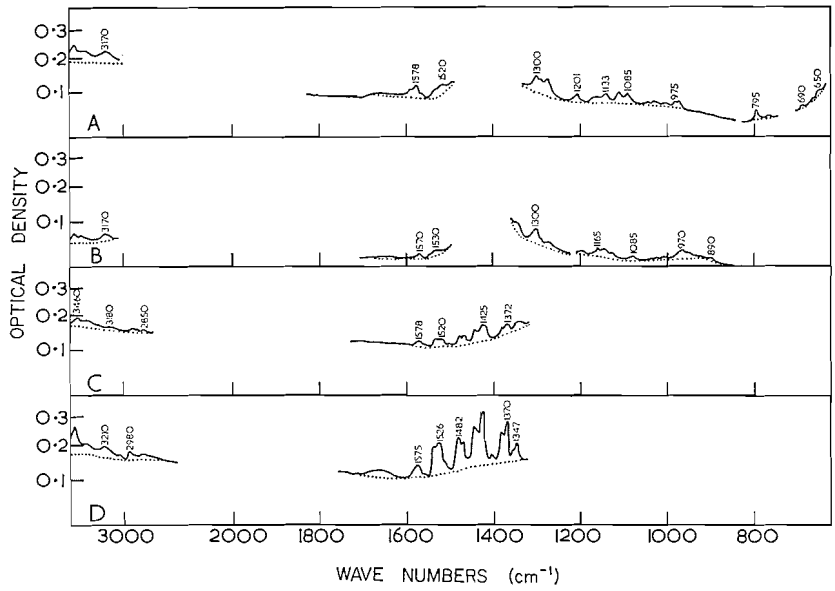

FIG. 4. Infrared spectra obtained from silver iodide formed in the presence of MCT.

MCT may ionize by two possible mechanisms to give either a negative nitrogen or a negative sulphur, or more probably a mesomeric anion:

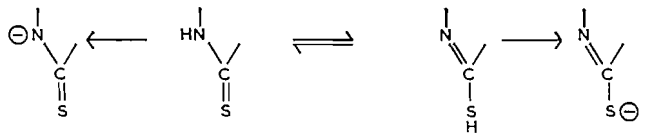

The close resemblance between the titration curves of benztriazole and MCT would infer that it is the NH group which is the group involved in ionization. This is supported by the spectra of the silver salt, since the N—H stretching frequency (3100–3140 cm^{-1}) disappears and the C=S band remains unchanged, at least in the case of MCTH, where a definite C=S assignment has been made. Results of ultraviolet spectra also suggested that the thione form HN—C=S is the stable one (18–20).

It is attractive to consider that adsorption of MCT on the surface of silver iodide occurs via an ion-exchange mechanism, viz. replacement by the MCT anion of the I^- on the surface, but this does not seem to be supported by the pK value or the spectra. For instance, from Fig. 4 it can be seen that in the case of silver iodide formed in the presence of MCT the N—H stretching vibration is retained. The particle size in this case was very small. Hence the scatter was small and good spectra were obtained in the 3000 cm^{-1} region.

In the case of preformed silver iodide sols coagulated by MCT, precise study of the region 3000–4000 cm^{-1} was not possible owing to scatter by the larger particles. However, the spectra appear to indicate that in this case the NH group is also retained. In this case many features of the spectra in the region 1480–1600 cm^{-1} have little resemblance to those of silver MCT, and it seems unlikely that the adsorbed species is an adsorbed silver MCT molecule.

Figure 1 shows that in solid MCT all N—H groups are involved in hydrogen bonding.

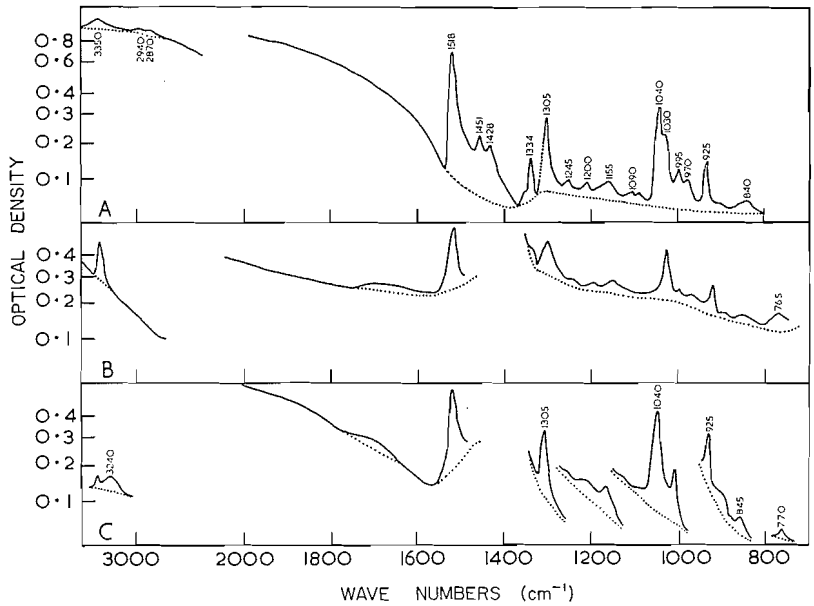

FIG. 5. Infrared spectra of (A) MCTH adsorbed on silver iodide powder, (B) silver iodide formed in the presence of MCTH, (C) MCTH adsorbed on preformed silver iodide sol.

However, in the case of silver iodide formed in the presence of MCT the greater proportion of the molecules appears to be adsorbed with free NH groups. Thus the strong sharp band at 3460 cm^{-1} (Fig. 4) is due to the stretching of free N—H groups on the surface. This would infer, therefore, that adsorption of the molecules responsible for this band cannot occur via the N—H group, for example, by hydrogen bonding of the N—H to the potential-determining iodide ion. In Fig. 4 the presence of adsorbed water is shown by the H—O—H deformation band at ca. 1650 cm^{-1}. The broad O—H stretching band accompanying this must lie beneath the sharp N—H band at 3460 cm^{-1}. The bands at 3390, 3200, and 3070 cm^{-1} are due to the stretching modes of N—H groups in varying degrees of hydrogen bonding, or to combination bands whose intensities have been increased by Fermi resonance with the N—H vibration. From the relative intensities of the free and hydrogen-bonded N—H groups there is clearly a high proportion of free N—H groups since the intrinsic intensity of the bonded N—H stretching band is far greater than that of the free. Although in very dilute solutions of MCT, in polar and non-polar solvents, there is a considerable amount of NH which is free from hydrogen bonding (Fig. 1A), the proportion of free groupings is even greater for material in the adsorbed state (Fig. 4).

One other possibility is that the MCT molecule is adsorbed to the silver iodide surface by means of the polarizable C=S bond. Unfortunately, it is not clear whether a definite band can be associated with the C=S bond in MCT. Bands between 800 and 1280 cm^{-1} do not seem to be greatly different for MCT, silver MCT, or MCT adsorbed on silver iodide particles. Since the C=S stretching mode would be expected to occur in the region 800–1300 cm^{-1} (16), the suggestion is that no great change has occurred in this mode.

In the spectral region 1300–1600 cm^{-1}, several bands which appear single in the MCT and silver MCT spectra (Fig. 1) are doubled in the spectrum of MCT adsorbed on silver iodide (Figs. 3 and 4). This splitting may be due to the heterogeneous nature of the surface of the silver iodide perturbing the molecular vibrations to varying degrees.

The spectra of the preformed sols coagulated with MCT are masked by scattering in the region 3000–4000 cm^{-1} but it does appear that NH groups are present and that most of these are hydrogen bonded; a broad band appears between 3200 and 3300 cm^{-1} (Fig. 3). If this assignment is correct, hydrogen bonding in these samples is not as strong as in crystalline MCT, where the frequency is displaced to 3050–3090 cm^{-1}. In Fig. 3D the band at 3200–3280 cm^{-1} due to weakly hydrogen-bonded molecules is more readily observed because of the lower scatter for this particular sample. The band at 3500 cm^{-1} may well be due to adsorbed water on the sample rather than to adsorbed molecules with free N—H groups.

Other differences also occur in the region 1450–1600 cm^{-1} of the spectra of the sol coagulated with MCT and that formed in the presence of MCT. In the former case the 3,4 C=N stretching band appears at the normal position (1575 cm^{-1}) found for MCT crystals, for MCT in solution in organic solvents, and for deuterated MCT (Fig. 1). However, the C=N stretching band of the thiolactam group was displaced from 1500 cm^{-1} to ca. 1480 cm^{-1} when MCT was used to coagulate a silver iodide sol. This is rather similar to the shift caused by deuteration or by solution in chloroform.

In the case of silver iodide formed in the presence of MCT the spectrum is considerably different in the region 1450–1600 cm^{-1} to that of MCT in the solid state or in solution. The double band at 1526 and 1536 cm^{-1} (Fig. 4) probably is that which occurs at 1545 cm^{-1} in the spectrum of silver MCT; two possibilities were considered for the interpretation of this band. If the band at 1545 cm^{-1} in the spectrum of silver MCT is due to the 3,4 C=N stretching mode (the weak band at 1580 cm^{-1} was ascribed to a small amount of unchanged MCT) then two forms of adsorbed MCT would occur when silver iodide is formed in the presence of MCT, one form with the 3,4 C=N stretching mode at 1575 cm^{-1}, as in the case of MCT adsorbed on preformed silver iodide particles, and the other form having the 3,4 C=N stretching band at 1526–1536 cm^{-1}, as in the case of silver MCT. The bands at 1471–1482 cm^{-1} and, perhaps, at 1428–1447 cm^{-1}, which appear abnormally strong, are then the C=N stretching bands of the two forms.

The alternative explanation assigned the 1580 cm^{-1} band of the silver MCT spectrum to the 3,4 C=N stretching mode, whose intensity was weakened by replacement of hydrogen by silver. The 1545 cm^{-1} band was then due to the C=N stretching mode. On this basis only one form of MCT need be considered when silver iodide is formed in the presence of the organic compound.

A weak but distinct band appears at 1530–1540 cm^{-1} in the spectrum of the preformed sol coagulated with MCT (Fig. 3). Thus in this system there is a small amount of surface material similar to that adsorbed on silver iodide formed in the presence of MCT.

It would appear that in the concentration range investigated MCT is physically adsorbed onto the surface of silver iodide. No evidence has been found that adsorption proceeds via formation of silver MCT on the surface, or that adsorption is preceded by formation of silver MCT in the liquid phase. Solubility conditions would in any case be unfavorable for the latter situation to occur. It would appear from the spectra, however, that the adsorption process is connected with the 3,4 C=N and the C=N group in the MCT molecule, since bands corresponding to the stretching motions of these groups are most strongly affected by adsorption; this would be consistent with physical adsorption via the C=S with consequent polarization of the bond. The high proportion of free NH groups (non-hydrogen-bonded) may be an indication that this grouping is directed away from the surface.

The lack of evidence for a chemisorption process involving either the breaking of the —NH or C═S bond is surprising in view of the fact that MCT will reverse the charge of silver iodide at a concentration of ca. 10^{-3} *M*, and above 10^{-1} *M* the silver iodide appears to dissolve to give a silver MCT complex. The nature of these complexes, however, does not appear to have been completely investigated. Certainly, from infrared spectra there appears little evidence for the formation of a chemisorbed complex on the surface of silver iodide and it seems unlikely that if a chemisorbed layer had been formed it would be removed easily by washing.

Adsorption of MCTH on Silver Iodide

The spectrum of MCTH adsorbed on silver iodide is very similar to that of the material in the bulk phase (cf. Figs. 2 and 5).

The frequency of the N—H stretching vibration of the thiolactam group in the adsorbed material (3350 cm^{-1}) is below that of MCTH in dilute solution in organic solvents (3450 cm^{-1}), showing that weak hydrogen bonding occurs in the former state. However, as in the case of adsorbed MCT considered above, the adsorbed MCTH is not as strongly hydrogen bonded as in the crystalline material, where the N—H stretching frequency is between 3050 and 3150 cm^{-1}.

The spectrum in the N—H stretching region of MCT adsorbed on a preformed silver iodide sol was different to that of silver iodide formed in the presence of MCT. In the case of MCTH, bands occurred at 3350 cm^{-1}, for both methods of sample preparation, suggesting that hydrogen bonding occurred with —NH but to a lesser extent than in the crystal of MCTH. Figures 5B and 5C indicate that there is more hydrogen bonding in the case of adsorption on a preformed sol than in the case of silver iodide formed in the presence of MCTH.

Only very slight changes were observed in other regions of the spectrum of adsorbed MCTH compared to that of the bulk material. The C═N stretching vibration (1520 cm^{-1}) is practically unaffected by adsorption. The C═S stretching frequency in the adsorbed state (1040 cm^{-1}) is slightly below that of MCTH in the solid (1050 cm^{-1}) but the effect is small and less than that accompanying the silver salt formation. It is clear that there has been little perturbation of the molecule by adsorption onto silver iodide.

REFERENCES

1. M. J. Jaycock, R. H. Ottewill, and M. C. Rastogi. Third International Congress of Surface Activity, Cologne. Vol. 2. 1960. p. 283.
2. R. H. Ottewill. *In* Encyclopedia of microscopy. *Edited by* G. L. Clark. Reinhold, New York. 1961. p. 135.
3. R. P. Eischens and W. A. Pliskin. Advan. Catalysis, **10**, 1 (1958).
4. R. H. Ottewill and M. C. Rastogi. Trans. Faraday Soc. **56**, 866 (1960).
5. B. Težak, E. Matijević, and K. F. Schulz. J. Phys. Colloid Chem. **55**, 1557, 1567 (1951).
6. R. H. Ottewill. Unpublished results.
7. G. J. Harmsen, J. van Schooten, and J. Th. G. Overbeek. J. Colloid Sci. **8**, 64 (1953).
8. M. St. C. Flett. J. Chem. Soc. **69**, 347 (1953).
9. M. G. Ettlinger. J. Am. Chem. Soc. **72**, 4699 (1950).
10. L. J. Bellamy. The infrared spectra of complex molecules. 2nd ed. Methuen and Co. Ltd., London. 1958.
11. J. Chatt, L. A. Duncanson, and L. M. Vinanzi. Suomen Kemistilehti, B, **29**, 75 (1956).
12. D. Hadži. J. Chem. Soc. **159**, 847 (1957).
13. R. Mecke, R. Mecke, and A. Luttringhaus. Chem. Ber. **90**, 975 (1957).
14. B. A. Gingras, R. L. Somorjai, and C. H. Bailey. Can. J. Chem. **39**, 973 (1961).
15. S. Refn. Spectrochim. Acta, **17**, 40 (1961).
16. L. J. Bellamy and P. E. Rogasch. J. Chem. Soc. 2218 (1960).
17. H. O. Dickinson. Private communication.
18. G. A. Reynolds and J. A. Van Allen. J. Org. Chem. 1478, **24** (1959).
19. R. A. Morton and A. L. Stubbs. J. Chem. Soc. 1321 (1939).
20. C. Hassan and R. F. Hunter. J. Chem. Soc. 1672 (1936).

THE NUCLEAR MAGNETIC RESONANCE SPECTRA OF PARA-SUBSTITUTED PHENOLS[1]

W. G. Paterson and N. R. Tipman
Department of Chemistry, University of Alberta, Edmonton, Alberta

Received June 25, 1962

ABSTRACT

The nuclear magnetic resonance spectra of a number of para-substituted phenols have been examined. The —OH chemical shifts, extrapolated to infinite dilution in benzene and in carbon tetrachloride, were found to be almost independent of the nature of the ring substituent. Approximately linear relationships were observed between the internal chemical shift of the ring protons and other physical properties.

INTRODUCTION

Nuclear magnetic resonance spectroscopy has been used extensively in the study of intermolecular hydrogen bonding in phenols (1–12). However, in nearly all instances, measurements were not extended to regions of very low concentration. The results quoted in the present paper indicate that caution should be taken in the extrapolation of chemical shift data to infinite dilution. The electric field theory of Buckingham (13) has been applied to para-substituted phenols and the predictions of the theory with regard to internal ring proton shifts have been qualitatively verified.

EXPERIMENTAL

The nuclear magnetic resonance spectra were obtained at approximately 40° C on a Varian A-60 analytical n.m.r. spectrometer operating at 60 Mc/sec. The line positions were measured by the usual audio-frequency side-band technique (14) using a Hewlett–Packard Model 200AB audio-oscillator and a Hewlett–Packard Model 521C frequency counter.

All the phenols were of reagent grade quality or better and were dried over a suitable desiccant before use. Small amounts of spectroscopic grade cyclohexane (mole fraction 0.01 or less) were used as internal reference and were taken into account in the calculation of mole fraction. Carbon tetrachloride, benzene, and acetone were dried by shaking repeatedly with anhydrous $MgSO_4$, followed by distillation in a protected atmosphere. A middle cut was collected. The moisture content of the solvents was negligible, as indicated by their infrared spectra recorded at high gain. Due to the high noise level in the n.m.r. spectra of very dilute solutions, and also to the uncertainties involved in the extrapolation of data to infinite dilution, a considerable error is quoted for the chemical shift measurements listed in Table I.

TABLE I

OH chemical shifts in para-substituted phenols

Solute	Solvent	—OH shift at infinite dilution*
C_6H_5OH	CCl_4	2.84±0.03†
p-ClC_6H_4OH	CCl_4	2.90±0.03‡
p-BrC_6H_4OH	CCl_4	2.91±0.03
p-IC_6H_4OH	CCl_4	2.92±0.03
C_6H_5OH	C_6H_6	2.32±0.02
p-ClC_6H_4OH	C_6H_6	2.22±0.02
p-BrC_6H_4OH	C_6H_6	2.21±0.02
p-IC_6H_4OH	C_6H_6	2.24±0.02
p-$CH_3OC_6H_4OH$	C_6H_6	2.14±0.02
C_6H_5OH	$(CH_3)_2CO$	6.75±0.03

*Expressed in p.p.m. to low field from cyclohexane as internal reference.
†Measured as 2.8 in reference 2.
‡Measured as 3.3 in reference 2.

[1]*Abstracted in part from the B.Sc. Research Report of N. R. Tipman, University of Alberta, 1962.*

RESULTS AND DISCUSSION

The variation of —OH chemical shift with concentration for solutions of several para-substituted phenols in carbon tetrachloride and in benzene is shown in Figs. 1 and 2.

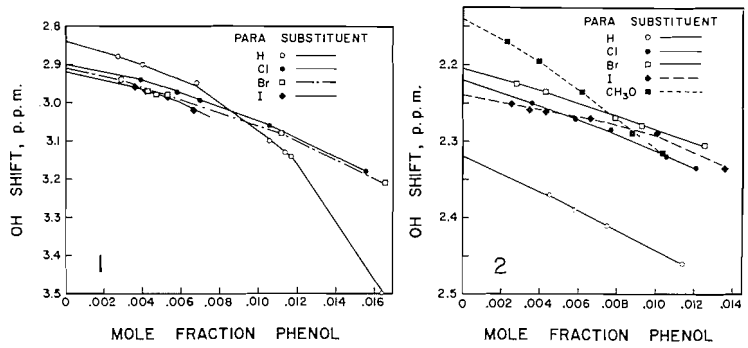

FIG. 1. Variation of —OH shift (in p.p.m. to low field from C_6H_{12} as internal reference) of para-substituted phenols with concentration in CCl_4.

FIG 2. Variation of —OH shift (in p.p.m. to low field from C_6H_{12} as internal reference) of para-substituted phenols with concentration in C_6H_6.

The —OH chemical shift at infinite dilution in a particular solvent appears to be almost independent of the nature of the ring substituent. The data are summarized in Table I.

The value of 2.84 p.p.m. for phenol in CCl_4 is in satisfactory agreement with the value of 2.8 p.p.m. reported by Huggins *et al.* (2), but their value of 3.3 p.p.m. for *p*-chlorophenol is in disagreement with the value of 2.90 p.p.m. in Table I. Their measurements on *p*-chlorophenol were not extended below 0.025 mole fraction, so their extrapolation is perhaps somewhat uncertain. Huggins *et al.* also reported the slopes at infinite dilution of the chemical shift vs. concentration curve. For phenol and *p*-chlorophenol, the limiting slopes differed by a factor of 2, which yielded 13 ± 7 and 9 ± 4, respectively, as the values of the dimerization equilibrium constant. In the present work (Fig. 1), it was found that the slopes were nearly the same. On the basis of infrared measurements, Maguire and West (15) reported recently that the dimerization equilibrium constants for phenol and *p*-chlorophenol were 7.22 and 6.24, respectively. These more accurate measurements substantiate the data reported in Table I and Figs. 1 and 2.

Due to the similarity of the extrapolated —OH shift values in a given solvent, a comparison of these data with Hammett or Taft substituent constants (16, 17) is unjustified. The shifts of the —OH signal to high field and low field observed in benzene and in acetone respectively, relative to that in carbon tetrachloride, are in the directions predicted by the well-known anisotropies of the benzene ring and the carbonyl group (18).

The n.m.r. spectra of the ring protons of para-substituted phenols in dilute acetone solution (approximately 3% by weight) consist, to a good approximation, of two superimposed AB spectra (19, 20). The intramolecular ring shifts and coupling constants of some para-substituted phenols are summarized in Table II. The ring shifts were compared with other data. No correlation was found with group electronegativity (21), suggesting that the ring shifts are due both to inductive and to resonance effects (20). The variation of ring shift with the Hammett substituent constant σ_p (16) is shown in Fig. 3. Although the points are widely scattered, a definite trend is apparent. No significant improvement in the plot was obtained with the modified constants proposed by Taft (17, 22).

TABLE II

Ring proton shifts and coupling constants in para-substituted phenols

Para substituent	Ring shift (p.p.m.)*	J_{HH}^{ortho} (cycles/sec)†
1. H	0.17‡	—
2. NO_2	1.155	9.2
3. Cl	0.343	9.2
4. Br	0.525	9.0
5. I	0.800	8.9
6. NH_2	−0.240	9.0
7. CHO	0.781	8.6
8. CH_3O	0.000	—
9. COOH	0.998	8.8
10. $COCH_3$	0.950	8.7
11. COC_6H_5	0.758	8.8
12. C_6H_5	0.563	8.7
13. $C(CH_3)_3$	0.458	8.8
14. CH_3	0.260§	8.6‖
15. OH	0.000	—

*Chemical shift between ortho ring protons. Error estimated as ±0.005 p.p.m.
†Error estimated as ±0.1 cycle/sec.
‡Reference 9.
§Measured as 0.261 p.p.m. in reference 11.
‖Measured as 8.5 cycles/sec in reference 11.

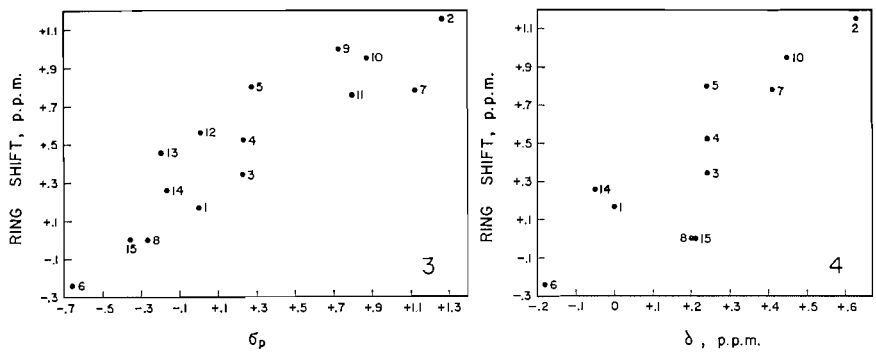

FIG. 3. Variation of internal ortho ring proton shift with Hammett substituent constant σ_p (16, 26). The numbering of points corresponds with that of Table II. The ring shift of p-$NH_2C_6H_4OH$ fits the correlation regardless of its sign.

FIG. 4. Comparison of observed ortho ring proton shift with the calculated contribution δ to this shift from the polarity of the para-substituent. The numbering of the points corresponds with that of Table II.

A theory proposed recently by Buckingham (13) indicates that the electric field E at a particular proton due to polar groups in other parts of the molecule can give rise to chemical shifts in the n.m.r. spectrum proportional to the first power of the electric field strength. The change $\Delta\sigma$ in the proton screening constant under these conditions is given by

$$[1] \qquad \Delta\sigma = -2\times10^{-12}E_z - 10^{-18}E^2,$$

where E_z is the component of E in the bond direction. Formulae were given by Buckingham for the calculation of E_z and E^2 at various positions in the ring and also for the differential ring shifts caused by the reaction field of the solvent. For phenol itself, a calculation such as that described above predicts a differential ring shift of 0.05 p.p.m., while the observed shift is 0.16 p.p.m. (Table II). In the case of p-nitrophenol, the calculated shift of 0.18 p.p.m. compares very poorly with the observed shift of 1.15 p.p.m.

Similarly, Buckingham (13) calculated that the ring shift between protons ortho and meta to the nitro group in nitrobenzene should be 0.29 p.p.m. in a mixture of equal volumes of cyclohexane and nitrobenzene, while the observed shift was actually 0.67 p.p.m. (23). Anomalies of this kind have been ascribed to a specific association between solute and solvent (13). However, if in the series p-XC_6H_4OH, the solute–solvent interaction and the reaction field from the polarized solvent remain approximately constant, then there should be a linear correlation between the observed ring shift and the calculated contribution to this shift from the polarity of X. The results plotted in Fig. 4 suggest that this is qualitatively true. Dipole moment data were taken from references 24 and 25.

ACKNOWLEDGMENTS

This work was supported in part by the National Research Council of Canada, whose financial assistance is greatly appreciated. The authors wish to express their thanks to Mr. R. Swindlehurst and Miss G. B. Stayura, who measured many of the spectra, and to Dr. R. J. Crawford for helpful discussion.

REFERENCES

1. R. L. Batdorf. Ph.D. Thesis, University of Minnesota, Minneapolis, Minn. 1955.
2. C. M. Huggins, G. C. Pimentel, and J. N. Shoolery. J. Phys. Chem. **60**, 1311 (1956).
3. I. Gränacher. Helv. Phys. Acta, **31**, 734 (1958).
4. E. D. Becker. J. Chem. Phys. **31**, 269 (1959).
5. M. Saunders and J. B. Hyne. J. Chem. Phys. **29**, 1319 (1958); **31**, 270 (1959).
6. R. Freymann, M. Freymann, M. Koechlin, M. Martin, and G. Mavel. Arch. Sci. (Geneva), **12**, Fasc. spéc., 207 (1959).
7. I. Gränacher and P. Diehl. Arch. Sci. (Geneva), **12**, Fasc. spéc., 238 (1959).
8. M. Martin and F. Hérail. Compt. Rend. **248**, 1994 (1959).
9. I. Gränacher. Helv. Phys. Acta, **34**, 272 (1961).
10. M. Martin and M. Quilbeuf. Compt. Rend. **252**, 4151 (1961).
11. I. Yamaguchi. Bull. Chem. Soc. Japan, **34**, 451, 744, 1602 (1961).
12. B. D. N. Rao, P. Venkateswarlu, A. S. N. Murthy, and C. N. R. Rao. Can. J. Chem. **40**, 963 (1962).
13. A. D. Buckingham. Can. J. Chem. **38**, 300 (1960).
14. J. T. Arnold and M. E. Packard. J. Chem. Phys. **19**, 1608 (1951).
15. M. M. Maguire and R. West. Spectrochim. Acta, **17**, 369 (1961).
16. L. P. Hammett. Physical organic chemistry. McGraw-Hill Book Co., Inc., New York. 1940.
17. R. W. Taft, Jr., R. E. Glick, I. C. Lewis, I. Fox, and S. Ehrenson. J. Am. Chem. Soc. **82**, 756 (1960).
18. L. M. Jackman. Applications of nuclear magnetic resonance spectroscopy in organic chemistry. Pergamon Press, London. 1959.
19. J. A. Pople, W. G. Schneider, and H. J. Bernstein. High-resolution nuclear magnetic resonance. McGraw-Hill Book Co., Inc., New York. 1959.
20. P. Diehl. Helv. Chim. Acta, **44**, 829 (1961).
21. B. P. Dailey and J. N. Shoolery. J. Am. Chem. Soc. **77**, 3977 (1955).
22. R. W. Taft, Jr. J. Am. Chem. Soc. **79**, 1045 (1957).
23. P. L. Corio and B. P. Dailey. J. Am. Chem. Soc. **78**, 3043 (1956).
24. Handbook of Chemistry and Physics. 34th ed. Chemical Rubber Publishing Co., Cleveland, Ohio. 1952.
25. C. P. Smyth. Dielectric constant and molecular structure. The Chemical Catalog Co., Inc., New York. 1931.
26. J. Hine. Physical organic chemistry. McGraw-Hill Book Co., Inc., New York. 1956.

N-MUSTARD DERIVATIVES OF ESTROGENS

THOMAS NOGRADY,[1] KITTY M. VAGI, AND VINCENT W. ADAMKIEWICZ
Department of Physiology, University of Montreal, Montreal, Que.

Received March 14, 1962

ABSTRACT

N-Mustard urethanes of estrone and stilbestrol, as well as an N-mustard-phosphoramidate of stilbestrol, were synthesized. Only the estrone derivative proved to be slightly active against an adenocarcinoma.

Efforts to influence the transport characteristics of nitrogen mustards resulted in the synthesis of a large number of compounds (1), several among them bearing steroid carriers (2–6). Most of the steroids used were, however, physiologically inactive in themselves, e.g. cholestene, ergostatriene, and stigmastadiene. 3β-[Bis-(β-chloroethyl)-aminoethyl]-Δ^5-cholestene (4) was reported to be inactive; 3-cholesteryl-N-[4′-N-bis-(β-chloroethyl)-aminophenyl]-carbamate (5) and 3-cholesteryl-[4′-N-bis-(β-chloroethyl)-aminophenyl]-sulphonate (6) were found to be nontoxic, but possessed a slight activity only. Steroid hormones were used as carriers by Burstein and Ringold (7) as well as by Rao and Price (8).

We prepared a few N-mustard derivatives of estrone and diethylstilbestrol, hoping to be able to influence estrogen-dependent tumors more selectively.

3-Esteryl-bis-(β-chloroethyl)-carbamate (I) was obtained from estrone and chloroformyl-bis-(β-chloroethyl) amine:

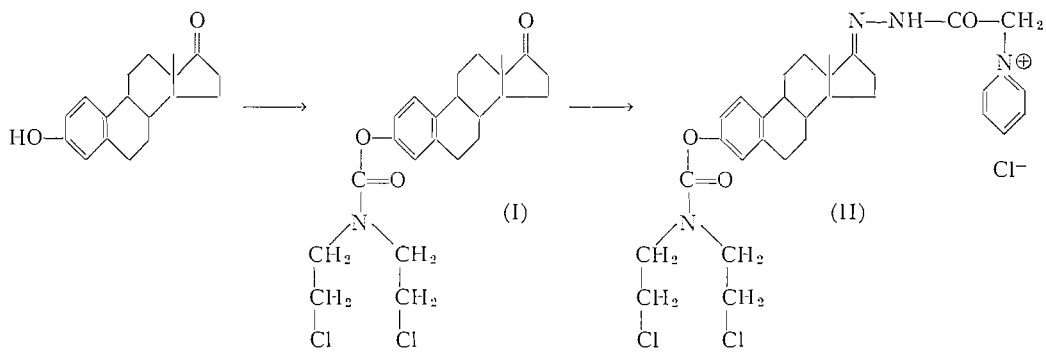

Due to its water insolubility, it was difficult to administer compound I to experimental animals. Therefore a water-soluble but amorphous hydrazone (II) with Girard's P reagent was also prepared.

The same urethane-type mustard (IV) (cf. ref. 9) was also synthesized from diethylstilbestrol, in the usual way.

Stilbestrol-phosphate is reported (10) to have a beneficial effect on prostate tumors, because the high phosphatase activity of prostatic tissue liberates stilbestrol selectively from the ester. It seemed, therefore, interesting to see a N-mustard-phosphate bound to stilbestrol. It was expected that a double selectivity should result: first, the selective

[1]*Present address: Department of Chemistry, Loyola College, Montreal 28, Que.*

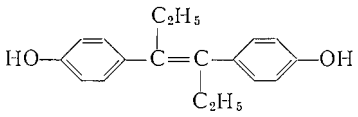

(III)

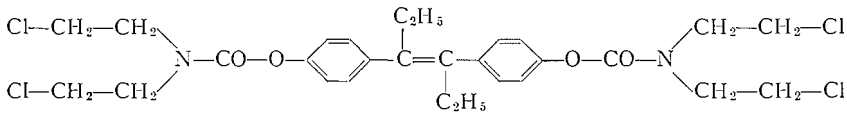

(IV)

accumulation of the compound in prostatic or mammary tissue, due to the carrier, and secondly, the preferential splitting of the phosphate bond at the sites of high phosphatase activity. Moreover, the "hidden" N-mustard group should be nontoxic at sites of low phosphatase activity, thus decreasing the general toxicity.

To test this hypothesis, the diethylstilbesteryl-phosphoramidic chloride (V) was prepared, according to the method of Friedman and Seligman (11). From this, we wished to prepare either the free phosphoric acid or an amide. After lengthy experimentation, it

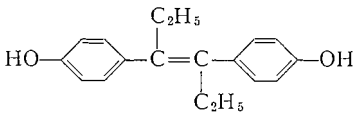

(III)

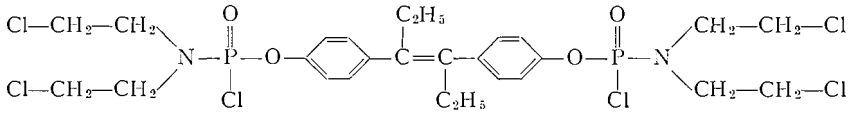

(V)

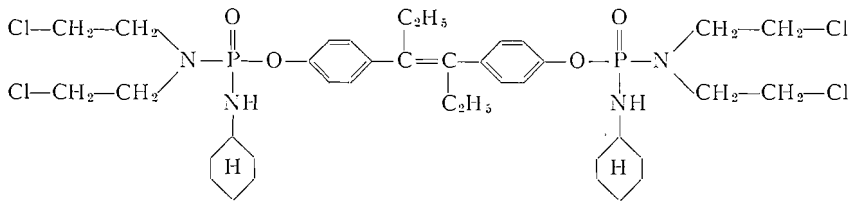

(VI)

was found that only the cyclohexyl amide (VI) could be obtained as a crystalline solid. The free acid and amides with aniline, piperidine, or morpholine were oily.

Pharmacological Results

Screened on mammary adenocarcinoma BN/10232, the estrone urethane (I) showed a 30% inhibition at a dosage level of 5 mg per day per mouse for 14 days, with a 15% mortality. Interestingly, the analogous stilbestrol derivative (IV) proved inactive at the

same dosage level, with a 5% mortality. Tested under similar circumstances, the stilbestrol-phosphoramidate (VI) was inactive too.

EXPERIMENTAL*

3-Esteryl-bis-(β-chloroethyl)-carbamate (I)

Ten grams of estrone (USP grade) and 7.8 g chloroformyl-bis-(β-chloroethyl)amine in 37 ml pyridine solution stood for 4 days at room temperature. When the solution was poured into ice water a solid crystallized out. The precipitate was filtered off, washed with water and methanol, and recrystallized from 250 ml isopropanol, yielding 10.02 g (52.4%) of colorless crystals, m.p. 143–145°. $[\alpha]_D^{20}+109.5°$ (*c* 2, chloroform). Anal. Calc. for $C_{23}H_{29}Cl_2NO_3$: C, 63.01; H, 6.67; N, 3.20. Found: C, 63.2; H, 6.9; N, 3.3.

Hydrazone with Girard's P Reagent (II)

Compound I (0.44 g) and Girard's P reagent (0.19 g) were refluxed in a mixture of 10 ml ethanol and 1 ml acetic acid, for 1 hour. On evaporation, the solution left a colorless water-soluble syrup which solidified to an amorphous precipitate when it was triturated with diisopropyl ether. In a few months it turned brown. Anal. Calc. for $C_{30}H_{37}Cl_3N_4O_3$: Cl, 17.5. Found: Cl, 17.1.

Diethylstilbesteryl bis-[di-(β-chloroethyl)]-carbamate (IV)

The solution of 3.14 g diethylstilbestrol (III) and 4.28 g (3.12 ml) of chloroformyl-bis-(β-chloroethyl)-amine in 10 ml dry pyridine stood at room temperature for 4 days. The solution was decanted from the precipitated pyridine hydrochloride, evaporated under reduced pressure, and the semisolid mass freed from the last traces of pyridine by azeotropic distillation with toluene. Recrystallized from methanol, it yielded 2.94 g (48.8%) colorless crystals, m.p. 139–140°. Anal. Calc. for $C_{28}H_{34}Cl_4N_2O_4$: C, 55.65; H, 5.67; N, 4.67. Found: C, 55.5; H, 5.9; N, 4.7.

Diethylstilbesteryl bis-[di-(β-chloroethyl)-phosphoramidic chloride] (V)

Diethylstilbestrol (1.57 g), bis-(β-chloroethyl)-phosphoramidic dichloride (2.60 g), and triethylamine (1.4 ml) were refluxed and stirred in 25 ml dry benzene for 1½ hours. After the reaction mixture was chilled, the separated triethylamine hydrochloride was filtered off (95.6% of the theoretical amount), and the benzene solution evaporated. The resulting colorless syrup (3.07 g, 86.1%) was used for further experiments. Anal. Calc. for $C_{26}H_{34}Cl_6N_2O_4P_2$: N, 3.93. Found: N, 3.78.

Diethylstilbesteryl bis-[N-di-(β-chloroethyl)-N'-cyclohexyl-phosphorodiamidate] (VI)

The phosphoramidic chloride (V) prepared from 7.6 g diethylstilbestrol was refluxed and stirred with 11.0 ml cyclohexylamine in 150 ml dry toluene for 4 hours, until neutral. The separated cyclohexylamine hydrochloride was filtered off from the hot reaction mixture. On cooling, the solution deposited 9.85 g of colorless crystals, which was recrystallized from 135 ml isopropanol, yielding 7.87 g (38.6%) of compound VI, melting at 206–208°. Anal. Calc. for $C_{38}H_{58}Cl_4N_4O_4P_2$: C, 54.16; H, 6.94; Cl, 16.38; N, 6.65. Found: C, 54.3; H, 7.0; Cl, 16.2; N, 6.7.

ACKNOWLEDGMENTS

This investigation was supported by the National Cancer Institute of Canada, the U.S. Department of Health, Education and Welfare, National Institutes of Health (Grant No. 2260), and the National Research Council of Canada (Grant No. MA 640).

We wish to thank Dr. R. Gaudry, research director of Ayerst, McKenna & Harrison Ltd. (Montreal) for his generous gifts of estrone and stilbestrol. The carcinostatic screening was done by Dr. R. Herne of Ayerst, McKenna & Harrison Ltd., and details will be published elsewhere. We thank Dr. Herne for permission to publish his findings.

REFERENCES

1. R. B. Ross and P. E. Swartzentruber. Literature survey of nitrogen mustards. Cancer Chemotherapy National Service Center, Bethesda, Md. 1959.
2. G. R. Vavasour, H. I. Bolker, and A. F. McKay. Can. J. Chem. **30**, 933 (1952).
3. G. G. Hazen. Doctoral Dissertation, University of Michigan, Ann Arbor, Mich. 1951; Chem. Abstr. **47**, 8761 (1953).
4. W. J. Gensler and G. M. Sherman. J. Org. Chem. **23**, 1227 (1958).
5. L. N. Owen, M. H. Benn, and A. M. Creighton. Brit. Emp. Cancer Campaign Annual Rept. **34**, 448 (1956).

**All melting points are uncorrected. Microanalyses by Dr. C. Daesslé, Microanalytical Laboratory, Montreal.*

6. J. F. DANIELLI, L. HAMILTON, M. S. MAY, and P. J. BERNARD. Brit. Emp. Cancer Campaign Annual Rept. **34**, 398 (1956).
7. S. H. BURSTEIN and H. I. RINGOLD. J. Org. Chem. **26**, 3084 (1961).
8. G. V. RAO and C. C. PRICE. J. Org. Chem. **27**, 205 (1962).
9. T. NOGRADY. J. Org. Chem. **26**, 4177 (1961).
10. H. DRUCKREY. Deut. Med. Wochschr. **76**, 655 (1954).
11. O. M. FRIEDMAN and A. M. SELIGMAN. J. Am. Chem. Soc. **77**, 1534 (1952).

KINETIC STUDY OF THE ISOMERIZATION OF *n*-BUTENES ON CHROMIA–ALUMINA*

Y. AMENOMIYA AND R. J. CVETANOVIĆ
Division of Applied Chemistry, National Research Council, Ottawa, Canada
Received July 17, 1962

ABSTRACT

Mutual interconversions of the three *n*-butenes on a chromia–alumina catalyst have been studied in a temperature range between 210 and 260° C and in a pressure range from about 10 to about 100 mm. Dependence of initial rates on the initial pressures of the reactants was determined experimentally. The initial rates of isomerization could be, in each case, expressed empirically by a rate equation conforming to the Langmuir–Hinshelwood formula. It was possible to explain the experimental results by assuming the existence of three different adsorbed species for the three *n*-butene isomers and their surface interconversions as the rate-determining step.

INTRODUCTION

Catalytic isomerization of butenes has been extensively investigated in attempts to contribute to the understanding of the mechanism of the catalytic isomerization of olefins. It is well known that the presence of hydrogen is necessary for the olefin isomerization on some metallic catalysts (1–6), while the reaction occurs in the absence of hydrogen on metal oxide, alkali, and acid catalysts (6–20). Several kinetic studies have been carried out on metallic catalysts and the mechanism of olefin isomerization has been discussed in conjunction with the mechanism of hydrogenation (2–5). On the other hand, relatively few kinetic studies of olefin isomerizations on oxide catalysts are available (12, 13, 18, 21).

Carbonium ions and carbanions have been postulated by many investigators as intermediates in the catalytic reactions of olefins and have been also recently invoked to explain the stereoselectivity in the catalytic isomerization of butenes (6, 15). It is felt, however, that further kinetic studies of these reactions, on catalytic materials of various types, are necessary, and the present work has, therefore, been carried out with the object of obtaining kinetic information on butene isomerization on a chromia–alumina catalyst. This catalyst is used commercially as a dehydro-isomerization catalyst.

EXPERIMENTAL

Catalyst

Chromia–alumina catalyst was prepared by mixing and grinding aluminum hydroxide and chromium hydroxide, both of which were spearately precipitated by adding ammonium hydroxide to the solutions of the respective nitrates. The composition of the catalyst was about 20% Cr_2O_3 and 80% Al_2O_3 by weight, as calculated from the loss on ignition of the two hydroxides. The catalyst was heated at 500° C for 1 hour, and crushed into pieces of convenient size. The same catalyst sample, weighing 0.0038 g, was used in all kinetic measurements. The surface area of the catalyst, determined by the B.E.T. method with nitrogen, was 100.5 m^2/g.

Research grade butenes of Phillips Petroleum Co. were used as reactants. They were twice condensed in liquid nitrogen traps followed by evacuation, and were kept in a 3-l. reservoir. The impurities in 1-butene and *cis*-butene were negligibly small, but *trans*-butene contained a small amount of *cis*-butene, which was subtracted from the amount of *cis*-butene produced.

Apparatus

The apparatus used consisted of a plunger-type glass circulating pump and a spiral-type reactor, as shown in Fig. 1. The reactants in the reaction system were circulated to prevent the reaction from becoming

**Issued as N.R.C. No. 7015.*

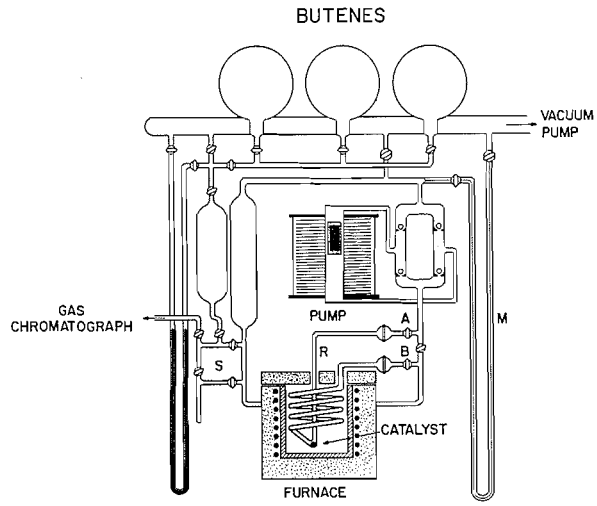

FIG. 1. Apparatus.

controlled by the diffusion of the reactant. Prior to the kinetic measurements lack of diffusion control was verified; it was observed that reaction rates were proportional to the amount of the catalyst up to 0.03 g at the pumping speed used subsequently in the kinetic measurements with 0.0038 g of the catalyst.

The reactor was provided with a spiral preheater made of quartz tubing about 160 cm in length, which assured only a very small drop in the catalyst temperature when the reactants were circulated through the reactor. This was checked by placing a thermocouple in place of the catalyst under conditions similar to those used in kinetic measurements. The reactor was placed in a stainless steel block furnace, the temperature of which was regulated to $\pm 0.5°$ C. The total volume of the reaction system was about 560 cc, of which about 90 cc was kept at the reaction temperature. A temperature range between 210 and 260° C was employed and the pressure of butenes was varied from 10 to 100 mm. The circulation pump was found to be sufficiently effective to homogenize the gases in the reaction system within 30 seconds.

Procedure

Before use the catalyst was heated up to 700° C and treated with 680 mm of circulating air at the same temperature for 2 hours, then evacuated for 1 hour at 700° C at a pressure below 10^{-4} mm and cooled to the reaction temperature *in vacuo*. The same treatment was repeated before each run in order to maintain the catalyst activity constant. Occasional experiments were carried out under the same conditions to check the constancy of catalyst activity (expts. 175, 176, 196, and 259). They showed that the activity of the catalyst remained constant in the course of 127 runs performed.

The reaction was started by opening the taps A and B (Fig. 1) after the circulating pump had been turned on. Gaseous samples were withdrawn into the small samplers S by expansion at intervals of several minutes (usually every 2–3 minutes), and were analyzed by gas chromatography. The change in total pressure resulting from the withdrawal of a sample was within 1%, and this effect on the rate of reaction in a run was neglected. Unless samples were taken, no pressure change was observed on the manometer M during the reaction (at least up to 30 minutes), and no hydrocarbons lower than C_4 were observed chromatographically. Therefore neither polymerization nor cracking appeared to take place to any appreciable extent.

Analysis

The products of the reactions of 1-butene and *cis*-butene were analyzed gas chromatographically on a 11-m column of dimethyl sulpholane on activated alumina, and those of *trans*-butene were analyzed on a 10-m column of propylene carbonate on firebrick. Correction factors for peak-area responses were obtained from standard samples.

RESULTS AND DISCUSSIONS

A trace of 1,3-butadiene was observed at reaction temperatures higher than 250° C, but the amount was so small (less than 0.1%) that the formation of this compound was neglected. No detectable amounts of *n*-butane, isobutane, or isobutene were observed, indicating that no hydrogenation or skeletal isomerization had occurred.

The results obtained are summarized in Tables I, II, and III. The pressure changes of each of the three butene isomers in the course of a run, obtained from gas chromato-

TABLE I

Isomerization of butene-1
(Amount of catalyst 0.0038 g)

Reaction temp. (°C)	Expt. No.	Initial pressure of butene-1 (mm)	Reaction time (min)	Final conversion (%)	Initial rate (mm/min)			Ratio of *trans/cis*
					$-dp_1/dt$	dp_t/dt	dp_c/dt	
259	133	77.5	7	4.62	2.00	1.02	1.02	1.11
	134	27.8	7	20.01	1.20	0.72	0.48	1.17
	135	42.1	7	14.63	1.43	0.74	0.69	1.11
	137	98.6	7	9.06	2.32	1.24	1.10	1.18
	139	31.3	5	14.15	1.10	0.57	0.56	1.15
	140	41.1	7.3	14.59	1.39	0.70	0.67	1.07
	141	121.8	6	6.54	2.67	1.37	1.28	1.07
	142	61.0	7	13.63	1.90	0.99	0.87	1.10
	175*	50.1	7	14.05	1.60	0.79	0.78	1.05
229	153	61.2	7	9.01	1.48	0.75	0.75	1.03
	154	80.6	7.2	8.81	1.74	0.89	0.87	1.02
	156	42.1	7	10.80	1.18	0.57	0.61	0.93
	157	21.1	7.5	17.33	0.72	0.37	0.39	0.92
	176*	51.3	7	10.61	1.30	0.65	0.67	0.95
	196*	42.3	8.2	12.35	1.20	0.62	0.59	0.96
	259*	44.7	8	12.54	1.20	—	—	1.02
210	159	41.5	7.5	10.91	0.98	0.47	0.49	0.98
	160	61.8	7.5	7.09	1.15	0.57	0.63	0.97
	161	83.8	7	6.41	1.36	0.67	0.72	0.94
	162	26.3	8	14.46	0.65	0.32	0.35	0.96
	173	51.4	7.5	8.89	1.03	0.47	0.56	0.95
	177	52.5	7.5	8.60	1.00	—	—	0.92

*These experiments were carried out in order to check the constancy of catalyst activity.

graphic analysis, have been plotted against reaction time, as shown, for example, in Fig. 2. The pressure decrease of the reactant and pressure increase of the products in

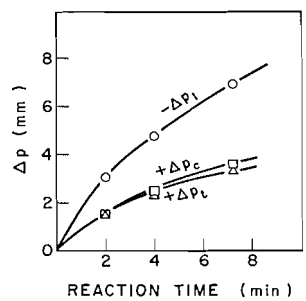

FIG. 2. Pressure changes as a function of reaction time (expt. 154, temp. 230° C, initial pressure of butene-1 80.6 mm, catalyst 0.0038 g).

the first minute are taken as the respective initial rates. These are listed in the sixth to eighth columns of the tables as dp_1/dt, dp_t/dt, and dp_c/dt, where p_1, p_t, and p_c represent the partial pressures of 1-butene, *trans*-butene, and *cis*-butene, respectively.

The ratios of the products given in the last column of the tables were obtained by

TABLE II

Isomerization of *cis*-butene-2
(Amount of catalyst 0.0038 g)

Reaction temp. (°C)	Expt. No.	Initial pressure of *cis*-butene (mm)	Reaction time (min)	Final conversion (%)	Initial rate (mm/min)			Ratio of 1/*trans*
					$-dp_c/dt$	dp_1/dt	dp_t/dt	
250	199	41.0	8	10.52	0.80	0.31	0.50	0.57
	201	25.0	10	16.67	0.59	0.24	0.40	0.58
	202	60.7	7.5	7.34	0.97	0.36	0.61	0.59
	203	84.9	8	7.77	1.24	0.38	0.88	0.42
	206	58.6	8	9.86	1.00	0.32	0.70	0.51
	207	89.2	8	7.97	1.29	0.38	0.92	0.44
	208	19.4	10	19.41	0.51	0.16	0.35	0.42
230	183	44.7	7	7.41	0.70	0.28	0.42	0.66
	184	64.0	7	6.73	0.86	0.35	0.51	0.68
	187	82.4	8	5.63	0.91	0.34	0.60	0.67
	189	38.8	9	9.86	0.66	0.24	0.43	0.66
	191	21.2	9.5	16.01	0.48	0.18	0.29	0.60
	192	98.3	6.3	4.17	1.00	0.39	0.60	0.67
	193	56.0	8	8.77	0.80	0.29	0.50	0.57
	194	16.6	10	17.23	0.40	0.16	0.26	0.70
210	210	37.0	10	8.81	0.48	0.20	0.28	0.67
	211	63.0	6	3.91	0.58	0.24	0.36	0.65
	212	81.0	8	5.13	0.70	0.27	0.47	0.58
	214	28.9	10	10.99	0.43	0.15	0.29	0.56
	215	51.7	9.2	5.86	0.56	0.22	0.37	0.55
	216	89.8	8	3.91	0.68	0.26	0.43	0.61
	217	23.1	10	15.35	0.41	0.11	0.31	0.34

TABLE III

Isomerization of *trans*-butene-2
(Amount of catalyst 0.0038 g)

Reaction temp. (°C)	Expt. No.	Initial pressure of *trans*-butene (mm)	Reaction time (min)	Final conversion (%)	Initial rate (mm/min)			Ratio of *cis*/1
					$-dp_t/dt$	dp_c/dt	dp_1/dt	
250	251	47.4	8	7.96	0.60	0.44	0.17	2.6
	252	63.8	8	6.87	0.73	0.51	0.22	2.3
	253	24.2	9	11.04	0.37	0.25	0.11	2.4
	255	44.6	8	9.23	0.64	0.48	0.17	2.9
	258	78.0	8	6.99	0.85	0.61	0.23	2.5
230	240	48.4	8.3	5.91	0.45	0.30	0.15	2.2
	241	62.1	8	5.48	0.55	0.38	0.18	2.2
	243	36.5	9	8.79	0.38	0.29	0.11	2.5
	246	91.0	8	4.79	0.70	0.48	0.21	2.2
	248	16.6	9	6.93	0.21	0.15	0.07	2.2
210	229	37.4	9.2	5.13	0.25	0.18	0.07	2.3
	230	27.9	9.2	7.33	0.26	0.18	0.08	2.3
	231	52.9	8	3.70	0.34	0.23	0.11	2.0
	232	71.6	8	3.82	0.41	0.28	0.13	2.2
	234	91.8	8	3.95	0.57	0.40	0.17	2.4
	236	32.5	9	6.67	0.26	0.18	0.08	2.4
	237	70.4	8	3.36	0.45	0.30	0.15	2.1
	238	95.3	8.8	4.55	0.59	0.42	0.18	2.4

extrapolating to zero conversion. These extrapolations are only approximate; as an example, the ratios of *trans*- to *cis*-butene-2 formed in the isomerization of 1-butene are

shown in Fig. 3, which contains all the experimental points taken independently of the pressure of butene-1 used. The good linearity in the figure of the plots of the product

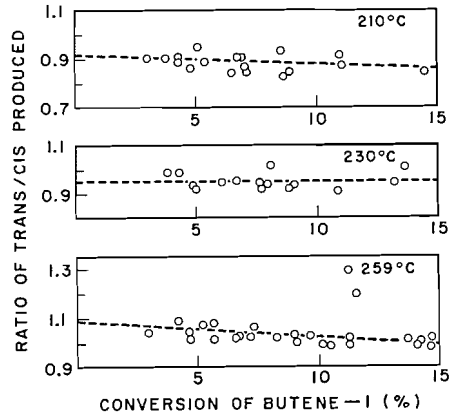

FIG. 3. Ratio of *trans*-butene-2/*cis*-butene-2 produced from butene-1 as a function of conversion.

ratio against conversion suggests that the reactions forming the two products are parallel rather than being consecutive.

In Fig. 4 the initial rates are plotted against the initial pressure of the reactant. From the shape of these curves the reaction orders of the reactant-consuming and the product-forming reactions seem to be between 1 and 0.

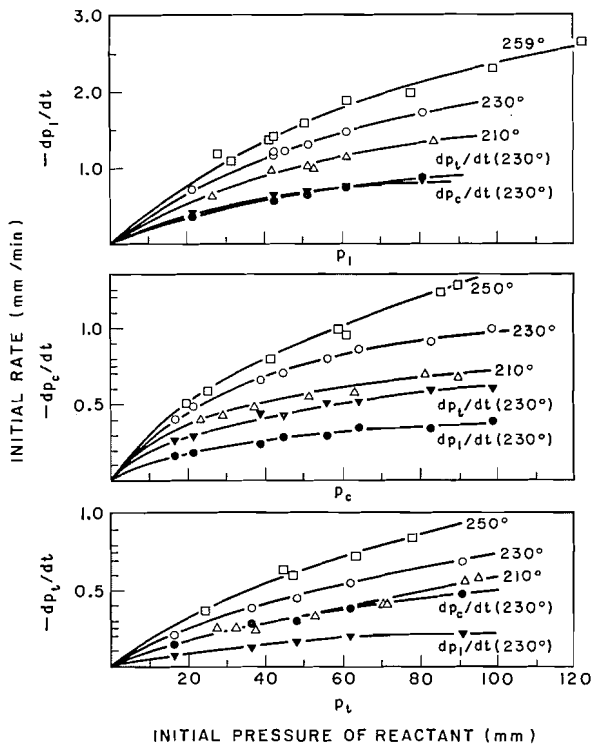

FIG. 4. Dependence of the initial rates on the initial pressure of the reactants. (Catalyst weight 0.0038 g. The rates of product formation at 230° C only are plotted.)

The mechanism shown in Fig. 5 is based on the assumption that there are three different adsorbed species for the three *n*-butene isomers. If it is assumed that the interconversions

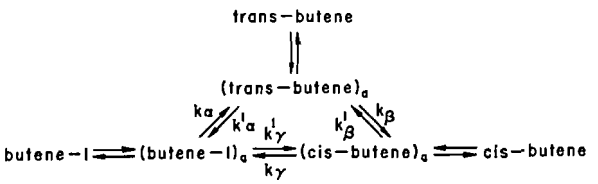

FIG. 5. The proposed mechanism of isomerization. (Subscript "a" denotes an adsorbed state.)

of the three *n*-butenes on the chromia–alumina catalyst proceed by this mechanism and that the rate-determining steps of these reactions are the respective surface reactions of the adsorbed molecules, the rates of the isomerization reactions are given by the equations

$$[1] \qquad -dp_1/dt = (dp_t/dt)+(dp_c/dt) = k_\alpha K_1 p_1/(1+K_1 p_1)+k_\gamma' K_1 p_1/(1+K_1 p_1) \quad \text{(from 1-butene)},$$

$$[2] \qquad -dp_c/dt = (dp_1/dt)+(dp_t/dt) = k_\gamma K_c p_c(1+K_c p_c)+k_\beta' K_c p_c/(1+K_c p_c) \quad \text{(from } cis\text{-butene)},$$

$$[3] \qquad -dp_t/dt = (dp_c/dt)+(dp_1/dt) = k_\beta K_t p_t/(1+K_t p_t)+k_\alpha' K_t p_t/(1+K_t p_t) \quad \text{(from } trans\text{-butene)},$$

where p stands for the partial pressures, K for the equilibrium constants of adsorption (simplified in the following to "adsorption constants") of the respective butenes, and k and k' for the rate constants of the respective surface reactions, as illustrated in Fig. 5. It is also assumed that the adsorption of the products is negligible because of their very small partial pressures in the initial stages of the reaction. In accord with the above equations, plots of the reciprocal initial rates against the reciprocal reactant pressure should be linear, and their intercepts and slopes should provide the various rate and adsorption constants. Such plots have been obtained in Fig. 6 by replotting the curves of Fig. 4. It is evident that the observed initial rates agree well with the above equations.

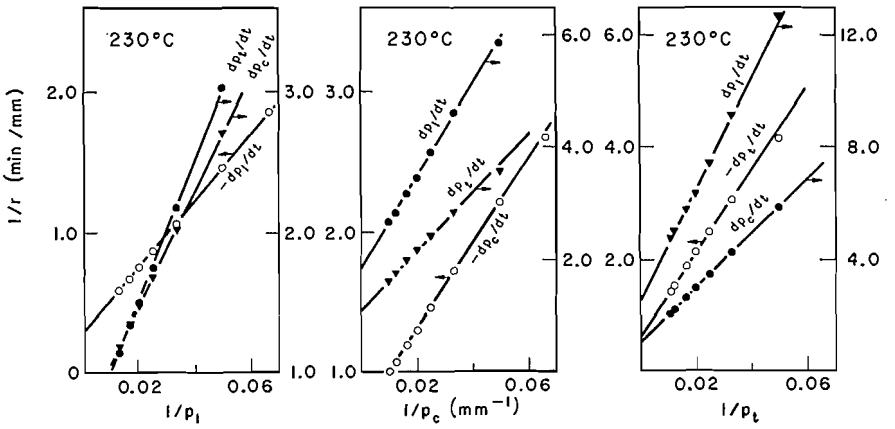

FIG. 6. Plots of the reciprocal initial rates vs. reciprocal pressures.

In the figures the rates of product formation are plotted as well as the rates of reactant consumption (the overall reaction). From the latter the adsorption constants can be obtained separately and should be identical with the values obtained from the rates of product formation.

The values obtained are shown in Table IV. It is seen in Table IV(i) that there is a fair agreement between the adsorption constants for butene-1 (K_1). The Arrhenius plot

TABLE IV

Values of the rate and adsorption constants*

(i) Isomerization of butene-1

Temp. (°C)	K_1 obtained from the plot of: dp_t/dt	dp_c/dt	$-dp_1/dt$	K_1, mean	k_α	k_γ'
259	0.0092	0.0104	0.0107	0.0101	2.56	2.22
250				0.0108†	2.43†	2.01†
230	0.0109	0.0144	0.0124	0.0126	1.90	1.61
210	0.0143	0.0133	0.0150	0.0142	1.22	1.39
Heat of adsorption				3.6		
Activation energy					7.9	5.0

(ii) Isomerization of *cis*-butene

Temp. (°C)	K_c	k_β'
250	0.0117	1.770
230	0.0222	0.893
210	0.0257	0.649
Heat of adsorption		10.4
Activation energy		12.6

(iii) Isomerization of *trans*-butene

Temp. (°C)	K_t obtained from the plot of: dp_1/dt	dp_c/dt	$-dp_t/dt$	K_t, mean	k_α'	k_β
250	0.0098	0.0082	0.0096	0.0092	0.571	1.562
230	0.0124	0.0098	0.0083	0.0102	0.408	1.020
210	0.0020	0.0025	0.0042		1.15	2.13

*The units are: k, mm/min; K, 1/mm; heat of adsorption and activation energy, kcal/mole.
†These values were obtained from the plots in Figs. 7 and 8.

of the mean value of K_1 is shown in Fig. 7, from which the heat of adsorption of butene-1 was found to be 3.6 kcal/mole. The Arrhenius plots of the rate constants k_α and k_γ' of the two surface reactions are given in Fig. 8. The activation energies are, respectively, 7.9 and 5.0 kcal/mole, as listed in the table.

The values of K_c calculated from the dp_1/dt plot are 0.0188, 0.0288, and 0.0296 at 210, 230, and 250° C, respectively, i.e., they show an increase rather than a decrease with temperature. However, the equilibrium composition of butene-1 in *n*-butenes is only about 10% at these temperatures and it might therefore be necessary in this case to consider the reverse reaction (butene-1 → *cis*-butene) as well. The values K_c and k_β' calculated from the dp_t/dt plot are shown in Table IV(ii), and their Arrhenius plots in Figs. 7 and 8, from which the heat of adsorption and the activation energy were found to be 10.4 and 12.6 kcal/mole respectively.

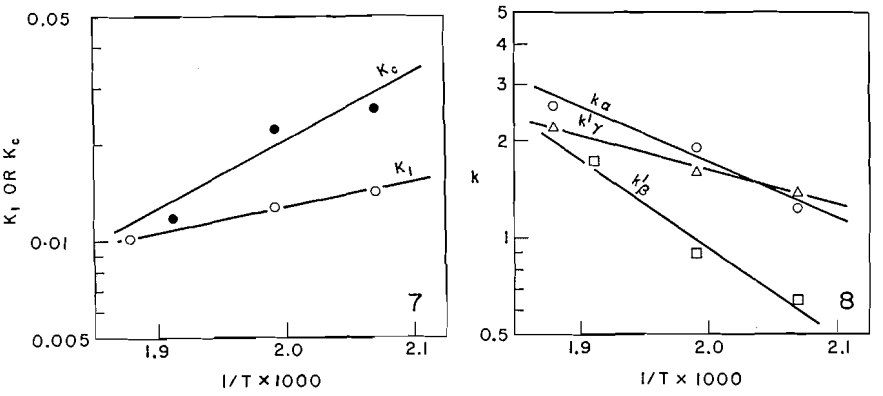

FIG. 7. Arrhenius plots of adsorption constants.
FIG. 8. Arrhenius plots of the rate constants.

It is seen in Table IV(iii) that the three K_t values obtained agree reasonably well with each other at 250 and 230° C, but at 210° C K_t, k_α', and k_β show abnormal values. The following discussion will be first confined to the values of constants at 250 and 230° C, ignoring for the moment the abnormality at 210° C.

When butene-1, *trans*-butene-2, and *cis*-butene-2 are equilibrated in the presence of the catalyst, the forward rates of surface reactions must be equal to their respective reverse reactions, that is,

$$k_\alpha K_1 p_1/(1+K_1p_1+K_tp_t+K_cp_c) = k_\alpha' K_t p_t/(1+K_1p_1+K_tp_t+K_cp_c),$$
$$k_\beta K_t p_t/(1+K_1p_1+K_tp_t+K_cp_c) = k_\beta' K_c p_c/(1+K_1p_1+K_tp_t+K_cp_c),$$
$$k_\gamma K_c p_c/(1+K_1p_1+K_tp_t+K_cp_c) = k_\gamma' K_1 p_1/(1+K_1p_1+K_tp_t+K_cp_c),$$

and therefore

[4] $$k_\alpha K_1 = k_\alpha' K_t (p_t/p_1)_e = k_\alpha' K_t/K_\alpha,$$

[5] $$k_\beta K_t = k_\beta' K_c (p_c/p_t)_e = k_\beta' K_c/K_\beta,$$

[6] $$k_\gamma K_c = k_\gamma' K_1 (p_1/p_c)_e = k_\gamma' K_1/K_\gamma,$$

where $(p_t/p_1)_e$, etc. are the equilibrium ratios of each pair of two isomers and are denoted by K_α, etc. These values are listed in Table V. In the above equations, values of $k_\alpha K_1$

TABLE V
Equilibrium constants*

Temp. (°C)	$K_\alpha = (p_1/p_t)_e$	$K_\beta = (p_t/p_c)_e$	$K_\gamma = (p_c/p_1)_e$
259	0.209	1.73	2.76
250	0.199	1.77	2.83
230	0.181	1.80	3.08
210	0.162	1.85	3.34

*Calculated from the data in "Selected Values of Physical and Thermodynamic Properties of Hydrocarbons and Related Substances" by F. D. Rossini (Carnegie Press, Pittsburgh, 1953).

and $k_\beta K_t$ can be calculated from Tables IV(i) and IV(iii), respectively, and can be compared with $k_\alpha' K_t/K_\alpha$ and $k_\beta' K_c/K_\beta$, which are calculated from the data in Tables IV(iii), IV(ii), and V. The results obtained are shown in Table VI. In agreement with

TABLE VI

Comparison of the values of the constants based on the proposed mechanism (Fig. 5)

Temp. (°C)	$k_\alpha' K_t$	K_α	$k_\alpha' K_t/K_\alpha$*	$k_\alpha K_1$†	$k_\beta' K_c$	K_β	$k_\beta' K_c/K_\beta$‡	$k_\beta K_t$§
250	0.00525	0.199	**0.0264**	**0.0262**	0.0207	1.77	**0.0117**	**0.0144**
230	0.00416	0.181	**0.0230**	**0.0239**	0.0198	1.80	**0.0110**	**0.0104**

*Calculated from Tables IV (iii) and V.
†Calculated from Table IV(i).
‡Calculated from Tables IV(ii) and V.
§Calculated from Table IV(iii).

equations [4] and [5], excellent agreement is seen between $k_\alpha K_1$ and $k_\alpha' K_t/K_\alpha$ and between $k_\beta K_t$ and $k_\beta' K_c/K_\beta$, all of which were obtained from independent reactions. This fact, as well as the linearity of plots in Fig. 6, indicates that the mechanism and the rate-determining steps assumed are consistent with the present results.

The abnormal values of K_t, k_α', and k_β at 210° cannot be explained in the same manner. They may have been caused partly by increased analytical uncertainties, since *trans*-butene is the predominant isomer under these conditions. It is also possible that at the lower temperature a change in the type of the rate-determining step might begin to occur.

Other mechanisms and rate-determining steps also considered but found to be inconsistent with the experimental results were: (1) only one adsorbed species common to the three isomers; (2) two different adsorbed species, one of which corresponds to butene-1, the other common to the two 2-butenes; (3) desorption of the products as the alternative rate-determining step in the mechanism of Fig. 5.

The formal kinetic treatment discussed here does not provide information on the nature of the three adsorbed species and these could be adsorbed organic ions as is frequently postulated. Equally well they could be physically adsorbed butene molecules, in which case the rate-determining step (k_α, k_β, k_γ, . . . , in Fig. 5) is their interaction with the active catalytic sites. Brouwer (21) has recently shown that the 1/*trans* ratio formed from *cis*-butene on γ-alumina varies greatly as the catalyst is poisoned with water or other substances. He has suggested that the catalytic surface has to meet different requirements for the double-bond shift and cis–trans isomerization. The double-bond shift is assumed to occur by the concerted "*hydrogen switch*" mechanism of Turkevich and Smith (11), while cis–trans isomerization proceeds by carbonium ion mechanism. Foster and Cvetanović (6, 20) had similarly considered dual function of the catalyst surface in the isomerization of *n*-butenes, with cis–trans isomerization involving predominantly the carbonium ion or the "associative" radical mechanism, and double-bond migration predominantly the carbanion, the "dissociative" radical, or the hydrogen switch mechanism, depending on the type of catalyst. All these processes could involve a slow interaction of a physically adsorbed olefin molecule with the active sites of the catalyst. Stereoselectivity in the catalytic isomerization of *n*-butenes is also found in the present work, as shown, for example, by initial formation from butene-1 of the thermodynamically less stable *cis*-butene in greater amounts than *trans*-butene-2. This is evident

from the data in Tables I, II, and III. In the present instance the stereoselectivity is associated with the magnitudes of the rate constants of the surface reactions. These are likely to depend on the acid properties of the surface of the catalyst, although no generalizations appear possible on the basis of the present results without additional experimental information.

REFERENCES

1. G. H. TWIGG. Trans. Faraday Soc. **35**, 934 (1939).
2. G. H. TWIGG. Proc. Roy. Soc. (London), A, **178**, 106 (1941).
3. G. H. TWIGG. Discussions Faraday Soc. **8**, 152 (1950).
4. V. H. DIBELER and T. H. TAYLOR. J. Phys. Chem. **55**, 1036 (1951).
5. Y. AMENOMIYA. J. Res. Inst. Catalysis, Hokkaido Univ. **9**, 1 (1961).
6. N. F. FOSTER and R. J. CVETANOVIĆ. J. Am. Chem. Soc. **82**, 4274 (1960).
7. V. N. IPATIEFF, H. PINES, and R. E. SCHAAD. J. Am. Chem. Soc. **56**, 2696 (1934).
8. R. H. EWELL and P. E. HARDY. J. Am. Chem. Soc. **63**, 3460 (1941).
9. W. W. MCCARTHY and J. TURKEVICH. J. Chem. Phys. **12**, 405 (1944).
10. H. H. VOGE, G. M. GOOD, and B. S. GREENSFELDER. Ind. Eng. Chem. **38**, 1033 (1946).
11. J. TURKEVICH and R. K. SMITH. J. Chem. Phys. **16**, 466 (1948).
12. R. G. HAY, J. COULL, and P. H. EMMETT. Ind. Eng. Chem. **41**, 2809 (1949).
13. P. J. LUCCHESI, D. L. BAEDER, and J. P. LONGWELL. J. Am. Chem. Soc. **81**, 3235 (1959).
14. H. PINES and W. O. HAAG. J. Org. Chem. **23**, 328 (1958).
15. W. O. HAAG and H. PINES. J. Am. Chem. Soc. **82**, 387 (1960).
16. H. PINES and W. O. HAAG. J. Am. Chem. Soc. **82**, 2471 (1960).
17. H. PINES and G. BENOY. J. Am. Chem. Soc. **82**, 2483 (1960).
18. W. O. HAAG and H. PINES. J. Am. Chem. Soc. **82**, 2488 (1960).
19. M. G. HAMPTON and R. J. CVETANOVIĆ. Can. J. Chem. **37**, 1417 (1959).
20. R. J. CVETANOVIĆ and N. F. FOSTER. Discussions Faraday Soc. **28**, 201 (1959).
21. D. M. BROUWER. J. Catalysis, **1**, 22 (1962).

ON THE EVALUATION OF CERTAIN TWO- AND THREE-CENTER MOLECULAR INTEGRALS OCCURRING IN ELECTROSTATIC CALCULATIONS

R. F. W. BADER
Department of Chemistry, University of Ottawa, Ottawa, Canada
Received June 29, 1962

ABSTRACT

A general method is developed for the evaluation of the three-center integrals which occur in the application of the Hellmann–Feynman theorem to the study of molecular binding. The method employs Gegenbauer polynomials for the series expansion of the radial dependence of the electric field. It is also shown that the same expansion greatly simplifies the evaluation of the two-center electrostatic penetration integrals. General formulae are presented for these latter integrals for all nonvanishing combinations of *s*, *p*, and *d* atomic orbitals for all principal quantum numbers.

I. INTRODUCTION

The Hellmann–Feynman theorem enables one to calculate the forces acting on a nucleus in a molecule if the electron density function is known. The integrals which occur in such calculations fall into three general classes when the electron density is expressed in terms of atomic orbitals. All three classes of integrals are of the general form

$$I = \int \mathscr{D}_{\alpha x}\phi_i\phi_j d\tau,$$

where $\mathscr{D}_{\alpha x}$ is the x-component of the electric field produced by a unit charge at nucleus α and ϕ_i and ϕ_j are atomic orbitals. It is the positioning of the two atomic orbitals with respect to atom α which distinguishes the three classes of integrals.

(*a*) When ϕ_i and ϕ_j are both situated on the same atom but not on atom α, the integral (I) represents the force exerted on nucleus α by the charge density on some other atom β. These are labelled penetration integrals. The penetration integrals may be evaluated by the method usually employed for two-center molecular integrals, i.e. expressing them in terms of spheroidal coordinates. However, in these cases a second coordinate transformation is necessary, to an orthogonal set obtained by a rotation of the λ and μ axes of the spheroidal set. The method is long and cumbersome and takes no advantage of the inherent symmetry of the integrals. We report here a new method which allows for their evaluation in terms of a few simple integrations about one center only. This method greatly reduces both the labor involved and the possibility of committing errors.

(*b*) When ϕ_i and ϕ_j are situated on different atoms neither of which is atom α, the result is a three-center integral. Hurley (1) has pointed out that this type of three-center one-electron integral is the most complicated type that can arise in the application of the Hellmann–Feynman theorem to polyatomic molecules. We describe in this paper a general method for the evaluation of such three-center integrals.

(*c*) When ϕ_i is situated on atom α and ϕ_j on some other atom, the integral (I) represents the force exerted on nucleus α by the charge density arising from the overlap of $\phi_{i(\alpha)}\phi_{j(\beta)}$. These integrals may be evaluated by expressing them in terms of spheroidal coordinates. The methods described in this paper offer no advantages in the evaluation of this third

type of integral. Coulson (2) and Bader and Jones (3) have given analytical expression for many of these integrals.

The basis of the present method is in the use of the Gegenbauer polynomials for the expansion of the radial dependence of the electric field about another atomic center. In both the two- and three-center integrals, $\mathscr{D}_{\alpha x}$ and $\mathscr{D}_{\alpha y}$ are expanded about center β (see Fig. 1):

$$[1] \qquad \mathscr{D}_{\alpha x} = \frac{\cos\theta_\alpha}{r_\alpha^2} = \frac{1}{r_\alpha^3}(\rho - r\cos\theta) = (\rho - r\cos\theta)\sum_{k=0}^{\infty}\frac{1}{\rho^3}\left(\frac{r}{\rho}\right)^k C_k^{3/2}(\cos\theta)$$

$$[2] \qquad \mathscr{D}_{\alpha y} = \frac{\sin\theta_\alpha\cos\phi}{r_\alpha^2} = \frac{1}{r_\alpha^3}(r\sin\theta\cos\phi) = (r\sin\theta\cos\phi)\sum_{k=0}^{\infty}\frac{1}{\rho^3}\left(\frac{r}{\rho}\right)^k C_k^{3/2}(\cos\theta).$$

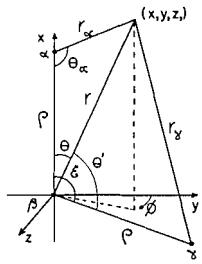

FIG. 1. The coordinate system for the two- and three-center integrals. The bond distance is designated by ρ and the bond angle by ξ.

(Both [1] and [2] are written for $\rho > r$; ρ and r are interchanged in the expressions when $r > \rho$.) The $C_k^{\nu}(\cos\theta)$ are Gegenbauer polynomials of the first kind. These particular polynomials permit the expansion of any inverse power of the distance. The Neumann expansion of r^{-1} in terms of Legendre polynomials is a special case of the more general expansion of $r^{-2\nu}$ in terms of the Gegenbauer polynomials, as the $C_k^{\nu}(\cos\theta)$ reduce to the $P_k(\cos\theta)$ when $\nu = 1/2$. The properties of the C_k^{ν} are well described by Whittaker and Watson (4), Magnus and Oberhettinger (5), and Prigogine (6). The $C_k^{\nu}(\cos\theta)$ may be related to the associated Legendre polynomials $P_k^m(\cos\theta)$ for any value of ν (5). Specifically, the relationship for $\nu = 3/2$ is

$$C_k^{3/2}(\cos\theta) = \frac{1}{\sin\theta}P_{k+1}^1(\cos\theta).$$

II. EVALUATION OF THE PENETRATION INTEGRALS

We shall consider first those integrals expressing the force directed along the bond axis:

$$P_{\parallel} = \int \mathscr{D}_{\alpha x}\phi_{i(\beta)}\phi_{j(\beta)}d\tau.$$

The ϕ_i are Slater atomic orbitals and may be expressed as

$$\phi_j(n,l,m) = N_n \exp(-ar)r^{n-1}\Theta_l^m(\cos\theta)\Phi_m(\phi),$$

where

$$\Theta_l^m(\cos\theta) = [\{(2l+1)/2\}\{(l-m)!/(l+m)!\}]^{1/2}P_l^m(\cos\theta)$$

are the normalized associated Legendre polynomials, and

$$\Phi_0(\phi) = (2\pi)^{-1/2};\ \Phi_m(\phi) = (\pi)^{-1/2}\begin{Bmatrix}\sin m\phi\\ \cos m\phi\end{Bmatrix}$$

$$N_n = (2a)^{n+1/2}/[(2n)!]^{1/2}.$$

When equation [1] is substituted for $\mathscr{D}_{ax}$ in $P_\parallel$ ($P_\parallel{}^0 = P_\parallel/N_nN_{n'}$) the result is

$$[3]\qquad P_\parallel{}^0 = \sum_{k=0}^{\infty}[\{\rho^{-(k+2)}A_{(u+k)}(\kappa,\rho)+\rho^{(k+1)}B_{(u-k-3)}(\kappa,\rho)\}\int\Theta_l{}^m\Theta_{l'}{}^{m'}P_{k+1}^1\,d\theta$$
$$-\{\rho^{-(k+3)}A_{(u+k+1)}(\kappa,\rho)+\rho^kB_{(u-k-2)}(\kappa,\rho)\}\int\Theta_l{}^m\Theta_{l'}{}^{m'}\cos\theta\,P_{k+1}^1\,d\theta]\int\Phi_m\Phi_{m'}d\phi,$$

where $u = n+n'$ (when $n = n'$, $u = 2n$); $\kappa = a+b$, the sum of the orbital exponents of ϕ_i and ϕ_j; and the $A_z(\kappa,\rho)$ and $B_z(\kappa,\rho)$ are the incomplete gamma functions defined by

$$A_z(\kappa,\rho) = \int_0^\rho e^{-\kappa r}r^z dr;\quad B_z(\kappa,\rho) = \int_\rho^\infty e^{-\kappa r}r^z dr.$$

Equation [3] terminates after the first few terms in any particular case due to the orthogonality and recurrence relationships of the Legendre polynomials. In Table I we have listed the resulting general formulae for all of the nonvanishing penetration integrals involving s, p, and d atomic orbitals of any principal quantum number.

TABLE I

Formulae* for the penetration integrals $P_\parallel = \int(\cos\theta_\alpha/r_\alpha^2)\cdot\phi_\beta(n,l,m)\phi_\beta(n',l',m')d\tau$

nlm	$n'l'm'$	$P_\parallel{}^0 = P_\parallel/N_nN_n{}'$
$ns\sigma$	$n's\sigma$	$[\rho^{-2}A_{(u)}]$
$np\sigma$	$n'p\sigma$	$[\rho^{-2}A_{(u)}+(6/5)\rho^{-1}A_{(u+2)}-(4/5)\rho B_{(u-3)}]$
$np\pi$	$n'p\pi$	$[\rho^{-2}A_{(u)}-(3/5)\rho^{-1}A_{(u+2)}+(2/5)\rho B_{(u-3)}]$
$nd\sigma$	$n'd\sigma$	$[\rho^{-2}A_{(u)}+(6/7)\rho^{-1}A_{(u+2)}+(10/7)\rho^{-6}A_{(u+4)}-(4/7)\rho B_{(u-3)}-(8/7)\rho^3B_{(u-5)}]$
$nd\pi$	$n'd\pi$	$[\rho^{-2}A_{(u)}+(3/7)\rho^{-4}A_{(u+2)}-(20/21)\rho^{-6}A_{(u+4)}-(2/7)\rho B_{(u-3)}+(16/21)\rho^3B_{(u-5)}]$
$nd\delta$	$n'd\delta$	$[\rho^{-2}A_{(u)}-(6/7)\rho^{-4}A_{(u+2)}+(5/21)\rho^{-6}A_{(u+4)}+(4/7)\rho B_{(u-3)}-(4/21)\rho^3B_{(u-5)}]$
$ns\sigma$	$n'p\sigma$	$(1/\sqrt{3})[2\rho^{-3}A_{(u+1)}-B_{(u-2)}]$
$ns\sigma$	$n'd\sigma$	$(1/\sqrt{5})[3\rho^{-1}A_{(u+2)}-2\rho B_{(u-3)}]$
$np\sigma$	$n'd\sigma$	$(1/\sqrt{15})[4\rho^{-3}A_{(u+1)}+(36/7)\rho^{-5}A_{(u+3)}-2B_{(u-2)}-(27/7)\rho^2B_{(u-4)}]$
$np\pi$	$n'd\pi$	$(1/\sqrt{5})[2\rho^{-3}A_{(u+1)}-(12/7)\rho^{-5}A_{(u+3)}-B_{(u-2)}+(9/7)\rho^2B_{(u-4)}]$

*Formulae for some particular cases ($n = n' = 1, 2$; $l = l' = 0, 1$ and $n = n' = 2$; $l = 0$, $l' = 1$) have been given previously (3).

The manner in which equation [3] reduces in a particular case will be illustrated for $n \neq n'$, $l = l' = 1$, and $m = m' = 0$. Consider first the two integrations over θ in equation [3]. When $l = l' = 1$ the first integral is zero unless k is an even integer and the second is zero unless k is odd. Thus equation [3] may be written

$$P_\parallel{}^0 = \frac{3}{2}\sum_{k=0,2,\ldots}^{\infty}[\{\rho^{-(k+2)}A_{(u+k)}+\rho^{(k+1)}B_{(u-k-3)}\}\int\cos^2\theta\,P_{k+1}^1\,d\theta$$
$$-\{\rho^{-(k+4)}\,A_{(u+k+2)}+\rho^{(k+1)}B_{(u-k-3)}\}\int\cos^3\theta\,P_{k+2}^1\,d\theta].$$

From the definition of $P_l{}^m(\cos\theta)$ in terms of $P_l(\cos\theta)$ and the recurrence relationship

$$zP_{k+1}'(z) = P_k{}'(z)+(k+1)P_{k+1}(z),$$

where the prime denotes (d/dz), one can show that

$$[4] \qquad \int \cos^2\theta\, P^1_{k+1}\, d\theta = \int \cos^3\theta\, P^1_{k+2}\, d\theta - (k+2)\int \sin\theta \cos^2\theta\, P_{k+2} d\theta.$$

The last integral in equation [4] is different from zero only for $k = 0$, when it has the value of 8/15. This result terminates the expansion after $k = 2$, and for $k = 2$ only $A_{(u+2)}$ remains. All succeeding terms are cancelled out, the B's within the same k term and the A's by the term which follows. The result is the expression listed in Table I for $np\sigma$, $n'p\sigma$.

We shall consider next the penetration integrals determining the force perpendicular to the bond axis:

$$P_\perp = \int \mathscr{D}_{\alpha\gamma}\phi_{i(\beta)}\phi_{j(\beta)}d\tau.$$

These integrals arise in the calculation of the forces operative in polyatomic molecules and play an important role in determining the equilibrium bond angles in such molecules. Substitution of equation [2] for $\mathscr{D}_{\alpha\gamma}$ into $P_\perp$ gives (again dividing out the normalizing factors)

$$P_\perp{}^0 = \sum_{k=0}^{\infty} \{\rho^{-(k+3)}A_{(u+k+1)} + \rho^k B_{(u-k-2)}\} \cdot \int \Theta_l{}^m \Theta_{l'}{}^{m'} P^1_{k+1} \sin\theta\, d\theta \int \cos\phi\, \Phi_m \Phi_{m'} d\phi.$$

The general formulae for all the nonvanishing $P_\perp$ integrals for s, p, and d orbital combinations are listed in Table II.

TABLE II

Formulae for the penetration integrals $P_\perp = \int (\sin\theta_\alpha \cos\phi/r_\alpha{}^2)\phi_\beta(n,l,m)\phi_\beta(n',l',m')d\tau$

nlm	$n'l'm'$	$P_\perp{}^0 = P_\perp/N_nN_n'$
$ns\sigma$	$n'p\pi$	$(1/\sqrt{3})[\rho^{-3}A_{(u+1)} + B_{(u-2)}]$
$np\sigma$	$n'p\pi$	$(3/5)[\rho^{-4}A_{(u+2)} + \rho B_{(u-3)}]$
$nd\sigma$	$n'p\pi$	$(1/\sqrt{15})[-\rho^{-3}A_{(u+1)} + (18/7)\rho^{-5}A_{(u+3)} - B_{(u-2)} + (18/7)\rho^2 B_{(u-4)}]$
$ns\sigma$	$n'd\pi$	$(\sqrt{3}/\sqrt{5})[\rho^{-4}A_{(u+2)} + \rho B_{(u-3)}]$
$np\sigma$	$n'd\pi$	$(1/\sqrt{5})[\rho^{-3}A_{(u+1)} + (12/7)\rho^{-5}A_{(u+3)} + B_{(u-2)} + (12/7)\rho^2 B_{(u-4)}]$
$nd\sigma$	$n'd\pi$	$(\sqrt{3}/7)[\rho^{-4}A_{(u+2)} + (10/3)\rho^{-6}A_{(u+4)} + \rho B_{(u-3)} + (10/3)\rho^3 B_{(u-5)}]$

III. EVALUATION OF THE THREE-CENTER INTEGRALS

The integrals are of the form (see Fig. 1)

$$I = \int \mathscr{D}_{\alpha z}\phi_{i(\beta)}\phi_{j(\gamma)}d\tau.$$

The technique employed in their evaluation is to expand both $\mathscr{D}_{\alpha z}$ (or $\mathscr{D}_{\alpha\gamma}$) and $\phi_{j(\gamma)}$ about center β. This is analogous to the method developed by Coulson (7, 8) for three-center integrals of the somewhat simpler form

$$\int \frac{1}{r_\alpha}\phi_{i(\beta)}\phi_{j(\gamma)}d\tau.$$

In the molecular integrals arising from the Hellmann–Feynman theorem, one must contend with the term $r_\alpha{}^{-3}$ from $\mathscr{D}_{\alpha z}$ as opposed to the $r_\alpha{}^{-1}$ considered previously. $\mathscr{D}_{\alpha z}$ is again expanded in terms of the Gegenbauer polynomials as given by equation [2] (or [3]

for $\mathscr{D}_{\alpha\gamma}$). The orbital $\phi_{j(\gamma)}$ is also expanded about center β using the method developed by Coulson (7, 8):

$$r_\gamma^{m-1}\exp(-cr_\gamma) = \sum_{n=0}^{\infty}\frac{2n+1}{(r\rho)^{1/2}}P_n(\cos\theta')\zeta_{m,n}(c,r;\rho).$$

The $\zeta_{m,n}$ are functions of c, r, and ρ and are fully described by Coulson and Barnett (8). The result of making these two substitutions is to transform the integral into a product of two integrals, one over the radial dependence and the other over the angular factors, which involves products of Gegenbauer and Legendre polynomials. Both integrations are over but one center and are therefore, easily effected.

An example of such a three-center integral arises in the calculation of the forces which determine the bond angle in H_2O and in NH_3. One is interested in determining the force operative on one of the hydrogen nuclei (center α) due to the charge density arising from the overlap of a $2p\pi$ orbital on the oxygen atom (center β) and the $1s$ orbital on another hydrogen atom. The integral is

$$I = \int\frac{\sin\theta_\alpha\cos^2\phi}{r_\alpha^2}r\sin\theta\exp(-br-cr_\gamma)d\tau.$$

On making the above-mentioned substitutions for $\mathscr{D}_{\alpha\gamma}$ and e^{-cr_γ} one obtains, upon some reduction,

$$I = \sum_{k=0}^{\infty}\sum_{n=0}^{\infty}R_{kn}(r)\cdot Q_{knm}(\theta,\phi),$$

where

$$R_{kn}(r) = \alpha^{-2}\tau^{-1/2}\left(\tau^{-(k+2)}\int_0^\tau t^{9/2+k}[\gamma_{n-1}(1,t;\tau)-\gamma_{n+1}(1,t;\tau)]e^{-\kappa t}dt + \tau^{(k+1)}\int_\tau^\infty t^{3/2-k}[\gamma_{n-1}(1,t;\tau)-\gamma_{n+1}(1,t;\tau)]e^{-\kappa t}dt\right)$$

(the $\gamma_n(1,t;\tau)$ are products of Bessel functions of imaginary argument, $t = cr$, $\kappa = b/c$, and $\tau = c\rho$), and where

$$Q_{knm} = \int_0^\pi\int_0^{2\pi}\sin^2\theta\, C_k^{3/2}(\cos\theta)P_n(\cos\theta')\cos^2\phi\sin\theta\, d\theta\, d\phi.$$

The $P_n(\cos\theta')$ may be expressed in terms of $P_n^m(\cos\theta)$ and $P_n^m(\cos\xi)$ by means of the well-known addition theorem for Legendre polynomials. Because of the Q_{knm} integral a large number of terms in the double sum vanish, the only terms remaining besides $n = k = 0$ and 1 being those where $k = n$ or $n-2$. Thus after the integrations over θ and ϕ, each $R_{kn}(r)$ is multiplied by some numerical constant and a trigonometric function of ξ. The advantage of this method is that a variation of the bond angle ξ entails no further work beyond looking up new sine and cosine values for this angle. When ξ goes to zero in the present example ($\theta = \theta'$) the integral is transformed into a two-center one of type (*c*) described in the introduction. This case of $\xi = 0$ can be put into an independent analytical

form and thus provides a valuable check of the method reported here. When $\xi = 0$, recurrence and orthogonality relationships give

$$Q_{knm} = Q_{kn} = (\pm 1)\frac{\pi}{(2n+1)}\frac{2(k+2)(k+1)}{2k+3}.$$

$$(+ \text{ when } k = n, - \text{ when } k = n-2)$$

The analytical expression for the case $\xi = 0$ gives a value of 0.02907 for the integral. After 12 terms in the expansion the present method yields an answer of 0.02909. (The slight difference in the final figure is due to round off error.) It should be pointed out that the case of $\xi = 0$ is in no ways a special one as the same expansions are employed as when $\xi \neq 0$. From these two results it is evident that the present method is capable of giving reliable answers for the three-center integrals which arise in applications of the Hellmann–Feynman theorem.

The author wishes to acknowledge helpful discussions of the three-center problem with Miss G. A. Jones, Professor V. Linis, and Dr. J. L. Howland. He also thanks Miss V. Zahradnitzky for checking the numerical work.

REFERENCES

1. A. C. HURLEY. Proc. Roy. Soc. (London), A, **235**, 224 (1956).
2. C. A. COULSON. Proc. Cambridge Phil. Soc. **38**, 210 (1942).
3. R. F. W. BADER and G. A. JONES. Can. J. Chem. **39**, 1253 (1961).
4. E. T. WHITTAKER and G. N. WATSON. A course of modern analysis. Cambridge University Press, Cambridge. 1950.
5. W. MAGNUS and F. OBERHETTINGER. Special functions of mathematical physics. Chelsea Publishing Co., New York. 1949.
6. I. PRIGOGINE. The molecular theory of solutions. North-Holland Publishing Co., Amsterdam. 1957.
7. C. A. COULSON. Proc. Cambridge Phil. Soc. **33**, 104 (1937).
8. C. A. COULSON and M. P. BARNETT. Phil. Trans. Roy. Soc. London, Ser. A, **243**, 221 (1951).

THE REACTION OF 4-PYRONES WITH HYDROXYLAMINE

PETER YATES[1]

Departments of Chemistry, University of Toronto, Toronto, Ontario, and Harvard University, Cambridge, Mass., U.S.A.

AND

MARGARET JEFRAIM JORGENSON[2]

Department of Chemistry, Harvard University, Cambridge, Mass., U.S.A.

AND

SUNIL KUMAR ROY

Department of Chemistry, University of Toronto, Toronto, Ontario

Received June 15, 1962

ABSTRACT

Treatment of 2,6-dimethyl-4-pyrone with hydroxylamine gives 4-hydroxyamino-2,6-lutidine 1-oxide. Under the influence of light or in weakly basic media this is converted in the presence of air to 4,4′-azoxydi-2,6-lutidine 1,1′-dioxide. In a strongly basic medium it is converted to 4,4′-azodi-2,6-lutidine 1,1′-dioxide. Similar results are obtained in the case of 2,6-diethyl-4-pyrone.

On treatment with hydroxylamine, 4-pyrones usually fail to give oximes (1). In some cases, no reaction occurs; this lack of reactivity can be attributed to the quasi-aromatic nature of the 4-pyrone ring system (I) (1, 2). In other cases, reaction proceeds via opening

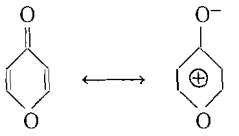

I

of the pyrone ring; for example, the methyl ether of comenic acid (II) forms the 4-hydroxypyridine-1-oxide derivative III (or its tautomer) (3). The reaction of 2,6-dimethyl-3,5-

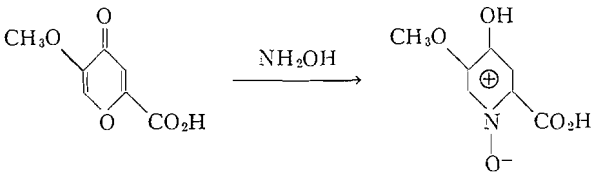

II III

dicarboethoxy-4-pyrone (IV) with hydroxylamine also must involve initial ring opening, but the intermediate in this case recloses to give an isoxazole derivative (V) (4). The following route seems probable:

[1]*To whom inquiries may be addressed at the University of Toronto, Toronto, Ontario.*
[2]*N.I.H. Fellow, 1957–58.*

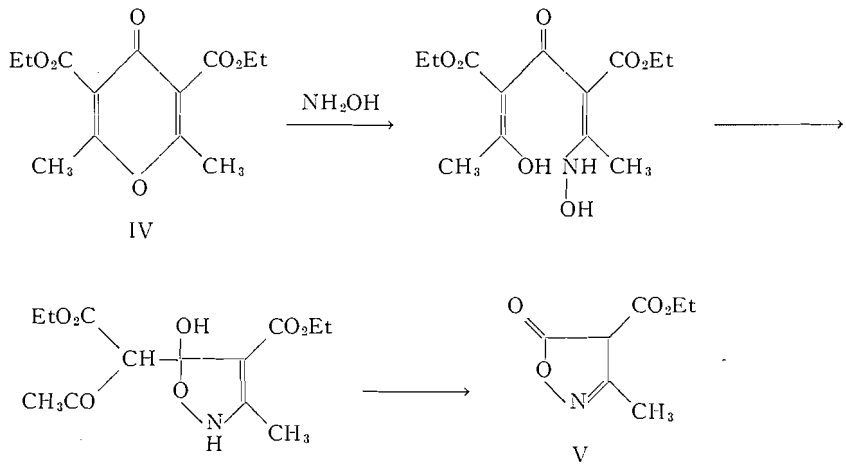

IV V

Related complexities often attend the reactions of 4-pyrones with other amines; thus, Ainsworth and Jones (5) have observed that 2,6-dialkyl-4-pyrones (VI) give pyrazole derivatives (VII) with phenylhydrazine and its derivatives.

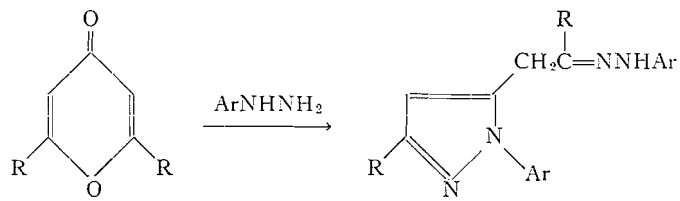

VI VII

In connection with studies on the oximes of the photodimers of 4-pyrones (6) we have had occasion to examine the reactions of hydroxylamine with 2,6-dimethyl- and 2,6-diethyl-4-pyrone and have found that here too simple derivative formation does not occur.

Treatment of 2,6-dimethyl-4-pyrone with an excess of hydroxylamine hydrochloride and pyridine in boiling ethanol gives two crystalline products. When pure these are colorless, but in the presence of traces of bases or of light they rapidly assume a yellow or pink color. Their elemental composition corresponds to the empirical formulae $C_7H_{10}N_2O_2$ and $C_7H_{10}N_2O_2.HCl$. The latter compound was demonstrated to be the hydrochloride of the former by the interconversion of the two products under mild conditions.

The ultraviolet spectrum (λ_{max}^{EtOH} 280 mμ (log ϵ 4.31), 215 mμ (shoulder, log ϵ 4.27)) of the free base, $C_7H_{10}N_2O_2$, closely resembles that of 4-amino-2,6-lutidine 1-oxide (VIII*a*)[3] (λ_{max}^{EtOH} 275 mμ (log ϵ 4.23), 210 mμ (apparent, log ϵ 4.21)). Its infrared spectrum (Nujol) shows strong bands at 3.10, 6.10, and 8.37 μ. This product is therefore assigned structure IX*a*, whose formation involves, in undetermined order, ring opening, reclosure, and oxime formation by the pyrone. This formulation is preferred to the tautomeric structure X on the basis of the presence of a very strong band at 8.37 μ in the infrared spectrum of the compound, which may be assigned to the N^+—O^- group (9), and of analogy to the case of 4-aminopyridine-1-oxide (VIII*b*) (10).

[3]*Prepared by hydrogenation of 4-nitro-2,6-lutidine 1-oxide (7); this compound has been prepared independently in similar fashion by other workers (8).*

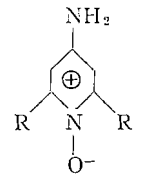

VIII*a*, R = CH_3
VIII*b*, R = H

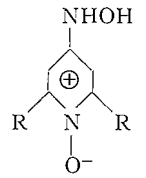

IX*a*, R = CH_3
IX*b*, R = C_2H_5

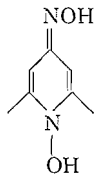

X

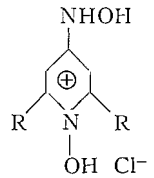

XI*a*, R = CH_3
XI*b*, R = C_2H_5

The ultraviolet spectrum of the hydrochloride, $C_7H_{10}N_2O_2.HCl$, is very similar to that of the parent base, and its infrared spectrum (λ_{max}^{Nujol} 3.20, 3.65 (sh), 3.80 (sh), 6.10 μ) shows only medium intensity absorption in the 7.5- to 8.5-μ region. This product is therefore considered to have structure XI*a*, rather than that derived by protonation of the nitrogen atom of the hydroxyamino group in IX*a*. The observed position of protonation is in accord with expectation based on theoretical considerations and on analogy with the case of VIII*b* (10, 11).

When either IX*a* or XI*a* is treated with aqueous 10% sodium hydroxide, a deep red coloration immediately occurs and an orange-red crystalline product, $C_{14}H_{16}N_4O_2$, is formed. The source and color of this compound suggested that it is the azo compound XII*a*. This view is supported by the close correspondence of its ultraviolet spectrum

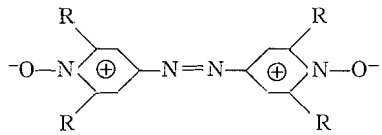

XII*a*, R = CH_3
XII*b*, R = H
XII*c*, R = C_2H_5

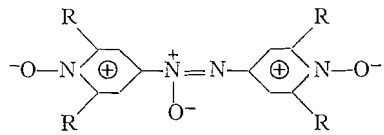

XIII*a*, R = CH_3
XIII*b*, R = H
XIII*c*, R = C_2H_5

to that of 4,4′-azodipyridine 1,1′-dioxide (XII*b*) (Table I). An independent synthesis of XII*a* was therefore carried out by the reduction of 4-nitro-2,6-lutidine 1-oxide with sodium nitrite and base (12):[4] the product was shown to be identical with that obtained from IX*a* or XI*a*.

TABLE I

Ultraviolet spectra

	λ_{max}^{EtOH} (mμ)	log ϵ
4,4′-Azodipyridine 1,1′-dioxide (XII*b*)*	405	4.5
	255	4.05
4,4′-Azodi-2,6-lutidine 1,1′-dioxide (XII*a*)	401	4.53
	258	4.12
4,4′-Azodi-2,6-diethylpyridine 1,1′-dioxide (XII*c*)	408	4.59
	260	4.16
4,4′-Azoxydipyridine 1,1′-dioxide (XIII*b*)*	395	4.4
	250	4.1
4,4′-Azoxydi-2,6-lutidine 1,1′-dioxide (XIII*a*)	393	4.39
	249	4.05
4,4′-Azoxydi-2,6-diethylpyridine 1,1′-dioxide (XIII*c*)	399	4.40
	252	4.04

*H. J. den Hertog, C. H. Henkens, and J. H. van Roon. Rec. Trav. Chim. **71**, 1145 (1952).

[4]*After this phase of our investigation had been completed, a report (8) became available to us which describes the preparation of XII*a *and XIII*a *from 4-nitro-2,6-lutidine 1-oxide by methods similar to those described here.*

Exposure of aqueous solutions of IX*a* or XI*a* to light leads to the formation of a yellow crystalline product, $C_{14}H_{16}N_4O_3$. The same product is obtained much more rapidly when these compounds are treated with dilute aqueous ammonia or with aqueous sodium bicarbonate. Its ultraviolet spectrum (Table I) and infrared spectrum are similar to those of XII*a*. It was established to be the azoxy compound XIII*a* by its independent synthesis by the reduction of 4-nitro-2,6-lutidine 1-oxide with zinc (12).[4]

The formation of the azoxy compound XIII*a* from the hydroxylamine derivative IX*a* is analogous to the formation of azoxybenzene from *N*-phenylhydroxylamine. One route for the latter reaction has been found to involve oxidation of the hydroxylamine with atmospheric oxygen (13). This has been shown also to be the case for the present reaction, since it was found that XI*a* is not converted to the azoxy compound by the action of light nor by aqueous sodium bicarbonate when air is rigidly excluded from the reaction system. The formation of the azoxy compound can then be suggested to occur by the following route, analogous to that proposed for the formation of azoxybenzene (13(*a*), 14):

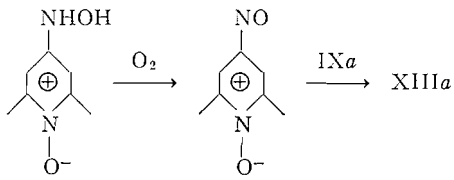

IX*a* XIV

The photochemically induced oxidation of the hydroxyamino compound IX*a* to the nitroso compound XIV may be analogous to other autoxidation reactions, which are accelerated by light (15). The formation of XIII*a* in the presence of either aqueous ammonia or sodium bicarbonate (pH 7–9) proceeds in the absence of light. The pH of the reaction solution plays a critical role in the dark reaction, for at pH 5–6 no azoxy compound is formed, while at pH 12–13 (aqueous sodium hydroxide) only the azo compound XII*a* is formed; however, the data available at present do not permit the designation of the function of the basic reagents in the formation of the azoxy compound.[5]

The formation of the azo compound at pH 12–13 was found to proceed in the absence of both air and light.[6] It is possible that this reaction involves proton abstraction from IX*a* by hydroxide ion to form XV. Formation of the azo compound XII*a* could then occur either by α-elimination to give XVI followed by reaction of this with unchanged hydroxyamino compound IX*a* (route A) or by hydride transfer to IX*a* to give the disproportionation products XIV and VIII*a* followed by condensation of these (route B). The fact that no azoxy compound is formed under the strongly basic conditions militates against, but does not exclude, the intermediacy of the nitroso compound XIV in this case; route A is therefore preferred.

The reaction of 2,6-diethyl-4-pyrone with hydroxylamine hydrochloride and pyridine follows a similar course to that of the 2,6-dimethyl compound, giving the hydroxyamino compound IX*b*. Treatment of this product with aqueous 10% sodium hydroxide yields the azo compound XII*c*. In the case of IX*b*, unlike that of IX*a*, treatment with concentrated aqueous ammonia in the presence of air yields a mixture of azoxy compound

[5]*Bases have also been found to accelerate the oxidation of N-phenylhydroxylamine by air (13). The influence of pH on the autoxidation of amines is known to be complex (16).*

[6]*In the absence of air, N-phenylhydroxylamine gives azoxybenzene and aniline when treated with aqueous sodium hydroxide, while on treatment with ethanolic hydroxide it gives azobenzene as the sole product (13(b)).*

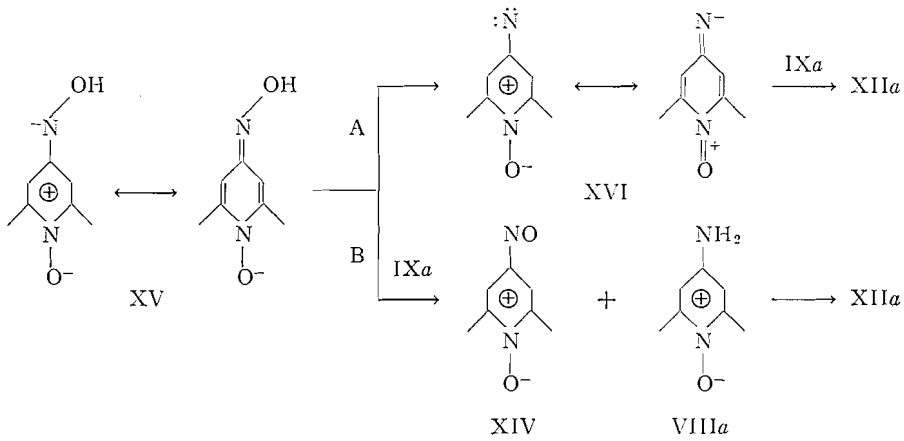

(XIII*c*) and azo compound (XII*c*) in comparable quantities. However, the azoxy compound is the sole product when an aqueous solution of IX*b* is irradiated. The structures XII*c* and XIII*c* are assigned to these products on the basis of their origin and elemental analyses and the correspondence of their infrared and ultraviolet spectra (Table I) to those of the azo and azoxy compounds obtained in the 2,6-dimethyl series.[7]

EXPERIMENTAL[8]

Reaction of 2,6-Dimethyl-4-pyrone with Hydroxylamine. Formation of IXa and XIa[9]

A mixture of 2,6-dimethyl-4-pyrone (20.0 g, 0.16 mole), hydroxylamine hydrochloride (20.0 g, 0.28 mole), dry pyridine (120 ml), and ethanol (120 ml) was boiled under reflux for 6 hours. The ethanol was then removed at room temperature under reduced pressure and the remaining solution was treated with water (50 ml) and cooled at 0° for 72 hours. The yellow solid (14.0 g) which separated was crystallized from a mixture of aqueous ethanol and chloroform to give IX*a* as pale yellow plates (2.7 g, 11%). This was recrystallized five times from methanol/acetone, giving colorless plates. The product did not melt sharply: when heated above 100° it turned yellow and a slow transition to a red-colored product occurred between 100° and 200°, followed by melting at ca. 200°.

Anal. Calc. for $C_7H_{10}N_2O_2$: C, 54.53; H, 6.54; N, 18.17. Found: C, 54.54; H, 6.66; N, 18.40.

λ_{max}^{Nujol} 2.85 (w), 3.10 (sh), 6.10 (vs), 8.37 (vs) μ; λ_{max}^{EtOH} 215 mμ (sh, log ϵ 4.27), 280 mμ (log ϵ 4.31).

Ethanol and chloroform were removed at room temperature under reduced pressure from the mother liquor from the first crystallization of IX*a*. The remaining yellow aqueous solution was treated with acetone and cooled at 0° for several days to give XI*a* as pale yellow plates (2.2 g, 9%). This was recrystallized seven times from aqueous acetone, giving colorless plates whose behavior on heating was similar to that of IX*a*.

Anal. Calc. for $C_7H_{11}ClN_2O_2$: C, 44.09; H, 5.82; Cl, 18.63; N, 14.70. Found: C, 44.04; H, 6.15; Cl, 18.35; N, 14.65.

λ_{max}^{Nujol} 3.20 (vs), 3.65 (sh), 3.80 (sh), 6.10 (vs), 8.30 (m), 8.45 (m); λ_{max}^{EtOH} 218 mμ (log ϵ 4.13), 280 mμ (log ϵ 4.27).

Reaction of XIa with Pyridine. Formation of IXa

A mixture of XI*a* (0.15 g) and dry pyridine (2 ml) was stirred until solution was complete (4–5 minutes). Most of the pyridine was removed under reduced pressure and the residue was dissolved in water (10 ml). The solution was treated with chloroform (70 ml) and the mixture was cooled at 0° for several hours, when a solid (0.072 g) separated. This was shown to be identical with IX*a* by infrared spectral comparison.

Reaction of IXa with Hydrochloric Acid. Formation of XIa

A solution of IX*a* (0.10 g) in dilute hydrochloric acid (1:10; 10 ml) was treated with acetone (70 ml). The solution was cooled at 0° for several days, when a solid (0.044 g) separated, which was shown to be identical with XI*a* by infrared spectral comparison.[10]

[7]*After this manuscript had been completed, Dr. A. R. Katritzky, Cambridge University, kindly drew our attention to the fact that related results have recently been reported for the case of 4-pyrone (17).*

[8]*Melting points are uncorrected.*

[9]*These products were found to be very sensitive to light and bases (vide infra); their preparation and purification were carried out in acid-washed glassware in the dark or in subdued light.*

[10]*For storage, it was found advantageous to convert IXa to the hydrochloride.*

4-Amino-2,6-lutidine 1-Oxide (VIIIa)

A solution of 4-nitro-2,6-lutidine 1-oxide (7) (0.51 g) in ethanol (75 ml) was hydrogenated over 5% palladium–charcoal (0.053 g). After 1 hour 3 molar equiv. of hydrogen had been absorbed. The solution was then filtered and the ethanol was removed under reduced pressure. The residue was recrystallized from ethanol/benzene to give VIII*a* as white needles, m.p. 265° decomp. (lit. (8) m.p. 264–266°); λ_{max}^{Nujol} 2.80, 3.00, 5.90 (sh), 6.05, 8.35, 8.45 μ; λ_{max}^{EtOH} 275 mμ (log ϵ 4.23), 210 mμ (apparent, log ϵ 4.21).

Reaction of XIa with Aqueous Bases[11]

(i) pH 12–13. Formation of XIIa

A solution of XI*a* (0.30 g) in water (20 ml) was brought to pH 12–13 with aqueous 10% sodium hydroxide. The resulting dark red solution immediately deposited a fluffy, orange-red solid (0.20 g, 90%). Crystallization from aqueous ethanol afforded XII*a* as orange-red needles, m.p. 257–259° decomp.

Anal. Calc. for $C_{14}H_{16}N_4O_2$: C, 61.75; H, 5.92; N, 20.58. Found: C, 61.50; H, 5.91; N, 20.31.

$\lambda_{max}^{CHCl_3}$ 3.0 (w), 4.1 (w), 6.18, 6.40, 6.86, 7.28, 8.82 μ.

When this experiment was performed with the rigid exclusion of oxygen, XII*a* was again obtained in 80% yield. The same product was also obtained when the reaction was carried out in the dark.

The azoxy compound XIII*a* was recovered unchanged after treatment with aqueous 10% sodium hydroxide.

(ii) pH 7–9. Formation of XIIIa

A solution of XI*a* (0.055 g) in water (10 ml) was brought to pH 7–8 with aqueous 10% sodium bicarbonate. During 30 minutes a yellow solid (0.037 g, 85%) was deposited. Crystallization from aqueous ethanol gave XIII*a* as yellow needles, m.p. 248–250° decomp.

Anal. Calc. for $C_{14}H_{16}N_4O_3$: C, 58.32; H, 5.59; N, 19.44. Found: C, 58.22; H, 5.56; N, 19.31.

$\lambda_{max}^{CHCl_3}$ 3.0 (w), 4.1 (w), 6.19, 6.45, 6.71, 7.26, 8.75, 9.12 μ.

The azo compound XII*a* was recovered unchanged after subjection to the conditions of this experiment.

When XI*a* was treated with aqueous 10% sodium bicarbonate with the exclusion of oxygen, no reaction occurred.

Treatment of an aqueous solution of XI*a* with dilute aqueous ammonia at pH 8–9 in the presence of air also gave XIII*a* (70%); the reaction proceeded in both the presence and absence of light. Concentration of the aqueous mother liquor in this case gave further XIII*a* and a trace of the azo compound XII*a*, identified by infrared spectral comparison and mixture melting point.

Effect of Light on XIa.[11] *Formation of XIIIa*

When an aqueous solution of XI*a* (pH 5–6) was exposed to daylight it turned yellow and slowly deposited yellow needles of XIII*a*, identified by infrared spectral comparison and melting point. When oxygen was rigidly excluded from the solution, no reaction occurred.

4,4′-Azodi-2,6-lutidine 1,1′-Dioxide (XIIa)

An authentic sample of this compound was prepared by the reduction of 4-nitro-2,6-lutidine 1-oxide (7) with aqueous sodium nitrite and sodium hydroxide according to the method used by Ochiai (12) for the preparation of 4,4′-azodipyridine 1,1′-dioxide from 4-nitropyridine 1-oxide. The product crystallized from ethanol as orange-red needles, m.p. 257–259° decomp. (lit. (8) m.p. 248° decomp.).[12] This was shown by infrared spectral comparison and a mixture melting point determination to be identical with the product, m.p. 257–259° decomp., obtained from XI*a*.

4,4′-Azoxydi-2,6-lutidine 1,1′-Dioxide (XIIIa)

An authentic sample of this compound was prepared by the reduction of 4-nitro-2,6-lutidine 1-oxide (7) in aqueous solution with zinc according to the method used by Ochiai (12) for the preparation of 4,4′-azoxydipyridine 1,1′-dioxide from 4-nitropyridine 1-oxide. The product crystallized from ethanol as yellow needles, m.p. 248–250° decomp. (lit. (8) m.p. 233° decomp.).[12] This was shown by infrared spectral comparison and a mixture melting point determination to be identical with the product, m.p. 248–250° decomp., obtained from XI*a*.

Reaction of 2,6-Diethyl-4-pyrone with Hydroxylamine. Formation of IXb

A solution of 2,6-diethyl-4-pyrone (5 g, 0.033 mole) and hydroxylamine hydrochloride (5 g, 0.072 mole) in ethanol (30 ml) and pyridine (30 ml) was boiled under reflux for 6 hours. The reaction mixture was freed from solvent under reduced pressure. The brown oily residue was dissolved in water (20 ml) and cooled at 0° for 72 hours, when a viscous oil separated. The aqueous solution was decanted and cooled at 0° for a further 48 hours, giving a yellow solid deposit (1.2 g, 20%). Several crystallizations from ethanol/acetone gave IX*b* as colorless flakes. This product did not melt sharply; when heated at 135° it turned yellow and melted with decomposition at ca. 170°.

[11]*Similar results were obtained with the parent compound, IXa.*

[12]*The melting points of the azo and azoxy compounds are very sensitive to the rate of heating; we have also obtained melting points similar to those reported earlier (8).*

Anal. Calc. for $C_9H_{14}N_2O_2$: C, 59.32; H, 7.74; N, 15.38. Found: C, 59.06; H, 7.79; N, 15.41.
λ_{max}^{Nujol} 3.2 (sh), 3.75 (sh), 6.12 (s), 8.45 (m), 8.56 (m) μ.

Reaction of IXb with Aqueous Bases

(i) pH 12–13. Formation of XIIc

A solution of IX*b* (0.10 g) in water (4 ml) was brought to pH 12–13 with aqueous 10% sodium hydroxide. The azo compound XII*c* (0.060 g, 65%) precipitated rapidly and after crystallization from aqueous ethanol was obtained as red needles, m.p. 176–177°.

Anal. Calc. for $C_{18}H_{24}N_4O_2$: C, 65.83; H, 7.37; N, 17.07. Found: C, 65.54; H, 7.46; N, 16.97.
$\lambda_{max}^{CHCl_3}$ 2.95 (w), 4.1 (w), 6.20, 6.41, 6.83, 8.82 μ.

(ii) pH 7–9. Formation of XIIc and XIIIc

When aqueous solutions of IX*b* were brought to pH 7–9 with either aqueous 10% sodium bicarbonate or dilute aqueous ammonia, an orange-colored product was deposited which was shown to be a mixture of the azo compound XII*c* and the azoxy compound XIII*c* by infrared spectral comparison.

Irradiation of IXb. Formation of XIIIc

A solution of IX*b* (0.10 g) in water (10 ml) was irradiated with a fluorescent lamp for 60 hours. A red crystalline solid (0.055 g) separated. The aqueous mother liquor was extracted with ethyl acetate and the extract was dried and freed of solvent under reduced pressure, giving an orange solid (0.021 g). The combined solid material (80%) was crystallized three times from aqueous ethanol and once from petroleum ether (b.p. 60–70°) to give XIII*c* as orange needles, m.p. 127–128°.

Anal. Calc. for $C_{18}H_{24}N_4O_3$: C, 62.77; H, 7.02; N, 16.27. Found: C, 62.61; H, 7.09; N, 16.11.
$\lambda_{max}^{CHCl_3}$ 2.95 (w), 4.1 (w), 6.18, 6.46, 6.75, 8.76, 9.05 μ.

ACKNOWLEDGMENTS

We gratefully acknowledge fellowship support (M. J. J.) from the National Institutes of Health, United States, and a grant, which supported part of this work, from the National Research Council, Canada.

REFERENCES

1. L. F. CAVALIERI. Chem. Rev. **41**, 525 (1947).
2. J. FRIED. *In* Heterocyclic compounds. Vol. I. *Edited by* R. C. Elderfield. John Wiley and Sons, Inc., New York, N.Y. 1950. p. 342.
3. A. PERATONER and A. TAMBURELLO. Gazz. Chim. Ital. **41**, I, 666 (1911).
4. F. PALAZZO. Gazz. Chim. Ital. **34**, I, 458 (1904); **36**, I, 596 (1906).
5. C. AINSWORTH and R. G. JONES. J. Am. Chem. Soc. **76**, 3172 (1954).
6. P. YATES and M. J. JORGENSON. J. Am. Chem. Soc. **80**, 6150 (1958). P. YATES and E. S. HAND. Tetrahedron Letters, 669 (1961).
7. M. ISHIKAWA. J. Pharm. Soc. Japan, **65**, No. 3A, 6 (1945).
8. T. KATO and F. HAMAGUCHI. Pharm. Bull. (Tokyo), **4**, 174 (1956).
9. A. R. KATRITZKY and J. N. GARDNER. J. Chem. Soc. 2192 (1958). A. R. KATRITZKY and A. R. HANDS. J. Chem. Soc. 2195 (1958).
10. H. H. JAFFÉ. J. Am. Chem. Soc. **77**, 4445 (1955). J. N. GARDNER and A. R. KATRITZKY. J. Chem. Soc. 4375 (1957).
11. H. HIRAYAMA and T. KUBOTA. J. Pharm. Soc. Japan, **73**, 140 (1953). H. H. JAFFÉ. J. Am. Chem. Soc. **76**, 3527 (1954).
12. E. OCHIAI and I. SUZUKI. J. Pharm. Soc. Japan, **67**, 30 (1947). E. OCHIAI. J. Org. Chem. **18**, 534 (1953).
13. (*a*) E. BAMBERGER. Ber. **33**, 113 (1900).
(*b*) E. BAMBERGER and F. BRADY. Ber. **33**, 271 (1900).
14. Y. OGATA, M. TSUCHIDA, and Y. TAKAGI. J. Am. Chem. Soc. **79**, 3397 (1957).
15. C. WALLING. Free radicals in solution. John Wiley and Sons, Inc., New York, N.Y. 1957. Ch. 9.
16. J. E. LUVALLE, D. B. GLASS, and A. WEISSBERGER. J. Am. Chem. Soc. **70**, 2223 (1948).
17. F. PARISI, P. BOVINA, and A. QUILICO. Gazz. Chim. Ital. **90**, 903 (1960).

STEROIDS AND RELATED PRODUCTS

XIX.[1] THE SYNTHESIS OF 3,9,12,20-TETRAOXYGENATED 9,12-*seco* STEROIDS. PART III.[2] 11-AZA STEROIDS. PART I[3]

CH. R. ENGEL AND S. RAKHIT[4]
Department of Chemistry, Laval University, Quebec, Que.
Received July 9, 1962

ABSTRACT

The smooth conversion of 3β-acetoxy-5α-pregnane-12,20-dione (IV), readily available from hecogenin (I), to $\Delta^{9(11)}$-3β,20β-diacetoxy-5α-pregnan-12-one (VIII) is reported. Ozonolysis of this product in ethyl acetate gave, in almost 90% yield, 3β-hydroxy-20β-acetoxy-9-oxo-9,12-*seco*-11-nor-5α-pregnan-12-oic acid (XI), further characterized by its ester derivatives XI*a* and XI*b*. The conversion of the *seco* acid XI to $\Delta^{8(9)}$-3β-hydroxy-20β-acetoxy-9-amino-9,12-*seco*-11-nor-5α-pregnen-12-oic acid lactam (12 → 9) (XII) and thence to $\Delta^{8(9)}$-N-acetyl-3β,20β-diacetoxy-11-aza-5α-pregnene (XIV*a*), the first 11-aza steroids to be known, is described. On the other hand, $\Delta^{9(11)}$-3β,20β-diacetoxy-5α-pregnen-12-one (VIII) is readily transformed to the 9α,11α-glycol VII with osmium tetroxide and thence, with periodic acid, to 3β,9α-dihydroxy-20β-acetoxy-11-oxo-11,12-*seco*-5α-pregnan-12-oic acid (X), characterized as the methyl ester X*a* and diacetoxy methyl ester X*b*, and easily converted to the acetoxy hydroxy keto dicarboxylic *seco* acid XIII. In the course of this work it is shown that, whereas ketalization of the saturated 12,20-diketone IV with ethylene glycol and boron trifluoride etherate gives a good yield of the 12-monoketal (in accordance with the reports of the literature), treatment of the analogous 16-unsaturated 12,20-diketone with the same reagents under the same conditions leads not to ketal formation but to addition of ethylene glycol in position 16.

In Part II of this study (2) we showed that the opening of ring C of the steroid molecule, by ozonolysis of a 9,11-unsaturated 12-ketone, proceeded with significantly better yields in the case of a trans fusion of rings A and B than in the case of a cis fusion of these rings (cf. also ref. 3). We were thus able to prepare 3β,20α-dihydroxy-9-oxo-9,12-*seco*-11-nor-5α-pregnan-12-oic acid, the 20-epimer of the saponification product of XI, in 17% yield, from the corresponding $\Delta^{9(11)}$-12-ketone.

We intended to use 3,20-dioxygenated 9-oxo-9,12-*seco*-12-pregnanoic acids as starting materials for the synthesis of 11-aza steroids. The investigation of such compounds appears attractive not only in view of the chemical and biological interest of natural steroid alkaloids but also in consideration of the possible biological importance of certain aza derivatives of steroid hormones. Among the great number of aza derivatives of steroid hormones, the synthesis of which can be contemplated, we regard of greatest interest those in which the nitrogen function occupies a position of established biological importance. Such compounds should not only be investigated for their hormone-like activities but also for their hormone-antagonistic properties. To date no true 11-aza steroids, with an unexpanded C-ring, have been described, in spite of the biological significance of the 11-position, primarily with respect to gluco-corticoid activity. This, however, is not surprising since such 11-aza steroids cannot be obtained by a simple Beckmann rearrangement of readily available steroids and because of the difficulty of the synthesis of ring C-*seco* derivatives suitable for further transformations to 11-aza derivatives.[5]

[1] *For the previous paper of this series, see ref. 1.*
[2] *For Part II of this series, see ref. 2.*
[3] *Some of the results reported in this paper were presented in communications before the XXIXth and XXXth Congresses of the French Canadian Association for the Advancement of Science, Ottawa, October 1961, and Montreal, November 1962.*
[4] *National Research Council of Canada Postdoctorate Fellow, 1960–1962. Present address: Worcester Foundation for Experimental Biology, Shrewsbury, Mass., U.S.A.*
[5] *Valuable lists of references on aza steroids are contained in the article by Mazur (4) on 12a-aza-C-homo steroids and in that by Jacobs and Brownfield (5) on 6-aza steroids.*

Under the circumstances, a reinvestigation and improvement of the synthesis of 3,20-dioxygenated 9-oxo-9,12-*seco*-12-pregnanoic acids seemed called for. At first, the yields of the actual opening of ring C, by ozonolysis of a 9,11-unsaturated 12-ketone, were, even in the A/B-trans series, still not very satisfactory. Furthermore, our previous synthesis made use of a somewhat tedious partial acetylation, in positions 3β and 20α, of 5α-pregnane-3β,12β,20α-triol (2). As we endeavor to show in this paper, we have now surmounted both these difficulties and we were also able to introduce, with concomitant recyclization, a nitrogen function in lieu of the 11-carbon atom.

As in our previous experiments, 3β-acetoxy-5α-pregnane-12,20-dione (IV), readily available from hecogenin (I) through the Δ^{16}-12,20-diketone II, served as starting material. Instead of reducing this product to a 3,12,20-triol, protecting the alcohol functions in positions 3 and 20 by partial esterification, and reoxidizing the unprotected 12-hydroxy group to a 12-ketone (2), we protected the 12-ketone by preferential ketalization with ethylene glycol and the boron trifluoride ether complex (6, 7), reduced the 12-monoketal V with lithium aluminum hydride or with sodium borohydride to the 3β,20β-dihydroxy ketal VI (7), removed the 12-ketal protection by an exchange reaction with acetone in the presence of *p*-toluenesulphonic acid (cf. ref. 8), and acetylated the thus-obtained 3β,20β-dihydroxy 12-ketone IX (cf. ref. 7) to the diacetate IX*a* (7). Be effecting the ketalization reaction in a homogeneous medium we were able to raise the yield of this step from the 57%, obtained by following the procedure of Petrow's group (7), to 74%. The British authors did not establish the configuration of the 20-hydroxy function of compounds VI, IX, and IX*a*, formed by metal hydride reduction of the ketone V; with the help of molecular rotational differences, we can, however, assign without hesitation the β-configuration to this hydroxyl function. Indeed, acetylation of the 20-hydroxy group results in an increment of molecular rotation of 145° (cf. ref. 7), which is in excellent agreement with a β-configuration, but which contrasts with the results obtained upon acetylation of a 20α-hydroxy group (9). Thus, the reduction of a 20-ketone with metal hydrides, in the presence of a 12-ethylenedioxy substituent, takes the same stereochemical course as in the presence of a 12α-acetoxy function (3) but differs stereochemically from the reduction of a 20-ketone in the presence of a 12α-hydroxy or a 12-keto function (2, 10). We consider these findings of interest and we shall discuss them in connection with their implications on the conformation of the methyl ketone side chain in the following paper of this series (11).

We also investigated the possibility of partial ketalization of the 16-unsaturated 12,20-diketone II. Since α,β-unsaturated ketones are ketalized less readily than the corresponding saturated ketones, one could consider the possibility of increasing the selectivity of ketalization in position 12 by using the unsaturated diketone II as the substrate. However, since the Δ^{16}-20-keto moiety of the diketone II assumes predominantly a *s*-trans conformation (cf. ref. 12),[6] the 12-keto function is markedly hindered; it is therefore not surprising that under the previously described reaction conditions, the 12-ketone is not attacked. It is furthermore understandable that no ketalization in position 20 occurs. We found that, under the circumstances, ethylene glycol is added to the Δ^{16}-double bond (compare III); the spectra of the reaction product and of its acetate, III*a*, show the absence of the Δ^{16}-20-keto chromophore and agree in every respect with the

[6]*As a matter of fact, the α,β-unsaturated diketone II does not exist wholly in the s-trans conformation, as indicated by the ratio of the integrated band intensities of the 20-*C=O *and 16,17-*C=C *stretching vibrations in the infrared (5.18; for values of fixed s-cisoid and fixed s-transoid systems, see ref. 13) and by the extinction coefficient of the ultraviolet absorption band of the Δ^{16}-20-keto moiety (8150; for mean values of s-cisoid and s-transoid systems, compare refs. 13 and 14).*

proposed structure. The analytical data of the adduct III*a*, including an acetyl determination, are in excellent agreement with the assigned constitution; the tetranitromethane test indicates the absence of a double bond; furthermore, even prolonged and vigorous treatment of the acetylated reaction product (compare III*a*) with acetone and *p*-toluenesulphonic acid does not restore the chromophore of the α,β-unsaturated ketone, which also demonstrates that the absence of this chromophore in the adducts III and III*a* is not due to ketalization of the 20-ketone. By analogy with the findings of Mattox (15) and Gould *et al.* (16), who described the acid-catalyzed addition of monohydric alcohols to Δ^{16}-20-ketones, we can assume that the 16-hydroxyalkyl moiety of compound III occupies the α-configuration.[7]

We now reverted to the main pathway of our synthesis and introduced, as previously (2, 3), the $\Delta^{9(11)}$-double bond into the diacetoxy ketone IX*a*, with selenium dioxide (19), achieving a yield of 85%. Ozonolysis of the resulting unsaturated diacetoxy ketone, VIII, under conditions analogous to those employed in the previous experiments of the series (2, 3), in ethyl acetate – acetic acid, gave a 67.5% yield of crystalline 3β-hydroxy-20β-acetoxy-9-oxo-9,12-*seco*-11-nor-5α-pregnan-12-oic acid (XI), further characterized by its methyl ester derivative, XI*a*, and its diacetoxy methyl ester, XI*b*. We were able to raise the yield of the ozonolysis reaction further, to almost 90%, by performing the reaction in ethyl acetate without the addition of acetic acid. We have thus solved the problem of synthesizing in high yield, by a simple route, a 3,20-dioxygenated 9,12-*seco*-9-keto-12-pregnanoic acid suitable for transformations to 11-aza steroids.

As a matter of interest, we wished to study the possibility of applying the osmium tetroxide – periodate fission of double bonds, discovered by Pappo *et al.* (20), to the transformation of $\Delta^{9(11)}$-12-keto steroids to ring C-*seco* derivatives. However, this procedure gave unsatisfactory results and no well-defined reaction product could be isolated from the obtained mixture apart from appreciable amounts of starting material. We therefore prepared and isolated the diacetoxy keto glycol VII, employing the usual osmium tetroxide oxidation in pyridine, under the conditions described by Baran (21). We assign the 9α,11α-configuration to the glycol VII, since attack from the α-side is much less hindered than attack from the β-side; Hirschmann *et al.* (22) have attributed the same configuration to a glycol obtained by osmium tetroxide oxidation of a 9,11-double bond. Treatment of glycol VII with periodic acid in dioxane–water gave an amorphous aldehydo acid to which we assign the structure of 3β,9α-dihydroxy-20β-acetoxy-11-oxo-11,12-*seco*-5α-pregnan-12-oic acid (X). The product gave with diazomethane a crystalline methyl ester, X*a*, which afforded upon treatment with acetic anhydride in pyridine, at room temperature, the 3β,20β-diacetoxy methyl ester X*b*; oxidation of the amorphous dihydroxy acetoxy aldehydo acid X with chromic acid, in acetone and sulphuric acid, gave the crystalline 20β-acetoxy-9α-hydroxy-3-oxo-11,12-*seco*-5α-pregnane-11,12-dioic acid (XIII). When the oxidation of glycol VII was carried out in methanol–water, an appreciable part of the reaction product consisted of methyl ester X*a*.

Although the *seco* aldehydo acid X and the *seco* dicarboxylic acid XIII present considerable interest as intermediates for the synthesis of 11-aza steroids, we decided to study first, as originally planned, the transformation of 9-oxo-9,12-*seco*-12-pregnanoic acids of type XI to 11-aza pregnane derivatives. Since we had found (23) that even in the A/B-trans series the 9-keto function of 9-keto-9,12-*seco*-12-acids of type XI was extremely resistant to oxime formation,[8] we attempted to transform the *seco* keto acid

[7] *Adams et al. (17) reported that in the presence of a 12-ketone the base-catalyzed addition of methanol to Δ^{16}-20-ketones (cf. ref. 18) is markedly facilitated.*

[8] *Wieland and Posternak (24) reported already in 1931 that an analogous 3,20-non-oxygenated seco keto acid of the A/B-cis series did not yield an oxime.*

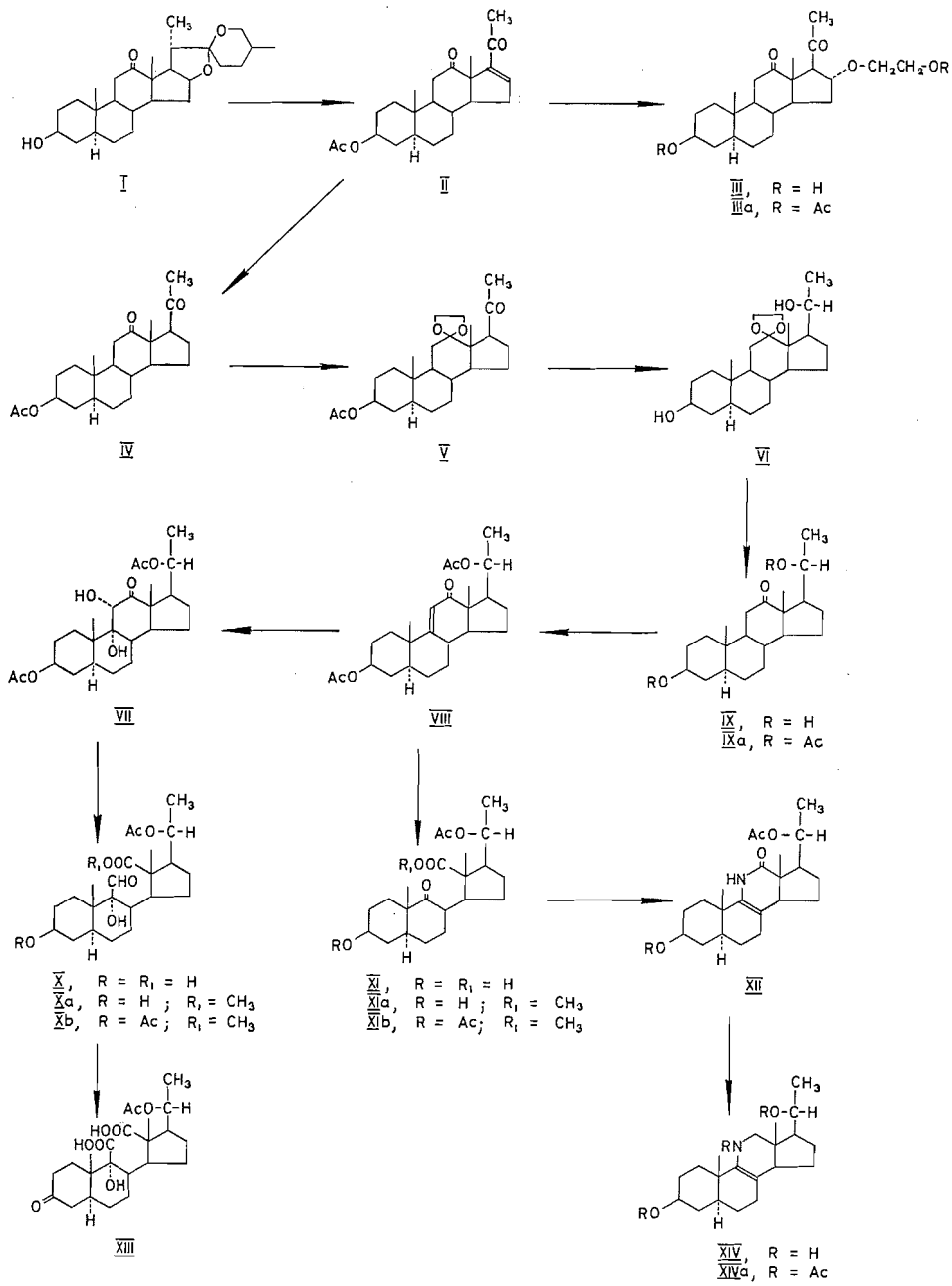

XI to the unsaturated lactam XII, by treatment with alcoholic ammonia in a sealed tube (cf. ref. 5). The lactam XII was indeed formed in very good yield (77.5%) and could be reduced by prolonged treatment with lithium aluminum hydride in boiling tetrahydrofuran to $\Delta^{8(9)}$-3β,20β-dihydroxy-11-aza-5α-pregnene (XIV), characterized as the N-acetyl-3β,20β-diacetate XIV*a*. The spectral and analytical data of the compounds XII and XIV*a*, *which represent the first known 11-aza steroids with an unexpanded C-ring*, fully

corroborate the assigned structures. In subsequent papers of this series we shall describe other reactions of the 9-keto-9,12-*seco*-12-acid XI, the reduction of the unsaturated 11-aza steroids XII and XIV*a*, and the preparation of further 11-aza derivatives.

EXPERIMENTAL[9, 10, 11]

3β-Acetoxy-16α-(2-acetoxyethoxy)-5α-pregnane-12,20-dione (IIIa)

A suspension of 530 mg of Δ^{16}-3β-acetoxy-5α-pregnene-12,20-dione (II) (13, 25; cf. also refs. 2 and 26), m.p. 178–180°, in 4 cc of freshly distilled ethylene glycol and 0.7 cc of boron trifluoride etherate, was shaken at room temperature for 72 hours. Subsequently, the dark brown solution was stirred into a cold sodium bicarbonate solution and the precipitate was extracted with ether. The organic layer was washed with water and was dried over sodium sulphate. Removal of the solvent afforded the crude amorphous product of the addition of ethylene glycol to the Δ^{16}-double bond (compare III) which showed no ultraviolet absorption typical of an α,β-unsaturated ketone, and the infrared spectrum of which revealed the hydrolysis of the 3-acetate; ν_{max}^{KBr} 3430 cm^{-1} (broad dihydroxy band), 1706 cm^{-1} (broad 12,20-diketo band), 1066 and 1045 cm^{-1} (complex hydroxy and ether bands). The crude product was acetylated with 2 cc of acetic anhydride in 4 cc of pyridine, at room temperature, for 16 hours. The usual working up yielded 435 mg of a yellow amorphous product which, upon crystallization from ether, gave 200 mg of the diacetylated addition product (III*a*), m.p. 121–122°. The mother liquors were dissolved in petroleum ether – benzene (4:1) and absorbed on 10 g of aluminum oxide, activity III. Elutions with petroleum ether – benzene mixtures (1:1 and 1:4) yielded another 155 mg of crystalline diacetate III*a*, m.p. 120–121° (total yield 60%). A sample was recrystallized three times from ether–hexane for analysis. Colorless needles; m.p. 124.5–125.5°; $[\alpha]_D^{25}$ 42° (*c*, 1.000 in $CHCl_3$); ν_{max}^{KBr} 1745 cm^{-1} (diacetate), 1705 cm^{-1} (12,20-diketone), 1245 cm^{-1} (broad diacetate band), 1040 cm^{-1} (16-ether band); tetranitromethane test negative; no ultraviolet absorption band between 225 and 260 mμ. Anal. Calc. for $C_{26}H_{38}O_7$: C, 67.51; H, 8.28; saponifiable CH_3CO, 18.6. Found: C, 67.53; H, 8.38; saponifiable CH_3CO (after 90 minutes alcoholic 1 *N* KOH), 17.24.

Hydrolysis

A portion of 110 mg of the 16-ether derivative III*a* was dissolved in 12.5 cc of absolute acetone and treated for 18 hours, at room temperature, with 40 mg of *p*-toluenesulphonic acid. Subsequently, the mixture was refluxed for 2 hours with exclusion of moisture and was worked up in the usual fashion. The resulting product (97 mg) showed no ultraviolet absorption typical of an α,β-unsaturated ketone and consisted of crude starting material, III*a*, from which the pure product was isolated by chromatography on aluminum oxide.

3β-Acetoxy-12-ethylenedioxy-5α-pregnan-20-one (V) (cf. Ref. 7)

(a) Ketalization without Solvent

According to the procedure of Kirk *et al.* (7), a suspension of 530 mg of 3β-acetoxy-5α-pregnane-12,20-dione (IV) (12, cf. also ref. 2), m.p. 180–182°, in 3.4 cc of freshly distilled ethylene glycol and 0.7 cc of boron trifluoride etherate was shaken at room temperature for 72 hours. The mixture was poured into ice water and the solid precipitate was extracted with dichloromethane. The organic solution was washed with sodium bicarbonate solution and with water and was dried over sodium sulphate. Removal of the solvent yielded 540 mg of a yellow amorphous product, the infrared spectrum of which indicated that partial hydrolysis in position 3 had occurred. The material was acetylated in the usual fashion with 2 cc of acetic anhydride in 5 cc of pyridine at room temperature. Thus, 550 mg of a yellow amorphous product was obtained. Crystallization from ether gave 50 mg of 3β-acetoxy-12-ethylenedioxy-5α-pregnan-20-one (V), m.p. 157–158°. The mother liquors were chromatographed on 45 g of aluminum oxide, activity III. Elutions with petroleum ether – benzene (1:1) yielded 330 mg of crude monoketal V, m.p. 145–149°, which, upon crystallization from ether, gave 290 mg of pure monoketal, m.p. 158–159° (total yield 57%). A sample was recrystallized twice from ether–hexane for analysis. Small prisms; m.p. 158–160°; $[\alpha]_D^{25}$ 99.8° (*c*, 0.850 in $CHCl_3$); ν_{max}^{KBr} 1735 and 1245 cm^{-1} (acetate), 1701 cm^{-1} (20-ketone), 1060 cm^{-1} (12-ketal). Anal. Calc. for $C_{25}H_{38}O_5$: C, 71.74; H, 9.18. Found: C, 71.89; H, 9.01.

(b) Ketalization in Dichloromethane Solution

A solution of 530 mg of 3β-acetoxy-5α-pregnane-12,20-dione (IV), m.p. 180–182°, in 2 cc of absolute dichloromethane was stored at room temperature, for 72 hours, with 3.4 cc of freshly distilled ethylene glycol and 0.7 cc of boron trifluoride etherate. Large quantities of water and dichloromethane were added and the mixture was worked up as described under (*a*). The resulting product was reacetylated as described above and gave 590 mg of a yellow amorphous product which yielded, upon crystallization from ether, 420 mg of 3β-acetoxy-12-ethylenedioxy-5α-pregnan-20-one (V), m.p. 155–157°. The mother liquors were chromato-

[9]*The melting points were taken in evacuated capillaries and the temperatures were corrected.*

[10]*We are indebted to Dr. C. Daesslé, Montreal, Que., Canada, and to Mr. A. Bernhardt, Mülheim, Germany, for the microanalyses, and we extend to them our sincere appreciation.*

[11]*If not otherwise stated, non-alkaline aluminum oxide Woelm and Davison's silica gel No. 923 were used for chromatography.*

graphed on 6 g of aluminum oxide, activity III. Elutions with petroleum ether – benzene (1:1) yielded another 30 mg of monoketal V (total yield 74%). The twice-recrystallized product melted at 158–160°, $[\alpha]_D^{24}$ 100.2° (*c*, 0.850 in $CHCl_3$). The melting point was not depressed upon admixture of a sample of the ketal prepared as described under (*a*) and the infrared spectra of both products were identical.

3β,20β-Dihydroxy-12-ethylenedioxy-5α-pregnane (VI) (7)

(a) Reduction with Sodium Borohydride

According to the procedure of Kirk *et al.* (7), 250 mg of 3β-acetoxy-12-ethylenedioxy-5α-pregnan-20-one (V), m.p. 155–157°, was reduced with sodium borohydride, in methanol, in the presence of sodium hydroxide (compound V dissolved in 30 cc of methanol, 150 mg of sodium hydroxide, and 60 mg of sodium borohydride in 6 cc of 50% methanol). The usual working up afforded 205 mg (98% yield) of crystalline dihydroxy ketal VI, m.p. 195–196°; no carbonyl absorption in the infrared. A sample was recrystallized twice from methanol–ether for analysis. Small prisms; m.p. 198–200°; $[\alpha]_D^{24}$ 39.6° (*c*, 1.000 in $CHCl_3$); ν_{max}^{KBr} 3485 and 3410 cm^{-1} (3,20-dihydroxy groups), 1058 cm^{-1} (12-ketal). Anal. Calc. for $C_{23}H_{38}O_4$: C, 72.97; H, 10.12. Found: C, 72.88; H, 10.11.

(b) Reduction with Lithium Aluminum Hydride

A solution of 3.7 g of 3β-acetoxy-12-ethylenedioxy-5α-pregnan-20-one (V), m.p. 155–157°, in 250 cc of absolute tetrahydrofuran, was added over a period of 25 minutes and with vigorous stirring to a slurry of 1.9 g of lithium aluminum hydride in 300 cc of absolute tetrahydrofuran. While the stirring was continued, the mixture was refluxed for 1 hour and was subsequently stored at room temperature for another 16 hours. The excess reagent was decomposed by addition of moist ethyl acetate and, subsequently, of ice water. A cold solution of ammonium chloride was added and the organic layer was washed with cold water until neutral. The solution was dried over sodium sulphate and the solvent was removed. There was obtained 3.26 g (98%) of crystalline 3β,20β-dihydroxy-12-ethylenedioxy-5α-pregnane (VI), m.p. 196–198°. The melting point was not depressed upon admixture of the sample prepared as described under (*a*) and the infrared spectra of both products were identical.

3β,20β-Dihydroxy-5α-pregnan-12-one (IX) (7)

A solution of 3.6 g of 3β,20β-dihydroxy-12-ethylenedioxy-5α-pregnane (VI), m.p. 196–198°, in 155 cc of absolute acetone was refluxed, for 40 minutes, with 450 mg of *p*-toluenesulphonic acid. The volume of the solution was reduced *in vacuo* to approximately 50 cc and the product was poured into an iced sodium bicarbonate solution. The precipitate was extracted with dichloromethane and the organic layer was washed with water and was dried over sodium sulphate. Removal of the solvent afforded 3.24 g of a yellow amorphous material which gave, upon crystallization from acetone, 2.24 g of crystalline 3β,20β-dihydroxy-5α-pregnan-12-one (IX), m.p. 232–233°. The mother liquors were chromatographed on 30 g of aluminum oxide, activity III. Elutions with benzene–ether (4:1) afforded 500 mg of the dihydroxy ketone IX, m.p. 231–233° (total yield 86.5%). A sample was recrystallized twice from dichloromethane–acetone for analysis. Plates; m.p. 232.5–234°; $[\alpha]_D^{24}$ 88.5° (*c*, 0.867 in $CHCl_3$); ν_{max}^{KBr} 3450 and 3400 cm^{-1} (3,20-dihydroxy groups), 1692 cm^{-1} (hydrogen-bonded 12-ketone). Anal. Calc. for $C_{21}H_{34}O_3$: C, 75.41; H, 10.24. Found: C, 75.30; H, 10.06.

Diacetate IXa (cf. Ref. 7)

A solution of 18.9 g of 3β,20β-dihydroxy-5α-pregnan-12-one (IX), m.p. 231–233°, in 60 cc of pyridine and 40 cc of acetic anhydride was heated, for 16 hours, to 100°. After cooling, 100 cc of methanol was slowly added while the flask was shaken in an ice bath. The product was poured into 1.5 liters of cold water and the precipitate was extracted with ether. The ethereal solution was washed with cold 2 *N* hydrochloric acid, with water, cold sodium bicarbonate solution, and again with water and was dried over sodium sulphate. Upon removal of the solvent, 21.9 g of a yellowish amorphous product was obtained. Crystallization from ether–hexane afforded 16 g of 3β,20β-diacetoxy-5α-pregnan-12-one (IX*a*), m.p. 135–136°. The mother liquors (5.35 g) were absorbed on 150 g of aluminum oxide, activity III. Elutions with petroleum ether – benzene mixtures (1:1 and 1:4) and with pure benzene yielded another 4.5 g of diacetate IX*a*, m.p. 134–136° (total yield 90%). A sample was recrystallized twice from ether–hexane for analysis. Needles; m.p. 135–136°; $[\alpha]_D^{24}$ 98.5° (*c*, 1.000 in $CHCl_3$); ν_{max}^{KBr} 1740 cm^{-1} (3,20-diacetate band), 1715 cm^{-1} (12-ketone), 1255 cm^{-1} (3,20-diacetate band). Anal. Calc. for $C_{25}H_{38}O_5$: C, 71.75; H, 9.15. Found: C, 71.85; H, 9.04.

$\Delta^{9(11)}$-3β,20β-Diacetoxy-5α-pregnen-12-one (VIII)

To a solution of 16 g of 3β,20β-diacetoxy-5α-pregnan-12-one (IX*a*), m.p. 135–136°, in 140 cc of a 0.0006 *N* hydrogen chloride solution in acetic acid, 12 g of selenium dioxide was added. The mixture was refluxed for 20 hours, cooled, and diluted with 1.5 liters of ether. The product was filtered over sodium sulphate and celite and the filtrate was washed with water, iced dilute hydrochloric acid, cold sodium carbonate solution, and again with water, and was dried over sodium sulphate. Upon removal of the solvent, 15.7 g of a yellow amorphous product was obtained, which was absorbed on 450 g of aluminum oxide, activity III. Elutions with petroleum ether – benzene yielded 13.85 g (86.9%) of crystalline $\Delta^{9(11)}$-3β,20β-diacetoxy-5α-pregnen-12-one (VIII), m.p. 128–132°. Recrystallization from ether afforded 13.71 g (86%) of the pure unsaturated

diacetoxy ketone VIII, m.p. 132–133°. A sample was recrystallized twice from ether for analysis. Needles; m.p. 133–134°; $[\alpha]_D^{25}$ 69° (*c*, 1.000 in $CHCl_3$); λ_{max}^{EtOH} 238 mμ (log ε 4.19); ν_{max}^{KBr} 1735 cm^{-1} (3,20-diacetate band), 1682 and 1602 cm^{-1} ($\Delta^{9(11)}$-12-keto doublet), 1250 and 1240 cm^{-1} (3,20-diacetate). Anal. Calc. for $C_{25}H_{36}O_5$: C, 72.08; H, 8.71. Found: C, 72.07; H, 8.80.

3β-Hydroxy-20β-acetoxy-9-oxo-9,12-seco-11-nor-5α-pregnan-12-oic Acid (XI)

(a) By Ozonolysis In Ethyl Acetate – Acetic Acid

At −10°, a stream of oxygen containing 5.1% of ozone was passed at a rate of 180 cc per minute, for a period of 3 hours, through a solution of 800 mg of $\Delta^{9(11)}$-3β,20β-diacetoxy-5α-pregnen-12-one (VIII), m.p. 132–133°, in 25 cc of ethyl acetate and 25 cc of acetic acid. To the product there were added 0.7 cc of a 30% hydrogen peroxide solution and 1 cc of water, and the mixture was shaken repeatedly and was stored at room temperature for 16 hours. Water and ether were added and the organic product was extracted with ether. The ethereal solution was washed with water, then six times with cold 2 *N* sodium hydroxide solution, and again with water. The solution was dried over sodium sulphate and the solvent was removed. Thus 200 mg of neutral material was obtained. The sodium hydroxide washings were combined with the first water washings following the sodium hydroxide extraction and the solution was acidified with cold 2 *N* sulphuric acid to the Congo-blue reaction. The organic product was extracted with ether, the ethereal solution was washed repeatedly with water and was dried over sodium sulphate. Removal of the solvent afforded 510 mg (67.5%) of crystalline 3β-hydroxy-20β-acetoxy-9-oxo-9,12-*seco*-11-nor-5α-pregnan-12-oic acid (XI), m.p. 210–212°. A sample was recrystallized three times from dichloromethane–ether for analysis. Plates; m.p. 211–212°; $[\alpha]_D^{25}$ −30.6° (*c*, 1.000 in $CHCl_3$); λ_{max}^{EtOH} 290 mμ (log ε 1.48); ν_{max}^{KBr} 3400 cm^{-1} (broad, associated OH bands), 1725 cm^{-1} (acetate), 1708 (shoulder) and 1700 cm^{-1} (9-keto-12-acid bands), 1245 cm^{-1} (acetate). Anal. Calc. for $C_{22}H_{34}O_6$: C, 66.98; H, 8.69. Found: C, 66.69; H, 8.53.

(b) By Ozonolysis in Pure Ethyl Acetate

Two batches of 3 g each of $\Delta^{9(11)}$-3β,20β-diacetoxy-5α-pregnen-12-one (VIII), m.p. 132–133°, were dissolved in 60 cc of ethyl acetate each. Both batches were ozonized separately as described under (*a*), at −10°, with an oxygen stream containing 5% of ozone and flowing at a rate of 170 cc per minute, for 3 hours. Each batch was treated with 2 cc of a 30% hydrogen peroxide solution and with 4 cc of water and was left at room temperature for 16 hours. The reaction products were worked up as described under (*a*). The combined neutral fractions of both batches amounted to 55 mg and the combined acid fractions to 5.75 g .Recrystallization of the acidic material from dichloromethane gave 5 g (87.5% yield) of the *seco* acid XI, m.p. 212–214°. The identity of this product with the material prepared as described under (*a*) was established by a mixed melting point and by comparison of the infrared spectra.

Methyl Ester XIa

At 0°, 10 cc of a 2% ethereal diazomethane solution was added slowly to a solution of 310 mg of *seco* acid XI, m.p. 212–214°, in 14 cc of absolute ether and 6 cc of absolute methanol, and the resulting mixture was allowed to warm to room temperature. After 14 hours, the excess reagent was destroyed with a few drops of acetic acid and the solution was taken to dryness *in vacuo*. Thus, 320 mg of crystalline methyl ester XI*a*, m.p. 137–139°, was obtained (quantitative yield). A portion was recrystallized three times from ether–hexane for analysis. Needles; m.p. 139–141°; $[\alpha]_D^{25}$ −40.5° (*c*, 1.000 in $CHCl_3$); ν_{max}^{KBr} 3520 cm^{-1} (3-hydroxy band), 1730 cm^{-1} (broad, multiple acetate and methyl ester band), 1712 cm^{-1} (9-ketone), 1250 cm^{-1} (broad, multiple ester bands). Anal. Calc. for $C_{23}H_{36}O_6$: C, 67.49; H, 8.87. Found: C, 67.51; H, 8.94.

Diacetoxy Methyl Ester XIb

A portion of 290 mg of methyl ester XI*a* was acetylated in the usual fashion with 2 cc of acetic anhydride in 5 cc of pyridine, at room temperature, for 16 hours. Thus there was obtained 300 mg (94% yield) of crystalline diacetoxy methyl ester XI*b*, m.p. 101–102°. A sample was recrystallized three times from ether–hexane for analysis. Needles; m.p. 105–106°; $[\alpha]_D^{25}$ −45.1° (*c*, 0.950 in $CHCl_3$); ν_{max}^{KBr} 1730 cm^{-1} (broad acetate and methyl ester bands), 1715 cm^{-1} (shoulder, 9-ketone), 1252 and 1260 cm^{-1} (broad ester and acetate bands). Anal. Calc. for $C_{25}H_{38}O_7$: C, 66.64; H, 8.50. Found: C, 66.52; H, 8.32.

3β,20β-Diacetoxy-9α,11α-dihydroxy-5α-pregnan-12-one (VII)

To a solution of 5 g of $\Delta^{9(11)}$-3β,20β-diacetoxy-5α-pregnen-12-one (VIII), m.p. 132–133°, in 85 cc of pyridine, a solution of 5 g of osmic acid in 9 cc of pyridine was added. The mixture was stored in the dark, at room temperature, for 6 days, and subsequently a solution of 10 g of sodium sulphite in 150 cc of water was added (cf. ref. 21); the resulting ratio of pyridine – water – sodium sulphite amounted to 35:30:2. The mixture was stored for 1 hour, by which time the color turned from dark brown to orange. The product was extracted with chloroform, the chloroform solution was washed with cold dilute hydrochloric acid, water, cold sodium bicarbonate solution, and again with water and was dried over sodium sulphate. Removal of the solvent afforded 5.35 g of an amorphous material, which was crystallized from acetone–ether to give 4.35 g of 3β,20β-diacetoxy-9α,11α-dihydroxy-5α-pregnan-12-one (VII), m.p. 185–186°. The mother liquors (1 g) were absorbed on 30 g of aluminum oxide, activity III. Elutions with petroleum ether – benzene (1:1 and 1:4), pure benzene, and benzene–ether (4:1) afforded 960 mg of crystalline VII, m.p. 179–183°; one recrystallization from acetone–ether gave 800 mg of pure glycol VII, m.p. 185–186° (total yield 95.5%). A

sample was recrystallized twice from ether–acetone for analysis. Rods; m.p. 186–187°; $[\alpha]_D^{25}$ 60° (*c*, 1.000 in $CHCl_3$); ν_{max}^{KBr} 3520 and 3475 cm^{-1} (9,11-diol), 1720 cm^{-1} (broad diacetate band), 1715 cm^{-1} (shoulder, 12-ketone), 1260 and 1250 cm^{-1} (3,20-diacetate). Anal. Calc. for $C_{25}H_{38}O_7$: C, 66.84; H, 8.50. Found: C, 67.15; H, 8.62.

20β-Acetoxy-3β,9α-dihydroxy-11-oxo-11,12-seco-5α-pregnan-12-oic Acid (X)

(a) By Periodic Acid Oxidation of Glycol VII in Methanol–Water

To a solution of 2 g of 3β,20β-diacetoxy-9α,11α-dihydroxy-5α-pregnan-12-one (VII), m.p. 185–186°, in 150 cc of methanol, a solution of 5 g of periodic acid dihydrate in 20 cc of water was added, with stirring. The mixture was stirred at room temperature and in the dark for 20 hours and was neutralized with a sodium carbonate solution. After concentration *in vacuo* the product was acidified with 2 *N* hydrochloric acid to the Congo-blue reaction and the resulting mixture was extracted with ether. The ethereal solution was extracted six times with a 2 *N* sodium hydroxide solution and was then washed until neutral and dried over sodium sulphate. Removal of the solvent afforded 1.015 g of an amorphous neutral product showing no ultraviolet absorption maximum typical of an α,β-unsaturated ketone and representing crude *dihydroxy acetoxy aldehydo methyl ester Xa (vide infra)*. The first water washings of the neutral ethereal solution were combined with the sodium hydroxide extracts and acidified with cold 2 *N* hydrochloric acid to the Congo-blue reaction. The product was extracted with ether and the ethereal solution was washed repeatedly with water and was dried over sodium sulphate. Removal of the solvent afforded 855 mg (43%) of crude *acid X* which resisted all attempts of crystallization.

(b) By Periodic Acid Oxidation in Dioxane–Water

A solution of 200 mg of periodic acid dihydrate in 5 cc of water was added, with stirring, to a solution of 300 mg of 3β,20β-diacetoxy-9α,11α-dihydroxy-5α-pregnan-12-one (VII), m.p. 185–186°, in 50 cc of dioxane. The mixture was stored at room temperature, in the dark, for 18 hours and was worked up as described under (*a*). Thus 5 mg of an amorphous neutral product and 280 mg (99% yield) of amorphous aldehydo acid X were obtained; positive Tollens reaction; ν_{max}^{KBr} 3520 and 3430 cm^{-1} (very broad, multiple, highly associated hydroxyl bands), 1735 cm^{-1} (20-acetate), 1721 and 1716 cm^{-1} (broad double band of 11-aldehyde and 12-acid), 1245 cm^{-1} (acetate); a comparison of the infrared spectra of the samples prepared as described under (*a*) and (*b*) revealed the identity of the products.

Methyl Ester Xa

To a solution of 225 mg of the above-described dihydroxy acetoxy aldehydo acid X in 35 cc of absolute ether and 15 cc of absolute methanol, 15 cc of a 1.5% ethereal diazomethane solution was added, at 0°. The temperature of the reaction mixture was allowed to rise to 25° and the product was stored for another 14 hours at this temperature. The excess reagent was destroyed with acetic acid and the solvent was removed *in vacuo*. Thus, 240 mg of a semicrystalline residue was obtained. Crystallization from ether gave 85 mg of pure methyl ester X*a*, m.p. 149–150°. A sample was recrystallized once from ether–acetone for analysis. Needles; m.p. 151–152°; $[\alpha]_D^{25}$ −12° (*c*, 1.000 in $CHCl_3$); λ_{max}^{EtOH} 295 mμ (log ε 1.6); ν_{max}^{KBr} 3560 cm^{-1} (hydroxyl groups), 1740–1735 cm^{-1} (acetate and methyl ester), 1718 cm^{-1} (shoulder, 11-aldehyde), 1255 and 1245 cm^{-1} (ester groups). Anal. Calc. for $C_{24}H_{38}O_7 . CH_3COCH_3$: C, 65.29; H, 8.91. Found: C, 65.19; H, 8.89.

Diacetoxy Methyl Ester Xb

(*a*) A portion of 160 mg of the mother liquors of the crystallization of methyl ester X*a* was acetylated in the usual fashion with 1 cc of acetic anhydride in 2 cc of pyridine, at room temperature. The resulting 185 mg of amorphous product was crystallized from ether and afforded 160 mg of the diacetoxy methyl ester X*b*, m.p. 185–187°. A further recrystallization from ether yielded 140 mg of pure product melting at 191–192°. The product showed a positive Tollens reaction. A sample was recrystallized from ether–hexane for analysis. Needles; m.p. 190–192°; $[\alpha]_D^{25}$ −15° (*c*, 1.000 in $CHCl_3$); ν_{max}^{KBr} 3520 cm^{-1} (hydroxy group), 2750 cm^{-1} (C—H stretching of aldehyde), 1730–1720 cm^{-1} (broad, multiple 11-aldehyde, acetate, and methyl ester bands), 1245 cm^{-1} (broad, multiple ester bands). Anal. Calc. for $C_{26}H_{40}O_8$: C, 64.98; H, 8.39. Found: C, 64.58; H, 8.31.

(*b*) The neutral product (1.01 g) obtained during the periodic acid oxidation of glycol VII in methanol–water (*vide supra*), was dissolved in 5 cc of absolute pyridine and acetylated with 2 cc of acetic anhydride, at room temperature, for 16 hours. The usual working up afforded 1.1 g of amorphous product which, upon crystallization from ether, gave 300 mg of authentic crystalline diacetoxy methyl ester X*b*, m.p. 185–187°, identified by the comparison of the infrared spectra and by a mixed melting point with the product prepared as described under (*a*). Recrystallization raised the melting point to 190–192°. The mother liquors of the first crystallization failed to give a well-defined product upon chromatography on aluminum oxide.

20β-Acetoxy-9α-hydroxy-3-oxo-11,12-seco-5α-pregnane-11,12-dioic Acid (XIII)

To a solution of 280 mg of the crude, amorphous dihydroxy acetoxy aldehydo acid X (obtained by periodic acid oxidation of glycol VII in dioxane–water) in 15 cc of absolute acetone, 1 cc of an 8 *N* chromic acid solution in sulphuric acid (cf. ref. 27) was added and the mixture was stored at room temperature for 10 minutes. The excess chromic acid was decomposed by addition of methanol and the product was poured

into ice water. The precipitate was extracted with dichloromethane, the organic solution was washed with water and was dried over sodium sulphate. Removal of the solvent afforded 270 mg of a semicrystalline material which gave, upon crystallization from dichloromethane–ether, 150 mg of the crystalline hydroxy acetoxy keto dicarboxylic acid XIII, m.p. 193–194°. A sample was recrystallized once from dichloromethane–ether for analysis. Needles; m.p. 194–195°; $[\alpha]_D^{25}$ −18° (*c*, 1.000 in $CHCl_3$). Anal. Calc. for $C_{23}H_{34}O_7$: C, 65.38; H, 8.11. Found: C, 65.49; H, 8.24.

$\Delta^{8(9)}$-3β-Hydroxy-20β-acetoxy-9-amino-9,12-seco-11-nor-5α-pregnen-12-oic Acid Lactam (12 → 9) (XII)

Through a solution of 1.65 g of 3β-hydroxy-20β-acetoxy-9-oxo-9,12-*seco*-11-nor-5α-pregnan-12-oic acid (XI), m.p. 212–214°, in 35 cc of ethanol, ammonia gas was passed for a period of 1 hour, at 0°. Subsequently, the solution was heated in a sealed tube at 145°, for 15 hours. The product was taken to dryness *in vacuo* and the dark brown amorphous residue (1.6 g) was taken up in a mixture (4:1) of benzene – ethyl acetate and was absorbed on 160 g of silica gel, deactivated by addition of 10% water. Elutions with benzene – ethyl acetate mixtures (70:30 and 50:50) afforded 1.2 g (77.5%) of the crystalline unsaturated lactam XII, m.p. 161–163°. A sample was recrystallized three times from acetone–hexane for analysis. Small plates; m.p. 165–167°; $[\alpha]_D^{25}$ 205° (*c*, 0.800 in $CHCl_3$); λ_{max}^{EtOH} 254 mμ (log ε 3.95); ν_{max}^{KBr} 3350 cm^{-1} (hydroxy group), 3250 cm^{-1} (N—H stretching), 1665 and 1653 cm^{-1} (lactam), 1630 cm^{-1} (double bond), 1240 cm^{-1} (acetate). Anal. Calc. for $C_{22}H_{33}NO_4$: C, 70.36; H, 8.86; N, 3.74. Found: C, 70.64; H, 8.70; N, 3.89.

$\Delta^{8(9)}$-3β,20β-Diacetoxy-11-aza-N-acetyl-5α-pregnene (XIVa)

A solution of 500 mg of the unsaturated lactam XII, m.p. 161–163°, in 100 cc of absolute tetrahydrofuran was added with stirring and with the exclusion of moisture to a slurry of 1 g of lithium aluminum hydride in 200 cc of absolute tetrahydrofuran. The mixture was refluxed with stirring for 18 hours and was subsequently cooled; the excess reagent was decomposed by careful addition of ice. The inorganic salts were filtered off and washed several times with tetrahydrofuran. The organic filtrate and the washings were combined and dried over sodium sulphate. Removal of the solvent afforded 400 mg of a yellow amorphous material which resisted crystallization and which represented crude *$\Delta^{8(9)}$-11-aza pregnene-3β,20β-diol (XIV)*. The product was dissolved in 4 cc of pyridine and treated with 4 cc of acetic anhydride at 100°, for 16 hours. The excess acetic anhydride was decomposed by addition of methanol and the solvents were removed under reduced pressure. The dark brown residue was taken up in ethyl acetate, the solution was washed with cold water, cold sodium bicarbonate solution, and again with water and was dried over sodium sulphate. Removal of the solvent gave 450 mg of a dark brown oil. The product was dissolved in a petroleum ether – benzene (1:1) mixture and was absorbed on 12 g of aluminum oxide, activity III. Elutions with petroleum ether – benzene (1:4) and pure benzene gave 135 mg of *$\Delta^{8(9)}$-3β,20β-diacetoxy-N-acetyl-11-aza-5α-pregnene (XIVa)*, m.p. 225–228°. A sample was recrystallized three times from ether–dichloromethane for analysis. Small prisms; m.p. 235–237°; $[\alpha]_D^{25}$ 64.2° (*c*, 0.700 in $CHCl_3$); ν_{max}^{KBr} 1745 cm^{-1} (acetate bands), 1645 cm^{-1} (amide), 1245–1240 cm^{-1} (broad acetate bands). Anal. Calc. for $C_{26}H_{39}NO_5$: C, 70.08; H, 8.82; N, 3.14. Found: C, 69.90; H, 8.91; N, 3.38.

ACKNOWLEDGMENTS

We extend sincerest thanks to Mrs. J. Capitaine and Mr. D. Capitaine for their devoted and expert assistance, and we express our gratitude to the National Research Council of Canada, the Schering Corporation, Bloomfield, N.J., and the Schering Corporation Ltd., Montreal, for financial support of this project.

REFERENCES

1. J. Capitaine, R. Deghenghi, and Ch. R. Engel. J. Med. Pharm. Chem. In press (1963).
2. Ch. R. Engel, S. Rakhit, and W. W. Huculak. Can. J. Chem. **40**, 921 (1962).
3. Ch. R. Engel and W. W. Huculak. Can. J. Chem. **37**, 2031 (1959).
4. R. H. Mazur. J. Am. Chem. Soc. **81**, 1454 (1959).
5. T. L. Jacobs and R. B. Brownfield. J. Am. Chem. Soc. **82**, 4033 (1960).
6. W. J. Adams, D. N. Kirk, D. K. Patel, V. Petrow, and I. A. Stuart-Webb. J. Chem. Soc. 2298 (1954).
7. D. N. Kirk, D. K. Patel, and V. Petrow. J. Chem. Soc. 1046 (1957).
8. H. Schinz and G. Schäppi. Helv. Chim. Acta, **30**, 1483 (1947).
9. L. H. Sarett. J. Chem. Soc. **71**, 1175 (1949).
10. G. Just and R. Nagarajan. Can. J. Chem. **39**, 548 (1961).
11. S. Rakhit and Ch. R. Engel. Can. J. Chem. This issue.
12. G. P. Mueller, R. E. Stobaugh, and R. S. Winniford. J. Am. Chem. Soc. **75**, 4888 (1953).
13. R. I. Erskine and E. S. Waight. J. Chem. Soc. 3425 (1960).
14. L. Dorfman. Chem. Rev. **53**, 47 (1953).
15. V. R. Mattox. J. Am. Chem. Soc. **74**, 4340 (1952).
16. D. Gould, F. Gruen, and E. B. Hershberg. J. Am. Chem. Soc. **75**, 2510 (1953).

17. W. J. ADAMS, D. N. KIRK, D. K. PATEL, V. PETROW, and I. A. STUART-WEBB. J. Chem. Soc. 2209 (1954).
18. D. K. FUKUSHIMA and T. G. GALLAGHER. J. Am. Chem. Soc. **73**, 196 (1951).
19. E. SCHWENK and E. STAHL. Arch. Biochem. **14**, 125 (1947).
20. R. PAPPO, D. S. ALLEN, JR., R. U. LEMIEUX, and W. S. JOHNSON. J. Org. Chem. **21**, 478 (1956).
21. J. S. BARAN. J. Org. Chem. **25**, 257 (1960).
22. R. HIRSHMANN, C. ST. SNODDY, JR., and N. L. WENDLER. J. Am. Chem. Soc. **75**, 3252 (1953).
23. W. W. HUCULAK. M.Sc. Thesis, University of Western Ontario, London, Ont. 1959.
24. H. WIELAND and TH. POSTERNAK. Z. Physiol. Chem. **197**, 17 (1931).
25. R. B. WAGNER, J. A. MOORE, and R. F. FORKER. J. Am. Chem. Soc. **72**, 1856 (1950).
26. M. E. WALL, H. E. KENNEY, and E. S. ROTHMAN. J. Am. Chem. Soc. **77**, 5665 (1955).
27. K. BOWDEN, J. M. HEILBRON, E. R. H. JONES, and B. C. L. WEEDON. J. Chem. Soc. 39 (1946).

THE CONFORMATIONS OF THE 20-KETO SIDE CHAIN OF C_{21}-STEROIDS[1]

S. RAKHIT[2] AND CH. R. ENGEL[3]

A number of important steroid hormones, such as progesterone, the mineralo-corticoids, and the gluco-corticoids, possess a two-carbon keto side chain. Whereas progesterone has a simple 21-methyl-20-keto side chain, the corticoids all bear a hydroxyl substituent at position 21. The biological activity of such steroids is markedly influenced by substituents on the carbon atoms adjacent to the 20-carbonyl group, for instance, by the presence of an additional hydroxy function in position 17, the point of origin of the side chain. It is well known that C_{21}-steroids exhibit marked hormonal activity only if the side chain occupies the β-configuration. The study of models, particularly of the Stuart type, shows clearly that the methyl keto side chain, or the derived ketol side chain, cannot rotate completely freely around the C_{17}—C_{20} single bond and that there exist four preferred conformations, which we designate as A_1, A_2, B_1, and B_2 (compare Fig. 1).[4] These conformations can readily be subjected to small rotational transformations but are separated from each other by energy barriers (the conversions $A_1 \rightleftarrows B_1$ and $A_2 \rightleftarrows B_2$ are achieved with greater ease than the conversions $A_1 \rightleftarrows A_2$ and $B_1 \rightleftarrows B_2$.

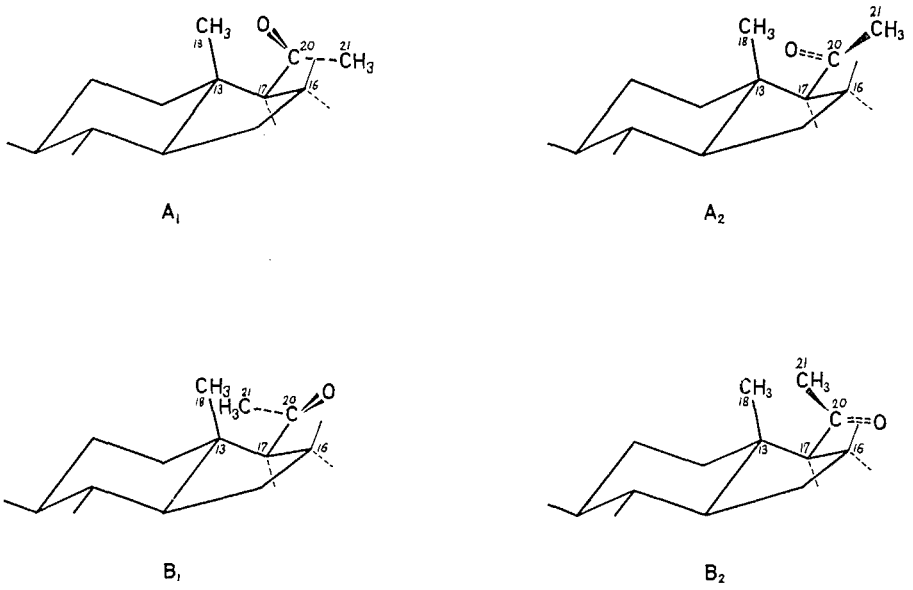

FIG. 1. Preferred conformations of the 20-keto side chain of C_{21}-steroids.

[1]*This communication represents paper XX in our series on Steroids and Related Products (for Paper XIX, see ref. 1). The main aspects of the problems discussed in this note were related in a communication presented before the XXIXth Congress of the French Canadian Association for the Advancement of Science, Ottawa, October 1961.*

[2]*National Research Council of Canada postdoctorate fellow, 1960–1962. Present address: Worcester Foundation for Experimental Biology, Shrewsbury, Mass., U.S.A.*

[3]*Correspondence should be addressed to this author.*

[4]*The drawings of ring D are only approximations; in this paper we do not intend to take issue with the problem of the actual conformation of ring D of individual steroids (cf. ref. 2).*

The question in which of these main conformations individual C_{21}-20-keto steroids predominantly exist merits attention, both as a matter of stereochemical interest and because of the biochemical and biological implications of the problem. The 20-keto function of C_{21}-hormones seems indeed to play an important role in their biological action and it is therefore logical to assume that the geometry of this group should be of biological significance. The contact or interaction of this function with a receptor should be influenced by its position in space, its distances from other centers, and its "availability" or "inavailability" for biochemical actions.

As we have already briefly indicated in a previous publication (3), the stereochemical course of metal hydride reductions, particularly of lithium aluminum hydride reduction, of 20-keto steroids can shed some light on the conformation of the side chain. Just and Nagarajan (4) reported recently that the reduction of 3α,12α-dihydroxypregnan-20-one with lithium aluminum hydride gives a high yield of the 20α-hydroxy derivative (58.5% in tetrahydrofuran, 65.8% in diethyl ether), in contradistinction to the reduction of the corresponding 3α,12α-diacetate, which gives predominantly the 20β-alcohol (5), in contradistinction also to the stereochemical course of metal hydride reductions of the majority of 20-keto steroids (cf. ref. 6, pp. 568 and 622 and the pertinent references therein). As an explanation, Just and Nagarajan put forward the hypothesis that in the course of the reduction of the 12α-hydroxy-20-ketone there is formed an intermediate aluminum complex which links the oxygen functions in positions 12 and 20 in a bridge-like fashion

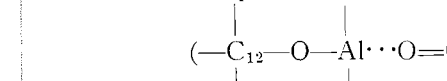

($-C_{12}-O-Al\cdots O=C_{20}-$). In order to make such a link possible, the 20-keto side chain must assume a conformation which should induce, according to Cram's rule (7), the predominant formation of a 20α-alcohol upon lithium aluminum hydride reduction. This assumption was further corroborated by our own experiments. We were able to show that lithium aluminum hydride reduction of a 12,20-diketone leads, practically exclusively, to a 12β,20α-diol (3), whereas the reduction of a 12-ethylenedioxy-20-ketone affords in high yield the 20β-alcohol (1). This fits well Just and Nagarajan's theory, since a 12,20-diketone should lend itself readily to the formation of an intermediate complex of the aluminum species with the oxygen atoms in positions 12 and 20 and should hence be expected to yield predominantly a 20α-alcohol; on the other hand, the formation of such a complex is not likely with a 12-ethylenedioxy group and, consequently, the methyl ketone side chain should, in this instance, not be forced into a conformation inducive to the formation of a 20α-alcohol.[5] Furthermore, if the aluminum hydride reagent were to form two distinct complexes with the oxygen functions in positions 12 and 20, the steric repulsion between these two complexes would result in a side-chain conformation inducive to reduction to a 20β-alcohol. As a matter of fact, the high stereospecificity of the reduction of a 12-ethylenedioxy-20-ketone with lithium aluminum hydride could be accounted for by the steric repulsion between the 12-ketal group and the complex formed between the aluminum hydride and the 20-ketone.

Just and Nagarajan had already pointed out that their theory provided an explanation for the finding that 17α-hydroxy-20-ketones are reduced by lithium aluminum hydride predominantly to 20α-alcohols (8, 9, cf. also ref. 10). As we endeavor to show in this

[5]*The great stereospecificity of the reduction of the 12,20-diketone as compared to that of the reduction of an 12α-hydroxy-20-ketone is understandable if one considers that the geometry of the* C=O *bond of a 12-ketone and, especially, of a 12β-hydroxy derivative (predominantly formed by metal hydride reduction of a 12-ketone) lends itself better to the formation of a bridge complex with the 20-oxygen atom than the geometry of the* C—O *bond of a 12α-hydroxy derivative.*

paper, the axis of the carbonyl group of 17α-hydroxy-21-methyl-20-keto steroids is almost coplanar with the C—O link of the 17α-hydroxy function. If an aluminum hydride link between the 17α-hydroxy group and the 20-carbonyl function is to be formed in the course of lithium aluminum hydride reduction, the side chain must undergo a rotation around the C_{17}—C_{20} bond in order to accommodate the aluminum species between the two oxygen functions. In this instance the formation of two distinct complexes of aluminum hydride with the oxygen functions in positions 17 and 20 would have the same result: the repulsion between these two complexes would drive the side chain into another conformation. The rotation of the side chain should occur towards conformation A_2, since the passage to conformation B_1 would require the clearing of a higher energy barrier. Hydride attack on a complex of the aluminum species with the 20-carbonyl function in conformation A_2, should afford predominantly the 20α-alcohol, which corresponds indeed to the experimental facts.

The stereochemical course of lithium aluminum hydride reduction of Δ16-*20-keto steroids* can also be explained readily by the consideration of the conformation of the side chain. Mueller *et al.* (11) showed that this conformation is of the *s*-trans type (cf. also ref. 1).[6]

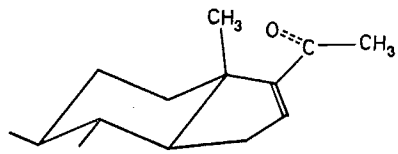

The conformation of the methyl ketone side chain of Δ16-20-keto steroids thus resembles conformation A_2 of the saturated products and should result in the predominant formation of 20α-alcohols upon reduction with aluminum hydrides, which is indeed the case (cf. ref. 12).[7]

As a corollary of these considerations it can be concluded that if the molecule does not contain groups which, by the formation of intermediate complexes or by other compelling steric factors, force the side chain out of its "normal" conformation, the hydride attack will occur on a complex having a conformation similar to that of the original 20-keto side chain. Thus, the stereochemical analysis of the lithium aluminum hydride reduction products of such 20-ketones should allow one to draw direct conclusions on the predominant conformation of the original side chain. In the absence of "interfering" oxygen functions (such as 12-hydroxy and 12-keto groups, a 17α-hydroxy function, or a 16,17-unsaturation) lithium aluminum hydride reduction yields predominantly 20β-alcohols; according to Cram's rule this is only possible if the intermediate complex of the carbonyl

[6]*In the absence of a 12-keto or 12-acetoxy function and consequently in the absence of repulsion between such groups and the 20-keto function, the ratio of s-trans conformation to s-cis conformation is even higher. Thus, the ratio of the integrated band intensities of the 20-C=O and 16,17-C=C stretching vibrations is 6.63 in the case of Δ16-3α-acetoxypregnene-11,20-dione, as compared to 5.18 in the case of Δ16-3β-acetoxy-5α-pregnene-12,20-dione; the extinction coefficient of the ultraviolet absorption maximum of the unsaturated ketone of Δ16-3α-acetoxypregnene-11,20-dione is 9050, that of Δ16-pregnene-3,20-dione 9800, as compared to 8510 for Δ16-3β-acetoxy-5α-pregnene-12,20-dione (our own unpublished results, cf. also footnote 6 of ref. 1).*

[7]*Shapiro et al. (12) suggested that the predominant formation of 20α-alcohols upon lithium aluminum hydride reduction of 16-unsaturated 20-ketones is due to a lesser hinderance of the 20-carbonyl function of such products as compared to that of the saturated compounds. In fact, in the s-trans conformation the unsaturated ketones are considerably hindered, which seems to be borne out by chemical evidence (cf. ref. 1); however, it is possible that the (small) portion of the ketone which occupies the s-cis conformation reacts rapidly with lithium aluminum hydride, that the equilibrium between the s-cis and s-trans forms is constantly restored, and that consequently the whole reaction takes place as if the side chain would occupy the s-cis conformation. Our own explanation would make such an assumption superfluous, since it rationalizes the predominant formation of the 20α-epimer without postulating a shift to the s-cis conformation.*

group with the aluminum hydride species exists predominantly in either conformation B_1 or B_2. As just pointed out, we can assume that in these instances the conformation of the original 20-keto side chain will be similar. In other words, the fact that, in the absence of groups which interfere with the geometry of intermediate complexes, lithium aluminum hydride reduction of 20-keto steroids yields predominantly 20β-alcohols allows us to conclude that the conformation of the original 20-keto side chain of such compounds must be, predominantly, either of type B_1 or B_2. A choice between these two conformations can, however, not be made on the basis of the stereochemical analysis of the reduction products, since both conformations should be inducive to the formation of 20β-alcohols.[8, 9]

Physical data are in agreement with our conclusions. Thus Djerassi *et al.* (14) have shown, by the application of the "axial halo keto rule" (15), that *17α-bromo-* and *17α-chloro-20-keto steroids* (cf. partial formula I) exist in a conformation of type B, in contra-

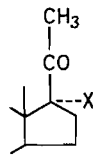

I, X = Br, Cl

distinction to 18-nor-20-keto steroids, the general conformation of which appears to be of type A (16, 17, cf. also ref. 18).[10] Djerassi *et al.* do not discuss specifically the two conformations B_1 and B_2; however, in this instance an assignment can be made readily on the grounds of spectral evidence. Indeed, if 17α-halo-20-ketones were to exist in conformation B_2, the C_{17}—X and C_{20}—O bonds would be almost coplanar and, as in the case of cyclic equatorial α-halo ketones, the resulting dipole interaction should be noticeable in the infrared (cf. refs. 20 and 21). However, the carbonyl frequency of the 20-keto group is hardly changed by the introduction of a 17α-halo substituent (cf. for instance ref. 20). We can thus conclude that the *actual conformation of 17α-halo-20-keto pregnanes is of type B_1.*

In a recent publication, Allinger and DaRooge (22) established, with the help of dipole moment measurements, that even in the absence of a 17α-halogen substituent the 21-methyl-20-keto side chain of the progesterone type (compare partial formula II) occupies the general conformation B. These authors briefly considered the choice between the two

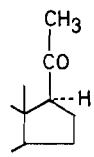

II

[8]*An inspection of models demonstrates that conformation B_2 should be particularly favorable for the reduction to a 20β-alcohol, the intermediate complex being particularly little hindered; but this does in no way mean that conformation B_2 represents the actual conformation of the majority of 20-keto steroids.*

[9]*In connection with their work on 18-oxygenated 20-keto pregnane derivatives, Heusler and Wettstein arrived independently at somewhat similar conclusions, which they published in an article (13) which appeared after our presentation before the Congress of the Canadian Association for the Advancement of Science. In their discussion, the Swiss authors do not consider conformation B_2.*

[10]*In this connection it seems of interest to point out that 18-nor- and 18,19-bis-nor-progesterones show only low progestational activity (18, 19).*

possible conformations B_1 and B_2, but dismissed, almost perfunctorily, the possibility of conformation B_2. Quite correctly, they point out that in this conformation the geometry of the C_{18}- and C_{21}-methyl groups resembles that of 1,3-diaxial methyl groups on a cyclohexane ring, an arrangement with a high energy content (cf. ref. 23). While we tend to agree that conformation B_1 is probably energetically more favored than conformation B_2, the difference between the energy contents of the two conformations seems less drastic than it would appear from Allinger's and DaRooge's article. Indeed, while the geometry of the C_{18}- and C_{21}-methyl groups of conformation B_2 is *similar* to that of a diaxial 1,3-dimethyl cyclohexane, it is by no means identical. As can be seen quite readily by inspection of models, particularly of the Stuart type, the interaction between the C_{18}- and C_{21}-methyl groups of conformation B_2 is definitely less severe than that of diaxial 1,3-dimethyl cyclohexane substituents (compare Fig. 2). Furthermore, in the alternative

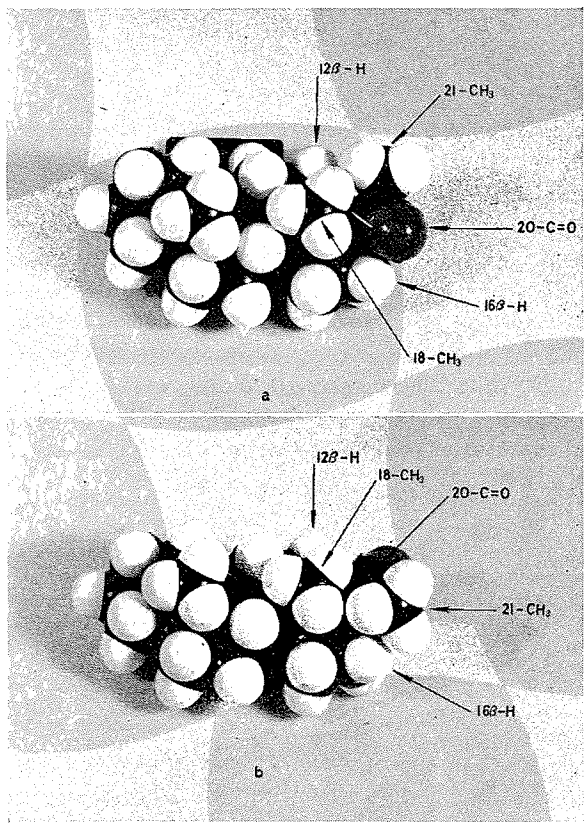

FIG. 2. Stuart models of 20-keto C_{21}-steroids: (*a*) conformation B_1; (*b*) conformation B_2.

conformation, B_1, there also exists an interaction between the hydrogen atoms of the two methyl groups (although it is smaller than in the case of conformation B_2) and an interaction between the 21-methyl group and the 12β-hydrogen atom; and there exists a marked interaction between the oxygen atom of the carbonyl group and the 16β-hydrogen atom (cf. Fig. 2). We can readily see that the last-mentioned interaction should not be neglected if we consider that a somewhat similar (although more severe) interaction between the 20-oxygen function and the C_{18}-methyl group must be responsible for the

fact that 21-methyl-20-ketones of the natural series (with an angular C_{18}-methyl substituent) do not generally exist in conformation A_1. (In the case of conformation A_2, another factor of thermodynamic instability has to be considered: an interaction between the 21-methyl group and the 16β-hydrogen atom.) As long as we are not in possession of further experimental evidence, our dismissal of conformation B_2 for 21-methyl-20-ketones should, therefore, be formulated with some caution.[11]

On the other hand, it seems logical to admit that *17α-hydroxy-21-methyl-20-ketones* (of the type of 17α-hydroxyprogesterone, cf. partial formula III) *exist to a considerable extent in conformation B_2*. This is indeed the only conformation which allows for the marked

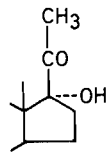

III

hydrogen bonding which can be observed between the 17α-hydroxy group and the 20-carbonyl function (27). Since lithium aluminum hydride reduction of 17α-hydroxy-21-methyl-20-ketones affords predominantly 20α-alcohols and since conformation B_2 is inducive to the formation of 20β-alcohols, we must conclude that during the reduction shift a to conformation A_2 occurs. We have already discussed this point above.

The case of *12β-hydroxy-21-methyl-20-keto steroids* is somewhat similar: the marked hydrogen bonding between the 12-hydroxy function and the 20-keto group (cf. refs. 28, 29) allows only for one predominant conformation: *conformation A_2*.

It is interesting that while the preferred conformation of 17α-hydroxy-21-methyl-20-keto steroids seems to be conformation B_2, compounds with a *dihydroxyacetone side chain*, i.e. with an additional hydroxy substituent in position 21 (cf. partial formula IV), as

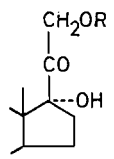

IV, R = H
IVa, R = Ac

well as 21-acetate derivatives of such products, exist predominantly in a different conformation, namely B_1. If products of this structure were to occur in conformation B_2, their infrared spectra should reveal, as in the case of the 21-unsubstituted 17α-hydroxy-20-ketones, pronounced hydrogen bonding between the 20-carbonyl function and the 17α-hydroxy group. This is not the case (27). On the other hand, lithium aluminum hydride

[11]*If biological data could be used as evidence in the determination of the exact conformation of the side chain of 17-unsubstituted 21-methyl-20-ketones, they would speak in favor of conformation B_1. Bulky 17α-substituents, which should definitely not favor conformation B_2, increase in general progestational activity (cf. ref. 24); thus 17α-bromoprogesterone is a highly active luteoid (25), whereas 17α-hydroxyprogesterone, which occurs to a considerable extent in conformation B_2 (vide infra), is almost inactive (26). It would not be unreasonable to assume that progesterone, the actual hormone of the corpus luteum, should also exist in conformation B_1, in which particularly active compounds occur, and not in conformation B_2, in which the almost inactive 17α-hydroxyprogesterone predominantly exists. Needless to emphasize, this argument has only limited value since the activating and deactivating actions of various substituents are generally due to a multitude of distinct factors.*

reduction of compounds of type IV*a* yields predominantly 20β-alcohols (30–33), which indicates that the general conformation of the side chain is of type B. Since the conformation cannot be of type B_2, we must assume that, in contradistinction to the 21-desoxy compounds, products of the type of cortisol and cortisone exist mainly in *conformation* B_1.[12]

By analogy, we can assume that the conformation of 17-unsubstituted 21-hydroxy-20-keto steroids, such as desoxycorticosterone, is of the general type B, probably of type B_1.[12, 13]

We may summarize the preferred conformations of various types of 20-keto C_{21}-steroids in Table I.[14, 15]

TABLE I

Substituents					Preferred conformation
12	13	16	17α	21	
H_2	CH_3	H_2	Br or Cl	H_3	B_1
H_2	CH_3	H_2	H	H_3	B (B_1?)
H_2	CH_3	H_2	OH	H_3	B_2
12α-H, 12β-OH	CH_3	H_2	H	H_3	A_2
H_2	CH_3	H_2	OH	OH, H_2	B_1
H_2	CH_3	H_2	H	OH, H_2	B (B_1?)
H_2	CH_3	$\Delta^{16,17}$	$\Delta^{16,17}$	H_3	A_2
H_2	H	H_2	H	H_3	A

In conclusion, it might be of interest to point out that the predominant side-chain conformation of products which exhibit marked hormonal activity always seems to be of the general type B, probably of the particular type B_1.[16] Whereas a coincidental relationship cannot be ruled out, we believe that the geometry of a group biologically as significant as the 20-keto side chain of C_{21}-steroids should be a factor of some consequence with respect to biological activity. One might be tempted to consider that conformations of the general type B, and in particular of type B_1, are favorable for hormonal action.

ACKNOWLEDGMENT

We express sincere thanks to the National Research Council of Canada for the generous support of our studies.

[12]*In a recent oral communication (cf. ref. 34), presented after the preparation of this manuscript, Birmingham, Ward, and Traikov advanced that the study of the near-infrared spectra of 17α,21-dihydroxy-20-ketones and of 21-acetoxy-17α-hydroxy-20-ketones suggests some hydrogen bonding between the 17α-hydroxy group and the 20-carbonyl function. This would mean that such compounds exist to some extent in conformation* B_2.

[13]*Such an assumption is relatively safe. Indeed, if not even a 17α-hydroxy substituent can induce, by hydrogen bonding, the ketol side chain to assume conformation* B_2, *ketols without this 17α-substituent should have even less reason to exist in this conformation. One could stretch this argument even further in favor of a more definite establishment of conformation* B_1 *for 20-ketones unsubstituted in both the 17 and 21 positions; however, the situation is not completely analogous because a 21-hydroxy or a 21-acetoxy substituent exercises, as we have seen, a marked influence on the conformation of the side chain.*

[14]*We have not discussed the conformation of 16α,17α-epoxy-20-keto steroids. Their reduction with lithium aluminum hydride leads to a mixture of 20-alcohols in which the β-epimer predominates, but to a lesser extent than in the absence of the epoxy group (31). This is not surprising since a 17α-hydroxy derivative is formed during the reduction. Furthermore, the geometry of the side chain is not the same as in the case of ring-D-saturated steroids. The available evidence points to conformation B for 16,17-epoxy-20-steroids; for obvious steric reasons conformation* B_1 *seems more probable. Likewise, one has to be cautious when interpreting the predominant reduction to a 20α-alcohol of 17α-acetoxy-20-keto steroids (9); one has to consider that during the reduction an aluminum hydride complex with a 17α-oxygen function is formed; we have seen that in the presence of such a substituent the main reduction product is a 20α-alcohol.*

[15]*In this article we are not discussing the side-chain conformations of 18-oxygenated steroids. For certain aspects we refer to the already cited article by Heusler and Wettstein (13) and to their preceding article (35).*

[16]*We refer only to products belonging to the groups discussed in Table I.*

1. CH. R. ENGEL and S. RAKHIT. Can. J. Chem. This issue.
2. F. V. BRUTCHER, JR., and W. BAUER, JR. J. Am. Chem. Soc. **84**, 2236 (1962).
3. CH. R. ENGEL, S. RAKHIT, and W. W. HUCULAK. Can. J. Chem. **40**, 921 (1962).
4. G. JUST and R. NAGARAJAN. Can. J. Chem. **39**, 548 (1961).
5. CH. R. ENGEL and W. W. HUCULAK. Can. J. Chem. **37**, 2031 (1959).
6. L. F. FIESER and M. FIESER. Steroids. Reinhold Publishing Corp., New York, and Chapman and Hall, Ltd., London. 1960.
7. D. J. CRAM and F. A. A. ELHAFEZ. J. Am. Chem. Soc. **74**, 5828 (1952).
8. H. HIRSHMANN and F. B. HIRSHMANN. J. Biol. Chem. **187**, 137 (1950).
9. R. B. TURNER. J. Am. Chem. Soc. **75**, 3489 (1953).
10. D. K. FUKUSHIMA and E. D. MEYER. J. Org. Chem. **23**, 174 (1958).
11. G. P. MUELLER, R. E. STOBAUGH, and R. S. WINNIFORD. J. Am. Chem. Soc. **75**, 4888 (1953).
12. E. L. SHAPIRO, D. GOULD, and E. B. HERSHBERG. J. Am. Chem. Soc. **77**, 2912 (1955).
13. K. HEUSLER and A. WETTSTEIN. Helv. Chim. Acta, **45**, 347 (1962).
14. C. DJERASSI, I. FORNAGUERA, and O. MANCERA. J. Am. Chem. Soc. **81**, 2383 (1959).
15. C. DJERASSI and W. KLYNE. J. Am. Chem. Soc. **79**, 1506 (1957).
16. C. DJERASSI, L. A. MITSCHER, and B. J. MITSCHER. J. Am. Chem. Soc. **81**, 947 (1959).
17. C. DJERASSI. Private communication.
18. G. STORK, H. N. KHASTGIR, and A. J. SOLO. J. Am. Chem. Soc. **80**, 6457 (1958).
19. R. ANLIKER, M. MÜLLER, M. PERELMAN, J. WOHLFART, and H. HEUSSER. Helv. Chim. Acta, **42**, 1071 (1959).
20. R. N. JONES, D. A. RAMSAY, F. HERLING, and K. DOBRINER. J. Am. Chem. Soc. **74**, 2828 (1952).
21. E. J. COREY. J. Am. Chem. Soc. **75**, 2301 (1953).
22. N. L. ALLINGER and M. A. DAROOGE. J. Am. Chem. Soc. **83**, 4256 (1961).
23. N. L. ALLINGER and M. A. MILLER. J. Am. Chem. Soc. **83**, 2145 (1961).
24. CH. R. ENGEL. Abstracts, 1st International Congress of Endocrinology, Copenhagen. 1960. p. 913.
25. CH. R. ENGEL and H. JAHNKE. Can. J. Biochem. Physiol. **35**, 1047 (1957).
26. J. FRIED, W. R. KESSLER, and A. BORMAN. Ann. N.Y. Acad. Sci. **71**, 494 (1958).
27. R. N. JONES, P. HUMPHRIES, F. HERLING, and K. DOBRINER. J. Am. Chem. Soc. **74**, 2820 (1952).
28. M. E. WALL and S. SEROTA. Tetrahedron, **10**, 238 (1960).
29. R. NAGARAJAN and G. JUST. Can. J. Chem. **39**, 1274 (1961).
30. L. H. SARETT, M. FEURER, and K. FOLKERS. J. Am. Chem. Soc. **73**, 1777 (1951).
31. P. L. JULIAN, E. W. MEYER, W. J. KARPEL, and W. COLE. J. Am. Chem. Soc. **73**, 1982 (1951).
32. C. DJERASSI, G. ROSENKRANZ, J. PATAKI, and S. KAUFMANN. J. Biol. Chem. **194**, 115 (1952).
33. R. ANTONUCCI, S. BERNSTEIN, M. HELLER, R. LENHARD, R. LITTELL, and J. H. WILLIAMS. J. Org. Chem. **18**, 70 (1953).
34. M. K. BIRMINGHAM, P. J. WARD, and H. TRAIKOV. Proc. Can. Federation Biol. Soc. **5**, 14 (1962).
35. J. SCHMIDLIN and A. WETTSTEIN. Helv. Chim. Acta, **45**, 331 (1962).

RECEIVED JULY 16, 1962.
DEPARTMENT OF CHEMISTRY,
LAVAL UNIVERSITY,
QUEBEC, QUE.

THE PURIFICATION OF SOLVENTS FOR ULTRAVIOLET ABSORPTION SPECTROSCOPY

SERGE N. VINOGRADOV

The purification of hydrocarbons for use as solvents in ultraviolet absorption spectroscopy is usually achieved through repeated and prolonged shaking with concentrated sulphuric acid or sulphuric acid – nitric acid mixture, washing with water, and finally distillation or passage through a column of suitable adsorbent such as alumina or silica gel (1–4). In the course of the purification of a large number of hydrocarbons ranging from pentane to tetradecane and cyclopentane to cyclooctane, for use in 5 to 10 cm thicknesses in the 2500–2600 Å region, the following procedure was found to be not only thorough but also quick and convenient. About 200–300 ml of the hydrocarbon was shaken in a 500-ml separatory funnel with about 100 ml of a 1:1 by volume mixture of

1. CH. R. ENGEL and S. RAKHIT. Can. J. Chem. This issue.
2. F. V. BRUTCHER, JR., and W. BAUER, JR. J. Am. Chem. Soc. **84**, 2236 (1962).
3. CH. R. ENGEL, S. RAKHIT, and W. W. HUCULAK. Can. J. Chem. **40**, 921 (1962).
4. G. JUST and R. NAGARAJAN. Can. J. Chem. **39**, 548 (1961).
5. CH. R. ENGEL and W. W. HUCULAK. Can. J. Chem. **37**, 2031 (1959).
6. L. F. FIESER and M. FIESER. Steroids. Reinhold Publishing Corp., New York, and Chapman and Hall, Ltd., London. 1960.
7. D. J. CRAM and F. A. A. ELHAFEZ. J. Am. Chem. Soc. **74**, 5828 (1952).
8. H. HIRSHMANN and F. B. HIRSHMANN. J. Biol. Chem. **187**, 137 (1950).
9. R. B. TURNER. J. Am. Chem. Soc. **75**, 3489 (1953).
10. D. K. FUKUSHIMA and E. D. MEYER. J. Org. Chem. **23**, 174 (1958).
11. G. P. MUELLER, R. E. STOBAUGH, and R. S. WINNIFORD. J. Am. Chem. Soc. **75**, 4888 (1953).
12. E. L. SHAPIRO, D. GOULD, and E. B. HERSHBERG. J. Am. Chem. Soc. **77**, 2912 (1955).
13. K. HEUSLER and A. WETTSTEIN. Helv. Chim. Acta, **45**, 347 (1962).
14. C. DJERASSI, I. FORNAGUERA, and O. MANCERA. J. Am. Chem. Soc. **81**, 2383 (1959).
15. C. DJERASSI and W. KLYNE. J. Am. Chem. Soc. **79**, 1506 (1957).
16. C. DJERASSI, L. A. MITSCHER, and B. J. MITSCHER. J. Am. Chem. Soc. **81**, 947 (1959).
17. C. DJERASSI. Private communication.
18. G. STORK, H. N. KHASTGIR, and A. J. SOLO. J. Am. Chem. Soc. **80**, 6457 (1958).
19. R. ANLIKER, M. MÜLLER, M. PERELMAN, J. WOHLFART, and H. HEUSSER. Helv. Chim. Acta, **42**, 1071 (1959).
20. R. N. JONES, D. A. RAMSAY, F. HERLING, and K. DOBRINER. J. Am. Chem. Soc. **74**, 2828 (1952).
21. E. J. COREY. J. Am. Chem. Soc. **75**, 2301 (1953).
22. N. L. ALLINGER and M. A. DAROOGE. J. Am. Chem. Soc. **83**, 4256 (1961).
23. N. L. ALLINGER and M. A. MILLER. J. Am. Chem. Soc. **83**, 2145 (1961).
24. CH. R. ENGEL. Abstracts, 1st International Congress of Endocrinology, Copenhagen. 1960. p. 913.
25. CH. R. ENGEL and H. JAHNKE. Can. J. Biochem. Physiol. **35**, 1047 (1957).
26. J. FRIED, W. R. KESSLER, and A. BORMAN. Ann. N.Y. Acad. Sci. **71**, 494 (1958).
27. R. N. JONES, P. HUMPHRIES, F. HERLING, and K. DOBRINER. J. Am. Chem. Soc. **74**, 2820 (1952).
28. M. E. WALL and S. SEROTA. Tetrahedron, **10**, 238 (1960).
29. R. NAGARAJAN and G. JUST. Can. J. Chem. **39**, 1274 (1961).
30. L. H. SARETT, M. FEURER, and K. FOLKERS. J. Am. Chem. Soc. **73**, 1777 (1951).
31. P. L. JULIAN, E. W. MEYER, W. J. KARPEL, and W. COLE. J. Am. Chem. Soc. **73**, 1982 (1951).
32. C. DJERASSI, G. ROSENKRANZ, J. PATAKI, and S. KAUFMANN. J. Biol. Chem. **194**, 115 (1952).
33. R. ANTONUCCI, S. BERNSTEIN, M. HELLER, R. LENHARD, R. LITTELL, and J. H. WILLIAMS. J. Org. Chem. **18**, 70 (1953).
34. M. K. BIRMINGHAM, P. J. WARD, and H. TRAIKOV. Proc. Can. Federation Biol. Soc. **5**, 14 (1962).
35. J. SCHMIDLIN and A. WETTSTEIN. Helv. Chim. Acta, **45**, 331 (1962).

RECEIVED JULY 16, 1962.
DEPARTMENT OF CHEMISTRY,
LAVAL UNIVERSITY,
QUEBEC, QUE.

THE PURIFICATION OF SOLVENTS FOR ULTRAVIOLET ABSORPTION SPECTROSCOPY

SERGE N. VINOGRADOV

The purification of hydrocarbons for use as solvents in ultraviolet absorption spectroscopy is usually achieved through repeated and prolonged shaking with concentrated sulphuric acid or sulphuric acid – nitric acid mixture, washing with water, and finally distillation or passage through a column of suitable adsorbent such as alumina or silica gel (1–4). In the course of the purification of a large number of hydrocarbons ranging from pentane to tetradecane and cyclopentane to cyclooctane, for use in 5 to 10 cm thicknesses in the 2500–2600 Å region, the following procedure was found to be not only thorough but also quick and convenient. About 200–300 ml of the hydrocarbon was shaken in a 500-ml separatory funnel with about 100 ml of a 1:1 by volume mixture of

concentrated nitric and sulphuric acids, twice, for 30 seconds each time, then shaken two or three times for 15 seconds with 100 ml concentrated sulphuric acid, washed three times with distilled water, dried over anhydrous calcium sulphate, and passed through ca. 60 cm of silica gel (Davison grade 12, mesh size 60–200) packed in an ordinary 50-ml burette. This amount of silica gel was sufficient for the purification of 200–300 ml of hydrocarbon; it usually was possible to observe visually the progress of the adsorbed, slightly yellowish impurities down the column. In the case of the low-boiling hydrocarbons it was found best to chill the mixture before shaking because of the large amount of heat evolved. It was observed that in most cases shaking with concentrated sulphuric acid (unless very lengthy) and (or) passage through a silica gel column did not result in sufficient improvement in the transmission of the hydrocarbons in the 2500 Å region. Prolonged shaking (>1 minute) with the acid mixture was found to be superfluous for our purposes. It may be necessary perhaps in cases where the best possible transmission is desired at wavelengths down to 2100 Å.

Figure 1 shows some typical results obtained with the method described above. The compounds used were reagent grade or had a stipulated purity of better than 99 mole%.

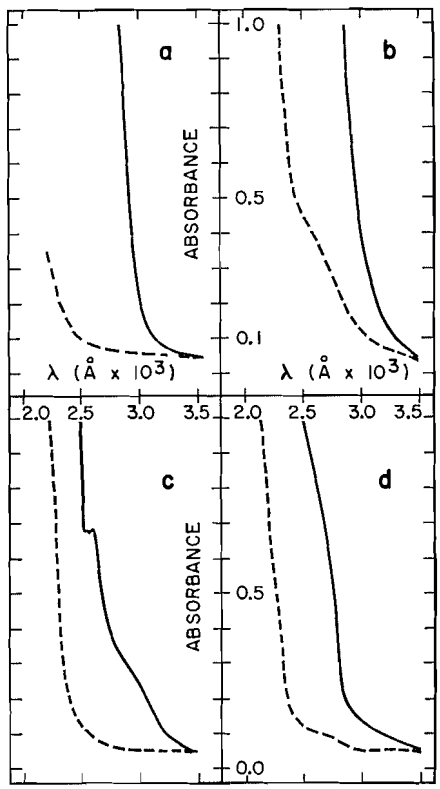

FIG. 1. The spectra of some ultraviolet solvents: (*a*) *n*-hexane, 5 cm; (*b*) *n*-tetradecane, 2 cm; (*c*) cyclohexane, 5 cm; (*d*) FC-75, 5 cm. —— original solvent; – – – purified solvent.

The hydrocarbons thus purified were at least as good as or better than the available and much more expensive Eastman Kodak or Matheson, Coleman and Bell spectrograde solvents. FC-75 is a mixture of isomers of the perfluorinated cyclic ether $C_8F_{16}O$ available commercially from Minnesota Mining and Manufacturing Company.

In conclusion, it should be noted that the limiting factor with respect to the time required by the procedure is the rate of passage of the solvent through the silica gel column.

1. G. HESE and H. SCHILDKNECHT. Angew. Chem. **67**, 737 (1955).
2. W. J. POTTS, JR. J. Chem. Phys. **30**, 809 (1952).
3. A. WEISSBERGER and E. S. PROSKAUER. Technique of organic chemistry. Vol. VII. 2nd ed. Interscience Publishers Inc. 1955.
4. K. B. WIBERG. Laboratory technique in organic chemistry. McGraw-Hill Book Co. 1960.

RECEIVED JULY 20, 1962.
CHEMISTRY DEPARTMENT,
UNIVERSITY OF ALBERTA,
EDMONTON, ALBERTA.

THE FRANCK–CONDON PRINCIPLE AND THE IONIZATION OF MOLECULES

JACQUES E. COLLIN

Ionization potentials obtained by electron impact or photon impact are generally discussed with reference to the Franck–Condon principle for both ground and ionic states concerned. By doing so it is admitted that the interaction time of the ionizing particle and the molecule, and the time necessary for the electron to leave the interested bond region of the molecule, were short, compared to the time of a complete vibration, considering only here diatomics.

In a recent paper, Stevenson (1) indicated that the particularly well-known case of hydrogen seemed to be in conflict with the Franck–Condon principle; this conclusion was based on a careful consideration of potential curves and observed ionization potentials. It was shown that, although the Franck–Condon principle would predict the highest probability for the transition to the vibrationally excited $v = 2$ state of the ion, the experimental data gave the 0–0 transition. This was later explained, thanks to the beautiful work of Marmet and Kerwin, who showed that it was mainly a matter of sensitivity of the detecting device (2).

The H—H bond being strong and the atoms light, the fundamental frequency is very high: 4276 cm^{-1}. This is thus a case where non-applicability of the Franck–Condon principle might be encountered, but Marmet and Kerwin's work lead to the theoretically expected relative cross sections for the 0–0, 0–1, 0–2 transitions.

In the case of heavier molecules, particularly the halogens having low fundamental frequencies, differences between electron or photon impact ionization potentials and those obtained by ultraviolet spectroscopy should be increasing, at least if there is an important modification of internuclear distance in the ion. This is indeed found experimentally.

Very few experimental data on vibrational quantum levels of ionic states of simple molecules are known. They have been summarized in Table I, where vibrational frequencies, ionization potentials, equilibrium distances, most probable ionization-calculated transitions, and most probable experimental values are given. Vibrational overlap integrals estimations, admitting the harmonic approximation, have been used for the calculated transition probabilities (3–6). It is interesting to compare the most probable theoretical transitions with those deduced from the experimental ionization potentials determined by mass spectrometry or photoionization:

In conclusion, it should be noted that the limiting factor with respect to the time required by the procedure is the rate of passage of the solvent through the silica gel column.

1. G. HESE and H. SCHILDKNECHT. Angew. Chem. **67**, 737 (1955).
2. W. J. POTTS, JR. J. Chem. Phys. **30**, 809 (1952).
3. A. WEISSBERGER and E. S. PROSKAUER. Technique of organic chemistry. Vol. VII. 2nd ed. Interscience Publishers Inc. 1955.
4. K. B. WIBERG. Laboratory technique in organic chemistry. McGraw-Hill Book Co. 1960.

RECEIVED JULY 20, 1962.
CHEMISTRY DEPARTMENT,
UNIVERSITY OF ALBERTA,
EDMONTON, ALBERTA.

THE FRANCK–CONDON PRINCIPLE AND THE IONIZATION OF MOLECULES

JACQUES E. COLLIN

Ionization potentials obtained by electron impact or photon impact are generally discussed with reference to the Franck–Condon principle for both ground and ionic states concerned. By doing so it is admitted that the interaction time of the ionizing particle and the molecule, and the time necessary for the electron to leave the interested bond region of the molecule, were short, compared to the time of a complete vibration, considering only here diatomics.

In a recent paper, Stevenson (1) indicated that the particularly well-known case of hydrogen seemed to be in conflict with the Franck–Condon principle; this conclusion was based on a careful consideration of potential curves and observed ionization potentials. It was shown that, although the Franck–Condon principle would predict the highest probability for the transition to the vibrationally excited $v = 2$ state of the ion, the experimental data gave the 0–0 transition. This was later explained, thanks to the beautiful work of Marmet and Kerwin, who showed that it was mainly a matter of sensitivity of the detecting device (2).

The H—H bond being strong and the atoms light, the fundamental frequency is very high: 4276 cm^{-1}. This is thus a case where non-applicability of the Franck–Condon principle might be encountered, but Marmet and Kerwin's work lead to the theoretically expected relative cross sections for the 0–0, 0–1, 0–2 transitions.

In the case of heavier molecules, particularly the halogens having low fundamental frequencies, differences between electron or photon impact ionization potentials and those obtained by ultraviolet spectroscopy should be increasing, at least if there is an important modification of internuclear distance in the ion. This is indeed found experimentally.

Very few experimental data on vibrational quantum levels of ionic states of simple molecules are known. They have been summarized in Table I, where vibrational frequencies, ionization potentials, equilibrium distances, most probable ionization-calculated transitions, and most probable experimental values are given. Vibrational overlap integrals estimations, admitting the harmonic approximation, have been used for the calculated transition probabilities (3–6). It is interesting to compare the most probable theoretical transitions with those deduced from the experimental ionization potentials determined by mass spectrometry or photoionization:

TABLE I

	ν (cm^{-1})*	ν^+ (cm^{-1})*	r_0*	$r_0{}^+$*	$h\nu$ (ev)	$h\nu^+$ (ev)	EI†	PI†	SP†	Δ_1	Δ_2	Transition	
												Calc.	Expt.
H_2	4276	2297	0.749	1.06	0.53	0.27	15.49 15.37	15.427	15.427	0.06–0.05	0.06–0.05	0–2	0–0
N_2	2359	2207	1.094	1.116	0.29	0.26	15.62	15.59	15.572	0.03	0.05	0–0	0–0
O_2	1580	1876	1.204	1.121	0.19_6	0.23_2	12.24	12.14	12.13	0.10	0.11	0–1	0–0
CO	2168	2214	1.128	1.112	0.26_9	0.27_4	14.08	14.04	14.01	0.04	−0.07	0–0	0–0
NO	1904	2377	1.15	1.06	0.23_6	0.29_4	9.41 9.25	9.24	—	0.17	—	0–1	0–0
F_2	892	—	—	—	0.11	—	16.16 15.83	15.7	—	0.46 0.13	—	—	0–4 ? 0–1 ?
Cl_2	565	645	1.983	1.89	0.07	0.081	11.65 11.63‡	11.48	11.32	0.17	0.33	0–2	0–4 ?
Br_2	324	—	2.28	—	0.04	—	10.69	10.55	(12.8)	0.18	—	—	0–4 ?
I_2	214	—	2.66	—	0.02_6	—	9.32 9.35	9.28	(10.0)	0.04	—	—	0–0 0–1 ?
HF	4141	—	0.916	—	0.51	—	15.97	—	—	—	—	—	0–0 ?
HCl	2860	2675	1.277	1.315	0.34_4	0.33_1	12.62	12.74	(12.90) (13.75)	−0.12	—	—	0–0
HBr	2649	—	1.414 1.459	—	0.32_8	—	11.69	11.62	(12.64) (12.04)	0.07	—	—	0–0
HI	2309	—	—	—	0.28_6	—	10.39	10.38	10.38	0.01	0.01	—	0–0

NOTE: r_0 and $r_0{}^+$ are in angstroms; EI (electron impact), PI (photon impact), and SP (spectroscopic) are in ev; Δ_1 and Δ_2 are the differences (EI−PI) and (EI−SP); the calc. and expt. transitions represent the most probable calculated and experimentally observed vibrational transitions (see text); and ν^+, $h\nu^+$, $r_0{}^+$ refer to the ionic state.

*Reference 8.
†Reference 9.
‡Reference 7.

	Vibrational transition probability		
	Theoretical	Lowest experimental	Most probable experimental
H_2	0–2	0–0	0–2
N_2	0–0	0–0	—
O_2	0–1	0–0	—
CO	0–0	0–0	—
NO	0–1	0–0	0–1
Cl_2	0–2	0–4	—

At first glance, the experimental and theoretical results coincide only in two cases: N_2 and CO. In one other case, Cl_2, one gets experimentally too high a value, and in three cases, O_2, H_2, NO, too low a value. The H_2 low value appears to correspond to the 0–0 transition, which has a non-negligible probability (4/10 of the most probable 0–2 transition), as Kerwin and Marmet have shown. A similar situation exists for NO and was examined by Cloutier and Schiff (4). For Cl_2, the discrepancy is serious and unexpected indeed. The 0–2 transition is theoretically the most probable, but the 0–0 transition is quite probable too (3/4 that for 0–2) and the same situation as in hydrogen is found. On the contrary the experimental evidence corresponds to a higher transition. The vibrational quantum is quite small ($0.081v$) however, and one or two vibrational jumps might have been missed, due to experimental errors, although the reproducibility of the measurements is good and the same results have been found by different authors. Thus simple application of the Franck–Condon principle appears difficult. It should be noted that the ionic state Cl_2^+ has an equilibrium distance considerably shorter than that for the molecular ground state, the difference being of the order of 5%.

For fluorine, the lack of experimental data on vibrational frequencies for ionic states does not allow a safe discussion. Assuming a variation similar to that for chlorine, however, it seems that the most probable transition is the 0–1 one.

The case of Br_2, as well as of I_2, is similar, but it becomes difficult to discuss the ionization potential differences, the vibrational quanta being of the order of magnitude of the thermal energy of the molecules. The experimental data, however, seem always to indicate a transition to a higher vibrationally excited state of the ion; apparently, as in Cl_2^+, the nuclear distance is shorter in the ion.

For the corresponding hydracids, the 0–0 transition appears to be the most probable, although, at least for HCl, the nuclear distance has undergone a variation of 3.5%. The spectroscopic ionization potential, however, is not very well known and the interpretation must be considered as tentative. For the variation of the distances in the ion, the following may be observed. In all cases where the 0–0 transition is observed and the ionic nuclear distance is known the variation in nuclear separation from the molecule to the ion is not greater than 3%. When there is a transition mainly to an excited vibrational state of the ion and when the nuclear distances are known, the variation of the latter has been found to be 30, 9, 8, and 4.5% respectively for H_2, O_2, NO, and Cl_2, the case of hydrogen being an extreme one. These facts may be used to estimate the nuclear distances in the molecular ions when no spectroscopic data are available, which is the case for F_2, Br_2, I_2, HF, HBr, and HI. It may be anticipated that in F_2^+, Br_2^+ (perhaps also I_2^+) the nuclear distance in the ion is considerably shorter than that in the molecule itself. On the contrary, in the acids HF, HBr, and HI, it may be expected that the nuclear distances are much the same in the molecule and in the molecular ion.

On the basis of experimental data, we also calculated the dissociation energies of the molecular ion, $D(A—B^+)$, and we obtained the values given in Table II.

TABLE II

Dissociation energies (kcal/mole)

	D(A—B)	$D(A—B)^{+}_{B^{+}}$	Transition
HF	135	158	0–0
HCl	102	108	0–0
HBr	87	93	0–0
HI	71	74–78	0–0
F_2	37	77	0–4 ?
Cl_2	57	97	0–2 or 0–4 ?
Br_2	45.4	83	0–4 ?
I_2	35.5	80	0–1

It is obvious that $D(A—B)^{+}_{B^{+}}$, leading to B^{+}, is much higher than D(A—B) in the halogens themselves, whereas for the hydracids, one gets very much the same value for both molecular and ionic states. This is precisely the case when the 0–0 transition is positively observed, as was expected since there must not be important changes in nuclear distances. On the contrary, for the halogens the considerable increase of the dissociation energy in the ion should result in a considerable shortening of the bond distance. It is then expected that the transition to vibrationally excited states will have a greater probability.

If one thus takes these considerations into account, it seems that the Franck–Condon principle is fairly well respected and discrepancies between accurately determined ionization potentials obtained by electron impact or photoionization and spectroscopic ionization potentials might be taken as a means of evaluating the modification of internuclear distances in the ions when no better means are available.

1. D. P. Stevenson. J. Am. Chem. Soc. **82**, 5961 (1960).
2. P. Marmet and L. Kerwin. Can. J. Phys. **38**, 972 (1960).
3. J. Momigny. Unpublished data.
4. G. G. Cloutier and H. I. Schiff. J. Chem. Phys. **31**, 793 (1959).
5. L. Kerwin, P. Marmet, and G. G. Clarke. Mass Spectrometry Conference, Oxford. 1961.
6. M. Krauss. J. Chem. Phys. **26**, 1776 (1957).
7. D. C. Frost and C. A. McDowell. Can. J. Chem. **38**, 407 (1960).
8. G. Herzberg. Spectra of diatomic molecules. Van Nostrand.
9. K. Watanabe, T. Nakayama, and J. Mottl. Final rept. on ionization potentials. Contract DA-04-200-ORD480 and 737. 1959. R. W. Kiser. Tables of ionization potentials. Kansas State University. 1960.

Received August 2, 1962.
Laboratoire de Spectrométrie de Masse,
Université de Liège,
Liège, Belgique.

THE SYNTHESIS OF LIGNIN MODEL SUBSTANCES: 5-HYDROXYVANILLIN AND 5-HYDROXYACETOGUAIACONE

S. K. Banerjee, M. Manolopoulo, and J. M. Pepper

In connection with studies on the oxidation of lignin it became necessary to prepare various lignin model substances, one of which was 5-hydroxyvanillin (II).

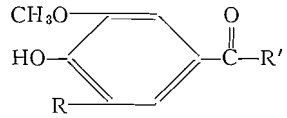

(I) R = R′ = H (IV) R = H, R′ = CH_3

(II) R = OH, R′ = H (V) R = OH, R′ = CH_3

(III) R = I, R′ = H (VI) R = I, R′ = CH_3

TABLE II

Dissociation energies (kcal/mole)

	D(A—B)	$D(A—B)^{+}_{B^{+}}$	Transition
HF	135	158	0–0
HCl	102	108	0–0
HBr	87	93	0–0
HI	71	74–78	0–0
F_2	37	77	0–4 ?
Cl_2	57	97	0–2 or 0–4 ?
Br_2	45.4	83	0–4 ?
I_2	35.5	80	0–1

It is obvious that $D(A—B)^{+}_{B^{+}}$, leading to B^{+}, is much higher than D(A—B) in the halogens themselves, whereas for the hydracids, one gets very much the same value for both molecular and ionic states. This is precisely the case when the 0–0 transition is positively observed, as was expected since there must not be important changes in nuclear distances. On the contrary, for the halogens the considerable increase of the dissociation energy in the ion should result in a considerable shortening of the bond distance. It is then expected that the transition to vibrationally excited states will have a greater probability.

If one thus takes these considerations into account, it seems that the Franck–Condon principle is fairly well respected and discrepancies between accurately determined ionization potentials obtained by electron impact or photoionization and spectroscopic ionization potentials might be taken as a means of evaluating the modification of internuclear distances in the ions when no better means are available.

1. D. P. Stevenson. J. Am. Chem. Soc. **82**, 5961 (1960).
2. P. Marmet and L. Kerwin. Can. J. Phys. **38**, 972 (1960).
3. J. Momigny. Unpublished data.
4. G. G. Cloutier and H. I. Schiff. J. Chem. Phys. **31**, 793 (1959).
5. L. Kerwin, P. Marmet, and G. G. Clarke. Mass Spectrometry Conference, Oxford. 1961.
6. M. Krauss. J. Chem. Phys. **26**, 1776 (1957).
7. D. C. Frost and C. A. McDowell. Can. J. Chem. **38**, 407 (1960).
8. G. Herzberg. Spectra of diatomic molecules. Van Nostrand.
9. K. Watanabe, T. Nakayama, and J. Mottl. Final rept. on ionization potentials. Contract DA-04-200-ORD480 and 737. 1959. R. W. Kiser. Tables of ionization potentials. Kansas State University. 1960.

Received August 2, 1962.
Laboratoire de Spectrométrie de Masse,
Université de Liège,
Liège, Belgique.

THE SYNTHESIS OF LIGNIN MODEL SUBSTANCES: 5-HYDROXYVANILLIN AND 5-HYDROXYACETOGUAIACONE

S. K. Banerjee, M. Manolopoulo, and J. M. Pepper

In connection with studies on the oxidation of lignin it became necessary to prepare various lignin model substances, one of which was 5-hydroxyvanillin (II).

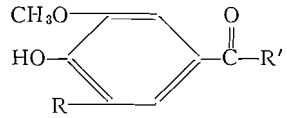

(I) R = R′ = H (IV) R = H, R′ = CH_3

(II) R = OH, R′ = H (V) R = OH, R′ = CH_3

(III) R = I, R′ = H (VI) R = I, R′ = CH_3

An examination of the reported syntheses (1, 2, 3, 4) indicated that no simple method was available other than those requiring heated autoclaves. A study was made, therefore, of the most promising procedure, which involved the copper-catalyzed hydrolysis of 5-halovanillin. It was early shown that 5-iodovanillin (III) underwent reaction much more readily than either the 5-bromo- or 5-chloro-derivatives. A satisfactory synthesis of II could indeed be obtained under reflux conditions, thus avoiding the need for reactions under pressure as had been recommended by previous workers. Of importance was the recognition that both the effectiveness of the catalyst as well as the nature of the products obtained were markedly dependent on the particular copper that was used. The authors maintained that only if a reproducible catalyst could be described would a synthetic procedure be of real value. This desire was achieved by the discovery that the addition of cupric ions provided the necessary catalytic activity for this alkaline hydrolysis reaction.

A study of the ratio of reactants, and the time and temperature of the reaction, resulted in a procedure whereby complete conversion of 5-iodovanillin (III) was achieved. The major product was 5-hydroxyvanillin (II) but in all cases a minor amount of the reductive dehalogenation product, vanillin (I), was also formed. The separation and identification of these products was made using both paper and gas–liquid chromatography. Separation and purification of the required II was readily achieved by recrystallization from benzene. The yield of purified product was 65–70% based on III.

This ready conversion of vanillin to 5-hydroxyvanillin prompted the attempt to similarly convert another lignin oxidation product, acetoguaiacone (IV) (also known as acetovanillone), to the previously unreported 5-hydroxyacetoguaiacone (V). No difficulty was experienced in this synthesis. The only modification involved an increase in the time of reflux from 4.5 to 6.5 hours in order to convert all the 5-iodoacetoguaiacone (VI). As expected, the only other product to accompany the major product (V), but in much less amount, was the reductive dehalogenation compound, acetoguaiacone (IV). The structure of V was confirmed by analyses, absorption spectra, and conversion, by methylation, to the previously known 3,4,5-trimethoxyphenyl methyl ketone. The yield of recrystallized product was 45–50%.

A more complete discussion of the significance of the role of the copper catalyst and of the mechanism of formation of the products in such copper-catalyzed alkaline dehalogenation reactions is being prepared.

EXPERIMENTAL

Melting points are uncorrected. The infrared spectrum was measured using a Perkin–Elmer Model 21 instrument with sodium chloride optics.

Paper Chromatography

5-Hydroxyvanillin, vanillin, and 5-iodovanillin were separated by descending chromatography using Whatman No. 1 paper and the solvent system of *n*-butanol saturated with 2% ammonia. A saturated solution of 2,4-dinitrophenylhydrazine in 1 *N* hydrochloric acid was the spray reagent. For these compounds the R_f values were 0.38, 0.50, and 0.48 respectively.

Gas–Liquid Chromatography

A Beckman GC-2 chromatograph, with a thermal conductivity detector unit, was used after some modification to place the injection system as close as possible to one end of the column, and to make it more comparable electronically to the GC-2A. The column was made from 3 ft×1/4 in. I.D. copper tubing and packed with Apiezon N grease on Fluoropak 80 (Wilkens Instrument and Research Inc.) in the ratio of 3 to 17. The chromatographic separations were effected at 220° using 30 p.s.i. helium carrier gas at a flow rate of 0.9 cc/second. Under these conditions the retention times for vanillin, 5-hydroxyvanillin, and 5-iodovanillin were 2.25, 4.7, and 12.0 minutes respectively, and for acetoguaiacone, 5-hydroxyacetoguaiacone, and 5-iodoacetoguaiacone they were 3.0, 6.7, and 19.5 minutes respectively.

5-Hydroxyvanillin

5-Iodovanillin (2.8 g), hydrated cupric sulphate (1.6 g), and 4 *N* sodium hydroxide (76 ml) were refluxed (105°) for 4.5 hours with continuous stirring under nitrogen. After cooling to 60–70°, the mixture was filtered under suction and the residue washed with hot water (3×10 ml). The alkaline solution was cooled to 10° and acidified to pH 3–4, by the dropwise addition of concentrated hydrochloric acid. During this addition the mixture was stirred continuously and the temperature maintained below 25°.

The resulting mixture, which contained a small amount of precipitate, was extracted continuously with ether for 16 hours. After being dried over anhydrous magnesium sulphate, the ether was removed (60–65°) to leave a dark gray product, 1.5 g. All but 0.10 g was dissolved in hot benzene, from which, after concentration to 75 ml, 5-hydroxyvanillin crystallized (1.15 g, 68%), m.p. 128–129°. Recrystallization from benzene, with charcoaling, gave a chromatographically pure product, m.p. 133–134°; reported 132–134° (2). With the exception of traces of 5-hydroxyvanillin the mother liquors contained only vanillin as indicated by gas–liquid chromatography.

5-Hydroxyacetoguaiacone

5-Iodoacetoguaiacone (2.9 g) (5), hydrated copper sulphate (1.6 g), and 4 *N* sodium hydroxide (76 ml) were refluxed (105°) for 6.5 hours with continuous stirring under nitrogen. As a result of a procedure similar to that used for the isolation of II, an ether extract (1.3 g) was obtained. Of this, 0.3 g was sparingly soluble in boiling benzene but the remainder crystallized on cooling of the benzene solution to yield crude 5-hydroxyacetoguaiacone (0.8 g, 44%), m.p. 162–166°. A sample recrystallized from *n*-hexane–ethanol (5:1) melted at 166–167°. Calc. for $C_9H_{10}O_4$: C, 59.33; H, 5.53%. Found: C, 58.99; H, 5.64%. Infrared spectrum (KBr disk) (main peaks only): 3500–3300 (s), 1657 (m), 1600 (s), 1528 (m), 1470 (m), 1357 (s), 1320 (s), 1200 (s), 870 cm^{-1} (m). Methylation with alkaline dimethylsulphate gave 3,4,5-trimethoxyphenyl methyl ketone, m.p. 77–78°; mixed m.p. with an authentic sample, 77–78°. The infrared spectrum was identical with that of the authentic sample.

ACKNOWLEDGMENTS

Grateful acknowledgment is made of the financial assistance provided by the National Research Council.

1. E. Späth and H. Roder. Monatsh. **43**, 93 (1922).
2. W. Bradley, R. Robinson, and G. Schwarzenbach. J. Chem. Soc. 793 (1930).
3. I. A. Pearl and D. L. Beyer. J. Am. Chem. Soc. **74**, 4262 (1952).
4. R. A. McIvor. M.A. Thesis, University of Saskatchewan, Saskatoon, Sask. 1949.
5. L. W. Crawford, E. O. Eaton, and J. M. Pepper. Can. J. Chem. **34**, 1562 (1956).

Received July 23, 1962.
Department of Chemistry,
University of Saskatchewan,
Saskatoon, Saskatchewan.

THE *p*-BROMOPHENYLOSAZONES OF 3- AND 5-*O*-METHYL-D-XYLOSE AND AN APPLICATION OF THIN-LAYER CHROMATOGRAPHY

D. A. Applegarth, G. G. S. Dutton, and Y. Tanaka

In connection with our study of the monomethyl ethers produced in the partial methylation of D-xylose diethyl dithioacetal (1) it was necessary to prepare crystalline derivatives of the 3- and 5-*O*-methyl ethers. The only derivative reported (2) for the latter compound is the *p*-bromophenylosazone and the preparation of this osazone from both ethers has been described by Levene and Raymond (3). These authors reported that 3-*O*-methyl-D-xylose *p*-bromophenylosazone melted at 153–155° C with darkening and softening at 142–143° and that 5-*O*-methyl-D-xylose *p*-bromophenylosazone melted at 170–171° C and had $[\alpha]_D$ $-50° \rightarrow -30°$ (24 hours). We are in agreement with the figures quoted but find that the data for the two isomers have inadvertently been transposed in the original article.

5-Hydroxyvanillin

5-Iodovanillin (2.8 g), hydrated cupric sulphate (1.6 g), and 4 *N* sodium hydroxide (76 ml) were refluxed (105°) for 4.5 hours with continuous stirring under nitrogen. After cooling to 60–70°, the mixture was filtered under suction and the residue washed with hot water (3×10 ml). The alkaline solution was cooled to 10° and acidified to pH 3–4, by the dropwise addition of concentrated hydrochloric acid. During this addition the mixture was stirred continuously and the temperature maintained below 25°.

The resulting mixture, which contained a small amount of precipitate, was extracted continuously with ether for 16 hours. After being dried over anhydrous magnesium sulphate, the ether was removed (60–65°) to leave a dark gray product, 1.5 g. All but 0.10 g was dissolved in hot benzene, from which, after concentration to 75 ml, 5-hydroxyvanillin crystallized (1.15 g, 68%), m.p. 128–129°. Recrystallization from benzene, with charcoaling, gave a chromatographically pure product, m.p. 133–134°; reported 132–134° (2). With the exception of traces of 5-hydroxyvanillin the mother liquors contained only vanillin as indicated by gas–liquid chromatography.

5-Hydroxyacetoguaiacone

5-Iodoacetoguaiacone (2.9 g) (5), hydrated copper sulphate (1.6 g), and 4 *N* sodium hydroxide (76 ml) were refluxed (105°) for 6.5 hours with continuous stirring under nitrogen. As a result of a procedure similar to that used for the isolation of II, an ether extract (1.3 g) was obtained. Of this, 0.3 g was sparingly soluble in boiling benzene but the remainder crystallized on cooling of the benzene solution to yield crude 5-hydroxyacetoguaiacone (0.8 g, 44%), m.p. 162–166°. A sample recrystallized from *n*-hexane–ethanol (5:1) melted at 166–167°. Calc. for $C_9H_{10}O_4$: C, 59.33; H, 5.53%. Found: C, 58.99; H, 5.64%. Infrared spectrum (KBr disk) (main peaks only): 3500–3300 (s), 1657 (m), 1600 (s), 1528 (m), 1470 (m), 1357 (s), 1320 (s), 1200 (s), 870 cm^{-1} (m). Methylation with alkaline dimethylsulphate gave 3,4,5-trimethoxyphenyl methyl ketone, m.p. 77–78°; mixed m.p. with an authentic sample, 77–78°. The infrared spectrum was identical with that of the authentic sample.

ACKNOWLEDGMENTS

Grateful acknowledgment is made of the financial assistance provided by the National Research Council.

1. E. Späth and H. Roder. Monatsh. **43**, 93 (1922).
2. W. Bradley, R. Robinson, and G. Schwarzenbach. J. Chem. Soc. 793 (1930).
3. I. A. Pearl and D. L. Beyer. J. Am. Chem. Soc. **74**, 4262 (1952).
4. R. A. McIvor. M.A. Thesis, University of Saskatchewan, Saskatoon, Sask. 1949.
5. L. W. Crawford, E. O. Eaton, and J. M. Pepper. Can. J. Chem. **34**, 1562 (1956).

Received July 23, 1962.
Department of Chemistry,
University of Saskatchewan,
Saskatoon, Saskatchewan.

THE *p*-BROMOPHENYLOSAZONES OF 3- AND 5-*O*-METHYL-D-XYLOSE AND AN APPLICATION OF THIN-LAYER CHROMATOGRAPHY

D. A. Applegarth, G. G. S. Dutton, and Y. Tanaka

In connection with our study of the monomethyl ethers produced in the partial methylation of D-xylose diethyl dithioacetal (1) it was necessary to prepare crystalline derivatives of the 3- and 5-*O*-methyl ethers. The only derivative reported (2) for the latter compound is the *p*-bromophenylosazone and the preparation of this osazone from both ethers has been described by Levene and Raymond (3). These authors reported that 3-*O*-methyl-D-xylose *p*-bromophenylosazone melted at 153–155° C with darkening and softening at 142–143° and that 5-*O*-methyl-D-xylose *p*-bromophenylosazone melted at 170–171° C and had $[\alpha]_D$ $-50° \rightarrow -30°$ (24 hours). We are in agreement with the figures quoted but find that the data for the two isomers have inadvertently been transposed in the original article.

The formation of *p*-bromophenylosazones was found to be rapid; the relatively long heating periods used earlier (3) are disadvantageous, promoting tar formation. Thin-layer chromatography was found to be ideally suited to determining the optimum reaction conditions. A variety of sugars was tested, and it is concluded that a 5–10 minute reaction period of the free base and the sugar in acetic acid is optimal for preparation of these derivatives. It is likely that phenylhydrazine and other substituted phenylhydrazines behave similarly.

EXPERIMENTAL

3-O-Methyl-D-xylose

This was prepared from 3-*O*-methyl-1,2-*O*-isopropylidene-D-glucose by a reported procedure (4). The compound had m.p. and mixed m.p. 101° and $[\alpha]_D^{22}$ 16° with an R_f in butanone–water azeotrope of 0.23. *p*-Bromophenylhydrazine (85 mg) and 3-*O*-methyl-D-xylose (25 mg) were dissolved in glacial acetic acid (0.75 ml) and the solution diluted with water (0.5 ml). When the solution was heated on the steam bath for 5 minutes, then cooled to room temperature, a mass of orange-yellow crystals separated. After it was washed with aqueous acetic acid, the osazone was recrystallized from ethyl acetate – petroleum ether (30–60°). 3-*O*-Methyl-D-xylose *p*-bromophenylosazone had m.p. 174–175° and $[\alpha]_D^{23}$ −55° → −27° (*c*, 0.5 in pyridine–ethanol, 2:3) (24 hours). Anal. calc. for $C_{18}H_{20}N_4O_3Br_2$: C, 43.2; H, 4.0; N, 11.2%. Found: C, 43.44; H, 3.97; N, 11.0%.

5-O-Methyl-D-xylose

This was prepared from 3,5-anhydro-1,2-*O*-isopropylidene-D-xylose by reaction with sodium methoxide as previously described (3). 1,2-*O*-Isopropylidene-5-*O*-methyl-D-xylose (m.p. 85°) was hydrolyzed with sulphuric acid (1 *N*) on the steam bath for 1 hour and the solution deionized with Duolite A4 resin. Chromatographic examination of the resulting sirup showed four components having R_f values 0.32 (VS), 0.19 (W), 0.09 (W), and 0.04 (W). Separation on a cellulose–hydrocellulose column gave 5-*O*-methyl-D-xylose as a chromatographically pure sirup with R_f 0.32 in butanone–water. 5-*O*-Methyl-D-xylose (293 mg), *p*-bromophenylhydrazine hydrocloride (1.2 g), and anhydrous sodium acetate (0.5 g) were dissolved in water and the solution heated for 3 hours on the steam bath. On cooling, the *p*-bromophenylosazone was obtained in poor yield and was recrystallized from ethanol–water, m.p. 152–154° C with softening at about 140° C. When the osazone was purified on a column of florisil and recrystallized from benzene – petroleum ether (30–60°) the m.p. was 153–155° C.

General Procedure

p-Bromophenylosazones were prepared from the following representative sugars: D-glucose, D-galactose, D-mannose, D-xylose, L-arabinose, maltose, 3-*O*-methyl-D-glucose (5), 6-*O*-methyl-D-galactose (6), 3,4-di-*O*-methyl-L-xylose (7) as follows. The sugar (25 mg) and *p*-bromophenylhydrazine (85 mg) were dissolved in glacial acetic acid (0.75 ml) and the solution diluted with water (0.5 ml). The reaction mixture was heated on the steam bath and samples were spotted on a thin plate of silica gel with calcium sulphate binder (Camag. apparatus) at zero time, 5, 10 . . . minutes and the plates developed once in benzene–methanol (9:1 v/v) (about 40 minutes). Unchanged reagent, after aerial oxidation, showed as a brown spot having an R_f of about 0.75 and the *p*-bromophenylosazones as bright yellow spots. Approximate R_f values for the osazones were pentoses 0.10, hexoses 0.04, monomethylpentoses 0.24, monomethylhexoses 0.18, dimethylpentoses 0.29.

The derivative from maltose had R_f 0.00 and further heating gave a faster yellow component streaking to an R_f of 0.10, presumably due to hydrolysis.

Glucose and mannose formed a pale yellow precipitate in the cold and this was replaced by a bright yellow precipitate which separated from the hot solution. For other sugars it was necessary to cool the solution before the product separated. In all cases crystalline solids were obtained and although these were not further examined they were judged to be the *p*-bromophenylosazones from their color and chromatographic behavior.

ACKNOWLEDGMENTS

We gratefully acknowledge the financial support of The Research Corporation and the Pioneering Research Program of The Institute of Paper Chemistry. One of us (Y. T.) thanks the National Research Council for the award of a studentship and we are indebted to Mrs. A. Aldridge for the analyses.

1. G. G. S. DUTTON and Y. TANAKA. To be published.
2. G. G. MAHER. *In* Advances in carbohydrate chemistry. Vol. 10. Academic Press, New York. 1955. p. 258.

3. P. A. LEVENE and A. L. RAYMOND. J. Biol. Chem. **102**, 331 (1933).
4. G. W. HUFFMAN, B. A. LEWIS, F. SMITH, and D. R. SPRIESTERSBACK. J. Am. Chem. Soc. **77**, 4346 (1955).
5. W. L. GLENN, G. S. MYERS, and G. A. GRANT. J. Chem. Soc. 2568 (1951).
6. K. FREUDENBERG and K. SMEYKAL. Ber. **59**, 100 (1926).
7. G. G. S. DUTTON and K. J. PIERRE. To be published.

RECEIVED JUNE 21, 1962.
DEPARTMENT OF CHEMISTRY,
UNIVERSITY OF BRITISH COLUMBIA,
VANCOUVER, B.C.

SOME EXAMPLES OF THE USE OF OXYGEN AS A DIAGNOSTIC TEST FOR THE TRIPLET STATE IN CHEMICAL REACTIONS[1,2]

D. W. SETSER,[3] D. W. PLACZEK,[3] R. J. CVETANOVIĆ,[4] AND B. S. RABINOVITCH[4,5]

It is known that oxygen in the gas phase may remove triplet-state species and may do this by both chemical and physical quenching (1, 2). Indeed, it is commonly believed that oxygen interacts efficiently with the triplet-state molecules, as is definitely known in some cases (1–4), and has been used in photochemical systems as a diagnostic test (see, for example, ref. 5) for the presence of triplet-state species.

This note describes some experiments on the application of oxygen as a scavenger of triplet-state species. These are the excited molecules of some olefins and of cyclopropane produced by mercury photosensitization. Vibrationally excited lowest electronically excited triplet states of these molecules are presumably formed in these reactions. The results show that information of considerable value is gained by scavenging with oxygen, but a cautionary remark must also be made, namely, that even relatively very large amounts of oxygen should not be expected to scavenge triplet biradical intermediates in a manner comparable to the well-known efficiency of small amounts of oxygen for removing alkyl radicals and for inhibiting formation of their conventional products.

Isomerization of Cyclopropane

The $Hg(^3P_1)$ photosensitized geometric isomerization of cyclopropane-d_2 is believed to proceed via the formation of the triplet state (6). Added amounts of oxygen up to 14% (expt. *a*, *b*, *c*, Table I) have obviously not quenched reaction, particularly when cognizance is taken of the high relative quenching cross section of O_2 (7) (cyclopropane:O_2 = 1.1:13.2). The present result can be due simply to rapid internal conversion of the excited (isomerized) cyclopropane to the ground singlet state, or to similar collision-induced transitions in which the cyclopropane reactant, which is present in larger amount, acts preponderantly as the deactivating inert gas.

Isomerization of trans-Ethylene-d_2

The $Hg(^3P_1)$ photosensitized decomposition of ethylene-d_2 to acetylene (8) and its geometric and structural isomerization (9) is believed to proceed via the biradical triplet state and with collisional inert gas inhibition of the decomposition (8, 9).[6]

[1]*Issued as N.R.C. No. 6959.*
[2]*Supported in part by the National Science Foundation, U.S.A.*
[3]*University of Washington, Seattle, Washington.*
[4]*Applied Chemistry Division, National Research Council, Ottawa, Ontario.*
[5]*Visiting Scientist, Applied Chemistry Division, National Research Council, Ottawa. John Simon Guggenheim Memorial Fellow, 1961–62, and International Award Fellow, Petroleum Research Fund, American Chemical Society, 1961–62.*
[6]*It is interesting to note that triplet acetylene is the initial product in the interpretation made in ref. 8.*

3. P. A. LEVENE and A. L. RAYMOND. J. Biol. Chem. **102**, 331 (1933).
4. G. W. HUFFMAN, B. A. LEWIS, F. SMITH, and D. R. SPRIESTERSBACK. J. Am. Chem. Soc. **77**, 4346 (1955).
5. W. L. GLENN, G. S. MYERS, and G. A. GRANT. J. Chem. Soc. 2568 (1951).
6. K. FREUDENBERG and K. SMEYKAL. Ber. **59**, 100 (1926).
7. G. G. S. DUTTON and K. J. PIERRE. To be published.

RECEIVED JUNE 21, 1962.
DEPARTMENT OF CHEMISTRY,
UNIVERSITY OF BRITISH COLUMBIA,
VANCOUVER, B.C.

SOME EXAMPLES OF THE USE OF OXYGEN AS A DIAGNOSTIC TEST FOR THE TRIPLET STATE IN CHEMICAL REACTIONS[1,2]

D. W. SETSER,[3] D. W. PLACZEK,[3] R. J. CVETANOVIĆ,[4] AND B. S. RABINOVITCH[4,5]

It is known that oxygen in the gas phase may remove triplet-state species and may do this by both chemical and physical quenching (1, 2). Indeed, it is commonly believed that oxygen interacts efficiently with the triplet-state molecules, as is definitely known in some cases (1–4), and has been used in photochemical systems as a diagnostic test (see, for example, ref. 5) for the presence of triplet-state species.

This note describes some experiments on the application of oxygen as a scavenger of triplet-state species. These are the excited molecules of some olefins and of cyclopropane produced by mercury photosensitization. Vibrationally excited lowest electronically excited triplet states of these molecules are presumably formed in these reactions. The results show that information of considerable value is gained by scavenging with oxygen, but a cautionary remark must also be made, namely, that even relatively very large amounts of oxygen should not be expected to scavenge triplet biradical intermediates in a manner comparable to the well-known efficiency of small amounts of oxygen for removing alkyl radicals and for inhibiting formation of their conventional products.

Isomerization of Cyclopropane

The $Hg(^3P_1)$ photosensitized geometric isomerization of cyclopropane-d_2 is believed to proceed via the formation of the triplet state (6). Added amounts of oxygen up to 14% (expt. *a*, *b*, *c*, Table I) have obviously not quenched reaction, particularly when cognizance is taken of the high relative quenching cross section of O_2 (7) (cyclopropane:O_2 = 1.1:13.2). The present result can be due simply to rapid internal conversion of the excited (isomerized) cyclopropane to the ground singlet state, or to similar collision-induced transitions in which the cyclopropane reactant, which is present in larger amount, acts preponderantly as the deactivating inert gas.

Isomerization of trans-Ethylene-d_2

The $Hg(^3P_1)$ photosensitized decomposition of ethylene-d_2 to acetylene (8) and its geometric and structural isomerization (9) is believed to proceed via the biradical triplet state and with collisional inert gas inhibition of the decomposition (8, 9).[6]

[1]*Issued as N.R.C. No. 6959.*
[2]*Supported in part by the National Science Foundation, U.S.A.*
[3]*University of Washington, Seattle, Washington.*
[4]*Applied Chemistry Division, National Research Council, Ottawa, Ontario.*
[5]*Visiting Scientist, Applied Chemistry Division, National Research Council, Ottawa. John Simon Guggenheim Memorial Fellow, 1961–62, and International Award Fellow, Petroleum Research Fund, American Chemical Society, 1961–62.*
[6]*It is interesting to note that triplet acetylene is the initial product in the interpretation made in ref. 8.*

TABLE I

Expt.	Reactor $l \times r$ (mm)	Time* (hr)	Gas pressure (atm) *trans*-Δ-d_2	Gas pressure (atm) O_2	Products *cis*-Δ-d_2 (%)	Products Polym. or oxygen prods.† (%)
a	35×3.7	8	1.3		25	38
b	35×3.7	8	1.3	0.2	17	28
c	23×3.7	10	2.0	0.1	15.8	10‡

Expt.	Reactor $l \times r$ (mm)	Time* (hr)	Gas pressure (atm) *trans*-$C_2H_2D_2$	Gas pressure (atm) N_2	Gas pressure (atm) O_2	Products $C_2H_2D_2$ Cis (%)	Asym. (%)	Acetylene (%)	Polym. etc.† (%)
d	98×0.57	12	5		0.35	14.1	—	—	—
e	98×0.57	12	5			15.6			
f	32×1.57	0.75	3		10	7.1	—	—	23
g	16×2.2	0.5	1		10	2.4	—	—	32
h	96×0.57	1.0	10		10	14.7	—	—	28
i	33×2.2	0.092	1	1		34.2	3.0	—	—
j	33×2.2	0.092	1		1	25.8	4.2	—	21§
k	33×2.2	0.092	1	2		31.7	2.0	—	—
l	33×2.2	0.092	1		2	16.6	3.4	—	—
m	98×0.57	12	5			12.8			
n	98×0.57	12	5		18	<1	—	—	Extensive

*Period of irradiation under conditions of constant light intensity for each set of experiments under comparison in the text.
†Defined as the percentage loss of cyclopropane or of ethylene plus acetylene, as appropriate.
‡A decline of percentage polymerization with rise of total pressure is characteristic of the reaction even in the absence of oxygen (see ref. 6).
§Believed to be unreliable value.

The following scheme (9) is largely (10) adequate:

$$\text{trans} \xrightarrow{\text{Hg}(^3P_1)} T^* \longrightarrow \text{cis} + \text{trans}$$
$$T^* \xrightarrow{k_i} E^* \xrightarrow{k_M} \text{asym} + \text{cis} + \text{trans}$$
$$E^* \xrightarrow{k_s} A^* \xrightarrow{k_M} \text{acetylene} (+ H_2, \text{HD, or } D_2)$$

where T* is believed to be the T state of ethylene, E* is another triplet species such as ethylidine, and A* is a triplet acetylene product molecule.

The isomerization reactions are particularly useful: although added O_2 inhibits acetylene formation by quenching triplet intermediates by both physical or chemical (reaction) mechanisms, the cis and asymmetric isomerization products can be inhibited below normal yields only by chemical quenching and not by physical deactivation of the intermediate triplet states by the "inert" gas. In short, the rate laws for the formation of decomposition and isomerization products differ in their dependence on *total* quenching (11). However, if a triplet acetylene product is also chemically quenched by O_2 *after* formation, then all the products might behave similarly with respect to effects due to O_2.

In practice, low percentages of oxygen appear to have only negligible effect on decomposition and isomerization in this system (runs *d* and *e*, Table I). The experiments were

TABLE II

Products from *trans*-$C_2H_2D_2$ in absence and presence of O_2

Run	% reaction*	Pressure (cm) $C_2H_2D_2$	Pressure (cm) O_2	Cell†	Time (min)	Products (%) Cis	Products (%) Asym.	Products (%) Acet.	Products (reduced‡) Cis	Products (reduced‡) Asym.	Products (reduced‡) Acet.	Difference §(%) Cis	Difference §(%) Asym.	Difference §(%) Acet.	Difference §(%) Max.‖
12	29.0	2	0	A	10	5.04	4.58	14.8	1.00	0.908	2.94				
13	17.8	1	1	A	10	2.84	2.68	9.36	0.434	0.410	1.43	56.6	54.9	51.2	45
14	29.9	2	0	A	10	5.28	4.03	15.3	1.00	0.765	2.90				
19	26.8	2	0	A	10	4.66	4.25	13.3	0.882	0.804	2.52				
16	24.1	1.5	0.5	A	10	4.29	3.72	11.8	0.720	0.624	1.98	28.0¶ 18.3	18.2 22.6	31.8 21.4	21.5
15	21.1	1	1	A	10	3.74	2.68	9.87	0.547	0.392	1.44	45.3¶ 38.2	48.8 51.4	50.4 42.9	45
17	26.4	1	0	A	5	3.12	2.82	17.4	1.00	0.903	5.58				
18	25.1	0.5	0.5	A	5	3.79	2.95	14.5	0.936	0.728	3.58	6.4	19.4	35.8	45
21	22.3	8	0	B	15	6.61	4.98	4.12	1.00	0.755	0.624				
22	11.2	6	2	B	15	3.19	1.26	3.51	0.427	0.162	0.470	57.3	78.9	24.5	21.5
20	10.5	4	4	B	15	3.21	1.27	2.78	0.375	0.148	0.325	62.5	80.3	47.9	45
24	19.6	16	0	B	30	7.30	3.42	1.56	1.00	0.469	0.213				
23	13.0	8	8	B	30	4.20	2.96	1.55	0.444	0.284	0.164	55.6	33.3	28.3	45
26	12.2	4	12	B	30	4.21	2.33	1.54	0.379	0.210	0.138	62.1	55.3	35.3	71
27	21.2	4	0	A	20	5.23	4.64	6.08	1.00	0.887	1.16				
28	18.7	3	1	A	20	4.75	4.22	5.00	0.804	0.714	0.846	19.6	19.5	27.2	21.4
29	14.5	2	2	A	20	4.26	3.22	2.76	0.628	0.475	0.407	37.2	46.5	65.0	45
o	22	2	0	C	5	3.6	3.2	11.6	1.00	0.888	3.22				
p	24	1	1	C	6	4.3	2.8	12.9	0.789	0.514	2.37	21.1	42.1	26.4	45
q	14.3	8	0	D	10	4.5	3.0	2.3	1.00	0.666	0.510				
r	11.2	4	4	D	10	3.6	1.8	2.2	0.616	0.308	0.377	38.4	53.8	26.1	45

*Percentage of *trans*-$C_2H_2D_2$ converted in the reaction to (isolated) 2× *cis*, *asym*, and acetylene products. Oxygenated products were not analyzed.
†A: 210 mm long, 9 mm radius, 54 cc; B: 190 mm long, 4 mm radius, 9.5 cc; C: as A but different optical geometry; D: 4.5 cc.
‡Corrected for quenching of mercury by O_2, assuming $\sigma_{O_2}/\sigma_{C_2H_4} = 13{:}24$.
§Percentage decline in the quantum yields (after correction for quenching of mercury by O_2).
‖Maximum possible decline in quantum yields if O_2 is completely efficient as a chemical quencher.
¶The first row is compared to run 14, the second to run 19.

conducted in the manner previously described (6) with the following important modification. The light from the 2537 Å resonance lamp transmitted *through* the reaction cell (used in a constant-geometry arrangement) was monitored by a photomultiplier cell. The light intensity was constant and remained so during each run for all comparable series of pure ethylene and ethylene–O_2 experiments. This signifies that there was *no* mercury depletion by reaction with oxygen species such that *less* light was absorbed in the cell for O_2 runs. There was therefore a constant light energy input to the system for all runs of a series.

Polymerization (runs *f*, *g*, and *h*, Table I) is enhanced considerably (compare ref. 5) in the presence of high percentages of O_2 at high pressures. At least part of the polymerization may occur due to the presence of O_2^* or due to O-atom formation rather than, or in addition to, attack of O_2 on the triplet species. It is of interest to note, however, that very extensive isomerization is still found even at high percentages of oxygen (runs *i* and *j*, *k* and *l*), in amounts which, if not subjected to (or not accessible to) quantitative scrutiny, might (erroneously) lend themselves to the qualitative interpretation that O_2 has little effect and that reaction is somewhat reduced, mainly insofar as part of the excited mercury is quenched by O_2.

Runs *m* and *n*, and also *e*, *f*, and *g*, illustrate that the isomerization which is still found in the presence of O_2 does not apparently arise via an excited oxygen molecule or oxygen atom (12) catalysis process. Thus, all of the above results presumably signify an efficiency of less than unity for oxygen inhibition of triplet-intermediate processes in the sense that these are not extinguished by large proportions of O_2 in the way that alkyl radical products are by smaller amounts of O_2.

The most unequivocal data for quantitative interpretation of the role of O_2 were those obtained at lower pressures and summarized in Table II. The relative amounts of the decomposition and isomerization products are given in Table III, taking in each case

TABLE III

Relative amounts of products in absence and presence of O_2 (*cis*-$C_2H_2D_2$ taken as unity)

	Pressure (cm)			Products		
Run	Total	$C_2H_2D_2$	O_2	Cis	Asym.	Acetylene
17	1	1	0	1	0.94	5.57
18	1	0.5	0.5	1	0.78	3.83
12	2	2	0	1	0.91	2.94
14	2	2	0	1	0.79	2.98
19	2	2	0	1	0.91	2.86
16	2	1.5	0.5	1	0.87	2.75
13	2	1	1	1	0.94	3.30
15	2	1	1	1	0.74	2.71
27	4	4	0	1	0.89	1.16
28	4	3	1	1	0.89	1.06
29	4	2	2	1	0.76	0.65
21	8	8	0	1	0.75	0.63
q	8	8	0	1	0.67	0.51
22	8	6	2	1	0.40	1.10
20	8	4	4	1	0.46	1.00
r	8	4	4	1	0.50	0.61
24	16	16	0	1	0.47	0.21
23	16	8	8	1	0.70	0.37
26	16	4	12	1	0.55	0.36

cis-$C_2H_2D_2$ as unity. Apart from the large experimental error, it is evident that the relative product fractions of asym, cis, and of acetylene are grossly unaltered by the

presence of O_2, relative to runs at the same total pressure of pure ethylene. This means either that chemical deactivation of T* and E* by O_2 cannot be occurring significantly, since the *cis-* plus *asym*-ethylene product percentages should then decline relatively, or that if cis and asymmetric production is inhibited by O_2 then the acetylene product A* is similarly destroyed. That the latter explanation is required is evident from Table II. The percentage difference of the normalized yields of products in the presence of oxygen from those obtained under comparable conditions with pure ethylene should be compared with the calculated maximum possible difference in the last column. The latter has been obtained by correcting for the quenching of the excited mercury atoms by O_2 (with use of the ratio 13:24[7] as a mean of several possible values for the relative quenching cross sections of O_2:C_2H_4) and assuming unit chemical quenching efficiency for O_2.

The comparison shows that O_2 has considerable efficiency per collision for inhibition of the formation of the products, i.e., for reaction with T*, E*, and A*. The data show large and apparently random error and fluctuations but the preceding conclusion seems justified.

The efficiency of ethylene for deactivation of the excited state has heretofore referred only to vibrational de-excitation (8, 9). The considerable chemical quenching efficiency of O_2 demands that ethylene be efficient for electronic de-excitation as well. Of course, all statements of efficiency are relative, only ethylene and O_2 being compared.

Isomerization of Butenes

A related finding is an isolated experiment wherein the $Hg(^3P_1)$ photosensitized isomerization of *cis*-butene-2 at 25° and 2 atm total pressure was not completely inhibited with 20% oxygen, although all characteristic radical products were eliminated.

In the $Hg(^3P_1)$ photosensitized isomerization of butene-1 (13), another triplet process, the addition of 6% of O_2 to the system reduced significantly, but did not completely inhibit, the isomerization to methylcyclopropane.

Conclusion

In the above reactions, there is good evidence for chemical removal of triplet-state molecules by O_2. A fact worth stressing, however, is that the mere presence of O_2, in amounts enormously greater than trace, does not necessarily completely inhibit reaction in these examples where triplet mechanisms are believed to occur. The inefficiency of oxygen in this respect may in large part be due to very fast competing unimolecular or collision-induced reactions of the excited species, and in part, depending upon circumstances, due to some inefficiency of chemical reaction of oxygen with triplet species. Since methyl radicals and nitric oxide, for example, are fairly inefficient (14) for recombination, this latter finding need not be considered exceptional in nature.

High Pressures and Product Yield

In the course of this work at high pressures, the authors reverted to very small reactors which were tubes of diameter 1 and 4 mm. In experiments with *trans*-ethylene-d_2, under conditions of constant vessel size and irradiation, it was found that although the yield of cis products was roughly constant from 0.2–1 atm (11), it declined markedly at pressures above 2 atm. The results in these vessels are interpreted to mean inefficient absorption of the resonance radiation at the higher pressure, due to line shift and pressure broadening (15). A similar result was also found with *cis*-butene-2 (1 atm) and added nitrogen,

[7]*This number is obtained by comparison with the original data on oxygen of Zemansky (7). Some confusion on the oxygen base, which exists in the literature, will be discussed by one of us (R. J. C., Progr. in Chem. Kinet., to be published).*

although in careful experiments with similar *cis*-butene-2 – N_2 mixtures, in a vessel of diameter 5 cm, no such decline occurred at nitrogen pressures up to 4 atm—as is reasonable in view of the longer light path.

We call attention to this difficulty as a reminder to others who may work at high pressure.

1. G. PORTER. Proc. Chem. Soc. 291 (1959).
2. R. M. HOCHSTRASSER and G. B. PORTER. Quart. Rev. (London), **14**, 146 (1960).
3. G. W. LUCKEY and W. A. NOYES, JR. J. Chem. Phys. **19**, 227 (1951). J. HEICKLEN. J. Am. Chem. Soc. **81**, 3863 (1959). R. SRINIVASAN and W. A. NOYES, JR. J. Am. Chem. Soc. **82**, 5591 (1960).
4. H. M. FREY. J. Am. Chem. Soc. **82**, 5947 (1960).
5. R. SRINIVASAN. J. Am. Chem. Soc. **83**, 4346 (1961).
6. D. W. SETSER, B. S. RABINOVITCH, and E. G. SPITTLER. J. Chem. Phys. **35**, 1840 (1961).
7. B. DE B. DARWENT and M. H. PHIBBS. J. Chem. Phys. **22**, 110 (1954). M. W. ZEMANSKY. Phys. Rev. **36**, 919 (1930).
8. D. J. LE ROY and E. W. R. STEACIE. J. Chem. Phys. **9**, 829 (1941). K. J. LAIDLER. J. Chem. Phys. **15**, 712 (1947).
9. A. B. CALLEAR and R. J. CVETANOVIĆ. J. Chem. Phys. **24**, 873 (1956).
10. P. AUSLOOS and R. GORDEN. J. Chem. Phys. **36**, 5 (1962).
11. D. W. SETSER and B. S. RABINOVITCH. To be published.
12. R. J. CVETANOVIĆ. Unpublished results with O atoms.
13. R. J. CVETANOVIĆ and L. C. DOYLE. J. Chem. Phys. **37**, 543 (1962).
14. D. M. MILLER and E. W. R. STEACIE. J. Chem. Phys. **19**, 73 (1952).
15. A. C. G. MITCHELL and M. W. ZEMANSKY. Resonance radiation and excited atoms. Cambridge University Press. 1934.

RECEIVED JUNE 21, 1962.
DEPARTMENT OF CHEMISTRY,
UNIVERSITY OF WASHINGTON,
SEATTLE, WASH., U.S.A.
AND
DIVISION OF APPLIED CHEMISTRY,
NATIONAL RESEARCH COUNCIL,
OTTAWA, CANADA

THE CHEMISTRY OF ALUMINUM–NITROGEN COMPOUNDS
III. THE STRUCTURE AND PYROLYSIS OF $Me_3Al{:}Me_2NN{=}NNMe_2$

NEIL R. FETTER, FREDERICK E. BRINCKMAN, JR.,* AND DONALD W. MOORE†

INTRODUCTION

In a survey of reactions between tetramethyltetrazene (TMT) and aluminum alkyls published recently (1) we reported a complex, for which elemental analysis implied the formula $Al(NMe_2)_3$. However, the physical properties of this material did not agree with those published by other authors (2, 3, 4).

Further study of the reaction between tetramethyltetrazene and trimethylaluminum has shown that $Al(NMe_2)_3$ is not formed, but rather the simple 1:1 adduct, $Me_3Al{:}Me_2NN{=}NNMe_2$, and the other products obtained, i.e. $Me_2Al{-}NMe_2$ and a red polymer do not arise from a second reaction route as proposed (1), but only from the decomposition of this adduct. Not only have $Me_2Al{-}NMe_2$ and red polymer been obtained from decomposition under mild conditions, but nitrogen, tetramethyltetrazene, and small quantities of methyl azide and methane were also obtained.

**Present address: Research and Development Department, U.S. Naval Propellant Plant, Indian Head, Maryland.*
†*Chemistry Division, U.S. Naval Ordnance Test Station, China Lake, California.*

although in careful experiments with similar *cis*-butene-2 – N_2 mixtures, in a vessel of diameter 5 cm, no such decline occurred at nitrogen pressures up to 4 atm—as is reasonable in view of the longer light path.

We call attention to this difficulty as a reminder to others who may work at high pressure.

1. G. PORTER. Proc. Chem. Soc. 291 (1959).
2. R. M. HOCHSTRASSER and G. B. PORTER. Quart. Rev. (London), **14**, 146 (1960).
3. G. W. LUCKEY and W. A. NOYES, JR. J. Chem. Phys. **19**, 227 (1951). J. HEICKLEN. J. Am. Chem. Soc. **81**, 3863 (1959). R. SRINIVASAN and W. A. NOYES, JR. J. Am. Chem. Soc. **82**, 5591 (1960).
4. H. M. FREY. J. Am. Chem. Soc. **82**, 5947 (1960).
5. R. SRINIVASAN. J. Am. Chem. Soc. **83**, 4346 (1961).
6. D. W. SETSER, B. S. RABINOVITCH, and E. G. SPITTLER. J. Chem. Phys. **35**, 1840 (1961).
7. B. DE B. DARWENT and M. H. PHIBBS. J. Chem. Phys. **22**, 110 (1954). M. W. ZEMANSKY. Phys. Rev. **36**, 919 (1930).
8. D. J. LE ROY and E. W. R. STEACIE. J. Chem. Phys. **9**, 829 (1941). K. J. LAIDLER. J. Chem. Phys. **15**, 712 (1947).
9. A. B. CALLEAR and R. J. CVETANOVIĆ. J. Chem. Phys. **24**, 873 (1956).
10. P. AUSLOOS and R. GORDEN. J. Chem. Phys. **36**, 5 (1962).
11. D. W. SETSER and B. S. RABINOVITCH. To be published.
12. R. J. CVETANOVIĆ. Unpublished results with O atoms.
13. R. J. CVETANOVIĆ and L. C. DOYLE. J. Chem. Phys. **37**, 543 (1962).
14. D. M. MILLER and E. W. R. STEACIE. J. Chem. Phys. **19**, 73 (1952).
15. A. C. G. MITCHELL and M. W. ZEMANSKY. Resonance radiation and excited atoms. Cambridge University Press. 1934.

RECEIVED JUNE 21, 1962.
DEPARTMENT OF CHEMISTRY,
UNIVERSITY OF WASHINGTON,
SEATTLE, WASH., U.S.A.
AND
DIVISION OF APPLIED CHEMISTRY,
NATIONAL RESEARCH COUNCIL,
OTTAWA, CANADA

THE CHEMISTRY OF ALUMINUM–NITROGEN COMPOUNDS
III. THE STRUCTURE AND PYROLYSIS OF $Me_3Al{:}Me_2NN{=}NNMe_2$

NEIL R. FETTER, FREDERICK E. BRINCKMAN, JR.,* AND DONALD W. MOORE†

INTRODUCTION

In a survey of reactions between tetramethyltetrazene (TMT) and aluminum alkyls published recently (1) we reported a complex, for which elemental analysis implied the formula $Al(NMe_2)_3$. However, the physical properties of this material did not agree with those published by other authors (2, 3, 4).

Further study of the reaction between tetramethyltetrazene and trimethylaluminum has shown that $Al(NMe_2)_3$ is not formed, but rather the simple 1:1 adduct, $Me_3Al{:}Me_2NN{=}NNMe_2$, and the other products obtained, i.e. $Me_2Al{-}NMe_2$ and a red polymer do not arise from a second reaction route as proposed (1), but only from the decomposition of this adduct. Not only have $Me_2Al{-}NMe_2$ and red polymer been obtained from decomposition under mild conditions, but nitrogen, tetramethyltetrazene, and small quantities of methyl azide and methane were also obtained.

**Present address: Research and Development Department, U.S. Naval Propellant Plant, Indian Head, Maryland.*
†*Chemistry Division, U.S. Naval Ordnance Test Station, China Lake, California.*

The $Me_3Al{:}Me_2NN{=}NNMe_2$ adduct reacts quantitatively with trimethylamine to form $Me_3Al{:}NMe_3$ and the free tetramethyltetrazene; reaction with D_2O gives rise to the expected amount of CH_3D required for the $Al(CH_3)_2CH_3$ moiety. The proton resonance spectrum of the adduct shows that it is symmetrically bonded to the aluminum atom in a unique "cyclic" structure.

EXPERIMENTAL

Apparatus and Reagents

The apparatus and starting materials employed have been described previously (1, 5). The elemental analyses were performed by the Schwarzkopf Microanalytical Laboratory, Woodside, New York.

N.M.R. Spectra

The proton resonance spectra were obtained with a Varian Associates Model V-4302 Spectrometer at 60 Mc. The samples containing 10% by weight of benzene for internal reference purposes were vacuum sealed into 5-mm Pyrex tubes and maintained at −15° C before spectra were taken at room temperature.

Reaction of Tetramethyltetrazene with Trimethylaluminum at 25° C

By means of vacuum transfer, 2.78 g (24.0 mmoles) of tetramethyltetrazene was added to a 50-ml flask containing 1.71 g (23.8 mmoles) of Me_3Al dissolved in 25 ml of *n*-heptane. After transfer, the mixture was allowed to warm from −196° C to room temperature and it then stood at approximately 25° C for 36 hours. Apparently a period of 20 hours is required for completion of this reaction, for if the solvent is removed shortly after the mixture reaches room temperature, a violent explosion will follow. During this period the mixture acquired a faint yellow color. The solvent and any excess TMT were removed *in vacuo* and the remaining liquid vacuum transferred under high vacuum at room temperature. A −15° C cold finger was placed in the vacuum system to trap any $Me_2Al{-}NMe_2$ that formed and the collection flask was maintained at −78° C. Along with the liquid complex, 0.05 g of $Me_2Al{-}NMe_2$ and 0.48 g of red residue were obtained.

By raising the temperature of the collection flask to −30° C and pumping through a −196° C trap a trace of methyl azide, heptane, and TMT was also obtained. The methyl azide was characterized by comparison of the recovered gas with infrared spectrum of an authentic sample as published by Pierson, Fletcher, and Gantz (6).

Although the distilled complex was slightly yellow, a yield of approximately 80 mole% was obtained. By distilling it again under the conditions described above, a clear colorless liquid was obtained. This material turns slowly yellow at room temperature, but may be stored for at least 2 months at −10° C without discoloration. Because of its instability, elemental analysis of the complex is difficult; however, an analysis of a freshly distilled sample gave results which are in fair agreement with the empirical formula $Me_3Al{:}Me_2NN{=}NNMe_2$. Anal. Calc. for $C_7H_{21}N_4Al$: C, 44.65; H, 11.24; N, 29.76; Al, 14.32. Found: C, 41.32; H, 11.95; N, 27.13; Al, 13.93.

Reaction of $Me_3Al{:}Me_2NN{=}NNMe_2$ with Trimethylamine

In order to elucidate the analysis given above, 4.92 mmoles of trimethylamine was condensed on 0.407 g (2.16 mmoles) of $Me_3Al{:}Me_2NN{=}NNMe_2$ at −196° C. The mixture was allowed to warm to room temperature (25° C) and stand overnight. The reaction was quantitative* with the consumption of 2.5 mmoles of trimethylamine and the formation of white crystals. The crystals were vacuum sublimed at 50° C and the sublimate proved from its melting point (100–103° C) and infrared spectrum to be $Me_3Al{:}NMe_3$. Although some was lost during purification, approximately 0.2 g of TMT was recovered.

The reaction is then:

$$Me_3Al{:}Me_2NN{=}NNMe_2 + NMe_3 \xrightarrow{25^\circ\,C} Me_3Al{:}NMe_3 + Me_2NN{=}NNMe_2.$$

Reaction of $Me_3Al{:}Me_2NN{=}NNMe_2$ with Deuterium Oxide

Treatment of 0.514 g (3.23 mmoles) of $Me_3Al{:}Me_2NN{=}NNMe_2$ with an excess of D_2O resulted in evolution of a gas (213 cc STP) which proved to be CH_3D by infrared and mass spectrometric examination. These results indicate three aluminum–carbon bonds exist in the structural moiety $Al(CH_3)_2CH_3$ (Al/C: Calc. 1:3, found 1:2.94) and supports the 1:1 adduct structure.

**The slightly high value for the NMe_3 consumed (calc. 21 mmole) may be accounted for by the presence of TMT.*

Proton Resonance Studies of Me_3Al:$Me_2NN{=}NNMe_2$

The n.m.r. spectrum (Fig. 1) shows two sharp peaks in the ratio of approximately 4:3 and with chemica l shifts (in tau values) of 7.25 and 10.82 p.p.m. The larger, low-field peak represents all N-protons and the other all Al-protons. Weak lines representing decomposition products appear even in the freshly prepared material and increase with time at room temperature.

It should be noted that both N-methyl and Al-methyl chemical shifts are close to those of the uncomplexed compounds. The shift of TMT is 7.21 p.p.m. and Groenewage *et al.* (7) have reported a shift of 10.69 p.p.m. for the non-bridging methyls in trimethylaluminum dimer and 9.59 p.p.m. for the bridge methyls. The small difference between these values and those observed for the complex suggests only weak dative bonds between Me_3Al and TMT.

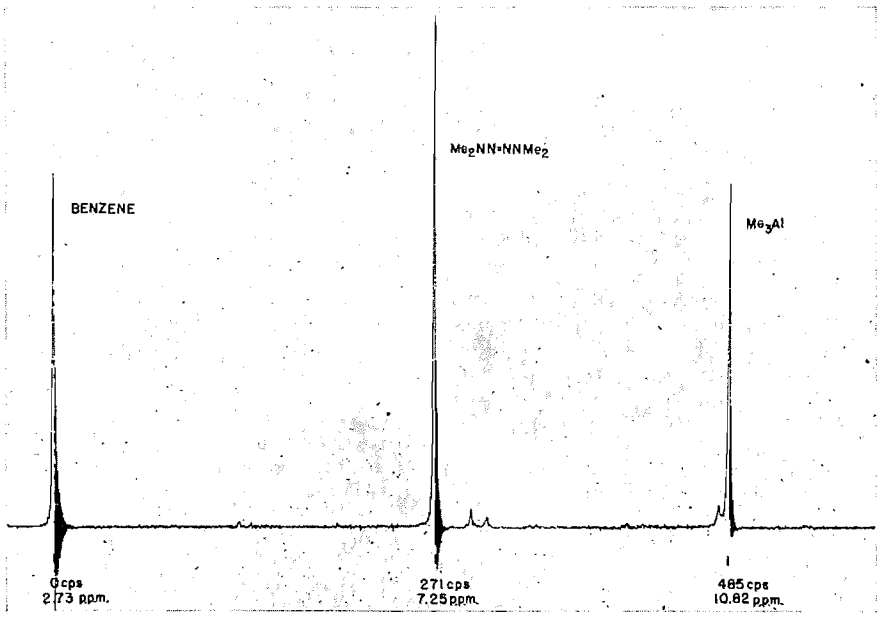

FIG. 1. N.M.R. spectrum of Me_3Al:$Me_2NN{=}NNMe_2$.

Pyrolysis of Me_3Al:$Me_2NN{=}NNMe_2$

To determine whether the compounds obtained in the reaction at 80° C resulted from the decomposition of Me_3Al:$Me_2NN{=}NNMe_2$ and not from an interaction of the starting materials and to obtain an exact mass balance of decomposition products, 0.416 g (2.21 mmoles) of the complex was heated under vacuum at 90° C for 18 hours. At the end of this period, gas evolution had ceased and the decomposition was assumed to be finished. In Table I are listed the quantities of materials obtained. The 0.050-g discrepancy between the starting weight of complex and the total recovered may be accounted for by the presence of a trace of stopcock grease in the flask containing the red residue.

TABLE I

Pyrolysis products of Me_3Al:$Me_2NN{=}NNMe_2$

Compound	g	Yield (wt. %)	mmoles
N_2	0.0835	20.0	2.88
CH_4	0.0045	1.1	0.28
CH_3N_2	0.0057	1.4	0.10
$Me_2NN{=}NNMe_2$	0.0620	14.8	0.54
$Me_2Al{-}NMe_2$	0.1195	28.8	1.09
Red polymer	0.1907	45.7	—
Total	0.4659		

DISCUSSION

It may be seen from the data presented above that the reaction scheme originally proposed for this reaction (1) does not proceed via multiple routes; instead, all of the

products obtained originate from the decomposition of an intermediate, $Me_3Al{:}Me_2NN{=}NNMe_2$. This complex is stable enough at room temperature that it may be purified by vacuum transfer but it must be maintained near $-10°$ C for prolonged storage. At room temperature the complex decomposes slowly over a period of weeks and at 90° C is 80% decomposed within an hour. In our first report of this reaction (1) a distillation temperature of 40° C was employed which was high enough to cause decomposition such that approximately equal amounts of $Me_3Al{:}Me_2NN{=}NNMe_2$, $Me_2Al{-}NMe_2$, and red polymer were recovered.

The two earlier elemental analyses (1) of the complex which agreed closely with the empirical formula for $Al(NMe_2)_3$ appear to have been fortuitous, i.e., the two samples had decomposed about the same degree before analysis. Even the freshly prepared sample, whose analysis is given above, has low nitrogen and carbon values, indicating some decomposition had occurred in the few days required to ship the sample to the analyst.

Subsequent analyses of the red polymer indicate that composition varies considerably and nothing can be said about its constitution at this point except that it contains hydrolyzable methyl groups, aluminum, and nitrogen. A sample of polymer was hydrolyzed with D_2O to see if $-AlCH_2Al-$ bonding was present; however, only CH_3D was obtained, indicating only terminal $Al{-}CH_3$ groups. Also, because the composition of the polymer is not known, it is difficult to fully elucidate the mechanism of pyrolysis.

However, the presence of methyl azide and $Me_2Al{-}NMe_2$, along with the proton resonance spectrum shown above, gives a clue to the structure of the complex. The n.m.r. spectrum of freshly prepared $Me_3Al{:}Me_2NN{=}NNMe_2$ is surprisingly simple with one peak at 7.25 p.p.m. upfield (benzene is taken as 2.73 p.p.m.) representing the protons on nitrogen methyl groups and another peak at 10.82 p.p.m. upfield representing the protons on aluminum methyl groups. The N-proton and Al-proton peaks are in the expected four to three ratio and their singularity indicates that N-protons are in an equivalent magnetic environment as are all Al-protons. It should also be noted that the molecular weight values (cryoscopic) of 193 and 199 obtained earlier (1) agree closely with that calculated for *monomeric* $Me_3Al{:}Me_2NN{=}NNMe_2$ (calc. 188.2).

Among the possible structures, Fig. 2 satisfies the n.m.r. data, and further, if asymmetric cleavage occurs, appears a reasonable precursor to the pyrolysis products $Me_2Al{-}NMe_2$ and methyl azide. Further work is in progress.

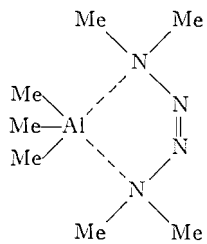

FIG. 2. Structural configuration of $Me_3Al{:}Me_2NN{=}NNMe_2$.

ACKNOWLEDGMENTS

The authors wish to acknowledge the assistance given by Dr. Peter J. Slota, Jr. and Dr. Charles P. Haber of the U. S. Naval Ordnance Laboratory, Corona, during this investigation.

The work was supported by funds from the Advance Research Projects Agency through the U. S. Navy Department, Bureau of Naval Weapons.

1. N. R. FETTER and B. BARTOCHA. Can. J. Chem. **40**, 342 (1962).
2. E. WIBERG and A. MAY. Z. Naturforsch. **106**, 234 (1955).
3. J. K. RUFF. J. Am. Chem. Soc. **83**, 2835 (1961).
4. P. LONGI, G. MAZZANTI, and F. BERNARDINI. Gazz. Chim. Ital. **90**, 180 (1960).
5. N. R. FETTER and B. BARTOCHA. Can. J. Chem. **39**, 2001 (1961).
6. R. H. PIERSON, A. N. FLETCHER, and E. C. GANTZ. Anal. Chem. **28**, 1218 (1956).
7. M. P. GROENWEGE, J. SMIDT, and H. DE VRIES. J. Am. Chem. Soc. **82**, 4425 (1960).

RECEIVED JUNE 7, 1962.
U.S. NAVAL LABORATORY,
CORONA,
CALIFORNIA, U.S.A.

EXOCELLULAR BACTERIAL POLYSACCHARIDE FROM XANTHOMONAS CAMPESTRIS NRRL B-1459

PART II. LINKAGE OF THE PYRUVIC ACID

J. H. SLONEKER AND DANUTE G. ORENTAS

Recently it was reported that the polysaccharide produced by the bacterium *Xanthomonas campestris* NRRL B-1459 contains 3.0–3.5% pyruvic acid (1). Previously, the only other polysaccharide reported to contain pyruvic acid as a constituent was a commercial red seaweed agar, which is composed of D-galactose, 3,6-anhydro-L-galactose, and 1% pyruvic acid attached to D-galactose as a 4,6-*O*-(1-carboxyethylidene) group (2). Polysaccharide B-1459 contains, in addition to pyruvic acid, D-glucose, D-mannose, D-glucuronic acid, and acetyl in the ratio 2.8:3.0:2.0:1.7 (3). Experimental evidence presented here indicates that the pyruvic acid in polysaccharide B-1459 is attached to certain of the glucose residues also by a 4,6-*O*-(1-carboxyethylidene) linkage.

EXPERIMENTAL

In order to isolate a compound that contained pyruvate, the polysaccharide was degraded by the technique of periodate oxidation and sodium borohydride reduction, followed by mild acid hydrolysis (4). This procedure hydrolyzes the acetal bond of periodate-oxidized glycosides without apparent cleavage of the pyruvate bond.

A 1.5-g sample of polysaccharide B-1459, which had consumed 1.2 moles of sodium metaperiodate per sugar unit and had been reduced with sodium borohydride, was hydrolyzed in 1 *N* hydrochloric acid for 24 hours at room temperature. The neutralized hydrolyzate was fractionated on a Dowex 1-X4, 300-mesh acetate column (2×40 cm) by exponential gradient elution starting with 1500 ml of water in the mixing chamber and introducing 3 *N* acetic acid. A fraction was obtained between 2.90 and 3.25 liters of effluent that contained 50% of the pyruvic acid applied. The fraction was lyophilized to dryness and the residue was neutralized with saturated barium hydroxide. The barium salt, precipitated as a soft gel from 70% ethanol upon addition of acetone, formed a white amorphous powder when dried. Calc. for $(C_7H_{11}O_6)_2Ba$: C, 33.7%; H, 4.27%; Ba, 26.4%. Found: C, 33.1%; H, 4.77%; Ba, 26.2%. The compound was not oxidized by periodate even under strong oxidation conditions. However, upon acid hydrolysis (1 *N* hydrochloric acid for 3 hours at 100° C) it was degraded to pyruvic acid and erythritol as shown by paper chromatography. Quantitative analysis (1, 5) of these products revealed that they are in a 1:1 ratio.

RESULTS AND DISCUSSION

The combined evidence indicates that the compound isolated from polysaccharide B-1459 is the barium salt of 1,3-*O*-(1-carboxyethylidene)-erythritol (II). The infrared and nuclear magnetic resonance spectra support this structure. In potassium bromide the infrared spectrum displays strong carboxyl ion absorption bands at 6.2 and 7.1 μ. Also, two strong bands are present at 8.5 and 9.4 μ. These bands are reported to be

1. N. R. FETTER and B. BARTOCHA. Can. J. Chem. **40**, 342 (1962).
2. E. WIBERG and A. MAY. Z. Naturforsch. **106**, 234 (1955).
3. J. K. RUFF. J. Am. Chem. Soc. **83**, 2835 (1961).
4. P. LONGI, G. MAZZANTI, and F. BERNARDINI. Gazz. Chim. Ital. **90**, 180 (1960).
5. N. R. FETTER and B. BARTOCHA. Can. J. Chem. **39**, 2001 (1961).
6. R. H. PIERSON, A. N. FLETCHER, and E. C. GANTZ. Anal. Chem. **28**, 1218 (1956).
7. M. P. GROENWEGE, J. SMIDT, and H. DE VRIES. J. Am. Chem. Soc. **82**, 4425 (1960).

RECEIVED JUNE 7, 1962.
U.S. NAVAL LABORATORY,
CORONA,
CALIFORNIA, U.S.A.

EXOCELLULAR BACTERIAL POLYSACCHARIDE FROM XANTHOMONAS CAMPESTRIS NRRL B-1459

PART II. LINKAGE OF THE PYRUVIC ACID

J. H. SLONEKER AND DANUTE G. ORENTAS

Recently it was reported that the polysaccharide produced by the bacterium *Xanthomonas campestris* NRRL B-1459 contains 3.0–3.5% pyruvic acid (1). Previously, the only other polysaccharide reported to contain pyruvic acid as a constituent was a commercial red seaweed agar, which is composed of D-galactose, 3,6-anhydro-L-galactose, and 1% pyruvic acid attached to D-galactose as a 4,6-*O*-(1-carboxyethylidene) group (2). Polysaccharide B-1459 contains, in addition to pyruvic acid, D-glucose, D-mannose, D-glucuronic acid, and acetyl in the ratio 2.8:3.0:2.0:1.7 (3). Experimental evidence presented here indicates that the pyruvic acid in polysaccharide B-1459 is attached to certain of the glucose residues also by a 4,6-*O*-(1-carboxyethylidene) linkage.

EXPERIMENTAL

In order to isolate a compound that contained pyruvate, the polysaccharide was degraded by the technique of periodate oxidation and sodium borohydride reduction, followed by mild acid hydrolysis (4). This procedure hydrolyzes the acetal bond of periodate-oxidized glycosides without apparent cleavage of the pyruvate bond.

A 1.5-g sample of polysaccharide B-1459, which had consumed 1.2 moles of sodium metaperiodate per sugar unit and had been reduced with sodium borohydride, was hydrolyzed in 1 *N* hydrochloric acid for 24 hours at room temperature. The neutralized hydrolyzate was fractionated on a Dowex 1-X4, 300-mesh acetate column (2×40 cm) by exponential gradient elution starting with 1500 ml of water in the mixing chamber and introducing 3 *N* acetic acid. A fraction was obtained between 2.90 and 3.25 liters of effluent that contained 50% of the pyruvic acid applied. The fraction was lyophilized to dryness and the residue was neutralized with saturated barium hydroxide. The barium salt, precipitated as a soft gel from 70% ethanol upon addition of acetone, formed a white amorphous powder when dried. Calc. for $(C_7H_{11}O_6)_2Ba$: C, 33.7%; H, 4.27%; Ba, 26.4%. Found: C, 33.1%; H, 4.77%; Ba, 26.2%. The compound was not oxidized by periodate even under strong oxidation conditions. However, upon acid hydrolysis (1 *N* hydrochloric acid for 3 hours at 100° C) it was degraded to pyruvic acid and erythritol as shown by paper chromatography. Quantitative analysis (1, 5) of these products revealed that they are in a 1:1 ratio.

RESULTS AND DISCUSSION

The combined evidence indicates that the compound isolated from polysaccharide B-1459 is the barium salt of 1,3-*O*-(1-carboxyethylidene)-erythritol (II). The infrared and nuclear magnetic resonance spectra support this structure. In potassium bromide the infrared spectrum displays strong carboxyl ion absorption bands at 6.2 and 7.1 μ. Also, two strong bands are present at 8.5 and 9.4 μ. These bands are reported to be

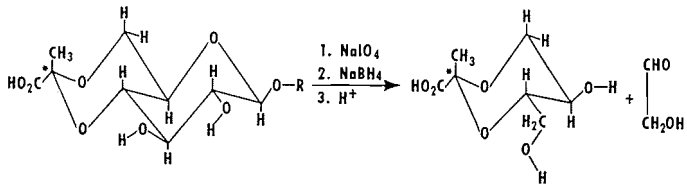

(I) (II)

R = Polysaccharide main chain
* = Configuration unknown

characteristic of a cyclic structure containing a —C—O—C—O—C— group (6). The n.m.r. spectrum shows several hydrogen resonances: CH_3 at 86, —CH—O and —CH_2—O at 218 and 226, and —OH at 332 c.p.s. ($(CH_3)_3Si(CH_2)_3SO_3H$ reference).

The erythritol that formed on hydrolysis of periodate-oxidized borohydride-reduced polysaccharide B-1459 can be derived only from the glucose moiety (7). Therefore, since the isolated pyruvate is bound to erythritol, it must be bound to glucose originally in the intact polymer. The pyruvate ketal of erythritol (II) can then arise under the conditions described from a glucose residue bearing pyruvic acid as a 4,6-*O*-(1-carboxyethylidene) group (I) provided that glucose exists as a side-chain unit.

ACKNOWLEDGMENTS

The authors are indebted to Dr. Allene Jeanes for her aid and encouragement and to Dr. Robert R. Bates for obtaining and interpreting the n.m.r. spectrum of II.

1. J. H. Sloneker and D. G. Orentas. Nature, **194**, 478 (1962).
2. S. Hirase. Bull. Chem. Soc. Japan, **30**, 68, 70 (1957).
3. J. H. Sloneker and A. Jeanes. Can. J. Chem. This issue.
4. I. J. Goldstein, G. W. Hay, B. A. Lewis, and F. Smith. Abstracts of Papers, 135th Meeting of the American Chemical Society, Boston, Mass. April, 1959. p. 3D.
5. M. Lambert and A. C. Neish. Can. J. Res. B, **28**, 83 (1950).
6. H. Tachamler and R. Leutner. Monatsh. **83**, 1502 (1952).
7. J. H. Sloneker, D. G. Orentas, and A. Jeanes. In preparation.

Received May 22, 1962.
Northern Regional Research Laboratory,
Agricultural Research Service,
U.S. Department of Agriculture,
Peoria, Ill., U.S.A.

SYNTHESIS AND PROPERTIES OF HOMOTAURINE

N. P. Sen

In the course of recent investigations in this laboratory, it became necessary to prepare homotaurine. The methods used were similar to those employed by Marvel *et al.* (1) (method I), and by Cortese (2) (method II) for the synthesis of taurine. The first method involved the preparation of 3-bromo-1-propanesulphonic acid followed by its ammonolysis to homotaurine, while in the second method, 3-bromopropylamine hydrobromide was first prepared, and it was then converted to homotaurine according to reaction 1:

$$HOCH_2CH_2CH_2NH_2 + HBr \rightarrow BrCH_2CH_2CH_2NH_3Br,$$

Reaction 1

$$BrCH_2CH_2CH_2NH_3Br + Na_2SO_3 \rightarrow HO_3SCH_2CH_2CH_2NH_2 + 2NaBr.$$

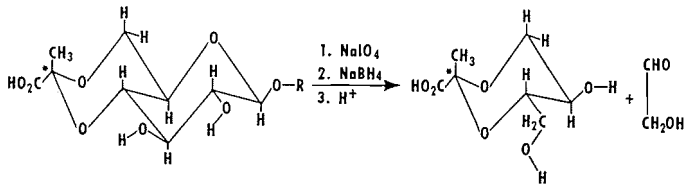

(I) (II)

R = Polysaccharide main chain
* = Configuration unknown

characteristic of a cyclic structure containing a —C—O—C—O—C— group (6). The n.m.r. spectrum shows several hydrogen resonances: CH_3 at 86, —CH—O and —CH_2—O at 218 and 226, and —OH at 332 c.p.s. ($(CH_3)_3Si(CH_2)_3SO_3H$ reference).

The erythritol that formed on hydrolysis of periodate-oxidized borohydride-reduced polysaccharide B-1459 can be derived only from the glucose moiety (7). Therefore, since the isolated pyruvate is bound to erythritol, it must be bound to glucose originally in the intact polymer. The pyruvate ketal of erythritol (II) can then arise under the conditions described from a glucose residue bearing pyruvic acid as a 4,6-*O*-(1-carboxyethylidene) group (I) provided that glucose exists as a side-chain unit.

ACKNOWLEDGMENTS

The authors are indebted to Dr. Allene Jeanes for her aid and encouragement and to Dr. Robert R. Bates for obtaining and interpreting the n.m.r. spectrum of II.

1. J. H. Sloneker and D. G. Orentas. Nature, **194**, 478 (1962).
2. S. Hirase. Bull. Chem. Soc. Japan, **30**, 68, 70 (1957).
3. J. H. Sloneker and A. Jeanes. Can. J. Chem. This issue.
4. I. J. Goldstein, G. W. Hay, B. A. Lewis, and F. Smith. Abstracts of Papers, 135th Meeting of the American Chemical Society, Boston, Mass. April, 1959. p. 3D.
5. M. Lambert and A. C. Neish. Can. J. Res. B, **28**, 83 (1950).
6. H. Tachamler and R. Leutner. Monatsh. **83**, 1502 (1952).
7. J. H. Sloneker, D. G. Orentas, and A. Jeanes. In preparation.

Received May 22, 1962.
Northern Regional Research Laboratory,
Agricultural Research Service,
U.S. Department of Agriculture,
Peoria, Ill., U.S.A.

SYNTHESIS AND PROPERTIES OF HOMOTAURINE

N. P. Sen

In the course of recent investigations in this laboratory, it became necessary to prepare homotaurine. The methods used were similar to those employed by Marvel *et al.* (1) (method I), and by Cortese (2) (method II) for the synthesis of taurine. The first method involved the preparation of 3-bromo-1-propanesulphonic acid followed by its ammonolysis to homotaurine, while in the second method, 3-bromopropylamine hydrobromide was first prepared, and it was then converted to homotaurine according to reaction 1:

$$HOCH_2CH_2CH_2NH_2 + HBr \rightarrow BrCH_2CH_2CH_2NH_3Br,$$

Reaction 1

$$BrCH_2CH_2CH_2NH_3Br + Na_2SO_3 \rightarrow HO_3SCH_2CH_2CH_2NH_2 + 2NaBr.$$

Both methods were found to work satisfactorily. However, since method I was not studied in detail, only method II will be described.

EXPERIMENTAL

3-Bromopropylamine hydrobromide.—Twenty-five grams (0.33 mole) of ice-cold 3-amino-1-propanol was added, through a dropping funnel, with vigorous stirring, to 175 ml (1.3 mole) of ice-cold hydrobromic acid in a 500-ml round-bottom flask. The flask was attached to a fractionating column and heated so that the solution refluxed with only a small portion of the liquid distilling off. This was continued for 16–18 hours, by which time about 125–130 ml of distillate had been collected and white fumes were starting to be given off. The distillation was discontinued at this point and the liquid was allowed to cool to about 70°. The hot mixture was poured into a beaker and 80 ml of acetone was added with stirring. The mixture was kept at 4° C overnight and the crystals of 3-bromopropylamine hydrobromide were collected on a filter and washed with acetone until colorless. The combined filtrate was concentrated under a vacuum and cooled, after it was seeded with a few crystals of the product. Thus, a second crop of the product was obtained. A third crop of less pure product could also be obtained. The total yield was 43.7 g (0.199 mole), 60.3% of the theoretical.

Homotaurine.—About 32.9 g (0.15 mole) of 3-bromopropylamine hydrobromide and 26 g (0.2 mole) of anhydrous sodium sulphite were dissolved in 95 ml of water. The mixture was concentrated on a hot plate (low heat) to a nearly dry cake; 24 hours were required for this operation. The residual cake was well triturated with 60 ml of concentrated HCl and the mixture filtered off on an asbestos mat. The solid on the mat was washed with ten 6-ml portions of concentrated HCl. The combined filtrate was concentrated to about 25 ml over a free flame. Then 95 ml of 95% ethanol was added to the hot solution with vigorous stirring and the mixture was allowed to cool. The precipitated crude product was filtered off. The crude product was dissolved in four times its weight of hot water, the water boiled with 1 g of Norite, the mixture filtered while hot, and the filtrate mixed with five volumes of 95% ethanol. When the filtrate was cooled, fine crystals of homotaurine were obtained. The product was filtered and dried in a vacuum desiccator. The total yield was 13.76 g (66%). The product gave only one ninhydrin spot on chromatographing in several solvents and had different R_f values than the chemicals from which it was synthesized. It decomposed at about 282–283° C. The product was found to be hygroscopic. Anal. Calc. for $C_3H_9O_3NS$: C, 25.86; H, 6.53; N, 10.00; S, 23.03. Found: C, 26.14; H, 6.61; N, 9.75; S, 23.24.

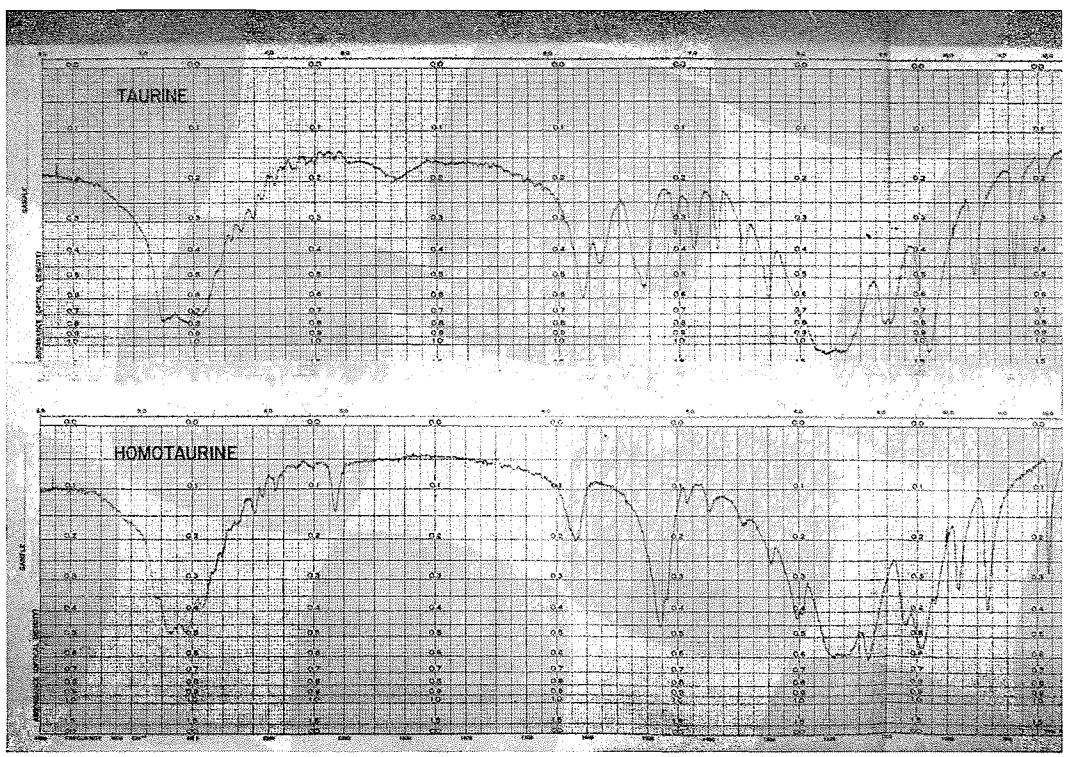

FIG. 1. Infrared spectra of taurine and homotaurine. KBr pellet.

Infrared spectra of taurine and homotaurine.—Figure 1 shows the infrared spectra of taurine and homotaurine. The series of low-intensity bands lying in the region from 3000–2400 cm^{-1} indicate the presence of an amino group. Two peaks near 1200–1160 cm^{-1} and 1050–1025 cm^{-1}, respectively, represent the presence of a sulphonic acid group.

Paper chromatography and paper electrophoresis of taurine and homotaurine.—Taurine and homotaurine, as indicated in Table I, have nearly identical R_f values in the solvent systems studied. Homotaurine can easily be distinguished from taurine, however, by paper electrophoresis, although the behavior of these two compounds is peculiar in a way. When 0.05 *N* NH_4OH (pH 10.95) solution was used as the electrolyte, taurine moved faster than homotaurine towards the anode. But when other basic solutions such as phosphate buffer and sodium hydroxide solution of the same pH, 10.95, were used these two compounds failed to separate from each other. On the other hand, use of a solution containing 0.001 equivalent of NaOH and 0.05 equivalent of NH_4OH per liter (final pH, 11.2) gave a clear separation of the two compounds. The results are noted in Table I. No. 3 Whatman paper was used as the supporting medium.

TABLE I

Paper chromatographic and electrophoretic data of taurine and homotaurine

	Electrophoresis cm/1000 volts hour, 0.05 *N* NH_4OH + 0.001 *N* NaOH, pH 11.2	R_f in solvent*				
		A	B	C	D	E
Taurine	8–8.2	0.10	0.28	0.49	0.41	0.43
Homotaurine	3–3.3	0.09	0.26	0.48	0.39	0.41

*A: Butanol – acetic acid – water (4:1:1); B: isopropanol – ammonium hydroxide – water (8:1:1); C: methanol–butanol–benzene–water (2:1:1:1); D: isobutyric acid – 0.5 *N* ammonium hydroxide (5:3); E: butanol–pyridine–water (1:1:1).

ACKNOWLEDGMENT

The author is indebted to Mrs. Zell of the Chemistry Department for taking the infrared spectra. The interest shown and many helpful suggestions given by Dr. P. L. McGeer is also gratefully acknowledged.

1. C. S. Marvel, C. F. Bailey, and M. S. Sparberg. J. Am. Chem. Soc. **49**, 1836 (1927).
2. F. Cortese. J. Am. Chem. Soc. **58**, 191 (1936).

Received June 28, 1962.
Kinsmen Laboratory of Neurological Research,
Faculty of Medicine,
University of British Columbia,
Vancouver, British Columbia.

THERMAL DECOMPOSITION OF SODIUM AZIDE CRYSTALS

E. A. Secco*

A study of the kinetics of thermal decomposition of sodium azide single crystals recently carried out in this laboratory has revealed some novel results on the progress of decomposition through the crystal.

Single crystals, transparent and colorless, of sodium azide in the form of platelets were obtained by crystallization from aqueous solution. Technical grade sodium azide was dissolved in distilled water and filtered. The solution was saturated by slow evaporation at 45–50° C and allowed to cool slowly (3–4 hours) to room temperature. The crystals

**On leave of absence from St. Francis Xavier University, Antigonish, Nova Scotia, and holder of a NATO Overseas Fellowship.*

Infrared spectra of taurine and homotaurine.—Figure 1 shows the infrared spectra of taurine and homotaurine. The series of low-intensity bands lying in the region from 3000–2400 cm^{-1} indicate the presence of an amino group. Two peaks near 1200–1160 cm^{-1} and 1050–1025 cm^{-1}, respectively, represent the presence of a sulphonic acid group.

Paper chromatography and paper electrophoresis of taurine and homotaurine.—Taurine and homotaurine, as indicated in Table I, have nearly identical R_f values in the solvent systems studied. Homotaurine can easily be distinguished from taurine, however, by paper electrophoresis, although the behavior of these two compounds is peculiar in a way. When 0.05 *N* NH_4OH (pH 10.95) solution was used as the electrolyte, taurine moved faster than homotaurine towards the anode. But when other basic solutions such as phosphate buffer and sodium hydroxide solution of the same pH, 10.95, were used these two compounds failed to separate from each other. On the other hand, use of a solution containing 0.001 equivalent of NaOH and 0.05 equivalent of NH_4OH per liter (final pH, 11.2) gave a clear separation of the two compounds. The results are noted in Table I. No. 3 Whatman paper was used as the supporting medium.

TABLE I

Paper chromatographic and electrophoretic data of taurine and homotaurine

Electrophoresis cm/1000 volts hour, 0.05 *N* NH_4OH + 0.001 *N* NaOH, pH 11.2		R_f in solvent*				
		A	B	C	D	E
Taurine	8–8.2	0.10	0.28	0.49	0.41	0.43
Homotaurine	3–3.3	0.09	0.26	0.48	0.39	0.41

*A: Butanol – acetic acid – water (4:1:1); B: isopropanol – ammonium hydroxide – water (8:1:1); C: methanol–butanol–benzene–water (2:1:1:1); D: isobutyric acid – 0.5 *N* ammonium hydroxide (5:3); E: butanol–pyridine–water (1:1:1).

ACKNOWLEDGMENT

The author is indebted to Mrs. Zell of the Chemistry Department for taking the infrared spectra. The interest shown and many helpful suggestions given by Dr. P. L. McGeer is also gratefully acknowledged.

1. C. S. Marvel, C. F. Bailey, and M. S. Sparberg. J. Am. Chem. Soc. **49**, 1836 (1927).
2. F. Cortese. J. Am. Chem. Soc. **58**, 191 (1936).

Received June 28, 1962.
Kinsmen Laboratory of Neurological Research,
Faculty of Medicine,
University of British Columbia,
Vancouver, British Columbia.

THERMAL DECOMPOSITION OF SODIUM AZIDE CRYSTALS

E. A. Secco*

A study of the kinetics of thermal decomposition of sodium azide single crystals recently carried out in this laboratory has revealed some novel results on the progress of decomposition through the crystal.

Single crystals, transparent and colorless, of sodium azide in the form of platelets were obtained by crystallization from aqueous solution. Technical grade sodium azide was dissolved in distilled water and filtered. The solution was saturated by slow evaporation at 45–50° C and allowed to cool slowly (3–4 hours) to room temperature. The crystals

**On leave of absence from St. Francis Xavier University, Antigonish, Nova Scotia, and holder of a NATO Overseas Fellowship.*

were recovered by filtration, dried, and stored in a desiccator with P_2O_5. These crystals had the *c*-axis parallel to the plane of the plate.

A single crystal of sodium azide was selected from the batch of crystals, weighed, and placed in a quartz bucket. The bucket, with the crystal, was suspended in a conventional vacuum system and degassed at room temperature. Under a final holding vacuum of 2×10^{-6} mm Hg the bucket was lowered into the furnace at the required temperature.

The progress of the reaction was followed with a Pirani gauge connected to a Fielden Servograph previously calibrated with a McLeod gauge. After a fraction of the crystal had decomposed, the crystal was withdrawn and examined with a microscope and photographed.

Figure 1 shows a photograph by reflected light of a crystal partially decomposed at 275° C in vacuum. It is evident that decomposition begins on preferred crystallographic faces and moves towards the center of the crystal. The relative rates of reaction on the various edges can be judged by the amount of white residue. The white residue is porous in structure and chemically identical with the original salt. The other significant features to be noted are the sharp purple line of demarcation at the undecomposed azide and white residue interface and the absence of reaction on the surface except for a few imperfect surface growths.

The experimental results for the rate of decomposition of NaN_3 crystals fall approximately into three temperature regions: (*a*) low temperature, below 300° C, where the rate follows, after a rapid initial stage (ca. 5%), a linear relation, leaving a white residue in the shape of the original crystal; curve I of Fig. 2; (*b*) medium temperature, 300–345° C,

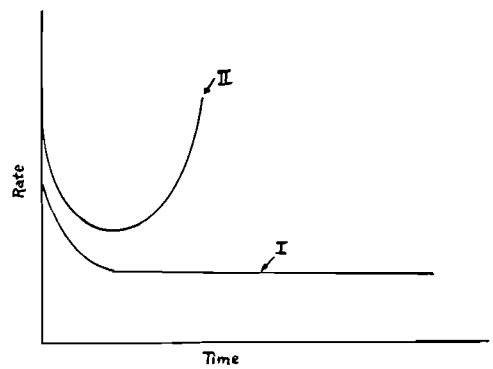

FIG. 2. Rate versus time curves at different temperatures.

where the rate is of the common sigmoid type, leaving a white residue; and finally (*c*) high temperature, above 350° C, where the decomposition follows two different linear rates, the latter being 100 times faster than the first, with no detectable residue; curve II of Fig. 2.

A more detailed account of this work will be reported later and these results will be discussed in the light of the early data on NaN_3 thermal decomposition (1) and the parallel case of ammonium perchlorate (2).

The author is indebted to the National Research Council of Canada for the award of a NATO Overseas Fellowship, to Dr. F. P. Bowden for providing laboratory facilities, and to Dr. A. Yoffe for helpful discussions.

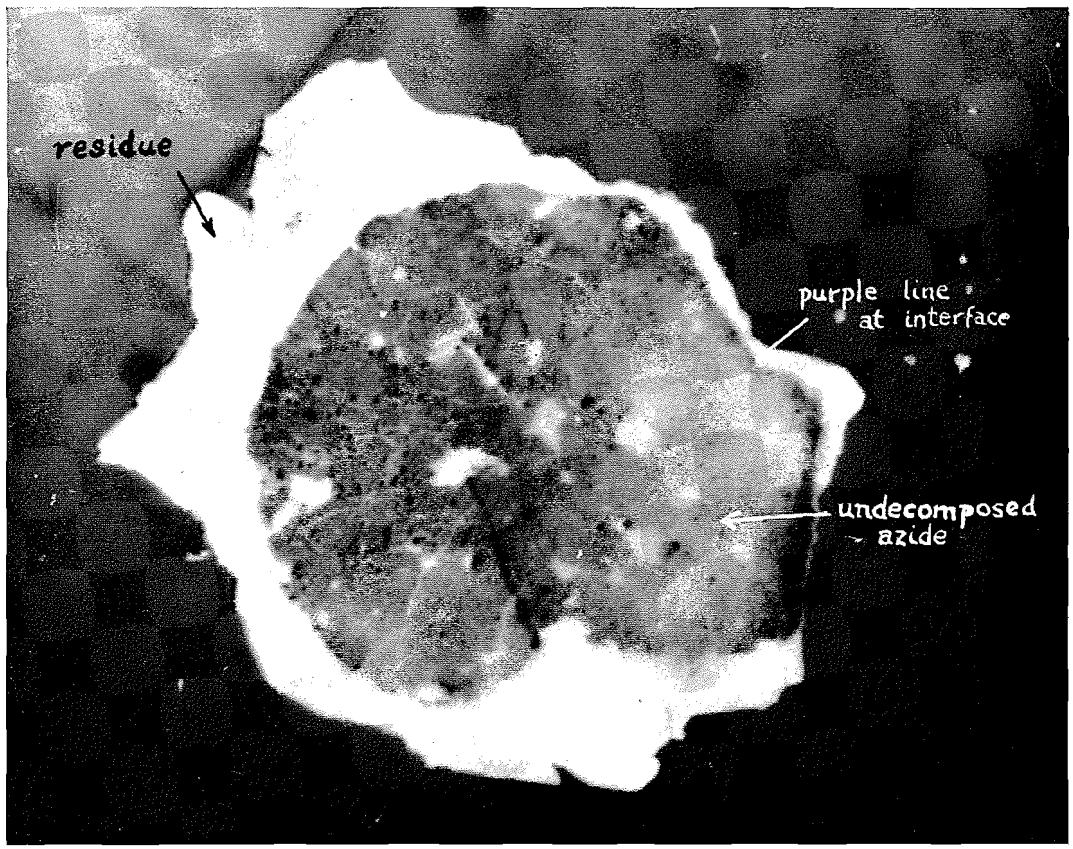

FIG. 1. Photograph (×20) of partially decomposed NaN_3 crystal showing white residue and central undecomposed crystal with purple line at interface.

1. W. E. GARNER and D. J. B. MARKE. J. Chem. Soc. 657 (1936).
2. L. L. BIRCUMSHAW and B. H. NEWMAN. Proc. Roy. Soc. (London), A, **227**, 115 (1954); A, **227**, 228 (1955).

RECEIVED JULY 20, 1962.
LABORATORY FOR THE PHYSICS AND CHEMISTRY OF SOLIDS,
CAVENDISH LABORATORY,
CAMBRIDGE, ENGLAND.

Canadian Journal of Chemistry

Issued by THE NATIONAL RESEARCH COUNCIL OF CANADA

VOLUME 40 DECEMBER 1962 NUMBER 12

THERMAL DECOMPOSITION OF MOLECULAR COMPLEXES

I. UREA–*n*-PARAFFIN INCLUSION COMPOUNDS[1]

H. G. MCADIE

Department of Chemistry, Ontario Research Foundation, Toronto, Ontario

Received July 16, 1962

ABSTRACT

The molecular complexes of urea and even-numbered *n*-paraffins up to C_{28} undergo thermal decomposition below the melting point of urea at temperatures which increase with the *n*-paraffin chain length. The decomposition is endothermal and is accompanied by changes in crystal structure, appearance, and by loss of the *n*-paraffin. Based on the enthalpy change a mechanism for the decomposition process is proposed.

The variety of molecular complexes now known provides the means for examining many molecules of different size and shape in an environment more or less isolated from others of their own kind. Within the canals which penetrate the structure of urea inclusion compounds, long-chain guest molecules are longitudinally isolated from one another by the canal walls but are permitted end-group interactions between successive chains, affording a means for comparing these interactions in different homologous series through their contribution to the thermal stability of the complex.

The decomposition of urea inclusion compounds at temperatures below the melting point of urea was first observed by Knight *et al.* (1) as a darkening of the normally translucent complex crystal when heated at a slow rate on a hot-stage microscope. The temperature at which darkening first occurred could be reproduced usually to $\pm 1.5°$ C provided optically suitable crystals were examined. For members of several homologous series the decomposition temperatures of the corresponding urea complexes were found to increase linearly with chain length up to about 18 carbon atoms. The thermal decomposition of the urea–*n*-paraffin series of complexes was not studied in this work, although a partial examination was made by Yata (2), who claimed values similar to those for the methyl esters reported by Knight. The decomposition of the even-numbered urea–*n*-paraffin complexes has been studied using differential thermal analysis (3–6), in which the samples were generally contaminated with free *n*-paraffin, and a discontinuity in the decomposition temperature – chain length curve was indicated in the vicinity of C_{18} to C_{20}. The present paper deals with the thermal decomposition of urea complexes of even-numbered *n*-paraffins in greater detail than previously, including an examination of the decomposition mechanism. Subsequent papers will describe the decomposition of other series of complexes in which there is increasing end-group interaction between successive guest molecules.

[1]*These results were presented in part at the 138th and 141st Meetings of the American Chemical Society.*

EXPERIMENTAL METHODS

Preparation of Complexes

The *n*-paraffins from C_{10} to C_{18} inclusive were fractionally distilled before use; C_{20}, C_{22}, and C_{28} were Eastman white label grade (or equivalent) used without further purification; C_{24} and C_{26} were research samples supplied by American Petroleum Institute Project 42. Other materials were reagent grade.

To prepare the complexes 5 g urea was dissolved in 20 g methanol, and 1 g *n*-paraffin added at room temperature. The mixture was warmed to 65° C and isopropanol added until the solution was homogeneous. On slow cooling crystallization of the complex was largely complete at temperatures above the melting point of the respective pure *n*-paraffin. The complex was filtered under suction and air-dried.

Visual Microscopy

The decomposition temperatures of the complexes were observed using polarized light and a calibrated Kofler micro hot-stage. The technique was similar to that of Knight *et al.* (1), a thin glass slide being substituted for the copper slide. A heating rate of 0.5° C min^{-1} was used to within 5° C of the decomposition temperature and reduced to 0.2° C min^{-1} thereafter. Results were generally reproducible to better than ±1° C over the multiple determinations made during a single heating period, provided careful selection of crystals was made initially. Slower heating rates did not improve this reproducibility. The average temperature at which opacity was first clearly distinguished was taken as the visual decomposition temperature, although the subjective evaluation of this point varied somewhat between operators.

X-Ray Diffraction

The presence of the hexagonal urea complex lattice was confirmed for all complexes by Debye–Scherrer powder patterns obtained using Cu $K\alpha$ radiation with a nickel filter.

Using a specially designed glancing-angle X-ray diffraction camera, containing a small copper block which could be held at a controlled temperature, it was possible to confirm the destruction of the hexagonal lattice at the decomposition temperature. A 0.5-mm lead-free glass capillary, open at one end, containing the complex was mounted on the copper block and a diffraction pattern obtained. It was then heated to a few degrees above the decomposition temperature and a second pattern obtained. The block was returned to room temperature before obtaining a final pattern.

Differential Thermal Analysis (DTA)

Part of this work was carried out on an instrument described earlier (7). Subsequently, a second instrument was constructed employing a horizontal furnace wound with 15-gauge Kanthal A wire, manually programmed by twin Variacs in series, and a palladium block having separate cavities for sample and reference material. The temperature of a thermal event was that of the block at that instant, measured on a calibrated potentiometric recorder. The differential temperature was sensed by a pair of Pt–Pt/13% Rh thermocouples amplified by a stabilized microvolt amplifier and displayed on a second recorder. Under normal operating conditions a sensitivity equivalent to 0.8 μv cm^{-1} of chart was used, although higher sensitivities were obtainable.

Samples were ground to pass a 325-mesh screen and diluted to 20% by weight in ignited α-alumina, which was also used as reference material.

Thermogravimetric Analysis (TGA)

A manually operated thermobalance was constructed from a standard analytical balance and a furnace of the same type as used in the DTA studies. The vertical core of this furnace was flushed with a preheated dry nitrogen stream at 50 cc min^{-1} and the appropriate buoyancy–temperature corrections made. A manually programmed heating rate of 1° C min^{-1} was used.

The sample holder was of the open-pan variety described by Garn and Kessler (8) with provision for measuring the pan temperature rather than that of the furnace. Approximately 0.3 g of −100 mesh complex was spread evenly over the pan to a depth of 2–3 mm. Weighings were made at 1° C intervals in sample block temperature.

RESULTS

Visual Decomposition Temperature

Average decomposition temperatures determined by the method of Knight *et al.* (1) are given in Table I together with the standard deviation in each case. Two sets of complexes were prepared, one of which was recrystallized from a methanol–isopropanol mixture containing a small amount of urea. The observed decomposition temperatures agreed within the standard deviation of a single sample so that recrystallization appears to have little effect on sample purity.

Although complexes decomposing above 120° C were increasingly difficult to observe

PLATE I

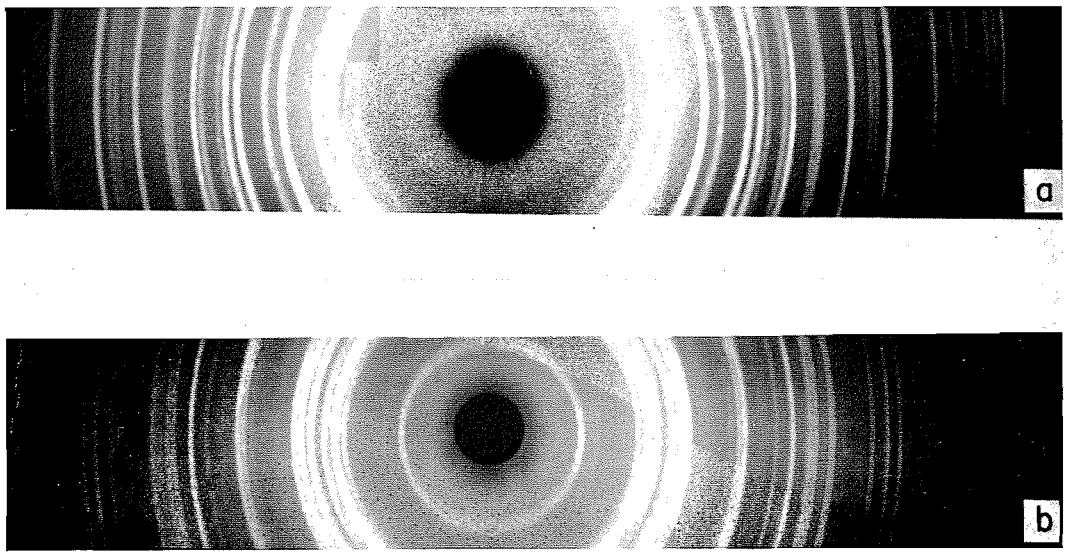

FIG. 1. Debye–Scherrer powder patterns of the tetragonal urea (*a*) and the hexagonal urea complex lattice (*b*).

TABLE I

Decomposition temperatures of urea–*n*-paraffin inclusion compounds (° C)

Carbon chain length (*n*)	Method: Visual	TGA	DTA (incipient)	DTA (peak)
10	46.1±1.6	56±1.0	72.8±1.2	81.5±1.1
12	60.0±0.5	73±1.0	85.3±0.3	91.2±1.7
14	79.4±0.0	86±1.0	96.2±0.7	101.7±2.3
16	96.3±0.3	95±0.5	103.0±1.3	108.1±0.7
18	113.8±0.0	104±0.0	110.0±2.0	114.2±1.5
20	118.4±0.2	113±5.0	113.9±0.9	117.9±0.4
22	121.7±0.5	120±3.0	119.3±0.7	123.2±0.8
24	124.3±0.6	123	121.4±0.1	125.3±1.6
26	126.2±0.7	123	123.3±0.2	130.0±0.1
28	—	—	125.3	131.2

by this technique due to sublimation of the urea, a discontinuity was apparent in the C_{18} region, which is beyond the region of linear behavior of complexes previously studied by this method.

X-Ray Diffraction Studies

While X-ray diffraction techniques do not permit the distinction of individual complexes, the method does differentiate clearly between the hexagonal lattice of the complex and the normal tetragonal lattice of urea as shown in Fig. 1. No evidence of the tetragonal lattice could be detected in patterns of the complexes prior to decomposition.

After accounting for lines due to copper in the patterns obtained using the glancing-angle camera, the patterns obtained before heating were characteristic of the hexagonal lattice and those obtained after heating were characteristic of the tetragonal lattice. Thus the complex was confirmed to be destroyed at the observed transition temperature.

However, if the sample capillary was sealed prior to heating, the pattern above the decomposition temperature was again that of tetragonal urea, while on cooling the pattern slowly reverted to that of the hexagonal lattice, indicating re-formation of the complex under conditions where the *n*-paraffin could not escape. It was also noticed that there was an improved definition in the tetragonal urea pattern resulting after decomposition, suggesting that this material is in a finer state of subdivision than the complex from which it was formed and supporting earlier reports (1, 9) of increased surface area following complex decomposition.

Differential Thermal Analysis

The differential thermograms of a series of unrecrystallized complexes are shown in Fig. 2. The urea fusion endotherm provides a convenient internal calibration of each system with respect to temperature and to the enthalpy equivalence of peak area. A further indication of sample purity, beyond the absence of tetragonal urea lines in the diffraction patterns of the complexes, was the absence of any low-temperature phase transition and fusion endotherms such as were found with complexes contaminated with free *n*-paraffin (3–6).

The C_{10} complex, being somewhat unstable at room temperature, was partially decomposed during preparation of the DTA sample. At the longer chain lengths the complex decomposition endotherm became increasingly superimposed on the urea fusion endotherm and further resolution was unsuccessful.

The regular progression of the temperature of the complex decomposition endotherm

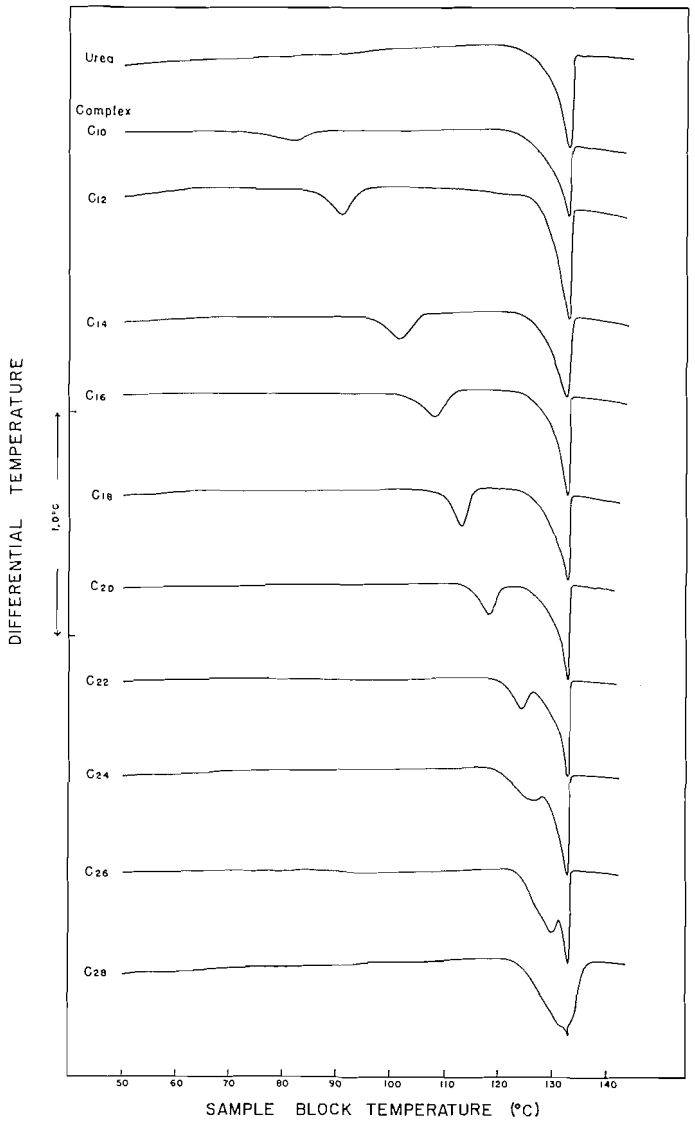

FIG. 2. Differential thermograms of urea and a series of urea–*n*-paraffin complexes.

with increasing chain length is given in Table I, again indicating the standard deviation over a series of samples of a given complex. The "incipient temperatures" were taken at the intersection of a projection of the thermogram base line with a projection of the low-temperature side of the endotherm (10). The discontinuity in the region of C_{18} is not as evident by this technique but, rather, a continuous curve is found asymptotically approaching the melting point of urea. In all cases temperatures were corrected to a value of 132.7° C for the peak of the urea fusion endotherm.

By comparison of the areas under the complex decomposition and urea fusion endotherms (Fig. 2), together with data on the ratio of urea to *n*-paraffin in the complex (11), and the heat of fusion of urea (12), an estimation of the heat of decomposition was made as follows:

$$\Delta H_d = m \cdot \frac{a_C}{a_U} \cdot \Delta H_f,$$

where

ΔH_d = heat of complex decomposition (kcal mole^{-1} *n*-paraffin),
m = molar ratio urea:*n*-paraffin,
a_C = area of complex decomposition peak,
a_U = area of urea fusion peak,
ΔH_f = heat of fusion (kcal mole^{-1} urea).

The results are given in Table II, and Fig. 3 shows a comparison with heats of reaction for three possible decomposition processes estimated from equilibrium data in the

TABLE II

Enthalpy and entropy of decomposition of urea–*n*-paraffin inclusion compounds

Carbon chain length (n)	Enthalpy		Entropy	
	Experimental (kcal mole^{-1} *n*-paraffin)	Least-squares fit (kcal mole^{-1} *n*-paraffin)	(e.u. mole^{-1} *n*-paraffin)	(e.u. mole^{-1} urea)
10	+ 9.9	+11.6	33.5	4.02
12	13.4	14.6	40.7	4.19
14	18.7	17.6	47.6	4.30
16	22.9	20.6	54.8	4.40
18	23.3	23.6	61.6	4.46
20	23.5	26.6	68.7	4.52
22	29.6	29.6	75.4	4.55

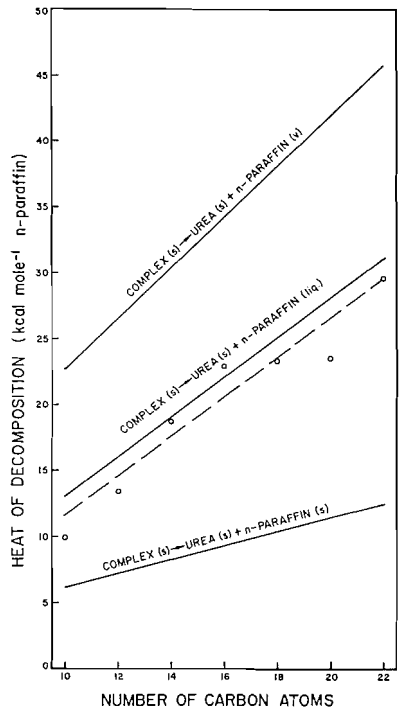

FIG. 3. Heat of decomposition of urea–*n*-paraffin complexes as a function of chain length. Solid lines represent data calculated from the literature; the broken line represents least-squares fit to experimental data (O).

literature (13–15). This comparison was possible only up to the C_{22} complex due to the extensive overlapping of the complex decomposition and urea fusion endotherms beyond this chain length. A least-squares fit of the experimental points indicates that the decomposition process is energetically equivalent to:

$$\text{complex (s)} = \text{urea (s)} + n\text{-paraffin (liq.)}.$$

An estimate of the entropy change accompanying decomposition, based on the observed enthalpy change at the transition temperature, is also shown in Table II.

Thermogravimetric Analysis

The loss in weight due to eventual vaporization of the *n*-paraffin after destruction of the complex made possible the study of this decomposition by TGA. Weight-loss curves are shown in Fig. 4, plotted as percentage of complex decomposition using an inverted ordinate so that decomposition in excess of 100% corresponds to degradation of the

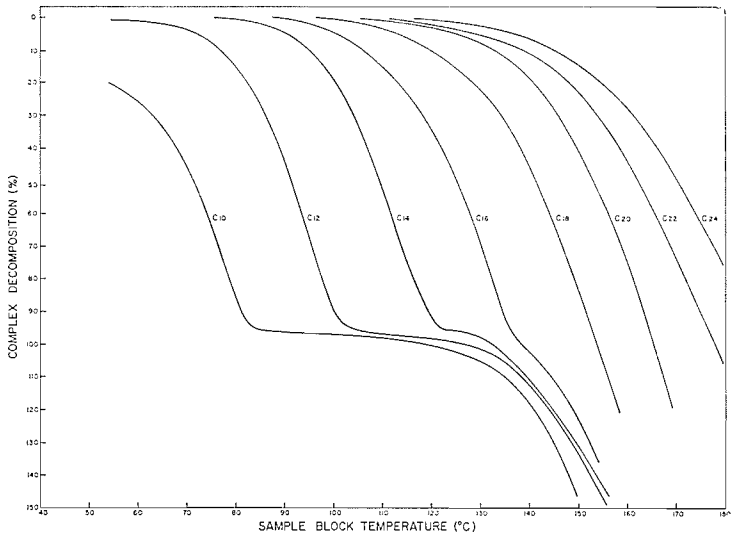

FIG. 4. Thermogravimetric analysis curves for a series of urea–*n*-paraffin complexes.

urea. At about 125° C urea begins to exhibit a measurable weight loss; consequently decomposition of the complexes above C_{16} could not be resolved into the two consecutive processes at a heating rate of 1° C min^{-1}. Decomposition temperatures, estimated at the point of incipient weight loss, appear in Table I. Due to urea degradation, decomposition temperatures determined by TGA reach essentially a constant value in the complexes of longer chain lengths.

DISCUSSION

It is evident that only "procedural decomposition temperatures" (16) have been determined in this work. Much of the variation in decomposition temperatures measured by different techniques is due to two factors: (i) sample environment and (ii) the point at which the decomposition process is observed.

Comparison of enthalpy changes involved (Fig. 3) indicates the decomposition process to be:

$$\text{complex (s)} = \text{urea (s)} + n\text{-paraffin (liq.)},$$

for which the equilibrium constant is $K = p/p_0$, where p is the decomposition pressure of the complex and p_0 the saturation vapor pressure of the pure n-paraffin. Although in none of the techniques used does a thermodynamic equilibrium exist, any factor which tends to alter p will also influence the decomposition temperature. In the cases of visual microscopy and TGA the sample is spread out as individual crystals or in a thin layer, respectively, so that the diffusion of liberated n-paraffin is relatively unimpeded. In DTA a narrow cylinder of compressed sample offers considerable impedence to diffusion of the large n-paraffin molecules and hence the decomposition temperatures are higher. Further, each technique observes a different stage of the decomposition process:

(i) TGA: the temperature at which continuous weight loss begins; sample is 1–2% decomposed;

(ii) visual: the temperature at which opacity is first clearly evident in the crystal, which is subjective, and the extent of decomposition will vary;

(iii) DTA: incipient temperatures probably correspond to about 5% decomposition; peak temperatures to 50–80% decomposition depending upon the reaction rate.

The combination of these factors tends to place the respective procedural decomposition temperatures in the observed relationship to one another.

The similarity in shape between the urea complex decomposition temperature curve and the melting point curve for the pure, even-numbered n-paraffins (Fig. 5), together with the observed enthalpy change during the decomposition process, support the suggested decomposition mechanism. Energetically (9, 11), the state of the n-paraffin chains

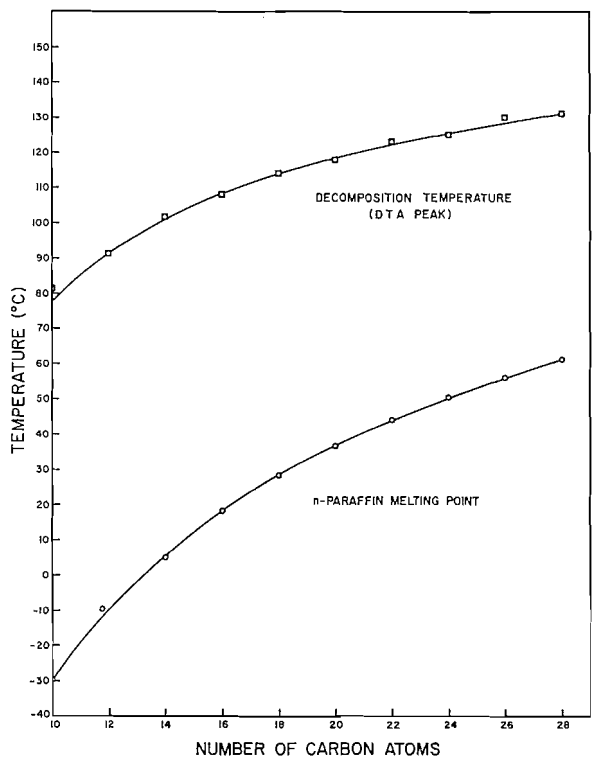

FIG. 5. Comparison of the decomposition temperature of urea–n-paraffin complexes and the melting points of pure n-paraffins as a function of chain length.

within the complex is similar to that in the pure solid. The bonds holding an *n*-paraffin molecule in the pure crystal lattice are associated with $(n-2)$ CH_2 groups, while the terminal CH_3 groups are repelled by the lattice (17). When the crystal melts, these $(n-2)$ intermolecular attractions must be broken by the potential of the terminal groups and the vibrational–rotational energy of the molecule as a whole. In the urea complex, the chain–chain interactions along the length of a chain are replaced by weak van der Waals interactions between the chain and the urea canal wall. These chains are in restricted motion within the canal (18) and it may be that once they acquire sufficient energy to permit substantially free rotation about the canal axis then the chain may escape. Unless its place is immediately filled by another chain, the hexagonal lattice cannot remain stable and rearranges to the tetragonal form.

The decomposition always occurs at a temperature above the melting point of the corresponding *n*-paraffin, which, therefore, emerges in a state energetically equivalent to that of the liquid and slowly vaporizes. This slow secondary vaporization is supported by the fact that the time required for loss of *n*-paraffin from a freely exposed decomposing sample is considerably greater than the time required for the completion of the enthalpy change even in the more confined DTA sample. The estimated entropy change accompanying decomposition *per mole of n-paraffin* increases rapidly with chain length, while the entropy change *per mole of urea* increases only slowly with chain length (Table II), indicating that it is largely associated with the transformation of the urea lattice resulting from removal of the *n*-paraffin chain.

These considerations of the decomposition mechanism apply for complexes which decompose at temperatures below the melting point of urea. Given a sufficiently long chain, the complex is stable up to the melting point of urea, at which temperature the urea cage simply melts, liberating the enclosed *n*-paraffin chain. As yet there is no definite evidence that urea in the hexagonal form will melt at a temperature measurably different from the melting point of urea in the tetragonal form.

ACKNOWLEDGMENTS

The writer wishes to acknowledge the kindness of Professor J. A. Dixon and the American Petroleum Institute Project 42 for supplying samples of *n*-C_{24} and *n*-C_{26}, and the technical assistance of T. J. Shannon and J. S. Haskill.

This work was carried out under a research grant to the Ontario Research Foundation from the Province of Ontario received through the Department of Economics and Development.

REFERENCES

1. H. B. KNIGHT, L. P. WITNAUER, J. E. COLEMAN, W. R. NOBLE, JR., and D. SWERN. Anal. Chem. **24**, 1331 (1952).
2. N. YATA. Bull. Chem. Soc. Japan, **32**, 991 (1959).
3. A. V. TOPCHIEV, L. M. ROZENBERG, N. A. NECHITAILO, and F. M. TERENT'EVA. Dokl. Akad. Nauk SSSR, **98**, 223 (1954).
4. L. M. ROZENBERG, E. M. TERENT'EVA, N. A. NECHITAILO, and A. V. TOPCHIEV. Dokl. Akad. Nauk SSSR, **109**, 1144 (1956).
5. A. V. TOPCHIEV, L. M. ROZENBERG, N. A. NECHITAILO, and E. M. TERENT'EVA. Zh. Neorgan. Khim. **1**, 1185 (1956).
6. I. R. KRICHEVSKII, G. D. EFREMOVA, and G. G. LEONT'EVA. Dokl. Akad. Nauk SSSR, **113**, 817 (1957).
7. W. E. P. FLECK, M. H. JONES, R. A. KUNTZE, and H. G. MCADIE. Can. J. Chem. **38**, 936 (1960).
8. P. D. GARN and J. E. KESSLER. Anal. Chem. **32**, 1900 (1960).
9. H. G. MCADIE and G. B. FROST. Can. J. Chem. **36**, 635 (1958).
10. R. C. MACKENZIE. The differential thermal investigation of clays. Mineralogical Society, London. 1957. p. 86.
11. A. E. SMITH. Acta Cryst. **5**, 224 (1952).

12. F. W. MILLER, JR. and H. R. DITTMAR. J. Am. Chem. Soc. **56**, 848 (1934).
13. O. REDLICH, C. M. GABLE, A. K. DUNLOP, and R. W. MILLAR. J. Am. Chem. Soc. **72**, 4161 (1950).
14. E. TERRES and S. NATH SUR. Brennstoff-Chem. **38**, 7 (1957).
15. F. D. ROSSINI, K. S. PITZER, R. L. ARNETT, R. M. BROWN, and G. C. PIMENTEL. Selected values of physical and thermodynamic properties of hydrocarbons and related compounds. Carnegie Press, Pittsburgh, Pa. 1953.
16. A. E. NEWKIRK. Anal. Chem. **32**, 1558 (1960).
17. C. G. GRAY. J. Inst. Petrol. **29**, 226 (1943).
18. D. F. R. GILSON and C. A. McDOWELL. Mol. Phys. 4, 125 (1961).

STRUCTURE OF THE EXTRACELLULAR POLYSACCHARIDE PRODUCED BY XANTHOMONAS ORYZAE*

A. MISAKI AND S. KIRKWOOD
Department of Agricultural Biochemistry, University of Minnesota, St. Paul, Minn., U.S.A.

AND

J. V. SCALETTI
Department of Animal Husbandry, University of Minnesota, St. Paul, Minn., U.S.A.

AND

F. SMITH
Department of Agricultural Biochemistry, University of Minnesota, St. Paul, Minn., U.S.A.

Received July 30, 1962

ABSTRACT

The extracellular polysaccharide isolated from cultures of *Xanthomonas oryzae* is composed of D-glucose (5 molecular proportions), D-glucuronic acid (2 molecular proportions), and D-mannose (5 molecular proportions). Acid hydrolysis of this polysaccharide, which contains 0.3% combined pyruvic acid, yields 2-*O*-β-D-glucopyranosyluronic acid D-mannose, which has been characterized as its crystalline fully methylated β-glycoside. Hydrolysis of the methylated polysaccharide gives 2,3,4,6-tetra-*O*-methyl-D-mannose (3 molecular proportions), 2,3,4-tri-*O*-methyl-D-glucuronic acid (1 molecular proportion), 2,3,6-tri-*O*-methyl-D-glucose (4 molecular proportions), 3,4,6-tri-*O*-methyl-D-mannose (2 molecular proportions), 2,6-di-*O*-methyl-D-glucose (3 molecular proportions), 2,3-di-*O*-methyl-D-glucose (1 molecular proportion). The polyalcohol derived from the polysaccharide by periodate oxidation followed by sodium borohydride reduction gives upon acid hydrolysis glycerol (2 molecular proportions), erythritol (1 molecular proportion), and D-glucose (1 molecular proportion). The general structural significance of these findings is discussed.

Xanthomonas oryzae (1) has long been known as a plant pathogenic microorganism responsible for the leaf blight disease of the rice plant (*Oryzae sativa*) in Japan and characterized by the fact that when growing on the natural host plant it is highly resistant to inhibitors. When this gram-negative organism was grown in a synthetic medium containing glucose or sucrose, under aerobic conditions, the medium became viscous due to the production of an extracellular polysaccharide which was composed of glucose, mannose, and glucuronic acid. After purification by copper hydroxide complex formation this acidic polysaccharide showed $[\alpha]_D$ −11° (in *N* NaOH) and had an equivalent weight of 988. Acid hydrolysis of the polysaccharide, which proceeded relatively slowly, was found to give rise to D-glucose (2.5 molecular proportions), D-mannose (2.7 molecular proportions), and D-glucuronic acid (1.0 molecular proportion), each of which was identified as the crystalline derivative.

Controlled acid hydrolysis furnished an aldobiouronic acid, 2-*O*-β-D-glucopyranosyluronic acid-D-mannose, recognized by its transformation into the characteristic crystalline methyl 2-*O*-[methyl (2,3,4-tri-*O*-methyl-β-D-glucosyl)uronate]-3,4,6-tri-*O*-methyl-D-mannoside (2).

Methylation of the *X. oryzae* polysaccharide first with methyl sulphate and sodium hydroxide and then with methyl iodide and silver oxide afforded a methylated derivative ($[\alpha]_D$ +44.5° ($CHCl_3$)). Hydrolysis of this methylated polysaccharide followed by column

*Paper No. 4875, Scientific Journal Series, Minnesota Agricultural Experiment Station, St. Paul 1, Minnesota.

chromatography (3) gave 2,3,4,6-tetra- (3 molecular proportions), 3,4,6-tri- (2 molecular proportions), and 3,4-di-*O*-methyl-D-mannose (2 molecular proportions); 2,3,6-tri- (4 molecular proportions) and 2,6-di-*O*-methyl-D-glucose (3 molecular proportions); and 2,3,4-tri- (1 molecular proportion) and 2,3-di-*O*-methyl-D-glucuronic acid (2 molecular proportions). Each of the above cleavage fragments was identified as a crystalline compound. In addition there was also produced approximately 1 molecular proportion of a mixture of 2- and 3-*O*-methyl-D-glucose, recognized only by paper electrophoresis.

The precise structure of the *X. oryzae* polysaccharide cannot be deduced from the data available so far but the general structural features of the polymer are apparent from the experimental findings. Inspection of the molar proportions of the cleavage fragments of the methylated polysaccharide (see Table I) shows that the molar ratio

TABLE I

Hydrolysis products of the methylated *Xanthomonas oryzae* polysaccharide

Component No.	Identity	Mol. props.	Structural feature indicated
1	2,3,4,6-Tetra-*O*-methyl-D-mannose	3	[D-Manp] 1 →
2	3,4,6-Tri-*O*-methyl-D-mannose	2	→ 2 [D-Manp] 1 →
3	2,3,6-Tri-*O*-methyl-D-glucose	4	→ 4 [D-Gp] 1 →
4	3,4-Di-*O*-methyl-D-mannose	2	→ 2, → 6 [D-Manp] 1 →
5	2,6-Di-*O*-methyl-D-glucose	3	→ 3, → 4 [D-Gp] 1 →
6	2,3,4-Tri-*O*-methyl-D-glucuronic acid	1	[D-GpA] 1 →
7	2,3-Di-*O*-methyl-D-glucuronic acid	2	→ 4 [D-GpA] 1 →

glucose:mannose:glucuronic acid is 2.3:2.3:1, a result in fairly good agreement with the corresponding ratio 2.5:2.7:1 calculated from the proportions of the glucose, mannose, and glucuronic acid formed by hydrolysis of the unmethylated polysaccharide. This deduction is in accord with the equivalent weight of 988 found for the polysaccharide, which corresponds to a repeating unit composed of one glucuronic acid residue and five hexose residues (calc. equiv. wt., 986). It seems reasonable to conclude from the above results that the molar ratio of glucuronic acid:glucose:mannose is approximately 1:2.5:2.5.

From the identity and proportions of the cleavage fragments of the methylated polysaccharide it is evident that the polymer possesses a highly branched structure. The exact proportions of the cleavage fragments of the methylated polysaccharide cannot be arrived at because the recovery (86% approx.) was not quantitative and also because of the formation of the mono-*O*-methyl glucose component, which for the present is regarded as an artifact probably derived from the 2,3,6-tri-*O*-methyl derivative and hence of no structural significance, since this would necessitate the formation of a much greater proportion of non-reducing terminal units than was actually encountered. Thus, for an average of about 17 to 18 sugar residues which make up the repeating unit of the polysaccharide there are 4 terminal non-reducing residues consisting of 3 units of mannose and 1 of glucuronic acid. There are also five residues, three of glucose and two of mannose, at which branching occurs in the polysaccharide. The remaining nine non-terminal

residues consist of two 1 → 2-linked mannose residues, five 1 → 4-linked glucose residues (this includes the mono-*O*-methyl fraction assumed to be derived from the 2,3,6-tri-*O*-methyl-D-glucose by demethylation), and two 1 → 4-linked glucuronic acid residues.

The identity of the components recorded in Table I coupled with the stability of the polysaccharide to acid hydrolysis show that all the building units in the polysaccharide are of the pyranose type. Moreover the negative specific optical rotation (−11°) of the polysaccharide indicates that many of the glycosidic bonds joining the sugar residues, all of which belong to the D-series, are of the β-type.

Support for these general structural features was furnished by periodate oxidation studies. Inspection of Table I will show that out of the repeating unit of 17 sugar residues consisting of (*a*) 3 terminal units of mannose and 1 of glucuronic acid, (*b*) 2 non-terminal units of mannose, 4 of glucose, and 2 of glucuronic acid, and (*c*) 2 branching units of mannose and 3 of glucose, only the 3 branching units of glucose, which give rise upon methylation and hydrolysis to 2,6-di-*O*-methyl-D-glucose (component 5), will be stable to periodate oxidation, whereas the remaining 14 will be cleaved.

Further consideration of the results in Table I will show that analysis of the polyalcohol, derived from the polysaccharide by periodate oxidation followed by reduction with sodium borohydride (4), should provide results in agreement with the following: (*a*) the erythritol must arise only from the 1 → 4-linked D-glucose units, (*b*) glycerol should be produced from the terminal, non-terminal, and also from the branching D-mannose residues, that is, from all the mannose building units, and (*c*) glucose surviving periodate cleavage should arise from the branching glucose residues joined through positions C_1, C_3, and C_4. Clearly, therefore, if the equimolar ratio of mannose to glucose as calculated from the compositional analysis is correct, then in the hydrolyzate of the *Xanthomonas* polyalcohol the sum of the molar proportions of erythritol and the molar proportions of periodate-stable glucose should be equal to the molar proportions of glycerol. This is borne out reasonably well by the experimental facts (see p. 2212).

The isolation, by graded acid hydrolysis of the polysaccharide, of an aldobiouronic acid composed of D-glucuronic acid joined to D-mannose by a 1 → 2-β linkage strongly suggests, if the repetitive structural feature of other polyuronides is generally applicable, that in the polysaccharide probably all of the units of glucuronic acid are joined to mannose residues in the same manner. Furthermore, the tentative identification of an aldotriouronic acid composed of 2-*O*-(β-D-glucopyranosyluronic acid)-D-mannose joined to a glucose residue indicates that some, although probably not all, of the aldobiouronic acid residues are joined to glucose in the following manner: D-GpA-(1 → 2)-D-Manp-(1 → 3 or 4)-D-Gp.

It is not yet possible to say whether the aldobiouronic acid residues constitute side chains directly attached to a glucomannan main chain or whether non-terminal 1 → 4-linked glucose units are interposed between the main chain and these aldobiouronic acid side chains but since three out of four terminal non-reducing units consist of mannose units it seems reasonably certain that two out of the three aldobiouronic acid side chains are terminated by mannose units, thus giving rise to the sequence D-Manp-(1 → 4)-D-GpA-(1 → 2)-D-Manp-(1 → 3 or 4)-D-Gp-1 →.

Structural deductions beyond this are not warranted until such time as oligosaccharides with and without glucuronic acid residues have been isolated. When these are forthcoming perhaps light will be thrown upon the unexpected property of this highly branched heteropolymer being insoluble in water, a property usually associated with either strictly linear character or repetitive and relatively simple side chains attached to linear chains.

The *X. oryzae* polysaccharide is similar to the extracellular polysaccharide derived from *Xanthomonas phaseoli* (5) and that from *Xanthomonas campestris* (6) inasmuch as they all contain D-glucose, D-mannose, and D-glucuronic acid. Another point of interest is that the polysaccharide from *X. oryzae* resembled that from *X. campestris* since both contained combined pyruvic acid, the former 0.3% and the latter 2.8 to 3.5% (7). Although the structural significance of the pyruvic acid in these polysaccharides is not yet understood, it appears to be present as a ketal group, as in the case of the red seaweed polysaccharides (8), since the pyruvic acid residues are removed by acid but not by alkali.

EXPERIMENTAL

All evaporations were carried out under reduced pressure at 40–50° C. Paper chromatography was performed by the descending method on filter paper (Whatman No. 1) using the following solvent systems: (A) 1-butanol:ethanol:water (4:1:5) (9), (B) ethyl acetate:pyridine:water (2.5:1:3.5) (10), (C) 1-butanol: acetic acid:water (2:1:1) (11), (D) butanone:water azeotrope (12).

Paper electrophoresis (13) was carried out on filter paper (Whatman No. 1) using 0.1 *M* borate buffer, 600 volts, for 3.5 hours. Chromatograms were sprayed with silver nitrate, *p*-anisidine trichloroacetic acid (11), or *p*-anisidine hydrochloride in 1-butanol saturated with water.

Production and Separation of Polysaccharide

The strain of *X. oryzae* was kindly provided by Dr. S. Matsunaka, National Institute of Agriculture, Tokyo, Japan. Preliminary experiments on cultural conditions showed that the following medium was suitable for polysaccharide production by the shaking flask culture technique: 3–5% glucose, 0.2% yeast extract (Difco), 0.1% L-glutamic acid, 0.2% $(NH_4)_2SO_4$, 0.07% Na_2HPO_4, 0.05% KH_2PO_4, 0.03% $MgSO_4$, and 0.1% NaCl (pH adjusted to 7.0 with NaOH). Each 400 ml of the medium was sterilized in a 2-l. Erlenmeyer flask for 30 minutes at 15 p.s.i., and inoculated with 20 ml of the preculture grown for 24 hours in the same medium at 25° C. The culture was mechanically shaken at 25° C for several days. Polysaccharide production proceeded smoothly, the cultural broth became viscous, and after 5 days no reducing sugars remained (tested with Fehling solution). At the end of this time, the broth (1.2 l.) was heated at 80° C to effect sterilization and clarified by centrifugation. The crude polysaccharide was precipitated by pouring the supernatant liquid into 3 volumes of ethanol. The polysaccharide was dissolved in water (200 ml), and the solution was centrifuged and treated with ethanol (3 vols.). The polysaccharide was then purified by copper hydroxide complex formation as follows: A solution of the polysaccharide in water (200 ml) was treated with Fehling solution (300 ml). The precipitated complex was collected (centrifuge) and washed repeatedly with 80% ethanol containing 4% hydrogen chloride until no more blue color remained in the precipitate.

The white precipitate thus obtained was washed successively with ethanol, diethyl ether, petroleum ether and dried *in vacuo* (yield 1.5 g or 5% based on the glucose present in the original culture medium).

The purified polysaccharide was a light fibrous material which showed $[\alpha]_D^{25}$ −11° in *N* sodium hydroxide (*c* 1.0). Whereas the crude polysaccharide precipitated directly with ethanol was soluble in water, the polysaccharide purified through its copper hydroxide complex and freed from salt was insoluble in water. Glass paper electrophoresis (14) showed that the polysaccharide was homogeneous.

When the polysaccharide was dissolved in sodium hydroxide (0.02 *N*) and dialyzed against water, the polysaccharide (salt form) was precipitated during the dialysis. These facts suggested that either the physical properties were changed during the purification process or the solubility of polysaccharide was greatly influenced by ions, especially OH^- ions.

Determination of the Equivalent Weight of the Polysaccharide

The purified and salt-free polysaccharide (67.2 mg) obtained by prolonged dialysis first against dilute sulphuric acid and then against water was dissolved in 0.01 *N* NaOH (20 ml) and the excess alkali was back-titrated with 0.01 *N* H_2SO_4. The result showed that the equivalent weight of the acidic polysaccharide was 988, which corresponded to 18.5% of glucuronic acid, or one unit of glucuronic acid for every five hexose units.

Hydrolysis of the Polysaccharide and Identification of the Components

The polysaccharide (120 mg) was hydrolyzed with *N* sulphuric acid in a sealed tube for 18 hours at 100° C. The solution was neutralized ($BaCO_3$), filtered, passed through Amberlite IR-120 (H^+ form) resin (1.5×10 cm), and evaporated to a sirup. Paper chromatography of this sirup using solvents A and B showed that the hydrolyzate contained glucose and mannose, a finding confirmed by paper electrophoresis. Chromatography (solvent C, time 35 hours) revealed the presence of glucuronolactone (R_{Rh} (mobility relative to that of L-rhamnose) 0.90), glucuronic acid (R_{Rh} 0.45), and an aldobiouronic acid (R_{Rh} 0.27) in addition to glucose and mannose.

Hydrolyzates of both the crude polysaccharide (precipitated from the cultural broth with ethanol) and the material purified through its copper hydroxide complex showed the same component sugars on paper chromatograms.

For identification of the component sugars, the hydrolyzate from the purified polysaccharide was passed through a column (1.5×10 cm) of Duolite A-4 (OH^- form) resin and the column was washed with water. The combined eluate and washing was evaporated to give a mixture of neutral sugars (86 mg). The anion column was then eluted with 0.2 *N* sodium hydroxide and the eluate was passed through Amberlite IR-120 (H^+ form). Evaporation of the acidic eluate gave a sirup which was found by paper chromatography (solvent C) to consist of glucuronic acid (10.2 mg) and aldobiouronic acid (8.1 mg).

Separation and Identification of the Neutral Components

A portion of the neutral fraction (25 mg) was subjected to paper electrophoresis. Each component was separated and freed from borate by treatment with 1% methanolic hydrogen chloride (13) followed by ion exchange resin. Evaporation of the solution in each case gave two sirupy components, D-glucose and D-mannose.

The glucose component (9.7 mg), which showed $[\alpha]_D^{25}$ +51° in water (*c*, 2.0), was treated with *p*-nitroaniline (15) in boiling methanolic hydrogen chloride (0.07%) for 15 minutes. This provided the *p*-nitroaniline derivative of D-glucose, which was recrystallized from methanol, m.p. and mixed m.p. 191–192° C (15).

The sirupy mannose component (11.9 mg), which showed $[\alpha]_D^{25}$ +14.4° in water (*c*, 3.0), was converted to D-mannose phenylhydrazone, in the usual way, m.p. and mixed m.p. 199–200° C (after recrystallization from ethanol) (16).

Identification of the Acidic Components

The D-glucuronic acid fraction (10.2 mg) was lactonized by heating for 1 hour at 80° C, and treated for 15 minutes with *p*-nitroaniline (10 mg) in boiling methanol (0.2 ml) containing hydrogen chloride (0.07%). Evaporation of the solvent afforded the crystalline *p*-nitroaniline derivative of D-glucuronolactone, which was recrystallized from methanol, m.p. and mixed m.p. 130° C (17).

Quantitative Determination of Component Sugars

For the quantitative determination of component sugars, the polysaccharide (45 mg) was completely hydrolyzed by heating (sealed tube) with 2 *N* sulphuric acid for 12 hours at 100° C. The D-glucose and D-mannose fractions were separated by paper electrophoresis, after previous passage of the hydrolyzate through an ion exchange resin as described above. Both sugars were determined colorimetrically by the phenol – sulphuric acid method (18), at 490 mμ, after previous removal of borate by treatment with methanolic hydrogen chloride (13). It was found that the molar ratio of D-mannose to D-glucose was 1.1:1.0. The D-glucuronic acid content was estimated by the carbazole method (19). Prior to the determination, partial hydrolysis of the polysaccharide (9.4 mg) was effected by treatment with 1.5 *N* sulphuric acid (1.5 ml) for 1 hour at 100° C in order to render the polysaccharide soluble. The hydrolyzate was diluted with water and an aliquot was used for the uronic acid determination. The polysaccharide contained 16.05% D-glucuronic acid, a result in fairly good agreement with that (18.5%) obtained by the titration method above. The lower figure obtained by the carbazole method may be due to decomposition caused by the pretreatment with acid. The molar ratio of the three components, D-glucose:D-mannose:D-glucuronic acid, was 2.5:2.7:1.0.

Isolation and Identification of 2-O-(β-D-Glucuronosyluronic acid)-D-mannose

The polysaccharide (800 mg) was refluxed with *N* sulphuric acid (40 ml) for 8 hours. The hydrolyzate was neutralized ($BaCO_3$), after which the neutral (580 mg) and acidic components (92 mg) were separated using ion exchange resins as described above.

Paper chromatographic separation of the acidic components so obtained using solvent C gave D-glucuronic acid (trace), an aldobiouronic acid (40 mg), an aldotriouronic acid (10.5 mg), and a trace of an unknown acidic oligosaccharide.

Identification of the Aldobiouronic Acid

The mobility of the aldobiouronic acid fraction on paper chromatography (R_{Rh} 0.275, solvent C) and on paper electrophoresis (M_g 0.82) coupled with its specific optical rotation, $[\alpha]_D^{25}$ −28.0° in water, showed that the aldobiouronic acid was probably 2-*O*-(β-D-glucuronic acid)-D-mannose, which has been isolated previously from the polysaccharide of *Brasenia schreberi* (20) and from *Virgilia oroboides* gum (2). Hydrolysis of the aldobiouronic acid with a cation exchange resin (IR-120, H^+ form) at 100° C, for 30 hours, followed by paper chromatography (solvents A and C) revealed the presence of D-glucuronolactone, D-glucuronic acid, D-mannose, and unchanged aldobiouronic acid.

Methylation of the Aldobiouronic Acid

The above aldobiouronic acid (40 mg) was dissolved in water (1 ml) and methylated with dimethyl sulphate (9 ml) and 30% (w/v) aqueous sodium hydroxide (25 ml) for 3 hours at 5° C and for 5 hours

at room temperature, thorough mixing being effected with a stream of nitrogen. The reaction mixture was heated for 20 minutes at 65° C, cooled (ice bath), and neutralized with 5 *N* sulphuric acid. Addition of ethanol (final concn. 60%) to precipitate sodium sulphate followed by filtration and evaporation of the solution gave a residue consisting of the partially methylated aldobiouronic acid and inorganic salts. The residue so obtained was subjected to a second methylation as before for 4 hours at room temperature and for 2.5 hours at 50–55° C. After acidifying the reaction mixture with 5 *N* H_2SO_4 the methylated product was extracted with chloroform (4×50 ml) (yield 35.3 mg). After a third methylation in the same way, the methylation of the aldobiouronic acid (25 mg) was completed with silver oxide (0.5 g) and methyl iodide (3 ml) under reflux for 10 hours. After evaporation of solvent, the residue was extracted with chloroform and the chloroform solution evaporated to a sirup. The sirup was dissolved in diethyl ether and the solution filtered to remove a trace of insoluble impurity. Slow evaporation of the solvent gave crystals of the fully methylated aldobiouronic acid (23 mg) which showed $[\alpha]_D^{25}$ −19° in methanol (*c*, 0.8) and had m.p. and mixed m.p. with an authentic specimen of methyl 2-*O*-[methyl (2,3,4-tri-*O*-methyl-β-D-glucosyl)uronate]-3,4,6-tri-*O*-methyl-D-mannoside 142–143° C (after recrystallization from a mixture of diethyl ether and petroleum ether (1:1)) (2).

Preparation of Amide

A portion of the above crystals was dissolved in methanol (2 ml) and the solution saturated with ammonia at 0° C. The reaction mixture was kept at room temperature overnight, and the solvent evaporated under reduced pressure. After the residue was dissolved in ethanol (0.5 ml) and diethyl ether and petroleum ether were added, there separated crystalline methyl 2-*O*-(2,3,4-tri-*O*-methyl-β-D-glucosyluronamide)-3,4,6-tri-*O*-methyl-D-mannoside (yield almost quantitative), which after recrystallization from a mixture of ethanol and diethyl ether had m.p. and mixed m.p. 186–187° C and $[\alpha]_D^{25}$ −64.4° in water (*c*, 0.9).

Examination of the Aldotriouronic Acid

This component (10.5 mg), judged to be an aldotriouronic acid from its mobility on chromatograms, *R* (aldobiouronic acid) 0.42, solvent C, showed $[\alpha]_D^{25}$ −4° in water (*c*, 2.5). Hydrolysis of this aldotriouronic acid with cation resin (IR-120, H^+ form) in water for 48 hours at 100° C gave D-mannose, D-glucose, aldobiouronic acid, and the original component, as revealed by chromatography.

It appears, therefore, that this fraction is an aldotriouronic acid, in which D-glucose is attached to 2-*O*-(β-D-glucopyranosyluronic acid)-D-mannose. The structure of this aldotriouronic acid remains to be determined.

The Presence of Pyruvic Acid in the Polysaccharide

In order to determine whether pyruvic acid was present in the polysaccharide as in the case of polysaccharides from some red seaweeds (8) and in *X. campestris* (7), the *X. oryzae* polysaccharide (500 mg) was hydrolyzed (7) with *N* sulphuric acid (20 ml) for 5 hours. After cooling, the solution was extracted with diethyl ether (5×100 ml). Evaporation of the diethyl ether gave a small residue which when examined by paper chromatography (solvent A) was found to contain a small proportion of pyruvic acid, detectable with a slightly alkaline bromphenol blue spray. The above residue was therefore dissolved in water (2 ml) and 0.5% 2,4-dinitrophenylhydrazine in 2 *N* hydrochloric acid (2 ml) was added. The reaction mixture, which showed a little turbidity after 30 minutes, was extracted with ethyl acetate (5 ml). The ethyl acetate layer was then extracted with 10% aqueous sodium carbonate solution (3×5 ml). Determination of the absorption spectrum of the solution showed a characteristic selective absorption band at 375 mμ (21) identical with that for the 2,4-dinitrophenylhydrazone of pyruvic acid. Since this absorption band is relatively non-specific for either pyruvic acid (370 mμ) or α-ketoglutaric acid (380 mμ), according to Koepsell (21), a portion of the above 2,4-dinitrophenylhydrazone in alkaline solution was re-extracted with ethyl acetate and the extract examined by paper chromatography using solvent A. This revealed a yellow component (R_f 0.37) (22) corresponding to that of the 2,4-dinitrophenylhydrazone of pyruvic acid; an unidentified faint yellow component (R_f 0.55), possibly a stereoisomer (23), was also detected. Because of the minute amount of 2,4-dinitrophenylhydrazone of pyruvic acid available, recrystallization was impossible.

The colorimetric determination of what is believed to be pyruvic acid in the polysaccharide was performed by measuring the yellow color of the 2,4-dinitrophenylhydrazone in alkaline solution at 375 mμ. This showed that the polysaccharide contained 0.31% of pyruvic acid. Because of the small amount it is not yet known whether pyruvic acid is present as a significant structural feature of the polysaccharide or whether it is a metabolic "birthmark".

Methylation of the Xanthomonas oryzae Polysaccharide

Since acetylation of the polysaccharide was difficult because of its insolubility in either pyridine or formamide the polysaccharide was methylated directly by the usual Haworth method.

The polysaccharide (2 g) was dissolved in 30% sodium hydroxide (80 ml) and the thick solution was stirred mechanically during the dropwise addition of dimethyl sulphate (25 ml) for 4 hours at 40° C; a second addition of dimethyl sulphate (40 ml) and 30% sodium hydroxide was made during a further 3 hours at 55° C, after which the mixture was heated for 30 minutes at 90–100° C. After cooling, the reaction mixture was neutralized with 5 *N* sulphuric acid, whereupon the partially methylated polysaccharide

separated as a curd on the surface of the liquid. After removal of as much of the methylated product as possible, the reaction mixture was dialyzed against water for 3 days and then evaporated to dryness. The partially methylated product and the residue from the dialyzate were combined and retreated with dimethyl sulphate (45 ml) and sodium hydroxide (120 ml) at 55° C as before. After decomposition of the excess of the dimethyl sulphate by heating, the reaction mixture was cooled, neutralized with dilute sulphuric acid, and treated with ethanol (final concn. 50% v/v). The precipitated salts were filtered and washed with 50% aqueous ethanol. Evaporation of the filtrate gave a residue which was dissolved in 80% aqueous 1,4-dioxane (30 ml) and methylated with dimethyl sulphate (45 ml) and 30% sodium hydroxide (110 ml). A slight excess of dilute sulphuric acid was added to the reaction mixture and the solution was extracted with chloroform (3×300 ml). The combined chloroform extracts were dried ($MgSO_4$), evaporated, and the residue again treated with dimethyl sulphate and 30% sodium hydroxide as before. The methylated product obtained in this manner was subjected to two treatments with Purdie reagents in the usual way using methyl iodide (30 ml) and silver oxide (3 g). The resulting fully methylated polysaccharide was dissolved in chloroform (10 ml) and precipitated by adding excess petroleum ether (60 ml). Yield 1.4 g, $[\alpha]_D^{25}$ +44.5° in chloroform (*c*, 1.8); found: OCH_3, 41.1%.

Hydrolysis of the Methylated Polysaccharide

A solution of the methylated polysaccharide (543 mg) in 3.7% methanolic hydrogen chloride (25 ml) was refluxed for 15 hours. The solution was neutralized (Ag_2CO_3), filtered, and evaporated. The mixture of methylated methyl glycosides was then hydrolyzed by heating with *N* sulphuric acid (20 ml) for 24 hours at 100° C; the solution was neutralized ($BaCO_3$), filtered, and evaporated to a dry residue (335 mg). Paper chromatography using solvents A and D revealed five components which corresponded to tetra-*O*-methylhexose (glucose or mannose), tri-*O*-methylhexose (glucose or mannose), 3,4-di-*O*-methylmannose, 2,6-di-*O*-methylglucose, and a mono-*O*-methylhexose, and one component (pink color with *p*-anisidine) remaining at the starting line which appeared to be a uronic acid derivative. The hydrolyzate was dissolved in water (20 ml) and passed first through an IR-120 (H^+ form) column (1×10 cm), then through a Duolite A-4 (OH^- form) column (1×10 cm). The eluate was evaporated to give the neutral methylated sugars as a sirup (yield, 261 mg). The acidic sugars were eluted from the anion column with dilute sodium hydroxide (see below).

Separation and Identification of Methyl Sugar Components

Neutral Components

The above mixture of the neutral sugars (260 mg) was dissolved in solvent D (1 ml) and put on the cellulose–hydrocellulose column (3) (3.5×38 cm) and fractionated with solvent D using an automatic fraction collector adjusted to collect 11 ml/20 min. Examination of the fractions of the eluate by paper chromatography gave the results in Table II.

TABLE II

Cleavage fragments of the methylated *Xanthomonas oryzae* polysaccharide

Fraction	Tube No.	Yield (mg)	Components
1	7–22	50.6	2,3,4,6-Tetra-*O*-methyl-D-mannose
2	27–32	13.2	3,4,6-Tri-*O*-methyl-D-mannose
3*	33–37	22.8	3,4,6-Tri-*O*-methyl-D-mannose (18.5 mg) 2,3,6-Tri-*O*-methyl-D-glucose (4.3 mg)
4	38–50	53.5	2,3,6-Tri-*O*-methyl-D-glucose
5	80–113	28.8	3,4-Di-*O*-methyl-D-mannose
6	145–200	40.3	2,6-Di-*O*-methyl-D-glucose
7†		13.7	2- and 3-*O*-Methyl-D-glucose
	Total	222.9	

*Quantitative separation on paper electrophoresis indicated that this fraction consisted of 18.5 mg of 3,4,6-tri-*O*-methyl-D-mannose and 4.3 mg of 2,3,6-tri-*O*-methyl-D-glucose.
†Eluted with 500 ml of solvent D:methanol (4:1).

Identification of 2,3,4,6-tetra-O-methyl-D-mannose.—Fraction 1 (50.6 mg), which was chromatographically identical with 2,3,4,6-tetra-*O*-methyl-D-glucose or -mannose (R_f 0.78, solvent D), showed $[\alpha]_D^{25}$ +12° in water (*c*, 1.5). A portion (23.4 mg) was heated with aniline (100 mg) in absolute ethanol (1 ml) for 6 hours under reflux. The solvent and excess aniline were evaporated *in vacuo*, giving a crystalline product (30 mg). Recrystallization from ethanol – diethyl ether gave *N*-phenyl 2,3,4,6-tetra-*O*-methyl-D-mannosylamine, m.p. and mixed m.p. 145–146° C, $[\alpha]_D^{25}$ −8° equilibrium value in methanol (*c*, 1.0) (24, 25).

Identification of 3,4,6-tri-O-methyl-D-mannose.—Fraction 2 (13.2 mg) showed a slightly higher R_f (0.58 in solvent D) on a paper chromatogram than fraction 4 (R_f 0.56) and a slightly different color with the *p*-anisidine spray reagent. Paper electrophoresis showed that fraction 2 consisted largely of 3,4,6-tri-*O*-

methyl-D-mannose (M_g 0.24) together with a trace of 2,3,6-tri-*O*-methyl-D-glucose (M_g 0.0). Upon nucleation with 3,4,6-tri-*O*-methyl-D-mannose fraction 2 crystallized immediately and after recrystallization from diethyl ether had m.p. and mixed m.p. 103–104° C, $[\alpha]_D^{25}$ +10° equilibrium value in water (*c*, 2.0) (25).

Identification of 2,3,6-tri-O-methyl-D-glucose.—Fraction 4 (53.5 mg), which corresponded to 2,3,6-tri-*O*-methyl-D-glucose, showed $[\alpha]_D^{25}$ +65° in water (*c*, 1.0), and R_f 0.56 (in solvent D). Paper electrophoresis showed that this fraction consisted mostly of 2,3,6-tri-*O*-methyl-D-glucose (M_g 0.0) with a trace of 3,4,6-tri-*O*-methyl-D-mannose (M_g 0.24). Upon standing at room temperature, fraction 4 crystallized slowly and after recrystallization from diethyl ether the 2,3,6-tri-*O*-methyl-D-glucose had m.p. and mixed m.p. 120–121° C (26).

A portion of the above material (20 mg), treated with *p*-nitrobenzoyl chloride (200 mg) in dry pyridine (2 ml) in the usual way, gave the characteristic di-*p*-nitrobenzoate, m.p. and mixed m.p. 190–191° C, $[\alpha]_D^{25}$ −34° in chloroform (*c*, 1.0) (27).

Identification of 3,4-di-O-methyl-D-mannose.—Fraction 5 (28.8 mg), which crystallized spontaneously, had R_f 0.32 (solvent D) and M_g 0.34 and corresponded to 3,4-di-*O*-methyl-D-mannose. After recrystallization from ethanol–ether, the 3,4-di-*O*-methyl-D-mannose had m.p. and mixed m.p. 80–81° C, $[\alpha]_D^{25}$ +5.4°, equilibrium value in water (*c*, 3.7) (28).

Identification of 2,6-di-O-methyl-D-glucose.—Fraction 6 (40.3 mg), which failed to crystallize, showed $[\alpha]_D^{25}$ +66° in water (*c*, 1.7) and R_f 0.18 (solvent D), corresponding to di-*O*-methyl-D-glucose. By paper electrophoresis, the migration (M_g 0.24) and color reaction with *p*-anisidine were identical with those of 2,6-di-*O*-methyl-D-glucose but differed from those shown by the 2,3-, 2,4-, and the 4,6-di-*O*-methyl derivatives. A portion of this sirup (6 mg) was dissolved in dry pyridine (2.5 ml), and *p*-phenylazobenzoyl chloride (150 mg) was added, and the mixture was kept for 48 hours at 40° C. The excess reagent was decomposed by addition of water and the mixture was evaporated to dryness. The residue was triturated with chloroform (10 ml) and filtered. The filtrate was passed through a zinc carbonate column (1×15 cm) under pressure. The column was washed with chloroform and the eluate was evaporated to a sirup. Trituration of this sirup with ethyl acetate afforded a crystalline azobenzoate derivative (22 mg), which was recrystallized from a mixture of ethyl acetate and petroleum ether, m.p. 210–211° C, undepressed upon mixture with authentic 1,3,4-tri-*O*-*p*-phenylazobenzoyl-2,6-di-*O*-methyl-D-glucose, and $[\alpha]_D^{25}$ −333° in chloroform (*c*, 0.5) (29).

Examination of the mono-O-methyl-D-glucose fraction.—After fraction 6 had emerged from the column, fraction 7 (13.7 mg) was eluted with solvent D containing 20% methanol (500 ml). Paper chromatography showed that this fraction was composed of a single component, R_f 0.07 (solvent D), which corresponded to mono-*O*-methyl-D-glucose, whereas paper electrophoresis revealed at least two components, one corresponding to 2-*O*-methyl-D-glucose (M_g 0.24) and the other to 3-*O*-methyl-D-glucose (M_g 0.60). There were not sufficient amounts of either of these materials for complete identification.

Acidic Components

After separation of the neutral sugar components, the acidic components adsorbed on Duolite A-4 column were eluted with 0.2 *N* sodium hydroxide (200 ml) and the eluate passed through an IR-120 (H^+ form) column (1×10 cm). The acidic eluate was evaporated to a sirup (yield 52 mg). On a paper chromatogram using solvent C, two pink spots (with *p*-anisidine spray reagent) were revealed, corresponding respectively to 2,3,4-tri-*O*-methyl-D-glucuronic acid (R_f 0.65) and 2,3-di-*O*-methyl-D-glucuronic acid (R_f 0.48). A slow-moving spot (R_f 0.30–0.33), probably a methylated aldobiouronic acid, was also detected. A portion (25 mg) of the above sirup was separated by paper chromatography (solvent C), giving 2,3,4-tri-*O*-methyl-D-glucuronic acid (6.0 mg) and 2,3-di-*O*-methyl-D-glucuronic acid (9.0 mg).

Identification of 2,3,4-tri-O-methyl-D-glucuronic acid.—The tri-*O*-methyluronic acid fraction was heated with methanolic hydrogen chloride (2.5%) for 12 hours under reflux, neutralized (Ag_2CO_3), and freed from solvent. Treatment of the sirupy residue with methanolic ammonia afforded crystalline methyl 2,3,4-tri-*O*-methyl-α-D-glucosiduronamide, m.p. and mixed m.p. 183° C (30).

Identification of 2,3-di-O-methyl-D-glucuronic acid.—The di-*O*-methyl-D-glucuronic acid fraction was treated with methanolic hydrogen chloride as described above and the product (4 mg) so formed was dissolved in ethanol (0.2 ml) containing freshly distilled phenylhydrazine (2 mg). The solution was heated for 20 minutes at about 80° C, after which the solvent was allowed to evaporate. The residue was heated for 8 hours at 110° C, after which the reaction mixture was extracted by refluxing with diethyl ether. Upon evaporation of the solvent a crystalline phenylhydrazide was formed. Recrystallization from acetone–petroleum ether gave the phenylhydrazide of methyl 2,3-di-*O*-methyl-D-glucosiduronic acid, m.p. and mixed m.p. 219–220° C (31).

Quantitative separation by paper chromatography and weighing of the two components showed that the molar ratio of 2,3,4-tri-*O*-methyl-D-glucuronic acid to 2,3-di-*O*-methyl-D-glucuronic acid was 1:1.7.

Periodate Oxidation and Reduction of the Polysaccharide

The polysaccharide (169 mg) was oxidized with 0.1 *M* sodium metaperiodate (100 ml) at room temperature (25° C) in the dark. At suitable intervals aliquots were removed and the periodate consumption was determined by the usual arsenite method (32); the formic acid production was determined by titration with 0.01 *N* sodium hydroxide (33) (a correction was applied for the presence of carboxyl groups by a blank

titration of the acidic polysaccharide itself; see p. 2207). The results showed that oxidation was complete after 10 days; the molar periodate consumption was 1.15 per hexose unit and the liberation of formic acid was 0.51 mole per hexose unit.

In another experiment, the polysaccharide (200 mg) was suspended in 0.1 *N* periodic acid (100 ml) and the oxidation was carried out at 10° C. After complete oxidation (25 days, periodate consumption 1.25 molecular proportions per hexose unit), the oxidized polysaccharide was separated (centrifuge), washed with water, then suspended in water (50 ml) and reduced with sodium borohydride (200 mg) as previously described (34), during which reaction the product dissolved. The excess of the sodium borohydride was decomposed by acidification with acetic acid and the polysaccharide polyalcohol was subjected to hydrolysis by refluxing for 12 hours with sulphuric acid (adjusted to concn. 0.15 *N*). After cooling, the hydrolyzate was neutralized with barium carbonate, filtered, and the filtrate was evaporated to dryness. Borate in the residue was removed by repeated evaporation with 1% methanolic hydrogen chloride at room temperature and subsequent deionization by passage first through cation exchange (IR-120, H^+ form) and then through the anion exchange (Duolite A-4, OH^- form) resin. The neutral solution was evaporated to a sirup (yield 139 mg) which was shown by paper chromatographic analysis (solvents A and B) to contain glucose, glycerol, and erythritol but little or no mannose.

Separation and Identification of the Products from the Polysaccharide Polyalcohol

A portion (50 mg) of the above hydrolyzate of the polyalcohol was fractionated by paper chromatography using solvent B. The zone of the paper containing each component was extracted with water (20 ml) and evaporated.

(i) Glucose

The glucose fraction (10 mg) was treated with acidified methanolic *p*-nitroaniline (20 mg) as described previously, and the crystalline *p*-nitroanilide of D-glucose was obtained, m.p. and mixed m.p. 190–192° C (15).

(ii) Glycerol

The glycerol fraction (5 mg) was dissolved in dry pyridine (1.5 ml), and *p*-nitrobenzoyl chloride (50 mg) was added. The solution was heated for 2 hours at 80–90° C, then poured into cold sodium bicarbonate solution (15 ml). After extraction with chloroform, the chloroform layer was washed with water and dried ($MgSO_4$). Upon evaporation of the chloroform extract, the crystalline tri-*p*-nitrobenzoate of glycerol was obtained, m.p. and mixed m.p. 191–192° C (after recrystallization from chloroform–ethanol at 0° C).

(iii) Erythritol

The erythritol fraction (8.5 mg) was dissolved in dry pyridine (1.5 ml), and *p*-nitrobenzoyl chloride (50 mg) was added. The mixture was kept for 24 hours at room temperature, poured into cold water (15 ml) saturated with sodium bicarbonate and the product was extracted with chloroform. The chloroform extract was washed with water, dried, and evaporated, when the crystalline tetra-*p*-nitrobenzoate of erythritol was obtained, m.p. and mixed m.p. 258–260° C (after recrystallization from acetone–ethanol).

Quantitative Determination of Glucose, Glycerol, and Erythritol

After separation of the hydrolyzate of the polyalcohol by paper chromatography in the manner described above, each component was extracted from the appropriate area of the paper with water (10 ml) and an aliquot of the solution was used for colorimetric determination. D-Glucose was determined by the phenol – sulphuric acid method (18) at 490 mμ, while glycerol and erythritol were determined by the chromotropic acid method at 570 mμ (35). The results showed that the molar ratio of glucose:glycerol:erythritol was 1.1:2.2:1.0, a result in agreement with the methylation findings.

ACKNOWLEDGMENT

The authors thank the National Science Foundation for support.

REFERENCES

1. BERGEY'S manual of determinative bacteriology. 7th ed. Williams & Wilkins Co., Baltimore. 1957. p.175.
2. F. SMITH and A. M. STEPHEN. J. Chem. Soc. 4892 (1961).
3. J. D. GEERDES, B. A. LEWIS, R. MONTGOMERY, and F. SMITH. Anal. Chem. **26**, 264 (1954).
4. M. ABDEL-AKHER, J. K. HAMILTON, R. MONTGOMERY, and F. SMITH. J. Am. Chem. Soc. **74**, 4970 (1952).
5. S. M. LESLEY and R. H. HOCHSTER. Can. J. Biochem. Physiol. **37**, 513 (1959).
6. A. JEANES, J. E. PITTSLEY, J. H. SLONEKER, and F. R. SENTI. Abstract, 136th American Chemical Society Meeting, Atlantic City, New Jersey. Sept., 1959. p. 7D. J. H. SLONEKER, A. JEANES, and R. J. DIMLER. Abstract, 137th Meeting, Cleveland, Ohio. April, 1960. p. 7D. P. R. WATSON, A. JEANES, and C. E. RIST. 137th Meeting, April, 1960, p. 8D.
7. J. H. SLONEKER and D. G. ORENTUS. Nature, **194**, 478 (1962).
8. S. HIRASE. Bull. Chem. Soc. Japan, **30**, 70 (1957).
9. S. M. PARTRIDGE and R. G. WESTALL. Biochem. J. **42**, 238 (1948).

10. M. A. JERMYN and F. A. ISHERWOOD. Biochem. J. **44**, 402 (1949).
11. L. HOUGH, J. K. N. JONES, and W. H. WADMAN. J. Chem. Soc. 1702 (1950).
12. L. A. BOGGS, L. S. CUENDET, I. EHRENTHAL, R. KOCH, and F. SMITH. Nature, **166**, 520 (1950).
13. D. R. BRIGGS, E. F. GARNER, R. MONTGOMERY, and F. SMITH. Anal Chem. **28**, 1333 (1956).
14. B. A. LEWIS and F. SMITH. J. Am. Chem. Soc. **79**, 3929 (1957).
15. F. WEYGAND, W. PERKOW, and P. KUHNER. Ber. **84**, 594 (1951).
16. E. FISCHER and J. HIRSCHBERGER. Ber. **21**, 1805 (1888).
17. J. K. HAMILTON, D. R. SPRIESTERSBACH, and F. SMITH. J. Am. Chem. Soc. **79**, 443 (1957).
18. M. DUBOIS, K. A. GILLES, J. K. HAMILTON, P. A. REBERS, and F. SMITH. Anal. Chem. **28**, 350 (1956).
19. Z. DISCHE. J. Biol. Chem. **167**, 189 (1947).
20. A. MISAKI and F. SMITH. J. Agr. Food Chem. **10**, 104 (1962).
21. H. J. KOEPSELL and E. S. SHARPE. Arch. Biochem. Biophys. **38**, 443 (1952).
22. D. CAVALLINI, N. FRONTALI, and G. TOSCHI. Nature, **163**, 568 (1949).
23. V. C. DEWEY and G. W. KIDDER. Proc. Soc. Exptl. Biol. Med. **80**, 302 (1952). H. B. STEWART. Biochem. J. **55**, XXVI (1953).
24. J. C. IRVINE and D. MCNICOLL. J. Chem. Soc. **97**, 1449 (1910).
25. W. N. HAWORTH, R. L. HEATH, and S. PEAT. J. Chem. Soc. 833 (1941).
26. J. C. IRVINE and E. L. HIRST. J. Chem. Soc. **121**, 1213 (1922).
27. P. A. REBERS and F. SMITH. J. Am. Chem. Soc. **76**, 6097 (1954).
28. G. O. ASPINALL and G. ZWEIFEL. J. Chem. Soc. 2271 (1957).
29. K. FREUDENBERG and G. HULL. Ber. B, **74**, 237 (1941). J. D. GEERDES, B. A. LEWIS, and F. SMITH. J. Am. Chem. Soc. **79**, 4209 (1957).
30. F. SMITH. J. Chem. Soc. 1724 (1939).
31. F. SMITH. J. Chem. Soc. 1035 (1940).
32. P. FLEURY and J. LANGE. J. Pharm. Chim. **17**, 107, 196 (1933).
33. A. L. PORTER and W. Z. HASSID. J. Am. Chem. Soc. **70**, 3488 (1948).
34. J. K. HAMILTON and F. SMITH. J. Am. Chem. Soc. **78**, 5907 (1956).
35. M. LAMBERT and A. C. NEISH. Can. J. Res. B, **28**, 83 (1950).

SYNTHESIS OF DIPEPTIDES CONTAINING 1-AMINOCYCLOALKYLCARBOXYLIC ACIDS

PART II[1]

PATRICE TAILLEUR AND LOUIS BERLINGUET
Département de Biochimie, Faculté de Médecine, Université Laval, Québec, Qué.

Received June 25, 1962

ABSTRACT

Six new dipeptides containing either 1-aminocyclopentanecarboxylic acid or 1-aminocyclohexanecarboxylic acid placed at either the N- or the C-terminal of L-phenylalanine or L-leucine have been synthesized. Two molecules of 1-aminocyclopentanecarboxylic acid were also linked with a peptide bond. These seven dipeptides were cyclized into the corresponding substituted 2,5-piperazinediones.

INTRODUCTION

The synthetic amino acid 1-aminocyclopentanecarboxylic acid has been shown to be an interesting amino acid. It is active against certain types of tumors (1–3). The biochemical studies done so far have not yet elucidated its mechanism of action (4), nor explained its toxicity. It is known that the alkylation of the cyclopentane ring destroys the antitumor activity of the compound. However, the incorporation of this synthetic amino acid into a short peptide chain preserves the antitumor effect (2), while lowering the toxicity.

In order to enhance the antitumor index, Connors and Ross (5) and Tailleur and Berlinguet (6) have recently reported the synthesis of a few short-chain peptides having glycine and DL-phenylalanine attached to 1-aminocyclopentanecarboxylic acid or to 1-aminocyclohexanecarboxylic acid. Shankman *et al.* (7) have just reported the synthesis of other peptides containing 1-aminocyclopentanecarboxylic acid.

Since these peptides were intended for biological assays, it was important to incorporate the L-form of the natural amino acids. We have synthesized six new dipeptides containing either 1-aminocyclopentanecarboxylic acid or 1-aminocyclohexanecarboxylic acid attached to L-leucine or L-phenylalanine. We have also prepared the dipeptide containing two molecules of 1-aminocyclopentanecarboxylic acid. The list of these peptides is given in Table I. For these syntheses the classical method of Sheehan and Hess (8) was used in which the N-carbobenzoxy derivative of one amino acid was condensed with the benzyl ester of the other amino acid in the presence of N,N′-dicyclohexylcarbodiimide. The protected dipeptides were then hydrogenolized in the presence of 10% palladium on carbon, and the free dipeptides isolated by two different procedures according to their solubilities.

During these manipulations, the free peptides had a strong tendency to cyclize into the corresponding diketopiperazines, especially when heated in anhydrous conditions. Therefore, one has to be careful when purifying the free peptide because in some cases the solubilities of the peptide and of the cyclized diketopiperazine are quite similar, the analytical values being also very close. We found that the separation by chromatography and the analysis by titration are the most reliable methods to detect traces of contamination by diketopiperazines.

In order to prevent this cyclization three methods can be used: (1) water can be added

[1]*For part I, see reference 6.*

TABLE I

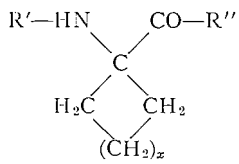

R′	R″	x	Name	
L-Leucyl-	-H	2	1-(L-Leucylamino)cyclopentanecarboxylic acid	(XI)
L-Leucyl-	-H	3	1-(L-Leucylamino)cyclohexanecarboxylic acid	(XII)
L-Phenylalanyl-	-H	2	1-(L-Phenylalanylamino)cyclopentanecarboxylic acid	(XIII)
L-Phenylalanyl-	-H	3	1-(L-Phenylalanylamino)cyclohexanecarboxylic acid	(XIV)
H-	-L-Phenylalanine	2	1-Aminocyclopentanecarbonyl-L-phenylalanine	(VIII)
H-	-L-Phenylalanine	3	1-Aminocyclohexanecarbonyl-L-phenylalanine	(IX)
H-	-1-Aminocyclopentane carboxylic acid	2	1-Aminocyclopentanecarbonyl-1-aminocyclopentanecarboxylic acid	(X)

to the ethanolic solution of the protected dipeptide before hydrogenolysis, (2) the hydrogenolysis can be done in acid medium where the liberated peptide would be ionized, thus preventing cyclization, and (3) if these conditions are not realized, care must be taken to avoid too much heating of the solutions especially if the content of water is low.

The spatial configuration of 1-aminocyclopentanecarboxylic acid and 1-aminocyclohexanecarboxylic acid seems to be responsible for the tendency to cyclize of the peptides containing these two amino acids attached to L-phenylalanine or L-leucine either by the C- or N-terminals. In fact, when those dipeptides are heated, they give a sublimate between 175° and 200° which melts between 175° and 195° depending on the peptide. The corresponding diketopiperazines obtained by different syntheses also give a sublimate between 175° and 200°. When these peptides are heated separately at 200° for a few minutes and then studied chromatographically they give two spots, one corresponding to the unchanged dipeptide and the other spot corresponding to the diketopiperazine. The dipeptide containing two molecules of 1-aminocyclopentanecarboxylic acid also cyclizes very easily by heating.

Preliminary testing of these peptides on tumors are now in progress and will be reported elsewhere.

EXPERIMENTAL

All melting points are uncorrected. The optical rotations were measured on a Rudolph polarimeter with a photoelectric cell alignment. The carbobenzoxy derivatives of L-leucine (9), L-phenylalanine (10), 1-aminocyclopentanecarboxylic acid (6), 1-aminocyclohexanecarboxylic acid (6), and the benzyl esters of L-phenylalanine (11), 1-aminocyclopentanecarboxylic acid (6), and 1-aminocyclohexanecarboxylic acid (6) were prepared according to published procedures.

N-Carbobenzoxydipeptide Benzyl Esters

The protected dipeptides were prepared as follows: to 0.01 mole of the N-carbobenzoxyamino acid dissolved in methylene chloride were added 0.011 mole of the appropriate amino acid benzyl ester and 0.011 mole of N,N′-dicyclohexylcarbodiimide. After 4 hours at room temperature, the N,N′-dicyclohexylurea formed was removed by filtration and the filtrate evaporated *in vacuo* on a water bath, after the addition of 2 ml of glacial acetic, which decomposes the excess of carbodiimide.

The oily residue was dissolved in 25 ml of ethyl acetate, and the solution filtered after 20 minutes to remove

the excess of N,N′-dicyclohexylurea formed after the addition of acetic acid. The filtrate was successively washed with 1 *N* hydrochloric acid, 1 *M* sodium carbonate, and water, and dried over anhydrous sodium sulphate. The solution was evaporated to dryness, and the N-carbobenzoxydipeptide benzyl ester was crystallized with the appropriate solvent system. The optical rotations were taken at 25° at a concentration of 2% in ethanol.

(I) Benzyl N-carbobenzoxy-1-(L-leucylamino)cyclopentanecarboxylate.—Yield: 3.7 g (78%), m.p. 116°, from ether–*n*-hexane, $[\alpha]_D$ −28°. Anal. Calc. for $C_{27}H_{34}N_2O_5$: N, 6.00%. Found: N, 6.08%.

(II) Benzyl N-carbobenzoxy-1-(L-leucylamino)cyclohexanecarboxylate.—Yield: 3.9 g (81%), m.p. 124–126°, from ether–*n*-hexane, $[\alpha]_D$ −31°. Anal. Calc. for $C_{28}H_{36}N_2O_5$: N, 5.85%. Found: 5.91%.

(III) Benzyl N-carbobenzoxy-1-(L-phenylalanylamino)cyclopentanecarboxylate.—Crude yield of the product which was isolated as an oil: 4.1 g (82%).

(IV) Benzyl N-carbobenzoxy-1-(L-phenylalanylamino)cyclohexanecarboxylate.—Crude yield of the product which was isolated as an oil: 4.0 g (78%).

(V) N-Carbobenzoxy-1-aminocyclopentanecarbonyl-L-phenylalanine benzyl ester.—Yield: 4.0 g (80%), m.p. 117°, from ethanol – petroleum ether, $[\alpha]_D$ −13°. Anal. Calc. for $C_{30}H_{32}N_2O_5$: N, 5.59%. Found: N, 5.58%.

(VI) N-Carbobenzoxy-1-aminocyclohexanecarbonyl-L-phenylalanine benzyl ester.—Yield: 4.2 g (82%), m.p. 98°, from ethanol – petroleum ether, $[\alpha]_D$ −9°. Anal. Calc. for $C_{31}H_{34}N_2O_5$: N, 5.44%. Found: 5.56%.

(VII) Benzyl N-carbobenzoxy-1-aminocyclopentanecarbonyl-1-aminocyclopentanecarboxylate.—Yield: 3.7 g (80%), m.p. 138°, from ethanol – petroleum ether. Anal. Calc. for $C_{27}H_{32}N_2O_5$: N, 6.03%. Found: N, 5.92%.

Free Dipeptides

The neutral equivalent values of the peptides were determined by titration with perchloric acid in glacial acetic acid, using crystal violet as indicator, according to Toennies and Callan (12). It was assumed that the molecular weight and the neutral equivalent are identical. The R_f values are for ascending chromatography in collidine–lutidine–water (1:1:2), the dipeptides and substituted diketopiperazines being detected by the Cl_2–KI–starch method of Rydon and Smith (13). The optical rotations were taken at 25° at a concentration of 1% in the given solvent.

(a) Peptides Soluble in Water

The appropriate N-carbobenzoxydipeptide benzyl ester (0.01 mole) was dissolved in 30 ml of hot ethanol containing 1 ml of glacial acetic acid. Then a suspension of 0.3 g of palladium (10%) on carbon in 6 ml of water was added. This hot solution was hydrogenolized at low pressure during 6 hours in a Parr apparatus, after which time the solution was heated if necessary to entirely dissolve the peptide, and the catalyst was removed by filtration. The clear filtrate was evaporated to a few milliliters, and then was added a mixture of water and ether to dissolve respectively the free dipeptide and the unreacted protected dipeptide. If at this stage there remains an insoluble product it is the substituted diketopiperazine. Being insoluble in both these solvents it is easily removed by filtration and can be identified by melting point and chromatography. The ethereal extract was decanted and discarded, and the aqueous fraction concentrated to allow the peptide to crystallize in the cold after the addition of acetone.

(VIII) 1-Aminocyclopentanecarbonyl-L-phenylalalanine.—Yield: 2.0 g (72%), m.p. 278–280° (subl. 180°), from water–acetone, $[\alpha]_D$ −2.0° (in water), R_f 0.64. Anal. Calc. for $C_{15}H_{20}N_2O_3$: N, 10.13%; mol. wt., 276. Found: N, 10.20%; mol. wt., 277.

(XIX) 1-Aminocyclohexanecarbonyl-L-phenylalanine.—Yield: 2.0 g (69%), m.p. 278–280° (subl. 180°), from water–acetone, $[\alpha]_D$ −1.3° (in water), R_f 0.67. Anal. Calc. for $C_{16}H_{22}N_2O_3$; N, 9.63%; mol. wt., 290. Found: N, 9.60%; mol. wt., 296.

(X) 1-Aminocyclopentanecarbonyl-1-aminocyclopentanecarboxylic acid.—Yield: 1.6 g (66%). The compound sublimates at 185° and does not decompose below 300°. It was recrystallized from water–acetone and had a R_f value of 0.54. Anal. Calc. for $C_{12}H_{20}N_2O_3$: N, 11.65%; mol. wt., 240. Found: N, 11.60%; mol. wt., 243.

(b) Peptides Insoluble in Water

The N-carbobenzoxydipeptide benzyl ester (0.01 mole) was dissolved in 20 ml of hot ethanol, and then 3.0 ml of 3.5 *N* hydrochloric acid and 0.3 g of palladium (10%) on carbon were added. This solution was hydrogenolized as described in the preceding part. After the water–ether treatment, there was no insoluble compound. The ethereal fraction was discarded and the water fraction neutralized with 3.5 *N* sodium hydroxide. The precipitated peptide was then filtered and washed with a little cold water, and recrystallized with the appropriate solvent system.

(XI) 1-(L-Leucylamino)cyclopentanecarboxylic acid.—Yield: 1.9 g (78%), m.p. 291–292° (subl.), from methanol–water, $[\alpha]_D$ +10.0° (in methanol), R_f 0.50. Anal. Calc. for $C_{12}H_{22}N_2O_3$: N, 11.54%; mol. wt., 242. Found: N, 11.45%; mol. wt., 241.

(XII) 1-(L-Leucylamino)cyclohexanecarboxylic acid.—Yield: 2.1 g (82%), m.p. 295–297° (subl.), from methanol–water, $[\alpha]_D$ +22.5° (in methanol), R_f 0.60. Anal. Calc. for $C_{13}H_{24}N_2O_3$: N, 10.92%; mol. wt., 256. Found: N, 10.87%; mol. wt., 260.

(XIII) 1-(L-Phenylalanylamino)cyclopentanecarboxylic acid.—Yield: 2.0 g (72%), m.p. 284–285° (subl. 180°), from aqueous ethanol 60%, $[\alpha]_D$ +57° (in glacial acetic acid), R_f 0.61. Anal. Calc. for $C_{15}H_{20}N_2O_3$: N, 10.13%; mol. wt., 276. Found: N, 9.98%; mol. wt., 279.

(XIV) 1-(L-Phenylalanylamino)cyclohexanecarboxylic acid.—Yield: 2.2 g (75%), m.p. 278° (subl. 180°),

from aqueous ethanol 60%, $[\alpha]_D$ +46° (in glacial acetic acid), R_f 0.63. Anal. Calc. for $C_{16}H_{22}N_2O_3$: N, 9.63%; mol. wt., 290. Found: N, 9.59%; mol. wt., 294.

Cyclization of Dipeptides into Substituted Diketopiperazines

The dipeptides (0.002 mole) were heated during 3 hours at 145° in 4 g of β-naphthol according to Lichtenstein (14).

The yellowish solutions so obtained were cooled and then thoroughly washed with four portions of 15 ml of ether to remove the β-naphthol. The insoluble 2,5-piperazinediones were crystallized with the appropriate solvent. The optical rotations were taken at 25° at a concentration of 0.2% in glacial acetic acid.

(XV) 1,4-Diazaspiro[4.5]decane-2,5-dione-3-benzyl.—(*a*) From 1-aminocyclopentanecarbonyl-L-phenylalanine: Yield: 0.41 g (79%), m.p. 287–289° (subl. 180°), from *n*-butanol, $[\alpha]_D$ +58°, R_f 0.90. Anal. Calc. for $C_{15}H_{18}N_2O_2$: N, 10.83%. Found: N, 10.78%. (*b*) From 1-(L-phenylalanylamino)cyclopentanecarboxylic acid: Yield: 0.42 g (80%), m.p. 289° (subl. 180°), from *n*-butanol, $[\alpha]_D$ +60°, R_f 0.91. Anal. Calc. for $C_{15}H_{18}N_2O_2$: N, 10.83%. Found: N, 10.87%.

(XVI) 1,4-Diazaspiro[5.5]undecane-2,5-dione-3-benzyl.—(*a*) From 1-aminocyclohexanecarbonyl-L-phenylalanine: Yield: 0.43 g (80%), m.p. 289–291° (subl. 180°), from *n*-butanol, $[\alpha]_D$ +59°, R_f 0.91. Anal. Calc. for $C_{16}H_{20}N_2O_2$: N, 10.28%. Found: N, 10.40%. (*b*) From 1-(L-phenylalanylamino)cyclohexanecarboxylic acid: Yield: 0.43 g (80%), m.p. 290–291° (subl. 180°), from *n*-butanol, $[\alpha]_D$ +56°, R_f 0.92. Anal. Calc. for $C_{16}H_{20}N_2O_2$: N, 10.28%. Found: N, 10.38%.

(XVII) 6,13-Diazaspiro[4.2.4.2]tetradecane-7,14-dione.—Yield: 0.36 g (82%), from 1-aminocyclopentanecarbonyl-1-aminocyclopentanecarboxylic acid. The compound, recrystallized from 75% acetic acid, began to sublime at 185°, and decomposed above 300°, R_f 0.92. Anal. Calc. for $C_{12}H_{18}N_2O_2$: N, 12.62%. Found: N, 12.70%.

(XVIII) 1,4-Diazaspiro[4.5]decane-2,5-dione-3-isobutyl.—Yield: 0.35 g (77%), from 1-(L-leucylamino)-cyclopentanecarboxylic acid, m.p. 289–293° (subl.), from *n*-butanol, $[\alpha]_D$ −10°, R_f 0.92. Anal. Calc. for $C_{12}H_{20}N_2O_2$: N, 12.51%. Found: N, 12.56%.

(XIX) 1,4-Diazaspiro[5.5]undecane-2,5-dione-3-isobutyl.—Yield: 0.38 g (80%), from 1-(L-leucylamino)-cyclohexanecarboxylic acid, $[\alpha]_D$ −20°, R_f 0.92. Anal. Calc. for $C_{13}H_{22}N_2O_2$: N, 11.76%. Found: N, 11.85%.

ACKNOWLEDGMENTS

The authors wish to thank the National Research Council for a studentship to one of them (P. T.) and the National Cancer Institute and the Medical Research Council for generous financial support.

RÉSUMÉ

On décrit la synthèse de six nouveaux dipeptides non-naturels. Ils contiennent d'une part un acide aminé de synthèse, soit l'acide amino-1 cyclopentane carboxylique, soit l'acide amino-1 cyclohexane carboxylique et, d'autre part, un acide aminé naturel, soit la L-phénylalanine, soit la L-leucine. On rapporte aussi la synthèse d'un dipeptide contenant deux molécules d'acide amino-1 cyclopentane carboxylique. Ces sept peptides furent cyclisés en pipérazinedione-2,5 substituées.

REFERENCES

1. F. MARTEL and L. BERLINGUET. Can. J. Biochem. Physiol. **37**, 433 (1959).
2. T. A. CONNORS, L. A. ELSON, and W. C. J. ROSS. Biochem. Pharmacol. **1**, 239 (1958).
3. R. B. ROSS, C. I. NOLL, W. C. J. ROSS, M. V. NADKARNI, B. H. MORRISON, JR., and H. W. BOND. J. Med. Pharm. Chem. **3**, 1 (1961).
4. L. BERLINGUET, N. BEGIN, L. M. BABINEAU, F. MARTEL, R. VALLEE, and R. O. LAFERTE. Can. J. Biochem. Physiol. **40**, 425 (1962). L. BERLINGUET, N. BEGIN, L. M. BABINEAU, and R. O. LAFERTE. Can. J. Biochem. Physiol. **40**, 433 (1962).
5. T. A. CONNORS and W. C. J. ROSS. J. Chem. Soc. 2119 (1960).
6. P. TAILLEUR and L. BERLINGUET. Can. J. Chem. **39**, 1309 (1961).
7. S. SHANKMAN, S. HIGA, F. LEW, and M. E. ROBERTS. J. Med. Pharm. Chem. **5**, 42 (1962).
8. J. C. SHEEHAN and G. P. HESS. J. Am. Chem. Soc. **77**, 1067 (1955).
9. M. BERGMANN, L. ZERVAS, and J. S. FRUTON. J. Biol. Chem. **115**, 589 (1936).
10. W. GRASSMAN and E. WUNSCH. Chem. Ber. **91**, 449, 462 (1958). W. GRASSMANN, E. WUNSCH, and A. RIEDEL. Chem. Ber. **91**, 455 (1958).
11. L. ZERVAS, M. WINITZ, and J. P. GREENSTEIN. J. Org. Chem. **22**, 1515 (1957).
12. G. TOENNIES and T. P. CALLAN. J. Biol. Chem. **125**, 259 (1938).
13. H. N. RYDON and P. W. G. SMITH. Nature, **169**, 922 (1952).
14. N. LICHTENSTEIN. J. Am. Chem. Soc. **60**, 560 (1938).

COORDINATION COMPLEXES OF METAL ALKOXIDES

PART II. METAL ALKOXIDE – ETHYLENEDIAMINE COMPLEXES[1]

M. S. BAINS[2] AND D. C. BRADLEY

Department of Chemistry, The University of Western Ontario, London, Ontario

Received July 26, 1962

ABSTRACT

Some complexes of titanium isopropoxide, titanium ethoxide, aluminum isopropoxide, tantalum isopropoxide, and zirconium isopropoxide with ethylenediamine (en) are described. Two complexes of titanium isopropoxide with ethylenediamine, i.e. $Ti(OPr^i)_4$,en and $Ti_2(OPr^i)_8$,en, were established by cryoscopic, X-ray powder photograph, and phase rule studies. The structure and stability of these complexes is discussed. Also isolated were $Ti_2(OEt)_8$,en; $Zr_2(OPr^i)_8$,en; $Ta_2(OPr^i)_{10}$,en, and $Al_2(OPr^i)_6$,en. Cryoscopic studies on the aluminum complex suggested that an octameric complex, $Al_8(OPr^i)_{24}$,$(en)_4$, is present in equilibrium with the dimer. The structural implications of the existence of these complexes are discussed.

Phase studies on the binary systems containing titanium tetraisopropoxide and pyridine, diethylamine, or *tert*-butyl acetate gave no clear indication of complex formation.

INTRODUCTION

In the previous publication in this series (1) it was mentioned that metal alkoxides form polymers or alkoxide salts in preference to addition compounds. Nevertheless, it is believed that the catalytic activity of metal alkoxides in numerous organic reactions (2) involves the ready formation of weak complexes between metal alkoxides and organic ligands. Our work with hydrazine (1) revealed that moderately stable complexes were formed by this ligand with metal alkoxides. Recently Cook (3) demonstrated by means of a tensiometric technique that two weak complexes, $Ti(OPr^i)_4$,$EtNH_2$ and $Ti(OPr^i)_4$, $2EtNH_2$, were formed in *n*-decane. The same author disclosed (3) that Gulledge had obtained crystalline $Ti(OPr^i)_4$,$EtNH_2$ from concentrated solution in cyclohexane. It thus seemed reasonable to suppose that ethylenediamine with its facility for chelation might form more stable complexes with metal alkoxides. In this paper we report the formation of several complexes involving ethylenediamine and metal alkoxides with particular reference to complexes involving titanium isopropoxide. The latter were studied using a variety of techniques. Phase studies on the systems involving $Ti(OPr^i)_4$ and pyridine, diethylamine, or isobutyl acetate are also described.

EXPERIMENTAL

Materials

Alkoxides

The metal alkoxides were prepared by the methods already described in the literature, i.e., aluminum isopropoxide (4, 5), titanium isopropoxide (6), titanium ethoxide (7), zirconium isopropoxide isopropylate (8), and tantalum isopropoxide (9) were purified by distillation under reduced pressure.

The purity of the above compounds was checked by the analytical methods given in the cited literature.

Solvents

Benzene and cyclohexane were of "Analytical Reagent" grade. These were dried azeotropically and stored over molecular sieve drying agent. Anhydrous diethyl ether, "Analytical Grade", was used directly from the cans in which it was supplied.

[1]*For Part I, see ref. 1.*

[2]*National Research Council Postdoctorate Fellow, 1959–1961. Present address: Department of Chemistry, The Panjab University, Chandigarh 3, India.*

Bases and Other Reagents

Pyridine was kept over potassium hydroxide pellets overnight and then distilled over fresh potassium hydroxide twice and collected at a constant temperature. Anhydrous diethylamine from an ampoule was kept over sodium metal and then distilled. *tert*-Butyl acetate was fractionally distilled three times. Ethylenediamine was purified from a 98% sample. It was kept over sodium hydroxide overnight and then the upper layer (base) was separated and distilled over sodium metal. The pure sample was analyzed by titration (found: 99.6, 99.8% purity).

Analytical Methods

Zirconium, titanium, tantalum, and aluminum were determined by the methods used in the references describing the preparation of the alkoxides. The alkoxide content was determined by the method developed by Bradley *et al.* (10) in the case of pure alkoxides.

Ethylenediamine was determined by acid titration in the case of titanium and tantalum alkoxide complexes. A weighed sample of the complex was dissolved in benzene (25 ml), and water was added to make the volume up to 200 ml. The titration was then performed using modified methyl orange as indicator. In the case of zirconium and aluminum alkoxide complexes, the sample was dissolved in the minimum amount of benzene, then a few milliliters of water was added, followed by 50 ml of cold, concentrated sodium hydroxide solution. This solution was then evaporated under reduced pressure and the volatile contents including water were collected in a clean cold-trap. The contents of the cold-trap were allowed to warm and then were titrated for the estimation of the ethylenediamine. To be sure of the reliability of this method blank experiments were performed using pure ethylenediamine (found: 99.8, 100.1% recovery).

Phase Studies

The liquidus for mixtures of $Ti(OPr^i)_4$ and ligand was obtained by determining melt points of a series of mixtures over the entire range of mole fractions. A slow rate of heating was ensured by surrounding the inner vessel by an air jacket. The temperature at which liquefaction appeared complete was measured to $\pm 0.1°$ C.

The results are shown graphically in Figs. 1 and 2.

X-Ray Powder Photographs

The compounds $Ti_2(OPr^i)_8$,en and $Ti(OPr^i)_4$,en were sealed into lithium glass capillaries of 0.5-mm diameter in the dry box. In the case of the latter compound great care was taken to avoid warming it during handling. The material was chilled before being filled into the capillary and was kept cool during the filling process; the powder photographs were taken immediately. The former compound was quite stable and could be handled easily under anhydrous conditions. A half-radian camera was used with Cu K_α radiation and a nickel filter. The calculated spacings for the more intense lines are given in Tables I and II.

Cryoscopy

A Beckmann apparatus was modified for use with compounds requiring rigorously anhydrous conditions and magnetic stirring was employed. The apparatus was cleaned and then dried in an oven at 150° C. Dry nitrogen was passed through the apparatus as it cooled. About 50 ml of solvent was weighed into the apparatus and the freezing point was determined in the usual manner. Weighed quantities of solute were introduced through a side arm whilst a countercurrent of nitrogen was maintained to exclude air. The following cryoscopic constants were used: benzene, 5.2; cyclohexane, 20.2.

The results are shown graphically in Fig. 3, where the number-average molecular weight of $Ti_2(OPr^i)_8$,en is plotted against molarity. The calculated data are given in Tables III and IV. The molecular weight of $Ti(OPr^i)_4$ was also determined over a range of concentrations and the results are given in Table V.

Preparation of Ethylenediamine Complexes with Metal Alkoxides

1. Aluminum Isopropoxide – Ethylenediamine Complex

To a solution of aluminum isopropoxide (10.0 g) in benzene, ethylenediamine (3.5 g) was added, but no precipitate appeared. The solution was evaporated at 0.1 mm pressure (10–11 hours at 30–35° C) and gave a fine powdery product whose analysis corresponded with the composition $Al_2(OPr^i)_6$,en (where en = ethylenediamine). Found: Al, 11.80, 11.85; en, 12.95, 12.90. $Al_2(OPr^i)_6$,en requires: Al, 11.55; en, 12.80%.

2. Tantalum Isopropoxide – Ethylenediamine Complex

To a freshly sublimed sample of tantalum isopropoxide (2 g) in benzene, an excess of ethylenediamine was added. After the mixture was allowed to stand for some time, benzene and volatile materials were removed under vacuum (0.1 mm). The residue was a sticky fluid mass which on warming melted to a clear liquid. When heated under reduced pressure the liquid gave a solid condensate which had an analysis corresponding to $Ta_2(OPr^i)_{10}$,en. Found: Ta, 35.67, 35.83; en, 5.93, 6.02. $Ta_2(OPr^i)_{10}$,en requires: Ta, 35.75; en, 5.93%.

The non-volatile residue was brown. Found: Ta, 38.86, 38.95; en, 6.18. [$Ta(OPr^i)_4$,$Ta(OPr^i)_5$,en] requires: Ta, 38.0; en, 6.29%.

3. Titanium Isopropoxide – Ethylenediamine Complex (2:1 Compound)

Titanium isopropoxide and ethylenediamine were mixed in equimolecular proportions and an exothermic reaction occurred. After drying *in vacuo* (0.1 mm) a white crystalline powder remained and its analysis

corresponded to $Ti_2(OPr^i)_8$,en. Found: Ti, 15.10, 15.32; en, 9.85, 9.80. $Ti_2(OPr^i)_8$,en requires: Ti, 15.29; en, 9.6%.

Other experiments were performed using an excess of ethylenediamine but the final solid product after drying *in vacuo* was always the complex $Ti_2(OPr^i)_8$,en. This compound sublimed at 60–64° C at 0.05 mm pressure. At temperatures above about 70° C the complex appeared to dissociate.

At a lower pressure (10^{-3} mm) the complex may readily be sublimed at around 40° C provided that the sublimate is cooled to about 12° C. The analysis of the sublimate agreed with the formula $Ti_2(OPr^i)_8$,en. Under normal pressure the complex melts at 75–76° C.

4. Titanium Isopropoxide – Ethylenediamine Complex (1:1 Compound)

Ethylenediamine (1.3 g) was added to a solution of titanium isopropoxide (2.83 g) in diethyl ether (50 ml) and after about 5 minutes the solution was cooled to induce crystallization. After the ethereal mother liquor was decanted off the white crystals were washed four times by decantation with ether (10 ml). The solvent was then removed under 40 mm pressure and the product thus obtained was the 1:1 complex $Ti(OPr^i)_4$,en. Found: Ti, 13.82, 13.83; en, 17.65, 17.80. $Ti(OPr^i)_4$,en requires: Ti, 13.95; en, 17.50%.

In another similar experiment the product had the following analysis: Found: Ti, 13.76, 14.09; en, 17.53, 17.70%.

5. Titanium Ethoxide – Ethylenediamine Complex

The addition of an excess of ethylenediamine (1 g) to a solution of redistilled titanium ethoxide (4 g) in benzene (25 ml) caused an exothermic reaction. The solution was allowed to stand for ½ hour and then the solvent was evaporated off *in vacuo* (0.1 mm). After drying *in vacuo* at room temperature a white crystalline solid remained which was shown by analysis to be $Ti_2(OEt)_8$,en. Found: Ti, 18.86, 18.85; en, 11.45, 11.50. $Ti_2(OEt)_8$,en requires: Ti, 18.60; en, 11.63%.

In a separate experiment where titanium ethoxide (10 g) was again treated with an excess of ethylenediamine (2 g) in ether a precipitate appeared. After about 10 minutes the solid product was filtered using a sintered-glass apparatus and washed three times with ether (20 ml). The ether was then removed by aspirating dry nitrogen through the product for 20 minutes. Found: Ti, 18.50, 18.40; en, 11.45%.

The product was then maintained at 0.1 mm pressure but no change in composition occurred. Found: Ti, 18.40, 18.45; en, 11.55, 11.40%.

6. Zirconium Isopropoxide – Ethylenediamine Complex

To a clear solution of zirconium isopropoxide (15 g) in ether (60 ml), ethylenediamine (2 g) was added, and a mild exothermic reaction occurred. After the system was warmed to 30–33° C for ½ hour, it was allowed to cool, when a large bulky precipitate appeared. When the system was cooled to 0° C it was filtered through an apparatus specially designed to exclude moisture. The solid product was washed with ether (15 ml, each) three times and then dried by aspirating with nitrogen. The white crystalline material amounted to about 75% yield and its analysis corresponded to the formula $Zr_2(OPr^i)_8$,en. Found: Zr, 25.75, 25.60; en, 8.35, 8.54. $Zr_2(OPr^i)_8$,en requires: Zr, 25.6; en, 8.41%.

DISCUSSION

Phase Studies

Among all the ligands used as the second component in the binary systems with titanium isopropoxide, only ethylenediamine clearly formed addition compounds. They are moderately stable compounds, which have been isolated by independent methods. The shape of the liquidus in this case is very interesting (Fig. 1) for the following reasons: (i) There is a sudden rise in the liquidus on both sides of the temperature–composition curve. The system has the melt point above or around 60° C when composition reaches 5–8 mole% of either component. (ii) Between these compositions the curve flattens out. (iii) The maximum temperature is just discernible at 33–34 mole% of ethylenediamine, corresponding to the composition $Ti_2(OPr^i)_8$,en. There are indications of a break at approximately 45 mole% ethylenediamine, corresponding with the formation of the 1:1 complex $Ti(OPr^i)_4$,en.

The flattening of the curve is presumably due to considerable dissociation of the respective complexes at these temperatures. The following type of general equilibria may be visualized:

$$Ti_2(OPr^i)_8,en \rightleftharpoons Ti(OPr^i)_4,en + Ti(OPr^i)_4 \quad [1]$$

$$3Ti(OPr^i)_4,en \rightleftharpoons Ti(OPr^i)_4,(en)_2 + Ti_2(OPr^i)_8,en. \quad [2]$$

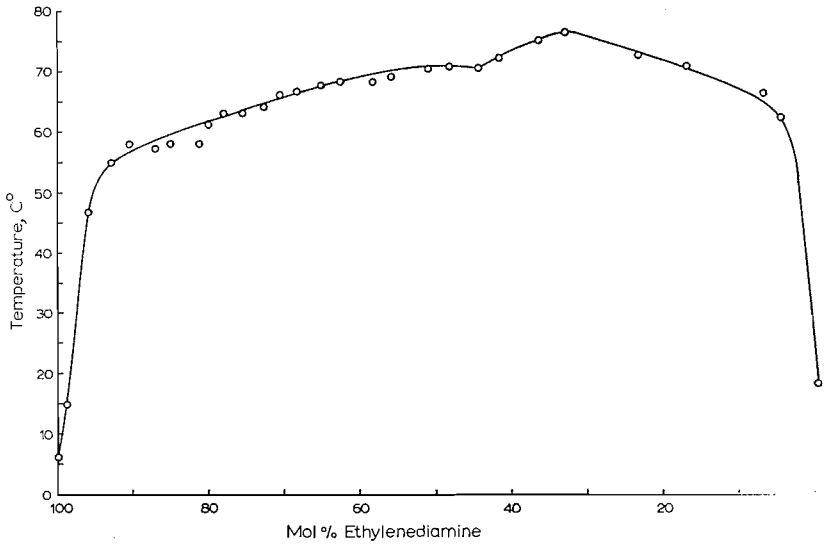

FIG. 1. Liquidus for the $Ti(OPr^i)_4$–$C_2H_4(NH_2)_2$ system.

In the case of the pyridine – titanium isopropoxide binary system (Fig. 2) there are indications of a break at approximately 50 mole% of pyridine, and the existence of a weak 1:1 complex could be inferred. The curves (Fig. 2) for the diethylamine – titanium isopropoxide and *tert*-butyl acetate – titanium isopropoxide systems do not give any clear indications of the formation of complexes, although there is a suspicion of a break corresponding to $Ti(OPr^i)_4,2Et_2NH$.

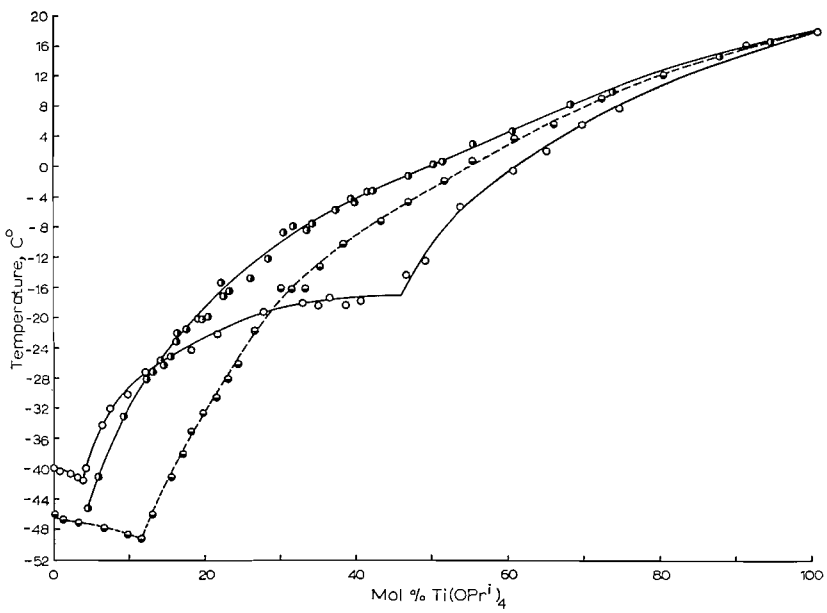

FIG. 2. $Ti(OPr^i)_4$ – *tert*-butyl acetate system, ◑–◑; $Ti(OPr^i)_4$–diethylamine system, ◒ - - ◒; $Ti(OPr^i)_4$–pyridine system, O–O.

X-Ray Studies

The X-ray powder diffraction patterns of $Ti_2(OPr^i)_8$,en (Table I) and $Ti(OPr^i)_4$,en (Table II) showed only two spacings in common (8.66 and 7.09 Å). The pattern was clearer and the lines in the pattern were generally more intense for $Ti_2(OPr^i)_8$,en than for $Ti(OPr^i)_4$,en. Comparison of the data in Tables I and II leaves no doubt that the two compounds are structurally distinct in the solid state.

TABLE I

X-Ray powder diffraction pattern spacings for $Ti_2(OPr^i)_8$,en

Intensity	V.I.	V.I.	V.I.	V.I.	V.I.	V.I.	W.	W.
Spacing *d* (Å)	8.66	7.20	7.09	5.64	4.34	3.90	3.89	3.54
Intensity	W.	W.	W.	V.I.	V.I.	V.I.	V.I.	W.
Spacing *d* (Å)	3.50	3.18	3.04	3.01	2.80	2.69	2.54	2.50
Intensity	W.	W.	W.	I.	I.	V.W.	V.W.	V.W.
Spacing *d* (Å)	2.34	2.28	2.08	1.900	1.852	1.594	1.506	1.442

NOTE: V.I., very intense; I., intense; W., weak; V.W., very weak.

TABLE II

X-Ray powder diffraction pattern spacings for $Ti(OPr^i)_4$,en

Intensity	V.I.	V.I.	W.	W.	I.	I.	I.	W.
Spacing *d* (Å)	8.66	7.09	5.44	4.43	3.88	3.49	3.16	2.99
Intensity	W.	W.	W.	V.W.	V.W.			
Spacing *d* (Å)	2.81	2.68	2.53	2.046	1.940			

Cryoscopic Results

Cryoscopic measurements were made on solutions of $Ti_2(OPr^i)_8$,en (A) in benzene and in cyclohexane and the results are illustrated in Fig. 3, in which molecular weight is

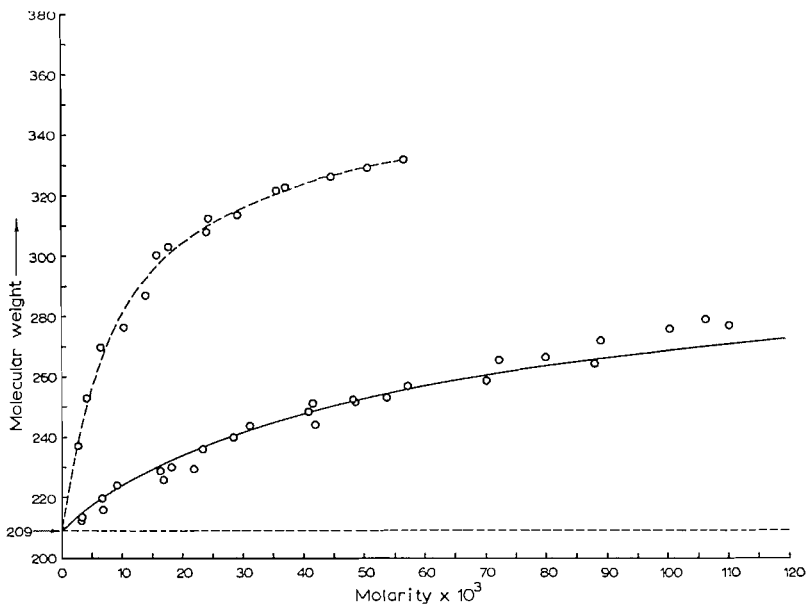

FIG. 3. Cryoscopic measurements on $Ti_2(OPr^i)_8$,en: in benzene, O—O; in cyclohexane, O - - O.

plotted as a function of molarity. In the case of cyclohexane solutions A began precipitating at about 66 mmoles/liter and the corresponding molecular weight was 340. But in contrast to this, at a concentration of 110 mmoles/liter of A in benzene the molecular weight is only 276. From the figure it is also clear that as the concentration approaches zero the molecular weight tends to the same value in both solutions.

The undissociated complex A should have a molecular weight of 628 whilst complete dissociation into three particles as shown in equation [3] requires an average molecular weight of 209.3 (horizontal dotted line in Fig. 3). Over the entire concentration range

$$Ti_2(OPr^i)_8,en \rightarrow 2Ti(OPr^i)_4 + en \qquad [3]$$

studied in benzene the molecular weight is lower than the 314 required for dissociation into the two molecular species indicated in equation [1]. However, in cyclohexane solution the molecular weight exceeds 314 at the higher concentrations.

The cryoscopic data are given in Tables III and IV for benzene and cyclohexane solutions respectively. To rationalize this data three equilibrium schemes were considered.

TABLE III

Cryoscopic measurements on $Ti_2(OPr^i)_8,en$ in benzene

$10^3 \times$molarity of $Ti_2(OPr^i)_8,en$	Mol. wt.	Average no. of particles/mole of $Ti_2(OPr^i)_8,en$	$10^2 \times K_B$ (moles/liter)
2.870	213.0	2.95	10.6
3.150	214.3	2.93	8.1
6.636	216.7	2.90	11.1
8.936	224.5	2.80	6.3
16.17	229.5	2.74	7.8
16.63	226.3	2.77	10.2
18.03	230.8	2.72	8.0
21.70	230.0	2.73	10.1
23.24	236.4	2.66	7.4
28.12	240.4	2.61	7.1
29.92	241.3	2.60	7.3
31.01	244.0	2.57	6.6
40.47	248.4	2.53	6.9
40.83	244.5	2.57	8.5
41.39	251.2	2.50	6.2
47.98	252.7	2.48	6.7
48.41	251.8	2.49	7.1
53.50	253.2	2.48	7.3
57.00	256.7	2.45	6.6
64.97	258.4	2.43	7.0
70.12	258.8	2.43	7.4
72.32	263.3	2.37	5.7
79.80	266.4	2.36	6.0
87.96	264.0	2.38	7.4
88.94	271.7	2.31	5.3
100.77	275.3	2.28	5.0
106.29	279.0	2.25	4.5
110.00	276.3	2.27	5.3

In the first case it is assumed that the complex A dissociates completely into $Ti(OPr^i)_4,en$ (B) and $Ti(OPr^i)_4$ (C). An equilibrium is then established between complex B and its components C and ethylenediamine (D) (equation [4]) with $K_B = [C][D]/[B]$. This

$$Ti_2(OPr^i)_8,en \xrightarrow[\text{dissociation}]{\text{complete}} Ti(OPr^i)_4,en + Ti(OPr^i)_4$$
$$\Big\Downarrow K_B$$
$$Ti(OPr^i)_4 + en \qquad [4]$$

TABLE IV

Cryoscopic measurements on $Ti_2(OPr^i)_8$,en in cyclohexane

$10^3\times$molarity of $Ti_2(OPr^i)_8$,en	Mol. wt.	Average no. of particles/mole of $Ti_2(OPr^i)_8$,en	$10^3\times K_A$ (moles/liter)	$10^3\times K_B$ (moles/liter)	$10^3\times K$ (moles^2/liter^2)
2.530	239.5	2.62	186	7.1	1.3
4.393	253.5	2.48	186	6.6	1.2
6.610	270.3	2.32	180	4.9	0.9
10.25	276.8	2.26	187	6.1	1.1
14.04	287.2	2.19	185	6.0	1.1
15.85	300.6	2.09	127	4.6	0.6
17.81	303.2	2.07	131	4.7	0.6
24.16	308.1	2.04	186	4.6	0.9
24.50	312.5	2.01	139	4.7	0.7
29.29	313.6	2.00	179	4.9	0.9
35.77	321.8	1.94	162	4.5	0.7
37.12	322.5	1.95	176	4.5	0.8
44.67	325.7	1.93	186	5.2	1.0
45.97	328.5	1.91	183	4.6	0.8
50.82	328.9	1.91	201	5.0	1.0
56.88	331.8	1.89	199	5.5	1.1

assumption leads to the conclusion that in benzene the molecular weight will always be less than 314. The data for benzene solution gave reasonable agreement for an equilibrium constant $K_B = 7\times10^{-2}$ mole/liter over the 40-fold range in concentration. Individual values of K_B calculated for each concentration are given in Table III. The solid line passing through the data for benzene solution in Fig. 3 is one calculated for $K_B = 7\times10^{-2}$ mole/liter. In view of the experimental difficulties involved the agreement seems to establish the equilibrium of equation [4].

A second scheme involving the equilibria shown in equation [5] applies to the solution of complex A in cyclohexane. By a trial and error technique the data in Table IV were

$$\begin{array}{ccc} Ti_2(OPr^i)_8,en & \overset{K_A}{\rightleftharpoons} & Ti(OPr^i)_4,en + Ti(OPr^i)_4 \\ & & \Big\uparrow\Big\downarrow K_B \\ & & Ti(OPr^i)_4 + en \end{array} \qquad [5]$$

fitted to values for the constants $K_A = [C][B]/[A]$ and K_B shown in the table. The overall constant $K = K_A \cdot K_B$ presented in the last column was calculated from the individual constants. Bearing in mind the experimental difficulties the agreement is satisfactory and there are no significant trends in the values of the equilibrium constants.

It is clear that whereas in benzene the complex B is the stable species and dissociation of complex A into complex B and alkoxide is complete, in cyclohexane both the species A and B are present in comparable concentrations. The slightly higher dielectric constant of benzene compared with cyclohexane should not contribute significantly as far as the dielectric nature of the solvent is concerned. However, it is possible that benzene by virtue of its π-electrons may act as a weak donor solvent towards titanium isopropoxide and thus tend to dissociate the complexes. In cyclohexane there are no π-electrons and hence less tendency to solvate the components of the complexes. Molecular weights were also determined on titanium isopropoxide in benzene and in cyclohexane (Table V). In benzene the alkoxide was monomeric over a threefold change in concentration. In cyclohexane the molecular weight increased slightly over a 10-fold increase in concentration but the data did not meet the requirements of any simple monomer–polymer equilibrium.

TABLE V

Molecular weights of $Ti(OPr^i)_4$ in benzene and in cyclohexane

Molarity in benzene	Mol. wt.	Number-average degree of polymerization	Molarity in cyclohexane	Mol. wt.	Number-average degree of polymerization
0.1086	281.0	0.988	0.0199_5	288.0	1.013
0.2759	285.5	1.004	0.0434_3	292.0	1.021
0.3305	286.0	1.006	0.0861_5	300.0	1.039
0.3453	286.3	1.007	0.1272	303.4	1.047
			0.1780	309.4	1.058

The tetrameric nature of aluminum isopropoxide was confirmed by molecular weight determinations in benzene (found: M.W., 810). Molecular weight determinations on $Al_2(OPr^i)_6$,en in benzene (Table VI) showed that the complex was binuclear at low

TABLE VI

Cryoscopic measurements on $Al_2(OPr^i)_6$,en in benzene

$10^2 \times$molarity of $Al_2(OPr^i)_6$,en	Mol. wt.	Average no. of aluminum atoms per osmotic particle	$10^6 \times K$ ($kg^3/mole^3$)
2.00	491.8	2.098	2.5
3.42	493.7	2.106	0.5
5.77	615.5	2.626	1.9
7.21	654.2	2.792	1.7
8.68	677.5	2.890	1.3
10.39	711.0	3.034	1.1

concentrations but the number-average degree of polymerization, n, increased with increase in concentration. A number of feasible equilibria were considered in an attempt to explain the concentration dependence of the number-average degree of polymerization. The best agreement was found for a system involving polymerization of $Al_2(OPr^i)_6$,en to an octameric species $Al_8(OPr^i)_{24}(en)_4$, viz. equation [6]. An average dissociation

$$4Al_2(OPr^i)_6,en \rightleftharpoons Al_8(OPr^i)_{24},(en)_4 \qquad [6]$$

constant $K \sim 1.5 \times 10^6$ $kg^3/mole^3$ was obtained from the calculated values shown in Table VI. The constancy of K is probably as good as can be expected in view of the limitations of the technique.

Structural Aspects of Metal Alkoxide – Ethylenediamine Complexes

The following new complexes have been identified and studied in more or less detail: $Ti_2(OEt)_8$,en; $Ti(OPr^i)_4$,en; $Ti_2(OPr^i)_8$,en; $Zr_2(OPr^i)_8$,en; $Ta_2(OPr^i)_{10}$,en; and $Al_2(OPr^i)_6$,en. The formulae of some of these compounds raise some interesting structural problems.

Since titanium tetraethoxide tends to trimerize due to alkoxide bridging it is not surprising that a complex $Ti_2(OEt)_8$,en is formed and the structures shown in Figs. 4 and 5 seem reasonable based on octahedral titanium. In particular Fig. 4 with the ethylenediamine behaving as a chelating ligand seems likely, although models do not rule out the structure in Fig. 5. The formation of ethylenediamine – titanium isopropoxide complexes was surprising because titanium tetraisopropoxide is monomeric, presumably because steric factors oppose polymerization through isopropoxide bridges (2). However, the phase studies and cryoscopic measurements show that $Ti_2(OPr^i)_8$,en and $Ti(OPr^i)_4$,en

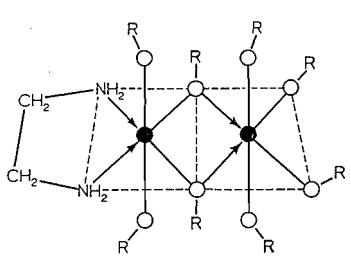

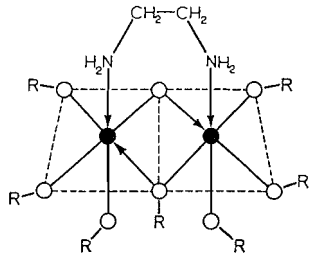

FIG. 4. Structure for $M_2(OR)_8$,en. ● = M (Ti or Zr); ○ = oxygen in OR; R = ethyl or isopropyl.
FIG. 5. Structure for $M_2(OR)_8$,en. ● = M (Ti or Zr); ○ = oxygen in OR; R = ethyl or isopropyl.

are rather weak complexes and it is also true that steric hindrance to coordination of ethylenediamine may be less than the steric hindrance to polymerization of the isopropoxide. There is the additional factor that ethylenediamine is a strong donor molecule. We presume that $Ti(OPr^i)_4$,en is the mononuclear chelate complex shown in Fig. 6 and

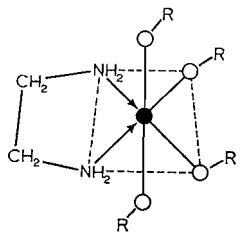

FIG. 6. Structure for $Ti(OPr^i)_4$,en. ● = Ti; ○ = oxygen in OR; R = isopropyl.

that $Ti_2(OPr^i)_8$,en has one of the structures shown in Figs. 4 and 5. Alternative structures may be formulated involving 5-coordinated titanium but we do not feel there is any justification for considering them seriously at present. Since the dimeric solvate $Zr_2(OPr^i)_8$,$(Pr^iOH)_2$ has been formulated as involving octahedral zirconium (2), it is logical to infer that $Zr_2(OPr^i)_8$,en has one of the structures shown in Figs. 4 and 5. With regard to the tantalum complex $Ta_2(OPr^i)_{10}$,en two possibilities are worthy of consideration. If the tantalum is octahedrally 6-coordinated then the ethylenediamine can only act as a chelate in a complex salt such as $[Ta(OPr^i)_4,en]^+[Ta(OPr^i)_6]^-$. The nature of the complex (e.g. volatile, soluble in benzene) suggested that it is not a salt. Thus, if the tantalum is 6-coordinated the ethylenediamine must form a flexible bridge between the two tantalum atoms as shown in Fig. 7. However, it is possible that the tantalum is 8-coordinated as shown in Fig. 8, with ethylenediamine acting as a chelating ligand. A cubic structure is shown for simplicity but there is no reason to exclude a square antiprismatic configuration for the 8-coordinated tantalums. A similar problem arises in assigning a structure to the aluminum complex $Al_2(OPr^i)_6$,en. If the aluminums are tetrahedrally 4-coordinated, as seems most likely, then the ethylenediamine must form a flexible bridge as shown in Fig. 9. It is not possible to construct a structure for $Al_2(OPr^i)_6$,en in which both aluminums are octahedral. However, if one aluminum is tetrahedrally coordinated and the other octahedrally coordinated the structure shown in Fig. 10 is a possibility, with the ethylenediamine acting as a chelating ligand. At

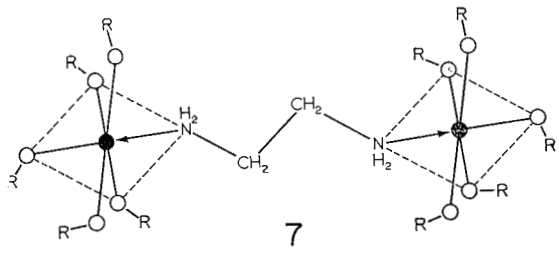

7

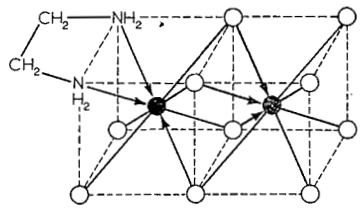

8

FIG. 7. Structure for $Ta_2(OPr^i)_{10}$,en. ● = Ta; ○ = oxygen in OR; R = isopropyl.
FIG. 8. Structure for $Ta_2(OPr^i)_{10}$,en. ● = Ta; ○ = oxygen in OPr^i (isopropyl groups omitted).

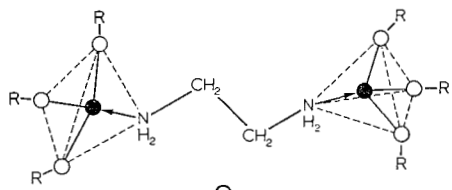

9

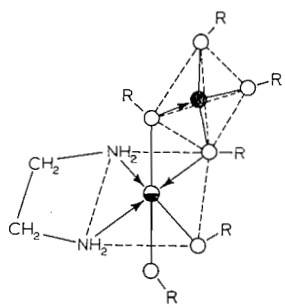

10

FIG. 9. Structure for $Al_2(OPr^i)_6$,en. ● = Al; ○ = oxygen in OR; R = isopropyl.
FIG. 10. Structure for $Al_2(OPr^i)_6$,en. ◒ = Al (octahedral); ● = Al (tetrahedral); ○ = oxygen in OR; R = isopropyl.

higher concentrations in benzene the complex $Al_2(OPr^i)_6$,en appears (from cryoscopic measurements) to polymerize to the octamer $Al_8(OPr^i)_{24}$,$(en)_4$. It is possible to construct an octamer containing octahedrally coordinated aluminum and with the ethylenediamine acting as a chelating ligand. An isomer of the octameric complex is shown in Fig. 11.

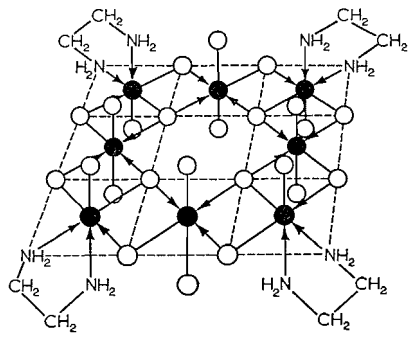

FIG. 11. Structure for $Al_8(OPr^i)_{24}$,$(en)_4$. ● = Al; ○ = oxygen in OPr^i (isopropyl groups omitted).

ACKNOWLEDGMENTS

We are grateful to the National Research Council for generous financial support for this work. We also thank Dr. G. Boone of the Geology Department for the use of the X-ray diffraction equipment.

REFERENCES

1. M. S. BAINS and D. C. BRADLEY. Can. J. Chem. **40**, 1350 (1962).
2. D. C. BRADLEY. Progress in inorganic chemistry. Vol. II. 1960. p. 321.
3. CHARLES M. COOK, JR. J. Am. Chem. Soc. **81**, 3828 (1959).
4. R. C. MEHROTRA. J. Indian Chem. Soc. **30**, 585 (1953).
5. W. G. YOUNG, W. H. HARTUNG, and F. S. CROSSLEY. J. Am. Chem. Soc. **58**, 100 (1936).
6. D. C. BRADLEY, R. C. MEHROTRA, and W. WARDLAW. J. Chem. Soc. 2027 (1952).
7. D. C. BRADLEY, D. C. HANCOCK, and W. WARDLAW. J. Chem. Soc. 2773 (1952).
8. D. C. BRADLEY and W. WARDLAW. J. Chem. Soc. 280 (1951).
9. D. C. BRADLEY, B. N. CHAKRAVARTI, A. K. CHATTERJEE, W. WARDLAW, and A. WHITLEY. J. Chem. Soc. 99 (1958).
10. D. C. BRADLEY, F. M. A. HALIM, and W. WARDLAW. J. Chem. Soc. 3450 (1950).

THE CARBOHYDRATE–PROTEIN LINKAGE IN GLYCOPROTEINS

PART II. THE SYNTHESIS OF N-L-SERYL-D-GLUCOSAMINE AND N-L-THREONYL-D-GLUCOSAMINE

J. K. N. Jones, J. P. Millington, and M. B. Perry

Department of Organic Chemistry, Queen's University, Kingston, Ontario

Received June 6, 1962

ABSTRACT

N-L-Seryl-D-glucosamine has been prepared by the condensation of *N*-carbobenzoxy-L-serine with D-glucosamine in the presence of dicyclohexyl carbodiimide followed by hydrogenolysis of the resulting *N*-(*N*-carbobenzoxy-L-seryl)-D-glucosamine to remove the *N*-carbobenzoxy protecting group.

N-L-Threonyl-D-glucosamine has been prepared by (*a*) the condensation of 1,3,4,6-tetra-*O*-acetyl-α- (and β-) D-glucosamine and *N*-carbobenzoxy-*O*-tetrahydropyranyl-L-threonine in the presence of diisopropyl carbodiimide followed by the removal of the protecting groups from the resulting *N*-(*N*-carbobenzoxy-*O*-tetrahydropyranyl-L-threonyl)-1,3,4,6-tetra-*O*-acetyl-α- (and β-) D-glucosamine, and (*b*) by the condensation of *N*-carbobenzoxy-L-threonine with D-glucosamine in the presence of dicyclohexyl carbodiimide followed by removal of the *N*-carbobenzoxy group from the resulting *N*-(*N*-carbobenzoxy-L-threonyl)-D-glucosamine by hydrogenolysis.

INTRODUCTION

As part of a program in this laboratory aimed at the determination of the nature of the carbohydrate–peptide bonds occurring in natural glycoproteins (1) the synthesis of model amino acid – glycose compounds linked by *N*-glycoside, *O*-glycoside, ester, and amide bonds is being undertaken. A study of the stability of these model compounds and of the conditions required for their successful paper chromatographic and electrophoretic separation will aid in the selection of experimental conditions required for the isolation of such derivatives from glycoproteins. The derivatives may subsequently be of use as reference compounds for the identification of the hydrolytic degradation products of glycoproteins and mucoproteins.

This paper records the synthesis of two *N*-amino acyl derivatives of D-glucosamine. The original methods used in the synthesis of this type of compound involved the reaction of *N*-carbobenzoxy amino acyl chlorides with fully *O*-acetylated 2-amino-2-deoxyaldohexoses (2) or the condensation of suitably protected 2-amino-2-deoxyhexoses with a *N*-carbobenzoxy amino acid derivative by the carbodiimide method (1, 3, 4). In either case the protecting groups must be subsequently removed in order to obtain the unsubstituted *N*-amino acyl aminohexose compounds.

A simple and convenient method for the preparation of amino acyl derivatives of glycoses has recently been reported by Kochetkov and his co-workers (5, 6) which involves the condensation of an unprotected glycose with a *N*-carbobenzoxy amino acid in the presence of carbodiimide. It was found that *N*-carbobenzoxy amino acids condensed readily with 2-amino-2-deoxyhexoses in the presence of dicyclohexyl carbodiimide in aqueous pyridine solution at room temperature to form *N*-(*N*-carbobenzoxy amino acyl)-hexosamines, the exclusive formation of the *N*-substituted derivatives under these conditions being attributed to the specific action of carbodiimide and the instability of *O*-acyl derivatives in aqueous pyridine solution. This procedure has now been applied to the synthesis of *N*-seryl-D-glucosamine and *N*-threonyl-D-glucosamine.

EXPERIMENTAL

All melting points were determined using the Fisher–Johns block and are uncorrected. Solutions were concentrated by rotary evaporation under reduced pressure below 40° C.

Paper chromatography was performed by the descending method on Whatman No. 1 paper, using butan-1-ol/ethanol/water (3:1:1 v/v). The following spray reagents were used to detect the compounds on the developed chromatograms: (A) 2% solution of *p*-anisidine hydrochloride in butan-1-ol (7), (B) 1% solution of silver nitrate in acetone, followed by 2% ethanolic sodium hydroxide solution (8), and (C) 2% ninhydrin in butan-1-ol (9). The rate of movement of the compounds on the chromatograms is given relative to that of D-glucosamine hydrochloride ($R_{GN.HCl}$) or *N*-acetyl-D-glucosamine (R_{GNAc}).

The infrared spectra of the compounds were measured as 0.8% dispersions in potassium bromide disks, or as 6% solutions in chloroform or methylene chloride, using the Perkin–Elmer Model 21 spectrophotometer.

1. N-L-Seryl-D-glucosamine

(a) N-(N-Carbobenzoxy-L-seryl)-D-glucosamine

The procedure of Kochetkov and his co-workers was followed (5, 6). D-Glucosamine hydrochloride (2.15 g, 0.01 mole) was dissolved in water (5 ml) and to the cooled, mechanically stirred solution was added 2 *N* sodium hydroxide solution (5 ml) followed by *N*-carbobenzoxy-L-serine (2.39 g, 0.01 mole) dissolved in dry redistilled pyridine, and dicyclohexyl carbodiimide (3.09 g, 0.015 mole) dissolved in pyridine (20 ml). The solution was allowed to warm to room temperature and stirring was continued for 24 hours. The precipitated dicyclohexyl urea (ca. 0.01 mole) was removed by filtration and the unreacted dicyclohexyl carbodiimide was removed by extraction with ether (2×50 ml).

The aqueous solution was concentrated to a small volume and the product which crystallized out was collected by filtration and was then recrystallized from methanol solution. The *N*-(*N*-carbobenzoxy-L-seryl)-D-glucosamine (38% yield) had m.p. 217° C (decomp.) and $[\alpha]_D^{23}$ +73.5° (*c*, 4.0 chloroform).

The compound had R_{GNAc} 2.09 on paper chromatograms and was free from D-glucosamine and L-serine. The infrared spectrum exhibited absorption bands at 3460 cm^{-1} (s, hydroxyl) and 1682 and 1495 cm^{-1} (amide). Anal. Found: C, 50.7; H, 6.5; N, 6.8%. $C_{17}H_{24}O_9N_2$ requires: C, 50.99; H, 6.04; N, 7.0%.

(b) N-(L-Seryl hydrochloride)-D-glucosamine

The *N*-carbobenzoxy group was removed from the *N*-(*N*-carbobenzoxy-L-seryl)-D-glucosamine by hydrogenolysis in dilute hydrochloric acid solution using palladized charcoal as a catalyst according to the procedure of Jones *et al.* (1). The *N*-(L-seryl hydrochloride)-D-glucosamine, obtained as fine crystals from methanol/ether mixture (85% yield), had $R_{GN.HCl}$ 0.55 on paper chromatograms and its infrared spectrum exhibited absorption bands at 3460 cm^{-1} (wide, hydroxyl), 1682 cm^{-1} (amide), and 1495 cm^{-1} (ionic nitrogen). Attempts to prepare the free amine failed since the initial product blackened before it could be isolated.

2. N-L-Threonyl-D-glucosamine

Method A

(a) N-Carbobenzoxy-L-threonine

N-Carbobenzoxy-L-threonine was prepared in 90% yield by the method of Moore *et al.* (3). The product after recrystallization from ethyl acetate had m.p. 102° C and $[\alpha]_D^{21}$ −4.3° (*c*, 4.25 acetic acid). Anal. Found: C, 57.0; H, 5.9; N, 5.6%. $C_{12}H_{15}O_5N$ requires: C, 56.91; H, 5.97; N, 5.53%.

(b) Methyl N-Carbobenzoxy-L-threonate

N-Carbobenzoxy-L-threonine (8.0 g) was dissolved in 2.5% methanolic hydrogen chloride solution (100 ml), and after 12 hours at room temperature the solution was neutralized by passage through a column of Duolite A4 (OH^-) ion-exchange resin. The solution was concentrated to a syrup which gave crystalline methyl *N*-carbobenzoxy-L-threonate (89% yield) having m.p. 90° C and $[\alpha]_D^{20}$ −16.1° (*c*, 4.25 methanol). Anal. Found: C, 57.9; H, 6.5; N, 5.3%. $C_{13}H_{17}O_5N$ requires: C, 58.42; H, 6.41; N, 5.24%.

(c) Methyl N-Carbobenzoxy-O-tetrahydropyranyl-L-threonate

The procedure of Iselin and Schwyzer (10) was followed. Hydrogen chloride (2 *N*) in anhydrous ethyl acetate (0.5 ml) was added to a solution of methyl *N*-carbobenzoxy-L-threonate (7.5 g) in purified 2,3-dihydro-4-pyran (4 g). The reaction mixture was kept at room temperature for 24 hours after which it was diluted with ether and then washed with dilute sodium bicarbonate solution followed by water. The ether solution was dried (anhyd. sodium sulphate), filtered, and then concentrated to a yellow oil (80% yield).

(d) Hydrolysis of Methyl N-Carbobenzoxy-O-tetrahydropyranyl-L-threonate

Methyl *N*-carbobenzoxy-*O*-tetrahydropyranyl-L-threonate (8.0 g) was dissolved in methanol (25 ml) and was then saponified by the addition of *N* methanolic sodium hydroxide solution (50 ml) according to the method of Iselin and Schwyzer (10) to yield *N*-carbobenzoxy-*O*-tetrahydropyranyl-L-threonine (4.21 g, 55% yield) as a yellow syrup which failed to crystallize. The syrup had equivalent weight 345 (theory 337) and its infrared spectrum showed absorption bands at 987 and 1125 cm^{-1} (tetrahydropyranyl group).

A second compound crystallized from the reaction product which had m.p. 183° C and equivalent weight 238. Anal. Found: C, 60.8; H, 5.7; N, 6.0%. $C_{12}H_{13}O_4N$ requires: C, 61.27; H, 5.57; N, 5.96%.

(e) 1,3,4,6-Tetra-O-acetyl-α- (and β-) D-glucosamine

These derivatives were prepared by the method described by Jones *et al.* (1). α-Anomer: 65% yield, m.p. 118° C, $[\alpha]_D^{20}$ +145° (*c*, 2 chloroform); β-anomer: 65% yield, m.p. 143° C, $[\alpha]_D^{20}$ +27° (*c*, 2 chloroform).

(f) N-(N-Carbobenzoxy-O-tetrahydropyranyl-L-threonyl)-1,3,4,6-tetra-O-acetyl-α- (and β-) D-glucosamine

N-Carbobenzoxy-*O*-tetrahydropyranyl-L-threonine (0.460 g), 1,3,4,6-tetra-*O*-acetyl-α-D-glucosamine (0.510 g), and diisopropyl carbodiimide (0.178 g) were dissolved in methylene chloride (6 ml) and the mixture was shaken mechanically at room temperature for 24 hours. The precipitated diisopropyl urea by-product was removed by filtration and the filtrate was washed with dilute hydrochloric acid, dilute sodium bicarbonate solution, and finally with water. The dried (anhyd. magnesium sulphate) methylene chloride solution on concentration gave a white solid (5% yield) which had m.p. 185° C and $[\alpha]_D^{20}$ +74.4° (*c*, 0.5 methanol).

The above procedure was repeated using 1,3,4,6-tetra-*O*-acetyl-β-D-glucosamine to give the β-anomer as a syrup (50% yield) which failed to crystallize. It had $[\alpha]_D^{20}$ +12.3° (*c*, 4.0 methanol).

The infrared absorption spectra of both the above products exhibited absorption bands at 1745 cm^{-1} (carbonyl, *O*-acetyl), 1670 cm^{-1} (amide I), 1555 cm^{-1} (amide II), 1130 and 987 cm^{-1} (tetrahydropyranyl group), and 695 cm^{-1} (phenyl group).

(g) N-(N-Carbobenzoxy-L-threonyl)-1,3,4,6-tetra-O-acetyl-β-D-glucosamine

N-(*N*-Carbobenzoxy-*O*-tetrahydropyranyl-L-threonyl)-1,3,4,6-tetra-*O*-acetyl-β-D-glucosamine (0.50 g) was heated in boiling 50% acetic acid solution (10 ml) for 10 minutes and the cooled solution was diluted with water and extracted with chloroform (4×20 ml). The dried (anhyd. magnesium sulphate) chloroform extract was concentrated to dryness to yield a syrup (0.25 g, 58% yield) which had $[\alpha]_D^{18}$ +30° (*c*, 3.0 chloroform) and whose infrared spectrum did not show absorption bands due to the tetrahydropyranyl group at either 1130 or 987 cm^{-1}.

(h) N-(N-Carbobenzoxy-L-threonyl)-D-glucosamine

N-(*N*-Carbobenzoxy-L-threonyl)-1,3,4,6-tetra-*O*-acetyl-β-D-glucosamine (100 mg) dissolved in dry methanol (4 ml) was treated with 0.4 *N* barium methoxide in methanol (2 ml) and the mixture was kept at 5° C for 24 hours. Slightly less than the equivalent amount of 0.01 *N* sulphuric acid was added to the reaction mixture, the precipitated barium sulphate was removed by filtration, and the filtrate was further deionized by passage through a column of mixed IR 120 (H^+) and Duolite A4 (OH^-) ion-exchange resins. On concentration of the methanol solution, *N*-(*N*-carbobenzoxy-L-threonyl)-D-glucosamine was obtained as a white solid (30 mg). It had m.p. 209° (decomp.) and $[\alpha]_D^{14}$ +20.4° (*c*, 2.8 methanol). On paper chromatography and detection with spray reagents A and B the compound was revealed as a single spot having R_{GNAc} 2.90 and was not contaminated with either D-glucosamine or L-threonine.

The infrared spectrum of the compound exhibited absorption bands at 3360 cm^{-1} (broad, hydroxyl group) and 1670 and 1550 cm^{-1} (amide) but no absorption band at 1745 cm^{-1} (carbonyl, *O*-acetyl).

Method B

(a) N-(N-Carbobenzoxy-L-threonyl)-D-glucosamine

The procedure of Kochetkov and his co-workers (5, 6) was used. D-Glucosamine hydrochloride (2.15 g, 0.01 mole) dissolved in water (5 ml) was cooled to 0° C and neutralized by the addition of 2 *N* sodium hydroxide solution (5 ml). The mechanically stirred solution was immediately treated with a solution of *N*-carbobenzoxy-L-threonine (2.53 g, 0.01 mole) in dry pyridine (7 ml) followed by a solution of dicyclohexyl carbodiimide (3.09 g, 0.015 mole) in dry pyridine (20 ml) and the stirring was continued for a further 24 hours. The precipitated dicyclohexyl urea was removed by filtration and the unreacted dicyclohexyl carbodiimide was removed by extraction with ether (2×50 ml). The *N*-(*N*-carbobenzoxy-L-threonyl)-D-glucosamine isolated from the concentrated aqueous solution was obtained as crystals which, after several recrystallizations from methanol (final yield 0.415 g), had m.p. 209° C (decomp.) and $[\alpha]_D^{20}$ +21.0° (*c*, 3.0 methanol). The compound was indistinguishable on paper chromatograms from the product obtained by method A and the infrared spectra of the two products were identical. Anal. Found: C, 51.7; H, 6.2; N, 6.7%. $C_{18}H_{26}O_9N_2$ requires: C, 52.17; H, 6.32; N, 6.76%.

(b) N-L-Threonyl-D-glucosamine

N-(*N*-Carbobenzoxy-L-threonyl)-D-glucosamine (25 mg) was dissolved in chloroform/ethanol mixture, and palladized charcoal (25 mg) was added. The mixture was shaken for 24 hours at room temperature in an atmosphere of hydrogen (1.3 atm). The catalyst was removed by filtration and the filtrate was concentrated to a dark yellow syrup (7 mg). On paper chromatography a single spot, which had $R_{GN.HCl}$ 0.44, was revealed by the ninhydrin spray whereas the silver nitrate spray revealed a series of spots indicating the presence of decomposition products.

(c) N-(L-Threonyl hydrochloride)-D-glucosamine

N-(*N*-Carbobenzoxy-L-threonyl)-D-glucosamine (28 mg) was subjected to hydrogenolysis as described above with the inclusion of *N* hydrochloric acid (0.7 ml) in the reaction mixture. The *N*-(L-threonyl

hydrochloride)-D-glucosamine (9.5 mg) was obtained as a clear syrup which failed to crystallize. The syrup had $[\alpha]_D^{20}$ −13° (*c*, 1.0 methanol) and on paper chromatograms it gave a single ninhydrin and silver nitrate positive spot having $R_{GN.HCl}$ 0.46. The infrared absorption spectrum of the compound showed a broad band at 3360 cm^{-1} due to hydroxyl and amino group absorption, but no bands due to the phenyl group corresponding to the original carbobenzoxy group.

Attempts to prepare the free amine from *N*-(L-threonyl hydrochloride)-D-glucosamine using Duolite A4 ($CO_3^=$) ion-exchange resin or Duolite A4 (OH^-) resin failed owing to the rapid decomposition of the initial product.

DISCUSSION

N-(L-Seryl hydrochloride)-D-glucosamine was prepared according to the general procedure of Kochetkov and his co-workers (5, 6). D-Glucosamine was condensed with *N*-carbobenzoxy-L-serine in aqueous pyridine solution in the presence of dicyclohexyl carbodiimide to give *N*-(*N*-carbobenzoxy-L-seryl)-D-glucosamine, from which the protecting *N*-carbobenzoxy group was removed by hydrogenolysis in the presence of dilute hydrochloric acid to yield *N*-(L-seryl hydrochloride)-D-glucosamine in 32% overall yield. The compound was stable in aqueous solution, but attempts to prepare the free *N*-L-seryl-D-glucosamine by careful neutralization with dilute alkali or by the use of mild basic ion-exchange resins failed owing to the rapid decomposition of the free amine under the conditions used.

The *N*-(L-seryl hydrochloride)-D-glucosamine was chromatographically identical with, and had an infrared spectrum indistinguishable from that of, the same derivative prepared earlier by Jones *et al.* (1) in greatly reduced overall yield by the condensation of *N*-carbobenzoxy-*O*-tetrahydropyranyl-L-serine with 1,3,4,6-tetra-*O*-acetyl-D-glucosamine in the presence of diisopropyl carbodiimide to give *N*-(*N*-carbobenzoxy-*O*-tetrahydropyranyl-L-seryl)-1,3,4,6-tetra-*O*-acetyl-D-glucosamine, from which the protecting groups were subsequently removed to yield the required product.

N-(L-Threonyl hydrochloride)-D-glucosamine was prepared in low overall yield by the condensation of *N*-carbobenzoxy-*O*-tetrahydropyranyl-L-threonine with 1,3,4,6-tetra-*O*-acetyl-D-glucosamine in the presence of diisopropyl carbodiimide to give *N*-(*N*-carbobenzoxy-*O*-tetrahydropyranyl-L-threonyl)-1,3,4,6-tetra-*O*-acetyl-D-glucosamine, from which the protecting groups were removed to yield the amino acyl-glycosamine derivative.

An unexpected crystalline product was obtained from the saponification product of methyl-*N*-carbobenzoxy-*O*-tetrahydropyranyl-L-threonate which had an equivalent weight of 238 and whose analysis agrees with the formula $C_{12}H_{13}O_4N$. The compound is tentatively identified as *N*-carbobenzoxy-2-amino-buten-3-oic acid, possibly formed by the elimination of a molecule of water from *N*-carbobenzoxy-L-threonine.

A greatly improved yield of *N*-(L-threonyl hydrochloride)-D-glucosamine was achieved when the general procedure of Kochetkov *et al.* (5, 6) was used. D-Glucosamine was condensed with *N*-carbobenzoxy-L-threonine in aqueous pyridine solution in the presence of dicyclohexyl carbodiimide to give *N*-(*N*-carbobenzoxy-L-threonyl)-D-glucosamine, which on hydrogenolysis in the presence of dilute hydrochloric acid afforded *N*-(L-threonyl hydrochloride)-D-glucosamine in 5% overall yield. The final products obtained by the two different routes were chromatographically identical and their infrared spectra were indistinguishable from each other.

Attempts to prepare *N*-L-threonyl-D-glucosamine by hydrogenolysis of the *N*-(*N*-carbobenzoxy-L-threonyl)-D-glucosamine in neutral media, or by neutralization of the *N*-(L-threonyl hydrochloride)-D-glucosamine by dilute alkali or by using mild basic ion-exchange resins failed to give a pure product owing to the rapid decomposition of the initial free amine. The hydrochloride salt, however, was stable in aqueous solution.

ACKNOWLEDGMENTS

We wish to thank the National Research Council of Canada (Grants T-39 and NRC 706), The National Institutes of Health, Bethesda, Md., U.S.A. (U.S.P.H.S. AM 04127-03), and Queen's University for financial assistance.

REFERENCES

1. J. K. N. JONES, M. B. PERRY, B. SHELTON, and D. J. WALTON. Can. J. Chem. **39**, 1005 (1961).
2. M. BERGMANN and L. ZERVAS. Ber. **65**, 1201 (1932).
3. J. A. MOORE, J. R. DICE, E. D. NICOLAIDES, R. D. WESTLAND, and E. L. WHITTLE. J. Am. Chem. Soc. **76**, 2884 (1954).
4. J. UKITA and S. SUZUKI. J. Pharm. Soc. Japan, **81**, 222 (1961).
5. N. K. KOCHETKOV, V. A. DEREVITSKAYA, and N. V. MOLODTSEV. Chem. Ind. (London), 1159 (1961).
6. N. K. KOCHETKOV, V. A. DEREVITSKAYA, L. M. LIKHOSHERSTOV, N. V. MOLODTSOV, and S. G. KARA-MURZA. Tetrahedron, **18**, 273 (1962).
7. L. HOUGH, J. K. N. JONES, and W. H. WADMAN. J. Chem. Soc. 1702 (1950).
8. W. E. TREVELYAN, D. P. PROCTER, and J. S. HARRISON. Nature, **166**, 444 (1950).
9. H. K. BERRY and L. CAIN. Arch. Biochem. **24**, 179 (1949).
10. B. ISELIN and R. SCHWYZER. Helv. Chim. Acta, **39**, 57 (1956).

COORDINATION COMPLEXES OF TITANIUM (IV) HALIDES

III. PREPARATION AND INFRARED SPECTRA OF THE COMPLEXES OF TITANIUM TETRACHLORIDE WITH UREA, THIOUREA, AND SOME OF THEIR DERIVATIVES[1]

ROLAND RIVEST

Department of Chemistry, University of Montreal, Montreal, Que.

Received June 19, 1962

ABSTRACT

The following coordination complexes of titanium (IV) have been prepared: $TiCl_4.2CO(NH_2)_2$, $TiCl_4.CO(NHCH_3)_2$, $TiCl_4.2CO(NHCH_3)_2$, $2TiCl_4.2NH_2CON(C_6H_5)_2$, $2TiCl_4.2CO(NHC_6H_5)_2$, $TiCl_4.2CS(NH_2)_2$, $2TiCl_4.CS(NHC_2H_5)_2$, $2TiCl_4.NH_2CSN(C_6H_5)_2$, and $2TiCl_4.CS(NHC_6H_5)_2$; their infrared spectra have been measured and their molecular weight determined. For urea and its derivatives the coordination to titanium (IV) is always through the oxygen atom. The phenyl derivatives of urea led to dinuclear complexes which were best explained by assuming halogen bridging between the titanium atoms. Thiourea and its derivatives gave complexes in which coordination occurred through one of the nitrogens in the case of thiourea and through both nitrogens in the case of the derivatives. Halogen bridging was again assumed to explain the formation of the dinuclear complexes.

INTRODUCTION

Many coordination complexes in which the donor bases were urea and thiourea have been reported. Quagliano and co-workers (1) have established that among the urea complexes, some coordinated through one of the nitrogen atoms and some through the oxygen atom of the urea molecule. We have prepared (2, 3) several coordination complexes of titanium (IV) halides with ordinary amides and found that in these complexes the donor atom was oxygen. It has been assumed, then, that coordination through nitrogen would hinder one of the two resonance forms of amides. In urea, the presence of two amino groups in the molecule leads to three resonating structures (4) of which only one would be hindered by coordination through one of the nitrogens. It seemed of interest to prepare and study the complexes formed by urea and its derivatives by reaction on titanium tetrachloride.

Quagliano (5) and his co-workers have prepared some thiourea complexes in which the sulphur atom of the ligand was exclusively involved as donor atom in coordination. Some addition compounds possessing a coordination bond between titanium (IV) and sulphur have been prepared, $TiCl_4.2H_2S$ being a good example of this.

The present investigation was undertaken to compare the relative donor abilities of sulphur and nitrogen toward coordination with titanium tetrachloride, by using thiourea and its derivatives as donor bases. Some substituted thioureas were studied to determine whether steric hindrance would lead to 5-coordinated complexes or to halogen-bridged complexes.

EXPERIMENTAL

Materials and Manipulations

Reagent grade titanium tetrachloride was purified by the method of Gilchrist (6) and the medium fraction was used for our experiment. Reagent grade urea (U); 1,3-dimethylurea (DMU); 1,1-diphenylurea (1,1-DPU); 1,3-diphenylurea (1,3-DPU); thiourea (TU); 1,3-diethylthiourea (DETU); 1,1-diphenylthiourea (1,1-DPTU); and 1,3-diphenylthiourea (1,3-DPTU) were dried over phosphorus pentoxide and used as such.

The solvents used for our experiments were anhydrous and their water content was checked by the Karl

[1]*Presented at the 45th Chemical Institute of Canada Annual Conference and Exhibition, Edmonton, May 27–30, 1962.*

Fisher method. The water-sensitive complexes were prepared and handled in a dry box continuously flushed with dry nitrogen. The method of analysis for chlorine, titanium, carbon, and hydrogen was described previously (9). Nitrogen was determined by the Kjeldahl method or the micro-Dumas method as specified in each case.

The infrared spectra were carried out on a Perkin–Elmer spectrophotometer model 21 using a sodium chloride prism. The spectra of the soluble complexes were determined in solutions of suitable solvents, and the spectra of the insoluble ones were taken as nujol mulls or using the KBr disk method.

The molecular weights were determined using two Gallenkamp ebulliometers, one for the solvent and the other one for the solution of the solute under investigation. This setup permitted simultaneous measurements and therefore eliminated possible errors due to change in atmospheric pressure.

The System $TiCl_4.2U$

Titanium tetrachloride was added in excess to a suspension of urea in methylene chloride. This reaction, being between a solid and a liquid, was very slow. After the suspension was stirred for 5 or 6 days, the reaction seemed to be complete and a yellow precipitate had replaced the urea crystals. The excess of titanium tetrachloride was washed out by methylene chloride on a sintered-glass filter and the precipitate was then dried under vacuum at room temperature. This precipitate was found to be insoluble in all the inert solvents. It melted with decomposition at about 215° C. The precipitate was then analyzed and the results are included in Table I.

TABLE I

Complexes	Analytical results found and calculated					
	Ti%	Cl%	N%*	C%	H%	M.W.
$TiCl_4.2U$	15.63	45.47	18.4*d*	7.76	3.36	—
	15.46	45.43	18.03	7.75	2.60	—
$TiCl_4.DMU$	17.11	49.56	10.04*k*	—	—	—
	17.24	51.04	10.04	—	—	—
$TiCl_4.2DMU$	13.42	37.58	14.92*k*	—	—	—
	13.09	38.90	15.30	—	—	—
$2TiCl_4.2(1,1\text{-DPU})$	11.93	34.28	—	—	—	760±60
	11.92	35.27	—	—	—	804
$2TiCl_4.2(1,3\text{-DPU})$	12.25	34.19	—	—	—	728±50
	11.92	35.27	—	—	—	804
$TiCl_4.2TU$	14.18	—	15.43*d*	6.37	3.01	—
	14.01	—	16.09	7.02	2.36	—
$2TiCl_4.1,3\text{-DETU}$	18.50	—	5.40	12.52	2.73	—
	18.72	—	5.48	11.82	2.36	—
$2TiCl_4.1,1\text{-DPTU}$	15.75	—	4.66*d*	25.69	2.16	470±40
	15.76	—	4.61	25.66	1.99	608
$2TiCl_4.1,3\text{-DPTU}$	15.64	—	4.58*d*	25.81	2.30	700±20
	15.76	—	4.61	25.66	1.99	608

**k*: Kjeldahl method; *d*: micro-Dumas method.

The System $TiCl_4.DMU$

Titanium tetrachloride in excess was added to a suspension of DMU. The reaction was quite slow, but after 2 days of agitation the reaction seemed to be complete and a yellow powder had replaced the white DMU crystals. The excess of titanium tetrachloride was removed by repeated washing with dichloroethane on a sintered-glass filter and the precipitate was dried under vacuum at room temperature. The precipitate is insoluble in non-polar organic solvents. Its melting point was found to be 209° C and it decomposed at 220°. The analytical results are included in Table I. They are in good agreement with the formula $TiCl_4.1DMU$.

If a 10% $TiCl_4$ solution in dichloroethane or cyclohexane was used instead of an excess of pure titanium tetrachloride, a different compound, $TiCl_4.2DMU$, was formed. This compound melted at 228° C and decomposed at 230° C. The analytical results are included in Table I.

When an excess of dimethylurea was used, many other pseudo addition compounds were obtained, but with no definite stoichiometry. Since there was no means of removing the excess of the donor base, it has not been possible to draw definite conclusions on these compounds.

The System $TiCl_4.1,1\text{-}DPU$

An excess of a 50% solution of titanium tetrachloride in methylene chloride was added to a suspension

of 5 g of the donor base in the same solvent. The compound so formed, being soluble, turned the solution a deep red color. After 2 days of agitation a dark orange precipitate was formed, which was filtered, washed, and dried as usual. It was then dissolved in CH_2Cl_2 and recrystallized, yielding orange crystals. The analytical results, indicating an acceptor–donor ratio of 1 to 1, are included in Table I. The melting point of this compound was found to be 89–90° C. The molecular weight determinations, included in Table I, indicated a 2:2 molar ratio.

The System $TiCl_4$.1,3-DPU

The technique used to prepare the complex $2TiCl_4$.2(1,3-DPU) was almost the same as the one used to prepare $2TiCl_4$.2(1,1-DPU). The brown complex thus obtained melted at 162–169° C. Its analytical results and its molecular weight values are included in Table I.

The System $TiCl_4$.1,3-DETU

Excess pure $TiCl_4$ was added to DETU dispersed in methylene chloride and cyclohexane. Dropwise addition of $TiCl_4$ led to a dark red coloration with adhesion of viscous material to the wall of the reacting flask. After 2 days of agitation, a brown powder extremely sensitive to moisture was obtained. The melting point was found to be 62°. The analytical results are included in Table I.

The System $TiCl_4$.TU

The technique used was the same as the one used to prepare $TiCl_4$.2U. The compound obtained was a dark brown powder melting with decomposition at around 130° C. The results of the elementary analyses are included in Table I.

The System $TiCl_4$.1,1-DPTU

An excess of pure titanium tetrachloride was added to a suspension of the donor base in cyclohexane. A dark brown suspension was obtained which was at first very viscous and which then separated into an orange-yellow powder after 2 days of agitation. The compound was filtered off, washed on the filter with cyclohexane, and dried under vacuum at room temperature. On recrystallization from a dichloroethane solution reddish brown crystals were obtained. It melted without decomposition at 126° C.

The System $TiCl_4$.1,3-DPTU

The technique used here was very similar to the one used to prepare $2TiCl_4$.1,1-DPTU. The powder obtained, however, was dark brown, and recrystallization from a dichloroethane solution led to orange-yellow crystals of which the melting point was found to be 109–112°. The analytical results are included in Table I.

INFRARED SPECTRA AND STRUCTURAL DISCUSSION

The infrared spectra of urea, substituted ureas, and their coordination complexes are included in Table II, and illustrated in Figs. 1, 2.

TABLE II

Infrared bands and assignment in the complexes of urea and derivatives

Band assignment	Urea*	$TiCl_4$.2U*	1,1-DPU†	$2TiCl_4$. 2(1,1-DPU)†	1,3-DPU‡	$2TiCl_4$. 2(1,3-DPU)
N—H stretching	3450 s 3350 s	3455 s 3340 s	3530 m 3410 m	3490 w 3370 w	3305 m	3342 m
C=O stretching	1683 s	1655 s	1690 vs	1622 vs	1650 s	1616 s
N—H deformation and aromatic ring vibrations	1629 vs	1635 vs 1615 s	1595 vs 1496	1550 sh 1535 sh 1505 vs 1426	1600 s 1560 s 1505 w	1600 s 1585 vs 1570 vs 1500 m

NOTE: vs = very strong, s = strong, m = medium, w = weak, sh = shoulder.
*KBr disks.
†Methylene chloride solutions.
‡Fluorolube mulls.

A comparison of the infrared spectrum of urea with that of its complex indicates that the N—H stretching frequency is unchanged in the complex, but that the absorption bands observed in the carbonyl frequency region are shifted to lower values; this is an indication that the oxygen atom of urea is involved in coordination. The formula is then simply $TiCl_4$.2U, in which the urea molecules probably occupy cis positions.

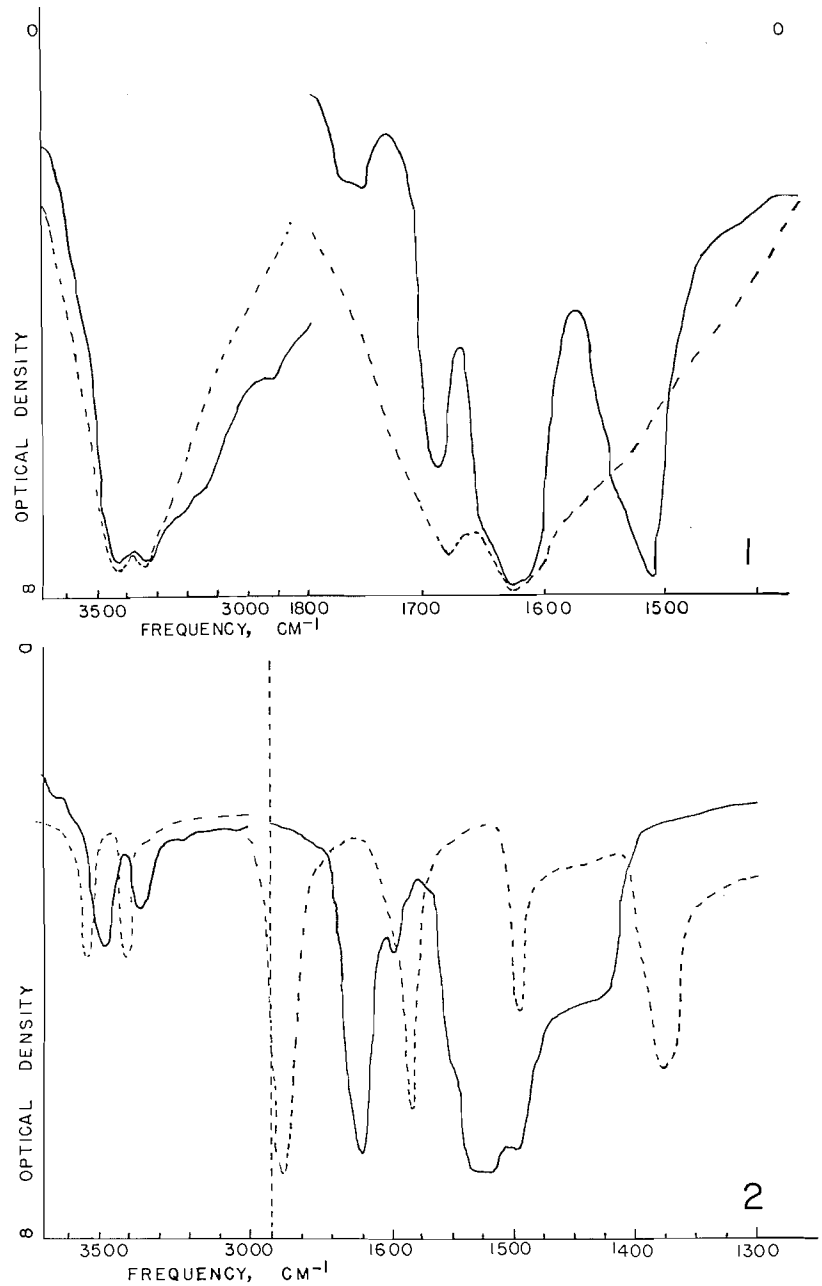

FIG. 1. Infrared spectra as KBr disks; – – – urea, —— $TiCl_4.2U$.
FIG. 2. Infrared spectra in methylene chloride solutions; – – – 1,1-DPU, —— $2TiCl_4.2(1,1\text{-DPU})$.

The changes in the spectra of the substituted urea when complexed to titanium (IV) are much larger. When 1,1-DPU is the donor base, complexing with titanium (IV) causes a bathochromic effect of some 40 cm^{-1} in the N—H stretching frequency region and of some 68 cm^{-1} in the carbonyl frequency region. Since molecular weight determinations of the complexes indicate dimeric values $2TiCl_4.2(1,1\text{-DPU})$, one could believe

that coordination in this compound takes place through oxygen and through one of the nitrogen atoms, probably of the NH_2 group. Then, two molecules of 1,1-DPU would act as bridging groups between the two $TiCl_4$ molecules. In such a case, however, the shift in the N—H stretching frequency should be much larger than 35 cm^{-1}. Quagliano (1) and co-workers have proposed 150 cm^{-1}. It seems, then, very reasonable to believe that the shift is due to intramolecular hydrogen bonding and that the dimeric nature of the complex is explained by assuming coordination through the oxygen, and halogen bridging between the two titanium (IV) atoms. This is illustrated schematically in Fig. 3, where it is shown that the two chlorines fill two coordinating positions each and where the broken lines indicate hydrogen bonding between the nitrogens.

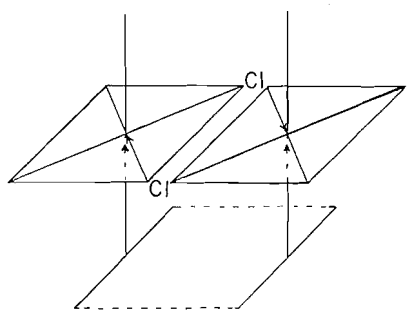

FIG. 3. Schematic representation of the complexes between $TiCl_4$ and 1,1-DPU and 1,3-DPU.

The complex formed with 1,3-DPU as donor base should have the same configuration as its analogue $2TiCl_4.2$(1,1-DPU). There is a difference in the sign of the N—H stretching frequency shift, but this difference is probably due to less favorable conditions for hydrogen bonding in the complex than in the pure 1,3-DPU. It is noticeable that the melting point of 1,3-DPU is considerably higher than that of 1,1-DPU, and this is certainly due to a difference in hydrogen bonding strength.

The infrared spectra of thiourea, substituted thioureas, and their coordination complexes are included in Tables III and IV and illustrated in Figs. 4, 5, and 6.

TABLE III

Infrared spectra and band assignment of TU and its complex as KBr disks and of DETU and its complex in methylene chloride solutions

Band assignment	TU	$TiCl_4.2TU$	DETU	$2TiCl_4.DETU$
N—H stretching	3400 s 3320 s 3200 s	3380 s 3330 s 3240 s 2935 s 2863 s	3420 s	3390 s
N—H deformation	1615 s	1648 s 1627 s	1567 sh 1550 vs 1535 vs 1500 vs 1484 sh	1640 sh 1620 vs 1588 sh 1535 sh 1520 s
C=S stretching and CN vibration	1470 m 1407 s	1470 m 1441 m	1385 m 1337 m	1393 m 1343 m

TABLE IV

Infrared spectra and band assignment in methylene chloride solutions

Band assignment	1,1-DPTU	$2TiCl_4$.1,1-DPTU	1,3-DPTU	$2TiCl_4$.1,3-DPTU
N—H vibration	3520 m 3385 m	3410 w 3315 m	3400	3280
NH deformation and aromatic ring vibrations	1593 vs 1498 s 1407 s	1630 vs 1597 w 1550 sh 1540 m 1495 w	1600 s 1550 sh 1540 sh 1530 sh 1590 vs 1495 vs	1615 s 1582 vs 1495 m
C=S stretching and CN vibration	1360 vs	1407 m 1275 sh	1353 s	1392 w

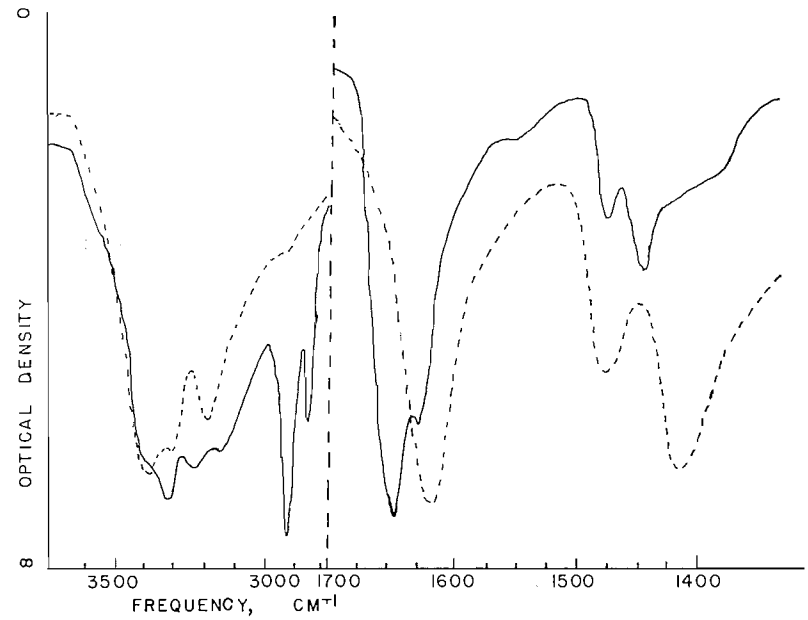

FIG. 4. Infrared spectra as KBr disks; - - - TU, —— $TiCl_4$.2TU.

The spectrum of thiourea when compared to the spectrum of $TiCl_4$.2TU shows a marked difference in the N—H stretching region and in the region attributed to NH_2 deformation and C=S stretching. A large negative shift observed in the N—H region combined with a positive shift in the C=S stretching region strongly suggests coordination through one of the nitrogens of thiourea. This would leave an uncoordinated nitrogen in each thiourea molecule and explain why the bands attributed to pure thiourea in the 3000 cm^{-1} region are still present in the spectrum of the complex. The formula proposed is simply, then, $TiCl_4$.2TU, in which the thioureas probably occupy cis positions on the titanium (IV) octahedron.

The complexes of substituted thioureas are quite interesting as monomeric species, especially because of their general formula $2TiCl_4$.1 donor base, which was confirmed by molecular weight determinations.

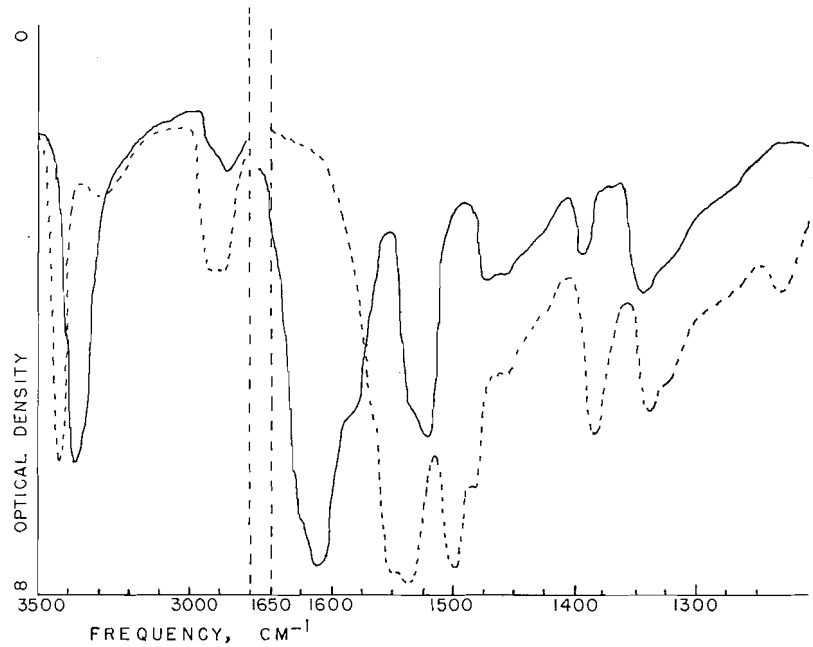

FIG. 5. Infrared spectra in methylene chloride solutions; - - - 1,3-DETU, —— $2TiCl_4$.1,3-DETU.

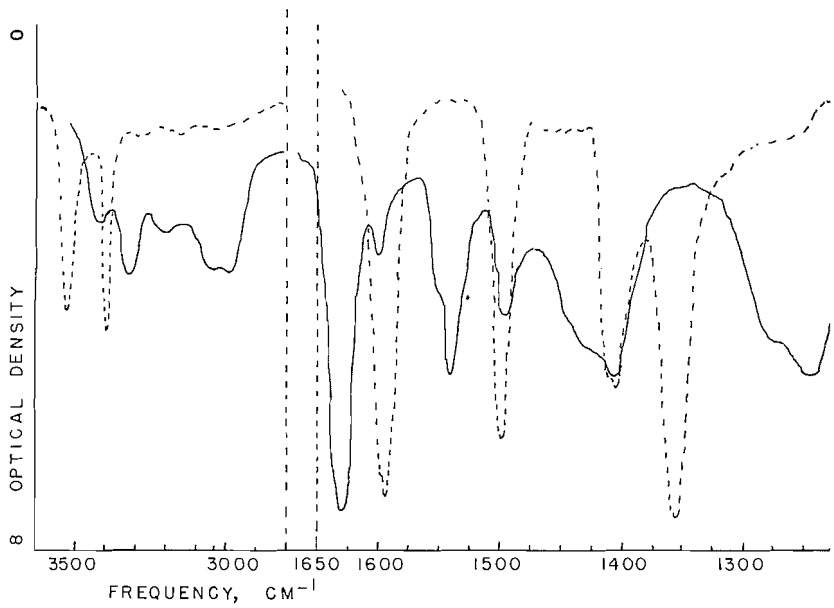

FIG. 6. Infrared spectra in methylene chloride solutions; - - - 1,1-DPTU, —— $2TiCl_4$.1,1-DPTU.

The infrared spectrum of the complex of DETU in methylene chloride solution showed only small differences from the spectrum of the pure donor base under the same condition. There is a negative N—H frequency shift of 30 cm^{-1}, a small positive shift for the NH deformation band and for the C=S stretching band. This is in agreement with the great

instability of this complex compound. Even if the perturbations in the spectrum are rather small, it is still believed that coordination involves the nitrogens of the ligand as donor atoms. If the donor atoms involved were one of the nitrogens and the sulphur atom, one should observe the original band at 3420 cm^{-1} in the spectrum of the complex molecule and the shifted band at lower frequency. This is not so. It seems, then, reasonable to assume that either the two titanium atoms have a coordination number of 5 and are held together by the bidentate DETU, or that they have a coordination number of 6 and the sixth position is occupied by halogen bridging of two chlorines.

For the system $2TiCl_4$.1,1-DPTU, the perturbation of the spectrum is much greater when going from the donor base to the complex. The N—H stretching frequency is shifted by 120 cm^{-1}, the N—H_2 deformation frequency is increased by about 30 cm^{-1}, and the C=S stretching is shifted to higher frequency by 37 cm^{-1} or to lower frequency by over 100 cm^{-1}. This last hypothesis is very unlikely because the shift due to complexing of the sulphur atom should be less than the one due to complexing of the oxygen atom and the carbonyl frequency shift observed in the spectrum of the complex $2TiCl_4$.2 (1,1-DPU) was found to be around 66 cm^{-1}. To find out if the presence of two phenyl groups on the donor atom would hinder the donor–acceptor reaction we have reacted diphenylamine and diphenyl ether with $TiCl_4$ and found that there was reaction in both cases. It seems quite reasonable to suppose that the two nitrogens of the 1,1-DPTU molecule are involved in coordination.

For the complex $2TiCl_4$.1,3-DPTU, the evidence of coordination through the two nitrogens of 1,3-DPTU is about the same, namely, a N—H frequency shift of 120 cm^{-1}, a N—H deformation frequency shift, and a positive shift for C=S stretching frequency. Moreover, since the original absorption band in the spectrum of 1,3-DPTU for the N—H stretching is not present in the spectrum of the complexes, it seems quite reasonable to believe that, in the complex, the two nitrogens are identical. This would not be true if only one nitrogen acted as donor atom. All the complexes prepared with the substituted thioureas can be represented by the following formula, in which R means a hydrogen, an alkyl, or an aryl radical:

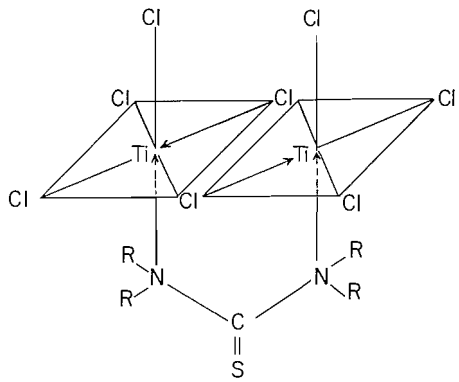

ACKNOWLEDGMENTS

The author is glad to thank Mr. Gilles Murphy for the preparation and analysis of some of the complexes and also the National Research Council of Canada for the financial support of this work.

SOMMAIRE

Les complexes suivants du titane (IV) ont été préparés: $TiCl_4.2CO(NH_2)_2$, $TiCl_4.CO(NHCH_3)_2$, $TiCl_4.2CO(NHCH_3)_2$, $2TiCl_4.2NH_2CON(C_6H_5)_2$, $2TiCl_4.2CO(NHC_6H_5)_2$, $TiCl_4.2CS(NH_2)_2$, $2TiCl_4.CS(NHC_2H_5)_2$, $2TiCl_4.NH_2CSN(C_6H_5)_2$, and $2TiCl_4.CS(NHC_6H_5)_2$. On a aussi mesuré leurs spectres infrarouges et déterminé leur poids moléculaire. L'urée et ses dérivés coordonne au titane (IV) par l'atome d'oxygène. Les dérivés phényl de l'urée donnent des complexes binucléaires dûs à la formation de ponts halogénés entre les titanes. La thiourée et ses dérivés ont donné des complexes pour lesquels la coordination implique un atome d'azote dans le cas de la thiourée et les deux atomes d'azote dans les autres cas. La formation de pont halogénés explique aussi dans ce cas la formation de complexes binucléaires.

REFERENCES

1. R. B. PENLAND, S. MIZUSHIMA, C. CURRAN, and J. V. QUAGLIANO. J. Am. Chem. Soc. **79**, 1575 (1957).
2. J. ARCHAMBAULT and R. RIVEST. Can. J. Chem. **36**, 1461 (1958).
3. J. ARCHAMBAULT and R. RIVEST. Can. J. Chem. **38**, 1331 (1960).
4. L. PAULING. The nature of the chemical bond. 3rd ed. Cornell University Press, Ithaca, N.Y. 1960. p. 286.
5. A. YAMAGUCHI, R. B. PENLAND, S. MIZUSHIMA, T. J. LANE, C. CURRAN, and J. V. QUAGLIANO. J. Am. Chem. Soc. **80**, 527 (1958).
6. N. S. CLABAUGH, R. T. LESLIE, and R. GILCHRIST. J. Res. Natl. Bur. Std. **55**, 261 (1955).

COORDINATION COMPLEXES OF TITANIUM (IV) HALIDES

IV. PREPARATION AND INFRARED SPECTRA OF THE COMPLEXES OF TITANIUM TETRACHLORIDE WITH CHLORINE-SUBSTITUTED ESTERS OF MONOBASIC ACIDS AS LIGANDS

SUMER CHAND JAIN AND ROLAND RIVEST
Department of Chemistry, University of Montreal, Montreal, Que.

Received June 29, 1962

ABSTRACT

Coordination complexes between titanium tetrachloride and some chlorine-substituted monoesters have been prepared.

Infrared spectra of these complexes and their melting points indicate that the strength of the coordination bonds decreases as the number of chlorines increases in the acid radical. When the substitution is in the alkyl radical, it is possible to prepare complexes of the formula $TiCl_4.2$ ester, since the chlorine substitution decreases the basic properties of the oxygen of the ether group in the ligand.

INTRODUCTION

Many coordination compounds between esters of monobasic acids and titanium tetrachloride have been reported previously (1–4). Physicochemical investigations on properties such as electrical conductance, viscosity, dipole moment, surface tension, density, specific heat, etc. have been carried out by Osipov (5, 6), Suchkov, and others but little work has been done on the effect of halogen substitution, in various esters, on complex formation.

Halogen substitution on the acid radical should lower the double-bond character of the carbonyl bond, thus weakening the bond between titanium (IV) and the carbonyl group. This should be evidenced by a lowering in the infrared carbonyl stretching frequency and also by a lowering in the melting points, since the melting point is the temperature at which almost all the sigma bonds are broken (7).

In order to prove these assumptions, we have prepared and studied the complexes formed between $TiCl_4$ and ethyl acetate, ethyl monochloroacetate, ethyl dichloroacetate, and ethyl trichloroacetate.

In a previous paper (3), it was postulated that the 1:1 addition compounds of monoester to titanium tetrachloride were due to the formation of a four-membered-ring chelate in which the two oxygens of the monoester were involved in coordination. It seemed of interest, then, to prepare some complexes in which the alkyl radical was substituted. β-Chloroethyl acetate was used for that purpose.

EXPERIMENTAL

Materials and Manipulations

Reagent grade titanium tetrachloride was purified by the method of Gilchrist (9), redistilled, and the medium fraction was used for our experiments.

The esters were dried over molecular sieves and used as such. The solvents used were normal hexane and methylene chloride, both of which were made absolutely dry by appropriate methods: normal hexane was kept dry with sodium wire, and methylene chloride, after being dried with phosphorus pentoxide, was distilled and kept in a dry box of very low humidity.

The complexes prepared were very sensitive to moisture and were, to avoid humidity, handled in the manner described in an earlier paper (8). The methods of analyses of titanium and chlorine have been described previously (8).

The infrared spectra measurements were carried out on a Perkin–Elmer infrared spectrophotometer,

Model 21, using a sodium chloride prism. The spectra were taken in solutions of suitable solvents and as nujol mulls.

Preparation of the Complexes

The preparation of these complexes was performed in normal hexane with solutions of the reactants ranging in concentration from 10 to 25%. The complexes prepared were yellow powders. The analytical results indicate that except for β-chloroethyl acetate, all the complexes are of 1:1 stoichiometric composition. Preparation of complexes of other molecular ratios have failed except for the specific case mentioned above. The analytical results of these complexes are included in Table I.

TABLE I

Analytical results

Ester in the complex	% Ti		% Cl (ionizable)		Melting point (°C)
	Theor.	Found	Theor.	Found	
CH_3CO_2Et*	17.24	17.28	51.0	50.85	110–111
CH_2ClCO_2Et	15.34	15.23	45.4	44.11	109–111
$CHCl_2CO_2Et$	13.81	13.40	40.94	41.05	82–84
CCl_3CO_2Et	12.56	12.48	37.21	37.20	23–24
$CH_3CO_2CH_2CH_2Cl$ (1:1 adduct)	15.34	14.60	45.40	44.82	78–80
$CH_3CO_2CH_2CH_2Cl$ (1:2 adduct)	11.02	11.50	32.61	32.60	74–76

*Et = ethyl.

INFRARED SPECTRA AND STRUCTURAL DISCUSSION

Nolin and Jones (10, 11) have studied extensively the spectra of methyl acetate and ethyl acetate, and by selective deuteration they were able to assign most of the infrared absorption frequencies. Lappert (12) has discussed also the infrared spectra of the carboxylic esters as ligands. From these papers it seemed that the infrared spectra of these esters contain three absorption bands that can be easily identified and that are likely to be influenced by coordination. These bands are the carbonyl stretching frequency at 1741 cm^{-1} and two skeletal vibrations, one at 1238 cm^{-1} and the other one at 1046 cm^{-1}, all these bands being from the spectrum of liquid ethyl acetate.

According to this skeleton:

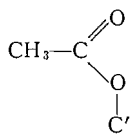

C—O would be represented by the 1238 cm^{-1} frequency, and C′—O by the 1046 cm^{-1} band. In the spectra of the complexes with halogenated esters as donor bases, it has not been possible to assign with reasonable certainty the band attributed to C—O in the 1250 cm^{-1} region because of the large number of bands with similar intensities in this region. However, the carbonyl frequencies ν_1 and C′—O frequencies ν_2 could be assigned easily and are given in Table II.

From this table, it can be seen that the presence of halogens in the acid or in the alkyl radical strongly influences the position of the two bands mentioned. The electronic pull of the chlorines decreases the double-bond character of the carbonyl bond and decreases the electronic density of the other bond. This effect is dependent upon the number of halogens on the acid radical, as is illustrated in Fig. 1. A bathochromic effect of ν_1 varying from 9 to 20 cm^{-1} and of ν_2 varying from 20 to 27 cm^{-1} is observed.

TABLE II

Infrared spectra in nujol mulls

Ester used in complex formation	Carbonyl stretching frequency (cm^{-1})		Shift (cm^{-1})	Stretching frequency of C'—O (cm^{-1})		Shift (cm^{-1})	Nature of adduct
	Pure ester	Complex		Pure ester	Complex		
Ethyl acetate	1748	1600	148	1052	1006	46	1:1
Ethyl monochloro-acetate	1757	1625	132	1032	998	34	1:1
Ethyl dichloroacetate	1762	1653	109	1027	1002	25	1:1
Ethyl trichloroacetate	1768	1663	105	1025	1015	10	1:1
β-Chloroethyl acetate	1748	1650	98	1043	1027	16	1:1
β-Chloroethyl acetate	1748	1650	98	1043	1033	10	1:2

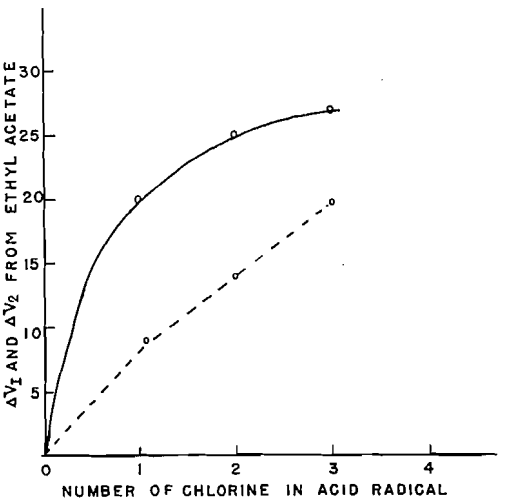

FIG. 1. Variation of the carbonyl stretching frequency and of the C—O frequency with respect to the number of chlorines in the acid radical; – – – $\Delta\nu_1$ variation, —— $\Delta\nu_2$ variation.

Walsh (13) and Cook (14) have proposed a relation between the ionization potential (IP) and the corresponding stretching frequency of a carbonyl group:

$$\nu_{C=O} = 49.351IP + 1249 \text{ cm}^{-1}. \quad [1]$$

This equation indicates that the smaller the carbonyl stretching frequency the smaller will be the ionization potential. Since the ionization potential is an indication of the electron availability, the smaller it is, the better will be the oxygen as a donor atom.

Since coordination to a Lewis acid usually causes a negative shift of the carbonyl frequency, the value of the shift should parallel the decrease in basic strength of the oxygen. Figure 2 is a plot of the bathochromic effect as a function of the number of chlorines on the acid radical. It indicates very clearly that the basicity decreases with an increase in the degree of halogen substitution. This is also indicated by a decrease in melting points, as shown in Table I. The fact that the melting point indicates breakage of the coordination bond can be illustrated by using the infrared spectrum of a complex taken at a temperature which is very close to its melting point. Ethyl trichloroacetate complex melting at 23–24° C was chosen for that purpose. Its infrared spectrum measured at room temperature is illustrated in Fig. 3; a peak in the 1768 cm^{-1} region due to the

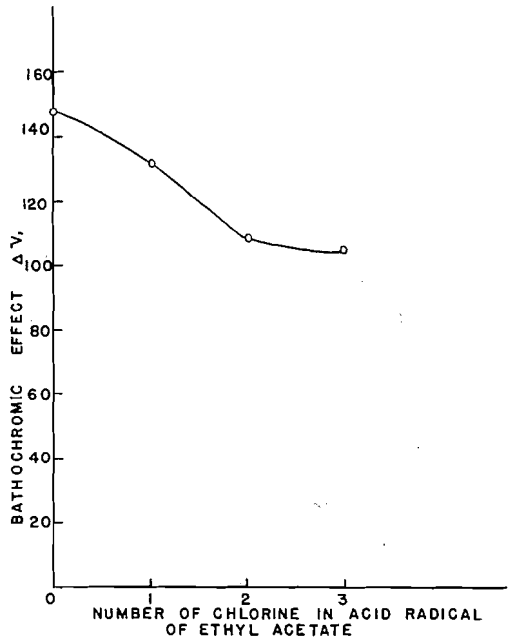

FIG. 2. Variation of the bathochromic effect as a function of the number of chlorines in the acid radical.

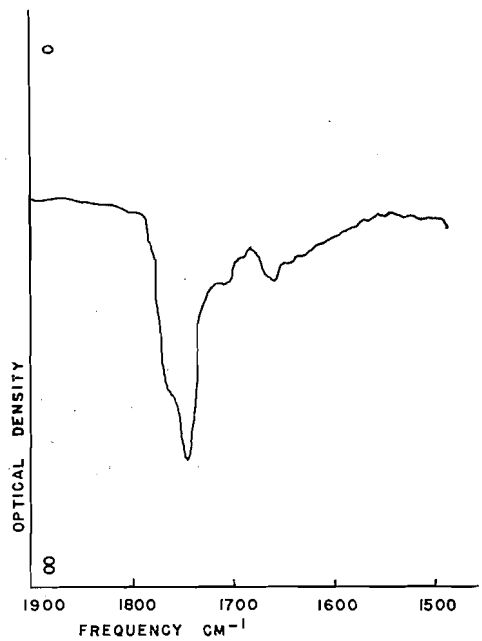

FIG. 3. Infrared spectrum of the trichloroacetate complex in nujol.

free ester is quite prominent in comparison with the one at 1663 cm^{-1} due to coordinated carbonyl group, thus indicating a very strong dissociation. This observation does not fit with the proposed reactions of Lysenko and Osipov (15), in which they presupposed that the dissociation in the liquid state proceeds according to the following scheme:

$$[TiCl_4.E]_2 \rightleftarrows [TiCl_2.2E][TiCl_6] \rightleftarrows [TiCl_2.2E]^{2+} + [TiCl_6]^{2-} \quad [2]$$

$$[TiCl_4.2E]_2 \rightleftarrows [TiCl_2.4E][TiCl_6] \rightleftarrows [TiCl_2.4E]^{2+} + [TiCl_6]^{2-}. \quad [3]$$

If this scheme were true, no uncoordinated carbonyl absorption bands would be observed in the infrared spectra of the species in the liquid state or in solution. Since we could not take the infrared spectra of all the complexes in the liquid state, we have taken them as solutions in methylene chloride. The results appear in Table III and are illustrated in Fig. 4. They indicate very clearly that as the melting point is approached, dissociation increases, this dissociation giving, always, uncoordinated carbonyl group.

TABLE III

Bathochromic effect of the carbonyl stretching frequency in methylene chloride solution

Ester in the complex	Carbonyl stretching frequency of C=O (cm^{-1})		Shift (cm^{-1})
	Pure ester	Complex	
CH_3CO_2Et	1738	1632	106
CH_2ClCO_2Et	1745	1650	95
$CHCl_2CO_2Et$	1755	1676	79
CCl_3CO_2Et	1765	1725	43
$CH_3CO_2CH_2CH_2Cl$	1745	1652	93

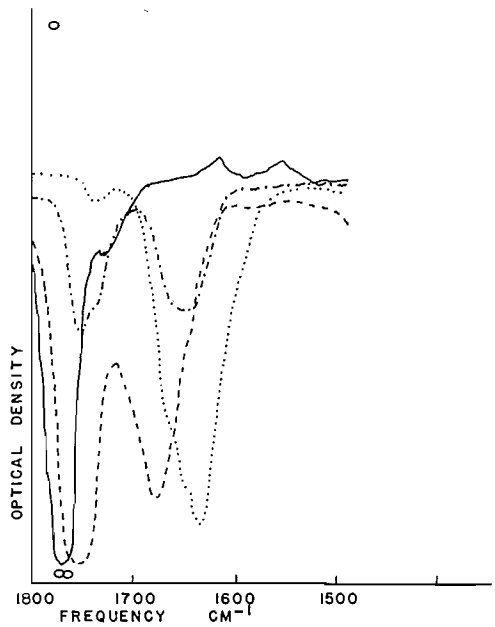

FIG. 4. Infrared spectra of the complexes in methylene chloride solutions; . . . ethyl acetate complex, •—• monochloroacetate complex, – – – dichloroacetate complex, —— trichloroacetate complex.

When the position of chlorine is shifted from the acid radical to the alkyl radical of the ester, the infrared spectra and the melting points again indicate some change in the donor properties of the ester. In Table IV, a comparison between complexes formed with

TABLE IV

Comparative data on addition complexes with isomeric esters (in nujol)

Ester in the complex	Shift in carbonyl stretching frequency (cm^{-1})	Shift in C—O stretching frequency (cm^{-1})	Melting point (°C)	Nature of adduct
$CH_2ClCOOEt$	132	34	109–110	1:1
$CH_3COOCH_2CH_2Cl$	98	16	78–80	1:1
$CH_3COOCH_2CH_2Cl$	98	10	74–76	1:2

isomeric esters, it is indicated that ethyl chloroacetate forms only a 1:1 addition compound. This was always observed even in experiments in which a large excess of the ester was used. This is different from the β-chloroethyl acetate, which gives 1:1 and 1:2 complexes. If one assumes that in the 1:1 addition compound there is formation of a four-membered-ring chelate, it is quite reasonable to believe that the replacement of one hydrogen by one chlorine would lead to a weaker coordinated bond of the oxygen of the ether group and facilitate the formation of the 1:2 complex.

ACKNOWLEDGMENT

The authors are indebted to the National Research Council of Canada for support of this work.

SOMMAIRE

Des complexes de coordination entre le tétrachlorure de titane et quelques monoesters chlorés ont été préparés. Les spectres infrarouges de ces complexes et leurs points de fusion indiquent que la force du lien de coordination diminue avec l'augmentation du nombre de chlores contenus dans le radical acide. Si la substitution a lieu sur le radical alkyl, il est possible de préparer des complexes de formule $TiCl_4.2$ ester, parce que la substitution d'un chlore à un hydrogène diminue les propriétés basiques de l'oxygène éthéré du ligand.

REFERENCES

1. E. Demarçay. Bull. Soc. Chim. France, **20**, 127 (1873).
2. D. C. Bradley, D. C. Hancock, and W. Wardlaw. J. Chem. Soc. 2773 (1952).
3. E. Rivet, R. Aubin, and R. Rivest. Can. J. Chem. **39**, 2343 (1961).
4. N. S. Kurnakov and E. B. Shternin. Bull. Acad. Sci. U.R.S.S. Classe Sci. Math. Nat., Ser. Khim. 467 (1936).
5. O. A. Osipov. Zh. Obshch. Khim. **26**, 322 (1956).
6. O. A. Osipov and V. Suchkov. Zh. Obshch. Khim. **22**, 1132 (1952).
7. J. Archambault. Ph.D. Thesis, University of Montreal, Montreal, Que. 1959. p. 73.
8. J. Archambault and R. Rivest. Can. J. Chem. **36**, 1331 (1960).
9. W. S. Clabaugh, R. T. Leslie, and R. Gilchrist. J. Res. Natl. Bur. Std. **55**, 261 (1955).
10. B. Nolin and R. N. Jones. Can. J. Chem. **34**, 1382 (1956).
11. B. Nolin and R. N. Jones. Can. J. Chem. **34**, 1392 (1956).
12. M. F. Lappert. J. Chem. Soc. 817 (1961).
13. A. D. Walsh. Trans. Faraday Soc. **43**, 158 (1947).
14. D. Cook. J. Am. Chem. Soc. **80**, 49 (1958).
15. Y. A. Lysenko and O. A. Osipov. Russ. J. Inorg. Chem. (English Transl.), 847 (1961).

STUDIES ON THE MECHANISM OF PERSULPHATE-INITIATED GRAFTING ONTO CELLULOSE

S. M. SANKALIA, D. K. RAY CHAUDHURI,* AND J. J. HERMANS†

Cellulose Research Institute, State University, College of Forestry, Syracuse, N.Y., U.S.A.

Received July 11, 1962

ABSTRACT

When the polymerization of vinyl acetate or acrylonitrile is initiated by persulphate in the presence of cellophane, grafting onto the cellulosic backbone occurs. This is proved by comparing the graft with a physical mixture of cellulose and homopolymer.

Some aspects of the mechanism of this grafting are studied by means of model compounds, in particular pinacol. It is found that the rate of polymerization of acrylonitrile initiated by persulphate is increased by the addition of pinacol, but decreases on addition of more pinacol. This may be explained by assuming that the radicals formed from the pinacol can terminate each other and that this reaction competes with the reaction between these radicals and the monomer. The amount of acetone formed by the persulphate oxidation of pinacol at low pinacol concentrations is about 0.5 mole per mole persulphate and decreases with increasing pinacol concentration. This indicates complexities that do not exist in the ceric ion oxidation of pinacol.

INTRODUCTION

It has been shown by Kolthoff and Miller (1) that the decomposition of persulphate ions produces sulphate ion radicals according to a first-order reaction. In addition, a decomposition takes place that does not produce radicals, but the rate of this second process is very small compared with that of the first when pH > 4.

Methanol accelerates the decomposition of persulphate (2), and it was shown by Kolthoff, Meehan, and Carr (3) that this is due to a reaction between persulphate ions and alcohol radicals (reaction [3]). This is demonstrated by the fact that the rate of

$$S_2O_8^{=} \rightarrow 2SO_4^{-}\cdot\text{; rate constant } k_0 \qquad [1]$$

$$SO_4^{-}\cdot + \text{Alc} \rightarrow HSO_4^{-} + \text{Alc}\cdot\text{; rate constant } k_1 \qquad [2]$$

$$\text{Alc}\cdot + S_2O_8^{=} \rightarrow \text{aldehyde} + HSO_4^{-} + SO_4^{-}\cdot \qquad [3]$$

decomposition of persulphate is reduced to the much lower value observed in the absence of methanol when a monomer is added to the system. In this case, the SO_4^{-} radicals produced by reaction [1] react with the monomer:

$$SO_4^{-}\cdot + M \rightarrow P\cdot\text{; rate constant } k_i. \qquad [4]$$

P· represents the polymer radical. This has been interpreted as meaning that reaction [2], and therefore also reaction [3], are suppressed. It is also possible, however, that only reaction [3] is suppressed and that the alcohol radicals react with monomer. This has an obvious bearing on the question as to whether polymerization initiated by persulphate in the presence of cellulose, starch, or other polyalcohols leads to grafting onto the polyalcohol. Haydel *et al.* (4) reported experiments with cotton in acrylonitrile vapor, but they refer to the process as deposition in and coating of the cotton, without investigating whether grafting occurred. Hayes (5) reported that grafting took place when the (emulsion) polymerization of butadiene was initiated by persulphate in the presence of highly cross-linked butadiene, and attributed this result to chain transfer. In principle, it cannot be excluded that chain transfer from a growing polymer chain to cellulosic

*Ontario Research Foundation, 43 Queen's Park, Toronto, Ontario.
†Present address: Chemstrand Research Center, Inc., Durham, N.C.

molecules (6) also takes place. However, cellulosic radicals may also be formed directly, since reaction [2] between SO_4^- radicals and methanol suggests that a similar reaction occurs between SO_4^- radicals and cellulose. The cellulosic radical formed could then initiate polymerization and form a graft. On the basis of the reactions established by Kolthoff, Meehan, and Carr, it may be expected that the likelihood of this type of grafting is determined by a competition between cellulose and monomer. For grafting to occur, it is necessary that reaction [2] takes place to an appreciable extent even when monomer is present and that the alcoholic radicals formed take part in the initiation of the polymerization. It may be expected, therefore, that the result will depend on the conditions of the experiment.

GRAFTING ONTO CELLOPHANE

Gel cellophane was soaked in an aqueous solution of persulphate and subsequently brought into contact with pure monomer. It is believed that this procedure creates conditions favorable to grafting. Since the monomer is a poor solvent for the persulphate, only small amounts of catalyst will diffuse from the gel into the monomer phase, so that little if any homopolymer is formed outside the cellophane. The concentration of cellulose in the gel being high, the rate of reaction [2] is large, so that the monomer which diffuses into the gel finds a high concentration of cellulosic radicals with which to react.

All experiments were done in a nitrogen atmosphere. After completion of the reaction, the film was thoroughly extracted with a solvent for the homopolymer, then dried in a vacuum oven at 60° C for 48 hours and weighed. The results are given in Table I. It is possible that part of the weight increase is due to homopolymer that could not be removed by solvent extraction. The following experiment shows, however, that an appreciable amount of graft was formed.

TABLE I

Monomer	c	Reaction time (hr)	Reaction temp. (°C)	G	H
Vinyl acetate	0.1	1.5	60	40.5	0.7
Vinyl acetate	0.1	1.5	50	15.4	
Vinyl acetate	0.1	4.8	60	80.7	1.0
Vinyl acetate	0.2	1.5	60	70.0	1.0
Acrylonitrile	0.1	0.4	50	84	2.7

NOTE: c = concentration of persulphate solution (mole/l.) used to soak film; G = % weight increase of film on basis of dry weight of cellophane; H = % homopolymer, on basis of total monomer used.

The product containing 80 g polyvinyl acetate per 100 g dry cellulose was hydrolyzed with 0.25 N alcoholic sodium hydroxide solution at about 50° C for 20 hours. This was done under nitrogen to minimize degradation of the cellulose. After conversion of the polyvinyl acetate chains to polyvinyl alcohol, the product was completely soluble in cupriethylenediamine. On acidifying this solution with 4% HCl, a precipitate resulted, which was washed with rochelle salt solution and then water. The infrared spectrum (KBr pellet) showed absorption in the region 12–13 μ, due to the presence of polyvinyl alcohol in the precipitate. This absorption is absent when the same procedure is followed with a physical mixture of 1 g dry cellophane and 0.8 g polyvinyl acetate. It follows that at least part of the weight increase was due to grafting.

To learn more about the possible mechanism of this grafting, studies were made with low molecular weight model compounds, as described in the next section.

STUDIES WITH LOW MOLECULAR WEIGHT COMPOUNDS

1. Serine Methyl Ester

The oxidation of the hydrochloride of serine methyl ester by persulphate in aqueous solution produces formaldehyde, as indicated by the color reaction with chromotropic acid (7). This suggests that the following radical is formed:

$$HOCH_2—\underset{\displaystyle NH_3Cl}{\underset{|}{CH}}—COOCH_3 \longrightarrow \cdot\underset{\displaystyle NH_3Cl}{\underset{|}{CH}}—COOCH_3.$$

Since this radical contains both an amine and an ester end group, it opens a possibility for checking whether this radical initiates polymerization. To explore this possibility, serine methyl ester was reacted with persulphate in the presence of acrylonitrile. The polymer formed was washed carefully. Infrared absorption revealed that it contained both NH_2 and $COOCH_3$ groups.

2. Pinacol

Pinacol was chosen as a model substance because its oxidation by ceric ions in aqueous solution has been studied in detail by Mino, Kaizerman, and Rasmussen (8), who found that in the absence of a monomer, each mole of ceric ion that is reduced to cerous ion produces 1 mole of acetone. In the presence of a monomer only half this amount of acetone is formed. This is explained by the following mechanism:

$$(CH_3)_2C(OH)—C(OH)C(CH_3)_2 + Ce^{IV} \rightarrow (CH_3)_2CO + \cdot C(OH)(CH_3)_2 + Ce^{III} + H^+.$$

In the absence of a monomer, the radical formed is oxidized to acetone by one more mole of Ce^{IV}, but when sufficient monomer is present, the alcoholic radical is used up to initiate the polymerization, and a second mole of ceric ion is used in the termination step without producing any acetone. For details see reference 8. It was hoped that similar, clear-cut, results would be found when pinacol was oxidized by persulphate.

Pinacol (Eastman Kodak) was purified by distillation at atmospheric pressure (b.p. 169.5–170.5° C). Acrylonitrile (Eastman Kodak) was freshly distilled, likewise at atmospheric pressure (b.p. 76.5–77.5° C), at the beginning of each experimental run when the solutions were prepared. The persulphate was Certified Fisher Reagent, 99.5% pure by iodometric titration (9). The reagents used for the titration were of Analytical Reagent grade.

All the experiments were carried out in a nitrogen stream at 50° C, in the presence of 0.05 *M* phosphate buffer, pH = 7. Loss of water or monomer was prevented by means of a reflux condensor. Samples were withdrawn at various times for analysis. In those cases in which acrylonitrile was present, the polymer formed precipitated. It was washed, dried, and weighed.

Table II shows the rate of persulphate decomposition under various conditions. The possible experimental error in this rate is about 10%. It is seen that the rate is increased by the presence of pinacol when no monomer is present, but this acceleration is very much smaller than that caused by methanol (3). When monomer is added, the rate of persulphate decomposition in the presence of pinacol is reduced again to that observed in the absence of pinacol. It even appears to drop slightly below this value, although it is not certain that this effect is outside the experimental error.

Figure 1 shows the monomer conversion as a function of time under the conditions listed in Table II. The inset in Fig. 1 gives the amount of polymer formed after 4 hours as a function of pinacol content, showing that the rate of polymerization first increases but subsequently decreases with increasing pinacol concentration.

TABLE II

Rate of decomposition (% per hour) of 0.01 *M* persulphate in various mixtures at 50° C, pH = 7

Pinacol (mole/l.)	Acrylonitrile (mole/l.)	Rate (% per hr)
0	0	0.79
0.05	0	1.17
0.10	0	1.30
0	0.3	0.72
0.05	0.3	0.71
0.10	0.3	0.67
~0.3	0.3	0.65

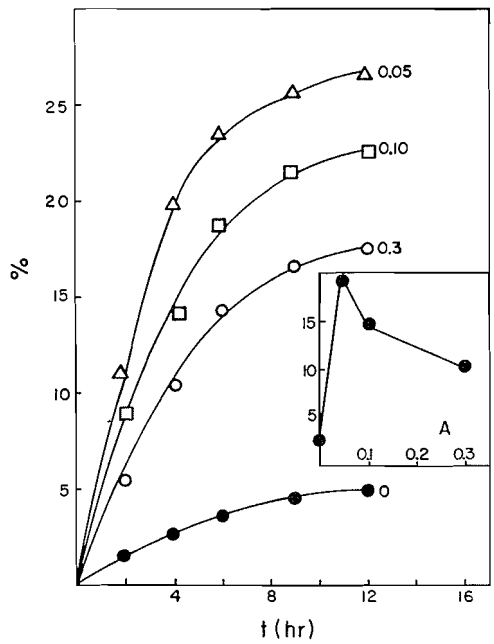

FIG. 1. Percent conversion of monomer as a function of time for pinacol concentrations 0–0.05–0.1 and about 0.3 *M*. Inset: % conversion after 4 hours as a function of pinacol concentration.

Some attempts were made to determine the amount of acetone formed, using the spectrophotometric method of Behre and Benedict (10). In analogy with the oxidation by ceric ions (8), it was hoped that the principal reaction would be

$$SO_4^{-}\cdot + (CH_3)_2C(OH)—C(OH)C(CH_3)_2 \rightarrow HSO_4^{-} + (CH_3)_2\dot{C}OH + (CH_3)_2CO,$$

followed, perhaps, by further oxidation (to acetone) of the radical formed. If this were correct, the amount of acetone produced for every mole of persulphate decomposed would be at least 2 mole. It was found, however, that only about 1/2 mole of acetone was formed for every mole of persulphate reduced when the pinacol concentration was 0.05 *M* and that this figure was decreased to about 1/3 mole acetone when the pinacol concentration was increased to 0.1 *M*. The persulphate concentration in both cases was 0.01 *M*, pH = 7, temp. 50° C. The result shows that some of the sulphate ion radicals are ineffective in the oxidation of pinacol (compare reaction [5] below) or else that products other than acetone are formed.

3. Glucose

The results with pinacol, although qualitatively similar to those found for methanol (3), suggest that, quantitatively, different alcohols may differ considerably in their behavior toward persulphate. A study with D-glucose showed that this alcohol, like the others, increased the rate of decomposition of persulphate. This effect was of the same order of magnitude as that observed with pinacol, but the addition of acrylonitrile this time did not reduce the rate of persulphate decomposition to the value found in the absence of glucose. The measurements were done at pH = 7 and at 50° C in an aqueous solution of persulphate, 0.01 *M*, and acrylonitrile, 0.3 *M*. In the presence of 0.1 *M* D-glucose, the rate of persulphate decomposition was 1.18% per hour. In the presence of 0.3 *M* glucose it was 1.83% per hour. These figures are to be compared with the value of about 0.7 in the absence of glucose (see Table II). The monomer conversion was the same within experimental error: about 30% after about 10 hours in both experiments.

DISCUSSION

In analogy with the mechanism proposed by Kolthoff, the following tentative explanation of the data is suggested.

Sulphate ion radicals are produced by reaction [1]. In the absence of reducing agents, these radicals disappear:

$$2SO_4^-\cdot \rightarrow \text{end products; rate constant } \lambda. \qquad [5]$$

The details of this reaction will not be considered. It may involve reaction with water under formation of OH radicals, which subsequently form H_2O_2. This would mean that one may have to consider reactions of alcohol and monomer with OH radicals instead of (or in addition to) reactions with $SO_4^-\cdot$. The reaction scheme would then become quite complicated, but the general conclusions arrived at would not be affected.

Reaction [3] accounts for the fact that the rate of decomposition of persulphate is increased by the presence of pinacol. This effect is not very large and is suppressed by acrylonitrile. The increase in the rate of polymerization on addition of alcohol indicates that reaction [2] is not suppressed. Alcohol radicals are formed and become progressively more important in the initiation step:

$$\text{Alc}\cdot + \text{M} \rightarrow \text{P}\cdot; \text{ rate constant } k_i'. \qquad [6]$$

However, as the concentration of these alcohol radicals is increased, there will also be an increased rate of termination, and this radical-destroying reaction,

$$2\text{Alc}\cdot \rightarrow \text{end products; rate constant } \mu, \qquad [7]$$

may eventually become so important that the rate of polymerization decreases again. This could explain why the rate of polymerization—although increased by the addition of pinacol—is decreased again on addition of more pinacol. This argument can be given in more quantitative terms, as follows. If we add the termination step

$$\text{P}\cdot + \text{P}\cdot \rightarrow \text{polymer; rate constant } k_t, \qquad [8]$$

the kinetics are supposed to be fully described by the reactions [1]–[8]. Of these reactions, [3] is suppressed by the presence of the monomer and will therefore be omitted. Then, if c is the concentration of persulphate, A that of the alcohol, m that of monomer, and if x, y, and r represent the concentrations of $SO_4^-\cdot$ radicals, alcohol radicals, and polymer radicals respectively,

$$2k_0c - 2\lambda x^2 - k_1Ax - k_tmx = 0 \qquad [9]$$

$$-2\mu y^2+k_1Ax-k_i'my = 0 \quad [10]$$

$$k_imx+k_i'my-2k_tr^2 = 0 \quad [11]$$

$$-dm/dt = m(k_ix+k_i'y+k_pr), \quad [12]$$

where k_p is the propagation rate constant. The equations [9], [10], and [11] give the expressions for dx/dt, dy/dt, and dr/dt respectively. They have been equated to zero on the (usual) assumption that "quasi steady state" conditions prevail. Eliminating r from equations [11] and [12], it is seen that the rate of polymerization for a given value of m is determined by the quantity

$$R = k_ix+k_i'y, \quad [13]$$

namely:

$$-dm/mdt = R+CR^{1/2},$$

where

$$C = k_p(m/2k_t)^{1/2}.$$

It will be shown that R increases on addition of alcohol but may decrease again on the addition of more alcohol. To this end, equations [9] and [10] are differentiated with respect to A at constant c and m. From the equations obtained one can solve for dx/dA and dy/dA, with the result

$$dx/dA = -(k_ix/N)(4\mu y+k_i'm) \quad [14]$$

$$dy/dA = (k_ix/N)(4\lambda x+k_im) \quad [15]$$

$$N = (4\mu y+k_i'm)(4\lambda x+k_im+k_iA).$$

This shows that dx/dA is negative and dy/dA positive for all values of A. Using the definition of R given in equation [13], it follows from equations [14] and [15] that

$$dR/dA = (4k_ix/N)(\lambda k_i'x-\mu k_iy). \quad [16]$$

At low alcohol concentrations, y is small so that dR/dA is positive. However, on increasing A, we know that x decreases and y increases, so that dR/dA will become smaller and may eventually become negative. This is the behavior found in Fig. 1 (inset).

CONCLUSION

The considerations in the preceding section are semiquantitative, because only a limited number of the possible reactions have been considered. A more complete reaction scheme would not, however, change the nature of the conclusions arrived at. The increase and subsequent decrease in the rate of polymerization when the pinacol concentration is increased may thus be considered as a natural consequence of the reactions involved.

These same reactions may have a bearing on the observation that the amount of acetone formed per mole of persulphate reduced decreases when the pinacol concentration is increased, but this statement is only tentative because the mechanism of the oxidation of pinacol by persulphate is not clear.

If our conjectures are correct, the results with glucose mean that in this case the reaction [3] is not suppressed by the presence of the monomer, even though the rate of polymerization is increased by the presence of the glucose. It must be borne in mind

that the oxidation of glucose by persulphate may be a complicated reaction in which several oxidation products and quite a few intermediates are formed. Any detailed speculation would be premature at the present stage.

The results obtained with the low molecular weight compounds indicate that grafting onto polymeric alcohols by the mechanism suggested in the introduction—although not firmly established—may be considered as a very likely process.

ACKNOWLEDGMENT

One of us (S. M. S.) is indebted to Morning Star Paisley, Hawthorne, N.J., for a grant-in-aid.

REFERENCES

1. I. M. KOLTHOFF and I. K. MILLER. J. Am. Chem. Soc. **74,** 4419 (1952).
2. C. MARIE and L. J. BUNEL. Bull. Soc. Chim. Paris, Ser. 3, **29**, 930 (1903).
3. I. M. KOLTHOFF, E. J. MEEHAN, and E. M. CARR. J. Am. Chem. Soc. **75**, 1439 (1953).
4. C. H. HAYDEL, H. J. JANSSEN, J. F. SEAL, H. L. E. VIX, and E. A. GASTROX. Textile Res. J. **27,** 975 (1957).
5. R. A. HAYES. J. Polymer Sci. **13**, 583 (1954).
6. D. K. RAY CHAUDHURI and J. J. HERMANS. J. Polymer Sci. **51**, 373 (1961).
7. C. E. BRICKER and H. R. JOHNSON. Ind. Eng. Chem., Anal. Ed. **17**, 400 (1945).
8. G. MINO, S. KAIZERMAN, and E. RASMUSSEN. J. Am. Chem. Soc. **81**, 1494 (1959).
9. I. M. KOLTHOFF and E. M. CARR. J. Am. Chem. Soc. **25**, 208 (1953).
10. J. A. BEHRE and S. R. BENEDICT. J. Biol. Chem. **70**, 487 (1926); **136**, 25 (1940).

HYDROLYSIS PRODUCTS OF PERIODATE-OXIDIZED PHOSPHOMANNAN Y-2448

ALLENE JEANES, J. E. PITTSLEY, P. R. WATSON, AND J. H. SLONEKER

Northern Regional Research Laboratory, Northern Utilization Research and Development Division, Agricultural Research Service, U.S. Department of Agriculture, Peoria, Ill., U.S.A.

Received May 17, 1962

ABSTRACT

Sequences of at least three α-1,3-linked mannose units have been shown to occur in phosphomannan Y-2448 through isolation of 3-O-[3-O-(α-D-mannopyranosyl)-α-D-mannopyranosyl]-D-mannose from partial acid hydrolyzates of both the native and the periodate-oxidized phosphomannan. 3-O-(α-D-Mannopyranosyl)-D-mannose has been obtained also. The mannosidic bond in these oligosaccharides appears to be more stable to acid hydrolysis than that by which the mannose 6-phosphate unit is held in this macromolecular polysaccharide derivative. It has been established that the D-mannose 6-phosphate unit is oxidized by periodate and that orthophosphate is the form which occurs in this phosphomannan.

The phosphomannan produced exocellularly by the yeast *Hansenula holstii* NRRL Y-2448 and isolated as the potassium salt is comprised of D-mannose, phosphate, and potassium in the molar ratio of 5:1:1 (1). The phosphate occurs in diester linkage between the carbon-6 position of one mannose unit (2) and the carbon-1 hemiacetal position of another (1, 2). Periodate oxidation indicates that 33% of the D-mannose units are linked through carbons-1 and -2, and 47% through carbons-1 and -3 (3).

Data from periodate oxidation of this phosphomannan indicate that significant structural information as well as saccharides heretofore unavailable might be obtained through hydrolysis of the periodate-oxidized product (3). The fact that inorganic phosphate could be eliminated by alkali from the periodate-oxidized but not from the native phosphomannan offered a means of establishing the form, either ortho or pyro, in which phosphate occurs in this unusual polysaccharide derivative. The absence of D-mannose 6-phosphate from among the products of acid hydrolysis would confirm other indications that this unit was oxidized by periodate (3). The fact that the mannose units were α-linked and that about 47% of them were inert to oxidation indicated an attractive source from which α-1,3-linked mannose oligosaccharides might be obtained by mild acid hydrolysis. Previously, 3-O-(α-D-mannopyranosyl)-D-mannose has been obtained only by acid reversion of D-mannose (4). Other members of this homologous series have not been reported.

RESULTS AND DISCUSSION

The form of phosphate that occurs in phosphomannan Y-2448 was shown to be ortho. Inorganic orthophosphate was demonstrated in phosphomannan which had been oxidized by periodate and subsequently treated with alkali, by paper chromatography and by a selective method of phosphorus analysis (5, 6). To avoid the possibility of hydrolysis of pyrophosphate, if it had been present, the conditions for all chemical reactions and physical operations were those under which inorganic pyrophosphate controls had been shown to be stable.

Several observations attested that the D-mannose 6-phosphate unit of phosphomannan Y-2448 is oxidized by periodate. Paper chromatography showed that this unit was not

among the products of autohydrolysis or of formic acid hydrolysis of the periodate-oxidized phosphomannan. Low molecular weight organic phosphate (possibly phosphoglyceraldehyde) and inorganic orthophosphate appeared during early stages of hydrolysis. Hydrolysis liberated inorganic orthophosphate from periodate-oxidized phosphomannan more rapidly and much more completely than from native phosphomannan.

Preliminary observations on acid hydrolysis of native phosphomannan (hydrogen form) showed that in 5 *N* formic acid at 100° C, maximum reducing power was reached in about 36 hours at a value 95% of that expected for complete hydrolysis to mannose. Products present at this time were D-mannose, D-mannose 6-phosphate, some inorganic orthophosphate, and traces of neutral oligosaccharides. After only 6 hours' hydrolysis under these conditions, substantial amounts of neutral di-, tri-, and tetra-saccharides were present in the hydrolyzate (Table I). Other work (2) has shown that the initial

TABLE I

Neutral saccharides in hydrolyzates of native and periodate-oxidized phosphomannan Y-2448*

Degree of polymerization	Native, hydrolyzed 5 *N* formic acid, 6 hours, 100° C		Periodate-oxidized, autohydrolyzed 72 hours, 100° C	
	Ratio by wt.	Mole ratio	Ratio by wt.	Mole ratio
1†	1.00‡	1.00	1.00‡	1.00
2	0.64	0.33	0.94	0.50
3	0.55	0.19	1.15	0.41
4	0.25	0.07	0.04	0.01
Higher	1.05	—	0.02	—

*Determined by quantitative paper chromatography.
†D-Mannose.
‡The weight of D-mannose found was assigned the value "1.00".

action of acid on native phosphomannan Y-2448 liberates oligosaccharide phosphomonoesters and that further hydrolysis produces D-mannose 6-phosphate in high yields.

When hydrolyzed in 5 *N* formic acid, the periodate-oxidized phosphomannan appeared to reach any given stage of partial hydrolysis about twice as fast as the native phosphomannan. When autohydrolyzed, the periodate-oxidized product depolymerized slowly enough that good yields of neutral di- and tri-saccharides were obtained (Table I). Autohydrolysis of the native phosphomannan progressed even more slowly, but permitted accumulation in hydrolyzates of neutral saccharides of D.P. 2, 3, and 4; at early stages of hydrolysis traces of a saccharide of D.P. 5 were also apparent. The neutral oligosaccharides from native and periodate-oxidized phosphomannans displayed identical chromatographic behavior.

These observations indicate that native phosphomannan Y-2448 has some sequences of at least four neutral mannose units and that these, as well as sequences of three units, are freed rather readily from mannose 6-phosphate units, which are believed to have been attached to (or near) them (3). Liberation of these neutral oligosaccharides apparently is not dependent on hydrolysis of the carbon-6 phosphate–ester bond since, under the conditions of hydrolysis (Table I), mannose 6-phosphate was found in the hydrolyzate of the native phosphomannan but essentially no inorganic phosphate was present. Thus, the glycosidic bond by which mannose 6-phosphate units are attached to mannose units seems more labile to hydrolysis than the bond joining the neutral mannose units. This appears to be contrary to the reported stabilization by phosphate of galactosidic bonds in di- and tri-saccharides terminated by galactose 6-phosphate (7).

In periodate-oxidized phosphomannan, the maximum sequence of units inert to periodate is restricted almost exclusively to three (Table I). Apparently, one unit in the sequence of four observed in the native phosphomannan has been oxidized by periodate. This possibility is in keeping with other structural details on phosphomannan Y-2448 (Fig. 1 of reference 3) as is also the indication (Table I) that the di-, tri-, and possibly even the mono-saccharides may originate mainly as blocks from the periodate-oxidized phosphomannan.

The identity of the neutral di- and tri-saccharides has been established as 3-O-(α-D-mannopyranosyl)-D-mannose and 3-O-[3-O-(α-D-mannopyranosyl)-α-D-mannopyranosyl]-D-mannose, respectively. The relatively high specific optical rotations, +57.6° and +79.8°, correlate with α-configurations. The specific optical rotation of the disaccharide is higher than that reported previously (4) and is the same as one (8) of the two values (4, 8) reported for 6-O-(α-D-mannopyranosyl)-D-mannose. However, lead tetraacetate oxidation (10) by a technique based on that of Perlin (11) gave results for the disaccharide in agreement with those previously reported for 3-O-(α-D-mannopyranosyl)-D-mannose (9) obtained by acid reversion of D-mannose (4), that is, about 1.6 moles of carbon dioxide were given off in 6 hours and D-arabinose was identified among the hydrolyzed oxidation products after both 2 and 20 hours. The trisaccharide produced 1.1 moles of carbon dioxide in 6 hours; after 20 hours' oxidation, both D-arabinose and D-mannose were present among the hydrolyzed oxidation products. These results are consistent with those expected for a 1,3-linked structure and eliminate the possibility of other linkages.

EXPERIMENTAL

Preparation of Materials, and Hydrolysis

Periodate-oxidized phosphomannan Y-2448, the product of a 240-hour oxidation at 4° C, was prepared as previously described (3). Excess periodate was removed by ethylene glycol (stoichiometric amount) and the solution was dialyzed against distilled water at 4° C until free of inorganic salts. Visking[1] dialysis tubing (1-7/8 S.S.) was washed repeatedly or boiled in water before use (5).

The dialysis residue was passed through Dowex 50X2, 50–100 mesh (H^+ form) cation exchange resin and then hydrolyzed at 0.3% concentration and 100° C in its own acidity (pH 2.5). At 72 hours' autohydrolysis, when the oligosaccharide concentrations were near their maxima, all phosphate was in the inorganic form. The hydrolyzate was used directly for qualitative paper chromatographic examination for organic phosphates but was deanionized (Dowex 3X4, 20–50 mesh) before quantitative paper chromatographic analysis and isolation of neutral oligosaccharides.

Dialyzates were neutralized and concentrated *in vacuo* at solution temperatures not exceeding 30° C.

Similarly, dialyzates were obtained from periodate-oxidized phosphomannan Y-2448 that had been treated with alkali or glycine buffer, to eliminate phosphate in inorganic form as previously described (3), and neutralized. These solutions were concentrated under conditions that did not hydrolyze inorganic pyrophosphate controls, that is, at solution temperatures not exceeding 30° C and at pH's in the range 6.5–8.5.

Native phosphomannan Y-2448 (1), decationized by Dowex 50X2, 50–100 mesh (H^+ form) exchange resin, hydrolyzed slowly in its own acidity (pH 2.2) at 100° C. Hydrolyzates obtained under these conditions were suitable for examination of products by paper chromatography, but for observations on rate and completeness of hydrolysis, a 0.2% concentration of decationized phosphomannan was treated with 5 *N* formic acid in sealed tubes at 100° C. Individual tubes were opened at chosen times, the hydrolyzate was transferred to a small flask, and formic acid was removed by evaporation, first *in vacuo* and then in the presence of toluene. Measurements of reducing power were made on these solutions (12). For isolation of products, larger amounts of hydrolyzate (from 0.65% phosphomannan concentration) were treated similarly except that for complete removal of formic acid, residues were taken to dryness, redissolved in water or ethanol, and dried again several times. Analysis showed that after 6 hours' hydrolysis essentially all the phosphate was in the organic form, but after 22 hours, 20% was inorganic. Phosphate and phosphate esters then were removed from hydrolyzates by use of Dowex 3X4, 20–50 mesh (amine form).

Paper Chromatography

Solvent systems used for separating the inorganic components of dialyzates were: (*a*) *n*-propyl alcohol –

[1]*Mention of trade names should not be construed as a recommendation or endorsement by the U.S. Department of Agriculture over those not mentioned.*

water – aqua ammonia (sp. gr. 0.90) (6:1:3) (13); and (*b*) the upper phase of *n*-butyl alcohol – pyridine – 1.5 *N* ammonium hydroxide (2:1:2) (14) (all v/v). Solvent systems used for separating carbohydrate components of hydrolyzates were: (*c*) *n*-butyl alcohol – pyridine – water (6:4:3) (15); (*d*) the upper phase of ethyl acetate – acetic acid – water (3:1:3) (16); and (*e*) ethyl acetate – acetic acid – water (3:3:1) (17) (all v/v).

Phosphate was detected by dipping chromatograms in an ammonium molybdate – perchloric acid reagent (18) and using ultraviolet light (2537 Å) to bring out the spots (19). Reducing sugars were detected by *o*-aminobiphenyl phosphate in glacial acetic acid (20).

For quantitative chromatography of hydrolyzates, Whatman No. 1 papers were spotted in triplicate with 1000–3000 μg of sugar per spot and the papers were irrigated for two 20-hour periods (15) with solvent *c*. The spots and corresponding blanks were eluted; the eluates were filtered through sintered glass and analyzed by the phenol – sulphuric acid method (21).

Isolation and Characterization of Oligosaccharides

For separation and isolation of neutral oligosaccharides, hydrolyzates were streaked on Whatman 3 MM paper and irrigated with solvent *c* for 40 hours. The sugars were eluted, the eluates were concentrated *in vacuo*, and the residues were taken up in water and filtered through decolorizing carbon. The sugars were precipitated several successive times from aqueous solution by ethanol and dried *in vacuo*.

On papergrams, the di- and tri-saccharides migrated slightly faster than the α-1,6-linked isomaltose and isomaltotriose (22). The di-, tri-, and tetra-saccharides did not show a positive reaction for phosphate when the papergram was dipped in an ammonium molybdate – perchloric acid reagent and irradiated with ultraviolet light under conditions known to detect difficultly hydrolyzable sugar phosphates (19). The di- and tri-saccharides reacted with triphenyltetrazolium chloride reagent, as would be expected from the presence of a free hydroxyl at carbon-2 in the reducing sugar units (23). Plots of log distance traveled (in solvent *c*) vs. D.P. for D-mannose and for the di-, tri-, and tetra-saccharides gave essentially straight lines. However, this rough indication of an homologous series (15) could be misleading in relation to the tetrasaccharide.

The disaccharide showed $[\alpha]_D^{25}$ +53.6° → +57.6° at 20 hours (*c*. 0.434, water). Anal. Calc. for $C_{12}H_{22}O_{11}$: C, 42.10; H, 6.49. Found: C, 41.42; H, 6.54.

The trisaccharide showed $[\alpha]_D^{25}$ +79.8° at 6 hours (*c*. 0.708, water). Anal. Calc. for $C_{18}H_{32}O_{16}$: C, 42.86; H, 6.39. Found: C, 43.54; H, 6.75.

Lead tetraacetate oxidation of the oligosaccharides was conducted by a technique (10) based on that of Perlin (11). Preparatory to paper chromatography in solvent *c*, oxidation solutions were treated with oxalic acid to remove lead ions and then were hydrolyzed by *N* hydrochloric acid for 2 hours at 100° C.

ACKNOWLEDGMENT

We are pleased to acknowledge that Mrs. Clara E. McGrew carried out the carbon and hydrogen analyses.

REFERENCES

1. A. JEANES, J. E. PITTSLEY, P. R. WATSON, and R. J. DIMLER. Arch. Biochem. Biophys. **92**, 343 (1961).
2. M. E. SLODKI. Biochim. Biophys. Acta, **57**, 525 (1962).
3. A. JEANES and P. R. WATSON. Can. J. Chem. **40**, 1318 (1962).
4. J. K. N. JONES and W. H. NICHOLSON. J. Chem. Soc. 27 (1958).
5. P. R. WATSON, J. E. PITTSLEY, and A. JEANES. Anal. Biochem. In press (1962).
6. R. L. DRYER, A. R. TAMMES, and J. I. ROUTH. J. Biol. Chem. **225**, 177 (1957).
7. H. WEINLAND. Z. Physiol. Chem. **306**, 56 (1956).
8. P. A. J. GORIN and A. S. PERLIN. Can. J. Chem. **37**, 1930 (1959).
9. A. J. CHARLSON and A. S. PERLIN. Can. J. Chem. **34**, 1200 (1956).
10. J. H. SLONEKER. Unpublished results.
11. A. S. PERLIN. Anal. Chem. **27**, 396 (1955).
12. N. NELSON. J. Biol. Chem. **153**, 375 (1944).
13. C. S. HANES and F. A. ISHERWOOD. Nature, **164**, 1107 (1949).
14. R. J. BLOCK, E. L. DURRUM, and G. ZWEIG. Paper chromatography and paper electrophoresis. Academic Press, New York. 1958. p. 415.
15. A. JEANES, C. S. WISE, and R. J. DIMLER. Anal. Chem. **23**, 415 (1951).
16. M. A. JERMYN and F. A. ISHERWOOD. Biochem. J. **44**, 402 (1949).
17. D. C. MORTIMER. Can. J. Chem. **30**, 653 (1952).
18. S. BURROWS, F. S. M. GRYLLS, and J. S. HARRISON. Nature, **170**, 800 (1952).
19. R. S. BANDURSKI and B. AXELROD. J. Biol. Chem. **193**, 405 (1951).
20. T. E. TIMELL, C. P. J. GLAUDEMANS, and A. L. CURRIE. Anal. Chem. **28**, 1916 (1956).
21. M. DUBOIS, K. A. GILLES, J. K. HAMILTON, P. A. REEBERS, and F. SMITH. Anal. Chem. **28**, 350 (1956).
22. A. JEANES, C. A. WILHAM, R. W. JONES, H. M. TSUCHIYA, and C. E. RIST. J. Am. Chem. Soc. **75**, 5911 (1953).
23. R. H. CÔTÉ. J. Chem. Soc. 2248 (1959).

PHYSICOCHEMICAL STUDIES OF WATER CHESTNUT STARCH (TRAPA BISPINOSA ROXB)

V. L. N. Murty, D. Choudhury, and P. Bagchi
Department of Macromolecules, Indian Association for the Cultivation of Science, Calcutta, India

Received June 25, 1962

ABSTRACT

The starch present in the kernel of water chestnut (*Trapa bispinosa* Roxb) has been isolated and obtained free from protein. Potentiometric titration showed that the starch contained 15% amylose. The starch was resolved into amylose and amylopectin through complex formation. The components were characterized by chemical and enzymic techniques. The average length of unit chain has been shown to be 22 in the amylopectin and 360 in amylose by both methylation and periodate oxidation studies. Molecular weights of the two components by viscosity and light scattering are also described.

Although the starchy nature of the kernel of water chestnut (*Trapa bispinosa* Roxb) has been reported (1) no detailed study of this material has been made previously. Those starches on which detailed structural investigations have been carried out belong either to the class of tuber starches or to the cereal variety. Water chestnut starch possesses the peculiarity that it originates from the kernel of an aquatic plant.

The starch was isolated in granular form, the use of reagents likely to cause degradation being avoided. The granules resembled those of potato starch in the X-ray powder diagram. Protein contamination was reduced to 0.7% under mild conditions (2). The purified starch showed an amylose content of 15% from the iodine affinity measurements, a value similar to that of other starches (cf. banana, pearl manioc, tapioca, etc. (3)). It was fractionated into its components, amylose and amylopectin, employing two methods. In the first thymol was used as the complexing agent for the initial precipitation (4) and butanol (5–7) for successive recrystallizations. The second method made use of aqueous pyridine as the precipitant for amylose, a 20% solution (7) being employed for the isolation of the amylopectin (the amylose fraction in this was discarded) and a 15% solution (8) for the isolation of amylose. The amylose obtained in the latter case was purified by successive reprecipitations as the butanol complex. The amylose obtained by the first method after five butanol recrystallizations showed a maximum iodine binding power of 19.5% and a blue value of 1.25, which could not be improved by further recrystallizations. In the second method the yield of amylose was poor and the blue value less (1.16). Hence the components obtained by the first method were used in further investigations. The properties of the components obtained are shown in Table I.

TABLE I

	Iodine affinity	Blue value	Purity*
Amylose	19.5	1.25	97.8
Amylopectin	0.10	0.06	97.5

*Determined by alkaline ferricyanide method.

It has been observed that the initial methylation of a polysaccharide is facilitated by converting it to an acetyl derivative and subjecting the latter to the action of dimethyl sulphate and alkali, when simultaneous deacetylation and methylation take place. Both

the components of water chestnut starch were, therefore, acetylated by dispersion in formamide (9) and then treatment with pyridine and acetic anhydride at room temperature (10). This method has been stated to cause minimum degradation (2). The acetylated products were directly methylated by repeated treatments with dimethyl sulphate and solid sodium hydroxide (11) and then by Purdie's method (12). The resulting methylated amylose and amylopectin showed no hydroxyl absorption band in the infrared spectrum.

Methanolysis and hydrolysis of the fully methylated amylopectin yielded a mixture which, on paper chromatographic examination, revealed the presence of 2,3,4,6-tetra-*O*-methyl-D-glucose, 2,3,6-tri-*O*-methyl-D-glucose, and 2,3-di-*O*-methyl-D-glucose together with a small amount of a mixture of probably 2,6- and 3,6-di-*O*-methyl-D-glucose. Trace amounts of monomethyl glucose and glucose were also obtained. The mixture of dimethyl sugars was resolved by paper chromatography into two fractions, the major component consisting of 2,3-di-*O*-methyl-D-glucose. All three sugars were identified through crystalline derivatives. The quantity of tetra-*O*-methyl glucose corresponds to the presence of one non-reducing terminal group per 20–21 glucose residues. The presence of other dimethyl sugars, probably 2,6- and 3,6-di-*O*-methylglucose, is not considered to have any structural significance, since they may have arisen from incomplete methylation of the polysaccharide and by demethylation during hydrolysis. Similar observations have been made in connection with methylation studies on amylopectin from malted barley (13) and rubber seed (2). The yield of formic acid during periodate oxidation on both the amylopectin and the whole starch corresponds to one non-reducing end group per 22 glucose residues in the amylopectin, a value in good agreement with that obtained from the methylation data. Estimation of the glucose obtained on hydrolysis of the periodate-oxidized amylopectin showed that 0.57% of the glucose residues was unattacked by periodate, indicating that at least 88% of the linkages between unit chains was of the $1 \rightarrow 6$ type. Small amounts (0.5–1.5%) of glucose have previously been detected in the hydrolyzate of periodate-oxidized starch from other sources (13(*a*)).

The structure of the amylopectin component of water chestnut starch was further confirmed by degradation studies with β-amylase. Soya bean was chosen as the source of β-amylase as it has been claimed that this enzyme is free from contamination by α-amylase and maltase (14). Purified β-amylase was prepared from soya bean by Peat, Pirt, and Whelan's method (15), which includes deactivation of Z-enzyme by heat treatment of the protein in acid medium. The enzyme preparation showed no maltase, α-amylase, or Z-enzyme activity. Stock β-amylase was also prepared by eliminating the heat treatment. Use of purified β-amylase under standard conditions led to 57% conversion to maltose, in agreement with the values (52–62%) found for amylopectins from other sources (16). The same conversion value was reached even when the digest was acted upon by stock β-amylase. The isolated β-limit dextrin contained 9–10 glucose residues, as determined by oxidation with periodate. The average length of the original external chains of the amylopectin was 15 anhydroglucose units.

The fully methylated amylose on methanolysis and hydrolysis furnished 2,3,4,6-tetra-*O*-methyl-D-glucose, 2,3,6-tri-*O*-methyl-D-glucose, and a mixture of di-*O*-methylglucoses. The presence of dimethyl sugars may be due to incomplete methylation or demethylation during hydrolysis and may not have any structural significance. Such an observation was made in the methylation studies of amyloses from other sources (17). The quantity of tetra-*O*-methylglucose corresponded to the presence of one non-reducing terminal group for every 370 glucose residues. The average chain length of the amylose obtained from periodate oxidation studies was 359, a value in good agreement with that obtained

from methylation data. The absence of glucose in the periodate-oxidized amylose is quite significant. The water chestnut amylose, therefore, consisted of an unbranched chain of ca. 360 glucose residues.

Treatment of the amylose with purified β-amylase led to 73% conversion to maltose, a value within the range (65–85%) observed in the case of amyloses prepared via complex formation (18, 19). That the observed conversion was not due to retrogradation was deduced from the fact that the limit was reached in the course of a few hours and could not be raised by further addition of the enzyme. Complete conversion to maltose was attained when the amylose was treated with stock β-amylase.

The intrinsic viscosities of the amylopectin in aqueous potassium hydroxide and of the acetate derivative in chloroform were 0.97 and 1.9 dl/g, respectively. Light scattering measurements on a solution of amylopectin acetate in chloroform, assuming a random coil model, gave a weight-average molecular weight of 23.6×10^6. It is interesting to note that the plot of HC/τ vs. C exhibited a negative slope. A negative slope at low concentration has been ascribed to association effects which decrease with decreasing concentration (20). Intrinsic viscosity measurements were made on both the water chestnut amylose and its acetylated product and the $\overline{\text{D.P.}}$ compared with the empirical relation of Cowie and Greenwood (21). A value of 430 for the $\overline{\text{D.P.}}$ of amylose was obtained against 370 and 360 from methylation and periodate oxidation studies respectively. Considering that the amylose was unfractionated and the solution viscosity measurements give $\bar{M}_v$ rather than $\bar{M}_n$ (given by end group assay methods such as methylation and periodate oxidation studies) the agreement is considered to be satisfactory.

The weight-average molecular weight of the amylose acetate as determined by light scattering was 6.7×10^6. Paschal and Foster (22) reported a value of 3×10^6 for a corn starch amylose which decreased to 4×10^5 on keeping for 24 hours. They attribute it to be due to disaggregation of an unusual type of aggregate. Water chestnut starch, therefore, appears to be similar in composition to starches from other sources. The detailed molecular architecture, size, and shape of the components are also of the same type.

EXPERIMENTAL

Paper chromatography was carried out by the descending method. Whatman No. 1 and No. 3 MM filter papers were used, the latter for preparative purposes. The solvent was allowed to run against the machine line. The following solvent mixtures were used for separating the sugars: (A) ethyl acetate:pyridine:water (8:2:1); (B) *n*-butanol:acetic acid:water (4:1:5), upper layer; (C) *n*-butanol:pyridine:benzene:water (5:3:1:3), upper layer; (D) ethyl methyl ketone – water azeotrope; (E) *n*-butanol:ethanol:water (4:1:5), upper layer. Aniline oxalate in water and ammonical silver nitrate were used as spray reagents.

Unless otherwise stated all evaporations were carried out *in vacuo* at 30–40° C. All the values of specific rotation given are at equilibrium except where mutarotation values are given.

Isolation and Purification of Starch

Fresh and middle-aged fruits of water chestnut were collected, peeled, and the pericarp removed. The kernel so obtained was minced into alcohol to inhibit enzymic activity and macerated in a "Kenmix 55" blender. The resulting slurry was filtered through a 100-mesh sieve and the filtrate centrifuged to yield a crude starch. The sediment was washed repeatedly with 0.1 *M* sodium chloride solution. The residue left on the sieve was macerated four times with 0.1 *M* sodium chloride in the blender and the resulting slurry filtered through a 100-mesh sieve; the fibrous material left on the sieve was rejected.

The starch products so obtained were combined, suspended in 0.1 *M* aqueous sodium chloride solution, and shaken with toluene (1/10 vol.) overnight to denature the protein. The brown toluene layer containing the protein was removed by centrifugation, this treatment being repeated four times. The sedimented starch formed two layers, the upper brown still containing protein. Further purification was effected by the method of Greenwood and Robertson (2). Salts were removed by washing with water followed by centrifugation, and the pure starch was stored under methanol at 5° C. The purified starch was then refluxed with aqueous methanol (80%) to remove residual fats and this material, after drying, was used for subsequent investigations. $[\alpha]_D^{25}$ +154° (*c*, 0.77 in *N* NaOH). Anal.: N, 0.014%; ash, 0.07%; blue value, 0.236.

Potentiometric Titration for Determination of Iodine Binding Powers

Iodine binding powers of water chestnut starch and its fractions were determined by a modification of the method of Schoch (24). A platinum electrode in conjunction with a saturated calomel half-cell was used. The potentials were measured with a Leeds Northrup potentiometer using a spot-type galvanometer. The total free iodine in the starch solution was plotted against the bound iodine and the iodine binding power was estimated by extrapolation of the linear portion of the titration curve to zero free iodine concentration. Calculation of the percentage of amylose was made from the observed iodine binding power of the starch, and the iodine binding power of the pure water chestnut amylose determined in a separate experiment (19.5%). Results showed water chestnut starch had 15% amylose content.

Estimation of Length of Unit Chain of Amylopectin

Starch (109.5 mg) was dispersed in water (50 ml) and subjected to oxidation by shaking with sodium metaperiodate (0.1 *M*, 50 ml) in the dark at 3° C. The liberated formic acid and the periodate consumption were estimated at regular intervals by the method of Fleury and Lange (25). The formic acid liberated corresponded to a chain length of 26 anhydroglucose residues in the starch. This value corresponded to a chain of 22 anhydroglucose residues in the amylopectin fraction.

Examination of the Amylopectin Fraction

Amylopectin had $[\alpha]_D^{25}$ +146.9° (*c*, 1.0 in *N* NaOH) and a blue value of 0.06. On hydrolysis this fraction yielded only glucose (97.6%). Potentiometric titration for the iodine binding power showed the presence of 0.53% amylose.

Periodate Oxidation of Amylopectin

The method described for the original starch was employed. The liberation of formic acid corresponded to 22 anhydroglucose units per mole of formic acid.

Determination of Glucose Residues Linked through C_1, C_4, and C_6

Amylopectin (0.5552 g) was dissolved in water (80 ml) containing potassium chloride (5 g), and sodium metaperiodate (30 ml, 0.3 *M*) was added. The reaction was allowed to proceed in the dark for 240 hours and the excess oxidant was destroyed with ethylene glycol. The oxidized amylopectin was dissolved in sodium hydroxide (30 ml, 0.2 *N*) and after the addition of sodium borohydride (0.25 g) the solution was left overnight. It was then neutralized with acetic acid, dialyzed, and evaporated to dryness. The resulting residue was hydrolyzed and the glucose estimated by quantitative paper chromatography. The results showed that 0.57% of the glucose residues in the amylopectin was unattacked by periodate.

Acetylation of the Amylopectin

Amylopectin (2 g) was dissolved in water and precipitated by the addition of ethanol. The precipitate was collected by filtration and washed with ethanol and ether. It was dispersed in formamide (9) (30 ml), and pyridine (50 ml) was added, followed by acetic anhydride (40 ml). The reaction was allowed to proceed at room temperature (10) for 2 hours. The partially acetylated amylopectin (acetyl content, 41%) was subjected to further acetylation as described above to give a product with $[\alpha]_D^{25}$ +165° (*c*, 1.0 in chloroform). Anal.: acetyl, 44.8%.

Methylation of the Amylopectin

The acetylated amylopectin (0.8 g) was dissolved in tetrahydrofuran (20 ml) and methylated (11) directly using dimethyl sulphate (15 ml) and solid sodium hydroxide (13 g). The partially methylated derivative was extracted with chloroform and subjected to methylation thrice by Purdie's method (12). $[\alpha]_D^{25}$ +198° (*c*, 0.5 in chloroform). Anal.: methoxyl, 43.5%.

Hydrolysis of the Methylated Amylopectin

The methylated amylopectin (300 mg) was refluxed with methanolic hydrogen chloride (20 ml, 1%) for 5 hours. The solution was evaporated to a syrup under reduced pressure and the resulting mixture of methyl glycosides was hydrolyzed with hydrochloric acid (30 ml, 0.5 *N*). The acid was neutralized with silver carbonate and solids were removed by filtration. The resulting solution, after deionization with Amberlite IR-120 (H) and Amberlite IR-45 (OH), was evaporated to a small quantity of a syrup. Examination by paper chromatography (solvent E) revealed the presence of 2,3,4,6-tetra-*O*-methyl-D-glucose, 2,3,6-tri-*O*-methyl-D-glucose, 2,3-di-*O*-methyl-D-glucose, and 2,6- and/or 3,6-di-methyl-D-glucose. Trace amounts of monomethylglucose and glucose were also detected. The mixture (ca. 250 mg) was resolved on sheets of Whatman No. 3 MM filter papers. The strips corresponding to tetra-, tri-, and di-*O*-methyl sugars were excised, eluted, and evaporated to dry syrups separately. They were present in a ratio of 11.9:214.1:18 respectively.

Characterization of O-Methyl Sugars

The 2,3,4,6-tetra-*O*-methyl-D-glucose fraction, $[\alpha]_D^{30}$ +82° (*c*, 0.2 in water), lit. +83°(13), was characterized as crystalline 2,3,4,6-tetra-*O*-methyl-*N*-phenyl-D-glucosylamine, m.p. and mixed m.p. 136–137°, lit. 136–138° (13).

The tri-*O*-methylglucose, $[\alpha]_D^{25}$ +67° (13), +70° (30), was characterized as the 1,4-di-*p*-nitrobenzoate derivative, m.p. 190–192° (26). The mixture of di-*O*-methyl sugars was resolved by paper chromatography. The major component was characterized as 2,3-di-*O*-methyl-D-glucose through its phenyl hydrazide, m.p. 160-162° C (13).

Quantitative Estimation of O-Methyl Sugars

A small portion of the methylated sugar mixture was resolved quantitatively and the tetra-, tri-, and di-*O*-methyl sugars were eluted and estimated by the alkaline hypoiodite method (27). The ratio was 1:17.7:1.9 respectively.

β-Amylolysis of the Amylopectin

Purified β-amylase was prepared from soya bean flour by the method of Peat, Pirt, and Whelan (15), in which the Z-enzyme is inactivated by a heat treatment of the protein in acid medium. Stock β-amylase containing Z-enzyme was also prepared by eliminating the heat treatment.

A digest was prepared by dissolving amylopectin (102.3 mg) in *N* sodium hydroxide solution (10 ml) and the pH was brought to 4.6 by acetate buffer. The concentration of enzyme was such that the reaction was complete in a few hours, but the digests were left for 24 hours before the concentration of the amylopectin and liberated maltose were separately estimated by the alkaline ferricyanide method (28). The amount of maltose liberated was 56.9%. No increase in the yield of maltose was noticed when the amylopectin was treated with stock β-amylase.

Isolation of Amylopectin β-Limit Dextrin

For isolation of amylopectin β-limit dextrin, the polysaccharide was incubated at pH 4.6 as described above (13). The formic acid produced on oxidation with periodate corresponded to one non-reducing end group per 9–10 anhydroglucose residues.

Measurement of Intrinsic Viscosity

The specific viscosity (η_{sp}) of the amylopectin in *M* potassium hydroxide solution was determined at several concentrations in an Ostwald viscometer at 35° C and the intrinsic viscosity [η] was determined graphically by extrapolation to zero concentration. Accurate dilutions were made to five concentrations and flow times were measured. The average of three readings was taken for each concentration. The concentrations were determined by hydrolyzing a portion and estimating the glucose by the alkaline ferricyanide method (28). Concentrations were expressed as g/100 ml. From the graph the intrinsic viscosity [η] of amylopectin in *M* potassium hydroxide was found to be 0.97 dl/g (average of two sets of readings). Intrinsic viscosity measurements were also made on the acetylated amylopectin in chloroform as in the above case. Concentrations were estimated by the dry weight method. [η], 1.96 dl/g (mean of two sets of measurements).

Light Scattering Measurements

Acetylated amylopectin was employed for the measurements. Solvent chloroform, twice distilled, was filtered through sintered glass G-5 under dust free conditions to remove any inherent dust particles. Measurements were taken with a Brice–Phoenix photometer (Model OM 1000 A) as described by Brice *et al.* (29). Turbidities (τ) were determined by the working standard method at 546 mμ. The dissymmetry ratio ($I_{45°}/I_{135°}$) was also measured. Turbidity of the solvent was measured first and successive aliquots of the clarified solution (passed through sintered glass G-4) were added to a known volume of the solvent in the scattering cell to form concentration series in the range of $(1\text{–}5)\times10^{-4}$ g/ml. Concentrations were determined by dry weight method. The molecular weight ($\bar{M}_w$) was calculated from the relationship

$$\frac{HC}{\tau} = \frac{1}{M(P_{90°})} + \frac{2B(P_{90°})C}{RT},$$

where

$$H = \frac{32\pi^3 n_0^2}{3N\lambda^4}\left(\frac{dn}{dc}\right)^2.$$

P_{90} is the particle scattering factor. *B* is a constant. The refractive index increment (dn/dc) was measured at 546 mμ with a Brice–Phoenix differential refractometer. From the plot of HC/τ vs. *C* and assuming a random coil model for the amylopectin acetate molecule the corrected molecular weight was to be 23.6×10^6.

Examination of Water Chestnut Amylose

Amylose had $[\alpha]_D^{25}$ +147.7° (*c*, 0.5 in *N* NaOH) and a blue value of 1.25. Potentiometric titration (23, 24) showed that the amylose had a maximum iodine affinity of 19.5%. Hydrolysis of the sample gave only glucose (97.8%).

Periodate Oxidation of Amylose

Amylose (0.1025 g) was subjected to periodate oxidation as described earlier. The formic acid corresponded to a chain length of 360 anhydroglucose residues, assuming the liberation of 3 moles of formic acid per mole of

amylose. Periodate-oxidized amylose after reduction and hydrolysis as described for amylopectin gave no spot corresponding to glucose on paper chromatographic examination.

Methylation of the Amylose

Acetylated amylose (0.8 g) was directly methylated by treatment with dimethyl sulphate and solid sodium hydroxide in tetrahydrofuran (11) and then thrice by Purdie's method (12), as described in the case of amylopectin. $[\alpha]_D^{28}$ +200° (*c*, 0.5 in chloroform). Anal.: —OCH_3, 44.5%.

Hydrolysis of the Methylated Amylose and Identification and Estimation of the Component Sugars

The methylated amylose (500 mg) after methanolysis and hydrolysis yielded a syrup which, on paper chromatographic examination, revealed the presence of a tetra-*O*-methylglucose, a tri-*O*-methylglucose, and several di-*O*-methylglucoses.

The neutral sugar mixture (450 mg) was resolved on Whatman No. 3 MM filter papers into pure components. The 2,3,4,6-tetra-*O*-methyl-D-glucose had $[\alpha]_D^{30}$ +81° (*c*, 0.1 in water) and moved at the same rate as an authentic sample on paper chromatograms.

The tri-*O*-methyl fraction, $[\alpha]_D^{30}$ +67° in water (*c*, 1.0 in water), lit. +70° (30), was identified as 2,3,6-tri-*O*-methyl-D-glucose by conversion to crystalline 2,3,6-tri-*O*-methyl-D-glucose-1,4-di-*p*-nitrobenzoate, m.p. 190–192° (26).

The mixture containing the di-*O*-methyl fraction on chromatographic examination gave spots corresponding to 2,3-, 2,6-, and/or 3,6-di-*O*-methyl-D-glucose. These were not further characterized. A small portion of the mixture was resolved quantitatively by paper chromatography and the tetra- and tri-*O*-methyl sugars were estimated by the alkaline hypoiodite method (27). The tetra- and tri-methyl sugars were present in the ratio of 1:370 respectively.

β-Amylolysis of Amylose

A digest was prepared with amylose (102.4 mg) and hydrolysis carried out at pH 4.6 with purified β-amylase. The liberated maltose was estimated as in the case of amylopectin at 35° C. A conversion limit of 73% for the liberation of maltose was obtained. Digests were also prepared with amylose and allowed to be acted upon by stock β-amylase; a conversion limit of 99.4% was reached.

Intrinsic Viscosity of the Amylose

Limiting viscosity numbers $[\eta]$ for both amylose in *M* potassium hydroxide and its acetate derivative in chloroform were determined at 35° C using the same technique used for the amylopectin. Concentrations were estimated as described in the earlier case. The intrinsic viscosities of the amylopectin and its acetate derivative were 0.59 and 1.38 dl/g, respectively.

Light Scattering Measurements

Measurements were carried out with a Brice–Phoenix Photometer (Model OM 1000 A) following the working standard method in the concentration series in the range $(3\text{–}15)\times10^{-4}$ g/ml. Acetylated amylose was employed and the technique was similar to that used for the acetylated amylopectin. The uncorrected molecular weight was 3.2×10^6. Assuming the random coil model for the amylose molecule the corrected molecular weight is 6.7×10^6.

REFERENCES

1. M. Shafee and J. L. Sarin. Ind. Eng. Chem. **29**, 1436 (1937).
2. C. T. Greenwood and J. S. M. Robertson. J. Chem. Soc. 3769 (1954).
3. M. L. Wolfrom. Advances in carbohydrate chemistry. Vol. II. Academic Press Inc., New York. 1956. Table II, p. 351.
4. W. N. Haworth, S. Peat, and P. E. Sagrott. Nature, **157**, 19 (1946).
5. R. S. Higginbotham and G. A. Morrison. Shirley Inst. Mem. **22**, 141 (1948).
6. R. S. Higginbotham and G. A. Morrison. Chem. Ind. (London), **25**, 45 (1947).
7. R. S. Higginbotham and G. A. Morrison. Shirley Inst. Mem. **22**, 148 (1948).
8. R. L. Whistler and G. E. Hilbert. J. Am. Chem. Soc. **67**, 1161 (1945).
9. J. F. Carson and W. D. Maclay. J. Am. Chem. Soc. **63**, 1015 (1946).
10. A. L. Potter and W. Z. Hassid. J. Am. Chem. Soc. **70**, 3774 (1948).
11. E. L. Falconer and G. A. Adams. Can. J. Chem. **34**, 338 (1956).
12. T. Purdie and J. C. Irvine. J. Chem. Soc. **83**, 1021 (1903).
13. G. O. Aspinall, E. L. Hirst, and W. McArthur. J. Chem. Soc. 3075 (1955).
13. (*a*) E. L. Hirst, J. K. N. Jones, and A. J. Roudier. J. Chem. Soc. 1779 (1948). W. G. Campbell, J. L. Frahn, E. L. Hirst, D. F. Packman, and E. G. V. Percival. J. Chem. Soc. 3489 (1951). C. E. Ballou and E. G. V. Percival. J. Chem. Soc. 1054 (1952).
14. E. J. Bourne, W. N. Haworth, A. Macey, and S. Peat. J. Chem. Soc. 924 (1948).
15. S. Peat, S. J. Pirt, and W. J. Whelan. J. Chem. Soc. 705, 714 (1952).
16. D. J. Manners. Quart. Rev. (London), **9**, 73 (1955).
17. I. C. McWilliam and E. G. V. Percival. J. Chem. Soc. 2259 (1951).
18. E. F. Neufeld and W. Z. Hassid. Arch. Biochem. Biophys. **59**, 405 (1955).
19. J. M. G. Cowie and C. T. Greenwood. J. Chem. Soc. 4640 (1957).

20. R. W. KERR, F. C. CLEVELAND, and W. J. KATZBECK. J. Am. Chem. Soc. **73**, 111 (1951).
21. J. M. G. COWIE and C. T. GREENWOOD. J. Chem. Soc. 2862 (1957).
22. E. F. PASCHALL and J. F. FOSTER. J. Polymer Sci. **9**, 73, 85 (1952).
23. E. J. WILSON, JR., T. J. SCHOCH, and C. S. HUDSON. J. Am. Chem. Soc. **65**, 1380 (1943).
24. F. L. BATES, D. FRENCH, and R. E. RUNDLE. J. Am. Chem. Soc. **65**, 142 (1943).
25. P. FLEURY and J. LANGE. J. pharm. chim. **17** (8), 107 (1933).
26. P. A. REBERS and F. SMITH. J. Am. Chem. Soc. **76**, 6097 (1954).
27. E. L. HIRST, L. HOUGH, and J. K. N. JONES. J. Chem. Soc. 928 (1949).
28. W. Z. HASSID. Ind. Eng. Chem. **9**, 228 (1937); **8**, 136 (1936).
29. B. A. BRICE, M. HALWER, and R. SPEISER. J. Opt. Soc. Am. **40**, 768 (1950).
30. J. C. IRVINE and E. L. HIRST. J. Chem. Soc. **121**, 1213 (1922).

SPECTROSCOPIC STUDIES OF KETO–ENOL EQUILIBRIA

PART 1. SOLVENT EFFECTS[1]

A. S. N. MURTHY, A. BALASUBRAMANIAN, AND C. N. R. RAO[2]

Department of Inorganic and Physical Chemistry, Indian Institute of Science, Bangalore, India

AND

T. R. KASTURI

Department of Organic Chemistry, Indian Institute of Science, Bangalore, India

Received July 23, 1962

ABSTRACT

Solvent effects on the keto–enol equilibria of ethyl acetoacetate, acetylacetone, ethyl cyclopentanone-2-carboxylate, and methyl 4-methylcyclopentane-1,2-dione-3,4,5-tricarboxylate have been studied by ultraviolet spectroscopy. The extent of enolization is mainly determined by the stabilization of the keto form by local association with polar or proton-donating solvent molecules, just as in the case of $n \rightarrow \pi^*$ transitions and infrared stretching frequencies. Solvent effects on infrared spectra reveal useful information regarding the characteristic frequencies of the tautomers.

Keto–enol tautomerism has been investigated extensively by ultraviolet (1), infrared (2), and n.m.r. (3) spectroscopy. Keto–enol equilibria are extremely solvent sensitive and the proportion of enol form is found to be much greater in non-polar solvents such as cyclohexane than in polar solvents such as alcohol or water. This is probably due to the stabilization of the keto form by polar solvents through local association. Recently in this laboratory we have investigated the solvent effects on the $n \rightarrow \pi^*$ transitions of several chromophores and have evaluated contributions from different factors (4). These studies clearly indicate that solvent effects on the $n \rightarrow \pi^*$ transitions are mainly controlled by local association between the solute and the solvent molecules and that the magnitude of the solvent blue shifts are determined by the polarity and/or proton-donating ability of the solvents. Studies of the solvent effects on infrared group frequencies have also shown that local association is an important factor in the determination of the solvent shifts (5). It was considered interesting to systematically investigate the keto–enol equilibria of a few systems in several solvents and correlate the observed effects with the solvent effects on the $n \rightarrow \pi^*$ transitions and the stretching vibration frequencies of carbonyl groups. We have now studied the keto–enol equilibria of ethyl acetoacetate, acetylacetone, ethyl cyclopentanone-2-carboxylate, and methyl 4-methylcyclopentane-1,2-dione-3,4,5-tricarboxylate (I) in solvents of varying degree of polarity or/and proton-donating ability.

EXPERIMENTAL

Commercial samples of ethyl acetoacetate and acetylacetone were used after suitable purification. Ethyl cyclopentanone-2-carboxylate was prepared by the procedure described in *Organic Syntheses* (6) and methyl 4-methylcyclopentane-1,2-dione-3,4,5-tricarboxylate was prepared according to the method of Chuang and Ma (7). All the solvents were purified and fractionated before use.

Ultraviolet absorption spectra were recorded with a Hilger Uvispek, model H 700, spectrophotometer. The infrared spectra were recorded with a Perkin–Elmer infrared spectrometer, model 137, with sodium chloride optics.

Percentage of the enol form was calculated from the extinction coefficient in the ultraviolet spectrum using the formula $100(\epsilon_o/\epsilon_a)$, where ϵ_o is the observed molar extinction coefficient and ϵ_a the assumed value for the chromophoric system of the enol form.

[1]*Taken in part from the Ph.D. Thesis of A. S. N. Murthy to be submitted to the Indian Institute of Science under the guidance of C. N. R. Rao.*

[2]*To whom all the correspondence should be addressed.*

RESULTS AND DISCUSSION

The ultraviolet absorption data and the percentage enol in the case of ethyl acetoacetate and acetylacetone are summarized in Table I and Fig. 1. The ϵ_a values for these are 16,000

TABLE I

Percentage of enol in the keto–enol equilibria of a few systems in different solvents

Solvent	Percentage of enol in: Ethyl acetoacetate (λ_{max} ~244mμ)	Acetylacetone (λ_{max} ~272 mμ)	Ethyl cyclopentanone-2-carboxylate (λ_{max} ~254 mμ)	Methyl 4-methylcyclopentane-1,2-dione-3,4,5-tricarboxylate† II (λ_{max} ~270 mμ)	Methyl 4-methylcyclopentane-1,2-dione-3,4,5-tricarboxylate† III (λ_{max} ~325 mμ)
Cyclohexane	43	88	22	34	49
Carbon tetrachloride	*	*	*	*	43
Dioxane	8	73	—	—	—
Diethyl ether	25	85	6	35	34
50% ether + 50% acetonitrile	6.5	68	—	—	—
75% ether + 25% acetonitrile	7	71	—	—	—
Acetonitrile	4	55	1.5	39	27
t-Butanol	10	80	5	35	41
i-Propanol	11	85	—	42	44
Ethanol	8	73	3	37	39
Methanol	6	70	2.5	38	38
Water	0.5	16	0.4	44	27

*Could not be determined because of solvent cutoff.
†The percentage-of-enol values for this compound are very approximate since the ϵ_a value is only arbitrary.

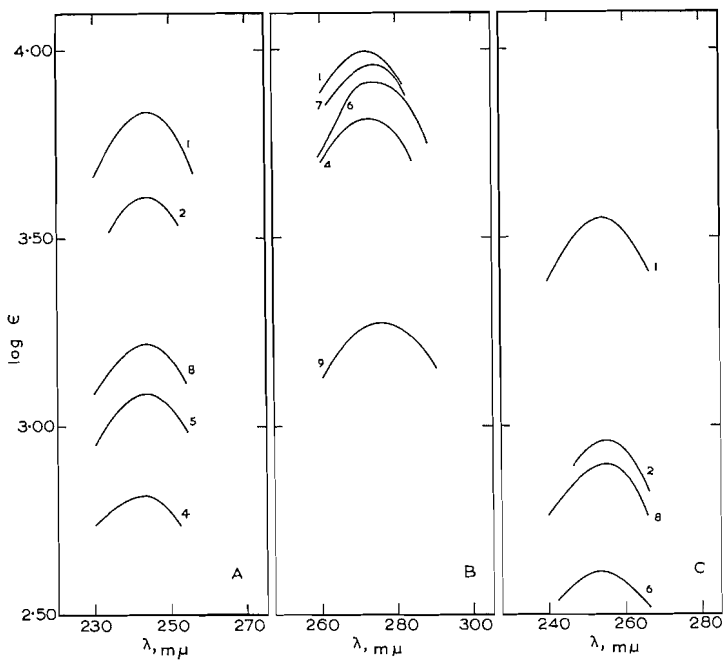

FIG. 1. Ultraviolet spectra of ethyl acetoacetate (A), acetylacetone (B), and ethyl cyclopentanone-2-carboxylate (C) in different solvents: (1) cyclohexane, (2) diethyl ether, (4) acetonitrile, (5) ethanol, (6) methanol, (7) *i*-propanol, (8) *t*-butanol, and (9) water.

and 12,000 respectively. In order to study the keto–enol equilibria in polar solvents of varying dielectric constant (which cannot donate protons), mixtures of acetonitrile and ether were employed. It was made certain that the observed extinction coefficients were not dependent on solute concentration, thereby indicating negligible association of the solute molecules in the enol form (8, 9). It can be seen that the percentage of enol is greatest in non-polar solvents and decreases with increasing polarity and/or proton-donating ability of the solvent. This trend in solvent effects is similar to that observed in the case of $n \rightarrow \pi^*$ transitions of chromophores (4). The $n \rightarrow \pi^*$ frequency of the carbonyl group increases with the polarity of the solvent, due to stabilization by local association. In the case of polar solvents which cannot donate protons, the solvent blue shifts are determined mainly by the dielectric constant of the solvent. In proton-donating solvents, however, the major contribution is due to hydrogen bonding. In the extreme case of water, where the carbonyl $n \rightarrow \pi^*$ frequency is highest, the percentage of enol is also lowest. In Fig. 2, the percentage of enol in ethyl acetoacetate has been plotted against

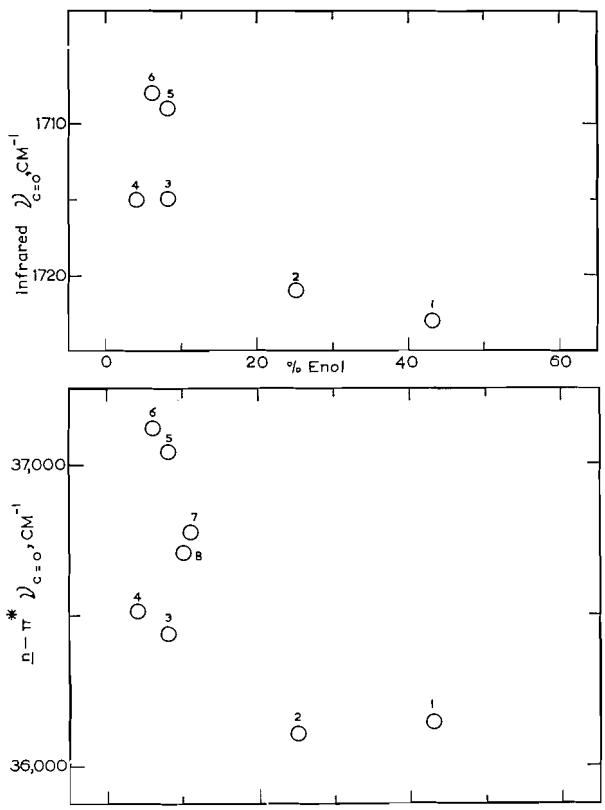

FIG. 2. Plots of percentage of enol of ethyl acetoacetate against the carbonyl infrared stretching frequency and the $n \rightarrow \pi^*$ frequency of acetone in different solvents: (1) cyclohexane, (2) diethyl ether, (3) dioxane, (4) acetonitrile, (5) ethanol, (6) methanol, (7) *i*-propanol, (8) *t*-butanol, and (9) water.

the $n \rightarrow \pi^*$ and the stretching vibration frequencies of the carbonyl group of acetone. It can be seen that the trends in these three quantities are similar, indicating that the stabilization of the carbonyl group by polar solvent molecules is the major controlling factor. In the case of polar solvents which cannot donate protons, the dielectric constant

of the solvent seems to be very important in the determination of the keto–enol equilibria, as indicated by the data obtained from acetonitrile and acetonitrile–ether mixtures.

Methyl 4-methylcyclopentane-1,2-dione-3,4,5-tricarboxylate (I) can give rise to two tautomeric species, II and III. The absorption maxima around 270 and 325 mμ (Fig. 3)

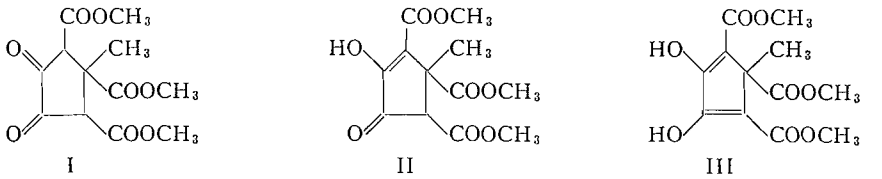

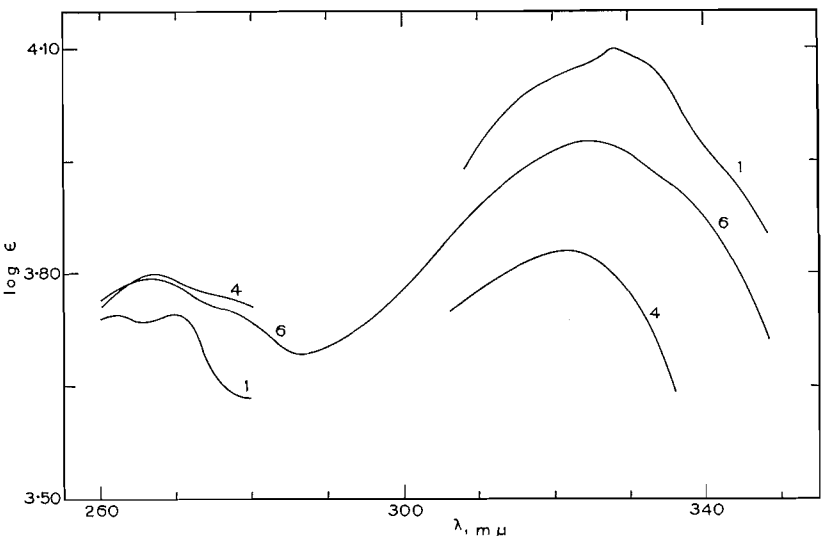

FIG. 3. Ultraviolet spectra of methyl 4-methylcyclopentane-1,2-dione-3,4,5-tricarboxylate in different solvents: (1) cyclohexane, (4) acetonitrile, and (6) methanol.

are assigned to the tautomers II and III respectively. The behavior of the model compound ethyl cyclopentanone-2-carboxylate is analogous to that of ethyl acetoacetate (Table I and Fig. 1). In compound I, the 270 mμ band (tautomer II) is nearly insensitive to the polarity of the solvent, whereas the intensity of the 325 mμ band (tautomer III) decreases with the polarity and/or proton-donating ability of the solvent (Fig. 3). The proportions of the two enol forms have been calculated by taking the ϵ_a values arbitrarily as 16,000 and 25,000, and the results are shown in Table I. It was considered worthwhile to study the solvent effects on the infrared spectra of these systems.

The double-bond regions in the infrared spectra of ethyl cyclopentanone-2-carboxylate and compound I in carbon tetrachloride and acetonitrile solutions are shown in Fig. 4. Ethyl cyclopentanone-2-carboxylate shows bands at 1750 cm^{-1} (ring ketone), 1730 cm^{-1} (β-keto ester), 1670 cm^{-1} (enolized β-keto ester), and 1620 cm^{-1} (C=C stretching) in carbon tetrachloride solution, where there is partial enolization (ca. 22%). In acetonitrile solution, where there is negligible enolization (<1%), bands are found around 1750, 1730, 1670, and 1620 (very weak) cm^{-1}. In carbon tetrachloride solution, I is present almost completely in the enolized form and distinct peaks are found in the double-bond region around 1750 cm^{-1} (ring ketone and saturated ester), 1680 cm^{-1} (enolized β-keto

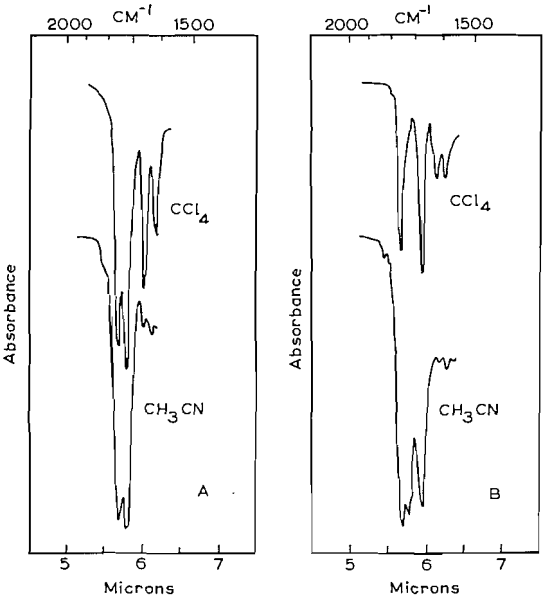

FIG. 4. The double-bond region in the infrared spectra of ethyl cyclopentanone-2-carboxylate (A) and methyl 4-methylcyclopentane-1,2-dione-3,4,5-tricarboxylate (B) in carbon tetrachloride and acetonitrile solutions.

ester), and 1618 and 1580 cm^{-1} (C=C stretching vibrations of II and III). In acetonitrile solution, where there is less enolization, the infrared spectrum shows bands around 1750 cm^{-1} (ring ketone and saturated ester), 1730 cm^{-1} (β-keto ester), 1680 cm^{-1} (weak, enolized β-keto ester), and 1600 cm^{-1} (very weak, C=C stretching). These results show how solvent effects on infrared spectra can also reveal interesting information regarding the two tautomers. Thus the C=O band due to the unenolized β-keto ester is only seen in acetonitrile solution in the case of compound I.

ACKNOWLEDGMENTS

The authors are thankful to Professors M. R. A. Rao and D. K. Banerjee for their interest in the work.

REFERENCES

1. C. N. R. RAO. Ultra-violet and visible spectroscopy—chemical applications. Butterworths, London. 1961.
2. L. J. BELLAMY. Infrared spectra of complex molecules. Methuen, London. 1958.
3. J. D. ROBERTS. Nuclear magnetic resonance. McGraw Hill, New York. 1959.
4. A. BALASUBRAMANIAN and C. N. R. RAO. Spectrochim. Acta. In press (1962).
5. L. J. BELLAMY and R. L. WILLIAMS. Trans. Faraday Soc. **55**, 14 (1959).
6. A. H. BLATT (*Editor*). Organic syntheses. Coll. Vol. II. John Wiley & Sons. 1947. p. 116.
7. C. K. CHUANG and C-M MA. Ber. **68B**, 882 (1935).
8. J. C. DEARDEN and W. F. FORBES. Can. J. Chem. **38**, 896 (1960).
9. C. N. R. RAO and A. S. N. MURTHY. J. Sci. Ind. Res. (India), **20B**, 290 (1961).

SPECTROSCOPIC STUDIES OF KETO–ENOL EQUILIBRIA

PART 2. ANOMALOUS ULTRAVIOLET ABSORPTION SPECTRA OF SATURATED 1,2-DICYANO ESTERS[1]

T. R. KASTURI AND B. N. MYLARI
Department of Organic Chemistry, Indian Institute of Science, Bangalore, India

AND

A. BALASUBRAMANIAN AND C. N. R. RAO[2]
Department of Inorganic and Physical Chemistry, Indian Institute of Science, Bangalore, India

Received July 23, 1962

ABSTRACT

1,2-Dicyano esters show an absorption band around 245 mμ in alcoholic solutions which is not found in non-polar and other polar solvents. This anomalous behavior has been found to be due to the unusual solvent dependence of the equilibrium between the keto and enol forms. The intensity of the absorption band in alcoholic solutions decreases with increase in concentration of the 1,2-dicyano ester, indicating association of the enol form. The keto–enol equilibrium is also found to be sensitive to the substituent R of the alcohol ROH.

INTRODUCTION

1,2-Dicyano esters are often prepared as synthetic intermediates by the addition of hydrocyanic acid to unsaturated cyano esters. Kasturi (1) observed that some of the 1,2-dicyano esters exhibited fairly intense absorption bands around 245 mμ even after

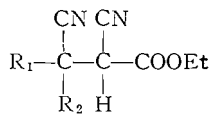

I

making certain, by infrared spectra, that there was no impurity of the parent olefin remaining. This is rather surprising since there is no absorbing chromophore in these derivatives (2). In this communication, we have reported the ultraviolet absorption spectra of several 1,2-dicyano esters and also certain model compounds, with a view to understanding the mechanism of absorption.

EXPERIMENTAL

The following 1,2-dicyano esters were studied and they were prepared by the addition of hydrocyanic acid to unsaturated cyano esters (for compound (i) see ref. 3; (ii), 4; (iii), 5; (iv), 6; (v), 6; (vii), 7; (viii), 1):

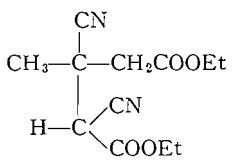

(i)

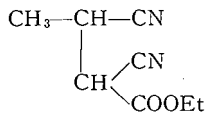

(ii)

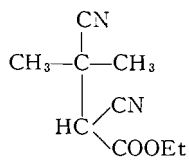

(iii)

[1]*Material taken from the Ph.D. Thesis of A. Balasubramanian submitted to the Indian Institute of Science under the guidance of C. N. R. Rao.*
[2]*To whom all the correspondence should be addressed.*

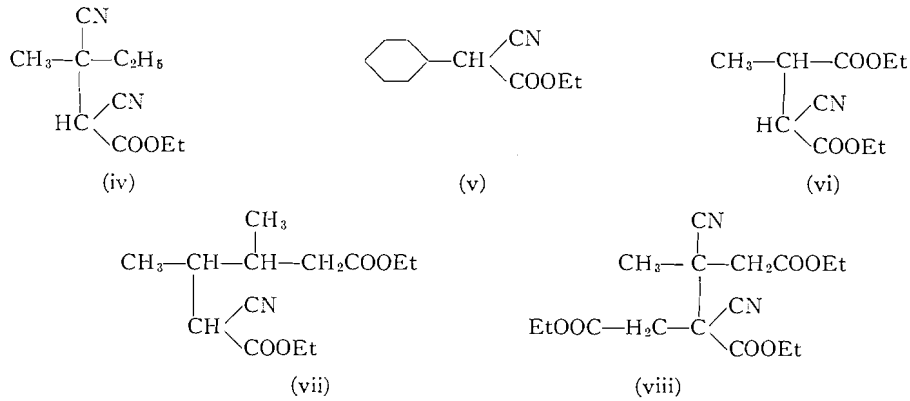

(iv) (v) (vi)

(vii) (viii)

These compounds were purified either by fractional distillation or by recrystallization before use. All the solvents employed were dried and distilled just before use.

The near-ultraviolet absorption spectra were recorded on a Hilger H700 UVispek spectrophotometer with matched quartz cells of 0.5-, 1.0-, 2.0-, and 4.0-cm path lengths. The infrared spectra were recorded on a Perkin-Elmer Infracord, model 137B, fitted with NaCl optics.

RESULTS AND DISCUSSION

The absorption data of several 1,2-dicyano esters in ethanol are summarized in Table I. First, it was considered that keto–enol tautomerism (I $\rightleftharpoons$ II) might be the possible cause

TABLE I

Near-ultraviolet absorption spectra of 1,2-dicyano esters (I) in ethanol

R_1	R_2	Concentration (moles liter^{-1})	λ_{max} (mμ)	ϵ_{max}
CH_3	H	6.017×10^{-3}	247	160
		6.017×10^{-4}	247	620
CH_3	CH_3	7.175×10^{-4}	247	1620
		3.6×10^{-4}	247	2240
CH_3	C_2H_5	1.03×10^{-3}	247	1520
		2.575×10^{-4}	247	2740
CH_3	$CH_2COOC_2H_5$	9.75×10^{-3}	242*	180
		6.5×10^{-5}	246	2020
Cyclohexyl		2.0564×10^{-3}	242*	160
		5.14×10^{-4}	246	260

*Shoulder.

of this absorption. But these derivatives fail to show any distinct absorption band in heptane and acetonitrile (Fig. 1). In simple compounds such as ethyl acetoacetate and

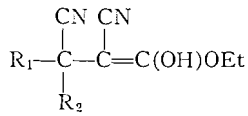

II

acetylacetone the band due to the enol form is much more intense in a non-polar solvent, such as heptane, than in alcohol or acetonitrile, since the keto form is more favored in polar or proton-donating solvents due to the stabilization of the C=O group (2, 8). But, the presence of the active hydrogen on the cyano ester residue is found to be necessary

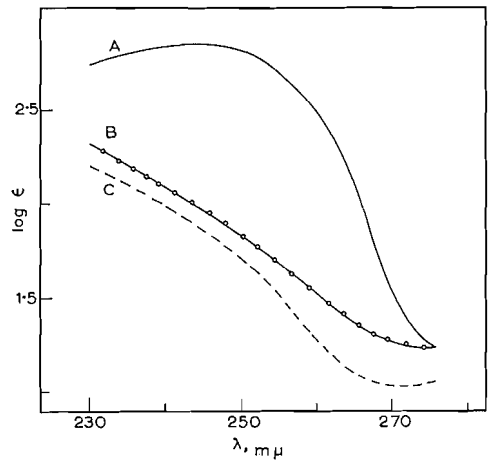

FIG. 1. The near-ultraviolet absorption spectra of a 1,2-dicyano ester (I, $R_1 = CH_3$, $R_2 = CH_2COOC_2H_5$) in heptane (C), acetonitrile (B), and ethanol (A).

for the absorption in these derivatives. Thus, derivatives III ($R_3 = CH_3$ or CH_2COOEt) do not absorb in the near-ultraviolet region.

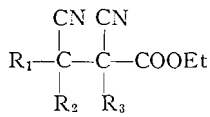

III

In view of these interesting results it was considered worthwhile to investigate the absorption spectra of a number of model compounds. A simple saturated dinitrile such as succinonitrile is transparent in the near-ultraviolet region. It is necessary to have a nitrile group on the carbon adjacent to the cyano ester moiety to observe this absorption (Table I). Thus, compounds IV and V do not absorb in the near-ultraviolet region.

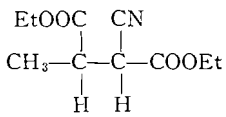

IV

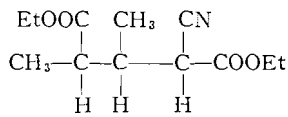

V

The 245 mμ band of 1,2-dicyano esters in ethanol is highly dependent on the concentration of the solute (Fig. 2 and Table I), unlike simple systems where there are keto–enol equilibria (8). The spectra recorded in different ethanol–heptane mixtures show that the extinction is also markedly dependent on the concentration of ethanol (Fig. 3). The extinction of the 245 mμ band is also found to be dependent on the substituent R of the alcohol ROH, the intensity generally decreasing in the order methanol, ethanol, *i*-propanol, and *t*-butanol (Table II). These results seem to point out that there is some solute association and also that the alcohol solvent is an important factor in the mechanism of the absorption.

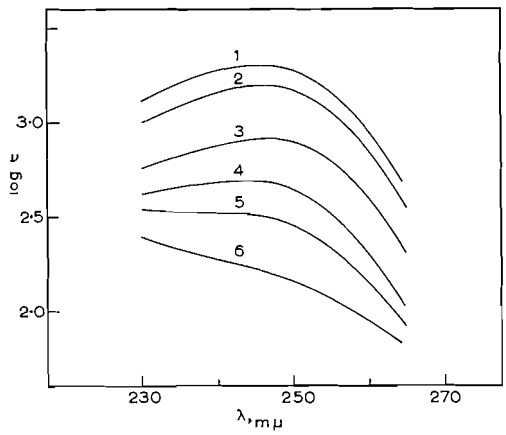

FIG. 2. Concentration dependence of the ultraviolet absorption spectrum of a 1,2-dicyano ester (I, $R_1 = CH_3$, $R_2 = CH_2COOC_2H_5$) in ethanol: (1) 6.5×10^{-5} *M*, (2) 2.5×10^{-4} *M*, (3) 6×10^{-4} *M*, (4) 2.4×10^{-3} *M*, (5) 5×10^{-3} *M*, and (6) 9.75×10^{-3} *M*.

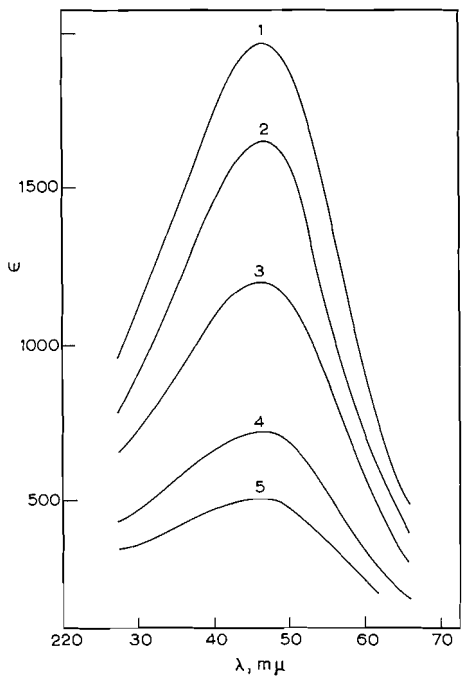

FIG. 3. The near-ultraviolet absorption of a 1,2-dicyano ester (I, $R_1 = CH_3$, $R_2 = CH_2COOC_2H_5$) in heptane–alcohol mixtures: (1) 0%, (2) 10%, (3) 40%, (4) 60%, and (5) 70% by volume of heptane.

Any mechanism offered to explain the absorption of 1,2-dicyano esters should necessarily explain the following observations:

(i) the necessity of the active hydrogen on the cyano ester moiety,
(ii) the necessity of the nitrile group on the adjacent carbon,
(iii) dependence of the extinction on the solute concentration, and
(iv) participation by the alcohol solvent.

TABLE II

Near-ultraviolet absorption spectra of a 1,2-dicyano ester
(I, $R_1 = CH_3$, $R_2 = CH_2COOC_2H_5$)

Alcohol	Concentration (moles liter^{-1})	λ_{max} (mμ)	ϵ_{max}
MeOH	4.024×10^{-4}	237*	560
	2.012×10^{-4}	237*	800
EtOH	4.98×10^{-3}	244*	320
	6.5×10^{-5}	246	2020
i-PrOH	1.163×10^{-3}	245	240
	5.817×10^{-4}	245	300
t-BuOH	1.102×10^{-2}	245–260	70
	6.17×10^{-4}	245–260	130

*Shoulder.

It is possible that tautomerism, I $\rightleftharpoons$ VI, may be the cause of the absorption of these derivatives in the near-ultraviolet region.

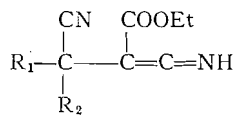

VI

In order to identify the nature of the species in alcohol media, infrared spectra of a 1,2-dicyano ester (I, $R_1 = CH_3$, $R_2 = CH_2COOEt$) were recorded in solutions of CCl_4 and 1:1 CCl_4–*i*-propanol mixture (Fig. 4). The most striking difference in the spectra in

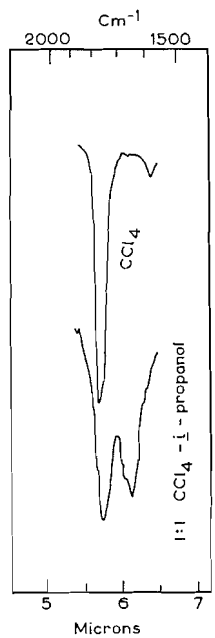

FIG. 4. The double-bond region of the infrared spectrum of a 1,2-dicyano ester (I, $R_1 = CH_3$, $R_2 = CH_3COOC_2H_5$) in CCl_4 and 1:1 CCl_4–*i*-propanol mixtures.

these two solvents is found in the double-bond stretching region. In the CCl_4–*i*-propanol solvent mixture, an intense band is found around 1650 cm^{-1} which can only be due to the C=C stretching vibration. A weak band around 2220 cm^{-1} (conjugated nitrile) is also seen in addition to the 2270 cm^{-1} band due to the saturated nitrile. If VI were the species, there should have been a fairly intense band around 2000 cm^{-1} due to the X=C=X type of group (9). These infrared results suggest that a keto–enol tautomerism (I $\rightleftharpoons$ II) with an unusual solvent dependence is responsible for the 247 mμ absorption of 1,2-dicyano esters in alcohol solvent. Apparently, the nitrile group of the cyano ester moiety is stabilized to a greater extent than the carbonyl group in alcohol solvents, probably due to the greater dipole moment associated with the nitrile group. The concentration dependence of the extinction may be explained in terms of association of the tautomer II, since the monomeric form may be quite unstable. The extent of such association as well as the associated species will vary with concentration and hence the concentration dependence of the extinction. At high concentrations of the solute, the species is only polymeric and the extinction is low.

ACKNOWLEDGMENTS

The authors are thankful to Professors D. K. Banerjee and M. R. A. Rao for their interest.

REFERENCES

1. T. R. Kasturi. Ph.D. Thesis, University of Bombay, Bombay, India. 1957. cf. D. K. Banerjee, T. R. Kasturi, P. Bagchi, A. R. Sen Gupta, and S. K. Das Gupta. J. Indian Inst. Sci. Golden Jubilee Res. Vol. 68 (1959).
2. C. N. R. Rao. Ultra-violet and visible spectroscopy—chemical applications. Butterworths, London. 1961.
3. P. C. Dutta, P. K. Dutta, and K. L. N. Sastry. J. Indian Chem. Soc. **31**, 881 (1954).
4. M. S. Newman and J. S. McPherson. J. Org. Chem. **19**, 1717 (1954).
5. A. Higson and J. F. Thorpe. J. Chem. Soc. 1465 (1906).
6. P. A. S. Smith and J. P. Harowitz. J. Am. Chem. Soc. **71**, 3418 (1949).
7. H. S. S. Iyengar and D. K. Banerjee. Unpublished results.
8. A. S. N. Murthy, A. Balasubramanian, T. R. Kasturi, and C. N. R. Rao. Can. J. Chem. This issue.
9. L. J. Bellamy. Infrared spectra of complex molecules. Methuen, London. 1958.

THE CRYSTALLINE FORM OF 1,3,5,7-TETRANITRO-1,3,5,7-TETRAZACYCLOOCTANE (HMX)

M. BEDARD, H. HUBER, J. L. MYERS, AND GEORGE F WRIGHT
Department of Chemistry, University of Toronto, Toronto, Ontario

Received August 11, 1962

ABSTRACT

The absorption spectra and dielectric constants of three of the four polymorphs of 1,3,5,7-tetranitro-1,3,5,7-tetrazacyclooctane (HMX) have been examined. The difference in absorption frequencies shows that these crystal forms are more distinctive than are most polymorphs. Likewise the distortion polarizations of HMX-I, -II, and -III are markedly different whereas identical distortion polarizations have been found among typical polymorphic systems. The distortion polarizations of HMX-II and -III also are unique because they are appreciably temperature dependent, although this electrical property ought to be temperature independent. Because of these unique behaviors we have postulated that the so-called HMX polymorphs actually are lattice-caged conformational modifications.

During the preparation of 1,3,5-trinitro-1,3,5-triazacyclohexane (RDX, Cyclonite, Hexogen) there is a contaminant formed in every process involving hexamethylenetetramine (1). This by-product, called HMX because of its high melting point (2), is known to be 1,3,5,7-tetranitro-1,3,5,7-tetrazacyclooctane (3). It has been found to exist in four polymorphic forms, HMX-I (β), -II (α), -III (γ), and -IV (δ) (4). The first three are workably stable at room pressure and temperature but HMX-IV transforms so readily that little has been done with it.

The classification as polymorphs has been derived from a consideration of physical properties. Only one graphic structure is required to explain the properties of HMX in solution. Only one melting point (280°) is known but solid-state transitions may be observed. The X-ray diffraction powder patterns of the polymorphs are quite distinctive, although frequently there is evidence of total or partial transformation during analysis of HMX-IV. However, the X-ray powder patterns of HMX-I, -II, and -III are quite as unique as those of the polymorphs of α- and β-resorcinol and of the 5-↑-hydroxy-6-↓-chloromercuri-1,4-↑↑-methylenecyclohexane-2-↑-3-↓-dicarboxylic acid polymorphs, which are included among others in Table I. Finally, the infrared spectra of the four forms of HMX in pellet dispersion are quite distinctive.

Indeed the infrared differences are so striking that they serve as well as the X-ray diffraction patterns for identification. The differences are apparent in the spectra of Fig. 1, the exact values of which are shown in Table I. In general the spectrum of HMX-I differs largely from those of HMX-II, -III, and -IV both in respect of the several methylene modes and also of the strong NNO_2 absorption in the 1300 cm^{-1} range.

It is of interest to compare the HMX spectra (Table II) with the spectra of the two substances shown in Table III. The two polymorphs of resorcinol, the structures of which are known, (5, 6) have very similar spectra; the notable difference (medium absorption at 1233 cm^{-1} in the beta but not in the alpha polymorph) is an expected one in view of the differences in hydrogen bonding that cause these crystalline modifications. The other pair of spectra shown in Table III depict the total effect of the crystal lattice because amorphous triphenylguanidine (obtained by quenching the molten substance on a cold metal plate (5), no X-ray diffraction pattern observed) is contrasted with the crystalline

TABLE I

X-Ray diffraction pattern identifications of crystal forms

Substance	d spacings, in angstroms, at relative intensities (I/I_1) using Cu $K\alpha$ nickel-filtered radiation
α-Resorcinol (stable)	(10) 4.44; (9) 4.87, 4.60; (8) 3.54, 3.43, 3.00; (6) 4.33; (4) 2.82, 2.53
β-Resorcinol (labile)	(10) 4.06; (9) 3.97, 3.21; (7) 4.91, 3.67; (6) 5.06; (5) 3.07; (4) 6.75, 6.28, 3.34
5-↑-Hydroxy-6-↓-chloro-mercuri-1,4-↑↑-methylene-cyclohexane-2-↑-3-↓-di-carboxylic acid, m.p. 183–184° C	(10) 4.21, 5.05; (9) 5.79; (8) 5.60; (7) 3.44; (6) 3.26, 3.14; (5) 3.03; (3) 2.39; (2) 2.74; (1) 2.66, 3.91
Same, m.p. 221–222° C	(10) 9.65; (9) 5.80; (8) 3.64; (7) 7.22; (6) 4.21, 4.25; (5) 4.56, 4.83, 5.26; (4) 3.22, 3.07; (3) 3.35, 3.50; (2) 2.94; (1) 2.82
Triphenyl guanidine (crystalline)	(10) 9.02; (9) 8.26; (8) 4.32; (7) 5.34; (6) 3.54; (5) 4.49; (4) 4.04; (3) 4.68; (2) 3.07; (1) 2.67
HMX-I	(10) 4.30, 2.79; (8) 3.86; (7) 3.41, 3.26, 5.53, 6.02; (6) 3.01, 2.41; (1) 4.84
HMX-II	(10) 5.37; (9) 3.60, 3.52, 2.74; (8) 5.94; (7) 4.53, 2.27; (6) 2.98; (5) 3.77
HMX-III	(10) 6.36; (9) 3.16; (8) 5.24; (7) 3.84; (6) 6.08; (5) 3.47; (4) 4.48; (3) 4.37; (2) 3.75; (1) 2.55
HMX-IV	(10) 3.64, 5.43; (9) 6.67; (8) 3.17, 3.48, 5.16; (7) 3.82; (6) 5.69; (5) 4.21; (4) 2.71; (3) 2.51; (2) 2.35, 2.22; (1) 2.15, 2.63
HMX–DMF, 1:1 complex	(10) 3.17, 5.18; (7) 3.98; (6) 4.35; (4) 6.80, 6.32, 3.02, 2.60, 2.46
1,5-Dinitro-1,5-diaza-3,7-dioxacyclooctane	(10) 4.68; (9) 3.34; (8) 5.38; (7) 2.83; (6) 2.95; (5) 2.60; (4) 2.37, 2.50; (3) 4.18, 2.68; (2) 2.04, 2.03; (1) 2.16, 2.24

TABLE II

Spectra of HMX-I, -II, -III, and -IV in the 3000–650 cm^{-1} range

	Wavelength (cm^{-1})
HMX-I	2999, 1575, 1460, 1432, 1385, 1348, 1280, 1239, 1202, 1148, 1090, 968, 949, 919, 864, 832, 773, 762
HMX-II	3030, 1575, 1545, 1455, 1415, 1394, 1368, 1323, 1270, 1218, 1111, 1090, 1034, 947, 919, 866, 849, 768, 754, 742, 714
HMX-III	3001, 1561, 1437, 1410, 1379, 1365, 1316, 1280, 1210, 1088, 1015, 967, 940, 911, 862, 840, 764, 751, 732, 707
HMX-IV	2993, 1715, 1551, 1440, 1409, 1375, 1308, 1267, 1242, 1212, 1105, 1088, 1011, 909, 864, 841, 763, 749, 733, 708

form. Although differences exist they are less than those among the HMX modifications. Moreover, in the "skeletal region" both substances of Table III show closely similar absorption by contrast with the marked difference in the 800–650 cm^{-1} region shown by HMX-I versus HMX-II, -III, and -IV.

These differences at the longer wavelength shown in Tables II and III are to be expected with the polymorphs and they ought to be even more characteristic in the 650–300 cm^{-1} region. However, this frequency range has not been favorable for examination of unstable species such as polymorphs because relatively high pressures (with consequent error due to strain) are required to pellet potassium chloride, which is used in order to utilize the spectrum at a frequency as low as 300 cm^{-1}. Of course, oils such as Nujol are transparent in this region but mulls are notoriously unreliable when precise comparisons are

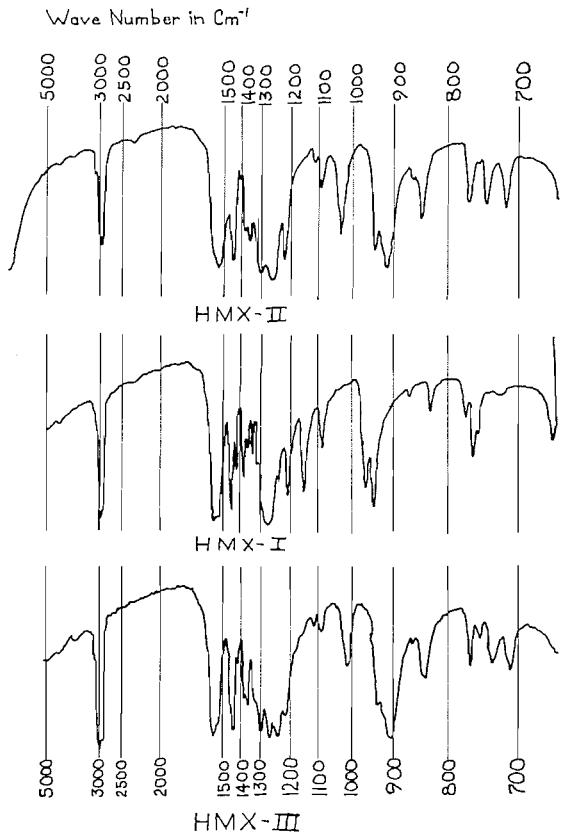

FIG. 1.

required. We have arrived at a compromise between these two media by use of polyethylene wax (molecular weight about 5000). A uniform mixture of the spectral candidate substance with this wax may be obtained and then pelleted easily (6000 p.s.i. for a pellet 2 cm²). Since polyethylene wax is suitably transparent (except for the CH_2 rocking mode at about 720 cm^{-1} at which frequency potassium bromide transmits) throughout the 300–900 cm^{-1} region it is the superior medium for examination of polymorphic substances.

The data of Table IV show absorptions in the 900–300 cm^{-1} region which are characteristically different for crystalline versus amorphous triphenylguanidine, for α- versus β-resorcinol, and for the differently melting polymorphs of 5-↑-hydroxy-6-↓-chloromercuri-1,4-↑↑-methylenecyclohexane-2-↓-3-↑-dicarboxylic acid (7). Nevertheless there are similarities which lattice force differences cannot conceal. By contrast the spectra of the HMX polymorphs I, II, and III are seen, in Table V, to be as different from one another as they are different from a number of other cyclic nitramines, which have been included for purposes of comparison. The distinctiveness is sufficient to suggest that phenomena other than simple polymorphism are involved with the HMX modifications.

The differences in extinction coefficient among polymorphs in the 900–300 cm^{-1} region ought to be the result of lattice force restriction on the structural absorption frequencies of the molecule. As such they ought to be sensitive to lattice dimension and, therefore, to variation in temperature. The polyethylene wax pellet is well adapted to temperature changes, so we have tested this variable from +40° to −39° in a special cell equipped

TABLE III

Spectral absorptions of *sym*-triphenylguanidine and resorcinol (3500–700 cm^{-1}) in potassium bromide

Triphenylguanidine				Resorcinol			
Crystalline		Amorphous		Alpha		Beta	
W.N.* (cm^{-1})	E_{max}	W.N. (cm^{-1})	E_{max}	W.N. (cm^{-1})	E_{max}	W.N. (cm^{-1})	E_{max}
692	20.73	694	21.94	681	7.19	688	6.87
740	11.13	742	18.77	744	6.33	742	4.66
751	18.77	755	20.73	781	6.59	776	4.52
765	12.17	—	—	—	—	806	3.80
840	3.73	834	3.98	851	4.52	846	3.69
—	—	854	2.78	864	2.74	855	4.52
—	—	885	1.54	971	5.47	969	5.66
—	—	897	3.48	1093	1.02	1083	1.63
906	4.80	901	4.25	1175	6.59	1170	6.59
963	1.09	963	1.09	—	—	1233	4.02
—	—	980	1.45	1325	6.59	1323	6.87
994	2.14	997	2.03	1412	6.59	1397	5.12
1029	2.67	1018	2.24	1511	6.09	1506	6.09
1075	4.66	1029	4.38	1639	5.67	1629	5.29
1111	0.99	1071	5.72	2702	2.32	2809	2.32
1160	2.14	1111	2.24	3378	5.87	3356	5.66
1179	3.73	1159	4.11				
1259	17.21	1179	7.14				
1326	20.73	1250	20.73				
1399	3.36	1330	18.77				
1451	14.75	1449	16.53				
—	—	1497	20.73				
1558	25.10	—	—				
1592	25.10	1587	25.10				
1647	18.77	—	—				
2941	10.21	3021	10.81				
3333	9.13	3226	9.65				
5155	8.88	—	—				

*W.N. = wave number.

with very thin latex rubber windows and have found (after correction for change of density) that absorption frequency is constant within our precision but that measurable differences in E_{max} occur for every absorption listed for HMX in Table VI. These differences appear greatest for the most dense (HMX-I) and least for the least dense (HMX-III) crystal modification, as would be expected if lattice restriction is effective. That is to say there is greater freedom for the molecule in HMX-III than in HMX-I. In consequence the thermal effects on lattice dimension will be more significant in HMX-I than in HMX-II and -III.

Since the dependence of extinction coefficient upon temperature has been interpreted in terms related to this geometry of the molecule it is of interest to consider the results of Table VI in view of those in Table VII. In Table VII are recorded the effects of decreasing temperature on part of the spectrum of *dd,ll*-2,5-dimethyl-2,5-dimethoxy-3,4-diphenylhexane. It may be seen that all of these skeletal absorptions are augmented by decreasing temperature and, therefore, are affected in the same way as the electrical moment (8) in benzene or carbon tetrachloride solution. But the higher dipole moment at the lower temperature is related to the most stable conformation that this tetrasubstituted ethane can assume. One may expect that as the population of this stable configuration becomes more preponderant the excitations characteristic of it will increase, with consequent narrowing of the absorption band to a greater peak.

TABLE IV

Spectral absorptions of *sym*-triphenylguanidine, resorcinol, and 5-↑-hydroxy-6-↓-chloromercuri-1,4-↑↑-methylenecyclohexane-2-↓-3-↑-dicarboxylic acid in polyethylene wax (700–300 cm^{-1})

Triphenylguanidine				Resorcinol				Hydroxychloromercurimethylene-cyclohexanedicarboxylic acid			
Crystalline		Amorphous		Alpha		Beta		Polymorph, m.p. 222°		Polymorph, m.p. 184°	
W.N. (cm^{-1})	E_{max}	W.N. (cm^{-1})	E_{max}	W.N. (cm^{-1})	E_{max}	W.N. (cm^{-1})	E_{max}	W.N. (cm^{-1})	E_{max}	W.N. (cm^{-1})	E_{max}
295	0.86	294	0.27	354	13.94	358	9.47	317	8.4	316	7.5
374	19.23	389	12.54	383	7.81	388	8.03	351	2.8	352	2.0
407	13.84	—	—	456	18.42	455	10.56	390	2.6	388	1.6
453	24.03	450	17.15	491	11.45	480	9.21	414	2.6	410	1.2
478	33.38	480	23.38	—	—	512	10.55	429	4.0	428	2.6
494	36.36	—	—	538	19.07	531	10.72	453	3.3	451	1.8
504	51.56	504	22.74	668	19.07	676	5.14	550	5.3	553	3.0
538	17.15	—	—					649	8.4	648	6.7
608	10.90	570	10.90					675	6.0	678	3.7
627	15.68	625	9.73					699	5.8	—	—
685	39.71	684	22.74					791	8.4	794	3.7
								841	1.8	—	—
								881	10.1	884	6.1

TABLE V

Spectral absorptions of cyclic nitramines in polyethylene wax (700–300 cm^{-1})

HMX-I	W.N. (cm^{-1})	354	375	382	416	437	597	625	656	761	772	830					
	E_{max}	4.86	6.85	12.35	8.66	12.70	29.15	20.83	15.82	23.38	14.58	13.79					
HMX-II	W.N. (cm^{-1})	374	397	450	598	622	644	745	767	847	861	881					
	E_{max}	13.31	7.01	13.72	30.05	16.85	29.21	11.35	26.15	25.45	17.33	11.73					
HMX-III	W.N. (cm^{-1})	381	404	418	461	478	605	617	646	711	755	770	846	851	871		
	E_{max}	6.81	6.51	6.21	6.21	6.91	29.63	31.37	9.75	9.94	12.72	19.10	20.74	20.74	13.12		
HMX–DMF,	W.N. (cm^{-1})	326	330	362	372	460	599	616	640	660	708	766	847	—	—		
1:1 complex	E_{max}	9.06	9.06	12.96	10.31	12.05	29.92	26.83	17.45	17.99	12.51	22.09	23.37	—	—		
QDX*	W.N. (cm^{-1})				384	414	433	515	591	612	632	653	698	744	761	794	824
	E_{max}				8.05	5.84	6.78	9.41	15.66	19.49	12.57	8.85	8.30	14.83	19.49	11.56	15.24
PS-2†	W.N. (cm^{-1})					—	443	460	484	—	678	—	784	844	866	—	—
	E_{max}					—	5.91	4.84	5.55	—	11.40	—	8.91	9.95	11.09	—	—
RDX‡	W.N. (cm^{-1})					408	458	484	585	591	601	669	702	755	785	848	881
	E_{max}					5.14	6.57	5.22	10.14	10.14	9.34	6.99	7.43	12.62	15.32	12.62	14.84
TAX§	W.N. (cm^{-1})					415	460	486	515	586	631	704	750	762	812	848	884
	E_{max}					5.90	7.11	8.72	8.00	14.69	8.00	8.47	13.90	13.15	10.58	13.90	20.46

*QDX is 1,3,5-trinitro-7-aceto-1,3,5,7-tetrazacyclooctane.
†PS-2 is 1,5-dinitro-3,7-dioxa-1,3,5,7-tetrazacyclooctane.
‡RDX is 1,3,5-trinitro-1,3,5-triazacyclohexane.
§TAX is 1,3-dinitro-5-aceto-1,3,5-triazacyclohexane.

TABLE VI

Variations in absorption spectra of HMX polymorphs with respect to temperature

W.N. (cm^{-1})	E_{max} of HMX absorption								
	I			II			III*		
	+40°	−39°	Diff.	+40°	−39°	Diff.	+40°	−39°	Diff.
353	0.51	1.45	+0.94						
373				5.49	7.45	+1.96			
382	5.49	9.90	+4.41						
396				4.81	7.24	+2.43			
417	2.32	4.30	+1.98						
436	4.58	9.73	+5.15						
450				5.67	6.23	0.56			
596	15.6	Total							
600				13.76	11.91	−1.85			
607							9.34	9.90	+0.56
616							9.91	11.40	+1.49
621				15.25	17.25	+2.00			
627	12.52	22.05	+9.53						
645				12.09	13.94	+1.85			
646							2.80	3.63	+0.83
770				7.94	6.82	−1.12			
768							5.57	5.73	0.16

*Because of the tendency of γ-HMX toward transformation the sample grinding was not as thorough as was used for HMX-I and -II. Consequently, some particle-size interference occurred below 600 cm^{-1}, and the lower-frequency absorptions have not been included because they are indistinct.

TABLE VII

Variation in absorption spectra of 2,5-dimethyl-2,5-dimethoxy-3,4-diphenylhexane in carbon disulphide with respect to temperature

W.N. (cm^{-1})	Temp. (°C)	E_{max}	ΔE_{max}
700	+40	44.1	
"	0	48.0	+ 3.9
"	−36	54.2	+10.1
724	+40	8.2	
"	0	9.8	+ 1.6
"	−36	10.5	+ 2.3
780	+40	12.0	
"	0	13.8	+ 1.8
"	−36	15.8	+ 3.8
1069	+40	44.1	
"	0	46.7	+ 2.6
1132	+40	23.7	
"	0	25.0	+ 1.3
1178	+40	23.2	
"	0	26.6	+ 3.4
1213	+40	12.9	
"	0	14.5	+ 1.6

Although this study of *dd,ll*-2,5-dimethyl-2,5-dimethoxy-3,4-diphenylhexane involves its solutions and as such is not directly applicable to the polymorphic solid states of HMX it does suggest that some relationship might be observed between infrared absorption and electrical polarization.

A method is available whereby the electrical polarization of crystalline solids (the distortion polarization) may be measured (9, 10). The method is not now applicable to solids melting below 50°, so crystalline dimethyldimethoxydiphenylhexane cannot be measured in this manner. However, the polymorphs of HMX are adequately high

melting, and reliable dielectric constants have been determined for HMX-I, -II, and -III. The distortion polarization may then be calculated from $(\epsilon-1)/(\epsilon+2)(M/D)$, where the density has been determined by air displacement (11).* Although polymorphic transformations are immanent under the manipulations required for this measurement it can be shown by X-ray or infrared analysis after the measurement that with care the transformation may be avoided. The results of the measurements are recorded, among others, in Table VIII, both as distortion polarizations (P_D) and as the residua after subtraction

TABLE VIII

Distortion polarizations

Polymorphs	d_4^{20}	ϵ	P_{E+A} (cc)	P_e* (cc)	P_A
α-Resorcinol (stable)	1.275	2.956	34.1	29.5	4.6
β-Resorcinol (labile)	1.298	3.032	34.2	29.5	4.7
5-↑-Hydroxy-6-↓-chloromercuri-1,4-↑↑-methylenecyclohexane-2-↑-3-↓-dicarboxylic acid, melting point 183–184° C	2.420	3.917	88.5	60.0	28.5
Same, melting point 221–222° C	2.453	4.019	88.9	60.0	28.9
Triphenylguanidine crystalline	1.135	2.964	100.0	89.5	10.5
Same, amorphous	1.154	3.036	100.6	89.5	11.1
HMX-I	1.9	3.087	63.6	58.3	5.3
HMX-II	1.87	4.671	87.0	58.3	28.7
HMX-III	1.82	3.867	79.5	58.3	21.2
HMX–DMF, 1:1 complex	1.72	3.180	87.8	78.1	9.7
1,5-Dinitro-1,5-diaza-3,7-dioxacyclooctane	1.693	3.790	59.2	42.3	16.9

*These electronic polarizations were calculated by summation of the constituent bond refractions.

of the electronic polarizations (P_E), which are equivalent to molecular refraction calculated from bond (12) or atom and group (13) refractions. These residua are called the atom polarizations (P_A). They include the electromagnetic polarizabilities at frequencies which atomic structures can follow and exclude polarizabilities due to orientation of the molecule as a whole. The latter are at any rate supposedly excluded in the solid state.

The atomic polarization (P_A) ordinarily may be expected to comprise only a small (2–5%) amount of the distortion polarization (P_{E+A}) because the energy corresponding to atomic and skeletal vibration is much less than that of electronic polarization. However, there are exceptions (not completely understood) where the atomic polarization is abnormally high. Such abnormalities seem to involve the presence of permanent dipoles (14, 15), although many substances with obvious dipoles do not display this abnormality (16). Whatever may be the cause, all of the substances listed in Table VIII show abnormally high atom polarizations. The first three of these substances have been chosen on the basis of high P_A in order that the effect of crystal lattice forces toward atom polarization might be discernible.

For the first three substances reported in the table the lattice forces seem not to be effective toward alteration of atom polarization within the precision of our measurements. The distortion polarizations (Table VIII) of α- and β-resorcinol are almost identical. Likewise the polymorphic forms of 5-↑-hydroxy-6-↓-chloromercuri-1,4-↑↑-methylenecyclohexane-2-↑-3-↓-dicarboxylic acid (7) differ in P_{E+A} by only 0.4 cc. Indeed the dis-

It is a consequence of the determinations that density determined by air displacement is less precise than the determinations by flotation. Moreover much more substance (0.5 g) is required for the air displacement method. However, problems of solubility and chemical reaction are obviated by air displacement. Consequently the air displacement method is more accurate and, therefore, is used whenever sufficient substance is available.

tortion polarization seems to be practically independent of lattice forces. This independence is exemplified by comparison of the amorphous triphenylguanidine (7) with its crystalline modification. The distortion polarization of the pair differs only by 0.6 cc. This difference is approximately the limit of the analytical precision.

Within this limit the crystal forms of these three typical substances do not affect their atom polarization. In contrast are the distortion polarizations found for HMX-I, -II, and -III. Assuming that their electronic polarizations are identical (58.3 cc) and calculable from bond refractions (12), as seems justified by earlier studies with nitramines (15), the atom polarization of HMX-I ($P_E-(\epsilon-1/\epsilon+2)(M/d)$) is 5.3 cc. On the same basis of calculation (ϵ = dielectric constant, M = molecular weight, and d = density), the atom polarization of HMX-II is 28.7 cc while that of HMX-III is 21.2 cc. No value has been determined for HMX-IV because of its great tendency to transform at room temperature.

The relative order of these atom polarizations (I < III < II) follows neither the order of densities nor the order of the thermal stabilities (I > II > III) and thus does not seem to be related simply to lattice packing or lattice energies. A more fruitful correlation may be sought from a previous study (15) where markedly high atom polarizations were found to exist among crystalline nitramines. These atom polarizations (4–7 cc per nitramino group) are not unexpected if they are due to charge separation because this group is responsible for large dipole moments in substances containing it (15).

A relationship of high atom polarization might have been predicted from the distortion polarizations of the alkali halides. The correlation ought to follow a function including ionic volume and charge separation, i.e. MF < MBr < MCl < MI, where M is an alkali metal ion, although the previous experimental evidence is equivocal. The predicted order was indeed found by Heydweiler (17) but not by Errera (18). To our satisfaction we have resolved this discrepancy by application of our wafer technique (8) to the crystalline sodium and potassium halides. In conformity with Errera we find the polarization to be independent of frequency between the limits of 0.5–5.0 mc but, as may be seen from Table IX we confirm Heydweiler (for the salts that he examined) rather than Errera in

TABLE IX

Distortion polarization of alkali metal halides at 20° C

Salt	d_4^{20}	$(M.R.)_D$* (cc) (P_A)	Dielectric constant			P_{E+A} (cc)		P_A (cc)
			Heydweiler	U. of T.	Errera	Errera	Heydweiler and U. of T.	
NaF	2.828	2.97†	3.94	3.950	4.9	8.4	7.4	4.4
NaCl	2.163	8.28	6.12	6.117	5.77	16.6	17.0	8.7
NaBr	3.213	11.46		5.878	5.99	20.1	19.8	8.2
NaI	3.659	16.16		6.551	6.60	26.6	26.6	10.4
KF	2.482	5.06	4.18	4.182	6.5	15.1	12.1	7.0
KCl	1.984	10.54	5.03	5.042	4.76	20.8	21.6	11.1
KBr	2.750	13.45	4.60	4.578	4.78	24.1	23.5	10.0
KI	3.123	18.73	5.60	5.607	4.94	30.2	32.2	13.6

*M.R. = molecular refraction.
†Calculated from square of refraction index (extrapolated to infinite wavelengths) as given by Errera.

respect of the order (F < Br < Cl < I) of the atom polarization of the sodium and potassium halides. Therefore, the preponderance of evidence supports the idea that

abnormally high atom polarization in (at least) an ionic crystal is related to the extent of charge separation among the atoms.

It is reasonable to presume that permanent charge separation in a covalent molecule likewise may contribute to the atom polarization. Indeed the nitramines (of which HMX is an example) in microcrystalline wafers show in general an amount of distortion polarization which cannot be accounted as electronic and so has been called atomic. This assignment of atom polarization amounts to about 7 cc per nitramino group (=NNO_2). Moreover the atom polarization is roughly additive, as is shown by the two nitramino groups in the linear N-methylnitramino-*bis*-ethane, I, the P_A of which is 14.5 cc.

However, if a relationship among nitramines exists in the solid state between charge separation and atom polarization it is not a simple one. When several nitramino groups are present in relatively fixed portions in a molecule (in contrast to I) the resultant atom polarization tends to be lowered. For example N,N′-dinitropiperazine, II, is found (15) to have an atom polarization ($P_D - P_E$) of 3.7 cc rather than of 14 cc expected (from group summation) such as occurs in the non-cyclic I. A limiting instance is that of 1,3-dinitro-1,3-diaza-5-oxacyclohexane, III, where no atom polarization at all is detectable ($P_D = P_E$).

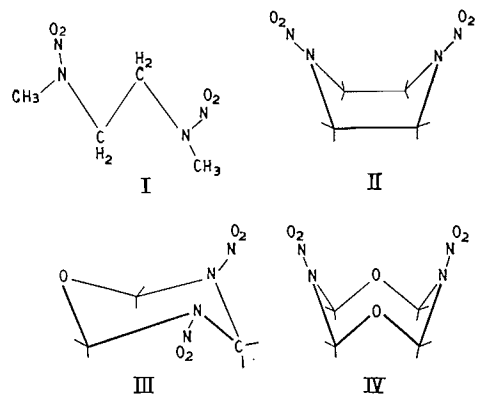

It is reasonable to draw from these observations the conclusion that when polar groups are in structural apposition they tend mutually to cancel the atom polarization of each group. The magnitude of this cancellation is in qualitative agreement with the expectation that the nitramino group is planar (or nearly so) as a consequence of resonance hybridization (19). The sp^2 character of the ring nitrogen disposes these groups equatorially and thus closely in apposition. On the other hand this sp^2 character might be expected to "fold" the molecule of 1,5-dinitro-1,5-diaza-3,7-dioxacyclooctane, IV, so that the atom polarizations of the nitramino group are geometrically additive rather than subtractive. It is tempting to attribute the 16.9 cc (Table VIII, $P_D - P_E$) of atom polarization found for IV entirely to this additive effect, but probably the geometry does not justify all of this magnitude. Flexibility of the molecule (to be discussed later) undoubtedly contributes as well.

It must be noted that these concepts are contradictory to the theory of Coop and Sutton (20), who attributed the appreciable difference between total and electronic polarization of a group of substances with opposed dipoles to atom polarization because inspection of the formulas indicated that orientation polarization could not occur. This theory became unacceptable to us when our "wafer" measurements showed that some

of these substances either showed no abnormality of atom polarization or else much less P_A (21, 15) than Coop and Sutton specified. Moreover certain of the substances, such as *p*-benzoquinone, tetramethylcyclobutane, and *p*-dinitrobenzene, were shown to have measurable orientation polarizations. In view of these experimental results we must at the present time favor our concept of group apposition rather than that of Coop and Sutton.

However, neither the theory of Coop and Sutton nor our own concept explains fully the difference in atom polarization shown by HMX-I, -II, and -III by contrast to the solid-state modifications of other substances in Table VIII. Therefore, we suggest for these HMX modifications some possible differences in conformation which would be labile in solution but may persist in the crystals. From at least five probable conformations we shall select three which are free from transannular methylene interaction. The conformation V has all four carbons in one plane and all aza nitrogens in another plane while in conformation VII all carbons are in one plane but two each of the aza nitrogens are in planes above and below the plane of methylene carbon. Intermediate between these extremes is VI, in which the four methylene carbons and two aza nitrogens as slightly puckered out of a plane and the remaining aza nitrogens are above this "plane".

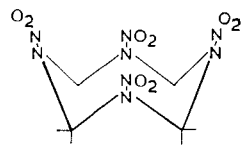

V, HMX-II (P_A, 28.7 cc)

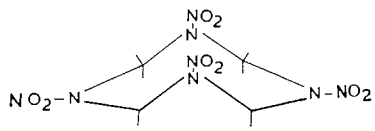

VI, HMX-III (P_A, 21.2 cc)

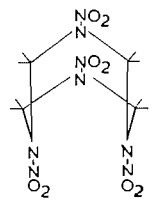

VII, HMX-I (P_A, 5.3 cc)

Assuming again that the NNO_2 group is chiefly planar the four groups in V ought to be geometrically additive while those in VII are subtractive. In VI two nitramino groups are strongly additive while the other two are weakly so. Therefore, V ought to represent HMX-II, VII corresponds to the low P_A of HMX-I, and the 21.2 cc atom polarization of HMX-III is best described by VI.

It is obvious by inspection that the amount of space occupied by these three conformers will be VI > V > VII. Although the density of lattice packing is not necessarily related to the volume of the molecules contained in the lattice it may be significant that the

structural assignments correspond with the densities (HMX-I > -II > -III) of the polymorphs.

The assignment of conformation V to HMX-II would seem nominally to be at variance with a recent single-crystal X-ray diffraction study (22) which favors conformation VI for this polymorph. The contradiction may be more apparent than real. Each scientific observer sees his evidence through the window of his method. The X-ray diffraction method "sees" mean position of electronic charge, which is assumed to be stagnant and centered by a nucleus. By contrast the reactance in an applied electrical field is accentuated by charge separation and thus "sees" preferentially the most strongly polar states of a system. It follows that different interpretations will be made if the structure of the substance is dynamic rather than static. But both X-ray and dielectric measurements agree that the difference in the HMX solid states is conformational. It remains to ascertain whether there is sufficient freedom in the crystal array to allow for that conformational motion which would cause the results of X-ray diffraction to differ from those of dielectric measurements.

Empty space in a crystal lattice is metastable at temperatures at which thermal agitation does not warrant its existence. The transformations of forms like HMX-II and -III into HMX-I at room temperature exemplify the metastability. However, it may be expected that other molecules might also fill these empty spaces if they were geometrically compatible with the space. The existence of a 1:1 molecular complex of HMX and dimethylformamide (23) therefore is not unexpected. In conformity with the expectation of a stoichiometric crystal complex (not a clathrate) is the analysis and the stability of HMX–dimethylformamide. An examination of the characteristic absorptions in the infrared spectral region shows a closer resemblance to HMX-II or -III than to HMX-I.

In absence of space-filling addenda one may assume that some conformational motion occurs within the lattice restriction which prevents transformation from HMX-III or -II to HMX-I at room temperature. If the interpretation of the HMX polymorphs is correct then these values ought to be temperature dependent.

In order to test this postulation several alterations in our technique for dielectric measurements have been necessary for the temperature range (−40 to +28°) which we have chosen. Instead of gold amalgam as a wafer surface layer we have used indium foil as the conductor. The foil-coated wafer is aligned on the flat Kovar metal cylindrical platform at the top of the non-grounded terminal D in Fig. 2. The sliding grounded terminal P not only completes the capacitance circuit but also transmits any change in thickness of the wafer assembly to the machinist's gauge K at the top. The temperature is measured by two thermistors situated as close to the wafer assembly as is possible. Ingress of moisture is prevented by dry nitrogen, in at N and out around the upper end of P.

The temperature may be lowered to −40° C by passage of dry air through the liquid-nitrogen-cooled coil at A and thence through the middle of three annuli and out at C. The outer, highly evacuated annulus is strip-silvered to reduce radiation and to shield the capacitance of the wafer which is being measured. The inner annulus, at atmospheric pressure, permits gradual and uniform heat exchange. About 1 hour is required to decrease the temperature to −40° after which the temperature is gradually increased to +28° during 5 hours by regulation of the airflow. Although the change in pellet thickness and capacitance is recorded during this interval (to detect abnormalities such as wafer fracture or foil separation) only the capacitance and thickness at −40° and +28° are used for calculation. Subsequently the dielectric constant and the thickness of the wafer are measured in the apparatus (Fig. 3) described previously (10).

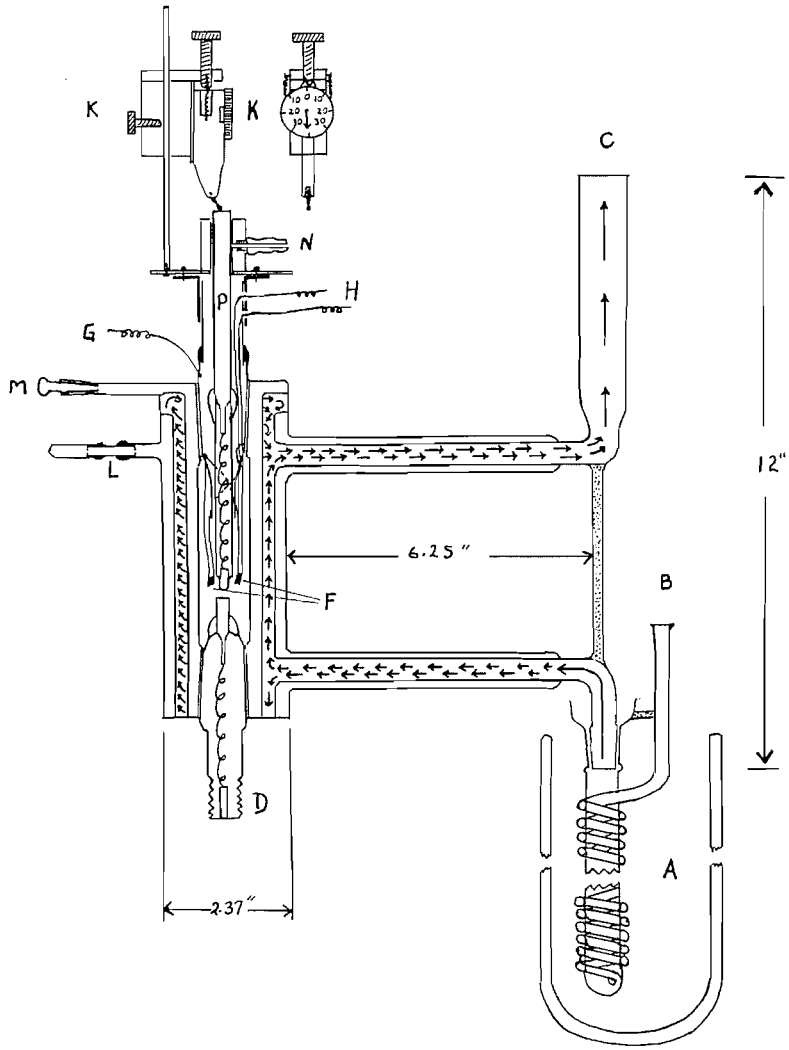

FIG. 2.

Since the measurement does not take into account the "edge effect" the dielectric constants derived at +28 and −40° are in error. For correction of the error a series of wafers of various thickness is examined and the apparent dielectric constants are plotted against thickness in order that the true dielectric constant may be ascertained by extrapolation to infinitesimal thickness (zero edge effect).

Several of these plots are shown in Fig. 4. It may be seen that the deviation is too great for graphic extrapolation and the method of least squares must be utilized. The least satisfactory of all the determinations is that of HMX-I. This latter result should not be considered to be typical because great difficulties were encountered in the preparation and maintenance of the wafers prepared for this polymorph even though 2% of polyethylene wax was incorporated for the purpose of consolidation.

The distortion polarizations calculated from the dielectric constants at +28° and −40° for a series of representative substances are shown in Table X. When the distortion

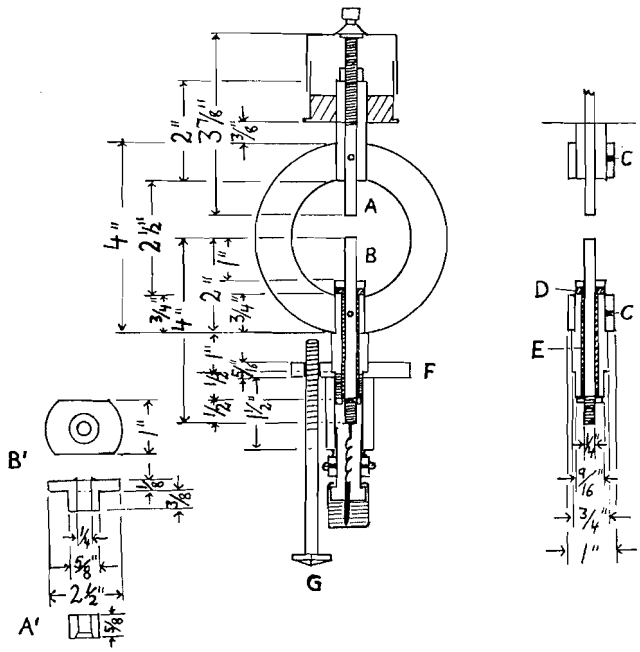

FIG. 3.

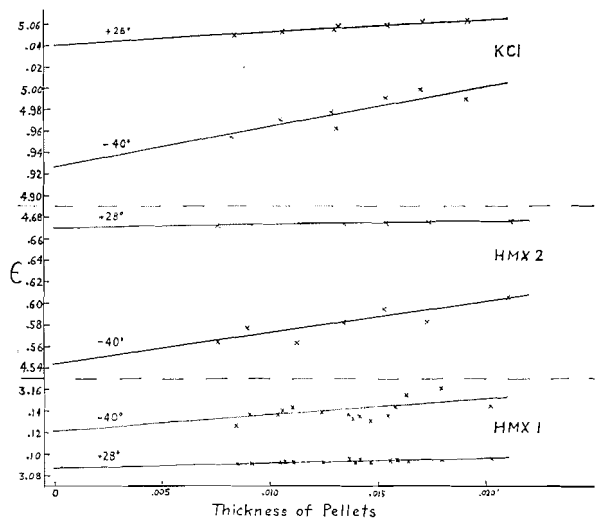

FIG. 4.

polarization is close in value to that of the temperature-invariant electronic polarization (i.e. when atom polarization is normally low) it ought to be the same at +28° and at −40°. Consequently the variations (+0.27 cc, +0.12 cc) over this temperature range for anthraquinone and hexachlorobenzene may be considered to be representative of experimental error. With this assignment of error the high atom polarization of zirconium acetylacetonate (10) must be declared invariant with respect to temperature. Likewise the appreciable atom polarization of sodium and potassium chlorides are temperature

TABLE X

Distortion polarization at $+28°$ (t_1) versus that at $-40°$ (t_2)

Substance	t (°C)	ϵ	d_4^{20}	P_D (cc)	ΔP_D (t_2-t_1)
Anthraquinone	t_1	3.200	1.421	62.0	
	t_2	3.217		62.3	+0.3
Zirconium acetylacetonate	t_1	2.937	1.412	135.3	
	t_2	2.938		135.4	+0.1
Hexachlorobenzene	t_1	2.832	2.044	52.8	
	t_2	2.839		52.9	+0.1
Sodium chloride	t_1	6.125	2.165	17.1	
	t_2	5.944		16.8	−0.3
Potassium chloride	t_1	5.040	1.984	21.6	
	t_2	4.927		21.3	−0.3
HMX-I	t_1	3.087	1.91	63.6	
P_A = 5.3 cc at 23°	t_2	3.118		64.1	+0.5
HMX-II	t_1	4.671	1.87	87.0	
P_A = 28.7 cc at 23°	t_2	4.544		85.8	−1.2
HMX-III	t_1	3.868	1.82	79.5	
P_A = 21.2 cc at 23°	t_2	3.776		78.2	−1.3

independent within our limit of error. These results are not unexpected in view of the commonly accepted concept of atom polarization.

On the other hand the ΔP_D of the HMX polymorphs is each beyond our limits of experimental error. Because of the difficulties in manipulation of HMX-I (exemplified by the ϵ vs. thickness plot of Fig. 4) we are reluctant to attach any meaning to the positive ΔP_D of 0.5 cc found for this polymorph. On the other hand the wafers of HMX-II and -III were prepared easily and the consequent plots of dielectric constant versus thickness are at least as good as those of the other substances listed in Table X. It seems clear that an appreciable diminution in distortion polarization is characteristic of HMX-II and -III at low temperatures. This behavior is the expected one if conformational motion were indeed occurring in these lattices of lesser density than that of the close-packed, centrosymmetrical HMX-I.

The extent of diminution in P_D with respect to temperature in HMX-II and -III is inversely related to the amount of "abnormality" in P_A. This might be interpretated as evidence of greater flexibility in HMX-III than in HMX-II. However, it seems more reasonable to attribute the higher ΔP_D in HMX-III to the geometry of our conformational assignments. It is a consequence of the symmetrical arrangement of the nitramino groups in conformation V, which we have assigned to HMX-II, that small deviations from this symmetry will be less effective in altering the resultant of the four directed dipoles than in the conformation VI, attributed to HMX-III, because the resultant of the axially aligned dipoles in VI will not be altered as much by small deviations in conformation as will be the resultant of the equatorial dipoles.

In summary the evidence from spectral absorption studies and electrical polarization studies seems to indicate that HMX-I, -II, and -III are lattice-caged conformational isomers which may undergo a restricted type of orientation polarization. On this basis it might be said that their abnormal P_D values do not involve high atom polarization and, indeed, that they are not properly to be classified as polymorphs. However, the etymological classification of natural phenomena is of less importance than the physical definition of these phenomena. Undoubtedly other crystals can be found in which conformational motion is detectable by the techniques of infrared spectroscopy and dielectric constant evaluation. We are searching for them.

EXPERIMENTAL

Temperature Coefficient of Distortion Polarization

A. Preparation of Wafers

Two techniques are used depending upon the physical characteristics of the candidate substance. According to method I the substance is first pressed at about half the usual compression (7500 lb dead load) in the die shown in the cross section in Fig. 5. Then the upper and lower (long and short) pistons are removed after the

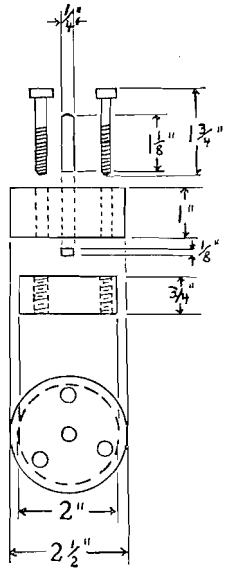

FIG. 5.

lower piston has been extruded slightly and disks of indium foil 0.01 inch thick and of diameter equal to that of the die cylinder are inserted onto both faces of the wafer *in situ*. The pistons are then reinserted and a maximum compression (15,000 lb dead load) is applied to the assembled die before the wafer is removed.

According to method II an indium disk is placed on the top of the small piston in the die and the finely powdered candidate substance is placed on top of it. The upper surface of the powder is now levelled by a circular motion of the upper piston. Then another indium disk is placed on top and the assembly is subjected to maximum compression.

By either of these methods the indium foil is likely to be extruded over the lateral wall of the wafer. This excess must be removed carefully by means of a very sharp knife. It is advisable to allow the wafers to "age" for 1 day during which time blisters may form on the surface. These blisters may be punctured with a needle and then flattened smoothly with a spoon-shaped tool. The reliability of a wafer also may be ascertained by cooling it quickly to $-40°$ in a test tube and then allowing it slowly to warm to room temperature.

B. Apparatus for Temperature-variant Measurement of Dielectric Constant

The cylindrical apparatus shown in Fig. 2 in cross section consists mainly of a lower electrode, an upper electrode, and a glass jacket. The jacket is triple walled. The outer annulus is highly evacuated and also is strip silvered; the silvering is continuous around top and bottom and it extends over the inner surface of the Kovar-glass seal, L, so that external grounding of L provides effective shielding from external influence. The middle annulus accommodates the cooling air which enters at B, is chilled by liquid nitrogen in A, and which leaves the apparatus at C. The inner annulus contains stagnant gas (usually air) at any desired pressure (usually atmospheric) but is variable by means of the tapered joint closure at M. The inside surface of this inner annulus is tooled and ground, and top as bottom, for 24/40 taper.

The lower electrode consists of a uniaxial fitting D surmounted by a 24/40 joint to which is sealed a Kovar rod platform upon which the test wafer is situated. The upper electrode is equipped with two thermistors F that are mutually grounded onto silver which is plated on the 24/40 cone. The insulated thermistor leads, H, are connected to two vacuum tube Wheatstone bridges off which the temperature can be read to $\pm 0.1°$ from a 10-turn potentiometer where a 6E5 magic eye tube indicates balance. The upper electrode is shown in more detail in Fig. 6, which depicts the guide platform as well as the internally grounded prolongation of the 24/40 joint and consists of a Trubore tube to which a rounded Kovar pin is sealed at

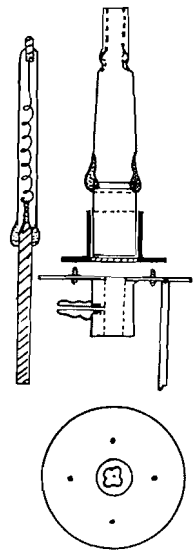

FIG. 6.

the bottom and a 5/16 Kovar rod is sealed at the top. Ground connection through this electrode is established by the interconnecting silver wire and the contact with the point of the machinist's gauge at the top. The dry nitrogen entrance at N blankets the interior of the assembly by emergence around the platform guide.

C. Apparatus for Room-temperature Measurement of the Dielectric Constant

This apparatus has already been described briefly (10). Constructional details are shown in Fig. 3 for a cross-sectional side view and end view. Also shown are polymethacrylate accessories A′, which slides on A as a centering device for the wafer, and B′, which slides on B for the same purpose as well as to catch droplets of gold amalgam when the latter is used as a wafer coating. It has been found necessary to install a rigidly attached ring, F, in which are threaded three equally spaced screws (one shown as G) which serve to keep the uniaxial connector under tension, thus to establish stability of the entire measuring device.

Insulation of the lower electrode is effected by means of the precisely concentric Steatite ring D and the glass tubing E. Around E at the bottom is a fiber insulating washer retained by a nut which completes the rigid assembly.

The lower electrode and upper electrode (which is the spindle of the 2 inch diameter Shardlaw head) are each secured into the soft steel ring which comprises the body of the apparatus by two Allen screws normal to each other. Adjustment to these screws compensates misalignment of the electrodes due to tightening of either screw.

Measurement of dielectric constant is accomplished by perfect alignment of the wafer coated either with indium foil or with the 15% gold amalgam. When the latter is used, about a minute should be allowed for the initially soft amalgam to become semirigid so that it can be brushed to concentricity with electrodes and wafer (the amalgam again becomes soft when it is rubbed in a mortar). After the oscillator circuit has been brought into balance with a fixed frequency (5 Mc) the wafer and coating are removed quickly and the air gap is closed until the oscillator is again in balance. This air gap dimension is then included with measurement of the uncoated wafer at the four quadrants and the center (these thicknesses being averaged) to give the dielectric constant, ϵ, as the ratio of thicknesses of substance and air.

D. Measurements from +28 to −40° with Wafers

With the lower electrode attached at D (Fig. 2) to the oscillator circuits the indium-coated wafer is installed concentrically on the top of D. The cooling jacket and grounded electrode assembly is added snugly and carefully.

The capacitance measurement is made by use of a connector comprised of a two-prong short-circuiting plug which may be repeatedly inserted and removed without capacitance alteration greater than 0.001 pf. A frequency balance is obtained with the test capacitor connected and then disconnected. The difference in capacitance is that of the candidate wafer after the cell capacitance (determined as described below) is subtracted.

An initial capacitance measurement is made at ambient temperature and then dry air, cooled by liquid nitrogen around A, is blown through the jacket and out at C. The change in dimension shown by the indicator dial K indicates, by communication via the grounded electrode E, the change in thickness of the wafer

assembly. After about 1 hour the temperature has been lowered to −40° C (as is indicated independently by the two thermistors F) and adjusted to constancy. The final thickness and the capacitance at −40° are determined. Now the temperature is raised slowly during 5–6 hours and is brought to constancy at intervals of 4° C for determination of capacitance. These intermediate measurements are made to detect any unusual deviation which would indicate that the wafer has developed a fault, but only the lowest and highest temperatures are utilized for the evaluation of temperature coefficient. After completion of measurement at the highest temperature the wafer is transferred to the device shown in Fig. 3, where apparent dielectric constant is determined in the usual manner, the foil being finally removed in order to measure the absolute thickness of the wafer and the indium foil at room temperature.

Although the change in thickness is closely followed in the determination it has been found to be worthwhile also to determine the coefficient of expansion of the candidate substance by temperature cycling of a comparatively thick wafer without indium foil in the apparatus of Fig. 2 while only the change in thickness is measured. Of course, the wafer must be sufficiently thin to ensure that its density is maximal.

The measurements described above would be in error because of dimensional and electrical variations in the apparatus of Fig. 2 had these not previously been determined. The change in capacitance of the apparatus with respect to temperature is made by maintaining the grounded electrode about 0.3 inch above the lower electrode while capacitance of the apparatus without a wafer is determined from +28 to −40°. In like manner the dimensional change of the apparatus in respect of temperature is made with observation of the indicator gauge K while the top and bottom electrodes are in direct contact, one with the other. Correction curves have been constructed for both of these variables and the capacitance of the cell is checked to ensure precision of assembly before every experiment.

E. Calculation of Distortion Polarization

The dielectric constant at −40° cannot be obtained directly because the air capacitance corresponding to capacitance of the wafer is not measured by the apparatus of Fig. 2. However, the air capacitance at +28° may be measured in the apparatus of Fig. 3. Then the distortion polarization P_D may be evaluated:

$$P_{D\rho} = \frac{(C_{S\rho} - C_{A\sigma})(H_\rho/H_\sigma)}{(C_{S\rho} + 2C_{A\sigma})(H_\rho/H_\sigma)M(1-3[H_\sigma - H_\rho])/d_\sigma},$$

where $\rho = -40°$, $\sigma = +28°$, C_S = capacitance of wafer, and C_A is the corresponding capacitance of air (C_S/ϵ) for thickness H of the wafer, density d, and molecular weight M.

X-Ray Diffraction Patterns

The d spacings in angstroms obtained with the HMX polymorphs and the various other compounds mentioned in this report are shown with their relative intensities (I/I_1) in Table 1. In all cases the diffraction patterns were determined using Cu $K\alpha$ radiations with a nickel filter.

Spectral Studies

For the spectral range 2500–700 cm^{-1} a Perkin–Elmer Model 21 instrument was used with potassium bromide pellets prepared in the usual manner. A Beckman IR-4 instrument was used from 900–300 cm^{-1}. Partial spectra were obtained in the latter range by the double-beam technique for a 1.7% solution of HMX in acetone (three strong bands at 597, 615–620, and 760 cm^{-1}) and for 2.25% solutions in dimethylformamide (four strong bands at 598, 615–620, 765, and 840–850 cm^{-1}). Complete spectra in the 900–300 cm^{-1} range were obtained by use of wafers prepared with polyethylene wax* (average molecular weight ca. 5000). This wax as received is comminuted in a Wiley Mill using an 80-mesh screen. The powder is tightly bottled. In order to prepare a wafer the candidate substance is ground to 1- to 10-μ size and then is mixed with the powdered wax to the desired concentration (1–25%) in a 15×150 mm test tube, the inside wall of which has been roughened to opacity by use of 300- to 500-mesh carborundum. The stoppered test tube is then rotated axially for 15 minutes (conveniently on Fisher Scientific Company motor-driven glass blowers' rollers). Enough of the mixture (190–200 mg) to make a wafer 0.4 mm thick is then introduced into the die shown in Fig. 7.

The body and lower plate of this die is fabricated from SPS-245 alloy steel inclusive of the bolts which hold the two taper-pinned halves of the body together. These parts are hardened to 45–50 Rockwell-C. The piston is made from high-carbon steel, case hardened and lapped to a fit in the body of ±0.0002 inch. The top of the plate and the bottom of the piston are finely surfaced to avoid adhesion of the completed wafer, and are wiped with Nujol before each use. The Nujol film must not be visible.

The mixture of sample and wax is evenly distributed in the die and then is pressed (without vacuum) under a dead load of 15,000 lb. Then the bottom plate is removed and the wafer is extruded carefully. It is mounted in a frame consisting of three pieces of filling card cut externally to fit into the IR-4 cell holder and internally so as to hold the wafer in the central card and to retain it with the outer cards, the three finally being stapled together. The "window" must be large enough to contain all of the light beam. These wafer holders may be filed together with reference wafers containing the same weight of wax. There is no mechanical or optical deterioration after 4 years of storage.

**Kindly donated by the Tennessee Eastman Company, Kingsport, Tennessee, U.S.A.*

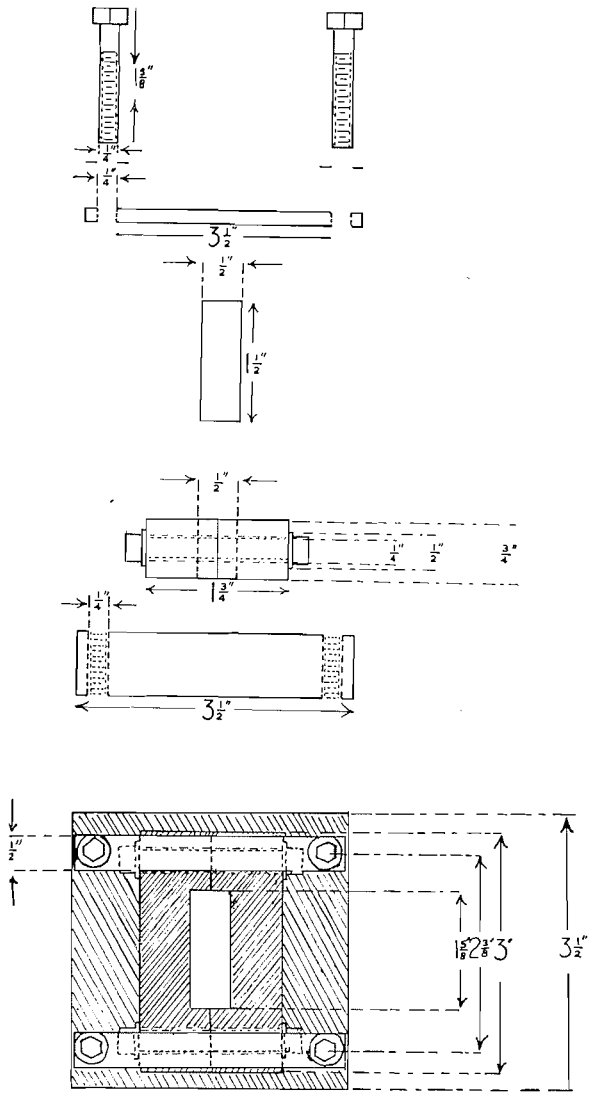

FIG. 7.

Temperature Coefficient of Infrared Absorption

1. Holders for Polyethylene Wax Pellets

The pellet holder for temperature-variable measurement is shown in Fig. 8. The median slotted plate A (into which the polyethylene wax pellet fits) is bounded by the brass plate B and by the bakelite plate C, which is drilled to accept the air inlet D at the bottom and the head thermistor E with its leads at the top. Over one side of detached A is stretched a cured latex rubber sheet of thickness 0.06 mm, supplied by courtesy of the Viceroy Rubber Co., Toronto. The rubber sheet is rendered non-tacky during this manipulation by a light layer of talc but the latter must be washed off by use of water–ethanol while the rubber sheet is held in its stretched condition. Then B is applied to A and secured by the eight screws so that the rubber cell window is firmly emplaced. A rubber window is similarly installed between A and C after small holes are made in it by hot wire so that the air inlet and the thermistor have access to the slot.

The pair of pellet holders used in the sample and reference beam of the Beckman IR-4 spectrometer are calibrated with respect to temperature by insertion in an empty 6-l. vacuum jar the cover of which holds (1) a glass tube of 40-mm O.D. to contain dry ice – acetone, (2) a motor-equipped 4×1 inch rotating rubber blade for air circulation, and (3) a precision thermometer between the two pellet holders which are hung

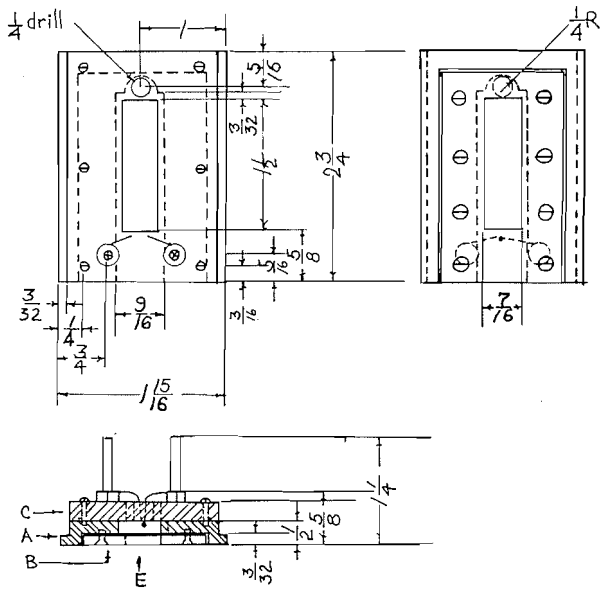

FIG. 8.

in close proximity to it. The thermistor leads from each holder are led each to its vacuum-tube-amplified Wheatstone bridge in which balance is indicated by a 6E5 magic eye tube.

Part of the air used for purging the IR-4 spectrometer (dried by a bed of pellet sodium hydroxide 4 ft long and then by a 30-inch length of Linde 3A molecular sieves) is divided by two valves into lines leading to water removal traps immersed in liquid nitrogen. Thence the two airstreams are led to separate copper coils immersed in a 5-l. spherical vacuum flask containing liquid nitrogen. The outlets of these copper tubes are connected to silvered and evacuated double-walled glass lines which carry the cold air through the cover that has been built over the IR-4 cell compartment and then to the air inlet tubes of the pellet holders in sample and reference path. With this equipment the pellet holders are reduced in temperature from 40° C to −39° C in 30 minutes by about 1 c.f.m. of cold airflow. Temperature regulation or temperature rise is controlled by the two valves.

2. Cooling Jackets for Standard Beckman Cells

The standard Beckman cells for use with solutions may be chilled to −40° *in situ* by use of the bakelite – polyurethane foam device shown in Fig. 9. The bottom and sides of the device form a yoke, A, which slips snugly (because of the foam) around the cell and provides air passage around the cell plates from bottom air inlet to top. After installation on the cell the yoke is retained by the bakelite bar B across the top, which bears a head thermistor like those used in the pellet holders (1, above) and also a vent for exit of cold air. About 1.5 c.f.m. of airflow is required to decrease the cell temperature to −40°.

Electrical Measurements

The distortion polarizations were determined according to an earlier report (10). It was found necessary with HMX to include 2% of Koroseal in order to make satisfactory pellets. Density of the polymorphs have been determined by flotation. After determination of dielectric constant each X-ray diffraction pattern was redetermined. The dipole moment of HMX was determined in dioxane at 20° C in equipment described earlier (9). Since $\Delta\epsilon/\Delta\omega = 9.80$ and $\Delta V/\Delta\omega = 0.445$ the total polarization is 519 cc. Subtraction of the additive group refractions of HMX (58.3 cc) enables an evaluation of electric moment as 4.68 D.

Preparation of Crystalline HMX Modifications

1. HMX-I

Several methods have been used to prepare this form but the preferred one is by cooling a hot saturated solution of HMX in acetone or acetonitrile. This method gives very pure beta crystals providing the solution is cooled in a stoppered flask and kept in agitation by means of a magnetic stirrer. Purity was confirmed by infrared and microscopic examination to ensure that the product was satisfactory for use. Calc. for $C_4H_8N_8O_8$: C, 16.2; H, 2.72. Found: C, 16.6; H, 2.96.

2. HMX-II

About 4 g of HMX was dissolved in 80 cc of 70% nitric acid by warming on a hot plate until slight fuming occurred. The flask was then insulated by wrapping lightly with a towel so that the contents cooled

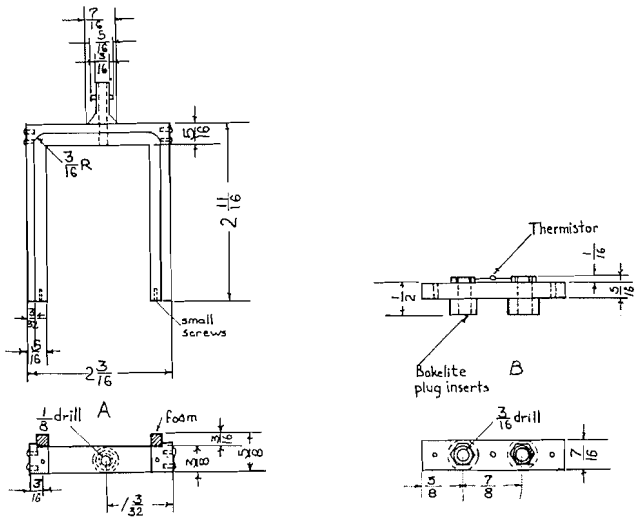

FIG. 9.

to room temperature in about ½ hour. The crystals were then filtered off, washed with water until free from acid, and dried in a vacuum oven at 50° C. The absence of other forms of HMX was confirmed by microscopic and infrared examination. Calc. for $C_4H_8N_8O_8$: C, 16.2; H, 2.72. Found: C, 16.5; H, 2.93.

3. HMX-III

About 1 g of finely ground beta HMX was dissolved by warming in 280 ml of 50% aqueous acetic acid. When dissolved, the flask and contents were cooled rapidly by swirling in an ice-water bath. The temperature dropped to 20° C in about 4 minutes. On filtration well-formed triangular plates were obtained. Microscopic and infrared examination showed the product to be free from other forms.

Some HMX-III was also prepared by steam-distilling off the solvent from a hot saturated solution of HMX in water-saturated cyclohexanone. After the cyclohexanone–water azeotrope had been stripped off at 96° C the precipitated HMX was filtered off and dried in a vacuum oven at 50° C .The product consisted of small, poorly defined crystals but its purity as shown by infrared examination was somewhat better than the product obtained from acetic acid. Calc. for $C_4H_8N_8O_8$: C, 16.2; H, 2.72. Found: C, 16.4; H, 2.92.

4. HMX-IV

Samples for X-ray diffraction studies of HMX-IV were prepared by sublimation of HMX-I at 180° C onto cold microscope slides. The slides were then washed with chloroform and vacuum-dried for 8 hours at 25° C. The reflections arranged in order of decreasing intensity (I/I_1) are: (10) 3.64, 5.43; (9) 6.67; (8) *3.17*, *3.48*, *5.16*; (7) *3.82*; (6) 5.69; (5) 4.21; (4) 2.71; (3) 2.51; (2) 2.35, 2.22; (1) 2.15, 2.63, where those in italics are very similar to lines found for HMX-III. The rest are not found among the reflections of the other polymorphs.

5. HMX–Dimethylformamide Complex

This form is prepared by simple crystallization from dimethylformamide (DMF). In the procedure used here a hot saturated solution was first prepared by adding ground HMX to about 100 ml of boiling DMF. The solution was then diluted with another 10 ml of DMF, poured into a petrie dish, and allowed to cool slowly. After filtration the crystals were dried in a vacuum oven at 50° C.

To prove that the product was a 1:1 HMX–DMF solvate, accurately weighed samples of about 2 g were refluxed in boiling water for 2 days. After cooling and filtration through a sintered-glass crucible the crystals were dried under vacuum to constant weight. The loss in weight in all experiments was 25.55% of the dry residue, giving a mole ratio of 1:1.02. Infrared examination of the residue revealed that it was completely converted to HMX-I.

The proportion of DMF present was also confirmed by dissolving a weighed sample in acetonitrile and then determining the quantity of DMF released by measuring the carbonyl absorption at 5.9 μ. With the aid of a calibration curve for DMF in acetonitrile it was shown that the mole ratio of DMF to HMX was exactly 1:1 even with a sample that had been finely ground.

The stability of this crystalline form is also shown by the following experiment: One gram of the complex was ground to about 20-μ size, let stand 1 year in a large bottle, and then was heated 1 hour at 80° C with 20 ml of water. After cooling, the system was filtered to remove HMX-I. The filtrate was treated with 5 ml of concentrated hydrochloric acid and then was evaporated to dryness, finally in an air stream. The residual

crystals were treated with $M/5$ aqueous triethanolamine picrate. Filtration removed 0.12 g of dimethylamine picrate, m.p. 157–158° C. A mixture melting point* with an authentic specimen was not lowered. Calc. for $C_7H_{15}N_9O_9$: C, 22.8; H, 4.09; N, 34.2. Found: C, 23.0; H, 4.09; N, 34.1.

When the complex was heated under observation through crossed Nicol prisms a transition was observed at 92° C. After a sample was heated under vacuum to 93° C during 1 hour and then cooled during 1 hour it had been transformed to HMX-I.

Stable and Labile Resorcinol

Resorcinol purified by crystallization from water was used as such (stable α form) or was heated to 70° C for 1 hour in a test tube which then was chilled quickly. The difference in melting point reported previously (5) could not be discerned, but the X-ray diffraction patterns (Table I) are distinctive and reproducible before and after pelleting. The densities, determined at 22° C by air displacement (11), are slightly different from those reported by Lautz (α, 1.271; β, 1.292 at 20° C).

Triphenylguanidine

After repeated crystallization from hot 95% ethanol to remove an insoluble impurity the substance melted at 143.8° C. We were unable to isolate the reported (5) polymorph, m.p. 138° C, but when the molten substance was poured onto a cold brass plate the amorphous form was obtained. This glass is stable at 25° C but it is converted to the crystalline form, m.p. 143.8° C, when it is maintained at 70° C for 3 hours.

ACKNOWLEDGMENTS

The authors are grateful to Peter Podleschka, Rudolph Deuringer, and Brigitte Kalnins for aid in the experimental work. The research has been supported by the Defence Research Board.

REFERENCES

1. W. P. Binnie, H. L. Cohen, and G. F Wright. J. Am. Chem. Soc. **72**, 4457 (1950).
2. W. J. Chute, D. C. Downing, A. F. McKay, G. S. Myers, and G. F Wright. Can. J. Res. B, **27**, 218 (1949).
3. W. E. Bachmann and J. C. Sheehan. J. Am. Chem. Soc. **71**, 1842 (1949).
4. W. C. McCrone. Anal. Chem. **22**, 1225 (1950).
5. H. Lautz. Z. Physik. Chem. **84**, 661 (1913).
6. A. F. Wells. Structural inorganic chemistry. Oxford University Press. 1945. p. 263.
7. M. J. Abercrombie, A. Rodgman, K. R. Bharucha, and G. F Wright. Can. J. Chem. **37**, 1328 (1959).
8. H. Sawatzky, G. K. White, and G. F Wright. Can. J. Chem. **37**, 1132 (1959).
9. C. C. Meredith and G. F Wright. Can. J. Technol. **33**, 182 (1955).
10. P. Podleschka, L. Westland, and G. F Wright. Can. J. Chem. **36**, 574 (1958).
11. M. V. George and G. F Wright. Can. J. Chem. **36**, 189 (1958).
12. A. J. Vogel, W. T. Cresswell, G. H. Jeffery, and J. Leicester. J. Chem. Soc. 514 (1952).
13. F. Eisenlohr. Z. Physik. Chem. **75**, 585 (1910); **79**, 129 (1912).
14. J. W. Smith. Electric dipole moments. Butterworth Publication. 1955. p. 270.
15. M. V. George and G. F Wright. J. Am. Chem. Soc. **80**, 1200 (1958).
16. M. V. George, R. W. Kierstead, and G. F Wright. Can. J. Chem. **37**, 679 (1959).
17. A. Heydweiler. Z. Physik, **3** (5), 308 (1920).
18. J. Errera. Z. Elektrochem. **36**, 818 (1930).
19. W. Costain and E. G. Cox. Nature, **160**, 826 (1947).
20. E. I. Coop and L. Sutton. J. Chem. Soc. 1269 (1938).
21. C. C. Meredith, L. Westland, and G. F Wright. J. Am. Chem Soc. **79**, 2385 (1957).
22. H. H. Cady, A. C. Larsen, and D. T. Cromer. Acta Cryst. In press (1962).
23. C. D. Bockman, Jr. Armour Research Foundation. Private communication.

**All melting points have been corrected against reliable standards.*

THE VIBRATIONAL MECHANISM OF THE FUNDAMENTAL NH_2 STRETCHING VIBRATIONS IN ANILINES*

PETER J. KRUEGER
Department of Chemistry, University of Alberta, Calgary, Alberta

Received July 27, 1962

ABSTRACT

The integrated intensities, frequencies, and half-band widths of the fundamental symmetric and asymmetric NH_2 stretching vibrations in 33 ortho-substituted anilines, measured in dilute carbon tetrachloride solution, have been examined in relation to the corresponding absorption band parameters for 31 meta- and para-substituted anilines, taking into consideration the electronic effects of the substituents. From an almost tetrahedral configuration in *p*-phenylenediamine, the calculated *s*-character of the nitrogen atom gradually increases as the substituent groups become more electron withdrawing, with a resultant increase in the apparent HNH angle and the NH force constant. Ortho substitution in general leads to enhanced HNH angle opening, probably because of intramolecular hydrogen bonding. The decrease in half-band width for both vibrational modes in ortho-substituted anilines with respect to corresponding values in meta and para compounds is ascribed to steric hindrance to solvation of the amino group.

The asymmetric intensities in ortho-substituted anilines are generally increased over corresponding values in meta and para compounds, unlike the behavior of the symmetric mode. These results are consistent with a vibrational mechanism taking into account the following factors for each mode: (i) the direction of the transition moment, (ii) the extent of nitrogen lone pair and aromatic π-electron participation, and (iii) the direct field effect of the ortho substituent.

INTRODUCTION

The vibrations localized in characteristic functional groups attached to the aromatic ring have in recent years been studied extensively as a function of electronic changes in the molecule. The frequencies of absorption maxima and the absorption intensities have been correlated with the Hammett σ constants (1, 2) of the substituents for the —OH stretching vibration in phenols (3), the C≡N stretching vibration in benzonitriles (4–6), the C=O stretching vibration in benzaldehydes, ethyl benzoates, and acetophenones (7, 8), the —NH stretching vibration in N-methylanilines (9), the two —NH_2 stretching vibrations in anilines (5, 9–12), and the C—O—C stretching vibration in anisoles (13).

For meta- and para-substituted benzene derivatives the frequency/σ correlations may be expressed by a Hammett-type equation (14),

$$[1] \qquad \nu = \nu_0 + \rho\sigma,$$

where ν is the observed group frequency in the substituted compound, ν_0 is the group frequency of the "parent" compound in the series, and ρ expresses the sensitivity of the frequency to substituent effects. These plots sometimes exhibit slight curvature as the frequency rises or falls with increasing electrophilic character of the substituents. A similar linear relationship has been sought (15) between ν and the electrophilic substituent constants σ^+ (16, 17). Rao and Venkataraghavan (14) have recently shown that a statistical evaluation of 18 sets of frequencies indicates that both σ and σ^+ correlate the frequencies equally well.

The integrated band intensities (A) of vibrations in functional groups in meta- and

Presented in part at the 13th Annual Mid-America Spectroscopy Symposium, Chicago, Illinois, April 30–May 3, 1962.

para-substituted benzenes have been correlated linearly through a logarithmic function so that

$$\log A = \log (A_0) + \rho'\sigma \quad [2]$$

or alternatively

$$\log A = \log (A_0^+) + \rho^+\sigma^+. \quad [3]$$

Statistical evaluation has indicated that the latter correlation is slightly better (14).

On the basis of a simple molecular orbital model Brown (18) has proposed that the quantity $A^{1/2}$ should be linearly related to the appropriate substituent constants σ or σ^+. Statistically this correlation appears to be as good as the correlation with log A (14). Brown suggests further that the success of these correlations indicates that the changes in electron distribution which occur in the molecule during vibrational distortions closely parallel those which occur in the formation of the transition state during chemical reactions.

In a previous publication Krueger and Thompson (5) showed that for a wide range of vibrational types the log A and ν values also correlated well with the inductive (σ_I) and resonance (σ_R) parameters deduced by Taft (19, pp. 594 ff.) on the basis that

$$\text{para-}\sigma_{\text{Hammett}} = \sigma_I + \sigma_R \quad [4]$$

as a first approximation. These relationships could be expressed explicitly as

$$\log A = \log (A_0) + \alpha\sigma_I + \beta\sigma_R \quad [5]$$

and

$$\nu = \nu_0 + \alpha'\sigma_I + \beta'\sigma_R, \quad [6]$$

where the α's and β's could be interpreted as the relative susceptibility of the correlated quantity to the inductive and resonance effects. The significance of this has been discussed.

The Hammett treatment of kinetic data is restricted to meta and para substituents to avoid complications due to the effect of neighboring groups, although Farthing and Nam (20) have made an attempt to extend it to ortho-substituted compounds. Krueger and Thompson (5) previously reported some spectroscopic measurements on ortho-substituted benzonitriles, anilines, phenols, ethyl benzoates, and benzaldehydes, and attempted to relate these values to those for meta- and para-substituted compounds. The substituent constants derived by Taft (19, p. 618) for ortho substituents were used in integrating all the data, since these σ_{ortho} values are on the same scale as the Hammett σ_{meta} and σ_{para} values. The additivity principle proposed by Jaffe (2) was used as a first approximation to get a $\sum\sigma$ value for compounds with several substituents. This was reasonably successful for the sterically favorable benzonitrile series, but a number of unexplained anomalies remained for the phenols and anilines.

The data available for the aniline series have now been re-examined and some conclusions drawn concerning the nature of the amino group and its response to ortho substitution. Further high-resolution infrared measurements have also been made on selected model compounds.

EXPERIMENTAL METHODS

A Perkin–Elmer 12C single-beam spectrometer was employed for the earlier measurements, using a LiF prism to improve the resolution in the 3-μ region. Standard absorption lines of water vapor and ammonia were used as frequency calibrants. The effective slit width was calculated to be about 8 cm^{-1} in this region. Quartz absorption cells up to 5 cm in length were used to keep the maximum aniline concentrations below 0.01 M in carbon tetrachloride. Measurements were made over a wide concentration range at several path lengths, the band areas determined by numerical integration, and the apparent intensities extrapolated to zero peak absorbance to eliminate slit effects (21). Since the true shape of liquid phase absorption bands is still in doubt, no "wing corrections" (22) were applied. Integration limits were set at those points where the recorder noise level became comparable with the residual absorbance. Due to slight overlapping of the two bands, a small amount of graphical separation was necessary.

The high-resolution measurements were made with a Beckman IR-7 spectrophotometer with a NaCl foreprism and a 75 lines/mm grating blazed at 12 μ. The instrument was calibrated as previously described (23) and the accuracy of the frequency measurements is believed to be limited only by the widths of the bands themselves. These measurements were made in the fourth grating order, where the slit width was calculated to be about 1 cm^{-1} in this region. A pair of matched 2-cm quartz cells was used. The use of a programmed slit, double-beam operation, linear absorbance, and linear frequency (cm^{-1}) recording permitted the direct evaluation of band areas by numerical integration. Slit width effects were found to be negligible in most cases (the calculated slit width is less than 5% of almost all the band widths measured), and the A and $\Delta\nu_{1/2}$[a] values reported are the averages of at least two completely independent measurements, except in a few cases where the small amount of material available precluded this.

Most of the compounds were commercial products, purified by recrystallization, sublimation, or fractional distillation under reduced pressure. A few were synthesized following standard procedures in the literature. "Spectrograde" carbon tetrachloride was used, and the solutions were made up volumetrically. In the high-resolution measurements the cell temperature was held at 25° C.

RESULTS

The detailed experimental results and the calculated parameters derived from them are given in Table I. In the graphical analyses points of special interest are numbered, and these refer to the respective compounds as listed in this table. For compounds where both high- and low-resolution intensity measurements were made the mean was used in the calculations.

For the purposes of this discussion the total electronic effect of the aromatic ring substituents on the NH_2 group is considered to be proportional to the additive sum of the substituent constants ($\sum\sigma$) as originally defined by Hammett (1) and Taft (19, p. 618). Wherever possible the more recent σ values from the critical analysis by McDaniel and Brown (24) were used. A few constants were taken from the review by Jaffe (2). For a number of ortho substituents σ values were estimated on the basis that $\sigma_{ortho} \approx \sigma_{para}$, since no kinetic data for them were available in the literature. The validity of this approximation is substantiated by the work of Taft and his associates.

Figure 1 shows plots of $\log_{10} A$ versus $\sum\sigma$ for the asymmetric and for the symmetric vibration. Considering that this presentation adjusts all the data for the varying electronic effects involved, the general conclusion can be drawn that for ortho compounds the symmetric intensities are not significantly different from those for meta and para compounds over most of the range. For the asymmetric vibration the intensities for ortho compounds are about 30–40% higher than the corresponding values for meta and para compounds. Only where the adjacent substituents are alkyl groups (and NH_2) is there no apparent increase in the asymmetric intensities, and a slight decrease in the symmetric intensities. Compounds 63 and 64 are extremely insoluble in CCl_4, and hence these intensities may be too low.

The frequency/$\sum\sigma$ correlations are shown in Fig. 2. Because of the two interacting vibrational modes, and the possibility that the geometry of the amino group may change in the aniline series, these are best discussed in terms of the HNH angle and the average NH stretching force constant.

TABLE I

Absorption band parameters for fundamental NH_2 stretching vibrations in substituted anilines

			Asymmetric vibration*				Symmetric vibration*						
No.	Substituents	$\Sigma\sigma$†	ν (cm^{-1})	$A\times10^{-6}$ (cm/mole, $\log_e$)	$\Delta\nu_{1/2}$[a] (cm^{-1})	$\partial M/\partial r$ (D/Å)	ν (cm^{-1})	$A\times10^{-6}$ (cm/mole, $\log_e$)	$\Delta\nu_{1/2}$[a] (cm^{-1})	$\partial M/\partial r$ (D/Å)	θ (°)	$k\times10^{-5}$ (dyne/cm)	b
1	4-$N(CH_3)_2$	−0.83	3453	2.33	42		3377	1.89	33				
			3456.5	*2.21*	*39.7*	0.62	*3379.5*	*1.41*	*30.1*	0.75	109.6	6.48	0.501
2	2-$N(CH_3)_2$	(−0.8)‡	Compound reacts rapidly with CCl_4										
3	4-NH_2	−0.66	3453	2.25§	39	0.61	3377	1.73§	29.5	0.77	109.4	6.47	0.499
4	2-NH_2	(−0.7)‡	*3487.5*	*2.45*§	*22.9*	0.64	*3351.5*	*1.17*§	*20.7*	0.65	112.2	6.39	0.523
5	2,4,6-tri-$C(CH_3)_3$	(−0.6)‡	*3517.5*	*4.11*	*28.1*	0.81	*3342.5*	*1.22*	*22.4*	0.70	115.8	6.77	0.551
6	2,4,6-tri-CH_3	−0.51‖	3479	2.37	36		3399	1.55	26.5				
			3479.5	*2.26*	*33.5*	0.62	*3399.5*	*1.44*	*24.6*	0.72	110.3	6.56	0.507
7	2,4,6-tri-$CH(CH_3)_2$	(−0.45)‡	*3481.5*	*2.24*	*40.1*	0.62	*3405*	*1.11*	*32.0*	0.61	109.3	6.58	0.499
8	2-OCH_3	−0.39‖	3487	4.16	39	0.80	3396	3.13	27	1.08	113.2	6.57	0.532
9	2-OCH_2CH_3	−0.35‖	3486	4.14	40	0.80	3396	3.11	27	1.07	112.9	6.57	0.529
10	2,6-di-CH_3	−0.34‖	3486	2.75	36		3404	1.91	26				
			3487.6	*2.47*	*31.8*	0.66	*3405*	*1.76*	*23.5*	0.81	110.9	6.59	0.513
11	2,5-di-$C(CH_3)_3$	(−0.3)‡	*3493.6*	*2.26*	*27.2*	0.60	*3402*	*1.34*	*21.0*	0.71	113.3	6.59	0.532
12	2,5-di-OCH_3	−0.27‖	*3492.5*	*4.07*	*34.8*	0.81	*3399*	*3.32*	*25.2*	1.12	113.8	6.59	0.537
13	4-OCH_3	−0.268	3460	2.67	41	0.66	3382	1.97	30.5	0.82	109.9	6.49	0.504
14	4-OCH_2CH_3	−0.24	3459	2.45	40	0.63	3381	1.87	30	0.80	109.9	6.49	0.504
15	3,4-di-CH_3	−0.239	3469	2.65	40	0.65	3387	2.29	28.5	0.90	110.9	6.52	0.513
16	2,5-di-OCH_2CH_3	−0.20‖	*3492*	*4.60*	*35.3*	0.86	*3399*	*3.83*	*25.2*	1.21	113.7	6.58	0.536
17	2-$C(CH_3)_3$	(−0.2)‡	*3496.5*	*2.54*	*27.3*	0.64	*3404*	*1.48*	*20.3*	0.75	113.5	6.60	0.534
18	4-$C(CH_3)_3$	−0.197	*3474*	*2.64*	*38.9*	0.67	*3391.5*	*2.25*	*27.3*	0.89	111.0	6.54	0.513
19	2-CH_3	−0.17‖	3482	2.79	36		3398	2.25	25				
			3482.5	*2.44*	*32.6*	0.66	*3398*	*2.00*	*23.4*	0.87	111.5	6.56	0.518
20	4-CH_3	−0.170	3470	2.51	41		3390	2.41	29				
			3471	*2.66*	*37.4*	0.66	*3389.5*	*2.15*	*26.9*	0.89	110.7	6.53	0.511
21	4-$CH(CH_3)_2$	−0.151	*3474*	*2.57*	*38.5*	0.66	*3392.5*	*2.26*	*27.4*	0.88	110.2	6.53	0.507
22	2-$CH(CH_3)_2$	(−0.15)‡	*3481*	*2.37*	*34.1*	0.63	*3397.6*	*1.86*	*24.3*	0.81	111.2	6.56	0.515
23	2-CH_2CH_3	(−0.15)‡	3480	2.71	37	0.66	3398	2.19	26	0.88	110.8	6.56	0.512
24	4-C_6H_5	−0.01	3483	3.07	39		3398	4.10	26.5				
			3485.5	*3.06*	*37.4*	0.71	*3399*	*3.69*	*25.2*	1.19	112.0	6.57	0.522
25	2-C_6H_5	(−0.01)‡	3481	4.16	44		3393	3.09	32				
			3483.6	*3.78*	*42.3*	0.80	*3394.6*	*2.64*	*30.9*	1.03	112.7	6.56	0.527
26	H	0	3479	2.91	39.5		3396	2.83	29.5				
			3481	*2.92*	*37.7*	0.69	*3395.6*	*2.66*	*26.7*	1.00	111.7	6.56	0.520
27	4-CH_2CN	+0.01	3487	(3.61)	39	0.75	3401	(3.82)	25.5	1.17	111.8	6.58	0.521
28	3,4-$(CH)_4$	+0.042	3481	3.21	38.5	0.71	3396	4.02	26	1.20	111.6	6.56	0.519
29	2,3-$(CH)_4$	(+0.04)‡	3475	1.95	34.5	0.56	3395	1.75	24.5	0.78	110.3	6.54	0.508
30	4-F	+0.062	3474	3.23	44.5	0.72	3394	3.21	31.5	1.05	110.3	6.54	0.508
31	3-CCH_2CH_3	+0.1	3482	2.95	39.5	0.68	3397	2.87	27.5	1.01	111.6	6.56	0.519
32	3-OCH_3	+0.115	3483	3.19	40	0.71	3398	3.23	27	1.08	111.6	6.56	0.519

TABLE I (*Concluded*)

No.	Substituents	$\Sigma\sigma$†	Asymmetric vibration*				Symmetric vibration*				θ (°)	$k\times10^{-5}$ (dyne/cm)	b
			ν (cm^{-1})	$A\times10^{-6}$ (cm/mole, log$_e$)	$\Delta\nu_{1/2}$§ (cm^{-1})	$\partial M/\partial r$ (D/Å)	ν (cm^{-1})	$A\times10^{-6}$ (cm/mole, log$_e$)	$\Delta\nu_{1/2}$§ (cm^{-1})	$\partial M/\partial r$ (D/Å)			
33	4-I	+0.18	*3490*	*3.39*	*35.9*	0.74	*3402*	*4.01*	*23.1*	1.21	112.4	6.59	0.525
34	2-Cl	+0.20‖	3494	4.62	31.5	0.84	3401	4.52	22	1.31	113.7	6.59	0.535
35	2-Br	+0.21‖	3491	4.78	31	0.86	3397	4.10	22	1.25	114.0	6.58	0.538
36	2-I	+0.21‖	*3485*	*4.45*	*25.7*	0.84	*3387.5*	*3.14*	*18.9*	1.11	115.0	6.55	0.525
37	4-Cl	+0.227	3482	3.17	38.5	0.71	3398	3.80	26.5	1.16	111.3	6.56	0.516
38	4-Br	+0.232	3485	3.33	38.5	0.72	3399	4.16	25.5	1.22	111.8	6.57	0.521
39	2-F	+0.24‖	*3493.5*	*3.90*	*31.7*	0.80	*3404*	*4.00*	*22.4*	1.22	112.7	6.60	0.528
40	3-F	+0.337	3492	3.59	36.5	0.75	3405	4.30	25.5	1.25	112.1	6.59	0.523
41	3-Cl	+0.373	3490	3.49	35.5	0.74	3402	3.96	25	1.20	112.4	6.58	0.525
42	3-$COCH_3$	+0.376	3486	3.67	38.5	0.76	3400	4.12	26	1.22	111.8	6.57	0.521
43	3-Br	+0.391	*3492.5*	*3.83*	*31.0*	0.74	*3404*	*3.78*	*22.4*	1.18	112.5	6.59	0.526
44	2,4-di-Cl	+0.43‖	3496	5.04	30.5	0.88	3402	5.04	21	1.39	114.0	6.60	0.537
45	3-CF_3	+0.43	3492	4.00	38	0.79	3404	4.56	26	1.27	112.3	6.59	0.525
46	4-SCN	+0.52	3500	4.62	34.5	0.85	3410	6.71	23.5	1.57	112.8	6.62	0.529
47	2-CF_3	(+0.54)‡	*3515.5*	*4.79*	*27.2*	0.89	*3426*	*5.34*	*19.1*	1.40	112.6	6.68	0.527
48	3-CN	+0.56	3495	4.26	32.5	0.81	3406	5.72	23	1.45	112.6	6.60	0.527
49	2,4,6-tri-Cl	+0.63‖	3503	6.37	28	0.97	3404	7.17	20	1.70	115.3	6.61	0.547
50	2-CN	+0.64¶	3504	5.38	29.5	0.91	3408	7.35	20.5	1.72	114.4	6.62	0.541
51	4-N=N—C_6H_5	+0.640	3498	4.56	34	0.84	3406	9.02	22	1.84	113.4	6.61	0.533
52	2,4,6-tri-Br	+0.65‖	3492	6.53	30	0.99	3394	6.47	21.5	1.61	115.1	6.57	0.546
53	4-$COOCH_2CH_3$	+0.678**	3500	4.06	33.5	0.79	3408	6.29	22.5	1.54	113.4	6.62	0.533
54	2-$COOCH_2CH_3$	(+0.68)‡	3506	9.02	26.5	1.11	3378	9.36	24.5	2.19	123.6	6.57	0.597
55	3-NO_2	+0.710	3497	4.94	33	0.87	3407	5.82	22.5	1.47	112.9	6.61	0.529
56	4-$COCH_3$	+0.874**	3502	4.56	33	0.84	3410	6.75	22	1.59	113.4	6.62	0.533
57	2-$COCH_3$	(+0.9)‡	*3503*	*7.57*	*21.5*	0.98	*3345*	*8.35*	*23.8*	2.51	133.4	6.52	0.638
58	4-CN	+1.000**	3505	5.12	33	0.89	3412	8.49	22	1.79	113.6	6.63	0.535
59	2,6-di-CN-3,5-di-CH_3	+1.14¶	3510	6.93	26	1.02	3409	11.08	19.5	2.12	115.8	6.64	0.551
60	2-NO_2	+1.22‖	3522	9.48	25.5	1.16	3400	9.02	17	2.09	121.7	6.64	0.587
61	4-NO_2	+1.27**	3509	4.62	34	0.84	3416	10.62	22.5	2.00	113.6	6.65	0.535
62	2,6-di-Cl-4-NO_2	+1.67‖**	3519	9.24	28	1.17	3412	13.73	21.5	2.42	117.4	6.66	0.561
63	2,6-di-NO_2	+2.44‖	*3478*	*(16.3)*	*17.3*	1.55	*3362*	*(8.83)*	*14.7*	2.01	120.3	6.49	0.579
64	2,4-di-NO_2	+2.49‖**	3520	(13.5)	16.5	1.37	3395	(19.9)	16	3.15	122.6	6.63	0.592
65	2,4,6-tri-NO_2	+3.71‖**	3457††	—	—	—	3344††	—	—	—	119.7	6.41	0.576

*High-resolution data in italics.
†Unless otherwise indicated the values used are from the critical analysis of Hammett substituent constants by McDaniel and Brown (24).
‡Estimated on the basis that $\sigma_{ortho} \simeq \sigma_{para}$.
§Intensities divided by a statistical factor of 2.
‖Involving σ_{ortho} value(s) according to Taft (19, p. 618).
¶Substituent constant for *o*-CN group obtained from correlation of quadrupole resonance frequencies (25).
**Involving special Hammett substituent constants for anilines according to Jaffe (2).
††Compound extremely insoluble in carbon tetrachloride; frequencies measured by Dyall (26) in CCl_4.

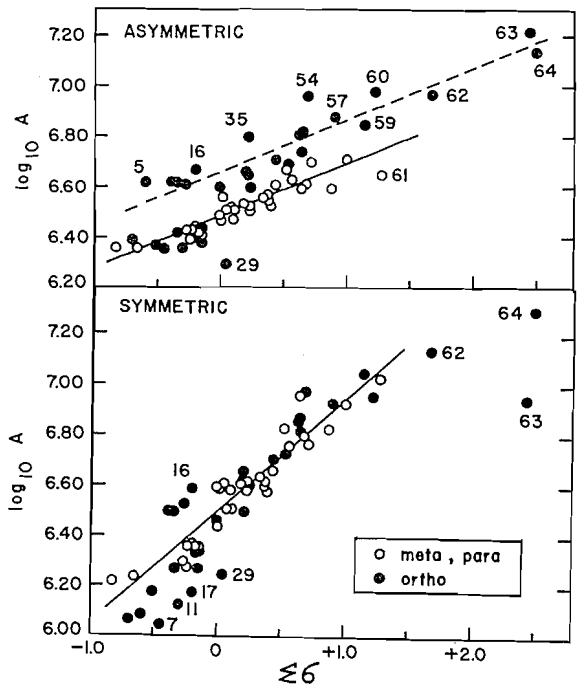

FIG. 1. Correlation of the intensity of the NH_2 stretching vibrations in substituted anilines with the electronic nature of the substituents. The units of A are cm mole^{-1} ($\log_e$).

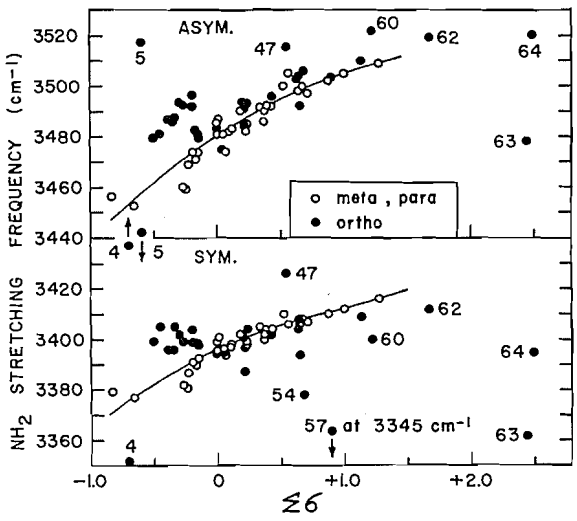

FIG. 2. The dependence of the NH_2 stretching frequencies on the electronic nature of the substituents in substituted anilines.

Our attention was first directed to a re-examination of the available data by a comparison of the apparent half-band widths ($\Delta\nu_{1/2}{}^a$), which are shown in Fig. 3 as a function of $\sum\sigma$. In general, both NH_2 bands are significantly narrower in ortho-substituted anilines than in meta- and para-substituted anilines. Since most of the band widths shown in

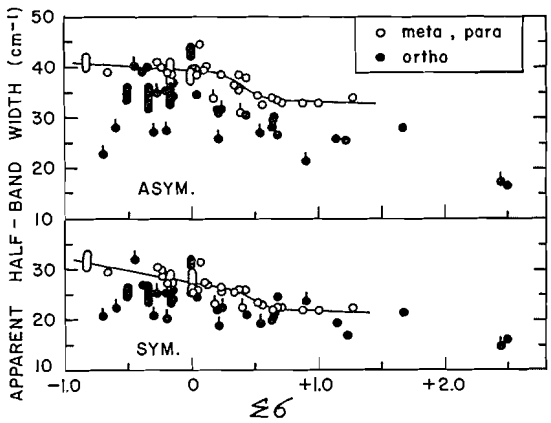

FIG. 3. The relationship of $\Delta\nu_{1/2}^{a}$ to the electronic nature and position of the substituents in substituted anilines. High-resolution measurements indicated by points with vertical tails, and by bottom ends of oval points.

Fig. 3 were obtained with an effective slit width of about 8 cm^{-1}, they will be somewhat wider than the limiting true widths, but relative values should still be correct. The extent of this distortion is also portrayed in Fig. 3, as indicated by the lower end of the elongated points, corresponding to measurements repeated with the better resolution of the grating spectrophotometer.

DISCUSSION

An interpretation of these observations is advanced along the lines of a simplified model for the two vibrational modes illustrated schematically in Fig. 4. The essential difference

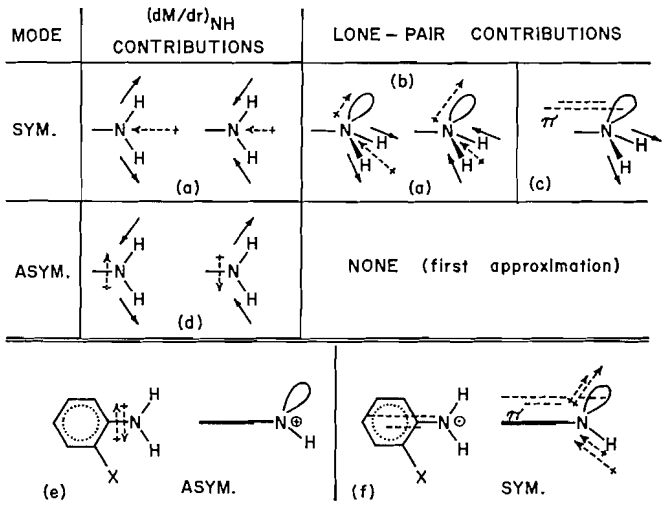

FIG. 4. A simple vibrational mechanism for the NH_2 group. (*a–d*) Contributions to the transition moment. (*e–f*) Orientation of the components of dipole moment change with respect to the aromatic system and ortho substituents. Solid arrows refer to atomic motion; broken arrows to dipole moment.

between these vibrational modes has previously been pointed out by Orville-Thomas, Parsons, and Ogden (27).

To a good approximation the only nuclei involved in the ν_s and ν_{as} vibrations are the nitrogen and hydrogen atoms. Thus changes in NH bond lengths during the vibration can be used to define the normal coordinate Q. The intensity of a fundamental infrared absorption band is proportional to $(\partial M/\partial Q)^2$, i.e. to the square of the variation of molecular dipole moment M with respect to the normal coordinate during the vibration. The dipole moment of the amino group in its equilibrium configuration can be separated into two NH bond moments, and a third component due to the atomic dipole of the lone-pair electrons. Coulson (28) has recently emphasized the importance of lone pair electron contributions to molecular dipole moment changes during vibrations, as well as the unexpected contributions that may be due to hybridization changes as the atoms move.

As the H atoms oscillate in the asymmetric mode the change in dipole moment is perpendicular to the symmetry axis of the NH_2 group, and parallel to the plane of the aromatic ring,* as summarized schematically in Fig. 4(*e*). The decrease in *s*-character of one nitrogen bonding orbital as that NH bond lengthens is exactly compensated by the increase in *s*-character of the other NH bond as it contracts. The *s*-character of the lone-pair orbital should remain unchanged, and $(\partial M/\partial Q)$ should depend on the small polarity changes in the NH bonds. During the second half of the vibrational cycle this small resultant dipole moment reverses sign, leading to contribution (*d*) in Fig. 4.

During the symmetric mode of vibration the s/p ratio of the nitrogen bonding orbitals will vary in phase, and this will give rise to a compensating change in *s*-character of the lone-pair orbital, as shown by contribution (*b*) in Fig. 4. Another component, (*a*), would be due to changes in the NH bond moments. Both (*a*) and (*b*) would lie in a plane along the CN bond and perpendicular to the aromatic ring. A third contribution, (*c*), to the net dipole moment change in the symmetric mode will arise from a variation of conjugation of the lone-pair electrons with the aromatic π-electrons during a vibrational cycle. When both H atoms move away from the N nucleus the *s*-character of the lone-pair orbital increases and it cannot combine as effectively with the π-orbitals (these have odd symmetry, whereas an *s*-orbital has even symmetry with respect to the plane of the ring). When the H atoms approach the N nucleus, the increase in *p*-character of the lone-pair orbital leads to more extensive interaction with the π-electrons. Thus the π-electron component of the permanent dipole of the aromatic part of the molecule contributes to the transition moment for this vibration as it varies in phase with the symmetric motion of the H atoms, to an extent determined by the hybridization of the N atom, i.e. leading to a very small contribution when the N atom is effectively sp^3, and a maximum when it is effectively sp^2. Figure 4(*f*) summarizes the contributions to $(\partial M/\partial Q)_s$.

A comparison of Fig. 4(*e*) and (*f*) shows that a substituent ortho to the NH_2 group might be expected to enhance A_{as} by a direct field effect if it were strongly electrophilic or nucleophilic, since the sign of the dipole that leads to contribution (*d*) reverses at every half cycle, and since the substituent group is almost directly in line with the direction of the transition moment. In the symmetric mode the ortho group is not intimately involved because it is well removed from the transition moment direction, and would likely only influence A_s by the inductive/resonance mechanism operating through the aromatic carbon skeleton and the π-electrons respectively. This factor also contributes to A_{as}, and is accounted for in the comparison on the σ basis. These views are borne out by Fig. 1. For the $\log_{10} A_{as}/\sum\sigma$ correlation the ortho compounds in which intensity

**On the basis of the absorption intensity of the 234-mμ ultraviolet band in substituted anilines, Wepster (29) has concluded that the lone-pair electrons of the amino group are oriented for maximum overlap with the aromatic π-electrons even with bulky tert-butyl groups in the 2,6-positions. Essery and Schofield (30) support this view on the basis of limited infrared measurements on a few ortho-alkyl anilines.*

enhancement is not observed are those where the substituents are 2,4,6-tri-CH_3, 2,4,6-tri-$CH(CH_3)_2$, 2,6-di-CH_3, 2,5-di-$C(CH_3)_3$, 2-$C(CH_3)_3$, 2-CH_3, 2-$CH(CH_3)_2$, and 2-CH_2CH_3. This is in harmony with the relatively low polarizing ability of alkyl groups. Some of the other deviations from the established patterns remain unexplained, but the effect of ortho substitution on the mechanical and electrical anharmonicity of these vibrations is being investigated in an attempt to provide some further information on the interaction mechanisms (31).

The apparent HNH bond angle (θ) and the NH stretching force constant (k) can be calculated from the two absorption frequencies of a primary amine by means of the valency force field equations of Linnett (32):

$$[7] \qquad 4\pi^2\nu_s^2 = k[1/m_H+(1+\cos\theta)/m_N]$$

$$[8] \qquad 4\pi^2\nu_{as}^2 = k[1/m_H+(1-\cos\theta)/m_N],$$

where m_H and m_N refer to the masses of the hydrogen and nitrogen atoms respectively. This treatment assumes that the nitrogen and hydrogen atoms move along the NH bond directions, and that the stretching force constant is much larger than the deformation and interaction force constants. McKean and Schatz (33) have shown that this would be a valid assumption for the ammonia molecule. Mason (34) has successfully applied these equations to a wide range of primary amines, and has found θ to vary from 104° in $LiNH_2$ to about 119° in heteroaromatic compounds such as 2-aminopyrimidine, 4-aminopyrimidine, and 3-amino-1,2,4-triazine. Although aniline itself was included in his study (θ = 111.8°), conclusive evidence for substituent effects on the hybridization state of the NH_2 group in the aromatic amine series has not been reported.

Figure 5 shows that for meta- and para-substituted anilines θ increases linearly with increasing electron-withdrawing power of the substituents, from a value of 109.6° in

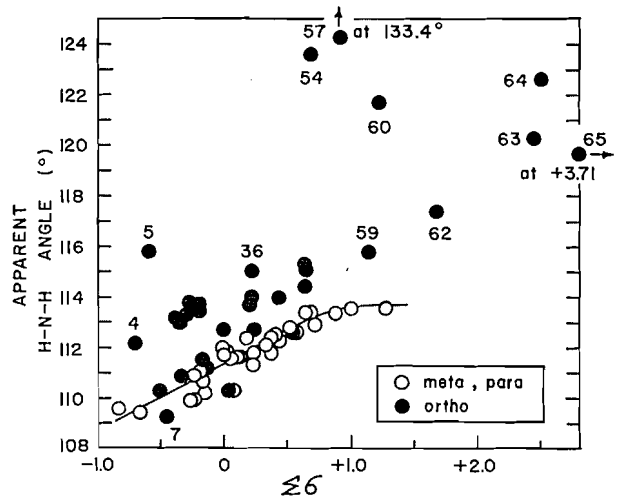

FIG. 5. The HNH bond angle in substituted anilines and its dependence on the electronic nature and position of ring substituents.

N,N-dimethyl-*p*-phenylenediamine and 109.4° in *p*-phenylenediamine (almost exactly sp^3) to a limiting value of 113.6°, which is reached in *p*-aminobenzonitrile and *p*-nitroaniline. This is in agreement with the predicted change in lone-pair conjugation with the

aromatic π-electrons. Ortho-substituted anilines show extensive HNH angle opening, except in those cases where the substituents involved are one or two methyl, ethyl, or isopropyl groups, or the CF_3 group. Undoubtedly there are a number of factors responsible for this increase in θ. For those cases where the angle is close to or exceeds 120°, as in 2,4,6-trinitroaniline (119.7°), 2,6-dinitroaniline (120.3°), 2-nitroaniline (121.7°), 2,4-dinitroaniline (122.6°), ethyl orthoanthranilate (123.6°), and 2-aminoacetophenone (133.4°), intramolecular hydrogen bonding is suggested, and similar interaction of a weak nature may account for the behavior of ortho-CN, -halogen, -OR, and $-NH_2$ groups. Weak bonding of an amino hydrogen atom to the π-electrons of an adjacent phenyl group can also be envisaged.

The increased apparent HNH angles for 2-nitro-, 2,4-dinitro, 2,6-dinitro-, and 2,4,6-trinitro-aniline are of interest in view of some recent controversy in the literature as to whether or not intramolecular hydrogen bonding is present in the first compound. Lutskii and Alexseeva (35), Moritz (36), and Farmer and Thompson (37) have concluded that there is intramolecular hydrogen bonding in 2-nitroaniline; Dyall (26) claims that solvent effect studies show it is absent in 2-nitro- and 2,4-dinitro-aniline, but present in 2,6-dinitro- and 2,4,6-trinitro-aniline. In view of the fact that the largest apparent HNH angle found in this work (133.4°) occurs in 2-aminoacetophenone, where hydrogen bonding is strongly favored because of the formation of a six-membered chelate ring, the enhanced angles in the nitroanilines also suggest a similar interaction mechanism.

The compound 1-naphthylamine (No. 29) appears to behave in an anomalous manner in that both A_s and A_{as} are smaller than expected, as is the calculated HNH angle. This suggests that the conjugation of the lone-pair electrons with the aromatic π-electrons is disturbed by some interference due to the *peri*-H atom. Elliott and Mason (38) have postulated "bending" of the nitrogen bonding orbital due to repulsion, and a slight twisting of the NH_2 group to reduce the conjugation. Narrower band widths for this compound support this view due to steric hindrance to solvation of the NH_2 group, as will be described later. 2-Naphthylamine (No. 28) behaves like a normal meta-substituted aniline.

A weakness in the calculation of θ for ortho-substituted anilines from equations [7] and [8] may arise in the underlying assumption that the two NH bonds be equivalent.* However, the fact that anilines which are symmetrically substituted in the 2,6-positions (compounds 5, 49, 52, 59, 62, 63, and 65) and thus should meet this requirement lead to similarly enhanced θ values provides some proof for the validity of the method. This variation in HNH angle in the aniline series can be further confirmed by applying the same type of calculation to the limiting cases of a primary alkyl amine (sp^3) and a primary acid amide (sp^2). Using the data of Orville-Thomas *et al.* (27) for methylamine in CCl_4 solution, the calculated HNH angle is 103.8°; and for acetamide in dilute $CHCl_3$ solution the measurements of Davies (39) lead to 120.3°.

For ortho-halogenated anilines, the apparent HNH angle is found to increase in the order F < Cl < Br < I. Intramolecular hydrogen bonding of the OH group in phenols to ortho-halogen atoms is well-known. Baker and Kaeding (40) have shown that the order of increasing hydrogen bond strength in the ortho-phenol series is really I < F < Br < Cl, which can be attributed to both the varying size of the halogens and an "orbital–orbital repulsive interaction" which increases in the order Cl < Br < I. These authors have also concluded that Badger's rule (41) does not apply in cases where the interacting groups

**We are indebted to a referee for pointing out that in all cases where $\theta > 120°$ the compound has a single ortho substituent, but for compounds 63 and 65, where two NO_2 groups flank the NH_2 group, the apparent HNH angle is almost exactly 120°, which tends to support this argument.*

are not free to take up their preferred orientation or interacting distance. In the aniline series the HNH . . . F interaction may be extremely weak because the small size of the fluorine prevents the H atom from getting close to its lone-pair orbitals. The increase in size of the halogens appears to more than offset the corresponding decrease in electronegativity.* The concept of intramolecular hydrogen bonding would account for the "normal" HNH angles in anilines with ortho-methyl, -ethyl, and -isopropyl groups. The large angle of 115.8° in 2,4,6-tri-*tert*-butylaniline could arise as the NH_2 group is forced into greater planarity with the aromatic ring by the bulky *tert*-butyl groups which flank it (see Fig. 9(*a*)). Qualitatively this could account for the marked increase in A_{as} relative to A_s in terms of NH bond moment contributions, the lone-pair conjugation being small because of the electron-donating characteristics of the three *tert*-butyl groups. To a lesser extent this could also account for A_{as} increases in 2-*tert*-butyl- and 2,5-di-*tert*-butyl-aniline.

The calculated NH stretching force constant increases smoothly with $\sum\sigma$ for meta- and para-substituted anilines (Fig. 6). The complex deviation of ortho-substituted

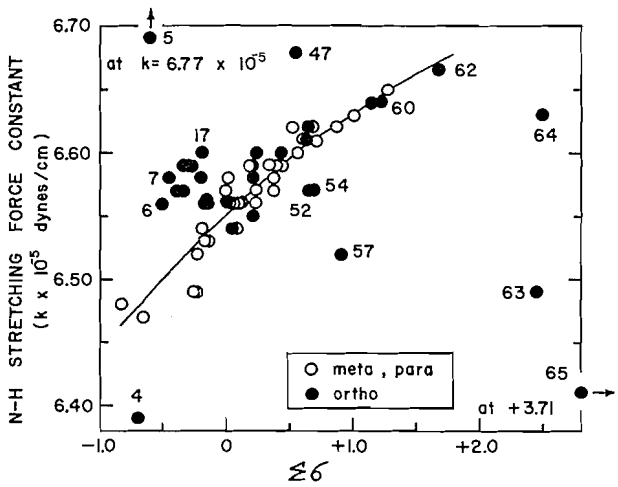

FIG. 6. The dependence of the calculated NH stretching force constant on the electronic nature and position of ring substituents in anilines.

compounds is a direct reflection of the dependence of the force constant on the effective charge on the nitrogen atom, as well as on its hybridization state (32, 42).

Once the bond angle θ is known, the contribution of $2s$ and $2p$ orbitals to the hybrid nitrogen bonding orbitals may be calculated (34). The coefficient b in the hybrid orbital

$$\psi_{\text{hybrid}} = b\psi_{2s} + \sqrt{(1-b^2)}\cdot\psi_{2p} \qquad [9]$$

can be used as a measure of s-character, and may be calculated from

$$b^2 = -\cos\theta/(1-\cos\theta) \qquad [10]$$

provided the two NH bonds are equivalent and the hybrid orbitals of N binding the H atoms are orthogonal. For meta and para anilines, k is a linear function of s-character (Fig. 7). This is in excellent agreement with Mason's calculations (34) based on Slater

Unambiguous data obtained by von R. Schleyer and West (P. von R. Schleyer and R. West. J. Am. Chem. Soc. **81, 3164 (1959)) for the intermolecular hydrogen bonding of methanol and phenol to alkyl halides confirms that the relative electron donor ability of the covalently bonded halogen atom increases in the order* F < Cl < Br < I.

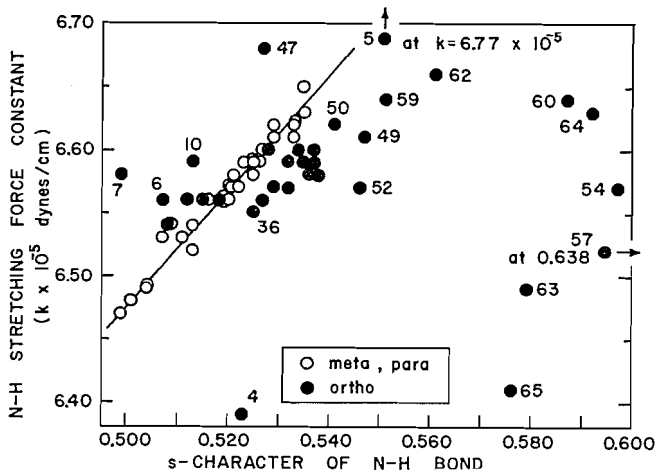

FIG. 7. Relation between the NH stretching force constant and the *s*-character of the hybrid orbitals bonding these atoms in substituted anilines. A *b* value of 0.500 corresponds to sp^3 hybridization of the N atom.

orbitals which show that the overlap integral (measuring the strength of the NH bond, as does the force constant) for a hybrid orbital of nitrogen according to equation [9] and a 1*s* orbital of hydrogen increases linearly with *b*. Figure 7 also shows that changes in the apparent HNH angle alone cannot account for the difference between the NH stretching force constants of ortho anilines and those for meta and para anilines. For a given HNH angle, an increase in the effective charge on the nitrogen atom should decrease its electronegativity and hence lower the NH stretching force constant and vice versa (34). Farmer and Thompson (37) have indicated that hydrogen bond formation with an amino hydrogen atom must induce a negative charge on the nitrogen atom. This would account for those points in Fig. 7 which are below the meta–para line.

The points above this line correspond to ortho-alkyl substituents (and *o*-CF_3). Since the bulkiest ortho-alkyl groups lead to the greatest increase in the NH force constant, a type of "internal specific solvation" of the amino group is suggested, whereby the effective dielectric environment of the amino group has acquired a larger hydrocarbon nature as CCl_4 molecules are crowded out. This should raise the NH force constant. The NH force constant for aniline in *n*-hexane does show a slight increase, whereas for 2,6-dimethylaniline in *n*-hexane it is identical with that calculated from frequencies obtained in CCl_4. Changes of force constant of less than 1% due to this effect would account for almost all of the positive deviations observed.

Crystallographic data available are in agreement with the concept of increasing sp^2 character of the amino nitrogen atom as ring substituents become more electrophilic. The C—N bond lengths (43) in *p*-hydroxyaniline, *p*-iodoaniline, and the *sym*-trinitrobenzene complex of *p*-nitroaniline are 1.47, 1.43, and 1.37 Å respectively, denoting increasing bond order. All three are classed as planar, with C_{2v} symmetry. The maximum displacement from the mean plane in the *p*-nitroaniline complex is given as 0.06 Å. Since the X-ray method is not suitable for the determination of H atom positions, these results are not at variance with the ideas advanced here. Recently Ritschl (44) has assigned the C—N stretching frequency in 10 anilines, and has shown that it increases linearly with the Hammett σ values of the substituents, also implying increasing bond order.

The integrated intensity (A) of a fundamental infrared absorption band depends on the square of the dipole moment change with the normal coordinate of the vibration ($\partial M/\partial Q$):

$$A = (N\pi/3c)(\partial M/\partial Q)^2, \quad [11]$$

where N is the Avogadro number and c is the velocity of light. If only the changes of NH bond moments with bond length (dM/dr) contributed to the transition moment, and if the contributions from both NH bond moments were equal and additive, then (dM/dr) could be calculated in two independent ways from the experimental intensities, using the expressions

$$(\partial M/\partial Q_s) = (2/\mu_s)^{1/2} \cos(\theta/2)\cdot(dM/dr) \quad [12]$$

$$(\partial M/\partial Q_{as}) = (2/\mu_{as})^{1/2} \sin(\theta/2)\cdot(dM/dr), \quad [13]$$

where the μ's are the effective reduced masses governing the amplitudes of vibration. These simplified expressions arise because the resultant NH bond dipole gradients in the symmetric and asymmetric stretching vibrations lie along the internal and external bisectors of the HNH angle respectively. Alternatively, the equations [12] and [13] can be used to estimate θ from the experimental intensities through

$$(A_s/A_{as}) = \tan^2(\theta/2). \quad [14]$$

Mason (34) attempted this for N-heteroaromatic primary amines, and found that these θ values never exceeded 92°, and were not even in the same relative order as the very reasonable θ values calculated from the frequencies. Further, Mason found that the two (dM/dr) values that could be derived independently from [12] and [13] did not agree, the calculation based on A_s always giving a larger value. The author concluded that because of the possibility of large lone-pair contributions to A_s, equation [13] may be a better approximation. It would fail insofar as the asymmetric vibration is anharmonic and has a small dipole moment gradient along the internal bisector of the HNH angle and small in-phase pulsations in s-character of the lone-pair orbital.

The present measurements and calculations lend strong support to this vibrational mechanism (Fig. 8). For p-phenylenediamine and N,N-dimethyl-p-phenylenediamine θ values of 109.4° and 109.6° respectively indicate virtual sp^3 hybridization, since $\theta = 106.8°$ in cyclohexylamine (34) and 106.78° in ammonia (45). With the lone-pair electrons localized on the nitrogen atom and effectively isolated from the π-electrons, the symmetric intensity is due to variation in the NH bond moments and in the atomic dipole. The NH bond moment component in the asymmetric mode exceeds the corresponding component in the symmetric mode for $\theta > 90°$. Table II gives the relative contributions of these bond moments, assuming a fixed vibrational amplitude and a fixed charge distribution in the bond. The numerical values are normalized to the contributions for $\theta = 90°$, where they are equal for both modes. Since $A_{as} > A_s$ for anilines with large negative substituent constants (9) it appears that the atomic dipole contribution is not large enough to outweigh the deficiency in the NH bond dipole component in the symmetric mode. The calculated values of (dM/dr) for these compounds from equations [12] and [13] are 0.8 and 0.6 D/Å respectively. The enhancement of 0.2 D/Å in the value based on A_s reflects the lone-pair contribution.

As the substituent constants become more positive and the HNH angle begins to

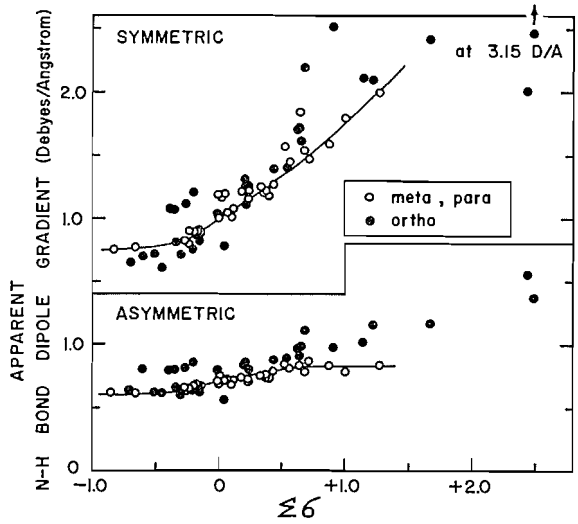

FIG. 8. The substituent dependence of the calculated NH bond moment gradients based on the intensities observed in the two vibrational modes.

TABLE II

Relative contributions of NH bond moments to the resultant dipole moment change in the NH_2 group, for a fixed vibrational amplitude, and fixed charges on the N and H atoms

	θ (°)	Asymmetric mode (dipole moment change along external bisector of ∠HNH)*	Symmetric mode (dipole moment change along internal bisector of ∠HNH)
	90°	1.00	1.00
(sp^3)	109.4°	1.16	0.83
	113.6°	1.20	0.79
(sp^2)	120°	1.25	0.71

*In the asymmetric mode this dipole moment change reverses sign after every half cycle of the vibration.

approach the trigonal angle of 120°, the lone-pair orbital becomes more extensively delocalized over the aromatic ring. Since the lone-pair conjugation will vary during a complete vibrational cycle, as already described, this should lead to a gradually increasing π-electron component as θ increases. This is no doubt a dominant factor in determining the intensities, and explains the pronounced rise in the apparent (dM/dr) values as calculated from A_s by a method neglecting this contribution (Fig. 8). When θ is large, the π-electron component ((*c*) in Fig. 4) more than outweighs the deficiency in the NH bond dipole contribution in the symmetric mode relative to the asymmetric mode (Table II). These results, as summarized in Table III, also explain the crossing of the log A_s/σ and log A_{as}/σ correlation lines near $\sigma = 0$ (parent compound, aniline*) previously reported by us (9).

The calculated (dM/dr) values based on A_{as} are probably reliable as far as order of magnitude is concerned. Figure 8 shows that this value rises slightly as θ increases, which is predicted (Table II). The bond dipole gradients for ortho-substituted anilines are slightly larger than those for corresponding meta and para anilines, as based on both A_s and A_{as}. This is a more sensitive plot than Fig. 1, symmetric stretching, which does not take into account HNH angle changes. Slight enhancement of (dM/dr) on ortho

**Coulson (46) has calculated the π-electron density on the nitrogen atom in aniline to be 1.91, using a molecular orbital method. This is consistent with an* HNH *angle of about 111.7°, as found in this work.*

TABLE III

Resultant dipole moment change in the NH_2 group

$\theta(°)$	b	σ	Contributions in vibrational modes*			Relative intensities	
			Asymmetric		Symmetric	Predicted	Observed A_{as}/A_s
109.4	0.499	-0.83 ($p-NH_2C_6H_4NH_2$)	d_{min}	$>$	resultant of $a_{max}+b$	$A_{as} > A_s$	1.30
111.7	0.520	0 ($C_6H_5NH_2$)	$d_{min}+\delta$	$\approx$	resultant of $(a_{max}-\delta)+c$	$A_{as} \approx A_s$	1.06
113.6	0.535	$+1.27$ ($p-NO_2C_6H_4NH_2$)	$\underbrace{d_{min}+\delta+\delta}_{d_{max}}$	$<$	resultant of $\underbrace{(a_{max}-\delta-\delta)}_{a_{min}}+c_{max}$	$A_{as} < A_s$	0.43

*Refer to Fig. 4 for the identity of the components.

substitution would be expected to show up in calculations based on both vibrational modes if intramolecular hydrogen bonding were involved. For 2,6-dinitroaniline, (dM/dr) based on the symmetric mode is unusually low (see also point No. 63 in Fig. 1, symmetric stretching), whereas the largest value is obtained from calculations based on the asymmetric mode. This must arise from abnormal charge fluctuations arising as the amino group is flanked on both sides by negatively charged oxygen atoms of the nitro groups.

Further evidence for this vibrational interpretation is provided by the log A_s and log A_{as} correlations with σ_I and σ_R according to equation [5] (5). For the asymmetric vibration, (α/β) was found to be 1.7, whereas for the symmetric vibration this ratio was 1.1, indicating that A_s is much more sensitive to the resonance effect than A_{as}.

In liquids and solutions collision broadening is considered to be the dominant factor contributing to vibrational band width, since Ramsay (22) has concluded that natural line widths would be $\sim 10^{-6}$ cm^{-1}, and Doppler broadening would lead to widths of only $\sim 10^{-3}$ cm^{-1}. The decrease in $\Delta\nu_{1/2}$ as the substituents become more electron withdrawing can be attributed generally to a rise in force constant, which makes the solvent perturbation of energy levels less significant. However, factors such as a certain amount of torsional libration of the $-NH_2$ group relative to the aromatic ring, without significant loss of π-electron overlap, cannot be excluded.* Such torsional motion would no doubt lead to band widening, and would decrease with increasing C—N bond order. Califano and Moccia (48) have assigned some of the additional vibrations of the $-NH_2$ group in a few substituted anilines, and Stewart (49) reports the $-NH_2$ torsional oscillation (twisting of the C—N bond) in the far infrared at ~ 290 cm^{-1}. Further studies on substituent effects on these vibrational modes are now in progress.

In ortho-substituted anilines the half-band widths are significantly narrower than those for corresponding meta and para compounds (Fig. 3). This narrowing is ascribed to a decrease in the number of effective collisions of solvent molecules with the amino group due to the shielding nature of the adjacent substituent(s). As expected, 2,4,6-tri-*tert*-butyl-, 2,5-di-*tert*-butyl-, and 2-*tert*-butyl-aniline (points 5, 11, and 17) show very extensive narrowing. Scale molecular models show that the NH_2 group must be vibrating in what is effectively a methyl cage in 2,4,6-tri-*tert*-butylaniline (shown schematically in Fig. 9(*a*)). Free rotation of the *tert*-butyl groups is not possible. Wepster and co-workers

*Jones, Forbes, and Mueller (47) have suggested that in ortho-substituted acetophenones the acetyl group may actually be in a state of minimum energy when it is displaced slightly from the plane of the ring.

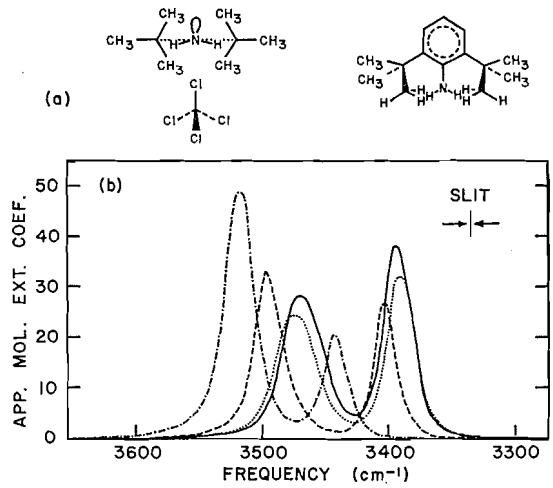

FIG. 9. (*a*) Steric hindrance to solvation in 2,6-di-*tert*-butylaniline. (*b*) Typical high-resolution amine absorption spectra (dilute CCl_4 solution); ——— aniline, . . . 4-*tert*-butylaniline, – – – 2-*tert*-butylaniline, – · – 2,4,6-tri-*tert*-butylaniline.

(50) report that the base strength of 2,6-di-*tert*-butylaniline is lower by a factor of 10^3 than would be expected, and Bartlett *et al.* (51) found that the pK_A of 2,4,6-tri-*tert*-butylaniline was <2 (in comparison with pK_A values of 4.14, 4.00, and 3.39 for aniline, *p*-*tert*-butylaniline, and *o*-*tert*-butylaniline respectively). Both anomalies were ascribed to steric hindrance to solvation. Very narrow bands are also observed in *o*-phenylenediamine. It is interesting to note that steric hindrance of ortho-alkyl groups has also been found to impair the chromatographic adsorption of anilines (52).

The spectacular increases in the integrated absorption intensity often observed for the fundamental hydrogenic stretching vibration on intermolecular hydrogen bond formation are not observed for the intramolecular association of ortho-substituted anilines. It is probable that for highly bent hydrogen bonds, charge transfer effects, which are largely responsible for the increase in band intensity, are of only secondary importance to the electrostatic interaction. For intermolecular association the increase in band width due to hydrogen bonding has not been satisfactorily explained for all systems, but factors such as a variety of absorbing species and a continuous range of configurations have found some support. The narrow band widths for ortho-substituted compounds are in agreement with the concept of intramolecular hydrogen bonding, since the interacting distance involved and the rotational configuration of the amino group are extremely restricted, especially as the lone-pair conjugation with the aromatic π-electrons increases. A further loss of degrees of freedom of the system occurs on hydrogen bond formation (40).

The high-resolution measurements indicate that almost all the NH_2 bands have some asymmetry on the low-frequency side. The significance of this is not known as yet. Cabana and Sandorfy (53) have pointed out a similar effect in the C≡N stretching vibration in benzonitriles, and have suggested an intramolecular Stark effect where highly polarizable groups are involved.

ACKNOWLEDGMENTS

Professor B. M. Wepster (Technische Hogeschool, Delft) and Professor L. R. C. Barclay (Mt. Allison University, Sackville, New Brunswick) generously supplied some

samples of ortho-substituted amines. The technical assistance of Mrs. G. D. Brown with the high-resolution measurements is gratefully acknowledged. The author is indebted to the Royal Dutch Shell Group for a Postgraduate Scholarship, during the tenure of which some of this work was done.

REFERENCES

1. L. P. HAMMETT. Physical organic chemistry. McGraw Hill, New York. 1940. Chap. VII.
2. H. H. JAFFE. Chem. Rev. **53**, 191 (1953).
3. P. J. STONE and H. W. THOMPSON. Spectrochim. Acta, **10**, 17 (1957).
4. H. W. THOMPSON and G. STEEL. Trans. Faraday Soc. **52**, 1451 (1956).
5. P. J. KRUEGER and H. W. THOMPSON. Proc. Roy. Soc. (London), Ser. A, **250**, 22 (1959).
6. M. F. A. E. SAYED. J. Inorg. Nucl. Chem. **10**, 168 (1959).
7. H. W. THOMPSON, R. W. NEEDHAM, and D. JAMESON. Spectrochim. Acta, **9**, 208 (1957).
8. R. N. JONES, W. F. FORBES, and W. A. MUELLER. Can. J. Chem. **35**, 504 (1957).
9. P. J. KRUEGER and H. W. THOMPSON. Proc. Roy. Soc. (London), Ser. A, **243**, 143 (1957).
10. M. S. C. FLETT. Trans. Faraday Soc. **44**, 767 (1948).
11. S. CALIFANO and R. MOCCIA. Gazz. Chim. Ital. **86**, 1014 (1956).
12. S. CALIFANO and R. MOCCIA. Gazz. Chim. Ital. **87**, 58 (1957).
13. G. K. GOLDMAN, H. LEHMAN, and C. N. R. RAO. Can. J. Chem. **38**, 171 (1960).
14. C. N. R. RAO and R. VENKATARAGHAVAN. Can. J. Chem. **39**, 1757 (1961).
15. C. N. R. RAO and G. B. SILVERMAN. Current Sci. (India), **26**, 375 (1957).
16. Y. OKAMOTO and H. C. BROWN. J. Org. Chem. **22**, 485 (1957).
17. H. C. BROWN and Y. OKAMOTO. J. Am. Chem. Soc. **80**, 4979 (1958).
18. T. L. BROWN. J. Phys. Chem. **64**, 1798 (1960).
19. R. W. TAFT, JR. *In* Steric effects in organic chemistry. *Edited by* M. S. Newman. John Wiley and Sons, New York. 1956.
20. A. C. FARTHING and B. NAM. *In* Steric effects in conjugated systems. *Edited by* G. W. Gray. Butterworths. 1958. p. 131.
21. R. A. RUSSELL and H. W. THOMPSON. Spectrochim. Acta, **9**, 133 (1957).
22. D. A. RAMSAY. J. Am. Chem. Soc. **74**, 72 (1952).
23. P. J. KRUEGER. Appl. Opt. **1**, 443 (1962).
24. D. H. MCDANIEL and H. C. BROWN. J. Org. Chem. **23**, 420 (1958).
25. P. J. BRAY and R. G. BARNES. J. Chem. Phys. **27**, 551 (1957).
26. L. K. DYALL. Spectrochim. Acta, **17**, 291 (1961).
27. W. J. ORVILLE-THOMAS, A. E. PARSONS, and C. P. OGDEN. J. Chem. Soc. 1047 (1958).
28. C. A. COULSON. *In* Proceedings of the conference on molecular spectroscopy. *Edited by* E. Thornton and H. W. Thompson. Pergamon Press. 1959. p. 183.
29. B. M. WEPSTER. *In* Steric effects in conjugated systems. *Edited by* G. W. Gray. Butterworths. 1958. p. 86.
30. J. M. ESSERY and K. SCHOFIELD. J. Chem. Soc. 3939 (1961).
31. P. J. KRUEGER. Unpublished results.
32. J. W. LINNETT. Trans. Faraday Soc. **41**, 223 (1945).
33. D. C. MCKEAN and P. N. SCHATZ. J. Chem. Phys. **24**, 316 (1956).
34. S. F. MASON. J. Chem. Soc. 3619 (1958).
35. A. E. LUTSKII and V. A. ALEXSEEVA. Zh. Obshch. Khim. **29**, 2992 (1959).
36. A. G. MORITZ. Spectrochim. Acta, **15**, 242 (1959).
37. V. C. FARMER and R. H. THOMPSON. Spectrochim. Acta, **16**, 559 (1960).
38. J. J. ELLIOTT and S. F. MASON. J. Chem. Soc. 1275 (1959).
39. M. DAVIES. Discussions Faraday Soc. **9**, 325 (1950).
40. A. W. BAKER and W. W. KAEDING. J. Am. Chem. Soc. **81**, 5904 (1959).
41. R. M. BADGER and S. H. BAUER. J. Chem. Phys. **5**, 839 (1937).
42. R. E. RICHARDS. Trans. Faraday Soc. 44, 40 (1948).
43. L. E. SUTTON (*Editor*). Tables of interatomic distances and configuration in molecules and ions. The Chem. Soc., London. 1958.
44. R. RITSCHL. Z. Chem. **1**, 285 (1961).
45. G. HERZBERG. Infrared and Raman spectra of polyatomic molecules. Van Nostrand, New York. 1945. p. 439.
46. C. A. COULSON. Valence. Oxford Univ. Press. 1952. p. 246.
47. R. N. JONES, W. F. FORBES, and W. A. MUELLER. Can. J. Chem. **35**, 504 (1957).
48. S. CALIFANO and R. MOCCIA. Gazz. Chim. Ital. **87**, 805 (1957).
49. J. E. STEWART. J. Chem. Phys. **30**, 1259 (1959).
50. J. BURGERS, M. A. HOEFNAGEL, P. E. VERKADE, H. VISSER, and B. M. WEPSTER. Rec. Trav. Chim. **77**, 491 (1958).
51. P. D. BARTLETT, M. ROHA, and R. M. STILES. J. Am. Chem. Soc. **76**, 2349 (1954).
52. J. K. CARLTON and F. B. O'NEAL. Talanta, **9**, 39 (1962).
53. A. CABANA and C. SANDORFY. Spectrochim. Acta, **16**, 335 (1960).

THE REDUCTION OF NITROBENZENE BY HYDROSULPHIDE ION IN AQUEOUS MEDIA[1]

O. J. Cope and R. K. Brown

Department of Chemistry, University of Alberta, Edmonton, Alberta

Received June 11, 1962

ABSTRACT

The reduction of nitrobenzene by sodium hydrosulphide and sodium hydrodisulphide in aqueous media at 50° has been examined. Goldschmidt's report of first-order dependence upon both nitrobenzene and hydrosulphide is corroborated. The action of hydrosulphide on nitrobenzene produces phenylhydroxylamine, which is reduced by hydrosulphide much more slowly than is nitrobenzene. As reaction progresses, nitrobenzene reduction produces yellow hydrodisulphide, which is responsible for the observed autocatalytic effect. Hydrodisulphide reduces phenylhydroxylamine more rapidly than it does the original nitrobenzene, and hence as reaction time is extended, phenylhydroxylamine disappears more rapidly than does nitrobenzene, yielding only aniline and some unreacted nitrobenzene towards the end of the reaction. Hydrosulphide reduction of phenylhydroxylamine to aniline produces thiosulphate but apparently no hydrodisulphide. Hydro*di*sulphide reduction of the phenylhydroxylamine leads only to conversion of the yellow hydrodisulphide to a colorless species, apparently thiosulphate. On the other hand hydrosulphide or hydrodisulphide reduction of nitrobenzene is accompanied by thiosulphate formation and some increase in hydrodisulphide. A comparison of the rate constants shows that under the conditions of the reaction, hydrodisulphide ion reduces nitrobenzene about seven times more rapidly than does hydrosulphide ion while phenylhydroxylamine is reduced two to three times more rapidly by hydrodisulphide than is nitrobenzene.

INTRODUCTION

The use of sodium hydrosulphide for the selective reduction of nitro groups in the aromatic nucleus is well known. This reagent has been prepared for this purpose by treatment of sodium monosulphide with 1 equivalent of sodium bicarbonate (1), or, in the form of more acidic systems, by bubbling hydrogen sulphide through a solution of the reducible substance containing a catalytic amount of ammonia (2). The addition of excess ammonium salts to a solution of hydrosulphide has also been employed to produce hydrosulphide under conditions designed to maintain a pH of 7.5 to 8.0 (3).

The only reported kinetic study of the hydrosulphide reduction is that of Goldschmidt and Larsen (4), who investigated the reduction in aqueous solution at 25° C of various nitro compounds by sodium hydrosulphide saturated with hydrogen sulphide. The conditions of their reaction resulted in conversion of the nitrobenzene to the corresponding N-phenylhydroxylamine along with complete precipitation of the sulphur formed according to equation (*a*). The rate of reduction was found to be first order in nitrobenzene, first order in hydrosulphide ion, and independent of hydrogen sulphide concentration.

$$C_6H_5NO_2 + 2NaHS + H_2O \rightarrow C_6H_5NHOH + 2S^0 + 2NaOH \qquad (a)$$

In a previous paper (5) we have shown that the $S_x^=$ species reduces nitrobenzene much faster than does the $S^=$, HS^-, or HS_x^- species. In the present work the reduction of nitrobenzene by sodium hydrosulphide has been studied in greater detail. Experimental conditions were devised which allowed at least a semiquantitative estimate to be made of the relative reducing abilities of HS^- and HS_2^-.*

[1]*Taken from the thesis of O. J. Cope submitted to the Graduate School of the University of Alberta in partial fulfillment of the requirements for the degree of Doctor of Philosophy.*

**For reasons indicated in the previous paper (5) the assumption is made that at low sulphur concentration compared with hydrosulphide ion concentration the predominating polysulphide species is* HS_2^-.

Normally reductions by hydrosulphide ion involve an increase in pH due to the formation of hydroxyl ions according to equation (*a*). This in turn gives rise to reaction (*b*) in which elemental sulphur is considered to be lost by conversion to sulphide and thiosulphate ions. Equation (*b*) has been utilized to account for thiosulphate ion formation *during* reductions of nitrobenzene with disulphide (6) and monosulphide ions (5). In

$$6OH^- + 4S^0 \rightarrow S_2O_3^= + 2S^= + 3H_2O \qquad (b)$$

his review of methods of reduction of nitro compounds Schröter (7) suggests that in the case of ammonium hydrosulphide reduction, thiosulphate formation occurs directly as the result of the two reactions (*c*) and (*d*). However, it is likely that the thiosulphate

$$RNO_2 + 6NH_4SH \rightarrow RNH_2 + 3(NH_4)_2S_2 + 2H_2O \qquad (c)$$

$$RNO_2 + (NH_4)_2S_2 + H_2O \rightarrow RNH_2 + (NH_4)_2S_2O_3 \qquad (d)$$

arises indirectly through a reaction such as (*b*) (6). If that is so, then by keeping the hydroxyl ion concentration low relative to the hydrosulphide ion concentration, it should be possible to minimize or eliminate the formation of thiosulphate ion, thus retaining the elemental sulphur either as S^0 or as HS_x^-, as has been done by Bullock and Forbes (6) for sulphide and disulphide reductions of nitro compounds.

It is important to operate under conditions which eliminate atmospheric oxygen to avoid the possibility of conversion of hydrosulphide to thiosulphate. Thiosulphate formation has been shown to occur when air is bubbled through a solution of sodium sulphide.

EXPERIMENTAL

Analytical Methods

The reductions were carried out using essentially the same apparatus and procedure as in the previous work with sodium monosulphide (5). The reflux condenser was dispensed with, however, as in trial experiments it was found that considerable condensation of hydrogen disulphide took place there, followed by decomposition and deposition of sulphur. The reaction mixture was at all times blanketed by nitrogen which had been passed through alkaline pyrogallol. Two hundred and fifty milliliters of an aqueous solution of nitrobenzene was pipetted into the reaction vessel and allowed to reach the thermostatted bath temperature (50.00±0.03° C). Then 50 ml of a 0.900 *M* sodium sulphide – ammonium chloride solution, first brought to 50° in a jacketted vessel, was introduced from an automatic pipette. The solution was thus 0.150 *M* with respect to hydrosulphide and 0.015 *M* or less in nitrobenzene. Time measurements were begun when all this solution had been added.

For spectrophotometric measurements of polysulphide in the visible region at 450 mμ, a portion of the reaction mixture was transferred by means of a warmed pipette to a glass-stoppered sample cell in the thermostatted cell compartment of a Beckman DU spectrophotometer. The glass cell, previously flushed with a stream of nitrogen, was filled *completely* with the solution so that no space was left between the solution surface and the stopper. It was important that the stopper fitted well (a small quantity of Apiezon grease was used) in order to exclude atmospheric oxygen and to prevent loss of H_2S and other volatile components of the reaction solution. The standard double thermospacer equipment was provided with an asbestos-coated wooden lid. It was found that once thermal equilibrium had been attained the temperature of the cell contents could be maintained quite well at 50.00±0.03° C.

The spectrophotometric method previously used for estimating the nitrobenzene concentration (5) was modified so that the 1-ml samples removed from the reaction mixture at timed intervals were diluted to 200 ml with 0.002 *M* aqueous hydrochloric acid. This procedure effectively "froze" the reaction and caused any polysulphide to be precipitated as sulphur, leaving a residual "blank" absorbance due to the inorganic components. This blank was found to be constant for the course of the reaction. However, as the precipitated sulphur appeared in a very finely divided form, it was necessary to allow the diluted sample to stand for 24 hours before the sulphur settled completely and absorption measurements at 267 mμ were made.

Preparation of Solutions

The water used was boiled and cooled in an atmosphere of nitrogen. Subsequently, all solutions were kept under nitrogen.

Na_2S–NH_4Cl Solutions

Two liters of a stock solution of 0.900 *M* sodium sulphide (from $Na_2S.9H_2O$) were prepared and solid ammonium chloride was added to the stirred solution until its pH had been reduced to 10.5 (at 25°). The solution, thus 0.944 *M* in ammonium chloride, was practically colorless and it was calculated that at this pH all the sulphide ion was in the protonated form. This stock solution was used throughout the experiments recorded here and was introduced into the reaction vessel via the automatic pipette under nitrogen pressure.

Polysulphide Solutions

Different amounts of sulphur were weighed into glass-stoppered Erlenmeyer flasks provided with magnetic stirring bars. The requisite volume of 0.150 *M* hydrosulphide solution was added and air expelled with a stream of nitrogen before the flasks were stoppered. In order to effect complete solution of the sulphur at room temperature it was necessary to have the mixtures stirred overnight. For absorbance measurements the solutions were introduced into the thermostatted cell, under the usual precautions of exclusion of air and attainment of thermal equilibrium (50.0° C).

Search for Organic Products of the Reduction of Nitrobenzene or Phenylhydroxylamine by Hydrosulphide or Hydrodisulphide Ion

A. Nitrobenzene Reduction by Hydrosulphide

Utility of vapor phase chromatography.—A Burrell Kromotog K-2 was used for all V.P.C. analyses. A 2.5-m column, containing a celite support coated with 20% of its weight of silicone rubber, at a temperature of 210° C, with a helium flow rate of 70 ml/min, gave good separation of a known mixture of aniline, phenylhydroxylamine, and nitrobenzene.

At elevated temperatures (120°) phenylhydroxylamine is known to decompose into products, two of which are believed to be aniline and azoxybenzene (8). Under our conditions, authentic azoxybenzene showed no retention band on the chart, whereas phenyl hydroxylamine gave two peaks of retention time 135 and 180 seconds. The second band was shown to be due to aniline. The identity of the first band was not established, although it may have been due to unchanged hydroxylamine. The important observation made was that the *ratio* of these two peaks under the conditions of our analysis was found to be constant at a value of second peak/first peak = 1.13±0.03, regardless of the original quantity of phenylhydroxylamine, or solvent used, or the presence of nitrobenzene or other possible reduction products of nitrobenzene. By calibration with authentic aniline and phenylhydroxylamine it was thus possible to analyze mixtures of aniline and phenylhydroxylamine by first measuring the area of the peak of retention time 135 seconds and multiplying it by the factor 1.13 to obtain the area of the peak for the aniline produced by phenylhydroxylamine's decomposition during the analysis. The difference between this calculated area and the actual area was due to additional aniline present with the phenylhydroxylamine *before* the V.P.C. determination. The analysis of several such synthetic mixtures did show clearly the presence of as little as 5% aniline originally present. Although this analysis was not highly accurate it did show qualitatively the presence or absence of phenylhydroxylamine and aniline as reduction products. This analysis was used in conjunction with infrared analyses for OH stretching at 3580 and 3700 cm^{-1} due to phenylhydroxylamine (9).

Analysis of the reaction mixture after 60 minutes' reduction.—The practically colorless mixture, 0.010 *M* in nitrobenzene and 0.150 *M* in hydrosulphide, was allowed to react. A slow development of yellow color (measurable at 450 mμ) due to hydrodisulphide occurred. After 60 minutes of reaction a 100-ml aliquot was extracted with ether, the ether extract dried ($MgSO_4$) and then freed of solvent. The residue was taken up in chloroform. Analysis by V.P.C. indicated the presence of very little aniline, approximately 1–2%, but much phenylhydroxylamine as well as unchanged nitrobenzene. Strong absorption in the infrared characteristic of phenylhydroxylamine corroborated these results.

Analysis of the reaction mixture after 18 hours' reduction.—A 100-ml aliquot of the above yellow reaction mixture, removed after 18 hours of reaction, when treated as above showed by V.P.C. analysis the presence only of aniline along with a small amount of unchanged nitrobenzene. No absorption in the infrared region due to phenylhydroxylamine could be detected.

Other organic reduction products of nitrobenzene.—A carbon tetrachloride solution of the extracted reduction products, taken at intervals during the course of the reaction, was at all times colorless. Measurements at the λ_{max} at which azoxybenzene and azobenzene absorb showed no increase in absorption, thus demonstrating that bimolecular reduction products were absent.

B. Phenylhydroxylamine Reduction by Hydrosulphide

An aqueous solution, 0.01 *M* in phenylhydroxylamine and 0.150 *M* in hydrosulphide, was allowed to react at 50°. No development of yellow color due to hydrodisulphide occurred throughout the course of reduction. A 100-ml aliquot was removed after 50 minutes of reaction time and analyzed. Vapor phase chromatography showed no significant formation of aniline, thus indicating no significant reduction during this time. The same results were obtained from an aliquot removed after 90 minutes of reaction.

After a 24-hour reaction period, however, a considerable amount of aniline had been produced, indicating that a slow reaction did occur between phenylhydroxylamine and sodium hydrosulphide.

C. Phenylhydroxylamine Reduction by Hydrodisulphide

An aqueous solution was prepared 0.01 *M* in phenylhydroxylamine and 0.150 *M* with respect to hydrosulphide ion, containing enough elemental sulphur predissolved in the sodium hydrosulphide solution to convert about 7–8% of the hydrosulphide to hydrodisulphide. The concentration of hydrodisulphide was measured by reference to a Beers' law plot of absorption at 450 mμ, versus concentration of sulphur in aqueous 0.150 *M* sodium hydrosulphide.

A continual decrease in absorption at 450 mμ occurred as reduction progressed. An aliquot removed after 70 minutes of reaction indicated by V.P.C. analysis that about 30% of the phenylhydroxylamine had been converted to aniline. After 1000 minutes of reaction approximately 90% of the hydroxylamine had become aniline.

Search for Inorganic Products of the Reaction of Nitrobenzene or Phenylhydroxylamine with Hydrosulphide or Hydrodisulphide Ions

General Procedure for Thiosulphate Estimation

An excess of a freshly prepared suspension of cadmium carbonate was used to precipitate sulphide and di- (or poly-) sulphide from a 100-ml aliquot of the reaction mixture. It was found necessary to remove the organic material (chiefly aniline) from the aliquot of the reaction mixture by ether extraction prior to the treatment with cadmium carbonate. If this was not done, complete precipitation of sulphide and disulphide could be brought about only by repeated treatments with cadmium carbonate. Moreover, the filtrations involved were hampered by the tendency of the precipitate to clog the porous plate of the filter, thus making the procedure quite time consuming. By prior removal of the aniline it was possible to obtain complete precipitation of the sulphide species by only one application of cadmium carbonate suspension, vigorously stirred with the aliquot for 10 minutes. Following the removal of all precipitate by filtration, it was found that the pH of the resultant solution was above 9, due to the presence of sodium carbonate. This base interfered in the titration with iodine by giving an indefinite end point. However, addition of ammonium chloride reduced the pH to a value less than 8 and permitted satisfactory titration of thiosulphate with 0.0500 *N* iodine to a starch end point.

Hydrodisulphide Estimation

This analysis was accomplished by measurement of the absorption at 450 mμ due to hydrodisulphide. A Beer's law plot of concentration of sulphur as hydrodisulphide (in 0.150 *M* hydrosulphide) versus absorption at 450 mμ gave a molar extinction coefficient of 35, which was then used to calculate the concentration of hydrodisulphide from absorption measurements. Details of the apparatus used are described at the beginning of the discussion of analytical methods.

RESULTS AND DISCUSSION

Products of the Reduction of Nitrobenzene and of Phenylhydroxylamine by Hydrosulphide and Hydrodisulphide

In previous work (5, and references therein) it had been established that the only organic reduction product of nitrobenzene by sodium sulphide or sodium disulphide was aniline. Since Goldschmidt and Larsen (4) had obtained N-phenylhydroxylamine as the principal product of the reduction of nitrobenzene by sodium hydrosulphide in water at 25°, it was necessary to determine the products of our reduction conditions. The analysis of aliquots of the reduction mixtures for organic products by vapor phase chromatography (see Experimental) and also by the use of infrared absorption at 3580 and 3700 cm^{-1} to detect the presence of phenylhydroxylamine is summarized in Table I. In addition, Table I includes the results of analyses for hydrodisulphide and thiosulphate.

The results (Table I) show clearly that hydrosulphide reduced phenylhydroxylamine extremely slowly, requiring 48 hours for near-completion of the reaction. No reduction apparently occurred for the first 90 minutes. On the other hand hydrosulphide with 8% of the hydrosulphide as hydro*di*sulphide reduced phenylhydroxylamine to the amine essentially completely in 1200 minutes. In both cases no hydrodisulphide accumulated. Instead the hydrodisulphide originally present was converted to a colorless species, most likely thiosulphate, since thiosulphate was found to increase during the reduction.

At the beginning of the reaction between *nitrobenzene* and hydrosulphide, only hydroxylamine was produced. Further reduction of the phenylhydroxylamine to aniline proceeded

TABLE I

Products obtained during the reduction of nitrobenzene or N-phenylhydroxylamine by sodium hydrosulphide or sodium hydrodisulphide in aqueous media at 50°

Initial reducible material (molarity)	Reducing agent (molarity)	Time of reduction (min)	Products of reduction				
			HS_2^-	$S_2O_3^=$	Phenylhydroxyl-amine	Aniline	Unchanged nitrobenzene
Nitrobenzene (0.010)	NaHS (0.150)	60 min	Increased by 0.0024 *M*	Increased by 0.0005 *M*	25%	~1%	75%
		3 hr	Increased to max. 0.0066 *M*		45%	20%	35%
		18 hr	Dropped to 0.0035 *M*	Increased by 0.0067 *M*	None	Practically all aniline	Trace
Phenylhydroxylamine (0.010)	NaHS (0.150)	50 min	None	Unchanged	Unchanged	None	—
		90 min	Trace	Unchanged	Unchanged	None	—
		24 hr	None	Increased	Considerably decreased	Much aniline	—
		48 hr	None	Increased	Small amount	Mostly aniline	—
Phenylhydroxylamine (0.010)	NaHS (0.150) containing 8% sulphur as HS_2^-	70 min	Decreased by 0.0026 *M*	Increased	60%	40%	—
		1000 min	Decreased by 0.0072 *M*	Increased by 0.0045 *M*	10%	90%	—

much more slowly than did its formation from nitrobenzene; hence phenylhydroxylamine accumulated during the first portion of the reaction. As the reduction of nitrobenzene progressed, hydro*di*sulphide also accumulated. The hydrodisulphide thus formed reduced phenylhydroxylamine more readily than it reduced nitrobenzene. Thus towards the *end* of the reduction of nitrobenzene by sodium hydrosulphide, the phenylhydroxylamine disappeared, leaving only aniline and some nitrobenzene yet to be reduced. Here again, as reduction progressed, thiosulphate ion increased. In fact, no increase in thiosulphate occurred unless reduction of either nitrobenzene or phenylhydroxylamine took place, in agreement with a similar observation in the case of nitrobenzene reduction by sulphide or disulphide ions (5). Also, in the case of nitrobenzene reduction by hydrosulphide, the amount of hydrodisulphide formed increased to a maximum after 3 hours' reaction, whereupon the total hydrodisulphide concentration decreased till the end of the reduction occurred. At this stage some hydrodisulphide still remained.

Autocatalytic Nature of Hydrosulphide Reduction of Nitrobenzene

In this work it was found that the reduction of nitrobenzene by hydrosulphide ion is also an autocatalytic process, but not to as marked an extent as for the analogous reduction by sulphide ion (5). This was shown by following the decrease of nitrobenzene (Fig. 1) or the increase in sulphur as hydrodisulphide (Fig. 2) during the reduction. In all cases an acceleration of rate is noted for the first portion of the reaction. In following the

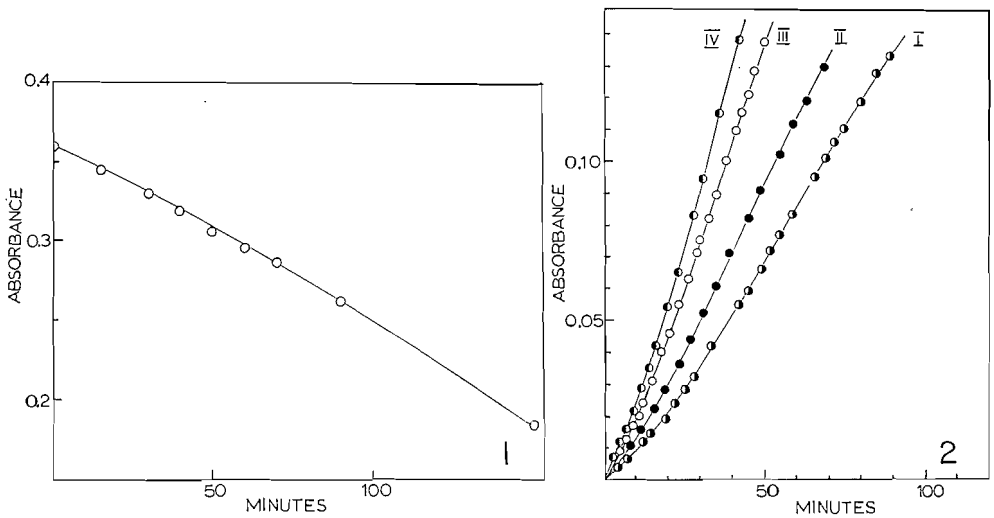

FIG. 1. Change in concentration of nitrobenzene (absorbance at 267 mμ) during reduction with aqueous sodium hydrosulphide at 50° C. Initial concentration of nitrobenzene and sodium hydrosulphide, 0.0098 *M* and 0.150 *M* respectively.

FIG. 2. Absorbance at 450 mμ of hydrodisulphide ion produced during the reduction of nitrobenzene by aqueous sodium hydrosulphide at 50° C. The initial concentration of nitrobenzene for all cases was 0.0094 *M*. Initial concentration of sodium hydrosulphide for runs I, II, III, and IV was 0.150 *M*, 0.200 *M*, 0.250 *M*, and 0.300 *M* respectively.

reduction by measurement of the absorption of nitrobenzene at 267 mμ, allowance for the absorption at 267 mμ due to phenylhydroxylamine was found to be necessary. Ogatas' technique (10) of acidification of the reduction mixture with hydrochloric acid and measurement of absorption of the residual nitrobenzene at 267 mμ was quite satisfactory for sulphide reductions of nitrobenzene (5) since the hydrochloride of aniline, the only reduction product, gave negligible absorption at this wavelength. However,

phenylhydroxylamine hydrochloride has an extinction coefficient at 267 mμ of 1.0×10^3 as compared with one of 7.4×10^3 for nitrobenzene. Since over the first 60 minutes of the hydrosulphide reduction of nitrobenzene, phenylhydroxylamine is essentially the only product, and the amount of hydro*di*sulphide produced is still small, simultaneous loss of phenylhydroxylamine by reduction due to hydrodisulphide would thus be very small. Hence for this first portion of the reduction it is true that 1 molecule of phenylhydroxylamine is produced as 1 molecule of nitrobenzene disappears. Setting the drop in absorbance at 267 mμ due to disappearance of nitrobenzene equal to X and the corresponding increase in absorbance due to phenylhydroxylamine as $(1.0\times10^3)/(7.4\times10^3)\cdot X$, the true decrease in absorption of nitrobenzene becomes $X = 1.15A_{obs}$, where A_{obs} is the observed decrease in absorption at 267 mμ. This factor has been used to obtain the corrected initial slopes in the plot of nitrobenzene absorption versus time in both Figs. 1 and 3.

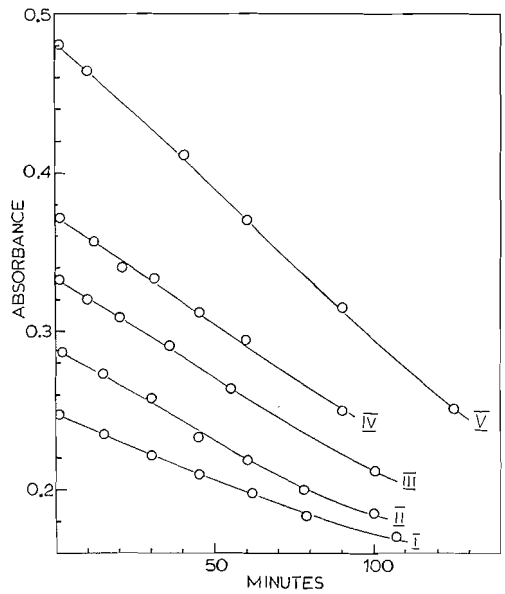

FIG. 3. Effect of change in the initial concentration of nitrobenzene on the rate of its reduction by aqueous 0.150 M hydrosulphide at 50° C. Initial concentration of nitrobenenze for runs I to V are 0.0068 M, 0.0079 M, 0.009 M, 0.0102 M, and 0.0132 M respectively.

Dependence of the Rate of Nitrobenzene Reduction on Nitrobenzene and on Hydrosulphide Ion Concentration

First-order dependence upon both hydrosulphide and nitrobenzene in the sodium hydrosulphide reduction of nitrobenzene in aqueous media was first pointed out by Goldschmidt and Larsen (4). This has been corroborated, over the limited range of concentration employed in this work. Initial slopes, obtained from the plots of nitrobenzene concentration versus time (Fig. 3), divided by the concentration of nitrobenzene gave a constant value (Table II). Similarly, by use of initial slopes of the plots of the appearance of hydrodisulphide ion versus time (Fig. 2), first-order dependence upon hydrosulphide ion concentration was illustrated (Table III). In the latter case, the upward drift of the figures in column 3 (Table III) may be due to the increase in ionic strength as one increases the sodium hydrosulphide concentration. A positive salt effect for the reaction has been found by Goldschmidt and Larsen (4).

TABLE II

Dependence of reduction of nitrobenzene by hydrosulphide ion on nitrobenzene concentration
(Initial hydrosulphide ion concentration, 0.150 M; solvent, H_2O; reaction temperature, 50.0°)

Initial nitrobenzene concentration (absorbance at 267 mμ)	Rate of decrease* in absorbance at 267 mμ, $\times 10^3$ (min^{-1})	Rate of decrease in absorbance ÷ absorbance of nitrobenzene, $\times 10^2$ (min^{-1})
0.482	1.94	4.03
0.373	1.51	4.05
0.334	1.33	3.98
0.289	1.15	3.97
0.248	1.01	4.06

*Obtained from initial slopes of plots in Fig. 3 multiplied by 1.15.

TABLE III

Dependence of rate of reduction of nitrobenzene by hydrosulphide ion on hydrosulphide ion concentration
(In water at 50°; nitrobenzene = 0.0094 M)

Initial hydrosulphide ion concentration (M)	Initial rate of HS_2^- increase, $\times 10^3$ (min^{-1})	Rate of HS_2^- decrease ÷ $[HS^-]$, $\times 10^2$ (min^{-1})
0.150	0.90	6.0
0.200	1.4	7.0
0.250	1.8	7.2
0.300	2.2	7.3

Comparison of Ease of Reduction of Nitrobenzene by Hydrosulphide and Hydrodisulphide

In order to test the relative reducing abilities of hydrosulphide and hydrodisulphide at the pH (10.3) and temperature (50°) of the solutions employed, one run was carried out wherein sufficient sulphur was predissolved in the 0.150 M solution of hydrosulphide to make it 0.0150 M in hydrodisulphide. Figure 4 shows that the deliberate addition of this sulphur as hydrodisulphide definitely accelerated the rate of reduction by a

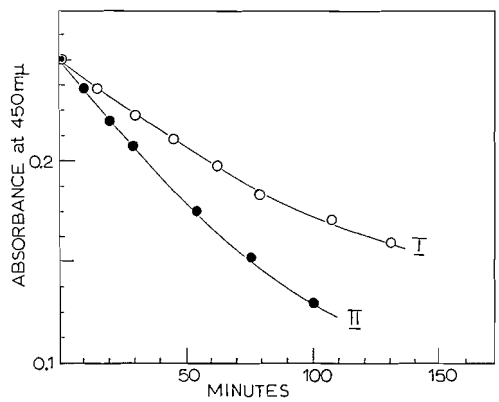

FIG. 4. The effect of addition of sulphur as hydrodisulphide to a solution of sodium hydrosulphide on the rate of reduction of nitrobenzene. Initial concentration of nitrobenzene, 0.0068 M. (I) Reduction by 0.150 M solution of sodium hydrosulphide. (II) Reduction by 0.150 M solution of sodium hydrosulphide containing 0.015 M of sulphur as hydrodisulphide.

factor of 1.8 (after correction for interference of phenylhydroxylamine at 267 mμ). This information is evidence that hydrodisulphide ion does reduce nitrobenzene more readily than does hydrosulphide ion and that hydrodisulphide is the entity responsible for the autocatalytic nature of the reaction. The conclusion made in our previous publication (5) that hydrodisulphide and hydrosulphide in aqueous ethanol possessed *comparable* reducing abilities must now be modified for the reduction in completely aqueous media. It is likely that in aqueous ethanol the hydrodisulphide is also somewhat more effective than is hydrosulphide but the difficulty and consequent error involved in estimating the interference of the hydrodisulphide at 267 mμ under those conditions (5) could readily have masked the relatively small increase in rate due to hydrodisulphide. In the *aqueous* media used in the present work there was no comparable difficulty in measuring the hydrodisulphide absorption (and concentration) and hence its interference at the λ_{max} of 267 mμ for nitrobenzene, since all polysulphide sulphur was completely removed by precipitation before absorption measurements were made.

The initial reduction, quite evident in Fig. 1 and in Fig. 4 (plot I), is due chiefly to HS^-. A small contribution may arise from the unavoidable traces of hydrodisulphide present. From absorption measurements, the highest concentration of this contaminating hydrodisulphide was 0.5% of the hydrosulphide. However, the fact that the rate of reduction was increased by a factor of only 1.8 when as much as 10% of the hydrosulphide was in the form of hydrodisulphide, shows that small traces of the latter as a contaminant could not have contributed much to the rate of reduction shown initially by the solution of sodium hydrosulphide.

Determination of Rate Constants for the Hydrosulphide and Hydrodisulphide Reduction of Nitrobenzene

An attempt has been made to obtain a quantitative comparison of the ability of sodium hydrosulphide and sodium hydrodisulphide to reduce nitrobenzene, as follows.

An approximate value of the rate constant (k_1) for hydrosulphide reduction of nitrobenzene in aqueous media can be obtained from the data in Table II. Using the expression $-dA_n/dt = k_1[HS^-]A_n$, where A_n is the concentration of nitrobenzene in terms of absorbance, and noting that the average value of $(-dA_n/dt)/A_n = 4.02\times10^{-3}$ min^{-1}, k_1 becomes 2.68×10^{-2} liter mole^{-1} min^{-1}. This figure may be slightly high since the contribution to the rate by traces of hydrodisulphide ion has been neglected for the reason stated in the preceding section.

From this value of k_1, and with the information available in Fig. 4, it is now possible to obtain a value for the hydro*di*sulphide reduction rate constant, k_2. Here it is assumed that the solution of elemental sulphur (S_8) in a large excess of sodium hydrosulphide produces only the species HS_2^-, although the solution may actually contain a *mixture* of higher polysulphides as contaminants (5). Accordingly, from Fig. 4, plot II, where $[HS^-] = 0.135\ M$, $[HS_2^-] = 0.015\ M$, $A_n = 0.500$, and the initial slope is $dA_n/dt = 3.5\times10^{-3}$ min^{-1}, appropriate substitution in the expression

$$-dA_n/dt = k_1[HS^-]A_n + k_2[HS_2^-]A_n$$

gives $k_2 = 1.92\times10^{-1}$ liter mole^{-1} min^{-1}.

Comparison of these rate constants shows that the sodium hydrodisulphide reduces nitrobenzene about seven times more rapidly than does sodium hydrosulphide.

Under our conditions, the sulphide ion is practically all in the protonated form as hydrosulphide. However, the extent of hydrolysis of the disulphide ion under these

conditions may be considerably less. The hydrolysis constant of the disulphide ion is not known, although Ogata (10) indicates that it is less than that of the sulphide ion. It is thus possible that in our solutions of sodium hydrosulphide containing as much as 10% of the hydrodisulphide, we are actually dealing with an appreciable concentration of the $S_2^=$ species, which is known to reduce nitrobenzene rapidly (5). This then may be the active species in our solution and it would be incorrect to attribute the rate expressed by $k_2 = 1.92\times10^{-1}$ liter mole^{-1} min^{-1} to the HS_2^- only. However, this can be taken into consideration using the expression

$$-dA_n/dt = A_n(k_1[HS^-]+k'[HS_2^-]+k''[S_2^=]).$$

Knowing that $[S_2^=] = [HS_2^-][OH^-]/K_h$, where K_h is the hydrolysis constant (unknown) of the disulphide ion, the observed rate constant is $k_2 = k'+k''[OH]/K_h$.

The Reduction of Phenylhydroxylamine by Hydrodisulphide Ion

The reduction of phenylhydroxylamine by aqueous sodium hydrosulphide containing hydrodisulphide is due essentially to the hydrodisulphide species. Hydrosulphide itself reduces the hydroxylamine very slowly (Table I). Certainly in the first 90 minutes of reaction, reduction with a mixture of hydrosulphide and hydrodisulphide occurs practically only by hydrodisulphide, with simultaneous decrease in the hydrodisulphide concentration. It has been possible to follow the reduction of phenylhydroxylamine during the first 90–100 minutes by measuring the decrease in absorption of hydrodisulphide at 450 mμ. The results are shown in Fig. 5.

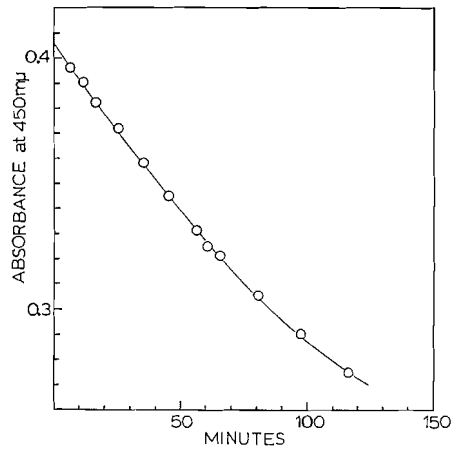

FIG. 5. Disappearance of hydrodisulphide ion during the reduction of a 0.010 M solution of N-phenylhydroxylamine by 0.150 M aqueous sodium hydrosulphide containing sufficient elemental sulphur to convert about 8% of the hydrosulphide to hydrodisulphide.

If it is assumed that the reaction between phenylhydroxylamine and hydrodisulphide is first order in each component, a value can be obtained for the rate constant k_3 for the disappearance of hydrodisulphide by use of the expression $-dA_{HS_2^-}/dt = k_3$[hydroxylamine][HS_2^-]. From a measurement of the initial rate, $dA_{HS_2^-}/dt = 2.00\times10^{-3}$ min^{-1}, obtained from Fig. 5, where $A_{HS_2^-}$ is the absorbance of hydrodisulphide, the concentration of the hydrodisulphide is 0.406 expressed as absorbance, and the concentration of phenylhydroxylamine is 0.010 M, substitution in the above expression gives $k_3 = 5.1\times10^{-1}$ liter mole^{-1} min^{-1}. This indicates that phenylhydroxylamine is reduced by hydrodisulphide about 2.7 times more rapidly than is nitrobenzene. This difference in rate

explains the findings in Table I, and the failure to find phenylhydroxylamine in nitrobenzene reduction by hydrodisulphide towards the end of the reaction.

Stoichiometry of the Overall Reduction of Nitrobenzene to Aniline by Sodium Hydrosulphide

The quantitative analyses of the initial reaction mixture and of the mixture obtained at the end of the reduction gave the results of Table IV. Thus both $S_2O_3^=$ and HS_2^- are produced during the reaction and are found at the end of the reduction in the concentration shown.

TABLE IV
(Compare Table I)

	Nitrobenzene	$S_2O_3^=$	HS_2^-
Initial concentration (M)	0.01	0.0035	0.0005
Final concentration (M)	0.00	0.0102	0.0035
Overall change (M)	−0.01	0.0067	0.0030

Assuming that HS^- reduction of nitrobenzene to aniline yields only HS_2^- one can write the following overall redox equation:

$$RNO_2 + 6HS^- + H_2O \rightarrow RNH_2 + 3HS_2^- + 3OH^-. \qquad (e)$$

On the other hand, the formation of only $S_2O_3^=$ is satisfied by the overall redox equation

$$4RNO_2 + 6HS^- + H_2O \rightarrow 4RNH_2 + 3S_2O_3^=. \qquad (f)$$

Equation (e) shows that the production of 1 mole of HS_2^- required 1/3 mole of nitrobenzene. Since in our reduction 0.0030 M of HS_2^- was produced, according to the preceding statement the amount of nitrobenzene consumed in this direction must have been 0.0010 M. The remainder of the nitrobenzene (0.0090 M) then gave $S_2O_3^=$ only. The stoichiometry of equation (f) shows that 1 mole of nitrobenzene yields 3/4 mole of $S_2O_3^=$. Accordingly, the 0.0090 M of nitrobenzene should yield 0.00675 M of the thiosulphate. The amount actually found (0.0067 M) agrees with this very well.

Stoichiometry of the Hydrodisulphide Reduction of Phenylhydroxylamine

Quantitative analysis of the initial and final reduction mixtures yielded the results of Table V.

TABLE V
(Compare Table I)

	Phenylhydroxylamine	$S_2O_3^=$	HS_2^-
Initial concentration (M)	0.010	0.0035	0.0116
Final concentration (M)	0.00	0.0080	0.0041
Overall change (M)	−0.01	0.0045	−0.0075

Reaction of either HS^- or HS_2^- with phenylhydroxylamine *apparently* failed to produce HS_2^-, but instead consumed any HS_2^- present. However, the amount of $S_2O_3^=$ increased considerably. The following overall redox equation agrees with these results but points out that 1 mole of phenylhydroxylamine yields 0.5 mole of $S_2O_3^=$:

$$2RNHOH + 2HS_2^- + 2OH^- \rightarrow 2RNH_2 + S_2O_3^= + 2HS^- + H_2O. \qquad (g)$$

The formation of 0.0045 mole of $S_2O_3^=$ from the reduction of 0.01 mole of phenylhydroxylamine supports this formulation. The slight decrease from the amount expected theoretically can be attributed to the simultaneous though much slower reduction of the phenylhydroxylamine by the HS^- (equation *h*) which is present in a concentration about 10

$$4RNHOH + 2HS^- \rightarrow 4RNH_2 + S_2O_3^= + H_2O \qquad (h)$$

times that of HS_2^-. Support for the view that HS^- also participates in the reaction is obtained from the quantitative data in Table V. Since only 0.0075 mole of HS_2^- was consumed, 0.0025 mole of HS^- must also have reacted to complete the supply of electrons required for the reduction of 0.01 mole of the phenylhydroxylamine to aniline. This gave 0.0025 mole of S^0, which by equation (*b*) must have led to the production of 1/4(0.0025) or 0.0006 mole of $S_2O_3^=$. The amount of $S_2O_3^=$ produced by these two paths then would be 1/2(0.0075)+0.0006 = 0.0044 *M*. The amount of $S_2O_3^=$ actually found (0.0045 *M*) is in very close agreement with this.

ACKNOWLEDGMENT

The authors would like to express their thanks to the National Research Council of Canada for its generous financial support.

REFERENCES

1. H. H. HODGSON and D. H WARD. J. Chem. Soc. 242 (1948).
2. G. D. PARKES and A. C. FARTHING. J. Chem. Soc. 1275 (1948).
3. E. LOWE. U.S. Patent No. 2,669,584 (1954).
4. H. GOLDSCHMIDT and H. LARSEN. Z. Physik. Chem. **71**, 437 (1910).
5. O. J. COPE and R. K. BROWN. Can. J. Chem. **39**, 1695 (1961).
6. J. L. BULLOCK and G. S. FORBES. J. Am. Chem. Soc. **55**, 232 (1933).
7. R. SCHRÖTER. Methoden der Organischen Chemie. Vol. II. 4th ed. Houben-Weyl, Stuttgart. 1957.
8. N. V. SIDGWICK. The organic chemistry of nitrogen. Clarendon Press, Oxford. 1937.
9. L. J. BELLAMY. The infra-red spectra of complex molecules. John Wiley and Sons, Inc., New York. 1958.
10. M. HOJO, Y. TAKAGI, and Y. OGATA. J. Am. Chem. Soc. **82**, 2459 (1960).

NUCLEAR MAGNETIC RESONANCE STUDIES

PART II. SOLVENT EFFECTS IN THE N.M.R. SPECTRA OF AROMATIC ALDEHYDES[1]

R. E. KLINCK AND J. B. STOTHERS

Department of Chemistry, University of Western Ontario, London, Ontario

Received August 15, 1962

ABSTRACT

The chemical shifts for the aromatic and formyl protons of a series of substituted benzaldehydes have been obtained in a number of solvents. Relative to the shifts observed in chloroform, pronounced effects are observed in acetone and benzene solutions. In general, the shielding of these nuclei is decreased in acetone and increased in benzene, while in benzene the magnitude of the solvent shift for a given proton depends markedly on the nature of the substituent group. These results can be rationalized in terms of a specific solute–solvent interaction in which the site of association is governed by the electron distribution in the solute molecule. The nature of the solvent interactions in this and related systems is discussed.

INTRODUCTION

In a recent paper (1) on the various factors contributing to the chemical shift of the formyl proton in aromatic aldehydes, some interesting solvent effects were presented and an interpretation based on the occurrence of specific solute–solvent associations was suggested. Further tests of this interpretation include a study of the solvent dependence of the chemical shifts of *all* the solute protons and an examination of the temperature dependence of the formyl shifts in these solvents. The present paper reports the results of these tests, all of which confirm the previous suggestions.

On the basis of the preliminary observations, it was suggested that in benzene solution a specific molecular complex is formed in which a benzene molecule tends to lie over a solute molecule while acting as a donor to the electron-deficient portion of the solute structure. This is to say that, on a time average, a solvent molecule is more closely associated with a particular part of the solute molecule. An example of complex formation in the chloroform–mesitylene system has been presented by Reeves and Schneider (2), who have detected its presence using both N.M.R. and other techniques. More recently, Abraham (3), Hatton and Richards (4, 5), and Hatton and Schneider (6) have discussed similar solute–solvent interactions involving a number of polar solutes in aromatic solvents.

In the case of acetone as solvent, the observed shifts, although qualitatively similar, are not so pronounced and may be rationalized in terms of a hydrogen-bonded complex involving one of the aromatic protons and the carbonyl oxygen of the solvent as suggested originally by Schaefer and Schneider (7).

In order to investigate these solute–solvent interactions in more detail, a series of para-substituted benzaldehydes was examined in acetone, benzene, and chloroform solutions and the chemical shifts of *all* solute protons determined. Throughout this study all chemical shift measurements were determined relative to an internal tetramethylsilane reference to eliminate effects due to the bulk diamagnetic susceptibility of the solvent as well as any non-specific effect of the solvent diamagnetic anisotropy. Because of solubility problems with some of the examples, all results are compared with those obtained in chloroform solution. We have found no evidence that this solvent causes differential shifts

[1]*These results were reported at the 45th Annual Conference of the Chemical Institute of Canada, Edmonton, Alberta, May 27–30, 1962.*

of the solute protons, although weak hydrogen bonding is to be expected between the solvent proton and the formyl oxygen atom. Therefore, differential shifts of the solute protons in benzene or acetone relative to chloroform solution would tend to confirm the existence of specific solute–solvent interactions as well as to provide evidence for their stereochemistry.

In benzene, the close approach of a solvent molecule to a given preferred site of the solute molecule should affect the solute protons in a predictable way, since the benzene molecule is anisotropic and exhibits a ring current effect arising from the induced (by the applied field) diamagnetic circulation of the mobile π-electrons around the ring. This secondary field tends to augment the applied field in the plane of the ring and to diminish it above and below this plane (8). The field experienced by a given proton in close proximity to an aromatic ring, therefore, will depend on the mutual orientation of the two groups, and one can predict with confidence, at least qualitatively, the way in which a given position within a solute molecule will be affected. Thus, if a molecular complex of the proposed geometry is involved in the present system, differential chemical shifts of the solute protons relative to their shifts in chloroform should indicate a preferred orientation of the solvent molecule(s). For example, in the case of a strong electron-withdrawing substituent, one can envisage an association of the donor solvent molecule with the opposite end of the solute molecule (i.e. lying over the carbon bearing the formyl group), while for an efficient electron-releasing group, association should be favored between the substituent group and the solvent. A suggested model for these two extreme cases is presented in Fig. 1. For the former case, one would expect both the formyl proton and the

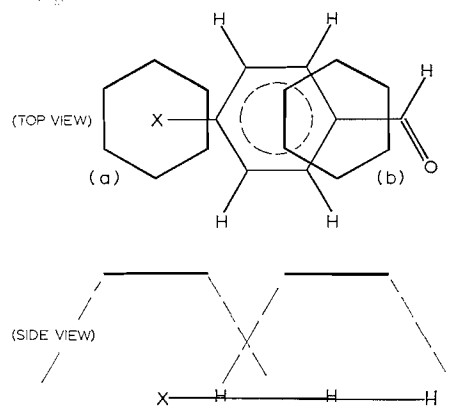

FIG. 1. Diagrammatic representation of the molecular complex formed by benzene with an aromatic aldehyde bearing (*a*) an electron-releasing group and (*b*) an electron-withdrawing group.

aromatic protons ortho thereto to experience a shielding effect while the meta protons would be affected to a lesser extent, whereas in the other extreme situation the shielding effect should be maximal at the substituent protons, if any, and would decrease progressively at the meta, ortho, and formyl positions, respectively. Indeed, it might be possible to realize a deshielding effect at the formyl proton.

For further evidence bearing on the nature of these associations in aromatic solvents, three additional series of experiments were carried out. First, the solvent effects of toluene, mesitylene, 1,3,5-triisopropylbenzene, nitrobenzene, and N,N-dimethylaniline on the formyl shifts of benzaldehyde and its *p*-nitro, *p*-formyl, and *p*-dimethylamino derivatives were determined for comparison with the shifts observed in benzene solutions. Secondly, the temperature dependence of these formyl shifts was measured in benzene and toluene.

Toluene was used in this study to allow observations over a wider temperature range (−35° to 100° C). Thirdly, the generality of these trends in acetone and benzene solutions was tested by an examination of the chemical shifts of the protons in a number of para-substituted toluenes and acetophenones.

EXPERIMENTAL

All of the compounds used in this study are commercially available and purification was effected by recrystallization or distillation before use. Similarly, the solvents employed were carefully purified before the solutions were prepared. Benzene-d_6 and chloroform-d were obtained from Merck, Sharp, and Dohme, with minimum deuterium content of 99.5%. To approximate "infinite dilution" conditions, 5 mole% solutions were used throughout and para-substituted compounds were chosen since these give rise to a nearly symmetrical A_2B_2 spectrum for the aromatic protons which can be analyzed approximately as a simple AB system to determine the chemical shifts of the aromatic protons. Since the benzene solvent peak obscures the aromatic proton pattern in some cases, benzene-d_6 was used to allow spectral analysis.

All spectra were obtained at 60 Mc/sec using a Varian spectrometer (DP-60) and were calibrated by interpolation between audio side bands of the internal tetramethylsilane signal placed on either side of the peak to be measured. The precision is estimated to be ±0.5 cycle/sec. To confirm certain assignments, some spin decoupling experiments were performed using an N.M.R. Specialties S.D. 60 unit operating at 4.3 and 56.4 Mc/sec (N^{14} and F^{19} resonance frequencies, respectively). The temperature studies were carried out using a Varian V-4340 Variable Temperature Probe Accessory.

RESULTS

Some typical data for the aromatic protons in some para-substituted benzaldehydes, acetophenones, and toluenes are listed in Table I, in which the internal chemical shift

TABLE I
Internal chemical shifts of aromatic protons,* $-(\nu_o-\nu_m)$ (in cycles/sec at 60 Mc/sec)

Substituent	Parent system	Solvent (5 mole%) Acetone	Chloroform (*n*-hexane)	Benzene
p-NO_2	Benzaldehyde	13.4	18.1	30.8
	Acetophenone	5.4	10.7	20.4
	Toluene	36.6 (35.9)	47.6 (49.1)	72.2 (72.2)
p-CN	Benzaldehyde	5.4	8.0	10.6
	Toluene	14.2 (15.6)	15.6 (13.5)	15.5 (15.6)
p-Cl	Benzaldehyde	−18.6	−18.8	−16.0
	Toluene	5.0 (5.3)	6.8 (9.4)	22.9 (23.1)
p-F	Benzaldehyde	−51.4	−41.8	−42.6
p-CH_3	Benzaldehyde	−24.6	−27.0	−29.6
	Acetophenone	−34.5 (−34.6)	−36.5 (−39.0)	−49.7 (−50)
p-CH_3O	Benzaldehyde	−46.2	−49.8	−58.0
	Acetophenone	−56.9	−59.9	−69.0
	Toluene	−15.9	−16.6	−11.0
p-NMe_2	Benzaldehyde	−55.4	−61.4	−83.4
	Acetophenone	−68.4	−73.6	−93.0
	Toluene	−20.0	−21.8	−25.0

*Positive values indicate that the ortho H is at higher field.

of the ring protons is given for benzene, acetone, and chloroform solutions. A related study by Schaefer and Schneider (7) compared the internal shifts of the aromatic protons of some para-substituted toluenes and fluorobenzenes in acetone, benzene, and *n*-hexane solutions. For comparative purposes, a few of their results are given in parentheses in Table I. It is to be noted that the data obtained in chloroform compare favorably with those in *n*-hexane. In general, it can be seen that benzene tends to increase the internal chemical shift while acetone tends to diminish it. The important point to note, however,

is that the two positions are affected differently in these solvents. The differential shifts of the solute protons are presented graphically in Figs. 2, 3, 4, and 5, in which the chemical

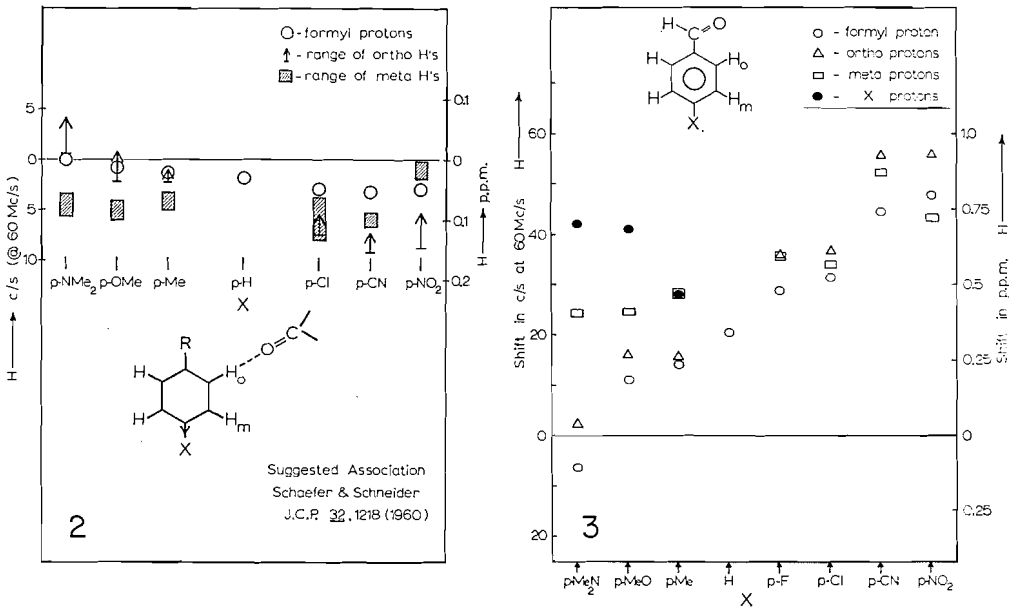

FIG. 2. Solvent shifts of some *p*-disubstituted benzenes in acetone (relative to chloroform).
FIG. 3. Solvent shifts for the protons of some *p*-substituted benzaldehydes in benzene solution (relative to chloroform).

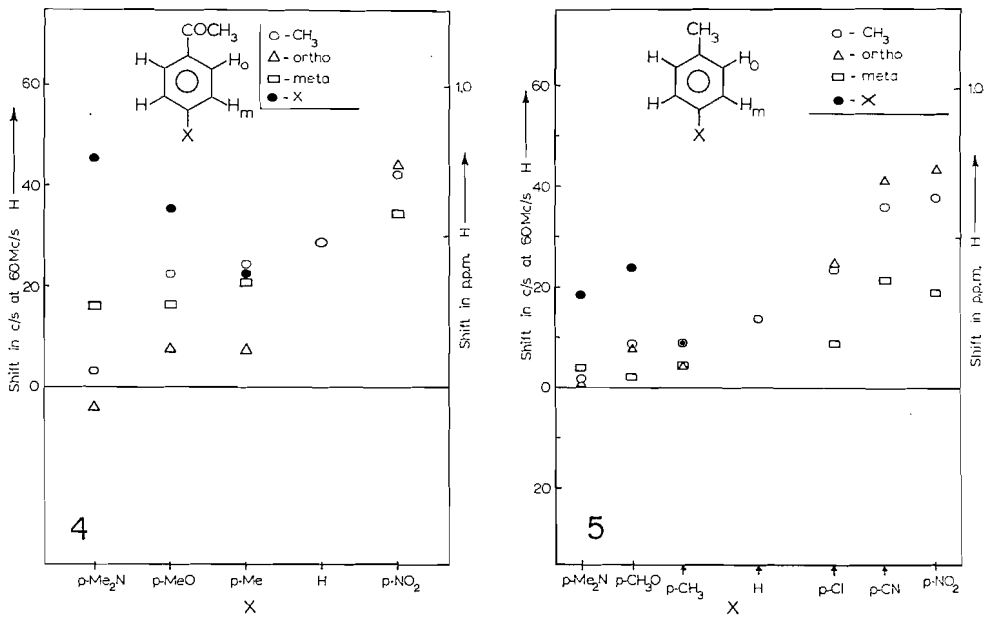

FIG. 4. Solvent shifts for the protons of some *p*-substituted acetophenones in benzene solution (relative to chloroform).
FIG. 5. Solvent shifts for the protons of some *p*-substituted toluenes in benzene solution (relative to chloroform).

shifts in acetone and benzene solution are shown relative to the shifts observed in chloroform. In the following, the ortho and meta positions will be considered relative to the parent grouping (CHO, $COCH_3$, and CH_3) unless otherwise indicated.

The effect of adding benzene to a chloroform solution of a solute exhibiting large shifts in an aromatic solvent was studied in the case of *p*-nitro- and *p*-dimethylamino-benzaldehyde and the chemical shift for the formyl and N-methyl protons is plotted for the various solvent compositions in Fig. 6. The chemical shifts of these protons as well as

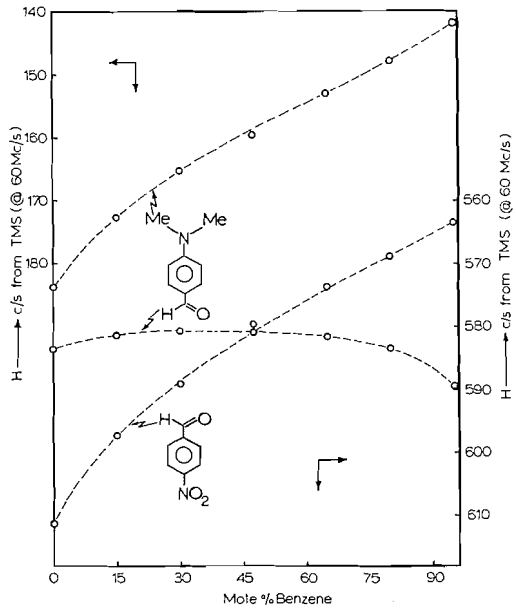

FIG. 6. Chemical shifts for the N-methyl and formyl protons of *p*-NMe_2- and *p*-NO_2-benzaldehyde in chloroform–benzene mixtures.

those of the formyl protons in benzaldehyde and terephthalaldehyde in a number of other aromatic solvents are listed in Table II and the temperature dependence of these shifts in toluene solution is indicated by the data in Table III.

TABLE II

Proton shifts of some substituted benzaldehydes in aromatic solvents (in cycles/sec from TMS at 60 Mc/sec; concn. 5 mole%)

	Substituent				
	Formyl protons				Methyl protons
Solvent	*p*-NO_2	*p*-CHO	*p*-H	*p*-NMe_2	*p*-NMe_2
Chloroform-*d*	611.2	608.8	600.8	583.8	183.5
Benzene	563.4	573.1	579.3	589.9	142.0
Toluene	562.4	570.4	576.2	584.5	144.2†
Mesitylene	561.1	566.6*	572.2	579.0	150.3
1,3,5-Triisopropylbenzene	569.8*	—	578.9	579.2	157.5
Nitrobenzene	611.2	609.2	602.7	591.3	175.5
N,N-Dimethylaniline	560.9	569.8	575.3	582.1	153

*2.5 mole% solutions.
†In toluene-d_8 solution.

TABLE III

Temperature dependence of proton shifts of some substituted benzaldehydes (in cycles/sec from TMS at 60 Mc/sec; concn. 5 mole% in toluene)

Temperature (°C)	Substituent				
	Formyl protons				Methyl protons*
	p-NO_2	*p*-CHO	*p*-H	*p*-NMe_2	*p*-NMe_2
100	568.7	576.1	580.6	584.7	145.5 (80°)
70	566.8	575.9	579.6	584.7	144.6
50	566.2	573.9	578.8	584.6	144.3
30	563.8	570.4	576.6	584.6	141.7
10	561.4	569.2	575.5	584.3	139.4
0	558.7	567.7	—	584.5	—
−20	551.3	—	572.0	584.5	—
−35	—	—	570.5	584.6	—
$d\nu/dT$† ((cycles/sec)/°C)	−0.100‡	−0.084‡	−0.072‡	0.00‡	−0.087§

*In benzene.
†The negative sign indicates a shift to low field with increasing temperature.
‡For the range 0–100° C.
§For the range 10–80° C.

DISCUSSION

(a) Acetone Solutions

From Fig. 2 and Table I, the results for various solutes in acetone solution show that one of the aromatic protons is, in general, affected to a greater extent than the other. In this solvent, Schaefer and Schneider (7) have suggested that one of the aromatic positions (that which is meta to the stronger electron-withdrawing group) is preferentially "hydrogen-bonded" to the carbonyl oxygen of a solvent molecule and so is deshielded relative to the other aromatic proton. (Their suggested model is included in Fig. 2.) Furthermore, a neighboring proton should be slightly affected by the close approach of the anisotropic carbonyl double bond and it is interesting that the formyl proton is shifted more in the *p*-NO_2, *p*-CN, and *p*-Cl derivatives, as expected for this model. In only one case is an up-field shift observed (*o*-protons in the *p*-dimethylamino derivatives). In all these examples, it is consistently observed that the proton meta to the stronger electron-withdrawing substituent appears at lower field in acetone solution *relative* to its shift in chloroform.

(b) Benzene Solutions

In benzene solution, the relative shifts of the solute protons appear to vary in a regular fashion in each of the three series of compounds (Figs. 3, 4, and 5). Again, since the relative chemical shifts of the solute protons change with different substituents, stereospecific interactions of some type are strongly indicated. An examination of the trends observed in these various series, therefore, will support or deny previous suggestions as to the nature of these associations.

For each of these series, the trend exhibited by the change in chemical shift for the aromatic protons is similar. For the *p*-dimethylamino derivatives, the meta proton is shielded more strongly, whereas the ortho proton is more strongly affected in the *p*-nitro derivatives. As noted previously (1), the parent grouping experiences an increased shielding as the electronic character of the substituent is changed progressively from a strong electron-releasing type to a strong electron-withdrawing species (i.e., *p*-NMe_2 to *p*-NO_2). In addition, those substituents bearing protons show the expected trend in that the shielding decreases as the electron-releasing power diminishes.

Presumably, in the benzaldehyde series, a strong electron-withdrawing substituent, such as the *p*-nitro group, aids association at the carbon bearing the formyl group since this carbon would be expected to be slightly positive. A benzene molecule(s) lying over this position would tend to shield the ortho and formyl protons strongly and the meta protons less strongly. At the other limit, the case of a strongly electron-donating grouping such as the *p*-NMe_2, the slightly positive substituent would attract a solvent molecule preferentially. Thus the N-methyl protons would be expected to experience a strong shielding effect which would be progressively smaller at the meta, ortho, and formyl protons, respectively. Indeed, the formyl proton appears to be slightly deshielded in the case of *p*-dimethylaminobenzaldehyde. The other substituents appear to give results intermediate between these two extremes. It is interesting to note that Hatton and Richards (6, 7) have recently presented evidence that similar complexes are involved in solutions of amides in aromatic solvents. In these cases the complexes appear to involve a close association between the aromatic ring of the solvent molecule and the slightly positive nitrogen atom in such a way that the electron-rich carbonyl group lies as far from the ring as possible.

An interesting comparison between the *p*-dimethylamino- and *p*-nitro-benzaldehydes can be made by an examination of the shift of the formyl and N-methyl protons as a chloroform solution of each is diluted with benzene in stages up to and including a pure benzene solvent. In all cases the solutes were present in a concentration of 5 mole% (Fig. 6). The changes in shift of the N-methyl protons in the *p*-dimethylamino compound and the formyl proton in the *p*-nitro compound can be seen to be virtually parallel while the shift of the formyl proton in the former is only slightly affected by these changes in solvent composition. Clearly the causes for these parallel shifts can be assumed to be similar.

The close similarity between the results obtained for the three series lends further support to the hypothesis that a complex with the proposed geometry is involved in solutions of aromatic solutes in aromatic solvents. Slight differences are observed in the substituted acetophenones relative to the aldehydes in that the methyl ketone protons are strongly shielded in four of the five cases examined. This could be taken as an indication that more than one solvent molecule tends to associate with a single ketone solute molecule.

In the substituted toluenes, the same general trend is still apparent, although the relative shifts are smaller for the compounds with electron-releasing substituents. These observations are consistent with the formation of a weaker complex in this than in the other series since the charges would be less highly developed.

(c) Other Aromatic Solvents

The shift of the aromatic formyl proton in solutions of a few other aromatic solvents was examined to determine the contribution of substituents in the solvent molecule to these interactions. According to the present model for the complex, the solvent molecule acts as a donor to the electron-deficient region of the solute molecule owing to the high π-electron density of the aromatic ring, and polar substituents would be expected to affect the stability of the complex in a predictable fashion. Electron-releasing substituents should stabilize the complex by rendering the solvent a better donor, whereas electron-withdrawing substituents should weaken the solute–solvent association. In addition to the polar effect, the substituents on the solvent molecule could conceivably introduce a steric factor such that complex formation at a given position on the solute molecule would be sterically hindered.

The formation of these complexes can be represented by the following equilibrium:

$$\text{solute} + \text{solvent} \rightleftharpoons \text{associated complex} \qquad [1]$$

and the substituent effects can be considered on the basis of this equation. Since the observed chemical shift of a given solute proton will be the weighted average of the shifts for that proton in each of the two extreme environments, any change in the equilibrium position will be reflected by the observed shift. Any factor favoring complex formation would be expected, in general, to give rise to an up-field shift and the reverse effect would be observed for any destabilizing factor.

An alternative view of the situation would consider the relative distances between the solute and solvent molecules in the complex. Since the ring current effect of a solvent molecule on a solute proton X Å from the center of the aromatic nucleus decreases as $1/X^3$, the solvent shift will decrease as this distance increases. Presumably, the weaker the complex, the greater is the distance between the interacting species, and therefore the interaction would be less specific with regard to a particular region of the solute molecule (i.e., a less stable complex). Thus a prediction of the effect of substituents in the aromatic solvent molecule would be the same as before.

To test for possible substituent effects the following aromatic solvents were chosen: for polar effects—nitrobenzene and N,N-dimethylaniline; for steric effects—toluene, mesitylene, and 1,3,5-triisopropylbenzene; as substrates, benzaldehyde and its *p*-nitro, *p*-formyl, and *p*-dimethylamino derivatives were selected. The results of these measurements are listed in Table II, in which the shifts in chloroform solution are included for comparison.

Considering first the results for benzaldehyde and its *p*-nitro and *p*-formyl derivatives (columns 2, 3, and 4), it is clear that the shielding of the formyl proton is increased in N,N-dimethylaniline and decreased in nitrobenzene relative to that observed in benzene solution. This is the expected behavior in terms of the present model. In the hydrocarbon solvents, the shielding increases slightly with increasing methylation of the solvent. This trend can be attributed to the polar characteristics of these solvents since their ability to act as donors would be enhanced slightly by substitution of hydrogen by methyl groups. Since the shifts are to higher field, no steric effect is evident. In 1,3,5-triisopropylbenzene, however, the shift is to lower field relative to that observed in mesitylene and an indication of steric interference would thereby be presented but for the fact that the isopropyl group is a poorer electron-releasing grouping than methyl. At any rate, evidence of steric hindrance of complex formation as a major factor appears to be lacking for these solutes in this series of solvents.

In the fourth case, *p*-dimethylaminobenzaldehyde (columns 5 and 6, Table II), the trend of the formyl shifts in the various solvents is not so clear cut. This is not unexpected since, on the basis of the evidence discussed earlier, association of the solvent appears to involve the substituent nitrogen atom and, hence, the solvating molecule(s) is relatively distant from the formyl proton. Furthermore, the contribution of dipolar resonance forms to the electron distribution in this solute will be greater than in the other examples and the possibility of other dipolar associations in nitrobenzene and dimethylaniline solutions cannot be dismissed. The solvent shifts of the N-methyl protons, on the other hand, appear to fit a pattern similar to that exhibited by the formyl protons in the other three examples, particularly in the polar solvents. Although it is not possible to determine this shift precisely in N,N-dimethylaniline, since a solvent peak appears in the same region, the N-methyl protons are significantly shielded. The fact that the shielding is less than

that observed in benzene solution might well be explained by steric hindrance to complex formation caused by the bulky substituent. Furthermore, in hydrocarbon solvents, the shielding of the N-methyl protons decreases with increasing alkyl substitution on the aromatic solvent; this trend is exactly analogous to that found for some N,N-dialkyl amides in aromatic solvents (5). In the present case, it seems reasonable that the alkyl groups of the solvent hinder its close approach to a solute molecule since one of the substituent groups would be forced to lie over the aromatic ring of the solute. In the previous examples, the aromatic rings would overlap instead and steric hindrance of complex formation would be much less. Indeed, in the case of terephthalaldehyde, the rings of solute and solvent would presumably be coaxially oriented in the complex.

(d) Temperature Effects

In the preceding discussion, evidence has been presented to confirm the existence of molecular complexes in solutions of a number of substituted benzenes in aromatic solvents and their formation has been represented by equation [1]. Since the equilibrium position in a given system will be temperature dependent (such that lowering the temperature favors complex formation), the observed chemical shift of a given solute proton should also be temperature dependent. In general, one would expect an increased shift to higher field as the temperature is lowered. To test this point, toluene solutions of benzaldehyde and its *p*-NO_2, *p*-CHO, and *p*-NMe_2 derivatives were examined at various temperatures and the chemical shifts of the formyl and N-methyl protons measured. The results are summarized in Table III.

Clearly, the shifts for the formyl protons in the first three examples are temperature dependent (last line of Table III) while the shift for the formyl proton in *p*-dimethylaminobenzaldehyde is not. It can be seen, however, that the N-methyl shift for the latter example changes with temperature in approximately the same way as other formyl shifts, although over a narrower temperature range. These results provide further proof of the stereospecificity of these solute–solvent interactions, since only those protons close to the solvating molecule(s) are affected by changes in temperature.

It is planned to extend the range of these temperature studies and to determine the chemical shift changes of all the solute protons in an effort to evaluate the parameters which govern the formation of these complexes.

CONCLUSIONS

On the basis of these results the original suggestion that a benzene solvent molecule(s) tends to form weak molecular complexes with substituted aromatic solutes appears to be substantiated. Strong evidence in support of this conclusion is provided by the observation that the solvent shifts of all the solute protons are interpretable, qualitatively at least, in terms of the ring current of a closely associated aromatic molecule occupying a preferred orientation which is governed by the substituents of the solute molecule. Furthermore, the effect of substituents on the aromatic solvent molecule is found to be completely in accord with this interpretation. Polar factors appear to dominate in the formation of these complexes while steric effects seem to be minor except possibly in the case of association between the solvent and the substituent grouping of the solute molecule. The temperature dependence of the solvent shifts also provides additional support for the formation of a stereospecific complex.

In acetone solution, the present results are in agreement with those expected for an association involving a type of "hydrogen bonding" between the aromatic protons and

the carbonyl oxygen atom of the solvent as was first suggested by Schaefer and Schneider (7). An alternative interpretation* of these relatively small effects would attribute the observed shifts to the polar effect of the acetone as discussed by Buckingham, Schaefer, and Schneider (9); but it is difficult to distinguish between these two possibilities when the shifts are small.

ACKNOWLEDGMENTS

This work was supported by grants from the National Research Council of Canada and the Petroleum Research Fund administered by the American Chemical Society. We wish to express our thanks to the donors of these funds. We also thank Farbenfabriken Bayer AG, Leverkusen, West Germany, for the generous sample of 1,3,5-triisopropylbenzene.

REFERENCES

1. R. E. KLINCK and J. B. STOTHERS. Can. J. Chem. **40**, 1071 (1962).
2. L. W. REEVES and W. G. SCHNEIDER. Can. J. Chem. **35**, 251 (1957).
3. R. J. ABRAHAM. Mol. Phys. **4**, 369 (1961).
4. J. V. HATTON and R. E. RICHARDS. Mol. Phys. **3**, 253 (1960).
5. J. V. HATTON and R. E. RICHARDS. Mol. Phys. **5**, 139, 153 (1962).
6. J. V. HATTON and W. G. SCHNEIDER. Can. J. Chem. **40**, 1285 (1962).
7. T. SCHAEFER and W. G. SCHNEIDER. J. Chem. Phys. **32**, 1218 (1960).
8. J. A. POPLE, W. G. SCHNEIDER, and H. J. BERNSTEIN. High resolution nuclear magnetic resonance. McGraw-Hill. 1959. pp. 180 ff.
9. A. D. BUCKINGHAM, T. SCHAEFER, and W. G. SCHNEIDER. J. Chem. Phys. **32**, 1227 (1960).

We are indebted to the Referee for this suggestion.

THE MERCURY-PHOTOSENSITIZED DECOMPOSITION OF METHANE[1]

R. A. BACK AND D. VAN DER AUWERA[2]

Division of Pure Chemistry, National Research Council of Canada, Ottawa, Canada

Received August 15, 1962

ABSTRACT

The mercury-photosensitized decomposition of methane has been studied at temperatures ranging from about 25 to 400° C, and pressures from about 100 to 1000 mm. Very low conversions and light intensities were employed, and it was shown that at temperatures of 120° C and above, the hydrogen produced was a direct measure of the primary yield of hydrogen atoms. The low, temperature-dependent quantum yield found in earlier studies persisted even under these conditions, and it seems necessary to postulate an inefficiency in the primary quenching process, involving essentially the quenching of $^3P_1$ mercury atoms by methane without decomposition of the methane.

Experiments with added ethylene showed that practically all the hydrogen produced in the decomposition of methane was scavengeable by ethylene, indicating that only atomic hydrogen was produced in the primary process. The rate of addition of hydrogen atoms to ethylene was estimated to be about 4×10^5 times faster than the rate of abstraction from methane at 120° C.

INTRODUCTION

There has been much evidence accumulated in recent years to suggest that the mercury-photosensitized decomposition of most of the alkanes proceeds by an initial reaction,

$$Hg^* + RH \rightarrow Hg + R + H,$$

with an efficiency close to unity. If care is taken to avoid (or make corrections for) the loss of hydrogen atoms by addition to olefins present, or by combination with radicals, the quantum yield of hydrogen formed by the reaction

$$H + RH \rightarrow H_2 + R$$

approaches a value close to 1, independent of temperature and pressure (1–3). Methane (4, 5) and neopentane (6) are the only apparent exceptions to this behavior.

An early study of the methane decomposition by Taylor *et al.* (4) showed a quantum yield of hydrogen which was about 0.004 at 98° C, and increased markedly with temperature to a maximum observed value of about 1 at 400° C. These experiments, and more recent ones made by Mains and Newton (5), were made under conditions (high conversion, high light intensity, doubtful purity of methane) such that complications by secondary reactions made it difficult to reach any conclusions about the efficiency of the primary quenching process or about the cause of the low quantum yield of hydrogen. The present work was undertaken to see whether, under suitable conditions, the decomposition could be made to follow the simple mechanism

$$CH_4 + Hg^* \rightarrow CH_3 + H + Hg \quad [1]$$

$$H + CH_4 \rightarrow CH_3 + H_2 \quad [2]$$

$$2CH_3 \rightarrow C_2H_6 \quad [3]$$

so that the hydrogen yield would become a measure of reaction [1]. To achieve this simple mechanism, two requirements must be fulfilled.

[1]*Issued as N.R.C. No. 7043.*

[2]*National Research Council of Canada Postdoctoral Fellow, 1959–61. Present address: Manufacture Belge de Lampes et de Materiel Electronique, Brussels, Belgium.*

(1) The light intensity must be low enough so that loss of hydrogen atoms in the second-order (in atoms and radicals) recombination reactions

$$H + CH_3 + M \rightarrow CH_4 + M \quad [4]$$

$$H + H + M \rightarrow H_2 + M, \quad [5]$$

which compete with reaction [2], and are favored by high intensity and high radical concentrations, may be neglected.

(2) Concentrations of products and impurities must be kept low enough so that only methane quenches $Hg(^3P_1)$ atoms, and so that secondary reactions such as

$$H + C_2H_6 \rightarrow H_2 + C_2H_5 \quad [6]$$

$$CH_3 + H_2 \rightarrow CH_4 + H \quad [7]$$

$$CH_3 + C_2H_6 \rightarrow CH_4 + C_2H_5 \quad [8]$$

are negligible compared to [2] and [3].

EXPERIMENTAL

The reaction was studied in a conventional cylindrical quartz vessel, 10 cm long and 5 cm in diameter, of about 200-ml volume, with plane windows at each end. In order to keep the percentage decomposition of methane low, the reaction vessel was made part of a closed flow circuit of about 4-l. volume, which included a thermosiphon as a circulating pump (7). In the flow circuit, the methane passed over a mercury saturator heated to 50° C, and through cold traps before and after the reaction vessel, which controlled the vapor pressure of mercury in the reaction system. The reaction vessel was contained in an air thermostat which operated up to temperatures of 200° C. For higher temperatures, a tubular metal furnace was placed directly around the reaction vessel. The mercury resonance lamp was made in the form of a tight, flat spiral of 1-cm tubing, about 5 cm in diameter, mounted outside the air thermostat 20 cm from and parallel to one end of the reaction vessel. From the spiral, the two arms leading to the electrodes were fitted with jackets through which water maintained at 24.3° C was circulated to control the vapor pressure of mercury in the lamp. The lamp was filled with a few millimeters of neon, and operated at a rather low current of 5 ma, a-c., controlled by a ballast resistor.

Methane (both Matheson C.P. and Phillips Research Grade were used) and other gases were handled in a conventional vacuum apparatus. Methane was purified by careful degassing at −210° C to remove traces of permanent gases, bulb-to-bulb distillation from −196 to −210° C to remove small amounts of C_2-hydrocarbons, and finally by treatment with bromine to remove traces of ethylene. A small quantity (about 1 ml) of bromine, carefully degassed, was condensed onto activated charcoal previously baked out under vacuum. Methane was condensed onto the same charcoal at −196° C, then warmed to give a pressure of about 600 mm over the charcoal and allowed to stand for 1 hour. Methane was finally distilled from the charcoal at a temperature low enough to give complete separation from the absorbed bromine.

The ethylene used was Phillips Research Grade, while ethylene-d_4 was supplied by Merck and Company, with a stated deuterium content of 99%.

The hydrogen produced in the reaction was analyzed by gas chromatography. After an irradiation, the methane and other products were transferred from the reaction vessel into a trap of much smaller volume (300 cc), first by condensation at −210° C, then by pumping for about 2 hours with a mercury diffusion pump and a Toepler pump until the residual pressure in the reaction vessel was less than 10^{-5} mm. The hydrogen, together with about 20 μmoles of methane, was removed from the trap by pumping for 10 minutes with another mercury diffusion pump and Toepler pump. These pumped the gases into a small, U-shaped volume (~10 cc) between two three-way stopcocks, from which the sample could be picked up by a stream of nitrogen and analyzed on a 6-ft column of silica gel at 0° C, which gave a good separation of hydrogen from the methane. Blank experiments showed that this analytical procedure recovered about 99% of samples of hydrogen added to methane in amounts comparable to the reaction products. In most of the experiments the yield of hydrogen was between 0.01 and 0.10 μmoles, corresponding to between 0.1 and 5 p.p.m. methane. An average overall reproducibility of 5% might be estimated for these measurements of hydrogen yield, with a rather better reproducibility for the larger quantities of hydrogen.

Hydrogen was the only product measured in most of the experiments. In a few instances, the ethane produced was measured by gas chromatography and found to be approximately equal to the hydrogen. No hydrocarbon products higher than ethane could be detected. The higher products observed by Mains and Newton (5) arose from secondary reactions of products, and would not be expected at the low conversions used in the present work.

Preliminary experiments were made to determine whether impurities, in particular ethylene, might be affecting the hydrogen yield. Analysis by gas chromatography and mass spectrometry showed small amounts

(~0.1%) of ethane, ethylene, and argon in both Phillips and Matheson methane. Careful distillation at −196 to −210° C reduced the ethane to <0.003%, and the ethylene to <0.01%. This purified methane was irradiated at 120° C, and the hydrgeon yield measured. Upon subsequent treatment of the methane with bromine, the hydrogen yield was approximately doubled, but could not be further increased by repeated treatment with bromine. The addition of a trace of ethylene sharply reduced the hydrogen yield, while subsequent treatment with bromine restored it to its original value. This same yield of hydrogen could be obtained with methane from either source, following the bromine treatment, and was quite reproducible. It was concluded that the ethylene content of methane purified by bromination was low enough so that it did not interfere in the reaction, and all subsequent experiments were made with methane purified in this way.

In all the experiments the concentration of hydrogen produced was low enough that the quenching of mercury by hydrogen was negligible, assuming quenching cross sections of 0.06 and 8.9×10^{-16} cm² for methane and hydrogen respectively (8, 9). One sample of methane was sometimes used for several experiments, the hydrogen being removed after each run but the ethane being retained. The accumulated ethane was always low enough that quenching by ethane ($\sigma = 0.42\times10^{-16}$ cm²) should have been negligible (8). The hydrogen yield was observed to be independent of conversion both in single experiments and in sequences of experiments starting with pure methane and allowing ethane to accumulate. This is further evidence that neither hydrogen nor ethane was quenching $Hg(^3P_1)$ atoms, or was affecting the hydrogen yield in any other way. It also supports the conclusion that residual ethylene impurity had no effect on the system, since any such ethylene should disappear quite rapidly by reaction with hydrogen atoms, so that the hydrogen yield would rise with increasing conversion. A few experiments, carried to much higher than normal conversions, did show an increase in hydrogen yield which may be attributed to quenching by-products.

The intensity of the 2537 Å resonance line absorbed in the system was measured by the mercury-photosensitized decomposition of propane at conversions less than 0.005%, assuming the quantum yield of hydrogen, which was independent of temperature and pressure, to be unity (1).

RESULTS AND DISCUSSION

Figure 1 shows the rate of hydrogen production as a function of methane concentration at four different temperatures, using constant light intensity and mercury vapor pressure.

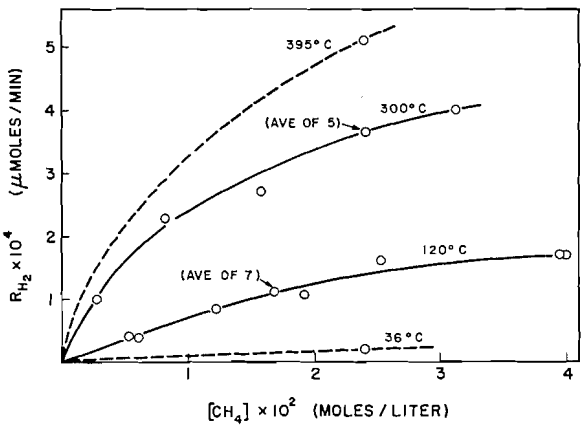

FIG. 1. Hydrogen production vs. methane pressure.

The strong temperature dependence observed by earlier workers was obviously confirmed. The reaction at 36° C was rather slow for practical purposes, while at 395° C some thermal decomposition of methane (probably a surface reaction) was becoming evident, and a small correction had to be made to the hydrogen yield. For these reasons, the reaction was studied in detail only at 120 and 300° C. At the highest methane pressures used (1000 mm), the hydrogen yield was not yet independent of pressure, although it appeared to be levelling out at values which are temperature dependent and which are much less than the hydrogen yield from propane under the same conditions (12×10^{-4} μmole/min).

The temperature dependence of the reaction is shown again in Fig. 2, where $\log_{10}$ of the quantum yield of hydrogen is plotted against the reciprocal of the absolute tem-

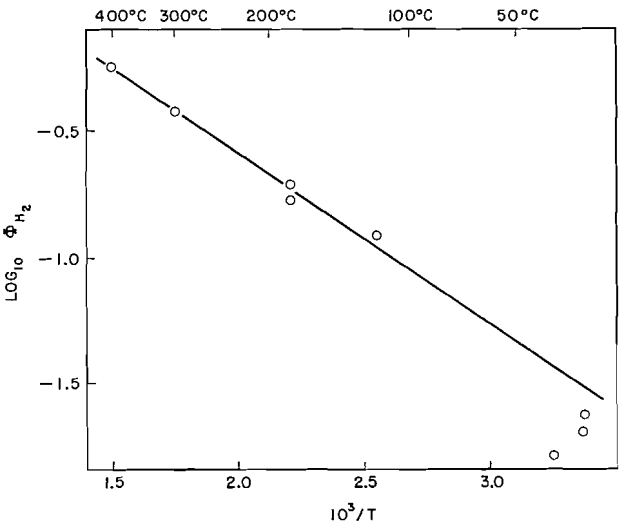

FIG. 2. Arrhenius plot of the quantum yield of hydrogen.

perature, with constant light intensity and constant methane concentration of 2.4×10^{-2} mole/liter. In obtaining these data, small corrections were made for measured differences in the absorption of the mercury resonance radiation in the propane and methane systems.

In Fig. 3, the hydrogen yield at constant methane concentration of 2.4×10^{-2} mole/liter is plotted against the light intensity for temperatures of 24, 120, and 300° C. The slopes of these log–log plots are 0.72, 0.98, and 1.00 respectively, so that the hydrogen yield at temperatures of 120° C and above appears to be close to a linear function of light

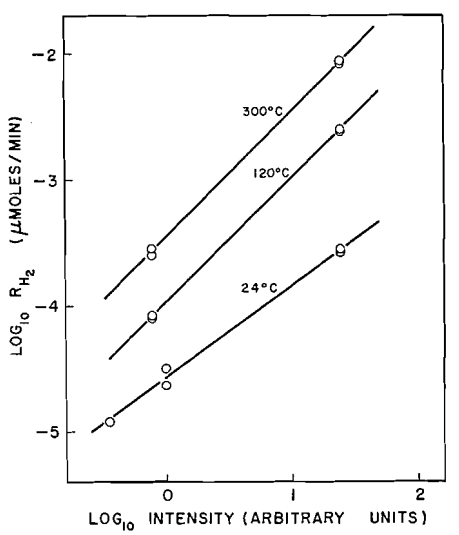

FIG. 3. Log–log plot of hydrogen yield vs. light intensity.

intensity. This linear dependence at the higher temperatures is most simply interpreted as indicating that every hydrogen atom produced in reaction [1] reacted with methane by reaction [2], while the less-than-linear dependence at 24° C suggests that reactions [4] and [5] were of some importance at the lower temperature. Some support is lent to this interpretation by a simple calculation of the relative rates of reactions [2], [4], and [5]. Since hydrogen and ethane were the only products, then $R_{H_2} = R_{C_2H_6}$, and the methyl radical concentration may be calculated, using the literature value (10) for k_3. Then, using Le Roy's values (11) for k_2 ($E_3 = 6.6$ kcal/mole, $P = 10^{-4}$), and assuming $E_4 = 0$ and $P_4 = 1$, the ratio of rates, R_2/R_4, was calculated to be 1.4, 6.6, and 54 at 24, 120, and 300° C respectively, for the *highest* light intensities shown in Fig. 3. These numbers are certainly compatible, within the considerable uncertainties of the calculations, with complete scavenging of hydrogen atoms by reaction [2] at the two higher temperatures, with some loss by reaction [4] at 24° C. If reactions [4] and [5] were not important at the higher temperatures, it also follows that the back reaction, [7], the reverse of [2], can have had no effect in the system. This is confirmed by the independence of hydrogen yield on conversion.

Loss of hydrogen atoms by reaction [5], proceeding in the gas phase, may be shown by similar calculations to be quite negligible. It is less easy to dispose of the possibility of recombination of hydrogen atoms on the surface, although the most reasonable calculation suggests that only a small fraction of atoms would have reached the wall before reacting. The occurrence of reaction [2] together with surface combination of atoms would probably not give a linear dependence of hydrogen yield on light intensity; it could only reduce the quantum yield of hydrogen to 0.5 at the most, and would not explain the dependence on light intensity at 24° C.

Thus it seems reasonably certain that at temperatures of 120° C and above all the hydrogen atoms formed in the primary process reacted with methane to form hydrogen, so that the yield of hydrogen should reflect the extent of the primary decomposition. It appears, therefore, that the low quantum yields of hydrogen observed in the present work are not due to loss of hydrogen through back reactions, but must be attributed to an inefficiency in the primary quenching process.[3]

An obvious cause of such an inefficiency could be the incomplete quenching of the $^3P_1$ mercury atoms by methane, with consequent escape of the resonance radiation from the reaction vessel. There is considerable uncertainty in the value of the quenching cross section of methane. It is undoubtedly very small, and there is some possibility that the quenching observed and attributed to methane was caused largely by traces of strongly quenching impurities such as ethylene, oxygen, and ethane. From Bates' data (8), it may be estimated that quenching should have been complete at a pressure of a few hundred millimeters of methane, which would rule out incomplete quenching as the cause of the low quantum yield. To further test this conclusion, experiments were made in which the partial pressure of mercury vapor was varied from 0.19 μ, the equilibrium pressure at 0° C, which was used in most of the work, to 25 μ. After a small correction was made for the increased primary absorption of light, the yield of hydrogen was found to be almost independent of mercury vapor pressure, decreasing slightly only at the highest pressure used. This decrease, which was more marked at lower temperatures, was probably due to the enhancement of reaction [4] caused by the higher local absorbed light intensity. If the low yield of hydrogen had been due to incomplete quenching, then an increase of

[3]*It should be noted that in previous work, all done with much higher light intensities and higher conversions, this was probably not true, and back reactions were probably important.*

the mercury vapor pressure by a factor of 10 or 100 should have sharply increased the hydrogen yield, as the resonance radiation would have been trapped much more effectively in the reaction vessel, with consequent improved chances of quenching by methane. Thus the evidence indicates that incomplete quenching of $^3P_1$ mercury does not account for the low quantum yields of hydrogen.

In Fig. 4 is shown the effect of added ethylene on the reaction at 120° C, with a methane pressure of 590 mm. The hydrogen yield was reduced to about one half by the addition of

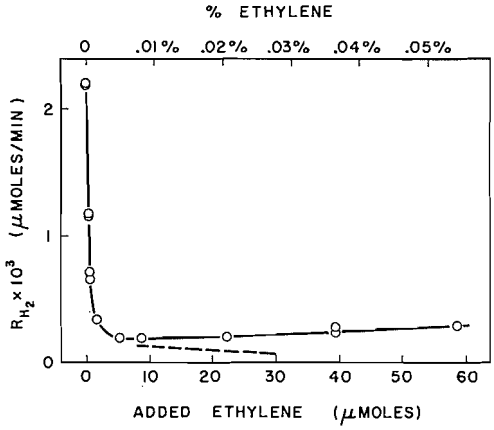

FIG. 4. The effect of added ethylene on the hydrogen yield at 120° C, with 590 mm pressure of methane.

2 p.p.m. ethylene, and fell to a minimum of about one tenth of its original value at about 50 p.p.m. As more ethylene was added, the hydrogen yield rose again slowly, presumably as ethylene itself was decomposed. The final, approximately linear part of the curve in Fig. 4 may be extrapolated to zero ethylene concentration to give a positive intercept which could be interpreted to indicate that some (about 7%) of the hydrogen from the methane decomposition was produced as molecular hydrogen and could not be scavenged by ethylene. However, experiments with C_2D_4 (Table I) showed that this was not so. The

TABLE I

Experiments with C_2D_4

C_2D_4 added (μmoles)	Composition of hydrogen produced		
	% H_2	% HD	% D_2
0.0	100	—	—
1.0	100	—	—
4.8	72	5	23
27.8	18	4	78

broken curve in Fig. 4 shows the yield of hydrogen from the methane decomposition corrected for hydrogen produced by the decomposition of ethylene, which was estimated from the yields of D_2 in Table I. The observed hydrogen yield is thus seen to be the sum of two curves: one, the hydrogen yield from the methane decomposition, which fell slowly to zero as scavenging of hydrogen atoms and quenching of $^3P_1$ mercury by ethylene became complete; the other, the hydrogen yield from the ethylene decomposition, which rose linearly at first, then more slowly, and would become constant when quenching by

ethylene was complete.[4] Thus the experiments with added ethylene may be completely explained in terms of reaction [1], yielding hydrogen atoms, as the only primary process in the methane decomposition.

The experiments with C_2D_4 also show that the initial rapid drop in the hydrogen yield was almost entirely due to the reaction

$$H + C_2H_4 \rightarrow C_2H_5 \qquad [9]$$

in competition with reaction [2], with competitive quenching of $Hg(^3P_1)$ only becoming important at higher concentrations of ethylene. The equation

$$(R_{H_2})_0/R_{H_2} = 1+k_9[C_2H_4]/k_2[CH_4],$$

where $(R_{H_2})_0$ is the hydrogen yield from pure methane, should describe the simple competition between reactions [9] and [2], and in Fig. 5, values of the left-hand side of this

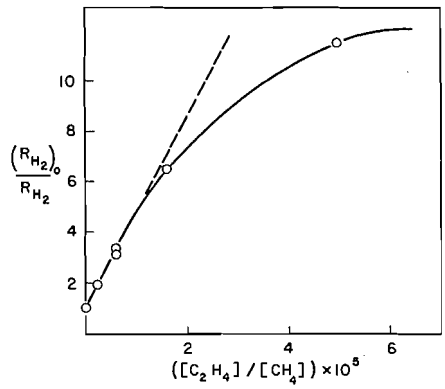

FIG. 5. Linear plot of the data from experiments with added ethylene.

equation are plotted against $[C_2H_4]/[CH_4]$. The experiments at the four lowest ethylene concentrations yielded a good straight line, and from its slope a value of $k_9/k_2 = 3.8\times10^5$ at 120° C may be estimated. At higher ethylene concentrations, of course, the data must fall off from the linear relation as quenching by ethylene becomes an important source of hydrogen. The large magnitude of k_9/k_2, and the consequent effectiveness of a few parts per million of ethylene, apparent in Fig. 4, emphasize the importance of trace impurities in the methane decomposition.

Finally, the conclusions to be drawn from the present study may be summarized. The low, temperature-dependent quantum yields of hydrogen observed in previous work on the mercury-photosensitized decomposition of methane have been found to persist even under conditions of low light intensity and low conversions, when the reaction was shown to follow the simple sequence of reactions [1], [2], and [3] at temperatures of 120° C and above. Both back reactions and incomplete quenching of $^3P_1$ mercury may be fairly certainly ruled out as causes of the low quantum yield, and it appears necessary to postulate an inefficiency in the primary quenching process. In the most general terms, a reaction,

$$CH_4 + Hg^* \rightarrow CH_4 + Hg, \qquad [10]$$

[4]*In one experiment in which 1700 μmoles (1.6%) of ethylene was added, so that quenching by ethylene should have been almost complete, 0.75×10^{-3} μmole/min of hydrogen was produced, corresponding to a quantum yield of about 2×10^{-2}. This is in fair agreement with previous studies of the ethylene decomposition (12), and the observed yields of D_2 from C_2D_4 are compatible with a final constant hydrogen yield of about this value.*

which quenches $^3P_1$ mercury in competition with reaction [1], but does not decompose methane, would seem to be required. The observed temperature dependence would then derive from a difference between the temperature dependences of reactions [1] and [10]. More specifically, one possible mechanism might involve a competition between collisional quenching and decomposition of an excited methane molecule,

$$\mathrm{Hg^* + CH_4 \rightarrow Hg + CH_4^*} \begin{cases} \nearrow \mathrm{CH_3 + H} & [1A] \\ \searrow + \mathrm{CH_4 \rightarrow 2CH_4} & [10A] \end{cases},$$

although the pressure dependence of the hydrogen yield (Fig. 1) does not support (but also does not disprove) this mechanism, which would predict a maximum in the plot of hydrogen yield against pressure.

A perhaps more likely mechanism is one which invokes two quite distinct reactions, for example,

$$\mathrm{Hg^* + CH_4 \rightarrow HgH + CH_3 \rightarrow Hg + H + CH_3} \qquad [1B]$$

and

$$\mathrm{Hg^* + CH_4 \rightarrow Hg + CH_4^* \rightarrow Hg + CH_4,} \qquad [10B]$$

where [10B] is a "physical" quenching process in which CH_4^*, probably vibrationally excited, is always deactivated by collision at the fairly high methane pressures used. Hydrogen abstraction reactions such as [1B], with HgH as an intermediate, have long been suggested in the mercury-photosensitized reactions of the alkanes (13), although there is almost no proof for or against their occurrence. The temperature dependence of the methane decomposition appears to favor this latter mechanism. Reaction [1] is exothermic by about 11 kcal/mole, and if it proceeded through an energy transfer process, as in [1A], an activation energy of about 3 kcal/mole, as observed, would seem most unlikely. Reaction [1B], on the other hand, might well show such an activation energy, although it is difficult to see why methane should be so much less reactive than ethane, as the difference in C—H bond energy is small compared to the exothermicities of both reactions. This raises the question of whether the primary process in the methane decomposition is qualitatively different from those of the higher alkanes, or is similar in mechanism but much slower because of the higher bond energy or some other property of the methane molecule. Molecular symmetry has been suggested as a cause of the low quantum yield of the mercury-photosensitized decomposition of methane and neopentane (6), since the latter has bond energies very similar to those of ethane but shows a much lower yield of hydrogen; however, it is difficult to see exactly what part symmetry could play in the process.

Another possible mechanism for the methane decomposition involves the quenching of mercury to the $^3P_0$ state as a primary process,

$$\mathrm{Hg(^3P_1) + CH_4 \rightarrow Hg(^3P_0) + CH_4,} \qquad [11]$$

followed by the rather slower reaction

$$\mathrm{Hg(^3P_0) + CH_4 \rightarrow Hg(^1S_0) + CH_3 + H.} \qquad [12]$$

The low yield of hydrogen would then be attributed to loss of $Hg(^3P_0)$ by the reactions

$$\mathrm{Hg(^3P_0) + wall \rightarrow Hg(^1S_0) + wall} \qquad [13]$$

$$\mathrm{Hg(^3P_0) \rightarrow} h\nu\ (2656\ \text{Å}) + \mathrm{Hg(^1S_0)} \qquad [14]$$

$$\mathrm{Hg(^3P_0) + CH_4 \rightarrow} h\nu\ (2656\ \text{Å}) + \mathrm{Hg(^1S_0) + CH_4.} \qquad [15]$$

Once the $^3P_1$ mercury has been quenched to the $^3P_0$ state, effective radiation trapping is no longer possible, and the observed independence of the hydrogen yield on mercury vapor pressure is explained. It is interesting that Bates (8) concluded from the quenching behavior of methane that quenching to the $^3P_0$ state was the main process. Reactions [13] and [14] have been recently shown to occur in a study (14) of the interaction of nitrogen with $Hg(^3P_1)$. Reaction [15] is kinetically equivalent to the general reaction, [10], and thus could account for the observed pressure dependence of the hydrogen yield. Kimbell and Le Roy (14) found it necessary to postulate a similar emission of the "forbidden" 2656 Å radiation induced by collision with nitrogen. The observed temperature dependence of the hydrogen yield would require reaction [12], which might or might not proceed through formation of HgH, to have an activation energy of about 3 kcal/mole.

The present results with methane do not distinguish clearly between the several possible causes of the inefficiency of the primary process, and, in this respect, an extension of the measurements to higher pressures, in the range from 1 to 10 atm, would be very useful, but it presents some experimental difficulties and is not planned at the present time. The whole problem of the nature of the primary process in the mercury-photosensitized decomposition of the alkanes is a very elusive one. A careful re-examination of quantum yields and quenching cross sections of a number of alkanes, in particular methane, ethane, and neopentane, over a wide range of pressure and temperature, and under conditions which prevent back reactions and internal scavenging by olefins, would seem to be required for its solution.

REFERENCES

1. R. A. BACK. Can. J. Chem. **37**, 1834 (1959).
2. R. J. CVETANOVIĆ, W. E. FALCONER, and K. R. JENNINGS. J. Chem. Phys. **35**, 1225 (1961).
3. R. L. STOCK and H. E. GUNNING. Can. J. Chem. **38**, 2295 (1960).
4. K. MORIKAWA, W. S. BENEDICT, and H. S. TAYLOR. J. Chem. Phys. **5**, 212 (1937).
5. G. J. MAINS and A. S. NEWTON. J. Phys. Chem. **65**, 212 (1961).
6. B. DEB. DARWENT and E. W. R. STEACIE. Can. J. Res. B, **27**, 181 (1949).
7. D. VAN DER AUWERA and R. A. BACK. Can. J. Chem. **40**, 385 (1962).
8. J. R. BATES. J. Am. Chem. Soc. **52**, 3825 (1930).
9. E. W. R. STEACIE. Can. J. Res. B, **18**, 44 (1940).
10. R. GOMER and G. B. KISTIAKOWSKI. J. Chem. Phys. **19**, 85 (1951).
11. E. W. R. STEACIE. Atomic and free radical reactions. 2nd ed. Reinhold, New York. 1954.
12. R. J. CVETANOVIĆ and A. B. CALLEAR. J. Chem. Phys. **23**, 1182 (1955); **24**, 873 (1956).
13. K. J. LAIDLER. The chemical kinetics of excited states. Clarendon Press, Oxford. 1955.
14. G. H. KIMBELL and D. J. LE ROY. Can. J. Chem. **38**, 1714 (1960).

A CONTINUOUS FLOW BETA SCINTILLATION DETECTOR FOR AQUEOUS SOLUTIONS[1]

R. TKACHUK

Grain Research Laboratory, Board of Grain Commissioners for Canada, Winnipeg, Manitoba

Received July 12, 1962

ABSTRACT

Counting of beta emitters in aqueous solutions was carried out with a detector whose detecting element is a packed column of a finely divided plastic scintillator. The efficiencies under practical operating conditions for C^{14}, Sr^{90}–Y^{90}, and K^{40} are 36, 74, and 82% at backgrounds of 27 ± 2 c.p.m.

INTRODUCTION

A need arose in this laboratory to determine continuously the activity of C^{14}-labelled amino acids and their derivatives in the effluents from ion exchange columns on a Spinco Model 120 automatic amino acid analyzer. A spiral capillary plastic scintillation flow detector as described by Funt and Hetherington (1) was first tried for this purpose. However, because of the low efficiency of 5.7% for C^{14}, and the small sample volume of 0.28 ml of this detector, useful results could not be obtained for the low specific activity of the compounds to be analyzed. The present report describes a detector which incorporates the useful features of the spiral capillary system and the method reported by Steinberg, who used a suspension of anthracene for C^{14}-assay of aqueous solutions, an efficiency as high as 54% being reached (2, 3).

The detecting element of the present system is a packed column of a finely divided plastic scintillator incorporated in a Lucite container. The detector is used in conjunction with a single multiplier tube and appropriate electronics, but with no refrigeration equipment. The features of this detection system are a direct reproducible measurement of C^{14}-activity in aqueous or alcoholic solutions without further sample preparation, and a good counting efficiency with low background which is not time dependent and not influenced by most impurity quenching effects nor by differences in counter filling compositions. Detectors with large sample volumes may be easily constructed. The detector may be used to monitor continuously the activity of ion exchange column effluents, or to measure the activities of single samples.

EXPERIMENTAL METHODS AND MATERIALS

Preparation of Scintillator

The plastic scintillator was prepared in the following manner. The plastic phosphor NE102 (Nuclear Enterprises, Winnipeg, Manitoba, Canada), in the form of lathe turnings, was initially reduced in size by treatment for 5–10 minutes in a Waring blendor operating at high speed. The more finely divided material was sieved out and further reduced in size by grinding with a mortar and pestle. A little water was judiciously added during the latter and subsequent procedures to eliminate the profound static electrical properties of the finely ground plastic. The 100- to 200-mesh fraction of nearly dry material was saved. The fines in the latter fraction were removed by settling in a graduated flask of water containing a little detergent. The main bulk of the resin was isolated by collecting on a sintered-glass funnel, washing with water, and air drying.

Construction of Detector

The detector was constructed from a $2\frac{1}{4} \times 2\frac{1}{4}$-inch block of Lucite by drilling three closely and evenly

[1]*Submitted as Paper No. 213, of the Grain Research Laboratory.*
Presented in part at the 45th Conference of the Chemical Institute of Canada, Edmonton, Alberta, May 27–30, 1962.

spaced holes in it, 0.48 cm in diameter and 3.7 cm deep. The holes were suitably interconnected with 0.5 mm diameter channels. The inlet and outlet connections were constructed by cementing into place a 20 gauge stainless steel hypodermic needle with an epoxyresin (Hysol (Canada) Ltd., Toronto, Ont., Canada). After small wads of Pyrex glass wool were placed in the bottom of the three holes, the detector was filled with increments of the previously prepared finely ground plastic scintillator. Each increment was settled in by tapping the Lucite block, and then firmly tamped in with an aluminum rod whose diameter was only slightly smaller than the hole being filled. When the columns were nearly full, disks of a Pyrex glass filter paper were firmly tamped in, and the columns of plastic scintillator sealed in with a piece of Lucite. The assembly was then trimmed into a semihemispherical shape, in accordance with good reflectance geometry for scattering out of the plane side as much as possible of the light originating in the plastic scintillator. (It is important to have the holes completely filled with a well-packed mass of plastic scintillator and glass filter paper; a loosely filled detector tends to clog and also to give unreproducible behavior.) The whole surface of the detector was then rubbed with a fine-textured sandpaper, in order to increase light reflection, and the semihemispherical surface was painted with a reflector TiO_2 paint (Nuclear Enterprises), until an opaque coat was obtained. The detector is illustrated in Fig. 1.

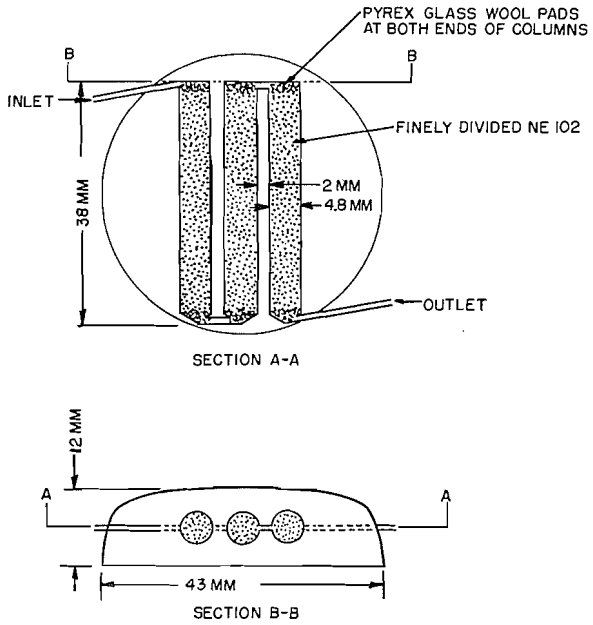

FIG. 1. Cross-sectional views of the flow detector.

Connections to the inlet and outlet of the detector were made with 22 gauge Teflon tubing (Pennsylvania Fluorocarbon Co., Philadelphia, Pa., U.S.A.), and the tubing was wired into place with copper wire. The whole assembly was checked for leaks by filling with water and then applying at least 100 p.s.i. pressure with a small hypodermic syringe. The detector was mounted with silicone fluid (Dow Corning 200, 60,000 centistokes) on a 2 inch diameter EMI 9536S multiplier tube inside a 2 inch thick lead castle. The detector was kept centered on the multiplier tube with the aid of a thick disk of pliable polystyrene foam. To prevent stray light from reaching the multiplier tube, the castle top was taped to the body of the castle with black opaque electrical tape, and the Teflon tubing connections leading to the detector were encased with black opaque spaghetti tubing. A small, easily replaceable filter, constructed from a piece of polyethylene tubing and Pyrex glass wool, was inserted into the inlet in order to remove the small amounts of suspended material that are usually found in solutions. The multiplier tube was kept at a constant temperature by running tap water through a coil incorporated in the castle body. The temperature of the multiplier tube during the winter months was approximately 7°.

Apparatus Used with the Detector

The detector was used with a white cathode follower-preamplifier (NE 5202A), a stabilized high-voltage supply (NE 5302), a non-blocking linear pulse amplifier (NE 5202), a single-channel differential pulse-height selector (NE 5102S), a rate meter (NE 5401), a Phillips scaler (PW 4032), a Baird-Atomic preset timer, and a Minneapolis-Honeywell Type 153 Electronik adjustable-span, adjustable-suppression recorder.

A liquid scintillation detector (NE 5503) was used to check the reliability of some of the measurements obtained with the flow detector. A 1000-watt Rayetheon Voltage Regulator was used to supply power for the whole system, which was enclosed in a grounded steel cabinet.

The above detection system was susceptible to some spurious interference from electrical relays and switches which were in the same room housing the detection system. The latter interference added approximately 0.5–3 c.p.m. to the background. The detector itself contributed approximately 14 c.p.m. to the background of the whole counting system. It was observed that occurrences of high humidity (or condensing moisture) gave rise to excessive spurious noise. This noise was eliminated by placing a drying agent, such as silica gel or Drierite, both in the castle compartment containing the multiplier tube and in the castle base which housed the preamplifier.

Labelled Materials

The gliadin-C^{14} was isolated from wheat which had been injected with acetate-2-C^{14} (4). C^{14}-Labelled amino acids were obtained by placing gliadin-C^{14} in a Pyrex test tube, adding 6 *N* redistilled HCl, freezing the mixture, evacuating to less than 0.5 μ pressure, sealing the tubing, and hydrolyzing for 22 hours at 120°. After hydrolysis, the HCl was removed by placing the tube, with its contents previously frozen, into a desiccator containing NaOH pellets and evacuating. Water was added to the residue, the humin removed by filtration, and the filtrate made up to volume with 0.2 *N* Na^+, pH 2.2 sodium citrate buffer containing BRIJ-35 detergent (Atlas Powder (Canada) Co., Brantford, Canada), and octanoic acid. S^{35}-Labelled amino acids were similarly obtained from wheat flour, the latter obtained from wheat injected with carrier-free $H_2S^{35}O_4$. S-(N-Ethylsuccinimido-1-C^{14})-cysteine was obtained by reacting N-ethylmaleimide-1-C^{14} (Schwarz Bioresearch, Inc.) with cysteine. A certified standard solution of C^{14} was obtained in the form of sodium carbonate from the Radiochemical Centre, Amersham, England.

RESULTS AND DISCUSSION

The effective scintillation-sensitive volume of the detector was determined by two different methods. In the first one, aliquots of S-(N-ethylsuccinimido-1-C^{14})-cysteine were successively introduced into the detector with an hypodermic syringe and the radioactivity noted. Plots of the activity versus the volume injected, as illustrated in Fig. 2, indicated that the volume was 1.02 ± 0.03 ml. In the second method, the activity of a solution occupying the whole detector volume was compared with the activity of the same solution passing through the detector at 0.500 ± 0.001 ml/min. The latter experiments indicated that the detector volume was 1.03 ± 0.08 ml. A value 1.02 ml was therefore used for the detector volume.

A representative integral bias curve for C^{14} is shown in Fig. 3, at the following operating conditions: multiplier tube voltage, 1000; amplifier gain, 5000; and temperature, 11.1°. The limiting efficiency was found to be 49%. At the lower bias setting of 7.50 v, which was chosen for routine counting of samples, the efficiency was 36.1% with a background of approximately 28 c.p.m.

The absolute efficiency of the detector for C^{14} was determined by injecting aliquots of a standard sodium carbonate-C^{14} solution into the detector with an hypodermic syringe and noting the resulting activity. The results, as illustrated in Fig. 4, indicated that the efficiency for C^{14} was 36.1%. The straight-line portion of the curve in Figs. 2 and 4 indicates that there is a linear relationship between the observed activity and the volume of activity injected into the detector. Higher efficiencies may be obtained by tighter packing of the plastic scintillator into the detector. The tighter packing, however, results in higher pressures necessary to introduce the sample into the detector. For example, to introduce a sample into a detector with an efficiency of 55% at the above operating conditions, a pressure of 100 p.s.i. was required for several minutes.

Repeated counts of the same aqueous C^{14}-solution over a period of several months gave an average count of 2129 ± 127 c.p.m. All the obtained counts were included in the latter average. When an equal volume of absolute ethanol was added to the above C^{14}-solution, the expected count was obtained.

Experiments with C^{14}-labelled wheat proteins and sodium carbonate-C^{14} indicated that

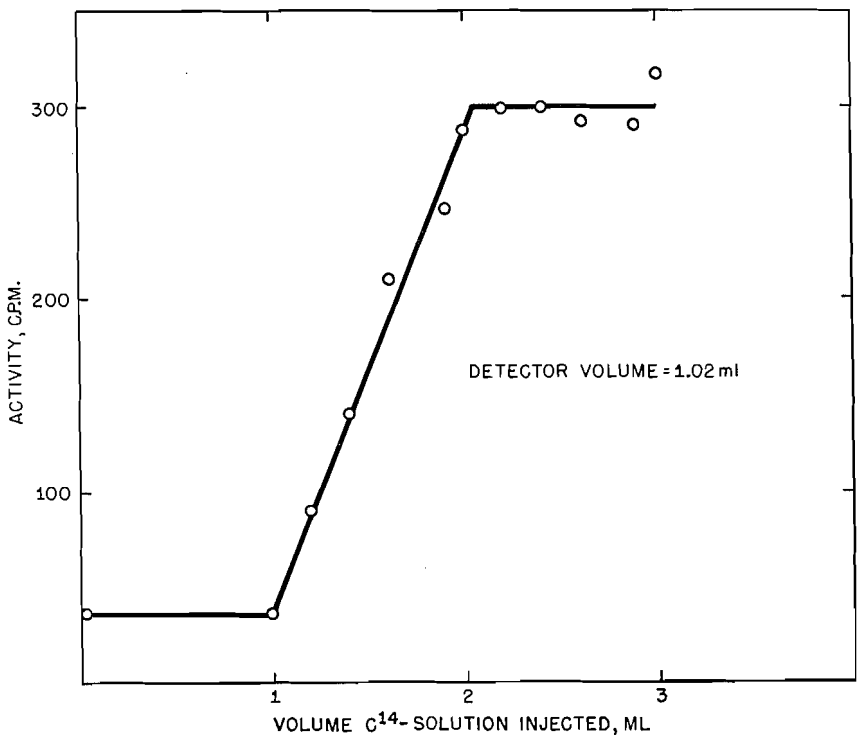

FIG. 2. Determination of detector volume by introduction of increments of a C^{14}-solution into the detector and determining the activity.

there was some retention of these substances on the detector. However, they were easily removed with weakly basic and acidic solutions respectively. The retention of sodium carbonate-C^{14} is illustrated by the skewed peak shown in Fig. 4, and the absence of a "flat top" to the curve (as in Fig. 2). When aqueous S^{35}-solutions containing sulphate-S^{35} were counted, however, the background usually increased from 5 to 15 c.p.m. The amount retained seemed to be a function of the amount of sulphate-S^{35} present and of the time the sample was kept in the detector. S^{35}-Activity retained could not be removed from the detector. It could be that under the acidic conditions of pH 2.2–3.5, at which most of solutions were counted, sulphonation of the polyvinyltoluene plastic scintillator might occur.

The quenching effects that are observed with this detector seem to be associated with the presence of those substances which have absorption spectra in the same region as the emission spectrum of the NE 102 plastic scintillator, which has a maximum at 4300 Å. Affirmative evidence for this assumption was obtained by counting $CuSO_4$ and $FeCl_3$ solutions containing the same amount of C^{14}. The data is given in Table I. These results are in agreement with those obtained by Steinberg, who used 2,4-dinitrophenol as a color quencher.

The efficiency of the detector for Sr^{90}–Y^{90} was determined by counting a solution of $SrCl_2$ made from a $Sr^{90}CO_3$ standard. An integral bias curve is illustrated in Fig. 5. At an amplifier gain of 5000, the limiting efficiency is 76%, and at a lower bias voltage of 7.5 v the efficiency is 72% with a background of 30 c.p.m.

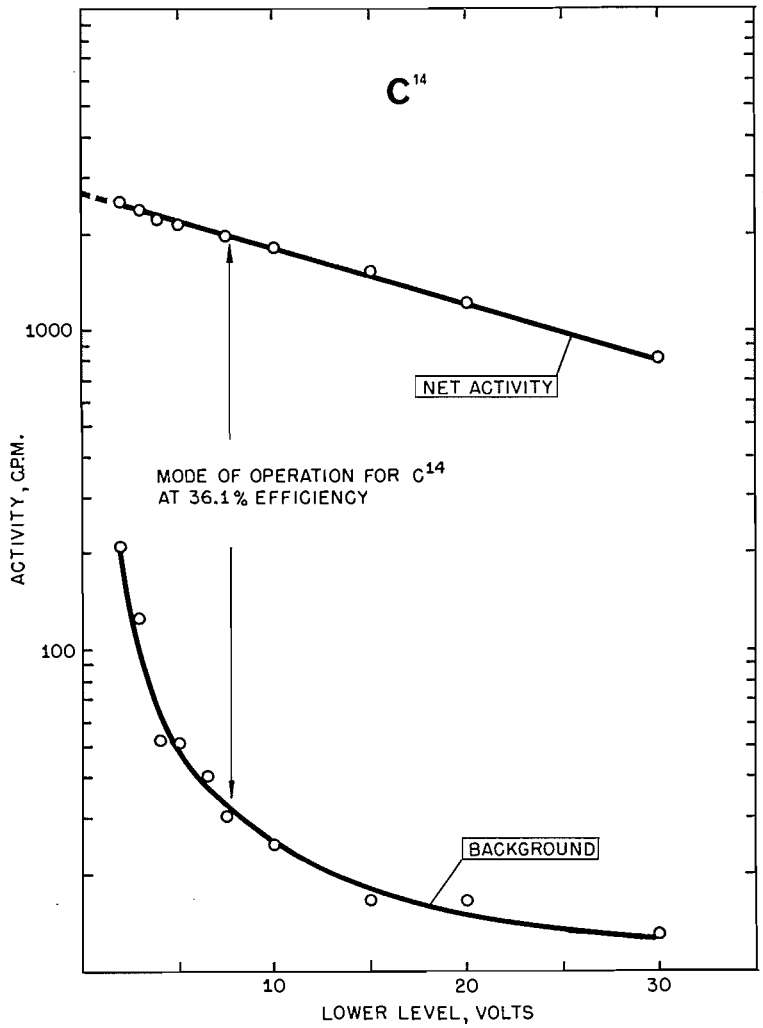

FIG. 3. Integral bias curve for a C^{14}-solution, with the 1.02 ml volume detector containing a total absolute activity of 5545 d.p.m. A multiplier tube voltage of 1000 v and an amplifier gain of 5000 was used. The temperature was 7°.

TABLE I

Activity of colored solutions

	Transmittance at 430 mμ (%)	Observed activity (c.p.m.)
Control solution	99.9	675
$CuSO_4$ solution	99.2	714
$FeCl_3$ solution	38.6	403

The detector efficiency for K^{40} was determined by counting a solution of naturally occurring KCl. The integral bias curve is illustrated in Fig. 6. It is seen that at an amplifier gain of 5000, the limiting efficiency is 93 and 83%, depending on whether the detector

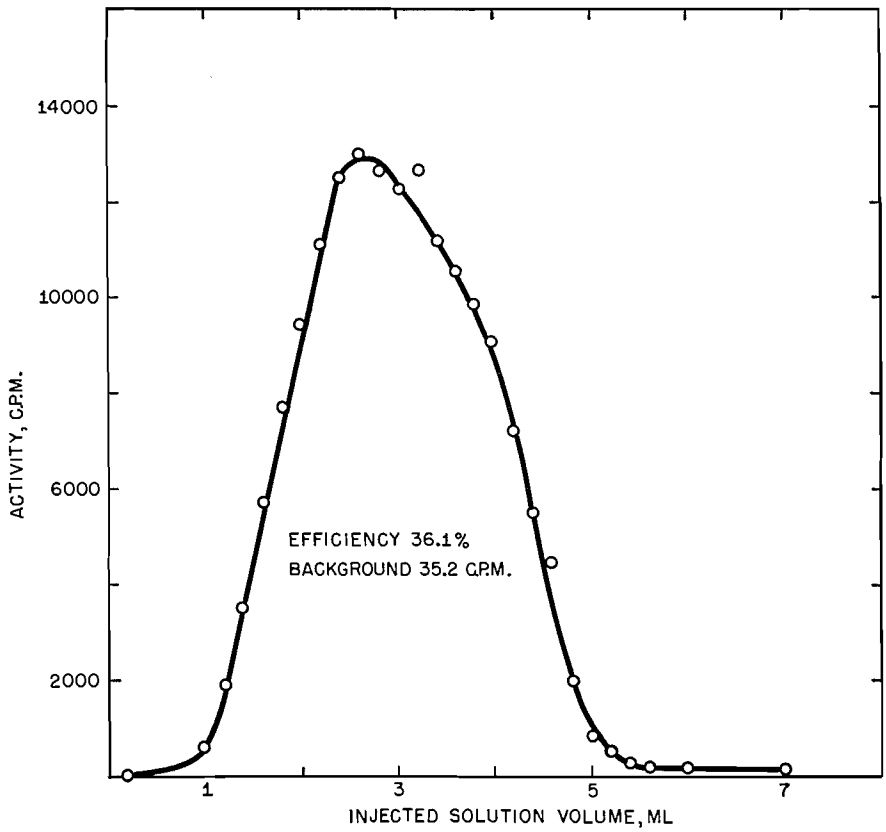

FIG. 4. Determination of detector efficiency by introduction into the detector of approximately 2 ml of a sodium carbonate-C^{14} standard solution (25,750 d.p.m./ml) followed by increments of water. The efficiency was calculated from the slope of the rising straight-line portion of the curve.

is sensitive only to the K^{40} β's or to K^{40} β's and γ's. It is unlikely that the detector would be sensitive to all of the 1.46 Mev γ's, because of the relatively low stopping power of the plastic phosphor. Evidence for this view was obtained by observing that a 5 μc Cs^{137} gamma source, when placed 3.8 cm from the geometrical center of the detector, gave a net count of only 1996 c.p.m. This activity is equivalent to an efficiency of approximately 2% for the 0.662 Mev γ's being emitted from this source. The absolute decay rate of 1692 and 209 d.p.m./g K was used for the K^{40} β- and γ-emission (5).

In the continuous flow experiments, effluents from ion exchange columns on a Spinco amino acid analyzer were monitored for their C^{14}- or S^{35}-activity. The detector was inserted into the effluent stream as it emerged from the ion exchange columns, by the use of encased Teflon tubing as described above for single sample operation. The use of the detector in conjunction with normal amino acid analyzer operation caused an increase of pressure of 4 p.s.i. on the buffer being pumped through the ion exchange columns at a rate of 30 ml/hr. Results from the analysis of a gliadin-C^{14} hydrolyzate are shown in Fig. 7. It is observed that the use of a detector with a 1.02-ml sample volume does not affect the resolution of the amino acids, nor cause any retention of the 18 C^{14}-labelled amino acids. These results are in agreement with those obtained independently, where the analysis of the above C^{14}-labelled amino acids was carried out with a vibrating reed

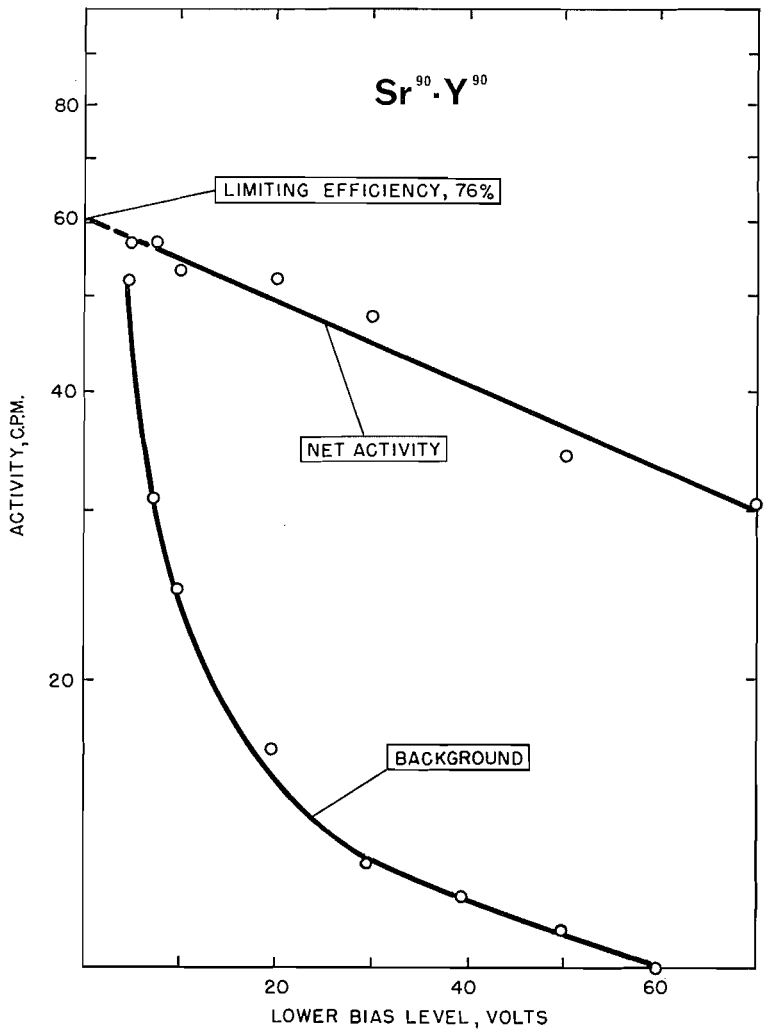

FIG. 5. Integral bias curve for a Sr^{90}–Y^{90} standard solution. The 1.02 ml volume detector contained a total absolute activity of 79.41 d.p.m. due to a mixture of Sr^{90}–Y^{90} at equilibrium. The multiplier tube voltage was 1000 v, the amplifier gain was 5000, and the temperature 6.9°.

electrometer. An analysis of an hydrolyzate from wheat flour labelled with S^{35} is illustrated in Fig. 8.

The reproducibility of the detector in the continuous flow mode of operation was checked by chromatography of a solution of S-(N-ethylsuccinimido-1-C^{14})-cysteine at various times over a period of several months. The activity was noted on the scaler and also from the size of the peak traced out by the recorder on the scintillation counter. The latter determination was done by tracing the peak from the chart paper onto bond paper and cutting out the traced peak and weighing it. The results were an average count of 4501 $\pm$136, equivalent to an average peak weight of 48.0$\pm$3.8 mg.

A single detector has been extensively used for a period of approximately 6 months. During the period, which included approximately 1 month of continuous operation, it gave constant and reproducible results. It would thus seem to be a fairly stable counting

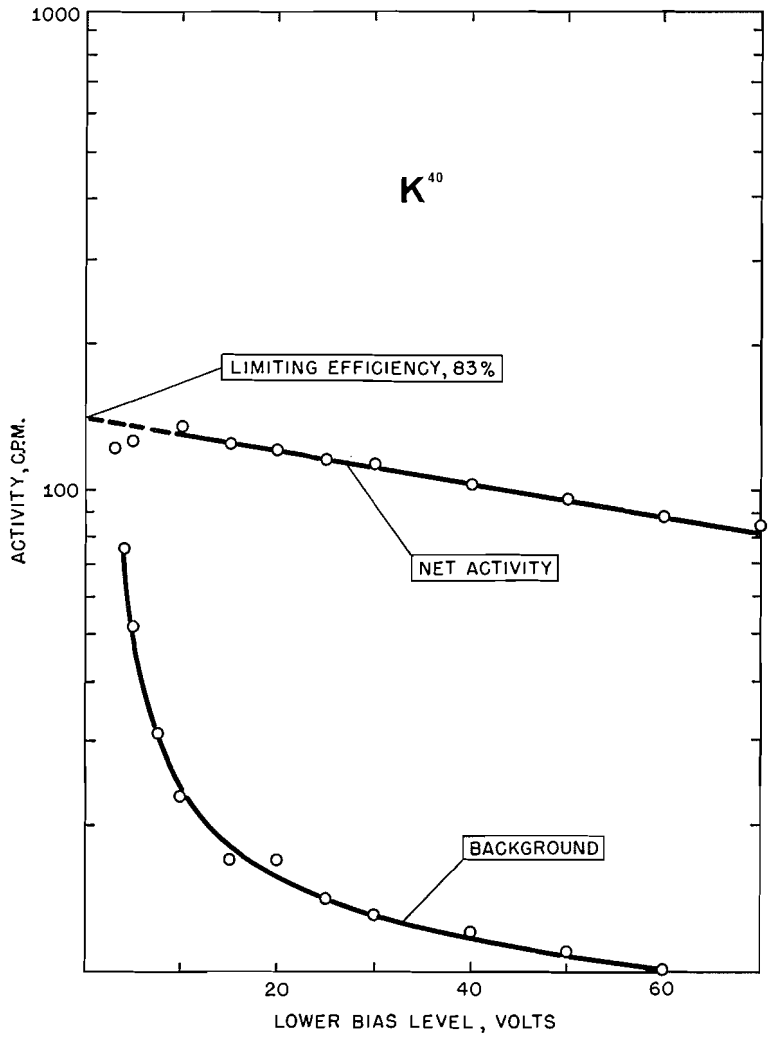

FIG. 6. Integral bias curve for K^{40}. The source of activity was 16.244 g of reagent grade KCl in 100 ml solution. Using the absolute decay rate of 1692 and 209 d.p.m./g K for K^{40} β's and γ's respectively, the limiting efficiencies are 93 and 83%, on the assumption that the detector is only sensitive to the 1.34 Mev K^{40} β's in the first instance, and sensitive both to the K^{40} β's and 1.46 Mev K^{40} γ's in the second instance. An efficiency of 100% under the present conditions is equivalent to 147 and 18 d.p.m. for the K^{40} β- and γ-emission. The multiplier tube voltage was 1000 v, the amplifier gain was 5000, and the temperature 6.9°.

device. Assuming that the detection limit is given by a net sample count equal to background, then its limit is approximately 35 $\mu\mu$c C^{14} per ml in the single sample and 70 $\mu\mu$c C^{14} per ml solution in the continuous flow mode of operation.

When the present work had been essentially completed two reports appeared dealing with an anthracene detector (6, 7), and in addition three commercial anthracene detectors have recently become available (Atomic Accessories Inc., New York, N.Y., U.S.A.; Nuclear-Chicago Corp., Des Plaines, Ill., U.S.A.; Packard Instrument Co., Inc., La Grange, Ill., U.S.A.). With the lack of sufficient detail, it is difficult to make a comparison of the two different detectors at the present time. It would seem, however, that the anthracene detector is slightly more efficient and may not retain sulphate ion. On the

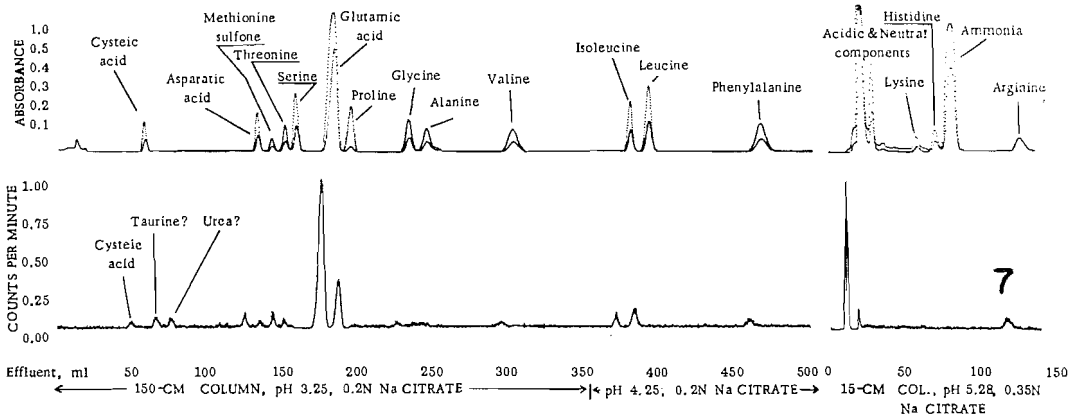

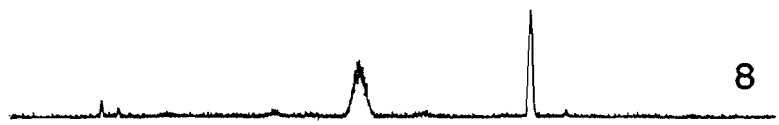

FIG. 7. Chromatographic (upper curve) with simultaneous C^{14}-radioactivity (lower curve) analysis record of a mixture of amino acids from a hydrolyzate of gliadin-C^{14}. The chromatographic analysis was obtained automatically in approximately 22 hours.

FIG. 8. S^{35}-Radioactivity record of a chromatographic separation of a hydrolyzate of wheat protein labelled with S^{35}. The two main peaks are due to cystine-S^{35} and methionine-S^{35}. The conditions are identical with those for the 150 cm column analysis illustrated in Fig. 7.

other hand, the anthracene will probably have to be replaced more often than the plastic scintillator in the detector because of solubility, and surface oxidation effects. The reported anthracene detector backgrounds have been slightly higher than observed for the present detector; however, this difference is probably not due to the detector but to the associated counting equipment.

ACKNOWLEDGMENTS

The author wishes to express his appreciation to Dr. A. J. Finlayson, Prairie Regional Laboratory, Saskatoon, for providing a sample of gliadin-C^{14} where C^{14} activity of the constituent amino acids had been previously determined by a vibrating reed electrometer; to Dr. I. H. Harley, Health and Safety Laboratory, New York, for providing the Sr^{90}–Y^{90} standard; to Dr. B. L. Funt, University of Manitoba, and Dr. W. Reid, Nuclear Enterprises, Winnipeg, for many helpful discussions; and to Nuclear Enterprises, Winnipeg, for providing a sample of NE 102 plastic scintillator.

REFERENCES

1. B. L. FUNT and A. HETHERINGTON. Science, **129**, 1429 (1959).
2. D. STEINBERG. Nature, **182**, 740 (1958).
3. D. STEINBERG. Nature, **183**, 1253 (1959).
4. E. BILINSKI and W. B. MCCONNELL. Can. J. Biochem. Physiol. **35**, 360 (1957).
5. L. T. ALDRICH and G. W. WETHERILL. Ann. Rev. Nucl. Sci. **8**, 257 (1958).
6. E. RAPKIN and L. E. PACKARD. Proceedings of the University of New Mexico Conference on Organic Scintillation Detectors. *Edited by* G. H. Daub, F. N. Hayes, and E. Sullivan. U.S. Government Printing Office, Washington 25, D.C. 1960. Report TID-7612, Instruments. E. Rapkin and J. A. Gibbs. Nature, **194**, 34 (1962).
7. E. SCHRAM and R. LOMBAERT. Anal. Biochem. **3**, 68 (1962).

BIOGENETIC STUDIES ON VOLUCRISPORIN[1]

G. READ,[2] L. C. VINING, AND R. H. HASKINS
Tha National Research Council of Canada, Prairie Regional Laboratory, Saskatoon, Saskatchewan

Received June 15, 1962

ABSTRACT

In experiments with C^{14}-labelled compounds, shikimic acid, phenylalanine, phenyllactic acid, and metatyrosine were found to be precursors of the terphenylquinone pigment volucrisporin. It is suggested that the pigment is biosynthesized by the self-condensation of two molecules of an unbranched phenylpropanoid intermediate, and that hydroxylation of the phenyl rings in the meta position occurs before the condensation step.

Several speculative schemes have been proposed for the biogenesis of terphenylquinone pigments. Kögl (1), as early as 1926, suggested that polyporic acid is formed from phenylacetic and oxalic acids. More recently Mittal and Seshadri (2) proposed that two branched C_6C_3 units such as 2-C-phenylglyceraldehyde might be involved in the formation of this pigment. Straight-chain phenylpropanoid compounds related to the common aromatic amino acids were considered to be more plausible intermediates by Read and Vining (3), who suggested that condensation of suitable pairs of such compounds would provide a general route to the terphenylquinones. The discovery of volucrisporin in saprophytic cultures of the hyphomycete *Volucrispora aurantiaca* Haskins (4) and elucidation of its structure as the terphenylquinone (III) (5) have provided the first practical opportunity to test these theories. Compounds of this class had previously been found only in the fruiting bodies of fungi growing in their natural environment, or in the slow-growing lichens (6).

V. aurantiaca has now been grown in the presence of various C^{14}-labelled substrates and the incorporation of radioactivity into the pigment examined. The results are shown in Tables I and II. The efficient utilization of the labelled carbon from D-glucose-1-C^{14},

TABLE I

Incorporation of C^{14}-labelled compounds into volucrisporin by *V. aurantiaca* PRL 1554

Compound added	Weight, mg	Specific activity, mμc/mmole	Volucrisporin, acetate isolated, mg	Specific activity, mμc/mmole	Dilution*
Glucose-1-C^{14}	100	105†	4.3	127	1.7
Shikimic acid-G-C^{14}	100	2,470	8.5	1,830	2.5
L-Phenylalanine-G-C^{14}	9.7	49,200†	19.8	5,880	16.8
Glycine-2-C^{14}	12.6	4,860†	11.4	‡	>200
Sodium pyruvate-2-C^{14}	100	5,500	6.4	‡	>500
Caffeic acid-β-C^{14}	34.5	19,600	37.2	‡	>2,000
Sodium acetate-1-C^{14}	10.4	96,900	29.5	‡	>3,500
L-Tyrosine-G-C^{14}	10.1	83,800†	12.6	‡	>5,000
Cinnamic acid-β-C^{14}	10.8	158,400	29.3	‡	>6,000
3,4-Dihydroxyphenylalanine-α-C^{14}	9.5	209,400	30.2	‡	>8,000

*Assuming incorporation of 2 moles of radioactive compound added per mole of volucrisporin.
†Specific activity calculated for total amount of compound in the growth medium. The values for glycine, phenylalanine, and tyrosine take into account an analysis of the total amino acid content of the peptone sample used.
‡Activity found in samples was not outside the limits of accuracy of the counting method.

[1]*Issued as N.R.C. No. 7054.*
[2]*National Research Council of Canada Postdoctorate Fellow, 1957–59. Present address: Washington Singer Laboratories, University of Exeter, Prince of Wales Road, Exeter, Devon, England.*

TABLE II

Incorporation of C^{14}-labelled compounds into volucrisporin by *V. aurantiaca* PRL 1952

Compound added	Weight, mg	Specific activity, mμc/mmole	Volucrisporin acetate isolated, mg	Specific activity, mμc/mmole	Dilution*
L-Phenylalanine-carboxyl-C^{14}	0.23	92,300†	30.0	24,400	7.6
DL-Phenyllactic acid-α-C^{14}	50	28,200	32.1	6,670	8.4
DL-Metatyrosine-carboxyl-C^{14}	50	34,800	6.6	1,600	43.5
Metahydroxycinnamic acid-α-C^{14}	50	39,300	9.8	‡	>10,000

*Assuming incorporation of 2 moles of radioactive compound added per mole of volucrisporin.
†The specific activity of phenylalanine was calculated by taking into account the total amount of this amino acid in free or bound form present in peptone.
‡Activity found in samples was not outside the limits of accuracy of the counting method.

shikimic acid-G-C^{14}, L-phenylalanine-G-C^{14}, L-phenylalanine-1-C^{14}, and DL-phenyllactic acid-2-C^{14} strongly supports the view that unbranched phenylpropanoid compounds are intermediates in the biosynthesis of volucrisporin. The results suggest further that these intermediates are formed via the shikimic acid pathway and that the whole phenylpropanoid skeleton is utilized. Since acetate and glycine were relatively poor precursors of the pigment, formation of the phenylpropanoid unit by the condensation of a benzaldehyde with glycine to give the corresponding α-amino-β-hydroxy acid, as has been demonstrated in some mammalian cells (7), does not appear to be involved to an appreciable extent.

Two schemes which have been put forward (3, 8) to account for the meta hydroxylation in volucrisporin involve reactions subsequent to the formation of the terphenyl skeleton. In view of the relatively low dilution of radioactivity in the pigment produced in the presence of labelled metatyrosine, it appears more probable that hydroxylation occurs before the terphenyl skeleton is formed. Only one other instance where metatyrosine has been found to participate in a biosynthetic pathway appears to have been recorded. Winstead and Suhadolnik (9) observed that the tritium-labelled amino acid is an effective precursor of the antibiotic gliotoxin in *Trichoderma viride*. Meta-hydroxylated compounds are produced from caffeic acid and its derivatives in some mammalian tissues (10). A similar process, in which the para hydroxyl is eliminated from a 3,4-dihydroxylated intermediate, does not seem to occur in *V. aurantiaca* since neither L-tyrosine nor DL-3,4-dihydroxyphenylalanine labelled with C^{14} were found to be incorporated into volucrisporin. It would appear that certain microorganisms may be capable of the direct meta hydroxylation of phenylalanine, or a closely related compound.

Cinnamic acid and its 3- and 3,4-hydroxy derivatives do not serve as precursors of volucrisporin. Although negative evidence of this kind must be accepted with reserve, it appears unlikely that they are biosynthetic intermediates. Phenyllactic acid, on the other hand, is incorporated almost as readily as phenylalanine. A reversible interconversion of phenyllactic acid, phenylalanine, and phenylpyruvic acid might be expected to occur (11) and, of these three compounds, it is suggested that phenylpyruvic acid is likely to be the most direct precursor of volucrisporin. Presumably it is converted to a suitably activated form of metahydroxyphenylpyruvic acid before dimerization. Derivatives of phenylpyruvic acid are more attractive as candidates for the condensing unit since, besides possessing a more highly activated methylene group, they might be expected to give rise more easily to other known terphenylquinone pigments, which all possess a 2,5-dihydroxylated quinone ring. Thus in the biosynthetic sequence for volucrisporin outlined in Scheme 1, polyporic acid (1), atromentin (12), leucomelone (13), and probably

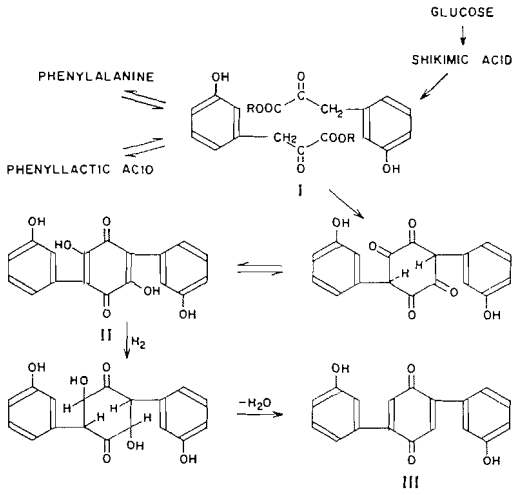

SCHEME 1.

thelephoric acid (14) would be derived from appropriately substituted phenylpropanoid compounds by a similar pathway terminating at an earlier stage corresponding to structure II.

Degradation of the volucrisporin produced when DL-phenyllactic acid-α-C^{14}, carboxyl-labelled L-phenylalanine, and DL-metatyrosine were fed to *V. aurantiaca* gave inactive metaacetoxybenzoic acid. It is concluded that the β-carbons in the phenylpropanoid precursors remain attached to the aromatic ring during formation of the pigment, becoming carbons 2 and 5 of the benzoquinone ring. There are two ways (Scheme 2, IV and V) by which unbranched phenylpropanoid units might condense to yield a terphenyl

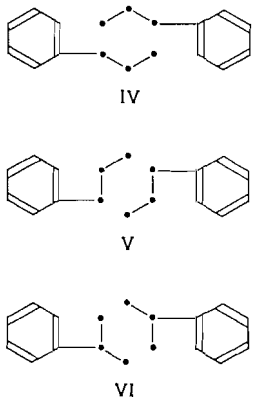

SCHEME 2.

skeleton. Moreover, a prior rearrangement of the carbon chain to give a branched intermediate (Scheme 2, VI) cannot be excluded, although this cannot take place by a migration of the phenyl group from the β- to the α-carbon, as in the biosynthesis of isoflavones (15). However, a rearrangement in which the carboxyl group migrates to the β-carbon as in the biosynthesis of tropic acid (16) is possible and would be difficult to detect by

degradation of the pigment since the labelling pattern would be the same as that for IV. Further work on the details of the biosynthetic process is in progress.

EXPERIMENTAL

C^{14}-Labelled Compounds

DL-Metatyrosine labelled in the carboxyl group was prepared from metahydroxybenzaldehyde and glycine-1-C^{14} by an azlactone synthesis using the procedure described by Sealock and co-workers (17). The crude product was purified by chromatography on a column of Dowex-1×8 (200–400 mesh) in the acetate form, developed with 0.1 *N* acetic acid. Crystallization of the amino acid from aqueous ethanol gave an analytically pure specimen in an overall yield of 50% based on glycine.

Metahydroxycinnamic acid-α-C^{14} was prepared by condensing metahydroxybenzaldehyde with malonic acid-2-C^{14} in the presence of pyridine as described by Pandya and Vahidy (18). The product after two crystallizations from aqueous ethanol was obtained in an analytically pure state, m.p. 197–198.5° C. The yield, based on malonic acid, was 94%.

DL-Phenyllactic acid-α-C^{14} was obtained in a yield of 65% by the action of nitrous acid on DL-phenylalanine-α-C^{14} using the method described by Wright and co-workers (19).

Shikimic acid-G-C^{14}, caffeic acid-β-C^{14}, cinnamic acid-β-C^{14} and DL-3,4-dihydroxyphenylalanine-α-C^{14} were prepared in this laboratory and kindly donated by Dr. A. C. Neish. The remaining compounds were purchased from the Atomic Energy Agency of Canada.

Culture

Experiments were carried out with two strains of PRL 1554 *V. aurantiaca*. Both were descendants of the original isolate (4). One strain was maintained in this laboratory and is referred to as PRL 1554; the other was maintained, probably under more constant conditions, in the American Type Culture Collection as ATCC 13128. It showed differences in pigmentation and manner of growth and is referred to as PRL 1952.

PRL 1554 was used in the early studies. The method of inoculation, nutrient medium, and conditions of growth were as described in a previous publication (5), except for the addition of the C^{14}-labelled compound to be tested. In a typical experiment a solution of glucose (10 g), peptone (1 g), soluble starch (0.2 g), soil extract (20 ml), and distilled water (180 ml) was dispensed in eight equal portions into 250-ml Erlenmeyer flasks and sterilized by autoclaving. Each flask was then supplemented aseptically with an aliquot (2 ml) of a filter-sterilized solution of the labelled compound,* and inoculated with a blended suspension in distilled water of *V. aurantiaca* grown on Difco potato-dextrose agar. Cultures were incubated at 25° C on a rotary shaker for 6 to 7 days.

PRL 1952 was used in later work after difficulty was encountered in obtaining adequate production of volucrisporin by PRL 1554. It gave appreciable yields of pigment on a simplified medium. In a typical experiment glucose (10 g) and peptone (1 g) were dissolved in distilled water (200 ml) and the C^{14}-labelled compound, dissolved in water (5 ml), was added. A small aliquot (2 ml) was removed for determination of the radioactivity, then aliquots of 25 ml were dispensed into 250-ml Erlenmeyer flasks, sterilized by autoclaving and inoculated with a suspension (1 ml) of washed, blended mycelium from a culture of *V. aurantiaca* grown in a glucose–peptone medium. Cultures were incubated on a rotary shaker for 11 days at 25° C.

Isolation of Volucrisporin

Appropriate cultures were pooled and filtered. The residual mycelium was washed, freeze-dried, and transferred to a Soxhlet thimble. After a preliminary Soxhlet extraction with petroleum ether (b.p. 30–60° C), it was extracted with acetone until the pigment was completely removed (3 to 6 hours). The acetone extract was dried by evaporation *in vacuo* and the residue washed successively with several portions of petroleum ether (b.p. 30–60° C), ether, and then water. The remaining deep red pigment was dried and then heated under reflux with acetic anhydride (2 ml) until completely dissolved. The orange-yellow solution was filtered while hot and water (0.5 ml) added. On cooling, yellow needles of volucrisporin diacetate separated. These were removed and recrystallized from acetic acid or a chloroform–ethanol mixture to constant melting point (219° C). Yields from 200 ml of culture medium varied between 5 and 40 mg. Measurement of radioactivity was carried out by total combustion of samples and estimation of the activity in the residual carbon dioxide in an electrometer.

Degradation of Volucrisporin

Volucrisporin acetate (2 mg) from experiments where L-phenylalanine-carboxyl-C^{14}, DL-metatyrosine-

**It was noted that glycerol, acetate, cinnamate, and phenylalanine at concentrations of 0.5 mg per ml of nutrient medium or higher severely depressed pigment formation and in some cases also the growth of the organism. Tests with various concentrations of phenylalanine showed growth to be unaffected at 1 mg per ml, but normal pigmentation was not obtained until the concentration was reduced to 0.25 mg per ml. Cinnamate gave normal growth and pigmentation at 0.08 mg per ml. At 0.25 mg per ml and above, growth was limited and no pigment was produced. The large variation in pigment yield in experiments where other C^{14}-labelled compounds were used may be attributed, at least in part, to their inhibitory effect.*

carboxyl-C^{14}, and DL-phenyllactic acid-α-C^{14} were used as precursors (Table II) was diluted with inactive carrier (60 mg) and dissolved in boiling acetic acid (5 ml). Chromium trioxide (200 mg) was added; the reaction mixture was heated under reflux for 10 minutes, then diluted with water and extracted with ether. Metaacetoxybenzoic acid (20 mg), m.p. 134° C, was obtained from the extract by sublimation, followed by crystallization from an ether – petroleum ether (b.p. 60–80° C) mixture.

In each instance the metaacetoxybenzoic acid contained no radioactivity.

ACKNOWLEDGMENTS

The authors wish to express their appreciation to Miss M. J. A. Gates and Mr. L. R. Nesbitt for expert technical assistance, and to Mr. J. Dyck for determining the radioactivity of numerous samples.

REFERENCES

1. F. KÖGL. Ann. **447**, 78 (1926).
2. O. P. MITTAL and T. R. SESHADRI. Current Sci. (India), **26**, 4 (1957).
3. G. READ and L. C. VINING. Chem. Ind. (London), 1547 (1959).
4. R. H. HASKINS. Can. J. Microbiol. **4**, 273 (1958).
5. P. V. DIVEKAR, G. READ, L. C. VINING, and R. H. HASKINS. Can. J. Chem. **37**, 1970 (1959).
6. R. H. THOMSON. Naturally occurring quinones. Butterworths Scientific Publications, London. **1957**, p. 26.
7. F. H. BRUNS. Biochem. Z. **331**, 54 (1958).
8. A. J. BIRCH. Proc. Chem. Soc. 3 (1962).
9. J. A. WINSTEAD and R. J. SUHADOLNIK. J. Am. Chem. Soc. **82**, 1644 (1960).
10. A. N. BOOTH, O. H. EMERSON, F. T. JONES, and F. DEEDS. J. Biol. Chem. **229**, 51 (1957).
11. A. C. NEISH. Ann. Rev. Plant Physiol. **11**, 55 (1960).
12. F. KÖGL and J. J. POSTOWSKY. Ann. **445**, 159 (1925).
13. M. AKAGI. J. Pharm. Soc. Japan, **62**, 129 (1942).
14. J. GRIPENBERG. Tetrahedron, **10**, 135 (1960).
15. H. GRISEBACH and W. D. OLLIS. Experientia, **17**, 4 (1961).
16. M. L. LOUDEN and E. LEETE. J. Am. Chem. Soc. **84**, 1510 (1962).
17. R. R. SEALOCK, M. E. SPEETER, and R. S. SCHWEET. J. Am. Chem. Soc. **73**, 5386 (1951).
18. K. C. PANDYA and T. A. VAHIDY. Proc. Indian Acad. Sci. Sect. A, **4**, 134 (1936); Chem. Abstr. **30**, 8149 (1936).
19. D. WRIGHT, S. A. BROWN, and A. C. NEISH. Can. J. Biochem. Physiol. **36**, 1037 (1958).

THE INFRARED SPECTRA OF N-ACYLTRIALKYLAMMONIUM HALIDES, IN RELATION TO THOSE OF AMIDE SALTS*†

DENYS COOK
Exploratory Research Laboratory, Dow Chemical of Canada, Limited, Sarnia, Ontario
Received July 19, 1962

ABSTRACT

N-Acyltrialkylammonium halides have been prepared from the trialkylamine and acid halides. The ionic solids so produced can be easily handled in inert atmospheres but are easily attacked by moisture. Their infrared spectra have strong carbonyl bands near 1800 cm^{-1}, showing that the R_3N^+ group, when attached to an acyl group, has strong electron-withdrawing characteristics, to a rather greater extent than the halogens in acid halides.

Structurally, the N-acyltrialkylammonium halides would be similar to protonated (or alkylated) amides, if such protonation (or alkylation) occurred at the nitrogen atom. Since all amide salts examined hitherto have carbonyl frequencies over 100 cm^{-1} lower than 1800 cm^{-1} it is concluded that this work offers further evidence that protonation in amides occurs at the oxygen atom.

INTRODUCTION

The N-acyltrialkylammonium halides can be isolated and examined by techniques which prevent contamination by moisture. Structurally they are interesting as they represent a class of carbonyl compounds RCOX where the X group contains a formal positive charge. The effect of this charge upon the vibrational spectrum, particularly the carbonyl frequency, a group frequency very sensitive to electronic and mechanical factors, is of wide interest (1, 2).

The N-acyltrialkylammonium halides would be very similar to protonated (or alkylated) amides if such protonation (or alkylation) occurred at the nitrogen atom, as has been claimed (3–5). The structure of an N-protonated amide would be as in I. If this

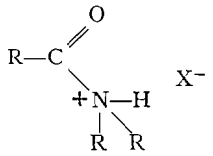

I

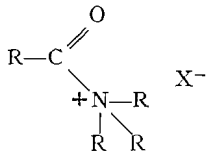

II

nitrogen hydrogen atom were replaced by a methyl group, structure II would result. Several compounds like II have been made by low-temperature reaction of an acyl halide and a trialkylamine or a pyridine derivative. It is not possible to make compounds like I by the same method since the dialkylamine reacts to form the amide, releasing hydrogen halide, which forms the amine hydrohalide rather than the amide hydrohalide, since the amine is usually more basic. The electronic or mechanical effect of replacing hydrogen in I with methyl as in II would not be expected to be significant.

Contribution No. 70.
†*Presented, in part, at the 45th Conference of the Chemical Institute of Canada, Edmonton, Alberta, May 29, 1962.*

EXPERIMENTAL

Trimethylamine was taken from a freshly opened bottle of Distillation Products Industries anhydrous material and was used without further purification, except for bulb-to-bulb distillation from anhydrous Na_2SO_4 on a high-vacuum line. Triethylamine, from the same source, was distilled, after standing over anhydrous Na_2SO_4, and a center cut boiling at 89.7° C was taken. Pyridine, from the Fisher Scientic Company, was dried over anhydrous Na_2SO_4 several weeks, then distilled in a Todd column at a reflux ratio of 50:1, the portion boiling at 115.4° C being collected. Acetyl chloride from the J. T. Baker Company and propionyl chloride from Distillation Products Industries were both distilled as above: their boiling points were 50.3 and 77.7° C respectively.

The procedure for making the compounds was as follows. Glass cells fitted with stopcocks were filled with the appropriate amount of each component in a dry box. These cells were then attached to a high-vacuum system and the liquids outgassed in the conventional manner. Freon 113, from a previously dried and outgassed stock contained in a flask on the vacuum line, was condensed onto the less volatile component, then the more volatile component was condensed onto that, by the use of liquid nitrogen. On warming to room temperature the solid compound was precipitated and excess Freon 113 removed by evacuation. Emulsions of these solids, in Nujol and Fluorolube, were prepared in a dry box. Small samples were sealed in tubes at the same time for melting point determination.

RESULTS

Tables I and II show the bands in the various spectra, and Fig. 1 shows a spectrum of the N-acetylpyridinium chloride and of the N-acetyltrimethylammonium chloride. Spectra of N,N-dicyclohexylacetamide hydrochloride and hydrobromide are shown in Fig. 2. Some of the bands from these materials and their deuterated analogues are shown in Table III.

TABLE I

Infrared bands in the spectra of N-acyltrialkylammonium halides

$(CH_3)_3\overset{+}{N}COCH_3\ Cl^-$	$(CH_3)_3\overset{+}{N}COCH_3\ Br^-$	$(CH_3)_3\overset{+}{N}COCH_2CH_3\ Cl^-$
3022m	3030w	3028m
3008m	3016m	3011m
2990m	2982w	2995m
2958m	2966m	2943w
		2890vw
2620m*	2710m	2618m
2480m*	2480m	2480w
1815s, sh		
1812s	1814s	1812vs
1473m	1486m	1476m
	1467m	1462m, sh
1414w		
1402w	1396m	1394m
1390w		
1356m	1358m	1368w
	1340w	1350w
	1258w	
1245w*	1246w	1250m
		1225w
1140m	1143s	1136m
1128m	1124w	
1112m	1116m	
		1082m
		1073m, sh
1039m	1046m	1038m
1005m	1003m	
988w*	978m	982m
952m	951m	946m, sh
940m	939m	935m
796s	795s	800s
718w	720w	723m
644m	640s	

*Bands marked thus are due to a small amount of amine hydrohalide.

TABLE II

Infrared bands in the spectra of N-acylpyridinium halides

$C_5H_5\overset{+}{N}COCH_2CH_3\ Cl^-$	$C_5H_5\overset{+}{N}COCH_3\ Cl^-$	$C_5H_5\overset{+}{N}COCH_2CH_3\ Cl^-$	$C_5H_5\overset{+}{N}COCH_3\ Cl^-$
3168w	3124m	1258w, b	1270w
3100w	3070m	1200w	1210w
3044w	3042s		1198w
3028w			1172s
3002m		1151m	1155m
	2962w	1125m, sh	
2928w	2947w	1120s	1118m
1796s	1804vs	1100m	
	1630m, sh	1090m	1080m
1619m	1622s	1076m	
1608m, sh	1610m, sh	1040m	1037m
	1575vw	1030m	1024m
	1532vw	1008m	1003w
	1482vw	958s	982m
1468m	1468s	863w	895vw
1460m, sh		781s	789s
1408w		754m	759s
1372w		742m	731s
1339w	1349m	682m	688m, sh
1325w	1332s	670s	679s
1290w	1292m		

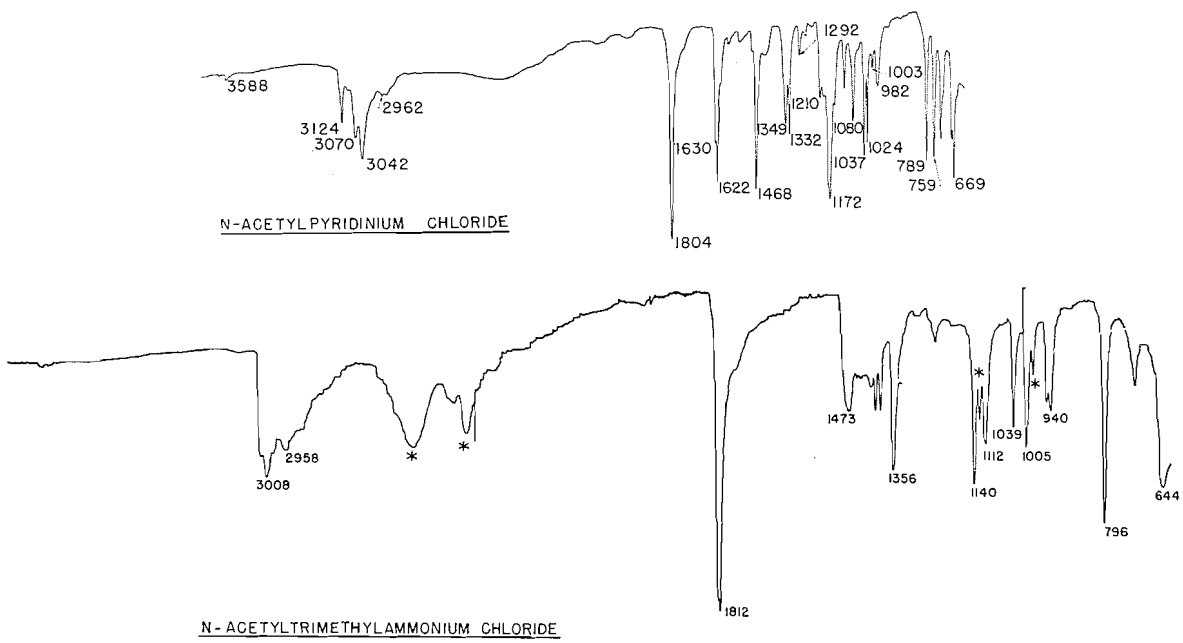

FIG. 1. Infrared spectrum of (*a*) N-acetylpyridinium chloride, (*b*) N-acetyltrimethylammonium chloride.

DISCUSSION

A strong band in the spectra of the N-acyltrialkylammonium halides at about 1800 cm^{-1} is attributed to the carbonyl stretching vibration in the salt. Its high frequency is an indication that the electron-withdrawing ability of the quaternary nitrogen atom is somewhat larger than that of the chlorine atom. Although the Taft sigma values (6)

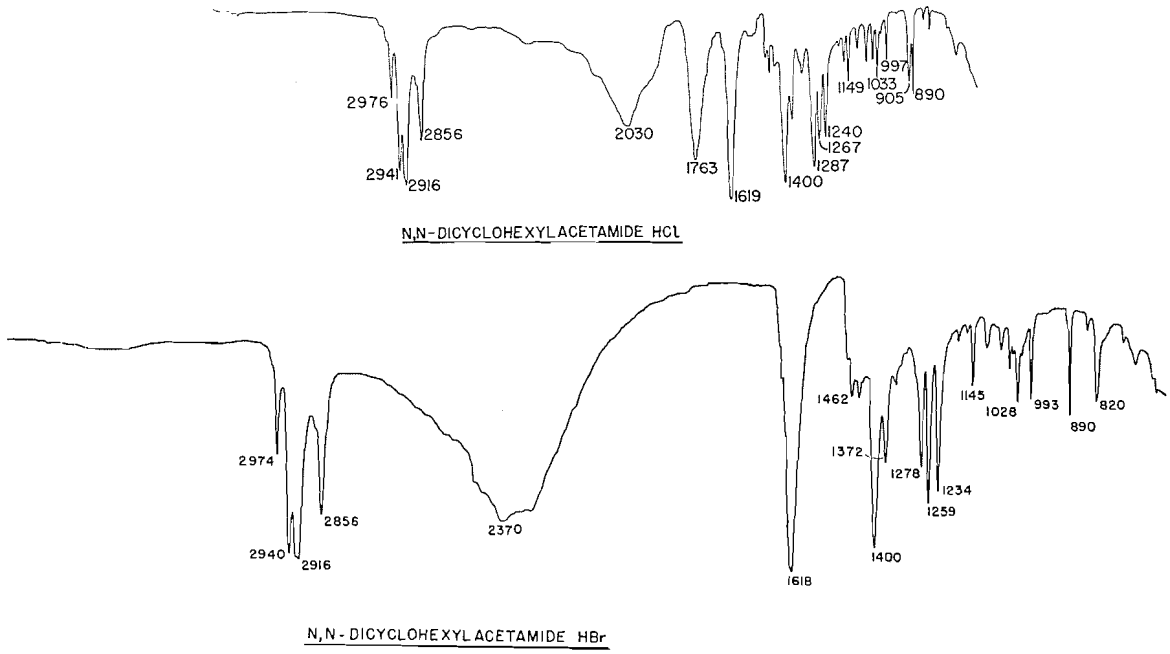

FIG. 2. Infrared spectrum of (*a*) N,N-dicyclohexylacetamide hydrochloride, (*b*) N,N-dicyclohexylacetamide hydrobromide.

TABLE III

Some bands in the infrared spectra of N,N-dicyclohexylacetamide salts

HCl	DCl		HBr	DBr		
2030			2370	1925	1.23	OH stretch
1763			2320	1822	1.27	Combination
1619	1616	1.0	1616	1620	1.0	CN stretch
1400	1300	1.08	1400	1300	1.08	CO stretch +
1287	1087	1.18	1278	1085	1.18	OH bend +
905						OH torsion

(inductive effect alone) are not equal, $NMe_3^+ = +0.86$, and $Cl = +0.47$, the diminution in the CCCl angle in the acid halide from the theoretical sp^2 hybridization value of 120° to about 110° (2) would account for an elevation of about 30 cm^{-1} in the carbonyl frequency. Similarly, in the N-acylammonium salts some slight hindrance between the nitrogen methyl group and that on the acyl group would be relieved by enlarging the angle CCN^+, which has the effect of lowering the carbonyl stretching frequency. When rough estimates are made for these effects, the frequencies and sigma values become reasonably proportional.

Very small differences are noted between the carbonyl frequencies of N-acylpyridinium and N-acyltrialkylammonium halides. It is likely then that formal charge on the nitrogen atom blocks the transmission of mesomeric effects from the rest of the molecule to the carbonyl group.

By contrast with the high carbonyl frequency in the N-acyltrialkylammonium halides, the amide salts have no band in this region at all. Instead, most amide salts show a strong band at a frequency between 1630 and 1730 cm^{-1} depending on the amide (5, 7–10). A medium band in the region of 1750 cm^{-1} in the HCl salts only should not be confused

with a carbonyl vibration frequency, as this is some combination band associated with the strong band between 2000 and 2400 cm^{-1} due to the hydrogen bond. Both these bands shift in the DCl salt, and the lower-frequency band is not seen in salts with other acids. These combination bands are well known but in some cases the very high intensity of this band occurring in a region where other bands are expected could be confusing.

In the N,N-dicyclohexylacetamide salts chosen as models for discussion, the combination band is at 1764 cm^{-1}, and another strong band is present at 1626 cm^{-1}. The next strong band at lower frequency is at 1400 cm^{-1}. In the past the 1626 cm^{-1} band has been assigned to the carbonyl group stretching vibration, and since it occurred at a lower frequency than the same band in the free amide at 1647 cm^{-1}, protonation was said to occur at the carbonyl oxygen atom. In a few amide hydrochlorides studied the new band attributed to the carbonyl group absorbed at a frequency higher than the carbonyl vibration in the free amide (5, 9, 10). For example, in acetamide hydrochloride the carbonyl vibration was assigned to a band at 1718 cm^{-1} in the solid (5), whereas the free amide absorbed at 1684 cm^{-1} in the solid state. This low value is due to hydrogen bonding, and in CCl_4 solution it absorbs at 1714 cm^{-1}. On this account, the protonation was said to take place at the nitrogen atom, and it became the fashion thereafter to attribute carbonyl frequencies in the salts at a higher frequency than in the free amide to N protonation, and at a lower frequency to O protonation.

This distinction is unrealistic, as the present work on the N-acyltrialkylammonium halides shows. The absence of the 1800 cm^{-1} bands in these amide salts definitely excludes the possibility of N-protonation. As stated earlier, the difference in effect between a $HN(CH_3)_2^+$ group (in the alleged N-protonated amide) and a $N(CH_3)_3^+$ (in the N-acyltrialkylammonium halide) on the carbonyl frequency (from a purely inductive or mesomeric viewpoint) should be small. Compare, for example, the carbonyl stretching frequencies of methyl isopropyl ketone, 1722 cm^{-1}, and methyl *tert*-butyl ketone, 1711 cm^{-1}, which are isoelectronic with the compounds just discussed.

Part of the confusion in interpretation of these amide salts also arose from the habit of assuming that the highest-frequency band in the carbonyl region came from the carbonyl stretching vibration. It has recently been shown that in 2,6-dimethyl-4-pyrone the higher-frequency band of a pair at 1678 and 1639 cm^{-1} arose from a ring mode (11), while the lower-frequency band was due to the true carbonyl stretching vibration. The same situation arises in the 4-pyridones (12, 13) and probably in many others. This situation is particularly likely to arise when the carbonyl group is attached to a system containing mobile π electrons, as in the compounds just mentioned. The amides afford another example of such a system, for the NR_2 group in the amide has electrons of π symmetry which can form an extended molecular orbital over the NCO atoms. All amides whose structures have been determined by the methods of X-ray or electron diffraction have been found to have a planar or nearly planar arrangement of heavy atom, with long CO bonds and short NC (O) bonds.

It is now quite reasonable to look for carbonyl bands at much lower frequencies than hitherto thought possible, and a likely assignment is the strong band at 1400 cm^{-1}. This is in a very similar place to that found in 4-pyrone (11) and 4-pyridone (13) salts, namely, about 1490 cm^{-1}. In different amide salts it has been recorded at a range of frequencies from 1395 to 1450 cm^{-1}. This low frequency indicates that the carbonyl group has a much lower force constant, and therefore bond order, in the salt than in the free amide, and that in valence bond language a large contribution from a structure III would be expected. An equivalent statement would be that binding due to π electrons was now much greater

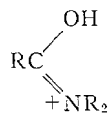

III

in the CN bond than in the CO bond. This leads very naturally to consideration of the assignment of the CN vibration. This must then be the band at between 1630 and 1730 cm^{-1} previously described, which is in keeping with our knowledge of the vibrational frequency of CN double bonds. In the amide salts, therefore, there is a reversal of assignments from the free amide. The amide I band is primarily CO stretching but contains some contribution from the CN stretching mode. The CN stretching vibration amide III is made up of contributions from the CO stretching mode and in secondary amides from the NH in-plane bending mode (14).

Corroborative evidence that these are the proper assignments comes from a consideration of the in-plane hydrogen bending mode of the protonated species. By replacement of HX with DX when preparing the amide salt, or by exchange with D_2O after preparation, new bands in the spectrum of the deuterated material were connected with bands which disappeared from the HX salt. Thus the band near 1280 cm^{-1} in the H salt is found near 1090 cm^{-1} in the D salt, the ratio of these frequencies being about 1.17. This low ratio indicates that a good deal of coupling takes place, probably with the CO stretching vibration. The shift of the absorption band due to this CO stretching vibration from 1400 to 1300 cm^{-1} is good evidence that these two are the coupled vibrations, though other coupling partners may also be present. Similar difficulties have been encountered in certain alcohols and phenols, and these have not yet been entirely resolved.

A comparison of the in-plane hydrogen bending frequency in the amide salts and in 4-pyrone salts (11) reveals some similarities. In 4-pyrone salts a band at 1340 cm^{-1} moves to about 1000 cm^{-1} in the deuterated species, and in the 2,6-dimethyl-4-pyrone salts the two frequencies are about 1300 and 1000 cm^{-1}. The band attributed to the carbonyl vibration is at 1490 cm^{-1}, which hardly shifts on deuteration. The ratio of the bending modes is about 1.30:1.35 and shows a fairly pure vibration. Absence of coupling is therefore inferred in the pyrone salts, and this is understandable since the two vibrations are further apart in frequency. Tertiary amine salts (15, 16) on the other hand have a hydrogen bending mode near 1420 cm^{-1} and the isotopic shift shows relative freedom from coupling in that the ratio is about 1.37.

Additional support for the assignment of the 1400 cm^{-1} band to the carbonyl stretching vibration was published recently (10). In an infrared study of propionamide hydrochloride containing O^{18}, the only band listed in the carbonyl region to show an isotopic shift was at 1487 cm^{-1} in the normal salt, and at 1480 cm^{-1} in the O^{18} salt. One other band showed a shift of 2 cm^{-1}, all others having zero shift. In the hydrobromide similar but not quite as clear-cut changes took place. In particular, a band at 1484 cm^{-1} shifted to 1479 cm^{-1} in the O^{18} salt. While these values may be slightly in doubt because of the possibility of confusion with NH bending modes, they do prove that the higher-frequency band near 1700 cm^{-1} does not move on isotopic substitution, and is therefore not associated with the oxygen atom.* They also strengthen the assignment of the protonated carbonyl group to bands in the 1400–1500 cm^{-1} region.

**This difficulty with* NH *modes was one of the reasons behind the choice of fully alkylated amides for this work.*

ACKNOWLEDGMENTS

The assistance of Miss C. D. Anderson in preparing some of the compounds and recording their spectra is gratefully acknowledged.

REFERENCES

1. D. Cook. J. Am. Chem. Soc. **80**, 49 (1958).
2. D. Cook. Can. J. Chem. **39**, 31 (1961).
3. L. Kahovec and K. Knollmüller. Z. Physik. Chem. **51**, 49 (1941).
4. C. H. Smith and J. D. Robinson. J. Am. Chem. Soc. **79**, 1349 (1957).
5. E. Spinner. Spectrochim. Acta, **15**, 95 (1959).
6. R. W. Taft, N. C. Deno, and P. S. Skell. Ann. Rev. Phys. Chem. **9**, 292 (1958).
7. E. H. White. J. Am. Chem. Soc. **77**, 6215 (1955).
8. R. Gompper and P. Altreuther. Z. Anal. Chem. **170**, 205 (1959).
9. R. Stewart and L. J. Muenster. Can. J. Chem. **39**, 401 (1961).
10. R. Stewart, L. J. Muenster, and J. T. Edward. Chem. Ind. (London), 1906 (1961).
11. D. Cook. Can. J. Chem. **39**, 1184 (1961).
12. L. J. Bellamy and R. E. Rogasch. Spectrochim. Acta, **16**, 30 (1960).
13. D. Cook. Eighth Ottawa Symposium on Applied Spectroscopy. Sept. 19, 1961.
14. T. Miyazawa, T. Shimanouchi, and S. Mizushima. J. Chem. Phys. **29**, 611 (1958).
15. E. A. V. Ebsworth and N. Sheppard. Spectrochim. Acta, **13**, 261 (1958).
16. R. H. Nuttall, D. W. A. Sharp, and T. C. Waddington. J. Chem. Soc. 4965 (1960).

THE KINETICS OF THE REACTION OF ORGANIC ISOTHIOCYANATES WITH 1-OCTANOL IN *o*-DICHLOROBENZENE

YOSHIO IWAKURA AND HISAO OKADA

Research Laboratory of Resources Utilization, Tokyo Institute of Technology, Ookayama, Meguro-Ku, Tokyo, Japan

Received June 25, 1962

ABSTRACT

The kinetics of the reaction of organic isothiocyanates with a large excess of 1-octanol in *o*-dichlorobenzene was examined at 90–140°. The rate of the reaction was first order with respect to the concentration of isothiocyanate, but the apparent second-order rate constants calculated varied according to the initial 1-octanol concentration. These facts can be explained by a reaction mechanism involving two molecules of 1-octanol in the transition state for the slow step of the reaction. The relative rate of the reaction of isothiocyanates with 1-octanol at 120° decreased in the order of benzyl, phenyl, allyl, ethyl, *n*-butyl, *n*-hexyl, isobutyl, and cyclohexyl isothiocyanate. The apparent energies of activation and log *A* were obtained as 13.5–16.5 kcal/mole and 4.65–6.46 (*A* in liter/mole min), respectively. Tributylamine had a slight catalytic effect, but dibutyltin dilaurate and ferric acetylacetonate had a strong catalytic action in these reactions.

INTRODUCTION

The addition reaction of organic isothiocyanates with alcohols gives thiourethanes:

$$R{-}N{=}C{=}S + R'{-}OH \rightarrow R{-}\overset{H}{N}{-}\overset{S}{\overset{\|}{C}}{-}O{-}R'. \quad [1]$$

Browne and Dyson (1, 2) compared the reactivity of various aromatic isothiocyanates with ethanol at its boiling point by isolating and weighing the products at different times. Zahradnik has studied the reaction of alkyl isothiocyanates with OH^- ions or alkylamines by using polarography (3, 4). It was an interesting problem for us to study the reactivity of organic isothiocyanates in the reaction with alcohols, to elucidate the mechanism of the reaction, and to determine the effective catalyst for this addition reaction.

In the present work, the kinetics of the reaction of organic isothiocyanates with a large excess of 1-octanol in *o*-dichlorobenzene at 90–140° has been studied, the reaction mechanism has been discussed, and the effect of catalysts on these reactions has been studied.

EXPERIMENTAL

Materials

Organic isothiocyanates, with the exception of commercial reagents, were synthesized in the following reactions, starting from the corresponding primary amines (5):

$$R{-}NH_2 + CS_2 + NaOH \rightarrow RNHCS_2Na + H_2O \quad [2]$$

$$RNHCS_2Na + ClCO_2C_2H_5 \rightarrow RNHCS_2CO_2C_2H_5 + NaCl \quad [3]$$

$$RNHCS_2CO_2C_2H_5 \rightarrow R{-}NCS + COS + C_2H_5OH. \quad [4]$$

The purification of the products was accomplished by fractional distillation. The boiling points observed are summarized in Table I.

Reagent grade 1-octanol was purified by fractional distillation, b.p. 87–91°/9 mm. *o*-Dichlorobenzene was dried over phosphorus pentoxide and distilled under reduced pressure, b.p. 68–75°/23 mm. Reagent grade tributylamine was dried over potassium hydroxide and fractionally distilled, b.p. 98–99°/19 mm. Free carboxylic acid was removed from commercial dibutyltin dilaurate by extraction of the latter three times with an equal volume of methanol. The slight amount of methanol remaining in the dilaurate was

TABLE I

Organic isothiocyanates

Isothiocyanate	Boiling point (°C/mm) Found	Literature*
Phenyl Commercial (special grade)	64.5–65.0/5	95/12
Benzyl	98–103/4	124–125/12
Allyl Commercial (special grade)	150.5–151.5	152
Ethyl	132–133	131–132
n-Butyl	170–172	167
i-Butyl	85/47	—
t-Butyl	140–143	140/770
n-Hexyl	117/33	136–138/96
Cyclohexyl	117/18	152–154/98

*References: Dictionary of Organic Compounds, Oxford University Press, New York, 1953; R. Zahradnik, Collection Czech. Chem. Commun., **24**, 3411 (1959).

then removed under reduced pressure at room temperature. Dibutyltin dilaurate was obtained as a slightly pale yellow liquid, m.p. 10–15°, n_D^{30} 1.4662. Ferric acetylacetonate was prepared from acetylacetone by the action of an aqueous solution of ferric chloride and sodium acetate. The product was obtained as a precipitate. On recrystallization from 60% methanol, the product was recovered as red needle-shaped crystals, m.p. 184–185°.

Procedure

The reaction vessel used was a long-necked, round-bottomed flask of approximately 50-ml capacity. A thermostat containing silicone oil (KF-96, Shin-etsu Chemical Industry Co. Ltd.) was controlled at 90–140 ±0.1° through the use of a decalin–mercury thermoregulator. Isothiocyanate or isothiocyanate–catalyst solution was prepared using a volumetric flask at a specified reaction temperature. After 1-octanol was brought to a specified temperature, a definite weight of 1-octanol was introduced into the reaction vessel. A kinetic run was initiated by adding isothiocyanate or isothiocyanate–catalyst solution to the reaction vessel and mixing rapidly. The total volume of the reaction mixture was about 30 ml in all cases. Disappearance of the isothiocyanate group was followed by a modification of the Stagg method (6) using di-*n*-butylamine in place of piperidine and titrating with 0.05 *N* hydrochloric acid – ethanol solution in the presence of bromphenol blue as indicator. Periodically 2-ml samples were pipetted from the reaction mixture and added to the 10-ml dibutylamine–acetone solution in a 100-ml glass-stoppered Erlenmeyer flask, and allowed to stand for about 30 minutes to react completely with the remaining isothiocyanate in the vessel. A blank determination on the dibutylamine solution was made at the beginning of each run.

RESULTS AND DISCUSSION

The reaction of benzyl isothiocyanate with a large excess of 1-octanol was carried out in *o*-dichlorobenzene at 100–120°. The apparent first-order rate constants were obtained by the method of least squares using the following equation:

$$\log [\text{concn. of R—NCS at time } t] = \log [\text{init. concn. of R—NCS}] - (k/2.303)t. \qquad [5]$$

The typical plot of equation [5] is shown in Fig. 1. From these plots the rate of reaction was shown to be apparently first order with respect to the concentration of isothiocyanate, and these results are summarized in Table II. If the reaction velocity is first order with respect to the concentration of isothiocyanate and 1-octanol respectively, the apparent second-order rate constants which were calculated by dividing the apparent first-order rate constants by the concentration of 1-octanol should show a constant value regardless of the concentration of 1-octanol. The second-order rate constants obtained in this experiment, however, varied according to the initial concentration of 1-octanol (see the last column in Table II). To compare the reactivity of several isothiocyanates, the reaction of the isothiocyanate (1 mole) with 1-octanol (35 moles) in *o*-dichlorobenzene was examined at 90–140°. The results are listed in Table III as the apparent second-order rate constants.

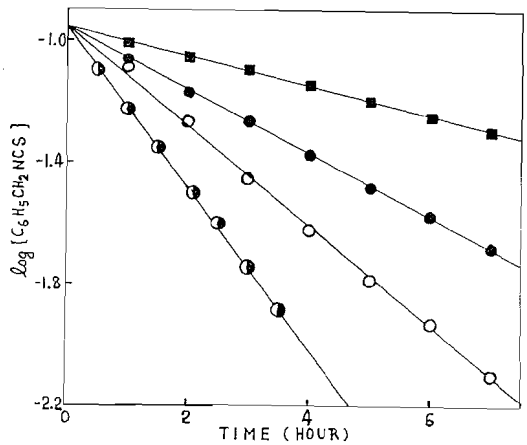

FIG. 1. Typical plots for the reaction of benzyl isothiocyanate with excess 1-octanol in *o*-dichlorobenzene at 120°. Initial concentration of 1-octanol: ■ 1.938, ● 2.907, ○ 3.876, ◑ 4.845 mole/liter.

TABLE II

The reaction of benzyl isothiocyanate with 1-octanol in *o*-dichlorobenzene

Reaction temp. (°C)	Init. concn. $C_6H_5CH_2NCS$ (mole/liter)	Init. concn. $C_8H_{17}OH$ (mole/liter)	Apparent first-order rate constant, $\times 10^4$ (min^{-1})	Apparent second-order rate constant, $\times 10^4$ (liter/mole min)
100	0.1100	1.971	7.00±0.10	3.55±0.04
	0.1098	2.957	14.3±0.1	4.83±0.03
	0.1112	3.942	22.0±0.2	5.58±0.05
	0.1087	4.928	31.5±0.2	6.39±0.04
110	0.1101	1.961	11.6±0.1	5.91±0.05
	0.1085	2.941	23.7±0.2	8.04±0.07
	0.1088	3.921	38.7±0.2	9.89±0.05
	0.1077	4.901	56.7±0.2	11.5±0.4
120	0.1095	1.938	18.4±0.1	9.51±0.05
	0.1089	2.907	39.5±0.3	13.6±0.1
	0.1246	3.876	68.3±1.5	17.6±0.4
	0.1109	4.845	101±1	20.8±0.2

TABLE III

The reaction of isothiocyanates with 1-octanol in *o*-dichlorobenzene
(Initial concentration: [R—NCS] = 0.11 mole/liter, $[C_8H_{17}OH]$ = 3.9 mole/liter)

	Apparent second-order rate constant, $\times 10^4$ (liter/mole min)					
Isothiocyanate	90°	100°	110°	120°	130°	140°
Phenyl	3.49±0.00	5.88±0.05	9.81±0.11	14.4±0.4		
Benzyl	3.08±0.03	5.58±0.05	9.89±0.05	17.6±0.4		
Allyl		3.34±0.06	5.94±0.04	10.3±0.9		
Ethyl		1.44±0.03	2.21±0.01	4.27±0.04	6.85±0.04	
n-Butyl			1.51±0.01	2.95±0.04	4.48±0.05	6.91±0.07
i-Butyl			1.15±0.01	2.05±0.00	3.07±0.04	5.08±0.06
n-Hexyl			1.47±0.04	2.78±0.03	4.78±0.15	6.84±0.08
Cyclohexyl				0.99±0.02	1.73±0.03	2.74±0.07

The apparent energies of activation and log A were calculated by the Arrhenius equation, and are listed in Table IV. The reactivity of organic isothiocyanates in the reaction with

TABLE IV

The apparent energies of activation and log A in the reaction of isothiocyanates with 1-octanol in *o*-dichlorobenzene

Isothiocyanate	Reactivity at 120°	Apparent energies of activation (kcal/mole)	log A (A in liter/mole min)
Phenyl	14.6	13.5±1.2	4.65±0.73
Benzyl	17.8	16.6±1.6	6.46±0.99
Allyl	10.4	16.4±2.4	6.14±1.36
Ethyl	4.3	15.8±3.0	5.43±1.69
n-Butyl	3.0	15.6±1.5	5.13±0.85
i-Butyl	2.1	15.2±1.6	4.75±0.87
n-Hexyl	2.8	16.3±0.8	5.47±0.42
Cyclohexyl	1.0	16.5±2.4	5.20±0.66

1-octanol at 120° decreased in the order of benzyl, phenyl, allyl, ethyl, *n*-butyl, *n*-hexyl, isobutyl, and cyclohexyl isothiocyanate. Reproducible results could not be obtained for the reaction of 1-octanol with *t*-butyl isothiocyanate.

In the reaction of isothiocyanates with a large excess of OH^- ion, the second-order rate constants which were calculated by dividing the apparent first-order rate constants obtained by the concentration of OH^- ion became almost constant, and a first-order decomposition mechanism of the complex has been proposed (3):

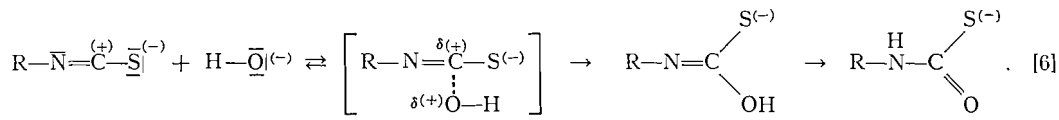

[6]

In the case of the addition reaction with a large excess of alkylamines, a similar reaction mechanism has been proposed (4):

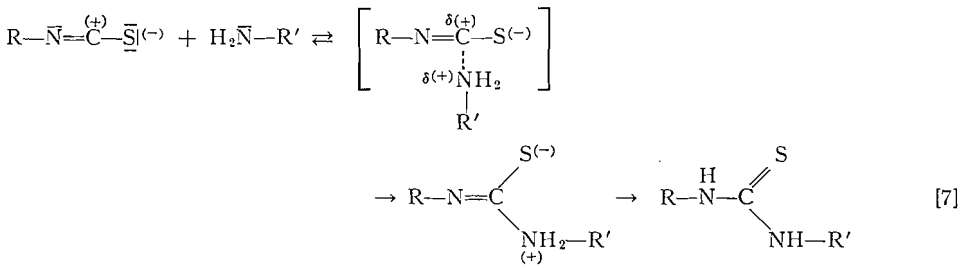

[7]

In the reaction of isothiocyanates with 1-octanol in *o*-dichlorobenzene, however, the simple second-order rate equation was not applicable. The values which were obtained as second-order rate constants did not become constant and varied according to the initial concentration of 1-octanol. Accordingly, the most probable mechanism is considered to be a bimolecular decomposition of the complex, that is, the reaction proceeds through the interaction of the complex with the 1-octanol molecule:

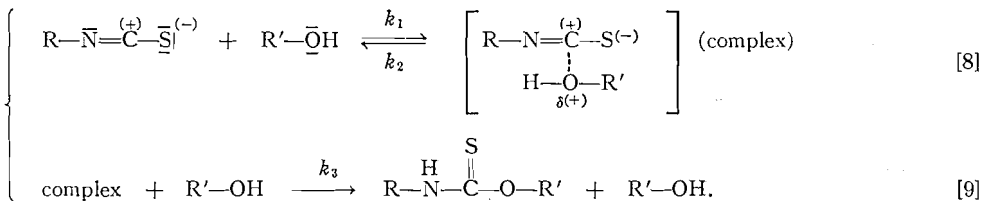

[8]

[9]

This reaction mechanism is similar to that of the reaction between organic isocyanates and alcohols (7, 8). Assuming a steady-state concentration of the complex in this kinetic scheme, the following equation was obtained:

$$\frac{d[\mathrm{RNHC(S)OR'}]}{dt} = \frac{k_1k_3[\mathrm{R{-}NCS}][\mathrm{R'{-}OH}]^2}{k_2+k_3[\mathrm{R'{-}OH}]}. \qquad [10]$$

The apparent second-order rate constants (k_{obs}) may now be related to the initial concentration of 1-octanol by the equation

$$k_{obs} = \frac{k_1k_3[\mathrm{R'{-}OH}]}{k_2+k_3[\mathrm{R'{-}OH}]}, \qquad [11]$$

$$\frac{1}{k_{obs}} = \frac{1}{k_1} + \frac{k_2}{k_1k_3[\mathrm{R'{-}OH}]}. \qquad [12]$$

If the assumed mechanism of equations [8] and [9] is consistent with the experimental results, a linear relationship between the values of $1/k_{obs}$ and $1/[\mathrm{R'{-}OH}]$ should be realized. The results of Table II are plotted in Fig. 2. As shown in Fig. 2, the linear

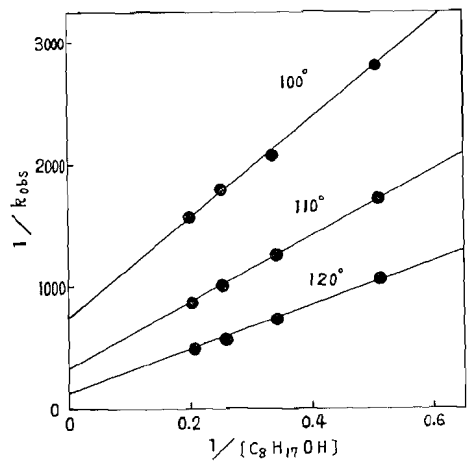

FIG. 2. Relationship between the apparent second-order rate constant and the initial concentration of 1-octanol in the reaction of benzyl isothiocyanate with 1-octanol in *o*-dichlorobenzene.

relationship is suitable, and this fact indicates that the presumed kinetic scheme and the derived kinetic equations are adequate. The individual rate constants k_1, and k_2/k_3, can be obtained as the intercept and the slope of these lines. The results are summarized in Table V. In the reaction of benzyl isothiocyanate with 1-octanol, the rate constant k_2 is larger than k_3 within the observed temperatures.

To examine the catalytic effect of tertiary amines and organometallic compounds in the reaction of isothiocyanates with alcohols, first the reaction of phenyl isothiocyanate with 1-octanol in the presence of tributylamine and then the reaction of ethyl isothiocyanate with 1-octanol in the presence of dibutyltin dilaurate or ferric acetylacetonate were investigated in *o*-dichlorobenzene at 120°.

Table V

The individual rate constants in the reaction of benzyl isothiocyanate with 1-octanol in *o*-dichlorobenzene

Reaction temp. (°C)	$k_1 \times 10^4$ (liter/mole min)	k_2/k_3
100	13.5±1.7	5.50±0.32
110	30.8±3.5	8.27±0.33
120	104±38	19.3±1.0

The catalytic action of tributylamine in the reaction of phenyl isothiocyanate with a large excess of 1-octanol in *o*-dichlorobenzene at 120° is shown in Table VI. The catalytic

TABLE VI

The tributylamine-catalyzed reaction of phenyl isothiocyanate with 1-octanol in *o*-dichlorobenzene at 120° (Initial concentration: $[C_6H_5NCS] = 0.11$ mole/liter, $[C_8H_{17}OH] = 3.9$ mole/liter)

Concn. of tributylamine (mole/liter)	Apparent second-order rate constant, $\times 10^4$ (liter/mole min)	Catalytic coefficient k_c
0.0000	14.4	—
0.0100	17.1	0.0270
0.0200	18.4	0.0200
0.0300	19.7	0.0177
0.0398	18.9	0.0113
0.0597	20.9	0.0109

coefficient is generally expressed in the following way:

$$k_{obs} = k_{0,\,obs} + k_c[\text{tributylamine}], \qquad [13]$$

where $k_{0,\,obs}$ is the apparent second-order rate constant in the absence of tributylamine and k_c is the catalytic coefficient. The values of k_c obtained are not constant, and decrease

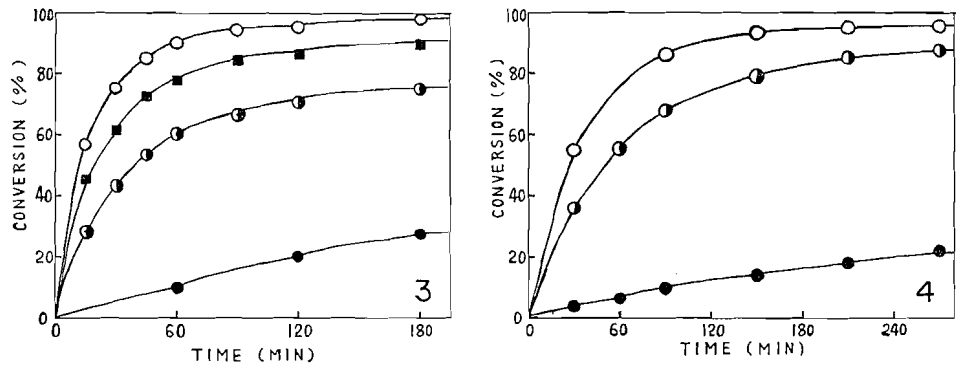

FIG. 3. Catalytic effect of dibutyltin dilaurate in the reaction of ethyl isothiocyanate with 1-octanol in *o*-dichlorobenzene at 120°. Initial concentration of ethyl isothiocyanate: 0.105 mole/liter; initial concentration of 1-octanol: 4.845 mole/liter; concentration of dibutyltin dilaurate: ● None, ◑ 0.0020, ■ 0.0040, ○ 0.0060 mole/liter.

FIG. 4. Catalytic effect of ferric acetylacetonate in the reaction of ethyl isothiocyanate with 1-octanol in *o*-dichlorobenzene at 120°. Initial concentration of ethyl isothiocyanate: 0.105 mole/liter; initial concentration of 1-octanol: 2.907 mole/liter; concentration of ferric acetylacetonate: ● None, ◑ 0.000269, ○ 0.000538 mole/liter.

as the concentration of tributylamine increases. This phenomenon may be explained by the Burkus hypothesis (9). The result shows that tributylamine had a slight catalytic effect in this reaction.

The catalytic actions of dibutyltin dilaurate and ferric acetylacetonate in the reaction of ethyl isothiocyanate with excess 1-octanol in *o*-dichlorobenzene at 120° were investigated. As shown in Figs. 3 and 4, these organometallic compounds have a strong catalytic action in this reaction; however, equation [5] was not applicable. More detailed kinetic evidence has not been obtained up to the present, and further work in this direction is in progress with a number of organometallic compounds.

REFERENCES

1. D. W. BROWNE and G. M. DYSON. J. Chem. Soc. 3285 (1931).
2. D. W. BROWNE and G. M. DYSON. J. Chem. Soc. 178 (1934).
3. R. ZAHRADNIK. Collection Czech. Chem. Commun. **24**, 3407 (1959).
4. R. ZAHRADNIK. Collection Czech. Chem. Commun. **24**, 3422 (1959).
5. M. L. MOORE and F. S. CROSSLEY. Organic syntheses. Coll. Vol. 3. John Wiley, New York. 1955. p. 599.
6. H. E. STAGG. Analyst, **71**, 557 (1946).
7. J. W. BAKER and J. B. HOLDSWORTH. J. Chem. Soc. 713 (1947).
8. J. W. BAKER and J. GAUNT. J. Chem. Soc. 9, 19, 24, 27 (1949).
9. J. BURKUS. J. Org. Chem. **26**, 779 (1961).

THE PREPARATION OF SUCROSE MONOESTERS*

R. U. LEMIEUX† AND A. G. MCINNES‡
Department of Chemistry, University of Ottawa, Ottawa, Ontario

Received July 16, 1962

ABSTRACT

The Snell procedure for the preparation of sucrose monoesters of the higher saturated fatty acids by transesterification of sucrose and methyl esters in N,N-dimethylformamide was found to yield variable results due to the use of solid potassium carbonate as catalyst and to impurities in the solvent. A kinetic study of the reaction revealed that yields of sucrose ester and rates of reaction were reproducible when conditions for homogeneous catalysis were established. The reaction followed first-order kinetics in methyl ester and sucrate ion and the rate of reaction was essentially independent of the sucrose concentration, the molecular weight of the fatty acid, and the nature of the metal sucrate used to catalyze the reaction. The activation energy for the reaction was 9.9 kcal mole^{-1}. Equilibrium constants for the principal reactions were determined, and it was established that only the thermodynamic product prevailed at any time throughout the transesterification reaction. A preparative method for the synthesis of sucrose monoesters was developed that gave yields of sucrose ester, based on the amount of methyl ester which had reacted, which were essentially quantitative. The product contained about 20% of di- and 80% of mono-ester.

INTRODUCTION

In 1954 Snell and co-workers developed a process for the preparation of fatty acid esters of sucrose (1) using the transesterification reaction, which was subsequently published in 1956 (2). The procedure was based on the reaction of sucrose with the methyl ester of a fatty acid, in N,N-dimethylformamide (DMF) solution, using solid potassium carbonate as a catalyst. The methanol formed in the reaction was removed *in vacuo* under conditions for fractional distillation. This process attracted considerable interest from industry as a means for the preparation of sucrose monoesters of the higher fatty acids for use as low-cost, non-ionic detergents (3, 4).

The elucidation of the structures of the sucrose monoesters formed and the determination of their relative amounts in the products obtained first attracted our attention to this process. However, when an attempt was made to prepare samples of sucrose monoester, by the original Snell procedure (2), for structural analysis, it soon became apparent that the product did not warrant such an investigation since it could not be prepared under fully controlled and reproducible conditions. For unknown reasons, highly variable yields were obtained and the products differed considerably in the degree of substitution, solubility, and color even when the reaction was performed under apparently identical experimental conditions (5). Although other workers have claimed more success in this respect a critical assessment of their results clearly indicates that they have been equally unsuccessful in preparing reproducibly a product in high yield (2, 6–8). Furthermore, the conclusions which the various workers have drawn (2, 6–11) from their experimental results are often in conflict, and in direct opposition to modern concepts on the mechanism of transesterification reactions. Snell and co-workers, for example, have claimed that sucrose monoester was esterified so much faster than sucrose that higher-substituted esters of sucrose accumulated in the first stage of the reaction and subsequently reacted with the excess sucrose to re-form sucrose monoesters (2). They also concluded that the concentration of sucrose monoester in the final product was

*This paper was submitted by A. G. McInnes as a portion of a thesis for the Ph.D. degree.
†Present address: Department of Chemistry, University of Alberta, Edmonton, Alberta.
‡Present address: Atlantic Regional Laboratory, National Research Council, Halifax, Nova Scotia.

dependent on the amount of solvent (DMF) in which the reaction was carried out (2), and on the concentration of water in the reaction solution (6). Moreover, their results indicated that the only effect of increasing the catalyst concentration was to increase the soap content in the product of reaction (2). Workers at the Herstein Laboratories (7, 8), on the other hand, have claimed that the sucrose monoester content was dependent on the catalyst concentration and was independent of the moisture content in the reaction solution. The latter workers also claimed that the cation of the catalyst chelates with the sucrose molecule, and that it was this chelate complex which was the effective catalyst in the reaction. They concluded that different cations produced a product with different sucrose mono- to di-ester ratio, and have suggested that this is in some way related to the ionic radius of the cation (7). For example, it was claimed that lithium produced only sucrose monoester whereas potassium produced sucrose diester also. This specificity was attributed to the fact that lithium, which has a smaller ionic radius than potassium, cannot form a chelate with two hydroxyl groups at the same time, in contrast to potassium (7). Furthermore, the sucrose diester concentration was found to increase with increasing cation–sucrose complex concentration (7, 8), at least for those catalysts with the necessary ionic radius. Herstein and his co-workers have also claimed that an equilibrium exists between sucrose, sucrose diester, and sucrose monoester in the reaction solution (7). In spite of this observation, however, they evaluated the optimal conditions for the transesterification reaction by orthogonal statistical design (7, 8), and reached the conclusion that although an equilibrium existed between sucrose, sucrose diester, and sucrose monoester, the concentration of the latter passed through a maximum with increasing sucrose concentration and then decreased with a further increase in the sucrose concentration. Komori and co-workers (9, 11) have reported that the rate of transesterification was dependent on the sucrose concentration.

In contrast to the above conclusions, mechanistic studies have established that transesterifications are reversible reactions (12) which exhibit first-order kinetics in ester and alkoxide ion (13). In view of the apparent contradictions and the important role the conditions for transesterification by the Snell procedure promise to have in carbohydrate chemistry, it was decided to conduct a careful kinetic study of the reaction and to determine the equilibrium constants for the principal reactions.

EXPERIMENTAL AND RESULTS

Materials

In all experiments the DMF was distilled from phosphorus pentoxide, and only the fraction boiling at 153–154° at atmospheric pressure was used. The sucrose, $[\alpha]_D$ +66.50 (*c*, 22; water), was stored over phosphorus pentoxide under reduced pressure. The methanol was dried by distillation from magnesium methoxide. The methyl myristate, methyl palmitate, and *n*-octadecane each had a purity greater than 99.5 mole% when analyzed by gas–liquid partition chromatography (GLPC). The methyl stearate contained 9.0 mole% of methyl myristate, methyl palmitate, and an unidentified ester having a retention volume corresponding to that expected for a C_{17} fatty acid methyl ester. Since these methyl esters contained no free fatty acid they were used without further purification. *n*-Octadecane was soluble to the extent of 4.5 g/300 ml of reaction solution at 80°. All other solvents were reagent grade.

Methyl myristate was used in all reactions unless otherwise specified.

Rate Measurements

All rates of reaction were determined by following the decrease in concentration of the methyl ester of a fatty acid by GLPC (14) using *n*-octadecane as an internal standard. The apparatus used for the analyses was a "Pye Argon Chromatograph", and some of the pertinent characteristics are listed below:

Column size, 4 ft, 5-mm I.D.	Resolution, up to 1000 theoretical plates/ft
Detector, ionization (80 μc radium D)	Limit of detection, 0.01 γ
Carrier gas, argon	Column packing, Celite 545:Apiezon 17 (9:1, w/w)
Sample size, 3–6 γ	Column temperature, 200° C

The calibration of apparatus is shown in Fig. 1 and the retention volumes at 200° of the methyl esters of myristic, palmitic, and stearic acids, relative to that (1.0) of *n*-octadecane, were 0.57, 1.38, and 3.22, respectively.

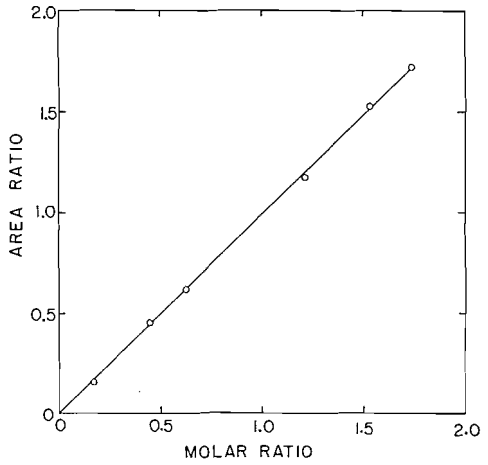

FIG. 1. The plot of the ratio of the areas obtained for standard mixtures of methyl-myristate and *n*-octadecane when analyzed by gas–liquid partition chromatography against the known molar ratio.

Standard Transesterification Reaction Conditions

The transesterification apparatus is shown in Fig. 2.

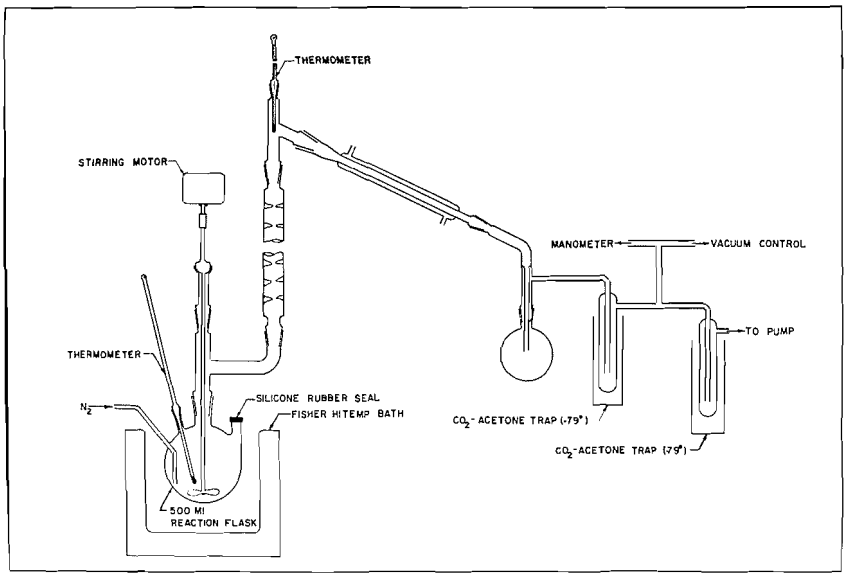

FIG. 2. The transesterification apparatus.

An attempt was made to remove the last traces of water from the reaction solution by conditioning the reactants in the following manner. Sucrose, 60 mmole, was dissolved in 300 ml of anhydrous DMF and conditioned at 80±0.5° at 75 mm pressure for 30 minutes. The oil-bath temperature was 89±1°, and the reaction solution was stirred mechanically and had a fine stream of dry nitrogen passing through it. A 50-ml volume of petroleum ether containing 20 mmole of methyl ester and 12.75 mmole of *n*-octadecane was then added to the DMF solution, and the petroleum ether was removed rapidly under reduced pressure. After 30 minutes the reaction solution temperature was again constant at 80° at 75 mm pressure. A

0.6-ml aliquot of the DMF solution was then taken and analyzed by GLPC (see below). The catalyst was then added to the reaction solution as a solid or as a methanolic solution at atmospheric or 75 mm pressure, respectively. In the former case a reaction temperature of 80° at 75 mm pressure was established as quickly as possible, and in the latter case the catalyst solution was injected into the reaction solution with a hypodermic syringe through the silicone rubber seal on the reaction vessel (see Fig. 2) while the apparatus was under reduced pressure. During the course of the transesterification reaction the temperature at the top of the Vigreaux column remained constant at 29±1°. The reaction solution had a total volume of 320 ml.

The progress of the reaction was followed by withdrawing at intervals of time 0.6-ml aliquots of the reaction solution, by means of a hypodermic syringe fitted with a 3-inch needle, through the silicone rubber seal (see Fig. 2) without disturbing the vacuum in the apparatus. These solutions were diluted with 0.6 ml of a 5% sodium chloride solution and the methyl ester and *n*-octadecane were extracted with 0.5-ml amounts of a 3:1 petroleum ether/ether solution. A 0.1-μl aliquot of the latter was then analyzed by GLPC. When standard mixtures of methyl myristate and *n*-octadecane in a 0.2 *M* solution of sucrose in DMF were analyzed in this manner the results were identical with those obtained using petroleum ether solutions of the compounds for calibration (see Fig. 1).

The yields of sucrose ester at the end of the reaction period were obtained, in duplicate, on 25-ml aliquots of the reaction mixture. Each aliquot was first cooled to 20° by the addition of solid carbon dioxide, and the *n*-octadecane and unreacted methyl ester were removed quantitatively by extracting the DMF solution with three 50-ml aliquots of petroleum ether. The DMF solution was then taken to dryness at 70° under reduced pressure and the residue was dissolved in 25 ml of *n*-butanol. The latter was washed with two 25-ml volumes of 5% sodium chloride solution to remove the catalyst (in the form of a metal carbonate) and unreacted sucrose, and the combined aqueous phase was re-extracted with 15 ml of *n*-butanol. Any sodium chloride in the combined *n*-butanol phase was precipitated by the addition of 40 ml of chloroform. After drying of the chloroform/*n*-butanol solution with 10 g of anhydrous sodium sulphate overnight the salts were removed by filtration, the latter being washed with a further 40 ml chloroform. The filtrate was taken to dryness under reduced pressure. Ethanol was then added and the mixture was evaporated in order to remove the last traces of *n*-butanol and DMF. The white residue of sucrose ester was dried under reduced pressure over phosphorus pentoxide.

The percentage yields of sucrose ester were based on the complete conversion of 20 mmole of methyl ester to sucrose monomyristate (denoted P) or on the amount of methyl myristate which had reacted (denoted P_I).

Routine Tests for the Presence of Impurities in the Sucrose Ester

The sucrose ester, 50 mg, was dissolved in 1 ml chloroform at room temperature. In the absence of sucrose and sodium chloride a clear solution free of insoluble residue was obtained. A 0.1-μl aliquot of the above chloroform solution was analyzed by GLPC for methyl ester and *n*-octadecane. An infrared spectrum of the above chloroform solution was taken. The presence of DMF or the anion of a fatty acid could be detected since they have characteristic absorptions, for the C=O stretching vibration, at approximately 1680 and 1560 cm^{-1}, respectively. An aqueous solution of the sucrose ester was also tested for chloride ion with silver nitrate.

All the samples of sucrose ester prepared using the above standard procedure gave negative results for these tests.

The Transesterification Reaction Using Solid Potassium Carbonate

The standard transesterification reaction conditions were used, and 4 meq of solid potassium carbonate were added to catalyze the reaction. Furthermore, the reaction was carried out (*a*) without mechanical stirring or nitrogen passing through the solution, (*b*) without mechanical stirring and with nitrogen passing through the solution, (*c*) with mechanical stirring and nitrogen passing through the solution, and (*d*) with the same reaction conditions as (*c*) except that the potassium carbonate had been impregnated on 1 g of Celite by admixing a 1-ml aliquot of an aqueous solution of potassium carbonate with 1 g of acid-washed Celite and drying the mixture at 180° for 48 hours before use.

Results for single experiments satisfying the above experimental conditions are given in Fig. 3. Reaction solutions (*a*), (*b*), (*c*), and (*d*) gave values of 41.2, 70.7, 87.8, and 79% for P after 7, 24, 7, and 4 hours, respectively. The corresponding values for P_I were 71.1, 70.5, 87.8, and 82.8%. Considerable variations in the rates of reaction and yields of sucrose ester were obtained when attempts were made to reproduce these results in duplicate experiments. Moreover, it was observed that all the solid potassium carbonate did not dissolve in any of the experiments. It was apparent that variable amounts went into solution.

The Effect of Water on the Transesterification Reaction at 80° using Solid Potassium Carbonate as Catalyst

The reaction conditions in (*c*) above were used.

The initial concentration of water in the reaction solutions were 0.01, 0.05, 0.25, and 1.25%, which corresponded to the addition of 0.42, 2.10, 10.5, and 52.5 mmole of water per meq of solid potassium carbonate. The water was added to the reaction solution after the usual 1-hour conditioning period, and

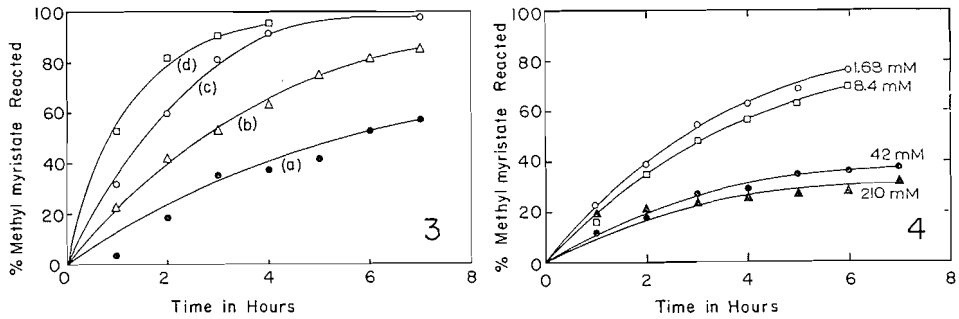

FIG. 3. Rates of transesterification at 80° using 4 meq of solid potassium carbonate as the catalyst. The reaction solutions were stirred mechanically in (*c*) and (*d*). A stream of nitrogen was passed through the solution in (*b*), (*c*), and (*d*). The catalyst in (*d*) was impregnated on Celite.

FIG. 4. The effect of adding 1.68, 8.4, 42, and 210 mmole of water on the rate of transesterification at 80°, using 4 meq of solid potassium carbonate as the catalyst. The reaction solutions were stirred mechanically, and scrubbed with a stream of nitrogen.

at the same time as the catalyst. The potassium carbonate did not dissolve completely in any of these experiments.

The effect of water on the rate of reaction is shown in Fig. 4. Yields of sucrose myristate of 82.2, 81.5, 31.0, and 32.3% for P, and 93.8, 87.7, 66.5, and 93.5% for P_I were obtained for the experiments containing 0.42, 2.10, 10.5, and 52.5 mmole of water, respectively.

Transesterification Reactions using Sodium Hydride and Saturated Solutions of Potassium Carbonate

The transesterification reaction was carried out in the usual manner using DMF or DMF plus sucrose solutions saturated with potassium carbonate. These solutions were prepared by heating 300 ml of DMF, or 300 ml of DMF containing 60 mmole of sucrose, with 4 meq of solid potassium carbonate at 80° for 18 and 6 hours, respectively. After removal of any solid material, by filtration, under anhydrous conditions, the filtrate was used for the transesterification reaction. Titration of aliquots of the DMF solution containing only potassium carbonate revealed that it was 0.0014 N in potassium ion. The latter solution gave only 9.9% reaction in 4 hours, and gave sucrose myristate values of 9.5 and 96.2% for P and P_I, respectively. The DMF plus sucrose solution of potassium carbonate, on the other hand, gave 56.0% reaction in 6 hours, and gave yields of sucrose myristate of 48.4 and 86.3% for P and P_I, respectively.

Another transesterification reaction carried out using 300 ml DMF, 60 mmole sucrose, 20 mmole methyl myristate, and 4 meq sodium hydride at 80°, at 190 mm pressure, on a rotary evaporator, gave 52% reaction in 6 hours, and sucrose myristate yields of 40.8 and 78.5% for P and P_I, respectively.

The Transesterification Reaction under Conditions for Homogeneous Catalysis

The yields of sucrose myristate as well as the rates of reaction are given in Table I.

All of the reactions reported in Table I were carried out in homogeneous solution at 80° under identical conditions of pressure and mechanical stirring, and with nitrogen bubbling through the reaction solution. In order to obtain homogeneous reaction conditions the catalyst (4 meq) was added to the reaction solution as a dilute solution in 5 ml anhydrous methanol or as a saturated methanolic or aqueous solution. Potassium carbonate, potassium methoxide, lithium methoxide, sodium methoxide, and potassium hydroxide were all used to catalyze the reaction.

The Effect of Sucrose Concentration on the Rate of Reaction at 80°

The rates for the standard transesterification reaction together with the yields of sucrose myristate are given for three concentrations of sucrose, namely 60, 40, and 20 mmole, respectively, in Table II. A saturated methanolic solution of potassium methoxide containing 4 meq of the latter in 0.68 ml solution was used as catalyst.

The Effect of Fatty Acid Chain Length on the Rate of Reaction at 80°

Potassium methoxide, 4 meq, in 5 ml anhydrous methanol was used to catalyze the reactions. The data for the three methyl esters are given in Table III. The pseudo first-order rate constants for the standard transesterification reaction using methyl myristate, methyl palmitate, and methyl stearate were found to be 3.33, 3.17, and 2.96×10^{-4} sec^{-1}, respectively.

The Effect of Gaseous Carbon Dioxide on the Rate of Transesterification at 80°

The standard transesterification reaction conditions were used except that gaseous carbon dioxide was passed through the solution for 150 minutes, and then replaced by a stream of nitrogen for a further 130

TABLE I

The rates of reaction at 80° using 4 meq of catalyst

Time (min)	Experimental number:* 1	2	3	4	5	6	7	8	9	10	11
	Percentage of methyl myristate reacted										
30	37.0	41.7	31.9	35.8	37.9	37.9	31.4	39.8	58.5	34.5	27.7
60	61.2	64.8	55.1	56.2	58.0	62.2	59.2	58.3	78.9	53.8	50.4
90	79.0	78.0	77.2	76.0	74.8	77.8	74.2	67.2	87.1	63.5	66.7
120	85.3	85.7	87.8	84.3	85.2	89.1	82.5	72.8	94.0	72.9	73.6
150	92.9	92.0	92.6	91.4	90.7	94.9	85.8	76.9	96.9	79.6	79.1
P	83.8	84.0	84.5	82.1	—	—	74.4	69.5	81.7	72.5	71.2
P_I	90.3	91.3	91.2	89.9	—	—	86.7	90.4	84.5	91.0	90.0

*Four milliequivalents of potassium carbonate, potassium methoxide, lithium methoxide, sodium methoxide, and potassium hydroxide in 5 ml anhydrous methanol were used in experiments 1 and 2, 3 and 4, 5, 6, and 7, respectively. Saturated methanolic solutions of potassium hydroxide (4 meq in 0.56 ml methanolic solution) and potassium methoxide (4 meq in 0.68 ml methanolic solution) were used in experiments 8 and 9, respectively. Saturated aqueous solutions of potassium hydroxide (4 meq in 0.26 ml aqueous solution) and potassium carbonate (4 meq in 0.329 ml of aqueous solution) were used in experiments 10 and 11, respectively.

TABLE II

The effect of sucrose concentration on the rate of reaction at 80°*

Time (min)	Percentage of methyl myristate reacted: 60 mmole sucrose, expt. 9	40 mmole sucrose, expt. 12	20 mmole† sucrose, expt. 13
30	58.5	55.0	38.5
60	78.9	75.1	57.6
90	87.1	83.5	76.8
120	94.0	91.4	83.9
150	96.9	95.5	84.8
P	81.7	84.5	68.7
P_I	84.5	89.0	76.5

*A saturated solution of potassium methoxide in methanol (4 meq in 0.68 ml methanolic solution) was used as catalyst.
†Substantial amounts of catalyst precipitated from solution and did not redissolve completely during the course of the reaction.

TABLE III

The effect of fatty acid chain length on the rate of reaction at 80°

Time (min)	Percentage of methyl ester reacted: Methyl myristate, expt. 14*	Methyl palmitate, expt. 15*	Methyl stearate, expt. 16*
30	43.3	43.8	42.4
60	67.5	68.6	63.1
90	84.9	81.7	79.6
120	91.6	89.8	88.7
150	95.5	92.4	—

*Four milliequivalents of potassium methoxide in 5 ml methanolic solution were used to form the catalyst.

minutes. Potassium carbonate, 4 meq, in 5 ml of anhydrous methanol was used as catalyst under conditions for homogeneous catalysis. After 150 minutes the sucrose myristate yield was 19.3 and 89.0% for P and P_I, respectively, whereas after 280 minutes the corresponding values for P and P_I were 84.7 and 88.6%, respectively.

The depression of the rate of reaction by gaseous carbon dioxide is shown graphically in Fig. 5.

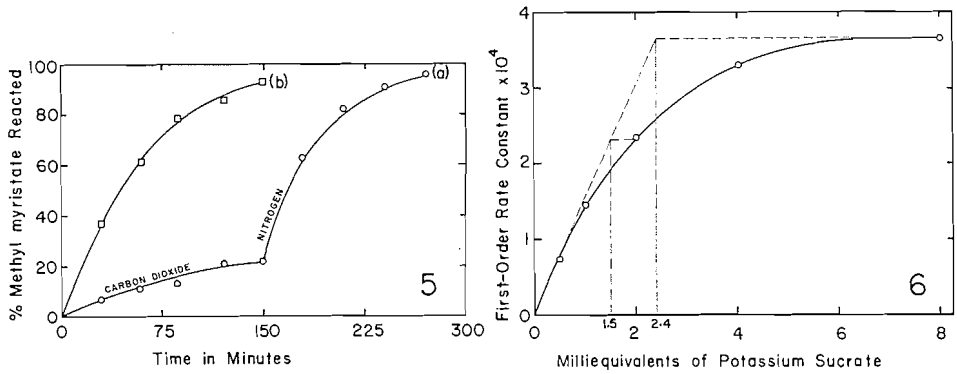

FIG. 5. Rates of transesterification reaction at 80° using 4 meq of potassium carbonate under conditions of homogeneous catalysis. In (*a*) streams of carbon dioxide and nitrogen were passed successively through the solution, whereas in (*b*) only nitrogen was used.

FIG. 6. The plot of the pseudo first-order rate constants for the standard transesterification reaction at 80° against the potassium sucrate concentration in 320 ml of reaction solution.

The Effect of Catalyst Concentration on the Rate of Transesterification at 80°

The standard transesterification reaction conditions were used except that 0.5, 1.0, 2.0, 4.0, and 8.0 meq of potassium methoxide in 5 ml of anhydrous methanol were used as catalyst, respectively. A precipitate of potassium sucrate was present during the entire reaction when more than 4 meq of potassium ion were used.

The plot of the pseudo first-order rate constants for the reactions at the different catalyst concentrations versus the catalyst concentrations is given in Fig. 6.

The Effect of Temperature on the Rate of Transesterification

The standard transesterification reaction was carried out at 80° (at 75 mm pressure) and 97° (at 140 mm pressure), respectively. Potassium methoxide, 2 meq, in 5 ml methanol was used as a source of catalyst. The pseudo first-order rate constants calculated for the data obtained at 80° and 97° and plotted in Fig. 7 were 2.36×10^{-4} and 4.51×10^{-4} sec^{-1}, respectively. Calculation by means of the Arrhenius equation (15) gave a value of 9.9 kcal $mole^{-1}$ for the energy of activation.

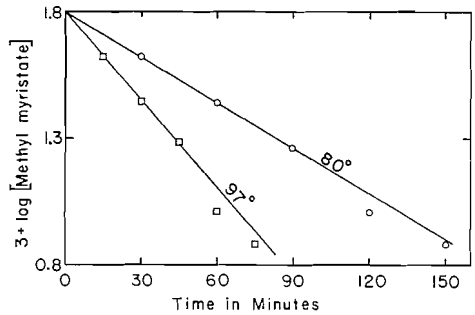

FIG. 7. The plot of the logarithm of the methyl myristate concentration against time for the standard transesterification reaction, at 80° and 97°, using 2 meq of potassium sucrate as catalyst.

Isolation of Sucrose Mono- and Di-myristate

Three standard transesterification reactions were carried out at 80° in the absence of *n*-octadecane and the sucrose myristate from the experiments combined. Four milliequivalents of potassium methoxide in 0.68 ml of anhydrous methanolic solution was used as catalyst. The products of the reaction were isolated by taking each reaction solution to dryness, at 70°, on a rotary evaporator, at the end of the reaction period of 150 minutes. The residue was then partitioned between *n*-butanol and 5% sodium chloride and the crude sucrose ester isolated as described above. The combined crude product weighed 26.57 g. The latter was then chromatographed on 250 g silicic acid (Mallinckrodt) using graded elution with methanol/

chloroform solutions. As the chromatogram developed the constituents were visible against a translucent background. The separation was also followed by taking infrared spectra of aliquots of the eluant. In this way it was possible to isolate three fractions containing methyl myristate, sucrose dimyristate, and sucrose monomyristate, as shown in Table IV.

TABLE IV

Chromatographic separation of sucrose myristates on silicic acid

Fraction	Solvent	Volume of solvent (ml)	Weight of fraction (g)	Compound*
I	Chloroform	2000	0.80	Methyl myristate
II	10% methanol/chloroform	250	7.95	Dimyristate
III	10% methanol/chloroform	1400	17.60	Sucrose monomyristate

*The residue from fraction I was actually collected in the first 700 ml of eluant and its infrared spectrum was identical with that of an authentic sample of methyl myristate.

The sucrose monomyristate (17.6 g) was precipitated from 100 ml acetone at −5° to yield 15.6 g of pure sucrose monomyristate as a white amorphous solid, m.p. 180–186°; $[\alpha]_D$ +36.7° (*c*, 4.8% in chloroform); saponification equivalent, 549 (theory, 552). Anal. calc. for $C_{28}H_{48}O_{12}$: C, 56.50%; H, 8.70%. Found: C, 56.36%; H, 8.63%.

The sucrose dimyristate (7.95 g) was precipitated first from methanol and then from acetone to yield 6.05 g sucrose dimyristate as a white amorphous solid, m.p. 139–145°; $[\alpha]_D$ +29.7° (*c*, 5.2% in chloroform); saponification equivalent, 376 (theory, 381). Anal. calc. for $C_{40}H_{74}O_{13}$: C, 63.0%; H, 9.77%. Found: C, 63.39%; H, 9.91%.

The infrared spectra for sucrose mono- and di-myristate were consistent with those expected for a mono- and di-fatty acid ester of a polyhydric alcohol. The two esters showed considerable differences in the relative intensities of the OH stretching and C=O stretching vibrations at 3500 and 1725 cm^{-1}, respectively, which could be used as a means of identification.

Determination of the Equilibrium Constant K_1

The equilibrium constant K_1 for the reaction

$$\text{sucrose} + \text{sucrose dimyristate} \rightleftarrows 2 \text{ sucrose monomyristate}$$

was estimated as follows at two different concentrations of sucrose.

Sucrose, 1 mmole, was dissolved in 15 ml anhydrous DMF at 80°, and 0.2 meq of potassium methoxide in 0.2 ml methanolic solution was added. The potassium sucrate which precipitated was redissolved by the addition of 5 ml anhydrous methanol and the solution was taken to dryness under reduced pressure. The residue was dried, under reduced pressure over phosphorus pentoxide, for 2 hours. Pure sucrose monomyristate, 1 mmole, was then added to the residue of sucrose and potassium sucrate, and the mixture was dissolved in 15 ml anhydrous DMF. The homogeneous reaction solution was at a temperature of 80° for 90 minutes. Care was taken at all times to exclude moisture from the reaction solution. At the end of t is period the catalyst was neutralized by the addition of 1 ml of a DMF solution containing 0.2 meq of potassium hydrogen phthalate. After taking the solution to dryness under reduced pressure, the sucrose myristates were isolated in the manner described above. Chromatography of the sucrose myristates (466.9 mg) on 10 g silicic acid using graded elution with methanol/chloroform solutions yielded 336.9 mg (0.61 mmole) of sucrose monomyristate, and 124.7 mg of sucrose "dimyristate". The separation was followed by comparing the infrared spectra of the sucrose ester in 5-ml fractions of the eluant from the chromatographic column with the infrared spectra of pure sucrose mono- and di-myristate. Seventeen fractions of 5% methanol/chloroform and 15 fractions of 10% methanol/chloroform were collected. The first 20 fractions contained sucrose dimyristate and the last 10 fractions contained sucrose monomyristate. The two intermediate fractions contained no sucrose ester, indicating that a complete separation of sucrose monomyristate from sucrose di- and higher myristates was achieved. On the assumption that only mono- and di-esters were formed, the yield of ester was 94%.

A second experiment, carried out under identical experimental conditions except that only 0.5 mmole of sucrose was used initially, yielded 434.0 mg of sucrose myristate. Chromatography of a sample of the latter (420.0 mg) on 10 g silicic acid, as described above, yielded 152.0 mg (0.199 mmole) of sucrose dimyristate and 267.0 mg (0.483 mmole) of sucrose monomyristate. The relative intensities of the hydroxyl and carbonyl stretching vibrations clearly indicated the product to contain some tri- and higher esters. On the assumption that only mono- and di-esters were formed, the yield of ester was 88%.

An estimate of the equilibrium constant, K_1, for the reaction

$$\text{sucrose} + \text{sucrose dimyristate} \rightleftarrows 2 \text{ sucrose monomyristate}$$

can be made using the above results and the assumption that only mono- and di-esters were formed. On this basis, the yields of the esters are corrected to 100% in order to use the following expression to calculate the equilibrium constant:

$$K_1 = [\text{sucrose monomyristate}]^2/[\text{sucrose}][\text{sucrose dimyristate}]$$
$$= 4M^2/(2Y-Z-M)(Z-M), \quad [1]$$

where M = moles of sucrose monomyristate at equilibrium, Y = total moles of sucrose in the system, and Z = total myristoyl groups in the system.

In the first experiment, $M = 0.61\times100/94 = 0.65$, $Y = 2$, and $Z = 1$; therefore $K_1 = 2.0$. In the second experiment, $M = 0.483\times100/88 = 0.55$, $Y = 1.5$, and $Z = 1$; therefore, $K_1 = 1.8$.

In all subsequent calculations a value of $K_1 = 2$ was assumed, since the error, introduced by ignoring the presence of higher-substituted sucrose myristates, was less for this value.

The Rate of Equilibration of C^{14}-Labelled Sucrose with Sucrose Mono- and Di-myristate

Uniformly C^{14}-labelled sucrose, 0.495 mmole, was equilibrated with 0.466 mmole of pure sucrose monomyristate, at 80°, in anhydrous DMF using 0.1 meq of potassium methoxide as catalyst. The reaction solution had a total volume of 5.5 ml and the procedure for preparation of the solutions was identical with that described above for the solutions used to determine the equilibrium constant K_1. Aliquots, 1 ml, of the reaction solution were taken at intervals of 10, 30, 45, and 65 minutes and the solvent removed rapidly (3 minutes) under reduced pressure. The residue was extracted with three 2-ml aliquots of chloroform and the combined chloroform extract was transferred quantitatively to a small chromatographic column containing 1 g silicic acid in chloroform. Elution with 25 ml 10% methanol/chloroform followed by removal of the solvent, under reduced pressure, yielded C^{14}-labelled sucrose myristates uncontaminated with C^{14}-labelled sucrose. The chromatographic procedure for isolating the C^{14}-labelled sucrose myristates was established by taking synthetic mixtures of sucrose monomyristate and sucrose di-myristate with C^{14}-labelled sucrose in anhydrous DMF, but in the absence of potassium sucrate, and recovering the corresponding sucrose ester in quantitative yield, and uncontaminated with C^{14}-labelled sucrose.

Another equilibration experiment using 0.475 mmole of sucrose dimyristate and 0.505 mmole sucrose in the presence of 0.1 meq of potassium sucrate was carried out under identical experimental conditions.

The specific activities of the C^{14}-labelled sucrose and sucrose myristates were determined by converting the compounds to barium carbonate by the apparatus and method of Calvin (16) except that a 0.2 M solution of barium hydroxide was used instead of sodium hydroxide. All samples were counted at infinite thickness, using a "Tracerlab (SC-50B) Automatic Flow Counter", and required 123.5 mg of barium carbonate for a planchet having an area of 4.94 cm^2. Under the experimental conditions used it was found that mock combustions gave a negligible blank of less than 0.3 mg of barium carbonate. All specific activities were calculated from the time taken for 10^4 disintegrations. However, since the composition of the sucrose myristates was not determined, the specific activities were calculated as the number of counts per minute per milligram of barium carbonate (c.p.m./mg $BaCO_3$). The C^{14}-labelled sucrose was found to have a specific activity of 8.475 c.p.m./mg $BaCO_3$.

The theoretical specific activities of the sucrose myristates, isolated after equilibration, were calculated in the following manner. The concentrations of sucrose monomyristate (M) and sucrose dimyristate were calculated by substituting the values for Y, Z, and K_1 into equation [1]. For example, these values were 0.961, 0.466, and 2.0, respectively, for the experiment using 0.495 mmole of C^{14}-labelled sucrose and 0.466 mmole of sucrose monomyristate. The calculated equilibrium concentrations of sucrose mono- and di-myristate were found to be 0.39 and 0.038 mmole, respectively. The theoretical specific activity was then calculated from the equation

$$A = 12fss^*/(d+m), \quad [2]$$

where A was the theoretical specific activity; s^* was the specific activity of the original C^{14}-labelled sucrose; s was the total moles of sucrose in the sucrose mono- and di-myristate; f was the fraction of the total moles of sucrose in the original reaction solution, whether present as sucrose myristate or free sucrose, which was C^{14}-labelled; d was the moles of barium carbonate obtained on combustion of the sucrose dimyristate; and m was the moles of barium carbonate obtained on combustion of the sucrose monomyristate.

The values of d, m, f, s, s^* in the above experiment were 1.52 mmole, 10.14 mmole, 0.5236, 0.428 mmole, and 8475, respectively. Substitution of these values into equation [2] gave a value for the theoretical specific activity, A, of 1950 c.p.m./mg $BaCO_3$ assuming random distribution of the sucrose molecules in the sucrose myristate.

A similar calculation for the experiment using 0.505 mmole of C^{14}-labelled sucrose and 0.475 mmole of sucrose dimyristate gave values for d, m, f, s, and s^* of 11.0 mmole, 10.40 mmole, 0.515, 0.675 mmole, and 8475, respectively, and a value of 1650 c.p.m./mg $BaCO_3$ for the theoretical specific activity A. The sucrose mono- and di-myristate concentrations at equilibrium were calculated to be 0.4 and 0.275 mmole, respectively.

The theoretical weight yields of the C^{14}-labelled sucrose myristates in 1 ml of the reaction solutions were calculated, assuming complete equilibration of the C^{14}-labelled sucrose and sucrose ester, from the

equilibrium concentrations of C^{14}-labelled sucrose mono- and di-myristate. The calculated yields were 44.4 and 78.1 mg/ml as compared with the highest experimental yields after 65 minutes' reaction of 38.3 and 72.2 mg/ml, respectively (see Table V).

The results of the equilibration studies are given in Table V.

TABLE V

Equilibration of C^{14}-labelled sucrose with sucrose monomyristate and sucrose dimyristate at 80°

	Sucrose monomyristate*		Sucrose dimyristate†	
Reaction time (min)	Yield of sucrose myristates (mg)	Specific activity of sucrose myristates (c.p.m./mg $BaCO_3$)	Yield of sucrose myristates (mg)	Specific activity of sucrose myristates (c.p.m./mg $BaCO_3$)
10	37.1	1216	71.7	1337
30	37.5	1404	70.7	1418
45	38.3	1432	70.3	1437
65	38.3	1471	72.2	1442
Theoretical specific activity		1950		1650

*Reaction carried out using sucrose monomyristate and C^{14}-labelled sucrose as reactants.
†Reaction carried out using sucrose dimyristate and C^{14}-labelled sucrose as reactants.

The Effect of Methanol Concentration on the Extent of Reaction at 80°

A standard transesterification reaction was carried out at 80° using 0.68 ml of a saturated methanolic solution containing 4 meq of potassium methoxide as catalyst. Two aliquots of the reaction mixture were taken at intervals and the percentage of methyl myristate which had reacted in one aliquot (0.6 ml) was determined by GLPC using *n*-octadecane as an internal standard. The other aliquot (2.0 ml) was transferred to a small, stoppered test tube (total volume 2.2 ml) and allowed to equilibrate at 80°. At the end of the equilibration period the percentage of methyl myristate which had reacted was determined once more. Care was taken at all times to exclude moisture from the reaction solutions. The results are given in Table VI.

TABLE VI

Effect of methanol concentration on the extent of reaction at 80°

Sample No.	1	2	3	4	5	6	7
Time (min)*	5	10	20	40	80	120	150
% methyl myristate reacted	11.0	24.7	44.2	65.8	84.2	90.2	94.5
Time (min) for the reaction to reach equilibrium	145	140	130	110	70	30	
% methyl myristate reacted	55.4	62.2	69.8	78.1	90.0	94.5	

*Samples were withdrawn from the reaction mixture at this time both for analysis and for storage at 80° in a closed system to achieve equilibrium.

Determination of the Equilibrium Constant K_2

The equilibrium constant K_2 for the reaction

$$\text{sucrose} + \text{methyl myristate} \rightleftarrows \text{sucrose myristates} + \text{methanol}$$

was determined by approaching the equilibrium from both sides of the reaction.

A transesterification reaction solution containing 3.18 mmoles of sucrose, 1.06 mmole of methyl myristate, 0.676 mmole of *n*-octadecane, 1 mmole of methanol, and 0.116 mmole of potassium sucrate in 17 ml of anhydrous DMF solution was brought to equilibrium at 80° in a 17.2-ml test tube fitted with a rubber serum cap. The rate of equilibration was determined by taking, at intervals, through the serum cap, with a calibrated microsyringe, 0.1-ml aliquots of the reaction solution and analyzing for methyl myristate by GLPC using the *n*-octadecane as an internal standard. It was assumed that the equilibrium condition had been reached when there was no further decrease in the concentration of methyl myristate. At the end of the equilibration period 10 mmole of methanol was added to the reaction solution and the solution analyzed for methyl myristate once more after an interval of 30 minutes. Since the concentration of methyl ester showed a significant increase this established that the catalyst was not destroyed during the equilibration period. It should be noted that care was taken to exclude moisture at all times from the reaction solution. The rate at which equilibrium was reached is shown in Fig. 8.

In another experiment, 1 mmole of sucrose monomyristate, 0.638 mmole of *n*-octadecane, 1 mmole of methanol, and 0.116 mmole of potassium sucrate were equilibrated at 80° in 15 ml of DMF solution contained in 15.1-ml test tube. The rate of equilibration was followed as described above, and is shown graphically in Fig. 8.

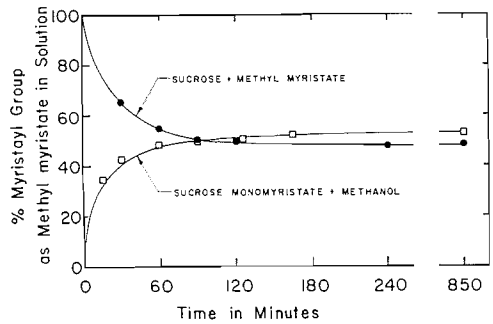

FIG. 8. The rate of equilibration of sucrose and methyl myristate with sucrose monomyristate and methanol in DMF solution at 80°. For the curve denoted by ● the reaction solution was 18.75, 6.25, 6.25, and 0.7×10^{-2} M in sucrose, methyl myristate, methanol, and alkoxide ion, respectively, whereas for the curve denoted by □ the solution was 6.25, 6.25, and 0.7×10^{-2} M in sucrose monomyristate, methanol, and alkoxide ion, respectively.

The data for the first experiment in Fig. 8 shows that 51.8% (0.549 mmole) of the methyl myristate had reacted at equilibrium to form sucrose myristates. If it was assumed that only sucrose mono- and di-myristate were formed in the reaction the equilibrium concentration of the former (0.468 mmole) could be calculated by substituting values for Y (3.18 mmole), Z (0.549 mmole), and $K_1 = 2$ into equation [1]. Setting R and X as the equilibrium and initial molar amounts of methanol and myristoyl group in the reaction solution, respectively, the molar amounts of the reactants and products in the reaction at equilibrium are, sucrose monomyristate = M, sucrose dimyristate = $(Z-M)/2$, methanol = R, sucrose = $(2Y-Z-M)/2$, and methyl myristate = $X-Z$. The other variables (Y, Z, and M) were defined previously in connection with equation [1]. The equilibrium constant, K_2, can be calculated from the expression

$$K_2 = \text{[sucrose myristates][methanol]/[sucrose][methyl myristate]}$$
$$= R(M+Z)/(2Y-Z-M)(X-Z).$$

A value of 0.577 for K_2 is obtained on substituting values (in mmole) for Y (3.18), X (1.06), M (0.468), R (1.549), and Z (0.549).

In the same way, the values (in mmole) of Y (1), X (1), M (0.31), R (0.472), and Z (0.472) which were obtained in a second experiment gave a value of 0.576 for K_2. In this experiment 52.8% (0.528 mmole) of the myristoyl group was converted to methyl myristate (see Fig. 8). Consequently, the methanol concentration (R) at equilibrium was 0.472 mmole, and 47.2% of methyl myristate had reacted to form sucrose myristate (see Fig. 8).

A solution of 60 mmole sucrose, 20 mmole methyl myristate, and 12.75 mmole *n*-octadecane in 300 ml DMF was maintained at 80° and 75 mm pressure, for 6 hours, with nitrogen passing through the solution. No catalyst was added to the reaction mixture. Analysis of the reaction solution by GLPC at 30-minute intervals revealed that the methyl myristate concentration remained constant over the entire reaction period.

The Preparation of Sucrose Myristates on a Preparative Scale

As a consequence of the kinetic studies of the reaction the following preparative procedure was developed.

Sucrose (60 mmole) was dissolved in anhydrous DMF at 80° and 65 mm pressure with vigorous and continuous stirring, and with a stream of nitrogen passing through the solution. After about 15 minutes the sucrose was completely dissolved and the solvent refluxed to a point in the Vigreaux column about 2 inches from the neck of the flask. Sodium methoxide solution (4 ml containing 4 meq) was added below the surface of the solution using a hypodermic syringe, in the usual manner. The evolution of methanol was rapid but caused no difficulties. After equilibrium was re-established, the oil-bath temperature was raised to 100°, whereupon the solution achieved a temperature of 80° and refluxed about half way up the Vigreaux column. The still head temperature was about 50°. The system was kept under these conditions for a further 15 minutes and then the methyl myristate (20 mmole) was added using a hypodermic syringe. The solution was then maintained at 80° for 150 minutes. During this reaction period approximately 50 ml of the DMF distilled over slowly.

At the end of the reaction period, glacial acetic acid (0.5 ml) was added to the stirred reaction solution, at atmospheric pressure, to stop the reaction. The solution was then taken to dryness at 70°, under reduced pressure, in 30 minutes, and the sucrose myristate isolated by partitioning the residue between *n*-butanol and 5% sodium chloride solution as described above. The residue of sucrose myristate (9.6 g) was then precipitated from acetone to yield sucrose myristates (9.2 g) as a white powder. Theory for pure sucrose monomyristate is 11.0 g.

DISCUSSION

Before the kinetic study of the transesterification reaction could be carried out it was first necessary to develop analytical methods for determining the rates and extents of the reaction, and the sucrose mono- and di-ester content in the product of the reaction.

The rates of reaction were determined by following the concentration of the methyl esters of the higher fatty acids in the reaction solution by GLPC using *n*-octadecane as an internal standard of constant concentration. In this way it was established that the concentration of methyl ester could be determined to within ±2% from 10 to 100% of the range of concentrations encountered (see Fig. 1). Methyl myristate was used for most of the kinetic studies since it had been used in this laboratory for previous investigations (5) and had a convenient retention volume relative to *n*-octadecane. Although Lovelock (17) had shown that the response of the ionization detector was not the same for hydrocarbons and methyl esters of fatty acids, due to differences in the magnitude of their ionization potentials, the methyl esters of myristic, palmitic, and stearic acids gave the same molar response as *n*-octadecane under our experimental conditions.

Although the catalyst was not neutralized before the product of reaction (sucrose ester) was isolated, the simple routine procedure which was developed gave high, reproducible yields of sucrose ester for reactions carried out under identical experimental conditions (see Table I). It was found, however, that the addition of an equivalent amount of acetic acid or potassium hydrogen phthalate neutralizes the catalyst without causing any significant inversion of sucrose or sucrose ester.

Of the other analytical methods used, one worthy of mention is the separation of sucrose monoester from higher esters of sucrose by chromatography on silicic acid using methanol/chloroform solutions as the developing phase. The recoveries were quantitative.

Equipped with these experimental procedures and analytical tools, we undertook a kinetic investigation of the reaction. It seemed desirable to begin with an examination of the procedure recommended by the Snell Laboratories (2, 6). Reactions performed by this procedure at 80° and initiated by the addition of solid potassium carbonate proceeded at unpredictable rates and to variable extents (see Fig. 3). It became evident that this situation was to an important degree dependent on the rate of dissolution of the catalyst since the rate of reaction was substantially increased (about twofold) by using very finely divided potassium carbonate distributed over Celite (see Fig. 3). Also, although the solid potassium carbonate did not dissolve completely in any of our experiments, it was apparent that variable amounts went into solution. The observations suggested that the rate and extent of dissolution of potassium carbonate were related to the presence of traces of water. In fact, the rate of reaction and yields of sucrose ester were influenced by the addition of water to the reaction solution (see Fig. 4). The exact nature of this effect was not established since it was later observed that homogeneous solutions of potassium carbonate in DMF or DMF containing sucrose could catalyze the formation of sucrose ester. These results suggested that a satisfactory solution to the problem would require conditions for homogeneous catalysis. Furthermore, identical specimens of the reagents were used for all experiments dealing with one reaction variable, since it was realized that different specimens of the reagents would be used during the investigation, which could affect the reproducibility of the results. In this way it was possible, for example, to compare the rates of reaction, even if they were not the absolute reaction rates, within a selected group of experiments.

It was decided, therefore, to add the potassium carbonate as a solution in methanol. At this point a surprising (to us) observation was made. When a saturated methanolic solution of potassium carbonate was prepared, under reflux, the titration of the solution revealed the presence of strong base. Furthermore, the amount of strong base increased the longer the solution was heated. It was apparent, therefore, that heating led to the loss of acid through the evolution of carbon dioxide. By analogy the reaction of sucrose with potassium carbonate should lead to the formation of potassium sucrate in high concentration. The formation of sucrose myristate using solid sodium hydride as the catalyst suggested, moreover, that sucrate ion was the reactive species which catalyzed the reaction. Consequently potassium methoxide should serve to initiate the catalysis at least as efficiently as potassium carbonate.

The procedure for the transesterification reaction was therefore modified to enable methanolic solution of the catalyst to be added to the reaction mixture. The methanol was then removed by distillation, under reduced pressure, to leave a homogeneous reaction solution. It was now found that the reaction proceeded at highly reproducible rates, and these were independent of the base used (see experiments 1–6, Table I). Furthermore, the infrared spectra of samples of sucrose ester (see experiments 1–4, Table I) were identical, indicating that the product composition was the same. The rates of reaction using the conditions for homogeneous catalysis were much superior to those obtained by other workers (2, 5, 6, 8, 9).

It was also demonstrated that aqueous solutions of potassium carbonate and hydroxide, or methanolic solutions of potassium hydroxide, led to the formation of detectable amounts of potassium soap, resulting in lower rates of reaction and yields of sucrose ester (see experiments 7, 8, 10, and 11, Table I). Superior initial rates of reaction were observed when a saturated solution of potassium methoxide was used (see experiments 9, 12; Tables I and II, respectively) instead of a dilute methanolic solution of potassium methoxide (see Table III) to catalyze the reaction. These results indicate that dry methanol is the solvent of choice for the preparation of potassium sucrate solutions, and that the discrepancy in the initial rates of reaction was related to the efficiency with which methanol was being removed from the reaction solution. This latter effect will, of course, be more critical in the initial stages of the reaction when the methanol concentration is highest, and is consistent with the observation of Komori and his associates (9) that the rate of transesterification increased when the pressure in the system was decreased. Under our experimental conditions a rapid and reproducible rate of removal of methanol could not be achieved by distillation alone. However, the introduction of a rapid rate of stirring, combined with a continuous stream of nitrogen as a carrier gas, was found to positively solve this problem, and this use resulted in highly reproducible rates of reaction. Moreover, the viscous nature of saturated methanolic solutions of potassium methoxide made them difficult to handle. Consequently, most of our experiments were carried out using dilute methanolic solutions.

The effectiveness of the procedure for the removal of the methanol from the reaction solution was tested by taking samples, at intervals, from a transesterification reaction and equilibrating them in sealed glass tubes at the reaction temperature. The data in Table VI clearly illustrate the necessity for efficient removal of methanol from the reaction solution. Furthermore, in view of the high rates of reaction obtained using our standard transesterification conditions it can be concluded that methanol was being removed rapidly in all of our experiments in which conditions for homogeneous catalysis prevailed.

Experiments directed at obtaining a direct measure of the equilibrium constant for the reaction

$$\text{sucrose} + \text{methyl myristate} \rightleftarrows \text{sucrose ester} + \text{methanol}$$

were carried out by approaching the equilibrium from both sides (see Fig. 8). The equilibrium constant, K_2, for this reaction was found to have a value of 0.57 in both cases. The close agreement is probably fortuitous, although it is not considered likely that the actual value will differ significantly from this value. This result is consistent with the observations of Fehland and Adkins (18) and Juvet and Wachi (19) that the formation of methyl ester is favored in reactions in which aliphatic alcohols are equilibrated with the methyl esters of fatty acids using base (18) or acid (19) catalysis.

It became obvious, early in the investigation, that the transesterification reaction followed pseudo first-order kinetics in the methyl ester of the fatty acid (see Fig. 7). Evidence that sucrate ion was the reactive species which catalyzed the reaction was provided when it was observed that sodium hydride catalyzed the reaction, and when the extent and rate of reaction, using a methanolic solution of potassium carbonate as catalyst, was strongly depressed when a stream of carbon dioxide was passed through the solution instead of the usual nitrogen (see Fig. 5). This requires that sucrose (SOH) and potassium carbonate react according to the following scheme,

$$\text{SOH} + \text{K}_2\text{CO}_3 \rightleftarrows \text{K.OS} + \text{KHCO}_3,$$

$$\text{SOH} + \text{KHCO}_3 \rightleftarrows \text{K.OS} + \text{H}_2\text{CO}_3,$$

$$\text{H}_2\text{CO}_3 \rightleftarrows \text{CO}_2 + \text{H}_2\text{O},$$

to form potassium sucrate (K.OS). Furthermore, the fact that equivalent amounts of potassium carbonate, potassium methoxide, sodium methoxide, and lithium methoxide gave identical rates of reaction can only be explained satisfactorily if sucrate ion is the effective catalyst for the reaction (see Table I).

The transesterification reaction must therefore be bimolecular and involve nucleophilic attack of the methyl ester by sucrate ion, as would be expected from the earlier studies (13) on the mechanism of base-catalyzed transesterifications.

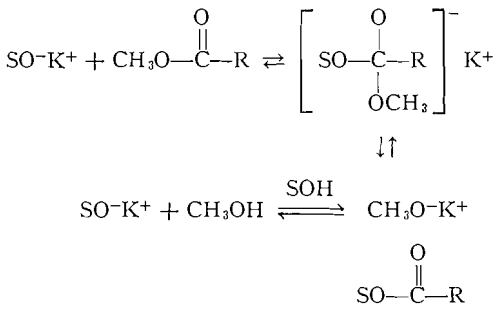

In view of this mechanism, the rate of the transesterification reaction should be dependent only on the concentrations of sucrate ion and methyl ester. However, the actual rate of reaction would also depend on the rate of re-formation of the methyl ester in the reverse direction, and this will depend on the efficiency with which the methanol is removed from the reaction solution. Since the methanol is kept at an insignificant low level under our experimental conditions (see above), the sucrate ion concentration should remain at virtually constant level throughout the course of the reaction.

Thus, the rate of reaction should be directly proportional to the sucrate ion concentration. It can be seen from Fig. 6 that this is the case for reaction solutions which were up to 3.125×10^{-3} M in potassium sucrate (1 meq of potassium sucrate per 320 ml of reaction solution). At higher concentrations of potassium sucrate the reactions behave in a non-ideal manner, and solid potassium sucrate precipitates from solution at concentrations in excess of 12.5×10^{-3} mole liter^{-1} (4 meq of potassium sucrate per 320 ml of reaction solution).

The downward drift may result from the association of the ionic substance at high concentrations in such a manner as to reduce the effective concentration.

In view of the above considerations the rate of reaction should be independent of the concentration of sucrose as long as methanol is being removed effectively. This was found to be the case and no appreciable rate difference was observed by doubling or halving the initial sucrose concentration (see Table II). Although the rate and extent of reaction was somewhat lower at the lowest concentration of sucrose (see experiment 13, Table II), it was observed that a precipitate of potassium sucrate was present during the entire reaction period. In view of the high rate of reaction, however, it is felt that if all the catalyst had been in solution the rates of reaction of the three concentrations of sucrose would have been identical. This is in contrast to the results of Komori and co-workers (9, 11), who claim that the rate of reaction was dependent on the sucrose concentration.

The chain length of the fatty acid (see Table III) and the nature of the cation have little effect on the rate of reaction. In the latter case, equivalent amounts of potassium carbonate, lithium methoxide, sodium methoxide, and potassium methoxide, as potential sources of sucrate ion, gave essentially the same rates of reaction (see Table I). The only possible gain that could be obtained by changing the cation would be in the solubility of the metal sucrate in the reaction solution. It was observed that lithium sucrate was the only catalyst which did not give an initial precipitate when it was added to the reaction mixture. The saturation levels of the metal sucrates, other than potassium sucrate, were not determined. These results are in contrast to the cation–sucrose complex theory of workers at the Herstein Laboratories, which must necessarily predict different rates of reaction for the different cations (7, 8).

Inspection of Fig. 6 reveals that the effective sucrate ion concentration is only 1.5 meq per 320 ml of reaction solution (4.96×10^{-3} mole liter^{-1}) when the pseudo first-order rate constant has a value of 2.36×10^{-4} sec^{-1} at the 2 meq level of potassium sucrate. Consequently, the corresponding second-order rate constant (k_r) for the reaction at 80° has a value of 5.03×10^{-3} mole liter^{-1}. From this value for k_r and the energy of activation (9.9 kcal mole^{-1}), the Arrhenius frequency factor (0.7×10^5 liter mole^{-1} sec^{-1}) was calculated (15). Using the transition-state theory (20), the following constants were calculated, $\Delta F^{\ddagger} = 22$ kcal mole^{-1}, $\Delta H^{\ddagger} = 9$ kcal mole^{-1}, and $\Delta S^{\ddagger} = -38$ entropy units. The low frequency factor and large negative entropy is usually associated with reactions in which there is electrorestriction of the solvent molecules due to the formation of a highly polar activated complex (21, 22). Reactions which exhibit this behavior also have negative volumes of activation, and the rates of reaction are accelerated by pressure (22). These phenomena are observed in the acid and base hydrolysis of esters and amides (23–25), and in the transesterification of esters with an alcohol using base catalysis (13, 26).

Using chromatographically pure samples of sucrose monomyristate, it was possible to establish the equilibrium constant K_1 for the reaction

$$\text{sucrose} + \text{sucrose dimyristate} \rightleftarrows 2 \text{ sucrose monomyristate}$$

to be approximately 2. Although the equilibrium was not approached from both sides, the values of K_1 were obtained at two different sucrose concentrations. The above expression neglects the formation of tri- or higher myristoyl sucroses. Our chromatographic analyses definitely indicate that such compounds are formed. However, their concentrations seemed negligible when two or more moles of sucrose were used per mole of myristoyl group.

The theoretical yield of sucrose monomyristate (M) corresponding to any initial concentration of sucrose (Y) and methyl myristate (Z) could be determined from a knowledge of K_1 provided it was assumed that there was quantitative conversion of the methyl myristate to sucrose mono- and di-myristate. Using a value of $K_1 = 2$, the quadratic equation [1] gave two solutions for M, only one of which was positive, namely,

$$M = \sqrt{(Y^2+2YZ-Z^2-Y)}.$$

If Y and M were expressed as multiples of Z (i.e., $Z = 1$), the above equation reduced to

$$M = \sqrt{(Y^2+2Y-1-Y)}.$$

Since this equation was satisfied by all values of Y from 0.5 to ∞, the effect of sucrose concentration on the yield of sucrose monomyristate could be shown graphically by plotting M/Z versus Y/Z. It should be noted, however, that this equation is only valid when an equilibrium exists exclusively between sucrose, sucrose dimyristate, and sucrose monomyristate. At concentrations of sucrose which are low relative to myristoyl group content substantial amounts of higher-substituted myristoyl esters of sucrose will be formed in their equilibrium proportions. Therefore, this equation can only be given values for $Y/Z \geqslant 2$ for which the concentration of sucrose esters with more than two myristoyl groups is not significant. Finally, the plot of M/Z against Y/Z must necessarily pass through the origin, as shown in Fig. 9.

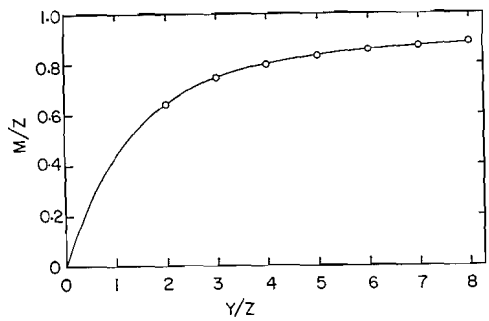

FIG. 9. The plot of the molar ratio of sucrose monomyristate/methyl myristate (M/Z) expected by calculation for the standard transesterification reaction conditions at 80° against the initial molar ratio of sucrose/methyl myristate (Y/Z).

From Fig. 9, it can be seen, for example, that 0.74, 0.80, and 0.83 mole of sucrose monomyristate are formed when 3, 4, and 5 moles of sucrose are used per mole of methyl myristate in the transesterification reaction. This corresponds to a 92, 93.7, and 95% yield of sucrose myristate (sucrose mono- and di-myristates), respectively, at the three sucrose concentrations. Thus, it is clear that little is gained by the use of a sucrose to methyl ester ratio greater than 3. However, in all of our experiments carried out under conditions for homogeneous catalysis (see Table I, experiments 1–4) the methyl myristate

had reacted to the extent of approximately 92% and gave a yield of sucrose myristates of approximately 83% by weight. From equation [1] it can be calculated that, under our standard conditions, 92% reaction would give 0.80 and 0.06 mole of sucrose mono- and di-myristates, respectively, corresponding to a theoretical weight yield of sucrose myristates of 87%, and a yield based on the amount of methyl myristate which had reacted of 94%. Furthermore, the preparative procedure which was developed as a result of our kinetic studies gave a yield of sucrose myristate of 84%. The experimental yields obtained during our investigations are therefore in excellent agreement with the predicted yield of 87%.

It was also established, using uniformly C^{14}-labelled sucrose, that the rate of the exchange reactions

$$\text{sucrose}^* + \text{sucrose dimyristate} \rightleftarrows \text{sucrose myristates}^*$$

and

$$\text{sucrose} + \text{sucrose monomyristate} \rightleftarrows \text{sucrose myristates}^*$$

was too rapid to expect any product control through kinetic control. In other words, at any time during the transesterification reaction, the product prevailing is the thermodynamic product under the conditions which prevail. From Table V it can be seen that approximately 65–80% of the theoretical activity was present in the isolated sucrose myristates after only 10 minutes' reaction. The discrepancy between the specific activity of the sucrose ester isolated after 65 minutes and the theoretical value is undoubtedly due to the presence of polysubstituted esters of sucrose. It is clear from these results that the sucrose esters formed in the transesterification reaction will have a higher sucrose monoester content in the initial stages of the reaction than at the completion of the reaction. We have not tested this prediction but make it with confidence. This is in direct contrast to the claims of other workers (2, 5–8) that the reaction proceeds by way of the rapid formation of sucrose diester. Furthermore, any claims that water (6) and the catalyst concentration (7, 8) influence the product composition are clearly not justified.

The fact that the rate constants for the transesterification remain virtually constant over the reaction period would suggest that little or no catalyst is used up in side reactions. The absence of soap in our reaction products is consistent with this observation. This is in contrast to the results of other workers who report that the catalyst is used up during the reaction, and that soap is formed in significant amounts (2, 5–8). The reason for this apparent discrepancy in the experimental results undobutedly lies in the fact that anhydrous conditions prevailed during this investigation, whereas the reaction solutions of other workers contained moisture.

ACKNOWLEDGMENTS

The authors wish to thank the Sugar Research Foundation, Inc., New York, for sponsoring this research as their Project 88.

REFERENCES

1. F. D. Snell. Personal communication.
2. L. Osipow, F. D. Snell, W. C. York, and A. Finchler. Ind. Eng. Chem. **48**, 1459 (1956).
3. L. F. Wiggins. Sugar and its industrial applications. The Royal Institute of Chemistry, London. 1960. Monograph No. 5.
4. Sucrose Ester Surfactants. Sugar Research Foundation Inc., New York. 1960.
5. J. M. Billy. Sucrose monoesters. M.Sc. Thesis, University of Ottawa, Ottawa, Ont. 1957.

6. L. OSIPOW, F. D. SNELL, and A. FINCHLER. J. Am. Oil Chemists' Soc. **34**, 185 (1957).
7. O. K. KONENENKO and I. L. KASTENBAUM. Abstracts of papers presented at the Am. Chem. Soc. St. Louis Meeting. 1961. Section 15D.
8. M. K. HERSTEIN. Personal communication.
9. S. KOMORI, M. OKAHARA, and E. SHINSUGI. J. Chem. Soc. Japan, Ind. Chem. Sect. **62**, 220 (1959).
10. K. MIHARA and K. TAKAOKA. J. Chem. Soc. Japan, Ind. Chem. Sect. **62**, 389 (1959); **62**, 393 (1959).
11. G. KOMORI, M. OKAHARA, and K. OKAMOTO. J. Am. Oil Chemists' Soc. **37**, 468 (1960).
12. H. ADKINS. Organic chemistry. *Edited by* H. Gilman. John Wiley and Sons Inc., London. 1943. Chap. 13.
13. R. W. TAFT, JR., M. S. NEWMAN, and F. H. VERHOEK. J. Am. Chem. Soc. **72**, 4511 (1950).
14. A. T. JAMES and A. J. P. MARTIN. Biochem. J. **50**, 679 (1952); **63**, 144 (1956).
15. S. GLASSTONE. The elements of physical chemistry. D. Van Nostrand Co. Ltd., New York. 1946. pp. 588, 607.
16. M. CALVIN. Isotopic carbon. John Wiley and Sons Inc., New York. 1948. pp. 79–81.
17. J. E. LOVELOCK. J. Chromatog. **1**, 35 (1958).
18. P. R. FEHLAND and H. ADKINS. J. Am. Chem. Soc. **57**, 195 (1935).
19. R. S. JUVET, JR. and F. M. WACHI. J. Am. Chem. Soc. **81**, 6110 (1959).
20. S. GLASSTONE, K. J. LAIDLER, and H. EYRING. The theory of rate process. McGraw-Hill Book Co., Inc., New York. 1941. pp. 195–197.
21. K. J. LAIDLER and P. A. LANDSKROENER. Trans. Faraday Soc. **52**, 200 (1956).
22. C. T. BURRIS and K. J. LAIDLER. Trans. Faraday Soc. **51**, 1497 (1955).
23. E. W. TIMM and C. N. HINSHELWOOD. J. Chem. Soc. 862 (1938).
24. I. MELOCHE and K. J. LAIDLER. J. Am. Chem. Soc. **73**, 1713 (1951).
25. G. GEISLER, F. ASNIGER, and C. HENNIG. Chem. Ber. **94**, 1008 (1961).
26. J. R. SCHAEFGEN, F. H. VERHOEK, and M. S. NEWMAN. J. Am. Chem. Soc. **67**, 253 (1945).

THE COMPOSITION OF THE SUCROSE MONOMYRISTATE PREPARED BY TRANSESTERIFICATION[1]

R. U. LEMIEUX[2] AND A. G. MCINNES[3]
Department of Chemistry, University of Ottawa, Ottawa, Ontario
Received July 16, 1962

ABSTRACT

The composition of the sucrose monomyristate which is obtained by reaction of sucrose with methyl myristate in dimethylformamide and in the presence of a basic catalyst was established by application of gas–liquid partition chromatography and nuclear magnetic resonance spectroscopy to appropriate derivatives. The substance is a mixture of 6′-myristoyl sucrose, 6-myristoyl sucrose, and unidentified isomeric esters in the relative proportions of 0.62:0.28:0.10, respectively.

INTRODUCTION

The first attempt to establish the structure of a fatty acid monoester of sucrose was made by Snell and co-workers (1) in 1956. Sucrose monolaurate, prepared by the transesterification reaction (2), was hydrolyzed with refluxing aqueous acid and a fraction containing glucose and fructose monolaurate was isolated. After deacylation, the ratio of the two hexoses was determined by visual inspection of the intensities of the spots developed on a paper chromatogram. Furthermore, 1 mole of sucrose monolaurate consumed 2.9 moles of periodate to yield 0.68 mole of formic acid. When sucrose monolaurate 3.15-tosylate was reacted with sodium iodide in acetone more than 71% of the tosyloxy groups were replaced by iodine. On the basis of these experimental observations, Snell concluded that at least 80% of the ester group was present at the 6-position of sucrose. It should be noted, however, that this work did not take into account the possibility that ester groups substituted on different positions in the sucrose molecule may undergo hydrolysis at very different rates in acid media. Also, no attempt was made to provide an explanation for the low yield of formic acid (68% of theory) obtained in the periodate oxidation. Moreover, Snell assumed that tosyloxy groups substituted on the three primary hydroxyl groups of sucrose would all react with iodide ion whereas it was established in this laboratory (3) that although tosyloxy groups at the 6- and 6′-positions of sucrose are replaceable by iodine, a tosyloxy group at the 1′-position is unreactive (3). A reinterpretation of Snell's results, on the basis that only the 6- and 6′-positions reacted, would require that none of the ester groups occupied either of these positions in sucrose.

Gee and Walker (4) also examined the structure of fatty acid monoesters of sucrose. A commercial sample of sucrose monostearate was methylated, the product was saponified, the solution was deionized, and the residue on evaporation was subjected to molecular distillation. Analysis of the distillate by gas–liquid partition chromatography (GLPC) revealed that it was a mixture of isomeric hepta-*O*-methyl sucroses and octa-*O*-methyl sucrose. The distillate was then subjected to methanolysis to yield a mixture of fully and partially methylated methyl fructosides and glucosides, which were subsequently analyzed by GLPC. It was concluded, on the basis of the analysis, that the stearoyl group was predominantly at the 6-position although appreciable substitution of stearate

[1]*This paper was submitted by A. G. McInnes as a portion of a thesis for the Ph.D. degree.*
[2]*Present address: Department of Chemistry, University of Alberta, Edmonton, Alberta.*
[3]*Present address: Atlantic Regional Laboratory, National Research Council, Halifax, Nova Scotia.*

at the 6′-position of sucrose was considered to be relatively unimportant. No attempt was made to explain the presence of octa-*O*-methyl sucrose in the distillate and analytical data to support the identification of the hepta-*O*-methyl sucroses were not provided. Since octa-*O*-methyl sucrose could only have formed during the methylation procedure by hydrolysis of sucrose monostearate, and the relative rates of hydrolysis of ester groups located on different positions in the sucrose molecule are not known, the composition proposed could not be accepted without reservation.

The failure of previous attempts to unambiguously establish the structure of a sucrose monester led us to reinvestigate the problem. The purpose of this communication is to report on the structure of an analytically pure sample of sucrose monomyristate.

EXPERIMENTAL AND RESULTS

The Tosylation of Sucrose Monomyristate

Pure sucrose monomyristate (0.6023 g) was reacted with *p*-toluenesulphonyl chloride (2.80 g) in anhydrous pyridine (20 ml) for 12 hours at room temperature. The excess *p*-toluenesulphonyl chloride was then destroyed by adding water (1 ml) to the reaction solution. After the latter was left standing at room temperature for 30 minutes, it was poured into ice water (50 ml) and extracted with five aliquots (20 ml) of chloroform. After being washed first with 2 *N* hydrochloric acid, then with sodium bicarbonate solution (20% w/v), and finally with distilled water, the chloroform solution was dried by filtration through paper wetted with chloroform. Removal of the chloroform under reduced pressure yielded a substance (1.48 g) which contained the amount of sulphur (12.28%) expected for a sucrose monomyristate containing 5.18 tosyl groups per sucrose unit.

Reaction of Sucrose Monomyristate "5.18-Tosylate" with Sodium Iodide

The sucrose monomyristate with a degree of tosylation of 5.18 (0.5396 g) was reacted with sodium iodide (0.6 g) in acetone (6 ml) for 15 hours at 105° in a sealed glass tube. After the reaction was complete, the sodium *p*-toluenesulphonate (0.1424 g) which had precipitated from the solution was collected. The filtrate was taken to dryness and the residue was extracted with three 15-ml amounts of chloroform. After extraction with sodium thiosulphate solution (10% w/v) and then with distilled water, the chloroform solution was dried. Evaporation under reduced pressure yielded sucrose 1.84-iodo, 3.34-tosylate (0.4474 g). Anal. Calc. for sucrose monomyristate 1.84-iodo, 3.34-tosylate: S, 8.43; I, 18.42%. Found: S, 8.30; I, 18.90%.

Methylation of Sucrose Monomyristate

Pure sucrose monomyristate (2.03 g) was methylated in anhydrous *N*,*N*-dimethylformamide (DMF) (60 ml) (5, 6) using methyl iodide (60 ml) and freshly prepared silver oxide (22 g). Finely divided anhydrous calcium sulphate (20 g) was added to the reaction solution to ensure anhydrous conditions for methylation and to reduce the possibility of ester hydrolysis. The reaction was assisted by vigorous agitation of the reaction solution on a mechanical shaker for 15 hours. At the end of the reaction period the solution was filtered free of solids and the clear filtrate was diluted with 150 ml of chloroform to precipitate silver iodide. The silver iodide was removed by filtration and the chloroform/DMF solution was taken to dryness *in vacuo* on a rotary evaporator. Drying under reduced pressure over phosphorus pentoxide left 2.39 g of crude methylated sucrose ester (quantitative yield). Since GLPC analysis revealed the presence of methyl myristate, a sample (2.35 g) was chromatographed on silicic acid (40 g) using graded elution with methanol/chloroform solutions as shown in Table I. Fraction 1 was shown (infrared and GLPC) to be pure methyl

TABLE I

Chromatography of methylated sucrose monomyristate on silicic acid

Fraction	Solvent	Volume (ml)	Weight of Residue (g)
1	Chloroform	150	0.0442*
2	"	100	0.1068
3	"	225	1.4985
4	10% methanol/chloroform	200	0.6909
5	Methanol	150	0.0030
		Total weight recovered	2.3434 (99.7% recovery)

*This material was collected in the first 100 ml of chloroform.

myristate and represented 1.9% of the total weight of the sample. Fraction 2 had an infrared spectrum virtually identical with those of fractions 3 and 4. Only the latter two fractions (2.1894 g, 91.6% theory) were combined for further examination. Their infrared spectra showed no absorption in the O—H stretching region and were consistent with that expected for hepta-*O*-methyl sucrose monomyristate.

Preparation of Hepta-O-methyl Sucrose

A sample (1.1200 g) of hepta-*O*-methyl sucrose monomyristate was transesterified with 10 ml of anhydrous methanol under reflux for 5 hours, using potassium methoxide (2 mmole) as catalyst. At the end of the reaction period the catalyst was converted to potassium carbonate by the addition of solid carbon dioxide and the methanol was removed under reduced pressure. The residue was extracted with 50 ml of chloroform and the extract was taken to dryness under reduced pressure. The residue was chromatographed on 10 g of silicic acid. Elution with 100 ml of chloroform yielded 0.3958 g of an oil (98.0% of theory) the infrared spectrum of which was identical with that of methyl myristate. Further elution with 5% methanol–chloroform (100 ml) yielded 0.6958 g of hepta-*O*-methyl sucrose (92% of theory) as a colorless oil. Anal. Calc. for $C_{19}H_{36}O_{11}$: methoxyl, 49.3%. Found: 48.4%. The infrared spectrum in carbon tetrachloride (0.0025 *M*) showed absorption in the O—H stretching region at 3485 cm^{-1}. The n.m.r. spectrum (Fig. 1) in carbon

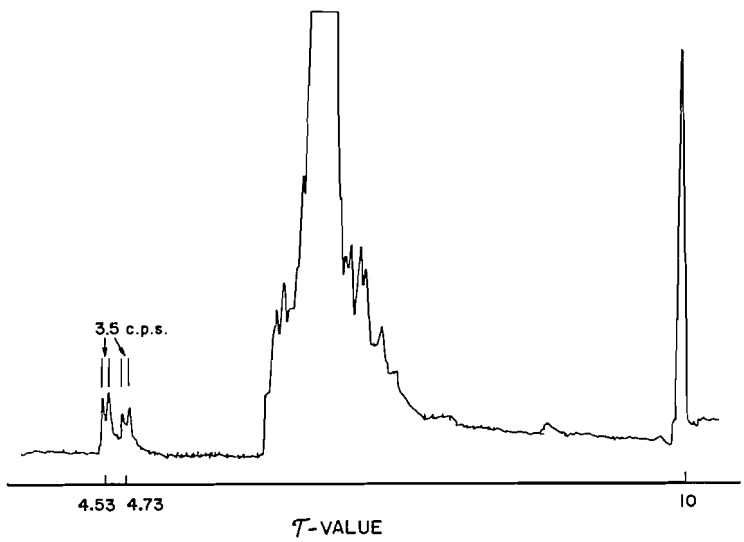

FIG. 1. The proton magnetic resonance spectrum of the mixture of hepta-*O*-methyl sucroses.

tetrachloride (20% w/v) had two doublets for two anomeric hydrogens (8, 9) with τ-values (7) of 4.73 and 4.53. Each doublet had a spacing of 3.5 c.p.s. and their relative intensities were 0.65 to 0.35, with the doublet at lower field having the greater intensity. All n.m.r. spectra were measured on a 60 Mc/s high-resolution Varian spectrometer.

Tosylation of Hepta-O-methyl Sucrose

Hepta-*O*-methyl sucrose (0.1566 g) was reacted with 0.27 g of *p*-toluenesulphonyl chloride in 2 ml of anhydrous pyridine for 12 hours. The hepta-*O*-methyl sucrose monotosylate (0.2172 g) was isolated in quantitative yield. Anal. Calc. for $C_{26}H_{42}SO_{13}$: S, 5.39%. Found: S, 5.15%. The infrared spectrum in chloroform (5% w/v) was consistent with that expected for a tosyl ester of a methylated sugar. The n.m.r. spectrum (Fig. 2) in carbon tetrachloride (20% w/v) possessed a quartet at an average τ-value of 2.55 for four aromatic protons (7). Two doublets with a combined intensity corresponding to one proton were in the region expected for signals from anomeric hydrogens. The relative intensities of the two doublets was 0.65:0.35.

The Preparation of Hepta-O-methyl Deoxysucrose from Hepta-O-methyl Sucrose Monotosylate

The hepta-*O*-methyl sucrose monotosylate (0.1019 g) was reacted with 0.6 g of sodium iodide in 6 ml of acetone at 105° for 15 hours. Hepta-*O*-methyl iododeoxysucrose (0.0916 g, 97% of theory) was isolated as an oil. The n.m.r. spectrum showed that only 10% of the tosyloxy groups had not been lost in the reaction with sodium iodide. The hepta-*O*-methyl iododeoxysucrose was dissolved in 6 ml of methanol containing 24 mg of diethylamine and the solution was reduced with hydrogen at atmospheric pressure for 4 hours using palladium on charcoal as catalyst. After clarification and deionization, the product was dried under reduced pressure. The yield based on hepta-*O*-methyl deoxysucrose was 0.061 g (87% of theory). Anal.

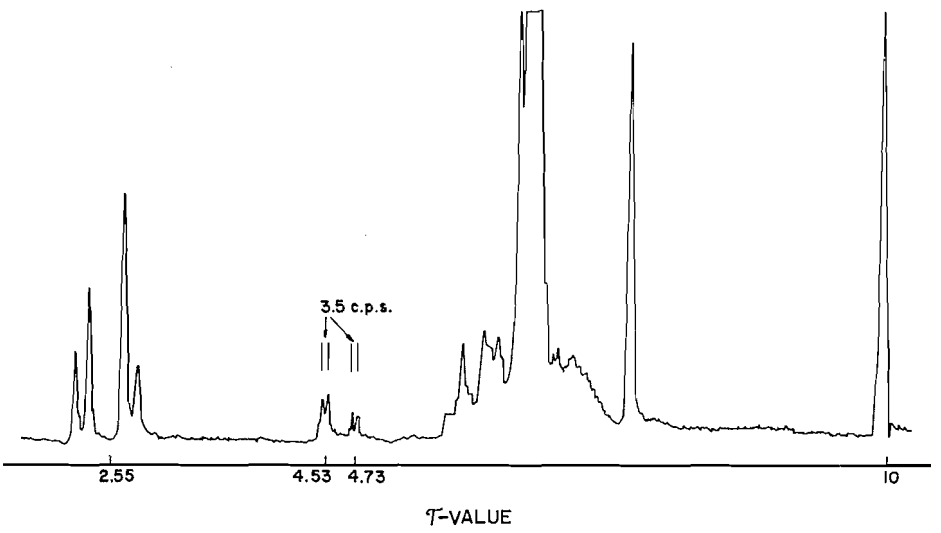

FIG. 2. The proton magnetic resonance spectrum of the mixture of the mono-*O*-tosyl hepta-*O*-methyl sucroses.

Calc. for $C_{19}H_{36}O_{10}$: C—CH_3, 6.37%. Found: 5.80%. The n.m.r. spectrum (Fig. 3) in carbon tetrachloride (20% w/v) showed that the aromatic protons (τ = 2.55) (7) had an intensity corresponding to only 0.4

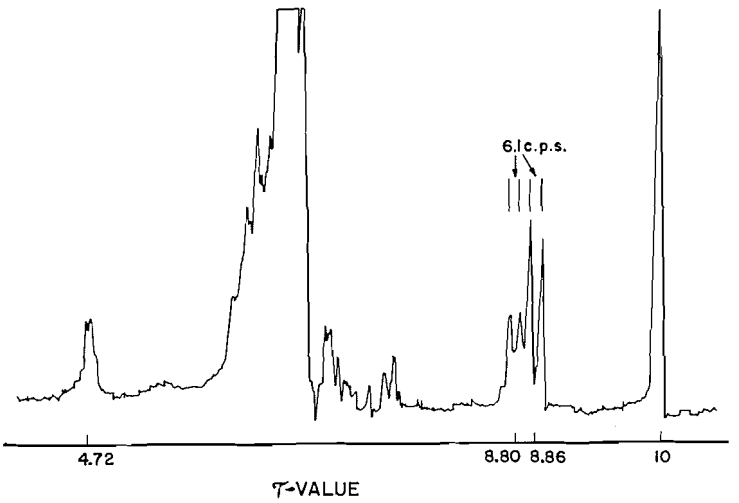

FIG. 3. The proton magnetic resonance spectrum of the mixture of deoxy hepta-*O*-methyl sucroses.

proton, and the anomeric hydrogens were present as an ill-defined quartet with an average τ-value of 4.72. Two doublets with a common spacing of 6.1 c.p.s. were present for the protons of methyl groups (7) at τ-values of 8.80 and 8.86, respectively. The total intensity of the two doublets corresponded to 2.8 protons (theory 3 protons) and the ratio of the intensities of the doublets was 0.65:0.35. The signal at highest field had the greater intensity.

Chromatography of Hydrolysis and Methanolysis Products of Hepta-O-methyl Sucrose

The method of Hayward (10) was used for the hydrolysis of 10 mg of hepta-*O*-methyl sucrose in 1 ml of 0.05 *N* sulphuric acid on a steam bath for 2 hours. At the end of the reaction period, the sulphuric acid was neutralized with solid barium carbonate and the aqueous solution was clarified by centrifugation. Aliquots of the supernatant solution were spotted on Schleicher and Schuell, orange ribbon 289, chromatographic

paper. The chromatogram was developed with *n*-butanol–ethanol–water, 5:1:4 (11), for 18 hours, using 2,3,4,6-tetra-*O*-methyl-D-glucose and 2,3,4-tri-*O*-methyl-D-glucose as standards. Two spray reagents were used, namely, 3% *p*-anisidine hydrochloride in moist *n*-butanol to detect both ketoses and aldoses and 3% resorcinol in *n*-butanol containing hydrochloric acid to detect ketoses only (11). Only three spots were present, with R_{TG} values (R_f value relative to that of 2,3,4,6-tetra-*O*-methyl glucose) of 0.81 (red-brown), 0.89 (yellow), and 1.00 (red-brown), when the *p*-anisidine hydrochloride spray was used. Two pink spots were present, with R_{TG} values of 0.89 and 1.00, when the resorcinol spray was used. Clearly, both 2,3,4,6-tetra-*O*-methyl-D-glucose and 1,3,4,6-tetra-*O*-methyl-D-fructose were present. 2,3,4-Tri-*O*-methyl-D-glucose produces a red-brown spot with $R_{TG} = 0.81$. For reasons which will become clearly apparent later on, the substance with $R_{TG} = 0.89$ must be 1,3,4-tri-*O*-methyl-D-fructose.

Hepta-*O*-methyl sucrose (13.2 mg) was reacted with 3% methanolic HCl (0.20 ml) for 5 hours at room temperature. Aliquots of the reaction mixture (0.1 μl) were analyzed by GLPC, on a "Pye Argon Chromatograph", using a Celite – butanediol succinate polyester (20% w/v) column (12) at 160° and using a flow rate of 60 ml of argon per minute. The analysis showed the presence of 10 methyl glycosides. The retention volumes of these compounds were calculated relative to that of methyl 2,3,4,6-tetra-*O*-methyl-α-D-glucopyranoside as shown in Table II. Only those compounds with relative retention volumes of 0.68, 0.73, 0.88, 1.00, 1.33, and 2.66 were present in significant amounts. The molar ratio of the pentamethyl glucosides to pentamethyl fructosides was found to be 0.69:0.31 as determined by their area ratios. Furthermore, the molar ratio of methyl 2,3,4-tri-*O*-methyl-β-D-glucopyranoside to that of the compounds with relative retention volumes of 1.33 and 2.66 (see Table II) was 0.34:0.66. The methanolysis products of octa-*O*-methyl sucrose are also shown in Table II.

TABLE II

Retention volumes of the products of methanolysis of hepta-*O*-methyl and octa-*O*-methyl sucrose relative to methyl 2,3,4,6-tetra-*O*-methyl-α-D-glucopyranoside

Compound	Standards	Octa-*O*-methyl sucrose	Hepta-*O*-methyl sucrose
Methyl 2,3,4,6-tetra-*O*-methyl-β-D-glucopyranoside	0.68	0.68	0.68
Methyl 1,3,4,6-tetra-*O*-methyl-β(?)-D-fructofuranoside		0.73	0.73
Methyl 1,3,4,6-tetra-*O*-methyl-α(?)-D-fructofuranoside		0.88	0.88
Methyl 2,3,4,6-tetra-*O*-methyl-α-D-glucopyranoside	1.00	1.00	1.00
Methyl 1,3,4-tri-*O*-methyl-β(?)-D-fructofuranoside*			1.33
Methyl 1,3,4-tri-*O*-methyl-α(?)-D-fructofuranoside*			1.49
Methyl 2,3,4-tri-*O*-methyl-β-D-glucopyranoside	1.81		1.81
Methyl 1,3,4-tri-*O*-methyl-β(?)-D-fructopyranoside*			1.91
Methyl 2,3,4-tri-*O*-methyl-α-D-glucopyranoside	2.38		2.38
Methyl 1,3,4-tri-*O*-methyl-α-(?)-D-fructopyranoside*			2.66

*These compounds were provisionally assigned these structures after the structure of hepta-*O*-methyl sucrose was known.

DISCUSSION

Sucrose monomyristate (6) was methylated using silver oxide and methyl iodide in dimethylformamide solution (5, 7(*a*)) and finely divided calcium sulphate as a drying agent. The crude yield was quantitative. However, chromatography on silicic acid showed the product to contain about 2% of the original myristoyl content as methyl myristate (see Table I). Pure hepta-*O*-methyl sucrose monomyristate was obtained in 92% yield from the chromatogram and the material was transesterified quantitatively to hepta-*O*-methyl sucrose with a methoxyl content, 48.2%, in good agreement with the theoretical value of 49.3%. Hydrolysis with 0.5 *N* sulphuric acid gave a product which was shown by chromatography to contain three components when sprayed with *p*-anisidine hydrochloride. Two of these spots (reddish brown), with R_{TG} values of 1.0 and 0.81, corresponded to 2,3,4,6-tetra-*O*-methyl glucose and 2,3,4-tri-*O*-methyl glucose. The third spot, with an R_{TG} value of 0.89, was yellow (ketose) and agreed with the reported value for 1,3,4-tri-*O*-methyl fructose (13). Therefore, it was evident that the hepta-*O*-methyl sucrose was almost entirely a mixture of only 2,3,4,1′,3′,4′,6′- and 2,3,4,6,1′,3′,4′-hepta-*O*-methyl sucroses.

Methanolysis of the mixture of hepta-*O*-methyl sucroses and GLPC analysis of the methyl glycosides revealed the presence of 10 compounds. The theoretical number of methyl glycosides which can be formed from the above mixture is 10 (see Table II). The relative amounts of the fully methylated D-glucopyranosides and D-fructofuranosides was 0.69:0.31. Since experience has shown that the methyl furanosides of fully, or partially, methylated hexoses have smaller retention volumes than the corresponding methyl pyranosides (12, 14), the compounds with relative retention volumes of 1.33 and 2.66 (see Table II) are probably the methyl furanoside and pyranoside of 1,3,4-tri-*O*-methyl-fructose, respectively. The relative amounts of these compounds to that of methyl 2,3,4-tri-*O*-methyl-β-D-glucopyranoside was found to be 0.66:0.34.

The nuclear magnetic resonance spectrum (Fig. 1) for the mixture of hepta-*O*-methyl sucroses showed two signals (doublets) for the anomeric hydrogen, at low field (16), with a common spacing of 3.5 c.p.s. The relative intensities of the two doublets was 0.65:0.35 and the doublet at lowest field had the greater intensity.

Reaction of the mixture of hepta-*O*-methyl sucroses with *p*-toluenesulphonyl chloride in pyridine produced hepta-*O*-methyl sucrose monotosylate in quantitative yield. The n.m.r. spectrum (Fig. 2) again showed the presence of two doublets for the anomeric hydrogen with a relative intensity of 0.65:0.35. When this monotosylate was treated with sodium iodide in acetone, at 105°, for 15 hours, hepta-*O*-methyl iododeoxysucrose was obtained in 97% yield. The nuclear magnetic resonance spectrum of this compound revealed that 90% of the tosyloxy groups had been replaced by iodine. Hydrogenolysis of the iodocompound produced in 87% yield an iodine-free compound the n.m.r. spectrum of which (Fig. 3) showed two signals in the form of doublets for C-methyl groups. The total intensity of these doublets relative to the total signal for anomeric hydrogen was 2.8 protons (theory 3 protons). The doublets had a spacing of 6.1 c.p.s., which is characteristic for methyl groups substituted on a carbon carrying one hydrogen (7(*b*)). The relative intensities of these signals were once again in the ratio of 0.65:0.35. Therefore, the methyl groups must be at the 6- and 6′-positions of sucrose since these are the only two positions in which a methyl group could be attached to a carbon atom bearing a hydrogen. Furthermore, the GLPC analysis of the products of methanolysis of the hepta-*O*-methyl sucroses showed that more pentamethyl glucoside was formed than pentamethyl fructoside. This can only mean that the myristoyl group was to a greater extent at the 6′- than at the 6-position of sucrose. It can be concluded, therefore, that sucrose monomyristate has about 0.62 of the myristoyl group at the 6′-position, 0.28 at the 6-position, and 0.10 at the other positions. It is likely that most of the latter fraction is on the third primary hydroxyl, namely, the 1′-position of sucrose. This is in direct contrast to the claims of other workers (1, 4) that sucrose monoester is substituted almost exclusively at the 6-position of sucrose.

The results obtained on the structure of sucrose monomyristate by first tosylating the ester and then reacting the tosylated product with sodium iodide in acetone were very misleading. A reaction sequence of this type revealed that 1.84 tosyloxy groups were replaced by iodine in sucrose monomyristate 5.18-tosylate. Since previous work in this laboratory had shown that only the 6- and 6′-positions in polysubstituted tosyl esters of sucrose were replaced by iodine (8), the above result would require 90% of the myristoyl groups to be at the other positions of sucrose. Since such an interpretation is erroneous, clearly secondary tosyloxy groups were replaced by iodine. Furthermore, it is apparent that the presence of the myristoyl group is required for the facile replacement. It is conceivable that the myristoyl groups at the 6- and 6′-positions participate in replacement at the 4- and 4′-positions. It is noteworthy in this respect that Helferich and Gnüchtel

(15) replaced the mesyloxy group in 4-*O*-mesyl-1,2,3,6-tetra-*O*-acetyl-β-D-glucose on heating the compound with sodium iodide in acetone. Methyl α-D-glucopyranoside tetramesylate underwent quantitative replacement of the 6-mesyloxy group (15). The relative amounts of the two isomeric mono-*O*-myristoyl sucroses together with the evidence (6) that they were formed as an equilibrium mixture requires the equilibrium constant, K_e, for the reaction

6-myristoyl sucrose $\rightleftarrows$ 6′-myristoyl sucrose

to be

$$K_e = \frac{0.62}{0.28} = 2.2.$$

This corresponds to a difference in standard free energy of approximately 0.6 kcal mole^{-1} at 80°, which likely arises mainly from the difference in the non-bonded interactions about the ester groupings. The pyranose ring of the glucose moiety of sucrose exists in the chair form wherein the atoms on neighboring carbons in the ring are in the staggered

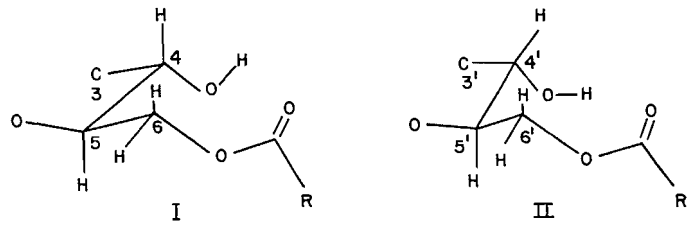

FIG. 4. The conformations of groups or atoms attached to the fourth and fifth carbon atoms in the glucose (I) moiety of 6-myristoyl sucrose, and the fructose (II) moiety of 6′-myristoyl sucrose.

relationship. Therefore, a staggering of the substituents on the 6-carbon with the substituents on the 5-carbon of the glucose molecule will cause an eclipsing of two of the substituents on the 6-carbon with the hydrogen and oxygen on the 4-carbon. This relationship is depicted in the conformational formula I (Fig. 4). On the other hand, the atoms on neighboring carbons in the furanose ring of the fructose moiety can only be in a partially staggered relationship. Therefore, in this case, a staggering of the substituents on carbons 5 and 6 will *not* eclipse the substituents on the 6-carbon with the hydrogen and the oxygen on the 4-carbon (see conformational formula II, Fig. 4). Thus, an acyloxy group at the 6′-position of the sucrose molecule will be in a less congested region of the sucrose molecule than an acyloxy group at the 6-position.

ACKNOWLEDGMENTS

The authors wish to thank the Sugar Research Foundation, Inc., New York, for sponsoring this research as their Project 88.

REFERENCES

1. W. C. YORK, A. FINCHLER, L. OSIPOW, and F. D. SNELL. J. Am. Oil Chemists' Soc. **33**, 424 (1956).
2. L. OSIPOW, F. D. SNELL, W. C. YORK, and A. FINCHLER. Ind. Eng. Chem. **48**, 1459 (1956).
3. R. U. LEMIEUX and J. P. BARETTE. Can. J. Chem. **38**, 655 (1960).
4. M. GEE and H. G. WALKER, JR. Chem. Ind. (London), 829 (1961).
5. R. KUHN, H. TRISCHMANN, and I. LÖW. Angew. Chem. **67**, 32 (1955).
6. R. U. LEMIEUX and A. G. MCINNES. Can. J. Chem. This issue.
7. (*a*) J. CROON and B. LINDBERG. Acta Chem. Scand. **13**, 593 (1959).
   (*b*) F. A. L. ANET. Can. J. Chem. **39**, 2262 (1961).

8. J. P. BARETTE. *p*-Toluenesulphonyl and anhydro derivatives of sucrose. Ph.D. Thesis, Ottawa University, Ottawa, Ont. 1960.
9. R. U. LEMIEUX and J. D. STEVENS. Unpublished work.
10. G. G. McKEOWN and L. O. HAYWARD. Can. J. Chem. **35**, 996 (1957).
11. L. HOUGH, J. K. N. JONES, and W. H. WADMAN. J. Chem. Soc. 1702 (1950).
12. C. T. BISHOP and F. P. COOPER. Can. J. Chem. **38**, 388 (1960).
13. E. L. HIRST and J. K. N. JONES. Discussions Faraday Soc. **7**, 268 (1949).
14. C. T. BISHOP. Personal communication.
15. B. HELFERICH and A. GNÜCHTEL. Ber. **71**, 712 (1938).
16. R. U. LEMIEUX, R. K. KULLNIG, H. J. BERNSTEIN, and W. G. SCHNEIDER. J. Am. Chem. Soc. **80**, 6098 (1958).

METAMECONINE AS A MODEL COMPOUND IN THE STUDY OF AROMATIC REACTIONS[1]

S. SAFE, MARJORIE ALLEN,[2] AND R. Y. MOIR

Department of Chemistry, Queen's University, Kingston, Ontario

Received August 9, 1962

ABSTRACT

Previous work had shown the somewhat unexpected course of nitration, bromination, and demethylation reactions of metameconine and its derivatives. The discovery that metameconine could easily be dinitrated enabled us to bring to light equally interesting results in the relative rates of reduction of the nitro groups, in the course of certain nucleophilic substitution reactions, in the activation of the methylene group, and in certain physical properties. Much of the work, past and present, now holds as its main interest the somewhat special character of a nitro group in the 7-position.

Metameconine (I), because its contrasting methylene and carbonyl groups are equivalently situated with respect to a pair of vacant positions and with respect to a pair of methoxyl groups, is beautifully adapted to the study of competing factors in aromatic reactions. Rây and Robinson (1) were the first to employ it in this way; we have followed their example, and the work of this paper, together with our previously reported experimental work, amounts to a qualitative survey of the possibilities of the system.

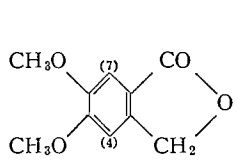

I

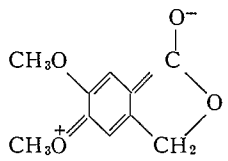

II

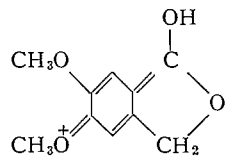

III

In one of the earliest tests of the new "electronic" theory of reactions, Rây and Robinson (1) predicted that metameconine should undergo nitration at position 7 (because of the depression of the directing influence of the methoxyl at position 5 by contributor II to the overall structure of metameconine) rather than at position 4 (suggested by the simple summation of the effects of the separate groups). This prediction was later verified (1–4). Ingold (5) generalized somewhat similar situations as characteristic of systems having a $+E$ group meta to a $-I-M$ group; his generalization has been applied to the present series by Blair and Newbold (6). Such systems often show differences between the directions of nitration and bromination, attributed by Ingold (5) to the greater steric requirements of bromination. Metameconine in particular is brominated at the 4-position (3), but Ingold's explanation is sufficiently less convincing for it than for the experimental examples cited by him to encourage consideration of other effects. Other differences between nitration and bromination are of course known; their importance is recognized and we hope to investigate them later, but in the absence of more quantitative data, only one is worth mentioning here because of its simplicity and because of its application in the quite different reaction of demethylation. Metameconine is much more likely to have its carbonyl protonated under the conditions of nitration than under those of

[1]*Presented in part at the Annual Meeting of the Chemical Institute of Canada in Montreal, August 4, 1961.*
[2]*Holder of a Scholarship from the National Research Council of Canada, 1960–61.*

bromination; the contributor III (more available in nitration than in bromination) would, of course, be more effective than the contributor II in suppressing the influence of the methoxyl at position 5.

This interest in the implications of our previous work on the electrophilic substitution reactions of metameconine was reawakened by a new observation. It was found that metameconine could easily be dinitrated in good yield to give 4,7-dinitrometameconine (IV) under conditions not much more severe than those required to produce high yields

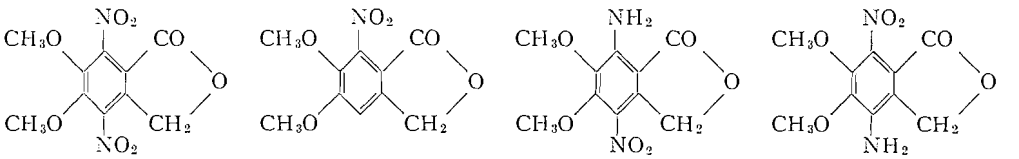

of easily purified 7-nitrometameconine (V) (1–3). Well-separated stages of nitration are commonplace, but few of the known examples involve insertion of the second nitro group para to the first. In fact, a moment's thought will show that, regardless of the course assumed for the dinitration, it is difficult to reconcile the experimental results with the great deactivation of the 4-position of V to be expected from the para nitro group. The existence of two unusual features in 7-nitrometameconine (V) is therefore of interest: (i) conjugation between the methoxyl at position 6 and the nitro group at position 7 is incompatible with the contributors corresponding to II and III, which also repress the activation of position 4; in the extreme limit, this effect would produce the delightful paradox of the *activation* for electrophilic substitution of position 4 by the insertion of a nitro group in the para position; (ii) the nitro group may be less deactivating than expected because of its lack of coplanarity with the ring. The existence of the second feature is confirmed in the discussion of the infrared spectra given later; because of this, the first effect is probably small.

The position of the two methoxyls in metameconine (I) permits the study of competitive effects in demethylation. Coordination with a proton (or some approximately equivalent association with an acid) is undoubtedly the first step in demethylation. Clearly, on account of the contribution of either II or III, coordination should be easier with the methoxyl at position 6 than with that at position 5, and if this is the determining step, demethylation of metameconine should occur preferentially at position 6. Previous work showed that metameconine is preferentially demethylated at position 6 (4), and the same argument may be extended to other demethylations. However, our further experimental work on the demethylation of halogenated metameconines (4, 7) showed that the second step is the determining step in still other reactions of this kind, and it is likely that further progress can be made only by more quantitative methods.

The discovery of the dinitration of metameconine enabled us to consider new types of competitive reactions. For example, which nitro group in 4,7-dinitrometameconine (IV) should be more subject to reduction? One current theory of the effect of substituents stresses that reduction is aided by electron withdrawal from the center to be reduced, and the obvious (but incautious) application of this theory suggests that 7-amino-4-nitrometameconine (VI) should be formed preferentially. The experimental result is the direct contrary: 7-amino-4-nitrometameconine (VI) is formed only in traces, and its isomer, 4-amino-7-nitrometameconine (VII), is formed in very high yield when IV is reduced with iron and acetic acid.

The remarkable substance VII forced several other unexpected results upon our attention. For example, diazotization of VII in hydrochloric acid, followed by reduction with hypophosphorous acid, gave 7-chlorometameconine (VIII) rather than the expected 7-nitrometameconine (V). Nucleophilic substitution of the nitro group by chlorine had,

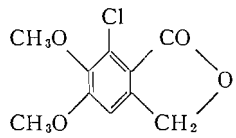

VIII

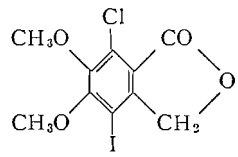

IX

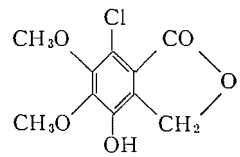

X

therefore, preceded the reduction of the diazonium group; other examples of this are, of course, known (8). We sought to avoid the nucleophilic reaction by the use of an acid with a less nucleophilic anion, but diazotization with nitrosylium bisulphate gave a diazonium salt whose great resistance to decomposition is recorded in the experimental part.

The easy displacement of the 7-nitro group made possible the formation of 7-chloro-4-iodometameconine (IX) by diazotization of VII in hydrochloric acid, followed by the addition of potassium iodide. The structure of the product was proved by its preferential reduction (4, 7) to the known 7-chlorometameconine (VIII) (7). One more surprise remained. The Ullmann reaction of IX with aqueous potassium hydroxide and copper gave only 7-chlorometameconine (VIII) in place of the expected 4-hydroxy-7-chlorometameconine (X). Reductive dehalogenation is a known side reaction of the Ullmann reaction (9, 10), but with the related 4-iodometameconine the normal substitution reaction predominated under similar conditions (10).

The unusual character of a nitro group in the 7-position of the metameconine system was further exemplified by the infrared spectra. A nitro group in the 7-position possessed a higher, sometimes a very much higher, stretching frequency than did a nitro group in the 4-position, suggesting that, in the solid state at least, the 7-nitro group was very far from being coplanar with the ring (11). Thus the dinitro compound IV showed peaks at 1547 and 1530 cm^{-1}, the minor isomer (VI) at 1512 cm^{-1}, and the major isomer (VII) at 1567 cm^{-1}; the conjugation between the nitro group and the amino group was, therefore, very much more effective in VI than in VII, in agreement with the assumed lack of coplanarity of the nitro group at position 7. Other bands in the infrared served to confirm the chemical proofs of structure. Thus hydrogen bonding should be more effective with the amino group of VI than of VII, whether one considers the greater opportunities for internal bonding in VI, the steric blocking of intermolecular bonding to the carbonyl in VII (7), or the greater effect of the nitro group in VI in reducing the shielding of the protons. In fact, the minor isomer from the reduction (VI) had its N—H stretching bands at 3466 and 3353 cm^{-1}, much lower than those of the major isomer (VII) at 3500 and 3402 cm^{-1}. Finally, whether due to resonance, or to the greater opportunities for hydrogen bonding, the compound assigned to VI should have a carbonyl stretching frequency lower than that of the compound thought to be VII; the experimental values were 1749 and 1758 cm^{-1}, respectively. The dinitro compound (IV) showed a band at 1772 cm^{-1}.

Hydroxyl groups do not appreciably bond with phthalide carbonyl groups ortho to them (7, 12), but the fact that VI has a much lower melting point than its geometrically

very similar isomer VII suggests strongly that the amino group in VI is internally bonded to carbonyl. At any rate, this analysis of the situation led one of us (S. S.) to suggest that VI might be more soluble than VII in water. There proved to be a large difference in the solubilities, and extraction of the mixed isomers with hot water led to a rapid separation of the isomers when previously the use of organic solvents had permitted only a very laborious separation of them.

The final item in our qualitative survey of competitive effects in metameconine concerned the activation of the methylene group by nitro groups. Rây and Robinson (1) reported that cotarnine readily condensed with 7-nitrometameconine (V), in which the nitro group is meta to the methylene. Hope and Robinson (13) had long before shown that in similar condensations the activating nitro group might be in any of the ortho, meta, or para positions. Our series of compounds seemed to provide us with the means for a further study of this interesting indifference to position. After a great deal of effort we succeeded in condensing cotarnine and 4,7-dinitrometameconine (IV) to the phthalide–isoquinoline derivative (XI). This proved to be a very labile compound indeed,

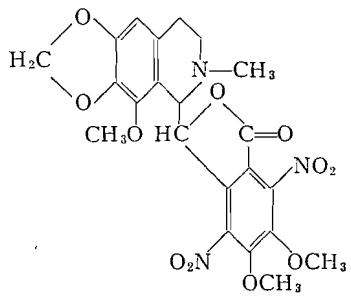

XI

easily reverting to its constituents. Clearly, the success of the condensation depended more upon the management of a mobile equilibrium than it did upon the increasing of the activation of the methylene to increase the rate of reactions. We feel, however, that this work has pointed to a new series of compounds interesting both for their relation to the natural phthalide–isoquinoline alkaloids and for the variety of steric effects possible in them.

EXPERIMENTAL

Infrared spectra were determined using potassium bromide disks containing 0.8% by weight of sample. The spectrometer was a Perkin–Elmer Model 21, with a sodium chloride prism; frequencies below 2000 cm^{-1} were corrected by repeated recalibrations with a polystyrene standard, but frequencies above 2000 cm^{-1} were not corrected. Melting points otherwise unspecified were determined on the Kofler Micro Hot Stage, and lowered 3–5° to agree with the precision capillary melting points of standard compounds. Melting points marked (P) were determined on the precision capillary apparatus (7); two interesting examples of large differences in the two melting points appear below.

4,7-Dinitrometameconine (IV)

Metameconine (I) (28 g, m.p. 154–157°) was added over a period of 1 hour to a mechanically stirred mixture of fuming nitric acid (80 ml, *d* 1.5) and concentrated sulphuric acid (20 ml) which had previously been cooled to 0°; though cooling was continued during the addition, the temperature at times rose as high as 8°. After stirring had been continued for 5 hours longer at 0°, the very dark, reddish reaction mixture was slowly poured onto ice with stirring. Next morning, the yellow precipitate was recovered, very thoroughly washed with water, and dried over sodium hydroxide in the desiccator, yield 25.3 g, m.p. 147.8–151.5°. Recrystallized with slow cooling from 50% aqueous acetic acid, the product was obtained as pale yellow flat plates, yield 22.3 g, or 54%; m.p. 153–154°.

In preliminary experiments, with the use of smaller proportions of the acids, 7-nitrometameconine (V) (1–3) was obtained from the crude nitration product by recrystallization from glacial acetic acid; dilution of the mother liquors with water gave a much larger crop of impure material, m.p. 134–151°. Part of this material was recrystallized six times from 50% aqueous acetic acid to give the analytical sample, m.p. 150.4–151.1° (P). Found: C, 42.51, 42.40; H, 2.88, 2.63; N, 10.68, 10.61; 10.10, 9.88% (repeat). Calc. for $C_{10}H_8O_8N_2$: C, 42.26; H, 2.84; N, 9.86%. The rest was nitrated again, giving after one recrystallization from dilute acetic acid a product of m.p. 153–154° in excellent yield.

Reduction of 4,7-Dinitrometameconine

Recrystallized 4,7-dinitrometameconine (22.5 g, m.p. 150–151°) was mechanically stirred with glacial acetic acid (500 ml) and iron powder (10 g). After 1 hour, the temperature had risen to 48°; after 3 hours, more iron powder (3 g) and acetic acid (100 ml) were added; stirring was then continued for another 11 hours. The red mixture was evaporated *in vacuo* on the rotary evaporator, the residue freed from acetic acid by two evaporations with water *in vacuo*, and then treated with water (200 ml). The insoluble residue was recovered, boiled with water, and filtered hot (the 7-amino-4-nitrometameconine passing into the filtrate). The material insoluble in the hot water was recrystallized from butanol with charcoal; slow cooling gave long bright yellow needles of pure *4-amino-7-nitrometameconine (VII)* in a yield of 15.3 g, or 76%; m.p. 230–231°. The analytical sample, obtained from an earlier run in which water extraction of the isomer was not used, after six recrystallizations from butanol (two with charcoal) had a melting point of 228.6–229.1° (P) (with slight decomposition). Found: C, 47.22, 47.05; H, 4.21, 4.01; N, 11.11, 10.95%. Calc. for $C_{10}H_{10}O_6N_2$: C, 47.24; H, 3.94; N, 11.02%.

The hot water extract of the crude reaction product deposited yellow crystals when cooled and concentrated; m.p. 165–171°. Two more recrystallizations from water gave small amounts of not quite pure *7-amino-4-nitrometameconine (VI)*. The analytical sample was recovered from an early run performed before the discovery of the efficient separation by water. The major isomer was isolated by recrystallization of the mixture from butanol; concentration of the mother liquors gave fractions, one of which was rich in the minor isomer. This fraction was recrystallized once from butanol, and then three times from water to give pure *7-amino-4-nitrometameconine (VI)*, m.p. 177.9–178.5° (P), yield 0.065 g (from 7.5 g of the dinitro compound). Found: C, 47.49, 47.19; H, 4.34, 4.12; N, 11.10%. Calc. for $C_{10}H_{10}O_6N_2$: C, 47.24; H, 3.94; N, 11.02%.

7-Chloro-4-iodometameconine (IX)

Concentrated hydrochloric acid (150 ml) and water (110 ml) were added to 4-amino-7-nitrometameconine (6 g) and the mixture stirred and warmed to 90° to dissolve as much solid as possible. With continued stirring, the mixture was cooled to 0° and kept at 0° during the diazotization. Sodium nitrate (2.7 g) in water (25 ml) was added over a period of 1 hour, the stirring continued for a further 2.5 hours, and the mixture then poured, with stirring, into a solution of potassium iodide (18 g) and urea (15 g) in water (35 ml). After the reaction had subsided, more urea was added, and then sulphur dioxide was passed in for about 1 hour to destroy the iodine formed. The yellow precipitate was recovered, washed with water, and dried; yield 4.0 g, or 48%; m.p. 148–150°. The analytical sample, made in a run in which the diazotization was allowed to proceed 10 hours to ensure the prior extrusion of the nitro group, was recrystallized twice from butanol with charcoal, and then four times from methanol; its melting point was 150.5–151.0° (P). Found: C, 33.89, 34.00; H, 2.29, 2.28; I, 35.69, 35.52%. Calc. for $C_{10}H_8O_4ClI$: C, 33.88; H, 2.28; I, 35.80%.

Under the microscope the analytical sample appeared to exhibit dimorphism, one set of crystals melting at 146° and another at 151°. The precision capillary method, in which the crystals were bathed in their own melt, gave the sharp melting point recorded above. Prolonged attempts to isolate one of the forms did not succeed in changing this behavior.

7-Chlorometameconine (VIII)

(a) By Reduction of the Iodo Compound

An aqueous solution of potassium hydroxide (36 ml, 10%) was heated with 7-chloro-4-iodometameconine (0.36 g) until the solid had dissolved. Zinc dust (1.44 g) was added and the mixture stirred and heated under reflux for 4.5 hours. The zinc was removed by filtration, the filtrate brought almost to boiling, and then slowly acidified with hydrochloric acid. The white crystals were recovered, washed, and dried in a desiccator; their yield was 0.205 g, or 88%, and their melting point (196.5–197.5°) was not depressed by admixture with known 7-chlorometameconine (7).

(b) By Ullmann Reduction of the Iodo Compound

Potassium hydroxide (5 g) dissolved in water (105 ml) was heated under reflux for 3 hours with 7-chloro-4-iodometameconine (1.1 g) and Kaulbaum's copper bronze catalyst (0.96 g). The solution was filtered hot, the filtrate reheated with charcoal, again filtered, and acidified cautiously with hydrochloric acid; after the solution had cooled, the resulting white precipitate was recovered and dried; yield 0.57 g, m.p. 190–197°. The crude material was recrystallized six times (once with charcoal) from water containing a little methanol; the pure sample had a melting point of 196.9–197.6° (P). Its infrared spectrum was identical with that of known 7-chlorometameconine. Found: C, 52.85, 52.58; H, 3.98, 3.85; Cl, 15.99%. Calc. for $C_{10}H_9O_4Cl$: C, 52.55; H, 3.94; Cl, 15.51%.

(c) From 4-Amino-7-nitrometameconine (VII)

Water (50 ml) and concentrated hydrochloric acid (10 ml) were heated to boiling, and 4-amino-7-nitrometameconine (crude, 0.67 g) was slowly added with stirring; the mixture was then cooled and kept at 0° during the addition of a solution of sodium nitrite (0.243 g) in water (15 ml). The addition required 50 minutes; hypophosphorous acid (5.4 ml of 50%) was then added dropwise during 30 minutes. Cooling and stirring were continued 90 minutes longer; the mixture was then kept 6 days in the refrigerator, the resulting precipitate recovered and recrystallized four times from aqueous acetic acid (50%), charcoal being used once. The purified material had a melting point of 195.2–195.8° (P) undepressed by admixture with known 7-chlorometameconine (7); the yield of pure material was 0.262 g, or 44%. Its infrared spectrum was identical with that of authentic material. Found: C, 52.50, 52.79; H, 4.21, 4.21 (N, 0.15%). Calc. for $C_{10}H_9O_4Cl$: C, 52.55; H, 3.94 (N, 0.00%).

Three other preparations gave the same compound in about the same yield.

Diazotization of VII in Absence of Chloride

Sodium nitrite (0.735 g) was added to concentrated sulphuric acid, the mixture warmed, then cooled to 0°. Glacial acetic acid (7.5 ml) was stirred with 4-amino-7-nitrometameconine (1.5 g) while concentrated sulphuric acid (3.9 ml) was slowly added; the clear yellow viscous paste was cooled to 0° and then added over a period of 2 hours to the cooled and stirred solution of the "nitrite". The following experiments showed the great stability of the diazonium group in this system. After excess "nitrous acid" had been destroyed with sulphamic acid, cold absolute ethanol (50 ml) was added slowly to the reaction mixture. There was some initial frothing. The stirrer was then removed and the mixture heated under reflux for 1.5 hours, then evaporated *in vacuo* to about one third its original volume, and poured onto ice with stirring. The yellow precipitate was twice crystallized from ethyl acetate – ligroin with charcoal, and dried; a small sample of the crystals decomposed at 171–172°, but without any violence. The infrared spectrum showed the very sharp, intense peak of the diazonium group at 2200 cm^{-1}.

An attempted diazotization in dilute aqueous sulphuric acid eventually gave back the unchanged amino compound.

Anhydrocotarnine-4,7-dinitro-5,6-dimethoxyphthalide (XI)

Cotarnine (2 g, m.p. 116–118°), purified 4,7-dinitrometameconine (2 g, m.p. 153–154°), and absolute ethanol (200 ml) were stirred together for 2 days at room temperature; the crystals which had deposited were then recovered and dried; their melting point of 152–154° was considerably depressed by admixture with the dinitro compound. The crystalline product was then treated with a mixture of methanol and chloroform (1:1), and filtered from insoluble plate-like crystals which did not melt below 250°. After being chilled in a bath of acetone and solid carbon dioxide, the filtrate yielded bright yellow crystals, m.p. 135–138°. Four more somewhat similar recrystallizations from methanol–chloroform (not above room temperature) gave the analytical sample, m.p. 135.8–136.4° (under the microscope; consistent melting points were obtained on the hot stage, but not in the capillary apparatus). The substance was very sensitive to light. Found: C, 53.04, 52.94; H, 4.65, 4.57; N, 8.19, 8.10%. Calc. for $C_{22}H_{21}O_{11}N_3$: C, 52.49; H, 4.21; N, 8.35%.

The product was very labile. An attempt to bring about the above condensation in boiling ethanol resulted in the recovery of nearly all of the 4,7-dinitrometameconine (identified by m.p. and mixture m.p.). The crude product obtained from condensations performed at lower temperatures suffered extensive decomposition when attempts were made to recrystallize it from boiling solvents (e.g. methanol). In one experiment, the very facile reversal of the condensation was shown. The crude product (m.p. 155–157°, giving a marked depression on admixture with 4,7-dinitrometameconine) was dissolved in acetic acid and the solution cautiously neutralized with ammonia. Long yellow needles separated; they were identified as pure 4,7-dinitrometameconine by their melting point (152–153°) and mixture melting point with authentic material. We did not succeed in isolating cotarnine from the decomposition product. The curious sharp drop in melting point attendant on purification of the condensation product was observed several times.

Two attempts to repeat the work of Rây and Robinson on the condensation of 7-nitrometameconine (V) with cotarnine gave only the original nitro compound, and in high yield; compare refs. 2–4.

ACKNOWLEDGMENTS

The work was made possible by Research Grant A-618 of the National Research Council of Canada. We wish to thank the Howard Smith Paper Company of Cornwall, Ontario, for the generous gift of the vanillin used as the raw material for our work.

REFERENCES

1. J. N. Rây and R. Robinson. J. Chem. Soc. **127**, 1618 (1925).
2. J. A. McRae, R. B. VanOrder, F. H. Griffiths, and T. E. Habgood. Can. J. Chem. **29**, 482 (1951).
3. R. H. Manske, J. A. McRae, and R. Y. Moir. Can. J. Chem. **29**, 526 (1951).
4. M. Allen, A. L. Promislow, and R. Y. Moir. J. Org. Chem. **26**, 2906 (1961).

5. C. K. INGOLD. Structure and mechanism in organic chemistry. Cornell University Press. 1953. p. 268.
6. J. BLAIR and G. T. NEWBOLD. J. Chem. Soc. 3935 (1954).
7. J. A. MCRAE, M. ALLEN, and R. Y. MOIR. Can. J. Chem. **39**, 995 (1961).
8. J. F. BUNNETT and R. E. ZAHLER. Chem. Rev. **49**, 273 (1951).
9. H. E. UNGNADE. Chem. Rev. **38**, 405 (1946).
10. J. A. MCRAE, R. Y. MOIR, J. J. URSPRUNG, and H. H. GIBBS. J. Org. Chem. **19**, 1500 (1954).
11. J. TROTTER. Can. J. Chem. **39**, 1638 (1961).
12. W. R. ALLISON and G. T. NEWBOLD. J. Chem. Soc. 3335 (1959)
13. E. HOPE and R. ROBINSON. Proc. Chem. Soc. **26**, 228 (1910).

NOTES

HYDROGEN ATOM RECOMBINATION IN THE FLOW SYSTEM ATTACHED TO A MASS SPECTROMETER AND USED FOR THE STUDY OF MERCURY-SENSITIZED REACTIONS

P. KEBARLE AND M. AVRAHAMI*

A flow system for the study of mercury-photosensitized reactions with a mass spectrometer has been developed by Lossing (1, 2). The primary decomposition of the compounds studied often leads to the formation of hydrogen atoms. An uncertainty has existed as to the fate of these atoms. The hydrogen atoms could be recombining in the flow system or could be reaching the ion source. In the ion source the atoms could be: (*a*) detected as hydrogen atoms, (*b*) adsorbed on the wall and not detected, (*c*) recombining on the wall and detected as hydrogen.

Experiments in which the sensitized decomposition of hydrogen and deuterium was studied in apparatus similar to that of Lossing were made so as to clear up some of these questions. The hydrogen at 1–10 μ Hg was added to the helium carrier gas (10 mm Hg). The reaction zone is defined by an annular resonance lamp of 3.5-cm length. In the flow tube, below the lamp, is a pinhole leading to the mass spectrometer ion source. The lamp could be moved relative to the sampling leak. When the lamp was 1 cm above the leak, the hydrogen decomposition measured at the leak was 7%. After the lamp was moved 12 cm† upstream the decomposition was only 0.9%. In order to demonstrate that the effect was due to downstream recombination, experiments with a 1:1 hydrogen–deuterium mixture were made. In a typical run, with the lamp in the low position, 16% of the hydrogen had disappeared; however, 19% HD was formed. Thus the unrecombined hydrogen was 6.5%, close to the value observed with hydrogen alone. When the lamp was in the upper position, the hydrogen decomposition was 13%, the HD 25%, i.e. the unrecombined hydrogen was 0.5%. These results clearly show that recombination occurs in the flow system.

A series of runs was made in which the position of the lamp was changed stepwise and the missing hydrogen determined. The results are summarized in Fig. 1. The missing hydrogen was multiplied by 2 and given as H atom concentration. The logarithmic plot gives reasonable straight lines, showing that the recombination is first order and thus occurs on the wall (3). The rate constant obtained is 490 ± 200 sec^{-1}. The error is estimated. The rate constant independent of the reactor tubing radius (3) is $k' = kr/2$ and for $r = 0.4$ cm $k' = 98$ cm/sec. It has been shown by Herzfeld (4) that the recombination coefficient γ does not depend on the presence of a carrier gas when the tubing is not too wide. Using, then, the general formula (3) $\gamma = 2kr/\bar{v}$ we obtain $\gamma = 1.5 \times 10^{-3}$ (silica). This agrees reasonably well with $\gamma = 0.75 \times 10^{-3}$ (pyrex) found by Wise (5) by an entirely different technique. Linnet (6) in a more comprehensive study of the recombination on clean silica and pyrex has shown that γ may be as low as 10^{-4}, depending on the pretreatment of the surface. Therefore the rate constant determined in the present experiments may be expected to give only order of magnitude estimates on the recom-

*University of Alberta postdoctoral fellow.
†*For the flow rate used, 1 cm corresponds to 0.4 millisecond.*

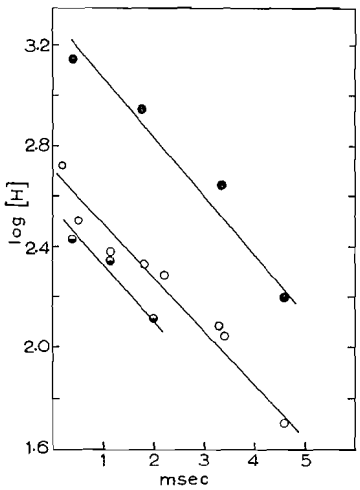

FIG. 1. Plot of downstream hydrogen atom decay giving first-order rate constant: ○, ● H_2 run at two different initial pressures; ◒ $H_2 + D_2$ run. [H] in mμ Hg.

bination of hydrogen atoms in the flow system, but from the results it is at least clear that the recombination is appreciable.

One still has to inquire about the fate of the hydrogen atoms in the ion source. It is evident that, in the experiments where the lamp was closest to the leak, hydrogen atoms were present in sufficient concentration to be detectable with the mass spectrometer. No positive detection could be achieved at mass 1. Since the sensitivity of the instrument at mass 1 could be quite low, while it was known to be adequate at mass 2, an experiment was made in which deuterium was decomposed. A small increase of the mass 2 peak was observed when the lamp was put on. A search of the upper mass range, with the lamp on, revealed no species which could make a contribution to mass 2. The appearance potential of the mass 2 species could not be measured since the concentration was too small, but it could be established that it was lower than that of hydrogen. Therefore, very probably, the peak was due to D atoms. Assuming that the sensitivity of D atoms was equal to half the sensitivity of hydrogen, a balance with the missing D_2 showed that at most 10% of the D atoms was detected. For a D atom pressure of 1 μ, on the high-pressure side of the leak, about 10^{13} atoms/sec enter the mass spectrometer. The instrument has an open ion source (2) and the surface area of the container is larger than 100 cm^2. If each atom were adsorbed on the first collision, it would take many hours before a monolayer (10^{15} atoms/cm^2) could build up. Thus the atoms would be missing, unless an appreciable part was ionized before colliding with a wall. Considering the particle beam, ion source, and pumping geometry, one can estimate that only about 1% of the particles is ionized before collision. Since in the experiment deuterium atoms could be detected, but incompletely, adsorption must occur after a few collisions. In contrast, alkyl radicals are known to withstand hundreds of collisions before adsorption or reaction (7, 8).

1. F. P. LOSSING, D. H. MARSDEN, and J. B. FARMER. Can. J. Chem. **34**, 701 (1956).
2. P. KEBARLE and F. P. LOSSING. Can. J. Chem. **37**, 389 (1959).
3. K. E. SHULER and K. J. LAIDLER. J. Chem. Phys. **17**, 1212 (1949).
4. F. A. PANETH and K. F. HERZFELD. Z. Elektrochem. **37**, 577 (1931).
5. B. J. WOOD and H. WISE. J. Chem. Phys. **29**, 1416 (1958).

6. M. GREEN, K. R. JENNINGS, J. W. LINNET, and D. SCHOFIELD. Trans. Faraday Soc. **55**, 2152 (1959).
7. A. J. B. ROBERTSON. Mass spectrometry. Methuen & Co., London. 1954. p. 108.
8. F. P. LOSSING and A. W. TICKNER. J. Chem. Phys. **20**, 907 (1952).

RECEIVED AUGUST 3, 1962.
CHEMISTRY DEPARTMENT,
UNIVERSITY OF ALBERTA,
EDMONTON, ALBERTA.

REACTIONS OF THE DIMER OF 2,4-TOLYLENE DIISOCYANATE

PRITAM SINGH AND JEAN L. BOIVIN

INTRODUCTION

In a previous paper (1) the uretidine-dione ring in 1,3-bis(4-methyl-3-*n*-butyl-carbamylphenyl)uretidine-2,4-dione was shown to change to an ureylene link by alkaline reduction. With hydrazine hydrate an unsymmetrically monosubstituted urea was obtained, while with hydroxylamine an oxime of the corresponding formamide was formed. Ammonium formate appeared to give the N-substituted amide with the ring unaffected. Further experiments are reported to verify the above reactions, using 1,3-bis[4-methyl-3-(N,N-dibenzylureido)phenyl]uretidine-2,4-dione (1).

DISCUSSION OF RESULTS

As expected, the reduction of 1,3-bis[4-methyl-3-(N,N-dibenzylureido)phenyl]uretidine-2,4-dione, I, by magnesium and methanol gave the symmetrically substituted urea, II. The uretidine-dione ring in the presence of alkali seemed to dissociate and one of the isocyanate groups might be hydrolyzed into an amino group, this latter reacting with the other isocyanate group to form a symmetrically substituted urea.

With ammonium formate, 1,3-bis(4-methyl-3-*n*-butyl-carbamylphenyl)uretidine-2,4-dione was cleaved to form a substituted biuret, by the addition of ammonia, rather than to form the 2,4-bis(N-formamido)uretidine as reported earlier. Although both compounds have the same carbon and hydrogen analysis and the presence of the ring cannot be detected by the carbonyl absorption in the infrared, the latter structure was arrived at when ammonia was found to give the same compound as ammonium formate. It appears that ammonium formate under the conditions used might be dissociating to give ammonia and formic acid, ammonia reacting with the ring.

Ammonium formate reacted in the same way with 1,3-bis[4-methyl-3-(N,N-dibenzylureido)phenyl]uretidine-2,4-dione to give the substituted biuret, IV. The compounds prepared by reaction with ammonia and ammonium formate showed no depression in a mixed melting point determination and the infrared absorption spectra were superimposable.

EXPERIMENTAL

N,N-Bis[4-methyl-3-(N,N-dibenzylureido)phenyl]urea, II

To a stirred suspension of 1,3-bis[4-methyl-3-(N,N-dibenzylureido)phenyl]uretidine-2,4-dione, I (1.0 g), in absolute methanol (30 ml), magnesium turnings (1.0 g) were added in small portions. Then the mixture was heated under reflux for 2 hours, cooled, and evaporated under reduced pressure. Hydrochloric acid (10%, 50 ml) was then added and the mixture warmed to 60° C; it was cooled, filtered, and washed free of acid with water. Crystallization from dimethylformamide–ethanol mixture gave a compound (0.62 g)

6. M. GREEN, K. R. JENNINGS, J. W. LINNET, and D. SCHOFIELD. Trans. Faraday Soc. **55**, 2152 (1959).
7. A. J. B. ROBERTSON. Mass spectrometry. Methuen & Co., London. 1954. p. 108.
8. F. P. LOSSING and A. W. TICKNER. J. Chem. Phys. **20**, 907 (1952).

RECEIVED AUGUST 3, 1962.
CHEMISTRY DEPARTMENT,
UNIVERSITY OF ALBERTA,
EDMONTON, ALBERTA.

REACTIONS OF THE DIMER OF 2,4-TOLYLENE DIISOCYANATE

PRITAM SINGH AND JEAN L. BOIVIN

INTRODUCTION

In a previous paper (1) the uretidine-dione ring in 1,3-bis(4-methyl-3-*n*-butyl-carbamylphenyl)uretidine-2,4-dione was shown to change to an ureylene link by alkaline reduction. With hydrazine hydrate an unsymmetrically monosubstituted urea was obtained, while with hydroxylamine an oxime of the corresponding formamide was formed. Ammonium formate appeared to give the N-substituted amide with the ring unaffected. Further experiments are reported to verify the above reactions, using 1,3-bis[4-methyl-3-(N,N-dibenzylureido)phenyl]uretidine-2,4-dione (1).

DISCUSSION OF RESULTS

As expected, the reduction of 1,3-bis[4-methyl-3-(N,N-dibenzylureido)phenyl]uretidine-2,4-dione, I, by magnesium and methanol gave the symmetrically substituted urea, II. The uretidine-dione ring in the presence of alkali seemed to dissociate and one of the isocyanate groups might be hydrolyzed into an amino group, this latter reacting with the other isocyanate group to form a symmetrically substituted urea.

With ammonium formate, 1,3-bis(4-methyl-3-*n*-butyl-carbamylphenyl)uretidine-2,4-dione was cleaved to form a substituted biuret, by the addition of ammonia, rather than to form the 2,4-bis(N-formamido)uretidine as reported earlier. Although both compounds have the same carbon and hydrogen analysis and the presence of the ring cannot be detected by the carbonyl absorption in the infrared, the latter structure was arrived at when ammonia was found to give the same compound as ammonium formate. It appears that ammonium formate under the conditions used might be dissociating to give ammonia and formic acid, ammonia reacting with the ring.

Ammonium formate reacted in the same way with 1,3-bis[4-methyl-3-(N,N-dibenzylureido)phenyl]uretidine-2,4-dione to give the substituted biuret, IV. The compounds prepared by reaction with ammonia and ammonium formate showed no depression in a mixed melting point determination and the infrared absorption spectra were superimposable.

EXPERIMENTAL

N,N-Bis[4-methyl-3-(N,N-dibenzylureido)phenyl]urea, II

To a stirred suspension of 1,3-bis[4-methyl-3-(N,N-dibenzylureido)phenyl]uretidine-2,4-dione, I (1.0 g), in absolute methanol (30 ml), magnesium turnings (1.0 g) were added in small portions. Then the mixture was heated under reflux for 2 hours, cooled, and evaporated under reduced pressure. Hydrochloric acid (10%, 50 ml) was then added and the mixture warmed to 60° C; it was cooled, filtered, and washed free of acid with water. Crystallization from dimethylformamide–ethanol mixture gave a compound (0.62 g)

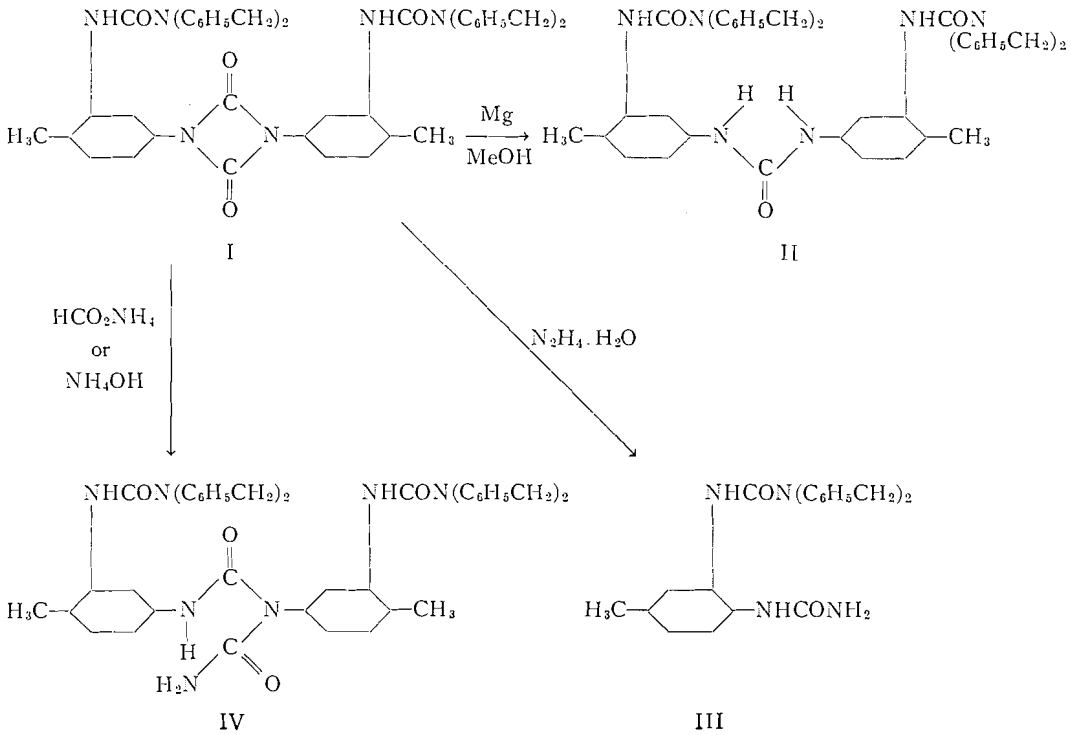

melting at 219–220° C. CO and NH absorptions for the disubstituted urea partial structure were obtained at 1660 cm^{-1} and 1620 cm^{-1} respectively. $\lambda_{max}^{HCON(CH_3)_2}$: 2660 Å, ϵ_{max}: 37,400, inflection point at 2900 Å. Calc. for $C_{45}H_{44}N_6O_3$: C, 75.4; H, 6.14; N, 11.7%. Found: C, 75.0; H, 6.77; N, 11.8%.

N-[4-Methyl-3-(N,N-dibenzylureido)phenyl]urea, III

To a solution of 1,3-bis[4-methyl-3-(N,N-dibenzylureido)phenyl]uretidine-2,4-dione (1.0 g), m.p. 197° C, in ethanol (95%, 20 ml) was added hydrazine hydrate (85%, 3 ml). After the reaction mixture was refluxed for 3 hours with constant stirring, it was cooled, and a crystalline material (0.8 g) melting at 147–150° C was obtained. Further purification by repeated crystallizations from cellosolve–alcohol gave a compound melting at 151–153° C. CO and NH absorption bands for the monosubstituted urea were at 1695 cm^{-1} (s) and 1635 cm^{-1} (s) respectively. Primary amine absorption was at 3340 cm^{-1} (m) and 3050 cm^{-1} (w). $\lambda_{max}^{HCON(CH_3)_2}$: 2860 Å, ϵ_{max}: 3140 and $\lambda_{max}^{HCON(CH_3)_2}$: 2660 Å, ϵ_{max}: 2340. Calc. for $C_{23}H_{24}N_4O_2$: C, 71.1; H, 6.16; N, 14.4%. Found: C, 71.1; H, 6.02; N, 14.6%.

1,3-Bis[4-methyl-3-(N,N-dibenzylureido)phenyl]biuret, IV

To a stirred solution of ammonium formate (1.0 g) in ethanol (30 ml) 1,3-bis[4-methyl-3-(N,N-dibenzylureido)phenyl]uretidine-2,4-dione (1.0 g) was added and the mixture refluxed for 2 hours with constant stirring. The clear solution obtained was evaporated to dryness and taken up with water. The solid was filtered, washed with water, and dried. Yield, 0.7 g. Further crystallization from ethanol gave an analytical sample, m.p. 118° C. CO and NH absorptions for the biuret were at 1720 cm^{-1} (s) and 1670 cm^{-1} (s) respectively. Primary amino group absorptions were at 3410 cm^{-1} (m), 3300 cm^{-1} (m), and 3050 cm^{-1} (m). λ_{max}^{EtOH}: 2300 Å, ϵ_{max}: 3470, inflection point at 2850 Å. Calc. for $C_{46}H_{45}N_7O_4$: C, 72.7; H, 5.9; N, 12.9%. Found: C, 72.5; H, 5.9; N, 13.0%. The same compound was also prepared in identical yield by substituting ammonium hydroxide (12 *N*, 2 ml) for ammonium formate, other reaction conditions being the same.

1,3-Bis[4-methyl-3-n-butyl-carbamylphenyl]biuret

To a solution of ammonium formate (3.0 g) in ethanol (30 ml) was added 1,3-bis[4-methyl-3-*n*-butylcarbamylphenyl]uretidine-2,4-dione (1.0 g) and the mixture refluxed for 2 hours with constant stirring. The solution was evaporated under reduced pressure and diluted with water to give a precipitate, which was filtered and washed with water. Yield, 0.8 g; m.p. 160–162° C. Three crystallizations from ethanol gave the analytical sample with a melting point of 164° C. Molecular weight by Rast method: 525. Free NH stretching frequencies for the primary amino group: 3410 cm^{-1} (m), 3250 cm^{-1} (m), and 3050 cm^{-1} (w). CO and NH absorptions were exhibited at 1720 cm^{-1} (s) and 1660 cm^{-1} (m). λ_{max}^{EtOH}: 2250 Å, ϵ_{max}: 75,900. Calc. for $C_{26}H_{35}N_5O_6$: C, 60.8; H, 6.82; N, 13.7%. Found: C, 60.5; H, 6.62; N, 13.9%.

The same compound was also prepared by substituting ammonium hydroxide (12 *N*, 2 ml) for ammonium formate. However, the yield in this case was lower (0.3 g). No depression of melting point was observed on a mixed melting point determination and the infrared spectra were superimposable.

1. P. Singh and J. L. Boivin. Can. J. Chem. **40**, 935 (1962).

Received June 25, 1962.
Department of Biochemistry,
Laval University,
Quebec, Que.,
and
Chemistry Section,
Canadian Armament Research and
Development Establishment,
Valcartier, Que.

KINETICS OF THE REACTIONS OF ATOMIC HYDROGEN
EFFECT OF DIFFUSION ON THE DETERMINATION OF H ATOM CONCENTRATION

W. R. Schulz and D. J. Le Roy

Voevodsky and Kondratiev (1) have recently criticized the results of Berlie and Le Roy (2) in their study of the kinetics of the reaction of atomic hydrogen with ethane, in which they used the method of Tollefson and Le Roy (3, 4). Their criticism is qualitatively correct, and it is the purpose of the present communication to make appropriate modifications in the theory of the method.

Briefly, the method consists in adding a reactant, say RH, to a gas stream containing about 1% H atoms and 99% H_2, and calculating the H atom concentration downstream from measurements of the rate of heat liberation on a detector which is operated as an isothermal calorimeter. As modified by Berlie and Le Roy (2), the detector is a flat spiral of tungsten or platinum wire extending over most of the cross section of the cylindrical reactor, so that all of the H atoms reaching that position combine on the detector. The difference between the wattage required to keep the detector at a given temperature (or resistance) in the absence of H atoms and in the presence of H atoms was defined as W_H. This can be related to the number of H atoms reaching the detector in unit time, n, by the expression

$$W_H = 4.184\Delta Hn/N, \qquad [1]$$

in which ΔH is the molar enthalpy of formation of atomic hydrogen and N is Avogadro's number. The quantity n was then related to the H atom concentration immediately in front of the detector by the expression

$$n = fA(H), \qquad [2]$$

in which f is the linear flow rate of the gas (almost pure H_2) and A is the cross-sectional area of the reactor.

Following this procedure, they measured W_H as a function of x_0, the distance of the detector from the RH inlet, and equated the rate of H atom consumption, $-d(H)/dt$, to $-(N/4.184\Delta HA)(dW_H/dx_0)$. It was necessary to assume that f remained constant (a reasonable assumption, since there is a negligible change in the total number of moles of gas) and that the H atom concentration between the inlet and the detector was not influenced by the diffusion gradient set up by the complete removal of H atoms at the detector.

The same compound was also prepared by substituting ammonium hydroxide (12 *N*, 2 ml) for ammonium formate. However, the yield in this case was lower (0.3 g). No depression of melting point was observed on a mixed melting point determination and the infrared spectra were superimposable.

1. P. Singh and J. L. Boivin. Can. J. Chem. **40**, 935 (1962).

Received June 25, 1962.
Department of Biochemistry,
Laval University,
Quebec, Que.,
and
Chemistry Section,
Canadian Armament Research and
Development Establishment,
Valcartier, Que.

KINETICS OF THE REACTIONS OF ATOMIC HYDROGEN
EFFECT OF DIFFUSION ON THE DETERMINATION OF H ATOM CONCENTRATION

W. R. Schulz and D. J. Le Roy

Voevodsky and Kondratiev (1) have recently criticized the results of Berlie and Le Roy (2) in their study of the kinetics of the reaction of atomic hydrogen with ethane, in which they used the method of Tollefson and Le Roy (3, 4). Their criticism is qualitatively correct, and it is the purpose of the present communication to make appropriate modifications in the theory of the method.

Briefly, the method consists in adding a reactant, say RH, to a gas stream containing about 1% H atoms and 99% H_2, and calculating the H atom concentration downstream from measurements of the rate of heat liberation on a detector which is operated as an isothermal calorimeter. As modified by Berlie and Le Roy (2), the detector is a flat spiral of tungsten or platinum wire extending over most of the cross section of the cylindrical reactor, so that all of the H atoms reaching that position combine on the detector. The difference between the wattage required to keep the detector at a given temperature (or resistance) in the absence of H atoms and in the presence of H atoms was defined as W_H. This can be related to the number of H atoms reaching the detector in unit time, n, by the expression

$$W_H = 4.184\Delta Hn/N, \qquad [1]$$

in which ΔH is the molar enthalpy of formation of atomic hydrogen and N is Avogadro's number. The quantity n was then related to the H atom concentration immediately in front of the detector by the expression

$$n = fA(\mathrm{H}), \qquad [2]$$

in which f is the linear flow rate of the gas (almost pure H_2) and A is the cross-sectional area of the reactor.

Following this procedure, they measured W_H as a function of x_0, the distance of the detector from the RH inlet, and equated the rate of H atom consumption, $-d(\mathrm{H})/dt$, to $-(N/4.184\Delta HA)(dW_H/dx_0)$. It was necessary to assume that f remained constant (a reasonable assumption, since there is a negligible change in the total number of moles of gas) and that the H atom concentration between the inlet and the detector was not influenced by the diffusion gradient set up by the complete removal of H atoms at the detector.

If the reactions removing atomic hydrogen are all first order in its concentration it is possible to take account of the diffusion effect in a fairly rigorous and simple manner for our experimental conditions. To treat the general case it would be necessary to extend the method of Wise and Ablow (5).

The recombination coefficient on the poisoned walls of the reactor is only of the order of 10^{-4} to 10^{-5} (4), and the total pressures used are of the order of 4 mm. It will therefore be assumed that the H atom concentration will be approximately uniform in any plane normal to the axis of the reactor (5). Equating the net rate of decrease in the H atom concentration in a volume element of cross section A and length dx at a distance x from the RH inlet to the rate of consumption, $k(\mathrm{H})$, it follows that

$$d^2(\mathrm{H})/dx^2-(f/D)d(\mathrm{H})/dx-(k/D)(\mathrm{H}) = 0, \qquad [3]$$

in which D is the diffusion coefficient of atomic hydrogen.

The general solution of [3] is

$$(\mathrm{H}) = C_1e^{-\beta_1 x}+C_2e^{\beta_2 x}, \qquad [4]$$

in which

$$\beta_1 = \frac{f}{2D}\left\{\left(1+\frac{4kD}{f^2}\right)^{1/2}-1\right\}, \qquad [5]$$

$$\beta_2 = \frac{f}{2D}\left\{\left(1+\frac{4kD}{f^2}\right)^{1/2}+1\right\}, \qquad [6]$$

and C_1 and C_2 are to be determined from the boundary conditions. It is convenient to set $(\mathrm{H}) = (\mathrm{H})_0$ at $x = 0$, the point at which the reactant RH is added, from which it follows that $C_1+C_2 = (\mathrm{H})_0$.

If the detector had no influence on H atom concentration one could set $(\mathrm{H}) = 0$ at $x = \infty$, from which it would follow that C_2 would be equal to zero and (H) would be equal to $(\mathrm{H})_0e^{-\beta_1 x}$. This was the procedure adopted by Dickens *et al.* (6) in dealing with the decay of oxygen atom concentration.

Since, in our method, the detector is designed to remove all H atoms reaching it we adopt the boundary condition $(\mathrm{H}) = 0$ at $x = x_0$. With this condition

$$(\mathrm{H}) = (\mathrm{H})_0\frac{e^{\beta_1(x_0-x)}-e^{-\beta_2(x_0-x)}}{e^{\beta_1 x_0}-e^{-\beta_2 x_0}}. \qquad [7]$$

The number of H atoms crossing any plane perpendicular to the axis per unit time is equal to $fA(\mathrm{H})-DAd(\mathrm{H})/dx$. In particular, the number reaching the plane of the detector per unit time will be equal to $-DA(d(\mathrm{H})/dx)_{x=x_0}$, since $(\mathrm{H}) = 0$ at $x = x_0$. Thus, from [1],

$$\frac{W_{\mathrm{H}}N}{4.184\Delta H} = -DA\,(d(\mathrm{H})/dx)_{x=x_0}, \qquad [8]$$

or

$$\frac{W_{\mathrm{H}}N}{4.184\Delta HDA} = (\mathrm{H})_0\frac{(\beta_1+\beta_2)e^{-\beta_1 x_0}}{1-e^{-(\beta_1+\beta_2)x_0}}. \qquad [9]$$

In general $(\mathrm{H})_0$ will depend on x_0 even when the rate of formation of H atoms in the dissociator and the flow rate are kept constant. However, if the values of x_0 are kept

large enough it seems reasonable to assume that $(H)_0$ will be relatively independent of x_0. In our previous procedure the slope of a plot of $-\ln W_H$ vs. x_0 was equated to the first-order rate constant divided by the flow rate. If we define the quantity obtained in this way as k^*, rather than the true rate constant k, then

$$[10] \qquad -\frac{d \ln W_H}{dx_0} \equiv k^*/f = \beta_1 + \frac{\beta_1+\beta_2}{e^{(\beta_1+\beta_2)x_0}-1} - \frac{d \ln (H)_0}{dx_0}.$$

The first approximation to β_1 will be k^*/f. The second term will be small compared to β_1; both it and the third term will vanish as x_0 increases and the two terms tend to cancel each other. It follows that β_1 can be equated to k^*/f if the values of x_0 are large enough for the slope of the $-\ln W_H$ vs. x_0 plot to become constant.

From [5] it is evident that the true rate constant, k, is related to β_1 by the expression

$$[11] \qquad k = \beta_1 f + \beta_1^2 D,$$

or, if the second and third terms of [10] can be neglected,

$$[12] \qquad k = k^* + (k^*)^2 D/f^2.$$

A test of [12] was made by carrying out a number of experiments over a range of values of D and f. No RH was added, so k is the rate constant for H atom consumption in the absence of reactant. The values of D were taken from Amdur (7), and are, of course, inversely proportional to the pressure. The pertinent data are given in Table I. The plots

TABLE I

Effect of flow rate and diffusion coefficient on $\beta_1 f$

Pressure (mm)	f (cm sec^{-1})	D (cm^2 sec^{-1})	$\beta_1 f$ (sec^{-1})	$\beta_1^2 D$ (sec^{-1})	D/f^2 (sec)
3.99	84.4	340.9	2.02	0.196	0.048
3.92	69.0	347.6	1.97	0.282	0.073
4.02	43.4	338.7	1.67	0.508	0.180
3.52	30.6	386.8	1.43	0.844	0.413
3.19	21.8	426.6	1.05	0.983	0.898

Least-squares value of $k = 2.27$ sec^{-1}

of $-\ln W_H$ vs. x_0 were linear over more than 20 cm but fell off close to the RH inlet, where the slope increased, indicating the importance of the second term in equation [10] for small values of x_0. The least-squares slopes of the linear portions of the curves were equated to β_1. In Fig. 1 is shown a plot of $\beta_1 f$ vs. $\beta_1^2 D$, i.e. k^* vs. $(k^*)^2 D/f^2$. The curve is linear, as predicted by the theory, and the least-squares slope of 1.15 is in good agreement with the predicted value of unity.

It should be emphasized that the present treatment is applicable to kinetic processes which are first order in the atom concentration. It has been assumed that W_H is dependent only on the H atom combination on the detector, i.e. that the H atom concentration is much greater than that of any radicals that might combine on the detector or of any excited molecules that might be deactivated on it (8). Gomer has pointed out (9) that any expansion or contraction occurring in a flow system may simulate a first-order reaction. However, under the conditions used in our experiments this effect would be negligible. The initial concentration of H atoms is only about 1%, and if they were completely removed, which is not the case, by combination or the conversion of a higher paraffin to methane the contraction would amount to about 0.5%.

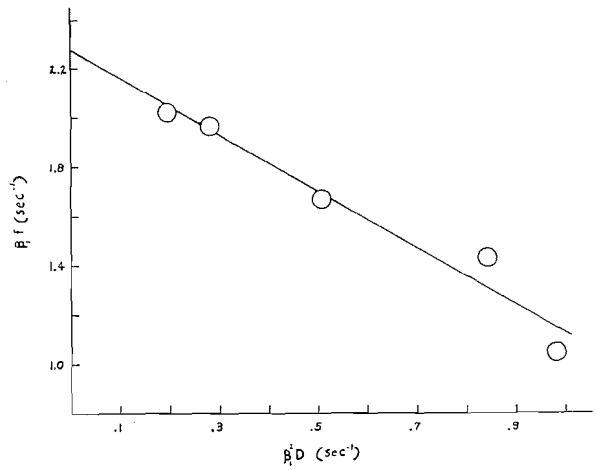

FIG. 1. Test of the relation $k = \beta_1 f + \beta_1^2 D$, or $k = k^* + (k^*)^2 D/f^2$.

The present treatment will be applied, in a forthcoming publication, to some recent work on the reaction of atomic hydrogen with propane.

1. V. V. VOEVODSKY and V. N. KONDRATIEV. Progress in reaction kinetics. Vol. I. G. Porter (*Editor*). Pergamon Press Ltd., Oxford. 1961.
2. M. R. BERLIE and D. J. LE ROY. Discussions Faraday Soc. **14**, 50 (1953).
3. E. L. TOLLEFSON and D. J. LE ROY. J. Chem. Phys. **16**, 1057 (1948).
4. J. R. DINGLE and D. J. LE ROY. J. Chem. Phys. **18**, 1632 (1950).
5. H. WISE and C. M. ABLOW. J. Chem. Phys. **35**, 10 (1961).
6. P. G. DICKENS, R. D. GOULD, J. W. LINNETT, and A. RICHMOND. Nature, **187**, 686 (1960).
7. I. AMDUR. J. Chem. Phys. **4**, 339 (1936).
8. J. E. MORGAN, L. F. PHILLIPS, and H. I. SCHIFF. Discussions of the Faraday Society, Cambridge. April, 1962.
9. R. GOMER. J. Chem. Phys. **19**, 284 (1951).

RECEIVED MARCH 22, 1962.
DEPARTMENT OF CHEMISTRY,
UNIVERSITY OF TORONTO,
TORONTO 5, ONTARIO.

THE STRUCTURE OF TUBEROSTEMONINE[1]

O. E. EDWARDS AND G. FENIAK[2]

The investigations of Götz, Bögri, and Gray (1) have established the structure of tuberostemonine as being either I or II. These formulations were consistent with the work of Professor Uyeo and his colleagues (2), and with the bulk of the evidence accumulated in these laboratories (3). We now present evidence that permits us to assign structure I to the alkaloid.

The n.m.r. spectrum of bisdehydrotuberostemonine (III or IV) in chloroform (3) had two apparent triplets at τ 5.45 and τ 6.9. These signals shifted to τ 6.1 and τ 7.65 in

[1]*Issued as N.R.C. No. 7036.*
[2]*National Research Council of Canada Postdoctorate Fellow.*

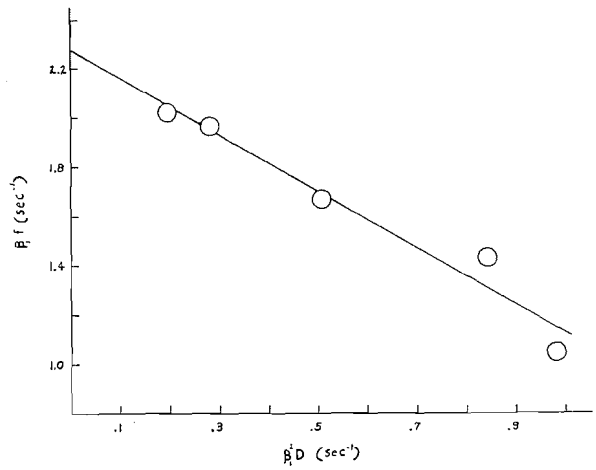

FIG. 1. Test of the relation $k = \beta_1 f + \beta_1^2 D$, or $k = k^* + (k^*)^2 D/f^2$.

The present treatment will be applied, in a forthcoming publication, to some recent work on the reaction of atomic hydrogen with propane.

1. V. V. VOEVODSKY and V. N. KONDRATIEV. Progress in reaction kinetics. Vol. I. G. Porter (*Editor*). Pergamon Press Ltd., Oxford. 1961.
2. M. R. BERLIE and D. J. LE ROY. Discussions Faraday Soc. **14**, 50 (1953).
3. E. L. TOLLEFSON and D. J. LE ROY. J. Chem. Phys. **16**, 1057 (1948).
4. J. R. DINGLE and D. J. LE ROY. J. Chem. Phys. **18**, 1632 (1950).
5. H. WISE and C. M. ABLOW. J. Chem. Phys. **35**, 10 (1961).
6. P. G. DICKENS, R. D. GOULD, J. W. LINNETT, and A. RICHMOND. Nature, **187**, 686 (1960).
7. I. AMDUR. J. Chem. Phys. **4**, 339 (1936).
8. J. E. MORGAN, L. F. PHILLIPS, and H. I. SCHIFF. Discussions of the Faraday Society, Cambridge. April, 1962.
9. R. GOMER. J. Chem. Phys. **19**, 284 (1951).

RECEIVED MARCH 22, 1962.
DEPARTMENT OF CHEMISTRY,
UNIVERSITY OF TORONTO,
TORONTO 5, ONTARIO.

THE STRUCTURE OF TUBEROSTEMONINE[1]

O. E. EDWARDS AND G. FENIAK[2]

The investigations of Götz, Bögri, and Gray (1) have established the structure of tuberostemonine as being either I or II. These formulations were consistent with the work of Professor Uyeo and his colleagues (2), and with the bulk of the evidence accumulated in these laboratories (3). We now present evidence that permits us to assign structure I to the alkaloid.

The n.m.r. spectrum of bisdehydrotuberostemonine (III or IV) in chloroform (3) had two apparent triplets at τ 5.45 and τ 6.9. These signals shifted to τ 6.1 and τ 7.65 in

[1]*Issued as N.R.C. No. 7036.*
[2]*National Research Council of Canada Postdoctorate Fellow.*

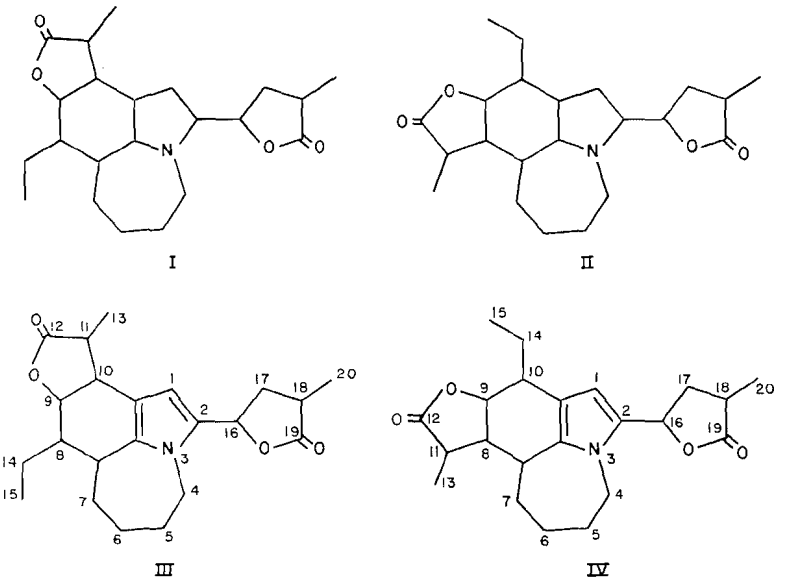

I II III IV

pyridine but retained their structure, confirming their true triplet character. Because of its chemical shift and the fact that it is a triplet, the signal at τ 5.45 can unambiguously be assigned to the hydrogen on C_9.[3,4] The similarity in the splitting of the signals at τ 5.45 and τ 6.9 (J = 6.5 c.p.s. in each case) suggested that the hydrogens responsible for these signals were on adjacent carbon atoms. If this were so, the signal at τ 6.9 would clearly be that of the hydrogen attached to C_{10}, which would be deshielded by the pyrrole ring and nearby oxygen atoms. The simplicity of this signal would not be consistent with structure IV for bisdehydrotuberostemonine since the C_{10} hydrogen in structure IV would give rise to at least a four-line multiplet.

It appeared that the spin decoupling technique could be used to establish whether the hydrogens giving rise to the signals at τ 5.45 and τ 6.9 were actually on adjacent carbon atoms. The method described by Kaiser (4) was used. It proved necessary to use an audiomodulation frequency of 85 c.p.s. rather than 92 c.p.s. (which corresponds to the chemical shift between the two signals) to avoid overlap of signals. The intensity of the decoupling magnetic field had to be increased to compensate for this. Under these conditions the upper side band of the τ 5.45 signal and the lower side band of the τ 6.9 signal were reduced to doublets (J = 6.5 c.p.s. in both cases) and there was no sign of other decoupling occurring in the vicinity of these signals. This proved that the two hydrogens in question were indeed on adjacent carbons. It follows that bisdehydrotuberostemonine has structure III and that tuberostemonine is correctly represented by I.

We are grateful to Dr. F. A. L. Anet for the spin decoupled spectrum and advice on its interpretation.

[3]*From its chemical shift, the quartet at τ 4.6 must also be due to a hydrogen of the type* H—C(|)—O—. *Since this signal is not present in the n.m.r. spectrum of the methyl ester of the acid obtained by hydrogenolysis of bisdehydrotuberostemonine (3), it must be due to the allylic hydrogen on* C_{16}.

[4]*The numbering system is based on that given for azepino[3,2,1-hi]indole in Patterson et al. (A. M. Patterson, L. T. Capell, and D. F. Walker. The ring index. American Chemical Society Publications, Washington. 1960).*

1. M. GÖTZ, T. BÖGRI, and A. H. GRAY. Tetrahedron Letters, **20**, 707 (1961).
2. T. SHINGU, Y. TSUDA, S. UYEO, Y. YAMATO, and (in part) H. HARADA. Chem. Ind. (London), 1191 (1962).
3. O. E. EDWARDS, G. FENIAK, and K. L. HANDA. Can. J. Chem. **40**, 455 (1962).
4. R. KAISER. Rev. Sci. Instr. **31**, 963 (1960).

RECEIVED AUGUST 15, 1962.
DIVISION OF PURE CHEMISTRY,
NATIONAL RESEARCH COUNCIL,
OTTAWA, CANADA.

ON PAOLONI'S NOTE ENTITLED: THE STRUCTURE OF CARBOLINES AND RELATED COMPOUNDS

R. A. ABRAMOVITCH

In a recent note (1), Paoloni has alleged that a phrase, quoted by Abramovitch and Adams (2) from his original paper (3), is not a *verbatim* translation of any sentence in that paper, "but is, on the best, the abstract of their interpretation of the last paragraph of p. 1532 of reference 2" (1). Both of these statements are incorrect. The phrase does indeed appear in Paoloni's original paper, on p. 1538, l. 16–18. The sentence, of which the phrase quoted is a part, appears in a discussion of the charge distributions as calculated by him, and reads as follows (my italics): "Su questa posizione si trova ora un eccesso negativo, che *illustra in maniera eloquente il compromesso tra la tendenza alla formazione del sestetto e quella al bilanciamento delle cariche*, sottolineata da R. Robinson[1] come una necessità strutturale" (3). The phrase italicized above was translated (2) as follows: "illustrate eloquently the compromise between the tendency to form the sextet and that to neutralize the charges".

1. L. PAOLONI. Can. J. Chem. **40**, 1717 (1962).
2. R. A. ABRAMOVITCH and K. A. H. ADAMS. Can. J. Chem. **39**, 2516 (1961).
3. L. PAOLONI. Gazz. Chim. Ital. **90**, 1530 (1960).

RECEIVED OCTOBER 16, 1962.
DEPARTMENT OF CHEMISTRY,
UNIVERSITY OF SASKATCHEWAN,
SASKATOON, SASKATCHEWAN.

1. M. GÖTZ, T. BÖGRI, and A. H. GRAY. Tetrahedron Letters, **20**, 707 (1961).
2. T. SHINGU, Y. TSUDA, S. UYEO, Y. YAMATO, and (in part) H. HARADA. Chem. Ind. (London), 1191 (1962).
3. O. E. EDWARDS, G. FENIAK, and K. L. HANDA. Can. J. Chem. **40**, 455 (1962).
4. R. KAISER. Rev. Sci. Instr. **31**, 963 (1960).

RECEIVED AUGUST 15, 1962.
DIVISION OF PURE CHEMISTRY,
NATIONAL RESEARCH COUNCIL,
OTTAWA, CANADA.

ON PAOLONI'S NOTE ENTITLED: THE STRUCTURE OF CARBOLINES AND RELATED COMPOUNDS

R. A. ABRAMOVITCH

In a recent note (1), Paoloni has alleged that a phrase, quoted by Abramovitch and Adams (2) from his original paper (3), is not a *verbatim* translation of any sentence in that paper, "but is, on the best, the abstract of their interpretation of the last paragraph of p. 1532 of reference 2" (1). Both of these statements are incorrect. The phrase does indeed appear in Paoloni's original paper, on p. 1538, l. 16–18. The sentence, of which the phrase quoted is a part, appears in a discussion of the charge distributions as calculated by him, and reads as follows (my italics): "Su questa posizione si trova ora un eccesso negativo, che *illustra in maniera eloquente il compromesso tra la tendenza alla formazione del sestetto e quella al bilanciamento delle cariche*, sottolineata da R. Robinson[1] come una necessità strutturale" (3). The phrase italicized above was translated (2) as follows: "illustrate eloquently the compromise between the tendency to form the sextet and that to neutralize the charges".

1. L. PAOLONI. Can. J. Chem. **40**, 1717 (1962).
2. R. A. ABRAMOVITCH and K. A. H. ADAMS. Can. J. Chem. **39**, 2516 (1961).
3. L. PAOLONI. Gazz. Chim. Ital. **90**, 1530 (1960).

RECEIVED OCTOBER 16, 1962.
DEPARTMENT OF CHEMISTRY,
UNIVERSITY OF SASKATCHEWAN,
SASKATOON, SASKATCHEWAN.